

VOLUME 23
1983
ACC. NOS. A83-10001 TO A83-50211

IAA

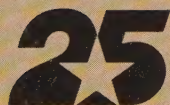
DOMESTIC & FOREIGN

International Aerospace Abstracts Annual Index 1983

Part One

PERIODICALS SCANNED
SUBJECT A-L

UIC
FEB 24 1984
LIBRARY



25th Anniversary
1958-1983

PRODUCED FOR THE
SCIENTIFIC AND TECHNICAL
INFORMATION
BRANCH

NASA





Digitized by the Internet Archive
in 2023

INTERNATIONAL AEROSPACE ABSTRACTS

TL
500
157

ANNUAL
CUMULATIVE
INDEX

PART 1

PERIODICALS SCANNED, SUBJECT INDEX, A — L

VOLUME 23

JANUARY — DECEMBER

1983

UIC
FEB 24 1984
LIBRARY

ACCESSION NUMBERS A83-10001 to A83-50211

INTERNATIONAL AEROSPACE ABSTRACTS is prepared and published semimonthly (except January, which has three issues) by the Technical Information Service, American Institute of Aeronautics and Astronautics, Inc., for the Institute and the National Aeronautics and Space Administration under Contract No. NASW-3520.

SUBSCRIPTION INFORMATION. Semi-monthly issues: United States and Possessions, 1 year, \$525 postpaid; all other countries, 1 year, \$750 postpaid. Cumulative index volume: United States and Possessions, 1 year, \$300 postpaid; all other countries, 1 year, \$425 postpaid. Full service subscription (semi-monthly issues and cumulative index): United States and Possessions, 1 year, \$750 postpaid; all other countries, 1 year, \$1050 postpaid.

EDITORIAL OFFICE: 555 West 57th Street, New York, NY 10019. SUBSCRIPTION OFFICES: 555 West 57th Street, New York, NY 10019; 1425 Third Avenue, Alpha, NJ 08865. Second-class postage paid at New York, NY, and at additional mailing offices. POSTMASTER: Send address changes to AIAA/TIS, 555 West 57th Street, New York, NY 10019. Copyright © 1984 by the American Institute of Aeronautics and Astronautics, Inc. (The index, however, may be reproduced for any bibliographic purpose.)
TELEPHONE: 212 247-6500

CONTENTS

PART 1

INTRODUCTION	iii
HOW TO OBTAIN PUBLICATIONS ANNOUNCED	iv
CROSS REFERENCES	iv
PERIODICALS SCANNED	v — xxi
SUBJECT INDEX, A — L	A1 — A884

PART 2

INTRODUCTION	iii
HOW TO OBTAIN PUBLICATIONS ANNOUNCED	iv
CROSS REFERENCES	iv
SUBJECT INDEX, M — Z	A885 — A1785

PART 3

INTRODUCTION	iii
HOW TO OBTAIN PUBLICATIONS ANNOUNCED	iv
PERSONAL AUTHOR INDEX	B1 — B1098
CONTRACT NUMBER INDEX	C1 — C39
MEETING PAPER & REPORT NUMBER INDEX	D1 — D16
ACCESSION NUMBER INDEX	E1 — E71

INTERNATIONAL AEROSPACE ABSTRACTS

Irene W. Bogolubsky, *Editor*
 Nanu Davis, *Abstracts Editor*
 Thomas Cheung, *Index Editor*

AIAA TECHNICAL INFORMATION SERVICE

Administrator, Barbara Lawrence
 Director—Technical, Irene W. Bogolubsky
 Director—Administrative, Dwain W. Smith
 Director—Library Resources, Patricia M. Marshall

INTRODUCTION

INTERNATIONAL AEROSPACE ABSTRACTS (IAA) is an abstracting and indexing service covering the world's published literature in the field of aeronautics and space science and technology. IAA is issued semimonthly, on the 1st and 15th of each month.

Coverage of Published Literature

The following types of publications are covered in IAA:

- Periodicals (including government-sponsored journals) and books.
- Meeting papers and conference proceedings issued by professional societies and academic organizations.
- Translations of journals and journal articles.

Coverage of Reports ("Unpublished" Literature)

Abstracts and indexes of report literature are issued in SCIENTIFIC AND TECHNICAL AEROSPACE REPORTS (STAR), which is published by the Scientific and Technical Information Branch, National Aeronautics and Space Administration.

By special arrangement between NASA and the American Institute of Aeronautics and Astronautics, IAA is issued in coordination with the twice-monthly schedule of STAR, which appears on the 8th and 23rd of each month.

IAA and STAR both utilize identical subject categories and indexes, which are described below.

Thus the two services provide comprehensive access to the national and international unclassified report and published literature of current significance to aerospace science and technology.

Arrangement of the Semi-monthly Issues

IAA is arranged in two major sections:

- (1) Abstracts Section. This section contains complete bibliographic citations with informative abstracts as required, arranged by appropriate subject categories to facilitate scanning. There are 75 subject categories, and the scope of each is outlined in the Table of Contents and again as they appear in the Abstracts Section. Each entry is prefixed by the IAA accession number.
- (2) Index Section. Five indexes are contained in this section: Subject, Personal Author, Contract Number, Meeting Paper and Report Number, and Accession Number. Each index is prefaced by explanatory notes.

Cumulative Index

A cumulative index appears each year. The Annual Cumulative Index, distributed in January, covers all 24 issues published from January to December.

The cumulative index contains the following sections: A—Subject Index, B—Personal Author Index, C—Contract Number Index, D—Meeting Paper and Report Number Index, and E—Accession Number Index.

Indexing Vocabulary

The 1982 Edition of the NASA THESAURUS (NASA SP-7051) is the authority for the indexing vocabulary that appears in the subject indexes to STAR and IAA. The NASA Thesaurus should be consulted for a total picture of the current indexing vocabulary and associated cross-reference structure. Copies of the NASA Thesaurus may be obtained from the National Technical Information Service (NTIS), Springfield, VA 22161 at a price of \$55. for the two-volume set.

Information regarding SCIENTIFIC AND TECHNICAL AEROSPACE REPORTS may be obtained from the following address:

National Aeronautics and Space Administration
Scientific and Technical Information Branch
Attention: Code NIT—44
Washington, DC 20546

how to obtain publications announced

Documents announced are available from the AIAA Technical Information Service as follows:

- Paper copies of accessions announced in IAA and STAR and of other documents in the TIS library are available at \$8.50 per document.
- Microfiche of documents announced in IAA are available at the rate of \$1.45 per microfiche for standing orders for all IAA microfiche, and at the rate of \$4.00 per microfiche for individual documents on demand. Documents available in this manner are identified by the symbol † following the accession number in the Abstracts Section and the symbol # in the Abstracts Section and in the Meeting Paper and Report Number and the Accession Number Indexes.
- Minimum air-mail postage to foreign countries is \$2.50.
- A number of publications, because of their special characteristics, are available only for reference in the library.

Address all inquiries and requests to:

Technical Information Service
American Institute of Aeronautics
and Astronautics, Inc.
555 West 57th Street, New York, NY 10019

Telephone: 212 247-6500

**PLEASE REFER TO THE ACCESSION NUMBER WHEN
REQUESTING PUBLICATIONS**

CROSS REFERENCES

The subject index includes two types of cross references to aid the user of the index in locating the material being sought:

1. "USE" references (U) direct the user to alternate headings under which material on the subject will be found, for example

COLUMBIUM
U NIOBIUM

2. "NARROWER TERM" references (NT) refer the user to more specific headings in the same subject area, for example

LUMINESCENCE
NT ELECTROLUMINESCENCE

The periodicals listed in this section contain material accessioned in *International Aerospace Abstracts* in 1983. The eight-digit hyphenated number at the end of a listing represents the ISSN number. The periodicals were received regularly in all but a few instances. In the case of titles preceded by an asterisk, only the articles announced in *International Aerospace Abstracts* are available. All announced articles can be obtained from the AIAA Technical Information Service.

BM —Bimonthly
BW —Biweekly
Irreg. —Irregular
M —Monthly

Q —Quarterly
SA —Semi-annual
SM —Semi-monthly
W —Weekly

Academia Scientiarum Fennica, Annales, Series A I - Mathematica. Helsinki. Irreg. 0066-1953

Académie des Sciences (Paris), Comptes Rendus, Série II - Mécanique, Physique, Chimie, Sciences de l'Univers, Sciences de la Terre. Académie des Sciences; Gauthier-Villars, Paris. W 0249-6305

**Académie des Sciences (Paris), Comptes Rendus, Vie Académique.* Académie des Sciences; Gauthier-Villars, Paris.

Académie Royale de Belgique, Classe des Sciences, Bulletin. Académie Royale de Belgique; Office International de Librairie, Brussels. BM 0001-4141

Académie Serbe des Sciences et des Arts, Bulletin, Classe des Sciences Techniques. Académie Serbe des Sciences et des Arts, Belgrade. Irreg.

ACM, Communications. Association for Computing Machinery, Baltimore, MD M 0001-0782

ACM Transactions on Graphics. Association for Computing Machinery, Inc., Baltimore, MD Q 0730-0301

Acoustical Society of America, Journal. Acoustical Society of America; American Institute of Physics, Inc., New York. M 0001-4966

Acta Aerodynamica Sinica. Chinese Aerodynamics Research Society, Beijing. Q

Acta Aeronautica et Astronautica Sinica. Chinese Society of Aeronautics and Astronautics, Beijing. Q

Acta Astronautica. International Academy of Astronautics; Pergamon Press, Inc., Elmsford, NY BM 0094-5765

Acta Astronomica. Polska Akademia Nauk; Państwowe Wydawnictwo Naukowe, Warsaw. Q 0001-5237

Acta Astronomica Sinica. Academia Sinica, Beijing. SA 0001-5245

Acta Geophysica Polonica. Polska Akademia Nauk; Państwowe Wydawnictwo Naukowe, Warsaw. Q 0001-5725

Acta Mechanica. Springer Verlag, Vienna. 8 issues per year 0001-5970

Acta Mechanica Solida Sinica. Chinese Society for Theoretical and Applied Mechanics, Beijing.

Acta Metallurgica. Pergamon Press, Inc., Elmsford, NY M 0001-6160

Acta Metallurgica Sinica. Academia Sinica, Beijing. Irreg. 0412-1961

Acta Physica Sinica. Academia Sinica, Beijing. BM 0512-4182

Acta Polytechnica Scandinavica, Chemistry Including Metallurgy Series. Scandinavian Council for Applied Research, Stockholm. Irreg. 0001-6853

Acta Polytechnica Scandinavica, Electrical Engineering

Series. Finnish Academy of Technical Sciences, Helsinki. Irreg. 0001-6845

Acta Polytechnica Scandinavica, Mathematics and Computer Science Series. Finnish Academy of Technical Sciences, Helsinki. Irreg. 0355-2713

Acta Technica. Akadémiai Kiadó, Budapest. Q 0001-7035

Acta Technica ČSAV. Československá Akademie Věd, Prague. BM 0001-7043

Acta Universitatis Lodzensis. Uniwersytet Lodzki, Lodz, Poland. Irreg. 0208-6026

Advances in Space Research. COSPAR, Paris; Pergamon Press, Inc., Elmsford, NY Irreg. 0273-1177

Aeronautical Journal. Royal Aeronautical Society, London. M 0001-9240

Aeronautical Quarterly. Royal Aeronautical Society, London. Q 0001-9259

Aeronautical Society of India, Journal. Aeronautical Society of India, New Delhi. Q 0001-9267

L'Aéronautique et l'Astronautique. Association Française des Ingénieurs et Techniciens de l'Aéronautique et de l'Espace and Société Française de l'Astronautique; Editions Air & Cosmos, Paris. BM 0001-9275

**Aerosol, Science and Technology.* Elsevier Science Publishing Co., Inc., New York, NY 4 issues per year

Aerospace (UK). Royal Aeronautical Society, London. M 0305-0831

Aerospace Dynamics. British Aerospace Dynamics Group, Stevenage, Herts., England. 3 issues per year 0263-2012

Aerospace Engineering (see *SAE in Aerospace Engineering*).

AIAA Journal. American Institute of Aeronautics and Astronautics, Inc., New York. M 0001-1452

AIAA Student Journal. American Institute of Aeronautics and Astronautics, Inc., New York. Q 0001-1460

AIChE Journal. American Institute of Chemical Engineers, New York. BM 0001-1541

Aircraft Engineering. Bunhill Publications, Ltd., London. M 0002-2667

Airet Cosmos. Paris. W 0044-6971

Air Force Magazine. Air Force Association, Washington, DC M 0730-6784

Air International. Fine Scroll, Ltd., London. M 0306-5634

Air Law. Kluwer B. V., Deventer, Netherlands. Q 0165-2079

Air Pollution Control Association, Journal. Air Pollution Control Association, Pittsburgh, PA M 0002-2470

- Airport Forum*. Bauverlag GmbH, Wiesbaden, West Germany. BM 0002-2802
- Airship*. Airship Association; London.
- **Akademiia Meditsinskikh Nauk SSSR, Vestnik*. Akademiia Meditsinskikh Nauk; Izdatel'stvo Meditsina, Moscow. M 0002-3027
- Akademiia Nauk Armianskoi SSR, Izvestiia, Mekhanika*. Akademiia Nauk Armianskoi SSR, Yerevan. BM 0002-3051
- Akademiia Nauk Azerbaidzhanskoi SSR, Doklady*. Akademiia Nauk Azerbaidzhanskoi SSR; Izdatel'stvo Elm, Baku. M 0002-3078
- Akademiia Nauk BSSR, Doklady*. Akademiia Nauk Belorusskoi SSR, Minsk. M 0002-354X
- Akademiia Nauk Gruzinskoi SSR, Soobshcheniia*. Akademiia Nauk Gruzinskoi SSR, Tiflis. M 0132-1447
- **Akademiia Nauk Kirgizskoi SSR, Izvestiia*. Akademiia Nauk Kirgizskoi SSR, Izdatel'stvo Ilim, Frunze. BM 0002-3221
- Akademiia Nauk SSSR, Doklady*. Akademiia Nauk SSSR; Izdatel'stvo Nauka, Moscow. 36 issues per year 0002-3264
- Akademiia Nauk SSSR, Izvestiia, Energetika i Transport*. Akademiia Nauk SSSR; Izdatel'stvo Nauka, Moscow. BM 0002-3310
- Akademiia Nauk SSSR, Izvestiia, Fizika Atmosfery i Okeana*. Akademiia Nauk SSSR; Izdatel'stvo Nauka, Moscow. M 0002-3515
- Akademiia Nauk SSSR, Izvestiia, Mekhanika Tverdogo Tela*. Akademiia Nauk SSSR; Izdatel'stvo Nauka, Moscow. BM 0572-3299
- Akademiia Nauk SSSR, Izvestiia, Mekhanika Zhidkosti i Gaza*. Akademiia Nauk SSSR; Izdatel'stvo Nauka, Moscow. BM 0568-5281
- Akademiia Nauk SSSR, Izvestiia, Metally*. Akademiia Nauk SSSR; Izdatel'stvo Nauka, Moscow. BM 0568-5303
- Akademiia Nauk SSSR, Izvestiia, Seriya Biologicheskaiia*. Akademiia Nauk SSSR; Izdatel'stvo Nauka, Moscow. BM 0002-3329
- Akademiia Nauk SSSR, Izvestiia, Seriya Fizicheskaiia*. Akademiia Nauk SSSR; Izdatel'stvo Nauka, Moscow. M 0367-6755
- **Akademiia Nauk SSSR, Sibirskoe Otdelenie, Izvestiia, Seriya Biologicheskikh Nauk*. Akademiia Nauk SSSR, Sibirskoe Otdelenie; Izdatel'stvo Nauka, Novosibirsk. 3 vols. per year
- Akademiia Nauk SSSR, Sibirskoe Otdelenie, Izvestiia, Seriya Tekhnicheskikh Nauk*. Akademiia Nauk SSSR, Sibirskoe Otdelenie; Izdatel'stvo Nauka, Novosibirsk. 3 issues per year. 0134-2428
- Akademiia Nauk Tadzhikskoi SSR, Doklady*. Akademiia Nauk Tadzhikskoi SSR; Izdatel'stvo Donish, Dushanbe. M 0002-3469
- Akademiia Nauk Tadzhikskoi SSR, Institut Astrofiziki, Biulleten'*. Akademiia Nauk Tadzhikskoi SSR; Izdatel'stvo Donish, Dushanbe. Irreg. 0321-4885
- Akademiia Nauk Turkmeniskoi SSR, Izvestiia, Seriya Fiziko-Tekhnicheskikh, Khimicheskikh i Geologicheskikh Nauk*. Akademiia Nauk Turkmeniskoi SSR; Izdatel'stvo Ylym, Ashkhabad. BM 0002-3507
- Akademiia Nauk Ukrainskoi RSR, Dopovidy, Seriya A - Fiziko-Matematichni ta Tekhnichni Nauki*. Akademiia Nauk Ukrainskoi RSR; Izdatel'stvo Naukova Dumka, Kiev. M 0002-3531
- Akademiia Nauk Ukrainskoi RSR, Dopovidy, Seriya B - Geologichni, Khimichni ta Biologichni Nauki*. Akademiia Nauk Ukrainskoi RSR; Izdatel'stvo Naukova Dumka, Kiev. M 0002-3523
- Akademiia Nauk Ukrainskoi RSR, Visnik*. Akademiia Nauk Ukrainskoi RSR; Izdatel'stvo Naukova Dumka, Kiev. M 0372-6436
- Akademiia Nauk Uzbekskoi SSR, Doklady*. Akademiia Nauk Uzbekskoi SSR, Tashkent. M 0134-4307
- Akustika i Ul'trazvukovaia Tekhnika*. Ministerstvo Vysshego i Srednego Spetsial'nogo Obrazovaniia USSR; Izdatel'stvo Tekhnika, Kiev. Irreg. 0321-477X
- Alta Frequenza* (English Edition). Associazione Elettrotecnica ed Elettronica Italiana, Milan. M 0002-6557
- American Ceramic Society, Bulletin*. American Ceramic Society, Inc., Columbus, OH M 0002-7812
- American Ceramic Society, Journal*. American Ceramic Society, Inc., Columbus, OH BM 0002-7820
- American Chemical Society, Journal*. American Chemical Society, Washington, DC BW 0002-7863
- American Helicopter Society, Journal*. American Helicopter Society, Inc., Washington, DC Q 0002-8711
- **American Journal of Physics*. American Association of Physics Teachers; American Institute of Physics, Inc., New York. M 0002-9505
- American Journal of Physiology*. American Physiological Society, Bethesda, MD M 0002-9513
- American Journal of Physiology: Regulatory, Integrative and Comparative Physiology* (see *American Journal of Physiology: Regulatory, Integrative and Comparative Physiology*).
- **American Journal of Physiology: Regulatory, Integrative and Comparative Physiology*. American Physiological Society, Bethesda, MD BM 0363-6119
- American Meteorological Society, Bulletin*. American Meteorological Society, Boston. M 0003-0007
- **American Mineralogist*. Mineralogical Society of America, Washington, DC BM 0003-004X
- American Scientist*. New Haven, CT M 0003-0996
- **Analytical Chemistry*. American Chemical Society, Washington, DC M 0003-2700
- Annales de Géophysique*. Centre National de la Recherche Scientifique, Paris. Q 0003-4029
- Annales des Télécommunications*. Centre National d'Etudes des Télécommunications, Issy-les-Moulineaux (Hauts-de-Seine), France. BM 0003-4347
- Annales Geophysicae*. European Geophysical Society; Gauthier-Villars, Paris. BM
- Antenny*. Nauchno-Tekhnicheskoe Obshchestvo Radiotekhniki i Elektrosviazi im. A. S. Popova; Izdatel'stvo Sviaz', Moscow. Irreg. 0320-9601
- **Applications of Surface Science*. North-Holland Publishing Co., Amsterdam. Q 0378-5963
- Applied Energy*. Applied Science Publishers, Ltd., Barking, Essex, England. Q 0306-2619
- Applied Mathematical Modelling*. IPC Science and Technology Press, Ltd., Guildford, Surrey, England. Q 0307-940X
- Applied Mathematics and Computation*. Elsevier/North-Holland Publishing Co., New York. Q 0096-3003
- Applied Mathematics and Optimization*. Springer Verlag, Inc., New York. Q 0095-4616
- Applied Mechanics Reviews*. American Society of Mechanical Engineers, New York. M 0003-6900
- **Applied Neurophysiology*. S. Karger AG, Basel. Q 0302-2773
- Applied Optics*. Optical Society of America; American Institute of Physics, Inc., New York. M 0003-6935
- Applied Physics A - Solids and Surfaces*. Deutsche physikalische Gesellschaft; Springer Verlag, Berlin, West Germany. M 0721-7250
- Applied Physics B - Photophysics and Laser Chemistry*. Deutsche physikalische Gesellschaft; Springer Verlag, Berlin, West Germany. M 0721-7269
- Applied Physics Communications*. Marcel Dekker, Inc., New York, NY 0277-9374

- Applied Physics Letters*. American Institute of Physics, Inc., New York. SM 0003-6951
- Applied Scientific Research*. Martinus Nijhoff, The Hague. BM 0003-6994
- Applied Spectroscopy*. Society for Applied Spectroscopy, Baltimore, MD BM 0003-7028
- Arabian Journal for Science and Engineering*. University of Petroleum and Minerals, Dhahran, Saudi Arabia. SA 0377-9211
- Archiv für Elektronik und Übertragungstechnik*. S. Hirzel Verlag, KG, Stuttgart, West Germany. M 0001-1096
- Archive for Rational Mechanics and Analysis*. Springer Verlag, Berlin, West Germany. Irreg. 0003-9527
- Archives for Meteorology, Geophysics, and Bioclimatology, Series A - Meteorology and Geophysics*. Springer Verlag, Vienna. Irreg. 0066-6416
- **Archives of Gerontology and Geriatrics*. Elsevier Biomedical Press, Amsterdam. 0167-4943
- Archiwum Automatyki i Telemechaniki*. Polska Akademia Nauk; Państwowe Wydawnictwo Naukowe, Warsaw. Q 0004-072X
- Archiwum Mechaniki Stosowanej*. Polska Akademia Nauk, Instytut Podstawowych Problemów Techniki; Państwowe Wydawnictwo Naukowe, Warsaw. BM 0373-2029
- **Arkhiv Anatomii, Gistologii i Embriologii*. Akademiia Meditsinskikh Nauk SSSR, Moscow; Izdatel'stvo Meditsina, Leningrad. M 0004-1947
- **Arkhiv Patologii*. Akademiia Meditsinskikh Nauk SSSR; Vsesoiuznoe Nauchnoe Obshchestvo Patologoanatomov; Izdatel'stvo Meditsina, Moscow. M 0004-1955
- Artificial Satellites - Planetary Geodesy*. Polska Akademia Nauk, Centrum Badan Kosmicznych; Państwowe Wydawnictwo Naukowe, Warsaw. Q 0208-841X
- ASCE, Transportation Engineering Journal*. American Society of Civil Engineers, New York. Q 0568-7891
- ASLE Transactions*. American Society of Lubrication Engineers, Park Ridge, IL Q
- ASME, Transactions, Journal of Applied Mechanics*. American Society of Mechanical Engineers, New York. Q 0021-8936
- ASME, Transactions, Journal of Dynamic Systems, Measurement, and Control*. American Society of Mechanical Engineers, New York. Q 0022-0434
- ASME, Transactions, Journal of Engineering for Power*. American Society of Mechanical Engineers, New York. Q 0022-0825
- ASME, Transactions, Journal of Engineering Materials and Technology*. American Society of Mechanical Engineers, New York. Q 0094-4289
- ASME, Transactions, Journal of Fluids Engineering*. American Society of Mechanical Engineers, New York. Q 0098-2202
- ASME, Transactions, Journal of Heat Transfer*. American Society of Mechanical Engineers, New York. Q 0002-1481
- ASME, Transactions, Journal of Lubrication Technology*. American Society of Mechanical Engineers, New York. Q 0022-2305
- ASME, Transactions, Journal of Mechanical Design*. American Society of Mechanical Engineers, New York. Q
- ASME, Transactions, Journal of Solar Energy Engineering*. American Society of Mechanical Engineers, New York. Q 0199-6231
- ASME, Transactions, Journal of Vibration, Acoustics, Stress, and Reliability in Design*. American Society of Mechanical Engineers, New York. Q
- Astrometriia i Astrofizika*. Akademiia Nauk Ukrainskoi SSR; Izdatel'stvo Naukova Dumka, Kiev. Irreg. 0582-8198
- Astronautics and Aeronautics*. American Institute of Aeronautics and Astronautics, Inc., New York. M 0004-6213
- Astronautik*. Hermann Oberth-Gesellschaft, e.V., Hannover, West Germany. Q 0004-6221
- Astronomical Institutes of Czechoslovakia, Bulletin*. Československá Akademie Věd, Prague. BM 0004-6248
- Astronomical Journal*. American Astronomical Society; American Institute of Physics, Inc., New York. M 0004-6256
- Astronomical Society of Australia, Proceedings*. Astronomical Society of Australia; Sydney University Press, Sydney. Annual 0066-9997
- **Astronomical Society of India, Bulletin*. Astronomical Society of India; Osmania University, Department of Astronomy, Hyderabad. Q
- Astronomical Society of Japan, Publications*. Astronomical Society of Japan c/o Tokyo Astronomical Observatory, Mitaka, Tokyo. Q 0004-6264
- Astronomical Society of the Pacific, Publications*. Astronomical Society of the Pacific, San Francisco. BM 0004-6280
- L'Astronomie*. Société Astronomique de France, Paris. BM 0004-6302
- Astronomische Gesellschaft, Mitteilungen*. Astronomische Gesellschaft, Hamburg; G. Braun GmbH, Karlsruhe, West Germany. SA 0374-1958
- Astronomische Nachrichten*. Akademie-Verlag, Berlin, East Germany. BM 0004-6337
- Astronomy*. AstroMedia Corp., Milwaukee, WI M 0091-6358
- Astronomy and Astrophysics*. Springer Verlag, Berlin, West Germany. SM 0004-6361
- Astronomy and Astrophysics Supplement Series*. European Southern Observatory; Astronomical Institute Lausanne and Geneva Observatory, Switzerland. M 0365-0138
- Astrophysical Journal, Part 1*. American Astronomical Society; University of Chicago Press, Chicago. M 0004-637X
- Astrophysical Journal, Part 2 - Letters to the Editor*. American Astronomical Society; University of Chicago Press, Chicago. M 0004-637X
- Astrophysical Journal Supplement Series*. American Astronomical Society; University of Chicago Press, Chicago. M 0067-0049
- Astrophysical Letters*. Gordon & Breach Science Publishers, Ltd., London. BM 0004-6388
- Astrophysics (Astrofizika)*. Consultants Bureau, New York. Q 0571-7132
- Astrophysics and Space Science*. D. Reidel Publishing Co., Dordrecht, Netherlands. M 0004-640X
- Atmospheric Environment*. Pergamon Press, Inc., Elmsford, NY M 0004-6981
- **Atomkernenergie/Kerntechnik*. Verlag Karl Thieme, Munich, West Germany.
- ATR/Australian Telecommunication Research*. Telecommunication Society of Australia, Melbourne. SA 0001-2777
- Australian Journal of Physics*. Commonwealth Scientific and Industrial Research Organization, Melbourne. BM 0004-9506
- Australian Mathematical Society, Journal, Series B - Applied Mathematics*. Australian Mathematical Society; John Wright & Sons, Ltd., Bristol, England. Q 0334-2700
- **Australian OCCA Proceedings and News*. Australian Oil & Colour Chemists Association, Malvern East, Victoria, Australia. M 0045-0774

- Automatica*. Pergamon Press, Ltd., Oxford. BM 0005-1098
- Automation and Remote Control (Automatika i Telemekhanika)*. Consultants Bureau, New York. BM 0005-1179
- Aviation, Space and Environmental Medicine*. Aerospace Medical Association, Washington, DC M 0095-0562
- Aviation Medicine*. Aero Medical Society of India, New Delhi. Bi-annual
- Aviation Week and Space Technology*. McGraw-Hill, Inc., New York. W 0005-2175
- Aviatsionnaia Tekhnika*. Ministerstvo Vysshego i Srednego Spetsial'nogo Obrazovaniia SSSR; Izdanie Kazanskogo Aviatsionnogo Instituta, Kazan. Q 0579-2975
- Beiträge aus der Plasmaphysik*. Akademie-Verlag, Berlin, East Germany. BM 0005-8025
- Beiträge zur Physik der Atmosphäre*. Friedr. Vieweg & Sohn GmbH, Braunschweig, West Germany. Q 0005-8173
- Bell System Technical Journal*. American Telephone and Telegraph Co., New York. 10 issues per year 0005-8580
- Bildmessung und Luftbildwesen*. Deutsche Gesellschaft für Photogrammetrie; Herbert Wichmann Verlag, Karlsruhe, West Germany. BM 0006-2421
- **Biofizika*. Akademiia Nauk SSSR; Izdatel'stvo Nauka, Moscow. BM 0006-3029
- **Biological Reviews*. Cambridge University Press, Cambridge. Q 0007-9723
- Bionika*. Akademiia Nauk Ukrainsoi SSR; Izdatel'stvo Naukova Dumka, Kiev. Irreg. 0374-6569
- **Biorheology*. Pergamon Press, Inc., Elmsford, NY BM 0006-355X
- **BioSystems*. North-Holland Publishing Co., Amsterdam. Q 0303-2647
- **Biotechnology and Bioengineering Symposia*. John Wiley & Sons, Inc., New York. Irreg. 0572-6565
- Biulleten' Eksperimental'noi Biologii i Meditsiny*. Akademiia Meditsinskikh Nauk SSSR; Izdatel'stvo Meditsina, Moscow. M 0006-4041
- B'lgarska Akademiia na Naukite, Spisanie*. B'lgarska Akademiia na Naukite, Sofia. 6 issues per year 0007-3989
- B'lgarsko Geofizichno Spisanie*. B'lgarska Akademiia na Naukite, Sofia. Q 0323-9918
- Bolgarskaia Akademiia Nauk, Doklady*. B'lgarska Akademiia na Naukite, Sofia. M 0266-8681
- **Botanicheskii Zhurnal*. Akademiia Nauk SSSR; Vsesoiuznoe Botanicheskoe Obshchestvo; Izdatel'stvo Nauka, Moscow. M 0006-8136
- Boundary-Layer Meteorology*. D. Reidel Publishing Co., Dordrecht, Netherlands. 8 issues per year 0006-8314
- **Brain Research*. Elsevier Scientific Publishing Co., Amsterdam. W 0006-8993
- British Interplanetary Society, Journal (Astronautics History)*. British Interplanetary Society, Ltd.; Space Education Aids, Ltd., London. M 0007-084X
- British Interplanetary Society, Journal (Infra-Red Astronomical Satellite)*. British Interplanetary Society, Ltd., London. M 0007-084X
- British Interplanetary Society, Journal (Interstellar Studies)*. British Interplanetary Society, Ltd.; Space Educational Aids, Ltd., London. M 0007-084X
- British Interplanetary Society, Journal (Soviet Astronautics)*. British Interplanetary Society, Ltd.; Space Educational Aids, Ltd., London. M 0007-084X
- British Interplanetary Society, Journal (Space Chronicle)*. British Interplanetary Society, Ltd.; Space Educational Aids, Ltd., London. M 0007-084X
- British Interplanetary Society, Journal (Space Technology)*. British Interplanetary Society, Ltd.; Space Educational Aids, Ltd., London. M 0007-084X
- Bulgarian Journal of Physics*. B'lgarska Akademiia na Naukite Sofia. BM 0323-9127
- Bulletin Géodésique*. Association Internationale de Géodésie. Q 0007-4632
- CAD/CAM Technology*. Society of Manufacturing Engineers, Computer and Automated Systems Association, Dearborn, MI Q
- **Calcified Tissue International*. Springer Verlag, New York. 3 issues per year 0008-0594
- Canadian Aeronautics and Space Journal*. Canadian Aeronautics and Space Institute, Ottawa. BM 0008-2821
- Canadian Electrical Engineering Journal*. Engineering Institute of Canada, Montreal. Q 0700-9216
- Canadian Journal of Physics*. National Research Council of Canada, Ottawa. SM 0008-4204
- Canadian Society for Mechanical Engineering, Transactions*. Canadian Society for Mechanical Engineering, Montreal. Q 0315-8977
- Celestial Mechanics*. D. Reidel Publishing Co., Dordrecht, Netherlands. 8 issues per year 0008-8714
- Ceramic Engineering and Science Proceedings*. American Ceramic Society, Inc., Columbus, OH BM 0196-6219
- Československý Časopis pro Fyziku, Sekce A*. Československá Akademie Věd, Prague. BM 0009-0700
- **Chemical Physics Letters*. Elsevier/North-Holland Publishing Co., Amsterdam. BW 0009-2614
- **Chest*. American College of Chest Physicians, Park Ridge, IL M 0012-3692
- Chile, Universidad, Departamento de Astronomía, Publicaciones*. Observatorio Astronómico Nacional, Santiago de Chile. Irreg.
- Chinese Astronomy and Astrophysics*. Pergamon Press, Inc., Elmsford, NY Q 0275-1062
- Chinese Institute of Engineers, Journal*. Chinese Institute of Engineers, Taipei, Taiwan, Republic of China. SA
- Chinese Journal of Space Sciences*. Scientific Publishers, Beijing. Q
- Chinese Physics*. American Institute of Physics, New York. Q 0273-429X
- Chinese Society of Mechanical Engineers, Journal*. Chinese Society of Mechanical Engineers, Taipei, Taiwan, Republic of China. SA
- CIDA*. Dirección General de Aviación Civil, Centro de Investigación y Difusión Aeronáutico-Espacial, Montevideo, Uruguay. Annual
- Circuits, Systems, and Signal Processing*. Birkhauser Boston, Inc., Cambridge, MA Q 0278-081X
- **Circuits Manufacturing*. Benwill Publishing Corp., Boston, MA M 0009-7306
- Cockpit*. Society of Experimental Test Pilots, Lancaster, CA Q
- Combustion and Flame*. Combustion Institute; American Elsevier Publishing Co., Inc., New York. BM 0010-2180
- Combustion Science and Technology*. Gordon & Breach Science Publishers, Ltd., London. BM 0010-2202
- Comments on Modern Physics, Part C - Comments on Astrophysics*. Gordon & Breach Science Publishers, Ltd., London. BM 0146-2970
- Communication and Broadcasting*. Marconi Co., Ltd., Chelmsford, Essex, England. 3 issues per year 0305-3601
- Communications on Pure and Applied Mathematics*. New York University, Courant Institute of Mathematical

- Sciences; Interscience Publishers, New York. BM 0010-3640
- Composites*. Iliffe Science and Technology Publications, Ltd., Guildford, Surrey, England. Q 0010-4361
- Composites Technology Review*. American Society for Testing and Materials, Philadelphia, PA Q
- Computer-Aided Design*. Butterworth Scientific, Ltd., Guildford, Surrey, England. Q 0010-4485
- Computer Graphics and Image Processing* (see *Computer Vision, Graphics, and Image Processing*).
- Computer Methods in Applied Mechanics and Engineering*. North-Holland Publishing Co., Amsterdam. 9 issues per year 0045-7825
- Computer Vision, Graphics, and Image Processing* (formerly *Computer Graphics and Image Processing*). Academic Press, New York. M 0734-189X
- Computers and Electrical Engineering*. Pergamon Press, Inc., Elmsford, NY Q 0045-7906
- Computers and Fluids*. Pergamon Press, Inc., Elmsford, NY Q 0045-7930
- Computers and Graphics*. Pergamon Press, Ltd., Oxford. Q 0097-8493
- Computers and Mathematics with Applications*. Pergamon Press, Ltd., Oxford. Q 0097-4943
- Computers and Structures*. Pergamon Press, Inc., Elmsford, NY BM 0045-7949
- Computing*. Springer Verlag, Vienna. 8 issues per year 0010-485X
- COMSAT Technical Review*. Communications Satellite Corporation, Washington, DC SA
- Contemporary Physics*. Taylor & Francis, Ltd., London. BM 0010-7514
- **Contributions to Mineralogy and Petrology*. Springer Verlag, Berlin, West Germany. 3 vols. per year 0010-7999
- Control and Computers*. International Association of Science and Technology for Development; Acta Press, Anaheim, CA Q 0315-8934
- The Controller*. International Federation of Air Traffic Controllers' Association, Geneva; Verlag W. Kramer & Co., Frankfurt am Main, West Germany. Q 0010-8073
- Corrosion*. National Association of Corrosion Engineers, Inc., Houston, TX M 0010-9312
- **Corrosion Science*. Pergamon Press, Ltd., Oxford. M 0010-938X
- CSELT - Rapporti Tecnici*. Centro Studi e Laboratori Telecomunicazioni, Torino. Q 0390-1815
- Czechoslovak Journal of Physics*. Československá Akademie Věd, Prague. M 0011-4626
- **Deep-Sea Research*. Pergamon Press, Inc., Elmsford, NY 0198-0149
- Defence Science Journal*. Indian Ministry of Defence, New Delhi. Q 0011-748X
- Delft Progress Report*. Delft University Press, Delft, Netherlands. Q
- DFVLR-Nachrichten*. Deutsche Forschungs- und Versuchsanstalt für Luft- und Raumfahrt, e.V., Porz-Wahn, West Germany. Irreg. 0011-4901
- Dinamika i Prochnost' Mashin*. Izdatel'stvo Khar'kovskogo Universiteta, Kharkov. Irreg.
- DISA Information*. DISA Elektronik A/S, Herlev, Denmark. Irreg. 0070-6639
- **Discovery*. Yale University, Peabody Museum of Natural History, New Haven, CT
- Displays*. Butterworth Scientific, Ltd., Guildford, Surrey, England. Q 0141-9382
- Dornier-Post* (English Edition). Dornier AG, Munich, West Germany. Q 0012-5563
- Earth and Planetary Science Letters*. Elsevier/North-Holland Publishing Co., Amsterdam. M 0012-821X
- Earth-Oriented Applications of Space Technology*. Pergamon Press, Inc., NY Q 0191-538X
- Eesti NSV Teaduste Akadeemia, Toimetised, Füüsika-Matemaatika*. Izdatel'stvo Periodika, Tallin. Q 0367-1429
- Electrical Communication*. International Telephone and Telegraph Corp., New York. Q 0013-4252
- Electrical Communication Laboratories, Review*. Nippon Telegraph & Telephone Public Corp., Tokyo. BM 0029-067X
- Electrochemical Society, Journal*. Electrochemical Society, Inc., New York. M 0013-4651
- Electronics and Communications in Japan* (*Denshi Tsushin Gakkai Ronbunshi*). Institute of Electronics and Communications Engineers in Japan; Scripta Publishing Co., Washington, DC 0424-8368
- Electronics Letters*. Institution of Electrical Engineers, London. BW 0013-5194
- Electrotechnical Laboratory, Researches*. Tokyo. 0366-9106
- Elektronnoe Modelirovanie*. Akademiia Nauk Ukrainskoi SSR; Izdatel'stvo Naukova Dumka, Kiev. BM 0204-3572
- Endocrinology*. Endocrine Society; J. B. Lippincott Co., Philadelphia, PA M 0013-7227
- Energetika*. Ministerstvo Vysshego i Srednego Spetsial'nogo Obrazovaniia SSSR, Izvestiia Vysshikh Uchebnykh Zavadenii; Belorusskii Politekhnikeskii Institut, Minsk. M 0579-2983
- Energy and Technology Review*. U. S. Department of Energy; University of California, Lawrence Livermore Lab., Livermore, CA M
- Energy Conversion and Management*. Pergamon Press, Inc., Elmsford, NY Q 0196-8904
- Energy Developments in Japan*. Rumford Publishing Co., Inc., Chicago, IL Q 0161-8091
- **Energy Progress*. American Institute of Chemical Engineers, New York. Annual 0278-4521
- Energy* (UK). Pergamon Press, Inc., Elmsford, NY Q 0360-5442
- Engineering Fracture Mechanics*. Pergamon Press, Inc., Elmsford, NY Q 0013-7944
- Engineering Management International*. Elsevier Scientific Publishing Co., Amsterdam. Q 0167-5419
- Entropie*. Editions Barthélemy & Cie., Paris. BM 0013-9084
- **Environmental Monitoring and Assessment*. D. Reidel Publishing Co., Dordrecht, Netherlands. 0167-6369
- Environmental Science and Technology*. American Chemical Society; ACS Publications, Washington, DC M 0013-936X
- EOS*. American Geophysical Union, Washington, DC M 0096-3941
- EPRI Journal*. Electric Power Research Institute, Palo Alto, CA BM
- Ergonomics*. Ergonomics Research Society, Nederlandse Vereniging voor Ergonomie, International Ergonomics Association; Taylor & Francis, Ltd., London. BM 0014-0139
- ESA Bulletin*. ESTEC, Noordwijk, Netherlands. Q 0376-4265
- ESA Journal*. ESTEC, Noordwijk, Netherlands. Q 0379-2285
- ESO Messenger*. European Southern Observatory, Munich, West Germany. Q 0722-6691
- **Experimental Gerontology*. Pergamon Press, Inc., Elmsford, NY BM 0531-5565
- Experimental Mechanics*. Society for Experimental Stress Analysis, Brookfield, CT M 0014-4851
- Experimental Techniques*. Society for Experimental Stress Analysis, Brookfield, CT M

Experiments in Fluids. Springer-Verlag GmbH & Co., Berlin, West Germany Q 0723-4864

**Farmakologiya i Toksikologiya.* Akademiia Meditsinskikh Nauk SSSR; Vsesoiuznoe Nauchnoe Obshchestvo Farmakologov; Izdatel'stvo Meditsina, Moscow. BM 0014-8318

Fatigue of Engineering Materials and Structures. Pergamon Press, Inc., Elmsford, NY Q 0160-4112

**Ferroelectrics.* Gordon & Breach Science Publishers, Ltd., London. 3 vols. per year 0015-0193

**Fibre Science and Technology.* Applied Science Publishers, Ltd., Barking, Essex, England. Q 0015-0568

Fizicheskaya Elektronika. Ministerstvo Vysshogo i Srednego Spetsial'nogo Obrazovaniia USSR; Izdatel'stvo L'vovskogo Universiteta, Lvov. Irreg.

Fizika. Ministerstvo Vysshogo i Srednego Spetsial'nogo Obrazovaniia SSSR; Izdatel'stvo Tomskogo Universiteta, Tomsk. M 0021-3411

Fizika Gorenii i Vzryva. Akademiia Nauk SSSR, Sibirskoe Otdelenie; Izdatel'stvo Nauka, Novosibirsk. BM 0430-6228

Fizika Metallov i Metallovedenie. Akademiia Nauk SSSR; Izdatel'stvo Nauka, Sverdlovsk. M 0015-3230

Fizika Molekul. Akademiia Nauk Ukrainkoi SSR, Institut Teoreticheskoi Fiziki; Izdatel'stvo Naukova Dumka, Kiev. Irreg. 0131-176X

Fiziko-Khimicheskaya Mekhanika Materialov. Akademiia Nauk Ukrainkoi SSR; Izdatel'stvo Naukova Dumka, Kiev. BM 0430-6252

Fiziologicheskii Zhurnal (Kiev). Akademiia Nauk Ukrainkoi SSR; Izdatel'stvo Naukova Dumka, Kiev. BM 0201-8489

Fiziologicheskii Zhurnal SSSR. Akademiia Nauk SSSR; Izdatel'stvo Nauka, Leningrad. M 0015-329X

Fiziologiya Cheloveka. Akademiia Nauk SSSR; Izdatel'stvo Nauka, Moscow. BM 0131-1646

Flight International. Royal Aero Club; IPC Business Press, Ltd., London. W 015-3710

Fluid Mechanics - Soviet Research. Scripta Publishing Corp., Washington, DC BM 0096-0764

Fluids Quarterly. Ann Arbor, MI Q 0015-4687

Forschung im Ingenieurwesen. Verein Deutscher Ingenieure; VDI-Verlag GmbH, Düsseldorf, West Germany. BM 0015-7899

Franklin Institute, Journal. Franklin Institute, Philadelphia, PA; Pergamon Press, Inc., Elmsford, NY M 0016-0032

Frequenz. Fachverlag Schiele & Schön, Berlin, West Germany. M 0016-1136

Functiones et Approximatio - Commentarii Mathematici. Poznan, Uniwersytet im. Adama Mickiewicza, Instytut Matematyki, Poznan, Poland. Irreg.

Fundamental'nye Osnovy Opticheskoi Pamiati i Sredy. Ministerstvo Vysshogo i Srednego Spetsial'nogo Obrazovaniia Ukrainkoi SSR; Izdatel'stvo Vishcha Shkola, Kiev. Irreg. 0201-8659

Fundamentals of Cosmic Physics. Gordon & Breach Science Publishers, Ltd., London. Q 0094-5846

Geliotekhnika. Akademiia Nauk Uzbekskoi SSR, Tashkent. BM 0130-0997

General Relativity and Gravitation. International Committee on General Relativity and Gravitation; Plenum Publishing Corp., New York. Q 0001-7701

Geochimica. Academia Sinica, Beijing. Q 0096-3089

Geochimica et Cosmochimica Acta. Geochemical Society and Meteoritical Society; Pergamon Press, Inc., Elmsford, NY M 0016-7037

Geodeziia, Kartografiia i Aerofotos'emka. Izdatel'stvo L'vovskogo Universiteta, Lvov. Irreg. 0435-3323

Geodeziia i Aerofotos'emka. Ministerstvo Vysshogo i Srednego Spetsial'nogo Obrazovaniia SSSR; Izdatel'stvo Instituta Inzhenerov Geodezii, Aerofotos'emki i Kartografii, Moscow. BM 0536-101X

Geodeziia i Kartografiia. Glavnoe Upravlenie Geodezii i Kartografii pri Sovete Ministrov SSSR; Izdatel'stvo Nedra, Moscow. M 0016-7126

Geofizicheskii Zhurnal. Akademiia Nauk Ukrainkoi SSR; Izdatel'stvo Naukova Dumka, Kiev. BM 0203-3100

Geokhimiia. Akademiia Nauk SSSR; Izdatel'stvo Nauka, Moscow. M 0016-7525

**Geological Magazine.* Cambridge University Press, Cambridge. BM 0016-7568

**Geological Society, Journal.* Geological Society of London; Scottish Academic Press, Ltd., Edinburgh. 6 issues per year 0016-7649

Geological Society of America, Bulletin. Geological Society of America, Boulder, CO M 0016-7606

**Geology.* Geological Society of America, Boulder, CO M 0091-7613

Geophysica Norvegica (Geofysiske Publikasjoner). Norwegian Academy of Sciences and Letters; Universitetsforlaget, Oslo. Irreg. 0332-5903

Geophysical and Astrophysical Fluid Dynamics. Gordon & Breach Science Publishers, Ltd., London. Q 0309-1929

Geophysical Journal. Royal Astronomical Society; Blackwell Scientific Publications, Ltd., Oxford. M 0016-8009

**Geophysical Prospecting.* European Association of Exploration Geophysicists, Netherlands; Blackwell Scientific Publications, Ltd., Oxford. BM 0016-8025

Geophysical Research Letters. American Geophysical Union, Washington, DC M 0094-8276

Geophysical Surveys. D. Reidel Publishing Co., Dordrecht, Netherlands. Q 0046-5763

Geomagnetizm i Aeronomiia. Akademiia Nauk SSSR; Izdatel'stvo Nauka, Moscow. BM 0016-7940

Geomagnitnye Issledovaniia. Izdatel'stvo Nauka, Moscow. Irreg.

Geo-Processing. Elsevier Scientific Publishing Co., Amsterdam. Q 0165-2273

**Geothermal Resources Council, Transactions.* Geothermal Resources Council, Davis, CA

Gerlands Beiträge zur Geophysik. Akademische Verlagsgesellschaft Geest & Portig, KG, Leipzig, East Germany. BM 0016-8696

**Gerontology.* S. Karger AG, Basel. BM 0304-324X

Gibridnye Vychislitel'nye Mashiny i Kompleksy. Akademiia Nauk Ukrainkoi SSR, Institut Elektrodinamiki; Izdatel'stvo Naukova Dumka, Kiev. Irreg. 0207-0111

**Gidrobiologicheskii Zhurnal.* Akademiia Nauk Ukrainkoi SSR; Izdatel'stvo Naukova Dumka, Kiev. BM

Gidromekhanika. Akademiia Nauk Ukrainkoi SSR; Izdatel'stvo Naukova Dumka, Kiev. Irreg. 0367-4088

Gigiena i Sanitariia. Ministerstvo Zdravookhraneniia SSSR; Izdatel'stvo Meditsina, Moscow. M 0016-9900

**Gigiena Truda i Professional'nye Zabolevaniia.* Ministerstvo Zdravookhraneniia SSSR; Izdatel'stvo Meditsina, Moscow. M 0016-9919

Grumman Aerospace Horizons. Grumman Aerospace Corp., Bethpage, NY Q 0095-7615

Heat Transfer - Japanese Research. Society of Chemical Engineers of Japan; Scripta Publishing Corp., Washington, DC Q 0096-0802

Heat Transfer - Soviet Research. American Society of Mechanical Engineers, New York. BM 0440-5749

Heat Transfer Engineering. Hemisphere Publishing Corp., Washington, DC Q 0145-7632

High-Speed Surface Craft. Kalerghi Publications, London. 10 issues per year

High Technology. Cox Broadcasting Corp., United Technical Publications, Inc., Garden City, NY M 0277-2981

High Temperature (Teplofizika Vysokikh Temperatur). Consultants Bureau, New York. BM 0018-151X

High Temperatures - High Pressures. Pion, Ltd., London. BM 0018-1544

Hokkaido University, Faculty of Engineering, Bulletin. Hokkaido University, Sapporo, Japan. Irreg. 0385-602X

Human Factors. Human Factors Society, Inc., Santa Monica, CA; The Johns Hopkins Press, Baltimore, MD BM 0018-7208

I & EC - Industrial and Engineering Chemistry, Fundamentals. American Chemical Society, Washington, DC Q 0196-4313

Icarus. Academic Press, Inc., New York. BM 0019-1035

IEE Proceedings, Part A - Physical Science, Measurement and Instrumentation, Management and Education, Reviews. Institution of Electrical Engineers, Hitchin, Herts., England. BM 0143-702X

IEE Proceedings, Part B - Electric Power Applications. Institution of Electrical Engineers, Hitchin, Herts., England. BM 0143-7038

IEE Proceedings, Part D - Control Theory and Applications. Institution of Electrical Engineers, Hitchin, Herts., England. BM 0143-7054

IEE Proceedings, Part E - Computers and Digital Techniques. Institution of Electrical Engineers, Hitchin, Herts., England. BM 0143-7062

IEE Proceedings, Part F - Communications, Radar and Signal Processing. Institution of Electrical Engineers, Hitchin, Herts., England. BM 0143-7070

IEE Proceedings, Part G - Electronic Circuits and Systems. Institution of Electrical Engineers, Hitchin, Herts., England. BM 0143-7089

IEE Proceedings, Part H - Microwaves, Optics and Antennas. Institution of Electrical Engineers, Hitchin, Herts., England. BM 0143-7097

IEE Proceedings, Part I - Solid-State and Electron Devices. Institution of Electrical Engineers, Hitchin, Herts., England. BM 0143-7100

IEEE, Proceedings. Institute of Electrical and Electronics Engineers, Inc., New York. M 0018-9219

IEEE Communications Magazine. Institute of Electrical and Electronics Engineers, Inc., New York BM 0163-6804

IEEE Control Systems Magazine. Institute of Electrical and Electronics Engineers, Inc., New York. Q 0272-1708

**IEEE Electron Device Letters.* Institute of Electrical and Electronics Engineers, Inc., New York, NY M 0193-8576

IEEE Journal of Oceanic Engineering. Institute of Electrical and Electronics Engineers, Inc., New York. Q 0364-9059

IEEE Journal of Quantum Electronics. Institute of Electrical and Electronics Engineers, Inc., New York. M 0018-9197

IEEE Journal of Solid-State Circuits. Institute of Elec-

trical and Electronics Engineers, Inc., New York. BM 0018-9200

IEEE Journal on Selected Areas in Communication. Institute of Electrical and Electronics Engineers, Inc., New York. BM 0733-8716

IEEE Spectrum. Institute of Electrical and Electronics Engineers, Inc., New York. M 0018-9235

IEEE Transactions on Acoustics, Speech, and Signal Processing. Institute of Electrical and Electronics Engineers, Inc., New York. BM 0096-3518

IEEE Transactions on Aerospace and Electronic Systems. Institute of Electrical and Electronics Engineers, Inc., New York. BM 0018-9251

IEEE Transactions on Antennas and Propagation. Institute of Electrical and Electronics Engineers, Inc., New York. BM 0018-926X

IEEE Transactions on Automatic Control. Institute of Electrical and Electronics Engineers, Inc., New York. BM 0018-9286

IEEE Transactions on Biomedical Engineering. Institute of Electrical and Electronics Engineers, Inc., New York. M 0018-9294

IEEE Transactions on Broadcasting. Institute of Electrical and Electronics Engineers, Inc., New York. Q 0018-9316

IEEE Transactions on Circuits and Systems. Institute of Electrical and Electronics Engineers, Inc., New York. M 0098-4094

IEEE Transactions on Communications. Institute of Electrical and Electronics Engineers, Inc., New York. M 0090-6778

IEEE Transactions on Components, Hybrids, and Manufacturing Technology. Institute of Electrical and Electronics Engineers, Inc., New York. BM 0148-6411

IEEE Transactions on Computer-Aided Design of Integrated Circuits and Systems. Institute of Electrical and Electronics Engineers, Inc., New York. Q 0278-0070

IEEE Transactions on Computers. Institute of Electrical and Electronics Engineers, Inc., New York. M 0018-9340

IEEE Transactions on Electrical Insulation. Institute of Electrical and Electronics Engineers, Inc., New York. Q 0018-9367

IEEE Transactions on Electromagnetic Compatibility. Institute of Electrical and Electronics Engineers, Inc., New York. Q 0018-9375

IEEE Transactions on Electron Devices. Institute of Electrical and Electronics Engineers, Inc., New York. M 0018-9383

IEEE Transactions on Engineering Management. Institute of Electrical and Electronics Engineers, Inc., New York. M 0018-9391

IEEE Transactions on Geoscience and Remote Sensing. Institute of Electrical and Electronics Engineers, Inc., New York. Q 0196-2892

IEEE Transactions on Industrial Electronics. Institute of Electrical and Electronics Engineers, Inc., New York. Q 0018-9421

IEEE Transactions on Industry Applications. Institute of Electrical and Electronics Engineers, Inc., New York. BM 0093-9994

IEEE Transactions on Information Theory. Institute of Electrical and Electronics Engineers, Inc., New York. BM 0018-9448

IEEE Transactions on Instrumentation and Measurement. Institute of Electrical and Electronics Engineers, Inc., New York. Q 0018-9456

IEEE Transactions on Magnetics. Institute of Electrical and Electronics Engineers, Inc., New York. Q 0018-9464

IEEE Transactions on Microwave Theory and Techniques. Institute of Electrical and Electronics Engineers, Inc., New York. M 0018-9480

INTERNATIONAL AEROSPACE ABSTRACTS

- IEEE Transactions on Nuclear Science.* Institute of Electrical and Electronics Engineers, Inc., New York. BM 0018-9499
- IEEE Transactions on Pattern Analysis and Machine Intelligence.* Institute of Electrical and Electronics Engineers, Inc., New York. Q 0162-8828
- IEEE Transactions on Plasma Science.* Institute of Electrical and Electronics Engineers, Inc., New York. Q 0093-3813
- IEEE Transactions on Power Apparatus and Systems.* Institute of Electrical and Electronics Engineers, Inc., New York. BM 0018-9510
- IEEE Transactions on Reliability.* Institute of Electrical and Electronics Engineers, Inc., New York. 5 issues per year 0018-9529
- IEEE Transactions on Software Engineering.* Institute of Electrical and Electronics Engineers, Inc., New York. Q 0098-5589
- IEEE Transactions on Sonics and Ultrasonics.* Institute of Electrical and Electronics Engineers, Inc., New York. BM 0018-9537
- IEEE Transactions on Systems, Man, and Cybernetics.* Institute of Electrical and Electronics Engineers, Inc., New York. M 0018-9472
- IEEE Transactions on Vehicular Technology.* Institute of Electrical and Electronics Engineers, Inc., New York. Q 0018-9545
- IHI Engineering Review.* Ishikawajima-Harima Heavy Industries Co., Ltd., Tokyo. SA 0018-9820
- IMA Journal of Applied Mathematics.* Institute of Mathematics and Its Applications; Academic Press, Inc., New York. Q 0272-4960
- IMA Journal of Numerical Analysis.* Institute of Mathematics and Its Applications; Academic Press, Inc., New York. Q 0272-4979
- Indian Academy of Sciences, Proceedings (Engineering Sciences).* Indian Academy of Sciences, Bangalore. 4 issues per vol. 0250-5983
- Indian Institute of Science, Journal, Section A - Engineering Technology.* Indian Institute of Science, Bangalore. M 0019-4964
- Indian Institute of Science, Journal, Section B - Physical and Chemical Sciences.* Indian Institute of Science, Bangalore. M 0019-4964
- Indian Journal of Radio and Space Physics.* Council of Scientific and Industrial Research, Indian National Science Academy, Delhi. Q 0367-8393
- **Indian National Science Academy, Proceedings, Part A.* Indian National Science Academy, New Delhi. BM 0073-6600
- Industrial Laboratory (Zavodskaya Laboratoriya).* Consultants Bureau, New York. M 0019-8447
- Infrared Physics.* Pergamon Press, Inc., Elmsford, NY BM 0020-0891
- Ingegneria.* Editore Ulrico Hoepli, Milan. M 0035-6263
- Ingenieur-Archiv.* Springer Verlag, Berlin, West Germany. BM 0020-1154
- **Inorganic Chemistry.* American Chemical Society, Washington, DC M 0020-1669
- Institut Teoreticheskoi Astronomii, Biulleten'.* Akademiia Nauk SSSR, Institut Teoreticheskoi Astronomii; Izdatel'stvo Nauka, Leningrad. Irreg. 0002-3302
- Institut Teoreticheskoi Astronomii, Trudy.* Akademiia Nauk SSSR, Institut Teoreticheskoi Astronomii; Izdatel'stvo Nauka, Leningrad. Irreg. 0568-6016
- Institute of Electronics and Communication Engineers of Japan, Transactions, Section E (English).* Tokyo. M 0387-236X
- Institution of Engineers (India), Journal, Electrical Engineering Division.* Institution of Engineers, Calcutta. BM 0020-3386
- Institution of Engineers (India), Journal, Electronics and Telecommunication Engineering Division.* Institution of Engineers, Calcutta. 3 issues per year 0020-3378
- Institution of Engineers (India), Journal, Mechanical Engineering Division.* Institution of Engineers, Calcutta. BM 0020-3408
- Institution of Mechanical Engineers, Proceedings, Part C - Mechanical Engineering Science* (formerly *Journal of Mechanical Engineering Science*). Mechanical Engineering Publications, Ltd., London. M 0263-7154
- Instituto de Tonantzintla, Boletín.* Instituto Nacional de Astrofísica, Óptica y Electrónica, Puebla, Pue., Mexico.
- Instytut Lotnictwa, Prace.* Instytut Lotnictwa, Wydawnictwo Naukowo-Techniczne, Warsaw. Q 0509-6669
- Interavia.* Interavia S. A., Geneva. M 0020-5168
- International Advances in Nondestructive Testing.* Gordon & Breach Science Publishers, New York. Annual 0140-072X
- International Communications in Heat and Mass Transfer* (formerly *Letters in Heat and Mass Transfer*). Pergamon Press, Inc., Elmsford, NY BM 0735-1933
- International Journal for Numerical Methods in Engineering.* John Wiley & Sons, Ltd., Chichester, Sussex, England. BM 0029-5981
- International Journal for Numerical Methods in Fluids.* John Wiley & Sons, Ltd., Chichester, Sussex, England. Q 0271-2091
- International Journal of Adhesion and Adhesives.* IPC Science and Technology Press, Ltd., Guildford, Surrey, England. Q 0143-7496
- International Journal of Ambient Energy.* Construction Press, Ltd., Hornby, Lancs., England. Q 0143-0750
- International Journal of Aviation Safety.* Capstan Press, Exeter, Devon, England. Q 0264-6803
- International Journal of Chemical Kinetics.* John Wiley & Sons, Inc., New York. M 0538-8066
- International Journal of Control.* Taylor & Francis, Ltd., London. M 0020-7179
- International Journal of Energy Research.* John Wiley & Sons, Ltd., Chichester, Sussex, England. Q 0363-907X
- International Journal of Engineering Science.* Pergamon Press, Inc., Elmsford, NY M 0020-7225
- International Journal of Fatigue.* IPC Business Press, Ltd., Haywards Heath, Sussex, England. Q 0142-1123
- International Journal of Fracture.* Noordhoff International Publishing, Leiden; Academic Book Services Holland, Groningen, Netherlands. BM 0376-9429
- International Journal of Heat and Mass Transfer.* Pergamon Press, Inc., Elmsford, NY M 0017-9310
- International Journal of Hydrogen Energy.* Pergamon Press, Inc., Elmsford, NY Q 0360-3199
- International Journal of Infrared and Millimeter Waves.* Plenum Publishing Corp., New York. Q 0195-9271
- International Journal of Mechanical Sciences.* Pergamon Press, Inc., Elmsford, NY M 0020-7403
- International Journal of Mini and Microcomputers.* ACTA Press, Anaheim, CA 0702-0481
- **International Journal of Multiphase Flow.* Pergamon Press, Ltd., Oxford. BM 0301-9322
- International Journal of Non-Linear Mechanics.* Pergamon Press, Inc., Elmsford, NY M 0020-7462
- **International Journal of Peptide and Protein Research.* Munksgaard, Copenhagen. BM 0300-9769
- International Journal of Quantum Chemistry, Quantum*

- Biology Symposium.* John Wiley & Sons, Inc., New York. Irreg. 0360-8832
- International Journal of Refractory and Hard Metals.* International Plansee Society for Powder Metallurgy; MPR Publishing Services, Ltd., Shrewsbury, England. Q 0263-4368
- International Journal of Remote Sensing.* Taylor & Francis, Ltd., London. Q 0143-1161
- International Journal of Robotics Research.* MIT Press, Cambridge, MA Q 0278-3649
- International Journal of Solar Energy.* Harwood Academic Publishers GmbH, Chur, Switzerland. BM 0142-5919
- International Journal of Solids and Structures.* Pergamon Press, Inc., Elmsford, NY M 0020-7683
- **International Journal of Systems Science.* Taylor & Francis, Ltd., London. M 0020-7721
- **International Journal of Theoretical Physics.* Plenum Publishing Corp., New York. M 0020-7748
- International Metals Reviews.* The Metals Society, London; American Society for Metals, Metals Park, OH Q 0308-4590
- Inzhenerno-Fizicheskii Zhurnal.* Akademiia Nauk Belorusskoi SSR; Izdatel'stvo Nauka i Tekhnika, Minsk. M 0021-0285
- Ionosfernye Issledovaniia.* Mezhdudedomstvennyi Geofizicheskii Komitet pri Prezidiume Akademii Nauk SSSR; Izdatel'stvo Nauka, Moscow. Irreg.
- Irish Astronomical Journal.* Observatory, Armagh, Northern Ireland. Q 0021-1052
- ISA Transactions.* Instrument Society of America, Pittsburgh, PA Q 0019-0578
- Ishikawajima-Harima Engineering Review.* Ishikawajima-Harima Heavy Industries Co., Ltd., Tokyo. BM 0578-7904
- Israel Journal of Technology.* Weizmann Science Press of Israel, Jerusalem. BM 0021-2202
- Issledovaniia po Uprugosti i Plastichnosti.* Izdatel'stvo Leningradskogo Universiteta, Leningrad. Irreg.
- Issledovanie Zemli iz Kosmosa.* Akademiia Nauk SSSR; Izdatel'stvo Nauka, Moscow. BM 0205-9614
- Istituto Italiano di Navigazione, Atti.* Istituto Italiano di Navigazione, Rome. Q
- ITC Journal.* International Institute for Aerial Survey and Earth Sciences, Enschede, Netherlands. Q 0303-2434
- Itoji Nauki i Tekhniki, Seriya Metallovedenie i Termicheskaiia Obrabotka.* VINITI, Moscow. Irreg. 0202-7739
- ITU Telecommunication Journal.* International Telecommunication Union, Geneva. M 0497-137X
- Japan Air Self Defence Force, Aeromedical Laboratory, Reports.* Aeromedical Laboratory, Tachikawa, Japan. Q 0023-2858
- Japan Institute of Light Metals, Journal.* Japan Institute of Light Metals, Tokyo. BM 0451-5994
- Japan Institute of Metals, Journal (Nippon Kinzoku Gakkai-si).* Japan Institute of Metals, Sendai. M 0021-4876
- Japan Institute of Metals, Transactions.* Japan Institute of Metals, Sendai. M 0021-4434
- Japan Society for Aeronautical and Space Sciences, Transactions.* Japan Society for Aeronautical and Space Sciences, Tokyo. Q 0549-3811
- Japan Society of Air Pollution, Journal (Taiki Osen Kenkyu).* Institute of Public Health, Tokyo. 3 issues per year
- Japan Society of Materials Science, Journal.* Society of Materials Science, Kyoto. M 0514-5163
- Japanese Journal of Applied Physics, Part 1.* Physical Society of Japan and Japan Society of Applied Physics, Tokyo. M 0021-4922
- Japanese Journal of Applied Physics, Part 2.* Physical Society of Japan and Japan Society of Applied Physics, Tokyo. M 0021-4922
- Jena Review.* VEB Verlag Technik, Berlin, East Germany. BM 0448-9497
- JETP Letters (ZHETF Pis'ma v Redaktsiiu).* American Institute of Physics, Inc., New York. SM 0021-3640
- Johns Hopkins APL Technical Digest.* Johns Hopkins University Applied Physics Lab., Baltimore, MD Q 0270-5214
- Journal de Mécanique Théorique et Appliquée.* Gauthier-Villars, Paris. BM 0750-7240
- **Journal of Adhesion.* Gordon & Breach Science Publishers, Ltd., London. Q 0021-8464
- Journal of Advanced Transportation.* Institute of Transportation, Durham, NC 3 issues per year
- Journal of Air Law and Commerce.* Southern Methodist University, School of Law, Dallas. Q 0021-8642
- Journal of Aircraft.* American Institute of Aeronautics and Astronautics, Inc., New York. BM 0021-8669
- Journal of Applied Meteorology (see Journal of Climate and Applied Meteorology).*
- Journal of Applied Physics.* American Institute of Physics, Inc., New York. M 0021-8979
- Journal of Applied Physiology: Respiratory, Environmental and Exercise Physiology.* American Physiological Society, Bethesda, MD M 0161-7567
- **Journal of Applied Polymer Science.* Interscience Publishers, New York. M 0021-8995
- Journal of Applied Psychology.* American Psychological Association, Washington, DC BM 0021-9010
- Journal of Astrophysics and Astronomy.* Indian Academy of Sciences, Bangalore. Q 0250-6335
- Journal of Atmospheric and Terrestrial Physics.* Pergamon Press, Inc., Elmsford, NY M 0021-9169
- Journal of Chemical Physics.* American Institute of Physics, Inc., New York. SM 0021-9606
- Journal of Climate and Applied Meteorology (formerly Journal of Applied Meteorology).* American Meteorological Society, Boston, MA M 0733-3021
- **Journal of Colloid and Interface Science.* Academic Press, Inc., New York. M 0021-9797
- Journal of Composite Materials.* Technomic Publishing Co., Inc., Westport, CT Q 0021-9983
- Journal of Computational Physics.* Academic Press, Inc., New York. M 0021-9991
- **Journal of Crystal Growth.* North-Holland Publishing Co., Amsterdam. BM 0022-0248
- Journal of Dispersion Science and Technology.* Marcel Dekker, Inc., NY 4 issues per year 0193-2691
- Journal of Elasticity.* Wolters-Noordhoff Publishing, Groningen, Netherlands. Q 0374-3535
- Journal of Electrical and Electronics Engineering, Australia.* Institution of Engineers, Australia, Barton; Institution of Radio and Electronics Engineers, Australia, Sydney. Q 0725-2986
- Journal of Energy.* American Institute of Aeronautics and Astronautics, Inc., New York. BM 0146-0412
- Journal of Engineering Mathematics.* Wolters-Noordhoff Publishing, Groningen, Netherlands. Q 0022-0833
- Journal of Engineering Mechanics.* American Society of Civil Engineers, New York BM 0733-9399
- Journal of Environmental Sciences.* Institute of Environmental Sciences, Mt. Prospect, IL BM 0022-0906
- Journal of Fire and Flammability.* Technomic Publishing Co., Inc., Westport, CT Q 0022-1104
- Journal of Fire Retardant Chemistry.* Technomic Publishing Co., Westport, CT Q
- Journal of Fire Sciences.* Technomic Publishing Co., Inc., Lancaster, PA BM 0734-9041

- Journal of Fluid Mechanics.* Cambridge University Press, London. SM 0022-1120
- Journal of Geomagnetism and Geoelectricity.* Society of Terrestrial Magnetism and Electricity, Kyoto, Japan. BM 0022-1392
- Journal of Geophysical Research.* American Geophysical Union, Washington, DC 36 issues per year 0148-0227
- Journal of Geophysics - Zeitschrift für Geophysik.* Deutsche Geophysikalische Gesellschaft; Springer Verlag, Berlin, West Germany. BM 0340-062X
- Journal of Guidance, Control, and Dynamics.* American Institute of Aeronautics and Astronautics, Inc., New York. BM 0731-5090
- **Journal of Heterocyclic Chemistry.* University Station, Provo, UT BM 0022-152X
- Journal of Lightwave Technology.* Institute of Electrical and Electronics Engineers, Inc., New York. Q 0733-8724
- Journal of Marine Research.* Sears Foundations for Marine Research; Yale University, New Haven, CT Q 0022-2402
- Journal of Materials Science.* Chapman & Hall, Ltd., London. M 0022-2461
- **Journal of Materials Science Letters.* Chapman & Hall, Ltd., London. M 0261-8028
- Journal of Mathematical and Physical Sciences.* Indian Institute of Technology, Madras. BM 0047-2557
- Journal of Mathematical Physics.* American Institute of Physics, Inc., New York. M 0022-2488
- Journal of Mechanical Engineering Science.* Institution of Mechanical Engineers, London. BM 0022-2542
- Journal of Metals.* AIME, Metallurgical Society, New York. M 0148-6608
- **Journal of Molecular Biology.* Academic Press, Ltd., London. 36 issues per year
- Journal of Molecular Evolution.* Springer Verlag, Berlin, West Germany. Q 0022-2844
- **Journal of Molecular Spectroscopy.* Academic Press, Inc., New York. M 0022-2852
- Journal of Navigation.* Royal Institute of Navigation; Scottish Academic Press, Edinburgh. Q 0020-3009
- Journal of Neurochemistry.* Pergamon Press, Ltd., Oxford. M 0022-3042
- Journal of Nondestructive Evaluation.* Plenum Publishing Corp., New York. Q 0195-9298
- **Journal of Non-Newtonian Fluid Mechanics.* Elsevier Scientific Publishing Co., Amsterdam. 8 issues per year 0377-0257
- Journal of Optics.* Masson, Editeur, Paris. BM 0150-536X
- Journal of Optimization Theory and Applications.* Plenum Publishing Corp., New York. M 0022-3239
- Journal of Physical Chemistry.* American Chemical Society, Washington, DC BW 0022-3654
- Journal of Physical Oceanography.* American Meteorological Society, Boston. BM 0022-3670
- Journal of Physics A - Mathematical and General.* Institute of Physics, London. M 0305-4470
- Journal of Physics B - Atomic and Molecular Physics.* Institute of Physics, London. 18 issues per year 0022-3700
- Journal of Physics D - Applied Physics.* Institute of Physics, London. 18 issues per year 0022-3727
- Journal of Physics E - Scientific Instruments.* Institute of Physics, London. M 0022-3735
- Journal of Plasma Physics.* Cambridge University Press, London. BM 0022-3778
- Journal of Power Sources.* Elsevier Sequoia S.A., Lausanne. Q 0378-7753
- Journal of Quality Technology.* American Society for Quality Control, Inc., Milwaukee, WI Q 0022-4065
- Journal of Quantitative Spectroscopy and Radiative Transfer.* Pergamon Press, Inc., Elmsford, NY M 0022-4073
- Journal of Research.* National Bureau of Standards; Supt. of Documents, Washington, DC BM
- Journal of Ship Research.* Society of Naval Architects and Marine Engineers, New York. Q 0022-4502
- Journal of Sound and Vibration.* British Acoustical Society; Academic Press, Inc. (London), Ltd., London. SM 0022-460X
- Journal of Space Law.* University of Mississippi School of Law, University, MS SA
- Journal of Spacecraft and Rockets.* American Institute of Aeronautics and Astronautics, Inc., New York. M 0022-4650
- Journal of Strain Analysis for Engineering Design.* Joint British Committee for Stress Analysis, Institution of Mechanical Engineers; Mechanical Engineering Publications, Ltd., London. Q 0309-3247
- Journal of Structural Mechanics.* Marcel Dekker, Inc., New York. Q 0360-1218
- Journal of Technical Physics.* Polska Akademia Nauk; Instytut Podstawowych Problemów Techniki; Państwowe Wydawnictwo Naukowe, Warsaw. Q 0324-8313
- Journal of Testing and Evaluation.* American Society for Testing and Materials, Philadelphia, PA BM 0090-3973
- Journal of the Astronautical Sciences.* American Astronautical Society, Inc., Washington, DC Q 0021-9142
- Journal of the Atmospheric Sciences.* American Meteorological Society, Boston. M 0022-4928
- **Journal of Theoretical Biology.* Academic Press, Ltd., London. M 0022-5193
- Journal of Thermal Stresses.* Hemisphere Publishing Corp., Washington, DC Q 0149-5739
- Journal of Vacuum Science Technology A.* American Vacuum Society; American Institute of Physics, Inc., Woodbury, NY Q 0734-2101
- JSME, Bulletin.* Japan Society of Mechanical Engineers, Tokyo. M 0021-3764
- **Kardiologiya.* Ministerstvo Zdravookhraneniia SSSR; Vsesoiuznoe Nauchnoe Kardiologicheskoe Obshchestvo; Izdatel'stvo Meditsina, Moscow. M 0022-9040
- **Kazanskii Meditsinskii Zhurnal.* Ministerstvo Zdravookhraneniia Tatarskoi Avtonomii SSR; Sovet Nauchnykh Meditsinskikh Obshchestv, Moscow.
- Khimiia i Tekhnologiya Topliv i Masel.* Ministerstvo Neftepererabatyvaiushchei i Neftekhimicheskoi Promyshlennosti SSSR, Akademiia Nauk SSSR, and Nauchno-Tekhnicheskoe Obshchestvo Nefianoi i Gazovoi Promyshlennosti; Izdatel'stvo Khimiia, Moscow. M 0023-1169
- **Khimiia i Zhizn'.* Akademiia Nauk SSSR, Moscow. M 0023-1142
- Khimiia Plazmy.* Atomizdat, Moscow. Irreg.
- Kibernetika i Vychislitel'naia Tekhnika.* Akademiia Nauk Ukrainskoi SSR; Izdatel'stvo Naukova Dumka, Kiev. Irreg. 0454-9910
- Kleinheubacher Berichte.* Fernmeldetechnischer Zentralamt, Darmstadt, West Germany. Irreg. 0343-5725
- Komety i Meteory.* Akademiia Nauk Tadzhikskoi SSR; Izdatel'stvo Donish, Dushanbe. Irreg. 0568-6199
- Kompozitsionnye Polimernye Materialy.* Akademiia Nauk Ukrainskoi SSR, Institut Khimii Vysokomolekuliarnykh Soedinenii; Izdatel'stvo Naukova Dumka, Kiev. Irreg. 0203-3275
- Korean Institute of Metals, Journal.* Korean Institute of Metals, Seoul. Q

- Kosmicheskie Issledovaniia.* Akademiia Nauk SSSR; Izdatel'stvo Nauka, Moscow. BM 0023-4206
- Kosmicheskie Luchi.* Izdatel'stvo Nauka, Moscow. Irreg. 0368-6485
- Kovové Materiály.* Slovenská Akademia Vied, Bratislava. BM 0023-432X
- Krymskaia Astrofizicheskaia Observatoriia, Izvestiia.* Akademiia Nauk SSSR; Izdatel'stvo Naukova Dumka, Moscow. BM
- Kvantovaia Elektronika.* Akademiia Nauk Ukrainkoi SSR, Institut Poluprovodnikov; Izdatel'stvo Naukova Dumka, Kiev. Irreg. 0368-7155
- Kyoto University, Faculty of Engineering, Memoirs.* Kyoto University, Kyoto. Q 0023-6063
- Kyushu University, Faculty of Engineering, Memoirs.* Kyushu University, Fukuoka, Japan. Q 0023-6160
- Kyushu University, Research Institute for Applied Mechanics, Reports.* Kyushu University, Fukuoka, Japan. Irreg. 0023-6195
- Kyushu University, Technology Reports.* Kyushu University, Faculty of Engineering, Fukuoka, Japan. 0023-2718
- **Laboratoires des Ponts et Chaussées, Bulletin de Liaison.* Laboratoire Central des Ponts et Chaussées, Paris. BM 0458-5860
- **Laboratornoe Delo.* Ministerstvo Zdravookhraneniia SSSR; Vsesoiuznoe Nauchnoe Obshchestvo Vrachei-Laborantov; Izdatel'stvo Meditsina, Moscow. M 0023-6749
- **Laboratory Animal Science.* American Association for Laboratory Animal Science, Joliet, IL BM 0023-6764
- Laser Focus.* Advanced Technology Publications, Inc., Newton, MA M 0023-8589
- **Leningradskii Universitet, Vestnik, Biologiia.* Izdatel'stvo Leningradskogo Universiteta, Leningrad. BM 0321-186X
- Leningradskii Universitet, Vestnik, Matematika, Mekhanika, Astronomiia.* Izdatel'stvo Leningradskogo Universiteta, Leningrad. Q 0024-0850
- Letters in Applied and Engineering Science.* Pergamon Press, Inc., Elmsford, NY BM 0020-7225
- Letters in Heat and Mass Transfer.* Pergamon Press, Inc., Elmsford, NY BM 0094-4548
- Lithos.* Universitetsforlaget, Oslo. Q 0024-4937
- Lubrication Engineering.* American Society of Lubrication Engineers, Park Ridge, IL M 0024-7154
- Luft- und Raumfahrt.* Deutsche Gesellschaft fur Luft- und Raumfahrt, Thalham, West Germany. Q 0173-6264
- Magnitnaia Gidromekhanika.* Akademiia Nauk Latvinskoi SSR; Izdatel'stvo Zinatne, Riga. Q 0025-0015
- Magnitosfernnye Issledovaniia.* Akademiia Nauk SSSR; Izdatel'stvo Radio i Sviazi, Moscow.
- ManTech Journal.* Army Materials and Mechanics Research Center, Watertown, MA; Battelle Metals and Ceramics Information Center, Columbus, OH Q
- Marconi Review.* Marconi Co., Ltd., Chelmsford, Essex, England. Q 0025-2883
- Matematicheskaia Fizika.* Akademiia Nauk Ukrainkoi SSR; Izdatel'stvo Naukova Dumka, Kiev. Irreg. 0542-9986
- Materialprüfung.* VDI-Verlag GmbH, Düsseldorf, West Germany. M 0025-5300
- Materials and Design.* Scientific and Technical Press, Ltd., Reigate, Surrey, England. BM 0261-3069
- Materials Evaluation.* American Society for Non-destructive Testing, Inc., Evanston, IL M 0025-5327
- Materials Letters.* North-Holland Publishing Co., Amsterdam. BM 0167-577X
- Materials Science and Engineering.* American Society for Metals, Metals Park, OH; Elsevier Sequoia S.A., Lausanne. M 0025-5416
- **Mathematical Geology.* Plenum Publishing Corp., New York. Irreg. 0020-5958
- Mathematical Methods in the Applied Sciences.* B. G. Teubner, Stuttgart, West Germany. Q 0170-4214
- **Mathematical Modelling.* Pergamon Press, Inc., Elmsford, NY BM 0270-0255
- Mathematics of Computation.* American Mathematical Society, Providence, RI Q 0025-5718
- Meccanica.* Italian Association of Theoretical and Applied Mechanics; Tamburini Editore, Milan. Q 0025-6455
- Mechanical Engineering.* American Society of Mechanical Engineers, New York. M 0025-6501
- Mechanics of Materials.* North-Holland Publishing Co., Amsterdam. Q 0167-6636
- Mechanika Teoretyczna i Stosowana.* Polskie Towarzystwo Mechaniki Teoretycznej i Stosowanej; Państwowe Wydawnictwo Naukowe, Warsaw. Q 0079-3701
- Mechanism and Machine Theory.* Pergamon Press, Ltd., Oxford. BM 0094-114X
- Médecine Aéronautique et Spatiale.* Société Française de Physiologie et de Médecine Aéronautiques et Cosmonautiques, Paris. Q
- **Medicine and Science in Sports and Exercise.* American College of Sports Medicine, Madison, WI 5 issues per year 0195-9131
- **Meditsinskaia Tekhnika.* Ministerstvo Meditsinskoi Promyshlennosti; Vsesoiuznoe Mediko-Tekhnicheskoe Obshchestvo; Izdatel'stvo Meditsina, Moscow. BM 0047-6617
- Mekhanika Giroskopicheskikh Sistem.* Ministerstvo Vysshego i Srednego Spetsial'nogo Obrazovaniia Ukrainkoi SSR; Izdatel'stvo Vischa Shkola, Kiev. Irreg. 0203-3711
- Mekhanika Kompozitnykh Materialov.* Akademiia Nauk Latvinskoi SSR; Izdatel'stvo Zinatne, Riga. 3 issues per year 0203-1272
- Mekhanika Tverdogo Tela.* Akademiia Nauk SSSR; Izdatel'stvo Nauka, Moscow. Irreg. 0321-1975
- Mémoires et Etudes Scientifiques de la Revue de Métallurgie.* Paris. M 0245-8292
- Metal Science.* Metals Society, London. M 0306-3453
- Metal Science and Heat Treatment (Metalovedenie i Termicheskaia Obrabotka Metallu).* Consultants Bureau, New York. BM 0026-0673
- Metall.* Metall-Verlag GmbH, Berlin, West Germany. M 0026-0746
- Metallofizika.* Akademiia Nauk Ukrainkoi SSR; Izdatel'stvo Naukova Dumka, Kiev. Irreg. 0204-3580
- Metallurgical Transactions A - Physical Metallurgy and Materials Science.* Metallurgical Society of the American Institute of Mining, Metallurgical and Petroleum Engineers, Inc., New York; American Society for Metals, Metals Park, OH M 0360-2133
- Metals Forum.* Pergamon Press, Inc., Elmsford, NY Q 0160-7952
- Metals Technology.* Metals Society, London. M 0307-1693
- Meteoritics.* Meteoritical Society and Arizona State University Bureau of Publications, Tempe, AZ Q 0026-1114
- Meteoritika.* Akademiia Nauk SSSR; Izdatel'stvo Nauka, Moscow. Irreg. 0369-2507
- Meteorological Society of Japan, Journal.* Meteorological Society of Japan c/o Japan

- Meteorological Agency, Tokyo. BM 0026-1165
Meteorologicheskii Issledovaniia. Sovetskoe Radio, Moscow. Irreg.
La Météorologie. Société Météorologique de France, Boulogne. Q 0026-1181
Meteorologiya i Gidrologiya. Glavnoe Upravlenie Gidrometeorologicheskoi Sluzhby; Gidrometeoizdat, Moscow. M 0130-2906
Meteorologiya, Klimatologiya i Gidrologiya. Ministerstvo Vysshogo i Srednego Spetsial'nogo Obrazovaniia Ukrainskoi SSR; Odesskii Gidrometeorologicheskii Institut; Izdatel'stvo Ob'edineniia Vishcha Shkola, Odessa. Irreg. 0130-2914
Meteorologische Rundschau. Verband Deutscher Meteorologischer Gesellschaften; Springer Verlag, Berlin, West Germany. BM 0026-1211
 **Micron*. Structural Publications, Ltd., London. Q 0047-7206
Microwave Journal. Horizon House, Inc., Dedham, MA M 0026-2897
MicroWaves (see *Microwaves & RF*).
Microwaves & RF (formerly *MicroWaves*). Hayden Microwaves Corp., Rochelle Park, NJ M
Military Electronics/Countermeasures. Hamilton Burr Publishing Co., Santa Clara, CA M 0164-4076
Mitsubishi Heavy Industries Technical Review. Mitsubishi Heavy Industries, Ltd., Tokyo. BM 0026-6817
Modern Geology. Gordon & Breach Science Publishers, Ltd., London. Q 0026-7775
 **Molecular and General Genetics*. Springer Verlag, New York. Q 0026-8925
Molecular Physics. Taylor & Francis, Ltd., London. M 0026-8976
Monthly Weather Review. U. S. Weather Bureau; Supt. of Documents, Washington, DC M 0027-0644
Moon and the Planets. D. Reidel Publishing Co., Dordrecht, Netherlands. 8 issues per year 0165-0807
Moskovskii Universitet, Vestnik, Seriya 1 - Matematika, Mekhanika. Izdatel'stvo Moskovskogo Universiteta, Moscow. BM 0579-9368
Moskovskii Universitet, Vestnik, Seriya 3 - Fizika, Astronomiya. Izdatel'stvo Moskovskogo Universiteta, Moscow. BM 0579-9392
- Nagoya University, Faculty of Engineering, Memoirs*. Nagoya University, Nagoya. SA 0027-7657
 **National Institute of Polar Research, Memoirs*. National Institute of Polar Research, Tokyo. Irreg. 0386-0744
 **National Weather Digest*. National Weather Association, Clinton, MD Irreg.
Nature. MacMillan (Journals), Ltd., London. W 0028-0836
 **Naturwissenschaften*. Max-Planck-Gesellschaft zur Förderung der Wissenschaften; Springer Verlag, Berlin, West Germany. M 0028-1042
 **Nauka i Zhizn'*. Vsesoiuznoe Obshchestvo Znanie; Izdatel'stvo Pravda, Moscow. M 0028-1263
Navigation. Institute of Navigation, Washington, DC Q 0028-1522
Navigation (Paris). Institut Français de Navigation, Paris. Q 0028-1530
NDT International. IPC Science and Technology Press, Ltd., Guildford, Surrey, England. BM 0308-9126
 **Neuropharmacology*. Pergamon Press, Inc., Elmsford, NY M 0028-3908
New Scientist. IPC Magazines, Ltd., London. W 0028-6664
New York Academy of Sciences, Annals. New York Academy of Sciences, New York. Irreg.
NHK Laboratories Note. Nippon Hoso Kyokai, Technical Research Laboratories, Tokyo. 10 issues per year 0027-657X
Noise Control Engineering (see *Noise Control Engineering Journal*).
Noise Control Engineering Journal (formerly *Noise Control Engineering*). Institute of Noise Control Engineering, Cedar Knolls, NJ BM 0093-9978
Northrop University Law Journal of Aerospace, Energy, and the Environment. Northrop University, Inglewood, CA Annual 0196-1489
Northwestern Polytechnical University, English Translation of Selected Papers. Northwestern Polytechnical University, Xian, Shaanxi, People's Republic of China. Irreg.
 **Nuclear Instruments and Methods*. North-Holland Publishing Co., Amsterdam. BW 0167-5087
 **Nucleic Acids Research*. I.R.L. Press, Ltd., Oxford. BM 0305-1048
Numerical Heat Transfer. Hemisphere Publishing Corp., Washington, DC Q 0149-5720
Nuovo Cimento, Lettere, Serie 2. Società Italiana di Fisica, Bologna.
Nuovo Cimento B, Serie 11. Società Italiana di Fisica; Editrice Compositori, Bologna.
Nuovo Cimento C, Geophysics and Space Physics. Società Italiana di Fisica, Bologna.
Nuovo Cimento C, Serie 1. Società Italiana di Fisica, Bologna.
- Observatoire de Genève, Publications, Série A*. Observatoire de Genève, Switzerland. Irreg.
 **Oftal'mologicheskii Zhurnal*. Ministerstvo Zdravookhraneniia Ukrainskoi SSR, Kiev. 8 issues per year 0030-0675
L'Onde Electrique. Société Française des Electroniciens; Masson & Cie., Paris. M 0030-2430
ONERA, TP. Office National d'Etudes et de Recherches Aérospatiales, Châtillon-Sous-Bagneux (Hauts-de-Seine), France. Irreg.
Optical and Quantum Electronics. Chapman & Hall, London. BM 0306-8919
Optical Engineering. Society of Photo-Optical Instrumentation Engineers, Redondo Beach, CA BM 0091-3286
Optical Society of America, Journal. Optical Society of America, Inc., Washington, DC; American Institute of Physics, Inc., New York. M 0030-3941
Optics and Lasers in Engineering. Applied Science Publishers, Ltd., Barking, Essex, England. Q 0143-8166
Optics Communications. Elsevier/North-Holland Publishing Co., Amsterdam. M 0030-4018
Optics Letters. Optical Society of America, Inc., Washington, DC M 0146-9592
Optimal Control Applications and Methods. John Wiley & Sons, Ltd., Chichester, Sussex, England. Q 0143-2087
Optoelektronika i Poluprovodnikovaia Tekhnika. Akademiia Nauk Ukrainskoi SSR, Institut Poluprovodnikov; Izdatel'stvo Naukova Dumka, Kiev. Irreg.
Origins of Life. D. Reidel Publishing Co., Dordrecht, Netherlands. Q 0302-1688
Ortung und Navigation. Deutsche Gesellschaft für Ortung und Navigation, e.V., Düsseldorf, West Germany. Q 0474-7550
Osaka Prefecture University, Bulletin, Series A - Engineering and Natural Sciences. University of Osaka Prefecture, Osaka, Japan. Irreg.
Osaka University, Technology Reports. Osaka University, Osaka, Japan. SA 0030-6177
Österreichische Akademie der Wissenschaften, mathematisch-naturwissenschaftliche Klasse, Sitzungsberichte, Abteilung 2. Österreichische

- Akademie der Wissenschaften; Springer Verlag, Vienna. 10 issues per year 0723-9319
- Otbor i Peredacha Informatsii.* Akademiia Nauk Ukrainskoi SSR; Izdatel'stvo Naukova Dumka, Kiev. Irreg. 0474-8662
- Oxidation of Metals.* Plenum Publishing Corp., New York. BM 0030-770X
- Papers in Meteorology and Geophysics.* Meteorological Research Institute, Tokyo. Q 0031-126X
- **Patologicheskaiia Fiziologiia i Eksperimental'naia Terapiia.* Akademiia Meditsinskikh Nauk SSSR; Vsesoiuznoe Obshchestvo Patofiziologov; Izdatel'stvo Meditsina, Moscow. BM 0031-2991
- Perception and Psychophysics.* Psychonomic Journals, Inc., Austin, TX M 0031-5117
- Periodica Polytechnica, Mechanical Engineering.* Budapest, Technical University, Budapest. Q 0324-6051
- Periodica Polytechnica, Transportation Engineering.* Budapest, Technical University, Budapest. Q 0303-7800
- Photo Interpretation.* Editions Technip, Paris. BM 0031-8523
- Photogrammetria.* International Society of Photogrammetry; Elsevier Publishing Co., Amsterdam. Q 0031-8663
- Photogrammetric Engineering and Remote Sensing.* American Society of Photogrammetry, Falls Church, VA M 0099-1112
- **Physica.* North-Holland Publishing Co., Amsterdam. Irreg.
- Physica Scripta.* Royal Swedish Academy of Sciences; Almqvist & Wiksell Periodical Co., Stockholm. M 0031-8949
- Physical Review A - General Physics, 3rd Series.* American Physical Society; American Institute of Physics, Inc., New York. M 0556-2791
- **Physical Review B - Solid State, 3rd Series.* American Physical Society; American Institute of Physics, Inc., New York. SM 0556-2805
- Physical Review D - Particles and Fields, 3rd Series.* American Physical Society; American Institute of Physics, Inc., New York. SM 0556-2821
- Physical Review Letters.* American Physical Society, New York. W 0031-9007
- Physical Society of Japan, Journal.* Physical Society of Japan, Tokyo. M 0031-9015
- **Physics and Chemistry of Minerals.* Springer Verlag, Marburg, West Germany. Q 0342-1791
- Physics Letters.* North-Holland Publishing Co., Amsterdam. W 0031-9163
- Physics of Fluids.* American Institute of Physics, Inc., New York. M 0031-9171
- Physics of the Earth and Planetary Interiors.* North-Holland Publishing Co., Amsterdam. 8 issues per year 0031-9201
- **Physics Teacher.* American Institute of Physics, Inc., New York. 9 issues per year 0031-921X
- Physics Today.* American Institute of Physics, Inc., New York. M 0031-9228
- **Physiologist, Supplement.* American Physiological Society, Bethesda, MD BM 0031-9376
- Planetary and Space Science.* Pergamon Press, Inc., Elmsford, NY M 0032-0633
- Plasma Physics.* Pergamon Press, Inc., Elmsford, NY M 0032-1028
- PMTF - Zhurnal Prikladnoi Mekhaniki i Tekhnicheskoi Fiziki.* Akademiia Nauk SSSR, Sibirskoe Otdelenie; Izdatel'stvo Nauka, Novosibirsk. BM 0044-4626
- Polish Academy of Sciences, Institute of Geophysics, Publications.* Państwowe Wydawnictwo Naukowe, Warsaw. Irreg. 0138-0184
- Politechnika Śląska, Zeszyty Naukowe, Matematyka - Fizyka.* Wydawnictwa Politechniki Śląskiej, Gliwice, Poland. Irreg. 0072-470X
- Pollution Atmosphérique.* Paris. Q 0032-3632
- Polymer Composites.* Society of Plastics Engineers, Inc., Broomfield Center, CT Q 0272-8397
- **Polymer Degradation and Stability.* Applied Science Publishers, Ltd., Barking, Essex, England. 0141-3910
- Polymer Engineering and Science.* Society of Plastics Engineers, Inc., Greenwich, CT M 0032-3888
- Polymer Engineering Reviews.* Elsevier Sequoia S.A., Lausanne. Q 0250-8079
- **Polymer Photochemistry.* Applied Science Publishers, Ltd., Barking, Essex, England. Q 0144-2880
- Poroshkovaia Metallurgiiia.* Akademiia Nauk Ukrainskoi SSR; Izdatel'stvo Naukova Dumka, Kiev. M 0032-4795
- Postępy Astronautyki.* Polskie Towarzystwo Astronautyczne, Lodz. Q 0373-5982
- Postępy Astronomii.* Polskie Towarzystwo Astronomiczne; Państwowe Wydawnictwo Naukowe, Warsaw. Q 0032-5414
- Powder Metallurgy International.* Verlag Schmid GmbH, Freiburg/Breisgau, West Germany. Q 0048-5012
- **Precambrian Research.* Elsevier Scientific Publishing Co., Amsterdam. Q
- **Preparative Biochemistry.* Marcel Dekker Journals, New York. 5 issues per year 0032-7484
- Priborostronenie.* Ministerstvo Vysshego i Srednego Spetsial'nogo Obrazovaniia SSSR; Izdatel'stvo Leningradskogo Instituta Tochnoi Mekhaniki i Optiki, Leningrad. M 0021-3454
- Priborostronenie (Kiev).* Ministerstvo Vysshego i Srednego Spetsial'nogo Obrazovaniia USSR; Izdatel'stvo Tekhnika, Kiev. Irreg. 0130-853X
- Prikladnaia Matematika i Mekhanika.* Akademiia Nauk SSSR; Izdatel'stvo Nauka, Moscow. BM 0032-8235
- Prikladnaia Mekhanika.* Akademiia Nauk Ukrainskoi SSR, Otdelenie Matematiki i Kibernetiki; Izdatel'stvo Naukova Dumka, Kiev. M 0032-8243
- Priroda.* Akademiia Nauk SSSR; Izdatel'stvo Nauka, Moscow. M 0032-874X
- Problemi na Tekhnicheskata Kibernetika i Robotikata.* B'lgarska Akademiia na Naukite, Sofia. 4 issues per vol. 0204-9848
- Problemy Bioniki.* Khar'kovskii Gosudarstvennyi Universitet, Kharkov. Irreg. 0555-2656
- **Problemy Endokrinologii.* Ministerstvo Zdravookhraneniia SSSR; Vsesoiuznoe Nauchnoe Obshchestvo Endokrinologov; Izdatel'stvo Meditsina, Moscow. BM
- Problemy Iadernoi Fiziki i Kosmicheskikh Luchei.* Khar'kovskii Gosudarstvennyi Universitet, Kharkov. Irreg. 0131-3142
- Problemy Kibernetiki.* Izdatel'stvo Nauka, Moscow. Irreg. 0555-277X
- Problemy Kontroli i Zashchita Atmosfery ot Zagriazneniia.* Akademiia Nauk Ukrainskoi SSR, Institut Tekhnicheskoi Teplofiziki; Izdatel'stvo Naukova Dumka, Kiev. Irreg. 0135-2253
- Problemy Kosmicheskoi Fiziki.* Izdatel'stvo Vischa Shkola, Kiev. Irreg. 0555-2796
- Problemy Mashinostroeniia.* Izdatel'stvo Naukova Dumka, Kiev. Irreg. 0131-2928
- Problemy Prochnosti.* Akademiia Nauk Ukrainskoi SSR, Institut Problem Prochnosti; Izdatel'stvo Naukova Dumka, Kiev. M 0556-171X
- Problemy Umstvennogo Truda.* Izdatel'stvo Moskovskogo Universiteta, Moscow. Irreg.
- Progress in Aerospace Sciences.* Pergamon Press, Ltd., Oxford. Q 0079-6026
- Progress in Quantum Electronics.* Pergamon Press, Inc., Elmsford, NY Q 0079-6727

- Promyshlennaia Teplotekhnika*. Akademiia Nauk Ukrainskoi SSR; Izdatel'stvo Naukova Dumka, Kiev. BM 0204-3602
- Propellants and Explosives* (see *Propellants, Explosives, Pyrotechnics*).
- Propellants, Explosives, Pyrotechnics* (formerly *Propellants and Explosives*). Verlag Chemie GmbH, Weinheim, West Germany. BM 0721-3115
- **Psikhologicheskii Zhurnal*. Akademiia Nauk SSSR; Izdatel'stvo Nauka, Moscow. BM
- Pure and Applied Geophysics*. Birkhäuser Verlag, Basel. BM 0033-4553
- Quarterly Journal of Mechanics and Applied Mathematics*. Oxford University Press, London. Q 0033-5614
- Quarterly of Applied Mathematics*. Brown University, Providence, RI. Q 0033-569X
- **Radiation Effects*. Gordon & Breach Science Publishers, Ltd., London. Q 0033-7579
- Radio and Electronic Engineer*. Institution of Electronics and Radio Engineers, London. M 0033-7722
- **Radiobiologiya*. Akademiia Nauk SSSR; Izdatel'stvo Nauka, Moscow. BM 0033-8192
- Radioelektronika*. Ministerstvo Vysshego i Srednego Spetsial'nogo Obrazovaniia SSSR; Izdatel'stvo Kievskogo Politekhnikheskogo Instituta, Kiev. M 0021-3470
- Radiofizika*. Ministerstvo Vysshego i Srednego Spetsial'nogo Obrazovaniia SSSR; Izdanie Gor'kovskogo Universiteta, Gorki. M 0021-3462
- Radio Research Laboratories, Journal*. Ministry of Posts and Telecommunications, Radio Research Laboratories, Tokyo. BM 0033-8001
- Radio Research Laboratories, Review*. Ministry of Posts and Telecommunications, Radio Research Laboratories, Tokyo. BM 0033-801X
- Radio Science*. American Geophysical Union, Washington, DC. M 0048-6604
- Radiotekhnika*. Nauchno-Tekhnicheskoe Obshchestvo Radiotekhniki i Elektrosviazi; Izdatel'stvo Sviaz', Moscow. M 0033-8486
- Radiotekhnika* (Kharkov). Izdatel'stvo Khar'kovskogo Gosudarstvennogo Universiteta, Kharkov. Irreg. 0485-8972
- Radiotekhnika i Elektronika*. Akademiia Nauk SSSR; Izdatel'stvo Nauka, Moscow. M 0033-8494
- RCA Review*. RCA Research Engineering, Princeton, NJ. Q 0033-6831
- La Recherche Aérospatiale* (English Edition). Office National d'Etudes et de Recherches Aérospatiales, Châtillon-sous-Bagneux (Hauts-de-Seine), France. BM 0379-380X
- Regional Journal of Energy, Heat and Mass Transfer*. Regional Centre for Energy, Heat and Mass Transfer for Asia and the Pacific; Indian Institute of Technology, Madras. Q
- Remote Sensing of Environment*. American Elsevier Publishing Co., Inc., New York. Q 0034-4257
- Reports on Progress in Physics*. Institute of Physics and the Physical Society, London. M 0034-4885
- Republic of China, National Science Council, Proceedings, Part A: Applied Sciences*. National Science Council, Taipei, Taiwan, Republic of China. Q 0250-1643
- Republic of China, National Science Council, Proceedings, Part B: Basic Science*. National Science Council, Taipei, Taiwan, Republic of China. Q 0250-6870
- Research Laboratory of Engineering Materials, Report*. Tokyo Institute of Technology, Research Laboratory of Engineering Materials, Tokyo. Irreg. 0385-3799
- Res Mechanica*. Applied Science Publishers, Ltd., Barking, Essex, England. Q 0143-0084
- Review of Scientific Instruments*. American Institute of Physics, Inc., New York. M 0034-6748
- Reviews of Geophysics and Space Physics*. American Geophysical Union, Washington, DC. Q 0034-6853
- Revista Brasileira de Física*. Sociedade Brasileira de Física, São Paulo, Brazil. 3 issues per year. 0374-4922
- Revista Mexicana de Astronomía y Astrofísica*. Universidad Nacional Autónoma de México, Instituto de Astronomía, Mexico, D.F. SA 0185-1101
- Revue d'Acoustique*. Groupement des Acousticiens de Langue Française, Paris.
- Revue Française de Mécanique*. Société Française des Mécaniciens, Paris. Q 0373-6601
- Revue Roumaine des Sciences Techniques, Série de Mécanique Appliquée*. Académie de la République Socialiste Roumaine, Bucharest. Q 0035-4074
- Revue Technique Thomson - CSF*. Thomson-CSF, Service de Documentation Technique; Masson & Cie., Paris. Q 0035-4279
- Rivista di Medicina Aeronautica e Spaziale*. Servizio di Sanità dell'Aeronautica Militare, Rome. Q 0035-631X
- Rivista di Meteorologia Aeronautica*. Servizio Meteorologico dell'Aeronautica, Rome. Q 0035-6328
- Robotica*. Cambridge University Press, Cambridge. Q 0263-5747
- Royal Astronomical Society, Monthly Notices*. Royal Astronomical Society, London; Blackwell Scientific Publications, Oxford. M 0035-8711
- Royal Astronomical Society of Canada, Journal*. Royal Astronomical Society of Canada, Toronto. BM 0035-872X
- Royal Meteorological Society, Quarterly Journal*. Royal Meteorological Society, London. Q 0035-9009
- Royal Society (London), Philosophical Transactions, Series A*. Royal Society, London. Irreg. 0080-4614
- Royal Society (London), Proceedings, Series A - Mathematical and Physical Sciences*. Royal Society, London. Irreg. 0080-4630
- Rozprawy Inżynierskie*. Polska Akademia Nauk, Instytut Podstawowych Problemów Techniki; Państwowe Wydawnictwo Naukowe, Warsaw. Q 0035-9408
- SAE Aerospace Information Report*. Society of Automotive Engineers, Inc., Warrendale, PA. Irreg.
- SAE Aerospace Recommended Practice*. Society of Automotive Engineers, Inc., Warrendale, PA. Irreg.
- SAE in Aerospace Engineering*. Society of Automotive Engineers, Inc., Warrendale, PA. Q 0736-2536
- SAFE Journal*. Survival and Flight Equipment Association, Canoga Park, CA. Q
- SAMPE Journal*. Society of Aerospace Material and Process Engineers; SAMPE Publications, Inc., Los Angeles. BM 0091-1062
- Satellite Communications*. Cardiff Publishing Co., Denver, CO. M 0147-7439
- **Scandinavian Journal of Statistics*. Almqvist and Wiksell International, Stockholm. 4 issues per year
- Science*. American Association for the Advancement of Science, Washington, DC. W 0036-8075
- Science Dimension*. National Research Council of Canada, Ottawa. 6 issues per vol. 0036-830X
- Sciences et Techniques de l'Armement (Mémorial de l'Artillerie Française)*. Ministère d'Etat Chargé de la Défense Nationale, Paris. Q
- Scientia Sinica*. Science Press, Beijing. BM 0250-7870

- Scientia Sinica, Series A - Mathematical and Technical Sciences.* Science Press, Beijing. M 0253-5831
- Scientific American.* Scientific American, Inc., New York. M 0036-8733
- Scripta Metallurgica.* Pergamon Press, Inc., Elmsford, NY M 0036-9748
- **Sedimentology.* International Association of Sedimentologists, Blackwell Scientific Publications, Ltd., Oxford. 0037-074X
- Seminar imeni I. G. Petrovskogo, Trudy. Izdatel'stvo Moskovskogo Universiteta, Moscow.* Irreg.
- Sensors and Actuators.* Elsevier Sequoia S.A., Lausanne, Switzerland. Q 0250-6874
- **Separation Science and Technology.* Marcel Dekker Journals, New York. 10 issues per year 0149-6395
- SIAM Journal on Applied Mathematics.* Society for Industrial and Applied Mathematics, Philadelphia, PA 8 issues per year 0036-1399
- SIAM Journal on Control and Optimization.* Society for Industrial and Applied Mathematics, Philadelphia, PA 6 issues per year 0363-0129
- SIAM Journal on Mathematical Analysis.* Society for Industrial and Applied Mathematics, Philadelphia, PA 8 issues per year 0036-1410
- Siemens Forschungs- und Entwicklungsberichte.* Siemens Aktiengesellschaft; Springer Verlag, Berlin, West Germany. BM 0370-9736
- Simulation.* Simulation Council, Inc., La Jolla, CA M 0037-5497
- Sky and Telescope.* Sky Publishing Corp., Cambridge, MA M 0037-6604
- Slovak Academy of Sciences, Geophysical Institute, Contributions.* VEDA, Bratislava.
- **SM Archives.* Martinus Nijhoff Publishers, The Hague. Q 0376-7426
- Società Astronomica Italiana, Memorie.* Gia Società degli Spettroscopisti Italiani, Milan. Q 0037-8720
- Société Française de Photogrammétrie et de Télédétection, Bulletin.* Société Française de Photogrammétrie et de Télédétection, Saint-Mandé, Val-de-Marne, France. Q 0244-6014
- Society for Experimental Biology and Medicine, Proceedings.* Society for Experimental Biology and Medicine, New York. 11 issues per year
- Society of Environmental Engineers, Journal.* Society of Environmental Engineers, London. Q 0374-356X
- **Soil Science.* Williams & Wilkins Co., Baltimore, MD M 0038-075X
- **Soil Science Society of America, Journal.* Soil Science Society of America, Madison, WI BM 0038-0776
- Solar Cells.* Elsevier Sequoia S.A., Lausanne. Q 0379-6787
- Solar Energy.* International Solar Energy Society, Victoria, Australia; Pergamon Press, Inc., Elmsford, NY BM 0038-092X
- Solar Energy Materials.* North-Holland Publishing Co., Amsterdam. Q 0165-1633
- Solar Physics.* Reidel Publishing Co., Dordrecht, Netherlands. M 0038-0938
- Solar System Research (Astronomicheskii Vestnik).* Consultants Bureau, New York. Q 0038-0946
- Solid Mechanics Archives.* University of Waterloo, Solid Mechanics Div., Waterloo, Ontario, Canada; Noordhoff International Publishing, Leiden, Netherlands. Q
- Solid-State Electronics.* Pergamon Press, Inc., Elmsford, NY M 0038-1101
- **Sovetskaia Meditsina.* Ministerstvo Zdravookhraneniia SSSR; Izdatel'stvo Meditsina, Moscow. M
- **Sovetskoe Zdravookhranenie.* Ministerstvo Zdravookhraneniia SSSR; Izdatel'stvo Meditsina, Moscow. M 0038-5239
- Soviet Astronomy (Astronomicheskii Zhurnal).* American Institute of Physics, Inc., New York. BM 0038-5301
- Soviet Astronomy Letters (Pis'ma v Astronomicheskii Zhurnal).* American Institute of Physics, Inc., New York. BM 0360-0327
- Soviet Journal of Nondestructive Testing (Defektoskopiia).* Consultants Bureau, New York. BM 0038-5492
- Soviet Journal of Optical Technology (Optiko-Mekhanicheskaiia Promyshlennost').* Optical Society of America, Inc., Washington, DC; American Institute of Physics, Inc., New York. M 0038-5514
- Soviet Journal of Plasma Physics (Fizika Plazmy).* American Institute of Physics, Inc., New York. BM 0360-0343
- Soviet Journal of Quantum Electronics (Kvantovaiia Elektronika /Moscow/).* American Institute of Physics, Inc., New York. M 0049-1748
- Soviet Physics - Acoustics (Akusticheskii Zhurnal).* American Institute of Physics, Inc., New York. Q 0038-562X
- Soviet Physics - Technical Physics (Zhurnal Tekhnicheskoi Fiziki).* American Institute of Physics, Inc., New York. M 0038-5662
- Soviet Physics - Uspekhi (Uspekhi Fizicheskikh Nauk).* American Institute of Physics, Inc., New York. BM 0038-5670
- Soviet Powder Metallurgy and Metal Ceramics (Poroshkovaia Metallurgiiia).* Consultants Bureau, New York. M 0038-5735
- Soviet Technical Physics Letters (Pis'ma v Zhurnal Tekhnicheskoi Fiziki).* American Institute of Physics, Inc., New York. M 0360-120X
- Space Communication and Broadcasting.* North-Holland Publishing Co., Amsterdam. Q 0167-9368
- Space Education.* British Interplanetary Society, Ltd., London. BA 0261-1813
- Spaceflight.* British Interplanetary Society, London. M 0038-6340
- Space Sciences Reviews.* D. Reidel Publishing Co., Dordrecht, Netherlands. 9 issues per year 0038-6308
- Space Solar Power Review.* Pergamon Press, Inc., Elmsford, NY Q 0191-9067
- Srpska Akademija Nauka i Umetnosti, Posebna Izdanja, Odeljenje Tehnichkikh Nauka.* Srpska Akademija Nauka i Umetnosti, Belgrade. Irreg.
- **Stain Technology.* Williams & Wilkins Co., Baltimore, MD BM 0038-9153
- Sterne und Weltraum.* Verlag Bibliographisches Institut AG, Mannheim, West Germany. M 0039-1263
- Studia Geophysica et Geodaetica.* Československa Akademie Věd, Geofysikální Ústav, Prague. Q 0039-3169
- Studies in Applied Mathematics.* MIT Press, Cambridge, MA Q 0022-2526
- Studii și Cercetări de Fizică.* Academia Republicii Socialiste Romine, Bucharest. 10 issues per year 0039-3940
- Studii și Cercetări de Mecanică Aplicată.* Academia Republicii Socialiste Romine, Bucharest. BM 0039-4017
- Sun at Work in Britain.* International Solar Energy Society; Pergamon Press, Inc., Elmsford, NY SA 0305-0254
- Sunworld.* International Solar Energy Society, Victoria, Australia. Q 0149-1938
- Surface Science.* North-Holland Publishing Co., Amsterdam. M 0039-6028
- Technical News.* Perkin-Elmer Corp., Wilton; Technical Publications, Optical Technology Div., Danbury, CT Q
- Technika Lotnicza i Astronautyczna.* Stowarzyszenie

- Inżynierów i Techników Polskich, Sekcja Lotnicza; Naczelna Organizacja Techniczna, Warsaw. M 0040-1145
- Technisch-ökonomische Information der Zivilen Luftfahrt.* Hauptverwaltung der zivilen Luftfahrt, Zentralflughafen Berlin-Schönefeld, East Germany. BM 0232-5012
- Technische Mitteilungen Krupp, Forschungsberichte.* Fried. Krupp GmbH, Essen, West Germany. Irreg. 0494-9382
- Technology Review.* Massachusetts Institute of Technology, Cambridge, MA 9 issues per year 0040-1692
- Tectonophysics.* Elsevier Publishing Co., Amsterdam. M 0040-1951
- Tekhnicheskaya Elektrodinamika.* Akademiia Nauk Ukrainskoi SSR, Otdelenie Fiziko-Khimicheskikh Problem Energetiki; Izdatel'stvo Naukova Dumka, Kiev. BM 0204-3599
- Telecommunications and Radio Engineering, Part 1 - Telecommunications, Part 2 - Radio Engineering (Elektrosviaz', Radiotekhnika).* Scripta Publishing Corp., Washington, DC M 0040-2508
- Tellus (see Tellus, Series A - Dynamic Meteorology and Oceanography; Tellus, Series B - Chemical and Physical Meteorology).*
- Tellus, Series A - Dynamic Meteorology and Oceanography (formerly Tellus).* Swedish Geophysical Society, Stockholm; Munksgaard International Publishers, Ltd., Copenhagen. 5 issues per year 0280-6495
- Tellus, Series B - Chemical and Physical Meteorology (formerly Tellus).* Swedish Geophysical Society, Stockholm; Munksgaard International Publishers, Ltd., Copenhagen. 5 issues per year 0280-6509
- Teoreticheskaya Elektrotekhnika.* L'vovskii Gosudarstvennyi Universitet; Izdatel'stvo Ob'edineniia Vischa Shkola, Lvov. Irreg.
- Teoreticheskaya i Prikladnaya Mekhanika.* Khar'kovskii Gosudarstvennyi Universitet; Izdatel'stvo Vischa Shkola, Kharkov. Irreg. 0136-4545
- **Teoriia i Praktika Fizicheskoi Kul'tury.* Komitet po Fizicheskoi Kul'ture i Sportu pri Sovete Ministrov SSSR; Izdatel'stvo Fizkul'tura i Sport, Moscow. M 0040-3601
- **Textile Research Journal.* Textile Research Institute, Princeton, NJ M 0040-5175
- **Theoretica Chimica Acta.* Springer Verlag, Berlin, West Germany. 2 vols. per year 0040-5744
- Thermal Engineering (Teploenergetika).* Pergamon Press, Inc., Elmsford, NY M 0040-6015
- **Thin Solid Films.* Elsevier Sequoia S.A., Lausanne. M 0040-6090
- Thin-Walled Structures.* Applied Science Publishers, Ltd., London. Q 0263-8231
- Thyssen Edelstahl Technische Berichte.* Thyssen Edelstahlwerke AG, Krefeld, West Germany. Irreg. 0340-5125
- Tokyo, University, Institute of Space and Astronautical Science, Report.* Tokyo, University, Institute of Space and Astronautical Science, Tokyo. Irreg. 0285-6808
- Tokyo, University, Tokyo Astronomical Observatory, Annals, Second Series.* Tokyo, University, Tokyo. Irreg. 0082-4704
- Tokyo Astronomical Observatory, Tokyo Astronomical Bulletin, Second Series.* Tokyo Astronomical Observatory, Tokyo. Q 0082-4690
- **Torino, Accademia delle Scienze, Classe di Scienze Fisiche, Matematiche e Naturali, Atti.* Turin. Irreg. 0001-4419
- Travaux Géophysiques.* Československa Akademie Věd, Geofyzikální Ústav, Prague. Irreg.
- TsAGI, Uchenye Zapiski.* Tsentral'nyi Aero-Gidrodinamicheskii Institut, Moscow. BM 0321-3429
- **Tsitologiya i Genetika.* Akademiia Nauk Ukrainskoi SSR, Institut Molekuliarnoi Biologii i Genetiki; Izdatel'stvo Naukova Dumka, Kiev. BM 0041-4883
- Ukrainskii Fizicheskii Zhurnal.* Akademiia Nauk Ukrainskoi SSR, Kiev. M 0503-1265
- Ultrasonics.* Iliffe Science & Technology Publications, Ltd., Guildford, Surrey, England. BM 0041-624X
- UNI Hannover.* Universität Hannover, Hannover, West Germany. SA 0171-2268
- Uspekhi Biologicheskoi Khimii.* Akademiia Nauk SSSR; Vsesoiuznoe Biokhimicheskoe Obshchestvo; Izdatel'stvo Nauka, Moscow. Irreg. 0502-8191
- Uspekhi Fiziologicheskikh Nauk.* Izdatel'stvo Nauka, Moscow. Q 0301-1798
- Uspekhi Mekhaniki - Advances in Mechanics.* Polish Scientific Publishers, Warsaw. Q 0137-3722
- **Uspekhi Sovremennoi Biologii.* Akademiia Nauk SSSR, Moscow. BM 0042-1324
- **Utah Science.* Utah State University of Agriculture and Applied Science, Logan, UT 3 issues per year 0042-1502
- Vacuum.* Pergamon Press, Ltd., Oxford. 0042-207X
- VDI-Forschungsheft.* Verein Deutscher Ingenieure; VDI-Verlag GmbH, Düsseldorf, West Germany. SM 0042-174X
- VDI-Z.* Verein Deutscher Ingenieure; VDI-Verlag GmbH, Düsseldorf, West Germany. SM 0042-1766
- VDI-Zeitschriften Fortschritt-Berichte, Reihe 7 - Strömungstechnik.* Verein Deutscher Ingenieure; VDI-Verlag GmbH, Düsseldorf. Irreg. 0341-1753
- Vertica.* Pergamon Press, Inc., Elmsford, NY Q 0360-5450
- Vertiflite.* American Helicopter Society, Inc., Washington, DC BM 0042-4455
- Vestnik Oftalmologii.* Ministerstvo Zdravookhraneniia SSSR; Vsesoiuznoe Nauchnoe Obshchestvo Oftalmologov; Izdatel'stvo Meditsina, Moscow. BM 0042-465X
- **Vestnik Otorinolaringologii.* Ministerstvo Zdravookhraneniia SSSR; Vsesoiuznoe Nauchnoe Obshchestvo Otorinolaringologov; Izdatel'stvo Meditsina, Moscow. BM 0042-4668
- Vision Research.* Pergamon Press, Inc., Elmsford, NY M 0042-6989
- Vissha Geodeziia.* B'lgarska Akademiia na Naukite, Sofia. Irreg. 0324-1114
- Vistas in Astronomy.* Pergamon Press, Inc., Elmsford, NY Q 0083-6656
- **VLSI Design.* Redwood Systems Group, Palo Alto, CA BM 0279-2834
- Voenno-Meditsinskii Zhurnal.* Tsentral'noe Voenno-Meditsinskoe Upravlenie Ministerstva Oborony SSSR; Izdatel'stvo Krasnaia Zvezda, Moscow. M 0026-9050
- Voprosy Dinamiki i Prochnosti.* Rzhskii Politekh-nicheskii Institut; Izdatel'stvo Zinatne, Riga. Irreg. 0321-236X
- **Voprosy Kurortologii, Fizioterapii i Lechebnoi Fizicheskoi Kul'tury.* Ministerstvo Zdravookhraneniia SSSR; Vsesoiuznoe Nauchnoe Obshchestvo Fizioterapevtov i Kurortologov; Vsesoiuznoe Nauchnoe Obshchestvo po Lechebnoi Fizkul'ture i Sportivnoi Meditsine; Izdatel'stvo Meditsina, Moscow. BM 0042-8787
- **Voprosy Meditsinskoi Khimii.* Akademiia Meditsinskikh Nauk SSSR; Izdatel'stvo Meditsina, Moscow. BM 0042-8809
- **Voprosy Neirokhirurgii.* Ministerstvo Zdravookhraneniia SSSR; Vsesoiuznoe Nauchnoe Obshchestvo Neirokhirurgov; Izdatel'stvo Meditsina, Moscow. BM 0042-8817

- * *Voprosy Pitaniia*. Ministerstvo Zdravookhraneniia SSSR; Vsesoiuznoe Nauchnoe Obshchestvo Gigienistov; Izdatel'stvo Meditsina, Moscow. BM 0042-8833
- * *Voprosy Psikhologii*. Akademiia Pedagogicheskikh Nauk SSSR; Izdatel'stvo Pedagogika, Moscow. BM 0042-8841
- Voprosy Teorii Plazmy*. Atomizdat. Irreg.
- * *Vrachebnoe Delo*. Ministerstvo Zdravookhraneniia Ukrainskoi SSR; Izdatel'stvo Zdoroviia, Kiev. M 0049-6804
- Vychislitel'naia i Prikladnaia Matematika*. Izdatel'stvo Kievskogo Universiteta, Kiev. Irreg. 0321-4117
- Vychislitel'naia Matematika i Programirovanie*. Akademiia Nauk Gruzinskoi SSR; Izdatel'stvo Metsniereba, Tiflis. Irreg. 0135-0730
- Wärme- und Stoffübertragung*. Springer Verlag, Berlin, West Germany. Q 0042-9929
- * *Washington Academy of Sciences, Journal*. Washington Academy of Sciences, Bethesda, MD Q 0043-0439
- Wave Motion*. North-Holland Publishing Co., Amsterdam. Q 0165-2125
- Wear*. Elsevier Sequoia S.A., Lausanne. M 0043-1648
- Weather*. Royal Meteorological Society, London. M 0043-1656
- Welding Journal*. American Welding Society, New York. M 0043-2296
- Welding Production (Svarochnoe Proizvodstvo)*. Welding Institute, Cambridge. M 0043-230X
- Wind Engineering*. Multi-Science Publishing Co., Ltd., London. Q 0309-524X
- Yamaguchi University, Faculty of Engineering, Memoirs*. Yamaguchi University, Tokiwadai, Ube, Japan. 0372-7661
- Zagadnienia Drgán Nielinowych*. Polska Akademia Nauk, Instytut Podstawowych Problemów Techniki; Państwowe Wydawnictwo Naukowe, Warsaw. Irreg. 0044-1597
- * *Zdravookhranenie Kirgizii*. Ministerstvo Zdravookhraneniia Kirgizskoi SSR, Frunze. BM
- * *Zdravookhranenie Rossiiskoi Federatsii*. Ministerstvo Zdravookhraneniia SSSR; Izdatel'stvo Meditsina, Moscow. M 0044-197X
- Zeitschrift für angewandte Mathematik und Mechanik*. Akademie-Verlag, Berlin, East Germany. M 0044-2267
- Zeitschrift für angewandte Mathematik und Physik*. Birkhäuser Verlag, Basel. BM 0044-2275
- Zeitschrift für Flugwissenschaften und Weltraumforschung*. Deutsche Gesellschaft für Luft- und Raumfahrt, e.V., and Deutsche Forschungs- und Versuchsanstalt für Luft- und Raumfahrt, e.V., Braunschweig, West Germany. BM 0342-068X
- Zeitschrift für Luft- und Weltraumrecht*. Institut für Luft- und Weltraumrecht; Carl Heymans Verlag, KG, Cologne, West Germany. Q 0340-8329
- Zeitschrift für Metallkunde*. Deutsche Gesellschaft für Metallkunde, e.V.; Riederer-Verlag GmbH, Stuttgart, West Germany. M 0044-3093
- Zeitschrift für Meteorologie*. Meteorologische Gesellschaft; Akademie-Verlag, Berlin, East Germany. Irreg. 0084-5361
- Zeitschrift für Naturforschung, Teil a*. Verlag der Zeitschrift für Naturforschung, Tübingen, West Germany. M 0340-4811
- Zeitschrift für Werkstofftechnik*. Deutsche Gesellschaft für Metallkunde; Verlag Chemie GmbH, Weinheim, West Germany. M 0049-8688
- Zhurnal Eksperimental'noi i Teoreticheskoi Fiziki*. Akademiia Nauk SSSR; Izdatel'stvo Nauka, Moscow. M 0044-4510
- Zhurnal Evoliutsionnoi Biokhimii i Fiziologii*. Akademiia Nauk SSSR; Izdatel'stvo Nauka, Leningrad. BM 0044-4529
- Zhurnal Mikrobiologii, Epidemiologii i Immunobiologii*. Ministerstvo Zdravookhraneniia SSSR; Vsesoiuznoe Nauchnoe Obshchestvo Mikrobiologov i Epidemiologov; Izdatel'stvo Meditsina, Moscow. M 0049-8726
- Zhurnal Nauchnoi i Prikladnoi Fotografii i Kinematografii*. Akademiia Nauk SSSR; Izdatel'stvo Nauka, Moscow. BM 0044-4561
- * *Zhurnal Nevropatologii i Psikhiiatrii im. S. S. Korsakova*. Ministerstvo Zdravookhraneniia SSSR; Vsesoiuznoe Nauchnoe Obshchestvo Nevropatologov i Psikhiatrov; Izdatel'stvo Meditsina, Moscow. M 0044-4588
- * *Zhurnal Obshchei Biologii*. Moscow. BM 0044-4596
- Zhurnal Prikladnoi Spektroskopii*. Izdatel'stvo Nauka i Tekhnika, Minsk. M 0514-7506
- * *Zhurnal Ushnykh, Nosovykh i Gorlovykh Boleznei*. Ministerstvo Zdravookhraneniia Ukrainskoi SSR; Ukrainskoe Nauchnoe Obshchestvo Otolaringologov; Izdatel'stvo Zdorov'ia, Kiev. BM 0044-4650
- Zhurnal Vychislitel'noi Matematiki i Matematicheskoi Fiziki*. Akademiia Nauk SSSR; Izdatel'stvo Nauka, Moscow. BM 0044-4669
- Zhurnal Vysshei Nervnoi Deiatel'nosti*. Akademiia Nauk SSSR; Izdatel'stvo Nauka, Moscow. BM 0044-4677
- Zpráva VZLÚ*. Výzkumný a Zkušební Letecký Ústav, Prague. Irreg.
- Zprávodaj VZLÚ*. Výzkumný a Zkušební Letecký Ústav, Prague. BM 0044-5355

The subject heading is the key to the subject content of the document. Titles of documents are followed by the *IAA* issue numbers, page numbers, and accession numbers under pertinent subject headings. When the title is insufficiently descriptive of document content, a title extension has been added (separated from the title by three hyphens) to better describe the content of the document. The titles, with title extensions if present, are arranged under each subject heading in ascending accession number order.

To illustrate:

Issue Number	Page Number	Accession Number
16	p2293	A83-36086

A

A STARS

- Spectroscopic investigations of Herbig-Ae-Be-Stars
01 p0123 A83-10356
- A search for magnetic fields in the symbiotic and VV
Cephei variables
02 p0246 A83-12131
- Photometric properties of Ap stars in the Geneva
system
02 p0247 A83-12521
- AN And - A detached eclipsing binary system with an
Am primary member
02 p0260 A83-12526
- Observed and computed UV spectral distribution of A
and F stars
02 p0261 A83-12539
- Stars of spectral types A and B in the southern galactic
halo. I - UVB photometry
02 p0249 A83-12915
- Spectral types in the direction of the Magellanic
Stream
03 p0401 A83-13307
- On the nature of the stellar population in the nucleus
of the Sd galaxy NGC 7793
03 p0414 A83-13336
- Mapping of iron and chromium on the surface of the
Ap star Epsilon Ursae Majoris
03 p0418 A83-13880
- A photoelectric investigation of Ap-stars in open clusters.
III - NGC 2362, NGC 2546, and NGC 3228
04 p0546 A83-15034
- Search for rapid variability of 53 Cam
04 p0546 A83-15110
- A study of X-ray emission from Ap and Am stars
05 p0694 A83-17028
- The discovery of 12.5-minute oscillations in the cool
magnetic Ap star, Gamma Equ
06 p0826 A83-18154
- Diffusion processes in Ap stars and white dwarfs
06 p0832 A83-18841
- Optical monitoring of Orion population stars. I - Results
for some T Tauri and Herbig Ae/Be stars
06 p0820 A83-18860
- Spectrographic material for RS Canum Venaticorum and
Algol binaries
06 p0836 A83-19061
- The near-infrared spectrum of the Herbig Ae-Be stars
06 p0844 A83-19497
- Variability and mass loss in IA O-B-A supergiants
07 p1010 A83-19858
- A method for spectroscopically detecting chemical
anomalies on the surface of an Ap star with a nonvariable
spectrum
07 p1006 A83-20659
- A study of peculiar A-type stars in the infrared
07 p1007 A83-20947
- On the photometric differences between luminous OBA
type stars in the LMC with and without P Cygni
characteristics
07 p1023 A83-21212
- Ultraviolet and visible photometric parameters for the
Am stars
07 p1009 A83-21235
- Spectral energy distributions and equivalent widths of
Balmer lines of B and A stars with rapid axial rotation -
Comparison with theoretical models
07 p1027 A83-21266

- Calcium in the atmospheres of peculiar stars
07 p1027 A83-21268
- Energy distributions in the spectra of 10 B to A stars
07 p1027 A83-21280
- HD 147010 - The Ap star in the reflection nebula vdB
102 in upper Scorpius region
08 p1185 A83-23104
- The z-distribution of Am stars
09 p1361 A83-24480
- Lists of photometric Am candidates
09 p1355 A83-24518
- A photometric study of southern Ap stars having right
ascensions on the order of 12 hr
09 p1355 A83-24520
- VBLOW photometry of the magnetic Ap stars HD 137949
/33 Lib/, HD 201601 /Gamma Equ/, HD 203006 /Theta
Mic/, and the peculiar shell star HD 190073
10 p1491 A83-25365
- Spectrophotometry of peculiar B and A stars. XV - Alpha
Andromedae, AR Aurigae, 36 Aurigae, 36 Lyncis, Phi
Herculis, HR 6127, and HR 6997
10 p1499 A83-25369
- Spectrophotometry of peculiar B and A stars. XIII - HD
51418, 53 Camelopardalis, 78 Virginis, and Kappa
Piscium
10 p1502 A83-25651
- Spectrophotometry of peculiar B and A stars. XIV - 56
Arietis, 41 Tauri, 25 Sextantis, HD 170973, HD 205087,
and HD 215441
10 p1502 A83-25661
- Spectrophotometry B, A, and F stars. III
10 p1497 A83-26380
- Mass loss in HR 1040 /A0 Ia/ - Analysis of Mg II lambda
2802 and H-alpha
10 p1509 A83-26381
- On the radii of Ap and Am stars
12 p1785 A83-29076
- Measurement of the absolute monochromatic flux from
Vega at 2.20 and 3.80 microns by comparison with a
furnace
13 p1942 A83-31705
- Properties of Am, Delta Del and Delta Sct stars in the
VBLOW system
13 p1959 A83-31738
- The Mg II h and k lines in Vega
13 p1959 A83-31742
- The spectrum of the star Ap HD 3473
14 p2108 A83-33269
- Diffusion, meridional circulation, and mass loss in Fm-Am
stars
15 p2268 A83-34633
- A photoelectric investigation of temporal changes in the
line at 4254.35 A (Cr I) in the spectrum of the Ap star
Alpha(2) CVn
17 p2601 A83-37703
- Studies of A and F stars in the region of the North
Galactic Pole. V - Interstellar reddening and the uvby-beta
intrinsic colour calibration
17 p2593 A83-38246
- Photoelectric photometry of peculiar and related stars.
II Delta-a-photometry of 339 southern Ap-stars
17 p2594 A83-38411
- Mapping of chemical elements on the surfaces of Ap
stars. I Solution of the inverse problem of finding local
profiles of spectral lines
17 p2611 A83-38558
- Three-micron emission features in Herbig Be/Ae stars
and related objects
19 p2909 A83-40722
- A physical study of the Ursa Major cluster (with special
attention to the peculiar A stars)
19 p2915 A83-41057
- Infrared magnitudes (JHKLM) for 105 chemically peculiar
A- and B-stars
19 p2910 A83-41065
- Light variations of the Am star 32 Vir
19 p2911 A83-41069
- Einstein Observations of X-ray emission from A stars
20 p3068 A83-42452
- Spectrophotometric studies of star HD 157978
20 p3062 A83-43651
- The magnetic field variation of the Ap star HR 465
20 p3077 A83-43662
- Notes on the heavily reddened and variable A-type
supergiant CD-33.12119 deg
21 p3228 A83-44410
- Infrared colors of the chemically peculiar stars of the
upper main sequence
21 p3223 A83-44436
- Confirmation among visual multiples of an increase of
Ap stars with age
21 p3237 A83-45546
- Photometric variability of B- and A-type supergiants
22 p3373 A83-46405
- Recent photometry of the central star of NGC 2346
22 p3375 A83-46578
- The dust envelope of the Herbig Ae star, AB Aur
23 p3519 A83-47449

- Four-colour uvby and H-beta photometry of A5 to G0
stars brighter than 8.3 m
24 p3642 A83-49317
- The discovery of 13.72-min oscillations in the cool
magnetic Ap star HD 217522
24 p3643 A83-49351
- Frequency analysis of the rapidly oscillating Ap star HR
1217 (HD 24712)
24 p3643 A83-49352
- Ap stars and galactic structure
24 p3663 A83-49607
- VBLOW photometry of the open cluster NGC 2516
24 p3645 A83-49850
- Photometric search for Ap-stars in open cluster. IV -
NGC 2287, Cr 121, NGC 2422 and supplementary
measurements in NGC 1662 and NGC 2516
24 p3668 A83-50087

A-6 AIRCRAFT

- The A6E /TRAM/ all-weather weapon system --- Target
Recognition and Attack Multisensor
01 p0008 A83-11260

A-7 AIRCRAFT

- Design and application of a multivariable, digital
controller to the A-7D Digitac II aircraft model
01 p0013 A83-11148
- Fatigue life evaluation of the A-7E arresting gear hook
shank
03 p0277 A83-13912
- Damage tolerance assessment of the A-7D aircraft
structure
08 p1044 A83-21771
- Battle damage and repair of an advanced composite
A-7 outer wing
20 p2927 A83-42547
- A7E/TF41 Engine Monitoring System (EMS)
[ASME PAPER 83-GT-91]
23 p3408 A83-47938

A-10 AIRCRAFT

- TF/TA by means of integrated FLIR and radar
sensors --- terrain following-terrain avoidance displays
using forward looking infrared imagery
01 p0010 A83-11240
- A-10 stall/post-stall testing - A status update
02 p0137 A83-11808
- Analysis of target coverage for an unstabilized 35 mm
panoramic strike camera
08 p1100 A83-22596
- War-time maintenance impact on aircraft availability
Quantifying the R&D investment payoff
[AIAA PAPER 83-2515]
23 p3392 A83-48359

A-300 AIRCRAFT

- Noise-reducing takeoff and landing procedures and the
potential for their operational use in the Airbus A300
[DGLR PAPER 82-032]
09 p1199 A83-24158
- Long-term operational testing of CFRP spoilers
23 p3391 A83-47205
- Design, construction, and operation of the calibration
model for the DNW wind tunnel
23 p3412 A83-47209
- Method of construction and fabrication procedures for
the A300-rudder unit, using a carbon-fiber type of
construction
23 p3391 A83-47211

ABDOMEN

- Computer tomography of organs of the abdominal
cavity
18 p2736 A83-40579

ABEL FUNCTION

- The Abel transformation in the thin-tape diffraction
problem
05 p0683 A83-17631
- Abel inversion with a simple analytic representation for
experimental data
07 p0988 A83-19984
- Inversion of Abel's integral equation for experimental
data
07 p0987 A83-20734
- On a class of integro-summator equations of diffraction
theory
18 p2741 A83-39490

ABERRATION

- Aberrations grazing incidence systems and their
reduction or toleration --- in astronomical X ray imagery
02 p0237 A83-12693
- Holographic aberration compensation with partially
coherent light
05 p0643 A83-16834
- The influence of orbital aberration on the position of
points on space photographs
05 p0645 A83-17682
- Rainbow holographic aberrations and the bandwidth
requirements
06 p0762 A83-18594
- Aberrative properties of a planar dielectric sheet ---
effects on antenna radiation patterns
06 p0742 A83-18675
- Axisymmetric reflectors of the stepped spherical type
06 p0781 A83-19194
- Beam aberration in phase conjugation by degenerate
four-wave mixing in optical waveguides
07 p0993 A83-20152

ABIOGENESIS

- Phase aberrations and laser output beam quality 08 p1108 A83-22450
- Aberrations in high power laser systems 08 p1108 A83-22452
- Simple infrared telescope with stray-light rejection 08 p1175 A83-22856
- Intracavity adaptive optic compensation of phase aberrations. III - Passive and active cavity study for a large N/eq/ resonator 09 p1271 A83-24087
- Unstable resonator with multiple outputs 10 p1435 A83-26880
- The effect of aberrations on the quality of the optical Fourier transformation 13 p1918 A83-30444
- Speckle interferometry and related techniques with advanced technology optical telescope 13 p1920 A83-31011
- Tests and quality of the 3.5 meter primary mirror of the Max-Planck-Institut fuer Astronomie's telescope at Calar Alto 13 p1920 A83-31012
- Cryogenic testing of mirrors for infrared space telescopes 13 p1939 A83-31026
- Investigation of the spherical and chromatic aberrations of the 400/2000 double wide-angle astrophotograph 14 p2095 A83-31839
- The field error and photometric system of the double long-focus astrophotograph of the Main Astronomical Observatory of the Academy of Sciences of the Ukrainian SSR 14 p2095 A83-31840
- Stellar spectrograph using aberration corrected concave holographic grating 14 p2017 A83-32009
- Aberrations of holographic toroidal grating systems 14 p2021 A83-32909
- X-ray spectrograph design 14 p2021 A83-32910
- On the nonlinear aberrations with self-deflection of a light beam in a moving medium 14 p2025 A83-33397
- The effect of phase distortions of the signal field on the current level of a photodetector 15 p2149 A83-35267
- Ray-trace analysis and data reduction methods for the Ritchey-Common test --- for optically flat surfaces 16 p2413 A83-36763
- Automated Foucault test for focus sensing 16 p2413 A83-36764
- Possible optical scheme of a telescope with a main spherical mirror with a diameter of 20-25 m 17 p2590 A83-37690
- A method of calculating the surface contour that accurately corrects the spherical aberration on the axis in a centered optical system 17 p2590 A83-37692
- Effect of optical aberrations on scanning Michelson interferometers 22 p3292 A83-46601
- Aberrated point-spread functions for rotationally symmetric aberrations 24 p3629 A83-49014
- Applied optics (2nd revised edition) --- Russian book 24 p3629 A83-49411

ABIOGENESIS

- Probing the presently tenuous link between comets and the origin of life 02 p0226 A83-11629
- Nucleoside and deoxynucleoside phosphorylation in formamide solutions --- under prebiotic conditions 02 p0226 A83-11631
- Comets and origin of life 03 p0384 A83-13403
- The abiogenic synthesis of amino acids under conditions imitating an ash-gas cloud during volcanic eruptions 06 p0800 A83-17987
- The possible role of soluble salts in chemical evolution 06 p0800 A83-18249
- Stages of emerging life - Five principles of early organization 06 p0801 A83-18250
- Criteria for the emergence and evolution of life in the solar system 06 p0801 A83-19406
- The abiogenic synthesis of peptides on organic matrices of the melanoid type 07 p0971 A83-19644
- The instability of the autogen --- theory of chemical evolution 12 p1767 A83-29425
- An investigation of the abiogenic synthesis of peptides in a model open system 13 p1908 A83-30100
- Cyano-bacterial symbiosis - A well into the past --- Y 13 p1895 A83-30320
- Impact of solar system exploration on theories of chemical evolution and the origin of life 13 p1908 A83-31155
- The concentrating of molecules in coacervate droplets and the origin of life 21 p3189 A83-44700
- Prebiotic evolution on a universal scale. I 23 p3500 A83-48054
- Prebiotic synthesis in atmospheres containing CH₄, CO, and CO₂. I - Amino acids 24 p3619 A83-49621

ABLATION

- Steady-state ablation of aluminum alloys by a CO₂ laser 01 p0054 A83-10701
- Comparison of different integration schemes based on the concept of characteristics as applied to the ablated blunt body problem 02 p0132 A83-13022

- Investigation of meteor ablation in the atmospheres of the earth, Mars, and Venus 03 p0432 A83-13211
- Two-station television observations of Perseid meteors 03 p0401 A83-13316
- One-dimensional finite element analysis of thermal ablation with pyrolysis 04 p0475 A83-15014
- Stationary shape of bodies ablating in hypersonic flow under the action of radiation heating 04 p0477 A83-15863
- Heat transfer with ablation in a finite slab subjected to time variant heat fluxes [AIAA PAPER 83-0582] 05 p0637 A83-16802
- Transient ablation of blunt bodies at the angle of attack [AIAA PAPER 83-0583] 05 p0637 A83-16803
- A steady state linear ablation problem 05 p0641 A83-17706
- Distribution of particle sizes which are formed in the process of modeling the ablation of meteoric material 09 p1367 A83-25281
- Hyperthermal environment simulation for development of thermal protection systems [SAE PAPER 820881] 10 p1381 A83-25774
- Two-dimensional deforming finite element methods for surface ablation [AIAA PAPER 83-1555] 14 p2012 A83-32773
- The cubic spline numerical solution of the ablation problem [AIAA PAPER 83-1556] 14 p2012 A83-32774
- Ablation of carbonaceous materials in a hydrogen-helium arc-jet flow [AIAA PAPER 83-1561] 14 p1998 A83-32778
- Laser wavelength effect on the thermal conductivity and ablation in plasmas created by a laser --- French thesis 15 p2232 A83-33700
- Charring ablation by finite element 15 p2159 A83-34237
- A quasi-three dimensional analysis of thermal ablation from a hypersonic missile 15 p2159 A83-34254
- Comparison of techniques for predicting 3-D viscous flows over ablated shapes [AIAA PAPER 83-0345] 16 p2292 A83-36051
- New aspects in single-body meteor physics 18 p2759 A83-39981
- Effect of low Reynolds number turbulence amplification on the Galileo probe flowfield 18 p2645 A83-40023
- Angular motion influence on reentry vehicle ablation or erosion asymmetry formation [AIAA PAPER 83-2111] 19 p2811 A83-41938
- A finite element analysis of heat transfer in solid with radiation and ablation 20 p2983 A83-43015
- The effect of nonequilibrium physical-chemical processes in the boundary layer on the ablation of quartz glass 23 p3452 A83-48665
- Choice of the initial configuration for a solid body which assures the fulfillment of a prescribed ablation law 24 p3579 A83-49668

ABLATIVE MATERIALS

- Surface recession measurements using a projected fringe technique 01 p0053 A83-11077
- A steady state linear ablation problem 05 p0641 A83-17706
- Ablation of a solid target by laser irradiation --- German thesis 09 p1348 A83-24848
- Ablative radome materials thermal-ablation and erosion modeling 09 p1239 A83-24964
- Ablative material development for Tomahawk Cruise Missile launch canister application [AIAA PAPER 83-1559] 14 p1985 A83-32776
- Appropriate finite element techniques for heat transfer problems with high gradients and ablation 15 p2159 A83-34236
- Experimental evaluation of ablative elastomeric insulators --- for thermal protection of liquid fueled propulsion system combustors 16 p2336 A83-35861
- Vented compression molding 17 p2516 A83-37367
- Tapewrapped phenolic composites reinforced with advanced carbon fabrics 18 p2657 A83-40231
- Experimental determination of vapor species from laser-ablated carbon phenolic composites 19 p2823 A83-40875
- Features of the effect of admixtures on the characteristics of a region perturbed by a body moving at hypersonic velocity 19 p2792 A83-41893
- Ablative thermal protection systems 20 p2969 A83-42257
- Nonequilibrium radiative heating of an ablating Jovian entry probe 20 p2930 A83-43452
- Optimization of fire blocking layers for aircraft seating [SAWE PAPER 1468] 20 p2931 A83-43742

ABLATIVE NOSE CONES

- A study of transport processes in a high-temperature boundary layer on an ablating graphite surface 19 p2842 A83-41259

- The base pressure of bodies of revolution with gas injection through the body surface into a supersonic flow 19 p2790 A83-41265
- Hypersonic dynamic testing of ablating models with three-degree-of-freedom gas bearings 23 p3412 A83-48135
- Thermochemical ablation of the glass-graphite surface of a blunt cone at the spreading line in a three-dimensional boundary layer 24 p3579 A83-49662

ABM

- U APOGEE BOOST MOTORS

ABORT APPARATUS

- Escape low and hot --- vertical-seeking, steerable ejection seat design for F-14A aircraft 13 p1806 A83-31587
- Performance assessment of a reclined ejection seat 17 p2462 A83-37879

ABORT TRAJECTORIES

- Ascent performance and abort analysis for a Future Space Transportation System [AIAA PAPER 83-2112] 19 p2817 A83-41939

ABORTED MISSIONS

- Environmental contamination in light of space law 05 p0692 A83-16973

ABRASION

- Abrasion cross sections for Ne-20 projectiles at 2.1 GeV/nucleon 08 p1163 A83-22280

ABRASION RESISTANCE

- Preliminary results on the abrasability of porous, sintered seal material [ASME PAPER 82-LUB-7] 03 p0298 A83-13504
- Ductility and the abrasive wear of an ultrahigh strength steel 15 p2141 A83-35242

ABRASIVES

- Metal transfer and wear in fine grinding 04 p0487 A83-16349

ABSORBENTS

- Operational test and evaluation of the molecular sieve On-Board Oxygen Generation System /OBOGS/ in the AV-8A 'Harrier' 04 p0525 A83-15417
- Materials that absorb microwave radiation --- Russian book 04 p0472 A83-15829
- Hydriding and dehydriding kinetics of Mg₂Ni above and below the structural phase transition 11 p1545 A83-27332
- The characterization of carbon dioxide absorbing agents for life support equipment; Proceedings of the Winter Annual Meeting, Phoenix, AZ, November 14-19, 1982 11 p1644 A83-28329
- Chemical and physical factors affecting the absorption capability of calcium hydroxide based carbon dioxide absorbents 11 p1645 A83-28333
- Carbon dioxide absorption dynamics of lithium hydroxide 11 p1645 A83-28334
- A theoretical model of CO₂ absorption in a mixed alkali bed under hyperbaric conditions 11 p1645 A83-28336
- Absorption of carbon dioxide by solid hydroxide sorbent beds in closed-loop atmospheric revitalization system 11 p1645 A83-28338
- The effect of boundary absorption on longitudinal dispersion in steady laminar flows 21 p3130 A83-44466

ABSORBERS (EQUIPMENT)

- Absorption refrigeration machines --- Thesis 02 p0243 A83-11525

ABSORBERS (MATERIALS)

- Studies of organic molecules as saturable absorbers at 193 nm 02 p0184 A83-12268
- The ultraviolet absorber on Venus - Amorphous sulfur 02 p0266 A83-12566
- Plane-wave scattering by bodies of revolution with absorbing coatings 04 p0466 A83-15728
- Interaction of electromagnetic radiation . and microstructural materials with regard to the production of spectral-selective solar absorbers --- German thesis 06 p0779 A83-18497
- Repetitive passive Q-switching and bistability in lasers with saturable absorbers 08 p1107 A83-22079
- Optical bistability of a CO₂ laser with intracavity saturable absorber Experiment and model 09 p1271 A83-23710
- Experimental study of the sound insulation of various shell configurations 10 p1477 A83-26297
- On the effect of absorbing materials on electromagnetic waves with large relative bandwidth 10 p1405 A83-26491
- Absorption and reshaping of 10.6 microns light in pure SF₆ using 1.5 ns, low-intensity incident pulses 11 p1582 A83-27610
- Propagation of sound in highly porous open-cell elastic foams 12 p1776 A83-28848
- Temperature distribution in uniform and layered microwave absorbers in waveguide 12 p1720 A83-29441

- Experimental and theoretical investigations of the influence of a saturation grating in an absorber on pulse generation in a passively mode-locked dye laser
16 p2359 A83-35887
- Problems in steady-state theory of a multimode laser with a selective saturable absorber
16 p2359 A83-35896
- Passive mode locking of a long pulse XeCl laser
22 p3299 A83-46724

ABSORPTANCE

- Theory of nonlinear optical absorption associated with free carriers in semiconductors
02 p0233 A83-12267
- Rapid simulated solar absorptance measurements on flat or curved surfaces
04 p0482 A83-15476
- Inorganic thermal control coatings - A review [AIAA PAPER 83-0074]
05 p0617 A83-16504
- Effect of the temperature dependence of optical properties of materials on their radiant heating
09 p1259 A83-24012
- Alpha-s/epsilon-H measurements of thermal control coatings over four years at geosynchronous altitude --- ratio of solar absorptance to infrared hemispherical emittance
15 p2127 A83-34909
- The effect of multiple-scattering in measuring the radiation properties of absorbing and scattering media [AIAA PAPER 83-1454]
15 p2161 A83-34910
- Total band absorptance, emissivity, and absorptivity of the pure rotational band of water vapor
16 p2411 A83-36800

ABSORPTION

- The effect of metal composition on the adsorption of zinc di-isopropylidithiophosphate
[ASLE PREPRINT 82-LC-4C-2]
03 p0302 A83-13242

ABSORPTION BANDS**U ABSORPTION SPECTRA****ABSORPTION COEFFICIENT****U ABSORPTIVITY****ABSORPTION COOLING**

- Simple analysis of a forced flow solar regeneration system
01 p0068 A83-10664
- Absorption refrigeration machines --- Thesis
02 p0243 A83-11525
- Fundamentals of solar energy conversion --- Textbook
13 p1869 A83-30153
- Energy balance of solar absorption and vapor compression cooling systems
14 p2046 A83-32350

ABSORPTION CROSS SECTIONS

- Lower and upper bounds on extinction cross sections of arbitrarily shaped strongly absorbing or strongly reflecting nonspherical particles
03 p0395 A83-14394
- Transmittance of the atmosphere in the /8-0/ and /9-0/ Schumann-Runge bands of oxygen
06 p0786 A83-18323
- Thermal emission rates and capture cross-section of majority carriers at titanium levels in silicon
06 p0814 A83-18959
- Determination of grain boundary barrier height and interface states by a focused laser beam
07 p0999 A83-19992
- Implication for stratospheric composition of a reduced absorption cross section in the Herzberg continuum of a molecular oxygen
07 p0958 A83-20088
- Fluorescence yields from photodissociation of OCS at 1060-1240 Å
07 p0882 A83-21056
- Abrasion cross sections for Ne-20 projectiles at 2.1 GeV/nucleon
08 p1163 A83-22280
- Study of sulfur-containing molecules in the EUV region.
II - Photoabsorption cross section of COS
09 p1343 A83-25131
- Study of sulfur-containing molecules in the EUV region.
III Photoexcitation of CS2
09 p1343 A83-25134
- Time-dependent gain and absorption in a 5 J UV preionized XeCl laser
10 p1428 A83-26024
- Temperature dependence of the excited-state absorption of alexandrite
10 p1429 A83-26031
- Sound scattering by a vortex
10 p1477 A83-26296
- Photodissociation of NH3 at 106-200 nm
11 p1655 A83-28527
- Radioactive ion beams for studying astrophysical nuclear reactions
13 p1917 A83-30178
- High resolution absorption cross section measurements and band oscillator strengths of the (1,0)-(12,0) Schumann-Runge bands of O2
13 p1917 A83-31537
- Electron capture into excited states of hydrogen
14 p2082 A83-32525
- Scattering and absorption of slow particles by a black hole
14 p2110 A83-33391
- Reversible photoinduced modification of electron-capture cross section at localized states in Alpha-Si:H
14 p2093 A83-33446

- Steady flow approximations to the helium r-process
15 p2263 A83-34541
- Interstellar photoelectric absorption cross sections, 0.03-10 keV
17 p2604 A83-37910
- Channels of energy losses in erbium laser glasses in the stimulated emission process
19 p2853 A83-41186
- Neutron capture rates in the r-process - The role of direct radiative capture --- in supernovas
19 p2920 A83-41639
- Total and partial cross sections for electron capture in collisions of hydrogen atoms with fully stripped ions
22 p3361 A83-45927
- Determination of stellar neutron-capture rates for radioactive nuclei with the aid of beta-delayed neutron emission
23 p3520 A83-47460
- Explicit Hilbert-space representations of atomic and molecular photoabsorption spectra - Computational studies of Stieltjes-Tchebycheff functions
24 p3625 A83-48826

ABSORPTION SPECTRA**NT FRAUNHOFER LINES****NT HERZBERG BANDS**

- Detection of the 1400 Å absorption in the ultraviolet spectrum of the DA white dwarf LB 3303
02 p0253 A83-11614
- The detection of ultraviolet photospheric absorption in the spectra of two Wolf-Rayet stars
02 p0253 A83-11615
- Concentration profiles of NH and OH in a stoichiometric CH4/N2O flame by laser excited fluorescence and absorption
02 p0152 A83-12081
- The interstellar absorption-line spectrum of Mu Ophiuchi
02 p0256 A83-12124
- Frequency locking to absorption lines by wave competition in a tunable ring dye laser
02 p0185 A83-12302
- Absorption spectra of deuterated water at DF laser wavelengths
02 p0211 A83-12601
- The infrared spectral properties of frozen volatiles --- in cometary nuclei
03 p0415 A83-13381
- Absorption spectra of toxic compounds at CO2 laser wavelengths
03 p0294 A83-13722
- Two Cr II multiplets around 1430 Å appearing in absorption in the spectrum of a solar active region
03 p0436 A83-13952
- Absorption spectra of typical space materials in the vacuum ultraviolet
03 p0395 A83-13972
- Stratospheric N2O mixing ratio profile from high-resolution balloon-borne solar absorption spectra and laboratory spectra near 1880/cm
03 p0359 A83-14395
- A catalog of equivalent widths of absorption lines in spectra of A1-G0-type stars
03 p0410 A83-14690
- Detection of the /8,8/ and /9,9/ absorption lines of ammonia - The hot molecular cloud toward Sgr B2
03 p0430 A83-14806
- Ly-alpha absorption at a high velocity in NGC1275
03 p0411 A83-14923
- An Effelsberg - Green Bank galactic H I absorption line survey. II - Results and interpretation
04 p0549 A83-15027
- The law of interstellar absorption in the wave-number interval 0.95/micron to 3.03/microns
04 p0550 A83-15042
- A structural interpretation of the infrared absorption spectra of a-Si:H:O alloys
04 p0541 A83-15515
- Further examples of companion galaxies with discordant redshifts and their spectral peculiarities
04 p0552 A83-15606
- VLA observations of H I absorption in the nuclei of Seyfert and active galaxies
04 p0552 A83-15609
- Are QSOs local objects. I - A new interpretation of the emission and absorption spectra of a few QSOs
04 p0556 A83-15967
- An interpretation of the near-ultraviolet absorption spectrum of SO2 - Implications for Venus, Io, and laboratory measurements
05 p0704 A83-16966
- Absorption lines, Faraday rotation, and magnetic field estimates for QSO absorption-line clouds
05 p0696 A83-16979
- Spectral characteristics of neodymium-activated yttrium aluminum garnet in the ultraviolet and visible ranges
05 p0648 A83-17044
- Generation of wide-band optical continuum in fiber waveguides
05 p0685 A83-17070
- 3.508 micron-HeXe-laser line absorption by formaldehyde monomer and dimer and by nitrogen dioxide monomer and dimer without and in the presence of argon
05 p0684 A83-17871
- The spectrum of 11 Cam in 1980 and 1981
06 p0817 A83-18016
- Radiative heating due to increased CO2 - The role of H2O continuum absorption in the 12-18 micron region
06 p0791 A83-18269

- The asymmetry of photospheric absorption lines. I - An analysis of mean solar line profiles
06 p0854 A83-18547
- Circumstellar material around rapidly rotating B stars. I - Nonemission-line stars
06 p0836 A83-19071
- Analysis of absorption spectra of 11 quasars with Z sub e greater than 2
06 p0837 A83-19206
- On the possibility of detecting very hot gas through absorption-line studies
06 p0839 A83-19268
- 21 centimeter H I absorption at z = 0.437 against the extended radio structure of 3C 196
06 p0839 A83-19271
- HD 207739 - A strange composite star
06 p0823 A83-19301
- The H I absorption in NGC 5128 /Centaurus A/
06 p0845 A83-19522
- Atmospheric spectroscopy studies
07 p0958 A83-19972
- Time variations of an absorption feature in the spectrum of the gamma-ray burst on 1980 April 19
07 p1011 A83-20015
- Investigation of nonlinear absorption in H2O vapors subjected to strong optical fields with linear and circular polarizations
07 p0991 A83-20128
- Ground-based infrared spectroscopic measurements of atmospheric hydrogen cyanide
07 p0956 A83-20212
- Further ultraviolet observations of interstellar gas associated with the supernova remnant S 147
07 p1017 A83-20931
- Spectrophotometry of the broad absorption-line QSO PHL 5200
07 p1019 A83-21106
- A non-spherically symmetric model for absorption regions near quasars
07 p1019 A83-21107
- Absorption by halo gas in the direction of M13
07 p1020 A83-21118
- Westerbork H I observations of the H II region W3
07 p1008 A83-21217
- The asymmetry of photospheric absorption lines. II - The asymmetry of medium-strong Fe I lines in quiet and active regions of the sun
07 p1038 A83-21243
- A survey of ultraviolet interstellar absorption lines
08 p1175 A83-22748
- Interstellar absorption toward HD 14633
08 p1183 A83-23051
- Versatile curved crystal spectrometer for laboratory extended X-ray absorption fine structure measurements
08 p1105 A83-23227
- Water vapor absorption at isotopic CO2 laser wavelengths
09 p1269 A83-24446
- Calculation of absorption by wings of the H2O monomer in the 8-13 micron atmospheric window
09 p1308 A83-25062
- Heterogeneous catalyzed photolysis via photoacoustic spectroscopy
09 p1297 A83-25189
- An absorption feature and filamentary structures in the central galaxy of the Centaurus cluster, NGC 4696
09 p1365 A83-25296
- Periphery of absorption bands as a specific form of the manifestation of intermolecular interaction in gases
10 p1478 A83-25521
- Collision-induced absorption spectra of simple molecular systems
10 p1448 A83-25523
- Investigation of absorption line profiles of molecular gases by methods of laser spectroscopy
10 p1419 A83-25525
- NGC 315 - High-velocity H I in an active elliptical galaxy
10 p1511 A83-26404
- Three-dimensional quantum dynamics of H2O and HOD photodissociation
10 p1480 A83-26459
- PKS 0119-046 and the origin of infalling absorption-line systems in quasars
10 p1515 A83-26747
- H I absorption in the peculiar galaxy UGC 6081
10 p1516 A83-26750
- Theory of time-delayed measurement - Subnatural linewidth spectroscopy
11 p1572 A83-27511
- Overlapping effect of atmospheric H2O, CO2 and O3 on the CO2 radiative effect
11 p1632 A83-27669
- Absorption bursts in the radio emission from the sun at decimeter wavelengths
11 p1691 A83-27991
- The optimal design for spectral gas analyzers of atmospheric pollution
11 p1573 A83-28201
- Spectroscopic survey of southern compact and bright-nucleus galaxies. V
11 p1680 A83-28257
- The ratio of deuterium to hydrogen in interstellar space. V The line of sight to Epsilon Persei
12 p1790 A83-28882
- A statistical study of the Lyman-alpha absorption lines of nine quasars
12 p1795 A83-29352
- The redshift distribution of quasar absorption lines and its origin
12 p1795 A83-29353
- Spectroscopy of three ultraviolet-excess galaxies
12 p1796 A83-29489
- The effect of laser radiation on absorption in the far wings of spectral lines
13 p1849 A83-30084
- Absorption-line spectroscopy of close pairs of QSOs
13 p1954 A83-31582

Absorption spectra of interstellar grains. III - On the origin of the '2200' hump 13 p1955 A83-31664
 Analysis of additional absorption components of MgII lines in Algal in terms of a model of gas stream 13 p1955 A83-31668
 A survey of formaldehyde in the Cepheus OB3 molecular cloud 13 p1958 A83-31709
 The effect of pressure on the absorption spectrum of solid oxygen 14 p2081 A83-32135
 Laser methods for the control of atmospheric gases and gases which pollute the atmosphere 14 p2052 A83-32560
 Quantitative intracavity spectroscopy 14 p2052 A83-32561
 An investigation of the possibilities for lowering the detection limits of elements in a graphite laser torch using the intracavity method for the registration of atomic absorption 14 p2020 A83-32826
 The dependence of the fluorescence and absorption spectra of anthracene vapor on concentration 14 p2082 A83-32828
 The absorption spectrum of (C-12)D2 in the 1.06-micron region 14 p2048 A83-32833
 Measurement of absorption line intensities with VUV monochromators 14 p2021 A83-32913
 The incidence of 21 centimeter absorption in QSO redshift systems selected for Mg II absorption - Evidence for a two-phase nature of the absorbing gas 14 p2104 A83-33185
 Characterisation of the 50-70 GHz band for space communications 14 p2003 A83-33473
 Interstellar absorption in three Bode fields in the Andromeda Nebula 15 p2253 A83-33702
 Electron scattering and absorption-line formation in type II supernova atmospheres 15 p2254 A83-33717
 Hydrogen vibration on Si(111) 7 x 7 - Evidence for a unique chemisorption site 15 p2131 A83-33897
 Wigner method studies of ozone photodissociation 15 p2227 A83-34015
 Ultraviolet absorption spectra of FNO₃ and HOF --- in stratosphere 15 p2194 A83-34041
 Common absorption systems in the spectra of the QSO pair Q0307-195A, B 15 p2259 A83-34117
 New absolute spectroscopic measurement of the solar equatorial rotation rate 15 p2281 A83-34308
 A new test of the cosmological interpretation of QSO redshifts 15 p2260 A83-34378
 AFGL trace gas compilation - 1982 version [AD-A130554] 15 p2201 A83-34456
 The X-ray absorption spectrum of 4U 1700-37 and its implications for the stellar wind of the companion HD 153919 15 p2268 A83-34637
 High-velocity iron absorption lines in supernova remnant 106 15 p2269 A83-34647
 Io's 4-micron band and the role of adsorbed SO₂ 15 p2275 A83-34723
 Quasar absorption spectra and molecular spectra - An attempt at identification 15 p2270 A83-34752
 Optical observations of the interstellar absorption lines towards the M8 nebula 15 p2272 A83-34790
 High-redshift objects as probes of nearby cosmic voids 15 p2272 A83-34792
 Absorption and emission line profile coefficients of multilevel atoms. I - Atomic profile coefficients. II Velocity-averaged profile coefficients 15 p2227 A83-34991
 N2 broadening parameters of ozone at 9.6 microns 15 p2203 A83-34995
 Rydberg series in the absorption spectrum of Te I limiting on 5s(2)5p(3) (4)S(0)3/2 15 p2228 A83-35296
 Photoexcitations in trans-(CH)_x - A Fourier-transform infrared study 16 p2420 A83-35748
 The Lyman-alpha absorption anomaly in satellite occultation measurements as a tracer for some thermospheric composition variations 16 p2378 A83-36117
 Photoinduced infrared activity in polyacetylene 16 p2421 A83-36565
 Observations of the MG II lambda 2800 spectral region in broad absorption line quasars 16 p2431 A83-36661
 Status of laboratory experiments on ice mixtures and on the 12 micron H₂O ice feature --- suggesting interstellar IR absorption 16 p2431 A83-36670
 The elliptical galaxy NGC 4696 - CCD observations of an absorbing lane 16 p2433 A83-36698
 Absorption measurements of H₂O at high temperatures using a CO laser 16 p2328 A83-36795
 Mrk 744 and Mrk 1066 - Two Seyfert galaxies with strong absorption-line spectra 17 p2596 A83-37306
 Neutral hydrogen absorption in the quasar 3C 268.4 - Possible evidence for galactic halo clouds 17 p2598 A83-37346
 Anomalous reddening of supernovae 17 p2603 A83-37888

The C₂H, C₂, and CN electronic absorption bands in the carbon star HD 19557 17 p2605 A83-37918
 Absorptivity of nitric oxide in the fundamental vibrational band 18 p2742 A83-39185
 Changes in interstellar atomic abundances from the galactic plane to the halo 18 p2768 A83-39630
 Low latitude absorption spectra 18 p2768 A83-39644
 Collision-induced absorption in the far infrared spectrum of Nitral 19 p2921 A83-40779
 Neutral hydrogen absorption in early spiral galaxies 19 p2920 A83-41645
 Neutral hydrogen absorption in Mrk 6, NGC 3810, 1506+34, and NGC 1068 20 p3063 A83-42180
 AFGL atmospheric absorption line parameters compilation - 1982 edition 20 p3016 A83-42207
 Observations of H1414 +089, QSO with extremely high velocity broad-absorption-line gas 20 p3058 A83-42317
 Total internal reflectance optoacoustic spectroscopy 20 p2989 A83-42582
 Absorption spectra, energy levels and crystal-field analysis of trivalent neodymium in the gamma phase of neodymium sesquisulfide (gamma-Nd₂S₃) 20 p3053 A83-42627
 On the optical properties of trans-polyacetylene 20 p3048 A83-42641
 Interstellar C₂ molecules in a Taurus dark cloud 20 p3074 A83-43091
 Interstellar proteins and the discovery of a new absorption feature at lambda = 2800 A 20 p3077 A83-43669
 Observations of asteroids in the 3- to 4-micron region 21 p3239 A83-44085
 The experimental measurement of total absorbance by the ozone 9.6 micron band 21 p3109 A83-44507
 The distribution of absorption lines in QSO spectra 21 p3232 A83-44731
 Spectroscopy of the QSO pair Q1228 + 076/Q1228 + 077 21 p3225 A83-44767
 The use of the extrapolation technique in the calibration of radiation-measuring devices in the region of strong band absorption for the rho-sigma-tau water-vapor bands from 0.91 to 0.98 microns 21 p3142 A83-45406
 Polarization of interstellar molecular radiofrequency absorption lines 22 p3376 A83-45633
 Optical studies of In(x)Ga(1-x)As-GaAs strained multiquantum well structures 22 p3365 A83-46730
 Wavelength-selective absorption enhancement in thin-film solar cells 22 p3319 A83-46735
 Neutral interstellar gas in the lower galactic halo 22 p3381 A83-46983
 Photoionisation spectrum of Te I - Autoionising series and relative cross section 23 p3506 A83-48584
 Nonlinear noise fields and strongly driven atomic transitions 24 p3587 A83-48839
ABSORPTION SPECTROSCOPY
 NT OPTOGALVANIC SPECTROSCOPY
 High-resolution atmospheric spectroscopy using a diode laser heterodyne spectrometer 03 p0327 A83-13984
 Spatially resolved IR absorption spectroscopy by optical Stark modulation 03 p0295 A83-14376
 Feasibility of determining concentrations of atmospheric pollutants by comparative absorption using lasers having a single emission line 05 p0659 A83-17057
 Laser absorption under saturation conditions with allowance for spectral hole burning 05 p0651 A83-17869
 High-performance transient absorption spectrometry on the nanosecond scale 08 p1105 A83-23228
 Shock-tube absorption measurements of OH using a remotely located dye laser 09 p1269 A83-24438
 Absorption of 9.6-micron CO₂ laser radiation by CO₂ at elevated temperatures 09 p1272 A83-24447
 Daytime mesospheric temperatures over the low-latitude station Thumba derived from rocket-borne solar Lyman-alpha absorption measurements 09 p1307 A83-24691
 Photophoretic spectroscopy - A search for the composition of a single aerosol particle 09 p1297 A83-25183
 The diffuse interstellar medium and the CES --- Coude Echelle Spectrograph 09 p1365 A83-25299
 Number density of the 5s states during the ionisation relaxation of shock heated krypton 10 p1479 A83-26176
 Resonance absorption measurements of atom concentrations in reacting gas mixtures. IX - Measurements of O atoms in oxidation of H₂ and D₂ 10 p1480 A83-26182
 Analysis method for Fourier transform spectroscopy 10 p1424 A83-26867
 Infrared absorption spectroscopy with color center lasers 11 p1653 A83-27529
 Frequency modulation spectroscopy and frequency domain optical memories 11 p1656 A83-27594

CW ultraviolet saturation spectroscopy of the 6p 3P₀-9s 3S₁ transition in Mercury at 246.5 nm 12 p1778 A83-29191
 An IR spectrometry experiment for the Spacelab I mission [ONERA, TP NO. 1983-98] 14 p1983 A83-31825
 Atomic absorption spectroscopy in studying metal vaporization --- Russian book 15 p2133 A83-34750
 Infrared absorption spectroscopy applied to stratospheric profiles of minor constituents [ONERA, TP NO. 1983-99] 16 p2380 A83-36150
 Spatially resolved tunable diode-laser absorption measurements of CO using optical Stark shifting 17 p2485 A83-37747
 Absorption of H₂S at DF laser wavelengths 19 p2852 A83-41108
 Measurement of the J = 0-1 rotational transitions of three isotopes of ArD(+) 20 p3045 A83-42642
 Remote sensing applications of pulsed photothermal radiometry 20 p2992 A83-43594
 Atomic absorption analysis in ferrous metallurgy --- Russian book 21 p3114 A83-45008
 Balloon-borne diode-laser absorption spectrometer for measurements of stratospheric trace species 22 p3288 A83-46079
 Remote measurements of atmospheric NO₂ concentration by means of a differential-absorption lidar 23 p3453 A83-47165
 The Hull coherent DIAL programme --- differential-absorption LIDAR 23 p3456 A83-47770
 Measurements of atmospheric trace gases by long path differential UV/visible absorption spectroscopy 23 p3456 A83-47778
 2.7 measurements of HONO, NO₃, and NO₂ by long-path differential optical absorption spectroscopy in the Los Angeles Basin 23 p3478 A83-47779
 Ozone and water vapor monitoring using a ground-based lidar system 23 p3481 A83-47794
 The unexpectedly high solubility of water in cryogenic liquids 24 p3570 A83-50114

ABSORPTIVE INDEX

U ABSORPTIVITY

ABSORPTIVITY

The estimation of the absorption coefficients of ozone adopted for the Dobson spectrophotometer in the new selected additional wavelengths 01 p0071 A83-10290
 Ozone absorption coefficients' role in Dobson instrument ozone measurement accuracy 03 p0357 A83-13542
 Optical absorption coefficient and minority carrier diffusion length measurements in low-cost silicon solar cell material 03 p0354 A83-13922
 Spectral selectivity of high-temperature solar absorbers. II Effects of interference 04 p0505 A83-15488
 Strong photoinduced infrared absorption in GaP 07 p0999 A83-20745
 Effect of the temperature dependence of optical properties of materials on their radiant heating 09 p1259 A83-24012
 Multiwavelength laser rate calorimetry on various infrared window materials 09 p1346 A83-24967
 Temperature dependence of the classical potential of intermolecular interaction and the light absorption coefficient in the wing of the 4.3 micron band of CO₂ 10 p1478 A83-25524
 Determination of absorption coefficients in shock heated propellant mixtures for laser-heated rocket thrusters 10 p1387 A83-26170
 Interpretation of temperature dependences of the absorption coefficient in the 8-12 micron atmospheric window on the basis of the generalized line profile 11 p1584 A83-28550
 Measurement of the indices of refraction and the absorption coefficients of dielectric materials in the millimeter wave region 11 p1664 A83-28717
 Experimental study of the pure rotational S₁ line of the H₂-He spectrum induced by an absorption defect collision due to collisional interference effects 12 p1778 A83-29390
 Optical transmission through aerosol deposits on diffusely reflective filters - A method for measuring the absorbing component of aerosol particles 13 p1880 A83-31454
 Studies of the gap states density in undoped and doped amorphous hydrogenated silicon 14 p2088 A83-32237
 The absorption coefficient of light in the wing of the 4.3 micron band of CO₂ 14 p2082 A83-32556
 Direct free-hole absorption induced in germanium by 1.06 micron picosecond pulses 14 p2093 A83-33428
 Absorption coefficient of electron cyclotron radiation in a plasma in the temperature range 5-20 keV 16 p2416 A83-35891

Total band absorptance, emissivity, and absorptivity of the pure rotational band of water vapor 16 p2411 A83-36800

Cyclotron absorption of finite-amplitude waves 16 p2417 A83-36932

Experimental investigation of absorption coefficient of cesium resonance doublets in a plasma of combustion products 18 p2746 A83-39859

Linear absorption coefficient of beryllium in the 50-300-A wavelength range --- bandpass filter materials for ultraviolet astronomy instrumentation 23 p3508 A83-47588

ABSTRACTS

Miami International Conference on Alternative Energy Sources, 5th, Miami Beach, FL, December 13-15, 1982, Proceedings of Condensed Papers 10 p1445 A83-25575

Bibliography of the moon and the planet (with name index) --- of articles on moon, planets and other solar system bodies 16 p2439 A83-36790

ABUNDANCE

Discovery of CaII absorption at 1840 A in IUE spectra of two helium-rich white dwarfs 01 p0125 A83-10928

Physical conditions and carbon monoxide abundance in the dark cloud B5 02 p0251 A83-11586

Metal abundances of RR Lyrae stars in globular clusters 02 p0251 A83-11592

The chemical composition of R Coronae Borealis and XX Camelopardalis 02 p0252 A83-11594

Primary nucleosynthesis in the galactic disk 02 p0252 A83-11599

Oscillator strengths for Y I and Y II and the solar abundance of yttrium 02 p0268 A83-11608

The abundance of the actinides in the cosmic radiation as measured on HEAO 3 02 p0272 A83-11619

Siderophiles in the Brachina meteorite - Impact melting 02 p0263 A83-11624

Terrestrial-type xenon in meteoritic troilite 02 p0263 A83-11625

Observations of the infrared fine-structure lines of S III at 18.71 and 33.47 microns in four H II regions 02 p0255 A83-12119

The interstellar absorption-line spectrum of Mu Ophiuchi 02 p0256 A83-12124

Element segregation in stellar outer layers 02 p0258 A83-12177

Sulfuric acid vapor and other cloud-related gases in the Venus atmosphere - Abundances inferred from observed radio opacity 02 p0266 A83-12564

A CO2-rich coma model applied to the neutral coma of Comet West 02 p0262 A83-12923

The carbon and nitrogen abundances in WN and WC Wolf-Rayet stars 03 p0412 A83-13306

Color differences and chemical abundances in lunar soils 03 p0432 A83-13367

Spectrophotometry of comets at optical wavelengths 03 p0416 A83-13393

The El'gygytgyn meteorite - Probable composition 03 p0434 A83-13896

Studies on the spectra of K-giants. I - Physical parameters and Fe and Ti abundances for 26 K-giants 03 p0419 A83-13927

The IUE spectrum of BD + 39 deg 4926 03 p0421 A83-14142

Two lithium-rich supergiants 03 p0421 A83-14144

The relationship between carbon monoxide abundance and visual extinction in interstellar clouds 03 p0423 A83-14192

Samples of the Milky Way --- isotopic abundances in Galactic cosmic rays 03 p0426 A83-14599

Investigation of the abundance of iron in the nondisturbed solar photosphere. I - Method for calculating theoretical profiles of Fe I. II - Determination of the abundance of Fe I 03 p0436 A83-14686

Carbon, nitrogen, and oxygen abundances in G8-K3 giant stars 03 p0430 A83-14802

Abundances in metal-poor stars. I - The globular clusters NGC 2808, NGC 3201, NGC 6397, and M 22 03 p0430 A83-14805

The solar abundance of tungsten 03 p0437 A83-14901

Abundances in metal-poor stars. II - The anomalous globular cluster Omega Centauri 04 p0550 A83-15041

Abundance of lithium in unevolved halo stars and old disk stars - Interpretation and consequences 04 p0550 A83-15043

Processes affecting abundances in the solar wind 04 p0574 A83-15121

An ultra-refractory inclusion from the Ormans carbonaceous chondrite 04 p0558 A83-15301

Carbon components and their isotopic compositions in the Allende meteorite 04 p0562 A83-15353

The variable carbon isotopic composition of type 3 ordinary chondrites 04 p0562 A83-15354

An inventory of particles from stratospheric collectors - Extraterrestrial and otherwise 04 p0563 A83-15366

Relationship between an iridium anomaly and the North American microtektite layer in core RC9-58 from the Caribbean Sea 04 p0563 A83-15370

Abundances of the elements in six stars in the globular cluster M22 04 p0553 A83-15620

The compositional classification of chondrites. III - Ungrouped carbonaceous chondrites 04 p0572 A83-16354

Solar-system abundances of the elements 04 p0572 A83-16357

On the C/H and D/H ratios in the atmospheres of Jupiter and Saturn 05 p0703 A83-16959

Atmospheric parameters and carbon abundance of white dwarfs of spectral types C2 and DC 06 p0826 A83-18093

Studies on the spectra of K-giants. II - Abundance determinations for K-giants from very strong iron lines 06 p0827 A83-18170

A search for the J = 1-0 transition of /C-14/O --- and Galactic abundance ratios for carbon isotopes 06 p0827 A83-18174

A kinematic and abundance survey at the galactic poles 06 p0833 A83-18859

Carbon, nitrogen, and iron-peak abundances for giants in the remote globular clusters NGC 7006 and Pal 13 06 p0835 A83-19051

Line identifications in the spectrum of HR 1100 06 p0821 A83-19068

Propagation effects in the hydrogen-to-helium ratio in the solar cosmic rays 06 p0856 A83-19170

The galactic abundance of deuterium - A test for cosmological models 06 p0837 A83-19215

The interstellar medium near the sun. III - Detailed analysis of the line of sight to lambda24 Scorpii 06 p0840 A83-19281

The ages and compositions of old clusters 06 p0840 A83-19283

The Cyanogen distribution of the red giants in M5 06 p0840 A83-19284

Evolutionary effects of helium diffusion in population II stars 06 p0840 A83-19286

The propagation of ultraheavy cosmic ray nuclei 06 p0858 A83-19297

A few relevant facts on the problem of the origin of the solar system 06 p0842 A83-19454

Condensation of grains --- relevance to astrophysical problems 06 p0842 A83-19455

Nuclear cosmochronology or the age of the elements 06 p0842 A83-19457

Chemical compositions of planetary nebulae 07 p1013 A83-20134

Dense cloud chemistry. II - The HCS+/+CS ratio 07 p1018 A83-20946

CN in dark clouds 07 p1020 A83-21119

Modeling of G333.6-0.2 as a spherical H II region 07 p1021 A83-21122

Measurements of stratospheric ethane in the Jovian South Polar Region from infrared heterodyne spectroscopy of the nu9 band near 12 microns 07 p1031 A83-21151

Non-resonance lines of neutral calcium in the spectra of Arcturus and Beta Virginis 07 p1024 A83-21227

Siderophile trace elements in the earth's oceanic crust and upper mantle 07 p0965 A83-21285

The lunar nearside highlands - Evidence of resurfacing 07 p1032 A83-21288

Evolution of Ca-Al-rich bodies in the earliest solar system 07 p1036 A83-21337

Growth by incorporation 07 p1036 A83-21337

Cloud height differences on Saturn 08 p1189 A83-22934

The isotopic composition and concentration of Ag in iron meteorites and the origin of exotic silver 08 p1190 A83-22995

Experimental investigation of the partitioning of phosphorus between metal and silicate phases - Implications for the earth, moon and eucrite parent body 08 p1190 A83-22997

Metal-deficient O9-B0 supergiants in the Small Magellanic Cloud 08 p1182 A83-23039

Interstellar absorption toward HD 14633 08 p1183 A83-23051

The depletion of calcium in the Rho Ophiuchi cloud 08 p1185 A83-23082

Excitation conditions in HII regions 09 p1361 A83-24514

A rediscussion of sulfur abundances in Magellanic Clouds and galactic H II regions 10 p1498 A83-25358

The abundance of M71 and 47 Tucanae 10 p1501 A83-25576

The abundance analysis of metal-poor late-type stars from a theoretical standpoint 10 p1501 A83-25578

The Cretaceous-Tertiary transition 10 p1448 A83-25650

ABUNDANCE

The chemical inhomogeneity of M22 10 p1502 A83-25711

Carbon and nitrogen abundances in giant stars of the metal-poor globular cluster M15 10 p1503 A83-25712

The hydrogen-depleted planetary nebulae Abell 30 and Abell 78 10 p1504 A83-25726

An analysis of the reflection spectrum of Jupiter from 1500 A to 1740 A 10 p1518 A83-25736

Interstellar abundances of oxygen and nitrogen 10 p1505 A83-25747

Iron and magnesium in the white dwarf GD 40 - A test of diffusion theory 10 p1509 A83-26384

The isotopic composition of solar flare noble gases 10 p1522 A83-26397

The polarization of millimeter-wave emission lines in dense interstellar clouds 10 p1513 A83-26713

Dependence of interstellar depletion on hydrogen column density - Possibilities and implications 10 p1513 A83-26716

Structure of dense molecular gas in TMC 1 from observations of three transitions of HC3N 10 p1513 A83-26717

Chemical separation in horizontal-branch stars 10 p1514 A83-26727

The cyanogen inhomogeneity of NGC 362 11 p1669 A83-27114

A laser-based technique for the measurement of hydrogen at local areas in metals 11 p1547 A83-27331

A new method for determining the helium abundance in the solar atmosphere /Invited Review/ 11 p1689 A83-27642

Effect of meteorologic conditions on total suspended particulate /TSP/ levels and elemental concentration of aerosols in a semi-arid zone /Beer-Sheva, Israel/ 11 p1613 A83-28093

Cosmological implications of helium and deuterium abundances on Jupiter and Saturn 11 p1686 A83-28388

Model-atmosphere analysis of high-dispersion spectra of four red giants and supergiants 12 p1790 A83-28879

The ratio of deuterium to hydrogen in interstellar space. V The line of sight to Epsilon Persei 12 p1790 A83-28882

Evolution of chemical abundances in massive stars. I - OB stars, Hubble-Sandage variables and Wolf-Rayet stars - Changes at stellar surfaces and galactic enrichment by stellar winds. II - Abundance anomalies in Wolf-Rayet stars in relation with cosmic rays and 22/Ne in meteorites 12 p1790 A83-28890

Oscillator strengths and Ne abundance in B stars 12 p1790 A83-28892

Comparison of mesospheric ozone abundances measured by the solar mesosphere explorer and model calculations 12 p1750 A83-28904

Interstellar carbon in meteorites 12 p1797 A83-28923

Helium on Venus - Implications for uranium and thorium 12 p1797 A83-28924

Mass spectrometry on the Venera 13 and Venera 14 landers Preliminary results 12 p1798 A83-29477

Venera 13 and Venera 14 gas-chromatography analysis of the Venus atmosphere composition 12 p1798 A83-29478

Spectroscopy of three ultraviolet-excess galaxies 12 p1796 A83-29489

Identification of Lanning 90 as a previously uncataloged cataclysmic variable 12 p1789 A83-29957

Helium abundance variations in the solar wind [AD-A129760] 13 p1964 A83-29991

The Corona Australis dark cloud 13 p1946 A83-30389

Methane abundance in the atmosphere of Uranus 13 p1961 A83-31201

Limits on Venus' SO2 abundance profile from interferometric observations at 3.4 mm wavelength 13 p1961 A83-31211

The ionization structure of planetary nebulae. III - NGC 7009 13 p1950 A83-31416

CNO abundances and the strengths of nova outbursts and hydrogen flashes on accreting white dwarfs 13 p1951 A83-31428

Barium from a mini r-process in supernovae 13 p1951 A83-31429

The r- and s-process nuclei in the early history of the galaxy - HD 122563 13 p1952 A83-31430

Temporal variations of nucleonic abundances in solar flare energetic particle events. I - Well-connected events 13 p1965 A83-31436

On the global distribution of Pluto's atmosphere 13 p1962 A83-31438

Cosmic-ray abundances of Sn, Te, Xe, and Ba nuclei measured on HEAO 3 13 p1953 A83-31446

Abundance analyses of main-sequence stars in a possible nitrogen deficient cluster NGC 6231 13 p1956 A83-31677

The pure rotation spectrum of the hydroxyl radical and the solar oxygen abundance 13 p1965 A83-31701

A survey of spectral morphology and rotational velocities among the helium-rich stars 14 p2105 A83-33197

The spectra of Wolf-Rayet stars. I - Optical line strengths and the hydrogen-to-helium ratios in WN type stars 14 p2105 A83-33201

The binary nature of the barium stars. II - Velocities, binary frequency, and preliminary orbits 14 p2099 A83-33204

Observations of ultraviolet carbon lines in the spectra of three DC white dwarfs 14 p2105 A83-33206

Extinct radioactivities - A three-phase mixing model --- for early solar system abundances 14 p2106 A83-33215

The discovery of nonradial instability strips for hot, evolved stars 14 p2106 A83-33229

Convective mixing length and the galactic carbon to oxygen ratio 14 p2107 A83-33241

Narrow-band photometry in the 1-4 micron region - Calibration and applications 14 p2100 A83-33258

The spectrum of the star Ap HD 3473 14 p2108 A83-33269

Ultraviolet observations of planetary nebulae - NGC 6572, NGC 5315 and BD + 30 deg 3639 14 p2109 A83-33280

Ultraviolet spectrum of the planetary nebula NGC 7662 14 p2109 A83-33281

Chemical enrichment in halo planetary nebulae 14 p2110 A83-33282

The chemical composition of NGC 288 14 p2110 A83-33460

Chemical abundances of the extreme-velocity RR Lyrae variable VY Serpentis 14 p2110 A83-33462

On nucleosynthesis in supernovae beyond the iron peak 15 p2254 A83-33716

The Hyades CN anomaly? 15 p2245 A83-33837

PL 1547.3-5612 - A pure nitrogen ring nebula 15 p2260 A83-34126

Density inhomogeneities and the deduced chemical composition of planetary nebulae 15 p2261 A83-34502

DDO photometry of the open cluster IC 4756 15 p2247 A83-34505

Reticon observations of the yellow symbiotic star AG Draconis 15 p2247 A83-34532

Emission features in the solar corona after the perihelion passage of Comet 1979 XI 15 p2281 A83-34533

Stellar chromospheric temperatures 15 p2262 A83-34539

Effect of variations of opacity and helium-hydrogen ratio on pulsational instability 15 p2263 A83-34548

Accuracy of abundance determinations by weighting functions method of curves of growth --- of stars 15 p2263 A83-34556

The chemical composition of Algol systems. II - The carbon and nitrogen abundances of the secondaries of U Cep and U Sge 15 p2265 A83-34593

Doubly ionized aluminium - A diagnostic of cooling gas in the galactic corona 15 p2266 A83-34600

Zinc as a tracer of metallicity in the interstellar medium 15 p2266 A83-34604

The M17 SW molecular cloud 15 p2267 A83-34627

The effect of a readily ionized element on stellar atmospheres 15 p2270 A83-34686

Pulsations of stellar models in H and He burning phases 15 p2272 A83-34778

CNO abundances from pre-maximum spectra of Nova Cygni 1975 16 p2429 A83-36543

Determination of natural radiative lifetimes of the 5p2 P state in Ga I and 6p2 P state in In I using a pulsed dye laser 16 p2410 A83-36653

The hydrogen-rich, cool DA white dwarf Ross 627 16 p2433 A83-36697

Note on technetium in stars 16 p2433 A83-36703

Nickel isotopic studies in meteorites 16 p2438 A83-36746

Ni isotopic compositions in Allende and other meteorites 16 p2438 A83-36747

The problem of rare gases in the Venus atmosphere 17 p2618 A83-37431

Energetic oxygen and sulfur ions in the Jovian magnetosphere and their contribution to the auroral excitation 17 p2618 A83-37580

A detailed analysis of F-type supergiants. I - The distribution of microturbulence and the abundance of elements in the atmospheres of the stars Gamma Cyg and Alpha UMi 17 p2601 A83-37701

A spectrophotometric investigation of the lithium star Xi Boo A 17 p2590 A83-37732

The stages of the irradiation of protoplanetary matter by cosmic rays 17 p2619 A83-37815

The chemical composition of stars in globular clusters 17 p2602 A83-37828

Fourier spectroscopy of the (C-12)2, (C-13)2, and (C-12)(C-13) (0-0) Swan bands 17 p2578 A83-37831

A comparison between observed and theoretical H-R diagrams for the young LMC star cluster NGC 1866 17 p2604 A83-37915

Methane on Triton and Pluto - New CCD spectra 17 p2619 A83-37935

The galactic abundance gradient --- in H II regions 17 p2606 A83-38237

On the carbon overabundance in the OBC-type stars 17 p2606 A83-38239

Spectrophotometry in the galactic supernova remnants RCW 86, 103 and Kepler 17 p2593 A83-38248

The galactic globular cluster system - Helium content versus metallicity 17 p2609 A83-38424

The canonical anticorrelation between Y and Z in galactic globular clusters and the case of the pulsators in M15 17 p2609 A83-38425

Carbon isotopic variation in spectral type II diamonds 17 p2545 A83-38603

Carbon isotopic variation within individual diamonds 17 p2545 A83-38604

Orbital and chemical properties of globular clusters and halo stars 18 p2770 A83-39667

Primordial nucleosynthesis and scale-covariant cosmology 18 p2774 A83-39736

Very massive stars - Evolution with mass loss. I - The hydrogen and helium burning phase 18 p2775 A83-39744

The cosmological relevance of light element abundances 18 p2776 A83-39772

Rare earth abundances in chondritic phosphates and their implications for early stage chronologies 18 p2780 A83-40348

Dependence of the velocity ellipsoid for nearby stars upon metallicity and spectral type 18 p2778 A83-40482

The solar mercury abundance 19 p2923 A83-40719

Abundances in metal-poor stars. III - Eleven field giants 19 p2914 A83-40721

The HCO(+)/HOC(+) abundance ratio in molecular clouds 19 p2919 A83-41625

Sulfur abundances in three halo planetary nebulae 19 p2919 A83-41629

Determinations of S III, O IV, and Ne V abundances in planetary nebulae from infrared lines 19 p2919 A83-41630

Abundances in globular cluster red giants. V - The metal-rich globular clusters 19 p2919 A83-41631

r-process abundances near the mass 130 peak 19 p2920 A83-41640

Selective nonresonant acceleration of He-3(2+) and heavy ions by H(+) cyclotron waves --- in solar flares 19 p2925 A83-41657

Some recent developments in the study of the elements and isotopes of the cosmic radiation 19 p2926 A83-42161

Spectrum analysis of the barium stars HD 83548 and HD 65699 20 p3065 A83-42384

Comparison of C(+) distributions with new interstellar sources of HCO emission 20 p3067 A83-42444

The evolution of large planetary nebulae and their central stars 20 p3067 A83-42447

Cross section for the reaction C-12(e,p)B-11; and its relevance to the formation of B-11 in active galaxies 20 p3068 A83-42464

Mg-26(p, n)Al-26 cross section measurements --- abundance anomalies in Allende meteorite 20 p3069 A83-42465

Lithium abundance and age spread in the Pleiades 20 p3072 A83-43059

Observations of interstellar C2 toward three heavily reddened stars 20 p3074 A83-43092

Hf chronometer for the early solar system 20 p3076 A83-43539

Abundance of cosmic-ray elements from sulfur to nickel as a function of atmospheric depth 20 p3083 A83-43668

Stellar deuterium abundance - A new upper limite in Canopus 21 p3228 A83-44406

Interstellar C2 in the Ophiuchus clouds 21 p3228 A83-44409

Abundance gradients in galaxies in the Sculptor and Centaurus groups 21 p3233 A83-44750

The effect of hyperfine structure on stellar abundance analysis 21 p3233 A83-44752

The helium abundance and the isotropy of the universe 21 p3234 A83-44766

Cosmogonical implications of elemental and isotopic abundances in atmospheres of the giant planets 21 p3241 A83-44991

The extraordinary extragalactic supernova remnant in NGC 4449. II - X-ray and optical investigations 21 p3236 A83-45533

The evolutionary state and pulsation characteristics of red variables in globular clusters 21 p3236 A83-45544

The ellipticities of globular clusters and the second parameter problem 21 p3237 A83-45556

Remote sensing by IR heterodyne spectroscopy 22 p3260 A83-46078

Abundances of carbon-bearing diatomic molecules in diffuse interstellar clouds 22 p3377 A83-46259

The magnetic fields of the helium-weak B stars 22 p3377 A83-46265

Abundance sensitive parameters for red giants in globular clusters 22 p3378 A83-46545

S stars in Omega Centauri 22 p3378 A83-46547

Composition of bulk samples and a possible pristine clast from Allan Hills A81005 22 p3387 A83-46877

Element identifications in the ultraviolet spectrum of HD 101065 22 p3382 A83-46993

Effect of molecules and grains on Rosseland mean opacities --- for stellar structure calculations 22 p3383 A83-47005

The Jovian spectrum in the 3-micron window 22 p3388 A83-47082

Significance of ultraheavy cosmic rays 23 p3539 A83-47738

Cosmic-ray isotopic composition 23 p3539 A83-47739

Cosmic ray sources 23 p3539 A83-47749

A detector to investigate the anomalous component of cosmic rays and its rarer constituents including a possible molecular ion component 23 p3540 A83-47756

The effect of cross-section uncertainties on the derivation of source abundances from cosmic-ray composition observations 23 p3540 A83-47760

Laboratory measurements of D/H ratios in interplanetary dust 23 p3529 A83-48084

Planetary nebulae; Proceedings of the Symposium, University College, London, England, August 9-13, 1982 24 p3638 A83-49126

Planetary nebulae - An introductory review 24 p3638 A83-49127

Molecules in planetary nebulae 24 p3651 A83-49134

Some recent results from UV observations 24 p3639 A83-49136

Type I planetary nebulae 24 p3652 A83-49143

Elemental abundances in planetary nebulae 24 p3652 A83-49144

Effects of dust formation on chemical abundances --- in planetary nebulae 24 p3652 A83-49145

Planetary nebulae in the Magellanic Clouds 24 p3640 A83-49156

Planetary nebulae in Local Group galaxies 24 p3640 A83-49157

On the nature of early-type stars in the galactic halo 24 p3660 A83-49383

Chemical and isotopic study of extraterrestrial particles from the ocean floor 24 p3672 A83-49398

Rb-Sr, Sm-Nd, K-Ca, O, and H isotopic study of Cretaceous-Tertiary boundary sediments, Caravaca, Spain 24 p3672 A83-49399

Planetary nebulae - IUE results 24 p3662 A83-49567

Star formation and abundance gradients in the galaxy 24 p3664 A83-49997

ESO Workshop on Primordial Helium, Garching, West Germany, February 2, 3, 1983, Proceedings 24 p3664 A83-50030

The origin of the light elements - A quite complex problem --- primordial abundances in universe 24 p3664 A83-50031

Primordial nucleosynthesis - A theorist's shopping list 24 p3665 A83-50032

Neutrinos, the He-4 abundance, and stellar evolution 24 p3665 A83-50033

The primordial helium abundance and the age of the universe 24 p3665 A83-50034

Nuclear uncertainties of element yields in the big bang 24 p3665 A83-50035

On the mass range of the first stars 24 p3665 A83-50036

Pregalactic synthesis of deuterium 24 p3665 A83-50037

Evolution of zero metal stars and early chemical enrichment of the Galaxy 24 p3665 A83-50038

Helium production by low and intermediate mass stars 24 p3665 A83-50040

The protosolar helium abundance 24 p3675 A83-50041

Helium and deuterium in the outer solar system 24 p3665 A83-50042

Helium abundances from young stars and open clusters 24 p3666 A83-50043

The helium abundance of halo dwarfs 24 p3666 A83-50044

Observational evidence for helium production in stars - The helium abundance of hot subdwarfs, central stars of planetary nebulae, very massive O-stars and OBN-stars 24 p3666 A83-50045

The helium abundances of G-K main sequence halo and disk stars, the helium galactic abundance evolution and the astrometric satellite Hipparcos 24 p3666 A83-50046

Primordial helium in galactic globular clusters 24 p3666 A83-50047

Globular cluster colour-magnitude diagrams - Possible evidence for helium abundance variations 24 p3666 A83-50048

Helium content in globular clusters - The R-method 24 p3666 A83-50049

Helium abundances in globular star clusters 24 p3666 A83-50050

Helium in supernova remnants 24 p3666 A83-50052

Determining helium abundances in H II regions 24 p3666 A83-50053

On the pregalactic He/H abundance ratio derived from planetary nebulae 24 p3667 A83-50054

He-4 determinations from radio recombination lines --- of interstellar matter 24 p3667 A83-50055

Primordial helium abundance determinations using galactic H II regions 24 p3667 A83-50056

Pregalactic helium abundance determination from extragalactic H II regions 24 p3667 A83-50057

Are three systematic observational effects on abundance determinations in giant extragalactic H II regions? 24 p3667 A83-50058

Abundance of lithium in old dwarf stars 24 p3667 A83-50060

The interstellar lithium abundance 24 p3667 A83-50061

Detection of the 3.46 cm line of interstellar He-3(+) (He-3(+)/H(+) ratios 24 p3667 A83-50062

Calculation of stellar structure. III - Solar models that satisfy the necessary conditions for a unique solution to the stellar structure equations 24 p3675 A83-50091

Infrared fluorescence of molecules in comets - The general synthetic spectrum 24 p3669 A83-50098

Mantle plume noble gas component in glassy basalts from Reykjanes Ridge 24 p3608 A83-50111

Chemical evolution of the galactic halo. II - Enrichment in primary elements 24 p3670 A83-50154

Pi Gruis - Molecular identifications and spectral classification 24 p3670 A83-50156

Measurement of the relative composition of the cosmic-ray iron group with lexan polycarbonate 24 p3676 A83-50163

AC (CURRENT)

U ALTERNATING CURRENT

AC GENERATORS

Digital computer simulation of 3-phase full-wave SCR bridge regulator 01 p0043 A83-11252

AC-1 AIRCRAFT

U DHC 4 AIRCRAFT

ACCELERATED LIFE TESTS

Accelerated life tests of aircraft thermocouples 01 p0009 A83-10442

Analysis of accumulated damage in accelerated fatigue testing by the increasing load methods 01 p0059 A83-10686

Results of the mission profile life test --- for J-series mercury ion engines 02 p0144 A83-12480

[AIAA PAPER 82-1905] Structural service life estimate for a reduced smoke rocket motor 02 p0148 A83-13088

Space environmental effects on materials 03 p0291 A83-14125

TF41/Lamilly accelerated mission test 04 p0449 A83-15319

Status cells - A demonstration of performance reproducibility, capacity retention, and cycle life for LiAl/FeS cells 04 p0506 A83-15868

Accelerated thermal cycling of spacecraft solar-cell modules 05 p0603 A83-17436

Pulsed laser diode reliability tests 07 p0917 A83-19707

Estimation of mixed Weibull parameters in life testing 07 p0943 A83-20517

Comparison of several accelerated laboratory tests for the determination of localized corrosion resistance of high-performance alloys 08 p1066 A83-22650

Nonparametric accelerated life testing 08 p1114 A83-22707

The influence of environmental effects on the mechanical properties of graphite/epoxy laminates 09 p1221 A83-23369

Accelerated aging studies of low density /hydrocarbon/ resin systems 09 p1222 A83-23646

Helicopter engine development - New standards for the '80s 09 p1208 A83-24837

Analytical description of the aging of polyamide 6 under fatigue fracture 09 p1239 A83-25023

Accelerated cycle life tests of Ni/Cd cells with ED nickel electrodes - Comparison of three separators 11 p1605 A83-27192

Long life Ni/Cd cells with zirconia separators - Accelerated cycle tests 11 p1605 A83-27193

Life test report for ETS-III battery 11 p1539 A83-27195

NiCd lifetime prediction for LEO 11 p1540 A83-27199

Outdoor and laboratory testing of photovoltaic modules 13 p1862 A83-31482

Accelerated weathering of photovoltaic modules employing natural sunlight 13 p1862 A83-31484

Aluminum/ammonia heat pipe gas generation and long term system impact for the Space Telescope's Wide Field Planetary Camera [AIAA PAPER 83-1428] 14 p2009 A83-32704

A study of the high-cycle fatigue of materials under plane cantilever bending 14 p1998 A83-33020

High-frequency fatigue testing of structural steels and alloys at 77 K 14 p1998 A83-33021

Canadian forces tracker aircraft full-scale fatigue test at the National Aeronautical Establishment 15 p2122 A83-33548

An approach to accelerated testing 15 p2173 A83-33549

Prediction of constant amplitude fatigue lives of precracked specimens from accelerated fatigue data 15 p2140 A83-34743

Statistical study of TBO and estimation of acceleration factors of ASMT for aircraft turbo-engine --- Accelerated Simulated Mission Endurance Testing 16 p2304 A83-35858

Accelerated Mission Testing of the F110 Engine [AIAA PAPER 83-1235] 16 p2308 A83-36298

Accelerated simulated mission endurance test of a turboshaft engine for military attack helicopter application [AIAA PAPER 83-1359] 16 p2309 A83-36357

Development of simulated mission endurance test acceleration factors in determining engine component serviceability and failure mode criticality [AIAA PAPER 83-1409] 16 p2310 A83-36398

Accelerated temperature aging of black chrome solar selective coatings 16 p2421 A83-36736

Optimum simple step-stress plans for accelerated life testing 17 p2517 A83-37291

Titanium fan disc Structural Life Prediction/Correlation program [SAE PAPER 821437] 17 p2522 A83-37985

The generation of random load sequences for serviceability tests on the basis of measured values stored in Markov transition matrices 18 p2697 A83-39257

A technique for the accelerated life testing of fan impellers 18 p2698 A83-39512

Qualification and durability tests - Applications for thermal collectors and photovoltaic modules 18 p2710 A83-40531

On the accelerated ageing of CFRP 20 p2946 A83-42802

Evaluation of a 90-mm bore bearing operating in a simulated space environment [ASLE PREPRINT 83-AM-1A-3] 20 p2999 A83-43332

Dust storm simulation for accelerated life testing of solar collector mirrors 21 p3168 A83-45063

Polymers in solar energy utilization 23 p3433 A83-47823

ACCELERATION (PHYSICS)

NT ANGULAR ACCELERATION

NT DECELERATION

NT ELECTRON ACCELERATION

NT HIGH ACCELERATION

NT HIGH GRAVITY ENVIRONMENTS

NT IMPACT ACCELERATION

NT LUNAR GRAVITATIONAL EFFECTS

NT PARTICLE ACCELERATION

NT PLASMA ACCELERATION

NT SPIN REDUCTION

Knee-ligament loading properties as influenced by gravity. I - Junction with bone of 3-G rodents 02 p0223 A83-12407

Ferromagnetic resonance g-factor measurement on LUNA 20 soil 03 p0432 A83-13297

Covariational analysis of the correlation between lunar relief and the acceleration due to gravity 03 p0432 A83-13369

The precise measurement of gravitational acceleration using a laser interferometric technique 04 p0481 A83-15275

ACCELERATION STRESSES (PHYSIOLOGY)

Investigation of the motion of the center of mass of an occupant under ejection accelerations 04 p0525 A83-15411

On one-dimensional acceleration waves in composite materials modeled as interpenetrating solid continua 06 p0776 A83-19000

Nonlinear hydrodynamic pressure on an accelerating plate 08 p1084 A83-22377

Rayleigh-Taylor instability with spatially varying acceleration - An illustration 08 p1168 A83-22378

The fourth test of General Relativity 09 p1357 A83-23855

Operational utilization study on new human centrifuge of JASDF. II - Capability and usability of the new systems 10 p1458 A83-26088

Operational utilization study on new human centrifuge of JASDF. III - Measurement of a three-axis acceleration force in human centrifuge 10 p1458 A83-26089

Operational utilization study on new human centrifuge of JASDF. IV - Test and evaluation of anti-g system 10 p1458 A83-26090

Exceedance statistics of accelerations resulting from thruster firings on the Apollo-Soyuz mission 15 p2126 A83-33746

On the analysis of motions perpendicular to the galactic plane 18 p2758 A83-39634

The maneuver acceleration parameter - A figure of merit for evaluating missile miss distance performance [AIAA PAPER 83-2199] 19 p2796 A83-41684

Determination of physically achievable accelerations in the problem of the spatial convergence of a material point --- for ergatic control system synthesis 20 p3035 A83-43502

Effect of deploying acceleration on a flexible antenna of a spin-satellite 21 p3099 A83-44015

The secular accelerations in Gylden's problem --- of lunar motion 24 p3643 A83-49391

High and low thrust acceleration 24 p3551 A83-49625

The effect of the acceleration of the external force on the evolution of a combustion site in a closed vessel 24 p3555 A83-49759

Optimum conditions for the acceleration of the flame of gas mixtures at discontinuous obstacles in large volume 24 p3555 A83-49768

Flow of a dipolar fluid due to suddenly accelerated flat plate 24 p3581 A83-50149

Finite difference analysis of MHD free-convection flow past an accelerated vertical porous plate 24 p3633 A83-50165

ACCELERATION PROTECTION

Studies on an acceleration platform and at the time of a simulated crash of helicopter anticrash seats 08 p1043 A83-22976

Study of +Gz protection given by an anti 'G' suit worn on top of a liquid cooled suit 09 p1324 A83-24003

Operational utilization study on new human centrifuge of JASDF. IV - Test and evaluation of anti-g system 10 p1458 A83-26090

Combining techniques to enhance protection against high sustained accelerative forces 12 p1766 A83-28932

ACCELERATION STRESSES (PHYSIOLOGY)

NT CENTRIFUGING STRESS

A comparison of some effects of three antmotion sickness drugs on nystagmic responses to angular accelerations and to optokinetic stimuli 04 p0521 A83-15533

Acceleration-induced ventricular tachycardia in asymptomatic men - Relation to mitral valve prolapse 06 p0797 A83-18196

Cinematography data systems at the Naval Biodynamics Laboratory 08 p1102 A83-22791

Targets for three-dimensional /3-D/ tracking of human impact test subjects 08 p1102 A83-22792

Medical standards for experimental human use in acceleration stress research 10 p1454 A83-25671

Effects of chronic acceleration on body composition 11 p1635 A83-27780

Altered auditory function in rats exposed to hypergravic fields 11 p1637 A83-27808

Influence of abdominal restriction on gas exchange during +Gz stress in dogs 11 p1637 A83-27809

The application of positive pressure breathing for improving +Gz acceleration tolerance 12 p1764 A83-28931

Combining techniques to enhance protection against high sustained accelerative forces 12 p1766 A83-28932

The effect of vision on the endurance by humans of the continuous action of Coriolis acceleration 12 p1764 A83-29273

Vibratory behavior of the lumbo-sacral joint after ablation of the pulposus nucleus 14 p2063 A83-32459

- An investigation of motion base cueing and G-seat cueing on pilot performance in a simulator
[AIAA PAPER 83-1084] 16 p2401 A83-36209
- The behavior of heart rate in flight under +Gz stimulation
Continuous monitoring using Holter's method and catecholamine excretion 17 p2561 A83-38944
- Cardiopulmonary responses to combined lateral and vertical acceleration 18 p2734 A83-40360
- The acquisition and validation of the surface electromyogram signal for evaluating muscle fatigue 21 p3187 A83-43998
- Pathophysiological effects of acceleration stress in the miniature swine 24 p3617 A83-48876
- ACCELERATION TOLERANCE**
- Positive G tolerance of Indian subjects - Effects of age and flying experience 09 p1323 A83-24004
- Circadian variations in tolerance to +Gz acceleration 11 p1642 A83-27783
- Human tolerance to rotation at different G's 11 p1642 A83-27784
- Enhancement of chronic acceleration tolerance by selection 11 p1637 A83-27804
- The application of positive pressure breathing for improving +Gz acceleration tolerance 12 p1764 A83-28931
- Combining techniques to enhance protection against high sustained accelerative forces 12 p1766 A83-28932
- The effect of vision on the endurance by humans of the continuous action of Coriolis acceleration 12 p1764 A83-29273
- Effects of strength training on g tolerance 21 p3186 A83-43989
- ACCELERATORS**
- Magnetic acceleration of interstellar probes 01 p0016 A83-10703
- Investigation of the jet parameters of a source of accelerated gas flow for an aerodynamic test facility 24 p3545 A83-49659
- ACCELEROMETERS**
- NT STRAIN GAGE ACCELEROMETERS
- A spaceborne superconducting gravity gradiometer for mapping the earth's gravity field 01 p0020 A83-10025
- Integrated optics strapdown inertial system 03 p0326 A83-13755
- Accelerometer-enhanced orbit control near the sun-earth L1 libration point [AIAA PAPER 83-0018] 05 p0601 A83-16467
- Concerning the measurement of aircraft acceleration 05 p0595 A83-16876
- The Venus stratosphere according to Venera-11 and Venera-12 accelerometer data 06 p0848 A83-18364
- Combination of accelerometer and photographically derived kinematic variables defining three-dimensional rigid body motion 08 p1102 A83-22793
- Measuring shock and vibration 09 p1270 A83-25141
- Improved accelerometers for high accuracy strapdown inertial navigation systems 11 p1576 A83-28783
- A simple fibre Fabry-Perot sensor 12 p1729 A83-29189
- An onboard navigator for the extremely low-altitude satellite utilizing accelerometers 13 p1812 A83-30167
- Investigation of the characteristics of the Venus stratosphere from acceleration measurements during the braking of the Venera-13 and Venera-14 probes 14 p2110 A83-31959
- Investigation of a combined rotor vibratory gyroscope with a common elastic rotor suspension 15 p2166 A83-35263
- Modern technology and airborne engine vibration monitoring systems [AIAA PAPER 83-1240] 16 p2302 A83-36303
- Redundancy Management of Shuttle flight control rate gyroscopes and accelerometers 17 p2474 A83-37123
- Acceleration measurements in a high G environment 17 p2509 A83-37131
- Kalman filter formulations for transfer alignment of strapdown inertial units 18 p2739 A83-40303
- Investigation of the characteristics of the Venusian stratosphere on the basis of Soviet-probe accelerometer measurements 20 p3078 A83-42891
- Computer analysis of the operation of a pendulum accelerometer 24 p3586 A83-50211
- ACCEPTABILITY**
- Card level acceptance testing 13 p1861 A83-31183
- ACCEPTANCE**
- U ACCEPTABILITY
- ACCEPTOR MATERIALS**
- Residual double acceptors in bulk GaAs 07 p0998 A83-19989

- Evidence that the gold donor and acceptor in silicon are two levels of the same defect 13 p1928 A83-30340
- A study of the 0.1-eV conversion acceptor in GaAs 16 p2419 A83-35443
- Three holes bound to a double acceptor - Be(+) in germanium 21 p3218 A83-45199
- ACCESS CONTROL**
- Effects of cache coherency in multiprocessors 05 p0679 A83-17242
- Communication protocol for a multisatellite communication system 07 p0907 A83-19725
- Demand Assignment Multiple Access /DAMA/ techniques for satellite communications 07 p0907 A83-19727
- Performance analysis for an adaptive polling access-control scheme employing a dynamic reservation protocol 07 p0908 A83-19738
- A conditional algorithm for setting a discrete device with memory to a definite state 24 p3622 A83-50206
- ACCESS TIME**
- A fast method to retrieve data from a large star catalogue file 01 p0113 A83-10138
- Comparison of various data allocation schemes in the memory of a multiprocessor computing system 11 p1647 A83-28625
- A data structure and algorithm based on a linear key for a rectangle retrieval problem 24 p3619 A83-49194
- ACCIDENT INVESTIGATION**
- NT AIRCRAFT ACCIDENT INVESTIGATION
- Preliminary overview analyses of U.S. Navy Aircrew Automated Escape Systems /AAES/-in-service usage data 04 p0444 A83-15405
- ACCIDENT PREVENTION**
- Potential for catastrophic rupture of large liquid oxygen storage tanks 20 p2961 A83-43238
- The missing element in wind shear protection [SAE PAPER 830715] 20 p2937 A83-43325
- Reflections on the Potomac 21 p3089 A83-44876
- ACCIDENT PRONENESS**
- An investigation of the connection between solar activity and the severity of the consequences of traffic accidents in Moscow 02 p0222 A83-11880
- ACCIDENTS**
- NT BIRD-AIRCRAFT COLLISIONS
- ACCLIMATIZATION**
- NT ALTITUDE ACCLIMATIZATION
- NT COLD ACCLIMATIZATION
- NT HEAT ACCLIMATIZATION
- ACCOMMODATION COEFFICIENT**
- An experimental study of the thermal accommodation coefficients of inert gases on a tungsten surface 04 p0457 A83-16169
- The gas-grain interaction in the interstellar medium - Thermal accommodation and trapping 07 p1021 A83-21120
- Determination of basic constants of satellite - Atmosphere interaction from the analysis of motion of 1974-70A 16 p2314 A83-36114
- ACCRETION**
- U DEPOSITION
- ACCRETION DISKS**
- Jitter in SS 433-A clue to the collimation mechanism 01 p0126 A83-10967
- Thick supercritical accretion disks and active galactic nuclei 01 p0128 A83-11340
- Transport of neutrinos, radiation and energetic particles in accretion flows 02 p0276 A83-12031
- On the orbital phase dependence of the turn-on times of Hercules X-1 02 p0256 A83-12132
- On the instability of thick accretion disks 02 p0257 A83-12136
- On the compatibility of thermal and hydrostatic equilibrium in thin radiative accretion disks 02 p0260 A83-12527
- Luminosity limits for funnels in thick accretion discs 03 p0414 A83-13325
- On the evolution of convective accretion disk models of the primordial solar nebula 03 p0425 A83-14213
- Transonic accretion flow in a thin disk around a black hole 03 p0427 A83-14713
- Transonic disk accretion of barytropic gas onto black holes 03 p0427 A83-14714
- Hydrodynamical calculations of accretion disks in close binary systems. I - Method. II - Models 03 p0428 A83-14765
- The UV spectrum of the old nova HR Del at different orbital phases 03 p0428 A83-14770
- Are thick accretion disks the 'central engine' for astrophysical jets 03 p0431 A83-14875
- Accretion and inner excretion disks in close binaries 04 p0551 A83-15108
- Herbig-Haro Objects 46 and 47 - Evidence for bipolar ejection from a young star 05 p0700 A83-17031

- Theoretical decay rates of cataclysmic variable eruptions 06 p0827 A83-18165
- Disk accretion by dynamical friction - A model for the dynamical evolution of giant molecular clouds 06 p0832 A83-18836
- Four-color photometry of RZ Ophiuchi and its accretion disk 06 p0841 A83-19288
- Thick accretion disks around black holes /Karl Schwarzschild Lecture 1981/ 06 p0846 A83-19529
- Model protoplanetary disks around F-G stars 07 p1015 A83-20672
- Rayleigh-Taylor instability with spatially varying acceleration - An illustration 08 p1168 A83-22378
- The time-dependence of non-planar accretion discs 09 p1364 A83-25003
- GX 339-4 - X-ray spectra of high and low states 10 p1498 A83-25352
- Comptonization effects in spherical accretion onto black holes 10 p1515 A83-26739
- The symbiotic star CH Cyg - The occasional transition from an unstable to a stable accretion disk 11 p1678 A83-27687
- Evolution of accretion tori orbiting black holes. I - Theory 11 p1682 A83-28281
- On disk accretion --- in binary stars and black holes 12 p1791 A83-28986
- Temperature profile of accretion disk around a Kerr black hole 12 p1795 A83-29354
- Accretion of jet streams and formation of asteroids 12 p1795 A83-29357
- Runaway instability in accretion disks orbiting black holes 12 p1795 A83-29449
- On the nature of SS 433 13 p1947 A83-31252
- A family of three-dimensional orbits in the restricted problem of three bodies - Application to inclined disks 13 p1942 A83-31653
- Accretion in cataclysmic binaries. I - Modified alpha-disks with convection. II - Observational data 13 p1955 A83-31654
- Thick disks with equatorial accretion. II 13 p1955 A83-31660
- A model for the standstill of the Z Camelopardalis variables 13 p1959 A83-31737
- On the influence of the 'alpha-turbulence' on the energy transport in accretion disks 13 p1960 A83-31755
- The ultraviolet excess of luminous quasars. II - Evidence for massive accretion disks 15 p2256 A83-34085
- The abnormal temperature profile of accreting disk around the Kerr black hole 15 p2262 A83-34527
- Ultraviolet and optical observations of the dwarf novae VW and WX Hydr during outburst 15 p2264 A83-34576
- High speed photometry of the dwarf nova V2051 Ophiuchi 15 p2264 A83-34579
- The bright mass ejection on the disk on October 14, 1980 15 p2285 A83-35229
- The distinction between Seyfert 1 and Seyfert 2 galaxies 17 p2610 A83-38552
- WBVR photometry of SS 433 - Spectra of the 'normal' star and the accretion disk 17 p2611 A83-38559
- Magnetic field in the spherical accretion of black holes 18 p2766 A83-39247
- Active galactic nuclei as clusters of accreting black holes 18 p2766 A83-39248
- Dissipation of thick accretion disks 18 p2774 A83-39742
- On the hypothesis of ejection of supermassive black holes from centers of galaxies and its application to quasar-galaxy associations 18 p2775 A83-39758
- Intrinsic polarization of a precessing, electron-scattering accretion disk, with applications to SS 433 18 p2777 A83-40476
- Compton heated winds and coronae above accretion disks. I Dynamics 20 p3066 A83-42437
- Compton heated winds and coronae above accretion disks. II Radiative transfer and observable consequences 20 p3067 A83-42438
- The relationship between the X-ray and optical luminosities for QSOs 20 p3071 A83-43045
- The high-energy spectrum of hot accretion disks 20 p3073 A83-43072
- The old-nova GK Per (1901). III - Accretion disc models 21 p3231 A83-44447
- The asymptotic mass distribution for an accreting system of particles 21 p3234 A83-44759
- The minimum mantle viscosity of an accreting earth 23 p3529 A83-47856
- The evolution of viscous disks. IV - Stream penetration effects --- dwarf novae accretion disks 24 p3658 A83-49362
- On the evolution of accretion disc flow in cataclysmic variables. I - The prospect of a limit cycle in dwarf nova systems 24 p3659 A83-49377
- The disk-star boundary layer and its effect on the accretion disk structure 24 p3669 A83-50095

ACCUMULATIONS

- Accumulation and fragmentation in protoplanetary and protosatellite systems 04 p0557 A83-16034
- Accumulation effects at contacts to n-type cadmium-mercury-telluride photoconductors 06 p0753 A83-18947

ACCUMULATORS

- NT DUST COLLECTORS
- NT SOLAR COLLECTORS
- NT SOLAR REFLECTORS
- e-guns and depressed collectors for two-stage free electron lasers 10 p1427 A83-26008

ACCURACY

- The effect of imbalance in a dynamically adjustable gyroscope on its dynamics and accuracy 01 p0050 A83-10688
 - Accuracy enhancement of a broadband A.T.E. 01 p0037 A83-10770
 - Horizontal displacement of simulated cloud particles by the propeller of an aeroplane --- particle measurement accuracy 02 p0216 A83-12944
 - Models of satellite motion and the precision of the numerical prediction of orbits 03 p0283 A83-13295
 - The accuracy of measuring angular coordinates by means of antenna arrays 04 p0467 A83-15751
 - Estimation of the accuracy of synthesis of approximately optimal control for a nonlinear plant 04 p0527 A83-15915
 - Precision measurement of the angles of a radio telescope 06 p0761 A83-18037
 - Accuracy of optical angle estimator operating through the turbulent atmosphere 06 p0736 A83-18584
 - The accuracy of mass-spectrometer soundings in investigations of the flame structure of condensed systems 07 p0928 A83-19956
 - Maximum precision of the measurement of gravity gradients 07 p0989 A83-20854
 - A difference scheme of second-order accuracy with a minimal pattern for hyperbolic equations 09 p1335 A83-23567
 - Software correctness and reliability 09 p1326 A83-24247
 - An accuracy goal for a comprehensive satellite wind measuring system 10 p1451 A83-25394
 - Potential accuracy of the goniometer section of a complex short-range navigation system 10 p1375 A83-26929
 - Analysis of the precision of inertial navigation systems --- German thesis 11 p1528 A83-28649
 - Sensing relative attitudes for automatic docking 13 p1809 A83-30169
 - Analysis of the accuracy and sensitivity of algorithms for the processing of multidimensional signals and noise 14 p2001 A83-32488
 - Increasing the accuracy of static deformation measurements 14 p2019 A83-32570
 - Observable degree and accuracy of various attitude determination for spinning satellite 17 p2478 A83-37453
 - On the accuracy of calculating the aerodynamic characteristics of thin wings and airfoils by the method of discrete vortices 17 p2448 A83-37519
 - The accuracy check in numerical integration of dynamical systems 17 p2591 A83-37788
 - Statistical models for meteorological data analysis 17 p2551 A83-38745
 - The effect of manufacturing imperfections on the accuracy of inertial navigation systems 21 p3097 A83-44631
 - Unbalanced-bridge computational techniques and accuracy for automated multichannel strain-measuring systems 21 p3141 A83-45147
 - The potential accuracy of distance measurements in passive detection and ranging 22 p3272 A83-45670
- ACEE PROGRAM**
- Nonlinear controller for the pitch-up region [AIAA PAPER 83-0064] 05 p0597 A83-16496
 - Developments in the NASA transport aircraft laminar flow program [AIAA PAPER 83-0090] 05 p0579 A83-16514
 - Scale model performance test investigation of mixed flow exhaust systems for an energy efficient engine /E3/ propulsion system [AIAA PAPER 83-0541] 05 p0597 A83-16776
- ACETATES**
- Formation of amino acids from reactor-irradiated ammonium acetate 17 p2563 A83-38892
 - Nonenzymatic phosphorylation of acetate by carbamyl phosphate - A model reaction for prebiotic activation of carboxyl groups 19 p2887 A83-42157
 - Photothermal degradation of ethylene/vinylacetate copolymer 22 p3270 A83-46717
 - Investigations of sodium acetate trihydrate for solar latent heat storage, controlling the melting point 24 p3601 A83-50179

ACETONE

- Laboratory measurements of dry deposition of acetone over adobe clay soil 09 p1297 A83-25186
- Heat transfer during the boiling of acetone and ethyl alcohol in a thermosiphon with porous capillary structures on the heat-transfer face 11 p1571 A83-28798

ACETYL COMPOUNDS

- Peroxyacetyl nitrate in the free troposphere 11 p1613 A83-28399
- The ubiquity of peroxyacetyl nitrate in the continental boundary layer 19 p2863 A83-41974
- World-wide ambient measurements of peroxyacetyl nitrate (PAN) and implications for plant injury 23 p3479 A83-48690

ACETYLENE

- Spectroscopic detection of acetylene and ethane in the terrestrial atmosphere using ground-based solar IR observations 04 p0508 A83-16447
- Acetylene terminated fluorenone and its use with fluorenone polyesters 05 p0619 A83-17572
- Photochemistry of acetylene at 1849 Å 08 p1053 A83-22217
- An improved version of processible acetylene-terminated oligomers for composites and coatings 09 p1237 A83-23619
- Direct measurements of O-atom reactions with HCN and C2H2 behind shock waves 10 p1391 A83-26183
- The absorption spectrum of (C-12)D2 in the 1.06-micron region 14 p2048 A83-32833
- HCN formation on Jupiter - The coupled photochemistry of ammonia and Acetylene 15 p2275 A83-34718
- Soot formation in pyrolysis of acetylene, allene and 1,3-butadiene 18 p2664 A83-39274

ACHONDRITES

- The Nilpena ureilite, an unusual polymict breccia - Implications for origin 02 p0262 A83-11548
- The Manegaon diogenite 03 p0434 A83-14321
- Petrology of EETA79006 and implications for the formation of polymict eucrites 03 p0435 A83-14323
- Chemical composition of the Howardite Parent Body deduced from Kapoeta primary 'mafic' magmas 04 p0562 A83-15358
- The polymict eucrites Elephant Moraine A79004 and A79011 and the regolith history of a basaltic achondrite parent body 04 p0562 A83-15359
- Primary igneous carbon in ureilites - Petrological implications 04 p0562 A83-15360
- Petrography and mineralogy of two basalts and olivine-pyroxene-spinel fragments in achondrite EETA79001 04 p0563 A83-15362
- Chronology and petrogenesis of young achondrites, Shergotty, Zagami, and ALHA77005 - Late magmatism on a geologically active planet 04 p0572 A83-16355
- Do oblique impacts produce Martian meteorites 07 p1034 A83-21313
- The metal content of the eucrite parent body - Constraints from the partitioning behavior of tungsten 07 p1035 A83-21332
- Oxygen isotopes in eucrites, shergottites, nakhlites, and chassignites 08 p1187 A83-21639
- A preliminary report on the achondrite meteorites in the 1979 U.S. Antarctic meteorite collection 11 p1686 A83-28759
- Petrology of igneous lithic clasts from polymict eucrites ALHA76005 and ALHA77302 14 p2112 A83-33071
- Moessbauer spectroscopy of pyroxenes from two meteorites (achondrites) 18 p2780 A83-40648
- The nomenclature of polymict basaltic achondrites 22 p3384 A83-46372
- Lithium in stone meteorites and stony irons 22 p3385 A83-46374
- Regolith breccia Allan Hills A81005 - Evidence of lunar origin, and petrography of pristine and nonpristine clasts 22 p3385 A83-46861
- Petrogenesis of the Elephant Moraine A79001 meteorite 22 p3384 A83-46372
- Multiple magma pulses on the shergottite parent body 24 p3671 A83-48810

ACID BASE EQUILIBRIUM

- The gas composition and the acid-base state of the blood in twins when breathing a hypoxic gas mixture 01 p0082 A83-10492
- Association of triethylammonium perchlorate with bases 01 p0023 A83-11322
- Rapid monitoring of the acid-base and gas composition of the blood 03 p0375 A83-14334
- The characteristics of the CO2 balance during physical loads in healthy untrained individuals 08 p1146 A83-22778
- An investigation of the genotypic conditionality of the gas composition and acid-base state indicators of the blood during various effects on the body 09 p1323 A83-25152
- Blood osmolality during in vivo changes of CO2 pressure 13 p1902 A83-30460
- Acid-base curve and alignment nomograms for swine blood 13 p1898 A83-30500

- The effect of alimentary alkalemia on the maximum duration of an anaerobic work and the concentration of lactate in the muscles and blood 16 p2398 A83-35906
- O2 transport during two forms of stagnant hypoxia following acid and base infusions 17 p2554 A83-36992
- Pulmonary gas exchange in cats under a heat load 17 p2555 A83-37247

ACID RAIN

- Fogwater composition in southern California [AIAA PAPER 83-0362] 05 p0659 A83-16671
 - Variations of delta S-34/SO4/, delta O-18/H2O/, and Cl/SO4 ratio in rainwater over northern Israel, from the Mediterranean coast to Jordan Rift Valley and Golan Heights 05 p0665 A83-17843
 - The chemistry of western Atlantic precipitation at the mid-Atlantic coast and on Bermuda 07 p0956 A83-20202
 - Estimation of sulfate deposition 07 p0957 A83-20811
 - Reversible and irreversible wet deposition processes involving atmospheric admixtures 09 p1294 A83-23547
 - The sources of sulfate in precipitation. I - Parameterization scheme and physical sensitivities 09 p1295 A83-24265
 - The sources of sulfate in precipitation. II - Sensitivities to chemical variables 09 p1296 A83-24266
 - Sulfur dioxide absorption, oxidation, and oxidation inhibition in falling drops - An experimental/modeling approach 09 p1298 A83-25194
 - Acidity of aerosol particles and of precipitation in the North Polar region and over the Atlantic 11 p1613 A83-28090
 - Acid rain in an Amazon rainforest 11 p1613 A83-28096
 - Pollutant transfer in upland regions by occult precipitation 11 p1613 A83-28393
 - HCl in rocket exhaust clouds - Atmospheric dispersion, acid aerosol characteristics, and acid rain deposition 11 p1613 A83-28698
 - Aqueous oxidation of SO2 by hydrogen peroxide 13 p1817 A83-30882
 - Cloud and precipitation chemistry research and Whiteface Mountain 13 p1873 A83-31527
 - Source contributions to acid precipitation in Texas 15 p2194 A83-34043
 - Measurement of weak organic acidity in precipitation from remote areas of the world 16 p2372 A83-36129
 - The mechanism of sulfate aerosol formation - Chemical and sulfur isotopic evidence 19 p2862 A83-41111
 - Effect of freezing on sulfur dioxide dissolved in supercooled droplets 19 p2863 A83-41973
 - Temporal variations in acid precipitation over New York State - What the 1965-1979 USGS data reveal 19 p2863 A83-41981
 - Acid clouds and precipitation in eastern Colorado 19 p2863 A83-41982
 - A separator for obtaining samples of cloud water in aircraft 19 p2849 A83-41983
 - Case studies of aerosol size distribution and chemistry during passages of a cold and a warm front 20 p3014 A83-43427
 - Modeling of multiphase atmospheric aerosols 20 p3015 A83-43429
 - Acid deposition-precursor emission relationship in the northeastern U.S.A. - The effectiveness of regional emission reduction 20 p3015 A83-43435
 - Aqueous-phase source of formic acid in clouds 20 p3028 A83-43555
 - Acid generation in the troposphere by gas-phase chemistry 22 p3320 A83-45922
 - Observations on the chemical composition of rain using short sampling times during a single event 23 p3479 A83-48683
 - The pH and ionic composition of stratiform cloud water 23 p3479 A83-48684
 - Electron microscopy of acidic aerosols collected over the northeastern United States 23 p3479 A83-48687
 - Some implications of acid rain field studies 24 p3602 A83-49684
 - Distribution of acidity in convective clouds due to the aqueous phase oxidation of sulfur dioxide by ozone - A numerical simulation 24 p3602 A83-49685
 - In-situ, rapid response measurement of H2SO4/(NH4)2SO4 aerosols in urban Houston - A comparison with rural Virginia 24 p3603 A83-50193
 - Size-differentiated composition of inorganic atmospheric aerosols of both marine and polluted continental origin 24 p3603 A83-50194
- ACIDITY**
- Reduction in acidity of RDX and its compositions by use of suitable additives 15 p2143 A83-33872

ACIDOSIS

- Strong and weak acidity of aerosols collected over the northeastern United States 16 p2372 A83-35765
Measurement of weak organic acidity in precipitation from remote areas of the world 16 p2372 A83-36129

ACIDOSIS

- Liquid ventilation in dogs - An apparatus for normobaric and hyperbaric studies 13 p1898 A83-30510

ACIDS

- NT ALANINE
NT AMINO ACIDS
NT ASCORBIC ACID
NT BUTYRIC ACID
NT CARBOXYLIC ACIDS
NT CHROMIC ACID
NT DEOXYRIBONUCLEIC ACID
NT FATTY ACIDS
NT FORMIC ACID
NT GLUTAMIC ACID
NT GLUTATHIONE
NT GLYCINE
NT GUANOSINES
NT HEXOGENES (TRADEMARK)
NT HYDROBROMIC ACID
NT HYDROCHLORIC ACID
NT HYDROCYANIC ACID
NT HYDROFLUORIC ACID
NT LACTIC ACID
NT MELANOIDIN
NT NITRIC ACID
NT NUCLEIC ACIDS
NT PALMITIC ACID
NT PAPAINE
NT PEPTIDES
NT PHOSPHORIC ACID
NT PYRUVATES
NT RIBONUCLEIC ACIDS
NT SULFONIC ACID
NT SULFURIC ACID
NT THYROXINE
NT TRYPTOPHAN
NT URIC ACID
Immunobiological properties of teichoic acids --- for diagnosing staphylococcal infections 01 p0081 A83-10556
Q branches in the rotational spectrum of HOCl 05 p0684 A83-17873
Evaluation of tetrafluoroethane-1,2-disulfonic acid as a fuel cell electrolyte 11 p1546 A83-28300
Energy Storage in a fuel cell with bipolar membranes burning acid and hydroxide 13 p1872 A83-31599

ACOUSTIC ATTENUATION

- NT SHOCK WAVE ATTENUATION
Radiation damping of acoustic-gravity waves in a nonisothermal atmosphere 03 p0362 A83-14828
Modal power distribution in ducts at high frequencies 04 p0532 A83-15285
Investigation of screech tone elimination in an underexpanded supersonic jet [AIAA PAPER 83-0646] 05 p0683 A83-16813
The nonlinear relaxation of a beam of relativistic electrons in a plasma - Nonlinear sound attenuation 05 p0686 A83-16891
Theoretical and experimental evaluation of transmission loss of cylinders --- as idealized aircraft fuselages 07 p0990 A83-19808
Eigensolutions for liners in uniform mean flow ducts 07 p0990 A83-19810
Path dependence of acoustic velocity and attenuation in experimentally deformed Westerly granite 07 p0959 A83-20096
Sound attenuation in ducts with lined walls of non-uniform acoustic impedance 08 p1162 A83-22074
Pressure wave attenuation due to anode mufflers in pulsed lasers 08 p1107 A83-22135
Pulsed visible laser flow and acoustics 08 p1108 A83-22459
Noise transmission characteristics of advanced composite structural materials [AIAA PAPER 83-0694] 10 p1473 A83-25915
Acoustic nonlinearities and power losses at orifices [AIAA PAPER 83-0739] 10 p1476 A83-25942
Experimental study of the sound insulation of various shell configurations 10 p1477 A83-26297
Measurement of acoustic modes and wall impedance in a turbofan exhaust duct [AIAA PAPER 83-0733] 11 p1651 A83-28015
Effect of flow on the acoustic performance of extended reaction lined ducts [AIAA PAPER 83-0778] 11 p1652 A83-28024
Propagation of sound in highly porous open-cell elastic foams 12 p1776 A83-28848
Discontinuation of periodic vortex formation behind a stabilizer in an acoustically damped chamber following mixture ignition 14 p1989 A83-32089

- Effect of sound absorbing wall linings on aerodynamic forces of a subsonic vibrating cascade 14 p2081 A83-33372

- Sound diffraction at wall impedance discontinuities in a circular cylinder - Investigated using Wiener-Hopf technique [AIAA PAPER 83-0730] 15 p2226 A83-33485
Sound propagation in ducts with impedance walls in the presence of an air flow. II - Optimization of acoustic attenuation in ducts 17 p2577 A83-37512
Asymptotic laws for the attenuation of weak continuous and shock waves in a dusty gas 19 p2842 A83-41257
The energetic balance of active noise attenuation 21 p3201 A83-44324

ACOUSTIC COMBUSTION

U COMBUSTION STABILITY

ACOUSTIC DELAY LINES

- Continuous separable regulation of group delay and phase of the carrier frequency of a signal in an acoustic delay line 01 p0038 A83-10807
Effect of nonuniform piezoelectric films on monolithic surface acoustic wave devices 01 p0039 A83-10986
A new type of laser probe --- for surface acoustic wave beam measurement 13 p1846 A83-30334
Analysis of the temperature stability of the frequency of a SAW oscillator 19 p2840 A83-41784
A Lamb wave voltage sensor 23 p3454 A83-47627

ACOUSTIC DUCTS

- A two-dimensional isoparametric Galerkin finite element for acoustic-flow problems [ASME PAPER 82-DET-97] 02 p0234 A83-12778
Development of a sound radiation model for a finite-length duct of arbitrary shape 03 p0391 A83-13134
Heat transfer and associated turbulent processes in pulsed turbulent flows under conditions of acoustical resonance 03 p0318 A83-14471
Boundary layer effects on sound in a circular duct 04 p0532 A83-15066
Modal power distribution in ducts at high frequencies 04 p0532 A83-15285
A comparison of measured and computed sound pressure levels in a non-uniform acoustically lined duct 04 p0533 A83-16344
Duct acoustics - A time dependent difference approach for steady state solutions 04 p0533 A83-16345
Acoustics in variable area duct - Finite element and finite difference comparisons to experiment 07 p0990 A83-19809

- Eigensolutions for liners in uniform mean flow ducts 07 p0990 A83-19810
Sound attenuation in ducts with lined walls of non-uniform acoustic impedance 08 p1162 A83-22074

ADAM - An axisymmetric duct aeroacoustic modeling system

- [AIAA PAPER 83-0666] 10 p1473 A83-25903
Uniform asymptotic approximations for duct eigenfunctions in a thin boundary layer flow [AIAA PAPER 83-0668] 10 p1473 A83-25905
An analysis of the two-dimensional acoustic field in a nonuniform duct carrying compressible flow [AIAA PAPER 83-0669] 10 p1473 A83-25906
An experimental investigation of sound radiation from a duct with a circumferentially varying liner [AIAA PAPER 83-0712] 10 p1475 A83-25928
Sound radiation from annular ducts/nozzles using modal decomposition of in-duct acoustic power [AIAA PAPER 83-0714] 10 p1475 A83-25929
Experimental investigation of modal power distribution in a duct at high frequency [AIAA PAPER 83-0731] 10 p1475 A83-25938
An evaluation of circumferentially segmented duct liners [AIAA PAPER 83-0732] 10 p1475 A83-25939
Experimental investigation of geometry and flow effects on acoustic radiation from duct inlets [AIAA PAPER 83-0713] 11 p1651 A83-28012
Measurement of acoustic modes and wall impedance in a turbofan exhaust duct [AIAA PAPER 83-0733] 11 p1651 A83-28015
Simplified modal analysis for sound propagation in segmented ducts [AIAA PAPER 83-0735] 11 p1651 A83-28017
Effect of flow on the acoustic performance of extended reaction lined ducts [AIAA PAPER 83-0778] 11 p1652 A83-28024
One-dimensional acoustic wave propagation in a particulate suspension 14 p2081 A83-33456
Friction drag measurements of acoustic surfaces [AIAA PAPER 83-1356] 16 p2296 A83-36414
Effect on the acoustic channel of a flaw detector due to the side surface of an object 22 p3303 A83-46323

- Experimental methods in compressor noise studies [ONERA, TP NO. 1983-79] 23 p3505 A83-48194

ACOUSTIC EMISSION

- Remote sensing applications for mine waste stability monitoring using the acoustic emission method 01 p0062 A83-10036
The AD-60S low-frequency acoustic flaw detector 01 p0049 A83-10358
Method, scientific, and technical fundamentals of metrological provisions for ultrasonic measuring transducers 01 p0049 A83-10359
Instantaneous determination of the locations of acoustic-emission signal sources in three coordinates 02 p0188 A83-12157
Generation of desired signals from acoustic drivers --- for aircraft engine internal noise propagation experiment 04 p0449 A83-15068
Characterization of stability mechanisms in advanced composites 04 p0454 A83-15181
The inverse problem of acoustic emission - Explicit determination of acoustic emission source time-functions 04 p0491 A83-15193
A case study of sensitivity of some pattern classifiers used in sorting acoustic emission signals 04 p0491 A83-15194
Quantitative acoustic emission for source characterization in metals 04 p0458 A83-15195
Acoustic emission during plastic deformation and crack growth in 2024 and 2124 aluminium alloys 04 p0458 A83-15196
Develop in-flight acoustic emission monitoring of aircraft to detect fatigue crack growth 04 p0447 A83-15197
Establishing signal processing and pattern recognition techniques for inflight discrimination between crack-growth acoustic emission and other acoustic waveforms 04 p0491 A83-15198
A study of the relationship between the acoustic emission parameters and the processes of elastic-plastic deformation and fracture of EI-602 alloy 04 p0459 A83-15466
Acceptance testing of graphite/epoxy composite parts using an acoustic emission monitoring technique 05 p0653 A83-16874
A new instrument for acoustic emission activity, with an application to the thermoelastic instability 05 p0644 A83-16922
A comparative study of the light transmission, acoustic emission, and thermal effects of a glass-reinforced plastic under mechanical loads 06 p0725 A83-18519
Acousto-ultrasonic evaluation of impact-damaged graphite epoxy composites 07 p0875 A83-20454
A study of the cracking of oxide films on MoSi2 using the method of acoustic emission 07 p0899 A83-20680
Radiation from a dislocation oscillating in a circular cylinder 07 p0948 A83-21169
Application of the statistical characteristics of acoustic-emission signals to measure the time rate of elementary emission events 07 p0943 A83-21403
Characteristics of the amplitude distribution of acoustic emission in the nucleation and propagation of fatigue cracks 07 p0943 A83-21405
Sensitivity of the method of acoustic leak detection in pneumatic tightness tests 07 p0943 A83-21408
Fracture mechanics, sub-critical events and structure of polypphase ceramics 08 p1069 A83-21722
Acoustic emission in rock fracture analysis 08 p1113 A83-21769
A study of stress corrosion cracking in high strength steels using acoustic emission techniques 08 p1064 A83-21770
Acoustic emission during the plastic deformation of aluminium alloys 2024 and 2124 08 p1065 A83-22014
Failure and acoustic-emission response of plasma-sprayed ZrO2-8 wt% Y2O3 coatings 08 p1072 A83-22274
Advanced methods for damage analysis in graphite-epoxy composites 09 p1222 A83-23648
Acoustic phenomena associated with a TEA laser discharge 09 p1271 A83-23664
Stable crack growth during fracture toughness testing in Ti-6Al-4V alloy 09 p1230 A83-23916
Acoustic inspection of explosion welded joints in titanium 10 p1436 A83-26220
Procedure for estimating the fatigue strength of gas turbine blades by method of acoustic emission 10 p1436 A83-26286
Fatigue crack advance presumably detected by acoustic emission signals 11 p1590 A83-28225
Determination of the coordinates of an acoustic emission source from the spectral components of its signal 11 p1590 A83-28519
Sound emission from moving sources in an inhomogeneous gaseous medium 12 p1777 A83-29257

On the origin of the first peak of acoustic emission in 7075 aluminium alloy 12 p1714 A83-29507

Application of the acoustic emission method in repeated determinations of fracture toughness characteristics 13 p1823 A83-31219

The use of the acoustic emission method for studying the strength and ductility of materials at low temperatures 14 p1997 A83-33014

Acoustic emission from thermally cycled plasma-sprayed oxides 15 p2173 A83-33517

Origin of acoustic emission in aged Al-Zn-Mg alloys. I - The base ternary alloy 16 p2334 A83-36566

Origin of acoustic emission in Al-Zn-Mg alloys. II Copper-containing quaternary alloys 16 p2334 A83-36567

Dynamic crack growth during pop-in fracture in 7075 aluminium alloy 17 p2489 A83-38123

The use of acoustic emission techniques to monitor fracture processes in high strength precipitation hardened aluminum alloys 17 p2491 A83-38525

The application of polyvinylidene fluoride as an acoustic emission transducer for fibrous composite materials 18 p2695 A83-39622

Acoustic emission characterization using AE (parameter) delay 18 p2695 A83-39623

Estimation of the dimensions of growing cracks and relaxation regions from acoustic signal parameters 18 p2701 A83-40109

The modelling of failure processes and the role of the matrix in the failure of carbon fibre reinforced epoxy resin 18 p2655 A83-40208

Fabrication cycle influence on the acoustic emission response of GFRP composites 18 p2660 A83-40270

Thickness and stacking sequence effect on the acoustic emission of CFRP 18 p2660 A83-40271

A contribution to non-destructive inspection of fibrous plastics composites with an emphasis on application of AE techniques 18 p2660 A83-40274

Effect of stacking sequence in cross-ply graphite/epoxy laminates on acoustic emission results 18 p2661 A83-40276

Estimation of extra useful life of objects by monitoring acoustic emission 20 p3000 A83-43181

Acoustic emission from graphite/epoxy composite laminates with special reference to delamination 21 p3106 A83-44126

Acoustic radiations from lightning 22 p3339 A83-45891

Location information of acoustic-emission signals 22 p3304 A83-46328

Analysis of the errors of location of acoustic-emission sources for one-dimensional objects 22 p3304 A83-46333

Turbulent sound generation in red dwarf stars 23 p3525 A83-47543

The transformation ratio of acoustic emission during irreversible deformation of crystals 24 p3590 A83-49058

The use of the acoustic emission method for analyzing the quality of protective coatings --- molybdenum disilicide coatings on Mo 24 p3568 A83-49082

The mechanism of acoustic emission from a turbulent gas flame 24 p3555 A83-49762

ACOUSTIC EXCITATION

Investigations of the excitation mechanism of thermoacoustic vibrations - The Rijke phenomenon --- German thesis 01 p0022 A83-10167

Jet noise and the effects of jet forcing 01 p0105 A83-10898

Natural frequencies of circular plates with partially free, partially clamped edges 01 p0060 A83-11039

Noise and flow structure of a tone-excited jet 03 p0391 A83-13136

The superposition principle in acoustics 04 p0533 A83-15450

Resonant entrainment of a confined pulsed jet 04 p0478 A83-16139

The organized shear layer due to oscillations of a turbulent jet through an axisymmetric cavity 04 p0480 A83-16343

The effect of acoustics and flow conditions in the wall boundary layer of a nozzle on the mixing layer of a submerged jet 06 p0760 A83-19429

Effect of excitation on coaxial jet noise 07 p0990 A83-19811

Acoustic fluidization and the scale dependence of impact crater morphology 07 p1034 A83-21317

An improved schlieren system and some new results on acoustically excited jets 08 p1162 A83-21806

Flow-excited resonances in covered cavities 09 p1340 A83-23339

Strain measurement of acoustically excited aircraft structures at elevated temperatures 09 p1265 A83-23366

Viscous stability of compressible axisymmetric jets 09 p1341 A83-24651

A model of the excitation of large scale fluctuations in a shear layer [AIAA PAPER 83-0724] 10 p1475 A83-25935

Tone generation by rotor-downstream strut interaction [AIAA PAPER 83-0767] 10 p1378 A83-25957

Nearfield observations of tones generated from supersonic jet flows [AIAA PAPER 83-0706] 10 p1478 A83-26449

Sound excitation and appearance of additional losses in a single-mode fiber-optic waveguide in the case of the transmission of amplitude-modulated optical waves 10 p1484 A83-26942

The velocity perturbations above the orifice of an acoustically excited cavity in grazing flow 12 p1777 A83-29235

Large-amplitude multimode response of clamped rectangular panels to acoustic excitation [AIAA 83-1033] 12 p1745 A83-29879

Oscillators of short high-power electric pulses for the electromagnetic acoustic excitation of ultrasound 13 p1860 A83-30841

Rotary flow of a fluid 13 p1842 A83-30908

Excitation of circular flow of a fluid by a rotating velocity field 13 p1842 A83-30909

On small forced oscillations of a nonlinear acoustic resonator 13 p1915 A83-31331

The effect of a standing acoustic wave transverse to the flow on a turbulent flame 14 p1989 A83-32087

The cancellation of a sound-excited Tollmien-Schlichting wave with plate vibration 14 p2013 A83-33377

Interaction of an acoustic disturbance and a two-dimensional turbulent jet - Experimental data 17 p2504 A83-37395

Time-resolved two-dimensional concentration measurements in an acoustically driven flow 19 p2841 A83-40856

Acoustic excitation of Tollmien-Schlichting waves in a supersonic boundary layer 19 p2790 A83-41256

The susceptibility of a boundary layer on blunted-nose bodies to acoustic flow oscillations 19 p2791 A83-41274

Acoustic enhancement of heat transfer in plane channels 20 p2929 A83-42751

Scattering of light and acoustic disturbances in the atomic iodine laser 20 p2995 A83-42795

Acoustic pulses excited by impacts on objects - Their analytical representation and spectra 20 p3000 A83-43645

ACOUSTIC FATIGUE

Sonic fatigue of advanced composite panels in thermal environments 08 p1055 A83-22166

The use of high-intensity ultrasonics --- Book 09 p1341 A83-24904

Design for prevention of acoustic fatigue --- of aircraft structures [AIAA 83-0973] 12 p1701 A83-29782

The effect of acoustic-thermal environments on advanced composite fuselage panels [AIAA 83-0955] 12 p1744 A83-29857

Acoustic fatigue test evaluation of adhesively bonded aluminum fuselage panels using FM 73/BR 127 adhesive/primer system [AIAA 83-0999] 12 p1744 A83-29874

Acoustic fatigue life analysis - Honeycomb panels subjected to diffuse and progressive random acoustic waves [AIAA 83-1000] 12 p1745 A83-29875

Monitoring of high power ultrasonic fatigue systems 16 p2367 A83-36178

ACOUSTIC GENERATORS

U SOUND GENERATORS

ACOUSTIC IMPEDANCE

A note on the calculation of sound propagation over impedance jumps and screens 02 p0234 A83-13006

Runge's theorem and far field patterns for the impedance boundary value problem in acoustic wave propagation 04 p0533 A83-16365

Sound attenuation in ducts with lined walls of non-uniform acoustic impedance 08 p1162 A83-22074

The measurement of the steady flow resistance of porous materials --- for noise suppression in aircraft turbofan engine ducts [AIAA PAPER 83-0779] 10 p1477 A83-25961

Simplified modal analysis for sound propagation in segmented ducts [AIAA PAPER 83-0735] 11 p1651 A83-28017

Surface acoustic admittance of highly porous open-cell, elastic foams 12 p1776 A83-28849

The velocity perturbations above the orifice of an acoustically excited cavity in grazing flow 12 p1777 A83-29235

Acoustic waves in a Rijke tube with radiation impedance 12 p1777 A83-29382

Sound diffraction at wall impedance discontinuities in a circular cylinder - Investigated using Wiener-Hopf technique [AIAA PAPER 83-0730] 15 p2226 A83-33485

Sound propagation in ducts with impedance walls in the presence of an air flow. II - Optimization of acoustic attenuation in ducts 17 p2577 A83-37512

Acoustic ground impedance meter 17 p2510 A83-37732

ACOUSTIC INSTABILITY

Stability of shock waves with a finite relaxation zone 04 p0475 A83-15097

Thermal conductivity measurement in high temperature argon by the shock perturbation and Mach reflection methods 10 p1415 A83-26153

Nearfield observations of tones generated from supersonic jet flows [AIAA PAPER 83-0706] 10 p1478 A83-26449

Derivation of the amplitude equations of acoustic modes of an unstable semi-infinite polytrope /Invited Review/ --- solar oscillations 11 p1689 A83-27649

Longitudinal modes of gas oscillations in the main combustion chamber of gas-turbine engines 18 p2641 A83-39169

The effect of inhomogeneity on the nonlinear stabilization of the acoustic oscillations of a heat-releasing medium in a limited volume 23 p3513 A83-48651

A coupled mode approach to modulation instability and envelope solitons 24 p3623 A83-48904

ACOUSTIC LEVITATION

Polymer coating of glass microballoons levitated in a focused acoustic field 20 p2962 A83-43258

Present and future capabilities of acoustic levitation and positioning devices 20 p2940 A83-43267

ACOUSTIC MEASUREMENT

NT NOISE MEASUREMENT

Ultrasonic inspection using the acoustic fields of elastic wave scattering by defects /liquid model/ 01 p0057 A83-10357

Wind tunnel measurements of blade/vane ratio and spacing effects on fan noise 04 p0533 A83-15317

Quantitative ultrasonic backscatter measurements in the presence of phase distortion 04 p0533 A83-16313

A comparison of measured and computed sound pressure levels in a non-uniform acoustically lined duct 04 p0533 A83-16344

Crack height measurement - An evaluation of the accuracy of ultrasonic timing methods 05 p0653 A83-16875

On the acoustic registration of cascades and single strongly ionized particles 06 p0764 A83-19350

Study of a measuring method for the dimensions of three-dimensional flaws during ultrasonic inspection 07 p0943 A83-21401

Application of the statistical characteristics of acoustic-emission signals to measure the time rate of elementary emission events 07 p0943 A83-21403

Multidetector intensity interferometers 08 p1092 A83-22327

Use of voltage and current amplifiers in ultrasonic apparatus 08 p1080 A83-22403

Sonic diagnostics of HF discharges 09 p1347 A83-23660

Experimental investigations concerning the noise produced by model propellers and propeller-driven small aircraft [DGLR PAPER 82-068] 09 p1206 A83-24182

Acoustic metrology and signal processing [ONERA, TP NO. 1982-123] 09 p1341 A83-24334

Acousto-elastic measurement of stress and stress intensity factors around crack tips 09 p1283 A83-25116

In-flight acoustic measurements in the engine intake of a Fokker F28 aircraft [AIAA PAPER 83-0677] 10 p1376 A83-25909

Sound radiation from annular ducts/nozzles using modal decomposition of in-duct acoustic power [AIAA PAPER 83-0714] 10 p1475 A83-25929

Acoustic measurements of a full-scale coaxial helicopter [AIAA PAPER 83-0722] 10 p1375 A83-25933

Near field acoustic measurements in natural and artificially excited high speed subsonic jets [AIAA PAPER 83-0725] 10 p1475 A83-25936

Flight effects on jet noise sources investigated by model experiments in the DNW [AIAA PAPER 83-0752] 10 p1476 A83-25951

Measurement of the energy characteristics of a sound field in an interferometer 11 p1650 A83-27451

Acoustic measurements on aerofoils moving in a circle at high speed [AIAA PAPER 83-0674] 11 p1650 A83-28003

Measurement of acoustic modes and wall impedance in a turbofan exhaust duct [AIAA PAPER 83-0733] 11 p1651 A83-28015

- The pseudo sound contribution to the pressure field under a turbulent boundary layer
[AIAA PAPER 83-0755] 11 p1652 A83-28020
- Direct measurement of transmission loss of aircraft structures using the acoustic intensity approach
11 p1530 A83-28185
- Direct measurement of sound from large scale structures in jet flows
[AIAA PAPER 83-0662] 11 p1653 A83-28197
- Acoustic measurements of the wind velocity at the Venera 13 and Venera 14 landing sites
12 p1798 A83-29482
- Rotor-vortex interaction noise
[AIAA PAPER 83-0720] 12 p1777 A83-29950
- A new type of laser probe --- for surface acoustic wave beam measurement 13 p1846 A83-30334
- Wind velocity at the Venus surface according to acoustic measurements 14 p1983 A83-31961
- Full-scale measurements of blade-vortex interaction noise 15 p2227 A83-33505
- Determination of in-plane residual stress states in plates using horizontally polarized shear waves
16 p2364 A83-35434
- Measurement of the acoustical properties of plastics
20 p3000 A83-43644
- An all fiber-optic sensor for surface acoustic wave measurements 22 p3287 A83-45735
- Long-wave acoustic flowmeter 24 p3586 A83-49925

ACOUSTIC MICROSCOPES

- Quantitative flaw characterization by means of the Scanning Laser Acoustic Microscope /SLAM/
04 p0493 A83-15227
- A description of the Bell Laboratories scanned acoustic microscope 04 p0482 A83-16321
- Comparison of NDE techniques for sintered-SiC components 08 p1113 A83-22265
- Confocal surface acoustic wave microscopy
08 p1101 A83-22754
- Directional acoustic microscopy for observation of elastic anisotropy 08 p1101 A83-22755
- High resolution acoustic microscopy in superfluid helium 14 p2022 A83-33443
- Simultaneous scanning optical and acoustic microscopy 16 p2356 A83-36478
- Energy leakage from Rayleigh waves on a fluid-loaded, layered half-space 17 p2576 A83-38046
- Non-destructive testing and acoustic microscopy of diffusion bonds 21 p3149 A83-44123

ACOUSTIC NOZZLES

- Sound radiation from annular ducts/nozzles using modal decomposition of in-duct acoustic power
[AIAA PAPER 83-0714] 10 p1475 A83-25929
- The force effect on a sphere of an underexpanded jet issuing from a transonic nozzle 13 p1842 A83-30678

ACOUSTIC PROPAGATION

- Acoustic-wave diffraction by a plate moving near a flat surface 01 p0105 A83-11319
- Acoustic waves in supernova remnants
02 p0257 A83-12135
- A finite element method for solving Helmholtz type equations in waveguides and other unbounded domains
03 p0390 A83-13567
- Boundary layer effects on sound in a circular duct
04 p0532 A83-15066
- Reflection of sound by a boundary layer
04 p0532 A83-15067
- The superposition principle in acoustics
04 p0533 A83-15450
- Second-harmonic diffraction field in nonlinear propagation of transversely limited surface acoustic wave beams
04 p0473 A83-16058
- Acoustic radiation pressure produced by a beam sound
04 p0533 A83-16311
- Gain and efficiency of a traveling wave heat engine
04 p0480 A83-16312
- Pressure transfer function of a JT15D nozzle due to acoustic and convected entropy fluctuations
04 p0533 A83-16319
- A comparison of measured and computed sound pressure levels in a non-uniform acoustically lined duct
04 p0533 A83-16344
- Sound source radiation in two-dimensional shear flow
07 p0990 A83-19812
- Numerical calculations of ultrasonic fields. I - Transducer near fields 07 p0942 A83-20269
- Sound attenuation in ducts with lined walls of non-uniform acoustic impedance
08 p1162 A83-22074
- Acoustic environment in large enclosures with a small opening exposed to flow 08 p1162 A83-22161
- New methods for optical, quasi-optical, acoustic and electromagnetic synthesis; Proceedings of the Meeting, San Diego, CA, August 25, 26, 1981
08 p1161 A83-22468

- Analysis of the effect of heated jet flow on the far field radiation from a noise source
[ASME PAPER 82-WA/NCA-4] 10 p1472 A83-25697
- Finite difference solutions to shocked acoustic waves
[AIAA PAPER 83-0671] 10 p1473 A83-25907
- Acoustic wave propagation through the shear layer of the DNW large open jet wind tunnel
[AIAA PAPER 83-0699] 10 p1474 A83-25919
- Acoustic nonlinearities and power losses at orifices
[AIAA PAPER 83-0739] 10 p1476 A83-25942
- Transformation of strong acoustic noise pulses
10 p1477 A83-26290
- Experimental investigation of geometry and flow effects on acoustic radiation from duct inlets
[AIAA PAPER 83-0713] 11 p1651 A83-28012
- Regimes of interaction of nonlinear waves in a low-viscosity medium --- sound propagation in gases and liquids 11 p1652 A83-28064
- The unique solvability of the null field equations of acoustics
[AD-A129263] 11 p1653 A83-28406
- A series expansion of the acoustic power radiated from planar sources 14 p2081 A83-33022
- A study on the transmission and reflection of an ultrasonic beam at machined surfaces pressed against each other 15 p2172 A83-33499
- Scaling analysis of thermoacoustic convection in a zero-gravity environment 15 p2156 A83-33745
- Principles of acoustic devices --- Book
15 p2163 A83-33750
- The effect of acoustic perturbations on the flow structure in a boundary layer with an unfavorable pressure gradient 16 p2289 A83-35705
- Acoustic signature from flames as a combustion diagnostic tool 19 p2820 A83-40860
- The effect of the dispersion and diffraction of surface acoustic waves on the characteristics of matched filters for PSK signals 19 p2840 A83-41783
- The propagation of ultrasonic waves in mixed media and application to mode B imagery for nondestructive control --- French thesis 19 p2855 A83-41814
- Collapse of acoustic waves in media with positive dispersion 20 p3049 A83-42286
- The finite-difference method in wave problems of acoustics --- Russian book 21 p3201 A83-45026
- Nonlinear theory for acoustic beams --- Russian book
21 p3201 A83-45028
- Nondestructive residual-stress measurement in a wide-flanged rolled beam by acoustoelasticity
21 p3162 A83-45171
- Effect of driven-wall motion on a turbulent boundary layer 22 p3247 A83-46429
- Weakly nonlinear high frequency waves
22 p3354 A83-47091
- The effect of plastic deformation on the acoustoelastic response of metals 23 p3469 A83-47599
- Nonstationarity in acoustic fields
23 p3505 A83-47628
- Focusing antennas usage in locating acoustic sources [ONERA, TP NO. 1983-75] 23 p3505 A83-48190
- The effect of inhomogeneity on the nonlinear stabilization of the acoustic oscillations of a heat-releasing medium in a limited volume 23 p3513 A83-48651
- Channelled acoustic waves - Elastic waves of a new type of polydomain ferroelectrics
24 p3634 A83-48866
- A coupled mode approach to modulation instability and envelope solitons 24 p3623 A83-48904
- A review of numerical methods in acoustic wave propagation [ONERA, TP NO. 1983-93] 24 p3625 A83-49410
- Nonlinear tridimensional propagation of acoustic waves in radiative gas dynamics 24 p3625 A83-49522
- On the effect of the correlation in phonon motion on the viscosity of impure dielectrics 24 p3636 A83-49755

ACOUSTIC PROPERTIES

- NT ACOUSTIC IMPEDANCE
- NT ACOUSTIC INSTABILITY
- NT ACOUSTIC SCATTERING
- NT ACOUSTIC VELOCITY
- NT SOUND INTENSITY
- The thermoacoustic effect in a resonance tube having one open end 02 p0233 A83-11516
- Acoustoelastic response of polycrystalline aggregates exhibiting transverse isotropy 07 p0945 A83-20266
- Acoustic properties of plasma-sprayed coatings and their applications to non-destructive evaluation
10 p1436 A83-25529
- A compact inflow control device for simulating flight fan noise
[AIAA PAPER 83-0680] 11 p1651 A83-28005
- A study of the acoustic properties of a ceramic material 13 p1825 A83-30062

- Optoacoustic characteristics of single-mode fiber waveguides 15 p2230 A83-33985
- The relationship between the aerodynamic and acoustic characteristics of coaxial jets 16 p2408 A83-35712
- On the acoustoelastic effect 17 p2576 A83-37728
- An evaluation of the effectiveness of methods for reducing the noise of jets 17 p2578 A83-37801
- Measurement of the acoustical properties of plastics
20 p3000 A83-43644

ACOUSTIC RADIATION**U SOUND WAVES****ACOUSTIC RETROFITTING**

- Evaluation of interior noise control treatments for high-speed propfan-powered aircraft
[AIAA PAPER 83-0693] 10 p1375 A83-25914
- Optimization of acoustic liners by the hybrid finite element-integral approach
[AIAA PAPER 83-0670] 10 p1478 A83-26917

ACOUSTIC SCATTERING

- Ultrasonic inspection using the acoustic fields of elastic wave scattering by defects /liquid model/
01 p0057 A83-10357
- A survey of the physical optics inverse scattering identity 01 p0104 A83-11369
- Reflection of sound by a boundary layer
04 p0532 A83-15067
- A calculation of the impulse responses of acoustically reflecting targets 04 p0531 A83-15073
- Ultrasonic defect classification using the Singularity Expansion Method 04 p0489 A83-15170
- Crack characterization by the combined use of time-domain and frequency-domain scattering data
04 p0491 A83-15199
- Optical probing of resonant ultrasonic scattering from machined flaws in plates 04 p0492 A83-15208
- Acoustic imaging with two dimensional arrays
04 p0493 A83-15229
- Quantitative ultrasonic backscatter measurements in the presence of phase distortion 04 p0533 A83-16313
- A least-square iterative technique for solving time-domain scattering problems
04 p0530 A83-16316
- Scattering by slender bodies of revolution
04 p0533 A83-16317
- Scattering of acoustic waves by rigid cylindrical objects with sharp corners 04 p0533 A83-16318
- Runge's theorem and far field patterns for the impedance boundary value problem in acoustic wave propagation
04 p0533 A83-16365
- Study of elastic-wave scattering by hollow imperfections in a solid medium 07 p0943 A83-21402
- Experimental investigation of the scattering effects of a sphere in a cylindrical resonant chamber
10 p1472 A83-25822
- The dependence of sound extinction on the parameters of thermal turbulence in the atmospheric boundary layer
10 p1451 A83-25823
- Scattering of an acoustic field by a free jet shear layer [AIAA PAPER 83-0698] 10 p1474 A83-25918
- Possibility of observing stimulated thermal scattering of sound
10 p1477 A83-26287
- Sound scattering by a vortex
10 p1477 A83-26296
- Sound propagation through fluctuating flows - Its significance in aeroacoustics
[AIAA PAPER 83-0697] 10 p1477 A83-26448
- On complex poles in scattering theory
16 p2407 A83-35698
- Stimulated scattering of sound by an acoustic flow of a viscous liquid 17 p2578 A83-37899
- Sound scattering by a vortex wake behind a cylinder
17 p2578 A83-38049
- Excitation of Tollmein-Schlichting waves during the scattering of acoustic and vortex perturbations in a boundary layer on a wavy surface
20 p2987 A83-43519
- Analysis of the elastic field of ultrasonic waves scattered by a cylindrical cavity 21 p3148 A83-43876
- Resonant acoustic scattering from elastic cylindrical shells 24 p3624 A83-48974
- A model relating ultrasonic scattering measurements through liquid-solid interfaces to unbounded medium scattering amplitudes 24 p3625 A83-48975

ACOUSTIC SIMULATION

- Simulation of the acoustic environment by a launch vehicle at lift-off and its vibratory effects on its structures [ONERA, TP NO. 1982-117] 09 p1212 A83-24328
- Simulation of propfan noise impact on a fuselage --- by newly developed siren
[AIAA PAPER 83-0715] 10 p1475 A83-25930
- Acoustic testing of missiles 11 p1531 A83-28163

ACOUSTIC SOUNDING

- Combined acoustic and radioacoustic probing of the atmospheric boundary layer 03 p0372 A83-14829
- Acoustic remote sensing of the boundary layer
08 p1141 A83-22991

- The spectrum of the scattering signal for the radioacoustic sounding system / RASS/ 09 p1310 A83-23406
- Acoustic remote sensing of internal waves in shallow water 15 p2208 A83-34153
- Temperature sounding in the planetary boundary layer by RASS System analysis and results 15 p2164 A83-34154
- Wave and turbulence structure in a disturbed nocturnal inversion 23 p3492 A83-48731
- ACOUSTIC STABILITY**
- U FREQUENCY STABILITY
- ACOUSTIC STREAMING**
- The dominant coherent structure of the circular jet organized by controlled perturbation 03 p0318 A83-14463
- Acoustic streaming in swirling flow and the Ranque-Hilsch /vortex-tube/ effect 04 p0479 A83-16259
- Control of turbulent boundary layer flows by sound [AIAA PAPER 83-0726] 10 p1475 A83-25937
- An interplay between acoustic waves and steady vortical flow [AIAA PAPER 83-0740] 10 p1476 A83-25943
- ACOUSTIC VELOCITY**
- A resonance method for measurement of longitudinal and transverse ultrasonic wave velocities and their attenuations 04 p0492 A83-15217
- Sound velocity and critical mass throughput in one- and two-component gas-liquid flows --- German thesis 06 p0761 A83-19621
- Path dependence of acoustic velocity and attenuation in experimentally deformed Westerly granite 07 p0959 A83-20096
- Optimization of the calculation of the elastic constants from velocity measurements with an ultrasonic wave 12 p1735 A83-29387
- Excitation of circular flow of a fluid by a rotating velocity field 13 p1842 A83-30909
- Ultrasonic wave velocities guided in a heterogeneous medium 17 p2578 A83-38067
- Numerical evaluation of the radiation from un baffled, finite plates using the FFT 18 p2742 A83-39975
- Evaluation of the effect of certain factors on the accuracy of acoustoelastic measurements of stresses in solids 19 p2855 A83-41976
- Increasing the accuracy of the measurements of ultrasound propagation time in stressed-strained solids 19 p2849 A83-41977
- Acoustic velocities of two-phase mixtures of cryogenic fluids 20 p2983 A83-43012
- Determination of the propagation velocity of perturbations in a pipeline in the case of the rotational-translational motion of a liquid with cavitation 24 p3578 A83-49651
- Determination of changes in the sound velocity in shock loaded Ti-6Al-4V with in-material manganin gauges 24 p3566 A83-49833
- ACOUSTIC VIBRATIONS**
- U SOUND WAVES
- ACOUSTICAL HOLOGRAPHY**
- Experiences regarding the accuracy of localization and reconstruction in the case of ultrasonic holography 09 p1270 A83-24943
- Acoustic imaging for diagnostics of chemically reacting systems [AIAA PAPER 83-0761] 10 p1476 A83-25955
- Optical reconstruction of wideband Fourier and Fresnel acoustic holograms 10 p1421 A83-26295
- Acoustical speckle interferometry 12 p1730 A83-29586
- Thermoelastic hologram for focused ultrasound 16 p2357 A83-36773
- Three-dimensional defect imaging by multifrequency acoustical holography 18 p2689 A83-39621
- ACOUSTICS**
- NT AEROACOUSTICS
- NT BIOACOUSTICS
- NT GEOMETRICAL ACOUSTICS
- NT MAGNETOACOUSTICS
- NT PSYCHOACOUSTICS
- NT UNDERWATER ACOUSTICS
- Acoustics of thunder - A quasi-linear model for tortuous lightning 04 p0519 A83-16315
- Acoustic crystals --- Russian book 15 p2238 A83-34165
- A comparison of two theories of acoustoelasticity 21 p3152 A83-44493
- A review of numerical methods in acoustic wave propagation [ONERA, TP NO. 1983-93] 24 p3625 A83-49410
- ACOUSTO-OPTICS**
- Coherent-optical synthesis of an antenna radiation pattern with a zero in a prescribed direction 02 p0166 A83-11686
- Transform receivers for ECM applications 02 p0167 A83-11922
- Fine delay estimation with time integrating correlators 02 p0168 A83-12308
- Gas laser mode-locking using an external acoustooptic modulator with a potential application to passive ring gyroscopes 02 p0185 A83-12589
- Adaptive optical processor 02 p0178 A83-12592
- Laser schlieren microphone for optoacoustic spectroscopy 02 p0178 A83-12600
- Real-time NDE of flaws using a digital acoustic imaging system 03 p0337 A83-13434
- Bulk and integrated acousto-optic spectrometers for molecular astronomy with heterodyne spectrometers 03 p0405 A83-13459
- Recent developments in infrared acousto-optic tunable filters 03 p0393 A83-13770
- A stable acousto-optical spectrometer for millimeter radio astronomy 03 p0330 A83-14759
- Scanning photoacoustic microscopy /SPAM/ of Si3N4 ceramic test bars 04 p0463 A83-15220
- Two-coordinate acoustooptic Q-switch for a YAG-Nd/3 + / laser with nonpolarized radiation 04 p0484 A83-15271
- The control of solid-state laser radiation by paratellurite acoustooptic devices 04 p0484 A83-15274
- Study of the absorption of pulsed CO2 laser radiation by air and by carbon dioxide 04 p0484 A83-15705
- An analysis of multicomponent electroacoustic transducers providing matched control of the acoustic field in Bragg acoustooptic devices in the short-wave portion of the microwave range 05 p0630 A83-17595
- Frequency-multiplexed and pipelined iterative optical systolic array processors 06 p0802 A83-18588
- Mode-medium interactions --- high power CO2 laser output instability 08 p1109 A83-22461
- Recent progress in acoustic processing by coherent optical techniques 08 p1167 A83-22810
- Chemical amplification of optoacoustic signals 08 p1162 A83-23269
- Correlation analysis of the optical fields in optoacoustic interaction 09 p1344 A83-24001
- Oscillations in an acoustooptic bistable device 09 p1345 A83-24638
- Coherent-optical processor for two-dimensional antenna arrays with a complex format of signal recording 09 p1345 A83-24920
- Singular value decomposition using iterative optical processors 10 p1483 A83-26632
- Interferometric acoustooptic signal processor for simultaneous direction finding and spectrum analysis 10 p1424 A83-26871
- Acoustooptical device with extremely high contrast ratio 10 p1424 A83-26872
- Sound excitation and appearance of additional losses in a single-mode fiber-optic waveguide in the case of the transmission of amplitude-modulated optical waves 10 p1484 A83-26942
- Mechanisms of acoustic wave generation by lasers 11 p1650 A83-27563
- Infra-red homodyne receiver with acousto-optically controlled local oscillator 11 p1657 A83-28616
- The construction of a spectrophone and a CO2 laser waveguide excited by a radiofrequency field for application to the detection of atmospheric trace species --- French thesis 11 p1585 A83-28654
- Acousto-optic measurements of effective refractive indices of guided modes in planar waveguides 12 p1779 A83-29459
- Improved acousto-optic modulators for CO2 heterodyne laser systems 12 p1732 A83-29467
- The effect of laser radiation on absorption in the far wings of spectral lines 13 p1849 A83-30084
- Acoustooptic excitation of surface electromagnetic waves by a light beam of finite aperture 14 p2003 A83-32119
- Optoacoustic characteristics of single-mode fiber waveguides 15 p2230 A83-33985
- Characteristics of the diffraction of light by regular reflections of an acoustic wave 15 p2231 A83-34707
- Simultaneous scanning optical and acoustic microscopy 16 p2356 A83-36478
- Triangular system solutions on an optical systolic processor 16 p2403 A83-36752
- Hybrid time and space integrating processors for spread spectrum applications 19 p2846 A83-41097
- Self-pulsing and chaos in acoustooptic bistability 19 p2900 A83-41305
- Theory of acoustooptic interaction in active resonators 19 p2854 A83-41774
- The influence of the divergence of ultrasonic waves in the acoustic line of an acoustooptic modulator on the spatial spectrum of a pulsed radio signal 19 p2900 A83-41782
- Acousto-optic phase modulator for single-mode fibres 20 p3047 A83-42479
- Total internal reflectance optoacoustic spectroscopy 20 p2989 A83-42582
- Photothermal measurements of thermal diffusivities 20 p2989 A83-42779
- Holographic installation for SAW visualization 20 p2990 A83-42910
- A real-time signal processor with high resolution using acousto-optic light deflectors and a prism 20 p3048 A83-42947
- LU and Cholesky decomposition on an optical systolic array processor 20 p3037 A83-43629
- Acousto-optic filters in astronomical spectrophotometry 21 p3139 A83-44811
- Multiwavelength operation of an acousto-optic deflector --- for laser flight simulation displays 21 p3140 A83-44839
- Asymmetry of diffraction orders during the diffraction of light by a surface acoustic wave 22 p3277 A83-45681
- Optoacoustic transducers with intensity-modulated inputs 22 p3287 A83-45699
- Broad-band ultrasonic sensor based on induced optical phase shifts in single-mode fibers 22 p3287 A83-45731
- An all fiber-optic sensor for surface acoustic wave measurements 22 p3287 A83-45735
- Heterodyne receiver on silicon - An exercise in integration 22 p3359 A83-46646
- Application of wide band Bragg cells for integrated optic (IO) spectrum analyzers 22 p3293 A83-46661
- Picosecond transient grating generation of tunable ultrasonic waves 22 p3298 A83-46671
- Properties of light transmission across an ultrasound beam with strong acoustooptical interaction 23 p3507 A83-47562
- Wide-band acoustooptical spectral analyzer of the autocollimation type 23 p3507 A83-47573
- Acoustic wave calibration for CO2 laser scattering experiments 23 p3461 A83-47647
- Processing signals the optical way 23 p3508 A83-47821
- Quantitative investigation of critical slowing down in all-optical bistability 23 p3509 A83-48324
- Acousto-optic frequency shifter for single-mode fibres 24 p3630 A83-49978
- ACQUISITION**
- NT DATA ACQUISITION
- NT TARGET ACQUISITION
- Acquisition and tracking performance of a PLL using a class of nonlinear filters 14 p2007 A83-32866
- ACRYLATES**
- Environmental testing of UV-cured acrylate-coated fibers 08 p1073 A83-22488
- Use of polymeric materials in the assembly of solar cells 13 p1872 A83-31610
- A possible mechanism for the reduction of voltage delay in the Li/SOC2 system via cyanoacrylate coatings on lithium 24 p3599 A83-49929
- ACRYLIC RESINS**
- Thermoelastic temperature changes in poly/methyl methacrylate/ at high hydrostatic pressure - Experimental 01 p0027 A83-10607
- USAF studying techniques to restore windshields 02 p0131 A83-12324
- Polymer matrices interpenetrated by a base of polyurethanes and acrylic polymers - Synthesis and properties --- French thesis 11 p1551 A83-28638
- Photooxidative degradation of clear ultraviolet absorbing acrylic copolymer surfaces 11 p1552 A83-28753
- ACRYLONITRILES**
- Oxidative stabilization of oriented acrylic fibres - Morphological rearrangements 05 p0619 A83-17561
- A theoretical analysis and interpretation of the vibrational spectra of polyacrylonitrile and polymethacrylonitrile 14 p1999 A83-32829
- Surface analyses of carbon fibers produced from polyacrylonitrile fibers at low carbonization temperatures 19 p2824 A83-41860
- The detection of vinyl cyanide in TMC-1 21 p3236 A83-45541
- On the relation between Young's modulus and orientation in carbon fibres 24 p3553 A83-48898
- ACTH**
- U ADRENOCORTICOTROPIN (ACTH)
- ACTINIDE SERIES**
- NT CALIFORNIUM ISOTOPES
- NT PLUTONIUM 238
- NT PLUTONIUM 244
- NT THORIUM
- NT THORIUM ISOTOPES
- NT URANIUM
- NT URANIUM ISOTOPES
- The abundance of the actinides in the cosmic radiation as measured on HEAO 3 02 p0272 A83-11619

ACTINIDE SERIES COMPOUNDS

Actinide microdistributions in the enstatite meteorites
07 p1035 A83-21329

ACTINIDE SERIES COMPOUNDS

NT URANIUM COMPOUNDS

NT URANIUM FLUORIDES

ACTINOGRAPHS

U ACTINOMETERS

ACTINOMETERS

NT DICKE RADIOMETERS

NT INFRARED DETECTORS

NT INFRARED SCANNERS

NT INFRARED SPECTROMETERS

NT INFRARED SPECTROPHOTOMETERS

NT MICROWAVE RADIOMETERS

NT PYRANOMETERS

NT RADIOMETERS

NT SOLAR SPECTROMETERS

NT SPECTROHELIOGRAPHS

NT SPECTROPHOTOMETERS

NT SPECTRORADIOMETERS

NT ULTRAVIOLET SPECTROMETERS

Meteorological and actinometrical observations at Baikal during the solar eclipse of 31 July 1981

09 p1316 A83-25061

Actinometric instruments for measuring the radiant flux density
16 p2355 A83-35593

ACTINOMYCETES

Nocardopsis antarcticus - A new species of actinomycetes isolated from the ice sheet of the Central Antarctica glacier
21 p3185 A83-45377

ACTIVATION

The characteristics, neuronal mechanisms, and functional significance of cortical inhibition
13 p1895 A83-30303

ACTIVATION (BIOLOGY)

An electroencephalographic investigation of the human cerebral cortex during the processing of the solution of visual-motor problems with training
01 p0083 A83-10530

The changes in the erythropoiesis-stimulating action of the erythrocytic factors during the blocking of cells of the mononuclear phagocyte system
07 p0972 A83-19921

The effect of the calmodulin inhibitor, trifluoroperazine, on the calcium activation of phosphorylases in the glycosomes of the skeletal muscles in rabbits
07 p0975 A83-20981

ACTIVATION ANALYSIS

NT NEUTRON ACTIVATION ANALYSIS

O-18 tracer studies of Al₂O₃ scale formation on NiCrAl alloys
01 p0024 A83-10249

Activation analysis in the Nuclear Physics Institute of the Academy of Sciences of the Uzbek SSR
06 p0727 A83-19419

ACTIVATION ENERGY

Thermal activation analysis of the structural stability of refractory alloys and computer simulation of the fracture process
01 p0024 A83-10391

Determination of the activation energies of monomolecular dissociation reactions by means of IR spectroscopy-N-nitrodimethylamine
01 p0023 A83-11323

The temperature and force dependence of the activation energy of cyclic creep for refractory alloys
03 p0301 A83-14730

Activation energy asymptotics applied to burning carbon particles
03 p0296 A83-14849

Compressive creep of Si₃N₄/MgO alloys
04 p0463 A83-15992

On the influence of the plate thickness on the boundary layer ignition for large activation energies
07 p0878 A83-19839

The asymptotic structure of a counterflow premixed flame for large activation energies
07 p0882 A83-21166

New temperature fluctuation method for direct determination of thermal activation energy of deep levels in semiconductors
12 p1782 A83-29475

Activation-energy asymptotics of the plane premixed flame
15 p2131 A83-34028

Theoretical implications of nonequal diffusivities of heat and matter on the stability of a plane premixed flame
15 p2132 A83-34029

The activation energy of conductivity in organic solids and liquids in relation to the cohesive energy density
21 p3216 A83-43948

Pressure-induced alpha-omega transformation in titanium Features of the kinetics data
24 p3559 A83-48910

ACTIVE CONTROL

Adaptive system for the active suppression of random wave fields
02 p0232 A83-11683

Adaptive system for the active suppression of random waves on the basis of near-field measurements
02 p0232 A83-11684

Quadratic synthesis of integrated active controls for an aeroelastic forward-swept-wing-aircraft
02 p0137 A83-12458

Nonlinear controller for the pitch-up region
05 p0597 A83-16496

[AIAA PAPER 83-0064]

Active control of a relaxed-static-stability airplane using a discrete model following technique
05 p0598 A83-16624

[AIAA PAPER 83-0279]

Fault isolation methodology for the L-1011 digital avionics flight control system
09 p1209 A83-24427

Experimental results for active structural control --- of large space structures
09 p1217 A83-24758

Development of an active optical mirror for astronomical applications
10 p1482 A83-25829

Active wavefront correction in large telescopes
10 p1482 A83-25830

Image quality and high resolution in future telescopes
10 p1482 A83-25832

Active optics - Don't build a telescope without it
13 p1920 A83-31007

Mirror control system for the University of California technical demonstration prototype
13 p1921 A83-31021

Telescope alignment with the absolute distance interferometer
13 p1921 A83-31023

Robust active vibration damping of finite element structures in space flight
13 p1868 A83-31624

Higher harmonic control for the jet smooth ride
14 p1977 A83-33096

Aircraft active controls - New era in design
16 p2311 A83-35773

A comparison of control techniques for large flexible systems
17 p2475 A83-37070

Active attitude control of a spinning symmetrical satellite in an elliptic orbit
17 p2475 A83-37073

Active flow control effects on boundary layer development around a protuberance at high subsonic speed
17 p2445 A83-37216

[AIAA PAPER 83-1737]

Aeroelastic interactions with flight control (A survey paper)
19 p2803 A83-41700

[AIAA PAPER 83-2219]

Control of forward swept wing aeroelastic instabilities using active feedback systems
19 p2803 A83-41701

[AIAA PAPER 83-2220]

Active control of parameter-excited rotor systems
20 p2998 A83-42982

Active control of large flexible spacecraft - A new design approach based on minimum information modelling of parameter uncertainties
21 p3196 A83-45133

Certification of the Lockheed 1011-500 active control system
22 p3255 A83-45850

An optimal active control system with Fourier transformed states for a flexible structure in space
23 p3421 A83-47250

[IAF PAPER 83-68]

Investigation of the unsteady airloads on airfoils with oscillating control in sub- and transonic flows
24 p3544 A83-49180

Active control of near frequency coalescence flutter
24 p3549 A83-49191

Active gust load alleviation and ride comfort improvement
24 p3549 A83-49193

ACTIVE GLACIERS

U GLACIERS

ACTIVE SATELLITES

NT SYNCOM SATELLITES

ACTIVE VOLCANOES

U VOLCANOES

ACTIVITY (BIOLOGY)

The effect of biostimulation amplification after the combined action of laser irradiation in the blue and red regions of the spectrum
01 p0078 A83-10456

The effect of emotional and pain stress on the activity of Na,K-ATPase in the heart muscle
01 p0079 A83-10535

The regulation of erythropoiesis /Status of the problem/
01 p0081 A83-10916

The effect of the solar-geomagnetic situation on monolayers of cells and the distant intercellular interactions at high latitudes
02 p0220 A83-11881

Low-strength ULF magnetic fields and the condition of the adaptive reserve in experimental animals
02 p0220 A83-11883

The self-purification of water depending on the physiological peculiarities of higher aquatic plants
03 p0373 A83-13289

The activity of prostaglandin synthetase in brain tissues during radiation sickness in experimental animals
03 p0375 A83-13639

The effect of a geomagnetic field and neuro-psychological stress on the electrical resistance in biologically active points of the skin
04 p0523 A83-15787

The comparative activity of neuropeptide modulators of memory before and after electroshocks in white rats
04 p0520 A83-15891

A new approach to the quantitative evaluation of reflex vestibular nystagmus
06 p0798 A83-18974

The activity of afferents during the effects of temperature on the skin of the forelegs of cats
08 p1145 A83-22114

The systemic determination of the activity of neurons in behavior
08 p1145 A83-22118

Daily rhythms of activity and temperature of Macaca nemestrina
11 p1641 A83-27843

The changes in the T and B immune systems in sailors during prolonged voyages
13 p1906 A83-30950

An investigation of the biological activity during irradiation of calf spleen extracts containing an inhibitor of DNase I
14 p2062 A83-32066

The content of bioelements in the tissues during the aging of an organism (Review of the literature)
15 p2210 A83-34942

The biological activity of lunar soil from Mare Fecunditatis during intratracheal injection
16 p2394 A83-35924

Devices for the study of the bioelectrical activity of the muscles of athletes
17 p2562 A83-38174

The pituitary gland and the resistance of the body to extreme actions
18 p2732 A83-40555

The change in the impulse activity of bulbar respiratory neurons in conditions of acute hypoxia
19 p2871 A83-40813

Functional state of chromatin and proliferative activity of meristematic cells in pea seedlings under various clinostatic conditions
19 p2878 A83-42053

The probabilistic principles of nervous activity
21 p3185 A83-45373

Rhythmic activity in sensory systems --- Russian book
23 p3494 A83-47148

Atmospheric composition - Influence of biology
24 p3604 A83-48760

ACTIVITY CYCLES (BIOLOGY)

Possible mechanisms for the organization of the structure of the sleep-wakefulness cycle according to the data of factor analysis
06 p0794 A83-18971

Material cycling and organic evolution
17 p2557 A83-38894

Global biology - An interdisciplinary scientific research program at NASA, Ames Research Center
23 p3474 A83-47264

[IAF PAPER 83-100]

ACTUATION

The design and evaluation of a hydraulic actuation system for a legged rough-terrain vehicle
11 p1552 A83-27485

ACTUATOR DISKS

Optimum performance of propeller wind turbine blades
04 p0507 A83-16109

The dynamic inducer as a cost-effective wind turbine system
06 p0779 A83-18457

The use of discontinuity surfaces of active and passive disk type for the mathematical modeling of unsteady flows in the circuit of a powerplant with a jet engine
17 p2450 A83-37636

ACTUATORS

Structural kinematics of in-parallel-actuated robot-arms [ASME PAPER 82-DET-105]
02 p0187 A83-12779

Individual blade control independent of a swashplate
04 p0446 A83-16027

Stabilization of a class of plants with possible loss of outputs or actuator failures
08 p1157 A83-22418

Fiber optics for aircraft engine/inlet control
08 p1046 A83-22494

Qualitative stability of large space structures with noncollocated actuators and sensors
09 p1217 A83-24756

Aggregation of large space structure dynamics with respect to actuator and sensor influences
09 p1217 A83-24784

The decentralized control of large flexible space structures
09 p1217 A83-24786

A new approach to pulse frequency modulated control --- mathematical models for analysis and design of control systems
10 p1465 A83-26522

An asymptotic analysis of interactions of feedback loops with parasitics in actuators and sensors
10 p1465 A83-26527

Multivariable approach to the problem of structural cross coupling of force feedback electrohydraulic actuators --- for structural testing of aircraft and their components
10 p1379 A83-26601

Optimum actuator placement, gain, and number for a two-dimensional grillage
12 p1770 A83-29827

[AIAA 83-0854]

A missile flight control system using boundary layer thrust vector control
16 p2293 A83-36246

[AIAA PAPER 83-1149]

Number and placement of control system actuators considering possible failures --- for large space structures
17 p2476 A83-37078

Displacement control of elastic structures - Integral control with a robustness property
17 p2565 A83-37090

Spillover prevention via proper synthesis/placement of actuators and sensors --- on large space structures 17 p2476 A83-37157

Electromechanical primary flight control activation systems for fighter/attack aircraft [SAE PAPER 821435] 17 p2463 A83-37983

The use of actuator-disc dynamic inflow for helicopter flap-lag stability 19 p2797 A83-41081

International Conference on Small and Special Electrical Machines, 2nd, London, England, September 22-24, 1981, Proceedings 19 p2839 A83-41472

An electromechanical primary flight control actuation system for military transport aircraft [AIAA PAPER 83-2195] 19 p2802 A83-41680

An analytical investigation of shape control of large space structures by applied temperatures 21 p3098 A83-43891

An analytical design of electrohydraulic position servo systems with variable structure 21 p3118 A83-44038

Electromechanical control systems 23 p3411 A83-47201

Active vibration control of a cantilevered beam - A study of control actuators --- for large space structures [IAF PAPER 83-ST-11] 23 p3423 A83-47388

Effect of aircraft configuration and control integration on surface actuation [AIAA PAPER 83-2487] 23 p3404 A83-48347

Bucking the current --- electric actuators for V/STOL aircraft 24 p3547 A83-48887

ACUITY

NT VISUAL ACUITY

ADA (PROGRAMMING LANGUAGE)

ADATLAS - The test language of the future 01 p0091 A83-10741

A predictive tracking EW preprocessor using standard computer instruction set architectures 01 p0088 A83-11133

Jovial language control procedures with a view toward Ada 01 p0092 A83-11198

ADA, an introduction: ADA reference manual, /July 1980/ --- Book 01 p0093 A83-11503

The process view of simulation in ADA 07 p0983 A83-19647

An attribute grammar for the semantic analysis of Ada --- Book 21 p3191 A83-45140

ADAPTATION

NT ALTITUDE ACCLIMATIZATION

NT COLD ACCLIMATIZATION

NT DARK ADAPTATION

NT HEAT ACCLIMATIZATION

NT LIGHT ADAPTATION

NT RETINAL ADAPTATION

The adaptation of the neuro-psychic system in sailors of the marine and inland waterway fleets to the conditions of sailing 01 p0085 A83-11405

Investigations of adaptation and solar activity 02 p0220 A83-11877

Poststress activation of the synthesis of nucleic acids and proteins, and its role in adaptive reactions of the body 03 p0373 A83-13597

Two types of adaptation reactions of the blood circulation apparatus 03 p0379 A83-13616

The adaptive properties of the major arterial vessels 03 p0379 A83-13620

The adaptive function of sleep, the causes and manifestations of its disruption --- Russian book 03 p0380 A83-13812

The dependence of the character of the recovery of pulse on the rhythm of the heart and the lability of the sinusoid nodes in athletes after step loads 03 p0382 A83-14355

The oxygen effect and the adaptive reactions of cells. IX - The dependence of the radioprotective effectiveness of gaseous hypoxia on its degree and duration in neonatal and adult mice 03 p0376 A83-14879

Biorhythmic criteria of nonspecific adaptive capability 04 p0523 A83-15786

The activity of the sympathetic-adrenal system as an indicator of athletes' adaptation to physical loads at high temperatures 05 p0672 A83-17154

The poststress activation of the synthesis of nucleic acids and proteins and its role in the adaptive reactions of the organism 05 p0670 A83-17184

Microbiochemical criteria for adaptive reactions in certain barrier systems of the organism 05 p0670 A83-17204

A study of the adaptation processes in the peripheral blood using methods of mathematical modeling --- leukocyte adaptation to microwaves 06 p0796 A83-19382

The adaptive possibilities of an operator in conditions of reduced-gravity simulation 07 p0981 A83-20327

Morphofunctional features of the cardiac neural structures in adapting to physical loads in experiments 07 p0975 A83-20994

Motion sickness - Acquisition and retention of adaptation effects compared in three motion environments 12 p1763 A83-28926

The phase character of the compensatory reactions of the cardiovascular system during active orthostatic tests 12 p1765 A83-29307

Spatial adaptation and line detectors 13 p1900 A83-30431

Cardiovascular adaptation to weightlessness [SAE PAPER 820830] 13 p1905 A83-30928

The role of the cerebral hemispheres in the realization of the adaptive mechanisms in humans (in conditions of sleep deprivation) 14 p2071 A83-33343

Toward a general theory of adaptation --- of biological and nonbiological systems 15 p2210 A83-34930

New data about the mechanisms of the adaptation to physical loads during ischemic heart disease and ways of using these data during the rehabilitation of patients with myocardial infarction 15 p2213 A83-34957

The use of the sound loading test in comprehensive audiological diagnosis 15 p2213 A83-34973

A model for prediction of resynchronization after time-zone flights 15 p2214 A83-34983

A stimulative mechanism of human adaptation to situations of sensory deprivation 15 p2215 A83-35048

Several indicators of the functional condition of the immune system in normal and pathological situations 16 p2400 A83-36842

Several characteristics of the adaptation process during vibrational loads in grinders 17 p2559 A83-38183

The biological role of the reactive inhibition of mitosis during stress 18 p2733 A83-40561

The stability of physiological and psychological functions of humans during the action of extreme factors --- Russian book 19 p2880 A83-40981

The conditions contributing to the sensorimotor adaptation of the eye movement system in humans 19 p2883 A83-41835

The hygienic aspects of the adaptation of an organism to environmental factors (review of the literature) 21 p3184 A83-45298

Evidence against saturation of contrast adaptation in the human visual system 22 p3349 A83-46755

Clinical possibilities in the evaluation of extreme effects --- on humans 23 p3496 A83-47102

Mathematical models of the readaptation of the human visual analyzer following short light flashes 23 p3497 A83-47111

The effect of the neuropeptides vasopressin and fragments of corticotrophin on the cardiovascular and respiratory system of humans at rest and during physical loading 23 p3497 A83-47116

Changes in the microcirculation in mesentery rats during hyperoxia 23 p3496 A83-48568

ADAPTERS

Stability analysis of Centaur-in-Shuttle composite corrugated adapters [AIAA 83-1003] 12 p1707 A83-29791

ADAPTIVE CONTROL

NT ACTIVE CONTROL

NT LEARNING MACHINES

NT SELF ADAPTIVE CONTROL SYSTEMS

Adaptive control of certain systems with the aid of the Liapunov function 01 p0094 A83-10454

A discrete model reference adaptive control system for a plant with input amplitude constraints 01 p0095 A83-10956

Continuous time adaptive identification and control algorithms via newly developed adaptive laws 01 p0095 A83-10960

Design of direct digital adaptive flight-mode control systems for high-performance aircraft 01 p0013 A83-11179

Adaptive power management - A hierarchical/control system with a central multiplex system --- for aircraft applications 01 p0012 A83-11202

Application of model reference adaptive control to a relaxed static stability transport aircraft 01 p0013 A83-11209

Scene classification of Landsat multispectral scanner data by means of the Adaptive Learning Network methodology 01 p0067 A83-11458

Adaptive system for the active suppression of random wave fields 02 p0232 A83-11683

Adaptive system for the active suppression of random waves on the basis of near-field measurements 02 p0232 A83-11684

Model reference adaptive control of bilinear systems 02 p0229 A83-11789

Explication of a simple output error based model reference adaptive controller 02 p0229 A83-11791

Optimal moments for switching operating cycles in an adaptive system with an identifier 03 p0386 A83-14098

Bounded error adaptive control 03 p0386 A83-14589

Stable model reference adaptive control in the presence of bounded disturbances 03 p0386 A83-14590

Global convergence of output error recursions in colored noise 03 p0386 A83-14592

Asymptotic behavior of an adaptive estimation algorithm with application to M-dependent data 03 p0387 A83-14595

Stochastic adaptive control and prediction based on a modified least squares - The general delay-colored noise case 03 p0387 A83-14596

Adaptive control of a coherent meter of angular velocity 04 p0481 A83-15145

Adaptive ultimately optimal control of linear stochastic object in correlated noise conditions 04 p0527 A83-15924

A plant parameter identifier for an adaptive system of nonsearching self-adjusting class 04 p0527 A83-15925

A model reference adaptive control system for discrete multivariable systems with time delays 04 p0528 A83-16147

Adaptive control of a class of linear stochastic systems with continuous and discrete unknown parameters 04 p0528 A83-16150

Robustness properties of model-reference adaptive control systems 04 p0529 A83-16193

An adaptive sensitive time control circuit implemented with a CCD sampled delay line for clutter rejection in a radar processor 04 p0474 A83-16449

Techniques of self-tuning 05 p0680 A83-17578

Model following and pole-placement self-tuners 05 p0680 A83-17579

Self-tuning control with linear input constraints 05 p0680 A83-17580

Self-tuning controller with integral action 05 p0681 A83-17581

Discrete model reference adaptive control of non-minimum phase systems 05 p0681 A83-17582

A continuous-time approach to discrete-time self-tuning control 05 p0681 A83-17583

Adaptive control and optimal input design - A realistic approach 05 p0681 A83-17584

Discrete adaptive control of a manipulator arm 05 p0681 A83-17585

A single receiver adaptive antenna system 06 p0738 A83-18622

Effects of element cross-polarisation in adpative antennas 06 p0739 A83-18626

Adaptive null steering by reflector antennas 06 p0739 A83-18631

The application of sub-optimal control methods to adaptive antennas for airborne communication systems 06 p0715 A83-18632

Adaptive antenna studies for HF communications 06 p0739 A83-18635

An adaptive MTI for weather clutter suppression 06 p0754 A83-19029

Implicit adaptive control for a class of MIMO systems --- with application to lateral dynamics of F-8 aircraft 06 p0719 A83-19031

Upper limits on the performance of the optimum processor in mismatched environment 06 p0803 A83-19037

Fast algorithms for time domain broadband adaptive array processing 06 p0748 A83-19041

Performance measures of an adaptive array in bandlimited noise 07 p0906 A83-19719

A failure mechanism in adaptive arrays 07 p0907 A83-19722

Optimum signal processing for adaptive arrays with broadband signals and interferers 07 p0907 A83-19723

Performance analysis for an adaptive polling access-control scheme employing a dynamic reservation protocol 07 p0908 A83-19738

Design of adaptive controllers using the method of Lyapunov functions 07 p0984 A83-19998

Convergence in distribution of LMS-type adaptive parameter estimates 07 p0984 A83-20721

Simultaneous identification and adaptive control of unknown systems over finite parameter sets 07 p0985 A83-20722

Second-order convergence analysis of stochastic adaptive linear filtering 07 p0985 A83-20723

Design of an adaptive observer and its application to an adaptive pole placement controller 07 p0985 A83-21163

Adaptive systems and time varying plants 07 p0985 A83-21164

Adaptive linear controller for robotic manipulators 08 p1157 A83-22417

Adaptive detection of targets in laser speckle noise 08 p1045 A83-22521

- An analog open-loop adaptive-array antenna system 08 p1077 A83-22733
- Batch covariance relaxation /BCR/ adaptive processing --- for low-sidelobe main antenna array 08 p1078 A83-22815
- Application of multivariable systems theory; Symposium, Plymouth, England, October 26-28, 1982, Collected Papers 08 p1158 A83-23171
- On the recursive identification of multivariable state space models 08 p1159 A83-23174
- Control - Demands mushroom as station grows 09 p1216 A83-24355
- Model reference adaptive control of large structural systems 09 p1327 A83-24433
- Conference on Decision and Control, 20th, and Symposium on Adaptive Processes, San Diego, CA, December 16-18, 1981, Proceedings. Volumes 1, 2 & 3 09 p1327 A83-24701
- Multi-domain adaptive parameter estimation 09 p1249 A83-24702
- Adaptive parameter estimation of large-scale systems by reduced-order modeling 09 p1327 A83-24710
- Control of robotic manipulator with adaptive controller 09 p1328 A83-24713
- Robust Lyapunov stability results and adaptive systems 09 p1328 A83-24724
- Rate of convergence in model reference adaptive control 09 p1328 A83-24725
- Robustness redesign of continuous-time adaptive schemes 09 p1329 A83-24726
- On satisfying Strict Positive Real condition for convergence by over-parameterization --- of stochastic adaptive control and recursive identification 09 p1329 A83-24727
- Direct adaptive pole placement with application to nonminimum phase systems 09 p1329 A83-24728
- On order overspecification for a direct adaptive pole placer 09 p1329 A83-24729
- Adaptive digital control implemented using residue number systems 09 p1332 A83-24774
- Model adaptive dual control of MIMO stochastic systems 09 p1332 A83-24777
- Adaptive control algorithm design for high-speed cameras 09 p1269 A83-24778
- A globally stable adaptive controller for multivariable systems 09 p1332 A83-24789
- Multivariable adaptive pole placement 09 p1333 A83-24790
- Multivariable self-tuning regulators 09 p1333 A83-24791
- Problems in the application of multivariable adaptive control to flexible spacecraft 09 p1217 A83-24792
- Design of a multivariable model following adaptive control system 09 p1333 A83-24793
- An adaptive servomechanism control strategy for a single-input single-output linear discrete system 09 p1334 A83-24803
- Internal model adaptive control 09 p1334 A83-24804
- On multiple model adaptive controllers and the minimax criterion 09 p1334 A83-24805
- Analytical verification of undesirable properties of direct model reference adaptive control algorithms 09 p1334 A83-24806
- Recent developments in digital control for helicopter powerplants 09 p1207 A83-24829
- Asymptotic reception of optical signals in conditions of indeterminacy 09 p1346 A83-25167
- Adaptive system for varying the range of sawtooth control voltage depending on the potential of the satellite body in a four-electrode probe experiment 10 p1386 A83-25337
- Self-tuning regulators - Non-parametric algorithms 10 p1461 A83-25399
- Static properties of dynamic systems that have controllers using a prediction model 10 p1461 A83-25465
- Optimal adaptive control of linear-quadratic-Gaussian systems 10 p1462 A83-25996
- An economical algorithm of adaptive control of a multidimensional static plant 10 p1462 A83-26068
- Continuous time relay-controlled model reference adaptive system 10 p1462 A83-26070
- Shock capturing using flux-corrected transport algorithms with adaptive gridding 10 p1415 A83-26161
- Control science and technology for the progress of society; Proceedings of the Eighth Triennial World Congress, Kyoto, Japan, August 24-28, 1981. Volume 1 - Control theory 10 p1463 A83-26501
- Extension of V. M. Popov's hyperstability theory of its application in adaptive system design 10 p1464 A83-26513
- A new method for synthesis of nonlinear parameter and state estimators for noisily disturbed processes 10 p1465 A83-26532
- Identification of high dimensional system by the general parameter method 10 p1466 A83-26534
- Theory and applications of adaptive control 10 p1466 A83-26540
- Stochastic control and identification enhancement for the flutter suppression problem 10 p1379 A83-26544
- Adaptive control based on explicit criterion minimization 10 p1467 A83-26547
- Exponential convergence of adaptive identification and control algorithms 10 p1467 A83-26548
- Schemes for multivariable parameter-adaptive deadbeat control 10 p1467 A83-26549
- Stochastic adaptive control - Randomly varying parameters and continually disturbed controls 10 p1467 A83-26550
- Design of a continuous-time adaptive regulator 10 p1467 A83-26551
- Adaptive identification and control of linear MIMO discrete systems in a noisy environment 10 p1467 A83-26552
- Minimum variance control harnessed for non-minimum-phase plants 10 p1467 A83-26553
- Adaptive control with forgetting factor 10 p1467 A83-26554
- Possible evolution of feedback types and their applications in control of nonstationary plants 10 p1467 A83-26555
- Combining model reference adaptive controllers and stochastic self-tuning regulators 10 p1468 A83-26556
- Design of model reference adaptive control systems with arbitrarily small error 10 p1468 A83-26557
- Synthesis of C(asterisk)-model reference adaptive flight controller 10 p1379 A83-26559
- On a problem of Optimal Model Reference Adaptive System 10 p1468 A83-26560
- A new solution to parameter adaptive estimation of random processes 10 p1468 A83-26561
- An adaptive observer with exponential rate of convergence for single-input single-output linear systems 10 p1468 A83-26562
- Two approaches for adaptive observer in multi-output systems 10 p1468 A83-26563
- Remote control of satellites and applied automation 10 p1382 A83-26597
- Development of adaptation and identification algorithms in adaptive digital aircraft control systems 10 p1379 A83-26600
- Self-tuning fly-by-wire control system 10 p1379 A83-26603
- Analysis of the performance of adaptive beam forming using perturbation sequences 10 p1405 A83-26833
- Vibration control of multi-mode rotor-bearing systems 11 p1586 A83-27100
- Adaptive array processing - A tutorial 11 p1553 A83-27901
- A complex gradient operator and its application in adaptive array theory 11 p1554 A83-27902
- Adaptive algorithms in the space and time domains --- signal processing for antenna arrays 11 p1554 A83-27903
- Convergence time of sidelobe cancellation systems 11 p1554 A83-27908
- Multifunction adaptive processor for small antenna arrays 11 p1554 A83-27909
- Problems associated with correlation-loop adaptive antennas employing hard limiting 11 p1554 A83-27910
- UHF circular arrays incorporating open-loop null steering for communications 11 p1554 A83-27911
- Direction finding using an adaptive null tracker 11 p1555 A83-27912
- Perturbation adaptive array processor for airborne application 11 p1527 A83-27913
- Coefficient perturbation adaptive HF array 11 p1555 A83-27914
- Adaptive antenna design considerations for satellite communication antennas 11 p1535 A83-27915
- Open-loop adaptivity for rotating antennas 11 p1555 A83-27917
- Experimental linear phased array with partial adaptivity 11 p1555 A83-27918
- Adaptive clutter suppression for airborne phased array radars 11 p1527 A83-27919
- The design of adaptive information-transfer systems for automatic control --- Russian book 12 p1769 A83-29333
- Adaptive zoning for singular problems in two dimensions 12 p1771 A83-29613
- Diagnostic analysis of vibration signals using adaptive digital filtering techniques [AIAA 83-0883] 12 p1770 A83-29831
- Synthesis of control systems with quasi-continuous generation of the control signal 13 p1910 A83-30077
- Some features of the operation of adaptive antenna systems intended for the receptions of FSK signals in a two-beam fluctuating field 13 p1828 A83-30279
- System for the computer-aided design of robot devices 13 p1906 A83-30619
- An engineering concept of adaptive control for manipulation robots via parametric sensitivity analysis 13 p1907 A83-30972
- Modal control for wavefront reconstruction in adaptive optics 13 p1920 A83-31009
- A model reference adaptive control system for discrete bilinear systems 14 p2074 A83-31931
- Game systems of adaptive control 14 p2076 A83-32962
- Adaptation and learning in systems of control and decision making --- Russian book 14 p2076 A83-33025
- An LSI adaptive array processor 15 p2216 A83-33887
- Design of adaptive robust estimation algorithms 15 p2220 A83-33899
- Using adaptive control to synthesize invariant and partially autonomous automatic stabilization systems 15 p2123 A83-33900
- Structural control research and experiments at NASA/LaRC 15 p2220 A83-33968
- Adaptive companded pulse-code-modulation 15 p2146 A83-35103
- Computational aspects of discrete time adaptive control 15 p2222 A83-35120
- A new approach to system diagnosis --- for fault identification in self-testing systems 15 p2218 A83-35140
- Superresolution of multiple noise sources in antenna beam 15 p2148 A83-35180
- Method for calculating the orientation angle of the workpiece for the control systems of adaptive industrial robots 15 p2143 A83-35265
- Aircraft active controls - New era in design 16 p2311 A83-35773
- Cancellation performance degradation of a fully adaptive Yagi array due to inner-element coupling 16 p2342 A83-36483
- Adaptive canceller for elevation angle estimation in the presence of multipath 16 p2343 A83-36577
- Adaptive companded pulse code modulation 16 p2344 A83-36609
- Adaptive control of satellite EIRP to reduce outage caused by fading --- Effective Isotropically Radiated Power 16 p2344 A83-36611
- Principles for the adaptation of logical integrating computing structures for the implementation of fuzzy algorithm 16 p2403 A83-36902
- Some critical questions about deterministic and stochastic adaptive control algorithms 16 p2406 A83-36978
- An adaptive identifier for discrete-time linear systems 17 p2565 A83-37088
- Proportional + integral + double integral adaptive laws for Liapunov MRAC --- Model Reference Adaptive Control 17 p2566 A83-37100
- Parameter-adaptive state space controller for nonlinear processes 17 p2566 A83-37111
- Adaptive control techniques for reducing settling time 17 p2566 A83-37112
- Model reference adaptive control with inexact model matching. I 17 p2568 A83-37126
- Adaptive control of nonlinear self-oscillating systems using MRAS technique 17 p2568 A83-37127
- Model reference adaptive control in the presence of measurement noise 17 p2568 A83-37128
- A model following algorithm for polynomial inputs 17 p2568 A83-37129
- Frequency-shaped penalty functions for robust control design 17 p2568 A83-37143
- Coordinate-parametric control system for spacecraft functioning algorithms 17 p2569 A83-37442
- An adaptive attitude control system for large-angle slew manoeuvres 17 p2477 A83-37449
- State synthesiser - A digital observer for spacecraft attitude control systems 17 p2569 A83-37452
- Adaptive systems with reduced models --- Book 17 p2569 A83-37494
- Asymptotically optimal automata with growing memory 18 p2738 A83-39513
- Approximation of solutions of strongly nonstationary stochastic extremal problems in continuous time. II Convergence of algorithms 19 p2889 A83-40899
- Prediction of adaptive array performance 19 p2826 A83-41145
- Orthogonal-mixing adaptive detection in incompletely specified noise 19 p2828 A83-41346
- High speed adaptive sidelobe canceller studies 19 p2831 A83-41383
- Increased data rates for communication systems with adaptive antennas 19 p2831 A83-41384

- The SINR performance of cascaded adaptive arrays
19 p2831 A83-41385
- Bootstrapping adaptive cross pol cancelers for satellite communications
19 p2831 A83-41386
- Adaptive acquisition of multiple access codes
19 p2833 A83-41407
- Control and its applications; Proceedings of the International Conference, Warwick, England, March 23-25, 1981
19 p2890 A83-41476
- Computer aided design in real-time adaptive control
19 p2890 A83-41481
- An adaptive mechanism for a non-linear control system
19 p2890 A83-41483
- A square-root algorithm for the adaptive control of multivariate systems
19 p2891 A83-41573
- Adaptive control of variable flow ducted rockets [AIAA PAPER 83-2202]
19 p2797 A83-41686
- Adaptive parameter estimation for a flexible structure Effects of spillover
[AIAA PAPER 83-2244]
19 p2891 A83-41720
- Parameter testing for lattice filter based adaptive modal control systems
[AIAA PAPER 83-2245]
19 p2892 A83-41721
- Adaptive control for large space structures
[AIAA PAPER 83-2246]
19 p2816 A83-41722
- The effect of the initial approximation on the convergence speed of processes of the adaptive adjustment of clutter-suppression systems
19 p2835 A83-41775
- Decentralization of the identification or control laws of adaptive systems with a large dimension reference model --- French thesis
19 p2892 A83-41812
- Experimental transonic studies of a three-dimensional adaptive-wall wind tunnel
20 p2928 A83-42548
- Electronic steering of antenna nulls for interference reduction
20 p2965 A83-43680
- Broadband adaptive array processing
20 p2965 A83-43682
- Recognition of cutting states for difficult-to-cut materials Application of pattern recognition technique
20 p3040 A83-43698
- Multiple-window parallel adaptive boundary finding in computer vision
21 p3192 A83-43952
- On adaptive regulation of flexible spacecraft
21 p3101 A83-45114
- Partitioning of Large Space Structures
21 p3103 A83-45132
- Synchronous and channel-sense asynchronous dynamic group-random-access schemes for multiple-access communications
22 p3272 A83-45738
- Adaptive control of a flexible beam using least square lattice filters
22 p3351 A83-46099
- Experimental implementation of parameter adaptive control on a free-free beam
22 p3351 A83-46100
- Global adaptive pole placement - Detailed analysis of a first-order system
22 p3351 A83-46368
- Model reference adaptive control of system having purely deterministic disturbances
22 p3351 A83-46369
- Adaptive manipulator control (movement learning algorithms)
22 p3352 A83-46399
- Extended discrete-time multivariable adaptive control using long-term predictor
23 p3502 A83-48644
- Adaptive diversity combining for improved millimeter wave communication through rain
24 p3571 A83-49859
- Zero-latency tracking of predictable targets by time-delay systems
24 p3621 A83-49898
- Stability analysis of adaptively controlled systems subject to bounded disturbances
24 p3621 A83-49921
- Convergence analysis of recursive identification algorithms with forgetting factor
24 p3621 A83-49922
- An adaptive robustizing approach to Kalman filtering
24 p3621 A83-49924
- ADAPTIVE CONTROL SYSTEMS**
- U. ADAPTIVE CONTROL**
- ADAPTIVE FILTERS**
- Digital stochastic iterative procedures for the adaptive adjustment of noise compensation systems - Analysis of convergence and convergence rate
01 p0031 A83-10412
- Analysis of digital adaptive rejection filters
01 p0038 A83-10806
- Synthesis of an adaptive analyzer of levels of nonstationary radio interference --- for decametric wave band
01 p0031 A83-10809
- Adaptive randomized detector of optical signals
01 p0031 A83-10812
- An adaptive transform image data compression scheme incorporating pattern recognition procedures
01 p0098 A83-11428
- Digital adaptive methods of signal processing
02 p0162 A83-11529
- The efficiency of an adaptive algorithm with regularization of the sampled correlation matrix --- for filter optimization
02 p0162 A83-11532
- Explication of a simple output error based model reference adaptive controller
02 p0229 A83-11791
- System identification techniques for adaptive signal processing
02 p0229 A83-11821
- An introduction to adaptive signal processing
02 p0163 A83-11914
- Adaptive optical processor
02 p0178 A83-12592
- Adaptive spatial/temporal/spectral filters for background clutter suppression and target detection
03 p0386 A83-13874
- Inertial navigation and optimal filtering --- Russian book
05 p0680 A83-17123
- Adaptive method for the real-time identification of a covariance matrix of measurement errors
06 p0803 A83-19178
- Calculation of the stationary characteristics of an adaptive transversal filter
06 p0754 A83-19340
- The use of adaptive filters for narrowband interference rejection
07 p0905 A83-19700
- Optimal adaptive smoothing in correlated noise conditions
07 p0984 A83-20000
- Adaptive filter with a time-domain implementation using correlation cancellation loops
07 p0993 A83-20158
- Fault detection by adaptive nonlinear filtering
07 p0984 A83-20501
- Second-order convergence analysis of stochastic adaptive linear filtering
07 p0985 A83-20723
- An adaptive digital filter as a sinusoidal noise canceller
07 p0921 A83-20820
- Rejection of pulsed CW interference in PN spread-spectrum systems using complex adaptive filters
07 p0915 A83-21196
- A new multiple-model adaptive filter for continuous-time stochastic distributed parameter systems
08 p1156 A83-22073
- Investigation of the noise immunity of analog-to-digital conversion by adaptive-averaging methods
08 p1156 A83-22123
- ARMA time series modeling - An effective method
08 p1158 A83-22730
- Self-adaptive filters for the integration of navigation data
09 p1204 A83-23374
- SNR enhancement of narrowband signals in colored noise using adaptive predictors
09 p1327 A83-24703
- Residual signal analysis - A subsystem approach to adaptive signal processing
09 p1249 A83-24704
- Convergence properties of LMS adaptive estimators with unbounded dependent inputs
09 p1330 A83-24743
- An unbiased adaptive method for retrieval of sinusoidal signals in colored noise
09 p1331 A83-24773
- An adaptive scheme for optimal target detection in variable clutter environment
09 p1200 A83-24779
- Self-adaptive filters for the integration of navigation data
09 p1335 A83-24866
- Random-search algorithms in the problem of the adaptation of an antenna array with discrete phase shifters
09 p1250 A83-24919
- Adaptive enhancement of finite bandwidth signals in white Gaussian noise
10 p1402 A83-25635
- Effectiveness of the frequency-adaptive parallel transmission of discrete signals
10 p1407 A83-26936
- Results of the simulation of an adaptive nonparametric linear classifier of polarization-shift-keyed signals
10 p1407 A83-26939
- Eigenfilter approaches to adaptive array processing
11 p1554 A83-27904
- Transversal filter techniques for adaptive array applications
11 p1554 A83-27905
- The rate of convergence of the parameters of adaptive filters with quasi-harmonic input signals
11 p1561 A83-27934
- Near-real-time flutter boundary prediction from turbulence excited response
[AIAA 83-0814]
12 p1741 A83-29814
- Method for the design of adaptive filters with limited size of the learning sample
14 p2003 A83-32112
- Performance of digital implementations of an adaptive processor
14 p2007 A83-33127
- Epsilon-separating nonlinear digital filter and its applications
15 p2220 A83-33519
- An adaptive filter using polynomial least squares methods
15 p2221 A83-35108
- Computational noise effects on adaptive filter algorithms
16 p2403 A83-35349
- Convergence of partitioned adaptive filters for systems with unknown biases
17 p2569 A83-37550
- Synthesis of adaptive tracking systems
17 p2570 A83-38483
- Estimation of the covariance matrix of stationary noise --- in adaptive systems of moving targets
18 p2674 A83-39431
- Flight test experience with pilot-induced-oscillation suppressor filters
[AIAA PAPER 83-2107]
19 p2806 A83-41936
- Estimation and identification of two-dimensional images
20 p2991 A83-43404
- Radar performance studies of adaptive lattice clutter-suppression filters
20 p2964 A83-43676
- A 'current' statistical model and adaptive tracking algorithm for maneuvering targets
20 p3040 A83-43697
- Devices for the discrimination of radar signals from noise --- Russian book
21 p3119 A83-43904
- Identification of structural dynamics systems using least-square lattice filters --- large space structures
21 p3103 A83-45467
- Adaptive Kalman filter for tracking maneuvering targets
21 p3197 A83-45474
- An analysis of the efficiency of adaptive systems utilizing correlation feedback for passive-noise suppression
22 p3271 A83-45659
- Evaluating the effectiveness of using adaptive algorithms in communication lines with fading
22 p3271 A83-45662
- A complex algorithm for linearly constrained adaptive arrays
23 p3443 A83-47843
- Synthesis of optimal weight distribution in adaptive antenna arrays
23 p3444 A83-48488
- Regularization of algorithms for the processing of signals and noise in adaptive antenna arrays
23 p3444 A83-48522
- Applicability of the relay correlator to radar signal processing
23 p3444 A83-48714
- ADAPTIVE OPTICS**
- Intracavity adaptive optics. III - HSURIA performance --- Half-Symmetrical Unstable Resonator with Intracavity Axicon
02 p0236 A83-12319
- Adaptive optical system referencing in the case of resolved targets illuminated through turbulence
02 p0215 A83-12591
- Adaptive optics
03 p0395 A83-14928
- Adaptive mirrors --- for astronomical telescopes
04 p0534 A83-15260
- A spatio-temporal light modulator with a DKDP crystal in an adaptive optical system
04 p0534 A83-15262
- Polarization control of an antireflection-coated GaAlAs laser diode by an external optical feedback
04 p0535 A83-16092
- An investigation of the dislocation density of a wave front in light fields having a speckle structure
05 p0647 A83-16889
- Quality of wavefront correction in adaptive transmitting systems
05 p0685 A83-17045
- Adaptive optics methods in interferometry
05 p0644 A83-17073
- Quantum noise in adaptive optical systems. I
05 p0685 A83-17589
- Quantum noise in adaptive optical systems. II
06 p0810 A83-19330
- Image compensation in the presence of thermal blooming --- extended target image reconstruction using adaptive optics
07 p0935 A83-20156
- Wavefront distortions in power optics; Proceedings of the Meeting, San Diego, CA, August 27, 28, 1981
08 p1107 A83-22449
- Aberrations in high power laser systems
08 p1108 A83-22452
- Pseudo-conjugation/compensation of high-power optical trains
08 p1164 A83-22464
- Adaptive optics - Problems and prospects
08 p1109 A83-22465
- Local optical correction system --- adaptive laser beam control
08 p1109 A83-22466
- A method for the numerical investigation of adaptive optical systems of aperture sensing
09 p1344 A83-23486
- Intracavity adaptive optic compensation of phase aberrations. III - Passive and active cavity study for a large N/eq resonator
09 p1271 A83-24087
- Development of an active optical mirror for astronomical applications
10 p1482 A83-25829
- Transient regime and correction with adaptive optics of thermal blooming
11 p1579 A83-27553
- Status of the European Southern Observatory new technology telescope project
13 p1937 A83-30988
- Deformable mirror with combined piezoelectric and electrostatic actuators
13 p1920 A83-31008
- Modal control for wavefront reconstruction in adaptive optics
13 p1920 A83-31009
- Four-wave mixer phase compensation performance --- for atmospheric turbulence-caused resolution improvement in large terrestrial telescopes
13 p1920 A83-31010
- Experiments with high bandwidth segmented mirrors
13 p1921 A83-31020
- Correction of angular displacements of optical beams
14 p2083 A83-31911

The phase-conjugation method in adaptive systems for the shaping of light beams 14 p2024 A83-32593
Real-time fringe-pattern analysis 14 p2021 A83-32912
Performance evaluation of an edge-actuated, modal, deformable mirror 14 p2085 A83-33176
Wave-front dislocations - Topological limitations for adaptive systems with phase conjugation 15 p2228 A83-33526
Stationary transform processing of digital images for data compression 19 p2847 A83-41105
Adaptive optical system for astronomical applications 21 p3206 A83-44808
Strehl's ratio for a two-wavelength continuously deformable optical adaptive transmitter 23 p3507 A83-47579

ADDERS (CIRCUITS)

U ADDING CIRCUITS

ADDING CIRCUITS

A new method for simultaneous complex addition and subtraction --- of two input optical signals with holographic grating 05 p0646 A83-17890

ADDITION RESINS

NT ACRYLIC RESINS
NT VINYL COPOLYMERS

ADDITION THEOREM

Fringe addition in moireanalysis 24 p3582 A83-49010

ADDITIVES

NT ADMIXTURES
NT ANTIOXIDANTS
NT OIL ADDITIVES
NT PLASTICIZERS
NT PROPELLANT ADDITIVES
NT PROPELLANT BINDERS
NT SOLID ROCKET BINDERS

The use of powdered metals as antifriction additions to plastic lubricants 01 p0027 A83-10459
Rate and additive influences on the oxidation of HCN 02 p0153 A83-13099

Formation mechanisms of keying or pegging yttrium oxide and increased plasticity of alumina scale on FeCrAlY 03 p0296 A83-13121
Some aspects of the detonation of explosive mixtures 06 p0726 A83-18005

The modification of Si phase in Al-Si eutectic alloys - Effect of element addition on microstructures of Al-Si and Al-Si-Ge eutectic alloys 07 p0885 A83-20275
Erosion resistance of Co-Cr-Al coatings containing active element additions 10 p1395 A83-25551
An EPR study of the reaction between poly(p-phenylene sulfide) and electron-acceptor dopants 13 p1825 A83-30951

In-situ optical measurement of additive effects on particulates in a sooting diffusion flame 14 p1991 A83-32943
Reduction in acidity of RDX and its compositions by use of suitable additives 15 p2143 A83-33872

The effect of products based on higher fatty acids on the performance characteristics of jet fuels 15 p2143 A83-34500
The probability distribution of passive-additive concentration in a mixing layer 17 p2505 A83-37631
The formation of NO(x) from nitrogen-containing additives in premixed methane flames 17 p2485 A83-38027

The influence of cobalt, iron and aluminum on the precipitation of metastable phases in the Ni-Ta system 20 p2955 A83-43471
The effect of doping on the photoconductivity of p-CdSiAs₂ single crystals 21 p3219 A83-45269

The effect of impurities on the current-amplification cut-off frequency of field-effect transistors 22 p3277 A83-45675
Effects of doping on transport and deep trapping in hydrogenated amorphous silicon 24 p3634 A83-48792

The effect of additives on the critical diameter of detonation of nitroesters 24 p3557 A83-49791

ADDRESSING

Addressing and control of high-speed logic circuits with picosecond light pulses 07 p0921 A83-20793
Some properties of the binary n-cube as a network interconnection structure 15 p2219 A83-35133

ADENINES

NT RIBONUCLEIC ACIDS

ADENOSINE DIPHOSPHATE

The activity of Ca²⁺/ATPase and enzymes of cAMP metabolism in the nerve tissue of rats during the early stages of acute radiation damage 06 p0796 A83-19383

ADENOSINE TRIPHOSPHATE

The effect of emotional and pain stress on the activity of Na,K-ATPase in the heart muscle 01 p0079 A83-10535

The effect of adeturon on the survival and the blood system of mice under the effect of various types of ionizing radiation 03 p0376 A83-14880

A circulating inhibitor of /Na⁺/ + /K⁺/ ATPase associated with essential hypertension 05 p0672 A83-17794

The updated experimental proteinoid model 07 p0976 A83-21050
Thermoelectric energy conversion could be an energy source of living organisms 19 p2875 A83-41168

ATP-regulated K(+) channels in cardiac muscle 23 p3495 A83-48088

ADENOSINES

NT ADENOSINE DIPHOSPHATE
NT ADENOSINE TRIPHOSPHATE
NT CYCLIC AMP

The effect of activators of cAMP accumulation on separate stages of the cell genome expression during acute radiation damage of the animal. V Investigations of the sedimentation characteristics of RNP-particles released from the cell nuclei of irradiated animals and of animals protected with serotonin 03 p0376 A83-14878

Peculiarities of the reaction of cortical pyramidal neurons to the cessation of oxygen supply by the effect of cAMP 04 p0520 A83-15890

The comparative radioprotective effect of adenylates during short-term and long-term gamma-irradiation 09 p1321 A83-24931
AMP synthesis in aqueous solution of adenosine and phosphorus pentoxide 17 p2563 A83-38891

ADHEROMETERS

U ADHESION TESTS

ADHESION

Adhesion of solids 06 p0805 A83-18144
Adhesion 6 --- Book 15 p2142 A83-33617
Mechanism of peg growth and influence on scale adhesion 24 p3563 A83-49495

ADHESION TESTS

The viscoelastic constitutive modelling of adhesives 01 p0027 A83-10242
Mechanical properties of adhesive systems at cryogenic and other temperatures 01 p0027 A83-11490
NDE of simulated Space Shuttle tile disbands 04 p0452 A83-15183

The effect of moisture and temperature on the properties of an epoxide-polyamide adhesive in relation to its performance in single lap joints 04 p0463 A83-15872
A three-point flexure test configuration for improved sensitivity to metal/adhesive interfacial phenomena 04 p0487 A83-15875

Improved surface pretreatments for adhesive bonding of titanium alloys 07 p0885 A83-20440
The structure of aluminum oxides used for corrosion resistance and primer adhesion 07 p0899 A83-20492

A study of the adhesive interaction between plasma-sprayed coatings of eutectic alloys on refractory steels 07 p0888 A83-20695
Fracture mechanisms in the peeling failure of adhesive joints 08 p1069 A83-21730

The conditions for the adhesion of freshly generated metal surfaces under load 13 p1819 A83-30018
Special features of the measurement of adhesion of steel fibers to a polymer matrix in a wide range of loading rates 13 p1816 A83-31221

Evaluation of the curing of structural adhesives by ultrasonic interface waves - Correlation with strength 13 p1826 A83-31617
The cohesive and adhesive strength of ice --- adhering to stainless steel, titanium, and anodized aluminum engineering structures 15 p2130 A83-35069

Cohesive and adhesive analog test specimens for solid propellant grain simulation [AIAA PAPER 83-1118] 16 p2338 A83-36229
The effect of adhesion on the elastic properties of a composite with a disperse filler 18 p2649 A83-39478

Improved chromatic acid anodize seal for optimum paint adhesion [SAE PAPER 820603] 22 p3301 A83-45864
Enhanced adhesion from high energy ion irradiation 22 p3365 A83-46703

A sodium hydroxide anodize surface pretreatment for the adhesive bonding of titanium alloys 23 p3432 A83-48151
Chemical interactions in the system anodized aluminum-primer-adhesive 23 p3427 A83-48152

ADHESIVE BONDING

The viscoelastic constitutive modelling of adhesives 01 p0027 A83-10242
Role of fibre surface-matrix combination in carbon fibre reinforced epoxy composites 02 p0149 A83-11669

The use of composite patches for repair of aircraft structural parts 02 p0131 A83-12968

Optimal cooling of cross-ply composite laminates and adhesive joints [ASME PAPER 82-WA/APM-24] 04 p0455 A83-15679

Mechanism of interfacial bond failure 04 p0463 A83-15873
Cold-setting adhesives for repair purposes using various surface preparation methods 04 p0463 A83-15874

National SAMPE Symposium and Exhibition, 27th, San Diego, CA, May 4-6, 1982, Proceedings 07 p0874 A83-20426
Seeding of FPL solution --- in preparation of aluminum surfaces for adhesive bonding 07 p0885 A83-20431

A sensible approach to process control of adhesive bonding 07 p0861 A83-20432
The alkaline peroxide prebond surface treatment for titanium - The development of a production process 07 p0885 A83-20433

Improved surface pretreatments for adhesive bonding of titanium alloys 07 p0885 A83-20440
Effect of moisture on adhesively bonded titanium structures 07 p0886 A83-20442

The effect of primer-adhesive compatibility on adhesive peel strength at low temperature 07 p0898 A83-20448
An evaluation of titanium bonding pretreatments with a wedge test method 07 p0886 A83-20450

Evaluation of titanium prebond treatments by stress durability testing 07 p0886 A83-20455
Service history of phosphoric acid anodized aluminum structure --- with adhesive bonding for aircraft construction 07 p0861 A83-20479

Surface characterization and failure analysis of thermally aged, polyimide bonded titanium 07 p0886 A83-20491
Primary bonded aircraft wing construction 07 p0861 A83-20493

Aging and performance of structural film adhesives. I - A comparison of two high-temperature curing, epoxy-based systems 07 p0900 A83-21048
Fracture mechanisms in the peeling failure of adhesive joints 08 p1069 A83-21730

Fabrication of thin glass mirrors on alnico magnets 08 p1112 A83-22866
Surface treatment of AM355 stainless steel for adhesive bonding 09 p1228 A83-23327

The performance of adhesive-bonded thin-gauge sheet-metal structures with particular reference to box-section beams 09 p1276 A83-23328
The design of bonded structure repairs 09 p1243 A83-23329

Polyimide adhesives to reduce thermal stresses in LSI ceramic packages 09 p1237 A83-23621
Weak boundary zones in metal bonds 09 p1237 A83-23626

An analysis of adhesive-bonded single-lap joints [ASME PAPER 83-APM-14] 10 p1441 A83-26436
On the analysis of adhesive joints in fiber reinforced composite plates and shells 11 p1591 A83-27430

Ultrasonic scanning and spectrum analysis for inspection of bond efficiency of metal-to-metal structural adhesive joints 11 p1590 A83-27898
The strength of S0115M glass ceramic and its joints made through optical contact 11 p1551 A83-28511

Optimization of bonded joints [AIAA 83-0906] 12 p1739 A83-29762
Effect of stitching on the strength of bonded composite single lap joints [AIAA 83-0969] 12 p1739 A83-29779

An evaluation of the random bending fatigue life of bonded aluminum joints using various adhesive/primer combinations [AIAA 83-0998] 12 p1744 A83-29873

Acoustic fatigue test evaluation of adhesively bonded aluminum fuselage panels using FM 73/BR 127 adhesive/primer system [AIAA 83-0999] 12 p1744 A83-29874

Free-volume relaxation during the molding of composite materials 13 p1816 A83-30087
Diatom molecules and metallic adhesion, cohesion, and chemisorption - A single binding-energy relation 13 p1817 A83-30921

Surface roughness effects on the stress analysis of adhesive joints 14 p2032 A83-32843
Some applications of ultrasonic methods for the quality control of nonmetallic objects 16 p2364 A83-36794

Adhesive bonding and composites 18 p2650 A83-40131
Physical properties of dihalocarbene modified rubbers 18 p2672 A83-40139

Anaerobic structural adhesives 18 p2672 A83-40140
Stress analysis and strength of adhesive bonded joints under bending loads 18 p2703 A83-40156

Hygrothermal effects on CFRP bonded systems 18 p2652 A83-40157

The effect of composite prebond moisture on adhesive-bonded CFRP-CFRP joints
20 p2947 A83-42807

Bonded aluminum honeycomb - Aircraft flight surface primary structure application
21 p3091 A83-43972

Fracture toughness of composite adherend adhesive joints under mixed mode I and III loading
21 p3115 A83-44121

Enhanced adhesion from high energy ion irradiation
22 p3365 A83-46703

Influence of late-breaking ligaments on crack propagation in compact specimens - A photoelastic study
22 p3306 A83-46808

A sodium hydroxide anodize surface pretreatment for the adhesive bonding of titanium alloys
23 p3432 A83-48151

Chemical interactions in the system anodized aluminum-primer-adhesive
23 p3427 A83-48152

Stress analysis of stepped-lap joints with bondline flaws
23 p3471 A83-48214

ADHESIVES

Reinforced plastics/composites adhesives and thermosets; Proceedings of the Sixth Annual Pacific Technical Conference and Displays, Los Angeles, CA, August 25-27, 1981
04 p0454 A83-16176

Rheological characterization of a toughened epoxy adhesive system as a quality control tool
07 p0942 A83-20446

High temperature adhesives
07 p0898 A83-20449

The effects of humidity on the processing and performance of a structural adhesive
07 p0899 A83-20453

Adhesive stress-strain properties relative to fatigue life of titanium bonded to graphite reinforced plastic
09 p1237 A83-23616

Characterization of room temperature curing adhesives
09 p1237 A83-23622

Silicone sealants as adhesives
09 p1237 A83-23624

An application of unsupported film adhesive to fabricate spacecraft structures
09 p1238 A83-23629

Characterization of two nitrile-epoxy structural adhesives
12 p1716 A83-29550

Assessment of chemical cure-shrinkage stresses in two technical resins
12 p1716 A83-29732

Evaluation of the curing of structural adhesives by ultrasonic interface waves - Correlation with strength
13 p1826 A83-31617

Adhesion 6 --- Book
15 p2142 A83-33617

Damage tolerance evaluation of adhesively laminated titanium
18 p2666 A83-39994

Anaerobic structural adhesives
18 p2672 A83-40140

On the thermoviscoelastic characterization of adhesives and composites
18 p2705 A83-40207

ADIABATIC CONDITIONS

Adiabatic vs. isothermal - Two pictures of galaxy origin
01 p0127 A83-11291

Formation of galaxies in G-variable cosmologies
01 p0127 A83-11294

Adiabatic heating at a dislocation pile-up avalanche
03 p0291 A83-14497

Calculation of long-range radio paths by the adiabatic method using a parabolic model of the ionosphere
05 p0663 A83-17611

The adiabatic invariant and evolution equations for the motion of a particle in a strongly nonuniform magnetic field
06 p0806 A83-19328

Adiabatic calorimetry for kinetics modeling of epoxy resin systems
07 p0898 A83-20445

Evolution of potential perturbations after decoupling /The adiabatic scenario/ --- in early Universe
07 p1016 A83-20763

Analysis of the large-scale structure of the universe
07 p1017 A83-20935

Small-angle anisotropy of the microwave background radiation in the adiabatic theory --- concerning structure of Universe
09 p1364 A83-25002

The ideal adiabatic cycle - A rational basis for Stirling engine analysis
11 p1684 A83-27264

Adiabatic oscillations of solar models with a high-Z convective core
11 p1689 A83-27644

Adiabatic oscillations of a differentially-rotating star - Second-order perturbation theory
11 p1677 A83-27656

Adiabatic density perturbations in a cosmological model with massive neutrinos
13 p1955 A83-31652

Adiabatic motion of an electron bunch in the magnetosphere
17 p2544 A83-38520

An accurate theoretical approximation for adiabatic condensation temperature
20 p3030 A83-42514

Experimental study of a toroidal plasma under the conditions for adiabatic Budker-Buneman instability
23 p3510 A83-47610

Ignition of crystalline hexogen with adiabatic compression of the adjacent gas pocket
24 p3557 A83-49792

ADIABATIC EQUATIONS

The adiabatic motion of charged dust grains in rotating magnetospheres --- and for ring systems of Jupiter and Saturn
06 p0847 A83-18276

Stellar structures with constant local adiabatic index under extreme relativistic conditions
18 p2774 A83-39735

ADIABATIC FLOW

A self-similar flow of self-gravitating gas behind a shock wave with increasing energy. I
04 p0557 A83-15978

Adiabatic shearing of incompressible fluids with temperature-dependent viscosity
10 p1414 A83-25873

On the use of adaptive grids in numerically calculating adiabatic flame speeds
15 p2132 A83-34032

ADIPOSE TISSUES

The effect of hypokinesia on lipid metabolism in adipose tissue
[IAF PAPER 83-189]
23 p3494 A83-47305

ADJOINTS

On the problem of observation spillover in self-adjoint distributed-parameter systems
08 p1156 A83-22044

A linear theory of thin-walled shells based on the concept of adjoint vectors
17 p2524 A83-38504

ADJUSTING

Automatic methods for the adjustment of faceted solar-energy concentrators and heliostats
04 p0503 A83-15131

A practical method of correcting monthly average temperature biases resulting from differing times of observation
18 p2722 A83-39127

ADJUSTMENT

U ADJUSTING

ADMITTANCE

U ELECTRICAL IMPEDANCE

ADMIXTURES

Reversible and irreversible wet deposition processes involving atmospheric admixtures
09 p1294 A83-23547

Features of the effect of admixtures on the characteristics of a region perturbed by a body moving at hypersonic velocity
19 p2792 A83-41893

ADP

U ADENOSINE DIPHOSPHATE

ADRENAL GLAND

The combined effect of noise, vibration, and high temperatures on the condition of the sympathetic-adrenal system in sailors
03 p0379 A83-13615

The significance of glucocorticoids in the regulation of the resynthesis of glycogen in the postexercise period and the mechanism of their action
04 p0520 A83-15898

A histochemical study of the rat spinal cord, spinal ganglia, and adrenal glands under local vibration
05 p0670 A83-17192

The peculiarities of the functional condition of the adrenal cortex in old rats during immobilization stress
05 p0672 A83-17600

The effect of adrenalectomy and hydrocortisone on the carbohydrate metabolism in the lungs and myocardium during chronic hypoxia
07 p0972 A83-19922

The characteristics of the mechanism of action of cyproheptadine /peritol/ on the activity of the hypothalamo-hypophyseal-adrenal system
07 p0974 A83-20979

The effect of azaperone on the dynamics of the stress-reaction and the content of catecholamines in the adrenal glands of rats during immobilization stress
07 p0975 A83-20984

The condition of the hypothalamic-hypophyseal-adrenal system during sudden cardiac death
09 p1322 A83-23982

The sympathicoadrenal system during hypoxic conditions
09 p1321 A83-25153

The effect of the pharmacological blocking of the alpha and beta adrenoreceptors on the development of experimental high-altitude acute pulmonary edema
09 p1322 A83-25171

Circadian rhythms of work capacity, the activity of the sympathoadrenal system and myocardial infarction
12 p1765 A83-29308

The function of the hypophyseal-adrenal system when exposed to a variable magnetic field of industrial frequency
15 p2210 A83-34931

The content of gonadotropin hormones and hydrocortisone in women during adaptation to conditions of high latitudes
23 p3497 A83-47104

ADRENAL METABOLISM

The changes in the content of corticosterone in the blood plasma of inbred mice after exposure to stress
01 p0080 A83-10541

The state of the adrenal cortex function in healthy individuals during changes in geomagnetic activity
02 p0222 A83-11882

ADSORPTION

Serotonin and the adrenocortical response to cold during the early postnatal development of rats
03 p0375 A83-14328

The activity of the sympathetic-adrenal system as an indicator of athletes' adaptation to physical loads at high temperatures
05 p0672 A83-17154

The reaction of the hypophyseal-adrenal system to emotional stress in patients with hypertension
05 p0674 A83-17200

Temperature and adrenocortical responses in rhesus monkeys exposed to microwaves
05 p0671 A83-17334

Current ideas about the mechanism of the action of glucocorticoid hormones
05 p0672 A83-17599

The adrenoreactivity of the vessels of the small intestine in cats during the process of high altitude adaptation
07 p0973 A83-20245

Clonidine as a counter measure for metabolic studies during weightlessness simulation
11 p1642 A83-27796

Effect of suspension hypokinesia/hypodynamia on glucocorticoid receptor levels in rat hindlimb muscles
11 p1640 A83-27836

Sympathoadrenal responses to cold and ketamine anesthesia in the rhesus monkey
13 p1898 A83-30496

The interaction of prostaglandins and the sympathetic-adrenal system
14 p2066 A83-33328

An evaluation of the condition and potential of athletes using indicators of humoral-hormonal reactions
16 p2398 A83-35904

Adrenocortical activity in athletes after repeated physical loads during the course of the day
16 p2398 A83-35909

The biological role of the reactive inhibition of mitosis during stress
18 p2733 A83-40561

The pattern of the changes in the concentration of catecholamines and acetylcholine in the blood during the prolonged action of a constant magnetic field with a high induction
21 p3186 A83-45379

On the functional state of the pituitary-adrenal-axis in rats under different conditions of motor activity
23 p3496 A83-48448

ADRENALINE

U EPINEPHRINE

ADRENERGICS

Beta adrenergic blockade and erythropoietic production in rats after hypoxia and hypovolemia
09 p1321 A83-23875

Effects of beta-adrenergic blockade on O2 uptake during submaximal and maximal exercise
13 p1904 A83-30497

The role of adrenergic mechanisms in the development of cerebrovascular disorders during acute myocardial ischemia
15 p2210 A83-34960

Cholinergic and adrenergic innervation of intracerebral arteries during ontogenesis in humans
17 p2560 A83-38194

The pharmacology of cardioactive compounds in early ontogenesis --- Russian book
21 p3184 A83-45027

ADRENOCORTICOTROPIN (ACTH)

An evaluation of the possibility of predicting the individual radiosensitivity of rats by their reaction to hypoxia and the administration of adrenocorticotropin
14 p2062 A83-32069

ADSORBENTS

The effect of the nature of the substrate on the emission properties and thermal stability of the adsorption systems cesium-oxygen film-metal
05 p0690 A83-16903

ADSORPTION

NT CHEMISORPTION

The electronic surface state and repolarization processes in barium titanate single crystals
01 p0110 A83-10848

High-temperature adsorption of air oxygen by silicon nitride powders
02 p0161 A83-13034

Performance testing of a three-bed molecular sieve oxygen generator
04 p0524 A83-15307

Adsorption and excess fission Xe - Adsorption of Xe on vacuum crushed minerals
04 p0564 A83-15376

Spouts in a bed of silica powder associated with fluidization by outgassing of adsorbed water
06 p0756 A83-18400

Interaction of metal ions and amino acids - Possible mechanisms for the adsorption of amino acids on homoionic smectite clays
12 p1712 A83-29556

Cluster studies of CO adsorption. III - CO on small Cu clusters
13 p1817 A83-30965

lo's 4-micron band and the role of adsorbed SO2
15 p2275 A83-34723

CO adsorption and the optical properties of interstellar grains
16 p2428 A83-36529

Drastic reduction of adsorption of CO and H2 on (111)-type Pd layers
16 p2328 A83-36990

Miniature J-T refrigerators using adsorption compressors
20 p2960 A83-43231

- Interaction of hydrogen chloride and water with oxide surfaces. III - Titanium dioxide 22 p3267 A83-46700
 Kinetics of hydrogen absorption by alpha-zirconium 23 p3429 A83-47635
 Ground state energy and structure of physisorbed monolayers of linear molecules 23 p3429 A83-47636

ADVANCED X RAY ASTROPHYSICAL FACILITY

U X RAY ASTROPHYSICS FACILITY

ADVANCED X RAY ASTROPHYSICS FACILITY

U X RAY ASTROPHYSICS FACILITY

ADVANCING GLACIERS

U GLACIERS

ADVECTION

- Errors in fixed and moving frame of references - Applications for conventional and Doppler radar analysis 02 p0214 A83-12327
 Algorithms for advection and shock problems 03 p0322 A83-14611
 The 5-min oscillations of the sun are incompatible with a rapidly-rotating core 05 p0709 A83-17797
 Testing subroutines solving advection-diffusion equations in atmospheric environments 06 p0756 A83-18374
 Multiply-upstream, semi-Lagrangian advective schemes - Analysis and application to a multi-level primitive equation model 08 p1139 A83-22288
 Selected comment on multiple Doppler analysis --- of radar scanned storm with advection error correction 11 p1628 A83-27051
 Estimation and correction of advection effects with single and multiple, conventional and Doppler radars 11 p1630 A83-27071
 On low-order non-linear stochastic-dynamic systems --- for atmospheric circulation 11 p1632 A83-28079
 Vector statistics of hourly wind advection data for energy transport applications 13 p1884 A83-30197
 Finite elements and characteristics applied to advection-diffusion equations 15 p2157 A83-33864
 A simple positive definite advection scheme with small implicit diffusion 15 p2204 A83-33881
 An analysis of finite-difference schemes for the numerical solution of the advection equation 18 p2723 A83-39438
 Solution of the advection-diffusion equation by the moments method --- applied to pollutant plumes 19 p2863 A83-41971
 General circulation of air parcels and transport characteristics derived from a hemispheric GCM. I - A determination of advective mass flow in the lower stratosphere 20 p3031 A83-43457
 An accurate variation of the two-step Lax-Wendroff integration of horizontal advection 21 p3179 A83-44398
 Three-dimensional wind field analysis from dual-Doppler radar data. II - Minimizing the error due to temporal variation 22 p3342 A83-46944

AE-C SATELLITE

U EXPLORER 51 SATELLITE

AE-D SATELLITE

U EXPLORER 54 SATELLITE

AE-E SATELLITE

U EXPLORER 55 SATELLITE

AERIAL EXPLOSIONS

- A large-scale explosion in an inhomogeneous terrestrial atmosphere with allowance for spectral radiation --- simulating Tunguska event 06 p0849 A83-19435
 Fuel-air explosions; Proceedings of the International Conference, McGill University, Montreal, Canada, November 4-6, 1981 19 p2820 A83-41523

AERIAL IMAGERY

U AERIAL PHOTOGRAPHY

AERIAL PHOTOGRAPHY

- Analyzing and mapping regional land use trends by combining Landsat and topographic data 01 p0066 A83-10119
 The utilization of infrared /IR/ aerial and space observations of Arctic seas in navigation and during the solution of other national-economic problems 01 p0077 A83-10836
 The use of nonstandard flight vehicles for topographic aerial photography 01 p0051 A83-10856
 Shape analysis of segmented objects using moments 01 p0097 A83-11422
 Elimination of seams from photomosaics 01 p0099 A83-11452
 A relational image data base system for remote sensing /LAND DBMS/ 01 p0067 A83-11462
 Image quality and lens aberrations of an aerial camera 02 p0177 A83-11989
 Mount St. Helens quick response damage assessment using high-altitude infrared photography 02 p0199 A83-12672
 Zoom 500 imagery analysis station 02 p0179 A83-12682

- Computer-assisted photo interpretation system 02 p0180 A83-12684
 Interpretation of aerial thermographic data 02 p0200 A83-12687
 Field evaluation of aerial infrared surveys for residential applications 02 p0200 A83-12688
 Relaxation matching applied to aerial images 02 p0200 A83-12889
 Line finding with subpixel precision 02 p0182 A83-12890
 Use of aerial photography with Loran C positioning to map offshore surface currents 03 p0372 A83-14093
 Spatial frequency pseudocolor filters 03 p0328 A83-14094
 Monitoring revision requirements for Canadian maps 03 p0346 A83-14237
 Environmental monitoring of the Athabasca Oil Sands Region 03 p0346 A83-14238
 Vegetation and human impact mapping for the management of the sunshine area, Canadian Rocky Mountains 03 p0346 A83-14242
 Ecological land classification in the Yukon 03 p0347 A83-14250
 Remote sensing applications for British Columbia wetlands using 35 mm aerial photography 03 p0347 A83-14251
 Aerial survey of crop losses due to grasshoppers /Orthoptera - Acrididae/ in Saskatchewan 03 p0347 A83-14255
 Predicting forest land attributes from aerial photo interpretation variables 03 p0347 A83-14259
 Construction and interpretation of a thermal inertia image using airborne data 03 p0348 A83-14260
 Remote sensing and waste management 03 p0400 A83-14263
 Remote sensing software for airborne image analysis 03 p0349 A83-14273
 Building a small format, in-house aerial photography system 03 p0329 A83-14274
 Cartographic aspects of dual-frequency dual-polarization SAR imagery 03 p0349 A83-14280
 The effects of haze on resolution on small scale aerial photography 03 p0329 A83-14283
 A system for the complex processing of aerial and space data for agriculture 03 p0350 A83-14301
 Determination of forest fire spread rates from infrared photographs 03 p0350 A83-14307
 A method for the digital processing of contour imagery 03 p0329 A83-14312
 Aerial camera vibration 03 p0330 A83-14663
 To mix or match - On choosing matched samples in comparative aerial surveys 03 p0351 A83-14664
 Aerial thermal infrared census of Canada geese in South Dakota 03 p0351 A83-14665
 Investigations of interpretability of images by different sensors and platforms for small scale mapping 03 p0352 A83-14943
 Remote determination of humus content in soils 04 p0502 A83-15889
 Optical coupling of two scanners for the processing of aerial and space images 05 p0645 A83-17681
 Mapping erosion with airphotos - Panchromatic or black and white infrared 05 p0657 A83-17839
 Super high altitude photography for coastal geomorphology --- from approximately 20 km altitude 05 p0657 A83-17840
 Some comparative aspects of SLAR and airphoto images for geomorphologic and geologic interpretation 05 p0657 A83-17842
 Method for additional correction of algorithm for the restoration of smeared images 07 p0929 A83-20558
 Landsat multitemporal color composites 07 p0952 A83-21433
 Direction dependant classification of airborne multispectral scanner data 08 p1125 A83-21914
 Monitoring recent changes in extent of natural forests in Kenya using remote sensing techniques 08 p1127 A83-21940
 Remote sensing methods of geological investigations in the USSR to date and in future 08 p1127 A83-21941
 The use of SPOT simulations in geology - Comparison with aerial photographs and Landsat images - Example: Camares area - Massif central - France 08 p1127 A83-21942
 Aerial survey of water quality - An Indian case study 08 p1128 A83-21949
 Renewal of land use data base with the aid of remote sensing 08 p1128 A83-21952
 Study of tidal vortices at the Naruto Strait through multi level remote sensing 08 p1143 A83-21956
 The development of a sampling procedure for urban land use mapping from aerial photographs - A study in Calabar, Nigeria 08 p1172 A83-21960
 Photointerpretation for land use planning --- using digital terrain models 08 p1129 A83-21966

- Low cost monitoring of land use and soil erosion in the humid tropics - An application of aerial photography 08 p1129 A83-21967
 An investigation methodology for territorial studies in unknown areas /East Kalimantan - Timur, Indonesia/ 08 p1129 A83-21968
 New results regarding aerotriangulation with statorscope data 08 p1092 A83-22033
 High performance image generators for reconnaissance applications 08 p1099 A83-22580
 Design versatility of the prism panoramic camera - The KS-116 and KA-95 cameras 08 p1099 A83-22582
 The KS-146A long range oblique photography /LOROP/ camera system 08 p1099 A83-22583
 Film still looks good --- advantages of conventional cameras for aerial reconnaissance 08 p1099 A83-22587
 Anatomy of a code block --- for aerial reconnaissance 08 p1100 A83-22592
 Motion-error immunity in photo coordinate determination - A novel approach to the absolute comparator 08 p1100 A83-22594
 Analysis of target coverage for an unstabilized 35 mm panoramic strike camera 08 p1100 A83-22596
 Quality metrics of digitally derived imagery and their relation to interpreter performance 08 p1150 A83-22893
 Monitoring of seasonal and yearly land-use changes on aerial photography and Landsat imagery - A case study in the Yemen Arab Republic 09 p1285 A83-24538
 Use of aerial photographs in land reclamation 09 p1285 A83-24541
 Use of remote sensing techniques to study geothermal resources in arid and semi-arid zones in Chile 09 p1288 A83-24577
 Evaluating the soil resources and potential of the Bahr El Jebel region in southern Sudan using Landsat 09 p1288 A83-24581
 Application of multispectral aerial photography in land use and land cover mapping of a part of El Fayoum depression northwestern Egypt 09 p1289 A83-24593
 Natural water containment site identification in the arid mountains of Djibouti 09 p1289 A83-24595
 Post-Aswan High Dam changes of the Nile Delta coast, east of Ras El Bar, interpreted from aerial photographs 09 p1289 A83-24600
 Remote sensing investigations on some fruit orchards in El Faiyoum Governorate, Egypt 09 p1290 A83-24615
 A survey of Brazil's semi-arid lands with the use of the remote sensing 09 p1290 A83-24618
 Structural geomorphology of Rajasthan basin, India-interpreted through Landsat imagery and aerial photos 09 p1291 A83-24626
 Some air-photo scale effects on Douglas-fir damage type interpretation 10 p1443 A83-25967
 Effects of blur and noise on digital imagery interpretability 10 p1456 A83-26322
 An analysis of natural features of the Colombian plans by remote sensing 11 p1601 A83-28148
 3D statistics of landforms from single air-photos - A hypothesis 11 p1601 A83-28172
 An aerial photographic method for estimating urban population 12 p1783 A83-29920
 A framework for analysis of temporal and spatial patterns of land use changes in Michigan's coastal zone 15 p2186 A83-34835
 Oregon's Statewide Landuse Inventory - Remote sensing input to geographic information systems 15 p2187 A83-34844
 The use of high altitude aerial photography (1:120,000) for range condition/trend determination 15 p2187 A83-34845
 Application of aerial thermography to determine physical states in wildlife 15 p2187 A83-34848
 A geographic data base for Texas pecan 16 p2370 A83-35740
 Photographic documentation of some distinctive cloud forms observed beneath a large cumulonimbus 16 p2387 A83-35743
 Autonomous earth feature classification - Shuttle and aircraft flight test results [AIAA PAPER 83-0417] 16 p2370 A83-36054
 The application of aerial techniques in geocryological explorations --- Russian book 16 p2370 A83-36446
 Constrained transform coding and surface fitting 16 p2405 A83-36610
 Identification of corn fields using multirate radar data 17 p2526 A83-37624
 Method for the production of color synthesized photographs and photoplans using a photorecifier 17 p2510 A83-37725
 Image quality of the new AGFA-Gevaert aerial-photography films 17 p2511 A83-38058

Application of remote sensing techniques in geological studies of various mineralized belts in India (national paper on IGCP-143) 17 p2527 A83-38130

Mineral exploration by remote sensing techniques in Nepal 17 p2527 A83-38132

Remote sensing and mineral exploration in China 17 p2527 A83-38135

The application of remote sensing techniques to regional geological survey in China 17 p2527 A83-38138

American Congress on Surveying and Mapping and American Society of Photogrammetry Convention; APS Annual Meeting, 48th, Denver, CO, March 14-20, 1982, Technical Papers 17 p2530 A83-38336

Aerial photograph interpretation to update and refine LUNR forest land classifications --- New York State Land Use and Natural Resource Inventory 17 p2530 A83-38338

The classification of forest species types using gradient analysis and spectral data 17 p2531 A83-38340

Automatic DTM generation from digitized image densities 17 p2531 A83-38342

Air photo interpretation of river system behavior 17 p2531 A83-38349

Characterization of lake water quality parameters with airborne multispectral scanner data - Flathead Lake, Montana 17 p2531 A83-38350

Mapping snow and ice and other land cover categories in south-central Alaska 17 p2532 A83-38355

Survey and analysis of present or potential environmental impact sites in Woburn, Massachusetts 17 p2536 A83-38359

The role of aerial photography in multiresource inventories Techniques and tests in applications research 17 p2532 A83-38362

The use of small scales for a stereoscopic dual chamber with a 'VHF-homing' system for the inventory and monitoring of natural renewable resources 17 p2533 A83-38447

The relationship between spectrometric and photographic methods for the remote sensing of earth resources 18 p2707 A83-40593

Some ground truth considerations in inland water quality surveys 20 p3010 A83-42960

New generation lens systems for the wild aviophot aerial camera system 21 p3135 A83-43895

Use of a chromogenic film for aerial photography of erosion features 21 p3135 A83-43896

An estimation-theoretic approach to terrain image segmentation 21 p3194 A83-44261

Aerial photography and scanning aerial methods in engineering geological investigations --- Russian book 21 p3166 A83-45013

Manual of remote sensing. Volume 2 - Theory, instruments and techniques /2nd edition/ 22 p3307 A83-45921

The influence of the image scale on the precision of morphotopo analysis from aerial photographs performed by a digital shape recognition analysis 22 p3308 A83-46117

Results from the Marine Remote Sensing Experiment in the North Sea (MARSEN), phase I 22 p3344 A83-46157

Qualitative and quantitative evaluation of airborne scanner imagery for pedological and agricultural purposes in north Germany 22 p3310 A83-46162

Remote sensing of arid and semiarid rangeland 22 p3310 A83-46163

Detection of oil on water surfaces by aerial remote sensing 24 p3581 A83-48934

Certain results of a comparison of airborne data with satellite measurements --- spectral brightness and albedo of deserts and agricultural regions 24 p3598 A83-49280

Cloud photogrammetry from aircraft 24 p3613 A83-49710

AERIAL RECONNAISSANCE

NT AIRBORNE INTEGRATED RECONNAISSANCE SYSTEM

Tarps test program set /parallel development of avionics and its support capability/ 01 p0014 A83-10755

Intelligent control of tactical target cueing --- by subsonic flight vehicles 02 p0133 A83-12879

Registration of a synthetic aperture radar /SAR/ reconnaissance image with a map reference data base 02 p0200 A83-12885

U.S. Army considers Aquila RPV ready to field 02 p0135 A83-13025

Aerospace reconnaissance and its exploitation /The 27th Chadwick Memorial Lecture/ 06 p0711 A83-18066

Airborne reconnaissance V; Proceedings of the Seminar, San Diego, CA, August 27, 28, 1981 08 p1099 A83-22573

Advanced tactical air reconnaissance system 08 p1041 A83-22575

Real-time reconnaissance - A systems look at advanced technology 08 p1043 A83-22576

Reconnaissance of the year 2000 and beyond 08 p1041 A83-22577

Future trends in the use of infrared line scanners for airborne reconnaissance 08 p1045 A83-22578

Digital reconnaissance imagery processing system for real-time and near-real-time imagery exploitation 08 p1099 A83-22579

High performance image generators for reconnaissance applications 08 p1099 A83-22580

Itek model 2KL sensor - The mini-electro-optical imaging system /Mini EOIS/ 08 p1099 A83-22581

Design versatility of the prism panoramic camera - The KS-116 and KA-95 cameras 08 p1099 A83-22582

The KS-146A long range oblique photography /LOROP/ camera system 08 p1099 A83-22583

Fourier transform image tracker and stabilizer 08 p1099 A83-22584

Hardware systems design of an airborne video bandwidth compressor 08 p1099 A83-22585

Film still looks good --- advantages of conventional cameras for aerial reconnaissance 08 p1099 A83-22587

Validation of a digital simulation of an optical matched filter correlator applied to aerial reconnaissance 08 p1100 A83-22589

Stimulus variables affecting dynamic target acquisition 08 p1045 A83-22590

CINNA - A system for preparing reconnaissance missions 08 p1044 A83-22591

Anatomy of a code block --- for aerial reconnaissance 08 p1100 A83-22592

Comparison of transform image coding techniques for compression of tactical imagery 08 p1100 A83-22597

Observations of optical lightning emissions from above thunderstorms using U-2 aircraft 08 p1141 A83-22703

Image quality experiments for TV reconnaissance at reduced transmission bandwidth 08 p1105 A83-22902

Development of a mini RPV - Stabileye 11 p1529 A83-28180

Canadian forces tracker aircraft full-scale fatigue test at the National Aeronautical Establishment 15 p2122 A83-33548

Airborne reconnaissance in the civilian sector - Agricultural monitoring from high-altitude powered platforms 18 p2706 A83-39939

Digital line-artifact removal --- image processing 21 p3134 A83-43868

Mapping and analysis of aerial conductivity measurements from INPUT system over geothermal areas 22 p3314 A83-46233

AERIAL RUDDERS

Configuration development for a highly maneuverable experimental aircraft with negative sweep rudder units [DGLR PAPER 82-035] 09 p1203 A83-24160

On the critical speed of empennage flutter with allowance for the rudder 12 p1704 A83-29286

Method of construction and fabrication procedures for the A300-rudder unit, using a carbon-fiber type of construction 23 p3391 A83-47211

AEROACOUSTICS

Tests of a thermal acoustic shield with a supersonic jet 01 p0105 A83-10183

Jet noise and the effects of jet forcing 01 p0105 A83-10898

Noise measurement at an obstacle in a wind tunnel [AAAF PAPER NT 81-10] 02 p0234 A83-11771

Noise and flow structure of a tone-excited jet 03 p0391 A83-13136

A note on the general scaling of helicopter blade-vortex interaction noise [ONERA, TP NO. 1982-32] 03 p0391 A83-13375

Aeroacoustical characteristics of a mechanical noise suppressor in a nozzle configuration with a central tailcone 03 p0391 A83-13590

Nonlinear self-excited acoustic oscillations within fixed boundaries 03 p0391 A83-14582

Generation of desired signals from acoustic drivers --- for aircraft engine internal noise propagation experiment 04 p0449 A83-15068

Length and time scales relevant to sound generation in excited jets 04 p0533 A83-15298

Propeller noise at model- and full-scale 04 p0533 A83-15314

Novel airborne technique for aircraft noise measurements above the flight path 04 p0533 A83-15316

Acoustic capabilities of the German-Dutch wind tunnel DNW [AIAA PAPER 83-0146] 05 p0599 A83-16554

Vibration and acoustic environments for payload/cargo integration [AIAA PAPER 83-0329] 05 p0604 A83-16658

Strut or guide vane secondary flows and their effect on turbomachinery noise 06 p0807 A83-18414

The heating effect in resonance tubes --- German thesis 06 p0761 A83-19623

Acoustic environment in large enclosures with a small opening exposed to flow 08 p1162 A83-22161

A note on the tip noise of rotating blades 09 p1340 A83-23708

Experimental investigations concerning the noise produced by model propellers and propeller-driven small aircraft [DGLR PAPER 82-068] 09 p1206 A83-24182

Acoustic metrology and signal processing [ONERA, TP NO. 1982-123] 09 p1341 A83-24334

A boundary value problem in the propagation of sound in a rarefied gas 09 p1371 A83-24485

Viscous stability of compressible axisymmetric jets 09 p1341 A83-24651

Wall pressure fluctuations in attached boundary-layer flow 09 p1198 A83-24655

Analysis of the effect of heated jet flow on the far field radiation from a noise source [ASME PAPER 82-WA/NCA-4] 10 p1472 A83-25697

Near field pressure fluctuations of an elliptic jet [AIAA PAPER 83-0663] 10 p1472 A83-25901

Some new results on edge-tone oscillations in high-speed subsonic jets [AIAA PAPER 83-0665] 10 p1473 A83-25902

ADAM - An axisymmetric duct aeroacoustic modeling system [AIAA PAPER 83-0666] 10 p1473 A83-25903

In-flight acoustic measurements in the engine intake of a Fokker F28 aircraft [AIAA PAPER 83-0677] 10 p1376 A83-25909

Interaction of fan rotor flow with downstream struts [AIAA PAPER 83-0682] 10 p1377 A83-25912

Evaluation of interior noise control treatments for high-speed propfan-powered aircraft [AIAA PAPER 83-0693] 10 p1375 A83-25914

Scattering of an acoustic field by a free jet shear layer [AIAA PAPER 83-0698] 10 p1474 A83-25918

Acoustic wave propagation through the shear layer of the DNW large open jet wind tunnel [AIAA PAPER 83-0699] 10 p1474 A83-25919

An experimental study of supersonic jet shock-associated noise [AIAA PAPER 83-0708] 10 p1474 A83-25924

Experimental investigation of modal power distribution in a duct at high frequency [AIAA PAPER 83-0731] 10 p1475 A83-25938

Aeroacoustic computation of cylinder wake flow [AIAA PAPER 83-0736] 10 p1476 A83-25940

Sound radiation from a vibrating cylinder in flow [AIAA PAPER 83-0737] 10 p1476 A83-25941

An interplay between acoustic waves and steady vortical flow [AIAA PAPER 83-0740] 10 p1476 A83-25943

An experimental investigation of wake edge tones [AIAA PAPER 83-0741] 10 p1476 A83-25944

The prediction of the noise of supersonic propellers in time domain - New theoretical results [AIAA PAPER 83-0743] 10 p1377 A83-25945

Acoustic evaluation of DNW free jet shear layer correction using a model jet [AIAA PAPER 83-0757] 10 p1476 A83-25954

Tone generation by rotor-downstream strut interaction [AIAA PAPER 83-0767] 10 p1378 A83-25957

Prediction of high bypass ratio engine static and flyover jet noise [AIAA PAPER 83-0773] 10 p1378 A83-25958

Modified jet noise source model for twin-jet shielding analysis [AIAA PAPER 83-0776] 10 p1477 A83-25960

The measurement of the steady flow resistance of porous materials --- for noise suppression in aircraft turbofan engine ducts [AIAA PAPER 83-0779] 10 p1477 A83-25961

Airfoil self noise - Effect of scale [AIAA PAPER 83-0785] 10 p1477 A83-25966

Sound propagation through fluctuating flows - Its significance in aeroacoustics [AIAA PAPER 83-0697] 10 p1477 A83-26448

Nearfield observations of tones generated from supersonic jet flows [AIAA PAPER 83-0706] 10 p1478 A83-26449

On discrete tones generated by an impinging underexpanded rectangular jet [AIAA PAPER 83-0729] 10 p1478 A83-26919

Theoretical study on the design of low noise rotor blade section 10 p1478 A83-26966

- Sound generation by instability waves in a low Mach number jet
[AIAA PAPER 83-0661] 11 p1650 A83-28001
- Measurements of the scattering of sound by a line vortex
[AIAA PAPER 83-0676] 11 p1650 A83-28004
- The influence of inlet design on the aeroacoustic performance of a JT15D turbofan engine as measured in the NASA-Ames 40 x 80 foot wind tunnel
[AIAA PAPER 83-0681] 11 p1531 A83-28006
- The acoustic response of a propeller subjected to gusts incident from various inflow angles
[AIAA PAPER 83-0692] 11 p1651 A83-28010
- Incidence angle effects on convected gust airfoil noise
[AIAA PAPER 83-0765] 11 p1652 A83-28022
- Noise generation by a finite span swept airfoil
[AIAA PAPER 83-0768] 11 p1652 A83-28023
- Effect of flow on the acoustic performance of extended reaction lined ducts
[AIAA PAPER 83-0778] 11 p1652 A83-28024
- Regimes of interaction of nonlinear waves in a low-viscosity medium --- sound propagation in gases and liquids
11 p1652 A83-28064
- Shock-associated noise in supersonic jets
12 p1777 A83-28957
- Flow-acoustic interaction near a flexible wall
12 p1777 A83-29230
- The velocity perturbations above the orifice of an acoustically excited cavity in grazing flow
12 p1777 A83-29235
- A study of helicopter rotor noise, with special reference to tail rotors, using an acoustic wind tunnel
12 p1777 A83-29403
- Acoustic wave radiated by head-on collision of two vortex rings
12 p1777 A83-29595
- Aeroacoustics of supersonic porous plug-nozzle flows
[AIAA PAPER 83-0775] 13 p1915 A83-31325
- Effects of artificial excitation upon a low Reynolds number Mach 2.5 jet
14 p2081 A83-32996
- The aerodynamics of hypersonic velocities (On flows with low Mach numbers)
16 p2288 A83-35535
- Edge tones in high-speed flows and their application to multiple-jet mixing
16 p2408 A83-36077
- Derivation of the fundamental equation of sound generated by moving aerodynamic surfaces
16 p2408 A83-36096
- Mathematical models of the acoustic properties of propellers
16 p2311 A83-36792
- Method for calculating jet noise in the presence of a shielding surface
17 p2577 A83-37253
- The aerodynamics of propellers and rotors using an acoustic formulation in the time domain
[AIAA PAPER 83-1821] 17 p2455 A83-38653
- Intensity of focused sonic booms in straight flight at constant altitude
18 p2742 A83-39424
- Acoustic interaction with a turbulent plane jet - Some effects on turbulent structure
19 p2897 A83-40851
- Acoustic excitation of Tollmien-Schlichting waves in a supersonic boundary layer
19 p2790 A83-41256
- Universities - Have they a role in aeronautical research?
Noise research
20 p3044 A83-42617
- Aeroacoustic flight test of four single engine propellers
[SAE PAPER 830731] 20 p2936 A83-43328
- An aeroacoustic model for high-speed, unsteady blade-vortex interaction
20 p3044 A83-43437
- Instrumentation and signal analysis --- for aeronautical acoustics noise reduction research
[ONERA, TP NO. 1983-33] 21 p3201 A83-44311
- Low speed performance of a supersonic axisymmetric mixed compression inlet with auxiliary inlets
[AIAA PAPER 83-1414] 21 p3088 A83-45516
- Nonstationarity in acoustic fields
23 p3505 A83-47628
- Experimental methods in compressor noise studies
[ONERA, TP NO. 1983-79] 23 p3505 A83-48194
- Helicopter noise
[ONERA, TP NO. 1983-80] 23 p3506 A83-48195
- Noise generation by a low-Mach-number jet
24 p3625 A83-49462
- Noise generated by airfoil profiles placed in a uniform laminar flow
24 p3625 A83-49463
- Nonlinear tridimensional propagation of acoustic waves in radiative gas dynamics
24 p3625 A83-49522
- AEROASSIST**
- Radiation enhancement by nonequilibrium in earth's atmosphere --- for aero-assisted OTV
[AIAA PAPER 83-0410] 05 p0607 A83-16698
- Chemical nonequilibrium effects on flowfields for aeroassist orbital transfer vehicles
[AIAA PAPER 83-0214] 05 p0602 A83-17913
- Aerodynamic characteristics of generalized bent biconic bodies for aero-assisted, orbital-transfer vehicles
[AIAA PAPER 83-1512] 14 p1970 A83-32749
- Thermal-protection requirements for near-earth aero-assisted orbital-transfer vehicle missions
[AIAA PAPER 83-1513] 14 p1982 A83-32750
- System technology analysis of aeroassisted orbital transfer vehicles - Moderate lift/drag
[AIAA PAPER 83-2108] 19 p2809 A83-41474
- Optimization and closed loop guidance of drag modulated aeroassisted orbital transfer
[AIAA PAPER 83-2093] 19 p2810 A83-41923
- Optimal control of orbital transfer vehicles
[AIAA PAPER 83-2092] 19 p2811 A83-41927
- Aerocapture and aeroassisted orbital transfer - A high performance leverage space technology
20 p2943 A83-42827
- Optimal aeroassisted return from high earth orbit with plane change
[IAF PAPER 83-330] 23 p3417 A83-47344
- AEROBES**
- Investigation of the localization of dehydrogenases in aerobic and anaerobic bacteria at the submicroscopic level
01 p0078 A83-10421
- AEROBRACING**
- Physical parameters of meteoroids undergoing quasicontinuous crushing in the atmosphere. I - Methods of parameter determination
03 p0432 A83-13373
- Trajectory analysis of radiative heating for planetary missions with aerobraking of spacecraft
[AIAA PAPER 83-0407] 05 p0602 A83-16696
- Base heating on an aerobraking orbital transfer vehicle
[AIAA PAPER 83-0408] 05 p0607 A83-16697
- Low L/D aerobrake test at Mach 10
[AIAA PAPER 83-1509] 14 p1970 A83-32746
- Aerothermodynamic design considerations of an aerobraked spacecraft
[AIAA PAPER 83-1510] 14 p1982 A83-32747
- Aerodynamic characteristics of generalized bent biconic bodies for aero-assisted, orbital-transfer vehicles
[AIAA PAPER 83-1512] 14 p1970 A83-32749
- Three-dimensional nonequilibrium viscous shock-layer flows over complex geometries
[AIAA PAPER 83-0212] 16 p2292 A83-36048
- Hypersonic flows over bionics using a variable-effective-gamma, Parabolized-Navier-Stokes code
[AIAA PAPER 83-1666] 17 p2443 A83-37177
- Aerobraking of a low L/D manned vehicle from Geo return to rendezvous with the Space Shuttle
[AIAA PAPER 83-2110] 19 p2811 A83-41937
- AEROCAPTURE**
- Heating analysis of bent-nose bionics at high angles of attack using the parabolized Navier-Stokes equations
[AIAA PAPER 83-1507] 14 p1970 A83-32744
- Three-dimensional nonequilibrium viscous shock-layer flows over complex geometries
[AIAA PAPER 83-0212] 16 p2292 A83-36048
- Hypersonic flows over bionics using a variable-effective-gamma, Parabolized-Navier-Stokes code
[AIAA PAPER 83-1666] 17 p2443 A83-37177
- Aerocapture and aeroassisted orbital transfer - A high performance leverage space technology
20 p2943 A83-42827
- Origin of the moon - Capture by gas drag of the earth's primordial atmosphere
20 p3079 A83-43590
- AERODYNAMIC AXIS**
- U AERODYNAMIC BALANCE**
- AERODYNAMIC BALANCE**
- Unbalance response analysis of a complete turbomachine
07 p0938 A83-19674
- F-104 CCV research flight test program
07 p0867 A83-20074
- Trim Tank system for optimizing drag at the center of gravity
[DGLR PAPER 82-030] 09 p1209 A83-24156
- Innovative concepts for tactical STOL
[AIAA PAPER 83-2129] 19 p2798 A83-41952
- The heading of a vehicle moving with roll and trim
19 p2897 A83-42020
- Philosophy of automated balance calculations
[SAWE PAPER 1470] 20 p2931 A83-43744
- AERODYNAMIC BRAKES**
- NT LEADING EDGE SLATS
- NT TRAILING-EDGE FLAPS
- NT WING FLAPS
- Aeroballistic characteristics of 3-ft-long parachute decelerators
12 p1696 A83-29019
- AERODYNAMIC BUZZ**
- U FLUTTER**
- AERODYNAMIC CENTER**
- U AERODYNAMIC BALANCE**
- AERODYNAMIC CHARACTERISTICS**
- NT AERODYNAMIC BALANCE
- NT AERODYNAMIC DRAG
- NT AERODYNAMIC STABILITY
- NT INTERFERENCE DRAG
- NT LIFT
- NT STATIC AERODYNAMIC CHARACTERISTICS
- NT SUPERSONIC DRAG

- Flow visualization reveals causes of Shuttle nonlinear aerodynamics
01 p0002 A83-10181
- The use of spline functions in problems of aerodynamics
01 p0002 A83-10441
- Extension of the Carafoli tracer method to profiles cascades
01 p0002 A83-10578
- Supersonic flow around a conical fuselage of arbitrary section isolated or equipped with a delta wing with subsonic leading edges
01 p0002 A83-10579
- The fundamental geometrical and aerodynamic characteristics of aircraft and rockets --- Russian book
01 p0003 A83-10669
- The supersonic wind tunnel installations at Peenemunde and Kockel and their contributions to the aerodynamics of rocket-powered vehicles
01 p0130 A83-11285
- Hyperballistic vehicle dynamics
02 p0132 A83-13078
- Synergetic maneuvering of winged spacecraft for orbital plane change
02 p0139 A83-13080
- The unsteady suction analogy and applications --- in predicting longitudinal dynamic stability derivatives for slender wings at high angles of attack
03 p0277 A83-13128
- Helicopter rotor performance evaluation using oscillatory airfoil data
03 p0278 A83-13172
- Principles of helicopter design and construction --- Serbo-Croatian book
03 p0281 A83-14042
- Survey of engineering computational methods and experimental programs for estimating supersonic missile aerodynamic characteristics
03 p0278 A83-14124
- Operation of a helicopter on sloping ground. I
03 p0280 A83-14618
- Transonic flow past an isolated profile and through a blade cascade - Phenomenological analysis
03 p0280 A83-14622
- Numerical investigation of the problem of viscous reacting gas flow past blunt bodies
04 p0441 A83-15078
- Concerning the center of pressure of bodies --- supersonic flow interactions with variable surface configurations
04 p0441 A83-15089
- The vortex theory of rotors
04 p0442 A83-15095
- A study of the effect of the transverse sweep of delta wings on their vortex structures and aerodynamic characteristics in separated flows at low subsonic velocities
04 p0442 A83-15096
- Unsteady Newton-Busemann flow theory. III - Frequency dependence and indicial response
04 p0476 A83-15149
- Aerodynamic characteristics of a slotted vs smooth-skin supercritical wing model
04 p0443 A83-15324
- Vibration of airfoils in sinusoidal oblique gust
[AIAA PAPER 83-0005] 05 p0577 A83-16457
- Aerodynamic investigation of closely coupled lifting surfaces with positive and negative stagger for general aviation applications
[AIAA PAPER 83-0057] 05 p0578 A83-16489
- Aerodynamic optimization, comparison, and trim design of canard and conventional high performance general aviation configurations
[AIAA PAPER 83-0058] 05 p0594 A83-16490
- Effects of various empennage parameters on the aerodynamic characteristics of a twin-engine afterbody model
[AIAA PAPER 83-0085] 05 p0579 A83-16511
- On the transonic aerodynamic characteristics of 10 percent thick airfoils with a plain flap
[AIAA PAPER 83-0091] 05 p0579 A83-16515
- On the flight derived/aerodynamic data base performance comparisons for the NASA Space Shuttle entries during the hypersonic regime
[AIAA PAPER 83-0115] 05 p0606 A83-16529
- Acoustic capabilities of the German-Dutch wind tunnel DNW
[AIAA PAPER 83-0146] 05 p0599 A83-16554
- A method for estimating the propulsion induced aerodynamic characteristics of STOL aircraft in ground effect
[AIAA PAPER 83-0169] 05 p0594 A83-16567
- Some observations on the aerodynamics of an airfoil with a jet exhausting from the lower surface
[AIAA PAPER 83-0173] 05 p0580 A83-16569
- Evaluation of missile aerodynamic characteristics for diversified configurations using rapid prediction techniques
[AIAA PAPER 83-0180] 05 p0581 A83-16573
- Missile Datcom status report - Body and fin alone methodology
[AIAA PAPER 83-0181] 05 p0581 A83-16574
- Compressible flow analysis about three-dimensional wing surfaces using a combination technique
[AIAA PAPER 83-0183] 05 p0581 A83-16575
- Numerical simulation of wing-fuselage aerodynamic interaction
[AIAA PAPER 83-0225] 05 p0582 A83-16595

High-speed characteristics of circulation control airfoils [AIAA PAPER 83-0265] 05 p0583 A83-16621

Aerodynamic characteristics of a jet controlled projectile [AIAA PAPER 83-0392] 05 p0585 A83-16689

Low-speed investigation of the maneuver capability of supersonic fighter wings [AIAA PAPER 83-0426] 05 p0585 A83-16708

Techniques for roll tailoring for missiles with wrap-around fins [AIAA PAPER 83-0463] 05 p0598 A83-16731

Aerodynamic features of turbulent flames [AIAA PAPER 83-0470] 05 p0636 A83-16737

On the aerodynamics of over-the-wing nacelles supported on 'stub-wings' [AIAA PAPER 83-0538] 05 p0595 A83-16774

Flow fields and aerodynamic characteristics for hypersonic missiles with mid-fuselage inlets [AIAA PAPER 83-0542] 05 p0587 A83-16777

Calculation of fundamental aerodynamic derivatives of aircraft 05 p0589 A83-16882

Application of the PANAIR production code to a complex canard/wing configuration [AIAA PAPER 83-0009] 05 p0590 A83-17902

Three-dimensional Euler solutions for long-duct nacelles [AIAA PAPER 83-0089] 05 p0590 A83-17905

An evaluation of aerodynamics modeling of spinning light airplanes [AIAA PAPER 83-0368] 05 p0598 A83-17922

The multi-sweep method for the maximum likelihood identification of many parameters 06 p0802 A83-18370

Spin prediction techniques 06 p0719 A83-18401

Effects of spanwise blowing and reverse thrust on fighter low-speed aerodynamics 06 p0712 A83-18410

Trailing edge flap influence on leading edge vortex flap aerodynamics 06 p0712 A83-18411

The impact of data processing on wind tunnel testing [ONERA, TP NO. 1982-92] 06 p0720 A83-18429

Smoke visualization in wind tunnels 06 p0763 A83-18813

Aerodynamic characteristics of polygonal lifting bodies at supersonic speeds 06 p0713 A83-19571

Research on contaminated wings, current issues --- concerning icing conditions and aerodynamic effects [AIAA PAPER 83-0277] 06 p0715 A83-19584

Nonlinear observers for evaluating the state variables of the longitudinal motion of an aircraft --- German thesis 06 p0719 A83-19622

Space Shuttle entry aerodynamic comparisons of flight 1 with preflight predictions 07 p0869 A83-20414

A test stand for studying transient phenomena in aerodynamic turbomachine cascades 07 p0868 A83-20913

Leading edge vortex flap aerodynamics 07 p0863 A83-21004

Effective aerodynamic parameter evaluation from free flight tests 07 p0866 A83-21005

The capture region of a coasting pursuer 07 p0987 A83-21010

Aerodynamics of wrap-around fins 07 p0863 A83-21011

2-D coordinate grid generation by a vortex singularity method 07 p0864 A83-21018

Numerical calculations of nonlinear aerodynamics of wing-body configurations 07 p0864 A83-21022

Curved lifting-line theory for thin planar wings 07 p0864 A83-21024

Wind tunnel investigation of the transonic aerodynamic characteristics of forward swept wings--- supersonic cruise aircraft research 08 p1042 A83-22153

Acoustic environment in large enclosures with a small opening exposed to flow 08 p1162 A83-22161

Aerodynamic tests of Darrieus wind turbine blades 08 p1132 A83-23128

Design, construction, and testing of an experimental propeller in the 750 PS performance class [DGLR PAPER 82-066] 09 p1206 A83-24180

The aerodynamic characteristics of caret wings at subsonic flight speeds 09 p1197 A83-24241

Computation of hypersonic viscous flow over a body with mass transfer and/or spin 09 p1198 A83-24878

Store separation from cavities at supersonic flight speeds 09 p1198 A83-24882

On aerodynamic design of the Savonius windmill rotor 11 p1610 A83-27325

Aerodynamics of guided missiles 11 p1526 A83-28162

The extended Kalman filter and its use in estimating aerodynamic derivatives 11 p1531 A83-28183

Dynamics of soft deceleration systems --- parachutes 11 p1597 A83-28469

Comparison of laser anemometer measurements and theory in an annular turbine cascade with experimental accuracy determined by parameter estimation 12 p1695 A83-28833

Shock reflection transition in three-dimensional steady flow about interfering bodies 12 p1696 A83-28960

Unified panel flutter theory with viscous damping effects 12 p1734 A83-28968

Heavy-lift airship dynamics 12 p1704 A83-29016

Approximate calculation of the aerodynamic characteristics of a cylindrical body of small aspect ratio in an incompressible flow 12 p1696 A83-29287

Wind tunnel correlation study of aerodynamic modeling for F/A-18 wing-store tip-missile flutter [AIAA 83-1028] 12 p1703 A83-29877

Supersonic flow past a body with prescribed oscillations of its surface 13 p1803 A83-30002

Aerodynamic performance of a Wells air turbine 13 p1869 A83-30191

Approximate aerodynamic analysis for horizontal axis wind turbines 13 p1870 A83-30194

Calculation of fundamental aerodynamic derivatives of aircraft. II 13 p1804 A83-30516

Displacement effects in transonic airfoil flows 13 p1804 A83-30638

X-29 - Advanced technology demonstrator 13 p1806 A83-31051

On the theory of the horizontal-axis wind turbine 13 p1871 A83-31077

The aerodynamic characteristics of a square parachute 13 p1804 A83-31398

Unique flight characteristics of the AD-1 oblique-wing research airplane 14 p1975 A83-32588

Aerodynamic characteristics of generalized bent biconic bodies for aero-assisted, orbital-transfer vehicles [AIAA PAPER 83-1512] 14 p1970 A83-32749

Compressible helicoidal surface theory for propeller aerodynamics and noise 14 p1971 A83-32986

The effect of windstream on the aerodynamic characteristics of an airfoil moving near a perturbed surface 14 p1972 A83-33006

Coupled flap-lag-torsional dynamics of hingeless rotor blades in forward flight 15 p2121 A83-33506

ACV lift air systems - More puff for less power 15 p2242 A83-34861

Calculation of subsonic flow past rectangular wings and their combinations on the basis of a discrete vortex scheme 16 p2288 A83-35541

The relationship between the aerodynamic and acoustic characteristics of coaxial jets 16 p2408 A83-35712

Aerodynamic optimization theory of A 3-D axial-flow rotor-blading via optimal control 16 p2291 A83-35839

Investigation of flow through high cambered supersonic compressor cascade 16 p2291 A83-35845

Optimization of the plane compressor blade aerodynamic design 16 p2291 A83-35857

Some aerodynamic and noise studies of flow in centrifugal fans 16 p2408 A83-35864

Numerical calculation of nonlinear aerodynamics of wing-body configurations 16 p2293 A83-36076

The aerodynamic design and performance of the General Electric/NASA EEE fan --- Energy Efficient Engine [AIAA PAPER 83-1160] 16 p2306 A83-36252

STOL wind tunnel test results for a tactical supercruiser [AIAA PAPER 83-1224] 16 p2294 A83-36291

Application of 3D aerodynamic/combustion model to combustor primary zone study [AIAA PAPER 83-1265] 16 p2308 A83-36316

Aerodynamic measurements about a rotating propeller with a laser velocimeter [AIAA PAPER 83-1354] 16 p2295 A83-36355

The motion dynamics of parachute systems --- Russian book 16 p2296 A83-36450

AFTI/F-111 mission adaptive wing technology demonstration program [AIAA PAPER 83-1057] 16 p2301 A83-36468

Wind tunnel tests of over-the-wing nacelles --- supported on 'stub-wings' 16 p2296 A83-36916

Correction to the wing source velocity error in Woodward's USSAERO code 16 p2297 A83-36920

A comparison of minimizing strategies for maximum likelihood identification --- stability and control derivatives of wide body aircraft 17 p2565 A83-37085

Experimental and computational investigation of the flow in the leading edge region of a swept wing [AIAA PAPER 83-1762] 17 p2446 A83-37233

Unsteady aerodynamic characteristics of a profile in the transonic flow of an ideal gas 17 p2446 A83-37251

Concerning a type of separated flow on a rectangular wing of small aspect ratio 17 p2447 A83-37260

On the accuracy of calculating the aerodynamic characteristics of thin wings and airfoils by the method of discrete vortices 17 p2448 A83-37519

AERODYNAMIC CHARACTERISTICS

Use of the panel method to calculate the distributed aerodynamic characteristics of a wing with pylon and nacelle at low speeds 17 p2448 A83-37520

The effect of slot suction on the aerodynamic characteristics of an airfoil at transonic velocities 17 p2449 A83-37552

Separated flows at the leeward side of a delta wing and body of revolution in supersonic flow 17 p2449 A83-37553

The effect of unsteadiness on the aerodynamic and thermal characteristics of bodies braking in a gas 17 p2449 A83-37554

On an experimental possibility of investigating the hydrodynamic interaction of particles at low Reynolds numbers 17 p2505 A83-37556

Computational study of an unregulated air intake of a hypersonic ramjet engine with three-dimensional deceleration of the flow at freestream Mach numbers of 5-7 17 p2449 A83-37559

Subsonic compressible-gas separated flow past a low-aspect-ratio wing 17 p2450 A83-37626

Aerodynamic characteristics of thin wings in a nonequilibrium hypersonic gas flow 17 p2450 A83-37640

A study of the control properties of axial fans on the basis of theoretical characteristics of plane cascades 17 p2451 A83-37807

Performance assessment of a reclined ejection seat 17 p2462 A83-37879

Low-speed aerodynamic characteristics of a generic forward-swept-wing aircraft [SAE PAPER 821467] 17 p2451 A83-37998

Experimental evaluation of inlet turbulence, wall boundary layer, surface finish, and fillet radius on small axial turbine state performance [SAE PAPER 821475] 17 p2469 A83-38C01

Comparison of NACA 6-series and 4-digit airfoils for Darrieus wind turbines 17 p2535 A83-38013

Determination of regime coefficients for thin bodies from the data of numerical and laboratory experiments --- aerodynamic coefficients of plate in rarefied gas 17 p2452 A83-38095

Aerodynamic properties of a two-dimensional inextensible flexible airfoil [AIAA PAPER 83-1796] 17 p2453 A83-38635

Application of a full potential method for predicting supersonic flow fields and aerodynamic characteristics [AIAA PAPER 83-1802] 17 p2453 A83-38637

Aerodynamic characteristics of a two-dimensional moving spoiler in subsonic and transonic flow [AIAA PAPER 83-1809] 17 p2454 A83-38642

The impact of strakes on a vortex-flapped delta wing [AIAA PAPER 83-1814] 17 p2454 A83-38647

PAN AIR modeling studies --- higher order panel method for aircraft design [AIAA PAPER 83-1830] 17 p2455 A83-38660

Application of forward sweep wings to an air combat fighter [AIAA PAPER 83-1833] 17 p2465 A83-38662

X-29 forward swept wing aerodynamic overview [AIAA PAPER 83-1834] 17 p2465 A83-38663

Qualification of the Datcom for sweptforward wing platforms A summary of work to date [AIAA PAPER 83-1836] 17 p2455 A83-38665

Aerodynamics characteristics of a canard controlled high fineness ratio missile [AIAA PAPER 83-1839] 17 p2470 A83-38668

Analysis of surface pressure distributions on two elliptic missile configurations [AIAA PAPER 83-1841] 17 p2456 A83-38670

A method for predicting low-speed aerodynamic characteristics of transport aircraft [AIAA PAPER 83-1845] 17 p2456 A83-38673

Powered lift aerodynamics of USB STOL aircraft --- Upper Surface Blowing [AIAA PAPER 83-1848] 17 p2456 A83-38676

Some lessons from NACA/NASA aerodynamic studies following World War II [AIAA PAPER 83-1856] 17 p2443 A83-38683

Thrust reverser effects on the tail surface aerodynamics of an F-18 type configuration [AIAA PAPER 83-1860] 17 p2457 A83-38687

Aerodynamics critical to the operations of tactical fighters from bomb damaged runways [AIAA PAPER 83-1861] 17 p2465 A83-38688

Atmospheric determination for Shuttle aerodynamic studies 17 p2552 A83-38757

Dynamic analysis of the Magnus Aerospace Corporation LTA 20-1 heavy-lift aircraft [AIAA PAPER 83-1977] 17 p2466 A83-38908

Wind tunnel demonstration of an optimized LTA system with 65 percent power reduction and neutral static stability [AIAA PAPER 83-1981] 17 p2466 A83-38910

Dynamics of the STARS aerostat [AIAA PAPER 83-1990] 17 p2470 A83-38916

Comparison of panel method formulations and its influence on the development of QUADPAN, an advanced low-order method

[AIAA PAPER 83-1827] 18 p2632 A83-39097

Convergence characteristics of nonlinear vortex-lattice methods for configuration aerodynamics

[AIAA PAPER 83-1882] 18 p2637 A83-39421

The aerodynamic characteristics at the mid-span of a circular cylinder with tangential blowing

18 p2684 A83-39457

Aerodynamics of wraparound fins

18 p2638 A83-40007

Equivalent angle-of-attack method for estimating nonlinear aerodynamics of missile fins

18 p2638 A83-40010

Comprehensive missile aerodynamics programs for preliminary design

18 p2638 A83-40025

Recent improvements in prediction techniques for supersonic weapon separation

19 p2789 A83-41041

Dynamics of the Venera 13 and 14 descent modules in the parachute segment of descent

19 p2809 A83-41238

The effect of a boundary layer on the nonstationary aerodynamic characteristics of blunted cones in supersonic flows

19 p2790 A83-41255

The maximum aerodynamic efficiency of conical wing-body combinations at high supersonic speeds

19 p2790 A83-41266

Aerodynamic development of a spinning submunition dispenser

[AIAA PAPER 83-2082] 19 p2805 A83-41916

Aerodynamic characteristics of missile control fins in nonlinear flow fields

[AIAA PAPER 83-2083] 19 p2792 A83-41917

Filtering flight data prior to aerodynamic system identification

[AIAA PAPER 83-2098] 19 p2798 A83-41928

Direct optimization methods in real-time parameter identification of missile aerodynamic characteristics

[AIAA PAPER 83-2102] 19 p2893 A83-41931

Experimental and analytical investigation of the subsonic aerodynamics of slender wings with leading-edge vortex flaps

[AIAA PAPER 83-2113] 19 p2793 A83-41940

Aerodynamics of pointed forebodies at high angles of attack

[AIAA PAPER 83-2117] 19 p2793 A83-41942

Dynamics of forebody flow separation and associated vortices

[AIAA PAPER 83-2118] 19 p2793 A83-41943

Circulation-controlled elliptical airfoil

20 p2928 A83-42537

The calculation of two-dimensional transonic flow over aerofoils including boundary layer and wake effects

[SAE PAPER 830708] 20 p2930 A83-43318

Wing modification for increased spin resistance

[SAE PAPER 830720] 20 p2937 A83-43327

A general solution to the problem of jet flow past a wedge

20 p2931 A83-43520

Estimation of parameters involved in high angle-of-attack aerodynamic theory using spin flight test data

[AIAA PAPER 83-2086] 20 p2937 A83-43809

Estimation of nonlinear aerodynamics from transport airplane certification maneuvers - A system identification approach

[AIAA PAPER 83-2065] 20 p2938 A83-43811

Aerodynamic aspects of aircraft dynamics at high angles of attack

21 p3085 A83-43964

Experimental work on the aerodynamics of integrated slender wings for supersonic flight

21 p3086 A83-44360

An explicit Lagrangian scheme for solving plane and axisymmetric aerodynamic problems, and the mesh rezoning

21 p3130 A83-44558

The influence of the 3-dimensional transition-section onto the aerodynamical uniformity in test section

21 p3087 A83-44567

Finite volume calculation of three-dimensional potential flow around a propeller

21 p3089 A83-44577

Calculation of three-dimensional transonic flow over thin body (wing)

22 p3250 A83-46499

Studies concerning model technology in the European Transonic Wind Tunnel (ETW)

23 p3412 A83-47197

Commercial aircraft with reduced longitudinal stability and active tail planes, and the unsteady aerodynamics of rapidly adjusted control surfaces

23 p3412 A83-47213

A configuration to improve the aerodynamics and scope of can-annular combustors

[ASME PAPER 83-GT-37] 23 p3406 A83-47898

Measurements of heat transfer distribution over the surfaces of highly loaded turbine nozzle guide vanes

[ASME PAPER 83-GT-53] 23 p3394 A83-47910

Large-scale wind-tunnel investigation of a close-coupled canard-delta-wing fighter model through high angles of attack

[AIAA PAPER 83-2554] 23 p3399 A83-48373

Efficient computational grid generation for three-dimensional aircraft configurations

[AIAA PAPER 83-2557] 23 p3405 A83-48376

Aerodynamic and thermal characteristics of three-dimensional star-shaped bodies in a rarefied gas

23 p3400 A83-48672

The basic aerodynamics of floatation

23 p3453 A83-48679

Comments on the theory of local interaction in a rarefied gas

24 p3543 A83-48926

Vortex sheet shortening in the Smith model for slender delta wings with leading-edge separation

24 p3544 A83-49025

International Symposium on Aeroelasticity, Nuremberg, West Germany, October 5-7, 1981, Collected Papers

[DGLR BERICHT 82-01] 24 p3543 A83-49176

Flow visualization by light sheet

[ONERA, TP NO. 1983-105] 24 p3583 A83-49416

Characteristics of the ground vortex developed by various V/STOL jets at forward speeds

[AIAA PAPER 83-2494] 24 p3545 A83-49585

Application of slender wing benefits to military aircraft

[AIAA PAPER 83-2566] 24 p3545 A83-49596

Forces and moments acting on axisymmetric bodies rotating arbitrarily in free molecular flow

24 p3545 A83-49657

Calculation of the aerodynamic characteristics of bodies in transition flow

24 p3545 A83-49658

Investigation of the jet parameters of a source of accelerated gas flow for an aerodynamic test facility

24 p3545 A83-49659

AERODYNAMIC CHORDS

U AIRFOIL PROFILES

U CHORDS (GEOMETRY)

AERODYNAMIC COEFFICIENTS

Problems concerning the external aerodynamics of air-breathing missiles

[ONERA, TP NO. 1982-93] 03 p0279 A83-14542

Ballistic entry motion, including gravity - Constant drag coefficient case

03 p0283 A83-14839

Determination of aerodynamic coefficients for a re-entry body by means of an extended Kalman filter

04 p0451 A83-15544

A simple tandem disk model for a cross-wind machine

04 p0506 A83-15800

Critical evaluation of eight semiempirical aerodynamic coefficient prediction programs for missiles and stores

[AIAA PAPER 83-0185] 05 p0581 A83-16576

An experimental investigation of control surface effectiveness and real-gas simulation for bionics

[AIAA PAPER 83-0213] 05 p0591 A83-17912

Aerodynamic estimation techniques for aerostats and airships

06 p0712 A83-18404

Calculation of symmetric vortex separation affecting subsonic bodies at high incidence

08 p1042 A83-22137

Moment coefficient of the NACA 65 profile in delay cascades

09 p1198 A83-24509

Aerodynamic characteristics for a slender missile with wrap-around fins

09 p1198 A83-24881

Three-dimensional supersonic ideal-gas flow past a body with a tail assembly

11 p1526 A83-27721

Airplane model structure determination from flight data

12 p1704 A83-29023

Calculation of unsteady aerodynamic coefficients using transonic time domain methods

[AIAA 83-0885] 12 p1697 A83-29833

General equations of motion for an elastic wing and method of solution

[AIAA 83-0921] 12 p1743 A83-29847

Aerodynamic characteristics of a circulation controlled elliptical airfoil with blown jets

[AIAA PAPER 83-1794] 17 p2453 A83-38633

Accuracy criteria for evaluating supersonic missile aerodynamic coefficient predictions

18 p2638 A83-40005

Determination of aerodynamic parameters of a fighter airplane from flight data at high angles of attack

[AIAA PAPER 83-2066] 19 p2804 A83-41904

Computational method of the drag of axisymmetric afterbodies in subsonic flow

[AIAA PAPER 83-2079] 19 p2792 A83-41913

Identification of aerodynamic coefficients using flight testing data

[AIAA PAPER 83-2099] 19 p2798 A83-41929

Calibration of the aerodynamic coefficient identification package measurements from the shuttle entry flights using inertial measurement unit data

[AIAA PAPER 83-2100] 19 p2818 A83-41930

Apparent-mass coefficients for isosceles triangles and cross sections formed by two circles --- in slender body fuselage aerodynamics

21 p3091 A83-43973

Mathematical modeling of unsteady separated flow past a circular cylinder

23 p3452 A83-48667

AERODYNAMIC CONFIGURATIONS

NT WING NACELLE CONFIGURATIONS

Problems concerning supersonic flow past bodies of prismatic configurations

04 p0443 A83-16394

Pan Air versus S/HABP - An evaluation of two diverse approaches to supersonic missile aerodynamic analysis

--- Advanced Panel Pilot Code and Supersonic/Hypersonic Arbitrary Body Program

[AIAA PAPER 83-0008] 05 p0578 A83-16460

Calculation of supersonic flow over realistic configurations by an updated low-order panel method

[AIAA PAPER 83-0010] 05 p0578 A83-16461

Evaluation of missile aerodynamic characteristics for diversified configurations using rapid prediction techniques

[AIAA PAPER 83-0180] 05 p0581 A83-16573

Aerodynamic characteristics of a jet controlled projectile

[AIAA PAPER 83-0392] 05 p0585 A83-16689

A component buildup aerodynamic prediction approach for airbreathing missiles

[AIAA PAPER 83-0461] 05 p0586 A83-16729

Slender body theory and optimization procedures for transonic lifting wing bodies

[AIAA PAPER 83-0184] 05 p0591 A83-17911

Transonic flow simulation of prop-fan configurations

[AIAA PAPER 83-0187] 06 p0714 A83-19582

Computer-enhanced analysis of a jet in a cross stream

07 p0924 A83-19804

Transonic airfoil calculations using solution-adaptive grids

07 p0863 A83-19824

Oil flow separation patterns on an ogive forebody

09 p1198 A83-24662

Three-dimensional supersonic ideal-gas flow past a body with a tail assembly

11 p1526 A83-27721

Parametric study of hypersonic three-dimensional configurations

11 p1527 A83-28537

Development and validation of the V/STOL aerodynamics and stability and control manual

12 p1696 A83-29020

Approximate calculation of the aerodynamic characteristics of a cylindrical body of small aspect ratio in an incompressible flow

12 p1696 A83-29287

The problem of an optimum wing of constant seaworthiness

14 p1972 A83-33003

A study of the motion of thin-section wings of complex configurations near a solid surface

14 p1972 A83-33005

Equations of the necessary extremum condition for a class of incorrect extreme-value problems --- for optimization of aerodynamic configurations

14 p1972 A83-33011

ADI methods for solution of the transient heat conduction problems in spherical geometry

15 p2159 A83-34234

Aerodynamic design of propan powered transports

[AIAA PAPER 83-1213] 16 p2300 A83-36285

Calculation of transonic axisymmetric flow past bodies of revolution

17 p2450 A83-37627

Aerodynamic development for efficient military cargo transports

[AIAA PAPER 83-1822] 17 p2464 A83-38654

Hover and transition flight performance of a twin tilt-nacelle V/STOL configuration

[AIAA PAPER 83-1824] 17 p2465 A83-38656

The evaluation of the rolling moments induced by wraparound fins

[AIAA PAPER 83-1840] 17 p2470 A83-38669

A multiple separation model for multielement airfoils

[AIAA PAPER 83-1844] 17 p2456 A83-38672

On the conceptual design of supersonic cruising aircraft with subsonic wing leading edges

17 p2466 A83-38950

Accuracy criteria for evaluating supersonic missile aerodynamic coefficient predictions

18 p2638 A83-40005

Unconventional commuter configurations - A design investigation

[SAE PAPER 830710] 20 p2933 A83-43320

The aerodynamics of small RPV's

20 p2934 A83-43710

Optimum configuration for a 10-passenger business turbofan jet airplane

21 p3091 A83-43967

New developments in open separation --- of three dimensional boundary layers

22 p3250 A83-47016

Development of aerodynamical technology for large civil aviation aircraft

23 p3391 A83-47204

Optimization of waverider configurations generated from axisymmetric conical flows

23 p3398 A83-48134

Subsonic airplane configurations for maximum range for endurance

[AIAA PAPER 83-2536] 23 p3405 A83-48370

AERODYNAMIC DRAG

NT SUPERSONIC DRAG

Comparison of computational and experimental jet effects 01 p0002 A83-10185

The artificial earth satellite motion in an oblate, rotating atmosphere with symmetrical diurnal effect 01 p0017 A83-10269

Ballistic entry motion, including gravity - Constant drag coefficient case 03 p0283 A83-14839

Reductions in parachute drag due to forebody wake effects 04 p0443 A83-15315

Iterative optimal subcritical aerodynamic design code including profile drag [AIAA PAPER 83-0012] 05 p0578 A83-16462

SAMID, an interactive system for the analysis and constrained minimization of induced drag of aircraft configurations [AIAA PAPER 83-0095] 05 p0594 A83-16519

The design of a human-powered vehicle [AIAA PAPER 83-0649] 05 p0621 A83-16816

The air drag perturbation of satellite in an orbit with small-eccentricity 05 p0602 A83-16857

Piloting techniques on the backside --- of drag curve 05 p0598 A83-16927

Turbulent diffusion of particles in a gas-suspension flow in different directions of the component motion 05 p0638 A83-16951

Aerodynamic drag in two-phase flows 05 p0589 A83-17408

The effects of turbulence and surface roughness on the drag of spheres in thin jets 06 p0711 A83-18067

Aerodynamic estimation techniques for aerostats and airships 06 p0712 A83-18404

Full scale test of the C22 target in the ONERA S1MA wind tunnel [ONERA, TP NO. 1982-95] 06 p0717 A83-18430

Altitude transitions in energy climbs 10 p1379 A83-26604

Body with minimum wave drag in a twisted hypersonic flow 11 p1526 A83-27712

An experimental investigation of the wake of an axisymmetric body with a slanted base 11 p1526 A83-27873

Motion of an earth satellite. II - Nonlinear perturbations 11 p1532 A83-28034

Parametric study of hypersonic three-dimensional configurations 11 p1527 A83-28537

Calculation of drag and heat transfer for viscous quasi-stabilized flow of supercritical helium in a pipe 11 p1570 A83-28552

Induced drag of a slender wing in a nonuniform stream 12 p1696 A83-28970

An onboard navigator for the extremely low-altitude satellite utilizing accelerometers 13 p1812 A83-30167

Investigation of the possibility of reducing aerodynamic drag by a mechanism of initial vortex formations 13 p1804 A83-30723

A semi-empirical approach for the prediction of aft-body drag of supersonic projectiles with base bleeding 15 p2119 A83-33489

Determining the form drag contribution to the total stress of the atmospheric flow over ridged sea ice 15 p2203 A83-33498

Determination of basic constants of satellite - Atmosphere interaction from the analysis of motion of 1974-70A 16 p2314 A83-36114

A technique to determine lift and drag polars in flight 16 p2296 A83-36913

Unsteady flow field, lift and drag measurements of impulsively started elliptical cylinder and circular-arc airfoil [AIAA PAPER 83-1711] 17 p2502 A83-37205

Calculation of the aerodynamic efficiency of winglets 17 p2446 A83-37257

Calculation of transonic axisymmetric flow past bodies of revolution 17 p2450 A83-37627

The wake drag of bodies with a conical tail section 17 p2452 A83-38093

An aftbody drag prediction technique for military airlifters [AIAA PAPER 83-1787] 17 p2452 A83-38627

Axisymmetric bluff-body drag reduction using circumferential grooves [AIAA PAPER 83-1788] 17 p2453 A83-38628

Inviscid drag calculations for transonic flows [AIAA PAPER 83-1928] 18 p2635 A83-39380

The hydrodynamic forces acting on a cylinder set in motion in an impulsive manner 19 p2843 A83-41264

The aerodynamics of a sphere outgassing in a rarefied gas flow 19 p2791 A83-41268

Drag on a sphere oscillating in a dusty gas 19 p2843 A83-41543

On the behavior of a body with a frontal circulation zone in unsteady flow (the computational model) 19 p2791 A83-41885

Aerodynamic drag of a cone in two-phase flow 19 p2792 A83-41899

Computational method of the drag of axisymmetric afterbodies in subsonic flow [AIAA PAPER 83-2079] 19 p2792 A83-41913

LDA measurements of separated flows and a simple calculation method for the drag of a sharp-edged cylinder 20 p2929 A83-43006

Experimental wing and canard jet-flap aerodynamics [AIAA PAPER 83-0081] 23 p3398 A83-48211

Drag of wings with cambered airfoils and partial leading-edge suction 23 p3398 A83-48220

Wave drag prediction using a simplified supersonic area rule 23 p3399 A83-48222

The effect of heat release and injection on the structure of a laminar hypersonic flow behind a body 23 p3399 A83-48534

AERODYNAMIC FORCES

NT AERODYNAMIC DRAG

NT AERODYNAMIC INTERFERENCE

NT AERODYNAMIC LOADS

NT BLAST LOADS

NT GUST LOADS

NT LIFT

NT SUPERSONIC DRAG

NT WING LOADING

Development and trial of a rotary balance for the 3 M low speed wind tunnels of West Germany 01 p0015 A83-11082

Experimental forces and moments on cone-derived waveriders for freestream M = 3 to 5 02 p1332 A83-13092

A new approach to weapon separation aerodynamics 03 p0278 A83-13164

Linear/nonlinear behavior in unsteady transonic aerodynamics 04 p0442 A83-15280

Nonlinear aerodynamic modeling of flap oscillations in transonic flow - A numerical validation [AIAA PAPER 81-0073] 04 p0442 A83-15290

Optimum performance of propeller wind turbine blades 04 p0507 A83-16109

Maximum vortex-induced side force revisited --- for aerodynamic design [AIAA PAPER 83-0458] 05 p0586 A83-16727

A component buildup aerodynamic prediction approach for airbreathing missiles [AIAA PAPER 83-0461] 05 p0586 A83-16729

An exploratory study of finite difference grids for transonic unsteady aerodynamics [AIAA PAPER 83-0503] 05 p0587 A83-16752

Some applications of a generalized aerodynamic forces and moments theory [AIAA PAPER 83-0543] 05 p0587 A83-16778

The effect of backlash and trailing-edge strips on the flutter speed of a two-dimensional model of a tailplane with tab 06 p0716 A83-18068

The effect of aerodynamic coupling between the blades of a cascade on the aerodynamic damping of blade vibrations and the onset of blading flutter 06 p0777 A83-19312

Numerical prediction of dynamic forces on arbitrarily pitched airfoils 07 p0862 A83-19801

Application of the matrix method of forces for the calculation of aircraft structures 08 p1123 A83-23221

Development of the basic methods needed to predict helicopters' aeroelastic behaviour [ONERA, TP NO. 1982-75] 08 p1124 A83-23248

Influence of leading-edge thrust on twisted and cambered wing design for sruersonic cruise 12 p1696 A83-29018

The coupled aeroelastic response of turbomachinery blading to aerodynamic excitations [AIAA 83-0844] 12 p1742 A83-29822

Double multiple streamtube model with recent improvements --- for predicting aerodynamic loads and performance of Darricus vertical axis wind turbines 13 p1870 A83-30195

A three degree-of-freedom, typical section flutter analysis using harmonic transonic air forces [AIAA PAPER 83-0960] 14 p2032 A83-32797

Effect of sound absorbing wall linings on aerodynamic forces of a subsonic vibrating cascade 14 p2081 A83-33372

Effects of Reynolds number and corner radius on two-dimensional flow around hexadecagonal cylinders [AIAA PAPER 83-1705] 17 p2502 A83-37202

Aerodynamic design for improved maneuverability by the use of three-dimensional transonic theory [AIAA PAPER 83-1859] 17 p2465 A83-38686

Unsteady aerodynamic forces and flutter analysis for a wing-aileron-tab configuration 20 p3008 A83-43688

Apparent-mass coefficients for isosceles triangles and cross sections formed by two circles --- in slender body fuselage aerodynamics 21 p3091 A83-43973

Computation of aerodynamic forces on bodies with non-circular cross-section in supersonic viscous flow [AIAA PAPER 83-2077] 21 p3089 A83-45519

Determination of the suction-force distribution and its effect on the aerodynamic design of a wing for supersonic flow 22 p3250 A83-46495

On the energy characteristics of the aerodynamic matrix and the relationship to possible flutter 23 p3398 A83-48144

Progress in the semi-empirical prediction of the aerodynamic forces due to large amplitude oscillations of an airfoil in attached or separated flow [ONERA, TP NO. 1983-111] 24 p3545 A83-49422

AERODYNAMIC HEAT TRANSFER

NT HYPERSONIC HEAT TRANSFER

NT SUPERSONIC HEAT TRANSFER

Three-dimensional recoiling/optimal entry, with minimum heating of the vehicle 01 p0017 A83-10583

Orbiter entry leeside heat-transfer data analysis [AIAA PAPER 83-0484] 05 p0586 A83-16745

Estimates of turbulent boundary layer behind a shock wave moving with uniform velocity in air [AIAA PAPER 83-0567] 05 p0637 A83-16794

Shock strength modification for reduced heat transfer to lifting re-entry vehicles 10 p1372 A83-26160

Effects of nonequilibrium and surface catalysis on Shuttle heat transfer - A review [AIAA PAPER 83-1485] 15 p2127 A83-34916

Heat-transfer non-uniformities downstream of three-dimensional boundary layer trips 20 p2976 A83-42718

Flow past and radiant heating of blunt bodies moving at angles of attack alpha greater than or equal to 0 deg 20 p2929 A83-42878

Measurements of heat transfer distribution over the surfaces of highly loaded turbine nozzle guide vanes [ASME PAPER 83-GT-53] 23 p3394 A83-47910

AERODYNAMIC HEATING

NT SHOCK HEATING

Entry vehicle performance in low-heat-load trajectories 02 p0139 A83-13079

An investigation of gap heating due to stepped tiles in zero pressure gradient regions of the Shuttle Orbiter Thermal Protection System [AIAA PAPER 83-0120] 05 p0606 A83-16533

Base heating on an aerobraking orbital transfer vehicle [AIAA PAPER 83-0408] 05 p0607 A83-16697

Aerodynamic heating and surface temperatures on vehicles for computer-aided design studies [AIAA PAPER 83-0411] 05 p0585 A83-16699

Aerothermodynamic parameter estimation from Space Shuttle thermocouple data during transient flight test maneuvers [AIAA PAPER 83-0482] 05 p0607 A83-16743

Space Shuttle heating analysis with variation in angle of attack and surface condition [AIAA PAPER 83-0486] 05 p0586 A83-16747

Chemical nonequilibrium effects on flowfields for aeroassist orbital transfer vehicles [AIAA PAPER 83-0214] 05 p0602 A83-17913

Comparison of computational and flight data concerning heat transfer for axisymmetric bodies moving along a trajectory at freestream Mach of not greater than 5 06 p0713 A83-19570

Thermostructural evaluation of spinel infrared IIR/domes 09 p1239 A83-24966

Flight measurements of temperature and pressure on rescued nose cones of the M100 and Obolako meteorological rockets 11 p1634 A83-28373

Unsteady boundary layer with self-induced pressure near a rapidly heated section of the surface of a flat plate in supersonic flow 11 p1527 A83-28536

Heating measurements on Space Shuttle Orbiter models with differentially deflected elevons [AIAA PAPER 83-1534] 14 p2011 A83-32763

Experimental aerodynamic heating to simulated Shuttle tiles [AIAA PAPER 83-1536] 14 p2011 A83-32764

Expanded uses of infrared scanning data in aerodynamic heating materials tests [AIAA-PAPER 83-1542] 14 p1979 A83-32766

Two-dimensional deforming finite element methods for surface ablation [AIAA PAPER 83-1555] 14 p2012 A83-32773

The cubic spline numerical solution of the albatron problem [AIAA PAPER 83-1556] 14 p2012 A83-32774

Analysis of aerothermal loads on spherical dome protuberances [AIAA PAPER 83-1557] 14 p1971 A83-32775

Comparisons of STS-1 experimental and predicted heating rates 15 p2125 A83-33729

Benchmark determination of Shuttle Orbiter entry aerodynamic heat-transfer data 15 p2119 A83-33730

- An empirical method for computing leeside centerline heating on the Space Shuttle Orbiter
15 p2120 A83-33731
Analysis of STS-2 experimental heating rates and transition data
15 p2125 A83-33732
Review of helicopter icing protection systems
[AIAA PAPER 83-2529] 23 p3401 A83-48367
- AERODYNAMIC INTERFERENCE**
Support interference in static and dynamic tests --- of wind tunnel models at high angles of attack
01 p0014 A83-11074
Numerical simulation of wing-fuselage interference
03 p0277 A83-13129
Airframe effects on a top-mounted fighter inlet system
03 p0278 A83-13166
The interference of oblique shocks of a particular family in a hypersonic flow
04 p0441 A83-15090
Thrust reversing effects on horizontal tail effectiveness of twin-engine fighter aircraft
[AIAA PAPER 83-0086] 05 p0594 A83-16512
Propulsion installation characteristics for turbofan transports
[AIAA PAPER 83-0087] 05 p0579 A83-16513
A transonic analysis of propfan slipstream effect on a supercritical wing
[AIAA PAPER 83-0186] 05 p0581 A83-16577
A multi-grid method for the computation of viscid/inviscid interactions on airfoils
[AIAA PAPER 83-0234] 05 p0582 A83-16602
Advances in methods for predicting store aerodynamic characteristics in proximity to an aircraft
[AIAA PAPER 83-0266] 05 p0584 A83-16622
Investigation of the effects of upstream sidewall boundary-layer removal on a supercritical airfoil
[AIAA PAPER 83-0386] 05 p0585 A83-16686
Support-ting interference on boattail pressure drag for Reynolds numbers up to 70×10^6 to the 6th
[AIAA PAPER 83-0387] 05 p0599 A83-16687
On the aerodynamics of over-the-wing nacelles supported on 'stub-wings'
[AIAA PAPER 83-0538] 05 p0595 A83-16774
Application of panel methods to external stores at supersonic speeds
06 p0712 A83-18409
Full scale test of the C22 target in the ONERA S1MA wind tunnel
[ONERA, TP NO. 1982-95] 06 p0717 A83-18430
The transonic wind tunnel Braunschweig of DFVLR
07 p0867 A83-19663
Theory of resistance interference of airfoil wings and engine exhaust
07 p0862 A83-19667
Fuselage-lifting surfaces interaction in unsteady subsonic flow --- French thesis
08 p1041 A83-22093
Overview of aero-optical phenomena --- in pulsed and continuous wave laser-target interactions
08 p1108 A83-22453
An interaction algorithm for three-dimensional turbulent subsonic aerodynamic juncture region flow
09 p1198 A83-24659
Aerodynamics of asymmetric sabot discard
09 p1198 A83-24892
Some new results on edge-tone oscillations in high-speed subsonic jets
[AIAA PAPER 83-0665] 10 p1473 A83-25902
Subsonic dynamic stall in pitching and plunging oscillations including large ground interference effects
[AIAA 83-0889] 12 p1697 A83-29836
Special mesh for determining aerodynamic interference between casing walls and rotating blade rows of subsonic and transonic turbines and compressors
13 p1804 A83-30512
Wind tunnel tests of over-the-wing nacelles --- supported on 'stub-wings'
16 p2296 A83-36916
Wake interference of a row of normal flat plates arranged side by side in a uniform flow
17 p2505 A83-37571
Optimization of Darrieus turbines with an upwind and downwind momentum model
17 p2536 A83-38016
Parametric study of factors affecting the fuel efficiency of advanced turboprop airplanes
[AIAA PAPER 83-1823] 17 p2464 A83-38655
Surface pressures induced on a flat plate with in-line and side-by-side dual jet configurations
[AIAA PAPER 83-1849] 17 p2456 A83-38677
2-D elliptic grid generation using a singularity method and its application to transonic interference flows
17 p2458 A83-38808
Plume/flowfield jet interaction effects on the Space Shuttle Orbiter during entry
18 p2646 A83-40009
Interference during flow around a wing and an axisymmetric nacelle
19 p2791 A83-41879
Studies of light-twin wing-body interference
[SAE PAPER 830709] 20 p2930 A83-43319
Combined four-wall interference assessment in two-dimensional airfoil tests
21 p3093 A83-45576
- AERODYNAMIC LIFT**
U LIFT

AERODYNAMIC LOADS

- NT BLAST LOADS
NT GUST LOADS
Aerodynamic loads and performance of the Darrieus rotor
01 p0068 A83-10657
Problems of temperature compensation during direct measurement of aerodynamic pressures
01 p0051 A83-11053
Development of analytical and experimental techniques for determining store airload distributions
02 p0132 A83-13077
Calculation of steady and unsteady transonic flows using parametric differentiation and an extended integral equation method
[AIAA PAPER 83-0232] 05 p0582 A83-16600
Loads environment for payload/cargo integration
[AIAA PAPER 83-0328] 05 p0604 A83-16657
Parametrically excited non-linear multidegree-of-freedom systems with repeated natural frequencies
06 p0773 A83-18392
The analysis of operational stresses --- on aircraft during flight
06 p0775 A83-18596
Experimental comparison of simulation methods of aeronautic type loading
[ONERA, TP NO. 1982-130] 06 p0775 A83-18598
Prediction of the aerodynamic loads on helicopter blades in hovering and axial flight using lifting line theory
07 p0864 A83-21016
Blade loading and rotation effects on compressor rotor wake near end walls
08 p1042 A83-22138
The simulation of fatigue loads in aeronautics
08 p1048 A83-23241
Maneuver load control for reducing the design loads of modern combat aircraft
[DGLR PAPER 82-046] 09 p1209 A83-24169
Aerodynamic loads on a Darrieus rotor blade
10 p1446 A83-26628
Some effects of size on non-rigid airships
11 p1530 A83-28192
On the determination of the load-carrying capacity of the glass-plastic propeller blade of an aircraft
12 p1703 A83-29294
Airfoil shape and thickness effects on transonic airloads and flutter
[AIAA 83-0959] 12 p1702 A83-29860
A discretized asymptotic method for unsteady helicopter rotor airloads
[AIAA 83-0989] 12 p1697 A83-29867
Anti-flutter control concept using a reduced non-linear dynamic model of elastic structure aircraft
[AIAA 83-0993] 12 p1704 A83-29870
On measuring transonic dips in the flutter boundaries of a supercritical wing in the wind tunnel
[AIAA 83-1031] 12 p1703 A83-29878
Determination of horizontal tail load and hinge moment characteristics from flight data --- on Learjet Model 55 Longhorn
13 p1805 A83-30162
Double multiple streamtube model with recent improvements --- for predicting aerodynamic loads and performance of Darrieus vertical axis wind turbines
13 p1870 A83-30195
Aerodynamic theory for wing with side edge passing subsonically through a gust
14 p1971 A83-32977
Pressure pulsations during flow past blunt bodies
16 p2288 A83-35537
Loads and pressures due to underexpanded jets impinging on wedges
16 p2288 A83-35619
Maximum loading capability of axial flow compressors
[AIAA PAPER 83-1163] 16 p2306 A83-36254
Experimental research on the design of highly loaded axial fans --- German thesis
17 p2447 A83-37498
Aerodynamic loads on the rear part of a fuselage behind a swept wing in supersonic flow
17 p2450 A83-37562
The lateral response of an airship to turbulence
[AIAA PAPER 83-1989] 17 p2459 A83-38915
The LANN program - An experimental and theoretical study of steady and unsteady transonic airloads on a supercritical wing
[AIAA PAPER 83-1686] 18 p2632 A83-39099
JT9D performance deterioration results from a simulated aerodynamic load test
19 p2800 A83-41040
Preliminary supersonic analysis methods including high angle of attack
21 p3085 A83-43969
Unsteady airloads on supercritical wings
24 p3544 A83-49179
Investigation of the unsteady airloads on airfoils with oscillating control in sub- and transonic flows
24 p3544 A83-49180
- AERODYNAMIC MOMENTS**
U STABILITY DERIVATIVES
AERODYNAMIC NOISE
Tests of a thermal acoustic shield with a supersonic jet
01 p0105 A83-10183
Noise measurement at an obstacle in a wind tunnel
[AAAF PAPER NT 81-10] 02 p0234 A83-11771

- Study of fan noise sources through thin film pressure transducers
02 p0136 A83-12350
Noise and flow structure of a tone-excited jet
03 p0391 A83-13136
Method of multiple scales and the problem of aerodynamically generated sound
04 p0533 A83-16100
Free stream noise and transition measurements in a Mach 3.5 pilot quiet tunnel
[AIAA PAPER 83-0042] 05 p0598 A83-16482
Investigation of screech tone elimination in an underexpanded supersonic jet
05 p0683 A83-16813
On the radially non-compact source model for subsonic jet noise
05 p0683 A83-16929
Strut or guide vane secondary flows and their effect on turbomachinery noise
06 p0807 A83-18414
Sound source radiation in two-dimensional shear flow
07 p0990 A83-19812
Radiation from a double layer jet --- aerodynamic noise
07 p0990 A83-20364
Conventional profile coaxial jet noise prediction
08 p1162 A83-22128
Analysis of airfoil noise with an array of near- and far-field sensors
09 p1340 A83-23473
A theoretical and experimental study of propeller noise
[ONERA, TP NO. 1982-122] 09 p1340 A83-24333
Shock waves ahead of a fan with nonuniform blades
09 p1341 A83-24665
Fluctuating pressure measurements on the fan blades of a turbofan engine during ground and flight tests
[AIAA PAPER 83-0679] 10 p1377 A83-25911
An experimental study of windturbine noise from blade-tower wake interaction
[AIAA PAPER 83-0691] 10 p1473 A83-25913
On the shock cell structure and noise of supersonic jets
[AIAA PAPER 83-0703] 10 p1474 A83-25923
Simulation of propfan noise impact on a fuselage --- by newly developed siren
[AIAA PAPER 83-0715] 10 p1475 A83-25930
Near field acoustic measurements in natural and artificially excited high speed subsonic jets
[AIAA PAPER 83-0725] 10 p1475 A83-25936
Flight effects on jet mixing noise - Scaling laws predicted for single jets from flight simulation data
[AIAA PAPER 83-0748] 10 p1476 A83-25950
Flight effects on jet noise sources investigated by model experiments in the DNW
[AIAA PAPER 83-0752] 10 p1476 A83-25951
Acoustic evaluation of DNW free jet shear layer correction using a model jet
[AIAA PAPER 83-0757] 10 p1476 A83-25954
Porous-plug flowfield mechanisms for reducing supersonic jet noise
[AIAA PAPER 83-0774] 10 p1378 A83-25959
Analysis of jet-airframe interaction noise
[AIAA PAPER 83-0783] 10 p1376 A83-25964
Airfoil self noise - Effect of scale
[AIAA PAPER 83-0785] 10 p1477 A83-25966
Near-field frequency - Domain theory for propeller noise
[AIAA PAPER 83-0688] 11 p1651 A83-28007
Comparison of broadband noise mechanisms, analyses, and experiments on helicopters, propellers, and wind turbines
[AIAA PAPER 83-0690] 11 p1651 A83-28009
On the mechanism of screech tone generation in underexpanded rectangular jets
[AIAA PAPER 83-0727] 11 p1651 A83-28014
Influence of surface compliance on boundary layer noise
[AIAA PAPER 83-0738] 11 p1652 A83-28018
Experimental investigation of surface roughness generated flow noise
[AIAA PAPER 83-0786] 11 p1652 A83-28025
A new measurement method for separating airborne and structureborne aircraft interior noise
11 p1652 A83-28186
Direct measurement of sound from large scale structures in jet flows
[AIAA PAPER 83-0662] 11 p1653 A83-28197
Wind tunnel noise reduction at Mach 5 with a rod-wall sound shield --- for prevention of premature boundary layer transition on wind tunnel models
[AIAA PAPER 82-0570] 12 p1704 A83-28952
Shock-associated noise in supersonic jets
12 p1777 A83-28957
Noise emission and propagation in an air flow
[ONERA, TP NO. 1983-95] 12 p1777 A83-29385
Turbulence measurements relevant to sound generation of moving jets
[AIAA PAPER 83-0664] 12 p1777 A83-29525
Acoustic wave radiated by head-on collision of two vortex rings
12 p1777 A83-29595

Compressible helicoidal surface theory for propeller aerodynamics and noise 14 p1971 A83-32986

Method of calculating optimum angular blade pitches in fan with unequally pitched blades 14 p1972 A83-33090

Constraints on the invariant functions of axisymmetric turbulence 16 p2351 A83-36083

Derivation of the fundamental equation of sound generated by moving aerodynamic surfaces 16 p2408 A83-36096

In-flight acoustic test results for the SR-2 and SR-3 advanced-design propellers [AIAA PAPER 83-1214] 16 p2307 A83-36286

An experimental study of the impingement of a supersonic annular jet on an obstacle 19 p2790 A83-41260

Low flight speed acoustic results for a supersonic inlet with auxiliary inlet doors [AIAA PAPER 83-1415] 21 p3201 A83-45517

Rotational flow of a weakly viscous fluid 22 p3280 A83-45976

Subsonic and transonic propeller noise [ONERA, TP NO. 1983-76] 23 p3505 A83-48191

AERODYNAMIC STABILITY

Dynamic simulation in wind tunnels 01 p0014 A83-11079

Development and trial of a rotary balance for the 3 M low speed wind tunnels of West Germany 01 p0015 A83-11082

Evaluation of component buildup methods for missile aerodynamic predictions 02 p0132 A83-13076

A new concept for aircraft dynamic stability testing 04 p0449 A83-15310

A look at the Russell 'Lobe' parachute - The first ultra-stable parachute design 04 p0444 A83-15434

Simplified analysis techniques to support the determination of Shuttle aerodynamics [AIAA PAPER 83-0117] 05 p0606 A83-16531

Effects of large oscillation amplitude on axisymmetric vehicle longitudinal static and dynamic stability in hypersonic flow [AIAA PAPER 83-0215] 05 p0581 A83-16587

Flight testing of the Space Shuttle 05 p0605 A83-16972

Dynamic stability of a buoyant quad-rotor aircraft 08 p1047 A83-22160

Stability of steady sideslip equilibria for high alpha --- supersonic fighter aircraft 09 p1209 A83-24031

Pressure measurements of a rotating liquid for impulsive coning motion 09 p1263 A83-24877

A closed-form analysis of rotor blade flap-lag stability in hover and low-speed forward flight in turbulent flow [AIAA 83-0986] 12 p1702 A83-29864

Measured inplane stability characteristics in hover for an advanced bearingless rotor [AIAA 83-0987] 12 p1702 A83-29865

Active suppression of aeroelastic instabilities on a forward swept wing [AIAA 83-0991] 12 p1704 A83-29869

Stability study of a tilt-rotor aircraft model 13 p1806 A83-31172

Alleviation of the subsonic pitch-up of delta wings 14 p1969 A83-32583

Effects of friction dampers on aerodynamically unstable rotor stages [AIAA PAPER 83-0848] 14 p1976 A83-32791

Certain aspects of the optimum design of hydrodynamic lifting complexes 14 p1972 A83-33002

Analysis of results of aerodynamic studies on the Venera 13 and 14 descent modules 19 p2809 A83-41237

Control of forward swept wing aeroelastic instabilities using active feedback systems [AIAA PAPER 83-2220] 19 p2803 A83-41701

Coupled static stability analysis for nonlinear aerodynamics [AIAA PAPER 83-2069] 19 p2805 A83-41906

New flying qualities criteria for relaxed static longitudinal stability [AIAA PAPER 83-2104] 19 p2806 A83-41933

An improved method for predicting lateral-directional dynamic stability characteristics [SAE PAPER 830711] 20 p2937 A83-43321

Formulation and solution of rotary-wing aeroelastic stability and response problems 20 p2933 A83-43673

Investigations of hingeless rotor stability 20 p2933 A83-43674

Aeroservoelasticity in the time domain --- for YF-16 aircraft 21 p3093 A83-43965

Accelerated method for the computer calculation of a nonlinear oscillatory system 21 p3200 A83-45212

The effect of elastically suspended masses on the stability of elastic panels in supersonic flow 21 p3164 A83-45369

Space Shuttle response to ascent wind profiles 21 p3097 A83-45464

Aeromechanical stability of a hingeless rotor in hover and forward flight - Analysis and wind tunnel tests 24 p3548 A83-50141

AERODYNAMIC STALLING

A half-wing near a wall at high angles of attack in a pulsed flow [AAAF PAPER NT 81-12] 02 p0132 A83-11773

A-10 stall/post-stall testing - A status update 02 p0137 A83-11808

Helicopter rotor performance evaluation using oscillatory airfoil data 03 p0278 A83-13172

Concerning dynamic stall --- of laminar flow near leading edges of airfoils 04 p0442 A83-15150

A dynamic model for aircraft poststall departure [AIAA PAPER 83-0367] 05 p0595 A83-16674

Laser holographic interferometry for an unsteady airfoil in dynamic stall [AIAA PAPER 83-0388] 05 p0643 A83-16688

Shock-induced dynamic stall [AIAA PAPER 83-0547] 05 p0588 A83-16782

Aeroelasticity of helicopter rotors in forward flight 05 p0654 A83-17316

Spin prediction techniques 06 p0719 A83-18401

Helicopter-rotor aeroelastic equilibrium under nonlinear aerodynamic forces 09 p1202 A83-23679

A discrete tracking control law for nonlinear plants --- applied to F-8 aircraft stall recovery 10 p1378 A83-26503

Airplane model structure determination from flight data 12 p1704 A83-29023

Subsonic dynamic stall in pitching and plunging oscillations including large ground interference effects [AIAA 83-0889] 12 p1697 A83-29836

A model of axial impeller stall 16 p2292 A83-35878

Maximum loading capability of axial flow compressors [AIAA PAPER 83-1163] 16 p2306 A83-36254

Configuration development of a research aircraft with post-stall maneuverability 16 p2301 A83-36915

Flight at supersonic attitudes [SAE PAPER 821469] 17 p2470 A83-38000

Modeling of turbulent flow fields through cascade of airfoils at stall conditions [AIAA PAPER 83-1743] 17 p2452 A83-38091

Interacting flow theory and trailing edge separation - No stall 18 p2633 A83-39214

Poststall flight in close combat [AIAA PAPER 83-2120] 19 p2806 A83-41945

Designed to be stalled --- T-46A training aircraft 22 p3254 A83-46349

Half model testing applied to wings above and below stall 22 p3248 A83-46455

The effect of a leading-edge slat on the dynamic stall of an oscillating airfoil [AIAA PAPER 83-2533] 23 p3399 A83-48368

Progress in the semi-empirical prediction of the aerodynamic forces due to large amplitude oscillations of an airfoil in attached or separated flow [ONERA, TP NO. 1983-111] 24 p3545 A83-49422

AERODYNAMIC VEHICLES

U AIRCRAFT

AERODYNAMICS

NT AEROTHERMODYNAMICS

NT HYPERSONICS

NT ROTOR AERODYNAMICS

NT SUPERSONICS

Application of pulse code modulation technology to aircraft dynamics data acquisition 01 p0008 A83-10182

Extension of the lifting body theory to evolution on random trajectories at subsonic velocities 01 p0002 A83-10576

Design considerations for aerodynamically quenching gas sample probes [ASME PAPER 82-HT-39] 02 p0172 A83-12794

Applications of flow visualization techniques in aerodynamics [ONERA, TP NO. 1982-68] 03 p0330 A83-14528

Supersonic flow past a thin wedge traversed by an external plane shock wave front 03 p0280 A83-14894

A new approach to optimization for aerodynamic applications 04 p0443 A83-15325

A perspective of theoretical and applied computational fluid dynamics [AIAA PAPER 83-0037] 05 p0632 A83-16477

Computational Transonic Equivalent Strip method for applications to unsteady three-dimensional aerodynamics [AIAA PAPER 83-0261] 05 p0583 A83-16617

A fast viscous correction method for unsteady transonic flow about airfoils [AIAA PAPER 83-0264] 05 p0583 A83-16620

Hypersonic Mach number and real gas effects on Space Shuttle Orbiter aerodynamics [AIAA PAPER 83-0343] 05 p0584 A83-16668

75th anniversary of the establishment of the Aerodynamic Experimental Institute of Goettingen 05 p0577 A83-16896

Bringing aerodynamics to America --- Book 05 p0710 A83-17114

Concerning impingement of shock waves on permeable baffles 05 p0589 A83-17418

A solution to the problem of multiparameter optimization in calculating flow around bodies with injection 06 p0712 A83-18143

A finite state aerodynamic model for a lifting surface in incompressible flow 07 p0862 A83-19802

Certain effects and paradoxes in aerodynamics and hydraulics --- Russian book 07 p0925 A83-20379

The aerodynamics of flexible membranes 08 p1042 A83-22990

The relationship between the aerodynamics of a combustion chamber and the dynamics of heat release 09 p1205 A83-23446

Investigation of landing gear alternatives for high performance aircraft 09 p1202 A83-24030

The German-Dutch wind tunnel as an aid in aircraft development [DGLR PAPER 82-050] 09 p1210 A83-24173

Shock tube simulation of pulsed flow aerodynamic windows 10 p1371 A83-26138

Oscillations of impinging shear layers 12 p1695 A83-28953

DYSCO - An executive control system for dynamic analysis of synthesized structures [AIAA 83-0944] 12 p1768 A83-29773

Flutter analysis of a transport wing using XTRAN3S [AIAA 83-0922] 12 p1743 A83-29848

Fundamentals of flight --- Book 13 p1803 A83-30152

Certain aspects of the kinetic theory of reacting gases and its applications to relaxation aerodynamics 13 p1932 A83-30667

The use of kinetic theory for describing disperse media 13 p1933 A83-30670

The principles of aerodynamic aircraft design 13 p1806 A83-30924

Perturbation methods in mechanics 14 p1972 A83-33001

Second approximation of quadrupole wing theory in lifting surface theory 14 p1972 A83-33004

Impingement of an oblique shock wave on a cylinder 15 p2156 A83-33727

The aerodynamics of hypersonic velocities (On flows with low Mach numbers) 16 p2288 A83-35535

Turbulence modeling for computational aerodynamics 16 p2293 A83-36079

Unsteady aerodynamics in open cavities applications to rocket propulsion [AIAA PAPER 83-1314] 16 p2295 A83-36335

Calculation of afterbody flows with a composite velocity formulation [AIAA PAPER 83-1736] 17 p2445 A83-37215

Experience with hybrid aerodynamic methods [AIAA PAPER 83-1819] 17 p2455 A83-38651

Smart aerodynamic optimization [AIAA PAPER 83-1863] 17 p2457 A83-38690

Global PNS solutions for laminar and turbulent flow - Parabolized Navier-Stokes equations around boattail, flat plate and NACA 0012 airfoil geometries [AIAA PAPER 83-1911] 18 p2635 A83-39369

The motion of compressible fluids and inhomogeneous media 19 p2845 A83-41877

An electrical balance for aerodynamic investigations 19 p2849 A83-41883

The impact of computational aerodynamics on aircraft design [AIAA PAPER 83-2060] 19 p2798 A83-41901

An application of parameter identification to the oscillatory motion of an airplane at high C(L) [AIAA PAPER 83-2067] 19 p2804 A83-41905

Influence of airplane components on rotational aerodynamic data for a typical single-engine airplane [AIAA PAPER 83-2135] 19 p2793 A83-41957

Annual Mini-Symposium on Aerospace Science and Technology, 9th, USAF, Institute of Technology, Wright-Patterson AFB, OH, March 22, 1983, Proceedings 20 p2927 A83-42526

Universities - Have they a role in aeronautical research? Aerodynamics 20 p2928 A83-42621

Processing of infrared thermal images for aerodynamic research [ONERA, TP NO. 1983-32] 21 p3137 A83-44310

Finite element methods in aerodynamics 21 p3086 A83-44551

Unsteady turbulent shear flows; Proceedings of the Symposium, Toulouse, France, May 5-8, 1981 22 p3281 A83-46426

Publication on the occasion of the 65th birthday of Prof. Dr.-Ing. Erich Truckenbrodt; Scientific Colloquium, Technische Universität München, Munich, West Germany, February 1, 1982, Reports

- 22 p3284 A83-46482
The way to the supercritical wing
22 p3250 A83-46483
Numerical aerodynamics - Replacement of analytical solutions and/or the experiment by the supercomputer?
22 p3250 A83-46485
An experimental investigation of endwall heat transfer and aerodynamics in a linear vane cascade
[ASME PAPER 83-GT-52] 23 p3394 A83-47909
Aerodynamic tests on centrifugal process compressors
Influence of diffuser diameter ratio, axial stage pitch and impeller cut-back
[ASME PAPER 83-GT-172] 23 p3396 A83-47973
Recent applications of a laser velocimeter in the Langley 4by 7-meter Wind Tunnel
24 p3586 A83-50145

AEROELASTIC RESEARCH WINGS

The design, testing and analysis of aeroelastically tailored transonic flutter model wings
[AIAA 83-1027] 12 p1702 A83-29876

AEROELASTICITY

- Prediction of transonic flutter for a supercritical wing by modified strip analysis 01 p0058 A83-10190
Swept composite wing aeroelastic divergence experiments 01 p0009 A83-10193
Quadratic synthesis of integrated active controls for an aeroelastic forward-swept-wing-aircraft
02 p0137 A83-12458
Nonlinear flapping vibrations of rotating blades
02 p0197 A83-13004
In-flight deflection measurement of the HiMAT aeroelastically tailored wing 03 p0281 A83-13167
An analytical pilot rating method for highly elastic aircraft 03 p0282 A83-14843
Flutter of a buckled plate as an example of chaotic motion of a deterministic autonomous system
04 p0501 A83-16339
Numerical prediction of choking flutter of axial compressor blades
[AIAA PAPER 83-0006] 05 p0596 A83-16458
Limit amplitude of galloping cables --- effects of separated flow on Shuttle tank cable trays
[AIAA PAPER 83-0132] 05 p0682 A83-16545
Investigation of dynamic characteristics of an elastic wing due to correction of mass and stiffness matrices
[AIAA PAPER 83-0653] 05 p0595 A83-16818
Aeroelasticity of helicopter rotors in forward flight
05 p0654 A83-17316
Dynamic analysis of constant-lift and free-tip rotors
06 p0773 A83-18386
Stability of two-bladed aeroelastic rotors on flexible supports 06 p0717 A83-18387
Model attitude and deformation measurement in wind tunnel
[ONERA, TP NO. 1982-91] 06 p0762 A83-18428
Aeroelastic behavior of hypersonic re-entry vehicles
[AIAA PAPER 83-0033] 06 p0723 A83-19577
A finite state aerodynamic model for a lifting surface in incompressible flow 07 p0862 A83-19802
Flutter of orthotropic panels in supersonic flow using affine transformations 07 p0944 A83-19821
A test stand for studying transient phenomena in aerodynamic turbomachine cascades
07 p0868 A83-20913
The aeroelastic behavior of curved helicopter blades in hovering and axial flight 07 p0866 A83-21017
Design, analyses, and model tests of an aeroelastically tailored lifting surface 08 p1044 A83-22155
The aerodynamics of flexible membranes
08 p1042 A83-22990
Development of the basic methods needed to predict helicopters' aeroelastic behaviour
[ONERA, TP NO. 1982-75] 08 p1124 A83-23248
Helicopter-rotor aeroelastic equilibrium under nonlinear aerodynamic forces 09 p1202 A83-23679
Friction damping of flutter in gas turbine engine airfoils 09 p1206 A83-24038
State-space aeroelastic modeling and its application in flutter calculation 10 p1442 A83-26761
Dynamics of soft deceleration systems --- parachutes 11 p1597 A83-28469
Optimum cone angles in aeroelastic flutter 11 p1599 A83-28720
The coupled aeroelastic response of turbomachinery blading to aerodynamic excitations
[AIAA 83-0844] 12 p1742 A83-29822
Flutter and forced response of mistuned rotors using standing wave analysis
[AIAA 83-0845] 12 p1742 A83-29823
Calculation of unsteady small disturbance transonic flow at arbitrary reduced frequency using an extended integral equation method.
[AIAA 83-0884] 12 p1697 A83-29832

Effects of viscosity on transonic-aerodynamic and aeroelastic characteristics of oscillating airfoils
[AIAA 83-0888] 12 p1697 A83-29835

- Aeroelastic tailoring of rotor blades for vibration reduction in forward flight
[AIAA 83-0916] 12 p1701 A83-29844
Aeroelastic considerations for continuous patrol/high altitude surveillance platforms
[AIAA 83-0924] 12 p1702 A83-29850
Buffeting of a slender circular beam in axial turbulent flows
[AIAA 83-0928] 12 p1744 A83-29854
Active suppression of aeroelastic instabilities on a forward swept wing
[AIAA 83-0991] 12 p1704 A83-29869
Anti-flutter control concept using a reduced non-linear dynamic model of elastic structure aircraft
[AIAA 83-0993] 12 p1704 A83-29870
Wind tunnel correlation study of aerodynamic modeling for F/A-18 wing-store tip-missile flutter
[AIAA 83-1028] 12 p1703 A83-29877
On measuring transonic dips in the flutter boundaries of a supercritical wing in the wind tunnel
[AIAA 83-1031] 12 p1703 A83-29878
Comparison of frequency determination techniques for cantilevered plates with bending-torsion coupling
[AIAA 83-0953] 12 p1745 A83-29885
Performance of an angular flange aeroelastic wind energy converter 13 p1870 A83-30200
Aeroelastic stability of an elastic circulation control rotor blade in hover
[AIAA PAPER 83-0985] 14 p1975 A83-32785
Effect of tensile force on the fundamental frequency of coupled vibrations of a rotating slender beam under aerodynamic couplings 14 p2032 A83-32920
Coupled flap-lag-torsional dynamics of hingeless rotor blades in forward flight 15 p2121 A83-33506
Nonlinear supersonic flutter of panels considering shear deformation and rotary inertia 15 p2176 A83-34315
Integro-differential equations of the dynamics of elastic systems in nonstationary flows --- flight vehicle dynamics in turbulent nonseparated flow 16 p2366 A83-35933
Coupled flap-lag-torsional dynamics of hingeless rotor blades in forward flight 16 p2298 A83-35948
The effect of a normal shock on the aeroelastic stability of a panel
[ASME PAPER 83-APM-28] 17 p2447 A83-37381
Plane flow past an air-supported soft cylindrical shell 17 p2522 A83-38099
Aerodynamic properties of a two-dimensional inextensible flexible airfoil
[AIAA PAPER 83-1796] 17 p2453 A83-38635
X-29 forward swept wing aerodynamic overview
[AIAA PAPER 83-1834] 17 p2465 A83-38663
The dynamics of a helicopter rotor structure
18 p2639 A83-39485
Aeroelastic optimization of orthotropic rectangular flat panels 19 p2855 A83-40675
Transonic time-response analysis of 3-degree-of-freedom conventional and supercritical airfoils 19 p2789 A83-41047
Optimization of structures subjected to aeroelastic instability phenomena 19 p2859 A83-41541
Aeroelastic interactions with flight control (A survey paper)
[AIAA PAPER 83-2219] 19 p2803 A83-41700
Control of forward swept wing aeroelastic instabilities using active feedback systems
[AIAA PAPER 83-2220] 19 p2803 A83-41701
Pilot modeling and closed-loop analysis of flexible aircraft in the pitch tracking task
[AIAA PAPER 83-2231] 19 p2803 A83-41709
A modal analysis of flexible aircraft dynamics with handling qualities implications
[AIAA PAPER 83-2074] 19 p2805 A83-41911
Numerical analysis of natural, coupled, longitudinal-lateral vibrations of an asymmetric aeroplane 20 p3001 A83-42334
Formulation and solution of rotary-wing aeroelastic stability and response problems 20 p2933 A83-43673
Investigations of hingeless rotor stability 20 p2933 A83-43674
Aeroservoelasticity in the time domain --- for YF-16 aircraft 21 p3093 A83-43965
Nonlinear aeroelasticity 21 p3150 A83-44027
Optical design and aeroelastic investigation of segmented windmill rotor blades 21 p3166 A83-44028
The effect of elastically suspended masses on the stability of elastic panels in supersonic flow 21 p3164 A83-45369
Performing literal calculation with a micro-computer -- symbolic calculations applied to aeroelasticity problem 22 p3350 A83-45980

- Substructuring and wave propagation - An efficient technique for impeller dynamic analysis
[ASME PAPER 83-GT-150] 23 p3409 A83-47969
Flutter of mistuned turbomachinery rotors
[ASME PAPER 83-GT-153] 23 p3465 A83-47979
Inverse problem of the two-dimensional theory of elasticity in the hydrodynamic formulation 23 p3473 A83-48535
Problem of the motion of a thin airfoil near a wavy boundary 24 p3576 A83-48945
International Symposium on Aeroelasticity, Nuremberg, West Germany, October 5-7, 1981, Collected Papers [DGLR BERICHT 82-01] 24 p3543 A83-49176
Aeroelasticity at separated flow - Concepts and prospects 24 p3544 A83-49177
Survey of aeroelastic wind tunnel and flight testing methods at MBB 24 p3550 A83-49181
Practical applications of system identification in flutter testing 24 p3550 A83-49182
Experience from flight flutter testing with tip vanes on Airbus 24 p3547 A83-49183
Survey of the state of the art in modern ground vibration testing 24 p3550 A83-49184
Calculation of modal characteristics from measured quasi-normal mode information 24 p3591 A83-49185
Structural optimization with aeroelastic constraints - A survey of US applications 24 p3593 A83-49188
Aeroelastic considerations for automatic structural design procedures 24 p3547 A83-49189
The F-4 flutter suppression program 24 p3547 A83-49192
Parametric tip effects for conformable rotor applications 24 p3548 A83-50140

AEROEMBOLISM

The effects of various gases on cortical and spinal somatosensory evoked potentials at pressures up to 10 bar 07 p0974 A83-20777

AEROLOGY

A comparison of calculated and radar-located precipitation in GATE 19 p2868 A83-41586

AEROMAGNETISM

U GEOMAGNETISM

AEROMAGNETO FLUTTER

U FLUTTER

AEROMANEUVERING

A small parameter method in problems of maneuvering space vehicles with aerodynamic efficiency 15 p2127 A83-34849
Analytic solution for a cruising plane change maneuver
[AIAA PAPER 83-2095] 19 p2810 A83-41924

AERONAUTICAL ENGINEERING

- Aeronautical research - Some current influences and trends /The Second Sir Frederick Page Lecture/
02 p0131 A83-12851
The design of a packet switched network for aeronautical data interchange 03 p0281 A83-14862
Highlights of the new national aeronautical research and technology policy 04 p0441 A83-16374
Aerospace highlights 1982 04 p0576 A83-16375
Bringing aerodynamics to America --- Book 05 p0710 A83-17114
Operator influences on aircraft design 13 p1803 A83-31813
Bring cohesion to handling-qualities engineering 16 p2298 A83-35772
Eight steps needed to reach the aeronautical policy goals 18 p2632 A83-40304
Computer-aided engineering - The AI connection 18 p2738 A83-40307
Universities - Have they a role in aeronautical research? Noise research 20 p3044 A83-42617
Universities - Have they a role in aeronautical research? Contribution to RAES discussion evening --- university department planning for aeronautical research 20 p3056 A83-42620
New computers will aid advanced designs 21 p3190 A83-44102
Technology transfer from the aircraft sector to other sectors as exemplified by helicopter technology 23 p3391 A83-47190
The increase in the cost effectiveness of the construction of and preparation of manufacturing processes for flight equipment through integrated and graphic data processing-CAD/CAM 23 p3440 A83-47191
Aircraft design (3rd revised and enlarged edition) --- Russian book 23 p3403 A83-48100
Consolidated TPS implementation today and tomorrow --- quality Test Program Sets for aircraft industry [AIAA PAPER 83-2495] 23 p3468 A83-48350
- AERONAUTICS**
Helicopter evolution 06 p0711 A83-18384
Israel Annual Conference on Aviation and Astronautics, 24th, Tel Aviv and Haifa, Israel, February 17, 18, 1982, Collection of Papers 07 p0862 A83-21001

- Deutsche Forschungs- und Versuchsanstalt fuer Luft- und Raumfahrt, Annual Report 1981 --- Book
09 p1195 A83-23850
- Aeronautics - A coop aerospace education program at University of Sherbrooke, Canada
[AIAA PAPER 83-2474] 23 p3513 A83-48340
- AERONOMY**
Copernicus measurement of the Jovian Lyman-alpha emission and its aeronomic significance
02 p0264 A83-12142
- A pioneer-class Mars aeronomy mission
[AIAA PAPER 83-0520] 05 p0600 A83-16765
- International Geomagnetic Reference Field - The third generation
09 p1302 A83-23711
- Shuttle Entry Air Data System concepts applied to Space Shuttle Orbiter flight pressure data to determine air data - STS 1-4
[AIAA PAPER 83-0118] 11 p1537 A83-28348
- Instruments and analysis techniques for space physics; Proceedings of the Workshop, Ottawa, Canada, May 16-June 2, 1982
13 p1813 A83-30751
- On the possibility to measure the high altitude light ion concentrations with Eiscat
13 p1883 A83-31716
- The aeronomic dissociation of water vapor by solar H Lyman-alpha radiation
15 p2196 A83-33947
- Generation of ultra-violet oxygen emissions with wavelengths of 1304 and 1356 A by electron collision and some aeronomic consequences
15 p2200 A83-34416
- International Union of Geodesy and Geophysics, General Assembly, 18th, Hamburg, West Germany, August 15-27, 1983, U.S. National Committee Report
17 p2586 A83-38265
- U.S. contributions to auroral aeronomy, 1979-1982
17 p2541 A83-38276
- Aeronomy of the inner planets
17 p2622 A83-38278
- The Arcad-3 project--- aboard Franco-Soviet AUREOL-3 satellite
18 p2715 A83-39571
- The AUREOL-3 satellite
18 p2645 A83-39572
- Electron precipitation and related aeronomy of the Jovian thermosphere and ionosphere
20 p3077 A83-42407
- Positive and negative ions in the stratosphere
21 p3170 A83-44235
- Positive ion composition measurements between 33 and 20 km altitude
21 p3170 A83-44236
- Variation of aeronomic parameters during the period from the equinox to summer
21 p3175 A83-45241
- Symposium on Coordinated Observations of the ionosphere and the Magnetosphere in the Polar Regions, 4th, Tokyo, Japan, February 23-25, 1981, Proceedings
22 p3329 A83-46501
- Structure of the upper and middle atmosphere; Proceedings of the Meeting, Leeds, England, August 23-27, 1982
24 p3603 A83-48751
- A point of view on semi-empirical thermospheric models
24 p3603 A83-48752
- AEROPHYSICS**
U ATMOSPHERIC PHYSICS
- AEROS SATELLITE**
EUV indices for low solar activity
09 p1368 A83-23415
- AEROSOLS**
NT FOG
Remote determination of cloud properties from solar photometric data
01 p0074 A83-10043
- Detection of regional air pollution episodes utilizing satellite data in the visual range
01 p0069 A83-10044
- Combustion-related pollutants of polydisperse single-composition aerosols and advection fog formation
01 p0070 A83-10226
- More about the influence of the aerosol correction on the results of total ozone amount
01 p0070 A83-10289
- Aerosol technology: Properties, behavior, and measurement of airborne particles --- Book
01 p0072 A83-10874
- Laser transit anemometer measurements with unseeded backscatter
01 p0051 A83-11057
- Aerosol characterization of a smoldering source
02 p0203 A83-11829
- The coincidence tracker - Electronic equipment for a time-of-flight wind-speed measurement system
02 p0177 A83-12009
- Normalized scattering diagram for atmospheric aerosols with Junge particle size distribution
02 p0206 A83-12304
- Correlation between surface and cloud base CCN spectra in Montana --- Cloud Condensation Nuclei
02 p0216 A83-12953
- Horizontal wind vector determination from the displacement of aerosol distribution patterns observed by a scanning lidar
02 p0216 A83-12959
- Aerosol minima --- in Arctic
03 p0357 A83-13546
- An optical-radar model of continental aerosols --- Russian book
03 p0358 A83-13821
- The effects of haze on resolution on small scale aerial photography
03 p0329 A83-14283
- Infrared spectrum of a single aerosol particle by photothermal modulation of structure resonances
03 p0356 A83-14379
- Marine sediment tolerances for remote sensing of atmospheric aerosols over water
03 p0373 A83-14380
- Comparison between albedo changes and lidar-measured aerosol changes for a set of aerosol events
03 p0370 A83-14641
- On short term variations of zenith polarization during twilight
03 p0361 A83-14645
- Rayleigh scattering measurements of the gas concentration field in turbulent jets
04 p0481 A83-15286
- Thermal self-defocusing of a CW CO2-laser beam during the interaction with water aerosol
04 p0484 A83-15734
- A simple method to compute the change in earth-atmosphere radiative balance due to a stratospheric aerosol layer
04 p0510 A83-15939
- Arctic haze and the Arctic gas and aerosol sampling program /AGASP/
[AIAA PAPER 83-0439] 05 p0659 A83-16714
- Physical and optical properties of dust particles
[AIAA PAPER 83-0549] 05 p0659 A83-16784
- Effects of aerosols on photosynthesis
05 p0659 A83-16850
- Self-excitation of surface oscillations of droplets in an electromagnetic wave field
05 p0649 A83-17063
- Twilight IR brightening over India due to El Chichon's eruption in Mexico
05 p0665 A83-17791
- Fine-dispersion aerosol and climate
06 p0788 A83-17998
- The effect of troposphere aerosol on the integral albedo of the system consisting of the atmosphere and the underlying surface
06 p0782 A83-17999
- Photophoretic force on particles for low Knudsen number
06 p0786 A83-18586
- Lidar measurements of natural and artificial aerosol during PUKK
06 p0787 A83-18997
- Satellite methods for detecting and investigating the aerosols in the earth's atmosphere
06 p0787 A83-19372
- Lidar observations of dust layers' transience in the stratosphere following the El Chichon volcanic eruption
07 p0958 A83-20090
- Spatial changes in the induced fluctuations of the intensity of radiation used to probe a bleachable aerodisperse medium
07 p0988 A83-20106
- Snow chemistry on James Ross Island /Antarctic Peninsula/
07 p0956 A83-20201
- Air-sea particle exchange at a nearshore oceanic site
07 p0956 A83-20204
- Balloon-borne observations of stratospheric aerosol and condensation nuclei during the year following the Mt. St. Helens eruption
07 p0959 A83-20205
- Particles and gases in the emissions from the 1980-1981 volcanic eruptions of Mt. St. Helens
07 p0959 A83-20206
- Volcanic aerosol phosphorus, chlorine, and sulfur at Kilauea, Hawaii
07 p0960 A83-20208
- Ice nucleus characteristics of Mount St. Helens effluents
07 p0969 A83-20210
- Lipids in aerosols from the tropical North Pacific - Temporal variability
07 p0960 A83-20214
- Study of the particulate sulfur-light scattering relationship using in situ aerosol thermal analysis
07 p0957 A83-20222
- Estimation of sulfate deposition
07 p0957 A83-20811
- The stratospheric aerosol and its effect on the earth's climate
07 p0970 A83-20887
- Results of a statistical analysis of the backscattering of light with model indicatixes --- remote sensing of atmospheric aerosols
07 p0963 A83-20896
- Numerical simulation of fog formation and liquid water content on polydisperse multi-composition aerosols due to combustion-related pollutants
07 p0963 A83-21038
- Enormous increase of stratospheric aerosols over Fukuoka due to volcanic eruption of El Chichon in 1982
07 p0967 A83-21557
- EOSAEL 82 - A library of battlefield obscuration models
08 p1093 A83-22352
- Effect of the aerosol on fog microstructure
08 p1140 A83-22355
- Extinction by clouds consisting of polydisperse and randomly oriented nonspherical particles at arbitrary wavelengths
08 p1135 A83-22356
- Atmospheric effects on electro-optical, infrared, and millimeter wave systems performance; Proceedings of the Meeting, San Diego, CA, August 27, 28, 1981
08 p1098 A83-22540
- Transmission effects of explosion-produced dust clouds on downward viewing airborne platforms
08 p1132 A83-22543
- Measurements of the phase function of natural particles
08 p1076 A83-22547
- Optical properties of model aerosols growing into fogs
08 p1135 A83-22551
- Aerosol modeling in the marine boundary layer
08 p1136 A83-22552
- Modified gamma aerosol model for the marine environment
08 p1136 A83-22553
- Satellite measurements of aerosols over oceans
08 p1136 A83-22554
- Impact of aerosol modeling on performance calculations of electro-optic /EO/ systems operating in marine environments
08 p1136 A83-22555
- NASA multipurpose airborne DIAL system and measurements of ozone and aerosol profiles--- Differential Absorption Lidar
08 p1101 A83-22615
- The effect of tropospheric aerosols on the earth's radiation budget - A parameterization for climate models
08 p1142 A83-23009
- Approximate determination of the statistical error in lidar measurements of wind velocity by accounting for the evolution of the aerosol non-uniformities
08 p1143 A83-23245
- New H2SO4 and HSO3 vapour measurements in the stratosphere - Evidence for a volcanic influence
08 p1138 A83-23264
- Global distribution of stratospheric aerosols by satellite measurements
09 p1306 A83-24675
- On the estimation of the concentration of aerosols in the upper layer of the Venus clouds
09 p1366 A83-25038
- Heterogeneous atmospheric chemistry --- Book
09 p1297 A83-25176
- Common problems in nucleation and growth, chemical kinetics, and catalysis --- in earth atmosphere
09 p1308 A83-25177
- Effect of the mechanism of gas-to-particle conversion on the evolution of aerosol size distributions
09 p1308 A83-25178
- Neutral and charged clusters in the atmosphere - Their importance and potential role in heterogeneous catalysis
09 p1297 A83-25179
- Structural studies of isolated small particles using molecular beam techniques --- atmospheric aerosols
09 p1308 A83-25181
- Chemical reactions with aerosols
09 p1297 A83-25182
- Photophoretic spectroscopy - A search for the composition of a single aerosol particle
09 p1297 A83-25183
- Electron beam studies of individual natural and anthropogenic microparticles - Compositions, structures, and surface reactions
09 p1297 A83-25184
- Reactions of gases on prototype aerosol particle surfaces
09 p1297 A83-25185
- Kinetics of reactions between free radicals and surfaces /aerosols/ applicable to atmospheric chemistry
09 p1297 A83-25187
- Observation of sulfate compounds on filter substrates by means of X-ray diffraction
09 p1297 A83-25190
- Theoretical limitations on heterogeneous catalysis by transition metals in aqueous atmospheric aerosols
09 p1298 A83-25196
- The relative importance of various urban sulfate aerosol production mechanisms - A theoretical comparison
09 p1298 A83-25199
- Sulfate in the atmospheric boundary layer - Concentration and mechanisms of formation
09 p1299 A83-25201
- Water vapor and temperature dependence of aerosol sulfur concentrations at Fort Wayne, Indiana, October 1977
09 p1299 A83-25202
- Evidence for aerosol chlorine reactivity during filter sampling
09 p1299 A83-25203
- The possible role of heterogeneous aerosol processes in the chemistry of CH4 and CO in the troposphere
09 p1299 A83-25204
- The First GARP Global Experiment, Volume 2 - Polar aerosols, extensive cloudiness, and radiation --- Russian book
09 p1316 A83-25226
- The optical properties of the atmosphere over the Arctic basin
09 p1316 A83-25230
- Atmospheric aerosols in the polar regions
09 p1316 A83-25231
- Aerosol measurements in the Arctic and in a volcanic region
09 p1309 A83-25232
- Cloud and aerosol effects in radiant heat transfer --- in planetary atmospheres
09 p1367 A83-25260

Inverse problems in the laser probing of atmospheric aerosols 09 p1309 A83-2561

Venus -Mesospheric hazes of ice, dust, and acid aerosols 10 p1518 A83-25507

Regularizing the solution of the laser sounding equation of atmospheric aerosols by means of a stabilizing functional 10 p1425 A83-25567

Shock tube measurements of IR radiation in hot gas/particle mixtures 10 p1416 A83-26189

Aerosol mode of ball lightning 10 p1451 A83-26465

Estimation regarding the feasibility of using larger distances in measurements with L2F systems in flight tests --- Laser-two-Focus 10 p1431 A83-26487

Effects of the El Chichon volcanic cloud in the stratosphere on the polarization of light from the sky 10 p1451 A83-26640

Propagation of laser radiation in water aerosol in conditions of the dispersal of this aerosol 10 p1434 A83-26778

Peculiarities of laser radiation and solid aerosol interaction 11 p1612 A83-27607

The usefulness of a bulk refractive index for the calculation of the scattering properties of mixtures of aerosol particles at wavelength 530 nm 11 p1615 A83-27973

Acidity of aerosol particles and of precipitation in the North Polar region and over the Atlantic 11 p1613 A83-28090

An analysis of the surface production of sea-salt aerosols 11 p1616 A83-28091

A comprehensive study of physical and chemical parameters of the Arctic summer aerosol; results from the Swedish expedition Ymer-80 11 p1613 A83-28092

Effect of meteorologic conditions on total suspended particulate /TSP/ levels and elemental concentration of aerosols in a semi-arid zone /Beer-Sheva, Israel/ 11 p1613 A83-28093

The removal of particulate matter from the atmosphere - The physical mechanisms 11 p1619 A83-28344

HCl in rocket exhaust clouds - Atmospheric dispersion, acid aerosol characteristics, and acid rain deposition 11 p1613 A83-28698

Stratospheric sulfuric acid fraction and mass estimate for the 1982 volcanic eruption of El Chichon 12 p1751 A83-28912

Optical properties of the ash from El Chichon volcano 12 p1751 A83-28913

Lidar observations of the El Chichon dust cloud at 23 deg S 12 p1751 A83-28914

Sulfuric acid vapour derivations from negative ion composition data between 25 and 34 km 12 p1751 A83-28916

Computations of Mie scattering applied to the observation of stratospheric aerosol 12 p1754 A83-29540

Space observations of aerosols and ozone; Proceedings of the Topical Meeting, Ottawa, Canada, May 16-June 2, 1982 12 p1754 A83-29557

The effect of aerosols on climate and aerosol climatology on the basis of observations from space 12 p1759 A83-29558

The role of aerosols in the climate system - Results of numerical experiments in climate models 12 p1759 A83-29559

Passive remote sensing of aerosols from space now and in the future 12 p1754 A83-29560

Most suitable conditions for aerosol monitoring from space 12 p1754 A83-29561

On the influence of rough water surfaces on polarimetric investigations of aerosols from space 12 p1730 A83-29562

Laser sounding of aerosols using airborne and space facilities 12 p1755 A83-29563

Spaceborne lidar measurement accuracy - Simulation of aerosol, cloud, molecular density, and temperature retrievals 12 p1755 A83-29564

Retrieval of aerosol characteristics from scattering and extinction measurements 12 p1755 A83-29565

Retrieval of aerosol optical characteristics from polarization measurements of reflected solar radiation above the oceans 12 p1755 A83-29566

Remote monitoring of aerosols from space 12 p1755 A83-29567

Investigation of the atmospheric aerosols by the visible and IR channels of the AVHRR radiometer on NOAA-6 12 p1755 A83-29568

Aerosol observations from Nimbus-7 CZCS along the South African West Coast --- Coastal Zone Color Scanner 12 p1755 A83-29569

Satellite measurements of tropospheric aerosols 12 p1755 A83-29570

Validation of aerosol measurements by the satellite sensors SAM II and Sage 12 p1755 A83-29572

Retrieval of aerosol size distribution from extinction measurements and verification with observations at a tropical station 12 p1755 A83-29573

Can turbidity measurements be used for the estimation of aerosol parameters? 12 p1755 A83-29574

Rocket studies of atmospheric scattering and the aerosol size distribution in the troposphere and lower stratosphere over Thumba 12 p1756 A83-29575

Determination of aerosol optical depth from ground measurements 12 p1730 A83-29576

The characterization of atmospheric spread functions affecting satellite remote sensing of the earth's surface 12 p1748 A83-29578

A method for estimating cross radiance 12 p1748 A83-29579

Climatic influence of background and volcanic stratosphere aerosol models 12 p1756 A83-29580

Radiation-aerosols interaction - Applications to remote sensing and for calculation of the radiative balance --- French thesis 12 p1756 A83-29949

A kinetic model for a fine anhydrous aerosol in the troposphere 13 p1873 A83-30027

Diffusion mechanism of the interaction of aerosol drops and the possibility of controlling this mechanism by means of electromagnetic radiation 13 p1874 A83-30043

Monitoring aerosol elemental composition in particle size fractions of long-range transport 13 p1874 A83-30180

PIXE analysis of aerosol in the workplace 13 p1872 A83-30181

Theory of thermophoresis of moderately large aerosol particles 13 p1933 A83-30820

Unusual behavior in the condensation nuclei concentration at 30 km 13 p1877 A83-30885

A decade of stratospheric sulfate measurements compared with observations of volcanic eruptions 13 p1877 A83-30887

Lidar- and balloon-borne particle counter comparisons following recent volcanic eruptions 13 p1877 A83-30888

Measurement of stratospheric aerosol near Sanriku (39 deg N, 142 deg E) in Japan on May 31, 1979 13 p1877 A83-30889

An aerosol and gas sampling apparatus for remote observatory use 13 p1847 A83-30905

Effects of CCN concentrations on stratus clouds 13 p1893 A83-31044

They dance in the air --- properties of atmospheric aerosols 13 p1880 A83-31317

Optical transmission through aerosol deposits on diffusely reflective filters - A method for measuring the absorbing component of aerosol particles 13 p1880 A83-31454

Application of the 2-D discrete-ordinates method to multiple scattering of laser radiation 13 p1857 A83-31460

Aerosol effects on regional radiative balance 13 p1880 A83-31505

Gross mechanisms of smoke aerosol production from solids, liquids and gases 13 p1818 A83-31521

A simple hourly clear-sky solar radiation model based on meteorological parameters 13 p1894 A83-31611

The effect of the stratospheric aerosol layer on the total radiation 14 p2051 A83-32372

Relation between observed aerosol optical thicknesses and calculated values from size distribution measurements 14 p2057 A83-32439

Simultaneous determination of complex refractive index and size distribution of airborne and water-suspended particles from light scattering measurements 14 p2052 A83-32440

Measurements of infrared optical properties of Al₂O₃ rocket particles 14 p1985 A83-32780

[AIAA PAPER 83-1568] Aerosol formation in a mixing layer --- for flow visualization 15 p2163 A83-33660

Inverse problems of lidar sensing of the atmosphere --- Book 15 p2195 A83-33768

Soot carbon and excess fine potassium - Long-range transport of combustion-derived aerosols 15 p2193 A83-34003

Atmospheric trace element concentrations in Jerusalem, Israel 15 p2194 A83-34045

The measurement of the humidity spectrum and of the concentration of the cloud condensation nuclei 15 p2164 A83-34055

A model experiment concerning particle scavenging by cloud and rain drops 15 p2205 A83-34058

The influence of aerosol and meteorological parameters on maximum supersaturation and activation of particles in a cloud 15 p2205 A83-34059

The influence of atmospheric aerosol on the life cycle radiation fog 15 p2205 A83-34066

Retrieval of stratospheric aerosol size distribution from atmospheric extinction of solar radiation at two wavelengths 15 p2201 A83-34459

Photography and photographic-photometry of the solar aureole 15 p2281 A83-34460

Modelling atmospheric aerosol backscatter at CO₂ laser wavelengths. I - Aerosol properties, modeling techniques, and associated problems. II - Modeled values in the atmosphere. III - Effects of changes in wavelength and ambient conditions 15 p2201 A83-34461

The distribution of the disperse fraction of a polydisperse jet injected into a gas flow 15 p2161 A83-34472

Elements of the theory of light scattering and optical radar --- Russian book 15 p2170 A83-34573

Increasing backscattered light from the stratospheric aerosol layer after Mt. El Chichon eruption - Laser radar measurement at Nagoya (35 deg N, 137 deg E) 15 p2202 A83-34728

Aerosol concentrations and size distribution in the troposphere and lower stratosphere over Thumba 15 p2202 A83-34745

Polarization properties of the surface and atmosphere of Mars 15 p2276 A83-34769

Nonintrusive laser-based particle diagnostics [AIAA PAPER 83-1514] 15 p2165 A83-34919

On the definition of collision efficiency of atmospheric particles 16 p2387 A83-35495

Strong and weak acidity of aerosols collected over the northeastern United States 16 p2372 A83-35765

Water and acid soluble trace metals in atmospheric particles 16 p2379 A83-36126

Droplet phase (heterogeneous) and gas phase (homogeneous) contributions to secondary ambient aerosol formation as functions of relative humidity 16 p2379 A83-36127

The 1980 eruptions of Mount St. Helens - Physical and chemical processes in the stratospheric clouds 16 p2380 A83-36146

Atmospheric trace elements at Enewetak Atoll. I Concentrations, sources, and temporal variability 16 p2380 A83-36147

Transport of mineral aerosol from Asia over the North Pacific Ocean 16 p2380 A83-36148

Characterization of the atmospheric aerosol over the eastern equatorial Pacific 16 p2380 A83-36149

Radiometric levitation of spherical carbon aerosol particles using a Nd:YAG laser 16 p2413 A83-36761

Modeling the effect of temperature changes in the stratosphere on the growth of drops of a sulfate aerosol 16 p2382 A83-36870

A numerical investigation of the transport of coagulating aerosols in the atmosphere of a city 16 p2372 A83-36875

Determination of the charging current of a plate in an aerosol flow when a liquid film is separated from its surface 17 p2503 A83-37266

Circumglobal transport of the El Chichon volcanic dust cloud 17 p2540 A83-37773

Design and performance of the Stratospheric Aerosol and Gas Experiment II (SAGE II) instrument 17 p2511 A83-38056

Saturn's equatorial haze 17 p2620 A83-38113

Remote sensing of atmospheric gases and particulates by lidar 17 p2515 A83-38363

Measured aerosol size distributions and calculated EM extinction in air masses moving off the east coast 17 p2550 A83-38730

Model of marine aerosol generation via whitecaps and wave disruption 17 p2554 A83-38731

A field study to relate marine aerosol particles with satellite detected radiance 17 p2550 A83-38732

On the accuracy of IR extinction predictions made by the Navy Aerosol Model 17 p2546 A83-38740

Intercomparison of PMS particle size spectrometers --- Particle Measuring Systems, Inc. 17 p2546 A83-38741

Aerosols in the clouds on Venus - Preliminary Venera 14 data 17 p2623 A83-38836

Number, mass and volume distributions of mineral aerosol and soils of the Sahara 18 p2711 A83-39121

Modeling the effect of stratospheric aerosols on climate 18 p2723 A83-39437

Mt. St. Helens' aerosols - Some tropospheric and stratospheric effects 18 p2716 A83-39686

On the aerosol particle size distribution spectrum in Alaskan air mass systems - Arctic haze and non-haze episodes 18 p2729 A83-40043

Organic films on atmospheric aerosol particles, fog droplets, cloud droplets, raindrops, and snowflakes 18 p2719 A83-40329

Molecular state of sulfate aerosols in the remote Everest highlands 18 p2711 A83-40647

The mechanism of sulfate aerosol formation - Chemical and sulfur isotopic evidence 19 p2862 A83-41111

Tropospheric oxalate 19 p2862 A83-41112

The possibility of the formation of aerosol in the chemical reaction between SO₂ and NH₃ in conditions of the Venus atmosphere 19 p2923 A83-41240

A laser method for investigating aerosol systems
19 p2854 A83-41588

Mathematical modeling of the formation and transport of ammonium nitrate aerosol
19 p2863 A83-41970

The atmospheric aerosol system - An overview
20 p3015 A83-42176

Laser radar observations in mid-Wales of aerosols from the el Chichon eruption
20 p3017 A83-42332

Production rate of airborne sea-salt sulfur deduced from chemical analysis of marine aerosols and precipitation
20 p3021 A83-42853

Relationships between Pb and Pb-210 in aerosol and precipitation at a semiremote site in northern Wisconsin
20 p3014 A83-42854

The function and response of an improved stratospheric condensation nucleus counter
20 p2990 A83-42858

The effect of an acoustic wave on the aerosol capture efficiency of a granular bed
20 p3014 A83-42977

Physico-chemical mechanisms for generation of aerosols with a high temperature aerosol - An example of volcanic aerosols
20 p3014 A83-42978

Correlations between meteorological data and water-soluble sulphur compounds in fine aerosols
20 p3014 A83-43424

Kinetics of SO₂ oxidation over carbonaceous particles in the presence of H₂O, NO₂, NH₃ and O₃
20 p3014 A83-43425

Comparison of calculated and observed super- and sub-micrometer aerosol mass concentrations using St. Louis RAPS data base --- Regional Air Pollution Study
20 p3014 A83-43426

Case studies of aerosol size distribution and chemistry during passages of a cold and a warm front
20 p3014 A83-43427

Atmospheric pollution studies at Kanpur-suspended particulate matter
20 p3015 A83-43428

Modeling of multiphase atmospheric aerosols
20 p3015 A83-43429

Determination of ambient aerosol and gaseous sulfur using a continuous FPD. III - Design and characterization of a monitor for airborne applications --- flame photometric detector
20 p2991 A83-43434

Particle size distribution of n-alkanes nA Pb-210 in aerosols off the coast of Peru
20 p3028 A83-43556

Combined sounding of the atmosphere by aerosol and Raman lidars
20 p2992 A83-43791

Chemical laser amplifier using a photon-branched reaction in an aerosol medium
20 p2998 A83-43808

Elemental carbon in the atmosphere - Cycle and lifetime
21 p3171 A83-44376

SO₂ and SO₄(2-) in the arctic - Interpretation of observations at three Norwegian arctic-subarctic stations
21 p3171 A83-44377

The possibility of the visual monitoring of the state of the ozonosphere from an orbital station
21 p3177 A83-45396

Infrared absorption by natural organic aerosol
22 p3321 A83-45635

Electrooptical investigations of the effect of the humidification processes of various types of aerosols on the dipole characteristics of the particles
22 p3321 A83-45636

The dependence of the Q-ranch profile of the Raman spectrum of water vapor on temperature
22 p3322 A83-45638

The effect of modulated electromagnetic radiation on the temperature regime of a monodisperse aerosol medium
22 p3322 A83-45642

Optical emission from photoexcitation of aerosol particles produced by reaction of ozone with 1,3-butadiene
22 p3328 A83-46065

Mauna Loa sky conditions - Bench mark and present
22 p3374 A83-46408

The coefficient of haze as a measure of particulate elemental carbon
22 p3321 A83-46775

On the form of stationary size distributions established by coagulation and sedimentation --- for atmospheric particles
22 p3341 A83-46859

Stratospheric aerosol mass and latitudinal distribution of the El Chichon eruption cloud for October 1982
22 p3333 A83-46883

Refractive index and size distribution of aerosols as estimated from light scattering measurements
22 p3334 A83-46947

Spatial and temporal variations of tropospheric aerosol volume distributions
22 p3334 A83-46948

Characteristics of the restoration of the microstructure of an atmospheric aerosol from multiple-frequency sounding data
23 p3480 A83-47167

The High Spectral Resolution Lidar
23 p3458 A83-47803

Wide-area air pollution measurement by the NIES large lidar
23 p3458 A83-47809

Spatial changes in the stratospheric aerosol associated with the north polar vortex
23 p3482 A83-47858

Variability of the size distributions of aerosol particles near the earth's surface
23 p3485 A83-48558

The spatial and temporal variability of absorption coefficients of the tropospheric aerosol in the spectral region of 0.4-2.2 microns
23 p3492 A83-48561

The dynamic range of a resonance spectrophone
23 p3459 A83-48562

Aerosol composition at Chacaltaya, Bolivia, as determined by size-fractionated sampling
23 p3486 A83-48666

Electron microscopy of acidic aerosols collected over the northeastern United States
23 p3479 A83-48687

Elemental composition of aerosols collected with airborne cascade impactors
23 p3479 A83-48688

Apportioning light extinction coefficients to chemical species in atmospheric aerosol
23 p3479 A83-48689

Theory of thermophoresis of nonvolatile liquid aerosol particles
24 p3575 A83-48861

Retrieval of the optical properties of aerosols from aureole and extinction data
24 p3604 A83-49002

Aerosol backscattering of a laser beam
24 p3588 A83-49004

Forward multiple scattering corrections as a function of detector field of view --- laser beam propagation through atmospheric aerosols
24 p3588 A83-49005

Background variability of the aerosol and ion composition of the atmospheric surface layer
24 p3604 A83-49109

Electromagnetic wave damping in a nonequilibrium aerosol plasma
24 p3632 A83-49115

Certain characteristics of the radiation balance in the cloudless atmosphere and at the ocean surface depending on the dustiness of the atmosphere
24 p3605 A83-49281

Electrification of metallic bodies in aerosol flows in the case of the fragmentation of solid disperse particles during collisions with the body
24 p3624 A83-49532

The effect of solution concentrations in sulfate aerosols
24 p3602 A83-49688

Aerosol spectra observed in maritime stratus cloud layers
24 p3611 A83-49689

Contact ice nucleation by submicron atmospheric aerosols
24 p3612 A83-49692

In-situ, rapid response measurement of H₂SO₄/(NH₄)₂SO₄ aerosols in urban Houston - A comparison with rural Virginia
24 p3603 A83-50193

Size-differentiated composition of inorganic atmospheric aerosols of both marine and polluted continental origin
24 p3603 A83-50194

AEROSPACE ENGINEERING

NT AERONAUTICAL ENGINEERING

The centenary of Robert Hutchings Goddard, 1882-1982
02 p0276 A83-12646

Polysulfide sealants for aerospace. I - Theory and background
03 p0302 A83-13562

Survey of engineering computational methods and experimental programs for estimating supersonic missile aerodynamic characteristics
03 p0278 A83-14124

The agency's approach to normalisation and standards --- for ESA space technology
05 p0621 A83-17435

Moisture resistance of conformal coatings
09 p1237 A83-23620

Celion/Larc-160 graphite/polyimide composite processing techniques and properties
09 p1222 A83-23635

Analysis, design, and test of a graphite/polyimide Shuttle orbiter body flap segment
09 p1216 A83-23637

Implementation of operational aspects in the European Spacelab system engineering
10 p1381 A83-26596

1982 advances in aerospace structures and materials; Proceedings of the Winter Annual Meeting, Phoenix, AZ, November 14-19, 1982
11 p1591 A83-27426

Superplastic forming and diffusion bonding
11 p1589 A83-28176

Integrating computer programs for engineering analysis and design
11 p1647 A83-28350

[AIAA PAPER 83-0597]

Getting the picture through computer graphics
11 p1525 A83-28691

Tethers open new space options
11 p1534 A83-28692

National Aerospace Meeting, Moffett Field, CA, March 24, 25, 1982, Proceedings
11 p1528 A83-28776

On the dynamic response and collapse of slender guyed booms for space application
12 p1742 A83-29818

[AIAA 83-0821]

Fundamentals of flight --- Book
13 p1803 A83-30152

The technical 'productivity gap'
13 p1933 A83-30831

The challenge of the 80's: Some environment-sensitive technologies - Status and problems
13 p1827 A83-31477

Survey of usage of technical report components to establish their most effective organization
15 p2239 A83-34800

Buckling of continuous filament composite isogrid panels
18 p2704 A83-40183

Theory and experiment
18 p2704 A83-40183

Development of advanced composite fabrication for aerospace structures
18 p2661 A83-40278

From outer space to the great ocean's depths - An adventure in high performance composite materials
18 p2661 A83-40288

Synthesis of insensitive regulators with comparative evaluations in aerospace applications
19 p2891 A83-41704

[AIAA PAPER 83-2224]

Annual Mini-Symposium on Aerospace Science and Technology, 9th, USAF, Institute of Technology, Wright-Patterson AFB, OH, March 22, 1983, Proceedings
20 p2927 A83-42526

Problems of mechanics and heat transfer in space technology
20 p2939 A83-42876

Methodological problems in the development of space systems for the remote sensing of earth resources
20 p3010 A83-42889

Metrication of aerospace engineering computer programs
20 p3037 A83-43745

[SAWE PAPER 1475]

Automatix incorporated in aerospace applications
21 p3119 A83-44862

[SME PAPER MS83-230]

Spot peening for advanced aerospace design; Proceedings of the Aerospace Congress and Exposition, Anaheim, CA, October 25-28, 1982
22 p3302 A83-45872

Optical data processing for aerospace applications
23 p3500 A83-47657

Aeronautics - A coop aerospace education program at University of Sherbrooke, Canada
23 p3513 A83-48340

[AIAA PAPER 83-2474]

Formulation of a helicopter preliminary design course
23 p3404 A83-48363

[AIAA PAPER 83-2521]

Methods for teaching aerospace vehicle design
24 p3637 A83-49582

AIAA PAPER 83-2475]

AEROSPACE ENVIRONMENTS

NT CISLUNAR SPACE

NT DEEP SPACE

NT INTERPLANETARY SPACE

NT INTERSTELLAR SPACE

Space: Mankind's fourth environment; Proceedings of the Thirty-second International Astronautical Congress, Rome, Italy, September 6-12, 1981
01 p0016 A83-11330

The Space Shuttle's uncertain environment
03 p0284 A83-13174

Space environmental effects on materials
03 p0291 A83-14125

Oxygen atom reaction with Shuttle materials at orbital altitudes - Data and experiment status
05 p0617 A83-16503

[AIAA PAPER 83-0073]

Development of a new integral solar cell protective cover
05 p0657 A83-16506

[AIAA PAPER 83-0076]

Gallium arsenide ICs in space and nuclear radiation environments
05 p0623 A83-16565

[AIAA PAPER 83-0165]

Plasma diagnostics package assessment of the STS-3 orbiter environment and systems for science
05 p0604 A83-16612

[AIAA PAPER 83-0253]

Calculation of cosmic-ray induced soft upsets and scaling in VLSI devices
05 p0629 A83-17541

Fiber optics in adverse environments; Proceedings of the Seminar, San Diego, CA, August 25-27, 1981
08 p1164 A83-22475

Spatial disorientation in the naval aviation environment
08 p1149 A83-22979

ZOT - A white thermal control coating for space environment: Considerations --- Zinc-Ortho Titanate
09 p1236 A83-23607

Space applications of gallium arsenide solar cells
11 p1541 A83-27258

Recent topics in physics of hot plasmas in space environment
11 p1680 A83-28247

Materials in space - Working in a vacuum
12 p1705 A83-29552

The application of free-electron lasers to the transmission of energy in space
13 p1856 A83-31141

Space environmental effects on graphite/epoxy composites
14 p1987 A83-33121

The cohesive and adhesive strength of ice --- adhering to stainless steel, titanium, and anodized aluminum engineering structures
15 p2130 A83-35069

The effect of open-space exposure on the physicochemical properties of a carbon composite
16 p2323 A83-35504

Development of environmental criteria guidelines for aerospace vehicle design
17 p2546 A83-38754

Bringing AI up to the space challenge
18 p2737 A83-40306

- Life sciences and Space Research XX(1); Proceedings of the Workshops and Topical Meeting, Ottawa, Canada, May 16-June 2, 1982 19 p2871 A83-40826
- Effect of HZE particles and space hadrons on bacteriophages 19 p2871 A83-40834
- Unique biological aspects of radiation hazards - An overview 19 p2873 A83-40847
- Determining the concentration of two dominant types of ions with the aid of a cylindrical Langmuir probe --- in aerospace environments 19 p2817 A83-41593
- Improved active phase separator for He II space cooling systems 20 p2962 A83-43246
- Materials processing in the reduced gravity environment of space; Proceedings of the Annual Meeting, Boston, MA, November 16-18, 1981 20 p2939 A83-43251
- Hexanitrostilbene and its properties 21 p3117 A83-44074
- Canadarm and the Space Shuttle 21 p3096 A83-44602
- Materials processing in the reduced-gravity environment of space 22 p3257 A83-45895
- Study of satellite situations mission 24 p3551 A83-49624

AEROSPACE INDUSTRY

- NT AIRCRAFT INDUSTRY
- Economic and industrial aspects of the conquest of space 01 p0111 A83-10438
- Application of simulation and zero-one programming for analysis of numerically controlled machining operations in the aerospace industry 07 p0902 A83-19648
- Advances in laser and MIAB welding techniques 07 p0940 A83-20523
- The development of standards for the common ICAO Data Interchange Network /CIDIN/ 08 p1075 A83-22027
- Techniques for assessing product reliability in polymeric materials used in aerospace electronic circuitry 09 p1236 A83-23604
- The effect of fluoride contamination on the durability of PAA surfaces --- preparation of aluminum alloy surfaces for adhesive bonding by phosphoric acid anodize solution 09 p1230 A83-23625
- How to reduce the drilling cost for the aerospace industry 09 p1273 A83-23638
- Cost engineering --- programs in aerospace industry 11 p1666 A83-28181
- Cost factors and approach methodology in selecting structural materials and manufacturing technologies [AIAA 83-0791] 12 p1783 A83-29730
- Titanium powder metallurgy components for advanced aerospace applications [AIAA 83-0982] 12 p1715 A83-29789
- Changing the course of U.S. aviation 13 p1803 A83-30830
- High-technology factory of the future 13 p1827 A83-31052
- Aluminum-lithium alloys 14 p1995 A83-32876
- Al-Li-X alloys - An overview 14 p1995 A83-32880
- Recent advancements in titanium near-net-shape technology 15 p2171 A83-33633
- Vacuum hot pressing of large near net shape spar fittings 15 p2171 A83-33635
- Effect of heat-treatment on the fatigue behavior 15 p2135 A83-33636
- Aspects of metallography and manufacturing technology regarding the superplastic forming of TiAl6V4 15 p2136 A83-33961
- Improved methods for characterizing material-induced contamination --- of spacecraft [AIAA PAPER 83-1496] 15 p2130 A83-34918
- Commercial Titan ELV - Filling a need in the national Space Transportation System [AIAA PAPER 83-1193] 16 p2315 A83-36269
- The Space Transportation Company Inc. [SAE PAPER 821368] 17 p2586 A83-37961
- Air industry cooperation 18 p2631 A83-39692
- Manufacturer's liability in international aerospace - A view from the United States 18 p2753 A83-39696
- Implications of international space law for private enterprise 22 p3368 A83-45813
- Brush plating in aerospace applications [SAE PAPER 820612] 22 p3302 A83-45870
- Economics of telecommunications space segments [IAF PAPER 83-234] 23 p3514 A83-47317
- The reaction motors division - Thiokol Chemical Corporation --- management history of aerospace rocket engine products [IAF PAPER 83-289] 23 p3415 A83-47330

AEROSPACE MEDICINE

- Major medical results of the Salyut-6 - Soyuz 185-day space flight 01 p0084 A83-11281
- Metabolism during hypodynamia --- Russian book 02 p0221 A83-11950
- Agricultural aviation in India - A perspective with accent on aero-medical problems 02 p0223 A83-12258

- The effect of adeturon on the survival and the blood system of mice under the effect of various types of ionizing radiation 03 p0376 A83-14880
- Prevalence of selected pathology among currently certified active airmen 04 p0521 A83-15535
- Medical fitness examination of commercial pilots - New criteria for evaluation of vestibular tests 04 p0522 A83-15539
- Prediction of threshold pain skin temperature from thermal properties of materials in contact 04 p0522 A83-15540
- Flight simulation - Avionic systems and aero medical aspects; Proceedings of the International Conference, London, England, April 6, 7, 1982 04 p0441 A83-16326
- Pilots are treated and rest here 05 p0673 A83-17178
- Clinical aviation medicine --- Book 05 p0674 A83-17300
- Psychotherapies and chemotherapies in aeronautic psychopathology - Indications, contraindications, and occurrences involving capacity 06 p0797 A83-18331
- Numerical and psychopathological data bearing upon 700 certifications of civil aviation flight personnel 06 p0799 A83-18333
- Pilot deafness - Statistical study of military pilot hearing 06 p0797 A83-18336
- The problem of presbyopia in pilots and its correction with eyeglasses 06 p0798 A83-18338
- The lipid balance of technical flight personnel between 50 and 55 years old in commercial and civil aviation 06 p0798 A83-18340
- Pleurodesis - The results of treatment for spontaneous pneumothorax in the Royal Air Force 07 p0978 A83-20786
- Sudden incapacitation - USAF experience, 1970-80 07 p0978 A83-20787
- International Congress on Aerospace Medicine, 29th, Nancy, France, September 7-11, 1981, Scientific Reports 08 p1147 A83-22951
- What is to be thought of induced hyperglycemia in aviation medicine in 1981 08 p1147 A83-22952
- Blood eosinophilia in aviators 08 p1147 A83-22954
- A study of the psychophysiological behavior in a group of airline pilots after the operational age limit /60 years/ 08 p1150 A83-22955
- A presentation of a new protocol for the evaluation of color sense in aeronautics 08 p1147 A83-22956
- The pressure problems of the middle ear in flight personnel - The importance of impedance metric examinations 08 p1147 A83-22958
- Extrastyles and the fitness of flight personnel - The contribution of the stress EKG tests 08 p1147 A83-22961
- Disease risk factors and the flight surgeon - A strategy to keep pilots flying 08 p1147 A83-22963
- Cardiac localizations of sarcoidosis - The importance of the continuous electrocardiogram 08 p1148 A83-22964
- The detection of drug addiction among flight personnel 08 p1148 A83-22965
- An experimental study of the encephalic hemodynamic variations connected with flight and position with respect to the flight axes on Alouette III in a healthy subject 08 p1148 A83-22966
- The nutritional and microbiological aspects of the onboard meal for pilots of international airlines 08 p1148 A83-22967
- A study of the physiological behavior in a real-world situation of 70 front line air traffic controllers with regard to the neurovegetative, neuromuscular, and ophthalmologic modifications, and alertness 08 p1148 A83-22968
- Remarks on the systematic tonal audiometry of the ground personnel in charge of airspace security 08 p1148 A83-22972
- Spinal traumas /dorsal spinal fractures and lumbar disk hernias/ occurring after rapid vibratory phenomena /pumping/ in air combat pilots 08 p1148 A83-22973
- Electroretinography in space 08 p1149 A83-22985
- Verification trials for a primate physiological experimentation model intended for Spacelab 08 p1146 A83-22986
- Multiple hormonal changes during water immersion - An analog of weightlessness 08 p1149 A83-22988
- The organization of medical facilities for flight safety 09 p1322 A83-23975
- Positive G tolerance of Indian subjects - Effects of age and flying experience 09 p1323 A83-24004
- Decompression sickness - USAF experience 1970-80 10 p1455 A83-25674
- Changes in the loco-regional cerebral blood flow /r.C.B.F./ during a simulation of weightlessness 11 p1641 A83-27349

Comparison of cardiovascular effects of space flight and its analogs using computer simulations 11 p1642 A83-27792

- Space Motion Sickness - Phenomenology, countermeasures, and mechanisms 12 p1763 A83-28927
- Correction of changes in fluid-electrolyte metabolism in manned space flights 12 p1763 A83-28928
- Problems in aerospace medicine posed by mitral valve prolapse 14 p2067 A83-32451
- The pathology of crisis and medical transport of mental patients in acute conditions 14 p2067 A83-32453
- Medical problems peculiar to airline pilots 14 p2067 A83-32461
- Maxillary intrasinus benign expansive processes that inflate and/or destroy the sinus bony walls (five case studies) interest in their knowledge for aeronautical medicine 14 p2067 A83-32462
- Aviation medicine training for aircrew in the 1980's 14 p2067 A83-32463
- Education in aerospace medicine at the German Air Force Institute of Aviation Medicine 14 p2063 A83-32464
- The influence of waterproofing failure on the thermal insulation of sealed flightsuits used in military aviation 14 p2072 A83-32467
- Physiological and behavioral effects of tilt-induced body fluid shifts 14 p2068 A83-32685
- Automatic activity and workload during learning of a simulated aircraft carrier landing task 14 p2071 A83-32690
- A model for prediction of resynchronization after time-zone flights 15 p2214 A83-34983
- Development of an occupational health data base system 15 p2239 A83-34990
- The problems of health protection in polar expeditions and their importance for space flights 15 p2214 A83-35049
- Color vision and vision at low light levels 16 p2396 A83-35577
- Procedures for the examination of the visual acuity and of the visual field in civil aeronautics 16 p2396 A83-35578
- Vertebral lesions after the aircraft crashes 16 p2396 A83-35579
- Vertebral lesions after pilot ejection from fighter aircraft 16 p2397 A83-35580
- The spine of the parachutist 16 p2397 A83-35581
- The spine and the helicopter 16 p2397 A83-35582
- The pilot seat and the vertebral column 16 p2397 A83-35583
- Problems of fitness posed by vertebral pathology in flight personnel 16 p2397 A83-35584
- Practical aspects of the medical check-up of nonprofessional pilots 16 p2397 A83-35585
- Barotraumatism and a Killian polyp in a parachutist 16 p2397 A83-35587
- Vital questions of the psychophysiological training of pilots 17 p2561 A83-38203
- The behavior of heart rate in flight under +Gz stimulation 17 p2561 A83-38203
- Continuous monitoring using Holter's method and catecholamine excretion 17 p2561 A83-38944
- Etiological aspects of indispositions in flight 17 p2561 A83-38945
- The Air Canada programme for rehabilitation of the alcoholic employee/pilot 18 p2734 A83-40352
- Return to flying after head injuries - A review 18 p2734 A83-40355
- Methazolamide and acetazolamide in acute mountain sickness 18 p2734 A83-40357
- The characteristics of aerospace medical expertise for diseases of the eye 19 p2884 A83-42024
- Space Station and the life sciences [AIAA PAPER 83-7089] 19 p2884 A83-42078
- Smoke/fumes in the cockpit 21 p3187 A83-43997
- Effects of spaceflight on trabecular bone in rats 21 p3183 A83-44863
- Bone resorption and mineral excretion in rats during spaceflight 21 p3184 A83-44866
- Age-specific morbidity among Navy-pilots 24 p3618 A83-48880
- Psychiatric assessment of female fliers at the U.S. Air Force School of Aerospace Medicine (USAFSAM) 24 p3618 A83-48883
- Personality profiles of pilots 24 p3618 A83-48884

AEROSPACE SAFETY

- Land development, tall buildings and airport operations [AIAA PAPER 83-1581] 14 p1978 A83-33353
- Space safety and rescue 1979-1981: Worldwide disaster response, rescue and safety employing space-borne systems 19 p2807 A83-40761
- Orbital debris management - International cooperation for the control of a growing safety hazard [IAF PAPER 83-254] 23 p3415 A83-47324

Safety of space activities
[IAF PAPER 83-255] 23 p3515 A83-47325

AEROSPACE SCIENCES

Twenty-five years which have prepared the future in space 01 p0016 A83-10426

Space: Mankind's fourth environment; Proceedings of the Thirty-second International Astronautical Congress, Rome, Italy, September 6-12, 1981 01 p0016 A83-11330

Aerospace highlights 1982 04 p0576 A83-16375

Global implications of space activities; Proceedings of the Conference, Aspen, CO, August 30-September 4, 1981 05 p0710 A83-17349

UNISPACE 82 and beyond 07 p1002 A83-21390

The Second United Nations conference on the exploration and peaceful uses of outer-space / UNISPACE 82/ 07 p1002 A83-21391

NGOs at UNISPACE 82 --- nongovernmental organizations 07 p1002 A83-21392

Report of the second United Nations conference on the exploration and peaceful uses of outer space 07 p1002 A83-21394

Certain aspects of the development of space scientific instrumentation 10 p1386 A83-25327

Space stations of the imagination 13 p1808 A83-31050

Survey of usage of technical report components to establish their most effective organization 15 p2239 A83-34800

Role and impact of space research in developing countries; Proceedings of the Workshop, Ottawa, Canada, May 16-June 2, 1982 18 p2787 A83-39825

Transfer of space science and technology - A Third World point of view 18 p2751 A83-39826

Space sciences in developing countries - The Indian experience 18 p2787 A83-39829

Status of space science and technology - An Australian perspective 18 p2787 A83-39832

Basic space sciences - The Latin American experience 18 p2787 A83-39833

Basic space sciences in Africa 18 p2788 A83-39835

Impact of space research and technology on small countries 18 p2788 A83-39836

Experiences of the GDR in space sciences and technology 18 p2788 A83-39837

Annual Mini-Symposium on Aerospace Science and Technology, 9th, USAF, Institute of Technology, Wright-Patterson AFB, OH, March 22, 1983, Proceedings 20 p2927 A83-42526

The world in space: A survey of space activities and issues --- Book 21 p3093 A83-45091

Space technology - Apollo: The driver and the driven 21 p3221 A83-45601

Space technology -- Computers: Learning from dinosaurs 21 p3191 A83-45602

A cooperative educational program in aerospace science and technology for the high school and middle school - Model for international implementation [IAF PAPER 83-439] 23 p3513 A83-47381

Soviet space science 23 p3416 A83-48628

AEROSPACE SYSTEMS

The Avdel MBC aerospace blind riveting system 01 p0056 A83-10870

Vibration of a two layered ring on periodic radial supports 01 p0061 A83-11041

ICIASF '81; International Congress on Instrumentation in Aerospace Simulation Facilities, Dayton, OH, September 30, 1981, Record 01 p0051 A83-11051

NAECON 1982; Proceedings of the National Aerospace and Electronics Conference, Dayton, OH, May 18-20, 1982, Volumes 1, 2 & 3 01 p0001 A83-11083

A high speed 10MHz multiplex data bus interface 01 p0042 A83-11152

Aerodynamic heating and surface temperatures on vehicles for computer-aided design studies [AIAA PAPER 83-0411] 05 p0585 A83-16699

The agency's approach to normalisation and standards --- for ESA space technology 05 p0621 A83-17435

The reliability of aviation systems --- Russian book 10 p1436 A83-25621

Recent advances in interpretation of corona test results 11 p1602 A83-27154

Applications of dynamic impedance measurements to aerospace battery cells 11 p1605 A83-27197

Development of improved hydrogen recombination in sealed nickel-cadmium aerospace cells 11 p1540 A83-27198

The NASA program in Space Energy Conversion Research and Technology 11 p1610 A83-27326

Time domain response envelope for structural dynamic systems [AIAA 83-0818] 12 p1707 A83-29817

Aerospace Testing Seminar, 6th, Los Angeles, CA, March 11-13, 1981, Proceedings 13 p1809 A83-31176

Personnel training for precision cleaning of aerospace hardware to military standard 1246 A levels 13 p1865 A83-31519

Digital control system design for a precision pointing system [AAS PAPER 83-003] 21 p3103 A83-44163

Optical data processing for aerospace applications 23 p3500 A83-47657

Flight-control designer becomes metallurgician 24 p3619 A83-48892

AEROSPACE TECHNOLOGY TRANSFER

Economic and industrial aspects of the conquest of space 01 p0111 A83-10438

Domestic satellite communications systems - Background and projections 04 p0466 A83-15664

Global implications of space activities; Proceedings of the Conference, Aspen, CO, August 30-September 4, 1981 05 p0710 A83-17349

Face to face for industry on NASA high technology 07 p1003 A83-20649

Technology transfer - A case history of success 07 p1003 A83-20650

New technologies from developments in air transport and space travel 09 p1369 A83-24188

[DGLR PAPER 82-074] 09 p1369 A83-24188

Assessing the user environment for Landsat in developing countries 15 p2187 A83-35277

Technology and engine demonstrator programs [AIAA PAPER 83-1064] 16 p2310 A83-36464

New technologies from aerospace development 18 p2631 A83-39343

Role and impact of space research in developing countries; Proceedings of the Workshop, Ottawa, Canada, May 16-June 2, 1982 18 p2787 A83-39825

Transfer of space science and technology - A Third World point of view 18 p2751 A83-39826

A critical look at space technology and the developing world 18 p2752 A83-39827

The evolution of space technology and its economic impact Reflection on the transposition of the European model in the countries of the Third World 18 p2752 A83-39828

The status of space science and technology in developed countries - The European experience 18 p2643 A83-39830

Impact of space research and technology on small countries --- developing nations 18 p2705 A83-39831

Impact of space research and technology on small countries (A case study for Austria) 18 p2788 A83-39834

Impact of space research and technology on small countries 18 p2788 A83-39836

Earth survey satellites and cooperative programs 18 p2706 A83-39844

25 years of NASA - Reflections and projections-applications [AAS PAPER 83-153] 20 p2943 A83-43761

The significance of a strong value-added industry to the successful commercialization of Landsat [AAS PAPER 83-185] 20 p3011 A83-43769

The future of space - Looking ahead in space 21 p3094 A83-45610

Application of advanced CAD/CAM procedures in areas other than air transport technology 23 p3440 A83-47189

Technology transfer from the aircraft sector to other sectors as exemplified by helicopter technology 23 p3391 A83-47190

Use of flight engine technology in stationary industrial gas turbines and diesel motors 23 p3464 A83-47203

The application of aeronautical technology to the construction of machines and vehicles 23 p3392 A83-47214

The commercial Centaur family [IAF PAPER 83-233] 23 p3514 A83-47316

The fruits of space exploration - Cornucopia or Armageddon --- prospects for prevention of space militarization [IAF PAPER 83-244] 23 p3414 A83-47321

Communications satellites - The experimental years [IAF PAPER 83-302] 23 p3419 A83-47335

Heat resistant explosives produced in Hungary with possible space applications [IAF PAPER 83-357] 23 p3429 A83-47356

AEROSPACE VEHICLES

NT FLEXIBLE SPACECRAFT

The ideas of F. A. Tsander and an assessment of the application of jet engines for the acceleration of aerospace vehicles 08 p1052 A83-22657

Integrating computer programs for engineering analysis and design [AIAA PAPER 83-0597] 11 p1647 A83-28350

Polysulfide sealants for aerospace. II - Application and handling 12 p1716 A83-29242

Aerospace technology demonstrators/research and operational options [AIAA PAPER 83-1054] 16 p2300 A83-36465

AEROSPACEPLANES

Air Force Aeronautical Systems the 1990's - A major shift [AIAA PAPER 83-2433] 24 p3543 A83-49576

AEROSTATICS

A simplified procedure for predicting the performance of inherently compensated aerostatic thrust bearings 24 p3590 A83-48823

Steady-state characteristics of aerostatic porous rectangular thrust bearings incorporating the effects of velocity slip, anisotropy and tilt 24 p3590 A83-48825

AEROSTATS

U AIRSHIPS

AEROTHERMOCHEMISTRY

Gaseous emissions of gas turbine combustors [AIAA PAPER 83-0242] 05 p0596 A83-16608

An aerothermochemical model of carbon-carbon composite nozzle recession [AIAA 83-0910] 12 p1709 A83-29764

Effects of nonequilibrium and surface catalysis on Shuttle heat transfer - A review [AIAA PAPER 83-1485] 15 p2127 A83-34916

An Eulerian-Lagrangian method for turbulent combustion [ONERA, TP NO. 1983-16] 16 p2327 A83-36426

Nonequilibrium hypersonic air flow past blunt bodies 17 p2450 A83-37630

A study of transport processes in a high-temperature boundary layer on an ablating graphite surface 19 p2842 A83-41259

Thermochemical ablation of the glass-graphite surface of a blunt cone at the spreading line in a three-dimensional boundary layer 24 p3579 A83-49662

AEROTHERMODYNAMICS

Thermodynamics of the turbulent atmosphere and parameterization of fluxes 01 p0074 A83-10219

Surface recession measurements using a projected fringe technique 01 p0053 A83-11077

Flow behavior and heat transfer around a circular cylinder at high blockage ratios 03 p0315 A83-13344

Some characteristics of turbulent flows at elevated temperatures 03 p0318 A83-14468

An exact solution for a high-temperature jet stream 04 p0480 A83-16390

Axial-compressor flow distortion with water ingestion [AIAA PAPER 83-0004] 05 p0596 A83-16456

Introductory aerothermodynamics of advanced space transportation systems [AIAA PAPER 83-0406] 05 p0585 A83-16695

Aerothermodynamic parameter estimation from Space Shuttle thermocouple data during transient flight test maneuvers [AIAA PAPER 83-0482] 05 p0607 A83-16743

Estimates of turbulent boundary layer behind a shock wave moving with uniform velocity in air [AIAA PAPER 83-0567] 05 p0637 A83-16794

The heating effect in resonance tubes --- German thesis 06 p0761 A83-19623

Improved fault detection in the hot section of turbojet engines by individual monitoring procedures 07 p0867 A83-19666

Influence coefficients of variable geometry free gas turbine engines 08 p1111 A83-22321

Analysis of viscous dissipation effect on thermal entrance heat transfer in laminar pipe flows with convective boundary conditions 08 p1086 A83-23123

Momentum and heat transfer in power-law fluid flow over two-dimensional or axisymmetrical bodies 08 p1087 A83-23143

Atmospheric definition for Shuttle aerothermodynamic investigations 09 p1212 A83-24883

The effect of the mechanisms of heterogeneous catalytic reactions on the heat flux in hypersonic flow past a blunted body 13 p1804 A83-30675

Heat waves near meteor bodies moving in the atmosphere at hypersonic velocities 13 p1880 A83-31329

Aerothermal environment in control surface gaps in hypersonic flow - An overview [AIAA PAPER 83-1483] 14 p1970 A83-32732

An assessment of the Space Shuttle Orbiter thermal environment using flight data [AIAA PAPER 83-1488] 14 p1980 A83-32734

Aerothermodynamic design considerations of an aerobraked spacecraft [AIAA PAPER 83-1510] 14 p1982 A83-32747

- Thermal-protection requirements for near-earth
aero-assisted orbital-transfer vehicle missions
[AIAA PAPER 83-1513] 14 p1982 A83-32750
- Analysis of aerothermal loads on spherical dome
protuberances
[AIAA PAPER 83-1557] 14 p1971 A83-32775
- Parabolized Navier-Stokes solutions for hypersonic flow
fields
[AIAA PAPER 83-0580] 16 p2293 A83-36061
- Radio-physical and gasdynamic problems of passage
through an atmosphere --- Russian book on spacecraft
reentry trajectories and communications
16 p2314 A83-36444
- Developing mass spectrometric techniques for boundary
layer measurement in hypersonic high enthalpy test
facilities
18 p2689 A83-39937
- Thermal processes in resonance tubes
19 p2845 A83-41890
- Numerical computation of the matrix Riccati equation
for heat propagation during Space Shuttle reentry
20 p3041 A83-42550
- On a scheme for solving the equations of a viscous
heat-conducting gas
21 p3133 A83-45216
- Numerical determination of the parameters in
high-entropy layers on slightly blunt bodies in supersonic
flow
21 p3088 A83-45220
- The H-theorem and the Onsager principle for the steady
Boltzmann equation
21 p3220 A83-45221
- Integrated thermal-structural approach for shells of
revolution
21 p3164 A83-45596
- The Tunguska event - No cometary signature in
evidence
22 p3385 A83-46387
- Diffusion of heat as a passive contaminant in a slightly
pulsating jet
22 p3283 A83-46450
- Inclusion of dynamic factors in a thermodynamic model
of climate and numerical forecasting of mean monthly air
temperature in the troposphere
23 p3488 A83-47153
- Aerodynamic loss penalty produced by film cooling
transonic turbine blades
[ASME PAPER 83-GT-77] 23 p3395 A83-47930
- Calculation of macroparameters in the Monte Carlo
method of direct statistical simulation --- of molecular gas
dynamics
23 p3513 A83-48501
- High-temperature physical-chemical processes in the
atmosphere during thunderstorms
23 p3485 A83-48504
- Asymptotic theory of three-dimensional hypersonic
radiating-gas flow past bodies
23 p3399 A83-48531
- The effect of heat release and injection on the structure
of a laminar hypersonic flow behind a body
23 p3399 A83-48534
- Aerodynamic and thermal characteristics of
three-dimensional star-shaped bodies in a rarefied gas
23 p3400 A83-48672
- The destruction of temperature fluctuations in a turbulent
plane jet
24 p3577 A83-49465
- Investigation of unsteady temperature fields of
nonaxisymmetric nozzle inserts
24 p3579 A83-49667
- Zonally asymmetric aspects of large-scale
thermodynamic forcing by cumulus convection
24 p3613 A83-49705

AFC (CONTROL)

U AUTOMATIC FREQUENCY CONTROL

AFCS (CONTROL SYSTEM)

U AUTOMATIC FLIGHT CONTROL

AFFERENT NERVOUS SYSTEMS

- The activity of afferents during the effects of temperature
on the skin of the forelegs of cats
08 p1145 A83-22114
- Afferent activity in the cardiac branches of vagus nerves
after intracoronary and intravenous administration of
anticardiac cytotoxic serum
13 p1895 A83-30301
- The role of the afferent nerve in the regulation of the
repair regeneration of bone tissue
18 p2732 A83-40554

AFFINITY

- Electron affinities of the alkali dimers - Na₂, K₂, and
Rb₂
20 p3045 A83-42635

AFRICA

- The possibilities of using aerospace remote sensing
techniques in the North Sahelian regions of Africa
08 p1128 A83-21963
- Atmospheric turbidity over Africa - Disturbed by the El
Chichon eruption
09 p1306 A83-24345
- Basic space sciences in Africa
18 p2788 A83-39835
- Broadcasting aspects of a projected African regional
satellite telecommunications system
21 p3122 A83-45432

AFRICAN RIFT SYSTEM

- Remote sensing and ground observations of NW-SE
dextral strike-slip movements in the
Tanganyika-Rukwa-Malawi transform zone of the East
African Rift
17 p2526 A83-38069

AFTERBODIES

- Comparison of computational and experimental jet
effects
01 p0002 A83-10185
- Laser velocimetric analysis of the flow downstream of
missile aft-bodies
[ONERA, TP NO. 1982-94] 03 p0279 A83-14543
- Effects of various empennage parameters on the
aerodynamic characteristics of a twin-engine afterbody
model
[AIAA PAPER 83-0085] 05 p0579 A83-16511
- A computational investigation of supersonic
axisymmetric flow over boattails containing a centered
propulsive jet
[AIAA PAPER 83-0462] 05 p0586 A83-16730
- Numerical simulation of transonic flow about isolated
afterbodies
[AIAA PAPER 83-0498] 05 p0586 A83-16750
- Measurements on a projectile with an asymmetric
afterbody at transonic speeds
[AIAA PAPER 83-0545] 05 p0587 A83-16780
- Comparison of subsonic/transonic afterbody flow
prediction methods
06 p0712 A83-18408
- Evolution of shock-induced pressure on a
flat-face/flat-base body and afterbody flow separation
10 p1372 A83-26159
- A semi-empirical approach for the prediction of aft-body
drag of supersonic projectiles with base bleeding
15 p2119 A83-33489
- Vectored thrust afterbody nozzles for future combat
aircraft
16 p2305 A83-35859
- Empennage/afterbody integration for single and
twin-engine fighter aircraft
[AIAA PAPER 83-1126] 16 p2293 A83-36235
- Analysis of viscous transonic flow over aircraft
forebodies and afterbodies
[AIAA PAPER 83-1366] 16 p2295 A83-36362
- Flow over a biconic configuration with an afterbody
compression flap - A comparative numerical study
[AIAA PAPER 83-1668] 17 p2444 A83-37179
- Calculation of afterbody flows with a composite velocity
formulation
[AIAA PAPER 83-1736] 17 p2445 A83-37215
- An afterbody drag prediction technique for military
airlifters
[AIAA PAPER 83-1787] 17 p2452 A83-38627
- Axisymmetric bluff-body drag reduction using
circumferential grooves
[AIAA PAPER 83-1788] 17 p2453 A83-38628
- Assessment of NASA and RAE viscous-inviscid
interaction methods for predicting transonic flow over
nozzle afterbodies
[AIAA PAPER 83-1789] 17 p2453 A83-38629
- Computational method of the drag of axisymmetric
afterbodies in subsonic flow
[AIAA PAPER 83-2079] 19 p2792 A83-41913
- ONERA research on afterbody viscid/inviscid interaction
with special emphasis on base flows
[ONERA, TP NO. 1983-26] 21 p3085 A83-44305
- Three-dimensional flow over a conical afterbody
containing a centered propulsive jet - A numerical
simulation
[AIAA PAPER 83-1709] 21 p3088 A83-45518

AFTERBURNERS

U AFTERBURNING

AFTERBURNING

- Calculation of pressure losses in the diffusers of mixing
afterburners
09 p1205 A83-23445
- Effect of initial conditions on constant pressure mixing
between two turbulent streams
11 p1567 A83-27875

AFTERGLOWS

NT HELIUM AFTERGLOW

- Optical emissions induced by spacecraft - Atmosphere
interactions
07 p0869 A83-21551
- Test wave diagnostics in the afterglow of a microwave
discharge
13 p1927 A83-31574

AFTERIMAGES

- Temporal integration following intensification of
long-lasting visual displays
19 p2884 A83-40749

AGC (CONTROL)

U AUTOMATIC GAIN CONTROL

AGE DETERMINATION

U CHRONOLOGY

AGE FACTOR

- The age-related peculiarities of the development of
hypoxia in skeletal muscles during acute hypoxic
hypoxia
01 p0078 A83-10483
- The determination of the normal /desirable/ body weight
for males 40-59 years of age according to the findings
of an epidemiological study of cardiovascular diseases
01 p0083 A83-10513
- Dependence of the structural lability of the outer
membrane of liver mitochondria on the age and sex of
rats
03 p0375 A83-14358

- The oxygen effect and the adaptive reactions of cells.
- IX - The dependence of the radioprotective effectiveness
of gaseous hypoxia on its degree and duration in neonatal
and adult mice
03 p0376 A83-14879
- Age-related patterns of lateral movement preferences
05 p0673 A83-17156
- The relationship between the patient's age, the function
of certain of his regulatory systems, and myocardial
infarction
05 p0673 A83-17160
- The peculiarities of the functional condition of the adrenal
cortex in old rats during immobilization stress
05 p0672 A83-17600
- The effects of age on normal saccadic characteristics
and their variability
05 p0675 A83-17748
- Does heat acclimation lower the rate of metabolism
elicited by muscular exercise
06 p0796 A83-18191
- Ocular functions and incidence of acute mountain
sickness in women at altitude
07 p0977 A83-20779
- Response of age forty and over military personnel to
an unsupervised, self-administered aerobic training
program
07 p0977 A83-20783
- The functional morphology of the submaxillary salivary
glands of rats during age-related disorders of endocrine
regulation
07 p0974 A83-20978
- Histometric indicators of the structure of the femoral
and crural muscles of children, adolescents, and young
men
07 p0978 A83-20991
- A study of the psychophysiological behavior in a group
of airline pilots after the operational age limit /60 years/
08 p1150 A83-22955
- Positive G tolerance of Indian subjects - Effects of age
and flying experience
09 p1323 A83-24004
- Stereo acuity rating in different age groups as tested
on Titmus optical stereo tests
09 p1323 A83-24007
- The histochemical and ultrastructural characteristics of
the neuron reactions of mammillary nuclei in old animals
to injections of adrenaline
09 p1321 A83-25154
- Effects of age and sex on hormonal responses to
weightlessness simulation
11 p1643 A83-27841
- Increased hematuria following hypergravic exposure in
middle-aged women
11 p1643 A83-27844
- The effect of hypoxia on the functional condition of the
external respiratory system in mature and old age
12 p1765 A83-29310
- Effect of age on benzodiazepine-induced behavioural
convulsions in rats
12 p1763 A83-29711
- The characteristics of the interaction of the
vestibular-oculomotor and the visual systems in young
animals
14 p2063 A83-32565
- The age characteristics of cortical auditory evoked
potentials
14 p2071 A83-33341
- The turnover of mitochondrial proteins in the livers of
rats of various ages
15 p2211 A83-34964
- The atmosphere of Canopus. II - A chemical composition.
Determination of the mass, radius, luminosity, and age
17 p2603 A83-37890
- The optimal speed of cyclic locomotion in individuals
of different ages
17 p2559 A83-38172
- Age-related changes of interneuronal connections in the
cerebral cortex of humans
17 p2560 A83-38193
- The sensitivity by age of animals to electromagnetic
fields at microwave frequencies
17 p2557 A83-38928
- Age discrimination of airline pilots - Effects of the bona
fide occupational qualification
18 p2753 A83-39046
- Age-related peculiarities of the functional condition of
the vascular system in patients with bronchial asthma in
the case of mountain-climate therapy
18 p2735 A83-40569
- The dependence of the topography of the hepatic veins
on the external form of the liver, its sizes, and age
18 p2736 A83-40583
- Age-related characteristics of the vestibular response
according to cupulometry data
19 p2880 A83-41425
- Differences in the response of systemic blood circulation
to loading tests depending on the sex and age of the
subject
19 p2881 A83-41431
- Age-related changes of the auditory perception of
ultrasound
19 p2883 A83-41842
- Age-related characteristics of the prostaglandin system
in several organs
19 p2879 A83-42096
- The functional condition of the brain during early forms
of arterial hypertension in young individuals
21 p3187 A83-44661
- Atherosclerosis and age --- Russian book
21 p3188 A83-45005
- Experimental injury of the aorta of rabbits of various
ages by immune complexes
21 p3185 A83-45342
- Age-related characteristics of the postirradiation
regeneration of the blood system
23 p3495 A83-48206
- Comparative cardiovascular responses to 70 head up
tilt in pilots and non-pilots
23 p3499 A83-48691
- Age-specific morbidity among Navy-pilots
24 p3618 A83-48880

AGE HARDENING

U PRECIPITATION HARDENING

AGGLOMERATION

Motion of small particles in a field of oscillating shock waves 10 p1416 A83-26188
A pocket model for aluminum agglomeration in composite propellants 12 p1717 A83-28962
Kinematics of molecular clouds - Evidence for agglomeration in spiral arms 18 p2769 A83-39646

AGGREGATES

Chained aggregation - A geometric analysis --- of large scale systems 10 p1469 A83-26576
The characteristics of the aggregation of erythrocytes in various animals and in humans 19 p2871 A83-40814

AGING (BIOLOGY)

Is cell aging caused by respiration-dependent injury to the mitochondrial genome 02 p0220 A83-11834
Psychological and electroencephalographic changes with aging in relation to aircrew performance 02 p0225 A83-12253
Growth and aging of the lens 05 p0670 A83-17196
Effects of ageing on cardiorespiratory changes to moderate physical exercise 09 p1323 A83-24005
The content of bioelements in the tissues during the aging of an organism (Review of the literature) 15 p2210 A83-34942
Heredity, aging, and longevity of humans 18 p2735 A83-40572
Experiments with air-dried seeds of *Arabidopsis thaliana* (L) Heynh. and *Crepis capillaris* (L) Wall., aboard Salyut 6 19 p2872 A83-40841
Role of metabolic rate and DNA-repair in *Drosophila* aging Implications for the mitochondrial mutation theory of aging 19 p2877 A83-41861
Effects of simulated increased gravity on the rate of aging of rats - Implications for the rate of living theory of aging 21 p3183 A83-44575
Antioxidants, metabolic rate and aging in *Drosophila* 21 p3183 A83-44600

AGING (MATERIALS)

NT AGING (METALLURGY)

The modelling of hydrothermal aging in glass fibre reinforced epoxy composites 01 p0022 A83-10700
The aging of alpha-LiIO₃ single crystals under laser irradiation 01 p0055 A83-10819
The effect of physical aging on the time-dependent properties of carbon-fiber-reinforced epoxy composites 02 p0150 A83-12064
The effect of physical aging on the deformation properties of polycarbonates 02 p0160 A83-12366
The creep behavior of inhomogeneously aging bodies 05 p0656 A83-17774
A viscoplasticity theory for inhomogeneously aging bodies 06 p0778 A83-19602
Aging and performance of structural film adhesives. I - A comparison of two high-temperature curing, epoxy-based systems 07 p0900 A83-21048
Hygrothermal aging effects on the micromechanisms of crack extension in glass fibre and carbon fibre composites 08 p1053 A83-21679
Accelerated aging studies of low density /hydrocarbon/ resin systems 09 p1222 A83-23646
Analytical description of the aging of polyamide 6 under fatigue fracture 09 p1239 A83-25023
Statistical analysis of aging-induced degradation /or lifetime/ variations in /Al, Ga/As/GaAs double-heterostructure lasers 10 p1429 A83-26028
Aging embrittlement behavior of Al-Zn-Mg alloy after stress-corrosion treatment 13 p1825 A83-31603
The asymptotic behavior of the stress-strain state of inhomogeneously aging bodies near the tip of a crack 14 p2030 A83-32352
Aging studies on carboxy terminated polybutadiene (CTPB) binder and propellant 18 p2673 A83-40013
Hygrothermal ageing of fibrous composites 18 p2657 A83-40229
On the accelerated ageing of CFRP 20 p2946 A83-42802
A study of the thermo-oxidative process and stability of graphite and glass-PMR polyimide composites 22 p3262 A83-46285
Environmental aging of epoxy composites 22 p3263 A83-46288
Photochemical ageing of Kevlar 49 22 p3270 A83-46708
Nonlinear creep problems for variable-boundary aging bodies 23 p3472 A83-48464
AGING (METALLURGY)
A study of the processes of second phase precipitation in titanium alloy VT30 02 p0155 A83-12204
Softening schedules for aging pressed semifinished products made from high-strength aluminum alloy V95pch 03 p0296 A83-13252

Structure and fracture character of V95 alloy sheets in relation to impurity content and aging conditions 03 p0297 A83-13254

Increasing the corrosion resistance of alloy AK8 03 p0297 A83-13257

The effect of the initial structure on the characteristics of beta solid solution decomposition in high-strength titanium alloy VT22 03 p0300 A83-14157
Effect of aging on the temperature at which martensitic transformation initiates in a TiNi intermetallic compound 04 p0459 A83-15702

Decomposition processes in an Al-5 percent Zn-1 percent Mg alloy. III - Reversion of GP-zones 05 p0617 A83-17953

Relationships between the structure and the mechanical properties of Inconel 718 06 p0729 A83-18600

The aging response of a high-strength P/M aluminum alloy 06 p0731 A83-19091

Influence of hot isostatic processing and heat treatment variables on the tensile properties of cast Transage 175 alloy, Ti-2.5Al-13V-7Sn-2Zr 07 p0886 A83-20471
Characteristics of concentration changes occurring in the solid solution of deformed Ni-7.1 wt% Al alloy during rapid heating 07 p0890 A83-20917

Control of the mechanical properties of alloy D16 sheets by the eddy-current method taking the kinetics of aging into account 07 p0891 A83-21419

The role of aging in the modeling of elevated temperature deformation 09 p1232 A83-24064

Effect of long-term exposure at elevated temperatures on the structure and properties of a Nimonic PE 16 superalloy 10 p1393 A83-25419

Superconducting properties of a liquid-infiltration Nb-Nb₃Sn composite formed during a low-temperature reaction 10 p1489 A83-26216

The crystallographic aspects of the decomposition of supersaturated solid solutions based on aluminum 10 p1399 A83-26792

A study of coalescence processes in Al - 2.8 pct Li alloy 13 p1821 A83-30739

Solution of gamma-prime phase in nickel heat-resistant aging alloys 13 p1823 A83-31214

The characteristics of Au-Ge-based ohmic contacts to n-GaAs including the effects of aging 14 p2006 A83-32671

Grain boundary segregation in Ni and binary Ni alloys doped with sulfur 14 p1993 A83-32677

Metallography of fatigue crack initiation in an overaged high-strength aluminum alloy 14 p1994 A83-32681

Transmission electron microscopy studies of structural changes in 13Ni-15Co-10Mo maraging steel as a result of aging 16 p2329 A83-35605

Origin of acoustic emission in aged Al-Zn-Mg alloys. I - The base ternary alloy 16 p2334 A83-36566

Origin of acoustic emission in Al-Zn-Mg alloys. II Copper-containing quaternary alloys 16 p2334 A83-36567

Accelerated temperature aging of black chrome solar selective coatings 16 p2421 A83-36736

The effectiveness of the artificial aging of low-alloy duralumin 16 p2335 A83-36889

Effects of microstructure and aging treatment on the fatigue crack growth behavior of high strength P/M aluminum alloy X7091 17 p2487 A83-37837

A study of the aging of tungsten-zirconium-carbon alloys 19 p2822 A83-42072

Structural transformations during the aging of Ni-Cr-Nb alloys 20 p2955 A83-43495

The aging response of a welded iron-based superalloy 22 p3268 A83-45727

A TEM study of microstructural changes during retrogression and reaging in 7075 aluminum 22 p3269 A83-46397

The effect of plastic deformation on phase transformations during the aging of VT3-1 titanium alloy 23 p3431 A83-47179

Properties of maraging steels VNS-2 and EP817 after aging 24 p3559 A83-48807

Characteristics of the precipitation of the gamma-prime phase in 40KhNYu alloy 24 p3560 A83-49068

Long-term ageing characteristics of Hastelloy alloy X 24 p3567 A83-50067

AGITATION

NT ULTRASONIC AGITATION

AGREEMENTS

Article 22 of the Warsaw Convention - In a state of limbo 09 p1351 A83-25118
The legal regime of the airspace above the exclusive economic zone 09 p1351 A83-25119
Air cargo - Liability limitations of the Warsaw Convention for loss of cargo are unenforceable in United States courts 09 p1351 A83-25121

AGRICULTURAL AIRCRAFT

Thunder power for executive and ag-aircraft 01 p0011 A83-10866

Agricultural aviation in India - A perspective with accent on aero-medical problems 02 p0223 A83-12258
Putting the microlight to work 09 p1195 A83-23686

AGRICULTURE

Action plan for remote sensing applications for rice production --- Book [IFAORS-207] 03 p0345 A83-14121

A procedure to overlay thematic map and domain land survey system data to geometrically-corrected Landsat images and its application to agricultural land use studies in western Canada 03 p0345 A83-14231

Potentials of Landsat-D and SPOT-1 for crop identification in the maritimes 03 p0346 A83-14240

Landsat for delineation and mapping of saline soils in dryland areas in southern Alberta 03 p0348 A83-14261

Office automation in resource-management - The future is now --- agricultural land use map dissemination 03 p0348 A83-14269

A system for the complex processing of aerial and space data for agriculture 03 p0350 A83-14301

The possibilities of using aerospace remote sensing techniques in the North Sahelian regions of Africa 08 p1128 A83-21963

Quantifying agricultural indicators of desert encroachment 09 p1285 A83-24542

Urban encroachment on agricultural land 09 p1285 A83-24544

Agricultural resource assessment in tropical arid Djibouti 09 p1290 A83-24605

Some aspects of land transformation in the western Mediterranean desert of Egypt 15 p2181 A83-33553

Assessment of modified surface temperatures and solar reflectance using meteorological satellite and aircraft data 15 p2194 A83-33558

Mapping recent agricultural developments in China from satellite data 15 p2181 A83-33562

Canadian Landsat studies for monitoring agricultural intensification and urbanization - A summary 15 p2182 A83-33566

The evolution of land use over a 10 year period in France Results and methodology 15 p2182 A83-33568

Some aspects of large-scale land transformation due to urbanization and agricultural development in recent Japan 15 p2182 A83-33570

Photointerpretation for agricultural purposes --- Russian book 16 p2370 A83-36445

Comparison of simulated data of SPOT and Landsat-D sensors Application to an agricultural region 17 p2529 A83-38162

Estimation of shelter temperatures from operational satellite sounder data --- for farm crop monitoring 18 p2706 A83-39131

Airborne reconnaissance in the civilian sector - Agricultural monitoring from high-altitude powered platforms 18 p2706 A83-39939

The utility of remote sensing in agricultural statistics 22 p3310 A83-46160

Multispectral observations of agricultural fields in the Kiskoeer test-area 22 p3310 A83-46161

A statistical model for radar images of agricultural scenes 22 p3312 A83-46191

Image enhancement for determination of agricultural fields using Digital-SLAR data 22 p3313 A83-46211

Investigation of signs of erosion of agricultural lands on the basis of aerial and space remote sensing data (using the southwestern spurs of the Gissar ridge as an example) 24 p3598 A83-48935

Information about the environment from spaceborne observations and the national-economic significance and cost effectiveness of this information 24 p3598 A83-49291

AGRISTARS PROJECT

AgRISTARS - Plans and first-year achievements --- Agriculture and Resources Inventory Surveys Through Aerospace Remote Sensing 01 p0065 A83-10095

Research advances in satellite-aided crop forecasting 08 p1126 A83-21930

Enhanced crop discrimination using the mid-IR (1.55-1.75 microns) 17 p2530 A83-38165

Comparisons among a new soil index and other two- and four-dimensional vegetation indices 17 p2531 A83-38341

AGROCLIMATOLOGY

Spectral distribution of solar radiation in the Nordic countries 18 p2713 A83-39115

AGROMETEOROLOGY

Retrieval of near-surface temperatures from satellite data 18 p2722 A83-39130

The Group Agromet Monitoring Project (GAMP) - Application of Meteosat data for rainfall, evaporation, soil-moisture and plant-growth monitoring in Africa 21 p3165 A83-43980

AGT

U AUTOMATED GUIDEWAY TRANSIT VEHICLES

AH-1G HELICOPTER

The significant elements of the reliability and maintainability programs for the modernized Cobra helicopter weapons/weapons control systems
13 p1863 A83-31499

AH-64 HELICOPTER

Fault Detection/Location System for intermediate and tail rotor gearboxes 09 p1274 A83-24835
Apache on the war path - The Hughes AH-64 in production at last 14 p1974 A83-31939

AILERONS

Decomposition method for minimizing the weight of the load-carrying structure of a swept wing with allowance for the conditions of static strength and prescribed aileron efficiency 17 p2520 A83-37514
Unsteady aerodynamic forces and flutter analysis for a wing-aileron-tab configuration 20 p3008 A83-43688

AIR

NT ALVEOLAR AIR
NT COMPRESSED AIR
NT EXPIRED AIR
NT HIGH TEMPERATURE AIR

Research on oxidation by air and tempering of Raney nickel electrocatalysts for the H₂ anodes of alkali combustion materials cells --- German thesis
06 p0726 A83-18494

The oxidation of ultrafine powders of boron, vanadium, and chromium carbides 09 p1240 A83-25067
Oxidation of SO₂ by NO₂ and air in an aqueous suspension of carbon 09 p1298 A83-25193
Electron kinetics in the atmosphere in conditions of repeated air breakdown 14 p2049 A83-31864
Evaluation of advanced airplane fire extinguishants [AIAA PAPER 83-1141] 17 p2459 A83-38076
A comparison of microvoid sizes in nickel base alloys tested in air and in the presence of hydrogen 18 p2668 A83-40614

The oxidation behavior of a model molybdenum/tungsten-containing alloy in air alone and in air with trace levels of NaCl(g) 20 p2952 A83-42241
Picosecond air breakdown studies at 0.53 micron 20 p3051 A83-43598
The Atmospheric Lifetime Experiment. II - Calibration 24 p3606 A83-49329

AIR BAG RESTRAINT DEVICES

Air bag impact attenuation system for the AQM-34V remote piloted vehicle 01 p0008 A83-10188

AIR BEARINGS

U GAS BEARINGS

AIR BLASTS

U AERIAL EXPLOSIONS

AIR BREATHING BOOSTERS

Istra - An air-breathing ballistic space transport vehicle for Europe
[DGLR PAPER 82-075] 09 p1213 A83-24189
Fully reusable launch vehicle with airbreathing booster [IAF PAPER 83-376] 23 p3419 A83-47364

AIR BREATHING ENGINES

NT BRISTOL-SIDDELEY BS 53 ENGINE
NT GAS TURBINE ENGINES
NT J-79 ENGINE
NT JET ENGINES
NT PULSEJET ENGINES
NT RAMJET ENGINES
NT SUPERSONIC COMBUSTION RAMJET ENGINES
NT T-56 ENGINE
NT T-64 ENGINE
NT TF-41 ENGINE
NT TURBOFAN ENGINES
NT TURBOJET ENGINES
NT TURBOPROP ENGINES

Problems concerning the external aerodynamics of air-breathing missiles

[ONERA, TP NO. 1982-93] 03 p0279 A83-14542
The flow field in a suddenly enlarged combustion chamber 04 p0476 A83-15288

A component buildup aerodynamic prediction approach for airbreathing missiles

[AIAA PAPER 83-0461] 05 p0586 A83-16729
Viscous primary/secondary flow analysis for use with nonorthogonal coordinate systems 05 p0588 A83-16785

[AIAA PAPER 83-0556] 05 p0588 A83-16785
International Symposium on Air Breathing Engines, 6th, Paris, France, June 6-10, 1983, Symposium Papers 16 p2302 A83-35801

Closed-loop engine fuel system simulation [SAE PAPER 821374] 17 p2468 A83-37964

Axisymmetric nose inlet effects on supersonic airflows 18 p2638 A83-40008

Strong pressure waves in air-breathing engines 23 p3398 A83-48216

AIR CARGO

The United Nations Convention on International Multimodal Transport of Goods /1980/ - Discussion of the operations of pick-up and delivery with particular attention to the air mode 06 p0816 A83-18100

Air cargo - Liability limitations of the Warsaw Convention for loss of cargo are unenforceable in United States courts 09 p1351 A83-25121

Overview of the air cargo industry 14 p1973 A83-33369

Aircraft design trends for cargo compatibility [AIAA PAPER 83-1609] 14 p1973 A83-33370

Airport - Air cargo compatibility [AIAA PAPER 83-1610] 14 p1973 A83-33371

New concept for low cost VTOL cargo delivery capability [AIAA PAPER 83-2207] 19 p2794 A83-41691

Are the principles of the Warsaw Convention endangered by recent U.S. court decisions? 20 p3057 A83-43126

The implications of the United Nations Convention on International Multimodal Transport of Goods (Geneva, 1980) for International Civil Aviation 22 p3367 A83-45804

International Forum for Air Cargo, 11th, New York, NY, September 27-30, 1982, Proceedings 22 p3251 A83-45900

Challenges for military airlift in the 1990's [AIAA PAPER 83-2437] 23 p3400 A83-48327

AIR CONDITIONING

The hygienic characteristic of the air environment in buildings during artificial ionization 01 p0086 A83-11396

Solar operated water-ammonia absorption heat pump for air-conditioning - Modelling and simulation 15 p2192 A83-34674

A mathematical model on the thermal behaviour of an aircraft cabin --- Thesis 22 p3254 A83-46691

AIR CONDITIONING EQUIPMENT

Shuttle orbiter flash evaporator operational flight test performance [SAE PAPER 820883] 13 p1812 A83-30926

Thermal control system for a Manned Space Station [SAE PAPER 820836] 13 p1906 A83-30933

An integrated regenerative air revitalization system for spacecraft [SAE PAPER 820846] 13 p1907 A83-30937

AIR CONDUCTIVITY

Regular measurements of the air's electrical conductivity 11 p1634 A83-28732

An analysis of multiyear variations in atmospheric electrical quantities in the atmospheric surface layer on the basis of observational data 11 p1634 A83-28733

Results from regular observations of the electrical conductivity of air at Verkhnee Dubrovo 11 p1634 A83-28735

Elaborating methods for measuring atmospheric electrical quantities 11 p1575 A83-28737

Conductivity, ion production rate, and light flashes in air under the effect of a short pulse of relativistic electrons 19 p2902 A83-41794

AIR COOLING

Evaluation of air-cooled Si₃N₄ vanes 08 p1072 A83-22263

Features of the selection of the basic parameters of cooled GTE turbines 08 p1046 A83-22655

A nonstationary approach to the investigation of heat transfer in the cooling ducts of turbine blades 09 p1258 A83-23429

Low power, air-cooled DC-Link aircraft generation systems 11 p1530 A83-27324

Optimization of the jet cooling of a rotating disk 19 p2844 A83-41567

Results of an experimental study of the thermal state of blades in turbines with partial root cooling 19 p2801 A83-42138

Thermodynamic efficiency of air injection into the radial clearance of the turbine of a turbojet engine 19 p2801 A83-42139

A study of the thermal state of porous turbine blades in a straight nozzle cascade 19 p2794 A83-42148

Cooling of a rotating disk by means of an impinging jet 20 p2978 A83-42739

Combined forced and free convection between parallel plates 20 p2979 A83-42752

Film cooling effectiveness of discrete holes measured by mass transfer and laser interferometer 20 p2983 A83-43017

Heat transfer characteristics for jet array impingement with initial crossflow [ASME PAPER 83-GT-28] 23 p3393 A83-47891

Heat transfer and friction loss characteristics of pin fin cooling configuration [ASME PAPER 83-GT-123] 23 p3448 A83-47952

Developments in air cooling of gas turbine vanes and blades [ASME PAPER 83-GT-160] 23 p3409 A83-47984

Temperature profile development in turbulent mixing of coolant jets with a confined hot cross flow [ASME PAPER 83-GT-220] 23 p3448 A83-48019

Effectiveness measurements for a cooling film disrupted by a single jet

[ASME PAPER 83-GT-250] 23 p3397 A83-48037

AIR CURRENTS

NT JET STREAMS (METEOROLOGY)

NT MERIDIONAL FLOW

NT VERTICAL AIR CURRENTS

Mesoscale structures of vortices in polar air streams 02 p0218 A83-13058

The inclusion of moist downdraft effects in the Arakawa-Schubert cumulus parameterization 03 p0368 A83-14445

A numerical simulation of an atmospheric vortex street 04 p0516 A83-15856

Eastward and westward flows over topography in nonlinear and linear barotropic models 04 p0516 A83-15933

Seasonality in Southern Hemisphere eddy statistics at 500 mb 04 p0517 A83-15935

On the causes of formation of two intertropical convergence zones in the western part of the Pacific Ocean and in the Indian Ocean 04 p0517 A83-16012

Numerical simulation of land-breeze-induced snowbands along the western shore of Lake Michigan 06 p0791 A83-18461

New technology for improved clean room operations 13 p1865 A83-31520

Air motion and precipitation growth in a major snowstorm 21 p3179 A83-44397

AIR CUSHION LANDING SYSTEMS

LCAC - from test craft to production design --- air cushion vehicles for amphibious assault landing operations [AIAA PAPER 83-0622] 08 p1173 A83-22423

Design and experimentation within the Mobility Development Laboratory (MDL) utilizing the Static and Dynamic Test Machines 20 p2938 A83-42549

AIR CUSHION VEHICLES

U GROUND EFFECT MACHINES

AIR DEFENSE

NT ANTIMISSILE DEFENSE

Tactical three-dimensional air surveillance radar 01 p0003 A83-10259

Development of a simulator certification /SIMCERT/ methodology for SAC --- Air Force aircrew training regulation 10 p1459 A83-26306

Missile guidance design tradeoffs for high-altitude air defense 13 p1812 A83-30168

The evolution and state of the art in air defense radar antennas 20 p2964 A83-42825

Missile guidance electromagnetic sensors 24 p3546 A83-48769

Broadband sensors for lethal defense suppression 24 p3570 A83-48770

Semi-active radar guidance 24 p3546 A83-48771

AIR DROP OPERATIONS

C-141 operations in Bright Star 82 02 p0133 A83-12224

AIR DUCTS

Cast titanium inlet duct development [AIAA 83-0951] 12 p1695 A83-29776

AIR FILTERS

An investigation of the shielding effectiveness of FPP-15 fabric relative to bacterial aerosols 05 p0677 A83-17201

Evidence for aerosol chlorine reactivity during filter sampling 09 p1299 A83-25203

Aviation filters for fuels, oils, hydraulic fluids, and air --- Russian book 12 p1700 A83-28813

An affbody drag prediction technique for military airlifters [AIAA PAPER 83-1787] 17 p2452 A83-38627

The effect of an acoustic wave on the aerosol capture efficiency of a granular bed 20 p3014 A83-42977

Calibration and tests of the filter-collection method for measuring clean-air, ambient levels of nitric acid 20 p2991 A83-43432

AIR FLOW

NT AIR CURRENTS

NT JET STREAMS (METEOROLOGY)

NT MERIDIONAL FLOW

NT VERTICAL AIR CURRENTS

On a geophysical inviscid vortex 01 p0075 A83-10496

Structure of air flow separation over wind wave crests 01 p0075 A83-10725

Response of stratified flow in the lee of the Olympic Mountains 02 p0218 A83-13061

Numerical simulation of air flow over and around a long mountain range 03 p0367 A83-14421

Numerical simulation of the airflow over Lake Michigan for a major lake-effect snow event 03 p0368 A83-14438

A single-level, numerical model suitable for complex terrain 03 p0369 A83-14452

Heat transfer and associated turbulent processes in pulsed turbulent flows under conditions of acoustical resonance 03 p0318 A83-14471

A new use for NWC's wind machine - Parachute testing 04 p0449 A83-15309

Emission characteristics of refractory materials --- as electrodes in aerodynamic generators 04 p0506 A83-16019

Numerical modelling of the mesoscale airflow downwind of the Alps - Two case studies under cyclogenetic conditions 04 p0518 A83-16153

Prediction of liquid fuel spray capture by v-gutter downstream of plain orifice injector under uniform cross air-flow [AIAA PAPER 83-0153] 05 p0596 A83-16559

Field observations of stratified atmospheric flow above an obstacle 06 p0788 A83-18237

Momentum balance of gravity flows 06 p0789 A83-18255

Non-linear effect in high speed rotor noise 06 p0807 A83-18393

A synoptic climatology of northwest flow severe weather outbreaks. I - Nature and significance 06 p0792 A83-18468

Investigation of supersonic air ejectors. II - Effects of throat-area-ratio on ejector performance 07 p0863 A83-20285

Flow widening through a Darrieus wind turbine - Theory and experiment 07 p0955 A83-21082

An experimental study of unsteady heat transfer from a flat plate to an oscillating air flow 08 p1084 A83-22239

On the predictability of quasi-geostrophic flow - The effects of beta and baroclinicity 08 p1142 A83-23002

An experimental investigation of the dispersion of a gas jet in a coflowing stream of air 08 p1042 A83-23215

A yawmeter for steady and low-frequency unsteady flows 08 p1106 A83-23296

Atmospheric definition for Shuttle aerothermodynamic investigations 09 p1212 A83-24883

Numerical simulation of the airflow over Lake Michigan for a major lake-effect snow event 10 p1451 A83-25392

Cyclic wave action in the stable operation of a Hartmann-Sprenger tube 10 p1414 A83-26144

Supercell flow inferred from single-Doppler radar and environmental data 11 p1623 A83-26997

On the simulation of the hypervelocity regime of flow past bodies in wind tunnels 11 p1526 A83-27714

The acoustic response of a propeller subjected to gusts incident from various inflow angles [AIAA PAPER 83-0692] 11 p1651 A83-28010

An experimental determination of the turbulent Prandtl number in the inner boundary layer for air flow over a flat plate 11 p1569 A83-28377

Analytical method for determining the nonequilibrium parameters of an air plasma in a Laval nozzle 13 p1922 A83-30044

Aerodynamic performance of a Wells air turbine 13 p1869 A83-30191

Airflow resistivity instrument for in situ measurement on the earth's ground surface 14 p2020 A83-32824

Determining the form drag contribution to the total stress of the atmospheric flow over ridged sea ice 15 p2203 A83-33498

Case study of a hailstorm in Colorado. III - Airflow from triple-Doppler measurements 16 p2384 A83-35466

Experimental study of the air flow through labyrinth seal 16 p2361 A83-35860

Sound propagation in ducts with impedance walls in the presence of an air flow. II - Optimization of acoustic attenuation in ducts 17 p2577 A83-37512

The use of stereophotogrammetry for studying the stress-strain state of a soft spherical shell in air flow 17 p2522 A83-37808

Plane flow past an air-supported soft cylindrical shell 17 p2522 A83-38099

Dynamic behaviour and stability of thermistor air flowmeters 17 p2512 A83-38531

The use of pressure fluctuations on the nose of an aircraft for measuring air motion 18 p2721 A83-39118

Stochastic simulation of atmospheric trajectories 18 p2722 A83-39123

On the effect of a large temperature difference on the velocity and temperature profiles for the turbulent flow of air in a tube 18 p2685 A83-39852

The kinematics of orographic airflow during Sierra storms 18 p2729 A83-40037

Calculation of shock-layer parameters for the hypersonic flow of equilibrium-dissociated air around bodies with bends of the generatrix 19 p2791 A83-41881

Turbulent heat transfer in the entrance region of a concentric annulus with inner cylinder rotation 20 p2975 A83-42701

Modification of the turbulent temperature field in strongly heated air flows 20 p2977 A83-42726

Experimental mixed convection from a large, vertical plate in a horizontal flow 20 p2980 A83-42754

Study of convective heat transfer in gas turbine combustion chambers 20 p2984 A83-43024

Properties of a constricted-tube air-flow levitator 20 p2940 A83-43266

Aerodynamic-wave break-up of liquid sheets in swirling airflows and combustor modules [AIAA PAPER 83-1204] 21 p3133 A83-45511

Demands on the air system of modern aircraft engines 22 p3255 A83-46491

Supersonic stabiliation of a tangential shear in a thin atmosphere 22 p3285 A83-46938

A model for radial flow in a tube-dome junction of a telescope 23 p3508 A83-47846

Combustion experiments with a new burner air distribution concept [ASME PAPER 83-GT-31] 23 p3406 A83-47893

A compact diffuser system for annular combustors [ASME PAPER 83-GT-43] 23 p3407 A83-47903

Penetration and break-up behaviour of a discrete liquid jet in a cross flowing airstream - A further study [ASME PAPER 83-GT-170] 23 p3448 A83-47971

Experimental investigation of fuel distribution in a transverse stream [ASME PAPER 83-GT-207] 23 p3410 A83-48008

On the energy characteristics of the aerodynamic matrix and the relationship to possible flutter 23 p3398 A83-48144

The calculation of the film vaporization of hydrocarbons in a hot-air flow 23 p3430 A83-48494

Interaction of shock waves of air with a porous screen 23 p3452 A83-48658

Calculation of the attached mass for a supersonic gas jet 24 p3576 A83-48938

Hydrodynamic visualization of the flow phenomena characterizing air intakes [ONERA, TP NO. 1983-103] 24 p3583 A83-49414

AIR FREIGHT

U AIR CARGO

AIR INLETS

U AIR INTAKES

AIR INTAKES

NT ENGINE INLETS

NT HYPERSONIC INLETS

NT INLET AIRFRAME CONFIGURATIONS

NT SUPERSONIC INLETS

X-wire sounding in an air inlet at high angle of attack [AAAF PAPER NT 81-15] 02 p0132 A83-11775

Numerical studies of the formation and destruction of vortices in a motored four-stroke piston-cylinder configuration [AIAA PAPER 83-0497] 05 p0652 A83-16749

On the choice of the optimal total wedge angle for the air intake of a hypersonic ramjet engine 08 p1046 A83-22656

Experimental investigations in transonic highly separated, turbulent flow 15 p2119 A83-33665

The swirl in an S-duct of typical air intake proportions 16 p2289 A83-35620

Swirl characteristics of an S-shaped air intake with both horizontal and vertical offsets 16 p2289 A83-35621

The effect of the geometrical parameters of an air intake with a central body on drag relative to the fluid streamline in the case when there is an incompressible-gas flow around it 17 p2448 A83-37531

Application of numerical methods to the calculation of the characteristics of supersonic and hypersonic jet-engine air intakes 17 p2448 A83-37532

Investigation of the parameters of a boundary layer before the inlet of a supersonic air intake mounted under the surface of a triangular plate 17 p2448 A83-37533

Comparison of computational and experimental data concerning flow past axisymmetric air intakes in regimes with an expelled shock wave 17 p2449 A83-37541

Computational study of an unregulated air intake of a hypersonic ramjet engine with three-dimensional deceleration of the flow at freestream Mach numbers of 5-7 17 p2449 A83-37559

Numerical investigation of three-dimensional transonic flow through air intakes disturbed by a missile plume [AIAA PAPER 83-1854] 17 p2457 A83-38682

Determining compressor-inlet airflow in the compact multimission aircraft propulsion simulators in wind-tunnel applications [AIAA PAPER 83-1231] 18 p2642 A83-39104

Survey of inlet development for supersonic aircraft [AIAA PAPER 83-1164] 18 p2638 A83-40473

Low flight speed acoustic results for a supersonic inlet with auxiliary inlet doors [AIAA PAPER 83-1415] 21 p3201 A83-45517

Hydrodynamic visualization of the flow phenomena characterizing air intakes [ONERA, TP NO. 1983-103] 24 p3583 A83-49414

AIR JETS

Use of breakdown coefficients in turbulent jets to determine the universal exponent mu 03 p0363 A83-13273

Low-level circulations induced by an upper-level jet in a fine mesh numerical model 03 p0367 A83-14433

The dominant coherent structure of the circular jet organized by controlled perturbation 03 p0318 A83-14463

Investigations on the effects of discrete wingtip jets [AIAA PAPER 83-0546] 05 p0587 A83-16781

The effects of turbulence and surface roughness on the drag of spheres in thin jets 06 p0711 A83-18067

The effect of acoustics and flow conditions in the wall boundary layer of a nozzle on the mixing layer of a submerged jet 06 p0760 A83-19429

Flames with impinging jets 07 p0882 A83-21423

Principles governing the mixing of transverse jets 09 p1196 A83-23439

The pressure on a flat surface of arbitrary orientation past which a strongly underexpanded jet of rarefied gas flows 09 p1197 A83-24484

A numerical and experimental investigation of turbulent heat transport of an axisymmetric jet impinging on a flat plate [ASME PAPER 82-WA/HT-55] 10 p1413 A83-25695

Near field acoustic measurements in natural and artificially excited high speed subsonic jets [AIAA PAPER 83-0725] 10 p1475 A83-25936

Penetration into a supersonic flow of a jet injected through a convex cylindrical surface 11 p1526 A83-27722

On the mechanism of screech tone generation in underexpanded rectangular jets [AIAA PAPER 83-0727] 11 p1651 A83-28014

Axial wavenumber measurements in axisymmetric jets 12 p1696 A83-28974

Effects of artificial excitation upon a low Reynolds number Mach 2.5 jet 14 p2081 A83-32996

Loads and pressures due to underexpanded jets impinging on wedges 16 p2288 A83-35619

The introduction of tangential or perpendicular nonisothermal plane jets into a turbulent crossflow for the purpose of film cooling 16 p2350 A83-35799

Effect of air, liquid and injector geometry variables upon the performance of a plain-jet airblast atomizer 16 p2351 A83-35809

Edge tones in high-speed flows and their application to multiple-jet mixing 16 p2408 A83-36077

Acoustic interaction with a turbulent plane jet - Some effects on turbulent structure 19 p2897 A83-40851

Optimization of the jet cooling of a rotating disk 19 p2844 A83-41567

The effect of cold air jet injection upon the film cooling effectiveness of combustion chamber walls for different injection geometries 20 p2978 A83-42738

Heat transfer from a turbulent, swirling, impinging jet 20 p2979 A83-42747

The effect of ordered structure of turbulence on momentum, heat and mass transfer of impinging round jets 20 p2984 A83-43020

Air jet levitation furnace system for observing glass microspheres during heating and melting 20 p2963 A83-43265

A critical study of the erosion of an aluminum alloy by solid spherical particles at normal impingement 21 p3112 A83-44375

An experimental investigation into the effect of changes in the geometry of a slot nozzle on the heat transfer characteristics of an impinging air jet 21 p3131 A83-44851

Cooling airflow studies at the leading edge of a film-cooled airfoil [ASME PAPER 83-GT-82] 23 p3447 A83-47935

AIR LAND INTERACTIONS

An evaluation of four thermal models used in thermal inertia analysis --- for thermal mapping from remotely sensed data 01 p0065 A83-10098

Two-dimensional field of thermal turbulence at the edge of an escarpment 01 p0075 A83-10723

Math modeling for prediction of infrared signatures 01 p0106 A83-11221

The relationship between the cloud amount and the temperature when averaged over a large space 02 p0213 A83-11978

The influence of mountains and the beta-effect on wave motion in the atmosphere 02 p0213 A83-11981

Response of stratified flow in the lee of the Olympic Mountains 02 p0218 A83-13061

The influence of ground moisture conditions in North America on summer climate as modeled in the GISS GCM 02 p0218 A83-13062

Measuring γ sub T/-squared, γ sub Q/-squared, and C sub TQ in the unstable surface layer, and relations to the vertical fluxes of heat and moisture --- atmospheric temperature and humidity 03 p0363 A83-13274

Numerical simulation of air flow over and around a long mountain range 03 p0367 A83-14421

Numerical studies of atmospheric flows over and around large-scale mountains 03 p0367 A83-14422

A model of Martian slope winds - Implications for eolian transport 04 p0566 A83-15569

Seasonal carbon dioxide exchange between the regolith and atmosphere of Mars - Experimental and theoretical studies 04 p0568 A83-15588

Dynamics of the baroclinic unstratified planetary boundary layer over land and sea 04 p0515 A83-15721

Numerical study of terrain-induced mesoscale motions in a mixed layer 04 p0516 A83-15932

The effects of moisture on trapped mountain lee waves 04 p0517 A83-15934

Quasistatic approximation of atmospheric dynamics. VI - Rossby waves over orographically modified terrain 04 p0510 A83-16035

Dust loading of the normal atmosphere [AIAA PAPER 81-0548] 05 p0659 A83-16783

Field observations of stratified atmospheric flow above an obstacle 06 p0788 A83-18237

Arid soils as a source of atmospheric carbon monoxide 07 p0959 A83-20198

Characterization of trace gases in 1980 volcanic plumes of Mt. St. Helens 07 p0960 A83-20215

Satellite imagery characteristics for surveys for the protection of oases against sand invasion 08 p1128 A83-21950

Questions concerning the atmospheric circulation over the Antarctic 08 p1140 A83-22420

Optical characteristics of windblown dust 08 p1135 A83-22542

The amplification and capture of atmospheric solitons by topography - A theory of the onset of regional blocking 08 p1142 A83-23003

A radar study of topographic effects 11 p1629 A83-27060

Pollutant transfer in upland regions by occult precipitation 11 p1613 A83-28393

The upslope effect 13 p1888 A83-30565

Tropographic effects and weather forecasting in the Colorado PROFS mesonet network area --- Prototype Regional Observing and Forecasting Service 13 p1890 A83-30589

An effort to simulate magnetospheric-ionospheric effects in the presence of seismic phenomena 13 p1880 A83-31328

Airflow resistivity instrument for in situ measurement on the earth's ground surface 14 p2020 A83-32824

The spatial problem of the flow around an obstacle of an incompressible stratified fluid (numerical modeling) --- atmospheric air flow around mountains 14 p2058 A83-32853

Io's atmosphere - Pressure control by regolith cold trapping and surface venting 15 p2274 A83-33931

The numerical simulation of the interaction of cloud formation and lee waves 15 p2206 A83-34067

Observations and models of simple nocturnal slope flows 16 p2384 A83-35467

Transient planetary waves simulated by GFDL spectral general circulation models. I - Effects of mountains. II - Effects of nonlinear energy transfer 16 p2386 A83-35485

Nonlinear interactions in a two-layer, quasi-geostrophic, low-order model with topography. I - Zonal flow-forced wave interactions 16 p2381 A83-36489

Numerical calculations and wind tunnel experiments on gas diffusion in thermally stratified flow over a ridge 16 p2390 A83-36495

Some problems of heat-transfer climatology in energetically active zones of the Atlantic Ocean 16 p2392 A83-36848

Numerical and analytical investigations of three-dimensional lee waves 17 p2553 A83-38763

Surface influence upon vertical profiles in the nocturnal boundary layer 18 p2721 A83-39014

The effects of orographically determined vertical motions and surface friction on the development and motion of baroclinic waves in numerical models with different vertical resolution 18 p2723 A83-39259

The albedo of the underlying surface-cloudy atmosphere system 18 p2723 A83-39439

A simple scheme for daytime estimates of the surface fluxes from routine weather data 18 p2724 A83-39675

A model for the Priestley-Taylor parameter alpha --- of atmospheric boundary layer 18 p2724 A83-39680

The kinematics of orographic airflow during Sierra storms 18 p2729 A83-40037

A laboratory experiment on the dynamics of the land and sea breeze 18 p2729 A83-40038

Observations of liquid water in orographic clouds over Elk Mountain 18 p2729 A83-40042

Hurricane Allen and island obstacles 18 p2730 A83-40047

Terrain classification and derived meteorological parameters for interregional transport models 19 p2863 A83-41985

The influence of poloidal motions and latent heat release on the equilibrium ice extent in a simple climate model 21 p3180 A83-44703

Numerical studies of major and minor stratospheric warmings caused by orographic forcing 21 p3180 A83-44708

A boundary-layer-scale model of mountain upslope flow [AD-A130312] 22 p3340 A83-46226

Elevated mixed layers in the regional severe storm environment - Conceptual model and case studies 23 p3491 A83-47413

Reconstructing the components of the radiation balance of the earth's surface on the basis of satellite data 23 p3483 A83-48101

AIR LAUNCHING

Operational software evaluation for the Air Launched Cruise Missile fly-off 01 p0093 A83-11248

Air-launched Shuttle concepts 09 p1218 A83-25127

Facility problems due to test tailoring --- at Pacific Missile Test Center 13 p1811 A83-31479

AMRAAM - Tomorrow's Sparrow 14 p1969 A83-32844

Propulsion for an air launched space sortie system [AIAA PAPER 83-1188] 16 p2319 A83-36266

AIR LAW

Existing time limit for overwater operations - Its validity 03 p0281 A83-13170

Recent developments in aviation case law 03 p0400 A83-13429

An overview of relevant issues in mid-air crash litigation 03 p0400 A83-13431

Defendant's discovery plan in mid-air crash litigation 03 p0400 A83-13432

Developing the plaintiff's discovery plan in mid-air collision litigation 03 p0400 A83-13433

The Montreal Agreement of 1966 and the Malta Agreement of 1965 05 p0692 A83-16975

The United Nations Convention on International Multimodal Transport of Goods /1980/ - Discussion of the operations of pick-up and delivery with particular attention to the air mode 06 p0816 A83-18100

Cockpit visibility and contrail detection 07 p0982 A83-20623

Problems of representation of air traffic controllers in mid-air litigation 07 p1002 A83-21547

On the constitutionality of seizing aircraft without a hearing pursuant to Section 903/b/ of the Federal Aviation Act of 1958 - Procedural due process up in the air 07 p1002 A83-21548

Nationality of airlines - A hidden force in the international air regulation equation 07 p1003 A83-21549

Limitations on air carrier liability - An inadvertent return to common law principles 07 p1003 A83-21550

Official liability for insufficient airworthiness - Comments in connection with a supreme-court decision 08 p1171 A83-21898

Additional remarks with respect to the American decree of regarding the suspension of foreign certificates of airworthiness 08 p1171 A83-21899

Article 22 of the Warsaw Convention - In a state of limbo 09 p1351 A83-25118

The legal regime of the airspace above the exclusive economic zone 09 p1351 A83-25119

Air cargo - Liability limitations of the Warsaw Convention for loss of cargo are unenforceable in United States courts 09 p1351 A83-25121

International aspects of air traffic control liability. I 11 p1666 A83-27968

Airline safety and labor relations law - Balancing rights and responsibility 15 p2240 A83-34475

Weather after the event --- for aircraft accident investigation 17 p2550 A83-38729

Pilot judgment - Current developments in evaluation and training and future issues in aviation cases 18 p2736 A83-39042

Legislative developments affecting the aviation industry 1981-1982 18 p2752 A83-39043

Aircraft crashworthiness in the United States - Some legal and technical parameters 18 p2752 A83-39044

Strict liability in military aviation cases - Should it apply? 18 p2753 A83-39045

Age discrimination of airline pilots - Effects of the bona fide occupational qualification 18 p2753 A83-39046

Airline liability for the involuntary violation of immigration laws 18 p2753 A83-39694

Public interest under the Federal Aviation Act of 1958 and the Airline Deregulation Act of 1978 18 p2753 A83-39695

Manufacturer's liability in international aerospace - A view from the United States 18 p2753 A83-39696

Airport use and access 18 p2753 A83-39698

International aspects of air traffic control liability. II 19 p2907 A83-40900

The role of the Air Force in the transfer of general-aviation-traffic control from ITAV to AA/V/TAG 19 p2795 A83-41226

Are the principles of the Warsaw Convention endangered by recent U.S. court decisions? 20 p3057 A83-43126

The Memorandum of Understanding between the United States and Certain ECAC Member States on Pricing Regime between U.S. and Europe 20 p3057 A83-43127

Annals of air and space law. Volume 7 22 p3367 A83-45802

The interpretation of international conventions supporting a uniform law in international relations 22 p3367 A83-45803

The implications of the United Nations Convention on International Multimodal Transport of Goods (Geneva, 1980) for International Civil Aviation 22 p3367 A83-45804

Security of International Civil Aviation - Role of ICAO 22 p3367 A83-45805

With regards to the Warsaw Convention - A bad process for false problems --- legal liability in airlaw 22 p3367 A83-45806

Comfort criteria and/or national requirements in the issuance of a license for air service in Canada 22 p3367 A83-45807

Aircraft crashworthiness and the manufacturer's tort liability in the United States 22 p3367 A83-45808

On the lack of physical bases for defining a boundary between air space and outer space 22 p3368 A83-45818

Essays in air law 22 p3368 A83-45826

The Warsaw Convention - Past, present and future 22 p3369 A83-45827

Some thoughts on the economic significance of limited liability in air passenger transport 22 p3369 A83-45828

From aerostats to DC-10s - Recognition of certificates of airworthiness 22 p3369 A83-45829

Unlawful interference with civil aviation 22 p3369 A83-45830

Passenger liability in international carriage by air - Lines of development 22 p3369 A83-45831

Interchange of aircraft --- international lease regulations 22 p3369 A83-45832

Liability and insurance for damage caused by foreign aircraft to third parties on the surface - A possible new approach to an old problem 22 p3369 A83-45835

Air safety - Enforcement of the Federal Aviation Regulations 22 p3369 A83-45836

International multimodal transport - A legal labyrinth 22 p3369 A83-45837

The 'legislative hearing' on IATA traffic conferences Creative procedure in a high stakes setting 22 p3370 A83-45838

The right to fly - Review at random 22 p3370 A83-45840

The right to be heard - The British practice --- refusal or revocation of licenses in air transport 22 p3370 A83-45841

The legal status of the aircraft commander - Ups and downs of a controversial personality in international law 22 p3370 A83-45842

Montreal Protocol - The most recent attempt to modify the Warsaw Convention 24 p3637 A83-49026

International relations in civil aviation --- Russian book 24 p3637 A83-49200

AIR MASSES

A simple model for relative air mass 03 p0370 A83-14644

Performance and temperature stability of an air mass flowmeter based on a self-heated thermistor 04 p0481 A83-15100

Modification of convective snow-clouds in landing the Japan sea coastal region 04 p0518 A83-16016

Structure of the cold front observed in SESAME-AVE III and its comparison with the Hoskins-Bretherton frontogenesis model --- Severe Environmental Storms And Mesoscale Experiment - Atmospheric Variability Experiment 06 p0790 A83-18261

Vertical air mass flux properties in the northeast Colorado hailstorm of 22 July 1976 11 p1623 A83-26996

Linear non-divergent mass-wind laws on the sphere 11 p1633 A83-28080

Measured aerosol size distributions and calculated EM extinction in air masses moving off the east coast 17 p2550 A83-38730

Stochastic simulation of atmospheric trajectories 18 p2722 A83-39123

On the aerosol particle size distribution spectrum in Alaskan air mass systems - Arctic haze and non-haze episodes 18 p2729 A83-40043

General circulation of air parcels and transport characteristics derived from a hemispheric GCM. I - A determination of advective mass flow in the lower stratosphere 20 p3031 A83-43457

The construction of the integral characteristics of the static stability of the atmosphere 22 p3338 A83-45640

The effect of atmospheric attenuators with structured vertical distributions on air mass determinations and Langley plot analyses 22 p3341 A83-46858

AIR NAVIGATION

NT ALL-WEATHER AIR NAVIGATION

NT AREA NAVIGATION

NT NAP-OF-THE-EARTH NAVIGATION

Fundamentals of radio navigation --- Russian book 01 p0003 A83-10668

Optimality of the measurement of navigation parameters on the basis of signals of difference-ranging systems 01 p0004 A83-10805

NAECON 1982; Proceedings of the National Aerospace and Electronics Conference, Dayton, OH, May 18-20, 1982. Volumes 1, 2 & 3 01 p0001 A83-11083

Integrated CNI avionics maximizes reliability --- communications, navigation, and cooperative identification 01 p0042 A83-11089

Gravity modeling for airborne applications 01 p0004 A83-11090

Integrated CNI - A new testing challenge --- Communication, Navigation and Identification 01 p0004 A83-11095

ICNIA - Lessons learned on sensor integration --- Integrated Communication Navigation Identification Avionics 01 p0004 A83-11096

Software optimization of a Kalman filter for an AP-120B array processor 01 p0091 A83-11111

Integrated CNI avionics logistics considerations 01 p0103 A83-11157

Programmable filter technology for integrated communication, navigation and identification systems 01 p0042 A83-11214

Comparison of some matching methods --- for aircraft and missile navigation 01 p0007 A83-11219

Advanced terrain following radar for LANTIRN --- Low Altitude, Navigation, Targeting Infrared at Night 01 p0007 A83-11241

Stability of the decentralized estimation in the JTIDS relative navigation 01 p0008 A83-11253

Timing a LORAN-C chain 02 p0133 A83-12225

Bootstrap stereo error simulations --- autonomous aerial navigation using terrain images 02 p0134 A83-12895

Observations regarding the MNPS in the North Atlantic and considerations concerning their applicability in the European air space. I 02 p0133 A83-13011

An auxiliary passive microwave navigation system [ONERA, TP NO. 1982-83] 03 p0281 A83-14535

Loran-C RNAV - The best near-term solution to air operations in northeastern North America 06 p0716 A83-18822

Lasers in aviation --- Russian book 07 p0936 A83-20384

Suboptimal filters for INS alignment on a moving base 07 p0865 A83-21019

Evaluation of the sensitivity and intrusion of workload estimation techniques in piloting tasks emphasizing mediational activity 07 p0980 A83-21075

CINNA - A system for preparing reconnaissance missions 08 p1044 A83-22591

Human aspects of integrated navigation in the air 09 p1323 A83-23370

Aircraft separation assurance - Systems design 09 p1199 A83-23371

Possible improvements in meteorology for aircraft navigation 09 p1199 A83-23373

Self-adaptive filters for the integration of navigation data 09 p1204 A83-23374

Integrated navigation: Actual and potential - Sea-air-space; Proceedings of the International Congress, Paris, France, September 21-24, 1982. Volumes 1 & 2 09 p1200 A83-24851

Integration of navigation resources in modern avionics systems 09 p1200 A83-24852

A multifunction integrated approach to providing aircraft inertial data 09 p1200 A83-24853

Carrier Aircraft Inertial Navigation System /CAINS/ integrated system approach 09 p1201 A83-24854

The Integrated Inertial Navigation System - AN/ASN-132 09 p1201 A83-24855

Technical and operational evaluation of wide-area coverage navigation systems in the continental United States 09 p1201 A83-24857

The laser gyro - Myth or panacea 09 p1270 A83-24858

New on board equipments /PMS, FMS/ and the ATC system - Evolution or revolution 09 p1204 A83-24859

Study of an on-board trajectory system for in-flight checking of air-navigation and landing radio aids 09 p1201 A83-24860

Navstar equipments accuracy compared with experimental results 09 p1201 A83-24861

Experiments of Omega for aviation 09 p1201 A83-24862

Human aspects of integrated navigation in the air 09 p1323 A83-24864

Possible improvements in meteorology for aircraft navigation 09 p1315 A83-24865

Self-adaptive filters for the integration of navigation data 09 p1335 A83-24866

The role of advanced navigation in future air traffic management 09 p1201 A83-24867

Main technical and operational characteristics of navigation systems with a view to identifying a mixed radionavigation system 09 p1201 A83-24869

Integrated navigation system for the Augusta 129 attack helicopter 09 p1202 A83-24870

Flight tests of integrated navigation by least squares adjustment 09 p1202 A83-24871

Integrated navigation by supplementing MLS with DAS --- DME-based Azimuth System 09 p1202 A83-24872

Simple integrated navigation systems 09 p1202 A83-24873

Viewpoints on selection of collision avoidance systems 09 p1202 A83-24874

Application of multiple model estimation to a recursive terrain height correlation system 10 p1374 A83-26264

An integrated multisensor aircraft track recovery system for remote sensing 10 p1374 A83-26266

Advances related to the measurement and representation of real multipath propagation --- for radio navigation and instrument landing applications 10 p1374 A83-26485

Potential accuracy of the goniometer section of a complex short-range navigation system 10 p1375 A83-26929

Estimation of the mutual influence of a group of radio-electronic devices --- for air navigation 10 p1375 A83-26934

The Navsat aeronavigation system - Possible control-segment concepts 11 p1535 A83-27371

Development and testing of Skyship 500 11 p1530 A83-28191

A multifunction integrated approach to providing aircraft inertial data 11 p1528 A83-28595

National Aerospace Meeting, Moffett Field, CA, March 24, 25, 1982, Proceedings 11 p1528 A83-28776

Guidance and flight control demonstration in a helicopter flight environment using a laser-gyro inertial navigation system 11 p1528 A83-28779

Radar detection of low level wind shear affecting aircraft terminal navigation 11 p1529 A83-28784

Integration and flight demonstrations of the Integrated Inertial Sensor Assembly /IISA/ 11 p1529 A83-28785

Fault/maneuver tolerance of aided GPS demodulation/navigation processors in the non-precision approach environment 11 p1529 A83-28787

FAA helicopter NAVSTAR GPS flight testing 11 p1529 A83-28788

Reliability of NAVSTAR GPS for civil aviation 11 p1529 A83-28791

Institute of Navigation, Annual Meeting, 38th, U.S. Air Force Academy, Colorado Springs, CO, June 14-17, 1982, Proceedings 12 p1700 A83-29201

B-52 operations in the Bright Star 82 exercise 12 p1699 A83-29204

The laser gyro as a self-contained inertial navigation aid 12 p1729 A83-29208

Flight testing the Low Cost Inertial Guidance System 12 p1700 A83-29210

Advanced navigation systems and fuel conservation 15 p2120 A83-33545

A theoretical framework for analysis of lateral position errors in VOR jet-route systems 15 p2121 A83-35273

Omega application in the Indonesian region 16 p2298 A83-35599

Performance capabilities of photographic flight navigation and sensor orientation systems 16 p2298 A83-36122

The future of civil avionics 17 p2461 A83-37819

Avionics analyzed. III - The hidden sensors 17 p2461 A83-38471

The Air Force Global Weather Central computer flight planning system 17 p2552 A83-38761

Radio-navigation prerequisites for IFR operation of regional airports and civil airfields 17 p2461 A83-38932

Navigation for balloon payloads - Recent experience with OMEGA in the US and a new slant range system 18 p2639 A83-39814

Utilization of the Trident radar system for air navigation, photogrammetry, and geodesy at the National Geographic Institute: First results - Ongoing tests 18 p2639 A83-40623

Digital Instrumentation Analysis and Navigation System (DIANS) for system identification [AIAA PAPER 83-2091] 19 p2799 A83-41922

Meteorology for the pilot (4th revised and enlarged edition) --- Russian book 21 p3178 A83-43907

Evolution of map display optical systems 21 p3092 A83-44830

National Aerospace Meeting, Arlington, VA, March 22-25, 1983, Proceedings 22 p3252 A83-46952

Use of commercial Omega/VLF in naval aviation 22 p3252 A83-46953

Minimizing pilot work load in an advanced development, low-cost Omega/VLF/RNAV system 22 p3252 A83-46954

Flight test evaluation of Loran-C in Alaska 22 p3252 A83-46955

Improved system reliability through master independent operation --- for Loran C 22 p3252 A83-46956

Status of the TCAS program 22 p3255 A83-46959

Applications of time transfer using Navstar GPS 22 p3253 A83-46964

The Navstar GPS 22 p3253 A83-46965

Post-flight compensation for a master navigator error 22 p3253 A83-46966

Comparison of simple position resets and Kalman filter position updates for correcting inertial navigation system errors 22 p3253 A83-46967

State of the art and development potential of fiberoptic rotation sensors --- for inertial navigation 23 p3405 A83-47187

DAS, a DME-supported multifunction system with a wide applications range for distance and angle measurements with data transfer 23 p3401 A83-47199

Air traffic control simulation in the airport area 23 p3401 A83-47200

Principles and present status --- of Navstar GPS for sea and air navigation 23 p3401 A83-48733

Integrated navigation systems for aircraft 23 p3402 A83-48735

AIR PIRACY

Security of International Civil Aviation - Role of ICAO 22 p3367 A83-45805

Unlawful interference with civil aviation 22 p3369 A83-45830

AIR POLLUTION

NT GLOBAL AIR POLLUTION

NT INDOOR AIR POLLUTION

Detection of regional air pollution episodes utilizing satellite data in the visual range 01 p0069 A83-10044

Investigation of the tribochemical influence of air pollution on the rolling friction of various materials being used in a newly developed railroad measuring post --- German thesis 01 p0056 A83-10175

Combustion-related pollutants of polydisperse single-composition aerosols and advection fog formation 01 p0070 A83-10226

Destruction of polyvinyl chloride under extrusion --- toxic hazards in industry 01 p0029 A83-11404

Laser monitoring of atmospheric NO using ultraviolet differential-absorption techniques 02 p0203 A83-11565

Evidence for a central Eurasian source area of arctic haze in Alaska 02 p0203 A83-11626

The effect of ordered vertical velocities and of the earth's surface on the trajectories of particles of polluted air in the atmosphere 02 p0205 A83-12000

The influence of equivalence ratio variation on pollutant formation in a gas turbine type combustor 02 p0136 A83-13095

Carbon monoxide measurements in the troposphere 03 p0355 A83-13351

Modification of a commercial NOx detector for high sensitivity 03 p0328 A83-14168

A study of atmospheric diffusion from the Landsat imagery 03 p0350 A83-14504

The satellite power system - Assessment of the environmental impact on middle atmosphere composition and on climate 03 p0360 A83-14517

A study of mesospheric rocket contrails and clouds produced by liquid-fueled rockets 03 p0290 A83-14518

Prediction of corridor effect from the launching of the satellite power system --- air pollutant concentration into narrow band of latitude 03 p0360 A83-14519

Analysis of multiple jets in a cross-flow [ASME PAPER 82-WA/FE-4] 04 p0478 A83-16140

Air quality mathematical modeling in the presence of strong point emissions 04 p0507 A83-16156

The equivalence of the criteria for normative SO₂ limit values in the urban region recommended by the Austrian Academy of Sciences Commission on protecting air purity 04 p0508 A83-16225

Spectroscopic detection of acetylene and ethane in the terrestrial atmosphere using ground-based solar IR observations 04 p0508 A83-16447

IR optical properties of thin CO, NO, CH₄, HCl, N₂O, O₂, N₂ and Ar cryofilms [AIAA PAPER 83-0244] 05 p0684 A83-16610

Atmospheric diffusion of a passive contaminant in a spatially homogeneous flow with transverse velocity [AIAA PAPER 83-0272] 05 p0633 A83-16623

Fogwater composition in southern California [AIAA PAPER 83-0362] 05 p0659 A83-16671

Effects of aerosols on photosynthesis 05 p0659 A83-16850

A study of the descriptive statistics of turbulent pollution concentration fields in atmospheric air and of meteorological elements for cities with developed industry 05 p0659 A83-16954

Feasibility of determining concentrations of atmospheric pollutants by comparative absorption using lasers having a single emission line 05 p0659 A83-17057

Automatic laser radar systems for measurement of atmospheric pollutants 05 p0651 A83-17281

A statistical plume model with first-order decay 05 p0659 A83-17438

A Lagrangian long-range transport model with atmospheric boundary layer chemistry 05 p0667 A83-17443

Radar observations of a plume from an elevated continuous point source 05 p0667 A83-17445

The effect of troposphere aerosol on the integral albedo of the system consisting of the atmosphere and the underlying surface 06 p0782 A83-17999

Atmospheric-dispersion experiments in the near and medium field /Fourth European Community Campaign, Turbigo, Italy, September 1979/ 06 p0781 A83-18137

Testing subroutines solving advection-diffusion equations in atmospheric environments 06 p0756 A83-18374

Point discharge current studies near a large pollution source 06 p0781 A83-18417

Laser resonant optoacoustic gas-analyzer for the monitoring of trace contaminants of the atmosphere 06 p0764 A83-19183

A comparative study of two trajectory models of long-range transport --- of air pollution 07 p0956 A83-19850

A climatological model for the determination of air pollutant concentrations at a topographically complex site 07 p0956 A83-20199

The origins of sulfur compounds in the atmosphere of a zone of high productivity /Gulf of Guinea/ 07 p0956 A83-20203

Air-sea particle exchange at a nearshore oceanic site 07 p0956 A83-20204

Characterization of trace gases in 1980 volcanic plumes of Mt. St. Helens 07 p0960 A83-20215

Optimal weighting of data to detect climatic change - Application to the carbon dioxide problem 07 p0969 A83-20216

Study of the particulate sulfur-light scattering relationship using in situ aerosol thermal analysis 07 p0957 A83-20222

The influence of large-scale advection on the vertical distribution of stratospheric source gases in 44 degree and 41 degree north 07 p0957 A83-20224

VOC compliant aircraft and transportation primers --- Volatile Organic Compound 07 p0898 A83-20430

Estimation of sulfate deposition 07 p0957 A83-20811

Numerical simulation of fog formation and liquid water content on polydisperse multi-composition aerosols due to combustion-related pollutants 07 p0963 A83-21038

The origin and nature of 'prompt' nitric oxide in flames 08 p1056 A83-22344

Studies of a diffusion flame matrix burner in a combustion chamber with heat exchanger 09 p1225 A83-23334

Simultaneous interpretation of wind speed and direction to study air-pollution from smoke, at the National Observatory of Athens, Greece 09 p1294 A83-23549

Detection of trace quantities of dimethylacetamide during the curing process of a polyimide film 09 p1237 A83-23623

The sources of sulfate in precipitation. II - Sensitivities to chemical variables 09 p1296 A83-24266

On the relationship between the greenhouse effect, atmospheric photochemistry, and species distribution 09 p1296 A83-24268

Chlorocarbon emission scenarios - Potential impact on stratospheric ozone 09 p1296 A83-24270

Effect of coupled anthropogenic perturbations on stratospheric ozone 09 p1296 A83-24271

The seasonal variation of the atmospheric SO₂ to SO₄^{-/-} conversion rate 09 p1296 A83-24279

Several models for optimizing the behavior of atmospheric pollution sources 09 p1297 A83-24940

Electron beam studies of individual natural and anthropogenic microparticles - Compositions, structures, and surface reactions 09 p1297 A83-25184

Laboratory measurements of dry deposition of acetone over adobe clay soil 09 p1297 A83-25186

Kinetics of reactions between free radicals and surfaces /aerosols/ applicable to atmospheric chemistry 09 p1297 A83-25187

Oxidation of SO₂ by NO₂ and air in an aqueous suspension of carbon 09 p1298 A83-25193

Sulfur dioxide absorption, oxidation, and oxidation inhibition in falling drops - An experimental/modeling approach 09 p1298 A83-25194

The relative importance of various urban sulfate aerosol production mechanisms - A theoretical comparison 09 p1298 A83-25199

Sulfate in the atmospheric boundary layer - Concentration and mechanisms of formation 09 p1299 A83-25201

Water vapor and temperature dependence of aerosol sulfur concentrations at Fort Wayne, Indiana, October 1977 09 p1299 A83-25202

Atmospheric aerosols in the polar regions 09 p1316 A83-25231

Aerosol measurements in the Arctic and in a volcanic region 09 p1309 A83-25232

The structure of mathematical models in environmental hydrodynamics problems 09 p1299 A83-25245

Methodological and systems engineering aspects of environmental pollution monitoring --- Russian book 09 p1299 A83-25248

Regularizing the solution of the laser sounding equation of atmospheric aerosols by means of a stabilizing functional 10 p1425 A83-25567

New application of dependence between mean times of sampling and maximal air pollutant concentrations 10 p1446 A83-25568

Monitoring of pollutants in the environment --- Russian book 10 p1446 A83-25607

Methodology for the investigation of the long-range transport of sulfur compounds 10 p1446 A83-25608

Evaluation of the transport of sulfur dioxide and sulfates over the territory of the USSR 10 p1447 A83-25609

The global cycle of benz/a/pyrene 10 p1447 A83-25611

Current methods for the determination of iodine in the atmosphere 10 p1447 A83-25612

Peculiarities of laser radiation and solid aerosol interaction 11 p1612 A83-27607

Atmospheric balance of sulphur above an equatorial forest 11 p1615 A83-27671

Seasonal variations of Cd, Pb, Cu and Ni levels in snow from the eastern Arctic Ocean 11 p1613 A83-27673

An investigation of the atmospheric HNO₃-NH₃-NH₄NO₃ equilibrium relationship in a cool, humid climate 11 p1613 A83-27675

The optimal design for spectral gas analyzers of atmospheric pollution 11 p1573 A83-28201

Separate determination of the nitrogen oxides NO, NO₂, and NO_x/ in city air by an automatic gas analyzer and a chemical method 11 p1613 A83-28202

Features in using lidars for measuring the dust content of air 11 p1573 A83-28203

Calculation of the parameter for the quality of the least-squares fit in investigating atmospheric pollution by resonance absorption 11 p1613 A83-28204

The removal of particulate matter from the atmosphere - The physical mechanisms 11 p1619 A83-28344

Short and middle range remote sensing of atmospheric gases using Raman lidar --- French thesis 11 p1585 A83-28640

Ozone measurements from a network of remote sites 11 p1613 A83-28697

HCl in rocket exhaust clouds - Atmospheric dispersion, acid aerosol characteristics, and acid rain deposition 11 p1613 A83-28698

Concentration of selected vapor and particulate-phase substances in the Lincoln and Holland Tunnels 11 p1613 A83-28699

The electrical conductivity of air over the Indian Ocean 11 p1620 A83-28729

Regular measurements of the air's electrical conductivity 11 p1634 A83-28732

Results from regular observations of the electrical conductivity of air at Verkhnee Dubrovo 11 p1634 A83-28735

Photochemical ozone formation in urban and point-source plumes 12 p1750 A83-29093

A study of turbulent energy over complex terrain (state, 1978) 12 p1757 A83-29127

A wind tunnel study of the flow field within and around open-top chambers used for air pollution studies 12 p1750 A83-29134

Spectral ranges for determining the concentration of hydrogen bromide and hydrogen fluoride in the earth's atmosphere 13 p1872 A83-30036

The distribution of radioactive carbon-14 of anthropogenic origin between the atmosphere and ocean since 1963 13 p1872 A83-30297

Tracing bomb C-14 in the atmosphere 1962-1980 13 p1876 A83-30878

Nonlinear response of stratospheric ozone column to chlorine injections 13 p1872 A83-30880

Selected man-made halogenated chemicals in the air and oceanic environment 13 p1873 A83-30883

A decade of stratospheric sulfate measurements compared with observations of volcanic eruptions 13 p1877 A83-30887

An aerosol and gas sampling apparatus for remote observatory use 13 p1847 A83-30905

They dance in the air --- properties of atmospheric aerosols 13 p1880 A83-31317

Cloud and precipitation chemistry research and Whitetace Mountain 13 p1873 A83-31527

A survey of laser and selected optical systems for remote measurement of pollutant gas concentrations 13 p1848 A83-31595

The interaction between air pollution dispersion and residential heating demands 13 p1873 A83-31596

The NO/NO₂/O₃ photostationary state in Claremont, California 13 p1873 A83-31597

Modeling the carbon cycle using the method of fractional-order derivatives 14 p2051 A83-32366

Laser methods for the control of atmospheric gases and gases which pollute the atmosphere 14 p2052 A83-32560

Pulmonary effects of ozone exposure during exercise: dose-response characteristics 14 p2069 A83-32818

The absorption spectrum of (C-12)D₂ in the 1.06-micron region 14 p2048 A83-32833

A model calculation of the coefficients of turbulent diffusion in a nonstratified atmospheric surface layer 14 p2058 A83-32854

Spectroscopic measurements of the total content of CO, CH₄, and N₂O in the atmosphere in the Arctic region 14 p2053 A83-32861

An approximation method for predicting changes in the level of atmospheric pollution in a city 14 p2048 A83-33042

Ozone precursor monitor for investigating air pollution 15 p2162 A83-33488

Toxic substances in the atmospheric environment - A critical review 15 p2193 A83-33502

The atmospheric oxidation of flue gases from a coal-fired power plant - A comparison between smog chamber and airborne plume sampling 15 p2193 A83-33503

Sulphur dioxide precipitation scavenging 15 p2194 A83-34042

Atmospheric trace element concentrations in Jerusalem, Israel 15 p2194 A83-34045

Halocarbon measurements in the Southern Hemisphere since 1977 15 p2194 A83-34046

Aircraft survey of the secondary photochemical pollutants covering the Tokyo metropolitan area 15 p2194 A83-34047

The measurement of H₂SO₄ and other sulfate species at Tuxedo, New York with a thermal analysis flame photometric detector and simultaneously collected quartz filter samples 15 p2194 A83-34048

Relevance of mixed layer scaling for daytime dispersion based on raps and other field programs --- Regional Air Pollution Study 15 p2194 A83-34049

Hydrogen peroxide and sulfur (IV) in Los Angeles cloud water 15 p2194 A83-34050

Remote sensing data integration into a geographic information system for the creation of a biogenic hydrocarbon inventory of the San Francisco Bay area 15 p2185 A83-34819

Air pollutants and forest decline 16 p2372 A83-35764

Strong and weak acidity of aerosols collected over the northeastern United States 16 p2372 A83-35765

The effects of fuel properties upon pollutants present in gas turbine aero-engines 16 p2338 A83-35813

Effect of sand erosion on the performance deterioration of a single stage axial flow compressor 16 p2304 A83-35854

A JT8D low emissions combustor by radial zoning [AIAA PAPER 83-1324] 16 p2309 A83-36339

A numerical investigation of the transport of coagulating aerosols in the atmosphere of a city 16 p2372 A83-36875

Remote sensing of atmospheric gases and particulates by lidar 17 p2515 A83-38363

An application of model testing for the study of rocket exhaust cloud properties 17 p2483 A83-38706

ALPHA-1/ alarm airborne lidar systems and measurements 17 p2495 A83-38747

Incorporation of planetary boundary layer dynamics in a numerical model of long-range air pollutant transport 18 p2720 A83-39011

Estimating plume dispersion - A comparison of several Sigma schemes 18 p2721 A83-39111

Stability of the surface layer and its relation to the dispersion of primary pollutants in St. Louis 18 p2711 A83-39122

Meteorological tracer techniques for parameterizing atmospheric dispersion 18 p2727 A83-39885

Increase and seasonal cycles of nitrous oxide in the earth's atmosphere 18 p2720 A83-40644

Henry's Law constants and the air-sea exchange of various low molecular weight halocarbon gases 18 p2705 A83-40645

Molecular state of sulfate aerosols in the remote Everest highlands 18 p2711 A83-40647

Tropospheric oxalate 19 p2862 A83-41112

Simultaneous detection of FC-11, FC-12 and FC-22, through 8 to 13 micrometers IR solar observations from the ground 19 p2862 A83-41113

Analysis of the error associated with grid representation of point sources --- for pollutant dispersion 19 p2863 A83-41969

Mathematical modeling of the formation and transport of ammonium nitrate aerosol 19 p2863 A83-41970

Solution of the advection-diffusion equation by the moments method --- applied to pollutant plumes 19 p2863 A83-41971

Trace gas profiles to 3000 m over Antarctica 19 p2863 A83-41972

Effect of freezing on sulfur dioxide dissolved in supercooled droplets 19 p2863 A83-41973

The ubiquity of peroxyacetyl nitrate in the continental boundary layer 19 p2863 A83-41974

A separator for obtaining samples of cloud water in aircraft 19 p2849 A83-41983

Determination of ethylene and other reactive hydrocarbons in the atmospheric air at Trombay, Bombay by gas chromatography using a chemiluminescent detector 19 p2849 A83-41984

Terrain classification and derived meteorological parameters for interregional transport models 19 p2863 A83-41985

Seasonal averages of net decay rate of SO2 over northern Europe 19 p2864 A83-41988

Numerical stimulation of photochemical air pollution over the Ise Bay District 20 p3013 A83-42202

Eye-safe tracking of oil fog plumes by UV lidar 20 p2988 A83-42211

General circulation model experiments on the climatic effects due to a doubling and quadrupling of carbon dioxide concentration 20 p3031 A83-42843

A dynamic model for the production of H(+), NO3(-), and SO4(2-) in urban fog 20 p3013 A83-42844

A two-dimensional photochemical model of the atmosphere. I Chlorocarbon emissions and their effect on stratospheric ozone 20 p3013 A83-42845

A two-dimensional photochemical model of the atmosphere. II The tropospheric budgets of the anthropogenic chlorocarbons CO, CH4, CH3Cl and the effect of various NO(x) sources on tropospheric ozone 20 p3013 A83-42846

The mechanism of NO3 and HONO formation in the nighttime chemistry of the urban atmosphere 20 p3013 A83-42848

The photochemistry of anthropogenic nonmethane hydrocarbons in the troposphere 20 p3013 A83-42849

Factors influencing the loss of fertilizer nitrogen into the atmosphere as N2O 20 p3014 A83-42851

C-13/C-12 records in Northern Hemispheric trees during the past 500 years - Anthropogenic impact and climatic superpositions 20 p3022 A83-42866

Physico-chemical mechanisms for generation of aerosols with a high temperature aerosol - An example of volcanic aerosols 20 p3014 A83-42978

Acetonitrile in the atmosphere 20 p3026 A83-43208

A mesoscale atmospheric dispersion model for predicting ambient air concentration and deposition patterns for single and multiple sources 20 p3014 A83-43422

Evaluation of an episodic regional transport model for a multi-day sulfate episode 20 p3014 A83-43423

Correlations between meteorological data and water-soluble sulphur compounds in fine aerosols 20 p3014 A83-43424

Kinetics of SO2 oxidation over carbonaceous particles in the presence of H2O, NO2, NH3 and O3 20 p3014 A83-43425

Comparison of calculated and observed super- and sub-micrometer aerosol mass concentrations using St. Louis RAPS data base --- Regional Air Pollution Study 20 p3014 A83-43426

Atmospheric pollution studies at Kanpur-suspended particulate matter 20 p3015 A83-43428

Modeling of multiphase atmospheric aerosols 20 p3015 A83-43429

Some environmental effects of forest fires in interior Alaska 20 p3015 A83-43430

Methods and results of gas chromatographic-mass spectrometric determination of volatile organic substances in an urban atmosphere 20 p3015 A83-43431

Calibration and tests of the filter-collection method for measuring clean-air, ambient levels of nitric acid 20 p2991 A83-43432

Determination of ambient aerosol and gaseous sulfur using a continuous FPD. III - Design and characterization of a monitor for airborne applications --- flame photometric detector 20 p2991 A83-43434

Acid deposition-precursor emission relationship in the northeastern U.S.A. - The effectiveness of regional emission reduction 20 p3015 A83-43435

Particle size distribution of n-alkanes nda Pb-210 in aerosols off the coast of Peru 20 p3028 A83-43556

Gas-phase NO2 and NO3 clustering with C2H5ONO2 and SO2 molecules - Experimental and semi-empirical MO studies --- ion chemistry of lower atmosphere 21 p3202 A83-44237

SO2 and SO4(2-) in the arctic - Interpretation of observations at three Norwegian arctic-subarctic stations 21 p3171 A83-44377

The seasonal response of a general circulation model to changes in CO2 and sea temperatures 21 p3179 A83-44393

An air pollution analytic transport model admitting the surface and inversion layer effect 21 p3169 A83-44489

Gaseous contaminants in the atmosphere and changes of the global climate 21 p3169 A83-45334

Possibilities for an improvement in short-distance diffusion modeling --- of air pollution 21 p3169 A83-45403

Smog chamber studies of NO(x) transformation rate and nitrate/precursor relationships 21 p3110 A83-45619

Methods of estimating wind fields for the simulation of atmospheric dispersion 22 p3339 A83-45713

Determination of particulate and gaseous arsenic compounds in the atmosphere at trace levels 22 p3320 A83-45714

Physicochemical characterization of trace metal compounds in airborne particulate matter 22 p3320 A83-45715

Acid generation in the troposphere by gas-phase chemistry 22 p3320 A83-45922

A gaseous tracer model for air pollution from residential wood burning 22 p3321 A83-45924

Optical emission from photoexcitation of aerosol particles produced by reaction of ozone with 1,3-butadiene 22 p3328 A83-46065

Sensor technology for future atmospheric observation systems 22 p3321 A83-46169

Mauna Loa sky conditions - Bench mark and present 22 p3374 A83-46408

The coefficient of haze as a measure of particulate elemental carbon 22 p3321 A83-46775

Calculated droplet size distributions and opacities of condensed sulfuric acid aerosols 22 p3321 A83-46898

Surface ozone and peroxyacetyl nitrate (PAN) observations at rural locations in Alberta, Canada 22 p3321 A83-46899

PAN concentrations in ambient air in New Jersey 22 p3321 A83-46900

Spatial and temporal variations of tropospheric aerosol volume distributions 22 p3334 A83-46948

A systems model of the interaction of radiation effects, transport, and photochemistry of trace gases in the stratosphere 23 p3478 A83-47154

Remote measurements of atmospheric NO2 concentration by means of a differential-absorption lidar 23 p3453 A83-47165

Atmospheric-pollution monitoring through conductivity measurements 23 p3454 A83-47419

Differential-absorption measurements with fixed-frequency IR and UV lasers --- for pollution monitoring and control 23 p3455 A83-47768

Remote sensing of hydrazine compounds using a dual mini-TEA CO2 laser DIAL system --- differential-absorption LIDAR 23 p3456 A83-47769

2.7 measurements of HONO, NO3, and NO2 by long-path differential optical absorption spectroscopy in the Los Angeles Basin 23 p3478 A83-47779

Ground-based ultraviolet differential absorption lidar (DIAL) system and measurements 23 p3457 A83-47782

Pollution monitoring using Nd:YAG based lidar systems 23 p3457 A83-47784

Optical remote sensing of environmental pollution and danger by molecular species using low-loss optical fiber network system 23 p3508 A83-47802

Wide-area air pollution measurement by the NIES large lidar 23 p3458 A83-47809

The reaction of gas phase N2O5 with water vapor 23 p3479 A83-47861

Emissions variability and traversing on production RB211 engines [ASME PAPER 83-GT-141] 23 p3409 A83-47966

Dispersion limitations of oxidation in power plant plumes during long-range transport 23 p3479 A83-48085

Mesoscale air pollution dispersion modelling 23 p3479 A83-48681

Modelling of long-range transport of sulphur over Europe A two-year model run and some model experiments 23 p3479 A83-48682

The pH and ionic composition of stratiform cloud water 23 p3479 A83-48684

Electron microscopy of acidic aerosols collected over the northeastern United States 23 p3479 A83-48687

Elemental composition of aerosols collected with airborne cascade impactors 23 p3479 A83-48688

Apportioning light extinction coefficients to chemical species in atmospheric aerosol 23 p3479 A83-48689

World-wide ambient measurements of peroxyacetyl nitrate (PAN) and implications for plant injury 23 p3479 A83-48690

Tracer experiments with turbulently dispersed air ions 23 p3479 A83-48730

Atmospheric composition - Influence of biology 24 p3604 A83-48760

Influence of peroxyacetyl nitrate (PAN) on odd nitrogen in the troposphere and lower stratosphere 24 p3602 A83-48761

Investigation of the background concentration of ozone in the atmospheric surface layer 24 p3604 A83-49106

Background variability of the aerosol and ion composition of the atmospheric surface layer 24 p3604 A83-49109

Measurements of the concentration of carbon monoxide in the atmospheric surface layer using tunable diode lasers 24 p3583 A83-49110

Development of instrumentation for monitoring natural ultraviolet radiation 24 p3583 A83-49111

The atmospheric lifetime experiment. I - Introduction, instrumentation, and overview 24 p3606 A83-49328

The atmospheric lifetime experiment. III - Lifetime methodology and application to three years of CFCL3 data 24 p3606 A83-49330

The Atmospheric Lifetime Experiment. VI - Results for carbon tetrachloride based on 3 years data 24 p3607 A83-49332

Some implications of acid rain field studies 24 p3602 A83-49684

Characterization of the transport and dispersion of pollutants in a narrow mountain valley region by means of an atmospheric tracer 24 p3602 A83-50187

Forecasting peak ozone levels 24 p3602 A83-50188

On the treatment of point source emissions in urban air quality modeling 24 p3602 A83-50189

A long-range atmospheric tracer field test 24 p3616 A83-50190

Aircraft observations of regional transport of ozone in the northeastern United States 24 p3603 A83-50191

Measurements of benzene, toluene and xylenes in urban air 24 p3603 A83-50192

In-situ, rapid response measurement of H2SO4/(NH4)2SO4 aerosols in urban Houston - A comparison with rural Virginia 24 p3603 A83-50193

Size-differentiated composition of inorganic atmospheric aerosols of both marine and polluted continental origin 24 p3603 A83-50194

AIR QUALITY

The hygienic characteristic of the air environment in buildings during artificial ionization

- 01 p0086 A83-11396
- Air quality mathematical modeling in the presence of strong point emissions 04 p0507 A83-16156
- Intercomparisons of upper air and surface winds in an urban region 06 p0781 A83-18238
- A framework for evaluating air quality models 06 p0781 A83-18240
- July 1981 NASA workshop on passive remote sensing of the troposphere 09 p1283 A83-24889
- Air monitoring - Research needs 21 p3169 A83-45616
- Laboratory evaluation of an airborne ozone instrument that compensates for altitude/sensitivity effects 21 p3092 A83-45618

AIR SAMPLING

- Correlation between surface and cloud base CCN spectra in Montana --- Cloud Condensation Nuclei 02 p0216 A83-12953
- Arctic haze and the Arctic gas and aerosol sampling program /AGASP/ [AIAA PAPER 83-0439] 05 p0659 A83-16714
- Acetonitrile in the lower troposphere 07 p0959 A83-20197
- Characterization of trace gases in 1980 volcanic plumes of Mt. St. Helens 07 p0960 A83-20215
- Innovative air data system for the Space Shuttle Orbiter 07 p0872 A83-20421
- Global circulation of volcanic debris of Mt. St. Helens - Evidence from the change of chemical constituents in the surface air 09 p1304 A83-23898
- Semiautomatic nondispersive infrared analyzer apparatus for CO2 air sample analyses 09 p1295 A83-24258
- Preliminary study of CO2 variations at Amsterdam Island /Terroire des Terres Australes et Antarctiques Francaises/ 09 p1295 A83-24259
- Interpretation of atmospheric CO2 measurements at Mt. Cimone /Italy/ related to wind data 09 p1295 A83-24260
- Sampling strategy to obtain data used in models of global annual CO2 increase and global carbon cycle 09 p1295 A83-24262
- Selection of CO2 concentration data from whole-air sampling at three locations between 1968 and 1974 09 p1295 A83-24263
- Evidence for aerosol chlorine reactivity during filter sampling 09 p1299 A83-25203
- An investigation of the atmospheric HNO3-NH3-NH4NO3 equilibrium relationship in a cool, humid climate 11 p1613 A83-27675
- Palladium-silicondioxide-silicon structures as hydrogen sensors in electrolytes 12 p1712 A83-29464
- On the quasi-biennial oscillation in equatorial stratospheric temperatures and total ozone 12 p1756 A83-29581
- Monitoring aerosol elemental composition in particle size fractions of long-range transport 13 p1874 A83-30180
- Stratospheric N2O, CF2Cl2, and CFC13 composition studies utilizing in situ cryogenic, whole air sampling methods [AD-A128389] 13 p1873 A83-30891
- An aerosol and gas sampling apparatus for remote observatory use 13 p1847 A83-30905
- Characterization of the atmospheric aerosol over the eastern equatorial Pacific 16 p2380 A83-36149
- Trace gas profiles to 3000 m over Antarctica 19 p2863 A83-41972
- Calibration and tests of the filter-collection method for measuring clean-air, ambient levels of nitric acid 20 p2991 A83-43432
- Air monitoring - Research needs 21 p3169 A83-45616
- Determination of particulate and gaseous arsenic compounds in the atmosphere at trace levels 22 p3320 A83-45714
- Physicochemical characterization of trace metal compounds in airborne particulate matter 22 p3320 A83-45715
- PAN concentrations in ambient air in New Jersey 22 p3321 A83-46900
- Aerosol composition at Chacaltaya, Bolivia, as determined by size-fractionated sampling 23 p3486 A83-48686
- On the concentration of mercury in the atmosphere in background regions 24 p3604 A83-49108
- Interstitial CCN measurements --- Cloud Condensation Nuclei 24 p3611 A83-49687
- Aircraft observations of regional transport of ozone in the northeastern United States 24 p3603 A83-50191

AIR SEA ICE INTERACTIONS

The use of model experiments performed in natural conditions to study the interaction of petroleum products with the ocean and atmosphere

- 01 p0069 A83-10834
- The utilization of infrared /IR/ aerial and space observations of Arctic seas in navigation and during the solution of other national-economic problems 01 p0077 A83-10836
- A one-dimensional model of the atmosphere considered as a climatic system block comprising the ocean, the atmosphere, and the ice cover 03 p0371 A83-14826
- Origin, nature and world climate effect of Arctic Ocean ice-cover [AD-A130919] 03 p0344 A83-14922
- A possible marine mechanism for internally generated long-period climate cycles 04 p0517 A83-15944
- Momentum and heat transfers in the surface layer over a frozen sea 06 p0788 A83-18059
- Global mean sea level - Indicator of climate change 08 p1144 A83-22325
- Norwegian remote sensing experiment in a marginal ice zone 13 p1894 A83-31198
- Atmosphere - Sea ice interactions in the Beaufort/Chukchi Sea and in the European sector of the Arctic 15 p2208 A83-33497
- Determining the form drag contribution to the total stress of the atmospheric flow over ridged sea ice 15 p2203 A83-33498
- Variability of antarctic sea ice and changes in carbon dioxide 15 p2208 A83-33775
- Sensitivity studies with a coupled ice-ocean model of the marginal ice zone 20 p3032 A83-43475
- The influence of poloidal motions and latent heat release on the equilibrium ice extent in a simple climate model 21 p3180 A83-44703
- Mathematical model of the glaciers-ocean-atmosphere system 24 p3610 A83-49556

AIR SEA INTERACTIONS

U AIR WATER INTERACTIONS

AIR SICKNESS

U MOTION SICKNESS

AIR TO AIR MISSILES

NT SPARROW MISSILES

- Development and evaluation of advanced air-to-air missile fire control algorithms and displays 01 p0006 A83-11191
- Air-to-air missiles - Flight test in the 80's 02 p0134 A83-11805
- Phoenix missile system - Still the one to beat 04 p0441 A83-16452
- Thirty years of fighter armament 07 p0866 A83-20600
- Algorithm development for infra-red air-to-air guidance systems - How to separate the wheat from the chaff: A simple approach to target detection 11 p1528 A83-28178
- On the certainty of synergistic effects --- in environmental reliability testing 13 p1862 A83-31480
- Analysis of missile response to gunfire environment --- vibration and shock effects on captive-carry configuration aboard aircraft 13 p1806 A83-31495
- AMRAAM - Tomorrow's Sparrow 14 p1969 A83-32844
- Multicriteria optimization of air-to-air missiles 17 p2460 A83-37133
- Identification of a nonlinear polynomial model for an air-to-air missile using the GMDH algorithm 17 p2460 A83-37134
- Nonlinear generalized likelihood ratio algorithms for maneuver detection and estimation 17 p2461 A83-37136
- Investigation of time-to-go algorithms for air-to-air missiles 17 p2461 A83-37137
- Numerical investigation of three-dimensional transonic flow through air intakes disturbed by a missile plume [AIAA PAPER 83-1854] 17 p2457 A83-38682
- New target models for homing missile guidance [AIAA PAPER 83-2166] 19 p2795 A83-41662
- Design of an integrated strapdown guidance and control system for a tactical missile [AIAA PAPER 83-2169] 19 p2796 A83-41665
- An eccentric two-target differential game model for qualitative air-to-air combat analysis [AIAA PAPER 83-2122] 19 p2789 A83-41947

AIR TO AIR REFUELING

- The KC-10A - USAF's newest range extender 03 p0281 A83-14700
- C-141 operations in Operation Bright Star 82 12 p1699 A83-29203
- Validation of the KC-10 refueling boom digital control system [SAE PAPER 821421] 17 p2463 A83-37978

AIR TO AIR ROCKETS

U AIR TO AIR MISSILES

AIR TO SURFACE MISSILES

- B-52 roles in sea control 07 p0862 A83-20646

AIR TRAFFIC

- Modeling the spatial distribution of aircraft on visual flight rules 09 p1200 A83-24040
- Air traffic and requirements for future passenger aircraft [DGLR PAPER 82-024] 09 p1195 A83-24151
- Height measurement by quadrilateration 18 p2674 A83-39252

AIR TRAFFIC CONTROL

NT RADAR APPROACH CONTROL

- Use of aircraft-derived data to assist in ATC tracking systems. II - Some practical tracking filters 02 p0133 A83-11557
- Observations regarding the MNPS in the North Atlantic and considerations concerning their applicability in the European air space. I 02 p0133 A83-13011
- Collision risk models 02 p0133 A83-13012
- A procedure for the utilization of the signals of a DME transponder to determine the position of an aircraft from the ground 02 p0134 A83-13016
- An overview of relevant issues in mid-air crash litigation 03 p0400 A83-13431
- A nonlinear smoothing procedure for the reconstruction of flight trajectories on the basis of radar data 03 p0280 A83-14494
- Center Weather Service Unit - The future of aviation weather services [AIAA PAPER 83-0445] 05 p0666 A83-16718
- Air traffic management - Current problems and future concepts; Proceedings of the Spring Convention, London, England, May 12, 13, 1982 05 p0593 A83-17726
- NATS - Taking stock --- National Air Traffic Services in United Kingdom 05 p0593 A83-17727
- Air traffic management - The impact at the airport 05 p0593 A83-17728
- National air traffic services implementation plans 05 p0593 A83-17729
- Air traffic management research at the Royal Signals and Radar Establishment 05 p0593 A83-17730
- The capability and potential role of airborne avionics systems in air traffic management 05 p0593 A83-17731
- Human factors of future air traffic control systems 05 p0677 A83-17732
- The impact of new air traffic systems on the flight deck 05 p0593 A83-17733
- Some advances in ground systems for air traffic control 05 p0593 A83-17734
- Air traffic flow management over Europe 05 p0593 A83-17735
- Fuel savings in air transport 06 p0714 A83-19150
- Performance analysis of a dwell-time processor for monopulse beacon radars 08 p1044 A83-22726
- Reply correlation test analysis in monopulse beacon radars 08 p1044 A83-22727
- Aircraft separation assurance - Systems design 09 p1199 A83-23371
- The role of advanced navigation in future air traffic management 09 p1199 A83-23372
- Air traffic control for tomorrow - Problems and solutions 09 p1200 A83-23494
- Instrument Landing Systems /ILS/ at GDR airports. II 09 p1200 A83-23495
- New on board equipments /PMS, FMS/ and the ATC system - Evolution or revolution 09 p1204 A83-24859
- Aircraft separation assurance - Systems design 09 p1201 A83-24863
- The role of advanced navigation in future air traffic management 09 p1201 A83-24867
- Structure and mode of operation of an interactive onboard four-dimensional flight path control system 10 p1378 A83-26478
- Conflict recognition and collision probability in connection with horizontal evasion maneuvers 10 p1373 A83-26481
- Advantages of statistically interrogating onboard anticollision systems 10 p1374 A83-26482
- Air traffic flow control systems - Modelling and evaluation 10 p1374 A83-26602
- Data transmission in the case of secondary radar /Mode S/ 11 p1527 A83-27124
- International aspects of air traffic control liability. I 11 p1666 A83-27968
- Automation of preplanning as a means for improving quality in connection with flight operational control. I 12 p1699 A83-29372
- Energy conservation in air transportation - The Canadian Air Traffic Control Effort 12 p1699 A83-29393
- Analysis of in-trail following dynamics of CDTI-equipped aircraft --- Cockpit Displays of Traffic Information 13 p1807 A83-30161
- Air traffic control into the 21st century 13 p1805 A83-30275

Advanced navigation systems and fuel conservation 15 p2120 A83-33545

On the use of height rules in off-route airspace 15 p2121 A83-35274

Computer model of a collision-avoidance system for air traffic control 15 p2121 A83-35275

All weather heliports and airway system - The future need 16 p2312 A83-36073

The man-vehicle systems research facility - A new NASA aeronautical R & D facility [AIAA PAPER 83-1098] 16 p2312 A83-36218

Development of airborne collision avoidance algorithms compatible with the national airspace system 17 p2461 A83-37141

The future of civil avionics 17 p2461 A83-37819

Helicopter IFR - The economics of schedule regularity [SAE PAPER 821501] 17 p2459 A83-38009

Short-term prediction of high reflectivity contours for aviation safety 17 p2550 A83-38726

Meteorological data requirements for fuel efficient flight 17 p2552 A83-38760

Air traffic control problems in the field of general aviation 17 p2460 A83-38931

Automation of preplanning as a means for enhancing quality in operational flight control. II 18 p2638 A83-39222

The COMPAS system for more efficient approach traffic --- for aircraft 18 p2639 A83-39345

Helicopter IFR approaches into major terminals using RNAV, MLS, and CDTI 19 p2794 A83-41042

The role of the Air Force in the transfer of general-aviation-traffic control from ITAV to AAVV/TAG 19 p2795 A83-41226

Instrument-approach technique for poor-visibility landings 19 p2795 A83-41228

Safety in the skies 19 p2794 A83-41467

Mixing 4D equipped and unequipped aircraft in the terminal area [AIAA PAPER 83-2240] 19 p2796 A83-41717

Human factors in air traffic control 21 p3189 A83-44881

Status of the TCAS program 22 p3255 A83-46959

Air traffic control simulation in the airport area 23 p3401 A83-47200

Improvements in SSR 23 p3401 A83-47655

Analysis of general aviation accidents using ATC radar records 23 p3400 A83-48218

AIR TRAFFIC CONTROLLERS (PERSONNEL)

Human factors of future air traffic control systems 05 p0677 A83-17732

Problems of representation of air traffic controllers in mid-air litigation 07 p1002 A83-21547

A study of the physiological behavior in a real-world situation of 70 front line air traffic controllers with regard to the neurovegetative, neuromuscular, and ophthalmologic modifications, and alertness 08 p1148 A83-22968

Analysis of continuous electrocardiographic tracing of air traffic controllers recorded during work 08 p1148 A83-22969

A preliminary study using surface electromyography of the behavior of air traffic controllers according to the density of traffic 08 p1148 A83-22971

Remarks on the systematic tonal audiometry of the ground personnel in charge of airspace security 08 p1148 A83-22972

The measurement of risk indicators for coronary heart disease in Air Traffic Control Officers - A screening study in a healthy population 10 p1454 A83-25672

The current technique for radar control room lighting of the French Air Force 14 p2071 A83-32457

The human element in air traffic control - Aeromedical aspects, problems, and prescriptions 15 p2214 A83-34981

Evaluation of system performance in the air-traffic-control workplace 17 p2563 A83-38933

International aspects of air traffic control liability. II 19 p2907 A83-40900

The changes in the cardiac rhythm of air traffic controllers using automated systems 23 p3497 A83-47112

AIR TRANSPORTATION

Fuel savings in air transport 06 p0714 A83-19150

The transport aircraft of tomorrow - A single element of an overall system 06 p0711 A83-19410

The development of standards for the common ICAO Data Interchange Network /CIDIN/ 08 p1075 A83-22027

International Congress on Aerospace Medicine, 29th, Nancy, France, September 7-11, 1981, Scientific Reports 08 p1147 A83-22951

Economic conditions and key points of BMFT air transport research requirements in the eighties [DGLR PAPER 82-044] 09 p1196 A83-24168

New technologies from developments in air transport and space travel [DGLR PAPER 82-074] 09 p1369 A83-24188

Energy conservation in air transportation - The Canadian Air Traffic Control Effort 12 p1699 A83-29393

Planning intra-airport transportation - A framework for decision making [AIAA PAPER 83-1585] 14 p1978 A83-33356

Concepts for a future joint airlift development program [AIAA PAPER 83-1591] 16 p2297 A83-36951

USAF mobility requirements --- User requirements [AIAA PAPER 83-1588] 16 p2297 A83-36954

A study of dirigibles for use in the Peruvian Selva Central region [AIAA PAPER 83-1970] 17 p2459 A83-38902

The preliminary design of a very large pressure airship for civilian and military applications [AIAA PAPER 83-2005] 17 p2466 A83-38923

The activity of the Italian Air Rescue Service in the transport of high-risk patients in emergency situations 17 p2557 A83-38943

Flight frequency determination 22 p3251 A83-46776

AIR WATER INTERACTIONS

NT AIR SEA ICE INTERACTIONS

On the circulation of the western Gulf of Mexico - A satellite view 01 p0076 A83-10113

Structure of air flow separation over wind wave crests 01 p0075 A83-10725

A model for the formation of a temperature inversion layer in a thin atmosphere stratum adjacent to water 01 p0076 A83-10910

The Marangoni wave in ripples on an air-water interface covered by a spreading film 01 p0069 A83-11047

On some characteristics of the atmospheric boundary layer in the Indian Ocean during the GARP cruise 02 p0212 A83-11846

The exchange of CO2 between the ocean and atmosphere 02 p0205 A83-11980

Aircraft observations of marine stratocumulus during JASIN --- Joint Air-Sea Interaction Experiment 02 p0215 A83-12940

Satellite estimates of ocean-air heat fluxes during cold air outbreaks 02 p0218 A83-13059

Comments on 'Planetary-scale atmospheric phenomena associated with the Southern Oscillation' 02 p0218 A83-13063

Effects of mesoscale atmospheric convection cells on the waters of the East China Sea 03 p0363 A83-13270

Marine sediment tolerances for remote sensing of atmospheric aerosols over water 03 p0373 A83-14380

Numerical simulation of the airflow over Lake Michigan for a major lake-affected snow event 03 p0368 A83-14438

Lake-effect disturbances over Lake Michigan - Some numerical results 03 p0368 A83-14439

An operational turbulence closure model forecast system 03 p0369 A83-14451

A comparison of spectral and cospectral characteristics of dynamic and thermal turbulent fields in weakly stratified boundary layers 03 p0319 A83-14475

On the use of laser profilometry for ocean wave studies 03 p0373 A83-14502

The relationship between atmospheric pressure fields and the sea level at the Kuril Islands 03 p0372 A83-14832

Dynamics of the baroclinic unstratified planetary boundary layer over land and sea 04 p0515 A83-15721

Assessment of the separate effects of baroclinicity and thermal stability in the atmospheric boundary layer over the sea 04 p0516 A83-15857

The interactive evolution of the oceanic and atmospheric boundary layers in the source regions of the trades 06 p0790 A83-18260

The origins of sulfur compounds in the atmosphere of a zone of high productivity /Gulf of Guinea/ 07 p0956 A83-20203

Air-sea particle exchange at a nearshore oceanic site 07 p0956 A83-20204

Reflectance contrast observed by Landsat between a calm and a rough sea 07 p0971 A83-21434

The numerical simulation of the turbulent boundary layers at a rough, air-water interface 08 p1089 A83-23196

Royal Society, Discussion on the Joint Air-Sea Interaction Project /JASIN/, London, England, June 2, 3, 1982, Proceedings 09 p1309 A83-23351

Transfer processes at the air-sea interface 09 p1317 A83-23352

Mass, momentum, sensible heat and latent heat budgets for the lower atmosphere 09 p1309 A83-23353

The structure of the turbulent atmospheric boundary layer 09 p1309 A83-23354

Boundary layer structure in relation to large-scale flow - Some remarks on the JASIN observations 09 p1310 A83-23357

Lake-effect snow storms on Lake Michigan, USA 09 p1312 A83-23956

Preliminary study of CO2 variations at Amsterdam Island /Territoire des Terres Australes et Antarctiques Francaises/ 09 p1295 A83-24259

Tropospheric NO/x/ and O3 budgets in the equatorial Pacific 09 p1305 A83-24264

A subsatellite experiment in the Arctic --- atmospheric radiation study 09 p1316 A83-25233

Numerical simulation of the airflow over Lake Michigan for a major lake-effect snow event 10 p1451 A83-25392

Transport of certain substances through the atmosphere-ocean interface in the region of the Bering Sea 10 p1447 A83-25610

Sea surface winds from sun glitter observations 10 p1452 A83-25972

A coupled ice-ocean model of upwelling in the marginal ice zone 10 p1452 A83-26348

Observation of internal waves in the ocean 10 p1453 A83-26812

Methane flux across the air-water interface - Air velocity effects 11 p1615 A83-27670

On the response of ocean currents to atmospheric cooling 11 p1635 A83-28084

An analysis of the surface production of sea-salt aerosols 11 p1616 A83-28091

Interrelationship of temperature fields in the ocean-atmosphere system /Considering the example of the North Atlantic/ 11 p1633 A83-28205

Distribution of ocean surface temperature in connection with features of atmospheric processes and hydrometeorological fields /According to POLYMODE data/ 11 p1634 A83-28208

El Nino Southern Oscillation phenomena 11 p1634 A83-28394

Marine biological controls on atmospheric CO2 and climate 11 p1600 A83-28400

Modelling the height, temperature and relative humidity of a well-mixed planetary boundary layer over a water surface 12 p1758 A83-29131

Statistical reliability and the seasonal cycle - comments on 'Bottom pressure measurements across the Antarctic Circumpolar Current and their relation to the wind' 12 p1759 A83-29527

The thermohaline driving mechanism of oceanic jet streams 12 p1761 A83-29553

The dynamics of singular geostrophic vortices in a two-level model of the atmosphere (ocean) 13 p1873 A83-30026

The shape of the spectrum of the energy-carrying components of the water surface in the weakly turbulent theory of wind waves 13 p1894 A83-30031

The effect of waves on the vertical profiles of wind velocity and on momentum fluxes in the atmospheric surface layer at sea 13 p1883 A83-30033

The modeling of certain long-period atmospheric processes 13 p1884 A83-30292

A simulation of the carbon cycle in the system atmosphere-ocean-biosphere in the framework of linear and diffusion models 13 p1874 A83-30296

The distribution of radioactive carbon-14 of anthropogenic origin between the atmosphere and ocean since 1963 13 p1872 A83-30297

The thermal interaction between the ocean and the atmosphere at the surface in the trade-wind zone in the North Atlantic 13 p1884 A83-30300

The influence of coastal shape on winter mesoscale air-sea interaction 13 p1891 A83-30801

A model of tropical ocean-atmosphere interaction 13 p1891 A83-30807

Uptake of excess CO2 by an outcrop-diffusion model of the ocean 13 p1869 A83-30877

Tracing bomb C-14 in the atmosphere 1962-1980 13 p1876 A83-30878

Some comments on the exchange of CO2 across the air-sea interface 13 p1869 A83-30879

On the production of Aitken nuclei from breaking waves and their role in the atmosphere --- maritime aerosols from ocean whitecap bubble bursting 13 p1893 A83-31043

The cosmic horizons of climatology 13 p1893 A83-31315

Three-dimensional numerical model of wind-wave interaction 13 p1894 A83-31341

A simple model of the ocean climate 13 p1894 A83-31349

Thermodynamic model of the seasonal evolution of the ocean-atmosphere system 13 p1894 A83-31350

Modeling the carbon cycle using the method of fractional-order derivatives 14 p2051 A83-32366

AIRBORNE EQUIPMENT

Factors affecting the variability of the structure of the upper ocean layer in the tropics

14 p2059 A83-32373
Investigation of the characteristics of wind waves on the basis of variations of intrinsic and scattered radiation of the sea surface 14 p2059 A83-32502
The dependence of wave parameters on the velocity of wind, the duration of its action, and the acceleration in the theory of weakly turbulent wind waves

14 p2059 A83-32859
The transfer of momentum from wind to waves

14 p2059 A83-32863
Low-frequency current and temperature variability from Gulf Stream frontal eddies and atmospheric forcing along the southeast U.S. outer continental shelf

14 p2059 A83-33076
Oceanographic studies. Number 35 --- Russian book

15 p2208 A83-34351
Investigation of atmospheric processes of different scale in the POLYMODE experiment 15 p2206 A83-34352
Characteristics of thermobaric fields in the southwest part of the North Atlantic in the summer of 1977

15 p2206 A83-34353
Characteristics of the variability of atmospheric processes during the period of the experiment in the POLYMODE area 15 p2206 A83-34355
The excitation of inertial oscillations by atmospheric effects --- on ocean dynamic processes

15 p2209 A83-34357
Solar-tropospheric connections and the cold film of the world ocean 15 p2203 A83-34775

Effect of wind-generated waves on the transfer of solar radiation in the atmosphere-ocean system

15 p2209 A83-34994
Typical influences of moisture on profile measurements in the marine atmospheric surface layer

16 p2388 A83-35796
Determining latent heat flux at sea - A comparison between wind-wave interaction and profile methods

16 p2388 A83-35797
Gas-liquid interface behaviour in a pulse-tube thruster --- in hydrofoils and surface effect ships

16 p2362 A83-36320
[AIAA PAPER 83-1278]
Vertical profile of wind speed over the open sea

16 p2390 A83-36493
The effect of islands on low frequency equatorial motions 16 p2393 A83-36976

Estimation of the average exchanges in momentum and latent heat between the atmosphere and the oceans with Seasat observations 16 p2393 A83-36982

Model of marine aerosol generation via whitecaps and wave disruption 17 p2554 A83-38731

Convection model for stratus cloud over a warm water surface 18 p2720 A83-39012

Comparison of parameters of wave storm zones in the Pacific Ocean with cloud information from satellites

18 p2724 A83-39443
Sea pressure waves 18 p2731 A83-39444
The effect of sea roughness and atmospheric inhomogeneity on the microwave emission of the atmosphere-sea surface system

18 p2720 A83-40598
Henry's Law constants and the air-sea exchange of various low molecular weight halocarbon gases

18 p2705 A83-40645
Certain characteristics of the structure and dynamics of hydrophysical fields in the zone of the Lomonosov current at 18 deg 30 min W 19 p2870 A83-42103

On the thermal structure of the upper layer of the ocean 19 p2870 A83-42104

Measurement of heat flux through the ocean surface 19 p2870 A83-42112

Meteorological conditions in the Atlantic FGGE study area 19 p2869 A83-42121

The role of sea surface temperature in large-scale air-sea interaction 20 p3029 A83-42504

The ocean --- chemical composition 20 p3032 A83-42820

Air-sea fluxes of transient atmospheric species 20 p3021 A83-42850

Production rate of airborne sea-salt sulfur deduced from chemical analysis of marine aerosols and precipitation 20 p3021 A83-42853

Relationships between Pb and Pb-210 in aerosol and precipitation at a semiremote site in northern Wisconsin 20 p3014 A83-42854

Computation of turbulent flow over a moving wavy boundary 21 p3128 A83-43927

The possible link between net surface heating and El Nino 21 p3182 A83-43985

Atmospheric chloroform (CHCl₃) - Ocean-air exchange and global mass balance 21 p3169 A83-44378

The seasonal response of a general circulation model to changes in CO₂ and sea temperatures 21 p3179 A83-44393

Variations of zonal mean sea surface temperature and large-scale air-sea interaction 21 p3182 A83-44394

A new approach to evaluation of the atmospheric effects on upwelling radiance from the ocean 21 p3182 A83-44399

A general circulation model study of January climate anomaly patterns associated with interannual variation of equatorial Pacific sea surface temperatures 21 p3180 A83-44702

Boundary layer evolution in the region between shore and cloud edge during cold-air outbreaks 21 p3180 A83-44705

Oxygen and carbon dioxide exchange between the Arctic Ocean and the atmosphere 21 p3182 A83-45398

The effect of the stratification of the atmospheric boundary layer over water on the energy flux to waves 22 p3338 A83-45641

Emissivity of the sea surface 22 p3342 A83-45643

A practical approach to flux measurements of long duration in the marine atmospheric surface layer 22 p3338 A83-45710

Numerical simulation of the atmospheric response to equatorial Pacific sea surface temperature anomalies 22 p3340 A83-46844

Effect of two different atmospheric models of the absorptive rate of excess atmospheric carbon by the sea 22 p3333 A83-46881

The near-surface circulation of the North Pacific using satellite tracked drifting buoys 22 p3344 A83-46908

Interannual variability of the equatorial Pacific - Revisited 22 p3344 A83-46910

Boundary-layer structure over tropical oceans from TIROS-N infrared sounder observations 22 p3342 A83-46951

Dynamical interaction of sensible heat released by sea surface to the outburst of the cold air [IAF PAPER 83-104] 23 p3493 A83-47267

The wind field in the western Indian Ocean and the related ocean circulation 23 p3493 A83-47412

Large-scale thermal anomalies in the California current during the 1982-1983 El Nino 23 p3493 A83-47857

Dimethyl sulfide in the equatorial Pacific Ocean - A natural source of sulfur to the atmosphere 23 p3493 A83-47860

The spatial and temporal structure of internal inertial-gravity and topographic waves in the sea at frequencies close to the inertial frequency 23 p3493 A83-48563

The response of the ocean to changes in the greenhouse effect 23 p3493 A83-48564

Heat and mass transfer through a water/vapor interface with allowance for radiation --- in ocean-atmosphere interactions 24 p3616 A83-48947

Certain characteristics of the radiation balance in the cloudless atmosphere and at the ocean surface depending on the dustiness of the atmosphere 24 p3605 A83-49281

Use of long-lived radon daughters as indicators of exchange between the free troposphere and the marine boundary layer 24 p3610 A83-49345

Radiation tides in the ocean and atmosphere 24 p3608 A83-49545

AIRBORNE EQUIPMENT

NT AIRBORNE/SPACEBORNE COMPUTERS

NT LIGHT AIRBORNE MULTIPURPOSE SYSTEM

NT TERCOM

Airborne laser ranging system for monitoring regional crustal deformation 01 p0047 A83-10024

Remote mineralogical analysis using a high-resolution airborne spectroradiometer - Preliminary results of the Mark II system 01 p0062 A83-10035

Use of reflectance spectra of native plant species for interpreting airborne multispectral scanner data in the East Tintic Mountains, Utah 01 p0063 A83-10060

In-flight lightning data measurement system for fleet application - Flight test results 01 p0009 A83-11087

Airborne electronic terrain map display - An update 01 p0010 A83-11135

Computer simulation of waveforms on time division command/response multiplex data buses 01 p0042 A83-11150

Aircraft power management control system designed for fast response and high reliability 01 p0012 A83-11151

Investigation of constant turn-rate dynamics models in filters for airborne vehicle tracking 01 p0096 A83-11190

High voltage equipment parts evaluation tests --- for airborne power supplies 01 p0042 A83-11204

Ka-band passive/active airborne radar 01 p0007 A83-11239

Synthetic aperture radar signal processing for airborne applications 02 p0162 A83-11524

Use of aircraft-derived data to assist in ATC tracking systems. II - Some practical tracking filters 02 p0133 A83-11557

Horizontal displacement of simulated cloud particles by the propeller of an aeroplane --- particle measurement accuracy 02 p0216 A83-12944

Air Force Geophysics Laboratory /AFGL/ infrared sky survey experiments 03 p0405 A83-13454

Airborne measurements of infrared atmospheric radiance and sky noise 03 p0324 A83-13461

The aviation and radioelectronic equipment of the Yak-18T aircraft --- Russian book 03 p0282 A83-13814

Passive bathymetry with airborne multispectral scanner 03 p0372 A83-14288

On the use of laser profilometry for ocean wave studies 03 p0373 A83-14502

Performance testing of a three-bed molecular sieve oxygen generator 04 p0524 A83-15307

Novel airborne technique for aircraft noise measurements above the flight path 04 p0533 A83-15316

OBOGS and OBIGGS - The application of molecular sieves to aircrew breathing and aircraft survivability --- On-Board Oxygen Generator System and On-Board Inert Gas Generator System 04 p0525 A83-15430

Color selection and verification testing for airborne color CRT displays 04 p0524 A83-16128

Airborne electronic colour displays 04 p0448 A83-16133

The perception of colour on electro-optical displays 04 p0524 A83-16328

ASPJ update counters the changing threat --- Airborne Self-Protection Jammer System 05 p0592 A83-16866

A note on errors and uncertainties in NCAR aircraft pyrogeometer data from MONEX 05 p0644 A83-17275

The problem of the maximum data compression in an information system with large data flows 05 p0623 A83-17657

Measurements of ocean surface spectrum from an aircraft using the two-frequency microwave resonance technique 05 p0646 A83-17710

Passive microwave detection of river-plume fronts in the German Bight 05 p0646 A83-17713

Airborne operation of an infrared low-level wind shear prediction system 06 p0791 A83-18412

Experimental feasibility of the airborne measurement of absolute oil fluorescence spectral conversion efficiency 06 p0793 A83-18581

Effects of finite wire scatterers in the field of VOR 06 p0716 A83-19039

Minimum angular vibration design of airborne electro-optical packages 07 p0944 A83-19820

Assault breaker breaks out --- airborne radar targeting and weapons delivery systems 07 p0862 A83-20645

Influence of suspended inorganic sediment on airborne laser fluorosensor measurements 07 p0971 A83-20830

Hardware systems design of an airborne video bandwidth compressor 08 p1099 A83-22585

Graphite/epoxy material characteristics and design techniques for airborne instrument application 08 p1055 A83-22595

Observations of optical lightning emissions from above thunderstorms using U-2 aircraft 08 p1141 A83-22703

Navy real-time signal processor development - Second generation planned service standard 08 p1154 A83-22821

Spatial calibration of a multispectral data base --- of airborne scanner systems 08 p1045 A83-22882

Possible improvements in meteorology for aircraft navigation 09 p1199 A83-23373

Viewpoints on selection of collision avoidance systems 09 p1202 A83-24874

A materials study to find an advanced optical window material for 8 to 12 micron airborne applications 09 p1345 A83-24956

Gallium arsenide infrared windows for high-speed airborne applications 09 p1345 A83-24958

A study on airborne integrated display system and human information processing 10 p1456 A83-26086

The processing of synthetic aperture radar signals 10 p1404 A83-26473

Simultaneous observation of precipitation by the airborne microwave rain-scatterometer/radiometer and the ground-based weather radar system 11 p1625 A83-27018

Simulations of airborne Doppler radar 11 p1629 A83-27069

Technical and operational evaluation of wide-area coverage navigation systems in the continental United States 11 p1528 A83-28594

Laser sounding of aerosols using airborne and space facilities 12 p1755 A83-29563

Ultralight sounder - An airborne system for studying the planetary boundary layer 13 p1803 A83-30787

Analysis of missile response to gunfire --- vibration and shock on captive-carry configuration aboard aircraft 13 p1806 A83-31511

All-electric vs conventional aircraft - The production/operational aspects 14 p1974 A83-32576

Reducing the cost for airborne instrumentation hardware testing 14 p1978 A83-32928

The airborne Knollenberg cloud droplet spectrometer probes of DFVLR 15 p2164 A83-34054

Aerial testing of an N2 laser fluorosensor system 15 p2169 A83-34467

Optical photometry with the Kuiper Airborne Observatory 15 p2247 A83-34509

The NCAR Research Aviation Facility fleet workshop 18-19 February 1982, Boulder, Colo 16 p2287 A83-35744

Effect of suction on the wake structure of a three-dimensional turret [AIAA PAPER 83-1738] 17 p2445 A83-37217

Simulate airborne radar environments 17 p2461 A83-37821

A prospectus on airborne laser mapping systems 17 p2530 A83-38168

Geometric constraints in multispectral scanner data 17 p2532 A83-38361

Thunderstorm top structure observed by aircraft overflights with an infrared radiometer 18 p2724 A83-39681

Feasibility test of an airborne pulse-Doppler meteorological radar 18 p2726 A83-39872

ASTROPLANE - A European airborne observatory for infrared astronomy 18 p2762 A83-40455

Astroplane - The Airbus proposal 18 p2762 A83-40456

ASTROPLANE - A working group of the European Science Foundation 18 p2762 A83-40457

Airborne radar and the three PRFs --- Pulse Repetition Frequency 19 p2795 A83-40759

Numerical processing of an airborne thermal experiment conducted on an Oblako meteorological rocket, with Emmons' spot theory taken into account 19 p2791 A83-41271

A separator for obtaining samples of cloud water in aircraft 19 p2849 A83-41983

An overview of airborne optical communications 20 p2932 A83-42574

Neodymium YAG laser in airborne systems 20 p2936 A83-42835

Preprocessing of side-looking airborne radar data 20 p2990 A83-42968

Determination of ambient aerosol and gaseous sulfur using a continuous FPD. III - Design and characterization of a monitor for airborne applications --- flame photometric detector 20 p2991 A83-43434

Airborne radar tracking system based on optimal filtering theory 20 p2932 A83-43696

A versatile thermal imager for RPV applications 20 p2936 A83-43720

Imaging sensors for an RPV payload 20 p2936 A83-43721

A multi-function radar system for RPVs 20 p2932 A83-43722

Remote sensing --- of earth resources 21 p3165 A83-43820

Aircraft-borne lightning sensor 21 p3134 A83-43867

New generation lens systems for the wild aviophot aerial camera system 21 p3135 A83-43895

Improvements in cloud photogrammetry using airborne, side-looking, time-lapse cameras 22 p3307 A83-45707

Comment on 'Laboratory Evaluation of an airborne ozone instrument that compensates for altitude/sensitivity effects' 22 p3287 A83-45925

Airborne measurements of laser backscatter from the ocean surface 22 p3342 A83-46074

Marine gravity measurement from fixed wing aircraft 22 p3288 A83-46111

New results of airborne measurements with a sensitive high resolution 90 GHz radiometer 22 p3309 A83-46124

Modeling and deconvolution for reconstruction of airborne gamma ray radiometer data 22 p3288 A83-46125

The Delta-K ocean wave spectrometer - Aircraft measurements and theoretical system analysis 22 p3288 A83-46158

Observations of rainfall rates by the airborne microwave rain-scatterometer/radiometer 22 p3340 A83-46168

On the design and operation of a SLAR system with digital recording 22 p3289 A83-46181

Status of the TCAS program 22 p3255 A83-46959

Airborne CO2 laser heterodyne sensor for monitoring regional ozone distributions 23 p3456 A83-47773

Remote sensing of tropospheric gases and aerosols with airborne DIAL system 23 p3478 A83-47783

Mineralogic information from a new airborne thermal infrared multispectral scanner 23 p3475 A83-47816

Spatial and temporal variations of cloud liquid water determined by aircraft and microwave radiometer measurements in northern Colorado orographic storms 24 p3615 A83-49724

Cumulus convection as observed from an airborne infrared radiometer 24 p3615 A83-49726

AIRBORNE INFECTION

An investigation of the shielding effectiveness of FPP-15 fabric relative to bacterial aerosols 05 p0677 A83-17201

AIRBORNE INTEGRATED RECONNAISSANCE SYSTEM

Remote sensing software for airborne image analysis 03 p0349 A83-14273

AIRBORNE SURVEILLANCE RADAR

A ray tracing computer analysis program /RAYCAP/ for airborne surveillance radar applications 01 p0007 A83-11243

A technique to empirically model clutter signals in airborne pulse Doppler radar 01 p0008 A83-11251

Propagation effects on a VHF radar [ONERA, TP NO. 1982-96] 03 p0308 A83-14545

Advanced tactical air reconnaissance system 08 p1041 A83-22575

Radar - Reflections on radio waves 08 p1078 A83-23250

An adaptive scheme for optimal target detection in variable clutter environment 09 p1200 A83-24779

Doppler radar and aircraft measurements of thunderstorm turbulence 11 p1627 A83-27043

Adaptive clutter suppression for airborne phased array radars 11 p1527 A83-27919

Weibull-distributed sea clutter 20 p2965 A83-43687

Status of the TCAS program 22 p3255 A83-46959

AIRBORNE/SPACEBORNE COMPUTERS

Computer support system 01 p0088 A83-10787

Air data systems for airplanes of the 1990's 01 p0004 A83-11099

Technology upgrade to ALR-46 and ALR-69 radar warning receivers 01 p0005 A83-11102

Embedded microprocessors for avionics applications 01 p0088 A83-11104

Marconi avionics standard central air data computer 01 p0009 A83-11119

The U.S. Air Force and U.S. Navy Standard Central Air Data Computer 01 p0009 A83-11120

Terrain following/terrain avoidance for advanced penetrating aircraft 01 p0006 A83-11146

A prototype parallel computer architecture for advanced avionics applications 01 p0088 A83-11153

An AN/APN-194/V/ radar altimeter/MIL-STD-1553 interface circuit 01 p0010 A83-11186

Jovial language control procedures with a view toward Ada 01 p0092 A83-11198

Integrated and transferable hardware/software checkout --- of digitally controlled flight systems 01 p0093 A83-11249

Distributed processing and fiber optic communications in air data measurement 01 p0011 A83-11258

The A6E /TRAM/ all-weather weapon system --- Target Recognition and Attack Multisensor 01 p0008 A83-11260

Some thoughts on the development of computer-based systems --- airborne equipment design to cost 02 p0135 A83-11807

Software and system level tests of a test flight mercury ion thruster subsystem [AIAA PAPER 82-1912] 02 p0145 A83-12485

Autonomous star cataloging for space surveillance missions 03 p0406 A83-13468

Spacelab software for science applications 03 p0285 A83-13710

Celestial navigation in the computer age --- Book 03 p0280 A83-14116

Operational planning of the process of earth survey by satellites 03 p0350 A83-14314

Attitude control of a satellite with a rotating solar array 03 p0287 A83-14845

The history of Apollo onboard guidance, navigation, and control 04 p0453 A83-16114

Semantic definitions of spacecraft command and control languages using hierarchical graphs 04 p0527 A83-16117

Spacecraft computer resource margin management --- of Project Galileo Orbiter in-flight reprogramming task 04 p0527 A83-16118

Digital electronic engine control system - F-15 flight test 06 p0718 A83-18406

Flight evaluation of modifications to a digital electronic engine control system in an F-15 airplane [AIAA PAPER 83-0537] 06 p0718 A83-19593

Fault tolerant techniques for a multiple microprocessor-based space borne packet switch 07 p0906 A83-19714

Microcomputer-based improvements to the AFSATCOM System 07 p0906 A83-19716

On-board process - An overview 07 p0910 A83-19771

The automated cockpit 07 p0866 A83-20849

The software-implemented fault tolerance /SIFT/ approach to fault tolerant computing 08 p1155 A83-22825

Computer-generated images in visual simulation and avionic technologies 08 p1047 A83-22835

Data systems - Optical bus will connect distributed system 09 p1215 A83-24352

Flight management systems and data links 09 p1209 A83-24424

Recent developments in digital control for helicopter powerplants 09 p1207 A83-24829

Carrier Aircraft Inertial Navigation System /CAINS/ integrated system approach 09 p1201 A83-24854

Experimental system for computer network via satellite /CS/. II - Communication protocols 10 p1403 A83-26078

Experimental system for computer network via satellite /CS/. V - Data collecting and processing system 10 p1403 A83-26081

Computer control of the Infra-Red Astronomical Satellite /IRAS/ 10 p1384 A83-26583

Software for automatic control of spacecraft instruments 10 p1382 A83-26598

Development of adaptation and identification algorithms in adaptive digital aircraft control systems 10 p1379 A83-26600

Application of redundant processing to Space Shuttle 10 p1381 A83-26610

OAO-3 end of mission power subsystem evaluation 11 p1538 A83-27133

On board computing - Intelligent modules add a new dimension to satellite control systems 11 p1645 A83-28169

On the routes - Boeing 757 with British Airways 12 p1701 A83-29241

Space Shuttle primary onboard software - STS-1 to operational use 13 p1909 A83-30157

Microcomputer applications in space-borne instruments 13 p1815 A83-30776

The use of onboard computers for satellite testing 13 p1815 A83-31187

Cost effective development of a Shuttle-based astronomical instrument control system 14 p1984 A83-32040

Integrated verification and testing system (IVTS) for HAL/S programs 15 p2219 A83-33971

Some aspects of development of power plant optimum control to increase aircraft fuel efficiency 16 p2303 A83-35841

Flight management concepts development for fuel conservation 16 p2304 A83-35843

Compensation for time delay in flight simulator visual-display systems [AIAA PAPER 83-1080] 16 p2312 A83-36222

F/A-18A Inflight Engine Condition Monitoring System (IECMS) [AIAA PAPER 83-1237] 16 p2308 A83-36300

Computer performance monitoring during the Centaur launch countdown 17 p2472 A83-37060

HIMAT onboard flight computer system architecture and qualification 17 p2467 A83-37061

Design and analysis of a digitally controlled integrated flight/fire control system 17 p2460 A83-37063

Space station automation and autonomy - Advantages and problems 17 p2476 A83-37096

System design approaches to integrated controls 17 p2460 A83-37103

A microprocessor-based position control system for a telescope secondary mirror 17 p2476 A83-37433

Space Telescope pointing control 17 p2480 A83-37434

The attitude and orbit control system for GIOTTO, ESA's Halley encounter mission 17 p2476 A83-37435

The L-SAT attitude and orbit control subsystem 17 p2477 A83-37437

Validation techniques for spot attitude control system development 17 p2477 A83-37439

Validation of the in-orbit checkout of the IRAS gyroscopes using computer simulations 17 p2481 A83-37475

The HEAO experience - design through operations 17 p2473 A83-37482

Ground support software for the Exosat onboard computer 17 p2472 A83-37489

Interfacing Spacelab payloads for the first mission and the development of the processor interface adaptor (PIA) 17 p2482 A83-37873

The GEMPAK Barnes interactive objective map analysis scheme --- General Meteorological Software Package 17 p2548 A83-38709

Scientific French and Franco-Soviet experiment control and data transmission aboard the AUREOL-3 satellite 18 p2647 A83-39573

French-Soviet data processing system for Arcad-3 experiments 18 p2648 A83-39587

Guidance and control of a balloon-borne X-ray telescope with onboard and ground based computers 18 p2641 A83-39823

Flight management computers (FMS) 19 p2801 A83-40881

Autonomous failure detection and correction on Landsat-4 [AIAA PAPER 83-2265] 19 p2817 A83-41735

Digital Instrumentation Analysis and Navigation System (DIANS) for system identification [AIAA PAPER 83-2091] 19 p2799 A83-41922

Low cost antenna pointing system --- with computerized control for transmission from aircraft to satellite 20 p3038 A83-42575

Digital simulation and control of the Machan UMA 20 p2932 A83-43718

A low-risk hardened computer for today's spacecraft programs 21 p3190 A83-43999

Space technology - Computers: Learning from dinosaurs 21 p3191 A83-45602

The layer model and error control for satellite communications 22 p3273 A83-45756

Testing for space and weapon products; Proceedings of the Symposium, London, England, January 18, 1983 22 p3303 A83-45821

On target with confidence automated testing of guided weapons 22 p3303 A83-45822

Flight clearance of the Jaguar-fly-by-wire aircraft. II 22 p3255 A83-45846

A method of designing fault tolerant software 22 p3350 A83-45847

Certification of digital systems for civil aircraft 22 p3252 A83-45848

Modern digital air-data computer 23 p3405 A83-47186

New approaches to planetary exploration - Spacecraft and information systems design [IAF PAPER 83-348] 23 p3415 A83-47354

Integrated control system concept for high-speed aircraft [AIAA PAPER 83-2564] 24 p3549 A83-50074

AIRBUS

U EUROPEAN AIRBUS

AIRCRAFT

Aircraft leasing practices in the United States - A few observations 09 p1351 A83-25120

Evidence for the production of ice particles in clouds due to aircraft penetrations 24 p3612 A83-49691

AIRCRAFT ACCIDENT INVESTIGATION

Defendant's discovery plan in mid-air crash litigation 03 p0400 A83-13432

Developing the plaintiff's discovery plan in mid-air collision litigation 03 p0400 A83-13433

Human factors dilemmas in the quest for aviation safety 04 p0444 A83-15423

A method for investigating human factor aspects of aircraft accidents and incidents 04 p0523 A83-15899

Heavy rain influence on airplane accidents 06 p0714 A83-18415

Aircraft accident survivors as witnesses 07 p0865 A83-20788

General aviation accident rates and pilot community population size - An examination of rural-urban differences 12 p1766 A83-28935

Studies of damage involving aircraft components --- accident-causing metallic component fractures 12 p1699 A83-29371

Naval aviation mishaps and fatigue 15 p2215 A83-34985

Weather after the event --- for aircraft accident investigation 17 p2550 A83-38729

Analysis of rapid interval GOES data for the 9 July 1982 New Orleans airliner crash 17 p2553 A83-38767

Pilot judgment - Current developments in evaluation and training and future issues in aviation cases 18 p2736 A83-39042

Legislative developments affecting the aviation industry 1981-1982 18 p2752 A83-39043

Aircraft crashworthiness in the United States - Some legal and technical parameters 18 p2752 A83-39044

Experiences in medical coverage of airport disasters at Logan International Airport in Boston 18 p2638 A83-40356

International aspects of air traffic control liability. II 19 p2907 A83-40900

Reflections on the Potomac 21 p3089 A83-44876

Flight data recorders - An investigator's tool 21 p3092 A83-44877

The Jetstar overrun at Luton 21 p3089 A83-44880

Airports as a threat to public safety --- Book 22 p3251 A83-46420

Hazards of loose harness during flying 23 p3499 A83-48693

AIRCRAFT ACCIDENTS

NT BIRD-AIRCRAFT COLLISIONS

Stress coping and the U.S. Navy aircrew factor mishap 02 p0225 A83-12408

Observations regarding the MNPS in the North Atlantic and considerations concerning their applicability in the European air space. I 02 p0133 A83-13011

Recent developments in aviation case law 03 p0400 A83-13429

An overview of relevant issues in mid-air crash litigation 03 p0400 A83-13431

Extension of service life of rigid transfer lines /SMDC/ --- explosive components for aircraft escape systems 03 p0303 A83-14173

The role of endogenous circadian rhythmicity in Air-Force flight accidents due to pilot error 04 p0521 A83-15402

An analysis of the fatality rate data from 'jettison-canopy' and 'through-the-canopy' ejections from automated airborne escape systems 04 p0443 A83-15403

The human factor in mishaps - Psychological anomalies of attention 04 p0523 A83-15413

The United States Navy's injury experience in aircraft mishaps 04 p0445 A83-15441

Negative transfer - A threat to flying safety 04 p0523 A83-15541

The Montreal Agreement of 1966 and the Malta Agreement of 1965 05 p0692 A83-16975

The development and application of a full-scale wide-body test article to study the behavior of interior materials during a post crash fuel fire 06 p0719 A83-18373

Aerodynamic penalties of heavy rain on landing airplanes 06 p0714 A83-18403

Heavy rain influence on airplane accidents 06 p0714 A83-18415

Pilot performance and stress - Search for a killer 07 p0979 A83-20075

Problems of representation of air traffic controllers in mid-air litigation 07 p1002 A83-21547

Official liability for insufficient airworthiness - Comments in connection with a supreme-court decision 08 p1171 A83-21898

Optimum siting of NEXRAD to detect hazardous weather at airports 09 p1313 A83-24037

Pilot fatigue - A deadly cover-up --- Book 09 p1199 A83-24901

Conflict recognition and collision probability in connection with horizontal evasion maneuvers 10 p1373 A83-26481

The design of wind shear filters 10 p1378 A83-26483

Crashing for safety 13 p1805 A83-31588

Flight experience and naval aircraft mishaps 14 p2071 A83-32691

Vertebral lesions after the aircraft crashes 16 p2396 A83-35579

Status of FAA crash dynamics program - Transport category aircraft [SAE PAPER 82-1483] 17 p2459 A83-38002

An FAA analysis of aircraft emergency evacuation demonstrations [SAE PAPER 82-1486] 17 p2459 A83-38005

CAT detection and forecasting using operational NMC analysis data 17 p2553 A83-38765

Basilar skull fracture in U.S. Army aircraft accidents --- helmet design for pilot protection 18 p2737 A83-40359

A simulation study of the low-speed characteristics of a light twin with an engine-out [AIAA PAPER 83-2128] 19 p2806 A83-41951

The survivable aircraft fire 20 p2931 A83-43407

Analysis of aircraft dynamic behavior in a crash environment 21 p3091 A83-43966

Analysis of general aviation accidents using ATC radar records 23 p3400 A83-48218

AIRCRAFT ANTENNAS

Antenna couplers - The aircraft interface 01 p0004 A83-10738

The solution of 'real-world' aircraft EMC problems using the AAPG computer program 01 p0041 A83-11085

A technique for predicting antenna-to-antenna isolation and electromagnetic compatibility for aircraft 01 p0007 A83-11235

Properties of phase synchronizing sources for a radio camera 03 p0328 A83-14008

Airframe multipath effects in airborne adaptive antenna arrays 06 p0715 A83-18627

The application of sub-optimal control methods to adaptive antennas for airborne communication systems 06 p0715 A83-18632

A novel precise method of measuring the efficiency of arbitrary low-gain antennas 06 p0740 A83-18643

Near and far field airborne antenna pattern analysis 06 p0715 A83-18645

An asymptotic high frequency analysis of the radiation from sources on perfectly-conducting structures with an impedance surface patch 06 p0715 A83-18647

Recent examples of conformal microstrip antenna arrays for aerospace applications 06 p0715 A83-18672

Radiation patterns of a quarter-wave monopole on a finite ground plane --- for aircraft antennas 06 p0715 A83-18682

Perturbation adaptive array processor for airborne application 11 p1527 A83-27913

Low cost antenna pointing system --- with computerized control for transmission from aircraft to satellite 20 p3038 A83-42575

Laboratory and in flight passive dischargers characterization --- for elimination of electrostatic radiation interference [ONERA, TP NO. 1983-54] 23 p3400 A83-48176

AIRCRAFT APPROACH SPACING

Analysis of in-trail following dynamics of CDTI-equipped aircraft --- Cockpit Displays of Traffic Information 13 p1807 A83-30161

AIRCRAFT BASES

U MILITARY AIR FACILITIES

AIRCRAFT BRAKES

NT LEADING EDGE SLATS

NT TRAILING-EDGE FLAPS

NT WING FLAPS

Review of NASA antiskid braking research [SAE PAPER 821393] 17 p2463 A83-37969

AIRCRAFT CABINS

U AIRCRAFT COMPARTMENTS

AIRCRAFT CARRIERS

A review of naval aviation on-board oxygen generating systems 04 p0526 A83-15432

CTOL, STOAL, V/STOL - An operational comparison for forward deployed CVNs 08 p1043 A83-22157

The swath ship option as a V/STOL aircraft carrier [AIAA PAPER 83-0621] 08 p1172 A83-22170

Preliminary shipboard optical turbulence measurements 08 p1166 A83-22556

On the feasibility of real-time prediction of aircraft carrier motion at sea 10 p1463 A83-26265

Simulation evaluation of flight controls and display concepts for VTOL shipboard operations [AIAA PAPER 83-2173] 19 p2789 A83-41668

Extended pilot-vehicle-task models for Navy missions [AIAA PAPER 83-2233] 19 p2885 A83-41711

Integrated flight control systems development - The F/A-18A Automatic Carrier Landing System [AIAA PAPER 83-2162] 19 p2804 A83-41765

Carrier landing simulation results of precision flight path controllers in manual and automatic approach [AIAA PAPER 83-2072] 19 p2796 A83-41909

Evaluation of control and display configurations for helicopter shipboard operations [AIAA PAPER 83-2486] 23 p3405 A83-48346

AIRCRAFT COMMUNICATION

Integrated CNI avionics maximizes reliability --- communications, navigation, and cooperative identification 01 p0042 A83-11089

Integrated CNI - A new testing challenge --- Communication, Navigation and Identification 01 p0004 A83-11095

ICNIA - Lessons learned on sensor integration --- Integrated Communication Navigation Identification Avionics 01 p0004 A83-11096

Voice techniques on board aircraft - An experimental approach 01 p0005 A83-11123

Integrated CNI avionics logistics considerations 01 p0103 A83-11157

Fiber optics wavelength division multiplexing for aircraft applications 01 p0006 A83-11181

High speed data link concepts for military aircraft 01 p0010 A83-11233

The development of radio engineering 05 p0621 A83-16898

USAF ground fiber optic development program 07 p0906 A83-19711

Obscuration by helicopter-produced snow clouds 08 p1043 A83-22357

ARINC 429 digital data communications for commercial aircraft 09 p1200 A83-24435

A Differential Omega/VLF Navigator 09 p1201 A83-24856

Characterization of the dynamical response of receivers to fading 10 p1404 A83-26471

Data transmission in the case of secondary radar / Mode S/ 11 p1527 A83-27124

Probabilistic estimation of the efficiency of radio systems in the presence of interference 13 p1829 A83-30731

An overview of airborne optical communications 20 p2932 A83-42574

Wide-beam atmospheric optical communication for aircraft application using semiconductor diodes 21 p3090 A83-44159

AIRCRAFT COMPARTMENTS

The development and application of a full-scale wide-body test article to study the behavior of interior materials during a post crash fuel fire 06 p0719 A83-18373

Safety requirements and trends in the passenger aircraft cabin area [DGLR PAPER 82-043] 09 p1199 A83-24167

Evaluation of interior noise control treatments for high-speed propfan-powered aircraft [AIAA PAPER 83-0693] 10 p1375 A83-25914

Noise source identification in airplane cabins using acoustic intensity technique [AIAA PAPER 83-0716] 10 p1475 A83-25931

Performance decrement at cabin altitudes - A replication 10 p1455 A83-26303

Synchrophasing for cabin noise reduction of propeller-driven airplanes [AIAA PAPER 83-0717] 11 p1529 A83-28013

Choice of optimal cabin capacity --- statistical model for optimal number of seats in passenger aircraft 12 p1699 A83-29968

Ground and in-flight testing of new portable oxygen generators 14 p2072 A83-32465

Effectiveness of seat cushion blocking layer materials against cabin fires [SAE PAPER 821484] 17 p2459 A83-38003

A mathematical model on the thermal behaviour of an aircraft cabin --- Thesis 22 p3254 A83-46691

AIRCRAFT CONFIGURATIONS

Departure susceptibility and uncoordinated roll-reversal boundaries for fighter configurations 01 p0012 A83-10176

The fundamental geometrical and aerodynamic characteristics of aircraft and rockets --- Russian book 01 p0003 A83-10669

The water tunnel - A helpful simulation facility for the aircraft industry 01 p0014 A83-11080

A numerical simulation of three-dimensional transonic flows of compressible perfect fluids around aircraft by use of the finite element and least squares methods [AAAF PAPER NT 81-23] 02 p0169 A83-11779

Military potential of the ABC 02 p0134 A83-12097

The UH-60A Black Hawk - A world-wide force multiplier 02 p0135 A83-12934

Airframe effects on a top-mounted fighter inlet system 03 p0278 A83-13166

Problems concerning supersonic flow past bodies of prismatic configurations 04 p0443 A83-16394

PAN AIR applications to complex configurations --- computer program for predicting subsonic and supersonic linear potential flows [AIAA PAPER 83-0007] 05 p0577 A83-16459

Aerodynamic investigation of closely coupled lifting surfaces with positive and negative stagger for general aviation applications [AIAA PAPER 83-0057] 05 p0578 A83-16489

SAMID, an interactive system for the analysis and constrained minimization of induced drag of aircraft configurations [AIAA PAPER 83-0095] 05 p0594 A83-16519

A method for estimating the propulsion induced aerodynamic characteristics of STOL aircraft in ground effect [AIAA PAPER 83-0169] 05 p0594 A83-16567

Three-dimensional grid generation using elliptic equations with direct grid distribution control [AIAA PAPER 83-0448] 05 p0636 A83-16720

Numerical computation of transonic flow about wing-fuselage configurations on a vector computer [AIAA PAPER 83-0499] 05 p0587 A83-16751

On the aerodynamics of over-the-wing nacelles supported on 'stub-wings' [AIAA PAPER 83-0538] 05 p0595 A83-16774

Regular or catastrophic evolution of steady flows depending on parameters --- in aerodynamics 05 p0638 A83-17318

Finite-volume solutions to the Euler equations in transonic flow [AIAA PAPER 81-1265] 06 p0712 A83-18405

The Hummercraft 07 p0866 A83-21033

Configuration development for a highly maneuverable experimental aircraft with negative sweep rudder units [DGLR PAPER 82-035] 09 p1203 A83-24160

Delta canard configuration at high angle of attack 09 p1210 A83-24650

The response of aircraft to pulse excitation 15 p2122 A83-34312

KC-135/CFM56 re-engine - The best solution [AIAA PAPER 83-1374] 16 p2309 A83-36367

The F-16 - A technology demonstrator, a prototype, and a flight demonstrator. [AIAA PAPER 83-1063] 16 p2301 A83-36467

Configuration development of a research aircraft with post-stall maneuverability 16 p2301 A83-36915

Wind tunnel tests of over-the-wing nacelles --- supported on 'stub-wings' 16 p2296 A83-36916

Configuration studies for future fighters 17 p2462 A83-37859

NGT sub-scale flight demonstrator - A cost-effective approach to aircraft development --- Next Generation Trainer [SAE PAPER 821341] 17 p2462 A83-37952

Effects of nacelle position and shape on performance of subsonic cruise aircraft [AIAA PAPER 83-1124] 17 p2464 A83-38079

PAN AIR modeling studies --- higher order panel method for aircraft design [AIAA PAPER 83-1830] 17 p2455 A83-38660

Comparison of panel method formulations and its influence on the development of QUADPAN, an advanced low-order method [AIAA PAPER 83-1827] 18 p2632 A83-39097

Inviscid drag calculations for transonic flows [AIAA PAPER 83-1928] 18 p2635 A83-39380

Solution of the Euler equations for complex configurations [AIAA PAPER 83-1929] 18 p2635 A83-39381

B-1B manufacturing - Avco modifies prototype processes for production 18 p2632 A83-40333

Subsonic roll oscillation experiments on the Standard Dynamics Model [AIAA PAPER 83-2134] 19 p2806 A83-41956

A grid overlapping scheme for flowfield computations about multicomponent configurations 20 p2930 A83-43443

Unsteady aerodynamic forces and flutter analysis for a wing-aileron-tab configuration 20 p3008 A83-43688

Design, construction, and operation of the calibration model for the DNW wind tunnel 23 p3412 A83-47209

PAN AIR applications to complex configurations --- computer program for predicting subsonic and supersonic linear potential flows 23 p3399 A83-48221

Wave drag prediction using a simplified supersonic area rule 23 p3399 A83-48222

Effect of aircraft configuration and control integration on surface actuation [AIAA PAPER 83-2487] 23 p3404 A83-48347

Efficient computational grid generation for three-dimensional aircraft configurations [AIAA PAPER 83-2557] 23 p3405 A83-48376

Characteristics of the ground vortex developed by various V/STOL jets at forward speeds [AIAA PAPER 83-2494] 24 p3545 A83-49585

Exploratory low-speed wind-tunnel investigation of advanced commuter configurations including an over-the-wing propeller design [AIAA PAPER 83-2531] 24 p3548 A83-49590

AIRCRAFT CONSTRUCTION

U AIRCRAFT STRUCTURES

AIRCRAFT CONSTRUCTION MATERIALS

NT AIRFRAME MATERIALS

Materials for the manufacture of aircraft instruments and structures --- Russian book 01 p0021 A83-10466

High temperature aerospace materials prepared by powder metallurgy 02 p0153 A83-11508

A production engineers view of advanced composite materials 02 p0149 A83-11800

The use of composite materials in aircraft propellers 02 p0136 A83-12966

The impact of composite technology on commercial transport aircraft 02 p0135 A83-12969

Softening schedules for aging pressed semifinished products made from high-strength aluminum alloy V95pch 03 p0296 A83-13252

Polysulfide sealants for aerospace. I - Theory and background 03 p0302 A83-13562

The ULS experimental ultralight glider made of polymer composites. I - Genesis of the program and construction of the glider 03 p0281 A83-14621

Application of the ultrasonic testbed to graphite/organic composites 04 p0454 A83-15179

Helicopter technology for the 1990s 04 p0446 A83-16372

The application of energy saving concepts to future fighter/attack aircraft design [AIAA PAPER 83-0092] 05 p0594 A83-16516

Evolution of the application of composite materials to helicopters 06 p0716 A83-18376

AIRCRAFT CONSTRUCTION MATERIALS

Composite technology in the UK helicopter industry 06 p0716 A83-18377

Development of a structural, bird impact resistant, de-cised wing leading edge for the de Havilland Dash 8 aircraft using fibre-reinforced composites 06 p0717 A83-18823

A new high impact resin system for advanced composites with 300 F / 150 C/ properties 07 p0875 A83-20429

Material characterization and specification development for 350 F curing epoxy-graphite materials 07 p0875 A83-20443

Acousto-ultrasonic evaluation of impact-damaged graphite epoxy composites 07 p0875 A83-20454

The development of advanced composite front fuselage technology 07 p0865 A83-20464

High performance, low viscosity resin systems 07 p0899 A83-20465

Applications for Nextel in the aerospace industry 07 p0899 A83-20466

Superplastic forming/weld-brazing of titanium skin-stiffened compression panels 07 p0886 A83-20467

Low cost fabrication of sheet structure using a new beta titanium alloy, Ti-15V-3Cr-3Al-3Sn 07 p0886 A83-20469

Polyimide composites - Grumman application case histories 07 p0876 A83-20475

Service history of phosphoric acid anodized aluminum structure --- with adhesive bonding for aircraft construction 07 p0861 A83-20479

Damage tolerance and reparability of advanced composite structures 07 p0876 A83-20484

Advanced composite materials in aerobatic aircraft 07 p0865 A83-20496

Fabrication of aircraft components using prepried broadgoods layed-up in the flat and subsequently formed - Cost benefits and resource utilization enhancements 09 p1195 A83-23602

An improved version of processible acetylene-terminated oligomers for composites and coatings 09 p1237 A83-23619

An analysis of delamination in drilling composite materials 09 p1273 A83-23640

Advanced composites structures at Hughes Helicopters, Inc 09 p1202 A83-23645

Thermal performance of aircraft polyurethane seat cushions 09 p1238 A83-23849

Investigations concerning the structural design of a forward swept wing for a combat aircraft [DGLR PAPER 82-036] 09 p1203 A83-24161

Developmental trends in helicopter design [DGLR PAPER 82-065] 09 p1203 A83-24179

Noise transmission characteristics of advanced composite structural materials [AIAA PAPER 83-0694] 10 p1473 A83-25915

Smooth contact between a rigid indenter and an initially stressed orthotropic beam 11 p1592 A83-27441

Development of a mini RPV - Stableye 11 p1529 A83-28180

Advanced design structural considerations when introducing new materials and construction methods 12 p1701 A83-29394

Characterization of two nitrile-epoxy structural adhesives 12 p1716 A83-29550

An aerothermochemical model of carbon-carbon composite nozzle recession [AIAA 83-0910] 12 p1709 A83-29764

Carbon/epoxy laminates under combined fastener bearing and tension bypass loading [AIAA 83-0967] 12 p1710 A83-29778

Properties and application benefits of low density aluminum alloys [AIAA 83-0981] 12 p1715 A83-29788

Statistical modeling of ballistic damage and residual strength in composite structures [AIAA 83-1002] 12 p1711 A83-29790

Repairing composite structures 13 p1803 A83-30074

Development of structural materials for the new generation of aircraft 13 p1805 A83-30511

First design details of the all-composite Lear Fan 13 p1806 A83-30829

Composite materials applications in the manufacture of helicopters - Design and problems of helicopters 14 p1974 A83-31822

Processing of fatigue test results for corrosion-affected structural materials 14 p1992 A83-32074

The residual strength of prefabricated structures made of pressed panels of D16chT alloy and its modifications 14 p2029 A83-32075

A perspective on the development of aluminum-lithium alloys 14 p1996 A83-32881

Alloying additions and property modification in aluminum-lithium - X systems 14 p1996 A83-32884

Microstructure and deformation of rapidly solidified Al-3Li alloys containing incoherent dispersoids

14 p1996 A83-32885
The design and mechanical properties of rapidly solidified Al-Li-X alloys 14 p1996 A83-32887
V378A polyimide resin - A new composite matrix for the 1980's 14 p1987 A83-33116
Effects of extreme aircraft storage and flight environments on graphite/epoxy

14 p1987 A83-33122
Technology status for an advanced supersonic transport [SAE PAPER 820955] 15 p2122 A83-33627
Influence of hydrogen additions on high-temperature superplasticity of titanium alloys 15 p2135 A83-33639

Highly stressed materials, with aviation considered as an example --- Book 15 p2135 A83-33951
Materials in the mirror of aviation criteria 15 p2122 A83-33952

Material, structural component, service life --- of aircraft construction materials 15 p2136 A83-33953
Structural members made of high-strength cast aluminum and their properties --- and reduction of aircraft production costs 15 p2136 A83-33954

High-strength aluminum high-quality casting alloy in aeronautics and astronautics 15 p2136 A83-33955
Light aircraft and sailplane structures in reinforced plastics 16 p2299 A83-36065

Smooth contact between a rigid indenter and an initially stressed orthotropic beam 16 p2366 A83-36092
XB-70 technology advancements [AIAA PAPER 83-1048] 16 p2300 A83-36460

The effectiveness of the artificial aging of low-alloy duralumin 16 p2335 A83-36889
Elevated temperature aluminum alloys for aerospace 17 p2488 A83-37843

Development of Al-Li-X alloys using rapidly solidified powders 17 p2489 A83-37851
New metal technologies in airframe construction 17 p2516 A83-37861

Advanced aluminum alloy for transport aircraft - Why and what are the benefits [SAE PAPER 821345] 17 p2489 A83-37954

Design of an aerobatic aircraft wing using advanced composite materials [SAE PAPER 821346] 17 p2463 A83-37955
Composite materials in aircraft structures 18 p2650 A83-40130

On mechanical fastening in graphite epoxy composite 18 p2652 A83-40155

Experimental investigation of anisotropic laminate structural behavior 18 p2652 A83-40167

Distributions of fatigue life and fatigue strength in notched specimens of a carbon eight-harness-satin laminate 18 p2655 A83-40201

Impact damage tolerance of composites reinforced with Kevlar aramid fibers 18 p2656 A83-40214

Hybrid composite application to the Boeing 767 wing/body fairing 18 p2640 A83-40244

Development of advanced composite fabrication for aerospace structures 18 p2661 A83-40278

Kevlar aramid as a fiber reinforcement with emphasis on aircraft 18 p2661 A83-40286

New insights in structural design of composite rotor blades for helicopters 18 p2640 A83-40287

Advanced composites for advanced aircraft 18 p2662 A83-40342

Fatigue crack initiation and propagation in several nickel-base superalloys at 650 C 19 p2821 A83-41199

Fracture anomalies of a casting magnesium alloy in low-cycle fatigue 19 p2822 A83-41595

A modified chemical-stress crazing test method 20 p2958 A83-42545

Design, fabrication, and qualification of composite carbon/epoxy horizontal stabilizer components 20 p2927 A83-42546

Universities - Have they a role in aeronautical research? Structures and materials 20 p3002 A83-42618

The environmental degradation of notched CFRP in compression 20 p2947 A83-42806

The in-service flight testing of some carbon fibre-reinforced plastic components 20 p2933 A83-42808

The survivable aircraft fire 20 p2931 A83-43407
Optimization of fire blocking layers for aircraft seating [SAE PAPER 1468] 20 p2931 A83-43742

Design-to-cost in the application of advanced composite technology [SAE PAPER 1480] 20 p3056 A83-43749

Application of finite element analysis techniques to the derivation of advanced composite structure weight [SAE PAPER 1490] 20 p3009 A83-43757

Polar-scan - A nondestructive test method for the inspection of layer orientation and stacking order in advanced fiber composites 21 p3148 A83-43828

A critical commentary on magnetic particle inspection 21 p3148 A83-43829

Pin joints in composites 21 p3151 A83-44053
Composite helicopter structure tested for crashworthiness 21 p3091 A83-44875

Fiber-reinforced plastics in aviation and space flight 21 p3107 A83-45088

Shot peening for advanced aerospace design; Proceedings of the Aerospace Congress and Exposition, Anaheim, CA, October 25-28, 1982 22 p3302 A83-45872

The application of shot peen forming technology to commercial aircraft wing skins [SAE PAPER 821456] 22 p3247 A83-45875

Composites in commercial aircraft 22 p3262 A83-46281

Consideration on the fatigue damage of specimens used for composite critical components qualification 22 p3305 A83-46307

Design impact of composites on fighter aircraft. I - They force a fresh look at the design process 22 p3254 A83-46347

Safe structures for future aircraft 22 p3254 A83-46350

Method of construction and fabrication procedures for the A300-rudder unit, using a carbon-fiber type of construction 23 p3391 A83-47211

Composite interphase characterization 23 p3427 A83-47424

Depot level reparability, maintainability, and supportability of advanced composites [AIAA PAPER 83-2516] 23 p3404 A83-48360

Impact of composites on fighter aircraft. II - Composites New look to the aircraft production line 24 p3543 A83-48889

Material selection for the new-technology commercial transport - The designer's dilemma [AIAA PAPER 83-2477] 24 p3553 A83-49583

Developments in UK rotor blade technology [AIAA PAPER 83-2525] 24 p3548 A83-49589

AIRCRAFT CONTROL

NT HELICOPTER CONTROL

Departure susceptibility and uncoordinated roll-reversal boundaries for fighter configurations 01 p0012 A83-10176

Experiment control in problems of minimax estimation --- for aircraft longitudinal control 01 p0094 A83-10455

Integrated perceptual information for designers 01 p0029 A83-11136

Design and application of a multivariable, digital controller to the A-7D Digitac II aircraft model 01 p0013 A83-11148

Integrated airframe/propulsion controls technology 01 p0013 A83-11175

Design of direct digital adaptive flight-mode control systems for high-performance aircraft 01 p0013 A83-11179

Sensor snap and narrow field-of-view inset for terrain avoidance flight 01 p0010 A83-11188

Evaluating cockpit components with hand displacement time scores 01 p0086 A83-11189

Advanced automatic terrain following/terrain avoidance control concepts study 01 p0013 A83-11254

F-18 Hornet high angle of attack /AOA/ program 02 p0137 A83-11809

Implementation of the DAST ARW II control laws using an 8086 microprocessor and an 8087 floating-point coprocessor --- drones for aeroelasticity research 02 p0227 A83-11910

An analytical pilot rating method for highly elastic aircraft 03 p0282 A83-14843

Cross-coupling between longitudinal and lateral aircraft dynamics in a spiral dive 04 p0449 A83-15312

Nonlinear controller for the pitch-up region [AIAA PAPER 83-0064] 05 p0597 A83-16496

Effects of control saturation on the command response of statically unstable aircraft [AIAA PAPER 83-0065] 05 p0598 A83-16497

'A total G-force environment dynamic flight simulator' - A new dimension in flight simulation [AIAA PAPER 83-0139] 05 p0599 A83-16548

Total simulation for airline applications /Line Oriented Flight Training/ 05 p0676 A83-17306

A proposed simple and safe aircraft take-off or landing procedure with wing roughness or protuberances [AIAA PAPER 83-0604] 06 p0718 A83-19594

Nonlinear observers for evaluating the state variables of the longitudinal motion of an aircraft --- German thesis 06 p0719 A83-19622

Extended perfect model following --- control system synthesis technique 07 p0984 A83-20289

Application of vector performance optimization to a robust control loop design for a fighter aircraft 07 p0867 A83-21160

Realistic 'feel' in flight simulators is based on precise control loading 08 p1048 A83-23240

Maneuver load control for reducing the design loads of modern combat aircraft [DGLR PAPER 82-046] 09 p1209 A83-24169

The construction of augmented tracking regulators for piloting highly maneuverable aircraft [ONERA, TP NO. 1982-118] 09 p1209 A83-24329

A unifying framework for longitudinal flying qualities criteria 09 p1209 A83-24429

Control characteristics of a buoyant quad-rotor research aircraft 09 p1203 A83-24430

The attainability domain of a coasting vehicle 10 p1380 A83-26073

Automatic return in multifunction control logic --- for fighter cockpits 10 p1459 A83-26317

Integrated control/display unit vs. dedicated control heads for radio tuning in a KC-135 flight simulator 10 p1459 A83-26318

Cognitive task performance time during tracking 10 p1457 A83-26333

The Special Research Area of Flight Control, Colloquium, Brunswick, West Germany, September 9, 10, 1981, Reports 10 p1374 A83-26476

Integrated flight path control system 10 p1378 A83-26477

Structure and mode of operation of an interactive onboard four-dimensional flight path control system 10 p1378 A83-26478

Procedure for an evaluation of control systems on the basis of human factor considerations 10 p1460 A83-26479

The design of wind shear filters 10 p1378 A83-26483

A discrete tracking control law for nonlinear plants --- applied to F-8 aircraft stall recovery 10 p1378 A83-26503

Synthesis of C(asterisk)-model reference adaptive flight controller 10 p1379 A83-26559

Development of adaptation and identification algorithms in adaptive digital aircraft control systems 10 p1379 A83-26600

Self-tuning fly-by-wire control system 10 p1379 A83-26603

Altitude transitions in energy climbs 10 p1379 A83-26604

Development and validation of the V/STOL aerodynamics and stability and control manual 12 p1696 A83-29020

Airplane model structure determination from flight data 12 p1704 A83-29023

On the synthesis of the optimal control of a certain hydromagnetic process --- with applications in flight vehicle and temperature control 12 p1769 A83-29285

Solution of the fundamental control problem /FCP/ --- for aircraft 12 p1704 A83-29291

Test demonstration of digital control of wing/store flutter 13 p1805 A83-30163

A core software concept for integrated control 13 p1909 A83-30170

Excessive roll damping can cause roll ratchet 13 p1808 A83-30171

Globally stable nonlinear flight control system 14 p1977 A83-32425

The definition of short-period flying qualities characteristics via equivalent systems 14 p1977 A83-32578

Sidestick controller design requirements 14 p1977 A83-32934

Advanced navigation systems and fuel conservation 15 p2120 A83-33545

Bring cohesion to handling-qualities engineering 16 p2298 A83-35772

Aircraft active controls - New era in design 16 p2311 A83-35773

Use of flight test results to improve the flying qualities simulation of the B-52H weapon system trainer [AIAA PAPER 83-1091] 16 p2300 A83-36215

Definition of vectored nonaxisymmetric nozzle plumes --- for aircraft thrust vector control [AIAA PAPER 83-1290] 16 p2297 A83-36924

Piloted simulation of hover and transition of a vertical attitude takeoff and landing aircraft	17	p2462	A83-37064
Integrated control techniques	17	p2566	A83-37102
System design approaches to integrated controls	17	p2460	A83-37103
Role of standards with integrated control	17	p2566	A83-37104
Model reference adaptive control in the presence of measurement noise	17	p2568	A83-37128
A variable structure approach to robust control of VTOL aircraft	17	p2470	A83-37145
The all electric airplane-benefits and challenges	17	p2463	A83-37982
[SAE PAPER 821434]	17	p2463	A83-37982
Hover and transition flight performance of a twin tilt-nacelle V/STOL configuration	17	p2465	A83-38656
[AIAA PAPER 83-1824]	17	p2465	A83-38656
High angle-of-attack flight dynamics of a forward-swept wing fighter configuration	17	p2470	A83-38666
[AIAA PAPER 83-1837]	17	p2470	A83-38666
Dynamic analysis of the Magnus Aerospace Corporation LTA 20-1 heavy-lift aircraft	17	p2466	A83-38908
[AIAA PAPER 83-1977]	17	p2466	A83-38908
Flight test of the HX-1 radio-controlled hybrid airship	17	p2466	A83-38917
[AIAA PAPER 83-1992]	17	p2466	A83-38917
Wind tunnel evaluation of tactical aircraft stability and control as affected by nozzle thrust reverser parameter variations	18	p2642	A83-39103
[AIAA PAPER 83-1228]	18	p2642	A83-39103
Control configured vehicle as a new generation aircraft	19	p2801	A83-40884
Application of optimal control theory to aircraft gust load alleviation	19	p2802	A83-41484
Guidance and Control Conference, Gatlinburg, TN, August 15-17, 1983, Collection of Technical Papers	19	p2891	A83-41659
Integrated airframe/propulsion control system architectures (IAPSA) study	19	p2797	A83-41660
[AIAA PAPER 83-2158]	19	p2797	A83-41660
Robust fault detection, isolation, and accommodation to support integrated aircraft control	19	p2802	A83-41661
[AIAA PAPER 83-2161]	19	p2802	A83-41661
Simulation evaluation of flight controls and display concepts for VTOL shipboard operations	19	p2789	A83-41668
[AIAA PAPER 83-2173]	19	p2789	A83-41668
Flight-test results using nonlinear control with the F-8C digital fly-by-wire aircraft	19	p2802	A83-41669
[AIAA PAPER 83-2174]	19	p2802	A83-41669
Robustness analysis of a multiloop flight control system	19	p2802	A83-41675
[AIAA PAPER 83-2189]	19	p2802	A83-41675
The use of singular value gradients and optimization techniques to design robust controllers for multiloop systems	19	p2891	A83-41677
[AIAA PAPER 83-2191]	19	p2891	A83-41677
An advanced control system for a next generation transport aircraft	19	p2802	A83-41679
[AIAA PAPER 83-2194]	19	p2802	A83-41679
Impact of aircraft structural dynamics on integrated control design	19	p2798	A83-41698
[AIAA PAPER 83-2216]	19	p2798	A83-41698
Optimal symmetric flight with an intermediate vehicle model	19	p2798	A83-41715
[AIAA PAPER 83-2238]	19	p2798	A83-41715
Restructurable controls for aircraft	19	p2804	A83-41728
[AIAA PAPER 83-2255]	19	p2804	A83-41728
Robustness of a decoupled multivariable digital flight control system	19	p2804	A83-41738
[AIAA PAPER 83-2272]	19	p2804	A83-41738
Tradeoff studies in multiobjective insensitive design of airplane control systems	19	p2804	A83-41739
[AIAA PAPER 83-2273]	19	p2804	A83-41739
MIMO controller design for longitudinal decoupled aircraft motion --- Multi-Input/Multi-Output	19	p2804	A83-41740
[AIAA PAPER 83-2274]	19	p2804	A83-41740
Comparison of the Bode envelope criterion with other criteria	19	p2805	A83-41910
[AIAA PAPER 83-2073]	19	p2805	A83-41910
A modal analysis of flexible aircraft dynamics with handling qualities implications	19	p2805	A83-41911
[AIAA PAPER 83-2074]	19	p2805	A83-41911
Sensitivity of digital flight control design to parameter estimation error	19	p2805	A83-41921
[AIAA PAPER 83-2089]	19	p2805	A83-41921
Status of the development of handling criteria for VSTOL transition	19	p2806	A83-41932
[AIAA PAPER 83-2103]	19	p2806	A83-41932
New flying qualities criteria for relaxed static longitudinal stability	19	p2806	A83-41933
[AIAA PAPER 83-2104]	19	p2806	A83-41933
Comparison of fixed-base and in-flight simulation results for lateral high order systems	19	p2806	A83-41934
[AIAA PAPER 83-2105]	19	p2806	A83-41934
F/A-18 high angle of attack departure resistant criteria for control law development	19	p2806	A83-41950
[AIAA PAPER 83-2126]	19	p2806	A83-41950
Separation of time scales in aircraft trajectory optimization	19	p2799	A83-41958
[AIAA PAPER 83-2136]	19	p2799	A83-41958
Circulation-controlled elliptical airfoil	20	p2928	A83-42537
Fail-operational DAFCS for business/commuter aircraft --- Digital Automatic Flight Control System	20	p2937	A83-43324
[SAE PAPER 830714]	20	p2937	A83-43324
Conditions of the generalized similarity of simulators to aircraft	20	p3036	A83-43505
Application of factor-analysis methods to evaluate the quality of ergatic control systems --- of aircraft landing by human operator	20	p3036	A83-43508
Nonlinear control law for piloting aircraft in the air-to-ground attack phase	21	p3093	A83-44315
[ONERA, TP NO. 1983-37]	21	p3093	A83-44315
An optimal control approach to pilot/vehicle analysis and the Neal-Smith criteria	21	p3093	A83-45462
Electromechanical control systems	23	p3411	A83-47201
Advancing electronic technology impact on integrated propulsion/airframe controls design and development	23	p3402	A83-47985
[ASME PAPER 83-GT-161]	23	p3402	A83-47985
F-14 aircraft and propulsion control integration evaluation	23	p3411	A83-48029
[ASME PAPER 83-GT-234]	23	p3411	A83-48029
Integrated control system concept for high-speed aircraft	24	p3549	A83-50074
[AIAA PAPER 83-2564]	24	p3549	A83-50074
AIRCRAFT DESIGN			
NT HELICOPTER DESIGN			
The use of bicubic spline surfaces to represent aircraft wings and propellers --- German thesis	01	p0008	A83-10170
Departure susceptibility and uncoordinated roll-reversal boundaries for fighter configurations	01	p0012	A83-10176
Combat survivability with advanced aircraft propulsion development	01	p0008	A83-10179
Air bag impact attenuation system for the AQM-34V remote piloted vehicle	01	p0008	A83-10188
Analytical design of thin-wall wings at the drafting stage	01	p0058	A83-10453
The use of nonstandard flight vehicles for topographic aerial photography	01	p0051	A83-10856
Designing a mini-RPV for a world endurance record	01	p0001	A83-11000
Rationalizing Tacair force development in the next decade	01	p0002	A83-11116
Integrated perceptual information for designers	01	p0029	A83-11136
Application of model reference adaptive control to a relaxed static stability transport aircraft	01	p0013	A83-11209
Optimization of aircraft structures	02	p0189	A83-11857
Quadratic synthesis of integrated active controls for an aeroelastic forward-swept-wing-aircraft	02	p0137	A83-12458
Nomogram for take-off performance of the V/STOL airplane	02	p0134	A83-12665
Recent progress in V/STOL technology	02	p0131	A83-12852
ACA-ECA or pipedream; Industry needs it - but who will pay	02	p0135	A83-13017
Numerical study of flowfields about asymmetric external conical corners	03	p0277	A83-13130
Noise and detectability characteristics of small-scale remotely piloted vehicle propellers	03	p0282	A83-13162
Tomorrow's Tomcat	03	p0281	A83-14324
The ULS experimental ultralight glider made of polymer composites. I - Genesis of the program and construction of the glider	03	p0281	A83-14621
The KC-10A - USAF's newest range extender	03	p0281	A83-14700
The A310 - Even better than expected	04	p0445	A83-14952
Open seat ejection at high dynamic pressure - A radical approach	04	p0445	A83-15308
Some recent applications of high-lift computational methods at Boeing	04	p0443	A83-15313
Design for global damage tolerance and associated mass penalties	04	p0496	A83-15321
MPES update 1981 --- Navy Maximum Performance Ejection System program	04	p0445	A83-15425
Advanced escape system design for future combat aircraft	04	p0446	A83-15436
Microwave measurements for an attitude reference system design --- thrust vector controlled escape systems	04	p0447	A83-15438
The next generation - The Stencil S45 ejection seat development program	04	p0446	A83-15440
System identification and aircraft flutter	04	p0497	A83-15546
Human engineering in aircraft and system design	04	p0446	A83-16127
Highlights of the new national aeronautical research and technology policy	04	p0441	A83-16374
Aerospace highlights 1982	04	p0576	A83-16375
Iterative optimal subcritical aerodynamic design code including profile drag	05	p0578	A83-16462
[AIAA PAPER 83-0012]	05	p0578	A83-16462
GASAP - A general aviation airplane analysis and synthesis program	05	p0594	A83-16488
[AIAA PAPER 83-0054]	05	p0594	A83-16488
Aerodynamic optimization, comparison, and trim design of canard and conventional high performance general aviation configurations	05	p0594	A83-16490
[AIAA PAPER 83-0058]	05	p0594	A83-16490
Efficiency improved turboprop	05	p0596	A83-16491
[AIAA PAPER 83-0059]	05	p0596	A83-16491
A root locus based flutter synthesis procedure	05	p0653	A83-16495
[AIAA PAPER 83-0063]	05	p0653	A83-16495
Circulation controlled STOL wing optimization	05	p0579	A83-16509
[AIAA PAPER 83-0082]	05	p0579	A83-16509
The application of energy saving concepts to future fighter/attack aircraft design	05	p0594	A83-16516
[AIAA PAPER 83-0092]	05	p0594	A83-16516
Computational wing design for an advanced trainer	05	p0594	A83-16517
[AIAA PAPER 83-0093]	05	p0594	A83-16517
Design of optimum propellers	05	p0581	A83-16578
[AIAA PAPER 83-0190]	05	p0581	A83-16578
An interactive method for surface fitting three-dimensional bodies	05	p0581	A83-16591
[AIAA PAPER 83-0220]	05	p0581	A83-16591
Active control of a relaxed-static-stability airplane using a discrete model following technique	05	p0598	A83-16624
[AIAA PAPER 83-0279]	05	p0598	A83-16624
A new hybrid approach to supersonic aircraft analysis --- and flow field prediction	05	p0584	A83-16666
[AIAA PAPER 83-0340]	05	p0584	A83-16666
Subsonic surface panel method for airframe analysis and wing design	05	p0584	A83-16667
[AIAA PAPER 83-0341]	05	p0584	A83-16667
A supersonic maneuver wing designed for nonlinear attached flow	05	p0585	A83-16707
[AIAA PAPER 83-0425]	05	p0585	A83-16707
Solar drones scan the earth	05	p0595	A83-16872
Calculation of fundamental aerodynamic derivatives of aircraft	05	p0589	A83-16882
The intricate patterns of stress	05	p0654	A83-17282
Application of the PANAIR production code to a complex canard/wing configuration	05	p0590	A83-17902
[AIAA PAPER 83-0009]	05	p0590	A83-17902
Slender body theory and optimization procedures for transonic lifting wing bodies	05	p0591	A83-17911
[AIAA PAPER 83-0184]	05	p0591	A83-17911
The inverse design of closed airfoils in transonic flow	05	p0591	A83-17929
[AIAA PAPER 83-0504]	05	p0591	A83-17929
Boeing gains real-time flight data	06	p0719	A83-18270
Rockwell B-1B design to be studied in new cab	06	p0719	A83-18271
Computer models cut USAF test costs	06	p0719	A83-18274
How decisions are made - Major considerations for aircraft programs	06	p0717	A83-18398
Effects of spanwise blowing and reverse thrust on fighter low-speed aerodynamics	06	p0712	A83-18410
V/STOL - A practical weapon system	06	p0711	A83-18808
Designing patrol aircraft for the crew	06	p0800	A83-18811
Development of a structural, bird impact resistant, de-cised wing leading edge for the de Havilland Dash 8 aircraft using fibre-reinforced composites	06	p0717	A83-18823
Military propulsion technology. II - Supersonic V/STOL technology shapes up	06	p0718	A83-18949
The General Dynamics F-16 XL fighter aircraft	06	p0717	A83-19411
US Navy STOVL - Waiting in the wings	06	p0717	A83-19450
Theory of resistance interference of airfoil wings and engine exhaust	07	p0862	A83-19667
A superelement analysis of stiffened shells --- Russian book on aircraft fuselage structures	07	p0865	A83-20392
Curvature transitions of composite curves and surfaces	07	p0862	A83-20398
Questions regarding details of computer-aided design --- German thesis	07	p0862	A83-20398
The development of advanced composite front fuselage technology	07	p0865	A83-20464
Advanced composite materials in aerobatic aircraft	07	p0865	A83-20496
The future for fighter aircraft	07	p0862	A83-20597

- Technology and modern fighter aircraft - The evolutionary F-16 07 p0865 A83-20598
 NGT - The Next Generation Trainer 07 p0866 A83-20599
 Thirty years of fighter armament 07 p0866 A83-20600
 USAF's design guide coming out next month 07 p1001 A83-20647
 Dynamics of air combat 07 p0862 A83-21026
 Operator influences on aircraft design 07 p0866 A83-21032
 Design, analyses, and model tests of an aerodynamically tailored lifting surface 08 p1044 A83-22155
 Analysis of aero-optic interface phenomena 08 p1042 A83-22588
 Initial design of stringer stiffened bend boxes using geometric programming 08 p1123 A83-23149
 Ergonomic analysis and evaluation procedures for cockpit operating positions 09 p1324 A83-23496
 Microlights - The state of the art 09 p1195 A83-23685
 Note on non-linear dynamic response of a clamped orthotropic circular plate to pulse excitations 09 p1278 A83-23707
 Aviation system technology from the point of view of the aircraft manufacturer [DGLR PAPER 82-025] 09 p1195 A83-24152
 Development trend in general aviation [DGLR PAPER 82-026] 09 p1195 A83-24153
 Alternative wing concepts for a long-distance aircraft of the nineties [DGLR PAPER 82-029] 09 p1202 A83-24155
 Performance-increasing modifications on transonic passenger plane wings [DGLR PAPER 82-031] 09 p1203 A83-24157
 Configuration development for a highly maneuverable experimental aircraft with negative sweep rudder units [DGLR PAPER 82-035] 09 p1203 A83-24160
 Investigations concerning the structural design of a forward swept wing for a combat aircraft [DGLR PAPER 82-036] 09 p1203 A83-24161
 Design and manufacture of the Tornado carbon-fiber reinforced plastics taileron [DGLR PAPER 82-038] 09 p1203 A83-24162
 Integrated avionics/weapon system for air/ground missions [DGLR PAPER 82-039] 09 p1200 A83-24163
 Economic conditions and key points of BMFT air transport research requirements in the eighties [DGLR PAPER 82-044] 09 p1196 A83-24168
 Maneuver load control for reducing the design loads of modern combat aircraft [DGLR PAPER 82-046] 09 p1209 A83-24169
 Design and implementation of an active load alleviation system, taking into account the example of a modern transport aircraft [DGLR PAPER 82-045] 09 p1209 A83-24170
 The consideration of operational aspects for utility-/commuter aircraft, taking into account the example of the Dornier 228 [DGLR PAPER 82-047] 09 p1199 A83-24171
 New technology in general aviation [DGLR PAPER 82-048] 09 p1203 A83-24172
 The German-Dutch wind tunnel as an aid in aircraft development [DGLR PAPER 82-050] 09 p1210 A83-24173
 Performance improvements of single-engine business airplanes by the integration of advanced technologies [DGLR PAPER 82-064] 09 p1203 A83-24178
 Design, construction, and testing of an experimental propeller in the 750 PS performance class [DGLR PAPER 82-066] 09 p1206 A83-24180
 Development of four profiles for an experimental propeller in the performance class of 750 PS [DGLR PAPER 82-067] 09 p1197 A83-24181
 The cost definition phase of a new commercial aircraft programme 09 p1196 A83-24425
 Control characteristics of a buoyant quad-rotor research aircraft 09 p1203 A83-24430
 The ATR 42 will keep its promises 09 p1203 A83-25115
 Homebuilt airplanes - The sky's the limit 09 p1196 A83-25122
 Now is the time for new fighters 09 p1204 A83-25137
 A hybrid facility for the simulation, development, and validation of ECS microprocessor based controls [SAE PAPER 820867] 10 p1379 A83-25766
 ECS schemes for All Electric Airliners [SAE PAPER 820870] 10 p1375 A83-25769
 Thermal design of integrated avionic racks for aircraft [SAE PAPER 820871] 10 p1375 A83-25770
 Thermal design of standard avionic enclosures [SAE PAPER 820878] 10 p1373 A83-25772
 State-space aeroelastic modeling and its application in flutter calculation 10 p1442 A83-26761
 Development of a mini RPV - Stabileye 11 p1529 A83-28180
 Some effects of size on non-rigid airships 11 p1530 A83-28192
 Preliminary report on the engineering development of the Magnus Aerospace Corp LTA 20-1 heavy-lift aircraft 11 p1530 A83-28193
 Investigation of possible LTA craft application to solve national economy problems 11 p1527 A83-28194
 An overview of two nonlinear supersonic wing design studies [AIAA PAPER 83-0182] 11 p1527 A83-28349
 Parametric study of hypersonic three-dimensional configurations 11 p1527 A83-28537
 Propulsion system installation design for high-speed prop-fans 12 p1703 A83-29014
 Design and development of the RF-5E aircraft 12 p1700 A83-29015
 Influence of leading-edge thrust on twisted and cambered wing design for sursersonic cruise 12 p1696 A83-29018
 The application of a sub-scale flight demonstrator as a cost effective approach to aircraft development 12 p1701 A83-29395
 Dash 8 - Canada's new commuter 12 p1701 A83-29675
 An optimality criterion method for structures with stress, displacement and frequency constraints [AIAA 83-0939] 12 p1739 A83-29769
 A building block approach to design verification testing of primary composite structure [AIAA 83-0947] 12 p1739 A83-29775
 Design for prevention of acoustic fatigue --- of aircraft structures [AIAA 83-0973] 12 p1701 A83-29782
 An analytical comparison of two wing structures for Mach 5 cruise airplanes [AIAA 83-0974] 12 p1701 A83-29806
 Design of the flutter suppression system for DAST ARW-1R - A status report [AIAA 83-0990] 12 p1702 A83-29868
 The design, testing and analysis of aeroelastically tailored transonic flutter model wings [AIAA 83-1027] 12 p1702 A83-29876
 AFTI/F-16 aeroservoelastic analyses and ground test with a digital flight control system [AIAA 83-0994] 12 p1704 A83-29888
 Computational fluid dynamics of airfoils and wings 12 p1698 A83-29927
 Steady-state solution of the Euler equations for transonic flow 12 p1698 A83-29929
 Transonic flows with viscous effects 12 p1698 A83-29935
 Military potential of TiltRotor aircraft 12 p1700 A83-29969
 Fundamentals of flight --- Book 13 p1803 A83-30152
 Prediction of turbulent flows - A Boeing view 13 p1804 A83-30643
 First design details of the all-composite Lear Fan 13 p1806 A83-30829
 Modern propellers for commuter airlines [SAE PAPER 820719] 13 p1807 A83-30874
 The Dash 8 - Design considerations [SAE PAPER 820728] 13 p1806 A83-30875
 The principles of aerodynamic aircraft design 13 p1806 A83-30924
 X-29 - Advanced technology demonstrator 13 p1806 A83-31051
 Advanced propeller technology for new commuter aircraft [SAE PAPER 820720] 13 p1807 A83-31803
 Design considerations for ease of maintenance in commuter aircraft [SAE PAPER 820722] 13 p1803 A83-31804
 Advanced technology for SAAB-Fairchild 340 aircraft [SAE PAPER 820729] 13 p1806 A83-31805
 The CAC-100 - Design features --- passenger commuter transport aircraft [SAE PAPER 820730] 13 p1806 A83-31806
 Operator influences on aircraft design 13 p1803 A83-31813
 New aircraft. I --- for military use 14 p1974 A83-31821
 AM-X - The export challenger with a foot in two continents 14 p1974 A83-31940
 The B-1 gets airborne again 14 p1974 A83-31941
 New life for the dragon lady --- U-2 aircraft design and production 14 p1974 A83-32398
 Globally stable nonlinear flight control system 14 p1977 A83-32425
 Flight tests verify predictions for F-20 14 p1974 A83-32475
 Sun-powered aircraft designs 14 p1974 A83-32577
 Type A V/STOL - One aircraft for all support missions? 14 p1974 A83-32580
 Use of simulated ice shapes in known icing certification 14 p1973 A83-32936
 Perturbation methods in mechanics 14 p1972 A83-33001
 Certain aspects of the optimum design of hydrodynamic lifting complexes 14 p1972 A83-33002
 The history of V/STOL aircraft. II 14 p1969 A83-33097
 Towards a renewal of the propeller in aeronautics [AIAA PAPER NT 82-01] 14 p1976 A83-33159
 Impact of new technology on future short-haul transports [AIAA PAPER 83-1604] 14 p1976 A83-33367
 Short haul technology - Refining the turboprop [AIAA PAPER 83-1606] 14 p1973 A83-33368
 Aircraft design trends for cargo compatibility [AIAA PAPER 83-1609] 14 p1973 A83-33370
 The Dash 8 development program 15 p2121 A83-33546
 A complete introduction to the revolutionary new way to fly ultralights --- Book 15 p2119 A83-33622
 Technology status for an advanced supersonic transport [SAE PAPER 820955] 15 p2122 A83-33627
 Applications of advanced upper surface blowing propulsive-lift technology [SAE PAPER 820956] 15 p2122 A83-33628
 Prop-fan powered aircraft - An overview [SAE PAPER 820957] 15 p2122 A83-33629
 Materials in the mirror of aviation criteria 15 p2122 A83-33952
 Recent studies at NASA-Langley of vortical flows interacting with neighboring surfaces 15 p2120 A83-33972
 SAAB-Fairchild 340 - Transatlantic frontrunner 16 p2298 A83-35623
 Aircraft design philosophy. I - Lee Begin of Northrop 16 p2298 A83-35624
 Aircraft active controls - New era in design 16 p2311 A83-35773
 Design and development of a small gasturbine engine: Results today - A basis for design criteria of a next generation 16 p2303 A83-35829
 Inlet, engine, airframe controls integration development for supercruising aircraft 16 p2304 A83-35842
 Light aircraft and sailplane structures in reinforced plastics 16 p2299 A83-36065
 The history of V/STOL aircraft 16 p2299 A83-36074
 Progress in propulsion system/airframe structural integration [AIAA PAPER 83-1123] 16 p2300 A83-36234
 Aerodynamic design of propan powered transports [AIAA PAPER 83-1213] 16 p2300 A83-36285
 Aircraft Prototype and Technology Demonstrator Symposium, Dayton, OH, March 23, 24, 1983, Proceedings 16 p2287 A83-36457
 Prototyping for fun and profit --- military aircraft design [AIAA PAPER 83-1045] 16 p2287 A83-36458
 From new technology development to operational usefulness B-36, B-58, F-111/FB-111 [AIAA PAPER 83-1046] 16 p2287 A83-36459
 XB-70 technology advancements [AIAA PAPER 83-1048] 16 p2300 A83-36460
 Variable sweep wing design [AIAA PAPER 83-1051] 16 p2300 A83-36461
 The application of low-cost demonstrators for advanced fighter technology evaluation [AIAA PAPER 83-1052] 16 p2300 A83-36462
 YAV-8B flight demonstration program [AIAA PAPER 83-1055] 16 p2300 A83-36466
 The F-16 - A technology demonstrator, a prototype, and a flight demonstrator. [AIAA PAPER 83-1063] 16 p2301 A83-36467
 AFTI/F-111 mission adaptive wing technology demonstration program [AIAA PAPER 83-1057] 16 p2301 A83-36468
 Design for testing of a low altitude night-in-weather attack system [AIAA PAPER 83-1061] 16 p2298 A83-36470
 The Northrop Flying Wing prototypes [AIAA PAPER 83-1047] 16 p2287 A83-36471
 Large jet aircraft validation and demonstrations - An overview of Boeing experience [AIAA PAPER 83-1049] 16 p2301 A83-36472
 The F-5 story - Prototype and technology demonstrator [AIAA PAPER 83-1062] 16 p2301 A83-36473
 AFTI/F-16 technology demonstrator [AIAA PAPER 83-1059] 16 p2301 A83-36474
 Generalized maximum specific range performance 16 p2301 A83-36918
 The future of the manned aircraft 16 p2287 A83-36960

A comparison of minimizing strategies for maximum likelihood identification --- stability and control derivatives of wide body aircraft	17	p2565	A83-37085
The impact of CFD on development test facilities - A National Research Council projection --- computational fluid dynamics	17	p2503	A83-37234
Optimal mass distribution between the stages of a two-stage aircraft for maximization of the flight cruise range	17	p2462	A83-37267
New technologies for general aviation	17	p2443	A83-37856
Dornier Do 24 TT(technology tested) experimental amphibian	17	p2462	A83-37857
Alpha Jet - Further version for the international market	17	p2467	A83-37858
Configuration studies for future fighters	17	p2462	A83-37859
Aerodynamic simulation - A key technology not only for aviation	17	p2451	A83-37860
NGT sub-scale flight demonstrator - A cost-effective approach to aircraft development --- Next Generation Trainer	17	p2462	A83-37952
[SAE PAPER 821341]	17	p2462	A83-37952
Design of an aerobatic aircraft wing using advanced composite materials	17	p2463	A83-37955
[SAE PAPER 821346]	17	p2463	A83-37955
Cabin noise weight penalty requirements for a high-speed propfan-powered aircraft - A progress report	17	p2463	A83-37958
[SAE PAPER 821360]	17	p2463	A83-37958
Supersonic STOVL research aircraft	17	p2463	A83-37965
[SAE PAPER 821375]	17	p2463	A83-37965
Impact protection in air transport passenger seat design	17	p2459	A83-37967
[SAE PAPER 821391]	17	p2459	A83-37967
The all electric airplane-benefits and challenges	17	p2463	A83-37982
[SAE PAPER 821434]	17	p2463	A83-37982
Design aspects of systems in all-electric aircraft	17	p2463	A83-37984
[SAE PAPER 821436]	17	p2463	A83-37984
Aircraft super integrated power unit	17	p2469	A83-37995
[SAE PAPER 821461]	17	p2469	A83-37995
Low-speed aerodynamic characteristics of a generic forward-swept-wing aircraft	17	p2451	A83-37998
[SAE PAPER 821467]	17	p2451	A83-37998
Aircraft flexible tanks general design and installation recommendations	17	p2464	A83-38102
[SAE ARP 1664]	17	p2464	A83-38102
New aircraft, II	17	p2464	A83-38329
Advanced airfoil design for general aviation propellers	17	p2453	A83-38631
[AIAA PAPER 83-1791]	17	p2453	A83-38631
Design and true Reynolds number 2-D testing of an advanced technology airfoil	17	p2453	A83-38632
[AIAA PAPER 83-1792]	17	p2453	A83-38632
An extension of a transonic wing/body code to include underwing pylon/nacelle effects	17	p2454	A83-38639
[AIAA PAPER 83-1805]	17	p2454	A83-38639
Aerodynamic development for efficient military cargo transports	17	p2464	A83-38654
[AIAA PAPER 83-1822]	17	p2464	A83-38654
Parametric study of factors affecting the fuel efficiency of advanced turboprop airplanes	17	p2464	A83-38655
[AIAA PAPER 83-1823]	17	p2464	A83-38655
Design study for remotely piloted, high-altitude airplanes powered by microwave energy	17	p2465	A83-38657
[AIAA PAPER 83-1825]	17	p2465	A83-38657
PAN AIR modeling studies --- higher order panel method for aircraft design	17	p2455	A83-38660
[AIAA PAPER 83-1830]	17	p2455	A83-38660
High aspect ratio forward sweep for transport aircraft	17	p2455	A83-38661
[AIAA PAPER 83-1832]	17	p2455	A83-38661
Application of forward sweep wings to an air combat fighter	17	p2465	A83-38662
[AIAA PAPER 83-1833]	17	p2465	A83-38662
X-29 forward swept wing aerodynamic overview	17	p2465	A83-38663
[AIAA PAPER 83-1834]	17	p2465	A83-38663
A multiple separation model for multielement airfoils	17	p2456	A83-38672
[AIAA PAPER 83-1844]	17	p2456	A83-38672
Powered lift aerodynamics of USB STOL aircraft --- Upper Surface Blowing	17	p2456	A83-38676
[AIAA PAPER 83-1848]	17	p2456	A83-38676
An assessment of PANDORA using a Canard/Wing/Body configuration --- Preliminary Automated Numerical Design of Realistic Aircraft	17	p2456	A83-38678
[AIAA PAPER 83-1850]	17	p2456	A83-38678
Some lessons from NACA/NASA aerodynamic studies following World War II	17	p2443	A83-38683
[AIAA PAPER 83-1856]	17	p2443	A83-38683
Status review of a supersonically-biased fighter wing-design study	17	p2465	A83-38684
[AIAA PAPER 83-1857]	17	p2465	A83-38684
SC3 - A wing concept for supersonic maneuvering	17	p2457	A83-38685
[AIAA PAPER 83-1858]	17	p2457	A83-38685
Aerodynamic design for improved maneuverability by the use of three-dimensional transonic theory	17	p2465	A83-38686
[AIAA PAPER 83-1859]	17	p2465	A83-38686
The combination of a geometry generator with transonic design and analysis algorithms	17	p2457	A83-38689
[AIAA PAPER 83-1862]	17	p2457	A83-38689
Smart aerodynamic optimization	17	p2457	A83-38690
[AIAA PAPER 83-1863]	17	p2457	A83-38690
Improved method for transonic airfoil design-by-optimization	17	p2457	A83-38691
[AIAA PAPER 83-1864]	17	p2457	A83-38691
Computational aerodynamic design methodology	17	p2457	A83-38692
[AIAA PAPER 83-1865]	17	p2457	A83-38692
Supercritical inlet design	17	p2457	A83-38693
[AIAA PAPER 83-1866]	17	p2457	A83-38693
Effect of buoyancy and power design parameters on hybrid airship performance	17	p2465	A83-38907
[AIAA PAPER 83-1976]	17	p2465	A83-38907
Dynamic analysis of the Magnus Aerospace Corporation LTA 20-1 heavy-lift aircraft	17	p2466	A83-38908
[AIAA PAPER 83-1977]	17	p2466	A83-38908
Development of the Magnus Aerospace Corporation's rotating-sphere airship	17	p2466	A83-38922
[AIAA PAPER 83-2003]	17	p2466	A83-38922
On the conceptual design of supersonic cruising aircraft with subsonic wing leading edges	17	p2466	A83-38950
[AIAA PAPER 83-1977]	17	p2466	A83-38950
Transonic Euler simulations by means of finite element explicit schemes	18	p2635	A83-39378
[AIAA PAPER 83-1924]	18	p2635	A83-39378
Inviscid drag calculations for transonic flows	18	p2635	A83-39380
[AIAA PAPER 83-1928]	18	p2635	A83-39380
Fracture mechanics in design - Particular reference to the thickness effect on the risk of unstable fracture	18	p2699	A83-39547
[AIAA PAPER 83-1928]	18	p2699	A83-39547
Airborne reconnaissance in the civilian sector - Agricultural monitoring from high-altitude powered platforms	18	p2706	A83-39939
[AIAA PAPER 83-1928]	18	p2706	A83-39939
Design, manufacture and test of graphite composite wing box test structure	18	p2641	A83-40291
[AIAA PAPER 83-1928]	18	p2641	A83-40291
Computer-aided engineering - The AI connection	18	p2738	A83-40307
[AIAA PAPER 83-1928]	18	p2738	A83-40307
Advanced composites for advanced aircraft	18	p2662	A83-40342
[AIAA PAPER 83-1928]	18	p2662	A83-40342
F-16XL - GD hatches a new Falcon	18	p2641	A83-40621
[AIAA PAPER 83-1928]	18	p2641	A83-40621
JVX - The world's first production tilt-rotor?	18	p2641	A83-40622
[AIAA PAPER 83-1928]	18	p2641	A83-40622
Finite-element analysis of the T-38 canopy	19	p2797	A83-41044
[AIAA PAPER 83-1928]	19	p2797	A83-41044
Frogfoot - A new Shurtumovik on trial	19	p2797	A83-41320
[AIAA PAPER 83-1928]	19	p2797	A83-41320
A new approach to exact model-matching with applications to aircraft systems	19	p2890	A83-41477
[AIAA PAPER 83-1928]	19	p2890	A83-41477
Control law design for ejection seats	19	p2797	A83-41688
[AIAA PAPER 83-2204]	19	p2797	A83-41688
Impact of aircraft structural dynamics on integrated control design	19	p2798	A83-41698
[AIAA PAPER 83-2216]	19	p2798	A83-41698
An integrated maneuver enhancement and gust alleviation mode for the AFTI/F-111 MAW aircraft	19	p2803	A83-41699
[AIAA PAPER 83-2217]	19	p2803	A83-41699
Aeroleastic interactions with flight control (A survey paper)	19	p2803	A83-41700
[AIAA PAPER 83-2219]	19	p2803	A83-41700
The impact of computational aerodynamics on aircraft design	19	p2798	A83-41901
[AIAA PAPER 83-2060]	19	p2798	A83-41901
Computational aerodynamics applications to transport aircraft design	19	p2792	A83-41902
[AIAA PAPER 83-2061]	19	p2792	A83-41902
Computational aerodynamic design of fighter aircraft Progress and pitfalls	19	p2798	A83-41903
[AIAA PAPER 83-2063]	19	p2798	A83-41903
Experimental and analytical investigation of the subsonic aerodynamics of slender wings with leading-edge vortex flaps	19	p2793	A83-41940
[AIAA PAPER 83-2113]	19	p2793	A83-41940
Flight path/nose pointing - A required criterion in future fighter aircraft design	19	p2798	A83-41948
[AIAA PAPER 83-2123]	19	p2798	A83-41948
Innovative concepts for tactical STOL	19	p2798	A83-41952
[AIAA PAPER 83-2129]	19	p2798	A83-41952
Parametric study of critical constraints for a canard configured medium range transport using conceptual design optimization	19	p2799	A83-41963
[AIAA PAPER 83-2141]	19	p2799	A83-41963
Development of compatible numerical software for application to aircraft dynamic analysis	20	p3038	A83-42538
[AIAA PAPER 83-2141]	20	p3038	A83-42538
State space model concept for evaluating survivability methodologies for aircraft design	20	p2932	A83-42567
[AIAA PAPER 83-2141]	20	p2932	A83-42567
Vector optimization applied to survivability methodology evaluation --- for aircraft design	20	p3042	A83-42568
[AIAA PAPER 83-2141]	20	p3042	A83-42568
Progress in supersonic cruise technology	20	p2927	A83-43025
[AIAA PAPER 83-2141]	20	p2927	A83-43025
World aeronautical research - III	20	p2927	A83-43033
[SAE PAPER 830710]	20	p2927	A83-43033
Unconventional commuter configurations - A design investigation	20	p2933	A83-43320
[SAE PAPER 830710]	20	p2933	A83-43320
Design consideration for lighting modern commercial aircraft	20	p2933	A83-43322
[SAE PAPER 830712]	20	p2933	A83-43322
Aircraft night lighting systems	20	p2936	A83-43323
[SAE PAPER 830713]	20	p2936	A83-43323
Flight investigation of natural laminar flow on the Bellanca Skyrocket II	20	p2933	A83-43326
[SAE PAPER 830717]	20	p2933	A83-43326
Development of low cost RPVs under Indian conditions	20	p2934	A83-43701
[SAE PAPER 830717]	20	p2934	A83-43701
A rocket-boosted sea launched target system	20	p2934	A83-43702
[SAE PAPER 830717]	20	p2934	A83-43702
A low signature RPV	20	p2934	A83-43703
[SAE PAPER 830717]	20	p2934	A83-43703
AN/USD-502 (CL 289) reconnaissance drone system	20	p2934	A83-43704
[SAE PAPER 830717]	20	p2934	A83-43704
ASAT - The U.K.'s new turbo jet R.P.V.	20	p2934	A83-43707
[SAE PAPER 830717]	20	p2934	A83-43707
The aerodynamics of small RPV's	20	p2934	A83-43710
[SAE PAPER 830717]	20	p2934	A83-43710
Extended uses of the Aquila RPV system	20	p2934	A83-43716
[SAE PAPER 830717]	20	p2934	A83-43716
Algorithmic mass-factoring of finite element model analyses	20	p3009	A83-43733
[SAWE PAPER 1451]	20	p3009	A83-43733
Theory of transport aircraft weight fractions	20	p2935	A83-43734
[SAWE PAPER 1452]	20	p2935	A83-43734
Grumman's forward swept wing feasibility studies and X-29A technology demonstrator	20	p2935	A83-43736
[SAWE PAPER 1454]	20	p2935	A83-43736
Optimizing tail size and wing location within loadability constraints	20	p2935	A83-43740
[SAWE PAPER 1466]	20	p2935	A83-43740
An introduction to the Boeing 767-200 and the 767 Weight Control Program	20	p2935	A83-43741
[SAWE PAPER 1467]	20	p2935	A83-43741
Weight reduction for fuel economy	20	p2935	A83-43743
[SAWE PAPER 1469]	20	p2935	A83-43743
Life cycle cost applications to conceptual designs	20	p3056	A83-43748
[SAWE PAPER 1479]	20	p3056	A83-43748
Design-to-cost in the application of advanced composite technology	20	p3056	A83-43749
[SAWE PAPER 1480]	20	p3056	A83-43749
Weight control program for a graphite/epoxy aircraft	20	p2948	A83-43752
[SAWE PAPER 1485]	20	p2948	A83-43752
Advanced technology wing structure	20	p3009	A83-43754
[SAWE PAPER 1487]	20	p3009	A83-43754
LEONARDO - A computer-aided engineering system	20	p3037	A83-43755
[SAWE PAPER 1488]	20	p3037	A83-43755
Application of finite element analysis techniques to the derivation of advanced composite structure weight	20	p3009	A83-43757
[SAWE PAPER 1490]	20	p3009	A83-43757
V/STOL;STOL;CTOL comparisons	20	p2935	A83-43759
[SAWE PAPER 1499]	20	p2935	A83-43759
Analysis of aircraft dynamic behavior in a crash environment	21	p3091	A83-43966
[SAWE PAPER 1499]	21	p3091	A83-43966
Optimum configuration for a 10-passenger business turboprop jet airplane	21	p3091	A83-43967
[SAWE PAPER 1499]	21	p3091	A83-43967
Bonded aluminum honeycomb - Aircraft flight surface primary structure application	21	p3091	A83-43972
[SAWE PAPER 1499]	21	p3091	A83-43972
Design, fabrication and test of a composite elevator	21	p3151	A83-44046
[SAWE PAPER 1499]	21	p3151	A83-44046
Wing tip devices for energy conservation and other purposes Experimental and analytical work in progress at the Lockheed-Georgia Company	21	p3086	A83-44358
[SAWE PAPER 1499]	21	p3086	A83-44358
Design of transonic shock-free airfoil	21	p3087	A83-44572
[SAWE PAPER 1499]	21	p3087	A83-44572
Counter-rotation propellers - A feasibility study	21	p3092	A83-44874
[SAWE PAPER 1499]	21	p3092	A83-44874
Design impact of composites on fighter aircraft. I - They force a fresh look at the design process	22	p3254	A83-46347
[SAWE PAPER 1499]	22	p3254	A83-46347
Designed to be stalled --- T-46A training aircraft	22	p3254	A83-46349
[SAWE PAPER 1499]	22	p3254	A83-46349
The way to the supercritical wing	22	p3250	A83-46483
[SAWE PAPER 1499]	22	p3250	A83-46483
Numerical aerodynamics - Replacement of analytical solutions and/or the experiment by the supercomputer?	22	p3250	A83-46485
[SAWE PAPER 1499]	22	p3250	A83-46485
Problems in determining aircraft polar curves from test-flight data	22	p3254	A83-46489
[SAWE PAPER 1499]	22	p3254	A83-46489
Determination of the suction-force distribution and its effect on the aerodynamic design of a wing for supersonic flow	22	p3250	A83-46495
[SAWE PAPER 1499]	22	p3250	A83-46495
F-16XL shows advances in range, ride	22	p3254	A83-46924
[SAWE PAPER 1499]	22	p3254	A83-46924
Design of a candidate flutter suppression control law for DAST ARW-2 --- Drones for Aerodynamic and Structural Testing Aeroelastic Research Wing	23	p3402	A83-47125
[AIAA PAPER 83-2221]	23	p3402	A83-47125

The increase in the cost effectiveness of the construction of and preparation of manufacturing processes for flight equipment through integrated and graphic data processing-CAD/CAM 23 p3440 A83-47191
Development and testing of a high-technology amphibious flying vehicle 23 p3402 A83-47192
Development of aerodynamical technology for large civil aviation aircraft 23 p3391 A83-47204
Design, construction, and operation of the calibration model for the DNW wind tunnel 23 p3412 A83-47209

Commercial aircraft with reduced longitudinal stability and active tail planes, and the unsteady aerodynamics of rapidly adjusted control surfaces 23 p3412 A83-47213

Propulsion system screening for survivability and effectiveness [ASME PAPER 83-GT-200] 23 p3410 A83-48003

Propulsion system integration as applied to business jet aircraft [ASME PAPER 83-GT-227] 23 p3403 A83-48024

STOL fighter technology program [ASME PAPER 83-GT-243] 23 p3403 A83-48033

Aircraft design (3rd revised and enlarged edition) --- Russian book 23 p3403 A83-48100

Model test and full-scale checkout of dry-cooled jet runup sound suppressors 23 p3413 A83-48217

Advanced lightweight, fire retardant floor paneling for aircraft [AIAA PAPER 83-2442] 23 p3403 A83-48330

Light aircraft wing structure optimization [AIAA PAPER 83-2446] 23 p3403 A83-48332

Aircraft synthesis using numerical optimization methodology [AIAA PAPER 83-2458] 23 p3500 A83-48336

Conceptual kinematic design using homogeneous coordinate transformations [AIAA PAPER 83-2460] 23 p3500 A83-48337

Future aircraft development for commuter and third-level operations [AIAA PAPER 83-2464] 23 p3403 A83-48338

The prospects and potential of all electric aircraft [AIAA PAPER 83-2478] 23 p3411 A83-48341

Effect of aircraft configuration and control integration on surface actuation [AIAA PAPER 83-2487] 23 p3404 A83-48347

STOL attack aircraft design based on an upper surface blowing concept [AIAA PAPER 83-2535] 23 p3405 A83-48369

Subsonic airplane configurations for maximum range for endurance [AIAA PAPER 83-2536] 23 p3405 A83-48370

Wing extensions for improving climb performance [AIAA PAPER 83-2556] 23 p3405 A83-48375

Efficient computational grid generation for three-dimensional aircraft configurations [AIAA PAPER 83-2557] 23 p3405 A83-48376

Von Mises wing optimization [AIAA PAPER 83-2558] 23 p3405 A83-48377

Structural optimization with aeroelastic constraints - A survey of US applications 24 p3593 A83-49188

Aeroelastic considerations for automatic structural design procedures 24 p3547 A83-49189

A very large cargo aircraft design project 24 p3547 A83-49436

Conceptual design of transport aircraft 24 p3547 A83-49475

Air Force Aeronautical Systems the 1990's - A major shift [AIAA PAPER 83-2433] 24 p3543 A83-49576

Design integration of laminar flow control for transport aircraft [AIAA PAPER 83-2440] 24 p3547 A83-49577

Civil transport aircraft design methodology [AIAA PAPER 83-2463] 24 p3547 A83-49579

High speed propeller for the Lear Fan 2100 [AIAA PAPER 83-2465] 24 p3549 A83-49580

The development of a generalized advanced propeller analysis system [AIAA PAPER 83-2466] 24 p3549 A83-49581

An overview of V/STOL aircraft development [AIAA PAPER 83-2491] 24 p3548 A83-49584

A McDonnell Douglas perspective - Commercial aircraft for the next generation [AIAA PAPER 83-2502] 24 p3548 A83-49587

Army family of light rotorcraft (LHX) concept formulation [AIAA PAPER 83-2552] 24 p3548 A83-49592

Application of slender wing benefits to military aircraft [AIAA PAPER 83-2566] 24 p3545 A83-49596

AIRCRAFT DETECTION
Use of aircraft-derived data to assist in ATC tracking systems. II - Some practical tracking filters 02 p0133 A83-11557

A procedure for the utilization of the signals of a DME transponder to determine the position of an aircraft from the ground 02 p0134 A83-13016

Noise and detectability characteristics of small-scale remotely piloted vehicle propellers 03 p0282 A83-13162

Terrain effect in monostatic, multistatic, and network radar 09 p1244 A83-23412

Aircraft contrast signatures in the infrared spectral region 22 p3292 A83-46598

AIRCRAFT ENERGY EFFICIENCY PROGRAM

U ACEE PROGRAM

AIRCRAFT ENGINES

NT HELICOPTER ENGINES

NT TF-34 ENGINE

NT TF-41 ENGINE

NT VARIABLE CYCLE ENGINES

Accelerated life tests of aircraft thermocouples 01 p0009 A83-10442

Fuel property effects on Air Force gas turbine engines - Program genesis 01 p0028 A83-10653

Effect of oxygen addition on ignition of aero-gas turbine at simulated altitude facility 01 p0011 A83-10660

The theory of aircraft engines --- Russian book 01 p0011 A83-10675

Thunder power for executive and ag-aircraft 01 p0011 A83-10866

Engines for future combat aircraft 01 p0011 A83-10867

Digital engine control for V/STOL and V/TOL aircraft 01 p0012 A83-10871

Adaptive power management - A hierarchical/control system with a central multiplex system --- for aircraft applications 01 p0012 A83-11202

On the design and test of an advanced containment structure for PM machines --- in aircraft electrical power systems 01 p0012 A83-11206

A 400 Hz starter/generator system --- for aircraft engines 01 p0012 A83-11207

Rotaries for GA - NASA gets serious 02 p0136 A83-11627

Repair of the auxiliary power plants of aircraft --- Russian book 02 p0136 A83-11949

Rolls-Royce engine status report 02 p0136 A83-12933

Assessment of inflow control structure effectiveness and design system development 03 p0281 A83-13161

The icing of aircraft gas turbine engines 03 p0280 A83-14619

Powerplants. I --- turbofan engine design for aircraft 04 p0449 A83-14951

Generation of desired signals from acoustic drivers --- for aircraft engine internal noise propagation experiment 04 p0449 A83-15068

Retirement for cause inspection system design 04 p0488 A83-15159

Sounding propagation in multistage axial flow turbomachines 04 p0533 A83-15289

Rolls-Royce RB 211-535 power plant 04 p0449 A83-15311

A method of predicting the performance deterioration of a compressor cascade due to sand erosion [AIAA PAPER 83-0178] 05 p0596 A83-16572

Effectiveness of turbine engine diagnostic systems [AIAA PAPER 83-0535] 05 p0597 A83-16773

The module concept in a mathematical model of a turboprop engine 05 p0597 A83-16878

New thrusts in engine design 05 p0597 A83-17236

Powerplants. II --- review of current aircraft turbofan engines 06 p0718 A83-18147

Application of optimization to aircraft engine disk synthesis 06 p0718 A83-18213

How decisions are made - Major considerations for aircraft programs 06 p0717 A83-18398

Digital electronic engine control system - F-15 flight test 06 p0718 A83-18406

NAPC gyroscopic moment test facility 06 p0720 A83-18407

The Pratt & Whitney PW100 - Evolution of the design concept 06 p0718 A83-18821

Military propulsion technology. I - Fighter power - The need for tomorrow 06 p0718 A83-18948

Military propulsion technology. III - Materials are the key --- for fighter aircraft engines 06 p0730 A83-18950

Fabrication technology for aircraft engines --- Russian book 07 p0861 A83-20381

Precision casting for gas turbine engines 07 p0941 A83-21347

Automated machining of turbine blades by Rolls-Royce 07 p0941 A83-21348

Cleaning gas turbine compressors - Some service experience with a wet-wash system 07 p0867 A83-21350

The corrosion resistance of protective coatings 07 p0891 A83-21454

Fatigue failure under fretting conditions 07 p0894 A83-21481

Internal performance prediction for advanced exhaust systems --- for tactical aircraft 08 p1046 A83-22156

Compact installation for testing vectored-thrust engines 08 p1047 A83-22158

High bypass ratio engine noise component separation by coherence technique 08 p1046 A83-22159

Advances in high-speed rolling-element bearings --- for aircraft engine and transmission application 08 p1111 A83-22319

Fiber optics for aircraft engine/inlet control 08 p1046 A83-22494

Theory and design of flight-vehicle engines --- Russian book 08 p1046 A83-22651

Current problems in the testing of aircraft engines 08 p1046 A83-22652

Errors in the experimental determination of the parameters of supersonic combustion ramjet engines 08 p1046 A83-22653

The effect of the nonuniformity of supersonic flow with shocks on friction and heat transfer in the channel of a hypersonic ramjet engine 08 p1046 A83-22654

Features of the selection of the basic parameters of cooled GTE turbines 08 p1046 A83-22655

On the choice of the optimal total wedge angle for the air intake of a hypersonic ramjet engine 08 p1046 A83-22656

Numerical calculation of the separation and connection of two-dimensional supersonic flows in channels with discontinuous boundaries 08 p1046 A83-22658

Gas turbine combustor modelling for calculating pollutant emission 08 p1046 A83-23142

Design of an integrated control system for a supersonic aircraft power plant 08 p1046 A83-23175

PW 4000 - A radically new jet engine being developed in the USA 08 p1046 A83-23239

Evaluation of the technical state of aircraft gas-turbine engines from thermodynamic parameters with allowance for the natural scatter of state parameters 09 p1205 A83-23430

Statistical estimation of the mean time-to-failure of an aircraft engine as a function of the cause of failure 09 p1205 A83-23433

A method for calculating the parameters of a turbojet engine in the autorotation regime 09 p1205 A83-23434

A system of criteria for evaluating the energy efficiency of an engine at the state of technical proposals 09 p1205 A83-23437

Determination of the region of efficient use for microturbines with working medium recirculation 09 p1205 A83-23440

A finite-element study of the stress-strain state of the turbofan rotor of an aircraft gas-turbine engine 09 p1205 A83-23515

Microlights - The state of the art 09 p1195 A83-23685

Turbofan engine blade pressure and acoustic radiation at simulated forward speed 09 p1205 A83-24026

Effect of variable guide vanes on the performance of a high-bypass turbofan engine 09 p1205 A83-24028

Tactical aircraft engine usage - A statistical study 09 p1206 A83-24033

Performance improvements of single-engine business airplanes by the integration of advanced technologies [DGLR PAPER 82-064] 09 p1203 A83-24178

Jet engines for airliners of the next generation [DGLR PAPER 82-069] 09 p1206 A83-24183

The maintenance of modern engines in civil aviation [DGLR PAPER 82-070] 09 p1206 A83-24184

Some aspects of the engine design of future fighter planes [DGLR PAPER 82-071] 09 p1206 A83-24185

Development trends regarding jet engines for future combat aircraft [DGLR PAPER 82-072] 09 p1206 A83-24186

On the design philosophy of fighter aircraft engines [DGLR PAPER 82-073] 09 p1206 A83-24187

Digital engine control unit - Future employment possibilities [DGLR PAPER 82-085] 09 p1206 A83-24197

Prospects for the use of heat exchangers in aircraft gas turbines [DGLR PAPER 82-088] 09 p1207 A83-24200

U.S. Army/Detroit Diesel Allison Advanced Technology Demonstrator Engine 09 p1208 A83-24836

Rotary engines 09 p1369 A83-25140

NASA clean catalytic combustor program [ASME PAPER 82-JPGC-GT-11] 09 p1227 A83-25269

In-flight acoustic measurements in the engine intake of a Fokker F28 aircraft [AIAA PAPER 83-0677] 10 p1376 A83-25909

Noise transmission through sidewall treatments applicable to twin-engine turboprop aircraft [AIAA PAPER 83-0695] 10 p1473 A83-25916

Specification, design, and test of aircraft engine isolators for reduced interior noise [AIAA PAPER 83-0718] 10 p1377 A83-25932

PW4000 uses JT9D, new technology 10 p1378 A83-26072

Three-dimensional elastoplastic finite element analysis 10 p1442 A83-26767

Optimization of the oil-change period for aircraft systems and units 10 p1401 A83-26922

A steady state performance model for general aviation spark-ignition piston engines 11 p1530 A83-27163

A samarium cobalt motor-controller for mini-RPV propulsion 11 p1530 A83-27187

Transient performance of permanent magnet synchronous motors 11 p1560 A83-27189

Discharge rate capability of nickel-cadmium aircraft batteries 11 p1530 A83-27190

Effect of initial conditions on constant pressure mixing between two turbulent streams 11 p1567 A83-27875

The influence of inlet design on the aeroacoustic performance of a JT15D turbofan engine as measured in the NASA-Ames 40 x 80 foot wind tunnel [AIAA PAPER 83-0681] 11 p1531 A83-28006

Preliminary report on the engineering development of the Magnus Aerospace Corp LTA 20-1 heavy-lift aircraft 11 p1530 A83-28193

The interaction between a separated blade and the armor ring 11 p1531 A83-28510

Analysis of engine usage data for tactical systems [AIAA PAPER 81-1370] 12 p1703 A83-29011

On the routes - Boeing 757 with British Airways 12 p1701 A83-29241

Evaluation of the productivity of an automated system for the testing of aircraft engines 12 p1703 A83-29277

Calculation of the depth and hardness of the carburization layer of cylindrical parts --- for aircraft engines 12 p1713 A83-29282

An overview of turbine engine structural design - Development trends in the Air Force [AIAA 83-0952] 12 p1703 A83-29777

Maintenance of large engines CF6s for the Airbus A310 13 p1807 A83-30073

PMUX - The interface for engine data to AIDS --- propulsion multiplexer Aircraft Integrated Data System 13 p1807 A83-30158

Institute of environmental sciences aircraft engine combustor casing life simulation for increased reliability 13 p1807 A83-31493

A review of commuter propulsion technology [SAE PAPER 820716] 13 p1807 A83-31801

Design features of a new commuter turboprop engine [SAE PAPER 820717] 13 p1807 A83-31802

Advanced technology for SAAB-Fairchild 340 aircraft [SAE PAPER 820729] 13 p1806 A83-31805

The integration of internal combustion engines of the General Aviation - Problems raised by ventilation and exhaust [AAAF PAPER NT 82-16] 14 p1976 A83-33167

The influence of defects on the operational strength of disks and wheels in engines 15 p2174 A83-33964

Thermal cycling in compact plate-fin heat exchangers --- in aircraft gas turbines 15 p2123 A83-34253

AR.318 - Italy's low-cost GA turboprop 16 p2302 A83-35675

International Symposium on Air Breathing Engines, 6th, Paris, France, June 6-10, 1983, Symposium Papers 16 p2302 A83-35801

The effects of fuel properties upon pollutants present in gas turbine aero-engines 16 p2338 A83-35813

The prediction of performance of turbojet engine with distorted inlet flow and its experimental studies 16 p2303 A83-35832

Cost effective performance restoration of high by-pass engines 16 p2303 A83-35833

Numerical computation of turbulent flow around the spinner of a turbofan engine 16 p2291 A83-35838

Some aspects of development of power plant optimum control to increase aircraft fuel efficiency 16 p2303 A83-35841

The transient performance of turbojet engines and axial compressors 16 p2304 A83-35847

Development of a turbojet engine simulator for scale model wind tunnel testing of multi-mission aircraft 16 p2304 A83-35848

Propulsion system simulation technique for scaled wind tunnel model testing 16 p2311 A83-35850

Experimental study of a high-through-flow transonic axial compressor stage 16 p2291 A83-35853

Effect of sand erosion on the performance deterioration of a single stage axial flow compressor 16 p2304 A83-35854

Effect of humidity on jet engine axial-flow compressor performance 16 p2304 A83-35856

Statistical study of TBO and estimation of acceleration factors of ASMT for aircraft turbo-engine --- Accelerated Simulated Mission Endurance Testing 16 p2304 A83-35858

Ground simulation of engine operation at altitude 16 p2312 A83-35863

The effect of variation of diffuser design on the performance of centrifugal compressors 16 p2305 A83-35866

Component life reduction due to use of AVGS in gas turbine engines 16 p2305 A83-35869

Life estimation methods of gas turbine rotating components 16 p2305 A83-35870

Containment of turbine engine fan blades 16 p2305 A83-35871

Investigation methods on residual stresses in aero engines components 16 p2305 A83-35879

Stress analysis of critical areas of low-pressure compressor-disc assembly of a developmental aero-engine 16 p2305 A83-35880

Propulsion control sensor sharing opportunities [AIAA PAPER 83-0536] 16 p2318 A83-36059

Simulator fidelity and flight test data - Improving the flight performance of the B-52H WST production unit flight station simulator [AIAA PAPER 83-1075] 16 p2299 A83-36204

Progress in propulsion system/airframe structural integration [AIAA PAPER 83-1123] 16 p2300 A83-36234

Simulation of advanced engine lubrication and rotor dynamics systems - Rig design and fabrication [AIAA PAPER 83-1133] 16 p2306 A83-36238

The performance of single-shaft gas turbine load compressor auxiliary power units [AIAA PAPER 83-1159] 16 p2306 A83-36251

A survey of trends in modern turbine technology [AIAA PAPER 83-1174] 16 p2306 A83-36260

Analytical design and experimental verification of S-duct diffusers for turboprop installations with an offset gearbox [AIAA PAPER 83-1211] 16 p2294 A83-36283

Advanced turboprop and dual cycle engine performance benefits and installation options on a Mach 0.7 shorthaul transport aircraft [AIAA PAPER 83-1212] 16 p2307 A83-36284

A Monte Carlo simulation of the engine development process [AIAA PAPER 83-1230] 16 p2307 A83-36294

Nondestructive evaluation methods for implementation of damage-tolerant designed gas turbine engine components [AIAA PAPER 83-1232] 16 p2307 A83-36295

Aircraft engine inlet pressure distortion testing in a ground test facility [AIAA PAPER 83-1233] 16 p2307 A83-36296

Deterioration trending enhances jet engine hardware durability assessment and part management [AIAA PAPER 83-1234] 16 p2308 A83-36297

Accelerated Mission Testing of the F110 Engine [AIAA PAPER 83-1235] 16 p2308 A83-36298

Integrated propulsion-aircraft control evaluation for a current Navy fighter [AIAA PAPER 83-1236] 16 p2308 A83-36299

F/A-18A Inflight Engine Condition Monitoring System (IECMS) [AIAA PAPER 83-1237] 16 p2308 A83-36300

Flight/propulsion control system integration [AIAA PAPER 83-1238] 16 p2308 A83-36301

United Kingdom military engine usage, condition and maintenance systems experience [AIAA PAPER 83-1239] 16 p2308 A83-36302

Modern technology and airborne engine vibration monitoring systems [AIAA PAPER 83-1240] 16 p2302 A83-36303

Comparison of an experience with full authority digital engine controls in rotary wing and jet-lift VSTOL aircraft [AIAA PAPER 83-1241] 16 p2308 A83-36304

Results of tests of a rectangular vectoring/reversing nozzle on an F100 engine [AIAA PAPER 83-1285] 16 p2308 A83-36322

Advanced techniques for gas and metal temperature measurements in gas turbine engines [AIAA PAPER 83-1291] 16 p2302 A83-36325

Application of thin film strain gages and thermocouples for measurement on aircraft engine parts [AIAA PAPER 83-1292] 16 p2302 A83-36326

Development trends in engine durability --- for USAF aircraft gas turbines [AIAA PAPER 83-1297] 16 p2309 A83-36329

Development and application of a liquid-cooled V-8 piston engine for general aviation aircraft [AIAA PAPER 83-1342] 16 p2309 A83-36347

Performance capability of a Compact Multimission Aircraft Propulsion Simulator [AIAA PAPER 83-1358] 16 p2312 A83-36356

KC-135/CFM56 re-engine - The best solution [AIAA PAPER 83-1374] 16 p2309 A83-36367

Introducing the Rolls-Royce Tay [AIAA PAPER 83-1377] 16 p2309 A83-36368

The impact of engine usage on life cycle cost [AIAA PAPER 83-1406] 16 p2310 A83-36395

LCC evaluation of advanced engine damage tolerance goals for a hot-section disk --- in aircraft engines [AIAA PAPER 83-1407] 16 p2310 A83-36396

Configuration selection and technology transition in 5000 SHP class engines [AIAA PAPER 83-1411] 16 p2310 A83-36400

Fighter engine cycle selection [AIAA PAPER 83-1300] 16 p2310 A83-36412

Friction drag measurements of acoustic surfaces [AIAA PAPER 83-1356] 16 p2296 A83-36414

Propulsion prototypes at General Electric [AIAA PAPER 83-1053] 16 p2310 A83-36463

Technology and engine demonstrator programs [AIAA PAPER 83-1064] 16 p2310 A83-36464

The F-5 story - Prototype and technology demonstrator [AIAA PAPER 83-1062] 16 p2301 A83-36473

Advanced propulsion controls - A total system view 16 p2311 A83-36612

Electrohydraulic fuel-flow regulator for gas-turbine-engine control systems 16 p2311 A83-36793

V/STOL status from the engine technology viewpoint 16 p2311 A83-36912

Generalized maximum specific range performance 16 p2301 A83-36918

An update on high output lightweight diesel engines for aircraft applications [AIAA PAPER 83-1339] 16 p2311 A83-36925

Reliability analysis of a dual-redundant engine controller 17 p2517 A83-37289

Supersonic flow field analysis for a twin-engine aircraft model 17 p2448 A83-37521

Some aspects of Prop-Fan propulsion systems analysis [SAE PAPER 821358] 17 p2467 A83-37956

Inlet design for high-speed proptans [SAE PAPER 821359] 17 p2451 A83-37957

Supersonic STOVL research aircraft [SAE PAPER 821375] 17 p2463 A83-37965

Development of thrust augmentation technology for the Pegasus vectored thrust engine [SAE PAPER 821390] 17 p2468 A83-37966

Full Authority Fault Tolerant Electronic Engine Control systems for advanced high performance engines (FAFTEEC) [SAE PAPER 821398] 17 p2468 A83-37972

Developments in performance monitoring and diagnostics in aircraft turbine engines [SAE PAPER 821400] 17 p2468 A83-37973

Microcomputer brings digital power to the small aircraft gas turbine [SAE PAPER 821402] 17 p2468 A83-37975

Implementation and integration of process planning [SAE PAPER 821424] 17 p2493 A83-37981

Design aspects of systems in all-electric aircraft [SAE PAPER 821436] 17 p2463 A83-37984

The recipe for re-engining jet transports [SAE PAPER 821441] 17 p2463 A83-37989

Re-engining the 737 [SAE PAPER 821442] 17 p2463 A83-37990

727, B-52 retrofit with PW2037 meeting today's requirements [SAE PAPER 821443] 17 p2463 A83-37991

Re-engining applications of T56 derivative engines [SAE PAPER 821444] 17 p2464 A83-37992

Re-engining studies on the P-3 aircraft [SAE PAPER 821445] 17 p2464 A83-37993

The application of a liquid-cooled V-8 piston engine to general aviation aircraft [SAE PAPER 821446] 17 p2468 A83-37994

Super integrated power unit (SIPU) for the F-16 engine start system [SAE PAPER 821462] 17 p2469 A83-37996

Propulsion system integration configurations for future prop-fan powered aircraft [AIAA PAPER 83-1157] 17 p2469 A83-38081

Procedure for the calculation of basic emission parameters for aircraft turbine engines [SAE AIR 1533] 17 p2469 A83-38104

V/STOL from the propulsion viewpoint (7th Sir Sydney Camm Memorial Lecture) 17 p2470 A83-38869

Regional airline turboprop engine technology [AIAA PAPER 83-1158] 18 p2641 A83-39101

B-1B manufacturing - General Electric F101 production
 nears 18 p2632 A83-40332

Survey of inlet development for supersonic aircraft
 [AIAA PAPER 83-1164] 18 p2638 A83-40473

JVX - The world's first production tilt-rotor?
 18 p2641 A83-40622

Blade loss transient dynamic analysis of
 turbomachinery 19 p2800 A83-40864

JT9D performance deterioration results from a simulated
 aerodynamic load test 19 p2800 A83-41040

Use of mixed performance criteria in gas turbine engine
 controller design 19 p2800 A83-41482

Large scale aeroengine compressor test facility
 19 p2807 A83-41534

Method of thermodynamic function control and of
 damage analysis regarding aircraft engines with the aid
 of flight data recording systems --- German thesis
 19 p2800 A83-41850

A criterial approach to estimating the accumulation of
 the working medium mass and energy in the gas-air circuit
 of gas-turbine engines when analyzing transient regimes
 19 p2800 A83-42126

An analysis of the parameters determining the maximum
 thrust of ramjet engines 19 p2800 A83-42127

A study of the characteristics of short hydrodynamic
 dampers of aircraft engine motors with allowance for
 turbulization of the working fluid in the damper clearance
 19 p2800 A83-42129

Characteristics of the occurrence and elimination of a
 stall in an axial-flow compressor in the presence of a
 rotating irregularity at the inlet 19 p2800 A83-42132

Experimental investigation of a model of the internal
 exhaust gas mixer configuration of a turbofan engine in
 the reverse-thrust mode 19 p2801 A83-42146

PW100 - Canada's commuter turboprop
 20 p2936 A83-42524

Operation of an aircraft engine using liquefied methane
 fuel 20 p2927 A83-43239

A range of lightweight engines for RPV's
 20 p2937 A83-43719

Final evaluation of multi-viscosity oils designed for
 aircraft reciprocating engines
 [SAE PAPER 830707] 21 p3116 A83-44685

Reengineering the key to aircraft renewal
 [AIAA PAPER 83-1372] 21 p3091 A83-45514

Dynamic distortion in a short s-shaped subsonic diffuser
 with flow separation --- Lewis 8 by 6 foot Supersonic Wind
 Tunnel [AIAA PAPER 83-1412] 21 p3092 A83-45515

Engine power simulation for transonic flow-through
 nacelles 21 p3089 A83-45594

Electronic control of aircraft turbine engine
 21 p3093 A83-45600

Demands on the air system of modern aircraft engines
 22 p3255 A83-46491

Development of new combustion chamber technologies
 for future alternative combustion fuels
 23 p3406 A83-47183

Increased energy exploitation in cooled
 high-temperature turbines 23 p3406 A83-47202

Use of flight engine technology in stationary industrial
 gas turbines and diesel motors 23 p3464 A83-47203

The construction and testing of pilot installations for
 making diffusion connections and for depositing layers on
 high-alloy engine components 23 p3440 A83-47206

A new-technology gas generator for medium-power
 shaft-turbine engines 23 p3406 A83-47217

Combustion experiments with a new burner air
 distribution concept
 [ASME PAPER 83-GT-31] 23 p3406 A83-47893

The Rolls-Royce annular vaporizer combustor
 [ASME PAPER 83-GT-49] 23 p3407 A83-47908

A small engine high temperature core research
 programme [ASME PAPER 83-GT-56] 23 p3407 A83-47912

The purpose, the principles and the problems of fault
 tolerant systems --- for aircraft gas turbine engines
 [ASME PAPER 83-GT-59] 23 p3407 A83-47915

Investigation of F/A-18A engine throttle usage and
 parametric sensitivities [ASME PAPER 83-GT-64] 23 p3407 A83-47919

Investigation of fixed-rake sampling system for the
 assessment of emission characteristics of gas turbine
 engines [ASME PAPER 83-GT-72] 23 p3407 A83-47925

Test experience with turbine-end foil bearing equipped
 gas turbine engines [ASME PAPER 83-GT-73] 23 p3407 A83-47926

Automated diagnostic system for engine maintenance
 --- vibration data extraction from gas turbine engines
 [ASME PAPER 83-GT-103] 23 p3408 A83-47943

Measurement and analyses of heat flux data in a turbine
 stage. II - Discussion of results and comparison with
 predictions [ASME PAPER 83-GT-122] 23 p3408 A83-47951

Aircraft usage and effects on engine life
 [ASME PAPER 83-GT-143] 23 p3409 A83-47967

Integrated flight and propulsion operating modes for
 advanced fighter engines [ASME PAPER 83-GT-194] 23 p3410 A83-47999

A comparison of Navy and contractor gas turbine
 acquisition cost [ASME PAPER 83-GT-198] 23 p3410 A83-48001

A three-dimensional model for the prediction of shock
 losses in compressor blade rows [ASME PAPER 83-GT-216] 23 p3410 A83-48016

An historical review of propeller developments
 23 p3411 A83-48173

Saving fuel with the wide-chord fan
 23 p3411 A83-48174

Strong pressure waves in air-breathing engines
 23 p3398 A83-48216

Design concepts for low cost composite engine
 frames [AIAA PAPER 83-2445] 23 p3411 A83-48331

Preliminary design engine thermodynamic cycle
 selection for advanced fighters [AIAA PAPER 83-2480] 23 p3411 A83-48343

Subsonic diffuser development of advanced tactical
 aircraft [AIAA PAPER 83-1168] 24 p3544 A83-49300

Integrated flight/propulsion control system architectures
 for a high speed aircraft [AIAA PAPER 83-2563] 24 p3549 A83-49595

The formation of carbon monoxide during turbulent
 diffusion combustion --- for aircraft gas turbine combustion
 chambers 24 p3569 A83-49769

AIRCRAFT EQUIPMENT

NT AIRCRAFT HYDRAULIC SYSTEMS

NT AIRCRAFT LIGHTS

NT AIRCRAFT TIRES

NT BOMBING EQUIPMENT

NT EJECTION SEATS

NT FLYING EJECTION SEATS

NT TERCOM

Ice detector evaluation for aircraft hazard warning and
 undercooled water content measurements
 01 p0009 A83-10187

Aircraft systems test requirements analysis
 01 p0014 A83-10737

On-line certification for ATE systems
 01 p0001 A83-10785

Methods for minimizing the effects of lightning transients
 on aircraft electrical systems 01 p0009 A83-11088

Color, pictorial display formats for future fighters
 01 p0010 A83-11134

Video stand-alone instrument multi-function cockpit
 display system 01 p0010 A83-11172

Video distribution requirements for future tactical
 aircraft 01 p0006 A83-11182

A cost effective approach to design evaluation of
 advanced system display switchology
 01 p0093 A83-11200

Real-time infrared image processing --- onboard
 aircraft 01 p0011 A83-11459

Mass-produced laser gyros 02 p0176 A83-11628

Comparison of respirator protection factors measured
 by two quantitative fit test methods 02 p0226 A83-12409

Life development of components/systems of aircraft
 02 p0188 A83-12657

Weather radar radomes and their maintenance
 02 p0131 A83-12658

Electric power supply of aircraft --- Russian book
 03 p0282 A83-14115

Operational test and evaluation of the molecular sieve
 On-Board Oxygen Generation System /OBOGS/ in the
 AV-8A 'Harrier' 04 p0525 A83-15417

Advanced Aircrew Display Symposium, 5th, Patuxent
 River, MD, September 15, 16, 1981, Proceedings
 04 p0447 A83-16126

Colour flight deck displays 04 p0448 A83-16336

Aircraft electrical equipment --- Russian book
 05 p0597 A83-17125

USAF studies fighters for dual-role, all-weather
 operations 05 p0595 A83-17276

The JA37 /VIGGEN/ pilot training concepts ATD
 preliminary use and 'signs' of effectiveness --- Aircraft
 Training Device System 05 p0676 A83-17310

Application of software design standards to commercial
 aircraft equipment 05 p0592 A83-17312

Software aspects in certification of new European civil
 transport aircraft 05 p0679 A83-17314

Long-range Falcon - Flight-test Dassault Falcon 50
 06 p0716 A83-18074

The transport aircraft of tomorrow - A single element
 of an overall system 06 p0711 A83-19410

Electrical, avionics, and sensor equipment of the Yak-40
 aircraft /2nd revised and enlarged edition/ --- Russian
 book 07 p0866 A83-20390

Systemic aspects of flying weapons systems as factors
 in planning [DGLR PAPER 82-028] 09 p1195 A83-24154

Selected topics in licensing Airbus A310
 [DGLR PAPER 82-042] 09 p1199 A83-24166

Aircraft vehicle equipment improvements via
 microprocessors [SAE PAPER 820868] 10 p1375 A83-25767

Advantages of statistically interrogating onboard
 anticollision systems 10 p1374 A83-26482

Estimation regarding the feasibility of using larger
 distances in measurements with L2F systems in flight
 tests --- Laser-two-Focus 10 p1431 A83-26487

Low power, air-cooled DC-Link aircraft generation
 systems 11 p1530 A83-27324

Aviation filters for fuels, oils, hydraulic fluids, and air ---
 Russian book 12 p1700 A83-28813

On the routes - Boeing 757 with British Airways
 12 p1701 A83-29241

Application of the nonlinear finite element method to
 crashworthiness analysis of aircraft seats
 [AIAA 83-0929] 12 p1699 A83-29855

Changing the course of U.S. aviation
 13 p1803 A83-30830

Design for random - An example --- vibration testing
 power supply for drone aircraft 13 p1861 A83-30856

Flight operations: A study of flight deck management
 --- Book 15 p2120 A83-33767

Design aspects of systems in all-electric aircraft
 [SAE PAPER 821436] 17 p2463 A83-37984

Aircraft super integrated power unit
 [SAE PAPER 821461] 17 p2469 A83-37995

Guide for qualification testing of aircraft air valves
 [SAE ARP 986A] 17 p2443 A83-38101

Transfiling and maintenance of oxygen cylinders
 [SAE AIR 1059A] 17 p2471 A83-38103

Mixing 4D equipped and unequipped aircraft in the
 terminal area [AIAA PAPER 83-2240] 19 p2796 A83-41717

The application of gyroscopes in remotely piloted
 vehicles 20 p2936 A83-43708

The development of quartz-membrane pressure
 transducers at the Aeronautical Research and Test
 Institute 20 p2993 A83-43815

Flight clearance of the Jaguar fly by wire aircraft. I
 22 p3254 A83-45845

On-board weight and center-of-gravity measurement
 system with tire-pressure monitoring 23 p3402 A83-47216

Maintenance aspects of modern avionics
 23 p3392 A83-47654

The GTCP331, a 600 hp auxiliary power unit program
 --- for advanced transport aircraft [ASME PAPER 83-GT-188] 23 p3409 A83-47994

General aviation goes digital - Many advantages, but
 some problems 23 p3406 A83-48640

Bucking the current --- electric actuators for V/STOL
 aircraft 24 p3547 A83-48887

Improvement of a captive trajectory system by using
 optical distance sensors --- store separation from aircraft
 [ONERA, TP NO. 1983-115] 24 p3550 A83-49426

Army family of light rotorcraft (LHX) concept
 formulation [AIAA PAPER 83-2552] 24 p3548 A83-49592

Direct-current power supply units GVG 800/350
 24 p3549 A83-50115

AIRCRAFT FUEL SYSTEMS

The effect of the jet fuel temperature on wear rates
 during the friction of sliding and rolling 04 p0464 A83-16145

Optimal processing of the correction data of an aircraft
 fuel-measurement system 06 p0718 A83-19177

Trim Tank system for optimizing drag at the center of
 gravity [DGLR PAPER 82-030] 09 p1209 A83-24156

Future fuels for turbojet engines and their impacts on
 combustion chambers and fuel systems [DGLR PAPER 82-089] 09 p1242 A83-24201

Flight testing with hot JP-4 fuel --- in helicopter suction
 fuel systems 09 p1208 A83-24831

Thermal stability of alternative aircraft fuels
 [AIAA PAPER 83-1143] 16 p2339 A83-36243

Testing of antimisting kerosene in the DC-10/KC-10 fuel
 system simulator [SAE PAPER 821485] 17 p2492 A83-38004

Performance tests of two inert gas generator concepts
 for airplane fuel tank inerting [AIAA PAPER 83-1140] 17 p2464 A83-38078

Aircraft flexible tanks general design and installation
 recommendations [SAE ARP 166A] 17 p2464 A83-38102

AIRCRAFT FUELS

Estimation of aircraft fuel consumption
 01 p0008 A83-10186

Impacts of broadened-specification fuels on aircraft
 turbine engine combustors 01 p0028 A83-10655

Tests of blending and correlation of distillate fuel properties	01	p0028	A83-11050
Fuel for future transport aircraft	07	p0901	A83-20082
Effect of broad properties fuel on injector performance in a reverse flow combustor			
[AIAA PAPER 83-0154]	07	p0867	A83-21079
Radiation and smoke from the gas turbine combustor using heavy fuels	09	p1242	A83-23877
Degradation and characterization of antimisting kerosene	09	p1242	A83-24035
Ground contamination by fuel jettisoned from aircraft in flight			
[AD-A128451]	09	p1294	A83-24041
Application of digital image analysis techniques to antimisting fuel spray characterization			
[ASME PAPER 82-WA/HT-23]	10	p1401	A83-25690
Is LH2 the high cost option for aircraft fuel	11	p1552	A83-27215
Effective generalized conductivity of three-phase cellular systems --- with kerosene-air-water fuel mixture example	12	p1775	A83-29270
Some fuel effects on carbon formation in gas turbine combustors	12	p1717	A83-29392
Further studies on the prediction of spray evaporation rates --- for aircraft fuels	16	p2338	A83-35811
Component life reduction due to use of AVGAS in gas turbine engines	16	p2305	A83-35869
Thermal stability of alternative aircraft fuels			
[AIAA PAPER 83-1143]	16	p2339	A83-36243
Operational effects of increased freeze point fuels in military airplanes			
[AIAA PAPER 83-1139]	17	p2492	A83-38077
Aviation gasoline - Issues and answers	20	p2959	A83-43316
[SAE PAPER 830705]	20	p2959	A83-43316
Autogas flight test in a Cessna 150 airplane			
[SAE PAPER 830706]	20	p2933	A83-43317
Model of a cryogenic liquid-hydrogen pipeline for an airport ground distribution system	20	p3013	A83-43641
The effect of hydrocarbon structure upon fuel sooting tendency in a turbulent spray diffusion flame			
[ASME PAPER 83-GT-90]	23	p3440	A83-47937
A vortex venturi for reverting antimisting fuel properties			
[ASME PAPER 83-GT-137]	23	p3409	A83-47964
Drop size measurements in evaporating realistic sprays of emulsified and neat fuels			
[ASME PAPER 83-GT-231]	23	p3440	A83-48027
An airline view of LH2 as a fuel for commercial aircraft	23	p3440	A83-48598

AIRCRAFT GUIDANCE

The reliability analysis of a dual, physically separated, communicating IMU system	01	p0005	A83-11128
DC-9 Super 80 digital flight guidance system simulation techniques for certification	05	p0592	A83-17305
Software design for the Douglas DC-9 Super 80 digital flight guidance system	05	p0592	A83-17311
Automation of on-board flightpath management	07	p0867	A83-21002
Flight management systems and data links	09	p1209	A83-24424
Integration of navigation resources in modern avionics systems	09	p1200	A83-24852
Technical and operational evaluation of wide-area coverage navigation systems in the continental United States	09	p1201	A83-24857
Guidance control systems for aircraft on airport surfaces			
[AIAA PAPER 83-1579]	16	p2297	A83-36953
Development of 4-D time-controlled guidance laws using singular perturbation methodology	17	p2461	A83-37149
DC-9 Super 80 Digital Flight Guidance System integrated system testing			
[SAE PAPER 821364]	17	p2467	A83-37959
Mixing 4D equipped and unequipped aircraft in the terminal area			
[AIAA PAPER 83-2240]	19	p2796	A83-41717
4 D fuel-optimal guidance in the presence of winds			
[AIAA PAPER 83-2242]	19	p2796	A83-41719

AIRCRAFT HAZARDS

Ice detector evaluation for aircraft hazard warning and undercooled water content measurements	01	p0009	A83-10187
AEHP for advanced technology aircraft --- Atmospheric Electricity Hazard Protection	01	p0001	A83-11086
Design of an aircraft ice detector using microcomputer electronics to enhance system availability	01	p0009	A83-11097
A similarity analysis of the droplet trajectory equation	03	p0315	A83-13133
Conflict of interest wind modeling in aircraft response study	03	p0281	A83-13158

Corona type sensor for aircraft electrical potential measurement			
[ONERA, TP NO. 1982-73]	03	p0282	A83-14530
Atmospheric electricity and air transport safety			
[ONERA, TP NO. 1982-82]	03	p0280	A83-14534
The Air Force Flight Test Center Palletized Airborne Water Spray System			
[AIAA PAPER 83-0030]	05	p0594	A83-16472
Aircraft icing roughness features and its effect on the icing process			
[AIAA PAPER 83-0111]	05	p0666	A83-16527
NASA Lewis Research Center's program on icing research			
[AIAA PAPER 83-0204]	05	p0577	A83-16582
Applications of Doppler radar to aviation operations - JAWS experiences			
[AIAA PAPER 83-0205]	05	p0666	A83-16583
Heavy rain influence on airplane accidents	06	p0714	A83-18415
Remote sensing of problem birds in aviation	08	p1043	A83-21876
Management of bird problem in Indian airlines	08	p1043	A83-21877
Bird strikes to aircraft and associated hazards and problems regarding the safety of aircraft operations	08	p1043	A83-21878
Wind shear detection with a modified airport surveillance radar	11	p1627	A83-27040
A contribution to airworthiness certification of gas turbine disks	16	p2305	A83-35872
Preliminary results of the AFGL icing study			
[AD-A129843]	17	p2549	A83-38718
The LLP lightning locating system --- Lightning Location and Protection	17	p2549	A83-38720
Specification of slant wind shear with an offset tower observation system	17	p2552	A83-38749
The short-range forecasting of meteorological conditions of the icing of aircraft on the ground and the runway at the Sofia airport	19	p2868	A83-41585
F/RF-4 transparency baseline bird impact test program	20	p2932	A83-42533
Induced currents at the resonant frequency in the Rocket Triggered Lightning Investigation	20	p3030	A83-42534
FOD hazard from tire-lofted debris --- Foreign Object Damage	20	p2931	A83-42557
Observations of severe in-flight environments on airplane composite structural components	20	p2933	A83-43330
Theoretical and experimental studies of the electromagnetic coupling mechanisms between aircraft and consecutive lightning strikes, both direct and nearby	21	p3089	A83-44318
[ONERA, TP NO. 1983-44]	21	p3089	A83-44318
The diagnosis and evaluation of turbulence which influences the flight of aircraft, according to rawinsonde network observation data	21	p3181	A83-45326
A systematic characterization of the effects of atmospheric electricity on the operational conditions of aircraft			
[ONERA, TP NO. 1983-59]	23	p3400	A83-48180
Microphysical influences on aircraft icing	24	p3546	A83-49722

AIRCRAFT HYDRAULIC SYSTEMS

A study of the structural strength and ductility of nickel screens --- for aircraft hydraulic system filters	07	p0940	A83-20910
Determination of the sensitivity of U.S. Air Force aircraft hydraulic system components to particulate contamination	16	p2362	A83-36910
Calculation of the flow rate characteristic of a jet-throttling hydraulic distributor with allowance for the ejection properties of a tube-plate system	19	p2799	A83-42128
Emergency power for the F-16 aircraft	23	p3410	A83-47995
[ASME PAPER 83-GT-189]	23	p3410	A83-47995
AIRCRAFT INDUSTRY			
Rethinking automation in NDT applications	09	p1275	A83-23920
Aviation system technology from the point of view of the aircraft manufacturer			
[DGLR PAPER 82-025]	09	p1195	A83-24152
The ATR 42 will keep its promises	09	p1203	A83-25115
Advanced technology for future regional transport aircraft	11	p1529	A83-27499
Materials in the mirror of aviation criteria	15	p2122	A83-33952
Legislative developments affecting the aviation industry 1981-1982	18	p2752	A83-39043
Aircraft crashworthiness in the United States - Some legal and technical parameters	18	p2752	A83-39044
Strict liability in military aviation cases - Should it apply?	18	p2753	A83-39045
Aircraft crashworthiness and the manufacturer's tort liability in the United States	22	p3367	A83-45808

Ten years of promoting the development of air transport research	23	p3391	A83-47185
Technology transfer from the aircraft sector to other sectors as exemplified by helicopter technology	23	p3391	A83-47190
Design and technology influences - 'Maturity' at introduction of the 214ST			
[AIAA PAPER 83-2528]	23	p3404	A83-48366
LHX - The US Army wants 5,000 - Industry needs the business	23	p3405	A83-48642
Civil transport aircraft design methodology			
[AIAA PAPER 83-2463]	24	p3547	A83-49579
A McDonnell Douglas perspective - Commercial aircraft for the next generation			
[AIAA PAPER 83-2502]	24	p3548	A83-49587
Transport aircraft requirements - How much? How soon? How to pay?			
[AIAA PAPER 83-2504]	24	p3546	A83-49588

AIRCRAFT INSTRUMENTS

NT ALTIMETERS			
NT ANEMOMETERS			
NT APPROACH INDICATORS			
NT ATTITUDE INDICATORS			
NT AUTOMATIC PILOTS			
NT FLIGHT RECORDERS			
NT GYROCOMPASSES			
NT HOT-WIRE ANEMOMETERS			
NT POSITION INDICATORS			
NT RADIO ALTIMETERS			
NT RADIO DIRECTION FINDERS			
NT SONIC ANEMOMETERS			
NT SPACECRAFT POSITION INDICATORS			
NT SPEED INDICATORS			
NT TACHOMETERS			
Materials for the manufacture of aircraft instruments and structures --- Russian book	01	p0021	A83-10466
Advanced multiple output air data sensor for angle of attack, pilot and static pressure measurements	01	p0009	A83-11098
The reliability analysis of a dual, physically separated, communicating IMU system	01	p0005	A83-11128
Secondary air data measurement technology --- pressure transducers for RPVs, drones, cruise missiles and fighter backup systems	01	p0011	A83-11261
The complete book of cockpits	02	p0135	A83-11575
Visual scanning behavior and pilot workload	02	p0225	A83-12405
Trend analysis concerning the displays and the keyboard of GPS navigation receivers for different applications	02	p0135	A83-13010
The aviation and radioelectronic equipment of the Yak-18T aircraft --- Russian book	03	p0282	A83-13814
Corona type sensor for aircraft electrical potential measurement			
[ONERA, TP NO. 1982-73]	03	p0282	A83-14530
Advanced P-3 flight station studies	04	p0447	A83-15429
Development and testing of a microwave radiometric vertical sensor for application to a vertical seeking aircrew escape system	04	p0447	A83-15437
Ergonomic aspects of aircraft keyboard design - The effects of gloves and sensory feedback on keying performance	04	p0526	A83-15900
Airborne electronic colour displays	04	p0448	A83-16133
Concerning the measurement of aircraft acceleration	05	p0595	A83-16876
An instrument for recording the exceeding of specified levels of an operational parameter of an aircraft	05	p0596	A83-16880
Multifunction display simulation facility	05	p0596	A83-17302
Computer-based pre-simulator training	05	p0676	A83-17308
Microwave Ice Accretion Measurement Instrument /MIAMI/	08	p1045	A83-22163
Calibration support of the AN/AAM-60 common forward-looking infrared /FLIR/ test bench	08	p1104	A83-22886
Increasing flight safety under shear wind conditions by modifying thrust regulation systems and existing cockpit instrumentation	09	p1209	A83-24159
[DGLR PAPER 82-033]	09	p1209	A83-24159
Aircraft laboratory for optical observations in experiments involving active effects upon the earth's ionosphere and magnetosphere	10	p1447	A83-25334
Human factors in the application of large screen electronic displays to transport flight station design	10	p1376	A83-26312
Doppler radar and aircraft measurements of thunderstorm turbulence	11	p1627	A83-27043
Flight deck display	11	p1530	A83-27123

Analysis of the precision of inertial navigation systems
 --- German thesis 11 p1528 A83-28649
 Development and test of an integrated sensory system for advanced aircraft 13 p1807 A83-30159
 Sidestick controller design requirements 14 p1977 A83-32934
 Performance capabilities of photographic flight navigation and sensor orientation systems 16 p2298 A83-36122
 Advanced display techniques for training the multi-member tactical air crew
 [AIAA PAPER 83-1079] 16 p2302 A83-36207
 GE's APG-67 - Fighter radar with a future 16 p2298 A83-36625
 Alpha Jet - Further version for the international market 17 p2467 A83-37858
 The use of pressure fluctuations on the nose of an aircraft for measuring air motion 18 p2721 A83-39118
 A history of electronic flight instruments - through tomorrow 19 p2799 A83-41532
 The Airborne Laser Ranging System - Its capabilities and applications 19 p2848 A83-41560
 Functional development of the 757/767 digital cat. IIIB Autoland System
 [AIAA PAPER 83-2192] 19 p2796 A83-41762
 Selecting measurements and controls in log problems 21 p3192 A83-44004
 Application and experience of colour CRT flight deck displays 21 p3091 A83-44688
 Four-dimensional flight management using colour CRT displays 21 p3091 A83-44689
 Aircraft keyboard ergonomics - A review 21 p3189 A83-44691
 Evolution of map display optical systems 21 p3092 A83-44830
 Improvement of the measurement system for the survey of class-II ILS installations 21 p3090 A83-45401
 Space technology - The art and science of ergonomics 21 p3092 A83-45605
 Laboratory evaluation of an airborne ozone instrument that compensates for altitude/sensitivity effects 21 p3092 A83-45618
 Military systems acceptance criteria --- for digital avionics systems 22 p3247 A83-45844
 Flight clearance of the Jaguar fly by wire aircraft. I 22 p3254 A83-45845
 Plating on glass for hermetic seal
 [SAE PAPER 820613] 22 p3302 A83-45871
 A new generation of navigation and landing aids for aviation 23 p3401 A83-47188
 Central operating and display unit for avionics systems 23 p3401 A83-47193
 Integrated navigation systems for aircraft 23 p3402 A83-48735

AIRCRAFT LANDING

NT CRASH LANDING
 NT SKID LANDINGS
 Conflict of interest wind modeling in aircraft response study 03 p0281 A83-13158
 Fuel-optimal aircraft trajectories with fixed arrival times 04 p0446 A83-16115
 Information requirements for pilot supervision of automatic landing in low visibility conditions 04 p0524 A83-16129
 Helmet mounted display symbology for helicopter landing on small ships 04 p0448 A83-16134
 Aerodynamic penalties of heavy rain on landing airplanes 06 p0714 A83-18403
 A proposed simple and safe aircraft take-off or landing procedure with wing roughness or protuberances
 [AIAA PAPER 83-0604] 06 p0718 A83-19594
 The learning behaviour of trainee pilots during aircraft-landing - A simulator study 07 p0981 A83-19662
 A concept for reducing helicopter IFR landing weather minimums - Onshore 07 p0865 A83-21034
 Real time estimation of ship motions using Kalman filtering techniques 08 p1158 A83-22720
 Noise-reducing takeoff and landing procedures and the potential for their operational use in the Airbus A300
 [DGLR PAPER 82-032] 09 p1199 A83-24158
 Applications of head-up displays in commercial transport aircraft 09 p1204 A83-24428
 Observers as noise filters in an automatic aircraft landing system 09 p1209 A83-24434
 On the feasibility of real-time prediction of aircraft carrier motion at sea 10 p1463 A83-26265
 A visual channel theory approach to pilot performance and simulator imagery 10 p1456 A83-26311
 Adjacent channel interference in the case of the precision distance measuring system DME/P 10 p1374 A83-26480
 The design of wind shear filters 10 p1378 A83-26483

Operation of ILS during snow and ice conditions 11 p1527 A83-27969
 Automatic activity and workload during learning of a simulated aircraft carrier landing task 14 p2071 A83-32690
 Dynamic taxi response (have bounce) testing of the C-5A aircraft
 [AIAA PAPER 83-1024] 14 p1975 A83-32783
 All-weather small-deck operations in the U.S. Navy
 [SAE PAPER 821503] 17 p2459 A83-38010
 DFVLR-remote slant visual range (SVR) and wind vector measuring systems 17 p2552 A83-38750
 The COMPAS system for more efficient approach traffic --- for aircraft 18 p2639 A83-39345
 Simulated fan-beam radar imagery --- use in assessing aircraft approach-to-landing paths 18 p2675 A83-40302
 Extended pilot-vehicle-task models for Navy missions
 [AIAA PAPER 83-2233] 19 p2885 A83-41711
 Carrier landing simulation results of precision flight path controllers in manual and automatic approach
 [AIAA PAPER 83-2072] 19 p2796 A83-41909
 Application of factor-analysis methods to evaluate the quality of ergatic control systems --- of aircraft landing by human operator 20 p3036 A83-43508
 Improvement of the measurement system for the survey of class-II ILS installations 21 p3090 A83-45401

AIRCRAFT LAUNCHING DEVICES

Sky Hook to help ships launch Harrier 03 p0282 A83-13575
 Launch and recovery techniques for RPVs 20 p2934 A83-43715

AIRCRAFT LIGHTS

Design consideration for lighting modern commercial aircraft
 [SAE PAPER 830712] 20 p2933 A83-43322
 Aircraft night lighting systems
 [SAE PAPER 830713] 20 p2936 A83-43323

AIRCRAFT MAINTENANCE

Repair of the auxiliary power plants of aircraft --- Russian book 02 p0136 A83-11949
 USAF studying techniques to restore windshields 02 p0131 A83-12324
 Reliability and maintainability aspects of a 'fleet' of prototype helicopters 02 p0131 A83-12654
 Life development of components/systems of aircraft 02 p0188 A83-12657
 Weather radar radomes and their maintenance 02 p0131 A83-12658
 The use of composite patches for repair of aircraft structural parts 02 p0131 A83-12968
 Analysis of bonded repairs to damaged fibre composite structures 03 p0291 A83-13200
 The cleaning of the exterior of the aircraft 03 p0277 A83-14325
 Application of fatigue-strength analysis to the evaluation of the consequences of local damage and the effects of wing-shell repairs. III - An example of the application of fatigue-strength analysis using a specific fatigue wear 03 p0342 A83-14620
 Cold-setting adhesives for repair purposes using various surface preparation methods 04 p0463 A83-15874
 The remanufacturers --- of passenger aircraft 06 p0711 A83-18075
 Aircraft inspection using radiography 07 p0861 A83-20478
 Damage tolerance and reparability of advanced composite structures 07 p0876 A83-20484
 Demonstration of reparability and repair quality on graphite/epoxy structural subelements 07 p0861 A83-20485
 Elevated temperature repairs of advanced composite structures 07 p0877 A83-20499
 Cleaning gas turbine compressors - Some service experience with a wet-wash system 07 p0867 A83-21350
 Analysis and repair of flaws in thick structures 08 p1115 A83-21654
 The design of bonded structure repairs 09 p1243 A83-23329
 The maintenance of modern engines in civil aviation
 [DGLR PAPER 82-070] 09 p1206 A83-24184
 Fault isolation methodology for the L-1011 digital avionics flight control system 09 p1209 A83-24427
 Full-flow debris monitoring and fine filtration for helicopter propulsion systems 09 p1208 A83-24838
 A qualitative methodology for studying Air Force maintenance 10 p1457 A83-26327
 Optimization of the oil-change period for aircraft systems and units 10 p1401 A83-26922
 Maintenance of large engines CF6s for the Airbus A310 13 p1807 A83-30073
 Repairing composite structures 13 p1803 A83-30074

Design considerations for ease of maintenance in commuter aircraft 13 p1803 A83-31804
 [SAE PAPER 820722] 13 p1803 A83-31804
 Cost effective performance restoration of high by-pass engines 16 p2303 A83-35833
 Statistical study of TBO and estimation of acceleration factors of ASMT for aircraft turbo-engine --- Accelerated Simulated Mission Endurance Testing 16 p2304 A83-35858
 Major hot section component salvaged through advanced repair methods
 [SAE PAPER 821489] 17 p2469 A83-38007
 Maintenance according to technical conditions --- for aircraft 18 p2631 A83-39221
 Simulation which simulates less 18 p2642 A83-40619
 Battle damage and repair of an advanced composite A-7 outer wing 20 p2927 A83-42547
 Impact of new technology on engineering and maintenance systems --- of airlines 21 p3085 A83-45078
 Design of the Eastern Air Lines plating shop 22 p3256 A83-45866
 Electroless nickel applications in aircraft maintenance
 [SAE PAPER 820609] 22 p3301 A83-45867
 Maintenance aspects of modern avionics 23 p3392 A83-47654
 EAGLE/DTA - A life cycle cost model for damage tolerance assessment --- Engine/Aircraft Generalized Life cycle cost Evaluator 23 p3407 A83-47929
 [ASME PAPER 83-GT-76] 23 p3407 A83-47929
 Aircraft usage and effects on engine life
 [ASME PAPER 83-GT-143] 23 p3409 A83-47967
 Built-In Test Equipment (BITE) on the Garrett model GTCP331 APU digital electronic control unit --- for gas turbine aircraft auxiliary power system
 [ASME PAPER 83-GT-186] 23 p3409 A83-47992
 Enhanced aircraft structural maintenance using organic depot damage tolerance analysis
 [AIAA PAPER 83-2450] 23 p3392 A83-48333
 New concepts for intermediate level maintenance --- of avionics by ATE 23 p3468 A83-48353
 [AIAA PAPER 83-2498] 23 p3468 A83-48353
 Wartime maintenance impact on aircraft availability
 Quantifying the R&D investment payoff
 [AIAA PAPER 83-2515] 23 p3392 A83-48359
 Depot level reparability, maintainability, and supportability of advanced composites
 [AIAA PAPER 83-2516] 23 p3404 A83-48360
 Scheduled depot maintenance of naval aircraft - How often?
 [AIAA PAPER 83-2517] 23 p3392 A83-48361
 Designing for supportability and cost effectiveness
 [AIAA PAPER 83-2499] 24 p3543 A83-49586
 Demonstration of mobile accelerator neutron radiography for in situ detection of moisture and corrosion in aircraft structures
 [AIAA PAPER 83-2449] 24 p3591 A83-50073

AIRCRAFT MANEUVERS

Minimum-time 180 deg turns of aircraft 01 p0012 A83-10250
 Advanced automatic terrain following/terrain avoidance control concepts study 01 p0013 A83-11254
 Recovery curves in partially fatigued muscle 01 p0084 A83-11259
 Military potential of the ABC 02 p0134 A83-12097
 The influence of differential physical conditioning regimens on simulated aerial combat maneuvering tolerance
 [AD-A126486] 02 p0223 A83-12406
 The maneuvering flight path display - An update 04 p0447 A83-16130
 Development of a flight test maneuver autopilot for a highly maneuverable aircraft
 [AIAA PAPER 83-0061] 05 p0597 A83-16493
 Decoupling of high gain multivariable tracking systems
 [AIAA PAPER 83-0280] 05 p0592 A83-16625
 Computation of optimal feedback strategies for interception in a horizontal plane
 [AIAA PAPER 83-0281] 05 p0577 A83-16626
 Optimization of variable-altitude flyback maneuvers --- for rocket-propelled lifting vehicles
 [AIAA PAPER 83-0282] 05 p0594 A83-16627
 Variable dimension filter for maneuvering target tracking 06 p0803 A83-19033
 Advanced composite materials in aerobatic aircraft 07 p0865 A83-20496
 Supersonic maneuvers without superbooms 07 p0864 A83-21021
 Dynamics of air combat 07 p0862 A83-21026
 Aircraft maneuver mechanics with turning of the power-plant thrust vector 08 p1047 A83-22076
 Configuration development for a highly maneuverable experimental aircraft with negative sweep rudder units
 [DGLR PAPER 82-035] 09 p1203 A83-24160

Maneuver load control for reducing the design loads of modern combat aircraft
[DGLR PAPER 82-046] 09 p1209 A83-24169

Conflict recognition and collision probability in connection with horizontal evasion maneuvers
10 p1373 A83-26481

Fault/maneuver tolerance of aided GPS demodulation/navigation processors in the non-precision approach environment
11 p1529 A83-28787

Impact damping and airplane towing
15 p2120 A83-33625

A high speed wind tunnel test evaluation of STOL dedicated advanced exhaust nozzle concepts
[AIAA PAPER 83-1225] 16 p2294 A83-36292

Dynamics of air combat
16 p2287 A83-36914

A collision avoidance tool for aircraft pilots
17 p2461 A83-37142

Design of an aerobatic aircraft wing using advanced composite materials
[SAE PAPER 821346] 17 p2463 A83-37955

The effects of non-linear kinematics in optimal evasion
19 p2889 A83-40674

The effects of engine and height-control characteristics on helicopter handling qualities
19 p2802 A83-41078

A comparative evaluation of some maneuvering target tracking algorithms
[AIAA PAPER 83-2168] 19 p2891 A83-41664

An integrated maneuver enhancement and gust alleviation mode for the AFTI/F-111 MAW aircraft
[AIAA PAPER 83-2217] 19 p2803 A83-41699

Robustness of a decoupled multivariable digital flight control system
[AIAA PAPER 83-2272] 19 p2804 A83-41738

Pursuit-evasion between two realistic aircraft
[AIAA PAPER 83-2119] 19 p2894 A83-41944

Poststall flight in close combat
[AIAA PAPER 83-2120] 19 p2806 A83-41945

Flight path/nose pointing - A required criterion in future fighter aircraft design
[AIAA PAPER 83-2123] 19 p2798 A83-41948

The application and results of a new flight test technique
[AIAA PAPER 83-2137] 19 p2799 A83-41959

The optimal evasive maneuver of a fighter against proportional navigation missiles
[AIAA PAPER 83-2139] 19 p2807 A83-41961

Estimation of nonlinear aerodynamics from transport airplane certification maneuvers - A system identification approach
[AIAA PAPER 83-2065] 20 p2938 A83-43811

Extracting the comprehensive characteristics in terms of similar parameters from flight test
21 p3091 A83-44570

Problems in determining aircraft polar curves from test-flight data
22 p3254 A83-46489

AIRCRAFT MODELS

Design and application of a multivariable, digital controller to the A-7D Digitac II aircraft model
01 p0013 A83-11148

A technique for predicting antenna-to-antenna isolation and electromagnetic compatibility for aircraft
01 p0007 A83-11235

A new concept for aircraft dynamic stability testing
04 p0449 A83-15310

Helicopter vibration reduction by local structural modification
04 p0500 A83-16028

Active control of a relaxed-static-stability airplane using a discrete model following technique
[AIAA PAPER 83-0279] 05 p0598 A83-16624

75th anniversary of the establishment of the Aerodynamic Experimental Institute of Goettingen
05 p0577 A83-16896

Researchers study methods to combat effects of wind shear
08 p1043 A83-22175

A comparison of model helicopter rotor Primary and Secondary blade/vortex interaction blade slap
[AIAA PAPER 83-0723] 10 p1475 A83-25934

Flight effects for jet-airframe interaction noise
[AIAA PAPER 83-0784] 10 p1376 A83-25965

Airplane model structure determination from flight data
12 p1704 A83-29023

Measured inplane stability characteristics in hover for an advanced bearingless rotor
[AIAA 83-0987] 12 p1702 A83-29865

Stability study of a tilt-rotor aircraft model
13 p1806 A83-31172

Experiment of a shockless transonic airfoil partially modified from an arbitrary airfoil
14 p1969 A83-32514

An axisymmetric nacelle and turboprop inlet analysis including power simulation
14 p1970 A83-32584

Performance capability of a Compact Multimission Aircraft Propulsion Simulator
[AIAA PAPER 83-1358] 16 p2312 A83-36356

Identification of aerodynamic coefficients using flight testing data
[AIAA PAPER 83-2099] 19 p2798 A83-41929

AIRCRAFT NOISE

NT JET AIRCRAFT NOISE

NT SONIC BOOMS

Advanced facility for processing aircraft dynamic test data
01 p0013 A83-10189

Noise generated by a propeller or a helicopter rotor
02 p0136 A83-12343

Noise and detectability characteristics of small-scale remotely piloted vehicle propellers
03 p0282 A83-13162

Noise transmission into semicylindrical enclosures through discretely stiffened curved panels
04 p0532 A83-15069

Novel airborne technique for aircraft noise measurements above the flight path
04 p0533 A83-15316

Procedure for evaluation of engine isolators for reduced structure-borne noise transmission
04 p0449 A83-15320

Non-linear effect in high speed rotor noise
06 p0807 A83-18393

Noise of a model helicopter rotor due to ingestion of isotropic turbulence
06 p0807 A83-18397

Theoretical and experimental evaluation of transmission loss of cylinders --- as idealized aircraft fuselages
07 p0990 A83-19808

Aerosound from corner flow and flap flow
[AIAA PAPER 81-2039] 07 p0990 A83-19813

Noise-reducing takeoff and landing procedures and the potential for their operational use in the Airbus A300
[DGLR PAPER 82-032] 09 p1199 A83-24158

Experimental investigations concerning the noise produced by model propellers and propeller-driven small aircraft
[DGLR PAPER 82-068] 09 p1206 A83-24182

A theoretical and experimental study of propeller noise
[ONERA, TP NO. 1982-122] 09 p1340 A83-24333

Acoustic metrology and signal processing
[ONERA, TP NO. 1982-123] 09 p1341 A83-24334

On high frequency broadband noise from model helicopter rotors
[AIAA PAPER 83-0673] 10 p1473 A83-25908

Flight effects on fan noise with static and wind tunnel comparisons
[AIAA PAPER 83-0678] 10 p1377 A83-25910

Interaction of fan rotor flow with downstream struts
[AIAA PAPER 83-0682] 10 p1377 A83-25912

Noise transmission through nonlinear sandwich panels
[AIAA PAPER 83-0696] 10 p1474 A83-25917

Effects of nonlinear propagation on long-range noise attenuation
[AIAA PAPER 83-0700] 10 p1474 A83-25920

Uncertainty of flyover noise data
[AIAA PAPER 83-0701] 10 p1474 A83-25921

An experimental investigation of sound radiation from a duct with a circumferentially varying liner
[AIAA PAPER 83-0712] 10 p1475 A83-25928

Noise source identification in airplane cabins using acoustic intensity technique
[AIAA PAPER 83-0716] 10 p1475 A83-25931

An evaluation of circumferentially segmented duct liners
[AIAA PAPER 83-0732] 10 p1475 A83-25939

Sources of installed turboprop noise
[AIAA PAPER 83-0744] 10 p1377 A83-25946

Farfield inflight measurements of high-speed turboprop noise
[AIAA PAPER 83-0745] 10 p1377 A83-25947

Flyover noise measurements for turbo-prop aircraft
[AIAA PAPER 83-0746] 10 p1377 A83-25948

Helicopter flight noise tests about the influence of rotor-rotational and forward speed changes on the characteristics of the immitted sound
[AIAA PAPER 83-0672] 11 p1650 A83-28002

Measurements of the scattering of sound by a line vortex
[AIAA PAPER 83-0676] 11 p1650 A83-28004

Near-field frequency - Domain theory for propeller noise
[AIAA PAPER 83-0688] 11 p1651 A83-28007

Measurements and predictions of turboprop noise at high cruise speed
[AIAA PAPER 83-0689] 11 p1651 A83-28008

Comparison of broadband noise mechanisms, analyses, and experiments on helicopters, propellers, and wind turbines
[AIAA PAPER 83-0690] 11 p1651 A83-28009

Synchrophasing for cabin noise reduction of propeller-driven airplanes
[AIAA PAPER 83-0717] 11 p1529 A83-28013

Application of 3-signal coherence to core noise transmission
[AIAA PAPER 83-0759] 11 p1652 A83-28021

Direct measurement of transmission loss of aircraft structures using the acoustic intensity approach
11 p1530 A83-28185

A new measurement method for separating airborne and structureborne aircraft interior noise
11 p1652 A83-28186

Noise emission and propagation in an air flow
[ONERA, TP NO. 1983-95] 12 p1777 A83-29385

A study of helicopter rotor noise, with special reference to tail rotors, using an acoustic wind tunnel
12 p1777 A83-29403

Advanced turboprop cargo aircraft systems study
14 p1974 A83-32582

Time-of-day corrections in measures of aircraft noise exposure
14 p2081 A83-33024

Full-scale measurements of blade-vortex interaction noise
15 p2227 A83-33505

In-flight acoustic test results for the SR-2 and SR-3 advanced-design propellers
[AIAA PAPER 83-1214] 16 p2307 A83-36286

Mathematical models of the acoustic properties of propellers
16 p2311 A83-36792

Sampling strategies for monitoring noise in the vicinity of airports
17 p2578 A83-37731

DFVLR research on helicopter noise
18 p2631 A83-39346

Aeroacoustic flight test of four single engine propellers
[SAE PAPER 830731] 20 p2936 A83-43328

Aircraft trajectories for reduced noise impact
21 p3089 A83-43971

Nonstationarity in acoustic fields
23 p3505 A83-47628

Subsonic and transonic propeller noise
[ONERA, TP NO. 1983-76] 23 p3505 A83-48191

Helicopter noise
[ONERA, TP NO. 1983-80] 23 p3506 A83-48195

Operational military helicopter interior noise and vibration measurements with comparisons to ride quality criteria
[AIAA PAPER 83-2526] 23 p3404 A83-48364

AIRCRAFT NOISE PREDICTION

U NOISE PREDICTION (AIRCRAFT)

AIRCRAFT PARTS

Preventing the strength failure of machines by vibrodiagnostic techniques.
06 p0770 A83-19313

Elevated temperature repairs of advanced composite structures
07 p0877 A83-20499

Design of an advanced 500-HP helicopter transmission
09 p1208 A83-24834

Reliability of aircraft splines with or without a wear induction period
[ASME PAPER 82-WA/DE-4] 10 p1436 A83-25700

The expansion of conical blanks by means of an elastic medium --- pressing technique for aircraft under-wing fuel tank parts
12 p1733 A83-29288

On the determination of the load-carrying capacity of the glass-plastic propeller blade of an aircraft
12 p1703 A83-29294

Studies of damage involving aircraft components --- accident-causing metallic component fractures
12 p1699 A83-29371

Titanium powder metallurgy components for advanced aerospace applications
[AIAA 83-0982] 12 p1715 A83-29789

Landing gear design handbook
13 p1805 A83-30143

Measuring and processing of undercarriage loading spectra of the L-39 aircraft
13 p1805 A83-30513

Development of process models to produce a dual-property titanium alloy compressor disk
15 p2134 A83-33634

Effect of processing on fatigue life of Ti-6Al-4Al-4V castings
15 p2135 A83-33641

Numerical simulation of electrothermal de-icing systems
[AIAA PAPER 83-0114] 16 p2297 A83-36043

Some applications of ultrasonic methods for the quality control of nonmetallic objects
16 p2364 A83-36794

In-flight computation of helicopter transmission fatigue life expenditure
16 p2301 A83-36921

Method for calculating jet noise in the presence of a shielding surface
17 p2577 A83-37253

Influence of airplane components on rotational aerodynamic data for a typical single-engine airplane
[AIAA PAPER 83-2135] 19 p2793 A83-41957

Determination of full pressure losses in stepped annular diffusers with rectilinear outer walls and a uniform velocity field at the inlet
19 p2800 A83-42130

A critical commentary on magnetic particle inspection
21 p3148 A83-43829

Process planning at Sikorsky
21 p3119 A83-44872

Selecting shock and vibration isolators
22 p3302 A83-46346

Aircraft design (3rd revised and enlarged edition) --- Russian book 23 p3403 A83-48100

AIRCRAFT PERFORMANCE

NT HELICOPTER PERFORMANCE

A-10 stall/post-stall testing - A status update 02 p0137 A83-11808

Identification of the causes of aircraft performance shortfalls in fleet operations 02 p0131 A83-12659

Nomogram for take-off performance of the V/STOL airplane 02 p0134 A83-12665

ACA-ECA or pipedream; Industry needs it - but who will pay 02 p0135 A83-13017

Selected results from the quiet short-haul research aircraft flight research program 03 p0281 A83-13165

Tomorrow's Tomcat 03 p0281 A83-14324

The A310 - Even better than expected 04 p0445 A83-14952

The 'Flying Peanut' - Revolutionary design promises high performance 04 p0447 A83-16400

Experimental study of a four-jet impingement flow using visualization techniques --- with applications to high performance VTOL aircraft [AIAA PAPER 83-0171] 05 p0633 A83-16568

Segmented vortex flaps [AIAA PAPER 83-0424] 05 p0585 A83-16706

Review of factors affecting aircraft wet runway performance [AIAA PAPER 83-0274] 05 p0595 A83-17915

Long-range Falcon - Flight-test Dassault Falcon 50 06 p0716 A83-18074

Powerplants. II --- review of current aircraft turbofan engines 06 p0718 A83-18147

The future for fighter aircraft 07 p0862 A83-20597

Technology and modern fighter aircraft - The evolutionary F-16 07 p0865 A83-20598

NGT - The Next Generation Trainer 07 p0866 A83-20599

CTOL, STOAL, V/STOL - An operational comparison for forward deployed CVNs 08 p1043 A83-22157

Investigation of landing gear alternatives for high performance aircraft 09 p1202 A83-24030

Performance improvements of single-engine business airplanes by the integration of advanced technologies [DGLR PAPER 82-064] 09 p1203 A83-24178

Some aspects of the engine design of future fighter planes [DGLR PAPER 82-071] 09 p1206 A83-24185

Calculation of the average slipstream of a propeller and its effect on the performance of an aircraft [ONERA, TP NO. 1982-120] 09 p1197 A83-24331

Homebuilt airplanes - The sky's the limit 09 p1196 A83-25122

Now is the time for new fighters 09 p1204 A83-25137

The extended Kalman filter and its use in estimating aerodynamic derivatives 11 p1531 A83-28183

Investigation of possible LTA craft application to solve national economy problems 11 p1527 A83-28194

Integrated systems evaluated on F-15 11 p1528 A83-28700

Fleet planning models --- in airline operations 12 p1699 A83-29967

Military potential of TiltRotor aircraft 12 p1700 A83-29969

Determination of horizontal tail load and hinge moment characteristics from flight data --- on Learjet Model 55 Longhorn 13 p1805 A83-30162

New life for the dragon lady --- U-2 aircraft design and production 14 p1974 A83-32398

Flight tests verify predictions for F-20 14 p1974 A83-32475

Performance estimation for light propeller airplanes 14 p1975 A83-32589

Performance flight testing --- Book 15 p2122 A83-33621

Aircraft design philosophy. I - Lee Begin of Northrop 16 p2298 A83-35624

Preliminary investigation on the performance of regenerative turbofan with inter-cooled compressor and its influence to aircraft 16 p2303 A83-35830

Propulsion system simulation technique for scaled wind tunnel model testing 16 p2311 A83-35850

Simulator fidelity and flight test data - Improving the flight performance of the B-52H WST production unit flight station simulator [AIAA PAPER 83-1075] 16 p2299 A83-36204

Development and application of a liquid-cooled V-8 piston engine for general aviation aircraft [AIAA PAPER 83-1342] 16 p2309 A83-36347

Introducing the Rolls-Royce Tay [AIAA PAPER 83-1377] 16 p2309 A83-36368

From new technology development to operational usefulness B-36, B-58, F-111/FB-111 [AIAA PAPER 83-1046] 16 p2287 A83-36459

Variable sweep wing design [AIAA PAPER 83-1051] 16 p2300 A83-36461

YAV-8B flight demonstration program [AIAA PAPER 83-1055] 16 p2300 A83-36466

A technique to determine lift and drag polars in flight 16 p2296 A83-36913

Configuration development of a research aircraft with post-stall maneuverability 16 p2301 A83-36915

Generalized maximum specific range performance 16 p2301 A83-36918

New technologies for general aviation 17 p2443 A83-37856

Re-engining the 737 [SAE PAPER 821442] 17 p2463 A83-37990

Re-engining applications of T56 derivative engines [SAE PAPER 821444] 17 p2464 A83-37992

V/STOL from the propulsion viewpoint (7th Sir Sydney Camm Memorial Lecture) 17 p2470 A83-38869

Effect of buoyancy and power design parameters on hybrid airship performance [AIAA PAPER 83-1976] 17 p2465 A83-38907

F-16XL - GD hatches a new Falcon 18 p2641 A83-40621

JVX - The world's first production tilt-rotor? 18 p2641 A83-40622

US fighter options 18 p2641 A83-40665

Frogfoot - A new Shтурmovik on trial 19 p2797 A83-41320

Determination of aerodynamic parameters of a fighter airplane from flight data at high angles of attack [AIAA PAPER 83-2066] 19 p2804 A83-41904

Applications of state estimation in aircraft flight-data analysis [AIAA PAPER 83-2087] 19 p2798 A83-41919

The SKYEYE R-4E surveillance system 20 p2934 A83-43705

The tasks and organization of the flight testing of airplanes and helicopters --- Russian book 21 p3091 A83-43901

Aerodynamic aspects of aircraft dynamics at high angles of attack 21 p3085 A83-43964

Optimum configuration for a 10-passenger business turbofan jet airplane 21 p3091 A83-43967

Extracting the comprehensive characteristics in terms of similar parameters from flight test 21 p3091 A83-44570

A model-based investigation of manipulator characteristics and pilot/vehicle performance 21 p3189 A83-45463

Designed to be stalled --- T-46A training aircraft 22 p3254 A83-46349

F-16XL shows advances in range, ride 22 p3254 A83-46924

Performance of a forward swept wing fighter utilizing thrust vectoring [AIAA PAPER 83-2482] 23 p3404 A83-48344

AIRCRAFT PILOTS

NT TEST PILOTS

Acquisition and analysis of the EMG power spectra - A reproducible technique for assessment of muscle fatigue --- electromyogram 01 p0086 A83-11107

Pilot workload in the night attack mission 01 p0086 A83-11187

Prevalence of selected pathology among currently certified active airmen 04 p0521 A83-15535

Safety attitudes of a general aviation pilot population 04 p0523 A83-15542

The psychiatric point of view on pilot headaches 06 p0797 A83-18335

Pilot deafness - Statistical study of military pilot hearing 06 p0797 A83-18336

Statistical data and the sound environment of Air Force aircrews 06 p0798 A83-18337

The problem of presbyopia in pilots and its correction with eyeglasses 06 p0798 A83-18338

The lipidic balance of technical flight personnel between 50 and 55 years old in commercial and civil aviation 06 p0798 A83-18340

Sudden incapacitation - USAF experience, 1970-80 07 p0978 A83-20787

Blood eosinophilia in aviators 08 p1147 A83-22954

A study of the psychophysiological behavior in a group of airline pilots after the operational age limit /60 years/ 08 p1150 A83-22955

Disease risk factors and the flight surgeon - A strategy to keep pilots flying 08 p1147 A83-22963

The nutritional and microbiological aspects of the onboard meal for pilots of international airlines 08 p1148 A83-22967

Spinal traumas /dorsal spinal fractures and lumbar disk hernias/ occurring after rapid vibratory phenomena /pumping/ in air combat pilots 08 p1148 A83-22973

Some observations on bail out injuries 08 p1148 A83-22975

Unusual ejection injury - A case report 09 p1323 A83-24008

Timolol maleate - Side effects on healthy nonglaucomatous volunteers 12 p1764 A83-28937

Medical problems peculiar to airline pilots 14 p2067 A83-32461

Automatic activity and workload during learning of a simulated aircraft carrier landing task 14 p2071 A83-32690

Locus of control, self-serving biases, and attitudes towards safety in general aviation pilots 15 p2215 A83-34980

Procedures for the examination of the visual acuity and of the visual field in civil aeronautics 16 p2396 A83-35578

The spine and the helicopter 16 p2397 A83-35582

The pilot seat and the vertebral column 16 p2397 A83-35583

Practical aspects of the medical check-up of nonprofessional pilots 16 p2397 A83-35585

A description of an experimental protocol for the study of the seat comfort of an aircraft pilot 16 p2402 A83-35586

Piloted simulation of hover and transition of a vertical attitude takeoff and landing aircraft 17 p2462 A83-37064

The behavior of heart rate in flight under +Gz stimulation Continuous monitoring using Holter's method and catecholamine excretion 17 p2561 A83-38944

The Air Canada programme for rehabilitation of the alcoholic employee/pilot 18 p2734 A83-40352

The characteristics of aerospace medical expertise for diseases of the eye 19 p2884 A83-42024

Effects of strength training on g tolerance 21 p3186 A83-43989

The legal status of the aircraft commander - Ups and downs of a controversial personality in international law 22 p3370 A83-45842

Age-specific morbidity among Navy-pilots 24 p3618 A83-48880

Personality profiles of pilots 24 p3618 A83-48884

The direct electrical stimulation of the upper urinary tract in case of ureteroliths in flight crew personnel 24 p3618 A83-49071

AIRCRAFT POWER SOURCES**U AIRCRAFT ENGINES****AIRCRAFT PRODUCTION**

A high order language for the analysis of experimental data 01 p0089 A83-11196

CAM networks for the factory of the future [AIAA PAPER 83-0217] 05 p0679 A83-16588

Plastic tooling for advanced composites 07 p0876 A83-20481

Fabrication of aircraft components using prepried broadgoods layed-up in the flat and subsequently formed - Cost benefits and resource utilization enhancements 09 p1195 A83-23602

Ceramic tooling in aircraft fabrication 09 p1195 A83-23603

Aviation system technology from the point of view of the aircraft manufacturer [DGLR PAPER 82-025] 09 p1195 A83-24152

Pre-planned product improvement /P3I/ the T64-GE-418 derivative engine 09 p1207 A83-24826

Changing the course of U.S. aviation 13 p1803 A83-30830

High-technology factory of the future 13 p1827 A83-31052

Apache on the war path - The Hughes AH-64 in production at last 14 p1974 A83-31939

AM-X - The export challenger with a foot in two continents 14 p1974 A83-31940

New life for the dragon lady --- U-2 aircraft design and production 14 p1974 A83-32398

All-electric vs conventional aircraft - The production/operational aspects 14 p1974 A83-32576

Comparison of properties of joints prepared by ultrasonic welding and other means 14 p2031 A83-32586

Lasers in aircraft construction --- Russian book 15 p2169 A83-34170

SAAB-Fairchild 340 - Transatlantic frontrunner 16 p2298 A83-35623

Aircraft production technology (2nd revised and enlarged edition) --- Russian textbook 16 p2287 A83-36443

Close-range photogrammetry for aircraft quality control 17 p2493 A83-38347

New insights in structural design of composite rotor blades for helicopters 18 p2640 A83-40287

B-1B manufacturing - Rockwell management plan saving costs, time 18 p2632 A83-40331

B-1B manufacturing - General Electric F101 production nears 18 p2632 A83-40332

B-1B manufacturing - Avco modifies prototype processes for production 18 p2632 A83-40333

Aircraft crashworthiness and the manufacturer's tort liability in the United States 22 p3367 A83-45808

Automated bonding process for load-bearing aircraft cellular structural components in light contour systems 23 p3391 A83-47198

AIRCRAFT PRODUCTION COSTS

Will technology make the helicopter competitive 07 p0866 A83-21574

Cost control of aircraft manufacture - A modern approach 08 p1171 A83-23148

Fabrication of aircraft components using preplied broadgoods layed-up in the flat and subsequently formed - Cost benefits and resource utilization enhancements 09 p1195 A83-23602

How to reduce the drilling cost for the aerospace industry 09 p1273 A83-23638

The cost definition phase of a new commercial aircraft programme 09 p1196 A83-24425

Structural members made of high-strength cast aluminum and their properties --- and reduction of aircraft production costs 15 p2136 A83-33954

High-strength aluminum high-quality casting alloy in aeronautics and astronautics 15 p2136 A83-33955

A tubular braided composite main rotor blade spar 16 p2299 A83-35949

The application of low-cost demonstrators for advanced fighter technology evaluation [AIAA PAPER 83-1052] 16 p2300 A83-36462

A critical look at the development and application of airframe cost models [SAWE PAPER 1478] 20 p2935 A83-43747

A comparison of Navy and contractor gas turbine acquisition cost [ASME PAPER 83-GT-198] 23 p3410 A83-48001

Comparative cost of military aircraft - Fiction versus fact [AIAA PAPER 83-2565] 23 p3392 A83-48378

Impact of composites on fighter aircraft. II - Composites New look to the aircraft production line 24 p3543 A83-48889

AIRCRAFT RELIABILITY

AEHP for advanced technology aircraft --- Atmospheric Electricity Hazard Protection 01 p0001 A83-11086

Integrated CNI avionics maximizes reliability --- communications, navigation, and cooperative identification 01 p0042 A83-11089

Air data systems for airplanes of the 1990's 01 p0004 A83-11099

Reliability and maintainability aspects of a 'fleet' of prototype helicopters 02 p0131 A83-12654

Existing time limit for overwater operations - Its validity 03 p0281 A83-13170

Tentative principles of the evaluation of the airworthiness of aircraft of one-of-a-kind design 03 p0280 A83-14623

The remanufacturers --- of passenger aircraft 06 p0711 A83-18075

Aircraft inspection using radiography 07 p0861 A83-20478

Official liability for insufficient airworthiness - Comments in connection with a supreme-court decision 08 p1171 A83-21898

Additional remarks with respect to the American decree of regarding the suspension of foreign certificates of airworthiness 08 p1171 A83-21899

Ground tests for obtaining the airworthiness certificate for an automatic terrain-following system [DGLR PAPER 82-040] 09 p1200 A83-24164

The reliability of aviation systems --- Russian book 10 p1436 A83-25621

Reliability of aircraft spines with or without a wear induction period [ASME PAPER 82-WA/DE-4] 10 p1436 A83-25700

Development and testing of Skyship 500 11 p1530 A83-28191

Benefits of mission profile testing 13 p1862 A83-31481

A contribution to airworthiness certification of gas turbine disks 16 p2305 A83-35872

Mathematical models of the acoustic properties of propellers 16 p2311 A83-36792

A model for determining the reliability of an aircraft wing structure 17 p2521 A83-37638

Durability and damage tolerance control plans for U.S. Air Force aircraft 19 p2797 A83-41045

A summary of NASA/FAA experiments concerning helicopter IFR airworthiness criteria 19 p2794 A83-41079

State space model concept for evaluating survivability methodologies for aircraft design 20 p2932 A83-42567

Vector optimization applied to survivability methodology evaluation --- for aircraft design 20 p3042 A83-42568

Development of a mathematical model of a flight vehicle and the experimental verification of its reliability 20 p2933 A83-42888

From aerostats to DC-10s - Recognition of certificates of airworthiness 22 p3369 A83-45829

Certification of avionic systems; Proceedings of the Symposium, London, England, April 27, 1982 22 p3247 A83-45843

Military systems acceptance criteria --- for digital avionic systems 22 p3247 A83-45844

Flight clearance of the Jaguar fly by wire aircraft. I 22 p3254 A83-45845

Flight clearance of the Jaguar-fly-by-wire aircraft. II 22 p3255 A83-45846

Certification of digital systems for civil aircraft 22 p3252 A83-45848

Helicopter avionic systems certification 22 p3255 A83-45849

Certification of the Lockheed 1011-500 active control system 22 p3255 A83-45850

Airplane reliability in a nutshell 23 p3467 A83-47614

The purpose, the principles and the problems of fault tolerant systems --- for aircraft gas turbine engines [ASME PAPER 83-GT-59] 23 p3407 A83-47915

AIRCRAFT SAFETY

Atmospheric electricity and air transport safety [ONERA, TP NO. 1982-82] 03 p0280 A83-14534

SAFE Association, Annual Symposium, 19th, Las Vegas, NV, December 6-10, 1981, Proceedings 04 p0524 A83-15401

Prediction of threshold pain skin temperature from thermal properties of materials in contact 04 p0522 A83-15540

Engineering safety analysis via destructive numerical experiments 04 p0500 A83-16198

Applications of Doppler radar to aviation operations - JAWS experiences [AIAA PAPER 83-0205] 05 p0666 A83-16583

Electromagnetic environment simulation for TCAS avionics --- Threat Alert and Collision Avoidance Systems 05 p0592 A83-17304

Aerodynamic penalties of heavy rain on landing airplanes 06 p0714 A83-18403

Safety requirements and trends in the passenger aircraft cabin area [DGLR PAPER 82-043] 09 p1199 A83-24167

The AH-64 nitrogen inerting unit 10 p1375 A83-25895

Radar detection of low level wind shear affecting aircraft terminal navigation 11 p1529 A83-28784

Improved fatigue life tracking procedures for Navy aircraft structures [AIAA 83-0805] 12 p1703 A83-29807

Crashing for safety 13 p1805 A83-31588

Airport pavement management - A total system [AIAA PAPER 83-1600] 14 p1978 A83-33363

The influence of defects on the operational strength of disks and wheels in engines 15 p2174 A83-33964

Development of airborne collision avoidance algorithms compatible with the national airspace system 17 p2461 A83-37141

A collision avoidance tool for aircraft pilots 17 p2461 A83-37142

Status of FAA crash dynamics program - Transport category aircraft [SAE PAPER 821483] 17 p2459 A83-38002

Evaluation of advanced airplane fire extinguishants [AIAA PAPER 83-1141] 17 p2459 A83-38076

Recent technical advances at the National Severe Storms Forecast Center that will improve short-term aviation advisories 17 p2550 A83-38723

Short-term prediction of high reflectivity contours for aviation safety 17 p2550 A83-38726

Aircraft crashworthiness in the United States - Some legal and technical parameters 18 p2752 A83-39044

Powder pack protection for aircraft dry bays 20 p2931 A83-42558

Aviation gasoline - Issues and answers [SAE PAPER 830705] 20 p2959 A83-43316

The missing element in wind shear protection [SAE PAPER 830715] 20 p2937 A83-43325

Optimization of fire blocking layers for aircraft seating [SAWE PAPER 1468] 20 p2931 A83-43742

General aviation safety - How safe? Its implication for flying and theory training 21 p3089 A83-44878

Security of International Civil Aviation - Role of ICAO 22 p3367 A83-45805

Air safety - Enforcement of the Federal Aviation Regulations 22 p3369 A83-45836

Enhanced aircraft structural maintenance using organic depot damage tolerance analysis [AIAA PAPER 83-2450] 23 p3392 A83-48333

NOTAR - The viable alternative to a tail rotor [AIAA PAPER 83-2527] 23 p3404 A83-48365

Ultralight aircraft safety and regulation 24 p3546 A83-48885

AIRCRAFT SPECIFICATIONS

Blackjack - Soviet B-1 or better 04 p0447 A83-16373

Dash 8 - Canada's new commuter 12 p1701 A83-29675

CF34 upgrades Challenger capabilities 15 p2122 A83-35315

Dashing ahead in commuterliners 17 p2464 A83-38470

Suggested changes in large aircraft flying qualities criteria [AIAA PAPER 83-2071] 19 p2805 A83-41908

AIRCRAFT SPIN

An evaluation of aerodynamics modeling of spinning light airplanes [AIAA PAPER 83-0368] 05 p0598 A83-17922

Autorotation --- in fluid dynamics 13 p1804 A83-31079

F/A-18 high angle of attack departure resistant criteria for control law development [AIAA PAPER 83-2126] 19 p2806 A83-41950

Wing modification for increased spin resistance [SAE PAPER 830720] 20 p2937 A83-43327

Estimation of parameters involved in high angle-of-attack aerodynamic theory using spin flight test data [AIAA PAPER 83-2086] 20 p2937 A83-43809

AIRCRAFT STABILITY

NT HOVERING STABILITY

VTOL aircraft stability 01 p0012 A83-10577

Application of model reference adaptive control to a relaxed static stability transport aircraft 01 p0013 A83-11209

A-10 stall/post-stall testing - A status update 02 p0137 A83-11808

F-18 Hornet high angle of attack /AOA/ program 02 p0137 A83-11809

Application of matrix singular value properties for evaluating gain and phase margins of multiloop systems --- stability margins for wing flutter suppression and drone lateral attitude control 02 p0230 A83-12457

A new concept for aircraft dynamic stability testing 04 p0449 A83-15310

Effects of control saturation on the command response of statically unstable aircraft [AIAA PAPER 83-0065] 05 p0598 A83-16497

Active control of a relaxed-static-stability airplane using a discrete model following technique [AIAA PAPER 83-0279] 05 p0598 A83-16624

Estimating roll coupling instability for highly augmented aircraft [AIAA PAPER 83-0366] 05 p0598 A83-16673

Calculation of the lift distribution and aerodynamic derivatives of quasi-static elastic aircraft 06 p0712 A83-18151

Stability of steady sideslip equilibria for high alpha --- supersonic fighter aircraft 09 p1209 A83-24031

Increasing flight safety under shear wind conditions by modifying thrust regulation systems and existing cockpit instrumentation [DGLR PAPER 82-033] 09 p1209 A83-24159

Control characteristics of a buoyant quad-rotor research aircraft 09 p1203 A83-24430

Study on longitudinal dynamic characteristics of pilot-airplane system - Approach to the method for studying PIO problem --- Pilot-Induced Oscillation 10 p1379 A83-26762

Development and validation of the V/STOL aerodynamics and stability and control manual 12 p1696 A83-29020

Airplane model structure determination from flight data 12 p1704 A83-29023

Near-real-time flutter boundary prediction from turbulence excited response [AIAA 83-0814] 12 p1741 A83-29814

Calculation of fundamental aerodynamic derivatives of aircraft. II 13 p1804 A83-30516

Stability study of a tilt-rotor aircraft model 13 p1806 A83-31172

Dynamic stability of a flight vehicle near a perturbed surface 14 p1977 A83-33008

The corkscrew phenomenon on the prototype of the Epsilon --- training aircraft for French airforce [AAAF PAPER NT-82-15] 14 p1977 A83-33166

Using adaptive control to synthesize invariant and partially autonomous automatic stabilization systems 15 p2123 A83-33900

Application of maximum likelihood estimation to the identification of the stability derivatives of a wide body transport aircraft 15 p2123 A83-35121

In-flight simulation at the U.S. Air Force and Naval Test Pilot Schools [AIAA PAPER 83-1078] 16 p2299 A83-36206

- Stability of aircraft motion in critical cases
17 p2470 A83-37066
- Bifurcation and limit cycle analysis of nonlinear systems with an application to aircraft at high angles of attack
17 p2470 A83-37080
- High angle-of-attack flight dynamics of a forward-swept wing fighter configuration
[AIAA PAPER 83-1837] 17 p2470 A83-38666
- Thrust reverser effects on the tail surface aerodynamics of an F-18 type configuration
[AIAA PAPER 83-1860] 17 p2457 A83-38687
- Wind tunnel evaluation of tactical aircraft stability and control as affected by nozzle thrust reverser parameter variations
[AIAA PAPER 83-1228] 18 p2642 A83-39103
- Training pilots for testing airplanes with modern flight control systems
18 p2736 A83-40340
- An application of parameter identification to the oscillatory motion of an airplane at high C(L)
[AIAA PAPER 83-2067] 19 p2804 A83-41905
- Coupled static stability analysis for nonlinear aerodynamics
[AIAA PAPER 83-2069] 19 p2805 A83-41906
- Divergence suppression system for a forward swept wing configuration with wing-mounted stores
[AIAA PAPER 83-2125] 19 p2806 A83-41949
- Aerodynamic aspects of aircraft dynamics at high angles of attack
21 p3085 A83-43964
- Ground simulation investigation of helicopter decelerating instrument approaches
21 p3090 A83-45461
- The method of pole displacement in the artificial stabilization of dynamic systems
22 p3352 A83-46500
- Conceptual kinematic design using homogeneous coordinate transformations
[AIAA PAPER 83-2460] 23 p3500 A83-48337
- ### AIRCRAFT STRUCTURES
- NT AFTERBODIES
- NT AIRFRAMES
- NT CENTERBODIES
- NT FOREBODIES
- NT FUSELAGES
- NT PLASTIC AIRCRAFT STRUCTURES
- Materials for the manufacture of aircraft instruments and structures --- Russian book
01 p0021 A83-10466
- The Avdel MBC aerospace blind riveting system
01 p0056 A83-10870
- Optimization of aircraft structures
02 p0189 A83-11857
- Water-displacing organic corrosion inhibitors - Their effect on the fatigue characteristics of aluminum alloy bolted joints
02 p0148 A83-12014
- USAF studying techniques to restore windshields
02 p0131 A83-12324
- Anisotropic beam theory and applications
02 p0195 A83-12756
- The impact of composite technology on commercial transport aircraft
02 p0135 A83-12969
- The Canadair challenger advanced composite material program
02 p0151 A83-12971
- Prediction capability and improvements of the numerical notch analysis for fatigue loaded aircraft and automotive components
03 p0340 A83-13907
- Principles of helicopter design and construction --- Serbo-Croatian book
03 p0281 A83-14042
- Problems of the statics and dynamics of modern engineering structures - Current status and prospects
03 p0304 A83-14726
- Develop in-flight acoustic emission monitoring of aircraft to detect fatigue crack growth
04 p0447 A83-15197
- Establishing signal processing and pattern recognition techniques for inflight discrimination between crack-growth acoustic emission and other acoustic waveforms
04 p0491 A83-15198
- Design for global damage tolerance and associated mass penalties
04 p0496 A83-15321
- A program system for dynamic analysis of aeronautical structures /HAJIF-II/
04 p0497 A83-15545
- An evaluation of fretting at small slip amplitudes
05 p0614 A83-17254
- Fatigue spectrum sensitivity of composite joints --- in aircraft structures
06 p0716 A83-17964
- The remanufacturers --- of passenger aircraft
06 p0711 A83-18075
- Calculation of the lift distribution and aerodynamic derivatives of quasi-static elastic aircraft
06 p0712 A83-18151
- Fatigue sensitivity of composite structure for fighter aircraft
06 p0717 A83-18402
- Icing analysis of an unprotected aircraft radome
06 p0791 A83-18413
- The analysis of operational stresses --- on aircraft during flight
06 p0775 A83-18596
- Effect of moisture on adhesively bonded titanium structures
07 p0886 A83-20442
- Aircraft inspection using radiography
07 p0861 A83-20478
- The structure of aluminum oxides used for corrosion resistance and primer adhesion
07 p0899 A83-20492
- Primary bonded aircraft wing construction
07 p0861 A83-20493
- Electrical discharge machining of aluminum honeycomb core
07 p0940 A83-20500
- Analysis and repair of flaws in thick structures
08 p1115 A83-21654
- Damage tolerance assessment of the A-7D aircraft structure
08 p1044 A83-21771
- Progress in the practical applications of fracture mechanics
08 p1119 A83-21796
- An improved methodology for predicting random spectrum load interaction effects on fatigue crack growth
08 p1065 A83-21802
- Sonic fatigue of advanced composite panels in thermal environments
08 p1055 A83-22166
- Improvement of the accuracy of temperature measurement by resistance thermometers --- for in-flight aircraft structures monitoring
08 p1092 A83-22186
- Eddy current impedance plane analysis
08 p1114 A83-22410
- Initial design of stringer stiffened bend boxes using geometric programming
08 p1123 A83-23149
- Application of the matrix method of forces for the calculation of aircraft structures
08 p1123 A83-23221
- The simulation of fatigue loads in aeronautics
08 p1048 A83-23241
- The design of bonded structure repairs
09 p1243 A83-23329
- Strain measurement of acoustically excited aircraft structures at elevated temperatures
09 p1265 A83-23366
- Sealants - Uses in composite structures
09 p1236 A83-23615
- Advanced composites structures at Hughes Helicopters, Inc
09 p1202 A83-23645
- Developmental trends in helicopter design
[DGLR PAPER 82-065] 09 p1203 A83-24179
- Impact-resistant transparencies for marine service --- windscreens for aircraft
[ASME PAPER 82-WA/OCE-4] 10 p1400 A83-25686
- 'Scaling' analysis of the ice accretion process on aircraft surfaces
[ASME PAPER 82-WA/HT-39] 10 p1373 A83-25693
- Noise transmission characteristics of advanced composite structural materials
[AIAA PAPER 83-0694] 10 p1473 A83-25915
- Statistical determination of a flaw detection probability curve
10 p1437 A83-26763
- Multi-level substructural analysis in modal synthesis - Two improved substructural assembling techniques
10 p1442 A83-26764
- Application of laser holographic interferometry to vibration analysis of aircraft beam structure model
10 p1442 A83-26765
- An analysis of the durability characteristics of aircraft structures on the basis of fracture mechanics
11 p1597 A83-28477
- The effect of anisotropy, thickness, and operating time on the crack growth in pressed and rolled products of D16chT and V95pchT1 alloys
11 p1549 A83-28478
- An alternating method for analysis of surface-flawed aircraft structural components
12 p1734 A83-28966
- On an algorithm for solving the incomplete eigenvalue problem in the vibration analysis of complex structures of fuselage type
12 p1735 A83-29278
- The use of multiple coordinate systems to form stiffness matrices of thin-walled structures on the basis of hybrid computational schemes
12 p1735 A83-29283
- Helicopter flight testing, simulation and real-time analysis
12 p1701 A83-29391
- Reproducible processing and reliable repeatability in carbon fibre composites
12 p1710 A83-29715
- Improved damage-tolerance analysis methodology
[AIAA 83-0863] 12 p1738 A83-29751
- Design, fabrication and test of graphite/polyimide composite joints and attachments
[AIAA 83-0907] 12 p1739 A83-29763
- A building block approach to design verification testing of primary composite structure
[AIAA 83-0947] 12 p1739 A83-29775
- Design for prevention of acoustic fatigue --- of aircraft structures
[AIAA 83-0973] 12 p1701 A83-29782
- Improved fatigue life tracking procedures for Navy aircraft structures
[AIAA 83-0805] 12 p1703 A83-29807
- Anti-flutter control concept using a reduced non-linear dynamic model of elastic structure aircraft
[AIAA 83-0993] 12 p1704 A83-29870
- Large-amplitude multimode response of clamped rectangular panels to acoustic excitation
[AIAA 83-1033] 12 p1745 A83-29879
- Experimental verification of properties of S-N fatigue life gages for the purpose of a use of the gages as indicators of the relative severity of operating conditions
13 p1808 A83-30514
- Composite materials applications in the manufacture of helicopters - Design and problems of helicopters
14 p1974 A83-31822
- Engineering property comparisons of 7050-T73651 7010-T7651 and 7010-T73651 aluminum alloy plate
14 p1992 A83-32340
- Material, structural component, service life --- of aircraft construction materials
15 p2136 A83-33953
- Structural members made of high-strength cast aluminum and their properties --- and reduction of aircraft production costs
15 p2136 A83-33954
- Automatic eddy current bolt-hole scanning system
16 p2363 A83-35760
- Light aircraft and sailplane structures in reinforced plastics
16 p2299 A83-36065
- On the formulation of the finite-element method in heat-conduction problems for aircraft structures
17 p2520 A83-37515
- The effect of stringers on the stress-strain state near a hole or crack in an anisotropic plate
17 p2520 A83-37516
- Analytical control of the shape of the polygons used in the finite-element method
17 p2521 A83-37644
- Manufacturing methods for composite graphite hole generation
[SAE PAPER 821418] 17 p2516 A83-37976
- Composite materials in aircraft structures
18 p2650 A83-40130
- The comparison of the results of service-spectrum tests with the help of the relative Miner rule --- fatigue life analysis of aircraft structures
18 p2696 A83-40471
- Numerical analysis of natural, coupled, longitudinal-lateral vibrations of an asymmetric aeroplane
20 p3001 A83-42334
- Residual strength predictions for ballistically damaged aircraft
20 p3001 A83-42540
- Undetectable critical defects in safety-of-flight structure
20 p2999 A83-42544
- Universities - Have they a role in aeronautical research? Structures and materials
20 p3002 A83-42618
- Development of a mathematical model of a flight vehicle and the experimental verification of its reliability
20 p2933 A83-42888
- Observations of severe in-flight environments on airplane composite structural components
20 p2933 A83-43330
- Three theorems of weight characteristics of statically determinate and indeterminate structures and their application
20 p3009 A83-43691
- Bonded aluminum honeycomb - Aircraft flight surface primary structure application
21 p3091 A83-43972
- Pulsed holographic nondestructive testing on aircraft
21 p3149 A83-44828
- Annual Airline Plating and Metal Finishing Forum, 18th, Orlando, FL, March 16-18, 1982, Proceedings
22 p3301 A83-45863
- Composites in commercial aircraft
22 p3262 A83-46281
- Safe structures for future aircraft
22 p3254 A83-46350
- Detection of cracks under installed fasteners in aircraft structures
22 p3304 A83-46769
- Automated riveter for spherical aircraft cell structures
23 p3391 A83-47182
- Automatized bonding process for load-bearing aircraft cellular structural components in light contour systems
23 p3391 A83-47198
- Advanced lightweight, fire retardant floor paneling for aircraft
[AIAA PAPER 83-2442] 23 p3403 A83-48330
- A new approach to fault-tolerant helicopter swashplate control
[AIAA PAPER 83-2485] 23 p3412 A83-48345
- Depot level reparability, maintainability, and supportability of advanced composites
[AIAA PAPER 83-2516] 23 p3404 A83-48360
- Strength-flutter structural optimization of a supersonic cruise combat aircraft
24 p3547 A83-49190
- The effect of damage in structural elements on the ground resonance of a helicopter
24 p3547 A83-49446
- Demonstration of mobile accelerator neutron radiography for in situ detection of moisture and corrosion in aircraft structures
[AIAA PAPER 83-2449] 24 p3591 A83-50073

AIRCRAFT SURVIVABILITY

- Combat survivability with advanced aircraft propulsion development 01 p0008 A83-10179
- Computer models for determining countermeasures effectiveness of expendables in air-to-air engagements 01 p0103 A83-11162
- Maximizing survivability and effectiveness of air-to-ground gunnery using a moveable gun 01 p0006 A83-11192
- OBOGS and OBIGGS - The application of molecular sieves to aircrew breathing and aircraft survivability --- On-Board Oxygen Generator System and On-Board Inert Gas Generator System 04 p0525 A83-15430
- Tactical air war - A SIMSCRIPT model 07 p0987 A83-19649
- State space model concept for evaluating survivability methodologies for aircraft design 20 p2932 A83-42567
- Vector optimization applied to survivability methodology evaluation --- for aircraft design 20 p3042 A83-42568
- Development of low cost RPVs under Indian conditions 20 p2934 A83-43701
- Analysis of aircraft dynamic behavior in a crash environment 21 p3091 A83-43966
- Propulsion system screening for survivability and effectiveness [ASME PAPER 83-GT-200] 23 p3410 A83-48003
- Correlation of flight test and analytic M-on-N air combat exchange ratios --- Many-on-Many 23 p3392 A83-48219

AIRCRAFT TIRES

- Recent aircraft tire thermal studies [SAE PAPER 821392] 17 p2463 A83-37968
- Analysis of a thin-walled pressurized torus in contact with a plane --- aircraft tires study [AIAA PAPER 82-0702] 19 p2856 A83-40869
- FOD hazard from tire-lofted debris --- Foreign Object Damage 20 p2931 A83-42557
- The durability of aircraft tyres 21 p3116 A83-44879
- On-board weight and center-of-gravity measurement system with tire-pressure monitoring 23 p3402 A83-47216

AIRCRAFT WAKES

- NT HELICOPTER WAKES
- NT PROPELLER SLIPSTREAMS
- NT SLIPSTREAMS
- Evolution of aircraft trailing vortices in a stratified fluid [AIAA PAPER 83-0564] 05 p0588 A83-16792
- A higher order panel method applied to vortex sheet roll-up 09 p1198 A83-24658
- NASA aerial applications wake interaction research --- particle trajectories in aircraft induced wakes 12 p1699 A83-28899
- A version of a single-beam laser time-of-flight method for measuring flight velocity 17 p2510 A83-37642
- Wake characteristics and interactions of the canard/wing lifting surface configuration of the X-29 forward-swept wing flight demonstrator [AIAA PAPER 83-1835] 17 p2455 A83-38664
- Computational and experimental study of trailing vortices [AIAA PAPER 83-1868] 17 p2458 A83-38694
- Measurements of an aircraft wake vortex system using a meteorological tower 17 p2552 A83-38751
- Motion of aircraft trailing vortices near the ground [AIAA PAPER 83-2130] 19 p2793 A83-41953
- The calculation of two-dimensional transonic flow over aerofoils including boundary layer and wake effects [SAE PAPER 830708] 20 p2930 A83-43318
- NASA wake interactions research and applications [SAE PAPER 830764] 20 p2930 A83-43329

AIRCROWS

- U FLIGHT CREWS

AIRDROPS

- C-141 operations in Operation Bright Star 82 12 p1699 A83-29203

AIRFIELD SURFACE MOVEMENTS

- Transient response of taxiing aircraft [AIAA 83-0927] 12 p1702 A83-29853
- Time-of-day corrections in measures of aircraft noise exposure 14 p2081 A83-33024
- Planning intra-airport transportation - A framework for decision making [AIAA PAPER 83-1585] 14 p1978 A83-33356
- Guidance control systems for aircraft on airport surfaces [AIAA PAPER 83-1579] 16 p2297 A83-36953
- TALIS - A proposed system for taxiway control --- Taxiing Aircraft Location and Identification System 17 p2462 A83-38934

AIRFIELDS

- U AIRPORTS

AIRFOIL CHARACTERISTICS

- U AIRFOILS

AIRFOIL PROFILES**NT WING PROFILES**

- The use of spline functions in problems of aerodynamics 01 p0002 A83-10441
- Extension of the Carafoli tracer method to profiles cascades 01 p0002 A83-10578
- An oscillating rig for the generation of sinusoidal flows 02 p0137 A83-12008
- Numerical experiments on the leading-edge flowfield 03 p0277 A83-13131
- Experimental investigation on film cooling of a gas turbine blade 03 p0282 A83-13346
- Calculation method for transonic separated flows over airfoils including spoiler effects [ONERA, TP NO. 1982-66] 03 p0279 A83-14526
- Flow past a profile at angle of attack to a transonic flow 04 p0441 A83-15083
- Automated ultrasonic dimensional and defect inspection of complex geometry gas turbine airfoil shapes 04 p0488 A83-15158
- Analytical profiling of turbine blades 04 p0449 A83-16010
- Influence of multidroplet size distribution on icing collection efficiency [AIAA PAPER 83-0110] 05 p0666 A83-16526
- A multigrid method for the Euler equations [AIAA PAPER 83-0124] 05 p0580 A83-16537
- Autotoration of an elliptic airfoil [AIAA PAPER 83-0130] 05 p0580 A83-16543
- A multi-grid method for the computation of viscid/inviscid interactions on airfoils [AIAA PAPER 83-0234] 05 p0582 A83-16602
- A viscous-inviscid interactive procedure for rotational flow in cascades of two-dimensional airfoils of arbitrary shape [AIAA PAPER 83-0256] 05 p0583 A83-16614
- A fast viscous correction method for unsteady transonic flow about airfoils [AIAA PAPER 83-0264] 05 p0583 A83-16620
- High-speed characteristics of circulation control airfoils [AIAA PAPER 83-0265] 05 p0583 A83-16621
- Laser holographic interferometry for an unsteady airfoil in dynamic stall [AIAA PAPER 83-0388] 05 p0643 A83-16688
- Experimental investigation of the confluent boundary layer of a multielement low speed airfoil [AIAA PAPER 83-0566] 05 p0588 A83-16793
- An experimental investigation of the low Reynolds number performance of the Lissaman 7769 airfoil [AIAA PAPER 83-0647] 05 p0588 A83-16814
- Studies of aerofoils and blade tips for helicopters 05 p0589 A83-17317
- Derivation and solution of the transonic integral equation for lifting flows 05 p0590 A83-17553
- The inverse design of closed airfoils in transonic flow [AIAA PAPER 83-0504] 05 p0591 A83-17929
- The development of thermal boundary layers in airfoil-cascade flows with off-design angles of attack 06 p0713 A83-19155
- The stability of a preseparation boundary layer at the leading edge of a thin profile 06 p0713 A83-19432
- The far nonlinear field in transonic flows past nonlifting profiles 06 p0713 A83-19442
- Critical angle of incidence for the flow around spheroids 07 p0862 A83-19668
- Transonic airfoil calculations using solution-adaptive grids 07 p0863 A83-19824
- 2-D coordinate grid generation by a vortex singularity method 07 p0864 A83-21018
- The effect of the nonisothermality of an airfoil surface on the local values of the heat transfer coefficient 09 p1196 A83-23438
- Development of four profiles for an experimental propeller in the performance class of 750 PS [DGLR PAPER 82-067] 09 p1197 A83-24181
- Shear center in airfoil sections with special reference to circular arc airfoil blades [ASME PAPER 82-WA/DE-19] 10 p1439 A83-25699
- On the application of linearized theory to multi-element aerofoils. I - Tandem flat plate aerofoils 11 p1526 A83-27874
- Instantaneous turbulence profiles in the wake of an oscillating airfoil 12 p1695 A83-28951
- A fuzzy algorithm to compute transonic profile flow 12 p1696 A83-28973
- Calculation of equilibrium temperature on a profile with variable heat capacity 12 p1783 A83-29290
- The coupled aeroelastic response of turbomachinery blading to aerodynamic excitations [AIAA 83-0844] 12 p1742 A83-29822
- Airfoil shape and thickness effects on transonic airloads and flutter [AIAA 83-0959] 12 p1702 A83-29860
- Computational fluid dynamics of airfoils and wings 12 p1698 A83-29927

- Development of two airfoil sections for helicopter rotor blades 13 p1805 A83-31623
- Experiment of a shockless transonic airfoil partially modified from an arbitrary airfoil 14 p1969 A83-32514
- A new facility and technique for two-dimensional aerodynamic testing 14 p1977 A83-32585
- A three degree-of-freedom, typical section flutter analysis using harmonic transonic air forces [AIAA PAPER 83-0960] 14 p2032 A83-32797
- A multigrid finite element method for the calculation of transonic potential flows [ONERA, TP NO. 1983-18] 16 p2296 A83-36427
- Experimental studies of the boundary layer on an airfoil at low Reynolds numbers [AIAA PAPER 83-1671] 17 p2444 A83-37181
- Unsteady aerodynamic characteristics of a profile in the transonic flow of an ideal gas 17 p2446 A83-37251
- Comparison of NACA 6-series and 4-digit airfoils for Darrieus wind turbines 17 p2535 A83-38013
- Aerodynamic characteristics of a circulation controlled elliptical airfoil with blown jets [AIAA PAPER 83-1794] 17 p2453 A83-38633
- A multiple separation model for multielement airfoils [AIAA PAPER 83-1844] 17 p2456 A83-38672
- The combination of a geometry generator with transonic design and analysis algorithms [AIAA PAPER 83-1862] 17 p2457 A83-38689
- Transonic time-response analysis of 3-degree-of-freedom conventional and supercritical airfoils 19 p2789 A83-41047
- Theoretical gust response prediction of a Joukowski airfoil 20 p2928 A83-42536
- Circulation-controlled elliptical airfoil 20 p2928 A83-42537
- A study of the unsteady flow field of an airfoil with deflected spoiler [AIAA PAPER 83-2131] 20 p2931 A83-43810
- Design of transonic shock-free airfoil 21 p3087 A83-44572
- Combined four-wall interference assessment in two-dimensional airfoil tests 21 p3093 A83-45576
- Experiments on a flow with swept separation and reattachment of a boundary layer 22 p3286 A83-47020
- Flow in a turbine cascade. I - Losses and leading-edge effects [ASME PAPER 83-GT-68] 23 p3395 A83-47921
- The lift on an aerofoil in starting flow 23 p3398 A83-48121
- Drag of wings with cambered airfoils and partial leading-edge suction 23 p3398 A83-48220
- Wing loading on a 60 degree delta wing with vortex flaps [AIAA PAPER 83-2555] 23 p3399 A83-48374
- Inverse problem of the two-dimensional theory of elasticity in the hydrodynamic formulation 23 p3473 A83-48535
- Interaction between the outer inviscid flow and the boundary layer on transonic airfoils 24 p3544 A83-49021
- Investigation of the unsteady airloads on airfoils with oscillating control in sub- and transonic flows 24 p3544 A83-49180
- Structural optimization with aeroelastic constraints - A survey of US applications 24 p3593 A83-49188
- Noise generated by airfoil profiles placed in a uniform laminar flow 24 p3625 A83-49463

AIRFOIL SECTIONS**U AIRFOIL PROFILES****AIRFOIL THICKNESS****U AIRFOIL PROFILES****AIRFOILS**

- NT AERIAL RUDDERS
- NTAILERONS
- NTARROW WINGS
- NTBEARINGLESS ROTORS
- NTCAMBERED WINGS
- NTCARET WINGS
- NTCIRCULATION CONTROL AIRFOILS
- NTCRUCIFORM WINGS
- NTDELTA WINGS
- NT ELEVATORS (CONTROL SURFACES)
- NT ELEVONS
- NT EXTERNALLY BLOWN FLAPS
- NT FIXED WINGS
- NT FLAPS (CONTROL SURFACES)
- NT FLEXIBLE WINGS
- NT GAW-2 AIRFOIL
- NT HORIZONTAL TAIL SURFACES
- NT INFINITE SPAN WINGS
- NT JET FLAPS
- NT LAMINAR FLOW AIRFOILS
- NT LEADING EDGE SLATS
- NT LOW ASPECT RATIO WINGS
- NT OBLIQUE WINGS

NT PROPELLER BLADES
 NT RECTANGULAR WINGS
 NT RIGID ROTORS
 NT RIGID WINGS
 NT RING WINGS
 NT ROTARY WINGS
 NT SLENDER WINGS
 NT SPOILERS
 NT SUPERCRITICAL WINGS
 NT SUPERSONIC AIRFOILS
 NT SWEEP FORWARD WINGS
 NT SWEEP WINGS
 NT SWEPTBACK WINGS
 NT TABS (CONTROL SURFACES)
 NT THIN AIRFOILS
 NT THIN WINGS
 NT TIP DRIVEN ROTORS
 NT TRAILING-EDGE FLAPS
 NT TRAPEZOIDAL WINGS
 NT TWISTED WINGS
 NT UNCAMBERED WINGS
 NT UNSWEEP WINGS
 NT VARIABLE SWEEP WINGS
 NT VORTEX FLAPS
 NT WING FLAPS
 NT WINGS
 The far field of an airfoil 01 p0002 A83-10573
 Wall interference evaluation from pressure measurements on control surfaces 03 p0278 A83-13169
 Helicopter rotor performance evaluation using oscillatory airfoil data 03 p0278 A83-13172
 Convergence and stability of a collocation method for the generalized airfoil equation 03 p0278 A83-13844
 Experiments on the role of amplitude and phase modulations during transition to turbulence 03 p0321 A83-14576
 Methods for solving Euler's equations for airfoil and intake flow 03 p0279 A83-14604
 Explicit and implicit corrected viscosity schemes for the computation of steady transonic flows 03 p0279 A83-14606
 A fast pseudo-time integration scheme for the solution of the steady transonic flow problem 04 p0441 A83-15015
 Concerning dynamic stall --- of laminar flow near leading edges of airfoils 04 p0442 A83-15150
 The use of an error index to improve numerical solutions for unsteady lifting airfoils 04 p0442 A83-15281
 Subsonic potential flow past a circle and the transonic controversy 04 p0443 A83-16366
 Vibration of airfoils in sinusoidal oblique gust [AIAA PAPER 83-0005] 05 p0577 A83-16457
 The performance of a circulation control airfoil at transonic speeds [AIAA PAPER 83-0083] 05 p0579 A83-16510
 On the transonic aerodynamic characteristics of 10 percent thick airfoils with a plain flap [AIAA PAPER 83-0091] 05 p0579 A83-16515
 An analytical evaluation of the icing properties of several low and medium speed airfoils [AIAA PAPER 83-0109] 05 p0579 A83-16525
 Measurements of the near wake of an airfoil in unsteady flow [AIAA PAPER 83-0127] 05 p0580 A83-16540
 Unsteady flows about a Joukowski airfoil in the presence of moving vortices [AIAA PAPER 83-0129] 05 p0580 A83-16542
 Unsteady flow separation and attachment induced by pitching airfoils [AIAA PAPER 83-0131] 05 p0580 A83-16544
 Passive shock wave/boundary layer control for transonic airfoil drag reduction [AIAA PAPER 83-0137] 05 p0580 A83-16546
 Some observations on the aerodynamics of an airfoil with a jet exhausting from the lower surface [AIAA PAPER 83-0173] 05 p0580 A83-16569
 A separation model for two-dimensional airfoils in transonic flow [AIAA PAPER 83-0298] 05 p0584 A83-16638
 Flow measurements of an airfoil with deflected spoiler [AIAA PAPER 83-0365] 05 p0584 A83-16672
 A fast finite element method for transonic potential flow calculations [AIAA PAPER 83-0507] 05 p0587 A83-16755
 Flow over flat and axisymmetric bodies moving at high variable velocities 05 p0589 A83-17413
 The transonic wind tunnel Braunschweig of DFVLR 07 p0867 A83-19663
 Numerical prediction of dynamic forces on arbitrarily pitched airfoils 07 p0862 A83-19801
 Quadrature formulas for chordwise integrals of lifting surface theories 08 p1042 A83-22146
 Numerical prediction of turbulent boundary layer development on a two-dimensional curved wall 08 p1089 A83-23198

Analysis of airfoil noise with an array of near- and far-field sensors 09 p1340 A83-23473
 Control of turbulent boundary layer flows by sound [AIAA PAPER 83-0726] 10 p1475 A83-25937
 Airfoil self noise - Effect of scale [AIAA PAPER 83-0785] 10 p1477 A83-25966
 Incidence angle effects on convected gust airfoil noise [AIAA PAPER 83-0765] 11 p1652 A83-28022
 Coordinate generation with precise controls over mesh properties 12 p1772 A83-29631
 A multigrid algorithm for steady transonic potential flows around aerofoils using Newton iteration 12 p1697 A83-29656
 Flutter analysis of a transport wing using XTRAN3S [AIAA 83-0922] 12 p1743 A83-29848
 Transonic interference effects in testing of oscillating airfoils [AIAA 83-1032] 12 p1698 A83-29883
 Shock-free configurations in two- and three-dimensional transonic flow 12 p1698 A83-29928
 Numerical solutions for unsteady aerofoils using internal singularity distributions 12 p1698 A83-29971
 Displacement effects in transonic airfoil flows 13 p1804 A83-30638
 Low-Reynolds-number airfoils 13 p1804 A83-31082
 Transonic flow calculations using the Euler equations 14 p1971 A83-32981
 Numerical simulation of airfoil ice accretion [AIAA PAPER 83-0112] 16 p2297 A83-36042
 Prediction of stagnation flow heat transfer on turbomachinery airfoils [AIAA PAPER 83-1173] 16 p2294 A83-36259
 Natural laminar flow data from full-scale flight and wind-tunnel experiments 16 p2296 A83-36409
 Application of internal singularity distribution approach to multi-element aerofoil problems 16 p2296 A83-36615
 Finite-difference simulation of transonic separated flow using a full potential boundary layer interaction approach [AIAA PAPER 83-1689] 17 p2502 A83-37189
 Unsteady flow field, lift and drag measurements of impulsively started elliptic cylinder and circular-arc airfoil [AIAA PAPER 83-1711] 17 p2502 A83-37205
 Experimental research on cavitation erosion for an oscillating wing profile --- German thesis 17 p2493 A83-37497
 On the accuracy of calculating the aerodynamic characteristics of thin wings and airfoils by the method of discrete vortices 17 p2448 A83-37519
 The effect of slot suction on the aerodynamic characteristics of an airfoil at transonic velocities 17 p2449 A83-37552
 Repairing gas turbine hot section airfoils today [SAE PAPER 821487] 17 p2469 A83-38006
 Modeling of turbulent flow fields through cascade of airfoils at stall conditions [AIAA PAPER 83-1743] 17 p2452 A83-38091
 Advanced airfoil design for general aviation propellers [AIAA PAPER 83-1791] 17 p2453 A83-38631
 Design and true Reynolds number 2-D testing of an advanced technology airfoil [AIAA PAPER 83-1792] 17 p2453 A83-38632
 Boundary layer characteristics of the Miley airfoil at low Reynolds numbers [AIAA PAPER 83-1795] 17 p2453 A83-38634
 Aerodynamic properties of a two-dimensional inextensible flexible airfoil [AIAA PAPER 83-1796] 17 p2453 A83-38635
 Conformal grid generation for multielement airfoils 17 p2458 A83-38800
 Grid generation by elliptic partial differential equations for a tri-element Augmentor-Wing airfoil 17 p2458 A83-38803
 Marching grid generation using parabolic partial differential equations 17 p2574 A83-38810
 Airfoil generation with a desktop computer using Lighthill's exact inverse method [AIAA PAPER 83-1867] 18 p2632 A83-39096
 Interacting flow theory and trailing edge separation - No stall 18 p2633 A83-39214
 Interactions of airfoils with gusts and concentrated vortices in unsteady transonic flow [AIAA PAPER 83-1691] 18 p2633 A83-39267
 Transonic flow calculations using triangular finite elements [AIAA PAPER 83-1922] 18 p2635 A83-39376
 A flexible grid embedding technique with application to the Euler equations [AIAA PAPER 83-1944] 18 p2636 A83-39391
 Comparison of supercritical airfoil flow calculations with wind-tunnel results [AIAA PAPER 83-1688] 18 p2638 A83-40472

An experimental study of the development of a supersonic zone near the leading edge of an airfoil oscillating in subsonic flow [AIAA PAPER 83-2133] 19 p2793 A83-41955
 The satellite sail --- suspended airfoil into upper atmosphere from space shuttle by long tether 20 p2945 A83-42539
 Pressure loss and heat transfer through multiple rows of short pin fins 20 p2975 A83-42709
 A view of the triple deck --- low speed boundary layer theory 20 p2930 A83-43120
 Unified unsteady supersonic/hypersonic theory of flow past double wedge airfoils 21 p3086 A83-44465
 The influence of free-stream disturbances on low Reynolds number airfoil experiments 21 p3088 A83-44676
 A turbulent flow Navier-Stokes analysis for an airfoil oscillating in pitch 22 p3248 A83-46437
 Unsteady Kutta condition of a plunging airfoil 22 p3248 A83-46438
 Experimental analysis of the wake behind an isolated cambered airfoil 22 p3248 A83-46443
 Turbulence structures in the wake of an oscillating airfoil 22 p3248 A83-46446
 Viscid-inviscid interaction analysis on airfoils with an inverse boundary layer approach 22 p3249 A83-46474
 Cooling airflow studies at the leading edge of a film-cooled airfoil [ASME PAPER 83-GT-82] 23 p3447 A83-47935
 Development of controlled diffusion airfoils for multistage compressor application [ASME PAPER 83-GT-211] 23 p3397 A83-48012
 The effect of a leading-edge slat on the dynamic stall of an oscillating airfoil [AIAA PAPER 83-2533] 23 p3399 A83-48368
 A least squares finite element scheme for transonic flow around harmonically oscillating airfoils 24 p3543 A83-48872

AIRFRAME MATERIALS

Composites in the construction of the Lear Fan 2100 aircraft 12 p1710 A83-29718
 Design, analysis and test of composite curved frames for helicopter fuselage structure [AIAA 83-1005] 12 p1741 A83-29805
 Development of structural materials for the new generation of aircraft 13 p1805 A83-30511
 The effect of microstructure and moisture on the low cycle fatigue and fatigue crack propagation of two Al-Li-X alloys 14 p1996 A83-32889
 Fatigue of composite bolted joints under dual load levels 18 p2703 A83-40158

AIRFRAMES

Prediction of jet exhaust noise on airframe surfaces during low-speed flight 03 p0282 A83-13160
 Airframe effects on a top-mounted fighter inlet system 03 p0278 A83-13166
 Subsonic surface panel method for airframe analysis and wing design [AIAA PAPER 83-0341] 05 p0584 A83-16667
 An improved methodology for predicting random spectrum load interaction effects on fatigue crack growth 08 p1064 A83-21794
 Investigation of landing gear alternatives for high performance aircraft 09 p1202 A83-24030
 Analysis of jet-airframe interaction noise [AIAA PAPER 83-0783] 10 p1376 A83-25964
 Flight effects for jet-airframe interaction noise [AIAA PAPER 83-0784] 10 p1376 A83-25965
 Microeconomic models for process development 15 p2172 A83-33650
 On improving the fatigue performance of a double-shear lap joint 15 p2180 A83-34744
 Inlet, engine, airframe controls integration development for supercruising aircraft 16 p2304 A83-35842
 New metal technologies in airframe construction 17 p2516 A83-37861
 Re-engineing the 737 [SAE PAPER 821442] 17 p2463 A83-37990
 The in-service flight testing of some carbon fibre-reinforced plastic components 20 p2933 A83-42808
 A critical look at the development and application of airframe cost models [SAWE PAPER 1478] 20 p2935 A83-43747
 Enhanced aircraft structural maintenance using organic depot damage tolerance analysis [AIAA PAPER 83-2450] 23 p3392 A83-48333

AIRGLOW
 NT GEOCORONAL EMISSIONS
 NT NIGHTGLOW
 NT TWILIGHT GLOW
 Mg/+/- morphology from visual airglow experiment observations 02 p0208 A83-12396
 Airglow at a height below 40 km in the vacuum ultraviolet 03 p0356 A83-13216

Ultraviolet spectroscopy of the zodiacal light	05	p0694	A83-17022
Emission photometric system for scanning dynamic processes in upper atmosphere	06	p0761	A83-18022
Emission of the earth's nocturnal atmosphere according to Salyut-6 observations	07	p0964	A83-21177
Optical emissions induced by spacecraft - Atmosphere interactions	07	p0869	A83-21551
Space Shuttle glow observations	07	p0869	A83-21552
Observations of optical emissions on STS-4	07	p0870	A83-21553
Visible glow induced by spacecraft-environment interaction	07	p0870	A83-21554
Remote ground-based observations of terrestrial airglow emissions and thermospheric dynamics at Calgary, Alberta, Canada	08	p1135	A83-22360
Intersystem collisional transfer of excitation in low altitude aurora	10	p1448	A83-25553
Conjugate studies of an isolated equatorial irregularity region	11	p1618	A83-28320
[AD-A127561] Thermospheric odd nitrogen. I - NO, N/4S/, and O/3P/ densities from rocket measurements of the NO delta and gamma bands and the O2 Herzberg I bands	11	p1618	A83-28323
Particle and optical measurements aboard the Aureol-3 spacecraft (ARCAD 3 project)	13	p1814	A83-30764
Airglow atmospheric imager on board the 'IK-Bulgaria-1300' satellite	13	p1815	A83-30771
Visible continuum emission and gravity waves	13	p1881	A83-31536
Artificial glow and additional ionization in the upper ionosphere in the field of a high-power radio wave	14	p2049	A83-31855
The extreme ultraviolet day airglow	15	p2196	A83-33942
Solrad 11 observations of the far-ultraviolet background	15	p2245	A83-34116
Dynamics of the dayside aurora	16	p2373	A83-35365
Analysis of gravity-wave induced instabilities and turbulence viscosity parameters from optical emissions	16	p2374	A83-35377
Geometry of depleted plasma regions in the equatorial ionosphere	17	p2539	A83-37606
Ionospheric conditions affecting the evolution of equatorial plasma depletions	19	p2864	A83-41118
Analysis of airglow image data	20	p3016	A83-42310
Observations of large scale F-region irregularities using airglow emissions at 7774 A and 6300 A	21	p3170	A83-44245
The NO + O continuum and excitation mechanism of the oxygen green line in the lower thermosphere	21	p3171	A83-44285
Electron impact excitation of lambda 7990-A multiplet	22	p3355	A83-46061
Optical emission from photoexcitation of aerosol particles produced by reaction of ozone with 1,3-butadiene	22	p3328	A83-46065
OH airglow phenomena during the 5-6 July 1982 total lunar eclipse	22	p3328	A83-46082
Simultaneous observation of tropical arc, SAR arc and Aurora during geomagnetic storm from IC-Bulgaria-1300 satellite	23	p3484	A83-48446
Determination of atmospheric composition and temperature from the U.V. airglow	24	p3603	A83-48753
AIRLINE OPERATIONS			
Identification of the causes of aircraft performance shortfalls in fleet operations	02	p0131	A83-12659
Airline economics --- Book	03	p0400	A83-14000
Airline planning: Corporate, financial, and marketing --- Book	03	p0400	A83-14046
Chicago to spend \$1 billion to expand O'Hare, Midway airports	04	p0450	A83-15825
The Montreal Agreement of 1966 and the Malta Agreement of 1965	05	p0692	A83-16975
International civil aviation in the South Pacific: A perspective --- Book	05	p0591	A83-17116
Total simulation for airline applications /Line Oriented Flight Training/	05	p0676	A83-17306
Operator influences on aircraft design	07	p0866	A83-21032
Limitations on air carrier liability - An inadvertent return to common law principles	07	p1003	A83-21550
Air traffic and requirements for future passenger aircraft	09	p1195	A83-24151
[DGLR PAPER 82-024] Jet engines for airliners of the next generation	09	p1206	A83-24183
[DGLR PAPER 82-069] Forecasting in air transport - A critical review of the techniques available	12	p1699	A83-29966

Fleet planning models --- in airline operations	12	p1699	A83-29967
Air traffic control into the 21st century	13	p1805	A83-30275
Identifying aircraft and airport compatibility - A straightforward approach to complexity	14	p1978	A83-33354
[AIAA PAPER 83-1582] Interaction of the small commuter operation within the hub terminal	14	p1973	A83-33355
[AIAA PAPER 83-1584] Overview of the air cargo industry	14	p1973	A83-33369
[AIAA PAPER 83-1607] Airport - Air cargo compatibility	14	p1973	A83-33371
[AIAA PAPER 83-1610] Worldwide aviation outlook --- for passenger and freight traffic 1982-1992	16	p2297	A83-36952
[AIAA PAPER 83-1597] AFOS terminal forecast monitoring system - Operational aspects --- Automation of Field Operations and Services	17	p2548	A83-38702
Cloud encounter statistics in the 28.5-43.5 KFT altitude region from four years of GASP observations	17	p2550	A83-38733
Operational aspects of Delta air lines meteorological department	17	p2551	A83-38746
Automated systems of control in civil aviation of the USSR	18	p2639	A83-39219
Maintenance according to technical conditions --- for aircraft	18	p2631	A83-39221
Airline liability for the involuntary violation of immigration laws	18	p2753	A83-39694
Public interest under the Federal Aviation Act of 1958 and the Airline Deregulation Act of 1978	18	p2753	A83-39695
Airport use and access	18	p2753	A83-39698
Safety in the skies	19	p2794	A83-41467
Flight management systems - What are they and why are they being developed?	19	p2803	A83-41712
[AIAA PAPER 83-2235] The Memorandum of Understanding between the United States and Certain ECAC Member States on Pricing Regime between U.S. and Europe	20	p3057	A83-43127
Philosophy of automated balance calculations	20	p2931	A83-43744
[SAWE PAPER 1470] SITELCOM-82 - Telecommunications and data processing in the air transport industry; Proceedings of the Conference, Monte Carlo, Monaco, March 2-4, 1982	21	p3090	A83-45076
ARGHOS - A tool for schedule planning --- for airlines	21	p3090	A83-45077
Impact of new technology on engineering and maintenance systems --- of airlines	21	p3085	A83-45078
SITA - Advanced telecommunications services --- for air transport industry	21	p3090	A83-45079
The role of information systems in airline management functions	21	p3221	A83-45080
Airline common databases and data processing applications	21	p3190	A83-45081
Some thoughts on the economic significance of limited liability in air passenger transport	22	p3369	A83-45828
Airline subsidies --- a historical review	22	p3369	A83-45833
Deregulation of aviation in the United States	22	p3369	A83-45834
The Freedom of Information Act - Its impact on civil aviation	22	p3370	A83-45839
The right to be heard - The British practice --- refusal or revocation of licenses in air transport	22	p3370	A83-45841
International Forum for Air Cargo, 11th, New York, NY, September 27-30, 1982, Proceedings	22	p3251	A83-45900
Flight frequency determination	22	p3251	A83-46776
Future aircraft development for commuter and third-level operations	23	p3403	A83-48338
[AIAA PAPER 83-2464] Airline requirements for future civil transport aircraft	23	p3401	A83-48354
[AIAA PAPER 83-2501] An airline view of LH2 as a fuel for commercial aircraft	23	p3440	A83-48598
Montreal Protocol - The most recent attempt to modify the Warsaw Convention	24	p3637	A83-49026
AIRPORT BEACONS			
NT DISCRETE ADDRESS BEACON SYSTEM			
AIRPORT LIGHTS			
U.S. sets own standards for airport lighting	16	p2311	A83-35625
AIRPORT PLANNING			
Chicago to spend \$1 billion to expand O'Hare, Midway airports	04	p0450	A83-15825

Impact of stretching wide-bodied aircraft on existing airport facilities	14	p1978	A83-33351
[AIAA PAPER 83-1578] Land development, tall buildings and airport operations	14	p1978	A83-33353
[AIAA PAPER 83-1581] Identifying aircraft and airport compatibility - A straightforward approach to complexity	14	p1978	A83-33354
[AIAA PAPER 83-1582] Planning intra-airport transportation - A framework for decision making	14	p1978	A83-33356
[AIAA PAPER 83-1585] Airport - Air cargo compatibility	14	p1973	A83-33371
[AIAA PAPER 83-1610] TALIS - A proposed system for taxiway control --- Taxing Aircraft Location and Identification System	17	p2462	A83-38934
AIRPORT SURFACE DETECTION EQUIPMENT			
Low-level wind shear detection and warning - A systems update	05	p0666	A83-16717
[AIAA PAPER 83-0444]			
AIRPORTS			
NT HELIPORTS			
Air traffic management - The impact at the airport	05	p0593	A83-17728
Instrument Landing Systems /ILS/ at GDR airports. II	09	p1200	A83-23495
Optimum siting of NEXRAD to detect hazardous weather at airports	09	p1313	A83-24037
Wind shear detection with a modified airport surveillance radar	11	p1627	A83-27040
Aircraft noise and the airport community	14	p2048	A83-33352
[AIAA PAPER 83-1580] Interaction of the small commuter operation within the hub terminal	14	p1973	A83-33355
[AIAA PAPER 83-1584] Integration of ground and air services through use of STOLmobiles	14	p2095	A83-33357
[AIAA PAPER 83-1587] Thermal properties of some asphaltic concrete mixes	14	p1978	A83-33361
[AIAA PAPER 83-1598] Evaluation of properties of recycled asphalt concrete hot mix	14	p1978	A83-33362
[AIAA PAPER 83-1599] Airport pavement management - A total system	14	p1978	A83-33363
[AIAA PAPER 83-1600] Nondestructive airfield pavement testing using laser technology	14	p1978	A83-33364
[AIAA PAPER 83-1601] Standardized pavement strength reporting system - ACN/PCN --- Aircraft Classification Number/Pavement Classification Number	14	p1978	A83-33365
[AIAA PAPER 83-1602] The prediction of the dissipation of radiation fogs over Sofia airport	15	p2206	A83-34415
Sampling strategies for monitoring noise in the vicinity of airports	17	p2578	A83-37731
An evaluation of interactive computer display systems for short-range terminal forecasting applications	17	p2548	A83-38711
[AD-A129839] Air traffic control problems in the field of general aviation	17	p2460	A83-38931
Radio-navigation prerequisites for IFR operation of regional airports and civil airfields	17	p2461	A83-38932
Airport use and access	18	p2753	A83-39698
Experiences in medical coverage of airport disasters at Logan International Airport in Boston	18	p2638	A83-40356
Model of a cryogenic liquid-hydrogen pipeline for an airport ground distribution system	20	p3013	A83-43641
Airfield coatings incorporating polymer materials - Repair and maintenance --- Russian book	21	p3093	A83-45029
Airports as a threat to public safety --- Book	22	p3251	A83-46420
Air traffic control simulation in the airport area	23	p3401	A83-47200
AIRS (RECONNAISSANCE SYS)			
U AIRBORNE INTEGRATED RECONNAISSANCE SYSTEM			
AIRSHIPS			
NT HEAVY LIFT AIRSHIPS			
75th anniversary of the establishment of the Aerodynamic Experimental Institute of Goettingen	05	p0577	A83-16896
Aerodynamic estimation techniques for aerostats and airships	06	p0712	A83-18404
Development and testing of Skyship 500	11	p1530	A83-28191
Some effects of size on non-rigid airships	11	p1530	A83-28192
1983 LTA technology assessment	16	p2300	A83-36406
[AIAA PAPER 83-1617]			

- Lighter-Than-Air Systems Conference, Anaheim, CA, July 25-27, 1983, Collection of Technical Papers
17 p2443 A83-38901
- A study of dirigibles for use in the Peruvian Selva Central region
[AIAA PAPER 83-1970] 17 p2459 A83-38902
- The use of non-rigid airships for Maritime patrol in Canada
[AIAA PAPER 83-1971] 17 p2459 A83-38903
- The utility of small aerostats for surveillance missions
[AIAA PAPER 83-1973] 17 p2460 A83-38904
- Barriers and possibilities for the use of airships in developing countries
[AIAA PAPER 83-1974] 17 p2460 A83-38905
- Applications and market potentials for the light utility airship concept
[AIAA PAPER 83-1975] 17 p2443 A83-38906
- Effect of buoyancy and power design parameters on hybrid airship performance
[AIAA PAPER 83-1976] 17 p2465 A83-38907
- Application of the panel method to airships
[AIAA PAPER 83-1978] 17 p2458 A83-38909
- Wind tunnel demonstration of an optimized LTA system with 65 percent power reduction and neutral static stability
[AIAA PAPER 83-1981] 17 p2466 A83-38910
- Patterning techniques for inflatable LTA vehicles --- Lighter Than Air
[AIAA PAPER 83-1983] 17 p2466 A83-38911
- Thermal effects on a high altitude airship
[AIAA PAPER 83-1984] 17 p2460 A83-38912
- Measurement of helium gas transmission through aerostat material
[AIAA PAPER 83-1986] 17 p2483 A83-38913
- The lateral response of an airship to turbulence
[AIAA PAPER 83-1989] 17 p2459 A83-38915
- Dynamics of the STARS aerostat
[AIAA PAPER 83-1990] 17 p2470 A83-38916
- Flight test of the HX-I radio-controlled hybrid airship
[AIAA PAPER 83-1992] 17 p2466 A83-38917
- Recent progress of lighter-than-air programs in Japan
[AIAA PAPER 83-1993] 17 p2466 A83-38918
- Tethered aerostat operations in arctic weather
[AIAA PAPER 83-1998] 17 p2466 A83-38919
- Flight testing and operational demonstrations of a modern non-rigid airship
[AIAA PAPER 83-1999] 17 p2466 A83-38920
- The stable sensor platform (SSP) tethered balloon series
[AIAA PAPER 83-2000] 17 p2460 A83-38921
- The preliminary design of a very large pressure airship for civilian and military applications
[AIAA PAPER 83-2005] 17 p2466 A83-38923
- AIRSPACE**
Observations regarding the MNPS in the North Atlantic and considerations concerning their applicability in the European air space. I 02 p0133 A83-13011
- Collision risk models 02 p0133 A83-13012
- NATS - Taking stock --- National Air Traffic Services in United Kingdom 05 p0593 A83-17727
- The legal regime of the airspace above the exclusive economic zone 09 p1351 A83-25119
- For delimiting outer space 15 p2240 A83-34661
- Delimitation of air space and outer space - Is it necessary? 15 p2240 A83-34662
- Juridical spatialism or fictionalism? 15 p2240 A83-34663
- Why it is not necessary to define a boundary between air space and outer space 15 p2240 A83-34664
- Delimitation of air space and outer space - Is such a boundary needed now? 15 p2241 A83-34665
- On the use of height rules in off-route airspace 15 p2121 A83-35274
- Measurements of an aircraft wake vortex system using a meteorological tower 17 p2552 A83-38751
- AIRSPEED**
An improved jet noise scaling law which incorporates phase differences due to flight effects
[AIAA PAPER 83-0747] 10 p1476 A83-25949
- Helicopter flight noise tests about the influence of rotor-rotational and forward speed changes on the characteristics of the imitted sound
[AIAA PAPER 83-0672] 11 p1650 A83-28002
- Medical problems peculiar to airline pilots 14 p2067 A83-32461
- Airspeed calibrations on a stretch YC-141B aircraft 14 p1975 A83-32931
- A true air speed sensor for miniature unmanned aircraft 16 p2302 A83-36613
- Optimal mass distribution between the stages of a two-stage aircraft for maximization of the flight cruise range 17 p2462 A83-37267
- A version of a single-beam laser time-of-flight method for measuring flight velocity 17 p2510 A83-37642
- Flutter investigation of a repaired T-38 horizontal stabilizer using NASTRAN 20 p3002 A83-42541
- Thrust augmenting ejectors. I 21 p3089 A83-45586
- Application of optimal control synthesis to integrated vertical flight path and airspeed control for an advanced fighter
[AIAA PAPER 83-2560] 24 p3549 A83-49594
- AIRWORTHINESS**
U AIRCRAFT RELIABILITY
- AIRWORTHINESS REQUIREMENTS**
U AIRCRAFT RELIABILITY
- AITKEN NUCLEI**
Numerical study of the effect of CCN on the size distribution of cloud droplets. I - Cloud droplets in the stage of condensation growth --- Cloud Condensation Nuclei 04 p0518 A83-16017
- On the production of Aitken nuclei from breaking waves and their role in the atmosphere --- maritime aerosols from ocean whitecap bubble bursting 13 p1893 A83-31043
- ALANINE**
Piezooptical properties of crystals of triglycine sulfate doped with L-alpha-alanine 13 p1930 A83-31304
- The effect of growth conditions on the polarization of triglycine sulfate doped with L-alpha-alanine 13 p1930 A83-31306
- Asymmetrical radical formation in D- and L-alanines irradiated with tritium-beta-rays 17 p2563 A83-38897
- ALARMS**
U WARNING SYSTEMS
- ALASKA**
Evidence for a central Eurasian source area of arctic haze in Alaska 02 p0203 A83-11626
- Forecasting foehn winds at Anchorage, Alaska 13 p1888 A83-30566
- ALBEDO**
NT COSMIC RAY ALBEDO
- NT EARTH ALBEDO
- NT LUNAR ALBEDO
- 50 per cent more output power from an albedo-collecting flat panel using bifacial solar cells 03 p0354 A83-13700
- Infrared photometry of periodic comets Encke, Chernykh, Kearns-Kwee, Stephan-Oterma, and Tuttle 03 p0407 A83-13826
- Comparison between albedo changes and lidar-measured aerosol changes for a set of aerosol events 03 p0370 A83-14641
- Diurnal radiation budget - Four months assembled into an annual mean 03 p0370 A83-14646
- Mars: Definition and characterization of global surface units with emphasis on composition 04 p0568 A83-15581
- Investigations of the apparent temperature of snow cover in the submillimeter wavelength region 04 p0502 A83-15816
- The outer satellites of Jupiter 04 p0570 A83-16230
- Diameters and albedos of satellites of Uranus 05 p0693 A83-16847
- Diameters of Triton and Pluto 05 p0693 A83-16848
- Ice in Comet Bowell 08 p1186 A83-23275
- A preliminary global oceanic cloud climatology from satellite albedo observations 09 p1314 A83-24275
- The albedo of Uranus 10 p1494 A83-25735
- Albedo, internal heat flux, and energy balance of Saturn 11 p1684 A83-27359
- Diffuse reflection and transmission of radiation for Rayleigh phase function 12 p1775 A83-29077
- Methane abundance in the atmosphere of Uranus 13 p1961 A83-31201
- Io - The near-infrared monitoring program, 1979-1981 14 p2112 A83-32609
- Refining a radiation model of a stratiformis cloud 14 p2058 A83-32856
- Fragmentation of prestellar clouds by molecule formation 14 p2109 A83-33278
- Ice and snow feedbacks and the latitudinal and seasonal distribution of climate sensitivity 16 p2386 A83-35489
- A determination of the composition of the Saturnian stratosphere using the IUE 16 p2436 A83-35736
- Stellar magnitude and albedo data of Venus 17 p2616 A83-37404
- Some optical properties of the Venus surface 17 p2616 A83-37408
- Albedo asymmetry of Iapetus 17 p2623 A83-38601
- Estimating the solar zenith dependence of the clear-sky planetary albedo for land surfaces from the GOES satellite 20 p3010 A83-43474
- Effects of stepwise variation of albedo on reflectivity and transmissivity of an isotropically scattering slab 23 p3513 A83-48622
- ALBERTA**
Intraplate stress orientations from Alberta oil-wells 22 p3323 A83-45786
- ALCOHOLS**
NT BISPHENOLS
- NT ETHYL ALCOHOL
- NT METHYL ALCOHOLS
- NT POLYVINYL ALCOHOL
- Lithium cycling behavior in 2-methyltetrahydrofuran with alcohol additives --- in lithium batteries 07 p0880 A83-19890
- Interactions of alcohol and caffeine on human reaction time 15 p2215 A83-34984
- ALDEHYDES**
NT FORMALDEHYDE
- ALDOLASE**
The transport and turnover of aldolase in rat livers during total body irradiation with X-rays 09 p1321 A83-24927
- ALDOSTERONE**
A low-renin form of hypertension - Characteristics of the functional relationships of the renin-aldosterone pressor system 19 p2881 A83-41439
- Effect of prolonged exercise at altitude on the renin-aldosterone system 20 p3034 A83-43482
- Renin-aldosterone and angiotensin-converting enzyme during prolonged altitude exposure 22 p3347 A83-45984
- ALFVEN WAVES**
U MAGNETOHYDRODYNAMIC WAVES
- ALGAAS**
U ALUMINUM GALLIUM ARSENIDES
- ALGAE**
NT CHLORELLA
- Field investigation of techniques for remote laser sensing of oceanographic parameters 10 p1419 A83-25643
- The application of SPOT simulated data to the remote sensing of an intertidal environment 17 p2534 A83-38457
- Effect of high atmospheric CO2 concentration on delta C-13 of algae - A possible cause for the average depletion of C-13 in Precambrian reduced carbon 17 p2557 A83-38895
- An extraterrestrial habitat on earth - The algal mat of Don Juan Pond 19 p2885 A83-40832
- Single cell algae and higher plant cell cultures used in space biology [IAF PAPER 83-185] 23 p3494 A83-47302
- ALGAL BLOOM**
U ALGAE
- ALGEBRA**
NT ADJOINTS
- NT BANACH SPACE
- NT BINOMIAL THEOREM
- NT CANONICAL FORMS
- NT CUBIC EQUATIONS
- NT DUFFING DIFFERENTIAL EQUATION
- NT DYADICS
- NT EIGENVALUES
- NT EIGENVECTORS
- NT GROUP THEORY
- NT HERMITIAN POLYNOMIAL
- NT HILBERT SPACE
- NT LIE GROUPS
- NT LINEAR EQUATIONS
- NT LINEAR TRANSFORMATIONS
- NT MATRICES (MATHEMATICS)
- NT MONGE-AMPERE EQUATION
- NT NONLINEAR EQUATIONS
- NT NONLINEAR EVOLUTION EQUATIONS
- NT POLYNOMIALS
- NT QUADRATIC EQUATIONS
- NT QUARTIC EQUATIONS
- NT SPINOR GROUPS
- NT STATE VECTORS
- NT STIFFNESS MATRIX
- NT STOKES THEOREM (VECTOR CALCULUS)
- NT STRESS TENSORS
- NT TENSORS
- NT VECTOR SPACES
- NT VECTORS (MATHEMATICS)
- NT VORTICITY
- Poisson brackets compatible with algebraic geometry and Korteweg-de Vries dynamics over a set of finite-gap potentials 02 p0232 A83-11651
- Moving frames and prolongation algebras 07 p0988 A83-21043
- On a method of designing processors for searching for the roots of algebraic equations 08 p1151 A83-22181
- Organization of the solution of systems of linear algebraic equations in pipeline computing systems 08 p1154 A83-22185
- Equilibrium points of the Riccati equation - Geometric structure 09 p1329 A83-24736

A general precompiler for algebraic manipulation 12 p1768 A83-29110

Geometry of the algebraic Riccati equation. I [AD-A129991] 13 p1911 A83-31355

Algebra related to the N-soliton solution of the Benjamin-Ono equation 14 p2077 A83-32508

Soliton and algebraic equation 14 p2077 A83-32509

Symmetric linear systems - An application of algebraic systems theory 16 p2405 A83-36454

On the question of using the method of false perturbations in astronomical practice 16 p2427 A83-36862

Controller scheduling - A possible algebraic viewpoint 17 p2565 A83-37093

An algebraically derived nonlinear control theory 17 p2566 A83-37098

A linear algebra approach to the analysis of rigid body velocity from position and velocity data 17 p2575 A83-37546

Algebraic grid generation 17 p2573 A83-38782

Automatic algebraic coordinate generation 17 p2564 A83-38793

Three-dimensional algebraic grid generation [AIAA PAPER 83-1904] 18 p2739 A83-39363

Algebraic criterion of absolute stability 20 p3039 A83-42919

A method for solving a system of equations encountered in problems of electrodynamics --- for multi-discrete element antennas 22 p3272 A83-45693

Quaternion algebra applied to polygon theory in three dimensional space --- Thesis 22 p3353 A83-46697

ALGERIA

Analysis of multitemporal Landsat 2 imagery of the Annaba zone of Algeria - April 28, 1977 and February 28, 1978 /Earthnet 20 834/ 11 p1600 A83-28145

Remote sensing and cartography for soil use in Algeria: Comparative study of the interpretation of analog imagery /aerial photographs/ and of data treatment of digitized versions of the same images and spacial imagery - Application to the mouth of the Isser wadi /coastal Kabylie/ - Algeria 11 p1600 A83-28146

ALGORITHMS

Continuous time adaptive identification and control algorithms via newly developed adaptive laws 01 p0095 A83-10960

Fast firmware algorithms for square root, sine/cosine, and exponential 01 p0087 A83-11149

Advanced automatic terrain following/terrain avoidance control concepts study 01 p0013 A83-11254

A two-stage method of fitting conic arcs and straight-line segments to digitized contours 01 p0098 A83-11427

An iterative algorithm for multiple threshold detection --- in image processing 01 p0098 A83-11434

Object growing algorithm for cavity measurement in structural materials 01 p0053 A83-11443

A simple contour matching algorithm 01 p0100 A83-11471

Digital adaptive methods of signal processing 02 p0162 A83-11529

Analysis of algorithms of the spatial-temporal processing of signals in the presence of noise 02 p0162 A83-11543

A generalization of algebraic surface drawing 02 p0226 A83-11783

Adapting iterative algorithms developed for symmetric systems to nonsymmetric systems 03 p0388 A83-14088

Statistical synthesis of an algorithm for the computer-aided processing of cardiac signals 03 p0384 A83-14329

Algorithms for advection and shock problems 03 p0322 A83-14611

Range of applicability of inversion algorithms --- for ultrasonic flaw detection 04 p0490 A83-15174

Inversion algorithms for crack-like flaws 04 p0492 A83-15204

A study of textures by modeling pole figures --- crystal structure computerized simulation for metal microstructure study 04 p0459 A83-15472

Computer-aided design within the framework of the algorithmic selection procedure for the design with catalogs --- German thesis 04 p0487 A83-15844

A practical algorithm for the solution of triangular systems on a parallel processing system 05 p0678 A83-17241

On the analysis and synthesis of VLSI algorithms 05 p0678 A83-17246

Architecture for scientific software. II - Analysis of a quadratic programming algorithm 05 p0680 A83-17319

Algorithm of the two-dimensional Fourier transformation with a mixed base 06 p0802 A83-18031

An algorithm for optimum structural design without line search 06 p0772 A83-18219

The recursive-iterative algorithm for solving the characteristic equation for stabilized spacecraft. II 06 p0723 A83-18353

Steady-state performance of an adaptive sequential routing algorithm 07 p0911 A83-19775

Partitioned matrix algorithms for VLSI arithmetic systems 07 p0982 A83-20249

Algorithmization of computations in a discretely observed gravitational field 07 p0962 A83-20602

Development of mixed time partition procedures for thermal analysis of structures 07 p0949 A83-21445

On the design of algorithms for VLSI systolic arrays 07 p0923 A83-21542

Evaluation of peak location algorithms with subpixel accuracy for mosaic focal planes 08 p1050 A83-22448

Modified FFT algorithms with a reduced number of multiplication operations 08 p1154 A83-23169

Picard's method for solving nonlinear two-point boundary value problem in optimal control theory 09 p1326 A83-23976

Parallel computations of Boolean functions 09 p1327 A83-24246

Evaluation of Seasat SMMR wind speed measurements 09 p1314 A83-24297

A new recursive partitioned estimation algorithm derived from Extended Least Squares technique 09 p1330 A83-24744

A convection parameterization scheme based on a direct algorithm of dry convective adjustment --- for atmospheric models 09 p1315 A83-24939

Algorithm for the optimal planning of spacecraft operation 09 p1211 A83-25030

The modular structure of algorithms and programs in problems involving continuous medium mechanics and computer structure 09 p1326 A83-25239

Latice implementation of some recursive parameter-estimation algorithms 10 p1461 A83-25395

A time efficient finite differences algorithm for the solution of the meridional flow in turbo compressor impellers 10 p1413 A83-25683

[ASME PAPER 82-WA/FE-3] Conditional sampling with a laser velocimeter --- for tone-excited jet and rotating propeller blade [AIAA PAPER 83-0756] 10 p1420 A83-25953

A radio guidance algorithm for M Series rockets that are used to launch Japanese scientific satellites 10 p1382 A83-26593

Frequency limitations and optimal step size for the two-point central difference derivative algorithm with applications to human eye movement data 10 p1460 A83-26650

A stable smoothing algorithm --- for digital processing of radar signals 11 p1556 A83-27948

Supervisory control of a multilegged robot 11 p1648 A83-28098

Spectral factorization by optimal gain iteration 12 p1770 A83-28998

A multigrid algorithm for steady transonic potential flows around aerofoils using Newton iteration 12 p1697 A83-29656

Black box multigrid 12 p1773 A83-29658

General relaxation schemes in multigrid algorithms for higher-order singularity methods 12 p1773 A83-29660

A robust Feasible Directions algorithm for design synthesis [AIAA 83-0938] 12 p1773 A83-29768

Construction of algorithms for the automatic control of the force operations of manipulator robots 13 p1910 A83-30089

Efficient square root algorithm for measurement update in Kalman filtering 13 p1910 A83-30156

Binary trees and parallel scheduling algorithms 13 p1909 A83-30795

Finite element, boundary element and coupled analysis of unbounded problems in elastostatics 13 p1868 A83-31641

On an algorithm for the simulation of a vector random process 14 p2076 A83-32966

Pseudo-updated constrained solution algorithm for nonlinear heat conduction 14 p2012 A83-32989

Fabry-Perot interferograms for amplitude and phase modulated light 15 p2163 A83-33755

A numerical algorithm for solving inverse problems of two-dimensional wave equations 15 p2223 A83-33819

Error free computation - A direct method to convert finite-segment p-adic numbers into rational numbers 15 p2217 A83-33903

A simple approach to the error analysis of division-free numerical algorithms 15 p2217 A83-33904

Recent developments in the analysis and design of extended surface 15 p2157 A83-33994

Unconditionally stable implicit-explicit algorithms for coupled thermal stress waves 15 p2176 A83-34317

An algorithm of flight simulation on a dynamic stand of support type 15 p2123 A83-34429

Designing efficient parallel algorithms for multiple-output computations with fan-in constraints 15 p2218 A83-35113

Systolic and SIMD algorithms for digital filtering 15 p2219 A83-35148

Computational noise effects on adaptive filter algorithms 16 p2403 A83-35349

Performance evaluation of algorithms for mildly nonlinear elliptic problems 16 p2406 A83-35644

Algorithms, software, and architecture of multiprocessor computing systems --- Russian book 16 p2404 A83-36442

A modified algorithm for determining structural controllability 16 p2405 A83-36455

A simple efficient hidden line algorithm 16 p2404 A83-36558

A quasi-Newton versus a homotopy method for nonlinear structural analysis 16 p2369 A83-36560

Simple M-factor algorithm for improved estimation of the basic maximum usable frequency of radio waves reflected from the ionospheric F-region 16 p2342 A83-36576

A method of stabilizing the clean algorithm --- for deconvolution of Fourier synthesis point spread functions from radio astronomy images 16 p2425 A83-36646

Some critical questions about deterministic and stochastic adaptive control algorithms 16 p2406 A83-36978

A recursive algorithm by using eigenvector method for identifying multivariable linear time-invariant systems 17 p2565 A83-37086

Investigation of time-to-go algorithms for air-to-air missiles 17 p2461 A83-37137

Fast Fourier transform and convolution algorithms /2nd revised edition/ 17 p2571 A83-37175

On the attitude estimation of earth observation satellites 17 p2478 A83-37454

Numerical prediction of the motion of high-altitude geodetic satellites 17 p2472 A83-37724

Algorithms for determining invertible two- and three-dimensional quadratic isoparametric finite element transformations 17 p2572 A83-38569

An iterative algorithm for solving inverse problems in structural dynamics 17 p2525 A83-38571

An algorithm for engineering design optimization 17 p2575 A83-38573

Efficient solution of the Euler and Navier-Stokes equations with a vectorized multiple-grid algorithm [AIAA PAPER 83-1893] 18 p2634 A83-39359

Noise immunity of selection algorithms in the whole 18 p2674 A83-39426

An algorithm for solving the nonisothermal thermoplasticity problem on the basis of the finite element method 18 p2698 A83-39502

Algorithm for investigating the stability of rings of variable thickness under nonuniform loading 18 p2702 A83-40120

Algorithm improvements for optical eigenfunction computers 19 p2893 A83-41095

The paralleling of algorithms for the simulation of nonlinear systems of large dimensionality 19 p2888 A83-41422

Algorithms for real-time flutter identification [AIAA PAPER 83-2223] 19 p2859 A83-41703

Reduction method for verifying the correctness of parallel algorithms of logic control 19 p2893 A83-42021

Algorithm for the fast computation of the two-dimensional discrete Fourier transformation 20 p3041 A83-42903

A paradigm for the design of parallel algorithms with applications 20 p3038 A83-43114

A causal model for analyzing distributed concurrency control algorithms 20 p3038 A83-43116

Algorithm for determining the dimensions of flaws in the theory of eddy-current flaw detection by superposed transducers 20 p3000 A83-43179

Hardware-based Fourier transforms - Algorithms and architectures 20 p3037 A83-43681

Design of optimal algorithms of simultaneous multialternative detection and estimation of parameters with unknown probabilities of the signals to be detected 22 p3352 A83-46398

A simple algorithm for the nonlinear dynamic analysis of networks 23 p3470 A83-48160

Comparative analysis of the efficiency of practical realizations of the Kalman algorithm --- for microwave landing systems 23 p3406 A83-48518

Regularization of algorithms for the processing of signals and noise in adaptive antenna arrays 23 p3444 A83-48522

ALIGNMENT

- Asymptotically optimal test algorithms in problems of recognition 24 p3620 A83-49124
- A data structure and algorithm based on a linear key for a rectangle retrieval problem 24 p3619 A83-49194
- A linear test algorithm of pattern recognition 24 p3620 A83-49538
- A conditional algorithm for setting a discrete device with memory to a definite state 24 p3622 A83-50206
- ALIGNMENT**
- NT SELF ALIGNMENT
- The effect of test system misalignment in the dynamic tension test 01 p0026 A83-10649
- Optical alignment measurements at Goddard Space Flight Center 02 p0139 A83-12311
- Large space structures, alignment, and extravehicular activities /EVA/ crew support 09 p1213 A83-23585
- Telescope alignment with the absolute distance interferometer 13 p1921 A83-31023
- Linear crater chains - Indication of a volcanic organ 16 p2439 A83-36786
- Kalman filter formulations for transfer alignment of strapdown inertial units 18 p2739 A83-40303

ALIPHATIC COMPOUNDS

- NT ACETONE
- NT ACETYL COMPOUNDS
- NT ACETYLENE
- NT ACRYLATES
- NT ACRYLONITRILES
- NT ADENOSINE DIPHOSPHATE
- NT ADENOSINE TRIPHOSPHATE
- NT ADENOSINES
- NT ALKANES
- NT ALKYL COMPOUNDS
- NT ALKYLATES
- NT ANTHRACENE
- NT BUTADIENE
- NT CARBON TETRACHLORIDE
- NT CELLULOSE
- NT CHLOROETHYLENE
- NT CHLOROFORM
- NT CYANOGEN
- NT CYCLIC HYDROCARBONS
- NT DEXTRANS
- NT ETHANE
- NT ETHYL ALCOHOL
- NT ETHYLENE
- NT FATTY ACIDS
- NT FORMIC ACID
- NT GLUCOSE
- NT GLUCOSIDES
- NT GLUTAMATES
- NT GLUTAMIC ACID
- NT GLUTATHIONE
- NT GLYCERIDES
- NT GLYCEROLS
- NT GLYCOGENS
- NT HEPTANES
- NT HEXOGENES (TRADEMARK)
- NT HYDRAZINES
- NT KETONES
- NT LACTATES
- NT LACTIC ACID
- NT METHANE
- NT METHYL ALCOHOLS
- NT METHYL COMPOUNDS
- NT METHYLHYDRAZINE
- NT NITRATE ESTERS
- NT NITROAMINES
- NT NITROSAMINE
- NT NUCLEOSIDES
- NT PALMITIC ACID
- NT. PARAFFINS
- NT PENTANES
- NT PROPANE
- NT PROPYL COMPOUNDS
- NT PROPYLENE
- NT STEARATES
- NT THIOLS
- NT VINYLIDENE
- Thiol-catalyzed formation of lactate and glycerate from glyceraldehyde --- significance in molecular evolution 20 p3036 A83-42398
- Amplified spontaneous emission in doped alkali-halides 21 p3145 A83-44814
- ALKALI METAL COMPOUNDS**
- Bragg-reflection profiles of graphite and alkali-graphite intercalation compounds - Comparison of double-axis and triple-axis spectrometer results 07 p0932 A83-21380
- The characterization of carbon dioxide absorbing agents for life support equipment; Proceedings of the Winter Annual Meeting, Phoenix, AZ, November 14-19, 1982 11 p1644 A83-28329
- Carbon dioxide scrubbing materials in life support equipment 11 p1644 A83-28330
- ALKALI METALS**
- NT CESIUM
- NT CESIUM VAPOR
- NT LITHIUM
- NT LITHIUM ISOTOPES
- NT POTASSIUM
- NT POTASSIUM ISOTOPES
- NT RUBIDIUM
- NT RUBIDIUM ISOTOPES
- NT SODIUM
- NT SODIUM VAPOR
- Filtration coefficient and hydraulic permeability of Nafion 125 membranes in metal alkali solutions 10 p1390 A83-26056
- New optically pumped alkali metal dimer lasers 11 p1579 A83-27555
- Peculiar asymmetry in the wings of self-broadened Li and Na first resonance lines 11 p1654 A83-27847
- Nonlinear optical indication in frequency-stabilization systems --- for metal vapor lasers 11 p1583 A83-27955
- Resonant extinction of lidar returns from the alkali metal layers in the upper atmosphere 13 p1880 A83-31465
- An instrument for absolute or relative measurement of wavenumbers of a continuous or pulsed laser - The sigmameter. Application to the spectroscopic study of the D lines of a series of alkaline radioactive isotopes --- French thesis 17 p2512 A83-38432
- Electrical conductivity of alkali metal vapors in the neighborhood of the critical point 18 p2747 A83-39864
- Proposal for high-power radiative-collisional lasers [AD-A122225] 19 p2850 A83-40671
- Double radio-optical resonance in alkali-metal vapors 19 p2854 A83-41795
- Electron affinities of the alkali dimers - Na₂, K₂, and Rb₂ 20 p3045 A83-42635
- Black-body radiation shifts in ground and metastable levels of Mg and Ca 24 p3626 A83-49524
- Intercalation of alkali metals in graphite under high pressure 24 p3569 A83-49554
- ALKALIES**
- NT LITHIUM HYDROXIDES
- NT SODIUM HYDROXIDES
- A theoretical model of CO₂ absorption in a mixed alkali bed under hyperbaric conditions 11 p1645 A83-28336
- An ab initio study of core-valence correlation --- in atoms 20 p3045 A83-42636
- ALKALINE BATTERIES**
- Pelletized lithium-metal sulphide cells. II - Some operating characteristics of pelletized LiAl-FeS cells 01 p0068 A83-10792
- Investigation and production control of Li/SO₂ cells by the galvanostatic pulse method 01 p0068 A83-10796
- Zinc electrode morphology in alkaline solutions. I - Study of alternating voltage modulation on a rotating disk electrode 04 p0456 A83-15867
- Research on oxidation by air and tempering of Raney nickel electrocatalysts for the H₂ anodes of alkali combustion materials cells --- German thesis 06 p0726 A83-18494
- Cross-linked polyvinyl alcohol films as alkaline battery separators 07 p0881 A83-20576
- Electrolyte film structure on battery separator and electrode materials 07 p0954 A83-20577
- Large nickel alkaline batteries 11 p1604 A83-27176
- Alkaline regenerative fuel cell energy storage system for manned orbital satellites 11 p1540 A83-27206
- Zinc electrode morphology in alkaline solutions. II - Study of alternating charging current modulation on pasted zinc battery electrodes 20 p2951 A83-43418
- Thermoelectric energy conversion with solid electrolytes 21 p3166 A83-43983
- The choice of low-temperature hydrogen fuel cells: Acidic - or alkaline 21 p3168 A83-45424
- On the suppression of self discharge of the zinc electrodes of zinc-air cells and other related battery systems 24 p3599 A83-49931
- ALKALINE EARTH METALS**
- NT BARIUM ISOTOPES

ALKALINE EARTH OXIDES

- NT BERYLLIUM OXIDES
- NT CALCIUM OXIDES
- NT MAGNESIUM OXIDES
- ALKALOIDS**
- NT ATROPINE
- NT HYOSCINE
- NT MORPHINE
- NT NICOTINAMIDE
- Ionizing radiation decreases veratridine-stimulated uptake of sodium in rat brain synaptosomes 15 p2209 A83-33776
- ALKALOSIS**
- The effect of alimentary alkalemia on the maximum duration of anaerobic work and the concentration of lactate in the muscles and blood 16 p2398 A83-35906
- ALKANES**
- NT ETHANE
- NT HEPTANES
- NT METHANE
- NT PARAFFINS
- NT PENTANES
- NT PROPANE
- Fluid flow in the contact line region of a mixture of alkanes - 98 percent hexane and 2 percent octane [AIAA PAPER 83-1528] 14 p2011 A83-32759
- Particle size distribution of n-alkanes nda Pb-210 in aerosols off the coast of Peru 20 p3028 A83-43556
- ALKENES**
- NT BUTADIENE
- NT ETHYLENE
- NT PROPYLENE
- NT VINYLIDENE
- ALKYL COMPOUNDS**
- Thick film formation by zinc dialkyldithiophosphates 06 p0734 A83-18200
- Use of column V alkyls in organometallic vapor phase epitaxy (OMVPE) 22 p3266 A83-46608
- ALKYLATES**
- A comparative analysis of the effect of alkylating agents, ionizing radiation, and ultraviolet light on the mammalian cell progression in the mitotic cycle. I - The effect of N-methyl-N'-nitro-N-nitrosoguanisine on the passing of various phases of the cycle by HeLa cells 06 p0796 A83-19378
- A comparative analysis of the effect of alkylating agents, ionizing radiation, and ultraviolet radiation on the progression of mammalian cells through the mitotic cycle. II - The effect of gamma-radiation and N-methyl-N'-nitro-N-nitrosoguanidine on DNA synthesis in HeLa cells 09 p1321 A83-24928
- ALKYLATION**
- A quantitative determination of the hemodepressive effect of some alkylating agents 03 p0374 A83-13633
- ALKYNES**
- NT ACETYLENE
- ALL SKY PHOTOGRAPHY**
- ASCORECORD 3 DP two-coordinate measuring instrument in the service of the European Fireball Programme 02 p0183 A83-13046
- ALL-WEATHER AIR NAVIGATION**
- USAF studies fighters for dual-role, all-weather operations 05 p0595 A83-17276
- Environmental control of an aircraft pod mounted electronics system [SAE PAPER 820869] 10 p1375 A83-25768
- All weather heliports and airway system - The future need 16 p2312 A83-36073
- The integration of multiple avionic sensors and technologies for future military helicopters 18 p2639 A83-40301
- ALL-WEATHER LANDING SYSTEMS**
- General conditions of operational and technical utilization of ILS during Category III operations 02 p0134 A83-13008
- All-weather small-deck operations in the U.S. Navy [SAE PAPER 821503] 17 p2459 A83-38010
- ALLERGIC DISEASES**
- The state of the vestibular-analyzer function in patients with infectious-allergic bronchial asthma 03 p0381 A83-14337
- ALLOCATIONS**
- NT RESOURCE ALLOCATION
- ALLTROPY**
- Composition of the surfaces of the Galilean satellites 04 p0570 A83-16232
- ALLOYS**
- NT ALUMINUM ALLOYS
- NT ANTIMONY ALLOYS
- NT ASTROLOY (TRADEMARK)
- NT AUSTENITIC STAINLESS STEELS
- NT BEARING ALLOYS
- NT BERYLLIUM ALLOYS
- NT BINARY ALLOYS
- NT BISMUTH ALLOYS

NT BORON ALLOYS
 NT BRASSES
 NT CARBON STEELS
 NT CAST ALLOYS
 NT CHROMIUM ALLOYS
 NT CHROMIUM STEELS
 NT COBALT ALLOYS
 NT COPPER ALLOYS
 NT ERBIUM ALLOYS
 NT EUTECTIC ALLOYS
 NT FERRITIC STAINLESS STEELS
 NT GERMANIUM ALLOYS
 NT GOLD ALLOYS
 NT HAFNIUM ALLOYS
 NT HASTELLOY (TRADEMARK)
 NT HEAT RESISTANT ALLOYS
 NT HIGH STRENGTH ALLOYS
 NT HIGH STRENGTH STEELS
 NT INCONEL (TRADEMARK)
 NT INDIUM ALLOYS
 NT IRON ALLOYS
 NT LEAD ALLOYS
 NT LIGHT ALLOYS
 NT LITHIUM ALLOYS
 NT LOW CARBON STEELS
 NT MAGNESIUM ALLOYS
 NT MANGANESE ALLOYS
 NT MANGANIN (TRADEMARK)
 NT MARAGING STEELS
 NT MARTENSITIC STAINLESS STEELS
 NT MERCURY AMALGAMS
 NT MOLYBDENUM ALLOYS
 NT MONOTECTIC ALLOYS
 NT NICHROME (TRADEMARK)
 NT NICKEL ALLOYS
 NT NICKEL STEELS
 NT NIMONIC ALLOYS
 NT NIOBIUM ALLOYS
 NT PALLADIUM ALLOYS
 NT PLATINUM ALLOYS
 NT QUATERNARY ALLOYS
 NT RARE EARTH ALLOYS
 NT REFRACTORY METAL ALLOYS
 NT RHENIUM ALLOYS
 NT RUTHENIUM ALLOYS
 NT SHAPE MEMORY ALLOYS
 NT SILICON ALLOYS
 NT STAINLESS STEELS
 NT STEELS
 NT TANTALUM ALLOYS
 NT TERNARY ALLOYS
 NT THORIUM ALLOYS
 NT TIN ALLOYS
 NT TITANIUM ALLOYS
 NT TUNGSTEN ALLOYS
 NT UDIMET ALLOYS
 NT VANADIUM ALLOYS
 NT WASPALOY
 NT WROUGHT ALLOYS
 NT YTTRIUM ALLOYS
 NT ZINC ALLOYS
 NT ZIRCALOYS (TRADEMARK)
 NT ZIRCONIUM ALLOYS
 A compendium of sources of fracture toughness and fatigue crack growth data for metallic alloys. II
 03 p0301 A83-14822
 Japan Congress on Materials Research, 25th, Tokyo, Japan, October 1981, Proceedings
 05 p0610 A83-17086
 Relations between chemistry, solidification behaviour, and microstructure in IN 100
 07 p0894 A83-21485
 Selecting parts and materials for sterilized electronics --- for medical and interplanetary landing craft instruments
 09 p1324 A83-23612
 Dislocation creep in subgrain-forming pure metals and alloys
 09 p1231 A83-24052
 Deformation and dislocation behaviour in metals and single-phase alloys at elevated temperatures
 09 p1231 A83-24054
 Work hardening and recovery rates of internal stress in pure metals and alloys
 09 p1231 A83-24056
 A new simple casting technique - The Flying Wheel Casting
 09 p1274 A83-24123
 Advanced alloys and metal/ceramic composites from lunar source materials
 11 p1531 A83-27345
 Thermal and transformation stresses
 12 p1746 A83-29902
 Plasticity of metals and alloys with special properties
 13 p1820 A83-30681
 The mechanical properties and stability of alloys
 14 p1991 A83-31945
 Dispersed crystalline powders - An analysis of the scientific-technical literature
 14 p1992 A83-32144
 Strengthening of metals and alloys
 14 p1994 A83-32805

Mechanical tests of structural alloys at cryogenic temperatures
 14 p1997 A83-33012
 A study of the elastic characteristics of structural alloys over a wide temperature range
 14 p1998 A83-33017

Atomic absorption spectroscopy in studying metal vaporization --- Russian book
 15 p2133 A83-34750
 Superplasticity - A review of data
 16 p2335 A83-36959

Some aspects of micro-alloying
 17 p2489 A83-38122
 The effect of crack closure and estimation of the cyclic fracture toughness of structural alloys
 19 p2856 A83-40803

Heat treatment, structure and properties of nonferrous alloys --- Book
 19 p2822 A83-41465
 Phase transformations and structure of metals and alloys --- Russian book
 19 p2822 A83-41993
 Thermodynamic analyses of the high temperature corrosion of alloys in gases containing more than one reactant
 20 p2949 A83-42242
 Influence of oxide scales on high temperature corrosion erosion behavior of alloys
 20 p2952 A83-42243
 Some effects of environment on high temperature mechanical behavior of alloys
 20 p2953 A83-42245
 Influence of diffusion and convective transport on dendritic growth in dilute alloys
 20 p3054 A83-43298

Metallurgy and metallography of nonferrous alloys
 20 p2955 A83-43489

Influence of the microstructure on the corrosion behavior of magnetron sputter-quenched amorphous metallic alloys
 21 p3217 A83-44611
 Mechanical alloying
 22 p3268 A83-45896
 The metal chemistry of complex alloying --- Russian book
 23 p3431 A83-47098

Order of magnitude analysis of convective effects in dendritic solidification --- of alloys
 [IAF PAPER 83-150]
 23 p3413 A83-47290

Electronic structure and ordering in transition alloys and compounds
 [ONERA, TP NO. 1983-64]
 23 p3432 A83-48185

Plastic deformation of strain-hardenable metals and alloys The governing equations and calculations
 23 p3472 A83-48463

Studies on the corrosion resistance of MCrAlY alloys at high temperatures
 24 p3564 A83-49506

ALMUCANTAR

U ELEVATION ANGLE

ALOHA SYSTEM

A discrete model for the distribution of users and the signal-capture effect in ALOHA networks
 06 p0749 A83-19569

Experimental system for computer network via satellite /CS/. II - Communication protocols
 10 p1403 A83-26078

Diversity ALOHA - A random access scheme for satellite communications
 13 p1827 A83-36225
 Increasing the efficiency of the cyclic phasing of contiguous classes of cyclic codes
 13 p1829 A83-30730

Dynamic frame length ALOHA

Application of catastrophe theory to a slotted ALOHA communication system
 16 p2343 A83-36580

Analysis and stability considerations in a reservation multiaccess system
 16 p2343 A83-36606
 On the capacity of multihop slotted ALOHA networks with regular structure
 19 p2825 A83-40893

On the capacity of single-hop slotted ALOHA networks for various traffic matrices and transmission strategies
 19 p2826 A83-40894
 Improving stability and delay characteristics of multiple access systems employing ALOHA type channels
 19 p2828 A83-41333

An iterative scheme for performance modeling of slotted ALOHA packet radio networks
 19 p2832 A83-41397
 Traffic control in satellite-aided slotted-ALOHA system using HDLC procedure for an error recovery --- High-Level Data Link Control
 22 p3275 A83-46916

ALPHA DECAY

Measurement of the Be-7/pi gamma/B-8 reaction cross section at low energies --- solar neutrinos
 07 p1037 A83-20815

ALPHA JET AIRCRAFT

Alpha Jet - Further version for the international market
 17 p2467 A83-37858

ALPHA PARTICLES

Measurements of the properties of solar wind plasma relevant to studies of its coronal sources
 04 p0574 A83-15118
 Thermal and suprathreshold protons and alpha particles in the earth's plasma sheet
 06 p0782 A83-18289

Computer analysis of the significance of surface boundary conditions on the collection of alpha-induced charge --- carrier transport simulation
 06 p0753 A83-18960

Acceleration of low-energy protons and alpha particles at interplanetary shock waves
 09 p1357 A83-23753
 Accelerator simulation of astrophysical processes
 13 p1944 A83-30179

An alpha particle instrument with alpha, proton, and X-ray modes for planetary chemical analyses
 16 p2357 A83-36718

Collection of charge from alpha-particle tracks in silicon devices
 18 p2678 A83-40381
 The effect of alpha particles on bacteriophage T4Br(+)
 19 p2872 A83-40835

ALPHA RADIATION

U ALPHA PARTICLES

ALPHANUMERIC CHARACTERS

NT BINARY DIGITS

Investigating the correlation between reading errors and degraded numerics - Or, do missing dots call the shots
 01 p0085 A83-11168
 Evaluation of alternative alphanumeric keying logics
 02 p0225 A83-12087

The display capacity of alphanumeric information on visual display units with restrictions in the electrical or visual channel --- Dutch book
 03 p0383 A83-14113

ALPINE METEOROLOGY

Numerical modelling of the mesoscale airflow downwind of the Alps - Two case studies under cyclogenetic conditions
 04 p0518 A83-16153
 Digital radar information in the Swiss Meteorological Institute
 11 p1624 A83-27003

Orographic trough or low in the Alpine region /and their effect on weather in the CSR/
 11 p1633 A83-28114

The use of satellite picture data in the fields of forecasting and research at the Swiss Meteorological Institute
 14 p2055 A83-31849

ALPS MOUNTAINS (EUROPE)

Orographic trough or low in the Alpine region /and their effect on weather in the CSR/
 11 p1633 A83-28114

ALSEP

U APOLLO LUNAR SURFACE EXPERIMENTS PACKAGE

ALTERATION

U REVISIONS

ALTERNATING CURRENT

Dipolar field propulsion - Principles and concepts [AIAA PAPER 82-1933]
 02 p0146 A83-12499
 Zinc electrode morphology in alkaline solutions. I - Study of alternating voltage modulation on a rotating disk electrode
 04 p0456 A83-15867

Probe characterization in ac field measurements of surface crack depth
 07 p0929 A83-20267
 A.C. field measurements - A new method for detecting and measuring fatigue cracks
 08 p1112 A83-21761

Crack depth measurements using AC potential drop
 08 p1113 A83-22408
 AC model for MOS transistors from transient-current computations
 09 p1252 A83-23349

Crack shape evolution studies in threaded connections using A.C.F.M. --- Alternating Current Field Measurement
 11 p1590 A83-27858
 The influence of skin depth on crack measurement by the ac field technique
 12 p1733 A83-29140

ac characteristics in ac/dc/dc conversion
 14 p2006 A83-32427
 Josephson-junction circuit analysis via integral manifolds
 15 p2151 A83-33928

Zinc electrode morphology in alkaline solutions. II - Study of alternating charging current modulation on pasted zinc battery electrodes
 20 p2951 A83-43418

ALTERNATING CURRENT GENERATORS

U AC GENERATORS

ALTERNATORS (GENERATORS)

U AC GENERATORS

ALTIMETERS

NT LASER ALTIMETERS

NT RADIO ALTIMETERS

Relief of the Memnonia Fossae-Margaritifer Sinus region according to Mars-5 CO2 altimetry data
 06 p0848 A83-18365

Global mean sea surface computation using GEOS 3 altimeter data
 07 p0971 A83-20238

Southern Hemisphere western boundary current variability revealed by GEOS 3 altimeter
 07 p0971 A83-20545

Absolute measurement by satellite altimetry of dynamic topography of the Pacific Ocean
 08 p1144 A83-23277

Optimal design of a baro/radio supported inertial altitude system [DGLR PAPER 82-041]
 09 p1204 A83-24165

On the wave number spectrum of oceanic mesoscale variability observed by the SEASAT altimeter
 15 p2207 A83-33490

Global mesoscale variability from collinear tracks of SEASAT altimeter data 15 p2207 A83-33491
 Satellite altimetry determination of differences between mean sea-level heights and testing geopotential models 17 p2525 A83-38145
 Satellite altimetry --- geodetic applications 17 p2482 A83-38306
 Development of active microwave sensors in Japan --- for remote sensing satellites 22 p3260 A83-46115

ALTITUDE

NT FLIGHT ALTITUDE
 NT HIGH ALTITUDE
 NT LOW ALTITUDE
 NT SEA LEVEL

The law governing the variation of the anomalous gravitational field with the survey altitude 04 p0510 A83-16037

Solar altitude frequency tables 08 p1136 A83-22617
 Collinear-track altimetry in the Gulf of Mexico from Seasat - Measurements, models, and surface truth 09 p1318 A83-24290

An analytic version of Jacchia's 1977 model atmosphere 12 p1752 A83-29101
 Performance capabilities of photographic flight navigation and sensor orientation systems 16 p2298 A83-36122

ALTITUDE ACCLIMATIZATION

The changes in the hemodynamics of dogs during exercise of different intensities in the acute adaptation to high altitude 01 p0079 A83-10529

The antihypoxic effectiveness of alimentary fasting 02 p0219 A83-11521

Augmentation of the resistance of the myocardium to pituitrin damage via adaptation to hypoxia 03 p0373 A83-13598

Prophylactics for mountain sickness 03 p0382 A83-14499

The adaptation of the heart to chronic high-altitude hypoxia 04 p0522 A83-15780

The correlation of the parameters of the cardiac rhythm with the physical work capacity of humans during the adaptation to high-altitude hypoxia 04 p0522 A83-15781

Adaptation and resistance to hypoxia in light of the functional activity of the antisystems 05 p0669 A83-17161

The improvement of the myocardial resistance to pituitrin via adaptation to hypoxia 05 p0670 A83-17186

The prevention of disorders of the contractile function of the heart during stress by means of preliminary adaptation of the animals to hypoxia 07 p0972 A83-19920

The adrenoreactivity of the vessels of the small intestine in cats during the process of high altitude adaptation 07 p0973 A83-20245

Chemoreceptor sensitivity in adaptation to high altitude 07 p0977 A83-20780

The content of ubiquinone and vitamin E in rat tissues during experimental focal myocarditis and hypoxic hypoxia 07 p0974 A83-20980

The sympathoadrenal system during hypoxic conditions 09 p1321 A83-25153

The problem of tissue adaptation to hypoxia 09 p1322 A83-25168

The architectonics of the arterial bed in the brain hemispheres of rats during normal conditions and after a stay at a 'height' of 5600 m 10 p1454 A83-26788

The content of endogenous serotonin in the lymph organs of rats during the adaptation to high-altitudes and the pattern of radiation sickness 11 p1641 A83-28763

The pathological and physiological characteristics of the deficiencies of the mitral valve in animals as a consequence of high-altitude hypoxia 11 p1641 A83-28764

The response of the lymph and blood coagulation systems to gamma-radiation at high altitudes 14 p2062 A83-32064

Barometric pressures at extreme altitudes on Mt. Everest Physiological significance 14 p2068 A83-32811

Heart function and certain mechanisms for its regulation when simulating the adaptation to hypoxia by administering 2,4-dinitrophenol 15 p2210 A83-34958

Age-related peculiarities of the functional condition of the vascular system in patients with bronchial asthma in the case of mountain-climate therapy 18 p2735 A83-40569

Acclimatization to high altitude in goats with ablated carotid bodies 19 p2875 A83-41132

The working capacity of humans in mountains --- Russian book 21 p3186 A83-43922

The characteristics of the immunological reactivity of humans in conditions of a mountain climate 21 p3188 A83-45341

Maximal exercise at extreme altitudes on Mount Everest 22 p3347 A83-45983

The interaction of cardiac ventricles in intact dogs during 3-5 days of high altitude adaptation 23 p3496 A83-48566

Changes in the microcirculation in mesentery rats during hyperoxia 23 p3496 A83-48568

ALTITUDE CONTROL

Automatic control of balloon altitude 18 p2641 A83-39809

ALTITUDE SICKNESS

Prophylactics for mountain sickness 03 p0382 A83-14499

Survival following accidental decompression to an altitude greater than 74,000 feet /22,555 m/ 04 p0522 A83-15538

Ocular functions and incidence of acute mountain sickness in women at altitude 07 p0977 A83-20779

Acute mountain sickness, antacids, and ventilation during rapid, active ascent of Mount Rainier 14 p2068 A83-32684

Methazolamide and acetazolamide in acute mountain sickness 18 p2734 A83-40357

Renin-aldosterone and angiotensin-converting enzyme during prolonged altitude exposure 22 p3347 A83-45984

ALTITUDE SIMULATION

An AN/APN-194/V/ radar altimeter/MIL-STD-1553 interface circuit 01 p0010 A83-11186

An experimental study of the effects of hypobaric hypoxia on the cerebral blood flow and the metabolism of the brain 06 p0794 A83-18342

Separated measurement of gas flows through different compartments of a partially pressurized suit 06 p0800 A83-18345

A rheological investigation of the circulatory system during high-altitude hypoxia and an orthostatic test 06 p0798 A83-19374

Performance decrement at cabin altitudes - A replication 10 p1455 A83-26303

Hemorrhagic tolerance of rats at sea level after acute exposure to high altitude 12 p1762 A83-28934

Laboratory evaluation of an airborne ozone instrument that compensates for altitude/sensitivity effects 21 p3092 A83-45618

ALTITUDE TESTS

NT HIGH ALTITUDE TESTS

ALTITUDE TOLERANCE

Effect of change in P50 on exercise tolerance at high altitude - A theoretical study 05 p0671 A83-17329

Metabolic effect of intermittent exposure to altitude stress on rats and guinea pigs 10 p1453 A83-25670

Hemorrhagic tolerance of rats at sea level after acute exposure to high altitude 12 p1762 A83-28934

ALU (COMPUTER COMPONENTS)

U ARITHMETIC AND LOGIC UNITS

ALUMINA

U ALUMINUM OXIDES

ALUMINATES

A new calcium-aluminate from a refractory inclusion in the Leoville carbonaceous chondrite 04 p0558 A83-15302

Hot-pressed MgAl2O4 for ultraviolet /UV/, visible, and infrared /IR/ optical requirements 09 p1345 A83-24953

ALUMINIZING

U ALUMINUM COATINGS

ALUMINUM

NT ALUMINUM 26

NT POWDERED ALUMINUM

NT SINTERED ALUMINUM POWDER

The size of grains formed during dynamic recrystallization in ultrasonically loaded aluminum 02 p0155 A83-12205

Electron-microscope investigation of aluminum steel in a highly coercive state 03 p0298 A83-13267

TEM observations of dislocation emission at crack tips in aluminum 03 p0298 A83-13679

Transient processes in metal droplet combustion 03 p0295 A83-14123

A study of the mechanism of the steady-state creep of aluminum under compression 03 p0300 A83-14161

A study of polygonization in aluminum deformed by cyclic bending using low-angle X-ray scattering 03 p0300 A83-14163

Lueders deformation in ultrafine-grained pure aluminum 04 p0458 A83-15000

Contribution to the determination of forming limit curves for titanium and aluminum - Proposal of an intrinsic criterion --- French thesis 04 p0459 A83-15840

Optical and electrical characterization of multiply doped silicon - A study of the Si/In,Al/ system 04 p0542 A83-16065

Experimental investigation of pressure and velocity coupled response functions of aluminized and non-aluminized solid propellants [AIAA PAPER 83-0478] 05 p0620 A83-16741

The ET in orbit as a space system material resource [IAF PAPER 82-392] 05 p0603 A83-16924

Cyclic creep behavior of pure aluminum 05 p0614 A83-17089

On the preparation of glass-fibre reinforced aluminum by powder hot extrusion 05 p0611 A83-17110

Diffusivity and growth rate of silicon in solid-phase epitaxy with an aluminum medium 05 p0691 A83-17768

Transmission electron microscopy studies on the oxidation of aluminum 05 p0617 A83-17952

Experimental ionization rate coefficients of aluminum and silicon ions 06 p0811 A83-18818

The production of dispersion strengthened aluminum parts by powder forging 06 p0731 A83-19087

Seeding of FPL solution --- in preparation of aluminum surfaces for adhesive bonding 07 p0885 A83-20431

Service history of phosphoric acid anodized aluminum structure --- with adhesive bonding for aircraft construction 07 p0861 A83-20479

Electromigration transport mobility associated with pulsed direct current in fine-grained evaporated Al-0.5%Cu thin films 07 p0921 A83-20744

Evolution of Ca-Al-rich bodies in the earliest solar system Growth by incorporation 07 p1036 A83-21337

An experimental study of the Dugdale model --- relation between crack tip displacement and applied load 08 p1119 A83-21787

An investigation of the distributions of the equilibrium charge states in carbon, the emission spectroscopy and the mean radiative lifetimes of aluminum ions /Al VI-X/ 08 p1163 A83-21986

Study on composite flywheels for energy storage 08 p1131 A83-22701

Novel fine line patterning technique for submicron devices based on selective oxidation of aluminum 08 p1169 A83-22763

Strain hardening of aluminium at high strains 08 p1068 A83-23225

Effect of strain-amplitude change on low-cycle fatigue behavior of pure aluminium at 77 K 09 p1228 A83-23300

Weak boundary zones in metal bonds 09 p1237 A83-23626

A microscopic approach of the aluminum creep rate at intermediate temperature 09 p1231 A83-24053

Effects of plastic prestrain on the creep of aluminum under biaxial stress 09 p1233 A83-24078

Hot-rolled silicon carbide-aluminum composites 10 p1388 A83-25627

Static and fatigue testing of 2024 Al-SiC /F-9/ T-4 [ASME PAPER 82-WA/AERO-2] 10 p1388 A83-25677

Evidence of population inversion in Li-like aluminum ions in a laser produced plasma 11 p1577 A83-27522

On the structure of tilt grain boundaries in cubic metals. I - Symmetrical tilt boundaries. II - Asymmetrical tilt boundaries. III - Generalizations of the structural study and implications for the properties of grain boundaries 11 p1551 A83-28807

High temperature deformation mechanism of aluminum 12 p1713 A83-29413

Observations of cyclic grain boundary migration in aluminum after large numbers of fatigue cycles 12 p1714 A83-29510

An evaluation of the random bending fatigue life of bonded aluminum joints using various adhesive/primer combinations [AIAA 83-0998] 12 p1744 A83-29873

Acoustic fatigue test evaluation of adhesively bonded aluminum fuselage panels using FM 73/BR 127 adhesive/primer system [AIAA 83-0999] 12 p1744 A83-29874

Low cycle fatigue behavior of aluminum/stainless steel composites [AIAA 83-0806] 12 p1711 A83-29886

Allowing for temperature in descriptions of the delayed fracture of inelastic materials 13 p1865 A83-30056

Optical properties of codeposited aluminum-silicon composite films 13 p1918 A83-30211

Suppressing Al outdiffusion in implantation amorphized and recrystallized silicon on sapphire films 13 p1929 A83-30347

The deformation behavior of the components of the composite aluminum-fibers of steel with special properties 13 p1816 A83-30684

Effect of the structure on the strength of the fibrous composite aluminum-carbon strip 13 p1816 A83-31217

Hydrogen in pure aluminum solidified unidirectionally 13 p1824 A83-31601

Microstructure of aluminium during creep at intermediate temperatures. III - The rate controlling process 13 p1825 A83-31650

Dissolved metal species mechanism for initiation of crevice corrosion of aluminum. I - Experimental investigations in chloride solutions. II - Mathematical model 14 p1993 A83-32628

Variable anodic thermal control coating on aluminum [AIAA PAPER 83-1492] 14 p1985 A83-32737

Low cycle fatigue of aluminum at elevated temperatures 15 p2138 A83-34133

Doubly ionized aluminium - A diagnostic of cooling gas in the galactic corona 15 p2266 A83-34600

Laser annealing of submicrometer NMOS test structures and devices 15 p2152 A83-34696

The cohesive and adhesive strength of ice --- adhering to stainless steel, titanium, and anodized aluminum engineering structures 15 p2130 A83-35069

Transport of mineral aerosol from Asia over the North Pacific Ocean 16 p2380 A83-36148

Fatigue limits of Cu and Al up to 10 to the 10th loading cycles 16 p2332 A83-36189

The effect of microstructure on the fatigue crack growth behavior near threshold in Cu and Al 16 p2333 A83-36198

Variations in ductility produced by strain rate changes in tensile testing 16 p2334 A83-36568

Initial strain field and fatigue crack initiation mechanics [ASME PAPER 83-APM-20] 17 p2519 A83-37385

Long-range surface-plasmon modes in silver and aluminum films 17 p2576 A83-37945

Fracture strains in biaxially loaded 2024 aluminum tubes 17 p2491 A83-38527

Replacement textures in CAI and implications regarding planetary metamorphism 17 p2623 A83-38851

Laser-controlled chemical etching of aluminum 18 p2693 A83-40055

Hygrothermal effects on CFRP bonded systems 18 p2652 A83-40157

Interfacial interactions in aluminium matrix stainless steel fibre composites 18 p2667 A83-40250

Influence of the interface on transverse strength, creep behaviour, and impact behaviour of boron and silicon carbide fibre reinforced aluminum 18 p2659 A83-40253

Mechanical properties of SiC fiber reinforced Al composites 18 p2659 A83-40259

Fabrication of carbon fiber reinforced aluminum composites by roll diffusion bonding method 18 p2659 A83-40262

Squeeze casting of silicon carbide fiber reinforced aluminum 18 p2659 A83-40263

Fabricaton of SiC fiber-aluminum composite materials 18 p2659 A83-40264

Initial oxidation of metals and alloys 20 p2948 A83-42228

Novel titanium-aluminum joints for cryogenic cold finger structures 20 p2960 A83-43229

Temperature dependence of the absorptivity of aluminum targets at the 10.6 microns wavelength 20 p2957 A83-43785

Special features of the ultrasonic inspection of purity of aluminum A9999 22 p3269 A83-46329

The principles governing the superplastic behavior of aluminum in torsion 24 p3560 A83-49039

Steady state and transient creep of Al at 400 K - An analysis in terms of recovery controlled by thermally activated glide 24 p3566 A83-49600

Work-hardening rates during the high temperature creep of aluminum determined from the instantaneous strain on sudden stress changes 24 p3567 A83-49875

ALUMINUM ALLOYS

Rapid solidification --- for alloy design and process control 01 p0023 A83-10213

Protection of Fe-Cr-Al alloys in sulfidizing environments by means of an alpha-Al2O3 scale 01 p0024 A83-10245

Application of X-ray energy dispersive analyses /EDAX/ to determine the penetration depth of one oxide phase /NiAl2O4/ in a two-phase oxide internal oxidation zone /NiAl2O4+Al2O3/ of a binary alloy /Ni-Al/ 01 p0024 A83-10248

Correlation between fracture toughness Kc for a plane stress system and mechanical properties 01 p0024 A83-10298

Determining the temperature to which sheets of alloy D16T have been heated from the structure and properties 01 p0025 A83-10445

Steady-state ablation of aluminium alloys by a CO2 laser 01 p0054 A83-10701

The Avdel MBC aerospace blind riveting system 01 p0056 A83-10870

Microstructural study of a high-strength stress-corrosion resistant 7075 aluminum alloy 02 p0153 A83-11663

Structural inhomogeneties of AlSi alloys rapidly quenched from the melt 02 p0153 A83-11665

Comments on 'The influence of Mg contents on the formation and reversion of Guinier-Preston zones in Al-4.5 at percent Zn-xMg alloys' 02 p0154 A83-11671

Threshold stresses in materials containing dispersed particles 02 p0149 A83-11864

The effect of grain structure on the fracture behavior and tensile properties of an Al-Li-Cu alloy 02 p0154 A83-11865

Water-displacing organic corrosion inhibitors - Their effect on the fatigue characteristics of aluminum alloy bolted joints 02 p0148 A83-12014

High temperature thermodynamic study of the molybdenum-rich regions of the Mo-Al system 02 p0155 A83-12058

A study of the structure and properties of aluminum-magnesium alloys with high magnesium contents after various deformation and heat treatment schedules 02 p0155 A83-12203

Critical grain size corresponding to the superplastic transition 02 p0156 A83-12207

Research of hydrogen-induced cracking and stress corrosion cracking in an aluminum alloy 02 p0156 A83-12222

Fracture diagrams for the case of monotonic loading at elevated temperatures --- in aluminum alloys 02 p0156 A83-12326

The structure of rapidly solidified Al-Fe-Cr alloys 02 p0157 A83-12412

The early stage of Ni3Al layer growth in NiAl/Ni diffusion couples 02 p0157 A83-12413

The significance of the dimensionless constant in the rate equation for superplastic flow 02 p0157 A83-12416

Rapid-solidification phenomena 02 p0158 A83-12929

Changes in the volume of Al-Zn compacts during liquid-phase sintering 02 p0159 A83-13027

A nuclear gamma resonance study of Ti3Al containing Fe-57 impurity 02 p0159 A83-13039

New high-strength aluminum alloy V950ch 03 p0296 A83-13251

Softening schedules for aging pressed semifinished products made from high-strength aluminum alloy V95pch 03 p0296 A83-13252

Effect of zirconium additives on the properties of plates of type V95pch alloy 03 p0296 A83-13253

Structure and fracture character of V95 alloy sheets in relation to impurity content and aging conditions 03 p0297 A83-13254

Effect of composition and structure on the properties of wrought aluminum alloys of the D16 type 03 p0297 A83-13255

Effect of particles of the insoluble phase Al9FeNi on the kinetics of fatigue crack propagation in alloy AK4-1 03 p0297 A83-13256

Increasing the corrosion resistance of alloy AK8 03 p0297 A83-13257

Effect of silicon on the structure and properties of heat resistant aluminum alloy D21 03 p0297 A83-13258

Effect of rapid cooling in crystallization on the structure and properties of sintered alloy 1201 03 p0297 A83-13259

Powdered aluminum alloys 03 p0297 A83-13260

Structure and properties of large slabs of alloy 1201 03 p0297 A83-13261

Heat resistant and corrosion resistant aluminum alloys hardened with oxide phase 03 p0297 A83-13262

Recovery treatment of Al27-1 alloy 03 p0297 A83-13264

Aluminum-lead antifriction alloys produced under conditions of compensation of gravitational segregation by electromagnetic forces 03 p0298 A83-13268

Variations of various fracture parameters during the process of subcritical crack growth 03 p0298 A83-13341

Metastable phases in vapour-deposited Al-Ru alloys 03 p0298 A83-13680

Low-cycle fatigue damage accumulation of aluminum alloys 03 p0299 A83-13903

Fatigue fracture properties of a Mg-Al-Zn alloy 03 p0300 A83-14600

The fracture of constituent particles during fatigue 03 p0301 A83-14705

Fracture toughness of high-strength laminate sheets containing plastic layers of high elastic modulus 03 p0293 A83-14728

The J contour integral in the plastic region 03 p0343 A83-14729

Intergranular corrosion mechanism in Al-Mn alloys 04 p0457 A83-14963

Creep response of strip-cast Al-1wt.%Mn-1wt.%Mg alloy to thermomechanical treatment 04 p0457 A83-14996

The evolution of a defect structure and its relation to the deformation parameters in Ti-Al-Nb-Zr alloy at 4.2 K 04 p0457 A83-14997

Role of the strain history on the flow law for high temperature creep 04 p0457 A83-14998

Quantitative acoustic emission for source characterization in metals 04 p0458 A83-15195

Acoustic emission during plastic deformation and crack growth in 2024 and 2124 aluminium alloys 04 p0458 A83-15196

Crack closure effects in ultrasonic NDE for real part-through fatigue cracks in Al-alloy 04 p0458 A83-15206

An ultrasonic investigation of precipitation hardening phenomena in 2219 aluminum alloy 04 p0458 A83-15216

Nondestructive evaluation of materials by optical correlation 04 p0492 A83-15219

On the properties of the superplastic aluminium-calcium alloy as material for solar collectors 04 p0505 A83-15496

Oxide film rupture, reanodization, and stress corrosion cracking in aluminum 04 p0460 A83-15866

The influence of the method of supersaturation on the course of precipitation hardening of chill castings made of aluminum silicon alloys 04 p0460 A83-15991

Nature of subsurface damage in an aluminium-22 wt% silicon during dry sliding wear 04 p0460 A83-15995

Effect of defect structure upon the mechanical behavior of beta-LiAl through dislocation damping and hardness studies 04 p0460 A83-16002

The influence of grain structure on the ductility of the Al-Cu-Li-Mn-Cd alloy 2020 04 p0460 A83-16004

Influence of corrosion deposits on near-threshold fatigue crack growth behavior in 2XXX and 7XXX series aluminum alloys 04 p0460 A83-16005

Thermal expansion of the directionally solidified Ni3Al-Ni3Nb eutectic alloy and its constituent phases 04 p0461 A83-16006

Microstructural influence on fatigue crack growth near threshold in 7075 Al alloy 04 p0461 A83-16251

The effect of aluminum oxide particles and precipitate type on near-threshold fatigue crack propagation rate in P/M 7XXX aluminum alloys 04 p0461 A83-16255

The role of transfer and back transfer of metals in the wear of binary Al-Si alloys 04 p0462 A83-16347

Effect of technological and metallurgical factors on the properties of welded joints in 01205 alloy 05 p0613 A83-16885

A study of the structural precipitation kinetics in the alloys Al-8 percent Zn-1 percent Mg and Al-15 percent Zn-2 percent Mg 05 p0613 A83-16948

Influence of tensile pre-strain on fatigue crack closure in aluminum alloy 2017-T3 05 p0614 A83-17095

Some properties of foamed material-aluminum composites 05 p0611 A83-17108

Working property in rolling a Zn-Al alloy containing helical tungsten fibers 05 p0611 A83-17109

Effect ion implantation on fretting fatigue in Ti-6Al-4V alloy 05 p0614 A83-17257

Effect of residual stresses on fatigue crack growth rates in weldments of aluminum alloy 5456 plate 05 p0615 A83-17262

Characterization of fracture surface, pores and inclusions in sintered Ti-6Al-4V 05 p0615 A83-17548

Influence of structural parameters on oxidation of austenitic Fe-Ni-Cr-Al alloys 05 p0615 A83-17562

Bidirectional torsion and dynamic recovery in aluminium-zinc-silicon alloy 05 p0616 A83-17568

The growth of small fatigue cracks in 7075-T6 aluminum 05 p0616 A83-17674

Anti-phase domain boundary tubes in Ni3Al --- crystal defect structures 05 p0616 A83-17792

A study of cumulative fatigue damage in aluminum alloy 2011-T3 05 p0616 A83-17864

Internal stress measurements during the saturation fatigue of polycrystalline aluminum 05 p0616 A83-17865

The effect of environment on fatigue crack growth behavior of 2021 aluminum alloy 05 p0616 A83-17894

An evaluation of overload models on the retardation behavior in a Ti-6Al-4V alloy 05 p0616 A83-17896

Decomposition processes in an Al-5 percent Zn-1 percent Mg alloy. III - Reversion of GP-zones 05 p0617 A83-17953

Mechanisms of the microbial corrosion of aluminum alloys 06 p0726 A83-18550

New metallurgic processes based on the rapid solidification and diffusion of metals 06 p0729 A83-18742

Metastable equilibriums during the solidification of alloys 06 p0729 A83-18743

A unified description of micro and macroscopic fatigue crack behaviour 06 p0776 A83-18938

Gel electrode imaging of fatigue cracks in aluminum alloys 06 p0730 A83-18941

Production of high quality parts by hot pressing metal particulates 06 p0769 A83-19081

Wear resistance of dynamically compacted aluminium-steel and Al-steel-Pb alloy mixtures 06 p0731 A83-19089

Powder metallurgy processing of high strength commercial aluminum alloys 06 p0731 A83-19090

The aging response of a high-strength P/M aluminum alloy 06 p0731 A83-19091

Processing effects on microstructure and elevated temperature properties of an ODS Fe-Al-Mo P/M alloy 06 p0732 A83-19099

A study of the effect of cyclic block loading on the deformation characteristics and strength of structural materials under plane stressed state. I - Resistance to elastic-plastic deformation 06 p0733 A83-19306

The relationship between the time to failure and the minimum creep rate during long-term loading under plane stressed state 06 p0733 A83-19309

A study of the short-term strength of boron-composite-reinforced tubular specimens at room and cryogenic temperatures 06 p0725 A83-19310

The effect of superplastic deformation on subsequent service properties of fine grained 7475 Al 07 p0883 A83-19672

Morphological studies on the Li-Al electrode in fused salt electrolytes --- in Li-Al/FeS cells 07 p0879 A83-19877

The self-propagating high-temperature synthesis of aluminides. I - A thermodynamic analysis 07 p0883 A83-19964

The properties of rolled powder-metallurgy-alloy products 07 p0883 A83-19966

Reactions and diffusion between an Al film and a Ti substrate 07 p0874 A83-20252

The importance of surface layer on fatigue behavior of a Ti-6Al-4V-alloy 07 p0884 A83-20254

The modification of Si phase in Al-Si eutectic alloys - Effect of element addition on microstructures of Al-Si and Al-Si-Ge eutectic alloys 07 p0885 A83-20275

Precipitation of T1 phase in /alpha + T1/ type Al-4.2%Cu-1.3%Li alloy 07 p0885 A83-20294

Rapidly solidified structure and grain refinement of aluminum containing titanium 07 p0885 A83-20295

Evaluation of titanium prebond treatments by stress durability testing 07 p0886 A83-20455

Electrical discharge machining of aluminum honeycomb core 07 p0940 A83-20500

Laser beam welding of aluminum alloy 5456 07 p0940 A83-20525

The effect of absorbed hydrogen on torsional fatigue of 2024-T351 aluminum alloy 07 p0887 A83-20633

Microstructure of fiber and particulate SiC in 6061 Al composites 07 p0877 A83-20634

The thermodynamic principles of calorizing 07 p0887 A83-20679

The fatigue resistance of aluminum alloy 1201 under programmed and random high-frequency loading 07 p0890 A83-20906

A study of the structure of liquid aluminum-silicon alloys. I - Hypoeutectic and eutectic melts 07 p0890 A83-20916

Characteristics of concentration changes occurring in the solid solution of deformed Ni-7.1 wt% Al alloy during rapid heating 07 p0890 A83-20917

An electron microscopy study of the structure of V-Al alloys 07 p0890 A83-20919

Nuclear gamma resonance of Fe-57 impurity atoms in Ti3Al 07 p0890 A83-20920

Control of the mechanical properties of alloy D16 sheets by the eddy-current method taking the kinetics of aging into account 07 p0891 A83-21419

The effect of soaking times on the mechanical properties of rapidly solidified aluminium alloys 07 p0896 A83-21571

Microstructures and strengthening of aluminium alloys 07 p0896 A83-21605

Microstructures in cold-rolled polycrystalline aluminium 07 p0897 A83-21608

Dynamics of microstructural changes in a superplastic aluminum alloy 07 p0897 A83-21611

The effects of very high cumulative deformation on structure and mechanical properties of aluminium 07 p0897 A83-21615

The fracture toughness of high strength engineering alloys containing short cracks 08 p1058 A83-21655

Anisotropy of bulk-formability in 2024-T351 aluminum plates and bars 08 p1058 A83-21664

Mechanisms and criteria for cleavage 08 p1058 A83-21666

Slip plane facets in fatigued aluminum alloys 08 p1058 A83-21667

The influence of dispersoids on fatigue crack propagation in Al-Mg-Si alloys 08 p1058 A83-21669

Fatigue crack initiation and propagation in Ti-6Al and Ti-6Al-4V 08 p1058 A83-21671

Experimental determination of high loading rate effects on fracture toughness of aluminum alloys 08 p1058 A83-21673

Application of the equivalent initial damage method to fretting fatigue 08 p1059 A83-21691

The effect of overloads upon fatigue crack tip opening displacement and crack tip opening/closing loads in aluminum alloys 08 p1060 A83-21709

Fatigue crack propagation response in extruded and cast aluminum alloys 08 p1060 A83-21710

The metallography of fatigue in the high strength aluminum alloy 7010 08 p1060 A83-21711

R ratio influence and overload effects on fatigue crack mechanisms 08 p1060 A83-21714

Crack growth mechanism maps 08 p1117 A83-21731

Experimental procedure for fast measurement of threshold in fatigue crack propagation 08 p1062 A83-21734

The fracture characteristics of Al and Al-5% Mg at elevated temperatures 08 p1062 A83-21747

The effect of overloading on fatigue crack propagation in two aluminum alloys and an austenitic stainless steel 08 p1063 A83-21754

Influence of specimen geometry on delayed retardation phenomena of fatigue crack growth in HT80 steel and A5083 aluminum alloy 08 p1063 A83-21755

Mode II fatigue crack growth in aluminum alloys and mild steel 08 p1063 A83-21759

An improved methodology for predicting random spectrum load interaction effects on fatigue crack growth 08 p1065 A83-21802

On the Ti-Al phase diagram 08 p1065 A83-22013

Acoustic emission during the plastic deformation of aluminum alloys 2024 and 2124 08 p1065 A83-22014

The effect of dispersoids on the ductile fracture toughness of Al-Mg-Si alloys 08 p1065 A83-22015

Influence of thermomechanical processing on elevated temperature slow plastic flow properties of B2 aluminide Fe-39.8at.% Al 08 p1065 A83-22017

Fatigue behavior of solution-treated and quenched Ti-6Al-4V 09 p1228 A83-23344

Fatigue considerations in use of aluminum alloys 09 p1228 A83-23425

A study of the effect of stresses below the fatigue limit on the life of D16T alloy under programmed loading 09 p1228 A83-23501

Characteristics of the spalling fracture of aluminum and aluminum alloys D16 and AMg6 in the temperature range -196 to 600 C 09 p1229 A83-23510

Mechanical properties of a high-strength aluminum alloy under impact loading 09 p1229 A83-23511

Enthalpies of formation of liquid aluminum-silicon alloys 09 p1229 A83-23518

A metastable phase diagram for Al-Sc in the aluminum-rich region 09 p1229 A83-23525

Sealants - Uses in composite structures 09 p1236 A83-23615

Evaluation of the P2 and PAA treatments --- sulfuric acid-ferric sulfate etching and phosphoric acid anodizing 09 p1238 A83-23627

Effects of GTA dressing on the fatigue properties of aluminum alloy welded, butt jointed and fillet welded plates 09 p1274 A83-23650

The influence of metallurgical factors on the fracture toughness of 7010 and 7050 aluminum alloys 09 p1230 A83-23677

The effect of strain and concurrent grain growth on the superplastic behaviour of the Ti-6Al-4V alloy 09 p1230 A83-23871

Stable crack growth during fracture toughness testing in Ti-6Al-4V alloy 09 p1230 A83-23916

Monotectic solidification structure of Al-In alloys 09 p1231 A83-23919

The effect of instantaneous strain on creep measurements at apparent constant structure 09 p1231 A83-24057

Dislocation dynamics and viscosity effects associated with a plane stress wave in metals 09 p1233 A83-24208

The effect of alloying on the physical properties, electron structure, and phase stability of titanium alloys 09 p1234 A83-24378

The effect of hydrogen plasticization in alloys of titanium with aluminum 09 p1235 A83-24397

The deformation resistance of pressed strips of powder-metallurgy alloys 09 p1236 A83-25063

Fracture properties of aluminum alloys 10 p1393 A83-25322

Cavity growth and failure in superplastic alloys 10 p1393 A83-25402

Ni-Al and Ni-Ta phase diagrams 10 p1393 A83-25403

Study of the constitutive creep laws using biaxial relaxation tests 10 p1393 A83-25416

Serrated flow in a commercial AA2036 aluminium alloy 10 p1394 A83-25420

Fatigue crack evolution in overaged Ni-14.4at.% alloy with coherent precipitates 10 p1394 A83-25423

Effect of grain flow on creep properties of heat-resistant aluminium-alloy forgings 10 p1394 A83-25473

Characterization of copper in phosphoric-acid-anodized 2024-T3 aluminum by Auger electron spectroscopy and Rutherford backscattering 10 p1395 A83-25547

Methods of producing dispersion-strengthened cast alloys based on aluminum 10 p1395 A83-25629

Comparative evaluation of the effect of titanium and aluminum on properties of creep-resisting metal deposited by the argon-arc method 10 p1397 A83-26223

Physical metallurgy of recycling wrought aluminum alloys 10 p1398 A83-26276

The effect of ITMT's and P/N processing on the microstructure and mechanical properties of the X7091 alloy --- Intermediate Thermal Mechanical Treatments 10 p1398 A83-26281

Orientation relationships between bcc Mo and fcc gamma in a Ni-Al-Mo-W superalloy 10 p1398 A83-26284

The crystallographic aspects of the decomposition of supersaturated solid solutions based on aluminum 10 p1399 A83-26792

Nucleation during solidification of aluminum-titanium alloys 10 p1399 A83-26890

Incipient fracture in shock-loaded lamellar metal alloy composites with and without microstructural defects 11 p1547 A83-27436

A dilatometric study of the growth of Ti-Al compacts during liquid-phase sintering 11 p1547 A83-27922

Overload induced crack growth rate attenuation behavior in aluminum alloys 11 p1548 A83-28223

Superplasticity in Al-Li based alloys 11 p1548 A83-28224

Growth of thin ribbons of aluminum-base regular eutectic compositions and a study of their microstructures 11 p1548 A83-28367

The effect of anisotropy, thickness, and operating time on the crack growth in pressed and rolled products of D16chT and V95pchT1 alloys 11 p1549 A83-28478

The use of linear fracture mechanics for processing the results of residual strength tests 11 p1597 A83-28479

A diagram for the discrete growth of a fatigue crack under self-similarity conditions 11 p1597 A83-28480

The shielding of excess phases during fracture under plane strain conditions and its effect on the fracture toughness 11 p1549 A83-28481

The effect of block cyclic loading on the deformability and strength of structural materials under conditions of plane stressed state. II - The limiting states /yield and strength/ 11 p1549 A83-28504

The effect of prior elastic-plastic cyclic deformation on the mechanical characteristics of 1201 alloy at cryogenic temperatures 11 p1550 A83-28517

The strengthening of steel-aluminum composites in the transverse direction 11 p1544 A83-28524

Development of preferential intergranular oxides in nickel-aluminum alloys at high temperatures 11 p1550 A83-28668

The morphological and structural development of internal oxides in nickel-aluminum alloys at high temperatures 11 p1550 A83-28669

A model for the behavior of the titanium alloy Ti-6 percent Al-4 percent V in the hot forging regime 11 p1551 A83-28808

Effect of some casting parameters on surface segregation in the case of continuous casting involving aluminum 12 p1713 A83-29368

Subsurface plastic deformation in machining 6Al-2Sn-4Zr-2Mo titanium alloy 12 p1713 A83-29400

Stress fluctuations accompanying strain rate change in an aluminum alloy 2017 12 p1714 A83-29414

Tensile properties of directionally solidified Ni-Al-Ti-(Ta) gamma/gamma prime eutectic alloys 12 p1714 A83-29415

On the origin of the first peak of acoustic emission in 7075 aluminum alloy 12 p1714 A83-29507

The effect of dispersoids on the micromechanisms of crack extension in Al-Mg-Si alloys 12 p1714 A83-29509

Laser welding of aluminum and aluminum alloys 12 p1733 A83-29524

A recommended procedure for determining the strain rate sensitivity in superplasticity --- of metal alloys 12 p1714 A83-29721

Ion implantation effect on fatigue crack initiation in Ti-24V 12 p1714 A83-29724

A brittle to ductile transition in NiAl of a critical grain size 12 p1714 A83-29726

A crack-tip strain model for the growth of small fatigue cracks --- in engineering alloys 12 p1715 A83-29727

Microsegregation and extended solid solutions after rapid solidification of aluminum alloys 12 p1715 A83-29728

Properties and application benefits of low density aluminum alloys [AIAA 83-0981] 12 p1715 A83-29788

The relaxation of residual stresses during fatigue 12 p1715 A83-29907

Metallographic features of the subdendritic structure of aluminum alloy ingots 13 p1819 A83-30065

The effect of the chemical composition on the high-cycle and low-cycle fatigue behavior of D16 and V95 alloy sheets under pulsating tension 13 p1819 A83-30068

Experimental study of the fatigue fracture of the aluminum alloy AU4G1-T3 and the austenitic stainless steel Type 316 --- French thesis 13 p1819 A83-30144

Optimum design of multilayer panels on the basis of a vector of quality criteria 13 p1866 A83-30309

Effects of cooling rate and modifier concentration on modification of Al-Si eutectic alloys 13 p1820 A83-30324

Stress corrosion and hydrogen induced cracking behaviour in an Al alloy 13 p1820 A83-30325

Ion-induced amorphous and crystalline phase formation in Al/Ni, Al/Pd, and Al/Pt thin films 13 p1928 A83-30338

Light alloys containing lithium --- Russian book 13 p1820 A83-30424

The effect of scandium on the high-temperature ductility of the binary alloy Al-6.5 pct Mg 13 p1821 A83-30695

The effect of scandium on the mechanical properties of Al-6.5 pct Mg alloy 13 p1821 A83-30696

A study of coalescence processes in Al - 2.8 pct Li alloy 13 p1821 A83-30739

Use of oblique wide-beam probe for inspection of strips with normal waves 13 p1860 A83-30835

Observation of voids and cracks on ductile fracture process in tensile test of 5083 aluminum alloy plate 13 p1822 A83-30842

Localized corrosion of aluminum vacuum brazing T-joints 13 p1822 A83-30844

Spall studies of differently treated 2024 Al specimens. 13 p1824 A83-31376

The effect of environment on the growth of small fatigue cracks 13 p1824 A83-31539

Application of the graining process for the fabrication of chopped carbon fiber-aluminum composite 13 p1816 A83-31602

Aging embrittlement behavior of Al-Zn-Mg alloy after stress-corrosion treatment 13 p1825 A83-31603

Interaction between SiC fibers and aluminum alloys 13 p1816 A83-31604

The role of the environment on the corrosion cracking of Al-Mg and Al-Li-Mg alloys 14 p1992 A83-32072

Processing of fatigue test results for corrosion-affected structural materials 14 p1992 A83-32074

The residual strength of prefabricated structures made of pressed panels of D16chT alloy and its modifications 14 p2029 A83-32075

Engineering property comparisons of 7050-T73651, 7010-T7651 and 7010-T73651 aluminum alloy plate 14 p1992 A83-32340

On the cyclic behavior of cast and extruded aluminum alloys. I - Fatigue crack propagation 14 p1992 A83-32342

On the cyclic behavior of cast and extruded aluminum alloys. B - Fractography 14 p1992 A83-32343

Subsurface damage during dry sliding wear of Al-Al3Ni eutectic alloy 14 p1993 A83-32623

Morphology of ductile metals eroded by a jet of spherical particles impinging at normal incidence 14 p1993 A83-32624

Chemistry and distribution of phases produced by solid state SiC/NiCrAl reaction 14 p1985 A83-32676

The effect of loading mode on the stress-corrosion cracking of aluminum alloy 5083 14 p1994 A83-32680

Metallography of fatigue crack initiation in an overaged high-strength aluminum alloy 14 p1994 A83-32681

Thermal coupling on aluminum alloy surfaces in vacuum at 10.6 micrometer --- pulsed CO2 laser-duraluminum target interaction [AIAA PAPER 83-1441] 14 p2024 A83-32712

Aluminum-lithium alloys 14 p1995 A83-32876

Aluminum-lithium dispersion alloys 14 p1995 A83-32877

Overview of D.C. casting --- Direct-Chill solid-liquid interface shape prediction using heat transfer models 14 p1995 A83-32878

Casting problems specific to aluminum-lithium alloys 14 p2028 A83-32879

Al-Li-X alloys - An overview 14 p1995 A83-32880

A perspective on the development of aluminum-lithium alloys 14 p1996 A83-32881

Microstructural characteristics of Al-Li alloys 14 p1996 A83-32882

Relationship between microstructure and mechanical properties of aluminum-lithium-magnesium alloys 14 p1996 A83-32883

Alloying additions and property modification in aluminum-lithium - X systems 14 p1996 A83-32884

Microstructure and deformation of rapidly solidified Al-3Li alloys containing incoherent dispersoids 14 p1996 A83-32885

Toughness and ductility of aluminum-lithium alloys prepared by powder metallurgy and ingot metallurgy 14 p1996 A83-32886

The design and mechanical properties of rapidly solidified Al-Li-X alloys 14 p1996 A83-32887

A comparison of microstructure and tensile properties of P/M and I/M Al-Li-X alloys --- Powder Metallurgy and Ingot Metallurgy 14 p1996 A83-32888

The effect of microstructure and moisture on the low cycle fatigue and fatigue crack propagation of two Al-Li-X alloys 14 p1996 A83-32889

Microstructure, deformation, and corrosion-fatigue behavior of a rapidly solidified Al-Li-Cu-Mn alloy 14 p1996 A83-32890

High temperature oxidation studies of Al-3wt pctLi, Al-4.2wt pctMg and Al-3wt pctLi-2wt pctMg alloys 14 p1996 A83-32891

The influence of microstructure on the corrosion of Al-Li, Al-Li-Mn, Al-Li-Mg and Al-Li-Cu alloys in 3.5 percent NaCl solution 14 p1997 A83-32892

HVEM in situ deformation of Al-Li-X alloys --- High Voltage Electron Microscope 14 p1997 A83-32948

Effect of processing on fatigue life of Ti-6Al-4Al-4V castings 15 p2135 A83-33641

Some aspects of welding on the structure and properties of titanium alloys 15 p2135 A83-33645

Structural members made of high-strength cast aluminum and their properties --- and reduction of aircraft production costs 15 p2136 A83-33954

High-strength aluminum high-quality casting alloy in aeronautics and astronautics 15 p2136 A83-33955

Development of technical cracks on Al-2024-T3 in the case of one-stage and non-one-stage vibratory stresses 15 p2136 A83-33957

Studies of the microstructure and mechanical properties of Al-10Mn and Al-10Mn-2.5Si made by powder metallurgy techniques 15 p2136 A83-33958

Comparison of microstructure and mechanical properties of Al-Li-X alloys made by conventional and by powder-metallurgy procedures 15 p2136 A83-33959

A study of alloying element redistribution during the diffusion annealing of titanium alloys 15 p2137 A83-34016

Micromechanics of crack propagation in Ti-6Al and Ti-6Al-4V 15 p2139 A83-34480

Temperature dependence of creep crack growth in aluminum alloy RR58 15 p2139 A83-34487

Prediction of constant amplitude fatigue lives of precracked specimens from accelerated fatigue data 15 p2140 A83-34743

High temperature internal oxidation behaviour of dilute Ni-Al alloys 15 p2140 A83-35068

Experimental study on the effects of specimen sizes on erosion 15 p2141 A83-35245

A study of the structure of liquid aluminum-silicon alloys. II - Hypereutectic melts 15 p2141 A83-35308

On the serration in Al-Mg alloys at elevated temperatures 16 p2329 A83-35604

Fatigue crack initiation and microcrack propagation in X7091 type aluminum P/M alloys 16 p2329 A83-35691

Wear debris due to mode II opening of mode I fatigue cracks in an aluminum alloy 16 p2330 A83-35693

An experimental study of the failure of elastoplastic cylindrical shells under combined loading 16 p2365 A83-35929

Heat evolution investigated by a liquid crystal film technique during fracture in metals 16 p2330 A83-35978

Fatigue crack growth rates for very short cracks developing at fastener holes in 7075 and 7010 aluminum alloys 16 p2330 A83-35982

Embrittlement of P/M X7091 and I/M 7175 aluminum alloys by mercury solutions 16 p2330 A83-35983

Microstructure of in-situ composites 16 p2324 A83-35999

Determination of prefracture damage and failure prediction in corrosion-fatigued Al-2024-T4 by X-ray diffraction methods 16 p2331 A83-36163

Effects of high frequency loading on materials 16 p2331 A83-36181

The prediction of fatigue life using ultrasound testing 16 p2367 A83-36184

Near-threshold fatigue crack growth determination at ultrasonic frequencies 16 p2333 A83-36197

The structure and properties of Al-Zn-Mg alloys --- Russian book 16 p2333 A83-36435

On statistical moments of fatigue crack propagation 16 p2368 A83-36501

Crack closure studies under constant amplitude loading 16 p2333 A83-36508

Origin of acoustic emission in aged Al-Zn-Mg alloys. I - The base ternary alloy 16 p2334 A83-36566

Origin of acoustic emission in Al-Zn-Mg alloys. II Copper-containing quaternary alloys 16 p2334 A83-36567

Influence of stress cycling on creep behaviour of an Al-Mg alloy under strain ageing conditions 16 p2334 A83-36727

The structure and properties of powder metallurgy aluminum alloys with transition metals 16 p2334 A83-36885

The effect of the stress pattern on the ductility of aluminum-alloy powder compacts 16 p2334 A83-36886

Plastic deformation of sheets and bands of aluminum alloys during continuous hardening 16 p2334 A83-36887

The effectiveness of the artificial aging of low-alloy duralumin 16 p2335 A83-36889

A study of the hardening of cast aluminum containing refractory tungsten compounds 16 p2335 A83-36893

A study of the inhomogeneity of deformation in AD1-M aluminum alloy 16 p2335 A83-36894

The principles governing changes in the hot brittleness of aluminum alloys of the system Al-Cu-Mg 16 p2335 A83-36895

Stress corrosion cracking 17 p2486 A83-37172

Anodic films on aluminum 17 p2486 A83-37173

A study relating slip steps and substructure produced during creep of an Al-Zn alloy 17 p2486 A83-37298

High-strength powder metallurgy aluminum alloys; Proceedings of the Symposium, Dallas, TX, February 17, 18, 1982 17 p2487 A83-37832

Fatigue crack initiation and microcrack propagation in X7091 type aluminum P/M alloys 17 p2487 A83-37834

Fatigue of high-strength powder metallurgy aluminum alloys 17 p2487 A83-37835

Investigation of the fatigue and crack propagation properties of X7091-T7E69 extrusion 17 p2487 A83-37836

Effects of microstructure and aging treatment on the fatigue crack growth behavior of high strength P/M aluminum alloy X7091 17 p2487 A83-37837

Effect of defects in aluminum P/M 17 p2487 A83-37838

The effect of recrystallization on the microstructure and fatigue properties of a 2XXX-type P/M alloy 17 p2487 A83-37839

Fatigue crack tip plasticity and crack growth mechanics in powder metallurgy and wrought aluminum alloys 17 p2488 A83-37840

Stress-corrosion cracking and hydrogen embrittlement in P/M X7091 and I/M 7075 17 p2488 A83-37841

Consolidation of metalworking preforms of X7091 (CT-91) aluminum powder 17 p2488 A83-37842

Elevated temperature aluminum alloys for aerospace 17 p2488 A83-37843

Microstructure/strength/fatigue crack growth relations in high temperature P/M aluminum alloys 17 p2488 A83-37844

Influence of powder morphology on the mechanical properties of rapidly solidified aluminum alloys 17 p2488 A83-37845

The effect of solidification microstructure on the strength, ductility and toughness of dispersion-hardened Al P/M alloys 17 p2488 A83-37846

Development of duplex Al-Zn-Mg/Al-Mn high modulus P/M aluminum alloys 17 p2488 A83-37847

The mechanical behavior of mechanically alloyed Al alloys 17 p2488 A83-37848

The effect of heat treatment on the mechanical properties of a mechanically alloyed 2000 series aluminum alloy 17 p2488 A83-37849

Heat treatment, microstructure and mechanical property correlations in Al-Li-Cu and Al-Li-Mg PM alloys 17 p2489 A83-37850

Development of Al-Li-X alloys using rapidly solidified powders 17 p2489 A83-37851

A high strength Al Li-Mn alloy with high modulus 17 p2489 A83-37852

New metal technologies in airframe construction 17 p2516 A83-37861

Advanced aluminum alloy for transport aircraft - Why and what are the benefits [SAE PAPER 821345] 17 p2489 A83-37954

Dynamic crack growth during pop-in fracture in 7075 aluminum alloy 17 p2489 A83-38123

Dislocation dynamics in aluminum and in aluminum-based alloys investigated by TEM and NMR techniques 17 p2490 A83-38379

The influence of microstructure on the scatter of the fatigue strength of the titanium alloy TiAl6V4 17 p2491 A83-38473

Creep behavior of aluminum-nickel alloys 17 p2491 A83-38475

The use of acoustic emission techniques to monitor fracture processes in high strength precipitation hardened aluminum alloys 17 p2491 A83-38525

Thermal and superconducting properties of an aluminum alloy for gravitational wave antennae below 1 K 17 p2492 A83-38864

Kinetic aspects of the solidification of aluminum-zinc alloys 18 p2665 A83-39048

The effects of load ratio on environmentally assisted fatigue crack growth 18 p2665 A83-39078

Prediction of the fatigue life of Duralumin specimens 18 p2665 A83-39499

Separate processing of the results of low-cycle and high-cycle fatigue tests --- of aluminum alloys 18 p2665 A83-39500

Fracture of an aluminum alloy at the prespalling stage 18 p2666 A83-39504

Determination of zones of crack distribution in flexible specimens --- of aluminum alloys 18 p2666 A83-39509

Stress analysis and strength of adhesive bonded joints under bending loads 18 p2703 A83-40156

Tensile and compressive deformation and fracture behavior of the Al-Al₃Ni eutectic composites at elevated temperatures 18 p2667 A83-40255

Mechanical behavior of silicon carbide whisker reinforced aluminum alloys 18 p2659 A83-40266

Mechanical behavior of aluminum alloys reinforced with B and SiC filaments, and properties of B-Al alloy composite as a high speed rotor cylinder 18 p2660 A83-40269

New method of preparation of dispersion-hardening materials Improvement of mechanical properties of as-cast eutectics followed by heavy deformation 18 p2667 A83-40280

Discontinuous gamma-prime coarsening in a Ni-Al-Mo base superalloy 18 p2669 A83-40628

Deuterium transport and trapping in aluminum alloys 18 p2669 A83-40629

Microstructure and mechanical properties of rapidly quenched L1(2) alloys in Ni-Al-X systems 18 p2669 A83-40632

Observations of grain boundary sliding during superplastic deformation 18 p2669 A83-40635

Oxide scale induced cleavage fracture in an ODS Fe-Cr-Al alloy 18 p2670 A83-40639

Flow localization accompanying the intergranular fracture of Ni₃Al 18 p2670 A83-40641

Fatigue crack growth rate of Ti-6Al-4V prealloyed powder compacts 18 p2670 A83-40642

Thermal stability in microstructure and rupture strength of directionally solidified Ni-Al-Ti eutectic alloys 19 p2819 A83-40775

The cyclic fracture toughness, K_{IIc}, of aluminum alloys 19 p2821 A83-40802

Some effects of material property data selection on crack propagation analyses 19 p2821 A83-41200

Studies in the ternary system Ti-Ta-Al and in the quaternary system Ti-Ta-Al-C 19 p2821 A83-41316

The formation of aligned spheres in miscibility gap systems --- during directional solidification of monotelectics 19 p2822 A83-42027

Fatigue crack micromechanisms in ingot and powder metallurgy 7XXX aluminum alloys in air and vacuum 19 p2822 A83-42028

The development and growth of protective alpha-Al₂O₃ scales on alloys 20 p2952 A83-42235

Growth and microstructures of oxide scales and subscales on Ni-Al gamma-solid solution alloys 20 p2952 A83-42236

An investigation of residual stress of oxide scale affected by the addition rare earth elements in Fe-Cr-Al alloys at 1200 C and 1350 C 20 p2952 A83-42237

Radiative properties of metals at cryogenic temperatures 20 p2974 A83-42694

Determination of stable crack growth resistance of ductile material using an RDCB specimen --- Reinforced Double Cantilever Beam 20 p2954 A83-42830

Aluminum-air battery development - Toward an electric car 20 p3057 A83-42976

Solidification of hypermonotectic Al-In alloys under microgravity conditions 20 p2942 A83-43304

A study of a cellular phase transformation in the ternary Ni-Al-Mo alloy system 20 p2954 A83-43341

Control of superplastic cavitation by hydrostatic pressure --- in aluminum alloys 20 p2954 A83-43342

Development of forming limits for superplastic formed fine grain 7475 Al 20 p2954 A83-43343

Structure and properties of rapidly solidified 7075 P/M aluminum alloy modified with nickel and zirconium 20 p2954 A83-43344

The effect of grain size on fatigue growth of short cracks 20 p2954 A83-43346

The effect of particle shape and size on erosion of aluminum alloy 1100 at 90 deg impact angles 20 p2955 A83-43408

The cyclic stress-strain response of polycrystalline Al-Zn-Mg alloy and commercial alloys based on this system 20 p2955 A83-43469

An electron-microscopy study of Al-Si alloys following rapid solidification 20 p2955 A83-43491

Modification of aluminum-silicon alloys in the light of new studies 20 p2955 A83-43493

The effect of structural transformations on the properties of the aluminum alloy VAD23 20 p2955 A83-43494

Matrix alloys for composite materials based on aluminum, magnesium, and titanium 20 p2948 A83-43498

High resolution lattice images of G.P. zones in an Al-3.97 wt pct Cu alloy --- Guinier-Preston 20 p2956 A83-43613

High resolution electron microscopy studies on the precipitation in an Al-4 percent Cu alloy 20 p2956 A83-43614

Evaluation of fracture toughness of thermomechanical-processed 7079 alloy using double torsion bend test 20 p2957 A83-43635

Tear test on 7075 and 7475 alloys by use of kahn type specimens 20 p2957 A83-43636

Mechanical properties of superplastic Al-Zn eutectoid-base alloys having ultrafine-grained structures 20 p2957 A83-43637

Bonded aluminum honeycomb - Aircraft flight surface primary structure application 21 p3091 A83-43972

Uniaxial and biaxial transient creep behavior of aluminum alloy 21 p3111 A83-44057

Decomposition processes in Al-Zn-Mg alloys 21 p3111 A83-44119

Relationship between grain boundary segregation and heat-treatment parameters in an aluminum alloy 21 p3111 A83-44338

Hydrogen embrittlement of 7075 series aluminum alloys 21 p3112 A83-44368

A critical study of the erosion of an aluminum alloy by solid spherical particles at normal impingement 21 p3112 A83-44375

Effect of iron content on the structure and properties of the AK7 alloy 21 p3112 A83-44477

Stainless steel reinforcing filaments 21 p3112 A83-44480

Structure and mechanical properties of Al-Si alloys obtained by crystallization under pressure 21 p3112 A83-44481

Mechanical properties of A8 and A85 aluminum at elevated temperatures 21 p3112 A83-44482

Effect of magnesium on the thermal stability of the polygonized structure of Al-Zn-Mg alloys 21 p3112 A83-44483

Fracture toughness tests on an aluminum alloy using a chevron notch bend specimen 21 p3113 A83-44899

Plane-stress fracture testing of finite sheets under biaxial loads 21 p3161 A83-45161

Crack-tip stresses as computed from strains determined by stereomaging 21 p3161 A83-45163

Recovery behavior of hydrogen charged 7075-T6 aluminum 22 p3268 A83-45625

Tensile and toughness properties of Arc-welded 5083 and 6082 aluminum alloys 22 p3268 A83-45728

A constant amplitude fatigue study of an aluminum powder metallurgy alloy 22 p3269 A83-46024

A TEM study of microstructural changes during retrogression and reaging in 7075 aluminum 22 p3269 A83-46397

Corrosion behavior of SiC/Al metal matrix composites 22 p3265 A83-46694

Influence of zero-gravity state on crystallization of metallic materials [IAF PAPER 83-160] 23 p3414 A83-47296

Unidirectional solidification behaviors at high cooling rates in Al-Fe-Mn ternary eutectic alloys 23 p3431 A83-47651

Precipitation in Ni-Mo-Al in-situ composite 23 p3431 A83-47848

Fatigue induced changes in surface residual stress --- in alloys 23 p3432 A83-47852

The effect of water vapor on fatigue crack tip mechanics in 7075-T651 aluminum alloy 23 p3432 A83-48147

On the transition from near-threshold to intermediate growth rates in fatigue 23 p3432 A83-48149

Chemical interactions in the system anodized aluminium-primer-adhesive 23 p3427 A83-48152

Ordered structures in Ti Al alloys in the composition range from AB to AB₃ [ONERA, TP NO. 1983-65] 23 p3432 A83-48186

Effect of zirconium content on properties of type D16 alloy plates 24 p3559 A83-48804

The sulfidation behavior of nickel chromium and nickel-aluminum binary alloys with and without yttrium 24 p3565 A83-49514

The effect of Hf additions on oxidation behaviour of Ni₃Al 24 p3565 A83-49515

Influence of nitrogen and carbon in the base steel on the transformation temperature of the alloy layer of an aluminized steel sheet for high temperature use 24 p3566 A83-49519

Influence of stress cycling on creep behaviour of an Al-Mg alloy under strain ageing conditions 24 p3566 A83-49598

Effect of Cu addition on intergranular corrosion of Al-5.5 percent Zn-2.5 percent Mg alloy 24 p3566 A83-49860

Stress corrosion cracking and intergranular corrosion of 2017 aluminum alloy 24 p3566 A83-49861

Effect of thermomechanical treatment on mechanical properties of 2024 aluminum alloy 24 p3566 A83-49862

Mixed-mode crack opening in fatigue 24 p3567 A83-49874

The microstructure of an aluminum alloy at early stages of spall damage 24 p3567 A83-49913

On the processes responsible for the degradation of the aluminium-lithium electrode used as anode material in lithium aprotic electrolyte batteries 24 p3600 A83-49933

Interface stability in vacuum infiltrated stainless steel and nichrome reinforced aluminum composites 24 p3554 A83-50072

ALUMINUM ANTIMONIDES

Investigation of the thermoelectromotive force in Al(x)(n1-x)Sb solid solutions 13 p1928 A83-30272

ALUMINUM ARSENIDES

Direct observation of picosecond light pulses from a pulse-current pumped semiconductor laser 01 p0054 A83-10615

Ion implantation of Si and Be in Al(0.48)In(0.52)As 20 p3052 A83-42593

ALUMINUM BORON COMPOSITES

Compliance of a unidirectionally reinforced inelastic material 02 p0150 A83-12353

Mechanisms of fatigue damage in boron/aluminum composites 03 p0292 A83-14557

Deformation characteristics of metal composites with brittle fibers during bending 03 p0293 A83-14817

The effect of liquid media on the strength of an aluminum-matrix composite 04 p0455 A83-15394

Room-temperature tensile strength of boron-aluminum composite as a function of annealing temperature and time 08 p1054 A83-22100

The effect of interface structure on the strength of fibrous composite materials 09 p1224 A83-23943

Room-temperature tensile strength of fibres in boron-aluminum, boron-titanium and graphite-aluminum composites as a function of annealing temperature and time 09 p1225 A83-25148

Micromechanical predictions of crack initiation, propagation and crack growth resistance in boron/aluminum composites 10 p1389 A83-25879

Notched unidirectional boron/aluminum - Effect of matrix properties 10 p1389 A83-25881

Damage accumulation in the matrix of an Al-B composite under cyclic deformation 11 p1544 A83-28493

Mathematical modeling of damage in unidirectional composites 14 p1986 A83-32344

Strengthening effect and interfacial adhesion of boron and silicon carbide fibre reinforced aluminum 18 p2659 A83-40252

Bending characteristics of boron-aluminum composites 18 p2660 A83-40268

Mechanical behavior of aluminum alloys reinforced with B and SiC filaments, and properties of B-Al alloy composite as a high speed rotor cylinder 18 p2660 A83-40269

ALUMINUM CARBIDES

Effect of the structure on the strength of the fibrous composite aluminum-carbon strip 13 p1816 A83-31217

Interface interaction in aluminum-carbon system 18 p2658 A83-40247

Formation of intermetallic compound in composite materials 18 p2658 A83-40248

ALUMINUM COATINGS

Structure of the coating on a nickel alloy after chromoaluminizing in vacuum 01 p0025 A83-10449

The influence of different deposition parameters on the aluminum content in alloy coatings obtained by cathodic sputtering [ONERA, TP NO. 1982-86] 03 p0300 A83-14538

Metal coated fibers for use in the radiation environment 05 p0685 A83-17480

The thermodynamic principles of calorizing 07 p0887 A83-20679

A study of the effectiveness of certain refractory diffusion coatings on nickel alloys 07 p0888 A83-20690

High temperature stability of pack aluminide coatings on IN38LC 07 p0941 A83-21459

The high-temperature corrosion of aluminum-rich coatings in an atmosphere of sulfur vapor containing oxygen 08 p1068 A83-23243

Effect of ion-plated aluminum coating on hydrogen gas embrittlement of ultrahigh strength maraging steel 09 p1230 A83-23918

The production of clad rolled sheets from secondary aluminum powder 09 p1236 A83-25064

Microstructure and hot corrosion resistance of aluminide coating on a nickel-base superalloy in 738LC 15 p2137 A83-33973

Hot corrosion of aluminide coatings on nickel-base superalloys in oxidizing and reducing conditions [ONERA, TP NO. 1983-12] 16 p2333 A83-36422

Removable volatile protective coatings for aluminised mirrors used in far-ultraviolet space astronomy 18 p2649 A83-40663

Oxidation of aluminide coatings on unalloyed titanium 20 p2953 A83-42258

Photodeposition of aluminum oxide and aluminum thin films 21 p3219 A83-45489

Aluminide coatings on superalloys [ONERA, TP NO. 1983-68] 23 p3432 A83-48189

Protective coatings against hot corrosion 24 p3590 A83-49479

Hot corrosion resistance of nickel-base superalloys and aluminide coatings to molten Na2SO4-NiSO4-NaCl salt 24 p3564 A83-49503

Influence of nitrogen and carbon in the base steel on the transformation temperature of the alloy layer of an aluminized steel sheet for high temperature use 24 p3566 A83-49519

ALUMINUM COMPOUNDS

NT ALUMINATES

NT ALUMINUM ANTIMONIDES

NT ALUMINUM ARSENIDES

NT ALUMINUM CARBIDES

NT ALUMINUM HYDRIDES

NT ALUMINUM NITRIDES

NT ALUMINUM OXIDES

NT ALUMINUM SILICATES

NT ANDESITE

NT BERYL

NT FELDSPARS

NT LITHIUM ALUMINUM HYDRIDES

NT MONTMORILLONITE

NT SAPPHIRE

Magnetic and crystallographic characteristics of R2Ni2Ga and R2Ni2Al compounds --- rare earth compounds 03 p0299 A83-14153

The texture in diffusion-grown layers of trialuminides MeAl3 (Me = Ti, V, Ta, Nb, Zr, Hf) and VNi3 15 p2140 A83-34798

Ca-Al-rich chondrules and inclusions in ordinary chondrites 17 p2623 A83-38593

The influence of pack aluminized coatings on the creep behavior of Nimonic 105 20 p2953 A83-42256

ALUMINUM GALLIUM ARSENIDES

Room-temperature CW operation in the visible spectral range of 680-700 nm by AlGaAs double heterojunction lasers 01 p0055 A83-10983

Low loss poly/methyl methacrylate-d5/ core optical fibers 01 p0106 A83-10985

A study of silicon and GaAs solar cells, and their optical coupling by means of a dichroic mirror --- French thesis 02 p0200 A83-11764

Optical phase modulation in an injection locked AlGaAs semiconductor laser 02 p0184 A83-12168

Narrow strip AlGaAs lasers using double current confinement 02 p0185 A83-12276

Raman scattering characterization of Ga/1-x/Al/x/As/GaAs heterojunctions - Epilayer and interface 02 p0243 A83-12289

GHz bandwidth /GaAl/As semiconductor lasers and optical detectors for signal processing applications 03 p0331 A83-13766

High-power single-mode AlGaAs laser diodes 03 p0331 A83-13875

Theoretical analysis of single-mode AlGaAs-GaAs double heterostructure lasers with channel-guide structure 03 p0332 A83-13920

Continuous wave high-power, high-temperature semiconductor laser phase-locked arrays 03 p0333 A83-14932

Locking bandwidth asymmetry in injection-locked GaAlAs lasers 04 p0483 A83-15231

Polarization control of an antireflection-coated GaAlAs laser diode by an external optical feedback 04 p0535 A83-16092

Single-mode lasers for optical communications 04 p0486 A83-16213

Pulsed-power performance and stability of 880 nm GaAlAs/GaAs oxide-stripe lasers 04 p0486 A83-16215

A survey of optical nonlinearities - Theory and observation in /AlGa/As injection lasers 04 p0486 A83-16216

Forward bias voltage characteristics for /GaAl/As and /GaIn/ /AsP/ lasers 04 p0486 A83-16222

Catastrophic degradation level of visible and infrared GaAlAs lasers 05 p0647 A83-16941

Determination of the parameters of injection laser amplifiers based on GaAlAs heterostructures from superluminescence characteristics 05 p0649 A83-17060

GaAs/GaAlAs heterojunction bipolar transistors with cutoff frequencies above 10 GHz 05 p0624 A83-17285

Numerical simulation of GaAs/GaAlAs heterojunction bipolar transistors 05 p0624 A83-17294

The effect of Al-GaAs interaction on the technology of self-aligned gallium arsenide MESFETs 05 p0631 A83-17771

High-performance single-mode AlGaAs Gaussian channel substrate planar laser diodes 06 p0765 A83-18566

Anomalous tuning of single mode AlGaAs diode lasers 06 p0765 A83-18901

Radiation effects on modulation-doped GaAs-Al/x/Ga/1-x/As heterostructures 06 p0815 A83-19263

Pulsed laser diode reliability tests 07 p0917 A83-19707

Characteristics of modulation-doped Al/x/Ga/1-x/As/GaAs field-effect transistors - Effect of donor-electron separation 07 p0918 A83-19987

Properties of diode lasers with intensity noise control 07 p0935 A83-20161

Measurement of the linewidth enhancement factor alpha of semiconductor lasers 07 p0937 A83-21363

Optically integrated coherently coupled Al/x/ Ga/1-x/As lasers 07 p0937 A83-21367

Frequency stabilization of GaAlAs laser using a Doppler-free spectrum of the Cs-D2 line 07 p0938 A83-21593

Prediction of transverse-mode selection in double heterojunction lasers by an ambipolar excess carrier diffusion solution 08 p1107 A83-22332

AlGaAs/GaAs heterojunction charge-coupled devices /CCDs/ for visible/near infrared imaging applications 08 p1080 A83-22604

Effects of 140 Mbit/s operation on degradation of GaAlAs DH lasers 09 p1272 A83-24113

Detection at Gbit/s rates with a TJS GaAlAs laser 10 p1425 A83-25426

Noise and longitudinal mode characteristics of /GaAl/As TS lasers with reduced facet reflectivities 10 p1429 A83-26029

Lattice parameter changes in Al/0.39/Ga/0.61/As due to O, Ge, Si, and S doping 10 p1488 A83-26059

Use of a superlattice to enhance the interface properties between two bulk heterolayers 10 p1489 A83-26214

Submicrostructures generated in semiconductors by athermal laser processing 11 p1661 A83-27561

Light sensitivity of Al/0.25/Ga/0.75/As/GaAs modulation-doped structures grown by molecular beam epitaxy - Effect of substrate temperature 11 p1664 A83-28603

The study and manufacture of Ga-Al-As double heterojunction laser diodes emitting in the visible spectrum --- French thesis 11 p1585 A83-28627

Study of electronically active defects in GaAlAs:Sn devices and their role in degradation --- French thesis 13 p1830 A83-30129

Picosecond Al(x)Ga(1-x) As modulation-doped optical field-effect transistor sampling gate 13 p1832 A83-30341

Measurement of high electron drift velocity in a submicron, heavily doped graded gap Al(x)Ga(1-x)As layer 13 p1929 A83-31056

Passive mode locking of buried heterostructure lasers with nonuniform current injection 13 p1852 A83-31057

Low-current-threshold (GaAl)As visible lasers with emission wavelengths below 750 nm 13 p1857 A83-31378

GaAs/GaAlAs active-passive-interference laser 13 p1858 A83-31768

Role of photoluminescence in the efficiency of a Ga(1-x)Al(x)As-GaAs solar cell 14 p2043 A83-32269

Electroabsorption by Stark effect on room-temperature excitons in GaAs/GaAlAs multiple quantum well structures 14 p2093 A83-33442

Positive feedback model of defect formation in gradually degraded GaAlAs light emitting devices 15 p2237 A83-33678

Magnetoresistance anisotropy due to the 2D-electron subsystem at a GaAs/AlGaAs interface 15 p2237 A83-33784

Degenerate four-wave mixing in room-temperature GaAs/GaAlAs multiple quantum well structures 15 p2230 A83-33840

Double heterojunction Al(x)Ga(1-x)As/GaAs bipolar transistors (DHBJT's) by MBE with a current gain of 1650 15 p2151 A83-33916

(GaAl)As/GaAs heterojunction bipolar transistors with graded composition in the base 15 p2152 A83-34516

Fractional quantization of the Hall effect 16 p2420 A83-35750

Synthetic nonlinear semiconductors 16 p2420 A83-35957

Dispersion of the refractive index of GaAs and Al(x)Ga(1-x)As 16 p2420 A83-35970

Fabrication of GaAs bistable optical devices 16 p2412 A83-36069

Polarisation-dependent gain-current relationship in GaAs-AlGaAs MOW laser diodes --- Multi-Quantum-Well 16 p2360 A83-36481

Electric and photoelectric properties of graded-band-gap Ga(1-x)Al(x)As p-n structures 17 p2535 A83-37055

Reliability of constricted double-heterojunction AlGaAs diode lasers 18 p2693 A83-40052

Planar structure AlGaAs/GaAs PIN photodiode grown by MOCVD 18 p2679 A83-40388

Streak camera study of short pulse generation in an optically pumped GaAs/(GaAl)As laser 19 p2850 A83-40735

Anomalous longitudinal mode behavior of a deep Zn-diffused GaAs/GaAlAs laser 19 p2850 A83-40736

High-speed GaAlAs/GaAs p-i-n photodiode on a semi-insulating GaAs substrate 19 p2836 A83-40742

Long-lived GaAlAs laser diodes with multiple quantum well active layers grown by organometallic vapor phase epitaxy 19 p2850 A83-40744

A nondestructive method for predicting laser emission wavelength from photocurrent spectra of GaAlAs double heterostructure wafers 19 p2851 A83-40930

High-efficiency and high-power AlGaAs/GaAs laser 19 p2851 A83-40935

Graded barrier single quantum well lasers - Theory and experiment 19 p2851 A83-40937

Observation of changes of laser beam characteristics in aged oxide-defined narrow-stripe lasers 19 p2852 A83-40943

Isolation spectra for laser diode optical switch 19 p2900 A83-41278

A dual-stripe phase-locked diode laser 19 p2853 A83-41288

Low cost process for ohmic contacts on GaAs/Ga(1-x)Al(x)As concentrator solar cells based on palladium and gold deposition 20 p2965 A83-42353

High pressure measurements on photopumped low threshold Al(x)Ga(1-x)As quantum well lasers 20 p2994 A83-42595

Transient capacitance spectroscopy on large quantum well heterostructures 20 p3053 A83-42614

Investigation of the refractive index profiles of multilayer Ga(1-x)Al(x)As laser heterostructures 20 p2997 A83-43796

Femtosecond relaxation of photoexcited nonequilibrium carriers in Al(x)Ga(1-x)As 21 p3216 A83-43890

Modulation characteristics of constricted double-heterojunction AlGaAs laser diodes 21 p3144 A83-44216

Small-radii curved rib waveguides in GaAs/GaAlAs using electron-beam lithography 21 p3205 A83-44222

GaAlAs p-n junction waveguide modulator 21 p3205 A83-44224

Interfacial chemistry of electrical contacts on GaAs and Al0.3Ga0.7As 21 p3109 A83-44614

Optical stability of narrow stripe, proton-isolated AlGaAs double heterostructure lasers with gain guiding 21 p3147 A83-45485

Nonlinear optics with a diode-laser light source 22 p3356 A83-45963

Theoretical analysis of solar cells based on graded band-gap structures 22 p3318 A83-46277

Cascade AlGaAs-GaAs solar cell research using molecular beam epitaxy 22 p3319 A83-46606

Narrow diffused stripe GaAs/GaAlAs lasers for high speed integrated optical transmitters 22 p3297 A83-46655

Tunneling in the reverse dark current characteristic of Be-implanted GaAlAsSb avalanche photodetectors 22 p3365 A83-46656

Modification of optical properties of GaAs-Ga(1-x)Al(x)As superlattices due to band mixing 22 p3365 A83-46725

AlGaAs/GaAs cascade solar cell computer modeling under high solar concentration 23 p3478 A83-48616

1.5 GHz operation of an Al(x)Ga(1-x)As/GaAs modulation-doped photoconductive detector 23 p3446 A83-48712

GaAlAs buried-heterostructure lasers grown by a two-step MOCVD process 24 p3590 A83-49963

ALUMINUM GRAPHITE COMPOSITES

Auger and electron energy-loss study of the Al/SiC interface 05 p0611 A83-16947

Hot extrusion of aluminum composite containing dispersed graphite particles - Study of properties of particle-dispersed aluminum composite II 05 p0611 A83-17103

Computer simulation of the fracture of composite materials with various degrees of physicochemical interaction between the components 07 p0874 A83-19971

Aluminum-matrix composites reinforced with carbon fibers 14 p1986 A83-32146

Fibre composites of aluminium with graphite 16 p2325 A83-36525

Electrical resistivity of an aluminium-graphite composite between 77 K and 300 K 24 p3553 A83-48897

ALUMINUM HYDRIDES

Theoretical study of AlH₃ / + - Spin splitting, core polarization, and interstellar chemistry 08 p1180 A83-22219

Astrophysical molecules of AlH and CaH - RKR potential and dissociation energies --- Rydberg-Klein-Rees 18 p2764 A83-39192

ALUMINUM ISOTOPES**NT ALUMINUM 26****ALUMINUM NITRIDES**

Comments on 'Kinetics of densification during hot-pressing of aluminium nitride' 02 p0159 A83-11672

The mechanical properties of a material obtained from ultrafine aluminum-nitride powders 07 p0884 A83-19970

Improvements on the electrical and luminescent properties of reactive molecular beam epitaxially grown GaN films by using AlN-coated sapphire substrates 08 p1169 A83-22759

Effect of hot-pressing temperature on the thermal diffusivity/conductivity of SiC/AlN composites 09 p1225 A83-25208

Investigation of phase stability in the system SiC-AlN 12 p1717 A83-29974

Formation of alpha-Si₃N₄ solid solutions in the system Si₃N₄-AlN-Y₂O₃ 16 p2337 A83-36949

The thermophysical properties of a material based on aluminum nitride and yttrium oxide 17 p2492 A83-38871

Chemical preparation of ultra-fine aluminum nitride by electric-arc plasma 18 p2671 A83-39054

Reactively RF magnetron sputtered AlN films as gate dielectric 20 p2967 A83-42609

Properties and ion implantation of Al(x)Ga(1-x)N epitaxial single crystal films prepared by low pressure metalorganic chemical vapor deposition 21 p3220 A83-45499

High temperature reactions and microstructures in the Al₂O₃-AlN system 23 p3434 A83-48259

An experimental plan for the nitridation of Si+Al compacts 23 p3434 A83-48262

Sintering of aluminium nitride with low oxide addition 23 p3435 A83-48272

Hot pressing of aluminium nitride 23 p3436 A83-48275

Thermal shock resistance of two nitrogen ceramics 23 p3438 A83-48298

ALUMINUM OXIDES**NT SAPPHIRE**

Application of X-ray energy dispersive analyses /EDAX/ to determine the penetration depth of one oxide phase /NiAl₂O₄/ in a two-phase oxide internal oxidation zone /NiAl₂O₄+Al₂O₃/ of a binary alloy /Ni-Al/ 01 p0024 A83-10248

O-18 tracer studies of Al₂O₃ scale formation on NiCrAl alloys 01 p0024 A83-10249

Enhancement of the diffusional creep of polycrystalline Al₂O₃ by simultaneous doping with manganese and titanium 02 p0159 A83-11668

J series thruster isolator failure analysis [AIAA PAPER 82-1907] 02 p0144 A83-12482

Formation mechanisms of keying or pegging yttrium oxide and increased plasticity of alumina scale on FeCrAlY 03 p0296 A83-13121

The surface temperature and the concentration of alumina particles in the detonation products of a gas mixture 03 p0295 A83-14063

The effect of temperature and alumina additions on the particle dispersity and morphology during the reduction of molybdenum trioxide 03 p0302 A83-14813

Fracture toughness of polycrystalline beta-alumina 03 p0303 A83-14921

Switching behaviour of Al₂O₃-n GaAs MISFETs 04 p0470 A83-15248

The effect of aluminum oxide particles and precipitate type on near-threshold fatigue crack propagation rate in P/M 7XXX aluminum alloys 04 p0461 A83-16255

Metal transfer and wear in fine grinding 04 p0487 A83-16349

Transformation toughening of beta double prime-alumina by incorporation of zirconia 05 p0619 A83-17558

Increase of crack resistance during slow crack growth in Al₂O₃ bend specimens 05 p0619 A83-17566

Critical microstructures for microcracking in Al₂O₃-ZrO₂ composites 06 p0733 A83-17954

Dependence of fracture toughness of alumina on grain size and test technique 06 p0734 A83-18051

Possibility of determining the dispersed composition of a two-phase flow from small-angle light scattering 06 p0757 A83-18448

Properties of cold extruded aluminum-Al₂O₃ powder materials 06 p0731 A83-19088

The stressed state of cylindrical specimens during thermal-stability testing 07 p0897 A83-19969

Observation of the population inversion of O VIII levels in a laser plasma 07 p0996 A83-20126

Microstructure and grain-boundary composition of hot-pressed silicon nitride with yttria and alumina 07 p0898 A83-20166

Rhombohedral twinning in alumina 07 p0898 A83-20168

A biaxial-flexure test for evaluating ceramic strengths 07 p0898 A83-20169

The structure of aluminum oxides used for corrosion resistance and primer adhesion 07 p0899 A83-20492

Boride-thermic synthesis of materials 07 p0873 A83-20682

The dependence of the permeability of detonation-sprayed aluminum oxide coatings on the composition of the detonation gas mixture 07 p0900 A83-20693

Phase transformations during detonation spraying and their effect on the wear resistance of aluminum oxide coatings 07 p0900 A83-20694

Plasma-sprayed coatings of refractory oxides and oxide compositions 07 p0900 A83-20696

High-temperature protective coatings based on aluminosilicophosphate systems 07 p0900 A83-20711

Sputtering of Al₂O₃ and LiNbO₃ in the electronic stopping region [BAP-24] 07 p0901 A83-21057

Viscous flow behavior of four iron-containing silicates with alumina, effects of composition and oxidation condition 07 p0965 A83-21322

The fracture toughness-microstructure relationship of alumina-based ceramics 08 p1069 A83-21768

Application of the J concept to alumina at high temperatures 08 p1070 A83-22192

Effect of doping simultaneously with iron and titanium on the diffusional creep of polycrystalline Al₂O₃ 08 p1071 A83-22195

Determination of residual surface stresses caused by grinding in polycrystalline Al₂O₃ 08 p1071 A83-22199

Effect of Y₂O₃ and Al₂O₃ on the oxidation resistance of Si₃N₄ 08 p1072 A83-22258

Radiation processes in corundum crystals 09 p1349 A83-23450

Titanium-containing powder-metalurgy alloys with special physical properties --- microwave absorbers 09 p1235 A83-24405

Nitrogen-stabilized aluminum oxide spinel /ALON/ 09 p1345 A83-24954

Flaws responsible for slow cracking in the delayed fracture of alumina 09 p1240 A83-25205

Transformation strengthening of beta double prime-Al₂O₃ with tetragonal ZrO₂ 09 p1240 A83-25210

Structure and spectra of H₂O in hydrated beta-alumina 09 p1227 A83-25212

Hydration of lithium beta-alumina 09 p1227 A83-25213

The structure and interdiffusional degradation of aluminide coatings on oxide-dispersion-strengthened alloys 10 p1394 A83-25541

Characterization of copper in phosphoric-acid-anodized 2024-T3 aluminum by Auger electron spectroscopy and Rutherford backscattering 10 p1395 A83-25547

50-GHz IC components using alumina substrates 10 p1408 A83-25803

Spectroscopic and luminescent investigation of third group metal oxides 11 p1581 A83-27596

Optical fibres with an Al₂O₃-doped silicate core composition 12 p1779 A83-29471

Microchemistry and microstructure of a multiphase aluminosilicate ceramic 12 p1716 A83-29505

Measurements of infrared optical properties of Al₂O₃ rocket particles [AIAA PAPER 83-1568] 14 p1985 A83-32780

A supersaturation model for the degradation of sodium beta/beta (double prime)-aluminas 16 p2326 A83-35977

Theoretical and experimental study of momentum and heat transfer between alumina particles and a d.c. plasma jet 16 p2362 A83-36878

Processing-related fracture origins. I - Observations in sintered and isostatically hot-pressed Al₂O₃/ZrO₂ composites 16 p2337 A83-36945

Processing-related fracture origins. II - Agglomerate motion and cracklike internal surfaces caused by differential sintering 16 p2337 A83-36946

Processing-related fracture origins. III - Differential sintering of ZrO₂ agglomerates in Al₂O₃/ZrO₂ composite 16 p2337 A83-36947

The formation of solid solutions in vacuum condensates of the system Al₂O₃-ZrO₂ 17 p2492 A83-37575

Plastic deformation and wear process at a surface during unlubricated sliding 17 p2516 A83-37822

Observations on the fracture and deformation behaviour during annealing of residually stressed polycrystalline aluminium oxides 18 p2671 A83-39058

Microstructure, adhesion and growth kinetics of protective scales on metals and alloys 18 p2666 A83-39731

The high temperature creep of dispersion strengthened Ni-Al₂O₃ alloy 18 p2667 A83-40258

High-performance alumina fiber and alumina/aluminum composites 18 p2659 A83-40261

Slow crack growth behavior in transformation-toughened Al₂O₃-ZrO₂(Y₂O₃) ceramics 19 p2823 A83-40907

Tensile property evaluation of polycrystalline alumina filaments and their composites 19 p2819 A83-41032

The development and growth of protective alpha-Al₂O₃ scales on alloys 20 p2952 A83-42235

Diffusion processes in Al₂O₃ scales - Void growth, grain growth, and scale growth 20 p2952 A83-42238

Coatings containing chromium, aluminum, and silicon for high temperature alloys 20 p2953 A83-42260

Anomalous electric-field-induced damping of ultrasound in superionic crystals 20 p3051 A83-42265

Photodeposition of aluminum oxide and aluminum thin films 21 p3219 A83-45489

Sialon X-phase --- crystal structure 23 p3436 A83-48278

Friction and wear of iron and nickel in sodium hydroxide solutions 24 p3559 A83-48922

Factors influencing residual surface stresses due to a stress-induced phase transformation --- in alumina-zirconia ceramics [ACS PAPER 83-B-82] 24 p3567 A83-48960

Al₂O₃ scales on ODS alloys --- oxide dispersion strengthened 24 p3563 A83-49490

ALUMINUM SILICATES**NT ANDESITE****NT MONTMORILLONITE**

Andalusite traveling-wave masers for the middle part of the millimeter wave band 01 p0054 A83-10413

Thermal and mechanical properties of multilic substrates for low-cost solar cells obtained by dry-pressing 12 p1749 A83-29506

ALUMINUM 26

A direct measurement of the distribution in depth of Al-26 in the Estacado meteorite 02 p0267 A83-12849

Accelerator mass spectrometry measurement of cosmogenic Al-26 in terrestrial and extraterrestrial matter 08 p1187 A83-23293

Nucleosynthesis of Al-26 at low stellar temperatures 17 p2598 A83-37331

Mg-26(p, n)Al-26 cross section measurements --- abundance anomalies in Allende meteorite 20 p3069 A83-42465

Recent cosmic ray exposure history of ALHA 81005 22 p3386 A83-46868

ALVEOLAR AIR

The blood flow in bronchial vessels during hypoxia 01 p0078 A83-10481

Dynamic response of local pulmonary blood flow to alveolar gas tensions - Analysis 13 p1789 A83-30473

ALVEOLI
The surfactant system of the lungs in experimental
papa-in-induced emphysema 05 p0670 A83-17188
Ascorbate uptake by isolated rat alveolar macrophages
and type II cells 13 p1897 A83-30464
Hypoxic constriction of alveolar and extra-alveolar
vessels in isolated pig lungs 17 p2555 A83-36994

AMALGAMS
U MERCURY AMALGAMS

AMALTHEA
Amalthea --- Voyager observations 04 p0570 A83-16231
Pioneer 11 observations of trapped particle absorption
by Amalthea 06 p0847 A83-18279
Amalthea - Implications of the temperature observed
by Voyager 15 p2275 A83-34724

AMAZON REGION (SOUTH AMERICA)
The utilization of SLAR and the Landsat satellites in
geomorpho-pedological surveys performed in the
Venezuelian Amazon - Methodology and initial results 08 p1126 A83-21924
Acid rain in an Amazon rainforest 11 p1613 A83-28096

AMBIENT TEMPERATURE
An indirect method of measuring temperature 08 p1091 A83-21982
Establishment of the optimal irradiance of man at low
ambient temperatures in the workplace 17 p2561 A83-38929

AMBIGUITY
The Ambiguity function as a polar display of the OTF 08 p1167 A83-23150
Airborne radar and the three PRFs --- Pulse Repetition
Frequency 19 p2795 A83-40759
Ambiguities in spaceborne synthetic aperture radar
systems 19 p2861 A83-41146

AMBIPOLAR DIFFUSION
Structure of the electron density profile in the vicinity
of localized inhomogeneities in the case of ambipolar
diffusion of magnetized recombining plasma 04 p0537 A83-15859
Electric field and space charge density distributions in
the processes of ambipolar plasma diffusion with volume
recombination 05 p0687 A83-16902
A numerical study of the effects of ambipolar diffusion
on the collapse of magnetic gas clouds 05 p0698 A83-16997
Prediction of transverse-mode selection in double
heterojunction lasers by an ambipolar excess carrier
diffusion solution 08 p1107 A83-22332
Open-circuit voltages across two junctions in
n/+/-p-p/+/- solar cells under high illumination levels 11 p1611 A83-27976
Ambipolarity in the motion of ionospheric plasma 11 p1620 A83-28745
Nonintrinsic ambipolar diffusion in turbulence theory 17 p2581 A83-37027

AMBIT
U FIELD THEORY (PHYSICS)

AMIDES
NT NICOTINAMIDE
NT POLYIMIDES
NT THIOUREAS
NT UREAS
Nucleoside and deoxynucleoside phosphorylation in
formamide solutions --- under prebiotic conditions 02 p0226 A83-11631
Oxidative peptide /and amide/ formation from Schiff
base complexes 06 p0800 A83-18247
Epitaxial crystallization of nylon 6 cast from solution on
the surface of poly(p-phenylene terephthalamide)
filament 13 p1817 A83-31796

AMINES
NT AMPHETAMINES
NT ANILINE
NT CATECHOLAMINE
NT CATECHAMINE
NT DIAMINES
NT HYOSCINE
NT NITROAMINES
NT NITROSAMINE
NT SEROTONIN
Synthesis and characterization of bisimide amines and
bisimide amine-cured epoxy resins 01 p0027 A83-11486
Theoretical study of NH2 - Potential curves, transition
moments, and photodissociation cross sections 05 p0684 A83-17655
The effect of short-term hypothermia on the monoamine
oxidase enzyme system in the rat brain 06 p0795 A83-18989
Polyamine formation by arginine decarboxylase as a
transducer of hormonal, environmental and stress stimuli
in higher plants 11 p1639 A83-27830

A regenerable solid amine CO2 concentrator for space
station [SAE PAPER 820847] 13 p1907 A83-30938
The aminergic control of the cerebral arteries 14 p2063 A83-32099
Synthesis and characterization of bisimide amines and
bisimide amine-cured epoxy resins 19 p2823 A83-40924
Effects of chronic hypoxia on pulmonary vascular
responses to biogenic amines 20 p3033 A83-43487
Formation and photochemistry of methylamine in
Jupiter's atmosphere 22 p3388 A83-47083

AMINO ACIDS
NT ALANINE
NT GLUTAMIC ACID
NT GLUTATHIONE
NT GLYCINE
NT MELANOIDIN
NT PAPAIN
NT PEPTIDES
NT POLYPEPTIDES
NT PYRUVATES
NT THYROXINE
NT TRYPTOPHAN
An evolutionary model for the insect vitellins 01 p0081 A83-11034
Formation and catalytic activity of high molecular weight
soluble polymers produced by heating amino acids in a
modified sea medium 02 p0219 A83-11632
Amino acids from the Late Precambrian Thule Group,
Greenland 02 p0219 A83-11636
Template directed reactions of 2-aminoadenylic acid
derivatives 02 p0148 A83-11842
The effect of radiation on the pool of free amino acids
in the tissues of rats 03 p0377 A83-14885
The abiogenic synthesis of amino acids under conditions
imitating an ash-gas cloud during volcanic eruptions 06 p0800 A83-17987
Formation of amino acids from models of Titan and more
oxidized atmospheres 06 p0801 A83-19407
The peripheral and central effects of
gamma-aminobutyric acid on the vascular
thermoregulatory reaction in rabbits 07 p0973 A83-20361
The updated experimental proteinoid model 07 p0976 A83-21050
On the reported optical activity of amino acids in the
Murchison meteorite 08 p1191 A83-23283
Synthesis of amino acids in weight bearing and
non-weight bearing leg muscles of suspended rats 11 p1640 A83-27838
Highly efficient peptide formation from
N-acetylaminocacyl-AMP anhydride and free amino acid 12 p1767 A83-29422
Radiolysis of aqueous solutions of hydrogen cyanide
(pH about 6) - Compounds of interest in chemical evolution
studies 12 p1767 A83-29424
Interaction of metal ions and amino acids - Possible
mechanisms for the adsorption of amino acids on
homoionic smectite clays 12 p1712 A83-29556
Potentiation of oxygen toxicity in rats by dietary protein
or amino acid deficiency 13 p1897 A83-30461
Tissue ammonia and amino acids in rats at various
oxygen pressures 13 p1897 A83-30472
Changes in kinin kallikrein system in rabbits with
experimental atherosclerosis treated with protein
hydrolysate 'Hydroprot' 14 p2061 A83-31820
The effect of exogenous amino acids on the cardiac
contractile function and the metabolism of nitrogen
compounds during anoxia 14 p2066 A83-33336
Formation of amino acids from reactor-irradiated
ammonium acetate 17 p2563 A83-38892
Amino acids in meteorites 19 p2886 A83-42030
The atmosphere of the primitive earth and the prebiotic
synthesis of organic compounds 19 p2886 A83-42033
A novel way for the formation of alpha-amino acids and
their derivatives in an aqueous medium 19 p2887 A83-42036
Changes in the amino acid code 19 p2877 A83-42039
Evolution of the amino acid code - Inferences from
mitochondrial codes 20 p3033 A83-42397
The evolutionary pattern of aromatic amino acid
biosynthesis and the emerging phylogeny of pseudomonad
bacteria 20 p3033 A83-42399
Prebiotic synthesis in atmospheres containing CH4, CO,
and CO2. I - Amino acids 24 p3619 A83-49621

AMMINES
Quantum chemical studies of a model for peptide bond
formation. II - Role of amine catalyst in formation of
formamide and water from ammonia and formic acid 19 p2819 A83-41865

AMMONIA
Absorption refrigeration machines --- Thesis 02 p0243 A83-11525

Raman gain in 12-micron NH3 lasers 02 p0183 A83-11560
Investigation of pressure shifts of frequencies in a system
of successive transitions of the /N-14/H3 molecule in the
nu2-excited vibrational state 02 p0234 A83-11692
Detection of the /8,8/ and /9,9/ absorption lines of
ammonia - The hot molecular cloud toward Sgr B2 03 p0430 A83-14806
Airborne spectroscopy of Jupiter in the 100- to 300/cm
region - Global properties of ammonia gas and ice haze 05 p0703 A83-16961
The effect of ammonia ice on the outgoing thermal
radiance from the atmosphere of Jupiter 05 p0703 A83-16962
Photochemistry of NH3, CH4 and PH3 - Possible
applications to the Jovian planets 06 p0801 A83-19403
Quantum chemical studies of a model for peptide bond
formation Formation of formamide and water from
ammonia and formic acid 07 p0976 A83-21052
Small rotating clouds of stellar mass in Orion molecular
cloud 1 08 p1185 A83-23081
Infrared laser optogalvanic spectroscopy of molecules 09 p1227 A83-25132
M dependence in the analysis of NH3-He microwave
double resonance experiments 09 p1343 A83-25133
Dense cores in dark clouds. II - NH3 observations and
star formation 10 p1504 A83-25727
VLA observations of warm NH3 associated with mass
outflows in W51 10 p1508 A83-26368
High-pressure NH3-N2 laser 10 p1434 A83-26689
Thermal infrared constraints on ammonia ice particles
as candidates for clouds in the atmosphere of Saturn 11 p1684 A83-27361
An investigation of the atmospheric
HNO3-NH3-NH4NO3 equilibrium relationship in a cool,
humid climate 11 p1613 A83-27675
New CW two-photon pumped and Raman FIR laser lines
in /N-14/H3 and /N-15/H3 11 p1583 A83-27848
Photodissociation of NH3 at 106-200 nm 11 p1655 A83-28527
The ground state far infrared spectrum of NH3 12 p1778 A83-29526
Tissue ammonia and amino acids in rats at various
oxygen pressures 13 p1897 A83-30472
Muscle fiber composition and blood ammonia levels after
intense exercise in humans 13 p1903 A83-30480
A photoelectron spectroscopic study of (3 + 1) resonant
multiphoton ionization of NO and NH3 13 p1916 A83-30964
The nuclear hyperfine structure of deuterated
ammonia 13 p1958 A83-31730
Measurements of the dissociative recombination
coefficients of O2(+), NO(+), and NH4(+) in the
temperature range 200-600 K 14 p2082 A83-32524
The effect of nonrigidity in the rotational structure of
the spectra of molecules of water vapor and ammonia
(Calculation of the dependence of rotational and centrifugal
constants on vibration with great amplitude) 14 p2082 A83-32558
Aluminum/ammonia heat pipe gas generation and long
term system impact for the Space Telescope's Wide Field
Planetary Camera [AIAA PAPER 83-1428] 14 p2009 A83-32704
Ammonia and ammonium concentrations in the antarctic
atmosphere 15 p2197 A83-34044
The NH3 spectrum in Saturn's 5 micron window 15 p2274 A83-34114
Observations of NH3 and H2O in the Pelican Nebula
hotspot 15 p2265 A83-34595
Detection of interstellar NH3 in the far-infrared - Warm
and dense gas in Orion-KL 15 p2269 A83-34648
Solar operated water-ammonia absorption heat pump
for air-conditioning - Modelling and simulation 15 p2192 A83-34674
HCN formation on Jupiter - The coupled photochemistry
of ammonia and Acetylene 15 p2275 A83-34718
Study of the deep cloud structure in the equatorial region
of Jupiter from Voyager infrared and visible data 15 p2275 A83-34719
Elastic and inelastic scattering of high-energy electrons
and X-rays by NH3, CH4 and H2O molecules 16 p2409 A83-35333
Energy disposal in charge transfer reactions producing
NH3(-) - Dependence of the NH3(+) + H2O reaction
on NH3(+) internal energy 16 p2327 A83-36520
Ammonia as a molecular cloud thermometer 16 p2431 A83-36678
Nitric oxide formation in an ammonia-doped
methane-oxygen low pressure flame 17 p2485 A83-38028
Three gas clumps near the edge of the visible Orion
Nebula 18 p2773 A83-39722
Uranus - Variability of the microwave spectrum 18 p2779 A83-39933

Hydroxyl concentration measurements in the NH₃-NO₂ reaction in postflame gases 18 p2664 A83-40311

Observation of period doubling in an all-optical resonator containing NH₃ gas 19 p2900 A83-41156

Intracavity pumped NH₃ laser using a very small cavity 19 p2853 A83-41184

The possibility of the formation of aerosol in the chemical reaction between SO₂ and NH₃ in conditions of the Venus atmosphere 19 p2923 A83-41240

Momentum transfer cross sections for the low-energy electron scattering by NH₃ molecules 19 p2898 A83-41293

Clumping in Orion KL - 2-arcsecond maps of ammonia 20 p3065 A83-42380

First detection of the ground-state J(K) = 1(0)-0(0) submillimeter transition of interstellar ammonia 20 p3069 A83-42473

Two-photon-ionization mass spectroscopy of ammonia clusters in a pulsed supersonic nozzle beam 20 p3044 A83-42631

Ammonia toward DR21 - A weak maser in ortho-NH₃? 21 p3229 A83-44428

Identification of forbidden transitions in the nu-4 band of (N-14)H₃ by intracavity laser-Stark spectroscopy 22 p3355 A83-45966

VLA observations of extragalactic NH₃ in IC 342 22 p3381 A83-46981

Infrared studies of molecular ions. I - The nu₃ band of NH₄(+) 23 p3506 A83-47637

The nu₃ vibrational spectrum of the free ammonium ion NH₄(+) 23 p3506 A83-47638

A 1.5 W CW optically pumped 12.08 microns NH₃ laser 23 p3462 A83-48317

The reaction NH₂ + PH₃ yields NH₃ + PH₂ - Absolute rate constant measurement and implication for NH₃ and PH₃ photochemistry in the atmosphere of Jupiter 24 p3672 A83-49343

Ammonia observations of the Herbig-Haro objects HH24-27 24 p3658 A83-49359

Ammonia absorption toward W3(OH) - 0.3 arcsec resolution maps in the (2,2) line 24 p3668 A83-50078

AMMONIUM BROMIDES

Effect of ammonium halides on the combustion of polystyrene 21 p3116 A83-44666

AMMONIUM CHLORIDES

Effect of ammonium halides on the combustion of polystyrene 21 p3116 A83-44666

AMMONIUM COMPOUNDS

NT AMMONIUM BROMIDES

NT AMMONIUM CHLORIDES

NT AMMONIUM NITRATES

NT AMMONIUM PERCHLORATES

NT AMMONIUM SULFATES

Formation of amino acids from reactor-irradiated ammonium acetate 17 p2563 A83-38892

AMMONIUM NITRATES

An investigation of the atmospheric HNO₃-NH₃-NH₄NO₃ equilibrium relationship in a cool, humid climate 11 p1613 A83-27675

Mathematical modeling of the formation and transport of ammonium nitrate aerosol 19 p2863 A83-41970

AMMONIUM PERCHLORATES

Association of triethylammonium perchlorate with bases 01 p0023 A83-11322

An improved model for the combustion of AP composite propellants 03 p0303 A83-13142

Combustion of condensed two-component systems with spatially separated components 03 p0294 A83-14052

Combustion response to compositional fluctuations --- of composite solid propellants [AIAA PAPER 83-0476] 05 p0619 A83-16740

The mechanism for the thermal decomposition of ammonium perchlorate --- Russian book 05 p0620 A83-17139

The mechanism for the thermal decomposition of ammonium perchlorate 05 p0620 A83-17140

The topographic characteristics of the thermal decomposition of ammonium perchlorate 05 p0620 A83-17141

The nucleation mechanism during the low-temperature decomposition of ammonium perchlorate 05 p0620 A83-17142

On the question of the mechanism for the thermal decomposition of ammonium perchlorate 05 p0620 A83-17143

Thermal decomposition of tetraethylammonium perchlorate 06 p0726 A83-18458

Fine ammonium perchlorate manufacture by the use of the vibro-energy mill wet grinding process 09 p1240 A83-23830

Processing modifications for improved propellants - Coated oxidizers 09 p1241 A83-23838

Techniques in the formulation and handling of composite and very-low-density explosives 09 p1242 A83-23845

Unified model of catalyzed and uncatalyzed decomposition of ammonium perchlorate 14 p1999 A83-32940

Bonding agents for AP and nitramine/HTPB composite propellants [AIAA PAPER 83-1199] 16 p2340 A83-36275

Effects of AP particle size on combustion response to crossflow [AIAA PAPER 83-1270] 16 p2340 A83-36317

Ignition of composite solid propellant at subatmospheric pressures 18 p2673 A83-40313

Catalyzed and inhibited decomposition of ammonium perchlorate 20 p2959 A83-43456

Ammonium ion rotation in ammonium perchlorate as studied by infrared spectroscopy 23 p3506 A83-47631

Changes in the reactivity of a solid substance at the interface of the reagent and the product of the topochemical reaction --- thermal decomposition of ammonium perchlorate 23 p3430 A83-48506

Characteristics of the initiation of fast chemical reactions in oxidizer-combustible mixtures 24 p3557 A83-49790

AMMONIUM SULFATES

Infrared spectrum of a single aerosol particle by photothermal modulation of structure resonances 03 p0356 A83-14379

Structural studies of new series of crystals 13 p1928 A83-30316

AMOR ASTEROID

Missions to the asteroid Anteros and the space of true anomalies 18 p2642 A83-39474

AMORPHOUS MATERIALS

Radial distribution studies in a diamond anvil pressure cell 01 p0028 A83-10643

Structural and thermal analysis studies of magnetron sputter-deposited amorphous metallic /Mo_{0.6}Ru_{0.4}/82B18 films 02 p0243 A83-12649

A two-dimensional phase separation on the spherical surface of the metallic glass Au₅₅Pb_{22.5}Si_{22.5} 03 p0399 A83-14937

Amorphous solid and bipolaronic ground-state 04 p0540 A83-15507

Structural difference rule for amorphous alloy formation by ion mixing 05 p0690 A83-16945

Fracture behavior of polymers by Charpy impact tests 05 p0618 A83-17100

Mechanical properties of ductile Fe-Ni-Zr and Fe-Ni-Zr /Nb or Ta/ amorphous alloys containing fine crystalline particles 05 p0615 A83-17559

Normalization of fatigue crack propagation behavior in polymers 08 p1068 A83-21677

Fracture mechanical studies of the strength resulting from polymer interdiffusion 08 p1068 A83-21696

Amorphous glassy plasma in dense stellar matter 08 p1185 A83-23085

Ion mixing to produce amorphous Mo-Ru superconducting films 10 p1489 A83-26217

Computer simulation of the optical behaviour of amorphous silicon solar cells 11 p1611 A83-27979

Kinetics of crystallization of ZrF₄-BaF₂-LaF₃ glass by differential scanning calorimetry 12 p1717 A83-29972

Hard carbon coatings with low optical absorption 13 p1825 A83-30326

Ion-induced amorphous and crystalline phase formation in Al/Ni, Al/Pd, and Al/Pt thin films 13 p1928 A83-30338

Possibility of amorphous glassy state in astrophysical dense plasmas 13 p1947 A83-30422

The effect of gamma-irradiation on amorphous silicon field effect transistors 14 p2007 A83-33142

Interfacial electrical properties of ion-beam sputter deposited amorphous carbon on silicon 15 p2238 A83-33920

Lattice images of amorphous-like Ni-B films prepared by the electroless plating method 16 p2328 A83-35601

Crystallization of amorphous Si₃N₄ prepared by the thermal decomposition of Si(NH)₂ 16 p2336 A83-35985

Physical properties of disordered structures (Molecular-kinetic and thermodynamic processes in inorganic glasses and polymers) --- Russian book 16 p2337 A83-36438

Contacts between amorphous metals and semiconductors 17 p2500 A83-38881

On the nature of craze development and breakdown during fatigue 18 p2671 A83-39059

Light-induced effects in indium tin oxide/n-i-p hydrogenated amorphous silicon solar cells 18 p2707 A83-39463

Electron-diffraction evidence for threefold coordination in amorphous hydrogenated carbon films 19 p2823 A83-40955

RF-plasma deposited amorphous hydrogenated hard carbon thin films - Preparation, properties, and applications. 20 p3048 A83-42610

The lattice images of amorphous-like Ni-B alloy films prepared by electroless plating method 20 p2956 A83-43615

The structure of boron in boron fibres 21 p3116 A83-44342

Influence of the microstructure on the corrosion behavior of magnetron sputter-quenched amorphous metallic alloys 21 p3217 A83-44611

Low-loss integrated optical waveguides fabricated by nitrogen ion implantation 22 p3360 A83-46720

AMORPHOUS SEMICONDUCTORS

Features of the Raman spectra of noncrystalline semiconductor compounds of the type Hg/Ge/-As/Sb/-S-I 01 p0110 A83-10847

Structural features and the stimulated crystallization of amorphous films of chalcogenide semiconductors 01 p0110 A83-10849

Production and properties of amorphous films of nonstoichiometric As_x/S_{1-x}/ composition 01 p0110 A83-10850

Recent progress of amorphous-silicon solar-cell technology in Japan 02 p0201 A83-11803

Meaning of the photovoltaic band gap for amorphous semiconductors 02 p0243 A83-12267

Reversible photoinduced changes in the low-temperature photoconductivity of hydrogenated amorphous silicon 02 p0243 A83-12293

Properties of amorphous silicon solar cells 02 p0202 A83-12321

Valency control of glow discharge produced a-SiC:H and its application to heterojunction solar cells 03 p0354 A83-13649

Structural aspects and numerical modeling of diffusion in gold/chalcogenide /GeTe₄/ thin layers --- French thesis 03 p0399 A83-14106

Preparation and characteristics of a-Si:Cl:H films 04 p0539 A83-15478

Schottky barriers on p-type a-Si:H 04 p0539 A83-15486

Effect of discharge conditions on characteristics of hydrogenated amorphous silicon deposited by DC glow discharge decomposition 04 p0539 A83-15498

A role of the lowest unoccupied molecular orbital of the local structure of amorphous materials 04 p0540 A83-15501

EXAFS investigation of dilute Cu impurities in amorphous As₂Se₃ 04 p0540 A83-15502

Paramagnetism in X-irradiated chalcogenide glasses and crystals 04 p0540 A83-15503

Index of refraction of the glassy As_x/Te_{100-x}/ system 04 p0535 A83-15504

The relationship between transient and steady-state photoconductivity in amorphous semiconductors 04 p0540 A83-15505

Electronic correlations and transient effects in disordered systems 04 p0540 A83-15506

Recent advances in amorphous silicon solar cells 04 p0505 A83-15510

The residual voltage in fast electrophotography of a-SiH_x/ 04 p0540 A83-15511

Effects of prolonged illumination on the properties of hydrogenated amorphous silicon 04 p0540 A83-15512

Light-induced metastable effects in hydrogenated amorphous silicon 04 p0540 A83-15513

Luminescence fatigue and light-induced electron spin resonance in amorphous silicon-hydrogen alloys 04 p0541 A83-15514

Chemical bonding in amorphous semiconductors 04 p0541 A83-15516

Studies of thin-film growth of sputtered hydrogenated amorphous silicon 04 p0541 A83-15517

The role of hydrogen in amorphous silicon films deposited by the pyrolytic decomposition of silane 04 p0541 A83-15519

Optical absorption above the optical gap of amorphous silicon hydride 04 p0541 A83-15520

Studies of the band tails in a-Si:H by photomodulation spectroscopy 04 p0541 A83-15523

States in the gap of amorphous hydrogenated silicon 04 p0541 A83-15524

PAS study of gap-state profiles of P-doped and undoped a-Si:H --- photoacoustic spectroscopy 04 p0541 A83-15525

Influence of interface states on field effect and capacitance-voltage characteristics of metal/oxide/a-Si:H structures 04 p0541 A83-15526

Some problems in determination of gap-state density in amorphous silicon 04 p0541 A83-15527

What is the majority carrier drift mobility in a-Si alloys
04 p0541 A83-15528

Defects in amorphous Si-n films prepared by RF sputtering
04 p0542 A83-15529

Electronic properties of doped glow-discharge amorphous germanium
04 p0542 A83-15530

Defects in amorphous III-V compounds
04 p0542 A83-15531

Chemical modification of amorphous arsenic
04 p0542 A83-15532

Hydrogenated a-Si(x)/Ge/1-x/- A potential solar cell material
04 p0542 A83-15871

The population of localized states and the photoconductivity of disordered systems
04 p0542 A83-15920

Changes in photovoltaic and dark electrical properties of hydrogenated amorphous silicon diodes induced by forward bias carrier injection
04 p0542 A83-16021

Optical conductivity of amorphous Ta and beta-Ta films
04 p0543 A83-16079

Effect of hydrogen on the deposition rate for planar RF magnetron sputtering of hydrogenated amorphous silicon
04 p0543 A83-16082

Temperature distribution in a plate produced by a moving heat source --- with application to recrystallization of amorphous silicon thin films
05 p0690 A83-16769

[AIAA PAPER 83-0530]
Anodic oxidation of a-Si:H films
06 p0814 A83-18567

Spectroscopic detection of silylene in the infrared multiphoton decomposition of silane --- amorphous silicon film deposition chemistry
07 p0881 A83-19979

Origin of the difference in the open circuit voltage between p-i-n type and n-i-p type hydrogenated amorphous silicon solar cells
07 p0953 A83-19991

A study of defects in amorphous silicon films
07 p0999 A83-20735

Theory and experiment on the surface-photovoltage diffusion-length measurement as applied to amorphous silicon
07 p0999 A83-20738

Photoconductivity in amorphous Si:H:Cl films
07 p0999 A83-20741

Highly conductive and transparent amorphous tin oxide
07 p1000 A83-20754

Amorphous silicon - A new semiconductor material for solar cells
07 p0955 A83-21627

Photocapacitance of mobile carriers in hydrogenated amorphous silicon solar cells
08 p1131 A83-22765

Effect of an SiC layer on p-i-n amorphous silicon solar cells
08 p1131 A83-22909

Amorphous silicon bibliography update - Introduction
08 p1170 A83-22915

Transient photoconductivity studies of the light soaked state of hydrogenated amorphous silicon
10 p1488 A83-25982

Electronic properties of amorphous silicon selenium films
10 p1488 A83-25984

Amorphous silicon photovoltaic modules
10 p1446 A83-26064

On the mechanism of light-induced effects in hydrogenated amorphous silicon alloys
10 p1489 A83-26209

Electrical and optical properties of sputtered amorphous silicon films prepared under a reduced pumping speed
10 p1489 A83-26211

Silicon melt, regrowth, and amorphization velocities during pulsed laser irradiation
10 p1490 A83-26269

Optical picosecond studies of carrier dynamics in amorphous semiconductors
11 p1661 A83-27604

Microscopic processes in low-power laser annealing of ion-implanted Ge
11 p1661 A83-28068

Optical and electrical properties of amorphous silicon films prepared by photochemical vapor deposition
13 p1870 A83-30339

Heat of crystallization and melting point of amorphous silicon
13 p1825 A83-30344

Photoconductivity enhancement by light trapping in rough amorphous silicon
13 p1870 A83-30349

Photovoltaically active p layers of amorphous silicon
13 p1870 A83-30352

Photoinduced structural transformations in complex chalcogenide glasses
13 p1929 A83-30446

Moessbauer spectroscopy of amorphous silicon-tin-hydrogen alloys
13 p1931 A83-31387

Barrier at the interface between amorphous silicon and transparent conducting oxides and its influence on solar cell performance
13 p1871 A83-31389

Studies of the gap states density in undoped and doped amorphous hydrogenated silicon
14 p2088 A83-32237

Influence of light exposure on the transport properties of a-Si:H films
14 p2088 A83-32238

Study of gap states in a-Si:H by transient current spectroscopy
14 p2089 A83-32251

High efficiency tandem type solar cells consisting of a-Si:H and a-SiGe:H
14 p2042 A83-32263

The photovoltaic advanced research and development program in the United States
14 p2042 A83-32265

Amorphous silicon solar cells produced by a consecutive, separated reaction chamber method
14 p2043 A83-32277

Charge collection in a-Si:H solar cells
14 p2043 A83-32278

Large area and high efficiency A-Si:H solar cell
14 p2044 A83-32284

Post-hydrogenated CVD amorphous silicon p-i-n diodes for photovoltaic applications
14 p2005 A83-32285

Stability of amorphous silicon solar cells with pin structure
14 p2044 A83-32286

Large area hydrogenated amorphous silicon for photovoltaic application
14 p2044 A83-32289

Novel plasma chemical methods for doping a-Si:H
14 p2044 A83-32290

Electronic properties of doped amorphous SiO(x)
14 p2089 A83-32291

Impurity diffusion in amorphous silicon and its implications for solar cells
14 p2005 A83-32336

Pd/a-Si:H metal-insulator-semiconductor Schottky barrier diode for hydrogen detection
15 p2150 A83-33845

Optically enhanced amorphous silicon solar cells
15 p2189 A83-33847

Electrical characteristics of amorphous iron-tungsten contacts on silicon
15 p2238 A83-33851

Computer simulation of amorphous silicon based alloy p-i-n solar cells
15 p2189 A83-33919

Variable minority carrier transport model for amorphous silicon solar cells
15 p2192 A83-34667

Measurement of boron diffusivity in hydrogenated amorphous silicon by using nuclear reaction B-10(n, alpha)Li-7
16 p2418 A83-35437

Mobility-lifetime product and interface property in amorphous silicon solar cells
16 p2418 A83-35442

Laser processing of silicon
16 p2420 A83-35993

High performance hydrogenated amorphous silicon solar cells made at a high deposition rate by glow discharge of disilane
16 p2371 A83-36774

Theory of electron-hole kinetics in amorphous semiconductors under illumination - Application to solar cells
17 p2584 A83-38213

Deep traps in metal-insulator-chemically vapor-deposited amorphous Si(n)x diodes
17 p2584 A83-38214

Thickness dependence of kink temperature and band bending in amorphous silicon
17 p2585 A83-38954

Workshop on Light-induced Change in a-Si:H and its Effect on Solar Cell Stability, San Diego, CA, September 24, 25, 1982
18 p2707 A83-39461

Stability of P-I-N hydrogenated amorphous silicon solar cells to light exposure
18 p2707 A83-39462

Light-induced effects in amorphous silicon material and devices
18 p2749 A83-39464

Light-induced instability of amorphous silicon photovoltaic cells
18 p2707 A83-39465

Effects of optical stress on the properties of sputtered amorphous silicon solar cells and thin films
18 p2707 A83-39466

Analysis of photo-induced changes in the performance of amorphous silicon solar cells
18 p2708 A83-39467

Staebler-Wronski effects in hydrogenated amorphous Si(1-x)Ge(x)
18 p2749 A83-39469

The effect of light soaking on the low temperature photoconductivity of hydrogenated amorphous silicon
18 p2749 A83-39470

The interpretation of photoconductivity measurements in hydrogenated amorphous silicon
18 p2750 A83-39471

Origin of the photo-induced changes in hydrogenated amorphous silicon
18 p2750 A83-39473

Optical constants of amorphous hydrogenated carbon and silicon-carbon alloy films and their application in high temperature solar selective surfaces
18 p2708 A83-39931

Hydrogenated amorphous silicon produced by laser induced chemical vapor deposition of silane
19 p2903 A83-40743

Spectroscopic laser scanning analysis of photo-induced current on a-Si solar cells
19 p2862 A83-41286

Stability of Pd/Nb2O5/amorphous hydrogenated silicon solar cells
20 p3011 A83-42356

Anodic oxide gate a-Si:H MOSFET
20 p2966 A83-42480

a-Si:H MIS position sensitive detector by anodic oxidation processes
20 p2966 A83-42490

Effect of boron compensation on the photovoltaic properties of amorphous silicon solar cells
20 p3055 A83-43601

Generation and amplification of ultrashort laser pulses and applications to electron trapping in amorphous media
22 p3299 A83-46683

A study of built-in potential in a-Si solar cells by means of back-surface reflected electroabsorption
23 p3478 A83-48702

Electronic properties of non-crystalline materials
24 p3634 A83-48776

New types of high efficiency solar cells based on a-Si
24 p3598 A83-48787

Effects of doping on transport and deep trapping in hydrogenated amorphous silicon
24 p3634 A83-48792

Reduction in the localized band-gap states in amorphous silicon by annealing and hydrogen implantation
24 p3634 A83-48793

Theoretical modeling of amorphous silicon-based alloy p-i-n solar cells
24 p3634 A83-48914

A study of the parameters of traps in hydrogenated amorphous silicon by the method of volt-farad characteristics
24 p3635 A83-49047

Photostimulated exoemission and photoconductivity of hydrogenated amorphous silicon
24 p3635 A83-49069

Investigation of in-situ sputtered a-Si(H) by AES
24 p3636 A83-50180

Preparation and properties of sputtered a-Si:H:F films
24 p3636 A83-50185

AMPERAGE
U ELECTRIC CURRENT

AMPHETAMINES
The effect of amphetamine and amizyl on the interaction of the delayed reaction and the conditioned reflex differentiation in rhesus monkeys and capuchins
01 p0079 A83-10532

AMPHIBIOUS AIRCRAFT
Dornier Do 24 TT(technology testbed) experimental amphibian
17 p2462 A83-37857

Development and testing of a high-technology amphibious flying vehicle
23 p3402 A83-47192

AMPHIBIOUS VEHICLES
NT AMPHIBIOUS AIRCRAFT
LCAC--from test craft to production design--- air cushion vehicles for amphibious assault landing operations
[AIAA PAPER 83-0622]
08 p1173 A83-22423

AMPHIBOLES
Geochemistry and petrogenesis of Archaean metavolcanic amphibolites from Fiskenaeset, S. W. Greenland
04 p0514 A83-16353

Recognition of extraneous argon components through incremental-release (Ar-40)/(Ar-39) analysis of biotite and hornblende across the Grenvillian metamorphic gradient in southwestern Labrador
15 p2201 A83-34496

AMPLIFICATION
NT POWER GAIN
NT SOUND AMPLIFICATION
NT WAVE AMPLIFICATION
Preliminary announcement of an 85 percent efficient reflector antenna
10 p1406 A83-26841

Temporal measurement of the gain of a CuCl laser
11 p1585 A83-28702

Superconducting current injection transistor
13 p1832 A83-30354

Small-signal gain in lethargic and conventional laser amplifiers
19 p2853 A83-41198

AMPLIFICATION FACTOR
U AMPLIFICATION

AMPLIFIER DESIGN
Two methods for the analysis of multifrequency regimes of microwave amplifiers
01 p0036 A83-10414

Concerning convective and absolute instabilities in bounded media --- wave amplifier and generator theory
01 p0036 A83-10416

A maser operating in the middle part of the millimeter range
01 p0054 A83-10418

Broadband monolithic integrated power amplifiers in gallium arsenide
03 p0308 A83-13440

Monolithic GaAs FET low-noise amplifiers for X-band applications
03 p0308 A83-13441

Broadband microwave power amplifiers using lumped-element matching and distributed combining techniques
03 p0313 A83-13998

A design method of super-wideband pulse amplifiers
03 p0314 A83-14129

Statistical models of power-combining circuits for O-type traveling-wave tube amplifiers
04 p0469 A83-15138

Designing YIG drivers
04 p0474 A83-16426

Design of a XeF-pumped second Stokes amplifier for blue-green production in H2
05 p0651 A83-17877

On design and performance of lossy match GaAs MESFET amplifiers
06 p0752 A83-18765

Broad-band GaAs monolithic amplifier using negative feedback
06 p0753 A83-18774

4-GHz high-efficiency broadband FET power amplifiers
07 p0920 A83-20556

A network modeling and design method for a 2-18-GHz feedback amplifier
07 p0923 A83-21536

A simplified 'real frequency' technique applied to broad-band multistage microwave amplifiers 07 p0923 A83-21537

Phase control of pulsed broadband microwave amplifiers 08 p1079 A83-22000

Highly sensitive temperature-stable DC amplifier for space probe experiment 08 p1080 A83-22279

Parasitic channels of a superregenerative parametric amplifier 08 p1082 A83-23168

An ultra-low-drift dc amplifier for use with photomultipliers 09 p1267 A83-23743

Practical design of 2-4 GHz low intermodulation distortion GaAs FET amplifiers with flat gain response and low noise figure 09 p1255 A83-24348

A two-stage monolithic IF amplifier utilizing a TaO₅ capacitor 09 p1256 A83-24681

A monolithic GaAs DC to 2-GHz feedback amplifier 09 p1256 A83-24682

Injection locking performance of a 41-GHz 10-W power combining amplifier 10 p1409 A83-25811

Design and operation of a collective millimeter-wave free-electron laser 10 p1427 A83-26014

Line shape parameter analysis of individual vibrational-rotational transitions in a CO₂ laser amplifier 10 p1428 A83-26023

Low-power high-drive CMOS operational amplifiers 10 p1410 A83-26125

Improving the power-added efficiency of FET amplifiers operating with varying-envelope signals 10 p1410 A83-26340

Four MOSFETs deliver 600 W of RF power 11 p1562 A83-28155

A broad-band traveling-wave maser for the range 40-46.5 GHz 13 p1849 A83-30236

A simple model of a dematron 13 p1834 A83-30719

Improvement of signal-to-noise ratio in a combination of a linear and a nonlinear amplifier 13 p1834 A83-30784

Preamplifiers and clock drivers for the University of California at Los Angeles Reticon spectrometer 14 p2017 A83-32020

Low-noise, low power dissipation GaAs monolithic broad-band amplifiers 14 p2008 A83-33459

Effects of the collector current fall time on the class E tuned power amplifier 15 p2150 A83-33889

Exact analysis of class E tuned power amplifier with only one inductor and one capacitor in load network 15 p2151 A83-33893

Receiver design for digital fiber optic transmission systems using Manchester (biphase) coding 16 p2343 A83-36602

A fluidic/pneumatic interface amplifier 17 p2501 A83-37117

An unguided wave Cerenkov amplifier 17 p2497 A83-37754

On theory and performance of solid-state microwave distributed amplifiers 17 p2497 A83-37799

Novel design of travelling-wave FET 17 p2500 A83-38876

A two-stage monolithic buffer amplifier for 20 GHz satellite communication 18 p2676 A83-39272

Small-signal gain in lethargic and conventional laser amplifiers 19 p2853 A83-41198

High efficiency broadband FET power amplifier for C-band TWT replacement 19 p2839 A83-41335

On noise in distributed amplifiers at microwave frequencies 21 p3122 A83-43836

Some problems of designing the system of time control of the sensitivity of pulse-echo flaw detectors 22 p3303 A83-46324

Computer-aided design of infrared detector preamplifiers having switched feedback resistors 22 p3292 A83-46604

A study of optical amplification in a double heterostructure GaAs device using the density matrix approach 22 p3301 A83-46825

L-band transistor HPA with adaptive bias [IAF PAPER 83-62] 23 p3444 A83-47248

Radio-frequency amplified based on a dc superconducting quantum interference device 24 p3572 A83-48795

A 20 GHz band 0.5 W GaAs FET amplifier for satellite communications 24 p3574 A83-49858

AMPLIFIERS

NT BEAM PLASMA AMPLIFIERS

NT BROADBAND AMPLIFIERS

NT CARCINOTRONS

NT CROSSED FIELD AMPLIFIERS

NT CURRENT AMPLIFIERS

NT DIFFERENTIAL AMPLIFIERS

NT DISTRIBUTED AMPLIFIERS

NT FEEDBACK AMPLIFIERS

NT FLUID AMPLIFIERS

NT FREQUENCY MODULATION PHOTOMULTIPLIERS

NT INTERMEDIATE FREQUENCY AMPLIFIERS

NT LIGHT AMPLIFIERS

NT LINEAR AMPLIFIERS

NT MICROWAVE AMPLIFIERS

NT OPERATIONAL AMPLIFIERS

NT PARAMETRIC AMPLIFIERS

NT PHOTOMULTIPLIER TUBES

NT POWER AMPLIFIERS

NT PREAMPLIFIERS

NT PUSH-PULL AMPLIFIERS

NT TRANSISTOR AMPLIFIERS

NT TRAVELING WAVE AMPLIFIERS

NT VOLTAGE AMPLIFIERS

Test results of Spacelab 2 infrared telescope focal plane --- photoconductive detector fabrication and JFET transimpedance amplifier design 03 p0405 A83-13452

AMPLITUDE DISTRIBUTION ANALYSIS

Amplitude coherence in an absorption region --- measurement on millimeter wave transmission loss 03 p0307 A83-14033

Amplification characteristics of injection-locked oscillator having an opposite phase self-injection circuit 03 p0314 A83-14131

HR 6434 and the factors limiting pulsational amplitudes of delta Scuti stars 03 p0421 A83-14150

Determination of the vibrating phase by a time-averaged shadow moire method 03 p0395 A83-14396

The structure of the radiation pattern and the role of amplitude-phase distributions in curved antenna arrays 04 p0467 A83-15748

Structure of the spatial distribution of the amplitude and polarization characteristics of Pi2 geomagnetic pulsations in the region of the activation of auroras 05 p0663 A83-17615

Beamshaping of sectoral and pyramidal horns with stepped amplitude distribution 06 p0741 A83-18659

Measuring amplitude and phase of microirradiations by heterodyne speckle interferometry 07 p0930 A83-20796

Characteristics of the amplitude distribution of acoustic emission in the nucleation and propagation of fatigue cracks 07 p0943 A83-21405

Angular spectrum representation of scattered electromagnetic fields 08 p1161 A83-22668

Maximum-power and amplitude-equalizing algorithms for phase control in space diversity combining 09 p1248 A83-23872

Synthesis of an array with an amplitude or phase field distribution fixed on part of the aperture 09 p1251 A83-25163

On the synthesis of antenna arrays with a variable amplitude-phase distribution in certain radiators 13 p1828 A83-30716

A method for measuring amplitude and phase of each radiating element of a phased array antenna 17 p2494 A83-38033

A complex amplitude detector for radiofrequency signals analysis 21 p3127 A83-45418

AMPLITUDE MODULATION

Group time and bandwidth of signals modulated simultaneously in amplitude and frequency 01 p0032 A83-11335

Carrier recovery systems for arbitrarily mapped APK signals 03 p0312 A83-13867

Measurement of scattering parameters at 35 GHz using amplitude-modulated homodyne detection 04 p0474 A83-16212

High-rate amplitude and frequency modulation of semiconductor lasers 04 p0486 A83-16218

The parametric discrete Fourier transformation 06 p0802 A83-18028

The amplitude modulation of the short-period oscillations of the earth's electromagnetic field 06 p0787 A83-19421

Calculation of the frequency spectrum of an electron beam in a klystron with premodulation 07 p0921 A83-20855

Measurement of the linewidth enhancement factor alpha of semiconductor lasers 07 p0937 A83-21363

Amplitude modulation of a nonlinear progressive ionisation wave 09 p1347 A83-23661

The scattering of amplitude-modulated waves by bodies of complex shape 09 p1251 A83-25082

Feedback control of parametric instabilities 10 p1461 A83-25398

Contributions of amplitude and phase modulation to diffraction efficiency in three-dimensional reflective holograms 10 p1422 A83-26470

Electrostatic acceleration of a modulated electron beam 11 p1560 A83-27449

Conditions of amplitude self-modulation in a delay oscillator 11 p1561 A83-27943

Damping of large-amplitude plasma waves propagating perpendicular to the magnetic field 13 p1926 A83-31358

Connection for wave modulation

14 p2080 A83-32835

An automatically controlled predistorer for multilevel quadrature amplitude modulation 16 p2347 A83-36608

Direct amplitude modulation of short-cavity GaAs lasers up to X-band frequencies 17 p2514 A83-38042

Non-linear phenomena in the ionosphere traversed by high power radio wave 17 p2495 A83-38541

Enhanced frequency modulation in cleaved-coupled-cavity semiconductor lasers with reduced spurious intensity modulation 22 p3299 A83-46722

Cochannel and intersymbol interferences in QAM system 24 p3571 A83-49965

AMPLITUDE PROBABILITY ANALYSIS

U AMPLITUDE DISTRIBUTION ANALYSIS

AMPLITUDES

NT PULSE AMPLITUDE

NT SCATTERING AMPLITUDE

The method of differential amplitude approximation for solving dynamic viscoelasticity problems 01 p0059 A83-10683

The relationship between the amplitude and phase of wave fields 02 p0232 A83-11645

Investigation of fluctuations in a varactor frequency-tripler 04 p0471 A83-15738

A comparative analysis of the amplitude-frequency characteristics of the microphone potentials of humans as determined by experiments and with a mathematical model 12 p1764 A83-29304

Direct observational upper limit to gravitational radiation from millisecond pulsar PSR1937+214 15 p2261 A83-34383

Threshold singularities in the diffraction of electromagnetic waves by a periodic half-space 15 p2145 A83-34708

Propagation of magnetostatic waves in a structure with a tangentially magnetized anisotropic ferrite layer 15 p2152 A83-34711

Oscillation-amplitude fluctuations of a BWT operating in the short-wave part of the millimeter range 15 p2152 A83-34712

The effect of oscillation amplitudes on the noise of IMPATT-diode oscillators with uniformly doped GaAs 15 p2152 A83-34713

Determination of the form of the amplitude-frequency response of variable-length optical waveguides 15 p2232 A83-34885

Amplitude and phase errors involved in retrieving depolarized radar cross section measurements --- from remotely sensed natural surfaces 22 p3315 A83-46237

AMPOULES

Convective-diffusive transport in vapor growth ampoules 18 p2685 A83-39897

ANAEROBES

Investigation of the localization of dehydrogenases in aerobic and anaerobic bacteria at the submicroscopic level 01 p0078 A83-10421

The utilization of carbon monoxide by anaerobic bacteria 01 p0078 A83-10422

Effects of hyperbaric oxygen on anaerobic organisms 02 p0222 A83-12260

The effect of glucose concentration and pH on hydrogen production by Rhodopseudomonas sphaeroides VM 81 15 p2193 A83-35303

ANALGESIA

An investigation of the changes in the opiate-like, bombazine-like, and P-like substances in rats with stress-induced anesthesia 06 p0795 A83-18990

Analgesic intestinal peptides - New agents of bodily defense 07 p0975 A83-21000

ANALOG CIRCUITS

Automatic selection of switching paths 01 p0037 A83-10734

An examination of background noise in analog integrated circuits and components --- French thesis 02 p0166 A83-11765

Analog multipliers in radio-electronic equipment --- Russian book 04 p0472 A83-15832

Analysis of the effect of dispersion errors of memories on the precision of discrete spectral analysis 06 p0802 A83-19180

An analog open-loop adaptive-array antenna system 08 p1077 A83-22733

Noise in time-discrete analog filters 09 p1252 A83-23409

Realization of some analog functions with switchable feedback loops 09 p1253 A83-23694

Mode-fault diagnosis and a design of testability 09 p1333 A83-24796

Organization of the structure and computational process of a multiprocessor hybrid computing system with a network analog processor 12 p1768 A83-29346

Analog multifrequency fault diagnosis 15 p2151 A83-33923

Node-fault diagnosis and a design of testability
15 p2151 A83-33926

Integrated surface acoustic wave/field-effect transistor
high-speed analog memory 16 p2347 A83-36772

An algebraically derived nonlinear control theory
17 p2566 A83-37098

A system for analog-digital conversion with signal
processing in the frequency domain --- German thesis
17 p2563 A83-37502

Functional analog integrated microcircuits --- Russian
book 21 p3126 A83-45017

ANALOG COMPUTERS

Fully-parallel relaxation algebraic operations for optical
computers 02 p0236 A83-12398

Software for hybrid computing systems. I - Systems of
analog and hybrid programming automation
19 p2888 A83-41421

Software for hybrid systems. II - Systems software
24 p3620 A83-50202

ANALOG DATA

Analysis of systems containing multiple, irregular
sampling 01 p0095 A83-11131

Discrete-analog signal processing --- Russian book
03 p0311 A83-13815

Rapid acquisition techniques for Direct-Sequence
Spread Spectrum Systems using an analog detector
07 p0903 A83-19677

Video compression using sampled data analog
devices 08 p1078 A83-22813

Adaptive companded pulse-code-modulation
15 p2146 A83-35103

The transmission of analog information over digital
communications channels --- Russian book
23 p3443 A83-48425

ANALOG SIMULATION

Analog computer simulation of a Duffing oscillator and
comparison with statistical linearization
02 p0233 A83-12869

Identification of certain dynamic characteristics of a
helicopter-autopilot system by means of simulation
08 p1047 A83-23222

Modeling of optical impedance spectroscopy
11 p1572 A83-27530

Signal simulations, signal generators, and signal
integrity 13 p1835 A83-30973

A photovoltaic array simulator
14 p2047 A83-32845

Electronic circuits for the simulation of physical
processes in semiconductor structures by the method of
direct analogies 16 p2347 A83-36904

Laboratory simulation of tunable diode laser remote
measurement of atmospheric gases using topographic
targets 17 p2510 A83-37741

The modeling of inverse problems of heat conduction
with movable phase transition boundaries
19 p2844 A83-41571

Simulation of detonation cell kinematics using
two-dimensional reactive blast waves
24 p3580 A83-49836

A method for the simulation of the transfer of charge
carriers and the distribution of electrostatic potential in
semiconductor structures 24 p3575 A83-50208

ANALOG TO DIGITAL CONVERTERS

Data enhancement and analysis through mathematical
deconvolution of signals from scientific measuring
instruments 01 p0051 A83-11055

Design of a microprocessor-based A/D converter with
drift and offset correction 03 p0385 A83-13499

Prototype of an integrated-optics four-digit analog-digital
converter 05 p0685 A83-17062

Bandpass signal sampling and coherent detection
06 p0749 A83-19048

A symmetrical three-junction superconducting quantum
interference device 07 p0921 A83-20755

Investigation of the noise immunity of analog-to-digital
conversion by adaptive-averaging methods
08 p1156 A83-22123

Resolution improvement in an analog-to-digital converter
by the superposed dither signal
08 p1080 A83-22231

Switched-capacitor second-order noise-shaping coder
08 p1082 A83-22923

Design, fabrication, and evaluation of 2- and 3-bit GaAs
MESFET analog-to-digital converter IC's
09 p1256 A83-24678

An automatic test set for the dynamic characterization
of A/D converters 13 p1836 A83-31288

2-bit 1-Gsample/s electro-optic guided-wave
analogue-to-digital convertor system
13 p1838 A83-31780

6-bit 25 MHz NMOS parallel A/D convertor
13 p1838 A83-31786

Investigation of the characteristics of an integrated-optic
analog-to-digital converter 15 p2232 A83-34890

Digitech - A microcomputer-digitizer facility for
automated testing of motor performance during discrete
positioning movements 16 p2402 A83-35567

A system for analog-digital conversion with signal
processing in the frequency domain --- German thesis
17 p2563 A83-37502

Digital complex sampling 20 p2963 A83-42481

Picosecond transient digitizer for optical pulse analysis
22 p3360 A83-46651

ANALOGIES

NT HYDRAULIC ANALOGIES

ANALYSIS (MATHEMATICS)

NT ABEL FUNCTION

NT ANALYTIC FUNCTIONS

NT APPROXIMATION

NT ASYMPTOTES

NT ASYMPTOTIC SERIES

NT BANACH SPACE

NT BESSEL FUNCTIONS

NT BIHARMONIC EQUATIONS

NT BORN APPROXIMATION

NT BORN-OPPENHEIMER APPROXIMATION

NT BURGER EQUATION

NT CALCULUS

NT CALCULUS OF VARIATIONS

NT CAUCHY INTEGRAL FORMULA

NT CAUCHY-RIEMANN EQUATIONS

NT CHANDRASEKHAR EQUATION

NT CHEBYSHEV APPROXIMATION

NT COLLINEARITY

NT COMBINATORIAL ANALYSIS

NT COMPLEX VARIABLES

NT COMPOSITE FUNCTIONS

NT COMPUTATIONAL CHEMISTRY

NT COMPUTATIONAL FLUID DYNAMICS

NT CONFORMAL MAPPING

NT CONJUGATES

NT CONTINUITY (MATHEMATICS)

NT CONVOLUTION INTEGRALS

NT COSINE SERIES

NT CUBIC EQUATIONS

NT DIFFERENCE EQUATIONS

NT DIFFERENTIAL CALCULUS

NT DIFFERENTIAL EQUATIONS

NT DUFFING DIFFERENTIAL EQUATION

NT EDDINGTON APPROXIMATION

NT EINSTEIN EQUATIONS

NT ELLIPTIC DIFFERENTIAL EQUATIONS

NT ELLIPTIC FUNCTIONS

NT ENTIRE FUNCTIONS

NT ERROR ANALYSIS

NT EXISTENCE THEOREMS

NT EXPONENTIAL FUNCTIONS

NT EXTREMUM VALUES

NT FALKNER-SKAN EQUATION

NT FINITE DIFFERENCE THEORY

NT FINITE ELEMENT METHOD

NT FOKKER-PLANCK EQUATION

NT FOURIER ANALYSIS

NT FOURIER SERIES

NT FOURIER TRANSFORMATION

NT FOURIER-BESSEL TRANSFORMATIONS

NT FREDHOLM EQUATIONS

NT FUNCTION SPACE

NT FUNCTIONAL ANALYSIS

NT FUNCTIONAL INTEGRATION

NT GAMMA FUNCTION

NT GAUSS EQUATION

NT GREEN FUNCTION

NT HALF PLANES

NT HALF SPACES

NT HANKEL FUNCTIONS

NT HARMONIC ANALYSIS

NT HARMONIC FUNCTIONS

NT HARTREE APPROXIMATION

NT HELMHOLTZ VORTICITY EQUATION

NT HILBERT SPACE

NT HILBERT TRANSFORMATION

NT HILL DETERMINANT

NT HYPERBOLIC DIFFERENTIAL EQUATIONS

NT HYPERBOLIC FUNCTIONS

NT HYPERGEOMETRIC FUNCTIONS

NT HYPERPLANES

NT INTEGRAL CALCULUS

NT INTEGRAL EQUATIONS

NT INTEGRAL TRANSFORMATIONS

NT INTERPOLATION

NT ITERATION

NT J INTEGRAL

NT JACOBI INTEGRAL

NT JACOBI MATRIX METHOD

NT KERNEL FUNCTIONS

NT LAGUERRE FUNCTIONS

NT LAME WAVE EQUATIONS

NT LAPLACE TRANSFORMATION

NT LEAST SQUARES METHOD

NT LEGENDRE FUNCTIONS

NT LIAPUNOV FUNCTIONS

NT LIMITS (MATHEMATICS)

NT LINEAR EQUATIONS

NT LIOUVILLE EQUATIONS

NT LIOUVILLE THEOREM

NT LOGARITHMS

NT MACLAURIN SERIES

NT MATHIEU FUNCTION

NT MAXIMA

NT MEAN SQUARE VALUES

NT MEASURE AND INTEGRATION

NT MEROMORPHIC FUNCTIONS

NT MINIMA

NT MONGE-AMPERE EQUATION

NT MONTE CARLO METHOD

NT NAKED SINGULARITIES

NT NEUMANN PROBLEM

NT NEWTON-RAPHSON METHOD

NT NOMOGRAPHS

NT NONLINEAR EQUATIONS

NT NONLINEAR EVOLUTION EQUATIONS

NT NUMERICAL ANALYSIS

NT NUMERICAL DIFFERENTIATION

NT NUMERICAL INTEGRATION

NT ORTHOGONAL FUNCTIONS

NT OSEEN APPROXIMATION

NT PADE APPROXIMATION

NT PARABOLIC DIFFERENTIAL EQUATIONS

NT PARTIAL DIFFERENTIAL EQUATIONS

NT PARTICLE IN CELL TECHNIQUE

NT PARTITIONS (MATHEMATICS)

NT PERIODIC FUNCTIONS

NT PFAFF EQUATION

NT PHASE-SPACE INTEGRAL

NT POHLHAUSEN METHOD

NT POISSON EQUATION

NT POWER SERIES

NT PRONY SERIES

NT QUADRATIC EQUATIONS

NT QUARTIC EQUATIONS

NT RATIONAL FUNCTIONS

NT RAYLEIGH-RITZ METHOD

NT REAL VARIABLES

NT RELAXATION METHOD (MATHEMATICS)

NT RITZ AVERAGING METHOD

NT RUNGE-KUTTA METHOD

NT SCHWARZ-CHRISTOFFEL TRANSFORMATION

NT SERIES (MATHEMATICS)

NT SINE SERIES

NT SINGULAR INTEGRAL EQUATIONS

NT SINGULARITY (MATHEMATICS)

NT SOMMERFELD APPROXIMATION

NT SPHERICAL HARMONICS

NT STURM-LIOUVILLE THEORY

NT TAYLOR SERIES

NT TRIGONOMETRIC FUNCTIONS

NT VECTOR ANALYSIS

NT VLASOV EQUATIONS

NT VOLTERRA EQUATIONS

NT VORTICITY

NT WEIERSTRASS FUNCTIONS

NT WEIGHTING FUNCTIONS

NT WIENER HOPF EQUATIONS

NT ZONAL HARMONICS

Current problems of mathematical physics and
computational mathematics --- Russian book
07 p0988 A83-20302

ANALYSIS OF VARIANCE

The measurement of surface topography parameters
described by the composition of the random and
deterministic components 08 p1092 A83-22005

ANALYTIC FUNCTIONS

NT ENTIRE FUNCTIONS

Methods for practical calculations of light fields under
conditions of multiple scattering
09 p1347 A83-25257

New solutions of Einstein equations from analytic
mappings 10 p1471 A83-25408

The Sommerfeld half-plane problem revisited. II - The
factoring of a matrix of analytic functions
10 p1471 A83-25461

Numerical conformal mapping and analytic
continuation 10 p1470 A83-25875

The value distribution of holomorphic maps --- Russian
book 12 p1774 A83-29336

A generalization of the Hines' dispersion relation --- for
real atmosphere 16 p2377 A83-36108

ANALYTIC GEOMETRY

NT CONICS

NT LOCI

NT OBLATE SPHEROIDS

NT PARABOLAS

NT PROLATE SPHEROIDS

ANALYZERS

- NT SPHEROIDS
 NT TORUSES
 NT TRIGONOMETRY
 Exact expressions for radiative transfer in a three-dimensional rectangular geometry 04 p0532 A83-16438

ANALYZERS

- NT SIGNAL ANALYZERS
 Equipment for measuring ionospheric parameters by means of a cylindrical Langmuir probe and a planar retarding-potential analyzer on the Cosmos-900 satellite 10 p1386 A83-25335
 The optimal design for spectral gas analyzers of atmospheric pollution 11 p1573 A83-28201

ANAPHYLAXIS

- Environmentally induced cholinergic urticaria and anaphylaxis 15 p2214 A83-34989

ANATOMY

- NT ABDOMEN
 NT ADRENAL GLAND
 NT AORTA
 NT ARM (ANATOMY)
 NT ARTERIES
 NT BARORECEPTORS
 NT BLOOD VESSELS
 NT BONES
 NT BRAIN
 NT BRAIN STEM
 NT BRONCHI
 NT CAPILLARIES (ANATOMY)
 NT CARDIAC AURICLES
 NT CARDIAC VENTRICLES
 NT CARDIOVASCULAR SYSTEM
 NT CEREBRAL CORTEX
 NT CEREBRUM
 NT CHEMORECEPTORS
 NT CHEST
 NT CIRCULATORY SYSTEM
 NT COCHLEA
 NT COLLAGENS
 NT CONJUNCTIVA
 NT CONNECTIVE TISSUE
 NT CORNEA
 NT CRANIUM
 NT DIASTOLE
 NT DIGESTIVE SYSTEM
 NT EAR
 NT ELBOW (ANATOMY)
 NT ENDOCRINE GLANDS
 NT EOSINOPHILS
 NT ERYTHROCYTES
 NT EYE (ANATOMY)
 NT FEET (ANATOMY)
 NT FINGERS
 NT FOREARM
 NT GASTROINTESTINAL SYSTEM
 NT GLOMERULUS
 NT GRAVIRECEPTORS
 NT HAND (ANATOMY)
 NT HEAD (ANATOMY)
 NT HEART
 NT HEMATOPOIESIS
 NT HEMATOPOIETIC SYSTEM
 NT HIPPOCAMPUS
 NT HUMAN BODY
 NT INTESTINES
 NT INTRACRANIAL CAVITY
 NT JOINTS (ANATOMY)
 NT KIDNEYS
 NT KNEE (ANATOMY)
 NT LABYRINTH
 NT LEG (ANATOMY)
 NT LEUKOCYTES
 NT LIMBS (ANATOMY)
 NT LIVER
 NT LUNGS
 NT LYMPHOCYTES
 NT MIDDLE EAR
 NT MUSCULOSKELETAL SYSTEM
 NT MYOCARDIUM
 NT NECK (ANATOMY)
 NT NOSE (ANATOMY)
 NT OCULOMOTOR NERVES
 NT ORGANS
 NT OTOLITH ORGANS
 NT PANCREAS
 NT PHARYNX
 NT PHOTORECEPTORS
 NT PINEAL GLAND
 NT PITUITARY GLAND
 NT PROPRIOCEPTORS
 NT RESPIRATORY SYSTEM
 NT RETINA
 NT SALIVARY GLANDS
 NT SKULL
 NT SPLEEN
 NT STOMACH
 NT SYSTOLE
 NT TEETH
 NT TESTES
 NT THERMORECEPTORS
 NT THYMUS GLAND
 NT THYROID GLAND
 NT TIBIA
 NT TORSO
 NT TRACHEA
 NT UTERUS
 NT VASCULAR SYSTEM
 NT VEINS
 NT VERTEBRAE
 NT VERTEBRAL COLUMN
 NT VESTIBULES
 NT WRIST
 The pathological anatomy of shock lung 01 p0081 A83-11390
- ANDES MOUNTAINS (SOUTH AMERICA)**
 Temporary lakes and salt plains in the high plateaus of the Andes /Bolivia/ - A continuing survey of periodic hydrologic phenomena using the geostationary satellite GOES-EST 03 p0360 A83-14574
- ANDESITE**
 Sulfide saturation of basalt and andesite melts at high pressures and temperatures 07 p0963 A83-21045
- ANDROMEDA GALAXIES**
 Bulge X-ray sources and Novae in M31 01 p0118 A83-10951
 Novae as sources of nitrogen in galaxies 02 p0253 A83-11612
 Gravitationally induced spurs in spiral galaxies - An example in M31 06 p0843 A83-19488
 The structure of spiral arm S6 in the Andromeda Nebula 07 p1007 A83-20666
 A radio continuum survey of M31 at 4850 MHz. I - Observations - List of sources 07 p1008 A83-21220
 Supernova remnants in M31 08 p1179 A83-21851
 The supernovae near the nuclei of M31 and the Galaxy 08 p1182 A83-23040
 Novae --- eruptive stars as precursors of planetary nebulae 09 p1353 A83-23909
 Diameter distribution and Sigma-D relation of SNRs in M31 and M33 12 p1785 A83-28894
 Photoelectric photometry of star clusters in M31. VIII 12 p1788 A83-29488
 Interstellar absorption in three Bode fields in the Andromeda Nebula 15 p2253 A83-33702
 Star complexes in the Andromeda Nebula 15 p2253 A83-33713
 Photoelectric catalogue of globular clusters in the Andromeda Nebula M31 and its companions NGC 147, NGC 185, and NGC 205 15 p2249 A83-34785
 Masses and mystery in the local group --- of galaxies 18 p2771 A83-39670
 Dynamics of the stellar component of the bulge of M31 19 p2918 A83-41617
 H-alpha observations of four novae in M31 21 p3226 A83-45534
 A high resolution HI survey of M31 24 p3640 A83-49204
 High velocity HI in the inner 5 kpc of M31 24 p3640 A83-49205
 Mass distribution and dark halos 24 p3654 A83-49215
- ANECHOIC CHAMBERS**
 Wind tunnel measurements of blade/vane ratio and spacing effects on fan noise 04 p0533 A83-15317
 Microwave anechoic chambers --- Russian book 07 p0902 A83-20380
- ANELASTICITY**
 Spurious mass loss in some mesometeorological models 06 p0789 A83-18241
 Anelastic response of the earth to a dip slip earthquake 07 p0957 A83-19869
 Anelastic relaxation controlled cyclic creep and cyclic stress rupture behavior of an oxide dispersion strengthened alloy 07 p0885 A83-20263
 Allowing for temperature in descriptions of the delayed fracture of inelastic materials 13 p1865 A83-30056
- ANEMIAS**
 Fluid shifts and erythropoiesis - Relevance to the 'anemia' of space flight 11 p1637 A83-27801
- ANEMOMETERS**
 NT HOT-FILM ANEMOMETERS
 NT HOT-WIRE ANEMOMETERS
 NT LASER ANEMOMETERS
 NT SONIC ANEMOMETERS
 Fibre-optic laser Doppler anemometer with Bragg frequency shift utilising polarisation-preserving single-mode fibre 02 p0177 A83-12010
 A high-resolution ionic anemometer for boundary-layer measurements --- in atmosphere 02 p0216 A83-12955

Initial results from the use of ionic anemometers under stratospheric balloons - Application to the high-resolution analysis of stratospheric motions 02 p0216 A83-12956

The use of multiple wall probes to identify coherent flow patterns in the viscous wall region 04 p0479 A83-16265

A dual focus fiber optic anemometer for measurements in wet steam 10 p1422 A83-26422
 Directional gas-flow measurement with pyroelectric anemometers (PA) 17 p2512 A83-38532

The dynamics of the constant temperature detector system 17 p2513 A83-38863

Raman anemometry, a method for component-selective velocity measurements of particles in a flow 20 p2990 A83-42950

ANEMOMETRY

U VELOCITY MEASUREMENT

ANESTHESIA

Regional circulatory responses to head-out water immersion in anesthetized dog 05 p0672 A83-17339

ANESTHETICS

NT CHLOROFORM
 NT METHYL CHLORIDE
 The antiarrhythmic effect of intramuscular and enteral injections of trimecain 03 p0374 A83-13630

ANGIOGRAPHY

Discordance of exercise thallium testing with coronary arteriography in patients with atypical presentations 07 p0978 A83-21053

Mechanisms of the regulation of high cardiac output in patients with hypertension (angiocardiographic investigation) 17 p2559 A83-38177

The diagnosis of changes in the vessels and membranes of eyes using fluorescent angiography 17 p2560 A83-38202

The elevation of the ST segment during physical loading Computer analysis, comparison with angiographic data, and clinical significance 18 p2735 A83-40547

ANGLE OF ATTACK

The measurement of impulsive forces on a wind tunnel model with a conventional strain gage balance 01 p0014 A83-11069

Support interference in static and dynamic tests --- of wind tunnel models at high angles of attack 01 p0014 A83-11074

Advanced multiple output air data sensor for angle of attack, pitot and static pressure measurements 01 p0009 A83-11098

X-wire sounding in an air inlet at high angle of attack [AAAF PAPER NT 81-15] 02 p0132 A83-11775

The unsteady suction analogy and applications --- in predicting longitudinal dynamic stability derivatives for slender wings at high angles of attack 03 p0277 A83-13128

Flow past a profile at angle of attack to a transonic flow 04 p0441 A83-15083

Concerning dynamic stall --- of laminar flow near leading edges of airfoils 04 p0442 A83-15150

Computation of supersonic viscous flows around pointed bodies at large incidence 05 p0578 A83-16474

[AIAA PAPER 83-0034] 05 p0578 A83-16475

High angle-of-attack calculations of the subsonic vortex flow on slender bodies 05 p0578 A83-16475

[AIAA PAPER 83-0035] 05 p0578 A83-16475

An analytical evaluation of the icing properties of several low and medium speed airfoils 05 p0579 A83-16525

[AIAA PAPER 83-0109] 05 p0579 A83-16525

Space Shuttle heating analysis with variation in angle of attack and surface condition 05 p0586 A83-16747

[AIAA PAPER 83-0486] 05 p0586 A83-16747

Transient ablation of blunt bodies at the angle of attack 05 p0637 A83-16803

[AIAA PAPER 83-0583] 05 p0637 A83-16803

The turbulence transport properties of a supersonic boundary layer on a sharp cone at angle-of-attack 05 p0591 A83-17927

[AIAA PAPER 83-0456] 05 p0591 A83-17927

The development of thermal boundary layers in airfoil-cascade flows with off-design angles of attack 06 p0713 A83-19155

The configuration of subsonic zones generated during supersonic flow past a spherically blunted cylinder at large angles of attack 06 p0713 A83-19443

An experimental investigation of heat transfer near the leading edge of inclined flat plate in hypersonic flow 08 p1041 A83-22071

Calculation of symmetric vortex separation affecting subsonic bodies at high incidence 08 p1042 A83-22137

Stability of steady sideslip equilibria for high alpha --- supersonic fighter aircraft 09 p1209 A83-24031

Delta canard configuration at high angle of attack 09 p1210 A83-24650

Oil flow separation patterns on an ogive forebody 09 p1198 A83-24662

Flat spin of slender bodies at high angles of attack
09 p1210 A83-24879

The attainability domain of a coasting vehicle
10 p1380 A83-26073

Hypersonic slender-wedge analysis with gradual change in angle of attack
11 p1526 A83-27864

Heating analysis of bent-nose biconics at high angles of attack using the parabolized Navier-Stokes equations [AIAA PAPER 83-1507]
14 p1970 A83-32744

Hypersonic viscous flows past general bodies at angle of attack and yaw
15 p2119 A83-33728

Three-dimensional turbulent boundary layers on bielliptic bodies in flows of a compressible gas at angle of attack
16 p2289 A83-35704

High angle-of-attack cascade measurements and analysis
16 p2292 A83-35875

Seven-hole cone probes for high angle flow measurement Theory and calibration
16 p2356 A83-36085

Stability of aircraft motion in critical cases
17 p2470 A83-37066

Bifurcation and limit cycle analysis of nonlinear systems with an application to aircraft at high angles of attack
17 p2470 A83-37080

Numerical simulation of hypersonic viscous flow over cones at very high incidence
[AIAA PAPER 83-1669]
17 p2444 A83-37180

The aerodynamic characteristics at the mid-span of a circular cylinder with tangential blowing
18 p2684 A83-39457

Nonequilibrium viscous shock-layer flows over blunt sphere-cones at angle of attack
18 p2638 A83-40006

Equivalent angle-of-attack method for estimating nonlinear aerodynamics of missile fins
18 p2638 A83-40010

Determination of aerodynamic parameters of a fighter airplane from flight data at high angles of attack
[AIAA PAPER 83-2066]
19 p2804 A83-41904

An investigation of the breakdown of the leading edge vortices on a delta wing at high angles of attack
[AIAA PAPER 83-2114]
19 p2793 A83-41941

Aerodynamics of pointed forebodies at high angles of attack
[AIAA PAPER 83-2117]
19 p2793 A83-41942

F/A-18 high angle of attack departure resistant criteria for control law development
[AIAA PAPER 83-2126]
19 p2806 A83-41950

Magnus effects at high angles of attack and critical Reynolds numbers
[AIAA PAPER 83-2145]
19 p2793 A83-41966

Wing modification for increased spin resistance
[SAE PAPER 830720]
20 p2937 A83-43327

Equivalent angle of attack for the lifting plane with linear camber-twist at low speeds
20 p2931 A83-43690

Estimation of parameters involved in high angle-of-attack aerodynamic theory using spin flight test data
[AIAA PAPER 83-2086]
20 p2937 A83-43809

Aerodynamic aspects of aircraft dynamics at high angles of attack
21 p3085 A83-43964

Preliminary supersonic analysis methods including high angle of attack
21 p3085 A83-43969

Effects of angle of attack on transonic flutter of a supercritical wing
23 p3403 A83-48213

Approximation to the optimization of a coast-glide trajectory
23 p3403 A83-48223

ANGLES (GEOMETRY)

NT ANGLE OF ATTACK

NT BRAGG ANGLE

NT ELEVATION ANGLE

NT GRAZING INCIDENCE

NT LEADING EDGE SWEEP

NT LOOK ANGLES (TRACKING)

NT SWEEP ANGLE

Precision measurement of the angles of a radio telescope
06 p0761 A83-18037

Possibility of determining the dispersed composition of a two-phase flow from small-angle light scattering
06 p0757 A83-18448

Accuracy of optical angle estimator operating through the turbulent atmosphere
06 p0736 A83-18584

Angles of multivariable root loci
[LIDS-P-1147]
06 p0803 A83-19320

Maximization of the accuracy of autonomous navigation in the case of the measurement of angles between directions from an artificial earth satellite to a known star and an unspecified ground reference point
09 p1215 A83-25043

Shock strength modification for reduced heat transfer to lifting re-entry vehicles
10 p1372 A83-26160

Optimum cone angles in aeroelastic flutter
11 p1599 A83-28720

Raindrop canting --- angle theory derived from drop response to wind shear
13 p1893 A83-31041

A worldwide examination of solar beam-slope angle values
19 p2861 A83-40768

ANGULAR ACCELERATION

The screen effect of the earth in the TETG - Theory of a screening experiment of a sample body at the equator, using the earth as a screen --- electrothermodynamic theory of gravitation
01 p0127 A83-11044

Gyro motion boundedness under uncertain angular acceleration about vehicle output axis
06 p0723 A83-19034

Vestibular and optokinetic reflexes in athletes
10 p1455 A83-26950

Control techniques to improve Space Shuttle solid rocket booster separation
13 p1811 A83-30164

Excessive roll damping can cause roll ratchet
13 p1808 A83-30171

Determination of higher order accelerations by a functional method
17 p2575 A83-37023

Secular variation of earth's gravitational harmonic J2 coefficient from Lageos and nontidal acceleration of earth rotation
17 p2545 A83-38597

ANGULAR CORRELATION

Precision measurement of the angles of a radio telescope
06 p0761 A83-18037

Excitation of atoms by collisions with ions - Photon-ion angle correlation measurements for determining the scattering amplitudes in magnetic substrates for He/ +/ + He and He/ +/ + Ne systems --- German thesis
06 p0808 A83-18524

On estimates of the galaxy correlation function
09 p1355 A83-25007

Isoplanatism with respect to the arrival angles of light rays in telescopes
16 p2426 A83-36856

ANGULAR DISTRIBUTION

Electron transverse velocity measurements in an intense relativistic electron beam diode
03 p0398 A83-13916

Interaction between a shock wave and a rarefaction wave in a problem concerning an angular piston
03 p0323 A83-14895

The angular divergence of radiation from flowing gas lasers
04 p0483 A83-15258

Reflected solar radiances from regional scale scenes
05 p0662 A83-17446

Determination of the temperature of the earth's surface on the basis of the angular structure of radiation in atmospheric windows
07 p0958 A83-19913

Angular spectrum representation of scattered electromagnetic fields
08 p1161 A83-22668

Angular and energy distribution of photons of the radiative scattering of a neutrino /antineutrino/ by an electron
09 p1344 A83-24205

Threshold structures in the cross sections of low-energy electron scattering of methane
09 p1343 A83-24825

The Venera 13 and Venera 14 spectrophotometry experiments
12 p1798 A83-28479

Angular distribution for electron excitation of the 4(2)S yields 4(2)P transition in Zn II - Comparison of experiment and theory
13 p1926 A83-30917

Photoelectron angular distributions of the N2O outer valence orbitals in the 19-31 eV photon energy range
15 p2227 A83-34012

Angle-resolved photoelectron spectroscopy of N2O measured as a function of photon energy from 14 to 70 eV
16 p2410 A83-36518

On angular distribution of radiation reflected from a ruffled sea
17 p2544 A83-38454

Modified likelihood function in the problem of determining the angular coordinates of sources by means of an antenna array
19 p2836 A83-42062

Angular and energy distributions of transition X-radiation
20 p3046 A83-43536

Angular distribution of electrons elastically scattered from O2 at 40-500 eV - A two-potential coherent approach
22 p3355 A83-45941

ANGULAR MOMENTUM

Stability of differential rotation in stars
01 p0126 A83-10943

Implications of gravitational interactions for the angular momenta of galaxies
01 p0126 A83-10965

The primeval magnetic field --- magnetic moment/intrinsic angular momentum relation
01 p0127 A83-11293

Cosmic turbulence and the angular momenta of astronomical systems
02 p0252 A83-11598

Nonlinear diffusive instabilities in differentially rotating stars
03 p0425 A83-14522

Rotational studies of late-type stars. I - Rotational velocities of solar-type stars
04 p0553 A83-15625

Estimated absolute dimensions and the inferred lifetime and angular momentum of W Ursae Majoris contact binaries
06 p0824 A83-18078

The structure of the atmospheric circulation of Venus, and possible irregularities in its rotation rate
07 p1030 A83-20661

Spinning fluids in general relativity
07 p0990 A83-21064

Consequences of a new experimental determination of the quadrupole moment of the sun for gravitation theory
08 p1186 A83-23238

The control of angular momentum for asymmetric rigid bodies
09 p1327 A83-24705

Angular momentum and star formation
10 p1495 A83-25852

Conservative mass transfer in close binary systems. I - Equations of motion for spin and orbital angular momenta
10 p1510 A83-26386

High orbital angular momentum states in H2 and D2
11 p1653 A83-27491

Clarification of the angular momentum/mass relation /J = pM-squared/ for astronomical objects
11 p1669 A83-27699

Loss of angular momentum in a binary system due to collisionless particles as monopoles or gravitinos - Does it exceed the gravitational radiation emission in the binary system PSR 1913 + 16?
12 p1792 A83-29037

A quest for initial parameters of the semi-detached eclipsing binary Mu(1)Sco
12 p1793 A83-29078

Comment on 'Dirac states for unit position and momentum Phase consistency of their angular momentum representations'
12 p1775 A83-29532

Artificial viscosity and the simulation of fragmentation --- of rotating self-gravitating clouds
13 p1945 A83-30368

Dynamics of gyro-elastic continua
[AIAA PAPER 83-0826]
14 p2032 A83-32795

Angular momentum loss and the evolution of cataclysmic binaries
14 p2106 A83-33212

Orbital periods of novae before eruption
15 p2257 A83-34096

The possible motions of a satellite about an oblate planet
15 p2246 A83-34391

Gravitational radiation from particles falling along the symmetry axis into a Kerr black hole - The momentum radiated
15 p2269 A83-34640

Interstellar magnetic fields
15 p2273 A83-35010

On the relativistic dynamics of spinning matter in space-time with curvature and torsion
16 p2427 A83-35615

Atmospheric angular momentum fluctuations, length-of-day changes and polar motion
16 p2376 A83-35638

Velocity-dependent factors for the Rubakov process for slowly moving magnetic monopoles
16 p2441 A83-35745

Variations in atmospheric angular momentum on global and regional scales and the length of day
16 p2381 A83-36157

Absolute synchronization - Faster-than-light particles and causality violation
16 p2407 A83-36551

The transfer of angular momentum by vortex disturbances during the loss of stability in a plane, axially symmetric shear flow
16 p2392 A83-36872

New control schemes for a magnetic attitude control system
17 p2478 A83-37455

Rotation and tidal interactions in BY Draconis binaries
19 p2914 A83-40724

Gravitational radiation from a particle with zero orbital angular momentum plunging into a Kerr black hole
19 p2916 A83-41171

Dynamic isolation via momentum compensation for precision instrument pointing
[AIAA PAPER 83-2176]
19 p2817 A83-41670

Optimal magnetic bearing control for high speed momentum wheels
[AIAA PAPER 83-2263]
19 p2855 A83-41733

Photoinduced angular motion of states and field splitting of levels
20 p3044 A83-42284

Rotation among Orion Ic G stars - Angular momentum loss considerations in pre-main-sequence stars
20 p3068 A83-42449

Internal rotation of the sun
20 p3082 A83-43542

The angular momentum of eclipsing binaries
20 p3062 A83-43663

Angular momentum transports in tropical cyclones
21 p3179 A83-44396

Gravitational lenses with angular momentum
21 p3228 A83-44407

The molecular weight barrier and angular momentum transport in radiative stellar interiors
21 p3230 A83-44440

The latitude-height structure of 40-50 day variations in atmospheric angular momentum
21 p3173 A83-44710

Three-body problem - A test of escape valid even for very small mutual distances
[IAF PAPER 83-319]
23 p3515 A83-47340

The angular momentum of celestial bodies and the fundamental dimensionless constants of nature
23 p3518 A83-47423

Angular momentum loss and the formation of W UMa systems
23 p3523 A83-47527

- Transfer of angular momentum in a galactic disk by the interaction of clouds of interstellar gas
24 p3653 A83-49166
- Relation between star formation and angular momentum in spiral galaxies
24 p3655 A83-49225
- ANGULAR MOTION**
- U ANGULAR VELOCITY**
- ANGULAR RESOLUTION**
- An angular approximation for the difference of two sines
01 p0102 A83-11109
- Concerning the resolving power of radar stations with antenna arrays
02 p0162 A83-11541
- A possibility of detecting optical radiation from superhigh-energy extensive air showers
02 p0276 A83-11761
- X-ray scattering of superpolished flat mirror samples
02 p0240 A83-12730
- Noise angle accuracy of several monopulse architectures
06 p0748 A83-19044
- High throughput non-dispersive hard X-ray spectrograph with angular resolution for cosmic bursts, transients, and sources
09 p1268 A83-24108
- Scientific importance of high angular resolution at infrared and optical wavelengths; Proceedings of the Conference, Garching, West Germany, March 24-27, 1981
10 p1494 A83-25826
- Atmospheric limitations to high angular resolution imaging
10 p1481 A83-25827
- Active optics in astronomy
10 p1481 A83-25828
- Development of an active optical mirror for astronomical applications
10 p1482 A83-25829
- Coherent large telescopes
10 p1494 A83-25836
- Rotation interferometry - A new technique for achieving high angular resolution
10 p1419 A83-25837
- Planets, asteroids and comets at high angular resolution
10 p1495 A83-25849
- The impact of high angular resolution observations on the study of pre main sequence objects
10 p1495 A83-25851
- Angular momentum and star formation
10 p1495 A83-25852
- Optical observations of active galaxies and quasars at high angular resolution
10 p1496 A83-25857
- Synthesis of a quasi-optimal meter of the angular coordinates of a point source of signals
10 p1407 A83-26931
- One-dimensional telescope aperture for brightness and velocity speckle interferometry measurements
13 p1939 A83-31029
- Current wisdom and future possibilities for gamma-ray sources within high-energy astronomy
18 p2755 A83-39277
- ANGULAR VELOCITY**
- Optical spectroscopy of HD102567 / 4U1145-61/
01 p0121 A83-10322
- Rotational velocity versus mass loss in Be stars
01 p0122 A83-10340
- Cosmic turbulence and the angular momenta of astronomical systems
02 p0252 A83-11598
- The vortex theory of rotors
04 p0442 A83-11595
- Adaptive control of a coherent meter of angular velocity
04 p0481 A83-15145
- Free rotation of a flight vehicle as a rigid body
04 p0531 A83-15382
- The axial distribution of the rotational velocity of a sunspot filament
05 p0707 A83-16853
- From the pendulum to the laser gyroscope
05 p0644 A83-16899
- Angular velocity of sunspots along the butterfly diagram
06 p0850 A83-18099
- Determination of the orientation of a sensor trihedron using angular information
07 p0988 A83-19938
- The structure of the atmospheric circulation of Venus, and possible irregularities in its rotation rate
07 p1030 A83-20661
- Effects of differential rotation on the gravitational figures of Jupiter and Saturn
08 p1189 A83-22935
- Rotational velocities and central velocity dispersions for a sample of S0 galaxies
08 p1182 A83-23035
- Construction of a complete solution for one problem of rigid-body dynamics
09 p1337 A83-23554
- Investigation of the sufficient and necessary conditions of the stability of the uniform rotations of a gyrost at about the principal axis
09 p1337 A83-23561
- Fibre-optic gyro for sensitive measurement of rotation
10 p1422 A83-26474
- Attitude estimation for a spinning satellite from gyroscope and star mapper data
10 p1385 A83-26589
- Asymptotic solution of the Navier-Stokes equations for the problems of the radial flow of a fluid in a gap formed by two rotating disks
11 p1569 A83-28532
- Solar rotation results at Mount Wilson
13 p1963 A83-29988
- Relationships between photospheric plasma angular velocity and solar activity
13 p1963 A83-29989

- On the depth dependence of the solar rotation velocity determined from Fraunhofer lines
15 p2281 A83-34307
- Another view of synodic solar rotation
15 p2281 A83-34309
- The evolution of spokes in Saturn's B ring
16 p2435 A83-35730
- Determination of higher order accelerations by a functional method
17 p2575 A83-37023
- Angular motion of a spinning projectile with a viscous liquid payload
17 p2470 A83-37067
- Recursive relationships for body axis rotation rates
17 p2575 A83-37074
- The choice of an astatic system for the regulation of the rotational velocity of a dc electric motor for azimuthal mountings of a gamma-telescope
17 p2496 A83-37720
- Daily variations of the photospheric equatorial rotation velocity of the sun and its absolute values in 1981 and 1982 as determined from measurements using a two-dimensional photodiode array
17 p2628 A83-38408
- Solar activity and rotation
18 p2783 A83-39228
- NGC 3200 - Is this what our Galaxy is like?
18 p2771 A83-39672
- The motions of the umbras in Hale active regions 16 862 and 16 863
18 p2785 A83-39979
- Angular motion influence on reentry vehicle ablation or erosion asymmetry formation
[AIAA PAPER 83-2111]
19 p2811 A83-41938
- Attitude determination and calibration for a three-dimensional angular velocimeter with the use of angular information
21 p3200 A83-45354
- Attitude determination for a rigid body
21 p3200 A83-45355
- State of the art and development potential of fiberoptic rotation sensors --- for inertial navigation
23 p3405 A83-47187
- Solar rotation 1947-1981 - Determined from sunspot data
23 p3530 A83-47454
- Nonlinear shell dynamics - Intrinsic and semi-intrinsic approaches
23 p3468 A83-47592
- ANHYDRIDES**
- NT INORGANIC PEROXIDES**
- NT ORGANIC PEROXIDES**
- NT PEROXIDES**
- NT SODIUM PEROXIDES**
- The dielectric properties of anhydride-cured epoxy potting compounds
07 p0899 A83-20458
- Tetrachlorophthalicanhydride based chloropolyesters for inhibition of double rocket propellants
[IAF PAPER 83-370]
23 p3439 A83-47362

ANIK B

U ANIK 2

ANIK C

U ANIK 3

ANIK SATELLITES

The program management of the Telesat space segment (A program manager's recollections)
[IAF PAPER 83-85]
23 p3513 A83-47259

ANIK 2

A ground loop attitude control system for Anik B
17 p2479 A83-37484

ANIK 3

Evaluation of a 14/12 GHz 90 Mbit digital satellite link
07 p0908 A83-19741

ANILINE

Fe/II/, Co/III/, Ni/II/, Cu/II/, Zn/II/, Cd/II/ and Hg/II/ complexes
of
4'-nitrobenzylidene-2-hydroxy-3,5-dinitroaniline
04 p0454 A83-16427

HPLC evaluation of MY 720 II --- High Performance Liquid Chromatography-tetraglycidylated methylenedianiline used in epoxy graphite composites
07 p0875 A83-20441

ANIMALS

NT BEETLES

NT BIRDS

NT CARIBOUS

NT DEER

NT DROSOPHILA

NT GRASSHOPPERS

NT HUMAN BEINGS

NT INSECTS

NT LOCUSTS

NT MAMMALS

NT MICROSPORES

NT PIGEONS

NT PRIMATES

NT PROTOZOA

NT PUPA

NT SPORES

NT SWINE

NT VERTEBRATES

NT WATERFOWL

NT WILDLIFE

ANISOTROPIC FLUIDS

Role of the pressure anisotropy in the relativistic pulsar wind
12 p1793 A83-29060

Contribution to the spectral study of slightly inhomogeneous and anisotropic turbulent flows --- French thesis
13 p1840 A83-30130

Quasi-axisymmetric circulation and superrotation in planetary atmospheres
13 p1962 A83-31750

Theory of radiation in an anisotropic plasma
18 p2746 A83-39741

Spatially self-similar cosmological model of Bianchi type-1(I)
18 p2775 A83-39749

ANISOTROPIC MEDIA**NT ANISOTROPIC FLUIDS**

Mean dyadic Green's function for remote sensing of a two layer random medium
01 p0063 A83-10066

Three dimensional crack analysis for an anisotropic body
01 p0059 A83-10709

Optimum control of the wave front and time profile of optical radiation propagating in a nonlinear medium
01 p0106 A83-10902

Stability of an economical difference scheme for the solution of a boundary value problem of diffraction
01 p0104 A83-11271

Dispersion relation for general anisotropic media
01 p0033 A83-11371

The pitch-angle anisotropy of solar protons according to stratospheric measurements
02 p0269 A83-11719

Frequency spectra and dynamics of long-period variations of isotropic and anisotropic fluxes --- of cosmic rays
02 p0273 A83-11728

Investigation of the anisotropy of ionospheric inhomogeneities by the differential-phase method
02 p0209 A83-12426

Radiative heat transfer in segregated media
[ASME PAPER 82-HT-16]
02 p0171 A83-12785

The effect of a strong gravitational wave on an anisotropic plasma
03 p0397 A83-13534

Hexagonal ferrites for millimeter wave applications
03 p0399 A83-13786

Interaction of waves in homogeneous media --- Russian book
03 p0390 A83-13822

Paraxial imaging and transforming in a medium with gradient-index Transmittance function
03 p0395 A83-14388

Initial results for multidimensional radiative transfer by the adding/doubling method
03 p0391 A83-14639

Anisotropy of the mechanical properties of deformed molybdenum
04 p0459 A83-15467

Stress function interface and boundary conditions in anisotropic materials
[ASME PAPER 82-WA/APM-4]
04 p0498 A83-15685

Equilibrium approximations in radiative heat transfer theory
04 p0479 A83-16170

Integral representation of electromagnetic fields in inhomogeneous anisotropic media
04 p0532 A83-16451

Filamentary instability of a relativistic electron beam in an anisotropic plasma
05 p0688 A83-17366

The most probable trajectories of rays in a plane-stratified scattering medium. I - A linear layer --- in ionosphere
05 p0663 A83-17612

Inverse Monte Carlo solutions for radiative transfer in inhomogeneous media
05 p0692 A83-17870

The use of the method of elementary cells for the numerical solution of elasticity problems. I - General principles of the elementary-cell method
06 p0777 A83-19316

Three-dimensional problem of backscattering in stratified, randomly inhomogeneous media
06 p0806 A83-19331

Approximate solution of the problem of the coefficient of reflection from a layer of a one-dimensional, randomly inhomogeneous medium
06 p0806 A83-19332

The singular edge in problems of diffraction by inhomogeneities with a gyrotropic medium
06 p0754 A83-19356

Emission from particles in periodic media
06 p0806 A83-19417

Inverse dynamic problems for an anisotropic elastic medium
07 p0944 A83-19632

Inverse ray tracing in elastic solids with unknown anisotropy
08 p1160 A83-22226

Weak and short waves in one-dimensional inhomogeneous materials with memory. II
08 p1160 A83-22228

A method of measuring the thermal conductivity of orthogonal anisotropic materials by a transient hot wire method
08 p1092 A83-22240

Reflection of electromagnetic waves at a biaxial-isotropic interface
08 p1161 A83-22330

An application of the Ambartsumian invariance principle to the investigation of extended lightguides with random inhomogeneities
09 p1344 A83-23484

The propagation of a soliton in a randomly inhomogeneous medium 09 p1336 A83-23485

A thermoelastic problem for a crack between dissimilar anisotropic media 09 p1278 A83-23669

Medium frequency linear vibrations of anisotropic elastic structures 09 p1278 A83-23680

Shearing in inhomogeneous media --- Russian book on fracture mechanics 09 p1278 A83-23823

Thermal stresses in anisotropic noncylindrical beams 09 p1280 A83-24511

A perturbation-theory method in the electrodynamic of inhomogeneous and nonstationary media /Review/ 09 p1339 A83-25078

The reconstruction of images scattered in an inhomogeneous medium --- Russian book 09 p1270 A83-25224

Surface waves in cubic elastic materials 10 p1437 A83-25304

A boundary integral equation for the solution of a class of problems in anisotropic inhomogeneous thermostatics and elastostatics 10 p1470 A83-25874

Submicrometer periodicity gratings as artificial anisotropic dielectrics 10 p1482 A83-25978

Scattering from a random slab 10 p1471 A83-26034

Radiation from a moving point charge in a drifting anisotropic plasma 10 p1486 A83-26041

Propagation of shock waves through nonuniform and random media 10 p1416 A83-26163

The interface crack between dissimilar anisotropic composite materials [ASME PAPER 83-APM-6] 10 p1441 A83-26443

The interface crack behavior in dissimilar anisotropic composites under mixed-mode loading [ASME PAPER 83-APM-7] 10 p1441 A83-26444

Deformations of anisotropic layered materials 10 p1442 A83-26818

On the nature of stress singularities in anisotropic layered composites 11 p1592 A83-27437

Exact solution to the formation and propagation problem of a non-stationary shock wave in bilinear media 11 p1567 A83-27723

Wave propagation in a medium with large-scale random irregularities 11 p1556 A83-27956

Theoretical stress analysis for a non-isotropic body of cylindrical configuration containing a row of cracks 11 p1596 A83-28447

Thermoelastic stress analysis of anisotropic composite sandwich plates by finite element method 11 p1599 A83-28721

An acoustic determination of the direction of the vibration of ordinary acoustic shear wave transducers 12 p1728 A83-29141

The carbonization of blends of pitches and resins to produce anisotropic carbon and the effects of pressure 12 p1712 A83-29504

The reproduction of atmospheric scattering indicatrices with an allowance made for the anisotropy of multiple effects 13 p1874 A83-30034

Operator calculation of anisotropic resonators with allowance for the optical mismatch of their elements 13 p1850 A83-30265

Radiation characteristics of a plane logarithmic spiral on a magnetized-plasma layer 13 p1828 A83-30284

Large anisotropic vibrational correlations in A15 Nb3Ge 13 p1929 A83-30922

A coordinate-free approach to wave reflection from a uniaxially anisotropic medium 13 p1914 A83-31144

Gas laser with a phase anisotropy in an axial magnetic field for arbitrary relative excitation of the active medium 14 p2022 A83-31902

A multi-dimensional differential approximation for absorbing/emitting and anisotropically scattering media with collimated irradiation [ASME PAPER 82-WA/HT-49] 14 p2008 A83-31937

The asymptotic behavior of the stress-strain state of inhomogeneously aging bodies near the tip of a crack 14 p2030 A83-32352

Radiative heat transfer in absorbing, emitting and anisotropically scattering boundary layer flows [AIAA PAPER 83-1504] 14 p2010 A83-32742

Magnetoresistance anisotropy due to the 2D-electron subsystem at a GaAs/AlGaAs interface 15 p2237 A83-33784

Solving fully 3-D nonlinear anisotropic multi-material heat conduction problems on a microcomputer 15 p2158 A83-34232

Padeapproximants for radiative transfer in inhomogeneous medium 15 p2226 A83-34537

Investigation of anisotropic problems in the mechanics of deformable bodies by the holographic moiremethod 16 p2355 A83-35512

Asymptotic laws of shock wave attenuation in inhomogeneous media 16 p2350 A83-35709

Instabilities of autowaves in excitable media connected with the phenomenon of critical curvature --- as in damaged regions of myocardial tissue 16 p2394 A83-36804

Beam propagation in uniaxial anisotropic media 17 p2580 A83-38048

Homogeneity conditions for elastic membranes 17 p2525 A83-38849

Application of the Monte Carlo method to solving statistical problems of radio-wave propagation in the randomly inhomogeneous ionosphere 18 p2674 A83-39434

Quasi-homogeneous states in composite materials with small-scale bends in the structure 18 p2701 A83-40112

Predicted elastic constants of transversely isotropic composites containing anisotropic fibers 18 p2652 A83-40160

Experimental investigation of anisotropic laminate structural behavior 18 p2652 A83-40167

Spatially homogeneous and anisotropic cosmological solution in Brans-Dicke theory 19 p2916 A83-41282

Applicability of the Bourret and Kraichnan approximations to solving problems of the propagation of coherent waves in a medium with strong random inhomogeneities 19 p2835 A83-41769

Investigation of anisotropic films by a resonance method 19 p2840 A83-41802

The dispersion properties of artificial anisotropic dielectrics 19 p2841 A83-41818

Emission from a moving charge during the instantaneous appearance of gyration in the medium 20 p3043 A83-42874

Fracture mechanics for delamination problems in composite materials 20 p3007 A83-43143

Performance of microstrip couplers on an anisotropic substrate with an isotropic superstrate 21 p3123 A83-43838

Light scattering from gaseous nitrous oxide - Effects of correlation between molecular and intermolecular axes upon the depolarization ratio in terms of the anisotropic potential choice 21 p3204 A83-44190

Coupled-mode analysis of anisotropic dielectric planar branching waveguides 21 p3205 A83-44227

The stressed state of an inhomogeneous orthotropic hollow cone 21 p3154 A83-44712

Practical single-polarisation anisotropic fibres 21 p3208 A83-44963

Phase distribution and ergodicity relative to the spatial variable in scattered fields 21 p3201 A83-45506

Electrodynamics of anisotropic waveguide structures --- Russian book 23 p3445 A83-48325

The beam propagation method - An analysis of its applicability --- to integrated optics 24 p3627 A83-48748

Transversely anisotropic optical fibers - Variational analysis of a nonstandard eigenproblem 24 p3628 A83-48968

A yield criterion for an anisotropic material characterized by the strength-differential effect --- for rolled metal sheets 24 p3592 A83-49034

Simple bounds for the stress intensity factors by the method of singular integral equations 24 p3595 A83-49868

ANISOTROPIC PLATES

Penny-shaped crack in a transversely isotropic plate of finite thickness 02 p0190 A83-12039

Survey of recent research in the analysis of composite plates 02 p0191 A83-12065

Calculation of the natural frequencies of anisotropic plates with holes 02 p0192 A83-12356

Bending waves in strongly anisotropic elastic plates 02 p0196 A83-12855

Residual stress measurement of laminated anisotropic plate by strain gauge method 02 p0197 A83-13067

Generalized dynamic problem of thermoelasticity and thermoviscoelasticity for an infinite cylindrically anisotropic plate 03 p0339 A83-13691

Bending of a semiinfinite anisotropic plate with curvilinear cracks 03 p0340 A83-14070

The effect of shear modulus on the elastic behavior of strongly anisotropic plates 03 p0343 A83-14736

Stress state for the off-axis tension of perforated materials 07 p0947 A83-21090

Central ductile crack in an orthotropic strip of finite width 08 p1120 A83-21818

Dynamic /transient/ analysis of layered anisotropic composite-material plates 08 p1123 A83-22944

Three-dimensional finite-element analysis of layered composite plates 11 p1591 A83-27432

Stress distribution in a strongly anisotropic elastic plane with a parabolic cutout 11 p1598 A83-28486

The application of the immersion method to the analysis of plates with variable-strength ribs 11 p1600 A83-28774

Buckling of anisotropic laminated cylindrical plates [AIAA 83-0979] 12 p1740 A83-29786

The finite-element method in solutions of boundary value problems for anisotropic plates of composite materials. I Refined theories for anisotropic plates and finite-element approximations 13 p1866 A83-30059

Elasto-plastic analysis of anisotropic plates and shells by the Semiloof element 13 p1868 A83-31639

Anisotropic elasto-plastic finite element analysis of thick and thin plates and shells 13 p1868 A83-31640

The mean transverse shear in stratified anisotropic plates [ONERA, TP NO. 1983-15] 16 p2368 A83-36425

Mixed mode fracture analysis of rectilinear anisotropic plates using singular boundary elements 16 p2369 A83-36555

The effect of stringers on the stress-strain state near a hole or crack in an anisotropic plate 17 p2520 A83-37516

Stability of nonlinear thermoelastic waves in spinning anisotropic membrane disks 18 p2703 A83-40169

A new method to determine the bending rigidities of anisotropic plates 18 p2662 A83-40293

The bending vibrations of an anisotropic free circular plate of regular symmetry 21 p3159 A83-44933

Optimization of openings in plates under plane stress 21 p3164 A83-45588

Low-velocity impact response of laminated plates 21 p3164 A83-45589

ANISOTROPIC SHELLS

Solution of the problem of the stressed state of an inhomogeneous hollow cone 10 p1439 A83-25592

Membrane theory for nonhomogeneous anisotropic shells of revolution 11 p1591 A83-27427

Achievement of a nonaxisymmetric membrane state in shells of revolution 11 p1599 A83-28543

The stability of inhomogeneous cylindrical shells --- Russian book 12 p1735 A83-29339

Calculation of the reliability of anisotropic shells on the basis of the probability of infrequent overshoots of the random vector field beyond the limiting surface 13 p1866 A83-30060

Elasto-plastic analysis of anisotropic plates and shells by the Semiloof element 13 p1868 A83-31639

Anisotropic elasto-plastic finite element analysis of thick and thin plates and shells 13 p1868 A83-31640

Description of finite deformations of thin shells by means of the coordinates of reference and actual configurations 15 p2178 A83-34438

On the applicability of the Kirchhoff-Love hypothesis to the elastoplastic calculation of nonuniformly heated shells 18 p2698 A83-39507

Variational theorem of a theory for shells that are inhomogeneous in the thickness direction 18 p2701 A83-40110

The thermal stressed state of curvilinearly orthotropic inhomogeneous bodies of revolution 21 p3154 A83-44711

A plasticity criterion an basic relationships for an anisotropic shell with different strenghts in tension and compression 21 p3162 A83-45303

ANISOTROPY

NT ELASTIC ANISOTROPY

NT PLASTIC ANISOTROPY

Relativistic cosmology for astrophysicists 01 p0127 A83-11288

Textural anisotropy features for texture analysis 01 p0101 A83-11475

Anisotropy of small atmospheric showers /with E sub 0 of approximately 10 to the 13th eV/ 02 p0273 A83-11725

Search for small-scale anisotropy in the cosmic microwave background 02 p0259 A83-12221

A simplified model for interpreting the Doppler spectrum of forward-scatter radar signals 03 p0307 A83-14032

Grand unified reactions and dissipation in anisotropic cosmologies 05 p0696 A83-16977

Dependence on declination of the intensity of cosmic ray showers with primary energies of about 10 to the 16th eV 05 p0709 A83-17268

Cosmic ray north-south anisotropy - The role of the interplanetary magnetic field 05 p0709 A83-17378

Local isotropy and anisotropy in a high-Reynolds-number turbulent boundary layer 06 p0758 A83-19023

The transport anisotropy effect in a turbulent plasma 06 p0813 A83-19188

Magnetic anisotropy and porosity of chondrites 07 p1028 A83-20098

Anisotropy of bulk-formability in 2024-T351 aluminum plates and bars 08 p1058 A83-21664

Small-angle anisotropy of the microwave background radiation in the adiabatic theory --- concerning structure of Universe 09 p1364 A83-25002

Models for elliptical galaxies. I - Oblate spheroids with anisotropy. II - Oblate spheroids with realistic rotation curves 09 p1364 A83-25004

- Quasi-periodic variations of cosmic-ray intensity and anisotropy --- Russian book 12 p1800 A83-28814
- Grain-boundary diffusion in metals 12 p1713 A83-29240
- The relationship between the anisotropy of high-modulus reinforcing fibers and the mechanical and thermophysical properties of fiber composites 13 p1815 A83-30063
- Gain anisotropy in low-pressure chemical lasers 13 p1857 A83-31456
- Early Brans-Dicke axisymmetric universe with magnetic field 13 p1958 A83-31731
- Characteristics of the anisotropy of the polarizability of molecules --- Russian book 15 p2227 A83-34700
- Large-scale anisotropy of the 3 K background radiation in density wave models 16 p2441 A83-36677
- Anisotropy in MHD turbulence due to a mean magnetic field 18 p2745 A83-39618
- On the effects of strong encounters in stellar systems. I - A basis for treating anisotropic systems 20 p3068 A83-42455
- Generation of static magnetic fields by a test charge in a plasma with an electron temperature anisotropy 21 p3210 A83-44129
- The helium abundance and the isotropy of the universe 21 p3234 A83-44766
- A unified theory of cosmic ray diurnal variations 22 p3390 A83-46893
- Gravitational anisotropies of gyromagnetic ratios and tests of general relativity 23 p3503 A83-47876
- The stability of axisymmetric galaxy models with anisotropic dispersions 24 p3641 A83-49248
- Kinematic modelling of NGC 3379 24 p3641 A83-49251
- Elasto-plastic analysis of an anisotropic rotating disc 24 p3597 A83-50146

ANNEALING

- NT LASER ANNEALING
- NT PULSE HEATING
- Gas saturation of the surface layers of welded joints of alloy OT4 after full and partial annealing in vacuum 01 p0025 A83-10448
- Rapid annealing of silicon with a scanning CW Hg lamp 01 p0109 A83-10646
- The effect of physical aging on the time-dependent properties of carbon-fiber-reinforced epoxy composites 02 p0150 A83-12064
- Certain characteristics of the flexural deformation and subsequent annealing of molybdenum single crystals 02 p0155 A83-12202
- Self-annealed ion implanted solar cells 02 p0202 A83-12290
- Effect of annealing conditions on grain growth in the complex Ti-1-x/Nb-x/C/0.5/N/0.5/ solid solutions 02 p0158 A83-12949
- The effect of heat treatment on element redistribution between the phase components of W-Ni-Fe alloy 02 p0159 A83-13032
- Ultrafine grain structures in alloys with recrystallization annealing 03 p0297 A83-13263
- Variations in the isotopic composition of xenon under the annealing and selective dissolution of material from the Tsarev meteorite 03 p0432 A83-13524
- Ordering kinetics and structural changes during the annealing of deformed NiPt alloy 03 p0299 A83-14154
- Thermal annealing of experimentally shocked feldspar crystals 04 p0564 A83-15375
- Mechanical instability of a cellular dislocation structure 04 p0459 A83-15469
- Optical properties of disordered silicon in the range 1-10 eV 04 p0541 A83-15521
- Optical properties of a-Si:H and a-SiC_{1-x}H_x films prepared by glow-discharge deposition 04 p0541 A83-15522
- Observation of an unusual martensitic-transformation sequence in TiNi 04 p0459 A83-15703
- Effects of annealing on the electrical properties of Cd/x/Hg/1-x/Te 04 p0543 A83-16085
- Effect of vacuum annealing temperature on the performance of welded joints in titanium structures 05 p0952 A83-16883
- Auger and electron energy-loss study of the Al/SiC interface 05 p0611 A83-16947
- Chemo-thermal treatment of alloy VT6 to improve antifriction properties 05 p0614 A83-17134
- Temperature effects on failure and annealing behavior in dynamic random access memories 05 p0626 A83-17506
- Thermal annealing of radiation damage in CMOS ICs in the temperature range -140 C to +375 C 05 p0627 A83-17515
- Rapid annealing in advanced bipolar microcircuits 05 p0627 A83-17516
- Oxidative stabilization of oriented acrylic fibres - Morphological rearrangements 05 p0619 A83-17561

- An investigation of heat-affected zone hot cracking in alloy 800 06 p0728 A83-18399
- Wear resistance of dynamically compacted aluminium-steel and Al-steel-Pb alloy mixtures 06 p0731 A83-19089
- Short time annealing --- in silicon processing 07 p0999 A83-20592
- Characteristics of concentration changes occurring in the solid solution of deformed Ni-7.1 wt% Al alloy during rapid heating 07 p0890 A83-20917
- The effect of low-temperature annealing on the initial temperature of martensitic transformation in a nickel-titanium intermetallic 07 p0890 A83-20921
- Investigation of preferred orientation and microstructure in oxide-dispersion-strengthened alloys 08 p1065 A83-22016
- Room-temperature tensile strength of boron-aluminum composite as a function of annealing temperature and time 08 p1054 A83-22100
- Effect of high-temperature vacuum annealing time on the structure and properties of titanium alloys 08 p1066 A83-22690
- Effect of diffusion welding thermal cycle on the strength of alloy VT20 08 p1067 A83-22696
- Flame annealing of arsenic and boron implanted silicon 08 p1170 A83-22768
- Enhancement of birefringence in polarisation-maintaining fibres by thermal annealing 08 p1167 A83-22921
- Fatigue behavior of solution-treated and quenched Ti-6Al-4V 09 p1228 A83-23344
- Effect of annealing in buffer gas at 800-1000 C on the mechanical properties of x 10 NiCrAlTi 32 20 type alloys 09 p1233 A83-24138
- Diffusion of nitrogen in alpha-Ti 10 p1397 A83-25980
- Reconstruction of objects from coded images by simulated annealing 10 p1420 A83-26110
- The effect of annealing on the structural and electronic properties of profiled silicon 11 p1663 A83-28363
- The effect of the annealing conditions on the cyclic fracture toughness of the magnesium alloy VMD-10 11 p1549 A83-28488
- Decomposition of the metastable beta phase in the textured alloy VT19 11 p1550 A83-28545
- The crystalline structure of gas-saturated beta titanium alloys 11 p1550 A83-28546
- Vacuum annealing effects in lithium niobate 12 p1782 A83-29170
- Distribution of impurity elements in titanium alloys 13 p1819 A83-30086
- A study of strength nonuniformity in the thickness direction of molybdenum alloys 13 p1821 A83-30691
- Lamination and microlamination in parts made of TsM2A alloy sheet --- molybdenum alloy 13 p1823 A83-31215
- Diffusion length of minority carriers in scanning electron beam annealed silicon 14 p2089 A83-32248
- Thin film Cu₂S/CdS junctions produced by evaporation and sputtering - Effect of thermal treatments in vacuum 14 p2089 A83-32297
- Comparison between various ion beam doping procedures and anneal techniques used in manufacturing silicon solar cells 14 p2091 A83-32325
- Optimization of pulsed electron beam annealing process for silicon solar cells 14 p2005 A83-32327
- Silicon solar cells by ion implantation - E-beam and self annealing 14 p2005 A83-32328
- A study of alloying element redistribution during the diffusion annealing of titanium alloys 15 p2137 A83-34016
- A study of the effect of annealing on the structure and mechanical properties of deformed tungsten 15 p2141 A83-35312
- Diffusion anomalies in cobalt alloys 15 p2141 A83-35313
- Low temperature annealing of Be-implanted GaAs 16 p2418 A83-35438
- Radiation effects on MOS devices - dosimetry, annealing, irradiation sequence, and sources 16 p2346 A83-36023
- Hydrogen embrittlement of titanium and its alloys 16 p2334 A83-36884
- Plastic deformation of sheets and bands of aluminum alloys during continuous hardening 16 p2334 A83-36887
- The relationship between the structure and cyclic fracture toughness of alpha titanium alloys 16 p2335 A83-36890
- Computer simulation for the intergranular corrosion of Alloy 800 16 p2335 A83-36899
- High-performance of Ni-Cr-Mo-W alloys 17 p2489 A83-38031

- Comparison between electron-beam and furnace rapid isothermal anneals of phosphorus-implanted solar cells 17 p2584 A83-38217
- Observations on the fracture and deformation behaviour during annealing of residually stressed polycrystalline aluminium oxides 18 p2671 A83-39058
- Corrosion behavior of annealed niobium-tantalum alloys 18 p2665 A83-39173
- Annealing of Hg₂Cl₂ crystals - Project of the experiment --- in space and terrestrial conditions 18 p2644 A83-39913
- Annealing behaviour of gamma-ray-induced electron traps in LEC n-InP 20 p3052 A83-42482
- Rapid thermal annealing of Se and Be implanted InP using an ultrahigh power argon arc lamp 20 p3055 A83-43605
- Application of thermal pulse annealing to ion-implanted GaAlAs/GaAs heterojunction bipolar transistors 21 p3123 A83-43851
- Rapid thermal annealing of Be, Si, and Zn implanted GaAs using an ultrahigh power argon arc lamp 21 p3220 A83-45500
- The electrical characteristics of thin film Cu(x)S-CdS solar cells and their dependence on the ambient atmosphere during annealing 23 p3477 A83-48198
- Study of deep-level defects and annealing effects in undoped and Sn-doped GaAs solar cells irradiated by one-MeV electrons 23 p3427 A83-48605
- Electrical characteristics of Be-implanted GaAs diodes annealed with an ultrahigh power argon arc lamp 24 p3572 A83-48788
- Reduction in the localized band-gap states in amorphous silicon by annealing and hydrogen implantation 24 p3634 A83-48793
- Study of defect annealing by supercritical proton beam irradiation and of radiation defect profiles in GaAs by the positron annihilation method 24 p3636 A83-49748
- ANNIHILATION REACTIONS**
- NT POSITRON ANNIHILATION
- Fractal basin boundaries, long-lived chaotic transients, and unstable-unstable pair bifurcation 10 p1471 A83-25794
- Experimental test of baryon conservation - A new limit on neutron-antineutron oscillations in oxygen 13 p1917 A83-30916
- Constraint on the photino mass from cosmology 13 p1949 A83-31357
- Fermion-induced monopole-antimonopole annihilation 13 p1954 A83-31606
- How can we approach the study of cosmology? 15 p2254 A83-33753
- The thermal pair annihilation spectrum - A detailed balance approach --- for cosmic plasma study 17 p2605 A83-37930
- Fast annihilation of oppositely directed magnetic fields in plasma 20 p3049 A83-42271
- ANNUAL VARIATIONS**
- Effects of the polarity change of the solar magnetic field in variations of cosmic rays 02 p0273 A83-11720
- Annual and semiannual oscillations of zonal wind at heights of 70-110 km 02 p0205 A83-11976
- Fluctuations on OTS-earth copolar link against diurnal and seasonal variations 02 p0163 A83-11983
- Spatial-temporal analysis of 60-year field variations according to data from the global network of observatories 02 p0210 A83-12441
- Seasonal variations in stratospheric NO₂ at 45 deg S 03 p0357 A83-13547
- Seasonal climatic sources of heat in the North Atlantic 03 p0373 A83-14833
- Two Mars years of surface changes seen at the Viking Landing sites 04 p0567 A83-15575
- Water vapor in Mars' arctic - Seasonal and spatial variability 04 p0569 A83-15590
- Martian North Polar Cap 1979-1980 04 p0569 A83-15591
- The seasonal CO₂ cycle on Mars - An application of an energy balance climate model 04 p0569 A83-15592
- Geographical and seasonal distribution of critical frequencies in the F₂-layer during a period of high solar activity 04 p0509 A83-15724
- The semiannual oscillation in the thermosphere as a conduction mode 05 p0661 A83-17403
- Fluctuations in tidal /24-, 12-h/ characteristics and oscillations /8-h-5-d/ in the mesosphere and lower thermosphere 05 p0665 A83-17785
- Quasi-biennial cyclicity as a parametric phenomenon in the climatic system 06 p0788 A83-17994
- Theory of the mesopause semiannual oscillation 06 p0782 A83-18253
- Heating of the Tibet Plateau and movements of the South Asian high during spring 06 p0792 A83-18471
- Comments on the gamma-ray burst log N /greater than S/ log S point of Beurle et al 06 p0858 A83-18888

Investigation of the relationship between the seasonal dynamics of the spectral brightness coefficients of certain sorts of wheat and plant physiological parameters 07 p0951 A83-19911

A stratospheric chemical instability 07 p0960 A83-20213

The Russian surface temperature data set 07 p0969 A83-20801

The influence of time of year and the colors of prairie flora bloom on their spectral behavior and that of the prairie where they are found 08 p1126 A83-21928

Multitemporal remote sensing of land use in the Sahelian region of Africa by Meteosat I 08 p1128 A83-21961

Seasonal variation of the atmospheric temperature at midlatitude - A revision of the CIRA 1972 model 08 p1138 A83-22061

Solar and lunar daily magnetic variations at Hyderabad, 1965-77 08 p1133 A83-22301

Solar and lunar seasonal variations in the American sector 08 p1133 A83-22302

Interpretation of seasonal variations of S and L --- solar and lunar geomagnetic variations 08 p1133 A83-22303

Studies of the external origin component of Sq by 'canonical' GDS analysis --- Geomagnetic Depth Sounding 08 p1134 A83-22313

Stationary waves in the winter stratosphere - Seasonal and interannual variability 08 p1143 A83-23016

Uncertainties regarding the transmission of time and frequency 09 p1336 A83-23401

The mean annual variation of the geopotential of the 500 mb surface for the Northern Hemisphere in wavenumber space 09 p1313 A83-24120

Three-dimensional tracer model study of atmospheric CO₂ - Response to seasonal exchanges with the terrestrial biosphere 09 p1305 A83-24254

Distribution of and changes in industrial carbon dioxide production 09 p1295 A83-24256

The seasonal variation of the atmospheric SO₂ to SO₄/- conversion rate 09 p1296 A83-24279

Monitoring of seasonal and yearly land-use changes on aerial photography and Landsat imagery - A case study in the Yemen Arab Republic 09 p1285 A83-24538

The seasonal cycle over the United States and Mexico 10 p1450 A83-25389

Inter-annual and seasonal variations in the structure and energetics of the atmosphere over northeast Brazil 11 p1633 A83-28088

The significance of the long-term pattern of geomagnetic activity for forecasting 11 p1616 A83-28116

Annual variations in the gradient of the electric field potential in the atmosphere and their relationship with the forms of atmospheric circulation 11 p1634 A83-28727

An analysis of multiyear variations in atmospheric electrical quantities in the atmospheric surface layer on the basis of observational data 11 p1634 A83-28733

Solar-activity indices for cycles No. 17-20 (1934-1977) --- Russian book 12 p1799 A83-28811

Diurnal respiratory rhythms in young healthy people in Siberia and the Far North 12 p1765 A83-29312

Features of radio-aurora observations at the high-latitude station Mirnyi 13 p1875 A83-30605

Seasonal and geographical variation of blocking 13 p1891 A83-30808

The distribution and annual cycle of ozone in the upper stratosphere 13 p1877 A83-30893

On the role of the seasonal cycle 13 p1892 A83-31032

The effect of the winter anomaly of the D-region according to measurements on the Kerguelen Islands 14 p2050 A83-31876

Seasonal differences of the effects of sudden ionospheric disturbances in the D region 14 p2050 A83-31877

Possible effects of distant field sources in Sq variations 14 p2051 A83-31889

The seasonal radiosensitivity of rats and dogs 14 p2062 A83-32059

The seasonal variation of the thermal structure of the atmosphere of Uranus 14 p2112 A83-32608

Gulf Stream meanders off North Carolina during winter and summer 1979 14 p2060 A83-33082

Physiological and biochemical methods for evaluating the functional condition of athletes in cyclical forms of sports 14 p2070 A83-33306

A possible explanation of the observed persistence of monthly mean circulation anomalies 15 p2204 A83-33882

Interannual variability and climatic noise in satellite-observed outgoing longwave radiation 15 p2195 A83-33884

Seasonal variation of monoterpenes in the atmosphere of a pine forest 15 p2194 A83-34040

Seasonal variations of harmonic constants of diurnal and semidiurnal waves of atmospheric pressure according to POLYMODE data 15 p2206 A83-34354

The spectrum of temperature oscillations in the neighborhood of the inertial frequency according to POLYMODE data --- Atlantic Ocean temperature measurement analysis 15 p2209 A83-34356

The solution for seasonal variations in the earth's rate of rotation 15 p2246 A83-34393

Range distribution of sporadic meteors and sunrise 15 p2200 A83-34408

Seasonal and solar-related cyclic variations of equatorial F-scattering 15 p2200 A83-34418

The effects of seasonal differences in climatic conditions on Landsat spectral signatures and associated land cover classification 15 p2185 A83-34817

Microwave radio meteorology - Seasonal fading distributions 16 p2383 A83-35411

Modes of variability in annual hemispheric water vapor and transport fields 16 p2385 A83-35474

Ice and snow feedbacks and the latitudinal and seasonal distribution of climate sensitivity 16 p2386 A83-35489

Annual cycle and spatial spectra of earth emitted radiation at large scales 16 p2386 A83-35490

Seasonal and solar activity dependent variations of the geomagnetic activity effect at high latitudes 16 p2378 A83-36116

Seasonal transport and turbulence in the lower thermosphere 16 p2378 A83-36118

Solar, geomagnetic and long term effects on thermospheric neutral kinetic temperatures at midlatitude 16 p2378 A83-36121

Sources, sinks, and seasonal cycles of atmospheric methane 16 p2379 A83-36130

Some features of annual variation in the equatorial geomagnetic field 16 p2382 A83-36733

The effect of orbital element variations on the mean seasonal daily insolation on Mars 16 p2426 A83-36788

Some results of ionospheric slab thickness observations at Luning 17 p2537 A83-37577

Delineation of seasonal changes of chlorophyll frontal boundaries in Mediterranean coastal waters with Nimbus-7 coastal zone color scanner data 17 p2554 A83-37623

The annual variation of the solar mean magnetic field 17 p2626 A83-37676

Autumn and winter anomalies in ionospheric absorption as measured by riometers 17 p2543 A83-38369

A practical method of correcting monthly average temperature biases resulting from differing times of observation 18 p2722 A83-39127

The effect of seasonal asymmetry on the filling of plasma tubes 18 p2714 A83-39334

The response of finite-amplitude wave motions to seasonal heating of a baroclinic shear flow 18 p2684 A83-39449

Interannual variations of mean monthly sea-level pressure in January 18 p2725 A83-39690

Coronal index of solar activity. IV - Years 1964-1970 18 p2785 A83-39978

Large-scale energy transformations in the high latitudes of the Northern Hemisphere 18 p2728 A83-40026

Troposphere-stratosphere (surface-55 km) monthly winter general circulation statistics for the Northern Hemisphere Four year averages 18 p2730 A83-40045

Increase and seasonal cycles of nitrous oxide in the earth's atmosphere 18 p2720 A83-40644

Analysis of solar-radiation characteristics at the EURELIOS power plant of Adrano 19 p2862 A83-41165

Acid clouds and precipitation in eastern Colorado 19 p2863 A83-41982

Seasonal averages of net decay rate of SO₂ over northern Europe 19 p2864 A83-41988

Variations of the geomagnetic field at at Mbour (Senegal) and Bangui (Central Africa) between 1955 and 1981 20 p3017 A83-42314

The season dependent distortions of the ring current 20 p3020 A83-42522

Interannual variations of global total ozone revealed from Nimbus 4 BUV and ground-based observations 20 p3021 A83-42864

Seasonal variation of solar atmospheric tides at meteor heights 20 p3027 A83-43403

Seasonal distributions of diabatic heating during the first GARP global experiment 21 p3172 A83-44470

Variation of aeronomic parameters during the period from the equinox to summer 21 p3175 A83-45241

The variability of the times of the spring reversals of the strato-mesospheric circulation 21 p3181 A83-45327

Analysis of the periodic variations of atmospheric pressure over Greece 21 p3181 A83-45408

Characteristics of seasonal variations of O(+) ion density troughs in the nighttime topside ionosphere 21 p3178 A83-45458

Some singularities and irregularities in the seasonal progression of the 700 mb height field 22 p3338 A83-45702

Latitudinal (seasonal) variations in the thermospheric midnight temperature maximum - A tidal analysis 22 p3328 A83-46058

Seasonal variations in the vertically integrated water vapor transport fields over the Southern Hemisphere 23 p3489 A83-47399

Interannual variability and predictability of 500 mb geopotential heights over the Northern Hemisphere 23 p3489 A83-47400

A comparative study of scintillation analysis over two line-of-sight paths at 6.7 GHz and 7.6 GHz 23 p3443 A83-47834

Ozone variability --- in atmosphere and possible causes 24 p3604 A83-48759

ANNULAR DUCTS

An experimental study of the mixing of countertwisted turbulent jets in the initial section of an annular duct 09 p1260 A83-24228

Sound radiation from annular ducts/nozzles using modal decomposition of in-duct acoustic power [AIAA PAPER 83-0714] 10 p1475 A83-25929

Sound propagation in segmented exhaust ducts - Theoretical predictions and comparison with measurements [AIAA PAPER 83-0734] 11 p1651 A83-28016

Heat transfer in a latent heat storage device with finned annular tube heat exchanger --- German thesis 11 p1570 A83-28665

ANNULAR FLOW

Characteristic time ignition model extended to an annular gas turbine combustor 01 p0011 A83-10666

Differential rotation driven by convection in a rapidly rotating annulus 02 p0174 A83-12978

A steady source-sink flow in a two-layer rotating fluid 02 p0174 A83-12979

Dynamic analysis of turbulent annular seals based on Hirs' lubrication equation [ASME PAPER 82-LUB-41] 03 p0336 A83-13520

The theory of rotating and oscillating blade rows in a subsonic flow through an annular channel 03 p0279 A83-14492

Stability of nonparallel developing flow in an annulus 03 p0323 A83-14698

Unsteady flow of a viscous fluid through an annulus 04 p0480 A83-16428

Aerodynamic performance of an annular classical airfoil cascade [AIAA PAPER 83-0179] 05 p0588 A83-16824

Calculation of parameters of a near wake produced by injection of an annular jet into the base region 05 p0590 A83-17424

Natural convection in a rotating annulus 08 p1090 A83-23209

Flow through rotating straight pipes of a circular cross section 10 p1413 A83-25780

Excitation of circular flow of a fluid by a rotating velocity field 13 p1842 A83-30909

An experimental study of entraining, stress-driven, stratified flow in an annulus 14 p2013 A83-33382

Combined convection in an annulus applied to a thermal storage problem 15 p2191 A83-34259

Effect of entry boundary layer thickness on secondary flows in an annular cascade of turbine nozzle and rotor blades 16 p2292 A83-35868

A numerical analysis of the development of a system of jets in the mixing region of countertwisted annular flows 19 p2844 A83-41569

Natural convection in a spherical annulus filled with heat generating fluid 20 p2972 A83-42677

Turbulent heat transfer in the entrance region of a concentric annulus with inner cylinder rotation 20 p2975 A83-42701

Heat transfer in a vertical rotating annulus - A numerical study 20 p2975 A83-42705

Numerical solution of natural convection in eccentric annuli 20 p2987 A83-43451

Pressure recovery of collectors with annular curved diffusers [ASME PAPER 83-GT-35] 23 p3394 A83-47896

A configuration to improve the aerodynamics and scope of can-annular combustors [ASME PAPER 83-GT-37] 23 p3406 A83-47898

A simple method for designing optimum annular diffusers [ASME PAPER 83-GT-42] 23 p3407 A83-47902

A compact diffuser system for annular combustors [ASME PAPER 83-GT-43] 23 p3407 A83-47903

Theory of blade design for large deflections. II - Annular cascades [ASME PAPER 83-GT-125] 23 p3396 A83-47954

ANNULAR NOZZLES

- A preliminary study of annular diffusers with constant diameter outer walls (suitable for turbine exits)
 [ASME PAPER 83-GT-218] 23 p3411 A83-48018
 Annular jets of different diameter ratios
 23 p3449 A83-48142
 Generation and size distribution of droplet in annular two-phase flow
 [ASME PAPER 83-FE-2] 23 p3450 A83-48227
 An experimental study of low Reynolds number turbulent circular jet flow
 [ASME PAPER 83-FE-36] 23 p3451 A83-48239
 Rarefied gas flow in a cylindrical annulus
 24 p3575 A83-48738

ANNULAR NOZZLES

- An experimental study of the impingement of a supersonic annular jet on an obstacle
 19 p2790 A83-41260

ANNULAR PLATES

- Effect of surface roughness on the squeeze film between rotating porous annular discs 01 p0056 A83-10500
 Buckling of polar orthotropic annular plates under inplane radial pressures 02 p0190 A83-12002
 Free vibrations and the stability of annular plates under nonuniform tension and compression
 04 p0497 A83-15390
 Variational solutions for the nonlinear deflexion of an annular membrane under axial load
 05 p0656 A83-17945
 Natural frequencies of transverse vibration of polar orthotropic variable thickness annular plates
 08 p1119 A83-21804
 Pulse load of annular plastic plates supported on both edges 08 p1120 A83-21812
 Stress intensity factors for a curvilinear cut in a circular ring 11 p1598 A83-28490
 Optimisation of cylindrically orthotropic annular plates with simply supported edges subjected to a constraint on fundamental frequency 24 p3591 A83-48899
 Numerical optimum design of elastic annular plates with respect to buckling 24 p3594 A83-49443
 Buckling of a heated thin non-homogeneous annular circular plate of variable thickness
 24 p3597 A83-50132

ANNULI

- Numerical simulation of natural convection in concentric and eccentric horizontal cylindrical annuli
 03 p0315 A83-13484
 Laminar and turbulent natural convection in the annulus between horizontal concentric cylinders
 03 p0315 A83-13485
 Far-field radiation patterns of elliptical apertures and its annuli 10 p1406 A83-26847
 Certain problems of the contact interaction of an elastic infinite plane having a round hole with ring-shaped patches 15 p2180 A83-35150
 On the penetration of an electromagnetic field through circular and annular holes 18 p2677 A83-40096
 Analysis of smooth and ribbed annular structural elements --- Russian book 21 p3150 A83-43923

ANODES

- NT CELL ANODES
 NT TUBE ANODES
 Toward the development of conduction path anodes for sorting signals from microchannel plates --- German thesis 01 p0049 A83-10468
 UPS and Schottky barrier study of TiO₂ electrochemical anodes --- for solar cells 04 p0504 A83-15481
 Investigation of the operation of a two-stage accelerator with an anode layer with one power source
 06 p0755 A83-19562
 Regenerative photoelectrochemical cells using polymer-coated n-GaAs photoanodes in contact with aqueous electrolytes 07 p0952 A83-19882
 Electrochemically deposited CdS and CdSe anodes for photoelectrochemical cells 07 p0000 A83-19883
 Plasma layers near the electrodes of a cesium diode - Anode layer 09 p1348 A83-23990
 Ralicon anodes fabricated by electron beam lithography for image photon counting detectors
 11 p1553 A83-27754
 Anode tufting, arc faulting and plasma nonuniformity in ion sources 12 p1780 A83-29034
 Voltammetric study of the anodic oxidation of sulfide ions in molten fluorides 14 p1989 A83-32630
 Lithium alloy-thionyl chloride cells - Performance and safety aspects 15 p2192 A83-34694

ANODIC COATINGS

- On the properties of the superplastic aluminium-calcium alloy as material for solar collectors
 04 p0505 A83-15496
 Oxide film rupture, reanodization, and stress corrosion cracking in aluminum 04 p0460 A83-15866
 Electrochemical impedance diagrams of alloy 600 at active-passive transition potentials
 09 p1230 A83-23917

- Variable anodic thermal control coating on aluminum [AIAA PAPER 83-1492] 14 p1985 A83-32737
 Anodic films on aluminium 17 p2486 A83-37173
 The total anodization of copper films on platinum - Use as selective surface absorbers at high temperature
 20 p3012 A83-42615
 A possible mechanism for the reduction of voltage delay in the Li/SOCl₂ system via cyanoacrylate coatings on lithium 24 p3599 A83-49929
 Influence of hydrogen reduction on photoelectro-chemical behavior of anodic oxidized n-TiO₂ layers 24 p3559 A83-50178

ANODIC STRIPPING

- The anodic dissolution of a Ni-base superalloy
 12 p1713 A83-29401

ANODIZING

- Oxide film rupture, reanodization, and stress corrosion cracking in aluminum 04 p0460 A83-15866
 Service history of phosphoric acid anodized aluminum structure --- with adhesive bonding for aircraft construction 07 p0861 A83-20479
 The effect of fluoride contamination on the durability of PAA surfaces --- preparation of aluminum alloy surfaces for adhesive bonding by phosphoric acid anodize solution 09 p1230 A83-23625
 Evaluation of the P2 and PAA treatments --- sulfuric acid-ferric sulfate etching and phosphoric acid anodizing 09 p1238 A83-23627
 Characterization of copper in phosphoric-acid-anodized 2024-T3 aluminum by Auger electron spectroscopy and Rutherford backscattering 10 p1395 A83-25547
 Effect of anodic growth temperature on native oxides of n-(Hg, Cd)Te 13 p1929 A83-31066
 Improved chromatic acid anodize seal for optimum paint adhesion
 [SAE PAPER 820603] 22 p3301 A83-45864
 A sodium hydroxide anodize surface pretreatment for the adhesive bonding of titanium alloys
 23 p3432 A83-48151

ANOMALIES

- NT GRAVITY ANOMALIES
 NT MAGNETIC ANOMALIES
 A method for spectroscopically detecting chemical anomalies on the surface of an Ap star with a nonvariable spectrum 07 p1006 A83-20659
 Experimental study of the photovoltaic effect in piezoelectric and ferroelectric crystals
 13 p1930 A83-31302
 The winter anomaly (WA) of short waves
 14 p2048 A83-31815
 A possible explanation of the observed persistence of monthly mean circulation anomalies
 15 p2204 A83-33882
 Some singularities and irregularities in the seasonal progression of the 700 mb height field
 22 p3338 A83-45702
 Tornados, dark days, anomalous precipitation, and related weather phenomena - A catalog of geophysical anomalies --- Book 22 p3339 A83-45914
 On the origin of low energy anomalous component of galactic cosmic rays 23 p3539 A83-47744
 The anomalous spectral shift of mixed pairs of galaxies 24 p3661 A83-49452

ANOMALOUS TEMPERATURE ZONES

- Relations between climatic anomalies - Teleconnections --- global correlation between local atmospheric phenomena 03 p0370 A83-14575
 A ubiquitous wavenumber-5 anomaly in the Southern Hemisphere during FGGE --- First Garp Global Experiment 06 p0792 A83-18472
 Characteristics of thermobaric fields in the southwest part of the North Atlantic in the summer of 1977
 15 p2206 A83-34353
 Peru costal currents during El Nino - 1976 and 1982
 22 p3344 A83-46802
 Large-scale thermal anomalies in the California current during the 1982-1983 El Nino 23 p3493 A83-47857

ANORTHOSITE

- Adcumulus growth of anorthosite at the base of the lunar crust 04 p0559 A83-15328
 Adsorption and excess fission Xe - Adsorption of Xe on vacuum crushed minerals 04 p0564 A83-15376
 Sixth foray for pristine nonmare rocks and an assessment of the diversity of lunar anorthosites
 07 p1032 A83-21296
 Petrology and comparative thermal and mechanical histories of clasts in breccia 62236
 07 p1033 A83-21298
 Pre-Keweenaw anorthosite inclusions in the Keweenaw Beaver Bay and Duluth Complexes, northeastern Minnesota 16 p2382 A83-36971
 Origin of Archean anorthosites - Evidence from the Bad Vermilion Lake anorthosite complex, Ontario
 22 p3332 A83-46705
 Antarctic meteorite ALHA81005 - Not just another lunar anorthositic norite 22 p3386 A83-46875

ANOXIA

- Peculiarities of the reaction of cortical pyramidal neurons to the cessation of oxygen supply by the effect of cAMP
 04 p0520 A83-15890
 The effect of exogenous amino acids on the cardiac contractile function and the metabolism of nitrogen compounds during anoxia 14 p2066 A83-33336
 The role of cellular membranes in the resistance of plants to hypoxia and anoxia 16 p2396 A83-36839

ANS

- U ASTRONOMICAL NETHERLANDS SATELLITE

ANTARCTIC ENVIRONMENT

- U ICE ENVIRONMENTS

ANTARCTIC REGIONS

- The application of microwave remote sensing for snow and ice research 01 p0064 A83-10088
 Investigations of the Arctic, the Antarctic and the world ocean; Conference-Seminar, Moscow, USSR, February 9-13, 1981, Reports 01 p0077 A83-10826
 The network of automatic magnetographs in the Antarctic Geographic Polygon project for the investigation of near-earth space 01 p0072 A83-10837
 Astronomy on ice 03 p0401 A83-13173
 Geology and terrestrial age of the Derrick Peak meteorite occurrence, Antarctica 03 p0434 A83-14318
 Echoing mixed-path whistlers near the dawn plasmopause, observed by direction-finding receivers at two Antarctic stations 03 p0362 A83-14750
 Research at United States Antarctic stations during the International Magnetosphere Study
 04 p0513 A83-16298
 IMS results in Antarctica 04 p0513 A83-16299
 Antarctic observations available for IMS correlative analyses 04 p0513 A83-16300
 Formulation and testing of a climatonomical simulation of the microclimate of the dry valleys and of the Little America V Station in Antarctica
 06 p0788 A83-18236
 A quantitative determination of the microorganisms in microbiological investigations of Antarctic glaciers
 06 p0794 A83-18350
 Snow chemistry on James Ross Island /Antarctic Peninsula/ 07 p0956 A83-20201
 Chemical weathering and diagenesis of a cold desert soil from Wright Valley, Antarctica - An analog of Martian weathering processes 07 p0951 A83-21325
 Questions concerning the atmospheric circulation over the Antarctic 08 p1140 A83-22420
 Surface elevation contours of Greenland and Antarctic ice sheets 09 p1305 A83-24286
 Interaction of the antarctic circumpolar current with bottom topography - An investigation using satellite altimetry 09 p1319 A83-24306
 The noble gas record in Antarctic and other meteorites 10 p1518 A83-25451
 Numerical simulation of the Weddell Sea pack ice
 10 p1453 A83-26349
 Extraterrestrials have landed on Antarctica
 11 p1686 A83-28386
 A preliminary report on the achondrite meteorites in the 1979 U.S. Antarctic meteorite collection
 11 p1686 A83-28759
 Cl-36 and Mn-53 in Antarctic meteorites and (Be-10)-(Cl-36) dating of Antarctic ice
 12 p1797 A83-29175
 Regime of the Filchner-Ronne ice shelves, Antarctica
 12 p1754 A83-29448
 Statistical reliability and the seasonal cycle - comments on 'Bottom pressure measurements across the Antarctic Circumpolar Current and their relation to the wind'
 12 p1759 A83-29527
 Features of radio-aurora observations at the high-latitude station Mirnyi 13 p1875 A83-30605
 Distribution of Antarctic Intermediate Water over the Blake Plateau 14 p2061 A83-33087
 Variability of antarctic sea ice and changes in carbon dioxide 15 p2208 A83-33775
 Correlated irregular magnetic pulsations and optical emissions observed at Siple Station, Antarctica
 15 p2195 A83-33936
 Ammonia and ammonium concentrations in the antarctic atmosphere 15 p2197 A83-34044
 Measurements of katabatic winds between Dome C and Dumont d'Urville 15 p2207 A83-34747
 Meteorites in Antarctica - Statistics on falls, concentration, recovery and alteration on ice-sheet
 15 p2276 A83-35002
 Meteorites from Mars? 16 p2437 A83-36571
 Further studies on single station climatology. III - Time spectral analysis of Halley Bay (Antarctic) rawinsonde data 16 p2391 A83-36585
 Spatial and temporal variations in Antarctic sea-ice (1973-82) 18 p2731 A83-39140
 Anomalously old Ar-40 - Ar-39 ages of Antarctic meteorites due to weathering 18 p2779 A83-39965

An extraterrestrial habitat on earth - The algal mat of Don Juan Pond 19 p2885 A83-40832

Characterization of a halotolerant-psychrolerant bacterium from dry valley antarctic soil 19 p2886 A83-40833

Martian gases in an Antarctic meteorite? 19 p2922 A83-40913

Trace gas profiles to 3000 m over Antarctica 19 p2863 A83-41972

Cosmogenic records in Antarctic meteorites 20 p3078 A83-43149

Measurement of the OH rotational temperature at Mawson, East Antarctica 20 p3024 A83-43164

Nocardiopsis antarcticus - A new species of actinomyces isolated from the ice sheet of the Central Antarctica glacier 21 p3185 A83-45377

Application of remote sensing techniques to study environmental conditions and natural resources in Antarctic Peninsula 22 p3313 A83-46206

Meaning of the vertical profile of ion temperure over the Antarctic 22 p3331 A83-46522

Terrestrial age of an antarctic meteorite by thermoluminescence technique 23 p3528 A83-47422

Catch a falling star - Meteorites and old ice 23 p3528 A83-47817

ANTARCTICA
U ANTARCTIC REGIONS

ANTENNA ARRAYS
NT LINEAR ARRAYS
NT STEERABLE ANTENNAS
NT YAGI ANTENNAS

Accuracy of the estimation of point-target coordinates and their derivatives 01 p0030 A83-10407

Commulating spot transmissive lens antenna 01 p0042 A83-11158

A note on utilizing far-field phase information 01 p0034 A83-11375

Experimental study of embedded insulated antennas 01 p0034 A83-11377

On an index for array optimization and the discrete prolate spheroidal functions 01 p0034 A83-11379

Approximate difference pattern response of the weighted multibeam array 01 p0034 A83-11381

Sidelobe control in cylindrical arrays 01 p0034 A83-11382

Beam shaping using nonlinear phase distribution in a uniformly spaced array 01 p0034 A83-11383

The gain/directive gain ratio of phased-array antennas with a spread of parameters 02 p0162 A83-11538

Concerning the resolving power of radar stations with antenna arrays 02 p0162 A83-11541

Statistics of the polarization structure of oblique-sounding signals in the aperture of a linear antenna array 02 p0162 A83-11542

VLA observations of the Seyfert galaxy NGC 1068 02 p0252 A83-11609

Resolution of monochromatic signal sources using a simple receiving antenna array 02 p0164 A83-11985

Mutual coupling compensation for small, circularly symmetric planar antenna arrays 02 p0164 A83-12006

Facilities for US radioastronomy 02 p0249 A83-13104

Progress in millimeter wave integrated-circuit imaging antenna arrays 03 p0327 A83-13780

A wide-band electrically small superdirective array 03 p0306 A83-14018

Planar array synthesis with prescribed pattern nulls 03 p0306 A83-14019

The synthesis of shaped patterns with series-fed microstrip patch arrays 03 p0313 A83-14024

Effects of phase and amplitude quantization errors on hybrid phased-array reflector antennas 03 p0306 A83-14030

Crosspolar levels of ring arrays in reflection at 45 deg incidence - Influence of lattice spacing 04 p0466 A83-15252

Simultaneous detection, resolution, and measurement of the parameters of signals on a noise background at the output of an antenna array - Synthesis of the algorithm 04 p0467 A83-15737

The structure of the radiation pattern and the role of amplitude-phase distributions in curved antenna arrays 04 p0467 A83-15748

The accuracy of measuring angular coordinates by means of antenna arrays 04 p0467 A83-15751

The suppression of the interference signal in a band of frequencies by means of an adaptive array 04 p0467 A83-15753

Moment method analysis of a T-shaped slot radiator in bifurcated waveguide 04 p0473 A83-16203

VLA observations of the 6-cm H2CO absorption towards Sgr A West 06 p0828 A83-18184

Circular arrays - Their properties and potential applications 06 p0737 A83-18602

Integrated multiband phased array antenna 06 p0737 A83-18603

Design studies for a thinned active planar array 06 p0737 A83-18605

A planar array antenna for TV broadcasting communications 06 p0737 A83-18607

A printed millimetre wave array using a low loss dielectric waveguide feeder 06 p0738 A83-18612

A waveguide slot array for use at millimetric frequencies 06 p0751 A83-18614

Q-band dielectric-loaded short backfire antenna arrays 06 p0738 A83-18615

Rotman lens fed multiple beam array 06 p0738 A83-18618

Primary-feed elements for multiple and contoured beam satellite antennas 06 p0738 A83-18619

A single receiver adaptive antenna system 06 p0738 A83-18622

The performance of adaptive antennas in HF communications 06 p0739 A83-18625

Effects of element cross-polarisation in adpative antennas 06 p0739 A83-18626

Airframe multipath effects in airborne adaptive antenna arrays 06 p0715 A83-18627

Adaptive null steering by reflector antennas 06 p0739 A83-18631

The application of sub-optimal control methods to adaptive antennas for airborne communication systems 06 p0715 A83-18632

Studies of null steering arrays incorporating multiplicative signal processing 06 p0739 A83-18633

Array-fed reflector antenna design and applications --- to spacecraft communication 06 p0722 A83-18639

In-orbit performance of the OTS-2 communication antennas 06 p0722 A83-18641

Recent examples of conformal microstrip antenna arrays for aerospace applications 06 p0715 A83-18672

A directional antenna element for use in a phase array with H-plane scanning - Requirements, realisation, nearfields 06 p0751 A83-18674

Synthesis of conformal HF and VHF directional arrays on spherical bodies using surface resonator techniques 06 p0743 A83-18679

A wideband UHF circular array 06 p0743 A83-18681

Radiation characteristics of radial waveguide fed slot arrays of various shapes 06 p0744 A83-18692

A printed array of symmetrical dipoles with a novel feeding configuration 06 p0751 A83-18693

Theoretical and experimental analysis of cylindrical dipoles with minimal mutual coupling 06 p0744 A83-18694

The improvement of sidelobe performance of slotted waveguide arrays 06 p0748 A83-18937

Fast algorithms for time domain broadband adaptive array processing 06 p0748 A83-19041

Excitation of an infinite periodic structure by a local harmonic source with an imprecisely specified frequency 06 p0749 A83-19333

Difference patterns of antenna arrays 06 p0749 A83-19358

The use of a two-dimensional fast Fourier transformation algorithm for processing information from a linear antenna array 06 p0749 A83-19359

Performance evaluation of antenna arrays with noisy carrier reference 07 p0870 A83-19683

Performance measures of an adaptive array in bandlimited noise 07 p0906 A83-19719

Array performance optimization using projection techniques 07 p0907 A83-19721

A failure mechanism in adaptive arrays 07 p0907 A83-19722

Optimum signal processing for adaptive arrays with broadband signals and interferers 07 p0907 A83-19723

Coupled phase-tracking loops for retrodirective array systems 07 p0908 A83-19736

A survey of millimetre-wavelength planar antenna arrays for military applications 07 p0913 A83-20182

Synthesis of circular polarization with nonresonant slots in the narrow wall of a rectangular waveguide 07 p0921 A83-20822

Surface fields excited by a vertical electric point source located on a conducting concave spherical surface 07 p0914 A83-20823

Concerning the radiation pattern in the problem of the excitation of an array of circular dielectric cylinders by a local source 07 p0915 A83-20871

Virtual center arraying 07 p0916 A83-21199

Edge effects in dipole phased arrays 08 p1076 A83-22236

Impedance parameters and radiation pattern of two coupled circular microstrip disk antennas 08 p1076 A83-22329

Self-complementary monopole-notch array antennas 08 p1077 A83-22624

An analog open-loop adaptive-array antenna system 08 p1077 A83-22733

Batch covariance relaxation /BCR/ adaptive processing --- for low-sidelobe main antenna array 08 p1078 A83-22815

Diffraction of electromagnetic waves by a two-dimensional periodic waveguide-dielectric array 09 p1244 A83-23451

An improved design procedure for small arrays of shunt slots 09 p1246 A83-23781

External and internal mutual impedance effects on the radiation patterns of circularly disposed arrays using antennafiers or passive monopoles 09 p1246 A83-23786

On the collimation phase error computation of a space-fed planar phased array 09 p1247 A83-23797

Wide-band nulling performance versus number of pattern constraints for an array antenna 09 p1247 A83-23799

A modular approach for the design of microstrip array antennas 09 p1254 A83-23807

Localization of multiple targets by sensor arrays - A modeling approach 09 p1334 A83-24812

Active antenna arrays /Review/ 09 p1250 A83-24905

The formation of the frequency-angular spectrum of the signals of linear antenna arrays using coherent optical processors based on spatial light modulators with multichannel optical addressing 09 p1345 A83-24906

A study of a combined multifrequency waveguide phased-array antenna 09 p1250 A83-24907

A comparative evaluation of the architectures of transmit phased-array antennas in terms of efficiency 09 p1250 A83-24908

A study of the possibility of the wide-angle matching of the waveguide radiators of planar phased-array antennas 09 p1250 A83-24911

Wave diffraction by an open waveguide structure with a homogeneous laminar filler 09 p1250 A83-24912

The use of a mathematical model of a phased-array antenna to measure the radiation pattern 09 p1250 A83-24913

A method for the numerical analysis of a printed-circuit spiral radiator of a phased-array antenna 09 p1250 A83-24914

The natural modes of a hexagonal array of gyromagnetic waveguides 09 p1256 A83-24916

Random-search algorithms in the problem of the adaptation of an antenna array with discrete phase shifters 09 p1250 A83-24919

Coherent-optical processor for two-dimensional antenna arrays with a complex format of signal recording 09 p1345 A83-24920

Characteristics of a stepwise waveguide radiator in an antenna array with a dielectric coating 09 p1250 A83-24921

Impedance and polarization characteristics of rectangular printed radiators in planar phased-array antennas 09 p1250 A83-24922

Reduction of the field scattered by receiving vibrators 09 p1250 A83-24923

Semicircular-waveguide radiator with circular polarization 09 p1257 A83-24925

Synthesis of an array with an amplitude or phase field distribution fixed on part of the aperture 09 p1251 A83-25163

A large RF radiating membrane for space application [SAE PAPER 820840] 10 p1382 A83-25753

Near-field and far-field patterns of phase-locked semiconductor laser arrays 10 p1426 A83-25979

Influence of signal level quantization at the input of a beam-forming system on the noise immunity of the receiving section 10 p1404 A83-26289

Studies of the Adcock direction finder in terms of phase-mode excitations around circular arrays 10 p1404 A83-26472

Direction finding with an array of antennas having diverse polarizations 10 p1405 A83-26827

Analysis of the loop-coupled log-periodic dipole array 10 p1405 A83-26831

The broad-band scattering response of periodic arrays 10 p1405 A83-26832

Analysis of the performance of adaptive beam forming using perturbation sequences 10 p1405 A83-26833

Bandwidth of a low sidelobe level multimode radiating coupled waveguide array 10 p1405 A83-26834

Evaluation of the efficiency of a two-position reception system using discrete algorithms in the frequency domain 10 p1407 A83-26927

The effect of random phase errors on losses and self-noise of phased-array antennas 10 p1407 A83-26928

Dual-frequency circularly polarised printed antenna composed of strips and slots 11 p1560 A83-27895

- Adaptive array processing - A tutorial
11 p1553 A83-27901
- A complex gradient operator and its application in adaptive array theory
11 p1554 A83-27902
- Adaptive algorithms in the space and time domains --- signal processing for antenna arrays
11 p1554 A83-27903
- Eigenfilter approaches to adaptive array processing
11 p1554 A83-27904
- Transversal filter techniques for adaptive array applications
11 p1554 A83-27905
- Comparison of directional and derivative constraints for beamformers subject to multiple linear constraints
11 p1554 A83-27907
- Convergence time of sidelobe cancellation systems
11 p1554 A83-27908
- Multifunction adaptive processor for small antenna arrays
11 p1554 A83-27909
- Problems associated with correlation-loop adaptive antennas employing hard limiting
11 p1554 A83-27910
- UHF circular arrays incorporating open-loop null steering for communications
11 p1554 A83-27911
- Direction finding using an adaptive null tracker
11 p1555 A83-27912
- Perturbation adaptive array processor for airborne application
11 p1527 A83-27913
- Coefficient perturbation adaptive HF array
11 p1555 A83-27914
- The rate of convergence of the parameters of adaptive filters with quasi-harmonic input signals
11 p1561 A83-27934
- A quasi-optimum algorithm for measuring the amplitudes and phases of signals at the outputs of the elements of a receive array antenna operating in an inhomogeneous medium
11 p1555 A83-27936
- Experimental study of the efficiency of rectenna elements
11 p1561 A83-27950
- Natural modes of a periodic array of rectangular longitudinally magnetized ferrite rods
11 p1561 A83-27966
- Analytical properties of a covariance noise matrix in the theory of receiving antenna arrays
11 p1558 A83-28681
- An antenna system with a passive scatterer
11 p1558 A83-28682
- The radiation pattern of a phased-array excited by a wideband signal
11 p1558 A83-28683
- A scanned antenna with an electrically controlled lens
11 p1559 A83-28684
- Synthesis of unequal arrays on the basis of the optimal choice of the discrete set of the possible values of the radiator coordinates
11 p1559 A83-28686
- An analytical method for calculating the parameters of a linear phased-array antenna
11 p1559 A83-28688
- Modes of resonance of the Jerusalem cross in frequency-selective surfaces
12 p1718 A83-29438
- Polarization selection of signals by antenna arrays with controlled field-polarization
13 p1827 A83-30277
- Phase synthesis of highly directional antenna arrays with a low sidelobe level on one side of the main lobe
13 p1827 A83-30278
- The effectiveness of two-dimensional self-focusing antenna arrays
13 p1828 A83-30281
- On the synthesis of antenna arrays with a variable amplitude-phase distribution in certain radiators
13 p1828 A83-30716
- Calculation of the characteristics of multichannel array-receiving systems
14 p2000 A83-32110
- Method for the design of adaptive filters with limited size of the learning sample
14 p2003 A83-32112
- Antenna arrays with filtering of interfering spatial radio signals by coherent-optical methods using controlled liquid-crystal transparencies
14 p2000 A83-32118
- Analysis of the efficiency of the spatial-temporal processing of radio signals in the presence of noise
14 p2000 A83-32480
- Test results with an experimental direction-finding system
14 p2002 A83-33128
- Analysis of the effect of fluctuations of the parameters of short-duration noise on the efficiency of spatial polarization processing
15 p2145 A83-34895
- The compression of pulses 'stretched' by an optically excited array
15 p2145 A83-34897
- Antenna Applications Symposium, Monticello, IL, September 23-25, 1981, Proceedings
15 p2145 A83-35076
- New advances in wide band dual polarization antenna elements for EW applications
15 p2121 A83-35087
- An algebraic synthesis method for $R(\sqrt{N})$ multibeam matrix network
15 p2126 A83-35093
- An analysis of annular, annular sector, and circular sector microstrip antennas
15 p2146 A83-35095
- Diagnostics of faulty elements of a phased-array antenna by the focusing method
15 p2147 A83-35153
- Optimization of an antenna radiation pattern in conditions of spatial noise
15 p2147 A83-35169
- Superresolution of multiple noise sources in antenna beam
15 p2148 A83-35180
- Directivity of planar array feeds for satellite reflector applications
15 p2126 A83-35181
- The synthesis of surface reactance using an artificial dielectric
15 p2154 A83-35182
- Performance degradation in fast frequency-scanned circular arrays
15 p2148 A83-35188
- Tracking antenna arrays for near-millimeter waves
15 p2148 A83-35189
- Directivity optimization for Yagi-Uda arrays of shaped dipoles
15 p2149 A83-35193
- Experimental study of the characteristics of coupled top-loaded microstrip monopoles
15 p2149 A83-35196
- Cancellation performance degradation of a fully adaptive Yagi array due to inner-element coupling
16 p2342 A83-36483
- A comparative study of feed impedances of a circular and three different spiral antenna arrays
16 p2344 A83-36731
- The handbook of antenna design. Volumes 1 & 2
17 p2493 A83-37158
- Electromagnetic waves in a doubly periodic array of circular longitudinally magnetized ferrite rods
17 p2494 A83-38477
- Synthesis and analysis of algorithms for the spatial-temporal processing of signals and noise using a Markov model of fluctuations of the weighting coefficients of the antenna array
17 p2494 A83-38482
- Estimation of the covariance matrix of stationary noise --- in adaptive systems of moving targets
18 p2674 A83-39431
- Choice of optimal geometric parameters for conical spiral antennas comprising a conductor with additional bends
18 p2674 A83-39433
- An optimization method of super-synthesis observation by 'number of weighted holes' --- for radio telescopes
18 p2760 A83-40385
- Irspc --- cooled grating array IR spectrometer for use with New Technology Telescope
18 p2690 A83-40431
- Low-sidelobe radar antennas
19 p2825 A83-40757
- Increased data rates for communication systems with adaptive antennas
19 p2831 A83-41384
- The SINR performance of cascaded adaptive arrays
19 p2831 A83-41385
- Problems in the optimization of computer-simulation methods for flaw detection in phased arrays
19 p2834 A83-41424
- Experimental study of a resonance antenna synthesized according to a prescribed radiation pattern
19 p2835 A83-41788
- Modified likelihood function in the problem of determining the angular coordinates of sources by means of an antenna array
19 p2836 A83-42062
- 4-layer inductive grid FSS at 45 deg incidence --- Frequency Selective Surfaces
20 p2963 A83-42478
- The evolution and state of the art in air defense radar antennas
20 p2964 A83-42825
- Analysis of queues in a radar system
20 p2964 A83-42913
- Optimization of director antennas
21 p3121 A83-44778
- Double-square frequency-selective surfaces and their equivalent circuit
21 p3121 A83-44958
- A numerical model for an electronically scanned antenna
21 p3121 A83-45274
- A theoretical study and an experimental evaluation of the mutual coupling effects in MIC array antennas
21 p3127 A83-45411
- Auxiliary propulsion requirements for large space systems
21 p3105 A83-45512
- [AIAA PAPER 83-1217]
21 p3105 A83-45512
- A frequency-independent parabolic log-periodic phased-array antenna
22 p3272 A83-45686
- Determination of the parameters of a system of radiators for the matrix description of an array antenna
22 p3272 A83-45692
- A method for solving a system of equations encountered in problems of electrodynamics --- for multi-discrete element antennas
22 p3272 A83-45693
- Loop antennas for directive transmission into a material half space
22 p3274 A83-46527
- Antennas for nonsinusoidal waves. III - Arrays
22 p3276 A83-46933
- A large deployable antenna structure for the ERS-1 satellite
23 p3422 A83-47359
- [IAF PAPER 83-361]
23 p3422 A83-47359
- Design of transverse slot arrays fed by a boxed stripline
23 p3442 A83-47826
- A complex algorithm for linearly constrained adaptive arrays
23 p3443 A83-47843
- Direction of arrival estimation using a sparse circular array and multiplicative beamforming
23 p3443 A83-47844
- An algorithm for the empirical optimization of antenna arrays
23 p3443 A83-47845
- Synthesis of optimal weight distribution in adaptive antenna arrays
23 p3444 A83-48488
- Regularization of algorithms for the processing of signals and noise in adaptive antenna arrays
23 p3444 A83-48522
- Performance of two tripole arrays as frequency-selective surfaces
23 p3444 A83-48710
- Methods of integral equations for the study of mathematical models of convex antenna arrays
24 p3570 A83-49271
- Numerical method for calculating plane semiinfinite structures
24 p3573 A83-49273
- Analysis of the element pattern shape for circular arrays
24 p3571 A83-49989
- ## ANTENNA COMPONENTS
- ### NT ANTENNA COUPLERS
- ### NT ANTENNA FEEDS
- New drive system for large antennas
06 p0750 A83-18000
- Synthesis of conformal HF and VHF directional arrays on spherical bodies using surface resonator techniques
06 p0743 A83-18679
- Millimetric wavelength components and coherent radar systems
07 p0918 A83-20176
- On the choice of the optimal density of vibrators for a rectenna
09 p1292 A83-23464
- Experimental study of the efficiency of rectenna elements
11 p1561 A83-27950
- An analysis of radiation patterns of corrugated corner reflector antenna systems
16 p2344 A83-36734
- ## ANTENNA COUPLERS
- ### NT COUPLING CIRCUITS
- ### NT DIPLEXERS
- Antenna couplers - The aircraft interface
01 p0004 A83-10738
- Mutual coupling between rectangular slot antennas on a conducting concave spherical surface
01 p0033 A83-11363
- Mutual coupling compensation for small, circularly symmetric planar antenna arrays
02 p0164 A83-12006
- Input impedance and mutual coupling of rectangular microstrip antennas
03 p0313 A83-14021
- Theory and design of a Ku-band TE₂₁-mode coupler
06 p0752 A83-18763
- Coupled phase-tracking loops for retrodirective array systems
07 p0908 A83-19736
- Calculation of multislot directional couplers, with allowance for the thickness of the common wall between waveguides of different width
08 p1082 A83-23154
- Analysis of the loop-coupled log-periodic dipole array
10 p1405 A83-26831
- Electromagnetic coupling to an infinite wire through a slot in a conducting plane
10 p1411 A83-26838
- Coupling of a high-Q gravitational-wave antenna with the resonator of a capacitive sensor of oscillations
11 p1572 A83-27454
- Synthesis of directional couplers with a fixed phase difference of output signals
11 p1564 A83-28689
- Laser-plasma antennas, concentrators, and directional couplers for the RF range
13 p1851 A83-30910
- Radiation losses of E-plane groove-guide bends
18 p2679 A83-40390
- Broadband microstrip directional coupler
24 p3574 A83-49977
- ## ANTENNA DESIGN
- Characteristics of receiving antennas consisting of independently loaded dipoles --- rectennas
01 p0039 A83-10911
- A circularly polarized compact flat source
01 p0032 A83-10924
- Commutating spot transmissive lens antenna
01 p0042 A83-11158
- Optimal beamforming for a linear array antenna
01 p0032 A83-11159
- Solution of operator equations by the method of multiparametric regularization
01 p0102 A83-11262
- A broad-band annular-ring microstrip antenna
01 p0033 A83-11361
- Low sidelobe aperture distributions for blocked and unblocked circular apertures
01 p0033 A83-11364
- A broad-band constant beamwidth corrugated rectangular horn
01 p0033 A83-11367
- A band-switched resonant quadrifilar helix
01 p0034 A83-11376
- Experimental study of embedded insulated antennas
01 p0034 A83-11377
- Theory of the frequency responses of uniform and quasi-taper helical antennas
01 p0034 A83-11378
- Approximate difference pattern response of the weighted multibeam array
01 p0034 A83-11381

- A multiple beam antenna concept for a 30/20 GHz satellite communications system 01 p0034 A83-11485
- Optimal state controller design for tracking antenna driving systems 02 p0229 A83-11790
- Frequency agile microstrip antennas 02 p0163 A83-11919
- A microprocessor controlled variable phase and amplitude antenna feed network unit 02 p0167 A83-11920
- Characteristics of modified spiral and helical antennas 02 p0164 A83-12003
- Progress in millimeter wave integrated-circuit imaging antenna arrays 03 p0327 A83-13780
- Offset near-field Gregorian antenna scanning beam analysis 03 p0305 A83-13999
- TE/11/-to-HE/11/ mode converters for small angle corrugated horns 03 p0305 A83-14003
- A curved-aperture corrugated horn having very low cross-polar performance 03 p0305 A83-14005
- Beam scanning and focal surfaces for parabolic cylinder reflectors 03 p0305 A83-14006
- Flanged parabolic antennas 03 p0305 A83-14007
- Analytic determination of the transient response of a thin-wire antenna based upon an SEM representation --- Singular Expansion Method 03 p0306 A83-14015
- A wide-band electrically small superdirective array 03 p0306 A83-14018
- Planar array synthesis with prescribed pattern nulls 03 p0306 A83-14019
- E-plane performance trade-offs in two-dimensional microstrip-patch element phased arrays 03 p0313 A83-14023
- Bispherical constrained lens antennas 03 p0306 A83-14028
- Effects of phase and amplitude quantization errors on hybrid phased-array reflector antennas 03 p0306 A83-14030
- A formulation of the finite-length narrow slot or strip equation 03 p0313 A83-14036
- A wide-band omnidirectional vertical shaped-beam collinear array 03 p0307 A83-14038
- Interference suppression techniques for microwave antennas and transmitters --- Book 03 p0307 A83-14118
- Improvement of front-to-back ratio by choke loaded at edge of parabolic antenna 03 p0307 A83-14127
- A design method of circularly polarized rectangular microstrip antenna by one-point feed 03 p0314 A83-14128
- Balanced helical antenna with tapered open ends 03 p0307 A83-14130
- Design of E-plane cosecant square beam horn antennas based on ray theory and their radiation characteristics 03 p0308 A83-14135
- Characteristics of annular-ring microstrip antenna 04 p0466 A83-15249
- Antenna synthesis on the basis of maximum directive gain 04 p0466 A83-15727
- Novel leaky-wave antenna for millimetre waves based on groove guide 04 p0468 A83-16025
- Dual offset reflectors shaped for zero crosspolarisation with asymmetric feed pattern 04 p0468 A83-16204
- Geometrical optical characteristics of the Schwarzschild scanning antenna - Comparison with the Cassegrain antenna 04 p0468 A83-16205
- Full-wave analysis of microstrip resonator and open-circuit end effect 04 p0473 A83-16208
- Mechanics of the flexible dipole antenna of WISP --- Waves in Space Plasma [AIAA PAPER 83-0433] 05 p0607 A83-16712
- Research on tunable antenna to detect continuous gravitational wave at low frequency 05 p0700 A83-17144
- A design of back-feed type circularly polarized microstrip disk antennas having symmetrical perturbation element by one-point feed 05 p0622 A83-17279
- Analysis, design and characteristics of X-band dielectric wedge waveguide antennas 05 p0622 A83-17341
- Design and development of an omnidirectional antenna with a collinear array of slots 05 p0622 A83-17343
- New drive system for large antennas 06 p0750 A83-18000
- Study on doubly curved shaped-beam reflector antenna theory 06 p0735 A83-18149
- Characteristics and design of high-gain dielectric circular antennas operated in X-band 06 p0736 A83-18425
- Theory and design considerations for a new millimetre-wave leaky groove-guide antenna 06 p0736 A83-18571
- Design studies for a thinned active planar array 06 p0737 A83-18605
- The crow's-nest antenna - A spatial array in theory and experiment 06 p0737 A83-18606
- Scattering by a conducting tube of finite length 06 p0737 A83-18608
- The determination of the fields reflected from a twist reflector following illumination by a plane wave 06 p0737 A83-18609
- A printed millimetre wave array using a low loss dielectric waveguide feeder 06 p0738 A83-18612
- A waveguide slot array for use at millimetric frequencies 06 p0751 A83-18614
- Structural simplification in applications of wire antenna modelling by moment methods 06 p0738 A83-18617
- Rotman lens fed multiple beam array 06 p0738 A83-18618
- The Quad aperture /hoop/column/ antenna for advanced communications missions in the 1990's 06 p0738 A83-18621
- A single receiver adaptive antenna system 06 p0738 A83-18622
- Some characteristics of multiple beam antennas - A review 06 p0739 A83-18624
- Designing Schwarzschild antenna systems 06 p0739 A83-18628
- A shaped offset dual reflector antenna with high gain and low sidelobe levels 06 p0739 A83-18630
- Adaptive null steering by reflector antennas 06 p0739 A83-18631
- An improved integrated SSR antenna system --- Secondary Surveillance Radar 06 p0740 A83-18636
- Transverse beam scanning for an offset dual-reflector system with symmetric main reflector 06 p0740 A83-18638
- Array-fed reflector antenna design and applications --- to spacecraft communication 06 p0722 A83-18639
- Near and far field airborne antenna pattern analysis 06 p0715 A83-18645
- The plane wave synthesis technique for antenna near-field/far-field transformation - Further development 06 p0740 A83-18649
- Low frequency performance of hemispherical coverage conical log-spiral antennas 06 p0722 A83-18654
- Feeds for reflector antennas - A review 06 p0741 A83-18656
- Optimisation methods applied to horn antennas 06 p0741 A83-18657
- Optimum performance indices of aperture antennas with and without pattern constraints 06 p0741 A83-18660
- Limits of VSWR for optimal broadband capacitively loaded cylindrical antennas versus their length 06 p0741 A83-18661
- Diffraction from cylindrically truncated planar surfaces with application to an aperture matched horn design 06 p0742 A83-18666
- Numerical methods for current analysis in microstrip planar antennas 06 p0751 A83-18670
- A theoretical and experimental investigation of the circularly polarised elliptical printed-circuit antenna 06 p0742 A83-18671
- Recent examples of conformal microstrip antenna arrays for aerospace applications 06 p0715 A83-18672
- A directional antenna element for use in a phase array with H-plane scanning - Requirements, realisation, nearfields 06 p0751 A83-18674
- High gain and broad band Yagi-Uda array antenna composed of twin-delta loops 06 p0743 A83-18680
- Analytical techniques for reduction of computational effort in reflector antenna analysis 06 p0743 A83-18683
- Offset dual reflector synthesis as a boundary-value problem 06 p0743 A83-18684
- Complex ray and evanescent wave analysis of parabolic reflector antennas 06 p0743 A83-18685
- GTD analysis of reflector antennas with general rim shapes 06 p0743 A83-18690
- Pattern prediction for a focused reflector antenna using GTD and near-field to far-field transformations 06 p0744 A83-18691
- A printed array of symmetrical dipoles with a novel feeding configuration 06 p0751 A83-18693
- Theoretical and experimental analysis of cylindrical dipoles with minimal mutual coupling 06 p0744 A83-18694
- Attenuation due to accretion of dust and sand on reflector antennas at microwave frequencies 06 p0744 A83-18696
- Theory and design of a Ku-band TE/21/-mode coupler 06 p0752 A83-18763
- The improvement of sidelobe performance of slotted waveguide arrays 06 p0748 A83-18937
- Optimization of coverage pattern for regional communications satellite 06 p0723 A83-19036
- A failure mechanism in adaptive arrays 07 p0907 A83-19722
- AJ/LPI at millimeter wavelengths --- Anti-Jamming/Low Probability of Intercept 07 p0909 A83-19753
- New doubly orthogonal functions and their application to pattern synthesis --- in antenna design 07 p0913 A83-20071
- A survey of millimetre-wavelength planar antenna arrays for military applications 07 p0913 A83-20182
- Design considerations for millimetre wave lens antennas 07 p0913 A83-20183
- A pole-zero modeling approach to linear array synthesis. I - The unconstrained solution 07 p0913 A83-20368
- Beam scanning in the offset Gregorian antenna 07 p0913 A83-20551
- Control of the radiation polarization of a system of two coherently excited plane logarithmic spirals 07 p0915 A83-20879
- Decoupling of antennas by means of plane elements 07 p0915 A83-20880
- Dynamic programming in problems of the synthesis of multichannel phasing devices 07 p0921 A83-20881
- Techniques for low sidelobe, high efficiency offset dual reflector antennas 07 p0915 A83-21072
- Several aspects related to the realisation of annular synthesis telescopes operating at millimetre wavelengths 08 p1174 A83-22026
- A laser range finder for the dimensional control of radio telescope antennas 08 p1092 A83-22225
- Minimax optimization of two-dimensional Cartesian and Fresnel lens phased arrays 08 p1161 A83-22474
- Batch covariance relaxation /BCR/ adaptive processing --- for low-sidelobe main antenna array 08 p1078 A83-22815
- Radar - Reflections on radio waves 08 p1078 A83-23250
- Diffraction of electromagnetic waves by a two-dimensional periodic waveguide-dielectric array 09 p1244 A83-23451
- The application of mathematical programming to problems of the diffraction synthesis of antennas 09 p1245 A83-23455
- On the choice of the optimal density of vibrators for a rectenna 09 p1292 A83-23464
- Improved pattern synthesis for equispaced linear arrays 09 p1246 A83-23691
- Broad-band microwave electronically scanned direction finder 09 p1246 A83-23777
- Dielectric and width effect on H-plane and E-plane coupling between rectangular microstrip antennas 09 p1246 A83-23780
- An improved design procedure for small arrays of shunt slots 09 p1246 A83-23781
- Matching properties of arbitrarily large dielectric covered phased arrays 09 p1246 A83-23782
- A wide-angle scanning optical antenna 09 p1246 A83-23783
- Fourier transform of a polygonal shape function and its application in electromagnetics 09 p1247 A83-23789
- Time domain modeling of nonlinear loads --- for wire antennas 09 p1253 A83-23792
- On the collimation phase error computation of a space-fed planar phased array 09 p1247 A83-23797
- Simple method for pattern nulling by phase perturbation 09 p1247 A83-23800
- A wide-band low-sidelobe disc-o-cone antenna 09 p1248 A83-23805
- A fading reduction method for maritime satellite communications 09 p1248 A83-23806
- A modular approach for the design of microstrip array antennas 09 p1254 A83-23807
- On some broad-band microstrip resonators 09 p1248 A83-23808
- Dielectric lens shaping and coma-correction zoning. I - Analysis 09 p1248 A83-23813
- A coma-corrected multibeam shaped lens antenna. II - Experiments 09 p1248 A83-23814
- Static shape determination and control for a large space antenna 09 p1328 A83-24722
- Optimization of a controlled-polarization antenna 09 p1250 A83-24909
- Synthesis of an array with an amplitude or phase field distribution fixed on part of the aperture 09 p1251 A83-25163
- Design of dielectric grating antennas for millimeter-wave applications 10 p1402 A83-25816
- The conical antenna as a sensor or probe 10 p1404 A83-26488
- Antennas for nonsinusoidal waves. I - Radiators 10 p1404 A83-26489
- Radiation characteristics of traveling-wave antennas excited by nonsinusoidal currents 10 p1404 A83-26490
- The loop antenna with a cylindrical core - Theory and experiment 10 p1405 A83-26826
- Analysis of the loop-coupled log-periodic dipole array 10 p1405 A83-26831

Constrained optimization of monopulse circular aperture distribution in the presence of blockage

10 p1375 A83-26835

Preliminary announcement of an 85 percent efficient reflector antenna

10 p1406 A83-26841

A new minimum blocking condition including subreflector and quadropod shadow for the design of dual reflector systems

10 p1406 A83-26842

A logarithmic reflection chart for presentation of antenna impedance

10 p1411 A83-26844

Effect of substrate thickness on the performance of a circular-disk microstrip antenna

10 p1406 A83-26846

Calculation of the cross-polarization in the far field of waveguide radiators

10 p1412 A83-26888

Allowance for antenna errors in the determination of the scattering matrix of a radar target

10 p1407 A83-26959

Algorithm for the calculation of the current distribution of electrically long curvilinear conductors

10 p1412 A83-26961

Dual-frequency circularly polarised printed antenna composed of strips and slots

11 p1560 A83-27895

A complex gradient operator and its application in adaptive array theory

11 p1554 A83-27902

Multifunction adaptive processor for small antenna arrays

11 p1554 A83-27909

Problems associated with correlation-loop adaptive antennas employing hard limiting

11 p1554 A83-27910

Perturbation adaptive array processor for airborne application

11 p1527 A83-27913

Adaptive antenna design considerations for satellite communication antennas

11 p1535 A83-27915

Experimental open-loop canceller for radar

11 p1555 A83-27916

Open-loop adaptivity for rotating antennas

11 p1555 A83-27917

Natural modes of a periodic array of rectangular longitudinally magnetized ferrite rods

11 p1561 A83-27966

Simple expressions model antenna radiation patterns

11 p1558 A83-28153

High stability communications hardware for spacecraft

11 p1562 A83-28184

Driving-point impedance of a linear cylindrical antenna

11 p1558 A83-28607

Rectangular dielectric resonator antenna

[AD-A129976]

11 p1558 A83-28608

The status and prospects in the development of methods for measuring the external parameters of antennas

/review/ 11 p1558 A83-28680

Synthesis of directional couplers with a fixed phase difference of output signals

11 p1564 A83-28689

Antenna optimization of single beam microwave systems for the solar power satellite

12 p1706 A83-29048

Multiple beam microwave systems for the solar power satellite

12 p1706 A83-29049

Microstrip linear array with polarisation control

12 p1719 A83-29439

Comparative analysis of large antenna spacecraft using the ideas system

[AIAA 83-0798]

12 p1707 A83-29731

Waveguide slot antenna with a coupled dipole above the slot

13 p1830 A83-31760

Performance of small primary feeds with trapezoidal and sinusoidal corrugations --- for reflector antennas

13 p1837 A83-31766

Single-element rectangular microstrip antenna for dual-frequency operation

13 p1830 A83-31767

Optoelectronically pulsed slot-line antennas

13 p1837 A83-31773

Effects of choke-load position on radiation properties in double-choked small horn antennas

13 p1830 A83-31778

Almost-periodic linear arrays

14 p2002 A83-33469

Open coaxial resonance structures --- Russian book

15 p2152 A83-34168

Dual frequency microstrip antenna

15 p2144 A83-34512

0.81 micron band AlGaAs/GaAs double-channel planar buried-heterostructure laser with large optical cavity

15 p2169 A83-34517

Reduction of sidelobe level of reflector antennas by covering feed struts with a periodic structure

15 p2144 A83-34518

Antenna Applications Symposium, Monticello, IL, September 23-25, 1981, Proceedings

15 p2145 A83-35076

Recent developments in millimeter-wave antennas

15 p2145 A83-35078

Shaped lens antennas

15 p2146 A83-35081

A geodesic lens antenna for 360 deg azimuthal coverage

15 p2146 A83-35085

A common-aperture X- and S-band four-function feedcone --- hornfeed design for antennas of Deep Space Network

15 p2126 A83-35086

New advances in wide band dual polarization antenna elements for EW applications

15 p2121 A83-35087

A rapid-tuning high-power pod-mounted VHF antenna system

15 p2121 A83-35088

Multimode planar spiral for DF applications

15 p2121 A83-35089

A network formulation for phased arrays - Application to log-periodic arrays of monopoles on curved surfaces

15 p2121 A83-35090

Alternate formulas for near-field computation

15 p2146 A83-35091

Optimization of the directivity of a parabolic reflector antenna

15 p2146 A83-35094

Synthesis of a resonant antenna

15 p2147 A83-35154

Cost optimization of the dimensions of the antennas of a solar power satellite system

15 p2193 A83-35167

Superresolution of multiple noise sources in antenna beam

15 p2148 A83-35180

The synthesis of surface reactance using an artificial dielectric

15 p2154 A83-35182

The singular integral problem in surfaces

15 p2148 A83-35187

Tracking antenna arrays for near-millimeter waves

15 p2148 A83-35189

Comparative analysis of a phase and an amplitude processor for amplitude monopulse systems

15 p2121 A83-35192

Directivity optimization for Yagi-Uda arrays of shaped dipoles

15 p2149 A83-35193

A new MIC slot-line aerial

15 p2149 A83-35194

Experimental study of the characteristics of coupled top-loaded microstrip monopoles

15 p2149 A83-35196

Primary-focus operation of shaped dual-reflector antennas

15 p2149 A83-35199

Numerical calculations of low-frequency TE fields in arbitrarily shaped inhomogeneous lossy dielectric cylinders

16 p2407 A83-35407

New monopulse tracking radar

16 p2342 A83-36009

Mutual coupling between short-circuited microstrip antennas

16 p2342 A83-36484

The handbook of antenna design. Volumes 1 & 2

17 p2493 A83-37158

Matching networks in linear phased arrays

17 p2497 A83-37791

Composite materials and deployable boom technology [SAE PAPER 821395]

17 p2480 A83-37970

A pyramidal horn antenna with identical E- and H-plane patterns

17 p2494 A83-38064

On the quality factor and energy center of antennas

17 p2494 A83-38476

Choice of optimal geometric parameters for conical spiral antennas comprising a conductor with additional bends

18 p2674 A83-39433

Design, analysis and testing of two concepts for a dimensional stable structure --- composite antenna tower for communication satellites

18 p2662 A83-40289

Deformation and stress of antenna made of glass fiber reinforced plastics under wind force

18 p2662 A83-40296

Analysis and design of frequency scanned transmission gratings

18 p2676 A83-40651

Low-sidelobe radar antennas

19 p2825 A83-40757

Substrate optimization for integrated circuit antennas

19 p2826 A83-41087

Prediction of adaptive array performance

19 p2826 A83-41145

Advanced 30/20 GHz multiple beam antenna for future communications satellites

19 p2830 A83-41367

Experimental study of a resonance antenna synthesized according to a prescribed radiation pattern

19 p2835 A83-41788

Sidelobe reduction for phased array antennas using digital phase shifters. I - One bit phase weighting. II - Two bit phase weighting

20 p2963 A83-42367

Studies on certain modified Luneberg lenses

20 p2963 A83-42369

4-layer inductive grid FSS at 45 deg incidence --- Frequency Selective Surfaces

20 p2963 A83-42478

Dielectric image line leaky wave antenna for broadside radiation

20 p2964 A83-42491

The evolution and state of the art in air defense radar antennas

20 p2964 A83-42825

Electronic steering of antenna nulls for interference reduction

20 p2965 A83-43680

Broadband adaptive array processing

20 p2965 A83-43682

High power and pointing accuracy from body-spun spacecraft

21 p3100 A83-44534

Optimization of director antennas

21 p3121 A83-44778

Double-square frequency-selective surfaces and their equivalent circuit

21 p3121 A83-44958

Complex geometrical optics for the study of reflector antennas

21 p3121 A83-45409

The Jacobi-Bessel and the pseudo-sampling techniques in the analysis of reflector antennas

21 p3121 A83-45410

The theory of three-dimensional bifocal antennas

22 p3271 A83-45650

A frequency-independent parabolic log-periodic phased-array antenna

22 p3272 A83-45686

Designing an umbrella-type folding antenna

22 p3272 A83-45688

Launching large antennas

22 p3258 A83-45721

Synthetic aperture radar antenna from CFRP

22 p3259 A83-46178

A large millimeter wave antenna

22 p3375 A83-46748

Antennas for nonsinusoidal waves. III - Arrays

22 p3276 A83-46933

Research and development of synthetic aperture radar

[IAF PAPER 83-94]

23 p3424 A83-47263

A large deployable antenna structure for the ERS-1 satellite

[IAF PAPER 83-361]

23 p3422 A83-47359

Control of reflector vibrations in large spaceborne antennas by means of movable dampers

23 p3423 A83-47598

Design of transverse slot arrays fed by a boxed stripline

23 p3442 A83-47826

The optimum feed voltage for a dipole antenna for pulse radiation

23 p3442 A83-47827

Off-axis scanning of cylindrical lenses

23 p3442 A83-47831

An imaging beam waveguide feed --- for mm wave antenna

23 p3445 A83-47833

An algorithm for the empirical optimization of antenna arrays

23 p3443 A83-47845

Unfurlable offset antenna design for L- and C-band application

23 p3423 A83-48139

Computer-aided design of radiating systems of antenna-radome type

23 p3444 A83-48523

Simplified linearly polarised contoured beam reflector antenna for a European coverage requirement

23 p3444 A83-48713

Far field radiated by short-circuited microstrip antenna acting at a quarter-wavelength resonance

23 p3444 A83-48720

Design of the log-periodic feed of a reflector antenna

24 p3570 A83-49269

Millimeter wave antenna technology

24 p3570 A83-49856

High-precision measurements on a compact antenna test range

24 p3571 A83-49967

ANTENNA FEEDS

A microprocessor controlled variable phase and amplitude antenna feed network unit

02 p0167 A83-11920

Offset near-field Gregorian antenna scanning beam analysis

03 p0305 A83-13999

Input impedance and mutual coupling of rectangular microstrip antennas

03 p0313 A83-14021

The impedance of an elliptical printed-circuit antenna

03 p0313 A83-14022

A design method of circularly polarized rectangular microstrip antenna by one-point feed

03 p0314 A83-14128

Contoured-beam synthesis for array-fed reflector antennas by field correlation

04 p0468 A83-16202

Dual offset reflectors shaped for zero crosspolarisation with asymmetric feed pattern

04 p0468 A83-16204

A design of back-feed type circularly polarized microstrip disk antennas having symmetrical perturbation element by one-point feed

05 p0622 A83-17279

Axially symmetric radiation patterns from flanged E-plane sectoral horn feeds

06 p0736 A83-18421

Rotman lens fed multiple beam array

A directional antenna element for use in a phase array with H-plane scanning - Requirements, realisation, nearfields 06 p0751 A83-18674

A printed array of symmetrical dipoles with a novel feeding configuration 06 p0751 A83-18693

Excess loss of TE/11/ modes in curved circular waveguide 06 p0751 A83-18698

Beam scanning in the offset Gregorian antenna 07 p0913 A83-20551

Combined E- and H-plane phase centers of antenna feeds 09 p1248 A83-23810

Symmetrical crossed rectangular horn for a circularly polarized multiple-beam reflector antenna 09 p1248 A83-23811

Hybrid-mode, shielded, offset parabolic antenna 09 p1248 A83-23874

High stability communications hardware for spacecraft 11 p1562 A83-28184

Horizontal dipole antenna above an imperfectly conducting ground fed by a two-wire line 13 p1828 A83-30648

Performance of small primary feeds with trapezoidal and sinusoidal corrugations --- for reflector antennas 13 p1837 A83-31766

Dual frequency microstrip antenna 15 p2144 A83-34512

0.81 micron band AlGaAs/GaAs double-channel planar buried-heterostructure laser with large optical cavity 15 p2169 A83-34517

Uplink depolarisation control in TV feeder link earth stations 15 p2144 A83-34520

A beam waveguide linearly polarized KU band feed system 15 p2146 A83-35079

A common-aperture X- and S-band four-function feedcone --- hornfeed design for antennas of Deep Space Network 15 p2126 A83-35086

An algebraic synthesis method for R(sq N) multibeam matrix network 15 p2126 A83-35093

Directivity of planar array feeds for satellite reflector applications 15 p2126 A83-35181

Propagation and radiation properties of corrugated cylindrical coaxial waveguides 15 p2148 A83-35183

A comparative study of feed impedances of a circular and three different spiral antenna arrays 16 p2344 A83-36731

A pyramidal horn antenna with identical E- and H-plane patterns 17 p2494 A83-38064

Control of large spaceborne antenna systems with flexible booms by mechanical decoupling 18 p2646 A83-39095

Helically corrugated circular waveguides as antenna feeders 18 p2676 A83-40398

Radiation characteristics of coaxial waveguides as a small primary feed 20 p2964 A83-42488

A compact septum polarizer --- for antenna feed waveguide 21 p3119 A83-43835

Design of transverse slot arrays fed by a boxed stripline 23 p3442 A83-47826

The optimum feed voltage for a dipole antenna for pulse radiation 23 p3442 A83-47827

Off-axis scanning of cylindrical lenses 23 p3442 A83-47831

An imaging beam waveguide feed --- for mm wave antenna 23 p3445 A83-47833

Design of the log-periodic feed of a reflector antenna 24 p3570 A83-49269

ANTENNA FIELDS

U ANTENNA RADIATION PATTERNS

ANTENNA RADIATION PATTERNS

NT SIDELOBES

A circularly polarized compact flat source 01 p0032 A83-10924

Commutating spot transmissive lens antenna 01 p0042 A83-11158

Optimal beamforming for a linear array antenna 01 p0032 A83-11159

A broad-band annular-ring microstrip antenna 01 p0033 A83-11361

A high-frequency analysis of radome-induced radar pointing error 01 p0033 A83-11365

Range distance requirements for measuring low and ultralow sidelobe antenna patterns 01 p0033 A83-11366

A broad-band constant beamwidth corrugated rectangular horn 01 p0033 A83-11367

A note on utilizing far-field phase information 01 p0034 A83-11375

A band-switched resonant quadrifilar helix 01 p0034 A83-11376

Theory of the frequency responses of uniform and quasi-taper helical antennas 01 p0034 A83-11378

On an index for array optimization and the discrete prolate spheroidal functions 01 p0034 A83-11379

Approximate difference pattern response of the weighted multibeam array 01 p0034 A83-11381

Beam shaping using nonlinear phase distribution in a uniformly spaced array 01 p0034 A83-11383

The radiation characteristics of longitudinal slot antennas 02 p0162 A83-11537

Concerning the resolving power of radar stations with antenna arrays 02 p0162 A83-11541

Coherent-optical synthesis of an antenna radiation pattern with a zero in a prescribed direction 02 p0166 A83-11686

Frequency agile microstrip antennas 02 p0163 A83-11919

Ground station antenna crosspolarisation measurements with an imperfectly polarised ancillary antenna 02 p0164 A83-11986

Characteristics of modified spiral and helical antennas 02 p0164 A83-12003

Receiving analysis of the shaped cylindrical reflector antenna 02 p0164 A83-12004

Radiation patterns of interfacial dipole antennas 02 p0165 A83-12631

Offset near-field Gregorian antenna scanning beam analysis 03 p0305 A83-13999

A curved-aperture corrugated horn having very low cross-polar performance 03 p0305 A83-14005

Flanged parabolic antennas 03 p0305 A83-14007

A wide-band electrically small superdirective array 03 p0306 A83-14018

Planar array synthesis with prescribed pattern nulls 03 p0306 A83-14019

The synthesis of shaped patterns with series-fed microstrip patch arrays 03 p0313 A83-14024

Radiation pattern computation of a spherical lens using Mie series 03 p0306 A83-14027

Radiation from aperture antennas radiating in the presence of a dielectric sphere 03 p0307 A83-14031

Regge poles, natural frequencies, and surface wave resonance of a circular cylinder with a constant surface impedance 03 p0307 A83-14034

A hybrid MM-geometrical optics technique for the treatment of wire antennas mounted on a curved surface 03 p0307 A83-14037

A wide-band omnidirectional vertical shaped-beam collinear array 03 p0307 A83-14038

Improvement of front-to-back ratio by choke loaded at edge of parabolic antenna 03 p0307 A83-14127

A design method of circularly polarized rectangular microstrip antenna by one-point feed 03 p0314 A83-14128

Balanced helical antenna with tapered open ends 03 p0307 A83-14130

Design of E-plane cosecant square beam horn antennas based on ray theory and their radiation characteristics 03 p0308 A83-14135

Far field radiated by rectangular patch microstrip antenna 04 p0465 A83-15233

Characteristics of the cross-polarized radiation of dielectric rod lenses 04 p0466 A83-15718

The structure of the radiation pattern and the role of amplitude-phase distributions in curved antenna arrays 04 p0467 A83-15748

European OTS satellite transmit antenna patterns 04 p0453 A83-16201

Contoured-beam synthesis for array-fed reflector antennas by field correlation 04 p0468 A83-16202

Geometrical optical characteristics of the Schwarzschild scanning antenna - Comparison with the Cassegrain antenna 04 p0468 A83-16205

Measurements of K-band antenna patterns 04 p0468 A83-16419

Analysis, design and characteristics of X-band dielectric wedge waveguide antennas 05 p0622 A83-17341

Design and development of an omnidirectional antenna with a collinear array of slots 05 p0622 A83-17343

The spatial characteristics of a multichannel device in the case of nonlinear processing 05 p0623 A83-17688

A phased horn with a main lobe of elliptical cross section 05 p0623 A83-17690

Study on doubly curved shaped-beam reflector antenna theory 06 p0735 A83-18149

Analysis of VOR antenna radiation patterns 06 p0735 A83-18348

Axially symmetric radiation patterns from flanged E-plane sectoral horn feeds 06 p0736 A83-18421

Sampling approach for fast computation of scattered fields 06 p0736 A83-18569

Generation of field scattered by imperfectly conducting objects from the solution of a perfectly conducting object 06 p0736 A83-18575

International Conference on Antennas and Propagation, 2nd, University of York, York, England, April 13-16, 1981, Proceedings. Part 1 - Antennas. Part 2 - Propagation 06 p0736 A83-18601

Circular arrays - Their properties and potential applications 06 p0737 A83-18602

ANTENNA RADIATION PATTERNS

The crow's-nest antenna - A spatial array in theory and experiment 06 p0737 A83-18606

A planar array antenna for TV broadcasting communications 06 p0737 A83-18607

Primary-feed elements for multiple and contoured beam satellite antennas 06 p0738 A83-18619

An aperture phase compensation technique for off-axis beam synthesis in parabolic reflector antennas 06 p0738 A83-18620

The use of multiple transmitting antennas to provide beamwidth reduction for H.F. pulse radars with sector coverage 06 p0738 A83-18623

Some characteristics of multiple beam antennas - A review 06 p0739 A83-18624

Effects of element cross-polarisation in adpative antennas 06 p0739 A83-18626

Airframe multipath effects in airborne adaptive antenna arrays 06 p0715 A83-18627

Characteristics of beam waveguides --- in satellite antenna feeds 06 p0739 A83-18629

Beam-forming in the nearfield of small spherical reflectors 06 p0740 A83-18637

Distance criteria in near-field and far-field antenna measurements 06 p0740 A83-18640

In-orbit performance of the OTS-2 communication antennas 06 p0722 A83-18641

Microwave diagnostics of the Chilbolton 25M antenna using the OTS satellite 06 p0740 A83-18642

Calibration of standard gain antennas using a spherical near-field technique 06 p0740 A83-18644

Near and far field airborne antenna pattern analysis 06 p0715 A83-18645

An asymptotic high frequency analysis of the radiation from sources on perfectly-conducting structures with an impedance surface patch 06 p0715 A83-18647

High-frequency scattering from offset reflectors 06 p0740 A83-18648

The plane wave synthesis technique for antenna near-field/far-field transformation - Further development 06 p0740 A83-18649

Spherical near-field measurements from a 'compact-range' viewpoint 06 p0740 A83-18650

Near-field probe-scanning antenna measurement facility 06 p0721 A83-18651

Quasi-real-time antenna near-field/far-field transformation without phase and amplitude recording 06 p0741 A83-18652

Computer simulations of inaccuracies in spherical near-field testing 06 p0741 A83-18653

Low frequency performance of hemispherical coverage conical log-spiral antennas 06 p0722 A83-18654

A ship-borne helical array antenna for maritime satellite communication 06 p0741 A83-18655

Optimisation methods applied to horn antennas 06 p0741 A83-18657

Beamshaping of sectoral and pyramidal horns with stepped amplitude distribution 06 p0741 A83-18659

Optimum performance indices of aperture antennas with and without pattern constraints 06 p0741 A83-18660

Effect of the polarization squint of small horn antennas 06 p0741 A83-18662

A family of two-reflector antennas with identical dielectric primary feeds 06 p0742 A83-18664

Maximum entropy resolution of two dimensional antenna distributions 06 p0742 A83-18669

A theoretical and experimental investigation of the circularly polarised elliptical printed-circuit antenna 06 p0742 A83-18671

Recent examples of conformal microstrip antenna arrays for aerospace applications 06 p0715 A83-18672

Aberrative properties of a planar dielectric sheet --- effects on antenna radiation patterns 06 p0742 A83-18675

Methods for improving the performance of radome covered reflector antennas 06 p0742 A83-18676

Satellite measurement of the effects of rain and sleet on the performance of a radome covered antenna 06 p0742 A83-18678

Synthesis of conformal HF and VHF directional arrays on spherical bodies using surface resonator techniques 06 p0743 A83-18679

High gain and broad band Yagi-Uda array antenna composed of twin-delta loops 06 p0743 A83-18680

Radiation patterns of a quarter-wave monopole on a finite ground plane --- for aircraft antennas 06 p0715 A83-18682

Analytical techniques for reduction of computational effort in reflector antenna analysis 06 p0743 A83-18683

Complex ray and evanescent wave analysis of parabolic reflector antennas 06 p0743 A83-18685

Fourier transform-iteration for antenna pattern synthesis 06 p0743 A83-18686

A novel technique for the computation of secondary patterns of reflector antennas 06 p0743 A83-18687

A generalized sampling and sampling-like technique for fast analysis of reflector antennas

06 p0743 A83-18688

The effect of undersampling and finite truncation of the antenna near-field data on the predicted far-field pattern

06 p0743 A83-18689

GTD analysis of reflector antennas with general rim shapes

06 p0743 A83-18690

Pattern prediction for a focused reflector antenna using GTD and near-field to far-field transformations

06 p0744 A83-18691

Radiation characteristics of radial waveguide fed slot arrays of various shapes

06 p0744 A83-18692

Analysis of monopole-antenna with rectangular reflector

06 p0744 A83-18695

Comparison of radiometric measurements at 11.4 and 35 GHz with propagation data on the OTS space-earth path at 11.8 GHz

06 p0745 A83-18705

Optimization of coverage pattern for regional communications satellite

06 p0723 A83-19036

The potential possibilities of antennas in terms of directional properties and field attenuation in the shadow zone

06 p0749 A83-19357

Difference patterns of antenna arrays

06 p0749 A83-19358

A failure mechanism in adaptive arrays

07 p0907 A83-19722

New doubly orthogonal functions and their application to pattern synthesis --- in antenna design

07 p0913 A83-20071

A pole-zero modeling approach to linear array synthesis. I - The unconstrained solution

07 p0913 A83-20368

Electromagnetic excitation of a truncated cone by a plane wave

07 p0914 A83-20775

Antenna beam patterns and dual-wavelength processing --- for radar hail detection

07 p0969 A83-20806

Concerning the radiation pattern in the problem of the excitation of an array of circular dielectric cylinders by a local source

07 p0915 A83-20871

Techniques for low sidelobe, high efficiency offset dual reflector antennas

07 p0915 A83-21072

A study of the radiation from an antenna in a Maxwellian magnetoplasma Application to the in situ sounding of the auroral ionosphere --- French thesis

07 p0964 A83-21093

Modeling of simple antennas near to and penetrating an interface

07 p0916 A83-21546

Edge effects in dipole phased arrays

08 p1076 A83-22236

Impedance parameters and radiation pattern of two coupled circular microstrip disk antennas

08 p1076 A83-22329

Aperture synthesis of monopulse antenna for radome analysis using limited measured pattern data

08 p1076 A83-22473

Self-complementary monopole-notch array antennas

08 p1077 A83-22624

The radiation of a horn antenna

08 p1078 A83-23152

Signal detection in a clutter environment in a bistatic system

08 p1078 A83-23156

Diffraction of electromagnetic waves by a two-dimensional periodic waveguide-dielectric array

09 p1244 A83-23451

Analysis of the radiation characteristics of an aperture antenna excited by a periodic pulsed signal

09 p1245 A83-23454

The application of mathematical programming to problems of the diffraction synthesis of antennas

09 p1245 A83-23455

On the choice of the optimal density of vibrators for a rectenna

09 p1292 A83-23464

Improved pattern synthesis for equispaced linear arrays

09 p1246 A83-23691

New results on coherent scattering from randomly rough conducting surfaces

09 p1246 A83-23776

A geometrical theory for the resonant frequencies and Q-factors of some triangular microstrip patch antennas

09 p1246 A83-23778

On the effect of substrate thickness and permittivity on printed circuit dipole properties

09 p1246 A83-23779

Dielectric and width effect on H-plane and E-plane coupling between rectangular microstrip antennas

09 p1246 A83-23780

A wide-angle scanning optical antenna

09 p1246 A83-23783

Coherent scattering of a spherical wave from an irregular surface --- antenna pattern effects

09 p1267 A83-23784

External and internal mutual impedance effects on the radiation patterns of circularly disposed arrays using antennafiers or passive monopoles

09 p1246 A83-23786

An efficient computational method for characterizing the effects of random surface errors on the average power pattern of reflectors

09 p1247 A83-23788

Fourier transform of a polygonal shape function and its application in electromagnetics

09 p1247 A83-23789

Wide-band nulling performance versus number of pattern constraints for an array antenna

09 p1247 A83-23799

Simple method for pattern nulling by phase perturbation

09 p1247 A83-23800

Symmetrical crossed rectangular horn for a circularly polarized multiple-beam reflector antenna

09 p1248 A83-23811

Hybrid-mode, shielded, offset parabolic antenna

09 p1248 A83-23874

Numerical analysis of 4-arm Archimedean spiral antenna

09 p1249 A83-24111

Prediction of scattering cross-section reductions due to plate orthogonality errors in trihedral radar reflectors

09 p1249 A83-24116

The use of a mathematical model of a phased-array antenna to measure the radiation pattern

09 p1250 A83-24913

Characteristics of a stepwise waveguide radiator in an antenna array with a dielectric coating

09 p1250 A83-24921

Impedance and polarization characteristics of rectangular printed radiators in planar phased-array antennas

09 p1250 A83-24922

Semicircular-waveguide radiator with circular polarization

09 p1257 A83-24925

The excitation of a perfectly conducting multihedral body

09 p1251 A83-25083

Dynamic measurements of the effective scattering cross sections of targets

09 p1251 A83-25161

Synthesis of an array with an amplitude or phase field distribution fixed on part of the aperture

09 p1251 A83-25163

Analysis of rim loaded Cassegrain antennas

10 p1401 A83-25502

Real axis integration of Sommerfeld integrals - Source and observation points in air

10 p1403 A83-26038

Radiation characteristics of traveling-wave antennas excited by nonsinusoidal currents

10 p1404 A83-26490

Analysis of microstrip wraparound antennas using dyadic Green's function

10 p1374 A83-26830

A GTD study of pyramidal horns for offset reflector antenna applications

10 p1406 A83-26837

Experimental investigation on a method of lowering the silhouette of conical log-spiral antenna

10 p1406 A83-26843

Effect of substrate thickness on the performance of a circular-disk microstrip antenna

10 p1406 A83-26846

Far-field radiation patterns of elliptical apertures and its annuli

10 p1406 A83-26847

Rotational symmetries of electromagnetic radiation fields

10 p1406 A83-26853

Spheroidal wave functions of large frequency parameters $c - kf$ and the radiation fields of a metallic prolate spheroid excited by any circumferential slot

10 p1383 A83-26854

A technique for determining antenna beam patterns using a ground target

11 p1571 A83-27082

The effects of mismatched antenna beam patterns on dual-wavelength processing --- for hail detection

11 p1630 A83-27083

Transformation of the matrix of generalized impedances in the case of frequency variation --- for antenna radiation pattern calculations

11 p1556 A83-27945

Simple expressions model antenna radiation patterns

11 p1558 A83-28153

Rectangular dielectric resonator antenna [AD-A129976]

11 p1558 A83-28608

The status and prospects in the development of methods for measuring the external parameters of antennas /review/

11 p1558 A83-28680

The radiation pattern of a phased-array excited by a wideband signal

11 p1558 A83-28683

Decoupling of antennas with the aid of underlying surfaces

11 p1559 A83-28685

Difference-channel cross-polarization patterns of parabolic antennas

11 p1559 A83-28687

A numerical analysis of the diffraction of radio waves --- Russian book

12 p1718 A83-28827

Grating lobe characteristics and associated impacts upon the solar power satellite microwave system

12 p1706 A83-29047

Parameters of the RT-3 radio telescope

12 p1788 A83-29299

Conically depressed microstrip patch antenna

12 p1736 A83-29437

Microstrip linear array with polarisation control

12 p1719 A83-29439

Polarization selection of signals by antenna arrays with controlled field-polarization

13 p1827 A83-30277

Phase synthesis of highly directional antenna arrays with a low sidelobe level on one side of the main lobe

13 p1827 A83-30278

Some features of the operation of adaptive antenna systems intended for the receptions of FSK signals in a two-beam fluctuating field

13 p1828 A83-30279

Electrodynamic analysis of a model of a two-reflector antenna with strict allowance for the interaction between reflectors

13 p1828 A83-30280

The effect of errors in the amplitude-phase distribution of a linear antenna on its scattering coefficient

13 p1828 A83-30282

Radiation characteristics of a plane logarithmic spiral on a magnetized-plasma layer

13 p1828 A83-30284

Energy and polarization characteristics of radiation from the open end of a circular waveguide

13 p1828 A83-30714

Determination of the effect of losses in the dielectric substrate on the radiation of a plane logarithmic spiral with a screen

13 p1828 A83-30715

On the synthesis of antenna arrays with a variable amplitude-phase distribution in certain radiators

13 p1828 A83-30716

Investigation of the band characteristics of waveguide radiators coupled with dielectric-cylinder filters

13 p1834 A83-30732

Laser-plasma antennas, concentrators, anad directional couplers for the rf range

13 p1851 A83-30910

Test of large aperture antennas using near-field techniques

13 p1829 A83-31194

The design of an automated, high-accuracy antenna test facility

13 p1829 A83-31280

Antenna gain measurements by an extended version of the NBS extrapolation method

13 p1829 A83-31281

A near-field antenna measurement system

13 p1830 A83-31282

A holographic surface measurement of the Texas 4.9-m antenna at 86 GHz

13 p1847 A83-31283

Precision measurement of antenna system noise using radio stars

13 p1940 A83-31284

Waveguide slot antenna with a coupled dipole above the slot

13 p1830 A83-31760

Effects of choke-load position on radiation properties in double-choked small horn antennas

13 p1830 A83-31778

Parameters of a radiating slot cut into the wall of a nonreciprocal waveguide

14 p1999 A83-32105

A microcomputer based control system for antenna measurements

14 p2019 A83-32399

Almost-periodic linear arrays

14 p2002 A83-33469

Recent developments in millimeter-wave antennas

15 p2145 A83-35078

Phased array alignment with planar near-field scanning or determining element excitation from planar near-field data

15 p2146 A83-35082

Small array illuminations for pattern nulling with sidelobe level control

15 p2146 A83-35083

A geodesic lens antenna for 360 deg azimuthal coverage

15 p2146 A83-35085

A common-aperture X- and S-band four-function feedcone --- hornfeed design for antennas of Deep Space Network

15 p2126 A83-35086

Multimode planar spiral for DF applications

15 p2121 A83-35089

Alternate formulas for near-field computation

15 p2146 A83-35091

Optimization of the directivity of a parabolic reflector antenna

15 p2146 A83-35094

An analysis of annular, annular sector, and circular sector microstrip antennas

15 p2146 A83-35095

Radiation efficiency of a slot in a conducting screen coated with a dielectric layer

15 p2147 A83-35155

Radiation from a dielectric-filled flange waveguide

15 p2153 A83-35156

Variations of the direction-finding characteristics in the case of the direction finding of the source of a signal with unmatched polarization

15 p2147 A83-35158

Optimization of an antenna radiation pattern in conditions of spatial noise

15 p2147 A83-35169

The resonant cylindrical dielectric cavity antenna

15 p2148 A83-35175

Directivity of planar array feeds for satellite reflector applications

15 p2126 A83-35181

Propagation and radiation properties of corrugated cylindrical coaxial waveguides

15 p2148 A83-35183

Performance degradation in fast frequency-scanned circular arrays

15 p2148 A83-35188

Comparative analysis of a phase and an amplitude processor for amplitude monopulse systems

15 p2121 A83-35192

A new MIC slot-line aerial

15 p2149 A83-35194

Experimental study of the characteristics of coupled top-loaded microstrip monopoles 15 p2149 A83-35196

Mutual coupling and radiation patterns of two slots asymmetrically located on a square plate 15 p2149 A83-35197

The electromagnetic field in a layered earth induced by an arbitrary stationary current distribution 16 p2341 A83-35410

Antenna pattern measurement with a geostationary satellite 16 p2342 A83-35553

An analysis of radiation patterns of corrugated corner reflector antenna systems 16 p2344 A83-36734

The handbook of antenna design. Volumes 1 & 2 17 p2493 A83-37158

Optimum coupling of a Gaussian beam to a corner reflector with a four-wavelength antenna 17 p2510 A83-37753

Radio-astronomy antennas for 3 deg K cosmic radiation measurements 17 p2494 A83-38059

A pyramidal horn antenna with identical E- and H-plane patterns 17 p2494 A83-38064

On the quality factor and energy center of antennas 17 p2494 A83-38476

Radiation from circular symmetric sources in warm plasma column --- electromagnetic transmission in plasma media 17 p2495 A83-38537

Radiation from an Alford loop antenna in two-component warm plasma --- on Ariel-3 satellite 17 p2495 A83-38543

Statistical generalization of the formula of ideal radio transmission to the case of long-range short-wave communications 18 p2674 A83-39530

Contribution to the understanding of pattern coverage of an open-circuited microstrip wraparound antenna acting at half-wavelength resonance 18 p2675 A83-40386

Radiation losses of E-plane groove-guide bends 18 p2679 A83-40390

The method of complex rays --- extended to antenna electromagnetic fields 19 p2894 A83-40797

Radiation from antennas configured for spatial telecommunications 19 p2825 A83-40799

Substrate optimization for integrated circuit antennas 19 p2826 A83-41087

Radiation of a strip antenna with a half-wavelength resonance mounted on a finite cylindrical conductor 19 p2835 A83-41557

On the maximum interdependence of absorbed and scattered powers --- by receiving antennas or structures covered with absorbing materials 19 p2835 A83-41770

Experimental study of a resonance antenna synthesized according to a prescribed radiation pattern 19 p2835 A83-41788

A two-component model of Delano type for wave fields scattered by bodies of complex shape 19 p2836 A83-41821

Studies on certain modified Luneberg lenses 20 p2963 A83-42369

Radiation characteristics of coaxial waveguides as a small primary feed 20 p2964 A83-42488

Dielectric image line leaky wave antenna for broadside radiation 20 p2964 A83-42491

Double-square frequency-selective surfaces and their equivalent circuit 21 p3121 A83-44958

A numerical model for an electronically scanned antenna 21 p3121 A83-45274

Radiation of an elementary slot vibrator situated on an ideally conducting strip 22 p3271 A83-45668

Method for retrieving the true backscattering coefficient from measurements with a real antenna 22 p3314 A83-46236

Radiation properties of a vacuum-insulated infinite flat slotted plate antenna in a cold isotropic homogeneous plasma 22 p3274 A83-46526

Loop antennas for directive transmission into a material half space 22 p3274 A83-46527

Transmitting antenna for direct broadcasting satellites with radio frequency beam fine pointing capability [IAF PAPER 83-76] 23 p3441 A83-47255

The optimum feed voltage for a dipole antenna for pulse radiation 23 p3442 A83-47827

An improvement in electrical characteristics of a short backfire antenna 23 p3443 A83-47838

The finite ground plane effect on the microstrip antenna radiation patterns 23 p3443 A83-47839

An algorithm for the empirical optimization of antenna arrays 23 p3443 A83-47845

Synthesis of optimal weight distribution in adaptive antenna arrays 23 p3444 A83-48488

Computer-aided design of radiating systems of antenna-radome type 23 p3444 A83-48523

Digital model of a radio-astronomical measuring complex 24 p3638 A83-48957

Numerical method for calculating plane semiinfinite structures 24 p3573 A83-49273

High-precision measurements on a compact antenna test range 24 p3571 A83-49967

Analysis of the element pattern shape for circular arrays 24 p3571 A83-49989

Reflector shapes for any predetermined antenna radiation pattern 24 p3571 A83-50117

ANTENNAS

NT AIRCRAFT ANTENNAS

NT CASSEGRAIN ANTENNAS

NT CYLINDRICAL ANTENNAS

NT DELTA ANTENNAS

NT DIPOLE ANTENNAS

NT DIRECTIONAL ANTENNAS

NT FURLABLE ANTENNAS

NT GRAVITATIONAL WAVE ANTENNAS

NT HELICAL ANTENNAS

NT HORN ANTENNAS

NT LENS ANTENNAS

NT LOG PERIODIC ANTENNAS

NT LOG SPIRAL ANTENNAS

NT LOOP ANTENNAS

NT MICROWAVE ANTENNAS

NT MISSILE ANTENNAS

NT MONOPOLE ANTENNAS

NT MONOPULSE ANTENNAS

NT OMNIDIRECTIONAL ANTENNAS

NT PARABOLIC ANTENNAS

NT PLASMA ANTENNAS

NT RADAR ANTENNAS

NT RADIO ANTENNAS

NT RECTENNAS

NT RHOMBIC ANTENNAS

NT SATELLITE ANTENNAS

NT SCHWARZSCHILD ANTENNAS

NT SLOT ANTENNAS

NT SPACECRAFT ANTENNAS

NT SPACETENNAS

NT SPHERICAL ANTENNAS

NT SPIRAL ANTENNAS

NT STEERABLE ANTENNAS

NT TWO REFLECTOR ANTENNAS

NT WAVEGUIDE ANTENNAS

NT YAGI ANTENNAS

Accuracy of the measurement of the angular coordinate in the case of discrete antenna-beam scanning 04 p0466 A83-15713

Antennas in conducting media /Review/ 04 p0466 A83-15726

International Conference on Antennas and Propagation, 2nd, University of York, York, England, April 13-16, 1981, Proceedings. Part 1 - Antennas. Part 2 - Propagation 06 p0736 A83-18601

Crosspolarisation properties of reflector antennas with random surface errors 08 p1074 A83-21974

The wide-band matching area for a small antenna 10 p1406 A83-26848

Electrodynamic analysis of a reflector in the form of a system of parallel conductors /the E-wave case/ 10 p1407 A83-26952

The effect of longitudinal waves on the input conductance of a ring aperture antenna 12 p1780 A83-29261

A computing model and its experimental testing for an evaluation of electromagnetic interferences created by interfering circuits on transmission or high-voltage lines above a dissipative ground 14 p2002 A83-32894

On the controllability and control law design for an orbiting large flexible antenna system [IAF PAPER 83-340] 23 p3422 A83-47349

Focusing antennas usage in locating acoustic sources [ONERA, TP NO. 1983-75] 23 p3505 A83-48190

ANTHRACENE

The dependence of the fluorescence and absorption spectra of anthracene vapor on concentration 14 p2082 A83-32828

Observation of proton and electron detachment from an anthracene molecule during pronounced IR many-photon superexcitation 20 p3044 A83-42274

Luminescence of strong exciton transitions 21 p3219 A83-45336

Resonance Raman scattering of light and characteristics of the formation of low-temperature luminescence in anthracene crystals 21 p3219 A83-45337

The longitudinal excitation of vapors of complex organic compounds by an electron beam 24 p3627 A83-49740

ANTHROPOMETRY

Applications of digital image acquisition in anthropometry 03 p0384 A83-13449

The 1981 Naval and Marine Corps aviation anthropometry survey and applications 04 p0525 A83-15414

Humanscale 7/8/9 --- Book on human factors engineering information 13 p1906 A83-30154

The individual variability of the putamen of the brain in humans 16 p2399 A83-36813

ANTIADRENERGICS

Opposing actions of dibutylryl cyclic AMP and GMP on temperature in conscious guinea-pigs 12 p1762 A83-29530

Effects of beta-adrenergic blockade on ventilation and gas exchange during exercise in humans 14 p2068 A83-32816

ANTIAIRCRAFT MISSILES

Tactical air war - A SIMSCRIPT model 07 p0987 A83-19649

Status and concerns for preferred orientation control of high performance anti-air tactical missiles [AIAA PAPER 83-2198] 19 p2802 A83-41683

The optimal evasive maneuver of a fighter against proportional navigation missiles [AIAA PAPER 83-2139] 19 p2807 A83-41961

ANTIBIOTICS

NT STREPTOMYCIN

The endocochlear potential of the inner ear and its changes under the influence of dihydrostreptomycin and etacrinic acid 01 p0078 A83-10514

A study of the protective properties of nicotinamide and cytochrome C during aminoglycoside ototoxicosis 09 p1321 A83-25155

Preliminary results of Cytos 2 experiment --- for bacteria antibiotic sensitivity during orbital flight [IAF PAPER 83-192] 23 p3494 A83-47307

ANTIBODIES

NT GAMMA GLOBULIN

Antibodies to streptococcal lipoproteinase in the blood of healthy persons 01 p0083 A83-10554

Adaptation and resistance to hypoxia in light of the functional activity of the antisystems 05 p0669 A83-17161

The genetics of immunoglobulins - Successes and problems 06 p0795 A83-18982

Immunoglobulin genes 14 p2065 A83-33326

Changes in the formation of antibodies caused by the administration of immunomodulators in the respiratory organs 19 p2876 A83-41833

Experimental injury of the aorta of rabbits of various ages by immune complexes 21 p3185 A83-45342

ASECS - Antigen-Specific Electrophoretic Cell Separation 22 p3266 A83-45763

Biosynthesis of tetrapyrrol pigments as possible precursors of the nickel-containing factor F430 of Methanosarcina vacuolata 23 p3496 A83-48513

ANTICHOLINERGICS

The effect of preparations acting mainly in the region of the peripheral M-choline reactive systems on bone marrow eosinophils 14 p2066 A83-33332

ANTICLINES

An example of a statistical analysis of the results of space imagery interpretation for the eastern part of the Fergana Valley 03 p0350 A83-14315

Analysis of the fault and block structure of the Bashkir anticlinorium on the basis of space photographs 10 p1443 A83-26803

ANTICLINORIA

U ANTICLINES

ANTICONVULSANTS

Effect of age on benzodiazepine-induced behavioural convulsions in rats 12 p1763 A83-29711

ANTICYCLONES

On the circulation of the western Gulf of Mexico - A satellite view 01 p0076 A83-10113

On the generation of convectively driven mesohighs aloft 03 p0368 A83-14446

Heating of the Tibet Plateau and movements of the South Asian high during spring 06 p0792 A83-18471

Questions concerning the atmospheric circulation over the Antarctic 08 p1140 A83-22420

Experimental investigations of small-scale turbulence and turbulent exchange in cyclones and anticyclones at middle latitudes 09 p1315 A83-25053

Evidence for anticyclonic rotation in left-moving thunderstorms 11 p1622 A83-26983

Dissipation length in stable layers --- atmospheric boundary layer energy parameterization 12 p1758 A83-29136

Anticyclone of 11 to 18 November 1969 - An example of anticyclone evolution over North America 13 p1889 A83-30577

The anti-cyclonic shear wave - A new geophysical wave 14 p2033 A83-33140

ANTIIDIURETICS

ADH responses to volume shifts in the low pressure system --- AntiDiuretic Hormone 11 p1636 A83-27781

Inhibition of hypoxia-induced ADH release by meclofenamate in the conscious dog --- AntiDiuretic Hormone 17 p2554 A83-36993

ANTIFERROMAGNETISM

Ferromagnetics --- Russian book 09 p1349 A83-23817

ANTIFRICTION BEARINGS

- Evidence for Ising and Potts transitions in the epsilon-zeta transformation of two-dimensional O₂
21 p3216 A83-43886

ANTIFRICTION BEARINGS

- NT BALL BEARINGS
NT ROLLER BEARINGS
Aluminum-lead antifriction alloys produced under conditions of compensation of gravitational segregation by electromagnetic forces 03 p0298 A83-13268
Chemicothermal treatment of alloy VT6 to improve antifriction properties 05 p0614 A83-17134
Self-lubricating antifriction materials (Review)
17 p2483 A83-38870
Optimal magnetic bearing control for high speed momentum wheels
[AIAA PAPER 83-2263] 19 p2855 A83-41733

ANTIGENS

- Experimental injury of the aorta of rabbits of various ages by immune complexes 21 p3185 A83-45342
Biosynthesis of tetrapyrrol pigments as possible precursors of the nickel-containing factor F43O of Methanosarcina vacuolata 23 p3496 A83-48513

ANTIGRAVITY

- Study of +Gz protection given by an anti 'G' suit worn on top of a liquid cooled suit 09 p1324 A83-24003
On a gravitational hypothesis
19 p2896 A83-41563
The functional system of antigravitation --- Russian book on physiological responses to decreased gravitation
24 p3617 A83-50075

ANTIHYPERTENSIVE AGENTS

- The hemodynamic responses of normotensive and hypertensive rats to injections of prostaglandins and indomethacin 01 p0079 A83-10538
The effect of clonidine on the central and renal hemodynamics of individuals with hypertension during the administration of orthostatic probes --- side effects of antihypertensive treatments 05 p0674 A83-17198
The effects of clonidine on the modifications in the systolic time intervals induced by extended decubitus in an antihypertensive position 08 p1149 A83-22983
Clonidine as a counter measure for metabolic studies during weightlessness simulation
11 p1642 A83-27796

- Hemodynamic indicators, the phasic pattern of the systole of the left and right ventricles of the heart, and the condition of pulmonary blood circulation and microcirculation in patients with hypertension during treatment with adelpheane esidex
17 p2559 A83-38178

- Drug therapy of hypertension in drivers
17 p2561 A83-38930

- The character of water-sodium changes in the bodies of patients with hypertension under the influence of various types of hypotensive therapies 19 p2881 A83-41427

- The therapeutic effect of the cardioselective beta-blocker tenormin and its effect on parameters of the central, intracardiac, and regional hemodynamics in patients with hypertension 19 p2881 A83-41428

ANTIMATTER

- NT ANTINEUTRINOS
NT ANTIPARTICLES
NT ANTIPROTONS
NT POSITRONS

- Antimatter and distant space flight
12 p1705 A83-29673
How can we approach the study of cosmology?
15 p2254 A83-33753

- Optimization of relativistic antimatter rockets
[AIAA PAPER 83-1343] 16 p2321 A83-36348

ANTIMISSILE DEFENSE

- Real-time modular distributed signal processing --- sensors for ballistic missile defense systems
08 p1051 A83-22828

ANTIMISTING FUELS

- Degradation and characterization of antimisting kerosene 09 p1242 A83-24035
Application of digital image analysis techniques to antimisting fuel spray characterization
[ASME PAPER 82-WA/HT-23] 10 p1401 A83-25690

- Feasibility of a full-scale degrader for antimisting kerosene
[AIAA PAPER 83-1137] 16 p2339 A83-36240
Testing of antimisting kerosene in the DC-10/KC-10 fuel system simulator
[SAE PAPER 82-1485] 17 p2492 A83-38004

- Rheological behavior of FM-9 solutions and correlation with flammability test results and interpretations --- fuel thickening additive
21 p3117 A83-44856

- A vortex venturi for reverting antimisting fuel properties
[ASME PAPER 83-GT-137] 23 p3409 A83-47964

ANTIMONIDES

- NT ALUMINUM ANTIMONIDES
NT GALLIUM ANTIMONIDES
NT INDIUM ANTIMONIDES

ANTIMONY

- The use of space images to study tectonics and to predict antimony-mercury mineralization in the Southern Tien Shan 07 p0950 A83-19905
Antimony doping in vacuum deposited thin film silicon photovoltaic cells 14 p2089 A83-32292
Incorporation of Sb in GaAs(1-x)Sb(x) (x less than 0.15) by molecular beam epitaxy 16 p2420 A83-36013
Effects of antimony additions on the fracture of nickel at 600 C 17 p2491 A83-38858
2P photoionization cross section of Sb1
24 p3627 A83-49751

ANTIMONY ALLOYS

- A two-dimensional phase separation on the spherical surface of the metallic glass Au55Pb22.5Sb22.5
03 p0399 A83-14937

ANTIMONY COMPOUNDS

- NT ALUMINUM ANTIMONIDES
NT GALLIUM ANTIMONIDES
NT INDIUM ANTIMONIDES

- Antimony sulphide thin films 14 p2090 A83-32306

ANTINEUTRINOS

- On the neutrino luminosity from a type II supernova
02 p0257 A83-12147
Neutrino energy production spectra in a relativistic plasma 21 p3231 A83-44449
Neutrino emission from black holes
21 p3231 A83-44450

ANTIOXIDANTS

- The effect of additive compositions on the oxidation stability of T-6 fuel 01 p0028 A83-10458
The mechanism of the stabilization of turbine oil by antioxidants 09 p1238 A83-23868
The effect of the antioxidant OP-6 on several model reactions of the blood coagulation system
16 p2395 A83-36830
Antioxidants, metabolic rate and aging in Drosophila
21 p3183 A83-44600
The effect of an antioxidant on the recovery of hemopoiesis and the aggregation of thrombocytes
21 p3186 A83-45380

ANTIPARTICLES

- NT ANTINEUTRINOS
NT ANTIPROTONS
NT POSITRONS
Matter and antimatter in the universe
01 p0123 A83-10377
Astrophysical consequences of neutron-antineutron oscillations 04 p0556 A83-15965
Constraint on the photino mass from cosmology
13 p1949 A83-31357
Neutron oscillation and the primordial magnetic field
20 p3070 A83-42785

ANTIPROTONS

- Comments on the origin of cosmic rays
02 p0272 A83-11702
A measurement of the antiproton flux in the cosmic rays 04 p0575 A83-16350
Prediction of interstellar antiproton flux using a nonuniform galactic disk model
17 p2629 A83-37338
On the origin of the low-energy cosmic-ray antiprotons
18 p2787 A83-40491
Antiprotons in the cosmic radiation
23 p3539 A83-47742

ANTIRADIATION DRUGS

- The effect of activators of cAMP accumulation on separate stages of the cell genome expression during acute radiation damage of the animal. V Investigations of the sedimentation characteristics of RNP-particles released from the cell nuclei of irradiated animals and of animals protected with serotonin
03 p0376 A83-14878

- The oxygen effect and the adaptive reactions of cells. IX - The dependence of the radioprotective effectiveness of gaseous hypoxia on its degree and duration in neonatal and adult mice
03 p0376 A83-14879

- The effect of adeturon on the survival and the blood system of mice under the effect of various types of ionizing radiation
03 p0376 A83-14880

- The modification with methylated hematoporphyrin of the combined effect of radiation and hyperthermia in experiments on asynchronous and synchronous cell cultures
03 p0376 A83-14881

- The toxicity and radioprotective effect of multicomponent combinations of sulfur-containing compounds
03 p0377 A83-14882

- The inhibitory effect of linoleic acid hydroperoxide on the activity of superoxide dismutase --- radioprotective substance
03 p0377 A83-14887

- The radioprotective effect of a gaseous hypoxic mixture on hemopoiesis in mice
03 p0377 A83-14889

- The comparative radioprotective effect of adenylates during short-term and long-term gamma-irradiation
09 p1321 A83-24931

- The application of methods of the mathematical theory of experiment in the development of multicomponent radioprotective preparations 23 p3495 A83-48202

- The effect of beta-mercaptoethylamine on the accumulation of DNA strand breaks in Bac. stearothermophilus exposed to gamma-radiation, UV radiation, and nitrosomethylurea treatment --- Mercapto Ethyl Amine 23 p3495 A83-48204

ANTIREFLECTION COATINGS

- Raising damage thresholds of gradient-index antireflecting surfaces by pulsed laser irradiation
01 p0055 A83-10977
Progress in extreme ultraviolet and soft X-ray multilayer coatings 02 p0238 A83-12704
Two-layer antireflection coatings for silicon solar cells
04 p0503 A83-15134

- Antireflection layers for GaAs solar cells
04 p0507 A83-16068
Polarization control of an antireflection-coated GaAlAs laser diode by an external optical feedback
04 p0535 A83-16092

- Noise and longitudinal mode characteristics of /GaAl/As TS lasers with reduced facet reflectivities
10 p1429 A83-26029

- Selective and uniform laser-induced failure of antireflection-coated LiNbO₃ surfaces
10 p1429 A83-26030

- Recent developments in ultraviolet filters and coatings
11 p1657 A83-27743

- Design of antireflection coatings for textured silicon solar cells
11 p1612 A83-27983

- Reactive sputtered Ta₂O₅ antireflection coatings
11 p1551 A83-27984

- Development of high reflectance coatings for ground-based astronomical instruments
13 p1921 A83-31014

- Use of tin oxide as an inexpensive antireflection coating for p on n polycrystalline silicon solar cells
15 p2189 A83-33918

- Efficient and durable AR coatings for Ge in the 8-11.5 micron band using synthesized refractive indices by evaporation of homogeneous mixtures
16 p2413 A83-36756

- Structural characterization of TiO₂ optical coatings by Raman spectroscopy 16 p2413 A83-36758

- Plasma-enhanced CVD silicon nitride antireflection coatings for solar cells 22 p3318 A83-46095

- Low cost and high performance antireflective (AR) coatings for solar cells 22 p3319 A83-46586

- Optical properties for an antireflection-coated LD optical switch
24 p3630 A83-49983

ANTISEPTICS

- Experimental data from a study of the toxic effect on embryos exerted by hexachlorophene - A component of antimicrobial fabrics and synthetic articles of everyday use 05 p0677 A83-17203

ANTISHIP MISSILES

- B-52 roles in sea control 07 p0862 A83-20646

ANTISHIP WARFARE

- B-52 roles in sea control 07 p0862 A83-20646

ANTISKID DEVICES

- Review of NASA antiskid braking research
[SAE PAPER 82-1393] 17 p2463 A83-37969

ANTISUBMARINE WARFARE

- LAMPS MK III acoustic target tracker
19 p2799 A83-41533

ANTISUBMARINE WARFARE AIRCRAFT

- NT P-3 AIRCRAFT
All-weather small-deck operations in the U.S. Navy
[SAE PAPER 82-1503] 17 p2459 A83-38010

ANTITANK MISSILES

- Assault breaker breaks out --- airborne radar targeting and weapons delivery systems 07 p0862 A83-20645
An antitank missile seeker employing an infrared Schottky barrier focal plane array
09 p1253 A83-23544

- A robot machining facility - An experiment in production engineering 11 p1589 A83-28166

- Fluidic control systems for projectiles
[AIAA PAPER 83-1151] 16 p2352 A83-36248

ANVIL CLOUDS

- The water budget of a tropical squall-line system
11 p1626 A83-27027
Corona point measurements in a thundercloud at Langmuir Laboratory 13 p1892 A83-30903
Lightning and precipitation in a small multicellular thunderstorm 16 p2390 A83-36155
Upper-level structure of Oklahoma tornadic storms on 2 May 1979. I - Radar and satellite observations
22 p3341 A83-46852

Upper-level structure of Oklahoma tornadic storms on 2 May 1979. II - Proposed explanation of 'V' pattern and internal warm region in infrared observations 22 p3341 A83-46853

Interpretation of satellite-observed thunderstorm anvil structure 24 p3615 A83-49729

ANVILS

Pressure concentrations due to plastic deformation of thin films or gaskets between anvils 01 p0028 A83-10610

Simple double diaphragm press for diamond anvil cells at low temperatures 06 p0735 A83-19235

AORTA

Oxygen toxicity in cultured aortic endothelium Selenium-induced partial protective effect 20 p3033 A83-43478

Experimental injury of the aorta of rabbits of various ages by immune complexes 21 p3185 A83-45342

Changes in vascular responsiveness following chronic exposure to cold in the rat 22 p3346 A83-45993

Circulating antibodies to aortic elastin and their significance in atherosclerosis in humans 23 p3499 A83-48674

APATITES

U CALCIUM PHOSPHATES

U MINERALS

APERTURES

NT IRISES (MECHANICAL APERTURES)

NT SYNTHETIC APERTURES

Visualization of near diffraction fields from apertures of complex shape on a liquid-film converter in the millimeter-wavelength range 01 p0049 A83-10420

Electromagnetic-wave diffraction by a periodic screen with apertures of arbitrary shape 01 p0031 A83-10804

Low sidelobe aperture distributions for blocked and unblocked circular apertures 01 p0033 A83-11364

A geometrical construction for Chebyshev Z-plane zeros 01 p0103 A83-11380

Electromagnetic transmission through apertures in a cavity in a thick conductor 03 p0306 A83-14016

Generalised hybrid-network parameters for electromagnetic coupling between dissimilar regions through a small aperture 04 p0473 A83-16206

Multiple-aperture three-dimensional image construction utilizing fringe-modulated speckle patterns 05 p0643 A83-16835

Speckle reduction by a rotating aperture at the Fourier transform plane 05 p0647 A83-17940

Imaging performance of annular apertures. IV - Apodization and point spread functions. V - Total and partial energy integral functions 06 p0810 A83-18590

Optimum performance indices of aperture antennas with and without pattern constraints 06 p0741 A83-18660

GTD analysis of reflector antennas with general rim shapes 06 p0743 A83-18690

Analytic continuation applied to microwave apertures 08 p1095 A83-22471

Liquid crystals as large aperture waveplates and circular polarizers 08 p1166 A83-22571

A method for the numerical investigation of adaptive optical systems of aperture sensing 09 p1344 A83-23486

Generalized network representations for small-aperture coupling between dissimilar regions 09 p1254 A83-23804

Constrained optimization of monopulse circular aperture distribution in the presence of blockage 10 p1375 A83-26835

Far-field radiation patterns of elliptical apertures and its annuli 10 p1406 A83-26847

An admittance solution for electromagnetic coupling through a small aperture 12 p1718 A83-29402

Aperture analysis of laser speckle interferograms 12 p1730 A83-29588

Theoretical and experimental study of the coupling of two waveguides by a large aperture 13 p1833 A83-30712

Increasing the numerical aperture of a glass-polymer light guide 13 p1919 A83-30814

Test of large aperture antennas using near-field techniques 13 p1829 A83-31194

Maximum power penetration through an electrically small aperture 15 p2149 A83-35191

Method for subaperture testing interferogram reduction --- for large optical systems 22 p3356 A83-45960

Approximate expressions for field penetration through circular apertures 22 p3276 A83-46932

High-precision measurements on a compact antenna test range 24 p3571 A83-49967

APNEA

U RESPIRATION

APOGEE BOOST MOTORS

Contamination measurements during the firing of the solid propellant apogee insertion motor on the P78-2 /SCATHA/ spacecraft 03 p0284 A83-13751

The MAGE family of European solid-propellant apogee boost motors --- for geostationary orbit transfer 11 p1542 A83-27369

ISA-2 - A facility for vacuum firing tests on solid-propellant motors 11 p1533 A83-27370

APOLLO FLIGHTS

NT APOLLO 14 FLIGHT

NT APOLLO 16 FLIGHT

NT APOLLO 17 FLIGHT

Effectiveness of HZE-particles onto different biological systems in the Biostack Experiments on Apollo 16, and 17 and on ASTP 23 p3494 A83-47764

APOLLO LUNAR SURFACE EXPERIMENTS PACKAGE

Apollo lunar seismic experiment - Final summary 04 p0560 A83-15338

APOLLO PROJECT

Earthquakes - on the moon 02 p0263 A83-11825

Space technology - Apollo: The driver and the driven 21 p3221 A83-45601

Space technology - Computers: Learning from dinosaurs 21 p3191 A83-45602

Space technology - Superproject management 21 p3221 A83-45606

The human presence in space 22 p3347 A83-45861

APOLLO SPACECRAFT

The history of Apollo onboard guidance, navigation, and control 04 p0453 A83-16114

APOLLO 14 FLIGHT

The magma ocean from the Fra Mauro shoreline - An overview of the Apollo 14 crust 07 p1032 A83-21294

APOLLO 16 FLIGHT

KREEP glass and the exotic provenance and formation of polymict breccia 66055 04 p0560 A83-15341

Petrologic variations in Apollo 16 surface soils 04 p0561 A83-15345

Modal petrology of six soils from Apollo 16 double drive tube core 64002 04 p0561 A83-15346

Comparative geochemistry of Apollo 16 surface soils and samples from cores 64002 and 60002 through 60007 04 p0561 A83-15351

The content of phosphoglycerides in Rhodoturla rubra in three of its phenotypes as influenced by the lunar environment during the flight of Apollo 16 06 p0794 A83-18369

APOLLO 17 FLIGHT

Studies of the content and the distribution of uranium of lunar mare basaltic fragments taken by Apollo 17 21 p3240 A83-44503

APPARATUS

U EQUIPMENT

APPENDAGES

NT ARM (ANATOMY)

NT ELBOW (ANATOMY)

NT FOREARM

NT HAND (ANATOMY)

NT KNEE (ANATOMY)

NT LEG (ANATOMY)

Dynamics of a spacecraft during extension of flexible appendages 09 p1216 A83-24431

APPLICATION

U UTILIZATION

APPLICATIONS OF MATHEMATICS

Cybernetics, applied mathematics --- Russian book 01 p0094 A83-10563

Criteria of applicability for the geometrical theory of diffraction 04 p0531 A83-15763

Mathematical methods for optimizing treatment and diagnosis in cardiology /current status and future prospects/ 05 p0674 A83-17199

Current problems of mathematical physics and computational mathematics --- Russian book 07 p0988 A83-20302

Applications of deformation analysis in geodesy and geodynamics 07 p0962 A83-20837

Mathematical method for the design of the intake branch in the case of centrifugal blade machines --- Book 09 p1263 A83-24850

Current problems in applied mathematics and mathematical modeling --- Russian book 09 p1309 A83-25238

Twenty-five years of maximum-entropy principle 20 p3043 A83-42941

Theory of spinors and its application in physics and mechanics --- Russian book 21 p3200 A83-45031

APPLICATIONS PROGRAMS (COMPUTERS)

International standards for software structures in astronomy 01 p0113 A83-10140

Development environment for the design and test of applications software for a distributed multiprocessor computer system 07 p0983 A83-19625

Program implementation in the application software package NOLINEAR 12 p1768 A83-29541

MIDAS - ESO's new image processing system 13 p1942 A83-31581

APPROACH

NT INSTRUMENT APPROACH

Handling qualities criteria for STOL flight path control for approach and landing [AIAA PAPER 83-2106] 19 p2806 A83-41935

APPROACH AND LANDING TESTS (STS)

Flight testing of the Space Shuttle 05 p0605 A83-16972

APPROACH CONTROL

NT RADAR APPROACH CONTROL

Assessment of advanced fighter powered approach simulations [AIAA PAPER 83-0141] 05 p0598 A83-16550

Integrated navigation by supplementing MLS with DAS --- DME-based Azimuth System 09 p1202 A83-24872

Integrated flight path control system 10 p1378 A83-26477

Structure and mode of operation of an interactive onboard four-dimensional flight path control system 10 p1378 A83-26478

Fault/maneuver tolerance of aided GPS demodulation/navigation processors in the non-precision approach environment 11 p1529 A83-28787

Thrust reverser effects on the tail surface aerodynamics of an F-18 type configuration [AIAA PAPER 83-1860] 17 p2457 A83-38687

Simulated fan-beam radar imagery --- use in assessing aircraft approach-to-landing paths 18 p2675 A83-40302

Instrument-approach technique for poor-visibility landings 19 p2795 A83-41228

Carrier landing simulation results of precision flight path controllers in manual and automatic approach [AIAA PAPER 83-2072] 19 p2796 A83-41909

Vectoring exhaust systems for STOL tactical aircraft [ASME PAPER 83-GT-212] 23 p3410 A83-48013

APPROACH INDICATORS

Evaluation of control and display configurations for helicopter shipboard operations [AIAA PAPER 83-2486] 23 p3405 A83-48346

APPROXIMATION

NT BORN APPROXIMATION

NT BORN-OPPENHEIMER APPROXIMATION

NT CHEBYSHEV APPROXIMATION

NT EDDINGTON APPROXIMATION

NT FINITE DIFFERENCE THEORY

NT FINITE ELEMENT METHOD

NT HARTREE APPROXIMATION

NT LEAST SQUARES METHOD

NT MEAN SQUARE VALUES

NT NEWTON-RAPHSON METHOD

NT NUMERICAL DIFFERENTIATION

NT OSEEN APPROXIMATION

NT PADE APPROXIMATION

NT PARTICLE IN CELL TECHNIQUE

NT POHLHAUSEN METHOD

NT RAYLEIGH-RITZ METHOD

NT RELAXATION METHOD (MATHEMATICS)

NT RITZ AVERAGING METHOD

NT SCHWARTZ METHOD

NT SOMMERFELD APPROXIMATION

Suggestions for optimal regulation of linear systems using approximation methods --- German thesis 01 p0094 A83-10472

An angular approximation for the difference of two sines 01 p0102 A83-11109

Approximation of an integral exponent by means of quadrature formulas 01 p0102 A83-11263

Difference approximations of derivatives and polynomial splines 01 p0102 A83-11270

The thin-substrate approximation for reflection from the end of a slab-loaded parallel-plate waveguide with application to microstrip patch antennas 01 p0033 A83-11360

Approximate difference pattern response of the weighted multibeam array 01 p0034 A83-11381

Analysis of algorithms of the spatial-temporal processing of signals in the presence of noise 02 p0162 A83-11543

Investigation of the brightness temperature of a rough surface in the Kirchhoff approximation --- for oceans 02 p0218 A83-11682

Approximate analysis of postbuckled through-width delaminations 02 p0191 A83-12061

Approximating shapes using parameterized curves 02 p0231 A83-12174

Physically motivated approximations in some inverse scattering problems 02 p0233 A83-12632

Bent approximations to synchrotron radiation optics 02 p0237 A83-12700

Approximation of the spectrum of an operator given by the magnetohydrodynamic stability of a plasma
03 p0397 A83-13570

Applications of transfinite /blending-function/ interpolation to the approximate solution of elliptic problems
03 p0388 A83-14085

Approximation of extremal surface elements /hyperbolic type/ by means of characteristic three-dimensional quadrilateral elements
03 p0388 A83-14493

Computation of a degree of controllability via system discretization --- with application to flexible spacecraft control
03 p0287 A83-14844

The Eikonal approximation in elastic wave scattering theory
04 p0489 A83-15162

On a modified differential approximation method in radiative gas dynamics
04 p0544 A83-15819

An approximation theory for nonlinear partial differential equations with applications to identification and control
04 p0530 A83-16194

The approximation of periodic functions --- Russian book
05 p0681 A83-17124

Isogeometric approximation of functions of one variable --- explicit spline method for CAD of curves and surfaces
05 p0682 A83-17641

Numerical analysis of the behavior of a quasi-periodic solution to a periodic differential equation by means of a method of sections
06 p0804 A83-17974

Theory of nonstationary kinetic ionization, recombination and population of excited states
06 p0811 A83-18438

Optical bistability based on self-focusing - An approximate analysis
06 p0810 A83-18905

An approximate solution to the non-self-similar problem concerning the motion of a piston following an instantaneous impact
06 p0760 A83-19441

On method of successive approximations in a class of problems of the general theory of plasticity
07 p0945 A83-20142

Concerning an additive model for parabolic equations with mixed derivatives
07 p0986 A83-20308

A method for the approximate calculation of the current errors of mismatch in two-coordinate pursuit tracking
07 p0981 A83-20328

Stability theory of difference approximations for multidimensional initial-boundary value problems
07 p0986 A83-20504

Preconditioning and two-level multigrid methods of arbitrary degree of approximation
07 p0986 A83-20508

Another self-similar blast wave - Early time asymptote with shock-heated electrons and high thermal conductivity --- in astrophysics
07 p1023 A83-21141

Modal solutions of active dielectric waveguides by approximate methods
07 p0924 A83-21626

Linear-quadratic optimal control of hereditary differential systems - Infinite dimensional Riccati equations and numerical approximations
08 p1157 A83-22244

Theoretical justification of the method of successive approximations for stationary problems of the mechanics of viscous fluids with free boundaries
09 p1261 A83-24323

Polynomial approximations and white noise integrals
09 p1331 A83-24771

A new nonlinear filtering approximation
09 p1331 A83-24772

Diophantine approximations and transcendental numbers --- Russian book
10 p1471 A83-25597

An effective dispersion theory for layered composites
10 p1441 A83-26441

On approximation by the interpolating series of G. Valiron
10 p1470 A83-26475

On the deformation of the cross section of a rectangular turbulent jet
11 p1567 A83-27708

Approximate methods for the calculation of Cauchy integrals of a special form --- Russian book
12 p1770 A83-28816

Approximate solutions for isothermal flows behind strong spherical shocks with variable energy
12 p1722 A83-29056

An improved solution to the fourth moment equation for intensity fluctuations --- for waves propagating through random media
12 p1775 A83-29598

Convergence of approximate solutions to conservation laws --- in parabolic systems and finite difference schemes
12 p1727 A83-29939

Methods for the synthesis of the stressed state in shell theory
13 p1865 A83-30003

Calculation of the reliability of anisotropic shells on the basis of the probability of infrequent overshoots of the random vector field beyond the limiting surface
13 p1866 A83-30060

Approximate method for calculating the characteristics of a magnetron at frequencies above the higher temporal harmonics
13 p1833 A83-30704

Approximate nonlinear theory of an orotron
13 p1833 A83-30711

Approximation of 2-D separable in denominator filters
13 p1910 A83-30873

Asymptotic formulas for local spline approximation on a uniform grid
13 p1912 A83-31335

The application of a modified form of the S sub N method to the calculation of swarm parameters of electrons in a weakly ionised equilibrium medium
13 p1926 A83-31369

Approximate method of solving the kinetic equation for moderately dense gases near a boundary temperature jump in a binary mixture
13 p1933 A83-31467

Approximate solution of the heat-conduction equation with nonlinear boundary conditions
13 p1843 A83-31469

Classification of difference schemes of gas dynamics by the method of differential approximation. I - One-dimensional case
13 p1844 A83-31592

A non-conforming piecewise quadratic finite element on triangles --- for flow computation
13 p1844 A83-31638

Theory of time-dependent intense-field collisional resonance fluorescence
14 p2079 A83-31925

The choice and use of normal approximations to transfer-function matrices of multivariable control systems
14 p2074 A83-31932

Modification of approximate methods for separating normal stresses on the basis of experimental determinations of their difference or sum
14 p2029 A83-32156

The selection of a zero-order approximation in the theory of vibrational-rotational interactions in molecules (Convergence of contact transformations)
14 p2082 A83-32563

Second approximation of quadrupole wing theory in lifting surface theory
14 p1972 A83-33004

Binary-single star scattering. II - Analytic approximations for high velocity
14 p2105 A83-33210

Multi-segments approximation to a three-dimensional curved line using the least-squares locating method.
14 p2022 A83-33345

Density-functional theory of correlations in dense plasmas Improvement on the hypernetted-chain scheme
16 p2415 A83-35665

An approximate method for solving a kinetic equation for moderately dense gases near a boundary - The slip of a binary mixture
16 p2350 A83-35711

On the relevance of the MHD approach to study the Kelvin-Helmholtz instability of the terrestrial magnetopause
16 p2376 A83-35785

On the localized stability of vortices
16 p2290 A83-35819

Curve fitting with conic splines
17 p2571 A83-38060

Determination of regime coefficients for thin bodies from the data of numerical and laboratory experiments --- aerodynamic coefficients of plate in rarefied gas
17 p2452 A83-38095

Approximations in magnetoionic theory
17 p2543 A83-38370

P-N approximation for radiative heat transfer in a nongray medium
19 p2841 A83-40874

Approximation of solutions of strongly nonstationary stochastic extremal problems in continuous time. II Convergence of algorithms
19 p2889 A83-40899

Radiation heat transfer - Interaction with conduction and convection and appropriate methods in radiation
20 p2970 A83-42655

Nucleation theory - Is replacement free energy needed? --- error analysis of capillary approximation
20 p3056 A83-43287

Approximate-factorization scheme of transonic small-disturbance potential equation
21 p3088 A83-44574

Method for the approximation of terms parameterizing macroexchange in equations of atmospheric dynamics
23 p3488 A83-47157

Approximation to the optimization of a coast-glide trajectory
23 p3403 A83-48223

APPROXIMATION METHODS

U APPROXIMATION

APSIDAL ANGLES

U APSIDES

APSIDES

NT PERIGEEES

NT PERIHELIONS

A photometric study of the eclipsing binary V 889 Aql
- An example of relativistic apsidal motion
04 p0546 A83-15039

Classical systems: The star RX Cas - The motion of the apsidal line
09 p1353 A83-23902

A new method for the analysis of apsidal motions in eclipsing binaries
16 p2424 A83-36544

AQUARID METEORIDS

Southern and Northern Hemisphere observations of the ETA Aquarid meteor shower in 1969-1978
04 p0546 A83-15103

Evolution of the orbits of Halley's comet, the Orionids, and the eta-Aquarids over 15,000 years
10 p1498 A83-26903

AQUATIC PLANTS

The self-purification of water depending on the physiological peculiarities of higher aquatic plants
03 p0373 A83-13289

Growth response and spectral characteristics of a short Spartina alterniflora salt marsh irrigated with freshwater and sewage effluent
10 p1443 A83-25645

Satellite and ship studies of coccolithophore production along a continental shelf edge
20 p3032 A83-42171

AQUEOUS SOLUTIONS

Investigations of the variations in the transmission spectra of aqueous solutions and their correlations with the parameters of a neutron counter --- solar effects on biosphere
02 p0221 A83-11895

Bromine reduction in a two-phase electrolyte
02 p0151 A83-12051

Protein single crystal growth in a microgravity field
02 p0138 A83-12996

Concerning the absence of magnetic-field effect on the dissolving of oxygen in aqueous solutions --- in biological systems
03 p0375 A83-14356

Diffusion length of minority carrier in n-type semiconductors - A photoelectrochemical determination in aqueous solvents
04 p0543 A83-16070

Free radicals induced by UV light in aqueous solutions of DNA with various amounts of protein at 77 K
06 p0796 A83-19377

Seeding of FPL solution --- in preparation of aluminum surfaces for adhesive bonding
07 p0885 A83-20431

Growth of aqueous solution droplets of HNO₃ and HCl in the atmosphere
08 p1133 A83-23008

Performance and operational analysis of a liquid desiccant open-flow solar collector
11 p1608 A83-27246

Dissolved metal species mechanism for initiation of crevice corrosion of aluminum. I - Experimental investigations in chloride solutions. II - Mathematical model
14 p1993 A83-32628

Embrittlement of P/M X7091 and I/M 7175 aluminium alloys by mercury solutions
16 p2330 A83-35983

Corrosion: Aqueous processes and passive films --- Book
17 p2486 A83-37170

Anodic films on aluminium
17 p2486 A83-37173

A novel way for the formation of alpha-amino acids and their derivatives in an aqueous medium
19 p2887 A83-42036

Studies on aqueous two phase polymer systems useful for partitioning of biological materials
20 p2951 A83-43277

A theory of electrophoresis of emulsion drops in aqueous two-phase polymer systems
20 p2951 A83-43278

AQUICULTURE

Application of remote sensing techniques in oceanographic studies of the British Columbia Salmon Fishery
03 p0347 A83-14258

AQUIFERS

Increasing summer peak power with aquifer storage
11 p1609 A83-27313

AQUASTOR - A computer model for cost analysis of aquifer thermal energy storage coupled with district heating or cooling systems
11 p1609 A83-27314

ARC DISCHARGES

Optical measurement of the velocity of dielectric surface arcs
05 p0618 A83-17495

Barriers to flashover discharge arcs on Teflon
05 p0618 A83-17496

Near-electrode processes in arc discharges --- Russian book
07 p0996 A83-20386

Axial and angular distribution of current density in a thermionic converter with nonisothermal electrodes
10 p1445 A83-25887

Space charge measurement using a small sphere as a probe
10 p1423 A83-26500

Arc suppression in excimer laser discharges
11 p1576 A83-27506

Movement of an arc spot in a magnetic field
13 p1926 A83-30821

The state of the theory of vacuum arc cathodes
15 p2237 A83-35272

Half-widths of neutral fluorine spectral lines
19 p2897 A83-40714

ARC GENERATORS

Movement of an arc spot in a magnetic field
13 p1926 A83-30821

ARC HEATING

Production of solar grade silicon in an arc furnace using high purity starting materials
14 p2045 A83-32308

HIPERARC - A high performance arc heater [AIAA PAPER 83-1560]
14 p1979 A83-32777

ARC JET ENGINES

Capacitor bank charging by series-parallel switching of solar arrays [AIAA PAPER 82-1878]
02 p0143 A83-12464

Mass reduction of capacitor bank for MPD thruster
[AIAA PAPER 82-1879] 02 p0143 A83-12465

Radiated emission noise of the plasma --- in Space
Experiments with Particle Accelerators payloads
[AIAA PAPER 82-1883] 02 p0241 A83-12468

Fast acting valve for a quasi-steady MPD arcjet
[AIAA PAPER 82-1886] 02 p0144 A83-12470

Thrust and efficiency of new K III MPD thruster
[AIAA PAPER 82-1887] 02 p0144 A83-12471

Current distribution in a quasi-steady MPD arcjet
[AIAA PAPER 82-1917] 02 p0145 A83-12489

MPD arcjet performance with various propellants
[AIAA PAPER 82-1885] 03 p0289 A83-13425

ARC LAMPS

Rapid annealing of silicon with a scanning CW Hg lamp
01 p0109 A83-10646

Laser scattering and current transport in an argon arc plasma --- German thesis
17 p2582 A83-37504

Rapid thermal annealing of Se and Be implanted InP using an ultrahigh power argon arc lamp
20 p3055 A83-43605

Rapid thermal annealing of Be, Si, and Zn implanted GaAs using an ultrahigh power argon arc lamp
21 p3220 A83-45500

Widening the energy and technological possibilities of equipment for light beam welding with the pulsed feed of arc xenon lamps
22 p3301 A83-45701

Electrical characteristics of Be-implanted GaAs diodes annealed with an ultrahigh power argon arc lamp
24 p3572 A83-48788

ARC MELTING

Vader - A new melting and casting technology
07 p0895 A83-21491

The effect of zirconium on the superconducting properties of alloys based on the solid solution Nb3Sn-Nb3Ge
13 p1819 A83-30070

ARC SPRAYING

Progress report - Large sprayed metal composite tooling
07 p0876 A83-20483

Ultrahigh vacuum arc method to form thin refractory metal films
07 p0941 A83-21381

Methods based on ultrasound and optics for the nondestructive inspection of thermally sprayed coatings
10 p1436 A83-25530

ARC WELDING

NT GAS TUNGSTEN ARC WELDING

NT PLASMA ARC WELDING

Effect of technological and metallurgical factors on the properties of welded joints in Ti200 alloy
05 p0613 A83-16885

Advances in laser and MIAB welding techniques
07 p0940 A83-20523

Development of a two-directional seam tracking system with laser sensor
07 p0940 A83-20524

Some problems of technology and equipment for the twin arc two side welding of ribbed panels of titanium alloys
07 p0940 A83-21028

GMAW - A versatile process on the move --- Gas Metal Arc Welding
09 p1274 A83-23649

Improving the quality of diffusion bonded joints in OT-1 alloy workpieces containing argon-arc welded joints
10 p1436 A83-26218

Use of pickling pastes for surface preparation of titanium alloys for argon arc welding
10 p1436 A83-26221

Comparative evaluation of the effect of titanium and aluminum on properties of creep-resisting metal deposited by the argon-arc method
10 p1397 A83-26223

Welding technology /2nd edition/ --- Book
13 p1858 A83-30142

Exploiting MIG-welding developments --- Book
15 p2171 A83-33630

Tensile and toughness properties of Arc-welded 5083 and 6082 aluminum alloys
22 p3268 A83-45728

ARCHAEOLOGY

Subsurface valleys and geoarchaeology of the eastern Sahara revealed by Shuttle radar
03 p0344 A83-13349

Using remote sensig in a predictive archaeological model - The Jackson purchase region, Kentucky
15 p2186 A83-34837

ARCHES

Load-frequency relations for a clamped shallow circular arch
03 p0338 A83-13148

Natural frequencies of out-of-plane vibration of arcs
04 p0499 A83-15694

Dynamic stability boundaries for a sinusoidal shallow arch under pulse loads
08 p1122 A83-22148

The stability of elastoplastic arches and cylindrical panels
10 p1442 A83-26821

Bimodal optimization of vibrating shallow arches
15 p2174 A83-34146

Natural frequencies of in-plane vibration of arcs
17 p2519 A83-37390

ARCHITECTURE (COMPUTERS)

System performance ramifications of ATS architectures
01 p0088 A83-10735

Distributed system architectures --- modular approach to ATE
01 p0088 A83-10736

Distributed ATE systems software
01 p0088 A83-10771

A predictive tracking EW preprocessor using standard computer instruction set architectures
01 p0088 A83-11133

A prototype parallel computer architecture for advanced avionics applications
01 p0088 A83-11153

Software development support system for advanced avionics applications incorporating a parallel machine architecture
01 p0087 A83-11164

Incorporating ISPS into a commercial CAD system
01 p0092 A83-11195

Life Cycle Cost analysis of standard avionics hardware and software
01 p1122 A83-11256

Architectures for neighborhood processing --- of images by computer serial array processors
01 p0090 A83-11446

A VLSI pyramid machine for hierarchical parallel image processing
01 p0090 A83-11447

PUMPS architecture for pattern analysis and image database management --- shared resource multiprocessor computer
01 p0090 A83-11448

ZMOB - Hardware from a user's viewpoint --- multiprocessor with architecture including 256 autonomous microprocessors
01 p0090 A83-11449

A simulation-aided multiple processor architecture design for BMD underlay terminal defense
02 p0226 A83-11904

Multimicroprocessor systems
02 p0227 A83-11916

Star - A local network system for real-time management of imagery data
02 p0228 A83-12242

Image processing on ZMOB
02 p0228 A83-12244

A pipelined pseudoparallel system architecture for real-time dynamic scene analysis
02 p0227 A83-12245

Content-addressable read/write memories for image analysis
02 p0227 A83-12246

PUMPS architecture for pattern analysis and image database management
02 p0227 A83-12247

PICCOLO logic for a picture database computer and its implementation
02 p0228 A83-12248

PICAP - A system approach to image processing
02 p0229 A83-12249

Architecture for scientific software. I - Data centralization
02 p0229 A83-12348

Application of a parallel processor to the solution of finite difference problems
03 p0385 A83-14086

On the choice of discretization for solving P.D.E.'s on a multi-processor
03 p0385 A83-14090

The ETH-Multiprocessor EMPRESS - A dynamically configurable MIMD system
05 p0679 A83-17237

Design of HM2p - A hierarchical multimicroprocessor for general-purpose applications
05 p0679 A83-17238

Wavefront array processor - Language, architecture, and applications
05 p0679 A83-17239

Architecture for scientific software. II - Analysis of a quadratic programming algorithm
05 p0680 A83-17319

Frequency-multiplexed and pipelined iterative optical systolic array processors
06 p0802 A83-18588

Pseudo-associative store with hardware hashing --- data-flow approach in parallel computing systems
07 p0982 A83-19624

A new architecture for adaptive transform compression of NTSC composite video signal
07 p0908 A83-19732

Digital image processing - A systems approach --- Book
07 p0928 A83-19925

Partitioned matrix algorithms for VLSI arithmetic systems
07 p0982 A83-20249

Automatic hardware synthesis
07 p0923 A83-21540

On the design of algorithms for VLSI systolic arrays
07 p0923 A83-21542

Real-time image computer configuration
08 p1152 A83-22528

Advanced architecture for graphics and image processing
08 p1152 A83-22530

System architecture of Vicom digital image processor
08 p1097 A83-22533

Processing display system architectures
08 p1152 A83-22534

Powerful hardware/software architecture for a minicomputer-based interactive image processing system
08 p1097 A83-22537

Digital reconnaissance imagery processing system for real-time and near-real-time imagery exploitation
08 p1099 A83-22579

Parallel processing algorithms and architectures for real-time signal processing
08 p1152 A83-22795

A 200 million operations per second /MOPS/ systolic processor
08 p1155 A83-22796

Systolic array processor implementation
08 p1153 A83-22798

Josephson technology special purpose systolic architecture signal processing application
08 p1153 A83-22802

Scattering arrays for matrix computations
08 p1153 A83-22804

Architecture of an advanced signal processor
08 p1153 A83-22806

Signal processing technology overview
08 p1153 A83-22807

A large scale integration based, signal processor - Its application and possible evolution
08 p1155 A83-22811

Neural analog information processing
08 p1158 A83-22812

Microprogrammable high-speed bit slice image processor
08 p1153 A83-22814

Programmable systems components - A comprehensive approach to signal processing
08 p1154 A83-22819

Advanced onboard signal processors for satellite communication systems
08 p1050 A83-22822

Architecture and applications of the HEP multiprocessor computer system
08 p1155 A83-22823

Motivation for a combined data flow-control flow processor
08 p1155 A83-22827

Methods of investigating data transmission networks --- Russian book
09 p1326 A83-23818

Multiprocessors and their impact on integrated navigation and avionics - A status-of-the-art paper
09 p1204 A83-24868

The real-time signal processor
10 p1408 A83-25638

The NYU ultracomputer - Designing an MIMD shared memory parallel computer --- Multiple Instruction Multiple Data stream
10 p1461 A83-26258

AML - A manufacturing language
11 p1646 A83-28100

Alternate architectures and technologies for Intelisat type DSI design --- digital speech interpolation
11 p1558 A83-28141

Vector computations on a parallel-pipelined processor
11 p1646 A83-28623

Design and implementation of the Delft Image Processor DIP-1 --- Thesis
11 p1575 A83-28641

The organization of circuit analysis on array architectures --- Thesis
11 p1564 A83-28648

Cooperative development of application specifications, giving particular attention to the realization of software for specific branches of the economy --- German thesis
11 p1647 A83-28661

Development and use of an integrated analysis capability
12 p1773 A83-29799

[AIAA 83-1017]

Computational systems and methods in the automation of investigations and control --- Russian book
13 p1910 A83-30616

An efficient parallel algorithm for the solution of large sparse linear matrix equations
13 p1908 A83-30790

A parallel-pipeline architecture of the fast polynomial transform for computing a two-dimensional cyclic convolution
13 p1908 A83-30794

Binary trees and parallel scheduling algorithms
13 p1909 A83-30795

New computer architectures tackle bottleneck --- processor-memory link bypass
14 p2073 A83-33141

An LSI adaptive array processor
15 p2216 A83-33887

A fully parallel mixed-radix conversion algorithm for residue number applications
15 p2217 A83-33911

Fully digit on-line networks
15 p2217 A83-33912

Digital image processing systems and remote sensing
15 p2183 A83-34159

I/O limitations of multi-chip VLSI systems
15 p2218 A83-35116

Implementing parallel applications on a multi-array processor architecture
16 p2404 A83-36423

[ONERA, TP NO. 1983-13]

Algorithms, software, and architecture of multiprocessor computing systems --- Russian book
16 p2404 A83-36442

Finite element computation with parallel VLSI
16 p2403 A83-36720

Parallel solution of finite element equations
16 p2403 A83-36721

Principles for the adaptation of logical integrating computing structures for the implementation of fuzzy algorithm
16 p2403 A83-36902

HiMAT onboard flight computer system architecture and qualification
17 p2467 A83-37061

Chip architecture - A revolution brewing
17 p2497 A83-37739

Systolic processor for computing the Wigner distribution
17 p2564 A83-38882

Divide-and-conquer for parallel processing
19 p2887 A83-41038

- Satellite relayed tracking and data acquisition for the 1990's 19 p2813 A83-41340
- Flight management systems - What are they and why are they being developed? 19 p2803 A83-41712 [AIAA PAPER 83-2235]
- Bit-level systolic array circuit for matrix vector multiplication 20 p3037 A83-43167
- Discrete Fourier transform processor based on the prime-factor algorithm 20 p3037 A83-43169
- Parallel architectures for computing cyclic convolutions 20 p3037 A83-43679
- Hardware-based Fourier transforms - Algorithms and architectures 20 p3037 A83-43681
- Matching the task to an image processing architecture --- for overcoming Von Neumann bottleneck 21 p3190 A83-44260
- Optical systolic array processor using residue arithmetic 22 p3350 A83-46834
- Integrated digital avionics systems - Promise and threats 24 p3572 A83-48890
- Flight-control designer becomes metalogician 24 p3619 A83-48892
- TOPPSY - A time overlapped parallel processing system 24 p3620 A83-49197
- Integrated flight/propulsion control system architectures for a high speed aircraft 24 p3549 A83-49595 [AIAA PAPER 83-2563]
- Integrated control system concept for high-speed aircraft [AIAA PAPER 83-2564] 24 p3549 A83-50074
- Method for choosing the required complete configuration of a multiprocessor computing complex 24 p3620 A83-50210

ARCTIC ENVIRONMENTS

U ICE ENVIRONMENTS

ARCTIC OCEAN

- Provision of ice information to icebreaker-transport vessels in the Arctic 01 p0077 A83-10827
- Tidal phenomena in Arctic Ocean ice /according to space data/ 01 p0077 A83-10832
- Some features of the spatial structure of the Arctic Ocean ice cover in connection with turbulent friction and geostrophic capture of tide waves 01 p0077 A83-10833
- The use of model experiments performed in natural conditions to study the interaction of petroleum products with the ocean and atmosphere 01 p0069 A83-10834
- The utilization of infrared /IR/ aerial and space observations of Arctic seas in navigation and during the solution of other national-economic problems 01 p0077 A83-10836
- Statistical properties of the atmospheric pressure field over the Arctic Ocean 02 p0214 A83-12234
- Origin, nature and world climate effect of Arctic Ocean ice-cover [AD-A130919] 03 p0344 A83-14922
- Norwegian remote sensing experiment in a marginal ice zone 13 p1894 A83-31198
- Atmosphere - Sea ice interactions in the Beaufort/Chukchi Sea and in the European sector of the Arctic 15 p2208 A83-33497
- Oxygen and carbon dioxide exchange between the Arctic Ocean and the atmosphere 21 p3182 A83-45398

ARCTIC REGIONS

- The application of microwave remote sensing for snow and ice research 01 p0064 A83-10088
- The methods and results for the laser probing of the upper atmosphere in the polar region 01 p0072 A83-10604
- Investigations of the Arctic, the Antarctic and the world ocean; Conference-Seminar, Moscow, USSR, February 9-13, 1981, Reports 01 p0077 A83-10826
- Using new methods in monitoring the thermal regime of the Arctic 01 p0075 A83-10828
- Evidence for a central Eurasian source area of arctic haze in Alaska 02 p0203 A83-11626
- Electrojets of the explosive phase of a substorm 02 p0210 A83-12436
- Aerosol minima --- in Arctic 03 p0357 A83-13546
- Predicting permafrost conditions with infrared sensing techniques 03 p0348 A83-14264
- Arctic haze and perturbations in the solar radiation fluxes at Barrow, Alaska 03 p0370 A83-14642
- Water vapor in Mars' arctic - Seasonal and spatial variability 04 p0569 A83-15590
- Arctic haze and the Arctic gas and aerosol sampling program /AGASP/ [AIAA PAPER 83-0439] 05 p0659 A83-16714
- Observation of ice crystal formation in lower Arctic atmosphere 06 p0790 A83-18266
- Distribution of types of radio auroras with respect to the auroral bulge 07 p0964 A83-21181
- Unusual manifestations of auroral activity 07 p0965 A83-21187

Sea ice classification from infrared thermometry over the North Water, winter 1980/81 08 p1143 A83-21957

Reliability of enhanced infrared /EIR/ geostationary satellite data at high latitudes 08 p1137 A83-22925

Ionospheric modification experiments in northern Scandinavia 09 p1299 A83-23304

The changes of the protein metabolism characteristics during the acclimatization of humans in the Arctic 09 p1322 A83-23974

Approximation of atmospheric radio noise in the Arctic by the Hall model 09 p1251 A83-25166

The results of aircraft investigations of cloudiness and radiation carried out over the eastern Arctic during the Second Observational Period of the Global Weather Experiment 09 p1316 A83-25228

A comparison between the calculated and measured characteristics of an advection fog and a stratus over ice 09 p1316 A83-25229

The optical properties of the atmosphere over the Arctic basin 09 p1316 A83-25230

Atmospheric aerosols in the polar regions 09 p1316 A83-25231

Aerosol measurements in the Arctic and in a volcanic region 09 p1309 A83-25232

A subsatellite experiment in the Arctic --- atmospheric radiation study 09 p1316 A83-25233

Some aspects of a method for the analysis of lineaments /on the basis of the interpretation of space photographs/ 10 p1444 A83-26807

A comprehensive study of physical and chemical parameters of the Arctic summer aerosol; results from the Swedish expedition Ymer-80 11 p1613 A83-28092

Vertical motions in synoptic atmospheric eddies according to data from a field experiment 14 p2056 A83-32371

Observation of wintertime clouds and precipitation in the Arctic Canada (POLEX-north). I - Characteristic features of clouds and precipitation 14 p2057 A83-32435

Observation of wintertime clouds and precipitation in the Arctic Canada (POLEX-north). II - Characteristic properties of precipitation particles 14 p2057 A83-32436

Observation of wintertime clouds and precipitation in the Arctic Canada (POLEX-north). III - Radar observation of precipitating clouds 14 p2057 A83-32437

The use of space imagery for geocryological mapping 14 p2034 A83-32492

Spectroscopic measurements of the total content of CO, CH₄, and N₂O in the atmosphere in the Arctic region 14 p2053 A83-32861

An innovative type of icebreaker for the arctic environment 15 p2242 A83-34856

Tethered aerostat operations in arctic weather [AIAA PAPER 83-1998] 17 p2466 A83-38919

Variations of the geomagnetic field in the northern polar cap, independent of the interplanetary magnetic field 18 p2714 A83-39339

On the aerosol particle size distribution spectrum in Alaskan air mass systems - Arctic haze and non-haze episodes 18 p2729 A83-40043

Human nutrition in the north 18 p2735 A83-40566

Low elevation angle site diversity satellite communications for the Canadian Arctic 19 p2831 A83-41381

Atmospheric bromine in the Arctic 20 p3021 A83-42852

SO₂ and SO₄(2-) in the arctic - Interpretation of observations at three Norwegian arctic-subarctic stations 21 p3171 A83-44377

The content of gonadotropin hormones and hydrocortisone in women during adaptation to conditions of high latitudes 23 p3497 A83-47104

Repeatability and continuous duration of meteorological conditions that are complex for aviation in the northern European territory of the USSR 23 p3486 A83-47130

Selection of the initial conditions for an artificial satellite for investigations of the north auroral regions 23 p3417 A83-48071

Physical properties of arctic stratus clouds 24 p3611 A83-49679

AREA

A method for the computation of inertial properties for general areas 20 p3038 A83-42796

AREA NAVIGATION

NAVSTAR GPS - State of development and future of this global navigation system 02 p0134 A83-13009

Accuracy and availability of various modern navigation procedures 02 p0134 A83-13013

The role of advanced navigation in future air traffic management 09 p1199 A83-23372

Multipath propagation in the radio field of aircraft navigation systems 09 p1199 A83-23414

Technical and operational evaluation of wide-area coverage navigation systems in the continental United States 09 p1201 A83-24857

Technical and operational evaluation of wide-area coverage navigation systems in the continental United States 11 p1528 A83-28594

Institute of Navigation, Annual Meeting, 38th, U.S. Air Force Academy, Colorado Springs, CO, June 14-17, 1982, Proceedings 12 p1700 A83-29201

VOR area navigation - Techniques and results 12 p1700 A83-29205

A Kalman filter algorithm for terminal-area navigation with sensors of moderate accuracy 21 p3090 A83-45460

The emerging need for improved helicopter navigation 22 p3252 A83-46930

Coping with impulse interference in an advanced development, low-cost Omega/VLF RNAV system 22 p3252 A83-46957

Status of area navigation 22 p3253 A83-46960

Operational and control display concepts for flight management systems in new generation transport aircraft [AIAA PAPER 83-2489] 23 p3405 A83-48348

ARGON

NT ARGON ISOTOPES

Measurements of collisional broadening and the shift of argon spectral lines using a tunable diode laser 01 p0105 A83-10203

Experimental investigation of an argon hollow cathode [AIAA PAPER 82-1890] 02 p0241 A83-12472

A thrust measurement of an ion engine system [AIAA PAPER 82-1915] 02 p0145 A83-12487

Metastable atom density in helium, neon, and argon glow discharges 04 p0538 A83-16059

Effect of argon pressure on the optical properties of sputtered solar selective surfaces 08 p1131 A83-22620

Energies and widths for the series 2s2p/6/nl /neon and magnesium/ and the series 3s3p/6/nl /argon/ 09 p1341 A83-23659

An accurate determination of the thermal conductivity of argon at high temperatures 10 p1415 A83-26152

Thermal conductivity measurement in high temperature argon by the shock perturbation and Mach reflection methods 10 p1415 A83-26153

Experimental study on the ionization of argon gas in a non-equilibrium state behind reflected shock waves 10 p1490 A83-26174

Improving the quality of diffusion bonded joints in OT-41 alloy workpieces containing argon-arc welded joints 10 p1436 A83-26218

Use of pickling pastes for surface preparation of titanium alloys for argon arc welding 10 p1436 A83-26221

Formation of highly excited Ar and Kr atoms in the case of asymmetric charge transfer of Ar(+) and Kr(+) ions with rare-gas atoms 13 p1915 A83-30019

Thermal conductivity of yttrium oxide in the temperature range 400-2100 C in different gaseous media 13 p1826 A83-31468

Effect of argon implantation on the activation of boron implanted in silicon 14 p2093 A83-33444

Mobilities of various mass-identified positive ions in helium, neon, and argon 20 p2950 A83-42637

Molecular velocity distribution functions in an argon normal shock wave at Mach number 7 22 p3366 A83-46008

Secondary ionisation processes in laser-induced cascade ionisation 24 p3627 A83-49837

ARGON ISOTOPES

Ar-40/Ar-39 and U-Th-Pb dating of separated clasts from the Abee E4 chondrite 08 p1188 A83-21641

Ar-39 recoil losses and presolar ages in Allende inclusions 13 p1962 A83-31589

Noble gas constraints on the layered structure of the mantle 14 p2051 A83-31922

Recognition of extraneous argon components through incremental-release (Ar-40)/(Ar-39) analysis of biotite and hornblende across the Grenvillian metamorphic gradient in southwestern Labrador 15 p2201 A83-34496

Eruption age of a Pleistocene basalt from Ar-40-Ar-39 analysis of partially degassed xenoliths 16 p2381 A83-36599

Constraints on evolution of earth's mantle from rare gas systematics 17 p2545 A83-38598

Anomalously old Ar-40 - Ar-39 ages of Antarctic meteorites due to weathering 18 p2779 A83-39965

I-Xe and Ar-40-Ar-39 analyses of silicate from the Eagle Station pallasite and the anomalous iron meteorite Enon 18 p2779 A83-39984

Measurement of the J = 0-1 rotational transitions of three isotopes of ArD(+) 20 p3045 A83-42642

ARGON LASERS

Density measurement in compressible flows using off-resonant laser-induced fluorescence 02 p0183 A83-13075

The effectiveness of stimulating argon laser therapy for some forms of macular dystrophy 03 p0378 A83-13605

Simultaneous multiple-point velocity measurements using laser-induced iodine fluorescence 05 p0646 A83-17884

Radiative lifetimes of excited Ar II states 06 p0809 A83-19011

Generation of continuous-wave 194-nm radiation by sum-frequency mixing in an external ring cavity 07 p0936 A83-20789

Laser-controlled etching of chromium-doped 100 line-type GaAs 10 p1390 A83-25986

New configurations for high-efficiency prism couplers with application to GeO2 optical waveguides 10 p1483 A83-26638

Plasma oscillations in an ion argon laser 13 p1925 A83-30818

International intercomparison of laser power measurements in the visible region 13 p1856 A83-31278

Theoretical investigation of the spectral properties of gas lasers 16 p2359 A83-35889

A kinetic model of the sustained discharge HgBr laser 17 p2514 A83-38207

Interferometric determination of slow movements --- thermal dilatation measurement on laser heated semiconductor surface 21 p3139 A83-44795

Intense proton beam excitation of the high pressure Ar/N2 laser 22 p3296 A83-46270

ARGON PLASMA

Discharge plasma in a multipole ion thruster [AIAA PAPER 82-1931] 02 p0146 A83-12497

Nonlinear effects in the interaction between microwave pulses and low-temperature argon plasma streams 03 p0397 A83-13192

Effect of recombination on the ion saturation current on a cylindrical probe immersed in an argon plasma 09 p1348 A83-23662

A theoretical study of ionization phenomena and radiative behaviors behind a strong shock in argon gas 10 p1487 A83-26967

Improved Ar(II) transition probabilities 15 p2236 A83-34993

The infrared emission spectrum of an argon plasma jet between 4 and 25 microns 15 p2236 A83-35240

Laser scattering and current transport in an argon arc plasma --- German thesis 17 p2582 A83-37504

Measurements of turbulent waves by means of microwave scattering and correlation techniques 18 p2688 A83-39090

Beam-plasma interactions in a positive ion-negative ion plasma 18 p2749 A83-40517

Spectroscopic studies of the dark space ahead of a shock wave in an argon plasma flow 20 p3050 A83-43583

ARGUMENTS (MATHEMATICS)

U INDEPENDENT VARIABLES

ARIANE LAUNCH VEHICLE

The future of the Ariane 01 p0018 A83-10432

The European launch vehicle Ariane: its commercial status - Its evolution 04 p0452 A83-15673

Simulation of the acoustic environment by a launch vehicle at lift-off and its vibratory effects on its structures [ONERA, PT NO. 1982-117] 09 p1212 A83-24328

Ariane uprated 14 p1980 A83-31924

Development and qualification of welding technology for AZ 5 G (AlZn 4.5 Mg 1) of the Ariane primary structure 15 p2123 A83-33956

Ariane 4 liquid boosters and first stage propulsion system [AIAA PAPER 83-1192] 16 p2319 A83-36268

The Ariane rocket resumes successfully 18 p2645 A83-39086

Ariane - Europe's expendable launcher 19 p2812 A83-41375

Operational aspects of the injection of spacecraft into geostationary orbit 21 p3095 A83-44042

The future for communication satellites of the PAM-D/half Ariane class 21 p3096 A83-45427

Development of the thrust augmented Viking engine and first stage DRAKKAR propulsion systems for the Anane 3 launcher [IAF PAPER 83-04] 23 p3425 A83-47229

Ariane 3 third stage propulsion systems and HM7 B engine development [IAF PAPER 83-387] 23 p3426 A83-47367

ARID LANDS

Arid soils as a source of atmospheric carbon monoxide 07 p0959 A83-20198

Mapping semi-arid vegetation in Northern Kenya from Landsat digital data 08 p1126 A83-21931

Satellite imagery characteristics for surveys for the protection of oases against sand invasion 08 p1128 A83-21950

Satellite imagery - Application to a highway project in an arid region - Prospects offered by SPOT simulation 08 p1172 A83-21970

Remote sensing of arid and semi-arid lands; Proceedings of the International Symposium on Remote Sensing of Environment, Cairo, Egypt, January 19-25, 1982. Volumes 1 & 2 09 p1284 A83-24526

Potential application of remote sensing to the study of arid and semi-arid lands in Argentina 09 p1284 A83-24529

Joint U.S.-Mexican activities in arid land management and desertification control 09 p1284 A83-24531

Spot and remote sensing applications for arid and semi-arid lands 09 p1284 A83-24532

Eolian sand bodies of the world --- classification techniques for Landsat imagery applications 09 p1284 A83-24533

Resource inventories of arid and semi-arid lands using Landsat 09 p1284 A83-24534

Dynamic modeling of vegetation change in arid lands 09 p1285 A83-24537

Monitoring of seasonal and yearly land-use changes on aerial photography and Landsat imagery - A case study in the Yemen Arab Republic 09 p1285 A83-24538

Reclamation of salt-affected soils in California 09 p1285 A83-24539

Analysis of man-induced and natural resources of an arid region in California 09 p1285 A83-24543

Remote sensing in range management - An approach for practical application in development 09 p1285 A83-24545

Applying Landsat and ancillary data to arid land inventories - A case study 09 p1285 A83-24546

Spectral remote sensing of rocks in arid lands 09 p1286 A83-24548

Quaternary geochronology of the Western Desert 09 p1286 A83-24549

Refugee settlements and vegetation change - A multistage Landsat data analysis of a semi-arid region in Kenya 09 p1286 A83-24560

Geology and structures study of the Nuba Mountains, Sudan, using Landsat images 09 p1287 A83-24561

Desert construction siting utilizing remote sensing technology 09 p1287 A83-24564

On attaining semi-aridity of North-Bengal in Bangladesh as viewed through the Landsat imageries 09 p1287 A83-24565

Application of remote sensing data to hydrogeological purposes in the Fezzan Region-Lybia 09 p1287 A83-24566

A Landsat-based inventory procedure for the estimation of irrigated land in arid areas 09 p1287 A83-24567

Tectonics of west central New Mexico and adjacent Arizona - A remote sensing and field study in arid and semi-arid areas 09 p1287 A83-24573

Remote sensing applications in road development project in Mauritania, Africa - A valuable tool for projects in arid and semi-arid environments 09 p1287 A83-24574

Urban expansion in the Nile River Valley and Delta 09 p1351 A83-24575

Use of remote sensing techniques to study geothermal resources in arid and semi-arid zones in Chile 09 p1288 A83-24577

Evaluating the soil resources and potential of the Bahr El Jebel region in southern Sudan using Landsat 09 p1288 A83-24581

Interpretation of weathered surfaces in arid regions using Landsat multispectral images 09 p1288 A83-24582

The feasibility of thermal inertia mapping for detection of perched water tables in semi-arid irrigated lands 09 p1288 A83-24583

Application of Landsat imagery in groundwater investigations in a semi-arid hard-rock region of the State of Gujarat /India/ 09 p1288 A83-24584

Processing of remotely sensed data for mapping thermal inertia, soil moisture and evapotranspiration in semi-arid areas 09 p1288 A83-24585

Use of vegetation indicators for crop group stratification and efficient full frame analysis 09 p1288 A83-24587

Monitoring arid land changes in the Turpan Depression, People's Republic of China 09 p1288 A83-24589

Landsat as an aid in consulting projects in the Middle East and Africa some examples of applications on VBB/SWECO projects 09 p1289 A83-24592

Natural water containment site identification in the arid mountains of Djibouti 09 p1289 A83-24595

Using Landsat imageries to make soil-vegetation maps for large areas in Mali, West Africa 09 p1289 A83-24596

Irrigated agricultural mapping and water demand estimation in arid environments from remote sensing 09 p1289 A83-24601

Soil degradation mapping from Landsat in North Africa and the Middle East 09 p1289 A83-24602

Agricultural resource assessment in tropical arid Djibouti 09 p1290 A83-24605

Drought-induced wind erosion in southwestern Kansas, U.S.A. - Integration of Landsat, Seasat, and airborne multispectral data 09 p1290 A83-24606

Monitoring land use and land use appropriateness in the central Sudan - A combination of Landsat data and statistical analysis of climatic data 09 p1290 A83-24608

Landsat image investigation of major surface structures, topography, and hydrology in Qatar 09 p1290 A83-24610

Assessment and management of land and water resources in drought prone areas from satellite derived data - An Indian example 09 p1290 A83-24611

The utility of Landsat for monitoring the ephemeral water and herbage resources of arid lands - An example of rangeland management in the Channel Country of Australia 09 p1290 A83-24614

Classification of surface sediments in Kuwait using Landsat data 09 p1290 A83-24616

Contrast enhancement applied to Guayule distribution in Mexico for commercial rubber production 09 p1290 A83-24617

A survey of Brazil's semi-arid lands with the use of the remote sensing 09 p1290 A83-24618

Multidisciplinary evaluation of satellite data, an effective and economic tool for reconnaissance mapping of semiarid regions 09 p1291 A83-24621

Monitoring the changing areal extent of irrigated lands of the Gafara Plain, Libya 09 p1291 A83-24622

Causes and effects of increasing aridity in Northwest Bangladesh 09 p1291 A83-24628

Environmental change detection in the Nile using multitemp Landsat imagery 09 p1291 A83-24630

Estimates of regional evapotranspiration in South-Eastern France using thermal and albedo data from the heat capacity mapping mission satellite 09 p1291 A83-24631

Particle size and spacing variations in desert surface sediments - Importance for remote sensing of arid regions 09 p1291 A83-24632

Faults and block boundaries interpreted in the western side of the Red Sea between Safaga and Um Gheig, Egypt, and their significance 09 p1292 A83-24636

Classification of arid geomorphic surfaces using Landsat spectral and textural features 10 p1443 A83-25968

Effect of meteorologic conditions on total suspended particulate /TSP/ levels and elemental concentration of aerosols in a semi-arid zone /Beer-Sheva, Israel/ 11 p1613 A83-28093

Analysis of coregistered Landsat, Seasat and SIR-A images of varied terrain types 12 p1748 A83-28909

Investigation of digital Landsat data for mapping soils under range vegetation 14 p2035 A83-32611

Space platform albedo measurements as indicators of change in arid lands 15 p2181 A83-33554

Measurement of changes in Sahelian surface cover using Landsat albedo images 15 p2181 A83-33555

Satellite monitoring of surface temperatures in semi-desert - Differences between anthropogenically impacted terrain and protected natural vegetation 15 p2181 A83-33557

Investigation using space imagery of geological engineering conditions in areas where recent aeolian deposits are widespread (with the southern Aral region taken as an example) 18 p2706 A83-40587

Utilization of remote-sensing methods for the mapping of tree and bush vegetation in the southern Kysyl-Kum 18 p2706 A83-40588

Remote sensing of arid and semiarid rangeland 22 p3310 A83-46163

ARIEL SATELLITES

NT ARIEL 3 SATELLITE

NT ARIEL 5 SATELLITE

'Whatever happened to ...' - A scientific review of three astronomy satellites in which BAe has been involved 11 p1533 A83-28177

Soft X-ray reflectivity measurements of the mirrors flown on the Ariel-6 satellite 12 p1708 A83-29075

ARIEL 3 SATELLITE

Radiation from an Alford loop antenna in two-component warm plasma --- on Ariel-3 satellite 17 p2495 A83-38543

ARIEL 5 SATELLITE

A survey of the bright galactic bulge X-ray sources 03 p0414 A83-13331

ARIES SOUNDING ROCKET

Development of a 1m-normal-incidence-EUV-Telescope 11 p1670 A83-27745

ARIP (IMPACT PREDICTION)

U COMPUTERIZED SIMULATION

U IMPACT PREDICTION

ARITHMETIC

ARITHMETIC

- NT FIXED POINT ARITHMETIC
 NT FLOATING POINT ARITHMETIC
 Error-correcting codes in binary-coded radix-r arithmetic 13 p1910 A83-30796
 On the conversion of Hensel codes to Farey rationals --- algorithms based on p-adic computer arithmetic 15 p2216 A83-33902
 A basis for the quantitative comparison of computer number systems 15 p2217 A83-33906
 The design of error checkers for self-checking residue number arithmetic 15 p2217 A83-33909
 Some methods of parallel organization of mass computations 16 p2403 A83-36903
 Simple coding scheme for modular arithmetic 21 p3190 A83-44969
 Residue arithmetic circuit design based on integrated optics 22 p3350 A83-46659
 Optical systolic array processor using residue arithmetic 22 p3350 A83-46834

ARITHMETIC AND LOGIC UNITS

- Vector computations on a parallel-pipelined processor 11 p1646 A83-28623
 CADAC - A controlled-precision decimal arithmetic unit 15 p2217 A83-33907
 Concurrent error detection in multiply and divide arrays 15 p2218 A83-33915

ARM (ANATOMY)

- NT ELBOW (ANATOMY)
 NT FOREARM
 Ergonomic evaluation of two-hand control location 02 p0225 A83-12088
 Integration function and modeling of the central nervous system in forearm movement control 03 p0384 A83-14126
 Controller design for flexible, distributed parameter mechanical arms via combined state space and frequency domain techniques 11 p1647 A83-27487

ARMATURES

- Twin-armature rotary-linear induction motor 14 p2006 A83-32426
 Theoretical performance of plasma driven railguns [AIAA PAPER 83-1751] 17 p2582 A83-37225

ARMED FORCES

- NT ARMED FORCES (FOREIGN)
 NT ARMED FORCES (UNITED STATES)
 NT NAVY
 Several indicators of the functional condition of the immune system in normal and pathological situations 16 p2400 A83-36842

ARMED FORCES (FOREIGN)

- An analysis of spinal injuries after ejections and crash landings in the IAF 02 p0223 A83-12254
 Pilots are treated and rest here 05 p0673 A83-17178
 The use of telecommunications satellites by the air, sea, and land military forces and by civil defense - Project SICRAL AM/136/80 19 p2812 A83-41227

ARMED FORCES (UNITED STATES)

- An investigation of motivational factors among base-level Air Force civil engineers 06 p0798 A83-17958
 USAF's design guide coming out next month 07 p1001 A83-20647
 Highlights of U.S. Air Force metallurgical research programs 10 p1397 A83-26121
 USAF mobility requirements --- User requirements [AIAA PAPER 83-1588] 16 p2297 A83-36954
 The incidence of refractive anomalies in the USAF rated population 18 p2734 A83-40358
 Navigation, guidance and control curriculum at the Air Force Academy [AAS PAPER 83-021] 21 p3220 A83-44167

AROMATIC COMPOUNDS

- Sooting tendency of fuels containing polycyclic aromatics in a research combustor 08 p1073 A83-23138
 Improvements of CdS film photoanodic behavior by sulfur organic reducing agents 14 p1990 A83-32635
 Laser action benzimidazoles in various aggregate states 14 p2024 A83-32827
 The evolutionary pattern of aromatic amino acid biosynthesis and the emerging phylogeny of pseudomonad bacteria 20 p3033 A83-42399

ARRAYS

- NT ANTENNA ARRAYS
 NT LINEAR ARRAYS
 NT MULTISPECTRAL LINEAR ARRAYS
 NT PHASED ARRAYS
 NT SOLAR ARRAYS
 NT STEERABLE ANTENNAS
 NT SYNTHETIC ARRAYS
 NT YAGI ANTENNAS
 Software optimization of a Kalman filter for an AP-120B array processor 01 p0091 A83-11111

Test results of Spacelab 2 infrared telescope focal plane --- photoconductive detector fabrication and JFET transimpedance amplifier design 03 p0405 A83-13452

Electromagnetic-wave diffraction by a doubly periodic array of semiinfinite dielectric rods 11 p1556 A83-27961

The organization of circuit analysis on array architectures --- Thesis 11 p1564 A83-28648
 Noise rejection in array data 15 p2223 A83-35144

ARRESTING GEAR

Fatigue life evaluation of the A-7E arresting gear hook shank 03 p0277 A83-13912

ARRHYTHMIA

A pharmacological evaluation of electrical processes in the myocardium 01 p0078 A83-10510
 The integral EKG, the ventricular gradient, the differential EKG, and their diagnostic possibilities 03 p0379 A83-13621
 The antiarrhythmic effect of intramuscular and enteral injections of trimetaz 03 p0374 A83-13630
 Mechanism for the appearance of spiral waves in active media, associated with the phenomenon of critical curvature --- in damaged myocardium tissues 03 p0376 A83-14364
 Mechanism for the appearance of the first extrasystole during short-lived atrial arrhythmia 03 p0376 A83-14366

Refractoriness of heart tissues during a decrease of fast sodium current - A comparison of the atrium and the ventricle 03 p0376 A83-14370
 The use of cordarone during acute myocardial infarctions 05 p0674 A83-17221
 The role of the kidneys in the pharmacokinetics of novocainamide 07 p0975 A83-20989
 Wolf-Parkinson-White syndrome in young, asymptomatic pilot's applicants 08 p1147 A83-22960
 The modeling of respiratory arrhythmia 09 p1324 A83-23864
 The energy balance of the myocardium and its correction by antiarrhythmics 13 p1895 A83-30407
 Human sinus arrhythmia as an index of vagal cardiac outflow 13 p1904 A83-30498
 The diagnostic value of a test with graded physical load for several heart rhythm disorders 14 p2071 A83-33337
 Predicting complex ventricular arrhythmias during various periods of myocardial infarction 15 p2213 A83-34953
 The characteristics of heart rhythm disorders in athletes with various types of vegetative regulation 19 p2882 A83-41447

Investigation of flow past an aircraft wing section in flight and in a wind tunnel 17 p2447 A83-37506

ARROW WINGS

Investigation of flow past an aircraft wing section in flight and in a wind tunnel 17 p2447 A83-37506

ARSENIC

Chemical modification of amorphous arsenic 04 p0542 A83-15532
 Flame annealing of arsenic and boron implanted silicon 08 p1170 A83-22768
 Solid solubility and precipitation of phosphorus and arsenic in silicon solar cells front layer 14 p2088 A83-32232
 Incoherent light-induced diffusion of arsenic into silicon from a spin-on source 22 p3365 A83-46736
 Measurement of differential cross sections of low-energy electrons elastically scattered by gaseous molecules. IV Effect of intramolecular double scattering as observed in the scattering of 100 and 500 eV electrons by As₄ 24 p3626 A83-49433

ARSENIC COMPOUNDS

NT ALUMINUM GALLIUM ARSENIDES
 NT ARSENIDES
 NT GALLIUM ARSENIDES
 NT INDIUM ARSENIDES
 NT PROUSTITE
 Production and properties of amorphous films of nonstoichiometric As_x/S_{1-x}/ composition 01 p0110 A83-10850
 Modification of vitreous As₂Se₃ --- by metallic impurities 04 p0540 A83-15500
 A role of the lowest unoccupied molecular orbital of the local structure of amorphous materials 04 p0540 A83-15501
 EXAFS investigation of dilute Cu impurities in amorphous As₂Se₃ 04 p0540 A83-15502
 Index of refraction of the glassy As_x/Te_{100-x}/ system 04 p0535 A83-15504
 Chalcogenide glasses - Promising materials for quantum electronics. I - The interaction and structure of As-S glasses 14 p2088 A83-32167
 Middle IR As-S and As-Se glass fibres with optical losses lower than 1 dB/m 19 p2900 A83-41280
 Determination of particulate and gaseous arsenic compounds in the atmosphere at trace levels 22 p3320 A83-45714

ARSENIDES

NT ALUMINUM ARSENIDES
 NT ALUMINUM GALLIUM ARSENIDES
 NT GALLIUM ARSENIDES
 NT INDIUM ARSENIDES
 NT PROUSTITE
 The effect of doping on the photoconductivity of p-CdSiAs₂ single crystals 21 p3219 A83-45269

ARTERIES

NT AORTA
 The automatic stabilization of pressure in the main arteries during changes in the blood flow 01 p0080 A83-10545
 The adaptive properties of the major arterial vessels 03 p0379 A83-13620
 Arterial hypertonia in miners working in deep mines 05 p0673 A83-17167
 The role of catecholamines in the development of spontaneous arterial hypertension in spontaneously hypertensive rats 08 p1146 A83-22119
 The architectonics of the arterial bed in the brain hemispheres of rats during normal conditions and after a stay at a 'height' of 5600 m 10 p1454 A83-26788
 The aminergic control of the cerebral arteries 14 p2063 A83-32099
 Hyperpnea of exercise at various PIO₂ in normal and carotid body-denervated ponies 14 p2064 A83-32820
 Comparative study of various noninvasive methods of arterial pressure recording 17 p2562 A83-38179
 Cholinergic and adrenergic innervation of intracerebral arteries during ontogenesis in humans 17 p2560 A83-38194
 Reversal of arterial-to-expired CO₂ partial pressure differences during rebreathing in goats 22 p3345 A83-45987
 Effects of hypoxia on norepinephrine release and metabolism in dog pulmonary artery 22 p3346 A83-45989

ARTERIOSCLEROSIS

The effect of xenogenous cerebrospinal fluid on the course of experimental hypercholesterolemia 05 p0670 A83-17187
 The identification of the variation of atherosclerosis plaques by invasive and non-invasive methods 11 p1643 A83-28760
 An investigation of the microcirculatory bed in flightcrew members with conjunctivitis during the initial appearance of cerebral atherosclerosis 13 p1905 A83-30949
 Social stress and atherosclerosis in normocholesterolemic monkeys 13 p1899 A83-31166
 Changes in kinin kallikrein system in rabbits with experimental atherosclerosis treated with protein hydrolysate 'Hydroprot' 14 p2061 A83-31820
 The phospholipid content of subfractions of high-density lipoproteins in women with angiographically documented atherosclerosis of the coronary arteries 18 p2735 A83-40543
 Coronary artery spasm induced in atherosclerotic miniature swine 19 p2873 A83-40904
 Atherosclerosis and age --- Russian book 21 p3188 A83-45005
 Circulating antibodies to aortic elastin and their significance in atherosclerosis in humans 23 p3499 A83-48674
 The walls of vessels in atherogenesis and thrombogenesis (Investigations in the USSR) --- Russian book 24 p3617 A83-49073

ARTHROPODS

NT BEETLES
 NT DROSOPHILA
 NT GRASSHOPPERS
 NT INSECTS
 NT LOCUSTS
 NT PUPA

ARTIFICIAL CARDIAC PACEMAKER

The changes in the activity of the intracardiac ganglionic-synaptic apparatus during the interaction of sympathetic and parasympathetic regulatory effects on the rhythm of the pacemaker 07 p0973 A83-20243

ARTIFICIAL CLOUDS

NT BARIUM ION CLOUDS
 NT CHEMICAL CLOUDS

ARTIFICIAL INTELLIGENCE

NT COGNITIVE PSYCHOLOGY
 NT EXPERT SYSTEMS
 Semantic questions pertaining to artificial intelligence 01 p0094 A83-10508
 Robots with artificial intelligence 01 p0086 A83-10914
 Symbolic pattern matching for target acquisition 01 p0008 A83-11460
 3-D machine perception; Proceedings of the Conference, Washington, DC, April 23, 24, 1981 03 p0324 A83-13444

Toward the robot eye - Isomorphic representation for machine vision	03	p0384	A83-13447
Perceptual capabilities, ambiguities, and artifacts in man and machine			
[AD-A109864]	03	p0383	A83-13450
PAR image processing system /PARIPS/ - A testbed for automating image interpretation	08	p1154	A83-22536
Pathways of evolution for man and machine	12	p1784	A83-29454
Bringing AI up to the space challenge	18	p2737	A83-40306
Computer-aided engineering - The AI connection	18	p2738	A83-40307
The role of automation and artificial intelligence	19	p2825	A83-42088
[AIAA PAPER 83-7104]			
Planning in time - Windows and durations for activities and goals	21	p3198	A83-43951
Robotics and artificial intelligence across the Atlantic and Pacific	21	p3118	A83-44077
Current status and future of intelligent industrial robots	21	p3118	A83-44079
Rigid body motion from depth and optical flow --- for computer vision	21	p3194	A83-44254
Robot planning with fuzzy sets	21	p3194	A83-44696

ARTIFICIAL RADIATION BELTS			
Optimal conditions for the creation of an artificial ionized region in the atmosphere by intersecting microwave beams	05	p0662	A83-17608

ARTIFICIAL RESPIRATION			
U RESUSCITATION			
ARTIFICIAL SATELLITES			
NT AEROS SATELLITE			
NT ANIK 2			
NT ANIK 3			
NT ARIEL SATELLITES			
NT ARIEL 3 SATELLITE			
NT ARIEL 5 SATELLITE			
NT ASTRONOMICAL NETHERLANDS SATELLITE			
NT ATS 1			
NT ATS 6			
NT BEACON SATELLITES			
NT BIOSATELLITES			
NT COMMUNICATION SATELLITES			
NT COMMUNICATIONS TECHNOLOGY SATELLITE			
NT COMSTAR SATELLITES			
NT COS-B SATELLITE			
NT COSMOS SATELLITES			
NT COSMOS 1129 SATELLITE			
NT DISCOVERER SATELLITES			
NT DYNAMICS EXPLORER SATELLITES			
NT DYNAMICS EXPLORER 1 SATELLITE			
NT DYNAMICS EXPLORER 2 SATELLITE			
NT ENVIRONMENTAL RESEARCH SATELLITES			
NT EOSS			
NT ERS-1 (ESA SATELLITE)			
NT ESA SATELLITES			
NT EUROPEAN COMMUNICATIONS SATELLITE			
NT EXOSAT SATELLITE			
NT EXPLORER 1 SATELLITE			
NT EXPLORER 12 SATELLITE			
NT EXPLORER 47 SATELLITE			
NT EXPLORER 50 SATELLITE			
NT EXPLORER 51 SATELLITE			
NT EXPLORER 54 SATELLITE			
NT EXPLORER 55 SATELLITE			
NT FRENCH SATELLITES			
NT GEODETIC SATELLITES			
NT GEOPHYSICAL SATELLITES			
NT GEOS SATELLITES (ESA)			
NT GEOS 1 SATELLITE			
NT GEOS 2 SATELLITE			
NT GEOS 3 SATELLITE			
NT GOES SATELLITES			
NT GRAVITY GRADIENT SATELLITES			
NT GRAVSAT SATELLITE			
NT HAWKEYE SATELLITES			
NT HEAO 1			
NT HEAO 2			
NT HEAO 3			
NT HELIOS A			
NT HELIOS SATELLITES			
NT HELIOS 1			
NT HELIOS 2			
NT HEOS SATELLITES			
NT HIPPARCOS SATELLITE			
NT INFRARED ASTRONOMY SATELLITE			
NT INTLSAT SATELLITES			
NT INTERCOSMOS SATELLITES			
NT INTERNATIONAL SUN EARTH EXPLORER 1			
NT INTERNATIONAL SUN EARTH EXPLORER 2			
NT INTERNATIONAL SUN EARTH EXPLORER 3			
NT INTERNATIONAL SUN EARTH EXPLORERS			
NT IRIS SATELLITES			
NT IUE			

NT L-SAT			
NT LAGEOS (SATELLITE)			
NT LANDSAT D PRIME			
NT LANDSAT SATELLITES			
NT LANDSAT 2			
NT LANDSAT 3			
NT LANDSAT 4			
NT LONG DURATION EXPOSURE FACILITY			
NT LUNAR ORBITER			
NT LUNAR SATELLITES			
NT MAGELLAN MISSION			
NT MAGSAT SATELLITES			
NT MAPSAT			
NT MARECS MARITIME SATELLITES			
NT MARISAT SATELLITES			
NT MARITIME SATELLITES			
NT MAROTS (ESA)			
NT METEOROLOGICAL SATELLITES			
NT METEOSAT SATELLITE			
NT MULTISPECTRAL RESOURCE SAMPLER			
NT NAVIGATION SATELLITES			
NT NAVSTAR SATELLITES			
NT NIMBUS SATELLITES			
NT NIMBUS 4 SATELLITE			
NT NIMBUS 5 SATELLITE			
NT NIMBUS 6 SATELLITE			
NT NIMBUS 7 SATELLITE			
NT NOAA SATELLITES			
NT NOAA 6 SATELLITE			
NT NOAA 7 SATELLITE			
NT NOVA SATELLITES			
NT OAO 3			
NT ORBITAL SPACE STATIONS			
NT ORBITAL WORKSHOPS			
NT OSO-8			
NT OTS (ESA)			
NT POGO			
NT PROGNOZ SATELLITES			
NT RCA SATCOM SATELLITES			
NT RELAY SATELLITES			
NT ROSAT MISSION			
NT SAGE SATELLITE			
NT SARSAT			
NT SAS-2			
NT SCATHA SATELLITE			
NT SEASAT SATELLITES			
NT SEASAT 1			
NT SHUTTLE PALLET SATELLITES			
NT SIRIO SATELLITE			
NT SOLAR MESOSPHERE EXPLORER			
NT SOLAR POWER SATELLITES			
NT SPOT (FRENCH SATELLITE)			
NT SYMPHONIE SATELLITES			
NT SYNCHRONOUS METEOROLOGICAL SATELLITE			
NT SYNCHRONOUS SATELLITES			
NT SYNCOM SATELLITES			
NT TD SATELLITES			
NT TD-1 SATELLITE			
NT TETHERED SATELLITES			
NT TIROS N SERIES SATELLITES			
NT TIROS SATELLITES			
NT TRANSIT SATELLITES			
NT VENERA SATELLITES			
NT VENERA 8 SATELLITE			
NT VENERA 9 SATELLITE			
NT VENERA 10 SATELLITE			
NT VENERA 11 SATELLITE			
NT VENERA 12 SATELLITE			
The artificial earth satellite motion in an oblate, rotating atmosphere with symmetrical diurnal effect	01	p0017	A83-10269
Classification of the results of the electrophotometry of artificial celestial bodies	03	p0286	A83-14684
On the stability of the inner planets, satellites and close binaries	04	p0547	A83-15600
Potentials on large spacecraft in LEO	05	p0607	A83-17489
Perturbations in the nodal period of artificial satellites caused by the terrestrial infrared radiation pressure	05	p0602	A83-17858
Algorithm for the estimation of the parameters of the relative motion of two satellites given a full complement of measurements	06	p0721	A83-18354
Satellite servicing from the Shuttle Orbiter	06	p0722	A83-18371
Electrostatic flow field of satellites moving in ionosphere	08	p1050	A83-21881
Free rotation of a circular ring about a diameter	09	p1339	A83-24820
Construction of an optimal filter in the problem of the flywheel control of an artificial earth satellite	09	p1218	A83-25041
Astronomy - The next space race	11	p1675	A83-28387
Expansion of the perturbation function in the problem of two fixed centers	13	p1809	A83-31270

Effects of tripropellant engines on earth-to-orbit vehicles			
[AIAA PAPER 83-1187]	16	p2318	A83-36265
Artificial satellite break-ups. II - Soviet anti-satellite programme	18	p2644	A83-39970
About attitude motion of a satellite with time dependent moments of inertia	23	p3423	A83-48070
A noncanonical analytic solution to the J2 perturbed two-body problem	24	p3550	A83-48763
An analytic solution for the J2 perturbed equatorial orbit	24	p3550	A83-48764
ARTILLERY			
NT PRECISION GUIDED PROJECTILES			
ARTS			
NT GRAPHIC ARTS			
ARYABHATA			
U INDIAN SPACECRAFT			
ARYL COMPOUNDS			
U AROMATIC COMPOUNDS			
ASCENT			
NT CLIMBING FLIGHT			
ASCENT PROPULSION SYSTEMS			
The Talos propulsion system	02	p0148	A83-12857
Design and performance of the external tank portion of the Space Shuttle main propulsion system	11	p1535	A83-27471
ASCENT TRAJECTORIES			
Ascent performance and abort analysis for a Future Space Transportation System			
[AIAA PAPER 83-2112]	19	p2817	A83-41939
Space Shuttle response to ascent wind profiles	21	p3097	A83-45464
The calculation of optimal paths with singular control segments --- for flight vehicle trajectories	23	p3501	A83-48246
ASCORBIC ACID			
The daily food ration and the ascorbic acid supply of the human body during work in an arid zone	23	p3496	A83-47103
ASCORBIC ACID METABOLISM			
Ascorbate uptake by isolated rat alveolar macrophages and type II cells	13	p1897	A83-30464
ASDE			
U AIRPORT SURFACE DETECTION EQUIPMENT			
ASHES			
NT FLY ASH			
Volcanic ash over Arizona in the spring of 1982 - Astronomical observations	11	p1621	A83-28769
Optical properties of the ash from El Chichon volcano	12	p1751	A83-28913
Analysis of Mount St. Helens ash from optical photoelectric photometry	22	p3329	A83-46418
ASPECT RATIO			
NT HIGH ASPECT RATIO			
NT LOW ASPECT RATIO			
Effect of aspect ratio on heat transfer in shallow enclosures			
[ASME PAPER 82-HT-44]	02	p0172	A83-12797
Effect of fiber-aspect ratio and orientation on the stress-strain behavior of aligned, short-fiber-reinforced, ductile epoxy	08	p1055	A83-22719
Alternative wing concepts for a long-distance aircraft of the nineties			
[DGLR PAPER 82-029]	09	p1202	A83-24155
Flow around a normal plate of finite width immersed in a turbulent boundary layer	10	p1418	A83-26630
Parametric study of hypersonic three-dimensional configurations	11	p1527	A83-28537
On the off-axis tension test for unidirectional composites	19	p2819	A83-41033
Effect of fiber aspect ratio on ultimate properties of short-fiber composites	22	p3264	A83-46297
ASPHALT			
Reflective properties of asphalt and concrete surfaces	08	p1126	A83-21925
Thermal properties of some asphaltic concrete mixes			
[AIAA PAPER 83-1598]	14	p1978	A83-33361
Evaluation of properties of recycled asphalt concrete hot mix			
[AIAA PAPER 83-1599]	14	p1978	A83-33362
ASPHERICITY			
Polishing and testing of aspheric diamond-turned surfaces	02	p0239	A83-12720
The polarization of supernova light - A measure of deviation from spherical symmetry	05	p0699	A83-17015
Generation of off-axis aspherics --- optical surfaces for telescopes	13	p1921	A83-31015
A two-mirror stigmatic system in which the figure of one of the mirrors is known	17	p2580	A83-37672
Evaluating concave and convex aspherical mirrors with a T-shaped spherometer	17	p2580	A83-37691
A method of calculating the surface contour that accurately corrects the spherical aberration on the axis in a centered optical system	17	p2590	A83-37692

- The design and study of the aspherical plate corrector of the view field for Cassegrain system
17 p2580 A83-38774
- ASPHYXIA**
The effect of mechanical asphyxiation on lipid peroxidation processes in the rat brain 05 p0670 A83-17185
The energy metabolism in the brains of rats exposed to mechanical asphyxia 07 p0972 A83-19923
- ASPIRATION**
U VACUUM
- ASSEMBLIES**
NT TAIL ASSEMBLIES
A three-dimensional pattern recognition technique for inspection of missing parts in assemblies
07 p0942 A83-20452
Multi-level substructural analysis in modal synthesis - Two improved substructural assembling techniques
10 p1442 A83-26764
Design ATE systems for complex assemblies
16 p2348 A83-36962
- ASSEMBLING**
NT ORBITAL ASSEMBLY
Robotics for assembly - Design of a feedback sensor, and its use in general insertion procedures --- French thesis
02 p0229 A83-11767
Assembling, setting up, and tuning the instruments of automatic control systems --- Russian book
02 p0230 A83-11972
Satellite assembly, integration, and test and analysis
13 p1810 A83-31189
- ASSEMBLY**
Stress level evaluation of a Printed Wiring Assembly containing large hybrid packages
13 p1837 A83-31486
Sensor-based robotic assembly systems - Research and applications in electronic manufacturing
21 p3118 A83-44070
- ASSEMBLY LANGUAGE**
Optimal scheduling of assembly language kernels for vector processors
15 p2219 A83-35129
- ASSESSMENTS**
NT DAMAGE ASSESSMENT
NT TECHNOLOGY ASSESSMENT
- ASSET GLIDERS**
Asset and prime - Gliding re-entry test vehicles
18 p2645 A83-39972
- ASSOCIATION REACTIONS**
Association of triethylammonium perchlorate with bases
01 p0023 A83-11322
On the n-dependence of the reaction rate for $C^+ + C/n$ yields $C^+/n + 1/$ in interstellar space
05 p0698 A83-16999
Temperature dependence of three-body association reactions from 45 to 400 K - The reactions $N_2^+ + N_2$ yields $Na^+ + N_2$ and $O_2^+ + N_2$ yields $O_4^+ + N_2$
10 p1391 A83-26458
Resonant and nonresonant processes in the formation of $CH(+) +$ by radiative association
17 p2578 A83-37342
Theory of molecular formation by radiative association in interstellar clouds
19 p2918 A83-41623
Laboratory measurements of the association rate coefficients of $NO(+)$, $O_2(+)$, $N(+)$, and $N_2(+)$ ions with N_2 and CO_2 at temperatures between 100 K and 400 K
20 p3024 A83-43165
Three-body association reactions of $NO(+)$ and $O_2(+)$ with N_2
21 p3109 A83-43957
Temperature dependence of associative detachment reactions
21 p3109 A83-43960
Association reactions of $Na(+)$ and some implications for interstellar chemistry
21 p3238 A83-45571
Associative ionization in collisions between two $Na(3P)$ atoms
22 p3361 A83-45926
- ASSOCIATIONS**
U ORGANIZATIONS
- ASSOCIATIVE PROCESSING (COMPUTERS)**
Pseudo-associative store with hardware hashing --- data-flow approach in parallel computing systems
07 p0982 A83-19624
An iterative approach to region growing using associative memories
21 p3191 A83-43956
- ASTEROID BELTS**
NT AMOR ASTEROID
NT ASTEROIDS
NT CERES ASTEROID
NT TORO ASTEROID
Nature of the Kirkwood gaps in the asteroid belt
08 p1176 A83-23259
Colonies in the asteroid belt, or a missing term in the Drake equation
19 p2908 A83-41509
A mechanism of formation for the Kirkwood gaps
22 p3376 A83-47089
- ASTEROID CAPTURE**
The Tunguska event - No cometary signature in evidence
22 p3385 A83-46387

ASTEROID MISSIONS

- Characteristics of a dual mission concept for intensive study of moon and Mars or moon and asteroids
[AIAA PAPER 83-0349] 05 p0601 A83-17920
Interplanetary navigation or the cosmic flipper
16 p2314 A83-35600
Missions to the asteroid Anteros and the space of true anomalies
18 p2642 A83-39474
- ASTEROIDS**
NT AMOR ASTEROID
NT CERES ASTEROID
NT TORO ASTEROID
Three characteristic parameters of orbits of Hilda-type asteroids
02 p0247 A83-12544
The eight-color asteroid survey - Standard stars
02 p0249 A83-12921
Observations of 1 Ceres and 2 Pallas at centimeter wavelengths
02 p0268 A83-12922
Physical studies of asteroids. VIII - Photoelectric photometry of the asteroids 42, 48, 93, 105, 145 and 245
03 p0403 A83-13366
An interesting difference in the distributions of the average motions of S- and C-asteroids
03 p0403 A83-13370
UBV photometry of the M-type asteroids 16 Psyche and 22 Kalliope
03 p0403 A83-13371
Do comets evolve into asteroids - Evidence from physical studies
03 p0404 A83-13402
Numerical determination of proper inclinations of Hilda-type asteroids
03 p0404 A83-13419
Statistics of the complete set of bright and faint asteroids
03 p0133 A83-13668
Poynting-Robertson drag and orbital resonance
03 p0407 A83-13839
A method for constructing explicit solutions to a simplified version of the spatial circular restricted three-body problem
03 p0408 A83-13898
Positions of main belt asteroids
03 p0410 A83-14723
The dependence of asteroid lightcurves on the orientation parameters and the shapes of asteroids
03 p0435 A83-14866
Physical studies of asteroids. IX - The light curve of the M asteroid 77 Frigga
03 p0411 A83-14870
The six-day rotation period of 1689 Floris-Jan - A new record among slowly rotating asteroids
04 p0545 A83-15031
On asteroid classifications in families
04 p0546 A83-15040
Variation of the mean and median inclinations in the numbered minor planet sample
04 p0546 A83-15104
The distribution of orbital eccentricities of minor planets
04 p0548 A83-16440
Calibration of the radiometric asteroid scale using occultation diameters
05 p0704 A83-16969
Photoelectric photometry of asteroids 33 Polyhymnia and 386 Siegena
05 p0693 A83-16970
Rotation of asteroids and planetary axial rotation theory
06 p0818 A83-18476
Asteroids --- their classification
06 p0850 A83-19471
Precursors to gamma-ray bursts in the asteroid impact scenario
07 p1012 A83-20024
Clay mineralogy of the Cretaceous-Tertiary boundary clay --- in search for asteroid ejecta
07 p1029 A83-20301
Positions of asteroids /1981/. II
07 p1006 A83-20562
Minor planet positions obtained at Cerro Calan Observatory during 1978-1980
07 p1006 A83-20567
A check for the pole coordinates of asteroid 22 Kalliope
07 p1008 A83-21203
Rotation periods and lightcurves of the asteroids 136 Austria and 238 Hypatia
07 p1009 A83-21252
On lost minor planets
07 p1009 A83-21272
Impact of an asteroid or comet in the ocean and extinction of terrestrial life
07 p0950 A83-21314
Remote comets and related bodies - VJHK colorimetry and surface materials
08 p1181 A83-22926
The asteroids as outcomes of catastrophic collisions
08 p1175 A83-22927
Complete fragmentation of the parent bodies of Themis, Eos, and Koronis families
08 p1175 A83-22928
The diameter of 88 Thisbe from its occultation of SAO 187124
09 p1352 A83-23324
Occultations of stars by solar system objects. III - A photographic search for occultations of faint stars by selected asteroids
09 p1352 A83-23325
The rotation of minor planets
09 p1353 A83-24013
Studies of small asteroids. III - Positions of asteroids obtained during September 1978 with the ESO Schmidt telescope
09 p1355 A83-24524
Digital speckle interferometry of Juno, Amphitrite and Pluto's moon Charon
09 p1367 A83-25301

- Planets, asteroids and comets at high angular resolution
10 p1495 A83-25849
The exact positions of certain minor planets
10 p1498 A83-26910
Clarification of the angular momentum/mass relation $/J = pM\text{-squared}/$ for astronomical objects
11 p1669 A83-27699
Laboratory simulation of photometric light curves of the asteroids
11 p1685 A83-28378
Physical studies of asteroids. X - Photoelectric light curves of the asteroids 219 and 512
11 p1686 A83-28384
Rotation properties of the high-numbered asteroids 1236 Thais and 1317 Silvette
12 p1797 A83-28888
Accretion of jet streams and formation of asteroids
12 p1795 A83-29357
The brightness variations of asteroid 216 Kleopatra
13 p1960 A83-30380
Photoelectric analysis of asteroid 216 Kleopatra
Implications for its shape
13 p1961 A83-31207
Speckle interferometry observations of the asteroids Juno and Amphitrite
13 p1943 A83-31751
Software simulations of the detection of rapidly moving asteroids by a charge-coupled device
14 p2095 A83-31990
Lightcurves and phase function of asteroid 44 Nysa during its 1979 apparition
14 p2097 A83-32601
Pole orientation of asteroid 44 Nysa via photometric astrometry, including a discussion of the method's application and its limitations
14 p2097 A83-32602
Worldwide photometry and lightcurve observations of 16 Psyche during the 1975-1976 apparition
14 p2097 A83-32604
Limb darkening of meteorites and asteroids
14 p2112 A83-32605
Asteroid rotation. IV
14 p2097 A83-32607
Summary of five missions at the ESO, La Silla - The discovery of 38 new asteroids with the large objective prism astrophotograph (GPO)
14 p2097 A83-32839
UBV photometry of the minor planets 86 Semele, 521 Brixia, 53 Kalyso and 113 Amalthea
14 p2097 A83-33052
Asteroid and comet bombardment of the earth
14 p2095 A83-33483
A note on the normalized period of libration of Trojan asteroids
15 p2246 A83-34388
The critical energy density and the inelasticity coefficient for asteroidal catastrophic collisions
15 p2250 A83-35029
High-velocity impact experiments needed to improve our understanding of the asteroids
15 p2250 A83-35030
Results of astrophysical investigations of asteroids (survey) I
16 p2437 A83-35751
The light curves of a freely precessing spheroidal minor planet
16 p2438 A83-36689
2 Pallas pole revisited
16 p2426 A83-36778
On the asteroidal conductivities as inferred from meteorites
16 p2438 A83-36782
Photoelectric photometry of 2 Pallas
17 p2589 A83-37369
Asteroids and comets
17 p2608 A83-38272
A qualitative investigation of the motion of asteroids of the Hecuba type
17 p2594 A83-38563
Infrared (JHK) photometry of asteroids. II
18 p2757 A83-39605
Remarkable modification of light curves for shadowing effects on irregular surfaces - The case of the asteroid 37 Fides
19 p2909 A83-40726
The R asteroids reconsidered
19 p2922 A83-40787
The large C-type asteroids 146 Lucina and 410 Chloris, and the small S-type asteroids 152 Atala and 631 Philippina - Rotation periods and lightcurves
19 p2910 A83-41061
Lightcurves and rotation periods for the asteroids 70 Panopaea and 235 Carolina
19 p2910 A83-41062
Physical studies of asteroids. XI - Photoelectric observations of the asteroids 2, 161, 216 and 276
19 p2911 A83-41070
Positions of minor planets. II
20 p3061 A83-43384
Observations of minor planets. II
20 p3061 A83-43391
HD 134518 - A main-sequence detached or a semi-detached eclipsing binary?
20 p3075 A83-43395
Results of astrophysical investigations of asteroids (Survey). II
20 p3061 A83-43410
Photoelectric photometry of asteroids 45, 120, 776, 804, 814, and 1982DV
21 p3222 A83-44084
Observations of asteroids in the 3- to 4-micron region
21 p3239 A83-44085
Evolutionary relation between meteorites, meteoroids and asteroids or comets
21 p3240 A83-44298
Asteroidal resources for space manufacturing
22 p3257 A83-45856

Asteroids and meteorites - Parent bodies and delivered samples 22 p3388 A83-47088
The rotation, color, phase coefficient, and diameter of 1915 Quetzalcoatl 22 p3388 A83-47090
Theory of the Trojan asteroids - IV 24 p3637 A83-48765
381 astrometric positions of minor planets obtained at the GPO telescope of ESO, La Silla, February/March, 1981 24 p3642 A83-49316
Positions of asteroids obtained with the CERGA Schmidt telescope 24 p3643 A83-49323
The classification of asteroids 24 p3646 A83-49999

ASTHMA

The state of the vestibular-analyzer function in patients with infectious-allergic bronchial asthma 03 p0381 A83-14337
Cerebral circulation and the hemodynamics of lesser circulation in patients with bronchial asthma in combination with systemic arterial hypertension 05 p0673 A83-17162
Age-related peculiarities of the functional condition of the vascular system in patients with bronchial asthma in the case of mountain-climate therapy 18 p2735 A83-40569

ASTIGMATISM

Fabrication of a 360 deg astigmatic rainbow hologram 21 p3136 A83-44153

ASTRONICS

The ionizing particle environment near earth --- effects on spacecraft microelectronics 05 p0606 A83-16563
[AIAA PAPER 83-0163] Single event upsets in space --- radiation effects on spacecraft microelectronic circuits 05 p0606 A83-16564
[AIAA PAPER 83-0164] Relating SGEMP photon test exposures to spacecraft survivability expectations 05 p0628 A83-17521
The natural radiation environment inside spacecraft 05 p0608 A83-17545
Characterization of a polyurethane as a space approved encapsulant for electronic components 07 p0920 A83-20486

ASTROBIOLOGY

U EXOBIOLOGY

ASTRODYNAMICS

Space: Mankind's fourth environment; International Astronautical Congress, 32nd, Rome, Italy, September 1981, Selected Papers 01 p0016 A83-11276
Dynamics of elliptical galaxies and other spheroidal components 02 p0246 A83-12189
Vlasov equation --- for galactic and stellar plasma dynamics 02 p0261 A83-12547
The mechanics of an anchored lunar satellite 03 p0283 A83-13215
The dynamical evolution of clusters of nonpoint bodies 03 p0419 A83-13897
A readjustment of lumped coefficients from inclination of 1974-70A 04 p0451 A83-15102
Comments on Aksnes' intermediary --- in theory of artificial satellite orbits 04 p0452 A83-16358
Reentry vehicle impact error from high altitude transient roll resonance 05 p0602 A83-16473
[AIAA PAPER 83-0032] On the fastest reorientation of the axis of rotation of a dynamically symmetric spacecraft 09 p1218 A83-25029
Geostationary satellite orbital geometry and coverage area variations due to the attitude control errors 10 p1380 A83-25504
The shadow equation, free of singularities at arbitrary orientations of the orbit 11 p1532 A83-28033
Linear perturbations of the coordinates of satellites in ellipsoidal orbits due to the effect of atmospheric drag in the standard gravitational field of the earth 11 p1532 A83-28053
Orbital perturbations due to radiation pressure for a spacecraft of complex shape 12 p1705 A83-29102
Expansion of the perturbation function in the problem of two fixed centers 13 p1809 A83-31270
A resonance problem of two degrees of freedom --- for artificial earth satellite orbits 15 p2124 A83-34390
The possible motions of a satellite about an oblate planet 15 p2246 A83-34391
Interplanetary navigation or the cosmic flipper 16 p2314 A83-35600
The dynamics of rich clusters of galaxies. II - The Perseus cluster 17 p2591 A83-37776
Change in trajectory by velocity impulses 17 p2472 A83-38623
Integrals of motion for the classical two-body problem with drag 18 p2644 A83-39568
Weak dynamical effects in the Uranian ring system 18 p2779 A83-39604
The stability of the permanent rotations of an asymmetric heavy rigid body 19 p2895 A83-41202

Spacecraft dynamics --- Book

19 p2810 A83-41825
The effect of low-velocity, low-mass intruders (collisionless gas) on the dynamical evolution of a binary system 20 p3064 A83-42200
A linear solution of the equations of motion of an earth-orbiting satellite based on a Lie-series 20 p2944 A83-43578
Lateral drift compensation for satellites in non-equatorial synchronous orbits through attitude control 21 p3099 A83-44017
Dynamics and control of large flexible spacecraft; Proceedings of the Third Symposium, Blacksburg, VA, June 15-17, 1981 21 p3101 A83-45101
Dynamics of flexible hybrid satellites - Evaluation and computation of a symbolic formalism 21 p3102 A83-45122
Multi-body dynamics analysis on small computers 21 p3190 A83-45123
An elegant Lambert algorithm --- for spacecraft orbit estimation [IAF PAPER 83-325] 23 p3417 A83-47341
Relativistic astrodynamics - The problem of payload optimization in a two-star exploration flight with an intermediate powered swing-by [IAF PAPER 83-327] 23 p3415 A83-47343
Dynamic modeling of flexible spacecraft - A general program for simulation and control [IAF PAPER 83-339] 23 p3421 A83-47348
Technical issues in dynamics and control of large space structures [IAF PAPER 83-403] 23 p3422 A83-47375
The implications of the orbital characteristics of the European Kepler project 23 p3417 A83-48052
A noncanonical analytic solution to the J2 perturbed two-body problem 24 p3550 A83-48763
An analytic solution for the J2 perturbed equatorial orbit 24 p3550 A83-48764
The influence of the magnitude equation in the proper motions of stars on the determination of stellar astronomical constants 24 p3638 A83-48929
The application of the Kolmogoroff-Feller equation to problems of stellar dynamics 24 p3650 A83-48930
Spiral structure - Density waves or material arms? 24 p3656 A83-49231
On the formation and dynamics of shells around elliptical galaxies 24 p3657 A83-49260
High and low thrust acceleration 24 p3551 A83-49625
Mathematical model of a moving system with low-stiffness elastic elements 24 p3624 A83-49670
The dynamics of elliptical rings --- of Saturn and Uranus 24 p3646 A83-49893

ASTROGRAPHY

Investigation of the spherical and chromatic aberrations of the 400/2000 double wide-angle astrophotograph 14 p2095 A83-31839
The field error and photometric system of the double long-focus astrophotograph of the Main Astronomical Observatory of the Academy of Sciences of the Ukrainian SSR -- 14 p2095 A83-31840
The photometric field error of the double wide-angle astrophotograph of the Main Astronomical Observatory of the Academy of Sciences of the Ukrainian Soviet Socialist Republic 14 p2095 A83-31843
Survey of the astrographic catalogue from 1 to 31 degrees of northern declination 22 p3373 A83-46386
Photographic position observations of Venus at the Main Astronomical Observatory of the Ukrainian Academy of Sciences in 1975 24 p3644 A83-49628

ASTROLABES

Results of astrolabe observations made at Paris - Time and latitude 1981 03 p0402 A83-13358
Results of observations made with the Astrolabe of Santiago from 1977 to 1980 09 p1354 A83-24516
Solar observations in 1981 with the astrolabe at CERGA 14 p2115 A83-33055
First astrolabe catalogue of Rio de Janeiro 17 p2587 A83-37276
The first astrolabe catalogue at Valinhos 17 p2587 A83-37281
Corrections for the gravitational deflection of light in the case of observations with an astrolabe 17 p2594 A83-38406
Time and latitude results of observations made at Merate Observatory with the astrolabe for the year 1982 19 p2910 A83-41058
Astrolabe measurements of the solar diameter 23 p3515 A83-47435
Observations of Jupiter with the CERGA astrolabe (February 1980-May 1981) 24 p3645 A83-49843
An analysis of solar observations with the CERGA astrolabe 24 p3675 A83-50097

ASTROLOY (TRADEMARK)

Necklace structure obtained by forging astroloy supersolidus-sintered preforms 02 p0154 A83-11666
P/M Astroloy obtained by forcing or hipping supersolidus sintered preforms 06 p0732 A83-19100
Time dependent low cycle fatigue of PM Astroloy at 1003 K 07 p0893 A83-21475
The nature and origin of previous particle boundary precipitates in P/M superalloys 07 p0895 A83-21501
Forging Astroloy supersolidus-sintered preforms - Necklace structure achievement 07 p0896 A83-21502
Properties and structures of hot isostatic pressed and hot isostatic pressed plus forged superalloys 09 p1236 A83-25286
Microstructures and mechanical properties of hot isostatically pressed powder metallurgy alloy APK-1 10 p1397 A83-25869
Application of electron beam welding to hot isostatically pressed nickel-base materials 15 p2137 A83-33966
Studies of nucleation mechanisms and the role of residual stresses in the grain boundary cavitation of a superalloy 17 p2491 A83-38857

ASTROMETRY

Spectra, dimensions and luminosities of radio sources in the Culgoora-3 list 01 p0117 A83-10868
Secular variation of the longitudes of nodes and arguments of the periastra of the component orbits in the multiple system Xi Uma 01 p0117 A83-10903
Precise optical positions of radio sources in the FK 4-system. II - Results from 28 sources on the northern hemisphere and a preliminary comparison of the optical-radio reference frame 01 p0117 A83-10937
Towards a new scale of extragalactic distances 01 p0118 A83-11337
Halley's comet during its 1835 return 01 p0118 A83-11338
Experiences with the U.S. Naval Observatory glass circles --- for astrometric instruments 02 p0247 A83-12529
Improved orbital elements for periodic comet Schorr /1918 III/ 02 p0247 A83-12536
The fourth meridian catalog of Besancon Observatory 03 p0402 A83-13355
An accurate derivation of the division corrections in a photoelectric meridian circle 03 p0402 A83-13356
Electronographic photometry in the galactic cluster M 37 03 p0402 A83-13364
Comet discoveries, statistics, and observational selection 03 p0403 A83-13378
Interferometer observations of double stars. I 03 p0408 A83-13882
On the correction of stellar proper motions for random error 03 p0408 A83-13892
Further observations of the elliptical galaxy NGC 5813 03 p0420 A83-13937
On standard polarized stars 03 p0410 A83-14208
Positions of main belt asteroids 03 p0410 A83-14723
Orientation of the JPL Ephemerides, DE 200/LE 200, to the dynamical equinox of J 2000 03 p0410 A83-14763
The angular diameter of Betelgeuse 04 p0545 A83-15030
On asteroid classifications in families 04 p0546 A83-15040
Very-long-baseline radio interferometry - The Mark III system for geodesy, astrometry, and aperture synthesis 05 p0693 A83-16938
Calibration of the radiometric asteroid scale using occultation diameters 05 p0704 A83-16969
On the detection of other planetary systems by astrometric techniques 05 p0693 A83-17011
Multiple telescope infrared interferometry 05 p0694 A83-17425
A method for the operational calculation of the expected number of stars in a given region of the celestial sphere 05 p0694 A83-17677
Distances of galaxies from the apparent size distribution of Dark Clouds. II - NGC 224, NGC 2841 and NGC 7331 05 p0695 A83-17861
Occultations of Jupiter by the moon in 1983 06 p0817 A83-18065
Seeing-independent definitions of the solar limb position 06 p0818 A83-18537
Interferometer observations of double stars. II 06 p0819 A83-18788
Cloudcroft occultation summary. II - April 1980-December 1981 --- lunar occultations of stars [AD-A123790] 06 p0820 A83-18875
Possible occultations by satellites of Uranus and Neptune - 1983-1985 06 p0820 A83-18876
The SAOC and the AGK3 --- Smithsonian Astronomical Observatory Catalog 06 p0821 A83-18877

Astrometric studies of nearby white dwarfs and suspected white dwarfs 07 p1004 A83-19865
 The distance, space motions, and revised absolute parameters of R Canis Majoris 07 p1004 A83-19866
 Positions of asteroids /1981/. II 07 p1006 A83-20562
 Positions, magnitudes, and colors for stars in the globular cluster M15 07 p1006 A83-20566
 Minor planet positions obtained at Cerro Calan Observatory during 1978-1980 07 p1006 A83-20567
 The color-magnitude diagram for stars in the central part of the globular cluster NGC 7089 /M 2/ 07 p1006 A83-20573
 Orientation of the FK 4 coordinates from the Washington observations of the sun and planets 07 p1007 A83-20673
 A check for the pole coordinates of asteroid 22 Kalliope 07 p1008 A83-21203
 On the methods for determining galaxy velocity dispersions 07 p1009 A83-21236
 Periodogram of nearly diurnal variations in the latitude of Gor'kii 07 p1027 A83-21273
 Type II supernovae photospheres and distances 08 p1177 A83-21838
 Evaluation of peak location algorithms with subpixel accuracy for mosaic focal planes 08 p1050 A83-22448
 Speckle interferometric measurements of binary stars. VIII 08 p1175 A83-22749
 The exciting stars of Herbig-Haro objects 08 p1183 A83-23056
 Timing observations of the millisecond pulsar 08 p1176 A83-23266
 Six clusters in Puppis-Vela 09 p1352 A83-23321
 Occultations of stars by solar system objects. III - A photographic search for occultations of faint stars by selected asteroids 09 p1352 A83-23325
 Santiago 67 Catalogue - Catalogue of 7610 stars declination zone -25 deg to -47 deg equinox 1950.0 09 p1353 A83-23900
 Classical systems: The star RX Cas - The motion of the apsidal line 09 p1353 A83-23902
 Eclipsing star systems with extended atmospheres and disk-shaped envelopes 09 p1358 A83-23903
 Young star groups 09 p1358 A83-23910
 Systems of galaxies --- properties, structure and evolution 09 p1358 A83-23914
 Diffraction of a two-dimensional electromagnetic beam wave by a thick slit pierced in a perfectly conducting screen --- for study of objective incident radiation used to obtain image of star 09 p1268 A83-24091
 An optimal procedure for non-parametric elimination of observational cutoff bias in complete samples --- of celestial objects 09 p1354 A83-24477
 Optical positions of four benchmark radio sources 09 p1354 A83-24481
 Automated observations of the sun. II - Methods of observation 09 p1369 A83-24488
 Results of observations made with the Astrolabe of Santiago from 1977 to 1980 09 p1354 A83-24516
 Studies of small asteroids. III - Positions of asteroids obtained during September 1978 with the ESO Schmidt telescope 09 p1355 A83-24524
 Observations of solar oscillations of low and intermediate degree 09 p1369 A83-24695
 Accuracy of measurement of star images on a pixel array 10 p1492 A83-25588
 Astrometric positions of Pluto from 1980 to 1982 10 p1493 A83-25652
 Precise optical positions for radio/optical astrometric sources in the southern hemisphere 10 p1493 A83-25654
 Membership in the open cluster NGC 6709 10 p1493 A83-25663
 Inner ring structures in galaxies as distance indicators. IV - Distances to several groups, clusters, the Hercules supercluster, and the value of the Hubble constant 10 p1502 A83-25701
 Multiple telescope interferometry 10 p1494 A83-25841
 The distance to M33 based on a new study of its Cepheids 10 p1516 A83-26752
 Determination of the mass of Jupiter from perturbations of the orbit of Comet P/Wolf in its sphere of action in 1922 10 p1498 A83-26797
 Determining the radius of pulsating variables 10 p1517 A83-26907
 The exact positions of certain minor planets 10 p1498 A83-26910
 Complex of programs for the astrometric reduction of photographic observations 10 p1498 A83-26915
 On the origin of oscillations in a solar diameter observed through the earth's atmosphere - A terrestrial atmospheric or a solar phenomenon 11 p1688 A83-27637
 Solar diameter/s/ 11 p1688 A83-27638

The HIPPARCOS space astrometry mission 11 p1670 A83-27732
 The use of a system of four radio telescopes in solving a number of problems of astrometry and geodynamics by means of VLBI 11 p1673 A83-28028
 A VLBI method for the simultaneous determination of arcs between superdistant radio sources and several parameters of astrometry and geodynamics 11 p1673 A83-28029
 Evaluation of the accuracy of the determination of the arc length between two quasars by the VLBI method using synchronous observations 11 p1673 A83-28035
 Construction of continuous Chebyshev approximations for planetary coordinates 11 p1673 A83-28037
 Improvement of the ephemerides of the inner planets and the moon using radar, laser, and meridian measurements during 1961-1980 11 p1673 A83-28044
 Observed radii and structural parameters of clusters in the SMC. II 12 p1784 A83-28870
 Astrometric studies of ten double or suspected multiple systems from plates taken with the Sproul 61-cm refractor 12 p1788 A83-29184
 Catalogue of 20457 star positions obtained by photography in the declination zone -48 deg to -54 deg (1950) 12 p1788 A83-29185
 The law of variation of the SS 433 precession period 1978-1981 12 p1796 A83-29492
 Comparison of earth rotation as inferred from radio interferometric, laser ranging and astrometric observations 13 p1874 A83-30218
 Positions of bright stars --- Russian book 13 p1936 A83-30625
 The secular variation of cometary magnitude 13 p1939 A83-31205
 Optical positions of quasars 13 p1942 A83-31710
 Astrometry and photometry of comet P/Halley in October and November 1982 13 p1943 A83-31727
 Star transits with a photoelectric micrometer applied to the transit instrument of Torino Observatory 13 p1943 A83-31752
 Selecting the optimal photoelectric unit for a transit instrument 14 p2014 A83-31841
 Modified Bowen-Walraven image slicer 14 p2018 A83-32029
 Methods of photoelectric astrometry 14 p2096 A83-32032
 Pole orientation of asteroid 44 Nyssa via photometric astrometry, including a discussion of the method's application and its limitations 14 p2097 A83-32602
 Photographic observations of visual double stars 14 p2097 A83-33051
 New optical positions and proper motions of late type stars associated with SiO masers 14 p2098 A83-33061
 Block adjustment in photographic astrometry 14 p2100 A83-33253
 The combination of photographic material obtained with different Schmidt telescopes for the determination of proper motions 14 p2100 A83-33254
 A proper motion survey in the area of the galactic cluster in Coma Berenices 14 p2100 A83-33255
 An analysis of coordinate transformation in Schmidt telescope photographic plates 14 p2100 A83-33256
 Astrometric and infrared speckle analysis of the visually unresolved binary BD +41.328 deg 14 p2101 A83-33467
 The Sirius group as a moving supercluster 15 p2245 A83-33831
 Parallaxes and proper motions of 25 stars from plates taken with the 61-cm Sproul refractor 15 p2245 A83-33838
 Cometary ephemerides for spacecraft flyby missions 15 p2249 A83-35017
 PMC 190 - A new Photoelectric Meridian Circle of Tokyo Astronomical Observatory. I - Determination of instrumental errors. II - Pinhole system for solar and lunar observations. 16 p2422 A83-35677
 A new automatic meridian circle PMC 190 16 p2424 A83-36629
 Observation of faint stars by a slit micrometer 16 p2425 A83-36662
 IUE observations of high velocity interstellar gas tentatively associated with Radio Loop II 16 p2431 A83-36663
 Sanduleak-Pesch's twin white dwarf object 16 p2433 A83-36702
 The effect of systematic differences between proper stellar motions on the determination of the solar motion parameters 16 p2426 A83-36857
 On the catalog of star positions in the NPZT program --- Northern photographic zenith tube 16 p2426 A83-36858
 Automatic photoelectric device with a laser interferometer for measuring photographs of limbs of meridian instruments 16 p2357 A83-36863

The brightest stars as extragalactic distance indicators 17 p2595 A83-37301
 Radial velocities of galaxies in neighborhoods of groups of galaxies. II 17 p2602 A83-37884
 On the connection between Seyfert galaxies and neighboring objects 17 p2603 A83-37886
 The astrometric position of T Tauri and the nature of its companion 17 p2592 A83-37941
 Holetschek's effect revisited --- cometary statistics 17 p2592 A83-38234
 Concentrations in the local association. I - The southern concentrations NGC 2516, IC 2602, Centaurus-Lupus and upper Scorpius --- young star clusters in Galaxy 17 p2593 A83-38255
 Kinematic parameters for Trapezium-type systems 17 p2613 A83-38839
 Summary results of the Shanghai-Effelsberg VLBI experiment 18 p2754 A83-39006
 The local group irregular galaxies LGS 3 and Pegasus 18 p2757 A83-39591
 The galactic extinction of extragalactic objects. I - The csc b law and the extinction coefficient 18 p2767 A83-39592
 The precision of velocity measurements from H I profiles 18 p2757 A83-39593
 Astrometry of the low-luminosity stars VB8 and VB10 18 p2757 A83-39602
 Proper motions of Herbig-Haro objects. III - HH-7 through -11, HH-12, and HH-32 18 p2757 A83-39603
 The coordination of space and ground-based parallax programs for improvement of the stellar luminosity function 18 p2767 A83-39629
 On the analysis of motions perpendicular to the galactic plane 18 p2758 A83-39634
 On the determination of R(O) --- distance to center of Milky Way Galaxy 18 p2758 A83-39636
 Determination of AR (R = distance to galactic center) --- product of Oort's rotational constant and distance to Galactic center 18 p2758 A83-39639
 The distance to the Hyades 18 p2759 A83-39783
 Dependence of the observed rate of meteors on the Zenith distance of the radiant 18 p2760 A83-39982
 Double galaxies - Redshift measurements, error analysis, and mean mass/luminosity ratio 18 p2778 A83-40485
 The position of the infrared source IRS 16 in the galactic center region relative to a visual field star 19 p2909 A83-40690
 The search for invisible companions of binary stars 19 p2910 A83-40754
 Spectroscopic orbit of the star HR96 19 p2910 A83-41056
 Micrometric measurements of southern double stars 19 p2911 A83-41072
 The effect of the ellipticity and unevenness of the pivots in a multipurpose astronomical instrument on observations for determining the azimuth by the direct method 19 p2854 A83-41552
 The introduction of the IAU 1980 nutation theory in the computation of the Earth Rotation Parameters by the Bureau International de l'Heure 19 p2860 A83-41561
 The planetary system of Barnard's star 19 p2911 A83-42163
 On the distance to M33 determined from magnitude corrections to Hubble's original Cepheid photometry 20 p3057 A83-42182
 High precision astrometry via very-long-baseline radio interferometry - Estimate of the angular separation between the quasars 1038 +528A and B 20 p3057 A83-42184
 Arcsecond positions for milliarcsecond VLBI nuclei of extragalactic radio sources. II - 207 sources 20 p3057 A83-42185
 A faint star astrometric grid for the galactic center 20 p3058 A83-42199
 Limits on the accuracy of determining q(0) from supernovae 20 p3070 A83-42786
 The contributions of the Zentralinstitut fuer Physik der Erde to the MERIT project --- Monitor Earth-Rotation and Intercompare the Techniques of observation and analysis 20 p3022 A83-43132
 Definitive orbital elements of the visual binary star ADS 5871 - STF 1037 20 p3061 A83-43379
 Stellar-statistical investigations in the vicinity of the sun 20 p3075 A83-43381
 Halley's Comet - Orbital elements evolution 20 p3061 A83-43390
 Correction of meteor radiants for zenith attraction 20 p3061 A83-43416
 New measurements of the solar diameter 20 p3082 A83-43541
 Solar radius change between 1925 and 1979 20 p3082 A83-43543
 Apsidal motion in the eclipsing binary AS Cam 20 p3062 A83-43657

New central velocity dispersions for the bulges of 53 spiral and S0 galaxies 21 p3227 A83-44114

DE 102 - A numerically integrated ephemeris of the moon and planets spanning forty-four centuries 21 p3223 A83-44454

On the apparent association of quasars and Arp's companion galaxies 21 p3233 A83-44744

Optical positions of Seyfert galaxies. - II 21 p3224 A83-44755

Improved parameters for 40 pulsars 21 p3225 A83-44769

SW Lacertae - A quadruple system --- W UMa-type eclipsing binary 21 p3225 A83-44869

A study of the period of U Ophiuchi 21 p3225 A83-44871

Positions of stars in regions of 14 southern galactic clusters 21 p3225 A83-44976

Precise positions in the FK4 system for ten optical counterparts of extragalactic radio sources 22 p3373 A83-46385

Temporal variations of the absolute magnitude of Halley's comet 22 p3375 A83-46576

Astrolabe measurements of the solar diameter 23 p3515 A83-47435

EV Lacertae - Is flare activity related to an unseen planet-like companion? 23 p3516 A83-47493

Distances of the central stars and their position in the HR diagram 24 p3639 A83-49154

Micrometer measurements of visual binaries 24 p3642 A83-49315

381 astrometric positions of minor planets obtained at the GPO telescope of ESO, La Silla, February/March, 1981 24 p3642 A83-49316

Contribution to the study of F, G, K, M binaries. II - Orbital elements of the single-line spectroscopic binaries HD 69148 and HD 85091 24 p3642 A83-49322

Positions of asteroids obtained with the CERGA Schmidt telescope 24 p3643 A83-49323

Solar activity and the conjunctions of Venus 24 p3674 A83-49451

A methodology for determination of extragalactic distances 24 p3661 A83-49453

Exact formulas for calculations concerned with proper motions 24 p3644 A83-49602

Status and trends in the development of astrometric studies. I 24 p3644 A83-49626

The possibility of using sparse reference-star grids to determine the optical positions of extragalactic radio sources 24 p3644 A83-49627

Determination of the minimum distance between the orbits of celestial bodies 24 p3645 A83-49630

A program for investigating the kinematics of stars in the main meridional section of the Galaxy 24 p3645 A83-49637

Standard photometric diameters of galaxies 24 p3645 A83-49842

Observations of Jupiter with the CERGA astrolabe (February 1980-May 1981) 24 p3645 A83-49843

Micrometric measurements of binary stars (first list) 24 p3646 A83-49852

CCD astrometry. I - Preliminary results from the KPNO 4-m/CCD parallax program 24 p3646 A83-49886

Saturn's pole - geometric correction based on voyager UVS and radio occultations 24 p3673 A83-49890

Workshop on Astronomical Measuring Machines, Edinburgh, Scotland, September 28-30, 1982, Proceedings 24 p3647 A83-50001

Sparse field stellar photometry 24 p3647 A83-50002

Crowded-field stellar photometry 24 p3647 A83-50003

Automated analysis on stellar fields with valley lines 24 p3647 A83-50004

Progress report on the Second Cape Photographic Catalogue (CP2) 24 p3647 A83-50008

Point spread functions from electronographic emulsions --- for astronomical photography 24 p3648 A83-50012

The calibration of photographic plates using stellar images 24 p3648 A83-50015

The helium abundances of G-K main sequence halo and disk stars, the helium galactic abundance evolution and the astrometric satellite Hipparcos 24 p3666 A83-50046

The fraction of the sky screened by local diffuse dust clouds 24 p3668 A83-50089

An analysis of solar observations with the CERGA astrolabe 24 p3675 A83-50097

ASTRONAUT MANEUVERING EQUIPMENT

HHMU's, AMU's, and MMU's - The development of astronaut maneuvering units 02 p0140 A83-11936

Lessons learned on the manned maneuvering unit modal survey using single point random excitation [AIAA PAPER 83-1022] 14 p1981 A83-32784

ASTRONAUT PERFORMANCE

The maiden voyage of 'Columbia', III 02 p0137 A83-12644

Astronauts can't stomach zero gravity 03 p0377 A83-13250

The effect of the radiation factor on the activity of operators --- of spacecraft 06 p0799 A83-18366

The stress ECG and the ambulatory continuous ECG in the selection of French astronauts 14 p2067 A83-32455

ASTRONAUT TRAINING

Orthostatic and antiorthostatic tests for French astronauts during training 14 p2067 A83-32456

Features of cosmonaut training 15 p2215 A83-34945

The evolution and present status of mental health standards for selection of USAF candidates for space missions 21 p3188 A83-43996

The Soviet cosmonaut team, 1960-1971 23 p3416 A83-48631

The Soviet cosmonaut team, 1971-1983 23 p3416 A83-48632

ASTRONAUTICS

Twenty-five years which have prepared the future in space 01 p0016 A83-10426

Man in space - Present and future 01 p0016 A83-10427

Space: Mankind's fourth environment; Proceedings of the Thirty-second International Astronautical Congress, Rome, Italy, September 6-12, 1981 01 p0016 A83-11330

Pioneers of rocketry and space travel in scientific literature - A statistical approach [IAF PAPER 82-284] 05 p0710 A83-17933

Israel Annual Conference on Aviation and Astronautics, 24th, Tel Aviv and Haifa, Israel, February 17, 18, 1982, Collection of Papers 07 p0862 A83-21001

Deutsche Forschungs- und Versuchsanstalt fuer Luft- und Raumfahrt, Annual Report 1981 --- Book 09 p1195 A83-23850

The British Interplanetary Society - The first 50 years (1933-1983) 23 p3540 A83-47329

[IAF PAPER 83-386] 23 p3540 A83-47329

A life devoted to astronautics (Dr. Olgierd Wolczek (1922-1982) - Biographical remarks ans scientific activity in astronautics and space physics) [IAF PAPER 83-292] 23 p3541 A83-47332

ASTRONAUTS

Astronauts for the Shuttle 05 p0676 A83-17574

Criteria for the evaluation of the physical aptitude - Their utilization for the classification of subjects 06 p0799 A83-18339

Astronauts and seamen - A legal comparison 07 p1002 A83-21389

ASTRONAVIGATION

Attitude determination, control and navigation of a spinning satellite 17 p2475 A83-37445

ASTRONOMICAL CATALOGS

Automated data retrieval in astronomy; Proceedings of the Sixty-fourth Colloquium, Universite de Strasbourg I, Strasbourg, France, July 7-10, 1981 01 p0113 A83-10126

The astronomical data base and retrieval system at NASA 01 p0113 A83-10127

The Soviet Center of Astronomical Data 01 p0113 A83-10128

Management of astronomical data at Kanazawa Data Center 01 p0113 A83-10129

Infrared astronomical data base and catalog of infrared observations 01 p0113 A83-10130

A fast method to retrieve data from a large star catalogue file 01 p0113 A83-10138

A process for retrieval of data from a compiled star catalogue 01 p0114 A83-10142

Responsibilities and practical limitations in the operation of an astronomical data center 01 p0114 A83-10144

The Bibliographical Star Index 01 p0114 A83-10148

A list of standard star designation 01 p0114 A83-10150

Dictionary of the nomenclature of celestial objects 01 p0114 A83-10151

Data retrieval in the metacatalogue of galaxies 01 p0115 A83-10157

The compiled catalogue of galaxies in machine-readable form and its statistical investigation 01 p0115 A83-10158

Data for the compilation of the 'Third Catalogue of Nearby Stars' 01 p0115 A83-10160

Fundamental data for FK4/FK4Sup stars 01 p0115 A83-10161

Remarks about the cataloguing of open cluster data 01 p0115 A83-10162

The new catalogue of optical HII-regions 01 p0115 A83-10163

ASTRONOMICAL CATALOGS

Catalogue of planetary nebulae and their nuclei 01 p0115 A83-10164

Galaxy photometry in the Virgo cluster. I 01 p0116 A83-10265

HI in the Small Magellanic Cloud re-examined. II 01 p0124 A83-10869

The cross-correlation of the Zwicky and Shane-Wirtanen catalogs of galaxies 02 p0245 A83-11610

Photoelectric observations of lunar occultations. XIII 02 p0249 A83-12920

The fourth meridian catalog of Besancon Observatory 03 p0402 A83-13355

An accurate derivation of the division corrections in a photoelectric meridian circle 03 p0402 A83-13356

Results of astrolabe observations made at Paris - Time and latitude 1981 03 p0402 A83-13358

Infrared astronomical data base and catalog of infrared observations 03 p0406 A83-13467

Autonomous star cataloging for space surveillance missions 03 p0406 A83-13468

A photometric map of interstellar reddening within 300 parsecs 03 p0406 A83-13552

The stars near at hand 03 p0406 A83-13557

The Shternberg stellar spectrophotometry - Detailed comparison with V-band and Johnson-Mitchell 13-color photometry 03 p0407 A83-13660

Flocculent and grand design spiral structure in field, binary and group galaxies 03 p0420 A83-13941

The intrinsic colours of stars in the ultraviolet 03 p0420 A83-13947

Luminosity classification of galaxies in the revised Shapley-Ames Catalog 03 p0409 A83-14136

An approximately 300 Mpc void of rich clusters of galaxies 03 p0422 A83-14177

A catalog of equivalent widths of absorption lines in spectra of A1-G0-type stars 03 p0410 A83-14690

Conversion of positions and proper motions from B1950.0 to the IAU system at J2000.0 03 p0411 A83-14785

A pool of faint stars applied to star catalogue formation 03 p0411 A83-14808

The initial mass function for massive stars 05 p0698 A83-17004

The second catalog of ephemerides for the relative radial velocities of the components of visual binary stars with known orbits --- Book 05 p0694 A83-17133

Catalogue of the Small Magellanic Cloud star members 05 p0694 A83-17664

A list of ultraviolet excess galaxies 05 p0695 A83-17819

Comments on the gamma-ray burst catalog of Mazets et al. /1981a/ 05 p0710 A83-17820

The connection of a catalogue of stars' with an extragalactic reference frame 06 p0817 A83-18086

New candidate Herbig-Haro objects 06 p0819 A83-18797

A kinematic and abundance survey at the galactic poles 06 p0833 A83-18859

The SAOC and the AGK3 --- Smithsonian Astronomical Observatory Catalog 06 p0821 A83-18877

Spectrographic material for RS Canum Venaticorum and Algol binaries 06 p0836 A83-19061

Distribution of the stars in the General Catalogue of Variable Stars 06 p0821 A83-19066

Line identifications in the spectrum of HR 1100 06 p0821 A83-19068

Effect of variable obscuration on the clustering of galaxies 06 p0839 A83-19265

Spectral classification --- of stellar objects 06 p0824 A83-19534

Optical identifications of flat-spectrum radio sources 07 p1003 A83-19853

HEAO A-2 soft X-ray source catalog 07 p1005 A83-20076

5 GHz observations of sources in the Arecibo 611 MHz survey 07 p1005 A83-20078

Inner ring structures in galaxies as distance indicators. III - Distances to 453 spiral and lenticular galaxies 07 p1013 A83-20080

The Case low-dispersion northern sky survey. I 07 p1005 A83-20081

Luminosity and motion of large proper motion stars. II - Stars with annual proper motion larger than 0.7 arc seconds 07 p1005 A83-20132

A study of visual double stars with early type primaries. II - Photometric results 07 p1006 A83-20575

A complete sample of intermediate-strength radio sources selected from the GB/GB2 1400-MHz surveys III - High-resolution observations and optical identifications of sources with normal or flat spectra 09 p1351 A83-23315

Santiago 67 Catalogue - Catalogue of 7610 stars declination zone -25 deg to -47 deg equinox 1950.0 09 p1353 A83-23900

Types of stellar variability 09 p1358 A83-23906

Morphology of the ionized gas in NGC 1313
09 p1355 A83-24525

On estimates of the galaxy correlation function
09 p1355 A83-25007

Status of evolution of F, G, and K field stars contained in the Fe/H abundance ratio catalogue
10 p1492 A83-25478

Membership in the open cluster NGC 6709
10 p1493 A83-25663

A survey by HEAO 1 of clusters of galaxies. III - The complete Abell catalog
10 p1496 A83-26351

Classification of intrinsic variables. IX - The Cepheid domain
11 p1668 A83-27110

The magnitude equation in right ascension between the FK 4 and recent catalogues of southern observations
11 p1678 A83-27698

Cosmogonic characteristics of almost-parabolic orbits
11 p1672 A83-27881

UBV photometry of FK4 and FK4 supplement stars
12 p1784 A83-28868

Supernova remnants in the Magellanic Clouds
12 p1786 A83-29092

21-cm observations of galaxies in groups and multiplets
12 p1787 A83-29178

Catalogue of 20457 star positions obtained by photography in the declination zone -48 deg to -54 deg (1950)
12 p1788 A83-29185

The Asiago catalogue of quasi stellar objects
12 p1788 A83-29275

Atlas of photometric standards of stellar fields --- Russian book
12 p1788 A83-29334

The spectrophotometry of bright stars --- Russian book
13 p1936 A83-30524

Positions of bright stars --- Russian book
13 p1936 A83-30625

The Horologium-Reticulum supercluster of galaxies
13 p1956 A83-31682

The AAO JHKL-prime photometric standards
13 p1942 A83-31702

The Jovian satellites J VI and J VII - Ephemerides for the years 1981-1990
14 p2112 A83-33065

A catalog of hierarchical subclustering in the Turner-Gott groups
14 p2098 A83-33153

General properties of Algol binaries
14 p2103 A83-33154

A deep near infrared objective prism survey for carbon stars toward the galactic center and anticenter
14 p2099 A83-33247

A proper motion survey in the area of the galactic cluster in Coma Berenices
14 p2100 A83-33255

A catalog and identification charts of the Pleiades flare stars
15 p2244 A83-33751

Catalog of H-alpha emission stars in the region of the Orion Nebula
15 p2244 A83-33752

Revised list of pulsating stars with ultra-short periods
15 p2247 A83-34530

Spectral energy distributions for seven standard stars used in compiling a spectrophotometric catalog
15 p2249 A83-34760

The problem of determining the orientations of coordinate systems and the periodic errors of star catalogs from ground-based optical observations
15 p2249 A83-34773

Photoelectric catalogue of globular clusters in the Andromeda Nebula M31 and its companions NGC 147, NGC 185, and NGC 205
15 p2249 A83-34785

The catalog of 1111 Northern PZT Stars compiled from meridian circle catalogs in the 1950s, (NPZT58)
16 p2423 A83-35679

Northern PZT stars catalog (NPZT74)
16 p2423 A83-35680

Groups of galaxies. III - The CfA survey
16 p2423 A83-35971

A survey of galaxy redshifts. IV - The data
16 p2423 A83-35972

Stellar spectrophotometric atlas, wavelengths from 3130 to 10800 A
16 p2424 A83-35973

A catalog of spectral classification and photometry of barium stars
16 p2424 A83-35975

The effect of systematic differences between proper stellar motions on the determination of the solar motion parameters
16 p2426 A83-36857

On the catalog of star positions in the NPZT program --- Northern photographic zenith tube
16 p2426 A83-36858

First astrolabe catalogue of Rio de Janeiro
17 p2587 A83-37276

Infrared photometry of the RS CVn binaries. II - JHKL light curves of HR 1099
17 p2587 A83-37277

The first astrolabe catalogue at Valinhos
17 p2587 A83-37281

WSRT radio observations at 1.4 GHz of 22 Abell clusters of distance class 5
17 p2587 A83-37282

Investigation of the systematic errors of the Belgrade NPZT and AGK3 catalogues
17 p2587 A83-37285

A catalog of high accuracy circular polarization measurements
17 p2591 A83-37830

An assessment of the completeness and correctness of the Abell catalogue
17 p2606 A83-38235

Photometric boxes in the four-color system
17 p2594 A83-38410

Near infrared observations of some of the IRC sources
18 p2754 A83-39201

The Mount Wilson halo mapping project
18 p2758 A83-39666

Catalog of magnetic field measurements --- of stars
19 p2910 A83-41068

Analysis of the Konus catalog of gamma-ray bursts with the thermal synchrotron model
20 p3073 A83-43069

Positions of minor planets. II
20 p3061 A83-43384

Radial velocities of planetary nebulae
21 p3222 A83-44113

A catalogue of extragalactic radio source identifications
21 p3225 A83-44978

Meridian observations made with the Carlsberg Automatic Meridian Circle at Brorfelde (Copenhagen University Observatory) 1981-1982
21 p3225 A83-44979

A catalogue of late-type supergiant stars in the Small Magellanic Cloud
21 p3226 A83-44981

JPL pulsar timing observations. II - Geocentric arrival times
22 p3372 A83-46266

Survey of the astrophysical catalogue from 1 to 31 degrees of northern declination
22 p3373 A83-46386

Very large spiral galaxies
22 p3374 A83-46540

Galaxy groups - Correlations between luminosities, velocity dispersions, and virial radii
23 p3519 A83-47456

Calculations of comet orbits from observations of 1980/81
23 p3517 A83-48064

Identification of the coordinates of a transient gamma-ray source with star-catalog coordinates
23 p3517 A83-48410

Atlas of main-line OH masers in the galactic longitude range 3 to 60 deg
24 p3638 A83-48986

New and misclassified planetary nebulae
24 p3638 A83-49128

Geometrical analysis of catalogs of galaxies
24 p3640 A83-49168

Micrometer measurements of visual binaries
24 p3642 A83-49315

381 astrometric positions of minor planets obtained at the GPO telescope of ESO, La Silla, February/March, 1981
24 p3642 A83-49316

Four-colour uvby and H-beta photometry of A5 to G0 stars brighter than 8.3 m
24 p3642 A83-49317

A catalogue of Jovian radio observations from January 1980 to December 1981
24 p3672 A83-49318

Four-colour photometry of eclipsing binaries. XVI - Light curves of VV Pyxidis
24 p3642 A83-49319

Four-colour photometry of eclipsing binaries. XVII - Light curves of DM Virginis
24 p3642 A83-49320

Catalogue of non stellar molecular maser sources and their probable infrared counterparts in the galactic plane
24 p3642 A83-49321

Positions of asteroids obtained with the CERGA Schmidt telescope
24 p3643 A83-49323

A photoelectric UBV catalogue of 610 stars in Puppis
24 p3643 A83-49367

A second catalog of the profile of the H-alpha line in 55 Be stars
24 p3645 A83-49839

Standard photometric diameters of galaxies
24 p3645 A83-49842

Galaxies rotation curves - A catalogue
24 p3645 A83-49845

VBLUW photometry of the open cluster NGC 2516
24 p3645 A83-49850

Micrometric measurements of binary stars (first list)
24 p3646 A83-49852

New binary stars (18th series) discovered at Nice
24 p3646 A83-49853

Environmental effects on the flattening distribution of galaxies
24 p3664 A83-49880

Trigonometric parallaxes for Southern Hemisphere stars
24 p3646 A83-49887

Progress report on the Second Cape Photographic Catalogue (CP2)
24 p3647 A83-50008

A catalogue of photometric sequences (suppl. 3) --- for astronomical photograph calibration
24 p3647 A83-50010

Galactic gamma radiation - The contribution from discrete sources
24 p3675 A83-50080

ASTRONOMICAL COORDINATES

Towards a new scale of extragalactic distances
01 p0118 A83-11337

ASCORECORD 3 DP two-coordinate measuring instrument in the service of the European Fireball Programme
02 p0183 A83-13046

The distribution of relative distances of double galaxies
03 p0426 A83-14693

Concerning a method for the determination of initial geodetic data
05 p0664 A83-17679

Positions of asteroids /1981/. II
07 p1006 A83-20562

Minor planet positions obtained at Cerro Calan Observatory during 1978-1980
07 p1006 A83-20567

Orientation of the FK 4 coordinates from the Washington observations of the sun and planets
07 p1007 A83-20673

Santiago 67 Catalogue - Catalogue of 7610 stars declination zone -25 deg to -47 deg equinox 1950.0
09 p1353 A83-23900

Gravitational three-body problem in 120 deg axial coordinates
09 p1339 A83-24437

Results of observations made with the Astrolabe of Santiago from 1977 to 1980
09 p1354 A83-24516

Estimation of reddening at low galactic latitudes from the Lick galaxy counts
09 p1363 A83-24990

Precise optical positions for radio/optical astrometric sources in the southern hemisphere
10 p1493 A83-25654

Coordinate systems --- of Jupiter
10 p1497 A83-26624

The exact positions of certain minor planets
10 p1498 A83-26910

Construction of continuous Chebyshev approximations for planetary coordinates
11 p1673 A83-28037

Certain problems in the construction of a reference celestial coordinate system
11 p1674 A83-28051

Report of the IAU working group on cartographic coordinates and rotational elements of the planets and satellites - 1982
12 p1787 A83-29119

Catalogue of 20457 star positions obtained by photography in the declination zone -48 deg to -54 deg (1950)
12 p1788 A83-29185

On the choice of the equatorial coordinates of celestial bodies from computer printouts during the calculation of their azimuths
12 p1706 A83-29322

Two newly discovered S stars in a list of faint red objects
12 p1797 A83-29953

Positions of bright stars --- Russian book
13 p1936 A83-30625

Method for automatic compensation of geometrical distortions in astronomical television equipment
13 p1919 A83-30869

Selenodetic network of reference points for the far side of the moon
13 p1961 A83-31099

Optical positions of quasars
13 p1942 A83-31710

The effect of the existence of a single coordinate system of curvature on the properties of the boundary between the R and T regions and the energy-momentum tensor --- in stellar gravitational collapse
14 p2102 A83-32131

Block adjustment in photographic astrometry
14 p2100 A83-33253

A proper motion survey in the area of the galactic cluster in Coma Berenices
14 p2100 A83-33255

An analysis of coordinate transformation in Schmidt telescope photographic plates
14 p2100 A83-33256

A catalog and identification charts of the Pleiades flare stars
15 p2244 A83-33751

Radio observations of interacting galaxies NGC 7714 (Markarian 538) - NGC 7715 (ARP 284, VV 51), and Radio quasar UB1
15 p2269 A83-34678

The problem of determining the orientations of coordinate systems and the periodic errors of star catalogs from ground-based optical observations
15 p2249 A83-34773

Sanduleak-Pesch's twin white dwarf object
16 p2433 A83-36702

On the catalog of star positions in the NPZT program --- Northern photographic zenith tube
16 p2426 A83-36858

Variances and correlations of errors of rectangular coordinates of selenodetic reference points
16 p2439 A83-36859

Accuracy of the external orientation of a selenodetic coordinate system
16 p2439 A83-36860

Determination of the orientation angles of a selenodetic coordinate system on the basis of photographic positional observations of the moon
16 p2439 A83-36861

Optical identifications of Parkes radio sources using UK Schmidt plates
17 p2593 A83-38253

Optically-selected quasar candidates in a field containing the South Galactic Pole
17 p2593 A83-38254

Determination of the coordinates of sources of solar radio bursts in the conical scanning mode
17 p2628 A83-38976

Proper motions of Herbig-Haro objects. III - HH-7 through -11, HH-12, and HH-32
18 p2757 A83-39603

Positions, magnitudes, and colors for stars in the globular cluster M92
19 p2910 A83-41053

Time and latitude results of observations made at Merate Observatory with the astrolabe for the year 1982
19 p2910 A83-41058

- A faint star astrometric grid for the galactic center
20 p3058 A83-42199
- Positions of stars in regions of 14 southern galactic clusters
21 p3225 A83-44976
- Orientation of geodetic networks by gyro azimuths
22 p3316 A83-46345
- Determination of the coordinates of transient gamma-ray sources on the basis of delays in the passage of transients at various points of space
23 p3517 A83-48409
- Identification of the coordinates of a transient gamma-ray source with star-catalog coordinates
23 p3517 A83-48410
- The alternative derivation of the precessional influence on equatorial star coordinates
24 p3644 A83-49603
- ### ASTRONOMICAL MAPS
- The new catalogue of optical HII-regions
01 p0115 A83-10163
- Mapping the Local Supercluster
01 p0115 A83-10206
- High dynamic range mapping of strong radio sources, with application to 3C84
01 p0115 A83-10208
- Extended and anisotropic high-velocity gas flows in the Orion-KL region
01 p0125 A83-10930
- The far-infrared disk of M51
02 p0250 A83-11581
- Detection of bipolar CO outflow in Orion
02 p0253 A83-11617
- MERLIN observations of superluminal radio sources --- Multi Element Radio Linked Interferometer Network
02 p0245 A83-11621
- The Clark Lake Teepee-Tee telescope
02 p0246 A83-11995
- Further morphological studies of QSOs
02 p0246 A83-12107
- A photometric map of interstellar reddening within 300 parsecs
03 p0406 A83-13552
- Mapping of iron and chromium on the surface of the Ap star Epsilon Ursae Majoris
03 p0418 A83-13880
- Confirmation of a conspiracy - Dual-band VLBI maps of the flat-spectrum radio source 2021 + 614
03 p0425 A83-14217
- The distribution of neutral atomic hydrogen in our galaxy beyond the solar circle
04 p0552 A83-15613
- Surface photometry of the H II region - S254-S257
04 p0547 A83-15962
- MERLIN observations of compact sources with very steep radio spectra
06 p0825 A83-18082
- A 2.2-micron map of NGC 5128
06 p0827 A83-18171
- The radio structure of 3C303 at 408 MHz
06 p0828 A83-18182
- The unprecedented light variations of NGC 2346
06 p0829 A83-18527
- Neutral hydrogen in two extremely isolated galaxies
06 p0829 A83-18534
- A photometric map of interstellar reddening within 100 PC
06 p0820 A83-18863
- A high-resolution 2.2 micron polarization map of OH 0739-14
07 p1007 A83-20934
- Asymmetric structure in the nuclei of NGC 1275 and 3C 345
07 p1020 A83-21110
- Ansaе and the precession of central stars in planetary nebulae - The cases of NGC 5189 and NGC 6826
07 p1008 A83-21208
- A radio continuum survey of M31 at 4850 MHz. I - Observations - List of sources
07 p1008 A83-21220
- High density molecular gas in the Rho Ophiuchi cloud
07 p1024 A83-21221
- The exciting stars of Herbig-Haro objects
08 p1183 A83-23056
- Further observations of radio sources from the BG survey. II - Mainly extragalactic
08 p1176 A83-23109
- A complete sample of intermediate-strength radio sources selected from the GB/GB2 1400-MHz surveys. III - High-resolution observations and optical identifications of sources with normal or flat spectra
09 p1351 A83-23315
- Radioastronomy measurement and reduction procedures for the detection of extensive continuum emission
09 p1352 A83-23390
- Reconstruction of a polarized brightness distribution by the maximum entropy method --- for astronomical maps
09 p1354 A83-24479
- The kinematics of the Ori A SO emission zone
09 p1363 A83-24996
- The arc second radio structure of 12 BL Lacertae objects
10 p1493 A83-25702
- The mass of Tycho's supernova remnant as determined from a high-resolution X-ray map
10 p1504 A83-25725
- Sensitive mapping of E and S0 galaxies in search of H I content differences between supernovae and non-supernovae producing galaxies
11 p1668 A83-27104
- H II regions in M33. I - Radio and H-alpha observations of the H II complex NGC595
11 p1669 A83-27679
- J = 2-1 CO and H2O observations of the molecular cloud G35.2-0.74
11 p1682 A83-28288
- Report of the IAU working group on cartographic coordinates and rotational elements of the planets and satellites - 1982
12 p1787 A83-29119
- Atlas of photometric standards of stellar fields --- Russian book
12 p1788 A83-29334
- 1733-565 - A compact radio galaxy at low galactic latitude
13 p1946 A83-30390
- Radio maps revealing shell structures in five supernova remnants
13 p1942 A83-31686
- High-resolution X-ray and radio maps of the millisecond pulsar
14 p2102 A83-31918
- The Cancer Cluster - An unbound collection of groups
14 p2098 A83-33181
- Ring ejection in type II supernovae - IE 0102.2-7219 in the small magellanic cloud
14 p2106 A83-33226
- Fine structure in high velocity clouds
14 p2109 A83-33274
- A catalog and identification charts of the Pleiades flare stars
15 p2244 A83-33751
- Catalog of H-alpha emission stars in the region of the Orion Nebula
15 p2244 A83-33752
- Global fringe search techniques for VLBI
15 p2245 A83-33839
- IR maps of M17 in the forbidden O III 88 micron and 52 micron lines and forbidden N III 57 micron line measurements
15 p2245 A83-34098
- Near-infrared spectroscopy and monochromatic isophotometry of NGC 6302
15 p2248 A83-34586
- The radio structure of Sgr A
16 p2431 A83-36676
- Multifrequency WSRT observations of the radio galaxy 3C 31 --- Westerbork Synthesis Radio Telescope
16 p2426 A83-36699
- WSRT radio observations at 1.4 GHz of 22 Abell clusters of distance class 5
17 p2587 A83-37282
- A rotating protocluster in W58 - HCO(+) aperture synthesis maps
17 p2597 A83-37317
- Are wide-angle radio-tail QSOs members of clusters of galaxies? I - VLA maps at 20 cm of 117 radio quasars
17 p2602 A83-37777
- Radio observations of the SNR Puppis A
17 p2593 A83-38245
- Studies of A and F stars in the region of the North Galactic Pole. V - Interstellar reddening and the uvby-beta intrinsic colour calibration
17 p2593 A83-38246
- Optical identifications of Parkes radio sources using UK Schmidt plates
17 p2593 A83-38253
- Radio observations of compact H II regions
18 p2757 A83-39594
- The Mount Wilson halo mapping project
18 p2758 A83-39666
- Molecular clouds in Orion and Monoceros
18 p2771 A83-39701
- Synthesis maps of millimeter molecular lines
18 p2758 A83-39714
- Mapping and imaging of the galactic centre in the near infrared
19 p2909 A83-40689
- Clumping in Orion KL - 2-arcsecond maps of ammonia
20 p3065 A83-42380
- The spectral and spatial distribution of radiation from Eta Carinae. III - A high-resolution 2.2 micron map and morphological considerations of the evolutionary status
20 p3067 A83-42441
- Far-infrared and submillimeter observations of stellar radiative and wind heating in S140 IRS
20 p3072 A83-43056
- Synthesis maps of ultraviolet observations of neutral interstellar gas
20 p3073 A83-43084
- Position angle variation of the major axis of some galaxies
20 p3061 A83-43378
- H2 densities and masses of the molecular clouds close to the galactic center
21 p3231 A83-44452
- The Cerro El Roble sample of faint ultraviolet excess objects in the South Galactic Pole
22 p3372 A83-46379
- A new radio map of the AD 1006 supernova remnant, G327.6 + 14.6
22 p3374 A83-46542
- Electronographic polarimetry - The Durham polarimeter
22 p3291 A83-46562
- VLBI maps of 3C 273 and 3C 345 at 2.3 GHz
22 p3376 A83-46972
- Large-scale radio structures of superluminal sources
23 p3526 A83-47870
- Radio observations of planetary nebulae
24 p3639 A83-49131
- High resolution maps with the VLA
24 p3639 A83-49132
- A high resolution HI survey of M31
24 p3640 A83-49204
- Ammonia observations of the Herbig-Haro objects
24 p3658 A83-49359
- ### ASTRONOMICAL MODELS
- #### NT DENSITY WAVE MODEL
- #### NT STELLAR MODELS
- Inhomogeneous cosmological models containing homogeneous inner hypersurface geometry - Changes of the Bianchi type
01 p0119 A83-10263
- Numerical values of fundamental constants and the anthropocentric principle --- universe models
01 p0113 A83-10824
- Topology of cosmological models near critical points
01 p0125 A83-10907
- Radio measurements in the fields of gamma-ray sources. I - CG 195 + 04
01 p0117 A83-10949
- Reflections on the formation of galaxies in the frame of Lemaitre's cosmology
01 p0127 A83-11289
- Theoretical models of the mass spectrum of interstellar clouds
02 p0251 A83-11587
- X-ray nebular models
02 p0253 A83-11992
- The halos of rich clusters of galaxies. I - An infall model for the Coma Cluster
02 p0254 A83-12102
- Stellar populations in the Galaxy
02 p0258 A83-12179
- Dynamics of elliptical galaxies and other spheroidal components
02 p0246 A83-12189
- Gravitation, phase transitions, and the big bang
02 p0259 A83-12220
- Dynamic coma models for comet Bennett 1970 II
02 p0247 A83-12530
- 3D models for self-gravitating, rotating magnetic interstellar clouds
02 p0260 A83-12537
- On the origin of the globular cluster system of M87
02 p0261 A83-12909
- Physical processes in jets from active galaxies
03 p0412 A83-13151
- The gravitational evolution of structure in a scale-free universe
03 p0412 A83-13301
- A model of the Cygnus Loop
03 p0413 A83-13322
- Inference of nebular density and luminosity structure from polarization maps
03 p0414 A83-13328
- A survey of the bright galactic bulge X-ray sources
03 p0414 A83-13331
- The infrared spectral properties of frozen volatiles --- in cometary nuclei
03 p0415 A83-13381
- Structure and origin of cometary nuclei
03 p0415 A83-13382
- Dynamical history of the Oort Cloud
03 p0403 A83-13400
- Conference on Mathematical Methods in Celestial Mechanics, 7th, Oberwolfach, West Germany, August 24-28, 1981, Proceedings
03 p0404 A83-13405
- Asymptotic breaking and restoration of symmetry in a statistical system of particles with short-range vector interaction and isotropic cosmological models
03 p0417 A83-13533
- Far-infrared spectrophotometry of Saturn and its rings
03 p0133 A83-13828
- Io - A volcanic flow model for the hot spot emission spectrum and a thermostatic mechanism
03 p0133 A83-13833
- On the history of the lunar orbit
03 p0407 A83-13837
- Hydrodynamical models of presolar nebula formation
03 p0418 A83-13838
- A theoretical study of Comet Halley's spectrum in the infrared range
03 p0407 A83-13841
- The dynamical destruction of shocked gas clouds
03 p0419 A83-13928
- Dissipationless galaxy formation and the r to the 1/4-power law
03 p0420 A83-13935
- A mass estimate for the companion to the 'Cartwheel' galaxy
03 p0421 A83-13953
- Relativistic precessing jets in quasars and radio galaxies - Models to fit high resolution data
03 p0422 A83-14183
- A thermal wind model for the broad emission line region of quasars
03 p0423 A83-14184
- The equivalence of the short periods measured in the spectrum of SS 433
03 p0424 A83-14205
- Secondary electron spectra in interstellar clouds, and the bremsstrahlung gamma-ray luminosity
03 p0439 A83-14211
- Transonic accretion flow in a thin disk around a black hole
03 p0427 A83-14713
- Transonic disk accretion of barytropic gas onto black holes
03 p0427 A83-14714
- Dynamical evolution of globular clusters. I
03 p0427 A83-14718
- Massive neutrino halos in an expanding universe
03 p0427 A83-14754
- Perturbation of the magnitude-redshift relation in an inhomogeneous relativistic model. II - Correction to the Hubble law behind clusters
03 p0427 A83-14758
- Terrestrial O2 lines used as wavelength references - Comparison of measurements and model computations
03 p0428 A83-14771
- Galactic neutrino models
03 p0429 A83-14778
- A model for interstellar extinction
04 p0548 A83-14979

A semiquantitative general-relativistic model of quasar Markarian 205 interpreted as a massive black hole ejected from NGC 4319 04 p0549 A83-14989

The crust of Venus - Theoretical models of chemical and mineral composition 04 p0559 A83-15327

A finite temperature λ -phi-4 model and a de Sitter-Friedmann transition in the early universe 04 p0551 A83-15597

Evolution of the size of components of class D II radio sources 04 p0551 A83-15598

Space-time curvature and cosmology 04 p0555 A83-15707

Multisheet models of the universe 04 p0555 A83-15901

A radial velocity survey of the H II region S101 04 p0556 A83-15952

Nucleosynthesis in bouncing cosmologies 04 p0557 A83-15977

Steady-state versus viscous cosmology 04 p0557 A83-15983

Structure and thermal evolution of the Galilean satellites 04 p0570 A83-16229

Giant voids in the universe 05 p0695 A83-16845

Are there black holes in quasars 05 p0696 A83-16862

Charged relativistic spheres 05 p0683 A83-16901

Formation of the Galilean satellites in a gaseous nebula 05 p0703 A83-16957

Mass-radius relationships in icy satellites after Voyager 05 p0703 A83-16958

Internal stresses in Phobos and other triaxial bodies 05 p0704 A83-16965

Dynamical models and our Virgocentric deviation from Hubble flow 05 p0696 A83-16976

The curvature of radio jets and tails in the intracuster media of Abell 1446 and 2220 05 p0696 A83-16981

On 'hot spots' and the question of very narrow collimation of radio jets 05 p0697 A83-16984

Triaxial equilibrium models for elliptical galaxies with slow figure rotation 05 p0697 A83-16987

Dynamo action in a supermassive rotator and the active galactic nuclei 05 p0697 A83-16988

The warping of disk galaxies. I - Theory 05 p0697 A83-16992

Comparison of gas dynamic model with steady solar wind flow around Venus 05 p0704 A83-17383

Formation of Jovian decametric S bursts by modulated electron streams 05 p0705 A83-17387

Spatial-kinematical models for planetary nebulae - NGC 2371-2 05 p0701 A83-17671

Inhomogeneous cosmological models with flat slices generated from the Einstein-de Sitter universe 05 p0702 A83-17852

Cosmological testing of Mach's principle 05 p0703 A83-17859

Chaos in the mixmaster universe 05 p0703 A83-17937

Physical conditions in H II/OH maser regions 06 p0825 A83-18088

Stationary spherical accretion into black holes - The transition from the optically thin to the optically thick regime 06 p0825 A83-18089

Lifetime of spurs in galaxies 06 p0825 A83-18090

Common properties of clusters of galaxies containing radio halos and implications for models of radio halo formation 06 p0825 A83-18092

Gowdy three-handle and S/3/ inhomogeneous cosmological models 06 p0828 A83-18324

Fast coherent oscillations in variable X-ray sources and bursts 06 p0829 A83-18540

Disk accretion by dynamical friction - A model for the dynamical evolution of giant molecular clouds 06 p0832 A83-18836

A self-similar flow in generalized Roche model with increasing energy 06 p0833 A83-18878

Approximate method of solving problems of radiation transfer in a cold plasma with strong magnetic field 06 p0838 A83-19228

Relaxation and tidal stripping in rich clusters of galaxies. I - Evolution of the mass distribution 06 p0839 A83-19267

The propagation of ultraheavy cosmic ray nuclei 06 p0858 A83-19297

In search of the large-scale structure of the universe 06 p0841 A83-19418

Planetesimals to planets 06 p0842 A83-19461

Preferred orbit planes in the gravitational field of a tumbling spheroidal galaxy 06 p0843 A83-19480

A simple theory of how spiral galaxies acquire their principal global properties 06 p0843 A83-19483

Bubbles, jets, and clouds in active galactic nuclei 06 p0843 A83-19484

Stability limits for 'isothermal' cores in globular cluster models - Two-component systems 06 p0844 A83-19490

Thick accretion disks around black holes /Karl Schwarzschild Lecture 1981/ 06 p0846 A83-19529

The motions of the stars and their significance in galactic astronomy /Karl Schwarzschild Lecture 1982/ 06 p0824 A83-19532

The impulsive flux transfer solar flare model 07 p1037 A83-20036

Curves for analysis of the two lowest rotational transitions of carbon monoxide using the large velocity gradient radiative transfer model 07 p1013 A83-20133

Chemical compositions of planetary nebulae 07 p1013 A83-20134

The spatial distribution of H II regions in NGC 4321 07 p1020 A83-21111

The effects of induced star formation on the evolution of the galaxy. II - The galactic ecosystem 07 p1020 A83-21117

The gas-grain interaction in the interstellar medium - Thermal accommodation and trapping 07 p1021 A83-21120

Modeling of G333.6-0.2 as a spherical H II region 07 p1021 A83-21122

The planetary nebula IC 3568 - A model based on IUE observations 07 p1021 A83-21124

Large-amplitude hydromagnetic waves in collisionless relativistic plasma - Exact solution for the fast-mode magnetoacoustic wave 07 p1023 A83-21143

Effects of drift on the transport of cosmic rays. VI - A three-dimensional model including diffusion 07 p1040 A83-21153

Rapid variability in 3C273 at 1 mm 07 p1008 A83-21202

Structure of molecular clouds. VI - The accuracy of the standard analysis 07 p1023 A83-21210

The Re-187 - Os-187 chronology and chemical evolution of the Galaxy 07 p1024 A83-21214

SiO isotopy emission from Orion - A model for IRe2 07 p1025 A83-21244

Holes in cosmology 07 p1026 A83-21253

The Newtonian potentials and dynamics of a stratified ellipsoid --- study of elliptical galaxies 07 p1026 A83-21258

Comparison of the pulsational and lateral oscillation modes of a homogeneous spherical system 07 p1026 A83-21259

The Monte Carlo method for multilevel problems of radiation transfer with allowance for processes in the continuum --- for astronomical models 07 p1027 A83-21279

Supernova remnants in M31 08 p1179 A83-21851

Stellar axisymmetric space-times - A new approach 08 p1160 A83-22209

The large-scale structure of the universe 08 p1181 A83-22686

Formation of complex molecules in TMC-1 --- Taurus Molecular Cloud 08 p1186 A83-23274

Trail of the Crab progenitor star 08 p1187 A83-23286

Cosmology --- theories and models of early universe 09 p1358 A83-23915

Pressure distribution at the inner boundary of an astropause caused by a compressible stellar wind 09 p1360 A83-24459

The O III/O II problem in medium and high excitation planetary nebulae 09 p1360 A83-24466

On the role of instabilities in unsteady-beam models of extended radio sources 09 p1362 A83-24982

A simple model for the distribution of light in spherical galaxies 09 p1363 A83-24988

Distribution of particle sizes which are formed in the process of modeling the ablation of meteoric material 09 p1367 A83-25281

Orbital evolution of the Galilean satellites - Capture into resonance 10 p1492 A83-25510

Anisotropic velocity dispersions in spherical galaxies 10 p1502 A83-25705

Cosmological constant and absence of particle creation 10 p1505 A83-25799

A mathematical model of solar flares 10 p1521 A83-25872

Models of massive black holes in the active galactic nuclei 10 p1507 A83-26231

The dynamics and fueling of active nuclei 10 p1508 A83-26359

The role of the gas in propagating star formation 10 p1508 A83-26363

A wind and shock model for active galactic nuclei 10 p1511 A83-26401

Far-ultraviolet diffuse emission lines from the interstellar medium 10 p1511 A83-26406

Magnetospheric models --- Jovian phenomena 10 p1520 A83-26621

Modeling of steady, rotational, transonic winds from rotating stars and galaxies 10 p1512 A83-26708

Comptonization effects in spherical accretion onto black holes 10 p1515 A83-26739

Propagation of solar disturbances - Theories and models 11 p1687 A83-27382

IMF control of the earth's magnetosphere 11 p1614 A83-27390

160-min oscillations of the sun as the mean of study of its internal structure 11 p1689 A83-27643

Mass scales in a universe of dust and blackbody radiation 11 p1679 A83-27989

Intergalactic and galactic magnetic fields - An updated test 11 p1679 A83-27990

Relation of the B sub z component of the interplanetary magnetic field to the generation of the semi-annual wave in Kp-indices 11 p1616 A83-28106

Evolution toward equipartition in galaxy clusters and its effect on virial M/L estimates 11 p1681 A83-28271

Time-dependence of the infrared spectra of nova dust shells 11 p1681 A83-28277

Evolution of accretion tori orbiting black holes. I - Theory 11 p1682 A83-28281

Why weakly non-linear effects are small in a zero-pressure cosmology 11 p1682 A83-28283

Intrinsic principal axes twists in N-body models of elliptical galaxies 11 p1675 A83-28294

A multi-fluid model of an H₂O-dominated dusty cometary atmosphere 11 p1683 A83-28382

The evolution of the moon - A finite element approach 11 p1686 A83-28385

Active galaxies and the diffuse gamma-ray background 11 p1694 A83-28389

Observed radii and structural parameters of clusters in the SMC. II 12 p1784 A83-28870

The evolution of shear and gravitational wave perturbations of Friedmann models and the isotropy of the universe 12 p1790 A83-28889

Cosmic rays from binary neutron stars 12 p1800 A83-28983

On disk accretion --- in binary stars and black holes 12 p1791 A83-28986

Emden-Chandrasekhar axisymmetric, solid-body rotating polytropes. II - Power series solutions to EC associated equations of degree 0 and 2 12 p1793 A83-29070

Asymptotic freedom and entropy in a perpetually oscillating universe 12 p1794 A83-29166

The supersonic nozzles of the galaxies 12 p1795 A83-29364

Runaway instability in accretion disks orbiting black holes 12 p1795 A83-29449

Self-regulating star formation - The rate limit set by ionizing photons 12 p1796 A83-29544

Development of a numerical model of a cosmic radio source with a continuous mission spectrum 13 p1944 A83-30273

Numerical simulations of collapsing, isothermal, magnetic clouds 13 p1945 A83-30365

Loss of water from Venus. I - Hydrodynamic escape of hydrogen 13 p1961 A83-31209

The apparent superluminal motion of the fine-structure components of 3C 120 13 p1948 A83-31256

Solid particles in an early stage of evolution of a protoplanetary cloud 13 p1949 A83-31274

Stellar orbits in a triaxial galaxy. I - Orbits in the plane of rotation 13 p1950 A83-31411

The formation of disc galaxies 13 p1953 A83-31552

Roche's limit in a galaxy. II - The effects of rotation 13 p1953 A83-31558

The Crab Nebula 13 p1953 A83-31563

Adiabatic density perturbations in a cosmological model with massive neutrinos 13 p1955 A83-31652

Thick disks with equatorial accretion. II 13 p1955 A83-31660

Core radii determination for eleven southern clusters of galaxies 13 p1955 A83-31665

The collapse of a fast rotating interstellar gas cloud 13 p1956 A83-31679

Stochastic effects in the chemical evolution of galaxies 13 p1956 A83-31687

The opacity of the universe and the strong equivalence principle 14 p2102 A83-32421

The weight, shape, and speed of the universe 14 p2103 A83-33049

Fragmentation of prestellar clouds by molecule formation 14 p2109 A83-33278

Ultraviolet spectrum of the planetary nebula NGC 7662 14 p2109 A83-33281

Observations and models 14 p2109 A83-33281

Light curves of some periodic comets 14 p2101 A83-33287

Statistical genesis of a lognormal distribution as a source of properties observed in the clumping of galaxies 15 p2253 A83-33703

Cosmological models with a quasistable de Sitter stage 15 p2253 A83-33705

- Nonlinear effects in a gravitating plasma disk subject to a poloidal magnetic field 15 p2254 A83-33721
- Black hole accretion - The quasar powerhouse 15 p2254 A83-33813
- An arbitrary-mesh computer program with applications to astrophysics 15 p2254 A83-33817
- Collisionless matter and galaxy formation 15 p2255 A83-33818
- Numerical solutions of high-frequency perturbations in Bianchi type IX models --- for formation of galaxies in homogeneous isotropic universe 15 p2255 A83-34079
- A note on the formation of clusters of galaxies 15 p2256 A83-34083
- The ultraviolet excess of luminous quasars. II - Evidence for massive accretion disks 15 p2256 A83-34085
- An exact viscous fluid FRW cosmology --- Friedmann-Robertson-Walker 15 p2261 A83-34491
- Density inhomogeneities and the deduced chemical composition of planetary nebulae 15 p2261 A83-34502
- Observations of the line profile of Paschen alpha in 3C 273 15 p2261 A83-34503
- Interstellar Ca II and Na I line profiles towards halo OB stars 15 p2264 A83-34585
- Tidal interactions of disc galaxies 15 p2266 A83-34607
- The infall of a star into a massive black hole 15 p2269 A83-34641
- Saturn's icy satellites - Thermal and structural models 15 p2275 A83-34722
- The stability of a rotating fluid cylinder as a figure of equilibrium --- as model for various celestial bodies 15 p2271 A83-34755
- Modelling the neutral gas environment of comets with special application to P/Halley 15 p2273 A83-35014
- Dust modelling of fast flyby missions - Implications of in situ measurements 15 p2128 A83-35022
- W-shaped occultation signatures - Inference of entwined particle orbits in charged planetary ringlets 16 p2435 A83-35729
- Collisional interactions of ring particles - The ballistic transport process --- in Saturn's rings 16 p2436 A83-35731
- Genetic relationship between the Taurid meteor swarm and comet Encke-Baklund 16 p2423 A83-35754
- On the spiral structure in the galactic distribution of CO clouds 16 p2428 A83-36541
- Models of the planetary nebulae II 2003, NGC 3242, 6210, and 7009 - Constraints on the ionizing radiation of the central star 16 p2431 A83-36669
- Onion-shell model of cosmic ray acceleration in supernova remnants 16 p2441 A83-36674
- A Keplerian method to estimate perturbations in the restricted three-body problem 16 p2426 A83-36785
- Internal motions in ten planetary nebulae 17 p2587 A83-37279
- Can secondary infall produce flat rotation curves? 17 p2596 A83-37314
- Simulation models for the evolution of cloud systems. I Introduction and preliminary simulations 17 p2596 A83-37315
- X-ray sources in molecular clouds 17 p2597 A83-37316
- Cyclic phase changes of interstellar medium 17 p2599 A83-37357
- Laboratory simulation of the interaction between the solar wind and Venus 17 p2618 A83-37429
- A model of the Crab nebula - The emission spectrum and the distribution of brightness 17 p2600 A83-37660
- The gravitational field and density distribution inside Mars 17 p2619 A83-37696
- The dynamics of rich clusters of galaxies. II - The Perseus cluster 17 p2591 A83-37776
- Instability of some black holes 17 p2605 A83-38047
- The Io-control of Jupiter's decametric radiation - The Alfven wave model 17 p2620 A83-38115
- Planetary rings - 2-2/3 centuries of nearly total ignorance, 4 years of information explosion 17 p2621 A83-38118
- The cometary atmosphere and its interaction with the solar wind 17 p2606 A83-38228
- An assessment of the completeness and correctness of the Abell catalogue 17 p2606 A83-38235
- Simulations of galaxy mergers. II 17 p2593 A83-38244
- Distance and model dependence of observational galaxy cluster concepts 17 p2610 A83-38427
- The dynamical role of a primordial electromagnetic field in spatially homogeneous, diagonal Bianchi type I-IX cosmologies 17 p2610 A83-38546
- The stability of a differentially rotating disk of stars 17 p2610 A83-38551
- Observable properties of non-axisymmetric galaxies. I Geometrical parameters 17 p2595 A83-38581
- The continuing case for a hierarchical cosmology 17 p2611 A83-38582
- A new model for barred spiral galaxies 17 p2611 A83-38588
- Why is M87 jet one sided in appearance? 17 p2612 A83-38599
- Shocks in spiral galaxies 17 p2612 A83-38828
- On the nonlinear theory for the stability of a rotating gravitating disk 17 p2614 A83-38848
- Entwined and parallel bundled orbits as alternative models for narrow planetary ringlets 17 p2624 A83-38947
- Cosmological models with S3 topology 17 p2614 A83-38951
- The central powerhouse of active galactic nuclei 18 p2766 A83-39249
- Dynamical role of magnetic field in radio jets 18 p2766 A83-39250
- Magnetic fields in galactic jets 18 p2766 A83-39251
- Galactic HII regions, anomalous 1720 MHz OH clouds and spiral structure in the Galaxy 18 p2769 A83-39653
- A model for the galaxy with rising rotational velocity 18 p2770 A83-39660
- Radial distribution of atomic and molecular hydrogen from propagating star formation 18 p2770 A83-39661
- Cloud-particle galactic gas dynamics and star formation 18 p2770 A83-39662
- A modal approach to spiral structure - Two examples --- of galaxy models 18 p2770 A83-39664
- Globular clusters and the distance to the galactic centre 18 p2771 A83-39668
- Globular clusters and the potential well of the Galaxy 18 p2771 A83-39669
- Orion's cloak as a model for supershells of gas around OB associations 18 p2771 A83-39702
- Quasi-stellar but nebular condensations in the core of the Orion Nebula 18 p2773 A83-39718
- A model for the emission spectrum of active galactic nuclei 18 p2774 A83-39740
- Dissipation of thick accretion disks 18 p2774 A83-39742
- Elliptical galaxies - Can rotation be effective in determining their shapes? 18 p2775 A83-39748
- Spatially self-similar cosmological model of Bianchi type-1(I) 18 p2775 A83-39749
- What is a spiral galaxy? 18 p2775 A83-39756
- The cosmological relevance of light element abundances 18 p2776 A83-39772
- Quantum gravity - A unified model of existence? 18 p2776 A83-39773
- Relativistic thermodynamics of irreversible processes in a static gravitational field; a theory of phenomenological heat conduction 18 p2777 A83-39780
- On the origin of the low-energy cosmic-ray antiprotons 18 p2787 A83-40491
- Triaxiality and the galactic center 19 p2913 A83-40700
- Comparison of galactic center with other galaxies 19 p2913 A83-40701
- Quiet starts for galaxy simulations 19 p2910 A83-40751
- Initial data for N black holes 19 p2915 A83-40888
- Compactification of Friedmann's hyperbolic model 19 p2915 A83-40978
- A charged black hole in a uniform magnetic field 19 p2916 A83-41306
- Frame dragging in Einstein and Einstein zero mass scalar cosmologies 19 p2916 A83-41307
- Beam models for radio sources. IV - Improved jet collimation 19 p2917 A83-41612
- Core collapse with strong encounters --- for celestial systems 19 p2920 A83-41636
- The wind instability of radio-galaxy clouds 19 p2921 A83-41819
- The molecular cloud-H II region complexes associated with Sh 90 and Sh 235 20 p3065 A83-42378
- Zero-curvature Friedmann-Robertson-Walker models as exact viscous magnetohydrodynamic cosmologies 20 p3066 A83-42428
- Dirac's large numbers hypothesis and continuous creation --- of universe 20 p3066 A83-42429
- Cometary globules in the Gum-Vela complex 20 p3069 A83-42783
- The quadrupole component of the relic radiation in a quasi-hyperbolic cosmological model 20 p3070 A83-42789
- Nonlinear evolution of large-scale structure in the universe 20 p3070 A83-43035
- The Riemann disks. I - Equilibrium and secular evolution 20 p3071 A83-43051
- The Riemann disks. II - Stability 20 p3071 A83-43052
- Analysis of the Konus catalog of gamma-ray bursts with the thermal synchrotron model 20 p3073 A83-43069
- Empirical indicators of the evolution of clusters of galaxies 20 p3074 A83-43131
- The rate of occurrence of dayside Pc 3,4 pulsations - The L-value dependence of the IMF cone angle effect 20 p3025 A83-43200
- The Markarian chain of galaxies in the constellation Virgo 20 p3075 A83-43387
- Magnitude-redshift relation in clusters, groups and pairs of galaxies 20 p3075 A83-43393
- Can population III stars generate primordial helium? 20 p3075 A83-43538
- A model of sporadic stellar wind increase of hard X-ray transient source 21 p3228 A83-44296
- Coronal and collisional - Radiative model of the plasma for the case of hydrogen glow discharge 21 p3212 A83-44353
- Structure of molecular clouds. VII - Energy balance in clouds with star formation (Type IIb) 21 p3229 A83-44417
- 3-D simulations of the collapse of nonspherical interstellar clouds 21 p3230 A83-44438
- Periodic orbits in elliptical galaxies 21 p3223 A83-44445
- Kinematical and chemical evolution of the galactic disc 21 p3233 A83-44754
- The quick convolution of galaxy profiles, with application to power-law intensity distributions 21 p3234 A83-44764
- Charged particle distributions in Jupiter's magnetosphere 22 p3384 A83-46028
- Detectability of globular cluster systems in distant galaxies 22 p3378 A83-46410
- Three-dimensional numerical model of the formation of large-scale structure in the Universe 22 p3378 A83-46539
- Asteroids and meteorites - Parent bodies and delivered samples 22 p3388 A83-47088
- Star-planet systems as progenitors of cataclysmic binaries Tidal effects 23 p3518 A83-47428
- Cosmic ray acceleration in supernova blast waves 23 p3518 A83-47436
- Special perturbations of rotating isothermal gas clouds with constant rotational velocity 23 p3519 A83-47451
- On the origin of low energy anomalous component of galactic cosmic rays 23 p3539 A83-47744
- The problem of the Grand Unification Theory --- in cosmology 23 p3503 A83-48058
- The cosmological problem as initial value problem on the observer's past light cone - Observations 23 p3526 A83-48059
- Some exact models for nonspherical collapse. I 24 p3651 A83-49096
- Some exact models for nonspherical collapse. II 24 p3651 A83-49097
- Ionization equilibrium in models of planetary nebulae 24 p3639 A83-49138
- Physical processes in nebular shells and the interpretation of nebular spectra 24 p3639 A83-49142
- Fast winds in planetary nebulae 24 p3652 A83-49149
- Evolution and mass distribution of central stars of planetary nebulae 24 p3652 A83-49152
- Rotation curve and mass model for the edge-on galaxy NGC 5907 24 p3641 A83-49211
- Vertical motion and the thickness of HI disks - Implications for galactic mass models 24 p3654 A83-49213
- Quasi-stationary spiral structure in galaxies 24 p3655 A83-49222
- Velocity structures in the vertical extensions of spiral arms 24 p3655 A83-49227
- Theories of warps --- in disk galaxies 24 p3656 A83-49233
- Instabilities of hot stellar discs 24 p3656 A83-49235
- Theoretical studies of gas flow in barred spirals galaxies 24 p3656 A83-49240
- Hydrodynamical models of offcentered barred spirals 24 p3657 A83-49244
- Formation of rings and lenses --- in disk galaxies 24 p3657 A83-49245
- Models of ellipticals and bulges 24 p3641 A83-49247
- The stability of axisymmetric galaxy models with anisotropic dispersions 24 p3641 A83-49248
- Scale-free models of elliptical galaxies 24 p3641 A83-49249
- New phenomena in triaxial stellar systems 24 p3641 A83-49250

- Kinematic modelling of NGC 3379 24 p3641 A83-49251
- Dust and gas in triaxial galaxies 24 p3657 A83-49255
- Simulations of galaxy mergers 24 p3642 A83-49259
- Hydrodynamic models of Herbig-Haro objects 24 p3658 A83-49358
- Time-dependent chemistry. I - Modelling of a static cloud --- in interstellar space 24 p3659 A83-49374
- Multiple scattering in the reflection nebula NGC 1999 and the nature of interstellar dust 24 p3659 A83-49376
- Inertia coefficient considerations and the structure of Jovian planets 24 p3672 A83-49396
- The cosmological evolution of general Bianchi models in the adiabatic regime 24 p3660 A83-49429
- Spectral observations and physical modeling of Sharpless 121 24 p3646 A83-49884
- Application of star count data to studies of galactic structure 24 p3664 A83-49885
- Galaxies in clusters - Alignments, formation from pancakes, and tidal forces 24 p3664 A83-49998
- The origin of the light elements - A quite complex problem --- primordial abundances in universe 24 p3664 A83-50031
- Primordial nucleosynthesis - A theorist's shopping list 24 p3665 A83-50032
- On the pregalactic He/H abundance ratio derived from planetary nebulae 24 p3667 A83-50054
- Structure of the cosmic microwave background 24 p3670 A83-50110
- Plane symmetric vacuum Bianchi type I cosmological model in Brans-Dicke theory 24 p3670 A83-50157
- ASTRONOMICAL NETHERLANDS SATELLITE**
- Absolute ultraviolet fluxes of elliptical galaxies as observed with the Astronomical Netherlands Satellite /ANS/ 03 p0415 A83-13363
- A readjustment of lumped coefficients from inclination of 1974-70A 04 p0451 A83-15102
- Observations of RR Lyrae with the ANS satellite 06 p0821 A83-19057
- Peculiar ultraviolet interstellar extinction 10 p1509 A83-26374
- ANS ultraviolet observations of dwarf Cepheids 12 p1797 A83-29958
- Diffuse light near Zeta Orionis and the Horsehead nebula, and anomalous extinction of HD 37903, as measured with the ANS 23 p3516 A83-47441

ASTRONOMICAL OBSERVATORIES

- NT GAMMA RAY OBSERVATORY**
- NT HEAO 01 p0124 A83-10846
- Experiences with the U.S. Naval Observatory glass circles --- for astrometric instruments 02 p0247 A83-12529
- Solar physics at the main astronomical observatory of the Ukrainian Academy of Sciences 02 p0270 A83-12581
- 15 years of astronomical research work with the 2-m reflecting telescope of the Ondrejov Observatory /CSSR/ 02 p0249 A83-13045
- The National Observatory of the Bulgarian People's Republic 02 p0249 A83-13047
- Inventory of major operational and planned ground-based astronomical telescopes of the countries represented in the European Science Foundation /second edition, 1982/ 03 p0402 A83-13357
- Groundbased infrared measurements using the AMOS/MOTIF facility 03 p0283 A83-13471
- Systematic effects in trigonometric parallaxes. III - Comparisons with spectroscopic and cluster parallaxes 06 p0818 A83-18169
- The ROSAT mission --- all-sky survey with imaging X-ray telescope 11 p1671 A83-27759
- The potential for far-infrared astronomy in Australia 13 p1936 A83-30399
- Fibre optic development at the AAO 13 p1936 A83-30400
- Status of the European Southern Observatory new technology telescope project 13 p1937 A83-30988
- Remote observing experiments at Kitt Peak National Observatory 13 p1939 A83-31005
- The photometric field error of the double wide-angle astrophotograph of the Main Astronomical Observatory of the Academy of Sciences of the Ukrainian Soviet Socialist Republic 14 p2095 A83-31843
- European Southern Observatory (ESO) coudechelle spectrometer 14 p2084 A83-32005

- European Southern Observatory (ESO) automatic prime focus camera and the general problem of remote control 14 p2018 A83-32027
- Summary of five missions at the ESO, La Silla - The discovery of 38 new asteroids with the large objective prism astrophotograph (GPO) 14 p2097 A83-32839
- Evaluating concave and convex aspherical mirrors with a T-shaped spherometer 17 p2580 A83-37691
- Color photography from Mauna Kea 17 p2595 A83-38616
- Sigma - A new gamma-ray space observatory with high angular resolution for 1985 and beyond --- Satellite d'Imagerie Gamma Monte sur Ariane 18 p2756 A83-39288
- Infrared astronomy at ESO 18 p2760 A83-40420
- Infrared instrumentation on Calar Alto --- mountain-based telescopes for photography 18 p2760 A83-40421
- The C.F.H. telescope as an infrared telescope 18 p2760 A83-40422
- The Tingo observatory --- infrared astronomy 18 p2760 A83-40423
- Astronomical capability of the U.K. infrared telescope 18 p2761 A83-40424
- The infrared photometer of the 2 m telescope at Pic du Midi Observatory 18 p2761 A83-40425
- The IR spectrophotometer for the Gornegrat telescope 18 p2761 A83-40428
- Reflective field optics for IR spectrophotometers 18 p2744 A83-40429
- A cooled grating spectrometer for Tingo 18 p2690 A83-40430
- Irspex --- cooled grating array IR spectrometer for use with New Technology Telescope 18 p2690 A83-40431
- IFU - A multi-detector IR spectrometer 18 p2690 A83-40432
- ASTROPLANE - A European airborne observatory for infrared astronomy 18 p2762 A83-40455
- ASTROPLANE - A working group of the European Science Foundation 18 p2762 A83-40457
- New concept for a guide star tracker [AIAA PAPER 83-2288] 19 p2818 A83-41748
- Low light level detectors in astronomy --- Book 21 p3226 A83-45095
- Mauna Loa sky conditions - Bench mark and present 22 p3374 A83-46408

ASTRONOMICAL PHOTOGRAPHY

- System software approaches to the analysis of multidimensional data structures 01 p0090 A83-10137
- Retrieval of astronomical information from Padova-Asiago Observatory plates archives 01 p0114 A83-10154
- Large scale photometric surveys using archival plates --- obtained from astronomical photography 01 p0114 A83-10155
- Photographic observations of supernova 1979c in NGC 4321 01 p0116 A83-10237
- Galactic clusters 01 p0124 A83-10569
- Precise optical positions of radio sources in the FK 4-system. II - Results from 28 sources on the northern hemisphere and a preliminary comparison of the optical-radio reference frame 01 p0117 A83-10937
- Accurate optical positions of M 82 knots 01 p0118 A83-10954
- Improved orbital elements for periodic comet Schorr /1918 III/ 02 p0247 A83-12536
- Detection and study of secondary structures in some planetary nebulae 02 p0247 A83-12545
- Astronomical observations with the automatic camera for astrophysics from JENA 02 p0249 A83-13048
- Enhancement of astronomical images using digital filtration methods 03 p0407 A83-13672
- A note on the Delta Aurigid meteor stream 03 p0434 A83-13840
- A comparison of galaxy images on new and old POSS prints 03 p0409 A83-14137
- The relationships between morphological type and quantitative measures in the cluster environment 03 p0421 A83-14140
- Photographic surface photometry of the Milky Way. IV - The Northern Milky Way in the ultraviolet spectral region 03 p0430 A83-14798
- The width of echelle orders in IUE images as derived with the astronomical image display and analysis /AIDA/ system in Tuebingen 03 p0411 A83-14799
- Photographic photometry of galaxies using the INMP. I - The lenticulars NGC404 and NGC524 --- Interactive Numerical Mapping Package 04 p0546 A83-15046
- Observations of bipolar planetary nebula 19W32 04 p0551 A83-15050
- An interactive procedure to solve the background subtraction problems in IUE high resolution spectra - Application to the image SWP 4616 04 p0547 A83-15972

- Absolute proper motions of selected blue objects in the area of the galactic north pole 05 p0695 A83-17862
- The Pic-du-Midi 2 meter telescope - First observations of the planets 06 p0817 A83-18064
- Spectroscopic identification of white dwarfs in galactic clusters. II - NGC 2516 06 p0830 A83-18548
- A new search technique for M and C stars 06 p0820 A83-18862
- Observations of the Orion nebula in H-alpha, forbidden N II and H-beta lines 06 p0834 A83-18892
- Some properties of the centers of cD galaxies 06 p0821 A83-19052
- Photographic photometry of the eclipsing binary AD Bootes 06 p0822 A83-19173
- An electronic camera with a remotely controlled shutter at the primary focus of the 3.60 m C.F.H. telescope 06 p0822 A83-19192
- Modulated Multiple Slit Camera for improved localization of gamma ray bursts 07 p1005 A83-20038
- Photographic surface photometry of the Milky Way. I - Data and reduction methods 07 p1005 A83-20559
- Photographic surface photometry of the Milky Way. III - Photometry of the central area of the Galaxy in the ultraviolet 07 p1006 A83-20560
- Monochromatic photographs of the Cygnus Loop with a fiber-optics image intensifier 07 p1006 A83-20656
- Variable extragalactic objects - Identification and analysis of a complete sample to B = 21 07 p1007 A83-20938
- Correlation between albedo and polarization characteristics of the moon - Application of digital image processing 07 p1031 A83-21271
- New results of a study of the effect of photographic irradiation in photographic positional observations of the major planets 07 p1009 A83-21274
- Automated supernova search 08 p1173 A83-21844
- Automated supernova search from photographic plates 08 p1174 A83-21845
- Observing white-light flares [AD-A126041] 08 p1191 A83-22400
- Confirmation of the luminous connection between NGC 4319 and Markarian 205 08 p1184 A83-23079
- Comparison of infrared and optical positions for sources in the direction of the galactic center 09 p1351 A83-23318
- Occultations of stars by solar system objects. III - A photographic search for occultations of faint stars by selected asteroids 09 p1352 A83-23325
- Optical observations of the LMC H II region N 11 09 p1354 A83-24466
- NGC 6240 - A unique interacting galaxy 09 p1361 A83-24475
- The Cambridge photographic atlas of the planets --- Book 09 p1366 A83-24898
- Faint star studies in the Magellanic Clouds. I - RICHFLD photographic photometry in NGC 2257 10 p1493 A83-25708
- The rediscovery of Halley's comet 10 p1496 A83-26123
- CCD photometry of the center of M31 10 p1508 A83-26364
- The exact positions of certain minor planets 10 p1498 A83-26910
- Orbital elements of 44 bright meteors 10 p1498 A83-26913
- Complex of programs for the astrometric reduction of photographic observations 10 p1498 A83-26915
- An atlas of H II regions in 125 galaxies 11 p1668 A83-27107
- Photography in the Washington system --- observations of star cluster 11 p1669 A83-27119
- Infrared array detectors --- for astronomical observation 11 p1537 A83-27734
- Analysis of optical imagery for Seyfert's Sextet and VV 172 12 p1784 A83-28880
- Deep forbidden O III interference filter imagery of the supernova remnants G65.3+5.7, G126.2+1.6, CTA 1, and VRO 42.05.01 12 p1786 A83-29091
- Astrometric studies of ten double or suspected multiple systems from plates taken with the Sproul 61-cm refractor 12 p1788 A83-29184
- Catalogue of 20457 star positions obtained by photography in the declination zone -48 deg to -54 deg (1950) 12 p1788 A83-29185
- A CCD imager search for possible material orbiting Saturn between 10 and 36 Saturnian radii 12 p1788 A83-29187
- Evolution of the Venera 13 imagery 12 p1798 A83-29485
- A concentration of quasars in the Sculptor region of the sky 12 p1788 A83-29708
- On the possibility of discovering flare stars in their quiet state 13 p1943 A83-30004
- Uniformity of UKSTU photographic plates --- UK Schmidt Telescope Unit 13 p1936 A83-30397

- The medium dispersion prism of the UK Schmidt Telescope 13 p1936 A83-30398
- Method for automatic compensation of geometrical distortions in astronomical television equipment 13 p1919 A83-30869
- Conceptual design of a coherent optical system of modular imaging collectors (COSMIC) --- telescope array deployed by space shuttle in 1990's 13 p1938 A83-30996
- Deformable mirror with combined piezoelectric and electrostatic actuators 13 p1920 A83-31008
- A search for objects near the earth-moon Lagrangian points 13 p1939 A83-31206
- Morphological and physical study of planetary nebulae 13 p1942 A83-31580
- Continuation of the TV study of the Venus surface from descent modules 14 p1983 A83-31955
- The first color panoramic pictures of the Venus surface transmitted by the Venera 13, 14 probes 14 p2014 A83-31956
- Processing of panoramic TV pictures of the Venus surface transmitted by the Venera-13 and Venera-14 descent modules 14 p2014 A83-31957
- On dynamic phenomena recorded on panoramic pictures of the Venus surface transmitted by the Venera 13, 14 probes 14 p2014 A83-31958
- Instrumentation in astronomy IV; Proceedings of the Fourth Conference, Tucson, AZ, March 8-10, 1982 14 p2014 A83-31976
- Optimization of charge-coupled device (CCD) imager performance for astronomy 14 p2015 A83-31987
- Royal Greenwich Observatory (RGO) charge-coupled device (CCD) camera 14 p2015 A83-31988
- Development of a dual microchannel plate intensified charge-coupled device (CCD) speckle camera 14 p2015 A83-31991
- Drift scan observations with a charge-coupled device (CCD) 14 p2016 A83-31994
- Applications of an infrared charge-coupled device Schottky diode array in astronomical instrumentation 14 p2016 A83-31996
- New two-dimensional photon camera 14 p2018 A83-32021
- Wide Field and Planetary Camera for Space Telescope 14 p2018 A83-32025
- Microchannel intensified electrography 14 p2018 A83-32028
- Total eclipses and the solar environment 14 p2115 A83-32840
- Photographic observations of visual double stars 14 p2097 A83-33051
- Optical identification of radio sources in a 8.5 x 8.5 zone near the south galactic pole 14 p2099 A83-33239
- Block adjustment in photographic astrometry 14 p2100 A83-33253
- The combination of photographic material obtained with different Schmidt telescopes for the determination of proper motions 14 p2100 A83-33254
- A proper motion survey in the area of the galactic cluster in Coma Berenices 14 p2100 A83-33255
- An analysis of coordinate transformation in Schmidt telescope photographic plates 14 p2100 A83-33256
- Optical emission from ring-shaped nebulae in the LMC 14 p2110 A83-33283
- Possible outburst objects Hertzprung and Popovic 14 p2110 A83-33461
- The velocity field in the central region of the galaxy Markaryan 538 15 p2252 A83-33701
- The structure and evolution of a solar flare as observed in 3.5-30 keV X-rays 15 p2280 A83-34296
- Emission features in the solar corona after the perihelion passage of Comet 1979 XI 15 p2281 A83-34533
- Photographic photometry in globular clusters - Comparison of techniques 15 p2249 A83-34788
- Preparing for Halley's comet 15 p2250 A83-35319
- Automatic photoelectric device with a laser interferometer for measuring photographs of limbs of meridian instruments 16 p2357 A83-36863
- Direct evidence of type III electron streams propagating in coronal streamers 17 p2624 A83-37351
- TV photometric observations of 10 extragalactic peculiar objects 17 p2589 A83-37685
- Optical identifications of Parkes radio sources using UK Schmidt plates 17 p2593 A83-38253
- Color photography from Mauna Kea 17 p2595 A83-38616
- Isophotes of a field in the Cygnus Loop photographed in the forbidden O III and forbidden N II + H-alpha lines 17 p2613 A83-38832
- High-resolution photography of the solar chromosphere. XVI H-alpha contrast profiles of active region loops 18 p2781 A83-39026
- Broad-band, high-resolution photograph of the solar corona February 16, 1980 18 p2782 A83-39033
- Stars of low to intermediate mass in the Orion Nebula 18 p2772 A83-39707
- Distribution of QSOs around NGC 1097 18 p2760 A83-40365
- Infrared instrumentation on Calar Alto --- mountain-based telescopes for photography 18 p2760 A83-40421
- Photometry of the cataclysmic variable V426 Ophiuchi 18 p2763 A83-40479
- A comparison of several image processing techniques applied to photographically recorded astronomical spectra 19 p2909 A83-40715
- Balloon-borne imagery of the solar granulation. IV - The centre-to-limb variation of the intensity fluctuations 19 p2924 A83-40725
- Exploration of the nocturnal sky by photography from the Salyut space station 19 p2864 A83-40753
- Objective-prism discoveries in the northern sky. I 20 p3058 A83-42190
- Alignment of faint galaxy images - Cosmological distortion and rotation 20 p3070 A83-43036
- The IC 698 group of galaxies 20 p3071 A83-43039
- Observations of minor planets. II 20 p3061 A83-43391
- Planetary companions of stars 20 p3061 A83-43392
- Correction of spherochromatism in Schmidt cameras 21 p3139 A83-44809
- Spot sensitometer for astronomical use 21 p3139 A83-44810
- Shell structure in NGC 5128 22 p3372 A83-45627
- Effects of photon noise on speckle image reconstruction with the Knox-Thompson algorithm --- in astronomy 23 p3459 A83-48312
- Investigation of the characteristics of the PKT-26 telescope 24 p3638 A83-48956
- Optical features associated with the extended HI envelope of M83 24 p3641 A83-49212
- A high resolution study of the optical jet of M 87 24 p3661 A83-49456
- Photographic position observations of Venus at the Main Astronomical Observatory of the Ukrainian Academy of Sciences in 1975 24 p3644 A83-49628
- CCD astrometry. I - Preliminary results from the KPNO 4-m/CCD parallax program 24 p3646 A83-49886
- Parallaxes and proper motions. XVI 24 p3646 A83-49888
- Workshop on Astronomical Measuring Machines, Edinburgh, Scotland, September 28-30, 1982, Proceedings 24 p3647 A83-50001
- The automated detection of variable objects 24 p3647 A83-50005
- The detection of variable stars in the south galactic cap 24 p3647 A83-50006
- Progress report on the Second Cape Photographic Catalogue (CP2) 24 p3647 A83-50008
- A preliminary investigation of proper motions of faint stars in the Hazard 8hr region 24 p3647 A83-50009
- Evaluation of optimal parameters for photographic plate measurement and data reduction --- in astronomical photography 24 p3647 A83-50011
- Point spread functions from electronographic emulsions --- for astronomical photography 24 p3648 A83-50012
- A straightforward method to calibrate photographic data using stellar images 24 p3648 A83-50014
- The calibration of photographic plates using stellar images 24 p3648 A83-50015
- Internal calibration of astronomical photographs 24 p3648 A83-50016
- Galaxy redshifts from objective prism spectra 24 p3648 A83-50023
- Automated stellar photometry 24 p3649 A83-50029
- Variable stars in NGC 6397 24 p3649 A83-50153
- ASTRONOMICAL PHOTOMETRY**
- NT STELLAR SPECTROPHOTOMETRY
- Remote determination of cloud properties from solar photometric data 01 p0074 A83-10043
- Large scale photometric surveys using archival plates --- obtained from astronomical photography 01 p0114 A83-10155
- Geneva photometric boxes. IV - A refined method for direct access --- to stellar color data 01 p0115 A83-10159
- The three-channel photon-counting high-speed photometer of Beijing Observatory 01 p0048 A83-10230
- Galaxy photometry in the Virgo cluster. I 01 p0116 A83-10265
- Radial-velocity and photometric variations of o And - Critical evaluation of possible periods 01 p0122 A83-10339
- Photometric observations of active nuclei 01 p0124 A83-10840
- Multiaperture photometry of galaxies. II - Near-infrared observations of six isolated objects 01 p0117 A83-10940
- Photometric properties of Ap stars in the Geneva system 02 p0247 A83-12521
- Photographic surface photometry of the Milky Way. II - Surface photometry in the region of the dark cloud 'Coalsack' in U,B,V,R 02 p0247 A83-12524
- The eight-color asteroid survey - Standard stars 02 p0249 A83-12921
- An expedition to East Siberia to observe the total solar eclipse on 31 July 1981 02 p0249 A83-13049
- Electronographic photometry in the galactic cluster M 37 03 p0402 A83-13364
- Physical studies of asteroids. VIII - Photoelectric photometry of the asteroids 42, 48, 93, 105, 145 and 245 03 p0403 A83-13366
- UBV photometry of the M-type asteroids 16 Psyche and 22 Kalliope 03 p0403 A83-13371
- Spectrophotometry of comets at optical wavelengths 03 p0416 A83-13393
- Infrared camera for 10-micron astronomy 03 p0324 A83-13457
- Far-infrared spectrophotometer for astronomical observations 03 p0405 A83-13462
- A photometric map of interstellar reddening within 300 parsecs 03 p0406 A83-13552
- Object Kuwano, a novae-like /symbiotic/ binary with a red giant - Photometry and polarimetry 03 p0406 A83-13651
- The Shternberg stellar spectrophotometry - Detailed comparison with V-band and Johnson-Mitchell 13-color photometry 03 p0407 A83-13660
- Photometric characteristics of the night sky in the Crimea 03 p0407 A83-13673
- Infrared photometry of periodic comets Encke, Chernykh, Kearns-Kwee, Stephan-Oterma, and Tuttle 03 p0407 A83-13826
- Far-infrared spectrophotometry of Saturn and its rings 03 p0133 A83-13828
- Infrared photometry of HM Sagittae 03 p0408 A83-13891
- A photometric study of Pluto near perihelion. I - U,B,V photometry 03 p0408 A83-13895
- Corrections to fundamental constants from photoelectric observations of lunar occultations 03 p0409 A83-13939
- Two-color CCD observations of the galactic center region 03 p0409 A83-14190
- Brightness of the physical nucleus of a comet 03 p0426 A83-14679
- Classification of the results of the electrophotometry of artificial celestial bodies 03 p0286 A83-14684
- Absolute photometry of the Crab Nebula 03 p0411 A83-14793
- Photometric observations of CN Orionis 03 p0411 A83-14807
- Photographic photometry of galaxies using the INMP. I - The lenticulars NGC404 and NGC524 --- Interactive Numerical Mapping Package 04 p0546 A83-15046
- Properties and nature of Be and shell stars. II - A notable correlation between the long-term spectral and photometric variations of V 1294 Aql /HD 184 279/ 04 p0551 A83-15109
- Abrupt cutoffs in the optical-infrared spectra of nonthermal sources 04 p0552 A83-15607
- Optical bursts from 4U/MXB 1636-53 04 p0554 A83-15635
- Surface photometry of the H II region - S254-S257 04 p0547 A83-15962
- A microprocessor-controlled, integrating photometer 04 p0548 A83-16378
- Color photometry of surface features on Ganymede and Callisto 05 p0704 A83-16963
- Maps of the rings of Uranus at a wavelength of 2.2 microns 05 p0704 A83-16964
- Calibration of the radiometric asteroid scale using occultation diameters 05 p0704 A83-16969
- Photoelectric photometry of asteroids 33 Polyhymnia and 386 Siegena 05 p0693 A83-16970
- Intermediate band filter spectrophotometry of bright galaxies. II - Data reductions 05 p0694 A83-17663
- On the inner ring of HII regions in NGC 3351 05 p0701 A83-17669
- Dwarf galaxies in the M81/82 group - New photometric data 05 p0695 A83-17853
- Computer-controlled high-speed photometry, taking into account the example of the occultation of 57 Orionis by the moon. I 05 p0695 A83-17855
- Computer-controlled fast photometry as applied to the occultation of 57 Orionis by the moon. II 05 p0695 A83-17863
- Spectroscopic and photometric observations of six possible Seyfert galaxies 06 p0818 A83-18158
- Multiaperture infrared photometry of extragalactic radio sources 06 p0828 A83-18180

Spectrophotometry of the nucleus of the galaxy Arakelyan 144 06 p0831 A83-18792

Photometry of the supernova in NGC 4536 06 p0819 A83-18794

The eclipsing binary CV Serpentis - U, B, V, R photometry and properties of the Wolf-Rayet component 06 p0831 A83-18800

U, B, V photometry of nests of interacting galaxies 06 p0819 A83-18826

A study of the two-dimensional luminosity distribution of NGC 3379 06 p0833 A83-18855

The color and surface brightness of the Leo II dwarf galaxy 06 p0820 A83-18857

A photometric map of interstellar reddening within 100 PC 06 p0820 A83-18863

Theory of the light curves of eclipsing systems with oscillating components. II 06 p0834 A83-18884

On the possibility of cluster membership for the cepheid V Centauri 06 p0822 A83-19073

CCD photometry of Abell clusters. I - Magnitudes and redshifts for 84 brightest cluster galaxies 06 p0842 A83-19476

Astronomical photometry --- Book 07 p1004 A83-19924

Photographic surface photometry of the Milky Way. I - Data and reduction methods 07 p1005 A83-20559

DQ Cephei, a Delta Scuti star of constant variability 07 p1006 A83-20565

Seasonal light curves of TY UMa - Observations and solutions 07 p1006 A83-20568

Spectrophotometry of four galaxies of high surface brightness 07 p1007 A83-20665

Variable extragalactic objects - Identification and analysis of a complete sample to $B = 21$ 07 p1007 A83-20938

A simple and accurate on-line data acquisition program --- for astronomical photometry 07 p1007 A83-21039

Spectrophotometry of the broad absorption-line QSO PHL 5200 07 p1019 A83-21106

A search for globular clusters around the edge-on late-type spiral galaxy NGC 253 07 p1020 A83-21114

Abnormal extinction and dust properties in M 16, M 17, NGC 6357 and the Ophiuchus dark cloud 07 p1025 A83-21241

Empirical calibration of the RGU-system. I - Photoelectric realization of the system and definition of standard stars 07 p1009 A83-21248

Interpretation of integrated-disk photometry of Callisto and Ganymede 07 p1032 A83-21290

An optimist's guide to supernovae 08 p1176 A83-21828

Remote comets and related bodies - VJHK colorimetry and surface materials 08 p1181 A83-22926

Photometry of the unlit face of Saturn's rings 08 p1175 A83-22936

Infrared mapping and UBVR photometry of the spiral galaxy NGC 1566 08 p1175 A83-23033

Infrared photometry of the halo of M87 08 p1176 A83-23080

Photometry of Pluto during the 1982 opposition 09 p1352 A83-23322

Proportional counter with automatic gas gain control for use in the FH X-ray photometer /Satellite AUOS-S/ 09 p1267 A83-24017

A sealed high pressure xenon filled imaging proportional counter with a sensitive area 30cm square 09 p1268 A83-24109

Calibrated B, V surface photometry of X-ray cD galaxies 09 p1360 A83-24469

RGU photometry of a southern starfield near the galactic centre /SA 158/ 09 p1354 A83-24515

Size of a gamma-ray burster optical emitting region 09 p1361 A83-24697

CCD camera observations of nearby rich clusters. I - R photometry of brightest galaxies 09 p1355 A83-24998

Interpretation of whole-disk photometry of Phobos and Deimos 09 p1366 A83-25073

The reconstruction of images scattered in an inhomogeneous medium --- Russian book 09 p1270 A83-25224

Age and metal abundance of a globular cluster, as derived from Stromgren photometry 09 p1364 A83-25289

TAURUS - The imaging Fabry-Perot at La Silla 09 p1356 A83-25290

Four-colour photometry of some globular cluster giants in the Galaxy and the Magellanic Clouds 10 p1492 A83-25487

Rotation, mass and excitation of the spiral galaxy NGC 3893 10 p1502 A83-25655

Determination of parameters of W UMa systems. IV - BV Dra, BW Dra, EM Lac, SW Lac 10 p1493 A83-25656

Principal components analysis of spectral data. I - Methodology for spectral classification --- of A and F type stars 10 p1493 A83-25657

Near infrared photometry. I - Homogenization of near-infrared data from southern bright stars 10 p1493 A83-25659

RGU photometry in a field of the galactic bulge 10 p1493 A83-25662

Photometric studies of composite stellar systems. V - Infrared photometry of star clusters in the Magellanic clouds 10 p1494 A83-25710

The albedo of Uranus 10 p1494 A83-25735

Optical spectrophotometry of the nuclear region of M51. II - Further evidence for nuclear activity 10 p1496 A83-26361

CCD photometry of the center of M31 10 p1508 A83-26364

The extragalactic background light at 4400 A 10 p1511 A83-26400

Atmospheric trajectory, orbit, and photometric light curve of the fragmented meteor No. 770533 10 p1498 A83-26902

On the change of period and light curves of DS Aqr 10 p1516 A83-26904

Photoelectric observations of four classical cepheids 10 p1498 A83-26905

Dwarf novae: Observational results and their interpretation. I - Light variations; basic model of a cataclysmic binary; outburst models 11 p1676 A83-27125

Theoretical interpretation of the ground-based photometry of Saturn's B ring 11 p1683 A83-27352

Spatially resolved methane band photometry of Saturn. II - Cloud structure models at four latitudes 11 p1684 A83-27362

Spectrophotometry of Saturn and its rings from 60 to 180 microns 11 p1684 A83-27363

Eight-color photometry of Hyperion, Iapetus, and Phoebe 11 p1684 A83-27366

The surface brightness of spiral galaxies. I - Spheroidal components and Freeman's law 11 p1680 A83-28258

V388 Cygni - A binary system in the rapid phase of mass exchange 11 p1681 A83-28272

The infrared variability and nature of symbiotic stars. III - R Aquarii. IV - RX Puppis. V - Seven more systems 11 p1675 A83-28284

The infrared spectrum and variability of Eta Carinae 11 p1682 A83-28285

Laboratory simulation of photometric light curves of the asteroids 11 p1685 A83-28378

An investigation of the heavily reddened young open cluster Tr 27 on the Walraven photometric systems 12 p1784 A83-28862

The globular cluster NGC 6544 12 p1784 A83-28865

UBV photometry of FK4 and FK4 supplement stars 12 p1784 A83-28868

Rotation properties of the high-numbered asteroids 1236 Thais and 1317 Silvette 12 p1797 A83-28888

A re-analysis of the eclipsing binary system VV Orionis --- for UVB and uvby observations 12 p1792 A83-29052

Three years of photometry of IM Pegasi = HR 8703 12 p1785 A83-29054

On the evolution of the spiral galaxies in the Virgo cluster 12 p1794 A83-29177

Photometry of Cepheids in the LMC and Magellanic Cloud abundances 12 p1794 A83-29179

Photoelectric photometry of star clusters in M31. VIII 12 p1788 A83-29488

Detailed photometry of the Cepheid AD Geminorum 12 p1789 A83-29954

The brightness variations of asteroid 216 Kleopatra 13 p1960 A83-30380

Recent optical observations of the X-ray source HO139-68; an AM-Herculis type binary system 13 p1946 A83-30384

Photoelectric analysis of asteroid 216 Kleopatra Implications for its shape 13 p1961 A83-31207

The flare activity of V 780 Tau 13 p1941 A83-31555

A generalized algorithm for efficient photometric reductions 13 p1941 A83-31569

Astrometry and photometry of comet P/Halley in October and November 1982 13 p1943 A83-31727

The Gum Nebula - New photometric and spectrophotometric results 13 p1958 A83-31735

The field error and photometric system of the double long-focus astrograph of the Main Astronomical Observatory of the Academy of Sciences of the Ukrainian SSR 14 p2095 A83-31840

Superconducting bolometers in astronomical IR equipment. II Threshold sensitivity 14 p2014 A83-31842

The photometric field error of the double wide-angle astrograph of the Main Astronomical Observatory of the Academy of Sciences of the Ukrainian Soviet Socialist Republic 14 p2095 A83-31843

Instrumentation in astronomy IV; Proceedings of the Fourth Conference, Tucson, AZ, March 8-10, 1982 14 p2014 A83-31976

Single photon counters for the infrared 14 p2014 A83-31977

Charge-coupled device (CCD)/transit instrument (CTI) deep photometric and polarimetric survey - A progress report 14 p2016 A83-31993

Texas Instruments' virtual phase charge-coupled device (CCD) imager operated in the frontside electron-bombarded mode 14 p2016 A83-31995

Proposal for advanced infrared spectrophotometers 14 p2016 A83-31997

Low noise spectrometer for the daily measurement of solar chromospheric flux 14 p2017 A83-32007

Design of a four-channel simultaneous visual infrared photometer 14 p2096 A83-32030

Methods of photoelectric astrometry 14 p2096 A83-32032

Resolution classifier --- Bayesian approach for astronomical images 14 p2096 A83-32034

Analysis of synthesized dim galaxy images 14 p2096 A83-32035

Multi-temperature analysis of hard X-ray spectra measured aboard the Prognos 5 satellite --- for solar flares 14 p2114 A83-32394

Pole orientation of asteroid 44 Nysa via photometric astrometry, including a discussion of the method's application and its limitations 14 p2097 A83-32602

Asteroid rotation. IV 14 p2097 A83-32607

UBV photometry of the minor planets 86 Semele, 521 Brixia, 53 Kalypso and 113 Amalthaea 14 p2097 A83-33052

The variability of the optical counterparts of four extragalactic radio sources 14 p2103 A83-33059

The variation of dust temperatures in Maffei 2 14 p2106 A83-33225

Central condensations in Seyfert galaxies. I 15 p2253 A83-33712

Surface photometry of NGC 4656/4657 15 p2245 A83-33829

A search for stars physically associated with the 16-day Cepheid X Cygni. I - Luminous stars in the field 15 p2245 A83-33832

The Hyades CN anomaly? 15 p2245 A83-33837

CCD photometry of Abell clusters. II - Surface photometry of 249 cluster galaxies 15 p2255 A83-34077

Blue compact dwarf galaxies. II - Near-infrared studies and stellar populations 15 p2257 A83-34092

Color-magnitude photometry of 47 Tucanae to $M(V) = +9$ 15 p2260 A83-34127

Comparison between 'normal' double and single galaxies 15 p2246 A83-34445

Spectroscopy of upper-main-sequence and blue straggler stars in the intermediate-age cluster NGC 2477 15 p2246 A83-34501

Optical photometry with the Kuiper Airborne Observatory 15 p2247 A83-34509

A portable high-speed photometer. I - Photometer controller 15 p2164 A83-34510

DDO photometry and metallic abundances of E and SO galaxies and globular clusters of the LMC and SMC 15 p2262 A83-34534

DDO integrated photometry of globular clusters and initial chemical evolution of the galaxy 15 p2262 A83-34536

High speed photometry of the dwarf nova V2051 Ophiuchi 15 p2264 A83-34579

Two-colour photometry of a sample of faint galaxies 15 p2248 A83-34606

NGC 1275 - A burgeoning elliptical galaxy 15 p2267 A83-34622

Synthesized colors and spectra for galaxies of normal chemical composition 15 p2270 A83-34753

Photographic photometry in globular clusters - Comparison of techniques 15 p2249 A83-34788

Comet West 1976 VI - Photopolarimetry by the Helios 2 Zodiacal Light Experiment 15 p2249 A83-35020

Surface photometry of edge-on galaxies. III - Luminosity distributions in eight galaxies 16 p2422 A83-35676

Results of astrophysical investigations of asteroids (survey) I 16 p2437 A83-35751

Phase functions of atmosphereless bodies of the solar system 16 p2437 A83-35752

Light curve variation and period changes of VW Cep 16 p2428 A83-36530

Photometry, kinematics, and dynamics of the barred spiral galaxy NGC 5383 16 p2430 A83-36649

Contribution to the reduction of photoelectric occultation observations using an integrated deconvolution method 16 p2425 A83-36651

The Beta Cephei eclipsing binary system 16 Lacertae 16 p2432 A83-36682

2 Pallas pole revisited 16 p2426 A83-36778

Covariance analysis of a charge carrier device processing algorithm for stellar sensors 17 p2474 A83-37062

Photometric observations of AC Boo 17 p2587 A83-37286

A statistical VLBI study of milli-arcsecond cores in extragalactic radio sources 17 p2588 A83-37304

Photoelectric photometry of 2 Pallas 17 p2589 A83-37369

Multicolor photometry of bright patches in the galaxy NGC 4303 17 p2589 A83-37655

The change in the physical conditions of the spots in the active region McMath 14943 during the period from September 12 to September 19, 1977 17 p2625 A83-37665

TV photometric observations of 10 extragalactic peculiar objects 17 p2589 A83-37685

Multicolor photometry of the galaxy Markarian 141, a component of a binary system 17 p2590 A83-37711

Calibrations of the reddening, luminosity, and abundance of old disk giants from photometry of stars in M67, NGC 3680, NGC 2420, and the Wolf 630 and Arcturus groups 17 p2591 A83-37782

The evolution of galaxies in clusters. III - Photometry of 17 intermediate redshift clusters 17 p2591 A83-37826

Differential photometry of the metallic-line eclipsing binary AN Andromedae 17 p2592 A83-38052

Optically-selected quasar candidates in a field containing the South Galactic Pole 17 p2593 A83-38254

Infrared (JHK) photometry of asteroids. II 18 p2757 A83-39605

A photometric and spectroscopic study of the short-period eclipsing binary BV Eridani 18 p2775 A83-39757

An F/20 millimeter photometer for tingo --- Telescopio Infrarosso Gornegrat 18 p2761 A83-40427

Infrared array photometer 18 p2691 A83-40448

Infrared raster scans and a self optimizing micro-processor system for IR-photometry 18 p2691 A83-40450

IRAS follow-up - Problems and prospects 18 p2763 A83-40464

Remarkable modification of light curves for shadowing effects on irregular surfaces - The case of the asteroid 37 Fides 19 p2909 A83-40726

Voyager photometry of Europa 19 p2922 A83-40782

Positions, magnitudes, and colors for stars in the globular cluster M92 19 p2910 A83-41053

NGC 6256, a galactic globular cluster 19 p2915 A83-41059

The large C-type asteroids 146 Lucina and 410 Chloris, and the small S-type asteroids 152 Atala and 631 Philippina - Rotation periods and lightcurves 19 p2910 A83-41061

Lightcurves and rotation periods for the asteroids 70 Panopaea and 235 Carolina 19 p2910 A83-41062

Physical studies of asteroids. XI - Photoelectric observations of the asteroids 2, 161, 216 and 276 19 p2911 A83-41070

YZ Cassiopeiae and the Utrecht photometric system 19 p2911 A83-41071

Probable association of UX Piscium with a galaxy 20 p3058 A83-42323

High-resolution polarization images of Crab Nebula with a charge-coupled device camera 20 p3059 A83-42330

Photometry of resolved galaxies. III - GR 8 20 p3059 A83-42436

CCD photometry of the BL Lacertae object 1400+162 and the associated group of galaxies 20 p3059 A83-43040

New light curve analyses for the eclipsing binaries u Her and UV Leo 20 p3074 A83-43380

Photometric classification of normal galaxies and their redshift determination 20 p3062 A83-43653

Photoelectric photometry of asteroids 45, 120, 776, 804, 814, and 1982DV 21 p3222 A83-44084

A near-infrared and optical study of X-ray selected Seyfert Galaxies. I - Observations 21 p3227 A83-44110

Luminosity distribution in galaxies. II - A study of accidental and systematic errors with application to NGC 3379 21 p3222 A83-44118

H 0139-68 - High-speed optical photometry of an AM-Herculis type binary system 21 p3224 A83-44728

Acousto-optic filters in astronomical spectrophotometry 21 p3139 A83-44811

High-resolution optical observations of NGC 3379. I - An analysis of previous data 21 p3225 A83-44980

The optical variability and spectrum of PKS 2155-304 21 p3235 A83-45528

Two-dimensional spectrophotometry of the cores of X-ray luminous clusters 21 p3235 A83-45529

Near-infrared spectrophotometry of planetary nebulae 21 p3236 A83-45540

A search for light-time effects in binary cepheids - AW Persei 21 p3226 A83-45551

A study of low surface brightness spiral galaxies. II Optical surface photometry, infrared photometry, and H II region spectrophotometry 22 p3377 A83-46262

Photoelectric comparison sequences in the fields of four BL Lacertae objects 22 p3372 A83-46378

Photometric variability of B- and A-type supergiants 22 p3373 A83-46405

Redshifts of five extragalactic radio sources 22 p3375 A83-46574

Multicolor surface photometry of Markarian Seyfert galaxies 22 p3381 A83-46980

Properties of young clusters near reflection nebulae 23 p3516 A83-47464

Twenty years of dedicated photometry of RS CVn at Catania Observatory 23 p3516 A83-47514

On the instrumental and atmospheric stray-light for solar observations 23 p3517 A83-47717

Outburst period-energy relations in cataclysmic novae 23 p3527 A83-48072

Recent work on bipolar nebulae 24 p3638 A83-49130

Narrow-band photometry of normal and Seyfert galaxies 24 p3653 A83-49160

The barred galaxy NGC 7741 24 p3656 A83-49243

Kinematics and evolution of NGC 5128 24 p3642 A83-49258

Four-colour uvby and H-beta photometry of A5 to G0 stars brighter than 8.3 m 24 p3642 A83-49317

The galactic extinction towards Maffei 1 24 p3643 A83-49360

CCD surface photometry of two southern active galaxies, NGC 1316 and 1052 24 p3659 A83-49378

The AM Herculis-type binary E1405-451 24 p3660 A83-49384

Infrared photometry of the RS CVn binaries. III - JHK light curves of UV Psc 24 p3645 A83-49841

Standard photometric diameters of galaxies 24 p3645 A83-49842

A photometric study of the eclipsing binary V478 Cygni 24 p3645 A83-49844

High-resolution optical observations of NGC 3379. II - On the derivation of the East-West profile 24 p3663 A83-49846

Pseudocepheids. II - Two variables in the Large Magellanic Cloud 24 p3646 A83-49882

The variable stars in the field of the globular cluster NGC 6681 24 p3646 A83-49883

Workshop on Astronomical Measuring Machines, Edinburgh, Scotland, September 28-30, 1982, Proceedings 24 p3647 A83-50001

Crowded-field stellar photometry 24 p3647 A83-50003

Automated analysis on stellar fields with valley lines 24 p3647 A83-50004

Absolute photometry using APM, Cosmos and the PDS --- Automatic Plate Measuring Facility 24 p3647 A83-50007

A catalogue of photometric sequences (suppl. 3) --- for astronomical photograph calibration 24 p3647 A83-50010

Intensity estimation from pixel data --- for stellar and galactic magnitude determination 24 p3648 A83-50013

A straightforward method to calibrate photographic data using stellar images 24 p3648 A83-50014

Photometric calibration of Schmidt plates 24 p3648 A83-50017

Automated two-dimensional galaxy photometry 24 p3648 A83-50018

Fast shape analysis of galaxies 24 p3648 A83-50019

Galaxy number-magnitude counts 24 p3648 A83-50020

Photometric studies of faint galaxies on deep UKST plates with COSMOS 24 p3648 A83-50021

Automated stellar photometry 24 p3649 A83-50029

Photometric research for Ap-stars in open cluster. IV - NGC 2287, Cr 121, NGC 2422 and supplementary measurements in NGC 1662 and NGC 2516 24 p3668 A83-50087

ASTRONOMICAL SPECTROSCOPY

On the behaviour of QSO space density beyond z = 3.5 01 p0118 A83-10952

Markarian 914 is a galactic object, lick H-alpha 233 01 p0118 A83-10969

ASTRONOMICAL SPECTROSCOPY

Extended regions of soft X-ray emission and background spectrum at Southern latitudes 01 p0118 A83-10972

A modular Fabry-Perot interferometer system for imagery and spectrometry 01 p0118 A83-11048

Clusters of galaxies --- optical observation data 01 p0127 A83-11290

Optical identification of Balmer-dominated supernova remnants in the Large Magellanic Cloud 02 p0250 A83-11582

The absolute H-beta flux from NGC 7027 02 p0251 A83-11585

On the statistical uncertainties associated with line profile fitting --- in astronomy 02 p0252 A83-11607

VLA observations of the Seyfert galaxy NGC 1068 02 p0252 A83-11609

A nuclear spectroscopic survey of disk galaxies. II - Galaxies with emission lines not excited by stellar photoionization 02 p0254 A83-12109

Gas in the galactic halo 02 p0258 A83-12184

Dynamics of elliptical galaxies and other spheroidal components 02 p0246 A83-12189

Wave instability in the polar region of Venus 02 p0264 A83-12241

2-4 micrometer spectroscopy of the compact H II region G 45.13 + 0.14 A 02 p0260 A83-12520

Spectroscopic observations of thirteen optically-selected QSOs in a large field centred around NGC 5334 02 p0247 A83-12541

Detection and study of secondary structures in some planetary nebulae 02 p0247 A83-12545

Complete samples of active extragalactic objects. II - A deep 1.452-GHz VLA survey centered on alpha = 08h 52m 15s, delta = +17deg 16 arcmin 02 p0248 A83-12906

A new intermediate Seyfert galaxy - X-ray, optical, and radio properties 02 p0248 A83-12907

Observations of 1 Ceres and 2 Pallas at centimeter wavelengths 02 p0268 A83-12922

15 years of astronomical research work with the 2-m reflecting telescope of the Ondrejov Observatory /CSSR/ 02 p0249 A83-13045

TAURUS: A wide-field imaging Fabry-Perot spectrometer for astronomy 03 p0401 A83-13324

Ultraviolet spectra of planetary nebulae. IX - High-dispersion observations of NGC 7662 03 p0402 A83-13334

Spectrophotometry of comets at optical wavelengths 03 p0416 A83-13393

Infrared spectroscopy in astronomy 03 p0405 A83-13453

Bulk and integrated acousto-optic spectrometers for molecular astronomy with heterodyne spectrometers 03 p0405 A83-13459

433 micron laser heterodyne observations of galactic CO from Mauna Kea 03 p0405 A83-13464

Stellar populations in the edge-on spiral galaxy NGC 4565. I - Surface brightness and color distributions 03 p0406 A83-13551

A nuclear spectroscopic survey of field disk galaxies 03 p0406 A83-13553

Object Kuwano, a novalike /symbiotic/ binary with a red giant - Spectroscopy 03 p0417 A83-13652

The calibration of a radio-independent search for BL Lac objects 03 p0408 A83-13929

Further observations of the elliptical galaxy NGC 5813 03 p0420 A83-13937

A study of the Chamaeleon dark cloud complex - Survey, structure and embedded sources 03 p0420 A83-13945

A search for diffuse band profile variations in the rho Ophiuchi cloud 03 p0423 A83-14194

Observations of 12-200 keV X-rays from GX 339.4 03 p0425 A83-14207

The ultraviolet spectrum of Herbig-Haro object 2H 03 p0425 A83-14219

On the spectrum of Comet Bradfield 1980 t 03 p0428 A83-14774

Discovery of a large, high-excitation planetary nebula at l = 136 deg, b = +5 deg 03 p0411 A83-14781

Kinematics of ring-shaped nebulae in the LMC. II - The radial velocity field of N 185 03 p0429 A83-14790

Absolute photometry of the Crab Nebula 03 p0411 A83-14793

Infrared emission and star formation in NGC 5253 03 p0429 A83-14794

Observations of energetic ions near the Venus ionopause 04 p0558 A83-14968

The infrared spectrum of interstellar dust --- noting spectroscopic similarity to transmittance of diatomaceous organisms 04 p0526 A83-14981

New high resolution radio observations of NGC 4258 04 p0545 A83-15032

III - VLA and WSRT observations of the anomalous arms 04 p0551 A83-15050

Observations of bipolar planetary nebula 19W32 04 p0551 A83-15050

A spectroscopic method for determining the luminosities of spiral galaxies and estimating their stellar population 04 p0551 A83-15601

Coma quasars 04 p0551 A83-15603

A spectroscopic investigation of the nebulosity around low-luminosity quasars 04 p0551 A83-15604

Structure of the M33 nucleus 04 p0552 A83-15611

The H II regions of Messier 8 04 p0552 A83-15615

Advances in detectors for astronomical spectroscopy 04 p0547 A83-15806

Spectroscopic equipment for the Space Telescope 04 p0547 A83-15807

X-rays from quasars and active galaxies 04 p0555 A83-15822

Spectroscopy of galaxies in distant clusters. I - First results for 3C 295 and 0024 + 1654 05 p0696 A83-16980

Neutral hydrogen observations towards the Puppis Window of the Milky Way 05 p0701 A83-17665

An HI survey of southern galaxies 05 p0694 A83-17667

Spatial-kinematical models for planetary nebulae - NGC 2371-2 05 p0701 A83-17671

Cosmological molecular hydrogen and the distortion of the relic radiation spectrum 05 p0710 A83-17804

NGC 6503 - Rotation, mass and physical conditions in galaxy nucleus 06 p0824 A83-18017

Systematic effects in trigonometric parallaxes. III - Comparisons with spectroscopic and cluster parallaxes 06 p0818 A83-18169

The Saturn spectrum in the EUV - Electron excited hydrogen 06 p0848 A83-18316

Thermoluminescence of the lunar surface 06 p0848 A83-18474

Near infrared spectroscopy of W 51 IRS-2 06 p0818 A83-18541

Spectrophotometry of the nucleus of the galaxy Arakelyan 144 06 p0831 A83-18792

Can planetary nebulae rotate 06 p0832 A83-18842

New bright Seyfert Galaxies 06 p0819 A83-18852

Medusa spectroscopy of A400, A576, A1767, and A2124 06 p0820 A83-18856

Visual and infrared observations of the distant Comets P/Stephan-Oterma /1980g/, Panther /1980u/, and Bowell /1980b/ 06 p0833 A83-18873

A search for frosts in Comet Bowell /1980b/ 06 p0833 A83-18874

Identification of some diffuse interstellar features 06 p0835 A83-18895

Calibration of an infrared spectrometer and a far-infrared photometer for astronomical applications under low background conditions 06 p0821 A83-18946

A spectroscopic study of the old nova HR Delphini 06 p0836 A83-19058

Spectral observations of M 82 06 p0822 A83-19204

Analysis of absorption spectra of 11 quasars with Z sub e greater than 2 06 p0837 A83-19206

Physical conditions in interacting galaxies, in components of isolated pairs, and in isolated galaxies 06 p0838 A83-19220

Observations of galaxies with ultraviolet continuum at 102 MHz 06 p0823 A83-19221

Are there any shock-heated galaxies 06 p0839 A83-19273

The Cyanogen distribution of the red giants in M5 06 p0840 A83-19284

The nuclear radio source of the X-ray Galaxy NGC 2110 06 p0823 A83-19299

Low frequency asymptotic spectra of multiple, decelerating adiabatic bursts 06 p0843 A83-19486

Laboratory millimeter and submillimeter spectrum of HOC 06 p0846 A83-19528

Optical identifications of flat-spectrum radio sources 07 p1003 A83-19853

Searches for far-infrared emission from dark clouds - Rho Ophiuchi, Heiles 2, L1529, and L183 07 p1010 A83-19860

Spectroscopic observations of two very red objects toward the galactic center 07 p1004 A83-19861

CO observations of the supernova remnant G78.2+2.1 07 p1010 A83-19862

Gamma-ray burst spectra 07 p1039 A83-20013

A third-generation small spectroscopy experiment for hard transient events 07 p1005 A83-20039

Infrared views of the giant planets 07 p1005 A83-20150

Ultraviolet spectroscopy and the composition of cometary ice 07 p1013 A83-20296

Flux density measurements of bright extragalactic sources at 36.8 GHz 07 p1006 A83-20564

Observations of the new OH maser source G43.2-0.1 07 p1007 A83-20670

Optical spectroscopy of 28 southern radio galaxies 07 p1007 A83-20949

Spectroscopy of the fuzz associated with four quasars 07 p1023 A83-21154

Optical spectroscopy of flat spectrum radio sources 07 p1008 A83-21213

Morphological study of three Abell's planetary nebulae - A33, A36, and A79 07 p1009 A83-21238

Optical supernova remnants in external galaxies 08 p1179 A83-21852

Optical spectrophotometry of the Cygnus Loop 08 p1174 A83-21853

An optical study of IC 1470 08 p1183 A83-23048

The depletion of calcium in the Rho Ophiuchi cloud 08 p1185 A83-23082

H I observations of active and interacting galaxies 09 p1356 A83-23316

Planetary nebulae 09 p1352 A83-23498

The galaxy continuum in the spectrum of Cygnus A 09 p1357 A83-23726

Spectroscopy of blue stellar objects 09 p1357 A83-23735

Planetary nebulae 09 p1358 A83-23912

Active extragalactic objects in the visible and ultraviolet regions 09 p1353 A83-24015

H I line studies of galaxies. II - The 21-cm-width as an extragalactic distance indicator 09 p1359 A83-24453

The Hubble sequence of masses 09 p1359 A83-24454

Fourier spectroscopy of the /C-12//C-13/ and /C-13/2 Phillips system 09 p1361 A83-24519

Observations of M42 in the O III 52 and 88-micron forbidden lines, the O I 63-micron forbidden line, and the N III 57-micron forbidden line 09 p1362 A83-24977

Velocity field and physical conditions in the active lenticular galaxy NGC 3998 09 p1363 A83-24989

Spatial studies of the middle infrared spectral features in NGC 7027 09 p1364 A83-25006

A measurement of the 'missing' Q/6/ line of H2 in Orion 09 p1364 A83-25008

HCN J - 1-0 observations in L 673 and S 235B - Two different cases of hyperfine anomalies 10 p1499 A83-25368

How to maintain the spatial distribution of interplanetary dust 10 p1500 A83-25375

A far-infrared Fabry-Perot interferometer and grating spectrometer for balloon-borne astronomy 10 p1419 A83-25458

Nuclear activity in the barred spiral galaxy NGC 3660 from radio, optical, and X-ray observations 10 p1500 A83-25488

Formaldehyde toward Cas A - Cloud sizes and H2 densities 10 p1501 A83-25496

H1340 no. 10 - A high-redshift QSO with very narrow emission lines 10 p1501 A83-25579

Quasar candidates near A1139, A1775, and 1633+33 10 p1501 A83-25581

The hydrogen-depleted planetary nebulae Abell 30 and Abell 78 10 p1504 A83-25726

Active optics in astronomy 10 p1481 A83-25828

Speckle interferometry, speckle holography, speckle spectroscopy, and reconstruction of high-resolution images from space telescope data 10 p1419 A83-25833

Resolution in normal galaxies 10 p1496 A83-25856

Optical observations of active galaxies and quasars at high angular resolution 10 p1496 A83-25857

Highly compact structures in galactic nuclei and quasars 10 p1496 A83-25858

Active nuclei - Observations, classifications, and observational constraints 10 p1506 A83-26228

Physical conditions in the emission regions of active galactic nuclei 10 p1506 A83-26230

The formation of permitted and forbidden lines in quasars 10 p1507 A83-26233

Why are broad emission lines seen in Seyfert galaxies and not in BL Lacertae objects 10 p1507 A83-26355

Theoretical study of silicon dicarbide --- in stellar spectra 10 p1510 A83-26398

X-ray, radio, and infrared observations of the 'rapid burster' /MXB 1730-335/ during 1979 and 1980 10 p1514 A83-26731

PKS 0119-046 and the origin of infalling absorption-line systems in quasars 10 p1515 A83-26747

H I absorption in the peculiar galaxy UGC 6081 10 p1516 A83-26750

Detection of sulfur in the galactic center 10 p1516 A83-26754

Source of the high-velocity molecular flow in Orion 10 p1516 A83-26755

An image-tube camera for cometary spectrography 10 p1498 A83-26911

X-ray and optical studies of emission-line Markarian galaxies 11 p1668 A83-27103

Observations of low redshift H I in Stephan's Quintet 11 p1668 A83-27105

Intensity and extinction irregularities in the H2 emission from Orion 11 p1676 A83-27120

High voltage power electronics packaging on NASA's Space Telescope 11 p1539 A83-27155

On the accuracy of frequency determination by an autoregressive spectral estimator --- of astronomical spectra 11 p1669 A83-27636

X-ray astronomy from the Space Shuttle 11 p1671 A83-27763

Spectroscopic survey of southern compact and bright-nucleus galaxies. V 11 p1680 A83-28257

Spectroscopic changes in the Seyfert galaxy NGC 3783 11 p1682 A83-28290

The 8-13 micron spectrum of IC 2165 11 p1682 A83-28292

Arc measurements of FeII transition probabilities 12 p1789 A83-28863

The compact H II region S235A - Observations and interpretation 12 p1789 A83-28876

Gamma-ray imaging with a rotating modulator 12 p1708 A83-28895

The use of derivative techniques in astronomical spectroscopy 12 p1786 A83-29080

Redshifts for 115 galaxies near the equator 12 p1787 A83-29176

21-cm observations of galaxies in groups and multiplets 12 p1787 A83-29178

A statistical study of the Lyman-alpha absorption lines of nine quasars 12 p1795 A83-29352

The redshift distribution of quasar absorption lines and its origin 12 p1795 A83-29353

Mass spectrometry on the Venera 13 and Venera 14 landers Preliminary results 12 p1798 A83-29477

The Venera 13 and Venera 14 spectrophotometry experiments 12 p1798 A83-29479

Spectroscopy of three ultraviolet-excess galaxies 12 p1796 A83-29489

Velocity standards that have variable velocities. I - HD 184467 12 p1789 A83-29956

High efficiency spectrographs for the EUV and soft X-rays 13 p1935 A83-30183

1733-565 - A compact radio galaxy at low galactic latitude 13 p1946 A83-30390

H76-alpha recombination line emission near Sgr A 13 p1947 A83-30392

Fibre optic development at the AAO 13 p1936 A83-30400

Photoelectric analysis of asteroid 216 Kleopatra Implications for its shape 13 p1961 A83-31207

Solar radiation scattered in the Venus atmosphere - The Venera 11, 12 data 13 p1961 A83-31210

Radial velocities of Cygnus Loop filaments 13 p1948 A83-31260

Spectroscopy of Nova Vulpeculae 1976 13 p1940 A83-31262

H I observations of the high-velocity system in NGC 1275 13 p1950 A83-31406

X-ray burst observations of Serpens X-1 13 p1951 A83-31426

The-micron spectrometry in sharpless-106 13 p1956 A83-31676

Remarkable kinematics of the ionized gas in the nucleus of NGC 1365 13 p1957 A83-31700

Detection of H2 emission in Herbig-Haro object No. 101 13 p1957 A83-31703

A survey of formaldehyde in the Cepheus OB3 molecular cloud 13 p1958 A83-31709

Instrumentation in astronomy IV; Proceedings of the Fourth Conference, Tucson, AZ, March 8-10, 1982 14 p2014 A83-31976

Application of a charge-coupled device (CCD) detector for coudespectroscopy 14 p2016 A83-31992

Stellar spectrograph using aberration corrected concave holographic grating 14 p2017 A83-32009

Faint Object Spectrograph (FOS) calibration 14 p2017 A83-32011

Multiple object fiber optic spectroscopy 14 p2017 A83-32012

Multiple object fiber optics spectrograph feed for the Hale telescope 14 p2017 A83-32013

Multi-aperture spectroscopy at Kitt Peak 14 p2017 A83-32014

Speckle spectroscopy; an application for the multi-anode microchannel array detector system 14 p2017 A83-32016

Ultra-high precision radial velocity spectrometer 14 p2017 A83-32017

Grazing incidence optics - New techniques for high sensitivity spectroscopy in the space ultraviolet 14 p2084 A83-32018

Performance of the International Ultraviolet Explorer for spectral imaging 14 p1983 A83-32019

New two-dimensional photon camera
14 p2018 A83-32021

Modified Bowen-Walraven image slicer
14 p2018 A83-32029

Solar corona photoelectric photometer using mica
etalons
14 p2096 A83-32031

High-resolution spectra of C2 Swan bands from comet
West 1976 VI
14 p2099 A83-33222

The microwave and far-infrared spectra of the CH
radical
14 p2083 A83-33234

The spectrum of the extragalactic background light
14 p2107 A83-33237

The H 166 alpha recombination line in the Carina
Nebula
14 p2109 A83-33276

Ultraviolet spectrum of the planetary nebula NGC 7662
Observations and models
14 p2109 A83-33281

X-ray diagnostics of globular clusters
15 p2251 A83-33595

IUE observations of supernova remnants
15 p2251 A83-33596

Reddening indicators for quasars and Seyfert 1
galaxies
15 p2256 A83-34086

Tentative confirmation of an aurora on Uranus
15 p2274 A83-34221

Kinematic structure of planetary nebulae. I - The highly
evolved nebula Abell 30, II - The Eskimo, NGC 2392
15 p2265 A83-34594

Optical and X-ray observations of faint quasars in an
optically selected sample
15 p2248 A83-34616

CO observations of the galaxies in the Leo triplet - NGC
3623, NGC 3627, and NGC 3628
15 p2267 A83-34624

The structure of bright-rimmed molecular clouds
15 p2267 A83-34625

A study of H-alpha velocities in NGC 1499, NGC 7000,
and IC 1318B/C
15 p2267 A83-34626

The soft X-ray spectrum of the Vela supernova
remnant
15 p2268 A83-34630

Velocity dispersions of knots in Vela X and Puppis A
15 p2268 A83-34631

Quasar absorption spectra and molecular spectra - An
attempt at identification
15 p2270 A83-34752

A search for very high energy gamma-ray transients from
Cygnus X-3 and PSR 0531
16 p2441 A83-36639

Absolute dimensions of eclipsing binaries. I - The
early-type detached system QX Carinae
16 p2430 A83-36645

Hydrogen line ratios of low redshift QSO's
16 p2430 A83-36658

The spatial power spectrum of galactic neutral hydrogen
from observations of the 21-cm emission line
16 p2432 A83-36696

The elliptical galaxy NGC 4696 - CCD observations of
an absorbing lane
16 p2433 A83-36698

Internal motions in ten planetary nebulae
17 p2587 A83-37279

Morphology of optical forms of N galaxies
17 p2588 A83-37308

Neutral hydrogen absorption in the quasar 3C 268.4 -
Possible evidence for galactic halo clouds
17 p2598 A83-37346

Venus spectroscopy in the 3000-8000 A region by
Veneras 9 and 10
17 p2617 A83-37416

Method for determining sky background brightness on
the basis of data from the Galaktika experiment
17 p2600 A83-37653

Multicolor photometry of bright patches in the galaxy
NGC 4303
17 p2589 A83-37655

Results of investigations of extragalactic radio sources
in the microwave range
17 p2600 A83-37663

Structure and stellar content of dwarf elliptical
galaxies
17 p2602 A83-37781

New galaxies with ultraviolet excess. IV
17 p2591 A83-37882

On Markaryan 6 and the problem of the intermediate
Sy 1.5 type
17 p2602 A83-37885

Spectroscopy of galaxies in distant clusters. II - The
population of the 3C 295 cluster
17 p2603 A83-37901

The effects of seeing on spectral line measurements
in Seyfert 1 galaxies
17 p2604 A83-37906

Hard X-ray observations of the Crab Nebula and
A0535+26 with a high energy resolution spectrometer
17 p2604 A83-37913

Evidence for inhomogeneous thermal sources of two
similar solar spike events of 1978 May 5 and December
4
17 p2627 A83-37926

Empirical improvement in accuracy of atomic oscillation
strengths calculated by Kurucz and Peytremann --- of
relevance to model stellar atmospheres
17 p2606 A83-38240

The Seyfert 1 galaxy NGC 4593. II - The pattern of
variability of the UV spectrum
17 p2592 A83-38242

The structure and dynamics of the bi-polar nebula
MZ-3
17 p2607 A83-38243

Further high-resolution observations of faint radio
sources and the angular size-flux density relation
17 p2593 A83-38249

The location of material producing Lyman-limit
discontinuities in QSO spectra
17 p2607 A83-38251

Three-dimensional structure of the Crab Nebula
17 p2607 A83-38257

The forbidden O III electron temperature and density
structure in the nucleus of NGC 1068
17 p2609 A83-38419

A sample of 25 extragalactic radio sources having a
spectrum peaked around 1 GHz
17 p2594 A83-38420

Effect of search lines on emission and absorption
redshift distribution of QSOs
17 p2611 A83-38587

Correlations between synchrotron and self-Compton
spectra
18 p2764 A83-39004

Diffuse radio emission from the Coma cluster of galaxies
at decametre wavelengths
18 p2764 A83-39191

Maximum entropy image reconstruction - A practical
non-information-theoretic approach --- for astronomical
spectrum restoration
18 p2754 A83-39200

Techniques for fine gamma-ray burst spectroscopy
18 p2757 A83-39300

Colliding and merging galaxies. II - SO galaxies with polar
rings
18 p2767 A83-39589

CO(J = 2-1) observations of galactic HII-regions
18 p2769 A83-39650

Synthesis maps of millimeter molecular lines
18 p2758 A83-39714

Observations of forbidden C I emission in Orion A (M42)
and Orion B (NGC 2024)
18 p2773 A83-39717

Energetic molecular flows in star-forming cloud cores
18 p2773 A83-39719

Shock waves in Orion
18 p2774 A83-39727

A photometric and spectroscopic study of the
short-period eclipsing binary BV Eridani
18 p2775 A83-39757

An atlas of QSO spectra
18 p2760 A83-40324

Radio data on clusters of galaxies from the Culgoora
circular array
18 p2760 A83-40326

A new InSb charge amplifier for application to a
spectrometer array
18 p2691 A83-40446

Depression of molecular emission in the line of sight
of Sgr A West
19 p2912 A83-40680

Spatial and spectral studies of the galactic center near
10 microns
19 p2908 A83-40686

Observations of gamma-ray line emission from the
galactic center region
19 p2913 A83-40692

Observations of the galactic center with the GSFC
low-energy gamma-ray spectrometer - Preliminary results
19 p2909 A83-40693

The intensity and spectrum of galactic center beta (+)
annihilation protons after Compton scattering
19 p2913 A83-40696

A comparison of several image processing techniques
applied to photographically recorded astronomical
spectra
19 p2909 A83-40715

Absolute spectrophotometry of Neptune - 3390 to 7800
A
19 p2921 A83-40777

Search for Wolf-Rayet features in the spectra of giant
HII regions. I - Observations in NGC 300, NGC 604, NGC
5457 and He2-10
19 p2910 A83-41066

Arp 102B - A new and unusual broad-line galaxy
19 p2918 A83-41615

Dense cores in dark clouds. IV - HC5N observations
19 p2919 A83-41626

Optical spectroscopy of the radio-loud nuclei of spiral
galaxies - Starbursts or monsters?
20 p3057 A83-42179

Neutral hydrogen absorption in Mrk 6, NGC 3810,
1506+34, and NGC 1068
20 p3063 A83-42180

A survey of H-alpha emission in normal galaxies
20 p3063 A83-42181

Narrow- and intermediate-band H-alpha and O I 7774
A photometry and reticon spectroscopy of SX
Cassiopeiae
20 p3058 A83-42322

The magellanic irregular galaxy DDO 155
20 p3067 A83-42440

A gravitationally stable Bok globule
20 p3067 A83-42442

Cyanoacetylene as a density probe of molecular
clouds
20 p3067 A83-42443

The evolution of large planetary nebulae and their central
stars
20 p3067 A83-42447

Observationally determined Fe II oscillator strengths ---
interstellar and quasar absorption spectra
20 p3069 A83-42466

First detection of the ground-state J(K) = 1(0)-0(0)
submillimeter transition of interstellar ammonia
20 p3069 A83-42473

Detection of radio emission from the
Becklin-Neugebauer object
20 p3069 A83-42474

Tracing the gas in galaxies
20 p3069 A83-42625

Time development of the emission lines and continuum
of NGC 4151
20 p3071 A83-43049

Carbon monoxide emission from planetary nebulae and
their possible precursors
20 p3071 A83-43054

Interstellar C2 molecules in a Taurus dark cloud
20 p3074 A83-43091

Electron excitation rates among fine structure levels in
O III
21 p3227 A83-44112

Quasi-simultaneous ultraviolet and optical observations
of PKS 2155-304 --- H2155-304
21 p3223 A83-44448

Spectroscopic observations of southern N-galaxy
candidates
21 p3224 A83-44745

Spectroscopy of the QSO pair Q1228 + 076/Q1228
+ 077
21 p3225 A83-44767

Neutral hydrogen observations of double spiral galaxies.
II NGC 3958/3963, NGC 5289/5290, NGC 5673/IC 1029,
NGC 5107/5112
21 p3226 A83-44982

The optical variability and spectrum of PKS 2155-304
21 p3235 A83-45528

An identification for 'Geminga' (2CG 195+04) 1E
0630+178 - A unique object in the error box of the
high-energy gamma-ray source
22 p3372 A83-45628

CS J = 5 - 4 observations of galactic molecular
clouds
22 p3379 A83-46558

High-resolution images of the Galactic Centre
22 p3375 A83-46560

The high-ionization optical spectrum of the Seyfert
galaxy Tololo 0109-383
22 p3379 A83-46568

An infrared and optical investigation of galactic nuclei
with compact radio sources
22 p3380 A83-46974

VLA observations of extragalactic NH3 in IC 342
22 p3381 A83-46981

Tentative detection of the CS(+) molecular ion in diffuse
interstellar clouds
23 p3518 A83-47426

Radio observations of Comet 1983 d
23 p3515 A83-47430

The Hydra I cluster of galaxies. II - First results from H
I observations
23 p3518 A83-47433

ESO 438-G 9 - A Seyfert galaxy with unusual
properties
23 p3519 A83-47444

Infrared objects near H2O masers in regions of active
star formation. III - Evolutionary phases deduced from IR
recombination line and other data
23 p3519 A83-47453

Multifrequency observations of OV236 (1921-293) reveal
an unusual spectrum --- BL Lacertae object, quasar
23 p3526 A83-47872

Neutrino spectroscopy of the solar interior
23 p3538 A83-48549

Spectral channel of a digital radio spectrometer with
an analysis band of 180 kHz
24 p3581 A83-48959

Survey of OH masers at 1665 MHz. II - Galactic longitude
340 deg to the galactic centre
24 p3650 A83-48984

H2O masers in the galactic plane. I - Longitude 340
deg to the galactic centre
24 p3650 A83-48985

Planetary nebulae; Proceedings of the Symposium,
University College, London, England, August 9-13, 1982
24 p3638 A83-49126

Planetary nebulae - An introductory review
24 p3638 A83-49127

Recent work on bipolar nebulae
24 p3638 A83-49130

Molecules in planetary nebulae
24 p3651 A83-49134

Observations of dust in planetary nebulae
24 p3639 A83-49135

Second Byurakan spectral sky survey. I - Quasistellar
and Seyfert objects
24 p3640 A83-49162

HI observations of the irregular galaxy IC 10
24 p3640 A83-49207

Recent TAURUS results on H-alpha velocities in M83
24 p3655 A83-49228

Observations of the neutral hydrogen in the barred spiral
galaxies NGC 3992 and NGC 4731
24 p3656 A83-49242

Neutral hydrogen observations of the dwarf elliptical
galaxies NGC 185 and NGC 205
24 p3642 A83-49254

High precision spectropolarimetry of stars and planets.
I The ROE spectropolarimeter
24 p3643 A83-49353

High precision spectropolarimetry of stars and planets.
II Spectropolarimetry of Jupiter and Saturn
24 p3643 A83-49354

Hyperfine structure measurements for lines of
astrophysical interest in Mn I
24 p3658 A83-49364

Observations of H2O maser emission in the Large
Magellanic Cloud
24 p3659 A83-49368

Gamma-ray line features from the Crab Nebula in the
energy range 50-2000 keV
24 p3659 A83-49370

OH maser emission at 4765 MHz in W3
24 p3659 A83-49371

Analysis of nebulosity in the planetary nebula NGC 40
24 p3660 A83-49382

Active galactic nuclei - IUE results on continuum,
emission and absorption lines
24 p3661 A83-49559

A new type of decametric radio emission from Jupiter
24 p3673 A83-49631
Spectral observations and physical modeling of
Sharpless 121 24 p3646 A83-49884
Large scale structure in the direction of the Indus
supercluster 24 p3649 A83-50024
Determining helium abundances in H II regions
24 p3666 A83-50053
Are three systematic observational effects on
abundance determinations in giant extragalactic H II
regions? 24 p3667 A83-50058
Observations of interstellar deuterium
24 p3667 A83-50059
A flare in the millimetre to IR spectrum of 3C273
24 p3669 A83-50105

ASTRONOMICAL TELESCOPES

NT INFRARED TELESCOPES
NT PYROHELIOMETERS
NT SPECTROSCOPIC TELESCOPES
NT ULTRAVIOLET TELESCOPES
NT X RAY TELESCOPES

The UK Schmidt Telescope Plate Catalogue and
problems associated with increasing numbers of plates
and users 01 p0114 A83-10153
Spectra, dimensions and luminosities of radio sources
in the Culgoora-3 list 01 p0117 A83-10868
The Clark Lake Teepee-Tee telescope
02 p0246 A83-11995
15 years of astronomical research work with the 2-m
reflecting telescope of the Ondrejov Observatory
/CSSR/ 02 p0249 A83-13045
Facilities for US radioastronomy
02 p0249 A83-13104
Ultraviolet, optical and infrared astronomy
02 p0250 A83-13105
Inventory of major operational and planned
ground-based astronomical telescopes of the countries
represented in the European Science Foundation /second
edition, 1982/ 03 p0402 A83-13357
Optical figuring process, Dupont 2.6-m telescope
03 p0410 A83-14381
Adaptive mirrors --- for astronomical telescopes
04 p0534 A83-15260
Studies with the Pinhole/Occluder Facility
[AIAA PAPER 83-0513] 05 p0692 A83-16759
Multiple telescope infrared interferometry
05 p0694 A83-17425
The Pic-du-Midi 2 meter telescope - First observations
of the planets 06 p0817 A83-18064
Tests of vacuum vs helium in a solar telescope
06 p0818 A83-18577
A photoelectric radial-velocity spectrometer on the 1.2-m
telescope of the Dominion Astrophysical Observatory
06 p0822 A83-19075
The processing of infrared sky noise by chopping,
nodding and filtering 07 p1008 A83-21211
One form of apodization of telescopes
07 p1009 A83-21275
Discovery of close binary stars using the one-meter
telescope on Mt. Sanglok 08 p1174 A83-22054
Self-null corrector test for telescope hyperbolic
secondaries 08 p1175 A83-22614
Development and evaluation of integrated infrared
arrays for astronomical applications
08 p1052 A83-22858
A study of a correlation tracking method to improve
imaging quality of ground-based solar telescopes
10 p1492 A83-25489
Active optics in astronomy 10 p1481 A83-25828
Development of an active optical mirror for astronomical
applications 10 p1482 A83-25829
Active wavefront correction in large telescopes
10 p1482 A83-25830
Honeycomb mirrors of borosilicate glass
10 p1436 A83-25831
Image quality and high resolution in future telescopes
10 p1482 A83-25832
On the deconvolution of brightness profiles of galaxies
from seeing - Application to NGC 3379 10 p1494 A83-25834
Coherent large telescopes 10 p1494 A83-25836
Rotation interferometry - A new technique for achieving
high angular resolution 10 p1419 A83-25837
A shearing, modulating interferometer --- for
astronomical observation 10 p1420 A83-25838
Multiple telescope interferometry
10 p1494 A83-25841
Two-telescope Michelson stellar interferometry at 2.2
microns 10 p1494 A83-25842
Interferometric connection of the Canada-France-Hawaii
3.6 metre telescope and the United Kingdom 3.8 metre
telescope on Mauna Kea 10 p1495 A83-25843
Interferometry with the multiple mirror telescope and
conventional telescopes 10 p1495 A83-25845
An investigation of the narrow-band photometric system.
I - Spectral classification 10 p1498 A83-26906

How to achieve diffraction limited resolution with large
space telescopes 11 p1656 A83-27727
FLUTE or TRIO - Different approaches to optical arrays
in space 11 p1536 A83-27728
Orbiting VLB 11 p1670 A83-27730
Infrared telescope in space - IRTs
11 p1670 A83-27739
Hadamard X-ray spectro-telescope
11 p1671 A83-27753
The Pinhole/Occluder Facility
11 p1672 A83-27768
An orientation platform for a balloon-borne telescope
11 p1537 A83-28575
The near infrared spectrophotometer for the 182 cm
Asiago telescope 12 p1785 A83-28993
Computer-controlled polishing of telescope mirror
segments 12 p1778 A83-29145
On the use of mosaic direct-vision prism for radial
velocity measurements 12 p1729 A83-29359
Analysis of the shift-and-add method for imaging through
turbulent media 12 p1779 A83-29375
International Conference on Advanced Technology
Optical Telescopes, Tucson, AZ, March 11-13, 1982,
Proceedings 13 p1936 A83-30976
Performance of the Multiple Mirror Telescope (MMT). I
- MMT The first of the advanced technology telescopes
13 p1828 A83-30977
Performance of the Multiple Mirror Telescope (MMT).
II Mechanical properties of the MMT
13 p1936 A83-30978
Performance of the Multiple Mirror Telescope (MMT).
III Seeing experiments with the MMT
13 p1937 A83-30979
Performance of the Multiple Mirror Telescope (MMT).
IV - MMT computer systems 13 p1937 A83-30980
Performance of the Multiple Mirror Telescope (MMT).
V Pointing and tracking of the MMT
13 p1937 A83-30981
Performance of the Multiple Mirror Telescope (MMT).
VI - MMT telescope collimation system
13 p1919 A83-30982
Performance of the Multiple Mirror Telescope (MMT).
VII Image shrinking in sub-arc second seeing at the MMT
and 2.3m telescopes 13 p1919 A83-30983
Performance of the Multiple Mirror Telescope (MMT).
VIII - MMT as an optical-infrared interferometer and phased
array 13 p1937 A83-30984
Performance of the Multiple Mirror Telescope (MMT).
IX - Doing science with the MMT
13 p1937 A83-30985
Performance of the Multiple Mirror Telescope (MMT).
X - The first submillimeter phased array
13 p1937 A83-30986
Scaling the Multiple Mirror Telescope (MMT) to 15
meters Similarities and differences
13 p1937 A83-30987
Status of the European Southern Observatory new
technology telescope project 13 p1937 A83-30988
University of Texas 7.6 meter telescope project
13 p1937 A83-30989
University of California ten meter telescope project
13 p1938 A83-30990
Infrared performance of the University of California Ten
Meter Telescope 13 p1938 A83-30991
Effects of primary mirror segmentation on telescope
image quality 13 p1919 A83-30992
Good imaging with very fast paraboloidal primaries - An
optical solution and some applications --- performance
improvement of astronomical telescopes
13 p1920 A83-30993
Coherent optical system of modular imaging collectors
(COSMIC) telescope array - Astronomical goals and
preliminary image reconstruction results
13 p1920 A83-30997
Optical system design study for the University of Texas
300-inch telescope 13 p1920 A83-30998
Dome induced image motion --- in astronomical
telescopes 13 p1920 A83-30999
Seeing and the design and location of a 15 meter
telescope 13 p1938 A83-31000
Wind loading of large astronomical telescopes
13 p1938 A83-31001
Structural analysis of the mirror of the University of Texas
7.6 m Telescope 13 p1938 A83-31002
New console design - An example --- for telescope
control 13 p1938 A83-31004
Remote observing experiments at Kitt Peak National
Observatory 13 p1939 A83-31005
Remote operation of telescopes - Long-distance
observation 13 p1939 A83-31006
Active optics - Don't build a telescope without it
13 p1920 A83-31007
Modal control for wavefront reconstruction in adaptive
optics 13 p1920 A83-31009

Four-wave mixer phase compensation performance ---
for atmospheric turbulence-caused resolution
improvement in large terrestrial telescopes
13 p1920 A83-31010
Tests and quality of the 3.5 meter primary mirror of the
Max-Planck-Institut fuer Astronomie's telescope at Calar
Alto 13 p1920 A83-31012
Manufacture of large glass honeycomb mirrors --- for
astronomical telescopes 13 p1921 A83-31013
Development of high reflectance coatings for
ground-based astronomical instruments
13 p1921 A83-31014
Generation of off-axis aspherics --- optical surfaces for
telescopes 13 p1921 A83-31015
Stressed mirror polishing experiment underway at Kitt
Peak National Observatory 13 p1921 A83-31018
Interferometric control of a beam expander consisting
of multiple telescopes 13 p1921 A83-31022
Telescope alignment with the absolute distance
interferometer 13 p1921 A83-31023
10 m telescope for submillimeter waves
13 p1939 A83-31024
Coherent array telescopes as a fifteen meter optical
telescope equivalent 13 p1939 A83-31025
Optimum shapes for lightweighted mirrors --- of
astronomical telescopes 13 p1921 A83-31027
One-dimensional telescope aperture for brightness and
velocity speckle interferometry measurements
13 p1939 A83-31029
Speckle imaging for planetary research
13 p1939 A83-31028
Fiber optics at ESO. I - Coupling of the CES with the
3.6 m telescope using a 40 m fiber link
13 p1922 A83-31576
Application of a charge-coupled device (CCD) detector
for coudespectroscopy 14 p2016 A83-31992
Charge-coupled device (CCD)/transit instrument (CTI)
deep photometric and polarimetric survey - A progress
report 14 p2016 A83-31993
Drift scan observations with a charge-coupled device
(CCD) 14 p2016 A83-31994
Use of a Fourier transform spectrometer on a
balloon-borne telescope and at the multiple mirror
telescope (MMT) 14 p2016 A83-32002
Coudeauxiliary telescope (CAT) - A low cost telescope
at the European Southern Observatory
14 p2095 A83-32006
Grens for a Ritchey-Chretien (R-C) telescope ---
grating-on-lens corrector optics
14 p2096 A83-32008
Multiple object fiber optic spectroscopy
14 p2017 A83-32012
Multiple object fiber optics spectrograph feed for the
Hale telescope 14 p2017 A83-32013
Multi-aperture spectroscopy at Kitt Peak
14 p2017 A83-32014
High-resolution spectroscopy with the multi-anode
microchannel array detector systems
14 p2017 A83-32015
European Southern Observatory (ESO) automatic prime
focus camera and the general problem of remote control
14 p2018 A83-32027
A computational system for the automatic and
simultaneous acquisition of radio telescope data from four
different directions 14 p2101 A83-33292
Optical photometry with the Kuiper Airborne
Observatory 15 p2247 A83-34509
High accuracy measurement of the instrumental
polarization of the solar coudetelescope at the Okayama
Astrophysical Observatory 16 p2423 A83-35684
Design and adjustment of polarization compensators for
coudesoptics of stellar telescopes
16 p2423 A83-35686
A new automatic meridian circle PMC 190
16 p2424 A83-36629
Isoplanatism with respect to the arrival angles of light
rays in telescopes 16 p2426 A83-36856
Covariance analysis of a charge carrier device
processing algorithm for stellar sensors
17 p2474 A83-37062
A two-mirror stigmatic system in which the figure of one
of the mirrors is known 17 p2580 A83-37672
Optical telescope 25 m in diameter with a main mosaic
mirror 17 p2589 A83-37689
Possible optical scheme of a telescope with a main
spherical mirror with a diameter of 20-25 m
17 p2590 A83-37690
Testing of a five-channel spectrophotometer on the
AZT-8 telescope 17 p2590 A83-37695
Optical systems for large telescopes
17 p2590 A83-37722
A helium-3 cooled bolometer system for one millimeter
continuum observations 17 p2510 A83-37751
Southern spectrophotometric standards for large
telescopes 17 p2593 A83-38252

The design and study of the aspherical plate corrector of the view field for Cassegrain system
17 p2580 A83-38774
A large aperture balloon-borne telescope for a submillimeter wavelength survey of the galactic plane
18 p2759 A83-39824
SOT - A new look at the sun
18 p2785 A83-40309
ESO Infrared Workshop, 2nd, Garching, West Germany, April 20-23, 1982, Proceedings
18 p2760 A83-40419
Future UKIRT instrumentation --- infrared telescope
18 p2690 A83-40434
A middle-infrared heterodyne spectrometer to be used at the Cassegrain-focus of medium-size and large astronomical telescopes
18 p2761 A83-40436
A new InSb charge amplifier for application to a spectrometer array
18 p2691 A83-40446
Very Large Telescope (VLT) studies at ESO
18 p2762 A83-40451
VLT versus space --- Very Large Telescope
18 p2762 A83-40452
Infrared observations from the NASA Airborne Observatories
18 p2762 A83-40454
ASTROPLANE - A European airborne observatory for infrared astronomy
18 p2762 A83-40455
The scientific case and feasibility of a three metre balloon telescope
18 p2762 A83-40459
Adaptive optical system for astronomical applications
21 p3206 A83-48808
The Couder telescope - Better than the Schmidt?
22 p3375 A83-46579
A model for radial flow in a tube-dome junction of a telescope
23 p3508 A83-47846
Investigation of the characteristics of the PKT-26 telescope
24 p3638 A83-48956
Visual observations with a zenith telescope for the simultaneous determination of time and latitude
24 p3644 A83-49606
Automated quasar detection
24 p3649 A83-50028

ASTRONOMY

NT GAMMA RAY ASTRONOMY
NT INFRARED ASTRONOMY
NT RADAR ASTRONOMY
NT RADIO ASTRONOMY
NT SPACEBORNE ASTRONOMY
NT ULTRAVIOLET ASTRONOMY
NT X RAY ASTRONOMY
NT X RAY SOURCES
Automated data retrieval in astronomy; Proceedings of the Sixty-fourth Colloquium, Universite de Strasbourg I, Strasbourg, France, July 7-10, 1981
01 p0113 A83-10126
The Soviet Center of Astronomical Data
01 p0113 A83-10128
Management of astronomical data at Kanazawa Data Center
01 p0113 A83-10129
The U.K. StarLink computer network
01 p0093 A83-10134
ASTRONET - The network for analysis and retrieval of astronomical data in Italy
01 p0113 A83-10135
New developments in data storage
01 p0087 A83-10136
On systems of standards --- set of estimates in astronomy
01 p0101 A83-10139
International standards for software structures in astronomy
01 p0113 A83-10140
The system SPORA --- software package oriented to research in astronomy
01 p0114 A83-10145
The Bibliographical Star Index
01 p0114 A83-10148
Aids to the retrieval and evaluation of astronomical data
01 p0114 A83-10149
Data in astronomy --- and its management
01 p0114 A83-10152
Be stars; Proceedings of the Symposium, Munich, West Germany, April 6-10, 1981
01 p0119 A83-10301
Reports on astronomy
01 p0112 A83-10465
Astrophysics and cosmic physics --- Russian book
01 p0124 A83-10838
The primeval magnetic field --- magnetic moment/intrinsic angular momentum relation
01 p0127 A83-11293
Annual review of astronomy and astrophysics. Volume 20 --- Book
02 p0258 A83-12176
The United States astronomical community
02 p0245 A83-12273
Astronomical research outside the United States
02 p0245 A83-12274
Astronomical challenges for the twenty-first century
02 p0259 A83-12275
Basic information and references --- concerning comets
03 p0416 A83-13404
Infrared astronomy - Scientific/military thrusts and instrumentation; Proceedings of the Meeting, Washington, DC, April 21, 22, 1981
03 p0405 A83-13451

Problems in modern astrophysics --- Russian book
03 p0401 A83-13823
Astronomic geology - Its subject and general problems
04 p0502 A83-15400
Studies in astronomical time series analysis. II - Statistical aspects of spectral analysis of unevenly spaced data
05 p0693 A83-17010
The realm of the nebulae --- Book
05 p0701 A83-17325
Information search and retrieval in the areas of astronomy and geodesy --- Russian book
07 p1001 A83-20375
Two-dimensional goodness-of-fit testing in astronomy
07 p1007 A83-20942
The historical supernovae
08 p1174 A83-21846
Photoelastic-modulator polarimeters in astronomy
08 p1174 A83-22569
Molecular emission bands in the ultraviolet spectrum of the red rectangle star HD 44179
08 p1183 A83-23053
Stars and star systems --- Russian book
09 p1358 A83-23901
Astronomy and astrophysics for the 1980's. Volume 1 - Report of the Astronomy Survey Committee. Volume 2 - Reports of the Panels --- Book
09 p1351 A83-24950
Gravitational lenses
10 p1505 A83-25899
Advanced space instrumentation in astronomy; Proceedings of the Fourth Symposium, Ottawa, Canada, May 20-22, 1982
11 p1669 A83-27726
The planet Venus
13 p1960 A83-30138
Investigation of the possibilities of predicting astroclimate
13 p1935 A83-30271
MIDAS - ESO's new image processing system
13 p1942 A83-31581
The design of polarimeters for astronomy
13 p1848 A83-31684
Regional Latin American Conference on Astronomy, 2nd, Merida, Venezuela, January 19-23, 1981, Proceedings
14 p2107 A83-33235
Method of calculating the expected background luminance from the moon for planning astronomical observations
15 p2244 A83-33788
International Astronomical Union, General Assembly, 18th, Patras, Greece, August 17-26, 1982, Proceedings
16 p2422 A83-36725
On the question of using the method of false perturbations in astronomical practice
16 p2427 A83-36862
The development of studies of Venus
17 p2615 A83-37402
The dependence of the reflectivity of mirrors having a coating of Al + Al₂O₃ on the thickness of the Al₂O₃ film in the spectral range from 1700 A to 10,000 A
17 p2580 A83-37673
Search for Extraterrestrial Life - A new Commission of the International Astronomical Union
18 p2754 A83-39609
Present status and new trends in scientific ballooning in India
18 p2640 A83-39817
Compendium in astronomy --- Book
19 p2907 A83-41470
Errors in the referencing of geophysical fields by astronomical methods
19 p2867 A83-42019

ASTROPHYSICS

NT SOLAR PHYSICS
Plasma astrophysics at Santa Barbara
01 p0119 A83-10207
The limits of electrodynamics - Paraphotons
01 p0106 A83-10814
Astrophysics and cosmic physics --- Russian book
01 p0124 A83-10838
Relativistic cosmology for astrophysicists
01 p0127 A83-11288
On the instability of thick accretion disks
02 p0257 A83-12136
On perturbations of magnetic field configurations --- in astrophysics
02 p0257 A83-12139
Annual review of astronomy and astrophysics. Volume 20 --- Book
02 p0258 A83-12176
Extra-solar astronomy with a 2.4 m normal incidence X-ray telescope at 0.1 arcsec resolution
02 p0247 A83-12726
High-energy astrophysics
02 p0245 A83-13103
Physical processes in jets from active galaxies
03 p0412 A83-13151
The problem of split comets in review
03 p0403 A83-13384
Kinetics of the isotropic expansion of a homogeneous electron-photon plasma
03 p0397 A83-13535
Problems in modern astrophysics --- Russian book
03 p0401 A83-13823
Nonlinear diffusive instabilities in differentially rotating stars
03 p0425 A83-14522
Nonlinear waves in superposed fluids --- related to astrophysical phenomena
04 p0549 A83-14982

Toroidal solutions of the Gegenbauer equation --- for space gravitational and plasma problems
04 p0532 A83-15961
Astrophysical consequences of neutron-antineutron oscillations
04 p0556 A83-15965
Nonlinear astrophysical dynamo - Three-mode interaction
04 p0557 A83-15981
Gravitational lenses
05 p0701 A83-17773
On equations of motion for cross term modified gravitational field equations
05 p0703 A83-17860
Containment of a diffuse ionized mass orbiting around a magnetized central body --- for solar system development
06 p0828 A83-18475
Propagation of spherical shock waves in an exponential medium with radiation heat flux
06 p0834 A83-18879
Comment on 'Note on the stability of parallel magnetic fields'
06 p0835 A83-18897
Condensation of grains --- relevance to astrophysical problems
06 p0842 A83-19455
The motions of the stars and their significance in galactic astronomy / Karl Schwarzschild Lecture 1982/
06 p0824 A83-19532
G and K stars as indicators of the galactic evolution
06 p0846 A83-19535
Gamma ray transients and related astrophysical phenomena; Proceedings of the Workshop, La Jolla, CA, August 5-8, 1981
07 p1010 A83-20001
Relativistic plasmas --- of electron gas with non-relativistic ions in astrophysics
07 p1011 A83-20017
Cosmology and astrophysics - Essays in honor of Thomas Gold --- Book
07 p1013 A83-20401
Perfect fluids in the Einstein-Cartan theory
07 p0990 A83-21065
The optical scalar equations in the presence of a refractive medium
07 p1023 A83-21142
On rotating charged dust in general relativity. IV
07 p1027 A83-21356
An optimist's guide to supernovae
08 p1176 A83-21828
Calculation of the rate coefficients for the electron impact excitation of the n = 2 terms of O IV
08 p1179 A83-21989
Uniformly accelerated particle metrics obtained by soliton techniques
08 p1180 A83-22211
Energy loss of slowly moving magnetic monopoles in matter
08 p1192 A83-22640
New limit on magnetic monopole flux
08 p1192 A83-22642
Amorphous glassy plasma in dense stellar matter
08 p1185 A83-23085
Physical processes determining the structure of stellar chromospheres. I
09 p1358 A83-24014
Astronomy and astrophysics for the 1980's. Volume 1 - Report of the Astronomy Survey Committee. Volume 2 - Reports of the Panels --- Book
09 p1351 A83-24950
Transition probabilities for forbidden lines in the 3p4 configuration. III --- in astrophysics
09 p1362 A83-24986
The binary model for type I supernovae - Theoretical rates
10 p1498 A83-25355
Evolution of a population III star of low mass
10 p1499 A83-25361
Evolution of very low-mass stars
10 p1499 A83-25364
Comments on the dynamical effects of radiative viscosity --- in astrophysics
10 p1503 A83-25719
Huygens' principle and radiation tails in a weak Schwarzschild field
10 p1517 A83-26945
Magnetic fields in astrophysics /Helen B. Warner Prize Lecture/
11 p1676 A83-27102
Atomic clocks for astrophysical measurements
11 p1572 A83-27729
Plasma in astrophysics
11 p1680 A83-28242
On the magnetization and origin of the millisecond pulsar 1937 + 214
11 p1683 A83-28395
Physical processes determining the structure of stellar chromospheres. II
12 p1794 A83-29298
Inverse Compton scattering in a strong magnetic field
12 p1795 A83-29358
On the solution of the time-dependent inertial-frame equation of radiative transfer in moving media to O(v/c) --- largest velocity dependent term
12 p1796 A83-29610
Kernel estimates as a basis for general particle methods in hydrodynamics
12 p1724 A83-29617
The mean number of scatterings during radiative transfer with frequency redistribution
13 p1943 A83-30094
Conference on the Application of Accelerators in Research and Industry, 7th, North Texas State University, Denton, TX, November 8-10, 1982, Proceedings
13 p1917 A83-30176
Radioactive ion beams for studying astrophysical nuclear reactions
13 p1917 A83-30178

Coherent gyromagnetic emission --- in astrophysical objects 13 p1944 A83-30362

High-velocity outflow sources in molecular clouds - The case for low-mass stars 13 p1950 A83-31412

Stability of an astrophysical plasma near the onset of electron runaway 13 p1954 A83-31648

Thick disks with equatorial accretion. II 13 p1955 A83-31660

The effect of the existence of a single coordinate system of curvature on the properties of the boundary between the R and T regions and the energy-momentum tensor --- in stellar gravitational collapse 14 p2102 A83-32131

The macroscopic vacuum effects in an inhomogeneous and nonstationary electromagnetic field 14 p2079 A83-32136

The luminosity-core mass relation - Why and how 14 p2105 A83-33211

Regional Latin American Conference on Astronomy, 2nd, Merida, Venezuela, January 19-23, 1981, Proceedings 14 p2107 A83-32335

Electron impact excitation of positive ions of astrophysical interest. I - Theoretical method 14 p2109 A83-33279

Achievements in space astrophysics; Proceedings of the Topical Meeting, Ottawa, Canada, May 16-June 2, 1982 15 p2250 A83-33581

The solar corona - A testing ground for plasma astrophysics 15 p2277 A83-33582

Energy balance and stability --- in stellar coronae 15 p2252 A83-33606

Coronal heating mechanisms 15 p2277 A83-33607

Black hole accretion - The quasar powerhouse 15 p2254 A83-33813

An arbitrary-mesh computer program with applications to astrophysics 15 p2254 A83-33817

Level surface approach for uniformly rotating, axisymmetric polytropes --- used for astronomical models 15 p2269 A83-34642

Pair creation in a strong magnetic field 15 p2270 A83-34687

Physics of stellar evolution and cosmology --- Book 15 p2272 A83-34875

International Astronomical Union, General Assembly, 18th, Patras, Greece, August 17-26, 1982, Proceedings 16 p2422 A83-36725

Black holes, white dwarfs, and neutron stars: The physics of compact objects --- Book 17 p2595 A83-37164

Random fluctuations, persistence, and quasi-persistence in geophysical and cosmological periodicities - A sequel 17 p2525 A83-38231

The transitions between normal and null states of radio pulsars 17 p2606 A83-38233

The hydrodynamics of magnetic nonequilibrium 17 p2583 A83-38529

Compressible, conductive, steady MHD flow in a gravitational field --- applied to mass flow in sunspots 18 p2784 A83-39733

Astronomische Gesellschaft, Scientific Meeting on Cosmology and Relativistic Astrophysics, Constance, West Germany, March 22-25, 1983, Reports 18 p2776 A83-39770

Galaxy formation 18 p2776 A83-39774

Recent developments in scalar-tensor theories of gravity 18 p2741 A83-39781

Excitation of the earth's eigen vibrations by gravitational radiation from astrophysical sources 19 p2915 A83-41164

The excitation of a cyclotron potential instability in the magnetospheres of pulsars 19 p2916 A83-41223

Compendium in astronomy --- Book 19 p2907 A83-41470

The dynamics of intermediate-scale magnetic fields 19 p2903 A83-42001

Astrophysical consequences of a violation of the strong equivalence principle 20 p3063 A83-42166

The physics of planetary nebulae --- Russian book 21 p3227 A83-43918

Kelvin-Helmholtz instabilities in a sheared compressible plasma --- plasma physics 21 p3233 A83-44757

Numerical fits to important rates in high temperature astrophysical plasmas 22 p3380 A83-46573

The moment of creation - Big Bang physics from before the first millisecond to the present universe --- Book 22 p3380 A83-46686

Remote quantum mechanical detection of gravitational radiation 22 p3380 A83-46752

The angular momentum of celestial bodies and the fundamental dimensionless constants of nature 23 p3518 A83-47423

A class of self-similar astrophysical explosions 23 p3520 A83-47458

Activity in red-dwarf stars; Proceedings of the Seventy-first Colloquium, Catania, Italy, August 10-13, 1982 23 p3520 A83-47476

Magnetic fields and activity of the sun and stars - An overview 23 p3520 A83-47477

Stellar activity and calcium emission variability 23 p3521 A83-47492

Activity correlations in close binary systems 23 p3523 A83-47522

A second-order correlation approximation for thermal conductivity and Prandtl number of free turbulence --- in stars 23 p3527 A83-48062

Variational principle for relativistic magnetohydrodynamics 24 p3650 A83-48844

Planetary nebulae; Proceedings of the Symposium, University College, London, England, August 9-13, 1982 24 p3638 A83-49126

The evolution of viscous disks. IV - Stream penetration effects --- dwarf novae accretion disks 24 p3658 A83-49362

Semiconvective diffusion and energy transport --- in stellar interiors 24 p3669 A83-50102

ASYMMETRY

Some characteristics of the asymmetry of circulation mechanisms of the Northern and Southern Hemispheres 06 p0788 A83-17996

The asymmetry of photospheric absorption lines. I - An analysis of mean solar line profiles 06 p0854 A83-18547

A theory of the lo phase asymmetry of the Jovian decametric radiation 09 p1365 A83-23756

Problem of the global asymmetry of the lunar sphere 09 p1367 A83-25279

Dynamic effects of the angular asymmetry of stellar motions in galaxies 10 p1516 A83-26901

Asymmetries in four powerful radio sources 13 p1958 A83-31708

Inflation does not explain time asymmetry --- of universe 18 p2777 A83-39958

A study of nonsymmetrical periodic motions of symmetrical dynamic systems 23 p3501 A83-48460

ASYMPTOTES

Another self-similar blast wave - Early time asymptote with shock-heated electrons and high thermal conductivity --- in astrophysics 07 p1023 A83-21141

Methods for the investigation of rigid-body motions and their application to the classification of motions 09 p1337 A83-23556

Large-parameter asymptotics of the solution of the Fock-Klein-Gordon equation in the case of a discontinuous initial condition 09 p1339 A83-24318

Asymptotic properties of the Benjamin-Ono equation 14 p2077 A83-32506

Asymptotic behavior of the closed loop poles of linear optimal multivariable systems 23 p3502 A83-48676

ASYMPTOTIC METHODS

An asymptotic expression of lift slope of elliptic wing with high aspect ratio 01 p0002 A83-10125

Asymptotic error behavior in the Gaussian quadrature procedure --- German thesis 01 p0101 A83-10166

Asymptotic solutions for the motion of a viscous incompressible fluid filling the cavity of a rotating body 01 p0047 A83-11268

Asymptotic expansions for the problem of boundary layer formation 01 p0047 A83-11273

A boundary value problem for the Laplace equation with nonclassical spectral asymptotics 01 p0103 A83-11317

Concerning a method for investigating spectral asymptotics and its application to shell theory 02 p0189 A83-11639

Geometrical theory of dispersion distortions of signals with limited spectrum 02 p0163 A83-11685

Tests against certain ordered multinomial alternatives 02 p0232 A83-11832

Numerical improvement of asymptotic solutions for shells of revolution with application to toroidal shell segments 02 p0194 A83-12741

Melnikov's method and averaging 03 p0389 A83-13418

Analysis of global expansion methods: Weakly asymptotically diagonal systems --- Book 03 p0387 A83-13500

Asymptotic breaking and restoration of symmetry in a statistical system of particles with short-range vector interaction and isotropic cosmological models 03 p0417 A83-13533

An asymptotic analysis on the cracked plates including transverse shear deformation 03 p0341 A83-14488

Asymptotic behavior of an adaptive estimation algorithm with application to M-dependent data 03 p0387 A83-14595

On a multi-time step procedure to accelerate time-asymptotic flow calculations 03 p0322 A83-14613

Activation energy asymptotics applied to burning carbon particles 03 p0296 A83-14849

Analogy between the wave motions of chemically active and two-phase media 03 p0323 A83-14896

Asymptotic methods in the extreme-value problems of mechanics --- Russian book 04 p0530 A83-15835

The asymptotics of the averaged characteristics of periodic elastic media with strongly varying properties 04 p0456 A83-16411

An asymptotic method of calculating large-scale atmospheric motions 05 p0667 A83-17223

An asymptotic analysis of free convection boundary layer on a horizontal flat plate due to small fluctuations in surface temperature 05 p0638 A83-17321

Asymptotics of the solution of the Cauchy problem for a class of singularly perturbed systems of integro-differential equations 05 p0682 A83-17833

The asymptotic theory of resonance charge exchange between diatomics 06 p0807 A83-18044

An asymptotic high frequency analysis of the radiation from sources on perfectly-conducting structures with an impedance surface patch 06 p0715 A83-18647

Analytical techniques for reduction of computational effort in reflector antenna analysis 06 p0743 A83-18683

Uniform asymptotic technique for analyzing wave propagation in inhomogeneous slab waveguides 06 p0748 A83-18771

Analytical methods of nonlinear mechanics --- Russian book 07 p0989 A83-20377

Error bounds and error asymptotic behavior for a class of interpolation quadratures --- German thesis 07 p0987 A83-20397

Asymptotic solution of the diatomic Boltzmann equation 07 p0926 A83-20531

The asymptotics of the average intensity of radiation for several models of stochastic media 07 p0990 A83-20891

Asymptotic solution of the transfer equation for linearly polarized X-ray and gamma radiation 07 p1026 A83-21264

Numerical computation of an important integral function in two-dimensional radiative transfer 07 p1001 A83-21397

Analytic asymptotic solution of the kinked crack problem 08 p1116 A83-21657

Asymptotic relations and period doubling bifurcations in a mean-field model of optical bistability 08 p1164 A83-21887

An asymptotic theory of natural convection --- French thesis 08 p1084 A83-22091

A proof of the cosmic censorship hypothesis 08 p1180 A83-22208

An asymptotic study of the macroscopic behavior of a mixture of two viscous fluids 08 p1085 A83-22770

Transient response of an infinite cylindrical antenna 09 p1247 A83-23802

Vortex sheets and concentrated vorticity - A variation on the theme of asymptotic modelling in fluid mechanics 09 p1261 A83-24335

An asymptotic solution near the separation point of a shock layer in the case of hypersonic flow around pointed bodies 09 p1197 A83-24483

Analytical verification of undesirable properties of direct model reference adaptive control algorithms 09 p1334 A83-24806

Design of multivariable optimal control systems using asymptotic root loci 09 p1335 A83-24814

The development of numerical methods for solving the radiative transfer equation 09 p1340 A83-25258

Aspects of plastic postbuckling behavior 10 p1437 A83-25312

Uniform asymptotic approximations for duct eigenfunctions in a thin boundary layer flow [AIAA PAPER 83-0668] 10 p1473 A83-25905

Asymptotic stability of non-linear multiparameter singularly perturbed systems 10 p1464 A83-26512

An asymptotic analysis of interactions of feedback loops with parasitics in actuators and sensors 10 p1465 A83-26527

The autocorrelation function and Doppler spectral moments - Geometric and asymptotic interpretations --- of meteorological radar data 11 p1625 A83-27020

The nonlinear three-wave system - Strange attractors and asymptotic solutions 11 p1659 A83-28237

Standard and asymptotic finite element methods for incompressible viscous flows 12 p1721 A83-28856

Magnetic alignment of interstellar dust grains for dominating magnetic effects 12 p1790 A83-28896

Methods for the study of 'pendulum'-type dynamic systems --- Russian book 12 p1775 A83-29340

The second-order asymptotic solution for the shell of zero Gaussian curvature with closed cross sections 12 p1747 A83-29941

Asymptotic formulas for local spline approximation on a uniform grid 13 p1912 A83-31335

Asymptotic behavior of solutions of the Cauchy problem for a KdV-type system for large times 13 p1914 A83-31346

A calculation of the asymptotic behavior of 'intensity coefficients' in approaching corner and conical points
14 p2077 A83-31895

A model reference adaptive control system for discrete bilinear systems
14 p2074 A83-31931

Uniform ultimate boundedness of the solutions of uncertain dynamic delay systems with state-dependent and memoryless feedback control
14 p2074 A83-31933

Asymptotic analysis of radiative transfer problems
14 p2093 A83-31934

On a method of the asymptotic theory of diffraction
14 p2079 A83-32104

The asymptotic behavior of the stress-strain state of inhomogeneously aging bodies near the tip of a crack
14 p2030 A83-32352

An asymptotic solution to the equations of motion for the wobblestone --- asymmetrical spinning top dynamics
14 p2080 A83-32360

Nonlinear eigenvalue problems on infinite intervals
14 p2077 A83-32834

Connection for wave modulation
14 p2080 A83-32835

The use of the asymptotic method of short-time space for solving systems of differential and algebraic equations
14 p2078 A83-33010

Asymptotic near-wall stress dissipation rates in a turbulent flow
14 p2013 A83-33376

Analysis of a turbulent boundary layer subjected to a strong adverse pressure gradient
14 p2014 A83-33451

Asymptotic solution for the diffraction of an electromagnetic plane wave by a cylinder-tipped half-plane
15 p2144 A83-33806

Activation-energy asymptotics of the plane premixed flame
15 p2131 A83-34028

Theoretical implications of nonequal diffusivities of heat and matter on the stability of a plane premixed flame
15 p2132 A83-34029

Asymptotic methods in the elasticity theory for an orthotropic body --- Russian book
15 p2180 A83-34575

A servo compensator design approach for variable structure systems
15 p2222 A83-35126

Some results on stability and stabilization of systems with retardation
15 p2222 A83-35127

The evolution of Tollmien-Schlichting waves near a leading edge. II - Numerical determination of amplitudes
16 p2348 A83-35346

Numerical-asymptotic solution of problems of the strength and vibrations of thin shells of revolution
16 p2365 A83-35547

An asymptotic theory of deflagrations and detonations. I - The steady solutions
16 p2325 A83-35694

Asymptotic laws of shock wave attenuation in inhomogeneous media
16 p2350 A83-35709

Analysis of transient natural convection flow at high Prandtl number using a matched asymptotic expansion technique
16 p2354 A83-36596

Asymptotic properties of a state density approximation for optimal control
17 p2567 A83-37115

Asymptotic expansions of singularly perturbed Chandrasekhar type of equations
17 p2571 A83-37146

Scaling and modeling of three-dimensional, pressure-driven, turbulent boundary layers [AIAA PAPER 83-1695]
17 p2502 A83-37193

Asymptotic unbounded root loci - Formulas and computation
17 p2571 A83-37548

An asymptotic method for solving the Boltzmann equation for low Knudsen numbers
17 p2585 A83-38096

On boundary value problems for the domain exterior to a thin or slender region
18 p2680 A83-39146

Approximation of solutions of strongly nonstationary stochastic extremal problems in continuous time. II
19 p2889 A83-40899

Convergence of algorithms
19 p2893 A83-41023

Nonlinear dispersive systems - Theory and examples
19 p2842 A83-41257

An asymptotic solution to a class of singularly perturbed problems of optimum control
19 p2889 A83-41201

Asymptotic laws for the attenuation of weak continuous and shock waves in a dusty gas
19 p2844 A83-41810

Allowance for finite Mach numbers in hypersonic asymptotics for blunt axisymmetric bodies
19 p2791 A83-41880

Exact solutions of certain dual integral equations and their asymptotic properties
20 p3042 A83-43374

Asymptotic expansions and Lie algebras for some nonlinear filtering problems
20 p3040 A83-43406

Asymptotic methods in the equations of mathematical physics --- Russian book
21 p3197 A83-43908

The Knudsen ion layer problem in the theory of the collisionless sheath
21 p3212 A83-44356

An asymptotic method for the theory of shells
21 p3153 A83-44659

The asymptotic mass distribution for an accreting system of particles
21 p3234 A83-44759

The asymptotic near-tip solution for mode-III crack in steady growth in power hardening media
21 p3157 A83-44904

The asymptotic behavior of singular perturbations in the problem of the dynamics of a rigid body with elastic and dissipative elements
21 p3200 A83-45356

An asymptotic integration method in problems concerning wave propagation in shells of revolution
21 p3163 A83-45368

On asymptotically stabilizing feedback control of bilinear systems
22 p3352 A83-46370

Asymptotic theory of turbulent separation
23 p3452 A83-48655

Approximate solution of the strongly magnetized hydrogenic problem with the use of an asymptotic property --- application to stellar magnetic fields
24 p3650 A83-48828

Asymptotically optimal test algorithms in problems of recognition
24 p3620 A83-49124

The asymptotic method in the problem of the nonlinear vibration of shells
24 p3596 A83-49907

The asymptotic solutions of compressible, nonsteady boundary layer
24 p3581 A83-50129

ASYMPTOTIC SERIES

Asymptotic formulas for the dielectric response function of a relativistic plasma
01 p0107 A83-10905

Asymptotic solutions of the laminar boundary-layer equations
03 p0323 A83-14675

The evolution of Tollmien-Schlichting waves near a leading edge
09 p1261 A83-24410

Series solutions of the dispersion relation for linear water waves
11 p1635 A83-28428

An asymptotic theory of condensed two-phase flame propagation
12 p1712 A83-29000

A second order theory for large deflections of slender beams
12 p1736 A83-29706

A discretized asymptotic method for unsteady helicopter rotor airloads
12 p1697 A83-29867

[AIAA 83-0989]
12 p1697 A83-29867

A simple model for radiation damping
14 p2102 A83-33045

Exchange energy of an electron gas of arbitrary dimensionality
16 p2422 A83-35695

Analysis and optimization of Rosenblatt-Parsen classifier with the aid of asymptotic expansions
19 p2889 A83-40898

Advanced boundary-layer theory in heat transfer
20 p2970 A83-42657

On the asymptotic structure of interaction in a laminar axisymmetric wake
23 p3451 A83-48653

ASYNCHRONOUS MOTORS

Asynchronous induction micromotors for automatic systems --- Russian book
10 p1408 A83-25618

ATAXITE

The composition and structure of plessite phases in the Chinga ataxite
05 p0706 A83-17463

Analytical electron microscope study of eight ataxites
07 p1035 A83-21330

ATHEROSCLEROSIS

U ARTERIOSCLEROSIS

ATHLETES

The practical application of hypnosis in the athletic activity of young athletes
01 p0082 A83-10506

The ensemble of circadian rhythms and the effectiveness of training activities conducted at various times of the day
01 p0083 A83-10518

Sport gastroenterology - Some results and prospects of development
01 p0083 A83-10519

The content of glycogen in muscles and the effect of the carbohydrate saturation method on the physical aerobic work capacity of athletes and nonathletes
01 p0083 A83-10520

The active and passive flexibility of athletes of various specialties
01 p0083 A83-10523

The treatment of trauma of the locomotor system in athletes /Study of the work of the athletic clinic for trauma in Austria/
01 p0084 A83-11385

The effect of physical exercise on changes of lysozyme in the blood of athletes
01 p0084 A83-11388

The W170 differentiating test --- arm and leg veloergometer tests
01 p0084 A83-11389

A technique for determining the functional condition of athletes by a method of electropuncture diagnostics
03 p0382 A83-14349

The methodological principles for the determination of physical work capacity in young athletes
03 p0382 A83-14352

Selection and prediction of the athletic results of young female long-jumpers
03 p0382 A83-14353

Means for increasing athletic fitness - Technical and applied military aspects of athletics --- Russian book
07 p0977 A83-20383

Variations in heart rate (pulse 'drift') in the course of work of constant aerobic intensity in athletes and nonathletes
12 p1765 A83-29316

The use of biochemical indicators in a controlled training process for highly-trained biathlon participants
14 p2070 A83-33308

The time of the development of an interference electromyogram as an indicator of the speed and strength of an athlete
15 p2212 A83-34948

An evaluation of the condition and potential of athletes using indicators of humoral-hormonal reactions
16 p2398 A83-35904

The cardiovascular system and the fitness for work of athletes --- Russian book
19 p2880 A83-40983

The characteristics of heart rhythm disorders in athletes with various types of vegetative regulation
19 p2882 A83-41447

The dependence of the pattern of emotional condition on the characteristics of the training load of heavy athletes
19 p2884 A83-41448

Effect of exercise on left ventricular diastolic filling in athletes and nonathletes
20 p3034 A83-43477

ATHODYETS

U RAMJET ENGINES

ATLANTIC OCEAN

Optical properties of the atmosphere above the Atlantic Ocean
01 p0075 A83-10830

Observations regarding the MNPS in the North Atlantic and considerations concerning their applicability in the European air space. I
02 p0133 A83-13011

The chemistry of western Atlantic precipitation at the mid-Atlantic coast and on Bermuda
07 p0956 A83-20202

The newfoundland basin - Ocean-continent boundary and Mesozoic seafloor spreading history
12 p1752 A83-29173

The thermal interaction between the ocean and the atmosphere at the surface in the trade-wind zone in the North Atlantic
13 p1884 A83-30300

Diagnostic and prognostic numerical circulation studies of the South Atlantic Bight
14 p2060 A83-33078

Eddy kinetic energy in the North Atlantic from surface drifters
15 p2207 A83-33492

Observations of near-surface currents and temperature in the central and western tropical Atlantic ocean
15 p2208 A83-33495

Oceanographic studies. Number 35 --- Russian book
15 p2208 A83-34351

Seasonal variations of harmonic constants of diurnal and semidiurnal waves of atmospheric pressure according to POLYMODE data
15 p2206 A83-34354

Characteristics of the variability of atmospheric processes during the period of the experiment in the POLYMODE area
15 p2206 A83-34355

The spectrum of temperature oscillations in the neighborhood of the inertial frequency according to POLYMODE data --- Atlantic Ocean temperature measurement analysis
15 p2209 A83-34356

Some problems of heat-transfer climatology in energetically active zones of the Atlantic Ocean
16 p2392 A83-36848

Variability of the ocean and atmospheric in the equatorial Atlantic (FGGE investigations)
19 p2869 A83-42101

Variability of the temperature and salinity of surface and subsurface waters in the equatorial Atlantic
19 p2869 A83-42102

Certain characteristics of the structure and dynamics of hydrophysical fields in the zone of the Lomonosov current at 18 deg 30 min W
19 p2870 A83-42103

Optical characteristics of equatorial-Atlantic waters
19 p2870 A83-42105

Spatial-temporal variability of the optical attenuation coefficient of sea water
19 p2870 A83-42106

Spectra of primary hydrooptical characteristics --- in equatorial Atlantic
19 p2870 A83-42107

Variability of the spectral coefficient of sea brightness
19 p2870 A83-42108

Investigation of the mesoscale spatial variability of the distribution of the optical properties of surface waters in the tropical Atlantic
19 p2870 A83-42109

On the structure of the ocean surface layer
19 p2870 A83-42110

Investigation of maps of ocean surface temperature
19 p2870 A83-42111

Measurement of heat flux through the ocean surface
19 p2870 A83-42112

Meteorological investigations during the voyages of the research vessels Akademik Kurchatov and Professor Shokman in the FGGE program
19 p2868 A83-42114

Variability of meteorological fields in the equatorial Atlantic
19 p2868 A83-42115

- Precipitation patterns in the equatorial Atlantic
19 p2868 A83-42117
- Radiation studies in the equatorial Atlantic
19 p2867 A83-42119
- The structure of the atmosphere in the equatorial zone of the Atlantic in the spring and summer of 1979
19 p2869 A83-42120
- Meteorological conditions in the Atlantic FGGE study area
19 p2869 A83-42121
- Retarding layers in the troposphere over the equatorial Atlantic
19 p2869 A83-42122
- Water-vapor content of the near-equatorial atmosphere over the Atlantic Ocean during March-August 1979
19 p2869 A83-42123
- Weather conditions in the center of the equatorial Atlantic in the spring of 1979
19 p2869 A83-42124
- Atlantic hurricane season of 1982
20 p3030 A83-42512
- Influence of the Mediterranean outflow on the isotopic composition of neodymium in waters of the North Atlantic
20 p3028 A83-43473
- Structure of South Atlantic anomaly in maximum of 21st solar cycle by satellite IC-Bulgaria-1300 data
23 p3485 A83-48447
- ATLAS CENTAUR LAUNCH VEHICLE**
- Computer performance monitoring during the Centaur launch countdown
17 p2472 A83-37060
- Launch vehicles for communications satellites
19 p2812 A83-41374
- Commercial Atlas/Centaur program
[IAF PAPER 83-21] 23 p3419 A83-47235
- ATLAS LAUNCH VEHICLES**
- NT ATLAS CENTAUR LAUNCH VEHICLE
- Atlas and Centaur adaptation and evolution - 27 years and counting
01 p0018 A83-11483
- ATMOSPHERE EXPLORER C**
- U EXPLORER 51 SATELLITE
- ATMOSPHERE EXPLORER D**
- U EXPLORER 54 SATELLITE
- ATMOSPHERE EXPLORER E**
- U EXPLORER 55 SATELLITE
- ATMOSPHERIC ABSORPTION**
- U ATMOSPHERIC ATTENUATION
- ATMOSPHERIC ATTENUATION**
- NT AURORAL ABSORPTION
- The estimation of the absorption coefficients of ozone adopted for the Dobson spectrophotometer in the new selected additional wavelengths
01 p0071 A83-10290
- Evaluation of the atmospheric content of particulate mass from visibility observations
01 p0072 A83-11046
- Estimations of attenuations of earth-satellite links in France
01 p0032 A83-11336
- Using site-diversity reception to overcome rain depolarization in millimeter wave satellite communications systems
01 p0033 A83-11370
- Deformation of the absorption curves of cosmic rays in the atmosphere and the polarity of the solar magnetic field
02 p0273 A83-11722
- Satellite communications research - The problems of propagation
02 p0163 A83-11820
- Theoretical random process for prediction of rain attenuation statistics in site diversity satellite links above 10 GHz
02 p0163 A83-11984
- Source regions deduced from attenuation bands in VLF saucers
02 p0208 A83-12388
- Absorption of fluxes of galactic cosmic rays in the atmosphere during 1961-1980
02 p0208 A83-12418
- Results of the VPI&SU Comstar experiment --- depolarization and attenuation due to rain
02 p0140 A83-12610
- An improved model for earth-space microwave attenuation distribution prediction
02 p0140 A83-12611
- A two-component rain model for the prediction of attenuation statistics
02 p0164 A83-12612
- Results of 11.7-GHz CTS rain attenuation measurements at Waltham, Massachusetts
02 p0140 A83-12617
- Microwave noise temperature and attenuation of clouds - Statistics of these effects at various sites in the United States, Alaska, and Hawaii
02 p0164 A83-12618
- Centimeter and millimeter wave attenuation and brightness temperature due to atmospheric oxygen and water vapor
02 p0165 A83-12619
- A simple model for the estimation of rain-induced attenuation along earth-space paths at millimeter wavelengths
02 p0141 A83-12620
- Diversity reception of Comstar satellite 19/29-GHz beacons with the Tampa Triad, 1978-1981
02 p0141 A83-12621
- Initial results from the VPI&SU SIRIO diversity experiment
02 p0141 A83-12622
- Measurements of satellite beacon attenuation at 11.7, 19.04, and 28.56 GHz and radiometric site diversity at 13.6 GHz
02 p0141 A83-12625
- Solid state components adapt to sensor environmental demands
02 p0168 A83-12973
- Horizon line scanning telephotometry
03 p0325 A83-13496
- Transmission of CO₂ in the atmosphere of Venus for the spectral region near 7 microns
03 p0434 A83-13836
- Below room temperature measurements of the 8-12 micron water vapor continuum absorption
03 p0358 A83-13980
- High-resolution atmospheric spectroscopy using a diode laser heterodyne spectrometer
03 p0327 A83-13984
- Atmospheric transmittance and radiance - The LOWTRAN 5 code
03 p0358 A83-13988
- Radar prediction of absolute rain fade distributions for earth-satellite paths and general methods for extrapolation of fade statistics to other locations
03 p0306 A83-14013
- A simple model for relative air mass
03 p0370 A83-14644
- Radiation damping of acoustic-gravity waves in a nonisothermal atmosphere
03 p0362 A83-14828
- Raindrop size distribution from microwave scattering measurements in equatorial and tropical climates
04 p0466 A83-15239
- Study of the absorption of pulsed CO₂ laser radiation by air and by carbon dioxide
04 p0484 A83-15705
- Up-link power control experiment --- of Japanese Medium-scale Broadcasting Satellite
04 p0468 A83-16421
- The transmission to space of the light produced by lightning in the clouds of Venus
05 p0704 A83-16967
- Transmission cutoff accompanying remote optical breakdown of the atmosphere by CO₂ laser pulses
05 p0687 A83-17064
- A semi-empirical formula for microwave depolarization versus rain attenuation on earth-space paths
05 p0622 A83-17273
- Transmittance of the atmosphere in the /8-0/ and /9-0/ Schumann-Runge bands of oxygen
06 p0786 A83-18323
- Sodar echoes and line of sight microwave propagation
06 p0736 A83-18349
- Satellite measurement of the effects of rain and sleet on the performance of a radome covered antenna
06 p0742 A83-18678
- Melting layer attenuation at 28.56 GHz from simultaneous Comstar beacon and 16.5 GHz polarization diversity radar observations --- below ice crystals or snow
06 p0744 A83-18701
- Propagation effects on microwave and millimetre-wave earth-satellite links
06 p0745 A83-18703
- Slant-path attenuation measurements in the range 12-30 GHz using OTS and passive radiometers at Martlesham Heath
06 p0745 A83-18704
- Attenuation and crosspolarisation on satellite-earth paths observed with O.T.S. beacons
06 p0745 A83-18709
- Propagation measurements along a slant satellite path using the OTS satellite
06 p0745 A83-18710
- Molecular absorption by atmospheric gases in the 100-1000 GHz region
06 p0808 A83-18713
- The measurement of scattering characteristics of individual water drops at 100 GHz
06 p0746 A83-18719
- Diversity- and single-site radiometric measurements of 12-GHz rain attenuation in different climates
06 p0746 A83-18721
- Prediction of 11 and 14 GHz rain attenuation on satellite-earth paths using passive radiometers
06 p0746 A83-18723
- The measurement of propagation characteristics of the atmosphere at 890 GHz using an open resonator technique
06 p0748 A83-18740
- Meteosat-VIS-channel - Signal reduction due to atmospheric water vapor and ozone
06 p0787 A83-18994
- Radio occultation of the atmosphere by means of sources of artificial and natural origin
06 p0787 A83-19352
- Spatial changes in the induced fluctuations of the intensity of radiation used to probe a bleachable aerodisperse medium
07 p0988 A83-20106
- Ground-based infrared spectroscopic measurements of atmospheric hydrogen cyanide
07 p0956 A83-20212
- Depolarization of 19-GHz signals --- from satellite beacons
07 p0871 A83-20552
- Rain attenuation considerations for satellite paths in Australia
07 p0915 A83-21029
- Submillimeter transmission of the atmosphere at Shorbulak, Eastern Pamirs
07 p0971 A83-21276
- Statistics of differential rain attenuation on adjacent earth-space propagation paths
08 p1074 A83-21646
- Statistical properties of tropical rainfall intensity measured in Nigeria, for microwave and millimetre wave applications
08 p1074 A83-21649
- An analytical model to calculate the atmospheric correction on infrared thermal signals
08 p1133 A83-21927
- Rainfall attenuation at 36 GHz and 55 GHz
08 p1076 A83-22248
- Objective summary of U.S. Army electro-optical modeling and field testing in an obscuring environment
08 p1093 A83-22351
- Millimeter wave atmospheric turbulence measurements - Preliminary results and instrumentation for future measurements
08 p1076 A83-22354
- Extinction by clouds consisting of polydisperse and randomly oriented nonspherical particles at arbitrary wavelengths
08 p1135 A83-22356
- Obscuration by helicopter-produced snow clouds
08 p1043 A83-22357
- Review of cirrus cloud optical properties and effects on infrared sensors
08 p1135 A83-22544
- Measurements of infrared and visible extinction in adverse weather
08 p1140 A83-22546
- Measurements of the phase function of natural particles
08 p1076 A83-22547
- Modified gamma aerosol model for the marine environment
08 p1136 A83-22553
- Impact of aerosol modeling on performance calculations of electro-optic /EO/ systems operating in marine environments
08 p1136 A83-22555
- Near millimeter wave /NMMW/ snow extinction - Atmospheric Sciences Laboratory-MMTRN model and data review
08 p1141 A83-22558
- Characteristics of near-millimeter wave propagation in snow
08 p1076 A83-22560
- Lidar calibration and extinction coefficients
08 p1077 A83-22612
- Multiwavelength sun-photometers for accurate measurements of atmospheric extinction in the visible and near-IR spectral range
08 p1101 A83-22621
- Determination of atmospheric water vapor content in moderate optical paths by radiometric measurements
08 p1136 A83-22853
- Overview of infrared measurement programs
08 p1103 A83-22862
- Distance errors related to atmospheric effects at signal frequencies greater than 100 MHz in the case of geodetic systems of measurement. I - Influence of the troposphere. II - Influence of the ionosphere
09 p1301 A83-23387
- Measurements of the absorption and brightness temperatures of the atmosphere in the millimeter wavelength range
09 p1301 A83-23481
- Atmospheric EHF window transparencies near 35, 90, 140, and 220 GHz
09 p1247 A83-23793
- Selection of optimum frequencies for atmospheric electric path length measurement by satellite-borne microwave radiometers
09 p1219 A83-23794
- A review of satellite communication and propagation experiments for frequencies above 10 GHz
09 p1249 A83-24646
- Spectroscopic measurements of the 'additional absorbing mass' in total and partial cloudiness
09 p1316 A83-25055
- The propagation of narrow light beams in rain
09 p1273 A83-25079
- The nonstationary scattering of spatially confined and ultrashort light pulses
09 p1273 A83-25256
- Effects of nonlinear propagation on long-range noise attenuation
[AIAA PAPER 83-0700] 10 p1474 A83-25920
- The dependence of rain attenuation statistics on meteorological parameters
10 p1451 A83-26043
- Extension of Lin empirical formula for the prediction of rain attenuation
10 p1403 A83-26045
- Nonlinear energy attenuation of pulsed CO₂ laser radiation in the atmospheric surface layer
10 p1434 A83-26776
- An S band radar for studying the effects of weather on the Sirio and Comstar satellite downlink signals
11 p1628 A83-27053
- Role of gas absorption in formation of fluctuations in parameters of cleared cloud medium and laser radiation
11 p1631 A83-27606
- Attenuation of high-frequency radio waves in the lower high-latitude ionosphere, artificially disturbed by high-power radio transmissions
11 p1615 A83-27951
- The use of resource sharing and coding to increase the capacity of digital satellites
11 p1557 A83-28135
- Various features of VLF waves generated by lightning discharge
11 p1619 A83-28429

A beam ratio technique for microwave observation of S-component sources --- from solar active regions	11	p1693	A83-28589
Retrieval of aerosol characteristics from scattering and extinction measurements	12	p1755	A83-29565
Validation of aerosol measurements by the satellite sensors SAM II and Sage	12	p1755	A83-29572
Can turbidity measurements be used for the estimation of aerosol parameters?	12	p1755	A83-29574
Simultaneous measurements of sea surface temperature by GMS-1 and GMS-2	12	p1761	A83-29701
The attenuation and scattering of infrared radiation by polydisperse systems comprising platelets and cylinders of ice	13	p1883	A83-30029
A survey of Australian sites suitable for telescopes operating at mm-wavelengths	13	p1936	A83-30402
Anomalous absorption by water vapour in the microwave region	13	p1894	A83-31546
Diffuse and global solar spectral irradiance under cloudless skies	13	p1882	A83-31613
An experimental study of atmospheric optical transmission	13	p1830	A83-31724
The winter anomaly (WA) of short waves	14	p2048	A83-31815
The UV-photometry experiment on the Venera-13 and Venera-14 descent modules	14	p2111	A83-31966
A statistical study of abnormal depolarization	14	p2000	A83-32419
Fluctuations of the parameters of an electromagnetic wave in a turbulent light absorbing atmosphere	14	p2052	A83-32559
Refining a radiation model of a stratiformis cloud	14	p2058	A83-32856
A system for spacecraft attitude determination using laser techniques	14	p1981	A83-33148
Measuring atmospheric scattering and extinction at 10 microns using a CO2 lidar	15	p2201	A83-34464
A temperature effect at the origin of the UV contrast in the clouds of Venus	16	p2435	A83-35358
Remote determination of cloud liquid water path from bandwidth-limited shortwave measurements	16	p2384	A83-35465
[AD-A130447]	16	p2342	A83-35519
Studies on the temperature of the medium at 11.7 GHz	16	p2376	A83-35788
Twilight observations from a balloon gondola - Preliminary results	16	p2376	A83-35788
Measurements of solar radiation absorption in the clear atmosphere during PUKK --- project for investigation of coastal climate	16	p2391	A83-36589
Calculation of the inversion curves by the Monte Carlo method --- for ozone attenuation coefficient determination	16	p2392	A83-36849
Simple method for estimating atmospheric absorption at 1 to 15 GHz	17	p2494	A83-37795
A comparative study of some aspects of low and middle latitude ionospheric absorption	17	p2545	A83-38540
Measured aerosol size distributions and calculated EM extinction in air masses moving off the east coast	17	p2550	A83-38730
Determination of the attenuation of visible, infrared, and millimeter waves in clouds on the basis of meteorological models	18	p2674	A83-39427
Preliminary results of the analysis of light refraction in the atmospheric boundary layer of Venus	19	p2923	A83-41236
Effect of adverse sand storms on millimeter electromagnetic wave propagation	19	p2827	A83-41330
A one kilowatt class direct broadcast satellite	19	p2829	A83-41352
AFGL atmospheric absorption line parameters compilation - 1982 edition	20	p3016	A83-42207
Attenuation of solar irradiance in the stratosphere	20	p3021	A83-42861
Spectrometer measurements between 191 and 207 nm	20	p3021	A83-42861
Telluric spectra from 4690 to 5525 A in a humid atmosphere	21	p3169	A83-43873
Characteristics of an anomalous component of cosmic rays in the stratosphere	21	p3245	A83-45229
Gaseous contaminants in the atmosphere and changes of the global climate	21	p3169	A83-45334
A model for rain attenuation prediction in single and site diversity earth-satellite links	21	p3122	A83-45416
Infrared absorption by natural organic aerosol	22	p3321	A83-45635
The rotational spectrum of water dimers (H2O)2 in atmospheric conditions	22	p3322	A83-45637
A method for predicting the rain-attenuation statistics of radiowaves in the range of 10-100 GHz - Horizontal terrestrial paths	22	p3271	A83-45645
Theory of low frequency wave propagation	22	p3273	A83-45889
Analysis of Mount St. Helens ash from optical photoelectric photometry	22	p3329	A83-46418
An algorithm for estimating rain rate by a dual-frequency radar	22	p3274	A83-46529
Electromagnetic wave propagation and scattering in rain and other hydrometeors	22	p3275	A83-46777
The effect of atmospheric attenuators with structured vertical distributions on air mass determinations and Langley plot analyses	22	p3341	A83-46858
Centimeter wave propagation experiments using the beacon signals of CS and BSE satellites	23	p3420	A83-47832
A statistical method for the calculation of molecular absorption --- in atmosphere near earth surface	23	p3485	A83-48560
The spatial and temporal variability of absorption coefficients of the tropospheric aerosol in the spectral region of 0.4-2.2 microns	23	p3492	A83-48561
Determination of excessive absorption by atmospheric water vapour at 22.235 GHz	24	p3606	A83-49310
Advanced communications satellite systems	24	p3551	A83-49855
Rain-induced amplitude scintillation on 8.2 km line-of-sight path at 30 GHz	24	p3571	A83-50120
ATMOSPHERIC BOUNDARY LAYER			
Relationships between structure functions and temperature ramps in the atmospheric surface layer	01	p0075	A83-10719
A switched continuous-wave sonic anemometer for measuring surface heat fluxes	01	p0050	A83-10722
Two-dimensional field of thermal turbulence at the edge of an escarpment	01	p0075	A83-10723
Similarity forms for ground-source surface-layer diffusion	01	p0075	A83-10724
Structure of air flow separation over wind wave crests	01	p0075	A83-10725
Variations of the refractive index in the atmospheric surface layer	01	p0072	A83-10854
A model for the formation of a temperature inversion layer in a thin atmosphere stratum adjacent to water	01	p0076	A83-10910
On some characteristics of the atmospheric boundary layer in the Indian Ocean during the GARP cruise	02	p0212	A83-11846
A climatological estimate of the radiative cooling of the atmosphere	02	p0213	A83-11977
The effect of ordered vertical velocities and of the earth's surface on the trajectories of particles of polluted air in the atmosphere	02	p0205	A83-12000
A simple model for nonlinear critical layers in an unstable baroclinic wave	02	p0213	A83-12226
Velocity spectra in the unstable planetary boundary layer	02	p0214	A83-12235
A finite-element model of the atmospheric boundary layer suitable for use with numerical weather prediction models	02	p0214	A83-12236
The properties of ionospheric O+/+ ions as observed in the magnetotail boundary layer and northern plasma lobe	02	p0207	A83-12383
A two-dimensional numerical study of horizontal roll vortices in an inversion capped planetary boundary layer	02	p0215	A83-12939
A diagnostic model for estimating winds at potential sites for wind turbines	02	p0216	A83-12954
A high-resolution ionic anemometer for boundary-layer measurements --- in atmosphere	02	p0216	A83-12955
Measuring /C sub T/-squared, /C sub Q/-squared, and C sub TQ in the unstable surface layer, and relations to the vertical fluxes of heat and moisture --- atmospheric temperature and humidity	03	p0363	A83-13274
On the definition of the flux of sensible heat --- in atmosphere	03	p0364	A83-13276
Transmission of CO2 in the atmosphere of Venus for the spectral region near 7 microns	03	p0434	A83-13836
Diurnal and seasonal variations in the atmospheric structure parameter /C n/-squared/ that affect the atmospheric modulation transfer function /MTF/	03	p0364	A83-13978
Simulation of the planetary boundary layer with the UCLA general circulation model	03	p0366	A83-14413
An operational turbulence closure model forecast system	03	p0369	A83-14451
A comparison of spectral and cospectral characteristics of dynamic and thermal turbulent fields in weakly stratified boundary layers	03	p0319	A83-14475
Dilatation effects in wind tunnel simulation of non adiabatic atmospheres	03	p0319	A83-14476
Combined acoustic and radioacoustic probing of the atmospheric boundary layer	03	p0372	A83-14829
Dynamics of the baroclinic unstratified planetary boundary layer over land and sea	04	p0515	A83-15721
A numerical simulation of an atmospheric vortex street	04	p0516	A83-15856
Assessment of the separate effects of baroclinicity and thermal stability in the atmospheric boundary layer over the sea	04	p0516	A83-15857
Numerical study of terrain-induced mesoscale motions in a mixed layer	04	p0516	A83-15932
Spectral scales in the atmospheric boundary layer	05	p0667	A83-17441
A Lagrangian long-range transport model with atmospheric boundary layer chemistry	05	p0667	A83-17443
The depth of the daytime mixed layer at two coastal sites - A model and its validation	06	p0788	A83-18057
Momentum and heat transfers in the surface layer over a frozen sea	06	p0788	A83-18059
Stability dependence of fluxes and bulk transfer coefficients in a tropical boundary layer	06	p0788	A83-18061
Atmospheric-dispersion experiments in the near and medium field /Fourth European Community Campaign, Turbigo, Italy, September 1979/	06	p0781	A83-18137
The turbulent wind flow over an embankment	06	p0789	A83-18239
Spurious mass loss in some mesometeorological models	06	p0789	A83-18241
Studies of the atmospheric stability characteristics during the solar eclipse of February 16, 1980	06	p0789	A83-18243
The interactive evolution of the oceanic and atmospheric boundary layers in the source regions of the trades	06	p0790	A83-18260
Entrainment and detrainment in a simple cumulus cloud model	06	p0790	A83-18262
Operational evaluation of a turbulence closure model forecast system	06	p0791	A83-18460
[AD-A125467]	06	p0791	A83-18460
A comparative study of simple numerical models of the atmospheric boundary layer	06	p0792	A83-18927
Lidar measurements of natural and artificial aerosol during PUKK	06	p0787	A83-18997
Radio-remote-sensing determination of the vertical temperature gradient in the atmospheric surface layer	07	p0970	A83-20866
The refraction in the atmospheric surface layer	07	p1031	A83-20890
Aerosol modeling in the marine boundary layer	08	p1136	A83-22552
Acoustic remote sensing of the boundary layer	08	p1141	A83-22991
Royal Society, Discussion on the Joint Air-Sea Interaction Project /JASIN/, London, England, June 2, 3, 1982, Proceedings	09	p1309	A83-23351
Mass, momentum, sensible heat and latent heat budgets for the lower atmosphere	09	p1309	A83-23353
The structure of the turbulent atmospheric boundary layer	09	p1309	A83-23354
The structure of an atmospheric warm front and its interaction with the boundary layer	09	p1310	A83-23355
Case studies of radiation in the cloud-capped atmospheric boundary layer	09	p1310	A83-23356
Boundary layer structure in relation to large-scale flow - Some remarks on the JASIN observations	09	p1310	A83-23357
The spectrum of the scattering signal for the radioacoustic sounding system /RASS/	09	p1310	A83-23406
Stratospheric sulfuric acid vapor - New and updated measurements	09	p1296	A83-24272
On a satellite scatterometer as an anemometer	09	p1219	A83-24294
The causes of the origin of mesosets and the calculation of the wind velocity at their axes in narrow zones of warm fronts	09	p1315	A83-24936
Methods for the passive probing of transparency in the atmospheric surface layer	09	p1315	A83-25054
Ozone concentration near the earth's surface during a total solar eclipse	09	p1308	A83-25060
Sulfate in the atmospheric boundary layer - Concentration and mechanisms of formation	09	p1299	A83-25201
Surface signatures of a dry nocturnal gust front	10	p1451	A83-25391
The dependence of sound extinction on the parameters of thermal turbulence in the atmospheric boundary layer	10	p1451	A83-25823
Prestorm boundary layer observations with Doppler radar	11	p1629	A83-27061
Wintertime cyclonic storms over the north east Pacific Ocean	11	p1630	A83-27073
Magnetic structure of the boundary layer --- explaining magnetospheric convection	11	p1614	A83-27391

Doppler-SODAR measured variations of mean and turbulent wind field during PUKK --- project for the investigation of the coastal climate

An analysis of the surface production of sea-salt aerosols
Errors in measuring the temperature-inversion characteristics of the atmospheric boundary layer during radio sounding
Regular measurements of the air's electrical conductivity
An analysis of multiyear variations in atmospheric electrical quantities in the atmospheric surface layer on the basis of observational data

Results from regular observations of the electrical conductivity of air at Verkhnee Dubrovo

Variability in atmospheric electrical quantities

Profile measurements in the atmospheric near-surface layer and the use of suitable universal functions for the determination of the turbulent energy exchange

Convective plumes in the atmospheric boundary layer as observed with an acoustic Doppler sodar

An interpolation method of randomly distributed atmospheric data in the height-time domain

Dissipation length in stable layers --- atmospheric boundary layer energy parameterization

Turbulent characteristics of a shallow convective internal boundary layer

A one-dimensional simulation of the stratocumulus-capped mixed layer

Retrieval of aerosol optical characteristics from polarization measurements of reflected solar radiation above the oceans

The effect of waves on the vertical profiles of wind velocity and on momentum fluxes in the atmospheric surface layer at sea

Thermally indirect motions in the convective atmospheric boundary layer

Parameterization of the surface fluxes of heat and momentum for the convective atmospheric boundary layer

Airborne measurements of the free convective internal boundary layer during the sea breeze

Three-dimensional space structure of turbulent eddy in the atmospheric boundary layer above the ocean

A heat-flux history length scale for the nocturnal boundary layer

Current sheets at the boundary of the magnetosphere

Diagnostic and prognostic numerical circulation studies of the South Atlantic Bight

An objective boundary layer characterization using satellite photographs

Rossby-number similarity in the atmospheric boundary layer over a slightly inclined terrain

Effects of baroclinicity on resistance laws for the atmospheric boundary layer over a slightly inclined terrain

Typical influences of moisture on profile measurements in the marine atmospheric surface layer

On the maintenance of the Marine boundary layer-free tropospheric gradient of transient tracers

Structure of the free convective internal boundary layer above the coastal area

Atmospheric boundary layers --- review of recent research

Model of marine aerosol generation via whitecaps and wave disruption

Surface influence upon vertical profiles in the nocturnal boundary layer

Temperature measurement with a sonic anemometer and its application to heat and moisture fluxes

A note on estimating the vertical eddy diffusion coefficient from Landsat imagery

Conditional sampling of turbulence in the atmospheric surface layer

Dynamical model simulation of the morning boundary layer development in deep mountain valleys

Retrieval of near-surface temperatures from satellite data

Modeling of the boundary of the plasmasphere and its parameters with allowance for convective motions

A model for the Priestley-Taylor parameter alpha --- of atmospheric boundary layer

Integral scales for the nocturnal boundary layer. I

Empirical depth relationships

Interannual variations of mean monthly sea-level pressure in January

Horizontal structure of the atmospheric boundary layer in the intertropical convergence zone

Reflection of light by a multilayered planetary atmosphere

Computation of turbulent flow over a moving wavy boundary

Boundary layer evolution in the region between shore and cloud edge during cold-air outbreaks

The formation of a stable layer of atoms and ions of metals in the upper atmosphere

Method for calculating radio-brightness temperature in problems of satellite meteorology

The effect of the stratification of the atmospheric boundary layer over water on the energy flux to waves

A practical approach to flux measurements of long duration in the marine atmospheric surface layer

A boundary-layer-scale model of mountain upslope flow

[AD-A130312]

The simulation of temperature-stratified atmospheric boundary layers in a wind tunnel

Boundary-layer structure over tropical oceans from TIROS-N infrared sounder observations

Calculation of the turbulent regime in the boundary layer of the ocean

Variability of the size distributions of aerosol particles near the earth's surface

A statistical method for the calculation of molecular absorption --- in atmosphere near earth surface

Wave and turbulence structure in a disturbed nocturnal inversion

Investigation of the background concentration of ozone in the atmospheric surface layer

On the concentration of mercury in the atmosphere in background regions

Background variability of the aerosol and ion composition of the atmospheric surface layer

Measurements of the concentration of carbon monoxide in the atmospheric surface layer using tunable diode lasers

The equation of refraction in the atmospheric surface layer

Boundary layer processes and cloud formation

An investigation of the interaction between developing convective systems and the boundary layer --- for south Florida cumulonimbus

Sensitivity of radiative-convective processes to boundary layer clouds

ATMOSPHERIC CHEMISTRY

The role of photochemistry and dynamics in the D region of the ionosphere

The global troposphere - Biogeochemical cycles, chemistry, and remote sensing

Temperature and third-body dependence of the rate constant for the reaction $O + O_2 \rightarrow M$ yields $O_3 + M$

NO infrared radiation in the upper atmosphere

Temperature and solar zenith angle control of D-region positive ion chemistry

[AD-A126882]

Handbook of physics. Volume 49 - Geophysics III. Part 6 --- Book

The neutral and ion chemistry of the upper atmosphere

Photochemistry of the stratosphere of Venus - Implications for atmospheric evolution

The chemistry of metastable species in the Venusian ionosphere

Atmospheric ozone and changes in the global climate --- Russian book

The photochemistry and dynamics of a dusty cometary atmosphere

The thermospheric heating efficiency under electron precipitation conditions

On the chemistry of H_2O , H_2 and meteoritic ions in the mesosphere and lower thermosphere

Carbon catalyzed SO_2 oxidation by NO_2

The atmospheres of Io and other satellites

H_2CN /plus/- nN_2 clustering formation and the atmosphere of Titan

Kinetics of the reaction of hydroxyl radicals with nitric acid

Kinetics of the reaction $O + HO_2$ yields $OH + O_2$ from 229 to 372 K

A Lagrangian long-range transport model with atmospheric boundary layer chemistry

Combined mass spectrometric composition measurements of positive and negative ions in the lower ionosphere. I - Positive ions

Q branches in the rotational spectrum of $HOCl$

The atmospheric neutral sodium layer. II - Diurnal variations

The prebiological paleoatmosphere - Stability and composition

Photochemistry of NH_3 , CH_4 and PH_3 - Possible applications to the Jovian planets

Organic syntheses from CH_4 - N_2 atmospheres - Implications for Titan

Formation of amino acids from models of Titan and more oxidized atmospheres

The chemistry of western Atlantic precipitation at the mid-Atlantic coast and on Bermuda

Volcanic aerosol phosphorus, chlorine, and sulfur at Kilauea, Hawaii

A stratospheric chemical instability

Rate constants for the reaction of OH with SO_2 at low pressure

Thermospheric neutral composition from auroral ion ratios

The possible effects of translationally excited nitrogen atoms on lower thermospheric odd nitrogen

The kinetics of the reaction of OH with ClO

Photodissociation of $HCHO$ in air - CO and H_2 quantum yields at 220 and 300 K

Photochemistry of acetylene at 1849 Å

The role of ion-molecule reactions in the conversion of N_2O_5 to HNO_3 in the stratosphere

Reversible and irreversible wet deposition processes involving atmospheric admixtures

The sources of sulfate in precipitation. I - Parameterization scheme and physical sensitivities

On the relationship between the greenhouse effect, atmospheric photochemistry, and species distribution

The seasonal variation of the atmospheric SO_2 to SO_4^{2-} conversion rate

A rocket observation of the 6300 Å/5200 Å intensity ratio in the dayside aurora - Implications for the production of $O(1D)$ via the reaction $N(2D) + O_2 \rightarrow NO + O(1D)$

Vibrational population distribution in the hydroxyl night airglow

July 1981 NASA workshop on passive remote sensing of the troposphere

Rate constant for the reaction of $O(3P)$ with HBr from 221 to 455 K

Heterogeneous atmospheric chemistry --- Book

Common problems in nucleation and growth, chemical kinetics, and catalysis --- in earth atmosphere

Effect of the mechanism of gas-to-particle conversion on the evolution of aerosol size distributions

Neutral and charged clusters in the atmosphere - Their importance and potential role in heterogeneous catalysis

Role of ions in heteromolecular nucleation - Free energy change of hydrated ion clusters

Structural studies of isolated small particles using molecular beam techniques --- atmospheric aerosols

Chemical reactions with aerosols	09	p1297	A83-25182	The atmospheric oxidation of flue gases from a coal-fired power plant - A comparison between smog chamber and airborne plume sampling	15	p2193	A83-33503	Modeling of multiphase atmospheric aerosols	20	p3015	A83-43429
Electron beam studies of individual natural and anthropogenic microparticles - Compositions, structures, and surface reactions	09	p1297	A83-25184	Methane photochemistry in the outer planets	15	p2273	A83-33550	The measurement of the photodissociation rate of NO ₂ in the atmosphere	20	p3027	A83-43432
Reactions of gases on prototype aerosol particle surfaces	09	p1297	A83-25185	Hydrogen peroxide and sulfur (IV) in Los Angeles cloud water	15	p2194	A83-34050	Aqueous-phase source of formic acid in clouds	20	p3028	A83-43555
Kinetics of reactions between free radicals and surfaces /aerosols/ applicable to atmospheric chemistry	09	p1297	A83-25187	In situ aircraft measurements of enhanced levels of N ₂ O associated with thunderstorm lightning	15	p2199	A83-34222	Three-body association reactions of NO(+) and O ₂ (+) with N ₂	21	p3201	A83-43957
Heterogeneous catalyzed photolysis via photoacoustic spectroscopy	09	p1297	A83-25189	Positive ion composition measurements and acetonitrile in the upper stratosphere	15	p2199	A83-34223	On the detectability of H ₂ S in Jupiter	21	p3239	A83-44087
Observation of sulfate compounds on filter substrates by means of X-ray diffraction	09	p1297	A83-25190	HCN formation on Jupiter - The coupled photochemistry of ammonia and Acetylene	15	p2275	A83-34718	Spectroscopy of molecular oxygen in the atmospheres of Venus and Mars	21	p3239	A83-44088
Atmospheric gases on cold surfaces - Condensation, thermal desorption, and chemical reactions	09	p1298	A83-25191	Aeronomy of the upper atmosphere of Venus	16	p2434	A83-35353	Positive and negative ions in the stratosphere	21	p3170	A83-44235
Incomplete energy accommodation in surface-catalyzed reactions	09	p1298	A83-25192	Droplet phase (heterogeneous) and gas phase (homogeneous) contributions to secondary ambient aerosol formation as functions of relative humidity	16	p2379	A83-36127	Gas-phase NO ₂ and NO ₃ clustering with C ₂ H ₅ ONO ₂ and SO ₂ molecules - Experimental and semi-empirical MO studies --- ion chemistry of lower atmosphere	21	p3202	A83-44237
Sulfur dioxide absorption, oxidation, and oxidation inhibition in falling drops - An experimental/modeling approach	09	p1298	A83-25194	Fogwater chemistry in an urban atmosphere	16	p2372	A83-36128	Stratospheric diffusion of active species in ozone chemistry The correspondence between the results of spectroscopic measurements and those from a numerical model	21	p3171	A83-44317
Theoretical limitations on heterogeneous catalysis by transition metals in aqueous atmospheric aerosols	09	p1298	A83-25196	Latitudinal variation of tropospheric ozone in a photochemical model	16	p2379	A83-36132	[ONERA, TP NO. 1983-39]	21	p3171	A83-44317
Evidence for heterogeneous reactions in the atmosphere	09	p1298	A83-25197	The 1980 eruptions of Mount St. Helens - Physical and chemical processes in the stratospheric clouds	16	p2380	A83-36146	Elemental carbon in the atmosphere - Cycle and lifetime	21	p3171	A83-44376
Soot-catalyzed atmospheric reactions	09	p1298	A83-25198	Simulation of NO _x partitioning along isobaric parcel trajectories	16	p2381	A83-36159	On the photodecomposition of ClONO ₂ in the middle ultraviolet	21	p3109	A83-44486
The relative importance of various urban sulfate aerosol production mechanisms - A theoretical comparison	09	p1298	A83-25199	Relative rate constants for the reactions of atomic oxygen with HO ₂ and OH radicals	16	p2327	A83-36711	Atmospheric chemistry; Dahlem Workshop, Berlin, West Germany, May 2-7, 1982, Report	21	p3165	A83-45094
Importance of heterogeneous processes to tropospheric chemistry - Studies with a one-dimensional model	09	p1298	A83-25200	Infrared absorption intensities of nitrous acid (HONO) fundamental bands	16	p2411	A83-36798	Estimation of the rate constant for the reaction N ₂ (+) + O from data on the ion and neutral composition of a diffuse arc	21	p3176	A83-45261
The possible role of heterogeneous aerosol processes in the chemistry of CH ₄ and CO in the troposphere	09	p1299	A83-25204	Summary of preliminary results of the Venera 13 and Venera 14 missions	17	p2616	A83-37406	Smog chamber studies of NO(x) transformation rate and nitrate/precursor relationships	21	p3110	A83-45619
Sulfur trioxide in the lower atmosphere of Venus	10	p1518	A83-25505	Composition of the Venus atmosphere	17	p2616	A83-37414	Acid generation in the troposphere by gas-phase chemistry	22	p3320	A83-45922
The clouds of Venus - Sulfuric acid by the lead chamber process	10	p1518	A83-25506	Photochemistry of the Venus atmosphere	17	p2617	A83-37415	Photochemistry of N ₂ (+) in the daytime F region	22	p3328	A83-46056
New application of dependence between mean times of sampling and maximal air pollutant concentrations	10	p1446	A83-25568	Basic theory and model calculations of the Venus ionosphere	17	p2617	A83-37425	Optical emission from photoexcitation of aerosol particles produced by reaction of ozone with 1,3-butadiene	22	p3328	A83-46065
Investigations of homogeneous nucleation in Fe, Si, Fe/Si, FeO/x/, and SiO/x/ vapors and their subsequent condensation	10	p1490	A83-26191	Neutral and ion composition of the thermosphere	17	p2541	A83-38277	Formation and photochemistry of methylamine in Jupiter's atmosphere	22	p3388	A83-47083
Measurements of metastable N/+//D-1 6584 A emission in the twilight thermosphere	11	p1618	A83-28322	Reactivity and structure of NO ₂ (+) produced by the N ₃ (+) + O ₂ reaction	17	p2486	A83-38467	OH(X ² I) state distribution from HNO ₃ and H ₂ O ₂ photodissociation at 193 nm	23	p3429	A83-47639
Thermospheric odd nitrogen. I - NO, N/4S/, and O/3P/ densities from rocket measurements of the NO delta and gamma bands and the O ₂ Herzberg I bands	11	p1618	A83-28323	Formation of sulfate in a cloud-free environment	18	p2711	A83-39117	Examination of wintertime latitudinal gradients in stratospheric NO ₂ using theory and LIMS observations	23	p3482	A83-47859
Theoretical performance of a vortex generator type of cloud droplet sampler	12	p1728	A83-28897	Asymmetries of the upper stratospheric ozone distribution between two hemispheres	18	p2718	A83-40046	Dimethyl sulfide in the equatorial Pacific Ocean - A natural source of sulfur to the atmosphere	23	p3493	A83-47860
Mesospheric ozone depletion during the solar proton event of July 13, 1982. II - Comparison between theory and measurements	12	p1751	A83-28906	Organic films on atmospheric aerosol particles, fog droplets, cloud droplets, raindrops, and snowflakes	18	p2719	A83-40329	The reaction of gas phase N ₂ O ₅ with water vapor	23	p3479	A83-47861
Sulfuric acid vapour derivations from negative ion composition data between 25 and 34 km	12	p1751	A83-28916	Organic material in the global troposphere	18	p2719	A83-40330	Phosphine photochemistry in Saturn's atmosphere	23	p3529	A83-47862
A second-order effect of stratospheric vertical motions	12	p1757	A83-28917	The ubiquity of peroxyacetyl nitrate in the continental boundary layer	19	p2863	A83-41974	Identification of deuterium ions in the ionosphere of Venus	23	p3529	A83-47864
Effect of recent rate data revisions on stratospheric modeling	12	p1751	A83-28918	Investigation of the dynamics and threshold behavior of negative ion-neutral reactions	20	p2949	A83-42578	The young sun and the atmosphere and photochemistry of the early earth	23	p3483	A83-48075
The photochemistry of the atmospheres of Mars and Venus --- Russian book	12	p1798	A83-29329	Production of O(1D) and O(3P) by vacuum ultraviolet photodissociation of molecular oxygen	20	p3020	A83-42608	High-temperature physical-chemical processes in the atmosphere during thunderstorms	23	p3485	A83-48504
Bulgaria-1300 UV day glow spectra, related to the ozone problem	12	p1756	A83-29693	A dynamic model for the production of H(+), NO ₃ (-), and SO ₄ (2-) in urban fog	20	p3013	A83-42844	Methodology for the analysis of peroxyacetyl nitrate (PAN) in the unpolluted atmosphere	23	p3486	A83-48685
Nonlinear response of stratospheric ozone column to chlorine injections	13	p1872	A83-30880	A two-dimensional photochemical model of the atmosphere. I Chlorocarbon emissions and their effect on stratospheric ozone	20	p3013	A83-42845	Electron microscopy of acidic aerosols collected over the northeastern United States	23	p3479	A83-48687
Aqueous oxidation of SO ₂ by hydrogen peroxide	13	p1817	A83-30882	A two-dimensional photochemical model of the atmosphere. II The tropospheric budgets of the anthropogenic chlorocarbons CO, CH ₄ , CH ₃ Cl and the effect of various NO(x) sources on tropospheric ozone	20	p3013	A83-42846	Apportioning light extinction coefficients to chemical species in atmospheric aerosol	23	p3479	A83-48689
A general circulation model study of atmospheric carbon monoxide	13	p1876	A83-30884	Photochemical reactions of water and carbon monoxide in earth's primitive atmosphere	20	p3036	A83-42847	Photodissociation effects of solar UV radiation	24	p3603	A83-48755
The Delta band dissociation of nitric oxide - A potential mechanism for coupling thermospheric variations to the mesosphere and stratosphere	13	p1877	A83-30894	The mechanism of NO ₃ and HONO formation in the nighttime chemistry of the urban atmosphere	20	p3013	A83-42848	Chemical budgets of the stratosphere	24	p3603	A83-48757
Day and night models of the Venus thermosphere	13	p1962	A83-31229	The photochemistry of anthropogenic nonmethane hydrocarbons in the troposphere	20	p3013	A83-42849	The ozone budget in the stratosphere - Results of a one-dimensional photochemical model	24	p3604	A83-48758
They dance in the air --- properties of atmospheric aerosols	13	p1880	A83-31317	Air-sea fluxes of transient atmospheric species	20	p3021	A83-42850	Influence of peroxyacetyl nitrate (PAN) on odd nitrogen in the troposphere and lower stratosphere	24	p3602	A83-48761
Cloud and precipitation chemistry research and Whiteface Mountain	13	p1873	A83-31527	Stratospheric negative ions - Detailed height profiles	20	p3023	A83-43151	A theoretical study of the height distribution of sodium in the mesosphere	24	p3606	A83-49308
The dissipation of a sodium cloud	13	p1882	A83-31627	Atmospheric sodium chemistry and diurnal variations - An up-date	20	p3026	A83-43207	The reaction NH ₂ + PH ₃ yields NH ₃ + PH ₂ - Absolute rate constant measurement and implication for NH ₃ and PH ₃ photochemistry in the atmosphere of Jupiter	24	p3672	A83-49343
Energy dependence of the O(-) transfer reactions of O ₃ (-) and CO ₃ (-) with NO and SO ₂	14	p1991	A83-33103	Kinetics of SO ₂ oxidation over carbonaceous particles in the presence of H ₂ O, NO ₂ , NH ₃ and O ₃	20	p3014	A83-43425	Distribution of acidity in convective clouds due to the aqueous phase oxidation of sulfur dioxide by ozone - A numerical simulation	24	p3602	A83-49685
Absolute rate constants for the hydroxyl radical reactions with CH ₃ SH and C ₂ H ₅ SH at room temperature	14	p1991	A83-33105	Case studies of aerosol size distribution and chemistry during passages of a cold and a warm front	20	p3014	A83-43427	Aircraft observations of regional transport of ozone in the northeastern United States	24	p3603	A83-50191

ATMOSPHERIC CIRCULATION

- Accuracy of operational snow and ice charts
01 p0074 A83-10090
- A radiation scheme for circulation and climate models
01 p0074 A83-10221
- Grouping of clouds in a numerical cumulus convection model
01 p0074 A83-10222
- On a geophysical inviscid vortex
01 p0075 A83-10496
- Meteorological effects in ionospheric processes /Survey/
01 p0071 A83-10589
- Fabry-Perot determinations of midlatitude F-region neutral winds and temperatures from 1975 to 1979
02 p0204 A83-11965
- The influence of mountains and the beta-effect on wave motion in the atmosphere
02 p0213 A83-11981
- On the effects of moisture on the Brunt-Vaisala frequency
02 p0213 A83-12230
- The significance of thermodynamic forcing by cumulus convection in a general circulation model
02 p0213 A83-12231
- A scale analysis of deep moist convection and some related numerical calculations
02 p0213 A83-12233
- Errors in fixed and moving frame of references - Applications for conventional and Doppler radar analysis
02 p0214 A83-12237
- Instability of the three-dimensional distorted stratospheric polar vortex at the onset of the sudden warming
02 p0214 A83-12239
- Investigation of processes in the thermosphere during magnetic disturbances
02 p0209 A83-12430
- Zonal mean circulation at the cloud level on Venus - Spring and fall 1979 OCPP observations --- Orbiter Cloud Photo Polarimeter
02 p0266 A83-12569
- A new tool for the three-dimensional sounding of the atmosphere - The helisonde
02 p0216 A83-12957
- A convergent method for solving the balance equation --- for atmospheric circulation analysis
02 p0217 A83-13053
- Mesoscale structures of vortices in polar air streams
02 p0218 A83-13058
- A review of downdrafts at the rear of tropical squall lines
03 p0363 A83-13222
- Effects of mesoscale atmospheric convection cells on the waters of the East China Sea
03 p0363 A83-13270
- Dynamical implications of the observed thermal contrasts in Venus' upper atmosphere
03 p0434 A83-13834
- The local dispersion relation for magneto-atmospheric waves --- in solar atmosphere
03 p0436 A83-14212
- A comparison of long-range predictions from Hough and statistical interpolation analyses
03 p0365 A83-14408
- Variational normal mode balancing in the Navy operational data assimilation system --- for numerical weather prediction
03 p0366 A83-14410
- Towards the optimum control of gravity waves and ageostrophic circulations for data assimilation
03 p0366 A83-14411
- Winter simulation of standing and travelling waves with the UCLA general circulation model
03 p0366 A83-14412
- Simulation of the planetary boundary layer with the UCLA general circulation model
03 p0366 A83-14413
- Variational analysis/forecast cycling based on the conservation of potential vorticity
03 p0366 A83-14415
- Formulation of a modal-split-explicit time integration method for use in the UCLA atmospheric general circulation model
03 p0366 A83-14416
- An examination of the characteristics of planetary scale systematic forecast errors
03 p0366 A83-14418
- Details of low latitude medium range numerical weather prediction using a global spectral model
03 p0366 A83-14419
- Numerical studies of atmospheric flows over and around large-scale mountains
03 p0367 A83-14422
- The effect of initial divergence on prediction of extratropical cyclogenesis
03 p0367 A83-14426
- Low-level circulations induced by an upper-level jet in a fine mesh numerical model
03 p0367 A83-14433
- An explicit mixed numerical method for mesoscale model
03 p0368 A83-14440
- An analysis of the LFM-11 simulations of the Presidents' Day Cyclone, February 18-19, 1979
03 p0368 A83-14442
- The effects of latent heat release on the May 20 Sesame '77 wave cyclone
03 p0368 A83-14443
- Large-scale effects of deep convection on the tropical boundary layer
03 p0368 A83-14444
- On the generation of convectively driven mesohighs aloft
03 p0368 A83-14446
- On the predictability of individual deep convective clouds
03 p0369 A83-14447
- A lateral boundary condition for cumulus models which simulates the mesoscale response to convection
03 p0369 A83-14448
- Formation of the low-level jet under an inversion
03 p0369 A83-14449
- Meteorological effects in the variations of ionospheric parameters. I - The lower thermosphere
03 p0361 A83-14741
- Influence of solar wind variability of the recurrence of droughts
03 p0363 A83-14918
- Long-period atmospheric waves excited by a periodic source
04 p0515 A83-15055
- The influence of the thermal characteristics of the underlying surface on the atmosphere as revealed by a small-component model
04 p0515 A83-15056
- Present wind activity on Mars - Relation to large latitudinally zoned sediment deposits
04 p0566 A83-15571
- Martian North Polar Cap 1979-1980
04 p0569 A83-15591
- Dynamics of the baroclinic unstratified planetary boundary layer over land and sea
04 p0515 A83-15721
- A seasonal global climate model with an equivalent meridional atmospheric circulation
04 p0515 A83-15852
- Analysis of the diurnal oscillation of surface geostrophic wind over Western Europe
04 p0516 A83-15855
- A numerical simulation of an atmospheric vortex street
04 p0516 A83-15856
- Simulation of laboratory vortex flow by axisymmetric similarity solutions
04 p0477 A83-15858
- Wave-interactions in quasi-geostrophic uniform potential vorticity flow
04 p0516 A83-15927
- A study of the adequacy of quasi-geostrophic dynamics for modeling the effect of cyclone waves on the larger scale flow
04 p0516 A83-15929
- Eastward and westward flows over topography in nonlinear and linear barotropic models
04 p0516 A83-15933
- Seasonality in Southern Hemisphere eddy statistics at 500 mb
04 p0517 A83-15935
- Planetary-scale characteristics of the atmospheric circulation during January and February 1979
04 p0517 A83-15936
- A note on the effect of horizontal momentum fluxes by unresolved synoptic-scale eddies in a low-resolution spectral general circulation model
04 p0517 A83-15943
- The energetics of the general circulation of the atmosphere in southern hemisphere during the IGY. I - The distribution of atmospheric energy
04 p0517 A83-16011
- On the causes of formation of two intertropical convergence zones in the western part of the Pacific Ocean and in the Indian Ocean
04 p0517 A83-16012
- Evidence of solar influence on the tropospheric circulation in summertime
04 p0518 A83-16014
- Quasistatic approximation of atmospheric dynamics. VI - Rossby waves over orographically modified terrain
04 p0510 A83-16035
- Baroclinic instability in the presence of mountains
04 p0519 A83-16159
- The existence of Hadley convective regimes of atmospheric motion
04 p0519 A83-16367
- Motion in the interiors and atmospheres of Jupiter and Saturn - Scale analysis, anelastic equations, barotropic stability criterion
05 p0703 A83-16960
- An asymptotic method of calculating large-scale atmospheric motions
05 p0667 A83-17223
- Geophysical fluid dynamics --- Book
05 p0640 A83-17650
- The diagnostic calculation and analysis of mean climatic sources for winter conditions in the Northern Hemisphere
06 p0787 A83-17993
- Some characteristics of the asymmetry of circulation mechanisms of the Northern and Southern Hemispheres
06 p0788 A83-17996
- Atmospheric-dispersion experiments in the near and medium field /Fourth European Community Campaign, Turbigo, Italy, September 1979/
06 p0781 A83-18137
- Intercomparisons of upper air and surface winds in an urban region
06 p0781 A83-18238
- Spurious mass loss in some mesometeorological models
06 p0789 A83-18241
- An experimental study of the boundary layer above a moderate relief near a mountain chain. I - The influence on a flow by a relief at middle to large scales
06 p0789 A83-18242
- On the measurement of atmospheric winds
06 p0761 A83-18244
- Momentum balance of gravity flows
06 p0789 A83-18255
- An analysis of three-dimensional mountain lee-waves in a stratified shear flow. II
06 p0790 A83-18256
- Internal dynamics of tornado-like vortices
06 p0790 A83-18257
- Global-scale weekly and monthly energetics during January and February 1979
06 p0790 A83-18259
- Structure of the cold front observed in SESAME-AVE III and its comparison with the Hoskins-Bretherton frontogenesis model --- Severe Environmental Storms And Mesoscale Experiment - Atmospheric Variability Experiment
06 p0790 A83-18261
- Atmospheric vacillations in a general circulation model. III - Analysis using transformed Eulerian-mean diagnostics
06 p0791 A83-18268
- Observation of atmospheric waves generated by cyclone centres
06 p0791 A83-18422
- Cyclone development in polar air streams over the winter time continent
06 p0792 A83-18469
- Cloud-cluster-scale circulations and the vorticity budget of synoptic-scale waves over the eastern Atlantic intertropical convergence zone
06 p0792 A83-18470
- A newly found jet in north Kenya /Turkana Channel/
06 p0792 A83-18473
- Stability of mean monsoon zonal flow
06 p0792 A83-18991
- Stability of a stationary Rossby wave embedded in the monsoon zonal flow
06 p0792 A83-18992
- The climatology of the geopotential of the 500 mb surface of the northern hemisphere as obtained by natural orthogonal functions in the wave number region
06 p0793 A83-19249
- Synoptic-scale vertical motion computed by the quasi-geostrophic omega-equation
06 p0793 A83-19250
- A description of the atmosphere of Venus
06 p0849 A83-19466
- The influence of large-scale advection on the vertical distribution of stratospheric source gases in 44 degree and 41 degree north
07 p0957 A83-20224
- About the reversal of mean zonal wind during the stratospheric warming of 1970-1971
07 p0969 A83-20225
- The structure of planetary waves up to the lower mesosphere based on data analyses and model calculations
07 p0969 A83-20226
- Effect of geomagnetic activity on the changes of atmospheric circulation in the northern hemisphere
07 p0950 A83-20601
- The structure of the atmospheric circulation of Venus, and possible irregularities in its rotation rate
07 p1030 A83-20661
- Investigation of clear air convective structures in the PBL using a dual Doppler radar and a Doppler sodar
07 p0969 A83-20808
- The dynamics of the moist atmosphere
07 p0970 A83-20885
- The spring and autumn transformations of the circulation regime of the meteor zone according to the data of multi-year radar, measurements in Kirgizia
07 p0970 A83-20895
- Enormous increase of stratospheric aerosols over Fukuoka due to volcanic eruption of El Chichon in 1982
07 p0967 A83-21557
- F-region neutral winds and temperatures at equatorial latitudes - Measured and predicted behaviour during geomagnetically quiet conditions
07 p0968 A83-21580
- Incremental linear normal mode initialization in four-dimensional data assimilation --- for numerical weather forecasting
08 p1138 A83-22284
- Diagnostic equations in isobaric coordinates
08 p1139 A83-22286
- A non-iterative procedure for the time integration of the balance equations --- for atmospheric models
08 p1139 A83-22287
- Multiply-upstream, semi-Lagrangian advective schemes - Analysis and application to a multi-level primitive equation model
08 p1139 A83-22288
- Numerical simulation of the development of mean monsoon circulation in July
08 p1139 A83-22291
- Thermodynamic and circulation characteristics of winter monsoon tropical mesoscale convection
08 p1139 A83-22292
- Significance of non-elliptic regions in balanced flows of the tropical atmosphere
08 p1139 A83-22295
- Vertical mass transport in cumulonimbus clouds on day 261 of GATE
08 p1140 A83-22297
- Development of a two-dimensional finite-element PBL model and two preliminary model applications
08 p1140 A83-22299
- The nonlinear spectral dynamics of large-scale atmospheric motions
08 p1140 A83-22419
- Questions concerning the atmospheric circulation over the Antarctic
08 p1140 A83-22420
- Feasibility and design considerations of a global wind sensing coherent infrared radar /WINDSAT/
08 p1051 A83-22503

- Effects of differential rotation on the gravitational figures of Jupiter and Saturn 08 p1189 A83-22935
- Finite-amplitude stability of a zonal shear flow 08 p1141 A83-23001
- The amplification and capture of atmospheric solitons by topography - A theory of the onset of regional blocking 08 p1142 A83-23003
- A conservation law for small-amplitude quasi-geostrophic disturbances on a zonally asymmetric basic flow 08 p1142 A83-23007
- Stationary waves in the winter stratosphere - Seasonal and interannual variability 08 p1143 A83-23016
- Baroclinic instability of the summer mesosphere - A mechanism for the quasi-two-day wave 08 p1143 A83-23017
- The structure of an atmospheric warm front and its interaction with the boundary layer 09 p1310 A83-23355
- Application of WKB theory to turbulence layers in the vicinity of critical levels --- in winter hemisphere for internal gravity wave propagation 09 p1311 A83-23888
- The instability of the gravity-inertia wave and its relation to low-level jet and heavy rainfall 09 p1311 A83-23889
- Eliassen-Palm flux diagnostics and the effect of the mean wind on planetary wave propagation for an observed sudden stratospheric warming 09 p1311 A83-23891
- A numerical experiment on the mountain and valley winds 09 p1311 A83-23892
- Global circulation of volcanic debris of Mt. St. Helens - Evidence from the change of chemical constituents in the surface air 09 p1304 A83-23898
- Cloud bands in the atmosphere 09 p1312 A83-23960
- An introduction to deep convective systems --- thunderstorm development 09 p1312 A83-23961
- The mean annual variation of the geopotential of the 500 mb surface for the Northern Hemisphere in wavenumber space 09 p1313 A83-24120
- Complex eigenvalue bounds in magnetoatmospheric shear flow. I 09 p1359 A83-24127
- Complex eigenvalue bounds in magnetoatmospheric shear flow. II 09 p1359 A83-24128
- Three-dimensional tracer model study of atmospheric CO2 - Response to seasonal exchanges with the terrestrial biosphere 09 p1305 A83-24254
- A numerical model of the zonally averaged dynamical and chemical structure of the middle atmosphere 09 p1296 A83-24267
- Small atmospheric perturbations for one model of temperature stratification 09 p1308 A83-25051
- A small-component model of the nonlinear interactions between internal gravity waves 09 p1308 A83-25052
- Extensive cloudiness and radiation 09 p1316 A83-25227
- Mathematical modeling of the general circulation of the atmosphere and ocean 09 p1309 A83-25244
- The relationship between convective adjustment, Hadley circulation and normal modes of the ANMRC spectral model 10 p1450 A83-25381
- On the nonlinear versus linearized lower boundary conditions for topographically forced stationary long waves 10 p1450 A83-25384
- Monsoon and teleconnection variability over Australasia during the Southern Hemisphere summers of 1973-77 10 p1450 A83-25386
- Relationships among the stratospheric and tropospheric zonal flows and the Southern Oscillation 10 p1450 A83-25387
- Numerical simulation of the airflow over Lake Michigan for a major lake-effect snow event 10 p1451 A83-25392
- A model of mean zonal flows in the major planets 10 p1517 A83-25415
- The Poker Flat MST radar system - Current status and capabilities --- Mesosphere-Stratosphere-Troposphere 11 p1621 A83-26977
- Wind variability in the stratosphere deduced from space antenna VHF radar measurements 11 p1621 A83-26979
- Evidence for anticyclonic rotation in left-moving thunderstorms 11 p1622 A83-26983
- Dynamical and microphysical observations in 2 Oklahoma squall lines. I - Radar measurements. II - In-situ measurements 11 p1622 A83-26984
- Combined radar and aircraft analysis of a Doppler radar 'black hole' region in an Oklahoma squall line 11 p1622 A83-26985
- Joint observations of gravity wave activity in vertical winds in the troposphere and lower stratosphere over a 63 km baseline obtained with clear-air VHF radars at Platteville and Sunset, Colorado 11 p1623 A83-26991
- A mechanism of gravity wave excitation observable with atmospheric radars 11 p1623 A83-26992
- Supercell flow inferred from single-Doppler radar and environmental data 11 p1623 A83-26997
- Dual Doppler observations of diffusion and rolls --- due to atmospheric circulation patterns 11 p1629 A83-27059
- Prestorm boundary layer observations with Doppler radar 11 p1629 A83-27061
- Simulated radar sampling of a realistically-scaled analytical model of the planetary boundary layer 11 p1629 A83-27062
- A 35 GHz meteorological Doppler radar with polarization diversity capability 11 p1630 A83-27077
- MECCA - A portable system for real-time acquisition and display of field data --- Mesoscale Experiment Command and Control Assimilator meteorological measurement system 11 p1630 A83-27087
- Thermal structure of Saturn from Voyager infrared measurements - Implications for atmospheric dynamics 11 p1684 A83-27360
- Dynamics of the middle atmosphere 11 p1631 A83-27404
- Circulation and waves in the middle atmosphere in winter 11 p1631 A83-27406
- On certain periodicities of atmospheric circulation 11 p1631 A83-27452
- On the influence of nonlinear wave-wave interaction in a 3-d primitive equation model for sudden stratospheric warmings 11 p1632 A83-27971
- On low-order non-linear stochastic-dynamic systems --- for atmospheric circulation 11 p1632 A83-28079
- Linear non-divergent mass-wind laws on the sphere 11 p1633 A83-28080
- On the effect of model resolution on numerical simulation of blocking --- in atmospheric circulation 11 p1633 A83-28081
- Spectral study of wintertime kinetic energy of the Northern Hemisphere in the troposphere 11 p1633 A83-28085
- Theoretical study of multiple equilibria in simple axisymmetric tropical circulations 11 p1633 A83-28087
- Orographic trough or low in the Alpine region /and their effect on weather in the CSR/ 11 p1633 A83-28114
- The dynamic response of the high-latitude thermosphere and geostrophic adjustment 11 p1618 A83-28318
- Annual variations in the gradient of the electric field potential in the atmosphere and their relationship with the forms of atmospheric circulation 11 p1634 A83-28727
- The interplanetary magnetic field and the earth's lower atmosphere 11 p1634 A83-28744
- A second-order effect of stratospheric vertical motions 12 p1757 A83-28917
- Experimental study of the boundary layer over a gentle terrain near a mountain range. III - Turbulence structure in the boundary layer near the ground analyzed by acoustic sounding 12 p1758 A83-29130
- Direct relations between solar activity and atmospheric circulation, its effect on changes of weather and climate 12 p1758 A83-29405
- On the extraction of atmospheric turbulence parameters from radar backscatter Doppler spectra. I - Theory 12 p1758 A83-29427
- Wind velocities estimated from Venera 13 and Venera 14 Doppler measurements - Initial results 12 p1798 A83-29481
- Statistical reliability and the seasonal cycle - comments on 'Bottom pressure measurements across the Antarctic Circumpolar Current and their relation to the wind' 12 p1759 A83-29527
- Multiyear characteristics of the circulation in the lower thermosphere over parts of Central Asia 13 p1873 A83-30032
- The calculation characteristics of multilevel predictive schemes and models of general atmospheric circulation 13 p1884 A83-30291
- Baroclinic prog biases in particular weather patterns and the use of analogs 13 p1886 A83-30544
- Mesoscale vorticity centers induced by mesoscale convective complexes 13 p1887 A83-30556
- An objective diagnostic aid in locating meteorologically significant boundaries 13 p1888 A83-30571
- Diagnosis of weather events via kinematic analysis 13 p1888 A83-30572
- Prospects for prediction of zonal wind oscillations 13 p1889 A83-30575
- Anticyclone of 11 to 18 November 1969 - An example of anticyclone evolution over North America 13 p1889 A83-30577
- The interactive role of subsynoptic scale jet streak and planetary boundary layer adjustments in organizing an apparently isolated convective complex 13 p1890 A83-30585
- A comparison of adiabatic and kinematic vertical motions using mesoscale data 13 p1890 A83-30586
- Ageostrophic winds and vertical motion fields accompanying upper level jet streak propagation during the Red River Valley tornado outbreak 13 p1890 A83-30587
- The analysis and kinetic energy balance of an upper-level wind maximum during intense convection 13 p1890 A83-30588
- The influence of coastal shape on winter mesoscale air-sea interaction 13 p1891 A83-30801
- A composite analysis of the boundary layer accompanying a tropical squall line 13 p1891 A83-30803
- Seasonal and geographical variation of blocking 13 p1891 A83-30808
- A general circulation model study of atmospheric carbon monoxide 13 p1876 A83-30884
- Evidence for quasi-periodic components in Dobson network total ozone records 13 p1877 A83-30892
- A general circulation model of a Venus-like atmosphere 13 p1961 A83-31031
- On the role of the seasonal cycle 13 p1892 A83-31032
- Effects of planetary wave propagation and finite depth on the predictability of atmospheres 13 p1892 A83-31033
- Ship waves and lee waves 13 p1892 A83-31038
- Anti-clockwise rotation of the wind hodograph. I - Theoretical study 13 p1893 A83-31045
- A note on orographically induced instabilities in two-layer models --- of atmosphere 13 p1893 A83-31046
- On changes in atmospheric circulation after the entry of the earth into a solar corpuscular system 13 p1879 A83-31267
- Concerning the correctness on the whole of boundary value problems for models of the dynamics of the atmosphere and the ocean 13 p1880 A83-31326
- A simple model of the ocean climate 13 p1894 A83-31349
- Ionospheric E-region drifts at Sibirskir during 1970-75 13 p1882 A83-31547
- Quasi-axisymmetric circulation and superrotation in planetary atmospheres 13 p1962 A83-31750
- A determination of the total photospheric velocity field on the basis of the Fraunhofer lines of various elements 14 p2113 A83-31830
- Method and results of an analysis of comma cloud developments by means of vorticity fields from upper tropospheric satellite wind data 14 p2055 A83-31848
- The role of circulation in the formation of the morning-evening asymmetry of thermospheric disturbances 14 p2051 A83-31887
- Vertical motions in synoptic atmospheric eddies according to data from a field experiment 14 p2056 A83-32371
- The energetics of the general circulation of the atmosphere in southern hemisphere during the IGY. II - The cycle of the energetics of the atmosphere in southern hemisphere 14 p2056 A83-32401
- On a 3-component truncated model of a barotropic non-divergent rotating atmosphere in spherical geometry 14 p2057 A83-32405
- On truncated models of barotropic vorticity equation in spherical geometry 14 p2057 A83-32406
- Some discussions on the baroclinic and barotropic instabilities over Indian region during summer 14 p2057 A83-32407
- The background of the equivalent barotropic model for tropics 14 p2057 A83-32408
- Stability properties of cylindrically curved mean flows --- in atmosphere 14 p2058 A83-32469
- Large-scale fluctuations in a long-range integration of the ECMWF spectral model --- of atmosphere 14 p2058 A83-32470
- Satellite observations of the southern hemisphere monsoon during winter MONEX 14 p2058 A83-32471
- The spatial problem of the flow around an obstacle of an incompressible stratified fluid (numerical modeling) --- atmospheric air flow around mountains 14 p2058 A83-32853
- Diagnostic and prognostic numerical circulation studies of the South Atlantic Bight 14 p2060 A83-33078
- Kinematics and correlation of the surface wind field in the South Atlantic Bight 14 p2059 A83-33079
- Investigation of a laboratory model of a developing convective vortex 14 p2059 A83-33398
- A numerical scheme to treat the open lateral boundary of a limited area model 15 p2203 A83-33879
- A simple positive definite advection scheme with small implicit diffusion 15 p2204 A83-33881
- A possible explanation of the observed persistence of monthly mean circulation anomalies 15 p2204 A83-33882
- The numerical simulation of the interaction of cloud formation and lee waves 15 p2206 A83-34067

Upper-atmosphere zonal winds from satellite orbit analysis 15 p2199 A83-34360
Impact of Monex-79 data on the objective analysis of the wind field over the Indian region 15 p2206 A83-34746
The possibility of modeling the wind field in a planetary boundary layer with an incorporated temperature inversion in the (quasi)-stationary case 15 p2207 A83-35097
In situ and remote sensing of thermospheric winds during the Energy Budget Campaign 16 p2374 A83-35375
Responses of the upper middle atmosphere (60-110 km) to the stratwarms of the four pre-map winters (1978/9-1981/2) 16 p2374 A83-35383
Instabilities in a stratified fluid having one critical level. I - Results. II - Explanation of gravity wave instabilities using the concept of overreflection. III - Kelvin-Helmholtz instabilities as overreflected waves 16 p2384 A83-35458
January and July simulations with a spectral general circulation model 16 p2384 A83-35461
The response of a spectral general circulation model to refinements in radiative processes 16 p2384 A83-35462
A model to determine open or closed cellular convection 16 p2384 A83-35463
Case study of a hailstorm in Colorado. III - Airflow from triple-Doppler measurements 16 p2384 A83-35466
Rossby-number similarity in the atmospheric boundary layer over a slightly inclined terrain 16 p2385 A83-35468
Effects of baroclinicity on resistance laws for the atmospheric boundary layer over a slightly inclined terrain 16 p2385 A83-35469
Nonlinear baroclinic instability - An approach based on Serrin's energy method 16 p2385 A83-35472
A study of stratospheric vortications and sudden warmings on a beta-plane. I - Single wave-mean flow interaction 16 p2385 A83-35473
Modes of variability in annual hemispheric water vapor and transport fields 16 p2385 A83-35474
A nonsymmetric equatorial inertial instability 16 p2385 A83-35476
Disturbances and eddy fluxes in Northern Hemisphere flows Instability of three-dimensional January and July flows 16 p2385 A83-35478
On symmetric stability and instability of zonal mean flows near the equator 16 p2386 A83-35481
Transient planetary waves simulated by GFDL spectral general circulation models. I - Effects of mountains. II - Effects of nonlinear energy transfer 16 p2386 A83-35485
A first order vorticity equation for tropical easterly waves 16 p2386 A83-35486
Charney's problem for baroclinic instability applied to barotropic instability 16 p2387 A83-35492
A note on the criteria for the onset of stationary parallel-plate convection subject to mean vertical motion 16 p2348 A83-35494
Theory of waves in the shear flows of an inhomogeneous compressible fluid 16 p2349 A83-35530
Saturn meteorology - A diagnostic assessment of thin-layer configurations for the zonal flow 16 p2436 A83-35735
The NCAR Research Aviation Facility fleet workshop 18-19 February 1982, Boulder, Colo 16 p2287 A83-35744
Some economical, explicit finite-difference schemes for the primitive equations 16 p2388 A83-36027
Interaction of the Monsoon and Pacific Trade Wind System at interannual time scales. I - The equatorial zone 16 p2388 A83-36033
Low-level monsoon dynamics derived from satellite winds 16 p2389 A83-36034
A comparison of methods for computing the sigma-coordinate pressure gradient force for flow over sloped terrain in a hybrid theta-sigma model 16 p2389 A83-36037
Preliminary data of the thermal regime and circulation in the upper mesosphere and mesopause 16 p2377 A83-36106
Model calculations of middle atmospheric wind and temperature fields 16 p2377 A83-36107
A mechanistic model of Eulerian, Lagrangian mean, and Lagrangian ozone transport by steady planetary waves 16 p2379 A83-36136
Variations in atmospheric angular momentum on global and regional scales and the length of day 16 p2381 A83-36157
Simulation of NOx partitioning along isobaric parcel trajectories 16 p2381 A83-36159
Analysis of the deep convective activity over the western Pacific and southeast Asia. I - Diurnal variation 16 p2390 A83-36491
Vertical profile of wind speed over the open sea 16 p2390 A83-36493

Interactions of isolated vortices. II - Modon generation by monopole collision 16 p2353 A83-36546
Influence of mean divergence, mean vorticity and height-dependent eddy viscosity on thermal instability 16 p2391 A83-36583
An analysis of geopotential height at 300 mbar in the frequency wavenumber domain along 50 deg N in observed and modelled January climate 16 p2391 A83-36584
A complex vortex-system observed by the AVHRR of NOAA 6 16 p2391 A83-36591
Spatial variability of meteorological parameters in the Bermuda Triangle 16 p2392 A83-36847
A global model of the ocean-atmosphere system and an investigation of its sensitivity to changes in CO2 concentration 16 p2392 A83-36864
The transfer of angular momentum by vortex disturbances during the loss of stability in a plane, axially symmetric shear flow 16 p2392 A83-36872
Thermal structure of the atmosphere of Venus 17 p2616 A83-37412
General circulation and the dynamical state of the Venus atmosphere 17 p2617 A83-37422
The atmospheric dynamics of Venus according to Doppler measurements by the Venera entry probes 17 p2617 A83-37423
Dynamics of the earth's thermosphere 17 p2541 A83-38274
Middle atmosphere dynamics 17 p2541 A83-38281
Atmospheric boundary layers --- review of recent research 17 p2547 A83-38319
Regimes of flow in a planet's atmosphere - A numerical study 17 p2547 A83-38463
Cloud encounter statistics in the 28.5-43.5 KFT altitude region from four years of GASP observations 17 p2550 A83-38733
Numerical and analytical investigations of three-dimensional lee waves 17 p2553 A83-38763
Wakes from arrays of buildings --- flight safety 17 p2508 A83-38766
The use of pressure fluctuations on the nose of an aircraft for measuring air motion 18 p2721 A83-39118
Stochastic simulation of atmospheric trajectories 18 p2722 A83-39123
Correlation analysis of Doppler radar data and retrieval of the horizontal wind 18 p2722 A83-39125
Improved cloud motion wind vector and altitude assignment using VAS --- Visible Infrared Spin-Scan Radiometer Atmospheric Sounder 18 p2722 A83-39132
A comparison of two types of atmospheric transport models Use of observed winds versus dynamically predicted winds 18 p2722 A83-39134
An analysis of finite-difference schemes for the numerical solution of the advection equation 18 p2723 A83-39438
Forecasting experiments with a model of the general circulation of the atmosphere 18 p2724 A83-39445
The response of finite-amplitude wave motions to seasonal heating of a baroclinic shear flow 18 p2684 A83-39449
On the mechanism of the effect of solar corpuscular radiation on the circulation of the lower atmosphere 18 p2724 A83-39489
Orbital forcing of the inception of the Laurentide ice sheet? 18 p2718 A83-39960
On the theory of the long-term variability of the atmosphere 18 p2728 A83-40027
A diagnostic study of the forcing of the Ferrel cell by eddies, with latent heat effects included 18 p2728 A83-40029
The effect of the interference of traveling and stationary waves on time variations of the large-scale circulation 18 p2728 A83-40030
Interactions between orographically and thermally forced planetary waves 18 p2728 A83-40031
A moist baroclinic model for monsoonal mid-tropospheric cyclogenesis 18 p2728 A83-40032
The behavior of stationary waves and the summer monsoon 18 p2728 A83-40033
A laboratory experiment on the dynamics of the land and sea breeze 18 p2729 A83-40038
Troposphere-stratosphere (surface-55 km) monthly winter general circulation statistics for the Northern Hemisphere Four year averages 18 p2730 A83-40045
Hurricane Allen and island obstacles 18 p2730 A83-40047
The relationships between macrocirculation processes in the atmosphere at levels from 10 to 100 km over Middle Asia 18 p2719 A83-40076
A disturbance of the upper atmosphere caused by flow around an isolated mountain 18 p2730 A83-40077

Relationships between the thermodynamic cycles of the troposphere and stratosphere at extratropical latitudes 18 p2730 A83-40084
A history of prevailing ideas about the general circulation of the atmosphere 18 p2730 A83-40318
Equatorial disturbance dynamo electric fields 19 p2864 A83-41117
Energy equation of non-equilibrium states in the earth's atmosphere 19 p2867 A83-41319
Changes in pressure and circulation fields during extreme periods 19 p2867 A83-41582
Three dimensional numerical models of the large scale circulation induced by the global models of the thermosphere 20 p3017 A83-42311
The large-scale circulation and heat sources over the Tibetan Plateau and surrounding areas during the early summer of 1979. I - Precipitation and kinematic analyses 20 p3029 A83-42502
On the relative motion of binary tropical cyclones 20 p3029 A83-42503
Variability of the Indian summer monsoon and tropical circulation features 20 p3029 A83-42505
A convergence analysis of a numerical method for solving the balance equation --- of atmospheric circulation 20 p3029 A83-42507
Analysis of nighttime drainage winds in Boulder, Colorado during 1980 20 p3030 A83-42510
Heat transfer in the atmosphere 20 p3030 A83-42658
The atmosphere --- dynamics and climatology 20 p3020 A83-42821
General circulation model experiments on the climatic effects due to a doubling and quadrupling of carbon dioxide concentration 20 p3031 A83-42843
Fifteen-day observation of mesospheric and lower thermospheric motions with the aid of the Arecibo UHF radar 20 p3021 A83-42865
Dynamics of artificial plasma clouds in 'Spolokh' experiments - Movement pattern 20 p3023 A83-43155
The viscous-like magnetospheric convection and the length of the earth's magnetotail 20 p3023 A83-43160
General circulation of air parcels and transport characteristics derived from a hemispheric GCM. I - A determination of advective mass flow in the lower stratosphere 20 p3031 A83-43457
The energy budgets for the eye and eye wall of a numerically simulated tropical cyclone 20 p3031 A83-43461
Martian great dust storms - Interpretive axially symmetric models 21 p3239 A83-44090
Sloping convection in the laboratory and in the atmospheres of Jupiter and Saturn 21 p3240 A83-44233
A theoretical study of small amplitude waves in the Martian lower atmosphere and a comparison made with those on earth 21 p3240 A83-44240
Dynamical processes in the atmosphere and the use of models 21 p3179 A83-44389
Numerical forecasts of stratospheric warming events using a model with a hybrid vertical coordinate 21 p3179 A83-44392
The seasonal response of a general circulation model to changes in CO2 and sea temperatures 21 p3179 A83-44393
An accurate variation of the two-step Lax-Wendroff integration of horizontal advection 21 p3179 A83-44398
Seasonal distributions of diabatic heating during the first GARP global experiment 21 p3172 A83-44470
African wave disturbances in a general circulation model 21 p3179 A83-44471
Barotropic wave propagation and instability, and atmospheric teleconnection patterns 21 p3180 A83-44701
A general circulation model study of January climate anomaly patterns associated with interannual variation of equatorial Pacific sea surface temperatures 21 p3180 A83-44702
Transformed Eliassen balanced vortex model 21 p3180 A83-44709
The latitude-height structure of 40-50 day variations in atmospheric angular momentum 21 p3173 A83-44710
The variability of the times of the spring reversals of the strato-mesospheric circulation 21 p3181 A83-45327
A rotary-spectrum analysis of the horizontal flow over central Europe 21 p3181 A83-45404
The construction of the integral characteristics of the static stability of the atmosphere 22 p3338 A83-45640
Specification of monthly precipitation in the western United States from monthly mean circulation 22 p3338 A83-45704

On the relation between the thunderstorm updraft and tornado formation 22 p3339 A83-45908

The shape, propagation and mean-flow interaction of large-scale weather systems 22 p3340 A83-46843

A new look at the energy cycle --- in atmosphere 22 p3341 A83-46848

Some dynamical properties of vortex streets in Saturn's atmosphere from analyses of Voyager images 22 p3387 A83-46880

Speculation on Martian north polar wind circulation and the resultant orientations of polar sand dunes 22 p3388 A83-47084

Calculation of the circulation, heat budget, and moisture cycle of the atmosphere for July on the basis of a model of the general circulation of the atmosphere 23 p3488 A83-47152

Inclusion of dynamic factors in a thermodynamic model of climate and numerical forecasting of mean monthly air temperature in the troposphere 23 p3488 A83-47153

Calculation of radiative heat influxes in a model of the general circulation of the atmosphere 23 p3488 A83-47156

Method for the approximation of terms parameterizing macroexchange in equations of atmospheric dynamics 23 p3488 A83-47157

Integration of equations of atmospheric dynamics using a semiimplicit dissipative scheme 23 p3488 A83-47158

Integration of the equations of atmospheric dynamics for long time periods using nested grids 23 p3488 A83-47159

Dynamical interaction of sensible heat released by sea surface to the outburst of the cold air [IAF PAPER 83-104] 23 p3493 A83-47267

The speed of recurring typhoons over the Western North Pacific ocean 23 p3489 A83-47401

Short-period atmospheric gravity waves - A study of their statistical properties and source mechanisms 23 p3489 A83-47402

Short-term planetary-scale interactions over the tropics and midlatitudes. II - Winter-MONEX period 23 p3490 A83-47406

The energy exchange between the baroclinic and barotropic components of atmospheric flow in the tropics during the FGGE summer 23 p3490 A83-47407

Estimates of the seasonal mean vertical velocity fields of the extratropical Northern Hemisphere 23 p3490 A83-47410

Diagnostic study of the momentum balance in the Northern Hemisphere winter stratosphere 23 p3491 A83-47411

Large-scale meteorological conditions associated with midlatitude, mesoscale convective complexes 23 p3491 A83-47414

The baroclinic processes of monsoon depressions 23 p3491 A83-47417

Large-scale thermal anomalies in the California current during the 1982-1983 El Nino 23 p3493 A83-47857

Steady, periodic, and aperiodic atmospheric flows 23 p3491 A83-48040

On the relevance of two-dimensional turbulence to geophysical fluid motions 23 p3448 A83-48041

The numerical forecast of the spectacular winter storm in Central Europe at the turn of the year 1978-1979 - A synoptic case study 23 p3491 A83-48056

On the intensity of atmospheric convection 24 p3609 A83-48812

Supra-annual variations of geopotential heights in the subtropical stratosphere 24 p3609 A83-48814

Analysis and interpretation of wave solutions of atmospheric dynamics for low latitudes 24 p3609 A83-49052

Simultaneous observations of the quasi 2-day wave in the northern and southern hemispheres 24 p3605 A83-49301

Upper atmosphere wind observations of waves and tides with the UNH meteor radar system at Durham 43 deg N (1977, 1978 and 1979) 24 p3606 A83-49311

Long and medium-scale waves in the lower stratosphere from satellite-derived microwave measurements 24 p3607 A83-49339

The stability of the flows of a homogeneous atmosphere of finite thickness 24 p3673 A83-49529

The Vorticity Area Index --- cyclonic activity measure 24 p3610 A83-49619

Some implications of acid rain field studies 24 p3602 A83-49684

A method of determining mesoscale air motions for cloud physical studies and its application to the water budget of a squall line 24 p3613 A83-49702

Zonally asymmetric aspects of large-sale thermodynamic forcing by cumulus convection 24 p3613 A83-49705

ATMOSPHERIC COMPOSITION

NT ATMOSPHERIC MOISTURE

NT IONOSPHERIC COMPOSITION

Total amount of atmospheric ozone and its vertical distribution - Beisk 1981 01 p0070 A83-10287

Measurements of total amount of atmospheric ozone and spectral atmospheric transparency on Spitsbergen - July 1980-July 1981 01 p0070 A83-10288

The effect of variations in the composition of a neutral atmosphere and in the flux of ultraviolet solar radiation during the cycle of solar activity on the structure of the upper ionosphere 01 p0071 A83-10590

The possible global budget of carbon dioxide 01 p0072 A83-11045

Evaluation of the atmospheric content of particulate mass from visibility observations 01 p0072 A83-11046

The global troposphere - Biogeochemical cycles, chemistry, and remote sensing 02 p0198 A83-11828

Temperature and solar zenith angle control of D-region positive ion chemistry [AD-A126882] 02 p0204 A83-11970

The exchange of CO₂ between the ocean and atmosphere 02 p0205 A83-11980

The abundances of CH₄, CH₃D, NH₃, and PH₃ in the troposphere of Jupiter derived from high-resolution 1100-1200/cm spectra 02 p0264 A83-12143

The neutral and ion chemistry of the upper atmosphere 02 p0206 A83-12152

Extreme ultraviolet observational data on the solar spectrum 02 p0269 A83-12155

On the two-dimensional transport of stratospheric trace gases in isentropic coordinates 02 p0214 A83-12240

Atomic carbon in the atmosphere of Venus 02 p0264 A83-12395

Noble gases in planetary atmospheres - Implications for the origin and evolution of atmospheres 02 p0265 A83-12556

Sulfuric acid vapor and other cloud-related gases in the Venus atmosphere - Abundances inferred from observed radio opacity 02 p0266 A83-12564

The composition and vertical structure of the lower cloud deck on Venus 02 p0266 A83-12565

The influence of thermospheric winds on exospheric hydrogen on Venus 02 p0266 A83-12570

Satellite observed ozone variations and solar activity 02 p0212 A83-13109

Solar mesosphere Explorer measurements of the El Chichon volcanic cloud 03 p0356 A83-13224

Infrared device for simultaneous measurement of fluctuations of atmospheric carbon dioxide and water vapor 03 p0324 A83-13275

The spectrum of Canopus. II - Analysis and composition 03 p0414 A83-13326

Carbon monoxide measurements in the troposphere 03 p0355 A83-13351

Methane - The record in polar ice cores 03 p0357 A83-13539

Seasonal variations in stratospheric NO₂ at 45 deg S 03 p0357 A83-13547

Atmospheric ozone and changes in the global climate --- Russian book 03 p0358 A83-13820

The satellite power system - Assessment of the environmental impact on middle atmosphere composition and on climate 03 p0360 A83-14517

A study of mesospheric rocket contrails and clouds produced by liquid-fueled rockets 03 p0290 A83-14518

Reconstructing the vertical profile of the ozone density in the atmosphere on the basis of measurements of the absorption of solar infrared radiation 03 p0362 A83-14830

Transport of aurorally produced N₂D⁺ by winds in the high latitude thermosphere 04 p0508 A83-14967

An inventory of particles from stratospheric collectors - Extraterrestrial and otherwise 04 p0563 A83-15366

Classification of the Johnson Space Center stratospheric dust collection 04 p0563 A83-15368

The tropospheric gas composition of Jupiter's north equatorial belt /NH₃, PH₃, CH₃D, GeH₄, H₂O/ and the Jovian D/H isotopic ratio 04 p0569 A83-15643

Arctic haze and the Arctic gas and aerosol sampling program /AGASP/ [AIAA PAPER 83-0439] 05 p0659 A83-16714

Dust loading of the normal atmosphere [AIAA PAPER 81-0548] 05 p0659 A83-16783

Physical and optical properties of dust particles [AIAA PAPER 83-0549] 05 p0659 A83-16784

On the C/H and D/H ratios in the atmospheres of Jupiter and Saturn 05 p0703 A83-16959

Airborne spectroscopy of Jupiter in the 100- to 300/cm region - Global properties of ammonia gas and ice haze 05 p0703 A83-16961

Feasibility of determining concentrations of atmospheric pollutants by comparative absorption using lasers having a single emission line 05 p0659 A83-17057

The origins of the plasma in the distant plasma sheet 05 p0660 A83-17390

Variations of delta S-34/SO₄²⁻, delta O-18/H₂O¹⁸, and Cl/SO₄ ratio in rainwater over northern Israel, from the Mediterranean coast to Jordan Rift Valley and Golan Heights 05 p0665 A83-17843

Atmospheric-dispersion experiments in the near and medium field /Fourth European Community Campaign, Turbigo, Italy, September 1979/ 06 p0781 A83-18137

Global empirical model of the Venus thermosphere 06 p0847 A83-18283

The atmospheric neutral sodium layer. II - Diurnal variations 06 p0785 A83-18313

The Venusian atmosphere 06 p0848 A83-19398

The prebiological paleoatmosphere - Stability and composition 06 p0801 A83-19402

A description of the atmosphere of Venus 06 p0849 A83-19466

Implication for stratospheric composition of a reduced absorption cross section in the Herzberg continuum of a molecular oxygen 07 p0958 A83-20088

Acetonitrile in the lower troposphere 07 p0959 A83-20197

A climatological model for the determination of air pollutant concentrations at a topographically complex site 07 p0956 A83-20199

Snow chemistry on James Ross Island /Antarctic Peninsula/ 07 p0956 A83-20201

The origins of sulfur compounds in the atmosphere of a zone of high productivity /Gulf of Guinea/ 07 p0956 A83-20203

Balloon-borne observations of stratospheric aerosol and condensation nuclei during the year following the Mt. St. Helens eruption 07 p0959 A83-20205

Particles and gases in the emissions from the 1980-1981 volcanic eruptions of Mt. St. Helens 07 p0959 A83-20206

Volcanic aerosol phosphorus, chlorine, and sulfur at Kilauea, Hawaii 07 p0960 A83-20208

Volcanic output of long-lived radon daughters 07 p0960 A83-20209

The role of active volcanism in enrichment of the atmosphere in chalcophile elements 07 p0960 A83-20211

Lipids in aerosols from the tropical North Pacific - Temporal variability 07 p0960 A83-20214

Characterization of trace gases in 1980 volcanic plumes of Mt. St. Helens 07 p0960 A83-20215

The global distribution of water vapor in the middle atmosphere of Venus 07 p1030 A83-20614

Supply of SO₂ for the atmosphere of Io 07 p1036 A83-21523

Thermospheric neutral composition from auroral ion ratios [AD-A126032] 07 p0968 A83-21579

Carbon monoxide in the Martian atmosphere 08 p1188 A83-22059

CO₂ lidar for measurements of trace gases and wind velocities 08 p1095 A83-22504

Primitive helium in diamonds 08 p1136 A83-22687

The abundance of CH₃D in the atmosphere of Titan, derived from 8- to 14-micron thermal emission 08 p1189 A83-22931

The abundance of water on Jupiter from the Voyager IRIS data at 5 microns 08 p1189 A83-22932

New H₂SO₄ and HSO₃ vapour measurements in the stratosphere - Evidence for a volcanic influence 08 p1138 A83-23264

Initial tests of an index based on AL values for modeling magnetic storm related perturbations of the thermosphere 09 p1304 A83-23775

Global circulation of volcanic debris of Mt. St. Helens - Evidence from the change of chemical constituents in the surface air 09 p1304 A83-23898

Numerical modeling of a zonally averaged stratospheric ozone field 09 p1305 A83-24215

Uncertainties of predictions of future atmospheric CO₂ concentrations 09 p1294 A83-24251

Feedback mechanisms in the climate system affecting future levels of carbon dioxide 09 p1294 A83-24252

On the radiocarbon record in banded corals - Exchange parameters and net transport of ¹⁴CO₂ between atmosphere and surface ocean 09 p1295 A83-24253

Three-dimensional tracer model study of atmospheric CO₂ - Response to seasonal exchanges with the terrestrial biosphere 09 p1305 A83-24254

Exponential growth and atmospheric carbon dioxide 09 p1295 A83-24255

Distribution of and changes in industrial carbon dioxide production 09 p1295 A83-24256

CO₂ and radon 222 as tracers for atmospheric transport 09 p1295 A83-24257

Preliminary study of CO₂ variations at Amsterdam Island /Terriore des Terres Australes et Antarctiques Francaises/ 09 p1295 A83-24259

Interpretation of atmospheric CO₂ measurements at Mt. Cimone /Italy/ related to wind data 09 p1295 A83-24260

Concentration of atmospheric carbon dioxide over Japan 09 p1295 A83-24261

Sampling strategy to obtain data used in models of global annual CO₂ increase and global carbon cycle 09 p1295 A83-24262

Selection of CO₂ concentration data from whole-air sampling at three locations between 1968 and 1974 09 p1295 A83-24263

Tropospheric NO_x/ and O₃ budgets in the equatorial Pacific 09 p1305 A83-24264

On the relationship between the greenhouse effect, atmospheric photochemistry, and species distribution 09 p1296 A83-24268

Absolute band strengths of halocarbons F-11 and F-12 in the 8- to 16-micron region 09 p1296 A83-24269

Chlorocarbon emission scenarios - Potential impact on stratospheric ozone 09 p1296 A83-24270

Effect of coupled anthropogenic perturbations on stratospheric ozone 09 p1296 A83-24271

Stratospheric sulfuric acid vapor - New and updated measurements 09 p1296 A83-24272

Simultaneous measurements of vertical distributions of stratospheric NO₃ and O₃ at different periods of the night 09 p1296 A83-24273

UV rocket spectroscopy measurement of the nighttime ozone distribution 09 p1305 A83-24274

Carbon monoxide mixing ratio inference from gas filter radiometer data 09 p1306 A83-24450

On the estimation of the concentration of aerosols in the upper layer of the Venus clouds 09 p1366 A83-25038

Aircraft-borne measurements of ozone content in the atmosphere during the solar eclipse of July 31, 1981 09 p1308 A83-25059

Ozone concentration near the earth's surface during a total solar eclipse 09 p1308 A83-25060

Evidence for heterogeneous reactions in the atmosphere 09 p1298 A83-25197

Importance of heterogeneous processes to tropospheric chemistry - Studies with a one-dimensional model 09 p1298 A83-25200

Aerosol measurements in the Arctic and in a volcanic region 09 p1309 A83-25232

Chromatographic and mass-spectrometric determinations of traces of organic substances in the atmosphere --- Russian book 09 p1299 A83-25250

Sulfur trioxide in the lower atmosphere of Venus 10 p1518 A83-25505

The properties of dimers and their role in the atmosphere 10 p1448 A83-25522

Current methods for the determination of iodine in the atmosphere 10 p1447 A83-25612

An analysis of the reflection spectrum of Jupiter from 1500 A to 1740 A 10 p1518 A83-25736

High-sensitivity atmospheric gas analysis based on intracavity laser detection of scattered radiation 10 p1392 A83-26685

Solar variability and minor constituents in the lower troposphere and in the mesosphere 11 p1615 A83-27405

Atmospheric balance of sulphur above an equatorial forest 11 p1615 A83-27671

Some characteristics of chemical precipitation 11 p1612 A83-27672

A comprehensive study of physical and chemical parameters of the Arctic summer aerosol; results from the Swedish expedition Ymer-80 11 p1613 A83-28092

Effect of meteorologic conditions on total suspended particulate /TSP/ levels and elemental concentration of aerosols in a semi-arid zone /Beer-Sheva, Israel/ 11 p1613 A83-28093

Features in using lidars for measuring the dust content of air 11 p1573 A83-28203

Peroxyacetyl nitrate in the free troposphere 11 p1613 A83-28399

Marine biological controls on atmospheric CO₂ and climate 11 p1600 A83-28400

Short and middle range remote sensing of atmospheric gases using Raman lidar --- French thesis 11 p1585 A83-28640

The construction of a spectrophone and a CO₂ laser waveguide excited by a radiofrequency field for application to the detection of atmospheric trace species --- French thesis 11 p1585 A83-28654

Solar Mesosphere Explorer - Scientific objectives and results 12 p1750 A83-28901

Ozone density distribution in the mesosphere /50-90 km/ measured by the SME limb scanning near infrared spectrometer 12 p1750 A83-28903

Comparison of mesospheric ozone abundances measured by the solar mesosphere explorer and model calculations 12 p1750 A83-28904

Mesospheric ozone depletion during the solar proton event of July 13, 1982. I - Measurement 12 p1750 A83-28905

Measurements of NO₂ in the earth's stratosphere using a limb scanning visible light spectrometer 12 p1751 A83-28908

Stratospheric sulfuric acid fraction and mass estimate for the 1982 volcanic eruption of El Chichon 12 p1751 A83-28912

Atomic nitrogen abundance in polar upper thermosphere 12 p1751 A83-28919

Spectral least squares quantification of several atmospheric gases from high resolution infrared solar spectra obtained at the South Pole 12 p1752 A83-29148

The photochemistry of the atmospheres of Mars and Venus --- Russian book 12 p1798 A83-29329

Mass spectrometry on the Venera 13 and Venera 14 landers Preliminary results 12 p1798 A83-29477

Venera 13 and Venera 14 gas-chromatography analysis of the Venus atmosphere composition 12 p1798 A83-29478

Periodic and aperiodic ozone variations in the middle and upper stratosphere 12 p1756 A83-29583

Solar eclipse induced variations in mesospheric ozone concentrations 12 p1756 A83-29584

Solar UV and ozone balloon measurements 12 p1747 A83-29585

Verification of satellite observations of stratospheric minor constituents 12 p1756 A83-29690

Validation of 9.6 microns ozone transmittances by spectral radiance satellite measurements 12 p1756 A83-29691

Spectral ranges for determining the concentration of hydrogen bromide and hydrogen fluoride in the earth's atmosphere 13 p1872 A83-30036

The development of research on atmospheric ozone in India 13 p1874 A83-30039

Monitoring aerosol elemental composition in particle size fractions of long-range transport 13 p1874 A83-30180

The global distribution of atmospheric carbon dioxide. I Aspects of observations and modeling. II - A review of provisional background observations, 1978-1980 13 p1876 A83-30876

Tracing bomb C-14 in the atmosphere 1962-1980 13 p1876 A83-30878

Some comments on the exchange of CO₂ across the air-sea interface 13 p1869 A83-30879

Correlative nature of ozone and carbon monoxide in the troposphere - Implications for the tropospheric ozone budget 13 p1876 A83-30881

Unusual behavior in the condensation nuclei concentration at 30 km 13 p1877 A83-30885

The contribution of volcanoes to the global atmospheric sulfur budget 13 p1877 A83-30886

A decade of stratospheric sulfate measurements compared with observations of volcanic eruptions 13 p1877 A83-30887

Stratospheric N₂O, CF₂Cl₂, and CFC13 composition studies utilizing in situ cryogenic, whole air sampling methods [AD-A128389] 13 p1873 A83-30891

An aerosol and gas sampling apparatus for remote observatory use 13 p1847 A83-30905

Ab initio studies of the CO₂-HF and N₂O-HF complexes 13 p1818 A83-30966

Limits on Venus' SO₂ abundance profile from interferometric observations at 3.4 mm wavelength 13 p1961 A83-31211

Day and night models of the Venus thermosphere 13 p1962 A83-31229

They dance in the air --- properties of atmospheric aerosols 13 p1880 A83-31317

The dissipation of a sodium cloud 13 p1882 A83-31627

Collisional vibrational quenching of O₂(+)(v) and other molecular ions in planetary atmospheres 13 p1917 A83-31636

On the possibility to measure the high altitude light ion concentrations with Eiscat 13 p1883 A83-31716

The radon cycle and its daughters - An application to the study of troposphere-stratosphere exchanges 13 p1883 A83-31720

An IR spectrometry experiment for the Spacelab I mission [ONERA, TP NO. 1983-98] 14 p1983 A83-31825

The role of circulation in the formation of the morning-evening asymmetry of thermospheric disturbances 14 p2051 A83-31887

Gas-chromatographic analysis of the chemical composition of the Venusian atmosphere on the descent modules of the Venera-13 and Venera-14 probes 14 p2111 A83-31962

Relation between observed aerosol optical thicknesses and calculated values from size distribution measurements 14 p2057 A83-32439

Spectroscopy of atmospheric gases --- Russian book 14 p2052 A83-32555

The absorption coefficient of light in the wing of the 4.3 micron band of CO₂ 14 p2082 A83-32556

Analysis of the influence of intramolecular interactions on the probability of vibration-rotation transitions in linear molecules 14 p2082 A83-32557

The effect of nonrigidity in the rotational structure of the spectra of molecules of water vapor and ammonia (Calculation of the dependence of rotational and centrifugal constants on vibration with great amplitude) 14 p2082 A83-32558

Laser methods for the control of atmospheric gases and gases which pollute the atmosphere 14 p2052 A83-32560

Quantitative intracavity spectroscopy 14 p2052 A83-32561

Probabilities for multiplet transitions in vibrational-rotational spectra --- of atmospheric gases 14 p2052 A83-32562

Spectroscopic measurements of the total content of CO, CH₄, and N₂O in the atmosphere in the Arctic region 14 p2053 A83-32861

The neutral composition of the high-latitude atmosphere 14 p2054 A83-33029

Seasonal variation of monoterpenes in the atmosphere of a pine forest 15 p2194 A83-34040

Source contributions to acid precipitation in Texas 15 p2194 A83-34043

Ammonia and ammonium concentrations in the antarctic atmosphere 15 p2197 A83-34044

Atmospheric trace element concentrations in Jerusalem, Israel 15 p2194 A83-34045

The influence of atmospheric aerosol on the life cycle radiation fog 15 p2205 A83-34066

The NH₃ spectrum in Saturn's 5 micron window 15 p2274 A83-34114

In situ aircraft measurements of enhanced levels of N₂O associated with thunderstorm lightning 15 p2199 A83-34222

Positive ion composition measurements and acetonitrile in the upper stratosphere 15 p2199 A83-34223

Stratospheric NO₂ and upper limits of CH₃Cl and C₂H₆ from measurements at 3.4 microns 15 p2200 A83-34386

AFGL trace gas compilation - 1982 version [AD-A130554] 15 p2201 A83-34456

Retrieval of stratospheric aerosol size distribution from atmospheric extinction of solar radiation at two wavelengths 15 p2201 A83-34459

Increasing backscattered light from the stratospheric aerosol layer after Mt. El Chichon eruption - Laser radar measurement at Nagoya (35 deg N, 137 deg E) 15 p2202 A83-34728

Correlative studies of satellite ozone sensor measurements 15 p2202 A83-34729

Optical properties of the Venusian atmosphere and radiative heat exchange 16 p2434 A83-35352

Modulation of day-side and neutral distributions at Venus Evidence of direct and indirect solar energy inputs 16 p2434 A83-35357

The variability of stratospheric nitrogen compounds observed by LIMS in the winter of 1978-1979 16 p2374 A83-35382

Comparative neutral composition instrumentation and new results --- for measurement of planetary atmospheres 16 p2317 A83-35399

A determination of the composition of the Saturnian stratosphere using the IUE 16 p2436 A83-35736

The NCAR Research Aviation Facility fleet workshop 18-19 February 1982, Boulder, Colo 16 p2287 A83-35744

Scientific programs for the Spacelab ESO13 grille spectrometer 16 p2317 A83-35784

Titan - Discovery of carbon monoxide in its atmosphere 16 p2437 A83-36016

Sighting of El Chichon sulfur dioxide clouds with the Nimbus 7 total ozone mapping spectrometer 16 p2377 A83-36018

An ultraviolet spectrograph using an echelle grating with cross-disperser for the measurement of stratospheric constituents [AIAA PAPER 83-0020] 16 p2356 A83-36040

The terrestrial upper atmosphere; Proceedings of the Workshop, Ottawa, Canada, May 16-June 2, 1982 16 p2377 A83-36101

Properties of the neutral density and composition in the thermosphere 16 p2378 A83-36115

The Lyman-alpha absorption anomaly in satellite occultation measurements as a tracer for some thermospheric composition variations

16 p2378 A83-36117

Water and acid soluble trace metals in atmospheric particles

16 p2379 A83-36126

Sources, sinks, and seasonal cycles of atmospheric methane

16 p2379 A83-36130

On the distribution of nitrogen dioxide in the high-latitude stratosphere

16 p2379 A83-36138

Stratospheric NO₂. III - The effects of large-scale horizontal transport

16 p2379 A83-36139

Atmospheric trace elements at Enewetak Atoll. I

Concentrations, sources, and temporal variability

16 p2380 A83-36147

Infrared absorption spectroscopy applied to stratospheric profiles of minor constituents

[ONERA, TP NO. 1983-99]

16 p2380 A83-36150

Latitudinal distribution of ten stratospheric species deduced from simultaneous spectroscopic measurements

16 p2381 A83-36151

Analysis of upper stratospheric ozone profile data from the ground-based Umkehr method and the Nimbus-4 BUV satellite experiment

16 p2381 A83-36152

Simultaneous detection of trace constituents in the middle atmosphere with a small He-cooled, high resolution Michelson interferometer (MIPAS)

16 p2356 A83-36588

Saturn's ionosphere - A corona of ice particles?

16 p2438 A83-36781

Composition of the Venus atmosphere

17 p2616 A83-37414

Photochemistry of the Venus atmosphere

17 p2617 A83-37415

Origin and evolution of the atmosphere of Venus

17 p2618 A83-37430

The problem of rare gases in the Venus atmosphere

17 p2618 A83-37431

The problem of the excess of noble gases in the atmosphere of Venus

17 p2619 A83-37816

The atmosphere of Canopus. II - Chemical composition. Determination of the mass, radius, luminosity, and age

17 p2603 A83-37890

Methane on Triton and Pluto - New CCD spectra

17 p2619 A83-37935

A hygienic evaluation of the chemical composition of air in living accommodations

17 p2562 A83-38201

Neutral and ion composition of the thermosphere

17 p2541 A83-38277

Minor constituents in the stratosphere and mesosphere

17 p2541 A83-38280

Remote sensing of atmospheric gases and particulates by lidar

17 p2515 A83-38363

Effect of high atmospheric CO₂ concentration on delta C-13 of algae - A possible cause for the average depletion of C-13 in Precambrian reduced carbon

17 p2557 A83-38895

Sensitivity of ozone retrievals in limb-viewing experiments to errors in line-width parameters

18 p2664 A83-39183

IR emission and NO concentration in the case of the significant heating of the upper atmosphere

18 p2713 A83-39322

The intercomparison ozone campaign held in France in June 1981 - Description of the campaign

18 p2716 A83-39785

Total atmospheric ozone measured by ground based high resolution infrared spectra - Comparison with Dobson measurements

18 p2716 A83-39786

Atmospheric trace species measured above Haute-Provence observatory

18 p2716 A83-39788

Measurements of the vertical distribution of ozone by ground-based microwave techniques at the Bordeaux observatory during the June 1981 intercomparison campaign

18 p2716 A83-39789

Measurement of the vertical ozone distribution by means of an in situ gas phase chemiluminescence ozonometer during the intercomparison ozone campaign, Gap, France, June 1981

18 p2716 A83-39790

GSFC optical ozonesonde results during the Gap, France, intercomparisons, June 1981

18 p2716 A83-39791

NASA-JSC measurements during la campagne d'intercomparaison d'ozonometres, Gap, France, June 1981

18 p2716 A83-39792

Stratospheric ozone measurements by solar ultraviolet absorption

18 p2716 A83-39793

Nimbus 7 total ozone mapping spectrometer (TOMS) data during the Gap, France, ozone intercomparisons of June 1981

18 p2717 A83-39794

Total ozone measurements derived from T.O.V.S. radiances --- Tiros Operational Vertical Sounder

18 p2717 A83-39795

Measurements of total ozone - Intercomparison of data from a variety of instruments, June 1981

18 p2717 A83-39796

Measurements of the ozone vertical distribution (0-25 km) comparison of various instruments, Gap - Observatoire de Haute-Provence, June 1981

18 p2689 A83-39797

Ozone profile intercomparison based on simultaneous observations between 20 and 40 km

18 p2689 A83-39798

Comparison of ozone vertical distributions measured by different techniques at mesospheric altitudes

18 p2717 A83-39799

Ozone variations observed during the International Ozone Rocket Sonde Intercomparison

18 p2717 A83-39845

Uranus - Variability of the microwave spectrum

18 p2779 A83-39933

Ionic composition of the earth's radiation belts

18 p2787 A83-39953

Organic material in the global troposphere

18 p2719 A83-40330

Increase and seasonal cycles of nitrous oxide in the earth's atmosphere

18 p2720 A83-40644

Henry's Law constants and the air-sea exchange of various low molecular weight halocarbon gases

18 p2705 A83-40645

Molecular state of sulfate aerosols in the remote Everest highlands

18 p2711 A83-40647

Tropospheric oxalate

19 p2862 A83-41112

Simultaneous detection of FC-11, FC-12 and FC-22, through 8 to 13 micrometers IR solar observations from the ground

19 p2862 A83-41113

Venera 13 and 14 - Mass spectroscopy of the atmosphere

19 p2923 A83-41241

Rare-gas isotopes in the atmospheres of the terrestrial planets and early stages of the evolution of the solar system

19 p2923 A83-41242

The atmospheric aerosol system - An overview

20 p3015 A83-42176

Laser radar observations in mid-Wales of aerosols from the El Chichon eruption

20 p3017 A83-42332

Factors influencing the loss of fertilizer nitrogen into the atmosphere as N₂O

20 p3014 A83-42851

Atmospheric bromine in the Arctic

20 p3021 A83-42852

Production rate of airborne sea-salt sulfur deduced from chemical analysis of marine aerosols and precipitation

20 p3021 A83-42853

Relationships between Pb and Pb-210 in aerosol and precipitation at a semiremote site in northern Wisconsin

20 p3014 A83-42854

Vapor phase and particulate selenium in the marine atmosphere

20 p3021 A83-42855

On some radiative features of the El Chichon volcanic stratospheric dust cloud and a cloud of unknown origin observed at Mauna Loa

20 p3021 A83-42856

Interannual variations of global total ozone revealed from Nimbus 4 BUV and ground-based observations

20 p3021 A83-42864

C-13/C-12 records in Northern Hemispheric trees during the past 500 years - Anthropogenic impact and climatic superpositions

20 p3022 A83-42866

CO₂ measurements with an infrared laser spectrometer on flask samples collected at Jungfraujoch high-altitude research station (3500 meters asl) and with light aircraft up to 8000 meters over Switzerland

20 p3022 A83-42867

On the variability of atmospheric carbon dioxide concentration at Barrow, Alaska during winter

20 p3022 A83-42868

Comparison of airborne CO₂ flask samples and measurements from the Mauna Loa Observatory during the HAMEC Project (June 1980)

20 p3022 A83-42869

Stratospheric negative ions - Detailed height profiles

20 p3023 A83-43151

Acetonitrile in the atmosphere

20 p3026 A83-43208

A re-evaluation of laser heterodyne radiometer CIO measurements --- for stratospheric chemistry studies

20 p3026 A83-43209

A mesoscale atmospheric dispersion model for predicting ambient air concentration and deposition patterns for single and multiple sources

20 p3014 A83-43422

Evaluation of an episodic regional transport model for a multi-day sulfate episode

20 p3014 A83-43423

Comparison of calculated and observed super- and sub-micrometer aerosol mass concentrations using St. Louis RAPS data base --- Regional Air Pollution Study

20 p3014 A83-43426

Atmospheric pollution studies at Kanpur-suspended particulate matter

20 p3015 A83-43428

Methods and results of gas chromatographic-mass spectrometric determination of volatile organic substances in an urban atmosphere

20 p3015 A83-43431

Variability of carbon monoxide in the Mars atmosphere

21 p3239 A83-44089

Positive ion composition measurements between 33 and 20 km altitude

21 p3170 A83-44236

Stratospheric diffusion of active species in ozone chemistry The correspondence between the results of spectroscopic measurements and those from a numerical model

[ONERA, TP NO. 1983-39]

21 p3171 A83-44317

Millimeter wave ground-based heterodyne detection of two minority atmospheric constituents

21 p3171 A83-44325

Atmospheric chloroform (CHCl₃) - Ocean-air exchange and global mass balance

21 p3169 A83-44378

An analysis of the U.S. Standard Atmosphere, 1976

21 p3173 A83-44581

Understanding the middle atmosphere via the laboratory - Ion cluster investigations

21 p3173 A83-44670

An incoherent scatter study of short- and long-term temperature and atomic oxygen variations in the thermosphere

21 p3173 A83-44671

A two-stage mechanism for escape of Na and K from Io

21 p3241 A83-44994

Gaseous contaminants in the atmosphere and changes of the global climate

21 p3169 A83-45334

The possibility of the visual monitoring of the state of the ozonosphere from an orbital station

21 p3177 A83-45396

Air monitoring - Research needs

21 p3169 A83-45616

Measurements of minor constituents in the middle atmosphere from IR limb emission spectra - A feasibility study

22 p3328 A83-46062

New technological developments for the remote detection of atmospheric hydroxyl radicals

22 p3288 A83-46072

Frequency-doubled CO₂ lidar measurement and diode laser spectroscopy of atmospheric CO₂

22 p3288 A83-46073

Balloon-borne remote sensing of stratospheric constituents

22 p3328 A83-46076

Balloon-borne diode-laser absorption spectrometer for measurements of stratospheric trace species

22 p3288 A83-46079

Tests of an inversion algorithm for spectrally resolved limb emission

22 p3328 A83-46080

Assessment of relative error sources in IR DIAL measurement accuracy

22 p3295 A83-46084

Spectral pattern recognition in IR remote sensing

22 p3288 A83-46085

Oxygen and ozone in the early earth's atmosphere

22 p3332 A83-46698

OH Pepsios --- polyetanol pressure-scanned interferometric optical spectrometer for atmospheric measurements

22 p3294 A83-46841

Stratospheric sulfate from El Chichon and the mystery volcano

22 p3333 A83-46882

Relationship between thermal-radiation characteristics and concentrations of trace gases in different layers of the atmosphere

23 p3488 A83-47160

Remote measurements of atmospheric NO₂ concentration by means of a differential-absorption lidar

23 p3453 A83-47165

Rocket-based investigations of O(3P), O₂(a¹-delta/g) and excited OH (v = 1, 2) during the solar eclipse of 26 February 1979

23 p3481 A83-47471

Airborne remote sensing measurements with a pulsed CO₂ DIAL system

23 p3455 A83-47767

Differential-absorption measurements with fixed-frequency IR and UV lasers --- for pollution monitoring and control

23 p3455 A83-47768

Remote measurement of trace gases with the JPL laser absorption spectrometer

23 p3456 A83-47771

Laser remote sensing measurements of atmospheric species and natural target reflectivities

23 p3456 A83-47772

Tunable laser heterodyne spectrometer measurements of atmospheric species

23 p3456 A83-47774

Interferometric measurements of atmospheric species

23 p3456 A83-47775

Gaseous correlation spectrometric measurements --- remote sensing of gases in atmosphere

23 p3456 A83-47777

Measurements of atmospheric trace gases by long path differential UV/visible absorption spectroscopy

23 p3456 A83-47778

2.7 measurements of HONO, NO₃, and NO₂ by long-path differential optical absorption spectroscopy in the Los Angeles Basin

23 p3478 A83-47779

Remote sensing of tropospheric gases and aerosols with airborne DIAL system

23 p3478 A83-47783

CO₂ DIAL sensitivity studies for measurements of atmospheric trace gases

23 p3457 A83-47788

Signal averaging limitations in heterodyne- and direct-detection laser remote sensing measurements

23 p3457 A83-47789

- High-resolution lidar system for measuring the spatial and temporal structure of the mesospheric sodium layer 23 p3457 A83-47791
- Remote sensing of OH in the atmosphere using the technique of laser-induced fluorescence 23 p3457 A83-47792
- Development of compact excimer lasers for remote sensing 23 p3461 A83-47796
- The young sun and the atmosphere and photochemistry of the early earth 23 p3483 A83-48075
- The storm-time variation of atmospheric disturbance from the data of a global network of vertical-incidence ionospheric sounding stations 23 p3484 A83-48391
- The response of the ocean to changes in the greenhouse effect 23 p3493 A83-48564
- Aerosol composition at Chacaltaya, Bolivia, as determined by size-fractionated sampling 23 p3486 A83-48686
- Elemental composition of aerosols collected with airborne cascade impactors 23 p3479 A83-48688
- Determination of atmospheric composition and temperature from the U.V. airglow 24 p3603 A83-48753
- Chemical budgets of the stratosphere 24 p3603 A83-48757
- Ozone variability --- in atmosphere and possible causes 24 p3604 A83-48759
- Atmospheric composition - Influence of biology 24 p3604 A83-48760
- Determination of H₂O and CH₄ profiles from data of a nadir to limb scanning balloon-borne radiometer 24 p3604 A83-48813
- Resolution of vertical mixing-ratio profiles of atmospheric constituents retrieved from solar spectra 24 p3582 A83-49006
- Background concentration of ozone, dust, and nitrogen and sulfur compounds in the atmosphere (according to worldwide data) 24 p3602 A83-49102
- On the concentration of mercury in the atmosphere in background regions 24 p3604 A83-49108
- Numerical simulation of the effects of changes of the gas composition of the atmosphere on climate 24 p3609 A83-49278
- A theoretical study of the height distribution of sodium in the mesosphere 24 p3606 A83-49308
- The atmospheric lifetime experiment. I - Introduction, instrumentation, and overview 24 p3606 A83-49328
- The Atmospheric Lifetime Experiment. II - Calibration 24 p3606 A83-49329
- The atmospheric lifetime experiment. III - Lifetime methodology and application to three years of CFCL3 data 24 p3606 A83-49330
- The Atmospheric Lifetime Experiment. IV - Results for CF₂Cl₂ based on three years data 24 p3606 A83-49331
- The Atmospheric Lifetime Experiment. VI - Results for carbon tetrachloride based on 3 years data 24 p3607 A83-49332
- On the temporal increase of tropospheric CH₄ 24 p3607 A83-49333
- A comparison of the results of a one-dimensional model and measurements of CH₄, H₂O, and nitrogen oxides in the stratosphere [ONERA, TP NO. 1983-97] 24 p3608 A83-49412
- Vertical ozone profiles determined from satellite METEOR spectrometer measurements 24 p3608 A83-49618
- ATMOSPHERIC CONDITIONS**
- U METEOROLOGY**
- ATMOSPHERIC CONDUCTIVITY**
- NT IONOSPHERIC CONDUCTIVITY**
- Schumann resonance effects of electrical conductivity perturbations in an exponential atmospheric/ionospheric profile 09 p1307 A83-24693
- The electrical conductivity of air over the Indian Ocean 11 p1620 A83-28729
- Regular measurements of the air's electrical conductivity 11 p1634 A83-28732
- Results from regular observations of the electrical conductivity of air at Verkhnee Dubrovo 11 p1634 A83-28735
- Variability in atmospheric electrical quantities 11 p1634 A83-28736
- Effects of propagation on the rise times and the initial peaks of radiation fields from return strokes 16 p2341 A83-35415
- Atmospheric-pollution monitoring through conductivity measurements 23 p3454 A83-47419
- ATMOSPHERIC CORRECTION**
- A method for the calculation of refraction corrections in the atmosphere 22 p3322 A83-45646
- On the instrumental and atmospheric stray-light for solar observations 23 p3517 A83-47717
- ATMOSPHERIC DENSITY**
- Variability of satellite refraction in the Northern Hemisphere atmosphere 01 p0072 A83-10855
- A model for the formation of a temperature inversion layer in a thin atmosphere stratum adjacent to water 01 p0076 A83-10910
- The propagation of strong-plane magnetogasdynamical shock waves in an optically-thin atmosphere 04 p0557 A83-15974
- The atmospheric neutral sodium layer. II - Diurnal variations 06 p0785 A83-18313
- The change in satellite orbital inclination due to a rotating oblate atmosphere with a diurnal variation in density 11 p1532 A83-27099
- Ozone densities in the lower mesosphere measured by a limb scanning ultraviolet spectrometer 12 p1750 A83-28902
- An analytic version of Jacchia's 1977 model atmosphere 12 p1752 A83-29101
- Upper atmosphere density from the motion of the ANS satellite 14 p2052 A83-32397
- Spectroscopic measurements of the total content of CO, CH₄, and N₂O in the atmosphere in the Arctic region 14 p2053 A83-32861
- Instantaneous integrated Raman scattering --- for enhanced lidar measurement of atmospheric constituents 14 p2054 A83-32918
- An approximation method for predicting changes in the level of atmospheric pollution in a city 14 p2048 A83-33042
- Vertical density and temperature structure over northern Europe 16 p2373 A83-35373
- Evaluation of selected global thermospheric density models during low solar flux conditions 16 p2378 A83-36113
- Properties of the neutral density and composition in the thermosphere 16 p2378 A83-36115
- Seasonal and solar activity dependent variations of the geomagnetic activity effect at high latitudes 16 p2378 A83-36116
- Ion-neutral collision frequency variations in the lower thermosphere from incoherent scatter measurements 17 p2545 A83-38538
- Sensitivity study of orbital atmospheric density models 17 p2546 A83-38755
- The spatial structure of air density variations according to scintillation observations 18 p2719 A83-40085
- Determination of particulate and gaseous arsenic compounds in the atmosphere at trace levels 22 p3320 A83-45714
- Physicochemical characterization of trace metal compounds in airborne particulate matter 22 p3320 A83-45715
- Tests of an inversion algorithm for spectrally resolved limb emission 22 p3328 A83-46080
- Surface ozone and peroxyacetyl nitrate (PAN) observations at rural locations in Alberta, Canada 22 p3321 A83-46899
- Ground-based ultraviolet differential absorption lidar (DIAL) system and measurements 23 p3457 A83-47782
- Development of compact excimer lasers for remote sensing 23 p3461 A83-47796
- Examination of wintertime latitudinal gradients in stratospheric NO₂ using theory and LIMS observations 23 p3482 A83-47859
- ATMOSPHERIC DIFFUSION**
- Similarity forms for ground-source surface-layer diffusion 01 p0075 A83-10724
- Diffusion in the high atmosphere 02 p0206 A83-12153
- A diffusive model of the turbulent mixing of dry and cloudy air 02 p0215 A83-12942
- Diffusion processes in the magnetopause boundary layer 03 p0357 A83-13545
- A study of atmospheric diffusion from the Landsat imagery 03 p0350 A83-14504
- Atmospheric diffusion of a passive contaminant in a spatially homogeneous flow with transverse velocity [AIAA PAPER 83-0272] 05 p0633 A83-16623
- Statistical performance of several mesoscale atmospheric dispersion models 05 p0667 A83-17442
- Radar observations of a plume from an elevated continuous point source 05 p0667 A83-17445
- Diffusional transport of ionospheric irregularities 05 p0663 A83-17622
- Testing subroutines solving advection-diffusion equations in atmospheric environments 06 p0756 A83-18374
- Investigation of meso-scale atmospheric transport by means of radar tracked tetroons during PUKK 06 p0793 A83-18998
- Characteristics of maximum concentrations --- of plumes and their atmospheric dispersal 07 p0956 A83-19849
- A comparative study of two trajectory models of long-range transport --- of air pollution 07 p0956 A83-19850
- Diffusion of small-scale artificial irregularities of the upper ionosphere 09 p1301 A83-23491
- Global circulation of volcanic debris of Mt. St. Helens - Evidence from the change of chemical constituents in the surface air 09 p1304 A83-23898
- CO₂ and radon 222 as tracers for atmospheric transport 09 p1295 A83-24257
- Methodology for the investigation of the long-range transport of sulfur compounds 10 p1446 A83-25608
- Evaluation of the transport of sulfur dioxide and sulfates over the territory of the USSR 10 p1447 A83-25609
- The use of a mesoscale numerical model for evaluations of pollutant transport and diffusion in coastal regions and over irregular terrain 10 p1451 A83-26099
- Dual Doppler observations of diffusion and rolls --- due to atmospheric circulation patterns 11 p1629 A83-27059
- HCl in rocket exhaust clouds - Atmospheric dispersion, acid aerosol characteristics, and acid rain deposition 11 p1613 A83-28698
- Diffusion mechanism of the interaction of aerosol drops and the possibility of controlling this mechanism by means of electromagnetic radiation 13 p1874 A83-30043
- The interaction between air pollution dispersion and residential heating demands 13 p1873 A83-31596
- Global distribution and southern hemispheric trends of atmospheric CCl₃F 14 p2056 A83-31920
- A model calculation of the coefficients of turbulent diffusion in a nonstratified atmospheric surface layer 14 p2058 A83-32854
- A simple positive definite advection scheme with small implicit diffusion 15 p2204 A83-33881
- Relevance of mixed layer scaling for daytime dispersion based on raps and other field programs --- Regional Air Pollution Study 15 p2194 A83-34049
- Aeronomy of the upper atmosphere of Venus 16 p2434 A83-35353
- Turbulence structure in convective boundary layers and implications for diffusion 16 p2387 A83-35792
- A generalization of the Hines' dispersion relation --- for real atmosphere 16 p2377 A83-36108
- Numerical calculations and wind tunnel experiments on gas diffusion in thermally stratified flow over a ridge 16 p2390 A83-36495
- Composition of the Venus atmosphere 17 p2616 A83-37414
- Eddy diffusion coefficients in the lower thermosphere 17 p2539 A83-37603
- Estimating plume dispersion - A comparison of several Sigma schemes 18 p2721 A83-39111
- Meteorological tracer techniques for parameterizing atmospheric dispersion 18 p2727 A83-39885
- Solution of the advection-diffusion equation by the moments method --- applied to pollutant plumes 19 p2863 A83-41971
- On puff models of turbulence diffusion at various scales of atmospheric movements 21 p3179 A83-44490
- Possibilities for an improvement in short-distance diffusion modeling --- of air pollution 21 p3169 A83-45403
- Turbulent diffusion from a linear source in a field of wind varying with height 23 p3488 A83-47161
- Ozone transport by diabatic and planetary wave circulations on a beta plane 24 p3607 A83-49338
- ATMOSPHERIC EFFECTS**
- The artificial earth satellite motion in an oblate, rotating atmosphere with symmetrical diurnal effect 01 p0017 A83-10269
- Portrait of an unusual group of sunspots 01 p0129 A83-10572
- An atmospheric exposure chamber for small animals 01 p0086 A83-11108
- Simulation study of multispectral estimation of sea-surface temperature from infrared observations 02 p0177 A83-12034
- Atmospheric effects on radiation reflected from soil and vegetation as measured by orbital sensors using various scanning directions 02 p0198 A83-12315
- The effect of atmospheric drag on the single-axis gravity gradient stabilization of an artificial satellite 03 p0287 A83-13203
- Atmospheric transmission; Proceedings of the Meeting, Washington, DC, April 21, 22, 1981 03 p0344 A83-13976
- Capabilities and limitations of atmospheric transmission field measurement systems 03 p0359 A83-13995
- Experimental and theoretical statistics of microwave amplitude scintillations on satellite down-links 03 p0305 A83-14010
- Evaluation of methods for estimating solar irradiance in Canada 03 p0370 A83-14633
- Non-LTE atmospheric radiance and transmittance 03 p0360 A83-14638
- Comparison between albedo changes and lidar-measured aerosol changes for a set of aerosol events 03 p0370 A83-14641

On short term variations of zenith polarization during twilight 03 p0361 A83-14645

Overlapping effects of atmospheric H₂O, CO₂ and O₃ on the CO₂ radiative effects 03 p0361 A83-14660

A tutorial assessment of atmospheric height uncertainties for high-precision satellite altimeter missions to monitor ocean currents 03 p0289 A83-14851

Search for rapid variability of 53 Cam 04 p0546 A83-15110

Multiple telescope infrared interferometry 05 p0694 A83-17425

Manifestation of the effect of large-scale ionospheric irregularities in the case of back-oblique sounding 05 p0662 A83-17606

Twilight IR brightening over India due to El Chichon's eruption in Mexico 05 p0665 A83-17791

Ambient airborne solids concentrations including volcanic ash at Hanford, Washington sampling sites subsequent to the Mount St. Helens eruption 07 p0960 A83-20207

A review of geodetic and geodynamic satellite Doppler positioning 07 p0871 A83-20836

Supersonic maneuvers without superbooms 07 p0864 A83-21021

Test tailoring in the 80's --- as applied to Sparrow air-to-air missile environment simulation 07 p0869 A83-21036

The effects of atmospheric turbulence on telescopic observations 07 p0100 A83-21525

Optical emissions induced by spacecraft - Atmosphere interactions 07 p0869 A83-21551

Enormous increase of stratospheric aerosols over Fukuoka due to volcanic eruption of El Chichon in 1982 07 p0967 A83-21557

Rain-induced vibration --- of space vehicle 08 p1050 A83-22145

EOSAEL 82 - A library of battlefield obscuration models 08 p1093 A83-22352

Millimeter wave propagation measurements at the Ballistic Research Laboratory 08 p1076 A83-22353

Simultaneous multispectral absolute radiometer and transmissometer system 08 p1093 A83-22358

Atmospheric propagation effects on coherent laser radars 08 p1096 A83-22509

Atmospheric effects on electro-optical, infrared, and millimeter wave systems performance; Proceedings of the Meeting, San Diego, CA, August 27, 28, 1981 08 p1098 A83-22540

Effects of atmospheric and man-made obscuration on visual contrast 08 p1135 A83-22541

Measurements of infrared and visible extinction in adverse weather 08 p1140 A83-22546

Measurements of the properties of wintertime fog and haze in West Germany - A preliminary report on project 'Meppen 80' 08 p1141 A83-22549

Contrast transmittance models for cloudy atmospheres 08 p1135 A83-22550

Model for resonant transmittance in the millimeter wave region 08 p1076 A83-22559

The change of limiting resolution of electro-optical systems due to atmospheric effects 08 p1098 A83-22561

Optimization of the equatorial transfer orbit with an allowance made for atmospheric drag 09 p1212 A83-24487

A review of satellite communication and propagation experiments for frequencies above 10 GHz 09 p1249 A83-24646

Effects of the El Chichon volcanic cloud in the stratosphere on the polarization of light from the sky 10 p1451 A83-26640

Propagation at 10 microns through smoke produced by atmospheric combustion of diesel fuel 10 p1447 A83-26641

Observation of global 160-min infrared / differential/ intensity variation of the sun 11 p1688 A83-27628

On the origin of oscillations in a solar diameter observed through the earth's atmosphere - A terrestrial atmospheric or a solar phenomenon 11 p1688 A83-27637

Fluctuations of optical radiation on an inclined path 11 p1556 A83-27944

Analysis of the shift-and-add method for imaging through turbulent media 12 p1779 A83-29375

Aerosol observations from Nimbus-7 CZCS along the South African West Coast --- Coastal Zone Color Scanner 12 p1755 A83-29569

Different atmospheric effects in remote sensing of uniform and nonuniform surfaces 12 p1748 A83-29577

The characterization of atmospheric spread functions affecting satellite remote sensing of the earth's surface 12 p1748 A83-29578

A method for estimating cross radiance 12 p1748 A83-29579

Radiation-aerosols interaction - Applications to remote sensing and for calculation of the radiative balance --- French thesis 12 p1756 A83-29949

Investigation of the possibilities of predicting astrolclimate 13 p1935 A83-30271

Correcting low-frequency solar radio source positions for ionospheric refraction 13 p1964 A83-30371

Active optics - Don't build a telescope without it 13 p1920 A83-31007

Deformable mirror with combined piezoelectric and electrostatic actuators 13 p1920 A83-31008

The interaction of the cretaceous-tertiary extinction bolide with the atmosphere, ocean, and solid earth 13 p1880 A83-31475

The influence of ionospheric refraction on radio astronomy interferometry 13 p1941 A83-31571

The possible effect of atmospheric wind regimes on results of sonde measurements of cosmic rays 14 p2055 A83-31853

Meteorological effects in the F₂-layer of the ionosphere 14 p2049 A83-31857

Explanation for the inverse partial polarization of fog glories compared with rainbows and fogbows 14 p2057 A83-32413

Overview of power-line radiation and its coupling to the ionosphere and magnetosphere 14 p2001 A83-32893

Method of calculating the expected background luminance from the moon for planning astronomical observations 15 p2244 A83-33788

Atmospheric effects in satellite imaging of mountainous terrain 15 p2183 A83-34466

Atmospheric angular momentum fluctuations, length-of-day changes and polar motion 16 p2376 A83-35638

Effect of humidity on jet engine axial-flow compressor performance 16 p2304 A83-35856

Determination of basic constants of satellite - Atmosphere interaction from the analysis of motion of 1974-70A 16 p2314 A83-36114

The influence of seeing on the observation of short period fluctuations in the solar atmosphere 16 p2440 A83-36648

The effects of seeing on spectral line measurements in Seyfert 1 galaxies 17 p2604 A83-37906

Detailed choice of the spectral bands --- for SPOT satellite instruments 17 p2529 A83-38160

Atmospheric constraint statistics for the Space Shuttle mission planning 17 p2553 A83-38771

Modeling the effect of stratospheric aerosols on climate 18 p2723 A83-39437

Mt. St. Helens' aerosols - Some tropospheric and stratospheric effects 18 p2716 A83-39686

Aperture synthesis in the infrared 18 p2762 A83-40453

Achievements and promise of balloon IR astronomy 18 p2762 A83-40458

The effect of sea roughness and atmospheric inhomogeneity on the microwave emission of the atmosphere-sea surface system 18 p2720 A83-40598

Effect of ice-induced cross-polarization on digital earth-space links 19 p2833 A83-41400

Power series for perturbations in the intermediate motion of artificial earth satellites caused by atmospheric attraction 19 p2809 A83-41548

Propagation effect on interferometer 21 p3222 A83-44292

Some considerations on a Michelson spatial interferometer in the far IR 21 p3137 A83-44380

A new approach to evaluation of the atmospheric effects on upwelling radiance from the ocean 21 p3182 A83-44399

Adaptive optical system for astronomical applications 21 p3206 A83-44808

Influence of the precipitations and clouds on the performance of a synthetic aperture radar 22 p3289 A83-46197

Mauna Loa sky conditions - Bench mark and present 22 p3374 A83-46408

The solar eclipse of 26 February 1979 - Introductory comments 23 p3480 A83-47465

A comparative study of scintillation analysis over two line-of-sight paths at 6.7 GHz and 7.6 GHz 23 p3443 A83-47834

Aerodynamic and thermal characteristics of three-dimensional star-shaped bodies in a rarefied gas 23 p3400 A83-48672

Near-circular satellite orbits in an oblate, diurnally varying atmosphere 24 p3551 A83-49878

ATMOSPHERIC ELECTRICITY

NT AURORAL ELECTROJETS
NT ELECTROJETS
NT EQUATORIAL ELECTROJET
NT IONOSPHERIC CURRENTS

AEHP for advanced technology aircraft --- Atmospheric Electricity Hazard Protection 01 p0001 A83-11086

Mid-latitude horizontal electric fields in the stratosphere during magnetically disturbed periods 02 p0204 A83-11964

Field-aligned currents and magnetic disturbances in the dayside polar region 02 p0204 A83-11966

A broadband VLF burst associated with ring current electrons 02 p0207 A83-12385

Atmospheric electricity and air transport safety [ONERA, TP NO. 1982-82] 03 p0280 A83-14534

Some remarks about a ball lightning model 03 p0361 A83-14743

Charge deposition on ice particles by positive streamers 04 p0518 A83-16018

Field-aligned currents in the magnetosphere 05 p0663 A83-17617

Pi 2 pulsations - High latitude results 05 p0664 A83-17780

Generation of conic ions by auroral electric fields 06 p0785 A83-18317

Point discharge current studies near a large pollution source 06 p0781 A83-18417

OTS propagation experiments with radar, electric field and thunder location data 06 p0744 A83-18699

Altitude, thickness and charge concentration of charged regions of four thunderstorms during trip 1981 based upon in situ balloon electric field measurements 07 p0958 A83-20093

Maxwell currents under thunderstorms 07 p0960 A83-20217

Lightning and surface rainfall during Florida thunderstorms 07 p0969 A83-20219

On the characteristics of some radiation fields from lightning and their possible origin in positive ground flashes 07 p0960 A83-20220

Changes in concentrations of cloud and precipitation particles in the highly electrified regions of thundercloud 07 p0969 A83-20221

A one-dimensional model of the atmospheric electric field near the Venusian surface 07 p1030 A83-20619

Solitary waves and double layers on auroral field lines 07 p0966 A83-21517

An empirical electric field model derived from Chatanika radar data 07 p0967 A83-21522

Dynamics of the global Sq-field --- current distribution and geomagnetic variations 08 p1134 A83-22305

Role of various charging mechanisms in thundercloud electrification 08 p1140 A83-22316

Electrification of convective clouds 08 p1140 A83-22317

VLF radiometeorology - A model for interdisciplinary cooperation 09 p1310 A83-23402

The mirror image relation in the vertical distributions of electric field and precipitation charge in winter thunderclouds 09 p1311 A83-23897

The periodic variations in the atmospheric electric, electrotelluric, and geomagnetic fields according to data from the observatory at Dusheti 09 p1304 A83-23981

A mechanism to explain the generation of earthquake lights 09 p1307 A83-24696

The connection between radiation belt and auroral processes 11 p1614 A83-27394

Electric fields in the ionosphere and magnetosphere 11 p1614 A83-27399

Electric currents and voltage drops along auroral field lines 11 p1614 A83-27400

Whistler observations of magnetospheric electric field in the night side plasma-sphere at low latitude 11 p1619 A83-28383

Annual variations in the gradient of the electric field potential in the atmosphere and their relationship with the forms of atmospheric circulation 11 p1634 A83-28727

Measurements of the electric field over the Atlantic and Indian Oceans 11 p1619 A83-28728

The potential of high atmospheric layers 11 p1620 A83-28730

Methods for carrying out electrical measurements high in the atmosphere 11 p1620 A83-28731

An analysis of multiyear variations in atmospheric electrical quantities in the atmospheric surface layer on the basis of observational data 11 p1634 A83-28733

Cyclical processes in the atmospheric electric field 11 p1620 A83-28734

Results from regular observations of the electrical conductivity of air at Verkhnee Dubrovo 11 p1634 A83-28735

Variability in atmospheric electrical quantities 11 p1634 A83-28736

Elaborating methods for measuring atmospheric electrical quantities 11 p1575 A83-28737

Observations of quasistatic electric fields on the GEOS and ISEE satellites 11 p1621 A83-28770

Injection of ions and electrons into the ionosphere and the magnetosphere - Application to measurement of the parallel electric field in the auroral zones --- French thesis 13 p1874 A83-30126

An instrument for DC electric field and AC electric and magnetic field measurements aboard 'INTERCOSMOS-BULGARIA-1300' satellite 13 p1813 A83-30757

A payload for the study of electric fields and electron density in the equatorial region 13 p1814 A83-30759

Measurement of electric fields in the ionosphere by incoherent scatter radar techniques 13 p1876 A83-30772

Radar auroral observations and ionospheric electric fields 13 p1876 A83-30773

Bars - A dual bistatic auroral radar system for the study of electric fields in the Canadian sector of the auroral zone 13 p1815 A83-30774

The effects of energetic particle precipitation on the atmospheric electric circuit 13 p1878 A83-30898

Acoustic and electric signals from lightning 13 p1892 A83-30899

Observations of unusual structures of high-latitude stratospheric electric fields 13 p1878 A83-30901

Corona point measurements in a thundercloud at Langmuir Laboratory 13 p1892 A83-30903

Deductions concerning accumulations of electrified particles in thunderclouds based on electric field changes associated with lightning 13 p1892 A83-30904

Evidence for electrostatic shocks as the source of discrete auroral arcs 13 p1879 A83-31242

Method for determining the electrical properties of the underlying surface on inhomogeneous paths from measurements of the fields of VLF radio stations 14 p2050 A83-31882

The electrical activity of the Venus atmosphere. I Measurements using descent modules 14 p2111 A83-31968

New descriptive temperature model --- for electrons and ions in ionosphere 16 p2375 A83-35396

Oscillating bipolar electric field changes due to close lightning return strokes 16 p2383 A83-35413

Lightning research from space 16 p2422 A83-35778

Electric-probe potential in the space plasma 16 p2416 A83-35943

Low-frequency (f less than about 1 Hz) stratospheric electrical noise measured by balloon-borne sensors 16 p2381 A83-36156

The electrical activity of the atmosphere of Venus 17 p2617 A83-37418

STARE radar observations of a Pg pulsation --- giant pulsations 17 p2538 A83-37592

Systematics of the equatorward diffuse auroral boundary 17 p2538 A83-37595

Middle atmospheric electrodynamics 17 p2541 A83-38279

Cloud electrification --- during thunderstorms 17 p2547 A83-38315

Lightning --- research in U.S. 17 p2547 A83-38316

The appearance of nonuniform electric fields and currents associated with auroral arcs 18 p2713 A83-39321

Measurements of the VLF electric and magnetic components of waves and DC electric field on board the AUREOL-3 spacecraft The TBF-ONCH experiment 18 p2715 A83-39580

Electrodynamics of the stratosphere using 5000 cu m superpressure balloons 18 p2640 A83-39818

Importance of electric field measurement over low latitudes at stratospheric heights by balloons 18 p2717 A83-39819

On the dynamics of the ring current 18 p2718 A83-39952

A numerical simulation of winter cumulus electrification. I Shallow cloud 18 p2729 A83-40040

Planetary lightning - Earth, Jupiter, and Venus 18 p2780 A83-40328

Optical signature of Venus lightning as seen from space 19 p2922 A83-40789

Parameters of the day side magnetopause and generation of the electric field in the magnetosphere 20 p3016 A83-42303

Variation in light intensity with height and time from subsequent lightning return strokes 20 p3030 A83-42839

Large amplitude middle atmospheric electric fields - Fact or fiction? 20 p3026 A83-43210

Simulation of auroral current sheet equilibria and associated V-shaped potential structures 20 p3026 A83-43213

Upward electron beams measured by DE-1 - A primary source of dayside region-1 Birkeland currents 20 p3026 A83-43215

Geos 2 plasma drift velocity measurements associated with a storm time Pc5 pulsation 20 p3027 A83-43216

The 300 MHz electromagnetic radiation and electrostatic field associated with lightning discharges [ONERA, TP NO. 1983-46] 21 p3178 A83-44320

Electrical activity of the Venus atmosphere. II - Measurements by Venus satellites 21 p3242 A83-45289

CRC handbook of atmospheric. Volumes 1 & 2 22 p3307 A83-45876

The physics of thunderclouds 22 p3339 A83-45877

The lightning current 22 p3339 A83-45878

Quasi-electrostatic fields within the atmosphere 22 p3325 A83-45879

Low frequency radio noise 22 p3273 A83-45881

Sferics in the stratosphere 22 p3339 A83-45885

Spatial relationship of field-aligned currents, electron precipitation, and plasma convection in the auroral oval 22 p3327 A83-46051

Polarization patterns of Pi 2 magnetic pulsations and the substorm current wedge 22 p3336 A83-47057

Atmospheric storm explanation of saturnian electrostatic discharges 23 p3529 A83-47875

A systematic characterization of the effects of atmospheric electricity on the operational conditions of aircraft [ONERA, TP NO. 1983-59] 23 p3400 A83-48180

High-temperature physical-chemical processes in the atmosphere during thunderstorms 23 p3485 A83-48504

Positive cloud to ground lightning return strokes 24 p3610 A83-49336

The optical power radiated by lightning return strokes 24 p3610 A83-49347

Temperature and humidity spectra in cloud- and cloud-free air and associated cloud electrical and microphysical characteristics 24 p3611 A83-49681

ATMOSPHERIC EMISSION

U AIRGLOW

ATMOSPHERIC ENERGY SOURCES

Numerical prediction of the onset of the planetary-scale monsoon 03 p0367 A83-14420

The energetics of the lower thermosphere in the presence of internal gravity waves 03 p0362 A83-14834

Long-period atmospheric waves excited by a periodic source 04 p0515 A83-15055

The atmospheric energy budgets over North America, the North Atlantic and Europe based on ECMWF analyses and forecasts 11 p1633 A83-28082

A study of energy conversion in the wave number domain 11 p1619 A83-28341

A study of energy, generation and conversion over North America 11 p1619 A83-28342

The analysis and kinetic energy balance of an upper-level wind maximum during intense convection 13 p1890 A83-30588

Large-scale energy transformations in the high latitudes of the Northern Hemisphere 18 p2728 A83-40026

Energy equation of non-equilibrium states in the earth's atmosphere 19 p2867 A83-41319

ATMOSPHERIC ENTRY

NT HYPERBOLIC REENTRY

NT HYPERSONIC REENTRY

NT SPACECRAFT REENTRY

NT UNCONTROLLED REENTRY (SPACECRAFT)

Physical parameters of meteoroids undergoing quasicontinuous crushing in the atmosphere. I - Methods of parameter determination 03 p0432 A83-13373

Computing the reflection of a point-blast wave from a plane 04 p0476 A83-15098

The survival of solar flare tracks in interplanetary dust silicates on deceleration in the earth's atmosphere 04 p0563 A83-15367

Galileo Atmospheric Entry Probe System - Design, development, and test [AIAA PAPER 83-0098] 05 p0605 A83-16520

Trajectory analysis of radiative heating for planetary missions with aerobraking of spacecraft [AIAA PAPER 83-0407] 05 p0602 A83-16696

Orbiter entry leeside heat-transfer data analysis [AIAA PAPER 83-0484] 05 p0586 A83-16745

The Tsarev stony-meteorite rain 05 p0705 A83-17452

Radiative heat transfer near the stagnation point of a blunt body with an intensely vaporizing surface in the three-dimensional hypersonic flow of a hydrogen-helium mixture 06 p0712 A83-18357

Galileo atmospheric entry probe mission description [AIAA PAPER 83-0100] 06 p0722 A83-19580

Innovative air data system for the Space Shuttle Orbiter 07 p0872 A83-20421

Anomalous infrasound from Space Shuttle II and Skylab I 08 p1048 A83-22229

Interaction between large cosmic bodies and atmosphere 11 p1600 A83-27346

An approximate analytical method for calculating the trajectories of a flight vehicle in the atmosphere 14 p1979 A83-32364

Comparisons of STS-1 experimental and predicted heating rates 15 p2125 A83-33729

Physical parameters of meteoroids undergoing quasicontinuous crushing in the atmosphere. II Interpretation of the parameters 16 p2437 A83-35753

The effect of unsteadiness on the aerodynamic and thermal characteristics of bodies braking in a gas 17 p2449 A83-37554

New aspects in single-body meteor physics 18 p2759 A83-39981

Plume/flowfield jet interaction effects on the Space Shuttle Orbiter during entry 18 p2646 A83-40009

Nonequilibrium radiative heating during outer planet atmospheric entry 18 p2687 A83-40022

Analysis of results of aerodynamic studies on the Venera 13 and 14 descent modules 19 p2809 A83-41237

Angular motion influence on reentry vehicle ablation or erosion asymmetry formation 19 p2811 A83-41938

A finite-volume, adaptive grid algorithm applied to planetary entry flowfields 20 p2930 A83-43440

The Tunguska event - No cometary signature in evidence 22 p3385 A83-46387

ATMOSPHERIC ENTRY SIMULATION

Reconstruction of the shuttle reentry air data parameters using a linearized Kalman filter [AIAA PAPER 83-2097] 19 p2810 A83-41926

ATMOSPHERIC HEAT BUDGET

Thermodynamics of the turbulent atmosphere and parameterization of fluxes 01 p0074 A83-10219

A climatological estimate of the radiative cooling of the atmosphere 02 p0213 A83-11977

The parameterization of longwave flux in energy balance climate models 02 p0213 A83-12229

Stability of Pluto's atmosphere 03 p0434 A83-13842

The mass balance in diagnostic studies - An example of analysed and forecast data calculations --- for atmospheric energy budget equations 04 p0516 A83-15854

A project for exploitation of a new form of solar energy: the wind chill. I - The importance to the energy field. II - Application for building heat and electricity production 06 p0781 A83-19238

Energy fluxes of the /1,1,1/ atmospheric oscillation 07 p0968 A83-21581

Mass, momentum, sensible heat and latent heat budgets for the lower atmosphere 09 p1309 A83-23353

Cloud and aerosol effects in radiant heat transfer --- in planetary atmospheres 09 p1367 A83-25260

Overlapping effect of atmospheric H₂O, CO₂ and O₃ on the CO₂ radiative effect 11 p1632 A83-27669

Inter-annual and seasonal variations in the structure and energetics of the atmosphere over northeast Brazil 11 p1633 A83-28088

Where does the O(1D) energy go? --- in lower thermosphere budget 15 p2196 A83-33945

Optical properties of the Martian atmosphere and radiative heat exchange 16 p2435 A83-35359

Some problems of heat-transfer climatology in energetically active zones of the Atlantic Ocean 16 p2392 A83-36848

The role of turbulence in the heat balance of the mesosphere and lower thermosphere 17 p2537 A83-37052

Variations of turbulent heat transfer in the mesosphere and lower thermosphere 17 p2537 A83-37053

The thermal balance of the middle and upper atmosphere of Venus 17 p2617 A83-37421

A study of heat and moisture budget over the Arabian Sea and their role in the onset and maintenance of summer monsoon 20 p3031 A83-43459

Seasonal variations of heat budgets in both the atmosphere and the sea in the Japan Sea area 20 p3031 A83-43460

A new look at the energy cycle --- in atmosphere 22 p3341 A83-46848

The influence of radiative transfer on the mass and heat budgets of ice crystals falling in the atmosphere 22 p3341 A83-46851

Diagnostic study of the momentum balance in the Northern Hemisphere winter stratosphere 23 p3491 A83-47411

A study of multiple stable layers in the nocturnal lower atmosphere 23 p3492 A83-48732

On the intensity of atmospheric convection
24 p3609 A83-48812

Synoptic forcing of the planetary boundary layer - A case study from the PUKK experiment --- project for investigation of coastal climate
24 p3609 A83-48815

Aircraft observations of 'turbulent fluxes' of momentum, heat and moisture in the sub-cloud layer and associated cloud microphysical and electrical characteristics
24 p3611 A83-49683

ATMOSPHERIC HEATING

Resonant electrodynamic heating and the thermal stability of coronal loops
01 p0129 A83-10950

Instability of the three-dimensional distorted stratospheric polar vortex at the onset of the sudden warming
02 p0214 A83-12239

Satellite estimates of ocean-air heat fluxes during cold air outbreaks
02 p0218 A83-13059

A numerical study of the influence of the planetary boundary layer and moisture on frontal structure
03 p0367 A83-14432

The effects of latent heat release on the May 20 Sesame '77 wave cyclone
03 p0368 A83-14443

A single-level, numerical model suitable for complex terrain
03 p0369 A83-14452

A time Fourier analysis of zonal averaged ozone heating rates
03 p0361 A83-14651

Overlapping effects of atmospheric H2O, CO2 and O3 on the CO2 radiative effects
03 p0361 A83-14660

The thermospheric heating efficiency under electron precipitation conditions
04 p0508 A83-14966

The interrelationship between tropospheric and stratospheric processes during the development of a tropical storm in November, 1979
04 p0515 A83-15059

The existence of Hadley convective regimes of atmospheric motion
04 p0519 A83-16367

The semiannual oscillation in the thermosphere as a conduction mode
05 p0661 A83-17403

Radiative heating due to increased CO2 - The role of H2O continuum absorption in the 12-18 micron region
06 p0791 A83-18269

Heating of the Tibet Plateau and movements of the South Asian high during spring
06 p0792 A83-18471

Temperature effects on the stratosphere of the April 4, 1982 eruption of El Chichon, Mexico
07 p0958 A83-20089

About the reversal of mean zonal wind during the stratospheric warming of 1970-1971
07 p0969 A83-20225

Energy fluxes of the /1,1,1/ atmospheric oscillation
07 p0968 A83-21581

Numerical simulation of the development of mean monsoon circulation in July
08 p1139 A83-22291

Stratospheric warming following the El Chichon volcanic eruption
08 p1138 A83-23276

Eliassen-Palm flux diagnostics and the effect of the mean wind on planetary wave propagation for an observed sudden stratospheric warming
09 p1311 A83-23891

Absolute band strengths of halocarbons F-11 and F-12 in the 8- to 16-micron region
09 p1296 A83-24269

Heating-rate measurements over 30 deg and 40 deg /half-angle/ blunt cones in air and helium in the Langley expansion tube facility
10 p1371 A83-26146

Dynamics and spectroscopy of asymmetrically heated coronal loops
10 p1522 A83-26742

Electrodynamics of the outer solar atmosphere
11 p1687 A83-27379

Dynamics of the middle atmosphere
11 p1631 A83-27404

On the influence of nonlinear wave-wave interaction in a 3-d primitive equation model for sudden stratospheric warmings
11 p1632 A83-27971

The usefulness of a bulk refractive index for the calculation of the scattering properties of mixtures of aerosol particles at wavelength 530 nm
11 p1615 A83-27973

A coupling phenomenon between mesospheric wind patterns and midwinter stratospheric warmings - Preliminary results
12 p1757 A83-29031

VHF radar observations in the stratosphere and mesosphere during a stratospheric warming
12 p1754 A83-29434

Thermal cavitons --- Langmuir waves in plasma density depressions
13 p1925 A83-30421

Heat waves near meteor bodies moving in the atmosphere at hypersonic velocities
13 p1880 A83-31329

The role of thermal conductivity in the process of a flare
14 p2114 A83-32536

Numerical simulation of the heating of the solar chromosphere by intense heat fluxes
14 p2115 A83-32538

Joule heating at high latitudes
15 p2196 A83-33941

Modulation of dayside on and neutral distributions at Venus Evidence of direct and indirect solar energy inputs
16 p2434 A83-35357

Energy deposition rates by charged particles measured during the energy budget campaign
16 p2372 A83-35363

Results from the LIMS experiment for the PMP-1 winter 1978/79 --- Limb Infrared Monitor of the Stratosphere
16 p2383 A83-35381

Responses of the upper middle atmosphere (60-110 km) to the stratwarms of the four pre-map winters (1978/9-1981/2)
16 p2374 A83-35383

A study of stratospheric vacillations and sudden warmings on a beta-plane. I - Single wave-mean flow interaction
16 p2385 A83-35473

On the mechanism for the development of polar lows
16 p2386 A83-35480

Stratospheric sudden coolings and the role of nonlinear wave interactions in preconditioning the circumpolar flow
16 p2386 A83-35483

Cumulus parameterization and rainfall rates. II
16 p2389 A83-36035

The geomagnetic variation in the upper atmosphere [AD-A129193]
16 p2378 A83-36111

The distribution of climatic changes with global warming
16 p2391 A83-36844

The role of turbulence in the heat balance of the mesosphere and lower thermosphere
17 p2537 A83-37052

The thermal balance of the middle and upper atmosphere of Venus
17 p2617 A83-37421

Dynamics of the earth's thermosphere
17 p2541 A83-38274

On the global mean temperature of the thermosphere
17 p2544 A83-38515

The response of finite-amplitude wave motions to seasonal heating of a baroclinic shear flow
18 p2684 A83-39449

Changes in pressure and circulation fields during extreme periods
19 p2867 A83-41582

Neutral and ion gas heating by auroral electron precipitation
20 p3019 A83-42421

Evaluation of upwelling infrared radiance in a nonequilibrium nonhomogeneous atmosphere
20 p3020 A83-42698

Numerical forecasts of stratospheric warming events using a model with a hybrid vertical coordinate
21 p3179 A83-44392

Seasonal distributions of diabatic heating during the first GARP global experiment
21 p3172 A83-44470

Numerical studies of major and minor stratospheric warmings caused by orographic forcing
21 p3180 A83-44708

The effect of stratospheric warming on the turbopause
21 p3176 A83-45270

A boundary-layer-scale model of mountain upslope flow [AD-A130312]
22 p3340 A83-46226

A static model of chromospheric heating in solar flares
22 p3389 A83-47002

Indirect effects of cumulus convection on large-scale radiative heating rates
24 p3613 A83-49704

ATMOSPHERIC IMPURITIES

U. AIR POLLUTION

ATMOSPHERIC IONIZATION

NT. AURORAL IONIZATION

The manifestation of solar activity features upon the decay of the 20th cycle in the ionization of the F2 layer
01 p0129 A83-10594

Observed composition of the ionosphere of Venus - Implications for the ionization peak and the maintenance of the nightside ionosphere
02 p0265 A83-12561

5577-A nightglow and electron fluxes in the nightside atmosphere of Venus
03 p0432 A83-13213

A simple model for relative air mass
03 p0370 A83-14644

Observations of parallel ion energization in the equatorial region
05 p0661 A83-17404

Optimal conditions for the creation of an artificial ionized region in the atmosphere by intersecting microwave beams
05 p0662 A83-17608

Stability of an ionized layer in a gas /the atmosphere/
10 p1449 A83-25989

Ionization curves, masses, and densities of 276 meteor bodies according to radar observations from five points
11 p1685 A83-27878

On the ionization of the mid-latitude lower ionosphere by precipitating hard electrons
11 p1617 A83-28119

An investigation of the mid-latitude ionospheric D-region under twilight conditions in summer
12 p1753 A83-29237

Artificial glow and additional ionization in the upper ionosphere in the field of a high-power radio wave
14 p2049 A83-31855

Electron kinetics in the atmosphere in conditions of repeated air breakdown
14 p2049 A83-31864

Modulation of dayside on and neutral distributions at Venus Evidence of direct and indirect solar energy inputs
16 p2434 A83-35357

Equatorial F-region ionization differences between March and September, 1979
16 p2375 A83-35388

Mesospheric ionisation over dip equator at sunrise
16 p2375 A83-35392

Electron energy deposition in the middle atmosphere
20 p3019 A83-42419

Escape and ionization of atomic oxygen from lo
20 p3078 A83-43078

Modelling of stratospheric ions - A first attempt
21 p3170 A83-44238

Measurements of cosmic-radiation absolute ionization in the atmosphere
21 p3244 A83-44304

Hypotheses on the physical mechanisms of VHF-UHF radiation from lightning
21 p3178 A83-44319

[ONERA, TP NO. 1983-45]
Cosmic rays in the upper atmosphere --- Russian book
21 p3174 A83-45019

Ionization by keV electron precipitation in the auroral zone
22 p3331 A83-46517

Origin of magnetospheric plasma
23 p3485 A83-48552

The accuracy of simple methods for determining the height of the maximum electron concentration of the F2-layer from scaled ionospheric characteristics
24 p3606 A83-49312

ATMOSPHERIC LASERS

Atmospheric- and supraatmospheric-pressure CO2 lasers with a self-maintained discharge
04 p0483 A83-15256

Transmission cutoff accompanying remote optical breakdown of the atmosphere by CO2 laser pulses
05 p0687 A83-17064

High-power continuously tunable atmospheric-pressure CO2 laser operating in the superregenerative amplification regime
14 p2023 A83-31915

ATMOSPHERIC MODELS

NT. REFERENCE ATMOSPHERES

Accuracy of operational snow and ice charts
01 p0074 A83-10090

Thermodynamics of the turbulent atmosphere and parameterization of fluxes
01 p0074 A83-10219

A radiation scheme for circulation and climate models
01 p0074 A83-10221

A comparison of model generated radiation fields with satellite measurements
01 p0075 A83-10223

Priorities for boundary layer research - Consideration by a working group of the Commission of Atmospheric Sciences
01 p0075 A83-10462

Relationships between structure functions and temperature ramps in the atmospheric surface layer
01 p0075 A83-10719

Similarity forms for ground-source surface-layer diffusion
01 p0075 A83-10724

A model for the formation of a temperature inversion layer in a thin atmosphere stratum adjacent to water
01 p0076 A83-10910

NO infrared radiation in the upper atmosphere
02 p0204 A83-11967

Sunrise effect on atmospherics and its relation to the direction of the night noise source
02 p0205 A83-11998

The abundances of CH4, CH3D, NH3, and PH3 in the troposphere of Jupiter derived from high-resolution 1100-1200/cm spectra
02 p0264 A83-12143

Diffusion in the high atmosphere
02 p0206 A83-12153

A simple model for nonlinear critical layers in an unstable baroclinic wave
02 p0213 A83-12226

The Charney stability problem with a lower Ekman layer
02 p0213 A83-12227

Inhibition of baroclinic instability in low-resolution models
02 p0213 A83-12228

The parameterization of longwave flux in energy balance climate models
02 p0213 A83-12229

The significance of thermodynamic forcing by cumulus convection in a general circulation model
02 p0213 A83-12231

Cloud thermodynamic models in saturation point coordinates
02 p0213 A83-12232

Velocity spectra in the unstable planetary boundary layer
02 p0214 A83-12235

A finite-element model of the atmospheric boundary layer suitable for use with numerical weather prediction models
02 p0214 A83-12236

On the two-dimensional transport of stratospheric trace gases in isentropic coordinates
02 p0214 A83-12240

Climate - Multiyear average
02 p0214 A83-12299

A quantitative model of geomagnetic activity
02 p0207 A83-12379

A three-dimensional model of the high-latitude F-region with allowance for the noncoincidence of geographical and geomagnetic coordinates
02 p0208 A83-12421

Dependence of an equinoctial analytical model of ionospheric electron density on solar activity 02 p0209 A83-12423

Allowance for nonstationary and nonlinear terms in the equations of motion in regard to the solution of problems of ionospheric modeling 02 p0209 A83-12424

Investigation of frequency distortions of the meteoric component of a signal scattered in the ionosphere 02 p0209 A83-12427

A simple model for the estimation of rain-induced attenuation along earth-space paths at millimeter wavelengths 02 p0141 A83-12620

Planetary wave modelling of the middle atmosphere - The importance of travelling wave components 02 p0215 A83-12937

A numerical study of thunderstorm electrification using a three dimensional model incorporating the ice phase 02 p0215 A83-12938

A two-dimensional numerical study of horizontal roll vortices in an inversion capped planetary boundary layer 02 p0215 A83-12939

A diffusive model of the turbulent mixing of dry and cloudy air 02 p0215 A83-12942

The influence of ground moisture conditions in North America on summer climate as modeled in the GISS GCM 02 p0218 A83-13062

A simple model illustrating baroclinic development 03 p0363 A83-13223

Markov-chain simulation of particle dispersion in inhomogeneous flows - The mean drift velocity induced by a gradient in Eulerian velocity variance 03 p0363 A83-13269

The spectrum of Titan in the far-infrared and microwave regions 03 p0133 A83-13827

The upper atmosphere of Uranus - A critical test of isotropic turbulence models 03 p0133 A83-13829

Transmission of CO₂ in the atmosphere of Venus for the spectral region near 7 microns 03 p0434 A83-13836

Whatever happened to band models --- for calculating atmospheric IR spectral transmittance 03 p0358 A83-13987

Atmospheric transmittance and radiance - The LOWTRAN 5 code 03 p0358 A83-13988

REALTRAN - Real-time implementation of atmospheric-transmittance codes 03 p0359 A83-13989

Atmospheric model for laser transmission in the infrared 03 p0359 A83-13990

Radiative cooling computed for model atmospheres 03 p0359 A83-14397

Conference on Numerical Weather Prediction, 5th, Monterey, CA, November 2-6, 1981, Preprints [AD-A125468] 03 p0365 A83-14401

Preliminary results of an assessment of FGGE 'special effort' data and its impact on GLAS model analyses and forecasts 03 p0365 A83-14402

The impact of manually derived bogus data on the analysis and forecast models at the Air Force Global Weather Central 03 p0365 A83-14404

Towards the optimum control of gravity waves and ageostrophic circulations for data assimilation 03 p0366 A83-14411

Simulation of the planetary boundary layer with the UCLA general circulation model 03 p0366 A83-14413

NOGAPS - Navy Operational Global Atmospheric Prediction System 03 p0366 A83-14414

Formulation of a modal-split-explicit time integration method for use in the UCLA atmospheric general circulation model 03 p0366 A83-14416

Predictability of quasi-geostrophic planetary waves in global and hemispheric domains 03 p0366 A83-14417

An examination of the characteristics of planetary scale systematic forecast errors 03 p0366 A83-14418

Numerical studies of atmospheric flows over and around large-scale mountains 03 p0367 A83-14422

A variational initialization for a meso-scale model 03 p0367 A83-14424

The effect of initial divergence on prediction of extratropical cyclogenesis 03 p0367 A83-14426

The impact of model moist processes on baroclinic wave energetics 03 p0367 A83-14427

A numerical study of the influence of the planetary boundary layer and moisture on frontal structure 03 p0367 A83-14432

On the predictability of tropical cyclone motion [AD-125566] 03 p0368 A83-14435

Assimilation of remotely-sensed rainfall rates in a moist primitive equation model 03 p0368 A83-14436

Numerical simulation of the airflow over Lake Michigan for a major lake-affected snow event 03 p0368 A83-14438

An explicit mixed numerical method for mesoscale model 03 p0368 A83-14440

NORAPS - The Navy Operational Regional Atmospheric Prediction System 03 p0368 A83-14441

An analysis of the LFM-11 simulations of the Presidents' Day Cyclone, February 18-19, 1979 03 p0368 A83-14442

Large-scale effects of deep convection on the tropical boundary layer 03 p0368 A83-14444

On the generation of convectively driven mesohighs aloft 03 p0368 A83-14446

On the predictability of individual deep convective clouds 03 p0369 A83-14447

A lateral boundary condition for cumulus models which simulates the mesoscale response to convection 03 p0369 A83-14448

Formation of the low-level jet under an inversion 03 p0369 A83-14449

A numerical simulation of a stratocumulus-topped mixed layer 03 p0369 A83-14450

An operational turbulence closure model forecast system 03 p0369 A83-14451

A single-level, numerical model suitable for complex terrain 03 p0369 A83-14452

Prediction of corridor effect from the launching of the satellite power system --- air pollutant concentration into narrow band of latitude 03 p0360 A83-14519

Baroclinic nonlinear exchanges of energy and potential enstrophy in the quasi-geostrophic two-layer model 03 p0369 A83-14520

A simple model for relative air mass 03 p0370 A83-14644

Results from a monex radiation experiment 03 p0370 A83-14649

Numerical experiments on the role of radiative processes in the development and maintenance of upper level clouds 03 p0371 A83-14653

Some remarks about a ball lightning model 03 p0361 A83-14743

Non-LTE resonance line polarization with partial redistribution effects --- in solar spectra 03 p0437 A83-14783

A one-dimensional model of the atmosphere considered as a climatic system block comprising the ocean, the atmosphere, and the ice cover 03 p0371 A83-14826

The photochemistry and dynamics of a dusty cometary atmosphere 03 p0431 A83-14865

Noctilucent clouds - Simulation studies of their genesis, properties and global influences 04 p0509 A83-14973

A conception of a normal-mode expansion procedure applied to a limited-area model. I - The derivation of dynamic equations in normal mode form --- in numerical weather forecasting 04 p0514 A83-15023

The influence of the thermal characteristics of the underlying surface on the atmosphere as revealed by a small-component model 04 p0515 A83-15056

Meteorological inputs to flight simulators 04 p0515 A83-15323

Impact induced dehydration of serpentine and the evolution of planetary atmospheres 04 p0564 A83-15374

A model of Martian slope winds - Implications for eolian transport 04 p0566 A83-15569

The seasonal CO₂ cycle on Mars - An application of an energy balance climate model 04 p0569 A83-15592

Atmospheric predictability experiments with a large numerical model 04 p0515 A83-15851

A seasonal global climate model with an equivalent meridional atmospheric circulation 04 p0515 A83-15852

A numerical simulation of an atmospheric vortex street 04 p0516 A83-15856

The baroclinic instability of highly structured one-dimensional basic states 04 p0516 A83-15926

Wave-interactions in quasi-geostrophic uniform potential vorticity flow 04 p0516 A83-15927

Planetary-scale waves in the Venus atmosphere 04 p0569 A83-15928

A study of the adequacy of quasi-geostrophic dynamics for modeling the effect of cyclone waves on the larger scale flow 04 p0516 A83-15929

Forced, stationary waves in a linear, stratified, quasi-geostrophic atmosphere 04 p0516 A83-15930

An analysis of wave-turbulence interaction 04 p0516 A83-15931

Numerical study of terrain-induced mesoscale motions in a mixed layer 04 p0516 A83-15932

Eastward and westward flows over topography in nonlinear and linear barotropic models 04 p0516 A83-15933

A simple method to compute the change in earth-atmosphere radiative balance due to a stratospheric aerosol layer 04 p0510 A83-15939

A note on the effect of horizontal momentum fluxes by unresolved synoptic-scale eddies in a low-resolution spectral general circulation model 04 p0517 A83-15943

Numerical study of the effect of CCN on the size distribution of cloud droplets. I - Cloud droplets in the stage of condensation growth --- Cloud Condensation Nuclei 04 p0518 A83-16017

Weather predictions by fine mesh models; Proceedings of the Third Course of the International School of Meteorology of the Mediterranean, Erice, Italy, October 17-30, 1981 04 p0518 A83-16151

Performance and limits of global models in the Mediterranean 04 p0518 A83-16152

Numerical modelling of the mesoscale airflow downwind of the Alps - Two case studies under cyclogenetic conditions 04 p0518 A83-16153

Analysis methods for meteorological observations 04 p0518 A83-16154

Initialization in presence of mountains --- atmospheric prediction models 04 p0518 A83-16155

Air quality mathematical modeling in the presence of strong point emissions 04 p0507 A83-16156

Fine mesh models in the U.K. Meteorological Office 04 p0519 A83-16157

Parametrisation in weather prediction models 04 p0519 A83-16158

ECMWF limited area model 04 p0519 A83-16160

Effects of aerosols on photosynthesis 05 p0659 A83-16850

The effect of ammonia ice on the outgoing thermal radiance from the atmosphere of Jupiter 05 p0703 A83-16962

Intense atmospheric vortices; Proceedings of the Joint Symposium, Reading, Berks., England, July 14-17, 1981 05 p0667 A83-17113

A modulated point-vortex model for geostrophic, beta-plane dynamics [AD-A126704] 05 p0639 A83-17355

A high-resolution model of the planetary boundary layer - Sensitivity tests and comparisons with SESAME-79 data 05 p0667 A83-17439

Statistical performance of several mesoscale atmospheric dispersion models 05 p0667 A83-17442

A non-geostrophic study in a barotropic system 05 p0668 A83-17554

The use of a single coupling function for the correction of model profiles of electron density in the ionosphere 05 p0662 A83-17604

The modeling of a large-scale region of disturbances arising during the vertical heating of the ionosphere by a field of high-power radio waves 05 p0662 A83-17605

Manifestation of the effect of large-scale ionospheric irregularities in the case of back-oblique sounding 05 p0662 A83-17606

Modification of stationary ionospheric current systems under strong ionospheric disturbances 05 p0662 A83-17609

Calculation of long-range radio paths by the adiabatic method using a parabolic model of the ionosphere 05 p0663 A83-17611

The consequences of high latitude particle precipitation on global thermospheric dynamics 05 p0665 A83-17782

An analysis of the applicability of an experimental model of the sporadic-E layer at high latitudes 05 p0666 A83-17950

Radiative-convective models of climate 06 p0788 A83-17997

On the criterion of comparison of MSIS and IRI models by means of optical data 06 p0782 A83-18024

The depth of the daytime mixed layer at two coastal sites - A model and its validation 06 p0788 A83-18057

Atmospheric parameters and carbon abundance of white dwarfs of spectral types C2 and DC 06 p0826 A83-18093

Formulation and testing of a climatonic simulation of the microclimate of the dry valleys and of the Little America V Station in Antarctica 06 p0788 A83-18236

Intercomparisons of upper air and surface winds in an urban region 06 p0781 A83-18238

A framework for evaluating air quality models 06 p0781 A83-18240

Spurious mass loss in some mesometeorological models 06 p0789 A83-18241

On two-layer models and the similarity functions for the PBL 06 p0789 A83-18246

Climate studies with a multi-layer energy balance model. I - Model description and sensitivity to the solar constant. II - The role of feedback mechanisms in the CO₂ problem 06 p0789 A83-18251

Internal dynamics of tornado-like vortices
06 p0790 A83-18257

Structure of the cold front observed in SESAME-AVE
III and its comparison with the Hoskins-Bretherton
frontogenesis model --- Severe Environmental Storms And
Mesoscale Experiment - Atmospheric Variability
Experiment 06 p0790 A83-18261

Entrainment and detrainment in a simple cumulus cloud
model 06 p0790 A83-18262

Case study of a hailstorm in Colorado. I - Radar echo
structure and evolution 06 p0790 A83-18263

Magnetic flux ropes in the Venus ionosphere -
Observations and models 06 p0847 A83-18282

Global empirical model of the Venus thermosphere
06 p0847 A83-18283

Testing subroutines solving advection-diffusion
equations in atmospheric environments
06 p0756 A83-18374

Numerical simulation of land-breeze-induced
snowbands along the western shore of Lake Michigan
06 p0791 A83-18461

Initial results from a mesoscale atmospheric simulation
system and comparisons with the AVE-SESAME I data
set --- Atmospheric Variability Experiment-Severe
Environmental Storms And Mesoscale Experiment
06 p0791 A83-18462

Description and evaluation of NORAPS - The Navy
Operational Regional Atmospheric Prediction System
06 p0791 A83-18463

Adaptation of P. D. Thompson's scheme to the constraint
of potential vorticity conservation --- modified
two-parameter baroclinic model for weather prediction
06 p0791 A83-18465

A parameterized model for global insolation under
partially cloudy skies 06 p0792 A83-18552

Models of the ionospheric D region at noon
06 p0786 A83-18730

A comparative study of simple numerical models of the
atmospheric boundary layer 06 p0792 A83-18927

A simple parameterization of moist convection for
large-scale atmospheric models
06 p0793 A83-18993

The growth of filaments by the condensation of coronal
arches 06 p0855 A83-19134

Formation of amino acids from models of Titan and more
oxidized atmospheres 06 p0801 A83-19407

A climatological model for the determination of air
pollutant concentrations at a topographically complex
site 07 p0956 A83-20199

A stratospheric chemical instability
07 p0960 A83-20213

A one-dimensional model of the atmospheric electric
field near the Venusian surface
07 p1030 A83-20619

Sensible heat flux estimated from routine meteorological
data by the resistance method 07 p0969 A83-20805

Modern exospheric theories and their observational
relevance --- kinetic theory 07 p1031 A83-20839

Zonal models of the atmosphere
07 p0970 A83-20886

Numerical simulation of fog formation and liquid water
content on polydisperse multi-composition aerosols due
to combustion-related pollutants
07 p0963 A83-21038

A global model of the neutral thermosphere in magnetic
coordinates based on AE-C data
07 p0967 A83-21520

Seasonal variation of the atmospheric temperature at
midlatitude - A revision of the CIRA 1972 model
08 p1138 A83-22061

ANMRC data assimilation for the Southern
Hemisphere 08 p1138 A83-22283

Incremental linear normal mode initialization in
four-dimensional data assimilation --- for numerical weather
forecasting 08 p1138 A83-22284

Numerical weather prediction studies from the FGGE
Southern Hemisphere data base
08 p1138 A83-22285

A non-iterative procedure for the time integration of the
balance equations --- for atmospheric models
08 p1139 A83-22287

Multiply-upstream, semi-Lagrangian advective schemes
- Analysis and application to a multi-level primitive equation
model 08 p1139 A83-22288

Significance of non-elliptic regions in balanced flows of
the tropical atmosphere 08 p1139 A83-22295

A study of the sensitivity of numerical forecasts to an
upper boundary in the lower stratosphere
08 p1139 A83-22296

Vertical mass transport in cumulonimbus clouds on day
261 of GATE 08 p1140 A83-22297

Development of a two-dimensional finite-element PBL
model and two preliminary model applications
08 p1140 A83-22299

On the predictability of quasi-geostrophic flow - The
effects of beta and baroclinicity
08 p1142 A83-23002

Theory of generation of ULF pulsations by ionospheric
modification experiments 09 p1300 A83-23308

Ionospheric effects of rocket exhaust products -
HEAO-C, Skylab 09 p1301 A83-23314

The relation between the stratification parameter mu and
the vertical temperature gradient in the planetary boundary
layer 09 p1311 A83-23550

A simple theoretical model for calculating and
parameterizing the ionospheric photoelectron flux
09 p1304 A83-23772

A two-dimensional model for ozone changes by
planetary waves in the stratosphere. I - Formulation and
the effect of temperature waves on the zonal mean ozone
concentration 09 p1304 A83-23890

A numerical experiment on the mountain and valley
winds 09 p1311 A83-23892

On the preferred mode of cumulus convection in a
conditionally unstable atmosphere
09 p1312 A83-23958

Toward a unified theory of atmospheric convective
instability 09 p1312 A83-23959

Precipitation in convective storms - An observational
and numerical study 09 p1313 A83-23971

The mean annual variation of the geopotential of the
500 mb surface for the Northern Hemisphere in
wavenumber space 09 p1313 A83-24120

Closure models for rotating two-dimensional
turbulence 09 p1314 A83-24129

Numerical modeling of a zonally averaged stratospheric
ozone field 09 p1305 A83-24215

Uncertainties of predictions of future atmospheric CO2
concentrations 09 p1294 A83-24251

Exponential growth and atmospheric carbon dioxide
09 p1295 A83-24255

The sources of sulfate in precipitation. II - Sensitivities
to chemical variables 09 p1296 A83-24266

A numerical model of the zonally averaged dynamical
and chemical structure of the middle atmosphere
09 p1296 A83-24267

On the relationship between the greenhouse effect,
atmospheric photochemistry, and species distribution
09 p1296 A83-24268

Atomic oxygen emissions observed from Pioneer
Venus 09 p1366 A83-24341

Field-aligned plasma flow in the quiet, mid-latitude
ionosphere deduced from topside soundings
09 p1306 A83-24687

A hemispheric barotropic quasi-geostrophic model of the
atmosphere with conservation of the degrees of potential
vorticity 09 p1315 A83-24934

The role of short waves and the accuracy of their initial
representation during forecasting by the spectral model
09 p1315 A83-24935

An investigation of the convergence of a moist
convective adjustment scheme
09 p1315 A83-24938

A convection parameterization scheme based on a direct
algorithm of dry convective adjustment --- for atmospheric
models 09 p1315 A83-24939

Several models for optimizing the behavior of
atmospheric pollution sources 09 p1297 A83-24940

Importance of heterogeneous processes to tropospheric
chemistry - Studies with a one-dimensional model
09 p1298 A83-25200

A comparison between the calculated and measured
characteristics of an advection fog and a stratus over
ice 09 p1316 A83-25229

A method of calculating fluxes and the influx of long-wave
and solar radiation in a model of low clouds and fogs
09 p1317 A83-25235

Modeling the optical properties of Venusian clouds
09 p1367 A83-25237

Mathematical modeling for molecular spectroscopy of
the atmosphere 09 p1309 A83-25240

Building a balanced model of the climate
09 p1317 A83-25241

Application of statistical modeling to the problem of the
optical sensing of the ocean-atmosphere system
09 p1320 A83-25243

Mathematical modeling of the general circulation of the
atmosphere and ocean 09 p1309 A83-25244

The structure of mathematical models in environmental
hydrodynamics problems 09 p1299 A83-25245

Diagnostic analysis and spectral energetics of a blocking
event in the GLAS climate model simulation
10 p1449 A83-25380

The relationship between convective adjustment, Hadley
circulation and normal modes of the ANMRC spectral
model 10 p1450 A83-25381

Autocorrelation of Northern Hemisphere geopotential
heights 10 p1450 A83-25388

Numerical simulation of the airflow over Lake Michigan
for a major lake-effect snow event
10 p1451 A83-25392

Modeling of atmospheric radio noise near
thunderstorms 10 p1449 A83-26039

The use of a mesoscale numerical model for evaluations
of pollutant transport and diffusion in coastal regions and
over irregular terrain 10 p1451 A83-26099

Aerosol mode of ball lightning
10 p1451 A83-26465

A mechanism of gravity wave excitation observable with
atmospheric radars 11 p1623 A83-26992

An improved model for the calculation of profiles of
C/n-squared and epsilon in the free atmosphere from
background profiles of wind, temperature and humidity
11 p1623 A83-26994

Modification of raindrop size distributions in subcloud
downdrafts 11 p1627 A83-27034

Radiative equilibrium model of Titan's atmosphere
11 p1685 A83-27368

On waves in non-isothermal, compressible, ionized and
viscous atmospheres 11 p1677 A83-27654

On the influence of nonlinear wave-wave interaction in
a 3-d primitive equation model for sudden stratospheric
warmings 11 p1632 A83-27971

A radiation model using hourly meteorological data with
results from GATE 11 p1632 A83-27972

On the effect of model resolution on numerical simulation
of blocking --- in atmospheric circulation
11 p1633 A83-28081

Lagged average forecasting, an alternative to Monte
Carlo forecasting 11 p1633 A83-28086

Theoretical study of multiple equilibria in simple
axisymmetric tropical circulations
11 p1633 A83-28087

Interpretation for the R-T coefficient method applied to
the propagation of electromagnetic waves through the
earth's ionosphere 11 p1616 A83-28108

A study of energy conversion in the wave number
domain 11 p1619 A83-28341

Update of PAGEOPH Vol. 119 /1980/81/ pp. 726-749
- 'Comparison of the Nimbus-4 BUV ozone data with the
Ames two-dimensional model' 11 p1619 A83-28345

Model-atmosphere analysis of high-dispersion spectra
of four red giants and supergiants
12 p1790 A83-28879

Effect of recent rate data revisions on stratospheric
modeling 12 p1751 A83-28918

Ion-beam-driven electrostatic ion cyclotron instabilities
12 p1751 A83-28920

On the use of spectral radiance models to obtain
irradiances on surfaces of arbitrary orientation
12 p1752 A83-28945

An analytic version of Jacchia's 1977 model
atmosphere 12 p1752 A83-29101

Improving the Eddy Kinetic Energy model for planetary
boundary layer description 12 p1758 A83-29129

Modelling the height, temperature and relative humidity
of a well-mixed planetary boundary layer over a water
surface 12 p1758 A83-29131

A one-dimensional simulation of the
stratocumulus-capped mixed layer
12 p1758 A83-29139

The role of aerosols in the climate system - Results of
numerical experiments in climate models
12 p1759 A83-29559

Most suitable conditions for aerosol monitoring from
space 12 p1754 A83-29561

On the influence of rough water surfaces on polarimetric
investigations of aerosols from space
12 p1730 A83-29562

The dynamics of singular geostrophic vortices in a
two-level model of the atmosphere (ocean)
13 p1873 A83-30026

A kinetic model for a fine anhydrous aerosol in the
troposphere 13 p1873 A83-30027

Numerical modeling of the influence of thermals on the
development of cumulus clouds
13 p1883 A83-30030

Ionospheric plasma cloud dynamics via regularized
contour dynamics. I - Stability and nonlinear evolution of
one-contour models 13 p1874 A83-30125

The calculation characteristics of multilevel predictive
schemes and models of general atmospheric circulation
13 p1884 A83-30291

The modeling of certain long-period atmospheric
processes 13 p1884 A83-30292

Prospects for prediction of zonal wind oscillations
13 p1889 A83-30575

Verification of MOS guidance for cloud amount, ceiling,
and visibility --- model output statistics
13 p1889 A83-30581

The interactive role of subsynoptic scale jet streak and
planetary boundary layer adjustments in organizing an
apparently isolated convective complex
13 p1890 A83-30585

Objective analysis and assimilation of observational data from FGGE --- First GARP Global experiment 13 p1891 A83-30804

The constraints of energy-conserving vertical finite difference on the hydrostatic equations in a NWP model --- Numerical Weather Prediction 13 p1891 A83-30805

Basic state energy budget analysis for phases 1, 2 and 3 of GATE 13 p1891 A83-30806

A model of tropical ocean-atmosphere interaction 13 p1891 A83-30807

The global distribution of atmospheric carbon dioxide. I Aspects of observations and modeling. II - A review of provisional background observations, 1978-1980 13 p1876 A83-30876

Nonlinear response of stratospheric ozone column to chlorine injections 13 p1872 A83-30880

A general circulation model study of atmospheric carbon monoxide 13 p1876 A83-30884

A general circulation model of a Venus-like atmosphere 13 p1961 A83-31031

Effects of planetary wave propagation and finite depth on the predictability of atmospheres 13 p1892 A83-31033

Thermally indirect motions in the convective atmospheric boundary layer 13 p1892 A83-31035

On resonant interactions between unstable and neutral baroclinic waves 13 p1892 A83-31037

A note on orographically induced instabilities in two-layer models --- of atmosphere 13 p1893 A83-31046

Methane abundance in the atmosphere of Uranus 13 p1961 A83-31201

Day and night models of the Venus thermosphere 13 p1962 A83-31229

Concerning the correctness on the whole of boundary value problems for models of the dynamics of the atmosphere and the ocean 13 p1880 A83-31326

An effort to simulate magnetospheric-ionospheric effects in the presence of seismic phenomena 13 p1880 A83-31328

Thermodynamic model of the seasonal evolution of the ocean-atmosphere system 13 p1894 A83-31350

A simple hourly clear-sky solar radiation model based on meteorological parameters 13 p1894 A83-31611

Diffuse and global solar spectral irradiance under cloudless skies 13 p1882 A83-31613

The dissipation of a sodium cloud 13 p1882 A83-31627

A simple model of the distant Jovian tail with magnetic flux loss 13 p1962 A83-31662

Modeling of ionospheric-plasmaspheric interactions with allowance for temperature anisotropy 14 p2049 A83-31863

Modeling of the development of current systems of a polar magnetic substorm 14 p2050 A83-31868

Electric field in the polar cap 14 p2050 A83-31871

Global distribution and southern hemispheric trends of atmospheric CCl₃F 14 p2056 A83-31920

Modeling the carbon cycle using the method of fractional-order derivatives 14 p2051 A83-32366

Numerical modeling of an atmospheric front with a cloud system and precipitation 14 p2056 A83-32367

Parameterization of the surface fluxes of heat and momentum for the convective atmospheric boundary layer 14 p2056 A83-32402

An analytic study on the horizontal motion of monsoon depressions 14 p2056 A83-32403

On a 3-component truncated model of a barotropic non-divergent rotating atmosphere in spherical geometry 14 p2057 A83-32405

On truncated models of barotropic vorticity equation in spherical geometry 14 p2057 A83-32406

The background of the equivalent barotropic model for tropics 14 p2057 A83-32408

A cloud formation process contradictory to the classical occlusion development investigated with satellite images and model output parameters 14 p2057 A83-32409

Stability properties of cylindrically curved mean flows --- in atmosphere 14 p2058 A83-32469

Large-scale fluctuations in a long-range integration of the ECMWF spectral model --- of atmosphere 14 p2058 A83-32470

On the theory of the katabatic slope wind 14 p2058 A83-32472

Numerical simulation of nonstationary hydrodynamic phenomena in solar flares 14 p2115 A83-32537

Numerical simulation of the heating of the solar chromosphere by intense heat fluxes 14 p2115 A83-32538

The seasonal variation of the thermal structure of the atmosphere of Uranus 14 p2112 A83-32608

A method of calculating the natural components of meteorological fields 14 p2058 A83-32852

Diagnostic and prognostic numerical circulation studies of the South Atlantic Bight 14 p2060 A83-33078

Kinematics and correlation of the surface wind field in the South Atlantic Bight 14 p2059 A83-33079

A non-reflective upper boundary condition for limited-height hydrostatic models 15 p2203 A83-33877

An upper boundary condition permitting internal gravity wave radiation in numerical mesoscale models 15 p2203 A83-33878

A numerical scheme to treat the open lateral boundary of a limited area model 15 p2203 A83-33879

A simple positive definite advection scheme with small implicit diffusion 15 p2204 A83-33881

A possible explanation of the observed persistence of monthly mean circulation anomalies 15 p2204 A83-33882

On the mathematical simulation of non-equilibrium cloud condensation rates 15 p2205 A83-34061

Detailed and parameterized modeling of cloud-microphysics in a stationary cloud model 15 p2205 A83-34064

A numerical model of the dynamics and microphysics of warm cumulus convection - Model description and preliminary results 15 p2205 A83-34065

The influence of atmospheric aerosol on the life cycle radiation fog 15 p2205 A83-34066

The numerical simulation of the interaction of cloud formation and lee waves 15 p2206 A83-34067

Validated band model for NO₂ molecular transmittance in the infrared 15 p2201 A83-34457

Modeling atmospheric aerosol backscatter at CO₂ laser wavelengths. I - Aerosol properties, modeling techniques, and associated problems. II - Modeled values in the atmosphere. III - Effects of changes in wavelength and ambient conditions 15 p2201 A83-34461

The DB white dwarfs. I - The He I 4388 + 4471 + 4516 blend 15 p2264 A83-34577

The atmosphere of Canopus. I - Model of the atmosphere and distribution of the microturbulence 15 p2270 A83-34682

Experimental study of a multiplicative model of multiple ionospheric reflections 15 p2145 A83-34896

A conception of normal mode expansion procedure applied to a limited-area model. II - Linear aspects. III - Derivation and theoretical discussion of a nonlinear approach --- of geostrophic balance 15 p2207 A83-35096

The possibility of modeling the wind field in a planetary boundary layer with an incorporated temperature inversion in the (quasi-)stationary case 15 p2207 A83-35097

Replacement of the present sub-peak plasma density profile by a unique expression 16 p2374 A83-35385

Implementation of a new characteristic parameter into the IRI sub-peak electron density profile 16 p2374 A83-35386

Latitudinal influences on the quiet daytime D-region [AD-A128591] 16 p2375 A83-35391

New descriptive temperature model --- for electrons and ions in ionosphere 16 p2375 A83-35396

F-region ion composition modeling 16 p2376 A83-35398

Instabilities in a stratified fluid having one critical level. I - Results. II - Explanation of gravity wave instabilities using the concept of overreflection. III - Kelvin-Helmholtz instabilities as overreflected waves 16 p2384 A83-35458

January and July simulations with a spectral general circulation model 16 p2384 A83-35461

The response of a spectral general circulation model to refinements in radiative processes 16 p2384 A83-35462

A model to determine open or closed cellular convection 16 p2384 A83-35463

A quasi-one-dimensional, time-dependent and non-precipitating cumulus cloud model - On the bimodal distribution of cumulus cloud height 16 p2384 A83-35464

Low-resolution numerical simulation of decaying two-dimensional turbulence 16 p2385 A83-35470

A study of stratospheric vacillations and sudden warmings on a beta-plane. I - Single wave-mean flow interaction 16 p2385 A83-35473

A nonsymmetric equatorial inertial instability 16 p2385 A83-35476

Thermally driven flow in a rotating spherical shell Axisymmetric states 16 p2385 A83-35479

Transient planetary waves simulated by GFDL spectral general circulation models. I - Effects of mountains. II - Effects of nonlinear energy transfer 16 p2386 A83-35485

On the choice of boundary conditions for the matching of kinetic to hydrodynamic polar wind models 16 p2376 A83-35787

Numerical experiments with a one-dimensional higher order turbulence model - Simulation of the Wangarda Day 33 case 16 p2387 A83-35795

Efficient three-dimensional global models for climate studies - Models I and II 16 p2388 A83-36026

Experiments in shower-top forecasting using an iterative one-dimensional cloud model 16 p2389 A83-36036

A comparison of methods for computing the sigma-coordinate pressure gradient force for flow over sloped terrain in a hybrid theta-sigma model 16 p2389 A83-36037

Proposal for a reference model of the middle atmosphere of the Southern Hemisphere 16 p2389 A83-36102

Model calculations of middle atmospheric wind and temperature fields 16 p2377 A83-36107

The geomagnetic variation in the upper atmosphere [AD-A129193] 16 p2378 A83-36111

Evaluation of selected global thermospheric density models during low solar flux conditions 16 p2378 A83-36113

Seasonal transport and turbulence in the lower thermosphere 16 p2378 A83-36118

Recent incoherent scatter radar results not incorporated in current thermospheric models 16 p2378 A83-36119

Latitudinal variation of tropospheric ozone in a photochemical model 16 p2379 A83-36132

CO₂ radiative parameterization used in climate models Comparison with narrow band models and with laboratory data 16 p2389 A83-36134

Parameterization of carbon dioxide 15-micron band absorption and emission 16 p2379 A83-36135

Simulation of NO_x partitioning along isobaric parcel trajectories 16 p2381 A83-36159

Nonlinear interactions in a two-layer, quasi-geostrophic, low-order model with topography. I - Zonal flow-forced wave interactions 16 p2381 A83-36489

Structure of the free convective internal boundary layer above the coastal area 16 p2390 A83-36494

Interactions of isolated vortices. II - Modon generation by monopole collision 16 p2353 A83-36546

Influence of mean divergence, mean vorticity and height-dependent eddy viscosity on thermal instability 16 p2391 A83-36583

An analysis of geopotential height at 300 mbar in the frequency wavenumber domain along 50 deg N in observed and modelled January climate 16 p2391 A83-36584

The influence of the differencing methods used on the solution of the barotropic nesting problem 16 p2391 A83-36587

Thermal structure of the atmosphere of Venus 17 p2616 A83-37412

Basic theory and model calculations of the Venus ionosphere 17 p2617 A83-37425

Physics of the interaction of the solar wind with the ionosphere of Venus - Flow/field models 17 p2618 A83-37427

A two-dimensional model of the ionosphere of Venus 17 p2618 A83-37585

Drift wave model for geomagnetic pulsations in a high beta plasma 17 p2538 A83-37593

Simple method for estimating atmospheric absorption at 1 to 15 GHz 17 p2494 A83-37795

Neutral and ion composition of the thermosphere 17 p2541 A83-38277

Modeling planetary magnetospheres 17 p2542 A83-38299

Regimes of flow in a planet's atmosphere - A numerical study 17 p2547 A83-38463

Dynamo region and the equatorial electrojet in the Jovian atmosphere 17 p2623 A83-38517

Statistical models for meteorological data analysis 17 p2551 A83-38745

Atmospheric determination for Shuttle aerodynamic studies 17 p2552 A83-38757

Numerical simulation of the atmosphere during a CAT encounter 17 p2553 A83-38764

Incorporation of planetary boundary layer dynamics in a numerical model of long-range air pollutant transport 18 p2720 A83-39011

Network to cell contrast at microwaves --- radio brightness temperature of solar atmosphere 18 p2782 A83-39034

The mid-latitude trough in the electron concentration of the ionospheric F-layer - A review of observations and modelling 18 p2712 A83-39069

Stochastic simulation of atmospheric trajectories 18 p2722 A83-39123

A radiative transfer model for surface radiation budget studies 18 p2751 A83-39184

The effects of orographically determined vertical motions and surface friction on the development and motion of baroclinic waves in numerical models with different vertical resolution 18 p2723 A83-39259

The effect of seasonal asymmetry on the filling of plasma tubes 18 p2714 A83-39334

Modeling of the boundary of the plasmasphere and its parameters with allowance for convective motions 18 p2714 A83-39335

Modeling the effect of stratospheric aerosols on climate 18 p2723 A83-39437

A model of a cloud ensemble with two zones of mass ejection from clouds 18 p2723 A83-39440

Forecasting experiments with a model of the general circulation of the atmosphere 18 p2724 A83-39445

A model for the Priestley-Taylor parameter alpha --- of atmospheric boundary layer 18 p2724 A83-39680

Simulation of transport and removal processes of the Saharan dust 18 p2725 A83-39685

Some essential details for application of Bleck's method to the collision-breakup equation --- raindrop development model 18 p2725 A83-39691

Interactions between orographically and thermally forced planetary waves 18 p2728 A83-40031

A moist baroclinic model for monsoonal mid-tropospheric cyclogenesis 18 p2728 A83-40032

The behavior of stationary waves and the summer monsoon 18 p2728 A83-40033

The mesoscale and microscale structure and organization of clouds and precipitation in midlatitude cyclones. VIII - A model for the "seeder-feeder" process in warm-frontal rainbands 18 p2729 A83-40035

A laboratory experiment on the dynamics of the land and sea breeze 18 p2729 A83-40038

Numerical modelling of the ionospheric filtration of an ULF micropulsation signal 19 p2866 A83-41318

The numerical modeling of the diurnal variations of meteorological elements in a large city 19 p2868 A83-41584

A regional scale modeling study of the sulfur oxides with a comparison to ambient and wet deposition monitoring data 19 p2863 A83-41986

Three dimensional numerical models of the large scale circulation induced by the global models of the thermosphere 20 p3017 A83-42311

Electron precipitation and related aeronomy of the Jovian thermosphere and ionosphere 20 p3077 A83-42407

Limitations of some common lateral boundary schemes used in regional NWP models --- Numerical Weaather Prediction 20 p3029 A83-42508

The atmosphere --- dynamics and climatology 20 p3020 A83-42821

Synoptic cloud variations in a low resolution spectral atmospheric model 20 p3030 A83-42840

General circulation model experiments on the climatic effects due to a doubling and quadrupling of carbon dioxide concentration 20 p3031 A83-42843

A model for the variations of the critical frequency of F2 layer during the negative phases of ionospheric storms 20 p3024 A83-43173

Reflection of MHD-waves in the PC4-5 period range at ionospheres with non-uniform conductivity distributions 20 p3026 A83-43204

Ring coupling model - Implications for substorm onsets 20 p3027 A83-43217

A mesoscale atmospheric dispersion model for predicting ambient air concentration and deposition patterns for single and multiple sources 20 p3014 A83-43422

Evaluation of an episodic regional transport model for a multi-day sulfate episode 20 p3014 A83-43423

Comparison of calculated and observed super- and sub-micrometer aerosol mass concentrations using St. Louis RAPS data base --- Regional Air Pollution Study 20 p3014 A83-43426

General circulation of air parcels and transport characteristics derived from a hemispheric GCM. I - A determination of advective mass flow in the lower stratosphere 20 p3031 A83-43457

Details of low latitude medium range numerical weather prediction using a global spectral model. I - Formation of a monsoon depression 20 p3031 A83-43458

Enhancement and initiation of a cumulus by a heat island 20 p3032 A83-43462

Modified method of estimating space-time spectra from polar-orbiting satellite data. I - The frequency transform method. II - The wavenumber transform method 20 p3032 A83-43463

An economical explicit time integration scheme for a primitive model --- of atmosphere 20 p3032 A83-43464

Modelling of stratospheric ions - A first attempt 21 p3170 A83-44238

A static structural model of the outer magnetosphere of Jupiter 21 p3240 A83-44286

Numerical computations of non-linear waves in solar atmosphere 21 p3243 A83-44303

Dynamical processes in the atmosphere and the use of models 21 p3179 A83-44389

African wave disturbances in a general circulation model 21 p3179 A83-44471

On puff models of turbulence diffusion at various scales of atmospheric movements 21 p3179 A83-44490

The ablation model of the sodium layer in the middle atmosphere 21 p3172 A83-44501

The relation between the onset times of the negative phase of ionospheric storms and the main phase of magnetic storms and a theoretical model 21 p3172 A83-44524

An analysis of the U.S. Standard Atmosphere, 1976 21 p3173 A83-44581

Modelling of the ion composition of the middle atmosphere 21 p3173 A83-44669

Boundary layer evolution in the region between shore and cloud edge during cold-air outbreaks 21 p3180 A83-44705

On baroclinic instability in the case of vanishing viscosity 21 p3132 A83-44943

An introduction to the theory of climate --- Russian book 21 p3180 A83-45010

Numerical experiments in the analysis of mathematical models of the ionosphere 21 p3174 A83-45233

Model ionograms of oblique sounding on the Nikolaev-Havana path 21 p3174 A83-45237

Mathematical model of the three-dimensional structure of the winter polar ionosphere and its variability 21 p3175 A83-45239

Modeling of the equatorial ionosphere in the hybrid model 21 p3176 A83-45258

Comparison of an empirical magnetic-field-model based on HEOS-1,2 data with an analytical two-dipole model of the magnetosphere 21 p3176 A83-45268

The effect of a heat source on the large-scale pressure and wind fields (a quasi-barotropic model) 21 p3181 A83-45330

The four-dimensional assimilation of synoptic information on the basis of a nonlinear filtration scheme --- for numerical weather forecasting 21 p3181 A83-45331

A comparison of the calculated and measured spectral radiances of the atmosphere toward the zenith 21 p3177 A83-45407

Bulk parameterization of the snow field in a cloud model 22 p3338 A83-45709

Modeling of the atmosphere for analysis of horizon sensor performance 22 p3261 A83-46599

The shape, propagation and mean-flow interaction of large-scale weather systems 22 p3340 A83-46843

Numerical simulation of the atmospheric response to equatorial Pacific sea surface temperature anomalies 22 p3340 A83-46844

Numerical experiments with a stochastic zonal climate model 22 p3340 A83-46846

Evaporation-limited tropical temperatures as a constraint on climate sensitivity 22 p3340 A83-46847

Horizontal energy propagation in a barotropic atmosphere with meridional and zonal structure 22 p3341 A83-46849

Effect of two different atmospheric models of the absorptive rate of excess atmospheric carbon by the sea 22 p3333 A83-46881

A technique for investigating graupel and hail development 22 p3342 A83-46940

Modeling the total electron content observations above Ascension Island 22 p3337 A83-47064

An analytic solution for the response of the neutral atmosphere to the high-latitude convection pattern 22 p3337 A83-47069

Climate theory and numerical weather forecasting 23 p3487 A83-47151

Calculation of radiative heat influxes in a model of the general circulation of the atmosphere 23 p3488 A83-47156

Method for the approximation of terms parameterizing macroexchange in equations of atmospheric dynamics 23 p3488 A83-47157

Numerical simulations of a case of explosive marine cyclogenesis 23 p3489 A83-47393

Stability of vertical discretization schemes for semi-implicit primitive equation models - Theory and application 23 p3489 A83-47394

Identification of systematic errors in a numerical weather forecast 23 p3489 A83-47396

Regional models of the atmosphere in middle latitudes 23 p3490 A83-47404

A model of the lower ionosphere above Red Lake, Canada, during the 26 February 1979 solar eclipse 23 p3480 A83-47467

Steady-state model of the D-region during the February 1979 eclipse 23 p3481 A83-47472

Steady, periodic, and aperiodic atmospheric flows 23 p3491 A83-48040

Modeling of the nonstationary processes of the ionosphere-magnetosphere coupling with allowance for their self-consistency 23 p3484 A83-48389

Magnetospheric tail dynamics 23 p3485 A83-48354

Mesoscale air pollution dispersion modelling 23 p3479 A83-48681

Structure of the upper and middle atmosphere; Proceedings of the Meeting, Leeds, England, August 23-27, 1982 24 p3603 A83-48751

A point of view on semi-empirical thermospheric models 24 p3603 A83-48752

Chemical budgets of the stratosphere 24 p3603 A83-48757

The ozone budget in the stratosphere - Results of a one-dimensional photochemical model 24 p3604 A83-48758

Non-LTE model atmosphere analysis of central stars 24 p3652 A83-49151

A spatially distributed model of the biosphere --- latitude distribution of atmospheric temperature and precipitation 24 p3609 A83-49276

Mathematical model of the glaciers-ocean-atmosphere system 24 p3610 A83-49556

Merging of moderate-sized convective cells on day 261 of GATE 24 p3613 A83-49701

Retrieval of microphysical and thermal variables in observed convective storms 24 p3616 A83-49731

The development of an upshear sloping updraft in thunderstorms 24 p3616 A83-49732

Forecasting peak ozone levels 24 p3602 A83-50188

ATMOSPHERIC MOISTURE

Comparison of sea-surface temperature observations from TIROS-N and ships in the North Indian Ocean during MONEX /May-July 1979/ 02 p0218 A83-12033

On the effects of moisture on the Brunt-Vaisala frequency 02 p0213 A83-12230

The significance of thermodynamic forcing by cumulus convection in a general circulation model 02 p0213 A83-12231

A scale analysis of deep moist convection and some related numerical calculations 02 p0213 A83-12233

Crystal size and orientation in ice grown by droplet accretion in wet and spongy regimes 02 p0214 A83-12238

Theoretical determination of the effects of multiple scattering by hydrometeors in monopulse systems at millimeter wavelengths 02 p0165 A83-12635

A diffusive model of the turbulent mixing of dry and cloudy air 02 p0215 A83-12942

Lidar monitoring of the water vapor cycle in the troposphere 02 p0216 A83-12958

Criteria for the formation and water content of cumulus clouds 03 p0364 A83-14097

The possibility of measuring the moisture content of the upper layers of the atmosphere using radiometric techniques 03 p0359 A83-14308

The impact of model moist processes on baroclinic wave energetics 03 p0367 A83-14427

A numerical study of the influence of the planetary boundary layer and moisture on frontal structure 03 p0367 A83-14432

Assimilation of remotely-sensed rainfall rates in a moist primitive equation model 03 p0368 A83-14436

The inclusion of moist downdraft effects in the Arakawa-Schubert cumulus parameterization 03 p0368 A83-14445

Algorithms used to retrieve surface-skin temperature and vertical temperature and moisture profiles from VISSR atmospheric sounder /VAS/ radiance observations 03 p0370 A83-14628

Quantitative interpretation of cloud radiances observed with a 94 GHz scanning radiometer 03 p0371 A83-14657

Equations for deep moist convection that include moisture phase transitions 03 p0371 A83-14827

Lidar identification of drop and crystal clouds 03 p0372 A83-14831

Remote sensing evidence for regolith water vapor sources on Mars 04 p0569 A83-15589

The effects of moisture on trapped mountain lee waves 04 p0517 A83-15934

The ECMWF humidity analysis and its general impact on global forecasts and on the forecast in the Mediterranean area in particular 04 p0519 A83-16161

A comparative study of the rates of development of potential graupel and hail embryos in high plains storms 06 p0790 A83-18265

Transient thermal change on a solid surface - Coupled diffusion of heat and moisture 06 p0775 A83-18804

A simple parameterization of moist convection for large-scale atmospheric models 06 p0793 A83-18993

Some characteristics of the field of total water-vapor and liquid-water content in the atmosphere over the ocean /according to satellite measurements/ 07 p0968 A83-19910

Comments on 'Information content of METEOSAT and Nimbus/THIR water vapor channel data - Altitude association of observed phenomena'

07 p0970 A83-20813

The dynamics of the moist atmosphere

07 p0970 A83-20885

Moisture sounding at millimeter wavelengths /94/183 GHz/ at high altitudes

08 p1098 A83-22557

Determination of atmospheric water vapor content in moderate optical paths by radiometric measurements

08 p1136 A83-22853

A water vapor-energy balance model designed for sensitivity testing of climatic feedback processes

08 p1142 A83-23004

A theoretical determination of capture efficiency of small cumular ice crystals by large cloud drops

08 p1142 A83-23010

Measured collection efficiencies for cloud drops --- collision and coalescence mechanisms

08 p1142 A83-23011

Estimation of liquid water amount in an extended cloud by Nimbus-5 microwave data

09 p1311 A83-23894

Attempt to directly simulate cloud-radiation interaction in the case of small cumuli

09 p1312 A83-23957

Total precipitable water and rainfall determinations from the Seasat scanning multichannel microwave radiometer

09 p1315 A83-24314

An investigation of the convergence of a moist convective adjustment scheme

09 p1315 A83-24938

A convection parameterization scheme based on a direct algorithm of dry convective adjustment --- for atmospheric models

09 p1315 A83-24939

Sulfur-dioxide/water equilibria between 0 and 50 C - An examination of data at low concentrations

09 p1298 A83-25195

Correlation of surface humidity and integrated atmospheric water vapour determined from infrared measurements --- at mountain sites

10 p1451 A83-25460

An improved model for the calculation of profiles of C/n²-squared and epsilon in the free atmosphere from background profiles of wind, temperature and humidity

11 p1623 A83-26994

Effect of size distribution variations on precipitation parameters determined by dual-measurement techniques

11 p1625 A83-27016

Doppler radar measurements of moisture divergence in a coastal cyclone

11 p1630 A83-27075

Overlapping effect of atmospheric H₂O, CO₂ and O₃ on the CO₂ radiative effect

11 p1632 A83-27669

An investigation of the atmospheric HNO₃-NH₃-NH₄NO₃ equilibrium relationship in a cool, humid climate

11 p1613 A83-27675

A radiation model using hourly meteorological data with results from GATE

11 p1632 A83-27972

On the calibration and temperature behaviour of single-beam infrared hygrometers

12 p1728 A83-29137

Venera 13 and Venera 14 measurements of the water vapor content in the Venus atmosphere

12 p1798 A83-29480

Validation of satellite-derived atmospheric temperature and water vapor concentration using radiosonde and rocketsonde measurements

12 p1760 A83-29685

The measurement of water vapour in thermal emission on studies of Nimbus-7 stratosphere flights for correlative studies of Nimbus-7

12 p1760 A83-29687

A nondeterministic method for allowing for moisture evolution in a numerical model for predicting meteorological elements

13 p1884 A83-30299

Relative humidity distribution in the vicinity of the warm conveyor belt

13 p1889 A83-30574

Stratospheric water vapor

13 p1892 A83-30902

Loss of water from Venus. I - Hydrodynamic escape of hydrogen

13 p1961 A83-31209

Water-vapor content in the Venusian atmosphere according to data from the Venera-13 and Venera-14 probes

14 p2111 A83-31963

The spectrophotometric experiment on the Venera-13 and Venera-14 descent modules. II - Preliminary results of spectrum analysis in the region of H₂O absorption bands

14 p2111 A83-31965

Hydrogen peroxide and sulfur (IV) in Los Angeles cloud water

15 p2194 A83-34050

Investigation of remote sensing possibilities of the lower atmosphere in the microwave range and some aspects of statistical data use

15 p2180 A83-35291

Modes of variability in annual hemispheric water vapor and transport fields

16 p2385 A83-35474

Comments on 'Skylab near-infrared observations of clouds indicating supercooled liquid water droplets'

16 p2387 A83-35496

Typical influences of moisture on profile measurements in the marine atmospheric surface layer

16 p2388 A83-35796

The impact of model moist processes on the energetics of extratropical cyclones

16 p2388 A83-36032

Cumulus parameterization and rainfall rates. II

16 p2389 A83-36035

Experiments in shower-top forecasting using an iterative one-dimensional cloud model

16 p2389 A83-36036

Droplet phase (heterogeneous) and gas phase (homogeneous) contributions to secondary ambient aerosol formation as functions of relative humidity

16 p2379 A83-36127

Internal-gravity-wave-like variations of temperature, humidity and wind observed in the troposphere downstream of heavy rainfall area

16 p2390 A83-36498

Determination of the parameters of the underlying surface and atmosphere from measurements of outgoing microwave radiation

16 p2391 A83-36846

Model for atmospheric corrections to microwave brightness temperature data

17 p2526 A83-37621

Measured cloud data obtained in Northwest and Great Lakes United States and northern Canada during icing certification tests

17 p2549 A83-38719

Low level water vapor fields from the VISSR Atmospheric Sounder (VAS) 'split window' channels

17 p2551 A83-38734

Results of combining the Profiler and VAS for determining temperature and moisture in the atmosphere --- VISSR Atmospheric Sounder

17 p2551 A83-38738

Temperature measurement with a sonic anemometer and its application to heat and moisture fluxes

18 p2687 A83-39015

Determination of supercooled liquid water content by measuring rim rate

18 p2721 A83-39116

Changes in the nature of fluctuations of temperature and liquid water content during the lifetime of a large-scale storm

18 p2722 A83-39133

Extrapolation of the Goff-Gratch formula for vapor pressure of liquid water at temperatures below 0 deg C

18 p2723 A83-39143

The field of the absolute humidity of air in a zone of frontal divisions

18 p2724 A83-39487

The use of high horizontal resolution satellite temperature and moisture profiles to initialize a mesoscale numerical weather prediction model - A severe weather event case study

18 p2725 A83-39687

Low-level water vapor fields from the VISSR Atmospheric Sounder (VAS) 'split window' channels

18 p2726 A83-39871

Profiling atmospheric water vapor by microwave radiometry

18 p2726 A83-39875

A steerable dual-channel microwave radiometer for measurement of water vapor and liquid in the troposphere

18 p2726 A83-39876

An automatic profiler of the temperature, wind and humidity in the troposphere

18 p2727 A83-39877

An analysis and comparison of five water droplet measuring instruments

18 p2727 A83-39883

The polarization structure of backscattering by water-droplet and ice clouds

18 p2730 A83-40080

Water vapor in the thermosphere

18 p2719 A83-40086

Determination of the atmospheric water vapour content above La Silla and the prospects for FIR observations

18 p2761 A83-40440

The role of seasonal reservoirs in the Mars water cycle. I Seasonal exchange of water with the regolith. II - Coupled models of the regolith, the polar caps, and atmospheric transport

19 p2921 A83-40776

Atmospheric water vapour measurements at Zelenchukskaya (U.S.S.R.) and La Silla (Chile)

19 p2867 A83-40890

High altitude atmospheric water vapour measurements in the Himalayan region

19 p2867 A83-40891

The measurement of moisture in the stratosphere by radiosondes

19 p2868 A83-41587

Water-vapor content of the near-equatorial atmosphere over the Atlantic Ocean during March-August 1979

19 p2869 A83-42123

Backscatter and extinction in water clouds

20 p3031 A83-42859

A study of heat and moisture budget over the Arabian Sea and their role in the onset and maintenance of summer monsoon

20 p3031 A83-43459

Telluric spectra from 4690 to 5525 A in a humid atmosphere

21 p3169 A83-43873

The climatological minimum in tropical outgoing infrared radiation - Contributions of humidity and clouds

21 p3179 A83-44395

Electrooptical investigations of the effect of the humidification processes of various types of aerosols on the dipole characteristics of the particles

22 p3321 A83-45636

Evaporation derived from optical and radio-wave scintillation --- for water balance and mesoscale meteorological studies

22 p3339 A83-46069

Influence of the atmosphere on the performance of a multichannel microwave radiometer

22 p3289 A83-46199

A note on the new type hygrometer using the photochemical reaction - H₂O + h- ν (Ly-alpha line)-metastable OH + H₂ and metastable OH-OH + h- ν (wavelength=309 nm)

22 p3331 A83-46520

Water budget of a mesoscale convective system in the tropics

22 p3341 A83-46857

Retrieval of clear sky moisture profiles using the 183 GHz water vapor line

22 p3342 A83-46950

Boundary-layer structure over tropical oceans from TIROS-N infrared sounder observations

22 p3342 A83-46951

Experimental thermal-microwave radiometric determination of the moisture content of a cloudy atmosphere

23 p3487 A83-47139

Information content, accuracy, and optimal conditions of indirect ground-based thermal-microwave radiometric measurements of the integral water-vapor content of the atmosphere, and the water content and effective temperature of clouds

23 p3487 A83-47140

A method for determining water-vapor content in the atmosphere on the basis of joint infrared and microwave radiometric measurements

23 p3487 A83-47141

Calculation of the circulation, heat budget, and moisture cycle of the atmosphere for July on the basis of a model of the general circulation of the atmosphere

23 p3488 A83-47152

Estimating surface temperatures from satellite thermal infrared data - A simple formulation for the atmospheric effect

23 p3475 A83-47224

Remote sensing of precipitable water by a thermal infrared multichannel approach

[IAF PAPER 83-105] 23 p3488 A83-47268

Seasonal variations in the vertically integrated water vapor transport fields over the Southern Hemisphere

23 p3489 A83-47399

Lidar system analysis for measurement of atmospheric species

23 p3457 A83-47787

Ozone and water vapor monitoring using a ground-based lidar system

23 p3481 A83-47794

Microwave spectroscopy of H₂O in the stratosphere and mesosphere

23 p3483 A83-48078

A two-frequency 1.35-cm radiometer

23 p3459 A83-48490

Assessment of the accuracy of the determination of atmospheric moisture content in the microwave range

24 p3609 A83-49286

Determination of excessive absorption by atmospheric water vapour at 22.235 GHz

24 p3606 A83-49310

An observational study of water vapor in the mid-latitude mesosphere using ground-based microwave techniques

24 p3610 A83-49341

A comparison of the results of a one-dimensional model and measurements of CH₄, H₂O, and nitrogen oxides in the stratosphere

[ONERA, TP NO. 1983-97] 24 p3608 A83-49412

Aircraft observations of 'turbulent fluxes' of momentum, heat and moisture in the sub-cloud layer and associated cloud microphysical and electrical characteristics

24 p3611 A83-49683

Water droplet growth at precritical radii

24 p3611 A83-49686

Interstitial CCN measurements --- Cloud Condensation Nuclei

24 p3611 A83-49687

The effect of solution concentrations in sulfate aerosols

24 p3602 A83-49688

An experimental study of the ice column habit transitions --- crystal growth in atmosphere

24 p3611 A83-49690

Cloud droplet spectra in summertime cumulus clouds

24 p3612 A83-49695

5500 miles of liquid water and drops size measurements in supercooled clouds below 10,000 feet agl

24 p3614 A83-49720

Radar and aircraft observations of generating cells --- tropospheric cumulus-like clouds generating ice crystals

24 p3615 A83-49723

ATMOSPHERIC NOISE

U ATMOSPHERICS

ATMOSPHERIC OPTICS

Measurements of total amount of atmospheric ozone and spectral atmospheric transparency on Spitsbergen - July 1980-July 1981

01 p0070 A83-10288

Optical properties of the atmosphere above the Atlantic Ocean

01 p0075 A83-10830

Construction of regional semiempirical models of the optical characteristics of the atmosphere

01 p0072 A83-11320

The optical properties of the Titan atmosphere and radiative heat transfer

02 p0263 A83-11643

The accuracy of the representation of a real scattering signal by the lidar equation 02 p0176 A83-11697

Normalized scattering diagram for atmospheric aerosols with Junge particle size distribution 02 p0206 A83-12304

Static-split telescope application to atmospheric turbulence measurement 02 p0178 A83-12345

Adaptive optical system referencing in the case of resolved targets illuminated through turbulence 02 p0215 A83-12591

An examination of reduction techniques for determining the Linke turbidity factor 02 p0212 A83-12960

Optics in ballistic missile defense /BMD/ 03 p0392 A83-13754

An optical-radar model of continental aerosols --- Russian book 03 p0358 A83-13821

Atmospheric transmission; Proceedings of the Meeting, Washington, DC, April 21, 22, 1981 03 p0344 A83-13976

An optical device for path-averaged measurements of Cn2 03 p0364 A83-13977

Diurnal and seasonal variations in the atmospheric structure parameter /C/n/-squared/ that affect the atmospheric modulation transfer function /MTF/ 03 p0364 A83-13978

Accurate frequency and intensity measurements of the infrared spectra of atmospheric molecules 03 p0294 A83-13981

Recent results in the analysis of high-resolution infrared atmospheric transmission spectra 03 p0358 A83-13983

Infrared /IR/ spectroscopy in support of atmospheric measurements 03 p0294 A83-13985

Multiple scattering atmospheric radiation models 03 p0358 A83-13986

Whatever happened to band models --- for calculating atmospheric IR spectral transmittance 03 p0358 A83-13987

Atmospheric transmittance and radiance - The LOWTRAN 5 code 03 p0358 A83-13988

REALTRAN - Real-time implementation of atmospheric-transmittance codes 03 p0359 A83-13989

Atmospheric model for laser transmission in the infrared 03 p0359 A83-13990

High-resolution lower atmospheric transmission predictions over long paths 03 p0359 A83-13991

Atmospheric spectral transmittance and radiance - FASCOD1B 03 p0359 A83-13992

Design and implementation of a broadband infrared atmospheric transmissometer 03 p0327 A83-13993

Limitations on the calibration of infrared /IR/ transmissometer 03 p0328 A83-13994

Optical studies of the earth's upper atmosphere in Abastumani 03 p0363 A83-14837

The influence of water vapor on the transparency of a cloudless atmosphere 04 p0515 A83-15057

Thermal self-defocusing of a CW CO2-laser beam during the interaction with water aerosol 04 p0484 A83-15734

Concerning the invariance of observation systems in viewing theory 04 p0482 A83-15882

Automated measurements of atmospheric visibility [AIAA PAPER 83-0436] 05 p0643 A83-16713

The frequency of cloud-free viewing intervals [AIAA PAPER 83-0441] 05 p0666 A83-16715

Physical and optical properties of dust particles [AIAA PAPER 83-0549] 05 p0659 A83-16784

Quality of wavefront correction in adaptive transmitting systems 05 p0685 A83-17045

Transmission cutoff accompanying remote optical breakdown of the atmosphere by CO2 laser pulses 05 p0687 A83-17064

Optical refraction in the earth's atmosphere /Horizontal paths/ --- Russian book 05 p0660 A83-17127

Atmospheric visibility from gigahertz to petahertz [AIAA PAPER 83-0352] 05 p0683 A83-17921

The effect of troposphere aerosol on the integral albedo of the system consisting of the atmosphere and the underlying surface 06 p0782 A83-17999

Effects on skylight at South Pole Station, Antarctica, by ice crystal precipitation in the atmosphere 06 p0778 A83-18585

On the origin of speckle boiling and its effects in stellar speckle interferometry 06 p0822 A83-19190

Evaluation of nonlinear distortions of the optical image of the earth's surface in the horizontally inhomogeneous atmosphere 07 p0951 A83-19914

Atmospheric spectroscopy studies 07 p0958 A83-19972

Reassessment of net radiation measurements in the atmosphere of Venus 07 p1030 A83-20615

The asymptotics of the average intensity of radiation for several models of stochastic media 07 p0990 A83-20891

The possibilities of measuring the optical characteristics of scattering media by moving lidars 07 p0963 A83-20892

Experimental and mathematical modeling of the conditions of the seeing of objects through a turbid-medium layer --- earth atmosphere 07 p0963 A83-20893

Results of a statistical analysis of the backscattering of light with model indicatrices --- remote sensing of atmospheric aerosols 07 p0963 A83-20896

Diffusion of a light wave in a polarized state propagating through the atmosphere 07 p0993 A83-21083

Rayleigh scattering and optical heterodyne detection - Application to atmospheric fluctuations --- French thesis 07 p0970 A83-21092

Effect of transparency fluctuations on the accuracy of lidar correlation measurements of statistically unhomogeneous atmosphere 08 p1133 A83-21874

Effect of the aerosol on fog microstructure 08 p1140 A83-22355

Atmospheric effects on electro-optical, infrared, and millimeter wave systems performance; Proceedings of the Meeting, San Diego, CA, August 27, 28, 1981 08 p1098 A83-22540

Optical characteristics of windblown dust 08 p1135 A83-22542

Review of cirrus cloud optical properties and effects on infrared sensors 08 p1135 A83-22544

Measurements of the properties of wintertime fog and haze in West Germany - A preliminary report on project 'Meppen 80' 08 p1141 A83-22549

Preliminary shipboard optical turbulence measurements 08 p1166 A83-22556

Experimental measurements of turbulence induced beam spread and wander at 1.06, 3.8, and 10.6 microns 08 p1110 A83-22562

Analysis of aero-optic interface phenomena 08 p1042 A83-22588

Observations of optical lightning emissions from above thunderstorms using U-2 aircraft 08 p1141 A83-22703

Balloon atmospheric mosaic measurements /BAMM/ IIA phenomenology and band selection 08 p1045 A83-22844

Laser transmissometer calibration of long-path atmospheric transmission measurements 08 p1104 A83-22889

Structure characteristics of refractive-index fluctuations on an oblique tropospheric path 09 p1245 A83-23452

An application of the Ambartsumian invariance principle to the investigation of extended lightguides with random inhomogeneities 09 p1344 A83-23484

Phase function in the scattering in arbitrary higher order --- of light in planetary atmospheres 09 p1365 A83-23896

Propagation model of laser beams in turbulence 09 p1271 A83-24084

K-distributed phase differences in turbulent random phase screens 09 p1267 A83-24085

Inner-scale size effect on the scintillations of light in the turbulent atmosphere 09 p1344 A83-24086

Atmospheric turbidity over Africa - Disturbed by the El Chichon eruption 09 p1306 A83-24345

Methods for the passive probing of transparency in the atmospheric surface layer 09 p1315 A83-25054

Spectroscopic measurements of the 'additional absorbing mass' in total and partial cloudiness 09 p1316 A83-25055

The propagation of narrow light beams in rain 09 p1273 A83-25079

The measurement of the dispersion of the intensity fluctuations during the reflection of multimode laser beams in the atmosphere 09 p1273 A83-25085

The optical properties of the atmosphere over the Arctic basin 09 p1316 A83-25230

The variability of the optical characteristics of cirrostratus clouds 09 p1317 A83-25234

Modeling the optical properties of Venusian clouds 09 p1367 A83-25237

Mathematical modeling for molecular spectroscopy of the atmosphere 09 p1309 A83-25240

Application of statistical modeling to the problem of the optical sensing of the ocean-atmosphere system 09 p1320 A83-25243

Climate as determined by observations from space 09 p1317 A83-25259

Cloud and aerosol effects in radiant heat transfer --- in planetary atmospheres 09 p1367 A83-25260

Inverse problems in the laser probing of atmospheric aerosols 09 p1309 A83-25261

Additional solar spectral data sets 10 p1520 A83-25450

Regularizing the solution of the laser sounding equation of atmospheric aerosols by means of a stabilizing functional 10 p1425 A83-25567

Estimation regarding the feasibility of using larger distances in measurements with L2F systems in flight tests --- Laser-two-Focus 10 p1431 A83-26487

Propagation of laser radiation in water aerosol in conditions of the dispersal of this aerosol 10 p1434 A83-26778

Numerical study of the propagation of intense laser radiation in the atmosphere 10 p1434 A83-26781

Thermal distortions of focused laser beams in the atmosphere 10 p1434 A83-26782

Thermal self-defocusing of laser beams in a turbulent medium 10 p1434 A83-26783

Nonlinear optics of the stratosphere and the laser chemistry of ozone 10 p1449 A83-26785

On the reduction of the distorting effect of the atmosphere in the digital processing of space imagery 10 p1444 A83-26822

Signal-to-noise ratio of heterodyne detection - Matrix formalism 10 p1425 A83-26874

Role of gas absorption in formation of fluctuations in parameters of cleared cloud medium and laser radiation 11 p1631 A83-27606

Kinetics of 'blurring' process accompanying CO2 laser radiation propagation in cloud medium 11 p1632 A83-27609

Fluctuations of optical radiation on an inclined path 11 p1556 A83-27944

Amplification of the mean intensity of backscattering in a turbulent atmosphere 11 p1632 A83-27957

Imitation model of ray propagation in a three-dimensional turbulent medium 11 p1583 A83-27962

Volcanic ash over Arizona in the spring of 1982 - Astronomical observations 11 p1621 A83-28769

Theory of optical-radiation diffraction by a nontransparent half-plane in a turbulent atmospheric layer 12 p1779 A83-29256

Passive remote sensing of aerosols from space now and in the future 12 p1754 A83-29560

Most suitable conditions for aerosol monitoring from space 12 p1754 A83-29561

Remote monitoring of aerosols from space 12 p1755 A83-29567

Monitoring of Saharan dust over the Atlantic using Meteosat-VIS-data 12 p1759 A83-29571

Can turbidity measurements be used for the estimation of aerosol parameters? 12 p1755 A83-29574

Determination of aerosol optical depth from ground measurements 12 p1730 A83-29576

Climatic influence of background and volcanic stratosphere aerosol models 12 p1756 A83-29580

Nonlinear spatial-frequency characteristics of a three-dimensional inhomogeneous scattering layer --- in atmospheric optics 13 p1918 A83-30006

Reconstruction of the profiles of atmospheric optical parameters on the basis of data from laser probing 13 p1873 A83-30028

The reproduction of atmospheric scattering indicatrices with an allowance made for the anisotropy of multiple effects 13 p1874 A83-30034

Modal control for wavefront reconstruction in adaptive optics 13 p1920 A83-31009

Four-wave mixer phase compensation performance --- for atmospheric turbulence-caused resolution improvement in large terrestrial telescopes 13 p1920 A83-31010

Optical transmission through aerosol deposits on diffusely reflective filters - A method for measuring the absorbing component of aerosol particles 13 p1880 A83-31454

Data on total and spectral solar irradiance 13 p1880 A83-31461

High spectral resolution lidar system with atomic blocking filters for measuring atmospheric parameters [AD-A129929] 13 p1857 A83-31463

Resonant extinction of lidar returns from the alkali metal layers in the upper atmosphere 13 p1880 A83-31465

An experimental study of atmospheric optical transmission 13 p1830 A83-31724

Calculations of the intensity of a partially coherent optical beam in a turbulent atmosphere 14 p2023 A83-31908

Lidar system for visibility monitoring 14 p2019 A83-32449

The atmospheric correction of remote-sensing images 14 p2035 A83-32499

Solar-radiation transfer in the atmosphere in the presence of semitransparent clouds --- satellite multispectral photography 14 p2035 A83-32500

Fluctuations of the parameters of an electromagnetic wave in a turbulent light absorbing atmosphere 14 p2052 A83-32559

Quantitative intracavity spectroscopy 14 p2052 A83-32561

Variation of atmospheric optical depth for remote sensing radiance calculations 14 p2053 A83-32613

The matrix coefficient for the brightness of radiation reflected by a semi-infinite absorptive medium with a greatly extended indicatrix of scattering

- 14 p2085 A83-32857
- Instantaneous integrated Raman scattering --- for enhanced lidar measurement of atmospheric constituents 14 p2054 A83-32918
- Inverse problems of lidar sensing of the atmosphere --- Book 15 p2195 A83-33768
- Photography and photographic-photometry of the solar aureole 15 p2281 A83-34460
- Transformation of visual target acquisition data between different meteorological and optical sight parameters - A simple method 15 p2231 A83-34462
- Elements of the theory of light scattering and optical radar --- Russian book 15 p2170 A83-34573
- Passage of a pulsed optical signal through an absorbing medium with strongly anisotropic scattering 15 p2231 A83-34705

Effect of wind-generated waves on the transfer of solar radiation in the atmosphere-ocean system

- 15 p2209 A83-34994
- Optimization of the processing of optical signals in the case of incoherent detection 15 p2232 A83-35162
- Optical properties of the Venusian atmosphere and radiative heat exchange 16 p2434 A83-35352
- Optical properties of the Martian atmosphere and radiative heat exchange 16 p2435 A83-35359
- Comparison of Monte Carlo calculations with observations of light scattering in finite clouds 16 p2387 A83-35491

Investigations of the optical properties of Saturn's atmosphere carried out at the Main Astronomical Observatory of the Ukrainian Academy of Sciences

- 16 p2436 A83-35737
- Measurement of faint lidar signals in the presence of an intense background during pulsed laser sounding of the atmosphere 16 p2360 A83-36125
- Infrared optical properties of a coal-fired power plant plume 16 p2372 A83-36760

Isoplanatism with respect to the arrival angles of light rays in telescopes

- 16 p2426 A83-36856
- Polarization contrast --- atmospheric visibility of objects 16 p2392 A83-36867
- A brief description of the brightness spectra of a cloudless sky 16 p2392 A83-36868
- Discrimination of growth and water stress in wheat by various vegetation indices through clear and turbid atmospheres 17 p2526 A83-37620
- On the accuracy of IR extinction predictions made by the Navy Aerosol Model 17 p2546 A83-38740
- Intercomparison of PMS particle size spectrometers --- Particle Measuring Systems, Inc. 17 p2546 A83-38741

Visibility measurement techniques - An update

- 17 p2551 A83-38742
- Distribution of illumination from a narrow light beam in a turbid atmosphere 17 p2515 A83-38978
- High-order series solution for unsteady thermal blooming with crosswind 18 p2692 A83-39147
- Number of terms required in the Fourier expansion of the reflection function for optically thick atmospheres 18 p2743 A83-39179

Design and verification of a cloud field optical simulator

- 18 p2727 A83-39886
- The polarization structure of backscattering by water-droplet and ice clouds 18 p2730 A83-40080
- The problem of the scattering of light by a horizontally inhomogeneous cloud 18 p2730 A83-40081
- A method for on-line corrections of the transmission function in solving the problem of the thermal probing of the atmosphere 18 p2719 A83-40082

Statistical characteristics of the spectral structure of the atmospheric thickness for different optical states of the atmosphere

- 18 p2719 A83-40595
- Interferometric displacement sensing in the open atmosphere 19 p2848 A83-41177
- Increasing the transillumination capacity of a laser beam in the atmosphere 19 p2854 A83-41768
- On the mean intensity of a wave reflected from a wavefront-reversal mirror in a turbulent medium 19 p2900 A83-41798

Experimental determination of solar-point sky radiance for the spectral range 0.4-1.0 micron

- 20 p3023 A83-43141
- Reflection of light by a multilayered planetary atmosphere 20 p3079 A83-43411
- Landsat-4 Thematic Mapper calibration and atmospheric correction [AAS PAPER 83-162] 20 p2992 A83-43763

Optimal detector of laser radiation pulses transmitted by a turbulent atmosphere

- 20 p3048 A83-43777
- Wide-beam atmospheric optical communication for aircraft application using semiconductor diodes 21 p3090 A83-44159

Modified Monte-Carlo method to evaluate multiple scattering effects on lightbeam transmission through a turbid atmosphere

- 21 p3144 A83-44794
- The effect of modulated electromagnetic radiation on the temperature regime of a monodisperse aerosol medium 22 p3322 A83-45642

The effect on heterodyne reception of motion of a source of optical radiation in the presence of atmospheric turbulence

- 22 p3271 A83-45654
- Inverse methods for remote determination of properties of optically thick atmospheres 22 p3328 A83-46067

Multicolor laser altimeter for barometric measurements over the ocean - Theoretical

- 22 p3259 A83-46070
- A quasi-continuous record of atmospheric opacity at $\lambda = 1.1$ mm over 34 days at Mauna Kea Observatory 22 p3332 A83-46745

El Chichon eruption cloud - Latitudinal variation of the spectral optical thickness for October 1982

- 22 p3333 A83-46884
- El Chichon eruption cloud - Comparison of lidar and optical thickness measurements for October 1982 22 p3334 A83-46885

Repeatability of visibility in atmospheric precipitation in the European territory of the USSR

- 23 p3486 A83-47133
- Method of determining optical atmospheric parameters based on space-imagery earth-surface [IAF PAPER 83-102] 23 p3480 A83-47265

Effects of atmospheric obscurants on the propagation of optical/IR radiation

- 23 p3442 A83-47785
- Spatial changes in the stratospheric aerosol associated with the north polar vortex 23 p3482 A83-47858

Intensity fluctuations in the case of the specular reflection of light beams in the turbulent atmosphere

- 23 p3463 A83-48482
- The surface illuminance and albedo of a planetary atmosphere with nearly conservative scattering 23 p3529 A83-48559

A statistical method for the calculation of molecular absorption --- in atmosphere near earth surface

- 23 p3485 A83-48560
- The dynamic range of a resonance spectrophone 23 p3459 A83-48562

Forward multiple scattering corrections as a function of detector field of view --- laser beam propagation through atmospheric aerosols

- 24 p3588 A83-49005
- Vertical variations of the albedo of the system including the underlying surface and the atmosphere 24 p3605 A83-49279

Seeing for solar observations on the Terskol Peak

- 24 p3645 A83-49638
- The equation of refraction in the atmospheric surface layer 24 p3608 A83-49639

ATMOSPHERIC PHYSICS

NT CLOUD PHYSICS

The UCL interactive planetary image processing system /IPIPS/ Application to remote sensing studies in planetary meteorology and oceanography

- 01 p0128 A83-10051
- A numerical study on the combined action of droplet coagulation, ice particle riming and the splintering process concerning maritime cumuli 01 p0074 A83-10220

The problem of energetics in the physics of the ionosphere and approaches to its solution

- 01 p0071 A83-10596
- The beginnings of magnetospheric physics 01 p0072 A83-11284

On the effects of moisture on the Brunt-Vaisala frequency

- 02 p0213 A83-12230
- Investigation of processes in the thermosphere during magnetic disturbances 02 p0209 A83-12430

Predicted electrical conductivity between 0 and 80 km in the Venusian atmosphere

- 02 p0265 A83-12563
- The aurora - New light on an old subject 03 p0356 A83-13175

On charge exchange and knock-on processes in the exosphere of Io

- 03 p0434 A83-14214
- A numerical study of the influence of the planetary boundary layer and moisture on frontal structure 03 p0367 A83-14432

The Tethered Satellite System technical aspects and prospective scientific missions

- 04 p0453 A83-15672
- The propagation of thermal radiation in the case of the random refraction of beams in a medium with fluctuating permittivity 04 p0531 A83-15733

Excitation of acoustic-gravity waves by sources moving in the atmosphere at an angle to the horizon

- 04 p0510 A83-15758
- The atmospheres of Io and other satellites 04 p0571 A83-16246

Solar and heliospheric physics space missions for the 1980's

- [AIAA PAPER 83-0516] 05 p0600 A83-16761

Physical climatology

- 05 p0668 A83-17699

Inverse Monte Carlo solutions for radiative transfer in inhomogeneous media

- 05 p0692 A83-17870

Infrasound of cosmic origin in the atmosphere

- 07 p0962 A83-20606
- The role of latent heat release in baroclinic waves - Without beta-effect 08 p1142 A83-23005

The evolution of a Rossby-wave packet in a three-dimensional baroclinic atmosphere

- 08 p1142 A83-23006
- Growth of aqueous solution droplets of HNO₃ and HCl in the atmosphere 08 p1133 A83-23008

Point explosion in an exponential atmosphere with a nonzero asymptote --- for stellar and planetary atmospheric models

- 09 p1359 A83-24221
- A numerical model of the zonally averaged dynamical and chemical structure of the middle atmosphere 09 p1296 A83-24267

The sign change in the radiant influx of heat near the earth's surface

- 09 p1316 A83-25056
- Sound emission from line vortices --- in atmosphere 09 p1308 A83-25058

Laser photofragment spectroscopy of N₂ / + - Evidence for predissociation of B²Σ_g u +

- 10 p1480 A83-26455
- Inter-annual and seasonal variations in the structure and energetics of the atmosphere over northeast Brazil 11 p1633 A83-28088

A note on the orientation and size of noctilucent cloud particles

- 11 p1616 A83-28095
- The removal of particulate matter from the atmosphere - The physical mechanisms 11 p1619 A83-28344

The physics of slow MHD waves in the ionospheric plasma --- Russian book

- 12 p1750 A83-28828
- Profile measurements in the atmospheric near-surface layer and the use of suitable universal functions for the determination of the turbulent energy exchange 12 p1758 A83-29128

Magneto-atmospheric waves

- 13 p1878 A83-31083
- Energy balance and stability --- in stellar coronae 15 p2252 A83-33606

Investigation of atmospheric processes of different scale in the POLYMODE experiment

- 15 p2206 A83-34352
- On the kinetic balance in the ca. maximal part of the daily F-region 15 p2201 A83-34447

Anisotropic propagation of magnetogasdynamic sonic waves in conducting and radiating atmosphere

- 15 p2235 A83-34546
- On the definition of collision efficiency of atmospheric particles 16 p2387 A83-35495

Solar wind energy dissipation in the upper atmosphere

- 16 p2377 A83-36110
- A numerical model of gravity wave breaking and stress in the mesosphere 16 p2380 A83-36140

Basic theory and model calculations of the Venus ionosphere

- 17 p2617 A83-37425
- Theory of hydromagnetic waves in the magnetosphere 17 p2540 A83-37774

Plasma waves in planetary magnetospheres

- 17 p2542 A83-38298
- A comparison between radiation fluxes and heat influxes calculated with various transmission functions in a clear sky 18 p2719 A83-40083

Bragg resonator in the ionospheric plasma with an artificial quasi-periodic lattice

- 19 p2866 A83-41792
- Resonant electron scattering by metastable nitrogen --- in earth thermosphere 20 p3023 A83-43154

The latitude-height structure of 40-50 day variations in atmospheric angular momentum

- 21 p3173 A83-44710
- The dependence of the Q-branch profile of the Raman spectrum of water vapor on temperature 22 p3322 A83-45638

Schumann resonances --- earth surface-ionosphere cavity resonator

- 22 p3325 A83-45880
- On the form of stationary size distributions established by coagulation and sedimentation --- for atmospheric particles 22 p3341 A83-46859

High-temperature physical-chemical processes in the atmosphere during thunderstorms

- 23 p3485 A83-48504

ATMOSPHERIC PRESSURE

NT CYCLOGENESIS

Differential absorption lidar measurements of atmospheric temperature and pressure profiles

- 01 p0073 A83-10004

A microwave pressure sounder --- for remote measurement of atmospheric pressure

- 01 p0047 A83-10005

Statistical properties of the atmospheric pressure field over the Arctic Ocean

- 02 p0214 A83-12234

Spatial variability of sea level pressure and 500 mb height anomalies over the Southern Hemisphere

- 02 p0217 A83-13055

A simple model illustrating baroclinic development

- 03 p0363 A83-13223

The changes in the hemopoietic system and the small intestine mucosa during the breathing of pure oxygen under atmospheric pressure 03 p0374 A83-13632

Dynamical implications of the observed thermal contrasts in Venus' upper atmosphere 03 p0434 A83-13834

The effects of latent heat release on the May 20 Sesame '77 wave cyclone 03 p0368 A83-14443

The relationship between atmospheric pressure fields and the sea level at the Kuril Islands 03 p0372 A83-14832

A measurement of the tidal variations of atmospheric pressure and their relationship with geomagnetic disturbances 03 p0362 A83-14835

Band-pass filtering of one year of daily mean pressures on Mars 04 p0568 A83-15586

Typical low-tropospheric pressure distributions over and around the plateau of Tibet [AD-A126740] 04 p0518 A83-16013

Monthly mean sea-level variability along the west coast of North America 05 p0669 A83-17233

The radiosensitivity of the organism during the irradiation of animals in an altered gaseous environment. V - The effect on animals of the combined action of radiation and pure oxygen at normal pressure 06 p0796 A83-19384

The composition of the products of the combustion of pyropowder at atmospheric pressure 07 p0880 A83-19954

Diagnostic equations in isobaric coordinates 08 p1139 A83-22286

Large scale pressure disturbances over the Indonesian Maritime Continent 09 p1311 A83-23893

On the effect of model resolution on numerical simulation of blocking --- in atmospheric circulation 11 p1633 A83-28081

Utilization of satellite and surface observations in a gravity wave study 13 p1887 A83-30554

Shuttle Orbiter Atmospheric Revitalization Pressure Control Subsystem [SAE PAPER 820882] 13 p1906 A83-30927

The automation of data origination in monthly weather forecasts 14 p2056 A83-32370

Barometric pressures at extreme altitudes on Mt. Everest Physiological significance 14 p2068 A83-32811

Force and duration of muscle twitch contractions in humans at pressures up to 70 bar 14 p2068 A83-32812

Comments on 'natural variability and predictability' 15 p2204 A83-33885

Io's atmosphere - Pressure control by regolith cold trapping and surface venting 15 p2274 A83-33931

Seasonal variations of harmonic constants of diurnal and semidiurnal waves of atmospheric pressure according to POLYMODE data 15 p2206 A83-34354

Characteristics of the variability of atmospheric processes during the period of the experiment in the POLYMODE area 15 p2206 A83-34355

Optimizing a remote sensing instrument to measure atmospheric surface pressure 15 p2167 A83-35295

A comparison of methods for computing the sigma-coordinate pressure gradient force for flow over sloped terrain in a hybrid theta-sigma model 16 p2389 A83-36037

Pressure distributions in the Dischma Valley during the field experiments DISKUS 16 p2391 A83-36582

Sea pressure waves 18 p2731 A83-39444

Interannual variations of mean monthly sea-level pressure in January 18 p2725 A83-39690

Correlations concerning turbulent natural convection Influence of pressure and nature of the gas 18 p2685 A83-39851

Optical and spectroscopic investigations of a pulsed near-surface discharge at atmospheric pressure 18 p2746 A83-39862

The effect of a heat source on the large-scale pressure and wind fields (a quasi-barotropic model) 21 p3181 A83-45330

Analysis of the periodic variations of atmospheric pressure over Greece 21 p3181 A83-45408

Multicolor laser altimeter for barometric measurements over the ocean - Theoretical 22 p3259 A83-46070

Multicolor laser altimeter for barometric measurements over the ocean - Experimental 22 p3259 A83-46071

Interannual variability and predictability of 500 mb geopotential heights over the Northern Hemisphere 23 p3489 A83-47400

Estimation of the analysis error variance of the 500 mb height analyses in the Northern Hemisphere, 1946-79 23 p3490 A83-47409

Atmospheric pressure and temperature profiling using near IR differential absorption lidar 23 p3457 A83-47781

The possibility of the remote sensing of atmospheric pressure by a satellite radiometric method 23 p3492 A83-48104

ATMOSPHERIC RADIATION

NT AIRGLOW

NT AURORAL ARCS

NT AURORAS

NT DAWN CHORUS

NT DAYGLOW

NT GEOCORONAL EMISSIONS

NT IONOSPHERIC NOISE

NT NIGHTGLOW

NT RADIO AURORAS

NT SKY RADIATION

NT STRATOSPHERE RADIATION

NT TROPOSPHERIC RADIATION

NT TWILIGHT GLOW

NT WHISTLERS

A comparison of model generated radiation fields with satellite measurements 01 p0075 A83-10223

Computer simulations of atmospheric Cerenkov radiation in large cosmic-ray showers 01 p0130 A83-11043

Investigation, evaluation and forecast of near-earth space radiation situation 01 p0130 A83-11280

Study of diffuse cosmic and atmospheric gamma radiation using a spark chamber in the energy range 4 MeV-100 MeV 02 p0271 A83-11606

Installation for the investigation of sporadic radio emission of the earth's ionosphere 02 p0176 A83-11731

Characteristics of inelastic interactions with high transverse momenta of secondary particles 02 p0274 A83-11747

A climatological estimate of the radiative cooling of the atmosphere 02 p0213 A83-11977

Simulation of mid-infrared clutter rejection. I - One-dimensional LMS spatial filter and adaptive threshold algorithms 02 p0177 A83-12305

Dynamical implications of the observed thermal contrasts in Venus' upper atmosphere 03 p0434 A83-13834

Conference on Atmospheric Radiation, 4th, Toronto, Canada, June 16-18, 1981, Preprints 03 p0360 A83-14626

Emission characteristics of earth and cloud surfaces as measured by the ERB scanning channels on the NIMBUS-7 satellite 03 p0370 A83-14647

Results from a monex radiation experiment 03 p0370 A83-14649

Optimum angular and spatial sampling of reflected radiance fields 03 p0361 A83-14650

The transfer of 3.7 micrometer radiation through model cirrus clouds 03 p0371 A83-14655

Some improvements to the infrared emissivity algorithm including a parameterization of the absorption by water vapor polymers 03 p0371 A83-14659

Electron-bombarded CCD detectors for ultraviolet atmospheric remote sensing [AIAA PAPER 83-0106] 05 p0609 A83-16524

The effect of ammonia ice on the outgoing thermal radiance from the atmosphere of Jupiter 05 p0703 A83-16962

A note on errors and uncertainties in NCAR aircraft pyrgeometer data from MONEX 05 p0644 A83-17275

Parameterization of outgoing infrared radiation derived from detailed radiative calculations 06 p0789 A83-18252

Generation of a radio signal by a low-power gamma-ray source in the atmosphere 06 p0787 A83-19338

On the characteristics of some radiation fields from lightning and their possible origin in positive ground flashes 07 p0960 A83-20220

Net global thermal emission from the Venusian atmosphere 07 p1030 A83-20613

Radiation budget parameters at the top of the earth's atmosphere derived from Meteosat data 07 p0962 A83-20809

The radiative energetics of the climate system 07 p0970 A83-20888

Estimation of the atmospheric path radiance from multispectral infrared images 08 p1133 A83-21926

Radiative transfer and 4.3 micron atmospheric clutter observations --- with balloon-borne sensors 08 p1051 A83-22849

Earth limb emission analysis of Spectral Infrared Rocket Experiment /SPIRE/ data at 2.7 micrometers 08 p1051 A83-22851

Review of some nonlocal-thermodynamic-equilibrium high-altitude 4.3 micron background effects 08 p1136 A83-22854

Case studies of radiation in the cloud-capped atmospheric boundary layer 09 p1310 A83-23356

Atomic nitrogen emissions from photodissociation of N2 09 p1304 A83-23773

ATMOSPHERIC RADIATION

On the relationship between the intensity of the sporadic radio emission of the earth's magnetosphere in the 0.7-2.3 MHz frequency range and fluxes of soft electrons /0.2-10 keV/ 09 p1307 A83-25035

The First GARP Global Experiment. Volume 2 - Polar aerosols, extensive cloudiness, and radiation --- Russian book 09 p1316 A83-25226

Extensive cloudiness and radiation 09 p1316 A83-25227

The results of aircraft investigations of cloudiness and radiation carried out over the eastern Arctic during the Second Observational Period of the Global Weather Experiment 09 p1316 A83-25228

A subsatellite experiment in the Arctic --- atmospheric radiation study 09 p1316 A83-25233

The variability of the optical characteristics of cirrostratus clouds 09 p1317 A83-25234

Climate as determined by observations from space 09 p1317 A83-25259

Cloud and aerosol effects in radiant heat transfer --- in planetary atmospheres 09 p1367 A83-25260

Influence of sea roughness and atmospheric inhomogeneities on microwave radiation of the atmosphere-ocean system 10 p1422 A83-26494

Overlapping effect of atmospheric H2O, CO2 and O3 on the CO2 radiative effect 11 p1632 A83-27669

On the use of spectral radiance models to obtain irradiances on surfaces of arbitrary orientation 12 p1752 A83-28945

A one-dimensional simulation of the stratocumulus-capped mixed layer 12 p1758 A83-29139

A two-channel radio telescope for the investigation of the radio emission of the atmosphere and the sea surface 12 p1729 A83-29253

Aerosol effects on regional radiative balance 13 p1880 A83-31505

Ultrashort-wave radio emission of the ionosphere of slowly-varying-component type and soft electrons in the auroral zone 14 p2050 A83-31881

The possible nature of the prethunderstorm electromagnetic radiation of convective clouds 14 p2059 A83-32864

The influence of atmospheric aerosol on the life cycle radiation fog 15 p2205 A83-34066

Discrete VLF emissions (7-9 kHz) displaying unusual banded and periodic structure --- from magnetosphere 15 p2199 A83-34361

Comparison of calculated and measured atmospheric radiation values for remote sensing purposes 15 p2203 A83-35100

IR-spectroscopy of ionosphere from stratospheric balloons 16 p2373 A83-35370

A new spectrometric measurement of atmospheric 60 micron emission 16 p2373 A83-35371

The Lyman-alpha absorption anomaly in satellite occultation measurements as a tracer for some thermospheric composition variations 16 p2378 A83-36117

The detection of internal waves in the atmosphere over the sea on the basis of variations in the microwave self-radiation of the atmosphere and sea surface 16 p2393 A83-36873

Atmospheric radiation - 1975-1983 17 p2543 A83-38317

A model for the Priestley-Taylor parameter alpha --- of atmospheric boundary layer 18 p2724 A83-39680

Flux of atmospheric neutrinos 18 p2786 A83-39926

Atmospheric neutrinos, astrophysical neutrons, and proton-decay experiments 18 p2787 A83-39927

The International Satellite Cloud Climatology Project (ISCCP) - The first project of the World Climate Research Programme 18 p2730 A83-40320

On solving the problem of the radiation correction of space imagery 18 p2692 A83-40600

Some radiation budget and cloud measurements derived from Meteosat 1 data 18 p2731 A83-40646

Geomagnetic-cutoff distribution functions for use in estimating detector response to neutrinos of atmospheric origin 19 p2925 A83-40960

Radiation studies in the equatorial Atlantic 19 p2867 A83-42119

Observational evidence of Z and L-O mode waves as the origin of auroral kilometric radiation from the Jikiken (EXOS-B) satellite 20 p3018 A83-42411

Evaluation of upwelling infrared radiance in a nonequilibrium nonhomogeneous atmosphere 20 p3020 A83-42698

A method to measure the daytime long wave radiation 20 p3028 A83-43466

Abundance of cosmic-ray elements from sulfur to nickel as a function of atmospheric depth 20 p3083 A83-43668

Identification of electromagnetic sources --- generated in magnetosphere 21 p3170 A83-44241

- Role of scattering in emergent planetary radiation 21 p3241 A83-44868
- A comparison of the calculated and measured spectral radiances of the atmosphere toward the zenith 21 p3177 A83-45407
- A method for determining water-vapor content in the atmosphere on the basis of joint infrared and microwave radiometric measurements 23 p3487 A83-47141
- Reconstructing the components of the radiation balance of the earth's surface on the basis of satellite data 23 p3483 A83-48101
- The possibility of the remote sensing of atmospheric pressure by a satellite radiometric method 23 p3492 A83-48104
- The diagnostic capabilities of natural magnetospheric radio emissions 23 p3484 A83-48379
- A two-frequency 1.35-cm radiometer 23 p3459 A83-48490
- Radiation studies in the atmosphere 24 p3605 A83-49277
- Certain characteristics of the radiation balance in the cloudless atmosphere and at the ocean surface depending on the dustiness of the atmosphere 24 p3605 A83-49281
- Estimates of the applicability of the black-body approximation to the emission of the atmosphere at the horizon 24 p3605 A83-49290
- ### ATMOSPHERIC REFRACTION
- #### NT RADIO WAVE REFRACTION
- Variations of the refractive index in the atmospheric surface layer 01 p0072 A83-10854
- Variability of satellite refraction in the Northern Hemisphere atmosphere 01 p0072 A83-10855
- A ray tracing computer analysis program /RAYCAP/ for airborne surveillance radar applications 01 p0007 A83-11243
- Studies on radio duct occurrence and properties 01 p0032 A83-11353
- An optical device for path-averaged measurements of C_n^2 03 p0364 A83-13977
- Optical refraction in the earth's atmosphere /Horizontal paths/ --- Russian book 05 p0660 A83-17127
- The measurement of propagation characteristics of the atmosphere at 890 GHz using an open resonator technique 06 p0748 A83-18740
- The refraction in the atmospheric surface layer 07 p1031 A83-20890
- The effects of atmospheric turbulence on telescopic observations 07 p1010 A83-21525
- Solar altitude frequency tables 08 p1136 A83-22617
- Structure characteristics of refractive-index fluctuations on an oblique tropospheric path 09 p1245 A83-23452
- Calculations of atmospheric refraction for spacecraft remote-sensing applications 09 p1306 A83-24448
- An improved model for the calculation of profiles of C/n^2 -squared and epsilon in the free atmosphere from background profiles of wind, temperature and humidity 11 p1623 A83-26994
- Peculiarities of laser radiation refraction in the clearing process of cloud medium 11 p1632 A83-27608
- The usefulness of a bulk refractive index for the calculation of the scattering properties of mixtures of aerosol particles at wavelength 530 nm 11 p1615 A83-27973
- A quantitative comparison of the refractive index structure parameter determined from refractivity measurements and amplitude scintillation measurements at 36 GHz 15 p2195 A83-33694
- Autonomous satellite navigation by stellar refraction [AIAA PAPER 83-2211] 19 p2814 A83-41695
- Refractive effects on very high frequency radio waves through a three-dimensional inhomogeneous ionosphere 21 p3170 A83-44283
- Anomalous microwave propagation through atmospheric ducts 21 p3120 A83-44499
- The reconstruction of meteorological parameters from intra-atmospheric measurements of the optical refraction of cosmic sources 22 p3338 A83-45634
- A method for the calculation of refraction corrections in the atmosphere 22 p3322 A83-45646
- Refractive index and size distribution of aerosols as estimated from light scattering measurements 22 p3334 A83-46947
- Radio propagation beyond the horizon observed at 1 and 3 GHz compared with predicted reflections from random rough layers 23 p3443 A83-47835
- The modeling and statistical investigation of the refractometric method for determining meteorological parameters from space 23 p3492 A83-48103
- Star line-of-sight refraction observations from the orbiting astronomical observatory Copernicus and deduction of stratospheric structure in the tropical region 24 p3607 A83-49342
- The equation of refraction in the atmospheric surface layer 24 p3608 A83-49639
- ### ATMOSPHERIC SCATTERING
- #### NT TROPOSPHERIC SCATTERING
- Geophysical inversion and remote probing are inverse scattering problems 01 p0048 A83-10110
- Stimulated scattering of whistler waves by ion acoustic waves in the magnetosphere 01 p0070 A83-10199
- More about the influence of the aerosol correction on the results of total ozone amount 01 p0070 A83-10289
- Multiple scattering calculations of rain effects 02 p0164 A83-12616
- Microwave noise temperature and attenuation of clouds - Statistics of these effects at various sites in the United States, Alaska, and Hawaii 02 p0164 A83-12618
- Multiple scattering of electromagnetic waves by rain 02 p0165 A83-12623
- Scattering by single ice needles and plates at 30 GHz 02 p0141 A83-12624
- Generalization of the Booker-Gordon formula to include multiple scattering 02 p0165 A83-12626
- Strong refraction near the Venus surface - Effects observed by descent probes 02 p0266 A83-12634
- Theoretical determination of the effects of multiple scattering by hydrometeors in monopulse systems at millimeter wavelengths 02 p0165 A83-12635
- Atmospheric transmission; Proceedings of the Meeting, Washington, DC, April 21, 22, 1981 03 p0344 A83-13976
- Multiple scattering atmospheric radiation models 03 p0358 A83-13986
- The effects of haze on resolution on small scale aerial photography 03 p0329 A83-14283
- Application of the airborne microwave rain-scattered/radiometer system to the remote sensing of rains and wind vector measurements over the ocean 03 p0364 A83-14293
- Algorithm for vertical ozone profile determination for the Nimbus-4 BUV data set 03 p0360 A83-14631
- Initial results for multidimensional radiative transfer by the adding/doubling method 03 p0391 A83-14639
- Effects of cloud shape on cloud field identification 03 p0371 A83-14656
- An estimate of the effect of the indicatrix of scattering on the mean free path lengths of photons in clouds 03 p0372 A83-14836
- The polarization of supernova light - A measure of deviation from spherical symmetry 05 p0699 A83-17015
- Self-excitation of surface oscillations of droplets in an electromagnetic wave field 05 p0649 A83-17063
- The most probable trajectories of rays in a plane-stratified scattering medium. I - A linear layer --- in ionosphere 05 p0663 A83-17612
- Comparison of calculated and measured values of electron fluxes for the wide-angle detector in the ARAKS experiment --- on ionospheric electron beam injection 06 p0786 A83-18368
- Propagation effects on microwave and millimetre-wave earth-satellite links 06 p0745 A83-18703
- The effects of shape on electromagnetic scattering by ice crystals 06 p0746 A83-18717
- De-polarisation due to non-symmetry in raindrops 06 p0746 A83-18718
- Study of the particulate sulfur-light scattering relationship using in situ aerosol thermal analysis 07 p0957 A83-20222
- Photographic surface photometry of the Milky Way. I - Data and reduction methods 07 p1005 A83-20559
- Rayleigh scattering and optical heterodyne detection - Application to atmospheric fluctuations --- French thesis 07 p0970 A83-21092
- Effect of the aerosol on fog microstructure 08 p1140 A83-22355
- Design and calibration of a coherent lidar for measurement of atmospheric backscatter 08 p1096 A83-22507
- Measurements of the phase function of natural particles 08 p1076 A83-22547
- Laser transmissometer calibration of long-path atmospheric transmission measurements 08 p1104 A83-22889
- Intensity and polarization line profiles in a semi-infinite Rayleigh-scattering planetary atmosphere. I - Integrated flux 08 p1190 A83-23107
- The dust cloud of the century 08 p1138 A83-23271
- Heterodyne detection through rain, snow, and turbid media - Effective receiver size at optical through millimeter wavelengths 09 p1249 A83-24445
- A new ionospheric scattering mechanism 09 p1307 A83-24692
- Light propagation in a disperse medium --- Russian book 09 p1346 A83-25251

- The scattering of light in an inhomogeneous atmosphere 09 p1364 A83-25254
- Topics in the theory of radiative transfer in horizontally inhomogeneous media --- scattering of sunlight in clouds 09 p1317 A83-25255
- The development of numerical methods for solving the radiative transfer equation 09 p1340 A83-25258
- Inverse problems in the laser probing of atmospheric aerosols 09 p1309 A83-25261
- Definitions of atmospheric radiance and transmittances in remote sensing 10 p1448 A83-25647
- Real axis integration of Sommerfeld integrals - Source and observation points in air 10 p1403 A83-26038
- Parametric identification of multiple scattering systems via the quasi-linearization 10 p1466 A83-26536
- Rain backscattering effects in coherent polarization-diversity radar signals 11 p1630 A83-27078
- The usefulness of a bulk refractive index for the calculation of the scattering properties of mixtures of aerosol particles at wavelength 530 nm 11 p1615 A83-27973
- Lidar observations of the El Chichon dust cloud at 23 deg S 12 p1751 A83-28914
- Computations of Mie scattering applied to the observation of stratospheric aerosol 12 p1754 A83-29540
- Retrieval of aerosol characteristics from scattering and extinction measurements 12 p1755 A83-29565
- Rocket studies of atmospheric scattering and the aerosol size distribution in the troposphere and lower stratosphere over thumba 12 p1756 A83-29575
- Nonlinear spatial-frequency characteristics of a three-dimensional inhomogeneous scattering layer --- in atmospheric optics 13 p1918 A83-30006
- The reproduction of atmospheric scattering indicatrices with an allowance made for the anisotropy of multiple effects 13 p1874 A83-30034
- A calculation of the characteristics of polarized radiation by the method of iterations 13 p1913 A83-30035
- Measurement of stratospheric aerosol near Sanriku (39 deg N, 142 deg E) in Japan on May 31, 1979 13 p1877 A83-30889
- Application of the 2-D discrete-ordinates method to multiple scattering of laser radiation 13 p1857 A83-31460
- Atmospheric scattering effects on ground-based measurements of thermospheric winds 13 p1881 A83-31532
- Diffuse and global solar spectral irradiance under cloudless skies 13 p1882 A83-31613
- The spectrophotometric experiment on the Venera-13 and Venera-14 descent modules. I - Method, results, and preliminary analysis of measurements 14 p2111 A83-31964
- Investigation of the structure of the Venus clouds using the nephelometers on the Venera-13 and Venera-14 probes 14 p2111 A83-31967
- Time-dependent aureole about a source in a multiple-scattering medium --- for solar blind UV communication and warning systems 15 p2201 A83-34458
- Measuring atmospheric scattering and extinction at 10 microns using a CO2 lidar 15 p2201 A83-34464
- Increasing backscattered light from the stratospheric aerosol layer after Mt. El Chichon eruption - Laser radar measurement at Nagoya (35 deg N, 137 deg E) 15 p2202 A83-34728
- Comparison of calculated and measured atmospheric radiation values for remote sensing purposes 15 p2203 A83-35100
- Twilight observations from a balloon gondola - Preliminary results 16 p2376 A83-35788
- Comparison of the bistatic cross-section and reflectivities of spherical and spheroidal raindrops at microwave frequencies 16 p2343 A83-36578
- Calculation of the inversion curves by the Monte Carlo method --- for ozone attenuation coefficient determination 16 p2392 A83-36849
- Solar scattered radiation measurements by Venus probes 17 p2617 A83-37420
- Vertical atmospheric profiles measured with lidar 17 p2540 A83-37743
- Theoretical model for calculating rain-induced crosspolarisation 17 p2495 A83-38878
- Intensity and polarization line profiles in a semi-infinite Rayleigh-scattering planetary atmosphere. II - Variations of equivalent width over the disk 18 p2779 A83-39190
- Vertical distribution of scattering hazes in Titan's upper atmosphere 19 p2921 A83-40778
- Particulate extinction models for sun photometer measurements taken at high mountain stations 19 p2865 A83-41162

The turbulent scattering channel - Effective heterodyne receiver size for optical through millimeter wavelengths 19 p2828 A83-41331

Effects of the El Chichon volcanic cloud in the stratosphere on the intensity of light from the sky 20 p3028 A83-42209

Particle size distributions from forward scattered light using the Chahine inversion scheme 20 p3046 A83-42213

Techniques for measuring radiance in sea and air 20 p2988 A83-42216

Time-dependent scattering in resonance lines 20 p3044 A83-42458

Backscatter and extinction in water clouds 20 p3031 A83-42859

Point spread functions in imaging a Lambert surface from zenith through a thin scattering layer 20 p3011 A83-42964

Fraunhofer diffraction by ice crystals suspended in the atmosphere 20 p3028 A83-43465

Role of scattering in emergent planetary radiation 21 p3241 A83-44868

Resonance-line scattering in the upper atmosphere of Venus according to ultraviolet measurements made from Venera-11 and Venera-12 21 p3242 A83-45281

Passive and active remote sensing of atmospheric precipitation 22 p3339 A83-46064

Inverse methods for remote determination of properties of optically thick atmospheres 22 p3328 A83-46067

Speckle statistics of atmospherically backscattered laser light 22 p3295 A83-46068

Target reflectance measurements for calibration of lidar atmospheric backscatter data 22 p3295 A83-46075

Multiple scattering of optical pulses in scale model clouds --- impact on optical communications 22 p3274 A83-46081

Most reliable messenger - MM-waves get through 22 p3275 A83-46757

Electromagnetic wave propagation and scattering in rain and other hydrometeors 22 p3275 A83-46777

Refractive index and size distribution of aerosols as estimated from light scattering measurements 22 p3334 A83-46947

The possibility of using the synthetic-aperture method in radar meteorology 23 p3487 A83-47145

The surface illuminance and albedo of a planetary atmosphere with nearly conservative scattering 23 p3529 A83-48559

Retrieval of the optical properties of aerosols from aureole and extinction data 24 p3604 A83-49002

Forward multiple scattering corrections as a function of detector field of view --- laser beam propagation through atmospheric aerosols 24 p3588 A83-49005

Light scattering by randomly oriented cubes and parallelepipeds --- for interpretation of observed data from planetary atmospheres 24 p3671 A83-49009

ATMOSPHERIC SHELLS

U ATMOSPHERIC STRATIFICATION

ATMOSPHERIC SOUNDING

Differential absorption lidar measurements of atmospheric temperature and pressure profiles 01 p0073 A83-10004

A microwave pressure sounder --- for remote measurement of atmospheric pressure 01 p0047 A83-10005

The promise of remote sensing in the atmospheric sciences 01 p0073 A83-10013

Lidar meteorology 01 p0073 A83-10016

Measurements of the inhomogeneities in the polar ionosphere made with an auto-oscillating sonde 01 p0050 A83-10602

The methods and results for the laser probing of the upper atmosphere in the polar region 01 p0072 A83-10604

Investigation of the upper layers of the atmosphere in the Arctic, Antarctic, and above the world ocean by means of meteorological rockets 01 p0075 A83-10829

Advanced sensors for spaceborne measurements of the earth's atmosphere 01 p0053 A83-11279

An experimental determination of the accuracy characteristics of meteorological measurements made by rocket 02 p0213 A83-11979

Stable and rugged etalon for the Dynamics Explorer Fabry-Perot interferometer. I - Design and construction 02 p0142 A83-12312

Stable and rugged etalon for the Dynamics Explorer Fabry-Perot interferometer. II - Performance 02 p0142 A83-12313

Visible and infrared spin scanning radiometer /VISSR/ atmospheric sounder /VAS/ ground data system 02 p0142 A83-12679

A new tool for the three-dimensional sounding of the atmosphere - The helisonde 02 p0216 A83-12957

Satellite remote sensing by the technique of computed tomography 02 p0217 A83-12962

Objective analysis of discontinuous satellite-derived data fields for grid point interpolation [AD-A122568] 02 p0217 A83-12965

Airborne measurements of infrared atmospheric radiance and sky noise 03 p0324 A83-13461

Spectral line inversion for sounding of stratospheric minor constituents by infrared heterodyne technique from balloon altitudes 03 p0325 A83-13723

Accurate frequency and intensity measurements of the infrared spectra of atmospheric molecules 03 p0294 A83-13981

Infrared /IR/ spectroscopy in support of atmospheric measurements 03 p0294 A83-13985

Local-area atmospheric sounding from satellites 03 p0369 A83-14524

HIRS-AMTS satellite sounding system test - Vertical resolving power 03 p0289 A83-14627

Algorithms used to retrieve surface-skin temperature and vertical temperature and moisture profiles from VISSR atmospheric sounder /VAS/ radiance observations 03 p0370 A83-14628

An evaluation of a new technique for estimating atmospheric total ozone from TOVS --- TIROS Operational Vertical Sounder 03 p0360 A83-14629

A climate index indicative of cloudiness derived from satellite infrared sounder data 03 p0371 A83-14658

Combined acoustic and radioacoustic probing of the atmospheric boundary layer 03 p0372 A83-14829

Lidar identification of drop and crystal clouds 03 p0372 A83-14831

Optical studies of the earth's upper atmosphere in Abastumani 03 p0363 A83-14837

SAGE - European ozonesonde comparison 03 p0363 A83-14924

Observations of the horizontal irregularity of F-layer nightglow in the region of the Brazilian anomaly 05 p0663 A83-17621

A new method for the laser sounding of the atmosphere based on the reception of an echo signal by the laser 05 p0645 A83-17632

The methodology for the lidar sounding of atmospheric temperature on the basis of Raman spectra 05 p0668 A83-17692

Earth limb altitude determination for the Solar Mesosphere Explorer [AIAA PAPER 83-0429] 05 p0603 A83-17926

Quiet-time electron precipitation at L = 4 in the South Atlantic anomaly 06 p0783 A83-18293

The Venus stratosphere according to Venera-11 and Venera-12 accelerometer data 06 p0848 A83-18364

Echsonde - Design and development 06 p0762 A83-18420

On the altitude profile retrieval of the troposphere refraction index according to the earth satellite radio data 06 p0747 A83-18739

Lidar measurements of natural and artificial aerosol during PUKK 06 p0787 A83-18997

First infrared measurement of atmospheric NO2 from the ground 07 p0958 A83-20092

Thermal structure of the atmosphere of Venus from Pioneer Venus radio occultations 07 p1030 A83-20617

Small-scale turbulence in the atmosphere of Venus 07 p1030 A83-20618

The evaluation of the receiver noise level of a lidar response 08 p1074 A83-21873

Model experiment in measuring the temperature and concentration of water vapours in air by spontaneous Raman scattering 08 p1091 A83-21875

National Oceanic and Atmospheric Administration's /NOAA/ pulsed, coherent, infrared Doppler lidar - Characteristics and data 08 p1096 A83-22506

Moisture sounding at millimeter wavelengths /94/183 GHz/ at high altitudes 08 p1098 A83-22557

Some scientific objectives of a satellite-borne lightning mapper 08 p1141 A83-22702

Balloon atmospheric mosaic measurements /BAMM/ IIA phenomenology and band selection 08 p1045 A83-22844

Infrared spectral radiance of the sky 08 p1136 A83-22850

The spectrum of the scattering signal for the radioacoustic sounding system /RASS/ 09 p1310 A83-23406

Discrepancies between balloon-borne IR atmospheric spectra and corresponding synthetic spectra calculated line by line around 825 per cm 09 p1306 A83-24440

Lidar measurements of the atmosphere 09 p1272 A83-24644

The lunar semi-diurnal tide observed by stratospheric sounding units on the TIROS-N series of satellites 09 p1307 A83-24689

Methods for the passive probing of transparency in the atmospheric surface layer 09 p1315 A83-25054

Application of statistical modeling to the problem of the optical sensing of the ocean-atmosphere system 09 p1320 A83-25243

Inverse problems in the laser probing of atmospheric aerosols 09 p1309 A83-25261

Regularizing the solution of the laser sounding equation of atmospheric aerosols by means of a stabilizing functional 10 p1425 A83-25567

Rocketborne cryogenic /10 K/ high-resolution interferometer spectrometer flight HIRIS - Auroral and atmospheric IR emission spectra [AD-A128358] 10 p1423 A83-26642

Method and device for the compression of spectrometric data 10 p1423 A83-26814

The Poker Flat MST radar system - Current status and capabilities --- Mesosphere-Stratosphere-Troposphere 11 p1621 A83-26977

The atmosphere of Titan - An analysis of the Voyager 1 radio occultation measurements 11 p1684 A83-27367

Errors in measuring the temperature-inversion characteristics of the atmospheric boundary layer during radio sounding 11 p1634 A83-28207

Short and middle range remote sensing of atmospheric gases using Raman lidar --- French thesis 11 p1585 A83-28640

The construction of a spectrophone and a CO2 laser waveguide excited by a radiofrequency field for application to the detection of atmospheric trace species --- French thesis 11 p1585 A83-28654

Methods for carrying out electrical measurements high in the atmosphere 11 p1620 A83-28731

Atmospheric sounding with meteorological balloons --- Russian book 12 p1758 A83-29326

Mesospheric turbulence intensities measured with a HF radar at 35 deg S. II 12 p1759 A83-29428

VHF radar observations in the stratosphere and mesosphere during a stratospheric warming 12 p1754 A83-29434

Radar meteorology: Active remote sensing of the atmosphere --- French book 12 p1759 A83-29537

Microprocessor based data acquisition and control system for a balloon borne quadrupole mass spectrometer 12 p1730 A83-29539

Space observations of aerosols and ozone: Proceedings of the Topical Meeting, Ottawa, Canada, May 16-June 2, 1982 12 p1754 A83-29557

The effect of aerosols on climate and aerosol climatology on the basis of observations from space 12 p1759 A83-29558

Laser sounding of aerosols using airborne and space facilities 12 p1755 A83-29563

Spaceborne lidar measurement accuracy - Simulation of aerosol, cloud, molecular density, and temperature retrievals 12 p1755 A83-29564

Periodic and aperiodic ozone variations in the middle and upper stratosphere 12 p1756 A83-29583

Weather satellites: Stereoscopy and Sounding; Proceedings of the Topical Meeting, Ottawa, Canada, May 16-June 2, 1982 12 p1759 A83-29676

Validation of the stratospheric sounding unit 12 p1708 A83-29686

Satellite-in situ measurement intercomparisons at Wallops Island, Virginia --- comparative atmospheric sounding 12 p1760 A83-29688

The use of VAS satellite data in weather analysis, prediction and diagnosis 13 p1887 A83-30560

Ultralight sounder - An airborne system for studying the planetary boundary layer 13 p1803 A83-30787

Lidar- and balloon-borne particle counter comparisons following recent volcanic eruptions 13 p1877 A83-30888

Measurement of stratospheric aerosol near Sanriku (39 deg N, 142 deg E) in Japan on May 31, 1979 13 p1877 A83-30889

Spectroscopic measurements of carbon monoxide in the stratosphere 13 p1877 A83-30890

The distribution and annual cycle of ozone in the upper stratosphere 13 p1877 A83-30893

Mid-latitude lidar observations of planetary waves in the middle atmosphere during the winter of 1981-1982 13 p1891 A83-30895

Remote sensing of atmospheric temperature by lidar on the basis of the rotational spectrum of Raman scattering 14 p2059 A83-32862

The neutral composition of the high-latitude atmosphere 14 p2054 A83-33029

Uses of Raman scattering for remote sensing of atmospheric properties of meteorological significance 14 p2021 A83-33171

Limiting payload deceleration during ground impact 15 p2122 A83-33726

Inverse problems of lidar sensing of the atmosphere --- Book 15 p2195 A83-33768

An evaluation of soundings, analyses and model forecasts derived from TIROS-N and NOAA-6 satellite data 15 p2204 A83-33883

Temperature sounding in the planetary boundary layer by RASS System analysis and results 15 p2164 A83-34154

Experimental studies of the neutralization of a charged vehicle in space and in the laboratory in Japan 15 p2126 A83-34210

Comment on 'Can the standard radiosonde system meet special atmospheric research needs?' 15 p2165 A83-34739

Aerosol concentrations and size distribution in the troposphere and lower stratosphere over Thumba 15 p2202 A83-34745

Investigation of remote sensing possibilities of the lower atmosphere in the microwave range and some aspects of statistical data use 15 p2180 A83-35291

The upper atmospheres of the earth and planets; Proceedings of the Topical Meeting, Ottawa, Canada, May 16-June 2, 1982 16 p2434 A83-35351

Energy deposition rates by charged particles measured during the energy budget campaign 16 p2372 A83-35363

Neutral winds in the polar atmosphere as measured from Dynamics Explorer 16 p2374 A83-35376

Mean zonal wind and temperature structure during the PMP-1 winter periods --- Preparatory Middle Atmosphere Program Project-1 16 p2383 A83-35380

Results from the LIMS experiment for the PMP-1 winter 1978/79 --- Limb Infrared Monitor of the Stratosphere 16 p2383 A83-35381

The variability of stratospheric nitrogen compounds observed by LIMS in the winter of 1978-1979 16 p2374 A83-35382

Measurements of upper atmosphere wind and temperature from meteorological rocket experiments during winter 1979 16 p2383 A83-35384

Scientific programs for the Spacelab ESO13 grille spectrometer 16 p2317 A83-35784

Controlling the IESO13 spectrometer for spacelab and its data retrieval 16 p2317 A83-35786

An ultraviolet spectrograph using an echelle grating with cross-disperser for the measurement of stratospheric constituents [AIAA PAPER 83-0020] 16 p2356 A83-36040

Properties of the neutral density and composition in the thermosphere 16 p2378 A83-36115

Measurement of faint lidar signals in the presence of an intense background during pulsed laser sounding of the atmosphere 16 p2360 A83-36125

The fine structure of the stratospheric flow revealed by differential sounding 16 p2389 A83-36137

Analysis of upper stratospheric ozone profile data from the ground-based Umkehr method and the Nimbus-4 BUV satellite experiment 16 p2381 A83-36152

Low-frequency (f less than about 1 Hz) stratospheric electrical noise measured by balloon-borne sensors 16 p2381 A83-36156

Comparison of sounding results using Soviet and French rockets in 1977 16 p2392 A83-36850

Laboratory simulation of tunable diode laser remote measurement of atmospheric gases using topographic targets 17 p2510 A83-37741

Case study of the March 24, 1976 Elton, Louisiana tornado using satellite infrared imagery, Doppler sounder, rawinsonde, and radar observations 17 p2547 A83-37758

Planetary atmospheres --- summary of Pioneer and Venus observations 17 p2621 A83-38267

New tools for magnetospheric research 17 p2541 A83-38295

Advances in remote sensing of the atmosphere 17 p2547 A83-38313

Techniques for diagnosing mesoscale phenomena affecting aviation using VAS satellite data 17 p2548 A83-38704

Results of combining the Profiler and VAS for determining temperature and moisture in the atmosphere --- VISSR Atmospheric Sounder 17 p2551 A83-38738

Atmospheric temperature sounding from space 17 p2551 A83-38739

Intercomparison of PMS particle size spectrometers --- Particle Measuring Systems, Inc. 17 p2546 A83-38741

ALPHA-1/airborne lidar systems and measurements 17 p2495 A83-38747

Measurements of an aircraft wake vortex system using a meteorological tower 17 p2552 A83-38751

The use of pressure fluctuations on the nose of an aircraft for measuring air motion 18 p2721 A83-39118

Remote sounding of cloud parameters from a combination of infrared and microwave channels 18 p2721 A83-39119

The Arcad-3 project --- aboard Franco-Soviet AUREOL-3 satellite 18 p2715 A83-39571

Auroral photometers aboard the Aureol-3 satellite - The Altair experiment 18 p2647 A83-39578

Severe storm observations using the Microwave Sounding Unit 18 p2725 A83-39683

EISCAT - The European incoherent scatter radar for studying the polar atmosphere 18 p2716 A83-39775

The intercomparison ozone campaign held in France in June 1981 - Description of the campaign 18 p2716 A83-39785

Total atmospheric ozone measured by ground based high resolution infrared spectra - Comparison with Dobson measurements 18 p2716 A83-39786

Atmospheric trace species measured above Haute-Provence observatory 18 p2716 A83-39788

Measurements of the vertical distribution of ozone by ground-based microwave techniques at the Bordeaux observatory during the June 1981 intercomparison campaign 18 p2716 A83-39789

Measurement of the vertical ozone distribution by means of an in situ gas phase chemiluminescence ozonometer during the intercomparison ozone campaign, Gap, France, June 1981 18 p2716 A83-39790

GSFC optical ozonesonde results during the Gap, France, intercomparisons, June 1981 18 p2716 A83-39791

NASA-JSC measurements during la campagne d'intercomparaison d'ozonometres, Gap, France, June 1981 18 p2716 A83-39792

Stratospheric ozone measurements by solar ultraviolet absorption 18 p2716 A83-39793

Nimbus 7 total ozone mapping spectrometer (TOMS) data during the Gap, France, ozone intercomparisons of June 1981 18 p2717 A83-39794

Measurements of the ozone vertical distribution (0-25 km) comparison of various instruments, Gap - Observatoire de Haute-Provence, June 1981 18 p2689 A83-39797

Ozone profile intercomparison based on simultaneous observations between 20 and 40 km 18 p2689 A83-39798

Comparison of ozone vertical distributions measured by different techniques at mesospheric altitudes 18 p2717 A83-39799

The radiation controlled balloon (RACCOON) 18 p2640 A83-39803

An atmospheric sounding balloon with ballast - An automatic numerical model for its manufacture and simulation of its evolution 18 p2640 A83-39804

Importance of electric field measurement over low latitudes at stratospheric heights by balloons 18 p2717 A83-39819

Low-level water vapor fields from the VISSR Atmospheric Sounder (VAS) 'split window' channels 18 p2726 A83-39871

Theoretical experiments on cumulus dynamics 18 p2729 A83-40039

He-Ne laser frequencies near 2.4 microns and their application to hydrogen fluoride detection 19 p2851 A83-40928

Atmospheric water vapor differential absorption measurements on vertical paths with a CO2 lidar 20 p3028 A83-42208

Combined sounding of the atmosphere by aerosol and Raman lidars 20 p2992 A83-43791

Measurements of the mean, solar-fixed temperature and cloud structure of the middle atmosphere of Venus 21 p3240 A83-44391

Fluxes of quasi-trapped charged particles according to data from a rocket experiment 21 p3245 A83-45295

Operation and experimental results of ionosphere Sounding Satellite-b (ISS-b, UME-2). I - Outline of ISS-b project 21 p3096 A83-45434

Passive radiometry for vertical sounding from meteorological satellites --- of lower atmosphere 22 p3260 A83-46077

Atmospheric soundings from a geostationary satellite 22 p3329 A83-46083

Microwave atmospheric sounder for earth limb observations from space 22 p3261 A83-46170

A compact high-resolution Michelson Interferometer for Passive Atmospheric Sounding (MIPAS) 22 p3290 A83-46241

Symposium on Coordinated Observations of the Ionosphere and the Magnetosphere in the Polar Regions, 4th, Tokyo, Japan, February 23-25, 1981, Proceedings 22 p3329 A83-46501

Methods of active and passive radar detection in meteorology 23 p3487 A83-47137

The use of model representations and empirical data in the problem of passive-active radar sounding of clouds and precipitation 23 p3487 A83-47138

Characteristics of the restoration of the microstructure of an atmospheric aerosol from multiple-frequency sounding data 23 p3480 A83-47167

BAS - The project of an earth-atmosphere-spectrophotometer for basic research [IAF PAPER 83-113] 23 p3453 A83-47274

Optimization of the propulsion for meteorological probe [IAF PAPER 83-377] 23 p3426 A83-47365

Optical and laser remote sensing 23 p3455 A83-47766

Remote sensing of hydrazine compounds using a dual mini-TEA CO2 laser DIAL system --- differential-absorption LIDAR 23 p3456 A83-47769

Remote detection of gases by gas correlation spectroradiometry 23 p3456 A83-47780

Signal averaging limitations in heterodyne- and direct-detection laser remote sensing measurements 23 p3457 A83-47789

Rayleigh and resonance sounding of the stratosphere and mesosphere 23 p3457 A83-47790

High-resolution lidar system for measuring the spatial and temporal structure of the mesospheric sodium layer 23 p3457 A83-47791

Remote sensing of OH in the atmosphere using the technique of laser-induced fluorescence 23 p3457 A83-47792

The NASA/Goddard balloon borne lidar system 23 p3458 A83-47795

Atmospheric remote sensing using the NOAA coherent lidar system 23 p3458 A83-47807

Coherent CO2 lidar systems for remote atmospheric measurements 23 p3458 A83-47808

The modeling and statistical investigation of the refractometric method for determining meteorological parameters from space 23 p3492 A83-48103

Atmospheric sounding using optical systems 24 p3605 A83-49284

An accurate radiative transfer model for use in the direct physical inversion of HIRS2 and MSU temperature sounding data 24 p3607 A83-49344

Non-contact sensing of atmospheric temperature, humidity, and supersaturation 24 p3584 A83-49709

NASA's AVE/VAS program 24 p3616 A83-50142

ATMOSPHERIC STRATIFICATION

Vertical displacements of stratification in the E-layer during sunrise 02 p0205 A83-11996

On the effects of moisture on the Brunt-Vaisala frequency 02 p0213 A83-12230

Response of stratified flow in the lee of the Olympic Mountains 02 p0218 A83-13061

The dynamics of a rotating mesometeorological convective turbulent vortex in an unstably stratified atmosphere 04 p0509 A83-15720

Horizontally propagating solitary waves in the upper atmosphere 04 p0509 A83-15723

On the nature of homogeneous auroral arcs 05 p0663 A83-17613

The depth of the daytime mixed layer at two coastal sites - A model and its validation 06 p0788 A83-18057

Waves in magnetic structures 06 p0853 A83-18126

Method of remote sensing of horizontal stratification due to an ionospherically reflected powerful radio wave 06 p0786 A83-18321

Propagation of vertically and horizontally polarized waves excited by distributions of electric and magnetic sources in irregular stratified spheroidal structures of finite conductivity - Generalized field transforms 08 p1161 A83-22281

Fluctuations of radio-wave emergence angles in the case of scattering in the spherically stratified ionosphere 09 p1245 A83-23469

The relation between the stratification parameter mu and the vertical temperature gradient in the planetary boundary layer 09 p1311 A83-23550

Small atmospheric perturbations for one model of temperature stratification 09 p1308 A83-25051

Perturbation theory for a spectrum of normal modes in a stratified inhomogeneous medium --- tropospheric propagation 12 p1718 A83-29258

Measurement of the height of the hydroxyl-emission layer in the Moscow area 14 p2051 A83-31884

The spatial problem of the flow around an obstacle of an incompressible stratified fluid (numerical modeling) --- atmospheric air flow around mountains 14 p2058 A83-32853

Some characteristics of the F2 layer at low and middle latitudes 15 p2200 A83-34419

A generalization of the Hines' dispersion relation --- for real atmosphere 16 p2377 A83-36108

The spectral properties of filamentary and physical nonhomogeneous prominences. III - The structure and stratification of physical conditions 16 p2440 A83-36853

Structure and parameters of the Venus atmosphere according to Venera probe data 17 p2616 A83-37413

- Retarding layers in the troposphere over the equatorial Atlantic 19 p2869 A83-42122
- Perturbation of the zonal flow by a local heat source 21 p3181 A83-45329
- The effect of the stratification of the atmospheric boundary layer over water on the energy flux to waves 22 p3338 A83-45641
- Repeatability of the multilayer tropopause above the Northern Hemisphere 23 p3487 A83-47135
- Stratification of air in the upper troposphere and lower stratosphere 23 p3487 A83-47136
- Relationship between thermal-radiation characteristics and concentrations of trace gases in different layers of the atmosphere 23 p3488 A83-47160
- Elevated mixed layers in the regional severe storm environment - Conceptual model and case studies 23 p3491 A83-47413
- A study of multiple stable layers in the nocturnal lower atmosphere 23 p3492 A83-48732
- ### ATMOSPHERIC TEMPERATURE
- #### NT AUROLAL TEMPERATURE
- #### NT IONOSPHERIC TEMPERATURE
- Differential absorption lidar measurements of atmospheric temperature and pressure profiles 01 p0073 A83-10004
- A technique for determining the temperature profile from VHF radar observations 01 p0074 A83-10019
- Horizontal correlation of satellite temperature errors 01 p0074 A83-10045
- Relationships between structure functions and temperature ramps in the atmospheric surface layer 01 p0075 A83-10719
- Using new methods in monitoring the thermal regime of the Arctic 01 p0075 A83-10828
- Fabry-Perot determinations of midlatitude F-region neutral winds and temperatures from 1975 to 1979 02 p0204 A83-11965
- Temperature and solar zenith angle control of D-region positive ion chemistry [AD-A126882] 02 p0204 A83-11970
- A climatological estimate of the radiative cooling of the atmosphere 02 p0213 A83-11977
- The relationship between the cloud amount and the temperature when averaged over a large space 02 p0213 A83-11978
- An experimental determination of the accuracy characteristics of meteorological measurements made by rocket 02 p0213 A83-11979
- The parameterization of longwave flux in energy balance climate models 02 p0213 A83-12229
- A scale analysis of deep moist convection and some related numerical calculations 02 p0213 A83-12233
- Physiological criteria of upper limits of body heating 02 p0223 A83-12256
- Measuring /C sub T/-squared, /C sub Q/-squared, and C sub TQ in the unstable surface layer, and relations to the vertical fluxes of heat and moisture --- atmospheric temperature and humidity 03 p0363 A83-13274
- The spectrum of Titan in the far-infrared and microwave regions 03 p0133 A83-13827
- The upper atmosphere of Uranus - A critical test of isotropic turbulence models 03 p0133 A83-13829
- Criteria for the formation and water content of cumulus clouds 03 p0364 A83-14097
- Lake-effect disturbances over Lake Michigan - Some numerical results 03 p0368 A83-14439
- HIRS-AMTS satellite sounding system test - Vertical resolving power 03 p0289 A83-14627
- Algorithms used to retrieve surface-skin temperature and vertical temperature and moisture profiles from VISSR atmospheric sounder /VAS/ radiance observations 03 p0370 A83-14628
- An observational study of the D-region winter anomaly and sudden stratospheric warmings 03 p0362 A83-14746
- The energetics of the lower thermosphere in the presence of internal gravity waves 03 p0362 A83-14834
- Some problems encountered in monitoring the global thermal regime of the Northern Hemisphere 04 p0515 A83-15053
- A simple method to compute the change in earth-atmosphere radiative balance due to a stratospheric aerosol layer 04 p0510 A83-15939
- Measurement of true mean temperature for determination of climatic trends 05 p0668 A83-17449
- The methodology for the lidar sounding of atmospheric temperature on the basis of Raman spectra 05 p0668 A83-17692
- Radiative-convective models of climate 06 p0788 A83-17997
- The effects of changing solar angles, cloud regimes, and air temperatures on the temperatures of contrasting surfaces 06 p0779 A83-18234
- Studies of the atmospheric stability characteristics during the solar eclipse of February 16, 1980 06 p0789 A83-18243
- A ubiquitous wavenumber-5 anomaly in the Southern Hemisphere during FGGE --- First Garp Global Experiment 06 p0792 A83-18472
- Airborne atmospheric temperature structure measurements of a Pacific coast marine inversion [AIAA PAPER 83-0278] 06 p0793 A83-19585
- Temperature effects on the stratosphere of the April 4, 1982 eruption of El Chichon, Mexico 07 p0958 A83-20089
- Optimal weighting of data to detect climatic change - Application to the carbon dioxide problem 07 p0969 A83-20216
- Thermal structure of the atmosphere of Venus from Pioneer Venus radio occultations 07 p1030 A83-20617
- The Russian surface temperature data set 07 p0969 A83-20801
- Radio-remote-sensing determination of the vertical temperature gradient in the atmospheric surface layer 07 p0970 A83-20866
- Effect of the stratospheric medium temperature on strong lines observed in the far infrared region 07 p0965 A83-21399
- Model experiment in measuring the temperature and concentration of water vapours in air by spontaneous Raman scattering 08 p1091 A83-21875
- Seasonal variation of the atmospheric temperature at midlatitude - A revision of the CIRA 1972 model 08 p1138 A83-22061
- Global mean sea level - Indicator of climate change 08 p1144 A83-22325
- The 15 August 1980 occultation by the Uranian system - Structure of the rings and temperature of the upper atmosphere 08 p1189 A83-22930
- Stratospheric warming following the El Chichon volcanic eruption 08 p1138 A83-23276
- Radiance measurements by means of artificial satellites, and the analysis of atmospheric integral scales 09 p1310 A83-23408
- Dual Fabry-Perot spectrometer measurements of daytime thermospheric temperature and wind velocity - Data analysis procedures 09 p1306 A83-24449
- Temperatures in the plasmasphere determined from VLF observations 09 p1307 A83-24690
- Daytime mesospheric temperatures over the low-latitude station Thumba derived from rocket-borne solar Lyman-alpha absorption measurements 09 p1307 A83-24691
- Small atmospheric perturbations for one model of temperature stratification 09 p1308 A83-25051
- Venus - Mesospheric hazes of ice, dust, and acid aerosols 10 p1518 A83-25507
- New observational constraints on the temperature inversions of Uranus and Neptune 10 p1518 A83-25517
- An improved model for the calculation of profiles of C/n/-squared and epsilon in the free atmosphere from background profiles of wind, temperature and humidity 11 p1623 A83-26994
- Thermal structure of Saturn from Voyager infrared measurements - Implications for atmospheric dynamics 11 p1684 A83-27360
- Statistical predictability and spectra of air temperature over the northern hemisphere 11 p1633 A83-28083
- Interrelationship of temperature fields in the ocean-atmosphere system /Considering the example of the North Atlantic/ 11 p1633 A83-28205
- A method for studying temperature fields during stratospheric warmings 11 p1633 A83-28206
- Errors in measuring the temperature-inversion characteristics of the atmospheric boundary layer during radio sounding 11 p1634 A83-28207
- Distribution of ocean surface temperature in connection with features of atmospheric processes and hydrometeorological fields /According to POLYMODE data/ 11 p1634 A83-28208
- Solar Mesosphere Explorer - Scientific objectives and results 12 p1750 A83-28901
- Temperature measurements in the earth's stratosphere using a limb scanning visible light spectrometer --- onboard Solar Mesosphere Explorer 12 p1751 A83-28907
- An analytic version of Jacchia's 1977 model atmosphere 12 p1752 A83-29101
- On the quasi-biennial oscillation in equatorial stratospheric temperatures and total ozone 12 p1756 A83-29581
- Validation of Nimbus-7 temperature-humidity infrared radiometer estimates of cloud type and amount 12 p1759 A83-29679
- Validation of satellite-derived atmospheric temperature and water vapor concentration using radiosonde and rocketsonde measurements 12 p1760 A83-29685
- Interpolation with respect to the vertical of the relative geopotential and temperature 13 p1884 A83-30293
- The thermal interaction between the ocean and the atmosphere at the surface in the trade-wind zone in the North Atlantic 13 p1884 A83-30300
- Quality and trends in national weather service forecasts 13 p1886 A83-30545
- The impact of mesoscale convective weather systems upon MOS temperature guidance --- Model Output Statistics 13 p1887 A83-30559
- Objectively predicting temperature in the low and middle troposphere 13 p1889 A83-30579
- Ultralight sounder - An airborne system for studying the planetary boundary layer 13 p1803 A83-30787
- Mid-latitude lidar observations of planetary waves in the middle atmosphere during the winter of 1981-1982 13 p1891 A83-30895
- The thermal structure and energy balance of the Uranian upper atmosphere 13 p1961 A83-31202
- High latitude neutral atmosphere temperature and concentration measurements from the first Eiscat incoherent scatter observations 13 p1883 A83-31717
- The effect of the winter anomaly of the D-region according to measurements on the Kerguelen Islands 14 p2050 A83-31876
- The role of circulation in the formation of the morning-evening asymmetry of thermospheric disturbances 14 p2051 A83-31887
- The dependence of air temperature and the temperature of precipitates on the amount of carbon dioxide in the atmosphere 14 p2056 A83-32365
- A note on the intercomparison between monthly mean radiance equivalent and rocketsonde temperatures 14 p2057 A83-32410
- A heat-flux history length scale for the nocturnal boundary layer 14 p2058 A83-32473
- Long-period oscillations in the atmosphere 14 p2058 A83-32851
- Remote sensing of atmospheric temperature by lidar on the basis of the rotational spectrum of Raman scattering 14 p2059 A83-32862
- An evaluation of soundings, analyses and model forecasts derived from TIROS-N and NOAA-6 satellite data 15 p2204 A83-33883
- A numerical model of the dynamics and microphysics of warm cumulus convection - Model description and preliminary results 15 p2205 A83-34065
- Characteristics of thermobaric fields in the southwest part of the North Atlantic in the summer of 1977 15 p2206 A83-34353
- Investigation of remote sensing possibilities of the lower atmosphere in the microwave range and some aspects of statistical data use 15 p2180 A83-35291
- Vertical density and temperature structure over northern Europe 16 p2373 A83-35373
- Mean zonal wind and temperature structure during the PMP-1 winter periods --- Preparatory Middle Atmosphere Program Project-1 16 p2383 A83-35380
- Results from the LIMS experiment for the PMP-1 winter 1978/79 --- Limb Infrared Monitor of the Stratosphere 16 p2383 A83-35381
- Measurements of upper atmosphere wind and temperature from meteorological rocket experiments during winter 1979 16 p2383 A83-35384
- Observations and models of simple nocturnal slope flows 16 p2384 A83-35467
- A barotropic planetary boundary layer 16 p2387 A83-35794
- Determining latent heat flux at sea - A comparison between wind-wave interaction and profile methods 16 p2388 A83-35797
- Comments on 'the relative effect of solar altitude on surface temperatures and energy budget components on two contrasting landscapes' 16 p2388 A83-35798
- Improved procedure for Raman lidar measurements of the atmospheric temperature 16 p2355 A83-35899
- Objective specifications of monthly mean surface temperature from mean 700 mb heights in winter 16 p2388 A83-36029
- The terrestrial upper atmosphere; Proceedings of the Workshop, Ottawa, Canada, May 16-June 2, 1982 16 p2377 A83-36101
- Proposal for a reference model of the middle atmosphere of the Southern Hemisphere 16 p2389 A83-36102
- Proposals for an Indian Standard Tropical Atmosphere up to 50 km 16 p2389 A83-36103
- Variations of mesopause temperatures in Europe 16 p2377 A83-36104
- Preliminary data of the thermal regime and circulation in the upper mesosphere and mesopause 16 p2377 A83-36106
- Model calculations of middle atmospheric wind and temperature fields 16 p2377 A83-36107

Properties of the mesosphere and thermosphere and comparison with CIRA 72 16 p2377 A83-36109

[AD-A129615] 16 p2377 A83-36109
Neutral temperatures from Thomson scatter measurements Comparisons with the CIRA(1972) [AD-A130290] 16 p2378 A83-36120

Solar, geomagnetic and long term effects on thermospheric neutral kinetic temperatures at midlatitude 16 p2378 A83-36121

The thermal structure of the atmospheric surface boundary layer on Mars as modified by the radiative effect of aeolian dust 16 p2437 A83-36158

Diurnal variations of satellite-measured black-body temperature areal distribution and eye diameter of mature typhoons 16 p2390 A83-36492

Structure of the free convective internal boundary layer above the coastal area 16 p2390 A83-36494

Internal-gravity-wave-like variations of temperature, humidity and wind observed in the troposphere downstream of heavy rainfall area 16 p2390 A83-36498

Pressure distributions in the Dischma Valley during the field experiments DISKUS 16 p2391 A83-36582

The distribution of climatic changes with global warming 16 p2391 A83-36844

Some problems of heat-transfer climatology in energetically active zones of the Atlantic Ocean 16 p2392 A83-36848

Comparison of sounding results using Soviet and French rockets in 1977 16 p2392 A83-36850

Radiative damping of temperature disturbances in the earth's upper atmosphere, with an allowance for deviations from local thermodynamic equilibrium 16 p2382 A83-36866

Modeling the effect of temperature changes in the stratosphere on the growth of drops of a sulfate aerosol 16 p2382 A83-36870

Variations of turbulent heat transfer in the mesosphere and lower thermosphere 17 p2537 A83-37053

Thermal structure of the atmosphere of Venus 17 p2616 A83-37412

The thermal balance of the lower atmosphere of Venus 17 p2617 A83-37419

The thermal balance of the middle and upper atmosphere of Venus 17 p2617 A83-37421

Dynamics of the earth's thermosphere 17 p2541 A83-38274

On the global mean temperature of the thermosphere 17 p2544 A83-38515

Results of combining the Profiler and VAS for determining temperature and moisture in the atmosphere --- VISSR Atmospheric Sounder 17 p2551 A83-38738

Atmospheric temperature sounding from space 17 p2551 A83-38739

Differential inversion --- for thermal emission spectrum of atmosphere [AD-A130984] 17 p2572 A83-38743

Temperature measurement with a sonic anemometer and its application to heat and moisture fluxes 18 p2687 A83-39015

Asymmetry in the diurnal variation of temperature and electron loss coefficient in the mesosphere 18 p2712 A83-39068

Ground-based remote sensing of temperature profiles by a combination of microwave radiometry and radar 18 p2721 A83-39113

A practical method of correcting monthly average temperature biases resulting from differing times of observation 18 p2722 A83-39127

Retrieval of near-surface temperatures from satellite data 18 p2722 A83-39130

Changes in the nature of fluctuations of temperature and liquid water content during the lifetime of a large-scale storm 18 p2722 A83-39133

Snow cover and temperature relationships in North America and Eurasia 18 p2723 A83-39139

Modeling the effect of stratospheric aerosols on climate 18 p2723 A83-39437

A two-dimensional model of the electrocoagulation-hygroscopic dissipation of warm fogs 18 p2724 A83-39442

The use of high horizontal resolution satellite temperature and moisture profiles to initialize a mesoscale numerical weather prediction model - A severe weather event case study 18 p2725 A83-39687

An automatic profiler of the temperature, wind and humidity in the troposphere 18 p2727 A83-39877

Troposphere-stratosphere (surface-55 km) monthly winter general circulation statistics for the Northern Hemisphere Four year averages 18 p2730 A83-40045

A method for on-line corrections of the transmission function in solving the problem of the thermal probing of the atmosphere 18 p2719 A83-40082

The problem of the predictability of the atmosphere and certain questions relating to the hydrodynamic theory of long-term weather prediction 19 p2867 A83-41580

Causes of the relative stability of the mean temperature of the earth's surface in the geological past 19 p2867 A83-42068

Global temperature variations in the troposphere and stratosphere, 1958-1982 20 p3029 A83-42501

An accurate theoretical approximation for adiabatic condensation temperature 20 p3030 A83-42514

The isolation of stratospheric temperature change due to the El Chichon volcanic eruption from nonvolcanic signals 20 p3031 A83-42857

Measurements of the mean, solar-fixed temperature and cloud structure of the middle atmosphere of Venus 21 p3240 A83-44391

An incoherent scatter study of short- and long-term temperature and atomic oxygen variations in the thermosphere 21 p3173 A83-44671

Comments on 'A theoretical study of a two-wavelength lidar technique for the measurement of atmospheric temperature profiles' 22 p3339 A83-45712

Lower thermospheric structure from Millstone Hill incoherent scatter radar measurements. I - Daily mean temperature. II Semidiurnal temperature component 22 p3328 A83-46057

Latitudinal (seasonal) variations in the thermospheric midnight temperature maximum - A tidal analysis 22 p3328 A83-46058

Tests of an inversion algorithm for spectrally resolved limb emission 22 p3328 A83-46080

Formation of noctilucent cloud particles and the temperature distribution at the polar mesopause 22 p3331 A83-46521

Numerical simulation of the atmospheric response to equatorial Pacific sea surface temperature anomalies 22 p3340 A83-46844

Numerical experiments with a stochastic zonal climate model 22 p3340 A83-46846

Evaporation-limited tropical temperatures as a constraint on climate sensitivity 22 p3340 A83-46847

Upper-level structure of Oklahoma tornadic storms on 2 May 1979. II - Proposed explanation of 'V' pattern and internal warm region in infrared observations 22 p3341 A83-46853

Observations of the 10-micron natural laser emission from the mesospheres of Mars and Venus 22 p3387 A83-47079

Distribution of deviations of geopotential from standard-atmosphere values above the Northern Hemisphere 23 p3486 A83-47134

Stratification of air in the upper troposphere and lower stratosphere 23 p3487 A83-47136

Information content, accuracy, and optimal conditions of indirect ground-based thermal-microwave radiometric measurements of the integral water-vapor content of the atmosphere, and the water content and effective temperature of clouds 23 p3487 A83-47140

Inclusion of dynamic factors in a thermodynamic model of climate and numerical forecasting of mean monthly air temperature in the troposphere 23 p3488 A83-47153

Atmospheric temperatures near the tropical tropopause Temporal variations, zonal asymmetry and implications for stratospheric water vapor 23 p3490 A83-47408

Infrared cooling in cloudy atmospheres - Precision of grid point selection for numerical models 23 p3491 A83-47416

Atmospheric pressure and temperature profiling using near IR differential absorption lidar 23 p3457 A83-47781

The modeling and statistical investigation of the refractometric method for determining meteorological parameters from space 23 p3492 A83-48103

A study of multiple stable layers in the nocturnal lower atmosphere 23 p3492 A83-48732

Determination of atmospheric composition and temperature from the U.V. airglow 24 p3603 A83-48753

Heat and mass transfer through a water/vapor interface with allowance for radiation --- in ocean-atmosphere interactions 24 p3616 A83-48947

Atmospheric temperature measurements using a pure rotational Raman lidar 24 p3582 A83-49007

A spatially distributed model of the biosphere --- latitude distribution of atmospheric temperature and precipitation 24 p3609 A83-49276

An accurate radiative transfer model for use in the direct physical inversion of HIRS2 and MSU temperature sounding data 24 p3607 A83-49344

Temperature and humidity spectra in cloud- and cloud-free air and associated cloud electrical and microphysical characteristics 24 p3611 A83-49681

ATMOSPHERIC TIDES

The relationship between interannual variability in the 200 mb tropical wind field and the southern oscillation 02 p0217 A83-13056

The role of cross-equatorial tropical cyclone pairs in the southern oscillation 02 p0218 A83-13057

Comments on 'Planetary-scale atmospheric phenomena associated with the Southern Oscillation' 02 p0218 A83-13063

A measurement of the tidal variations of atmospheric pressure and their relationship with geomagnetic disturbances 03 p0362 A83-14835

The semiannual oscillation in the thermosphere as a conduction mode 05 p0661 A83-17403

Fluctuations in tidal /24-, 12-h/ characteristics and oscillations /8-h-5-d/ in the mesosphere and lower thermosphere 05 p0665 A83-17785

Space-time distribution of the velocity of tidal motions, with allowance for Coriolis force 07 p0962 A83-20773

Solar and lunar seasonal variations in the American sector 08 p1133 A83-22302

Interpretation of seasonal variations of S and L --- solar and lunar geomagnetic variations 08 p1133 A83-22303

Sq and L currents in the ionosphere --- solar quiet and lunar tidal effects on ionospheric and geomagnetic variations 08 p1134 A83-22307

Validation of the stratospheric sounding unit 12 p1708 A83-29686

On the global distribution of Pluto's atmosphere 13 p1962 A83-31438

Does Venus breathe? 15 p2275 A83-34725

On the dynamic atmospheric response to the Chandler wobble forcing 16 p2386 A83-35484

The semi-diurnal tide at the equinoxes - MF radar observations for 1978-1982 at Saskatoon (52 deg N, 107 deg W) 16 p2386 A83-35487

High-latitude stratospheric winds near summer solstice - The diurnal and semidiurnal solar tides 16 p2389 A83-36141

On the extraction of tidal information from measurements covering a fraction of a day --- for upper atmosphere meteorology 19 p2865 A83-41128

Turbulence originating from convectively stable internal waves 20 p3020 A83-42838

Seasonal variation of solar atmospheric tides at meteor heights 20 p3027 A83-43403

Solar related waves in the Venusian atmosphere from the cloud tops to 100 km 21 p3241 A83-44707

Lower thermospheric structure from Millstone Hill incoherent scatter radar measurements. I - Daily mean temperature. II Semidiurnal temperature component 22 p3328 A83-46057

Latitudinal (seasonal) variations in the thermospheric midnight temperature maximum - A tidal analysis 22 p3328 A83-46058

On the mechanism of variations of the height of low cloud cover (an attempt at a mesoanalysis) 23 p3487 A83-47144

Upper atmosphere wind observations of waves and tides with the UNH meteor radar system at Durham 43 deg N (1977, 1978 and 1979) 24 p3606 A83-49311

Radiation tides in the ocean and atmosphere 24 p3608 A83-49545

ATMOSPHERIC TURBULENCE

NT CLEAR AIR TURBULENCE

NT GUSTS

NT LOW LEVEL TURBULENCE

Thermodynamics of the turbulent atmosphere and parameterization of fluxes 01 p0074 A83-10219

Frequency fluctuations of radio waves propagating in a turbulent atmosphere 01 p0030 A83-10402

Relationships between structure functions and temperature ramps in the atmospheric surface layer 01 p0075 A83-10719

Two-dimensional field of thermal turbulence at the edge of an escarpment 01 p0075 A83-10723

The small-scale turbulence spectrum of the high-latitude and equatorial ionosphere 02 p0203 A83-11679

Static-split telescope application to atmospheric turbulence measurement 02 p0178 A83-12345

Adaptive optical system referencing in the case of resolved targets illuminated through turbulence 02 p0215 A83-12591

A two-dimensional numerical study of horizontal roll vortices in an inversion capped planetary boundary layer 02 p0215 A83-12939

Markov-chain simulation of particle dispersion in inhomogeneous flows - The mean drift velocity induced by a gradient in Eulerian velocity variance 03 p0363 A83-13269

Vertical cross-spectra of horizontal velocity components at the Boulder Observatory 03 p0363 A83-13271

- Use of breakdown coefficients in turbulent jets to determine the universal exponent mu 03 p0363 A83-13273
- The spectrum of wind speed fluctuations encountered by a rotating blade of a wind energy conversion system 03 p0354 A83-13695
- The upper atmosphere of Uranus - A critical test of isotropic turbulence models 03 p0133 A83-13829
- Simulation of the planetary boundary layer with the UCLA general circulation model 03 p0366 A83-14413
- A numerical simulation of a stratocumulus-topped mixed layer 03 p0369 A83-14450
- A comparison of spectral and cospectral characteristics of dynamic and thermal turbulent fields in weakly stratified boundary layers 03 p0319 A83-14475
- Dilatation effects in wind tunnel simulation of non adiabatic atmospheres 03 p0319 A83-14476
- Atmospheric turbulence simulation cell for optical propagation experiment [ONERA, TP NO. 1982-84] 03 p0330 A83-14536
- Meteorological inputs to flight simulators 04 p0515 A83-15323
- The dynamics of a rotating mesometeorological convective turbulent vortex in an unstably stratified atmosphere 04 p0509 A83-15720
- An analysis of wave-turbulence interaction 04 p0516 A83-15931
- A study of the descriptive statistics of turbulent pollution concentration fields in atmospheric air and of meteorological elements for cities with developed industry 05 p0659 A83-16954
- Turbulent compressible convection in a deep atmosphere. I - Preliminary two-dimensional results --- of stars 05 p0699 A83-17017
- Adaptive optics methods in interferometry 05 p0644 A83-17073
- Spectral scales in the atmospheric boundary layer 05 p0667 A83-17441
- A non-geostrophic study in a barotropic system 05 p0668 A83-17554
- Generation of atmospheric turbulence by solar radiation 05 p0668 A83-17818
- The dynamic structure of the turbopause 05 p0666 A83-17948
- An international turbulence comparison experiment /ITCE 1976/ 06 p0761 A83-18058
- A technique for parameterization of the turbulence associated with precipitation events in a three-dimensional model of cloud convection 06 p0788 A83-18060
- Stability dependence of fluxes and bulk transfer coefficients in a tropical boundary layer 06 p0788 A83-18061
- Space-time turbulent characteristics in the atmospheric surface layer 06 p0789 A83-18245
- Entrainment and detrainment in a simple cumulus cloud model 06 p0790 A83-18262
- Noise of a model helicopter rotor due to ingestion of isotropic turbulence 06 p0807 A83-18397
- Operational evaluation of a turbulence closure model forecast system [AD-A125467] 06 p0791 A83-18460
- Accuracy of optical angle estimator operating through the turbulent atmosphere 06 p0736 A83-18584
- A comparative study of simple numerical models of the atmospheric boundary layer 06 p0792 A83-18927
- On the origin of speckle boiling and its effects in stellar speckle interferometry 06 p0822 A83-19190
- Small-scale turbulence in the atmosphere of Venus 07 p1030 A83-20618
- A critical evaluation of the aerodynamical error of a turbulence instrument 07 p0930 A83-20804
- Effects of volume averaging on the line spectra of vertical velocity from multiple-Doppler radar observations 07 p0969 A83-20807
- Non-resonance lines of neutral calcium in the spectra of Arcturus and Beta Virginis 07 p1024 A83-21227
- The effects of atmospheric turbulence on telescopic observations 07 p1010 A83-21525
- Millimeter wave atmospheric turbulence measurements - Preliminary results and instrumentation for future measurements 08 p1076 A83-22354
- Probabilistic diffraction limited imaging through turbulence 08 p1164 A83-22361
- Preliminary shipboard optical turbulence measurements 08 p1166 A83-22556
- The change of limiting resolution of electro-optical systems due to atmospheric effects 08 p1098 A83-22561
- Experimental measurements of turbulence induced beam spread and wander at 1.06, 3.8, and 10.6 microns 08 p1110 A83-22562
- Homogeneous and isotropic turbulence on the sphere --- in atmosphere 08 p1142 A83-23012
- Large-scale two-dimensional turbulence in the atmosphere 08 p1143 A83-23013
- Theory of equilibrium temperatures in radiative-turbulent atmospheres 08 p1143 A83-23014
- A simulation model for the analysis of the dynamic behavior of a helicopter rotor under nonstationary limit flight conditions 08 p1044 A83-23220
- The structure of the turbulent atmospheric boundary layer 09 p1309 A83-23354
- Simple algorithms for calculating optical communication performance through turbulence 09 p1245 A83-23581
- Remote determination of the structure constant profile from amplitude scintillation data using Tikhonov's regularized inverse method --- Fourier transform for solving convolution equations 09 p1311 A83-23795
- Application of WKB theory to turbulence layers in the vicinity of critical levels --- in winter hemisphere for internal gravity wave propagation 09 p1311 A83-23888
- A diagnostic study of the tornadic storm based on dual-Doppler wind measurements 09 p1313 A83-23968
- An experimental investigation of the factors governing the dynamic structure and intensity of atmospheric vortices 09 p1313 A83-23969
- Turbulence parameterization in a deep convection model --- for cloud physics 09 p1313 A83-23972
- Propagation model of laser beams in turbulence 09 p1271 A83-24084
- Inner-scale size effect on the scintillations of light in the turbulent atmosphere 09 p1344 A83-24086
- Closure models for rotating two-dimensional turbulence 09 p1314 A83-24129
- High frequency behavior of the tilt spectrum of atmospheric turbulence 09 p1249 A83-24439
- Experimental investigations of small-scale turbulence and turbulent exchange in cyclones and anticyclones at middle latitudes 09 p1315 A83-25053
- Local influences in the microturbulence of the wind 09 p1316 A83-25147
- The reconstruction of images scattered in an inhomogeneous medium --- Russian book 09 p1270 A83-25224
- The dependence of sound extinction on the parameters of thermal turbulence in the atmospheric boundary layer 10 p1451 A83-25823
- Atmospheric limitations to high angular resolution imaging 10 p1481 A83-25827
- Probability of diffraction-limited images in infrared through turbulence experimental results 10 p1420 A83-25839
- Imaging by dilute apertures in the presence of atmospheric turbulence 10 p1482 A83-25840
- Mutual coherence functions and intensities of backscattered signals in a turbulent medium 10 p1403 A83-26036
- Experimental investigations of fluctuations of optical signals and disturbances in the atmosphere 10 p1434 A83-26694
- The value of radar observations on the question of stratospheric turbulence transport 11 p1623 A83-26993
- An improved model for the calculation of profiles of C/n^2 -squared and epsilon in the free atmosphere from background profiles of wind, temperature and humidity 11 p1623 A83-26994
- Doppler radar and aircraft measurements of thunderstorm turbulence 11 p1627 A83-27043
- Estimation of turbulence severity in precipitation environments by radar 11 p1627 A83-27044
- Amplification of the mean intensity of backscattering in a turbulent atmosphere 11 p1632 A83-27957
- Imitation model of ray propagation in a three-dimensional turbulent medium 11 p1583 A83-27962
- A treatment of three dimensional incompressible turbulence 12 p1722 A83-29068
- An experimental study of the boundary layer over gentle terrain near a mountain range. II - Mean and turbulent characteristics of the boundary layer in unstable conditions 12 p1757 A83-29126
- A study of turbulent energy over complex terrain (state, 1978) 12 p1757 A83-29127
- Experimental study of the boundary layer over a gentle terrain near a mountain range. III - Turbulence structure in the boundary layer near the ground analyzed by acoustic sounding 12 p1758 A83-29130
- Turbulent characteristics of a shallow convective internal boundary layer 12 p1758 A83-29138
- Theory of optical-radiation diffraction by a nontransparent half-plane in a turbulent atmospheric layer 12 p1779 A83-29256
- Analysis of the shift-and-add method for imaging through turbulent media 12 p1779 A83-29375
- On the extraction of atmospheric turbulence parameters from radar backscatter Doppler spectra. I - Theory 12 p1758 A83-29427
- Mesospheric turbulence intensities measured with a HF radar at 35 deg S. II 12 p1759 A83-29428
- The turbulent dissipation of a cloud of heavy particles settling from a great height 13 p1872 A83-30295
- Fine Doppler resolution observations of thin turbulence structures in the troposphere at Millstone Hill 13 p1892 A83-30896
- Dome induced image motion --- in astronomical telescopes 13 p1920 A83-30999
- Seeing and the design and location of a 15 meter telescope 13 p1938 A83-31000
- Calculations of the intensity of a partially coherent optical beam in a turbulent atmosphere 14 p2023 A83-31908
- Correction of angular displacements of optical beams 14 p2083 A83-31911
- Three-dimensional space structure of turbulent eddy in the atmospheric boundary layer above the ocean 14 p2058 A83-32443
- Fluctuations of the parameters of an electromagnetic wave in a turbulent light absorbing atmosphere 14 p2052 A83-32559
- Investigation of a laboratory model of a developing convective vortex 14 p2059 A83-33398
- A theoretical study of radiative cooling in homogeneous and isotropic turbulence 15 p2156 A83-33671
- Receiver-aperture averaging effects for the intensity fluctuation of a beam wave in the turbulent atmosphere 15 p2168 A83-33811
- Relevance of mixed layer scaling for daytime dispersion based on raps and other field programs --- Regional Air Pollution Study 15 p2194 A83-34049
- Aperture averaging of scintillation for space-to-ground optical communication applications 15 p2144 A83-34454
- Monostatic diffraction-limited lidars - The impact of optical refractive turbulence 15 p2164 A83-34465
- Analysis of gravity-wave induced instabilities and turbulence viscosity parameters from optical emissions 16 p2374 A83-35377
- Low-resolution numerical simulation of decaying two-dimensional turbulence 16 p2385 A83-35470
- Stratified turbulence and the mesoscale variability of the atmosphere 16 p2385 A83-35471
- Turbulence structure in convective boundary layers and implications for diffusion 16 p2387 A83-35792
- Numerical experiments with a one-dimensional higher order turbulence model - Simulation of the Wangarda Day 33 case 16 p2387 A83-35795
- Seasonal transport and turbulence in the lower thermosphere 16 p2378 A83-36118
- Mesoturbulence --- in solar photosphere 16 p2440 A83-36852
- The role of turbulence in the heat balance of the mesosphere and lower thermosphere 17 p2537 A83-37052
- Variations of turbulent heat transfer in the mesosphere and lower thermosphere 17 p2537 A83-37053
- Spectral characteristics of different types of sporadic-E-layers and its low-frequency spectra 17 p2537 A83-37056
- Sizes of turbulence elements in the solar atmosphere 17 p2628 A83-38560
- The lateral response of an airship to turbulence [AIAA PAPER 83-1989] 17 p2459 A83-38915
- A note on estimating the vertical eddy diffusion coefficient from Landsat imagery 18 p2721 A83-39016
- Conditional sampling of turbulence in the atmospheric surface layer 18 p2721 A83-39110
- Procedure for generating ground wind environments for Shuttle liftoff studies 18 p2687 A83-40024
- HF Doppler measurements of mesospheric gravity wave momentum fluxes 18 p2718 A83-40044
- The scintillations for weak atmospheric turbulence using a partially coherent source 18 p2676 A83-40653
- Coupled flap-torsional response of a rotor blade in forward flight due to atmospheric turbulence excitations 19 p2801 A83-41073
- The establishment of hydrostatic and quasi-geostrophic balance in synoptic-scale disturbances in a polytropic turbulent atmosphere 19 p2867 A83-41581
- Turbulence originating from convectively stable internal waves 20 p3020 A83-42838
- Perturbation of the zonal flow by a local heat source 21 p3181 A83-45329
- The effect on heterodyne reception of motion of a source of optical radiation in the presence of atmospheric turbulence 22 p3271 A83-45654
- The influence of phase errors induced by the turbulent atmosphere on the spatial resolution in synthetic aperture radar systems 22 p3289 A83-46198
- The effect of the inertia of hydrometeors on the statistical characteristics of a radar signal 23 p3487 A83-47142
- Calculation of the turbulent regime in the boundary layer of the ocean 23 p3492 A83-47155

- Diagnostic study of the momentum balance in the Northern Hemisphere winter stratosphere
23 p3491 A83-47411
- The effects of target-induced speckle, atmospheric turbulence, and beam pointing jitter on the errors in remote sensing measurements
23 p3457 A83-47786
- Introduction to two-dimensional turbulence
23 p3448 A83-48038
- Scattering of a diffracted field by turbulent pulsations of the refractive index of the troposphere
23 p3443 A83-48481
- Intensity fluctuations in the case of the specular reflection of light beams in the turbulent atmosphere
23 p3463 A83-48482
- Radiation from fast particles in a turbulent medium --- cosmic ray showers
23 p3540 A83-48491
- Wave and turbulence structure in a disturbed nocturnal inversion
23 p3492 A83-48731
- Phase estimation based on the maximum likelihood criterion
24 p3582 A83-49016
- Dimension measurements for geostrophic turbulence
24 p3609 A83-49294
- Characteristics of downdrafts and turbulence within thunderstorms
24 p3616 A83-49734
- ATMOSPHERIC WINDOWS**
- Below room temperature measurements of the 8-12 micron water vapor continuum absorption
03 p0358 A83-13980
- Concerning the determination of the temperature of the ocean surface from multichannel satellite measurements of radiation in infrared atmospheric windows
03 p0372 A83-14316
- Infrared emissivity of water clouds
03 p0371 A83-14654
- Transparency of earth's atmosphere in the frequency region below 1 THz
04 p0510 A83-15815
- Scintillation fading in an absorption region
06 p0747 A83-18732
- Determination of the temperature of the earth's surface on the basis of the angular structure of radiation in atmospheric windows
07 p0958 A83-19913
- Submillimeter transmission of the atmosphere at Shorbulak, Eastern Pamirs
07 p0971 A83-21276
- An analytical model to calculate the atmospheric correction on infrared thermal signals
08 p1133 A83-21927
- Millimeter wave propagation measurements at the Ballistic Research Laboratory
08 p1076 A83-22353
- Atmospheric EHF window transparencies near 35, 90, 140, and 220 GHz
09 p1247 A83-23793
- Water vapor absorption at isotopic CO₂ laser wavelengths
09 p1269 A83-24446
- Calculation of absorption by wings of the H₂O monomer in the 8-13 micron atmospheric window
09 p1308 A83-25062
- Observation of global 160-min infrared /differential/ intensity variation of the sun
11 p1688 A83-27628
- Interpretation of temperature dependences of the absorption coefficient in the 8-12 micron atmospheric window on the basis of the generalized line profile
11 p1584 A83-28550
- Polarized microwave radiation transfer in precipitating cloudy atmospheres - Applications to window frequencies
13 p1878 A83-30900
- Efficient and durable AR coatings for Ge in the 8-11.5 micron band using synthesized refractive indices by evaporation of homogeneous mixtures
16 p2413 A83-36756

ATMOSPHERICS

- NT DAWN CHORUS
- NT HISS
- NT IONOSPHERICS
- NT WHISTLERS
- Atmospheric infrasound as a possible factor in the transferring of the effect of solar activity to the biosphere
02 p0221 A83-11891
- Sunrise effect on atmospheric and its relation to the direction of the night noise source
02 p0205 A83-11998
- Variations of atmospheric radio noise at 27 Kc/s in northern and central Europe during the period 1965-1975
04 p0509 A83-15025
- Low-frequency noise during an intense magnetic storm
06 p0786 A83-18367
- Hard limiter performance as a polarity detector for extremely polluted signals --- in Ioran C navigation systems
06 p0716 A83-19026
- The microwave radiation of lightning and thunderstorm atmospheric processes
09 p1310 A83-23392
- VLF radiometeorology - A model for interdisciplinary cooperation
09 p1310 A83-23402
- Progress in the large-scale determination and analysis of thunderstorm activity with the aid of atmospheric measurements
09 p1310 A83-23403
- Registration of thunderstorm centers by automatic atmospheric stations
09 p1314 A83-24277

- Approximation of atmospheric radio noise in the Arctic by the Hall model
09 p1251 A83-25166
- Modeling of atmospheric radio noise near thunderstorms
10 p1449 A83-26039
- Plasma waves in the Jovian magnetosphere
10 p1519 A83-26619
- A C-band weather radar system with spherics to serve multiple diverse users in the Canadian climate
11 p1631 A83-27096
- Various features of VLF waves generated by lightning discharge
11 p1619 A83-28429
- The different forms of atmospheric impulse and their conditions of propagation
14 p2052 A83-32412
- Radar observations of tornadoes and the field intensity of atmospherics
14 p2057 A83-32414
- Lightning and precipitation in a small multicellular thunderstorm
16 p2390 A83-36155
- Low-frequency (f less than about 1 Hz) stratospheric electrical noise measured by balloon-borne sensors
16 p2381 A83-36156
- Electron pitch-angle scattering by low frequency waves at the geomagnetic equator
17 p2545 A83-38602
- The struggle against sky noise in ground based and air-borne observations
18 p2691 A83-40438
- Development of a minicomputer atmospheric noise model
18 p2720 A83-40661
- VLF emissions at low latitudes and geomagnetic activity
19 p2866 A83-41564
- Hypotheses on the physical mechanisms of VHF-UHF radiation from lightning
21 p3178 A83-44319
- [ONERA, TP NO. 1983-45]
The 300 MHz electromagnetic radiation and electrostatic field associated with lightning discharges
21 p3178 A83-44320
- [ONERA, TP NO. 1983-46]
Spatial distribution of the polar chorus at high latitudes
21 p3176 A83-45265
- The global distribution of thunderstorm activity observed by the ionosphere Sounding Satellite (ISS-b)
21 p3182 A83-45451
- CRC handbook of atmospheric. Volumes 1 & 2
22 p3307 A83-45876
- Low frequency radio noise
22 p3273 A83-45881
- High frequency radio noise
22 p3273 A83-45882
- Atmospheric noise and its effects on telecommunication systems performance
22 p3273 A83-45883
- Sferics in the stratosphere
22 p3339 A83-45885
- Theory of low frequency wave propagation
22 p3273 A83-45889
- Instrumentation --- for atmospheric analysis
22 p3287 A83-45890
- Observation of HF noise in an intense aurora by the sounding rocket S-310JA-7
22 p3331 A83-46516
- Global distribution of atmospheric radio noise derived from distribution of lightning activity
22 p3275 A83-46918
- UHF interferometric imaging of lightning
23 p3492 A83-48177
- [ONERA, TP NO. 1983-55]
The peak electromagnetic power radiated by lightning return strokes
24 p3610 A83-49335
- Simultaneous pulses in light and electric field from stepped leaders near ground level
24 p3610 A83-49346

ATOM CONCENTRATION

- Metastable atom density in helium, neon, and argon glow discharges
04 p0538 A83-16059
- Atomic oxygen density deduced from limb-scans of the UV dayglow
05 p0659 A83-16469
- [AIAA PAPER 83-0021]
The effect of turbulence on the formation of large superequilibrium concentrations of atoms and free radicals in diffusion flames
06 p0727 A83-19426
- Resonance absorption measurements of atom concentrations in reacting gas mixtures. IX - Measurements of O atoms in oxidation of H₂ and D₂
10 p1480 A83-26182
- High latitude neutral atmosphere temperature and concentration measurements from the first Eiscat incoherent scatter observations
13 p1883 A83-31717
- The formation of a stable layer of atoms and ions of metals in the upper atmosphere
21 p3176 A83-45262

ATOMIC BATTERIES**U RADIOISOTOPE BATTERIES****ATOMIC BEAMS**

- Velocity-specific atomic-state selection in an atomic beam by continuous-wave optical pumping
05 p0651 A83-17881
- [AD-A127187]
Scattering of thermal He beams by crossed atomic and molecular beams. V - Anisotropic intermolecular potentials for He + CO₂, N₂O, C₂N₂
08 p1163 A83-22215
- Transient response in absorptive bistability
10 p1481 A83-25433
- Laser polarization of accelerated protons
15 p2228 A83-33785

- Superemission (collective spontaneous emission) of photons by atoms moving in a substance
16 p2361 A83-36966
- Diffraction of an atomic beam by standing-wave radiation
19 p2852 A83-40966
- Stabilization of a microwave oscillator using a resonance Raman transition in a sodium beam
20 p2965 A83-42346
- Semiconductor detector for the selective detection of atomic hydrogen
23 p3454 A83-47643
- Longitudinal Ramsey-fringe spectroscopy in a calcium beam --- for optical frequency standard
23 p3509 A83-48707
- Observation of absorptive bistability with two-level atoms in a ring cavity
24 p3628 A83-48847
- Generation of high-intensity precision ion and atom beams
24 p3632 A83-49553

ATOMIC CLOCKS

- Phase-locked loops used with masers - Atomic frequency standards
03 p0331 A83-13865
- Uncertainties regarding the transmission of time and frequency
09 p1336 A83-23401
- Atomic clocks for astrophysical measurements
11 p1572 A83-27729
- Optimal on-board clock control
11 p1573 A83-28140
- Performance of the four NRC long-beam primary cesium clocks Cs V, Cs VIA, Cs VIB, and Cs VIC
13 p1847 A83-31293
- On-board clock correction by drift prediction
19 p2832 A83-41392
- Modeling of frequency random walk instability and effects on spectral spreading
19 p2832 A83-41394
- Ultra-stable laser clock - Second generation
20 p2989 A83-42576
- Estimation of parameters in models for Cesium beam atomic clocks
20 p2990 A83-42944
- Estimating time from atomic clocks
20 p2990 A83-42945
- Test of the principle of equivalence by a null gravitational red-shift experiment
22 p3380 A83-46714

ATOMIC COLLISIONS

- Charge transfer at large scattering angles in asymmetric ion-atom collisions
01 p0105 A83-10195
- Measurements of collisional broadening and the shift of argon spectral lines using a tunable diode laser
01 p0105 A83-10203
- Electron impact cross sections for the 2,2P state excitation of lithium
03 p0391 A83-13225
- Atomic collisions in the presence of laser radiation - Time dependence and the asymptotic wave function
03 p0391 A83-13247
- Single and multiple ionization of sulfur atoms by electron impact --- in lo plasma torus
05 p0707 A83-17783
- Three-photon excitation of hydrogen Rydberg states
05 p0684 A83-17880
- Modified-independent-atom-model /MIAM/ calculations for e-CO₂ elastic scattering at 50-500 eV
06 p0807 A83-18040
- Correlation effects in collisional depolarisation and redistribution of radiation
06 p0808 A83-19010
- Experimental evidence for collision-induced superradiance
07 p0937 A83-20797
- A high-density effusive target of atomic hydrogen
08 p1162 A83-21981
- Binary encounter calculations for electron capture from noble gases by He/2+ /
08 p1167 A83-21987
- Energy loss of slowly moving magnetic monopoles in matter
08 p1192 A83-22640
- A new class of atomic states - The 'Wannier-ridge' resonances
09 p1342 A83-24143
- A determination of the potential of the interatomic interaction on the basis of the function for the single scattering of a gas by a surface
09 p1339 A83-24491
- Auger spectroscopy of quasi-molecules
09 p1343 A83-25089
- The superradiance of a polyatomic system with allowance for the Coulomb interaction
09 p1273 A83-25090
- Analysis of the far infrared H₂-He spectrum
09 p1343 A83-25214
- Spectral distribution of CO₂ vibrational states produced by collisions with fast hydrogen atoms from laser photolysis of HBr
10 p1478 A83-25555
- Coherent emission by relativistic particles interacting with atomic rows during reflection from a crystal surface
10 p1489 A83-26237
- A theoretical study on the mechanism of electronic to vibrational energy transfer in Hg/3P/ + CO
11 p1655 A83-28529
- Charge transfer reaction of O(3+) + H yields O(2+) + H(+) in low energy collision
12 p1777 A83-29005

- Experimental study of the pure rotational S1 line of the H2-He spectrum induced by an absorption defect collision due to collisional interference effects 12 p1778 A83-29390
- Excimer laser photolysis studies of translational-to-vibrational energy transfer in collisions of H and D atoms with CO [AD-A129931] 13 p1916 A83-30952
- Rotational and vibrational-rotational relaxation in collisions of CO2(01¹/0) with He atoms 13 p1916 A83-30953
- Laser studies of electronic energy transfer in atomic copper 13 p1851 A83-30957
- Oscillator strengths and collision strengths for S II --- atomic spectra of Io plasma torus 13 p1962 A83-31440
- Theory of time-dependent intense-field collisional resonance fluorescence 14 p2079 A83-31925
- Fine-structure transitions occurring in collisional redistribution of light 15 p2227 A83-33795
- The neutral particle impact de-excitation cross-section of the fine structure level P-3 sub one of atomic oxygen in the thermosphere 16 p2373 A83-35372
- Effects of autoionizing levels in highly ionized atoms 16 p2409 A83-35635
- Excited states created in charge transfer collisions between atoms and highly charged ions 16 p2409 A83-35636
- Redistribution - Why half a collision is better than a whole one --- spectra of scattered light from perturbed atomic system 17 p2484 A83-37075
- The 1D-3P transition in atomic oxygen induced by collisions with atomic hydrogen 17 p2578 A83-37341
- Charge transfer and ionisation processes involving multiply charged ions in collision with atomic hydrogen 18 p2742 A83-39447
- Rydberg atoms 18 p2743 A83-40003
- Balmer-alpha and Balmer-beta emission cross sections for low-energy H collisions with He and H2 18 p2743 A83-40408
- Proposal for high-power radiative-collisional lasers [AD-A122225] 19 p2850 A83-40671
- Transport properties of ground state nitrogen atoms 19 p2906 A83-40773
- Associative ionization in collisions between two Na(3P) atoms 22 p3361 A83-45926
- Total and partial cross sections for electron capture in collisions of hydrogen atoms with fully stripped ions 22 p3361 A83-45927
- Rb and Cs broadening of the Na resonance lines 24 p3626 A83-48835
- Electron collisional rate coefficients for low-level transitions in hydrogen 24 p3626 A83-49386
- ATOMIC ENERGY**
- U NUCLEAR ENERGY**
- ATOMIC ENERGY LEVELS**
- Effect of electronic excitations on laser heating of a stationary plasma 01 p0107 A83-10698
- Energy values and sum rules for hydrogenic atoms in magnetic fields of arbitrary strength using numerical wave functions - Comparison with variational results 02 p0257 A83-12145
- Measurement of relative oscillator strengths for Fe I: Transitions from levels /b-3/-F/2-4/ /2.61 eV-2.56 eV/ - Use of a multipass optical system 03 p0413 A83-13318
- Precision measurement of relative oscillator strengths for Ti II. I - Transitions from levels /a-4/-F/3/2-9/2/ /0.00-0.05 eV/, /b-4/-F/5/2-9/2/ /0.12-0.15 eV/ 03 p0413 A83-13319
- Precision measurement of relative oscillator strengths for Ti II. II - Transitions from levels /a-5/-F/1-4/ /0.81-0.84 eV/, /a-1/-D/2/ /0.90 eV/ and /a-3/-P/0-2/ /1.5-1.07 eV/ 03 p0413 A83-13320
- A mechanism for the formation and breakdown of O1 levels in the positive column of a glow discharge in O2 05 p0689 A83-17691
- Three-photon excitation of hydrogen Rydberg states 05 p0684 A83-17880
- Velocity-specific atomic-state selection in an atomic beam by continuous-wave optical pumping [AD-A127187] 05 p0651 A83-17881
- Wavefunctions and oscillator strengths for Si II 06 p0827 A83-18164
- Excitation rate coefficients from the ground state of atomic hydrogen to the n = 2 and n = 3 levels 06 p0811 A83-18185
- The spectrum of neutral sulfur /S I/ in the vacuum ultra-violet 06 p0808 A83-18817
- Light-induced drift in cascade excitation of levels --- laser effects on atomic energy levels 07 p0934 A83-20117
- Persistence of two-state resonances in a hydrogen atom under the influence of a periodic impulsive field 08 p1162 A83-21984
- Multiconfiguration Hartree-Fock Breit-Pauli results for 2P1/2-2P3/2 transitions in the boron sequence 08 p1162 A83-21985
- Energies and widths for the series 2s2p/6/nl /neon and magnesium/ and the series 3s3p/6/nl /argon/ 09 p1341 A83-23659
- A new class of optical multistabilities and instabilities induced by atomic coherence 10 p1481 A83-25434
- Photoionisation of krypton atoms in 'strong' electric fields 11 p1653 A83-27512
- The theory of the quadratic Zeeman effect for highly excited hydrogen atoms 11 p1654 A83-28056
- The ground state of an atom moving in a medium 11 p1654 A83-28067
- Laser techniques for spectroscopy of core-excited atomic levels 13 p1819 A83-31811
- Effects on partial frequency redistribution R(II) on the level population ratios in a resonance line --- for stellar spectrum analysis 15 p2271 A83-34776
- Absorption and emission line profile coefficients of multilevel atoms. I - Atomic profile coefficients. II Velocity-averaged profile coefficients 15 p2227 A83-34991
- Rydberg series in the absorption spectrum of Te I limiting on 5s(2)5p(3) (4)S(0)3/2 15 p2228 A83-35296
- Energy levels of atomic nitrogen calculated in a multiconfiguration optimized potential model 15 p2228 A83-35297
- Spectra of the ironlike ions from Y XIV to Ag XXII 15 p2228 A83-35298
- The neutral particle impact de-excitation cross-section of the fine structure level P-3 sub one of atomic oxygen in the thermosphere 16 p2373 A83-35372
- Excited states created in charge transfer collisions between atoms and highly charged ions 16 p2409 A83-35636
- Proton excitation of fine-structure transitions in Fe XIV 16 p2410 A83-35652
- Transition probability of the Si III 189.2-nm intersystem line 16 p2427 A83-35657
- Determination of natural radiative lifetimes of the 5p2 P state in Ga I and 6p2 P state in In I using a pulsed dye laser 16 p2410 A83-36653
- Radiative recombination of the ground state of lithium-like ions 17 p2578 A83-37934
- Proposed quantum-beats, quantum-eraser experiment 17 p2579 A83-38957
- Initiation of superfluorescence in a three-level 'sweep-gain' amplifier 19 p2853 A83-41178
- An ab initio study of core-valence correlation --- in atoms 20 p3045 A83-42636
- The current state of the theory of the spectra of multiply charged ions 21 p3213 A83-44651
- Second order perturbation theory for the hydrogen atom in crossed electric and magnetic fields 21 p3202 A83-45206
- Remote quantum mechanical detection of gravitational radiation 22 p3380 A83-46752
- Magnesium II line formation - The contribution of high atomic levels to the resonance lines 23 p3530 A83-47438
- Study of the autoionising states of the hydrogen atom in intense magnetic fields by the complex coordinate coupled-channel formalism 23 p3506 A83-48576
- Observation of absorptive bistability with two-level atoms in a ring cavity 24 p3628 A83-48847
- Rydberg atoms in 'circular' states 24 p3626 A83-49293
- Electron collisional rate coefficients for low-level transitions in hydrogen 24 p3626 A83-49386
- ATOMIC EXCITATIONS**
- A single quantum cannot be cloned 02 p0234 A83-11622
- Time resolved study of superelastic collisions in laser excited strontium vapor 02 p0241 A83-12399
- Measurement of the excited-atom density in a discharge in neon by laser resonance fluorescence 03 p0396 A83-13185
- A laser-based measurement of electron collision rates for excited states of ionised helium in a plasma 03 p0398 A83-14662
- Three-photon excitation of hydrogen Rydberg states 05 p0684 A83-17880
- Excitation rate coefficients from the ground state of atomic hydrogen to the n = 2 and n = 3 levels 06 p0811 A83-18185
- Theory of nonstationary kinetic ionization, recombination and population of excited states 06 p0811 A83-18438
- Excitation of atoms by collisions with ions - Photon-ion angle correlation measurements for determining the scattering amplitudes in magnetic substates for He/+/- + He and He/+/- + Ne systems --- German thesis 06 p0808 A83-18524
- Correlation effects in collisional depolarisation and redistribution of radiation 06 p0808 A83-19010
- Radiative lifetimes of excited Ar II states 06 p0809 A83-19011
- Electron impact excitation of forbidden transitions in Si IX 06 p0835 A83-19012
- The dynamic polarizability of highly excited hydrogen-like states 06 p0809 A83-19185
- Quantization rules and instabilities of highly excited hydrogen atom in a strong magnetic field 07 p0991 A83-20605
- A semiclassical study of laser-induced atomic fluorescence from Na2, K2 and NaK [AD-A127849] 07 p0991 A83-21051
- Atomic photoionization 07 p0992 A83-21068
- Measurement of the cross sections for excitation of a singly charged iron ion by electron impact --- stellar spectra 07 p1027 A83-21278
- Isotopically selective photoionization of mercury atoms 07 p0991 A83-21358
- The doubly excited autoionizing states of H2 08 p1163 A83-22220
- Effective collision strengths for electron excitation of the ground state of O VII to the 2/3/S and 2/3/P states 09 p1347 A83-23652
- A new class of atomic states - The 'Wannier-ridge' resonances 09 p1342 A83-24143
- Observation of resonantly enhanced sum-frequency generation involving sodium Rydberg states 10 p1429 A83-26113
- Stimulated Raman scattering by particles captured in a trap 10 p1431 A83-26651
- Vacuum ultraviolet monochromator calibration using measured atomic branching ratios 10 p1484 A83-26857
- Billiard ball echo model --- atomic recoil model of photo, Raman and grating echoes in gases 11 p1654 A83-27615
- Generation and application of coherent radiation at Lyman-alpha 11 p1583 A83-27619
- The theory of the quadratic Zeeman effect for highly excited hydrogen atoms 11 p1654 A83-28056
- Formation of highly excited Ar and Kr atoms in the case of asymmetric charge transfer of Ar(+) and Kr(+) ions with rare-gas atoms 13 p1915 A83-30019
- The threshold laws for electron-atom and positron-atom impact ionization 13 p1915 A83-30177
- Hydrogen and lithium atoms in a strong electric field 13 p1915 A83-30266
- Angular distribution for electron excitation of the 4(2)S yields 4(2)P transition in Zn II - Comparison of experiment and theory 13 p1926 A83-30917
- The possibility of achieving the breakdown of the vibrational temperature of nitrogen in a decaying plasma at high pressure 13 p1926 A83-31336
- Oscillator strengths and collision strengths for S II --- atomic spectra of Io plasma torus 13 p1962 A83-31440
- Line ratios for O VII --- solar spectra 13 p1965 A83-31712
- Laser techniques for spectroscopy of core-excited atomic levels 13 p1819 A83-31811
- The spectral properties of filamentary, physically inhomogeneous prominences. II - Hydrogen (second level excitation, ionization) 14 p2113 A83-31832
- The quantum beats of the coherent radiation of atoms in a magnetic field 14 p2082 A83-32138
- Sidebands in cooperative resonance fluorescence in collections of N three-level atoms in strong excitation laser fields 15 p2169 A83-34371
- Energy levels of atomic nitrogen calculated in a multiconfiguration optimized potential model 15 p2228 A83-35297
- The neutral particle impact de-excitation cross-section of the fine structure level P-3 sub one of atomic oxygen in the thermosphere 16 p2373 A83-35372
- Proton excitation of fine-structure transitions in Fe XIV 16 p2410 A83-35652
- Elastic scattering of electrons by hydrogen atoms in the 2S state 16 p2410 A83-35654
- Excitation mechanisms for hydrogen atoms in an inverse-brush-cathode discharge 16 p2415 A83-35668
- Observation of cavity-enhanced single-atom spontaneous emission 16 p2410 A83-35746
- Laser-modified electron scattering from a slowly ionising atom 17 p2579 A83-38366
- Collision strengths for the N = 2 excitation of hydrogenic ions 17 p2583 A83-38960
- Rydberg atoms 18 p2743 A83-40003
- Investigation of superelastic electron scattering by laser-excited Ba - Experimental procedures and results 18 p2743 A83-40407
- Density-functional theory of excitation spectra of semiconductors - Application to Si 19 p2905 A83-41159
- Photoionization of atoms near threshold 19 p2898 A83-41179

- Antibunching in the Franck-Hertz experiment --- subpicosecond light generation from space-charge limited electron beams colliding with atoms
19 p2900 A83-41189
- Dephasing in steady-state and time-varying spectroscopy
20 p3044 A83-42264
- Novel short-pulse photoionization electron source - Li (1s2s2p)4P0 deexcitation measurements in a plasma
21 p3209 A83-43885
- Electron excitation rates among fine structure levels in O III
21 p3227 A83-44112
- Effect of potential fluctuations in a plasma on the population of highly excited atomic states
21 p3211 A83-44145
- Quantum cyclotron resonance in silicon
21 p3216 A83-44383
- Electron-induced excitation and ionization of multiply-charged ions
21 p3213 A83-44652
- Dielectronic recombination
21 p3213 A83-44654
- Correlation and the 3s2 3p5 2P0 to 3s 3p6 2S, 3s2 3p5 2P0 to 3s2 3p4 3d2S transitions in Fe X
21 p3202 A83-44749
- Radiative transitions between highly-excited atomic states in the presence of a strong microwave field
21 p3202 A83-45205
- Electron impact excitation of lambda 7990-A multiplet
22 p3355 A83-46061
- Observations of self-induced Rabi oscillations in two-level atoms excited inside a resonant cavity - The ringing regime of superradiance
23 p3461 A83-47609
- Electron excitation of Ca XVII
23 p3506 A83-48580
- Atomic photoionization in a strong magnetic field
24 p3626 A83-48833
- Nonlinear noise fields and strongly driven atomic transitions
24 p3587 A83-48839
- Recent advances in atomic calculations and experiments of interest in the study of planetary nebulae
24 p3651 A83-49137
- Rydberg atoms in 'circular' states
24 p3626 A83-49293
- Electron collisional rate coefficients for low-level transitions in hydrogen
24 p3626 A83-49386
- The measurement of the cross sections of excitation of several quartet states of the cobalt atom by electron impact
24 p3626 A83-49737
- 2P photoionization cross section of Sb I
24 p3627 A83-49751

ATOMIC EXPLOSIONS

U NUCLEAR EXPLOSIONS

ATOMIC GASES

U MONATOMIC GASES

ATOMIC MASS

U ATOMIC WEIGHTS

ATOMIC PHYSICS

- Study of the energy relaxation of sputtered atoms in a plasma
04 p0536 A83-15701
- Conference on the Application of Accelerators in Research and Industry, 7th, North Texas State University, Denton, TX, November 8-10, 1982, Proceedings
13 p1917 A83-30176
- Production and physics of highly charged ions; Proceedings of the International Symposium, Stockholm, Sweden, June 1-5, 1982
16 p2409 A83-35626
- An EBIS for atomic physics experiments --- Electron Beam Ion Source
16 p2409 A83-35628
- Radiationless transitions to atomic M 1,2,3 shells - Results of relativistic theory
16 p2410 A83-35656

ATOMIC RECOMBINATION

NT OXYGEN RECOMBINATION

- Concerning sources of O/1D/ in Aurora - Electron impact and dissociative recombination
11 p1619 A83-28326
- Principal and dielectronic satellite line spectra for Ca XIX SMM observations --- Solar Maximum Mission
13 p1965 A83-31713
- Direct radiative recombination of electrons with atomic ions Cross sections and rate coefficients
16 p2415 A83-35655

ATOMIC SPECTRA

- Wavefunctions and oscillator strengths for Si II
06 p0827 A83-18164
- The spectrum of neutral sulfur /S I/ in the vacuum ultra-violet
06 p0808 A83-18817
- Correlation effects in collisional depolarisation and redistribution of radiation
06 p0808 A83-19010
- A determination of the collision relaxation constants for a forbidden transition by means of nonlinear polarization spectroscopy for a three-level gas in a magnetic field
06 p0809 A83-19541
- Internal motions in planetary nebulae - NGC 7354, 1289 and Hu 1-2
07 p1014 A83-20570

The use of precision oscillator strengths as a means for obtaining large numbers of moderately accurate gf-values --- spectral line intensity

- 07 p0991 A83-20926
- Atomic photoionization
07 p0992 A83-21068
- Non-resonance lines of neutral calcium in the spectra of Arcturus and Beta Virginis
07 p1024 A83-21227
- EUV branching ratios for ionized nitrogen and oxygen emissions
07 p0991 A83-21396
- An investigation of the distributions of the equilibrium charge states in carbon, the emission spectroscopy and the mean radiative lifetimes of aluminum ions /Al VI-X/
08 p1163 A83-21986
- Inner-shell transitions in Fe XIX-XXII in the X-ray spectra of solar flares and Tokamaks
08 p1192 A83-23075
- Density-dependent Si XII dielectronic satellite spectra
09 p1347 A83-23655
- Measurement of oscillator strengths in the ultraviolet by magneto-optical rotation
09 p1341 A83-23656
- K-alpha and K-beta spectra from M-shell-ionized ions produced in a vacuum spark
10 p1485 A83-25410
- Interaction of ruby laser radiation with thallium vapor
10 p1433 A83-26678
- Photoionisation of krypton atoms in 'strong' electric fields
11 p1653 A83-27512
- Peculiar asymmetry in the wings of self-broadened Li and Na first resonance lines
11 p1654 A83-27847
- Atomic calculations for Ca XVII - UV and X-ray lines
12 p1799 A83-28866
- Experimental study of the pure rotational S1 line of the H2-He spectrum induced by an absorption defect collision due to collisional interference effects
12 p1778 A83-29390
- Oscillator strengths and collision strengths for S II --- atomic spectra of Io plasma torus
13 p1962 A83-31440
- Moderately accurate oscillator strengths from NBS intensities. II --- for application to astronomical spectroscopy
13 p1917 A83-31690
- Principal and dielectronic satellite line spectra for Ca XIX SMM observations --- Solar Maximum Mission
13 p1965 A83-31713
- Collisional broadening of intra-Doppler resonances of selective reflection on the D2 line of cesium
14 p2082 A83-32619
- The extreme ultraviolet day airglow
15 p2196 A83-33942
- Atomic absorption spectroscopy in studying metal vaporization --- Russian book
15 p2133 A83-34750
- The non-LTE analysis of carbon lines in the spectra of hot stars. I - C III lambda 4650 and lambda 9710 A triplet lines in the spectra of O stars
15 p2271 A83-34763
- Improved Ar(II) transition probabilities
15 p2236 A83-34993
- Rydberg series in the absorption spectrum of Te I limiting on 5s(2)5p(3) (4)S(0)3/2
15 p2228 A83-35296
- Energy levels of atomic nitrogen calculated in a multiconfiguration optimized potential model
15 p2228 A83-35297
- Spectra of the ironlike ions from Y XIV to Ag XXII
15 p2228 A83-35298
- Empirical improvement in accuracy of atomic oscillator strengths calculated by Kurucz and Peytremann --- of relevance to model stellar atmospheres
17 p2606 A83-38240
- Line broadening in multiphoton processes with a resonant intermediate transition
18 p2743 A83-39924
- Half-widths of neutral fluorine spectral lines
19 p2897 A83-40714
- Theory of spontaneous-emission line shape in an ideal cavity
19 p2898 A83-41155
- The current state of the theory of the spectra of multiply charged ions
21 p3213 A83-44651
- High resolution spectroscopy using picosecond pulse trains
21 p3140 A83-44818
- General consideration of electronic transitions in many-electron atoms and ions
23 p3506 A83-48577
- Explicit Hilbert-space representations of atomic and molecular photoabsorption spectra - Computational studies of Stieltjes-Tchebycheff functions
24 p3625 A83-48826
- Moessbauer study of the lattice location of Co-57 implanted in graphite
24 p3636 A83-49756

ATOMIC STRUCTURE

- Mechanisms of defect formation and migration in semiconductors --- Russian book
02 p0242 A83-11924
- A structural interpretation of the infrared absorption spectra of a-Si:H:O alloys
04 p0541 A83-15515
- Optical properties of a-Si:H and a-SiC1-x:H films prepared by glow-discharge deposition
04 p0541 A83-15522
- Defects in amorphous III-V compounds
04 p0542 A83-15531

- Grain boundary diffusion mechanisms in metals
04 p0460 A83-16001
- Quantum-chemical modeling of smectite clays
07 p0873 A83-21044
- Electron coincidence spectroscopy - An introduction to momentum space chemistry
09 p1342 A83-24144
- The electrical properties and electron structure of niobium-molybdenum alloys
09 p1349 A83-24220
- The effect of alloying on the physical properties, electron structure, and phase stability of titanium alloys
09 p1234 A83-24378
- NMR studies of electronic structure in crystalline and amorphous Zr2PdH/x/
10 p1488 A83-25411
- Theory of silicon superlattices - Electronic structure and enhanced mobility
11 p1664 A83-28710
- Solution of the Schroedinger equation by a spectral method
12 p1776 A83-29633
- The features of the atomic structure of pure inorganic ferroelastics
13 p1928 A83-30311
- Observation and quasistatic analysis of structure in microwave ionization of highly excited helium atoms
13 p1915 A83-30597
- Energy levels of atomic nitrogen calculated in a multiconfiguration optimized potential model
15 p2228 A83-35297
- Multi-charged ion spectroscopy
16 p2414 A83-35629
- The electron structure and properties of solids --- Russian book
19 p2905 A83-41995
- New trend of atom resolution electron microscopy - Direct observations of atoms, vacancies and impurity atoms in crystal and on-line image analysis
20 p2992 A83-43609
- Many-beam imaging studies of crystal structure of ordered alloys
20 p2992 A83-43610
- Monatom-high level electron microscopy of metal surfaces
20 p2992 A83-43611
- Atomic structure of alloys rapidly quenched from the melt
20 p2956 A83-43612
- High resolution lattice images of G.P. zones in an Al-3.97 wt pct Cu alloy --- Guinier-Preston
20 p2956 A83-43613
- The structure of boron in boron fibres
21 p3116 A83-44342
- Nuclear magnetic resonance in compounds of variable composition --- Russian book
23 p3511 A83-47149
- Electronic structure and ordering in transition alloys and compounds
23 p3432 A83-48185
- Supplemental basis functions for the second transition row elements
24 p3552 A83-48800

ATOMIC THEORY

NT HEISENBERG THEORY

- Vibrations of the atomic nucleus
12 p1778 A83-29248
- Theory of spontaneous-emission line shape in an ideal cavity
19 p2898 A83-41155

ATOMIC WEIGHTS

- Sensitivity of determining the atomic number of materials on the basis of bremsstrahlung backscattering
02 p0188 A83-12162
- On corotating high-z HI --- in inner Galaxy
18 p2770 A83-39665

ATOMIZATION

U ATOMIZING

ATOMIZERS

- Effect of air, liquid and injector geometry variables upon the performance of a plain-jet airblast atomizer
16 p2351 A83-35809
- Influence of atomizer design features on mean drop size
19 p2800 A83-40865
- Spray characteristics of plain-jet airblast atomizers [ASME PAPER 83-GT-138]
23 p3448 A83-47965

ATOMIZING

NT GAS ATOMIZATION

NT LIQUID ATOMIZATION

- Atomization of impinging liquid jets in a supersonic crossflow
[AD-A130714]
07 p0924 A83-19806
- Flames with impinging jets
07 p0882 A83-21423
- The effect of fuel atomization on soot-free combustion in a prevaporizing combustor
16 p2303 A83-35812
- Rotary cup slurry atomization [AIAA PAPER 83-1363]
16 p2353 A83-36359
- Aerodynamic-wave break-up of liquid sheets in swirling airflows and combustor modules [AIAA PAPER 83-1204]
21 p3133 A83-45511

ATOMS

- NT HELIUM ATOMS
- NT HOT ATOMS
- NT HYDROGEN ATOMS
- NT METASTABLE ATOMS
- NT NEUTRAL ATOMS
- NT NITROGEN ATOMS
- NT OXYGEN ATOMS
- NT RECOIL ATOMS

ATP

U ADENOSINE TRIPHOSPHATE

ATROPHY

- Effect of hindlimb immobilization on the fatigability of skeletal muscle 14 p2064 A83-32813
- A clinical and electroneuromyographic investigation of vegetative neuromuscular syndromes 14 p2070 A83-33309
- Research on the adaptation of skeletal muscle to hypogravity Past and future directions 19 p2877 A83-42047

ATROPINE

- The effect of preparations acting mainly in the region of the peripheral M-choline reactive systems on bone marrow eosinophils 14 p2066 A83-33332

ATS

- NT ATS 1
- NT ATS 6

ATS 1

- Pacific Telecommunications after ATS-1 - Reflections on ATS-1's fifteenth birthday 07 p0903 A83-19652

ATS 6

- Ground-Satellite correlative study of a giant pulsation event 03 p0357 A83-13299
- Geostationary satellites ATS-6 and SMS/GOES - Description, position and data availability during IMS 04 p0511 A83-16283
- PC 4 - PC 1 magnetic pulsations at synchronous orbit and their relation to pulsations on the ground 05 p0660 A83-17393
- A threshold effect for spacecraft charging 06 p0723 A83-18322
- Observation of an IMF sector effect in the Y magnetic field component at geostationary orbit 07 p0968 A83-21582
- The interpretation of protons and electrons observations from ATS 6 satellite within the frame of McIlwain's electric field model 23 p3482 A83-48055

ATTACK AIRCRAFT

- NT A-6 AIRCRAFT
- NT A-7 AIRCRAFT
- NT A-10 AIRCRAFT
- NT AH-64 HELICOPTER
- NT ALPHA JET AIRCRAFT
- NT B-1 AIRCRAFT
- NT B-52 AIRCRAFT
- NT B-58 AIRCRAFT
- NT BOMBER AIRCRAFT
- NT F-4 AIRCRAFT
- NT F-5 AIRCRAFT
- NT F-8 AIRCRAFT
- NT F-14 AIRCRAFT
- NT F-15 AIRCRAFT
- NT F-16 AIRCRAFT
- NT F-17 AIRCRAFT
- NT F-18 AIRCRAFT
- NT F-104 AIRCRAFT
- NT F-111 AIRCRAFT
- NT FIGHTER AIRCRAFT
- NT JAGUAR AIRCRAFT
- NT YF-12 AIRCRAFT

- Pilot workload in the night attack mission 01 p0086 A83-11187
- Estimation of helicopter and target motion for the advanced attack helicopter fire control system 06 p0715 A83-18378
- Naval aviation mishaps and fatigue 15 p2215 A83-34985
- Design for testing of a low altitude night-in-weather attack system [AIAA PAPER 83-1061] 16 p2298 A83-36470
- Frogfoot - A new Shtrumovik on trial 19 p2797 A83-41320
- STOL attack aircraft design based on an upper surface blowing concept [AIAA PAPER 83-2535] 23 p3405 A83-48369

ATTENTION

- The human factor in mishaps - Psychological anomalies of attention 04 p0523 A83-15413
- The cortical evoked negative wave as a reflection of selective attention 06 p0799 A83-18967
- Incorporation of a test of selective attention in a pilot selection battery 10 p1457 A83-26335
- Naloxone augments electrophysiological signs of selective attention in man 21 p3189 A83-44996
- Attending to different levels of structure in a visual image 22 p3349 A83-45954
- Color segregation and selective attention in a nonsearch task 22 p3349 A83-45955

ATTENUATION

- NT ACOUSTIC ATTENUATION
- NT ATMOSPHERIC ATTENUATION
- NT AURORAL ABSORPTION
- NT MICROWAVE ATTENUATION
- NT RADAR ATTENUATION
- NT RADIO ATTENUATION

NT SHOCK WAVE ATTENUATION

NT SIDELOBE REDUCTION

NT WAVE ATTENUATION

- Wake vortex attenuation flight tests - A status report 02 p0134 A83-11806
- Measurement of laser beam divergence 13 p1844 A83-30202

ATTENUATION COEFFICIENTS

- Transmission characteristics of a pulsed laser beam in natural sea-water - Determination of the attenuation coefficients in the 415-660 nm spectral range 01 p0054 A83-10695
- Evaluation of the atmospheric content of particulate mass from visibility observations 01 p0072 A83-11046
- Microwave propagation in sand and dust storms 02 p0162 A83-11551
- Horizon line scanning telephotometry 03 p0325 A83-13496
- An analysis of the efficiency of a noise self-compensator with correlation feedback with respect to the suppression coefficient 04 p0470 A83-15143
- First measurement of a superconducting microstrip-line attenuation constant at 10 GHz 04 p0472 A83-16024
- An analytical model to calculate the atmospheric correction on infrared thermal signals 08 p1133 A83-21927
- Millimeter wave atmospheric turbulence measurements - Preliminary results and instrumentation for future measurements 08 p1076 A83-22354
- Extinction by clouds consisting of polydisperse and randomly oriented nonspherical particles at arbitrary wavelengths 08 p1135 A83-22356
- Lidar calibration and extinction coefficients 08 p1077 A83-22612
- Inverse-square wavelength dependence of attenuation in infrared polycrystalline fibers 10 p1482 A83-26116
- Investigation of the damping constant for profiles of neutral iron lines in the undisturbed solar photosphere 16 p2440 A83-36851
- Optical characteristics of equatorial-Atlantic waters 19 p2870 A83-42105
- Spatial-temporal variability of the optical attenuation coefficient of sea water 19 p2870 A83-42106
- Attenuation at 10.6 microns in loaded and unloaded polycrystalline KRS-5 fibers 24 p3629 A83-49017

ATTENUATORS

NT RESISTORS

NT THERMISTORS

- Precise calibration of a rotary vane attenuator at 35 GHz using a homodyne network analyser 04 p0470 A83-15244
- Cryogenic X-band ferrite phase shifter/attenuator 08 p1079 A83-21977
- Precision broad-band RF-switched radiometer for the Megahertz and lower Gigahertz range with IF attenuator 13 p1847 A83-31294
- Toward attenuation of self-sustained oscillations of a turbulent jet through a cavity 23 p3453 A83-48680

ATTITUDE (INCLINATION)

NT PITCH (INCLINATION)

NT ROLL

NT SATELLITE ORIENTATION

NT YAW

- Effects of tilt of a four-bar pattern on the minimum resolvable temperature difference /MRTD/ --- of FLIR detectors 08 p1105 A83-22899
- The orientation in space of spiral galaxies in the local supercluster 09 p1359 A83-24457
- Non-parallel operation of conical hydrostatic thrust bearings 15 p2172 A83-35243
- Attitude determination, control and navigation of a spinning satellite 17 p2475 A83-37445
- Attitude measurement and estimation of solar observation satellites 17 p2478 A83-37451
- Flight at supernormal attitudes [SAE PAPER 821469] 17 p2470 A83-38000
- Attitude determination for a rigid body 21 p3199 A83-44635

ATTITUDE CONTROL

NT DIRECTIONAL CONTROL

NT LATERAL CONTROL

NT LONGITUDINAL CONTROL

NT SATELLITE ATTITUDE CONTROL

NT THRUST VECTOR CONTROL

- The measurement of impulsive forces on a wind tunnel model with a conventional strain gage balance 01 p0014 A83-11069
- Control - Demands mushroom as station grows 09 p1216 A83-24355
- HEAO project - Revisited --- attitude control system design for spaceborne astronomy 10 p1385 A83-26585

- A sensitivity analysis of modal controller for flexible space structures 10 p1385 A83-26587
- Optimal solar pressure attitude control of spacecraft. I - Inertially-fixed attitude stabilization. II - Large-angle attitude maneuvers 11 p1536 A83-27341
- Space vehicle attitude determination and surface vessel position fixing - A common analytical solution 11 p1536 A83-28598

- Inertial upperstage attitude initialization and update on Space Shuttle 11 p1534 A83-28777
- Sensing relative attitudes for automatic docking 13 p1809 A83-30169

- Heating measurements on Space Shuttle Orbiter models with differentially deflected elevons [AIAA PAPER 83-1534] 14 p2011 A83-32763
- Development of a reaction wheel-based attitude control system for balloon-borne infrared astronomical observation 15 p2119 A83-34000
- Tiny engine combines muscle and fast response 16 p2318 A83-35766

- Comparison of electric and chemical thruster systems for secondary propulsion on a large space system [AIAA PAPER 83-1393] 16 p2322 A83-36383
- Modeling rotational dynamics of a flexible space platform for application of multilevel attitude control 17 p2476 A83-37108

- The attitude and orbit control system for GIOTTO, ESA's Halley encounter mission 17 p2476 A83-37435
- Space platform attitude control system 17 p2477 A83-37436

- State synthesiser - A digital observer for spacecraft attitude control systems 17 p2569 A83-37452
- Star detection and tracking using CCDs 17 p2481 A83-37464

- An advanced star tracker design using the charge injection device 17 p2481 A83-37465
- Ion attitude control circuit operational experience 17 p2478 A83-37466

- Recent advances in the control of large flexible spacecraft 17 p2478 A83-37468
- Damping-augmentation mechanism for flexible spacecraft 17 p2478 A83-37469

- Performance characterization of the dry tuned-gimbal gyro for application to precision spacecraft attitude reference systems 17 p2482 A83-37476
- Spin free analytic platform type guidance and control system --- for attitude control of rocket launcher 17 p2473 A83-37488

- Control of large spaceborne antenna systems with flexible booms by mechanical decoupling 18 p2646 A83-39095
- Digital homing guidance - Stability vs. performance trade-offs [AIAA PAPER 83-2167] 19 p2795 A83-41663

- Flight-test results using nonlinear control with the F-8C digital fly-by-wire aircraft [AIAA PAPER 83-2174] 19 p2802 A83-41669
- Attitude stabilization of flexible spacecraft during stationkeeping maneuvers [AIAA PAPER 83-2226] 19 p2815 A83-41706

- Attitude control for experiments in microgravity [AIAA PAPER 83-2261] 19 p2816 A83-41731
- Spacecraft dynamics --- Book 19 p2810 A83-41825

- Dynamic motion measurements of a magnetically suspended momentum wheel for spacecraft attitude control 21 p3098 A83-44007
- Digital control system design for a precision pointing system [AAS PAPER 83-003] 21 p3103 A83-44163

- The Voyager 2 scan platform anomaly [AAS PAPER 83-046] 21 p3100 A83-44173
- On-board estimation technology for space station - Current status and future developments. [AAS PAPER 83-067] 21 p3100 A83-44180

- Attitude determination for a rigid body 21 p3200 A83-45355
- Effects of energy addition and dissipation on dual-spin spacecraft attitude motion 21 p3103 A83-45466

- MACS - The ESA standard for guidance/control and robotics --- Modular Attitude Control Systems [IAF PAPER 83-346] 23 p3422 A83-47352
- Guidance and attitude control during the final approach of an autonomous rendez-vous process [IAF PAPER 83-359] 23 p3422 A83-47358

- A design study of a reaction control system for a V/STOL fighter/attack aircraft [ASME PAPER 83-GT-199] 23 p3410 A83-48002

ATTITUDE GYROS

- A powered gyroscope with electromagnetic bearings for the attitude control of orbital stations 09 p1219 A83-25048
- Attitude estimation for a spinning satellite from gyroscope and star mapper data 10 p1385 A83-26589

- Gyroscopic attitude and stabilization systems --- Russian book 12 p1727 A83-28819
 A new strapdown attitude algorithm 17 p2460 A83-37068
 Geopositioning accuracy of an autonomous navigation system using landmarks 17 p2474 A83-37107
 On the attitude estimation of earth observation satellites 17 p2478 A83-37454
 Space borne attitude measurement units 17 p2481 A83-37474
 Performance characterization of the dry tuned-gimbal gyro for application to precision spacecraft attitude reference systems 17 p2482 A83-37476
 Noise characterization and minimization of a precision gyroscopic rate sensor --- for Space Telescope 17 p2482 A83-37477
 Floated gyro dynamical behavior during slow testing [AIAA PAPER 83-2182] 19 p2848 A83-41674

ATTITUDE INDICATORS

- 'Light bar' attitude indicator 04 p0448 A83-16136
 Simulator studies to develop and improve flight attitude information 04 p0448 A83-16334
 A study on airborne integrated display system and human information processing 10 p1456 A83-26086
 The earth's horizon - A reference for sub arc minute attitude sensing on flexible space structures [AIAA PAPER 83-2179] 19 p2815 A83-41673

ATTITUDE STABILITY

- NT DIRECTIONAL STABILITY
 NT GYROSCOPIC STABILITY
 NT LATERAL STABILITY
 NT LONGITUDINAL STABILITY
 A high speed microprocessor unit for real-time platform stabilization of an EHF SATCOM antenna 01 p0042 A83-11103
 Model attitude and deformation measurement in wind tunnel [ONERA, TP NO. 1982-91] 06 p0762 A83-18428
 Control technology as applied to Space Telescope 09 p1218 A83-23592
 Dynamics of a spacecraft during extension of flexible appendages 09 p1216 A83-24431
 Attitude control system with wheels and magnetic torquers 10 p1384 A83-26582
 Spacecraft attitude sensing based on the earth's radiation 11 p1536 A83-27373
 Attitude perturbations of the Giotto spacecraft in the dust cloud of Comet Halley 14 p1979 A83-33472
 Space Shuttle stability and control derivatives estimated from the first entry 17 p2470 A83-37065
 A new strapdown attitude algorithm 17 p2460 A83-37068
 Magnetic roll/way attitude control of a momentum biased near polar orbit satellite 17 p2478 A83-37459
 The effect of flexible satellite elasticity on orientation accuracy 17 p2479 A83-37470
 Failure detection and correction in low orbit satellite attitude control system --- for SPOT earth observation satellite 17 p2479 A83-37492
 Attitude stability of flexible asymmetric dual spin spacecraft [AIAA PAPER 83-2177] 19 p2815 A83-41671
 Effect of deploying acceleration on a flexible antenna of a spin-satellite 21 p3099 A83-44015
 Attitude control and stability of a Space Station [AAS PAPER 83-065] 21 p3100 A83-44178

ATTRACTION

- Correction of meteor radiants for zenith attraction 20 p3061 A83-43416
 Dimensionality of attractors of the Navier-Stokes system and other evolutionary equations 24 p3624 A83-49548

AUDIO EQUIPMENT

- NT MICROPHONES
 Bus protocols for a digital audio distribution system 01 p0005 A83-11126

AUDIO VISUAL EQUIPMENT

- U TRAINING DEVICES
 U VISUAL AIDS

AUDIOLOGY

- Sensory systems: Hearing --- Russian book 07 p0972 A83-19926
 The asymmetry of the sensitivity of the auditory system of humans determined by a method of constant stimuli 12 p1764 A83-29301
 The use of the sound loading test in comprehensive audiological diagnosis 15 p2213 A83-34973
 The diagnostic informativity of drugs used for revealing intralabyrinthine hydrops according to data of audiological and biochemical investigations 19 p2883 A83-41828
 Age-related changes of the auditory perception of ultrasound 19 p2883 A83-41842

ADIOMETRY

- Extratympanic electrocochleography in clinical practice 01 p0083 A83-10515

- A study of the localization function and differential sensitivity of the auditory system in patients with brain lesions 01 p0083 A83-10517
 The verbal and aural functions of communication system operators 03 p0382 A83-13277
 The impairment of the defensive and adaptive mechanisms of the ear as a result of the exposure to noise 07 p0978 A83-20876
 The pressure problems of the middle ear in flight personnel - The importance of impedance examinations 08 p1147 A83-22958
 Remarks on the systematic tonal audiometry of the ground personnel in charge of airspace security 08 p1148 A83-22972
 The formalization of the choice of the acoustic stimulus parameters in a small automatic device for the examination and diagnosis of the functional condition of the auditory analyzer 14 p2073 A83-33312
 A bone telephone for measuring the audible threshold in an extended range of frequencies 14 p2073 A83-33313
 The use of the sound loading test in comprehensive audiological diagnosis 15 p2213 A83-34973
 Masking during speech audiometry and its diagnostic value 19 p2881 A83-41445

AUDITORY DEFECTS

- Current aspects of prophylaxis and treatment of hearing disorders in patients with Meniere's disease 05 p0672 A83-16950
 Pilot deafness - Statistical study of military pilot hearing 06 p0797 A83-18336
 Statistical data and the sound environment of Air Force aircrews 06 p0798 A83-18337
 The impairment of the defensive and adaptive mechanisms of the ear as a result of the exposure to noise 07 p0978 A83-20876
 Effect of length of service on ground crew hearing threshold 15 p2211 A83-33541
 The role of the osmolarity of the blood serum in the pathogenesis of Meniere's disease 15 p2211 A83-34423
 The use of the sound loading test in comprehensive audiological diagnosis 15 p2213 A83-34973
 The prevention of early forms of medication-induced ototoxicosis in experimental studies 19 p2875 A83-41442
 A test of the lateralization of ultrasound in the diagnosis of early forms of neurosensory amblycusia 19 p2881 A83-41444
 Masking during speech audiometry and its diagnostic value 19 p2881 A83-41445
 Electrostimulation for receptor lesions of the ear 19 p2882 A83-41446
 The role of magnesium in the pathogenesis of otosclerosis and the results of the conservative treatment of patients with otosclerosis by a method of inner ear electrophoresis of magnesium sulfate 19 p2876 A83-41827
 An investigation of the proteinase activity in the perilymph of patients with otosclerosis 19 p2883 A83-41830
 The use of focused ultrasound in the megahertz range in otology 19 p2883 A83-41840
 The condition of the vestibular apparatus in children with hereditary hearing defects 19 p2884 A83-41843

AUDITORY FATIGUE

- An experimental study of the dose dependence of the effect of noise 01 p0084 A83-11397
 The impairment of the defensive and adaptive mechanisms of the ear as a result of the exposure to noise 07 p0978 A83-20876
 Effect of length of service on ground crew hearing threshold 15 p2211 A83-33541
 A hygienic evaluation of the combined effect of infrasound and low-frequency noise on the auditory and vestibular analyzer of compressor operators 15 p2212 A83-34932

AUDITORY PERCEPTION

- The verbal and aural functions of communication system operators 03 p0382 A83-13277
 The observer's activities in a near-threshold region --- of auditory perception 03 p0383 A83-13287
 Sensory systems: Hearing --- Russian book 07 p0972 A83-19926
 Mathematical models of the hydrodynamics of the cochlea of the inner ear 07 p0972 A83-19927
 Mathematical models of the process of signal conversion on the periphery of the auditory system /Status and prospects of application/ 07 p0972 A83-19928
 Auditory mechanisms of rhythm analysis 07 p0976 A83-19929
 Neurophysiological manifestations of monaural phase sensitivity of the auditory system 07 p0972 A83-19931

- The evolution of the structural-functional organization of the organ of hearing of vertebrates 07 p0972 A83-19933
 Altered auditory function in rats exposed to hypergravic fields 11 p1637 A83-27808
 The asymmetry of the sensitivity of the auditory system of humans determined by a method of constant stimuli 12 p1764 A83-29301
 A comparative analysis of the amplitude-frequency characteristics of the microphone potentials of humans as determined by experiments and with a mathematical model 12 p1764 A83-29304
 The formalization of the choice of the acoustic stimulus parameters in a small automatic device for the examination and diagnosis of the functional condition of the auditory analyzer 14 p2073 A83-33312
 A bone telephone for measuring the audible threshold in an extended range of frequencies 14 p2073 A83-33313

AUDITORY SENSATION AREAS

- Age-related changes of the auditory perception of ultrasound 19 p2883 A83-41842
 Understanding the pulse repetition interval. I - Pulsed time-domain receivers 22 p3279 A83-46759

AUDITORY SIGNALS

- The observer's activities in a near-threshold region --- of auditory perception 03 p0383 A83-13287
 Correlation methods of the analysis of the reaction of individual neurons of the auditory system. I - The correlation of an auditory signal with impulse activity 07 p0972 A83-19930
 Evaluation of an experimental central warning system with a synthesized voice component 15 p2216 A83-34982
 Local cerebral blood flow increases during auditory and emotional processing in the conscious rat 19 p2873 A83-40906

AUDITORY STIMULI

- The functional asymmetry of the brain and the direct subjective evaluation of loudness 01 p0085 A83-10503
 The modality of an imperative signal and the characteristics of the contingent negative variation /CNV/. II --- signal anticipation effects on brain wave amplitudes 02 p0224 A83-12211
 Types of trace effects from the perception of verbal information 05 p0676 A83-17180
 The slow latent auditory evoked potential of humans 07 p0976 A83-19932
 A cytochemical investigation of the hearing system during acoustic stimulation 07 p0972 A83-19935
 The effect of tonal confirmation on the quality of carrying out pursuit tracking on a plane 07 p0981 A83-20339
 The features of the behavior and the delayed reactions to visual and auditory conditioned stimuli during various time intervals between signals 07 p0980 A83-20842
 Some improvements in the measurement of variable latency acoustically evoked potentials in human EEG 14 p2069 A83-33110
 The age characteristics of cortical auditory evoked potentials 14 p2071 A83-33341
 Brainstem auditory evoked potentials 16 p2398 A83-35902
 Differential loudness sensitivity, the strength of the nervous system, and the psychophysiological scale of loudness 16 p2399 A83-36821

AUDITORY TASKS

- The verbal and aural functions of communication system operators 03 p0382 A83-13277
 Incorporation of a test of selective attention in a pilot selection battery 10 p1457 A83-26335
 Compatibility and resource competition between modalities of input, central processing, and output --- in human task performance in military aircraft 15 p2215 A83-34075

AUGER EFFECT

- Static and transient behavior of pin-diodes at high injection levels --- German thesis 01 p0036 A83-10474
 Interatomic Auger transitions in maximal valent V and Cr compounds 21 p3109 A83-44618

AUGER SPECTROSCOPY

- Auger and electron energy-loss study of the Al/SiC interface 05 p0611 A83-16947
 Techniques for the correction of topographical effects in scanning Auger electron microscopy 07 p0929 A83-20748
 X-ray-excited Auger and photoelectron spectroscopy 09 p1225 A83-23856
 Auger spectroscopy of quasi-molecules 09 p1343 A83-25089
 Characterization of copper in phosphoric-acid-anodized 2024-T3 aluminum by Auger electron spectroscopy and Rutherford backscattering 10 p1395 A83-25547
 Segregation to interphase boundaries in liquid-phase sintered Tungsten alloys 10 p1396 A83-25866

Relative intensity changes of L3MM Auger transitions in maximal-valent V and Cr compounds under ion bombardment 12 p1778 A83-29543

Auger electrons in the auroral ionosphere 14 p2051 A83-31883

Analysis of Auger electron spectroscopy depth profiles of the copper/silver interface of mirrors 18 p2708 A83-39928

Studies of liquid metal surfaces using Auger spectroscopy 20 p2942 A83-43301

Low-temperature oxygen diffusion in alpha titanium characterized by Auger sputter profiling 21 p3113 A83-44608

AES study on the chemical composition of ferroelectric BaTiO₃ thin films RF sputter-deposited on silicon 21 p3217 A83-44609

Microanalytical investigation of sintered SiC. II - Study of the grain boundaries of sintered SiC by high resolution Auger electron spectroscopy 24 p3569 A83-50071

Investigation of in-situ sputtered α -Si(H) by AES 24 p3636 A83-50180

AUGMENTATION

NT STABILITY AUGMENTATION

NT THRUST AUGMENTATION

Enhancement of heat transfer 20 p2970 A83-42659

AURORAL ABSORPTION

The interplanetary magnetic field and the absorption of radio waves in the auroral zone 11 p1620 A83-28741

Spectra of irregularities of the high-latitude lower ionosphere according to phase VLF measurements 13 p1875 A83-30608

AURORAL ACTIVITY

U AURORAS

AURORAL ARCS

A neutral vortex induced by an auroral arc 02 p0209 A83-12429

On the nature of homogeneous auroral arcs 05 p0663 A83-17613

Importance of initial ionospheric conductivity on substorm onset 05 p0665 A83-17788

Characteristics of optical emissions and particle precipitation in polar cap arcs 08 p1137 A83-23112

Polar cap arcs and the open regions 08 p1137 A83-23115

Spatial variations of ionospheric conductivity and radar auroral amplitude in the eastward electrojet region during pre-substorm conditions 10 p1447 A83-25437

Intersystem collisional transfer of excitation in low altitude aurora 10 p1448 A83-25553

Measurements of the stability of energetic electron beams in the ionosphere 11 p1617 A83-28312

Numerically simulated two-dimensional auroral double layers 11 p1618 A83-28314

Three-dimensional current flow and particle precipitation in a westward travelling surge /observed during the barium-GEOS rocket experiment/ 11 p1618 A83-28316

Short wavelength stabilization of the gradient drift instability due to velocity shear --- in equatorial electrojet 12 p1779 A83-28921

The eastward motion of the radio aurora and auroral loops in the morning sector 13 p1875 A83-30603

Airglow atmospheric imager on board the 'IK-Bulgaria-1300' satellite 13 p1815 A83-30771

Mirror instability and the origin of morningside auroral structure 13 p1878 A83-31236

Evidence for electrostatic shocks as the source of discrete auroral arcs 13 p1879 A83-31242

Observations of non-linear processes in the ionosphere 15 p2198 A83-34191

Eddy intrusion of hot plasma into the polar cap and formation of polar-cap arcs 15 p2202 A83-34733

Ionospheric and field-aligned current systems in the auroral zone - A concise review 16 p2372 A83-35361

Dynamics of the dayside aurora 16 p2373 A83-35365

Auroral plasmas in the evening sector - Satellite observations and theoretical interpretations 16 p2382 A83-36620

Polar and auroral phenomena - A review of U.S. progress during 1979-1982 17 p2541 A83-38294

The appearance of nonuniform electric fields and currents associated with auroral arcs 18 p2713 A83-39321

Ground-based observations of subauroral energetic-electron arcs 19 p2865 A83-41122

Ionospheric characteristics of a detached arc in the evening-sector trough 19 p2865 A83-41123

Generation of auroral arc elements in an inverted-V arc due to ion cyclotron turbulence 20 p3019 A83-42426

Auroral beam/plasma interaction observed directly 20 p3023 A83-43159

Experimental modelling of satellite wakes in auroral arcs 20 p3050 A83-43205

Simulation of auroral current sheet equilibria and associated V-shaped potential structures 20 p3026 A83-43213

The auroral arc as an electrical discharge between the ionosphere and magnetosphere 21 p3175 A83-45242

Altitude and structure of an auroral arc acceleration region 22 p3327 A83-46050

Small-scale auroral Arc deformations 22 p3336 A83-47063

Simultaneous observation of tropical arc, SAR arc and Aurora during geomagnetic storm from IC-Bulgaria-1300 satellite 23 p3484 A83-48446

AURORAL ECHOES

On reducing the inherent noise in the double-pulse Doppler technique 07 p0913 A83-20371

Interpretation of auroral radar experiments using a kinetic theory of the two-stream instability 07 p0961 A83-20373

The use of the radio aurora to measure electric fields and currents in the auroral ionosphere 13 p1875 A83-30602

The eastward motion of the radio aurora and auroral loops in the morning sector 13 p1875 A83-30603

Observation of a radio-aurora storm by a chain of stations 13 p1875 A83-30604

Features of radio-aurora observations at the high-latitude station Mirny 13 p1875 A83-30605

N-S radio-aurora forms 13 p1875 A83-30606

A new radar auroral backscatter experiment 21 p3173 A83-44995

The dependence of the relative backscatter cross section of 1-m density fluctuations in the auroral electrojet on the angle between electron drift and radar wave vector 22 p3337 A83-47066

AURORAL ELECTROJETS

An isolated internal wave in the thermosphere generated by the auroral electrojet 01 p0071 A83-10597

Field-aligned current and the auroral electrojets in the post-noon quadrant 02 p0207 A83-12381

Dependence of magnetic activity on the orientation of the geomagnetic dipole relative to the interplanetary magnetic field 02 p0209 A83-12433

Electrojets of the explosive phase of a substorm 02 p0210 A83-12436

The nature of the source of packets of fading long-period geomagnetic pulsations 02 p0210 A83-12439

Relationship between field-aligned currents, diffuse auroral precipitation and the westward electrojet in the early morning sector 05 p0661 A83-17397

The nature of the vertical component of the geoelectric field during magnetic disturbances 05 p0664 A83-17626

Initial tests of an index based on AL values for modeling magnetic storm related perturbations of the thermosphere 09 p1304 A83-23775

Spatial variations of ionospheric conductivity and radar auroral amplitude in the eastward electrojet region during pre-substorm conditions 10 p1447 A83-25437

Intensity variations of the IGW source and the ionospheric response during the substorm of September 18, 1974 --- Internal Gravity Wave 11 p1615 A83-27952

Generation of the internal gravity waves of auroral electrojets 11 p1620 A83-28747

Certain effects of the dissipation of the auroral electrojet during magnetospheric substorms 11 p1621 A83-28751

N-S radio-aurora forms 13 p1875 A83-30606

Behavior of the energy spectrum in fast pulsations of fluxes of precipitating electrons 13 p1875 A83-30613

Polarization characteristics of Pi 2 pulsations and implications for their source mechanisms - Influence of the westward travelling surge 13 p1882 A83-31633

Ultrashort-wave radio emission of the ionosphere of slowly-varying-component type and soft electrons in the auroral zone 14 p2050 A83-31881

Quantitative study of substorm-associated VLF phase anomalies and precipitating energetic electrons 14 p2055 A83-33146

Ionospheric and Birkeland current distributions inferred from the MAGSAT magnetometer data 15 p2196 A83-33940

Ionospheric and field-aligned current systems in the auroral zone - A concise review 16 p2372 A83-35361

A note on the accuracy of the auroral electrojet indices 17 p2539 A83-37604

Polar and auroral phenomena - A review of U.S. progress during 1979-1982 17 p2541 A83-38294

Electrojet boundaries and electron injection boundaries 17 p2546 A83-38699

Notes on the auroral electrojet indices 20 p3015 A83-42178

The diurnal behaviour of the auroral current system 20 p3016 A83-42302

The relationship between indices AE and Dst --- reflecting intensities of equatorial ring current and auroral electrojet due to geomagnetic disturbances 21 p3173 A83-44583

The distorting effect of ionospheric polar electrojets on the Dst variation 21 p3175 A83-45244

Relative contribution of ionospheric conductivity and electric field to the auroral electrojets 22 p3336 A83-47060

The dependence of the relative backscatter cross section of 1-m density fluctuations in the auroral electrojet on the angle between electron drift and radar wave vector 22 p3337 A83-47066

Inferring electric fields and currents from ground magnetometer data - A test with theoretically derived inputs 22 p3337 A83-47077

The dependence of the indices of auroral electrojets on the IMF Bz component and on the solar wind velocity 23 p3484 A83-48385

AURORAL IONIZATION

Nonlinear evolution of convecting plasma enhancements in the auroral ionosphere. II - Small scale irregularities 06 p0785 A83-18319

Possible enhancement of previously unobserved /NII/ emissions in the mid-day aurora associated with nighttime substorm activity 07 p0967 A83-21561

Thermospheric neutral composition from auroral ion ratios [AD-A126032] 07 p0968 A83-21579

Auroral ion velocity distribution function - Generalized polynomial solution of Boltzmann's equation 07 p0968 A83-21586

Energetic oxygen and sulfur ions in the Jovian magnetosphere and their contribution to the auroral excitation 17 p2618 A83-37580

Ionospheric characteristics of a detached arc in the evening-sector trough 19 p2865 A83-41123

Estimation of the rate constant for the reaction N₂(⁺) + O from data on the ion and neutral composition of a diffuse arc 21 p3176 A83-45261

Interpretation of ionograms in the vicinity of the dayside auroral oval by ray tracing 22 p3332 A83-46532

Eclipse-related measurements of middle-atmosphere electrical parameters 23 p3481 A83-47474

AURORAL IRRADIATION

Impacts of solar and auroral storms on power line systems 14 p2053 A83-32899

AURORAL SPECTROSCOPY

Ultraviolet imaging for auroral zone remote sensing [AIAA PAPER 83-0019] 05 p0659 A83-16468

Satellite auroral/ionospheric UV imager [AIAA PAPER 83-0104] 05 p0608 A83-16522

Detection of auroral hydrogen Lyman-alpha emission from Uranus 05 p0704 A83-17037

Detailed correlations of magnetic field and riometer observations at L = 4.2 with pulsating aurora 05 p0660 A83-17394

Synthetic spectra for auroral studies - The N₂ Vegard-Kaplan band system 05 p0662 A83-17405

Differences in near UV /approximately 3400-4300 A/ optical emissions from midday cusp and nighttime auroras 06 p0785 A83-18312

Vertical distribution of glow in H-alpha and in the 1PGN2 band at polar-cusp latitudes 07 p0964 A83-21178

Ratio of the intensities of 5577-A and 4278-A auroral emissions in proton and electron polar-auroras 07 p0964 A83-21183

Rocketborne cryogenic /10 K/ high-resolution interferometer spectrometer flight HIRIS - Auroral and atmospheric IR emission spectra [AD-A128358] 10 p1423 A83-26642

N I /3466 A/ and N I /5200 A/ emissions from various nighttime and daytime auroras 11 p1618 A83-28317

Auger electrons in the auroral ionosphere 14 p2051 A83-31883

The extreme ultraviolet spectrum of dayside and nighttime aurorae - 800-1400 A 15 p2196 A83-33943

Dynamics of the dayside aurora 16 p2373 A83-35365

Rocket-borne EUV-visible emission measurements 16 p2373 A83-35369

U.S. contributions to auroral aeronomy, 1979-1982 17 p2541 A83-38276

Polar and auroral phenomena - A review of U.S. progress during 1979-1982 17 p2541 A83-38294

Auroral photometers aboard the Aureol-3 satellite - The Altair experiment 18 p2647 A83-39578

Power spectral analysis of auroral occurrence frequency 20 p3019 A83-42423

Electron impact excitation of lambda 7990-A multiplet 22 p3355 A83-46061

Dependence of auroral FUV emissions on the incidence electron spectrum and neutral atmosphere 22 p3337 A83-47067
 Simultaneous observation of tropical arc, SAR arc and Aurora during geomagnetic storm from IC-Bulgaria-1300 satellite 23 p3484 A83-48446
 Determination of atmospheric composition and temperature from the U.V. airglow 24 p3603 A83-48753

AURORAL TEMPERATURE

Joule heating and particle precipitation --- in auroral upper atmosphere 16 p2372 A83-35360

AURORAL ZONES

Distances from auroral zones to the magnetic and geographic equators 02 p0205 A83-11971
 Ionospheric ELF radio signal generation due to LF and/or MF radio transmissions. I - Experimental results 02 p0205 A83-12015
 Ionospheric ELF radio signal generation due to LF and/or MF radio transmissions. II - Interpretation 02 p0205 A83-12016

Recent results in auroral-zone scintillation studies 02 p0206 A83-12021

On the relationship of the plasmopause to the equatorward boundary of the auroral oval and to the inner edge of the plasma sheet 02 p0207 A83-12380
 Transport of aurorally produced $N/2D^+$ by winds in the high latitude thermosphere 04 p0508 A83-14967
 Auroral ion velocity distribution function - The Boltzmann model revisited 04 p0509 A83-14972
 Observations of inverted-V electron precipitation 04 p0510 A83-15824

Space environment monitoring by low-altitude operational satellites 04 p0512 A83-16287
 SBARMO-79; a multi-balloon campaign in the auroral zone 04 p0512 A83-16295
 On ion harmonic structure in auroral zone waves - The effect of ion conic damping of auroral hiss 05 p0661 A83-17398

Upgoing ion beams. I - Microscopic analysis --- of auroral plasma 05 p0661 A83-17399
 The anisotropy of high-latitude nighttime F region irregularities 05 p0661 A83-17402
 Pi 2 pulsations - High latitude results 05 p0664 A83-17780

Auroral hiss, Z mode radiation, and auroral kilometric radiation in the polar magnetosphere - DE 1 observations [AD-A125914] 06 p0784 A83-18302

Spiky ion acoustic waves in collisionless auroral plasma 06 p0784 A83-18306

Generation of conic ions by auroral electric fields 06 p0785 A83-18317

Particle simulations of electrostatic emissions near the lower hybrid frequency 06 p0785 A83-18320

SABRE - A U.K.-German auroral radar 06 p0747 A83-18738

Current-driven double layers and the auroral plasma 07 p0959 A83-20196

Effect of geomagnetic activity on the changes of atmospheric circulation in the northern hemisphere 07 p0950 A83-20601

The origins of Birkeland currents 07 p0962 A83-20840

A study of the radiation from an antenna in a Maxwellian magnetoplasma Application to the in situ sounding of the auroral ionosphere --- French thesis 07 p0964 A83-21093

Compatibility of Doppler measurements of the drift of auroral scattering at different frequencies 07 p0964 A83-21180

The auroral oval and the sector structure of the interplanetary magnetic field 07 p0964 A83-21184

Morphology of spatial patterns in Pi 1-2 magnetic field pulsation activity - A review 07 p0965 A83-21428

Acceleration of hydrogen ions and conic formation along auroral field lines 07 p0966 A83-21516

Solitary waves and double layers on auroral field lines 07 p0966 A83-21517

A sounding rocket observation of an apparent wake generated parallel electric field 07 p0967 A83-21521

Location and source of ionospheric high latitude troughs 07 p0968 A83-21584

Solar wind control of the low-latitude asymmetric magnetic disturbance field 09 p1303 A83-23768

A rocket observation of the 6300 A/5200 A intensity ratio in the dayside aurora - Implications for the production of $O(1D)$ via the reaction $N(2D) + O_2 \rightarrow NO + O(1D)$ 09 p1306 A83-24344

A possible mechanism of ion acceleration in the daytime polar cusps 09 p1308 A83-25046

The stratification of magnetospheric convection and its manifestations in the high-latitude ionosphere 10 p1448 A83-25605

Electric currents and voltage drops along auroral field lines 11 p1614 A83-27400

Observations of small-scale auroral vortices by the S3-2 satellite [AD-A127796] 11 p1618 A83-28315

Monte Carlo calculations of the $O^+ / +$ velocity distribution in the auroral ionosphere 11 p1619 A83-28328

The height distribution of parameters of the auroral ionosphere during a magnetic storm 11 p1621 A83-28749

Ion-beam-driven electrostatic ion cyclotron instabilities 12 p1751 A83-28920

Auroral riometer absorptions and the F-region disturbances observed over a wide range of latitudes 12 p1754 A83-29436

Injections of ions and electrons into the ionosphere and the magnetosphere - Application to measurement of the parallel electric field in the auroral zones --- French thesis 13 p1874 A83-30126

Investigation of the high-latitude ionosphere and magnetosphere of the earth --- Russian book 13 p1874 A83-30601

Nonlinear limiting mechanism of Buneman-Farley instability --- in auroral ionosphere 13 p1875 A83-30607

Dynamics of sporadic E layers during magnetic disturbances 13 p1875 A83-30610

The height distribution of electron density in the high-latitude F2-layer 13 p1875 A83-30611

Features of the relationship between the spatial-temporal behavior of pulsations of decreasing period with magnetic activity 13 p1876 A83-30614

Field and wave measurements aboard the Aureol-3 spacecraft 13 p1813 A83-30758

Bars - A dual bistatic auroral radar system for the study of electric fields in the Canadian sector of the auroral zone 13 p1815 A83-30774

Response of nightside auroral-oval boundaries to the interplanetary magnetic field 13 p1947 A83-31233

A theory of coherent radar spectra in the auroral E region 13 p1879 A83-31240

Effect of an electron beam on the current-convective instability --- in diffuse auroral plasmas 13 p1926 A83-31244

Auroral electron interaction with the atmosphere in the presence of conjugate field-aligned electrostatic potentials 13 p1879 A83-31245

Excitation of an electrostatic wave by a cold electron current sheet of finite thickness 13 p1881 A83-31530

Generation of ionospheric irregularities by thermal-source - A new mechanism 13 p1881 A83-31533

Electron density profiles according to rocket measurements over Hayes Island during magnetospheric substorms 14 p2049 A83-31859

The formation of weakly anisotropic irregularities in the high-latitude ionosphere 14 p2049 A83-31861

On the possibility that certain types of geomagnetic pulsations have an ionospheric origin 14 p2050 A83-31869

Dependence of vertical drifts of the ionospheric F-layer at the Leningrad observatory on magnetic activity in the auroral zone 14 p2050 A83-31879

First VHF auroral radar interferometer observations 14 p2053 A83-32696

An alternative interpretation of ion ring distributions observed by the S3-3 satellite 14 p2053 A83-32700

An investigation of the state of the high-latitude ionosphere during substorms 14 p2054 A83-33027

A kinetic model of the polar wind with a Landau collision integral 14 p2054 A83-33028

The neutral composition of the high-latitude atmosphere 14 p2054 A83-33029

The dynamics of the polar ionosphere in the auroral zone 14 p2054 A83-33031

The electron concentration in the auroral and subauroral zones according to rocket measurements 14 p2054 A83-33035

Highlights of the observations in the POLAR 5 electron accelerator rocket experiment 15 p2198 A83-34187

Interaction between natural particle beams and space plasmas 15 p2198 A83-34192

The Norwegian program using particle accelerators in space 15 p2124 A83-34214

Excitation of whistler waves by reflected auroral electrons 15 p2199 A83-34359

An Alfven wave approach to auroral field-aligned currents 15 p2200 A83-34365

Computer simulation of auroral kilometric radiation 15 p2202 A83-34738

Ionospheric and field-aligned current systems in the auroral zone - A concise review 16 p2372 A83-35361

Dynamics of the dayside aurora 16 p2373 A83-35365

Energy deposition in the polar ionosphere as determined by measurements aboard 'Interkosmos-Bulgaria-1300' satellite 16 p2373 A83-35368

Millstone Hill incoherent scatter observations of auroral convection over $\Lambda = 60-75$ deg. III - Average patterns versus K_p 17 p2537 A83-37576

Systematics of the equatorward diffuse auroral boundary 17 p2538 A83-37595

On the rotation of the polar cap potential pattern and associated polar phenomena 17 p2539 A83-37605

Loss cone fluxes and pitch angle diffusion at the equatorial plane during auroral radio absorption events 17 p2543 A83-38372

Electron pitch-angle scattering by low frequency waves at the geomagnetic equator 17 p2545 A83-38602

Global pattern of auroral ion precipitation - A review of the results from the Aureole-1 and Aureole-2 satellites 18 p2717 A83-39946

Heating of heavy ions on auroral field lines 19 p2865 A83-41121

The relationship of total Birkeland currents to the merging electric field 19 p2865 A83-41126

Ion acceleration in the supauroral region - A Monte Carlo model 19 p2865 A83-41129

Spectral behaviour of disturbances observed in the southern auroral zone 20 p3016 A83-42307

Observational evidence of Z and L-O mode waves as the origin of auroral kilometric radiation from the Jikiken (EXOS-B) satellite 20 p3018 A83-42411

Production of auroral zone E region irregularities by powerful HF heating 20 p3020 A83-42427

Generation of Alfvén-ion cyclotron waves on auroral field lines in the presence of heavy ions 20 p3025 A83-43195

A statistical study of the dynamics of the equatorward boundary of the diffuse aurora in the pre-midnight sector 20 p3026 A83-43214

Spatial distribution of the polar chorus at high latitudes 21 p3176 A83-45265

Spatial relationship of field-aligned currents, electron precipitation, and plasma convection in the auroral oval 22 p3327 A83-46051

A theoretical approach to the morphology and the dynamics of diffuse auroral zones 22 p3327 A83-46054

Parametric excitation and suppression of convective plasma instabilities in the high-latitude F region ionosphere 22 p3328 A83-46060

Characteristics of the inverted-V events observed by the Kyokko satellite --- auroral electron precipitation 22 p3330 A83-46510

VHF radar observation of auroral E-region irregularities associated with moving-arcs 22 p3330 A83-46511

Ionization by keV electron precipitation in the auroral zone 22 p3331 A83-46517

Time-sharing measurements of ionospheric electron temperature and electron density with the electric field using double probes - An experiment on the Antarctic sounding rocket S-310JA-7 22 p3331 A83-46518

HF Doppler measurement in the auroral ionosphere 22 p3332 A83-46524

Selection of the initial conditions for an artificial satellite for investigations of the north auroral regions 23 p3417 A83-48071

AURORAS
 NT AURORAL ARCS
 NT RADIO AURORAS

Characteristics of auroral electrons according to Meteor-satellite observations 02 p0209 A83-12428

The aurora - New light on an old subject 03 p0356 A83-13175

Observation of guided ULF-waves correlated with auroral particle precipitation theoretically explained by negative Landau damping 03 p0357 A83-13298

Pulsing hiss, pulsating aurora and micropulsations 03 p0361 A83-14744

IMS ground observations on optical aurora and ionospheric absorption made in Northern Europe, with examples of data handling 04 p0512 A83-16291

Examples of multi-instrumental studies on auroral phenomena 04 p0512 A83-16292

IMS results in Antarctica 04 p0513 A83-16299

A correlation between auroral kilometric radiation and field-aligned currents 05 p0661 A83-17396

Structure of the spatial distribution of the amplitude and polarization characteristics of Pi2 geomagnetic pulsations in the region of the activation of auroras 05 p0663 A83-17615

Pi2 magnetic pulsations, auroral break-ups, and the substorm current wedge - A case study 05 p0665 A83-17868

The Duga photometric device for investigating polar auroras and tropical arcs from the Salyut 6 space station 06 p0723 A83-18021

A relation between the altitude of the aurora and solar activity 06 p0784 A83-18307

Differences in near UV /approximately 3400-4300 A/ optical emissions from midday cusp and nighttime auroras 06 p0785 A83-18312

The origin of Northern Lights 06 p0787 A83-19394

Polar auroras. Number 30 - Complex investigations of the dynamics of polar auroras --- Russian book 07 p0964 A83-21176

Pulsating auroral bistructures and the conductivity of the magnetospheric plasma 07 p0965 A83-21185

Characteristics of gaps in discrete dayside auroras 07 p0965 A83-21186

Unusual manifestations of auroral activity 07 p0965 A83-21187

Bay-like disturbances according to integral-photometer data 07 p0965 A83-21188

Rocket and ground-based study of an auroral breakup event 08 p1137 A83-23117

A dynamic model for the auroral field line plasma in the presence of field-aligned current 09 p1304 A83-23769

Splitting and divergence of STARE auroral radar velocities 09 p1304 A83-23771

The connection between radiation belt and auroral processes 11 p1614 A83-27394

Concerning sources of O/1D/ in Aurora - Electron impact and dissociative recombination 11 p1619 A83-28326

Atomic nitrogen abundance in polar upper thermosphere 12 p1751 A83-28919

Auroral oval dynamics in relation to solar wind-magnetosphere interaction 12 p1756 A83-29703

Advances in auroral imaging from space 13 p1814 A83-30768

Radar auroral observations and ionospheric electric fields 13 p1876 A83-30773

High latitude neutral atmosphere temperature and concentration measurements from the first Eiscat incoherent scatter observations 13 p1883 A83-31717

Auroral X-ray and luminosity pulsations and microbursts measured during February 25, 1974 SAMBO-1 balloon flight 13 p1883 A83-31718

Dynamics of the establishment of the distribution function of N2 molecules in vibrational levels and the formation of NO in auroral arcs 14 p2051 A83-31885

Multiple fluorescent scattering of N2 ultraviolet emissions in the atmospheres of the earth and Titan 15 p2274 A83-33932

Correlated irregular magnetic pulsations and optical emissions observed at Siple Station, Antarctica 15 p2195 A83-33936

OI (7990 A) emission and radiative entrapment of auroral EUV 15 p2196 A83-33944

Tentative confirmation of an aurora on Uranus 15 p2274 A83-34221

Coordinated rocket campaign on Heiss Island --- for upper atmosphere sounding during auroral disturbances 16 p2372 A83-35362

Polar and auroral phenomena - A review of U.S. progress during 1979-1982 17 p2541 A83-38294

Electric conductivities, electric fields and auroral particle energy injection rate in the auroral ionosphere and their empirical relations to the horizontal magnetic disturbances 17 p2544 A83-38518

Electron precipitation and related aeronomy of the Jovian thermosphere and ionosphere 20 p3077 A83-42407

Neutral and ion gas heating by auroral electron precipitation 20 p3019 A83-42421

Electron precipitation equatorward of the auroral oval and the mantle aurora in the midday sector 20 p3023 A83-43161

PD 1 pearl-electron interactions on the L = 4.2 magnetic shell 20 p3024 A83-43191

Apparent electrostatic ion cyclotron waves in the diffuse aurora 20 p3025 A83-43196

Ring coupling model - Implications for substorm onsets 20 p3027 A83-43217

Lightning, auroras, nocturnal lights, and related luminous phenomena: A catalog of geophysical anomalies --- Book 22 p3325 A83-45913

The distribution of auroral electrostatic shocks below 8000-km altitude 22 p3327 A83-46049

A quantitative description of the spatial distribution and dynamics of the energy flux in the continuous aurora 22 p3327 A83-46053

Comparison between the arrival direction of auroral hiss and the location of aurora observed at Syowa Station 22 p3329 A83-46504

Modes of pulsating auroras and related geomagnetic pulsations 22 p3330 A83-46508

Magnetic and auroral substorms associated with storm sudden commencements and sudden impulses 22 p3330 A83-46509

Wave normal direction of auroral hiss observed by the S-310JA-5 rocket 22 p3331 A83-46515

Distribution of energy input due to auroral protons and electrons 22 p3334 A83-46917

The shift of the auroral electron precipitation boundaries in the dawn-dusk sector in association with geomagnetic activity and interplanetary magnetic field 22 p3336 A83-47058

Evidence for the E x B drift of pulsating auroras 22 p3336 A83-47059

The visual aurora as a predictor of solar activity 22 p3337 A83-47076

Auroral physics 23 p3485 A83-48555

AUSTENITE

Influence of structural parameters on oxidation of austenitic Fe-Ni-Cr-Al alloys 05 p0615 A83-17562

The influence of prior austenite grain size and stress ratio on near threshold fatigue crack growth behavior in high strength steel 08 p1061 A83-21716

Effect of tungsten on the properties of austenitic precipitation-hardening Fe-Cr-Ni alloys 13 p1823 A83-31213

AUSTENITIC STAINLESS STEELS

Influence of the gaseous environment on fatigue crack propagation in an austenitic steel 03 p0300 A83-14701

A unified, self-consistent theory for the plastic-creep deformation of metals 04 p0498 A83-15678

Statistical aspect of fatigue crack propagation from surface defects 05 p0614 A83-17093

A study of the feasibility of ultrasonic inspection of thick bimetallic welds in mildly alloyed steel and corrosion resistant austenitic steel --- French thesis 07 p0943 A83-21094

Fatigue crack initiation after different surface treatments in precipitation hardening alloys 08 p1058 A83-21668

Creep crack growth characterization of austenitic stainless steel 08 p1061 A83-21732

On the interaction of hardening and fatigue damage in the 316 stainless steel 08 p1062 A83-21736

Creep fracture behavior of austenitic stainless steels from 550 to 800 C 08 p1062 A83-21746

The effect of overloading on fatigue crack propagation in two aluminum alloys and an austenitic stainless steel 08 p1063 A83-21754

Dynamic in situ high voltage electron microscopy studies of tensile cracks in thin stainless steel films 10 p1395 A83-25546

Notch effect on torsional low-cycle fatigue 10 p1399 A83-26893

A theoretical examination of thermal radiation from rough surfaces - The development of a device for measuring emissivity and application to AISI 316 stainless steel --- French thesis 11 p1650 A83-28633

Experimental study of the fatigue fracture of the aluminum alloy AU4G1-T3 and the austenitic stainless steel Type 316 --- French thesis 13 p1819 A83-30144

On the description of cyclic hardening under complex loading histories 13 p1822 A83-31170

On the description of cyclic hardening under complex loading histories [ONERA, TP NO. 1983-7] 16 p2333 A83-36420

Stress corrosion cracking 17 p2486 A83-37172

Low cycle fatigue of tubular specimens 17 p2519 A83-37299

Condition for stable growth of branched cracks 18 p2696 A83-39082

The effect of titanium on creep strength in 2.25 pct Cr-1 pct Mo steels 18 p2669 A83-40634

Microfracture model for hydrogen embrittlement of austenitic steels 18 p2670 A83-40643

The effect of structural dispersity on the high-temperature strength of prestrained steels and alloys 19 p2821 A83-40804

The sulfidation properties of iron-nickel alloys at low sulfur pressures 24 p3565 A83-49512

AUSTRALIA

Case study - Australian national satellite system 07 p0903 A83-19653

A preliminary assessment of International Geomagnetic Reference Field models for Australia 09 p1302 A83-33720

Status of space science and technology - An Australian perspective 18 p2787 A83-39832

Deformation of the Australian plate - Preliminary findings from laser ranging to the LAGEOS satellite 22 p3317 A83-46363

AUSTRALITES

Beryllium-10 in Australasian tektites - Evidence for a sedimentary precursor 02 p0264 A83-12066

AUTOCATALYSIS

The possible role of assignment catalysts in the origin of the genetic code 02 p0219 A83-11634

Catalyzed and inhibited decomposition of ammonium perchlorate 20 p2959 A83-43456

AUTOCLAVING

Characterization of quick-cure and vacuum-bag cure composites 21 p3119 A83-45073

Applications of mass spectrometry techniques to autoclave curing of materials 24 p3559 A83-50143

AUTOCOLLIMATORS

U COLLIMATORS

AUTOCORRELATION

Filamentary structure in the Shane-Wirtanen galaxy distribution 05 p0700 A83-17025

Determination of the duration of fluctuating picosecond optical pulses 05 p0649 A83-17056

Measurement of picosecond ultraviolet laser pulsewidths using an electrical autocorrelator 07 p0937 A83-21368

Application of correlation technology to radio observation problems 09 p1244 A83-23413

Computational studies of first-Born scattering cross sections. I - Spectral properties of Bethe surfaces. II - Moment-theory approach 09 p1341 A83-23722

Measurement of autocorrelation functions in a bi-static incoherent scatter radar 09 p1249 A83-24694

Autocorrelation of Northern Hemisphere geopotential heights 10 p1450 A83-25388

Approximation of multivariable linear systems with impulse response and autocorrelation sequences 10 p1463 A83-26502

The autocorrelation function and Doppler spectral moments - Geometric and asymptotic interpretations --- of meteorological radar data 11 p1625 A83-27020

Real time monitoring of CW mode-locked dye laser pulses using a rapid-scanning autocorrelator 12 p1729 A83-29194

On the synthesis of a class of self-synchronizing signals 13 p1828 A83-30289

Autocorrelation compression filter for radio pulses with linear frequency modulation 13 p1829 A83-30729

Singular-value decomposition approach to time series modelling 14 p2075 A83-32429

Statistical efficiency of correlation-based methods for ARMA spectral estimation 14 p2075 A83-32430

Unifying approach to spectral estimation 14 p2075 A83-32432

Autocorrelation of ultrashort optical pulses using polarization interferometry 15 p2230 A83-33764

Third order autocorrelation study of amplified subpicosecond laser pulses 16 p2359 A83-35953

Generation of codes with good autocorrelation properties 19 p2827 A83-41276

Origin-of long-time tails in strongly chaotic systems 21 p3199 A83-43883

Applicability of the relay correlator to radar signal processing 23 p3444 A83-48714

AUTODYNES

Semiconductor synchronized oscillators and autodynes --- Russian book 15 p2152 A83-34166

Optimization of the autodyne mode of operation of Gunn-diodes 15 p2153 A83-34892

AUTOIONIZATION

Electron impact ionisation of N/2+ including autoionisation 01 p0106 A83-10205

The doubly excited autoionizing states of H2 08 p1163 A83-22220

Interactions between neutral dissociation and ionization continua in N2O 10 p1479 A83-25560

Electron impact ionization of complex ions 15 p2236 A83-34608

Effects of autoionizing levels in highly ionized atoms 16 p2409 A83-35635

Observation of autoionising states in H2 and D2 above 30 eV by electron impact 18 p2743 A83-40317

Dielectronic recombination 21 p3213 A83-44654

Possible origins for the 12 microns emission lines in the solar spectrum 23 p3530 A83-47508

Study of the autoionising states of the hydrogen atom in intense magnetic fields by the complex coordinate coupled-channel formalism 23 p3506 A83-48576

Photoionisation spectrum of Te I - Autoionising series and relative cross section 23 p3506 A83-48584

Dielectronic recombination at low temperatures --- in gaseous nebulae 24 p3668 A83-50086

AUTOMATA THEORY

The motion of planar rod systems --- for dynamic automata 01 p0086 A83-10452

Polynomial realization of a train of Boolean functions 01 p0096 A83-11318

Structural kinematics of in-parallel-actuated robot-arms [ASME PAPER 82-DET-105] 02 p0187 A83-12779

Dynamic-automaton models in the visualization of three-dimensional scenes 08 p1157 A83-22177

- Terraforming Mars and Venus using machine self-replicating systems /SRS/ 09 p1211 A83-23684
- Calculation of the parameters of the optical system of the image converter of an adaptive industrial robot 12 p1767 A83-29325
- Nonlinear walking and running of a biped walking machine 13 p1908 A83-31396
- Computer simulation complex for the investigation of systems for the control of the manipulators of autonomous robots 15 p2223 A83-35261
- Method for calculating the orientation angle of the workpiece for the control systems of adaptive industrial robots 15 p2143 A83-35265
- Asymptotically optimal automata with growing memory 18 p2738 A83-39513
- Theory of the invariance of binary nonstationary and nonlinear sequential machines 20 p3039 A83-42923
- Infinite-valued logic in problems of cybernetics --- Russian book 21 p3192 A83-43910
- Probability density for the time of signal detection by an automaton with a continuous set of states 23 p3501 A83-48517
- AUTOMATED GUIDEWAY TRANSIT VEHICLES**
- Microprocessor control for automated guideway transit vehicles 01 p0112 A83-11035
- Intelligence allocation and digital control for automated guideway transit systems 01 p0112 A83-11036
- Control and design aspects of magnetically suspended vehicles 10 p1491 A83-26605
- An experimental system for automatic guidance of ground vehicle following the commanded guidance route on map 10 p1469 A83-26606
- AUTOMATED PILOT ADVISORY SYSTEM**
- Advantages of statistically interrogating onboard anticollision systems 10 p1374 A83-26482
- Status of the TCAS program 22 p3255 A83-46959
- AUTOMATIC CONTROL**
- NT ACTIVE CONTROL
- NT ADAPTIVE CONTROL
- NT AUTOMATIC FLIGHT CONTROL
- NT AUTOMATIC FREQUENCY CONTROL
- NT AUTOMATIC GAIN CONTROL
- NT AUTOMATIC LANDING CONTROL
- NT CASCADE CONTROL
- NT DYNAMIC CONTROL
- NT FEEDBACK CONTROL
- NT FEEDFORWARD CONTROL
- NT LEARNING MACHINES
- NT NUMERICAL CONTROL
- NT OFF-ON CONTROL
- NT OPTIMAL CONTROL
- NT PROPORTIONAL CONTROL
- NT SELF ADAPTIVE CONTROL SYSTEMS
- NT SELF ALIGNMENT
- NT SEQUENTIAL CONTROL
- NT TIME OPTIMAL CONTROL
- Automatic change detection of synthetic aperture radar imagery 01 p0007 A83-11222
- Assembling, setting up, and tuning the instruments of automatic control systems --- Russian book 02 p0230 A83-11972
- Automatic methods for the adjustment of faceted solar-energy concentrators and heliostats 04 p0503 A83-15131
- Automated measurements of atmospheric visibility [AIAA PAPER 83-0436] 05 p0643 A83-16713
- The measurement and control of impact finishing processes 05 p0652 A83-16921
- Problems associated with the development of automatic control systems 05 p0681 A83-17658
- A cooled pyrheliometer with automatic compensation 07 p0931 A83-20964
- Automated machining of turbine blades by Rolls-Royce 07 p0941 A83-21348
- Automated supernova search from photographic plates 08 p1174 A83-21845
- Application of multivariable systems theory; Symposium, Plymouth, England, October 26-28, 1982, Collected Papers 08 p1158 A83-23171
- Optimizing the cutting of stock with the aid of computers --- Russian book 09 p1274 A83-23826
- The automation of control system design. Number 4 --- Russian book 09 p1326 A83-24225
- Asynchronous induction micromotors for automatic systems --- Russian book 10 p1408 A83-25618
- Correlation-extremal methods of navigation --- Russian book 10 p1462 A83-25620
- The modelling of hierarchical systems of spatial-temporal synchronous connections of the human brain 10 p1462 A83-25625
- Control science and technology for the progress of society; Proceedings of the Eighth Triennial World Congress, Kyoto, Japan, August 24-28, 1981. Volume 4. Part A - Mechanical systems and robots. Part B - Aerospace and transportation 10 p1380 A83-26577
- An experimental system for automatic guidance of ground vehicle following the commanded guidance route on map 10 p1469 A83-26606
- The design of adaptive information-transfer systems for automatic control --- Russian book 12 p1769 A83-29333
- Automated knurl inspection for rockets 12 p1733 A83-29374
- Multivariable system theory and design --- Book 12 p1770 A83-29536
- Synthesis of control systems with quasi-continuous generation of the control signal 13 p1910 A83-30077
- Construction of algorithms for the automatic control of the force operations of manipulator robots 13 p1910 A83-30089
- Geometrical criterion for the stability of discrete stationary systems with one nonlinearity 13 p1910 A83-30090
- Computational systems and methods in the automation of investigations and control --- Russian book 13 p1910 A83-30616
- Robot systems as higher forms of tools for the automation of investigations in extreme environments 13 p1906 A83-30618
- Smooth extremal problems in spectra of constant matrices 13 p1910 A83-30620
- Method for automatic compensation of geometrical distortions in astronomical television equipment 13 p1919 A83-30869
- Automated timekeeping II 13 p1847 A83-31291
- A microcomputer based control system for antenna measurements 14 p2019 A83-32399
- An automated on-orbit thermal acquisition device --- reusable heat rejectors for space platforms [AIAA PAPER 83-1465] 14 p1982 A83-32723
- Mathematical models of discrete systems of automatic control with indeterminate parameters 14 p2076 A83-32963
- Mathematical methods for the optimization of automatic-control-system devices and algorithms --- Russian book 15 p2220 A83-34175
- An automatic system for the medical monitoring of the functional condition of a human 15 p2215 A83-34947
- Time-optimization of automatic control systems --- Russian book 16 p2405 A83-36441
- Automatic photoelectric device with a laser interferometer for measuring photographs of limbs of meridian instruments 16 p2357 A83-36863
- Control of robot manipulators for handling and assembly in space 16 p2402 A83-36981
- American Control Conference, 1st, Arlington, VA, June 14-16, 1982, Proceedings. Volumes 1, 2 & 3 17 p2564 A83-37076
- Number and placement of control system actuators considering possible failures --- for large space structures 17 p2476 A83-37078
- Space station automation and autonomy - Advantages and problems 17 p2476 A83-37096
- Longitudinal control and a new spacing policy for automated transit vehicles 17 p2586 A83-37101
- Geopositioning accuracy of an autonomous navigation system using landmarks 17 p2474 A83-37107
- Automatic control in space 1982; Proceedings of the Ninth Symposium, Noordwijkerhout, Netherlands, July 5-9, 1982 17 p2476 A83-37432
- Automatic controls on board planetary probes 17 p2480 A83-37493
- Nonlinear parametric model of nonsearching self-adjusting systems with a reference model and its use in the design and analysis of the self-adjustment circuit 17 p2569 A83-37766
- Automatic control of balloon altitude 18 p2641 A83-39809
- Survey of radar ADT --- Automatic Detection and Tracking 19 p2825 A83-40755
- The analysis and design of nonlinear systems with the aid of functional power series 19 p2889 A83-40982
- Applications on nonlinear programming for automated optimum multivariable control system design [AIAA PAPER 83-2275] 19 p2892 A83-41741
- Automated processes for the evaluation of the efficiency of 'man-machine' systems 19 p2885 A83-41837
- Problems in the control of relativistic and quantum dynamic systems (physical and informational aspects) --- Russian book 21 p3195 A83-45033
- Unbalanced-bridge computational techniques and accuracy for automated multichannel strain-measuring systems 21 p3141 A83-45147
- Discrete nonlinear systems --- Russian book 21 p3197 A83-45201
- Automation of satellite control system and its effectiveness in actual operation --- with Ionosphere Sounding Satellite 21 p3098 A83-45445
- The changes in the cardiac rhythm of air traffic controllers using automated systems 23 p3497 A83-47112
- Automated bonding process for load-bearing aircraft cellular structural components in light contour systems 23 p3391 A83-47198
- The automated detection of variable objects 24 p3647 A83-50005
- Automated two-dimensional galaxy photometry 24 p3648 A83-50018
- AUTOMATIC CONTROL VALVES**
- NT PRESSURE REGULATORS
- AUTOMATIC DATA PROCESSING**
- U DATA PROCESSING
- AUTOMATIC FLIGHT CONTROL**
- NT AUTOMATIC LANDING CONTROL
- Software configuration control in a real-time flight test environment 01 p0009 A83-11144
- Economic modeling of fault tolerant flight control systems in commercial applications 01 p0013 A83-11156
- Integrated flight and fire control development and flight test on an F-15B aircraft 01 p0006 A83-11160
- Integrated airframe/propulsion controls technology 01 p0013 A83-11175
- A digital flight control system verification laboratory 01 p0015 A83-11178
- Applications of autopath technology to terrain/obstacle avoidance 01 p0008 A83-11255
- Software and system level tests of a test flight mercury ion thruster subsystem [AIAA PAPER 82-1912] 02 p0145 A83-12485
- Advanced fighter technology integrator /AFTI/ F-16 display mechanization 04 p0448 A83-16132
- Simulation of a terrain following system 04 p0445 A83-16333
- Qualification of the flight-critical AFTI/F-16 digital flight control system --- Advanced Fighter Technology Integration [AIAA PAPER 83-0060] 05 p0597 A83-16492
- DC-9 Super 80 digital flight guidance system simulation techniques for certification 05 p0592 A83-17305
- Software design for the Douglas DC-9 Super 80 digital flight guidance system 05 p0592 A83-17311
- The automated cockpit 07 p0866 A83-20849
- Automation of on-board flightpath management 07 p0867 A83-21002
- Application of vector performance optimization to a robust control loop design for a fighter aircraft 07 p0867 A83-21160
- The software-implemented fault tolerance /SIFT/ approach to fault tolerant computing 08 p1155 A83-22825
- Flight management systems and data links 09 p1209 A83-24424
- Improved observer design incorporating modal consideration --- for feedback application to flight control problems 09 p1332 A83-24787
- Multivariable stability margins for vehicle flight control systems 09 p1210 A83-24815
- New on board equipments /PMS, FMS/ and the ATC system - Evolution or revolution 09 p1204 A83-24859
- Human aspects of integrated navigation in the air 09 p1323 A83-24864
- Electronic devices in automatic systems --- Russian book on light vehicle control 10 p1408 A83-25624
- Automatic return in multifunction control logic --- for fighter cockpits 10 p1459 A83-26317
- Synthesis of C(asterisk)-model reference adaptive flight controller 10 p1379 A83-26559
- Remote control of satellites and applied automation 10 p1382 A83-26597
- On the routes - Boeing 757 with British Airways 12 p1701 A83-29241
- Determination of the optimal characteristic polynomial in automatic control systems --- of autopilots 12 p1769 A83-29289
- Stresses affecting the cockpit personnel and automation 12 p1767 A83-29373
- Globally stable nonlinear flight control system 14 p1977 A83-32425
- Using adaptive control to synthesize invariant and partially autonomous automatic stabilization systems 15 p2123 A83-33900
- Flight management concepts development for fuel conservation 16 p2304 A83-35843
- HiMAT onboard flight computer system architecture and qualification 17 p2467 A83-37061
- A variable structure approach to robust control of VTOL aircraft 17 p2470 A83-37145
- Meteorological data requirements for fuel efficient flight 17 p2552 A83-38760
- Flight management computers (FMS) 19 p2801 A83-40881

Flight management systems - What are they and why are they being developed?
[AIAA PAPER 83-2235] 19 p2803 A83-41712

Flight management systems - Where are we today and what have we learned?
[AIAA PAPER 83-2236] 19 p2803 A83-41713

Flight Management Systems III - Where are we going and will it be worth it?
[AIAA PAPER 82-2237] 19 p2804 A83-41714

Vertical flight path and speed control autopilot design using total energy principles
[AIAA PAPER 83-2239] 19 p2804 A83-41716

Mixing 4D equipped and unequipped aircraft in the terminal area
[AIAA PAPER 83-2240] 19 p2796 A83-41717

Robustness of a decoupled multivariable digital flight control system
[AIAA PAPER 83-2272] 19 p2804 A83-41738

A generalized stage-state method for centralized fault-tolerant flight control system
[AIAA PAPER 83-2301] 19 p2892 A83-41759

New results in fault latency modelling
[AIAA PAPER 83-2303] 19 p2888 A83-41760

Utilization of path length fuzing in the Peacekeeper Weapon System
[AIAA PAPER 83-2251] 19 p2810 A83-41763

Sensitivity of digital flight control design to parameter estimation error
[AIAA PAPER 83-2089] 19 p2805 A83-41921

Flight test experience with pilot-induced-oscillation suppressor filters
[AIAA PAPER 83-2107] 19 p2806 A83-41936

Fail-operational DAFCS for business/commuter aircraft --- Digital Automatic Flight Control System
[SAE PAPER 830714] 20 p2937 A83-43324

Digital simulation and control of the Machan UMA
20 p2932 A83-43718

A flight control and navigation system for small RVPs
20 p2932 A83-43723

Avionics analysed. IV - Aircraft grey matter
21 p3090 A83-44494

Four-dimensional flight management using colour CRT displays
21 p3091 A83-44689

On the structure and functions of the ISS-b satellite control systems
21 p3098 A83-45439

A Kalman filter algorithm for terminal-area navigation with sensors of moderate accuracy
21 p3090 A83-45460

Certification of the Lockheed 1011-500 active control system
22 p3255 A83-45850

The method of pole displacement in the artificial stabilization of dynamic systems
22 p3352 A83-46500

Operational and control display concepts for flight management systems in new generation transport aircraft
[AIAA PAPER 83-2489] 23 p3405 A83-48348

Voice-actuated avionics
24 p3546 A83-48891

Flight-control designer becomes metalogician
24 p3619 A83-48892

Application of optimal control synthesis to integrated vertical flight path and airspeed control for an advanced fighter
[AIAA PAPER 83-2560] 24 p3549 A83-49594

AUTOMATIC FREQUENCY CONTROL
Dynamic performance evaluation of a frequency tracking filter
07 p0916 A83-19681

AUTOMATIC GAIN CONTROL
Mitigation of pulsed RFI via automatic gain control
07 p0905 A83-19696

Characterization of the dynamical response of receivers to fading
10 p1404 A83-26471

Synthesis of adaptive tracking systems
17 p2570 A83-38483

Estimation of f0F2 from interferences appearing on AGC data of ISS-b topside sounder
21 p3178 A83-45447

AUTOMATIC LANDING CONTROL
Information requirements for pilot supervision of automatic landing in low visibility conditions
04 p0524 A83-16129

Applications of head-up displays in commercial transport aircraft
09 p1204 A83-24428

Observers as noise filters in an automatic aircraft landing system
09 p1209 A83-24434

Application of Monte-Carlo techniques to the 757/767 autoland dispersion analysis by simulation
[AIAA PAPER 83-2193] 19 p2802 A83-41678

Functional development of the 757/767 digital cat. IIIB Autoland System
[AIAA PAPER 83-2192] 19 p2796 A83-41762

Integrated flight control systems development - The F/A-18A Automatic Carrier Landing System
[AIAA PAPER 83-2162] 19 p2804 A83-41765

AUTOMATIC PATTERN RECOGNITION
U PATTERN RECOGNITION

AUTOMATIC PILOTS

Development of a flight test maneuver autopilot for a highly maneuverable aircraft
[AIAA PAPER 83-0061] 05 p0597 A83-16493

Closed-loop eigenvalue selection for reduced autopilot sensitivity to radome errors
[AIAA PAPER 83-0062] 05 p0592 A83-16494

Measurement of the frequency response of a digital autopilot
[AIAA PAPER 83-0326] 05 p0605 A83-16655

Identification of certain dynamic characteristics of a helicopter-autopilot system by means of simulation
08 p1047 A83-23222

Investigation of types of root loci of Fourth-order linear and linearized systems --- automatic pilot control system
11 p1647 A83-27448

Determination of the optimal characteristic polynomial in automatic control systems --- of autopilots
12 p1769 A83-29289

Adaptive control of nonlinear self-oscillating systems using MRAS technique
17 p2568 A83-37127

Modal synthesis of missile autopilot control law
17 p2476 A83-37152

DC-9 Super 80 Digital Flight Guidance System integrated system testing
[SAE PAPER 821364] 17 p2467 A83-37959

An adaptive mechanism for a non-linear control system
19 p2890 A83-41483

Status and concerns for preferred orientation control of high performance anti-air tactical missiles
[AIAA PAPER 83-2198] 19 p2802 A83-41683

Vertical flight path and speed control autopilot design using total energy principles
[AIAA PAPER 83-2239] 19 p2804 A83-41716

Direct design of multivariable control systems through singular value decomposition
[AIAA PAPER 83-2276] 19 p2892 A83-41742

The application and results of a new flight test technique
[AIAA PAPER 83-2137] 19 p2799 A83-41959

AUTOMATIC ROCKET IMPACT PREDICTORS

U COMPUTERIZED SIMULATION
U IMPACT PREDICTION

AUTOMATIC TEST EQUIPMENT

Structure and parameters of an automated system of radiometric flaw detection in articles of complex profile
01 p0049 A83-10361

Automatic plotting of the results of bench tests of turbine engines
01 p0011 A83-10444

AUTOTESTCON '81; Proceedings of the Conference, Orlando, FL, October 19-21, 1981
01 p0087 A83-10726

Maximizing ATE throughput
01 p0087 A83-10727

A data base solution to ATE resource management
01 p0087 A83-10728

Some management views on test program set /TPS/ salvageability
01 p0088 A83-10729

A systematic approach to comprehensive TPS diagnostics for electronic modules --- Test Program Set
01 p0037 A83-10730

Consolidated TPS implementation today and tomorrow
01 p0090 A83-10731

ATE support of RF line replaceable units
01 p0013 A83-10732

A modular interface switch for ATE applications
01 p0037 A83-10733

Automatic selection of switching paths
01 p0037 A83-10734

System performance ramifications of ATS architectures
01 p0088 A83-10735

Distributed system architectures --- modular approach to ATE
01 p0088 A83-10736

Aircraft systems test requirements analysis
01 p0014 A83-10737

Antenna couplers - The aircraft interface
01 p0004 A83-10738

The evolution of Navy Flight Line EW testers from AN/ALM-66 to AN/USM-406C
01 p0014 A83-10739

An Atlas implementation for the '80s
01 p0091 A83-10740

ADATLAS - The test language of the future
01 p0091 A83-10741

Voice ATLAS
01 p0091 A83-10742

UUT modeling
01 p0091 A83-10743

Data correlation of measurements made by automatic test systems
01 p0057 A83-10744

High speed signal acquisition and processing in EW ATE
01 p0031 A83-10745

Testing of complex ECM systems
01 p0057 A83-10746

Color graphics in ATE
01 p0028 A83-10747

Bubble technology for automatic test equipment/ground support equipment /ATE/GSE/ applications
01 p0037 A83-10748

Automatic testing of Constant Speed Drives
01 p0028 A83-10749

The first implementation of ATLAS for testing gas turbine engines
01 p0001 A83-10750

PETTS /Programmable Engine Trim Test Set/
01 p0014 A83-10752

The modular ATE/UUT interface
01 p0037 A83-10753

The rationale for a standard unit-under-test-interface
01 p0037 A83-10754

Testability - A quantitative approach
01 p0057 A83-10756

Is multi-port ATE in your future
01 p0028 A83-10758

All devices to all pins - Modular architecture and flexible switching provides this capability even for future upgrades
01 p0037 A83-10759

The microprocessor controlled ATE - A cost effective approach to dedicated automatic test equipment
01 p0088 A83-10760

The complete ATE decision system - A demonstration report
01 p0103 A83-10761

Cost-effective approaches for extending the useful life of ATE and test program sets
01 p0088 A83-10762

Emulation, a cost effective alternative for replacing obsolete ATE
01 p0088 A83-10763

ATE calibration by means of dynamic transport standards
01 p0050 A83-10764

ATS measurements today - How good are they
01 p0050 A83-10765

Field calibration of ATE via satellite
01 p0050 A83-10766

Conformance testing IEEE standard 488-1978 bus interface
01 p0037 A83-10767

Software quality assurance for automated calibration laboratories
01 p0091 A83-10768

Design considerations for a multiport multitest machine
01 p0029 A83-10769

Accuracy enhancement of a broadband A.T.E.
01 p0037 A83-10770

Distributed ATE systems software
01 p0088 A83-10771

A demonstration of microprogramming for increased ATE throughput
01 p0091 A83-10772

A test pattern generation technique for detection of digital circuits
01 p0038 A83-10773

Application of static Automatic Test Program Generators /ATPG/ to dynamic circuitry
01 p0038 A83-10775

Microprocessor controlled digital test subsystem tailored to automatic test program generator output
01 p0038 A83-10776

Development of maintenance concepts for Navy ATE
01 p0001 A83-10778

The ultimate ATE customer - The user
01 p0029 A83-10779

Lessons learned from maintenance applications of ATE
01 p0001 A83-10780

Description of a 3-port ATE system required for testing of electro-optical UUT's
01 p0038 A83-10781

Innovation in inertial ATE interfaces
01 p0017 A83-10782

Operator test control and interface evaluation
01 p0086 A83-10783

Calibration of third-generation ATE systems
01 p0091 A83-10784

On-line certification for ATE systems
01 p0001 A83-10785

Status of the calibration support of the Navy ATE
01 p0001 A83-10786

Increasing test programmer productivity
01 p0091 A83-10788

Commonly misunderstood ATE instrument specifications
01 p0050 A83-10789

Automatic fault diagnosis of a switching regulator
01 p0040 A83-11014

Design of an aircraft ice detector using microcomputer electronics to enhance system availability
01 p0009 A83-11097

An Automated Verification System for JOVIAL J73
01 p0089 A83-11166

Automatic change detection of synthetic aperture radar imagery
01 p0007 A83-11222

An automatic test generation system for complex digital logic
01 p0042 A83-11230

Testability using Logmod --- Logic Model method for functional analysis of system design
01 p0029 A83-11232

Signal classification for automatic industrial inspection
01 p0029 A83-11442

Operational summary of an electric propulsion long term test facility
[AIAA PAPER 82-1903] 02 p0139 A83-12478

Material-testing machine concepts for the integration of material testing into central in-service data acquisition
02 p0189 A83-12987

Development of Teal Ruby Experiment radiometric test requirements
03 p0325 A83-13728

On-line acquisition and analysis for holographic nondestructive evaluation 03 p0337 A83-13873

Automatic apparatus for nucleation investigations --- crystalline phase detection 03 p0329 A83-14171

An automated production holography test facility 04 p0488 A83-15157

Automated ultrasonic dimensional and defect inspection of complex geometry gas turbine airfoil shapes 04 p0488 A83-15158

Test bed for quantitative NDE - Inversion results 04 p0490 A83-15175

Quantitative Time-Of-Flight /TOF/ imaging for nondestructive evaluation by computerized ultrasonic tomography 04 p0493 A83-15224

An automatic system for the complex studies of low-temperature plasmas 04 p0537 A83-15919

ATE accomplishes receiver specification testing with increased speed and throughput 04 p0474 A83-16398

Automatic determination of frequency response parameters and distortion in resonant microwave cavities 06 p0750 A83-17970

Instrumentation for incremental voltage step electrochemical measurements 07 p0932 A83-21382

Automated inspection of metallized glass fiber 07 p0944 A83-21415

An automated measuring system for analyzing the development of fatigue cracks in the case of nonstationary loading 08 p1113 A83-22404

Automated testing systems with hydraulic force excitation /review/ 08 p1074 A83-22632

Electro-optical calibration considerations at intermediate maintenance levels 08 p1104 A83-22883

Infrared focal plane test station calibration 08 p1104 A83-22885

Rethinking automation in NDT applications 09 p1275 A83-23920

Self-tuning regulators - Non-parametric algorithms 10 p1461 A83-25399

Accuracy and precision of crack length measurements using a compliance technique 10 p1438 A83-25424

Evaluation of the productivity of an automated system for the testing of aircraft engines 12 p1703 A83-29277

Tradeoffs in level of automation in large-scale computerized test systems 13 p1861 A83-31190

The design of an automated, high-accuracy antenna test facility 13 p1829 A83-31280

A near-field antenna measurement system 13 p1830 A83-31282

An automatic test set for the dynamic characterization of A/D converters 13 p1836 A83-31288

Low-cost digital random vibration control (DRVC) technology demonstration 13 p1862 A83-31488

A microprocessor-based instrument for automatic solar cell characterization 14 p2004 A83-32204

Reducing the cost for airborne instrumentation hardware testing 14 p1978 A83-32928

The formalization of the choice of the acoustic stimulus parameters in a small automatic device for the examination and diagnosis of the functional condition of the auditory analyzer 14 p2073 A83-33312

A new transducer to monitor fatigue crack propagation 15 p2162 A83-33513

An investigation of a six-port microwave measurement system 15 p2153 A83-35084

A new approach to system diagnosis --- for fault identification in self-testing systems 15 p2218 A83-35140

Developments in test software philosophy and techniques 16 p2363 A83-35499

Automatic eddy current bolt-hole scanning system 16 p2363 A83-35760

Automated Foucault test for focus sensing 16 p2413 A83-36764

Design ATE systems for complex assemblies 16 p2348 A83-36962

A millimeter-wave automatic network analyzer 19 p2837 A83-40760

Design of algorithms to extract data from capacitance sensors to measure fastener hole profiles 19 p2855 A83-41026

Automatic fringe analysis with a computer image-processing system 19 p2847 A83-41106

Gas turbine engine cascade wind tunnel with automatic data acquisition and control 20 p2938 A83-42563

Automatic devices for the electromagnetic inspection of the thickness of the coating on small components 20 p2991 A83-43180

A micro-computer system for cell electrophoresis measurements 21 p3108 A83-43825

Flaw detector DVT-24 for the inspection of axial holes in deep drilling 21 p3135 A83-43880

A semi-automated in-plane loader for materials testing --- of fiber reinforced composites 21 p3108 A83-45162

Computer controlled decreasing Delta-K fatigue threshold test 21 p3162 A83-45184

Automatic laser photometer-polarimeter 21 p3141 A83-45310

Testing for space and weapon products; Proceedings of the Symposium, London, England, January 18, 1983 22 p3303 A83-45821

On target with confidence automated testing of guided weapons 22 p3303 A83-45822

MATE institutionalization --- Management of Automatic Test Equipment for weapon systems 22 p3303 A83-45823

Communications spacecraft payload testing 22 p3257 A83-45824

System functional testing of a communication satellite 22 p3257 A83-45825

Integration of electro-optical sensor computing systems 22 p3350 A83-46605

Automated diagnostic system for engine maintenance --- vibration data extraction from gas turbine engines [ASME PAPER 83-GT-103] 23 p3408 A83-47943

The Navy PATE program - A status report --- Propulsion Automatic Test Equipment [ASME PAPER 83-GT-109] 23 p3408 A83-47944

Avionics fault tree analyzer [AIAA PAPER 83-2452] 23 p3401 A83-48335

Consolidated TPS implementation today and tomorrow --- quality Test Program Sets for aircraft industry [AIAA PAPER 83-2495] 23 p3468 A83-48350

New concepts for intermediate level maintenance --- of avionics by ATE [AIAA PAPER 83-2498] 23 p3468 A83-48353

Microwave automatic impedance measuring schemes using three fixed probes 24 p3573 A83-48970

A photoelectric scanning system, OSS-50-1300, for measuring thermal deformations in specimens of degradable composites 24 p3585 A83-49918

A generator of test sequences for probabilistic systems of the fault diagnostics of digital devices 24 p3575 A83-50207

AUTOMATIC WEATHER STATIONS

Evolution of the NMC data assimilation system - September 1978-January 1982 02 p0217 A83-13052

The issue of reports from automatic meteorological stations in standard code form 04 p0514 A83-15024

Registration of thunderstorm centers by automatic atmospheric stations 09 p1314 A83-24277

Integrating non-first order automated meteorological observations into national weather forecasting and analysis programs 13 p1891 A83-30593

The LLP lightning locating system --- Lightning Location and Protection 17 p2549 A83-38720

Surface meteorological observations in severe thunderstorms. I - Design details of TOTO --- Tornado Observatory 18 p2727 A83-39884

AUTOMATION

Robots and image processing 02 p0161 A83-11795

A method of automated processing of flaw inspection results 02 p0188 A83-12164

Data base support for automated photo interpretation 02 p0200 A83-12888

Office automation in resource-management - The future is now --- agricultural land use map dissemination 03 p0348 A83-14269

Automation of the search for and recognition of reference zones for precise coordinate control of space imagery 03 p0350 A83-14311

Multidensity and its application to Landsat imagery 08 p1125 A83-21915

Automated navigation and collision avoidance for high-speed surface craft [AIAA PAPER 83-0631] 08 p1173 A83-22174

Rethinking automation in NDT applications 09 p1275 A83-23920

A system for the automated thermal design of instruments 09 p1260 A83-24234

Automated observations of the sun. II - Methods of observation 09 p1369 A83-24488

World survey of CAM --- Book 09 p1243 A83-25097

An automatic meter of the moduli of the coefficients of a reflection matrix for a quasi-optic path --- Russian book 09 p1257 A83-25100

NASA space power system automation 11 p1538 A83-27141

Model of a process of the design of complex systems and a method for its paralleling 12 p1769 A83-29349

The automation of data origination in monthly weather forecasts 14 p2056 A83-32370

Automated systems of control in civil aviation of the USSR 18 p2639 A83-39219

Automation of preplanning as a means for enhancing quality in operational flight control. II 18 p2638 A83-39222

Productivity goals drive office automation 18 p2752 A83-40308

Image processing in automatic systems for scientific investigations --- Russian book 19 p2889 A83-40986

Software for hybrid computing systems. I - Systems of analog and hybrid programming automation 19 p2888 A83-41421

The role of automation and artificial intelligence [AIAA PAPER 83-7104] 19 p2825 A83-42088

The automation of the design of optical systems --- Russian book 21 p3203 A83-43921

Automatic Incorporated in aerospace applications [SME PAPER MS83-230] 21 p3119 A83-44862

Automated riveter for spherical aircraft cell structures 23 p3391 A83-47182

Automated stellar photometry 24 p3649 A83-50029

AUTOMOBILE ACCIDENTS

An investigation of the connection between solar activity and the severity of the consequences of traffic accidents in Moscow 02 p0222 A83-11880

AUTOMOBILE ENGINES

Design of a low emission combustor for an automotive gas turbine [AIAA PAPER 83-0338] 05 p0652 A83-16664

Rotary engines 09 p1369 A83-25140

Catalyst durability evaluation for advanced gas turbine engines [ASME PAPER 82-JPGC-GT-21] 09 p1274 A83-25270

The relative attractiveness of electric and hybrid passenger cars 11 p1667 A83-27159

Acid fuel cell technologies for vehicular power plants 11 p1604 A83-27185

Status of solid polymer electrolyte fuel cell technology and potential for transportation applications 11 p1604 A83-27186

An assessment of the multifuel capability and alternative fuel potential of the automotive Stirling engine /ASE/ 11 p1587 A83-27273

50 kW Stirling engine 11 p1588 A83-27282

Manufacture and testing of fibre composite rotor components /Fibre composite flywheel development program for road vehicle applications/ 11 p1667 A83-27308

Possibilities of improving exhaust emissions and energy consumption in mixed hydrogen-gasoline operation 11 p1589 A83-27334

Fuel cell power plants for automotive applications 13 p1871 A83-31092

US Army Tank-Automotive Command (TACOM) adiabatic engine program [AIAA PAPER 83-1283] 16 p2362 A83-36321

Minimization of energy storage requirements for internal combustion engine hybrid vehicles 17 p2516 A83-37547

A study of the formation of nitrogen oxides during the combustion of a lean homogeneous mixture in the hybrid combustion chamber of an automotive gas-turbine engine 19 p2821 A83-42134

The energetic optimization of propulsion systems for electric vehicles --- Dutch thesis 21 p3221 A83-45075

Automotive gas turbine ceramic component testing [ASME PAPER 83-GT-112] 23 p3464 A83-47945

Ceramic Applications in Turbine Engines (CATE) development testing [ASME PAPER 83-GT-179] 23 p3465 A83-47990

Ceramic components for high-temperature vehicular gas turbines - State of the art of the German ceramic program [ASME PAPER 83-GT-205] 23 p3465 A83-48006

Component qualification and initial build of the AGT 100 advanced automotive gas turbine [ASME PAPER 83-GT-225] 23 p3465 A83-48023

Progress in net shape fabrication of alpha SiC turbine components [ASME PAPER 83-GT-238] 23 p3466 A83-48030

AUTOMOBILE FUELS

An assessment of the multifuel capability and alternative fuel potential of the automotive Stirling engine /ASE/ 11 p1587 A83-27273

Hydrogen as a fuel 15 p2193 A83-35302

Autogas flight test in a Cessna 150 airplane [SAE PAPER 830706] 20 p2933 A83-43317

AUTOMOBILES

NT ELECTRIC AUTOMOBILES

Prediction capability and improvements of the numerical notch analysis for fatigue loaded aircraft and automotive components 03 p0340 A83-13907

- An advanced electric vehicle powertrain
11 p1667 A83-27161
- AUTONOMIC NERVOUS SYSTEM**
NT SYMPATHETIC NERVOUS SYSTEM
The activity of tyrosine hydroxylase in the ganglia of the vegetative nervous system in rabbits during acute experimental emotional stress 01 p0080 A83-10542
An investigation of the relations between EEG and vegetative indicators in stress situations in patients with various types of depression 03 p0383 A83-13641
The peculiarities of the functioning of the cardiovascular system and its regulator mechanisms in swimmers depending on the initial condition of the vegetative nervous system 04 p0522 A83-15782
Surfactant homeostasis in the rat lung during swimming exercise 05 p0671 A83-17330
Autonomic contribution to heart rate recovery from exercise in humans 05 p0675 A83-17335
Performance predicted from baseline autonomic functioning --- of military pilots 10 p1455 A83-26308
A clinical and electroneuromyographic investigation of vegetative neuromuscular syndromes 14 p2070 A83-33309
Results of an experimental verification of the 'law' of initial value --- for prediction of physiological responses to work loads 16 p2399 A83-35913
Nonspecific esterases of the extramural ganglia of the autonomic nervous system in rabbits during acute experimental emotional stress 17 p2556 A83-38175
The characteristics of heart rhythm disorders in athletes with various types of vegetative regulation 19 p2882 A83-41447
- AUTONOMY**
Autonomy in military aircraft
[AAS PAPER 83-041] 21 p3097 A83-44168
Trends in Space Shuttle autonomy
[AAS PAPER 83-042] 21 p3096 A83-44169
Autonomy issues for an operational space station
[AAS PAPER 83-043] 21 p3095 A83-44170
Autonomy and fault tolerant design --- for satellite system and components 21 p3104 A83-44171
Planning for long term control of Space Station
[AAS PAPER 83-062] 21 p3096 A83-44175
- AUTOPILOTS**
U AUTOMATIC PILOTS
- AUTORADIOGRAPHY**
An autoradiographic investigation of protein synthesis by the muscles and interstitial elements of the myocardium during the formation of compensatory hyperfunction of the heart 07 p0974 A83-20976
The distribution of streptomycin in the structures of the inner ear following its parenteral administration (a histoautoradiographic investigation) 19 p2875 A83-41443
- AUTOREGRESSIVE PROCESSES**
Synthetic generation and estimation in random field models of images 01 p0101 A83-11474
Analysis of pulsations --- of geomagnetic fields 05 p0664 A83-17781
Estimation and choice of neighbors in spatial-interaction models of images 07 p0984 A83-20549
ARMA time series modeling - An effective method 08 p1158 A83-22730
Estimation and identification of two dimensional images 09 p1328 A83-24718
Recursive maximum likelihood estimation of autoregressive processes 10 p1462 A83-25636
Large sample identification and spectral estimation of noisy multivariate autoregressive processes 10 p1462 A83-25637
Statistical properties of multivariate autoregressive spectral analysis 10 p1466 A83-26538
On the accuracy of frequency determination by an autoregressive spectral estimator --- of astronomical spectra 11 p1669 A83-27636
Efficient algorithm for ARMA spectral estimation --- Auto Regressive Moving Average 14 p2075 A83-32428
Statistical efficiency of correlation-based methods for ARMA spectral estimation 14 p2075 A83-32430
Incoherent sequential detection of signals on a background of passive noise 14 p2000 A83-32481
The covariance least-squares algorithm for spectral estimation of processes of short data length 15 p2163 A83-33690
Fitting a linear autoregressive model for long-range forecasting 16 p2388 A83-36030
Generation of codes with good autocorrelation properties 19 p2827 A83-41276
Effects of mismatch and low rate for coding of autoregressive data by tree-searched DPCM 19 p2832 A83-41387
- AUTOROTATION**
A method for calculating the parameters of a turbojet engine in the autorotation regime 09 p1205 A83-23434
- Autorotation --- in fluid dynamics 13 p1804 A83-31079
- AUTOTROPHS**
A theoretical and experimental analysis of the turnover of substances in a closed microecosystem. II - The stable steady states and the limiting factors of turnover 03 p0384 A83-14326
- AUTUMN**
The spring and autumn transformations of the circulation regime of the meteor zone according to the data of multi-year radar, measurements in Kirgizia 07 p0970 A83-20895
Snow cover and temperature relationships in North America and Eurasia 18 p2723 A83-39139
- AUXILIARY EQUIPMENT (COMPUTERS)**
NT PLOTTERS
NT PRINTERS (DATA PROCESSING)
- AUXILIARY POWER SOURCES**
NT NUCLEAR AUXILIARY POWER UNITS
NT SPACE POWER REACTORS
Repair of the auxiliary power plants of aircraft --- Russian book 02 p0136 A83-11949
Space Shuttle Orbiter auxiliary power unit [SAE PAPER 820838] 10 p1387 A83-25752
The development of a central electrical generating system for transport vehicles 10 p1411 A83-26885
A parametric study of thermally augmented O₂/H₂ rocket engines [AIAA PAPER 83-1258] 16 p2319 A83-36312
Aircraft super integrated power unit [SAE PAPER 821461] 17 p2469 A83-37995
Super integrated power unit (SIPU) for the F-16 engine start system [SAE PAPER 821462] 17 p2469 A83-37996
Application of a hot gas high pressure rotary vane motor to aircraft APU starting [SAE PAPER 821464] 17 p2469 A83-37997
Small gas turbines and their applications in the field of high-speed surface craft 21 p3147 A83-44371
Hovercraft auxiliary power units (APUs) 21 p3147 A83-44372
Built-In Test Equipment (BITE) on the Garrett model GTC331 APU digital electronic control unit --- for gas turbine aircraft auxiliary power system [ASME PAPER 83-GT-186] 23 p3409 A83-47992
The GTC331, a 600 hp auxiliary power unit program --- for advanced transport aircraft [ASME PAPER 83-GT-188] 23 p3409 A83-47994
Emergency power for the F-16 aircraft [ASME PAPER 83-GT-189] 23 p3410 A83-47995
The prospects and potential of all electric aircraft [AIAA PAPER 83-2478] 23 p3411 A83-48341
Choice of parameters for a flywheel energy storage system --- for spacecraft 24 p3552 A83-49674
Direct-current power supply units GVG 800/350 24 p3549 A83-50115
- AUXILIARY PROPULSION**
Repair of the auxiliary power plants of aircraft --- Russian book 02 p0136 A83-11949
Qualification test results of IAPS 8 cm ion thrusters [AIAA PAPER 82-1954] 02 p0147 A83-12511
Propulsion systems for rotary wing aircraft with auxiliary propulsors 09 p1207 A83-24827
Shuttle Water Spray Boiler flight performance --- lubricant cooling for Orbiter Hydraulic System and APU [SAE PAPER 820885] 10 p1383 A83-25751
Auxiliary propulsion requirements for large space systems [AIAA PAPER 83-1217] 21 p3105 A83-45512
- AV-8A AIRCRAFT**
U HARRIER AIRCRAFT
- AVAILABILITY**
Techniques for system readiness analysis 01 p0103 A83-11155
Maintenance policies for equipments with planned interrupted operation 02 p0188 A83-12655
Determining the availability factor for a restorable technical system subject to two types of failure 03 p0337 A83-14099
Geostationary satellites ATS-6 and SMS/GOES - Description, position and data availability during IMS 04 p0511 A83-16283
On availability of a series-system with imperfect detectors 04 p0494 A83-16429
The practical tradeoff among bandwidth efficiency, modulation schemes, availability, and cost in satellite communication system design considerations 07 p0912 A83-19798
Bayesian reliability and availability - A review 07 p0942 A83-20515
Advanced DOD military satellite communications 19 p2833 A83-41403
Availability as a function of usage profile [AIAA PAPER 83-2287] 19 p2855 A83-41747
- Confidence limits for availability of maintained systems
Exact and Monte Carlo method 20 p2999 A83-42551
Estimating the inspection survivability 23 p3467 A83-47616
Wartime maintenance impact on aircraft availability
Quantifying the R&D investment payoff [AIAA PAPER 83-2515] 23 p3392 A83-48359
- AVAILANCE DIODES**
Millimeter-wave pulsed IMPATT diode oscillators /Review/ 01 p0043 A83-11305
Simulation of non steady-state transport in GaAs and InP millimeter IMPATT diodes 02 p0167 A83-11799
Solid state components adapt to sensor environmental demands 02 p0168 A83-12973
Novel optoelectronic devices prepared by molecular beam epitaxy 03 p0331 A83-13761
Silicon technology applicable to monolithic millimeter wave sources 03 p0310 A83-13783
Computer analysis of dc field and current-density profiles of DAR IMPATT diode --- Double Avalanche Region 05 p0631 A83-17764
Electroabsorption produced mixed injection and its effect on the determination of ionization coefficients --- in low noise avalanche photodiodes 05 p0691 A83-17769
High power CW single-drift IMPATT diodes at W-band 06 p0750 A83-17971
Broad-band bias-current-tuned IMPATT oscillator for 100-200 GHz 06 p0753 A83-18767
Broad-band characteristics of EHF IMPATT diodes 06 p0753 A83-18768
Sensitivity of avalanche photodetector receivers for long-wavelength optical communications 06 p0810 A83-19598
TRAPATT oscillators with active harmonic tuning --- German thesis 07 p0919 A83-20396
Manufacture and study of Diffused Gallium Arsenide IMPATT Diodes in the Ku-band --- German thesis 07 p0919 A83-20399
Controlled avalanche and transit time /CATT/ transistor Physical analysis and fundamental limitations --- French thesis 08 p1079 A83-22092
Practical comparison of optoelectronic sampling systems and devices 09 p1251 A83-23347
On the possibility of microwave generation in the case of avalanche processes in dipole domains 09 p1252 A83-23468
Measurement of series resistance in IMPATT diodes 09 p1256 A83-24500
A high-power W-band /90-99 GHz/ solid-state transmitter for high duty cycles and wide bandwidth 10 p1409 A83-25813
Si Impatts exhibit low noise at mm-waves 11 p1562 A83-28157
New GaAs Impatt theory explains mm-wave operation 11 p1562 A83-28158
Integral packaging for millimetre-wave GaAs IMPATT diodes prepared by molecular beam epitaxy 13 p1838 A83-31777
Single photon counters for the infrared 14 p2014 A83-31977
Staircase solid-state photomultiplier and avalanche photodiodes with enhanced ionization rates ratio 15 p2150 A83-33681
Optical comparator - A new application for avalanche phototransistors 15 p2229 A83-33684
The effect of oscillation amplitudes on the noise of IMPATT-diode oscillators with uniformly doped GaAs 15 p2152 A83-34713
Electronic frequency tuning of Trapatt oscillators 17 p2500 A83-38888
Impact ionization in (100)-, (110)-, and (111)-oriented InP avalanche photodiodes 18 p2750 A83-40064
Experimental observation of avalanche multiplication in charge-coupled devices 18 p2678 A83-40382
New progress in the development of a 94-GHz pretuned module silicon IMPATT diode 20 p2968 A83-43348
High efficiency GaInAs/Inp heterojunction IMPATT diodes 20 p2968 A83-43350
Radiation effects on semiconductor optical devices for space communications 22 p3278 A83-46615
Tunneling in the reverse dark current characteristic of Be-implanted GaAlAsSb avalanche photodetectors 22 p3365 A83-46656
High-performance avalanche photodiode with separate absorption 'grading' and multiplication regions 24 p3630 A83-49979
- AVALANCHES**
NT ELECTRON AVALANCHE
- AVERAGE**
NT MEAN
The relationship between the cloud amount and the temperature when averaged over a large space 02 p0213 A83-11978
Averaging of partial differential equations with rapidly oscillating coefficients 07 p0986 A83-20304

Nodal averaging technique in the optimality criterion approach using tapered finite elements
08 p1121 A83-21889
Processes in periodic media that cannot be described in terms of average characteristics
09 p1338 A83-24216
The effect of spatial and temporal averaging on sampling strategies for cloud amount data
10 p1451 A83-26100
Seasonal averages of net decay rate of SO₂ over northern Europe
19 p2864 A83-41988

AVIATION

U AERONAUTICS

AVIATORS

U AIRCRAFT PILOTS

AVIONICS

Antenna couplers - The aircraft interface
01 p0004 A83-10738
Tarps test program set / parallel development of avionics and its support capability/
01 p0014 A83-10755
The complete ATE decision system - A demonstration report
01 p0103 A83-10761
Testability assessment of a system design
01 p0029 A83-10777
Integrated CNI - A new testing challenge --- Communication, Navigation and Identification
01 p0004 A83-11095
ICNIA - Lessons learned on sensor integration --- Integrated Communication Navigation Identification Avionics
01 p0004 A83-11096
Air data systems for airplanes of the 1990's
01 p0004 A83-11099
Embedded microprocessors for avionics applications
01 p0088 A83-11104
A dynamic interface error performance simulation - IV&V for the F-4F OFF --- Independent Verification and Validation for Operational Flight Program
01 p0092 A83-11114
Testing of voice control device for aircraft avionics applications
01 p0005 A83-11122
Advanced speech technology in fighter cockpits - A new perspective on issues and applications
01 p0005 A83-11125
Analysis of systems containing multiple, irregular sampling
01 p0095 A83-11131
Color, pictorial display formats for future fighters
01 p0010 A83-11134
Integrated CNI avionics logistics considerations
01 p0103 A83-11157
A survey of avionics software support environments
01 p0087 A83-11163
Software development support system for advanced avionics applications incorporating a parallel machine architecture
01 p0087 A83-11164
Flat-panel video resolution LED display system
01 p0029 A83-11170
Video stand-alone instrument multi-function cockpit display system
01 p0010 A83-11172
AEDCS - A computer-aided system design tool for integrated avionics
01 p0089 A83-11176
Fiber optic aircraft multiplex systems - Planning for the 1990s
01 p0006 A83-11180
Fiber optics wavelength division multiplexing for aircraft applications
01 p0006 A83-11181
Future Navy data bus requirements - Modular approach for flexible evolution
01 p0006 A83-11184
An AN/APN-194/V// radar altimeter/MIL-STD-1553 interface circuit
01 p0010 A83-11186
Jovial language control procedures with a view toward Ada
01 p0092 A83-11198
Integrated electrical power and avionics control system
01 p0012 A83-11205
Requirements for debug capability of HOL-source code during software test in avionics laboratories
01 p0092 A83-11225
The design and implementation of the KC-135 Avionics Hot Bench Monitor
01 p0010 A83-11227
Advanced terrain following radar for LANTIRN --- Low Altitude, Navigation, Targeting Infrared at Night
01 p0007 A83-11241
Life Cycle Cost analysis of standard avionics hardware and software
01 p0112 A83-11256
The aviation and radioelectronic equipment of the Yak-18T aircraft --- Russian book
03 p0282 A83-13814
Atmospheric electricity and air transport safety [ONERA, TP NO. 1982-82]
03 p0280 A83-14534
Effective electromagnetic shielding in multilayer printed circuit boards
04 p0473 A83-16122
Flight simulation - Avionic systems and aero medical aspects; Proceedings of the International Conference, London, England, April 6, 7, 1982
04 p0441 A83-16326
Stimulation versus simulation --- as illustrated with Mission System Avionics for Airborne Early Warning Nimrod
04 p0445 A83-16332

The Northrop F-20 avionics mission simulator [AIAA PAPER 83-0142]
05 p0599 A83-16551
Fiberoptics technology and its application to propulsion control systems
05 p0595 A83-16772
Vibration isolation system development for the FB-111 tail pod electronics
05 p0595 A83-16932
Aircraft electrical equipment --- Russian book
05 p0597 A83-17125
Multifunction display simulation facility
05 p0596 A83-17302
Electromagnetic environment simulation for TCAS avionics --- Threat Alert and Collision Avoidance Systems
05 p0592 A83-17304
The capability and potential role of airborne avionic systems in air traffic management
05 p0593 A83-17731
The impact of new air traffic systems on the flight deck
05 p0593 A83-17733
Flight evaluation of modifications to a digital electronic engine control system in an F-15 airplane [AIAA PAPER 83-0537]
06 p0718 A83-19593
Electrical, avionic, and sensor equipment of the Yak-40 aircraft /2nd revised and enlarged edition/ --- Russian book
07 p0866 A83-20390
Fiber optic wavelength multiplexing for civil aviation applications
08 p1045 A83-22492
Computer-generated images in visual simulation and avionic technologies
08 p1047 A83-22835
The role of advanced navigation in future air traffic management
09 p1199 A83-23372
Integrated avionics/weapon system for air/ground missions [DGLR PAPER 82-039]
09 p1200 A83-24163
New displays for the next generation of civil aircraft - Airbus A 310 and A 300/600 color cathode tubes
09 p1204 A83-24374
Flight management systems and data links
09 p1209 A83-24424
Fault isolation methodology for the L-1011 digital avionic flight control system
09 p1209 A83-24427
ARINC 429 digital data communications for commercial aircraft
09 p1200 A83-24435
Integration of navigation resources in modern avionics systems
09 p1200 A83-24852
Multiprocessors and their impact on integrated navigation and avionics - A status-of-the-art paper
09 p1204 A83-24868
Environmental control of an aircraft pod mounted electronics system [SAE PAPER 820869]
10 p1375 A83-25768
Thermal design of integrated avionic racks for aircraft [SAE PAPER 820871]
10 p1375 A83-25770
Thermal design of standard avionic enclosures [SAE PAPER 820878]
10 p1373 A83-25772
Computer generated cockpit engine displays
10 p1376 A83-26309
Flight deck display
11 p1530 A83-27123
Development and test of an integrated sensory system for advanced aircraft
13 p1807 A83-30159
An assessment of external stores reliability testing
13 p1864 A83-31509
An in-depth evaluation of mission profile testing: Environmental engineering aspects - Reliability engineering aspects
13 p1864 A83-31510
The B-1 gets airborne again
14 p1974 A83-31941
All-electric vs conventional aircraft - The production/operational aspects
14 p1974 A83-32576
Propulsion control sensor sharing opportunities [AIAA PAPER 83-0536]
16 p2318 A83-36059
Real time simulation of mission environments for avionics systems integration [AIAA PAPER 83-1097]
16 p2312 A83-36217
Role of standards with integrated control
17 p2566 A83-37104
Redundancy Management of Shuttle flight control rate gyroscopes and accelerometers
17 p2474 A83-37123
The future of civil avionics
17 p2461 A83-37819
Avionics analyzed. III - The hidden sensors
17 p2461 A83-38471
The integration of multiple avionic sensors and technologies for future military helicopters
18 p2639 A83-40301
Simulation which simulates less
18 p2642 A83-40619
LHX system design for improved performance and affordability --- Light Helicopter
19 p2797 A83-41080
Advanced helicopter avionics
19 p2795 A83-41531
A history of electronic flight instruments - through tomorrow
19 p2799 A83-41532

Integrated airframe/propulsion control system architectures (IAPSA) study
19 p2797 A83-41660
[AIAA PAPER 83-2158]
Flight management systems - Where are we today and what have we learned?
19 p2803 A83-41713
[AIAA PAPER 83-2236]
Flight Management Systems III - Where are we going and will it be worth it?
19 p2804 A83-41714
[AIAA PAPER 82-2237]
Universities - Have they a role in aeronautical research? Flight mechanics, avionics and space
20 p2927 A83-42619
Lasers and avionic integration
20 p2995 A83-42836
The application of gyroscopes in remotely piloted vehicles
20 p2936 A83-43708
Man, machine and configuration - Human factors versus hardware in avionic display design
21 p3189 A83-44686
Application and experience of colour CRT flight deck displays
21 p3091 A83-44688
Aircraft keyboard ergonomics - A review
21 p3189 A83-44691
Certification of avionic systems; Proceedings of the Symposium, London, England, April 27, 1982
22 p3247 A83-45843
Military systems acceptance criteria --- for digital avionic systems
22 p3247 A83-45844
Flight clearance of the Jaguar fly by wire aircraft. I
22 p3254 A83-45845
Flight clearance of the Jaguar-fly-by-wire aircraft. II
22 p3255 A83-45846
A method of designing fault tolerant software
22 p3350 A83-45847
Certification of digital systems for civil aircraft
22 p3252 A83-45848
Helicopter avionic systems certification
22 p3255 A83-45849
Selecting shock and vibration isolators
22 p3302 A83-46346
Coherent, single-mode fiber optic for multifunction 10.6 micron helicopter avionics system
22 p3359 A83-46639
The Navstar GPS
22 p3253 A83-46965
Central operating and display unit for avionics systems
23 p3401 A83-47193
Studies and designs for a new helicopter cockpit
23 p3402 A83-47210
Maintenance aspects of modern avionics
23 p3392 A83-47654
Avionics fault tree analyzer [AIAA PAPER 83-2452]
23 p3401 A83-48335
Operational and control display concepts for flight management systems in new generation transport aircraft
23 p3405 A83-48348
[AIAA PAPER 83-2489]
New concepts for intermediate level maintenance --- of avionics by ATE
23 p3468 A83-48353
[AIAA PAPER 83-2498]
PAVE PILLAR - A new road to avionics reliability
23 p3401 A83-48643
Integrated digital avionic systems - Promise and threats
24 p3572 A83-48890
Voice-actuated avionics
24 p3546 A83-48891
Avionics built-in-test effectiveness and life cycle cost [AIAA PAPER 83-2448]
24 p3543 A83-49578
AVOIDANCE
NT COLLISION AVOIDANCE
Changes of sidman avoidance behaviour of rats induced by hypoxia
15 p2209 A83-33542
AXAF
U X RAY ASTROPHYSICS FACILITY
AXES (COORDINATES)
U COORDINATES
AXES (REFERENCE LINES)
NT AXES OF ROTATION
NT EARTH AXIS
AXES OF ROTATION
NT EARTH AXIS
Determination of the inclination of rotational axes and rotational velocity from the line profiles of rotating stars
01 p0122 A83-10337
An excursion into large rotations
04 p0531 A83-15004
Geometric methods for determining the axis of rotation and coordinates of the center of mass of a planet from orbital data
04 p0514 A83-16384
A vertical-axis wind turbine
05 p0658 A83-16881
A dynamic method for determining the axis of rotation and coordinates of the center of mass of a planet from orbital data
05 p0707 A83-17676
The construction of periodic orbits of satellites in a system of rotating axes. I
06 p0817 A83-17988
Stationary motions of two linked bodies
09 p1337 A83-23559

Investigation of the sufficient and necessary conditions of the stability of the uniform rotations of a gyrostat about the principal axis 09 p1337 A83-23561

Intrinsic principal axes twists in N-body models of elliptical galaxies 11 p1675 A83-28294

Pole orientation of asteroid 44 Nysa via photometric astrometry, including a discussion of the method's application and its limitations 14 p2097 A83-32602

The inertial motion of a gyrostat about a fixed center of mass 17 p2576 A83-38073

Whirl flutter analysis of a horizontal-axis wind turbine with a two-bladed teetering rotor 19 p2861 A83-40766

Stability of the stationary motions of the axis of a rotating rotor mounted in nonlinear bearings 19 p2895 A83-41203

Position angle variation of the major axis of some galaxies 20 p3061 A83-43378

Precise setting of devices in gimbal suspensions with misalignment of the axes 21 p3141 A83-45308

AXIAL COMPRESSION LOADS

The effect of oscillations on the stability of cylindrical shells under axial compression 01 p0059 A83-10690

A new class of solutions for buckling of a short cylindrical shell in pure bending 02 p0191 A83-12075

Long-term strength of composite compacts under programmed uniaxial tension-compression. I - A comparative analysis of some accumulated damage hypotheses. II - Modification of a hereditary long-term strength criterion 02 p0192 A83-12355

Efficient reinforcement of orthotropic viscoelastic cylindrical shells under axial compression 02 p0192 A83-12357

Nonlinear analysis of axially-loaded laminated cylindrical shells 02 p0194 A83-12743

The fracture mechanics of composite materials under axial compression - Brittle fracture 03 p0291 A83-14064

Determination of optimal reinforcement-parameters for cylindrical shells under axial compression that increases rapidly with time 03 p0341 A83-14074

Stability and vibrations of compressed, aeolotropic, composite cylindrical shells 04 p0499 A83-15689

The fracture mechanics of composite materials under axial compression - Plastic fracture 04 p0456 A83-16402

Experimental and theoretical correlations for elastic buckling of axially compressed stringer stiffened cylinders 05 p0655 A83-17720

Use of the phase method for evaluating defects in the form of developing microcracks 07 p0944 A83-21414

Maximum stiffness beam-columns 09 p1282 A83-25103

Plastic buckling of initially imperfect stiffened cylinders in axial compression 10 p1440 A83-26433

Dynamic stability of cylindrical sandwich panel subjected to axial compression 11 p1593 A83-27770

Stability of three-layer cylindrical shells with a discrete filler under axial compression 11 p1596 A83-28455

Experimental and theoretical correlations for elastic buckling of axially compressed ring stiffened cylinders 12 p1736 A83-29445

The selection of optimum parameters for stiffened cylindrical shells loaded by internal pressure and an axial compressive force 13 p1867 A83-31324

Buckle pattern of biaxially compressed simply supported orthotropic rectangular plates 13 p1868 A83-31619

Buckling and postbuckling of imperfect cylindrical shells under axial compression 15 p2180 A83-34568

The stability of composite sandwich shells with load-carrying layers of different stiffness under axial compression and external pressure 17 p2521 A83-37561

The stability of thin-walled ribbed conical shells 17 p2524 A83-38508

Stability of asymmetric three-layer cylindrical shells with a low-rigidity core under axial compression 18 p2701 A83-40106

Determination of critical dynamic axial compression stresses for rib-stiffened layered cylindrical shells 18 p2702 A83-40115

Coupling effect on axial compressive buckling of laminated composite cylindrical shells 18 p2704 A83-40187

Compressive fatigue damage accumulation near holes in graphite/epoxy laminates 18 p2655 A83-40203

Energy absorption of composite materials under crash conditions 18 p2705 A83-40216

Strain aging of Ti-6242 at hot-working temperatures 18 p2670 A83-40638

Buckling of sinusoidally corrugated plates under axial compression 19 p2856 A83-40878

Doubly symmetric interactive buckling of plate structures 20 p3001 A83-42519

Moisture and temperature effects on the instability of cylindrical composite panels 21 p3105 A83-43968

Plastic buckling of axially compressed circular cylindrical shells 21 p3152 A83-44249

Effective widths of plates loaded uniaxially 21 p3152 A83-44250

Three-dimensional stressed state of longitudinally corrugated elastic cylinders 21 p3163 A83-45359

AXIAL COMPRESSORS

U TURBOCOMPRESSORS

AXIAL FLOW

Stability of nonparallel developing flow in an annulus 03 p0323 A83-14698

Momentum theory, dynamic inflow, and the vortex-ring state 04 p0443 A83-16026

Dynamic behavior of turbulent flow in a widely-spaced co-axial jet diffusion flame combustor [AIAA PAPER 83-0575] 05 p0637 A83-16800

Boundary-layer transition on a rotating cone in axial flow 09 p1262 A83-24416

Interaction of fan rotor flow with downstream struts [AIAA PAPER 83-0682] 10 p1377 A83-25912

The analytic continuation of solutions of the generalized axially symmetric Helmholtz equation 10 p1470 A83-26775

Prediction of the surge line of axial multistage compressor 10 p1373 A83-26924

Buffeting of a slender circular beam in axial turbulent flows [AIAA 83-0928] 12 p1744 A83-29854

A sensor for flow measurements near the surface of a compressor blade 14 p2019 A83-32400

A model of axial impeller stall 16 p2292 A83-35678

Development of three-dimensional turbulent boundary layer in an axially rotating pipe 17 p2504 A83-37397

Experimental research on the design of highly loaded axial fans --- German thesis 17 p2447 A83-37498

Flow of an incompressible fluid in a partially filled, rapidly rotating cylinder with a differentially rotating endcap 18 p2680 A83-39207

The dynamics and heat and mass transfer of particles in a vortex chamber with an axial plasma flow 19 p2902 A83-41275

The uniqueness of polynomials representing the integral quantities of a compressible boundary layer on a cylinder rotating in a flow 21 p3129 A83-44323

Boundary layers on bodies of revolution spinning in axial flows 22 p3286 A83-47023

Effect on a developed turbulent boundary layer of a sudden local wall motion 22 p3286 A83-47024

Axial flow past a cylinder with uniform injection 23 p3451 A83-48499

Non-uniform flows in axial compressors due to tip clearance variation 24 p3548 A83-48824

AXIAL FLOW COMPRESSORS

U TURBOCOMPRESSORS

AXIAL FLOW PUMPS

NT TURBINE PUMPS

Fluid dynamics of inducers - A review 04 p0478 A83-16137

AXIAL FLOW TURBINES

Performance of the Wells turbine at starting 01 p0068 A83-10661

Numerical solution of subsonic and transonic cascade flows 02 p0132 A83-12901

Sounding propagation in multistage axial flow turbomachines 04 p0533 A83-15289

A comparison between the Craig-Cox and the Kacker-Okapuu methods of turbine performance prediction 06 p0718 A83-19025

Computing three-dimensional transonic gas flow through an axial-turbine stage 06 p0713 A83-19437

Isothermal models of gas-turbine combustors 08 p1057 A83-23097

Hydrodynamic visualization of the flow in a model of an axial flow turbomachine 09 p1261 A83-24336

Moment coefficient of the NACA 65 profile in delay cascades 09 p1198 A83-24509

On the definition of the axial velocity density ratio in theoretical and experimental cascade investigations 10 p1372 A83-26415

Application of a three-sensor hot-wire probe for incompressible flow 12 p1728 A83-28963

Aerodynamic performance of a Wells air turbine 13 p1869 A83-30191

Convective heat transfer in rotating cylindrical cavity [ASME PAPER 82-GT-151] 13 p1840 A83-30239

Turbulent boundary layer associated with periodic rotating wakes --- from axial flow turbomachine rotors 14 p1972 A83-33373

Axissymmetric vortex flow in a turbine stage under variable operating conditions 15 p2120 A83-34899

Blade-to-blade transonic flow calculation in axial turbomachines 16 p2290 A83-35837

Aerodynamic optimization theory of A 3-D axial-flow rotor-blading via optimal control 16 p2291 A83-35839

An experimental investigation of three-dimensional unsteady flow in an axial flow turbine [AIAA PAPER 83-1170] 16 p2294 A83-36257

Effects of interstage diffuser flow distortion on the performance of a 15.41-centimeter tip diameter axial power turbine [AIAA PAPER 83-1179] 16 p2307 A83-36263

A comprehensive method for preliminary design optimization of axial gas turbine stages. II - Code verification 16 p2309 A83-36393

Experimental evaluation of inlet turbulence, wall boundary layer, surface finish, and fillet radius on small axial turbine state performance [SAE PAPER 821475] 17 p2469 A83-38001

Numerical analysis of 3-D potential flow in axial flow turbomachines 18 p2684 A83-39458

Constraint on design parameters and twist of S1 surfaces in turbomachines 18 p2638 A83-40367

Experimental investigation of rotor wake traverse minima and their effects on the dynamic load of axial compressor and turbine cascades --- German thesis 19 p2859 A83-41807

Optimal design of the blading of axial turbines --- Russian book 21 p3147 A83-43924

Analytical and experimental study of flow through an axial turbine stage with a nonuniform inlet radial temperature profile [AIAA PAPER 83-1175] 21 p3088 A83-45510

Boundary layer and loss measurements on the rotor of an axial-flow turbine [ASME PAPER 83-GT-4] 23 p3392 A83-47878

The relative eddy in axial turbine rotor passages [ASME PAPER 83-GT-22] 23 p3393 A83-47887

Negative incidence flow over a turbine rotor blade [ASME PAPER 83-GT-23] 23 p3393 A83-47888

Calculation of three-dimensional, inviscid, rotational flow in axial turbine blade rows [ASME PAPER 83-GT-119] 23 p3395 A83-47948

Theory of blade design for large deflections. I Two-dimensional cascade [ASME PAPER 83-GT-124] 23 p3396 A83-47953

Wall boundary layer development near the tip region of an IGV of an axial flow compressor [ASME PAPER 83-GT-171] 23 p3396 A83-47972

AXIAL LOADS

NT AXIAL COMPRESSION LOADS

A numerical study of the buckling process and strength analysis of layered cylindrical shells under axial impact 02 p0192 A83-12358

A closed-form solution of a slant crack under biaxial loading 03 p0339 A83-13337

The rapid deformation of metals 04 p0458 A83-15386

Correlations between cavitation, creep and dilation for multiaxial loading 04 p0501 A83-16269

Effect of transverse direction strain on fracture of notched 0 deg/90 deg GRP laminate under biaxial fatigue 05 p0611 A83-17105

Variational solutions for the nonlinear deflexion of an annular membrane under axial load 05 p0656 A83-17945

Influence of load biaxiality on the fracture load of center cracked sheets 06 p0776 A83-18911

An analysis of the physical parameters of the steady-state creep of metals over a wide range of temperatures and stresses 07 p0889 A83-20901

Buckling of a thin-walled conical shell under axisymmetric loads beyond the elastic limit 07 p0947 A83-21087

Limitations and possible extensions to a nonlinear finite element shell-of-revolution model based on Reissner's shell theory 07 p0948 A83-21438

Plane stress fracture under biaxial loading 08 p1062 A83-21749

The effect of an axial force on a conical body 08 p1122 A83-22056

Shell-core method for the analysis of a long circular cylindrical sandwich shell subjected to axisymmetric loading 08 p1123 A83-22413

A note on transverse vibrations of continuous beams subject to an axial force and carrying concentrated masses 09 p1276 A83-23341

The strength of S0115M glass ceramic and its joints made through optical contact 11 p1551 A83-28511

Reduction of stress concentration around a hole in a uniaxially loaded plate 12 p1736 A83-29447

A Mohr-circle graphical method for stress intensity factors in cracked plates under different loadings 14 p2031 A83-32656

Viscoelastic characterization of a random fiber composite material employing micromechanics 14 p1988 A83-33297

- Local buckling of thin tensioned plate with a crack
14 p2033 A83-33374
- A nonlinear energy analysis for mixed mode fracture
17 p2518 A83-37271
- Fracture strains in biaxially loaded 2024 aluminum tubes
17 p2491 A83-38527
- The effect of biaxiality of loading in the orientation of caustics
18 p2699 A83-39538
- Reduced stiffness axial load buckling of cylinders
18 p2700 A83-39559
- Experimental and theoretical study of the elastoplastic buckling of cylindrical shells under axial impact
18 p2702 A83-40118
- Photoelastic determination of complex stress intensity factors for slant cracks under biaxial loading with higher-order term effects
19 p2860 A83-41998
- Buckling loads in the case of imperfect truncated conical shells under axial pressure
20 p3005 A83-42983
- Analysis of symmetrically loaded thin circular plates
20 p3008 A83-43672
- On crack branching and curving in a finite body
21 p3156 A83-44887
- The inclined crack under biaxial and uniaxial loading
21 p3157 A83-44900
- Plane-stress fracture testing of finite sheets under biaxial loads
21 p3161 A83-45161
- Inelastic buckling of cylindrical shells subjected to axial tension and external pressure
21 p3164 A83-45597
- Creep of thin-walled circular cylinder under axial force, bending, and twisting moments
[ASME PAPER 83-GT-154] 23 p3469 A83-47980
- The effect of biaxial loading on the size of a plastic zone near a crack
24 p3593 A83-49038
- AXIAL MODES**
- Single-axial-mode operation of a polarization-coupled stable/unstable-resonator Nd:YAG laser oscillator - Update
11 p1577 A83-27519
- AXIAL STRAIN**
- An analysis of cracking and the reliability of thin walled tubes under fatigue using the Weibull law
02 p0189 A83-11861
- An anisotropic plasticity model for inelastic multi-axial cyclic deformation
02 p0193 A83-12736
- Effects of friction in tensile and compressive stress problems for a rigid circular disk in an infinite plate
02 p0197 A83-13066
- A hollow oblate spheroid subjected to internal or external pressure and an oblate spheroid with a penny-shaped crack
03 p0343 A83-14819
- The load-carrying capacity of shells with softened regions
09 p1277 A83-23506
- Large deflections of circular plates of variable thickness
09 p1278 A83-23671
- Nonaxisymmetric buckling of nonshallow elastic shells of revolution
09 p1281 A83-25011
- A 'periodic' solution for an axisymmetric deformable elastic paraboloid of revolution
09 p1282 A83-25019
- Nonlinear statics and dynamics of thin axisymmetric shells by high precision finite elements
15 p2177 A83-34347
- The nonaxisymmetric deformation of flexible conical shells of variable thickness
16 p2365 A83-35926
- Analysis of shells of revolution subjected to axisymmetric deformation
17 p2524 A83-38506
- Numerical solution of axisymmetric problems in the dynamics of thin-walled orthotropic shells of revolution
17 p2524 A83-38507
- The nonstationary thermoelasticity problem for a cylinder weakened by a periodic system of penny-shaped cracks
17 p2524 A83-38510
- Stability loss and fracture of plates with cracks under biaxial tension
18 p2702 A83-40124
- An analysis of free-edge delamination in laminated composite under uniform axial strain
18 p2702 A83-40150
- Uniaxial and biaxial transient creep behavior of aluminum alloy
21 p3111 A83-44057
- Axisymmetric torsion of an elastic half-space with an elastic washer
21 p3154 A83-44720
- A class of integral equations for solving three-dimensional axisymmetric elasticity problems
21 p3163 A83-45358
- Experimental and numerical investigation of a turbulent boundary layer subjected to a sudden transverse strain
22 p3247 A83-46004
- Analysis of plane elastic-plastic shock-waves from the fourth-order anharmonic theory
23 p3474 A83-48603
- An extensometer for axial strain measurement at high temperature
23 p3459 A83-48604
- An analysis of nonstationary processes resulting from the nonaxisymmetric loading of multiple-layer finite cylinders
24 p3595 A83-49901

AXIAL STRESS

- A study of the stressed state of inhomogeneous cylindrical shells
01 p0059 A83-10679

- A study of residual stresses in boron filaments
02 p0150 A83-12351
- The role of the generalized fracture toughness in fracture mechanics
[ASME PAPER 82-PVP-21] 02 p0157 A83-12768
- Creep fracture by coupled power-law creep and diffusion under multiaxial stress
02 p0197 A83-12930
- Two decades of progress in the assessment of multiaxial low-cycle fatigue life
03 p0340 A83-13910
- Stability of thin plates with cracks under biaxial tension
03 p0340 A83-14071
- Axisymmetric flexure of circular sandwich plate including transverse shear facings
03 p0342 A83-14508
- Peripheral edge crack around a spherical cavity under uniaxial tension field
07 p0946 A83-20642
- Stress biaxiality effects on slow crack growth in polymethylmethacrylate
08 p1069 A83-21723
- Notes on the relationship between symmetric plane strain and torsion-free axis-symmetric problems
08 p1123 A83-22725
- Effects of plastic prestrain on the creep of aluminium under biaxial stress
09 p1233 A83-24078
- The elastic interaction between a tensioned strip and a loaded insert
09 p1282 A83-25018
- Efficient pulse shapes to deform beams with axial constraints
[ASME PAPER 82-WA/APM-6] 10 p1439 A83-25678
- Allowing for the coalescence of microcracks in a statistical kinetic model for the fracture of materials under uniaxial tension
13 p1866 A83-30057
- A Dugdale problem for a finite internally cracked plate
14 p2029 A83-32346
- Stability loss of compressed longitudinally reinforced cylindrical shells in the case of finite displacements with allowance for local buckling of rib-plates
15 p2178 A83-34439
- The effect of creep on the magnitude of elastic deformation in a laminated composite
16 p2323 A83-35506
- High temperature uniaxial tensile stress rupture strength of sintered alpha SiC
18 p2671 A83-39051
- Singular stresses in an infinite solid with a flat annular crack around a spherical cavity under tension
18 p2696 A83-39080
- Safety assessments in fracture-mechanics defect evaluation for biaxial stresses
18 p2696 A83-39256
- Analysis of the elastoplastic behavior of (0 deg/90 deg) and + Theta/-Theta bidirectionally fiber-reinforced ductile matrix composites in uniaxial loading
18 p2653 A83-40174
- On the knee-point of cross-ply composite
18 p2653 A83-40175
- Deformation and fracture of strongly textured Ti alloy sheets in uniaxial tension
18 p2669 A83-40630
- An annular crack in microelasticity
22 p3306 A83-46394
- Evaluation of a uniaxial nonlinear, second-order differential overstress model for rate-dependence, creep and relaxation
23 p3470 A83-48092
- The behaviour of fatigue cracks subject to applied biaxial stress - A review of experimental evidence
23 p3470 A83-48146
- Solution of certain equilibrium problems for an elastic parallelepiped in stresses
24 p3593 A83-49051
- The stability of plates near a sharp defect in the case of the initial biaxial plane stressed state
24 p3596 A83-49908
- AXISYMMETRIC BODIES**
- Finite element analysis of ideal flow over axisymmetric solid body / sphere/
01 p0045 A83-10277
- The energy-momentum pseudotensor of the gravitational field and the gravitational radiation emitted by an axisymmetric system
03 p0417 A83-13474
- Laser velocimetric analysis of the flow downstream of missile aft-bodies
[ONERA, TP NO. 1982-94] 03 p0279 A83-14543
- Stationary shape of bodies ablating in hypersonic flow under the action of radiation heating
04 p0477 A83-15863
- A formulation of radiation view factors from conical surfaces
[AIAA PAPER 83-0156] 05 p0633 A83-16560
- Effects of large oscillation amplitude on axisymmetric vehicle longitudinal static and dynamic stability in hypersonic flow
[AIAA PAPER 83-0215] 05 p0581 A83-16587
- Aerodynamic estimation techniques for aerostats and airships
06 p0712 A83-18404
- Axisymmetric reflectors of the stepped spherical type
06 p0781 A83-19194
- Comparison of computational and flight data concerning heat transfer for axisymmetric bodies moving along a trajectory at freestream Mach of not greater than 5
06 p0713 A83-19570

- Complex eigenfrequencies of axisymmetric perfectly conducting bodies - Radar spectroscopy
07 p0916 A83-21544
- Nonlinear analysis of the statics of thin axisymmetric shells by the finite element method
08 p1114 A83-21629
- Linear analysis by the finite element method of the dynamics of axisymmetric structures subjected to arbitrary loads
10 p1442 A83-26819
- An experimental investigation of the wake of an axisymmetric body with a slanted base
11 p1526 A83-27873
- Peculiarities in measuring the velocity vector using a laser anemometer in flow through axisymmetric models
13 p1848 A83-31470
- A nonlinear, semi-analytical finite element analysis for nearly axisymmetric solids
15 p2176 A83-34318
- Geometrically nonlinear formulation for the axis-symmetric transition finite elements
15 p2179 A83-34567
- Single- and multiple-crater induced nosetip transition
16 p2293 A83-36078
- Interaction of multiple supersonic jets with a transonic flow field
[AIAA PAPER 83-1680] 17 p2444 A83-37186
- Wind-tunnel simulation of the actual conditions of high-altitude flight
17 p2447 A83-37507
- A numerical study of slow nonisothermal flows past axisymmetrical bodies
17 p2506 A83-37805
- Allowance for finite Mach numbers in hypersonic asymptotics for blunt axisymmetric bodies
19 p2791 A83-41880
- On an approximate solution to the problem of unsteady flow around two-dimensional and axisymmetric bodies moving at high variable velocity
19 p2792 A83-41886
- Computational method of the drag of axisymmetric afterbodies in subsonic flow
[AIAA PAPER 83-2079] 19 p2792 A83-41913
- Heat transfer during ionized-gas flow past bodies
20 p2929 A83-42880
- Low speed performance of a supersonic axisymmetric mixed compression inlet with auxiliary inlets
[AIAA PAPER 83-1414] 21 p3088 A83-45516
- Analysis of turbulent flow past a class of semi-infinite bodies
[ASME PAPER 83-FE-32] 23 p3450 A83-48237
- Stability of the periodic oscillations of a nearly axisymmetrical satellite in the plane of an elliptical orbit
23 p3418 A83-48455
- Nonlinear creep problems for variable-boundary aging bodies
23 p3472 A83-48464
- Forces and moments acting on axisymmetric bodies rotating arbitrarily in free molecular flow
24 p3545 A83-49657
- Choice of the initial configuration for a solid body which assures the fulfillment of a prescribed ablation law
24 p3579 A83-49668
- AXISYMMETRIC DEFORMATION**
- U AXIAL STRAIN
- AXISYMMETRIC FLOW**
- NT ANNULAR FLOW
- On the total axial-symmetric expansion of a supersonic stream
01 p0003 A83-11329
- Friction and heat transfer from plates to normally-incident axisymmetric turbulent jets
02 p0170 A83-11874
- Heat transfer and microstructure of the boundary layer in the vicinity of the stagnation point of a jet flowing over a baffle
02 p0170 A83-11875
- Finite analytic numerical solution of axisymmetric Navier-Stokes and energy equations
[ASME PAPER 82-HT-42] 02 p0172 A83-12795
- The stability of swirling flows at large Reynolds number when subjected to disturbances with large azimuthal wavenumber
03 p0314 A83-13114
- Visualization study of the axisymmetric mixing layer of a high Reynolds number jet
03 p0320 A83-14482
- Flow of a conducting rotating fluid above a disc under uniform suction
03 p0323 A83-14724
- Obtaining axisymmetric flows from plane-parallel ones
04 p0475 A83-15087
- Axisymmetric vortex breakdown in rotating fluid within a container
04 p0476 A83-15696
- The organized shear layer due to oscillations of a turbulent jet through an axisymmetric cavity
04 p0480 A83-16343
- An exact solution for a high-temperature jet stream
04 p0480 A83-16390
- Calculation of the flow of a dust-laden gas over a disk and the flat end of a cylinder
05 p0639 A83-17406
- Flow over flat and axisymmetric bodies moving at high variable velocities
05 p0589 A83-17413
- Influence of small-amplitude undulations on turbulent convection in an axisymmetric pipe flow - Experiments and numerical prediction
05 p0641 A83-17704

A numerical study of the lateral interaction between an axisymmetric jet issuing into vacuum and an obstacle
06 p0760 A83-19431

Inviscid axisymmetric jet impingement with recirculating stagnation regions
08 p1042 A83-22130

Rapid distortion of small-scale turbulence by an axisymmetric contraction
08 p1084 A83-22381

A comparison of techniques for reconstructing axisymmetric reacting flow fields from absorption measurements
08 p1057 A83-22393

Momentum and heat transfer in power-law fluid flow over two-dimensional or axisymmetrical bodies
08 p1087 A83-23143

Semi-elliptic computation of axis-symmetric transonic flows
08 p1089 A83-23204

Natural convection in a rotating annulus
08 p1090 A83-23209

On the interaction of a sound pulse with the shear layer of an axisymmetric jet. II - Heated jets
09 p1340 A83-23704

Gas flow in an overexpanded axisymmetric nozzle
09 p1197 A83-24046

Mean flowfields in axisymmetric combustor geometries with swirl
09 p1263 A83-24668

Eddy viscosity in axisymmetric swirling jets
09 p1263 A83-25025

Axisymmetric flows in spin-up from rest of a stratified fluid in a cylinder
10 p1412 A83-25414

On the shock cell structure and noise of supersonic jets
[AIAA PAPER 83-0703]
10 p1474 A83-25923

Axially symmetric jet flows
11 p1564 A83-26975

Contouring of axisymmetric and plane nozzles for radial supersonic flow
11 p1526 A83-27713

Semi-elliptic computation of an axis-symmetric transonic nozzle flow
11 p1526 A83-27775

Modification of subsonic wakes using boundary layer and base mass transfer
12 p1695 A83-28954

Axial wavenumber measurements in axisymmetric jets
12 p1696 A83-28974

Joint probability density measurements in an axisymmetric parietal radial plane jet
12 p1723 A83-29376

Supersonic flow past a body with prescribed oscillations of its surface
13 p1803 A83-30002

Hydrodynamics and heat transfer in turbulent zero-momentum wakes
13 p1838 A83-30046

Numerical optimization studies of axisymmetric unsteady sprays
13 p1843 A83-31368

Quasi-axisymmetric circulation and superrotation in planetary atmospheres
13 p1962 A83-31750

Thin axisymmetric cavities in flow past a body in a longitudinal gravitational field
14 p2008 A83-32158

An axisymmetric nacelle and turboport inlet analysis including power simulation
14 p1970 A83-32584

Effects of artificial excitation upon a low Reynolds number Mach 2.5 jet
14 p2081 A83-32996

Numerical analysis of an axisymmetric viscous flow
14 p2013 A83-33375

Turbulent and mean flow measurements in an incompressible axisymmetric boundary layer with incipient separation
15 p2156 A83-33668

Generation of boundary-fitted curvilinear coordinate systems for a two-dimensional axisymmetric flow problem
15 p2157 A83-33825

Axisymmetric vortex flow in a turbine stage under variable operating conditions
15 p2120 A83-34899

Thermally driven flow in a rotating spherical shell
Axisymmetric states
16 p2385 A83-35479

On the investigation of axisymmetric discontinuous flows using interferometry
16 p2349 A83-35538

Axisymmetric flow in front of a transonic compressor with unique incidence condition
[ONERA, TP NO. 1983-51]
16 p2290 A83-35835

Constraints on the invariant functions of axisymmetric turbulence
16 p2351 A83-36083

A variation on McCormack's method for axisymmetric viscous compressible flows
16 p2352 A83-36093

Prediction of an axisymmetric combustor flow
[AIAA PAPER 83-1264]
16 p2326 A83-36315

Heat and mass transfer and hydrodynamics of swirling flows in axisymmetric channels --- Russian book
16 p2353 A83-36437

Numerical simulation of cold flow in an axisymmetric centerbody combustor
[AIAA PAPER 83-1741]
17 p2467 A83-37219

Application of numerical methods to the calculation of the characteristics of supersonic and hypersonic jet-engine air intakes
17 p2448 A83-37532

Comparison of computational and experimental data concerning flow past axisymmetric air intakes in regimes with an expelled shock wave
17 p2449 A83-37541

Calculation of transonic axisymmetric flow past bodies of revolution
17 p2450 A83-37627

Calculation of axisymmetric inlet flowfield using the Euler equations
[AIAA PAPER 83-1853]
17 p2457 A83-38681

Formation of a counter current region near a gravitating sphere in a steady Stokes flow of a viscous ideal gas
18 p2680 A83-39010

An integral model for confined axisymmetric turbulent jet mixing
[AIAA PAPER 83-1742]
18 p2680 A83-39098

Hydrodynamic instability of axisymmetric flows of an ideal fluid with an interface
19 p2844 A83-41579

Interference during flow around a wing and an axisymmetric nacelle
19 p2791 A83-41879

A method for calculating and analyzing the properties of a vertical nonisothermal jet with allowance for the buoyancy force
19 p2794 A83-42131

The principles governing the formation of circulation zones in the wake of mechanical and jet screens in confined flows
19 p2794 A83-42147

On the calculation of ducted propeller performance in axisymmetric flows --- Book
20 p2969 A83-42201

An analysis of the axisymmetric turbulent buoyant jet
20 p2973 A83-42685

Local heat transfer rates from two adjacent spheres in turbulent axisymmetric flow
20 p2976 A83-42719

Heat transfer augmentation in an axisymmetric impinging jet
20 p2979 A83-42744

Flow past and radiant heating of blunt bodies moving at angles of attack alpha greater than or equal to 0 deg
20 p2929 A83-42878

The gasdynamic momentum of flow in axisymmetric channels
20 p2982 A83-42886

Note on the axisymmetric sonic jet
20 p2930 A83-43123

An explicit Lagrangian scheme for solving plane and axisymmetric aerodynamic problems, and the mesh rezoning
21 p3130 A83-44558

Transformed Eliassen balanced vortex model
21 p3180 A83-44709

An investigation of the Mach disc and the Riemann wave formation in impulsive jets
21 p3132 A83-44947

The preferred-mode coherent structure in the near field of an axisymmetric jet with and without excitation
22 p3283 A83-46451

A summary of developments of the mean-stream-line method in China --- for design and calculation of flow channels
[ASME PAPER 83-GT-11]
23 p3393 A83-47883

Optimization of waverider configurations generated from axisymmetric conical flows
23 p3398 A83-48134

Isothermal predictions of recirculating turbulent flowfields of confined dual coaxial jets behind an axisymmetric bluff body
[ASME PAPER 83-FE-14]
23 p3450 A83-48232

Evolution of axisymmetric distributions of vorticity in an ideal incompressible stratified fluid (the linear description)
23 p3451 A83-48530

On the asymptotic structure of interaction in a laminar axisymmetric wake
23 p3451 A83-48653

Spinning modes on axisymmetric jets. I
24 p3578 A83-49469

Numerical calculation of mixed flows in plate nozzles --- for spacecraft engines
24 p3552 A83-49566

Investigation of unsteady temperature fields of nonaxisymmetric nozzle inserts
24 p3579 A83-49667

AXISYMMETRY

U SYMMETRY

AXLES

U SHAFTS (MACHINE ELEMENTS)

AXONS

The basal ganglia-circa 1982 - A review and commentary
02 p0222 A83-11826

AZIDES (INORGANIC)**NT HYDROGEN AZIDES**

The effect of the mode structure of laser radiation on the stability of lead azide
24 p3557 A83-49795

AZIMUTH

Investigation of azimuth effects in gamma families with total energies of 30-1000 TeV
02 p0274 A83-11740

Integrated navigation by supplementing MLS with DAS --- DME-based Azimuth System
09 p1202 A83-24872

An azimuth rate inertial navigation system
10 p1382 A83-26768

On the choice of the equatorial coordinates of celestial bodies from computer printouts during the calculation of their azimuths
12 p1706 A83-29322

High-order azimuthal modes in the open resonator
18 p2679 A83-40392

The effect of the ellipticity and unevenness of the pivots in a multipurpose astronomical instrument on observations for determining the azimuth by the direct method
19 p2854 A83-41552

Orientation of geodetic networks by gyro azimuths
22 p3316 A83-46345

AZO COMPOUNDS

NT RDX

Photochemical storage potential of azobenzenes
12 p1709 A83-28941

AZOLES

NT CARBAZOLES

NT PYRROLES

NT TRYPTOPHAN

Photoelectrochemical synthesis of thin polyazole films on semiconductors
02 p0151 A83-11660

Photochemical stability of UV-screening transparent acrylic copolymers of
23 p3433 A83-47824

A2F AIRCRAFT

U A-6 AIRCRAFT

B**B STARS**

Be stars; Proceedings of the Symposium, Munich, West Germany, April 6-10, 1981
01 p0119 A83-10301

Some photometric characteristics of Be stars / Review Paper/
01 p0116 A83-10302

A study of Be stars variability
01 p0120 A83-10303

Composite colour-magnitude and colour-colour diagrams for Be stars in open clusters
01 p0120 A83-10304

Statistical analysis of the data available for Be stars
01 p0116 A83-10305

Absolute magnitudes and intrinsic colours of non-supergiant Be stars
01 p0120 A83-10306

Luminosity classification of Be stars by Balmer line narrow band photometry
01 p0120 A83-10307

Long-term variation of Be stars on the color-magnitude diagram
01 p0120 A83-10308

Light variations in several broad-lined B stars
01 p0120 A83-10309

Correlations between BCD parameters of the continuous spectrum and the Balmer decrement of Be stars
01 p0120 A83-10310

Intrinsic reddening of Be stars and its relation with H-alpha emission intensities
01 p0120 A83-10311

BCD spectrophotometry of the Be-shell star 88 Her
01 p0120 A83-10312

Optical variations of the Be star HDE 245770/A 0535+26
01 p0120 A83-10313

Polarimetry and physics of Be star envelopes / Review paper/
01 p0120 A83-10314

Simultaneous spectroscopic and polarimetric observations of pi Aqr
01 p0120 A83-10315

Polarization in peculiar emission-line objects
01 p0116 A83-10316

Spectroscopic observations of Be stars in the photographic and visual regions / Review paper/
01 p0120 A83-10317

Statistical properties of Be stars
01 p0120 A83-10318

Observation of the H-alpha line of Be stars
01 p0120 A83-10319

On the radiation deficiency of shell stars in the Balmer continuum
01 p0121 A83-10320

Intensifier-dissector-scanner observations of the bright northern Be stars
01 p0116 A83-10321

Search for long-period radial velocity variations in some Be stars
01 p0116 A83-10323

Spectroscopic study of Pleione in 1977-1979 --- Be star
01 p0121 A83-10324

Radial velocity variations in 69 Orionis
01 p0121 A83-10327

Recent changes of the Be star HD 58050
01 p0121 A83-10328

On the problem of the chemical composition of Beta Lyrae
01 p0121 A83-10329

Spectroscopic observations of Be stars especially in the infrared
01 p0121 A83-10330

Oe star spectra in the red and near infrared
01 p0121 A83-10331

Infrared photometry of Be stars
01 p0116 A83-10332

Infrared emission from four Be stars optical counterparts of galactic X-ray sources
01 p0121 A83-10333

Rotation, expansion and duplicity of Be stars
01 p0121 A83-10335

The evolution of rapidly rotating B/Be stars
01 p0122 A83-10336

Determination of the inclination of rotational axes and rotational velocity from the line profiles of rotating stars
01 p0122 A83-10337

Be stars as interacting binaries
01 p0122 A83-10338

Radial-velocity and photometric variations of o And - Critical evaluation of possible periods
01 p0122 A83-10339

- Rotational velocity versus mass loss in Be stars
01 p0122 A83-10340
- X-ray observations of Be stars
01 p0122 A83-10341
- Be components in X-ray binaries
01 p0122 A83-10342
- Are classical Be stars sources of hard X-rays
01 p0116 A83-10343
- Ultraviolet observations, stellar winds, and mass loss for Be stars
01 p0122 A83-10344
- Variation of anomalous stages of ionization with spectral type for Be stars
01 p0122 A83-10345
- The expanding atmosphere of HD 218393
01 p0122 A83-10346
- Ultraviolet observations of interacting binary Be stars
01 p0122 A83-10347
- Recent changes in the ultraviolet spectrum of the Be star HR 2855
01 p0123 A83-10348
- Far-ultraviolet colors of B stars with and without emission lines
01 p0123 A83-10349
- Spectral energy distribution /119 - 685 nm/ in 16 shell stars and a tentative model for accreting Be stars
01 p0123 A83-10352
- Model atmospheres of Be stars
01 p0123 A83-10353
- Theoretical surface brightness distributions and continuum polarization of rapidly rotating B stars
01 p0123 A83-10355
- Spectroscopic investigations of Herbig-Ae-Be-Stars
01 p0123 A83-10356
- Sk 143 - An SMC star with a galactic-type ultraviolet interstellar extinction
01 p0125 A83-10929
- The theoretical expected galactic distribution of WR runaway stars
01 p0125 A83-10935
- The interstellar absorption-line spectrum of Mu Ophiuchi
02 p0256 A83-12124
- Stars of spectral types A and B in the southern galactic halo. I - UVB photometry
02 p0249 A83-12915
- Equivalent widths of spectral lines in B stars
03 p0414 A83-13359
- UBV-H-beta/ photometry of luminous stars between l equals 335 deg and l equals 6 deg
03 p0402 A83-13365
- A search for OB associations near southern long-period Cepheids. I - WZ Carinae, YZ Carinae, KK Centauri, and OO Centauri
03 p0406 A83-13554
- A photometric and spectroscopic study of faint OB stars in the Southern Milky Way
03 p0409 A83-13931
- Optical observations of ultraviolet objects. II - Classification and photometry /I = 0 to 145 deg/
03 p0409 A83-13932
- He I lines in B stars - Comparison of non-local thermodynamic equilibrium models with observations
03 p0424 A83-14200
- Ultraviolet emission in the Mg II h and k lines in Be stars
03 p0424 A83-14201
- Properties and nature of Be and shell stars: 7 B.88 Her - An important clue to understanding the Be phenomenon
03 p0430 A83-14801
- Properties and nature of Be and shell stars. II - A notable correlation between the long-term spectral and photometric variations of V 1294 Aql /HD 184 279/
04 p0551 A83-15109
- A comparison of the X-ray properties of X Persei and Gamma Cassiopeiae
04 p0554 A83-15629
- Structure and evolution of large groups of Massive Close Binary systems
04 p0557 A83-15979
- Ultraviolet extinction towards far OB associations
04 p0557 A83-15986
- Properties and nature of Be and shell stars 7A. 88 Her - Observational data, their reduction and basic evaluation
05 p0694 A83-17668
- Spectroscopic analysis of alpha Andromedae
05 p0702 A83-17812
- The spectrum of 11 Cam in 1980 and 1981
06 p0817 A83-18016
- Shell and photosphere of Sigma Ori E - New observations and improved model
06 p0825 A83-18083
- A survey of ultraviolet objects
06 p0818 A83-18178
- Mass loss from extreme helium stars
06 p0829 A83-18539
- Optical monitoring of Orion population stars. I - Results for some T Tauri and Herbig Ae/Be stars
06 p0820 A83-18860
- Spectrographic material for RS Canum Venaticorum and Algol binaries
06 p0836 A83-19061
- Circumstellar material around rapidly rotating B stars. I - Nonemission-line stars
06 p0836 A83-19071
- HD 207739 - A strange composite star
06 p0823 A83-19301
- The near-infrared spectrum of the Herbig Ae-Be stars
06 p0844 A83-19497
- Variability and mass loss in IA O-B-A supergiants
07 p1010 A83-19858
- Transient emission events in the early Be star 59 Cygni
07 p1010 A83-19859
- Formation of OB clusters - OH maser observations
07 p1021 A83-21128
- Explosive helium burning in supernovae - A source of r-process elements
07 p1022 A83-21140
- On the photometric differences between luminous OBA type stars in the LMC with and without P Cygni characteristics
07 p1023 A83-21212
- Neutral hydrogen in the Cas OB6 association
07 p1025 A83-21242
- The frequency of Be stars
07 p1025 A83-21250
- Spectral energy distributions and equivalent widths of Balmer lines of B and A stars with rapid axial rotation - Comparison with theoretical models
07 p1027 A83-21266
- Energy distributions in the spectra of 10 B to A stars
07 p1027 A83-21280
- Discovery of close binary stars using the one-meter telescope on Mt. Sangklo
08 p1174 A83-22054
- On the Balmer progression in the expanding shell of Pleione
08 p1185 A83-23106
- Be and shell stars observed with the 13-color photometric system
09 p1353 A83-23733
- Spectral fine analysis of the extreme helium star BD + 10.2179 deg
09 p1359 A83-24458
- Kinematical studies of open clusters and OB-associations from relative radial velocity observations. II - The Orion Belt region
09 p1360 A83-24465
- Spectroscopic observations of eclipsing binaries. V - Accurate mass determination for the B-type systems V539 Arae and Zeta Phoenixis
10 p1491 A83-25360
- Spectrophotometry of peculiar B and A stars. XV - Alpha Andromedae, AR Aurigae, 36 Aurigae, 36 Lyncis, Phi Herculis, HR 6127, and HR 6997
10 p1499 A83-25369
- Search for light variability of LSI + 61deg303
10 p1492 A83-25379
- Evidence for outburst in the shell star 17 Lep derived from ultraviolet spectra
10 p1501 A83-25499
- On the presence of O I lambda 1302 emission in Be stars
10 p1502 A83-25585
- Spectrophotometry of peculiar B and A stars. XIII - HD 51418, 53 Camelopardalis, 78 Virginis, and Kappa Piscium
10 p1502 A83-25651
- Spectrophotometry of peculiar B and A stars. XIV - 56 Arietis, 41 Tauri, 25 Sextantis, HD 170973, HD 205087, and HD 215441
10 p1502 A83-25661
- Spectrophotometry B, A, and F stars. III
10 p1497 A83-26380
- The 1980 outburst of 4U 0115+63 /V635 Cassiopeiae/
10 p1510 A83-26389
- NGC 6067 and three cepheids
11 p1668 A83-27111
- HRr 9070 - A nonradially pulsating Be star
11 p1676 A83-27116
- HD 129929 - A multiperiodic pulsating early-type star at intermediate galactic latitude
11 p1678 A83-27693
- Photometric and spectroscopic observations of an optical candidate for the X-ray source H 0544 - 665
11 p1675 A83-28276
- Evolution of chemical abundances in massive stars. I - OB stars, Hubble-Sandage variables and Wolf-Rayet stars - Changes at stellar surfaces and galactic enrichment by stellar winds. II - Abundance anomalies in Wolf-Rayet stars in relation with cosmic rays and 22/Ne in meteorites
12 p1790 A83-28890
- Oscillator strengths and Ne abundance in B stars
12 p1790 A83-28892
- High-resolution H-alpha observations of Gamma Cas and Pi Aqr
12 p1788 A83-29181
- HDE 283809 - A type B star toward the Taurus dark cloud
12 p1796 A83-29495
- Formation of OB clusters - W33 complex
13 p1950 A83-31417
- The ultraviolet reddening of Be stars
13 p1953 A83-31560
- The early B-type eclipsing binary FZ Cma (HD 52942) - A massive triple system
13 p1941 A83-31566
- R 66(Aeq) - An LMC B supergiant with a massive cool and dusty wind
13 p1954 A83-31567
- Ultraviolet spectroscopy of LSI + 61 303
13 p1957 A83-31706
- The Cygnus X region. XIII - The dark cloud between IC 1318b and c
13 p1959 A83-31743
- New polarization measurements of HD 183143, HD 204827, and Cyg OB 2 Sch. No. 12
13 p1943 A83-31757
- Massive eclipsing binary candidates
14 p2098 A83-33151
- A survey of spectral morphology and rotational velocities among the helium-rich stars
14 p2105 A83-33197
- Observation of ice mantles toward HD 29647
14 p2107 A83-33232
- Fourier transform spectroscopy of six stars
14 p2100 A83-33257
- Thirteen-color photometry of Be stars
14 p2100 A83-33260
- Transition region models for Be stars
14 p2108 A83-33266
- Ultraviolet continuum of a sample of Be stars
14 p2108 A83-33267
- Spectrophotometry of three peculiar emission-line stars
15 p2253 A83-33708
- Star complexes in the Andromeda Nebula
15 p2253 A83-33713
- X-ray properties of the Be/X-ray system 28 0114+650 = LSI + 65deg 010
15 p2258 A83-34104
- Episodic mass loss and narrow lines in gamma Cassiopeiae and in other early-type stars
15 p2258 A83-34107
- Orbital motion and mass flow in the interacting binary Be star HR 2142
15 p2247 A83-34507
- ANS spectrophotometry - Delta Pictoris as an upper-main-sequence algol system
15 p2247 A83-34508
- Interstellar Ca II and Na I line profiles towards halo OB stars
15 p2264 A83-34585
- A generalized method for deriving mass-loss rates - The first order moment of unsaturated P Cygni line profiles
15 p2272 A83-34780
- On the need for a new spectroscopic standard for MK spectral type B0 III
15 p2250 A83-35321
- Envelope structure of the cyclic V/R variable shell stars
16 p2429 A83-36630
- Multi-periodicity of the new variable B-type star HR 3562
16 p2425 A83-36636
- The absolute masses of 72 galactic clusters and 12 OB associations
16 p2429 A83-36640
- Radial velocities of bright southern stars. I - 139 B-type HR and FK stars
17 p2587 A83-37287
- H-alpha line profiles in B stars - Comparison of theory and observations
17 p2597 A83-37324
- The double-lined spectroscopic binary HD28475
17 p2589 A83-37371
- The application of atmospheric models to the investigation of B-G stars
17 p2600 A83-37656
- The behavior of emissions in the spectrum of Gamma Cassiopeia from September to November 1977 and in September and October 1979
17 p2601 A83-37708
- A spectral investigation of the eclipsing binary V822 Aql
17 p2601 A83-37709
- A study of B-type supergiants with the uvby, beta photometric system
17 p2591 A83-37783
- On the carbon overabundance in the OBC-type stars
17 p2606 A83-38239
- The age and dimensions of star complexes
17 p2613 A83-38830
- Kinematic parameters for Trapezium-type systems
17 p2613 A83-38839
- Photoelectric and spectral observations of Vela X-1 during the time of sudden changes in its X-ray pulse period
18 p2754 A83-38997
- Changes in interstellar atomic abundances from the galactic plane to the halo
18 p2768 A83-39630
- The velocity fields of gas and stars within five kpc of the sun
18 p2768 A83-39637
- A comparison of the velocity fields of young stellar objects and of Sharpless H II regions
18 p2758 A83-39638
- Chemical evolution of OB associations
18 p2774 A83-39726
- P Cygni stars as a intermediate stage between red supergiants and Wolf-Rayet stars
19 p2914 A83-40705
- Observations of an emission nebula associated with the carbon star UV Aur
19 p2914 A83-40716
- Three-micron emission features in Herbig Be/Ae stars and related objects
19 p2909 A83-40722
- Spectroscopic orbit of the star HR96
19 p2910 A83-41056
- Infrared magnitudes (JHKLM) for 105 chemically peculiar A- and B-stars
19 p2910 A83-41065
- Cool neutral hydrogen in the direction of an anonymous OB association
20 p3064 A83-42194
- Theoretical evolution of massive stellar aggregates
20 p3065 A83-42385
- Star formation within OB subgroups - Implosion by multiple sources
20 p3073 A83-43086
- AB Aurigae and its variable hydrogen lines
21 p3228 A83-44404
- A study of UV spectra of Zeta Aur/UV Cep stars. IV - System parameters and mass-loss of Delta Sge
21 p3228 A83-44416
- The bright stellar content of the giant galactic H II region NGC 3603
21 p3229 A83-44420
- Can shell phases of Be stars be predicted on the basis of rapid spectroscopic micro-variability?
21 p3229 A83-44422

Studies of the Carina Nebula. V - The near infrared excess of O-type stars and the anomalous extinction law in their environment 21 p3230 A83-44442

The Beta Cep variables - Fundamental radial pulsators 21 p3234 A83-44763

Radio images of the bipolar H II region S106 21 p3236 A83-45542

The magnetic fields of the helium-weak B stars 22 p3377 A83-46265

A study of the binary system 58 Persei 22 p3374 A83-46543

Molecules in celestial objects. IV - IUE observation of CO lines towards Be stars with low reddening 22 p3379 A83-46555

Enhanced polarization in the Ca II K line of the Be star Kappa Dra 24 p3660 A83-49385

A second catalog of the profile of the H-alpha line in 55 Be stars 24 p3645 A83-49839

Far ultraviolet colors of B and Be stars 24 p3669 A83-50100

Far ultraviolet colors of Beta Cephei stars 24 p3669 A83-50101

B-A-W DEVICES

U BULK ACOUSTIC WAVE DEVICES

B-1 AIRCRAFT

Blackjack - Soviet B-1 or better 04 p0447 A83-16373

Rockwell B-1B design to be studied in new cab 06 p0719 A83-18271

The B-1 gets airborne again 14 p1974 A83-31941

B-1B manufacturing - Rockwell management plan saving costs, time 18 p2632 A83-40331

B-1B manufacturing - General Electric F101 production nears 18 p2632 A83-40332

B-1B manufacturing - Avco modifies prototype processes for production 18 p2632 A83-40333

B-52 AIRCRAFT

B-52 roles in sea control 07 p0862 A83-20646

B-52 operations in the Bright Star 82 exercise 12 p1699 A83-29204

Use of flight test results to improve the flying qualities simulation of the B-52H weapon system trainer [AIAA PAPER 83-1091] 16 p2300 A83-36215

727, B-52 retrofit with PW2037 meeting today's requirements [SAE PAPER 821443] 17 p2463 A83-37991

B-58 AIRCRAFT

Flight testing the Hustler 500 14 p1975 A83-32930

BACILLUS

The biological effect of nonionizing radiation and the question of the effect of solar activity on organisms 02 p0220 A83-11885

BACK INJURIES

An analysis of spinal injuries after ejections and crash landings in the IAF 02 p0223 A83-12254

Biomechanical aspects of the fracture resistance of the vertebral column of humans under impact overloads in the head-pelvis direction 06 p0798 A83-18509

Spinal traumas /dorsal spinal fractures and lumbar disk hernias/ occurring after rapid vibratory phenomena /pumping/ in air combat pilots 08 p1148 A83-22973

Some observations on bail out injuries 08 p1148 A83-22975

Unusual ejection injury - A case report 09 p1323 A83-24008

Vertebral lesions after the aircraft crashes 16 p2396 A83-35579

Vertebral lesions after pilot ejection from fighter aircraft 16 p2397 A83-35580

The spine of the parachutist 16 p2397 A83-35581

The structural and functional bases of the compensation of functions in the case of spinal cord trauma --- Russian book 23 p3494 A83-47099

BACKGROUND NOISE

Simulation of background clutter --- causing target signature distortion 01 p0048 A83-10063

The use of radar methods of optimum detection for ultrasonic echo monitoring 01 p0049 A83-10370

Game-theoretical approach to the detection of radar signals on a background of unknown noise 01 p0030 A83-10408

Testing of voice control device for aircraft avionics applications 01 p0005 A83-11122

Detection of a signal on a background of non-Gaussian noise with unknown nonstationarity characteristics 02 p0162 A83-11531

An examination of background noise in analog integrated circuits and components --- French thesis 02 p0166 A83-11765

1.0 to 2.5 micrometer short wavelength infrared /SWIR/ linear array technology for low background applications 03 p0326 A83-13739

Phase-locked loops with limiter phase detectors in the presence of noise 03 p0312 A83-13860

Rigorous results on inverse source and inverse scattering theory --- for use in quantitative nondestructive evaluation 04 p0490 A83-15172

Quantization of signals on a background of noise 04 p0467 A83-15736

Simultaneous detection, resolution, and measurement of the parameters of signals on a noise background at the output of an antenna array - Synthesis of the algorithm 04 p0467 A83-15737

Signal processing for staring infrared images 08 p1094 A83-22439

Analysis of the effect of finite register length on the efficiency of digital filters for the detection of signals on a noise background 08 p1082 A83-23159

Target acquisition and extraction from cluttered backgrounds 09 p1204 A83-23531

An unbiased adaptive method for retrieval of sinusoidal signals in colored noise 09 p1331 A83-24773

A comparative analysis of the noise immunity of methods for processing FSK signals with split values of frequencies on a noise background 09 p1251 A83-25081

Optimal sample-at-a-time processing of signals on a background of noise with an arbitrary distribution 09 p1251 A83-25162

Experimental investigations of fluctuations of optical signals and disturbances in the atmosphere 10 p1434 A83-26694

Utilization of the decorrelation properties of discrete spectral transformations for the multialternative recognition of signals on a background of correlated noise 10 p1470 A83-26955

Combination of the dependent channels of the detection of a random signal on a background of noise with an unknown correlation matrix 11 p1555 A83-27937

An objective procedure for detecting and correcting errors in geophysical data. II - Multidimensional applications 13 p1877 A83-30897

A duality principle for state estimation with partially noise-corrupted measurements 14 p2074 A83-31929

Analysis of the efficiency of the spatial-temporal processing of radio signals in the presence of noise 14 p2000 A83-32480

Incoherent sequential detection of signals on a background of passive noise 14 p2000 A83-32481

Edge and line detection in multidimensional noisy imagery data 15 p2183 A83-33688

Detection of constant signals in skewed noise 15 p2222 A83-35137

Estimation of the efficiency of devices for the detection and recognition of signals 16 p2404 A83-35940

Measurement of faint lidar signals in the presence of an intense background during pulsed laser sounding of the atmosphere 16 p2360 A83-36125

Performance of a two-stage nonparametric conditional detector for Rician density 16 p2347 A83-36579

Measurement of the phase of a coherent-pulsed signal in the presence of correlated noise 17 p2495 A83-38500

Optimal reception of digital messages in a channel with variable parameters on a background of pulsed and fluctuation noise 20 p2964 A83-42901

Approximating point-set images by line segments using a variation of the Hough transform 21 p3190 A83-44271

Application of the one-dimensional Fourier transform for tracking moving objects in noisy environments 21 p3194 A83-44278

Identification of structural dynamics systems using least-square lattice filters --- large space structures 21 p3103 A83-45467

BACKGROUND RADIATION

Intergalactic gas in galactic clusters, the microwave background radiation and cosmology 01 p0124 A83-10839

Mach's principle and the microwave background --- in homogeneous cosmology 01 p0126 A83-10971

Extended regions of soft X-ray emission and background spectrum at Southern latitudes 01 p0118 A83-10972

Some aspects of gravitational waves in an isotropic background universe 01 p0127 A83-11295

Search for small-scale anisotropy in the cosmic microwave background 02 p0259 A83-12221

Application of JFets to low background focal planes in space 03 p0308 A83-13456

Low background spectral response of 30-130-micron detectors from blackbody measurements 03 p0324 A83-13458

Angular fluctuations in the temperature of the cosmic background radiation in a universe with massive neutrinos 03 p0439 A83-13886

Heat death and oscillation in model universes containing interacting matter and radiation 03 p0422 A83-14179

Large-scale background temperature and mass fluctuations due to scale-invariant primeval perturbations 04 p0554 A83-15646

The origin of the cosmic X-ray background 04 p0575 A83-16047

Ultraviolet spectrum of the sky background at different galactic latitudes 06 p0830 A83-18545

Simulation of IR images of natural backgrounds 06 p0762 A83-18595

Structure in the universe and fluctuations in the cosmic microwave background 07 p1015 A83-20761

Large-scale fluctuations in the mass distribution and the microwave background - Nature and evolution 07 p1016 A83-20762

The neutrino background in the early universe, and temperature fluctuations in the cosmic microwave radiation 07 p1026 A83-21257

Review of some nonlocal-thermodynamic-equilibrium high-altitude 4.3 micron background effects 08 p1136 A83-22854

An upper limit on the stochastic background of ultralow-frequency gravitational waves 08 p1184 A83-23076

Upper limits on the isotropic gravitational radiation background from pulsar timing analysis 08 p1184 A83-23077

Designing for stray radiation rejection --- of heat seeking missile components 09 p1204 A83-23536

The environmental background in gas-filled detectors for X-ray astronomy 09 p1268 A83-24107

The contribution of quasi-stellar objects to the cosmic X-ray background 09 p1361 A83-24472

Small-angle anisotropy of the microwave background radiation in the adiabatic theory --- concerning structure of Universe 09 p1364 A83-25002

The extragalactic background light at 4400 A 10 p1511 A83-26400

A Bragg crystal spectrometer for the soft X-ray diffuse background 11 p1573 A83-27757

A possible interpretation of the ultraviolet sky background radiation observed with the space experiment 'Galaktika' 11 p1694 A83-27987

Spectral observations of atmospheric gamma-ray background 13 p1967 A83-31473

Optical design of the Diffuse Infrared Background Experiment for NASA's Cosmic Background Explorer 14 p2084 A83-32037

The possible effect of the natural background of ionizing radiation on the development of mammals 14 p2062 A83-32057

The spectrum of the extragalactic background light 14 p2107 A83-33237

Preliminary results of a galactic background survey at 45 MHz 14 p2099 A83-33246

Method of calculating the expected background luminance from the moon for planning astronomical observations 15 p2244 A83-33788

Solrad 11 observations of the far-ultraviolet background 15 p2245 A83-34116

Limits from the timing of pulsars on the cosmic gravitational wave background 15 p2264 A83-34583

Lambda 6-cm observations of fluctuations in the 3 K cosmic microwave background 15 p2286 A83-34598

The soft X-ray diffuse background 15 p2286 A83-34623

Temperature fluctuations in the background radiation in the entropy theory of galaxy formation 15 p2269 A83-34680

The possible role of axial photons in attenuating the solar neutrino flux 15 p2286 A83-35317

Large-scale anisotropy of the 3 K background radiation in density wave models 16 p2441 A83-36677

2-165 keV observations of active galaxies and the diffuse background 17 p2596 A83-37307

The irregular distribution of galaxies and the anisotropies in the microwave background photons 17 p2598 A83-37343

Radio-astronomy antennas for 3 deg K cosmic radiation measurements 17 p2494 A83-38059

Cosmic rays and magnetic fields in the galaxy 18 p2786 A83-39655

Experimental limits of the extreme ultraviolet background 18 p2759 A83-39777

Gravitational scintillation, anisotropies of background radiation and density inhomogeneities of cosmic matter 18 p2777 A83-40364

The spectral features in the microwave background spectrum due to energy release in the early universe 19 p2914 A83-40707

Interaction of solar neutrinos with the cosmic background 20 p3082 A83-42276

A search for the Sunyaev-Zel'dovich effect at millimeter wavelengths --- cosmic background photon energy increase due to Compton scattering by high temperature galactic cluster plasma electrons

20 p3082 A83-42467

Far ultraviolet observations of the expanding shell in Eridanus

21 p3229 A83-44425

A method to improve the visibility of time-variable gamma-ray sources in structured background

21 p3245 A83-44451

Search for large-scale extension of the quasars 3C273, 3C345 and 3C380

21 p3223 A83-44453

Low-frequency measurement of the spectrum of the cosmic background radiation

21 p3245 A83-45200

Massive neutrinos and the anisotropy of the cosmic microwave background radiation

24 p3675 A83-49357

BACKINGS

U BACKUPS

BACKSCATTERING

An approximate model for backscattering and emission from land and sea

01 p0063 A83-10062

Radar spectral observations of snow

01 p0063 A83-10064

Radar reflectivity measurements of ocean surface with and without a surface coat of oil

01 p0069 A83-10105

A backscatter model for a randomly perturbed periodic surface --- furrowed soils in agricultural fields

01 p0065 A83-10107

A parametric study of tillage effects on radar backscatter

01 p0065 A83-10108

Measurement of soil moisture and roughness using the backscatter from microwaves --- German thesis

01 p0066 A83-10172

Crystal rocking-diffraction of backscattered and transmitted electrons as an alternative method to conventional electron diffraction, especially for obtaining energy-filtered diffraction pictures --- German thesis

01 p0048 A83-10174

Analysis of low-pressure chemical vapor deposited silicon nitride by Rutherford backscattering spectrometry

01 p0110 A83-10990

Laser transit anemometer measurements with unseeded backscatter

01 p0051 A83-11057

Experimental study of the frequency characteristics of gas ring lasers with additional feedback

01 p0056 A83-11344

Estimating wind speed from HF skywave radar sea backscatter

01 p0076 A83-11352

Sensitivity of determining the atomic number of materials on the basis of bremsstrahlung backscattering

02 p0188 A83-12162

Flanged parabolic antennas

03 p0305 A83-14007

A parameter review and assessment of attenuation and backscatter properties associated with dust storms over desert regions in the frequency range of 1 to 10 GHz

03 p0306 A83-14012

Microwave remote sensing: Active and passive. Volume 2 - Radar remote sensing and surface scattering and emission theory --- Book

03 p0328 A83-14040

Vertical ozone profile results from the Nimbus-4 BUV data

03 p0360 A83-14630

Algorithm for vertical ozone profile determination for the Nimbus-4 BUV data set

03 p0360 A83-14631

An optimum statistical technique for ozone profile retrieval from backscattered UV radiances

03 p0360 A83-14632

A simple relation between active and passive microwave remote sensing measurements of earth terrain

03 p0352 A83-14857

A backscatter model for a randomly perturbed periodic surface --- radar imagery of earth soil with row structure

03 p0352 A83-14859

Radar backscattering of microwaves by spongy ice spheres

04 p0517 A83-15942

Raman backscattering in an electron beam-plasma system

04 p0538 A83-16091

Quantitative ultrasonic backscatter measurements in the presence of phase distortion

04 p0533 A83-16313

Interaction and competition between forward and backscattering in stimulated Raman scattering

05 p0649 A83-17058

Dual-frequency microwave backscatter from the ocean at low grazing angles Comparison with theory

05 p0645 A83-17708

Three-dimensional problem of backscattering in stratified, randomly inhomogeneous media

06 p0806 A83-19331

Microwave interferometer for measurements of small displacements

07 p0929 A83-20546

Radar backscattering by melting snowflakes

07 p0970 A83-20812

Polarization backscatter analysis of field distributions using fiber optics

07 p0930 A83-20828

The effect of resonant backscattering in the magnetospheric plasma

07 p0962 A83-20863

Results of a statistical analysis of the backscattering of light with model indicatrices --- remote sensing of atmospheric aerosols

07 p0963 A83-20896

Compatibility of Doppler measurements of the drift of auroral scattering at different frequencies

07 p0964 A83-21180

Observation of suprathermal electrons produced by stimulated Raman scattering processes

08 p1168 A83-22376

Design and calibration of a coherent lidar for measurement of atmospheric backscatter

08 p1096 A83-22507

Laser and millimeter-wave backscatter of transmission cables

08 p1043 A83-22523

Determination of rain rate from a spaceborne radar using measurements of total attenuation

08 p1141 A83-22679

Electromagnetic backscattering from a layer of vegetation - A discrete approach

08 p1077 A83-22682

Mudrocks examined by backscattered electron microscopy

08 p1130 A83-23278

An augmented technique for backscattering amplitude inversion in the study of cavities and plane defects

09 p1275 A83-23474

The effect of the amplification of wave backscattering by rough surfaces

09 p1336 A83-23483

L band radar backscatter dependence upon surface wind stress - A summary of new Seasat-1 and aircraft observations

09 p1318 A83-24298

Characterization of copper in phosphoric-acid-anodized 2024-T3 aluminum by Auger electron spectroscopy and Rutherford backscattering

10 p1395 A83-25547

Laser light backscattering off an electron beam-plasma system

10 p1428 A83-26019

Mutual coherence functions and intensities of backscattered signals in a turbulent medium

10 p1403 A83-26036

Direct- and cross-polarized scatter from a turbulent laboratory plasma

10 p1486 A83-26050

Stimulated Raman scattering by particles captured in a trap

10 p1431 A83-26651

Rain backscattering effects in coherent polarization-diversity radar signals

11 p1630 A83-27078

Amplification of the mean intensity of backscattering in a turbulent atmosphere

11 p1632 A83-27957

On the reflectivity of a spherical screen

11 p1649 A83-27963

Stimulated Raman backscattering in the presence of ion-acoustic fluctuations

13 p1923 A83-30119

Radiative heat transfer in absorbing, emitting and anisotropically scattering boundary layer flows

[AIAA PAPER 83-1504] 14 p2010 A83-32742

Energy redistribution among internal states of nitric oxide molecules upon scattering from Pt(111) crystal surface

14 p1991 A83-33107

Electromagnetic scattering by magnetic spheres

15 p2224 A83-33805

Parametric interaction and backward wave oscillation in stimulated Compton scattering

15 p2169 A83-34372

Modelling atmospheric aerosol backscatter at CO2 laser wavelengths. I - Aerosol properties, modeling techniques, and associated problems. II - Modeled values in the atmosphere. III - Effects of changes in wavelength and ambient conditions

15 p2201 A83-34461

Fluctuations of a millimeter-wave beam on a path with back reflection

15 p2145 A83-34702

Theory of backward Rayleigh scattering in polarization-maintaining single-mode fibers and its application to polarization optical time domain reflectometry

16 p2412 A83-35967

The problem of backscattering in three-dimensional randomly inhomogeneous media

17 p2577 A83-38981

Parameters of artificial irregularities according to results of the observation of backscattering during oblique sounding

17 p2547 A83-38989

On the resonant backscattering of VLF waves in the magnetosphere

18 p2714 A83-39333

Effectiveness of the model of volume backscattering in the theory of radiation transfer in media with axisymmetric scattering indices

18 p2685 A83-39865

The polarization structure of backscattering by water-droplet and ice clouds

18 p2730 A83-40080

Scattering from randomly oriented circular discs with application to vegetation

18 p2707 A83-40654

Shadowing by non-Gaussian rough surfaces for which decorrelation implies statistical independence

18 p2676 A83-40655

Simultaneous determination of refractive index and size of spherical dielectric particles from light scattering data

20 p3046 A83-42214

Anomalous backscattering of optical radiation in a stratified solution

20 p2993 A83-42280

Backscatter and extinction in water clouds

20 p3031 A83-42859

Evaluation of the information content of the characteristics of radiation scattered by the surface of geometrical bodies

20 p3000 A83-43184

Brillouin backscattering in an electron beam-plasma system

21 p3212 A83-44348

Backscattering observation of radiation damage in optical fibers

21 p3207 A83-44822

Rayleigh backscattering in a fiber gyroscope with limited coherence sources

22 p3287 A83-45730

Backscattering cascade of beam modes off ambient density fluctuations

22 p3362 A83-46021

Speckle statistics of atmospherically backscattered laser light

22 p3295 A83-46068

Airborne measurements of laser backscatter from the ocean surface

22 p3342 A83-46074

Active microwave signatures of soil and crops - Significant results of three years of experiments

22 p3308 A83-46104

Review of approaches to the investigation of the scattering properties of material media --- radar remote sensing

22 p3311 A83-46182

The effects of vegetation cover on the radar and radiometric sensitivity to soil moisture

22 p3311 A83-46183

Scattering from a random layer of leaves in the physical optics limit

22 p3311 A83-46184

A multilayer model for radar backscattering from vegetation canopies

22 p3312 A83-46185

Wind influence on the backscattering coefficient from crops

22 p3312 A83-46186

Coherent measurements of radar backscatter from rare and vegetation covered soil in the 8-12.5 GHz band

22 p3312 A83-46187

Parametric studies of SAR-images by means of radar backscattering models

22 p3312 A83-46190

Method for retrieving the true backscattering coefficient from measurements with a real antenna

22 p3314 A83-46236

Amplitude and phase errors involved in retrieving copolarized radar cross section measurements --- from remotely sensed natural surfaces

22 p3315 A83-46237

Radar backscattering properties of corn and soybeans at frequencies of 1.6, 4.75, and 13.3 GHz

22 p3315 A83-46248

Rayleigh backscattering theory for single-mode optical fibers

23 p3508 A83-47584

A comparison between backscattering coefficients using Gaussian and non-Gaussian surface statistics

23 p3443 A83-47836

Features characterizing the backscattering of radio signals by ocean waves

23 p3493 A83-48102

Measurement of polarization mode coupling along a polarization-maintaining optical fiber using a backscattering technique

24 p3628 A83-48858

Aerosol backscattering of a laser beam

24 p3588 A83-49004

Scattering and backscattering of 1 MeV electrons [ONERA, TP NO. 1983-87]

24 p3627 A83-49406

BACKUPS

Emergency power for the F-16 aircraft [ASME PAPER 83-GT-189]

23 p3410 A83-47995

BACKWARD FACING STEPS

k-epsilon calculations of heat transfer in redeveloping turbulent boundary layers downstream of reattachment [ASME PAPER 82-HT-77]

02 p0173 A83-12806

Numerical calculations of turbulent heat transfer downstream of a rearward-facing step

08 p1089 A83-23199

Experimental and theoretical investigation of backward-facing step flow

09 p1262 A83-24420

Propagation of two-dimensional nonsteady detonation in a channel with backward-facing step

10 p1416 A83-26165

Low-frequency unsteadiness of a reattaching turbulent shear layer

15 p2155 A83-33663

Reattaching turbulent shear layers with perturbed structure [AIAA PAPER 83-0603]

16 p2351 A83-36063

Unsteady behavior of a reattaching shear layer [AIAA PAPER 83-1712]

17 p2502 A83-37206

Effect of a wall jet on the dynamic configuration of the wake behind a backward step in a steady flow

20 p2977 A83-42721

Temperature characteristics of turbulent, premixed flames stabilized on a step

21 p3110 A83-44974

Effects of expansion ratio on the calculation of parallel-walled backward-facing step flows - Comparison of four models of turbulence
[ASME PAPER 83-FE-10] 23 p3450 A83-48229

Calculation of deflected-walled backward-facing step flows Effects of angle of deflection on the performance of four models of turbulence
[ASME PAPER 83-FE-16] 23 p3450 A83-48233

The effect of upstream boundary layer thickness upon flow past a backward-facing step 24 p3579 A83-49807

BACKWARD WAVE TUBES

New developments regarding traveling-wave tubes and backward-wave oscillators in the millimeter-wavelength region. I - Electronic engineering 02 p0168 A83-12320

Analysis of the propagation of electron waves inside and outside the passband of periodic structures 04 p0471 A83-15741

The suppression of generation on the backward wave in microwave devices having an inhomogeneous slow-wave system 04 p0471 A83-15742

Characteristics of InSb mixers and backward wave oscillators in a submm heterodyne receiver 04 p0472 A83-15813

Quasi-static calculation of noise parameters of a magnetron-type backward wave tube 06 p0750 A83-18026

Analytical method for calculating the suppression of TWT self-excitation at the minus-first harmonic by means of a field-phase jump 06 p0750 A83-18030

The dispersion characteristics of generators of diffraction radiation in the millimeter-wavelength range 06 p0750 A83-18141

New developments regarding traveling-wave tubes and backward-wave oscillators in the millimeter-wavelength region. II - Electron optics and experimental results 06 p0755 A83-19614

Parasitic frequency modulation of a millimeter-wave BWT and its elimination 07 p0921 A83-20882

Propagation of magnetostatic waves in a structure with a tangentially magnetized anisotropic ferrite layer 15 p2152 A83-34711

Oscillation-amplitude fluctuations of a BWT operating in the short-wave part of the millimeter range 15 p2152 A83-34712

Stochastic self-oscillations and instability in a backward wave tube 17 p2499 A83-38491

Observation of the backward cyclotron wave in a spiral electron beam-plasma system 23 p3510 A83-47623

BACKWARD WAVES

Demonstration of a two-stage backward-wave-oscillator free-electron laser 19 p2852 A83-41157

Three-wave parametric processes in electron beams 23 p3445 A83-47566

BACTERIA

NT ACTINOMYCETES

NT BACILLUS

NT ESCHERICHIA

NT STEAROTHERMOPHILUS

NT STREPTOCOCCUS

Effects of hyperbaric oxygen on anaerobic organisms 02 p0222 A83-12260

Optimal tactics of antibacterial therapy for the trigger model of the injection process 03 p0382 A83-14367

A kinetic model of the electron and conformational transitions in the photosynthetic reaction centers of purple bacteria 07 p0974 A83-20966

Cyano-bacterial symbiosis - A well into the past --- Y 13 p1895 A83-30320

Role of bacterial endotoxins of intestinal origin in rat heat stress mortality 13 p1896 A83-30454

Hemophilic bacteria in the nasopharynx of healthy individuals 14 p2066 A83-33334

On the optical properties of bacterial grains - I. 15 p2216 A83-34549

The effect of glucose concentration and pH on hydrogen production by Rhodospseudomonas sphaeroides VM 81 15 p2193 A83-35303

Growth of 'black smoker' bacteria at temperatures of at least 250 C 16 p2394 A83-35992

2.8-3.6-micron spectra of micro-organisms with varying H2O ice-content 17 p2563 A83-38590

Comparative studies on biochemical properties of protein synthesis of an archaeobacteria, Thermoplasma sp 17 p2557 A83-38896

Characterization of a halotolerant-psychrololerant bacterium from dry valley antarctic soil 19 p2886 A83-40833

Physical determinants of radiation sensitivity in bacterial spores 19 p2872 A83-40836

Inactivation, mutation induction and repair in Bacillus subtilis spores irradiated with heavy ions 19 p2872 A83-40837

Inactivation probability of heavy ion-irradiated Bacillus subtilis spores as a function of the radial distance to the particle's trajectory 19 p2872 A83-40838

Effect of heavy ions on bacterial spores 19 p2872 A83-40839

Sequence of the 16S ribosomal RNA from Halobacterium volcanii, an archaeobacterium 19 p2873 A83-40914

Changes in symbiotic and associative interrelations in a higher plant-bacterial system during space flight 19 p2878 A83-42058

The evolutionary pattern of aromatic amino acid biosynthesis and the emerging phylogeny of pseudomonad bacteria 20 p3033 A83-42399

Methylotrophic bacteria - Biochemical diversity and genetics 22 p3345 A83-45724

Electrophoretic measurements on purple membrane particles 22 p3345 A83-45765

Reduction of molecular sulphur by methanogenic bacteria 23 p3495 A83-48081

Biosynthesis of tetrapyrrol pigments as possible precursors of the nickel-containing factor F43O of Methanosarcina vacuolata 23 p3496 A83-48513

BACTERICIDES

Simultaneous luminescent assessment of the phagocytic and bactericidal functions of the macrophages and neutrophils of human skin exudate 03 p0381 A83-14336

BACTERIOLOGY

Investigation of the localization of dehydrogenases in aerobic and anaerobic bacteria at the submicroscopic level 01 p0078 A83-10421

The utilization of carbon monoxide by anaerobic bacteria 01 p0078 A83-10422

Hybridization of the DNA of purple phototrophic bacteria 01 p0078 A83-10423

An investigation of the shielding effectiveness of FPP-15 fabric relative to bacterial aerosols 05 p0677 A83-17201

Experimental data from a study of the toxic effect on embryos exerted by hexachlorophene - A component of antimicrobial fabrics and synthetic articles of everyday use 05 p0677 A83-17203

Nocardiopsis antarcticus - A new species of actinomycetes isolated from the ice sheet of the Central Antarctica glacier 21 p3185 A83-45377

An investigation of methane monooxygenase from Methylococcus capsulatus 21 p3186 A83-45378

Electrophoretic measurements on purple membrane particles 22 p3345 A83-45765

Preliminary results of Cytos 2 experiment --- for bacteria antibiotic sensitivity during orbital flight [IAF PAPER 83-192] 23 p3494 A83-47307

BACTERIOPHAGES

Effect of HZE particles and space hadrons on bacteriophages 19 p2871 A83-40834

The effect of alpha particles on bacteriophage T4Br(+) 19 p2872 A83-40835

DNA fusion product of phage P2 with plasmid pBR322 - A new phasmid 21 p3183 A83-44860

BAFFLES

Heat transfer and microstructure of the boundary layer in the vicinity of the stagnation point of a jet flowing over a baffle 02 p0170 A83-11875

Concerning impingement of shock waves on permeable baffles 05 p0589 A83-17418

The standoff distance of a compression shock upon impingement of an underexpanded jet onto a spherical baffle 05 p0590 A83-17419

An approach to calculating the flow following impingement of an underexpanded jet onto an infinite planar baffle 05 p0590 A83-17420

The impingement of a jet, in its initial formation stage, on a planar baffle 05 p0590 A83-17421

Designing for stray radiation rejection --- of heat seeking missile components 09 p1204 A83-23536

Use of reflective baffles for control of aperture heat loads and stray radiation 22 p3357 A83-46590

A model for radial flow in a tube-dome junction of a telescope 23 p3508 A83-47846

BAGS

NT AIR BAG RESTRAINT DEVICES

NT GAS BAGS

BAJA CALIFORNIA

U LOWER CALIFORNIA (MEXICO)

BAKEOUT

U DEGASSING

BAKING

Phase genesis in heterogeneous inorganic coatings obtained by suspension baking 07 p0873 A83-20678

BALANCE

The effect of imbalance in a dynamically adjustable gyroscope on its dynamics and accuracy 01 p0050 A83-10688

BALLISTIC MISSILES

The regulation by the human foot of the balance of the mechanical sytem of the 'inverted pendulum' type. I - The significance of the speed of motion. II - The role of the position of the center of gravity and temporal programs 23 p3497 A83-47117

BALANCED AMPLIFIERS

U PUSH-PULL AMPLIFIERS

BALANCING

A minimum strain energy approach for obtaining optimal unbalance distribution in flexible rotors 03 p0335 A83-13491

On the possibility of balancing rotating flexible shafts 05 p0653 A83-17724

A computational technique for optimizing correction weights and axial location of balance planes of rotating shafts 11 p1589 A83-28121

Change in vibrations of an flexible rotor due to a change in bearings 18 p2695 A83-39423

Reduction of large flexible spacecraft models using internal balancing theory [AIAA PAPER 83-2292] 19 p2817 A83-41751

In situ balancing of flexible rotors using influence coefficient balancing and the unified balancing approach [ASME PAPER 83-GT-178] 23 p3465 A83-47989

BALL BEARINGS

Friction oxidation characteristics [ASLE PREPRINT 82-LC-3B-2] 03 p0334 A83-13236

The load-life relationship for M50 steel bearings with silicon nitride ceramic balls [ASLE PREPRINT 82-LC-3C-4] 03 p0334 A83-13239

A technique in the evaluation of thin, solid film lubricants under combined rolling and sliding contact [ASLE PREPRINT 82-LC-3D-1] 03 p0334 A83-13240

A vibration analysis of a bearing/cartridge interface for a fretting corrosion study [ASME PAPER 82-LUB-19] 03 p0335 A83-13510

Ball contact locus in an angular contact bearing [ASME PAPER 82-LUB-21] 03 p0336 A83-13511

Fluorescent dye penetrant inspection of silicon nitride bearing surfaces 04 p0462 A83-15176

Unstable vibrations of an unsymmetrical shaft at the secondary critical speed due to ball bearings 07 p0939 A83-20291

Surface roughness effects in point contact elastohydrodynamic lubrication 08 p1111 A83-22008

Advances in high-speed rolling-element bearings --- for aircraft engine and transmission application 08 p1111 A83-22319

Structural and microstructural changes in the inner races of ball bearings 09 p1276 A83-23346

Innovative features of long-life momentum and reaction wheel assemblies 10 p1385 A83-26591

Slip measurement in an angular contact ball bearing [ASME PAPER 81-LUB-33] 13 p1858 A83-30243

The performance and application of high speed long life LH2 hybrid bearings for reusable rocket engine turbomachinery [AIAA PAPER 83-1389] 16 p2362 A83-36379

An experimental study of ball bearings in the combined supports of the rotors of gas-turbine engines 19 p2855 A83-42144

Evaluation of a 90-mm bore bearing operating in a simulated space environment 20 p2999 A83-43332

A nonlinear effect in rolling bearings 21 p3148 A83-44639

A study of the moment of elastic unbalance in a gyroscopic instrument in the case of the main resonance 21 p3138 A83-44640

Effect of molecular weight distribution of mineral oils on life of thrust ball bearings 24 p3590 A83-48924

BALL LIGHTNING

Some remarks about a ball lightning model 03 p0361 A83-14743

Aerosol mode of ball lightning 10 p1451 A83-26465

High-temperature physical-chemical processes in the atmosphere during thunderstorms 23 p3485 A83-48504

BALLASTS (IMPEDANCES)

Operation of an inductively ballasted helical TE-CO2 laser 19 p2850 A83-40734

BALLISTIC MISSILES

NT INTERCONTINENTAL BALLISTIC MISSILES

NT MINUTEMAN ICBM

A simulation-aided multiple processor architecture design for BMD underlay terminal defense 02 p0226 A83-11904

Optics in ballistic missile defense /BMD/ 03 p0392 A83-13754

- Real-time modular distributed signal processing ...
sensors for ballistic missile defense systems
08 p1051 A83-22828
- Statistical modeling of ballistic damage and residual
strength in composite structures
[AIAA 83-1002] 12 p1711 A83-29790
- Roll resonance probability for ballistic missiles with
random configurational asymmetry
13 p1809 A83-30173
- Acceleration measurements in a high G environment
17 p2509 A83-37131
- Peacekeeper - Guidance system flight readiness
review
[AIAA PAPER 83-2269] 19 p2814 A83-41736
- Utilization of path length fuzing in the Peacekeeper
Weapon System
[AIAA PAPER 83-2251] 19 p2810 A83-41763
- Satrac - Review and update
21 p3097 A83-44693

BALLISTIC TRAJECTORIES

- Unstable Marangoni convection under microgravity
02 p0138 A83-12994
- Ballistic entry motion, including gravity - Constant drag
coefficient case
03 p0283 A83-14839
- Ballistic transport and velocity overshoot in
semiconductors. I - Uniform field effects
09 p1350 A83-24498
- Aerodynamics of asymmetric sabot discard
09 p1198 A83-24892
- Method of the complex postflight ballistic analysis of
the descent trajectories of Venera-type descent modules
09 p1212 A83-25032
- Collisional interactions of ring particles - The ballistic
transport process --- in Saturn's rings
16 p2436 A83-35731
- Missions to the asteroid Anteros and the space of true
anomalies
18 p2642 A83-39474
- Angular motion influence on reentry vehicle ablation or
erosion asymmetry formation
[AIAA PAPER 83-2111] 19 p2811 A83-41938

BALLISTIC VEHICLES

- Hyperballistic vehicle dynamics
02 p0132 A83-13078
- Istra - An air-breathing ballistic space transport vehicle
for Europe
[DGLR PAPER 82-075] 09 p1213 A83-24189

BALLISTICS

- NT INTERIOR BALLISTICS
- Estimating the propelling action of explosives
06 p0726 A83-18009
- Ballistic and overshoot electron transport in bulk
semiconductors and in submicronic devices
07 p0999 A83-20737
- Investigation of the geometry of the near-wakes of
centrally-ducted models on a compact ballistic test
stand
09 p1197 A83-24044
- Aeroballistic characteristics of 3-ft-long parachute
decelerators
12 p1696 A83-29019
- Ballistics and navigation of the automatic interplanetary
probes Venera-13 and Venera-14
14 p1981 A83-31952
- Unsteady quasi-ballistic motion of electrons through
semiconducting layers of submicron thickness
17 p2585 A83-38494

BALLOON FLIGHT

- New thermal and trajectory model for high-altitude
balloons
14 p1974 A83-32579
- Scientific ballooning - III; Proceedings of the Workshop,
Ottawa, Canada, May 16-June 2, 1982
18 p2631 A83-39801
- The theoretical advantages and practical considerations
of gas replenishment techniques in long-duration scientific
ballooning
[AD-A129841] 18 p2640 A83-39802
- The radiation controlled balloon (RACON)
18 p2640 A83-39803
- New systems for extending the useful float duration of
standard zero-pressure balloon flights
18 p2640 A83-39805
- Balloon materials and designs
18 p2640 A83-39806
- Instantaneous, predictable balloon system descent from
high altitude
18 p2640 A83-39808
- Automatic control of balloon altitude
18 p2641 A83-39809
- Global telecommunications needs for the long duration
balloon environment
18 p2639 A83-39810
- A review of geostationary satellite alternatives for
retrieving data from long duration balloon flights
18 p2639 A83-39812
- A global HF telecommand system for long duration
balloon flights
18 p2639 A83-39813
- Power supplies for long duration balloon flights
18 p2642 A83-39815
- A new static-launch method for plastic balloons
18 p2642 A83-39816

- Electrodynamics of the stratosphere using 5000 cu m
superpressure balloons
18 p2640 A83-39818
- Detection of solar neutrons on a long duration balloon
flight
18 p2784 A83-39820
- Long duration balloon flights - A probe for deep hard
X-ray astronomy investigation
18 p2759 A83-39821

BALLOON SOUNDING

- The pitch-angle anisotropy of solar protons according
to stratospheric measurements
02 p0269 A83-11719
- Spectral line inversion for sounding of stratospheric
minor constituents by infrared heterodyne technique from
balloon altitudes
03 p0325 A83-13723
- Recent results in the analysis of high-resolution infrared
atmospheric transmission spectra
03 p0358 A83-13983
- SBARMO-79; a multi-balloon campaign in the auroral
zone
04 p0512 A83-16295
- A measurement of the antiproton flux in the cosmic
rays
04 p0575 A83-16350
- Second-order scattering approximation to X-ray photon
transport at balloon altitudes
05 p0665 A83-17803
- Altitude, thickness and charge concentration of charged
regions of four thunderstorms during trip 1981 based upon
in situ balloon electric field measurements
07 p0958 A83-20093
- Balloon atmospheric mosaic measurements /BAMM/
IIA phenomenology and band selection
08 p1045 A83-22844
- Atmospheric sounding with meteorological balloons ---
Russian book
12 p1758 A83-29326
- Microprocessor based data acquisition and control
system for a balloon borne quadrupole mass
spectrometer
12 p1730 A83-29539
- Solar UV and ozone balloon measurements
12 p1747 A83-29585
- The measurement of water vapour in thermal emission
on studies of Nimbus-7 stratosphere flights for correlative
studies of Nimbus-7
12 p1760 A83-29687
- Stratospheric N₂O, CF₂Cl₂, and CFC13 composition
studies utilizing in situ cryogenic, whole air sampling
methods
[AD-A128389] 13 p1873 A83-30891
- Spectral observations of atmospheric gamma-ray
background
13 p1967 A83-31473
- Low energy gamma ray enhancement observed during a
stratospheric balloon flight
13 p1967 A83-31474
- Auroral X-ray and luminosity pulsations and microbursts
measured during February 25, 1974 SAMBO-1 balloon
flight
13 p1883 A83-31718
- Mass spectrometry in the stratosphere
16 p2354 A83-35402
- Balloon borne LIDAR measurements of stratospheric
hydroxyl radical
16 p2380 A83-36144
- Infrared absorption spectroscopy applied to
stratospheric profiles of minor constituents
[ONERA, TP NO. 1983-99] 16 p2380 A83-36150
- Low-frequency (f less than about 1 Hz) stratospheric
electrical noise measured by balloon-borne sensors
16 p2381 A83-36156
- The radiation controlled balloon (RACON)
18 p2640 A83-39803
- An atmospheric sounding balloon with ballast - An
automatic numerical model for its manufacture and
simulation of its evolution
18 p2640 A83-39804
- Balloon materials and designs
18 p2640 A83-39806
- Present status and new trends in scientific ballooning
in India
18 p2640 A83-39817
- Importance of electric field measurement over low
latitudes at stratospheric heights by balloons
18 p2717 A83-39819
- Balloon research and cooperative programmes
18 p2631 A83-39838
- Remote sensing of Arkansas tornadoes on 11 April 1976
from a satellite, a balloon and an ionospheric sounder
array
20 p3031 A83-42967
- Measurements of cosmic-radiation absolute ionization
in the atmosphere
21 p3244 A83-44304
- Measurement of charge composition of primary cosmic
ray using CR-39 plastic track detector
21 p3245 A83-44529
- Balloon-borne remote sensing of stratospheric
constituents
22 p3328 A83-46076
- X-ray intensity, ozone density, and VLF wave intensity
observed by scientific balloon experiments at Esrange
22 p3330 A83-46513
- Determination of H₂O and CH₄ profiles from data of a
nadir to limb scanning balloon-borne radiometer
24 p3604 A83-48813
- BALLOON-BORNE INSTRUMENTS**
- Measuring compact X-ray sources in the southern sky
with the ATI/MPE balloon experiment --- German thesis
01 p0123 A83-10479

- Initial results from the use of ionic anemometers under
stratospheric balloons - Application to the high-resolution
analysis of stratospheric motions
02 p0216 A83-12956

- A new tool for the three-dimensional sounding of the
atmosphere - The helisonde
02 p0216 A83-12957
- SAGE - European ozonesonde comparison
03 p0363 A83-14924
- Observations of a gamma-ray burst and other sources
with a large-area, balloon-borne detector
07 p1039 A83-20007
- 10 June 1974 transient
07 p1039 A83-20014
- Balloon-borne observations of stratospheric aerosol and
condensation nuclei during the year following the Mt. St.
Helens eruption
07 p0959 A83-20205
- Radiative transfer and 4.3 micron atmospheric clutter
observations --- with balloon-borne sensors
08 p1051 A83-22849
- Gamma ray detection with long NaI/Tl/ scintillator
bars
09 p1268 A83-24104
- Discrepancies between balloon-borne IR atmospheric
spectra and corresponding synthetic spectra calculated
line by line around 825 per cm
09 p1306 A83-24440
- Energy spectrum of cosmic ray primaries at super high
energies estimated from the recent balloon-borne
calorimeter measurements
09 p1369 A83-24700
- A far-infrared Fabry-Perot interferometer and grating
spectrometer for balloon-borne astronomy
10 p1419 A83-25458
- An orientation platform for a balloon-borne telescope
11 p1537 A83-28575
- Microprocessor based data acquisition and control
system for a balloon borne quadrupole mass
spectrometer
12 p1730 A83-29539
- The UTIC hard X-ray balloon-borne platform
13 p1936 A83-30396
- Unusual behavior in the condensation nuclei
concentration at 30 km
13 p1877 A83-30885
- Lidar- and balloon-borne particle counter comparisons
following recent volcanic eruptions
13 p1877 A83-30888
- Measurement of stratospheric aerosol near Sanriku (39
deg N, 142 deg E) in Japan on May 31, 1979
13 p1877 A83-30889
- Use of a Fourier transform spectrometer on a
balloon-borne telescope and at the multiple mirror
telescope (MMT)
14 p2016 A83-32002
- Limiting payload deceleration during ground impact
15 p2122 A83-33726
- Development of a reaction wheel-based attitude control
system for balloon-borne infrared astronomical
observation
15 p2119 A83-34000
- The use of stratospheric balloons in astronomy -
Sun-pointing nacelles for the study of the solar UV
spectrum
16 p2427 A83-36955
- Relative contribution of various secondary X-ray
components below 100 keV at balloon altitudes
17 p2512 A83-38545
- The observation of the galactic anticenter region by the
balloon borne gamma-ray telescope Natalya-1
18 p2785 A83-39282
- The position sensitive low energy detector on board the
ZEBRA telescope --- for gamma and X-ray astronomy
18 p2647 A83-39286
- An imaging telescope for soft gamma-ray astronomy -
The preliminary in-flight tests
18 p2756 A83-39287
- A directional gamma-ray telescope using coded aperture
techniques
18 p2756 A83-39289
- Figaro - An experiment for pulsar and variable source
studies in the MeV range
18 p2688 A83-39291
- GSFC optical ozonesonde results during the Gap,
France, intercomparisons, June 1981
18 p2716 A83-39791
- Scientific ballooning - III; Proceedings of the Workshop,
Ottawa, Canada, May 16-June 2, 1982
18 p2631 A83-39801
- Automatic control of balloon altitude
18 p2641 A83-39809
- Navigation for balloon payloads - Recent experience
with OMEGA in the US and a new slant range system
18 p2639 A83-39814
- A hard X-ray experiment for long-duration balloon
flights
18 p2641 A83-39822
- Guidance and control of a balloon-borne X-ray telescope
with onboard and ground based computers
18 p2641 A83-39823
- A large aperture balloon-borne telescope for a
submillimeter wavelength survey of the galactic plane
18 p2759 A83-39824
- Achievements and promise of balloon IR astronomy
18 p2762 A83-40458
- The scientific case and feasibility of a three metre balloon
telescope
18 p2762 A83-40459
- A balloon-borne cooled telescope for far IR astronomy
18 p2762 A83-40460

Balloon observation of the central bulge of our Galaxy
in near infrared radiation 19 p2912 A83-40683
Balloon-borne imagery of the solar granulation. IV - The
centre-to-limb variation of the intensity fluctuations 19 p2924 A83-40725
Stratospheric negative ions - Detailed height profiles 20 p3023 A83-43151
Balloon-borne diode-laser absorption spectrometer for
measurements of stratospheric trace species 22 p3288 A83-46079
The NASA/Goddard balloon borne lidar system 23 p3458 A83-47795
Determination of H₂O and CH₄ profiles from data of a
nadir to limb scanning balloon-borne radiometer 24 p3604 A83-48813

BALLOONS

NT HIGH ALTITUDE BALLOONS
NT JIMSPHERE BALLOONS
NT METEOROLOGICAL BALLOONS
NT MICROBALLOONS
NT SUPERPRESSURE BALLOONS
NT TETHERED BALLOONS
A steam balloon for the exploration of the atmosphere
of the planet Venus 05 p0705 A83-17451
A balloon and its basket in the Venus' atmosphere 15 p1214 A83-34271
Scientific ballooning - III; Proceedings of the Workshop,
Ottawa, Canada, May 16-June 2, 1982 18 p2631 A83-39801
Balloon film strain measurement 18 p2641 A83-39807
Present status and new trends in scientific ballooning
in India 18 p2640 A83-39817

BALMER SERIES

Luminosity classification of Be stars by Balmer line
narrow band photometry 01 p0120 A83-10307
Correlations between BCD parameters of the continuous
spectrum and the Balmer decrement of Be stars 01 p0120 A83-10310
On the radiation deficiency of shell stars in the Balmer
continuum 01 p0121 A83-10320
Intensifier-dissector-scanner observations of the bright
northern Be stars 01 p0116 A83-10321
The detection of ultraviolet photospheric absorption in
the spectra of two Wolf-Rayet stars 02 p0253 A83-11615
The spectrum of 11 Cam in 1980 and 1981 06 p0817 A83-18016
Simultaneous spectroscopy and photometry of RW
Aurigae 06 p0830 A83-18785
Reddening of the narrow-line regions of active galaxies
and the intrinsic Balmer decrement 06 p0835 A83-19053
Spectral energy distributions and equivalent widths of
Balmer lines of B and A stars with rapid axial rotation -
Comparison with theoretical models 07 p1027 A83-21266
On the Balmer progression in the expanding shell of
Pleione 08 p1185 A83-23106
Nebular dust and extinction in ionized nebulae. I - The
Balmer decrement 10 p1513 A83-26712
On the behavior of the Balmer lines in the spectrum of
P Cygni in 1971 10 p1517 A83-26946
Electric fields in coronal magnetic loops 11 p1692 A83-28581
Identification of Lanning 90 as a previously uncataloged
cataclysmic variable 12 p1789 A83-29957
The spectroscopic orbit of KR Aurigae 14 p2101 A83-33465
The spectral properties of filamentary and physical
nonhomogeneous prominences. III - The structure and
stratification of physical conditions 16 p2440 A83-36853
The origin of anomalous Balmer decrements in the
spectra of eruptive stars 17 p2600 A83-37657
The Balmer decrement in moving stellar envelopes 17 p2600 A83-37658
The relative intensities of hydrogen lines in moving
media --- stellar spectra 17 p2600 A83-37659
The formation of hydrogen lines in quiescent
prominences 17 p2625 A83-37669
Spectral analysis of the optical continuum in the 24 April
1981 flare 18 p2782 A83-39037
Balmer-alpha and Balmer-beta emission cross sections
for low-energy H collisions with He and H₂ 18 p2743 A83-40408
The spectrum of Nova Sagittarii 1982 in the transition
phase 22 p3373 A83-46406
Stimulated emission and the flat Balmer decrements of
cataclysmic variable stars 22 p3383 A83-47009
Angular intensity distribution of Balmer-alpha emission
excited by electron impact on H₂ 24 p3626 A83-49431
Nonlinear plasma spectroscopy of the hydrogen
Balmer-alpha line 24 p3627 A83-50196

BANACH SPACE

Thermodynamics based on the Hahn-Banach theorem
- The Clausius inequality 16 p2422 A83-36100
BAND STRUCTURE OF SOLIDS
Meaning of the photovoltaic band gap for amorphous
semiconductors 02 p0243 A83-12287
PAS study of gap-state profiles of P-doped and undoped
a-Si:H --- photoacoustic spectroscopy 04 p0541 A83-15525
Common anion heterojunctions - CdTe-CdHgTe 06 p0814 A83-18962
Donor discrimination and bound exciton spectra in InP 07 p1000 A83-20746
Observation of 'intrinsic' surface states at the
TiO₂-aqueous-electrolyte interface by sub-band-gap
electroreflectance spectroscopy 07 p1000 A83-20818
Direct bandgap, ionizing-radiation insensitive,
photodiode structures 08 p1165 A83-22487
Horizontal tunneling and surface band bending - An
external technique for wavelength tuning of
surface-emitting light-emitting diodes /LEDs/ 08 p1081 A83-22860
Enhanced bandgap resonant nonlinear susceptibility in
quantum-well heterostructures 08 p1167 A83-22917
Hydrides formed from intermetallic compounds of two
transition metals - A special class of ternary alloys 09 p1225 A83-23858
NMR studies of electronic structure in crystalline and
amorphous Zr₂PdH/x/ 10 p1488 A83-25411
Estimation of the band gap of InPO₄ 10 p1489 A83-26210
Frequency dependence of degenerate four-wave mixing
at the band edge of InAs 11 p1581 A83-27597
A semiempirical self-consistent field Hartree-Fock
crystal orbital approach to the infinite tetraza porphyrin
nickel/II system 11 p1661 A83-28072
Slip bands along the matrix-inclusion interface 11 p1598 A83-28491
Theory of silicon superlattices - Electronic structure and
enhanced mobility 11 p1664 A83-28710
The efficiency of a graded-band-gap solar cell 13 p1870 A83-30270
Staircase solid-state photomultiplier and avalanche
photodiodes with enhanced ionization rates ratio 15 p2150 A83-33681
Photoelectrochemical energy conversion involving
transition metal d-states and intercalation of layer
compounds 15 p2131 A83-33863
Synthetic nonlinear semiconductors 16 p2420 A83-35957
Current injection in multiquantum well lasers 16 p2359 A83-35958
New class of materials - Half-metallic ferromagnets 16 p2421 A83-36564
Electric and photoelectric properties of graded-band-gap
Ga(1-x)Al(x)As p-n structures 17 p2535 A83-37055
Influence of radiative recombination on the
minority-carrier transport in direct band-gap
semiconductors 17 p2496 A83-37617
InP surface states and reduced surface recombination
velocity 18 p2750 A83-40061
Density of gap states of silicon grain boundaries
determined by optical absorption 18 p2750 A83-40063
Energy-band distortion in highly doped silicon 18 p2750 A83-40377
Graded barrier single quantum well lasers - Theory and
experiment 19 p2851 A83-40937
Three-dimensional energy band in graphite and
lithium-intercalated graphite 19 p2904 A83-40971
Quantum cyclotron resonance in silicon 21 p3216 A83-44383
Angle-resolved photoemission studies of the CdS band
structure 21 p3218 A83-44620
Degenerate four-wave mixing due to intervalence band
transition in p-type mercury cadmium telluride 21 p3209 A83-45495
Modification of optical properties of
GaAs-Ga(1-x)Al(x)As superlattices due to band mixing 22 p3365 A83-46725
Optical studies of In(x)Ga(1-x)As-GaAs strained
multiquantum well structures 22 p3365 A83-46730
The metal-insulator transition in transition-metal
compounds 24 p3635 A83-49074
The metal-insulator transition in oxides and sulfides of
3d metals 24 p3635 A83-49075
Solid-state superlattices 24 p3635 A83-49445
Bistable cyclotron resonance in semiconductors 24 p3635 A83-49743
New negative-resistance device by a CHIRP
superlattice --- coherent heterointerfaces for reflection and
penetration 24 p3636 A83-49981

BANDPASS FILTERS

NT CRYSTAL FILTERS
NT TRACKING FILTERS

Design of FIR digital filters using tapped cascaded FIR
subfilters 02 p0167 A83-11822
Cascaded bandpass v-th-law devices 02 p0164 A83-11987
Band-pass filtering of one year of daily mean pressures
on Mars 04 p0568 A83-15586
Multichannel recovery of quadrature components of
bandpass signals 06 p0748 A83-19046
Bandpass signal sampling and coherent detection 06 p0749 A83-19048
Quadrature sampling with high dynamic range 06 p0749 A83-19049
Optimized low-insertion-loss millimetre-wave fin-line and
metal insert filters 07 p0919 A83-20178
Theory and design of narrow-passband stripline filters
with finite transmission zeros realized with extra cross
couplings 07 p0922 A83-21084
Digital filter structures for canonic signed-digit code
implementation by microprocessor 10 p1460 A83-25500
A simplified approach to the design of apodized SAW
filters 10 p1408 A83-25503
Computer-aided design of millimeter-wave E-plane
filters 10 p1409 A83-25805
A new method of quantized feedback for the
regeneration of digital signals 10 p1412 A83-26899
Microwave surface magnetoplasma waves 11 p1561 A83-27940
Composite thin-foil bandpass filter for EUV astronomy
Titanium-antimony-titanium 13 p1918 A83-30209
Resonant array bandpass filters for the far infrared 15 p2231 A83-34470
An ellipsoidal frequency selective surface 15 p2146 A83-35080
INTFIS - An interactive package for electronic filter
synthesis 16 p2403 A83-35323
Broad-band compensation for diffraction in surface
acoustic wave filters 16 p2345 A83-35649
Analysis of natural waves of planar lines --- German
thesis 17 p2496 A83-37503
Bandpass filters based on multilayer dielectric
structures 18 p2676 A83-39432
Low insertion-loss, temperature-compensated dielectric
filters for microwave integrated circuits 18 p2679 A83-40393
Design and performance of coplanar waveguide
bandpass filters 19 p2838 A83-41088
Measurement Assurance Program transmittance
standards for spectrophotometric linearity testing -
Preparation and calibration 20 p2990 A83-42946
Dielectric multilayer thin-film filters for WDM transmission
systems --- Wavelength Division Multiplexing in optical fiber
communication 21 p3204 A83-44213
Frequency-selective combine directional couplers
designed as novel filters and multiplexers 21 p3126 A83-44965
PRESTO - A programmable etalon spectrometer for
twilight observations 22 p3288 A83-46066
Acoustic surface wave band filters with weighted fan
transducers 23 p3445 A83-47569
Linear absorption coefficient of beryllium in the 50-300-A
wavelength range --- bandpass filter materials for ultraviolet
astronomy instrumentation 23 p3508 A83-47588
Design and optimization of digital filters without
multipliers 24 p3575 A83-50119
BANDWIDTH
NT BROADBAND
NT SPECTRAL LINE WIDTH
Bandwidth, field distribution, and optimal electrode
design for waveguide modulators 01 p0036 A83-10617
Operational sensitivity of EW receivers 01 p0007 A83-11234
Group time and bandwidth of signals modulated
simultaneously in amplitude and frequency 01 p0032 A83-11335
Bandwidth, scattered light, and temporal variability
effects in spectral solar radiometry 03 p0370 A83-14643
Rainbow holographic aberrations and the bandwidth
requirements 06 p0762 A83-18594
Bulk wave Bragg cells with 1 GHz bandwidth 06 p0753 A83-18935
TV bandwidth compression techniques using time
companded differentials and their applications to satellite
transmissions 07 p0909 A83-19743
Bandwidth of crossbar and multiple-bus connections for
multiprocessors 07 p0984 A83-20250
Image bandwidth compression by pre-compensative
interpolation 08 p1075 A83-22235
Hardware-constrained hybrid coding of video imagery 08 p1077 A83-22731
Image quality experiments for TV reconnaissance at
reduced transmission bandwidth 08 p1105 A83-22902

- Method to increase the bandwidth of heat fluximeters
08 p1106 A83-23236
- Interpretation of synthetic aperture radar measurements
of ocean currents 09 p1319 A83-24309
- A high-power W-band /90-99 GHz/ solid-state
transmitter for high duty cycles and wide bandwidth
10 p1409 A83-25813
- On the effect of absorbing materials on electromagnetic
waves with large relative bandwidth
10 p1405 A83-26491
- Bandwidth estimation for multimode optical fibers using
the frequency correlation function of speckle patterns
10 p1423 A83-26634
- Bandwidth of a low sidelobe level multimode radiating
coupled waveguide array 10 p1405 A83-26834
- Minimum bandwidth signals with some specified
waveform parameters 12 p1718 A83-29474
- Substrate optimization for integrated circuit antennas
19 p2826 A83-41087
- Image design - Generation of a prescribed image at
the output of a band-limited system
20 p3039 A83-42647
- Spectrum of a pulse sequence with a period modulated
by a narrow-band random process
21 p3120 A83-44775

BANG-BANG CONTROL**U OFF-ON CONTROL****BANGLADESH**

- On attaining semi-aridity of North-Bengal in Bangladesh
as viewed through the Landsat imageries
09 p1287 A83-24565

BANKING FLIGHT**U TURNING FLIGHT****BARCHANS****U DUNES****BARDEEN APPROXIMATION****U BARRIER LAYERS****U ELECTRICAL PROPERTIES****U SURFACE PROPERTIES****BARIUM****NT BARIUM ISOTOPES**

- Experimental evidence for collision-induced
superradiance 07 p0937 A83-20797
- The binary nature of the barium stars. II - Velocities,
binary frequency, and preliminary orbits
14 p2099 A83-33204

- Observations of magnetized plasma flow through
stationary background plasma 14 p2087 A83-33380
- A catalog of spectral classification and photometry of
barium stars 16 p2424 A83-35975

- Do all barium stars have a white dwarf companion?
17 p2604 A83-37917
- Investigation of superelastic electron scattering by
laser-excited Ba - Experimental procedures and results
18 p2743 A83-40407
- Spectrum analysis of the barium stars HD 83548 and
HD 65699 20 p3065 A83-42384

BARIUM COMPOUNDS**NT BARIUM FLUORIDES****NT BARIUM TITANATES**

- Asymmetry of conductivity along the polarization axis
in ferroelectric crystals 04 p0542 A83-15885

BARIUM FLUORIDES

- Experience related to the employment of a highly
sensitive humidity probe with miniature humidity sensor
on a barium fluoride basis - Comparison with a Lyman
alpha-hygrometer 18 p2723 A83-39260

BARIUM ION CLOUDS

- Barium-cloud drift and the determination of some
parameters of field-aligned currents from observations
made on Hayes Island 02 p0209 A83-12432
- The drift of barium ion clouds and the electric field over
Volgograd 14 p2051 A83-31886
- Dynamics of artificial plasma clouds in 'Spolokh'
experiments - Movement pattern
20 p3023 A83-43155

- Towards an artificial comet 21 p3227 A83-43977
- Development of the barium shaped charge technique
in Japan --- for studying magnetic field configurations in
upper atmosphere 22 p3270 A83-46525
- Analysis and numerical simulation of the effect of ion
Pedersen mobility on ionospheric barium clouds
22 p3336 A83-47062

BARIUM ISOTOPES

- 5s/2/5p/4f-5s5p/5/ transitions in Cs IV, Ba V, and La
VI 09 p1342 A83-24095
- Barium from a mini r-process in supernovae
13 p1951 A83-31429

BARIUM TITANATES

- The electronic surface state and repolarization
processes in barium titanate single crystals
01 p0110 A83-10848
- Photovoltaic properties of ferroelectric BaTiO₃ thin films
RF sputter deposited on silicon
04 p0473 A83-16078

Spectral response of nearly degenerate four-wave
mixing in photorefractive materials

- 06 p0810 A83-19257
- Crystal structure of the microwave dielectric resonator
Ba₂Ti₉O₂₀ 12 p1717 A83-29973
- Correlation of the electron spectra and temperatures
of phase transformations in solid solutions based on barium
titanate 13 p1930 A83-31305
- AES study on the chemical composition of ferroelectric
BaTiO₃ thin films RF sputter-deposited on silicon
21 p3217 A83-44609

BARKHAUSEN EFFECT

- The Barkhausen effect and viscous phenomena in
gadolinium molybdate single crystals
13 p1928 A83-30315

BAROCLINIC INSTABILITY

- A simple model for nonlinear critical layers in an unstable
baroclinic wave 02 p0213 A83-12226
- The Charney stability problem with a lower Ekman
layer 02 p0213 A83-12227
- Inhibition of baroclinic instability in low-resolution
models 02 p0213 A83-12228
- The baroclinic instability of highly structured
one-dimensional basic states 04 p0516 A83-15926
- Baroclinic instability in the presence of mountains
04 p0519 A83-16159
- On the predictability of quasi-geostrophic flow - The
effects of beta and baroclinicity
08 p1142 A83-23002

- The evolution of a Rossby-wave packet in a
three-dimensional baroclinic atmosphere
08 p1142 A83-23006

- Baroclinic instability of the summer mesosphere - A
mechanism for the quasi-two-day wave
08 p1143 A83-23017

- The structure of an atmospheric warm front and its
interaction with the boundary layer
09 p1310 A83-23355

- Vertical structure and dynamics of Mesoscale Wave
Disturbance (MWD) inferred from GOES satellite imagery
and ground truth data 13 p1887 A83-30553
- A note on orographically induced instabilities in two-layer
models --- of atmosphere 13 p1893 A83-31046

- Stability properties of cylindrically curved mean flows
--- in atmosphere 14 p2058 A83-32469
- Nonlinear baroclinic instability - An approach based on
Serrin's energy method 16 p2385 A83-35472

- Disturbances and eddy fluxes in Northern Hemisphere
flows Instability of three-dimensional January and July
flows 16 p2385 A83-35478

- Charney's problem for baroclinic instability applied to
barotropic instability 16 p2387 A83-35492
- The dynamics of localized vortex perturbations (vortex
charges) in a baroclinic fluid 16 p2392 A83-36865

- Space-time spectral analyses of Northern Hemisphere
geopotential heights 18 p2728 A83-40028
- A moist baroclinic model for monsoonal
mid-tropospheric cyclogenesis 18 p2728 A83-40032

- On baroclinic instability in the case of vanishing
viscosity 21 p3132 A83-44943
- The baroclinic processes of monsoon depressions
23 p3491 A83-47417

BAROCLINIC WAVES

- A simple model for nonlinear critical layers in an unstable
baroclinic wave 02 p0213 A83-12226
- The impact of model moist processes on baroclinic wave
energetics 03 p0367 A83-14427
- Baroclinic nonlinear exchanges of energy and potential
enstrophy in the quasi-geostrophic two-layer model
03 p0369 A83-14520

- Adaptation of P. D. Thompson's scheme to the constraint
of potential vorticity conservation --- modified
two-parameter baroclinic model for weather prediction
06 p0791 A83-18465

- The amplification and capture of atmospheric solitons
by topography - A theory of the onset of regional
blocking 08 p1142 A83-23003

- The role of latent heat release in baroclinic waves -
Without beta-effect 08 p1142 A83-23005
- Relative humidity distribution in the vicinity of the warm
conveyor belt 13 p1889 A83-30574

- On resonant interactions between unstable and neutral
baroclinic waves 13 p1892 A83-31037

- A baroclinic quasigeostrophic open ocean model
13 p1895 A83-31366

- Contribution of baroclinic mechanism in the formation
of the depression during MONEX-79
14 p2056 A83-32404

- Some discussions on the baroclinic and barotropic
instabilities over Indian region during summer
14 p2057 A83-32407

- The anti-cyclonic shear wave - A new geophysical
wave 14 p2033 A83-33140
- The excitation of inertial oscillations by atmospheric
effects --- on ocean dynamic processes
15 p2209 A83-34357

The effect of islands on low frequency equatorial
motions 16 p2393 A83-36976

The effects of orographically determined vertical motions
and surface friction on the development and motion of
baroclinic waves in numerical models with different vertical
resolution 18 p2723 A83-39259

The response of finite-amplitude wave motions to
seasonal heating of a baroclinic shear flow
18 p2684 A83-39449

Sloping convection in the laboratory and in the
atmospheres of Jupiter and Saturn
21 p3240 A83-44233

The energy exchange between the baroclinic and
barotropic components of atmospheric flow in the tropics
during the FGGE summer 23 p3490 A83-47407

BAROCLINITY

A simple model illustrating baroclinic development
03 p0363 A83-13223

Dynamics of the baroclinic unstratified planetary
boundary layer over land and sea
04 p0515 A83-15721

Assessment of the separate effects of baroclinicity and
thermal stability in the atmospheric boundary layer over
the sea 04 p0516 A83-15857

The hydromagnetic viscous boundary layer at the free
surface of a rotating baroclinic fluid
05 p0641 A83-17835

Effects of baroclinicity on resistance laws for the
atmospheric boundary layer over a slightly inclined
terrain 16 p2385 A83-35469

On the mechanism for the development of polar lows
16 p2386 A83-35480

BAROMETERS

New results regarding aerotriangulation with statoscope
data 08 p1092 A83-22033

Experimental calibration of the sphalerite
cosmobarometer 08 p1190 A83-22998

A low-power hypsometer-type barometer for remote
weather stations 10 p1423 A83-26496

Multicolor laser altimeter for barometric measurements
over the ocean - Theoretical 22 p3259 A83-46070

Multicolor laser altimeter for barometric measurements
over the ocean - Experimental 22 p3259 A83-46071

BAROMETRIC PRESSURE**U ATMOSPHERIC PRESSURE****BARORECEPTORS**

The hemodynamic responses of normotensive and
hypertensive rats to injections of prostaglandins and
indomethacin 01 p0079 A83-10538

Gravitational effects on human cardiovascular
responses to isometric muscle contractions
19 p2884 A83-42049

BAROTRAUMA

The peculiarities of the pathogenesis of decompression
barotrauma of the lungs 03 p0382 A83-14547

Survival following accidental decompression to an
altitude greater than 74,000 feet /22,555 m/
04 p0522 A83-15538

The pressure problems of the middle ear in flight
personnel - The importance of impedanceometric
examinations 08 p1147 A83-22958

Current barotraumatic otitis of the commercial flight
personnel in civil aviation 14 p2067 A83-32454

Hemodynamic effects of Dextran 40 on hemorrhagic
shock during hyperbaria and hyperbaric hypoxia
14 p2064 A83-32687

Barotraumatism and a Killian polyp in a parachutist
16 p2397 A83-35587

BAROTROPIC FLOW

Baroclinic nonlinear exchanges of energy and potential
enstrophy in the quasi-geostrophic two-layer model
03 p0369 A83-14520

Eastward and westward flows over topography in
nonlinear and linear barotropic models
04 p0516 A83-15933

Motion in the interiors and atmospheres of Jupiter and
Saturn - Scale analysis, anelastic equations, barotropic
stability criterion 05 p0703 A83-16960

A modulated point-vortex model for geostrophic,
beta-plane dynamics
[AD-A126704] 05 p0639 A83-17355

A non-geostrophic study in a barotropic system
05 p0668 A83-17554

A weakly non-linear theory of barotropic instability
09 p1311 A83-23887

A hemispheric barotropic quasi-geostrophic model of the
atmosphere with conservation of the degrees of potential
vorticity 09 p1315 A83-24934

A note on orographically induced instabilities in two-layer
models --- of atmosphere 13 p1893 A83-31046

Notes on the stationary vortex motions of a continuum
14 p2009 A83-32363

On a 3-component truncated model of a barotropic
non-divergent rotating atmosphere in spherical geometry
14 p2057 A83-32405

On truncated models of barotropic vorticity equation in spherical geometry 14 p2057 A83-32406

Some discussions on the baroclinic and barotropic instabilities over Indian region during summer 14 p2057 A83-32407

The background of the equivalent barotropic model for tropics 14 p2057 A83-32408

The influence of a costal headland on oceanic boundary currents 15 p2208 A83-34325

Barotropic instability of the polar night jet stream 16 p2385 A83-35477

Charney's problem for baroclinic instability applied to barotropic instability 16 p2387 A83-35492

A gas-dynamic analogy of the motion and equilibrium of magnetizable and polarizable media 16 p2415 A83-35713

A barotropic planetary boundary layer 16 p2387 A83-35794

The influence of the differencing methods used on the solution of the barotropic nesting problem 16 p2391 A83-36587

Absolute barotropic instability and monsoon depressions 18 p2729 A83-40034

Bounds on the growth of perturbations to non-parallel steady flow on the barotropic beta plane 18 p2729 A83-40036

African wave disturbances in a general circulation model 21 p3179 A83-44471

A critical layer dominated by non-parallel effects in a rotating barotropic flow 21 p3132 A83-44940

The effect of a heat source on the large-scale pressure and wind fields (a quasi-barotropic model) 21 p3181 A83-45330

Horizontal energy propagation in a barotropic atmosphere with meridional and zonal structure 22 p3341 A83-46849

The energy exchange between the baroclinic and barotropic components of atmospheric flow in the tropics during the FGGE summer 23 p3490 A83-47407

Steady, periodic, and aperiodic atmospheric flows 23 p3491 A83-48040

BAROTROPISM

NT PLANETARY WAVES

Barotropic wave propagation and instability, and atmospheric teleconnection patterns 21 p3180 A83-44701

Steady, periodic, and aperiodic atmospheric flows 23 p3491 A83-48040

BARRED GALAXIES

Flocculent and grand design spiral structure in field, binary and group galaxies 03 p0420 A83-13941

Wolf-Rayet stars and an extraordinary star-forming region in the barred spiral galaxy NGC 5430 deg 03 p0421 A83-14138

On the inner ring of HII regions in NGC 3351 05 p0701 A83-17669

Preferred orbit planes in the gravitational field of a tumbling spheroidal galaxy 06 p0843 A83-19480

Optical studies of H I-rich southern galaxies. II - The low-visibility spiral NGC 1079 07 p1010 A83-19856

Ordered and ergodic motions of stars in galaxies 07 p1008 A83-21215

Morphology of the ionized gas in NGC 1313 09 p1355 A83-24525

On the nature of orbits in realistic bar potentials 10 p1492 A83-25480

Nuclear activity in the barred spiral galaxy NGC 3660 from radio, optical, and X-ray observations 10 p1500 A83-25488

Flocculent and grand design spiral galaxies in groups - Time scales for the persistence of grand design spiral structures 10 p1512 A83-26705

The galaxy NGC 1365 13 p1941 A83-31577

Unusual rotation curve of the Galaxy NGC 2814 15 p2269 A83-34677

Photometry, kinematics, and dynamics of the barred spiral galaxy NGC 5383 16 p2430 A83-36649

Bulge-halo effects in barred galaxies 16 p2426 A83-36688

Radio continuum observations of the bar of NGC 1097 17 p2588 A83-37347

A new model for barred spiral galaxies 17 p2611 A83-38588

Distribution of QSOs around NGC 1097 18 p2760 A83-40365

Velocity fields in late-type galaxies from H-alpha Fabry-Perot interferometry. IV - Kinematics and dynamics of the SAB(s) spiral NGC 5236 (M83) 22 p3377 A83-46257

Disk stability --- and barred galaxies 24 p3641 A83-49234

Numerical experiments on the response mechanism of barred spirals 24 p3656 A83-49237

Onset of stochasticity in barred spirals 24 p3641 A83-49238

Attacking the problem of a selfconsistent bar --- stellar orbits in barred galaxies 24 p3641 A83-49239

Theoretical studies of gas flow in barred spirals galaxies 24 p3656 A83-49240

H I in the barred spiral galaxies NGC 1365 and NGC 1097 24 p3656 A83-49241

Observations of the neutral hydrogen in the barred spiral galaxies NGC 3992 and NGC 4731 24 p3656 A83-49242

The barred galaxy NGC 7741 24 p3656 A83-49243

Hydrodynamical models of offcentered barred spirals 24 p3657 A83-49244

Six quasars near the jets of NGC 1097 24 p3643 A83-49355

BARRICADES

U BARRIERS

BARRIER INJECTION TRANSIT TIME DIODES

U BARRITT DIODES

BARRIER LAYERS

Dependence of barrier height on energy gap in Au n-type GaAs/1-x/P/x/ Schottky diodes 02 p0242 A83-11784

New method for the determination of the surface barrier heights in MIS tunnel diodes /solar cells/ 02 p0167 A83-11990

Very narrow graded-barrier single quantum well lasers grown by metalorganic chemical vapor deposition 02 p0185 A83-12279

Planar doped barriers by molecular beam epitaxy for millimeter wave devices 03 p0310 A83-13785

Investigation of metal-insulator-metal-insulator-metal structures 04 p0472 A83-15910

Electrical properties of bulk-barrier diodes 05 p0631 A83-17758

Undoped, semi-insulating GaAs layers grown by molecular beam epitaxy 06 p0815 A83-19262

A conduction model for semiconductor-grain-boundary-semiconductor barriers in polycrystalline-silicon films 09 p1350 A83-24497

Formation of electrostatic potential barrier between different plasmas 12 p1780 A83-29100

Barrier height enhancement in semiconductor-insulator-semiconductor solar cells due to surface states and insulator charges 15 p2238 A83-34672

Lithium alloy-thionyl chloride cells - Performance and safety aspects 15 p2192 A83-34694

Schottky barrier height variation with metallurgical reactions in aluminum-titanium-gallium arsenide contacts 16 p2419 A83-35671

Characteristics of semiconductor gas sensors. I - Steady state gas response 17 p2512 A83-38535

BARRIERS

The turbulent wind flow over an embankment 06 p0789 A83-18239

Unstable flow in the region of the interaction of an underexpanded jet with a barrier 17 p2450 A83-37567

BARRITT DIODES

Optical injection locking of BARRITT oscillators 10 p1411 A83-26344

Fabrication and investigation of BARRITT diodes in the Ka-band --- German thesis 11 p1564 A83-28645

BARS

NT ELASTIC BARS

NT PRISMATIC BARS

Basic properties of elastic-plastic boundaries in stress wave propagation in a bar 03 p0341 A83-14484

SIF of surface cracks and fatigue crack propagation behaviour in a cylindrical bar 05 p0614 A83-17092

On the longitudinal vibrations of tapered bars 08 p1115 A83-21636

Compliance calibration of a family of short rod and short bar fracture toughness specimens 11 p1548 A83-28435

A numerical method for the correction of dispersion in pressure bar signals 15 p2166 A83-35252

Investigation of the fatigue and crack propagation properties of X7091-T7E69 extrusion 17 p2487 A83-37836

Fracture of notched polycarbonate under hydrostatic pressure 18 p2670 A83-39049

On the stress wave velocity of fiber reinforced rectangular bar by means of finite prism method 18 p2705 A83-40218

Optimal modification of shape for two-dimensional elastic bodies 20 p3001 A83-42521

BARYCENTER

U CENTER OF GRAVITY

BARYONS

Matter and antimatter in the universe 01 p0123 A83-10377

Limits on the neutrino number and baryon density of a realistic universe 11 p1694 A83-28286

Astrophysical consequences of barytinos 12 p1794 A83-29085

Experimental test of baryon conservation - A new limit on neutron-antineutron oscillations in oxygen 13 p1917 A83-30916

Use of final-energy sum rules to describe baryon properties in quantum chromodynamics and to estimate the proton lifetime in the SU(5) model 14 p2083 A83-32621

Mechanism of generating isothermal perturbation by a strong CP nonconservation --- in early universe 19 p2915 A83-40972

Upper limit for mediation of baryon decay by slow magnetic monopoles 21 p3245 A83-45056

BASALT

Petrology of EETA79006 and implications for the formation of polymict eucrites 03 p0435 A83-14323

The mare basalt magma source region and mare basalt magma genesis 04 p0559 A83-15331

The polymict eucrites Elephant Moraine A79004 and A79011 and the regolith history of a basaltic achondrite parent body 04 p0562 A83-15359

Petrography and mineralogy of two basalts and olivine-pyroxene-spinel fragments in achondrite EETA79001 04 p0563 A83-15362

Martian volcanic materials - Preliminary thickness estimates in the eastern Tharsis region 04 p0565 A83-15559

Geochemistry and petrogenesis of Archaean metavolcanic amphibolites from Fiskenaeset, S. W. Greenland 04 p0514 A83-16353

Sulfide saturation of basalt and andesite melts at high pressures and temperatures 07 p0963 A83-21045

Siderophile trace elements in the earth's oceanic crust and upper mantle 07 p0965 A83-21285

Homogeneity of lava flows - Chemical data for historic Mauna Loa eruptions 07 p0965 A83-21321

Eruption age of a Pleistocene basalt from Ar-40-Ar-39 analysis of partially degassed xenoliths 16 p2381 A83-36599

Pb, Sr, Nd and Hf isotopic evidence of multiple sources for Oahu, Hawaii basalts 18 p2718 A83-39957

Studies of the content and the distribution of uranium of lunar mare basaltic fragments taken by Apollo 17 21 p3240 A83-44503

Strontium isotope composition of volcanic rocks - Evidence for contamination of the Kirkpatrick Basalt, Antarctica 22 p3323 A83-45783

The nomenclature of polymict basaltic achondrites 22 p3384 A83-46372

Origin of lunar meteorite ALHA 81005 - Clues from the presence of terrae clasts and a very low-titanium mare basalt clast 22 p3385 A83-46862

Petrogenesis of the Elephant Moraine A79001 meteorite 24 p3671 A83-48810

Multiple magma pulses on the shergottite parent body 24 p3608 A83-50111

BASE FLOW

Analysis of combustion in recirculating flow for rocket exhausts in supersonic streams 02 p0148 A83-13087

Laser velocimetric analysis of the flow downstream of missile aft-bodies [ONERA, TP NO. 1982-94] 03 p0279 A83-14543

Navier-Stokes computations of the projectile base flow with and without base injection [AIAA PAPER 83-0224] 05 p0582 A83-16594

Calculation of parameters of a near wake produced by injection of an annular jet into the base region 05 p0590 A83-17424

Flow in the base region in a channel --- supersonic jet discharge from nozzle 09 p1197 A83-24042

Optical studies of shock generated transient supersonic base flows 10 p1371 A83-26142

The effect of an increase in the temperature factor of a cone on the parameters of the base region 17 p2451 A83-37811

Flow in the base region of a channel in non-self-similar regimes 19 p2792 A83-41894

ONERA research on afterbody viscid/inviscid interaction with special emphasis on base flows [ONERA, TP NO. 1983-26] 21 p3085 A83-44305

BASE HEATING

Base heating on an aerobraking orbital transfer vehicle [AIAA PAPER 83-0408] 05 p0607 A83-16697

Steady supersonic flow of a viscous heat-conducting gas past a cylinder with a flat end-face 08 p1041 A83-21630

Space Shuttle base heating [AIAA PAPER 83-1544] 14 p1981 A83-32767

An experimental investigation of turbulent base heat transfer in hypersonic flow 21 p3087 A83-44569

BASE PRESSURE

- Model for pure source flow chemical lasers
07 p0932 A83-19817
- Evolution of shock-induced pressure on a flat-face/flat-base body and afterbody flow separation
10 p1372 A83-26159
- An experimental investigation of the wake of an axisymmetric body with a slanted base
11 p1526 A83-27873
- Loads and pressures due to underexpanded jets impinging on wedges
16 p2288 A83-35619
- Simple model for base pressure effects in source flow chemical lasers
19 p2850 A83-40858
- The base pressure of bodies of revolution with gas injection through the body surface into a supersonic flow
19 p2790 A83-41265
- The effect of the solid phase and thermophysical characteristics of a central single supersonic jet of an engine on base pressure and temperature
24 p3552 A83-49665

BASES (FOUNDATIONS)

U FOUNDATIONS

BASIC (PROGRAMMING LANGUAGE)

- Statistical study of TBO and estimation of acceleration factors of ASMT for aircraft turbo-engine --- Accelerated Simulated Mission Endurance Testing
16 p2304 A83-35858

BASINS

U STRUCTURAL BASINS

BATCH PROCESSING

- A noninteractive procedure for land-use determination
10 p1443 A83-25642

BATHYMETERS

- Remote bathymetry using active and passive techniques
01 p0076 A83-10070
- Passive bathymetry with airborne multispectral scanner
03 p0372 A83-14288
- Bathymetric prediction from Seasat altimeter data
09 p1318 A83-24283
- Analysis of bathymetry and submarine topography off the coast of east-central Tunisia with Landsat multispectral data
09 p1289 A83-24599
- Passive bathymetric measurements of inland waters with an airborne multi-spectral scanner
09 p1290 A83-24607
- Bathymetric and oceanographic applications of Kalman filtering techniques
10 p1452 A83-26267
- A prospectus on airborne laser mapping systems
17 p2530 A83-38168
- Surface expression of bathymetry on Seasat synthetic aperture radar images
20 p3032 A83-42969
- Bathymetry estimates in the southern oceans from Seasat altimetry
20 p3033 A83-43548

BATHYMETRY

U BATHYMETERS

BATTERIES

U ELECTRIC BATTERIES

BATTERY CHARGERS

- Sealed nickel cadmium batteries --- Book
15 p2188 A83-33614
- Power conditioning system of an international amateur radio satellite
[IAF PAPER 83-61] 23 p3425 A83-47247
- BATTERY SEPARATORS**
U SEPARATORS
- BAUSCHINGER EFFECT**
Anisotropic yield surfaces in cyclic plasticity
13 p1867 A83-31544

BAY ICE

- Ice distribution and winter surface circulation patterns, Kachemak Bay, Alaska
02 p0198 A83-12038

BAYES THEOREM

- Algorithm for distinguishing between the trajectories of moving targets and for estimating their coordinates
02 p0162 A83-11533
- HP-41C programs for Bayesian binomial and exponential interval estimation with a uniform prior on the reliability
07 p0942 A83-20513
- Bayesian reliability and availability - A review
07 p0942 A83-20515
- Bayes' error probability for noisy and imprecise measurement in pattern recognition
08 p1157 A83-22350
- On Bayes estimation of reliability for the Birnbaum-Saunders fatigue life model
[AD-A128477] 08 p1114 A83-22708
- Resolution classifier --- Bayesian approach for astronomical images
14 p2096 A83-32034
- The application of pseudo-Bayesian estimators to remote sensing data - Ideas and examples
14 p2036 A83-33347
- A finitely additive white noise approach to nonlinear filtering
19 p2889 A83-41021
- Locally optimum and suboptimum detector performance in non-Gaussian noise
19 p2839 A83-41365

- A comparative evaluation of some maneuvering target tracking algorithms
[AIAA PAPER 83-2168] 19 p2891 A83-41664
- Bayesian estimates of vector quantities in the case of microstatistics
19 p2893 A83-42059
- A solution of the problem of nonlinear filtering in conditions of ambiguous measurements
22 p3350 A83-45658
- QUEST - A Bayesian adaptive psychometric method
22 p3348 A83-45951

BAYESIAN STATISTICS

U BAYES THEOREM

BAYS (TOPOGRAPHIC FEATURES)

- Passive microwave detection of river-plume fronts in the German Bight
05 p0646 A83-17713
- Temperature and current variability of a Gulf Stream meander observed off Onslow Bay, August 1977
14 p2060 A83-33084
- Temporal analysis of suspended solid in Tokyo Bay by Landsat data
15 p2183 A83-33580
- Numerical stimulation of photochemical air pollution over the Isle Bay District
20 p3013 A83-42202
- Synoptic effects on the local winds in Todos Santos Bay - A case study
23 p3491 A83-47415

BBGKY HIERARCHY

- The four-point function in the BBGKY hierarchy --- galaxy correlation in clustering pattern
03 p0422 A83-14178

BCC LATTICES

U BODY CENTERED CUBIC LATTICES

BEACON SATELLITES

- GaAs laser beacon for satellite communications
09 p1214 A83-23582

BEACONS

NT DISCRETE ADDRESS BEACON SYSTEM

NT RADAR BEACONS

NT RADIO BEACONS

NT RADIO DIRECTION FINDERS

BEAM CURRENTS

- Ion accelerator systems for high power 30-cm thruster operation
[AIAA PAPER 82-1893] 02 p0144 A83-12474
- Ion extraction capabilities of closely spaced grids
[AIAA PAPER 82-1894] 02 p0147 A83-12551
- Calculation of the frequency spectrum of an electron beam in a klystron with premodulation
07 p0921 A83-20855
- Improved ion containment using a ring-cusp ion thruster
[AIAA PAPER 82-1928] 07 p0873 A83-21100
- Theory of excitation of plasma traveling wave tubes
09 p1254 A83-23997
- Theory of beam-induced currents in semiconductors
10 p1489 A83-26212
- Operation of the J-series thruster using inert gas
[AIAA PAPER 82-1929] 10 p1388 A83-26625
- Characterization of grain boundaries in polycrystalline solar cells using a computerized electron beam induced current system
20 p2988 A83-42299
- Upward electron beams measured by DE-1 - A primary source of dayside region-1 Birkeland currents
20 p3026 A83-43215
- High-current pulsed proton source
23 p3507 A83-47555

BEAM INJECTION

- Injection-locking of TEA CO₂ lasers by an orthogonally-polarised injection source
02 p0185 A83-12400
- Radar observations of an intense plasma beam in the ionosphere /the Aelita-1 experiment/
03 p0361 A83-14685
- Comparison of calculated and measured values of electron fluxes for the wide-angle detector in the ARAKS experiment --- on ionospheric electron beam injection
06 p0786 A83-18368
- A free electron laser oscillator based on a cyclotron-undulator interaction
10 p1427 A83-26012
- Measurements of the stability of energetic electron beams in the ionosphere
11 p1617 A83-28312
- Direct observation of radiation belt electrons precipitated by the controlled injection of VLF signals from a ground-based transmitter
12 p1800 A83-28922
- Dynamics of a charged-particle beam --- injected into ionosphere along geomagnetic field lines
13 p1875 A83-30612
- Subsatellite studies of wave, plasma, and chemical injections from Spacelab
15 p2126 A83-33733
- Artificial electron beams as probes of the magnetosphere
15 p2195 A83-33742
- Artificial particle beams in space plasma studies; Proceedings of the Advanced Research Institute, Gellio, Norway, April 21-26, 1981
15 p2233 A83-34176
- The use of artificial electron beams as probes of the distant magnetosphere
15 p2197 A83-34177

- Recent observations of beam plasma interactions in the ionosphere and a comparison with laboratory studies of the beam plasma discharge
15 p2197 A83-34178
- On the use of artificially injected energetic electrons as indicators of magnetospheric electric fields parallel to the magnetic lines of force
15 p2197 A83-34180
- The French-Soviet experiments ARAKS - Main results --- Artificial Radiation and Aurora between Kerguelen and Soviet Union
15 p2197 A83-34181
- Stimulation of plasma waves by electron guns on the ISEE-1 satellite
15 p2233 A83-34185
- Highlights of the observations in the POLAR 5 electron accelerator rocket experiment
15 p2198 A83-34187
- Onboard radiometric photography of EXCEDE SPECTRAL's ejected-electron beam
15 p2128 A83-34190
- Laboratory simulation of injection particle beams in the ionosphere
15 p2198 A83-34193
- Electron beam injection and associated phenomena as observed in a large space simulation chamber
15 p2234 A83-34203
- Theory of beam plasma discharge
15 p2235 A83-34204
- Electron beam as a source of electrostatic waves
15 p2228 A83-34205
- The artificially injected charged particles as a tool for the measurement of the electric field in the magnetosphere
15 p2198 A83-34215
- Launching light from semiconductor lasers into plane-ended multimode optical fibers
20 p3046 A83-42220
- Excitation of electromagnetic fields by a modulated electron beam entering a plasma waveguide
21 p3210 A83-44135
- Current neutralization during the formation of annular relativistic electron beams in a neutral gas and a weakly ionized plasma
21 p3210 A83-44136
- Full wave calculation for a Gaussian VLF wave injection into the ionosphere
22 p3330 A83-46505
- BEAM INTERACTIONS**
Control of beam instability in bounded plasma systems
01 p0108 A83-11346
- Two-dimensional model of the interaction of a relativistic electron beam with fields excited in a plasma
02 p0240 A83-11535
- Propagation of an electromagnetic beam in an inhomogeneous plasma formed during the interaction of this beam with a thin dense-gas layer
02 p0240 A83-11681
- The interaction of a relativistic electron beam with a thin target --- French thesis
03 p0398 A83-13806
- Target design of an archival electron beam memory
04 p0526 A83-16051
- The nonlinear relaxation of a beam of relativistic electrons in a plasma - Nonlinear sound attenuation
05 p0686 A83-16891
- A theory for the two-beam instability in a plasma
05 p0689 A83-17587
- Optimal conditions for the creation of an artificial ionized region in the atmosphere by intersecting microwave beams
05 p0662 A83-17608
- Generalized expressions for momentum and energy losses of charged particle beams in non-Maxwellian multi-species plasmas and spherical symmetry
06 p0812 A83-18915
- Coherent scattering of a surface wave by an electron beam with a spatially modulated velocity
06 p0767 A83-19366
- Nonlinear stationary space-charge waves in beam-plasma systems
07 p0995 A83-20058
- Close-range interactions in intense electron beams
09 p1253 A83-23489
- The dependence of the sharpness of an interference pattern on the quantum state of the electromagnetic field
09 p1346 A83-25092
- Production of negative ions by dissociative electron attachment to SO₂
10 p1478 A83-25552
- Interaction of a relativistic electron beam with a plasma
10 p1487 A83-26696
- Investigation of a Laser Doppler anemometer with counterpropagating beams
11 p1574 A83-28562
- Coherent electromagnetic emission from an electron-ion beam
11 p1584 A83-28564
- Turbulent relaxation of counterstreaming plasma beams
Results of numerical simulation on the M-10 computer
13 p1923 A83-30097
- Steady-state turbulence with a narrow inertial range
13 p1923 A83-30121
- Electromagnetic radiation from beam-plasma instabilities
13 p1923 A83-30122
- Modeling of the interaction of a confined electron beam with an electromagnetic wave in distributed-emission magnetron-type systems
13 p1833 A83-30703
- Theoretical study of processes in a system with 'conjugate' M-type interaction
13 p1833 A83-30705

Nonlinear interaction of a modulated electron beam with electromagnetic waves in M-type devices 13 p1833 A83-30707

Theory of a resonance oscillator with relay interaction 13 p1834 A83-30735

The thermal self-focusing of a wave beam in an underdense plasma. I - The wave spectrum 13 p1927 A83-31649

The interaction of surface acoustic waves in piezoelectrics and electron beams 14 p2003 A83-32143

Detailed spectra of high-power broadband microwave emission from intense electron-beam-plasma interactions 14 p2087 A83-32849

Electron-photon coincidence technique for the absolute calibration of VUV detectors 14 p2021 A83-32914

Artificial particle beams in space plasma studies; Proceedings of the Advanced Research Institute, Geilo, Norway, April 21-26, 1981 15 p2233 A83-34176

Evidence for beam-stimulated precipitation of high energy electrons --- in magnetosphere 15 p2198 A83-34186

Observations of non-linear processes in the ionosphere 15 p2198 A83-34191

Transient effects in beam-plasma interactions in a space simulation chamber stimulated by a fast pulse electron gun 15 p2234 A83-34198

Radial dependence of HF wave field strength in the BPD column --- Beam Plasma Discharge 15 p2234 A83-34200

Laboratory beam-plasma interactions - Linear and nonlinear 15 p2234 A83-34201

The beam-plasma under space-like conditions 15 p2235 A83-34207

Plasma waves generated by rippled, magnetically focused electron beams surrounded by tenuous plasmas 15 p2235 A83-34208

Analysis of the interaction of an electron beam with back surface field solar cells 17 p2536 A83-38212

Microwave generation from rotating electron beams in magnetron-type waveguides 17 p2498 A83-38219

Stimulated Cerenkov emission from ultrarelativistic helical electron beams 17 p2499 A83-38492

Rotating electron beam in crossed fields - Space charge, nonlinear effects 17 p2500 A83-38987

The instability of an electron beam passing through a resistive medium 18 p2749 A83-40514

Eigenfunction analysis of the beam-plasma instability with finite radial dimensions 18 p2749 A83-40515

Beam-plasma interactions in a positive ion-negative ion plasma 18 p2749 A83-40517

Auroral beam/plasma interaction observed directly 20 p3023 A83-43159

Dynamics of the formation of optical striations --- by laser bombardment of plasma columns 21 p3210 A83-44142

Electromagnetic two-stream and filamentation instabilities for a relativistic beam-plasma system 22 p3362 A83-46020

The Desertron - Colliding beams at 20 TeV 23 p3507 A83-47815

Forced interaction between an electron beam and superpower electromagnetic radiation at the boundary between two media 23 p3463 A83-48434

BEAM NEUTRALIZATION

The influence of stray magnetic fields on ion beam neutralization 02 p0242 A83-12554

[AIAA PAPER 82-1945] 02 p0242 A83-12554

Effect of background electron plasma waves on ion-beam neutralization 03 p0396 A83-13179

Laser polarization of accelerated protons 15 p2228 A83-33785

BEAM PLASMA AMPLIFIERS

Nonlinear theory of the amplification of electromagnetic waves by an electron beam passing through a stratified inhomogeneous medium 02 p0241 A83-11690

A review of studies on ion thruster beam and charge-exchange plasmas 02 p0146 A83-12504

[AIAA PAPER 82-1944] 02 p0146 A83-12504

Intense wave beams in smoothly inhomogeneous nonlinear media 04 p0537 A83-15905

Relaxation oscillations in a plasma with an ultrarelativistic electron beam 04 p0537 A83-15907

A relativistic plasma microwave generator 04 p0472 A83-15909

Upgoing ion beams. I - Microscopic analysis --- of auroral plasma 05 p0661 A83-17399

Nonlinear theory for the interaction of intense electron beams with plasmas in waveguides 07 p0918 A83-20053

Mathematical modeling of systems for the formation and focusing of intense charged-particle beams 07 p0996 A83-20316

Theory of the parametric excitation of electromagnetic radiation in a plasma waveguide with an electron beam 07 p0921 A83-20872

Theory of excitation of plasma traveling wave tubes 09 p1254 A83-23997

Laser light backscattering off an electron beam-plasma system 10 p1428 A83-26019

Coherent electromagnetic emission from an electron-ion beam 11 p1584 A83-28564

Discrimination effects during the parametric interaction of waves in a relativistic electron beam plasma 11 p1584 A83-28569

Nonlinear energy flow in a beam-plasma system 11 p1660 A83-28696

The effect of the transverse dimensions of the electron beam on beam-plasma instability 13 p1922 A83-30007

Magnetic guiding, focusing and compression of an intense charge-neutral ion beam 13 p1924 A83-30124

Electron beam injection and associated phenomena as observed in a large space simulation chamber 15 p2234 A83-34203

Nonlinear theory of the instability of a modulated electron beam of low density in a plasma. I - Conservation laws of energy and momentum for electromagnetic waves in a nonequilibrium dispersive and dissipative medium in the case of a slow change of amplitude and phase of the wave 15 p2236 A83-35237

Dispersion characteristics for decaying or amplifying waves. I - An observational approach. II - Analysis of a beam-plasma system 16 p2414 A83-35422

Radiation generation by collective phenomena in semiconductors 16 p2358 A83-35522

Bernstein mode quasi-optical gyrokykotron [AD-A130124] 17 p2497 A83-37760

Fourier analysis of the wave number of unstable waves in a spiral beam-plasma system 20 p3050 A83-43397

Brillouin backscattering in an electron beam-plasma system 21 p3212 A83-44348

The longitudinal excitation of vapors of complex organic compounds by an electron beam 24 p3627 A83-49740

BEAM RIDER GUIDANCE

The Talos guidance system 02 p0141 A83-12858

BEAM SPLITTERS

Optical-waveguide hybrid coupler 02 p0235 A83-11567

Multilayer mirrors and beam splitters for soft X-rays 02 p0236 A83-12397

A two-grating method for combined beam splitting and frequency shifting in a two-component laser-Doppler velocimeter 05 p0645 A83-17352

Dichroic beam splitter for extreme-ultraviolet and visible radiation 05 p0651 A83-17878

Wavefront distortion introduced by sampling with a hole grating --- high power laser beam diagnostics 08 p1108 A83-22455

Near-millimeter wave polarizing duplexer/isolator 10 p1483 A83-26646

Optical heterodyne measurement of vibration phase 15 p2164 A83-34396

Optical splitter for dynamic range enhancement of optical multichannel detectors 19 p2847 A83-41098

Measurement of coherence of radiation from diffusely illuminated beam splitters 21 p3140 A83-44842

BEAM SWITCHING

Intracavity phase switching and phase-plane dynamics of a bistable optical device 02 p0236 A83-12404

Switching of reflection of light at nonlinear interfaces 03 p0394 A83-13793

Offset near-field Gregorian antenna scanning beam analysis 03 p0305 A83-13999

Gain-switched pulse generation with semiconductor lasers 04 p0486 A83-16219

Transient phenomena in optical bistability 11 p1656 A83-27531

New mechanism for bistable operation of closely coupled twin stripe lasers 13 p1858 A83-31783

One- and two-photon excited picosecond conductivity in CdS 14 p2083 A83-31949

Characterisation of electrical and optical base controlled switching in the V-groove isolated punch through mode mist --- Metal-Insulator (tunnel)-Silicon Thyristor 14 p2006 A83-32666

Temporal and spectral characteristics of rapidly gain-switched GaAs/GaAlAs buried-heterostructure lasers 15 p2170 A83-34522

An algebraic synthesis method for R(sq N) multibeam matrix network 15 p2126 A83-35093

Simultaneous ultraviolet laser triggering of two megawatt gas switches 18 p2677 A83-40059

Electron-bombarded semiconductor (EBS) switch 18 p2678 A83-40373

Packet communication system for a multi-beam beam switched satellite repeater 19 p2828 A83-41336

Radial isolated Blumlein electron beam generator 20 p3045 A83-42293

Quantitative investigation of critical slowing down in all-optical bistability 23 p3509 A83-48324

Electro-optic branching-waveguide switch with low drive voltage 24 p3628 A83-48855

BEAM WAVEGUIDES

The limiting parameters of solid-state switches employing resonant waveguide arrays 01 p0043 A83-11308

Stability of a short charged beam in a plasma waveguide 03 p0396 A83-13180

Characteristics of beam waveguides --- in satellite antenna feeds 06 p0739 A83-18629

Expansion of Gaussian modes and analysis about the beam waveguide 06 p0744 A83-18697

Diffraction of a wave beam by a closed cylindrical screen 09 p1251 A83-25086

Kinetic description of free streaming mode in an electron beam propagating through a tape helix waveguide 10 p1408 A83-25793

A beam waveguide linearly polarized KU band feed system 15 p2146 A83-35079

BEAMS (RADIATION)

NT ATOMIC BEAMS

NT ELECTRON BEAMS

NT ION BEAMS

NT LIGHT BEAMS

NT MOLECULAR BEAMS

NT NEUTRAL BEAMS

NT NEUTRINO BEAMS

NT NEUTRON BEAMS

NT PARTICLE BEAMS

NT PHOTON BEAMS

NT PROTON BEAMS

NT RADAR BEAMS

NT RELATIVISTIC ELECTRON BEAMS

Adaptive beam forming for radar 01 p0030 A83-10260

A new expression for the scattering of a Gaussian beam by a conducting cylinder 01 p0033 A83-11356

Beam shaping using nonlinear phase distribution in a uniformly spaced array 01 p0034 A83-11383

The angular beaming model of microstructure and the subpulse drifting phenomenon --- in pulsars 04 p0550 A83-15033

The propagation of thermal radiation in the case of the random refraction of beams in a medium with fluctuating permittivity 04 p0531 A83-15733

Acoustic radiation pressure produced by a beam sound 04 p0533 A83-16311

Coupling and imaging of Gaussian beams in parallel dielectric slab waveguides 06 p0749 A83-17967

Study on doubly curved shaped-beam reflector antenna theory 06 p0735 A83-18149

Beam-forming in the nearfield of small spherical reflectors 06 p0740 A83-18637

Beamshaping of sectoral and pyramidal horns with stepped amplitude distribution 06 p0741 A83-18659

Beam scanning in the offset Gregorian antenna 07 p0913 A83-20551

Comparison of directional and derivative constraints for beamformers subject to multiple linear constraints 11 p1554 A83-27907

A beam ratio technique for microwave observation of S-component sources --- from solar active regions 11 p1693 A83-28589

Antenna optimization of single beam microwave systems for the solar power satellite 12 p1706 A83-29048

Multiple beam microwave systems for the solar power satellite 12 p1706 A83-29049

Polarization and spectral characteristics of open resonators with internal inhomogeneities 15 p2170 A83-34706

Microwave radio meteorology - Fading by beam focusing 19 p2333 A83-41405

Surface acoustic wave measurements using an impulsive converging beam --- velocity and attenuation 20 p2989 A83-42589

Fundamentals of the radio-optic theory of resonance and guiding quasi-optic devices 22 p3355 A83-45682

An analysis of the multibeam altimeter 22 p3260 A83-46142

The terrestrial coverage of the geostationary satellite beam [IAF PAPER 83-73] 23 p3441 A83-47252

Direction of arrival estimation using a sparse circular array and multiplicative beamforming 23 p3443 A83-47844

Simplified linearly polarised contoured beam reflector antenna for a European coverage requirement 23 p3444 A83-48713

BEAMS (SUPPORTS)

NT BOX BEAMS

NT CANTILEVER BEAMS

NT CURVED BEAMS

NT I BEAMS

NT RECTANGULAR BEAMS

NT TIMOSHENKO BEAMS

Development of advanced composite materials and geodetic structures for future space systems

01 p0017 A83-11334
A note on nonlinear analysis of clamped-clamped beams

02 p0193 A83-12664
An analysis of an Euler-Bernoulli beam-column with arbitrary initial crookedness by transfer matrix methods

02 p0195 A83-12757
Vibrations of split beams

02 p0197 A83-13002
Modal cross-spectral terms may be important and an alternative method of analysis is preferable

02 p0197 A83-13003
Dynamic fracture of a beam or plate under tensile loading

03 p0339 A83-13338
A variational principle and an algorithm for limit analysis of beams and plates

04 p0495 A83-15013
Beam bending-torsion dynamic stiffness method for calculation of exact vibration modes

04 p0496 A83-15070
Stress function interface and boundary conditions in anisotropic materials

[ASME PAPER 82-WA/APM-4] 04 p0498 A83-15685
Simplified crushing analysis of thin-walled columns and beams

04 p0500 A83-16197
On the natural frequencies and modes of beams loaded by sloshing liquids

04 p0501 A83-16340
Effect of solar radiation disturbance on a flexible beam in orbit

[AIAA PAPER 83-0431] 05 p0607 A83-16710
Parametric instability of tapered beams by finite element method

05 p0655 A83-17723
The torsion-extension coupling in pretwisted elastic beams

05 p0656 A83-17874
Parametric vibrations of a horizontal beam with a concentrated mass at one end

05 p0656 A83-17946
Impact of a body on a mass attached to an elastically restrained beam

06 p0770 A83-18070
A general theory of optimal structural layouts

06 p0771 A83-18211
Application of Trefftz-Fichera's method for improvable bracketing of the natural angular eigenfrequencies of a beam subject to bending vibration

06 p0777 A83-19199
The method of initial parameters as applied to the flexural vibrations of beams with hinges and oscillators

06 p0777 A83-19317
Vibrations of nonuniform beams with one end elastically restrained against rotation

07 p0944 A83-19828
Lagrange-type formulation for finite element analysis of non-linear beam vibrations

08 p1120 A83-21805
Deflections of elastic-plastic hyperstatic beams under cyclic loading

08 p1120 A83-21810
Optimum elastic design of a reinforced beam

08 p1121 A83-21825
Equivalent G/E of helicopter rotor blades --- shear modulus to Young's modulus ratio

08 p1122 A83-22151
The prediction of the drag on structural beams

08 p1088 A83-23194
A note on transverse vibrations of continuous beams subject to an axial force and carrying concentrated masses

09 p1276 A83-23341
Fundamental frequency of an elastically restrained beam with discontinuous moment of inertia and an intermediate support

09 p1276 A83-23342
Thermal stresses in anisotropic noncylindrical beams

09 p1280 A83-24511
Experimental results for active structural control --- of large space structures

09 p1217 A83-24758
Maximum stiffness beam-columns

09 p1282 A83-25103
Efficient pulse shapes to deform beams with axial constraints

[ASME PAPER 82-WA/APM-6] 10 p1439 A83-25678
A linear theory for pretwisted elastic beams

[ASME PAPER 83-APM-9] 10 p1441 A83-26439
Application of laser holographic interferometry to vibration analysis of aircraft beam structure model

10 p1442 A83-26765
Stacbeam - An efficient, low-mass, sequentially deployable structure --- for satellite solar power

11 p1536 A83-27248
Contact between a rigid cylinder and an orthotropic beam under initial stress

11 p1591 A83-27433
Smooth contact between a rigid indenter and an initially stressed orthotropic beam

11 p1592 A83-27441
Vibration of sandwich beams with biomodular facings

11 p1592 A83-27442
Bending of orthotropic beams which are nonlinear in shear and compression

11 p1593 A83-27465
The excitation of a fluid-loaded plate stiffened by a semi-infinite array of beams

11 p1594 A83-27995
On random transverse vibrations of a rotating beam with a tip mass - Method of integral equations

11 p1594 A83-28407
A simple mixed formulation for elastica problems

11 p1600 A83-28724
Finite element modeling techniques for constrained layer damping

12 p1735 A83-28976
A second order theory for large deflections of slender beams

12 p1736 A83-29706
Nonlinear control of an experimental beam by IMSC --- Independent Modal-Space Control

[AIAA 83-0855] 12 p1770 A83-29828
Fractional calculus in the transient analysis of viscoelastically damped structures

[AIAA 83-0901] 12 p1743 A83-29841
Buffeting of a slender circular beam in axial turbulent flows

[AIAA 83-0928] 12 p1744 A83-29854
Experimental demonstration of static shape control --- for large space structure development

13 p1812 A83-30165
Coupled vibrations of beams - An exact dynamic element stiffness matrix

13 p1868 A83-31637
Saint-Venant's principle in elasticity

14 p2029 A83-32123
Effect of bending moment on the dynamic fracture of a beam or plate under tensile loading

14 p2031 A83-32653
Effect of shear and rotary inertia on dynamic fracture of a beam or plate in tensile loading

14 p2031 A83-32654
A study of shear factors in reduced-selective integration Mindlin beam elements

15 p2175 A83-34313
Minimum-weight design with displacements constraints in 2-dimensional elasticity

15 p2176 A83-34316
Field redistribution in finite elements - A mathematical alternative to reduced integration

15 p2179 A83-34561
Existence of solutions for dynamic problems of one-dimensional plastic structures

16 p2365 A83-35552
Smooth contact between a rigid indenter and an initially stressed orthotropic beam

16 p2366 A83-36092
On torsion of prismatic beams with longitudinal cavities

17 p2525 A83-38775
Further considerations on the problem of torsion and flexure of prismatic beams

18 p2700 A83-39555
Analysis of elastic anisotropy in CFRP laminate beam

18 p2652 A83-40164
The bending of a laterally cracked beam clamped at its ends

19 p2856 A83-40807
Comparison of damping material properties from various characterization tests

20 p3002 A83-42573
Vibrations of an elastic beam with a flexible support

20 p3005 A83-42992
Mathematical modelling of a flexible beam under gravity

21 p3150 A83-43982
Flexure of beams with certain curvilinear cross sections

21 p3152 A83-44463
A four-point shear test for graphite/epoxy composites

21 p3107 A83-45068
Nondestructive residual-stress measurement in a wide-flanged rolled beam by acoustoelasticity

21 p3162 A83-45171
Adaptive control of a flexible beam using least square lattice filters

22 p3351 A83-46099
Some recent advances in boundary element methods

22 p3352 A83-46419
A stress versus compliance constraint in a minimum weight design

23 p3470 A83-48161
On dynamics and stability of continuous systems subjected to a distributed moving load

23 p3473 A83-48496
BEAMSHAPING
U COLLIMATION

BEARING (DIRECTION)
Sunrise effect on atmospherics and its relation to the direction of the night noise source

02 p0205 A83-11998
Bearings-only passive ranging using Kalman-Bucy and Moore-Penrose methods

09 p1266 A83-23543
Direction finding with an array of antennas having diverse polarizations

10 p1405 A83-26827
BEARING ALLOYS
Aluminum-lead antifriction alloys produced under conditions of compensation of gravitational segregation by electromagnetic forces

03 p0298 A83-13268
BEARINGLESS ROTORS
Measured inplane stability characteristics in hover for an advanced bearingless rotor

[AIAA 83-0987] 12 p1702 A83-29865
Smooth and simple - The Bell Model 680 bearingless main rotor

14 p1975 A83-33098
Analytical and experimental investigation of a bearingless hub-absorber

19 p2797 A83-41077
Hingeless and bearingless main rotor in a fiber composite type of construction for dynamic systems of future helicopters

23 p3402 A83-47195
A jointless and bearingless tail rotor of fiber-reinforced-composite construction

23 p3402 A83-47215
BEARINGS
NT ANTIFRICTION BEARINGS

NT BALL BEARINGS
NT FOIL BEARINGS

NT GAS BEARINGS
NT JOURNAL BEARINGS

NT LIQUID BEARINGS
NT MAGNETIC BEARINGS

NT ROLLER BEARINGS
NT THRUST BEARINGS

Theory of lubrication with ferrofluids - Application to short bearings
[ASME PAPER 81-LUB-39] 02 p0186 A83-11940

Effects of amplitude of oscillation on the wear of dry bearings containing PTFE
[ASME PAPER 81-LUB-6] 02 p0186 A83-11942

Microscopic contour changes of tribological surfaces by chemical and mechanical action
[ASLE PREPRINT 82-LC-3B-3] 03 p0334 A83-13237

Linear force coefficients for squeeze-film dampers
[ASME PAPER 82-LUB-30] 03 p0336 A83-13514

The thermal behavior of oscillating squeeze films
[ASME PAPER 81-LUB-26] 06 p0768 A83-18388

Unbalance behavior of squeeze film damped multi-mass flexible rotor bearing systems
06 p0769 A83-18389

The effect of thin lubricant films and the methods of their application on the friction of several materials of bearings with a gaseous lubricant

07 p0939 A83-20321
Fracture and fatigue crack propagation in bearing steels

08 p1059 A83-21689
Effect of the fluid film profile on the performance of magnetohydrodynamic bearings

09 p1273 A83-23345
Vibration control of multi-mode rotor-bearing systems

11 p1586 A83-27100
Vibration analysis of rotor-bearing system by quasi-modal transformation - Analyses of complex eigenvalue and response history

14 p2028 A83-33093
Externally pressurized magnetohydrodynamic bearings under a non-uniform magnetic field

16 p2363 A83-36942
Change in vibrations of an flexible rotor due to a change in bearings

18 p2695 A83-39423
Stability of the stationary motions of the axis of a rotating rotor mounted in nonlinear bearings

19 p2895 A83-41203
The effect of fluid inertia in squeeze film damper bearings

A heuristic and physical description
[ASME PAPER 83-GT-177] 23 p3465 A83-47976

BEAT
U SYNCHRONISM

BEAT FREQUENCIES
Experimental study of the frequency characteristics of gas ring lasers with additional feedback

01 p0056 A83-11344
Precision collisional lineshapes by difference-frequency laser spectroscopy

03 p0294 A83-13982
Birefringence variation with temperature in elliptically clad single-mode fibers

03 p0395 A83-14386
NO2A2B2 state properties from Zeeman quantum beats

05 p0684 A83-17652
Temperature effects on the beat heating of a collisional magnetoplasma

18 p2745 A83-39612
Effect of wall scattering on SNR in off-axis differential-type laser Doppler velocimetry

24 p3581 A83-48747
BEAUFORT SEA (NORTH AMERICA)
Atmosphere - Sea ice interactions in the Beaufort/Chukchi Sea and in the European sector of the Arctic

15 p2208 A83-33497
BED REST
Hydro-electrolytic and hormonal modifications linked to extended decubitus in an antihorostatic position

08 p1149 A83-22982
The effects of clonidine on the modifications in the systolic time intervals induced by extended decubitus in an antihorostatic position

08 p1149 A83-22983
Evaluation of a Reverse Gradient Garment for prevention of bed-rest deconditioning

10 p1458 A83-25664
Hydroelectrolytic and hormonal modifications related to prolonged bedrest in antihorostatic position

11 p1641 A83-27344
Effects of antihorostatic position at -4 deg on hydromineral balance

11 p1642 A83-27797

Alterations in mitochondria and sarcoplasmic reticulum from heart and skeletal muscle of horizontally casted primates 11 p1640 A83-27835
Short term /1 and 3 day/ cardiovascular adjustments to suspension antiorthostasis in rats 11 p1640 A83-27842

Reduction in peak oxygen uptake after prolonged bed rest 11 p1643 A83-28757
Handgrip and general muscular strength and endurance during prolonged bedrest with isometric and isotonic leg exercise training 21 p3186 A83-43990

BEDROCK

Lead isotope systematics of some igneous rocks from the Egyptian Shield 22 p3332 A83-46704

BEDS (GEOLOGY)

NT SALT BEDS

BEDS (PROCESS ENGINEERING)

Two applications of a numerical approach of heat transfer process within rock beds 06 p0780 A83-18551

Applications of porous flow-through electrodes. I - An experimental study on the hydrogen evolution reaction on packed bed electrodes 07 p0954 A83-20587
Experimental investigation of metal hydride reaction beds 11 p1545 A83-27214

Thermal energy storage media for advanced compressed air energy storage systems 11 p1609 A83-27312
Modeling and evaluation of designs for solid hydrogen storage beds 11 p1610 A83-27333

Sintering of Si3N4-based materials using the powder bed technique 23 p3435 A83-48268

BETTER

The application of remote sensing in southern Alberta's mountain pine beetle management 03 p0347 A83-14257

BEHAVIOR

NT HUMAN BEHAVIOR

Intracerebroventricular injections of cholecystokinin decreases the activity of the dopaminergic and serotonergic systems in the brain 02 p0219 A83-11519

The systemic quantization of behavior --- of animals and humans 08 p1150 A83-22116

The systemic determination of the activity of neurons in behavior 08 p1145 A83-22118

Effect of age on benzodiazepine-induced behavioural convulsions in rats 12 p1763 A83-29711

Changes of sidman avoidance behaviour of rats induced by hypoxia 15 p2209 A83-33542

Endogenous opiates mediate radiogenic behavioral change 15 p2209 A83-34005

The effects of the electrical stimulation of the visual cortex of cats on the behavioral model of the placement of a paw on a support 19 p2871 A83-40811

BELL AIRCRAFT

NT UH-1 HELICOPTER

NT XV-15 AIRCRAFT

Smooth and simple - The Bell Model 680 bearingless main rotor 14 p1975 A83-33098

BELTRAMI FLOW

On the geometry of vortex lines in magnetofluid flows 23 p3510 A83-47604

BENARD CELLS

Long-lasting precipitation cells in stratiform clouds 09 p1312 A83-23955

Absence of equilibrium among close-packed twisted flux tubes 10 p1520 A83-25412

Studies of variations of cell parameters to be exceeded to confirm certain seeding hypotheses --- for cumulus clouds 11 p1626 A83-27031

Flatness change in the transition to turbulent convection 12 p1721 A83-29003

A model to determine open or closed cellular convection 16 p2384 A83-35463

A note on the criteria for the onset of stationary parallel-plate convection subject to mean vertical motion 16 p2348 A83-35494

Two-component Benard convection - Interfacial deformation, oscillatory instabilities and the onset of turbulence 18 p2685 A83-39892

Benard-Marangoni instability in a rotating liquid layer subjected to a transverse magnetic field 18 p2685 A83-39893

Growth of fluctuations near the Benard-Marangoni convective instability 19 p2845 A83-41997

Aspects of Galerkin approximations for hydrodynamic simulations 20 p2972 A83-42675

Magnetic-flux transport by a convecting layer - Topological, geometrical and compressible phenomena --- in solar magnetic field 20 p3081 A83-43094

Energy stability in the Benard problem for a fluid of second grade 21 p3130 A83-44467

BENCHES

U SEATS

BENDING

NT ELASTIC BENDING

Analysis of simply supported multilayer trapeziform plates 01 p0059 A83-10685

A study of transient plate bending displacements using a boundary integral equations method 02 p0189 A83-11859

Survey of recent research in the analysis of composite plates 02 p0191 A83-12065

A note on nonlinear analysis of clamped-clamped beams 02 p0193 A83-12664

An efficient triangular plate bending finite element for crash simulation 02 p0194 A83-12755

A comprehensive theory for planar bending of composite laminates 02 p0195 A83-12760

Deflections of inflated cylindrical cantilever beams subjected to bending and torsion 02 p0196 A83-12853

Deformation characteristics of metal composites with brittle fibers during bending 03 p0293 A83-14817

Approximation to bending trial functions for shell triangular finite elements in quadratic parametric representation 05 p0655 A83-17739

Quality of trial functions in quadratic isoparametric representation of an arc 07 p0949 A83-21441

Block overrelaxation methods for non-rectangular co-ordinates 07 p0949 A83-21442

Bends in nonradiative dielectric waveguides 07 p0922 A83-21526

Stress couple concentrations for cylindrically bent plates with circular holes or rigid inclusions [ASME PAPER 83-APM-5] 10 p1440 A83-26432

Sharp bends with low losses in dielectric optical waveguides 10 p1483 A83-26637

The mechanics of gravitropic bending in leafy dicot stems 11 p1638 A83-27817

Comparison of frequency determination techniques for cantilevered plates with bending-torsion coupling [AIAA 83-0953] 12 p1745 A83-29885

Bending effects on structural dynamic instabilities of transonic wings [AIAA 83-0920] 12 p1745 A83-29887

Plastic rotational factor and J-COD relationship of three point bend specimen 14 p1993 A83-32655

The durability of polymers in different stressed states 15 p2142 A83-35044

Fortran computer program for inextensional bending of a doubly curved shell triangular element 16 p2365 A83-35643

An optimally integrated four-node quadrilateral plate bending element 17 p2525 A83-38572

Tubular lap joints in composite cylindrical shells under external bending and shear 18 p2703 A83-40154

Measurement of curvature and bending stiffness of thin carbon composite plates using holographic interferometry 21 p3155 A83-44829

Some recent advances in boundary element methods 22 p3352 A83-46419

Mode coupling analysis of bending losses in hollow infrared waveguides 22 p3358 A83-46634

Internal and edge cracks in a plate of finite width under bending 23 p3469 A83-47596

A curvilinear triangular finite element for plate bending by a hybrid method of assumed displacements supplemented with assumed stresses 24 p3593 A83-49442

Effects of crack growth on the load-displacement characteristics of precracked specimens under bending 24 p3594 A83-49864

BENDING DIAGRAMS

Certain characteristics of the flexural deformation and subsequent annealing of molybdenum single crystals 02 p0155 A83-12202

An evaluation of certain properties of fiber-reinforced composites through bending tests 08 p1055 A83-22993

The resistance of structural materials to fracture during impact bending 14 p2033 A83-33015

A new method to determine the bending rigidities of anisotropic plates 18 p2662 A83-40293

Precision bending apparatus for high temperature measurement 19 p2819 A83-41289

BENDING FATIGUE

Life determination under dual-frequency loading. II - Proposed method --- for metals and welded joints 02 p0156 A83-12327

Fatigue life prediction on the basis of the characteristic parameters of the loading process 02 p0156 A83-12328

A study of polygonization in aluminum deformed by cyclic bending using low-angle X-ray scattering 03 p0300 A83-14163

The effects of humidity on fatigue due to shear stress in unidirectional composites - Attempts at interpretation and a summing up [ONERA, TP NO. 1982-98] 03 p0292 A83-14546

Fatigue fracture properties of a Mg-Al-Zn alloy 03 p0300 A83-14600

Oscillatory internal friction associated with hydride precipitation in alpha-titanium 04 p0462 A83-16257

Failure probability of hot-pressed silicon-nitride 05 p0618 A83-17098

Increase of crack resistance during slow crack growth in Al2O3 bend specimens 05 p0619 A83-17566

Gel electrode imaging of fatigue cracks in aluminum alloys 06 p0730 A83-18941

Determination of stress relaxation by damping measurements 07 p0946 A83-20522

Simple reverse bending machine for low cycle fatigue at elevated temperatures 08 p1106 A83-23232

Change in geometry of surface cracks during alternating tension and bending 09 p1280 A83-24137

An evaluation of the random bending fatigue life of bonded aluminum joints using various adhesive/primer combinations 12 p1744 A83-29873

A study of the high-cycle fatigue of materials under plane cantilever bending 14 p1998 A83-33020

Fracture morphology of graphite/epoxy composites 15 p2130 A83-34793

High-temperature bending tests on powder metallurgy materials during exploratory studies 17 p2484 A83-38873

Bending characteristics of boron-aluminum composites 18 p2660 A83-40268

High temperature fatigue failure in pressureless sintered silicon nitride 23 p3437 A83-48289

BENDING MOMENTS

Bending of a semiinfinite anisotropic plate with curvilinear cracks 03 p0340 A83-14070

Crack propagation in bending thin plates 03 p0342 A83-14567

Effect of shear and rotary inertia on dynamic fracture of a beam or plate in pure bending [ASME PAPER 82-WA/APM-9] 04 p0498 A83-15683

Interferometric determination of curvatures of flexed plate [ASME PAPER 82-WA/APM-27] 04 p0499 A83-15688

Effects of specimen size on strength of sintered silicon nitride 06 p0735 A83-19319

On exactness of the kinematical approach in the structural shakedown and limit analysis 06 p0778 A83-19325

Instability of short stiffened composite cylindrical shells under bending with prebuckling displacements 08 p1121 A83-21891

A corrugated core theory of sandwich plates 09 p1280 A83-24512

Large deflections of point loaded cantilevers with nonlinear behaviour 09 p1281 A83-24823

Impulsive loading of a cylindrical shell with transverse shear and rotary inertia 11 p1594 A83-28412

Numerical solution of two-dimensional boundary value problems of the statics of flexible conical shells 13 p1866 A83-30071

A shell structure under the effect of pulsed loading 13 p1866 A83-30072

Boundary integral equation solution of the Berger equation 13 p1866 A83-30447

Effect of bending moment on the dynamic fracture of a beam or plate under tensile loading 14 p2031 A83-32653

Boundary integral equations for bending of thin plates 15 p2174 A83-33857

Further applications of the singularity function method to plate problems 18 p2701 A83-40048

Stress analysis and strength of adhesive bonded joints under bending loads 18 p2703 A83-40156

A method for solving problems concerning the bending of a round plate with a crack 19 p2856 A83-40806

Water absorption of glass/epoxy laminates under bending stresses 20 p2947 A83-42809

The behaviour of a channel cantilever under combined bending and torsional loads 21 p3153 A83-44623

Creep of thin-walled circular cylinder under axial force, bending, and twisting moments [ASME PAPER 83-GT-154] 23 p3469 A83-47980

Finite strip method with X-spline functions 23 p3502 A83-48168

BENDING THEORY

An integral equation approach to finite deflection of elastic plates 01 p0060 A83-10861

A new class of solutions for buckling of a short cylindrical shell in pure bending 02 p0191 A83-12075

Our discrete-Kirchhoff and isoparametric shell elements for nonlinear analysis - An assessment 02 p0193 A83-12740

A family of hybrid plate elements 02 p0196 A83-12837

- An analytical and experimental study of the plate tearing mode of fracture 03 p0339 A83-13201
- Evaluation of a new quadrilateral thin plate bending element 03 p0342 A83-14709
- Alternative ways for formulation of hybrid stress elements 03 p0342 A83-14710
- Concerning the dynamic bending of plastic plates 04 p0499 A83-15877
- A mode solution for the finite deflections of a circular plate loaded impulsively 04 p0500 A83-16199
- Concerning a refined theory of plates in the case of finite deflections 04 p0502 A83-16406
- Higher order flexural transients in a beam 05 p0654 A83-17322
- An improved rectangular element for plate bending analysis 05 p0656 A83-17740
- Variational solutions for the nonlinear deflection of an annular membrane under axial load 05 p0656 A83-17945
- An elastic-plastic constitutive equation for transversely isotropic materials and its application to the bending of perforated circular plates 05 p0656 A83-17947
- The cantilever beam under tension, bending or flexure at infinity 06 p0776 A83-18999
- A study of the bending of a multilayer plate on the basis of a finite-shear theory 06 p0778 A83-19545
- Equations of the linear theory of shells with slowly varying curvatures 07 p0947 A83-21086
- Post-yield deflections of elastic-plastic beams under uniformly increasing loads 08 p1114 A83-21631
- Deflections of elastic-plastic hyperstatic beams under cyclic loading 08 p1120 A83-21810
- Pulse load of annular plastic plates supported on both edges 08 p1120 A83-21812
- Integral equation formulation for nonlinear bending of plates - Formulation by weighted residual method 08 p1121 A83-21860
- Stiffness matrix for a tapered triangular bending element 08 p1121 A83-21880
- Pure plastic bending of sheet laminates under plane strain condition 08 p1122 A83-21991
- Computations in limit analysis for plastic plates 08 p1123 A83-22942
- A note on locking in a shear flexible triangular plate bending element 08 p1123 A83-22947
- Large deflections of circular plates of variable thickness 09 p1278 A83-23671
- Three-dimensional finite-element analysis of layered composite plates 11 p1591 A83-27432
- In-plane thermal expansion and thermal bending coefficients of fabric composites 11 p1592 A83-27444
- Nonlinear bending of bimodular-material plates 11 p1544 A83-28410
- The development of a theory for the bending of layered plates with essentially different layer characteristics 11 p1598 A83-28508
- A simple mixed formulation for elastica problems 11 p1600 A83-28724
- A theory for stress analysis of composite laminates [AIAA 83-0833] 12 p1737 A83-29742
- An adaptive finite element technique for plate structures [AIAA 83-1009] 12 p1740 A83-29795
- An algorithm for constructing shape functions for a rectangular finite element 13 p1867 A83-31322
- A solution to the bending problem for a layered inhomogeneous hollow cylinder 14 p2029 A83-32152
- The stability of the plane bending mode of a composite rod with allowance for the initial irregularities 14 p2030 A83-32381
- Isoparametric finite difference energy method for plate bending problems 15 p2176 A83-34322
- Nonlinear bending analyses of heated sandwich plates and shells by the boundary element method 16 p2369 A83-36728
- A boundary integral equation method for thermal bending of plates 18 p2697 A83-39425
- Quasi-homogeneous states in composite materials with small-scale bends in the structure 18 p2701 A83-40112
- On elastic-plastic analysis of I-beams in bending and torsion 20 p3003 A83-42929
- Mathematical modelling of a flexible beam under gravity 21 p3150 A83-43982
- Flexure of beams with certain curvilinear cross sections 21 p3152 A83-44463
- The problem of the bending of a circular plate with a supporting rib of varying cross-section 21 p3162 A83-45301
- A twelfth order theory of transverse bending of transversely isotropic plates 21 p3164 A83-45399
- Solution of two-dimensional elasticity problems in regions with a remote external boundary 24 p3592 A83-49036

BENDING VIBRATION

- On the two frequency spectra of Timoshenko beams 01 p0060 A83-11037
- Small transverse vibrations of circular laminate plates 02 p0191 A83-12334
- Bending waves in strongly anisotropic elastic plates 02 p0196 A83-12855
- Improved numerical computation of uniform beam characteristic values and characteristic functions 02 p0197 A83-13001
- Nonlinear flapping vibrations of rotating blades 02 p0197 A83-13004
- A study of the dynamic behavior of flexible rotors --- French thesis 03 p0337 A83-14103
- Synthetic discrete method in structural analysis 03 p0341 A83-14487
- Beam bending-torsion dynamic stiffness method for calculation of exact vibration modes 04 p0496 A83-15070
- Rayleigh-Ritz vibration analysis of rectangular Mindlin plates subjected to membrane stresses 04 p0500 A83-16181
- Sampling statistics for vibrating rectangular plates 04 p0501 A83-16314
- Shock response of viscoelastically damped sandwich plates 04 p0501 A83-16341
- Investigation of the effect of initial deflection on the natural-vibration frequencies of rib-stiffened conical shells 04 p0502 A83-16409
- Parametric vibrations of a horizontal beam with a concentrated mass at one end 05 p0656 A83-17946
- The vibration of a multilayer cylindrical panel with anisotropic layers at large deflections 06 p0775 A83-18506
- A resonance-type machine for studying the fatigue properties of composite materials 06 p0762 A83-18518
- Numerical solution of the problem of the bending and free vibrations of a plate 06 p0776 A83-19120
- Application of Trefftz-Fichera's method for improvable bracketing of the natural angular eigenfrequencies of a beam subject to bending vibration 06 p0777 A83-19199
- The method of initial parameters as applied to the flexural vibrations of beams with hinges and oscillators 06 p0777 A83-19317
- Lowering of the first blade number harmonic cell vibrations of a helicopter by reduction of rotor blade retention forces via appropriate bending-torsion coupling of the rotor blade --- German thesis 06 p0714 A83-19619
- Bending vibrational behavior of laminated rotors --- German thesis 06 p0769 A83-19620
- An energy analysis of the stability of flexible filaments in coaxial flow 07 p0926 A83-20899
- The effect of the geometric parameters of a compressor cascade on the threshold of the self-excited flexural vibration of the blades due to cascade flutter 07 p0946 A83-20911
- The use of natural modes to describe the forced vibrations of asymmetric shafts on flexible supports 07 p0947 A83-21091
- Vibration and bending of a cracked plate 08 p1115 A83-21632
- Analysis of membranes stretched over a unilateral support 08 p1115 A83-21638
- Numerical values for integrals of products of simply supported plate functions 08 p1120 A83-21809
- Hydroelastic effects of separated flow 08 p1084 A83-22144
- Numerical analysis of flexural vibrations of rotors resting on elastic supports 11 p1589 A83-27724
- Generation of shock waves in one-dimensional systems by a moving source 11 p1599 A83-28544
- Calculation of the natural frequencies and steady state response of thin plates in bending by an improved rectangular element 11 p1600 A83-28726
- Buckled plate vibrations and large amplitude vibrations using high-order triangular elements 12 p1734 A83-28967
- Vibrations of a shallow shell with an attached mass distributed on part of its surface 12 p1735 A83-29276
- On the critical speed of empennage flutter with allowance for the rudder 12 p1704 A83-29286
- Dynamic tests of graphite/epoxy composites in hygrothermal environments 14 p1987 A83-33124
- A simple selectively integrated torsion-flexure coupled tapered beam element with transverse shear deformation 15 p2176 A83-34319
- Transverse vibrations of nonuniform rectangular orthotropic plates 16 p2366 A83-36097
- Determination of zones of crack distribution in flexible specimens --- of aluminum alloys 18 p2666 A83-39509

- Stability of the Shuttle on-orbit flight control system for a class of flexible payloads [AIAA PAPER 83-2178] 19 p2815 A83-41672
- Propagation of flexural waves in noncircular cylinders with initial stresses 19 p2860 A83-42007
- Subspace iteration for the eigenvalue problems of self-adjoint differential equations and its applications in the vibration analysis of structures 21 p3151 A83-44109
- Multiple mode nonlinear analysis of circular plates 21 p3153 A83-44549
- The bending vibrations of an anisotropic free circular plate of regular symmetry 21 p3159 A83-44933
- Flexural vibrations of rotor systems of branched configurations 21 p3148 A83-45321
- Selection of the optimum orientations of the axes of elastic symmetry of an orthotropic plate 21 p3163 A83-45367
- Response in passing through critical speed of arbitrarily distributed flexible rotor system. I - Case without gyroscopic effect. II - Case with gyroscopic effect 21 p3148 A83-45475
- Vibration of triangular plates 21 p3164 A83-45595
- Nonlinear flexural vibrations of initially deflected cross-ply laminated plates with elastically restrained edges 24 p3591 A83-48894
- The vibration of an elastic-plastic plate under the effect of normal impact loads 24 p3592 A83-49030
- The mechanism of elastic energy absorption in boron fibers 24 p3553 A83-49474
- Bending vibration of a simply supported rectangular plate with a crack parallel to one edge 24 p3594 A83-49865

BENDS (PHYSIOLOGY)

U DECOMPRESSION SICKNESS

BENIN

- Satellite data as a basis for planning studies of infrastructure and related rural development in Atacora Province, Benin, West Africa 15 p2181 A83-33560

BENZENE

- Backward stimulated Raman scattering in shock-compressed benzene 08 p1057 A83-22643
- Photochemical storage potential of azobenzenes 12 p1709 A83-28941

BERING SEA

- Nimbus 7 SMMR observations of the Bering Sea ice cover during March 1979 10 p1452 A83-26345
- The movement and decay of ice edge bands in the winter Bering Sea [AD-A128281] 10 p1452 A83-26347

BERMUDA

- Spatial variability of meteorological parameters in the Bermuda Triangle 16 p2392 A83-36847

BERYL

- A tunable emerald laser 02 p0184 A83-12263
- Temperature dependence of the excited-state absorption of alexandrite 10 p1429 A83-26031

BERYLLIUM

- NT BERYLLIUM 9
- NT BERYLLIUM 10
- Microplastic deformation of beryllium 03 p0300 A83-14160
- The technical state of dispersion hardening. I 06 p0727 A83-17961
- Measurement of the Be-7/pi gamma/B-8 reaction cross section at low energies --- solar neutrinos 07 p1037 A83-20815
- Beryllium optical mirrors by vapor deposition 08 p1112 A83-22865
- Beryllium microdeformation mechanisms 09 p1231 A83-24058
- Chemical vapor deposition of boron on a beryllium surface 10 p1394 A83-25527
- Beryllium application for spacecraft deployable solar array booms [AIAA 83-0867] 12 p1707 A83-29754
- Identification and resolution of a material defect in high strength beryllium [AIAA 83-0871] 12 p1715 A83-29755
- A Mossbauer study of commercial beryllium 13 p1822 A83-30743
- Ceramic-beryllium composites for gas bearings 14 p1986 A83-31916
- Successful applications of beryllium sheet materials to satellite structures [AIAA PAPER 83-0950] 14 p1994 A83-32786
- Design and fabrication of brazed beryllium assemblies [AIAA PAPER 83-0868] 14 p2028 A83-32789
- Magnetic dipole transitions in the beryllium isoelectronic sequence 15 p2236 A83-34554
- Low temperature annealing of Be-implanted GaAs 16 p2418 A83-35438
- Investigations of the constitution in the beryllium-rich region of the beryllium-cobalt-nickel system 18 p2665 A83-39174

Ion implantation of Si and Be in Al(0.48)In(0.52)As
20 p3052 A83-42593

Three holes bound to a double acceptor - Be(+) in germanium
21 p3218 A83-45199

Linear absorption coefficient of beryllium in the 50-300-A wavelength range --- bandpass filter materials for ultraviolet astronomy instrumentation
23 p3508 A83-47588

BERYLLIUM ALLOYS
Diffusion of carbon in beryllium
01 p0027 A83-11350

Atomic ordering in heterophase beryllium alloys
02 p0157 A83-12373

Problems arising with fatigue-testing at ultrasonic frequencies in single and double transducer systems
16 p2331 A83-36180

BERYLLIUM COMPOUNDS
NT BERYL
NT BERYLLIUM OXIDES

BERYLLIUM ISOTOPES
NT BERYLLIUM 9
NT BERYLLIUM 10

BERYLLIUM OXIDES
Flip-chip BeO technology applied to GaAs active aperture radars
03 p0308 A83-13442

BERYLLIUM 9
Production of the Be-9 isotope induced by neutrinos generated through gravitational stellar collapse
07 p1015 A83-20668

BERYLLIUM 10
Beryllium-10 in Australasian tektites - Evidence for a sedimentary precursor
02 p0264 A83-12066

Recent cosmic ray exposure history of ALHA 81005
22 p3386 A83-46868

BESSEL FUNCTIONS
NT HANKEL FUNCTIONS
The use of Bessel function and Jacobi polynomial in radial vibrations of a gas in an infinite cylindrical tube
08 p1091 A83-23217

BETA FACTOR
Stability theory of drift-type flute modes in finite-beta plasmas
05 p0688 A83-17362

The importance of B-gradient drift in high beta magnetospheric plasma instabilities
07 p0958 A83-20087

Influence of magnetic shear on the lower-hybrid drift instability in finite beta plasmas
07 p0997 A83-20536

High-beta theory of low-frequency magnetic pulsations
09 p1303 A83-23762

Nonlinear dynamics of low-beta plasma and drift-wave studies
11 p1659 A83-28235

A kinetic cross-field streaming instability
14 p2087 A83-33387

Electron temperature measurements using a 12-channel array probe
20 p3049 A83-42292

'Stabilization' of the lower-hybrid-drift instability in finite-beta plasmas
21 p3209 A83-43942

Influences of the ion temperature on the nonlinear electrostatic waves in magnetized plasma
21 p3212 A83-44514

Linear density drift instabilities in very low beta plasmas
21 p3214 A83-45191

BETA INTERACTIONS
U WEAK INTERACTIONS (FIELD THEORY)

BETA PARTICLES
Pathomorphological changes in the brain of rats after general beta-irradiation at various doses
01 p0079 A83-10531

Asymmetrical radical formation in D- and L-alanines irradiated with tritium-beta-rays
17 p2563 A83-38897

BIAS
NT RESPONSE BIAS
Optical biasing on quasi-interferometry with coded correlation filtering
02 p0177 A83-12306

Forward bias voltage characteristics for /GaAl/As and /GaIn/ /AsP/ lasers
04 p0486 A83-16222

Bias in observed nearby clusters of galaxies
07 p1008 A83-21206

Analysis of small-scale features in precipitation by bias measurements
11 p1629 A83-27056

Information from bias measurements --- on statistical characteristics of fluctuating radar signal
11 p1629 A83-27057

A new method of satellite attitude control using a bias-momentum
17 p2478 A83-37457

Convergence of partitioned adaptive filters for systems with unknown biases
17 p2569 A83-37550

BIBLIOGRAPHIES
Prospects for automated solution of the subject characterization problem in the bibliographic services
01 p0111 A83-10146

Stellar bibliography retrieving system in Japan
01 p0114 A83-10147

The Bibliographical Star Index
01 p0114 A83-10148

Survey of recent research in the analysis of composite plates
02 p0191 A83-12065

A compendium of sources of fracture toughness and fatigue crack growth data for metallic alloys. II
03 p0301 A83-14822

Heat transfer - A review of 1981 literature
05 p0682 A83-17701

A literature survey on numerical heat transfer
05 p0641 A83-17741

The Voyager mission and the origin of life - Selected references
06 p0801 A83-19409

Amorphous silicon bibliography update - Introduction
08 p1170 A83-22915

The physics of strength and plasticity: A systematic index of the major literature in Russian and in foreign languages 1970-1975. Number 2 - Current and special topics in the plastic deformation of materials --- Russian book
09 p1231 A83-23925

Noise-immune coding of discrete information --- bibliography 1972-1979
09 p1327 A83-24248

Remote sensing - Corrections and data enhancement. I
11 p1601 A83-28188

Bibliography of the moon and the planet (with name index) --- of articles on moon, planets and other solar system bodies
16 p2439 A83-36790

Cosmic-ray modulation and the anomalous component
17 p2630 A83-38285

The global atmospheric research program - 1979-1982
17 p2525 A83-38320

Interstellar travel and communication bibliography - 1982 update
18 p2754 A83-39610

Chemical evolution and the origin of life - Bibliography supplement 1981
19 p2887 A83-42160

A focused bibliography on robotics
21 p3118 A83-44076

Picture processing - 1982
21 p3194 A83-44262

BICARBONATES
U CARBONATES

BICRYSTALS
The growth and structure of niobium bicrystals
03 p0300 A83-14159

Mechanisms of cavity growth in creep
07 p0887 A83-20629

Grain boundary sliding and fracture of metal bicrystals at high temperatures
09 p1232 A83-24068

BIFURCATION (BIOLOGY)
Remarks on origins of biomolecular asymmetry
02 p0219 A83-11635

BIFURCATION (MATHEMATICS)
U BRANCHING (MATHEMATICS)

BIG BANG COSMOLOGY
Statistical correction of projection of radio-sources on the sky and application to the apparent size-redshift and linear size-line width relations
01 p0125 A83-10939

Origin and evolution of galaxies; Proceedings of the International School of Cosmology and Gravitation, Course, 7th, Erice, Italy, May 11-23, 1981
01 p0127 A83-11287

Relativistic cosmology for astrophysicists
01 p0127 A83-11288

Reflections on the formation of galaxies in the frame of Lemaitre's cosmology
01 p0127 A83-11289

Towards a new scale of extragalactic distances
01 p0118 A83-11337

Three-dimensional structure of the universe and regions devoid of galaxies
01 p0128 A83-11342

Gravitation, phase transitions, and the big bang
02 p0259 A83-12220

The era of superheavy-particle dominance and big bang nucleosynthesis
03 p0439 A83-13653

Massive neutrino halos in an expanding universe
03 p0427 A83-14754

A finite temperature lambda-phi-4 model and a de Sitter-Friedmann transition in the early universe
04 p0551 A83-15597

Cosmic density wave and its observable vestiges - Maximum scale of inhomogeneities in the distribution of galaxies and features in the distribution of absorption-line redshifts of quasars
05 p0702 A83-17850

'Maximally hard' universe and mass spectrum of primordial black holes
06 p0839 A83-19230

The new inflationary universe
07 p1013 A83-20297

Steady state cosmology revisited
07 p1013 A83-20402

The maximum density in heavy-neutrino clouds
07 p1014 A83-20651

The origin and evolution of galaxies; Proceedings of the International School of Cosmology and Gravitation, Course, 7th, Erice, Italy, May 11-23, 1981
07 p1015 A83-20757

Structure in the universe and fluctuations in the cosmic microwave background
07 p1015 A83-20761

Large-scale fluctuations in the mass distribution and the microwave background - Nature and evolution
07 p1016 A83-20762

The origin of primordial irregularities in the universe
07 p1026 A83-21255

How big is the universe today
08 p1180 A83-22213

The large-scale structure of the universe
08 p1181 A83-22686

Stars and star systems --- Russian book
09 p1358 A83-23901

Cosmology --- theories and models of early universe
09 p1358 A83-23915

Pregeometric origin of the big bang
10 p1506 A83-26092

Axions and the evolution of structure in the universe
10 p1507 A83-26271

Cosmological implications of helium and deuterium abundances on Jupiter and Saturn
11 p1686 A83-28388

Tracking back to the big bang
11 p1683 A83-28767

General vacuum-Universe solutions in Brans-Dicke cosmology
12 p1790 A83-28982

Parastatistics and the equation of state for the early universe
12 p1791 A83-28994

Cosmological consequences of the existence of the unit gravitational charge (Planck's constant x speed of light/h) exp 1/2
12 p1942 A83-29042

Cosmology and elementary particles
13 p1944 A83-30250

A timeless, boundless, equilibrium universe
13 p1947 A83-30403

Synthesis of the chemical elements --- cosmochemical evolution
13 p1947 A83-31153

Early Brans-Dicke axisymmetric universe with magnetic field
13 p1958 A83-31731

Can graininess in the early universe make galaxies?
14 p2103 A83-33178

Cosmological self-similar shock waves and galaxy formation
14 p2103 A83-33179

Collisionless matter and galaxy formation
15 p2255 A83-33818

Decay of long-lived particles in the early universe
15 p2286 A83-34612

Temperature fluctuations in the background radiation in the entropy theory of galaxy formation
15 p2269 A83-34680

Structurally stable approximations to Friedmann-Lemaitre world models --- as dynamic cosmological systems
15 p2272 A83-34781

Tolman's cosmological models
15 p2272 A83-34782

Physics of stellar evolution and cosmology --- Book
15 p2272 A83-34875

Hot big bang and quark gas
16 p2434 A83-36883

Direct dissipationless formation of filaments in the large-scale matter distribution
17 p2607 A83-38259

The continuing case for a hierarchical cosmology
17 p2611 A83-38582

The infrared luminosity-H I profile width-surface brightness relation, and the cosmological expansion
17 p2612 A83-38826

Elimination of the standard big bang singularity and particle horizon through quantum conformal fluctuations
17 p2614 A83-38962

Quantum gravity and the 'flatness problem' of the standard big bang universe
17 p2614 A83-38963

The expansion of the universe as a driving mechanism for the evolution of correlations
17 p2614 A83-38967

The cosmological relevance of light element abundances
18 p2776 A83-39772

A neutrino-dominated universe?
18 p2777 A83-39782

Inflation does not explain time asymmetry --- of universe
18 p2777 A83-39958

The spectral features in the microwave background spectrum due to energy release in the early universe
19 p2914 A83-40707

Massive cosmological neutrinos in the expanding universe
19 p2915 A83-40819

Spatially homogeneous and anisotropic cosmological solution in Brans-Dicke theory
19 p2916 A83-41282

Dirac's large numbers hypothesis and continuous creation --- of universe
20 p3066 A83-42429

Neutron oscillation and the primordial magnetic field
20 p3070 A83-42785

The helium abundance and the isotropy of the universe
21 p3234 A83-44766

Quantum effects of scalar and vector particles with variable mass in homogeneous and isotropic cosmology
21 p3235 A83-45381

Pair correlations in an expanding universe for a multicomponent system
21 p3235 A83-45526

Problems with the new inflationary universe
21 p3238 A83-45574

- The moment of creation - Big Bang physics from before the first millisecond to the present universe --- Book
22 p3380 A83-46686
- The large-scale structure of the universe
23 p3526 A83-47825
- The cosmological evolution of general Bianchi models in the adiabatic regime
24 p3660 A83-49429
- Gravitational instability for a multilayer medium in an expanding universe
24 p3660 A83-49430
- Primordial nucleosynthesis - A theorist's shopping list
24 p3665 A83-50032
- The primordial helium abundance and the age of the universe
24 p3665 A83-50034
- Nuclear uncertainties of element yields in the big bang
24 p3665 A83-50035
- Pregalactic synthesis of deuterium
24 p3665 A83-50037
- Primordial helium in galactic globular clusters
24 p3666 A83-50047
- Fragmentation of the universe
24 p3671 A83-50166

BIGHTS

U BAYS (TOPOGRAPHIC FEATURES)

BIHARMONIC EQUATIONS

- A study and variational approach to biharmonic equations applied in unbounded domains - Applications in mechanics
03 p0388 A83-14571
- A segmentation approach to grid generation using biharmonics
12 p1772 A83-29635
- Three dimensional grid generation using biharmonics
17 p2574 A83-38809
- Relaxation method for solving a difference biharmonic equation
21 p3198 A83-45214
- An analysis of the Volterra problem for the steady state creep material using complex stress and pseudo-stress functions
24 p3597 A83-50148

BILLETS

- Raman spectroscopic study of ultraoriented solid state extruded polyethylene
01 p0027 A83-10609
- Acoustic imaging of 3D carbon/carbon billets
22 p3304 A83-46770

BIMETALS

- Detection of surface cracks in bimetallic structures - A reliability evaluation of five ultrasonic techniques
04 p0458 A83-15212
- A study of the feasibility of ultrasonic inspection of thick bimetallic welds in mildly alloyed steel and corrosion resistant austenitic steel --- French thesis
07 p0943 A83-21094

BIMETRIC THEORIES

- Charged particle motion on and off the equatorial plane of a magnetic star in Rosen's bimetric gravity
18 p2775 A83-39754
- Kepler and two-body problems in bimetric Machian gravitation
18 p2763 A83-40625
- A bimetric Machian approach to gravitation
19 p2916 A83-41285

BINARY ALLOYS

- Mechanisms of the isothermal decomposition of beta-solid solution in two-phase martensitic titanium alloys
01 p0025 A83-10446
- Fabrication of niobium and niobium alloys
02 p0154 A83-11788
- High temperature thermodynamic study of the molybdenum-rich regions of the Mo-Al system
02 p0155 A83-12058
- Material parameters of $\ln(1-x)/Ga/x/As/y/P/1-y/$ and related binaries
04 p0542 A83-16064
- Structural difference rule for amorphous alloy formation by ion mixing
05 p0690 A83-16945
- The thermophysical characteristics of two-phase titanium alloys and the optimum heat treatment schedules
05 p0614 A83-16952
- Modeling the shock-wave behavior of multicomponent materials --- for powder metallurgy
06 p0727 A83-18011
- On certain macroscopic and microscopic aspects of plastic flow of ductile materials
06 p0728 A83-18482
- The self-propagating high-temperature synthesis of aluminides. I - A thermodynamic analysis
07 p0883 A83-19964
- On the prediction of lattice parameter vs. concentration for solid solutions extended by rapid quenching from the melt
07 p0887 A83-20635
- Interpretation of superplastic flow in terms of a threshold stress
07 p0896 A83-21570
- On the Ti-Al phase diagram
08 p1065 A83-22013
- Short-range stratification in Ti-Zr, Ti-Hf, and Zr-Hf alloys and lattice instability
08 p1068 A83-22783
- Structure formation in binary refractory carbide eutectics based on niobium and molybdenum
09 p1229 A83-23522
- The alpha double prime-to-beta reverse martensitic transformation in two-phase titanium alloys
09 p1234 A83-24390

- The diffusion constants of hydrogen, nitrogen, and carbon in solid solutions and binary phases with titanium
09 p1235 A83-24395

Ni-Al and Ni-Ta phase diagrams

- On the occurrence of modulated phases in binary and ternary rare earth metal trialuminides
10 p1393 A83-25403
- The effect of scandium on the high-temperature ductility of the binary alloy Al-6.5 pct Mg
13 p1821 A83-30695

- The effect of scandium on the mechanical properties of Al-6.5 pct Mg alloy
13 p1821 A83-30696
- Alloying additions and property modification in aluminum-lithium - X systems
14 p1996 A83-32884
- Gravitational influence on binary alloy melt equilibria
18 p2644 A83-39905

- The effect of solute on the homogeneous crystal nucleation frequency in metallic melts
20 p2946 A83-43309
- Finite element analysis of the effect of a non-planar solid-liquid interface on the lateral solute segregation during unidirectional solidification
20 p2943 A83-43312

Ultrafine filamentary composites

- Diffusion of chromium and silicon in nickel solid-solution alloys of the Ni-Cr-Si system
22 p3269 A83-46702
- Ordered structures on the bcc lattice with first, second, third and fifth neighbour interactions
23 p3512 A83-48184
- [ONERA, TP NO. 1983-63]
23 p3561 A83-49435
- Oxidation theory of alloys
24 p3561 A83-49478
- The sulfidation behavior of nickel chromium and nickel-aluminum binary alloys with and without yttrium
24 p3565 A83-49514

BINARY CODES

- Linear frequency modulation derived polyphase pulse compression codes
06 p0748 A83-19035
- Transform coding strategies at low rates --- for image transmission
07 p0907 A83-19729
- Coding tradeoffs for improved performance of FH/MFSK systems in partial band noise
07 p0909 A83-19751
- Anatomy of a code block --- for aerial reconnaissance
08 p1100 A83-22592
- Digital filter structures for canonic signed-digit code implementation by microprocessor
10 p1460 A83-25500
- 1-Gbit/s code generator and matched filter using an optical fiber tapped delay line
10 p1483 A83-26204
- US Navy begins shift to digital telemetry
11 p1558 A83-28159
- Black box multigrad
12 p1773 A83-29658
- Error-correcting codes in binary-coded radix-r arithmetic
13 p1910 A83-30796
- The formation of nonlinear binary sequences
14 p2075 A83-32477
- Estimation of the free distance of convolutional codes with rate 1/2
14 p2075 A83-32486
- Image source coding using median filter roots
15 p2223 A83-35147
- Three-position shift-keying in communication systems
21 p3120 A83-44770
- Optimal symbol-by-symbol detection for duobinary signaling
22 p3272 A83-45739
- Sets of complementary sequences
23 p3502 A83-48711

BINARY DATA

- Test generation using binary decision diagrams
01 p0038 A83-10774
- Choice of parameters of a multistage detector of binary-quantized pulsed signals, minimizing time expenditures on detection
01 p0031 A83-10808
- A fast technique for segmentation and recognition of binary patterns --- image processing algorithms
01 p0099 A83-11444
- The noise immunity of group transmissions of binary data given constraints on the composite signal
04 p0465 A83-15142
- Conditions of the transformation of a binary signal under the effect of noise of random pulsed sequence type
04 p0466 A83-15716
- Optimization and comparison of binary and multistep digital transmission systems with and without quantified feedback --- German thesis
06 p0751 A83-18498
- High accuracy matrix multiplication with outer product optical processor
07 p0983 A83-20826
- Optimal digital algorithms of data reception by symbol estimation
09 p1245 A83-23457
- Algorithms for processing a stream of binarily quantized signals with a known beginning and end of the envelope
14 p2001 A83-32489
- Detectors for multinomial input --- for signal detection
14 p2002 A83-33135
- Correlation of binarized images
14 p2077 A83-33138

- Conflict resolution protocols for random multiple-access channels with binary feedback
15 p2147 A83-35122
- Noise models for detection
19 p2828 A83-41345
- A new binary logarithm-based computing system
24 p3619 A83-48999

BINARY DIGITS

- A language for bitmap manipulation
02 p0228 A83-11782

BINARY FLUIDS

- Approximate equation of state for multicomponent gaseous mixtures
04 p0544 A83-15861
- Measurement of temperature conductivity of pure fluids and binary mixtures with the aid of dynamic light scattering in the general region of the critical point --- German thesis
06 p0757 A83-18521
- An asymptotic study of the macroscopic behavior of a mixture of two viscous fluids
08 p1085 A83-22770
- Unsteady concentration distribution and the flow of a binary mixture in a cone and plate viscometer
09 p1262 A83-24502
- Study of binary nucleation in a Ludwig tube
10 p1417 A83-26190
- Approximate method of solving the kinetic equation for moderately dense gases near a boundary temperature jump in a binary mixture
13 p1933 A83-31467
- First-order wetting transition at a liquid-vapor interface
16 p2327 A83-36523
- Two-component Benard convection - Interfacial deformation, oscillatory instabilities and the onset of turbulence
18 p2685 A83-39892
- Experimental studies of heat and mass exchange phenomena in the two-component heat pipe
20 p2981 A83-42767
- Diffusive separation of binary mixtures of CO₂-H₂ in a sonic-orifice expansion
21 p3128 A83-43934
- The wave equations for the coupling of propagation in inhomogeneous and bi-fluids plasmas
21 p3211 A83-44299
- Problems with a direct simulation Monte Carlo method applied to the shock structure in a binary gas mixture
21 p3132 A83-44945

BINARY MIXTURES

- NT BINARY FLUIDS
NT EUTECTIC ALLOYS
NT EUTECTICS
- Boundary conditions for equations of the two-temperature gas dynamics of a binary mixture with significantly different component masses
04 p0544 A83-15085
- Finite-amplitude convection in mixtures with concentration-dependent heat sources
06 p0760 A83-19427
- Problems with the computation of the shock structure in binary gas mixtures using the direct simulation Monte Carlo method
07 p0927 A83-21340
- Theory of multiple phase separations in binary mixtures - Phase diagrams, thermodynamic properties, and comparisons with experiments --- lattice-gas models of interacting organic liquids
08 p1056 A83-22222
- The dynamic tensile strength of ice and ice-silicate mixtures
08 p1129 A83-22367
- Diffusion slipping of a binary gas mixture of moderate density along a flat surface
09 p1259 A83-23983
- Cross-sectional concentration of particles during shock process propagating through a gas-particle mixture in a shock tube
10 p1416 A83-26187
- A semiempirical method for analysis of the reflectance spectra of binary mineral mixtures
12 p1749 A83-29964
- An approximate method for solving a kinetic equation for moderately dense gases near a boundary - The slip of a binary mixture
16 p2350 A83-35711
- Experimental study of the parameters of a binary-mixture plasma jet
24 p3632 A83-49660
- Transient processes during the impact initiation of trotyl-hexogen and trotyl-octogen mixtures
24 p3557 A83-49794

BINARY STARS

- NT COMPANION STARS
NT DWARF NOVAE
NT ECLIPSING BINARY STARS
- Optical variations of the Be star HDE 245770/A
0535+26
01 p0120 A83-10313
- On the problem of the chemical composition of Beta Lyræ
01 p0121 A83-10329
- Rotation, expansion and duplicity of Be stars
01 p0121 A83-10335
- Be stars as interacting binaries
01 p0122 A83-10338
- X-ray observations of Be stars
01 p0122 A83-10341
- Be components in X-ray binaries
01 p0122 A83-10342
- The expanding atmosphere of HD 218393
01 p0122 A83-10346

- Ultraviolet observations of interacting binary Be stars
01 p0122 A83-10347
- Evaluation of EUV spectra of X-ray binaries Cygnus X-1, Vela X-1, and X Persei --- German thesis
01 p0123 A83-10477
- Secular variation of the longitudes of nodes and arguments of the periastra of the component orbits in the multiple system Xi UMa
01 p0117 A83-10903
- The hot component of KS Persei /HD 30353/
01 p0117 A83-10931
- The theoretical expected galactic distribution of WR runaway stars
01 p0125 A83-10935
- Radial velocities of CH Cygni during the outburst started in 1977
01 p0117 A83-10942
- Evolution of low mass stars through mass loss - Transition from the main sequence to the degenerate phase
01 p0126 A83-10947
- Bulge X-ray sources and Novae in M31
01 p0118 A83-10951
- Why are essential parts of 'bursters' located in globular clusters
01 p0128 A83-11341
- QU Carinae - Orbital parameters and spectra for a nova-like variable
02 p0252 A83-11596
- H1409-45 - A recurrent soft X-ray transient
02 p0252 A83-11597
- Timing observations of the binary pulsar PSR 1913 + 16
02 p0253 A83-11616
- X-ray illumination of globular cluster puzzles --- globular cluster X ray sources as clues to Milky Way Galaxy age and evolution
02 p0255 A83-12117
- Infrared photometry of the X-ray binary 2A 1822-371 - A model for the ultraviolet, optical, and infrared light curve
02 p0256 A83-12128
- On the orbital phase dependence of the turn-on times of Hercules X-1
02 p0256 A83-12132
- Einstein Observatory pulse-phase spectroscopy of Hercules X-1
02 p0257 A83-12133
- The nature of the 1E1145.1-6141 optical counterpart
02 p0259 A83-12517
- The fastest runaway Wolf-Rayet star of Population I in the Galaxy, 209 BAC - Evidence for a low mass companion
02 p0260 A83-12535
- Observations of low-mass stars in the Pleiades - Has a pre-main sequence been detected
02 p0249 A83-12914
- Infrared photometry of Hyades dwarfs
02 p0249 A83-12916
- Photoelectric radial velocities. X - The orbits of four spectroscopic binaries in the Clube selected areas
03 p0401 A83-13309
- The ellipsoidal light curve of VV Puppis
03 p0413 A83-13312
- A survey of the bright galactic bulge X-ray sources
03 p0414 A83-13331
- A possible outburst on AM Canem Venaticorum
03 p0414 A83-13335
- Object Kuwano, a novalike /symbiotic/ binary with a red giant - Photometry and polarimetry
03 p0406 A83-13651
- Interferometer observations of double stars. I
03 p0408 A83-13882
- Is NGC 1851-UV5 a binary star in a globular cluster
03 p0421 A83-14139
- Spectral morphology in Trumpler 16
03 p0409 A83-14143
- The hot halo subdwarf binary system HZ-22
03 p0421 A83-14145
- Speckle interferometry of the spectroscopic binary 94 Aquarii A
03 p0421 A83-14148
- The evolved stellar system Sigma 2367
03 p0422 A83-14152
- The equivalence of the short periods measured in the spectrum of SS 433
03 p0424 A83-14205
- The mystery of the missing boundary layer --- ultraviolet and X-ray fields of cataclysmic binaries
03 p0425 A83-14222
- Models of convective interiors surrounded by thin radiative envelopes
03 p0427 A83-14716
- PS 74 - The discovery of a new SU UMa type dwarf nova with high orbital inclination
03 p0410 A83-14753
- The binary system Sirius in the context of stellar evolution
03 p0428 A83-14762
- Hydrodynamical calculations of accretion disks in close binary systems. I - Method. II - Models
03 p0428 A83-14765
- UBV-polarimetry of the X-ray binaries HD 77581 /4U 0900-40/, HD 153919 /4U 1700-37/ and of HD 152667
03 p0410 A83-14766
- Mass transfer in a low mass semidetached binary, taking into consideration nonequilibrium effects
03 p0429 A83-14779
- Contribution to the study of composite spectra. III - Spectral binaries, an intermediate class between visual binaries and spectroscopic binaries
03 p0429 A83-14786
- On the difference between the initial mass function of single stars and of primaries of binaries
03 p0429 A83-14791
- The theoretically expected X-ray luminosity and the binary nature of Wolf-Rayet runaway stars
03 p0429 A83-14792
- Photometric observations of CN Orionis
03 p0411 A83-14807
- Accretion and inner excretion disks in close binaries
04 p0551 A83-15108
- The semi-detached binary system RZ Draconis
04 p0546 A83-15596
- On the stability of the inner planets, satellites and close binaries
04 p0547 A83-15600
- A time-resolved spectroscopic study and modeling of the dwarf nova BV Centauri
04 p0554 A83-15631
- Simultaneous optical and X-ray bursts from 4U/MXB 1636-53
04 p0554 A83-15634
- The longitudinal distribution of sunspots and the RS CVn starspot model
04 p0556 A83-15966
- Spectroscopic observations of Delta Orionis
04 p0556 A83-15971
- Four years of photometry of DK Draconis = HR 4665
04 p0548 A83-15975
- Structure and evolution of large groups of Massive Close Binary systems
04 p0557 A83-15979
- Close binary systems before and after mass transfer. III - Spectroscopic binaries
04 p0557 A83-15980
- Observation of an outburst of the transient X-ray pulsar A0535+26 in 1980
05 p0699 A83-17007
- A study of X-ray emission from Ap and Am stars
05 p0694 A83-17028
- The second catalog of ephemerides for the relative radial velocities of the components of visual binary stars with known orbits --- Book
05 p0694 A83-17133
- Study of physical properties of spectroscopic binary stars
05 p0702 A83-17806
- V 505 Mon - One of the most massive binaries
05 p0694 A83-17810
- Estimated absolute dimensions and the inferred lifetime and angular momentum of W Ursae Majoris contact binaries
06 p0824 A83-18078
- NGC 2346 - A bipolar nebula produced by mass-loss from a binary system
06 p0828 A83-18177
- Has P Cygni generated a shock front which emits nonthermal radiation
06 p0829 A83-18526
- CI Cyg - The stage of case C mass transfer
06 p0829 A83-18530
- Interpretation of line profiles of the symbiotic star V 1016
06 p0818 A83-18538
- U, B, V photometry of the X-ray binary HD 77581 = 4U 0900-40
06 p0819 A83-18782
- Interferometer observations of double stars. II
06 p0819 A83-18788
- Beta Lyrae as a magnetic binary star
06 p0831 A83-18799
- Spectroscopic orbital elements of X-ray binary systems
06 p0819 A83-18837
- Kuwano's peculiar object: A nova-like /symbiotic/ binary system containing a red giant - Discussion of observational results
06 p0832 A83-18838
- Periodic perturbations in close binary systems due to rotational distortion
06 p0821 A83-18885
- Periodic perturbations in close binary systems due to tidal distortion /non-lagging tides/
06 p0834 A83-18886
- Periodic perturbations in close binary systems due to tidal lag
06 p0834 A83-18887
- BV Dra and BW Dra - Two contact systems in one visual binary
06 p0834 A83-18889
- A spectroscopic study of the old nova HR Delphini
06 p0836 A83-19058
- A search for resonance polarization in stars with enhanced Ca II H and K emission
06 p0821 A83-19062
- Gravitational radiation of the binary pulsar PSR 1913 + 16
06 p0837 A83-19210
- Influence of rotation and a binary companion on the frequency of the radial pulsations of a homogeneous star
06 p0837 A83-19216
- X Persei - Optical polarization variation on the 580 day binary-like period
06 p0841 A83-19287
- Observation of Centaurus X-3 by Hakucho
06 p0824 A83-19499
- Discovery of 13.5 s X-ray pulsations from LMC X-4 and an orbital determination
06 p0844 A83-19500
- Optical identification of the X-ray source E1405-451 - A 101.5 minute binary system with extremely rapid quasi-periodic variability
06 p0844 A83-19501
- Relativistic tidal forces
06 p0845 A83-19507
- A giant X-ray flare in the Hyades
06 p0845 A83-19525
- H2215-086 - King of the DQ Herculis stars
06 p0846 A83-19526
- Activity in the centers of galaxies
06 p0846 A83-19530
- The structure and outburst mechanisms of dwarf novae and their evolutionary status among cataclysmic variables
06 p0846 A83-19531
- Radial velocities and kinematics in star systems of the Milky Way
06 p0846 A83-19533
- Transient emission events in the early Be star 59 Cygni
07 p1010 A83-19859
- Micrometer observations of double stars and new pairs. XI
07 p1005 A83-20135
- The binary pulsars
07 p1013 A83-20405
- The importance of the binary pulsar for general relativity
07 p1013 A83-20406
- A study of visual double stars with early type primaries. I - Spectroscopic results
07 p1006 A83-20574
- A study of visual double stars with early type primaries. II - Photometric results
07 p1006 A83-20575
- The /a, M1/ diagram for spectroscopic binaries
07 p1014 A83-20658
- Why are no X-ray pulsars paired with Wolf-Rayet stars
07 p1015 A83-20669
- The evolution of dwarf binaries
07 p1015 A83-20671
- Photoelectric photometry of HD 5303
07 p1017 A83-20927
- Extreme variability in the Be-type, periodic recurrent X-ray transient A0538-66 - A highly eccentric interacting binary
07 p1018 A83-20945
- Area scanner observations of close visual double stars. I - Technique
07 p1007 A83-20952
- Sudden loss of mass from a binary gravitating system
07 p1019 A83-21047
- Ultraviolet spectroscopy of V1341 Cygni /equals Cygnus X-2/
07 p1022 A83-21133
- Time-resolved ultraviolet and optical spectroscopy of the pulsating X-ray source H2252-035
07 p1022 A83-21134
- A feature in the X-ray spectrum of Cygnus X-1 - A possible positron annihilation line
07 p1022 A83-21136
- Remarkable light changes of the active RSCVn system V 711 Tau /equals HR 1099/ during 1979-1981
07 p1009 A83-21222
- Alternate period changes in close binary systems
07 p1024 A83-21225
- V 1016 Cygni and HM Sagittae - Binary stellar systems
07 p1025 A83-21231
- Hercules X-1 - A random walk noise model for the 35-day turn-ons
07 p1025 A83-21232
- On the stability and evolution of contact binaries. II
07 p1025 A83-21234
- Periodogram of nearly diurnal variations in the latitude of Gorkii
07 p1027 A83-21273
- Discovery of close binary stars using the one-meter telescope on Mt. Sanglok
08 p1174 A83-22054
- Speckle interferometric measurements of binary stars. VIII
08 p1175 A83-22749
- Spectral and temporal effects of a plasma shell around an X-ray source
08 p1184 A83-23066
- A new AM Her-like X-ray source
08 p1176 A83-23268
- Can gamma-ray bursts originate from low-mass binaries
08 p1186 A83-23281
- White dwarfs and neutron stars in globular cluster X-ray sources
08 p1187 A83-23287
- A search for nebulosity around G61-29
09 p1357 A83-23727
- Evidence for spectroscopic periodicity in an X-ray burster
09 p1357 A83-23729
- A radio survey of cataclysmic variable stars using the very large array
09 p1353 A83-23739
- Radial-velocity orbits of HR 5553 and HR 6524
09 p1353 A83-23741
- Classical systems: The star RX Cas - The motion of the apsidal line
09 p1353 A83-23902
- Stars in late stages of evolution in close binary systems
09 p1358 A83-23904
- Orbital elements for the double-line spectroscopic binaries HD 104451 and HD 141458
09 p1358 A83-24021
- The open cluster Tombaugh 1 and its neighbouring Cepheid XZ Canis Majoris
09 p1354 A83-24023
- The infrared variability and nature of symbiotic stars. II - RR Tel
09 p1362 A83-24983
- The time-dependence of non-planar accretion discs
09 p1364 A83-25003
- IUE observations of W UMa-type stars
09 p1364 A83-25005
- The binary model for type I supernovae - Theoretical rates
10 p1498 A83-25355
- Search for light variability of LSI +61deg303
10 p1492 A83-25379
- Evidence for outburst in the shell star 17 Lep derived from ultraviolet spectra
10 p1501 A83-25499
- Simultaneous spectroscopy and photometry of the AM Herculis-like star H0139-68
10 p1502 A83-25584

Photoelectric photometry of GG Carinae
10 p1502 A83-25587

X-ray observations of 4U 1626-67 by the monitor counter on the Einstein /HEAO 2/ observatory
10 p1510 A83-26385

Conservative mass transfer in close binary systems. I - Equations of motion for spin and orbital angular momenta
10 p1510 A83-26386

High-energy X-ray observations of Vela X-1
10 p1497 A83-26388

The 1980 outburst of 4U 0115+63 /V635 Cassiopeiae/
10 p1510 A83-26389

Optical confirmation of a very compact bipolar nebula associated with the symbiotic star V1016 Cygni
10 p1511 A83-26407

Radial velocity studies of cataclysmic binaries. I - KR Aurigae
10 p1514 A83-26724

Rapid rotation and stellar activity in the triple system HD 165590
10 p1514 A83-26725

Identification and properties of the M giant/X-ray system HD 154791 = 2A 1704 +241
10 p1514 A83-26730

The effects of sudden mass loss and a random kick velocity produced in a supernova explosion on the dynamics of a binary star of arbitrary orbital eccentricity - Applications to X-ray binaries and to the binary pulsars
10 p1515 A83-26734

Dwarf novae: Observational results and their interpretation. I - Light variations; basic model of a cataclysmic binary; outburst models
11 p1676 A83-27125

Simultaneous X-ray/optical observations of GX339-4 during the May 1981 optically bright state
11 p1669 A83-27677

The symbiotic star CH Cyg - The occasional transition from an unstable to a stable accretion disk
11 p1678 A83-27687

IUE observations of the high velocity symbiotic star AG Draconis during active phase
11 p1678 A83-27694

Radial velocities for contact binaries. II - TZ Boo, XY Boo, TX Cnc, RZ Com, CC Com and Y Sex
11 p1680 A83-28252

Symbiotic and VV Cephei stars in the Small Magellanic Cloud
11 p1680 A83-28255

Revised orbits for 105 Herculis and Pi Cephei A and a model for the Pi Cephei system
11 p1674 A83-28261

The infrared variability and nature of symbiotic stars. III - R Aquarii. IV - RX Puppis. V - Seven more systems
11 p1675 A83-28284

On the variability of the two brightest stars in the galactic cluster IC 2391
12 p1789 A83-28861

The combined effect of mass loss and overshooting. III Evolutionary scenarios for massive close binaries
12 p1790 A83-28887

Cosmic rays from binary neutron stars
12 p1800 A83-28983

On disk accretion --- in binary stars and black holes
12 p1791 A83-28986

A mathematical solution of general relativistic binary systems
12 p1791 A83-28989

Five years of photometry of Lambda Andromedae
12 p1785 A83-28995

Loss of angular momentum in a binary system due to collisionless particles as monopoles or gravitinos - Does it exceed the gravitational radiation emission in the binary system PSR 1913+16?
12 p1792 A83-29037

Three years of photometry of IM Pegasi = HR 8703
12 p1785 A83-29054

On the stability of close binaries in hierarchical three-body systems
12 p1787 A83-29113

On the double averaged three-body problem
12 p1787 A83-29118

Astrometric studies of ten double or suspected multiple systems from plates taken with the Sproul 61-cm refractor
12 p1788 A83-29184

The instability of the SS 433 precession period
12 p1796 A83-29491

Velocity standards that have variable velocities. I - HD 184467
12 p1789 A83-29956

Magnetic white dwarfs in binary systems
13 p1944 A83-30357

Recent optical observations of the X-ray source HO139-68; an AM-Herculis type binary system
13 p1946 A83-30384

On the nature of SS 433
13 p1947 A83-31252

Stellar chromospheres as a random phenomenon
13 p1949 A83-31327

HR 7578 - A K dwarf double-lined spectroscopic binary with peculiar abundances
13 p1951 A83-31422

Stellar contributions to the hard X-ray galactic ridge
13 p1951 A83-31423

X-ray evidence for white dwarf binaries in globular clusters
13 p1952 A83-31444

High spatial resolution VLA observations of the R Aquarii jet
13 p1953 A83-31448

A family of three-dimensional orbits in the restricted problem of three bodies - Application to inclined disks
13 p1942 A83-31653

Accretion in cataclysmic binaries. I - Modified alpha-disks with convection. II - Observational data
13 p1955 A83-31654

The low mass main sequence stars
13 p1955 A83-31659

The IUE observation of the active binary II Pegasi = HD 224085
13 p1955 A83-31663

RY Geminorum - An algol binary with moderate circumstellar emission
13 p1955 A83-31669

On the tidal spin up and orbital circularization rate for the massive X-ray binary systems
13 p1956 A83-31685

The enigmatic composite system HD 45166-B8V + qWR or SdO
13 p1957 A83-31688

Phase-dependent UV spectra of UX Ursae Majoris
13 p1957 A83-31693

Optical and IR light curves of VV Puppis
13 p1957 A83-31699

Confirmation of periodic radio outbursts from LSI + 61 deg 303 = GT 0236 + 61
13 p1942 A83-31704

Non-LTE analysis of subluminescent O-star. V - The binary system HD 128220
13 p1959 A83-31745

X-ray observations of bright galactic bulge sources in the vicinity of GX 5-1
13 p1959 A83-31749

Some enigmatic binary stars. I
14 p2097 A83-32841

Photographic observations of visual double stars
14 p2097 A83-33051

Study of type F, G, K, and M binaries. I - Orbital elements of the double lined spectroscopic binaries HD 47415 and HD 210763
14 p2098 A83-33060

On the nature of Upsilon Sagittarii
14 p2105 A83-33200

Observational studies of the symbiotic stars. II Emission-line relative intensity variations in CI Cygni, BF Cygni, AX Persei, and V1016 Cygni
14 p2105 A83-33203

The binary nature of the barium stars. II - Velocities, binary frequency, and preliminary orbits
14 p2099 A83-33204

Spectroscopy of V711 Tauri (= HR 1099) - Fundamental properties and evidence for starspots
14 p2105 A83-33205

Binary-single star scattering. I - Numerical experiments for equal masses
14 p2105 A83-33209

Binary-single star scattering. II - Analytic approximations for high velocity
14 p2105 A83-33210

Angular momentum loss and the evolution of cataclysmic binaries
14 p2106 A83-33212

Approximations to the radii of Roche lobes
14 p2106 A83-33213

VLBI observations of a radio flare of Circinus X-1
14 p2099 A83-33228

A search for binaries among short-period southern Cepheids
14 p2100 A83-33250

Numerical results in the three-body problem
14 p2100 A83-33251

Polarimetric observations of southern binary systems
14 p2100 A83-33252

The Wolf-Rayet stars
14 p2108 A83-33263

Variations in the ultraviolet spectrum of the symbiotic star Z Andromedae
14 p2108 A83-33264

The spectroscopic orbit of KR Aurigae
14 p2101 A83-33465

Astrometric and infrared speckle analysis of the visually unresolved binary BD +41.328 deg
14 p2101 A83-33467

A 0538-66 - The most powerful X-ray star
15 p2244 A83-33540

High luminosity X-ray binaries - IUE results
15 p2251 A83-33589

X-ray diagnostics of globular clusters
15 p2251 A83-33595

U, B, V photometry of SMC X-1 and Centaurus X-3, and some parameter correlations for X-ray binaries
15 p2244 A83-33719

A photometric search for halo binaries. I - New observational data. II - Results
15 p2245 A83-33830

Infrared spectroscopy of symbiotic stars and the nature of their cool components
15 p2255 A83-33835

Flare activity in two F-type stars, 5 Ser and Omicron Aql
15 p2245 A83-33836

The central X-ray source in RCW 103 - Evidence for blackbody emission
15 p2258 A83-34103

X-ray properties of the Be/X-ray system 28 0114 + 650 = LSI + 65deg 010
15 p2258 A83-34104

The minimum period and the gap in periods of cataclysmic binaries
15 p2258 A83-34108

Further observations of the long-period binary pulsar PSR 0820 + 02
15 p2245 A83-34109

An X-ray survey on nine algol systems
15 p2260 A83-34128

A field guide to the binary stars
15 p2260 A83-34376

Is the millisecond pulsar formed from coalescence of a close neutron-star binary
15 p2260 A83-34382

Orbital motion and mass flow in the interacting binary Be star HR 2142
15 p2247 A83-34507

Reticon observations of the yellow symbiotic star AG Draconis
15 p2247 A83-34532

A 300-day periodicity of CYG X-1
15 p2247 A83-34558

A period-finding method for sparse randomly spaced observations of 'How long is a piece of string?' --- for variable stars
15 p2248 A83-34580

The binary nature of the Cepheid T Monocerotis
15 p2264 A83-34581

An analysis of V 861 Sco. I - Light-curve synthesis
15 p2265 A83-34589

The influence of gravitational wave momentum losses on the centre of mass motion of a Newtonian binary system
15 p2265 A83-34592

Encounters of binaries. I - Equal energies
15 p2265 A83-34596

Observations of suspected low-mass post-T Tauri stars and their evolutionary status
15 p2268 A83-34632

Diffusion, meridional circulation, and mass loss in Fm-Am stars
15 p2268 A83-34633

Rotational studies of late-type stars. III - Rotation among BY Draconis stars
15 p2268 A83-34634

A model of AM Canum venaticorum
15 p2271 A83-34762

Non-conservative evolution of low-mass, close binaries with gravitational radiation and systemic mass losses
15 p2272 A83-34777

Vibrational stability of the components of close binary systems
16 p2428 A83-36526

Optical photometry of massive X-ray binaries - 4U 1538-52/QV Nor
16 p2425 A83-36666

A search for periodicities in the radio flaring of Cyg X-3
16 p2433 A83-36701

Sanduleak-Pesch's twin white dwarf object
16 p2433 A83-36702

Binarity and the local stellar mass density
16 p2433 A83-36705

About some enigmatic binary stars
16 p2427 A83-36956

Infrared photometry of the RS CVn binaries. II - JHK light curves of HR 1099
17 p2587 A83-37277

The binary central star of the planetary nebula LT-5
17 p2588 A83-37319

A spectroscopic study of four late-type galactic WN stars
17 p2588 A83-37320

The question of duplicity
17 p2598 A83-37352

Explosive helium burning at constant pressures
17 p2598 A83-37352

Couderadial velocities of Zeta Herculis
17 p2589 A83-37370

The double-lined spectroscopic binary HD28475
17 p2589 A83-37371

The results of observations of the X-ray source Cyg X-3 at energies exceeding 10 to the 12th eV made at the Tien Shan installation for detecting Cerenkov flashes in extensive air showers
17 p2589 A83-37661

The activity of the X-ray source Cygnus X-3 in the years 1975-1978 at a wavelength of 1.35 cm
17 p2600 A83-37662

Spectral observations of HD 206267, identified with the X-ray source Cep X-4
17 p2601 A83-37681

Absolute spectrophotometry of Upsilon Sgr
17 p2589 A83-37683

Photometric investigations of the short-period brightness variability in Nova Cygni 1975 (V1500 Cyg) in a continuum
17 p2590 A83-37707

Do all barium stars have a white dwarf companion?
17 p2604 A83-37917

The correlated X-ray and optical time variability of TT Arietis
17 p2605 A83-37920

Irregular X-ray variability in the transient X-ray burst source MXB 1659-29
17 p2605 A83-37921

Evidence for an about 300 day period in Cygnus X-1
17 p2605 A83-37922

The broad-band X-ray spectrum of Cygnus X-2
17 p2605 A83-37923

Image reconstruction by the speckle-masking method
17 p2592 A83-37949

The symbiotic star H1-36
17 p2606 A83-38238

Post-collapse evolution of globular clusters
17 p2607 A83-38261

The formation of massive white dwarfs in cataclysmic binaries
17 p2608 A83-38409

111-day periodicity of X-ray transient AO535 + 26
17 p2612 A83-38609

Infrared variability of the X-ray binary AO535 + 262
17 p2613 A83-38834

The novallike star TT Arietis - A binary system with conical accretion?
17 p2614 A83-38843

HD 187282 - A possible Wolf-Rayet binary with a low-mass companion
17 p2614 A83-38844

Reflection effect in close binaries. II - Distribution of
emergent radiation from the irradiated component along
the line of sight 18 p2764 A83-39188

Spectroscopic binaries near the north galactic pole paper
7: HD 107742 18 p2754 A83-39189

Spectroscopic binaries near the north galactic pole. VI
- BD 33.2206 deg 18 p2754 A83-39196

Dwarf novae - Observational results and their
interpretation. II - Orbital periods, masses, inherent colors,
absolute magnitude 18 p2765 A83-39223

Photometry of magnetic stars 18 p2755 A83-39240

VLA observations of MWC 349 at 15 and 23 GHz
18 p2757 A83-39597

The photometric period of 39 AY Ceti 18 p2759 A83-39739

Five years of photometry of Sigma Geminorum
18 p2759 A83-39743

Variable infrared radiation from X-ray sources 4U 0115
+ 634 and A 0535 + 262 18 p2776 A83-39768

X-ray sources and pulsars 18 p2776 A83-39771

The distance to the Hyades 18 p2759 A83-39783

Intrinsic polarization of a precessing, electron-scattering
accretion disk, with applications to SS 433 18 p2777 A83-40476

V1343 Aquilae (SS 433) as a double-period variable
18 p2777 A83-40477

Rotation and tidal interactions in BY Draconis binaries
19 p2914 A83-40724

Fragmentation of a nonisothermal protostellar cloud
19 p2915 A83-40788

Spectroscopic orbit of the star HR96 19 p2910 A83-41056

Correlations and periodicities of equivalent widths in SS
433 19 p2915 A83-41067

Light variations of the Am star 32 Vir 19 p2911 A83-41069

Micrometric measurements of southern double stars
19 p2911 A83-41072

Measurement of coronal X-ray emission lines from
Capella 19 p2919 A83-41632

Constraints on the inclination and masses of the HDE
226868/Cygnus X-1 system from the observations
19 p2919 A83-41633

On the evolutionary status of bright, low-mass X-ray
sources 19 p2919 A83-41634

The evolution of a stripped giant-neutron star binary
19 p2920 A83-41635

Accretion powered X-ray pulsars 19 p2920 A83-41637

The effect of low-velocity, low-mass intruders
(collisionless gas) on the dynamical evolution of a binary
system 20 p3064 A83-42200

Ultraviolet observations of the transient X-ray sources
A0535 + 26 and A0620-00 20 p3059 A83-42328

Compton heated winds and coronae above accretion
disks. II Radiative transfer and observable
consequences 20 p3067 A83-42438

The precataclysmic nucleus of Abell 41 20 p3068 A83-42451

On the effects of strong encounters in stellar systems.
I - A basis for treating anisotropic systems 20 p3068 A83-42455

Gamma-rays and the production of energetic electrons
in enshrouding material - A model for the quiescent radio
emission from Cygnus X-3 20 p3068 A83-42456

Magnetism in the AM Herculis variable CW 1103+ 254
20 p3072 A83-43066

Cygnus X-1 - Optical variation on the 294 day X-ray
period 20 p3073 A83-43085

Definitive orbital elements of the visual binary star ADS
5871 - STF 1037 20 p3061 A83-43379

Discovery of a 6.1-ms binary pulsar PSR1953 + 29
20 p3061 A83-43549

On the origin of the 6.1-ms pulsar 20 p3076 A83-43550

Evolutionary history of the 6.1-ms pulsar 20 p3076 A83-43551

Is the 6-ms binary pulsar the remnant of a bright galactic
X-ray source? 20 p3076 A83-43552

Fate of very low-mass secondaries in accreting binaries
and the 1.5-ms pulsar 20 p3076 A83-43554

Spectrographic observations of the suspected Delta
Scuti variable Beta Ari 20 p3062 A83-43656

Nineteen new spectroscopic binaries and the rate of
binary stars among F-M supergiants 21 p3223 A83-44418

Stellar activity and the period gap in cataclysmic
variables 21 p3229 A83-44419

Optical photometry of massive X-ray binaries - Cen
X-3/V779 Cen 21 p3229 A83-44424

Statistics of binary stars. I - Multivariate analysis of
spectroscopic binaries 21 p3223 A83-44427

The possibility of non-synchronism of convective
secondaries in close binary stars 21 p3231 A83-44726

H 0139-68 - High-speed optical photometry of an
AM-Herculis type binary system 21 p3224 A83-44728

Radial velocities for contact binary systems. III - V566
Ophiuchi 21 p3224 A83-44756

A redetermination of the orbit of HD 123299 21 p3225 A83-44977

Gravitational radiation reaction in the binary pulsar and
the quadrupole-formula controversy 21 p3235 A83-45197

Discovery of a massive unseen star in LMC X-3 21 p3236 A83-45537

The massive WC6+O6-8 spectroscopic binary HD
94305 21 p3237 A83-45547

A search for light-time effects in binary cepheids - AW
Persei 21 p3226 A83-45551

A search for X-rays from runaway stars 21 p3237 A83-45552

Outer atmospheres of cool stars. XIII - Capella at critical
phases 21 p3237 A83-45553

On the nature of dwarf novae 21 p3237 A83-45554

Binaries as a heat source in stellar dynamics - Release
of binding energy 22 p3376 A83-45632

Computer simulations of gravitational encounters
between pairs of binary star systems 22 p3377 A83-46389

High-sensitivity observations of HD 44179 - The Red
Rectangle 22 p3373 A83-46404

A study of the binary system 58 Persei 22 p3374 A83-46543

Symbiotic stars - Spectrophotometry at 3-4 and 8-13
microns 22 p3375 A83-46550

HZ Her - The nature and origin of the emission lines
22 p3379 A83-46556

A model for A 0538-066 - The fast flaring pulsar
22 p3379 A83-46563

HEAO 1 high-energy X-ray observations of Centaurus
X-3 22 p3383 A83-46996

Star-planet systems as progenitors of cataclysmic
binaries Tidal effects 23 p3518 A83-47428

The equations that govern rotational and tidal
perturbations of stellar oscillations 23 p3518 A83-47434

The multiple system Beta Sco and the age of the Upper
Scorpius complex 23 p3519 A83-47447

Mass transfer in close binary systems - Original and
remnant masses 23 p3520 A83-47461

Two-spot modeling of synoptic light curves of II Peg
23 p3516 A83-47490

RS CVn stars - Photospheric phenomena and rotation
23 p3522 A83-47511

Twenty years of dedicated photometry of RS CVn at
Catania Observatory 23 p3516 A83-47514

Features of the wave-like distortion in some RS CVn
binaries 23 p3522 A83-47515

HK Lacertae 23 p3522 A83-47517

A flare-like event from the short-period system XY
UMa 23 p3522 A83-47519

RS CVn systems - The high energy picture 23 p3523 A83-47520

Preliminary results of a five-year survey of radio emission
from RS CVn and similar binaries 23 p3523 A83-47521

Activity correlations in close binary systems 23 p3523 A83-47522

IUE spectra of RS CVn stars 23 p3523 A83-47523

Angular momentum loss and the formation of W UMa
systems 23 p3523 A83-47527

Activity of contact binaries 23 p3523 A83-47528

Rotation-activity connections in main sequence
binaries 23 p3523 A83-47529

Numerical analysis of orbital period variations and a
mechanism for changes in the light curve of VW Cep
23 p3524 A83-47532

Interacting magnetospheres in RS CVn binaries -
Coronal heating and flares 23 p3525 A83-47549

Elliptic stellar disks - Equilibrium solutions in the
presence of a halo and in binary systems 24 p3653 A83-49165

Decay time of triple systems --- in evolution of binary
stars 24 p3640 A83-49169

Micrometer measurements of visual binaries 24 p3642 A83-49315

Contribution to the study of F, G, K, M binaries. II -
Orbital elements of the single-line spectroscopic binaries
HD 69148 and HD 85091 24 p3642 A83-49322

Analytic treatment of polarization by arbitrary scattering
mechanisms in circumstellar envelopes. II - Binary stars
24 p3658 A83-49361

The AM Herculis-type binary E1405-451 24 p3660 A83-49384

Ultraviolet observations of binary X-ray sources 24 p3662 A83-49564

IUE observations of cataclysmic variables 24 p3662 A83-49565

New results on symbiotic stars 24 p3662 A83-49566

Planetary orbits in double star systems 24 p3644 A83-49601

Micrometric measurements of binary stars (first list)
24 p3646 A83-49852

New binary stars (18th series) discovered at Nice
24 p3646 A83-49853

Parallaxes and proper motions. XVI 24 p3646 A83-49888

The topology of three-body scattering --- in celestial
mechanics 24 p3646 A83-49892

The ultraviolet variability of the symbiotic star HBV
475 24 p3668 A83-50084

The disk-star boundary layer and its effect on the
accretion disk structure 24 p3669 A83-50095

The runaway Wolf-Rayet star HD 143414 - Evidence
for a low-mass companion 24 p3649 A83-50099

BINARY SUMMATORS
U ADDING CIRCUITS
BINARY SYSTEMS (DIGITAL)
U DIGITAL SYSTEMS
BINARY SYSTEMS (MATERIALS)
NT BINARY ALLOYS
NT BINARY FLUIDS
NT BINARY MIXTURES
NT EUTECTIC ALLOYS
NT EUTECTICS
Energie / 4th revised and enlarged edition/ --- German
book 02 p0244 A83-12325

The technical state of dispersion hardening. I
06 p0727 A83-17961

Anomalous bulk viscosity of two-phase fluids and
implications for planetary interiors 09 p1366 A83-25071

A fracture criterion for edge-bonded bimaterial bodies
10 p1439 A83-25878

Special features of the formation of the joint between
platinum and titanium during vacuum diffusion bonding
10 p1397 A83-26219

Phase equilibria and thermodynamic studies in the
titanium-nickel and titanium-nickel-oxygen systems
10 p1399 A83-26894

The effect of creep on the magnitude of elastic
deformation in a laminated composite 16 p2323 A83-35506

New approach for analysis and prediction of liquid-vapor
coexistence densities including the critical region 20 p3055 A83-43236

Strong spherical two-phase blowoff of liquid metals into
vacuum 21 p3220 A83-43935

An analogy of the motion of a two-phase medium
consisting of an incompressible phase and a gas phase
with the motion of a gas 21 p1311 A83-44848

Ion mixing 22 p3364 A83-45899

High temperature reactions and microstructures in the
Al2O3-AlN system 23 p3434 A83-48259

The electroconductivity of composites with binary fillers
containing high-conductivity components 24 p3553 A83-49054

Enthalpy of formation and transformation in binary and
ternary systems of the metals iron, cobalt, nickel, and
molybdenum 24 p3561 A83-49434

BINAURAL HEARING
The slow latent auditory evoked potential of humans
07 p0976 A83-19932

Brainstem auditory evoked potentials 16 p2398 A83-35902

BINDERS (ADHESIVES)
U ADHESIVES
BINDERS (MATERIALS)
NT PROPELLANT BINDERS
NT SOLID ROCKET BINDERS
Rolvians - New binders for heat resistant high-strength
reinforced plastics 02 p0160 A83-12352

Controlling the thermomechanical characteristics of a
Rolvians-type binder --- thermally stable reactive
oligomer 06 p0734 A83-18517

Longitudinal elastic wave propagation in laminated
composites with bonds 06 p0776 A83-19147

Component interaction in a glass-ceramic layer
07 p0900 A83-20710

Castable-sprayable insulations for rocket motors
09 p1241 A83-23841

TNT as a component in plastic-bonded explosive
09 p1242 A83-23844

Elastomeric binders for electrodes --- in secondary
lithium cells 14 p1998 A83-32638

The effect of proton-electron irradiation on the properties
of composites with disperse reinforcement 18 p2650 A83-40111

BINOCULAR VISION
Phantom images of binocular vision in the system of
hemispheric relations 01 p0082 A83-10505

- Color vision is altered during the suppression phase of binocular rivalry 02 p0222 A83-12067
- The accuracy of binocular vergence for peripheral stimuli 05 p0675 A83-17747
- Maturation of potentials evoked by spatially structured stimuli and sensitivity of the visual system to deprivation 06 p0798 A83-18970
- Separate motion aftereffects from each eye and from both eyes 08 p1150 A83-23146
- Detection and identification of moving targets 11 p1644 A83-27900
- Functional organization of the second cortical visual area in primates 13 p1900 A83-31167
- Vertical fusional response to asymmetric disparities --- of retinal image stimulus 14 p2068 A83-32800
- The mechanisms of spatial vision --- Russian book 21 p3182 A83-43913
- Biocular magnifiers for use with cathode ray tube (CRT) displays 21 p3139 A83-44786
- A model of the working of a binocular visual system in the process of volume perception 23 p3497 A83-47110

BINOMIAL THEOREM

- HP-41C programs for Bayesian binomial and exponential interval estimation with a uniform prior on the reliability 07 p0942 A83-20513

BIOACOUSTICS

- Sensory systems: Hearing --- Russian book 07 p0972 A83-19926
- Mathematical models of the hydrodynamics of the cochlea of the inner ear 07 p0972 A83-19927
- The spectral-structural analysis of speech as one of the parameters of change in the functional condition of an operator 07 p0979 A83-20331
- Microwave-induced pressure waves in mammalian brains 14 p2065 A83-33109
- Early ultrastructural changes in the auditory labyrinth of frogs produced by the action of pulsed ultrasound 18 p2731 A83-39497
- The use of focused ultrasound in the megahertz range in otology 19 p2883 A83-41840

BIOASSAY

- A method for the assessment of enzyme activity in drug metabolism 03 p0381 A83-14335

BIOASTRONAUTICS

- Applications of digital image acquisition in anthropometry 03 p0384 A83-13449
- Cosmic radiobiology --- Russian book 03 p0380 A83-13818
- Radiobiological research in space 04 p0519 A83-15675
- A comparison of limb plethysmograph systems proposed for use on the Space Shuttle 06 p0799 A83-18187
- Effects of weightlessness on pulmonary function 11 p1641 A83-27782
- Static and dynamic mechanisms of space vestibular malaise 11 p1636 A83-27785
- Changes in weightlessness in calcium metabolism and in the musculoskeletal system 11 p1636 A83-27787
- The NASA Space Biology Program 11 p1636 A83-27790
- Alterations in glomerular and tubular dynamics during simulated weightlessness 11 p1636 A83-27795
- Some karyological observations on plants grown in space 11 p1639 A83-27824
- Bone mineral analysis of rat vertebra following space flight - Cosmos 1129 11 p1640 A83-27834
- Cardiovascular adaptation to weightlessness [SAE PAPER 820830] 13 p1905 A83-30928
- Fluid and electrolyte homeostasis in space - A primate model to look at mechanisms [SAE PAPER 820832] 13 p1898 A83-30930
- Space motion sickness and vestibular experiments in Spacelab [SAE PAPER 820833] 13 p1905 A83-30931
- Life sciences experiments for a space platform/station [SAE PAPER 820834] 13 p1898 A83-30932
- Physiological and behavioral effects of tilt-induced body fluid shifts 14 p2068 A83-32685
- Sensory conflict theory of space motion sickness - An anatomical location for the neuroconflict 14 p2068 A83-32695
- Rheographic investigations of the stroke volume of the heart in antiorthostatic hypokinesia 15 p2214 A83-35047
- Life sciences and space research XX(2): Proceedings of the Workshop and Topical Meeting, Ottawa, Canada, May 16-June 2, 1982 19 p2877 A83-42029
- The first dedicated life sciences mission - Spacelab 4 19 p2808 A83-42042
- Experimental and theoretical analysis of the influence of gravity at the cellular level - A review 19 p2877 A83-42043
- Changes in symbiotic and associative interrelations in a higher plant-bacterial system during space flight 19 p2878 A83-42058

- Space Station and the life sciences [AIAA PAPER 83-7089] 19 p2884 A83-42078
- Meteorology in a space colony 20 p2938 A83-42336
- Isoelectric focusing in space 20 p2940 A83-42381
- Effects of spaceflight on trabecular bone in rats 21 p3183 A83-44863
- Bone resorption and mineral excretion in rats during spaceflight 21 p3184 A83-44866
- Single cell algae and higher plant cell cultures used in space biology [IAF PAPER 83-185] 23 p3494 A83-47302
- Preliminary results of Cytos 2 experiment --- for bacteria antibiotic sensitivity during orbital flight [IAF PAPER 83-192] 23 p3494 A83-47307
- Cardiovascular exploration in microgravity. French-Soviet flight aboard Saliout VII - June 1982 [IAF PAPER 83-194] 23 p3498 A83-47308

BIOCHEMICAL OXYGEN DEMAND

- Certain biochemical indices in healthy humans under the effect of high concentrations of carbon monoxide and carbon dioxide in a sealed chamber 01 p0085 A83-11403
- Systemic analysis of the mechanisms of the regulation of the affinity of the blood for oxygen. I - Intraerythrocytic regulation of the affinity of hemoglobin for oxygen 08 p1146 A83-22120
- Very low altitude remote sensing of the water quality of rivers 16 p2370 A83-36574
- A device for the continuous determination of the oxygen demand and the water loss of small animals 19 p2879 A83-42098
- The physiological mechanisms for supplying the energy requirements of an organism during a decrease in the concentration of hemoglobin in the blood 23 p3496 A83-48567

BIOCHEMISTRY

- NT BACTERIOLOGY
- NT BIOGEOCHEMISTRY
- NT PHYSIOCHEMISTRY
- Molecular structure of r/GCG/d/TATACGC/ - A DNA-RNA hybrid helix joined to double helical DNA 01 p0077 A83-10209
- The role of Fc-receptors of lymphocytes, macrophages, and other mammalian cells during the immune processes 01 p0082 A83-11406
- The complement and its role in the regulation of immunological reactions 01 p0082 A83-11407
- Evolutionary roots of catalysis by nicotinamide and flavins in C-H oxidoreductases and in photosynthesis 02 p0219 A83-11633
- The biological effectiveness of a weak electromagnetic field of infrared frequency 02 p0221 A83-11887
- The biochemical mechanism of the reactions of living organisms to changes of solar activity 02 p0221 A83-11892
- The assay of glycosaminoglycans in the blood serum 03 p0375 A83-14333
- Present-day problems in the biochemistry of physical exercise and sport 05 p0673 A83-17157
- The effect of mechanical asphyxiation on lipid peroxidation processes in the rat brain 05 p0670 A83-17185
- Microbiochemical criteria for adaptive reactions in certain barrier systems of the organism 05 p0670 A83-17204
- Current ideas about the mechanism of the action of glucocorticoid hormones 05 p0672 A83-17599
- The possible role of soluble salts in chemical evolution 06 p0800 A83-18249
- A study of the adaptation processes in the peripheral blood using methods of mathematical modeling --- leukocyte adaptation to microwaves 06 p0796 A83-19382
- The molecular mechanisms of the action of endogenous and exogenous ethanol 12 p1762 A83-29272
- Highly efficient peptide formation from N-acetylaminocacyl-AMP anhydride and free amino acid 12 p1767 A83-29422
- Selective modification of glutathione metabolism 13 p1899 A83-31162
- A mathematical model for the regulation of glycolysis by the oxidation of pyruvate and fatty acids in the myocardium 14 p2064 A83-32957
- Physiological and biochemical methods for evaluating the functional condition of athletes in cyclical forms of sports 14 p2070 A83-33306
- The use of biochemical indicators in a controlled training process for highly-trained biathlon participants 14 p2070 A83-33308
- The leading problems of contemporary age physiology, biochemistry, and biophysics and the investigations of the school of A. V. Nagorny 14 p2065 A83-33322
- The formation of an organic matrix in distractional bone regenerate and the characteristics of its mineralization during experimental crus stretching 14 p2066 A83-33338

- The condition of glycolysis in the heart during necrosis produced after the preliminary action of stress 14 p2066 A83-33339

- Nitrate respiration in primitive eukaryotes 15 p2209 A83-34224
- Electron-microscope cytochemical study of ribonucleoprotein particles in cerebral cortex neurons in a posthypoxic period 16 p2395 A83-36812
- Comparative studies on biochemical properties of protein synthesis of an archaebacteria, *Thermoplasma* sp 17 p2557 A83-38896
- An extraterrestrial habitat on earth - The algal mat of Don Juan Pond 19 p2885 A83-40832
- Possible forms of life in environments very different from the earth 19 p2886 A83-41511
- The diagnostic informativity of drugs used for revealing intralabyrinthine hydrops according to data of audiological and biochemical investigations 19 p2883 A83-41828
- Short-term and long-term clinostat and vibration-induced biochemical changes in dwarf marigold stems 19 p2878 A83-42054
- Studies on aqueous two phase polymer systems useful for partitioning of biological materials 20 p2951 A83-43277
- A comparison of methods for quantitation of metabolites in skeletal muscle 20 p3033 A83-43488
- Selected works. The biochemistry of vitamins --- Russian book 21 p3182 A83-43914
- Methylotrophic bacteria - Biochemical diversity and genetics 22 p3345 A83-45724
- Electrophoresis '82: Proceedings of the Fourth International Conference, Athens, Greece, April 21-24, 1982 22 p3265 A83-45757
- Chemistry of lipids --- Russian book 23 p3427 A83-47147
- Sharp resonances in yeast growth prove nonthermal sensitivity to microwaves 23 p3494 A83-47612
- Prebiotic evolution on a universal scale. I 23 p3500 A83-48054
- Biosynthesis of tetrapyrrole pigments as possible precursors of the nickel-containing factor F430 of *Methanobacterium vacuolatum* 23 p3496 A83-48513

BIOCLIMATOLOGY

- The physiological mechanisms of the rehabilitative action of a mountain climate 01 p0078 A83-10480
- The effect of a mountain climate on the condition of the respiratory-hemodynamic function in miners suffering from the initial stages of pneumoconiosis 01 p0082 A83-10482
- An investigation of the shielding effectiveness of FPP-15 fabric relative to bacterial aerosols 05 p0677 A83-17201
- An attempt to prevent weather-aggravated cardiovascular diseases 07 p0978 A83-20995
- The dependence of the origin of acute disorders of the brain blood circulation on the changes of meteorological factors 15 p2212 A83-34929
- The problems of health protection in polar expeditions and their importance for space flights 15 p2214 A83-35049

BIOCONTROL SYSTEMS

- Common mechanism of the intratissue regulation of proliferation on the basis of the principle of the tissue-specific control of the oxidative phosphorylation of mitochondria 01 p0078 A83-10425
- A method for adaptive biocontrol in the multifaceted treatment of patients with cerebral arachnoiditis 01 p0083 A83-10525
- The voluntary regulation of alpha and theta EEG rhythms in humans 02 p0224 A83-12215
- The relation of psychic and neurophysiological phenomena and biofeedback 02 p0224 A83-12216
- Integration function and modeling of the central nervous system in forearm movement control 03 p0384 A83-14126
- The regulation of the defense functions of organisms --- Russian book 04 p0520 A83-15826
- Adaptation and resistance to hypoxia in light of the functional activity of the antistresses 05 p0669 A83-17161
- The regulation of the biosynthesis of serotonin in the central nervous system 06 p0795 A83-18983
- The changes in the activity of the intracardiac ganglionic-synaptic apparatus during the interaction of sympathetic and parasympathetic regulatory effects on the rhythm of the pacemaker 07 p0973 A83-20243
- Biofeedback as an important mechanism in the success of teaching humans to control the skin-galvanic reaction 07 p0979 A83-20330
- Multipulse control of saccadic eye movements 09 p1325 A83-24706
- The modelling of hierarchical systems of spatial-temporal synchronous connections of the human brain 10 p1462 A83-25625
- An investigation of the resonance characteristics of the cardiovascular system 12 p1765 A83-29309

Control of respiratory pattern in conscious dog - Effects of heat and CO2 13 p1897 A83-30482

A mathematical model for the regulation of glycolysis by the oxidation of pyruvate and fatty acids in the myocardium 14 p2064 A83-32957

An automatic system for the medical monitoring of the functional condition of a human 15 p2215 A83-34947

The directed correction of biorhythmic structure of movements in athletes 16 p2398 A83-35905

Syzers: the modeling of fundamental characteristics of molecular-biological organization - The correspondence between general properties of genetic processes and the structural peculiarities of macromolecular assemblies 16 p2395 A83-36810

The action of colyones on erythropoiesis (A quantitative evaluation) 16 p2396 A83-36841

A mathematical model of the mechanism of respiratory rhythmogenesis 17 p2558 A83-37241

The possible interactions of inspiratory and expiratory neuronal systems 17 p2555 A83-37242

The breathing patterns of humans during hypercapnia and hypoxia 17 p2558 A83-37243

The regulation of the breathing pattern during muscular activity in conditions of normal and altered chemoreceptor stimulation 17 p2558 A83-37244

The duration of inhalation and exhalation in growing hypercapnia and the effect of additional resistive inspiratory resistance 17 p2558 A83-37246

Breathing patterns during submaximal and maximal exercise in elite oarsmen 20 p3034 A83-43483

Effect of catecholamine depletion on ventilatory control in unanesthetized normoxic and hypoxic rats 20 p3033 A83-43486

The involuntary regulation of the GSR --- Galvanic Skin Response 23 p3497 A83-47108

The regulation by the human foot of the balance of the mechanical sytem of the 'inverted pendulum' type. I - The significance of the speed of motion. II - The role of the position of the center of gravity and temporal programs 23 p3497 A83-47117

BIOCONVERSION

Solar power applications - Alcohols 07 p0955 A83-21066

Thermoelectric energy conversion could be an energy source of living organisms 19 p2875 A83-41168

Reduction of molecular sulphur by methanogenic bacteria 23 p3495 A83-48081

BIODYNAMICS

A comparative analysis of the movement of traumatized and healthy extremities during running on a treadmill 01 p0083 A83-10521

The mechanical properties of the brain in the process of the development of postischemic edema 01 p0079 A83-10526

Methods for determining the morphometric characteristics of muscles during movement in humans 03 p0384 A83-13645

Investigation of the motion of the center of mass of an occupant under ejection accelerations 04 p0525 A83-15411

A standardized instrumentation methodology for assessing ejection seat performance 04 p0525 A83-15412

Several contemporary paths of the analytical investigation of the human neuromotor units 04 p0523 A83-15789

The dynamics of vertical eye movements in normal human subjects 06 p0797 A83-18192

Isometric muscle force response of the human lower limb 06 p0797 A83-18195

Biomechanical aspects of the fracture resistance of the vertebral column of humans under impact overloads in the head-pelvis direction 06 p0798 A83-18509

International Symposium of Biomechanics Cinematography and High Speed Photography, 2nd, San Diego, CA, August 24-26, 1981, Proceedings 08 p1102 A83-22790

Cinematography data systems at the Naval Biodynamics Laboratory 08 p1102 A83-22791

Targets for three-dimensional /3-D/ tracking of human impact test subjects 08 p1102 A83-22792

Combination of accelerometer and photographically derived kinematic variables defining three-dimensional rigid body motion 08 p1102 A83-22793

Locomotion in anthropomorphic mechanisms --- Russian book 09 p1324 A83-23825

Kinematic and kinetic parameters as information feedback in the acquisition of man-machine skills 10 p1458 A83-26338

The association between cancellous architecture and loading in bone - An optical data analytic view 11 p1636 A83-27786

Alterations in glomerular and tubular dynamics during simulated weightlessness 11 p1636 A83-27795

An investigation of the biodynamic properties of the human body under general low-frequency vibration 17 p2560 A83-38189

The regulation by the human foot of the balance of the mechanical sytem of the 'inverted pendulum' type. I - The significance of the speed of motion. II - The role of the position of the center of gravity and temporal programs 23 p3497 A83-47117

Zero-latency tracking of predictable targets by time-delay systems 24 p3621 A83-49898

BIOELECTRIC POTENTIAL

Electrophysiological analysis of delayed-response behavior --- Russian book 02 p0221 A83-12149

The contingent negative variation /CNV/ during the fulfillment of tasks at the reaction time. I 02 p0224 A83-12210

The modality of an imperative signal and the characteristics of the contingent negative variation /CNV/. II --- signal anticipation effects on brain wave amplitudes 02 p0224 A83-12211

The possible meaning of the rapidly proceeding processes of the spatial-temporal organization of the EEG in the formation of psychic activity 02 p0224 A83-12213

The reflection of the success of the solving of arithmetic and visual tasks in the spatial-temporal distribution of cerebral cortical biopotentials 02 p0224 A83-12214

The voluntary regulation of alpha and theta EEG rhythms in humans 02 p0224 A83-12215

The relation of psychic and neurophysiological phenomena and biofeedback 02 p0224 A83-12216

The changes in the monosynaptic reflex excitability in the period of the organization and fulfillment of voluntary motor responses 02 p0223 A83-12217

The effect of 8-methoxypsoralen and UV radiation on the electric stability of liposome membranes 03 p0375 A83-14360

An investigation of the role of the sympathetic nervous system in the neurotrophic control of muscle fiber membranes in frogs 04 p0520 A83-15892

The cortical evoked negative wave as a reflection of selective attention 06 p0799 A83-18967

Maturation of potentials evoked by spatially structured stimuli and sensitivity of the visual system to deprivation 06 p0798 A83-18970

Blocking the negative delta waves in the rabbit visual cortex by light flashes 06 p0795 A83-18972

The slow latent auditory evoked potential of humans 07 p0976 A83-19932

The visual function of the nonprojected sections of the cortex and its reflection in the evoked potentials 07 p0973 A83-20353

Evoked potentials /EP/ and the processing of sensory information in the visual system of humans 07 p0976 A83-20354

Electrophysiological investigations of color vision in humans 07 p0977 A83-20358

The effects of various gases on cortical and spinal somatosensory evoked potentials at pressures up to 10 bar 07 p0974 A83-20777

The transmembrane potentials of the heart cells of rats during fibrillation induced by a decrease in extracellular sodium 10 p1454 A83-26791

The interaction of plasma lipoproteins with bilateral lipid membranes - The role of the surface charge 13 p1895 A83-30405

Intracellular feedback in the processes of the electromechanical integration of the myocardium in mammals 14 p2063 A83-32100

The effect of changes of the electrolytic composition of the perilymph on the endocochlear potential 14 p2063 A83-32567

A low-noise low input impedance amplifier for magnetic measurements of nerve action currents 14 p2020 A83-32798

Some improvements in the measurement of variable latency acoustically evoked potentials in human EEG 14 p2069 A83-33110

The age characteristics of cortical auditory evoked potentials 14 p2071 A83-33341

The effect of spatial-structural stimulus parameters on the evoked potentials in the visual and posterior associative areas of the cortex in humans 14 p2071 A83-33342

The regulatory mechanisms of perception - The question of the regulation of sensitivity --- visual perception sensitivity in normal and psychopathic subjects 15 p2213 A83-34970

Brainstem auditory evoked potentials 16 p2398 A83-35902

A test for evaluating muscular fatigue 17 p2559 A83-38186

Comparison of the spatial response properties of the human retina and cortex as measured by simultaneously recorded pattern ERGs and VEPs 19 p2880 A83-40750

BIOELECTRICITY

Thermoelectric energy conversion could be an energy source of living organisms 19 p2875 A83-41168

Shadows of thought - Shifting lateralization of human brain electrical patterns during brief visuomotor task 19 p2884 A83-41225

Membrane, action, and oscillatory potentials in simulated protocells 19 p2876 A83-41853

The characteristics of the evoked electrical reactions of the nucleus lateralis posterior of the thalamus of rabbits and their dependence on the functional condition of the cortex and the reticular formation 19 p2879 A83-42092

The first cortical implant of a multiplexed multi-electrode semiconductor brain electrode 20 p3035 A83-42553

Direct cortical responses and the integrating activity of the brain 21 p3185 A83-45372

BIOELECTRICITY

Extratympanal electrocochleography in clinical practice 01 p0083 A83-10515

A method for adaptive biocontrol in the multifaceted treatment of patients with cerebral arachnoiditis 01 p0083 A83-10525

Long-term posttetanic potentiation in the hippocampus 01 p0081 A83-10917

The changes in the nerve and cardiac activity in animals of various ages during the application of electromagnetic fields of low frequency and low voltage 02 p0220 A83-11884

Measurement of the specific electrical resistance of the blood 03 p0381 A83-14330

A technique for determining the functional condition of athletes by a method of electropuncture diagnostics 03 p0382 A83-14349

The implantation of sarcoplasmic reticulum membranes in a planar lipid membrane 03 p0375 A83-14359

The electric reactions of the cat brain to light following the section of the optic tracts 05 p0672 A83-17636

The response of the neurons of the visual centers of the rabbit brain to electric stimuli and a combination of the latter with nonvisual stimuli 05 p0672 A83-17638

Spectral analysis and the interference EMG 07 p0980 A83-19626

Use of phase spectral information in assessment of frequency contents of ECG waveforms 07 p0980 A83-19627

Signal processing for recovery of cardiac conducting system activity 07 p0980 A83-19628

Goal-directed movements of cat's eyes in response to electrical stimulation of the lateral geniculate body 07 p0972 A83-19645

Correlation methods of the analysis of the reaction of individual neurons of the auditory system. I - The correlation of an auditory signal with impulse activity 07 p0972 A83-19930

Neurophysiological manifestations of monaural phase sensitivity of the auditory system 07 p0972 A83-19931

The processing of signals of neural ensembles using modernized analyzers of the pulse-amplitude type 07 p0982 A83-20346

Visualization of the electric field around a moving animal by numerical calculation 07 p0976 A83-21172

Striated organelles in hair cells of rat inner ear maculas - Description and implication for transduction 11 p1638 A83-27818

The reaction of neurons to prolonged stimulation Morphological investigations --- Russian book 12 p1762 A83-28818

The regulation of the central mechanisms of vision --- Russian book 12 p1762 A83-28823

The structural principles of interneural integration --- Russian book 12 p1762 A83-29332

The changes in the electrical activity of the stomach of rats following direct X-ray irradiation 14 p2062 A83-32068

The problem of the contractility of the myocardium 14 p2063 A83-32098

On the possibility to determine integral characteristics of the cardiac electric generator from extracardiac electric and magnetic measurements 14 p2072 A83-32799

An investigation of the electrical conductivity of biological systems 14 p2065 A83-33317

The polyfunctionality of visual rhodopsin 14 p2065 A83-33321

The biological effect of the electric component of an electromagnetic field in the VLF range 16 p2393 A83-35921

The protective effect of extracellular K(+) in the myocardium during disorders of energy generation 18 p2732 A83-40552

Gating currents in the membrane of the nerve fiber Pharmacological analysis 21 p3185 A83-45374

The effect of a constant magnetic field on the identified neurons and the glia-neuronal interrelations in isolated nerve system of the *Helix lucorum*

- 21 p3185 A83-45376
Rhythmic activity in sensory systems --- Russian book
23 p3494 A83-47148
ATP-regulated K(+) channels in cardiac muscle
23 p3495 A83-48088

BIOENGINEERING

- NT ANTHROPOMETRY
NT BIOINSTRUMENTATION
NT BIOMETRICS
NT BIOTELEMETRY
NT BODY MEASUREMENT (BIOLOGY)
NT CARDIOGRAPHY
NT ECHOCARDIOGRAPHY
NT ELECTROCARDIOGRAPHY
NT ELECTROENCEPHALOGRAPHY
NT ELECTROMYOGRAPHY
NT ELECTROPLETHYSMOGRAPHY
NT ELECTRORETINOGRAPHY
NT PLETHYSMOGRAPHY
NT VECTORCARDIOGRAPHY
Bioprocessing in space 05 p0600 A83-17284
Free flow field step focusing - A new method for preparative protein isolation 22 p3266 A83-45762
ASECS - Antigen-Specific Electrophoretic Cell Separation 22 p3266 A83-45763
Preparative density gradient electrophoresis of cells and cell organelles - A new separation chamber
22 p3266 A83-45764
A new detailed lipidogram - Methods and clinical applications 22 p3347 A83-45766

BIOGENESIS

- U BIOLOGICAL EVOLUTION

BIOGEOCHEMISTRY

- The global troposphere - Biogeochemical cycles, chemistry, and remote sensing 02 p0198 A83-11828
Environmental effects of an impact-generated dust cloud - Implications for the Cretaceous-Tertiary extinctions
06 p0779 A83-18816
Inorganic chemistry of earliest sediments - Biogeochemical chemical aspects of the origin and evolution of life
13 p1899 A83-31158
Biologically mediated isotope fractionations - Biochemistry, geochemical significance and preservation in the earth's oldest sediments
13 p1899 A83-31159
Organic molecules as chemical fossils - The molecular fossil record
13 p1899 A83-31160
Geobotanical techniques for discriminating serpentine rock types in Western United States
17 p2533 A83-38448
The use of hydroxyacids as geochemical indicators
17 p2547 A83-38852
Material cycling and organic evolution
17 p2557 A83-38894
Global biology - An interdisciplinary scientific research program at NASA, Ames Research Center
[IAF PAPER 83-100] 23 p3474 A83-47264
Atmospheric composition - Influence of biology
24 p3604 A83-48760
Glutathione reductase in evolution
24 p3617 A83-49620

BIOGRAPHY

- A life devoted to astronautics (Dr. Olgierd Wolczek (1922-1982) - Biographical remarks and scientific activity in astronautics and space physics)
[IAF PAPER 83-292] 23 p3541 A83-47332

BIOINSTRUMENTATION

- NT BIOTELEMETRY
A device for recording the spatial synchronization of phases of EEG waves 01 p0050 A83-10502
The automatic stabilization of pressure in the main arteries during changes in the blood flow
01 p0080 A83-10545
The longitudinal radioisotopic gamma-tomograph GPR-1 01 p0050 A83-10558
A device for investigating the mechanical properties of biological tissues 03 p0329 A83-14331
Rapid monitoring of the acid-base and gas composition of the blood 03 p0375 A83-14334
A device controlling the timing and frequency of physical loads 05 p0677 A83-17169
Design and fabrication of a portable device to measure the response time to a luminous stimulus
06 p0800 A83-18343
International Symposium of Biomechanics Cinematography and High Speed Photography, 2nd, San Diego, CA, August 24-26, 1981, Proceedings
08 p1102 A83-22790
Verification trials for a primate physiological experimentation model intended for Spacelab
08 p1146 A83-22986

Automatic measurement of body surfaces using rasterstereography. I - Image scan and control point measurement 10 p1420 A83-25971

- Optical devices for investigations of the eye --- Russian book 12 p1767 A83-29331
Liquid ventilation in dogs - An apparatus for normobaric and hyperbaric studies 13 p1898 A83-30510
The formalization of the choice of the acoustic stimulus parameters in a small automatic device for the examination and diagnosis of the functional condition of the auditory analyzer 14 p2073 A83-33312

A bone telephone for measuring the audible threshold in an extended range of frequencies

- 14 p2073 A83-33313
An investigation of the electrical conductivity of biological systems 14 p2065 A83-33317
Effects of detector coil size and configuration on measurements of the magnetoencephalogram

A force transducer based on stress effects in bipolar transistors 16 p2401 A83-35452

The determination of the minute volume of the blood by a thermal dilution method 19 p2876 A83-41845

A micro-computer system for cell electrophoresis measurements 21 p3108 A83-43825

Rapid purification of fluorescent enzymes by ultrafiltration 21 p3105 A83-44858

BIOLOGICAL ACTIVITY

- U ACTIVITY (BIOLOGY)

BIOLOGICAL ANALYSIS

- U BIOASSAY

BIOLOGICAL CELLS

- U CELLS (BIOLOGY)

BIOLOGICAL CLOCKS

- U RHYTHM (BIOLOGY)

BIOLOGICAL EFFECTS

- NT JET LAG

NT RELATIVE BIOLOGICAL EFFECTIVENESS (RBE)

The effect of biostimulation amplification after the combined action of laser irradiation in the blue and red regions of the spectrum 01 p0078 A83-10456

A comparison of the neural and immunological modulator properties of low molecular weight neuropeptides

- 01 p0080 A83-10551

Immunobiological properties of teichoic acids --- for diagnosing staphylococcal infections

- 01 p0081 A83-10556

Automation of a Crawford-cell exposure system

- 01 p0051 A83-10865

Molecular mechanisms for the participation of peptides in the functions of nerve cells

- 01 p0081 A83-10918

Investigations of adaptation and solar activity

- 02 p0220 A83-11877

The effect of the solar-geomagnetic situation on monolayers of cells and the distant intercellular interactions at high latitudes

- 02 p0220 A83-11881

Low-strength ULF magnetic fields and the condition of the adaptive reserve in experimental animals

- 02 p0220 A83-11883

The biological effect of nonionizing radiation and the question of the effect of solar activity on organisms

- 02 p0220 A83-11885

An investigation of the frequency dependence of the biological effectiveness of a magnetic field in the range of the micropulsations of the geomagnetic field /0.01-100 Hz/

- 02 p0221 A83-11886

The biological effectiveness of a weak electromagnetic field of infralow frequency

- 02 p0221 A83-11887

The reaction of a biological system to adequate or weak low-frequency electromagnetic fields

- 02 p0221 A83-11889

The solar-terrestrial links in biology and the phenomenon of frequency 'capture'

- 02 p0221 A83-11890

Atmospheric infrasound as a possible factor in the transferring of the effect of solar activity to the biosphere

- 02 p0221 A83-11891

The biochemical mechanism of the reactions of living organisms to changes of solar activity

- 02 p0221 A83-11892

The possible mechanism of the solar-biosphere connections --- effect on enzymes

- 02 p0221 A83-11894

The stimulating effect of a helium-neon laser in acute inflammatory processes of the eye

- 03 p0378 A83-13603

The effectiveness of stimulating argon laser therapy for some forms of macular dystrophy

- 03 p0378 A83-13605

The effect of helium-neon laser irradiation on the membranes of the retina

- 03 p0374 A83-13610

A quantitative determination of the hemodepressive effect of some alkylating agents

- 03 p0374 A83-13633

The cyclase system and lysosome enzyme activity in health and disease

- 03 p0374 A83-13637

Cosmic radiobiology --- Russian book

- 03 p0380 A83-13818

Occupational skin hazards from ultraviolet /UV/ exposures

- 03 p0380 A83-13973

Possible effects of stratospheric ozone reductions on solar UV-B radiation reaching the earth's surface

- 03 p0356 A83-14635

The comparative activity of neuropeptide modulators of memory before and after electroshocks in white rats

- 04 p0520 A83-15891

The effect of an electric field of industrial frequency on parameters of natural immunity

- 05 p0669 A83-17164

The genetic danger of microwaves of nonthermal intensity and its hygienic aspects

- 05 p0670 A83-17202

The biological effect of ultraviolet radiation

- 06 p0795 A83-18985

A comparative analysis of the effect of alkylating agents, ionizing radiation, and ultraviolet light on the mammalian cell progression in the mitotic cycle. I - The effect of N-methyl-N'-nitro-N-nitrosoguanine on the passing of various phases of the cycle by HeLa cells

- 06 p0796 A83-19378

Visualization of the electric field around a moving animal by numerical calculation

- 07 p0976 A83-21172

DNA damage during the action of ionizing radiation with different physical characteristics

- 09 p1321 A83-24926

The transport and turnover of aldolase in rat livers during total body irradiation with X-rays

- 09 p1321 A83-24927

The reaction of chronically irradiated dogs to radiation as evaluated by changes in the activity of cholinesterase

- 09 p1321 A83-24932

Thermodynamic properties of tissue impacted by CO2 laser

- 11 p1635 A83-27520

Calcium transport from the intestine and into bone in a rat model simulating weightlessness

- 11 p1640 A83-27832

The effects of direct-current magnetic fields on turtle retinas in vitro

- 13 p1899 A83-31165

The interaction of the cretaceous-tertiary extinction bolide with the atmosphere, ocean, and solid earth

- 13 p1880 A83-31475

Influence of magnetic field on the process of self-assembly of tubulin

- 14 p2061 A83-31819

The effect of activators of cAMP accumulation on the separate stages of genome expression in cells during acute radiation injuries of organisms. VI - Peculiarities of the inhibition of RNA synthesis on a template of isolated chromatin by separate fractions of histones from the liver of normal, irradiated and serotonin-treated rats

- 14 p2061 A83-32051

The changes in the electrical activity of the stomach of rats following direct X-ray irradiation

- 14 p2062 A83-32068

The dependence of the biological effects of microwave irradiation on the intensity and length of exposure

- 15 p2210 A83-34933

Morphological features and certain representations of the mechanism for the biological effect of magnetic fields

- 15 p2211 A83-34975

Results of our 15-year study into the biological effects of microwave exposure

- 15 p2211 A83-34986

The biological effect of the electric component of an electromagnetic field in the VLF range

- 16 p2393 A83-35921

The biological activity of lunar soil from Mare Fecunditatis during intratracheal injection

- 16 p2394 A83-35924

The biological role of the reactive inhibition of mitosis during stress

- 18 p2733 A83-40561

A quarantine protocol for analysis of returned extraterrestrial samples

- 19 p2885 A83-40830

Characterization of a halotolerant-psychrotolerant bacterium from dry valley antarctic soil

- 19 p2886 A83-40833

Effect of HZE particles and space hadrons on bacteriophages

- 19 p2871 A83-40834

The effect of alpha particles on bacteriophage T4Br(+)

- 19 p2872 A83-40835

Physical determinants of radiation sensitivity in bacterial spores

- 19 p2872 A83-40836

Inactivation, mutation induction and repair in *Bacillus subtilis* spores irradiated with heavy ions

- 19 p2872 A83-40837

Effect of heavy ions on bacterial spores

- 19 p2872 A83-40839

Heavy ion action on yeast cells - Inhibition of ribosomal-RNA synthesis, loss of colony forming ability and induction of mutants

- 19 p2872 A83-40840

Experiments with air-dried seeds of *Arabidopsis thaliana* (L) Heynh. and *Crepis capillaris* (L) Wallr., aboard Saljut 6

Results on artemia cysts, lettuce and tobacco seeds in the Biobloc 4 experiment flown aboard the Soviet biosatellite Cosmos 1129 19 p2872 A83-40842

Some results of the effect of space flight factors on *Drosophila melanogaster* 19 p2872 A83-40843

Genetic risks associated with radiation exposures during space flight 19 p2873 A83-40845

Radiation exposures during space flight and their measurement 19 p2880 A83-40846

Unique biological aspects of radiation hazards - An overview 19 p2873 A83-40847

Cataractogenesis from high-LET radiation and the Casarett model 19 p2873 A83-40848

Late skin damage in rabbits and monkeys after exposure to particulate radiations 19 p2873 A83-40849

The change of immunobiological reactivity following the combined effects of microwaves, infrared, and gamma-irradiation 19 p2874 A83-41017

Research on the adaptation of skeletal muscle to hypogravity Past and future directions 19 p2877 A83-42047

Biological effects of weightlessness and clinostatic conditions registered in cells of root meristem and cap of higher plants 19 p2878 A83-42056

The effect of beta-mercaptoethylamine on the accumulation of DNA strand breaks in *Bac. stearothermophilus* exposed to gamma-radiation, UV radiation, and nitrosomethylurea treatment --- Mercapto Ethyl Amine 23 p3495 A83-48204

Cryogenic liquids and aviation --- biological effects and safety hazards 23 p3499 A83-48695

BIOLOGICAL EVOLUTION

NT ABIOTIC GENESIS

The appearance of life in the marine environment 01 p0077 A83-10381

The moon and the ecosphere 01 p0129 A83-10704

Evolution from space /The Omni Lecture/ and others papers on the origin of life --- Book 01 p0087 A83-10880

An evolutionary model for the insect vitellins 01 p0081 A83-11034

The possible role of assignment catalysts in the origin of the genetic code 02 p0219 A83-11634

Amino acids from the Late Precambrian Thule Group, Greenland 02 p0219 A83-11636

Evolutionary and experimental principles of muscle hygiene 05 p0673 A83-17168

Oxidative peptide /and amide/ formation from Schiff base complexes 06 p0800 A83-18247

Voyager Mission: Implications for planetary biology; Proceedings of the Sixth Annual Colloquium on Chemical Evolution, University of Maryland, College Park, MD, October 4-6, 1981 06 p0801 A83-19401

Criteria for the emergence and evolution of life in the solar system 06 p0801 A83-19406

The chemical structure of DNA sequence signals for RNA transcription 06 p0796 A83-19408

The Voyager mission and the origin of life - Selected references 06 p0801 A83-19409

The evolution of the structural-functional organization of the organ of hearing of vertebrates 07 p0972 A83-19933

The updated experimental proteinoid model 07 p0976 A83-21050

Oligomerization of /guanosine 5'-phosphor/-2-methylimidazole on poly/C/ - An RNA polymerase model 11 p1543 A83-28761

Transitions and transversions in evolutionary descent - An approach to understanding 12 p1762 A83-29421

Highly efficient peptide formation from N-acetylaminocyl-AMP anhydride and free amino acid 12 p1767 A83-29422

Pathways of evolution for man and machine 12 p1784 A83-29454

Evolution of sleep: Stages of the formation of the 'wakefulness-sleep' cycle in vertebrates --- Book 13 p1895 A83-30140

Cosmochemistry and the origin of life; Proceedings of the Advanced Study Institute, Maratea, Italy, June 1-12, 1981 13 p1899 A83-31151

The largest molecules in space - Interstellar dust 13 p1947 A83-31154

The chemical composition and climatology of the earth's early atmosphere 13 p1878 A83-31156

The dating of the earliest sediments on earth --- containing biogenic markers 13 p1899 A83-31157

Inorganic chemistry of earliest sediments - Biogeochemical aspects of the origin and evolution of life 13 p1899 A83-31158

Organic molecules as chemical fossils - The molecular fossil record 13 p1899 A83-31160

The possible effect of the natural background of ionizing radiation on the development of mammals 14 p2062 A83-32057

The structure of the microtubule organizational centers in a comparative evolutionary aspect 14 p2065 A83-33318

Toward a general theory of adaptation --- of biological and nonbiological systems 15 p2210 A83-34930

Controlling the duration of photosynthetic charge separation with microwave radiation 16 p2394 A83-35998

Syzers: the modeling of fundamental characteristics of molecular-biological organization - The correspondence between general properties of genetic processes and the structural peculiarities of macromolecular assemblies 16 p2395 A83-36810

Thermal neutrons could be a cause of biological extinctions 65 Myr ago 17 p2557 A83-38605

Material cycling and organic evolution 17 p2557 A83-38894

Comparative studies on biochemical properties of protein synthesis of an archaeobacteria, *Thermoplasma* sp 17 p2557 A83-38896

The characteristics of the aggregation of erythrocytes in various animals and in humans 19 p2871 A83-40814

Origin of Espanola Island and the age of terrestrial life on the Galapagos Islands 19 p2864 A83-40902

Chemical evolution and the origin of life 19 p2887 A83-42037

Exponential evolution - Implications for intelligent extraterrestrial life 19 p2908 A83-42038

Changes in the amino acid code 19 p2877 A83-42039

Experimental studies related to the origin of the genetic code and the process of protein synthesis - A review 19 p2879 A83-42156

Stabilization of the yeast desaturase system by low levels of oxygen 19 p2879 A83-42159

Chemical evolution and the origin of life - Bibliography supplement 1981 19 p2887 A83-42160

The enchanted loom --- Book on evolution of intelligence 20 p3033 A83-42174

The biosphere --- life effects on planetary evolution 20 p3033 A83-42822

The efficiency of coupled processes in connection with geochemical and biogeological evolution 23 p3485 A83-48508

The thermodynamics of evolution. II - Chemical and biological oscillations and instabilities 23 p3513 A83-48600

Glutathione reductase in evolution 24 p3617 A83-49620

BIOLOGICAL MODELS

U BIONICS

BIOLOGICAL MODELS (MATHEMATICS)

Numerical investigation of a turbulent boundary layer for the case of a positive pressure gradient 01 p0045 A83-10457

The age-related peculiarities of the development of hypoxia in skeletal muscles during acute hypoxic hypoxia 01 p0078 A83-10483

An investigation of the effect of local vibration at fragmented doses for the substantiation of a model of a sparing regime --- for human body 01 p0083 A83-10528

Disturbances of conditioned reflex activity during hypokinesia in rats and the normalizing effect of motor loads 01 p0079 A83-10534

An analysis of the parameters of the immunoreactive curve 01 p0080 A83-10555

Investigating the correlation between reading errors and degraded numerics - Or, do missing dots call the shots 01 p0085 A83-11168

Anisotropic filtering operations for image enhancement and their relation to the visual system 01 p0099 A83-11451

The possible role of assignment catalysts in the origin of the genetic code 02 p0219 A83-11634

Electrophysiological analysis of delayed-response behavior --- Russian book 02 p0221 A83-12149

A theoretical and experimental analysis of the turnover of substances in a closed microecosystem. II - The stable steady states and the limiting factors of turnover 03 p0384 A83-14326

Mechanism for the appearance of spiral waves in active media, associated with the phenomenon of critical curvature --- in damaged myocardium tissues 03 p0376 A83-14364

Numerical study of the stochastic behavior of a simple biological system 03 p0376 A83-14365

Optimal tactics of antibacterial therapy for the trigger model of the injection process 03 p0382 A83-14367

A theoretical analysis of the regularities of the Bainbridge reflex --- heart rate acceleration by blood pressure increase 04 p0520 A83-15894

Mathematical methods for optimizing treatment and diagnosis in cardiology /current status and future prospects/ 05 p0674 A83-17199

BIOLOGICAL MODELS (MATHEMATICS)

Emotional stresses and their role in cerebrovisceral disturbances 05 p0672 A83-17598

A study of the adaptation processes in the peripheral blood using methods of mathematical modeling --- leukocyte adaptation to microwaves 06 p0796 A83-19382

Mathematical models of the hydrodynamics of the cochlea of the inner ear 07 p0972 A83-19927

Mathematical models of the process of signal conversion on the periphery of the auditory system /Status and prospects of application/ 07 p0972 A83-19928

Auditory mechanisms of rhythm analysis 07 p0976 A83-19929

The tracking function as a basic psychophysiological parameter of the activity of an operator /Review/ 07 p0981 A83-20340

The dynamics of oxygen transport from the capillaries to the nerve cells of the brain 08 p1145 A83-22104

The systemic quantization of behavior --- of animals and humans 08 p1150 A83-22116

A new technique of studying the effects of vibrations on the spine 08 p1148 A83-22977

Locomotion in anthropomorphic mechanisms --- Russian book 09 p1324 A83-23825

The modeling of respiratory arrhythmia 09 p1324 A83-23864

Multipulse control of saccadic eye movements 09 p1325 A83-24706

The model human processor - A model for making engineering calculations of human performance 10 p1459 A83-26323

The relationship between processing resource and subjective dimensions of operator workload 10 p1457 A83-26331

Computer simulation analysis of the behavior of renal-regulating hormones during hypogravic stress 11 p1642 A83-27794

Evaluation of the response of rat skeletal muscle to a model of weightlessness 11 p1640 A83-27837

Sudden cardiac death - A problem in topology 12 p1762 A83-29250

The specific characteristics of heat stress during the microwave irradiation of mammals (Theoretical analysis) 12 p1762 A83-29274

A comparative analysis of the amplitude-frequency characteristics of the microphone potentials of humans as determined by experiments and with a mathematical model 12 p1784 A83-29304

Mathematical modeling of global biospheric processes --- Russian book 12 p1747 A83-29338

The instability of the autogen --- theory of chemical evolution 12 p1767 A83-29425

The problem of sudden coronary death in the light of mathematical catastrophe theory 13 p1900 A83-30093

An investigation of the abiogenic synthesis of peptides in a model open system 13 p1908 A83-30100

The energy balance of the myocardium and its correction by antiarrhythmics 13 p1895 A83-30407

The relationship of the properties of model and natural channel permeability in biological membranes 13 p1896 A83-30411

The identification of subjective evaluations of the interaction of a human operator and technical facilities 14 p2072 A83-32954

A linear model of the general coordinates of the functional condition of a human operator, and their calculation and interpretation 14 p2072 A83-32956

A mathematical model for the regulation of glycolysis by the oxidation of pyruvate and fatty acids in the myocardium 14 p2064 A83-32957

A method for the calculation of the spatial position of the dipole generators of multipole model of the equivalent generator of the heart 14 p2073 A83-32958

An investigation of the hemodynamics of a human in an antiorthostatic position using a method of mathematical modeling 14 p2069 A83-32959

The possibilities of the investigation of nonlinear connections using digital simulation --- heliogeophysical effects on human physiological parameters 14 p2069 A83-32960

Toward a general theory of adaptation --- of biological and nonbiological systems 15 p2210 A83-34930

A model for prediction of resynchronization after time-zone flights 15 p2214 A83-34983

A study of human behavior in adverse stress 16 p2400 A83-35700

The recovery of temperature homeostasis of mammals under microwave irradiation 16 p2394 A83-35922

A definition of the concept of 'information' and the possibilities of its use in biology 16 p2405 A83-36801

Instabilities of autowaves in excitable media connected with the phenomenon of critical curvature --- as in damaged regions of myocardial tissue 16 p2394 A83-36804

The effect of the kinetics of erythrocyte destruction on the dynamic behavior of the erythropoiesis system

16 p2395 A83-36805

An ionic mechanism of the Myocardium staircase --- electromechanical coupling in myocardium cells

16 p2395 A83-36806

The recovery of the weighting functions of simple fields of the visual cortex with regard to nonlinearity

16 p2395 A83-36807

Syzers: the modeling of fundamental characteristics of molecular-biological organization - The correspondence between general properties of genetic processes and the structural peculiarities of macromolecular assemblies

16 p2395 A83-36810

The calculation of controlled eye movements during shifts of the fixation points

16 p2399 A83-36817

Mathematical modelling in studies of the pathology of the visual nerve

16 p2400 A83-36835

Expiratory and arterial partial pressure relations under different ventilation-perfusion conditions

17 p2558 A83-36996

A mathematical model of the mechanism of respiratory rhythmogenesis

17 p2558 A83-37241

A model for the development of genetic translation

17 p2557 A83-38899

'Unlearning' has a stabilizing effect in collective memories

18 p2738 A83-39966

The mathematical selection of information criteria for the differential diagnosis of renovascular hypertension and hypertension

19 p2881 A83-41436

Computer simulation of the main gel-fluid phase transition of lipid bilayers

20 p3033 A83-42639

Theoretical studies in isoelectric focusing --- mathematical modeling and computer simulation for biological purification process

20 p2951 A83-43280

Mathematical model of psychophysiological stress on a pilot, based on Wilder's biological law

20 p3036 A83-43506

Computer modeling of membrane structures and the distribution of admixture particles in a lipid bilayer

21 p3184 A83-45224

The probabilistic principles of nervous activity

21 p3185 A83-45373

The Lie transformation group model of visual perception

22 p3348 A83-45947

Attending to different levels of structure in a visual image

22 p3349 A83-45954

A model of the working of a binocular visual system in the process of volume perception

23 p3497 A83-47110

Mathematical models of the readaptation of the human visual analyzer following short light flashes

23 p3497 A83-47111

The relationship between blood flow, partial pressure, and oxygen demand in the human cortex (A theory of tissue gas exchange)

23 p3497 A83-47113

BIOLOGICAL RHYTHM

U RHYTHM (BIOLOGY)

BIOGNOMIS

Investigations of adaptation and solar activity

02 p0220 A83-11877

The effect of geomagnetic disturbances on human biorhythms

02 p0222 A83-11878

The sector structure of the interplanetary magnetic field and disturbances of the central nervous system

02 p0222 A83-11879

The state of the adrenal cortex function in healthy individuals during changes in geomagnetic activity

02 p0222 A83-11882

Low-strength ULF magnetic fields and the condition of the adaptive reserve in experimental animals

02 p0220 A83-11883

An investigation of the frequency dependence of the biological effectiveness of a magnetic field in the range of the micropulsations of the geomagnetic field /0.01-100 Hz/

02 p0221 A83-11886

The effect of magnetic fields on the radiosensitivity of mice. I - The effect of infralow frequency magnetic fields of low intensity on the survival of experimental animals after general irradiation with X-rays

03 p0377 A83-14888

The effect of a geomagnetic field and neuro-psychological stress on the electrical resistance in biologically active points of the skin

04 p0523 A83-15787

The use of a constant magnetic field in the treatment of dystrophies of the extremities

05 p0673 A83-17197

The effect of a magnetic field on the patterns of the frequency changes and the content of serotonin in the isolated heart of frogs

07 p0974 A83-20968

The effect of a magnetic field on the aggregation of rhodopsin molecules during the photooxidation of the photoreceptor membranes

13 p1896 A83-30410

Influence of magnetic field on the process of self-assembly of tubulin

14 p2061 A83-31819

On the possibility to determine integral characteristics of the cardiac electric generator from extracardiac electric and magnetic measurements

14 p2072 A83-32799

The effect of magnetotherapy on the cardiovascular system of patients with hypertension

15 p2213 A83-34971

Morphological features and certain representations of the mechanism for the biological effect of magnetic fields

15 p2211 A83-34975

Effects of detector coil size and configuration on measurements of the magnetoencephalogram

16 p2401 A83-35452

The effect of a constant magnetic field on the respiration of human skin during reparative and destructive processes

21 p3188 A83-45225

BIOMASS

Remote measurement of biomass

03 p0350 A83-14306

Determination of the humus content of soils from remote sensing data

09 p1283 A83-24223

Growth response and spectral characteristics of a short Spartina alterniflora salt marsh irrigated with freshwater and sewage effluent

10 p1443 A83-25645

Radiometric estimation of biomass and nitrogen content of Alicia grass

14 p2035 A83-32616

Remote sensing salt marsh biomass and stress detection

15 p2182 A83-33577

Seasonal spectral characteristics and aboveground biomass of the tidal marsh plant, Spartina alterniflora

16 p2370 A83-35742

Satellites for the study of ocean primary productivity

19 p2869 A83-42041

BIOMASS ENERGY PRODUCTION

New sources for fuel and materials --- from plants

05 p0658 A83-16937

Thermochemical conversion of biomass - Gasification by flash pyrolysis study

06 p0780 A83-18556

Biomass energy

06 p0780 A83-18560

Marine power - Accomplishments of the 1970s

11 p1606 A83-27223

Gaseous fuel generation by magma-thermal conversion of biomass

13 p1870 A83-30196

The effect of glucose concentration and pH on hydrogen production by Rhodospseudomonas sphaeroides VM 81

15 p2193 A83-35303

Use of pyrolysis-derived fuel in a gas turbine engine [ASME PAPER 83-GT-96]

23 p3440 A83-47942

BIOMECHANICS

U BIODYNAMICS

BIOMEDICAL DATA

Spectral analysis and the interference EMG

07 p0980 A83-19626

Measurements and imaging method of blood flow profile in human heart

08 p1151 A83-22237

Performance based biomedical standards for evaluation aircrew

08 p1150 A83-22957

An automatic system for the evaluation of the psychophysiological condition of an operator according to EKG parameters

09 p1324 A83-23863

A statistical analysis of motion sickness incidence data

10 p1455 A83-25673

BIOMETEOROLOGY

U BIOCLIMATOLOGY

BIOMETRICS

NT ANTHROPOMETRY

NT BODY MEASUREMENT (BIOLOGY)

NT CARDIOGRAPHY

NT ECHOCARDIOGRAPHY

NT ELECTROCARDIOGRAPHY

NT ELECTROENCEPHALOGRAPHY

NT ELECTROMYOGRAPHY

NT ELECTROPLETHYSMOGRAPHY

NT ELECTRORETINOGRAPHY

NT PLETHYSMOGRAPHY

NT VECTORCARDIOGRAPHY

A correlation analysis of macrometric parameters of the pulmonary heart during chronic nonspecific diseases of the lungs

01 p0084 A83-11391

Morphological criteria for the individual variability of the human brain

03 p0380 A83-13643

Histometric indicators of the structure of the femoral and crural muscles of children, adolescents, and young men

07 p0978 A83-20991

Wolf-Parkinson-White syndrome in young, asymptomatic pilot's applicants

08 p1147 A83-22960

The architectonics of the arterial bed in the brain hemispheres of rats during normal conditions and after a stay at a 'height' of 5600 m

10 p1454 A83-26788

The evaluation of the psychophysiological condition of a human operator in real time

14 p2072 A83-32953

Comparative study of various noninvasive methods of arterial pressure recording

17 p2562 A83-38179

The determination of the volume of rapidly circulating blood by a thermal dilution method

18 p2732 A83-40553

BIONICS

Computer tracking of moving objects using a Fourier-domain filter based on a model of the human visual system

01 p0097 A83-11420

Structural kinematics of in-parallel-actuated robot-arms [ASME PAPER 82-DET-105]

02 p0187 A83-12779

Perceptual capabilities, ambiguities, and artifacts in man and machine

03 p0383 A83-13450

Neural analog information processing

08 p1158 A83-22812

Locomotion in anthropomorphic mechanisms --- Russian book

09 p1324 A83-23825

Simplified robot arm dynamics for control

09 p1328 A83-24712

Control of the constrained planar simple inverted pendulum

10 p1461 A83-25397

An electronic model of the conditioned reflex

14 p2072 A83-32571

BIOPHYSICS

NT HEALTH PHYSICS

NT PUBLIC HEALTH

A device for investigating the mechanical properties of biological tissues

03 p0329 A83-14331

Concerning the absence of magnetic-field effect on the dissolving of oxygen in aqueous solutions --- in biological systems

03 p0375 A83-14356

The role of physical characteristics of laser radiation in the absorption of light by heme-containing biological molecules

03 p0376 A83-14369

Enhanced erythrocyte suspension layer stability achieved by surface tension lowering additives

11 p1546 A83-28762

Intracellular feedback in the processes of the electromechanical integration of the myocardium in mammals

14 p2063 A83-32100

The leading problems of contemporary age physiology, biochemistry, and biophysics and the investigations of the school of A. V. Nagornyi

14 p2065 A83-33322

Bone sound conduction in a widened frequency range according to data of the Moessbauer effect

19 p2883 A83-41829

Tibial changes in experimental disuse osteoporosis in the monkey

19 p2876 A83-41859

Photoreceptors: Their role in vision --- Book

19 p2877 A83-41989

BIOREGENERATION

U REGENERATION (PHYSIOLOGY)

BIOGENERATIVE LIFE SUPPORT SYSTEMS

U CLOSED ECOLOGICAL SYSTEMS

BIOSELLITES

Status of joint US/USSR experiments planned for the Cosmos '83 biosatellite mission

11 p1636 A83-27791

BIOSENSORS

U BIOINSTRUMENTATION

BIOSIMULATION

U BIONICS

BIOSPHERE

The effect of solar activity on the biosphere --- Russian book

02 p0220 A83-11876

Atmospheric infrasound as a possible factor in the transferring of the effect of solar activity to the biosphere

02 p0221 A83-11891

The acceleration of the oxidation of thiol compounds during increasing solar activity --- in biosphere

02 p0221 A83-11893

The possible mechanism of the solar-biosphere connections --- effect on enzymes

02 p0221 A83-11894

Investigations of the variations in the transmission spectra of aqueous solutions and their correlations with the parameters of a neutron counter --- solar effects on biosphere

02 p0221 A83-11895

Three-dimensional tracer model study of atmospheric CO₂ - Response to seasonal exchanges with the terrestrial biosphere

09 p1305 A83-24254

Mathematical modeling of global biospheric processes --- Russian book

12 p1747 A83-29338

A simulation of the carbon cycle in the system atmosphere-ocean-biosphere in the framework of linear and diffusion models

13 p1874 A83-30296

A megastructural end to Geologic Time

18 p2754 A83-39607

The Antaeus Project - An orbital quarantine facility for analysis of planetary return samples

19 p2812 A83-40829

Terraforming --- human transformation of solar system planets and natural satellites into earthlike biospheres

19 p2908 A83-41507

The biosphere --- life effects on planetary evolution

20 p3033 A83-42822

Reviews of space science - Legacy of the IGY

24 p3597 A83-48893

A spatially distributed model of the biosphere --- latitude distribution of atmospheric temperature and precipitation
24 p3609 A83-49276

BIOSYNTHESIS
The peculiarities of DNA metabolism in rat brains in the process of the elaboration of a conditioned reflex
01 p0080 A83-10552
The poststress activation of the synthesis of nucleic acids and proteins and its role in the adaptive reactions of the organism
05 p0670 A83-17184
The regulation of the biosynthesis of serotonin in the central nervous system
06 p0795 A83-18983
Polyamine formation by arginine decarboxylase as a transducer of hormonal, environmental and stress stimuli in higher plants
11 p1639 A83-27830
Synthesis of amino acids in weight bearing and non-weight bearing leg muscles of suspended rats
11 p1640 A83-27838
Syzers: the modeling of fundamental characteristics of molecular-biological organization - The correspondence between general properties of genetic processes and the structural peculiarities of macromolecular assemblies
16 p2395 A83-36810
Role of succinic acid in chemical evolution
17 p2563 A83-38900
The biosynthesis of cholesterol in the tissues of irradiated rats
18 p2731 A83-39520
Physiological mechanisms of the regulation of lipoprotein biosynthesis in the liver during physical loading and in various phases of the recovery period
18 p2733 A83-40563
The characteristics of the biosynthesis of nucleic acids during the activation of erythroid cell proliferation evoked by prolonged gamma-irradiation
19 p2874 A83-41009
The atmosphere of the primitive earth and the prebiotic synthesis of organic compounds
19 p2886 A83-42033
Prebiotic synthesis and reactions of nucleosides and nucleotides
19 p2887 A83-42035
A novel way for the formation of alpha-amino acids and their derivatives in an aqueous medium
19 p2887 A83-42036
Age-related characteristics of the prostaglandin system in several organs
19 p2879 A83-42096
Photochemical synthesis of biomolecules under anoxic conditions
19 p2887 A83-42158
The evolutionary pattern of aromatic amino acid biosynthesis and the emerging phylogeny of pseudomonad bacteria
20 p3033 A83-42399
Biosynthesis of tetrapyrrol pigments as possible precursors of the nickel-containing factor F430 of Methanosarcina vacuolata
23 p3496 A83-48513

BIOT METHOD
The Biot-Savart formula for an equilibrium plasma --- in magnetosphere
02 p0240 A83-11646

BIOTECHNOLOGY
USAF Aerospace Biotechnology Research and Development Program
04 p0525 A83-15420
Biotechnology in space laboratories
05 p0669 A83-17111
Biological applications of picosecond spectroscopy
13 p1845 A83-30214
A device for the formation and investigation of spherical artificial phospholipid membranes
13 p1895 A83-30305

BIOTELEMETRY
The changes in cardiac activity during physical exercises in an athletic arena and swimming pool following prolonged antithrostatic hypokinesia /based on biotelemetry data/
05 p0673 A83-17171
An infrared method for measuring the eyelid motion reaction
07 p0982 A83-20343
An automatic system for the medical monitoring of the functional condition of a human
15 p2215 A83-34947
A study of the strength and endurance of individual groups of muscles using a polyergocorographic device
15 p2213 A83-34949
The diagnostic value of ambulatory electrocardiographic monitoring
19 p2882 A83-41450

BIOTITE
Kimberlites in western Liberia - An overview of the geological setting in a plate tectonic framework
07 p0961 A83-20236
Redox state of earth's upper mantle from kimberlitic ilmenites
15 p2198 A83-34218
Recognition of extraneous argon components through incremental-release (Ar-40)/(Ar-39) analysis of biotite and hornblende across the Grenvillian metamorphic gradient in southwestern Labrador
15 p2201 A83-34496

BIPOLAR TRANSISTORS
Effects of dV/dt in MOSFET and bipolar junction transistor switches
01 p0041 A83-11020

The current status and the principal problems of developing microwave transistors /Review/
01 p0043 A83-11304
An examination of background noise in analog integrated circuits and components --- French thesis
02 p0166 A83-11765
Bipolar transistor action in ion implanted diamond
02 p0168 A83-12286
Bipolar transistor oscillators for measurements of material parameters
03 p0338 A83-14300
Current-voltage characteristic for bipolar p-n junction devices with drift fields, including correlation between carrier lifetimes and shallow-impurity concentration --- with implications for solar cells
04 p0543 A83-16069
GaAs/GaAlAs heterojunction bipolar transistors with cutoff frequencies above 10 GHz
05 p0624 A83-17285
Numerical simulation of GaAs/GaAlAs heterojunction bipolar transistors
05 p0624 A83-17294
An improved bipolar junction transistor model for electrical and radiation effects
05 p0626 A83-17488
Rapid annealing in advanced bipolar microcircuits
05 p0627 A83-17516
A comparison of radiation damage in transistors from cobalt-60 gamma rays and 2.2 MeV electrons
05 p0629 A83-17534
An analytical breakdown model for short-channel MOSFET's
05 p0630 A83-17753
A vertically isolated self-aligned transistor - VIST
05 p0631 A83-17757
Controlled avalanche and transit time /CATT/ transistor Physical analysis and fundamental limitations --- French thesis
08 p1079 A83-22092
A spaceborne experiment to determine the radiation sensitivity of microwave bipolar transistors
08 p1080 A83-22371
Molecular beam epitaxial double heterojunction bipolar transistors with high current gains
08 p1081 A83-22916
High-speed GaAlAs-GaAs heterojunction bipolar transistors with near-ballistic operation
08 p1082 A83-22922
Failure modes induced in TTL-LS bipolar logics by negative inputs
09 p1253 A83-23696
Physics of semiconductor power devices
09 p1254 A83-23853
S-band transistors for radar applications - Unique metallization and emitter ballasting design
11 p1583 A83-28592
High-speed GaAs heterojunction bipolar phototransistor grown by molecular beam epitaxy
13 p1837 A83-31759
Gigabit logic bipolar technology advanced super self-aligned process technology
13 p1837 A83-31761
Translinear logic - A new technique in bipolar technology
13 p1838 A83-31787
10 ns 8 x 8 multiplier LSI using super self-aligned process technology
15 p2216 A83-33891
Double heterojunction Al(x)Ga(1-x)As/GaAs bipolar transistors (DHBJT's) by MBE with a current gain of 1650
15 p2151 A83-33916
(GaAl)As/GaAs heterojunction bipolar transistors with graded composition in the base
15 p2152 A83-34516
A force transducer based on stress effects in bipolar transistors
18 p2688 A83-39554
A new high-power voltage-controlled differential negative resistance device - The Lambda bipolar power transistor
21 p3123 A83-43850
Application of thermal pulse annealing to ion-implanted GaAlAs/GaAs heterojunction bipolar transistors
21 p3123 A83-43851
Planar, ion-implanted bipolar devices in GaAs
21 p3127 A83-45172
GaP/Al(x)Ga(1-x)P heterojunction transistors for high-temperature electronic applications
24 p3572 A83-48917

BIPOLARITY
A technique for calculating shunt leakage and cell currents in bipolar stacks having divided or undivided cells
14 p2047 A83-32637
Recent work on bipolar nebulae
24 p3638 A83-49130

BIPROPELLANTS
U LIQUID ROCKET PROPELLANTS

BIRD-AIRCRAFT COLLISIONS
Development of a structural, bird impact resistant, de-iced wing leading edge for the de Havilland Dash 8 aircraft using fibre-reinforced composites
06 p0717 A83-18823
Remote sensing of problem birds in aviation
08 p1043 A83-21876
Management of bird problem in Indian airlines
08 p1043 A83-21877

Bird strikes to aircraft and associated hazards and problems regarding the safety of aircraft operations
08 p1043 A83-21878
Recent developments in polycarbonate coatings for advanced aircraft
09 p1239 A83-24959
Simulation of T-38 aircraft student canopy response to cockpit pressure and thermal loads using MAGMA --- Materially and Geometrically Nonlinear Analysis [AIAA 83-0942]
12 p1701 A83-29772
Analytical and experimental investigation of bird impact on fan and compressor blading [AIAA 83-0954]
12 p1704 A83-29856
F/RF-4 transparency baseline bird impact test program
20 p2932 A83-42533

BIRDS
NT PIGEONS
NT WATERFOWL
Aerial thermal infrared census of Canada geese in South Dakota
03 p0351 A83-14665

BIREFRINGENCE
Polarization properties of single-polarization fibers
02 p0235 A83-11572
Figures of merit for dispersive birefringent filter materials
02 p0236 A83-12303
Birefringence variation with temperature in elliptically clad single-mode fibers
03 p0395 A83-14386
Dynamic crack-tip stresses under stress wave loading - A comparison of theory and experiment
03 p0343 A83-14820
Extension of oblique-incidence method to photo-orthotropic elasticity
03 p0344 A83-14941
Procedure for the determination of the rheo-optical behavior of a photoplastic model material for dynamic experiments --- German thesis
04 p0499 A83-15843
Birefringence correction for single-mode fiber couplers
05 p0684 A83-16843
Stress-induced single-polarization single-mode fiber
05 p0684 A83-16844
Generalized model for wire grid polarizers
08 p1098 A83-22564
Electro-optic shutter devices utilizing lead lanthanum zirconate titanate /PLZT/ ceramic wafers
08 p1098 A83-22565
Optical pulse compression using polarizing techniques
08 p1166 A83-22570
Enhancement of birefringence in polarisation-maintaining fibres by thermal annealing
08 p1167 A83-22921
An analysis of ultraviolet magneto-optical spectra
09 p1341 A83-23657
Acousto-elastic measurement of stress and stress intensity factors around crack tips
09 p1283 A83-25116
Submicrometer periodicity gratings as artificial anisotropic dielectrics
10 p1482 A83-25978
Single-polarisation operation of highly birefringent bow-tie optical fibres
12 p1779 A83-29462
Birefringence of Zn(x)Cd(1-x)S near the isotropic point
13 p1918 A83-30207
A quasi-optical nulling method for material birefringence measurements at near-millimeter wavelengths
13 p1847 A83-31148
Measurement of fiber birefringence by wavelength scanning Effect of dispersion
15 p2230 A83-33766
The stress-optic effect in optical fibers
16 p2412 A83-35964
Novel polarisation phenomena on anisotropic multimode fibres
16 p2412 A83-36001
New single-mode single-polarisation optical fibre
16 p2412 A83-36487
Modal birefringence and polarization mode dispersion in single-mode fibers with stress-induced anisotropy
19 p2899 A83-40945
Investigation of a probe sensor of electric field strength with a Pockels-effect cell
19 p2849 A83-41816
Long range surface plasmons in birefringent media
20 p3046 A83-42206
Thermal properties of highly birefringent optical fibers and preforms
20 p3047 A83-42222
Wave precession as a consequence of the nonlinearly developed birefringence in plasmas
21 p3209 A83-43939
Fabrication of polarization-maintaining and absorption-reducing fibers
21 p3204 A83-44203
Performance of Lyot depolarizers with birefringent single-mode fibers
21 p3204 A83-44207
Practical single-polarisation anisotropic fibres
21 p3208 A83-44963
Polarimetric strain gauges using high birefringence fibre
21 p3208 A83-44968
Optical wave propagation in form-birefringent media and waveguides
22 p3356 A83-45732
Half-fringe photoelasticity - A new approach to whole-field stress analysis
22 p3306 A83-46809

- Birefringence and polarization mode dispersion caused by thermal stress in single-mode fibers with various core ellipticities 22 p3360 A83-46813
- Single-mode, single-polarization fibers made of birefringent material 23 p3508 A83-47583
- Combined reciprocal and non-reciprocal birefringence in optical monomode fibres 24 p3627 A83-48744
- Molecular deformation and stress-strain behavior of poly(bisphenol-A-diphenyl sulfone) 24 p3567 A83-48903
- 8 km-long polarisation-maintaining fibre with highly stable polarisation state 24 p3630 A83-49974
- Polarisation-preserving coupler with self aligning birefringent fibres 24 p3630 A83-49982
- Polarisation holding in coiled high-birefringence fibres 24 p3630 A83-49992

BIREFRINGENT COATINGS

- Calculations for experimental stress analysis --- Book 03 p0340 A83-14044
- Strain measurement with asymmetric oblique-incidence polariscope for birefringent coatings 21 p3161 A83-45157

BIREFRINGENT FILTERS

- Gyrotropic isoindex filter 02 p0178 A83-12597
- Birefringence of Zn(x)Cd(1-x)S near the isotropic point 13 p1918 A83-30207

BISMUTH

- NT BISMUTH ISOTOPES
- Production of electronically excited bismuth in a supersonic flow 07 p0936 A83-20726

BISMUTH ALLOYS

- Investigations concerning the electrochemical equilibrium in the system tin-bismuth-oxygen 09 p1233 A83-24124
- Response of MnBi-Bi eutectic to freezing rate changes 20 p2942 A83-43303
- A study of the coalescence process inside the miscibility gap in Zn-Bi alloys 20 p2942 A83-43306
- Gravitationally induced convection during directional solidification of off-eutectic Mn-Bi alloys 20 p2942 A83-43308
- Low gravity solidification structures in the tin-15 wt pct lead and tin-3 wt pct bismuth alloys 20 p2943 A83-43314

BISMUTH COMPOUNDS

- NT BISMUTH SULFIDES
- Photoelectrochemical processes in bismuth germanium oxide, Bi₂GeO₂₀ single crystals 07 p0954 A83-20581
- Coherent optical image delay device using a BSO phase-conjugate mirror and its applications 10 p1424 A83-26864
- Influence of freezing rate changes of MnBi-Bi eutectic microstructure --- effects of space processing 18 p2643 A83-39899
- Photovoltaic effect in thin Bi₂GeO₂₀ films 20 p3051 A83-42263
- Behaviour of AgBi(Cr₂O₇)₂ as a possible cathode for lithium cells 24 p3601 A83-49953

BISMUTH ISOTOPES

- The radon cycle and its daughters - An application to the study of troposphere-stratosphere exchanges 13 p1883 A83-31720

BISMUTH SULFIDES

- Photoelectrochemical behaviour of electrodeposited and pressure-sintered Bi₂S₃, Bi₂S₃-PbS and Bi₂S₃-Ag₂S semiconductor electrodes 08 p1131 A83-22905

BISMUTH 205**U BISMUTH ISOTOPES****BISPENOLS**

- Analysis of the puncture of a bisphenol-A polycarbonate disc 10 p1400 A83-26075
- Experimental study of the T-criterion in ductile fractures 11 p1596 A83-28445
- Variation of dynamic mechanical properties of polycarbonate as a result of deformation 22 p3270 A83-46903
- The curing of a bisphenol A-type epoxy resin with 1,8 diamino-p-menthane 22 p3270 A83-46905

BISTABLE AMPLIFIERS**U FLIP-FLOPS****BISTABLE CIRCUITS**

- Guided wave approaches to optical bistability 02 p0235 A83-12167
- Self-pulsing and chaos in a mean-field model of optical bistability 02 p0236 A83-12402
- Intracavity phase switching and phase-plane dynamics of a bistable optical device 02 p0236 A83-12404
- Intrinsic bistable guided-wave devices - Theory and applications 03 p0393 A83-13771
- Periodic oscillations and chaos in optical bistability - Possible guided-wave all-optical square-wave oscillators 03 p0394 A83-13792
- Closely coupled twin-stripe lasers 04 p0486 A83-16220

- A one-dimensional-map model for noise-induced transitions between bistable states 11 p1649 A83-28066

- Stochastic resonance in a bistable system 20 p3043 A83-43565

BISTATIC RADAR**U MULTISTATIC RADAR****BISTATIC REFLECTIVITY**

- Spaceborne bistatic synthetic aperture imaging radar 01 p0020 A83-10087
- Bistatic radar reflectivities of Pruppacher-and-Pitter form raindrops at 14.3 and 5.33 GHz 08 p1075 A83-22041
- Signal detection in a clutter environment in a bistatic system 08 p1078 A83-23156
- Measurement of autocorrelation functions in a bi-static incoherent scatter radar 09 p1249 A83-24694
- Reduction of bistatic scattering matrix measurements for inversely symmetric radar targets 10 p1405 A83-26828
- Comparison of the bistatic cross-section and reflectivities of spherical and spheroidal raindrops at microwave frequencies 16 p2343 A83-36578
- The results of investigation of some regions of Venus by bistatic radiolocalization [IAF PAPER 83-212] 23 p3528 A83-47310

BIT ERROR RATE

- 11-GHz MIC QPSK modulator for regenerative satellite repeater 06 p0752 A83-18766
- Mitigation of pulsed RFI via automatic gain control 07 p0905 A83-19696
- Adjacent channel interference degradation with minimum shift keyed modulation 07 p0905 A83-19698
- Error probabilities in lasercom PPM systems 07 p0905 A83-19705
- Error rates for narrowband Manchester coded digital FM 07 p0909 A83-19748
- Viterbi decoder VLSI integrated circuit for bit error correction 07 p0917 A83-19755
- The effects of transmitter/receiver clock time base instability on coherent communication system performance 07 p0871 A83-19770
- Soft error in MOS dynamic RAM 07 p0918 A83-20072

- S/N and error rate evaluation for an optical FSK-heterodyne detection system using semiconductor lasers 07 p0994 A83-21594
- PCM sounds on digital subcarrier in television for a satellite broadcasting system 12 p1718 A83-29412
- Performance of a direct sequence spread-spectrum system with long period and short period code sequences 13 p1827 A83-30224
- Bit error rate evaluation of GSTDN/TDRSS communication links 15 p2125 A83-33734
- Average error probability for DS-SSMA communications - The Gram-Charlier expansion approach --- Direct Sequence-Spread Spectrum Multiple Access 15 p2147 A83-35117

- Bit-error rate of PSK heterodyne optical communication system and its degradation due to spectral spread of transmitter and local oscillator 16 p2342 A83-36003
- Au-Mg improved ohmic contacts to p-GaAs 16 p2346 A83-36004
- Performance of narrow-band Manchester coded FSK with discriminator detection 16 p2343 A83-36604
- The effects of noise correlation and power imbalance on terrestrial and satellite DPSK channels 16 p2344 A83-36906

- Comparison of memory chip organizations vs reliability in virtual memories 17 p2517 A83-37290
- Biased Gaussian noise source for digital-transmission-system simulations 18 p2675 A83-40395

- Computer modeling of spectral efficiency and sidelobe buildup effects in nonlinear satellite links 19 p2830 A83-41366

- TDMA site diversity switching experiments with Japanese CS 19 p2831 A83-41380
- A selective-repeat ARQ scheme and its throughput analysis 19 p2832 A83-41398
- Hybrid diversities in a spread spectrum mobile communication system 19 p2833 A83-41409
- Optimal symbol-by-symbol detection for duobinary signaling 22 p3272 A83-45739

BIT SYNCHRONIZATION

- Linear phase-locked loop theory for cyclostationary input disturbances 03 p0311 A83-13854
- Local area time dissemination by carrier-current waves --- in construction of transmission network for timing signals 03 p0328 A83-14167
- The Sirio-1 timing experiment 04 p0469 A83-16450
- The effects of transmitter/receiver clock time base instability on coherent communication system performance 07 p0871 A83-19770

- Bit synchronisation based on the sensitivity function 08 p1075 A83-21999
- Orbital error analysis of time synchronization via geostationary broadcast satellite 08 p1048 A83-22039
- High-speed decoding technique for slip detection in data transmission systems using modified cyclic block codes 09 p1249 A83-24115
- Asynchronous and clocked control structures for VLSI based interconnection networks 13 p1909 A83-30792
- Landsat-D wideband unbalanced QPSK demodulator/bit synchronizer signal conditioner 19 p2813 A83-41359

- The optimization of Walsh signals for the fast synchronization of receivers 22 p3271 A83-45657
- A class of phase detector characteristics for symbol synchronizers yielding unbiased estimates 22 p3272 A83-45737

- Synchronous and channel-sense asynchronous dynamic group-random-access schemes for multiple-access communications 22 p3272 A83-45738
- Single-mode fiber systems for deep space communication network 22 p3360 A83-46657

BIVARIATE ANALYSIS

- Accuracy of univariate, bivariate, and a 'modified double Monte Carlo' technique for finding lower confidence limits of system reliability 08 p1114 A83-22712
- k-Dimensional polar quantizers for Gaussian sources 15 p2221 A83-35106

BL LACERTAE OBJECTS

- A rapid outburst of BL Lac at 2.72 GHz 01 p0126 A83-10955
- A search for short time variability in the radio emission from active galaxies 01 p0118 A83-10968
- Two multifrequency observations of the BL Lacertae object OJ 287 02 p0250 A83-11576
- Rapid variability of OJ 287 at 1.25 micron --- BL Lacertae object 03 p0413 A83-13308
- IUE observations of the BL Lac object AO 0235 + 164 03 p0408 A83-13926
- The calibration of a radio-independent search for BL Lac objects 03 p0408 A83-13929
- Variability of compact radio sources at a wavelength of 1 millimeter 03 p0422 A83-14181
- 1 millimeter continuum observations of quasars 03 p0422 A83-14182
- Multiperture infrared photometry of extragalactic radio sources 06 p0828 A83-18180
- Low frequency asymptotic spectra of multiple, decelerating adiabatic bursts 06 p0843 A83-19486
- The radio variability of BL Lacertae objects 07 p1010 A83-19852
- Flux density measurements of bright extragalactic sources at 36.8 GHz 07 p1006 A83-20564
- Optical spectroscopy of flat spectrum radio sources 07 p1008 A83-21213
- Optical positions of four benchmark radio sources 09 p1354 A83-24481
- The arc second radio structure of 12 BL Lacertae objects 10 p1493 A83-25702
- Opacity effects at radio wavelengths in the quasar 1308 + 326 10 p1504 A83-25737
- Studies of BL Lacertae objects with the Einstein X-ray observatory - The absolute volume density 10 p1507 A83-26354
- Why are broad emission lines seen in Seyfert galaxies and not in BL Lacertae objects 10 p1507 A83-26355

- The wavelength dependence of polarization in BL Lac objects 11 p1682 A83-28282
- The UV spectrum of the BL Lac object PKS 0521-36 13 p1956 A83-31683

- Extragalactic 1 millimeter sources - Simultaneous observations at centimeter, millimeter, and visual wavelengths 14 p2098 A83-33184

- High-redshift objects as probes of nearby cosmic voids 15 p2272 A83-34792
- TV photometric observations of 10 extragalactic peculiar objects 17 p2589 A83-37685
- The variability of 3C 273, OJ 287, and PKS 0735 + 17 in radio and optical emissions 17 p2601 A83-37710
- Observations of radio sources by the 22-m radio telescope at the Crimean Astrophysical Observatory and the 14-m radio telescope at the Radio Laboratory of the Helsinki University of Technology at millimeter wavelengths 17 p2590 A83-37712
- The discovery of an X-ray bright BL Lacertae object - 0414 + 009 17 p2592 A83-37936
- Is it possible to turn an elliptical radio galaxy into a BL Lac object? 17 p2607 A83-38262
- CCD photometry of the BL Lacertae object 1400 + 162 and the associated group of galaxies 20 p3059 A83-43040

- The nature of the nebula around BL Lacertae 21 p3222 A83-44401

- Quasi-simultaneous ultraviolet and optical observations of PKS 2155-304 = H2155-304 21 p3223 A83-44448
- Optical variability, absolute luminosity, and the Hubble diagram for QSOs 21 p3235 A83-45527
- The optical variability and spectrum of PKS 2155-304 21 p3235 A83-45528
- Photoelectric comparison sequences in the fields of four BL Lacertae objects 22 p3372 A83-46378
- Reverse stellar evolution, stellar ablation, and the origin of gas in quasars 22 p3380 A83-46973
- Multifrequency observations of OV226 (1921-293) reveal an unusual spectrum --- BL Lacertae object, quasar 23 p3526 A83-47872
- Far ultraviolet observations of BL Lac objects 24 p3661 A83-49560
- BLACK AND WHITE PHOTOGRAPHY**
- Mapping erosion with airphotos - Panchromatic or black and white infrared 05 p0657 A83-17839
- On the reduction of the distorting effect of the atmosphere in the digital processing of space imagery 10 p1444 A83-26822
- BLACK BODY RADIATION**
- Low background spectral response of 30-130-micron detectors from blackbody measurements 03 p0324 A83-13458
- Inner structure and entropy production 04 p0544 A83-14960
- A general upper limit on the mass and entropy production of a cluster of supermassive objects 04 p0549 A83-14994
- A black body for absolute stellar measurements 06 p0764 A83-19193
- New design for blackbody simulator cavities 08 p1104 A83-22877
- Mass scales in a universe of dust and blackbody radiation 11 p1679 A83-27989
- Questions about the experimental status of black-body radiation 12 p1775 A83-29041
- The central X-ray source in RCW 103 - Evidence for blackbody emission 15 p2258 A83-34103
- Hot big bang and quark gas 16 p2434 A83-36883
- Blackbody-pumped CO2 laser experiment [AIAA PAPER 83-1701] 17 p2513 A83-37198
- Non-absorption dips in the spectra of gamma-ray bursts 18 p2777 A83-39962
- Pulselike character of blackbody radiation from neutron stars 20 p3068 A83-42454
- Estimates of the applicability of the black-body approximation to the emission of the atmosphere at the horizon 24 p3605 A83-49290
- Black-body radiation shifts in ground and metastable levels of Mg and Ca 24 p3626 A83-49524
- BLACK HAWK ASSAULT HELICOPTER**
- U H-60 HELICOPTER
- BLACK HOLES (ASTRONOMY)**
- The external field of a rotating and charged body in the vector graviton metric theory 01 p0119 A83-10232
- A comparison of the entropies of collapsing stars and black holes 01 p0119 A83-10234
- The distribution of stars around a black hole - Numerical solution of the kinetic equation with collisions 01 p0125 A83-10932
- Thick supercritical accretion disks and active galactic nuclei 01 p0128 A83-11340
- Radiation from a black hole - A Vaidya-metric-based computation 02 p0254 A83-12027
- Theory of electron-positron showers in double radio sources 02 p0255 A83-12111
- The nature of the central parsec of the Galaxy 02 p0255 A83-12114
- Do black holes exist at the centres of globular clusters 02 p0260 A83-12525
- Transonic accretion flow in a thin disk around a black hole 03 p0427 A83-14713
- Transonic disk accretion of barytropic gas onto black holes 03 p0427 A83-14714
- High energy gamma-rays from black holes 03 p0439 A83-14721
- Are thick accretion disks the 'central engine' for astrophysical jets 03 p0431 A83-14875
- SS 433 - New results 03 p0431 A83-14929
- A semiquantitative general-relativistic model of quasar Markarian 205 interpreted as a massive black hole ejected from NGC 4319 04 p0549 A83-14989
- The passage of a star by a massive black hole 04 p0554 A83-15638
- Are there black holes in quasars 05 p0696 A83-16862
- The fluctuation of black hole's energy and the upper bound to the temperature of the radiation in the vicinity of black hole 05 p0701 A83-17147
- On crossing the Cauchy horizon of a Reissner-Nordstroem black-hole 06 p0824 A83-17972
- Stationary spherical accretion into black holes - The transition from the optically thin to the optically thick regime 06 p0825 A83-18089
- Null geodesics in the static Ernst space-time 06 p0828 A83-18328
- Observable blueshifts near compact objects 06 p0834 A83-18883
- Inhomogeneity of the early Universe and formation of primordial black holes 06 p0837 A83-19217
- 'Maximally hard' universe and mass spectrum of primordial black holes 06 p0839 A83-19230
- Thick accretion disks around black holes /Karl Schwarzschild Lecture 1981/ 06 p0846 A83-19529
- Activity in the centers of galaxies 06 p0846 A83-19530
- Vacuum polarization near the horizon of a black hole in the presence of boundaries 06 p0847 A83-19610
- Black hole explosions 07 p1013 A83-20404
- Black holes and the stability of gravitation 08 p1180 A83-22202
- Electromagnetic test fields near a Schwarzschild horizon 08 p1180 A83-22210
- The global hyperbolicity of the dependence domain of a closed achronal set in general relativity 09 p1338 A83-23597
- Evaluation of characteristic parameters for Schwarzschild, extreme Kerr, and Hawking black holes 09 p1356 A83-23683
- How to mine energy from a black hole 10 p1506 A83-26091
- Models of massive black holes in the active galactic nuclei 10 p1507 A83-26231
- Toward explaining Seyfert galaxies 10 p1507 A83-26357
- The dynamics and fueling of active nuclei 10 p1508 A83-26359
- Comptonization effects in spherical accretion onto black holes 10 p1515 A83-26739
- Vacuum polarization near a black hole creating particles 10 p1517 A83-26970
- Energy, momentum and angular momentum of gravitational radiation from a particle plunging into a non-rotating black hole 11 p1679 A83-28070
- Evolution of accretion tori orbiting black holes. I - Theory 11 p1682 A83-28281
- Active galaxies and the diffuse gamma-ray background 11 p1694 A83-28389
- A mathematical solution of general relativistic binary systems 12 p1791 A83-28989
- Astrophysical consequences of barytinos 12 p1794 A83-29085
- Temperature profile of accretion disk around a Kerr black hole 12 p1795 A83-29354
- Runaway instability in accretion disks orbiting black holes 12 p1795 A83-29449
- Polarisation of the vacuum near a black hole inside a spherical cavity 13 p1947 A83-30518
- Dustlike stages in the early universe, and constraints on the primordial black hole spectrum 13 p1948 A83-31254
- The structure of the inhomogeneity field and the formation of primordial black holes 13 p1948 A83-31255
- Thick disks with equatorial accretion. II 13 p1955 A83-31660
- Tidal compression of a star by a large black hole. I 13 p1959 A83-31747
- Mechanical evolution and nuclear energy release by proton capture 13 p1959 A83-31747
- Thin charged shells and the violation of the third law of black hole mechanics 14 p2102 A83-33044
- Scattering and absorption of slow particles by a black hole 14 p2110 A83-33391
- Nonlinear effects in a gravitating plasma disk subject to a poloidal magnetic field 15 p2254 A83-33721
- Stationary axially symmetric perturbations of the Reissner-Nordstrom black hole. I - Equations for the perturbations 15 p2254 A83-33771
- Magnetic monopoles and evaporating black holes 15 p2254 A83-33793
- Black hole accretion - The quasar powerhouse 15 p2254 A83-33813
- Does stellar collapse produce supernovae or black holes? 15 p2254 A83-33814
- Monte Carlo simulations of the evolution of galactic nuclei containing massive, central black holes 15 p2256 A83-34084
- The question of an upper bound on entropy --- in black holes and closed thermodynamic systems 15 p2239 A83-34138
- The abnormal temperature profile of accreting disk around the Kerr black hole 15 p2262 A83-34527
- An outline of approach linking black-hole-evaporation with quantum-field effects in flat spacetime 15 p2262 A83-34531
- A 300-day periodicity of CYG X-1 15 p2247 A83-34558
- The influence of gravitational wave momentum losses on the centre of mass motion of a Newtonian binary system 15 p2265 A83-34592
- Gravitational radiation from particles falling along the symmetry axis into a Kerr black hole - The momentum radiated 15 p2269 A83-34640
- The infall of a star into a massive black hole 15 p2269 A83-34641
- Black holes, white dwarfs, and neutron stars: The physics of compact objects --- Book 17 p2595 A83-37164
- Searching for black holes 17 p2588 A83-37368
- Instability of some black holes 17 p2605 A83-38047
- Are black holes necessary? 17 p2612 A83-38617
- The black hole formed by electromagnetic radiation 17 p2614 A83-38958
- Magnetic field in the spherical accretion of black holes 18 p2766 A83-39247
- Active galactic nuclei as clusters of accreting black holes 18 p2766 A83-39248
- Black holes in neutrino fields 18 p2767 A83-39529
- On the hypothesis of ejection of supermassive black holes from centers of galaxies and its application to quasar-galaxy associations 18 p2775 A83-39758
- The compact source at the galactic center 19 p2913 A83-40697
- Positron production near a 1,000,000 solar mass black hole 19 p2913 A83-40698
- Interaction of a rotating charged black-hole with a uniform magnetic field 19 p2915 A83-40730
- Initial data for N black holes 19 p2915 A83-40888
- Gravitational radiation from a particle with zero orbital angular momentum plunging into a Kerr black hole 19 p2916 A83-41171
- Local toroidal black holes that are static and axisymmetric 19 p2916 A83-41292
- A charged black hole in a uniform magnetic field 19 p2916 A83-41306
- The relationship between the X-ray and optical luminosities for QSOs 20 p3071 A83-43045
- The high-energy spectrum of hot accretion disks 20 p3073 A83-43072
- Super-Eddington luminosity characteristics of active galactic nuclei 21 p3230 A83-44439
- Neutrino emission from black holes 21 p3231 A83-44450
- Discovery of a massive unseen star in LMC X-3 21 p3236 A83-45537
- The dynamics of dissipatively heated spherical accretion --- onto black holes 21 p3238 A83-45561
- The influence of quantum effects on the structure of space-time near singularities in general relativity 23 p3504 A83-48445
- Occupation of quasi-bound states by electrons in a Schwarzschild field 24 p3651 A83-49066
- Black hole electromagnetic fields and negative energy states for charged particles 24 p3668 A83-50092
- BLACK SEA**
- Some features of the water circulation of the Black Sea according to Meteor-satellite data 07 p0971 A83-19909
- BLACKOUT (PHYSIOLOGY)**
- Successful reversal of presumed carbon monoxide-induced semicoma 18 p2734 A83-40362
- BLACKOUT (PROPAGATION)**
- NT ATMOSPHERICS
- NT COSMIC NOISE
- NT DAWN CHORUS
- NT ELECTROMAGNETIC NOISE
- NT HISS
- NT IONOSPHERIC CROSS MODULATION
- NT IONOSPHERIC NOISE
- NT IONOSPHERICS
- NT POLAR RADIO BLACKOUT
- NT SHOT NOISE
- NT THERMAL NOISE
- NT WHISTLERS
- NT WHITE NOISE
- BLADDERS (MECHANICS)**
- U DIAPHRAGMS (MECHANICS)
- BLADE SLAP NOISE**
- Theoretical and experimental study of helicopter rotor noise [ONERA, TP NO. 1982-74] 08 p1044 A83-23247
- A comparison of model helicopter rotor Primary and Secondary blade/vortex interaction blade slap [AIAA PAPER 83-0723] 10 p1475 A83-25934
- The prediction of the noise of supersonic propellers in time domain - New theoretical results [AIAA PAPER 83-0743] 10 p1377 A83-25945
- Noise generation by a finite span swept airfoil [AIAA PAPER 83-0768] 11 p1652 A83-28023
- Full-scale measurements of blade-vortex interaction noise 15 p2227 A83-33505

BLADE TIPS

- Full-scale measurements of blade-vortex interaction noise 16 p2298 A83-35947
- Aeroacoustic flight test of four single engine propellers [SAE PAPER 830731] 20 p2936 A83-43328
- An aeroacoustic model for high-speed, unsteady blade-vortex interaction 20 p3044 A83-43437
- Experimental methods in compressor noise studies [ONERA, TP NO. 1983-79] 23 p3505 A83-48194

BLADE TIPS

- Helicopter blade tips 02 p0132 A83-11778
- [AAAF PAPER NT 81-19] 02 p0132 A83-11778
- Studies of aerofoils and blade tips for helicopters 05 p0589 A83-17317
- An investigation of the aerodynamics of an RAE swept tip using a model rotor 06 p0712 A83-18426
- [ONERA, TP NO. 1982-76] 06 p0712 A83-18426
- The dynamic inducer as a cost-effective wind turbine system 06 p0779 A83-18457
- A note on the tip noise of rotating blades 09 p1340 A83-23708
- On high frequency broadband noise from model helicopter rotors 10 p1473 A83-25908
- [AIAA PAPER 83-0673] 10 p1473 A83-25908
- Turbine blade nonlinear structural and life analysis 12 p1703 A83-29024
- The structure of trailing vortices generated by model rotor blades 12 p1696 A83-29404
- Tip clearance flow in a compressor rotor passage at design and off-design conditions 16 p2291 A83-35855
- Numerical calculations of time dependent three-dimensional viscous flows in a blade passage with tip clearance 16 p2294 A83-36258
- [AIAA PAPER 83-1171] 16 p2294 A83-36258
- Heat transfer at the tip of an unshrouded turbine blade 20 p2975 A83-42706
- Non-uniform flows in axial compressors due to tip clearance variation 24 p3548 A83-48824
- Parametric tip effects for conformable rotor applications 24 p3548 A83-50140

BLANKING (CUTTING)

- The expansion of conical blanks by means of an elastic medium --- pressing technique for aircraft under-wing fuel tank parts 12 p1733 A83-29288

BLAST LOADS

- Instrumentation for the measurement of blast waves attenuated by water sheets 01 p0052 A83-11062
- The effects of firing a weapon on the air intake in a subsonic flow 02 p0132 A83-11772
- [AAAF PAPER NT 81-11] 02 p0132 A83-11772
- Dynamic spalling in rarefaction waves 03 p0339 A83-13596
- Computing the reflection of a point-blast wave from a plane 04 p0476 A83-15098
- Recording shock waves by means of Manganin transducers and the pressures of the graphite-diamond transition at elevated temperatures 06 p0761 A83-18010
- The propagation of powerful blast waves in a gas-particle mixture 07 p0878 A83-19633
- Blast waves in free air 09 p1264 A83-25272
- A shock-on-shock interaction model for multiconic interceptors 17 p2456 A83-38671
- [AIAA PAPER 83-1843] 17 p2456 A83-38671
- Deformation of a cylindrical shell during an explosion in the vicinity of a concentrated explosive charge 24 p3595 A83-49905

BLASTOFF

- U ROCKET LAUNCHING

BLEACHING

- Amplitude and phase nonlinear response of bleachable dyes using picosecond excitation 14 p2026 A83-33431

BLEED-OFF

- U PRESSURE REDUCTION

BLENDS

- U MIXTURES

BLINDNESS

- The electric reactions of the cat brain to light following the section of the optic tracts 05 p0672 A83-17636

BLISTERS

- Blister formation in Pd gate MIS hydrogen sensors 05 p0645 A83-17290

BLOCH BAND

- The Bloch-FET - A lateral surface superlattice device 05 p0690 A83-17289

BLOCK DIAGRAMS

- A class of codes with unequal protection of symbols, based on balanced incomplete solvable block-schemes 01 p0094 A83-10567
- 32K bit MNOS BORAM --- Block Oriented RAM 01 p0089 A83-11211

BLOCKING

- The characteristics of the mechanism of action of cyproheptadine /peritol/ on the activity of the hypothalamo-hypophysial-adrenal system 07 p0974 A83-20979
- Beta adrenergic blockade and erythropoietic production in rats after hypoxia and hypovolemia 09 p1321 A83-23875
- Diagnostic analysis and spectral energetics of a blocking event in the GLAS climate model simulation 10 p1449 A83-25380

BLOOD

- NT EOSINOPHILS
- NT ERYTHROCYTES
- NT LEUKOCYTES
- NT LYMPHOCYTES
- NT WHITE BLOOD CELLS
- The gas composition and the acid-base state of the blood in twins when breathing a hypoxic gas mixture 01 p0082 A83-10492
- The effect of physical exercise on changes of lysozyme in the blood of athletes 01 p0084 A83-11388
- Rapid monitoring of the acid-base and gas composition of the blood 03 p0375 A83-14334
- The role of the lung in the formation of the rheological properties of the blood 05 p0670 A83-17183
- The behavior of blood serum proteins separated by electrophoresis in animals during hypokinesia 06 p0795 A83-19373
- The effect of a high-pressure gaseous environment on the content of sodium, potassium, and water in the blood and tissues of white rats 07 p0973 A83-20246
- Acid-base curve and alignment nomograms for swine blood 13 p1898 A83-30500
- The characteristics of the changes of several biochemical parameters of the blood during the testing of the general endurance of middle distance runners 14 p2070 A83-33305
- The mechanism which provides for urea removal after protein loads 16 p2398 A83-35911
- Ultraviolet-irradiated blood - Photochemistry, immunological action 16 p2393 A83-35920
- The functional activity and metabolism of neutrophils of the blood under the effect of low-intensity microwaves 16 p2395 A83-36834
- The effect of thyroxin on the concentration of lipoproteins of various densities in the blood serum of rats 17 p2556 A83-38075
- The effect of low-frequency acoustic vibrations on the phospholipid composition of the whole blood and some tissues of animals 17 p2556 A83-38187
- The effect of a constant electromagnetic field on the EKG parameters and several indicators of the blood in experimental conditions 21 p3184 A83-45306
- The pattern of the changes in the concentration of catecholamines and acetylcholine in the blood during the prolonged action of a constant magnetic field with a high induction 21 p3186 A83-45379

BLOOD CIRCULATION

- NT BRAIN CIRCULATION
- NT CORONARY CIRCULATION
- NT ISCHEMIA
- NT OCULAR CIRCULATION
- NT PERIPHERAL CIRCULATION
- NT PULMONARY CIRCULATION
- Two types of adaptation reactions of the blood circulation apparatus 03 p0379 A83-13616
- The hemodynamic parallels between the types of central and cerebral blood circulation in individuals with normal arterial pressure 03 p0379 A83-13618
- The adaptive properties of the major arterial vessels 03 p0379 A83-13620
- The effects of hypotensive drugs on the humoral factors of the regulation of blood circulation 03 p0380 A83-13631
- Measurement of the specific electrical resistance of the blood 03 p0381 A83-14330
- The state of hepatic circulation under the combined effect of lead and electromagnetic fields 05 p0673 A83-17159
- The positive effect that reduced venous return has on blood circulation in cases of myocardial infarction 05 p0671 A83-17217
- A circulating inhibitor of /Na⁺/ + /K⁺/ + // ATPase associated with essential hypertension 05 p0672 A83-17794
- The coefficient of capillary filtration in the skeletal muscles during changes in their hemodynamics 07 p0973 A83-20360
- The substance 'P' and the microcirculatory system during stress --- peptide 07 p0975 A83-20987
- The determination of the circulating immune complexes in humans 07 p0978 A83-20999

- The effect of low frequency vibrations on the human cardio-circulatory system - A measurement technique and results for an 18 Hz sinusoidal vibration 08 p1149 A83-22978

- The physiology and pathology of the venous blood circulation of the lower extremities --- Russian book 09 p1322 A83-23822

- Comparison of cardiovascular effects of space flight and its analogs using computer simulations 11 p1642 A83-27792

- The reaction of the central blood circulation of healthy individuals to the decompression of various areas of the body 12 p1764 A83-29306

- An investigation of the microcirculatory bed in flightcrew members with conjunctivitis during the initial appearance of cerebral atherosclerosis 13 p1905 A83-30949
- Physiological assessment of right-side and left-side cardiohemodynamics in patients with hypertension 13 p1906 A83-31395

- The problem of microcirculation and eye pathology 15 p2210 A83-34940

- Hemodynamic shifts in response to isometric loads in humans in the case of various initial indicators of systemic blood circulation 16 p2398 A83-35910

- The characteristics of thermoregulation and blood circulation during prolonged exposure to low temperature 16 p2398 A83-35912
- O₂ transport during two forms of stagnant hypoxia following acid and base infusions 17 p2554 A83-36992

- The diagnosis of changes in the vessels and membranes of eyes using fluorescent angiography 17 p2560 A83-38202

- The determination of the volume of rapidly circulating blood by a thermal dilution method 18 p2732 A83-40553

- The blood supply of the trachea and bronchi of rats 18 p2733 A83-40584

- The change in the reaction of systemic and regional blood circulation to immobilization stress in rats in the case of pharmacological desympathization 19 p2871 A83-40816

- Circulating macromolecular complexes in rats following radiation, thermal, and combined trauma 19 p2874 A83-41011

- Hemodynamic interrelations of the systemic and pulmonary blood circulation in the case of hypertension 19 p2880 A83-41426

- Differences in the response of systemic blood circulation to loading tests depending on the sex and age of the subject 19 p2881 A83-41431

- The system of the regulation of the aggregation condition of the blood in patients with ischemic heart disease 19 p2882 A83-41453

- The development of several ideas of V. V. Parin in the physiology and the pathophysiology of blood circulation 19 p2875 A83-41461

- The effect of prostaglandin analogs on systemic blood circulation 19 p2879 A83-42097

- Three position of the body and the regulation of blood circulation --- Russian book 21 p3184 A83-45002

- High altitude physiology and medicine --- Book 21 p3188 A83-45090

BLOOD COAGULATION

- The response of the lymph and blood coagulation systems to gamma-radiation at high altitudes 14 p2062 A83-32064
- The role of erythrocytes in blood coagulation and in blood platelet formation 14 p2065 A83-33319
- The suppression of blood platelet aggregation with immune complexes. I - Clinical investigations 14 p2070 A83-33331
- The effect of the antioxidant OP-6 on several model reactions of the blood coagulation system 16 p2395 A83-36830
- The system of the regulation of the aggregation condition of the blood in patients with ischemic heart disease 19 p2882 A83-41453
- The effect of an antioxidant on the recovery of hemopoiesis and the aggregation of thrombocytes 21 p3186 A83-45380

BLOOD FLOW

- The automatic stabilization of pressure in the main arteries during changes in the blood flow 01 p0080 A83-10545
- The initial manifestations of the defects of blood supply to the brain /Review of the literature/ 03 p0380 A83-13642
- The rheology of the blood --- Russian book 04 p0520 A83-15828
- Models for a comparative functional analysis of gas exchange organs in vertebrates 05 p0671 A83-17326

The blood supply and oxygen consumption in the gastrocnemius muscle of cats during isometric tetanus under conditions of intraarterial infusions of noradrenaline 07 p0973 A83-20244

A viscosimeter for the investigation of the rheological characteristics of blood 07 p0931 A83-20998

The changes of the blood flow during longitudinal strains of the gastrocnemius muscle in cats 08 p1145 A83-22106

The interrelationship of the intracranial pressure, the blood volume of the skull cavity, and the total blood flow of the brain 08 p1145 A83-22108

The blood supply and the oxygen consumption of the gastrocnemius muscles of cats during isometric tetanus in conditions of a partial arterial occlusion 08 p1145 A83-22110

Measurements and imaging method of blood flow profile in human heart 08 p1151 A83-22237

Evaluation of a Reverse Gradient Garment for prevention of bed-rest deconditioning 10 p1458 A83-25664

The efficiency of the physiological changes of the heat conductance and the heat and mass transfer in the skin of humans during thermoregulation 10 p1455 A83-26789

Changes in the loco-regional cerebral blood flow /r.C.B.F./ during a simulation of weightlessness 11 p1641 A83-27349

Dynamic response of local pulmonary blood flow to alveolar gas tensions - Analysis 13 p1789 A83-30473

The aminergic control of the cerebral arteries 14 p2063 A83-32099

The radioisotope (Xe-133) inhalation method for determining the regional brain blood flow 15 p2212 A83-34928

An ultrasonic investigation of the blood flow in various parts of the vascular bed of the lungs of cats 15 p2211 A83-34966

The differential diagnosis of functional murmurs and defects of the heart using ultrasonic pulse Doppler detection 18 p2734 A83-40541

The role of collateral coronary blood flow in the compensation of regional disorders of the energy metabolism of heart muscle during experimental myocardial ischemia 18 p2732 A83-40544

Investigations of the microcirculatory bed of the brain in experimental conditions. II - Disorders of blood flow following craniocerebral trauma 18 p2733 A83-40575

The neural apparatus of the coronary arteries in normal conditions and in patients with ischemic heart disease 18 p2736 A83-40585

Local cerebral blood flow increases during auditory and emotional processing in the conscious rat 19 p2873 A83-40906

Computation of turbulent flow through constrictions 21 p3130 A83-44588

Rheological properties of the arterial and venous blood of rats following intravital icing of the extremities 21 p3185 A83-45325

The relationship between blood flow, partial pressure, and oxygen demand in the human cortex (A theory of tissue gas exchange) 23 p3497 A83-47113

Cardiovascular exploration in microgravity. French-Soviet flight aboard Saliout VII - June 1982 [IAF PAPER 83-194] 23 p3498 A83-47308

Effect of wall scattering on SNR in off-axis differential-type laser Doppler velocimetry 24 p3581 A83-48747

BLOOD PLASMA

Reduction in plasma calcium during exercise in man 01 p0082 A83-10212

The changes in the content of corticosterone in the blood plasma of inbred mice after exposure to stress 01 p0080 A83-10541

The use of chromatography for determining kallikrein and prekallikrein in canine blood serum 01 p0080 A83-10546

Antibodies to streptococcal lipoproteinase in the blood of healthy persons 01 p0083 A83-10554

The complement and its role in the regulation of immunological reactions 01 p0082 A83-11407

The 'volume-dependent' form of essential hypertension 03 p0379 A83-13617

The activity of renin in blood plasma, the indicators of central hemodynamics, and the water-electrolyte balance in patients with hypertension 03 p0379 A83-13622

The assay of glycosaminoglycans in the blood serum 03 p0375 A83-14333

The functional characteristics of the immune response stimulators circulating in the blood in a toxic affection of the liver 05 p0670 A83-17182

Plasma electrolyte content and concentration during treadmill exercise in humans 05 p0674 A83-17331

The role of the kidneys and extrarenal mechanisms in the regulation of the concentration of sodium in the blood plasma of rats during the intravenous injection of a hypertonic solution of sodium chloride 08 p1145 A83-22115

An investigation of human blood, erythrocytes, and plasma using the method of ESR at 77 K 08 p1150 A83-23022

An investigation of the genotypic conditionality of the gas composition and acid-base state indicators of the blood during various effects on the body 09 p1323 A83-25152

An evaluation of plasma volume expanders in the treatment of decompression sickness 10 p1453 A83-25668

Hormonal and renal responses to plasma volume expansion after horizontal restraint in the rhesus monkey 11 p1636 A83-27799

The relative contributions of gravity, buoyancy, and cold to the changes of human plasma volume during simulated weightlessness 11 p1643 A83-27802

Influence of abdominal restriction on gas exchange during +Gz stress in dogs 11 p1637 A83-27809

The level of endogenous ethanol and its connection with the voluntary consumption of alcohol by rats 11 p1641 A83-28525

The role of the middle hypothalamus structures in the regulation of the glucose content in the blood and the glycogen content in the liver 13 p1895 A83-30304

The interaction of plasma lipoproteins with bilateral lipid membranes - The role of the surface charge 13 p1895 A83-30405

Blood lactate threshold in some well-trained ischemic heart disease patients 13 p1902 A83-30452

Blood osmolality in vitro - Dependence on P(CO2), lactic acid concentration, and O2 saturation 13 p1902 A83-30459

Blood osmolality during in vivo changes of CO2 pressure 13 p1902 A83-30460

Plasma volume shifts during progressive arm and leg exercise 13 p1903 A83-30475

Muscle fiber composition and blood ammonia levels after intense exercise in humans 13 p1903 A83-30480

Anaerobic threshold, blood lactate, and muscle metabolites in progressive exercise 13 p1905 A83-30503

A calorimetric approach to investigating the effect of electromagnetic radiation at radio frequencies on the plasmatic membrane of erythrocytes 13 p1900 A83-31334

The activity of 5-nucleotidase in leukocytes, erythrocytes, and blood serum of rats with radiation sickness 14 p2062 A83-32061

The intensity of kinergetic reactions of the cardiovascular system for various levels of the activity of the kallikrein-kinin system in blood plasma 14 p2064 A83-32569

The effect of T and B lymphocytes on the phagocytotic activity of polymorphonuclear neutrophils in the peripheral blood of humans 14 p2070 A83-33333

The role of the osmolality of the blood serum in the pathogenesis of Meniere's disease 15 p2211 A83-34423

The determination of circulating immune complexes by a spectrophotometric method 15 p2213 A83-34950

Changes of the hormonal spectrum of the blood under the effect of microwaves in the centimeter range 18 p2733 A83-40571

The content of immunoglobulins in the blood serum of patients with various forms of chronic inflammation of the middle ear 19 p2883 A83-41826

Renin-aldosterone and angiotensin-converting enzyme during prolonged altitude exposure 22 p3347 A83-45984

BLOOD PRESSURE

NT DIASTOLIC PRESSURE

NT HYPERTENSION

NT HYPOTENSION

NT LOWER BODY NEGATIVE PRESSURE

NT SYSTOLIC PRESSURE

The automatic stabilization of pressure in the main arteries during changes in the blood flow 01 p0080 A83-10545

A comparison of the cardiovascular responses to isometric exercise of three different sized muscle groups 01 p0083 A83-11139

The use of prostaglandin E2 during the treatment of essential hypertension which proceeds with high blood pressure 03 p0379 A83-13623

Dynamics of heart rate and blood pressure in the evaluation of the functional condition of swimmers 03 p0382 A83-14350

A theoretical analysis of the regularities of the Bainbridge reflex --- heart rate acceleration by blood pressure increase 04 p0520 A83-15894

Attenuation of hypoxic pulmonary vasoconstriction by pulsatile flow in dog lungs 05 p0672 A83-17336

An investigation of the participation of the venous return in the pressor changes of systemic hemodynamics by means of the automatic control of its size 08 p1145 A83-22107

The distensibility of the veins of skeletal muscles during shifts in the level of hydrostatic venous pressure 08 p1145 A83-22109

Effects of ageing on cardiorespiratory changes to moderate physical exercise 09 p1323 A83-24005

Cardiovascular and endocrine effects of gravitational stresses /LBNP/ - The influence of angiotensin-converting enzyme inhibition with captopril 11 p1642 A83-27798

Comparative study of various noninvasive methods of arterial pressure recording 17 p2562 A83-38179

The semantic structure of interpersonal evaluations and self-evaluations in individuals with normal and elevated arterial pressure 19 p2885 A83-41838

The effect of controlled hyperthermia on several hemodynamic parameters in experimental conditions 21 p3185 A83-45324

Brain peptides and the regulation of blood pressure 21 p3185 A83-45375

BLOOD VESSELS

NT AORTA

NT ARTERIES

NT CAPILLARIES (ANATOMY)

NT GLOMERULUS

NT VEINS

The changes in the structural components of the walls of the small vessels and the composition of the peripheral blood during immune and hypoxic effects on the heart 01 p0078 A83-10487

The effect of tobacco smoking on the microcirculation in the vessels of the bulbar conjunctiva in healthy young individuals 01 p0082 A83-10509

The arterial vascular bed of the human mesenteric lymph nodes 03 p0380 A83-13644

The dependence of the character of the recovery of pulse on the rhythm of the heart and the lability of the sinusoid nodes in athletes after step loads 03 p0382 A83-14355

The adrenoreactivity of the vessels of the small intestine in cats during the process of high altitude adaptation 07 p0973 A83-20245

The changes in the venous endothelium after acute hemodynamic disorders 07 p0975 A83-20992

The formation of the vascular-receptor relations in the forearm muscles of humans 07 p0978 A83-20993

An ultrasonic investigation of the blood flow in various parts of the vascular bed of the lungs of cats 15 p2211 A83-34966

The diagnosis of changes in the vessels and membranes of eyes using fluorescent angiography 17 p2560 A83-38202

The blood supply of the trachea and bronchi of rats 18 p2733 A83-40584

The morphofunctional reorganization of the vessels of the microcirculatory bed under the influence of local cooling 23 p3497 A83-47114

The walls of vessels in atherogenesis and thrombogenesis (Investigations in the USSR) --- Russian book 24 p3617 A83-49073

BLOOD VOLUME

The 'volume-dependent' form of essential hypertension 03 p0379 A83-13617

The positive effect that reduced venous return has on blood circulation in cases of myocardial infarction 05 p0671 A83-17217

An evaluation of plasma volume expanders in the treatment of decompression sickness 10 p1453 A83-25668

ADH responses to volume shifts in the low pressure system --- AntiDiuretic Hormone 11 p1636 A83-27781

Hormonal changes in antihypertensive rats 11 p1637 A83-27800

The relative contributions of gravity, buoyancy, and cold to the changes of human plasma volume during simulated weightlessness 11 p1643 A83-27802

Effects of water immersion on plasma catecholamines in normal humans 13 p1902 A83-30465

Drinking and water balance during exercise and heat acclimation 13 p1903 A83-30471

Plasma volume shifts during progressive arm and leg exercise 13 p1903 A83-30475

Plasma volume, renin, and vasopressin responses to graded exercise after training 13 p1903 A83-30476

Blood volume and protein responses to skin heating and cooling in resting subjects 13 p1903 A83-30477

The adaptation of the body to physical load after a loss of blood 14 p2069 A83-33301

The determination of the minute volume of the blood by a thermal dilution method 19 p2876 A83-41845

Canine blood volume and cardiovascular function during hyperthermia 20 p3033 A83-43476

Effect of blood volume on forearm venous and cardiac stroke volume during exercise 22 p3347 A83-45959

BLOWDOWN WIND TUNNELS

Wind tunnel measurements with an electronically scanned multiport pressure sensor system 01 p0051 A83-11052

Transient ablation of blunt bodies at the angle of attack [AIAA PAPER 83-0583] 05 p0637 A83-16803

An experimental heat-transfer investigation of an advanced winged entry vehicle at Mach 10 [AIAA PAPER 83-0409] 06 p0714 A83-19589

A study of hypersonic low-density gas flows in low-pressure blowdown wind tunnels using pressure tanks 13 p1804 A83-30680

Single- and multiple-crater induced nosetip transition 16 p2293 A83-36078

BLOWERS

Effect of the volute casing on the flow in radial-flow blowers 09 p1263 A83-24649

BLOWING

A study of the efficiency of a gas screen on a rough surface 04 p0478 A83-16162

Laminar free convection on a vertical nonisothermal plate under strong injection 04 p0478 A83-16164

Effect of suction and blowing on boundary-layer transition [AIAA PAPER 83-0043] 05 p0578 A83-16483

Augmentation of fighter aircraft lift and STOL capability by blowing outboard from the wing tips [AIAA PAPER 83-0078] 05 p0578 A83-16507

The performance of a circulation control airfoil at transonic speeds [AIAA PAPER 83-0083] 05 p0579 A83-16510

Effect of pulsed slot suction on a turbulent boundary layer 07 p0863 A83-19825

Parameters for the simulation of high temperature blown shock layers 07 p0924 A83-19829

The erosion combustion of a solid fuel under various temperatures of the ventilating flow 07 p0901 A83-19951

A novel property of the displacement thickness in three-dimensional boundary-layer theory 14 p2013 A83-33381

Interaction of a jet at a lateral angle to a mainstream at low injection rates - An experimental study 16 p2290 A83-35818

Experimental investigation of the effects of wall suction and blowing on the performance of highly offset diffusers [AIAA PAPER 83-1169] 16 p2297 A83-36922

Theory of the combustion of condensed substances with blowing past them 18 p2663 A83-39163

The aerodynamic characteristics at the mid-span of a circular cylinder with tangential blowing 18 p2684 A83-39457

A study of heat and mass transfer in flows past bodies of various shapes with allowance for injection 19 p2844 A83-41577

The effect of Prandtl number on heat transfer from an isothermal rotating disk with blowing at the wall 24 p3578 A83-49574

BLOWN FLAPS**U EXTERNALLY BLOWN FLAPS****BLUE STARS**

The hot halo subdwarf binary system HZ-22 03 p0421 A83-14145

Absolute proper motions of selected blue objects in the area of the galactic north pole 05 p0695 A83-17862

U, B, V photometry of nests of interacting galaxies 06 p0819 A83-18826

Observations of RR Lyrae with the ANS satellite 06 p0821 A83-19057

H2215-086 -King of the DQ Hercules stars 06 p0846 A83-19526

Spectroscopy of blue stellar objects 09 p1357 A83-23735

Detection of a late B star companion of the bright cluster giant c Pup equals HD 63032 11 p1679 A83-27701

Objects with UV excess in the vicinity of the south galactic pole 14 p2099 A83-33238

Variations in the ultraviolet spectrum of the symbiotic star Z Andromedae 14 p2108 A83-33264

IUE observations of globular clusters and blue horizontal branch stars 15 p2244 A83-33594

Spectroscopy of upper-main-sequence and blue straggler stars in the intermediate-age cluster NGC 2477 15 p2246 A83-34501

The metal abundances of RR Lyrae stars in the globular clusters NGC 3201, NGC 4590, and NGC 6171 18 p2767 A83-39595

Identification of a blue object with a newly detected X-ray source 24 p3649 A83-50155

BLUFF BODIES

Methods for calculating the stabilization limits of a flame of inhomogeneous mixtures using a bluff body 02 p0136 A83-11512

Modification of vortex shedding in the synchronization range [ASME PAPER 81-WA/FE-25] 04 p0478 A83-16142

Investigation of wall induced modifications to vortex shedding from a circular cylinder 04 p0478 A83-16143

Limit amplitude of galloping cables --- effects of separated flow on Shuttle tank cable trays [AIAA PAPER 83-0132] 05 p0682 A83-16545

Nonlinear analysis of cavity flows around arbitrarily shaped bluff bodies in a constrained flow 06 p0758 A83-19020

Influence of the vortex shedding process on a bluff-body diffusion flame [AIAA PAPER 83-0335] 06 p0727 A83-19588

The prediction of the drag on structural beams 08 p1088 A83-23194

Optical studies of shock generated transient supersonic base flows 10 p1371 A83-26142

Flow around a normal plate of finite width immersed in a turbulent boundary layer 10 p1418 A83-26630

An experimental investigation of the wake of an axisymmetric body with a slanted base 11 p1526 A83-27873

Blockage effect on vortex shedding from bluff bodies 11 p1567 A83-28000

Turbulent shear flow behind hemisphere-cylinder placed on ground plane 15 p2119 A83-33664

Simultaneous CARS and luminosity measurements in a bluff-body combustor [AIAA PAPER 83-1481] 15 p2134 A83-34915

Similarity considerations of isothermal turbulent recirculating flowfields in axisymmetric bluff-body near wakes [AIAA PAPER 83-1203] 16 p2294 A83-36279

Influence of laminar flame speed on the blowoff velocity of bluff-body stabilized flames [AIAA PAPER 83-1327] 16 p2326 A83-36341

Numerical simulation of cold flow in an axisymmetric centerbody combustor [AIAA PAPER 83-1741] 17 p2467 A83-37219

Axisymmetric bluff-body drag reduction using circumferential grooves [AIAA PAPER 83-1788] 17 p2453 A83-38628

The effect of duct walls on the vortex formation in the wake of a bluff body 19 p2842 A83-41253

The principles governing the formation of circulation zones in the wake of mechanical and jet screens in confined flows 19 p2794 A83-42147

Heat transfer in a turbulent boundary layer behind a two-dimensional bluff body at different Pr numbers 20 p2977 A83-42722

A flying hot-wire system 21 p3138 A83-44681

Heat and mass transfer toward bluff bodies 21 p3133 A83-45348

Dynamic behavior of a bluff-body diffusion flame 21 p3110 A83-45584

BLUNT BODIES

Analysis of flows of an equilibrium dissociated, ionized, and radiating gas by the method of large particles 01 p0003 A83-11275

Comparison of different integration schemes based on the concept of characteristics as applied to the ablated blunt body problem 02 p0132 A83-13022

Blunt fin-induced shock wave/turbulent boundary-layer interaction 03 p0277 A83-13132

Turbulent boundary-layer flow over re-entry bodies including roughness effects 03 p0278 A83-13146

Numerical investigation of the problem of viscous reacting gas flow past blunt bodies 04 p0441 A83-15078

Flow of a rarefied gas past a sphere under the conditions of surface injection 04 p0442 A83-15099

Stationary shape of bodies ablating in hypersonic flow under the action of radiation heating 04 p0477 A83-15863

Transient ablation of blunt bodies at the angle of attack [AIAA PAPER 83-0583] 05 p0637 A83-16803

Approximate correction for the effect of injectants on the ionization level in the boundary layer of a blunt body and in its near wake 05 p0590 A83-17423

Radiative heat transfer near the stagnation point of a blunt body with an intensely vaporizing surface in the three-dimensional hypersonic flow of a hydrogen-helium mixture 06 p0712 A83-18357

The configuration of subsonic zones generated during supersonic flow past a spherically blunted cylinder at large angles of attack 06 p0713 A83-19443

The effect of particles on gas parameters in the flow of matter suspended in gas around a blunt body 09 p1197 A83-24238

Computation of hypersonic viscous flow over a body with mass transfer and/or spin 09 p1198 A83-24878

Heating-rate measurements over 30 deg and 40 deg /half-angle/ blunt cones in air and helium in the Langley expansion tube facility 10 p1371 A83-26146

Supersonic flow past a body with prescribed oscillations of its surface 13 p1803 A83-30002

The effect of the mechanisms of heterogeneous catalytic reactions on the heat flux in hypersonic flow past a blunted body 13 p1804 A83-30675

Knudsen layer characteristics for a highly cooled blunt body in hypersonic rarefied flow [AIAA PAPER 83-1424] 14 p1970 A83-32703

Computation of nonequilibrium, supersonic three-dimensional inviscid flow over blunt-nosed bodies 14 p1971 A83-32980

Hypersonic viscous flows past general bodies at angle of attack and yaw 15 p2119 A83-33728

Pressure pulsations during flow past blunt bodies 16 p2288 A83-35537

Single- and multiple-crater induced nosetip transition 16 p2293 A83-36078

The behaviour of excited atoms near stagnation streamline of a blunt body in an ionized gas 16 p2296 A83-36880

Theory of vortex interaction on a blunt cone 17 p2448 A83-37511

Structure of the flow of an inviscid gas near an isolated stagnation point 17 p2505 A83-37526

Nonequilibrium hypersonic air flow past blunt bodies 17 p2450 A83-37630

The effect of an increase in the temperature factor of a cone on the parameters of the base region 17 p2451 A83-37811

Unsteady regular reflection of a plane shock wave from a blunt body 18 p2632 A83-39156

Nosetip bluntness effects on cone frustum boundary layer transition in hypersonic flow [AIAA PAPER 83-1763] 18 p2633 A83-39265

Nonequilibrium viscous shock-layer flows over blunt sphere-cones at angle of attack 18 p2638 A83-40006

The effect of a boundary layer on the nonstationary aerodynamic characteristics of blunted cones in supersonic flows 19 p2790 A83-41255

The base pressure of bodies of revolution with gas injection through the body surface into a supersonic flow 19 p2790 A83-41265

A viscous shock layer near the surface of a blunted body in a divergent supersonic flow 19 p2791 A83-41269

Flow control in a shock layer on a body of revolution 19 p2845 A83-41878

Allowance for finite Mach numbers in hypersonic asymptotics for blunt axisymmetric bodies 19 p2791 A83-41880

Features of the effect of admixtures on the characteristics of a region perturbed by a body moving at hypersonic velocity 19 p2792 A83-41893

Heat transfer characteristics and boundary layer development about heating and cooling rotating blunt bodies at supersonic speeds 20 p2929 A83-42710

Heat-transfer non-uniformities downstream of three-dimensional boundary layer trips 20 p2976 A83-42718

Flow past and radiant heating of blunt bodies moving at angles of attack alpha greater than or equal to 0 deg 20 p2929 A83-42878

Similarity law for hypersonic flow past asymmetrically blunt bodies 20 p2929 A83-42879

Spectroscopic studies of the dark space ahead of a shock wave in an argon plasma flow 20 p3050 A83-43583

Influence of asymmetric transition on static stability of blunted cones 21 p3087 A83-44562

A simplified calculation method for the nonequilibrium wake of the blunt-cone body 21 p3087 A83-44568

Numerical determination of the parameters in high-entropy layers on slightly blunt bodies in supersonic flow 21 p3088 A83-45220

The force effect of a supersonic flow of a dust-filled gas on a blunt body 21 p3088 A83-45347

Calculation of a boundary layer with phase transformations --- oxygen condensation at cooled surface 24 p3579 A83-49661

Thermochemical ablation of the glass-graphite surface of a blunt cone at the spreading line in a three-dimensional boundary layer 24 p3579 A83-49662

BLUNT LEADING EDGES

Relaxation computation of transonic flows around wings with blunt leading-edge and discussion on its stability and convergence 04 p0443 A83-15543

Heat transfer from interrupted plates 09 p1259 A83-23879

Parametric study of hypersonic three-dimensional configurations 11 p1527 A83-28537

- The effect of the blunting of the leading edges on the characteristics of separated flow past delta wings of low aspect ratio 17 p2449 A83-37551
- The susceptibility of a boundary layer on blunted-nose bodies to acoustic flow oscillations 19 p2791 A83-41274

BLURRING

- Unconstrained single deblurring filter made from blurred PSF and doubly blurred PSF --- Point Spread Function 06 p0762 A83-18589
- Effects of blur and noise on digital imagery interpretability 10 p1456 A83-26322
- Design of two-dimensional digital filters for blurred image restoration 10 p1464 A83-26515
- Simple method for image deblurring 10 p1484 A83-26860
- Real-time image deblurring using four-wave mixing 24 p3628 A83-48750

BMC**U BONE MINERAL CONTENT****BO-105 HELICOPTER**

- Lowering of the first blade number harmonic cell vibrations of a helicopter by reduction of rotor blade retention forces via appropriate bending-torsion coupling of the rotor blade --- German thesis 06 p0714 A83-19619
- Bo 105 rotor blade influence on the Calipso FLIR in the mast-mounted observation platform Ophelia 08 p1044 A83-23249

BOATTAILS

- Numerical simulation of steady supersonic flow over spinning bodies of revolution 03 p0277 A83-13140
- Support-sting interference on boattail pressure drag for Reynolds numbers up to 70 x 10 to the 6th [AIAA PAPER 83-0387] 05 p0599 A83-16687
- A computational investigation of supersonic axisymmetric flow over boattails containing a centered propulsive jet [AIAA PAPER 83-0462] 05 p0586 A83-16730
- Measurements on a projectile with an asymmetric afterbody at transonic speeds [AIAA PAPER 83-0545] 05 p0587 A83-16780
- Global PNS solutions for subsonic strong interaction flows over a cone-cylinder-boattail geometry --- Parabolized Navier-Stokes equation 20 p2928 A83-42554
- Computational study of the Magnus effect on boattailed shell at supersonic speeds 22 p3249 A83-46473

BOD**U BIOCHEMICAL OXYGEN DEMAND****BODIES OF REVOLUTION**

- NT CELESTIAL SPHERE
- NT CONCENTRIC SPHERES
- NT CONICAL BODIES
- NT CYLINDRICAL BODIES
- NT FALLING SPHERES
- NT PARABOLIC BODIES
- NT ROTATING CYLINDERS
- NT ROTATING SPHERES
- NT SLENDER CONES
- NT SPHERES
- NT TORUSES
- Axisymmetric thermoplastic state of layered shells on the basis of the theory of small-curvature processes 01 p0059 A83-10680
- A study of the creep of thin-walled shells under nonstationary loading 01 p0059 A83-10681
- Generalized conic concentrators 02 p0236 A83-12310
- Numerical improvement of asymptotic solutions for shells of revolution with application to toroidal shell segments 02 p0194 A83-12741
- Numerical simulation of steady supersonic flow over spinning bodies of revolution 03 p0277 A83-13140
- The fundamental nonlinear equations of the theory of imperfect rib-stiffened shells of revolution 03 p0339 A83-13690
- Investigation of the thermoelastoplastic state of shells of revolution with allowance for creep deformations 03 p0340 A83-14067
- New computation method for characteristic modes --- eigenvalue equation solution for perfectly conducting object 04 p0466 A83-15234
- Plane-wave scattering by bodies of revolution with absorbing coatings 04 p0466 A83-15728
- Scattering by slender bodies of revolution 04 p0533 A83-16317
- Jet trajectories and surface pressures induced on a body of revolution with various dual jet configurations [AIAA PAPER 83-0080] 05 p0579 A83-16508
- Maximum vortex-induced side force revisited --- for aerodynamic design [AIAA PAPER 83-0458] 05 p0586 A83-16727
- Flow over flat and axisymmetric bodies moving at high variable velocities 05 p0589 A83-17413

- A study of the elastic-plastic state of bodies of revolution under variable nonisothermal loading with allowance for creep 06 p0778 A83-19543
- A note on the specification of freestream velocity in the calculation of the boundary layer flow around bodies of revolution at incidence 07 p0862 A83-19665
- Optimization of solutions of the equations of motion of shells of revolution to enhance the dynamic-stability parameters 07 p0946 A83-20897
- Limitations and possible extensions to a nonlinear finite element shell-of-revolution model based on Reissner's shell theory 07 p0948 A83-21438
- Application of the initial value method to analysis of elastic-plastic plates and shells of revolution 08 p1121 A83-21890
- Potential flow around a thin oblate body of revolution 08 p1085 A83-22743
- Motion of a Kovalevskaia gyroscope in the Delaunay case 09 p1337 A83-23555
- Nonaxisymmetric buckling of nonshallow elastic shells of revolution 09 p1281 A83-25011
- Radiation of sound by a body of revolution 10 p1477 A83-26292
- General relations for exact and inexact involute bodies of revolution 11 p1592 A83-27446
- Achievement of a nonaxisymmetric membrane state in shells of revolution 11 p1599 A83-28543
- The theory and analysis of shells of revolution --- Russian book 12 p1735 A83-29327
- Numerical solution of problems of the statics of layered shells of revolution in a refined formulation 13 p1867 A83-30720
- Splines in problems involving the stability and stressed state of shells of revolution 13 p1867 A83-30722
- Investigation of the possibility of reducing aerodynamic drag by a mechanism of initial vortex formations 13 p1804 A83-30723
- The scattering of a scalar wave by a thin oblate body of revolution 14 p2081 A83-33453
- A nonlinear, semi-analytical finite element analysis for nearly axisymmetric solids 15 p2176 A83-34318
- Application of the triple-deck theory of viscous-inviscid interaction to bodies of revolution 16 p2288 A83-35345
- Numerical-asymptotic solution of problems of the strength and vibrations of thin shells of revolution 16 p2365 A83-35547
- Separated flows at the leeward side of a delta wing and body of revolution in supersonic flow 17 p2449 A83-37553
- Calculation of transonic axisymmetric flow past bodies of revolution 17 p2450 A83-37627
- The possibility of the breakdown of the static stability of an axisymmetric body of revolution in the near-resonance regime --- in spacecraft reentry 17 p2472 A83-37637
- Analysis of shells of revolution subjected to axisymmetric deformation 17 p2524 A83-38506
- Numerical solution of axisymmetric problems in the dynamics of thin-walled orthotropic shells of revolution 17 p2524 A83-38507
- Numerical generation of three-dimensional coordinates between bodies of arbitrary shapes 17 p2574 A83-38806
- Substantiation of the method of nonorthogonal series and the solution of certain inverse diffraction problems 18 p2674 A83-39154
- Variational-difference method of calculating critical loads for shells of revolution 18 p2698 A83-39506
- Flow control in a shock layer on a body of revolution 19 p2845 A83-41878
- Flat spin of bodies with circular cross-section [AIAA PAPER 83-2147] 19 p2807 A83-41968
- The thermal stressed state of curvilinearly orthotropic inhomogeneous bodies of revolution 21 p3154 A83-44711
- The principal nonlinear and linearized equations of the theory of imperfect ribbed shells of revolution 21 p3154 A83-44718
- Solution of problems in the statics of shells of revolution with additional supports 21 p3155 A83-44847
- A boundary element solution to elasto-plastic torsion of solids of revolution 21 p3160 A83-45053
- A class of integral equations for solving three-dimensional axisymmetric elasticity problems 21 p3163 A83-45358
- An asymptotic integration method in problems concerning wave propagation in shells of revolution 21 p3163 A83-45368
- Integrated thermal-structural approach for shells of revolution 21 p3164 A83-45596
- New developments in open separation --- of three dimensional boundary layers 22 p3250 A83-47016
- Boundary layers on bodies of revolution spinning in axial flows 22 p3286 A83-47023

- Hybrid solutions for scattering from perfectly conducting bodies of revolution 23 p3442 A83-47828
- Vibration and radiation of a shell of revolution under circumferential loading 23 p3472 A83-48468
- Allowance for the principal types of elastic deformation nonlinearities in axisymmetric problems of the statics of shells of revolution 24 p3592 A83-49032
- A numerical study of the plastic adaptation of plates and shells of revolution by equilibrium finite elements 24 p3594 A83-49645
- A finite element study of the nonstationary temperature fields of bodies of revolution 24 p3596 A83-49909

BODY CENTERED CUBIC LATTICES

- Mechanisms of the isothermal decomposition of beta-solid solution in two-phase martensitic titanium alloys 01 p0025 A83-10446
- Direct conversion from amorphous to beta-Si3N4 under high pressure 02 p0160 A83-11677
- Development of complex textures during deformation of bcc metals 02 p0155 A83-12201
- The mode of plastic deformation of beta Ti-V alloys 03 p0298 A83-13850
- The effect of the initial structure on the characteristics of beta solid solution decomposition in high-strength titanium alloy VT22 03 p0300 A83-14157
- Infrared spectroscopic study of beta-sialons in the system Si3N4-SiO2-AlN 04 p0464 A83-15998
- Transformation toughening of beta double prime-alumina by incorporation of zirconia 05 p0619 A83-17558
- Supercooled beta phase decomposition in titanium alloy VT23 06 p0728 A83-18134
- Application of the double slip plane crack model to temperature and strain rate sensitive BCC metals 06 p0733 A83-19146
- Formation of beta-Si3N4 coatings by chemical vapor deposition 07 p0898 A83-20172
- Hydrogen-induced fracture phenomena in a BCC titanium alloy 08 p1061 A83-21717
- Effect of diffusion welding thermal cycle on the strength of alloy VT20 08 p1067 A83-22696
- Principles governing the decomposition of a metastable beta solid solution in beta titanium alloys 09 p1234 A83-24385
- Morphological features of the structure of alpha titanium alloys after cooling from the beta region at various rates 09 p1234 A83-24389
- Microstructure and tensile ductility in a beta heat treated titanium alloy 10 p1398 A83-26280
- On the Portevin-le Chatelier effect due to Snoek strain aging in the niobium oxygen system 10 p1398 A83-26283
- Orientation relationships between bcc Mo and fcc gamma in a Ni-Al-Mo-W superalloy 10 p1398 A83-26284
- Alpha-beta interface sliding in Ti-Mn alloys 10 p1398 A83-26285
- A study of the structure of grain boundaries with special misorientations in tungsten 10 p1399 A83-26795
- Decomposition of the metastable beta phase in the textured alloy VT19 11 p1550 A83-28545
- The crystalline structure of gas-saturated beta titanium alloys 11 p1550 A83-28546
- Micromechanics of solid solution effects in BCC alloys [AIAA 83-0976] 12 p1715 A83-29783
- The effect of two-stage aging on structural transformations in beta zirconium alloys 13 p1822 A83-30745
- Mechanical properties of BCC metals: Proceedings of the U.S.-Japan Seminar, Honolulu, HI, March 23-27, 1981 14 p1995 A83-32874
- Deformation martensite in VT22 titanium alloy 15 p2141 A83-35307
- A supersaturation model for the degradation of sodium beta/beta (double prime)-aluminas 16 p2326 A83-35977
- Distribution of aluminum, molybdenum, and zirconium among phases in Ti-Al-Mo-Zr alloys 16 p2335 A83-36898
- Some surprising features of the plastic deformation of body-centered cubic metals and alloys (Edward DeMille Campbell Memorial Lecture) 18 p2668 A83-40626
- An electron microscopy study of alpha-planar defects formed by boron in alloys of bcc refractory metals 19 p2822 A83-41978
- H NMR study of hydrogen motion in the beta phase of the Mg2NiH(x) system 21 p3109 A83-43962
- Ordered structures on the bcc lattice with first, second, third and fifth neighbour interactions [ONERA, TP NO. 1983-63] 23 p3512 A83-48184
- Evaluation of microstructure in beta-SiAlON materials by TEM methods and its correlation to some properties 23 p3436 A83-48277
- Oxidation behaviour of beta-prime sialons in oxygen and carbon dioxide 23 p3436 A83-48284

Lucas Syalons - Composition, structure, properties and uses 23 p3438 A83-48304

BODY COMPOSITION (BIOLOGY)

The content and distribution of glycogen in the brain following an experimental craniocerebral injury 01 p0079 A83-10527

The changes in the content of corticosterone in the blood plasma of inbred mice after exposure to stress 01 p0080 A83-10541

Variability of fiber type distributions within human muscles 05 p0674 A83-17328

Effects of chronic acceleration on body composition 11 p1635 A83-27780

Muscle fiber composition and blood ammonia levels after intense exercise in humans 13 p1903 A83-30480

The distribution of Na, K, Ca, P, and S in the vestibular apparatus and eye of the larvae of the fish *Brachydanio rerio* 15 p2210 A83-34937

Effects of weightlessness on body composition in the rat 21 p3184 A83-44867

BODY FLUIDS

NT BLOOD

NT CEREBROSPINAL FLUID

NT ENDOLYMPH

NT EOSINOPHILS

NT ERYTHROCYTES

NT LEUKOCYTES

NT LYMPH

NT LYMPHOCYTES

NT MUCUS

NT SWEAT

NT WHITE BLOOD CELLS

Sweat composition in exercise and in heat 05 p0675 A83-17332

Fluid shifts in vascular and extravascular compartments of humans during and after simulated weightlessness 11 p1642 A83-27793

Computer simulation analysis of the behavior of renal-regulating hormones during hypogravic stress 11 p1642 A83-27794

Alterations in glomerular and tubular dynamics during simulated weightlessness 11 p1636 A83-27795

Fluid shifts and erythropoiesis - Relevance to the 'anemia' of space flight 11 p1637 A83-27801

The relative contributions of gravity, buoyancy, and cold to the changes of human plasma volume during simulated weightlessness 11 p1643 A83-27802

Psychological stress induces sodium and fluid retention in men at high risk for hypertension 12 p1763 A83-28925

Correction of changes in fluid-electrolyte metabolism in manned space flights 12 p1763 A83-28928

Fluid shifts and muscle function in humans during acute simulated weightlessness 13 p1904 A83-30501

Fluid and electrolyte homeostasis in space - A primate model to look at mechanisms [SAE PAPER 820832] 13 p1898 A83-30930

The effect of changes of the electrolytic composition of the perilymph on the endocochlear potential 14 p2063 A83-32567

Physiological and behavioral effects of tilt-induced body fluid shifts 14 p2068 A83-32685

Canine blood volume and cardiovascular function during hyperthermia 20 p3033 A83-43476

Fluid and electrolyte homeostasis during prolonged exercise at altitude 20 p3034 A83-43481

A modified technique for estimation of ethanol in body fluids by gas liquid chromatography 23 p3499 A83-48694

BODY KINEMATICS

Structural kinematics of in-parallel-actuated robot-arms [ASME PAPER 82-DET-105] 02 p0187 A83-12779

Geometrical properties of the Euler-Poisson equations of a rigid body about a fixed point 03 p0390 A83-13423

Combination of accelerometer and photographically derived kinematic variables defining three-dimensional rigid body motion 08 p1102 A83-22793

On conditions of the existence of certain classes of solutions of the problem of the motion of a rigid body with a fixed point 09 p1337 A83-23551

Kinematic interpretation of the motion of a gyrostat in one solution of E. I. Kharlamova 09 p1337 A83-23552

Isoconic motions of a rigid body with a fixed point 09 p1337 A83-23553

Construction of a complete solution for one problem of rigid-body dynamics 09 p1337 A83-23554

Motion of a Kovalevskaja gyroscope in the Delaunay case 09 p1337 A83-23555

Methods for the investigation of rigid-body motions and their application to the classification of motions 09 p1337 A83-23556

On an attempt to generalize the Hess solution of the problem concerning the motion of a heavy rigid body with a fixed point 09 p1337 A83-23557

On certain motions of a system of three Lagrange gyroscopes 09 p1337 A83-23558

Formation of a library of mathematical models of complex surfaces of special form 12 p1768 A83-29293

Gyrational motion of disks during free-fall 13 p1839 A83-30107

Solving the find-path problem by good representation of free space 13 p1910 A83-31070

The motion of an ellipsoid along a rough plane with slip 14 p2079 A83-32359

An asymptotic solution to the equations of motion for the wobblestone --- asymmetrical spinning top dynamics 14 p2080 A83-32360

A linear algebra approach to the analysis of rigid body velocity from position and velocity data 17 p2575 A83-37546

The effects of non-linear kinematics in optimal evasion 19 p2889 A83-40674

The calculation of robot dynamics using articulated-body inertias 20 p2959 A83-43109

An approach for the generation of kinematic chains with multiple joints 21 p3147 A83-44030

The asymptotic behavior of singular perturbations in the problem of the dynamics of a rigid body with elastic and dissipative elements 21 p3200 A83-45356

Rotatory motion of a rigid body near libration points [IAF PAPER 83-342] 23 p3417 A83-47351

The dynamics of a rigid body on an absolutely rough plane 23 p3505 A83-48529

Position and velocity transformations between robot end-effector coordinates and joint angles 23 p3501 A83-48634

BODY MEASUREMENT (BIOLOGY)

NT ANTHROPOMETRY

NT ELECTROPLETHYSMOGRAPHY

Measurement of scoliosis by orthopedic surgeons and radiologists 06 p0797 A83-18198

Automatic measurement of body surfaces using rasterstereography. I - Image scan and control point measurement 10 p1420 A83-25971

BODY SIZE (BIOLOGY)

Humanscale 4/5/6 --- Book on human factors engineering information 13 p1906 A83-30155

The dependence of the topography of the hepatic veins on the external form of the liver, its sizes, and age 18 p2736 A83-40583

BODY TEMPERATURE

Physiological criteria of upper limits of body heating 02 p0223 A83-12256

The effects of rest and exercise in the cold on substrate mobilization and utilization 04 p0521 A83-15534

Heat loss and tissue metabolism in white mice during the recovery after acute hypothermia 04 p0520 A83-15896

Effects of exposure to low O₂ or high CO₂ environments on respiration in hibernating hamsters and ground squirrels 04 p0520 A83-16009

Temperature and adrenocortical responses in rhesus monkeys exposed to microwaves 05 p0671 A83-17334

A pronounced decrease in the metabolism of warm-blooded animals caused by endogenous substances from the tissues of hibernants in the state of hibernation 07 p0971 A83-19643

Short hyperdynamic profiles influence primate temperature regulation 11 p1637 A83-27807

Daily rhythms of activity and temperature of Macaca nemestrina 11 p1641 A83-27843

The circadian rhythm of the body temperature, arterial pressure, and heart rate 12 p1765 A83-29311

The thermal condition and systemic blood circulation of the human body in the case of moderate (physiological) levels of cooling 12 p1765 A83-29313

Unusual core temperature decrease in exercising heart-failure patients 13 p1903 A83-30478

Effect of cold exposure on various sites of core temperature measurements [AD-A130437] 13 p1904 A83-30502

Effect of triiodothyronine on body temperature at rest and during exercise in dogs 13 p1898 A83-30508

The changes in the liver and muscles due to the effect of physical exercise during overheating in different water regimes 14 p2061 A83-31974

Calorimetry with heat flux transducers - Comparison with a suit calorimeter 14 p2072 A83-32819

A review of the literature concerning resuscitation from hypothermia. II - Selected rewarming protocols 15 p2214 A83-34978

Head and/or torso cooling during simulated cockpit heat stress 15 p2216 A83-34979

The human element in air traffic control - Aeromedical aspects, problems, and prescriptions 15 p2214 A83-34981

The recovery of temperature homeostasis of mammals under microwave irradiation 16 p2394 A83-35922

Establishment of the optimal irradiance of man at low ambient temperatures in the workplace 17 p2561 A83-38929

Active diver thermal protection requirements for cold water diving 18 p2737 A83-40363

Impaired memory registration and speed of reasoning caused by low body temperature 19 p2880 A83-41133

Thermoelectric energy conversion could be an energy source of living organisms 19 p2875 A83-41168

A technique for the evaluation of the temperature profile during local cooling of the medulla oblongata 19 p2876 A83-41846

The regulation of the heat content of the body 23 p3497 A83-47106

BODY TEMPERATURE (NON-BIOLOGICAL)**U TEMPERATURE****BODY TEMPERATURE REGULATION****U THERMOREGULATION****BODY WEIGHT**

The determination of the normal /desirable/ body weight for males 40-59 years of age according to the findings of an epidemiological study of cardiovascular diseases 01 p0083 A83-10513

The dynamics of the growth of the results of heavy athletes in connection with psychomotor peculiarities of personality 01 p0085 A83-10522

Metabolic effect of intermittent exposure to altitude stress on rats and guinea pigs 10 p1453 A83-25670

Plasma volume shifts during progressive arm and leg exercise 13 p1903 A83-30475

BODY-WING AND TAIL CONFIGURATIONS

A comparison of trim drag for conventional and supercritical wings [AIAA PAPER 83-0094] 05 p0579 A83-16518

Experimental investigation of rolling moment for a body-wing-tail missile configuration with wrap around wings and straight tails at supersonic speeds [AIAA PAPER 83-2081] 19 p2805 A83-41915

Optimizing tail size and wing location within loadability constraints [SAWE PAPER 1466] 20 p2935 A83-43740

BODY-WING CONFIGURATIONS

The multilevel substructure and the local analysis of structure 03 p0341 A83-14485

A fast algorithm for the calculation of transonic flow over wing/body combinations 04 p0442 A83-15283

Some recent applications of high-lift computational methods at Boeing 04 p0443 A83-15313

Problems concerning supersonic flow past bodies of prismatic configurations 04 p0443 A83-16394

Calculation of supersonic flow over realistic configurations by an updated low-order panel method [AIAA PAPER 83-0010] 05 p0578 A83-16461

Numerical simulation of wing-fuselage aerodynamic interaction [AIAA PAPER 83-0225] 05 p0582 A83-16595

Multi-grid calculation of three-dimensional transonic potential flows [AIAA PAPER 83-0374] 05 p0585 A83-16679

Numerical computation of transonic flow about wing-fuselage configurations on a vector computer [AIAA PAPER 83-0499] 05 p0587 A83-16751

Transonic wing-body calculations using Euler equations [AIAA PAPER 83-0501] 05 p0589 A83-16828

Slender body theory and optimization procedures for transonic lifting wing bodies [AIAA PAPER 83-0184] 05 p0591 A83-17911

An evaluation of aerodynamics modeling of spinning light airplanes [AIAA PAPER 83-0368] 05 p0598 A83-17922

Leading edge vortex flap aerodynamics 07 p0863 A83-21004

Numerical calculations of nonlinear aerodynamics of wing-body configurations 07 p0864 A83-21022

Fuselage-lifting surfaces interaction in unsteady subsonic flow --- French thesis 08 p1041 A83-22093

Oil flow separation patterns on an ogive forebody 09 p1198 A83-24662

Computational treatment of three-dimensional transonic canard-wing interactions 12 p1696 A83-29021

Steady-state solution of the Euler equations for transonic flow 12 p1698 A83-29929

Calculation of transonic potential flow past three-dimensional configurations 12 p1698 A83-29930

A more accurate transonic computational method for wing-body configurations 14 p1971 A83-32982

Asymmetric flows in corner configurations 16 p2288 A83-35532

Numerical calculation of nonlinear aerodynamics of wing-body configurations 16 p2293 A83-36076

A supersonic velocity field in the region of interference between a wing and a body having a common apex
17 p2451 A83-37802

An extension of a transonic wing/body code to include underwing pylon/nacelle effects
[AIAA PAPER 83-1805] 17 p2454 A83-38639

The leading-edge vortex trajectories of close-coupled wing-canard configurations and their breakdown characteristics
[AIAA PAPER 83-1817] 17 p2455 A83-38649

An assessment of PANDORA using a Canard/Wing/Body configuration --- Preliminary Automated Numerical Design of Realistic Aircraft
[AIAA PAPER 83-1850] 17 p2456 A83-38678

Computational analysis for an advanced transport configuration with engine nacelle
[AIAA PAPER 83-1851] 17 p2465 A83-38679

Computation of transonic flow field over Wing-Body-Pylon-Store combinations
[AIAA PAPER 83-1852] 17 p2456 A83-38680

The combination of a geometry generator with transonic design and analysis algorithms
[AIAA PAPER 83-1862] 17 p2457 A83-38689

Numerical generation of composite three dimensional grids by quasilinear elliptic systems
17 p2574 A83-38804

Fast body-fitted grid generation around 3-D configurations
[AIAA PAPER 83-1936] 18 p2635 A83-39386

Numerical simulation of the leading-edge separation vortex for a wing and strake-wing configuration
[AIAA PAPER 83-1908] 18 p2637 A83-39408

Convergence characteristics of nonlinear vortex-lattice methods for configuration aerodynamics
[AIAA PAPER 83-1882] 18 p2637 A83-39421

Equivalent angle-of-attack method for estimating nonlinear aerodynamics of missile fins
18 p2638 A83-40010

Hybrid composite application to the Boeing 767 wing/body fairing
18 p2640 A83-40244

Rigid-body structural mode coupling on a forward swept wing aircraft
19 p2797 A83-41046

The maximum aerodynamic efficiency of conical wing-body combinations at high supersonic speeds
19 p2790 A83-41266

Studies of light-twin wing-body interference
[SAE PAPER 830709] 20 p2930 A83-43319

An efficient, full-potential implicit method based on characteristics for supersonic flows
20 p2930 A83-43442

Induced rolling moment on wings of a missile with tilt-wings in 'X-X' configuration at supersonic speeds
20 p2937 A83-43689

Estimation of parameters involved in high angle-of-attack aerodynamic theory using spin flight test data
[AIAA PAPER 83-2086] 20 p2937 A83-43809

Experimental work on the aerodynamics of integrated slender wings for supersonic flight
21 p3086 A83-44360

Experimental wing and canard jet-flap aerodynamics
[AIAA PAPER 83-0081] 23 p3398 A83-48211

BOEING AIRCRAFT

NT B-52 AIRCRAFT

NT BOEING 727 AIRCRAFT

NT BOEING 737 AIRCRAFT

NT BOEING 747 AIRCRAFT

NT BOEING 757 AIRCRAFT

NT BOEING 767 AIRCRAFT

NT C-135 AIRCRAFT

NT CH-46 HELICOPTER

NT CH-47 HELICOPTER

Boeing gains real-time flight data
06 p0719 A83-18270

Boeing Vertol - The leading edge of technology
14 p1969 A83-33095

Large jet aircraft validation and demonstrations - An overview of Boeing experience
[AIAA PAPER 83-1049] 16 p2301 A83-36472

BOEING MILITARY AIRCRAFT

U MILITARY AIRCRAFT

BOEING 727 AIRCRAFT

Researchers study methods to combat effects of wind shear
08 p1043 A83-22175

727, B-52 retrofit with PW2037 meeting today's requirements
[SAE PAPER 821443] 17 p2463 A83-37991

BOEING 737 AIRCRAFT

Re-engining the 737
[SAE PAPER 821442] 17 p2463 A83-37990

BOEING 747 AIRCRAFT

Wake vortex attenuation flight tests - A status report
02 p0134 A83-11806

Flight test of the 747-JT9D for airframe noise
03 p0281 A83-13163

Ground effects on aircraft noise for a wide-body commercial airplane
09 p1340 A83-24034

BOEING 757 AIRCRAFT

The cost definition phase of a new commercial aircraft programme
09 p1196 A83-24425

ARINC 429 digital data communications for commercial aircraft
09 p1200 A83-24435

On the routes - Boeing 757 with British Airways
12 p1701 A83-29241

Application of Monte-Carlo techniques to the 757/767 autoland dispersion analysis by simulation
[AIAA PAPER 83-2193] 19 p2802 A83-41678

Functional development of the 757/767 digital cat. IIIB Autoland System
[AIAA PAPER 83-2192] 19 p2796 A83-41762

BOEING 767 AIRCRAFT

ARINC 429 digital data communications for commercial aircraft
09 p1200 A83-24435

Hybrid composite application to the Boeing 767 wing/body fairing
18 p2640 A83-40244

Application of Monte-Carlo techniques to the 757/767 autoland dispersion analysis by simulation
[AIAA PAPER 83-2193] 19 p2802 A83-41678

Functional development of the 757/767 digital cat. IIIB Autoland System
[AIAA PAPER 83-2192] 19 p2796 A83-41762

An introduction to the Boeing 767-200 and the 767 Weight Control Program
[SAE PAPER 1467] 20 p2935 A83-43741

Composites in commercial aircraft
22 p3262 A83-46281

BOGOLIUBOV THEORY

Unified approach to weak turbulence
15 p2239 A83-34543

The Hamiltonian formalism of one-dimensional systems of hydrodynamic type and the Bogoliubov-Whitham averaging method
18 p2741 A83-39477

BOGS

U MARSHLANDS

BOHR THEORY

Bohr effect data for blood gas calculations
22 p3348 A83-45999

BOILER PLATE

Application of electric resistance probe method to non-destructive inspection
01 p0057 A83-10280

BOILERS

An experimental study and modeling of heat transfer in boilers of small and medium power --- French thesis
04 p0456 A83-15841

Long term elastoplastic behavior of solar boiler tubes
07 p0945 A83-20366

Regulation of a system with variable structure --- for boilers of solar powered central receivers
09 p1293 A83-24761

Dynamic instabilities in radiation-heated boiler tubes for solar central receivers
[ASME PAPER 82-WA/HT-8] 10 p1445 A83-25692

Shuttle Water Spray Boiler flight performance --- lubricant cooling for Orbiter Hydraulic System and APU
[SAE PAPER 820885] 10 p1383 A83-25751

Performance benefits of the direct generation of steam in line-focus solar collectors
15 p2189 A83-33989

Linear stability analysis of heated parallel channels
20 p2981 A83-42768

BOILING

NT FILM BOILING

NT LEIDENFROST PHENOMENON

NT NUCLEATE BOILING

Heat transfer during the boiling of acetone and ethyl alcohol in a thermosiphon with porous capillary structures on the heat-transfer face
11 p1571 A83-28798

A relationship between the flash point, boiling point and the lean limit of flammability of liquid fuels
16 p2325 A83-35791

Experimental study of flash boiling in liquid nitrogen
[AIAA PAPER 83-1378] 16 p2341 A83-36369

The effect of a porous coating on the convective heat transfer during boiling
18 p2684 A83-39475

Heat transfer 1982; Proceedings of the Seventh International Conference, Technische Universitaet Muenchen, Munich, West Germany, September 6-10, 1982. Volume 4 - General papers: Pool boiling, flow boiling, measuring techniques
20 p2980 A83-42757

Holographic interferometry studies of temperature profiles in thermal boundary layer in free convection and bubble boiling
20 p2980 A83-42760

The dryout region in frictionally heated sliding contacts
20 p2980 A83-42762

Critical heat flux in flow boiling of helium
20 p2981 A83-42769

BOLIDES

The Tsarev stony-meteorite rain
05 p0705 A83-17452

The interaction of the cretaceous-tertiary extinction bolide with the atmosphere, ocean, and solid earth
13 p1880 A83-31475

BOLKOW AIRCRAFT

NT BO-105 HELICOPTER

BOLTZMANN TRANSPORT EQUATION

BOLOGRAMS

U BOLOMETERS

BOLOMETERS

InSb heterodyne receivers for submillimeter astronomy
03 p0405 A83-13463

A consistent model for 1/f-noise in thin-film devices such as bolometers, Josephson junctions and SQUIDs
11 p1562 A83-28074

Phase-slip shot noise contribution to excess noise in superconducting bolometers
13 p1848 A83-31390

Superconducting bolometers in astronomical IR equipment. II Threshold sensitivity
14 p2014 A83-31842

A helium-3 cooled bolometer system for one millimeter continuum observations
17 p2510 A83-37751

The effect of self-heating on the dynamical response of bolometric detectors
17 p2513 A83-38862

He-3 bolometers for MM- and SUBMM-photometry
18 p2691 A83-40444

Improved fabrication techniques for infrared bolometers
22 p3293 A83-46742

BOLTS

Stress measurement at the threads of nut-bolt assemblies using the finite element method --- German thesis
04 p0487 A83-15846

Detection and measurement of cracks in threaded bolts with an a.c. potential difference method
07 p0943 A83-21355

Automatic eddy current bolt-hole scanning system
16 p2363 A83-35760

Calculation of the local compliance of elements of a multiple-row double-shear bolt joint
17 p2518 A83-37256

The use of the moiremethod to study the local compliance of the joined element of a double-shear bolt joint
17 p2518 A83-37270

Interaction of a sunk bolt with parts of a single-shear joint in conditions of radial tension
17 p2520 A83-37517

On mechanical fastening in graphite epoxy composite
18 p2652 A83-40155

Fatigue of composite bolted joints under dual load levels
18 p2703 A83-40158

BOLTZMANN DISTRIBUTION

Generalized polytropes - Stellar structure with a Boltzmann factor
04 p0549 A83-14986

A measure of the incompleteness of a statistical description and irreversibility Fluctuation-dissipation relation /FDR/ for multiparticle distribution functions
07 p1001 A83-20607

The statistical particle-in-cell method for multicomponent gases
09 p1350 A83-23571

BOLTZMANN TRANSPORT EQUATION

Global existence results for discrete velocity models of the Boltzmann equation in several dimensions
03 p0400 A83-14569

Transport theory of semiconductor energy conversion
04 p0544 A83-16087

Asymptotic solution of the diatomic Boltzmann equation
07 p0926 A83-20531

Auroral ion velocity distribution function - Generalized polynomial solution of Boltzmann's equation
07 p0968 A83-21586

Modern methods of numerical investigation of rarefied gas phenomena
08 p1085 A83-22992

Global solutions of nonstationary kinetic equations
09 p1350 A83-24322

The mathematical kinetics of reacting gases --- Russian book
09 p1227 A83-25220

Kinetic theory of evaporation and condensation for a cylindrical condensed phase
10 p1490 A83-25784

Fluctuation-dissipation relations in the scattering problem and the method of fluctuations in the kinetic theory of gases
10 p1490 A83-26246

A similarity solution of the linearized Boltzmann equation with application to thermophoresis of a spherical particle
11 p1665 A83-28431

Asymmetries in evaporation and condensation Knudsen layer problems
13 p1840 A83-30110

Collisional coupling of fluctuations in plasmas
13 p1925 A83-30520

Analytical methods for solving the Boltzmann equation
13 p1932 A83-30652

Demonstration and generalization of the Boltzmann kinetic theory
13 p1932 A83-30654

Exact solutions to the nonlinear Boltzmann equation and its models
13 p1932 A83-30655

A method for the integral transformation of the Boltzman equation - Analytical studies
13 p1932 A83-30658

On the effectiveness of models of the Boltzmann operator of intermolecular collisions
13 p1932 A83-30660

The application of a modified form of the S sub N method to the calculation of swarm parameters of electrons in a weakly ionised equilibrium medium
13 p1926 A83-31369

- Asymptotic near-wall stress dissipation rates in a turbulent flow 14 p2013 A83-33376
- Thermal relaxation and entropy for charged particles in a heat bath with fields 16 p2421 A83-35616
- An asymptotic method for solving the Boltzmann equation for low Knudsen numbers 17 p2585 A83-38096
- An analysis of the asymmetric part of electron-electron Boltzmann integral 17 p2583 A83-38208
- A method for obtaining closed-form systems of equations for macroparameters of distribution functions in the case of small Knudsen numbers 18 p2751 A83-39493
- The Boltzmann equation theory of charged particle transport 19 p2906 A83-41536
- H-theorem and trend to equilibrium in the kinetic theory of gases 21 p3220 A83-44942
- Boltzmann equation on a lattice global solution for non-Maxwellian gases 21 p3220 A83-44944
- The H-theorem and the Onsager principle for the steady Boltzmann equation 21 p3220 A83-45221
- A distribution function for a gas under conditions of escape flow 21 p3176 A83-45263
- Self-consistent kinetic theory for the Lorentz gas 22 p3366 A83-45938
- Invariant transformations of kinetic equations 23 p3512 A83-47176
- Scale-free models of elliptical galaxies 24 p3641 A83-49249
- Compatibility criteria for generalized Boltzmann equations 24 p3636 A83-49428

BOMBARDMENT

- The history of meteoritic bombardment in the early stage of the evolution of planetary bodies - Models and observational data 05 p0706 A83-17474

BOMBER AIRCRAFT

- NT A-6 AIRCRAFT 04 p0447 A83-16373
- NT B-1 AIRCRAFT 10 p1459 A83-26302
- NT B-52 AIRCRAFT 16 p2287 A83-36459
- NT B-58 AIRCRAFT 16 p2300 A83-36460
- Blackjack - Soviet B-1 or better 16 p2287 A83-36459
- Application of advanced speech technology /AST/ in manned penetration bombers 10 p1459 A83-26302
- From new technology development to operational usefulness B-36, B-58, F-111/FB-111 [AIAA PAPER 83-1046] 16 p2287 A83-36459
- XB-70 technology advancements [AIAA PAPER 83-1048] 16 p2300 A83-36460
- Comparison of color and black-and-white visual displays as indicated by bombing performance in the 2B35 TA-4J flight simulator 21 p3092 A83-44692

BOMBING EQUIPMENT

- A comparison of color versus black and white visual display as indicated by bombing performance in the 2B35 TA-4J flight simulator 10 p1376 A83-26313
- B-52 operations in the Bright Star 82 exercise 12 p1699 A83-29204

BOMBS

- Numerical studies of laminar flame propagation in spherical bombs 08 p1056 A83-22139

BOMBS (ORDNANCE)

- Aerodynamic development of a spinning submunition dispenser [AIAA PAPER 83-2082] 19 p2805 A83-41916

BOMBS (SAMPLERS)

- U SAMPLERS

BOND GRAPHS

- Alternative bond graph causal patterns and equation formulations for dynamic systems 17 p2569 A83-37545

BONDING

- NT ADHESIVE BONDING
- NT CERAMIC BONDING
- NT EXPLOSIVE WELDING
- NT METAL BONDING
- NT METAL-METAL BONDING
- NT REACTION BONDING
- NT RESIN BONDING
- Vibration and stability of sandwich beams with elastic bonding 06 p0774 A83-18395
- Dynamic coefficient of a two-layered thick beam with imperfect bonding 06 p0774 A83-18396
- Structural and functional changes in the hemoglobin of irradiated dogs 06 p0796 A83-19379
- Laser bonding of dissimilar semiconductors 11 p1560 A83-27564
- Increasing the numerical aperture of a glass-polymer light guide 13 p1919 A83-30814
- On fibre composites with intermittent interlaminar bonding 18 p2651 A83-40151

BONE DEMINERALIZATION

- Calcium-phosphorous metabolism and prevention of its disorders in hypokinetic rats 11 p1636 A83-27788

- The formation of an organic matrix in distractional bone regenerate and the characteristics of its mineralization during experimental crus stretching 14 p2066 A83-33338

- Effect of spaceflight on periosteal bone formation in rats 17 p2556 A83-37250
- Tibial changes in experimental disuse osteoporosis in the monkey 19 p2876 A83-41859
- Quantitative histochemistry of rat lumbar vertebrae following spaceflight 21 p3184 A83-44864

BONE MARROW

- An increase in the effectiveness of the transplantation of allogenic bone marrow 01 p0080 A83-10547
- The significance of cellular contacts for the differentiation of precursor cells of hemopoietic stroma in long-term bone marrow cultures 01 p0080 A83-10548
- Stromal bone-marrow cells and the hemopoietic environment 05 p0671 A83-17207
- The comparative investigation of the radiosensitivity of normal and regenerating tissues. I - The interphase death of cells and the degree of aplasia of regenerating and normal tissues of the bone marrow and spleen of C57B1 mice 14 p2062 A83-32055
- The effect of preparations acting mainly in the region of the peripheral M-choline reactive systems on bone marrow eosinophils 14 p2066 A83-33332
- The role of the afferent nerve in the regulation of the repair regeneration of bone tissue 18 p2732 A83-40554
- The mechanism of the regeneration of erythropoiesis in conditions of local irradiation of bone marrow 19 p2874 A83-41008
- The radiosensitivity of colony forming units in diffuse chambers contained in the bone marrow and the spleen of mice during gamma-irradiation at various conditions of oxygenation 23 p3495 A83-48205

- The mechanism of the regeneration of erythropoiesis in conditions of local irradiation of bone marrow 19 p2874 A83-41008

- The radiosensitivity of colony forming units in diffuse chambers contained in the bone marrow and the spleen of mice during gamma-irradiation at various conditions of oxygenation 23 p3495 A83-48205

BONE MINERAL CONTENT

- The effect of 24, 25-dihydroxycholecalciferol on the chemical composition of the bone tissue of rats during hypokinesia 06 p0795 A83-18987
- Calcium transport from the intestine and into bone in a rat model simulating weightlessness 11 p1640 A83-27832
- Bone mineral analysis of rat vertebra following space flight - Cosmos 1129 11 p1640 A83-27834
- Bone tissue of hypokinetic rats - Effects of 24,25-dihydroxycholecalciferol and varying phosphorus content in the diet 14 p2064 A83-32692
- The formation of an organic matrix in distractional bone regenerate and the characteristics of its mineralization during experimental crus stretching 14 p2066 A83-33338
- The effect of an insufficiency of iodine on the growth and formation of bone tissue 18 p2733 A83-40565
- Effects of spaceflight on trabecular bone in rats 21 p3183 A83-44863
- Effect of spaceflight on the non-weight-bearing bones of rat skeleton 21 p3184 A83-44865
- Bone resorption and mineral excretion in rats during spaceflight 21 p3184 A83-44866

BONES

- NT CEREBRUM
- NT CRANIUM
- NT INTRACRANIAL CAVITY
- NT SKULL
- NT TIBIA
- NT VERTEBRAE
- Electron-microscopic aspects of the selection of ultrasound intensity in ultrasonic therapy 01 p0081 A83-11394
- Histological and histochemical investigations of the locomotor system during general hypoxia 03 p0375 A83-13640
- Closed osteosynthesis and conservative therapy of fresh diaphyseal fractures of the crural bones 03 p0381 A83-14339
- The effects on rat bones of a prolonged centrifugation - Results of a morphometrical analysis 06 p0794 A83-18341
- The association between cancellous architecture and loading in bone - An optical data analytic view 11 p1636 A83-27786
- Changes in osteoblastic activity due to simulated weightless conditions 11 p1640 A83-27831
- Is suppression of bone formation during simulated weightlessness related to glucocorticoid levels 11 p1640 A83-27833
- The pattern of the functional condition of the vestibular analyzer in patients with cervical osteochondrosis combined with a vertebral artery syndrome 16 p2399 A83-36826
- Bone sound conduction in a widened frequency range according to data of the Moessbauer effect 19 p2883 A83-41829

- The cervical test in vertebral-basilar insufficiency 19 p2883 A83-41832
- Effects of spaceflight on trabecular bone in rats 21 p3183 A83-44863

BOOLEAN ALGEBRA**NT BOOLEAN FUNCTIONS**

- Interactive reductions in the number of states in Markov reliability analysis [AIAA PAPER 83-2304] 19 p2894 A83-41761

BOOLEAN FUNCTIONS

- Polynomial realization of a train of Boolean functions 01 p0096 A83-11318
- A language for bitmap manipulation 02 p0228 A83-11782
- Parallel computations of Boolean functions 09 p1327 A83-24246
- A combinatorial limit to the computing power of VLSI circuits 13 p1908 A83-30793
- Theory of the invariance of binary nonstationary and nonlinear sequential machines 20 p3039 A83-42923

BOOMS (EQUIPMENT)

- Two years of training with the first true three-dimensional simulator 08 p1047 A83-22833
- Beryllium application for spacecraft deployable solar array booms [AIAA 83-0867] 12 p1707 A83-29754
- On the dynamic response and collapse of slender guyed booms for space application [AIAA 83-0821] 12 p1742 A83-29818
- Composite materials and deployable boom technology [SAE PAPER 821395] 17 p2480 A83-37970
- Control of large spaceborne antenna systems with flexible booms by mechanical decoupling 18 p2646 A83-39095

BOOST**U ACCELERATION (PHYSICS)****BOOSTER ROCKET ENGINES**

- NT APOGEE BOOST MOTORS
- NT SPINNING SOLID UPPER STAGE
- Integrating engine performance and trajectory analysis in designing future Shuttle systems [AIAA PAPER 83-1189] 16 p2316 A83-36267
- Ariane 4 liquid boosters and first stage propulsion system [AIAA PAPER 83-1192] 16 p2319 A83-36268
- Ariane - Europe's expendable launcher 19 p2812 A83-41375
- Development of movable nozzle for solid rocket motor [AIAA PAPER 83-2285] 19 p2818 A83-41745
- The cost-effectiveness of modular and single-purpose rocket boosters and worldwide trends 20 p2944 A83-42566
- A rocket-boosted sea launched target system 20 p2934 A83-43702
- The cost-effectiveness of modular and single-purpose rocket boosters and worldwide trends [IAF PAPER 83-06] 23 p3418 A83-47230

BOOSTGLIDE VEHICLES

- Design study for remotely piloted, high-altitude airplanes powered by microwave energy [AIAA PAPER 83-1825] 17 p2465 A83-38657

BORANES**NT CARBORANE****BORATES**

- Densification of calcia-stabilized zirconia with borates 08 p1071 A83-22200

BORES**U CAVITIES****BORESCOPES****U ENDOSCOPES****BORESIGHT ERROR**

- Galileo spacecraft high gain antenna offset calibration 17 p2474 A83-37147
- Estimation of boresight error in autoboresighting a laser beam on a point target - Influence of weak statistical fluctuations 19 p2900 A83-41094
- Line of sight reconstruction for faster homing guidance [AIAA PAPER 83-2170] 19 p2796 A83-41666

BORIDES**NT CHROMIUM BORIDES****NT TITANIUM BORIDES**

- Surface structure of boride layers grown on Fe-C-Ni alloys 03 p0298 A83-13678
- Boring of nickel and other metals at temperatures below 670 C --- for electric vehicle batteries 07 p0880 A83-19892
- Interactions in the system metal-coating during fusion 07 p0889 A83-20708
- The high-temperature enthalpy and specific heat of borides in the system niobium-boron 11 p1548 A83-27925
- Effect of boride stress rupture properties of an Fe/NiCr-base alloy 13 p1820 A83-30323
- Structure and phase composition of nickel-boride composite coatings 21 p3113 A83-44485

- Physicochemical means of reducing the synthesis temperature of refractory coatings for nonmetallic materials 24 p3568 A83-49079
- The effect of the saturating medium composition on the growth kinetics and composition of a diffusion silicide coating on molybdenum 24 p3569 A83-49090
- BORN APPROXIMATION**
- Elastic wave scattering calculations, the Born Series and the matrix variational Pade approximant method --- for prediction of spherical voids and inclusions in NDT 04 p0488 A83-15161
- Range of applicability of inversion algorithms --- for ultrasonic flaw detection 04 p0490 A83-15174
- Time domain Born approximation --- for ultrasonic nondestructive tests 07 p0942 A83-20271
- Angular spectrum representation of scattered electromagnetic fields 08 p1161 A83-22668
- Electromagnetic backscattering from a layer of vegetation - A discrete approach 08 p1077 A83-22682
- Direct inversion of one-dimensional magnetotelluric data 09 p1308 A83-25069
- Relativistic calculation of atomic M-shell ionization by protons [AD-A130664] 13 p1918 A83-31351
- Inversion procedure for inverse scattering within the distorted-wave Born approximation 19 p2895 A83-40951
- Electron-induced excitation and ionization of multiply-charged ions 21 p3213 A83-44652
- Elastic scattering of electrons by hydrogen atoms in a laser field 24 p3626 A83-49432
- BORN-MAYER EQUATION**
- U BORN APPROXIMATION
- BORN-OPPENHEIMER APPROXIMATION**
- The equilibrium geometry, potential function, and rotation-vibration energies of CH₂ in the X3B1 ground state 10 p1480 A83-26454
- BORON**
- NT BORON FIBERS
- Dependence of hydrogen evolution from a Si-H on boron doping and substrate potential 04 p0541 A83-15518
- A study on combustion of boron powders through Bunsen flame [AIAA PAPER 83-0071] 05 p0612 A83-16502
- Diagnostics of single particle boron combustion [AIAA PAPER 83-0070] 05 p0613 A83-17904
- Plasma-spraying of a refractory coating on graphite 07 p0900 A83-20700
- Multiconfiguration Hartree-Fock Breit-Pauli results for 2P1/2-2P3/2 transitions in the boron sequence 08 p1162 A83-21985
- Flame annealing of arsenic and boron implanted silicon 08 p1170 A83-22768
- Chemical vapor deposition of boron on a beryllium surface 10 p1394 A83-25527
- The oxidation of silicon - Enhanced diffusion of boron for segregation at the Si-SiO₂ interface --- French thesis 11 p1664 A83-28635
- The ignition of disperse heterogeneous systems with consecutive reactions 14 p1988 A83-32082
- Implantation of boron and boron fluoride compounds into silicon for production of solar cells 14 p2005 A83-32331
- Effect of argon implantation on the activation of boron implanted in silicon 14 p2093 A83-33444
- Measurement of boron diffusivity in hydrogenated amorphous silicon by using nuclear reaction B-10(n, alpha)Li-7 16 p2418 A83-35437
- Boron particle ignition in a restricted thermodynamical equilibrium 16 p2338 A83-36087
- Quantum-chemical modeling of boron and noble gas dopants in silicon 17 p2584 A83-38211
- Cross section for the reaction C-12(e,p)B-11; and its relevance to the formation of B-11 in active galaxies 20 p3068 A83-42464
- Effect of boron compensation on the photovoltaic properties of amorphous silicon solar cells 20 p3055 A83-43601
- BORON ALLOYS**
- Constitution and properties of nickel-boron coatings 12 p1716 A83-29367
- The effects of B and Zr on the creep and fatigue crack growth behavior of a Ni-base superalloy 14 p1994 A83-32679
- Lattice images of amorphous-like Ni-B films prepared by the electroless plating method 16 p2328 A83-35601
- An electron microscopy study of alpha-planar defects formed by boron in alloys of bcc refractory metals 19 p2822 A83-41978
- Shape of growing crystals of primary phases in eutectic alloys of the systems Fe-Fe2B and Ni-Ni3B 21 p3112 A83-44476

BORON CARBIDES

- A study of the formation conditions and refractory properties of silicon carbide and boron carbide coatings on GMZ-grade graphite 07 p0900 A83-20706
- The oxidation of ultrafine powders of boron, vanadium, and chromium carbides 09 p1240 A83-25067
- Electrodeposition of Ni-B4 C dispersion coatings 17 p2483 A83-38051
- The effect of hot-pressing conditions on the structure and mechanical properties of boron carbide 23 p3439 A83-48525

BORON COMPOUNDS

- NT BORATES
- NT BORIDES
- NT BORON CARBIDES
- NT BORON FLUORIDES
- NT BORON NITRIDES
- NT BORON-EPOXY COMPOUNDS
- NT CARBORANE
- NT CHROMIUM BORIDES
- NT TITANIUM BORIDES
- Low frequency dielectric relaxation in boracites 12 p1709 A83-29555

BORON FIBERS

- A study of residual stresses in boron filaments 02 p0150 A83-12351
- Thermal expansion of fibers in the temperature range 20-470 K 06 p0725 A83-18514
- Prediction of fracture toughness of unidirectional metal matrix composites 18 p2654 A83-40196
- Strengthening effect and interfacial adhesion of boron and silicon carbide fibre reinforced aluminum 18 p2659 A83-40252
- Influence of the interface on transverse strength, creep behaviour, and impact behaviour of boron and silicon carbide fibre reinforced aluminum 18 p2659 A83-40253
- Bending characteristics of boron-aluminum composites 18 p2660 A83-40268
- The structure of boron in boron fibres 21 p3116 A83-44342
- The mechanism of elastic energy absorption in boron fibers 24 p3553 A83-49474

BORON FLUORIDES

- Implantation of boron and boron fluoride compounds into silicon for production of solar cells 14 p2005 A83-32331

BORON HYDRIDES**NT CARBORANE****BORON NITRIDES**

- Characteristics of the cold compaction of wurtzite-like boron nitride powders at high pressures 02 p0160 A83-13026
- The cold pressing of wurtzitic boron nitride powders at high pressures 09 p1239 A83-25065
- The effect of thermal shock on the substructure and strength of single-crystal cubic boron nitride 15 p2142 A83-35043

BORON REINFORCED MATERIALS**NT BORON-EPOXY COMPOUNDS**

- Compliance of a unidirectionally reinforced inelastic material 02 p0150 A83-12353
- The cyclic strength of reinforced magnesium-matrix composites 02 p0151 A83-13038
- A study of the short-term strength of boron-composite-reinforced tubular specimens at room and cryogenic temperatures 06 p0725 A83-19310
- Room-temperature tensile strength of boron-aluminum composite as a function of annealing temperature and time 08 p1054 A83-22100
- Room-temperature tensile strength of fibres in boron-aluminium, boron-titanium and graphite-aluminium composites as a function of annealing temperature and time 09 p1225 A83-25148
- Notched unidirectional boron/aluminum - Effect of matrix properties 10 p1389 A83-25881
- The structure of boron in boron fibres 21 p3116 A83-44342

BORON TRIFLUORIDE**U BORON FLUORIDES****BORON-EPOXY COMPOUNDS**

- The problem of a crack in an orthotropic strip 06 p0778 A83-19546
- Advanced design structural considerations when introducing new materials and construction methods 12 p1701 A83-29394
- The fracture mechanism of carbon and boron composites in interlayer shear 16 p2323 A83-35509

BOROSILICATE GLASS

- A compliant, high failure strain, fibre-reinforced glass-matrix composite 04 p0455 A83-15989
- The structural-chemical role of iron in the reaction processes of the soldering of titanium with iron-containing alkali-free aluminoborosilicate glasses 07 p0873 A83-20685

Honeycomb mirrors of borosilicate glass

- 10 p1436 A83-25831
- Manufacture of large glass honeycomb mirrors --- for astronomical telescopes 13 p1921 A83-31013

BOSE-EINSTEIN STATISTICS**U QUANTUM STATISTICS****BOSONS**

- NT ALPHA PARTICLES
- NT LIGHT BEAMS
- NT MESONS
- NT MUONS
- NT PHOTONS
- NT PIONS
- NT VECTOR MESONS
- Axions and the evolution of structure in the universe 10 p1507 A83-26271
- Limits to the number of neutrinos - A comment on the Z(0) discovery 21 p3203 A83-44198
- On the statistical distribution off massive fermions and bosons in a Friedmann universe 23 p3518 A83-47442

BOTANY**NT GEOBOTANY****BOULES**

- Recent developments in infrared acousto-optic tunable filters 03 p0393 A83-13770

BOUNDARIES

- NT FLUID BOUNDARIES
- NT FREE BOUNDARIES
- NT GAS-SOLID INTERFACES
- NT GRAIN BOUNDARIES
- NT JET BOUNDARIES
- NT LIQUID-LIQUID INTERFACES
- NT LIQUID-SOLID INTERFACES
- NT LIQUID-VAPOR INTERFACES
- International law of territorial boundaries of sea, air, and outer space 18 p2753 A83-39697
- Limitations of some common lateral boundary schemes used in regional NWP models --- Numerical Weather Prediction 20 p3029 A83-42508
- Multiple-window parallel adaptive boundary finding in computer vision 21 p3192 A83-43952

BOUNDARY ELEMENT METHOD

- Determination of thermal stresses in disks with the Boundary Element Method 01 p0058 A83-10574
- Interactive computer graphic preprocessing for three-dimensional boundary-integral element analysis 02 p0228 A83-12744
- A family of hybrid plate elements 02 p0196 A83-12837
- On the numerical solution of constrained variational problems by boundary and finite elements 04 p0529 A83-14958
- Three-dimensional grid generation using elliptic equations with direct grid distribution control [AIAA PAPER 83-0448] 05 p0636 A83-16720
- Curved elements with polynomials of varying degree 05 p0682 A83-17555
- Boundary element method in fracture mechanics 07 p0947 A83-20925
- Numerical solution of viscous flows using integral equation methods 08 p1085 A83-22649
- The boundary element method applied to the creeping motion of a sphere 08 p1087 A83-23182
- Elastic-plastic boundary element analysis as a linear complementarity problem 11 p1593 A83-27774
- A novel boundary infinite element 11 p1649 A83-28418
- The method of boundary interpolation in fracture mechanics problems 11 p1597 A83-28476
- A contribution to the solution of axisymmetric thermoelastic notch problems using the boundary integral equation method --- German thesis 11 p1599 A83-28646
- Finite element, boundary element and coupled analysis of unbounded problems in elastostatics 13 p1868 A83-31641
- Progress in boundary element methods. Volume 2 15 p2224 A83-33852
- Non-linear potential problems 15 p2225 A83-33853
- Wave propagation phenomena --- in fluids and structures 15 p2225 A83-33854
- Fracture mechanics stress analysis 15 p2173 A83-33855
- Linear isotropic elasticity with body forces 15 p2173 A83-33856
- Fluid structure interaction 15 p2157 A83-33858
- Viscoplasticity and creep using boundary elements 15 p2174 A83-33859
- Discontinuous boundary elements for heat conduction 15 p2158 A83-34228
- On the accuracy of the boundary element method for three-dimensional conduction problems 15 p2158 A83-34229

- The calculation of electromagnetic fields by numerical methods 16 p2406 A83-35517
- Mixed mode fracture analysis of rectilinear anisotropic plates using singular boundary elements 16 p2369 A83-36555
- Nonlinear bending analyses of heated sandwich plates and shells by the boundary element method 16 p2369 A83-36728
- Boundary element methods in creep and fracture --- Book 17 p2518 A83-37159
- Boundary-element program realization for the solution of two or three-dimensional thermoelastic problems with volume forces --- German thesis 17 p2520 A83-37500
- A new approach to free vibration analysis using boundary elements 17 p2522 A83-37734
- Three-dimensional curved crack in an elastic body 18 p2700 A83-39558
- Boundary element methods; Proceedings of the Third International Seminar, Irvine, CA, July 7-9, 1981 19 p2896 A83-41516
- The treatment of thermoelastic boundary-value problems by means of the boundary element method 20 p3006 A83-42998
- The solution of three-dimensional elasticity problems using the boundary-element method 20 p3006 A83-42999
- Boundary element method applied to photoelastic analysis 21 p3153 A83-44590
- A boundary element solution to elasto-plastic torsion of solids of revolution 21 p3160 A83-45053
- Some recent advances in boundary element methods 22 p3352 A83-46419

BOUNDARY INTEGRAL METHOD

- Three dimensional crack analysis for an anisotropic body 01 p0059 A83-10709
- Fundamental solutions for the collocation method in planar elastostatics 01 p0060 A83-10711
- An integral equation approach to finite deflection of elastic plates 01 p0060 A83-10861
- A study of transient plate bending displacements using a boundary integral equations method 02 p0189 A83-11859
- Interactive computer graphic preprocessing for three-dimensional boundary-integral element analysis 02 p0228 A83-12744
- Boundary integral equation method calculations of surface regression effects in flame spreading 03 p0294 A83-13488
- On the numerical solution of constrained variational problems by boundary and finite elements 04 p0529 A83-14958
- The scattering of elastic waves by isolated cracks using a new integral equation model 04 p0491 A83-15201
- Kinematic, integral, and thermal characteristics of the turbulent flow of a suspension in a gas under the effect of thermal nonstationarity 04 p0476 A83-15446
- Integral method to thermally developing laminar flow in a duct subjected to external radiation and convection [AIAA PAPER 83-0529] 05 p0637 A83-16768
- Two stress intensity factor calculation methods and solutions for various three-dimensional crack problems 08 p1116 A83-21660
- An integral method in laminar film condensation of plane and axisymmetric bodies 08 p1083 A83-21893
- A solution technique for indirect boundary integral equation in planar elasto-plastic problems 09 p1278 A83-23668
- Boundary solutions for the linear theory of structures and the generalization of the work theorem 09 p1280 A83-24510
- The boundary integral method for the solution of planar multirack problems of linear elastostatics --- German thesis 09 p1281 A83-24846
- A boundary integral equation for the solution of a class of problems in anisotropic inhomogeneous thermostatics and elastostatics 10 p1470 A83-25874
- Analysis of elastic torsion in a bar with circular holes by a special boundary integral method 10 p1440 A83-26435
- On random transverse vibrations of a rotating beam with a tip mass - Method of integral equations 11 p1594 A83-28407
- Waves in stratified homogeneous elastic media - The method of boundary integrals in nonstationary problems of dynamics --- Russian book 12 p1774 A83-28826
- Boundary integral equation solution of the Berger equation 13 p1866 A83-30447
- Fracture mechanics stress analysis 15 p2173 A83-33855
- Linear isotropic elasticity with body forces 15 p2173 A83-33856
- Boundary integral equations for bending of thin plates 15 p2174 A83-33857
- Discontinuous boundary elements for heat conduction 15 p2158 A83-34228

- New results in transient heat transfer analysis by the boundary integral equation method 15 p2159 A83-34250
- Boundary integral equations for inextensible materials 15 p2130 A83-34341
- Some observations on Kelvin's solution in classical elastostatics as a double tensor field with implications for Somigliana's integral 16 p2369 A83-36550
- A new approach to free vibration analysis using boundary elements 17 p2522 A83-37734
- A boundary integral equation method for thermal bending of plates 18 p2697 A83-39425
- Compression of an elastic cylinder between two rigid planes Application of the indirect fictitious-boundary integral method to a contact problem 18 p2697 A83-39455
- Three-dimensional curved crack in an elastic body 18 p2700 A83-39558
- Solution of external boundary-value elasticity problems using the method of boundary integral equations 19 p2857 A83-41210
- Surface integral numerical solution for general steady heat conduction in composite media 20 p2971 A83-42666
- A method for the computation of inertial properties for general areas 20 p3038 A83-42796
- Boundary integral equation method in thermoelasticity. I General analysis 20 p3003 A83-42837
- Boundary integral equations applied in the characterization of elastic materials 20 p3006 A83-42995
- Extension of a boundary integral equation method to plates with elastically supported edges 20 p3006 A83-42997
- Economical solution technique for boundary integral matrices 20 p3042 A83-43648
- Stress analysis by combination of holographic interferometry and boundary-integral method 21 p3161 A83-45160
- Three-dimensional boundary-layer calculations in design aerodynamics 22 p3251 A83-47034
- A method for measuring the integral characteristics of boundary layers 24 p3581 A83-48949

BOUNDARY LAYER COMBUSTION

- Combustion of a layer of fuel in a flow of oxidizer over its surface 03 p0295 A83-14058
- The nonuniqueness and instability of steady-state combustion modes in a boundary layer with intense injection 03 p0296 A83-14898
- On the influence of the plate thickness on the boundary layer ignition for large activation energies 07 p0878 A83-19839
- Numerical study of a confined premixed laminar flame - Oscillatory propagation and wall quenching 07 p0879 A83-19842
- The erosion combustion of a solid fuel under various temperatures of the ventilating flow 07 p0901 A83-19951
- The combustion of substances with a liquid reaction layer 07 p0880 A83-19953
- Premixed combustion in a turbulent boundary layer with injection 09 p1225 A83-23750
- Laser fluorescence measurements of the OH concentration in a combustion boundary layer 09 p1226 A83-24367
- Experimental investigation of shock initiated methane-combustion near a wall 10 p1391 A83-26200
- Numerical study of transient laminar combustion in boundary layer flow 15 p2161 A83-34267
- Laminar boundary layers behind detonation waves 18 p2684 A83-39450
- Phase transformations in an inverse wave of filtrational combustion 24 p3556 A83-49783

BOUNDARY LAYER CONTROL

- NT POROUS BOUNDARY LAYER CONTROL
- Flow characteristics around a circular cylinder with a slit. II Effect of boundary layer suction 02 p0175 A83-13069
- Passive shock wave/boundary layer control for transonic airfoil drag reduction [AIAA PAPER 83-0137] 05 p0580 A83-16546
- Turbulent drag reduction for external flows [AIAA PAPER 83-0227] 05 p0582 A83-16597
- Development of a radial diffuser with boundary layer control 07 p0863 A83-21009
- Control of turbulent boundary layer flows by sound [AIAA PAPER 83-0726] 10 p1475 A83-25937
- Optimization of heat transfer in an incompressible-fluid boundary layer with allowance for the heat-balance equation 12 p1723 A83-29279
- A missile flight control system using boundary layer thrust vector control [AIAA PAPER 83-1149] 16 p2293 A83-36246

- Boundary layer TVC for missile applications --- Thrust Vector Control [AIAA PAPER 83-1153] 16 p2293 A83-36249
- Experimental investigation of the effects of wall suction and blowing on the performance of highly offset diffusers [AIAA PAPER 83-1169] 16 p2297 A83-36922
- Active flow control effects on boundary layer development around a protuberance at high subsonic speed [AIAA PAPER 83-1737] 17 p2445 A83-37216
- An electrogasdynamics boundary layer on a dielectric plate 17 p2505 A83-37523
- The effect of a sudden change in the motion of a plate surface on flow in a laminar boundary layer in supersonic flow 17 p2450 A83-37634
- Self-similar solutions of the equations of a boundary layer on a moving surface 17 p2506 A83-37635
- Injection slot location for boundary-layer control in shock-induced separation 19 p2789 A83-41050
- A flight test of laminar flow control leading-edge systems [AIAA PAPER 83-2508] 23 p3404 A83-48356
- Design integration of laminar flow control for transport aircraft [AIAA PAPER 83-2440] 24 p3547 A83-49577
- BOUNDARY LAYER EQUATIONS**
- Numerical simulation of turbulent flows in three-dimensional boundary layers 02 p0170 A83-11873
- Boundary layer on finite wings and related bodies with consideration of the attachment line region 03 p0280 A83-14612
- Asymptotic solutions of the laminar boundary-layer equations 03 p0323 A83-14675
- Approximate integration of the nonstationary equations of a diffusion or thermal boundary layer 04 p0475 A83-15084
- A diffusion equation illustrating spectral theory for boundary layer stability [AD-A123209] 04 p0479 A83-16182
- The use of the method of generalized self-similarity for computing turbulent boundary layers 04 p0480 A83-16392
- Calculation method for three dimensional turbulent boundary layers 04 p0480 A83-16431
- Direct/inverse, compressible turbulent boundary-layer computations using a two-equation turbulence model [AIAA PAPER 83-0453] 05 p0636 A83-16724
- Branching of the Falkner-Skan solutions for gamma less than zero 05 p0642 A83-17942
- A new transformation and method of solution of laminar boundary layer equations 06 p0756 A83-18152
- The computation of the compressor cascade boundary layer 06 p0712 A83-18153
- Boundary layer calculations in the inverse mode for incompressible flows over infinite swept wings [AIAA PAPER 83-0454] 06 p0714 A83-19590
- A new multifold series general solution of the steady, laminar boundary layers. I - Theory of the multifold series expansion. II - Application theory of the Euler transformation 07 p0925 A83-20278
- About a turbulence model to predict heat transfer correlations 07 p0926 A83-21008
- A finite boundary method for fluid flow field computations 07 p0927 A83-21436
- A new type of boundary layer in a rapidly rotating gas 08 p1086 A83-23098
- Accurate solutions for laminar and turbulent boundary layers at very large pressure gradient parameters 08 p1089 A83-23195
- Application of the modified Lax-Wendroff method to the solution of unsteady self-similar problems of boundary layer theory 09 p1258 A83-23572
- Flow in the base region in a channel --- supersonic jet discharge from nozzle 09 p1197 A83-24042
- Exact solution of the thermal boundary-layer equations for an arbitrary heat-flux distribution on a surface in a flow 10 p1417 A83-26253
- Numerical calculation of local convective heat transfer coefficients over air-cooled vane surfaces 10 p1418 A83-26772
- The method of successive approximations in the problem of a boundary layer with longitudinal and transverse pressure differentials 12 p1723 A83-29284
- Nonsimilar boundary layers on the leeside of cones at incidence 13 p1804 A83-31591
- A novel property of the displacement thickness in three-dimensional boundary-layer theory 14 p2013 A83-33381
- Solution of the equations of an unsteady boundary layer 16 p2349 A83-35533
- Calculation of stresses on the free edge in composite plates undergoing mechanical and thermal loading [ONERA, TP NO. 1983-20] 16 p2368 A83-36429

- Numerical solutions of three-dimensional time-dependent compressible turbulent integral boundary-layer equations in general curvilinear coordinates
[AIAA PAPER 83-1674] 17 p2501 A83-37183
- Finite-difference simulation of transonic separated flow using a full potential boundary layer interaction approach
[AIAA PAPER 83-1689] 17 p2502 A83-37189
- Transformation of the equations of a three-dimensional boundary layer for numerical calculation
17 p2506 A83-37635
- Self-similar solutions of the equations of a boundary layer on a moving surface
17 p2506 A83-37635
- Coupled Euler/Integral Boundary Layer analysis in transonic flow
[AIAA PAPER 83-1806] 17 p2508 A83-38640
- Flow development in the vicinity of the sharp trailing edge on bodies impulsively set into motion. II
18 p2632 A83-39213
- An interacting boundary layer model for cascades
[AIAA PAPER 83-1915] 18 p2635 A83-39372
- A class of exact solutions of the laminar-boundary-layer equations
19 p2845 A83-41892
- Advanced boundary-layer theory in heat transfer
20 p2970 A83-42657
- A view of the triple deck --- low speed boundary layer theory
20 p2930 A83-43120
- A Meksyn series method for the Falkner-Skan equation with mass transfer
21 p3128 A83-44023
- Similarity solutions of the boundary-layer equations for a stretching wall
21 p3129 A83-44459
- A new method of boundary layer correction in the design of supersonic wind tunnel nozzle
21 p3087 A83-44561
- Prediction of sudden expansion flows using the boundary-layer equations
[ASME PAPER 83-FE-11] 23 p3450 A83-48230
- Calculation of a boundary layer with phase transformations --- oxygen condensation at cooled surface
24 p3579 A83-49661
- A time-dependent approach for calculating steady inverse boundary-layer flows with separation
24 p3580 A83-49879
- ## BOUNDARY LAYER FLOW
- NT BOUNDARY LAYER SEPARATION
- NT REATTACHED FLOW
- NT SECONDARY FLOW
- NT SEPARATED FLOW
- Free convection fluctuating boundary layer on a horizontal plate
01 p0044 A83-10124
- Transient extinction of counter flow diffusion flame
01 p0022 A83-10497
- Asymptotic expansions for the problem of boundary layer formation
01 p0047 A83-11273
- Higher order boundary layer approximations for some flows of a power law fluid - Related solutions
02 p0169 A83-11858
- Slow rotating stratified flow past obstacles of large height
02 p0173 A83-12856
- On the stability of almost parallel boundary layer flows
02 p0174 A83-13019
- Flows in diffusers interfered with wake behind a circular cylinder
02 p0174 A83-13068
- Turbulent boundary-layer flow over re-entry bodies including roughness effects
03 p0278 A83-13146
- Investigation of intermittent phenomena in two phase boundary layer
03 p0319 A83-14473
- Calculation method for transonic separated flows over airfoils including spoiler effects
[ONERA, TP NO. 1982-66] 03 p0279 A83-14526
- Rotation and curvature effects on Reynolds stresses in boundary-layers
[ONERA, TP NO. 1982-81] 03 p0320 A83-14533
- Compressible boundary-layer flow at a three-dimensional stagnation point with massive blowing
03 p0322 A83-14672
- Boundary-layer diffusion on a plate with inhomogeneous chemical properties
03 p0323 A83-14900
- Boundary layer effects on sound in a circular duct
04 p0532 A83-15066
- Reflection of sound by a boundary layer
04 p0532 A83-15067
- Correlation of the detachment of two-dimensional turbulent boundary layers
04 p0442 A83-15284
- Taylor-Goertler vortices in fully developed or boundary-layer flows Linear theory
04 p0479 A83-16267
- The unsteady collision of free-convective boundary layers
04 p0480 A83-16363
- New implicit boundary procedures - Theory and applications
[AIAA PAPER 83-0123] 05 p0579 A83-16536
- Effect of boundary layers on solid walls in three-dimensional subsonic wind tunnels
[AIAA PAPER 83-0144] 05 p0580 A83-16553
- A multi-grid method for the computation of viscid/inviscid interactions on airfoils
[AIAA PAPER 83-0234] 05 p0582 A83-16602
- A laser interferometer for measuring skin friction in three-dimensional flows
[AIAA PAPER 83-0385] 05 p0643 A83-16685
- Investigation of the effects of upstream sidewall boundary-layer removal on a supercritical airfoil
[AIAA PAPER 83-0386] 05 p0585 A83-16686
- A one-dimensional unsteady model of dual mode scramjet operation
[AIAA PAPER 83-0422] 05 p0597 A83-16705
- Grid adaption for problems with separation, cell Reynolds number, shock-boundary layer interaction, and accuracy
[AIAA PAPER 83-0449] 05 p0636 A83-16721
- Adaptive grids generated by elliptic systems --- for computational fluid dynamics
[AIAA PAPER 83-0451] 05 p0636 A83-16723
- Structure of turbulence in curved wall boundary layers
[AIAA PAPER 83-0457] 05 p0636 A83-16726
- Experimental investigation of the confluent boundary layer of a multielement low speed airfoil
[AIAA PAPER 83-0566] 05 p0588 A83-16793
- An asymptotic analysis of free convection boundary layer on a horizontal flat plate due to small fluctuations in surface temperature
05 p0638 A83-17321
- Approximate correction for the effect of injectants on the ionization level in the boundary layer of a blunt body and in its near wake
05 p0590 A83-17423
- Construction of pointwise bounds for solutions of the problem of flow on a uniformly heated moving continuous flat surface
05 p0640 A83-17552
- Boundary-layer development on circular cylinders
06 p0756 A83-18235
- The turbulent wind flow over an embankment
06 p0789 A83-18239
- Boundary-layer pressures and the Corcos model - A development to incorporate low-wavenumber constraints
06 p0757 A83-19013
- The effect of acoustics and flow conditions in the wall boundary layer of a nozzle on the mixing layer of a submerged jet
06 p0760 A83-19429
- A note on the specification of freestream velocity in the calculation of the boundary layer flow around bodies of revolution at incidence
07 p0862 A83-19665
- Critical angle of incidence for the flow around spheroids
07 p0862 A83-19668
- On spatial and temporal stability in three dimensional fluid flows
07 p0927 A83-21343
- A system for phase and intermittency measurements in periodically turbulent flows
08 p1091 A83-21980
- A new type of boundary layer in a rapidly rotating gas
08 p1086 A83-23098
- The modeling of heat transfer in a boundary layer
09 p1257 A83-23427
- Determination of the cavitation boundary in liquid flows through constricting devices
09 p1258 A83-23432
- Application of the modified Lax-Wendroff method to the solution of unsteady self-similar problems of boundary layer theory
09 p1258 A83-23572
- Supercritical airfoil boundary-layer and near-wake measurements
09 p1196 A83-24027
- Analysis of circulation-controlled airfoils in transonic flow
09 p1196 A83-24032
- Wall pressure fluctuations in attached boundary-layer flow
09 p1198 A83-24655
- Numerical modeling of diurnal convergence oscillations above sloping terrain
10 p1450 A83-25385
- Formation of streamwise vortices in the flow past a corner
10 p1371 A83-25569
- The effect of an elastic wall on the boundary layer
10 p1413 A83-25593
- Uniform asymptotic approximations for duct eigenfunctions in a thin boundary layer flow
[AIAA PAPER 83-0668] 10 p1473 A83-25905
- Control of turbulent boundary layer flows by sound
[AIAA PAPER 83-0726] 10 p1475 A83-25937
- Current studies at Calspan utilizing short-duration flow techniques
10 p1379 A83-26128
- Determination of shock tube boundary layer parameter utilizing flow marking
10 p1415 A83-26150
- Boundary layer influenced shock structure
10 p1415 A83-26154
- Exact solution of the thermal boundary-layer equations for an arbitrary heat-flux distribution on a surface in a flow
10 p1417 A83-26253
- Flow in a rectangular diffuser with local flow detachment in the corner region
11 p1565 A83-27410
- Boundary layer effects on impingement and erosion
11 p1566 A83-27425
- Plastic boundary layers induced by variable wall friction
11 p1567 A83-27866
- Influence of surface compliance on boundary layer noise
[AIAA PAPER 83-0738] 11 p1652 A83-28018
- Effect of flow on the acoustic performance of extended reaction lined ducts
[AIAA PAPER 83-0778] 11 p1652 A83-28024
- Mixed laminar convection on a vertical surface under conditions of strong injection
11 p1571 A83-28799
- The three-dimensional laminar asymptotic boundary layer with suction
12 p1721 A83-28847
- Modification of subsonic wakes using boundary layer and base mass transfer
12 p1695 A83-28954
- A technique for exact determination of the parietal pressure in a flow
12 p1724 A83-29389
- Elliptic-vortex method for incompressible flow at high Reynolds number
12 p1724 A83-29609
- Three-dimensional boundary conditions in supersonic flow
12 p1697 A83-29654
- Radiative heat transfer in absorbing, emitting and anisotropically scattering boundary layer flows
[AIAA PAPER 83-1504] 14 p2010 A83-32742
- Effect of turbulent boundary layer flow on optical transmission
[AIAA PAPER 83-1524] 14 p2085 A83-32755
- Theoretical studies of boundary layers --- Russian book
15 p2158 A83-34163
- Numerical study of transient laminar combustion in boundary layer flow
15 p2161 A83-34267
- A theoretical and experimental study of non-adiabatic wall effects on transonic shock/boundary layer interaction
[AIAA PAPER 83-1421] 15 p2120 A83-34901
- Three-dimensional flow studies on a slotted transonic wind tunnel wall
16 p2293 A83-36086
- Progress toward the analysis of supersonic inlet flows
[AIAA PAPER 83-1371] 16 p2295 A83-36366
- Unsteady nonsimilar laminar boundary-layer flows with heat and mass transfer
17 p2501 A83-37024
- Oblique instream streamline intersections
17 p2501 A83-37026
- Experimental studies of the boundary layer on an airfoil at low Reynolds numbers
[AIAA PAPER 83-1671] 17 p2444 A83-37181
- An experimental study of surface curvature effects on a supersonic turbulent boundary layer
[AIAA PAPER 83-1672] 17 p2444 A83-37182
- Stability experiments in rotating-disk flow
[AIAA PAPER 83-1760] 17 p2503 A83-37232
- Boundary layers on characteristic surfaces for time-dependent rotating flows
17 p2504 A83-37377
- On a method for the closure of the energy equation formulated relative to the total enthalpy in the case of turbulent flow in a boundary layer
17 p2505 A83-37530
- Investigation of the parameters of a boundary layer before the inlet of a supersonic air intake mounted under the surface of a triangular plate
17 p2448 A83-37533
- Allowing for the effect of a weak inhomogeneity in a boundary-layer flow on its stability characteristics
17 p2506 A83-37812
- Experimental evaluation of inlet turbulence, wall boundary layer, surface finish, and fillet radius on small axial turbine stage performance
[SAE PAPER 821475] 17 p2469 A83-38001
- The linear development of Goertler vortices in growing boundary layers
18 p2680 A83-39205
- Wall-function boundary conditions in the solution of the Navier-Stokes equations for complex compressible flows
[AIAA PAPER 83-1694] 18 p2633 A83-39268
- Developing mass spectrometric techniques for boundary layer measurement in hypersonic high enthalpy test facilities
18 p2689 A83-39937
- Calculation of two-dimensional diffusers
18 p2686 A83-39989
- Nonsimilar laminar incompressible boundary layer flow over a rotating sphere
19 p2843 A83-41542
- Global PNS solutions for subsonic strong interaction flows over a cone-cylinder-boattail geometry --- Parabolized Navier-Stokes equation
20 p2928 A83-42554
- Longitudinal vortices in wind tunnel wall boundary layers
20 p2928 A83-42622
- Convex curvature effects on the heated turbulent boundary layer
20 p2978 A83-42733
- A turbulent burst model for boundary layer flows with pressure gradient
20 p2978 A83-42736
- Numerical investigation of the propagation of a linear wave packet in a boundary flow
20 p2983 A83-43007
- Flow in a hypersonic boundary layer on a delta wing of finite length at angle of attack
20 p2931 A83-43522
- Computation of turbulent flow over a moving wavy boundary
21 p3128 A83-43927
- A method for experimental analysis of the shock-boundary layer interaction in cascades
[ONERA, TP NO. 1983-48] 21 p3086 A83-44322

- 3-D shock-boundary layer solution from Navier-Stokes equations 21 p3087 A83-44563
- Measurements of some features of turbulence in wall-proximity 21 p3132 A83-44973
- Combined four-wall interference assessment in two-dimensional airfoil tests 21 p3093 A83-45576
- On vortex formation and interaction with solid boundaries 22 p3280 A83-45902
- Unsteady turbulent shear flows; Proceedings of the Symposium, Toulouse, France, May 5-8, 1981 22 p3281 A83-46426
- A review of unsteady turbulent boundary-layer experiments 22 p3281 A83-46427
- Dynamic behavior of an unsteady turbulent boundary layer 22 p3281 A83-46428
- Prediction of boundary-layer characteristics of an oscillating airfoil 22 p3248 A83-46435
- On the turbulence-modeling requirements of three-dimensional boundary-layer flows 22 p3248 A83-46456
- Viscid-inviscid interaction analysis on airfoils with an inverse boundary layer approach 22 p3249 A83-46474
- Boundary layer calculations for cryogenic wind tunnel flows 22 p3250 A83-46478
- Entropy production rates from viscous flow calculations. I - A turbulent boundary layer flow [ASME PAPER 83-GT-70] 23 p3512 A83-47923
- Design of shock-free compressor cascades including viscous boundary layer effects [ASME PAPER 83-GT-134] 23 p3396 A83-47961
- Wall boundary layer development near the tip region of an IGV of an axial flow compressor [ASME PAPER 83-GT-171] 23 p3396 A83-47972
- Calculation of friction and heat transfer on the profile of a turbomachine cascade 23 p3399 A83-48449
- Second-order boundary-layer flow past sharp cones 23 p3399 A83-48625
- Boundary layer with self-induced pressure during the transonic flow past the corner point of an airfoil 24 p3545 A83-49526
- Turbulent shear flows behind two-dimensional obstacles placed on plane boundary 24 p3579 A83-49803
- The effect of upstream boundary layer thickness upon flow past a backward-facing step 24 p3579 A83-49807
- Propagation of finite amplitude disturbances in the weakly non-parallel boundary layer 24 p3580 A83-49832
- Hall effect in a boundary layer flow --- over MHD generator walls 24 p3633 A83-50150
- BOUNDARY LAYER NOISE**
- U AERODYNAMIC NOISE
- U BOUNDARY LAYERS
- BOUNDARY LAYER PLASMAS**
- A theory for spherical electric probes in a weakly ionized plasma at rest 04 p0536 A83-15092
- Transition from single to multiple double layers --- of plasma 05 p0688 A83-17351
- Appearance of electrodynamic boundary layers during the propagation of sound in a confined low-temperature plasma 07 p0994 A83-19638
- MHD channel electrical boundary-layer theory and applications 08 p1168 A83-23131
- Exit of boundary layer plasma from the distant magnetotail 09 p1305 A83-24342
- Magnetic structure of the boundary layer --- explaining magnetospheric convection 11 p1614 A83-27391
- Accuracy of mass spectrometric low-temperature plasma diagnostics 13 p1925 A83-30812
- The interaction of magnetic fields at the boundary of the earth's magnetosphere 14 p2052 A83-32534
- Helical wave and K-H instability in type I comet tails. II Waves of infinitesimal amplitude in compressible plasma 14 p2102 A83-32924
- The thermal boundary layer in dual flow arc plasmas [AIAA PAPER 83-1747] 17 p2581 A83-37222
- Kelvin-Helmholtz instability in boundary layer regions of the plasma sheet during magnetospheric substorm recovery 21 p3171 A83-44291
- Coupling mechanism of boundary sheaths and wave launcher in a collisionless plasma 21 p3214 A83-45189
- Plasma boundary motion and the ion-acoustic wave 21 p3214 A83-45195
- Nonlinearly induced radiation from an overdense plasma region 24 p3631 A83-48821
- BOUNDARY LAYER SEPARATION**
- Structure of air flow separation over wind wave crests 01 p0075 A83-10725
- Correlation of the detachment of two-dimensional turbulent boundary layers 04 p0442 A83-15284
- New skin friction and entrainment correlations for turbulent boundary layers 04 p0478 A83-16144

- Aerodynamic investigation of closely coupled lifting surfaces with positive and negative stagger for general aviation applications 05 p0578 A83-16489
- [AIAA PAPER 83-0057]
- Flow measurements of an airfoil with deflected spoiler [AIAA PAPER 83-0365] 05 p0584 A83-16672
- A computational method for subsonic compressible flow in diffusers 05 p0587 A83-16753
- [AIAA PAPER 83-0505]
- Shock-induced dynamic stall [AIAA PAPER 83-0547] 05 p0588 A83-16782
- The stability of a preseparation boundary layer at the leading edge of a thin profile 06 p0713 A83-19432
- Experimental investigation of turbulence properties in transonic shock/boundary-layer interactions 07 p0863 A83-19807
- An unsteady interactive separation process --- from downstream moving wall 08 p1042 A83-22131
- Modifying a general aviation airfoil for supercritical flight 09 p1196 A83-24039
- The structure of a separating turbulent boundary layer. IV - Effects of periodic free-stream unsteadiness 09 p1261 A83-24414
- A stall margin design method for planar and axisymmetric diffusers 10 p1413 A83-25685
- [ASME PAPER 82-WA/FE-8]
- Evolution of shock-induced pressure on a flat-face/flat-base body and afterbody flow separation 10 p1372 A83-26159
- Solutions to the boundary value problem with velocity correlations in stratified flow through circular pipe. I 14 p2012 A83-32968
- Separated trailing-edge flow at a transonic Mach number 14 p1971 A83-32976
- Analytical approximation of two-dimensional separated turbulent boundary-layer velocity profiles 14 p2012 A83-32997
- Turbulent and mean flow measurements in an incompressible axisymmetric boundary layer with incipient separation 15 p2156 A83-33668
- Boundary layer development in a supersonic intake 16 p2290 A83-35826
- Prediction of cascade performance in the presence of a separating boundary layer 16 p2292 A83-35876
- Experimental studies of the boundary layer on an airfoil at low Reynolds numbers [AIAA PAPER 83-1671] 17 p2444 A83-37181
- Topological structures of three-dimensional vortex flow separation [AIAA PAPER 83-1735] 17 p2445 A83-37214
- Investigation of flow past an aircraft wing section in flight and in a wind tunnel 17 p2447 A83-37506
- Boundary layer separation from the moving surface of a body in a supersonic gas flow 17 p2448 A83-37509
- Boundary layer separation over a rotating cylinder in a flow of an incompressible fluid 17 p2506 A83-37804
- Interacting flow theory and trailing edge separation - No stall 18 p2633 A83-39214
- The calculation of separation bubbles in interactive turbulent boundary layers 18 p2633 A83-39216
- The structure of a separating turbulent boundary layer. V Frequency effects on periodic unsteady free-stream flows 18 p2681 A83-39217
- Injection slot location for boundary-layer control in shock-induced separation 19 p2789 A83-41050
- Subsonic laminar separation at the breaking point of an airfoil 19 p2790 A83-41216
- Influence of temperature and concentration boundary layers at separation on heat and mass transfer in separated flows 20 p2976 A83-42715
- A view of the triple deck --- low speed boundary layer theory 20 p2930 A83-43120
- Boundary-layer and turbulence intensity measurements in a shock wave/boundary-layer interaction 20 p2930 A83-43455
- Vortices following two dimensional separation 22 p3247 A83-45903
- Experimental study of two- and three-dimensional boundary layer separation 22 p3248 A83-46432
- Some features of unsteady separating turbulent boundary layers 22 p3248 A83-46433
- Influence of wall vibrations on a flow with boundary-layer separation at a convex edge 22 p3282 A83-46444
- The development of vortices in a mixing layer 22 p3282 A83-46448
- Half model testing applied to wings above and below stall 22 p3248 A83-46455
- Finite-difference solutions for laminar boundary layer flows with separation 22 p3249 A83-46459
- A turbulent boundary layer approaching separation 22 p3249 A83-46475
- New developments in open separation --- of three dimensional boundary layers 22 p3250 A83-47016

- Wind tunnel investigations of some three-dimensional separated turbulent boundary layers 22 p3250 A83-47019
- Experiments on a flow with swept separation and reattachment of a boundary layer 22 p3286 A83-47020
- Three-dimensional boundary layers in turbomachines 22 p3286 A83-47021
- A three-dimensional law-of-the-wall including skewness and roughness effects --- for aerodynamic mixing length flow theory 22 p3286 A83-47033
- An evaluation of the final discussion of the IUTAM Symposium on three-dimensional boundary layers 22 p3286 A83-47036
- On the calculation of separation bubbles 23 p3449 A83-48119
- Asymptotic theory of turbulent separation 23 p3452 A83-48655
- Mathematical modeling of unsteady separated flow past a circular cylinder 23 p3452 A83-48667
- Study of turbulence modeling in transonic shock wave-boundary layer interaction [ONERA, TP NO. 1983-84] 24 p3544 A83-49403
- A time-dependent approach for calculating steady inverse boundary-layer flows with separation 24 p3580 A83-49879
- BOUNDARY LAYER STABILITY**
- Free convection fluctuating boundary layer on a horizontal plate 01 p0044 A83-10124
- Three-dimensional or unsteady boundary layers [AAAF PAPER NT 81-16] 02 p0169 A83-11776
- On the non-linear evolution of Goertler vortices in non-parallel boundary layers 02 p0170 A83-12173
- Velocity spectra in the unstable planetary boundary layer 02 p0214 A83-12235
- On the stability of almost parallel boundary layer flows 02 p0174 A83-13019
- Measurement of bursting period and test of surface renewal model in a turbulent boundary layer disturbed by a cylinder 03 p0318 A83-14462
- Upstream influence in sharp fin-induced shock wave turbulent boundary-layer interaction 04 p0442 A83-15296
- The resonant effect of time-dependent boundary distortion on the stability and secondary regimes of a viscous fluid flow 04 p0477 A83-15879
- A diffusion equation illustrating spectral theory for boundary-layer stability [AD-A123209] 04 p0479 A83-16182
- Effect of suction and blowing on boundary-layer transition [AIAA PAPER 83-0043] 05 p0578 A83-16483
- The unsteady boundary layer on an elliptic cylinder following the impulsive onset of translational and rotational motion [AIAA PAPER 83-0128] 05 p0580 A83-16541
- The development of a two-dimensional wavepacket in a growing boundary layer 06 p0755 A83-17973
- Studies of the atmospheric stability characteristics during the solar eclipse of February 16, 1980 06 p0789 A83-18243
- Convection and gravity waves in two layer models. I - Overstable modes driven in conducting boundary layers --- of solar and stellar models 06 p0835 A83-18934
- On the stability of boundary-layer flow over a spring-mounted piston 06 p0757 A83-19017
- The stability of a preseparation boundary layer at the leading edge of a thin profile 06 p0713 A83-19432
- On the OLP prediction of the unstable modes of the flat plate turbulent boundary layer 08 p1089 A83-23197
- Shock induced unsteady flat plate boundary layers and transitions 10 p1414 A83-26147
- Stability limits and transition times of wave-induced wall boundary layers 10 p1415 A83-26151
- Boundary layer behavior on rough surfaces in the presence of a turbulent wake 11 p1565 A83-27417
- Unsteady boundary layer with self-induced pressure near a rapidly heated section of the surface of a flat plate in supersonic flow 11 p1527 A83-28536
- On the role of wall-pressure fluctuations in deterministic motions in the turbulent boundary layer 12 p1723 A83-29232
- Stability of two-dimensional hyperbolic initial boundary value problems for explicit and implicit schemes 12 p1772 A83-29647
- Stability criteria for convection at small Prandtl numbers 14 p2009 A83-32516
- A theoretical model of the coherent structure of the turbulent boundary layer in zero pressure gradient 15 p2155 A83-33656
- The two-dimensional, viscous boundary-value problem for fluctuations in boundary layers [AIAA PAPER 83-0044] 15 p2158 A83-33998
- Solution of the equations of an unsteady boundary layer 16 p2349 A83-35533

The effect of an entropy layer on the propagation of unsteady perturbations in a boundary layer --- of hypersonic viscous gas 16 p2288 A83-35534

Further experiments on shock tube wall boundary-layer transition 16 p2352 A83-36095

Natural laminar flow data from full-scale flight and wind-tunnel experiments 16 p2296 A83-36409

The stability of a laminar boundary layer on an elastic surface 17 p2505 A83-37510

Mathematical modeling of unsteady coherent structures in the near-wall region of a turbulent boundary layer 17 p2506 A83-37632

Allowing for the effect of a weak inhomogeneity in a boundary-layer flow on its stability characteristics 17 p2506 A83-37812

Amplitude-dependent stability of boundary-layer flow with a strongly non-linear critical layer 17 p2509 A83-38924

Stability of the surface layer and its relation to the dispersion of primary pollutants in St. Louis 18 p2711 A83-39122

Laminar boundary layer stability experiments on a cone at Mach 8.1 - Sharp cone [AIAA PAPER 83-1761] 18 p2633 A83-39264

The hydrodynamic structure of accelerating turbulent boundary layers 19 p2842 A83-41252

Acoustic excitation of Tollmien-Schlichting waves in a supersonic boundary layer 19 p2790 A83-41256

Stability characteristics of a boundary gas layer recombining on a cooled wall 19 p2843 A83-41272

The susceptibility of a boundary layer on blunted-nose bodies to acoustic flow oscillations 19 p2791 A83-41274

Thermal instability of two-dimensional stagnation-point boundary layers 20 p2984 A83-43095

Excitation of instability waves in a boundary layer on a vibrating surface 20 p2987 A83-43518

Excitation of Tollmien-Schlichting waves during the scattering of acoustic and vortex perturbations in a boundary layer on a wavy surface 20 p2987 A83-43519

Instability of the boundary layer between a streaming plasma and a vacuum magnetic field 21 p3209 A83-43946

The formation of a stable layer of atoms and ions of metals in the upper atmosphere 21 p3176 A83-45262

The parametric excitation of internal waves and convective instabilities in a fluid layer heated from above 22 p3322 A83-45639

Unsteady adverse pressure gradient turbulent boundary layers 22 p2822 A83-46436

Generation of Taylor-Goertler vortices in decaying swirl flow [ASME PAPER 83-FE-17] 23 p3450 A83-48234

BOUNDARY LAYER TRANSITION

Numerical investigation of a turbulent boundary layer for the case of a positive pressure gradient 01 p0045 A83-10457

The Charney stability problem with a lower Ekman layer 02 p0213 A83-12227

A review of roughness-induced nosetip transition [AIAA PAPER 81-1223] 04 p0442 A83-15277

Effect of suction and blowing on boundary-layer transition [AIAA PAPER 83-0043] 05 p0578 A83-16483

Shuttle Orbiter boundary-layer transition - A comparison of flight and wind tunnel data [AIAA PAPER 83-0485] 05 p0586 A83-16746

Visualization studies of turbulent transition flows in a porous medium [AIAA PAPER 83-0654] 05 p0638 A83-16819

The turbulent motions of a fluid in a closed region in a strong magnetic field 06 p0814 A83-19555

On certain aspects of three-dimensional instability of parallel flows 07 p0927 A83-21353

Low Reynolds number flow between interrupted flat plates 09 p1259 A83-23878

Heat transfer from interrupted plates 09 p1259 A83-23879

The evolution of Tollmien-Schlichting waves near a leading edge 09 p1261 A83-24410

Boundary-layer transition on a rotating cone in axial flow 09 p1262 A83-24416

Boundary-layer transition on a rotating cone in still fluid 09 p1262 A83-24417

Invalidity of local thermodynamic equilibrium for electrons in the solar transition region. I - Fokker-Planck results 10 p1521 A83-25730

Stability limits and transition times of wave-induced wall boundary layers 10 p1415 A83-26151

The development of intermittent turbulence on a swept attachment line including the effects of compressibility 11 p1567 A83-27872

Wind tunnel noise reduction at Mach 5 with a rod-wall sound shield --- for prevention of premature boundary layer transition on wind tunnel models [AIAA PAPER 82-0570] 12 p1704 A83-28952

Flatness change in the transition to turbulent convection 12 p1721 A83-29003

Experimental study of the generation of Goertler vortices in an unsteady boundary layer 12 p1724 A83-29444

The cancellation of a sound-excited Tollmien-Schlichting wave with plate vibration 14 p2013 A83-33377

Turbulent spots, wave packets, and growth 14 p2013 A83-33378

Analysis of STS-2 experimental heating rates and transition data 15 p2125 A83-33732

Asymmetric flows in corner configurations 16 p2288 A83-35532

Unsteady, exponentially-varying standing waves in boundary layers [AIAA PAPER 83-0045] 16 p2351 A83-36041

Single- and multiple-crater induced nosetip transition 16 p2293 A83-36078

Further experiments on shock tube wall boundary-layer transition 16 p2352 A83-36095

The relative effects of Reynolds number and turbulence in transonic flow [AIAA PAPER 83-1726] 17 p2445 A83-37212

Subharmonic three-dimensional disturbances [AIAA PAPER 83-1759] 17 p2503 A83-37231

Boundary layer characteristics of the Miley airfoil at low Reynolds numbers [AIAA PAPER 83-1795] 17 p2453 A83-38634

Nosetip bluntness effects on cone frustum boundary layer transition in hypersonic flow [AIAA PAPER 83-1763] 18 p2633 A83-39265

Holographic measurement of transition and turbulent bursting in supersonic axisymmetric boundary layers [AIAA PAPER 83-1724] 18 p2633 A83-39269

The possibility of a quick determination of the onset of turbulence in a laminar boundary layer 19 p2791 A83-41578

Dynamics of forebody flow separation and associated vortices [AIAA PAPER 83-2118] 19 p2793 A83-41943

Heat-transfer non-uniformities downstream of three-dimensional boundary layer trips 20 p2976 A83-42718

Flight investigation of natural laminar flow on the Bellanca Skyrocket II [SAE PAPER 830717] 20 p2933 A83-43326

Synthetic method in thermal boundary layer transition 20 p2987 A83-43650

Processing of infrared thermal images for aerodynamic research [ONERA, TP NO. 1983-32] 21 p3137 A83-44310

Influence of asymmetric transition on static stability of blunted cones 21 p3087 A83-44562

Effect of surface roughness on the delayed transition on 9:1 heated ellipsoids 21 p3134 A83-45583

Numerical experiments on transition triggering off in a two-dimensional shear flow 22 p3282 A83-46439

On the force fluctuations acting on a circular cylinder in crossflow from subcritical up to transcritical Reynolds numbers 23 p3398 A83-48118

Interaction between the outer inviscid flow and the boundary layer on transonic airfoils 24 p3544 A83-49021

Transition prediction based on a differential field theory of turbulence 24 p3580 A83-49830

BOUNDARY LAYERS

NT ATMOSPHERIC BOUNDARY LAYER

NT COMPRESSIBLE BOUNDARY LAYER

NT HYPERSONIC BOUNDARY LAYER

NT INCOMPRESSIBLE BOUNDARY LAYER

NT LAMINAR BOUNDARY LAYER

NT PLANETARY BOUNDARY LAYER

NT SUPERSONIC BOUNDARY LAYERS

NT THERMAL BOUNDARY LAYER

NT THREE DIMENSIONAL BOUNDARY LAYER

NT TURBULENT BOUNDARY LAYER

NT TWO DIMENSIONAL BOUNDARY LAYER

Continuous temporal eigenvalue spectrum of an Ekman boundary layer 03 p0315 A83-13115

Diffusion processes in the magnetopause boundary layer 03 p0357 A83-13545

Laminar free convection on a vertical nonisothermal plate under strong injection 04 p0478 A83-16164

Optimally discretized finite elements for boundary-layer stresses in composite laminates 09 p1281 A83-24671

Free convection boundary layers over humps and indentations 11 p1569 A83-28405

Present seismic evidence for a boundary layer at the base of the mantle 12 p1757 A83-29962

Stress concentration layers in finite deformation of fibre-reinforced elastic materials 15 p2130 A83-34344

Determination of boundary-layer width from the minimum-energy condition --- for edge damped cylindrical shells 15 p2178 A83-34443

Dielectric currents in the low-latitude boundary layer and geomagnetic tail 15 p2202 A83-34734

Application of the triple-deck theory of viscous-inviscid interaction to bodies of revolution 16 p2288 A83-35345

Destabilization of a 650 km chemical boundary layer and its bearing on the evolution of the continental crust 21 p3171 A83-44363

A singular hybrid finite element analysis of boundary-layer stresses in composite laminates 23 p3470 A83-48098

The effect of nonequilibrium physical-chemical processes in the boundary layer on the ablation of quartz glass 23 p3452 A83-48665

BOUNDARY LUBRICATION

On the mechanism of lubrication by tricesylphosphate /TCP/ - The coefficient of friction as a function of temperature for TCP on M-50 steel [ASLE PREPRINT 82-LC-4C-1] 03 p0333 A83-13228

The effect of metal composition on the adsorption of zinc di-isopropylidithiophosphate [ASLE PREPRINT 82-LC-4C-2] 03 p0302 A83-13242

Overall characteristics of bearings lubricated with ferrofluids [ASME PAPER 82-LUB-14] 03 p0335 A83-13508

Finite-length solutions for rotodynamic coefficients of turbulent annular seals [ASME PAPER 82-LUB-42] 03 p0336 A83-13521

Surface roughness effects in point contact elastohydrodynamic lubrication 08 p1111 A83-22008

A thermic study of a lubricated Hertzian contact --- French thesis 13 p1858 A83-30151

Analysis of multirecess conical hydrostatic thrust bearings under rotation 21 p3147 A83-44373

BOUNDARY VALUE PROBLEMS

NT CAUCHY PROBLEM

NT DIRICHLET PROBLEM

NT NEUMANN PROBLEM

Asymptotic rates of convergence for the symmetric successive overrelaxation /SSOR/ iterative method by means of an associated eigenvalue problem 01 p0101 A83-10201

Fourier transform perturbation solution of elliptic equations with small nonlinearities 01 p0102 A83-10495

Three dimensional crack analysis for an anisotropic body 01 p0059 A83-10709

Solution of a free-boundary problem for elliptic equations 01 p0102 A83-11264

Stability of an economical difference scheme for the solution of a boundary value problem of diffraction 01 p0104 A83-11271

Certain boundary value problems for the multidimensional wave equation 01 p0102 A83-11314

Boundary value problems for a class of equations containing a derivative with respect to time 01 p0102 A83-11315

Concerning a method for solving boundary value problems for third-order equations 01 p0103 A83-11316

A boundary value problem for the Laplace equation with nonclassical spectral asymptotics 01 p0103 A83-11317

Solvability of boundary value problems for linear and quasi-linear B-elliptic equations 02 p0231 A83-11637

The boundary and initial values of the solutions to second-order parabolic equations 02 p0231 A83-11653

Partial regularity of suitable weak solutions of the Navier-Stokes equations 02 p0170 A83-12100

A Newton-Lanczos method for solution of nonlinear finite element equations 02 p0194 A83-12748

Boundary value problems of composite media 02 p0233 A83-12763

A down-stream boundary procedure for the Euler equations 02 p0174 A83-13021

Boundary manifolds for energy surfaces in celestial mechanics 03 p0404 A83-13409

Global sensitivity to velocity errors at the liberation points 03 p0405 A83-13420

A finite element method for solving Helmholtz type equations in waveguides and other unbounded domains 03 p0390 A83-13567

On a higher order accurate fully discrete Galerkin approximation to the Navier-Stokes equations 03 p0316 A83-13568

Eigenvalue problems on infinite intervals 03 p0387 A83-13569

Analysis of a multilevel iterative method for nonlinear finite element equations 03 p0387 A83-13571
 Generalization of I. Z. Shtokalo's method to boundary value problems for parabolic equations 03 p0387 A83-13688
 The first boundary value problem for the linearized Navier-Stokes equations 03 p0316 A83-13694
 Switching of reflection of light at nonlinear interfaces 03 p0394 A83-13793
 Solution of a unilateral problem using integral equations and finite elements --- French thesis 03 p0390 A83-13809
 Dissipationless galaxy formation and the r to the $1/4$ -power law 03 p0420 A83-13935
 Computing scattering amplitudes for arbitrary cylinders under incident plane waves 03 p0390 A83-14001
 Solving elliptic problems - 1930-1980 03 p0388 A83-14078
 Applications of transfinite /'blending-function'/ interpolation to the approximate solution of elliptic problems 03 p0388 A83-14085
 Mesh generation by conformal and quasiconformal mappings 03 p0388 A83-14089
 The existence and uniqueness of a solution for a boundary-value problem for an equation of mixed type in a rectangular domain 03 p0388 A83-14495
 A-posteriori error analysis and adaptive finite element methods for singularly perturbed convection-diffusion equations 03 p0388 A83-14496
 A note on a Runge-Kutta-Chebyshev method 03 p0388 A83-14511
 A new automatic mesh selection strategy for the solution of boundary value problems with selfadaptive difference methods 03 p0389 A83-14610
 Computation of eigenvalues using two-point boundary value problem codes 03 p0389 A83-14712
 Quasi-periodic boundary-value problems and their application to elasticity theory 03 p0343 A83-14899
 A comparison of different solar magnetic field extrapolation procedures 03 p0438 A83-14909
 Bounded motion for a modified three-body problem 04 p0545 A83-14985
 Applicability of the Boussinesq approximation to solve problems of nonstationary concentrational natural convection 04 p0475 A83-15093
 Separation of the boundary conditions of a shallow spherical shell 04 p0500 A83-16048
 New formulas for the electromagnetic field of a vertical electric dipole in a dielectric or conducting half-space near its horizontal interface [AD-A125370] 04 p0468 A83-16054
 Runge's theorem and far field patterns for the impedance boundary value problem in acoustic wave propagation 04 p0533 A83-16365
 The perturbation method in boundary value problems of the mechanics of deformable bodies 04 p0501 A83-16401
 An improved dislocation approach in solving three-dimensional boundary value problems 05 p0681 A83-17324
 On the nonexistence and existence of global solutions of boundary value problems for quasi-linear parabolic equations --- in propagation of thermal disturbances 05 p0640 A83-17642
 The stability of positive solutions of inverse problems of heat conduction 05 p0640 A83-17649
 Techniques for the solution of MHD generator flows [AIAA PAPER 83-0465] 05 p0689 A83-17928
 Concerning some boundary value problems for a third-order equation and extremal properties of its solutions 06 p0804 A83-17978
 On the theory of compressible fluids 06 p0756 A83-18071
 Behaviour of a thermodynamic model system under time-dependent periodic boundary conditions 06 p0815 A83-18138
 Application of perturbation method to optimal design of structures 06 p0771 A83-18209
 Offset dual reflector synthesis as a boundary-value problem 06 p0743 A83-18684
 Analysis of monopole-antenna with rectangular reflector 06 p0744 A83-18695
 A note on uniqueness in thermoelasticity with one relaxation time 06 p0775 A83-18803
 Existence of a generalized solution in thermoelasticity with two relaxation times. I 06 p0775 A83-18807
 Computer analysis of the significance of surface boundary conditions on the collection of alpha-induced charge --- carrier transport simulation 06 p0753 A83-18960
 Solution of bifurcation problems and limit load problems in certain nonlinear boundary-value problems of continuum mechanics 06 p0777 A83-19322
 On method of successive approximations in a class of problems of the general theory of plasticity 07 p0945 A83-20142

Projection methods in non-self-adjoint problems of mathematical physics 07 p0986 A83-20310
 Concerning a modification of the seminversion method --- for electromagnetic wave propagation 07 p0986 A83-20317
 An integral equation method for electromagnetic scattering of guided modes by boundary deformations of dielectric slab waveguides 07 p0913 A83-20367
 Stability theory of difference approximations for multidimensional initial-boundary value problems 07 p0986 A83-20504
 Collocation methods for boundary value problems on 'long' intervals 07 p0986 A83-20505
 Block Runge-Kutta methods for the numerical integration of initial value problems in ordinary differential equations. I - The nonstiff case. II - The stiff case 07 p0986 A83-20506
 Preconditioning and two-level multigrid methods of arbitrary degree of approximation 07 p0986 A83-20508
 General solution of a certain mixed boundary value crack problem 07 p0948 A83-21167
 Pointwise bounds for the solution of a nonlinear problem in heat conduction 08 p1083 A83-21866
 Application of the initial value method to analysis of elastic-plastic plates and shells of revolution 08 p1121 A83-21890
 Analysis of boundary value problems on infinite intervals 08 p1159 A83-22024
 On the convergence of the finite element approximation of eigenfrequencies and eigenvectors to Maxwell's boundary value problem 08 p1159 A83-22077
 Control of wave processes with distributed controls supported on a subregion 08 p1157 A83-22243
 Cascading bifurcations 08 p1161 A83-22740
 The application of boundary value techniques in the solution of the Navier-Stokes equation 08 p1087 A83-23179
 Symmetric marching technique /SMT/ for the efficient solution of discretized Poisson equation on non-rectangular regions 08 p1091 A83-23218
 The use of the theory of thermal regularity in investigating the effect of radiation on free convection 09 p1258 A83-23448
 Picard's method for solving nonlinear two-point boundary value problem in optimal control theory 09 p1326 A83-23976
 Diffraction of a two-dimensional electromagnetic beam wave by a thick slit pierced in a perfectly conducting screen --- for study of objective incident radiation used to obtain image of star 09 p1268 A83-24091
 Boundary value problem of Bitsadze-Samarski type for a second-order elliptic equation with operator coefficients 09 p1335 A83-24249
 Boundary value problems of mathematical physics and related questions in the theory of functions. 14 --- Russian book 09 p1339 A83-24316
 Stationary solutions of the Navier-Stokes equations in periodic tubes 09 p1260 A83-24319
 The finite-dimensionality of bounded invariant sets for the Navier-Stokes system and other dissipative systems 09 p1261 A83-24321
 Simple relationship between the geometric and Hamiltonian representations of integrable nonlinear equations 09 p1339 A83-24325
 A boundary value problem in the propagation of sound in a rarefied gas 09 p1341 A83-24485
 Boundary solutions for the linear theory of structures and the generalization of the work theorem 09 p1280 A83-24510
 Stability of a class of stochastic distributed parameter systems with random boundary conditions 09 p1334 A83-24807
 The frictionless contact of cracked elastic bodies 09 p1283 A83-25108
 Solution of large sparse nonlinear systems by monotone convergent iterations and applications 09 p1336 A83-25109
 On minimum-principles for the initial-boundary-value problem of elastic-plastic plates with moderate rotations 09 p1283 A83-25217
 On the inverse scattering and direct linearizing transforms for the Kadomtsev-Petviashvili equation 09 p1340 A83-25283
 Boundary value problems in plane strain plasticity 10 p1437 A83-25306
 On the nonlinear versus linearized lower boundary conditions for topographically forced stationary long waves 10 p1450 A83-25384
 The Sommerfeld half-plane problem revisited. II - The factoring of a matrix of analytic functions 10 p1471 A83-25461
 The emergence of solitons of the Korteweg-de Vries equation from arbitrary initial conditions 10 p1471 A83-25464

Convection induced by insulated boundaries in a square 10 p1413 A83-25781
 A boundary integral equation for the solution of a class of problems in anisotropic inhomogeneous thermostatics and elastostatics 10 p1470 A83-25874
 Riccati transformations in the back-and-forth shooting method for solving two-point boundary-value problems 10 p1465 A83-26524
 The analytic continuation of solutions of the generalized axially symmetric Helmholtz equation 10 p1470 A83-26775
 A study of a high-frequency polarized-wave field penetrating a plasma in a transition region with a diffused boundary 10 p1487 A83-26800
 Constraints in general relativity in the form of Maxwell equations 10 p1517 A83-26949
 On the nature of boundary conditions for crack tip stress 11 p1593 A83-27773
 Bounds for the singular values of a matrix 11 p1649 A83-27997
 Computable finite element error bounds for Poisson's equation 11 p1649 A83-27998
 Solution of some boundary value problems of elasticity theory in bipolar coordinates 11 p1594 A83-28196
 The unique solvability of the null field equations of acoustics 11 p1653 A83-28406
 [AD-A129263] Bounding theorems for Stress Intensity Factors 11 p1596 A83-28443
 The solution of nonlinear boundary value problems in the statics of flexible layered shells in the supercritical region 11 p1596 A83-28454
 A numerical implementation of the variational method for solving certain problems in hydrodynamics --- free-surface oscillations of ideal incompressible fluid in axisymmetric cavity 11 p1569 A83-28460
 Two-phase gas-solid particle flow past bodies with allowance for erosion 11 p1569 A83-28540
 The penalty function method and its applications to the numerical solution of boundary value problems 12 p1770 A83-28857
 Euler equations - Implicit schemes and boundary conditions 12 p1695 A83-28959
 Buckled plate vibrations and large amplitude vibrations using high-order triangular elements 12 p1734 A83-28967
 Error estimate for the modified Newton method with applications to the solution of nonlinear, two-point boundary-value problems 12 p1771 A83-29244
 Numerical solution of an elastic boundary layer problem using a multiple shooting technique 12 p1736 A83-29614
 Boundary-fitted coordinate systems for numerical solution of partial differential equations - A review 12 p1772 A83-29620
 Computational techniques for spherical boundary conditions --- thermodynamic systems 12 p1783 A83-29629
 Coordinate generation with precise controls over mesh properties 12 p1772 A83-29631
 Solution of burner-stabilized premixed laminar flames by boundary value methods 12 p1712 A83-29642
 Numerical boundary condition procedures and multigrid methods; Proceedings of the Symposium, NASA Ames Research Center, Moffett Field, CA, October 19-22, 1981 12 p1772 A83-29646
 Stability of two-dimensional hyperbolic initial boundary value problems for explicit and implicit schemes 12 p1772 A83-29647
 Implicit boundary conditions for the solution of the parabolized Navier-Stokes equations for supersonic flows 12 p1697 A83-29648
 Far field boundary conditions for compressible flows 12 p1725 A83-29649
 Stability analysis of numerical boundary conditions and implicit difference approximations for hyperbolic equations 12 p1772 A83-29650
 Fully implicit shock tracking 12 p1725 A83-29651
 Influence of boundary approximations and conditions on finite-difference solutions 12 p1772 A83-29652
 The choice of numerical boundary conditions for hyperbolic systems 12 p1772 A83-29653
 Boundary treatments for implicit solutions to Euler and Navier-Stokes equations 12 p1725 A83-29655
 Spectral multigrid methods for elliptic equations 12 p1773 A83-29663
 Group velocity interpretation of the stability theory of Gustafsson, Kreiss, and Sundstrom 12 p1776 A83-29665
 An open boundary condition for incompressible stratified flows 12 p1725 A83-29667
 The finite-element method in solutions of boundary value problems for anisotropic plates of composite materials. I Refined theories for anisotropic plates and finite-element approximations 13 p1866 A83-30059

Numerical solution of two-dimensional boundary value problems of the statics of flexible conical shells 13 p1866 A83-30071

Quasi-linear degenerate and nonuniformly elliptic and parabolic equations of second order --- Russian book 13 p1912 A83-30450

Horizontal dipole antenna above an imperfectly conducting ground fed by a two-wire line 13 p1828 A83-30648

The problem of boundary conditions in the kinetic theory of gases 13 p1932 A83-30661

Boundary conditions on a solid surface in a flow of a rarefied gas 13 p1932 A83-30662

The statistical mechanics of transport processes at a phase boundary and the problem of boundary conditions 13 p1932 A83-30663

The effect of boundary conditions on the flow of a polyatomic gas mixture in a supersonic nozzle --- in gasdynamic lasers 13 p1850 A83-30676

The electrostatic potential of a two-layer three-element symmetric array 13 p1833 A83-30718

Solution of boundary-value problems by the G-polynomial method 13 p1912 A83-30810

A coordinate-free approach to wave reflection from a uniaxially anisotropic medium 13 p1914 A83-31144

Guided-wave experiments with dielectric waveguides having finite periodic corrugation 13 p1836 A83-31145

Concerning the correctness on the whole of boundary value problems for models of the dynamics of the atmosphere and the ocean 13 p1880 A83-31326

A computational study of finite element methods for second order linear two-point boundary value problems 13 p1912 A83-31362

Calculation of critical branching points in two-parameter bifurcation problems 13 p1913 A83-31371

Approximate method of solving the kinetic equation for moderately dense gases near a boundary temperature jump in a binary mixture 13 p1933 A83-31467

Approximate solution of the heat-conduction equation with nonlinear boundary conditions 13 p1843 A83-31469

On two upwind finite-difference schemes for hyperbolic equations in non-conservative form 13 p1913 A83-31593

A calculation of the asymptotic behavior of 'intensity coefficients' in approaching corner and conical points 14 p2077 A83-31895

The diffraction of electromagnetic waves by surfaces with an admittance operator boundary condition 14 p1999 A83-32103

Conservation form, in general non steady coordinates, of the Navier-Stokes equations and boundary conditions for a moving boundary problem 14 p2008 A83-32149

An iteration method for solving stochastic boundary value elasticity problems 14 p2029 A83-32155

Boundary conditions in the theory of piezoceramic shells polarized along the coordinate lines 14 p2030 A83-32355

Algebra related to the N-soliton solution of the Benjamin-Ono equation 14 p2077 A83-32508

Nonlinear eigenvalue problems on infinite intervals 14 p2077 A83-32834

The application of iterated defect correction to variational methods for elliptic boundary value problems 14 p2078 A83-32842

Solutions to the boundary value problem with velocity correlations in stratified flow through circular pipe. I 14 p2012 A83-32968

Equations of the necessary extremum condition for a class of incorrect extreme-value problems --- for optimization of aerodynamic configurations 14 p1972 A83-33011

Oblique derivative boundary value problems for nonlinear elliptic systems of second order 14 p2078 A83-33155

Variational principles and free-boundary problems --- Book 15 p2223 A83-33749

The Dufort-Frankel Chebyshev method for parabolic initial boundary value problems 15 p2224 A83-33867

A numerical scheme to treat the open lateral boundary of a limited area model 15 p2203 A83-33879

Diffraction of plane harmonic waves by cracks 15 p2174 A83-34006

Influence of transport models and boundary conditions on flame structure 15 p2132 A83-34034

The fictitious domain method for the numerical solution of nonstationary thermal problems 15 p2158 A83-34227

Connectivity methods for free boundary problems - 2 phase heat flow 15 p2159 A83-34238

Non-linear boundary value problem in thermoelasticity 15 p2177 A83-34332

On uniqueness in finite elasticity 15 p2177 A83-34334

Local theorems of existence and uniqueness in finite elastostatics 15 p2177 A83-34345

Behavior of solutions of dynamic problems near the edge of a crack propagating at transonic velocity in an elastic medium 15 p2178 A83-34436

Utilization of the method of continuation with respect to the length of the integration segment for calculating circular corrugated plates 15 p2178 A83-34444

Performance evaluation of algorithms for mildly nonlinear elliptic problems 16 p2406 A83-35644

An approximate method for solving a kinetic equation for moderately dense gases near a boundary - The slip of a binary mixture 16 p2350 A83-35711

Two methods for the stress analysis of a rotating disk with cuts 16 p2366 A83-35932

Importance of inlet boundary conditions for numerical simulation of combustor flows [AIAA PAPER 83-1263] 16 p2308 A83-36314

On initial and boundary conditions for the Navier-Stokes equations in the Helmholtz form 17 p2505 A83-37529

Solution of problems in the dynamics of noncircular cylindrical shells in a liquid 17 p2521 A83-37573

Transformation of the equations of a three-dimensional boundary layer for numerical calculation 17 p2506 A83-37633

Alternative variational formulations for first order partial differential systems 17 p2571 A83-37769

Boundary conditions at grain boundaries 17 p2584 A83-38220

General boundary conditions for the wave equation around non-homogeneous scatterers 17 p2576 A83-38618

Elliptic grid generation 17 p2572 A83-38780

Solid mechanics applications of boundary fitted coordinate systems 17 p2525 A83-38786

On a multipoint boundary value problem for integrodifferential-extremal equations with deviating argument of ultraneutral type 17 p2575 A83-38866

On boundary value problems for the domain exterior to a thin or slender region 18 p2680 A83-39146

Possibility of the analytic solution of certain classical problems of diffraction theory 18 p2674 A83-39153

An error estimate for a finite-element approximation of an elliptic variational inequality formulation of a Hele-Shaw moving-boundary problem 18 p2739 A83-39254

Finite element analysis in computational fluid dynamics [AIAA PAPER 83-1918] 18 p2682 A83-39374

Stability analysis of intermediate boundary conditions in approximate factorization schemes 18 p2740 A83-39403

[AIAA PAPER 83-1898] 18 p2740 A83-39403

Initial data for N black holes 19 p2915 A83-40888

Nonlinear dispersive systems - Theory and examples 19 p2893 A83-41023

Solution of external boundary-value elasticity problems using the method of boundary integral equations 19 p2857 A83-41210

Boundary conditions for a fourth order hyperbolic difference scheme 20 p3041 A83-42494

On the simplified hybrid-combined method --- for solving boundary value problems of elliptic equations 20 p3041 A83-42495

Unigrid for multigrid simulation 20 p3041 A83-42496

Boundary conditions of the second-order differential equation and the Riccati equation 20 p3041 A83-42525

Analysis of viscous flows using multi-grid solution of Neumann pressure problem 20 p2969 A83-42531

Natural convection with volumetric energy sources in a fluid bounded by a spherical segment 20 p2972 A83-42676

A Liapunov theory for the existence and uniqueness of solutions to boundary value problems 20 p3042 A83-42939

On the post-buckling analysis of thin elastic shells 20 p3005 A83-42991

The treatment of thermoelastic boundary-value problems by means of the boundary element method 20 p3006 A83-42998

On the initial boundary-value problem of elastic-plastic plates with finite deformations 20 p3006 A83-43002

Diffusion across characteristic boundaries with critical points 20 p3043 A83-43121

Multipoint boundary value problem (MPBVP) and spline interpolation 20 p3042 A83-43170

Strict error estimation of numerical solution of compressible flow in two-dimensional space 20 p2985 A83-43171

Initial boundary value problem for one class of system of multidimensional nonlinear Schroedinger equations with wave operator 20 p3042 A83-43174

Two-dimensional modeling of the MIS grating solar cell 20 p3054 A83-43356

Thermal problems with radiation boundary conditions 20 p3007 A83-43373

Exact solutions of certain dual integral equations and their asymptotic properties 20 p3042 A83-43374

Solitary waves induced by boundary motion 21 p3199 A83-43826

An iterative extended boundary condition method for solving the absorption characteristics of lossy dielectric objects of large aspect ratios --- under exposure to incident plane wave radiation 21 p3189 A83-43833

Numerical analysis of moving boundary problem in matrix with a thin alternate matrix 21 p3197 A83-44012

On the stability of coronal magnetic loops 21 p3242 A83-44281

Boundary conditions for energetic particle transport at shocks 21 p3244 A83-44405

The effect of boundary absorption on longitudinal dispersion in steady laminar flows 21 p3130 A83-44466

The reflection and transmission of electromagnetic waves from the lossy plasma moving parallel to the interface 21 p3213 A83-44527

Reduction of the problem of diffraction by parallel half-planes to the Riemann boundary value problem 21 p3121 A83-44779

Solution of problems in the statics of shells of revolution with additional supports 21 p3155 A83-44847

Constrained finite elements for singular boundary value problems --- applied to fracture mechanics 21 p3160 A83-44987

On extrapolation boundary conditions for the numerical solution of hyperbolic difference schemes 21 p3198 A83-45054

Relaxation method for solving a difference biharmonic equation 21 p3198 A83-45214

Possibilities for an improvement in short-distance diffusion modeling --- of air pollution 21 p3169 A83-45403

An automatic orthonormalization method for solving stiff boundary-value problems 21 p3198 A83-45524

Introduction to multi-grid methods for the numerical solution of boundary value problems 22 p3352 A83-45767

Introduction to the method of finite elements 22 p3305 A83-45770

Nonlinear evolution of an obliquely propagating Langmuir wave - Boundary-value problem 22 p3361 A83-46011

Optimal control problems involving second boundary value problems of parabolic type 22 p3351 A83-46092

Systems of singular perturbation problems with a first order turning point 22 p3353 A83-46922

Singular perturbation problems with a singularity of the second kind 22 p3307 A83-46923

High-frequency scattering from the edges of impedance discontinuities on a flat plane 23 p3442 A83-47830

The cosmological problem as initial value problem on the observer's past light cone - Observations 23 p3526 A83-48059

Initial-value problems for Rossby waves in a shear flow with critical level 23 p3449 A83-48122

Nonlinear creep problems for variable-boundary aging bodies 23 p3472 A83-48464

Angular points of the boundaries of domains of attainability --- for dynamic control of linear systems 23 p3501 A83-48528

Mixed boundary value problems of the contouring of supersonic nozzles and channels 23 p3400 A83-48663

Solution of two-dimensional elasticity problems in regions with a remote external boundary 24 p3592 A83-49036

Bending vibration of a simply supported rectangular plate with a crack parallel to one edge 24 p3594 A83-49865

Singular integral equations in micropolar thermoelasticity 24 p3597 A83-50133

An analysis of the Volterra problem for the steady state creep material using complex stress and pseudo-stress functions 24 p3597 A83-50148

BOUSSINESQ APPROXIMATION

Applicability of the Boussinesq approximation to solve problems of nonstationary concentrational natural convection 04 p0475 A83-15093

Magnetic buoyancy and the Boussinesq approximation --- applied to solar magnetic field 06 p0835 A83-18931

Convection and gravity waves in two layer models. I - Overstable modes driven in conducting boundary layers - of solar and stellar models 06 p0835 A83-18934

An application of the modified zero-fourth-cumulant approximation to homogeneous axisymmetric Boussinesq turbulence 12 p1722 A83-29006

BOW SHOCK WAVES

- Nonlinear interfacial progressive waves near a boundary in a Boussinesq fluid 13 p1839 A83-30106
- On the first-order smoothing expression for the alpha-effect in dynamo theory 13 p1952 A83-31433
- An exact solution of the classical Boussinesq equation 14 p2077 A83-32507
- Two-soliton resonant interactions in one spatial dimension Solutions of Boussinesq type equation 14 p2080 A83-32511
- A statistical theory of thermally-driven turbulent shear flows, with the derivation of a subgrid model 17 p2507 A83-37877
- The evolution of large-horizontal-scale disturbances in marginally stable, inviscid, shear flows. I - Derivation of the amplitude evolution equations 19 p2842 A83-41022
- Nonlinear convection 20 p2982 A83-43005
- The parametric excitation of internal waves and convective instabilities in a fluid layer heated from above 22 p3322 A83-45639
- The elastostatic axisymmetric problem of a sphere containing a penny-shaped crack in a nonequatorial plane 24 p3591 A83-48869
- The multiple scales concept for modelling turbulent flows. II - Reynolds stresses and turbulent fluxes of a passive scalar contaminant, algebraic modelling, and a simplified model using the Boussinesq hypothesis 24 p3578 A83-49646
- BOW SHOCK WAVES**
- U BOW WAVES
- U SHOCK WAVES
- BOW WAVES**
- The two-dimensional structure of diffuse ions associated with the earth's bow shock 04 p0509 A83-15644
- Solar wind flow about the terrestrial planets. II - Comparison with gas dynamic theory and implications for solar-planetary interactions 06 p0847 A83-18278
- Observations of upstream ions and low-frequency waves on ISEE 3 06 p0782 A83-18284
- Electron velocity distributions near the earth's bow shock 06 p0782 A83-18285
- Evidence for specularly reflected ions upstream from the quasi-parallel bow shock 07 p0959 A83-20193
- Ions upstream of the earth's bow shock - A theoretical comparison of alternative source populations 09 p1303 A83-23759
- The oblique whistler instability in the earth's foreshock 09 p1303 A83-23760
- Ion acceleration at shocks in interplanetary space - A brief review of recent observations 11 p1676 A83-27385
- Lower hybrid drift instability with temperature gradient in a perpendicular shock wave 11 p1617 A83-28306
- Stability of electron distributions within the earth's bow shock 11 p1617 A83-28307
- A source of the backstreaming ion beams in the foreshock region 11 p1617 A83-28308
- Computer constructed imagery of distant plasma interaction boundaries 13 p1876 A83-30777
- Bow wave patterns 14 p2012 A83-32990
- Multiple spacecraft observations of interplanetary shocks Four spacecraft determination of shock normals 15 p2255 A83-33929
- The bow shock and the magnetosphere of Venus according to measurements from Venera 9 and 10 Orbiters 17 p2618 A83-37428
- Turbulence analysis of the Jovian upstream 'wave' phenomenon 17 p2618 A83-37584
- Factors controlling the location of the Venus bow shock 17 p2619 A83-37587
- Dependence of 50-keV upstream ion events at IMP 7 and 8 upon magnetic field bow shock geometry 17 p2599 A83-37588
- ISEE/IMP observations of simultaneous upstream ion events 17 p2599 A83-37589
- Energetic ions upstream of the earth's bow shock during an energetic storm particle event 17 p2538 A83-37597
- Bow shock structure from laboratory and satellite experimental results 17 p2544 A83-38516
- Dominant acceleration processes of ambient energetic protons (E greater than or equal to 50 keV) at the bow shock Conditions and limitations 17 p2544 A83-38523
- Modeling of interaction of artificially released lithium with the earth's bow shock 19 p2864 A83-41114
- Evolution of ion distributions across the nearly perpendicular bow shock - Specularly and non-specularly reflected-gyrating ions 20 p3017 A83-42405
- An investigation of oblique shock-shock interaction on a stationary model in a shock tube 21 p3087 A83-44560
- Structure of the quasi-parallel bow shock - Results of numerical simulations 22 p3325 A83-46031
- Observational evidence on the origin of ions upstream of the earth's bow shock 22 p3335 A83-47047

- Reflection of the solar wind ions at the earth's bow shock Energization 22 p3389 A83-47048

BOX BEAMS

- Initial design of stringer stiffened bend boxes using geometric programming 08 p1123 A83-23149
- The performance of adhesive-bonded thin-gauge sheet-metal structures with particular reference to box-section beams 09 p1276 A83-23328
- Properties of composite box beams under combined impact loading 18 p2705 A83-40222
- Design, manufacture and test of graphite composite wing box test structure 18 p2641 A83-40291

BRADYCARDIA

- Effects of hypercapnia, hypoxia, and rebreathing on heart rate response during apnea 13 p1902 A83-30462
- Roles of stress and adaptation in the elicitation of face-immersion bradycardia 13 p1903 A83-30484

BRAGG ANGLE

- Graded-layer-thickness Bragg X-ray reflectors 02 p0238 A83-12703
- An analysis of multicomponent electroacoustic transducers providing matched control of the acoustic field in Bragg acoustooptic devices in the short-wave portion of the microwave range 05 p0630 A83-17595
- Bragg-reflection profiles of graphite and alkali-graphite intercalation compounds - Comparison of double-axis and triple-axis spectrometer results 07 p0932 A83-21380
- A Bragg crystal spectrometer for the soft X-ray diffuse background 11 p1573 A83-27757
- Opto-optical light deflection 21 p3207 A83-44834
- Application of wide band Bragg cells for integrated optic (IO) spectrum analyzers 22 p3293 A83-46661
- Investigation of the effect of uniform compression on the angle of the optical axes of olivine single crystals 23 p3485 A83-48509
- Diffraction characteristics of planar absorption gratings 23 p3509 A83-48706

BRAIN

- NT BRAIN STEM
- NT CEREBRAL CORTEX
- NT CEREBRUM
- NT HIPPOCAMPUS
- The functional asymmetry of the brain and the direct subjective evaluation of loudness 01 p0085 A83-10503
- The ontogeny of the functional asymmetry of the human brain 01 p0082 A83-10507
- The stereospecificity of the effect of the isomers of flupentixol on the substrate inhibition of brain tyrosine hydroxylase 01 p0079 A83-10536
- The participation of the dopaminergic system of the brain in the realization of the generalization function 01 p0080 A83-10540
- A comparison of the neural and immunological modulator properties of low molecular weight neuropeptides 01 p0080 A83-10551
- The peculiarities of DNA metabolism in rat brains in the process of the elaboration of a conditioned reflex 01 p0080 A83-10552
- Intracerebroventricular injections of cholecystokinin decreases the activity of the dopaminergic and serotonergic systems in the brain 02 p0219 A83-11519
- The changes in the nerve and cardiac activity in animals of various ages during the application of electromagnetic fields of low frequency and low voltage 02 p0220 A83-11884
- The brain organization of emotional reactions and states 02 p0224 A83-12209
- The activity of prostaglandin synthetase in brain tissues during radiation sickness in experimental animals 03 p0375 A83-13639
- Morphological criteria for the individual variability of the human brain 03 p0380 A83-13643
- Serotonin and the adrenocortical response to cold during the early postnatal development of rats 03 p0375 A83-14328
- The role of central and peripheral serotonergic mechanisms 04 p0520 A83-15895
- The condition of the metabolism of the brain and liver during the experimental application of a microwave field of nonthermal intensities 05 p0669 A83-17166
- The effect of mechanical asphyxiation on lipid peroxidation processes in the rat brain 05 p0670 A83-17185
- Comparative brain oxygenation and mitochondrial redox activity in turtles and rats 05 p0671 A83-17327
- The electric reactions of the cat brain to light following the section of the optic tracts 05 p0672 A83-17636
- Structural foundations of the reliability of the functioning of cortical neurons 06 p0795 A83-18984
- The effect of short-term hypothermia on the monoamine oxidase enzyme system in the rat brain 06 p0795 A83-18989

- The effect of small doses of ethanol on the minute waves of ultralow activity and the temperature of the brain 07 p0973 A83-20241

- The asymmetry of the brain hemispheres from the viewpoint of the identification of visual forms 07 p0977 A83-20355

- Visual pathways and the system of brain activation --- Russian book 07 p0973 A83-20385

- Investigation of cAMP phosphodiesterase activity in brain tissue under general and local irradiation of the head and body of adult animals and embryos 07 p0974 A83-20843

- The effect of hypothermia on the glutamate dehydrogenase activity in the brain 07 p0975 A83-20982

- The modelling of hierarchical systems of spatial-temporal synchronous connections of the human brain 10 p1462 A83-25625

- A window on the sleeping brain --- paralysis inhibition during REM state 10 p1454 A83-26300

- The eye movements of cats induced by the electrical stimulation of the lateral geniculate body 10 p1454 A83-26786

- The architectonics of the arterial bed in the brain hemispheres of rats during normal conditions and after a stay at a 'height' of 5600 m 10 p1454 A83-26788

- Central effects of some peptide and non-peptide opioids and naloxone on thermoregulation in the rabbit 12 p1763 A83-29533

- The invariance of visual identification in the right and left hemispheres of the human brain 13 p1901 A83-30441

- Functional organization of the second cortical visual area in primates 13 p1900 A83-31167

- The character of protein synthesis in the brains of hibernating mammals 13 p1900 A83-31342

- Polymerization of brain tubulin in and around the area of application of an electric field 14 p2061 A83-31818

- The direct reactions of smooth muscles of the major cerebral arteries to acute hypoxia and hypercapnia 14 p2061 A83-31971

- The subcellular distribution of a Ca(2+) -dependent protein regulator in the gray matter of the brain of normal and X-irradiated rats 14 p2062 A83-32060

- The early changes in the activation of nucleoside diphosphatase in the brain and liver of rats following total-body gamma-irradiation at an absolutely lethal dose 14 p2062 A83-32062

- Microwave-induced pressure waves in mammalian brains 14 p2065 A83-33109

- The morphological changes in several nuclei of the midbrain during various periods of water deprivation in white rats 14 p2065 A83-33150

- A study of the fatty acid composition of the major brain 14 p2065 A83-33316

- Optics, the eye, and the brain 15 p2209 A83-33801

- The individual variability of the putamen of the brain in humans 16 p2399 A83-36813

- UDP-coenzymes in the tissues of the brain glia of humans 16 p2400 A83-36831

- The role of proteolysis in the processing and inactivation of neuropeptides - Its possible connection with certain functions of the brain 16 p2396 A83-36840

- Several peculiarities of the cytoarchitectonics of the midbrain tegmentum of humans 18 p2736 A83-40581

- Induction and deduction as the function of different hemispheres --- of brain 19 p2870 A83-40810

- Shadows of thought - Shifting lateralization of human brain electrical patterns during brief visuomotor task 19 p2884 A83-41225

- A technique for the evaluation of the temperature profile during local cooling of the medulla oblongata 19 p2876 A83-41846

- Exponential evolution - Implications for intelligent extraterrestrial life 19 p2908 A83-42038

- The lateralization of the hemisphere control of inhibition stability --- brain hemisphere specialization of visual signal discrimination from noise 19 p2879 A83-42091

- The changes in the content of catecholamines in the dopamine-synthesizing nuclei of the brain of rats in conditions of immobilization stress 19 p2879 A83-42093

- The enchanted loom --- Book on evolution of intelligence 20 p3033 A83-42174

- The functional condition of the brain during early forms of arterial hypertension in young individuals 21 p3187 A83-44661

- Neurogenic conception as a basis for the investigation of the cerebral pathogenesis of hypertension 21 p3187 A83-44662

- Brain peptides and the regulation of blood pressure 21 p3185 A83-45375

BRAIN CIRCULATION

A device for recording the spatial synchronization of phases of EEG waves 01 p0050 A83-10502

The role of serotonin in the pathogenesis of disorders of the brain circulation /Review/ 01 p0079 A83-10524

The changes of several cerebral hemodynamic indicators during the action of physical factors 01 p0084 A83-11395

An experimental study of the dose dependence of the effect of noise 01 p0084 A83-11397

An investigation of the role of deep brain structures in the regulation of intracerebral microcirculation 02 p0219 A83-11518

Structure of the sleep-wakefulness cycle during experimental insufficiency of cerebral circulation 03 p0373 A83-13599

The hemodynamic parallels between the types of central and cerebral blood circulation in individuals with normal arterial pressure 03 p0379 A83-13618

The initial manifestations of the defects of blood supply to the brain /Review of the literature/ 03 p0380 A83-13642

Cerebral circulation and the hemodynamics of lesser circulation in patients with bronchial asthma in combination with systemic arterial hypertension 05 p0673 A83-17162

The structure of the sleep-wakefulness cycle given an experimental insufficiency of cerebral circulation 05 p0670 A83-17189

An experimental study of the effects of hypobaric hypoxia on the cerebral blood flow and the metabolism of the brain 06 p0794 A83-18342

The local cerebral blood flow and the local vascular reactivity during brain contusions in an experiment under conditions of arterial normal tension and hypertension 06 p0795 A83-18978

The effect of strophanthine and celanide on the blood circulation and metabolism in the brain 07 p0975 A83-20983

The dynamics of oxygen transport from the capillaries to the nerve cells of the brain 08 p1145 A83-22104

The interrelationship of the intracranial pressure, the blood volume of the skull cavity, and the total blood flow of the brain 08 p1145 A83-22108

An experimental study of the encephalic hemodynamic variations connected with flight and position with respect to the flight axes on Alouette III in a healthy subject 08 p1148 A83-22966

Changes in the loco-regional cerebral blood flow /r.C.B.F./ during a simulation of weightlessness 11 p1641 A83-27349

Pulmonary complications during acute disorders of the cerebral blood circulation 14 p2070 A83-33311

The diagnostics, treatment, and prophylactic measures for the initial appearances of brain blood insufficiencies 15 p2212 A83-34927

The radioisotope (Xe-133) inhalation method for determining the regional brain blood flow 15 p2212 A83-34928

The dependence of the origin of acute disorders of the brain blood circulation on the changes of meteorological factors 15 p2212 A83-34929

The role of adrenergic mechanisms in the development of cerebrovascular disorders during acute myocardial ischemia 15 p2210 A83-34960

The application of euphylline electrophoresis with sinusoidal modulated currents in the treatment of patients with transitory disorders of the brain blood circulation 15 p2213 A83-34972

The cerebral blood circulation of patients with vibration disease during treatment at health resorts 17 p2560 A83-38191

Investigations of the microcirculatory bed of the brain in experimental conditions. II - Disorders of blood flow following craniocerebral trauma 18 p2733 A83-40575

Physiotherapy in the multiple therapy treatment of patients with vascular diseases of the brain 19 p2882 A83-41449

Computer tomography of the brain during migraine (Review) 19 p2883 A83-41463

The relationship between blood flow, partial pressure, and oxygen demand in the human cortex (A theory of tissue gas exchange) 23 p3497 A83-47113

The central noradrenergic regulation of cerebral blood flow 23 p3496 A83-48565

BRAIN DAMAGE

A study of the localization function and differential sensitivity of the auditory system in patients with brain lesions 01 p0083 A83-10517

A method for adaptive biocontrol in the multifaceted treatment of patients with cerebral arachnoiditis 01 p0083 A83-10525

The mechanical properties of the brain in the process of the development of postischemic edema 01 p0079 A83-10526

The content and distribution of glycogen in the brain following an experimental craniocerebral injury 01 p0079 A83-10527

Pathomorphological changes in the brain of rats after general beta-irradiation at various doses 01 p0079 A83-10531

Long-term posttetanic potentiation in the hippocampus 01 p0081 A83-10917

Regulation of the activity of enzymatic reactions in the brain in the presence of nervous system pathology 03 p0374 A83-13638

Computer tomography applied to the study of inflammatory diseases of the brain /a survey of the literature/ 05 p0673 A83-17179

The participation of the pallidum in the mechanisms of memory 06 p0794 A83-18968

Gradations of severity in the condition of patients with craniocerebral injuries and unified criteria for their determination 06 p0798 A83-18976

The importance of laboratory data for the differentiation of mild and moderately severe craniocerebral injuries 06 p0798 A83-18977

The local cerebral blood flow and the local vascular reactivity during brain contusions in an experiment under conditions of arterial normal tension and hypertension 06 p0795 A83-18978

Otoneurological symptoms in the differential diagnosis of mild and moderately severe craniocerebral injuries 06 p0798 A83-18979

The energy metabolism in the brains of rats exposed to mechanical asphyxia 07 p0972 A83-19923

The role of various cortical regions in visual-motor coordination 07 p0973 A83-20356

The role of peptide factors in the compensatory processes in the central nervous system 08 p1146 A83-22780

The role of the inferotemporal and inferoparietal cortices in the description of a visual image in monkeys 13 p1896 A83-30440

Multiparameter monitoring of the awake brain under hyperbaric oxygenation 13 p1897 A83-30486

Brainstem auditory evoked potentials 16 p2398 A83-35902

Computer tomography in the diagnosis of cranio-cerebral injuries 16 p2400 A83-36832

Return to flying after head injuries - A review 18 p2734 A83-40355

Investigations of the microcirculatory bed of the brain in experimental conditions. II - Disorders of blood flow following craniocerebral trauma 18 p2733 A83-40575

Computer tomography for tumors of the posterior regions of the third ventricle and the pineal body 18 p2733 A83-40577

The changes in the water-electrolyte metabolism in the brain of rats during gamma-irradiation of the head at high doses 19 p2874 A83-41012

BRAIN STEM

Brainstem auditory evoked potentials 16 p2398 A83-35902

BRAKES (FOR ARRESTING MOTION)

NT AERODYNAMIC BRAKES

NT AIRCRAFT BRAKES

NT LEADING EDGE SLATS

NT TRAILING-EDGE FLAPS

NT WHEEL BRAKES

NT WING FLAPS

Aeroballistic characteristics of 3-ft-long parachute decelerators 12 p1696 A83-29019

BRAKING

Timing of the Crab pulsar - Consequences of the large glitch of 1975 07 p1017 A83-20928

The dynamic braking of a linear induction motor at a variable speed 08 p1080 A83-22224

Review of NASA antiskid braking research [SAE PAPER 821393] 17 p2463 A83-37969

BRANCHING (MATHEMATICS)

Determination of the parameters of the attraction regime of a nonautonomous phase-locked loop system 01 p0035 A83-10286

Bifurcation and stability of the permanent rotations of a heavy solid whose center of mass is located near the principal plane of the inertia ellipsoid 03 p0391 A83-14893

On making large nonlinear problems small --- for thermal and structural applications 04 p0495 A83-15016

Branching of the Falkner-Skan solutions for gamma less than zero 05 p0642 A83-17942

Symmetry and bifurcation in three-dimensional elasticity. I 06 p0776 A83-18928

Solution of bifurcation problems and limit load problems in certain nonlinear boundary-value problems of continuum mechanics 06 p0777 A83-19322

On the analysis of Hopf bifurcations 07 p0989 A83-20641

Numerical solution of multiparameter eigenvalue problems 08 p1159 A83-21863

Asymptotic relations and period doubling bifurcations in a mean-field model of optical bistability 08 p1164 A83-21887

Perturbed bifurcation of stationary striations in a contaminated, nonuniform plasma 08 p1168 A83-22739

Cascading bifurcations 08 p1161 A83-22740

Cascade of period doublings of tori 08 p1162 A83-22948

Universal bifurcation problems --- in structural analysis of solids 10 p1471 A83-25305

Aspects of plastic postbuckling behavior 10 p1437 A83-25312

Fractal basin boundaries, long-lived chaotic transients, and unstable-unstable pair bifurcation 10 p1471 A83-25794

On the bifurcation phenomena and the problem of the loss of stability in the nonlinear control systems 10 p1464 A83-26510

Mechanism for chaos in the Duffing equation 10 p1472 A83-26969

Evolution with the mass parameter of families of asymmetric periodic solutions of the restricted three body problem 12 p1786 A83-29105

On the bifurcations of a certain family of periodic orbits 12 p1787 A83-29112

Bifurcations in a three-dimensional two-parameter autonomous oscillation system with a strange attractor 12 p1775 A83-29255

Calculation of critical branching points in two-parameter bifurcation problems 13 p1913 A83-31371

Splitting of steady multiple eigenvalues may lead to periodic cascading bifurcation 16 p2407 A83-35699

Bifurcation and limit cycle analysis of nonlinear systems with an application to aircraft at high angles of attack 17 p2470 A83-37080

Experimental study of the mechanism of the appearance and the structure of a strange attractor in an oscillator with inertial nonlinearity 17 p2499 A83-38486

Period doubling and chaos in partial differential equations for thermosolutal convection 17 p2576 A83-38606

Topology of the invariant manifolds of period-doubling attractors for some forced nonlinear oscillators 19 p2895 A83-41166

Bifurcations and phase transitions of self-gravitating and uniformly rotating fluid 21 p2322 A83-44737

Structure of the phase space and bifurcations of the equation of motions of a magnetized satellite in a circular-polar-orbit plane 21 p3103 A83-45278

Oscillatory bifurcations in singular perturbation theory. I Slow oscillations. II - Fast oscillations 22 p3353 A83-46921

Subharmonic and chaotic bifurcation structure in optical bistability 23 p3509 A83-48320

Application of the theory of bifurcations to the study of unsteady regimes of combustion 24 p3556 A83-49777

BRANCHING (PHYSICS)

Observation of bifurcation to chaos in an all-optical bistable system 05 p0686 A83-17935

EUV branching ratios for ionized nitrogen and oxygen emissions 07 p0991 A83-21396

Catastrophe theory in physics 09 p1338 A83-23852

Vacuum ultraviolet monochromator calibration using measured atomic branching ratios 10 p1484 A83-26857

Branded cracks at small angles /An addendum/ 11 p1595 A83-28438

Electro-optic branching-waveguide switch with low drive voltage 24 p3628 A83-48855

BRASSES

Stress corrosion cracking 17 p2466 A83-37172

BRAYTON CYCLE

Characteristics of a closed Brayton cycle piston engine 08 p1112 A83-23135

Direct contact droplet heat exchangers for thermal management in space 11 p1564 A83-27137

The design and construction of a low power gas turbine for solar energy conversion - An analytical model of operation of the installation in a variable mode --- French thesis 11 p1612 A83-28647

BRAZIL

A survey of Brazil's semi-arid lands with the use of the remote sensing 09 p1290 A83-24618

Two severe freezes in Brazil - Precursors and synoptic evolution 10 p1450 A83-25390

The drift of the Brazilian anomaly 21 p3176 A83-45255

BRAZILIAN SPACE PROGRAM

- Prelaunch estimates of near earth satellite lifetimes
Application to a proposed Brazilian satellite
13 p1809 A83-29998

BRAZING

- Effect of nickel plating on Fe-BCu-Mo and -W
02 p0155 A83-12074
Effect of heating time at high temperatures on the structure and properties of brazed joints
05 p0652 A83-16884
Superplastic forming/weld-brazing of titanium skin-stiffened compression panels
07 p0886 A83-20467
Localized corrosion of aluminum vacuum brazing T-joints
13 p1822 A83-30844
Design and fabrication of brazed beryllium assemblies [AIAA PAPER 83-0868]
14 p2028 A83-32789
Brazing under microgravity in a resistance heated furnace
20 p2943 A83-43313
Brazing of silicon nitride
23 p3437 A83-48286
Metals handbook. Volume 6 - Welding, brazing, and soldering /9th edition/
24 p3590 A83-50121

BREADBOARD MODELS

- Technology upgrade to ALR-46 and ALR-69 radar warning receivers
01 p0005 A83-11102
Evaluating Scroll refrigerant compressors for reducing size and weight of military aircraft ECS [SAE PAPER 820877]
10 p1375 A83-25771

BREAKAWAY

- U BOUNDARY LAYER SEPARATION

BREAKERS (ELECTRIC)

- U CIRCUIT BREAKERS

BREATHING APPARATUS

- NT OXYGEN MASKS
Human breathing patterns on mouthpiece or face mask during air, CO₂, or low O₂
03 p0378 A83-13579
Review of potassium superoxide characteristics and applications
11 p1644 A83-28331
Lithium hydroxide as a CO₂ scrubber in closed circuit breathing apparatus
11 p1645 A83-28335

BRECCIA

- The Nilpena ureilite, an unusual polymict breccia - Implications for origin
02 p0262 A83-11548
Fission track studies of xenolithic chondrites - Implications regarding brecciation and metamorphism
02 p0267 A83-12840
Subcrater lithification of polymict regolith breccias
04 p0560 A83-15340
KREEP glass and the exotic provenance and formation of polymict breccia 66055
04 p0560 A83-15341
Hydrothermally altered impact melt rock and breccia - Contributions to the soil of Mars
04 p0567 A83-15578
Petrological and thermal histories of a lunar breccia 73217 as inferred from pyroxene crystallization sequences, exsolution phenomena, and pyroxene geothermometry
07 p1033 A83-21297
Petrology and comparative thermal and mechanical histories of clasts in breccia 62236
07 p1033 A83-21298
Rock 67015 - A feldspathic fragmental breccia with KREEP-rich melt clasts
07 p1033 A83-21299
Geochemical studies of feldspathic fragmental breccias and the nature of North Ray Crater ejecta
07 p1033 A83-21300
Nature of the H chondrite parent body regolith - Evidence from the Dimmitt breccia
07 p1034 A83-21308
Radiation history of lunar microbreccias and lithic chondrules from Weston meteorite by track data
07 p1034 A83-21310
Mineralogy and petrology of the Abee enstatite chondrite breccia and its dark inclusions
08 p1187 A83-21640
Ar-40/Ar-39 and U-Th-Pb dating of separated clasts from the Abee E4 chondrite
08 p1188 A83-21641
Composition and origin of clasts and inclusions in the Abee enstatite chondrite breccia
08 p1188 A83-21645
Chemical characteristics and origin of H chondrite regolith breccias
09 p1367 A83-25175
Brecciated Muong Nong-type tektites
14 p2112 A83-33068
The Atlanta enstatite chondrite breccia
22 p3385 A83-46373
Regolith breccia Allan Hills A81005 - Evidence of lunar origin, and petrography of pristine and nonpristine clasts
22 p3385 A83-46861
Petrology of ALHA 81005, the first lunar meteorite
22 p3385 A83-46863
ALHA 81005 - Moon, Mars, petrography, and Giordano Bruno
22 p3385 A83-46864
The Adhi Kot breccia and implications for the origin of chondrules and silica-rich clasts in enstatite chondrites
24 p3673 A83-50174

BREEDER REACTORS

- NT EXPERIMENTAL BREEDER REACTOR 2

BREMSSTRAHLUNG

- Coherent bremsstrahlung from relativistic electrons axially channeled in crystals
01 p0054 A83-10815
Sensitivity of determining the atomic number of materials on the basis of bremsstrahlung backscattering
02 p0188 A83-12162
Electron transverse velocity measurements in an intense relativistic electron beam diode
03 p0398 A83-13916
Secondary electron spectra in interstellar clouds, and the bremsstrahlung gamma-ray luminosity
03 p0439 A83-14211
Absorption of HCN-laser rays with inverse bremsstrahlung in a krypton atom field --- German thesis
06 p0811 A83-18520
Spectrometer for momentum-resolved bremsstrahlung spectroscopy
06 p0764 A83-19232
Emission from particles in periodic media
06 p0806 A83-19417
On the interpretation of gamma-ray burst continua and possible cyclotron absorption lines
07 p1011 A83-20019
Stimulated bremsstrahlung effect in multimode laser radiation field
07 p0934 A83-20120
Polarization effects in the bremsstrahlung production of massive mesons in a magnetic field
07 p0992 A83-20857
Radiation of ultrarelativistic electrons in a charged plasma
09 p1348 A83-23998
Coulomb bremsstrahlung and cyclotron emissivity in hot magnetized plasmas --- of magnetic X-ray pulsar
09 p1360 A83-24460
Transition radiation and transition scattering
11 p1649 A83-28243
The bremsstrahlung of a slow electron at a Coulomb center in an external electromagnetic field
14 p2079 A83-32139
The retardation of ions in a degenerate electron gas
14 p2086 A83-32141
Bremsstrahlung emission in a non LTE plasma
15 p2233 A83-34139
Spatial variation for flares observed with the gamma ray spectrometer aboard the SMM satellite
15 p2284 A83-35223
Relation between the free-free and scattering cross sections and 'two-state resonances' in bremsstrahlung
16 p2408 A83-35329
Calculation of free-free Gaunt factors in hot dense plasmas
16 p2415 A83-35664
Stimulated bremsstrahlung masers
16 p2361 A83-36771
Quantized synchrotron radiation as a cause of gamma-ray bursts
17 p2629 A83-38050
Gravitational radiation of plasmas - Bremsstrahlung
18 p2744 A83-39522
Multiphoton absorption of the momentum of an electromagnetic wave in a plasma
18 p2744 A83-39523
Bremsstrahlung in plasmas
19 p2901 A83-40915
Thick-target bremsstrahlung interpretation of short time-scale solar hard X-ray features
20 p3080 A83-42461
Evaluation of the information content of the characteristics of radiation scattered by the surface of geometrical bodies
20 p3000 A83-43184
Effectiveness of intensifying screens in a mosaic semiconductor transducer, and the aperture characteristics of sensors
21 p3215 A83-43878
Inverse photoemission --- ultraviolet bremsstrahlung spectroscopy
21 p3110 A83-44621
Bremsstrahlung produced by electrons in a hot plasma
21 p3213 A83-44653
Comment on 'Stimulated bremsstrahlung masers'
22 p3299 A83-46741

BRIDGES (STRUCTURES)

- Progress in the practical applications of fracture mechanics
08 p1119 A83-21796

BRIDGMAN METHOD

- An analytical approach to thermal modeling of Bridgman-type crystal growth. I - One-dimensional analysis
05 p0638 A83-17235
Ground based studies for the space processing of lead-tin-telluride
20 p2943 A83-43310
Effect of variable thermal conductivity on isotherms in Bridgman growth
22 p3285 A83-46707

BRIGHTNESS

NT SOLAR GRANULATION

- Temporal variability of ultraviolet cloud features in the Venus stratosphere
02 p0266 A83-12568
Determining optical flow --- distribution of apparent movement velocities of image brightness patterns
02 p0182 A83-12897
Remote measurement of biomass
03 p0350 A83-14306
Brightness of the physical nucleus of a comet
03 p0426 A83-14679

- The structure of cometary dust tails. II - Tail brightness profiles and dust characteristics of comet Arend-Roland, 1957 III
05 p0695 A83-16855
Investigation of the relationship between the seasonal dynamics of the spectral brightness coefficients of certain sorts of wheat and plant physiological parameters
07 p0951 A83-19911
Methods for the recovery of the spectral density of the energy brightness of natural objects on the basis of integral measurements
07 p0951 A83-19916
Remote sensing brightness maps
07 p0951 A83-20149
Accuracy of measurement of star images on a pixel array
10 p1492 A83-25588
Observation of internal waves in the ocean
10 p1453 A83-26812
Manifestation of the 160-min solar oscillations in velocity and brightness /Optical and radio observations/
11 p1687 A83-27627
Diameter distribution and Sigma-D relation of SNRs in M31 and M33
12 p1785 A83-28894
Identification of snow cover and cloud cover on the basis of the spectral brightness of near infrared radiation measured from space
14 p2058 A83-32495
Io - The near-infrared monitoring program, 1979-1981
14 p2112 A83-32609
Phase functions of atmosphereless bodies of the solar system
16 p2437 A83-35752
Surface brightness and effective radius for elliptical galaxies
17 p2602 A83-37780
Comparisons among a new soil index and other two- and four-dimensional vegetation indices
17 p2531 A83-38341
Variability of the spectral coefficient of sea brightness
19 p2870 A83-42108

BRIGHTNESS DISCRIMINATION

- The spatial parameters of color vision in humans
07 p0977 A83-20357
Electrophysiological investigations of color vision in humans
07 p0977 A83-20358
Stimulus determinants of brightness and distinctness of subjective contours
22 p3349 A83-46756

BRIGHTNESS DISTRIBUTION

- Theoretical surface brightness distributions and continuum polarization of rapidly rotating B stars
01 p0123 A83-10355
Extended regions of soft X-ray emission and background spectrum at Southern latitudes
01 p0118 A83-10972
Photographic surface photometry of the Milky Way. II - Surface photometry in the region of the dark cloud 'Coalsack' in U,B,V,R
02 p0247 A83-12524
Comet head photometry - Past, present, and future
03 p0403 A83-13392
Stellar populations in the edge-on spiral galaxy NGC 4565. I - Surface brightness and color distributions
03 p0406 A83-13551
The nature of the radio emission from the star-gas-dust complex W1
03 p0417 A83-13655
Statistics of the complete set of bright and faint asteroids
03 p0133 A83-13668
Study of the sun's neutrino brightness curve with the help of a chlorine-argon neutrino detector
03 p0436 A83-13825
The Hubble diagram for quasars and quasars
03 p0426 A83-14694
Ultraviolet spectroscopy of the zodiacal light
05 p0694 A83-17022
A search for extended structures near the radio sources 3C 120 and 3C 273
06 p0831 A83-18791
A study of the two-dimensional luminosity distribution of NGC 3379
06 p0833 A83-18855
The color and surface brightness of the Leo II dwarf galaxy
06 p0820 A83-18857
The radio continuum morphology of NGC 4631 at 2.7 and 8.1 GHz
06 p0833 A83-18858
The structure of a type-II supernova remnant G 160.5 + 2.8 /HB-9/ observed at lambda = 12m
06 p0834 A83-18882
On the dynamics of the chromosphere above sunspots
06 p0855 A83-19129
Morphology of compact galaxies. II
06 p0836 A83-19202
Observations of the Coma Cluster of galaxies /A 1656/ at frequency 102.5 MHz
06 p0838 A83-19218
Variability and mass loss in IA O-B-A supergiants
07 p1010 A83-19858
Photographic surface photometry of the Milky Way. I - Data and reduction methods
07 p1005 A83-20559
Photographic surface photometry of the Milky Way. III - Photometry of the central area of the Galaxy in the ultraviolet
07 p1006 A83-20560
A newly discovered nearby planetary nebula of old age
07 p1021 A83-21123
V 1016 Cygni and HM Sagittae - Binary stellar systems
07 p1025 A83-21231

- Brightness of the photosphere and faculae at the limb based on eclipse observations 07 p1027 A83-21269
- Photometry of the unlit face of Saturn's rings 08 p1175 A83-22936
- Effects of subsurface volume scattering on the lunar microwave brightness temperature spectrum 08 p1189 A83-22941
- The brightening effect during nonlinear light scattering by static optical inhomogeneities 09 p1345 A83-24217
- Reconstruction of a polarized brightness distribution by the maximum entropy method --- for astronomical maps 09 p1354 A83-24479
- A simple model for the distribution of light in spherical galaxies 09 p1363 A83-24988
- Brightness oscillations of the sun's chromosphere in K and H-alpha 10 p1521 A83-25494
- On the deconvolution of brightness profiles of galaxies from seeing - Application to NGC 3379 10 p1494 A83-25834
- A model for calculating the brightness-field contrast of homogeneous objects 10 p1423 A83-26811
- The surface brightness of reflection nebulae - NGC 1432 and the 17 Tauri nebula 11 p1676 A83-27115
- Bending waves in Saturn's rings 11 p1683 A83-27353
- Determination of the physical parameters of the neutral coma of Comet Bennet / 1970 II/ 11 p1679 A83-27889
- The effect of solar activity on the brightness of Comet Bradfield 1974b 11 p1673 A83-27890
- On the function $\lambda/bd/r$, describing the relative mass loss of a comet nucleus 11 p1679 A83-27891
- The surface brightness of spiral galaxies. I - Spheroidal components and Freeman's law 11 p1680 A83-28258
- A test for transverse motions of clusters of galaxies 11 p1675 A83-28396
- Do magnetic transients exist in solar flares? 12 p1800 A83-29499
- Development of a numerical model of a cosmic radio source with a continuous mission spectrum 13 p1944 A83-30273
- The brightness variations of asteroid 216 Kleopatra 13 p1960 A83-30380
- Positions of bright stars --- Russian book 13 p1936 A83-30625
- Pairs of spiral galaxies with magnitude differences greater than one 13 p1943 A83-31736
- The electrophotometry of Saturn. I - The distribution of brightness over the equatorial regions in the spectral range of 0.3-0.6 micron 14 p2095 A83-31837
- The matrix coefficient for the brightness of radiation reflected by a semi-infinite absorptive medium with a greatly extended indicatrix of scattering 14 p2085 A83-32857
- The characteristics of a confined light beam in an absorptive medium having a narrow indicatrix of scattering 14 p2085 A83-32858
- Distribution of brightness over apparent discs of distorted stars 15 p2263 A83-34547
- Fluid motions in the solar chromosphere-corona transition region. III - Active region flows from wide slit Dopplergrams 17 p2624 A83-37334
- Method for determining sky background brightness on the basis of data from the Galaktika experiment 17 p2600 A83-37653
- Multicolor photometry of bright patches in the galaxy NGC 4303 17 p2589 A83-37655
- A model of the Crab nebula - The emission spectrum and the distribution of brightness 17 p2600 A83-37660
- The relationship between variations in the brightness of hydrogen flocculi in active regions on the sun 17 p2625 A83-37666
- The distribution of radio brightness over the solar disk 17 p2626 A83-37717
- Snow properties and two channel microwave measurements 17 p2534 A83-38458
- Turbulence in the neutral interstellar medium 18 p2777 A83-39778
- The Uranian satellites - Surface compositions and opposition brightness surges 19 p2922 A83-40781
- Surface brightness in double SS-type galaxies 19 p2911 A83-41562
- Neutral cometary atmospheres. IV - Brightness profiles in the inner coma of comet Kohoutek 1973 XII 20 p3059 A83-42463
- Out of ecliptic zodiacal cloud profile 20 p3081 A83-43158
- Sparse field stellar photometry 24 p3647 A83-50002
- Microwave emission signatures of snow in Finland 01 p0063 A83-10065
- Microwave radiance of early fall sea ice at 1.55 cm 01 p0076 A83-10091
- Investigation of the brightness temperature of a rough surface in the Kirchhoff approximation --- for oceans 02 p0218 A83-11682
- Centimeter and millimeter wave attenuation and brightness temperature due to atmospheric oxygen and water vapor 02 p0165 A83-12619
- An interpretation of OH maser observations in W3/OH/ 03 p0413 A83-13313
- Angular fluctuations in the temperature of the cosmic background radiation in a universe with massive neutrinos 03 p0439 A83-13886
- The transfer of 3.7 micrometer radiation through model cirrus clouds 03 p0371 A83-14655
- Multifrequency microwave radiometer measurements of soil moisture 03 p0351 A83-14855
- Martian dust mantling and surface composition - Interpretation of thermophysical properties 04 p0566 A83-15570
- The propagation of thermal radiation in the case of the random refraction of beams in a medium with fluctuating permittivity 04 p0531 A83-15733
- High-brightness ultraviolet radiation source based on a cumulative plasmadynamic discharge 05 p0687 A83-17079
- The effect of monomolecular surface films on the microwave brightness temperature of the sea surface 05 p0669 A83-17714
- The quiet sun brightness temperature at 127 MHz 06 p0854 A83-19126
- Brightness temperature of the 'quiet' sun in the millimeter range 06 p0856 A83-19327
- A model for microwave emission from vegetation-covered fields 07 p0951 A83-20223
- Rapid variability in 3C273 at 1 mm 07 p1008 A83-21202
- Effects of subsurface volume scattering on the lunar microwave brightness temperature spectrum 08 p1189 A83-22941
- Measurements of the absorption and brightness temperatures of the atmosphere in the millimeter wavelength range 09 p1301 A83-23481
- The quantitative expression of the function of the remote sensing of soil moisture 09 p1283 A83-24224
- A model function for ocean microwave brightness temperatures 09 p1320 A83-24311
- Polarization of interstellar radio-frequency lines and magnetic field direction 10 p1513 A83-26714
- On the determination of the physical characteristics of forest fires by methods of microwave radiometry 14 p2035 A83-32501
- Some recent results in the interpretation of high brightness temperature microwave spike emission 15 p2284 A83-35221
- Investigation of remote sensing possibilities of the lower atmosphere in the microwave range and some aspects of statistical data use 15 p2180 A83-35291
- Solar limb brightening measurements at 3.4 mm wavelength 16 p2440 A83-36686
- Model for atmospheric corrections to microwave brightness temperature data 17 p2526 A83-37621
- The connection of the changes in the radio brightness of the sun with the humps of the magnetic field and the flocculae during a minimum of solar activity 17 p2626 A83-37718
- Observations of galaxies of high surface brightness at 102 MHz 17 p2594 A83-38550
- Network to cell contrast at microwaves --- radio brightness temperature of solar atmosphere 18 p2782 A83-39034
- Satellite microwave radiances correlated with radar rain rates over land 18 p2728 A83-39963
- Scattering of thermal emission from a flat surface in a medium with fluctuating permittivity 19 p2861 A83-41804
- The generation mechanism of solar metre-wave moving type IV bursts 21 p3243 A83-44510
- Method for calculating radio-brightness temperature in problems of satellite meteorology 21 p3181 A83-45294
- A multi-frequency measurement of thermal microwave emission from soils - The effect of soil texture and surface roughness 22 p3308 A83-46103
- The effects of vegetation cover on the radar and radiometric sensitivity to soil moisture 22 p3311 A83-46183
- Influence of the atmosphere on the performance of a multichannel microwave radiometer 22 p3289 A83-46199
- The brightness temperature of sea ice and fresh-water ice in the frequency range 500 MHz to 37 GHz 22 p3313 A83-46205
- Variation of the microwave brightness temperature of sea surfaces covered with mineral and monomolecular oil films 22 p3321 A83-46235
- Transient brightenings of interconnecting loops. III Interpretation --- solar corona 23 p3537 A83-47725
- Source characteristics of main and post-burst-increase phases of solar bursts at 17 GHz 23 p3537 A83-47732
- Observations on the slowly varying component of solar radio emission at decameter wavelengths 23 p3538 A83-47733
- Estimating the temperature and height of overshooting thunderstorm tops from geostationary satellite infrared data 24 p3615 A83-49727
- BRILLOUIN EFFECT**
- Effect of nonlinear phase shifts on stimulated scattering of electromagnetic waves in plasmas 03 p0397 A83-13190
- Theory of nonlinear saturation of stimulated Brillouin scattering in a plasma 04 p0537 A83-15908
- Determination of the width of the gain profile of an iodine laser with the aid of stimulated Brillouin scattering 05 p0649 A83-17059
- Parametric instabilities in a magnetized plasma 05 p0687 A83-17266
- Stimulated Mandel'shtam-Brillouin scattering in a multimode glass fiber lightguide 07 p0933 A83-20046
- Theory of stimulated Brillouin scattering in a low-density plasma 07 p0933 A83-20047
- Reversal of the wavefront of nanosecond and subnanosecond light pulses in stimulated Brillouin scattering 07 p0935 A83-20121
- Time-resolved Thomson-scattering measurements of ion fluctuations driven by stimulated Brillouin scattering 07 p0998 A83-20816
- Stimulated Brillouin scattering of nonducted whistlers 08 p1168 A83-22389
- Laser with diffraction-limited divergence and Q switching by stimulated Brillouin scattering 10 p1431 A83-26655
- Laser pulse compression by stimulated Brillouin scattering in tapered waveguides 11 p1583 A83-27621
- Efficient phase conjugation by Brillouin enhanced four wave mixing 12 p1731 A83-29199
- Stimulated Raman backscattering in the presence of ion-acoustic fluctuations 13 p1923 A83-30119
- Stimulated Brillouin scattering in an inhomogeneous plasma with broad-bandwidth thermal noise 13 p1923 A83-30120
- Expansion of a multi-ion plasma into a vacuum 13 p1924 A83-30123
- Numerical study of phase conjugation in stimulated Brillouin scattering from an optical waveguide 15 p2229 A83-33530
- High-efficiency laser-pulse compression by stimulated Brillouin scattering 15 p2167 A83-33759
- Efficient phase conjugation under parametric-feedback conditions 15 p2167 A83-33778
- Resonatorless generation of a giant laser pulse 17 p2514 A83-37900
- The Brillouin-scattering method in quantum electronics and laser-induced damage 18 p2694 A83-40608
- Investigation of Brillouin light scattering in crystals and glasses with application to problems of quantum electronics and fiber optics 18 p2694 A83-40609
- Spectral peculiarities of the stimulated Brillouin scattering at the wave-front reversal 19 p2853 A83-41188
- Stimulated Raman and Brillouin scattering of a Gaussian electromagnetic beam in ordinary mode in a magnetoplasma 19 p2901 A83-41197
- Brillouin backscattering in an electron beam-plasma system 21 p3212 A83-44348
- Phase matching and frequency detuning effects in Brillouin enhanced four-wave mixing 21 p3144 A83-44805
- Pulse compression by stimulated Brillouin scattering 22 p3297 A83-46630
- Highly efficient, high-quality phase-conjugate reflection at 308 nm using stimulated Brillouin scattering 24 p3587 A83-48854
- BRISTOL-SIDDELEY BS 53 ENGINE**
- Supersonic Harrier - One step closer 04 p0449 A83-16371
- Development of thrust augmentation technology for the Pegasus vectored thrust engine [SAE PAPER 821390] 17 p2468 A83-37966
- BRITTLE MATERIALS**
- Fracture statistics of surface brittle materials under flexure 02 p0189 A83-11673
- The role of the generalized fracture toughness in fracture mechanics [ASME PAPER 82-PVP-21] 02 p0157 A83-12768

- Dynamic fracture of a beam or plate under tensile loading 03 p0339 A83-13338
Quantitative analysis of delayed fracture observed in stress rate tests on brittle materials 03 p0290 A83-13686
Indentation microfracture in the Palmqvist crack regime - Implications for fracture toughness evaluation by the indentation method 03 p0290 A83-13725
Probabilistic fracture mechanics 04 p0496 A83-15153
Surface instability and splitting in compressed brittle elastic solids containing crack arrays [ASME PAPER 82-WA/APM-16] 04 p0498 A83-15682
Effect of shear and rotary inertia on dynamic fracture of a beam or plate in pure bending [ASME PAPER 82-WA/APM-9] 04 p0498 A83-15683
Conditions for spontaneous cracking of a brittle matrix due to the presence of thermoelastic stresses 04 p0464 A83-16274
A simple method for evaluating the subcritical crack growth of brittle materials 05 p0618 A83-17099
Role of cracks in the creep deformation of brittle polycrystalline ceramics 05 p0619 A83-17560
Effect of Delta T- and spatially varying heat transfer coefficient on thermal stress resistance of brittle ceramics measured by the quenching method 07 p0898 A83-20171
Conditions for toughening of particulate brittle composites 08 p1054 A83-21744
A relationship between the fracture strength and the fracture surface markings of brittle plastic plates 08 p1070 A83-22070
New method of determining the onset of ring cracking 08 p1106 A83-23233
Flaws and defects of structural carbon fibers 09 p1238 A83-23950
Development of a microfracture model for high rate tensile damage 09 p1279 A83-24071
Curved crack growth in brittle solids under farfield compression 11 p1592 A83-27439
Rain erosion damage in brittle materials 11 p1551 A83-28439
The development of the foundations of fracture mechanics for materials with initial stresses 14 p2029 A83-32151
Thermodynamics of crack growth 15 p2179 A83-34478
Dynamic fatigue of brittle materials containing indentation line flaws 15 p2180 A83-35064
The role of microcracking during crack growth in brittle materials 16 p2365 A83-35571
Fatigue life of brittle superconducting alloys in normal and superconducting states 20 p2955 A83-43468
On crack branching and curving in a finite body 21 p3156 A83-44887
Statistical approach to time-dependent failure of brittle material 21 p3157 A83-44903
Characteristics of brittle fracture under general combined modes including those under bi-axial tensile loads 24 p3594 A83-49866

BRITTLINESS

- Precipitation hardening and the resistance to brittle fracture of low alloy steels containing vanadium 01 p0025 A83-10396
Effect of grain size on the brittleness of titanium 01 p0025 A83-10447
Energy criteria of the brittle fracture of materials with initial stresses 01 p0059 A83-10676
The nature of the cold brittleness of transition metals 03 p0339 A83-13265
Mechanisms and criteria for cleavage 08 p1058 A83-21666
The experimental evaluation on the brittle fracture characterization under the mixed mode 08 p1122 A83-22069
The topography of the core-region around cracks under modes I, II and III of fracture 09 p1282 A83-25050
Brittle fracture near holes --- Russian book 21 p3150 A83-43911
A probabilistic treatment of brittle fracture under nonmonotonically increasing stresses 21 p3159 A83-44923

BROADBAND

- Broadband infrared generation in liquid-bromine-core optical fibers 02 p0183 A83-11571
Wide-band mirrors for vacuum ultraviolet and soft X-ray radiation 02 p0232 A83-11656
Frequency agile microstrip antennas 02 p0163 A83-11919
A broadband VLF burst associated with ring current electrons 02 p0207 A83-12385
Fiber optic pulse compression concept for processing wide bandwidth radar signals 03 p0304 A83-13790

- Generation of wide-band optical continuum in fiber waveguides 05 p0685 A83-17070
Simple design of broadband monomode tapers between hollow and dielectric filled rectangular waveguides 06 p0749 A83-17968
Constraints on umbral core models as derived from broad-band intensity observations 06 p0851 A83-18111
Limits of VSWR for optimal broadband capacitively loaded cylindrical antennas versus their length 06 p0741 A83-18661
Application of optical fibers to wide-band differential interferometry 07 p0993 A83-20175
Morphology of spatial patterns in Pi 1-2 magnetic field pulsation activity - A review 07 p0965 A83-21428
Wide-band subharmonically pumped W-band mixer in single-ridge fin-line 07 p0923 A83-21531
Broadband transducers 08 p1093 A83-22402
Self-complementary monopole-notch array antennas 08 p1077 A83-22624
A computer-controlled broadband system for measuring scattered fields and for locating scattering centers 09 p1244 A83-23382
Broad-band microwave electronically scanned direction finder 09 p1246 A83-23777
Broad-band wide-angle quasi-optical polarization rotators --- for ground station antennas 09 p1246 A83-23785
A wide-band low-sidelobe disc-o-cone antenna 09 p1248 A83-23805
On some broad-band microstrip resonators 09 p1248 A83-23808
Optimization of lines with small inhomogeneities for wide-band matching 09 p1256 A83-24915
The broad-band circular polarization of sunspots, 0.37-4.5 microns 10 p1521 A83-25750
Optical reconstruction of wideband Fourier and Fresnel acoustic holograms 10 p1421 A83-26295
The broad-band scattering response of periodic arrays 10 p1405 A83-26832
The wide-band matching area for a small antenna 10 p1406 A83-26848
Ultra-wideband quadrature coupler 11 p1563 A83-28602
A monolithically integrated wide-tunable sine oscillator --- Thesis 11 p1564 A83-28642
Wideband millimeter-wave impedance measurements 13 p1836 A83-30974
Estimation of the probability of error in the reception of broadband signals 14 p2001 A83-32487
Broad spectral band color image deblurring 14 p2020 A83-32904
Broad-band compensation for diffraction in surface acoustic wave filters 16 p2345 A83-35649
Transport of broadband radiation through a nonlinear dispersive medium 16 p2407 A83-35661
Simultaneous observation of rotational coherent Stokes Raman scattering and coherent anti-Stokes Raman scattering in air and nitrogen 17 p2511 A83-37943
Ultra-wideband millimetre-wave self-oscillating mixer 20 p2966 A83-42366
Wideband heterodyne detection in the far infrared with extrinsic Ge photocoductors 20 p3048 A83-42583
Broadband adaptive array processing 20 p2965 A83-43682
Broad band electro-optic tuning of a CW dye laser 21 p3143 A83-44188
Fiber-optic gyroscopes with broad-band sources 21 p3136 A83-44210
Design of broadband (fast) systems of digital signals processing 21 p3190 A83-44773
Broad-band ultrasonic sensor based on induced optical phase shifts in single-mode fibers 22 p3287 A83-45731
Wide-band acoustooptical spectral analyzer of the autocollimation type 23 p3507 A83-47573
- BROADBAND AMPLIFIERS**
Broadband monolithic integrated power amplifiers in gallium arsenide 03 p0308 A83-13440
Broadband microwave power amplifiers using lumped-element matching and distributed combining techniques 03 p0313 A83-13998
A design method of super-wideband pulse amplifiers 03 p0314 A83-14129
On design and performance of lossy match GaAs MESFET amplifiers 06 p0752 A83-18765
Broad-band bias-current-tuned IMPATT oscillator for 100-200 GHz 06 p0753 A83-18767
Broad-band characteristics of EHF IMPATT diodes 06 p0753 A83-18768
Broad-band GaAs monolithic amplifier using negative feedback 06 p0753 A83-18774
Increasing the output power of generator-type broadband microwave transistors 06 p0755 A83-19363

- A compact broad-band multifunction ECM MIC module 07 p0923 A83-21533
A network modeling and design method for a 2-18-GHz feedback amplifier 07 p0923 A83-21536
A simplified 'real frequency' technique applied to broad-band multistage microwave amplifiers 07 p0923 A83-21537
Phase control of pulsed broadband microwave amplifiers 08 p1079 A83-22000
A monolithic GaAs DC to 2-GHz feedback amplifier 09 p1256 A83-24682
A broad-band traveling-wave maser for the range 40-46.5 GHz 13 p1849 A83-30236
Low-noise, low power dissipation GaAs monolithic broad-band amplifiers 14 p2008 A83-33459
Electromagnetic-wave propagation in a conducting waveguide loaded with a tape helix 24 p3572 A83-48963

BROADCASTING

- Legal-political discrimination in cross-border satellite-mediated TV advertising and publicity - Review of problems 01 p0112 A83-10400
DBS platforms - A viable solution 03 p0284 A83-13899
Three is not enough - Why the U.S. specified four DBS service areas 03 p0304 A83-13900
Japan's BSE program --- Broadcasting Satellite for Experimental purpose 04 p0468 A83-16415
Aspects of the satellite broadcasting experiments using the BSE and its in-orbit performance 04 p0468 A83-16416
High definition television broadcasting by satellite 04 p0469 A83-16423
Transmission system for the television broadcasting satellite 04 p0469 A83-16424
Operational broadcasting satellite in Japan 04 p0469 A83-16425
A planar array antenna for TV broadcasting communications 06 p0737 A83-18607
Feeds for reflector antennas - A review 06 p0741 A83-18656
Broadcasting satellites and the system of the United States Satellite Broadcasting Company 07 p0904 A83-19680
Systems and technology aspects of a direct broadcast satellite service for the United States 07 p0904 A83-19692
'RARC '83' - International planning for broadcasting satellites at 12 GHz 07 p0906 A83-19717
Broadcast satellites in Europe 10 p1402 A83-25800
The 'Orbita-RV' satellite sound broadcasting and newspaper column transmission system 10 p1402 A83-25876
Satellite television broadcasting systems in the USSR 10 p1402 A83-25877
The United Nations resolution from December 10, 1982 concerning the principles for direct television broadcasting by satellites 12 p1783 A83-29366
PCM sounds on digital subcarrier in television for a satellite broadcasting system 12 p1718 A83-29412
The broadcasting-satellite service - Freedom or control 15 p2144 A83-34652
Direct broadcasting satellites - International policy issues 15 p2240 A83-34653
A new service at the starting line - Direct broadcasting from satellites 15 p2144 A83-34654
Domestic broadcasting-satellite systems - The need for a common standard and the case for block allotment planning 19 p2829 A83-41349
Orbit utilization in the US Broadcast Satellite Service 19 p2829 A83-41350
A one kilowatt class direct broadcast satellite 19 p2829 A83-41352
12 GHz band satellite broadcasting receiver with direct converting system 19 p2829 A83-41353
New telecommunications for the developing world 21 p3220 A83-44530
Major developments in space law from 1957 to 1982 - A general survey 21 p3221 A83-44536
Broadcasting aspects of a projected African regional satellite telecommunications system 21 p3122 A83-45432
Data broadcast to microterminals via satellite using spread-spectrum techniques 21 p3122 A83-45433
On board and ground equipment for TV broadcast applications State of the art and evolution [IAF PAPER 83-75] 23 p3441 A83-47254
Transmitting antenna for direct broadcasting satellites with radio frequency beam fine pointing capability [IAF PAPER 83-76] 23 p3441 A83-47255
Satellite broadcasting - The best way to meet the needs of television education in China [IAF PAPER 83-308] 23 p3513 A83-47337

BROKEN SYMMETRY

Matter and antimatter in the universe 01 p0123 A83-10377

Remarks on origins of biomolecular asymmetry 02 p0219 A83-11635

The lepton Brusselator - Creation of structure in the early Universe 02 p0254 A83-12091

Asymptotic breaking and restoration of symmetry in a statistical system of particles with short-range vector interaction and isotropic cosmological models 03 p0417 A83-13533

Hidden supersymmetry in stochastic dissipative dynamics 04 p0532 A83-15911

Spontaneously broken complete relativity 07 p0988 A83-20045

Possible new long-range interaction and methods for detecting it 07 p0989 A83-20609

Grand unification and cosmology 07 p1015 A83-20759

Upper bound on gauge-fermion masses 07 p0992 A83-20814

The nonuniqueness of the limit transition from Brans-Dicke theory to Einstein theory 07 p0990 A83-20970

The Inflationary Universe lives 08 p1181 A83-22398

Classical upper bounds for grand-unified monopole masses 13 p1917 A83-30596

'Supergravity '81'; Proceedings of the First School, Trieste, Italy, April 22-May 6, 1981 13 p1915 A83-31400

The renormalized coupling constant in an open static Einstein universe 13 p1954 A83-31607

A scalar field with self-interaction leads to the absence of a singularity in cosmology 14 p2102 A83-32424

Forced and self-excited vibrations of gas-turbine assemblies with perfect and perturbed symmetry 16 p2311 A83-36791

Bifurcations and phase transitions of self-gravitating and uniformly rotating fluid 21 p3232 A83-44737

Quantum effects of scalar and vector particles with variable mass in homogeneous and isotropic cosmology 21 p3235 A83-45381

Problems with the new inflationary universe 21 p3238 A83-45574

BROMIDES

NT AMMONIUM BROMIDES

NT HYDROBROMIC ACID

NT POTASSIUM BROMIDES

Bound-free emission in HgBr 01 p0055 A83-10979

A study of the dynamics of UV laser photolysis of NOCl and NOBr 07 p0882 A83-21195

Service life of a copper bromide vapor laser 10 p1432 A83-26674

Cavity-dumped mercury-bromide laser 11 p1582 A83-27613

Pressure-induced disproportionation in CuBr 12 p1782 A83-29168

Enhanced HgBr(B2Sigma+ - X2Sigma+) emission at low pressures --- blue-green laser 13 p1852 A83-31062

A kinetic model of the sustained discharge HgBr laser 17 p2514 A83-38207

Characteristics of mercurous bromide and iodide visible lasers 20 p2995 A83-43104

Relative efficiency of Hg-200Br-79, HgBr-79, and HgBr electric discharge lasers 24 p3586 A83-48781

BROMINATION

Chemical reactions with aerosols 09 p1297 A83-25182

BROMINE

Broadband infrared generation in liquid-bromine-core optical fibers 02 p0183 A83-11571

Multiple-nucleon interactions of relativistic heavy nuclei of cosmic rays with Ag and Br nuclei, and characteristics of interactions with a high multiplicity of shower particles in the energy range of 4-400 GeV/nucleon 02 p0274 A83-11739

Bromine reduction in a two-phase electrolyte 02 p0151 A83-12051

A new brominated polymeric additive for flame retardant glass-filled polybutylene terephthalate 19 p2824 A83-41854

Atmospheric bromine in the Arctic 20 p3021 A83-42852

Anti-Stokes Raman laser emission at 149 nm in atomic bromine 24 p3587 A83-48853

Visible iodine and bromine laser, and coaxial discharge excited strong UV iodine laser 24 p3589 A83-49615

BROMINE COMPOUNDS

NT AMMONIUM BROMIDES

NT BROMIDES

NT HYDROBROMIC ACID

NT POTASSIUM BROMIDES

Inverse-square wavelength dependence of attenuation in infrared polycrystalline fibers 10 p1482 A83-26116

BRONCHI

The blood flow in bronchial vessels during hypoxia 01 p0078 A83-10481

The blood supply of the trachea and bronchi of rats 18 p2733 A83-40584

BRONCHIAL TUBE

NT PHARYNX

NT TRACHEA

BROWNIAN MOVEMENTS

Propagation of chaos and the Burgers equation 20 p3043 A83-43124

Radiation balance and the stochastic Van der Pol-Duffing equation 22 p3354 A83-46771

BRUCETON TEST

U STATISTICAL TESTS

BRUDERHEIM METEORITE

Limb darkening of meteorites and asteroids 14 p2112 A83-32605

BRUNT-VAISALA FREQUENCY

A generalization of the Hines' dispersion relation --- for real atmosphere 16 p2377 A83-36108

BRUSHES

NT BRUSHES (ELECTRICAL CONTACTS)

Increasing the fatigue strength of welded joints in PT3V alloy treated with mechanical brushes 10 p1397 A83-26224

BRUSHES (ELECTRICAL CONTACTS)

Brush plating in aerospace applications [SAE PAPER 820612] 22 p3302 A83-45870

BUBBLE MEMORY DEVICES

Bubble technology for automatic test equipment/ground support equipment /ATE/GSE/ applications 01 p0037 A83-10748

BUBBLE TECHNIQUE

Flow visualization study in low specific speed pump impeller passages 01 p0053 A83-11073

BUBBLES

Inertial forces on an expanding bubble in motion in a fluid 01 p0047 A83-10921

Mechanism of impact pressure generation from spark-generated bubble collapse near a wall 04 p0476 A83-15282

Dissolution of a stationary bubble in a glassmelt with reversible chemical reaction - Rapid forward reaction rate constant 06 p0735 A83-19318

Fixation of bubbles and drops of specified shapes in a liquid dielectric by an electric field 06 p0813 A83-19434

Experimental study of the shock generation at the collapse of cavitation bubble 07 p0925 A83-20284

Marangoni convection-induced bubble motion 08 p1086 A83-23124

Improved light-scattering cavitation nuclei classifier 08 p1106 A83-23229

Shock propagation in liquid-gas media 10 p1417 A83-26194

Bubble nucleation and growth in open-cycle OTEC subsystems 15 p2189 A83-33988

The calculation of separation bubbles in interactive turbulent boundary layers 18 p2633 A83-39216

The effect of temperature gradient on the motion of a bubble in reduced gravity 18 p2686 A83-39906

Thermocapillary migration of bubbles and droplets 18 p2686 A83-39907

Marangoni effects under electric fields 18 p2686 A83-39911

Bubble motion in a rotating liquid body --- ground based tests for space shuttle experiments 20 p2940 A83-43272

Thermocapillary motion of bubbles inside drops --- in free fall environment with axisymmetric surface temperature field 20 p2940 A83-43279

Experimental observation of the thermocapillary driven motion of bubbles in a molten glass under low gravity conditions 20 p2941 A83-43283

Preliminary study of the effects of a reversible chemical reaction on gas bubble dissolution --- for space glass refining 20 p2941 A83-43285

Bubble behavior in molten glass in a temperature gradient --- in reduced gravity rocket experiment 20 p2941 A83-43286

Cavitation research performed at the Ecole Nationale Supérieure des Techniques Avancées 20 p2987 A83-43725

The effect of gas bubble evolution on the energy efficiency in water electrolysis --- Thesis 22 p3266 A83-46688

On the calculation of separation bubbles 23 p3449 A83-48119

The collapse of a gas bubble attached to a solid wall by a shock wave and the induced impact pressure [ASME PAPER 83-FE-3] 23 p3450 A83-48228

BUCKLING

NT CREEP BUCKLING

NT ELASTIC BUCKLING

NT EULER BUCKLING

NT THERMAL BUCKLING

Post-buckling dynamic behavior of periodically supported imperfect shells 01 p0060 A83-10860

Tensile buckling of advanced turboprops [AIAA PAPER 82-0776] 01 p0060 A83-10900

Buckling of polar orthotropic annular plates under inplane radial pressures 02 p0190 A83-12002

Approximate analysis of postbuckled through-width delaminations 02 p0191 A83-12061

A numerical study of the buckling process and strength analysis of layered cylindrical shells under axial impact 02 p0192 A83-12358

Recent advances in reduction methods for instability analysis of structures 02 p0193 A83-12738

On the solution of elastic-plastic static and dynamic postbuckling collapse of general structure 02 p0194 A83-12746

An energy theory for postbuckling of composite plates under combined loading 02 p0195 A83-12758

A formulation and solution procedure for post-buckling of thin-walled structures 04 p0494 A83-15007

Stability and postbuckling analysis of nonlinear structures 04 p0494 A83-15008

A creep type strategy used for tracing the load path in elastoplastic post buckling analysis 04 p0494 A83-15009

Compressive failure and kinking in uniaxially aligned glass-resin composite under superposed hydrostatic pressure 04 p0455 A83-15994

Hybrid optimization of truss structures with strength and buckling constraints 06 p0771 A83-18207

On the buckling and vibration of antisymmetric angle-ply laminated circular cylindrical shells 07 p0946 A83-20639

Buckling of a thin-walled conical shell under axisymmetric loads beyond the elastic limit 07 p0947 A83-21087

Stability and postbuckling behavior of simply supported trapezoidal plates under compression 07 p0947 A83-21088

An iterative method for finite dimensional structural optimization problems with repeated eigenvalues 07 p0949 A83-21444

Buckling of a conical sandwich shell beyond the elastic limit under combined load 08 p1115 A83-21637

Initial postbifurcation behavior of a ring subjected to the simultaneous action of normal and constant-directional pressures 08 p1121 A83-21868

Instability of short stiffened composite cylindrical shells under bending with prebuckling displacements 08 p1121 A83-21891

Note on the postbuckling analysis of cross-ply laminated plates with elastically restrained edges and initial curvatures 08 p1123 A83-22414

Study on the elastic-plastic buckling strength of plate structures 08 p1123 A83-22422

Analysis of progressive plastic buckling in cylindrical shell as contact problem 08 p1123 A83-22772

The lateral buckling-fracture stability of thin-sheet structural components with deep cracks 09 p1280 A83-24648

The influence of inplane deformation on the buckling loads of isotropic elastic plates 09 p1283 A83-25218

Aspects of plastic postbuckling behavior 10 p1437 A83-25312

Experimental investigation of the buckling of shallow spherical shells 10 p1438 A83-25469

Plastic buckling of initially imperfect stiffened cylinders in axial compression 10 p1440 A83-26433

On the unsymmetric eigenproblem for the buckling of shells under pressure loading 10 p1440 A83-26434

Delamination buckling and growth in laminates [ASME PAPER 83-APM-3] 10 p1441 A83-26445

Influence of tangential displacements on the dynamic buckling of viscoplastic cylindrical shells 10 p1442 A83-26820

Viscoelastic effects in buckling of laminated plates subjected to hygrothermal conditions 11 p1591 A83-27428

Further comparison of the numerical and experimental buckling behaviors of composite panels 11 p1599 A83-28722

Buckled plate vibrations and large amplitude vibrations using high-order triangular elements 12 p1734 A83-28967

Stability analysis of a spherical shell of imperfect shape on the basis of an improved buckling pattern 12 p1735 A83-29292

Dynamics of delamination buckling [AIAA 83-0873] 12 p1738 A83-29757

- Postbuckling of long orthotropic plates in combined shear and compression
[AIAA 83-0876] 12 p1738 A83-29760
- Buckling behavior and imperfection sensitivity of composite panels
[AIAA 83-0877] 12 p1739 A83-29761
- Minimum weight design of structures with geometric nonlinear behavior
[AIAA 83-0937] 12 p1739 A83-29767
- Buckling of anisotropic laminated cylindrical plates
[AIAA 83-0979] 12 p1740 A83-29786
- Numerical solution of two-dimensional boundary value problems of the statics of flexible conical shells
13 p1866 A83-30071
- Buckle pattern of biaxially compressed simply supported orthotropic rectangular plates
13 p1868 A83-31619
- Local buckling of thin tensioned plate with a crack
14 p2033 A83-33374
- Effective widths in plate buckling
15 p2173 A83-33612
- Elastic stability, buckling and post-buckling behaviour
15 p2176 A83-34328
- A reinvestigation of post-buckling behaviour of elastic circular plates using a simple finite element formulation
15 p2179 A83-34566
- Buckling and postbuckling of imperfect cylindrical shells under axial compression
15 p2180 A83-34568
- Probabilistic methods in the theory of structures --- Book
17 p2575 A83-37161
- Fracture mechanics in design - Particular reference to the thickness effect on the risk of unstable fracture
18 p2699 A83-39547
- Buckling of continuous filament composite isogrid panels
Theory and experiment
18 p2704 A83-40183
- Compressive buckling of graphite-epoxy composite circular cylindrical shells
18 p2704 A83-40184
- Best angles against buckling for rectangular laminates
18 p2704 A83-40186
- Coupling effect on axial compressive buckling of laminated composite cylindrical shells
18 p2704 A83-40187
- The effect of the direction of shear on the buckling of laminated plates subjected to combined shear and compressive loading
18 p2704 A83-40188
- Buckling of sinusoidally corrugated plates under axial compression
19 p2856 A83-40878
- On the interaction between local and overall buckling of an asymmetric portal frame
19 p2857 A83-41154
- On buckling paradox
20 p3001 A83-42349
- Doubly symmetric interactive buckling of plate structures
20 p3001 A83-42519
- On the automatic solution of nonlinear finite element equations --- for structural analysis
20 p3003 A83-42933
- Buckling loads in the case of imperfect truncated conical shells under axial pressure
20 p3005 A83-42983
- Dynamics and stability of open conical shells
20 p3005 A83-42993
- Implementation of an improved bisection algorithm in buckling problems
20 p3008 A83-43647
- An equilibrium model finite element analysis for buckling of moderately thick plates
21 p3151 A83-44105
- Plastic buckling of axially compressed circular cylindrical shells
21 p3152 A83-44249
- Buckling by cumulative plastic deformations under cyclic additional loading
21 p3152 A83-44458
- On axial and lateral buckling of end-loaded anisotropic cantilever beams
21 p3152 A83-44464
- Inelastic buckling of cylindrical shells subjected to axial tension and external pressure
21 p3164 A83-45597
- Postbuckling behavior of inelastic inextensional rings under external pressure
[ASME PAPER 83-WA/APM-4] 23 p3468 A83-47593
- Nonaxisymmetric buckling and supercritical behavior of elastic spherical shells in the case of a double critical value of load
23 p3473 A83-48537
- Review of experimental techniques for thin-walled structures liable to buckling. II - Stable buckling
24 p3592 A83-48997
- A modification of Potter's method for diagonal matrices with common unknown
24 p3593 A83-49440
- Numerical optimum design of elastic annular plates with respect to buckling
24 p3594 A83-49443
- Compressive strength of fiber-reinforced materials
24 p3597 A83-50147

BUDGETING

- Activity distribution analysis --- for life cycle budgeting and program management
01 p0112 A83-11154
- ESA procedures to account for inflation
11 p1666 A83-27372
- Towards the starship Enterprise - Are the current trends in defence unit costs inexorable?
14 p2094 A83-31923

BUFFER STORAGE

- Buffering of optoelectronic memory and its effect on computer efficiency
11 p1646 A83-28624
- Integrated surface acoustic wave/field-effect transistor high-speed analog memory
16 p2347 A83-36772

BUFFERS (CHEMISTRY)

- Effect of annealing in buffer gas at 800-1000 C on the mechanical properties of x 10 NiCrAlTi 32 20 type alloys
09 p1233 A83-24138

- Theoretical studies in isoelectric focusing --- mathematical modeling and computer simulation for biologicals purification process
20 p2951 A83-43280

BUFFETING

- Wind-tunnel measurements of wing-buffet boundaries at subsonic and transonic speeds
01 p0002 A83-10440

- Buffeting of a slender circular beam in axial turbulent flows
[AIAA 83-0928] 12 p1744 A83-29854

BUILDING MATERIALS

U CONSTRUCTION MATERIALS

BUILDING STRUCTURES

U BUILDINGS

BUILDINGS

- Wakes from arrays of buildings --- flight safety
17 p2508 A83-38766

BULGARIA

- The National Observatory of the Bulgarian People's Republic
02 p0249 A83-13047

BULGING

- Bursting and bulging of carbon fibre composite discs
01 p0022 A83-10243

BULK ACOUSTIC WAVE DEVICES

- A bulk-acoustic-wave device for the convolution of microwave signals
04 p0469 A83-15140
- Bulk wave Bragg cells with 1 GHz bandwidth
06 p0753 A83-18935
- Suppression of bulk modes in SAW transversal filters by gold transducers
09 p1255 A83-24119
- Principles of acoustic devices --- Book
15 p2163 A83-33750
- Analysis of two-beam interferometry for bulk wave measurements
22 p3294 A83-46839
- Temperature stability of surface-generated bulk waves
23 p3446 A83-48722

BULK MODULUS

- Bulk modulus technique for determining void content changes due to solid propellant gas evolution
[AIAA PAPER 83-1119] 16 p2338 A83-36230
- Clausius-Mossotti-type approximation for elastic moduli of a three-dimensional, two-component composite
17 p2484 A83-38816
- Compression, nonstoichiometry and bulk viscosity of wuestite
21 p3174 A83-45061

BUNCHING

NT ELECTRON BUNCHING

- Antibunching in the Franck-Hertz experiment --- subpoissonian light generation from space-charge limited electron beams colliding with atoms
19 p2900 A83-41189

BUOYANCY

- Natural convection heat transfer between eccentric horizontal cylinders
[ASME PAPER 82-HT-43] 02 p0172 A83-12796
- Buoyancy flow limited mixed layer depth in oscillating grid turbulence
03 p0319 A83-14477
- Buoyancy-induced two-dimensional vertical flows in a thermally stratified environment
06 p0756 A83-18375
- Magnetic buoyancy and the Boussinesq approximation --- applied to solar magnetic field
06 p0835 A83-18931

- The stability and disturbance-amplification characteristics of vertical mixed convection flow
09 p1261 A83-24413
- Buoyant plane jets in thermally stratified media
[ASME PAPER 82-WA/HT-57] 10 p1413 A83-25696

- The thermohaline driving mechanism of oceanic jet streams
12 p1761 A83-29553
- A statistical theory of thermally-driven turbulent shear flows, with the derivation of a subgrid model
17 p2507 A83-37877

- Effect of buoyancy and power design parameters on hybrid airship performance
[AIAA PAPER 83-1976] 17 p2465 A83-38907
- Turbulence structure in stably stratified open-channel flow
18 p2680 A83-39204

- Buoyancy effects and the manifolding of single ended absorber tubes
19 p2861 A83-40765
- A method for calculating and analyzing the properties of a vertical nonisothermal jet with allowance for the buoyancy force
19 p2794 A83-42131

- Buoyancy effect on heat transfer in forced channel flows
20 p2971 A83-42661

- An analysis of the axisymmetric turbulent buoyant jet
20 p2973 A83-42685

- Measurements of the turbulent energy and temperature balances in an axisymmetric buoyant plume in a stably stratified environment
20 p2973 A83-42686
- Heat transfer mechanism in a thermally stratified turbulent flow
20 p2973 A83-42688
- Turbulent boundary layers on moving, nonisothermal continuous cylinders
20 p2976 A83-42717
- Mechanism for transition to turbulence in buoyant plume flow
23 p3451 A83-48623

BUOYS

- Determination of the statistical characteristics of surface currents by means of satellite-tracked drifting buoys
18 p2731 A83-40599

- The near-surface circulation of the North Pacific using satellite tracked drifting buoys
22 p3344 A83-46908
- Surface circulation of the southern ocean according to FGGE drifting-buoy data
23 p3493 A83-48510

BURGER EQUATION

- Solution of Burgers' equation with a large Reynolds number
01 p0045 A83-10710
- Comparison of time integration /finite difference and spectral/ for the non-linear Burgers equation
03 p0389 A83-14603
- Generation of atmospheric turbulence by solar radiation
05 p0668 A83-17818
- A comparison of two explicit time integration schemes applied to the transient heat equation
06 p0757 A83-18467

- The generalized Burgers' equation in radiative magnetogasdynamics
12 p1780 A83-29026
- A pseudospectral scheme for the numerical calculation of shocks
12 p1725 A83-29622
- Shock calculations and the numerical solution of singular perturbation problems
12 p1726 A83-29938
- A numerical study of the Burgers turbulence at extremely large Reynolds numbers
14 p2009 A83-32520
- MHD turbulence via extended Burgers' equation
15 p2235 A83-34544

- Nonlinear interaction of waves in media without dispersion in the presence of external distributed sources
15 p2226 A83-34704
- Generating exact solutions of the two-dimensional Burgers' equations
16 p2349 A83-35524
- Model of Burgers turbulence for turbulent ionization waves
18 p2747 A83-39916
- Propagation of chaos and the Burgers equation
20 p3043 A83-43124

- A comparison of finite element and finite difference solutions of the one- and two-dimensional Burgers' equations
21 p3132 A83-44989
- A theory of weak shocks
22 p3287 A83-47095

BURNERS

- Convective heat transfer from laminar and turbulent premixed flames
20 p2979 A83-42748
- Combustion experiments with a new burner air distribution concept
[ASME PAPER 83-GT-31] 23 p3406 A83-47893

BURNING

U COMBUSTION

BURNING PROCESS

U COMBUSTION

BURNING RATE

- Parametric study of acceleration effects on burning rates of metallized solid propellants
02 p0161 A83-13084
- An improved model for the combustion of AP composite propellants
03 p0303 A83-13142
- The effect of mechanical stresses on the combustion velocity of solid fuel mixtures
03 p0295 A83-14057
- Combustion of a layer of fuel in a flow of oxidizer over its surface
03 p0295 A83-14058
- Effect of burning rate modifiers on propellant performance - A theoretical study
04 p0464 A83-15474

- Effect of oxidizer particle size on burning rate and thermal decomposition of composite solid propellants
04 p0465 A83-16430

- Influence of confinement on flame acceleration due to repeated obstacles
07 p0878 A83-19836
- Laminar burning velocities of hydrogen-air and hydrogen-air-steam flames
07 p0878 A83-19837
- The erosion combustion of a solid fuel under various temperatures of the ventilating flow
07 p0901 A83-19951

- Features of the dynamics of gas combustion in closed vessels under various laws for the change in the flame surface
07 p0880 A83-19952
- Erosive burning of composite solid propellants - Mechanism, correlation, and grain design applications
[AIAA PAPER 81-1581] 07 p0902 A83-20418

- Flame propagation through dust clouds of carbon, coal, aluminium and magnesium in an environment of zero gravity
07 p0882 A83-21352

A fresh look at the classical approach to homogeneous solid propellant combustion modeling 08 p1073 A83-22345

On the numerical accuracy of homogeneous solid propellant combustion models 08 p1073 A83-22346

New procedure for incorporating burning moderators in double-base solid propellants 09 p1241 A83-23834

A simple insulation method of end-burning composite propellant and its application to the motors loaded with high burning rate propellants 09 p1242 A83-23842

Non-steady burning in a randomly layered composite propellant [AIAA PAPER 83-0477] 09 p1220 A83-24148

Burning rate measurements in solid rocket motors [AIAA PAPER 83-0481] 09 p1269 A83-24149

Some experiments on model composite solid propellants 13 p1826 A83-31675

The rules governing changes in combustion characteristics for competing reactions 14 p1989 A83-32092

Determination of mass transfer number of polymers from heats of gasification 15 p2142 A83-33725

Flames near rich flammability limits, with particular reference to the hydrogen - Air and similar systems 15 p2132 A83-34038

Criteria analysis of VHBR solid propulsion system for in-tube burning rocket application --- Very High Burning Rate [AIAA PAPER 83-1111] 16 p2318 A83-36226

A combustion theory for very high regression-rate solid propellant [AIAA PAPER 83-1196] 16 p2339 A83-36272

Model for double-base propellants combustion, without and with additives [AIAA PAPER 83-1197] 16 p2339 A83-36273

Combustion chemistry of nitrate ester-based propellants [AIAA PAPER 83-1198] 16 p2340 A83-36274

Effects of AP particle size on combustion response to crossflow [AIAA PAPER 83-1270] 16 p2340 A83-36317

Burning rate characterization from one motor firing - An analytical approach [AIAA PAPER 83-1315] 16 p2340 A83-36336

The detailed processes involved in flame spread over solid fuels 17 p2484 A83-37044

Prediction of metal fire spread in high pressure oxygen 17 p2484 A83-37047

Fire spread mechanisms along steel cylinders in high pressure oxygen 17 p2485 A83-38026

Effect of ammonium halides on the combustion of polystyrene 21 p3116 A83-44666

BURNING TIME

Features of the dynamics of gas combustion in closed vessels under various laws for the change in the flame surface 07 p0880 A83-19952

BURNOUT

Evaluation of a rocket burnout velocity from ground and free flight tests [AIAA PAPER 83-0036] 05 p0602 A83-16476

BURNS (INJURIES)

The microcirculatory condition during burn shock in rats after a prolonged limitation of motor activity 14 p2061 A83-31973

Emergency care for burns --- Russian book 23 p3498 A83-48150

BURNTHROUGH (FAILURE)

X-band burnout characteristics of GaAs MESFET's 07 p0923 A83-21535

BURSTS

NT GAMMA RAY BURSTS

NT RADIO BURSTS

NT SOLAR RADIO BURSTS

NT TYPE 2 BURSTS

NT TYPE 3 BURSTS

NT TYPE 4 BURSTS

The 27-day periodicity of outbursts of Comet Schwassman-Wachmann I 03 p0410 A83-14680

Simultaneous optical and X-ray bursts from 4U/MXB 1636-53 04 p0554 A83-15634

Optical bursts from 4U/MXB 1636-53 04 p0554 A83-15635

Stochastic regime of the stabilization of burst instability in a nonequilibrium plasma 04 p0536 A83-15760

Fast coherent oscillations in variable X-ray sources and bursts 06 p0829 A83-18540

Some topics on the X-ray pulsars and the X-ray bursts observed by the satellite Hakucho 07 p1012 A83-20026

Thermonuclear runaways in thick hydrogen rich envelopes of neutron stars 07 p1012 A83-20029

Solar hard X-ray images observed by Astro-A 07 p1036 A83-20032

Artificial microburst dielectrics produced in laser-sol interactions 07 p0994 A83-20050

Evidence for spectroscopic periodicity in an X-ray burster 09 p1357 A83-23729

Statistical description of a simulacrum for eruptive variables 11 p1678 A83-27700

On the nature of the two modes in the type II bursts of MXB 1730-335 --- X ray source 12 p1796 A83-29493

Prospects for the detection of gravity wave bursts 13 p1846 A83-30359

X-ray burst observations of Serpens X-1 13 p1951 A83-31426

A 0538-66 - The most powerful X-ray star 15 p2244 A83-33540

Ultraviolet and optical observations of the dwarf novae VW and WX Hydri during outburst 15 p2264 A83-34576

Irregular X-ray variability in the transient X-ray burst source MXB 1659-29 17 p2605 A83-37921

Comments on the Neyman and Beall formulas for 'contagious' type-A probability distributions applied to burst processes especially in the field of digital transmission 19 p2827 A83-41313

Thick-target bremsstrahlung interpretation of short time-scale solar hard X-ray features 20 p3080 A83-42461

Statistical characteristics of turbulent bursts 20 p2987 A83-43514

On the structure of wall-bounded turbulent flows 21 p3128 A83-43930

Development of flare morphology in X-rays, and the flare scenario 23 p3531 A83-47661

Relation between hard X-ray spectra and electron energy spectra --- of solar X-ray bursts 23 p3533 A83-47683

General aspects of hard X-ray flares observed by Hinotori Gradual burst and impulsive burst 23 p3534 A83-47688

Hard X-ray images of impulsive bursts --- of sun 23 p3534 A83-47690

Investigation of flow visualization techniques for detecting turbulent bursts 24 p3585 A83-49820

BUSHINGS

Calculation of the wear of a shaft-bushing pair 07 p0939 A83-19941

BUTADIENE

Soot formation in pyrolysis of acetylene, allene and 1,3-butadiene 18 p2664 A83-39274

Optical emission from photoexcitation of aerosol particles produced by reaction of ozone with 1,3-butadiene 22 p3328 A83-46065

BUTT JOINTS

Advances in laser and MIAB welding techniques 07 p0940 A83-20523

Development of a two-directional seam tracking system with laser sensor 07 p0940 A83-20524

Effects of GTA dressing on the fatigue properties of aluminum alloy welded, butt jointed and fillet welded plates 09 p1274 A83-23650

BUTYLENE OXIDES

U TETRAHYDROFURAN

BUTYRIC ACID

The peripheral and central effects of gamma-aminobutyric acid on the vascular thermoregulatory reaction in rabbits 07 p0973 A83-20361

BYPASS RATIO

Composite fan exit guide vanes for high bypass ratio gas turbine engines 03 p0282 A83-13159

New thrusts in engine design 05 p0597 A83-17236

Prediction of high bypass ratio engine static and flyover jet noise [AIAA PAPER 83-0773] 10 p1378 A83-25958

Cost effective performance restoration of high by-pass engines 16 p2303 A83-35833

Experimental results of a deflected thrust V/STOL nozzle research program [AIAA PAPER 83-0170] 19 p2794 A83-42100

BYPASSES

Solar array power management --- in spacecraft power supplies 11 p1539 A83-27148

C

C BAND

Satellite clusters and frequency reuse 07 p0904 A83-19690

Monolithic GaAs interdigitated couplers 09 p1256 A83-24683

Measurement of relative propagation delay between C- and K-band satellite loops 10 p1403 A83-26076

High efficiency broadband FET power amplifier for C-band TWTA replacement 19 p2839 A83-41335

20 x 20 IF switch matrix for SS-TDMA systems 19 p2839 A83-41369

CADMIUM SELENIDES

Unfurlable offset antenna design for L- and C-band application 23 p3423 A83-48139

C-5 AIRCRAFT

Dynamic taxi response (have bounce) testing of the C-5A aircraft [AIAA PAPER 83-1024] 14 p1975 A83-32783

C-130 AIRCRAFT

C-141 operations in Bright Star 82 02 p0133 A83-12224

C-135 AIRCRAFT

Two years of training with the first true three-dimensional simulator 08 p1047 A83-22833

KC-135/CFM56 re-engine - The best solution [AIAA PAPER 83-1374] 16 p2309 A83-36367

Flight software for optimal trajectories in transport aircraft [AIAA PAPER 83-2241] 19 p2796 A83-41718

C-140 AIRCRAFT

Farfield inflight measurements of high-speed turboprop noise [AIAA PAPER 83-0745] 10 p1377 A83-25947

C-141 AIRCRAFT

C-141 operations in Bright Star 82 02 p0133 A83-12224

C-141 operations in Operation Bright Star 82 12 p1699 A83-29203

Infrared observations from the NASA Airborne Observatories 18 p2762 A83-40454

CABIN ATMOSPHERES

NT SPACECRAFT CABIN ATMOSPHERES

A physiological and hygienic evaluation of vibration in the cabin of the Mi-4 helicopter 14 p2073 A83-33325

CABLES (ROPES)

Orbital ring systems and Jacob's ladders. I 01 p0016 A83-10702

The mechanics of an anchored lunar satellite 03 p0283 A83-13215

The stability of motion of a flexible cable with loads in a Newtonian force field 04 p0453 A83-15380

The dynamics of plane supporting structures - A computer-aided experimental analysis of structure dynamic problems with interactive method of test --- German thesis 04 p0499 A83-15847

Limit amplitude of galloping cables --- effects of separated flow on Shuttle tank cable trays [AIAA PAPER 83-0132] 05 p0682 A83-16545

Dynamic wind tunnel tests of the simulated Shuttle external cable trays 07 p0869 A83-20412

Dynamics of space cable systems 17 p2472 A83-37473

Dynamics of the orbital cable system [IAF PAPER 83-336] 23 p3417 A83-47346

CAD (DESIGN)

U COMPUTER AIDED DESIGN

CADMIUM

CW recombination laser action in a cadmium vapor arc 07 p0938 A83-21370

Seasonal variations of Cd, Pb, Cu and Ni levels in snow from the eastern Arctic Ocean 11 p1613 A83-27673

Noise of He-Cd laser and its suppression 21 p3143 A83-44156

CADMIUM COMPOUNDS

NT CADMIUM SELENIDES

NT CADMIUM SULFIDES

NT CADMIUM TELLURIDES

A semiconductor-insulator-semiconductor CdO-SiO₂-Si solar cell 08 p1131 A83-22912

The relation between performance and stability of Cd-Chalcogenide/Polysulfide photoelectrochemical cells. I - Model and the effect of photoetching 11 p1546 A83-28297

Preparation of high purity II-VI compounds by laser annealing 14 p2090 A83-32303

CADMIUM MERCURY TELLURIDES

U MERCURY CADMIUM TELLURIDES

CADMIUM NICKEL BATTERIES

U NICKEL CADMIUM BATTERIES

CADMIUM SELENIDES

Preparation and analysis of cross-sections of etched and unetched CdSe semiconductor thin films 04 p0504 A83-15477

Influence of deposition rate on the character of electrodeposited CdSe used for photoelectrochemical cells 04 p0505 A83-15499

Hot-electron luminescence in aged electrodeposited CdSe liquid-junction solar cell 05 p0658 A83-16946

Electrochemical studies of photocorrosion of n-CdSe 07 p0952 A83-19881

Electrophoretically deposited CdS and CdSe anodes for photoelectrochemical cells 07 p0000 A83-19883

Electrochemical solar cells using CdSe thin film electrodes 07 p0953 A83-19885

Characterization of the interface energetics for N-type cadmium selenide/nonaqueous electrolyte junctions 07 p0881 A83-20585

Chemical bath deposition of thin film cadmium selenide for photoelectrochemical cells 07 p0954 A83-20594
Structural and compositional characterization of mixed CdS-CdSe films grown by cathodic electrodeposition 10 p1446 A83-26055
Cascade heterophotocells using wide-gap A/II/B/VI/ compounds 10 p1446 A83-26239
Photochemical reactions in CdS(x)Se(1-x) single crystals 12 p1782 A83-29161
Factors affecting the efficiency of chemically deposited CdSe based photoelectrochemical cells 12 p1749 A83-29514
Investigations of the photographic characteristics of a photoelectrochromic device 13 p1846 A83-30445
Photovoltaic behaviour of CdSe thin film solar cells 14 p2089 A83-32301
Influence of polarized optical pumping on the ferromagnetism of CdCr₂Se₄ 15 p2237 A83-33798
Cold pressed cadmium selenide photoanodes for electrochemical solar cells 18 p2708 A83-39929
Photoelectrochemical solar cells - Temperature control by cell design and its effects on the performance of cadmium chalcogenide-polysulphide systems 20 p3012 A83-42359
A one-volt p-InP/n-CdSe regenerative photoelectrochemical cell 20 p3013 A83-43421
Time-resolved nonlinear luminescence spectroscopy by picosecond excitation correlation 21 p3219 A83-45491

CADMIUM SULFIDES

Spray pyrolysis processing 02 p0186 A83-11507
A p-i-n heterojunction model for the thin-film CuInSe₂/CdS solar cell 03 p0355 A83-14513
Use of test structures in the production of CdS/Cu₂S photovoltaic devices 04 p0504 A83-15455
Effect of temperature on the performance of the PEC cells formed with chemically deposited CdS films --- photoelectrochemical cells 04 p0505 A83-15491
Heat-treatment studies on thin-film CdS/Cu_x/S solar cells 04 p0507 A83-16084
Photovoltaic properties of cadmium sulfide/trivalent-metal phthalocyanine heterojunction devices 06 p0754 A83-19259
Electrophoretically deposited CdS and CdSe anodes for photoelectrochemical cells 07 p0000 A83-19883
Spatial, temporal, and power characteristics of a streamer CdS semiconductor laser 07 p0933 A83-20101
Compositional depth profiles of chemically Cd₂S//Zn,Cd/S heterojunction solar cells 08 p1130 A83-22339
Role of impurities in sintered CdS/Cu₂S solar cells 09 p1292 A83-23666
X-ray diffraction study of the dry formation of Cu₂S-CdS solar cells 10 p1444 A83-25448
Thermal and plasma-chemical conversion of cadmium into alpha-CdS 10 p1389 A83-25528
Structural and compositional characterization of mixed CdS-CdSe films grown by cathodic electrodeposition 10 p1446 A83-26055
Submillimeter emission of CdS crystals pumped by intense light 10 p1430 A83-26234
Photochemical reactions in CdS(x)Se(1-x) single crystals 12 p1782 A83-29161
Birefringence of Zn(x)Cd(1-x)S near the isotropic point 13 p1918 A83-30207
One- and two-photon excited picosecond conductivity in CdS 14 p2083 A83-31949
The lasing mechanism, active layer thickness, natural resonator effects, and the nature of the M and P bands of the emission spectrum of CdS pumped by a nitrogen laser - T = 4.2-420 K 14 p2023 A83-32163
Fabrication of large area Cu₂S/CdS thin film solar modules 14 p2041 A83-32230
Front contacts for large area high efficiency Cu₂S-CdS solar cells 14 p2041 A83-32231
Recent advances in ITO/InP and CdS/InP solar cells 14 p2041 A83-32240
The assessment of thin film Cu(x)S-CdS solar cells using cathodoluminescence techniques 14 p2041 A83-32254
Studies on CdS/n-InP PEC solar cells 14 p2042 A83-32258
Electrodeposited CdS/CdTe heterojunction solar cells 14 p2044 A83-32280
Thin film heterojunction CdS/Cu ternary alloys solar cells with minority carrier mirrors 14 p2044 A83-32281
Large area CdS/Cu(x)S thin film solar cells produced by electrophoretic deposition 14 p2044 A83-32282
Sprayed zinc-cadmium sulfide films for backwall Cu₂S/(Z nCd)S cells 14 p2044 A83-32283
Photovoltaic performance of CdS heterojunctions on polycrystalline silicon 14 p2044 A83-32293
Temperature dependence of the IV-characteristic of Cu₂S-CdS thin film solar cells and related phenomena 14 p2044 A83-32294

Continuous deposition of photovoltaic grade CdS sheet at the unit operations scale 14 p2044 A83-32295
Cu(x)S(p)-CdZnS(n)-CdS(n+) evaporated thin film solar cells 14 p2045 A83-32296
Thin film Cu₂S/CdS junctions produced by evaporation and sputtering - Effect of thermal treatments in vacuum 14 p2089 A83-32297
Airless sprayed CdS solar cells 14 p2045 A83-32298
Cadmium sulfide polyacetylene photovoltaic hererojunction 14 p2090 A83-32305
Improvements of CdS film photoanodic behavior by sulfur organic reducing agents 14 p1990 A83-32635
8.5 percent efficient screen-printed CdS/CdTe solar cell produced on a 5-cm x 10-cm glass substrate 14 p2047 A83-32838
Technology of all electroplated CdS:Cu(x)S solar cells 14 p2047 A83-32847
Sprayed CdS-Cu₂S solar cells. I - Formation of cuprous sulphide 14 p2047 A83-32848
Single crystal Cu₂S/CdS photovoltaic devices with optimum performance before a post barrier air bake 18 p2708 A83-39930
The CdS-CuInSe₂ solar cell interface - Thermodynamic considerations 20 p2949 A83-42352
X-ray photoelectron spectroscopy studies of copper diffusion behavior and related degradation phenomena in thin film CdS/Cu₂S solar cells 20 p3052 A83-42355
Degradation of the performance of Cu₂S/CdS solar cells due to a two-way solid state diffusion process 20 p3052 A83-42358
Effect of photoelectrochemical etching on charge collection efficiency in CdS - An electron beam induced current study 20 p3053 A83-42613
Sprayed CdS-Cu₂S solar cells. II - preparation of CdS by airless spray 21 p3167 A83-44328
Electrophysical properties of heterogeneous CdS photovaractor structures 21 p3217 A83-44595
Process control of vacuum-deposited CdS for the fabrication of reproducible 8 percent efficient solar cells 21 p3167 A83-44605
Electrical and optical properties of n-CdS/P-Si and n(Zn(x)-Cd(1-x)S)/P-Si heterojunction solar cells 21 p3167 A83-44607
Angle-resolved photoemission studies of the CdS band structure 21 p3218 A83-44620
Deep level impurities and current collection in CdS/CdTe thin-film solar cells 22 p3365 A83-46734
The electrical characteristics of thin film Cu(x)S-CdS solar cells and their dependence on the ambient atmosphere during annealing 23 p3477 A83-48198
Characterization of epitaxial films of CdTe and CdS grown by hot-wall epitaxy 24 p3636 A83-50182
Chemical deposition of Cd(1-x)Hg(x)S thin film electrodes for liquid-junction solar cells 24 p3602 A83-50186

CADMIUM TELLURIDES

Direct-gap group IV semiconductors based on tin 01 p0108 A83-10294
Electrolyte electroreflectance study of laser annealing effects of the CdTe/Hg/0.8/Cd/0.2/Te/111/ system 01 p0110 A83-10992
Epitaxial HgCdTe/CdTe photodiodes for the 1 to 3 micron spectral region 03 p0309 A83-13737
Electron and hole diffusion length investigation in CdTe thin films by SPV method --- Surface Photovoltage 04 p0539 A83-15495
CdTe/HgCdTe indium-diffused photodiodes 06 p0753 A83-18943
Common anion heterojunctions - CdTe-CdHgTe 06 p0814 A83-18962
Growth of CdTe films on sapphire by molecular beam epitaxy 07 p0998 A83-19985
Cadmium telluride films on foreign substrates 07 p1000 A83-20750
Laser-induced damage and two-photon absorption measurements in CdTe 09 p1273 A83-24974
Mechanism of current transfer in SIS solar cells based on polycrystalline cadmium telluride In₂O₃/pCdTe and ITO/pCdTe 14 p2087 A83-32044
Investigation of the electrophysical characteristics of SIS structures based on polycrystalline cadmium telluride 14 p2087 A83-32045
Photovoltaic effect in SnTe/CdTe junctions 14 p2089 A83-32255
High efficiency shallow p(+)/nn(+) cadmium telluride solar cells 14 p2042 A83-32264
Electrodeposited CdS/CdTe heterojunction solar cells 14 p2044 A83-32280
All thin film n-CdTe/ITO solar cell 14 p2090 A83-32302
8.5 percent efficient screen-printed CdS/CdTe solar cell produced on a 5-cm x 10-cm glass substrate 14 p2047 A83-32838

Grain boundary phenomena in n-type CdTe films grown by hot wall vacuum evaporation 17 p2584 A83-38215

Growth of CdTe films on silicon by molecular beam epitaxy 17 p2585 A83-38221
Selective electrochemical etching of p-CdTe (for photovoltaic cells) 18 p2750 A83-40065
Occurrence of the dynamic Jahn-Teller effect in CdTe:Co crystals 19 p2904 A83-40998
Photoelectrochemical solar cells - Temperature control by cell design and its effects on the performance of cadmium chalcogenide-polysulphide systems 20 p3012 A83-42359
Effect of deposition rate and substrate temperature on properties of CdTe film 20 p3054 A83-43396
Heteroepitaxial growth of CdTe on GaAs by laser assisted deposition 21 p3219 A83-45492
Deep level impurities and current collection in CdS/CdTe thin-film solar cells 22 p3365 A83-46734
Recent progress on LADA growth of HgCdTe and CdTe epitaxial layers --- laser assisted deposition 24 p3633 A83-48739
Effects of surface preparation on the properties of metal/CdTe junctions 24 p3635 A83-48915
Characterization of epitaxial films of CdTe and CdS grown by hot-wall epitaxy 24 p3636 A83-50182

CAFFEINE

Effect of caffeine on skeletal muscle function before and after fatigue 14 p2068 A83-32815
Interactions of alcohol and caffeine on human reaction time 15 p2215 A83-34984

CAI

U COMPUTER ASSISTED INSTRUCTION

CALCIFEROL

The effect of 24, 25-dihydroxycalciferol on the chemical composition of the bone tissue of rats during hypokinesia 06 p0795 A83-18987
Calcium-phosphorus metabolism and prevention of its disorders in hypokinetic rats 11 p1636 A83-27788
Bone tissue of hypokinetic rats - Effects of 24,25-dihydroxycholecalciferol and varying phosphorus content in the diet 14 p2064 A83-32692

CALCIFICATION

The cervical test in vertebral-basilar insufficiency 19 p2883 A83-41832

CALCITE

Shock-induced devolatilization of calcite 04 p0559 A83-15306

CALCIUM

NT CALCIUM ISOTOPES

One-photon laser spectroscopy of Rydberg series from metastable levels in calcium and strontium 01 p0105 A83-10197
Dielectronic satellite spectra for highly-charged helium-like ions. VII - Calcium spectra: Theory and comparison with SMM observations 03 p0420 A83-13948

A search for resonance polarization in stars with enhanced Ca II H and K emission 06 p0821 A83-19062

Non-resonance lines of neutral calcium in the spectra of Arcturus and Beta Virginis 07 p1024 A83-21227
Calcium in the atmospheres of peculiar stars 07 p1027 A83-21268

Evolution of Ca-Al-rich bodies in the earliest solar system
Growth by incorporation 07 p1036 A83-21337
Electron and local gas densities in diffuse interstellar clouds from measurements of Ca I absorption 08 p1183 A83-23082

The depletion of calcium in the Rho Ophiuchi cloud 08 p1185 A83-23082

A discharge-heated calcium vapor laser 11 p1582 A83-27602

Atomic calculations for Ca XVII - UV and X-ray lines 12 p1799 A83-28866

Principal and dielectronic satellite line spectra for Ca XIX SMM observations --- Solar Maximum Mission 13 p1965 A83-31713

Low noise spectrometer for the daily measurement of solar chromospheric flux 14 p2017 A83-32007
Reversible loss of gravitropic sensitivity in maize roots after tip application of calcium chelators 16 p2394 A83-36017

Ca II chromospheric emission and rotation of main sequence stars 16 p2429 A83-36633

The Ca II K emission from the sun as a star. I - Observational parameters 16 p2440 A83-36668

Catalog of profiles and equivalent widths of the Ca II K line in the spectra of metallic-line stars 17 p2589 A83-37654

Electron impact excitation of forbidden transitions in Ca XV 17 p2579 A83-38367

Replacement textures in CAI and implications regarding planetary metamorphism 17 p2623 A83-38851

The Ca II K emission from the sun as a star. II - The plage emission profile 20 p3080 A83-42382

- Effects of Ca additions on some Mg-alloy hydrides
21 p3110 A83-45422
- High spatial and temporal resolution observations of the solar Ca II H line
21 p3244 A83-45569
- Electron excitation of Ca XVII
23 p3506 A83-48580
- Longitudinal Ramsey-fringe spectroscopy in a calcium beam --- for optical frequency standard
23 p3509 A83-48707
- Ca XVII line ratios in solar flares
24 p3674 A83-49356

CALCIUM CARBONATES

NT CALCITE

CALCIUM COMPOUNDS

NT CALCITE

NT CALCIUM FLUORIDES

NT CALCIUM OXIDES

NT CALCIUM PHOSPHATES

NT CALCIUM SILICATES

NT CALCIUM SULFIDES

NT PEROVSKITES

A new calcium-aluminate from a refractory inclusion in the Leoville carbonaceous chondrite
04 p0558 A83-15302

On the properties of the superplastic aluminium-calcium alloy as material for solar collectors
04 p0505 A83-15496

CaLa2S4 - Ceramic window material for the 8 to 14 micron region
09 p1345 A83-24957

Chemical and physical factors affecting the absorption capability of calcium hydroxide based carbon dioxide absorbers
11 p1645 A83-28333

Ca-Al-rich chondrules and inclusions in ordinary chondrites
17 p2623 A83-38593

Astrophysical molecules of A1H and CaH - RKR potential and dissociation energies --- Rydberg-Klein-Rees
18 p2764 A83-39192

Electrochemical reduction of calcium chromate --- cathode material in Ca/CaCrO4/Fe thermally activated batteries
22 p3268 A83-46895

Hot corrosion of iron- and nickel-base superalloys caused by deposit of calcium sulfate
24 p3563 A83-49498

CALCIUM FLUORIDES

The effect of CaF2 addition on the oxidation of hot-pressed materials based on silicon nitride
02 p0161 A83-13035

Epitaxial InP/fluoride/InP(001) double heterostructures grown by molecular beam epitaxy
22 p3365 A83-46732

CALCIUM ISOTOPES

The sp-process and Allende isotope anomalies in calcium and titanium
06 p0850 A83-19506

Precise age determinations and petrogenetic studies using the K-Ca method
07 p1035 A83-21335

CALCIUM METABOLISM

Reduction in plasma calcium during exercise in man
01 p0082 A83-10212

The effect of 24, 25-dihydroxycalciferol on the chemical composition of the bone tissue of rats during hypokinesia
06 p0795 A83-18987

Passive binding of Ca/2+/- by fragments of the sarcolemmal reticulum of frog skeletal muscles
06 p0795 A83-18988

The activity of Ca/2+/- ATPase and enzymes of cAMP metabolism in the nerve tissue of rats during the early stages of acute radiation damage
06 p0796 A83-19383

The effect of the calmodulin inhibitor, trifluoroperazine, on the calcium activation of phosphorylases in the glycosomes of the skeletal muscles in rabbits
07 p0975 A83-20981

The relationship between isometric and isotonic contractile responses of the myocardium of mammals
08 p1145 A83-22111

Changes in weightlessness in calcium metabolism and in the musculoskeletal system
11 p1636 A83-27787

Calcium-phosphorous metabolism and prevention of its disorders in hypokinetic rats
11 p1636 A83-27788

Calcium transport from the intestine and into bone in a rat model simulating weightlessness
11 p1640 A83-27832

The subcellular distribution of a Ca(2+)-dependent protein regulator in the gray matter of the brain of normal and X-irradiated rats
14 p2062 A83-32060

Bone tissue of hypokinetic rats - Effects of 24,25-dihydroxycholecalciferol and varying phosphorus content in the diet
14 p2064 A83-32692

The effect of calcium on the diastolic phases in healthy individuals and in patients with heart failure
18 p2735 A83-40549

Changes in total body calcium balance with exercise in the rat
19 p2875 A83-41138

Calcium movements and the cellular basis of gravitropism
19 p2878 A83-42051

Quantitative histochemistry of rat lumbar vertebrae following spaceflight
21 p3184 A83-44864

Bone resorption and mineral excretion in rats during spaceflight
21 p3184 A83-44866

The effect of calcium ions on the temperature sensitivity of humans
23 p3498 A83-47118

CALCIUM OXIDES

Densification of calcia-stabilized zirconia with borates
08 p1071 A83-22200

Tunable visible lasers using defects in oxides
11 p1578 A83-27545

A flow-system comparison of the reactivities of calcium superoxide and potassium superoxide with carbon dioxide and water vapor
13 p1907 A83-30946

CALCIUM PHOSPHATES

Formation of pyrophosphate on hydroxyapatite with thioesters as condensing agents
05 p0613 A83-17234

CALCIUM SILICATES

Reduction in acidity of RDX and its compositions by use of suitable additives
15 p2143 A83-33872

CALCIUM SULFIDES

Progress in the development of ternary sulfides for use from 8 to 14 microns
09 p1345 A83-24955

CALCIUM 45

U CALCIUM ISOTOPES

CALCULATION

U COMPUTATION

CALCULATORS

Bidirectional coupling of a cracking test machine to a calculator
08 p1112 A83-21764

CALCULUS

NT ASYMPTOTIC SERIES

NT COLLINEARITY

NT CONTINUITY (MATHEMATICS)

NT COSINE SERIES

NT DIFFERENTIAL CALCULUS

NT FOURIER SERIES

NT FOURIER-BESSEL TRANSFORMATIONS

NT INTEGRAL CALCULUS

NT LIMITS (MATHEMATICS)

NT MACLAURIN SERIES

NT PADE APPROXIMATION

NT POWER SERIES

NT PRONY SERIES

NT SERIES (MATHEMATICS)

NT SINE SERIES

NT TAYLOR SERIES

NT VECTOR ANALYSIS

NT VORTICITY

Fractional calculus in the transient analysis of viscoelastically damped structures
12 p1743 A83-29841

CALCULUS OF VARIATIONS

Suggestions for optimal regulation of linear systems using approximation methods --- German thesis
01 p0094 A83-10472

Variational normal mode balancing in the Navy operational data assimilation system --- for numerical weather prediction
03 p0366 A83-14410

Questions of convergence, duality, and averaging for a class of functionals of the calculus of variations
06 p0804 A83-17976

The solution of the equations of the applied theory of elasticity by the method of variational iterations
15 p2178 A83-34433

An error estimate for a finite-element approximation of an elliptic variational inequality formulation of a Hele-Shaw moving-boundary problem
18 p2739 A83-39254

Optimisation of homogeneous thermal insulation layers
23 p3449 A83-48097

CALDERAS

Io - A volcanic flow model for the hot spot emission spectrum and a thermostatic mechanism
03 p0133 A83-13833

Episodic rifting and volcanism at Krafla in North Iceland - Growth of large ground fissures along the plate boundary
07 p0957 A83-19870

The Cerro Galan ignimbrite
08 p1138 A83-23255

Giant volcanic calderas
14 p2054 A83-33099

CALIBRATING

NT WIND TUNNEL CALIBRATION

Amplitude calibration of synthetic aperture radars - The effects of nonlinearities
01 p0048 A83-10085

Calibration of synthetic aperture radar
01 p0048 A83-10086

Galaxy photometry in the Virgo cluster. I
01 p0116 A83-10265

ATE calibration by means of dynamic transport standards
01 p0050 A83-10764

Field calibration of ATE via satellite
01 p0050 A83-10766

Software quality assurance for automated calibration laboratories
01 p0091 A83-10768

Calibration of third-generation ATE systems
01 p0091 A83-10784

Status of the calibration support of the Navy ATE
01 p0001 A83-10786

Absolute calibration of X-ray film by means of spaced X-ray emulsion chambers
02 p0176 A83-11746

Using small extensive air showers where the number of electrons is greater than about 10,000 on mountains for calibrating an interaction model
02 p0276 A83-11759

A revised and extended calibration for the Spinrad-Taylor scanner system
02 p0245 A83-11994

Timing a LORAN-C chain
02 p0133 A83-12225

Procedure for camera calibration with image sequences
02 p0182 A83-12899

Calibration of solar cells by the reference cell method - The spectral mismatch problem
03 p0353 A83-13580

Signal processing for large focal plane arrays
03 p0309 A83-13738

The calibration of a radio-independent search for BL Lac objects
03 p0408 A83-13929

Limitations on the calibration of infrared /IR/ transmissometer
03 p0328 A83-13994

Two methods for absolute calibration of dynamic pressure transducers
03 p0329 A83-14170

Precise calibration of a rotary vane attenuator at 35 GHz using a homodyne network analyser
04 p0470 A83-15244

The calibration of pyrheliometers and pyranometers for testing photovoltaic devices
04 p0482 A83-15459

Progress in the development of standard procedures for the global method of calibration of photovoltaic reference cells
04 p0504 A83-15460

Measurement of 2-port devices by a reflectometer system
04 p0473 A83-16207

Reduction of flow-measurement uncertainties in laser velocimeters with nonorthogonal channels
05 p0642 A83-16486

[AIAA PAPER 83-0051] Basic calibration of a partially-parabolic procedure aimed at centrifugal impeller analysis
05 p0583 A83-16616

[AIAA PAPER 83-0260] Calibration of standard gain antennas using a spherical near-field technique
06 p0740 A83-18644

Calibration of an infrared spectrometer and a far-infrared photometer for astronomical applications under low background conditions
06 p0821 A83-18946

The equivalent-width calibration of the KPNO echelle spectrograph
06 p0822 A83-19076

Brightness temperature of the 'quiet' sun in the millimeter range
06 p0856 A83-19327

Absolute instruments for the in situ metrological verification of radiation detectors
07 p0931 A83-20963

A low-temperature chamber for calibrating thermal radiation detectors
07 p0902 A83-20965

Simple absolute calibration method using laser sources for pulsed spectroscopic applications in the visible and UV
07 p0932 A83-21384

Quality of upwelling radiance retrieved from coastal zone colour scanner /CZCS/ data for ocean colour determination
08 p1050 A83-21954

Calibration and correction in pointing accuracy of 10-m antenna at 32 GHz
08 p1075 A83-22036

Lidar calibration and extinction coefficients
08 p1077 A83-22612

Contemporary infrared standards and calibration; Proceedings of the Meeting, San Diego, CA, August 25, 26, 1981
08 p1104 A83-22873

Silicon photodiode self-calibration as a basis for radiometry in the infrared
08 p1104 A83-22874

Infrared calibration facilities at Newark Air Force Station
08 p1047 A83-22875

Calibration of a transfer radiometer in support of the Navy forward looking infrared systems /FLIR/ program
08 p1104 A83-22876

Broadband lamp standard for ultraviolet /UV/, visible, and infrared calibration to 6.0 microns
08 p1104 A83-22878

Coherence effects in laser testing of long wavelength infrared /LWIR/ sensors
08 p1052 A83-22879

Calibration of spaceborne thermal detectors
08 p1052 A83-22881

Spatial calibration of a multispectral data base --- of airborne scanner systems
08 p1045 A83-22882

Electro-optical calibration considerations at intermediate maintenance levels
08 p1104 A83-22883

Considerations in the selection and use of calibration equipment for simulators used with thermal imaging systems
08 p1104 A83-22884

Infrared focal plane test station calibration
08 p1104 A83-22885

Calibration support of the AN/AAM-60 common forward-looking infrared /FLIR/ test bench
08 p1104 A83-22886

Radiometric calibration for the Earth Radiation Budget Experiment instruments 08 p1049 A83-22888
 Laser transmission calibration of long-path atmospheric transmission measurements 08 p1104 A83-22889
 Experimental calibration of the spherulite cosmoarometer 08 p1190 A83-22998
 The aerodynamic properties of the DISA nozzle unit for calibrating and testing hot-wire probes, in particular multiple sensor probes at moderate velocities 09 p1267 A83-23700
 Characteristics of the detectors of multi spectral scanner /MSS/ of Landsat in space environment 09 p1219 A83-23895
 Calibrated B, V surface photometry of X-ray cD galaxies 09 p1360 A83-24469
 Vacuum ultraviolet monochromator calibration using measured atomic branching ratios 10 p1484 A83-26857
 Compliance calibration of a family of short rod and short bar fracture toughness specimens 11 p1548 A83-28435
 Improved calibration of hot-wire anemometers 11 p1574 A83-28574
 Application of a three-sensor hot-wire probe for incompressible flow 12 p1728 A83-28963
 On the calibration and temperature behaviour of single-beam infrared hygrometers 12 p1728 A83-29137
 Calibration of the VIS-channel of Meteosat-2 12 p1708 A83-29692
 Calibration system for satellite and rocket-borne ion mass spectrometers in the energy range from 5 eV/charge to 100 keV/charge 13 p1813 A83-30254
 Active optics - Don't build a telescope without it 13 p1920 A83-31007
 Self-calibrating surface measuring machine --- for fabrication of aspheric optical elements 13 p1847 A83-31016
 Faint Object Spectrograph (FOS) calibration 14 p2017 A83-32011
 Photometric properties of the Texas Mkil electrographic camera 14 p2018 A83-32033
 Electron-photon coincidence technique for the absolute calibration of VUV detectors 14 p2021 A83-32914
 Narrow-band photometry in the 1-4 micron region - Calibration and applications 14 p2100 A83-33258
 Programmable and automatic calibrator for radio sources at 45 MHz 14 p2101 A83-33291
 Quantitative intensity measurements using a soft X-ray streak camera 14 p2022 A83-33417
 The galaxy as fundamental calibrator of the extragalactic distance scale. I - The basic scale factors of the galaxy and two kinematic tests of the long and short distance scales 15 p2255 A83-34076
 Development of methods for calibration and testing gyroscopic instruments for GW applications 16 p2354 A83-35498
 Seven-hole cone probes for high angle flow measurement Theory and calibration 16 p2356 A83-36085
 Solar cell and module performance assessment based on indoor calibration methods 18 p2710 A83-40527
 The calibration and performance of a microstrip six-port reflectometer 19 p2837 A83-41082
 Open-loop residuals and alternate trajectories as a means of validating IMU calibration and alignment performance [AIAA PAPER 83-2252] 19 p2811 A83-41727
 Calibration of the aerodynamic coefficient identification package measurements from the shuttle entry flights using inertial measurement unit data [AIAA PAPER 83-2100] 19 p2818 A83-41930
 Gold as a reliable internal pressure calibrant at high temperatures 20 p2959 A83-42596
 Measurement Assurance Program transmittance standards for spectrophotometric linearity testing - Preparation and calibration 20 p2990 A83-42946
 Amplitude calibration of spaceborne synthetic aperture radars --- Synthetic Aperture Radar 21 p3103 A83-43979
 Process for producing laser-formed video calibration markers 21 p3136 A83-44155
 Scanning radiometer for calibrating thermal imager test targets 21 p3138 A83-44782
 X-ray interferometer calibration of microdisplacement transducers 21 p3140 A83-44949
 Modified calibration technique of a five-hole probe for high flow angles 21 p3141 A83-44975
 Altitude determination and calibration for a three-dimensional angular velocimeter with the use of angular information 21 p3200 A83-45354
 Problems and solution methods in the calibration of radiometers for remote-sensing measurements of the earth 21 p3142 A83-45405

The use of the extrapolation technique in the calibration of radiation-measuring devices in the region of strong band absorption for the rho-sigma-tau water-vapor bands from 0.91 to 0.98 microns 21 p3142 A83-45406
 Solar radiation measurements - Calibration and standardization efforts 22 p3318 A83-45917
 Absolute radiometric calibration of advanced remote sensing systems 22 p3288 A83-46151
 Amplitude calibrating the Seasat SAR imagery 22 p3289 A83-46196
 An active radar calibration target 22 p3274 A83-46200
 Optical angle marker --- for calibrating inertial guidance test equipment 22 p3291 A83-46591
 Acoustic wave calibration for CO2 laser scattering experiments 23 p3461 A83-47647
 On-line calibration technique for laser diffraction droplet sizing instruments [ASME PAPER 83-GT-232] 23 p3458 A83-48028
 Physical calibration of instruments for the detection of transients --- of gamma-ray bursts by satellite detectors 23 p3425 A83-48403
 The Atmospheric Lifetime Experiment. II - Calibration 24 p3606 A83-49329
 A catalogue of photometric sequences (suppl. 3) --- for astronomical photograph calibration 24 p3647 A83-50010
 A straightforward method to calibrate photographic data using stellar images 24 p3648 A83-50014
 The calibration of photographic plates using stellar images 24 p3648 A83-50015
 Internal calibration of astronomical photographs 24 p3648 A83-50016
 Photometric calibration of Schmidt plates 24 p3648 A83-50017

CALIFORNIA

Analysis of man-induced and natural resources of an arid region in California 09 p1285 A83-24543
 Precise leveling across active faults in California 22 p3329 A83-46362

CALIFORNIUM

NT CALIFORNIUM ISOTOPES

CALIFORNIUM ISOTOPES

Cf-252 plasma desorption in ion implanted mica 15 p2133 A83-34381

CALIFORNIUM 252

U CALIFORNIUM ISOTOPES

CALLISTO

Radar properties of Europa, Ganymede, and Callisto 04 p0570 A83-16233
 Craters and basins on Ganymede and Callisto - Morphological indicators of crustal evolution 04 p0570 A83-16237
 Color photometry of surface features on Ganymede and Callisto 05 p0704 A83-16963
 Interpretation of integrated-disk photometry of Callisto and Ganymede 07 p1032 A83-21290
 Ganymede and Callisto 08 p1188 A83-22774
 Impact experiments on ice --- for understanding cratering on Callisto and Mimas 18 p2779 A83-40322

CALORIC REQUIREMENTS

Several indicators of the functional condition of the human body during a prolonged low-calorie diet consisting of canned foods 15 p2212 A83-34941

CALORIC STIMULI

A new approach to the quantitative evaluation of reflex vestibular nystagmus 06 p0798 A83-18974

CALORIMETERS

Calorimetric measurements of thermal control surfaces of operational satellites [AIAA PAPER 83-0075] 05 p0605 A83-16505
 Investigation of groups and nuclear interactions of muons by the spark-calorimeter method 06 p0858 A83-19344
 On the acoustic registration of cascades and single strongly ionized particles 06 p0764 A83-19350
 An instrument for studying the thermophysical properties of solids at low temperatures 07 p0931 A83-20961
 A continuous-flow microcalorimeter 11 p1576 A83-28800

CALORIMETRY

U HEAT MEASUREMENT

CALUTRONS

U CYCLOTRONS

CAM (MANUFACTURING)

U COMPUTER AIDED MANUFACTURING

CAMBER

NT CONICAL CAMBER

NT WING CAMBER

Vane camber and angle of incidence effects in fan noise generation [AIAA PAPER 83-0766] 10 p1377 A83-25956
 Experimental analysis of the wake behind an isolated cambered airfoil 22 p3248 A83-46443

CAMBERED WINGS

Load distribution on deformed wings in supersonic flow 01 p0002 A83-10180
 Influence of leading-edge thrust on twisted and cambered wing design for supersonic cruise 12 p1696 A83-29018
 Circulation-controlled elliptical airfoil 20 p2928 A83-42537
 Equivalent angle of attack for the lifting plane with linear camber-twist at low speeds 20 p2931 A83-43690
 Calculation of potential flow about arbitrary three dimensional wings using internal singularity distributions 23 p3398 A83-48143

CAMERA SHUTTERS

An improved schlieren system and some new results on acoustically excited jets 08 p1162 A83-21806
 New developments in subpicosecond optoelectronics 22 p3298 A83-46676

CAMERA TUBES

NT IMAGE ORTHICONS

NT RETURN BEAM VIDICONS

NT VIDICONS

Features characterizing the formation of signal and noise, common to all TV camera tubes of the superorthicon class 24 p3574 A83-49641

CAMERAS

NT DELFT CAMERA
 NT DIFFRACTION LIMITED CAMERAS
 NT FAINT OBJECT CAMERA
 NT HIGH SPEED CAMERAS
 NT LALLEMAND CAMERAS
 NT PANORAMIC CAMERAS
 NT PINHOLE CAMERAS
 NT SCHMIDT CAMERAS
 NT STREAK CAMERAS
 NT TELEVISION CAMERAS

Spacecraft imaging of planets - Camera systems from Mariner to Space Telescope 01 p0020 A83-10047
 ATLAS C - A cartographic free-flyer system --- satellite-borne metric camera for photomapping [AAS 82-115] 02 p0139 A83-11929
 Image quality and lens aberrations of an aerial camera 02 p0177 A83-11989
 Performance characteristics for the Orbiter camera payload system's large format camera /LFC/ 02 p0179 A83-12675
 Procedure for camera calibration with image sequences 02 p0182 A83-12899
 The numerical stereo camera 03 p0324 A83-13445
 Infrared camera for 10-micron astronomy 03 p0324 A83-13457
 Use of charge-coupled device /CCD/ detectors for imaging in the vacuum ultraviolet 03 p0288 A83-13966
 Building a small format, in-house aerial photography system 03 p0329 A83-14274
 Aerial camera vibration 03 p0330 A83-14663
 Modulated Multiple Slit Camera for improved localization of gamma ray bursts 07 p1005 A83-20038
 The KS-146A long range oblique photography /LOROP/ camera system 08 p1099 A83-22583
 Film still looks good --- advantages of conventional cameras for aerial reconnaissance 08 p1099 A83-22587

An image-tube camera for cometary spectroscopy 10 p1498 A83-26911
 Infrared array detectors --- for astronomical observation 11 p1537 A83-27734
 X-ray imaging techniques - Modulation collimator and coded mask 11 p1657 A83-27752
 Royal Greenwich Observatory (RGO) charge-coupled device (CCD) camera 14 p2015 A83-31988
 Development of a dual microchannel plate intensified charge-coupled device (CCD) speckle camera 14 p2015 A83-31991
 New two-dimensional photon camera 14 p2018 A83-32021
 Space telescope low scattered light camera - A model 14 p2096 A83-32026
 Photometric properties of the Texas Mkil electrographic camera 14 p2018 A83-32033
 Aluminum/ammonia heat pipe gas generation and long term system impact for the Space Telescope's Wide Field Planetary Camera [AIAA PAPER 83-1428] 14 p2009 A83-32704
 Onboard radiometric photography of EXCEDE SPECTRAL's ejected-electron beam 15 p2128 A83-34190
 An example of the performance of the space telescope planetary camera 15 p2247 A83-34511
 Image quality of active and passive scanners 16 p2356 A83-36123
 The electronic system of the Halley Multicolour Camera (HMC) 17 p2482 A83-37864

The use of 16 mm movie cameras for evaluation of the Space Shuttle remote manipulator system 17 p2482 A83-38358

New generation lens systems for the wild aviophot aerial camera system 21 p3135 A83-43895

The exploration of outer space with cameras: A history of the NASA unmanned spacecraft missions --- Book 21 p3241 A83-45096

Improvements in cloud photogrammetry using airborne, side-looking, time-lapse cameras 22 p3307 A83-45707

CANADA

Canadian Symposium on Remote Sensing, 7th, Winnipeg, Canada, September 8-11, 1981, Proceedings 03 p0345 A83-14226

The importance of remote sensing for Canada - Past achievements, future needs 03 p0345 A83-14227

A C-band weather radar system with spherics to serve multiple diverse users in the Canadian climate 11 p1631 A83-27096

Canadian Landsat studies for monitoring agricultural intensification and urbanization - A summary 15 p2182 A83-33566

Hydrogen energy in Canada - I Proceedings of the First Hydrogen Energy Symposium, University of Western Ontario, London, Canada, May 1, 1981 15 p2193 A83-35301

Aeronautics - A coop aerospace education program at University of Sherbrooke, Canada [AIAA PAPER 83-2474] 23 p3513 A83-48340

CANADAIR AIRCRAFT

CF34 upgrades Challenger capabilities 15 p2122 A83-35315

CANADAIR CF-104 AIRCRAFT

U CANADAIR AIRCRAFT

U F-104 AIRCRAFT

CANADIAN SPACE PROGRAMS

Low elevation angle site diversity satellite communications for the Canadian Arctic 19 p2831 A83-41381

The Canadian Radarsat program 22 p3307 A83-46113

The program management of the Telesat space segment (A program manager's recollections) [IAF PAPER 83-85] 23 p3513 A83-47259

CANADIAN SPACECRAFT

NT ANIK 2

NT ANIK 3

NT RADARSAT

CANARD CONFIGURATIONS

Aerodynamic optimization, comparison, and trim design of canard and conventional high performance general aviation configurations [AIAA PAPER 83-0058] 05 p0594 A83-16490

Application of the PANAIR production code to a complex canard/wing configuration [AIAA PAPER 83-0009] 05 p0590 A83-17902

A numerical transformation solution procedure for closely coupled canard-wing transonic flows [AIAA PAPER 83-0502] 06 p0714 A83-19591

Delta canard configuration at high angle of attack 09 p1210 A83-24650

Homebuilt airplanes - The sky's the limit 09 p1196 A83-25122

Computational treatment of three-dimensional transonic canard-wing interactions 12 p1696 A83-29021

Low-speed aerodynamic characteristics of a generic forward-swept-wing aircraft [SAE PAPER 821467] 17 p2451 A83-37998

The leading-edge vortex trajectories of close-coupled wing-canard configurations and their breakdown characteristics [AIAA PAPER 83-1817] 17 p2455 A83-38649

High aspect ratio forward sweep for transport aircraft [AIAA PAPER 83-1832] 17 p2455 A83-38661

Wake characteristics and interactions of the canard/wing lifting surface configuration of the X-29 forward-swept wing flight demonstrator [AIAA PAPER 83-1835] 17 p2455 A83-38664

Aerodynamics characteristics of a canard controlled high fineness ratio missile [AIAA PAPER 83-1839] 17 p2470 A83-38668

An assessment of PANDORA using a Canard/Wing/Body configuration --- Preliminary Automated Numerical Design of Realistic Aircraft [AIAA PAPER 83-1850] 17 p2456 A83-38678

Comprehensive missile aerodynamics programs for preliminary design 18 p2638 A83-40025

Roll divergence of a Canard-controlled missile with freely spinning tail [AIAA PAPER 83-2080] 19 p2805 A83-41914

Parametric study of critical constraints for a canard configured medium range transport using conceptual design optimization [AIAA PAPER 83-2141] 19 p2799 A83-41963

Experimental wing and canard jet-flap aerodynamics [AIAA PAPER 83-0081] 23 p3398 A83-48211

Large-scale wind-tunnel investigation of a close-coupled canard-delta-wing fighter model through high angles of attack [AIAA PAPER 83-2554] 23 p3399 A83-48373

CANCELLATION CIRCUITS

Investigation and design of a highly integrable echo cancellation procedure for duplex transmission 04 p0472 A83-16039

RF methods for adaptive cancellation of cross polarisation in microwave satellite systems 06 p0746 A83-18728

Design and performance of interference cancellation circuit --- for radio communications 07 p0914 A83-20821

Echo Cancellers - How to improve satellite circuit performance 07 p0914 A83-20846

Transversal filter techniques for adaptive array applications 11 p1554 A83-27905

Experimental open-loop canceller for radar 11 p1555 A83-27916

A study on the MTI weather radar system for rejecting ground clutter 13 p1894 A83-31670

A cascaded echo canceller 19 p2832 A83-41393

CANCER

The changes in the chromosome pattern of mouse lymphosarcoma cells during prolonged irradiation 14 p2061 A83-32054

Toxic substances in the atmospheric environment - A critical review 15 p2193 A83-33502

CANNING

Several indicators of the functional condition of the human body during a prolonged low-calorie diet consisting of canned foods 15 p2212 A83-34941

CANNONS

U GUNS (ORDNANCE)

CANNULAE

Arterial oxygen saturation at altitude using a nasal cannula 04 p0521 A83-15537

CANONICAL FORMS

Beam scanning in the offset Gregorian antenna 07 p0913 A83-20551

Covariance analysis of oscillatory systems under combined periodic and random forced vibrations 08 p1160 A83-21862

Canonical formalism for relativistic dynamics 08 p1160 A83-22010

Studies of the external origin component of Sq by 'canonical' GDS analysis --- Geomagnetic Depth Sounding 08 p1134 A83-22313

Two approaches for adaptive observer in multi-output systems 10 p1468 A83-26563

On the regularization of the Hill problem 11 p1673 A83-28031

New algorithms for quasi-periodic solutions --- of oscillating systems in celestial mechanics 11 p1673 A83-28040

Hamiltonian formulation of the gauge theory of gravitation Pure-gravity case. 12 p1792 A83-29046

Lagrange variational equations from Hori's method for canonical systems 12 p1771 A83-29123

Canonical and quasi-canonical probability models of class A interference 16 p2342 A83-35780

A singular perturbation canonical form of invertible systems Determination of multivariable root-loci 16 p2405 A83-36452

A second order Jupiter-Saturn planetary theory 16 p2439 A83-36787

Nested bases of invariants for minimal realizations of finite matrix sequences 22 p3351 A83-46094

The Lie-series method in the problem of the separation of motions in nonlinear mechanics 23 p3505 A83-48527

Relativistic canonical formalism and invariant one-particle distribution function in general relativity 24 p3636 A83-49061

The method of canonical transformations in classical electrodynamics 24 p3623 A83-49065

Block decompositions and block modal controls of multivariable control systems 24 p3621 A83-49920

CANOPIES

An analysis of the fatality rate data from 'jettison-canopy' and 'through-the-canopy' ejections from automated airborne escape systems 04 p0443 A83-15403

Preliminary generalized thoughts concerning jettisoned vs through-the-canopy ejection escape systems 04 p0444 A83-15406

The 3 ring canopy release system 04 p0444 A83-15416

Simulation of T-38 aircraft student canopy response to cockpit pressure and thermal loads using MAGMA --- Materially and Geometrically Nonlinear Analysis [AIAA 83-0942] 12 p1701 A83-29772

Net-skirt addition to a parachute canopy to prevent inversion 16 p2297 A83-36911

Finite-element analysis of the T-38 canopy 19 p2797 A83-41044

CANOPIES (VEGETATION)

Application of computer axial tomography /CAT/ to measuring crop canopy geometry --- corn and soybeans 01 p0065 A83-10096

Reflectance of a vegetation canopy using the Adding method 02 p0199 A83-12603

Effects of vegetation cover on the radar sensitivity to soil moisture 03 p0351 A83-14856

Reflectance differences between untreated and Mepiquat Chloride-treated, field-grown cotton through a growing season 05 p0657 A83-16909

A model for microwave emission from vegetation-covered fields 07 p0951 A83-20223

Plant formations cartography for the Republic of Senegal using remote sensing 08 p1127 A83-21936

Satellite remote sensing over Quebec for inventory of the vegetal canopy 08 p1127 A83-21938

Effects of vegetation cover on the microwave radiometric sensitivity to soil moisture 08 p1129 A83-22681

Electromagnetic backscattering from a layer of vegetation - A discrete approach 08 p1077 A83-22682

Multispectral radiometer to measure crop canopy characteristics 13 p1845 A83-30259

Dynamics of directional reflectance factor distributions for vegetation canopies 13 p1869 A83-31462

Extension of a uniform canopy reflectance model to include row effects 14 p2035 A83-32612

Remote sensing salt marsh biomass and stress detection 15 p2182 A83-33577

The relationships between the chlorophyll concentration, LAI and reflectance of a simple vegetation canopy --- leaf area index 15 p2187 A83-35280

Diurnal variations of vegetation canopy structure 15 p2188 A83-35281

Leaf water stress detection utilizing thematic mapper bands 3, 4 and 5 in soybean plants 15 p2188 A83-35283

Directional radiometric measurements of row-crop temperatures 15 p2188 A83-35284

The influence of soil salinity, growth form, and leaf moisture on the spectral radiance of *Spartina alterniflora* canopies 16 p2370 A83-35741

Seasonal spectral characteristics and aboveground biomass of the tidal marsh plant, *Spartina alterniflora* 16 p2370 A83-35742

Comments on 'the relative effect of solar altitude on surface temperatures and energy budget components on two contrasting landscapes' 16 p2388 A83-35798

Evaporation from a partially wet forest canopy 21 p3165 A83-44234

The effects of vegetation cover on the radar and radiometric sensitivity to soil moisture 22 p3311 A83-46183

A multilayer model for radar backscattering from vegetation canopies 22 p3312 A83-46185

Detecting forest canopy change due to insect activity using Landsat MSS 22 p3318 A83-46765

A technique for phenological observations in measurements of the spectral brightness coefficients of vegetation 23 p3476 A83-48111

The hot spot effect of a homogeneous vegetative cover 23 p3476 A83-48113

CANT

U SLOPES

CANTILEVER BEAMS

Determination of fracture toughness of ductile materials using a reinforced double cantilever beam specimen 01 p0026 A83-11030

Anisotropic beam theory and applications 02 p0195 A83-12756

Deflections of inflated cylindrical cantilever beams subjected to bending and torsion 02 p0196 A83-12853

Improved numerical computation of uniform beam characteristic values and characteristic functions 02 p0197 A83-13001

Rapid crack propagation and arrest in the DCB specimen - An improved numerical analysis --- Double Cantilever Beam 03 p0343 A83-14711

Influence of rotary inertia on the fundamental frequency of a cantilever beam 04 p0496 A83-15071

Effect of water on the interlaminar fracture behaviour of glass fibre-reinforced polyester composite 06 p0724 A83-17966

On the shear center of a prismatic bar with T- and channel-cross-section 06 p0771 A83-18150

Natural frequency of rotating beams using non-rotating modes 06 p0773 A83-18383

Vibration and stability of sandwich beams with elastic bonding 06 p0774 A83-18395

- The cantilever beam under tension, bending or flexure at infinity 06 p0776 A83-18999
- Double-cantilever-beam testing of a transversely isotropic fibrous silica material [ACS PAPER 61-B-81F] 07 p0898 A83-20170
- Dynamic fracture toughnesses of reaction-bonded silicon nitride 08 p1071 A83-22197
- Dynamic response analysis of structures with large degrees of freedom by step-by-step transfer matrix method 09 p1276 A83-23335
- Large deflections of point loaded cantilevers with nonlinear behaviour 09 p1281 A83-24823
- The prediction of material damping of laminated composites 12 p1709 A83-29396
- Dynamic tests of graphite/epoxy composites in hygrothermal environments 14 p1987 A83-33124
- Quasi-dynamical systems and the stabilization of elastic vibrations with controls whose range is restricted to a finite number of values 15 p2220 A83-33875
- A simple selectively integrated torsion-flexure coupled tapered beam element with transverse shear deformation 15 p2176 A83-34319
- Polycrystalline silicon micromechanical beams 15 p2143 A83-34698
- Design of dry-friction dampers for turbine blades 16 p2306 A83-35883
- A fatigue fracture model for metal-matrix composites 18 p2701 A83-40103
- Minimum slope/deflection design of rectangular cantilever beams 19 p2857 A83-40886
- A displacement formulation for the finite element elastic-plastic problem 19 p2857 A83-41153
- Optimal design of a passive vibration absorber for a truss beam [AIAA PAPER 83-2291] 19 p2816 A83-41750
- Determination of stable crack growth resistance of ductile material using an RDCB specimen --- Reinforced Double Cantilever Beam 20 p2954 A83-42830
- Subspace iteration for the eigenvalue problems of self-adjoint differential equations and its applications in the vibration analysis of structures 21 p3151 A83-44109
- Fracture toughness of composite adherend adhesive joints under mixed mode I and III loading 21 p3115 A83-44121
- Speckle-shear interferometry with double Dove prisms 21 p3136 A83-44189
- On axial and lateral buckling of end-loaded anisotropic cantilever beams 21 p3152 A83-44464
- The stress intensity factor for the double cantilever beam 21 p3158 A83-44914
- Active vibration control of a cantilevered beam - A study of control actuators --- for large space structures [IAF PAPER 83-ST-11] 23 p3423 A83-47388

CANTILEVER MEMBERS

- NT CANTILEVER BEAMS
- NT CANTILEVER PLATES
- Determination of the degree of defectiveness in structural components 02 p0191 A83-12156
- Application of multiple dynamic absorbers to reducing the vibration level of a complex cantilever structure 04 p0497 A83-15547
- Stability of short Beck and Leipholz columns on elastic foundation 16 p2366 A83-36098
- Vibrations of cantilevered circular cylindrical shells
- Shallow versus deep shell theory 16 p2369 A83-36958
- On the three-dimensional vibrations of the cantilevered rectangular parallelepiped 17 p2521 A83-37729
- Vibrations of cantilevered doubly-curved shallow shells 18 p2700 A83-39557
- The behaviour of a channel cantilever under combined bending and torsional loads 21 p3153 A83-44623
- Determination of the resonance frequency spectrum of the forced vibration of current leads 21 p3138 A83-44634
- Cascade flutter analysis of cantilevered blades [ASME PAPER 83-GT-129] 23 p3408 A83-47958
- Mathematical model of a moving system with low-stiffness elastic elements 24 p3624 A83-49670
- CANTILEVER PLATES**
- Free vibration of cantilever quadrilateral plates 10 p1439 A83-25825
- Comparison of frequency determination techniques for cantilevered plates with bending-torsion coupling [AIAA 83-0953] 12 p1745 A83-29885
- CANTILEVER WINGS**
- U WINGS
- CAP CLOUDS**
- Observations of liquid water in orographic clouds over Elk Mountain 18 p2729 A83-40042
- Elevated mixed layers in the regional severe storm environment - Conceptual model and case studies 23 p3491 A83-47413
- Ice crystal and ice nucleus measurements in cap clouds 24 p3614 A83-49713

CAPACITANCE

- The electrical characteristics of degenerate InP Schottky diodes with an interfacial layer 01 p0036 A83-10629
- A model for field-sensitive interface states 01 p0109 A83-10631
- Effects of stray capacitances between transformer windings on the noise characteristics in switching power converters 01 p0040 A83-11012
- Channeling photodiode - A new versatile interdigitated p-n junction photodetector 02 p0167 A83-12285
- Automatic capacitance-voltage /C-V/ plotter for solar cells 02 p0181 A83-12821
- Simple phenomenological modeling of transition-region capacitance of forward-biased p-n junction diodes and transistor diodes 03 p0313 A83-13925
- Bulk and interface gap states in a-Si:H - A comparative study of field effect and capacitance measurements on codeposited samples 04 p0539 A83-15487
- Influence of interface states on field effect and capacitance-voltage characteristics of metal/oxide/a-Si:H structures 04 p0541 A83-15526
- Status cells - A demonstration of performance reproducibility, capacity retention, and cycle life for LiAl/FeS cells 04 p0506 A83-15868
- The shape factor of the capacitance of a conductor 04 p0472 A83-16053
- The effect of parasitic capacitances on the circuit speed of GaAs MESFET ring oscillators 05 p0631 A83-17763
- Theory for nonequilibrium behavior of anisotropy graded heterojunctions 06 p0814 A83-18961
- Photocapacitance of mobile carriers in hydrogenated amorphous silicon solar cells 08 p1131 A83-22765
- Al-Si peaked Schottky barriers 08 p1170 A83-22903
- The performance of thick piezoelectric transducers as wide-band ultrasonic detectors 09 p1270 A83-25117
- Relaxation-phenomena in LiAl/FeS-cells 11 p1603 A83-27167
- Coupling of a high-Q gravitational-wave antenna with the resonator of a capacitive sensor of oscillations 11 p1572 A83-27454
- A reevaluation of the meaning of capacitance plots for Schottky-barrier-type diodes 11 p1564 A83-28712
- The electrical behavior of GaAs-insulator interfaces - A discrete energy interface state model 13 p1931 A83-31386
- The capacitance-voltage characteristics of m-i-n GaN light emitting diodes --- metal-insulator-n-type semiconductor 17 p2496 A83-37649
- Deep traps in metal-insulator-chemically vapor-deposited amorphous SiN(x) diodes 17 p2584 A83-38214
- Design of algorithms to extract data from capacitance sensors to measure fastener hole profiles 19 p2855 A83-41026
- Transient capacitance spectroscopy on large quantum well heterostructures 20 p3053 A83-42614
- Low-Intensity Differential Photocapacitance of MOS structures 21 p3127 A83-45173
- A study of the parameters of traps in hydrogenated amorphous silicon by the method of volt-farad characteristics 24 p3635 A83-49047
- Surface films on lithium in acetonitrile-sulphur dioxide solutions 24 p3558 A83-49937
- CAPACITANCE SWITCHES**
- Capacitor bank charging by series-parallel switching of solar arrays [AIAA PAPER 82-1878] 02 p0143 A83-12464
- Switched-capacitor second-order noise-shaping coder 08 p1082 A83-22923
- Switched-capacitor realization of a discrete Fourier transformer 15 p2151 A83-33925
- CAPACITORS**
- Reliability considerations for metallized plastic film capacitors under high-stress ac waveforms 01 p0040 A83-11009
- Mass reduction of capacitor bank for MPD thruster [AIAA PAPER 82-1879] 02 p0143 A83-12465
- Surface potential relaxation in a biased Hg/1-x/Cd/x/Te metal-insulator-semiconductor capacitor 07 p0918 A83-19993
- A two-stage monolithic IF amplifier utilizing a Ta2O5 capacitor 09 p1256 A83-24681
- Design of interdigitated capacitors and their application to gallium arsenide monolithic filters 10 p1410 A83-26341
- Tunneling current microscopy 13 p1846 A83-30350
- Electrical measurements on n(+)-GaAs-undoped Ga(0.6)Al(0.4)As-n-GaAs 13 p1836 A83-31065
- Capacitance transducers for nondestructive testing (2nd revised and enlarged edition) 21 p3135 A83-43920
- Techniques for improving the Si-SiO2 interface characterization 22 p3364 A83-46275

- Electric field induced effects at the Si-SiO2 interface
- Theory and experiment 22 p3364 A83-46276

CAPE KENNEDY LAUNCH COMPLEX

- KSC ground support operations and equipment for the space transportation system 11 p1533 A83-27474
- STS cargo processing at the Kennedy Space Center 11 p1533 A83-27475
- DOD/Shuttle payload ground handling operations at Kennedy Space Center 13 p1811 A83-31196
- Processing cargoes for the first two operational STS flights at KSC [IAF PAPER 83-23] 23 p3418 A83-47236
- CAPIES (LANDFORMS)**
- Cape Romain and the Charleston Bump - Historical and recent hydrographic observations 14 p2060 A83-33086

CAPILLARIES (ANATOMY)

- Significance of the measurement of colloidal-oncotic and hydrostatic pressures in lung capillaries for the diagnosis of edema of the lungs 05 p0673 A83-17177
- The dynamics of oxygen transport from the capillaries to the nerve cells of the brain 08 p1145 A83-22104

CAPILLARY CIRCULATION**U CAPILLARY FLOW****CAPILLARY FLOW**

- Verification of the oscillatory state of thermocapillary convection in a floating zone under low gravity 01 p0047 A83-11327
- The coefficient of capillary filtration in the skeletal muscles during changes in their hemodynamics 07 p0973 A83-20360
- The morphological characteristics of the myons of the masticatory muscle of mammals and humans 07 p0975 A83-20990
- Influence of gas inertia forces generated within the stabilizing restrictor on dynamic characteristics of externally pressurized thrust gas bearings. II - Case of turbulent flow at the capillary restriction 09 p1273 A83-23336
- Double perforated plate as a capillary barrier --- in liquid propellant propulsion systems in low-G environment [AIAA PAPER 83-1379] 16 p2317 A83-36370
- Vapor flow into a capillary propellant-acquisition device [AIAA PAPER 83-1380] 16 p2321 A83-36371
- Oscillatory thermocapillary convection in floating zones under normal- and micro-gravity 18 p2643 A83-39901
- Thermocapillary migration of bubbles and droplets 18 p2686 A83-39907
- Exact solutions of a free-boundary problem for the Stokes system 19 p2846 A83-42061
- Instabilities of dynamic thermocapillary liquid layers. I
- Convective instabilities 20 p2985 A83-43098
- Liquid materials and flow processes in reduced gravity 20 p2940 A83-43268
- Steady thermocapillary flows and their stability 20 p2986 A83-43270
- Thermocapillary motion of bubbles inside drops --- in free fall environment with axisymmetric surface temperature field 20 p2940 A83-43279
- Experimental observation of the thermocapillary driven motion of bubbles in a molten glass under low gravity conditions 20 p2941 A83-43283
- A magnetogasdynamic model for a capillary discharge with wall vaporization 21 p3215 A83-45350
- Rheology of reinforced thermoplastics and its application to injection-molding. IV - Transient injection capillary flow and injection-molding 22 p3265 A83-46901
- Thermocapillary convection in a two-layer system 23 p3452 A83-48669
- Flow of a gas mixture in a cylindrical channel at intermediate Knudsen numbers 24 p3576 A83-48940
- Direct method for investigating the dynamics of liquid-filled bodies 24 p3624 A83-49672
- CAPILLARY TUBES**
- The effect of the parameters of metal-fiber capillary structures on the maximum heat-transfer capability of thermal pipes 02 p0169 A83-11515
- Investigation of the characteristics of heat transfer in the heating zone of heat pipes with metal fiber capillary structures 04 p0477 A83-15865
- Surface tension effects in a space radiator condenser with capillary liquid drainage [AIAA PAPER 83-1525] 14 p2011 A83-32756
- CAPILLARY WAVES**
- NT BAROCLINIC WAVES
- NT GRAVITY WAVES
- Influence of acoustic fields on drop dynamics in an acoustic resonator 18 p2686 A83-39908
- CAPTIVE TESTS**
- NT STATIC FIRING
- NT STATIC TESTS
- CAPTURE CROSS SECTIONS**
- U ABSORPTION CROSS SECTIONS

CAPTURE EFFECT

- Dosimetric silica films - The influence of fields on the capture of positive charge 05 p0691 A83-17535
- Pioneer 11 observations of trapped particle absorption by the Jovian ring and the satellites 1979, J1, J2, and J3 06 p0847 A83-18280
- How galaxies acquire their neutrino haloes 08 p1187 A83-23285
- Criteria of hyperbolic and hyperbolic-elliptical motion in capture theory 11 p1673 A83-28032
- Hollow probe for measuring ion density in a slightly ionized plasma flow 12 p1728 A83-29008
- Impossibility of the capture of retrograde satellites in the restricted three-body problem 12 p1787 A83-29124
- Radioactive ion beams for studying astrophysical nuclear reactions 13 p1917 A83-30178
- Tidal compression of a star by a large black hole. I
- Mechanical evolution and nuclear energy release by proton capture 13 p1959 A83-31747
- Capture and eruption hypotheses for comets 20 p3061 A83-43413
- The rate of the He-3(p,e+ nu) - He-4 reaction --- source of high energy solar neutrinos 21 p3244 A83-45564

CARBAZOLES

- Effect of molecular rotation upon charge transport between disordered carbazole units 20 p3053 A83-42602

CARBIDES

- NT ALUMINUM CARBIDES
- NT BORON CARBIDES
- NT CHROMIUM CARBIDES
- NT HAFNIUM CARBIDES
- NT MOLYBDENUM CARBIDES
- NT NIOBIUM CARBIDES
- NT SILICON CARBIDES
- NT TANTALUM CARBIDES
- NT TITANIUM CARBIDES
- NT TUNGSTEN CARBIDES
- NT VANADIUM CARBIDES
- NT ZIRCONIUM CARBIDES
- A model for the formation of subboundaries in the matrix of eutectic alloys of the system M-MeC --- Ni or Co alloyed with Ta, Nb or Hf carbides 01 p0025 A83-10397
- X-ray powder diffraction evidence for the incorporation of W and Mo into M23C6 extracted from high-temperature alloys 02 p0154 A83-11670
- Controlling the structure of hard alloys and other heterophase materials produced by liquid-phase sintering. II - Optimum design principles for hard alloys 02 p0159 A83-13029
- Resistivity, superconductivity, and order-disorder transformations in transition metal carbides and hydrogen-doped carbides 04 p0543 A83-16075
- The constitution of cemented carbide systems 06 p0732 A83-19106
- Modeling the creep and fracture of the directionally solidified gamma/gamma-prime-MeC eutectic 08 p1068 A83-22786
- Reactions between Ni-Cr-B-Si matrixes and carbide additives in coatings during fusion treatment 10 p1400 A83-25533
- The temperature dependence of the ultimate stress for eutectic tungsten alloys with titanium, zirconium, and hafnium carbides 15 p2141 A83-35311
- Ni-base MC-carbide reinforced eutectic alloys for jet engine application 21 p3111 A83-44061
- Characteristics of the formation of plasma-sprayed coatings based on clad carbide powders 24 p3590 A83-49087
- CARBOHYDRATE METABOLISM**
- NT HYPERGLYCEMIA
- Concerning the interrelationship between protein, fat, and carbohydrate metabolisms 01 p0081 A83-10560
- Metabolism during hypodynamia --- Russian book 02 p0221 A83-11950
- The significance of glucocorticoids in the regulation of the resynthesis of glycogen in the postexercise period and the mechanism of their action 04 p0520 A83-15898
- Several metabolic effects of a glucose-insulin-potassium mixture on patients with acute myocardial infarctions 05 p0674 A83-17218
- Fate of exogenous glucose during exercise of different intensities in humans 05 p0675 A83-17338
- Current ideas about the mechanism of the action of glucocorticoid hormones 05 p0672 A83-17599
- An experimental study of the effects of hypobaric hypoxia on the cerebral blood flow and the metabolism of the brain 06 p0794 A83-18342
- The effect of adrenalectomy and hydrocortisone on the carbohydrate metabolism in the lungs and myocardium during chronic hypoxia 07 p0972 A83-19922
- The energy metabolism in the brains of rats exposed to mechanical asphyxia 07 p0972 A83-19923

- The effect of strophanthine and celanide on the blood circulation and metabolism in the brain 07 p0975 A83-20983
- Increased gluconeogenesis in hyper-G stressed rats 11 p1637 A83-27805
- Biochemical changes in rat liver after 18.5 days of spaceflight (41566) 12 p1763 A83-29546
- Effect of denervation and reinnervation on oxidation of 6-(C-14) glucose by rat skeletal muscle homogenates 12 p1763 A83-29551
- The role of the middle hypothalamus structures in the regulation of the glucose content in the blood and the glycogen content in the liver 13 p1895 A83-30304
- Effect of glycogen depletion on the ventilatory response to exercise 13 p1903 A83-30474
- Certain characteristics of the metabolism of hexosephosphates 16 p2399 A83-36828
- UDP-coenzymes in the tissues of the brain glia of humans 16 p2400 A83-36831
- The role of collateral coronary blood flow in the compensation of regional disorders of the energy metabolism of heart muscle during experimental myocardial ischemia 18 p2732 A83-40544
- The participation of an insulin-dependent cytoplasmic regulator in carbohydrate metabolism during immobilization 19 p2871 A83-40818
- Carbohydrate feeding during prolonged strenuous exercise can delay fatigue 19 p2880 A83-41141
- Lactate in human skeletal muscle after 10 and 30 s of supramaximal exercise 20 p3034 A83-43479
- Effects of exercise and lack of exercise on glucose tolerance and insulin sensitivity 20 p3035 A83-43485
- Androgens enhance in vivo 2-deoxyglucose uptake by rat striated muscle 22 p3346 A83-46706
- Effect of confinement in small space flight size cages on insulin sensitivity of exercise-trained rats 24 p3617 A83-48881
- CARBOHYDRATES**
- NT ADENOSINE DIPHOSPHATE
- NT ADENOSINE TRIPHOSPHATE
- NT ADENOSINES
- NT CELLULOSE
- NT DEXTRANS
- NT GLUCOSE
- NT GLUCOSIDES
- NT GLYCOGENS
- NT NUCLEOSIDES
- The abundance of CH3D in the atmosphere of Titan, derived from 8- to 14-micron thermal emission 08 p1189 A83-22931
- Shock formation of HCO/+ / 10 p1513 A83-26718
- CARBON**
- NT CARBON ISOTOPES
- NT CARBON 12
- NT CARBON 13
- NT CARBON 14
- NT GLASSY CARBON
- Diffusion of carbon in beryllium 01 p0027 A83-11350
- Sorption of noble gases by solids, with reference to meteorites. I - Magnetite and carbon 02 p0262 A83-11546
- Sorption of noble gases by solids, with reference to meteorites. II - Chromite and carbon. III - Sulfides, spinels, and other substances; on the origin of planetary gases 02 p0262 A83-11547
- Electrical conduction in carbon-polymer composites 02 p0149 A83-11785
- Atomic carbon in the atmosphere of Venus 02 p0264 A83-12395
- On C3 molecules in diffuse interstellar clouds 03 p0414 A83-13327
- Diurnal and seasonal variations in the atmospheric structure parameter /C/n/-squared/ that affect the atmospheric modulation transfer function /MTF/ 03 p0364 A83-13978
- Carbon, nitrogen, and oxygen abundances in G8-K3 giant stars 03 p0430 A83-14802
- Activation energy asymptotics applied to burning carbon particles 03 p0296 A83-14849
- Carbon catalyzed SO2 oxidation by NO2 04 p0456 A83-15300
- Carbon-oxygen plasma - Parameter domain for a strong screening effect --- in red giant stars 04 p0555 A83-15951
- Influence of tantalum alloying additives on the solid solubility limit of carbon in molybdenum 04 p0461 A83-16173
- H atom detection and energy analysis by use of thin foils and TOF technique --- Time Of Flight 05 p0644 A83-16923
- Atmospheric parameters and carbon abundance of white dwarfs of spectral types C2 and DC 06 p0826 A83-18093

- A quantitative model for carbon incorporation in Czochralski silicon melts 07 p0880 A83-19894
- A quantitative study of the relationship between interfacial carbon and line dislocation density in silicon molecular beam epitaxy 07 p0998 A83-19896
- Profiles and shifts of the C I 5052-A line in the granulation spectrum --- of sun 07 p1038 A83-21239
- Problems of carbon oxidation 08 p1056 A83-22320
- Dielectronic recombination cross section for C/1+ / 08 p1168 A83-22645
- The effect of carbon, phosphorus, and silicon on the structure and properties of NM27 alloy 09 p1229 A83-23521
- Photodissociation and radiative processes in interstellar C2 09 p1356 A83-23658
- The diffusion constants of hydrogen, nitrogen, and carbon in solid solutions and binary phases with titanium 09 p1235 A83-24395
- Can C IV emission be used as a luminosity indicator --- of quasars 09 p1362 A83-24987
- Charge exchange of C/6+ / and O/8+ / ions with hydrogen atoms - Strong coupling calculation 10 p1486 A83-25885
- Combustion of carbon particles, initiated by laser radiation 10 p1392 A83-26777
- Gaseous equilibria in the C-H-O ternary system at 500-2000 K, 0.1-10 atm 11 p1666 A83-28670
- Some fuel effects on carbon formation in gas turbine combustors 12 p1717 A83-29392
- RECLAS - Resonant-enhanced CARS from C2 produced by laser ablation of soot particles 13 p1844 A83-30201
- Plasma shifts of the Lyman lines to shorter wavelengths in C VI 13 p1926 A83-30919
- Radiative association and the synthesis of long carbon chain molecules in interstellar clouds 13 p1953 A83-31451
- Convective mixing length and the galactic carbon to oxygen ratio 14 p2107 A83-33241
- Interfacial electrical properties of ion-beam sputter deposited amorphous carbon on silicon 15 p2238 A83-33920
- Distribution of forbidden neutral carbon emission in the ring nebula (NGC 6720) 15 p2257 A83-34093
- The non-LTE analysis of carbon lines in the spectra of hot stars. I - C III lambda 4650 and lambda 9710 A triplet lines in the spectra of O stars 15 p2271 A83-34763
- A surge observed in H alpha and C IV 15 p2285 A83-35228
- Resonance-enhanced coherent anti-Stokes Raman scattering in C2 16 p2327 A83-36416
- [ONERA, TP NO. 1983-1] CNO abundances from pre-maximum spectra of Nova Cygni 1975 16 p2429 A83-36543
- Profiles and intensity ratios of the C I lambda 1548, 1550 emission lines in planetary nebulae 16 p2433 A83-36706
- Radiometric levitation of spherical carbon aerosol particles using a Nd:YAG laser 16 p2413 A83-36761
- Copernicus observations of C I - Pressures and carbon abundances in diffuse interstellar clouds 17 p2604 A83-37908
- The strength of the C IV 1550 A resonance lines in planetary nebulae 17 p2608 A83-38413
- Atomic carbon in Orion 18 p2772 A83-39705
- Diffusion induced grain boundary migration in Ni-C alloys 18 p2668 A83-40615
- Electron-diffraction evidence for threefold coordination in amorphous hydrogenated carbon films 19 p2823 A83-40955
- Carbon diffusion in Ti-Nb alloys 19 p2822 A83-42071
- A study of the aging of tungsten-zirconium-carbon alloys 19 p2822 A83-42072
- RF-plasma deposited amorphous hydrogenated hard carbon thin films - Preparation, properties, and applications. 20 p3048 A83-42610
- Interstellar C2 molecules in a Taurus dark cloud 20 p3074 A83-43091
- Observations of interstellar C2 toward three heavily reddened stars 20 p3074 A83-43092
- Eikonal phase shift analyses of carbon-carbon scattering 20 p3046 A83-43580
- Interstellar C2 in the Ophiuchus clouds 21 p3228 A83-44409
- Absorption of carbon from residual gases during Ti implantation of alloys 21 p3115 A83-45490
- The carbon-oxygen system at present and in the Precambrian 22 p3323 A83-45782
- Abundances of carbon-bearing diatomic molecules in diffuse interstellar clouds 22 p3377 A83-46259
- The coefficient of haze as a measure of particulate elemental carbon 22 p3321 A83-46775
- Synthesis of chain molecules in regions with partially ionized carbon 22 p3382 A83-46987
- Some recent results from UV observations 24 p3639 A83-49136

Influence of nitrogen and carbon in the base steel on the transformation temperature of the alloy layer of an aluminized steel sheet for high temperature use
24 p3566 A83-49519

CARBON COMPOUNDS

NT ALUMINUM CARBIDES
NT BORON CARBIDES
NT CALCITE
NT CARBIDES
NT CARBONATES
NT CHLOROCARBONS
NT CHROMIUM CARBIDES
NT DOLOMITE (MINERAL)
NT HAFNIUM CARBIDES
NT HALOCARBONS
NT MOLYBDENUM CARBIDES
NT NIOBIUM CARBIDES
NT POLYCARBONATES
NT SILICON CARBIDES
NT SODIUM CARBONATES
NT TANTALUM CARBIDES
NT TITANIUM CARBIDES
NT TUNGSTEN CARBIDES
NT VANADIUM CARBIDES
NT ZIRCONIUM CARBIDES
Dense cloud chemistry. II - The HCS/+/CS ratio
07 p1018 A83-20946
Experimental determination of vapor species from laser-ablated carbon phenolic composites
19 p2823 A83-40875
Results of apparent atomic oxygen reactions on Ag, C, and Os exposed during the Shuttle STS-4 orbits
19 p2820 A83-41125
Tentative detection of the CS(+) molecular ion in diffuse interstellar clouds
23 p3518 A83-47426

CARBON CYCLE

The possible global budget of carbon dioxide
01 p0072 A83-11045
Sampling strategy to obtain data used in models of global annual CO₂ increase and global carbon cycle
09 p1295 A83-24262
A simulation of the carbon cycle in the system atmosphere-ocean-biosphere in the framework of linear and diffusion models
13 p1874 A83-30296
The effect of the variability of temperature and organic matter on the carbon cycle in the ocean
13 p1894 A83-30298
The global distribution of atmospheric carbon dioxide. I Aspects of observations and modeling. II - A review of provisional background observations, 1978-1980
13 p1876 A83-30876
Modeling the carbon cycle using the method of fractional-order derivatives
14 p2051 A83-32366
Material cycling and organic evolution
17 p2557 A83-38894
Elemental carbon in the atmosphere - Cycle and lifetime
21 p3171 A83-44376

CARBON DIOXIDE

Effects of carbon dioxide inhalation on psychomotor and mental performance during exercise and recovery
02 p0222 A83-12089
A CO₂-rich coma model applied to the neutral coma of Comet West
02 p0262 A83-12923
Absorption at 10 micron in CO₂-He and CO₂-N₂ mixtures at elevated temperatures
03 p0392 A83-13497
Noninvasive cardiac output determination using inhaled oxygen-15-labeled carbon dioxide
03 p0378 A83-13577
Transmission of CO₂ in the atmosphere of Venus for the spectral region near 7 microns
03 p0434 A83-13836
Formaldehyde formation in a H₂O/CO₂ ice mixture under irradiation by fast ions
03 p0424 A83-14196
Overlapping effects of atmospheric H₂O, CO₂ and O₃ on the CO₂ radiative effects
03 p0361 A83-14660
Parameterization of the radiative flux divergence in the 15 micron CO₂ band in the 30-75 km layer
03 p0362 A83-14752
The seasonal CO₂ cycle on Mars - An application of an energy balance climate model
04 p0569 A83-15592
Photoelectron spectroscopy of carbon dioxide
05 p0683 A83-17651
Modified-independent-atom-model /MIAM/ calculations for e-CO₂ elastic scattering at 50-500 eV
06 p0807 A83-18040
Climate studies with a multi-layer energy balance model. I - Model description and sensitivity to the solar constant. II - The role of feedback mechanisms in the CO₂ problem
06 p0789 A83-18251
Radiative heating due to increased CO₂ - The role of H₂O continuum absorption in the 12-18 micron region
06 p0791 A83-18269
Stimulated Raman scattering in a multipass cell filled with CO₂
07 p0935 A83-20125

Parameters of CO₂ bands near 3.6 microns
07 p0881 A83-20164
Optimal weighting of data to detect climatic change - Application to the carbon dioxide problem
07 p0969 A83-20216
Chemoreceptor sensitivity in adaptation to high altitude
07 p0977 A83-20780
Earth limb emission analysis of Spectral Infrared Rocket Experiment /SPIRE/ data at 2.7 micrometers
08 p1051 A83-22851
Unimolecular reaction paths of electronically excited species. IV - The Cl(II) 2Sigma plus g state of CO₂/plus/
08 p1163 A83-22999
Cross sections for electron impact excitation of the low-lying electron states of CO₂
08 p1163 A83-23021
On the radiocarbon record in banded corals - Exchange parameters and net transport of 14CO₂ between atmosphere and surface ocean
09 p1295 A83-24253
Temperature dependence of the classical potential of intermolecular interaction and the light absorption coefficient in the wing of the 4.3 micron band of CO₂
10 p1478 A83-25524
Spectral distribution of CO₂ vibrational states produced by collisions with fast hydrogen atoms from laser photolysis of HBr
10 p1478 A83-25555
Radiative-convective heat transfer during turbulent flow of carbon dioxide in a plane channel
11 p1570 A83-28793
Control of respiratory pattern in conscious dog - Effects of heat and CO₂
13 p1897 A83-30482
The effect of nonequilibrium on the expansion of CO₂ issuing into a rarefied medium
13 p1842 A83-30679
Uptake of excess CO₂ by an outcrop-diffusion model of the ocean
13 p1869 A83-30877
Some comments on the exchange of CO₂ across the air-sea interface
13 p1869 A83-30879
A flow-system comparison of the reactivities of calcium superoxide and potassium superoxide with carbon dioxide and water vapor
13 p1907 A83-30946
Rotational and vibrational-rotational relaxation in collisions of CO₂(01/1/0) with He atoms
13 p1916 A83-30953
Density-functional theory for solid nitrogen and carbon dioxide at high pressure
13 p1929 A83-30958
Climatic effects of atmospheric carbon dioxide
13 p1893 A83-31200
The absorption coefficient of light in the wing of the 4.3 micron band of CO₂
14 p2082 A83-32556
Analysis of the influence of intramolecular interactions on the probability of vibration-rotation transitions in linear molecules
14 p2082 A83-32557
Intermolecular potentials from NMR data - H₂-N₂O and H₂-CO₂
15 p2227 A83-33631
Two-photon Raman excitation and coherent anti-Stokes Raman spectroscopy probing of population changes in polyatomic molecules - A novel nonlinear optical technique for vibrational-relaxation studies
15 p2227 A83-33757
Does Venus breathe?
15 p2275 A83-34725
Dry ice II, a new polymorph of CO₂
16 p2437 A83-35996
CO₂ radiative parameterization used in climate models
Comparison with narrow band models and with laboratory data
16 p2389 A83-36134
Parameterization of carbon dioxide 15-micron band absorption and emission
16 p2379 A83-36135
The vibrationally averaged, temperature-dependent structure of polyatomic molecules. I - CO₂
16 p2410 A83-36521
Electrochemical measurements on the photoelectrochemical reduction of aqueous carbon dioxide on p-gallium phosphide and p-gallium arsenide semiconductor electrodes
16 p2328 A83-36741
A hygienic evaluation of the chemical composition of air in living accommodations
17 p2562 A83-38201
Dissociation of CO₂(2+) ions into O(+) and O(+) fragments
17 p2486 A83-38469
Production of O(-) from CO₂ by dissociative electron attachment
19 p2898 A83-41863
Non luminous gas radiation - Approximate emissivity models
20 p2974 A83-42692
Laboratory measurements of the association rate coefficients of NO(+), O₂(+), N(+), and N₂(+) ions with N₂ and CO₂ at temperatures between 100 K and 400 K
20 p3024 A83-43165
Determination of the third derivatives of the dipole moment function for CO₂
21 p3203 A83-45385
Nonequilibrium plasmachemical process of CO₂ decomposition in a supersonic microwave discharge
21 p3215 A83-45397
Oxygen and carbon dioxide exchange between the Arctic Ocean and the atmosphere
21 p3182 A83-45398

Effect of two different atmospheric models of the absorptive rate of excess atmospheric carbon by the sea
22 p3333 A83-46881
Observations of the 10-micron natural laser emission from the mesospheres of Mars and Venus
22 p3387 A83-47079
Ground state energy and structure of physisorbed monolayers of linear molecules
23 p3429 A83-47636
Electron transport coefficients in weakly ionized nonequilibrium plasma of CO₂:N₂ mixtures
24 p3632 A83-49112
Radiation characteristics of vibrationally nonequilibrium CO₂ gas in the spectral region 12-19 microns
24 p3626 A83-49117

CARBON DIOXIDE CONCENTRATION

The possible global budget of carbon dioxide
01 p0072 A83-11045
Certain biochemical indices in healthy humans under the effect of high concentrations of carbon monoxide and carbon dioxide in a sealed chamber
01 p0085 A83-11403
The exchange of CO₂ between the ocean and atmosphere
02 p0205 A83-11980
Infrared device for simultaneous measurement of fluctuations of atmospheric carbon dioxide and water vapor
03 p0324 A83-13275
Seasonal carbon dioxide exchange between the regolith and atmosphere of Mars - Experimental and theoretical studies
04 p0568 A83-15588
The dependence of the resonator efficiency of a CO₂ gasdynamic laser on the laser mixture parameters
04 p0486 A83-16387
The molten carbonate carbon dioxide concentrator - Cathode performance at high CO₂ utilization --- in manned space station cabin atmospheres
07 p0879 A83-19880
The effect on the human body of a high concentration of carbon dioxide and hypokinesia
07 p0978 A83-20883
A sealed 100-Hz CO₂ TEA laser using high CO₂ concentrations and ambient-temperature catalysts
08 p1107 A83-21983
Effects of increased CO₂ concentrations on surface temperature of the early earth
08 p1138 A83-23256
Uncertainties of predictions of future atmospheric CO₂ concentrations
09 p1294 A83-24251
Feedback mechanisms in the climate system affecting future levels of carbon dioxide
09 p1294 A83-24252
Three-dimensional tracer model study of atmospheric CO₂ - Response to seasonal exchanges with the terrestrial biosphere
09 p1305 A83-24254
Exponential growth and atmospheric carbon dioxide
09 p1295 A83-24255
Distribution of and changes in industrial carbon dioxide production
09 p1295 A83-24256
CO₂ and radon 222 as tracers for atmospheric transport
09 p1295 A83-24257
Semiautomatic nondispersive infrared analyzer apparatus for CO₂ air sample analyses
09 p1295 A83-24258
Preliminary study of CO₂ variations at Amsterdam Island /Terroire des Terres Australes et Antarctiques Francaises/
09 p1295 A83-24259
Interpretation of atmospheric CO₂ measurements at Mt. Cimone /Italy/ related to wind data
09 p1295 A83-24260
Concentration of atmospheric carbon dioxide over Japan
09 p1295 A83-24261
Sampling strategy to obtain data used in models of global annual CO₂ increase and global carbon cycle
09 p1295 A83-24262
Selection of CO₂ concentration data from whole-air sampling at three locations between 1968 and 1974
09 p1295 A83-24263
Overlapping effect of atmospheric H₂O, CO₂ and O₃ on the CO₂ radiative effect
11 p1632 A83-27669
Marine biological controls on atmospheric CO₂ and climate
11 p1600 A83-28400
Oxygen uptake and elimination of nonmetabolic CO₂ excess in an initial period of heavy muscular exercise
12 p1765 A83-29315
Blood osmolality in vitro - Dependence on P(CO₂), lactic acid concentration, and O₂ saturation
13 p1902 A83-30459
The global distribution of atmospheric carbon dioxide. I Aspects of observations and modeling. II - A review of provisional background observations, 1978-1980
13 p1876 A83-30876
Collisional vibrational quenching of O₂(+) (v) and other molecular ions in planetary atmospheres
13 p1917 A83-31636
The dependence of air temperature and the temperature of precipitates on the amount of carbon dioxide in the atmosphere
14 p2056 A83-32365

Modeling the carbon cycle using the method of fractional-order derivatives 14 p2051 A83-32366

Variability of antarctic sea ice and changes in carbon dioxide 15 p2208 A83-33775

A global model of the ocean-atmosphere system and an investigation of its sensitivity to changes in CO2 concentration 16 p2392 A83-36864

Effect of high atmospheric CO2 concentration on delta C-13 of algae - A possible cause for the average depletion of C-13 in Precambrian reduced carbon 17 p2557 A83-38895

Acclimatization to high altitude in goats with ablated carotid bodies 19 p2875 A83-41132

General circulation model experiments on the climatic effects due to a doubling and quadrupling of carbon dioxide concentration 20 p3031 A83-42843

CO2 measurements with an infrared laser spectrometer on flask samples collected at Jungfraujoch high-altitude research station (3500 meters asl) and with light aircraft up to 8000 meters over Switzerland 20 p3022 A83-42867

On the variability of atmospheric carbon dioxide concentration at Barrow, Alaska during winter 20 p3022 A83-42868

Comparison of airborne CO2 flask samples and measurements from the Mauna Loa Observatory during the HAMEC Project (June 1980) 20 p3022 A83-42869

The seasonal response of a general circulation model to changes in CO2 and sea temperatures 21 p3179 A83-44393

Frequency-doubled CO2 lidar measurement and diode laser spectroscopy of atmospheric CO2 22 p3288 A83-46073

Active measures for reducing the global climatic impacts of escalating CO2 concentrations [IAF PAPER 83-106] 23 p3488 A83-47269

The response of the ocean to changes in the greenhouse effect 23 p3493 A83-48564

CARBON DIOXIDE LASERS

Scaling laws for the mode purity of simple TEA CO2 lasers 01 p0054 A83-10696

Steady-state ablation of aluminum alloys by a CO2 laser 01 p0054 A83-10701

Sources of photoionization in transversely excited atmospheric CO2 lasers 01 p0055 A83-10978

A Michelson interferometer for high resolution of shot start movement using a CO2 laser 01 p0052 A83-11068

Multifunction CO2 NOE sensor - A status report --- Nap-Of-the-Earth 01 p0010 A83-11147

The use of the pulse-repetition mode of a CO2 electroionization laser for laser welding 02 p0187 A83-11957

Injection-locking of TEA CO2 lasers by an orthogonally-polarised injection source 02 p0185 A83-12400

Rapidly tunable CO2 TEA laser 02 p0185 A83-12590

High repetition rate mini TEA CO2 laser using a semiconductor preionizer 02 p0185 A83-12816

Observation of vapor generation preceding the ignition of liquid n-decane and l-decene by CO2 laser radiation 02 p0152 A83-13094

Influence of the active-medium inhomogeneity and of aperture stops on the output-beam parameters of a CO2 laser 03 p0330 A83-13585

Absorption spectra of toxic compounds at CO2 laser wavelengths 03 p0294 A83-13722

Titanium ignition by the emission of a CO2 laser 03 p0299 A83-14062

Miniature, sealed TEA-CO2 lasers with integral semiconductive preionization 03 p0332 A83-14166

Operating efficiencies in pulsed carbon dioxide lasers 03 p0333 A83-14934

High-pressure tunable CW waveguide CO2 lasers 04 p0483 A83-15255

Atmospheric- and supraatmospheric-pressure CO2 lasers with a self-maintained discharge 04 p0483 A83-15256

The angular divergence of radiation from flowing gas lasers 04 p0483 A83-15258

Gas breakdown on the surface of metallic mirrors due to radiation from a pulsed /periodic pulsed/ CO2 laser 04 p0484 A83-15263

Study of the absorption of pulsed CO2 laser radiation by air and by carbon dioxide 04 p0484 A83-15705

Thermal self-defocusing of a CW CO2-laser beam during the interaction with water aerosol 04 p0484 A83-15734

Ion aging effects on the dissociative-attachment instability in CO2 lasers 04 p0484 A83-15792

Theory of rotating mirror Q-switching in a helical transversely excited CO2 laser 04 p0485 A83-16056

The dependence of the resonator efficiency of a CO2 gasdynamic laser on the laser mixture parameters 04 p0486 A83-16387

Dual-wavelength correlation measurements with an airborne pulsed carbon dioxide lidar system 05 p0643 A83-16831

Passive frequency stability of pulsed CO2 lasers 05 p0647 A83-16919

Polarization coupling effects in transversely excited atmospheric CO2 lasers - Application to single axial mode operation 05 p0648 A83-16943

Numerical investigation of the nozzle flow of a vibrationally nonequilibrium medium of a CO2 gasdynamic laser 05 p0649 A83-17050

Wavefront reversal in a population-inverted carbon dioxide gas caused by light-induced heating 05 p0649 A83-17052

Approximate method for calculations of unstable telescopic resonators --- carbon dioxide gasdynamic laser design 05 p0649 A83-17061

Transmission cutoff accompanying remote optical breakdown of the atmosphere by CO2 laser pulses 05 p0687 A83-17064

Technological CW CO2 laser with a nonself-sustained discharge 05 p0649 A83-17067

Investigation of preionization CO and CO2 lasers operating in the active zone of a stationary nuclear reactor 05 p0650 A83-17085

An experimental study of the possibility of using a CO2 laser for changing the cornea refraction /A preliminary report/ 05 p0671 A83-17211

lasma fluctuations at critical density in a CO2 laser plasma interaction 05 p0688 A83-17364

High-temperature selective gasdynamic continuous CO2 laser 06 p0765 A83-18450

Small signal gain measurements for the 00/0/1-02/0/0 and 00/0/1-10/0/0 bands in a flowing-gas CW CO2 laser 06 p0766 A83-18945

A 10 cm aperture, high quality TEA CO2 laser 06 p0766 A83-18956

Experimental verification of a computational model for a combustion-product CO2-GDL for high stagnation temperatures 06 p0767 A83-19556

The effect of the quantum current on the relaxation of paired modes of the CO2 molecule 06 p0809 A83-19557

Characteristics of Schottky diodes at 10.6 microns 07 p0918 A83-19988

Infrared to visible up-conversion using GaP light-emitting diodes 07 p0992 A83-19990

Rapid-flow combined-action industrial CO2 laser 07 p0933 A83-20104

Investigation of the active medium in a fast-flow closed-cycle industrial CO2 laser 07 p0933 A83-20105

Divergence of radiation from an electric-discharge CO2 laser having an unstable resonator 07 p0934 A83-20108

Investigation of the vibrational temperature kinetics in a TEA CO2 laser 07 p0934 A83-20113

Amplification in a waveguide CO2 laser employing an RF electrodeless discharge 07 p0935 A83-20129

Calculation of the energy characteristics of a pulse-periodic electron-beam-controlled CO2 laser with a cooled active mixture 07 p0935 A83-20131

Injection locking of wide-aperture TEA CO2 lasers 07 p0935 A83-20151

Advances in laser and MIAB welding techniques 07 p0940 A83-20523

Metal drilling investigation by means of different high power laser radiation 07 p0940 A83-21031

A sealed 100-Hz CO2 TEA laser using high CO2 concentrations and ambient-temperature catalysts 08 p1107 A83-21983

Repetitive passive Q-switching and bistability in lasers with saturable absorbers 08 p1107 A83-22079

Pressure wave attenuation due to anode mufflers in pulsed lasers 08 p1107 A83-22135

Determination of laser frequencies by mixing experiments between two submillimeter lasers 08 p1107 A83-22245

New CH3OH laser lines pumped with a fine-tuned high-power CO2-TEA laser 08 p1107 A83-22247

Mode-medium interactions --- high power CO2 laser output instability 08 p1109 A83-22461

Phase grating effects in pulsed CO2 electric discharge lasers 08 p1109 A83-22462

Multifunction CO2 laser radar technology 08 p1045 A83-22502

CO2 lidar for measurements of trace gases and wind velocities 08 p1095 A83-22504

National Oceanic and Atmospheric Administration's /NOAA/ pulsed, coherent, infrared Doppler lidar - Characteristics and data 08 p1096 A83-22506

Experimental studies with a coherent CO2 laser radar 08 p1096 A83-22510

Frequency-stabilized transversely excited atmospheric /TEA/ CO2 lasers for coherent infrared radar systems 08 p1109 A83-22515

Electronically scanned coherent CO2 laser radar techniques 08 p1096 A83-22516

Programmable transmitters for coherent laser radars 08 p1109 A83-22517

Digital processor for coherent CO2 systems 08 p1097 A83-22520

Acoustic phenomena associated with a TEA laser discharge 09 p1271 A83-23664

Optical bistability of a CO2 laser with intracavity saturable absorber Experiment and model 09 p1271 A83-23710

Experimental comparison of heterodyne and direct detection for pulsed differential absorption CO2 lidar 09 p1272 A83-24444

Water vapor absorption at isotopic CO2 laser wavelengths 09 p1269 A83-24446

Absorption of 9.6-micron CO2 laser radiation by CO2 at elevated temperatures 09 p1272 A83-24447

A rangefinder for coherent detection with a CW CO2 laser - Study and design 09 p1272 A83-24643

Free electron laser small signal gain measurement at 10.6 microns 10 p1427 A83-26009

Line shape parameter analysis of individual vibrational-rotational transitions in a CO2 laser amplifier 10 p1428 A83-26023

Fluid-dynamical aspects of laser-metal interaction 10 p1416 A83-26172

Thermooptic-conversion method for detecting the spatial mode structure of a TEA CO2 laser beam 10 p1430 A83-26245

Application of advanced millimeter/far-infrared sources to collective Thomson scattering plasma diagnostics 10 p1487 A83-26647

Influence of rotational relaxation in a CO2 amplifier on the shape of a short amplified pulse 10 p1432 A83-26668

Investigation of the optical inhomogeneities of the active medium of a fast-flow CO2 laser with mixing 10 p1433 A83-26677

Electric-discharge CW industrial CO2 laser 10 p1433 A83-26687

Thermal action of laser radiation on imidization 10 p1392 A83-26690

Nonlinear energy attenuation of pulsed CO2 laser radiation in the atmospheric surface layer 10 p1434 A83-26776

Performance testing of a Gigahertz modulator for 10 microns --- possible use in spaceborne optical communication 11 p1656 A83-27517

Thermodynamic properties of tissue impacted by CO2 laser 11 p1635 A83-27520

High performance DF-CO2 chain-reaction laser 11 p1579 A83-27572

High-power electro-ionization CO2 - Lasers for laser technology 11 p1580 A83-27574

Review of laser technology at M.I.T. Lincoln Laboratory 11 p1580 A83-27575

Corona preionization technique for CO2 TEA lasers 11 p1580 A83-27580

Pulse formation and amplification in an absorbing medium by optical phase switching 11 p1582 A83-27600

Parametric study of intersatellite CO2 laser data links 11 p1535 A83-27605

Peculiarities of laser radiation refraction in the clearing process of cloud medium 11 p1632 A83-27608

Kinetics of 'blurring' process accompanying CO2 laser radiation propagation in cloud medium 11 p1632 A83-27609

Absorption and reshaping of 10.6 microns light in pure SF6 using 1.5 ns, low-intensity incident pulses 11 p1582 A83-27610

Improved performance and rotational spectral characteristics of a doped helical TEA CO2 laser 11 p1583 A83-27623

The construction of a spectrophone and a CO2 laser waveguide excited by a radiofrequency field for application to the detection of atmospheric trace species --- French thesis 11 p1585 A83-28654

Helical-flow CO2 laser 11 p1585 A83-28705

Electron drift velocities in gas mixtures of He, N2, and CO2 11 p1655 A83-28707

The physics of electric-discharge CO2-lasers --- Russian book 12 p1731 A83-28815

Stabilisation of carbon dioxide lasers using the Stark effect 12 p1731 A83-29154

LIMP in continuously coupled unstable resonator --- Laser Induced Medium Perturbation effect in pulsed carbon dioxide laser 12 p1731 A83-29155

Pulse evolution and mode selection characteristics in a TEA-CO2 laser perturbed by injection of external radiation 12 p1731 A83-29195

High power TEA CO₂ laser tuned by a holographic grating 12 p1731 A83-29196

Operating characteristics of a transverse-excited 16 microns CO₂ laser with profile electrodes and UV-preionization 12 p1732 A83-29408

Improved acousto-optic modulators for CO₂ heterodyne laser systems 12 p1732 A83-29467

Investigation of the gain in a CO₂ GDL behind wedge-shaped and contoured nozzles. I - The experimental setup, the repetitively pulsed system for gain measurement 13 p1849 A83-30042

The effect of laser radiation on absorption in the far wings of spectral lines 13 p1849 A83-30084

Effect of outgassing on the performance of a TE CO₂ laser sealed in an acrylic chamber 13 p1849 A83-30258

Runaway self-absorption in multikilowatt CO₂ lasers 13 p1850 A83-30328

Inverse Lamb dip spectroscopy using microwave modulation sidebands of CO₂ laser lines 13 p1850 A83-30333

High-repetition-rate CO₂-lasers 13 p1850 A83-30645

Dissociation of CO₂ in a nonequilibrium plasma 13 p1925 A83-30647

Interpretation of vibrational relaxation channels on the basis of gas-dynamic measurements 13 p1850 A83-30668

The effect of boundary conditions on the flow of a polyatomic gas mixture in a supersonic nozzle --- in gasdynamic lasers 13 p1850 A83-30676

Effects of optical irregularities in the active medium on angular divergence of a beam in a CW supersonic DF-CO₂ chemical laser 13 p1851 A83-30819

Breakdown of dynamic equilibrium between the symmetric and deformation mode levels in CO₂ caused by excitation in an electrical discharge 13 p1915 A83-30828

Ab initio studies of the CO₂-HF and N₂O-HF complexes 13 p1818 A83-30966

Progress in absolute distance interferometry 13 p1851 A83-31019

Radio-frequency-excited carbon dioxide metal waveguide laser 13 p1857 A83-31457

Influence of a counterpressure on the operation of a CO₂ gasdynamic laser emitting of 18.4 microns 14 p2023 A83-31914

High-power continuously tunable atmospheric-pressure CO₂ laser operating in the superregenerative amplification regime 14 p2023 A83-31915

Thermal coupling on aluminum alloy surfaces in vacuum at 10.6 micrometer --- pulsed CO₂ laser-duraluminum target interaction [AIAA PAPER 83-1441] 14 p2024 A83-32712

Growth and saturation of the two-plasmon decay instability 14 p2087 A83-33390

Dynamics of the CO₂ upper laser level as measured with a tunable diode laser 14 p2027 A83-33435

Spectral dependence of reversible optically induced transitions in organometallic compounds 14 p2086 A83-33439

Laser welding of a titanium alloy 15 p2135 A83-33643

Efficient lasing of a TEA CO₂ laser with ultraviolet preionization and utilizing unconventional transitions 15 p2168 A83-33977

Modelling atmospheric aerosol backscatter at CO₂ laser wavelengths. I - Aerosol properties, modeling techniques, and associated problems. II - Modeled values in the atmosphere. III - Effects of changes in wavelength and ambient conditions 15 p2201 A83-34461

Measuring atmospheric scattering and extinction at 10 microns using a CO₂ lidar 15 p2201 A83-34464

A study of the CO₂-GDL gain behind wedge-shaped and contoured nozzles. II - Measurement results. Comparison of experimental data with calculations 15 p2169 A83-34474

Miniature 250 Hz, TEA CO₂ laser using H₂ buffered gas mixture 15 p2170 A83-35251

Catalysed recombination of CO and O₂ in sealed CO₂ TEA laser gases at temperatures down to -27 C 15 p2170 A83-35254

Numerical analysis of an optically pumped D₂O far infrared laser 16 p2358 A83-35430

Theory of transient self-focusing of a CO₂ laser pulse in a cold dense plasma 16 p2358 A83-35432

Density and temperature variations in pulsed discharge lasers 16 p2358 A83-35453

Realization of 90- and 180 degree hybrids for optical frequencies 16 p2411 A83-35520

Electrooptic interaction in oversized waveguide modulators 16 p2315 A83-35521

Scaling laws for the intrapulse frequency stability of an injection mode selected TEA CO₂ laser 16 p2360 A83-35961

Cathode materials for sealed CO₂ waveguide lasers 16 p2360 A83-35962

Mode selection and frequency tuning by injection in pulsed TEA-CO₂ lasers 16 p2360 A83-35963

High-power, long-pulse CO₂ laser transversely excited by a damped oscillating discharge through dielectric electrodes 17 p2513 A83-36998

Blackbody-pumped CO₂ laser experiment [AIAA PAPER 83-1701] 17 p2513 A83-37198

An experimental study of downstream mixing CO₂ laser [AIAA PAPER 83-1703] 17 p2513 A83-37200

A new stabilization system for optically pumped CW far infrared lasers 17 p2514 A83-37752

Calculation of optimal lasing regimes for CW supersonic electroionization CO lasers 18 p2692 A83-39516

The effect of diffusion on the energy characteristics of molecular lasers 18 p2693 A83-39525

Molecular gas lasers: Physics and application 18 p2693 A83-39983

Ignition of composite solid propellant at subatmospheric pressures 18 p2673 A83-40313

A preliminary study of a retroreflective mirror resonator 18 p2693 A83-40345

Operation of an inductively ballasted helical TE-CO₂ laser 19 p2850 A83-40734

Recording of interferograms on normal high resolution plates using a CO₂ laser at 10.6 microns 19 p2847 A83-41103

Observation of period doubling in an all-optical resonator containing NH₃ gas 19 p2900 A83-41156

Accelerated precipitation of water fogs due to acoustic action of a CO₂ laser pulse 20 p3028 A83-42278

Yield of excited iodine atoms during many-photon dissociation of CF₃I and (CF₃)₃CI 20 p2993 A83-42287

Trends in the development of the application of CO₂-lasers in Materials Technology 20 p2999 A83-43627

A selfsustained discharge multiatmospheric CO₂ laser with electron-beam preionization 20 p2995 A83-43633

Formation of free fluorine atoms by laser-collisional initiation of the CH₃F + F₂ reaction 20 p2997 A83-43789

Investigation of the optical homogeneity of the active medium of an atmospheric-pressure electron-beam-controlled CO₂ laser during stimulated emission 20 p2997 A83-43792

Calculation of the maximum output power of a continuous-flow CO₂ laser 20 p2997 A83-43794

Chemical laser amplifier using a photon-branched reaction in an aerosol medium 20 p2998 A83-43808

Maximum input energy for an externally sustained CO₂ laser discharge 21 p3143 A83-44144

CO₂ laser rangefinders 21 p3090 A83-44812

Improved welding penetration of a 10-kW industrial laser 21 p3146 A83-45480

Degenerate four-wave mixing due to intervalence band transition in p-type mercury cadmium telluride 21 p3209 A83-45495

Forward CW CO₂-laser scattering on a high density plasma column 22 p3362 A83-46267

Reliability factors in gas lasers 22 p3296 A83-46612

Polycrystalline KRS-5 infrared fibers for power transmission 22 p3357 A83-46622

Carbon dioxide waveguide laser design for maximum output power at specified frequency offset 22 p3299 A83-46747

Atmospheric-pressure electroionization CO₂ laser using CO₂-N₂-H₂O mixtures 22 p3300 A83-46785

Spectrophone stabilization and offset tuning of a carbon dioxide waveguide laser 22 p3300 A83-46816

Carbon dioxide laser-induced fast signals from silicon photodiodes 22 p3301 A83-46826

Fine tuning lasers by means of an intracavity interferometer enclosing an absorbing gas 23 p3461 A83-47620

High-speed, low-cost laser-triggered plasma shutter 23 p3461 A83-47644

Acoustic wave calibration for CO₂ laser scattering experiments 23 p3461 A83-47647

Airborne remote sensing measurements with a pulsed CO₂ DIAL system 23 p3455 A83-47767

Remote sensing of hydrazine compounds using a dual mini-TEA CO₂ laser DIAL system --- differential-absorption LIDAR 23 p3456 A83-47769

Laser remote sensing measurements of atmospheric species and natural target reflectivities 23 p3456 A83-47772

Airborne CO₂ laser heterodyne sensor for monitoring regional ozone distributions 23 p3456 A83-47773

Review of NDRE remote sensing program and development of high pressure RF excited CO₂ waveguide lasers 23 p3462 A83-47799

Tactical and atmospheric coherent laser radar technology 23 p3462 A83-47806

Simultaneous measurement of magnetic field direction and ion temperature in a plasma by collective scattering with a CO₂ laser 24 p3630 A83-48786

Properties of the corona generated by the incidence of intense CO₂ laser pulses on spherical targets 24 p3631 A83-48820

High-power, subpicosecond 10-micron pulse generation 24 p3587 A83-48851

Optimization of corona-discharge photoionization sources for CO₂ lasers 24 p3587 A83-48909

Several generation parameters of a CO₂ gasdynamic laser with a high-temperature regenerative-heat-transfer heater of the working gas 24 p3588 A83-48936

Effect of a CO₂ laser pulse on transmission through fog at visible and IR wavelengths 24 p3588 A83-49003

Polarization of reflected 10.6-microns radiation from sublimed sulfur targets --- of carbon dioxide lidar 24 p3582 A83-49013

A study of the emission spectrum of a TEA CO₂ laser with an intracavity absorber 24 p3588 A83-49048

Electric-discharge CO₂-laser based on products of the reaction of oxygen and carbon 24 p3588 A83-49055

Thermal defocusing (LIMP) in stable CO₂ resonators 24 p3589 A83-49835

CARBON DIOXIDE REMOVAL

The characterization of carbon dioxide absorbing agents for life support equipment; Proceedings of the Winter Annual Meeting, Phoenix, AZ, November 14-19, 1982 11 p1644 A83-28329

Carbon dioxide scrubbing materials in life support equipment 11 p1644 A83-28330

Review of potassium superoxide characteristics and applications 11 p1644 A83-28331

Air revitalization compounds - A literature survey 11 p1644 A83-28332

Chemical and physical factors affecting the absorption capability of calcium hydroxide based carbon dioxide absorbents 11 p1645 A83-28333

Carbon dioxide absorption dynamics of lithium hydroxide 11 p1645 A83-28334

Lithium hydroxide as a CO₂ scrubber in closed circuit breathing apparatus 11 p1645 A83-28335

A theoretical model of CO₂ absorption in a mixed alkali bed under hyperbaric conditions 11 p1645 A83-28336

Model for the absorption rate of gaseous CO₂ by solid hydroxides 11 p1645 A83-28337

Absorption of carbon dioxide by solid hydroxide sorbent beds in closed-loop atmospheric revitalization system 11 p1645 A83-28338

Applications of permeable membranes as carbon dioxide scrubbers 11 p1645 A83-28339

An integrated regenerative air revitalization system for spacecraft [SAE PAPER 820846] 13 p1907 A83-30937

A regenerable solid amine CO₂ concentrator for space station [SAE PAPER 820847] 13 p1907 A83-30938

CO₂ concentration using a molten carbonate electrochemical cell [SAE PAPER 820874] 13 p1907 A83-30947

CARBON DIOXIDE TENSION

NT HYPERCAPNIA

NT HYPOCAPNIA

The gas composition and the acid-base state of the blood in twins when breathing a hypoxic gas mixture 01 p0082 A83-10492

The characteristics of the CO₂ balance during physical loads in healthy untrained individuals 08 p1146 A83-22778

Possible limits on the composition of the Archaean Ocean 13 p1874 A83-30221

Effect of glycogen depletion on the ventilatory response to exercise 13 p1903 A83-30474

Time course of posthyperventilation breathing in humans depends on alveolar CO₂ tension 13 p1903 A83-30491

Acid-base curve and alignment nomograms for swine blood 13 p1898 A83-30500

Reversal of arterial-to-expired CO₂ partial pressure differences during rebreathing in goats 22 p3345 A83-45987

Influence of body CO₂ stores on ventilatory dynamics during exercise 22 p3347 A83-45988

CARBON DISULFIDE

Photodissociation yields of CS₂ at 1060-1520 A 06 p0807 A83-18042

The spectral characteristics and nature of the radiation emitted by explosions in an enclosed region. II - Explosions of mixtures of CS₂/O₂ --- 1/4 07 p0880 A83-19962

Study of sulfur-containing molecules in the EUV region. III Photoexcitation of CS₂ 09 p1343 A83-25134

- Response of liquid carbon disulfide to shock compression Equation of state at normal and high densities 20 p3055 A83-42638
- CARBON FIBER REINFORCED PLASTICS**
- Bursting and bulging of carbon fiber composite discs 01 p0022 A83-10243
- Prediction of the stress-strain curve of a short-fibre reinforced thermoplastic 02 p0149 A83-11662
- A production engineers view of advanced composite materials 02 p0149 A83-11800
- Toughening epoxy resin matrix for glass and carbon fiber composites 02 p0149 A83-11852
- The effect of physical aging on the time-dependent properties of carbon-fiber-reinforced epoxy composites 02 p0150 A83-12064
- The effects of humidity on fatigue due to shear stress in unidirectional composites - Attempts at interpretation and a summing up [ONERA, TP NO. 1982-98] 03 p0292 A83-14546
- Behaviour of fibers in carbon reinforced thermoplastic polymers during sliding wear 05 p0611 A83-17102
- Joining of components moulded in carbon fibre-reinforced thermoplastics 06 p0724 A83-17963
- Temperature dependence of elastic constants of CFRP 06 p0724 A83-17965
- Calculating the elastic characteristics of a unidirectional fiber composite by the method of sections 06 p0725 A83-18501
- The interlayer strength criteria for carbon composites under cyclic loads 06 p0725 A83-18502
- Length distribution of ruptured fibers in unidirectional composites 06 p0725 A83-18516
- An improved high temperature carbon fiber finish for polyimide composites 07 p0875 A83-20428
- A new high impact resin system for advanced composites with 300 F /150 C/ properties 07 p0875 A83-20429
- High temperature thermoplastic matrices for advanced composites 07 p0876 A83-20477
- Tensile fatigue of carbon fiber reinforced plastics 07 p0877 A83-20924
- Hygrothermal aging effects on the micromechanisms of crack extension in glass fibre and carbon fiber composites 08 p1053 A83-21679
- Study on composite flywheels for energy storage 08 p1131 A83-22701
- Effects of processing on the mechanical properties of carbon short-fiber reinforced polycarbonate 08 p1055 A83-22718
- Development of solvent insensitive graphite reinforced thermoplastic composites 09 p1221 A83-23609
- Adhesive stress-strain properties relative to fatigue life of titanium bonded to graphite reinforced plastic 09 p1237 A83-23616
- An analysis of delamination in drilling composite materials 09 p1273 A83-23640
- Fracture tough composites - The effect of toughened matrices on the mechanical performance of carbon fiber reinforced laminates 09 p1222 A83-23642
- Damageability evaluation of organic and carbon fiber plastics by nondestructive technique 09 p1224 A83-23947
- Design and manufacture of the Tornado carbon-fiber reinforced plastics taileron [DGLR PAPER 82-038] 09 p1203 A83-24162
- A corrugated core theory of sandwich plates 09 p1280 A83-24512
- Composite materials - Some recent developments 10 p1389 A83-26122
- A Monte Carlo simulation of the strength of laminated hybrid composites 10 p1389 A83-26965
- Bending of orthotropic beams which are nonlinear in shear and compression 11 p1593 A83-27465
- A study of the strength characteristics of the carbon composite KJU-3L 11 p1544 A83-28483
- A morphological study of the fracture mechanisms of unidirectionally reinforced thermoplastics 11 p1544 A83-28512
- Temperature dependent dynamic shear properties of CFRP 12 p1710 A83-29719
- Carbon/epoxy laminates under combined fastener bearing and tension bypass loading [AIAA 83-0967] 12 p1710 A83-29778
- An accumulated-damage fracture criterion for a three-component layered composite 13 p1865 A83-30055
- The effect of the molding pressure on the overall physicomachanical properties of carbon composites 13 p1815 A83-30061
- Fracture toughness of unidirectional glass/carbon hybrid composites 13 p1816 A83-31616
- Distributions of fatigue life and fatigue strength in notched specimens of a carbon eight-harness-satin laminate 13 p1816 A83-31621
- Control of the material properties and structural application of carbon fibre reinforced plastics [AIAA PAPER 83-0859] 14 p1986 A83-32790
- Environmental exposure of carbon/epoxy composite material systems 14 p1987 A83-33123
- The effect of open-space exposure on the physicomachanical properties of a carbon composite 16 p2323 A83-35504
- The fracture of composites with allowance for the effects of temperature and humidity 16 p2323 A83-35508
- The fracture mechanism of carbon and boron composites in interlayer shear 16 p2323 A83-35509
- Electroplated carbon/graphite fibers 16 p2325 A83-36900
- Microstructure (microtexture), Structure and surface studies of some carbon fibers 18 p2650 A83-40133
- How the interface controls the properties of fibre composites 18 p2651 A83-40143
- The effect of fibre surface treatment on the compressive strength of CFRP laminates 18 p2651 A83-40145
- Hygrothermal effects on CFRP bonded systems 18 p2652 A83-40157
- Strength tests of CFRP joint assembly models for tailplane structure 18 p2703 A83-40159
- Analysis of elastic anisotropy in CFRP laminate beam 18 p2652 A83-40164
- Vibration characteristics of laminated composite plates 18 p2703 A83-40170
- The compressive behaviour of carbon fibre reinforced plastic 18 p2653 A83-40171
- The mechanical properties of carbon fiber SMC --- Sheet Molding Compound 18 p2653 A83-40178
- Effects of carbon fiber strain and resin characteristics on optimum composite performance 18 p2653 A83-40181
- A study on fracture mechanism of unidirectional fibrous composites 18 p2654 A83-40190
- On fracture behavior during crack propagation in carbon-fiber composites 18 p2654 A83-40192
- Distributions of fatigue life and fatigue strength in notched specimens of a carbon eight-harness-satin laminate 18 p2655 A83-40201
- Fatigue behaviour of carbon fiber reinforced epoxy composite materials with edge notch 18 p2655 A83-40202
- The modelling of failure processes and the role of the matrix in the failure of carbon fibre reinforced epoxy resin 18 p2655 A83-40208
- Creep behaviour of carbon-epoxy (+ or - 45 deg)2s laminates 18 p2655 A83-40209
- Effect of defect on the behaviour of composites 18 p2656 A83-40215
- The initiation of fracture in fiber-composites at elevated loading rates 18 p2656 A83-40217
- Impact behaviour of quasi-isotropic CFRP laminate 18 p2656 A83-40220
- Performance of carbon fibre reinforced epoxy composites under different environments 18 p2656 A83-40225
- Tapewrapped phenolic composites reinforced with advanced carbon fabrics 18 p2657 A83-40231
- The strength of aligned short-fiber carbon, glass, and hybrid carbon/glass composites 18 p2657 A83-40234
- Statistical aspects of fibre and bundle strength in hybrid composites 18 p2658 A83-40240
- Thickness and stacking sequence effect on the acoustic emission of CFRP 18 p2660 A83-40271
- Fractography of carbon/epoxy angle-ply laminates 18 p2660 A83-40273
- Vibro-punching Kevlar aramid and carbon fiber reinforced composites 18 p2661 A83-40284
- Design, analysis and testing of two concepts for a dimensional stable structure --- composite antenna tower for communication satellites 18 p2662 A83-40289
- A new construction method of carbon fibre hybrid GRP moulds in vacuum forming process 18 p2662 A83-40290
- A new method to determine the bending rigidities of anisotropic plates 18 p2662 A83-40293
- On the accelerated ageing of CFRP 20 p2946 A83-42802
- The effect of moisture on the shear properties of carbon fibre composites 20 p2947 A83-42804
- Effect of moisture on the notch sensitivity of carbon fibre composites 20 p2947 A83-42805
- The environmental degradation of notched CFRP in compression 20 p2947 A83-42806
- The effect of composite prebond moisture on adhesive-bonded CFRP-CFRP joints 20 p2947 A83-42807
- The in-service flight testing of some carbon fibre-reinforced plastic components 20 p2933 A83-42808
- Environmental resistance of carbon fibre-reinforced polyether etherketone 20 p2947 A83-42810
- The effects of environmental exposure on the fatigue behaviour of CFRP laminates 20 p2947 A83-42813
- Post-impact fatigue performance of carbon fibre laminates with non-woven and mixed-woven layers 20 p2948 A83-42814
- An experimental study of the effect of prestressed loose carbon strands on composite strength 20 p2948 A83-43142
- Measurement of curvature and bending stiffness of thin carbon composite plates using holographic interferometry 21 p3155 A83-44829
- Estimation of the extent of damage in reinforced composites under mechanical loading 21 p3163 A83-45320
- Synthetic aperture radar antenna from CFRP 22 p3259 A83-46178
- Long-term operational testing of CFRP spoilers 23 p3391 A83-47205
- Method of construction and fabrication procedures for the A300-rudder unit, using a carbon-fiber type of construction 23 p3391 A83-47211
- An approach to the evaluation of the impact resistance of a carbon composite 23 p3428 A83-48436
- In-plane and interlaminar shear fatigue characterization of unidirectional GFRP and CFRP, including moisture effects [ONERA, TP NO. 1983-109] 24 p3553 A83-49420
- CARBON FIBERS**
- Role of fibre surface-matrix combination in carbon fibre reinforced epoxy composites 02 p0149 A83-11669
- Carbon fibre-reinforced silicon nitride composite 04 p0455 A83-15990
- Metallic conductivity and air stability in copper chloride intercalated carbon fibers 04 p0473 A83-16095
- Oxidative stabilization of oriented acrylic fibres - Morphological rearrangements 05 p0619 A83-17561
- Thermal expansion of fibers in the temperature range 20-470 K 06 p0725 A83-18514
- Plastic composites for electromagnetic interference shielding applications 08 p1055 A83-22717
- Status and recent developments in Celion carbon fibers 09 p1221 A83-23614
- The preparation and properties of mesophase pitch-based carbon fibers 09 p1222 A83-23643
- Flaws and defects of structural carbon fibers 09 p1238 A83-23950
- The effects of pressure on the carbonization of pitch and pitch/carbon fiber composites 12 p1709 A83-29503
- The carbonization of blends of pitches and resins to produce anisotropic carbon and the effects of pressure 12 p1712 A83-29504
- Reproducible processing and reliable repeatability in carbon fiber composites 12 p1710 A83-29715
- Carbon fibers produced by pyrolysis of natural gas in stainless steel tubes 13 p1825 A83-30337
- Effect of the structure on the strength of the fibrous composite aluminum-carbon strip 13 p1816 A83-31217
- Application of the grainning process for the fabrication of chopped carbon fiber-aluminum composite 13 p1816 A83-31602
- Aluminum-matrix composites reinforced with carbon fibers 14 p1986 A83-32146
- Thermomechanical characterization of graphite/polyimide composites 14 p1987 A83-33117
- Studies of fabrication of carbon fiber reinforced aluminum matrix composite 16 p2324 A83-35606
- ACM reinforcement fiber production and its application in Japan 18 p2650 A83-40132
- Microstructure (microtexture), Structure and surface studies of some carbon fibers 18 p2650 A83-40133
- Residual stress in high modulus carbon fibers 18 p2650 A83-40134
- Analysis of the elastoplastic behavior of (0 deg/90 deg) and + Theta/-Theta) bidirectionally fiber-reinforced ductile matrix composites in uniaxial loading 18 p2653 A83-40174
- New composite materials with a carbon-titanium carbide hybrid matrix for high temperature application 18 p2658 A83-40245
- Interface interaction in aluminum-carbon system 18 p2658 A83-40247
- Formation of intermetallic compound in composite materials 18 p2658 A83-40248
- Prospects of metal nitride intermediate layer for FRM 18 p2659 A83-40251
- Fabrication of carbon fiber reinforced aluminum composites by roll diffusion bonding method 18 p2659 A83-40262
- Tribological behavior of carbon fiber reinforced metals 18 p2660 A83-40267
- Lower-curing-temperature PMR polyimides 19 p2823 A83-40923

Surface analyses of carbon fibers produced from polyacrylonitrile fibers at low carbonization temperatures
19 p2824 A83-41860

An experimental study of the effect of prestressed loose carbon strands on composite strength
20 p2948 A83-43142

Strain modulation measurements of stiffening effects in carbon fibers
23 p3454 A83-47649

On the relation between Young's modulus and orientation in carbon fibres
24 p3553 A83-48898

Protective coatings for carbon-fiber materials
24 p3553 A83-49091

A study of the deformation properties of an isotropic carbon material at elevated temperatures
24 p3554 A83-49666

CARBON ISOTOPES

NT CARBON 12
NT CARBON 13
NT CARBON 14

Isotopic anomalies of H2 and C in the peat from the Tunguska meteorite impact area
02 p0263 A83-11960

Carbon components and their isotopic compositions in the Allende meteorite
04 p0562 A83-15353

The variable carbon isotopic composition of type 3 ordinary chondrites
04 p0562 A83-15354

Fourier spectroscopy of the $^{12}\text{C}/^{13}\text{C}$ and $^{13}\text{C}/^{12}\text{C}$ Phillips system
09 p1361 A83-24519

The C-12/C-13 ratio in Jupiter from the Voyager infrared investigation
10 p1518 A83-25515

Further analysis of the possible effects of isotope-selective photodissociation on interstellar carbon monoxide
10 p1513 A83-26715

Spectral characteristics of carbon monoxide laser with different isotopic compositions
14 p2023 A83-31912

A high-precision mass spectrometer for stable carbon isotope analysis at the nanogram level
15 p2166 A83-35255

Preparation of nanogram quantities of deuteromethane for stable carbon isotope analysis -- using mass spectrometer
15 p2166 A83-35256

Carbon isotopic variation within individual diamonds
17 p2545 A83-38604

C-13/C-12 records in Northern Hemispheric trees during the past 500 years - Anthropogenic impact and climatic superpositions
20 p3022 A83-42866

A method for the identification and elimination of contamination during carbon isotopic analyses of extraterrestrial samples
22 p3385 A83-46375

CARBON MONOXIDE

The utilization of carbon monoxide by anaerobic bacteria
01 p0078 A83-10422

Rotational excitation of N2, CO and H2O by low-energy electron collisions
01 p0105 A83-10858

Certain biochemical indices in healthy humans under the effect of high concentrations of carbon monoxide and carbon dioxide in a sealed chamber
01 p0085 A83-11403

Combustion characteristics of hydrogen-carbon monoxide based gaseous fuels
01 p0023 A83-11491

Measurements of intensities and self- and foreign-gas-broadened half-widths of spectral lines in the CO fundamental band
02 p0234 A83-11574

Physical conditions and carbon monoxide abundance in the dark cloud B5
02 p0251 A83-11586

Energetic activity in a star-forming molecular cloud core - A disk constrained bipolar outflow in NGC 2071
02 p0251 A83-11590

Detection of bipolar CO outflow in Orion
02 p0253 A83-11617

Observations of C-12O/J=2-1/ emission in the Large and Small Magellanic Clouds
02 p0255 A83-12112

Conversion from $^{12}\text{C}/^{12}\text{O}$ integrated intensity at 2.6 millimeter wavelength to hydrogen column density -- for probing interstellar medium
02 p0256 A83-12122

Mathematical modeling of homogeneous-heterogeneous reactions in monolithic catalysts
02 p0152 A83-13093

The Bubble Nebula - Far-infrared and radio molecular observations of NGC 7635
03 p0412 A83-13304

Carbon monoxide measurements in the troposphere
03 p0355 A83-13351

433 micron laser heterodyne observations of galactic CO from Mauna Kea
03 p0405 A83-13464

Noninvasive cardiac output determination using inhaled oxygen-15-labeled carbon dioxide
03 p0378 A83-13577

The relationship between carbon monoxide abundance and visual extinction in interstellar clouds
03 p0423 A83-14192

Loss of CO/ + / ions by reaction with H2 in OMC-1
03 p0428 A83-14760

Intensities, half-widths and shapes of spectral lines in the fundamental band of CO at low temperatures
04 p0534 A83-16436

Long contact effect between active nitrogen and carbon monoxide - N2 dissociation to N/S-4/
05 p0613 A83-17872

Theory of rotational branch structure with application to N2 and CO
06 p0807 A83-18041

Low-energy electron scattering from CO. III - Analytic method for outer region in frame-transformation theory
06 p0808 A83-18045

CO J = 3 - 2 and submillimetre continuum observations of two molecular outflow sources
06 p0825 A83-18091

CO J = 2 - 1 observations of a sample of star-formation regions in the southern galactic plane
06 p0827 A83-18173

A search for the J = 1-0 transition of $^{13}\text{C}/^{14}\text{O}$ --- and Galactic abundance ratios for carbon isotopes
06 p0827 A83-18174

Analysis of absorption spectra of 11 quasars with Z sub e greater than 2
06 p0837 A83-19206

Dense cores in dark clouds. I - CO observations and column densities of high-extinction regions
06 p0844 A83-19493

CO observations of the supernova remnant G78.2 + 2.1
07 p1010 A83-19862

Curves for analysis of the two lowest rotational transitions of carbon monoxide using the large velocity gradient radiative transfer model
07 p1013 A83-20133

Arid soils as a source of atmospheric carbon monoxide
07 p0959 A83-20198

Highly excited J = 16 to 15/ rotational transitions of CO, at 162.8 microns, in the Orion cloud
07 p1019 A83-20955

Excitation energy dependence in the photoemission satellite structures in solid CO and N2
07 p0991 A83-21193

Carbon monoxide in the Martian atmosphere
08 p1188 A83-22059

Photodissociation of HCHO in air - CO and H2 quantum yields at 220 and 300 K
08 p1163 A83-22216

CO emission in directions of some millimeter wavelength continuum sources
08 p1182 A83-23045

Molecular gas in the W33 region
08 p1183 A83-23047

The high-velocity molecular flows near young stellar objects
08 p1183 A83-23052

Interactions between pre-main-sequence objects and molecular clouds. I - Elias 1-12
08 p1183 A83-23054

Semiclassical vibrational spectra for diatomic molecules - Application to HF, CO, and NO
09 p1342 A83-24131

Carbon monoxide mixing ratio inference from gas filter radiometer data
09 p1306 A83-24450

Direct measurements of N2 broadened linewidths in the CO fundamental at low temperatures
09 p1342 A83-24639

Potential energy surface for the study of inelastic collisions between nonrigid CO and H2
09 p1343 A83-25135

The possible role of heterogeneous aerosol processes in the chemistry of CH4 and CO in the troposphere
09 p1299 A83-25204

Comparison of photon stimulated dissociation of gas phase and chemisorbed CO
10 p1389 A83-25556

Vibrational relaxation of gaseous CO/v = 1/ and N2/v = 1/ from 300 K to liquid temperatures - A comparison with liquid state relaxation
10 p1389 A83-25563

Collision dynamical information from pressure broadening measurements - Application to carbon monoxide
10 p1479 A83-25564

J = 2-1 CO observations of molecular clouds with high-velocity gas - Evidence for clumpy outflows
10 p1504 A83-25728

CO + O chemiluminescence - Rate coefficient and spectral distribution
10 p1480 A83-26181

On vibrational excitations of interstellar molecules
10 p1509 A83-26370

CO emission and the optical disk in the giant Sc galaxy M101
10 p1511 A83-26405

On the formation of HCO/ + / and HOC/ + / from the reaction between H3/ + / and CO
10 p1392 A83-26461

Further analysis of the possible effects of isotope-selective photodissociation on interstellar carbon monoxide
10 p1513 A83-26715

CO emission in the outer Galaxy between longitudes 50 deg and 72 deg
10 p1516 A83-26753

Gas-kinetic magnetic resonance in N2 and CO gases
11 p1654 A83-28062

A theoretical study on the mechanism of electronic to vibrational energy transfer in Hg/3P/ + CO
11 p1655 A83-28529

Monte Carlo calculation of emitted radiation in the vibrational-rotational CO band from a cylindrical supersonic molecular-gas jet in the absence of local thermodynamic equilibrium
11 p1584 A83-28549

Observations of the 1-0 transition of CO towards southern HII regions
13 p1946 A83-30387

Correlative nature of ozone and carbon monoxide in the troposphere - Implications for the tropospheric ozone budget
13 p1876 A83-30881

A general circulation model study of atmospheric carbon monoxide
13 p1876 A83-30884

Spectroscopic measurements of carbon monoxide in the stratosphere
13 p1877 A83-30890

Excimer laser photolysis studies of translational-to-vibrational energy transfer in collisions of H and D atoms with CO
13 p1916 A83-30952

[AD-A129931]
Cluster studies of CO adsorption. III - CO on small Cu clusters
13 p1817 A83-30965

Pressure broadening of CO infrared lines perturbed by H2 and He
13 p1916 A83-30968

Fluorescence excitation of CO in comets
13 p1940 A83-31439

High-density gas associated with 'molecular jets' - NGC 1333 and NGC 2071
13 p1953 A83-31449

Electron-impact excitation of the Cameron system (a(3)pi yields x(1) Sigma) transition of CO
13 p1917 A83-31534

Spectroscopic measurements of the total content of CO, CH4, and N2O in the atmosphere in the Arctic region
14 p2053 A83-32861

A simple model for carbon monoxide in laminar and turbulent hydrocarbon diffusion flames
14 p1990 A83-32939

Warm H I halos around molecular clouds
15 p2257 A83-34099

CO observations of the galaxies in the Leo triplet - NGC 3623, NGC 3627, and NGC 3628
15 p2267 A83-34624

The structure of bright-rimmed molecular clouds
15 p2267 A83-34625

Catalysed recombination of CO and O2 in sealed CO2 TEA laser gases at temperatures down to -27 C
15 p2170 A83-35254

Inner-shell photoionisation in molecules - The carbon monoxide case
16 p2409 A83-35332

Titan - Discovery of carbon monoxide in its atmosphere
16 p2437 A83-36016

Observation of a new electronic state of carbon monoxide using LIF on highly vibrationally excited CO(X 1Sigma +)
16 p2410 A83-36517

CO adsorption and the optical properties of interstellar grains
16 p2428 A83-36529

On the spiral structure in the galactic distribution of CO clouds
16 p2428 A83-36541

Intensity, transition moment, and bandshapes for the second overtone of compressed CO
16 p2410 A83-36796

Drastic reduction of adsorption of CO and H2 on (111)-type Pd layers
16 p2328 A83-36990

Spatially resolved tunable diode-laser absorption measurements of CO using optical stark shifting
17 p2485 A83-37747

Far-infrared and CO observations of NGC 6357 and regions surrounding NGC 6357 and NGC 6334
17 p2591 A83-37784

Regions of low molecular column density near the galactic plane
17 p2602 A83-37829

Metastable excitation measurements in CO and N2 by high-resolution electron impact, using a low work function detector
17 p2579 A83-38368

Infrared and microwave fluorescence of carbon monoxide in comets
17 p2608 A83-38412

Dissociation of CO2(2+) ions into CO(+) and O(+) fragments
17 p2486 A83-38469

CO 1-0 band isotopic lines as intensity standards
18 p2742 A83-39176

Evidence for heterogeneous mechanisms in the active nitrogen-CO reaction
18 p2664 A83-39178

The distribution of molecular clouds in the Galaxy
18 p2769 A83-39645

(C-13)O in the galactic plane - The cloud-to-cloud velocity dispersion in the inner galaxy
18 p2769 A83-39647

How confidently do we know the CO rotation curve of the outer Galaxy?
18 p2769 A83-39648

CO(J = 2-1) observations of galactic HII-regions
18 p2769 A83-39650

Distribution of CO in the southern Milky Way
18 p2769 A83-39651

Molecular clouds in Orion and Monoceros
18 p2771 A83-39701

CO and shocks related to the evolution of the Orion Nebula
18 p2771 A83-39704

Millimeter-wavelength lines from the Orion plateau source
18 p2772 A83-39709

Far-infrared CO line emission from Orion-KL
18 p2772 A83-39712

Two micron observations of C-12O and C-13O in the red giant sources IRS 7, IRS 12, and IRS 19
19 p2912 A83-40688

Does CO condense on dust in molecular clouds?
19 p2914 A83-40718

Far-infrared and CO observations of Cep F - Implications for star formation in Cepheus OB3
20 p3064 A83-42196

Photochemical reactions of water and carbon monoxide in earth's primitive atmosphere
20 p3036 A83-42847

Carbon monoxide emission from planetary nebulae and their possible precursors
20 p3071 A83-43054

Lineshifts in the first overtone band of CO self-perturbed and perturbed by N2 at 298, 193, and 133 K
20 p3045 A83-43581

Variability of carbon monoxide in the Mars atmosphere
21 p3239 A83-44089

Millimeter wave ground-based heterodyne detection of two minority atmospheric constituents
21 p3171 A83-44325

Molecules in celestial objects. IV - IUE observation of CO lines towards Be stars with low reddening
22 p3379 A83-46555

Electron energy-loss spectroscopy of carbon monoxide. II - The energy region 11 to 20 eV
23 p3506 A83-48581

Measurements of the concentration of carbon monoxide in the atmospheric surface layer using tunable diode lasers
24 p3583 A83-49110

The CO rotation curve of the Milky Way - Accuracy and implications
24 p3654 A83-49209

Oscillatory regime of the gas-phase oxidation of carbon monoxide
24 p3554 A83-49537

The formation of carbon monoxide during turbulent diffusion combustion --- for aircraft gas turbine combustion chambers
24 p3569 A83-49769

CARBON MONOXIDE LASERS

Vacuum ultraviolet generation in phase matched carbon monoxide
02 p0185 A83-12403

Continuous-wave reaction-product chemical lasers /review/
05 p0648 A83-17038

Carbon monoxide laser with selective and nonselective resonators
05 p0648 A83-17048

Time-resolved Thomson-scattering measurements of ion fluctuations driven by stimulated Brillouin scattering
07 p0998 A83-20816

High gain CO chemical laser produced in a shock tunnel
10 p1429 A83-26168

Experimental investigation of the optimum specific input energy on a subsonic CO EDL --- Electric Discharge Laser
11 p1580 A83-27577

Calculation of the probabilities of vibrational-vibrational transfer between isotopic modifications of CO molecules
11 p1584 A83-28531

New applications of CO lasers
13 p1851 A83-30823

Spectral characteristics of carbon monoxide laser with different isotopic compositions
14 p2023 A83-31912

Tunable sealed-off CW CO laser at room temperature
14 p2023 A83-31950

Continuous-wave industrial electron-beam-controlled CO laser of 10 kW output power
15 p2168 A83-33976

Absorption measurements of H2O at high temperatures using a CO laser
16 p2328 A83-36795

Investigation of the power stability of a CW carbon monoxide laser
20 p2997 A83-43793

CARBON MONOXIDE POISONING

Evidence of genetic differences in acute hypoxia survival
07 p0974 A83-20781

Successful reversal of presumed carbon monoxide-induced semicoma
18 p2734 A83-40362

Carbon monoxide and human performance in a single and dual task methodology
21 p3187 A83-43993

CARBON STARS

A possible CH subdwarf
01 p0118 A83-11498

Numerical studies of nonispherical carbon combustion models --- of stars during nuclear burning
02 p0253 A83-11618

Strong CN stars in the globular cluster NGC 1851
02 p0248 A83-12910

The carbon and nitrogen abundances in WN and WC Wolf-Rayet stars
03 p0412 A83-13306

The structure of the carbon-burning deflagration front in a degenerate stellar core
03 p0418 A83-13878

A comparison of observed and theoretical luminosity functions of carbon stars and late M giants
04 p0553 A83-15627

On the formation of carbon star characteristics and the production of neutron-rich isotopes in asymptotic giant branch stars of small core mass
04 p0555 A83-15651

Fourier spectroscopy of the C-12C-13 and /C-13/2 Ballik-Ramsay system --- in cool carbon star atmospheres
05 p0700 A83-17023

Carbon stars in clusters in the galaxy and the Magellanic Clouds
06 p0826 A83-18159

The eclipsing binary CV Serpentis - U, B, V, R photometry and properties of the Wolf-Rayet component
06 p0831 A83-18800

A new search technique for M and C stars
06 p0820 A83-18862

Carbon stars in Local Group galaxies
06 p0839 A83-19274

Radiative transfer in dust clouds. III - Circumstellar dust shells around late M giants and supergiants. IV - Circumstellar dust shells around carbon stars
07 p1018 A83-20953

Shell ejection from the variable carbon star HV 2379
07 p1019 A83-20956

Carbon-oxygen white dwarf presupernova models
08 p1177 A83-21836

The ultraviolet spectra of three N-type carbon stars
08 p1183 A83-23060

Does a 2,200 A hump observed in an artificial carbonaceous composite account for UV interstellar extinction
08 p1187 A83-23282

A faint carbon star near the north galactic pole
09 p1357 A83-23734

Near infrared spectroscopy and infrared photometry of a new WC9 star
10 p1499 A83-25367

Accurate radial velocities for carbon stars in Draco and Ursa Minor - The first hint of a dwarf spheroidal mass-to-light ratio
10 p1504 A83-25739

Theoretical study of silicon dicarbide --- in stellar spectra
10 p1510 A83-26398

SIS maser emission from IRC + 10 deg 216
10 p1513 A83-26720

Carbon stars and the seven dwarfs --- stellar evolution in dwarf spheroidal galaxies
10 p1514 A83-26728

The pulsation of carbon Miras
11 p1677 A83-27682

Symbiotic and VV Cephei stars in the Small Magellanic Cloud
11 p1680 A83-28255

A proposed observational test of the temperature structure in hot stellar atmospheres
12 p1796 A83-29496

The dust around the carbon star IRC +10216
13 p1951 A83-31418

Active chromosphere in the carbon star TW Horologium
13 p1954 A83-31578

A deep near infrared objective prism survey for carbon stars toward the galactic center and anticenter
14 p2099 A83-33247

The C2H, C2, and CN electronic absorption bands in the carbon star HD 19557
17 p2605 A83-37918

On the carbon overabundance in the OBC-type stars
17 p2606 A83-38239

Low-frequency excited-carbon radio lines toward Cassiopeia A
17 p2613 A83-38835

Observations of an emission nebula associated with the carbon star UV Aur
19 p2914 A83-40716

The detection of H2 in cool carbon stars
19 p2921 A83-41651

Speckle interferometry of IRC +10216 in the fundamental vibration-rotation lines of CO
20 p3060 A83-43088

The massive WC6+O6-8 spectroscopic binary HD 94305
21 p2327 A83-45547

Notes on the open cluster NGC 1252 with the variable carbon star TW Horologii as a probable member
22 p3373 A83-46402

Slippery evidence on the Galaxy's invisible heavy halo
22 p3380 A83-46577

The distribution of carbon and M-type giants in the Magellanic Clouds
24 p3664 A83-49881

CARBON STEELS

NT LOW CARBON STEELS

Environmental fatigue crack growth analysis based on elastic-plastic fracture mechanics
[ASME PAPER 82-PVP-23] 02 p0196 A83-12769

Quantitative evaluation of fatigue strength of metals containing various small defects or cracks
03 p0338 A83-13197

An evaluation of fretting at small slip amplitudes
05 p0614 A83-17254

Effect of surface residual stresses on the fretting fatigue of a 4130 steel
05 p0615 A83-17264

Structural and microstructural changes in the inner races of ball bearings
09 p1276 A83-23346

Fracture properties of carbon and alloy steels
10 p1392 A83-25320

Characterization and corrosion behavior of duplex-chromized steel for the sulfur container in Na-S cells
10 p1394 A83-25537

CARBON TETRACHLORIDE

The Atmospheric Lifetime Experiment. VI - Results for carbon tetrachloride based on 3 years data
24 p3607 A83-49332

CARBON 12

The effect of heavy ions on mammalian cells. II - The evaluation of the relative biological effectiveness of accelerated ions of helium, carbon, and neon according to cytogenetic parameters
06 p0796 A83-19381

Freezing of a carbon-oxygen white dwarf
16 p2432 A83-36685

Fourier spectroscopy of the (C-12)2, (C-13)2, and (C-12)(C-13) (0-0) Swan bands
17 p2578 A83-37831

CARBON 13

A carbon-13 and proton nuclear magnetic resonance study of some experimental referee broadened-specification /ERBS/ turbine fuels
01 p0028 A83-11482

Interstellar carbon in meteorites
12 p1797 A83-28923

Fourier spectroscopy of the (C-12)2, (C-13)2, and (C-12)(C-13) (0-0) Swan bands
17 p2578 A83-37831

Carbon isotopic variation in spectral type II diamonds
17 p2545 A83-38603

Effect of high atmospheric CO2 concentration on delta C-13 of algae - A possible cause for the average depletion of C-13 in Precambrian reduced carbon
17 p2557 A83-38895

CARBON 14

A search for the J = 1-0 transition of /C-14/O --- and Galactic abundance ratios for carbon isotopes
06 p0827 A83-18174

On the radiocarbon record in banded corals - Exchange parameters and net transport of 14CO2 between atmosphere and surface ocean
09 p1295 A83-24253

The distribution of radioactive carbon-14 of anthropogenic origin between the atmosphere and ocean since 1963
13 p1872 A83-30297

Tracing bomb C-14 in the atmosphere 1962-1980
13 p1876 A83-30878

Some comments on the exchange of CO2 across the air-sea interface
13 p1869 A83-30879

CARBON-CARBON COMPOSITES

The Magnuswirl turbine wheel - The unique solution for the high temperature cruise missile
09 p1274 A83-23647

Analysis of transient thermal responses in a carbon-carbon composite
11 p1543 A83-27459

Stresses during fabrication of cylindrically woven carbon-carbon composites
11 p1543 A83-27462

Nonlinear behavior and failure mechanisms of three-dimensional carbon-carbon composites
11 p1544 A83-27463

Micromechanical modeling of 3D composites with interface failure
11 p1544 A83-27464

Structure in carbon/carbon fibre composites as studied by microscopy and etching with chromic acid
12 p1709 A83-29502

An aerothermochemical model of carbon-carbon composite nozzle recession
12 p1709 A83-29764

[AIAA 83-0910]

Space Shuttle carbon-carbon composite hot structure
12 p1707 A83-29765

[AIAA 83-0913]

Hypervelocity erosion of carbon-carbon composites by laser simulation
14 p1986 A83-32711

[AIAA PAPER 83-1440]

Nonstationary thermal behavior of directional reinforced composites - Limit of application of thermal property homogenization
14 p1986 A83-32725

[AIAA PAPER 83-1471]

Damage and fracture of tridirectional composites
18 p2704 A83-40194

Microstructure and fracture behaviour of unidirectionally reinforced carbon fiber/carbon composites
18 p2661 A83-40282

An inelastic finite element model of 4D carbon-carbon composite
19 p2819 A83-40866

Ultrasonic strength inspection of carbon-carbon composite materials
20 p2948 A83-43561

Acoustic imaging of 3D carbon/carbon billets
22 p3304 A83-46770

CARBONACEOUS CHONDRITES

On neutron-induced and other noble gases in Allende inclusions
02 p0267 A83-12842

An ultra-refractory inclusion from the Ormans carbonaceous chondrite
04 p0558 A83-15301

A new calcium-aluminate from a refractory inclusion in the Leoville carbonaceous chondrite
04 p0558 A83-15302

Carbon components and their isotopic compositions in the Allende meteorite
04 p0562 A83-15353

- Impact induced dehydration of serpentine and the evolution of planetary atmospheres
04 p0564 A83-15374
- Crystallization sequences of Ca-Al-rich inclusions from Allende - An experimental study
04 p0572 A83-16352
- The compositional classification of chondrites. III - Ungrouped carbonaceous chondrites
04 p0572 A83-16354
- Solar-system abundances of the elements
04 p0572 A83-16357
- Presolar matter in meteorites
06 p0849 A83-19458
- Computed tomographic analysis of meteorite inclusions
07 p1029 A83-20298
- Extinct I-129 in C3 chondrites
07 p1035 A83-21334
- The nature and origin of type B1 and B2 Ca-Al-rich inclusions in the Allende meteorite
07 p1036 A83-21336
- Evolution of Ca-Al-rich bodies in the earliest solar system
07 p1036 A83-21337
- A comparative study of the isotopic composition of xenon in the new meteorite Kaydun and in the carbonaceous chondrites Mighei /C2M/, Kainsaz /C30/ and Efremovka /C3V/
08 p1188 A83-22787
- Interstellar carbon in meteorites
12 p1797 A83-28923
- Barium from a mini r-process in supernovae
13 p1951 A83-31429
- Ar-39 recoil losses and presolar ages in Allende inclusions
13 p1962 A83-31589
- Limb darkening of meteorites and asteroids
14 p2112 A83-32605
- Classification of the Allan Hills A77307 meteorite
14 p2112 A83-33066
- Ni isotopic compositions in Allende and other meteorites
16 p2438 A83-36747
- Replacement textures in CAI and implications regarding planetary metamorphism
17 p2623 A83-38851
- Refractory inclusions in the Murchison meteorite
17 p2624 A83-38855
- Amino acids in meteorites
19 p2886 A83-42030
- Discovery of s-process Nd in Allende residue
20 p3078 A83-43093
- Terrestrial fission xenon - Choice of primordial isotopic composition
22 p3329 A83-46376
- Fe-Ni-S-O layer phase in C2M carbonaceous chondrites - A hydrous sulphide?
23 p3529 A83-48079
- Isotopic composition of carbonaceous-chondrite kerogen Evidence for an interstellar origin of organic matter in meteorites
24 p3673 A83-50173
- CARBONACEOUS MATERIALS**
NT PEAT
- Determination of chromium in chromium oxide layers synthesized on the surface of carbonaceous solid substances
08 p1057 A83-22626
- Ablation of carbonaceous materials in a hydrogen-helium arc-jet flow
[AIAA PAPER 83-1561]
14 p1998 A83-32778
- Solar gasification of carbonaceous materials
15 p2190 A83-34069
- Kinetics of SO₂ oxidation over carbonaceous particles in the presence of H₂O, NO₂, NH₃ and O₃
20 p3014 A83-43425
- Ceramics from polymer pyrolysis, opportunities and needs - A materials perspective
[ACS PAPER 13-B-81]
21 p3115 A83-44093
- Catalytically deposited carbon solar selective absorber
22 p3319 A83-46582
- CARBONACEOUS METEORITES**
NT ORGUEIL METEORITE
- Primary igneous carbon in ureilites - Petrological implications
04 p0562 A83-15360
- Shock-metamorphosed carbonaceous material in impactites
05 p0706 A83-17471
- On the asteroidal conductivities as inferred from meteorites
16 p2438 A83-36782
- Interstellar matter in meteorites
18 p2779 A83-39088
- CARBONATES**
NT CALCITE
- NT DOLOMITE (MINERAL)
- NT POLYCARBONATES
- NT SODIUM CARBONATES
- The effect of thickness on the performance of molten carbonate fuel cell cathodes
04 p0506 A83-15869
- The molten carbonate carbon dioxide concentrator - Cathode performance at high CO₂ utilization --- in manned space station cabin atmospheres
07 p0879 A83-19880
- Molten carbonate fuel cell performance model
07 p0953 A83-19884
- Simple porous electrode models for molten carbonate fuel cells
07 p0953 A83-19891

- Porous perovskite electrode as molten carbonate cathode --- in fuel cells
07 p0955 A83-20596
- Coating applications for the molten carbonate fuel cell
10 p1445 A83-25538
- Studies of the reduction of oxygen on gold in molten Li₂CO₃-K₂CO₃ at 650 C
10 p1390 A83-26054
- Composite salt/ceramic media for thermal energy storage applications
11 p1610 A83-27319
- CO₂ concentration using a molten carbonate electrochemical cell
[SAE PAPER 820874]
13 p1907 A83-30947
- Energy dependence of the O(-) transfer reactions of O₃(-) and CO₃(-) with NO and SO₂
14 p1991 A83-33103
- The cycling behaviour and stability of the lithium electrode in propylene carbonate and acetonitrile electrolytes
24 p3600 A83-49950
- Galvanostatic cycling of lithium-titanium disulphide cells in propylene carbonate and propylene carbonate-acetonitrile electrolytes
24 p3558 A83-49951
- CARBONIZATION**
- The carbonization of blends of pitches and resins to produce anisotropic carbon and the effects of pressure
12 p1712 A83-29504
- Surface analyses of carbon fibers produced from polyacrylonitrile fibers at low carbonization temperatures
19 p2824 A83-41860
- CARBONYL COMPOUNDS**
- Fluorescence yields from photodissociation of OCS at 1060-1240 A
07 p0882 A83-21056
- Study of sulfur-containing molecules in the EUV region. II - Photoabsorption cross section of COS
09 p1343 A83-25131
- Separation of lower carbonyl compounds as their 2,4-dinitrophenylhydrazones by high-performance liquid chromatography and analytical application from jet engine exhaust
10 p1388 A83-26087
- Submillimeter-wave laser emission in carbonyl fluoride
11 p1578 A83-27549
- A comparative study of permeable metal powder and fiber materials
11 p1548 A83-27924
- Resonance interactions of carbonyl vibrations in helical polynucleotides
19 p2819 A83-41815
- CARBORANE**
- Synthesis and thermal stability of carborane-containing phosphazenes
23 p3427 A83-47640
- CARBOXYL GROUP**
- Nonenzymatic phosphorylation of acetate by carbamyl phosphate - A model reaction for prebiotic activation of carboxyl groups
19 p2887 A83-42157
- CARBOXYLIC ACIDS**
NT ALANINE
- NT FORMIC ACID
- NT HEXOGENES (TRADEMARK)
- NT LACTIC ACID
- NT TRYPTOPHAN
- Role of succinic acid in chemical evolution
17 p2563 A83-38900
- CARBURIZING**
- Calculation of the depth and hardness of the carburization layer of cylindrical parts --- for aircraft engines
12 p1713 A83-29282
- Oxidation of carburized Hastelloy X
18 p2670 A83-40640
- Modeling of diffusion processes during carburization of alloys --- surface precipitation reactions
20 p2954 A83-42523
- Case depth requirements in carburized gears
20 p2999 A83-43409
- CARCINOGENS**
- An evaluation of the carcinogenic effect of radiation at the cellular level
06 p0796 A83-19380
- The global cycle of benz/a/pyrene
10 p1447 A83-25611
- Reductive destruction of hydrazines as an approach to hazard control
12 p1712 A83-29094
- Radiation safety standards - Space hazards vs. terrestrial hazards
19 p2885 A83-40844
- CARCINOMA**
U CANCER
- CARCINOTRONS**
- A low noise heterodyne receiver for astronomical observations operating around 0.63 mm wavelength
04 p0547 A83-15812
- Experimental investigation of a relativistic carcinotron
09 p1254 A83-23993
- Relativistic electron beam diagnostics and microwave emission in a carcinotron
16 p2347 A83-36927
- CARDIAC AURICLES**
- Mechanism for the appearance of the first extrasystole during short-lived atrial arrhythmia
03 p0376 A83-14366
- Static and dynamic components of the heterometric regulation of myocardial contractions of the auricle and ventricle
04 p0520 A83-15893

CARDIAC VENTRICLES

- The pulmonary circulation and the right ventricular function in experimental models of high-altitude acute edema of the lungs
01 p0080 A83-10543
- A correlation analysis of macroscopic parameters of the pulmonary heart during chronic nonspecific diseases of the lungs
01 p0084 A83-11391
- Refractoriness of heart tissues during a decrease of fast sodium current - A comparison of the atrium and the ventricle
03 p0376 A83-14370
- Static and dynamic components of the heterometric regulation of myocardial contractions of the auricle and ventricle
04 p0520 A83-15893
- The positive effect that reduced venous return has on blood circulation in cases of myocardial infarction
05 p0671 A83-17217
- A method for the quantitative evaluation of the contractile function of the myocardium
05 p0675 A83-17695
- Wolf-Parkinson-White syndrome in young, asymptomatic pilot's applicants
08 p1147 A83-22960
- The importance of determining the systole timing of the left ventricle in the selection of flight personnel
08 p1147 A83-22962
- Central hemodynamics during stepwise increasing water immersion
08 p1149 A83-22984
- The transmembrane potentials of the heart cells of rats during fibrillation induced by a decrease in extracellular sodium
10 p1454 A83-26791
- Physiological assessment of right-side and left-side cardiohemodynamics in patients with hypertension
13 p1906 A83-31395
- Characteristics of the left ventricular blood expulsion phase during arterial hypertension and aortic stenosis
17 p2559 A83-38176
- Hemodynamic indicators, the phasic pattern of the systole of the left and right ventricles of the heart, and the condition of pulmonary blood circulation and microcirculation in patients with hypertension during treatment with adelphane esidrex
17 p2559 A83-38178
- Effect of exercise on left ventricular diastolic filling in athletes and nonathletes
20 p3034 A83-43477
- The interaction of cardiac ventricles in intact dogs during 3-5 days of high altitude adaptation
23 p3496 A83-48566
- CARDIOGRAMS**
- Correlations between ejection times measured from the carotid pulse contour and the impedance cardiogram
24 p3617 A83-48877
- CARDIOGRAPHY**
NT ECHOCARDIOGRAPHY
- NT ELECTROCARDIOGRAPHY
- NT VECTORCARDIOGRAPHY
- Assessment of central hemodynamics during arm-crank exercise
01 p0083 A83-11138
- Mechanism for the appearance of the first extrasystole during short-lived atrial arrhythmia
03 p0376 A83-14366
- The application of noninvasive methods for the study of patients with ischemic heart disease
16 p2400 A83-36838
- CARDIOLOGY**
- Noninvasive cardiac output determination using inhaled oxygen-15-labeled carbon dioxide
03 p0378 A83-13577
- The antiarrhythmic effect of intramuscular and enteral injections of trimetazolin
03 p0374 A83-13630
- The relationship between the patient's age, the function of certain of his regulatory systems, and myocardial infarction
05 p0673 A83-17160
- Significance of the measurement of colloidal-oncotic and hydrostatic pressures in lung capillaries for the diagnosis of edema of the lungs
05 p0673 A83-17177
- Mathematical methods for optimizing treatment and diagnosis in cardiology /current status and future prospects/
05 p0674 A83-17199
- The condition of the hypothalamic-hypophyseal-adrenal system during sudden cardiac death
09 p1322 A83-23982
- A histopathological study on hearts in ischaemic heart disease fatalities
09 p1323 A83-24009
- The metrological possibilities of the tetrapolar transthoracic impedance rheoplethysmography method in clinical conditions
13 p1906 A83-30306
- Human sinus arrhythmia as an index of vagal cardiac outflow
13 p1904 A83-30498
- The therapeutic effect of the cardioselective beta-blocker tenormin and its effect on parameters of the central, intracardiac, and regional hemodynamics in patients with hypertension
19 p2881 A83-41428
- The diagnostic value of ambulatory electrocardiographic monitoring
19 p2882 A83-41450
- CARDIOVASCULAR SYSTEM**
NT AORTA
- NT ARTERIES
- NT BLOOD VESSELS

NT CAPILLARIES (ANATOMY)
 NT CARDIAC AURICLES
 NT CARDIAC VENTRICLES
 NT DIASTOLE
 NT EOSINOPHILS
 NT ERYTHROCYTES
 NT GLOMERULUS
 NT HEART
 NT HEMATOPOIESIS
 NT HEMATOPOIETIC SYSTEM
 NT LEUKOCYTES
 NT LYMPHOCYTES
 NT MYOCARDIUM
 NT SYSTOLE
 NT VEINS

The determination of the normal /desirable/ body weight for males 40-59 years of age according to the findings of an epidemiological study of cardiovascular diseases

A comparison of the cardiovascular responses to isometric exercise of three different sized muscle groups

An evaluation of the effects of aerobics on patients with border-line states with the help of investigations of the sympathetic-adrenal system

The effect of sinusoidal modulated currents on the cardiorespiratory system and the physical capacity of athletes

Comparison of hemodynamic responses to static and dynamic exercise

Role of impact velocity and chest compression in thoracic injury

An attempt to prevent weather-aggravated cardiovascular diseases

The effect of low frequency vibrations on the human cardio-circulatory system - A measurement technique and results for an 18 Hz sinusoidal vibration

Repeated exposures to high levels of plus g accelerations - Consequences for the myocardium and the cardiovascular system

Effects of ageing on cardiorespiratory changes to moderate physical exercise

Echocardiography in assessment of cardiovascular problems of Air Force personnel

Evaluation of a Reverse Gradient Garment for prevention of bed-rest deconditioning

Changes in the loco-regional cerebral blood flow /r.C.B.F./ during a simulation of weightlessness

Comparison of cardiovascular effects of space flight and its analogs using computer simulations

Effects of antiorthostatic position at -4 deg on hydromineral balance

The value of echocardiography in diagnosing diseases of the cardiovascular system

The phase character of the compensatory reactions of the cardiovascular system during active orthostatic tests

An investigation of the resonance characteristics of the cardiovascular system

Effects of hypercapnia, hypoxia, and rebreathing on circulatory response to apnea

Cardiovascular responses to treadmill exercise in rats

Effects of training

Cardiovascular adaptation to weightlessness

[SAE PAPER 820830]

Vasopressin and the cardiovascular system

The intensity of kininergic reactions of the cardiovascular system for various levels of the activity of the kallikrein-kinin system in blood plasma

Cardiovascular responses to exercise as functions of absolute and relative work load

The interrelation of the parameters of the cardiorespiratory system in athletes during various conditions

The effect of magnetotherapy on the cardiovascular system of patients with hypertension

The relationship between aerobic fitness and certain cardiovascular risk factors

Indicators of the cardiovascular system function during the work activity of scientific workers

Cardiopulmonary responses to combined lateral and vertical acceleration

The cardiovascular system and the fitness for work of athletes --- Russian book

Effects of hyperbaric oxygen exposure at 31.3 ATA on spontaneously beating cat hearts

Parameters of the vegetative regulation of the cardiovascular system during the early development of hypertension

The nature of 'congestive' excitation during emotional stress as a basis for cardiovascular disorders

Physiotherapy in the multiple therapy treatment of patients with vascular diseases of the brain

Gravitational effects on human cardiovascular responses to isometric muscle contractions

The observation of influence on the characteristics of cardiovascular response during bed rest

The pharmacology of cardioactive compounds in early ontogenesis --- Russian book

The condition of the pulmonary blood flow and central hemodynamics in healthy humans during the breathing of a helium-oxygen mixture

The effect of the neuropeptides vasopressin and fragments of corticotrophin on the cardiovascular and respiratory system of humans at rest and during physical loading

Cardiovascular exploration in microgravity. French-Soviet flight aboard Saliout VII - June 1982

[IAF PAPER 83-194]

CARET WINGS

The aerodynamic characteristics of caret wings at subsonic flight speeds

CARETS (TEST SITE)

U. CENTRAL ATLANTIC REGIONAL ECOL TEST SITE

CARGO

NT AIR CARGO

Vibration and acoustic environments for payload/cargo integration

[AIAA PAPER 83-0329]

CARGO AIRCRAFT

NT C-5 AIRCRAFT

NT C-130 AIRCRAFT

NT C-135 AIRCRAFT

NT C-140 AIRCRAFT

NT C-141 AIRCRAFT

NT YC-14 AIRCRAFT

The KC-10A - USAF's newest range extender

The Air Force Flight Test Center Palletized Airborne Water Spray System

[AIAA PAPER 83-0030]

Advanced turboprop cargo aircraft systems study

Aerodynamic development for efficient military cargo transports

[AIAA PAPER 83-1822]

New concept for low cost VTOL cargo delivery capability

[AIAA PAPER 83-2207]

International Forum for Air Cargo, 11th, New York, NY, September 27-30, 1982, Proceedings

A very large cargo aircraft design project

CARGO SPACECRAFT

Space sail liner --- interplanetary solar-powered cargo vehicle

The electromagnetic environment for the Space Shuttle orbiter

[AIAA PAPER 83-0332]

Environmental protection system for the Shuttle External Tank Aft Cargo Carrier

[SAE PAPER 820880]

Satellite handling for the Shuttle

A Shuttle Derived Vehicle launch system

[SAE PAPER 821342]

Processing cargoes for the first two operational STS flights at KSC

[IAF PAPER 83-23]

CARIBOU AIRCRAFT

U. DHC 4 AIRCRAFT

CARBIOUS

Digital colour enhancement of Landsat data for mapping vegetation of barrenground caribou winter range in northern Manitoba

CARNITINE

Effects of acute moderate-intensity exercise on carnitine metabolism in men and women

CARNOT CYCLE

Classical thermodynamics of homogeneous systems based upon Carnot's general axiom

CARRIER DENSITY (SOLID STATE)

Thermodynamics based on the Hahn-Banach theorem

- The Clausius inequality

CAROTENE

Efficient femtosecond optical Kerr shutter

CAROTID SINUS BODY

Effect of hypoxia and hypercapnia on catecholamine content in cat carotid body

Acclimatization to high altitude in goats with ablated carotid bodies

CAROTID SINUS REFLEX

The direct reactions of smooth muscles of the major cerebral arteries to acute hypoxia and hypercapnia

Hyperpnea of exercise at various PIO2 in normal and carotid body-denervated ponies

CARRIER DENSITY (SOLID STATE)

The electrical characteristics of degenerate InP Schottky diodes with an interfacial layer

Effects of gate metals on interface effects in metal oxide semiconductor systems after electron trapping

Relationship between carrier-induced index change and feedback noise in diode lasers

Bulk and interface gap states in a-Si:H - A comparative study of field effect and capacitance measurements on codeposited samples

Studies of the band tails in a-Si:H by photomodulation spectroscopy

States in the gap of amorphous hydrogenated silicon

Some problems in determination of gap-state density in amorphous silicon

Field ionization of deep levels in semiconductors with applications to Hg/1-x/Cd/x/ Te p-n junctions

Theory of open circuit photo-voltage in degenerate abrupt p-n junctions

Role of the conductivity of the confining layers in DH-laser spatial hole burning effects

Prediction of transverse-mode selection in double heterojunction lasers by an ambipolar excess carrier diffusion solution

Use of magnetic circular dichroism for nondestructive measurement of charge carrier concentration in wideband semiconductors

A model for the collection of minority carriers generated in the depletion region of a Schottky barrier solar cell

On the possibility of microwave generation in the case of avalanche processes in dipole domains

Non-destructive characterisation of n-type InP epitaxial layers by infrared reflectivity measurements

Carrier distribution and low-field resistance in short n/+/-n/-/-n/+/- and n/+/-p/-/-n/+/- structures

Transient photoconductivity studies of the light soaked state of hydrogenated amorphous silicon

Temperature and field dependence of the generation of interface states in the Si-SiO2 system after high-field stress

Defects in electron irradiated, gallium-doped silicon --- in solar cells

Light sensitivity of Al/0.25/Ga/0.75/As/GaAs modulation-doped structures grown by molecular beam epitaxy - Effect of substrate temperature

The effect of photon transfer on the distribution of nonequilibrium charge-carriers in a semiconductor

Stability of amorphous silicon solar cells with pin structure

Carrier conduction in a-Si:H solar cells

Picosecond transient orientational and concentration gratings in germanium

Complete experimental evaluation of the carrier dependence of the refractive index from the frequency modulation spectra of single mode injection lasers

Numerical simulation of nonstationary processes in semiconductor diode structures in the case of the ballistic motion of electrons

Numerical and experimental study of a GaAs transferred electron device without transit-time limitation

A correlation of atomic and electrical measurements of Cr and residual donors in thermally processed semi-insulating GaAs

Minority carrier recombination in heavily-doped silicon

- Fractional quantization of the Hall effect
16 p2420 A83-35750
- The quantized Hall effect
16 p2420 A83-35763
- Density of the gap states in undoped and doped glow discharge a-Si:H
16 p2421 A83-36740
- Beam-propagation analysis of stripe-geometry semiconductor lasers - Threshold behavior
17 p2514 A83-38043
- Staebl-Wronski effects in hydrogenated amorphous Si(1-x)Ge(x)
18 p2749 A83-39469
- The interpretation of photoconductivity measurements in hydrogenated amorphous silicon
18 p2750 A83-39471
- Photo-induced changes in the bulk density of gap states in hydrogenated amorphous silicon associated with the Staebler-Wronski effect
18 p2750 A83-39472
- On the optical evaluation of the EL2 deep level concentration in semi-insulating GaAs
18 p2750 A83-40062
- Generalized theory of conduction in Schottky barriers
19 p2836 A83-40670
- Models of the static and dynamic behavior of stripe geometry lasers
19 p2851 A83-40931
- Field ionised impurity scattering in an AlGaAs/GaAs two-dimensional electron gas
20 p3052 A83-42485
- Analysis of a multistable semiconductor light amplifier
20 p2994 A83-42791
- Femtosecond relaxation of photoexcited nonequilibrium carriers in Al(x)Ga(1-x)As
21 p3216 A83-43890
- Effect of grain size on the resistivity of polycrystalline material
23 p3512 A83-48611
- Bulk minority carrier diffusion length and photogenerated carrier profile in silicon photovoltaic cells
24 p3635 A83-48916

CARRIER FREQUENCIES

- Continuous separable regulation of group delay and phase of the carrier frequency of a signal in an acoustic delay line
01 p0038 A83-10807
- Carrier arraying with coupled phase-locked loops for tracking improvement
03 p0312 A83-13862
- Carrier recovery systems for arbitrarily mapped APK signals
03 p0312 A83-13867
- Dynamic performance evaluation of a frequency tracking filter
07 p0916 A83-19681
- Noise analysis of a PSK carrier recovery DPLL
11 p1559 A83-26973
- Generation and reception of spread-spectrum signals
14 p2002 A83-33075
- Observations on the spectral response of a driven unlocked SAW delay line oscillator
16 p2345 A83-35650

CARRIER INJECTION

- Static and transient behavior of pin-diodes at high injection levels --- German thesis
01 p0036 A83-10474
- Comparative studies of tunnel injection and irradiation on metal oxide semiconductor structures
01 p0109 A83-10633
- The MAJIC-FET - A high speed power switch with low on-resistance --- Modulated Admittance Junction Injection Controlled
02 p0167 A83-11798
- A two-dimensional analysis of transfer in a charge injection infrared sensor --- French thesis
03 p0310 A83-13801
- Calculated threshold current of GaAs quantum well lasers
03 p0331 A83-13918
- Locking bandwidth asymmetry in injection-locked GaAlAs lasers
04 p0483 A83-15231
- FM sideband injection locking of diode lasers
04 p0483 A83-15240
- An investigation of the magnetically sensitive properties of integral circuit elements having injection feed
04 p0471 A83-15744
- Changes in photovoltaic and dark electrical properties of hydrogenated amorphous silicon diodes induced by forward bias carrier injection
04 p0542 A83-16021
- A novel buried-drain DMOSFET structure
05 p0631 A83-17761
- Electroabsorption produced mixed injection and its effect on the determination of ionization coefficients --- in low noise avalanche photodiodes
05 p0691 A83-17769
- Investigation of transient electronic transport in GaAs following high energy injection
06 p0814 A83-18757
- Theory of triangular-barrier bulk unipolar diodes including minority-carrier effects
09 p1255 A83-24493
- Optical injection locking of BARITT oscillators
10 p1411 A83-26344
- Series resistance analysis of concentrator cells under high injection conditions
14 p2004 A83-32246
- A PISO JCCD filter with high-speed linear charge injection --- serial-in, parallel-out junction charge coupled devices
15 p2151 A83-33890
- Double-injection currents and the field effect in p(+)nn(+) silicon-on-sapphire diodes
16 p2346 A83-35946

- Electrojet boundaries and electron injection boundaries
17 p2546 A83-38699
- An empirical model for device degradation due to hot-carrier injection
21 p3124 A83-43857
- Simulation of GaAs submicron FET with hot-electron injection structure
21 p3126 A83-44967

CARRIER MOBILITY

- NT ELECTRON MOBILITY
- NT HOLE MOBILITY
- Temperature dependence of the Hall factor and the conductivity mobility in p-type silicon
01 p0109 A83-10628
- What is the majority carrier drift mobility in a-Si alloys
04 p0541 A83-15528
- Photocapacitance of mobile carriers in hydrogenated amorphous silicon solar cells
08 p1131 A83-22765
- Non-destructive characterisation of n-type InP epitaxial layers by infrared reflectivity measurements
09 p1349 A83-23667
- Use of a superlattice to enhance the interface properties between two bulk heterolayers
10 p1489 A83-26214
- Light sensitivity of Al_{0.25}Ga_{0.75}As/GaAs modulation-doped structures grown by molecular beam epitaxy - Effect of substrate temperature
11 p1664 A83-28603
- Mobility-lifetime product and interface property in amorphous silicon solar cells
16 p2418 A83-35442
- Fractional quantization of the Hall effect
16 p2420 A83-35750
- Conductivity of inversion layers in InSb MIS structures below the 'mobility threshold'
20 p3051 A83-42275
- Peripheral photoresponse of a p-n junction
20 p3053 A83-42612
- Resistivity and mobility of GaP at 300 K
20 p3054 A83-43358
- Effect of the velocity-field peak on I-V characteristics of GaAs FET's
21 p3127 A83-45181
- Position-dependent effective masses in semiconductor theory
22 p3365 A83-46712
- Estimation of alloy scattering potential in ternaries from the study of two-dimensional electron transport
24 p3634 A83-48794

CARRIER MODULATION

U MODULATION

CARRIER ROCKETS

U LAUNCH VEHICLES

CARRIER TO NOISE RATIOS

- Phase-noise effects on QPSK carriers in burst transmission
02 p0163 A83-11558
- Performance evaluation of antenna arrays with noisy carrier reference
07 p0870 A83-19683
- Evaluation of a 14/12 GHz digital satellite link as the facility between digital switches
07 p0908 A83-19742
- Line-rate energy dispersal waveforms for FM TV
07 p0910 A83-19763
- Intermodulation spectra for 2-carrier-level SPC system
07 p0916 A83-21575
- The use of resource sharing and coding to increase the capacity of digital satellites
11 p1557 A83-28135
- Staircase solid-state photomultiplier and avalanche photodiodes with enhanced ionization rates ratio
15 p2150 A83-33681
- Subcoded information carriers - Hybrid moiresystem
23 p3508 A83-47580

CARRIER TRANSPORT (SOLID STATE)

- Simulation of non steady-state transport in GaAs and InP millimeter IMPATT diodes
02 p0167 A83-11799
- Process for high photocurrent in IBC solar cells --- Interdigitated Back Contact
02 p0202 A83-12059
- Solar cell device physics --- Book
03 p0353 A83-13501
- Planar doped barriers by molecular beam epitaxy for millimeter wave devices
03 p0310 A83-13785
- Optical absorption coefficient and minority carrier diffusion length measurements in low-cost silicon solar cell material
03 p0354 A83-13922
- Structural aspects and numerical modeling of diffusion in gold/chalcogenide /GeTe4/ thin layers --- French thesis
03 p0399 A83-14106
- Electron and hole diffusion length investigation in CdTe thin films by SPV method --- Surface Photovoltage
04 p0539 A83-15495
- Schottky revisited --- model limitations and steps for extending treatment to solar cell structures
04 p0540 A83-15509
- Transport mechanisms for Mg/Zn3P2 junctions
04 p0543 A83-16071
- Diodes formed by laser drilling and diffusion
04 p0473 A83-16090
- The inverse population of the light-hole band on pumping at cyclotron resonance
05 p0690 A83-16895
- Semiconductor structures for repeated velocity overshoot
05 p0690 A83-17295

- Electron transport in GaAs n/+/-p/-n/+/- submicron diodes
05 p0624 A83-17296
- On the mechanism of carrier transport in metal-thin-oxide semiconductor diodes on polycrystalline silicon
06 p0751 A83-18752
- Investigation of transient electronic transport in GaAs following high energy injection
06 p0814 A83-18757
- Computer analysis of the significance of surface boundary conditions on the collection of alpha-induced charge --- carrier transport simulation
06 p0753 A83-18960
- Evidence for low diffusivity and mobility of minority carriers in highly doped Si and interpretation
06 p0814 A83-19261
- Radiation effects on modulation-doped GaAs-Al/x/Ga/1-x/As heterostructures
06 p0815 A83-19263
- Ballistic and overshoot electron transport in bulk semiconductors and in submicron devices
07 p0999 A83-20737
- Theory and experiment on the surface-photovoltage diffusion-length measurement as applied to amorphous silicon
07 p0999 A83-20738
- Determination of effective surface recombination velocity and minority-carrier lifetime in high-efficiency Si solar cells
07 p0999 A83-20740
- Cadmium telluride films on foreign substrates
07 p1000 A83-20750
- Quantum transport in a single layered structure for impurity scattering
07 p1000 A83-21372
- Absence of the Gunn effect in p-In_{0.53}Ga_{0.47}As
07 p1000 A83-21374
- Computer simulation of carrier transport in planar doped barrier diodes
08 p1081 A83-22762
- Effect of grain boundaries on the minority carrier diffusion length in InP solar cells
08 p1170 A83-22908
- Carrier lifetimes in silicon epitaxial layers deposited on oxygen-implanted substrates
08 p1082 A83-22920
- Carrier distribution and low-field resistance in short n/+/-n/-n/+/- and n/+/-p/-n/+/- structures
09 p1350 A83-24496
- Ballistic transport and velocity overshoot in semiconductors. I - Uniform field effects
09 p1350 A83-24498
- Theory of beam-induced currents in semiconductors
10 p1489 A83-26212
- Optical picosecond studies of carrier dynamics in amorphous semiconductors
11 p1661 A83-27604
- Grain boundary effects in polycrystalline silicon solar cells. I - Solution of the three-dimensional diffusion equation by the Green's function method. II - Numerical calculation of the limiting parameters and maximum efficiency
11 p1611 A83-27981
- Diffusion length determination in n/+/-p-p/+/- structure based silicon solar cells from the intensity dependence of the short-circuit current for illumination from the p/+/- side
11 p1612 A83-27982
- Minority carrier diffusion length measurements - A review and comparison of techniques
11 p1663 A83-28448
- Forces acting on free carriers in semiconductors of inhomogeneous composition I, II
11 p1663 A83-28449
- The effect of photon transfer on the distribution of nonequilibrium charge-carriers in a semiconductor
13 p1832 A83-30269
- Electron transport in InP at high electric fields
13 p1929 A83-30353
- Measurement of high electron drift velocity in a submicron, heavily doped graded gap Al(x)Ga(1-x)As layer
13 p1929 A83-31056
- Effect of reabsorbed recombination radiation on the diffusion length of minority carriers in wide-band-gap semiconductors
13 p1931 A83-31385
- Grain boundaries and intragrain defects dependence of local and global electronic and photovoltaic properties of CGE polysilicon
14 p2088 A83-32233
- Validity of the effective lifetime concept in polycrystalline silicon
14 p2088 A83-32235
- Diffusion length of minority carriers in scanning electron beam annealed silicon
14 p2089 A83-32248
- Cu(x)S(p)-CdZnS(n)-CdS(n+) evaporated thin film solar cells
14 p2045 A83-32296
- Grain boundary photocurrent enhancement in solar cells made by laser diffusion
14 p2046 A83-32332
- An improved derivation of solar cell parameters in terms of transition probabilities
14 p2046 A83-32335
- Impurity diffusion in amorphous silicon and its implications for solar cells
14 p2005 A83-32336
- Calculation of velocity overshoot, velocity autocorrelation and hot electron noise in semiconductors from the small signal microwave mobility
14 p2006 A83-32668
- On the physics and modeling of small semiconductor devices. IV - Generalized, retarded transport in ensemble Monte Carlo techniques
14 p2092 A83-32669

Effect of argon implantation on the activation of boron implanted in silicon 14 p2093 A83-33444

Determination of diffusion length of electron beam induced minority carriers in polycrystalline GaAs 15 p2238 A83-33844

Variable minority carrier transport model for amorphous silicon solar cells 15 p2192 A83-34667

Electronic circuits for the simulation of physical processes in semiconductor structures by the method of direct analogies 16 p2347 A83-36904

Influence of radiative recombination on the minority-carrier transport in direct band-gap semiconductors 17 p2496 A83-37617

Temperature dependence of electrical transport properties of n-type solar grade polycrystalline silicon 17 p2584 A83-38210

An experimental study of unsteady transport phenomena in GaAs --- French thesis 17 p2585 A83-38430

SEM-EBIC and traveling light spot diffusion length measurements - Normally irradiated charge-collecting diode 18 p2678 A83-40371

An As-P/n(+)-n(-)/ double diffused drain MOSFET for VLSI's 18 p2678 A83-40380

Implications of velocity overshoot in heterojunction transit-time diodes 18 p2679 A83-40387

On the effective minority carrier diffusion length of polycrystalline silicon solar cells 20 p3052 A83-42357

Simple method for the determination of the minority carrier diffusion length in metal/insulator/semiconductor solar cells 20 p3052 A83-42361

Schottky barriers on single-crystal indium telluride 21 p3127 A83-45176

Effect of the velocity-field peak on I-V characteristics of GaAs FET's 21 p3127 A83-45181

Acoustic and optical-phonon-limited mobilities in p-type silicon within the deformation-potential theory 21 p3219 A83-45497

Kinetic phenomena in nondegenerate narrow-gap semiconductors --- Russian book 23 p3511 A83-47121

High-field transport properties of In_{0.765}Ga_{0.235}As_{0.5}P_{0.5} 23 p3512 A83-48703

Current oscillations in semiconductor diodes under streaming instability conditions 23 p3512 A83-48719

Effects of doping on transport and deep trapping in hydrogenated amorphous silicon 24 p3634 A83-48792

Estimation of alloy scattering potential in ternaries from the study of two-dimensional electron transport 24 p3634 A83-48794

Investigation of a two-dimensional model of an MOS structure 24 p3575 A83-50203

A method for the simulation of the transfer of charge carriers and the distribution of electrostatic potential in semiconductor structures 24 p3575 A83-50208

CARRIER WAVES

Local area time dissemination by carrier-current waves --- in construction of transmission network for timing signals 03 p0328 A83-14167

Combined effect of the carrier recovery and symbol timing recovery error on the P/e/ performance of QPR and offset QPR systems --- quadrature partial response 05 p0621 A83-17271

Spatial carriers with orthogonal subcodes --- signal coding and decoding for optical communication 15 p2230 A83-33810

A coupled phase-locked loops system for carrier tracking improvement 19 p2814 A83-41395

CARRINGTON ROTATION

U SOLAR ROTATION

CARTAN SPACE

Perfect fluids in the Einstein-Cartan theory 07 p0990 A83-21065

Spinning fluids in the Einstein-Cartan theory 16 p2408 A83-36989

Cosmological term in a nonsingular cosmological model of the Einstein-Cartan gravitation theory 24 p3651 A83-49067

CARTESIAN COORDINATES

Determination of the transformation parameters of spatial rectangular coordinates --- for space geodesy and photogrammetry 01 p0072 A83-10851

Controlling the motion of a moving robot using a neuroid network 03 p0385 A83-13475

Exact expressions for radiative transfer in a three-dimensional rectangular geometry 04 p0532 A83-16438

Boundary-fitted coordinate systems for numerical solution of partial differential equations - A review 12 p1772 A83-29620

A note on the mathematical formulation of the problem of numerical coordinate generation 17 p2571 A83-37768

Coordinate transformations via multifacet holographic optical elements 21 p3134 A83-43871

CARTOGRAPHY

U MAPPING

CARTRIDGE ACTUATED DEVICES

U ACTUATORS

U EXPLOSIVE DEVICES

CASCADE CONTROL

A study of an arbiter function in the structures of a shared bus --- French thesis 02 p0166 A83-11700

Cascaded bandpass v-th-law devices 02 p0164 A83-11987

Self-tuning controller with integral action 05 p0681 A83-17581

A method of analyzing nonlinear phenomena in radio-receiving apparatus 09 p1257 A83-25159

GG-pseudo-band method for the design of multivariable control systems 10 p1464 A83-26520

Schemes for multivariable parameter-adaptive deadbeat control 10 p1467 A83-26549

Applications of Laurent expansions in multivariable control systems 10 p1469 A83-26571

A singular perturbation canonical form of invertible systems Determination of multivariable root-loci 16 p2405 A83-36452

A new approach for the design of multivariable feedback systems 16 p2405 A83-36453

Reconstructable states of linear multivariable systems with unknown inputs 16 p2405 A83-36456

The SINR performance of cascaded adaptive arrays 19 p2831 A83-41385

A cascaded echo canceller 19 p2832 A83-41393

A numerical method for the analysis of harmonic balance conditions in multiloop non-linear feedback systems 19 p2891 A83-41489

CASCADE FLOW

Extension of the Carafoli tracer method to profiles cascades 01 p0002 A83-10578

Measurements in shear layers in transonic flows with a laser transit anemometer 01 p0003 A83-10697

Optical methods of flow diagnostics in turbomachinery 01 p0053 A83-11076

Optimal design of the lateral feed of a turbomachine [AAAF PAPER NT 81-04] 02 p0169 A83-11770

Numerical solution of subsonic and transonic cascade flows 02 p0132 A83-12901

An improved method for calculating isentropic transonic flows in two-dimensional turbine cascades of arbitrary smooth profiles 03 p0278 A83-13492

Potential flow analysis of an arbitrary cascade using a conformal transformation into a row of circular cylinders 03 p0278 A83-13564

Baroclinic nonlinear exchanges of energy and potential enstrophy in the quasi-geostrophic two-layer model 03 p0369 A83-14520

Transonic flow past an isolated profile and through a blade cascade - Phenomenological analysis 03 p0280 A83-14622

Sounding propagation in multistage axial flow turbomachines 04 p0533 A83-15289

Analytical profiling of turbine blades 04 p0449 A83-16010

Development of secondary flow and vorticity in curved ducts, cascades, and rotors, including effects of viscosity and rotation 04 p0478 A83-16141

Experimental evaluation of shockless supercritical airfoils in cascade [AIAA PAPER 83-0003] 05 p0577 A83-16455

A viscous-inviscid interactive procedure for rotational flow in cascades of two-dimensional airfoils of arbitrary shape [AIAA PAPER 83-0256] 05 p0583 A83-16614

Solution procedures for accurate numerical simulations of flow in turbomachinery cascades [AIAA PAPER 83-0257] 05 p0583 A83-16615

An implicit, transonic, full-potential code for cascade flow on H-grid topology [AIAA PAPER 83-0506] 05 p0587 A83-16754

Aerodynamic performance of an annular classical airfoil cascade [AIAA PAPER 83-0179] 05 p0588 A83-16824

Numerical study of the dependence of the efficiency of the gas-screen cooling of perforated gas-turbine blades on cascade parameters 05 p0589 A83-16955

Modeling rotating stall by vortex dynamics [AIAA PAPER 83-0002] 05 p0590 A83-17901

The computation of the compressor cascade boundary layer 06 p0712 A83-18153

The development of thermal boundary layers in airfoil-cascade flows with off-design angles of attack 06 p0713 A83-19155

The effect of aerodynamic coupling between the blades of a cascade on the aerodynamic damping of blade vibrations and the onset of blading flutter 06 p0777 A83-19312

Computing three-dimensional transonic gas flow through an axial-turbine stage 06 p0713 A83-19437

Experimental determination of blade forces through stationary and nonstationary pressure measurements on interfering double cascades --- German thesis 06 p0714 A83-19616

The effect of the geometric parameters of a compressor cascade on the threshold of the self-excited flexural vibration of the blades due to cascade flutter 07 p0946 A83-20911

Cascading bifurcations 08 p1161 A83-22740

A finite element solution of compressible flow through cascades of turbomachines 08 p1089 A83-23203

Low frequency flows through an array of airfoils 09 p1196 A83-23703

Hydrodynamic visualization of the flow in a model of an axial flow turbomachine 09 p1261 A83-24336

On the definition of the axial velocity density ratio in theoretical and experimental cascade investigations 10 p1372 A83-26415

Probe investigations in the proximity of a wall in supersonic flow 10 p1372 A83-26416

1 MHz bandwidth, real-time Schlieren techniques in a linear transonic cascade 10 p1422 A83-26419

Three dimensional holographic flow visualization 10 p1422 A83-26420

Optical methods for performance evaluation of two-dimensional transonic turbine profiles in steam 10 p1422 A83-26421

Loss measurements using a fast traverse in an ILPT transient cascade --- Isentropic Light Piston Cascade Tunnel 10 p1372 A83-26423

The response of a multistage compressor to an azimuthal distortion 10 p1378 A83-26923

Prediction of the surge line of axial multistage compressor 10 p1373 A83-26924

Performance deterioration on turbomachinery with presence of solid particles 11 p1525 A83-27477

On the self-excited circumferential nonuniformity of a potential fluid flow near a circular cascade of profiles 11 p1569 A83-28534

Comparison of laser anemometer measurements and theory in an annular turbine cascade with experimental accuracy determined by parameter estimation 12 p1695 A83-28833

Computations of unsteady transonic cascade flows 12 p1696 A83-28975

A comparison of experimental and numerical results obtained for the secondary flow in a large turbine cascade 12 p1696 A83-29157

Viscous-inviscid interactions in cascades 15 p2120 A83-33790

Axisymmetric vortex flow in a turbine stage under variable operating conditions 15 p2120 A83-34899

Profile losses during the release of air onto the surface of nozzle vanes 16 p2288 A83-35590

Blade-to-blade transonic flow calculation in axial turbomachines 16 p2290 A83-35837

Numerical computation of turbulent flow around the spinner of a turbofan engine 16 p2291 A83-35838

Aerodynamic optimization theory of A 3-D axial-flow rotor-blading via optimal control 16 p2291 A83-35839

Computation of blade cascade aerodynamic losses due to detached shock waves [ONERA, TP NO. 1983-53] 16 p2291 A83-35844

Investigation of flow through high cambered supersonic compressor cascade 16 p2291 A83-35845

A contribution to the calculation of secondary flows in an axial flow compressor 16 p2291 A83-35852

Optimization of the plane compressor blade aerodynamic design 16 p2291 A83-35857

Effect of entry boundary layer thickness on secondary flows in an annular cascade of turbine nozzle and rotor blades 16 p2292 A83-35868

High angle-of-attack cascade measurements and analysis 16 p2292 A83-35875

Prediction of cascade performance in the presence of a separating boundary layer 16 p2292 A83-35876

The effect of flow fluctuations on the characteristics of turbine cascades 16 p2293 A83-36124

Experimental research on the design of highly loaded axial fans --- German thesis 17 p2447 A83-37498

The use of discontinuity surfaces of active and passive disk type for the mathematical modeling of unsteady flows in the circuit of a powerplant with a jet engine 17 p2450 A83-37636

A study of the control properties of axial fans on the basis of theoretical characteristics of plane cascades 17 p2451 A83-37807

Modeling of turbulent flow fields through cascade of airfoils at stall conditions [AIAA PAPER 83-1743] 17 p2452 A83-38091

Fast generation of three-dimensional computational boundary-conforming periodic grids of C-type --- for turbine blades and propellers 17 p2573 A83-38799

An interacting boundary layer model for cascades [AIAA PAPER 83-1915] 18 p2635 A83-39372

Constraint on design parameters and twist of S1 surfaces in turbomachines 18 p2638 A83-40367

Freestream turbulence effects on compressor cascade wake 19 p2789 A83-41051

Experimental investigation of rotor wake traverse minima and their effects on the dynamic load of axial compressor and turbine cascades --- German thesis 19 p2859 A83-41807

A study of the thermal state of porous turbine blades in a straight nozzle cascade 19 p2794 A83-42148

The rule of forbidden signals and apparent Mach numbers in supersonic compressor cascades 20 p2928 A83-42560

Analytical method for predicting compressor stage performance 20 p2928 A83-42561

Effect of particle presence on the incompressible inviscid flow through a two dimensional compressor cascade 20 p2928 A83-42562

Flow visualization investigation of choking cascade turns 20 p2989 A83-42564

Design of supercritical cascades with high solidity 20 p2930 A83-43446

A numerical method for weakening shock wave strength in transonic cascade flow fields 20 p2931 A83-43695

A method for experimental analysis of the shock-boundary layer interaction in cascades [ONERA, TP NO. 1983-48] 21 p3086 A83-44322

Unsteady transonic cascade with a subsonic leading-edge locus 21 p3088 A83-44931

Calculation of a laminar-turbulent two-dimensional turbine blade boundary layer including surface curvature effects 22 p3249 A83-46464

Three-dimensional boundary layers in turbomachines 22 p3286 A83-47021

Matrix solution of compressible flow on S1 surface through a turbomachine blade row with splitter vanes or tandem blades [ASME PAPER 83-GT-10] 23 p3393 A83-47882

An experimental and computational study of transonic three-dimensional flow in a turbine cascade [ASME PAPER 83-GT-12] 23 p3393 A83-47884

A streamline curvature method for calculating S1 stream surface flow [ASME PAPER 83-GT-16] 23 p3393 A83-47885

The relative eddy in axial turbine rotor passages [ASME PAPER 83-GT-22] 23 p3393 A83-47887

Measurements of secondary flows within a cascade of curved blades and in the wake of the cascade [ASME PAPER 83-GT-24] 23 p3393 A83-47889

A test facility for the investigation of steady and unsteady transonic flows in annular cascades [ASME PAPER 83-GT-34] 23 p3393 A83-47895

Experience with the development of an Euler code for rotor rows [ASME PAPER 83-GT-36] 23 p3394 A83-47897

An experimental investigation of endwall heat transfer and aerodynamics in a linear vane cascade [ASME PAPER 83-GT-52] 23 p3394 A83-47909

Flow in a turbine cascade. I - Losses and leading-edge effects [ASME PAPER 83-GT-68] 23 p3395 A83-47921

Flow in a turbine cascade. II - Measurement of flow trajectories by ethylene detection [ASME PAPER 83-GT-69] 23 p3395 A83-47922

Effect of particle presence on the incompressible inviscid flow through a two dimensional compressor cascade [ASME PAPER 83-GT-95] 23 p3395 A83-47941

Modifications of the Ives-Iliuteroza conformal-mapping procedure for turbomachinery cascades [ASME PAPER 83-GT-116] 23 p3395 A83-47947

Heat transfer and friction loss characteristics of pin fin cooling configuration [ASME PAPER 83-GT-123] 23 p3448 A83-47952

Theory of blade design for large deflections. I Two-dimensional cascade [ASME PAPER 83-GT-124] 23 p3396 A83-47953

Theory of blade design for large deflections. II - Annular cascades [ASME PAPER 83-GT-125] 23 p3396 A83-47954

An investigation of the flow characteristics and of losses in radial nozzle cascades [ASME PAPER 83-GT-126] 23 p3396 A83-47955

Cascade flutter analysis of cantilevered blades [ASME PAPER 83-GT-129] 23 p3408 A83-47958

Design of shock-free compressor cascades including viscous boundary layer effects [ASME PAPER 83-GT-134] 23 p3396 A83-47961

Redesign and performance analysis of a transonic axial compressor stator and equivalent plane cascades with subsonic controlled diffusion blades [ASME PAPER 83-GT-208] 23 p3397 A83-48009

Calculation of friction and heat transfer on the profile of a turbomachine cascade 23 p3399 A83-48449

On the question of the power law of the decay of grid turbulence 23 p3452 A83-48671

The use of coloured smoke to visualize secondary flows in a turbine-blade cascade 24 p3545 A83-49466

Numerical analysis of turbulent separated flow in a cascade of airfoils 24 p3545 A83-49531

CASCADE RANGE (CA-OR-WA)

Response of stratified flow in the lee of the Olympic Mountains 02 p0218 A83-13061

Particles and gases in the emissions from the 1980-1981 volcanic eruptions of Mt. St. Helens 07 p0959 A83-20206

Ice nucleus characteristics of Mount St. Helens effluents 07 p0969 A83-20210

CASCADE WIND TUNNELS

The NAL transonic cascade tunnel 01 p0015 A83-11081

Aerodynamic performance of an annular classical airfoil cascade [AIAA PAPER 83-0179] 05 p0588 A83-16824

An experimental investigation of turbulent wake behind 'S'-shaped profiles 07 p0926 A83-20502

Design of a flexible nozzle for probe calibration purposes 10 p1372 A83-26413

High angle-of-attack cascade measurements and analysis 16 p2292 A83-35875

Theoretical and experimental investigations involving plane turbine cascades with sweep and dihedral --- German thesis 19 p2791 A83-41806

Gas turbine engine cascade wind tunnel with automatic data acquisition and control 20 p2938 A83-42563

Experimental cascade analysis of a transonic compressor rotor blade section [ASME PAPER 83-GT-209] 23 p3397 A83-48010

CASCADES

Light-induced drift in cascade excitation of levels --- laser effects on atomic energy levels 07 p0934 A83-20117

CASCADES (FLUID DYNAMICS)

U FLUID DYNAMICS

CASCADE MOSFET

U FIELD EFFECT TRANSISTORS

CASE HISTORIES

Liquorhea via fistula in the area of the cochlear window 01 p0083 A83-10516

The therapeutic aspect of military pilot certification 06 p0797 A83-18334

Unusual ejection injury - A case report 09 p1323 A83-24008

CASES (CONTAINERS)

NT ROCKET ENGINE CASES

Major hot section component salvaged through advanced repair methods [SAE PAPER 821489] 17 p2469 A83-38007

CASING

Effect of the volute casing on the flow in radial-flow blowers 09 p1263 A83-24649

Institute of environmental sciences aircraft engine combustor casing life simulation for increased reliability 13 p1807 A83-31493

CASSEGRAIN ANTENNAS

LAMMR: A new generation satellite microwave radiometer - Its concepts and capabilities --- Large Antenna Multichannel Microwave Radiometer 01 p0021 A83-10116

A multiple beam antenna concept for a 30/20 GHz satellite communications system 01 p0034 A83-11485

Peak gain of a Cassegrain antenna with secondary position adjustment 03 p0306 A83-14029

Contoured-beam synthesis for array-fed reflector antennas by field correlation 04 p0468 A83-16202

Geometrical optical characteristics of the Schwarzschild scanning antenna - Comparison with the Cassegrain antenna 04 p0468 A83-16205

The determination of the fields reflected from a twist reflector following illumination by a plane wave 06 p0737 A83-18609

The analysis of a flat plate twist reflector Cassegrain aerial using GTD 06 p0715 A83-18646

A family of two-reflector antennas with identical dielectric primary feeds 06 p0742 A83-18664

A novel technique for the computation of secondary patterns of reflector antennas 06 p0743 A83-18687

Radar - Reflections on radio waves 08 p1078 A83-23250

Combined E- and H-plane phase centers of antenna feeds 09 p1248 A83-23810

Analysis of rim loaded Cassegrain antennas 10 p1401 A83-25502

A beam waveguide linearly polarized KU band feed system 15 p2146 A83-35079

Primary-focus operation of shaped dual-reflector antennas 15 p2149 A83-35199

Diffraction by the secondary reflector of a Cassegrain antenna of revolution 19 p2825 A83-40795

An analysis of diffraction effects in a Cassegrain antenna with a mesh subreflector 22 p3272 A83-45689

CASSEGRAIN OPTICS

Self-null corrector test for telescope hyperbolic secondaries 08 p1175 A83-22614

Performance of the Multiple Mirror Telescope (MMT). I - MMT The first of the advanced technology telescopes 13 p1828 A83-30977

Multiple object fiber optic spectroscopy 14 p2017 A83-32012

Refractive field correctors for the Starlab ultraviolet telescope 14 p2096 A83-32039

Optical systems for large telescopes 17 p2590 A83-37722

The design and study of the aspherical plate corrector of the view field for Cassegrain system 17 p2580 A83-38774

A middle-infrared heterodyne spectrometer to be used at the Cassegrain-focus of medium-size and large astronomical telescopes 18 p2761 A83-40436

CASSIOPEIA A

Optical studies of Cassiopeia A. VI - Observations during the period 1976-1980 14 p2098 A83-33192

High-velocity, asymmetric Doppler shifts of the X-ray emission lines of Cassiopeia A 14 p2104 A83-33193

Supernova shell structure and the spur of the Crab 16 p2429 A83-36626

Low-frequency excited-carbon radio lines toward Cassiopeia A 17 p2613 A83-38835

CAST ALLOYS

The effect of the characteristics of interstitial solid solution decomposition on the fine structure and properties of cast alloys of molybdenum 01 p0025 A83-10393

Fabrication of niobium and niobium alloys 02 p0154 A83-11788

Structure and properties of large slabs of alloy 1201 03 p0297 A83-13261

Recovery treatment of Al27-1 alloy 03 p0297 A83-13264

Creep response of strip-cast Al-1wt.%Mn-1wt.%Mg alloy to thermomechanical treatment 04 p0457 A83-14996

Cast transage 175 titanium alloy for durability critical structural components 04 p0458 A83-15318

The influence of the method of supersaturation on the course of precipitation hardening of chill castings made of aluminum silicon alloys 04 p0460 A83-15991

Reversible reaction between MC and M/23C/6/ in a NiCrWTi cast superalloy 07 p0885 A83-20274

Superalloy technology - Today and tomorrow 07 p0891 A83-21452

High cycle fatigue properties of cast nickel base superalloys IN 738LC and IN 939 07 p0892 A83-21463

Some interactions of creep and fatigue in IN 738 LC at 850 C 07 p0893 A83-21472

Factors influencing the creep behaviour of a cast Ni-Cr-base alloy 07 p0893 A83-21474

High temperature fatigue of a superalloy for cast turbine wheel 07 p0893 A83-21478

Mechanisms of high cycle fatigue of cast nickel base alloys 07 p0894 A83-21482

Grain boundary pore chains in cast nickel base superalloys 07 p0894 A83-21486

The effect of hot corrosion on creep and fracture behaviour of cast nickel-based superalloy IN738LC 07 p0895 A83-21490

Hot Isostatic Pressing of alloy IN-718 07 p0895 A83-21500

Fatigue crack propagation response in extruded and cast aluminum alloys 08 p1060 A83-21710

Metallographic aspects of creep fracture in a cast Ni-Cr-base alloy 08 p1062 A83-21745

A theory for the formation of closed shrinkage cavities during alloy solidification in large volumes 09 p1229 A83-23519

A theoretical consideration of the microstructural origins of friction stress in a cast gamma prime-strengthened superalloy 09 p1232 A83-24063

New developments in foundry engineering --- Russian book 10 p1395 A83-25628

Methods of producing dispersion-strengthened cast alloys based on aluminum 10 p1395 A83-25629

High temperature low cycle fatigue of IN 738 and application of strain range partitioning 10 p1398 A83-26282

Investigation of the solidification of titanium castings by means of a conduction MHD pump 12 p1732 A83-29271

Effect of multiple crack propagation on the high temperature low cycle fatigue of a cast nickel-base alloy 12 p1714 A83-29725

Distribution of impurity elements in titanium alloys 13 p1819 A83-30086

On the cyclic behavior of cast and extruded aluminum alloys. I - Fatigue crack propagation 14 p1992 A83-32342

On the cyclic behavior of cast and extruded aluminum alloys. B - Fractography 14 p1992 A83-32343

Segregation and structure in rapidly solidified cast metals 14 p1994 A83-32802

Casting problems specific to aluminum-lithium alloys 14 p2028 A83-32879

Toughness and ductility of aluminum-lithium alloys prepared by powder metallurgy and ingot metallurgy 14 p1996 A83-32886

Structural members made of high-strength cast aluminum and their properties --- and reduction of aircraft production costs 15 p2136 A83-33954

High-strength aluminum high-quality casting alloy in aeronautics and astronautics 15 p2136 A83-33955

Effect of cyclic stress on creep rupture strength of a cast superalloy with high Al and Ti contents 15 p2137 A83-34002

Low cycle fatigue behaviour of cast nickel-base superalloy IN738LC at room temperature 15 p2140 A83-34742

A study of the hardening of cast aluminum containing refractory tungsten compounds 16 p2335 A83-36893

The solidification point volume increment in solidification front dynamics --- of cast alloys in spaceborne experiments 18 p2643 A83-39903

New method of preparation of dispersion-hardening materials Improvement of mechanical properties of as-cast eutectics followed by heavy deformation 18 p2667 A83-40280

Fracture anomalies of a casting magnesium alloy in low-cycle fatigue 19 p2822 A83-41595

The effect of the natural convection on the transition from columnar to equiaxed crystals 20 p3054 A83-43311

Fracture toughness measurement of cast magnesium alloy by cylindrical specimen with ring-shaped crack 21 p3111 A83-44107

A study of the structure and physicomechanical properties of magnesium alloys under various conditions of solidification by the Stepanov method 21 p3114 A83-45340

Development of the single crystal alloys CM SX-2 and CM SX-3 for advanced technology turbine engines [ASME PAPER 83-GT-244] 23 p3432 A83-48034

CASTIGLIANO VARIATIONAL THEOREM

Castigliano's theorem and its limits 08 p1121 A83-21859

CASTING

NT INVESTMENT CASTING

NT PROPELLANT CASTING

NT SLIP CASTING

Vader - A new melting and casting technology 07 p0895 A83-21491

Precision casting of turbine blades and vanes 07 p0941 A83-21494

Ceramic tooling in aircraft fabrication 09 p1195 A83-23603

Developments in titanium alloy casting technology 09 p1230 A83-23745

A new simple casting technique - The Flying Wheel Casting 09 p1274 A83-24123

Effect of some casting parameters on surface segregation in the case of continuous casting involving aluminum 12 p1713 A83-29368

Low cost processes for cast silicon solar cells 14 p2045 A83-32313

Overview of D.C. casting --- Direct-Chill solid-liquid interface shape prediction using heat transfer models 14 p1995 A83-32878

Squeeze casting of silicon carbide fiber reinforced aluminum 18 p2659 A83-40263

CASTING SOLVENTS

U PLASTICIZERS

CASTINGS

NT INGOTS

NT PROPELLANT CASTING

Investigation of the surface grain refinement for superalloys castings 07 p0895 A83-21499

Effect of processing on fatigue life of Ti-6Al-4Al-4V castings 15 p2135 A83-33641

The effects of weld-repair and hot isostatic pressing on the fracture properties of Ti-5Al-2.5Sn ELI castings 15 p2135 A83-33642

Correlation of solar cell electrical properties with material characteristics of silicon cast by the ubiquitous crystallization process 15 p2192 A83-34695

CATABOLISM

Age-related characteristics of the prostaglandin system in several organs 19 p2879 A83-42096

CATALOGS (PUBLICATIONS)

NT ASTRONOMICAL CATALOGS

CATALYSIS

NT AUTOCATALYSIS

Evolutionary roots of catalysis by nicotinamide and flavins in C-H oxidoreductases and in photosynthesis 02 p0219 A83-11633

Monopole catalysis of nucleon decay in neutron stars 02 p0259 A83-12219

Tunnel effect in molecules in strong magnetic fields of neutron stars 04 p0556 A83-15956

Catalytic method of accurate localization of small leaks 07 p0932 A83-21407

Common problems in nucleation and growth, chemical kinetics, and catalysis --- in earth atmosphere 09 p1308 A83-25177

Neutral and charged clusters in the atmosphere - Their importance and potential role in heterogeneous catalysis 09 p1297 A83-25179

Photoassisted heterogeneous catalysis - Definition and hydrocarbon and chlorocarbon oxidations 09 p1297 A83-25188

Heterogeneous catalyzed photolysis via photoacoustic spectroscopy 09 p1297 A83-25189

Incomplete energy accommodation in surface-catalyzed reactions 09 p1298 A83-25192

Theoretical limitations on heterogeneous catalysis by transition metals in aqueous atmospheric aerosols 09 p1298 A83-25196

Soot-catalyzed atmospheric reactions 09 p1298 A83-25198

NASA clean catalytic combustor program [ASME PAPER 82-JPGC-GT-11] 09 p1227 A83-25269

Reductive destruction of hydrazines as an approach to hazard control 12 p1712 A83-29094

Effects of nonequilibrium and surface catalysis on Shuttle heat transfer - A review [AIAA PAPER 83-1485] 15 p2127 A83-34916

Enantioselective catalysis as a possible path for optical activation of organic compounds in nature 17 p2557 A83-38898

Catalytically deposited carbon solar selective absorber 22 p3319 A83-46582

Catalysis in solar energy --- development of photoelectrochemical cells 22 p3320 A83-46794

CATALYSTS

NT ELECTROCATALYSTS

A sealed 100-Hz CO₂ TEA laser using high CO₂ concentrations and ambient-temperature catalysts 08 p1107 A83-21983

Decomposition of nitromethane over NiO and Cr₂O₃ catalysts 08 p1057 A83-22394

Catalytic combustion of propane/air mixtures on platinum 11 p1546 A83-28600

The removal of metals from a jet fuel using a manganese catalyst 11 p1552 A83-28775

Unified model of catalyzed and uncatalyzed decomposition of ammonium perchlorate 14 p1999 A83-32940

Quantum chemical studies of a model for peptide bond formation. II - Role of amine catalyst in formation of formamide and water from ammonia and formic acid 19 p2819 A83-41865

CATALYTIC ACTIVITY

Formation and catalytic activity of high molecular weight soluble polymers produced by heating amino acids in a modified sea medium 02 p0219 A83-11632

Catalytic autothermal reforming increases fuel cell flexibility 02 p0201 A83-11794

Mathematical modeling of homogeneous-heterogeneous reactions in monolithic catalysts 02 p0152 A83-13093

Photostimulated generation and emission of singlet oxygen from the surface of oxides doped with transition metal ions 07 p0878 A83-19642

A model for the transient behavior of catalytic combustors 09 p1226 A83-24364

Gas-phase ignition of premixed fuel by catalytic bodies in stagnation flow 09 p1226 A83-24368

Catalyst durability evaluation for advanced gas turbine engines [ASME PAPER 82-JPGC-GT-21] 09 p1274 A83-25270

Catalytic combustion with steam injection [ASME PAPER 82-JPGC-GT-23] 09 p1294 A83-25271

Flow of a gas mixture near a catalytic surface 13 p1932 A83-30669

The effect of the mechanisms of heterogeneous catalytic reactions on the heat flux in hypersonic flow past a blunted body 13 p1804 A83-30675

Catalysed recombination of CO and O₂ in sealed CO₂ TEA laser gases at temperatures down to -27 C 15 p2170 A83-35254

Features of the simulation of the catalytic properties of surfaces in subsonic and hypersonic flows 17 p2447 A83-37508

Catalytic mechanism of histone in peptide formation from phenylalanyl adenylate 17 p2557 A83-38893

Thiol-catalyzed formation of lactate and glycerate from glyceraldehyde --- significance in molecular evolution 20 p3036 A83-42398

CATAPULTS

NT ROCKET CATAPULTS

CATARACTS

Possible dependence of complications of intracapsular cataract extraction on the phases of the moon 05 p0674 A83-17210

Cataractogenesis from high-LET radiation and the Casarett model 19 p2873 A83-40848

CATASTROPHE THEORY

Resonant electrodynamic heating and the thermal stability of coronal loops 01 p0129 A83-10950

Polarization catastrophe model of static electrification and spokes in the B-ring of Saturn 07 p1028 A83-20083

Catastrophe theory in physics 09 p1338 A83-23852

The problem of sudden coronary death in the light of mathematical catastrophe theory 13 p1900 A83-30093

Application of catastrophe theory to a slotted ALOHA communication system 16 p2343 A83-36580

Generation of a countable set of homoclinic flows through bifurcation 20 p3043 A83-43564

A plain man's guide to bifurcations 22 p3353 A83-45694

CATCHERS

Scattering of Al₂O₃ and LiNbO₃ in the electronic stopping region [BAP-24] 07 p0901 A83-21057

CATCHMENT AREAS

U WATERSHEDS

CATECHOLAMINE

NT EPINEPHRINE

The role of catechol-o-methyltransferase in catecholamine transformations in the hypothalamus of rats at long-term intervals after irradiation 03 p0377 A83-14886

The effect of azaperone on the dynamics of the stress-reaction and the content of catecholamines in the adrenal glands of rats during immobilization stress 07 p0975 A83-20984

An investigation of the participation of the venous return in the pressor changes of systemic hemodynamics by means of the automatic control of its size 08 p1145 A83-22107

The role of catecholamines in the development of spontaneous arterial hypertension in spontaneously hypertensive rats 08 p1146 A83-22119

The sympathoadrenal system during hypoxic conditions 09 p1321 A83-25153

Effect of hyperoxia on metabolic and catecholamine responses to prolonged exercise 13 p1902 A83-30456

Effects of water immersion on plasma catecholamines in normal humans 13 p1902 A83-30465

Sympathoadrenal responses to cold and ketamine anesthesia in the rhesus monkey 13 p1898 A83-30496

Effect of hypoxia and hypercapnia on catecholamine content in cat carotid body 14 p2064 A83-32822

The interaction of prostaglandins and the sympathic-adrenal system 14 p2066 A83-33328

The behavior of heart rate in flight under +Gz stimulation Continuous monitoring using Holter's method and catecholamine excretion 17 p2561 A83-38944

Effects of various levels of hypoxia on plasma catecholamines at rest and during exercise 18 p2734 A83-40361

The changes in the content of catecholamines in the dopamine-synthesizing nuclei of the brain of rats in conditions of immobilization stress 19 p2879 A83-42093

Effect of catecholamine depletion on ventilatory control in unanesthetized normoxic and hypoxic rats 20 p3033 A83-43486

The pattern of the changes in the concentration of catecholamines and acetylcholine in the blood during the prolonged action of a constant magnetic field with a high induction 21 p3186 A83-45379

CATHODE GLOW

Structural and compositional characterization of mixed CdS-CdSe films grown by cathodic electrodeposition 10 p1446 A83-26055

Excitation mechanisms for hydrogen atoms in an inverse-brush-cathode discharge 16 p2415 A83-35668

The hollow cathode glow discharge analysed by optogalvanic and other studies --- Thesis 22 p3267 A83-46689

CATHODE RAY TUBES

Color selection and verification testing for airborne color CRT displays 04 p0524 A83-16128

- The perception of colour on electro-optical displays
04 p0524 A83-16328
- Colour flight deck displays
04 p0448 A83-16336
- Evaluation of the perceptual attributes of emissive and non-emissive display designs using computer simulation
05 p0677 A83-16870
- Multifunction display simulation facility
05 p0596 A83-17302
- Electronic visualizations and means of protection for the visual function - A method of study
06 p0800 A83-18344
- Calligraphic/raster color display for simulation
08 p1102 A83-22832
- New displays for the next generation of civil aircraft - Airbus A 310 and A 300/600 color cathode tubes
09 p1204 A83-24374
- Multifunction screens for cathode ray tubes
09 p1257 A83-25114
- Computer generated cockpit engine displays
10 p1376 A83-26309
- Human factors in the application of large screen electronic displays to transport flight station design
10 p1376 A83-26312
- Laser cathode ray tube with a semiconductor double-heterostructure screen
15 p2163 A83-33921
- Operator's activities at CRT terminals - A behavioural approach
16 p2400 A83-35564
- Application and experience of colour CRT flight deck displays
21 p3091 A83-44688
- Four-dimensional flight management using colour CRT displays
21 p3091 A83-44689
- Biocular magnifiers for use with cathode ray tube (CRT) displays
21 p3139 A83-44786

CATHODES

NT CELL CATHODES

NT HOLLOW CATHODES

NT PHOTOCATHODES

NT THERMIONIC CATHODES

Radial ion acceleration at a virtual cathode formed in a neutral gas by a relativistic electron beam
03 p0392 A83-13178

The hydrogen evolution process on a Ni-28 percent Mo alloy
06 p0728 A83-18146

Plasma layers near the electrodes of a cesium diode - Cathode layer
09 p1348 A83-23989

Hydrogen absorption and embrittlement of tantalum at cathodic deposition
10 p1399 A83-26897

On the nature of explosive electron emission
13 p1830 A83-30016

The morphology of silicon electrodeposits on graphite substrates --- in solar cells
14 p2091 A83-32629

Elastomeric binders for electrodes --- in secondary lithium cells
14 p1998 A83-32638

The state of the theory of vacuum arc cathodes
15 p2237 A83-35272

Cathode materials for sealed CO₂ waveguide lasers
16 p2360 A83-35962

Explosive-emission mechanism for producing a cathode spot and extreme energy characteristics of a nanosecond volume discharge in nitrogen
21 p3210 A83-44141

CATHODIC COATINGS

Electrodeposition of Ni-B₄C dispersion coatings
17 p2483 A83-38051

Chromium oxides as cathodes for lithium cells
24 p3600 A83-49943

CATHODOLUMINESCENCE

Study of the thermal conversion of semi-insulating GaAs:Cr with cathodoluminescence, photoluminescence, and secondary ion mass spectrometry
07 p1000 A83-20747

The assessment of thin film Cu(x)S-CdS solar cells using cathodoluminescence techniques
14 p2041 A83-32254

The anomalous kinetics of cathode luminescence in GaN:Zn
19 p2903 A83-40822

CATIONS

NT METAL IONS

Gravity-induced emf in superionic conductor RbAg₄I₅
22 p3364 A83-45621

CAUCHY INTEGRAL FORMULA

Bounds for the dislocation densities and the stress intensity factors in elastic crack problems
02 p0190 A83-12042

The numerical evaluation of one-dimensional Cauchy principal value integrals
06 p0804 A83-18899

A generalization of the concept of Cauchy-type principal value integrals for plane elasticity crack problems
08 p1121 A83-21865

Branched cracks at small angles /An addendum/
11 p1595 A83-28438

Approximate methods for the calculation of Cauchy integrals of a special form --- Russian book
12 p1770 A83-28816

A natural interpolation formula for Cauchy-type singular integral equations with generalized kernels
12 p1772 A83-29643

Monotonicity methods for nonlinear singular integral and integro-differential equations
18 p2740 A83-39987

Further convergence results for the weighted Galerkin method of numerical solution of Cauchy-type singular integral equations
20 p3041 A83-42497

A class of integral equations for solving three-dimensional axisymmetric elasticity problems
21 p3163 A83-45358

CAUCHY PROBLEM

Approximation of extremal surface elements /hyperbolic type/ by means of characteristic three-dimensional quadrilateral elements
03 p0388 A83-14493

Generalized solutions of the inverse Kolmogoroff equation, corresponding to the stochastic Navier-Stokes system
05 p0638 A83-17136

Asymptotics of the solution of the Cauchy problem for a class of singularly perturbed systems of integro-differential equations
05 p0682 A83-17833

The Cauchy problem for the equation of internal waves
06 p0758 A83-19117

Net-stress analysis in creep mechanics
06 p0778 A83-19324

Large-parameter asymptotics of the solution of the Fock-Klein-Gordon equation in the case of a discontinuous initial condition
09 p1339 A83-24318

Global solutions of nonstationary kinetic equations
09 p1350 A83-24322

Instability and the ill-posed Cauchy problem in elasticity
10 p1437 A83-25310

The analytic continuation of solutions of the generalized axially symmetric Helmholtz equation
10 p1470 A83-26775

Exact solutions to the nonlinear Boltzmann equation and its models
13 p1932 A83-30655

On an algorithm for the simplified integration of dynamic systems --- for flight trajectory analysis
13 p1914 A83-30724

Asymptotic behavior of solutions of the Cauchy problem for a KdV-type system for large times
13 p1914 A83-31346

Completeness of derivatives of squared Schroedinger eigenfunctions and explicit solutions of the linearized KdV equation
17 p2572 A83-38464

Upwind schemes and boundary conditions with applications to Euler equations in general geometries
19 p2789 A83-40752

Reduction of the problem of diffraction by parallel half-planes to the Riemann boundary value problem
21 p3121 A83-44779

The small dispersion limit of the Korteweg-de Vries equation. II
22 p3353 A83-47092

CAUCHY-RIEMANN EQUATIONS

A nonstationary relaxation method for the Cauchy-Riemann and 1-D Euler equations [AIAA PAPER 83-1901]
18 p2683 A83-39418

CAUSTIC LINES

Evolution of singularities of potential flows in collisionless media and transformations of caustics in three-dimensional space
05 p0683 A83-17135

The effect of random irregularities on the field strength of radio waves in the region of caustics
05 p0663 A83-17624

CAUSTICS

U ALKALIES

CAUSTICS (OPTICS)

Dynamic crack-tip stresses under stress wave loading - A comparison of theory and experiment
03 p0343 A83-14820

Inversion of scattering data of the shadow region of discontinuities
04 p0492 A83-15205

The exact form of caustics in mixed-mode fracture - A comparison with approximate solutions
07 p0948 A83-21342

The influence of geometrical imperfections in the method of caustics --- for stress intensity factor determination
18 p2696 A83-39085

The effect of biaxiality of loading in the orientation of caustics
18 p2699 A83-39538

The caustics of gravitational 'lenses'
20 p3071 A83-43047

On the behaviour of test matter in the neighbourhood of caustics of homogeneous cosmological models
20 p3074 A83-43377

CAVITATION

U CAVITATION FLOW

CAVITATION CORROSION

Mechanism of impact pressure generation from spark-generated bubble collapse near a wall
04 p0476 A83-15282

Correlations between cavitation, creep and dilation for multiaxial loading
04 p0501 A83-16269

Mechanics and mechanisms of intergranular cavitation in creeping alloys
06 p0728 A83-18478

Introduction to the viewpoint set on creep cavitation
07 p0886 A83-20626

Intergranular cavitation in creeping alloys

07 p0887 A83-20627

Models of creep cavitation and their interrelationships

07 p0887 A83-20628

Mechanisms of cavity growth in creep

07 p0887 A83-20629

Mechanisms of intergranular cavity nucleation and growth during creep
07 p0887 A83-20630

Continuous cavity nucleation and creep fracture
07 p0887 A83-20631

Chemically driven cavity growth
07 p0887 A83-20632

The influence of applied coatings on the creep fracture of IN 738 LC
07 p0894 A83-21488

Dynamics of microstructural changes in a superplastic aluminum alloy
07 p0897 A83-21611

Creep damage concepts and applications to design life prediction
09 p1233 A83-24080

Cavitation and Polyphase Flow Forum-1982; Proceedings of the Third Joint Thermophysics, Fluids, Plasma, and Heat Transfer Conference, St. Louis, Mo, June 7-11, 1982
11 p1566 A83-27420

Dynamics and mechanism of cavitation erosion on perspex and epoxy resin tested in a rotating disk device
11 p1551 A83-27422

Experimental research on cavitation erosion for an oscillating wing profile --- German thesis
17 p2493 A83-37497

Cavitation erosion characteristics of poly(methyl methacrylate) in a rotating disk device
19 p2824 A83-41851

CAVITATION FLOW

High-speed motion picture camera experiments of cavitation in dynamically loaded journal bearings [ASME PAPER 82-LUB-18]
03 p0335 A83-13509

Mechanism of impact pressure generation from spark-generated bubble collapse near a wall
04 p0476 A83-15282

New method for monitoring and correlating cavitation noise to erosion capability
04 p0478 A83-16138

Two- and three-dimensional rotational structures in a cavitating wake
06 p0756 A83-18145

Creep cavitation of grain interfaces
06 p0728 A83-18483

Nonlinear analysis of cavity flows around arbitrarily shaped bluff bodies in a constrained flow
06 p0758 A83-19020

Experimental study of the shock generation at the collapse of cavitation bubble
07 p0925 A83-20284

The suppression of creep cavitation and slow crack growth in Si-Al-O-N ceramics
08 p1070 A83-21781

Improved light-scattering cavitation nuclei classifier
08 p1106 A83-23229

Determination of the cavitation boundary in liquid flows through constricting devices
09 p1258 A83-23432

Spurious solutions in driven cavity calculations
09 p1259 A83-23725

Visualization studies of a shear driven three-dimensional recirculating flow
11 p1565 A83-27411

Cavitation and Polyphase Flow Forum-1982; Proceedings of the Third Joint Thermophysics, Fluids, Plasma, and Heat Transfer Conference, St. Louis, Mo, June 7-11, 1982
11 p1566 A83-27420

The initial stages of cavitation damage and erosion on copper and brass tested in a rotating disk device
11 p1547 A83-27421

Lagrangian pressure fluctuations in a jet
11 p1566 A83-27423

A scheme for the analysis of a developed cavitation flow past a wedge
11 p1567 A83-27719

Driven cavity flows by efficient numerical techniques
12 p1726 A83-29669

Oil leakage and friction forces of reciprocating O-ring seals considering cavitation
13 p1859 A83-30249

Bubble nucleation and growth in open-cycle OTEC subsystems
15 p2189 A83-33988

Effects of triaxial stressing on creep cavitation of grain boundaries
16 p2335 A83-36961

The calculation of separation bubbles in interactive turbulent boundary layers
18 p2633 A83-39216

High-speed motion picture camera experiments of cavitation in dynamically loaded journal bearings [ASME PAPER 82-LUB-18]
18 p2695 A83-39944

Bubble motion in a rotating liquid body --- ground based tests for space shuttle experiments
20 p2940 A83-43272

Cavitation research performed at the Ecole Nationale Supérieure des Techniques Avancées
20 p2987 A83-43725

On the calculation of separation bubbles
23 p3449 A83-48119

Toward attenuation of self-sustained oscillations of a turbulent jet through a cavity
23 p3453 A83-48680

The effect of regime and structural parameters of an inclined Archimedean screw forepump on the volume of cavitation cavities, their elasticity, and cavitation resistance 24 p3578 A83-49652

Dependence of the head of a centrifugal inclined Archimedean screw pump on the volume of cavitation cavities in the flow area of the pump 24 p3579 A83-49653

CAVITIES

Measurement of the periodicity of internal surfaces by ultrasonic testing 01 p0057 A83-10694

Asymptotic solutions for the motion of a viscous incompressible fluid filling the cavity of a rotating body 01 p0047 A83-11268

Object growing algorithm for cavity measurement in structural materials 01 p0053 A83-11443

Electromagnetic transmission through apertures in a cavity in a thick conductor 03 p0306 A83-14016

Finite-difference analysis of EM fields inside complex cavities driven by large apertures 03 p0308 A83-14549

The diffraction of a nonstationary transverse wave by a cylindrical cavity 04 p0497 A83-15385

Numerical calculation of two-dimensional natural convection in isothermal open cavities 05 p0641 A83-17742

New design for blackbody simulator cavities 08 p1104 A83-22877

Flow-excited resonances in covered cavities 09 p1340 A83-23339

A unifying view of the kinetics of creep cavity growth 09 p1279 A83-24066

Cavitation in nickel during oxidation and creep 09 p1232 A83-24067

Models for intergranular creep crack growth by diffusion 09 p1279 A83-24069

Creep crack extension by grain-boundary cavitation 09 p1279 A83-24070

Cavitation and creep crack growth in low alloy steels 09 p1233 A83-24077

Effect of cavities on creep 09 p1283 A83-25206

Crack and cavity nucleation at interfaces during creep 10 p1396 A83-25861

The effects of segregation on the kinetics of intergranular cavity growth under creep conditions 10 p1396 A83-25862

Amplification of non-linear standing waves in a cylindrical cavity with varying cross section 10 p1414 A83-26143

Dynamic stress concentration around a circular hole in an infinite elastic strip 10 p1440 A83-26430

Interaction of a P-wave with a laterally stiffened slot 10 p1440 A83-26431

Analysis of elastic torsion in a bar with circular holes by a special boundary integral method [ASME PAPER 83-APM-15] 10 p1440 A83-26435

A numerical implementation of the variational method for solving certain problems in hydrodynamics --- free-surface oscillations of ideal incompressible fluid in axisymmetric cavity 11 p1569 A83-28460

A study of flow in a short cavity with one-way fluid inlet and outlet 11 p1570 A83-28794

Nonlinear resonant interactions in internal cavity flows 12 p1721 A83-28972

Convective heat transfer in rotating cylindrical cavity [ASME PAPER 82-GT-151] 13 p1840 A83-30239

Thin axisymmetric cavities in flow past a body in a longitudinal gravitational field 14 p2008 A83-32158

Manufacturing methods for composite graphite hole generation [SAE PAPER 821418] 17 p2516 A83-37976

Constitutive behavior and crack tip fields for materials undergoing creep-constrained grain boundary cavitation 17 p2492 A83-38860

Singular stresses in an infinite solid with a flat annular crack around a spherical cavity under tension 18 p2696 A83-39080

The dynamics of a rigid body having an ellipsoidal cavity filled with a magnetic fluid --- in theory of neutron stars 19 p2916 A83-41209

Evaluation of effective emissivities of nonisothermal cavities 20 p2988 A83-42217

Natural convection heat transfer in cavities and cells 20 p2971 A83-42662

Numerical study of the interaction of natural convection with radiation in nongray gases in a narrow vertical cavity 20 p2972 A83-42674

Natural convection in an open cavity 20 p2973 A83-42681

Control of superplastic cavitation by hydrostatic pressure --- in aluminum alloys 20 p2954 A83-43342

Development of forming limits for superplastic formed fine grain 7475 Al 20 p2954 A83-43343

The effect of regime and structural parameters of an inclined Archimedean screw forepump on the volume of cavitation cavities, their elasticity, and cavitation resistance 24 p3578 A83-49652

CAVITONS

Thermal cavitons --- Langmuir waves in plasma density depressions 13 p1925 A83-30421

Coherence in chaos turbulence 19 p2901 A83-40963

CAVITY RESONATORS

A study of secondary-emission microwave discharges with large electron transit angles 01 p0104 A83-11300

Reflection properties and applications of resonant optical cavities 02 p0235 A83-11564

Intracavity adaptive optics. III - HSURIA performance --- Half-Symmetrical Unstable Resonator with Intracavity Axiicon 02 p0236 A83-12319

Nonlinear self-excited acoustic oscillations within fixed boundaries 03 p0391 A83-14582

Numerical analysis of shielded dielectric resonators including substrate, support disc and tuning post 04 p0470 A83-15237

Uniaxially strained ZnO/SiO₂/Si SAW resonators 04 p0470 A83-15246

Automatic determination of frequency response parameters and distortion in resonant microwave cavities 06 p0750 A83-17970

Loaded Q's and field profiles of tapered axisymmetric gyrotron cavities 06 p0752 A83-18759

A multiple-device cavity oscillator using both magnetic and electric coupling mechanisms 06 p0753 A83-18769

A finite element analysis of planar circulators using arbitrarily shaped resonators 06 p0753 A83-18772

Synthesis of a waveguide field-converter 06 p0755 A83-19361

Multistability at microwave frequencies 08 p1079 A83-22011

Frequency-shift of self-trapped light --- due to decrease in resonant frequency of plasma cavity 08 p1168 A83-22391

Simulation and study of efficiency-optimized interaction processes in multicavity klystrons 09 p1252 A83-23463

Nonlinear analysis of a diffraction-radiation generator with two field spots 09 p1270 A83-23472

Intracavity adaptive optic compensation of phase aberrations. III - Passive and active cavity study for a large N/eq resonator 09 p1271 A83-24087

A study of the characteristics of a cylindrical resonator with a two-layer filler 09 p1256 A83-24918

A new class of optical multistabilities and instabilities induced by atomic coherence 10 p1481 A83-25434

Mode control in a submillimetre open resonator with a variable iris 10 p1425 A83-25459

Radiation exchange and oscillations in a pair of cavities sharing a partial reflector 10 p1482 A83-26002

Cylindrical resonators --- shock wave production in jet nozzles 10 p1380 A83-26162

Single-axial-mode operation of a polarization-coupled stable/unstable-resonator Nd:YAG laser oscillator - Update 11 p1577 A83-27519

On a single-cavity regenerative power-combining system 11 p1561 A83-27938

Image line Gunn diode combiner oscillators 11 p1563 A83-28593

Rectangular dielectric resonator antenna [AD-A129976] 11 p1558 A83-28608

Representation of coupled-cavity slow-wave structures by equivalent circuits 12 p1719 A83-29418

Shielded dielectric resonators 12 p1720 A83-29461

Determination of loaded, unloaded, and external quality factors of a dielectric resonator coupled to a microstrip line 13 p1831 A83-30228

Optimization of an electrodynamic basis for determination of the resonant frequencies of microwave cavities partially filled with a dielectric 13 p1831 A83-30234

Design and preparation of high-Q niobium reentrant cavities for physics measurements 13 p1845 A83-30252

Investigation of cylindrical resonators containing annular inhomogeneities 13 p1832 A83-30276

Theoretical analysis of the possibilities of an open-cavity klystron 13 p1833 A83-30710

Two-cavity klystron uses single-cavity tuning 13 p1835 A83-30913

A compact hydrogen maser with exceptional long-term stability 13 p1856 A83-31292

On the complex resonant frequency of open dielectric resonators 14 p2008 A83-33458

8 GHz tunable Gunn oscillator in WR-137 waveguide 15 p2150 A83-33870

Open coaxial resonance structures --- Russian book 15 p2152 A83-34168

The resonant cylindrical dielectric cavity antenna 15 p2148 A83-35175

Observation of cavity-enhanced single-atom spontaneous emission 16 p2410 A83-35746

Resonant frequencies, Q-factor, and susceptance slope parameter of waveguide circulators using weakly magnetized open resonators 17 p2497 A83-37798

Integration decrement method for measuring Q of microwave resonators 17 p2500 A83-38889

A proposal of a new dielectric resonator construction for MIC's 19 p2838 A83-41085

Theory of spontaneous-emission line shape in an ideal cavity 19 p2898 A83-41155

Magnetostatic wave tunable resonators 20 p2967 A83-42823

Scattering matrix description of microwave resonators 21 p3123 A83-43837

Schumann resonances --- earth surface-ionosphere cavity resonator 22 p3325 A83-45880

Observations of self-induced Rabi oscillations in two-level atoms excited inside a resonant cavity - The ringing regime of superradiance 23 p3461 A83-47609

Diffractional Q-factor of weakly conical resonators of gyrotrons 23 p3445 A83-48492

Highly stable FET DROs using new linear dielectric resonator material --- Dielectric Resonator Oscillators 23 p3446 A83-48723

A 3M-device cavity-type power combiner 24 p3573 A83-48967

CCD

U CHARGE COUPLED DEVICES

CDMA

U CODE DIVISION MULTIPLE ACCESS

CEILING (ARCHITECTURE)

Towards wind-aided flame spread along a horizontal charring slab - The steady-flow problem 17 p2484 A83-37048

CEILINGS (METEOROLOGY)

Verification of numerically produced flight weather products 17 p2548 A83-38705

CEILOMETERS

U CLOUD HEIGHT INDICATORS

CELESTIAL BODIES

NT A STARS

NT ACHONDRITES

NT AMOR ASTEROID

NT ANDROMEDA GALAXIES

NT AQUARIUS METEOROIDS

NT ASTEROID BELTS

NT ASTEROIDS

NT AUSTRALITES

NT B STARS

NT BARRED GALAXIES

NT BINARY STARS

NT BL LACERTAE OBJECTS

NT BLUE STARS

NT BOLIDES

NT BRUDERHEIM METEORITE

NT CALLISTO

NT CARBON STARS

NT CARBONACEOUS CHONDRITES

NT CARBONACEOUS METEORITES

NT CASSIOPEIA A

NT CEPHEID VARIABLES

NT CERES ASTEROID

NT CHARON

NT CHONDRITES

NT COMET HEADS

NT COMET NUCLEI

NT COMET TAILS

NT COMETS

NT COMPANION STARS

NT CRAB NEBULA

NT DEIMOS

NT DISK GALAXIES

NT DWARF GALAXIES

NT DWARF NOVAE

NT DWARF STARS

NT EARLY STARS

NT EARTH (PLANET)

NT ECLIPSING BINARY STARS

NT ELLIPTICAL GALAXIES

NT ENCKE COMET

NT EUROPA

NT EXTARS

NT EXTRAGALACTIC RADIO SOURCES

NT EXTRASOLAR PLANETS

NT FLARE STARS

NT GALACTIC CLUSTERS

NT GALAXIES

NT GALILEAN SATELLITES

NT GANYMEDE

NT GAS GIANT PLANETS

NT GEMINID METEORIDS
 NT GIACOBINI-ZINNER COMET
 NT GIANT STARS
 NT GLOBULAR CLUSTERS
 NT GUM NEBULA
 NT HALLEY'S COMET
 NT HERBIG-HARO OBJECTS
 NT HORIZONTAL BRANCH STARS
 NT HOT STARS
 NT IAPETUS
 NT INFRARED STARS
 NT IO
 NT IRAS-ARAKI-ALCOCK COMET
 NT IRON METEORITES
 NT JUPITER (PLANET)
 NT JUPITER RINGS
 NT JUPITER SATELLITES
 NT KOHOOTEK COMET
 NT LATE STARS
 NT M STARS
 NT MAGNETIC STARS
 NT MAIN SEQUENCE STARS
 NT MARS (PLANET)
 NT MERCURY (PLANET)
 NT METALLIC STARS
 NT METEORITES
 NT METEOROID DUST CLOUDS
 NT METEOROID SHOWERS
 NT METEORIDS
 NT MICROMETEORITES
 NT MICROMETEORIDS
 NT MILKY WAY GALAXY
 NT MOON
 NT MRKOS COMET
 NT NATURAL SATELLITES
 NT NEBULAE
 NT NEPTUNE (PLANET)
 NT NEUTRON STARS
 NT NOVAE
 NT O STARS
 NT ORGUEIL METEORITE
 NT ORION NEBULA
 NT ORIONID METEORIDS
 NT PECULIAR STARS
 NT PERSEID METEORIDS
 NT PHOBOS
 NT PLANETARY NEBULAE
 NT PLANETS
 NT PLUTO (PLANET)
 NT PRAESEPE STAR CLUSTERS
 NT PROTOPLANETS
 NT PROTOSTARS
 NT PULSARS
 NT QUASARS
 NT RADIO GALAXIES
 NT RADIO METEORS
 NT RADIO SOURCES (ASTRONOMY)
 NT RADIO STARS
 NT RED DWARF STARS
 NT RED GIANT STARS
 NT REFERENCE STARS
 NT REFLECTION NEBULAE
 NT RHEA (ASTRONOMY)
 NT S STARS
 NT SATURN (PLANET)
 NT SATURN RINGS
 NT SCHWASSMANN-WACHMANN COMET
 NT SEYFERT GALAXIES
 NT SOLAR SYSTEM
 NT SPIRAL GALAXIES
 NT SPORADIC METEORIDS
 NT STAR CLUSTERS
 NT STARS
 NT STONY METEORITES
 NT SUBDWARF STARS
 NT SUBGIANT STARS
 NT SUN
 NT SUPERGIANT STARS
 NT SUPERMASSIVE STARS
 NT SUPERNOVAE
 NT T TAURI STARS
 NT TAURID METEORIDS
 NT TEKITES
 NT TERRESTRIAL PLANETS
 NT TITAN
 NT TORO ASTEROID
 NT TRITON
 NT TUNGUSK METEORITE
 NT URANUS (PLANET)
 NT URANUS RINGS
 NT VARIABLE STARS
 NT VENUS (PLANET)
 NT VIRGO GALACTIC CLUSTER
 NT WEST COMET
 NT WHITE DWARF STARS

NT WHITE HOLES (ASTRONOMY)
 NT WOLF-RAYET STARS
 NT ZODIACAL DUST
 Dictionary of the nomenclature of celestial objects
 01 p0114 A83-10151
 Interaction between a magnetized plasma flow and a strongly magnetized celestial body with an ionized atmosphere - Energetics of the magnetosphere
 02 p0258 A83-12180
 Mid- and far-infrared extinction coefficients of hydrous silicate minerals
 05 p0707 A83-17808
 Investigation in the whole of the rotational motion of a rigid body
 06 p0806 A83-19116
 An optimal procedure for non-parametric elimination of observational cutoff bias in complete samples --- of celestial objects
 09 p1354 A83-24477
 Interaction between large cosmic bodies and atmosphere
 11 p1600 A83-27346
 A model for negative polarization of light by cosmic bodies without atmospheres
 13 p1940 A83-31275
 The equilibrium structure of loaded rotating polytropes --- in astronomical bodies study
 18 p2764 A83-39000
 IRAS follow-up - Problems and prospects
 18 p2763 A83-40464
 Time and latitude results of observations made at Merate Observatory with the astrolabe for the year 1982
 19 p2910 A83-41058
 Determination of the minimum distance between the orbits of celestial bodies
 24 p3645 A83-49630

CELESTIAL GEODESY

Miniature interferometer terminals for earth surveying /MITES/ - Geodetic results and multipath effects
 01 p0070 A83-10022
 Astronomical observations with the automatic camera for astrogodesy from JENA
 02 p0249 A83-13048
 Precision of the determination of the mutual location of points on the basis of satellite observations
 03 p0356 A83-13296
 Concerning the processing and the accuracy estimation of results of very long baseline interferometry in a single system of coordinates --- for geodesy
 04 p0514 A83-16380
 On the question of correlation in satellite geodesy networks
 04 p0514 A83-16382
 Expansion of planetary gravitational potential in a system of fundamental solutions of the Laplace equation
 04 p0514 A83-16383
 Geometric methods for determining the axis of rotation and coordinates of the center of mass of a planet from orbital data
 04 p0514 A83-16384
 Allowance for the influence of geopotential in the high-precision numerical integration of artificial-earth-satellite orbits
 04 p0453 A83-16385
 Determination of disturbing components of the pressure force of solar radiation reflected from the earth, with allowance for the shadow effect in the case of intermediate satellite-motion
 08 p1048 A83-22094
 Power series for determining satellite motion perturbations caused by solar radiation reflected from the earth, with allowance for the shadow effect
 08 p1048 A83-22095
 Recursive formulas for determining the intermediate coordinates of quasi-polar satellites
 08 p1048 A83-22096
 Recursive formulas for determining perturbing accelerations in intermediate satellite motion
 08 p1048 A83-22097
 Distance errors related to atmospheric effects at signal frequencies greater than 100 MHz in the case of geodetic systems of measurement. I - Influence of the troposphere. II - Influence of the ionosphere
 09 p1301 A83-23387
 The global stress field in the lithosphere obtained from the satellite gravitational harmonics
 12 p1752 A83-29222
 Secular variation of earth's gravitational harmonic J2 coefficient from Lageos and nontidal acceleration of earth rotation
 17 p2545 A83-38597
 Directions of axes of the earth's ellipsoid of inertia derived from satellite orbit dynamics
 19 p2860 A83-41317
 The effect of the ellipticity and unevenness of the pivots in a multipurpose astronomical instrument on observations for determining the azimuth by the direct method
 19 p2854 A83-41552
 Nodal period of a satellite perturbed by the earth's oblateness
 21 p3094 A83-43981
 International Symposium on Geodetic Networks and Computations, Munich, West Germany, August 31-September 5, 1981, Proceedings. Volume 4 - Modern observation techniques for terrestrial networks
 22 p3315 A83-46336
 Modern observation techniques for terrestrial networks
 22 p3316 A83-46337

Geodesy and the global positioning system
 22 p3252 A83-46338
 New method for the reduction of satellite data applicable to geodesy
 22 p3316 A83-46339
 Consequences of Gravsat and GPS - New concept of geodetic networks
 22 p3316 A83-46340
 On the use of orbital methods for development of satellite geodetic networks
 22 p3316 A83-46341
 International Symposium on Geodetic Networks and Computations, Munich, West Germany, August 31-September 5, 1981, Proceedings. Volume 7 - Combination of horizontal, vertical and gravity networks
 22 p3316 A83-46351
 Combination of horizontal, vertical and gravity networks - A review
 22 p3316 A83-46352
 A contribution to 3D-operational geodesy. I - Principle and observational equations of terrestrial type. II - Concepts of solution
 22 p3317 A83-46354
 Test computations of three-dimensional geodetic networks with observables in geometry and gravity space
 22 p3317 A83-46357
 Three-dimensional adjustment of geodetic networks using gravity field data
 22 p3317 A83-46358
 An investigation on the optimization of the space objects Observations for the East-European satellite triangulation
 22 p3259 A83-46364
 Satellite technology developments in gravity research [IAF PAPER 83-223]
 23 p3414 A83-47314
 Orbital rates of earth satellites at resonances to test the accuracy of earth gravity field models
 24 p3550 A83-48768

CELESTIAL MECHANICS

Motion of the sun in the interstellar medium
 01 p0124 A83-10845
 Cosmic turbulence and the angular momenta of astronomical systems
 02 p0252 A83-11598
 Conference on Mathematical Methods in Celestial Mechanics, 7th, Oberwolfach, West Germany, August 24-28, 1981, Proceedings
 03 p0404 A83-13405
 Central configurations of four bodies with one inferior mass
 03 p0404 A83-13406
 Motion near total collapse in the planar isosceles three-body problem
 03 p0404 A83-13408
 Boundary manifolds for energy surfaces in celestial mechanics
 03 p0404 A83-13409
 Analysis of some degenerate quadruple collisions
 03 p0389 A83-13410
 Quasi-periodic solutions of the plane three-body problem near Euler's orbits
 03 p0404 A83-13416
 The determination of the derivatives in Brown's lunar theory
 03 p0405 A83-13421
 The Liapunov transformation of Hill's equation and its dynamic interpretation
 03 p0390 A83-13424
 The problem of hyperbolic meteors
 03 p0426 A83-14676
 Theory for the motion of all the planets - The VSOP82 solution
 03 p0410 A83-14761
 On the stability of the inner planets, satellites and close binaries
 04 p0547 A83-15600
 Characteristics of resonant periodic orbits
 04 p0547 A83-15968
 On resonance in celestial mechanics /A survey/
 04 p0548 A83-16359
 The equilibrium of a galactic bar. II - Stellar-dynamical counterparts of the s-type Riemann ellipsoids
 05 p0697 A83-16993
 An analytic solution to the classical two-body problem with drag
 06 p0720 A83-17990
 The Fourier-Chebyshev approximation for time series with a great many terms --- for describing motions of celestial bodies
 06 p0817 A83-17991
 Translation effect of reference system on harmonic coefficients of gravitational potential
 06 p0817 A83-18018
 Relativistic perturbations of the moon in ELP 2000
 06 p0817 A83-18084
 Method for constructing families of three-dimensional periodic orbits in the Hill problem
 06 p0721 A83-18351
 Is there a ring around Milky Way
 06 p0828 A83-18419
 Motion of a particle in the gravitational field of a periodic variable star
 06 p0819 A83-18849
 The translational-rotational motion of two rigid bodies - Existence conditions for plane motion
 07 p1006 A83-20662
 The Newtonian potentials and dynamics of a stratified ellipsoid --- study of elliptical galaxies
 07 p1026 A83-21258
 Analytical theory of the libration of the moon
 08 p1190 A83-23125
 Symmetries in the three body problem
 09 p1353 A83-24018
 On the equatorial orbits of a satellite of a triaxial attracting rigid body
 09 p1212 A83-25044

Conservative mass transfer in close binary systems. I -
Equations of motion for spin and orbital angular
momenta 10 p1510 A83-26386
Equations of motion of the problem of two bodies with
variable masses 11 p1669 A83-27453
The modified Encke method --- for orbit calculation
11 p1672 A83-27884
On the regularization of the Hill problem
11 p1673 A83-28031
Questions concerning the solution of a system of
condition equations --- for calculation of planetary orbital
elements 11 p1673 A83-28038
New algorithms for quasi-periodic solutions --- of
oscillating systems in celestial mechanics
11 p1673 A83-28040
On the integration of functions of elliptical motion
11 p1673 A83-28043
Method for determining an orbit parameter from two
positions of a celestial body using an auxiliary orbit
11 p1674 A83-28045
Intermediate orbits with fourth-order tangency to
trajectories of perturbed motion
11 p1674 A83-28047
The use of the uniform approximation of the coordinates
of perturbing bodies in the Taylor-Steffensen numerical
integration method 11 p1674 A83-28048
The linking of two apparitions of Comet
Schwassmann-Wachmann 3 /1930 VI/ and the evolution
of its orbit over 200 years /1800-2000/
11 p1674 A83-28049
Investigation of encounters of Comet Chernykh /1978
IV/ with Jupiter in 1978-1981 and with Saturn in
1981-1984 11 p1674 A83-28052
Some applications of the Jacobi integral in fixed axes
--- for three body problem 11 p1674 A83-28195
Loss of angular momentum in a binary system due to
collisionless particles as monopoles or gravitinos - Does
it exceed the gravitational radiation emission in the binary
system PSR 1913+16? 12 p1792 A83-29037
The KS-transformation in hypercomplex form
12 p1786 A83-29103
Families of asymmetric periodic solutions of the
restricted problem of three bodies for the sun-Jupiter mass
ratio and their relationship with the symmetric families.
12 p1786 A83-29104
Evolution with the mass parameter of families of
asymmetric periodic solutions of the restricted three body
problem 12 p1786 A83-29105
On the stability of close binaries in hierarchical
three-body systems 12 p1787 A83-29113
Solution of equations of problem of motion of a heavy
rigid body about a fixed point in the Kowalevskaya's case
using theta-function 12 p1775 A83-29115
The rotation number of bounded orbits in a central
field 12 p1787 A83-29116
Stability criteria in many-body systems. V - On the totality
of possible hierarchical general four-body systems
12 p1787 A83-29117
On the double averaged three-body problem
12 p1787 A83-29118
About the non-existence of additional analytical integral
in the problem of satellite's motion under the gravitational
attraction of a triaxial rigid body 12 p1787 A83-29120
On the stability of the solar system 12 p1794 A83-29297
Comets, planet X and the orbit of Neptune 12 p1789 A83-29709
Libration points of central configurations 13 p1940 A83-31273
Reaction deceleration of comet nuclei and their relation
to the structure of meteor swarms 13 p1940 A83-31344
Periodic motions of a satellite in the gravitational field
of a rotating rigid body 13 p1809 A83-31397
Theory for the motion of the four giant planets - The
TOP 82 solution 13 p1941 A83-31556
An observational study of the dynamics of binary
galaxies 13 p1942 A83-31696
The evolution of clusters of galaxies. I - Very rich
clusters 14 p2104 A83-33180
Approximations to the radii of Roche lobes 14 p2106 A83-33213
Numerical results in the three-body problem 14 p2100 A83-33251
On the equilibrium configurations of prolate,
axisymmetric stellar systems 15 p2257 A83-34091
Orbital period changes in Centaurus X-3 15 p2258 A83-34105
Direct perturbations of the planets on the moon's motion
Results and comparisons 15 p2246 A83-34389
Periodic orbits in a three-dimensional potential 16 p2425 A83-36675
The light curves of a freely precessing spheroidal minor
planet 16 p2438 A83-36689

The planar inverse problem with four monoparametric
families of curves --- for coplanar cofocal elliptical orbits
in autonomous gravitational field 16 p2426 A83-36691
Some particular solutions of the restricted problem of
three rigid bodies --- in circular orbit 17 p2594 A83-38566
Stability and integrability in the planar general three-body
problem 18 p2757 A83-39606
Velocity distribution of stars and relaxation in the galactic
disk 18 p2768 A83-39640
Masses and mystery in the local group --- of galaxies
18 p2771 A83-39670
Expansion theory for the elliptic motion of arbitrary
eccentricity and semi-major axis . V - Elliptic expansions
in terms of the sectorial variables for the first four
categories 18 p2759 A83-39747
Orbital evolution and origin of the Martian satellites
19 p2910 A83-40785
Series summation under recurrent relations in problems
involving the motion of artificial earth satellites
19 p2810 A83-41550
The effect of low-velocity, low-mass intruders
(collisionless gas) on the dynamical evolution of a binary
system 20 p3064 A83-42200
The lunar ephemeris ELP 2000 20 p3059 A83-42383
Local regularization of the magnetic-binary problem ---
charged particle motion and two body problem with
magnetic dipoles 20 p3061 A83-43570
The gravitational potential due to uniform disks and
rings 20 p3061 A83-43571
Discrete mechanics - Some remarks --- numerical
method in celestial mechanics 20 p3062 A83-43573
Special cases in the problem of two rigid bodies
20 p3062 A83-43574
Generalized f and g series and convergence of the power
series solution of the n-body problem 20 p3062 A83-43575
Equations of motion of the restricted problem of three
bodies with variable mass 20 p3062 A83-43579
The elimination of the critical terms of a first order
Uranus-Neptune theory by Hori's method. II 20 p3062 A83-43584
Resonant effects during the tidal encounter of disc
galaxies 21 p3232 A83-44732
Escape velocities of interacting spherical galaxies 21 p3234 A83-44870
On a class of intermediate orbits 21 p3095 A83-45290
Further studies on criteria for the onset of dynamical
instability in general three-body systems 22 p3373 A83-46388
Distribution of cometary binding energies based on the
assumption of steady state 22 p3379 A83-46564
The angular momentum of celestial bodies and the
fundamental dimensionless constants of nature 23 p3518 A83-47423
Angular momentum loss and the formation of W UMa
systems 23 p3523 A83-47527
Symmetric rectilinear periodic orbits of three bodies 24 p3637 A83-48762
Three-dimensional regions of stability about the
triangular equilibrium points 24 p3638 A83-48766
The application of the Kolmogoroff-Feller equation to
problems of stellar dynamics 24 p3650 A83-48930
Simulations of galaxy mergers 24 p3642 A83-49259
The secular accelerations in Gylden's problem --- of lunar
motion 24 p3643 A83-49391
Regularization and linearization of the equations of
motion in central force-fields 24 p3551 A83-49395
The topology of three-body scattering --- in celestial
mechanics 24 p3646 A83-49892
The dynamics of elliptical rings --- of Saturn and
Uranus 24 p3646 A83-49893
CELESTIAL NAVIGATION
NT ASTRONAVIGATION
A process for retrieval of data from a compiled star
catalogue 01 p0114 A83-10142
Celestial navigation in the computer age --- Book
03 p0280 A83-14116
Celestial views from nonrelativistic and relativistic
interstellar spacecraft 09 p1210 A83-23681
Maximization of the accuracy of autonomous navigation
in the case of the measurement of angles between
directions from an artificial earth satellite to a known star
and an unspecified ground reference point 09 p1215 A83-25043
On the choice of the equatorial coordinates of celestial
bodies from computer printouts during the calculation of
their azimuths 12 p1706 A83-29322
Autonomous satellite navigation by stellar refraction
[AIAA PAPER 83-2211] 19 p2814 A83-41695
CELESTIAL OBSERVATION
U ASTRONOMY

CELESTIAL REFERENCE SYSTEMS
Towards a new scale of extragalactic distances
01 p0118 A83-11337
A pool of faint stars applied to star catalogue
formation 03 p0411 A83-14808
Translation effect of reference system on harmonic
coefficients of gravitational potential 06 p0817 A83-18018
The connection of a catalogue of stars with an
extragalactic reference frame 06 p0817 A83-18086
Orientation of the FK 4 coordinates from the Washington
observations of the sun and planets 07 p1007 A83-20673
Precise optical positions for radio/optical astrometric
sources in the southern hemisphere 10 p1493 A83-25654
Optical positions of quasars 13 p1942 A83-31710
Conditions of the construction and accuracy
characteristics of reference grids on planets and
satellites 16 p2435 A83-35502
Variances and correlations of errors of rectangular
coordinates of selenodetic reference points 16 p2439 A83-36859
Accuracy of the external orientation of a selenodetic
coordinate system 16 p2439 A83-36860
Determination of the orientation angles of a selenodetic
coordinate system on the basis of photographic positional
observations of the moon 16 p2439 A83-36861
The first astrolabe catalogue at Valinhos 17 p2587 A83-37281
Regions of low molecular column density near the
galactic plane 17 p2602 A83-37829
Precise positions in the FK4 system for ten optical
counterparts of extragalactic radio sources 22 p3373 A83-46385
CELESTIAL SPHERE
A fast method to retrieve data from a large star catalogue
file 01 p0113 A83-10138
A method for the operational calculation of the expected
number of stars in a given region of the celestial sphere
05 p0694 A83-17677
CELL ANODES
Oxygen evolution improvement at a Cr-doped SrTiO3
photoanode by a Ru-oxide coating 04 p0505 A83-15493
The preparation of TiO2 thick film anodes for
photoelectrochemical solar cells 04 p0505 A83-15494
Research on oxidation by air and tempering of Raney
nickel electrocatalysts for the H2 anodes of alkali
combustion materials cells --- German thesis 06 p0726 A83-18494
Cold pressed cadmium selenide photoanodes for
electrochemical solar cells 18 p2708 A83-39929
On the suppression of self discharge of the zinc
electrodes of zinc-air cells and other related battery
systems 24 p3599 A83-49931
On the processes responsible for the degradation of the
aluminium-lithium electrode used as anode material
in lithium aprotic electrolyte batteries 24 p3600 A83-49933
Characterization of the chemistry at the anode and
cathode in the Li/SO2 battery system 24 p3600 A83-49948
The anodic passivation of lithium 24 p3558 A83-49956
CELL CATHODES
The effect of thickness on the performance of molten
carbonate fuel cell cathodes 04 p0506 A83-15869
Precipitate formation during sea water electrolysis
04 p0506 A83-16040
The molten carbonate carbon dioxide concentrator -
Cathode performance at high CO2 utilization --- in manned
space station cabin atmospheres 07 p0879 A83-19880
Porous perovskite electrode as molten carbonate
cathode --- in fuel cells 07 p0955 A83-20596
Defects in nsutite (gamma-MnO2) and dry-cell battery
efficiency 18 p2708 A83-39964
Electrochemical reduction of calcium chromate ---
cathode material in Ca/CaCrO4/Fe thermally activated
batteries 22 p3268 A83-46895
Chromium oxides as cathodes for lithium cells 24 p3600 A83-49943
Behaviour of various cathode materials for nonaqueous
lithium cells 24 p3600 A83-49944
Characterization of the chemistry at the anode and
cathode in the Li/SO2 battery system 24 p3600 A83-49948
Behaviour of AgBi(Cr2O7)2 as a possible cathode for
lithium cells 24 p3601 A83-49953

CELL DIVISION

A comparative analysis of the effect of alkylating agents, ionizing radiation, and ultraviolet light on the mammalian cell progression in the mitotic cycle. I - The effect of N-methyl-N'-nitro-N-nitrosoguanisine on the passing of various phases of the cycle by HeLa cells

06 p0796 A83-19378

Some karyological observations on plants grown in space

11 p1639 A83-27824

CELLS (BIOLOGY)

NT AXONS

NT CHROMOSOMES

NT COLLAGENS

NT EOSINOPHILS

NT ERYTHROCYTES

NT HEMATOPOIESIS

NT HEMOGLOBIN

NT LEUKOCYTES

NT LYMPHOCYTES

NT MACROPHAGES

NT MITOCHONDRIA

NT NEURONS

NT OXYHEMOGLOBIN

The effect of biostimulation amplification after the combined action of laser irradiation in the blue and red regions of the spectrum

01 p0078 A83-10456

The functional differentiation of the vascular smooth muscle cells and the basal tonus of the vessels

01 p0078 A83-10486

Cloning higher plants from aseptically cultured tissues and cells

02 p0219 A83-11823

Is cell aging caused by respiration-dependent injury to the mitochondrial genome

02 p0220 A83-11834

How stems bend up

02 p0220 A83-11836

The effect of the solar-geomagnetic situation on monolayers of cells and the distant intercellular interactions at high latitudes

02 p0220 A83-11881

The implantation of sarcoplasmic reticulum membranes in a planar lipid membrane

03 p0375 A83-14359

The relationship between peroxide oxidation and cell respiration

03 p0376 A83-14368

The oxygen effect and the adaptive reactions of cells. IX - The dependence of the radioprotective effectiveness of gaseous hypoxia on its degree and duration in neonatal and adult mice

03 p0376 A83-14879

The modification with methylated hematoporphyrin of the combined effect of radiation and hyperthermia in experiments on asynchronous and synchronous cell cultures

03 p0376 A83-14881

Photobiological aspects of the damage of cells by radiation

03 p0377 A83-14927

The hair cells of the inner ear

04 p0521 A83-16046

Stromal bone-marrow cells and the hemopoietic environment

05 p0671 A83-17207

The structure of DNA and the transformation of cells

06 p0795 A83-18980

The biological effect of ultraviolet radiation

06 p0795 A83-18985

Factors which determine the differences in the biological effectiveness of ionizing radiation with various physical characteristics

06 p0796 A83-19376

The pattern of the conductivity and the permeability of cells at short periods following gamma-irradiation

09 p1321 A83-24930

The transmembrane potentials of the heart cells of rats during fibrillation induced by a decrease in extracellular sodium

10 p1454 A83-26791

The mode of gravity sensing in plant cells

11 p1638 A83-27811

Quantitation of chlorpromazine-bound calmodulin during chlorpromazine inhibition of gravitropism

11 p1638 A83-27815

Striated organelles in hair cells of rat inner ear maculas - Description and implication for transduction

11 p1638 A83-27818

Microbodies in the living cell

12 p1762 A83-29249

Information contained in protein shapes

12 p1763 A83-29547

Interrelated striated elements in vestibular hair cells of the rat

13 p1895 A83-30022

Hypoxic pulmonary hypertension in the mast cell-deficient mouse

13 p1897 A83-30485

Selective modification of glutathione metabolism

13 p1899 A83-31162

The mechanism of the degradation of chromatin in the thymocytes of irradiated rats. VI - The postirradiation changes in the activity of poly(ADP-ribose)-polymerase

14 p2061 A83-32052

The changes in the chromosome pattern of mouse lymphosarcoma cells during prolonged irradiation

14 p2061 A83-32054

The comparative investigation of the radiosensitivity of normal and regenerating tissues. I - The interphase death of cells and the degree of aplasia of regenerating and normal tissues of the bone marrow and spleen of C57B1 mice

14 p2062 A83-32055

The role of changes in the oxygen concentration by the modification of the reproductive death of cells in vitro. II The modification of the radiosensitivity during changes in the rate of oxygen absorption by the cells

14 p2062 A83-32058

Intracellular feedback in the processes of the electromechanical integration of the myocardium in mammals

14 p2063 A83-32100

The role of suprachiasmatic nuclei of the anterior hypothalamus in the organization of the circadian rhythms of locomotor activity in rats

14 p2063 A83-32564

The internalization and intracellular conversions of biologically active polypeptides and their receptors

14 p2065 A83-33320

Ultrastructural changes of acinar cells of the pancreas due to the effects of cold

14 p2066 A83-33329

A threshold molecular quantum regulator

16 p2394 A83-36802

An ionic mechanism of the Woodwors staircase --- electromechanical coupling in myocardium cells

16 p2395 A83-36806

The secretory activity of acinar cells of the pancreas at various times of the day and the sequence of the maturation process of secretory granules

16 p2395 A83-36814

The hypertrophy of cells and hyperplasia of ultrastructures in spleen parenchyma of mice as a consequence of acute stress

16 p2395 A83-36833

The role of cellular membranes in the resistance of plants to hypoxia and anoxia

16 p2396 A83-36839

Disorders of the contractile function of the myocardium and the ultrastructure of the cardiomyocytes following emotional and painful stress

17 p2556 A83-38195

The decrease in the functional ability of the hypertrophic heart due to disorders of cellular adaptation to oxygen

18 p2731 A83-39496

A theoretical analysis of the effect of the photoreactivation of E. Coli cells irradiated by gamma-rays

19 p2874 A83-41004

The role of changes in the concentration of oxygen in the case of the reproductive death of cells in vitro. III - The modification of the radiosensitivity by oxygen-reducing compounds

19 p2874 A83-41005

An investigation of the potential radiation damages of chromosomes in the cells of mammals with the aid of chemical modification and premature chromosome condensation

19 p2874 A83-41010

Membrane, action, and oscillatory potentials in simulated protocells

19 p2876 A83-41853

Experimental and theoretical analysis of the influence of gravity at the cellular level - A review

19 p2877 A83-42043

Gravity and positional homeostasis of the cell

19 p2877 A83-42044

Gravity and the cells of gravity receptors in mammals

19 p2877 A83-42046

Calcium movements and the cellular basis of gravitropism

19 p2878 A83-42051

The effect of small temperature gradients on flow in a continuous flow electrophoresis chamber

20 p2951 A83-43276

A micro-computer system for cell electrophoresis measurements

21 p3108 A83-43825

ASECS - Antigen-Specific Electrophoretic Cell Separation

22 p3266 A83-45763

Preparative density gradient electrophoresis of cells and cell organelles - A new separation chamber

22 p3266 A83-45764

Single cell algae and higher plant cell cultures used in space biology

[IAF PAPER 83-185]

Damages of the superhelical structures of nuclear DNA by gamma-rays and heavy ions

23 p3495 A83-48201

Radiation damage and the theory of T-cells of mice - The dynamics of suppressor cells after the effect of radiation

23 p3495 A83-48203

CELLULAR MATERIALS (NON BIOLOGICAL)

U FOAMS

CELLULOSE

Linkage between gravity perception and response in the grass leaf-sheath pulvinus

11 p1638 A83-27812

CELLULOSE NITRATE

The composition of the products of the combustion of pyropowder at atmospheric pressure

07 p0880 A83-19954

A fresh look at the classical approach to homogeneous solid propellant combustion modeling

08 p1073 A83-22345

Characterisation of NC/NG propellant pastes

09 p1241 A83-23835

On an integral method for solving problems of the thermal theory of the ignition of condensed substances

19 p2820 A83-42067

CEMENTS

Creep of Kevlar 49 fibre and a Kevlar 49-cement composite

24 p3554 A83-50066

CEMS SYSTEM

U CENTRAL ELECTRONIC MANAGEMENT SYSTEM

CENSORED DATA (MATHEMATICS)

Analysis of maximum-likelihood estimation on a randomly censored sample with a small fraction of failures in the example of exponential distributions

01 p0103 A83-10296

A tentative procedure of parameter estimation of Weibull distribution from the Type I censored samples

05 p0653 A83-17094

Estimators for the 2-parameter Weibull distribution with progressively censored samples

17 p2517 A83-37295

Shrunken estimators of Weibull shape parameter in censored samples

23 p3467 A83-47617

CENTAUR LAUNCH VEHICLE

NT ATLAS CENTAUR LAUNCH VEHICLE

Atlas and Centaur adaptation and evolution - 27 years and counting

01 p0018 A83-11483

Galileo 1986 on Centaur

07 p0868 A83-20644

Stability analysis of Centaur-in-Shuttle composite corrugated adapters

[AIAA 83-1003]

The Centaur G-Prime - Meeting mission needs today for tomorrow's space environment

[SAWE PAPER 1557]

The commercial Centaur family

[IAF PAPER 83-233]

CENTAUR PROJECT

Chemical orbit transfer vehicles - Options for the future

[IAF PAPER 83-11]

CENTAUR VEHICLE

U CENTAUR LAUNCH VEHICLE

CENTAURUS CONSTELLATION

Concentrations in the local association. I - The southern concentrations NGC 2516, IC 2602, Centaurus-Lupus and upper Scorpius --- young star clusters in Galaxy

17 p2593 A83-38255

Optical photometry of massive X-ray binaries - Cen X-3/V779 Cen

21 p3229 A83-44424

HEAO 1 high-energy X-ray observations of Centaurus X-3

22 p3383 A83-46996

Taurus observations of the emission-line velocity field of Centaurus A (NGC 5128)

24 p3642 A83-49257

Centaurus A - The nearest active galaxy

24 p3660 A83-49444

CENTER OF GRAVITY

On a stationary solution for the motion of a rigid body about a fixed point under the influence of a Newtonian force field

07 p0988 A83-20200

Trim Tank system for optimizing drag at the center of gravity

[DGLR PAPER 82-030]

Modeling rotational dynamics of a flexible space platform for application of multilevel attitude control

17 p2476 A83-37108

The employment of a miniature calculating device for the determination of the center of gravity

18 p2642 A83-39220

The component of 29.8 years in polar motion and Delta I.o.d. and oscillation of earth's inner core --- Length Of Day

20 p3010 A83-43172

Optimizing tail size and wing location within loadability constraints

[SAWE PAPER 1466]

On-board weight and center-of-gravity measurement system with tire-pressure monitoring

23 p3402 A83-47216

CENTER OF MASS

Bifurcation and stability of the permanent rotations of a heavy solid whose center of mass is located near the principal plane of the inertia ellipsoid

03 p0391 A83-14893

Investigation of the motion of the center of mass of an occupant under ejection accelerations

04 p0525 A83-15411

The reduction of a system of differential equations for the motion of a satellite that is dynamically compressed relative to the center of mass to a special form

04 p0451 A83-15771

The effect of displacing the center of a protective sphere on the oscillations of a body acted upon by Lorentz forces under conditions of resonance --- stability of rotating electrostatically protected satellite under resonant vibration

04 p0452 A83-15772

Geometric methods for determining the axis of rotation and coordinates of the center of mass of a planet from orbital data

04 p0514 A83-16384

A dynamic method for determining the axis of rotation and coordinates of the center of mass of a planet from orbital data 05 p0707 A83-17676

On an analogy to the Steklov case for a balanced gyrostat in a Newtonian gravitational force field 07 p0988 A83-20145

Nonlinear resonances in the problem of the motion of a body near the center of mass when acted upon by Lorentz forces 09 p1212 A83-24486

A study of the dynamic characteristics of thin-walled structures with attached loads 09 p1281 A83-25014

Method for determining the velocity of the center of mass of a spacecraft on the basis of results of trajectory measurements 09 p1215 A83-25040

The effect of dissipative magnetic moment on the rotation of a satellite relative to its center of mass 15 p2127 A83-34426

The inertial motion of a gyrostat about a fixed center of mass 17 p2576 A83-38073

The calculation of optimal paths with singular control segments --- for flight vehicle trajectories 23 p3501 A83-48246

CENTER OF PRESSURE

Concerning the center of pressure of bodies --- supersonic flow interactions with variable surface configurations 04 p0441 A83-15089

CENTERBODIES

Single- and double-wall cylinder noise reduction 12 p1777 A83-29017

Do centre-bodies improve the performance of horizontal-axis, sail-type wind-turbines? 15 p2192 A83-34673

Numerical simulation of cold flow in an axisymmetric centerbody combustor [AIAA PAPER 83-1741] 17 p2467 A83-37219

CENTIMETER WAVES

Numerical simulation of soil brightness temperatures at wavelength of 21 cm 01 p0062 A83-10038

The galactic center - Structure and kinematics from 21-cm line measurements 01 p0125 A83-10941

Observations of 1 Ceres and 2 Pallas at centimeter wavelengths 02 p0268 A83-12922

The resolution of P Cygni's stellar wind 03 p0424 A83-14199

Solar eclipse observations of a magnetic loop structure at 2, 3.2, 8.2 and 21 cm 04 p0574 A83-15599

The morphological changes of neurons of the central nervous system during the experimental action on the body of electromagnetic waves in the centimeter range 05 p0669 A83-17165

Radio observations of the 1968 September solar eclipse 06 p0856 A83-19165

21 centimeter H I absorption at $z = 0.437$ against the extended radio structure of 3C 196 06 p0839 A83-19271

A distance scale from the infrared magnitude/H I velocity-width relation. IV - The morphological type dependence and scatter in the relation; the distances to nearby groups 07 p1019 A83-21101

6 centimeter observations of solar bursts with 0.1 s time constant and arcsec resolution 07 p1038 A83-21149

A survey of the distribution of wavelength 2.8 cm radio continuum in nearby galaxies. III - A small sample of irregular and blue compact galaxies 07 p1025 A83-21246

Statistics of differential rain attenuation on adjacent earth-space propagation paths 08 p1074 A83-21646

Observations of H-alpha and microwave brightening caused by a distant solar flare 08 p1192 A83-23073

VLA source counts at 6-cm wavelength 08 p1187 A83-23291

The statistical characteristics of the field of centimeter and millimeter waves above the sea surface 09 p1245 A83-23480

A search for neutral hydrogen in radio galaxies 10 p1492 A83-25477

Ice crystal observations at 1.8 cm wavelength using a polarization diversity radar 11 p1629 A83-27066

A high-latitude H I-cloud with optical emission 12 p1785 A83-28883

Redshift quantization in compact groups of galaxies 14 p2104 A83-33182

X-ray studies of quasars with the Einstein Observatory. III The 3CR sample 14 p2104 A83-33183

The incidence of 21 centimeter absorption in QSO redshift systems selected for Mg II absorption - Evidence for a two-phase nature of the absorbing gas 14 p2104 A83-33185

Lambda 6-cm observations of fluctuations in the 3 K cosmic microwave background 15 p2286 A83-34598

21 centimeter observations of supercluster galaxies - The bridge between Coma and A1367 15 p2266 A83-34613

Microwave cineholography 15 p2165 A83-35166

The development of local radio sources and burst activity on the sun in the short-wave part of the centimeter range 17 p2625 A83-37670

The variability of 3C 273, OJ 287, and PKS 0735 + 17 in radio and optical emissions 17 p2601 A83-37710

The distribution of radio brightness over the solar disk 17 p2626 A83-37717

A model of the spectrum of the slowly varying component of solar radio emission from active regions 18 p2780 A83-39002

102-MHz observations of Seyfert galaxies 18 p2763 A83-40488

Changes of the hormonal spectrum of the blood under the effect of microwaves in the centimeter range 18 p2733 A83-40571

The distribution of 6 centimeter H₂CO in Orion Molecular Cloud 1 20 p3074 A83-43090

The Hydra I cluster of galaxies. II - First results from H I observations 23 p3518 A83-47433

Magnetic development of flaring regions at centimeter wavelengths 23 p3530 A83-47509

Spatial characteristics of microwave bursts --- from solar flares 23 p3533 A83-47678

Dual frequency observations of flares with the VLA 23 p3533 A83-47679

A two-frequency 1.35-cm radiometer 23 p3459 A83-48490

Comparison of global 21 cm velocity profiles with H-alpha rotation curves 24 p3640 A83-49206

5-cm radar echoes and their microphysical significance in Florida cumuli 24 p3612 A83-49697

CENTRAL AMERICA

Geologic observations of the northern boundary of the Caribbean plate across central America as seen by Seasat and SIR-A 08 p1128 A83-21947

CENTRAL ATLANTIC REGIONAL ECOL TEST SITE

From ecological test site to geographic information system Lessons for the 1980's 15 p2185 A83-34825

CENTRAL ELECTRONIC MANAGEMENT SYSTEM

Management of astronomical data at Kanazawa Data Center 01 p0113 A83-10129

CENTRAL EUROPE

The development and persistence of a cumulo-nimbus-cluster over central Europe observed by Meteosat 2 17 p2547 A83-38513

CENTRAL NERVOUS SYSTEM

NT BRAIN

NT BRAIN STEM

NT CEREBRAL CORTEX

NT CEREBRUM

NT HIPPOCAMPUS

NT SPINAL CORD

NT SPINE

NT THALAMUS

The basal ganglia-circa 1982 - A review and commentary 02 p0222 A83-11826

The sector structure of the interplanetary magnetic field and disturbances of the central nervous system 02 p0222 A83-11879

Oxygen toxicity 02 p0222 A83-12261

Combined light and electron microscopic investigations of the connections in the central nervous system - A review of current methodological approaches 03 p0375 A83-13646

Integration function and modeling of the central nervous system in forearm movement control 03 p0384 A83-14126

The morphological changes of neurons of the central nervous system during the experimental action on the body of electromagnetic waves in the centimeter range 05 p0669 A83-17165

Diseases of the nervous system in miners of the far north and problems of prevention 05 p0673 A83-17193

The regulation of the biosynthesis of serotonin in the central nervous system 06 p0795 A83-18983

An investigation of the changes in the opiate-like, bombesin-like, and P-like substances in rats with stress-induced anesthesia 06 p0795 A83-18990

The effects of various gases on cortical and spinal somatosensory evoked potentials at pressures up to 10 bar 07 p0974 A83-20777

Timing of neuron development in the rodent vestibular system 11 p1638 A83-27819

Ionizing radiation decreases veratridine-stimulated uptake of sodium in rat brain synaptosomes 15 p2209 A83-33776

Integral determination of changes in central nervous system functioning during mental work 17 p2561 A83-38927

The sensitivity by age of animals to electromagnetic fields at microwave frequencies 17 p2557 A83-38928

The significance of the strength of the central nervous system in the variability of the reaction in sick persons to acebutolol 18 p2736 A83-40578

The fitness for work of humans and the problems of its increase 19 p2882 A83-41458

CENTRAL NERVOUS SYSTEM DEPRESSANTS

The neurophysiological bases of narcosis - The general and selective effects of narcotic substances on the neuronal structures of the central nervous system 16 p2394 A83-35923

CENTRAL NERVOUS SYSTEM STIMULANTS

Further studies and the comparative characteristics of potential stimulants of higher nervous activity 03 p0374 A83-13634

CENTRAL PROCESSING UNITS

NT ARITHMETIC AND LOGIC UNITS

A note on using finite differences on the ICL distributed array processor 01 p0090 A83-10712

A predictive tracking EW preprocessor using standard computer instruction set architectures 01 p0088 A83-11133

Incorporating ISPS into a commercial CAD system 01 p0092 A83-11195

The real-time image processing problem 01 p0053 A83-11218

Architectures for neighborhood processing --- of images by computer serial array processors 01 p0090 A83-11446

Interactive computer graphic preprocessing for three-dimensional boundary-integral element analysis 02 p0228 A83-12744

Cellular array processing simulation 02 p0228 A83-12881

Residue-based image processor for very large scale integration /VLSI/ implementation 02 p0182 A83-12900

CPU coverage evaluation using automatic fault injection 03 p0385 A83-14842

The use of the intraperiod symmetry of harmonic basis functions to compute the discrete Fourier transformation 06 p0802 A83-18039

Experience with the parallel solution of partial differential equations on a distributed computing system 07 p0983 A83-20247

Performance analysis of a dwell-time processor for monopulse beacon radars 08 p1044 A83-22726

A 200 million operations per second /MOPS/ systolic processor 08 p1155 A83-22796

Interactive graphical preprocessing of three-dimensional framed structures 11 p1646 A83-28718

Organization of the structure and computational process of a multiprocessor hybrid computing system with a network analog processor 12 p1768 A83-29346

Designing efficient parallel algorithms for multiple-output computations with fan-in constraints 15 p2218 A83-35113

Some properties of the binary n-cube as a network interconnection structure 15 p2219 A83-35133

Experiments in automatic microcode generation 19 p2888 A83-41037

Fast special-purpose processors for the computation of elementary functions 19 p2888 A83-41423

CENTRIFUGAL COMPRESSORS

Numerical calculation of the laminar flow in the inlet of the axial sealing gap of radial-flow compressors 07 p0864 A83-21339

Choice of the optimal system of shock waves in the inlet part of the diffuser of a supersonic centrifugal compressor 08 p1043 A83-23223

A solution to inverse problem of quasi three-dimensional flow in centrifugal impeller 09 p1257 A83-23331

Mathematical method for the design of the intake branch in the case of centrifugal blade machines --- Book 09 p1263 A83-24850

Comparison between probe and laser measurements at the outlet of a centrifugal impeller 10 p1421 A83-26418

Flow measurements using a laser two-focus anemometer in a high-speed centrifugal and a multistage axial compressor 12 p1695 A83-28835

18:1 pressure ratio axial/centrifugal compressor demonstration program 12 p1732 A83-29013

An analysis of the natural vibrations of the rotors of centrifugal compressor machines 13 p1859 A83-30310

Modular method for centrifugal compressor performance prediction 13 p1804 A83-31169

Investigation of the combined regulation of the intermediate stage of a centrifugal compressor by an axial regulating apparatus and a two-row diffuser 14 p2028 A83-33149

Contribution to centrifugal compressor impeller design 16 p2305 A83-35865

The effect of variation of diffuser design on the performance of centrifugal compressors 16 p2305 A83-35866

- NASA low-speed centrifugal compressor for fundamental research 16 p2312 A83-36353 [AIAA PAPER 83-1351]
- Simplified inverse design of a straight vaneless diffuser of radial stage [ASME PAPER 83-GT-2] 23 p3392 A83-47877
- On the influence of the diffuser inlet shape on the performance of a centrifugal compressor stage [ASME PAPER 83-GT-9] 23 p3406 A83-47881
- Alternative vaneless diffusers and collecting volutes for turbocharger compressors [ASME PAPER 83-GT-32] 23 p3464 A83-47894
- Distinction between different types of impeller and diffuser rotating stall in a centrifugal compressor with vaneless diffuser [ASME PAPER 83-GT-61] 23 p3395 A83-47917
- Performance evaluation of centrifugal compressor impellers using three-dimensional viscous flow calculations [ASME PAPER 83-GT-62] 23 p3395 A83-47918
- A CAD method for centrifugal compressor impellers [ASME PAPER 83-GT-65] 23 p3395 A83-47920
- Effect of relative velocity distribution on efficiency and exit flow of centrifugal impellers [ASME PAPER 83-GT-74] 23 p3447 A83-47927
- Blade vibration measurements on centrifugal compressors by means of telemetry and holographic interferometry [ASME PAPER 83-GT-131] 23 p3408 A83-47959
- Substructuring and wave propagation - An efficient technique for impeller dynamic analysis [ASME PAPER 83-GT-150] 23 p3409 A83-47969
- Aerodynamic tests on centrifugal process compressors Influence of diffuser diameter ratio, axial stage pitch and impeller cut-back [ASME PAPER 83-GT-172] 23 p3396 A83-47973
- Vibration analysis of radial compressor impellers [ASME PAPER 83-GT-156] 23 p3469 A83-47982
- Two focus laser velocimeter applied to measurements in an experimental centrifugal compressor [ONERA, TP NO. 1983-113] 24 p3583 A83-49424
- CENTRIFUGAL FORCE**
- Stresses in rotating disc with eccentric hole 02 p0196 A83-12873
- V2 dependence of the centrifugal constants of the H2O molecule in the Morse oscillator model 04 p0534 A83-15706
- Wet classification in the centrifugal force field --- German thesis 07 p0925 A83-20395
- Operational utilization study on new human centrifuge of JASDF. III - Measurement of a three-axis acceleration force in human centrifuge 10 p1458 A83-26089
- Operational utilization study on new human centrifuge of JASDF. IV - Test and evaluation of anti-g system 10 p1458 A83-26090
- The effect of perturbations in Coriolis and centrifugal forces on the nonlinear stability of equilibrium points in the restricted problem of three bodies 15 p2246 A83-34395
- The problem of the origin of the centrifugal force according to Mach's principle 15 p2262 A83-34526
- Satellite orbit perturbations due to the deforming potential of centrifugal forces 18 p2645 A83-39977
- A method for investigating the damping capacity of the blades of turbomachines under the effect of high temperatures and centrifugal forces 19 p2859 A83-41598
- A study of the damping capacity of rods in a centrifugal force field 21 p3148 A83-45322
- CENTRIFUGAL PUMPS**
- Basic calibration of a partially-parabolic procedure aimed at centrifugal impeller analysis [AIAA PAPER 83-0260] 05 p0583 A83-16616
- Dynamic response of a centrifugal liquid oxygen rocket pump [ASME PAPER 83-FE-24] 23 p3426 A83-48235
- The effect of regime and structural parameters of an inclined Archimedean screw forepump on the volume of cavitation cavities, their elasticity, and cavitation resistance 24 p3578 A83-49652
- Dependence of the head of a centrifugal inclined Archimedean screw pump on the volume of cavitation cavities in the flow area of the pump 24 p3579 A83-49653
- CENTRIFUGES**
- NT HUMAN CENTRIFUGES
- Composite engine inlet particle separator swirl frame --- CAD for T700 helicopter engine centrifugal filter 09 p1208 A83-24841
- A shock tube driver with a 'cyclone' separator 10 p1380 A83-26130
- CENTRIFUGING**
- Centrifugal mixing - A comparison of temperature profiles in nonrecirculating swirling and nonswirling flames 02 p0152 A83-12076

- Drop motion in a rotating immiscible liquid body 18 p2686 A83-39909
- CENTRIFUGING STRESS**
- The influence of differential physical conditioning regimens on simulated aerial combat maneuvering tolerance [AD-A126486] 02 p0223 A83-12406
- Knee-ligament loading properties as influenced by gravity. I - Junction with bone of 3-G rodents 02 p0223 A83-12407
- The effects on rat bones of a prolonged centrifugation - Results of a morphometrical analysis 06 p0794 A83-18341
- Repeated exposures to high levels of plus g accelerations - Consequences for the myocardium and the cardiovascular system 08 p1146 A83-22981
- Increased gluconeogenesis in hyper-G stressed rats 11 p1637 A83-27805
- Short hyperdynamic profiles influence primate temperature regulation 11 p1637 A83-27807
- Application of experimentally derived pilot perceptual angular response transfer functions [AIAA PAPER 83-1100] 16 p2402 A83-36220
- CENTROIDS**
- The theory of flaw centroids and low-frequency phase shifts - A review 04 p0489 A83-15169
- On estimation of image signal-to-noise ratio and centroid of coherent laser radar target images 08 p1096 A83-22512
- CEPHALAGIA**
- U HEADACHE
- CEPHEID VARIABLES**
- On the change of period of DY Pegasi 01 p0115 A83-10229
- Metal abundances of RR Lyrae stars in globular clusters 02 p0251 A83-11592
- A search for magnetic fields in the symbiotic and VV Cephei variables 02 p0246 A83-12131
- The X-ray transient 3A 1431-409 - A highly active RS CVn system 03 p0414 A83-13332
- A search for OB associations near southern long-period Cepheids. I - WZ Carinae, YZ Carinae, KK Centauri, and OO Centauri 03 p0406 A83-13554
- The light curve of the eclipsing binary system CX Cephei and the properties of the Wolf-Rayet component 03 p0418 A83-13661
- Peculiarities of the Cepheid distribution in the Large Magellanic Cloud 03 p0408 A83-13877
- HR 6434 and the factors limiting pulsational amplitudes of delta Scuti stars 03 p0421 A83-14150
- The mass of the anomalous cepheid in the globular cluster NGC 5466 03 p0424 A83-14203
- The very small amplitude Cepheids HD 9250 and HD 14662 03 p0411 A83-14787
- The nonadiabatic analysis of nonradial modes of stellar oscillation in the presence of slow rotation 04 p0554 A83-15636
- Four years of photometry of DK Draconis = HR 4665 04 p0548 A83-15975
- A PRC relation for delta Scuti stars --- Period Radius Color 05 p0702 A83-17815
- Increased evidence for overtone pulsation in galactic cepheids - SU Cassiopeiae 06 p0836 A83-19065
- On the possibility of cluster membership for the cepheid V Centauri 06 p0822 A83-19073
- Intermediate-band photometry of stars in three clusters containing classical Cepheids 07 p1004 A83-19863
- DQ Cephei, a Delta Scuti star of constant variability 07 p1006 A83-20565
- Pulsational mode-typing in line profile variables. V - Multimodes and 'moving shells' in Nu Eridani and other Beta Cephei stars 07 p1022 A83-21132
- Spectroscopic and photometric analysis of the WN7 eclipsing binary CQ Cephei 08 p1183 A83-23061
- The structural properties of Cepheid velocity curves 08 p1184 A83-23064
- HR 5960 - New observations and period search 09 p1357 A83-23738
- An application of discriminant analysis to variable and nonvariable stars 09 p1353 A83-23742
- Cepheids --- luminosity-color-age study 09 p1353 A83-23908
- The open cluster Tombaugh 1 and its neighbouring Cepheid XZ Canis Majoris 09 p1354 A83-24023
- Resonance effects in radial pulsators 09 p1361 A83-24474
- A spectrographic study of the Beta Cephei star 16 Lacertae 10 p1491 A83-25366
- The double-mode Cepheid CO Aur 10 p1499 A83-25370
- Einstein observations of three classical Cepheids 10 p1494 A83-25714
- The light and velocity curves of classical Cepheids - Theory versus observation 10 p1510 A83-26387
- The distance to M33 based on a new study of its Cepheids 10 p1516 A83-26752

- Photoelectric observations of four classical cepheids 10 p1498 A83-26905
- Classification of intrinsic variables. IX - The Cepheid domain 11 p1668 A83-27110
- NGC 6067 and three cepheids 11 p1668 A83-27111
- A discussion on the reddening of long period Cepheids in the Magellanic Clouds 11 p1677 A83-27680
- Revised orbits for 105 Herculis and Pi Cephei A and a model for the Pi Cephei system 11 p1674 A83-28261
- HR 6522 - A previously unknown multiperiodic Delta Scuti star 12 p1784 A83-28859
- A reanalysis of the data of three classical Cepheids - V381 Cen, V500 Sco, and SV Vel 12 p1791 A83-28991
- A study of the variability of the Delta Scuti stars. V Photoelectric photometry of the bright star HR 2557 12 p1786 A83-29086
- Blue edges of the Delta-Scuti instability strip - Theory in comparison with observations 12 p1794 A83-29087
- Photometry of Cepheids in the LMC and Magellanic Cloud abundances 12 p1794 A83-29179
- Detailed photometry of the Cepheid AD Geminorum 12 p1789 A83-29954
- ANS ultraviolet observations of dwarf Cepheids 12 p1797 A83-29958
- New observations of the beat Cepheid variable AX Velorum 13 p1945 A83-30375
- Global value of Hubble constant 13 p1946 A83-30382
- The CQ Cephei system - U, B, V, R photometry, period variation, and mass loss by the Wolf-Rayet component 13 p1940 A83-31261
- Star formation and interstellar matter in the Large Magellanic Cloud 13 p1954 A83-31579
- AQ Leonis revisited --- electrophotometry of double-mode RR Lyrae variable 13 p1942 A83-31666
- Simultaneous spectroscopic and photoelectric observations of Beta Cephei stars. I - nu and Beta Centauri 13 p1942 A83-31667
- Properties of Am, Delta Del and Delta Sct stars in the VBLUW system 13 p1959 A83-31738
- A search for binaries among short-period southern Cepheids 14 p2100 A83-33250
- Interstellar absorption in three Bade fields in the Andromeda Nebula 15 p2253 A83-33702
- A search for stars physically associated with the 16-day Cepheid X Cygni. I - Luminous stars in the field 15 p2245 A83-33832
- Revised list of pulsating stars with ultra-short periods 15 p2247 A83-34530
- The binary nature of the Cepheid T Monocerotis 15 p2264 A83-34581
- A search for Beta Cephei stars in NGC 6231 15 p2265 A83-34591
- Theoretical blue limits of the instability strip for Delta Scuti-type stars 15 p2271 A83-34765
- Delta Scuti variables. I - Theoretical evolution sequences for standard models and models with two-zone envelopes 16 p2429 A83-36641
- Delta Scuti variables. II - Comparison of theoretical evolution sequences with observational data 16 p2430 A83-36642
- The Beta Cephei eclipsing binary system 16 Lacertae 16 p2432 A83-36682
- VBLUW photometry of Cepheids in the Magellanic Clouds made in 1971-1978 17 p2587 A83-37283
- The near-infrared Cepheid distance scale. I - Preliminary galactic calibration 17 p2588 A83-37325
- A photoelectric investigation of temporal changes in the line at 4254.35 A (Cr I) in the spectrum of the Ap star Alpha(2) CVn 17 p2601 A83-37703
- Beat Cepheids. IV - AX Velorum and mode energy transfer 17 p2606 A83-38232
- The canonical anticorrelation between Y and Z in galactic globular clusters and the case of the pulsators in M15 17 p2609 A83-38425
- The radial pulsation modes of the Delta Scuti stars, and their nonuniform period distribution 17 p2610 A83-38554
- The age and dimensions of star complexes 17 p2613 A83-38830
- Scanner observations of the classical Cepheids RT Aur and T Vul 18 p2764 A83-39187
- The metal abundances of RR Lyrae stars in the globular clusters NGC 3201, NGC 4590, and NGC 6171 18 p2767 A83-39595
- Intermediate band and (R,I) observations of long-period cepheids 18 p2757 A83-39596
- Cepheids and spiral structure 18 p2778 A83-40490
- Period determination of the Delta Scuti star HR 5005 19 p2910 A83-41063

SUBJECT INDEX

Determination of radii of cepheids. II - Radial velocities and dimensions of AD Gem 19 p2910 A83-41064

On the distance to M33 determined from magnitude corrections to Hubble's original Cepheid photometry 20 p3057 A83-42182

The spectroscopic parallax of stock 14 20 p3058 A83-42321

A photometric classification of pulsating variables with periods between one and three days 20 p3059 A83-42391

Secondaries of eclipsing binaries. V - Ek Cephei 20 p3060 A83-43064

On the variability of RZ Cephei 20 p3061 A83-43382

Spectrographic observations of the suspected Delta Scuti variable Beta Ari 20 p3062 A83-43656

Period-luminosities relation of classical Cepheids 20 p3077 A83-43666

The intrinsic properties of 29 Cepheids in the Magellanic Clouds 21 p3228 A83-44414

The Beta Cep variables - Fundamental radial pulsators 21 p3234 A83-44763

A search for light-time effects in binary cepheids - AW Persei 21 p3226 A83-45551

The behavior of H-alpha in the 16-day cepheid X Cygni 22 p3378 A83-46413

A photometric and spectrographic study of YZ Bootis 22 p3374 A83-46415

On the secular variation of amplitudes in double-mode Cepheids 22 p3379 A83-46565

The multiple system Beta Sco and the age of the Upper Scorpius complex 23 p3519 A83-47447

The VW Cephei system 23 p3524 A83-47530

A bright spot and a serendipitous stellar flare on the contact-binary VW Cep 23 p3524 A83-47531

The light curve changes of VW Cephei 23 p3527 A83-48063

Three-colour electrophotometry of Dy Peg 23 p3517 A83-48442

Frequency analysis of Beta Cephei variables in NGC 6231 24 p3659 A83-49373

The variable stars in the field of the globular cluster NGC 6681 24 p3646 A83-49883

CEPSTRA

Analytical expressions of 2-D complex cepstrum 24 p3621 A83-49986

CEPSTRAL ANALYSIS

Cepstrum analysis of interfering delayed signals as a tool for detecting gravitational lenses 06 p0830 A83-18777

Analytical expressions of 2-D complex cepstrum 24 p3621 A83-49986

CERAMAL PROTECTIVE COATINGS

U CERAMETS

U PROTECTIVE COATINGS

CERAMALS

U CERAMETS

CERAMIC BONDING

Effect of fractional composition of starting mixtures on the properties of self-bonded silicon carbide 03 p0302 A83-14224

The structural-chemical role of iron in the reaction processes of the soldering of titanium with iron-containing alkali-free aluminoborosilicate glasses 07 p0873 A83-20685

Dynamic fracture toughnesses of reaction-bonded silicon nitride 08 p1071 A83-22197

Polyimide adhesives to reduce thermal stresses in LSI ceramic packages 09 p1237 A83-23621

New method for solid-state bonding between ceramics and metals 19 p2818 A83-40911

The effect of silicon particle size on the nitriding behaviour of reaction bonded Si3N4 compacts 23 p3434 A83-48261

Microstructure of densified reaction bonded silicon nitride 23 p3435 A83-48271

Contribution of the strength-porosity relationship of reaction bonded silicon nitride 23 p3436 A83-48280

CERAMIC COATINGS

A structural study of detonation-sprayed tungsten carbide-cobalt coatings 02 p0159 A83-13030

The formation of nickel-plated titanium carbide coatings and the effect of spraying conditions on the coating structure and properties 02 p0151 A83-13031

The influence of superficially applied oxide powders on the high-temperature oxidation behavior of Cr2O3-forming alloys 03 p0296 A83-13124

Infrared emission spectrophotometric study of the changes produced by TiN coating of metal surfaces in an operating EHD contact [ASLE PREPRINT 82-LC-3C-3] 03 p0333 A83-13229

The surface temperature and the concentration of alumina particles in the detonation products of a gas mixture 03 p0295 A83-14063

Powder selection for plasma sprayed coatings in diesel engine applications 06 p0733 A83-19109

A study of the high-temperature creep and long-term strength of a niobium alloy with a complex coating in an oxidizing medium 07 p0887 A83-20683

Complex silicide coatings on niobium 07 p0888 A83-20689

Phase transformations during detonation spraying and their effect on the wear resistance of aluminum oxide coatings 07 p0900 A83-20694

Component interaction in a glass-ceramic layer 07 p0900 A83-20710

Reducing the gas permeability of porous ceramics by means of magnesium oxide coatings 07 p0900 A83-20712

Suppression of the solid-state reaction between Ni-base alloys and Si-base ceramics 08 p1053 A83-22253

Improved uniformity of multiphase ceramic-metal plasma-sprayed coats 08 p1053 A83-22269

Use of fiber-like materials to augment cycle life of thick, thermoprotective-seal coatings --- for gas turbine engine components 08 p1072 A83-22271

Some inelastic effects of thermal cycling on ZrO2-Y2O3 materials 08 p1072 A83-22272

Creep of plasma-sprayed-ZrO2 thermal-barrier coatings 08 p1072 A83-22273

Failure and acoustic-emission response of plasma-sprayed ZrO2-8 wt% Y2O3 coatings 08 p1072 A83-22274

ZOT - A white thermal control coating for space environment: Considerations --- Zinc-Ortho Titanate 09 p1236 A83-23607

Metallurgical coatings 1981; Proceedings of the Eighth International Conference, San Francisco, CA, April 6-10, 1981. Volumes 1 & 2 10 p1388 A83-25526

Chemical vapor deposition of boron on a beryllium surface 10 p1394 A83-25527

Plasma- and vacuum-plasma-sprayed Cr3C2 composite coatings 10 p1400 A83-25531

Thermal barrier coatings for thermal insulation and corrosion resistance in industrial gas turbine engines 10 p1400 A83-25542

Characterization of ZrO2-Y2O3 thermal barrier coatings by Raman spectroscopy 10 p1400 A83-25543

Tribological and protective coatings by chemical vapour deposition 10 p1435 A83-25549

Optical properties of CVD-coated TiN, ZrN and HfN 12 p1779 A83-29511

An electrostatic charge decay technique for nondestructive evaluation of nonmetallic materials 12 p1734 A83-29591

Acoustic emission from thermally cycled plasma-sprayed oxides 15 p2173 A83-33517

High-temperature composites - Status and future directions 18 p2650 A83-40129

Recent developments in high temperature coatings for gas turbine airfoils 20 p2953 A83-42254

Improved performance thermal barrier coatings 20 p2957 A83-42261

High temperature corrosion resistance of ceramic thermal barrier coatings 20 p2957 A83-42262

Structure and phase composition of nickel-boride composite coatings 21 p3113 A83-44485

GATOR-GARD applied coatings extend service lives of critical aerospace components 22 p3301 A83-45869

Strain isolated ceramic coatings [ASME PAPER 83-GT-223] 23 p3465 A83-48021

Thermal stability of compositions consisting of molybdenum disilicide, quartz, and glass 24 p3568 A83-49080

A study of the interaction between coatings and alloys based on refractory metals 24 p3560 A83-49081

Modern techniques for depositing thermally sprayed ceramic coatings with specified performance characteristics 24 p3568 A83-49084

Development and characterization of multilayer heat-insulating coatings based on plasma-sprayed thermoreactive metal-ceramic compositions 24 p3568 A83-49086

Heat resistance of coatings based on aluminoborosilicate glass and disilicides of refractory metals 24 p3569 A83-49092

Effect of bond metal on durability of thermal barrier coating 24 p3565 A83-49518

CERAMIC MATRIX COMPOSITES

A comparative study of permeable metal powder and fiber materials 11 p1548 A83-27924

Processing-related fracture origins. I - Observations in sintered and isostatically hot-pressed Al2O3/ZrO2 composites 16 p2337 A83-36945

Processing-related fracture origins. II - Agglomerate motion and cracklike internal surfaces caused by differential sintering 16 p2337 A83-36946

Processing-related fracture origins. III - Differential sintering of ZrO2 agglomerates in Al2O3/ZrO2 composite 16 p2337 A83-36947

Density and deposition rate of chemically vapour-deposited Si3N4-TiN composites 21 p3106 A83-44125

Metallic infiltration of reaction bonded silicon nitride 23 p3436 A83-48285

CERAMICS

NT CERAMIC MATRIX COMPOSITES

NT PYROCERAM (TRADEMARK)

Hot isostatic pressing of niobium carbide 01 p0027 A83-10218

Comments on 'Kinetics of densification during hot-pressing of aluminium nitride' 02 p0159 A83-11672

X-ray analysis of the transformed zone in partially stabilized zirconia /PSZ/ 02 p0159 A83-11675

Direct conversion from amorphous to beta-Si3N4 under high pressure 02 p0160 A83-11677

Ceramic materials as mirrors for synchrotron radiation 02 p0238 A83-12708

The load-life relationship for M50 steel bearings with silicon nitride ceramic balls [ASLE PREPRINT 82-LC-3C-4] 03 p0334 A83-13239

High-temperature ceramic heat exchanger element for a solar thermal receiver 03 p0352 A83-13476

Microstructure of Si3N4-TiN composites prepared by chemical-vapour deposition 03 p0291 A83-13687

Influence of machining on strength properties of turbine materials 03 p0302 A83-13800

A combination of statistics and subcritical crack extension 03 p0342 A83-14703

Fabrication and characterization of Si3N4 ceramics without additives by high pressure hot-pressing 03 p0303 A83-14920

The fatigue behavior of SiSiC 04 p0462 A83-15125

The application of the state-of-the-art NDE techniques to defect detection in silicon carbide structural ceramics 04 p0463 A83-15177

Tensile testing of silicon nitride 04 p0463 A83-15178

Nondestructive evaluation of ceramics 04 p0463 A83-15213

Probabilistic failure prediction for ceramics 04 p0463 A83-15214

Infrared spectroscopic study of beta-sialons in the system Si3N4-SiO2-AlN 04 p0464 A83-15998

Japan Congress on Materials Research, 25th, Tokyo, Japan, October 1981, Proceedings 05 p0610 A83-17086

HIP treatment on non-oxide ceramics 05 p0617 A83-17097

A simple method for evaluating the subcritical crack growth of brittle materials 05 p0618 A83-17099

Creep of ceramics. I - Mechanical characteristics 05 p0619 A83-17557

Role of cracks in the creep deformation of brittle polycrystalline ceramics 05 p0619 A83-17560

The effect of iron, aluminium, calcium on the vitrification of grain-boundary phases in nitrogen ceramics 05 p0619 A83-17570

Characterization and crystallization of Y-Si-Al-O-N glass 06 p0734 A83-18053

Slow growth of microcracks - Evidence for one type of ZrO2 toughening 06 p0734 A83-18054

The mechanical properties of a material obtained from ultrafine aluminum-nitride powders 07 p0884 A83-19970

Microstructure and grain-boundary composition of hot-pressed silicon nitride with yttria and alumina 07 p0898 A83-20166

Processing ternary sulfide ceramics - Powder preparation, sintering, and hot-pressing 07 p0898 A83-20167

A biaxial-flexure test for evaluating ceramic strengths 07 p0898 A83-20169

Effect of Delta T- and spatially varying heat transfer coefficient on thermal stress resistance of brittle ceramics measured by the quenching method 07 p0898 A83-20171

The effect of thin lubricant films and the methods of their application on the friction of several materials of bearings with a gaseous lubricant 07 p0939 A83-20321

Applications for Nextel in the aerospace industry 07 p0899 A83-20466

The effect of materials and processes on package reliability 07 p0920 A83-20473

Ceramic SrTiO3 photoanodes - Enhancement of photoactivity through donor doping 07 p0954 A83-20579

Microanalytical investigation of sintered SiC. I - Bulk material and inclusions 07 p0901 A83-21563

High-temperature fracture of hot-pressed AlN ceramics 07 p0901 A83-21567

The solid-state reaction of silicon nitride with an Ni-base alloy 07 p0874 A83-21568

Characterization of AlN ceramics containing long-period polytypes 07 p0901 A83-21569

Deformation of polycrystalline materials at high temperatures 07 p0874 A83-21604

Fracture mechanics, sub-critical events and structure of polypase ceramics 08 p1069 A83-21722

Fracture strength and toughness of engineering nitrogen ceramics 08 p1069 A83-21741

Fractographic identification of subcritical to critical crack growth transition mechanisms in ceramics 08 p1069 A83-21743

High and medium frequency nondestructive testing of the thermal shock resistance of ceramics 08 p1069 A83-21767

The fracture toughness-microstructure relationship of alumina-based ceramics 08 p1069 A83-21768

The influence of microstructure and geometric factors on the stress state and the fracture toughness of ceramics 08 p1070 A83-21780

The suppression of creep cavitation and slow crack growth in Si-Al-O-N ceramics 08 p1070 A83-21781

Physics of fracture /The Sosman Lecture/ --- crack propagation and crack-tip phenomena in structural ceramics 08 p1070 A83-22188

Application of the J concept to alumina at high temperatures 08 p1070 A83-22192

Controlled flaws in ceramics - A comparison of Knoop and Vickers indentation 08 p1070 A83-22193

Annual Conference on Composites and Advanced Ceramic Materials, 6th, Cocoa Beach, FL, January 17-21, 1982, Proceedings 08 p1071 A83-22251

Suppression of the solid-state reaction between Ni-base alloys and Si-base ceramics 08 p1053 A83-22253

Self-propagating high temperature synthesis - A Soviet method for producing ceramic materials 08 p1071 A83-22254

Injection molding ceramics 08 p1111 A83-22255

Formation of silicon carbide and silicon nitride by vapor-phase reaction 08 p1071 A83-22256

Initial characterization of partially stabilized HfO₂ single crystals 08 p1072 A83-22257

Design considerations for fabrication of sintered alpha-SiC components 08 p1072 A83-22261

Cyclic rig and engine testing of ceramic turbine components 08 p1072 A83-22262

A ceramic nozzle for the NASA-Langley 2.4-m /8.0-ft/ high temperature structures tunnel 08 p1072 A83-22264

Comparison of NDE techniques for sintered-SiC components 08 p1113 A83-22265

Refractory-ceramic-fiber composites - Progress, needs, and opportunities 08 p1055 A83-22267

Comparison of static, cyclic, and thermal-shock fatigue in ceramic composites 08 p1055 A83-22268

Ceramic tooling in aircraft fabrication 09 p1195 A83-23603

Mechanisms of creep deformation and fracture in single and two-phase Si-Al-O-N ceramics 09 p1238 A83-24072

Emerging optical materials; Proceedings of the Conference, San Diego, CA, August 25, 26, 1981 09 p1345 A83-24951

Development of a new family of improved infrared /IR/ dome ceramics 09 p1239 A83-24952

Nitrogen-stabilized aluminum oxide spinel /ALON/ 09 p1345 A83-24954

CaLa₂S₄ - Ceramic window material for the 8 to 14 micron region 09 p1345 A83-24957

Thermal shock testing of optical ceramics 09 p1221 A83-24965

Toughened optical materials 09 p1239 A83-24970

Flaws responsible for slow cracking in the delayed fracture of alumina 09 p1240 A83-25205

Effect of cavities on creep 09 p1283 A83-25206

Cylindrical piezoelectric transducer with controllable characteristics 10 p1421 A83-26291

Flexible ceramic powder separators for molten salt electrolyte galvanic cells 11 p1603 A83-27168

Composite salt/ceramic media for thermal energy storage applications 11 p1610 A83-27319

Continuum theory of dilatant transformation toughening in ceramics 12 p1716 A83-29025

Tribological properties of sintered polycrystalline and single-crystal silicon carbide 12 p1716 A83-29397

Strength and fracture toughness of reaction-bonded Si₃N₄ 12 p1716 A83-29398

Microchemistry and microstructure of a multiphase aluminosilicate ceramic 12 p1716 A83-29505

Thermal and mechanical properties of multilic substrates for low-cost solar cells obtained by dry-pressing 12 p1749 A83-29506

Kinetics of crystallization of ZrF₄-BaF₂-LaF₃ glass by differential scanning calorimetry 12 p1717 A83-29972

Effect of indenter geometry on controlled-surface-flaw fracture toughness 12 p1717 A83-29975

A study of the acoustic properties of a ceramic material 13 p1825 A83-30062

Method of examining subcritical crack growth in ceramics during the double twisting of specimens 13 p1825 A83-31220

Interaction between SiC fibers and aluminum alloys 13 p1816 A83-31604

Ceramic-beryllium composites for gas bearings 14 p1986 A83-31916

Chemistry and distribution of phases produced by solid state SiC/NiCrAl reaction 14 p1985 A83-32676

Ceramic tube development for solar receiver applications [AIAA PAPER 83-1501] 14 p2047 A83-32740

Theory of fatigue for brittle flaws originating from residual stress concentrations 14 p2032 A83-32974

Determination of threshold stress intensity for crack growth at high temperature in silicon carbide ceramics 14 p1999 A83-32975

Injection molding ceramics to high green densities 15 p2170 A83-33515

Electrical behaviour of doped-yttria stabilized zirconia ceramic materials 15 p2134 A83-35065

A fracture mechanics analysis of indentation-induced Palmqvist crack in ceramics 16 p2336 A83-35572

Comparative study of the temperature dependence of hardness and compressive strength in ceramics 16 p2336 A83-35979

Crystallization of amorphous Si₃N₄ prepared by the thermal decomposition of Si(NH)₂ 16 p2336 A83-35985

Silicon carbide (SiSiC), a new material for apparatus construction 16 p2336 A83-36000

High-temperature static fatigue in ceramics 16 p2337 A83-36169

Heat transfer performance of ceramic regenerator matrices with sine-duct shaped passages 16 p2353 A83-36592

Intergranular crack-deflection toughening in silicon carbide 16 p2337 A83-36948

Formation of alpha-Si₃N₄ solid solutions in the system Si₃N₄-AlN-Y₂O₃ 16 p2337 A83-36949

Compressive creep and oxidation resistance of an Si₃N₄ material fabricated in the system Si₃N₄-Si₂N₂O₂-Y₂Si₂O₇ 16 p2337 A83-36950

High-temperature bending tests on powder metallurgy materials during exploratory studies 17 p2484 A83-38873

Mechanical properties and fracture behaviour of ZrO₂-Y₂O₃ ceramics 18 p2670 A83-39050

Formation and characterization of oxynitride glasses in the Si-Ca-Al-O-N and Si-Ca-Al,B-O-N systems 18 p2671 A83-39056

On some transport properties of strontium-doped lanthanum chromite ceramics 18 p2671 A83-39057

The variation of hardness in Lucas Syalon ceramics 18 p2671 A83-39061

Reaction sintering (RS) of mixed zircon-based powders as a route for producing ceramics containing zirconia with enhanced mechanical properties 18 p2671 A83-39062

Analysis of flexure strength data of ceramics 18 p2672 A83-39996

High-temperature composites - Status and future directions 18 p2650 A83-40129

Slow crack growth behavior in transformation-toughened Al₂O₃-ZrO₂(Y₂O₃) ceramics 19 p2823 A83-40907

Dynamic fatigue of a machinable glass-ceramic 19 p2823 A83-40908

Silicon carbide yarn stimulates development of new composites 19 p2819 A83-41034

Studies on the metastable phase retention and hardness in zirconia ceramics 20 p2958 A83-42782

Ceramics from polymer pyrolysis, opportunities and needs - A materials perspective [ACS PAPER 13-B-81] 21 p3115 A83-44093

Siloxanes, silanes, and silazanes in the preparation of ceramics and glasses [ACS PAPER 17-B-81] 21 p3115 A83-44095

Preparation and properties of monolithic and composite ceramics produced by polymer pyrolysis [ACS PAPER 19-B-81] 21 p3115 A83-44097

On subcritical crack growth in ceramics as influenced by grain size and energy-dissipative mechanisms 21 p3116 A83-44122

X-ray diffraction analysis at high temperature on two ceramic systems 21 p3116 A83-44127

Microstructures and subcritical crack growth in oxidized hot-pressed Si₃N₄ 21 p3116 A83-44331

Observations on the characteristics of a fluidized bed for the thermal shock testing of brittle ceramics 21 p3116 A83-44333

Sub-eutectoid aged Mg-PSZ alloy with enhanced thermal up-shock resistance 21 p3116 A83-44335

A probabilistic treatment of brittle fracture under nonmonotonically increasing stresses 21 p3159 A83-44923

Automotive gas turbine ceramic component testing [ASME PAPER 83-GT-112] 23 p3464 A83-47945

Ceramic Applications in Turbine Engines (CATE) development testing [ASME PAPER 83-GT-179] 23 p3465 A83-47990

Effect of grinding variables on strength of hot pressed silicon nitride [ASME PAPER 83-GT-203] 23 p3465 A83-48004

Ceramic components for high-temperature vehicular gas turbines - State of the art of the German ceramic program [ASME PAPER 83-GT-205] 23 p3465 A83-48006

X-ray tomography applied to NDE of ceramics [ASME PAPER 83-GT-206] 23 p3458 A83-48007

Progress in net shape fabrication of alpha SiC turbine components [ASME PAPER 83-GT-238] 23 p3466 A83-48030

Progress in nitrogen ceramics; Proceedings of the Second Advanced Study Institute, University of Sussex, Brighton, England, July 27-August 7, 1981 23 p3433 A83-48251

Nitrogen ceramics 1976-1981 23 p3433 A83-48252

Silicate structures and atomic substitution 23 p3427 A83-48253

The characterization of alpha-prime-sialons and the alpha-beta relationships in sialons and silicon nitrides 23 p3434 A83-48254

The structural characterisation of sialon polytypoids 23 p3434 A83-48255

Calculation of phase equilibria in systems based on Si₃N₄ 23 p3434 A83-48256

Solid-liquid reactions in part of the system Si, Al, Y/N, O 23 p3434 A83-48258

High temperature reactions and microstructures in the Al₂O₃-AlN system 23 p3434 A83-48259

Liquid phase sintering 23 p3435 A83-48265

Sintering of silicon nitride - A review 23 p3435 A83-48266

Sintering of Si₃N₄-based materials using the powder bed technique 23 p3435 A83-48268

Densification and transformation mechanisms in nitrogen ceramics 23 p3435 A83-48269

Sintering of reaction bonded silicon nitride 23 p3435 A83-48270

Sintering of aluminium nitride with low oxide addition 23 p3435 A83-48272

Stress assisted hot formation of ceramics 23 p3435 A83-48273

A gas pressure sintering process for producing dense Si₃N₄ 23 p3435 A83-48274

Hot pressing of aluminium nitride 23 p3436 A83-48275

The microstructure of nitrogen ceramics 23 p3436 A83-48276

The kinetics of gas-solid reactions and environmental degradation of nitrogen ceramics 23 p3436 A83-48281

Thermodynamic mechanism for cation diffusion through an intergranular phase - Application to environmental reactions with nitrogen ceramics 23 p3436 A83-48282

Oxidation kinetics of hot-pressed silicon nitride 23 p3436 A83-48283

Oxidation behaviour of beta-prime sialons in oxygen and carbon dioxide 23 p3436 A83-48284

Time-temperature effects in nitride and carbide ceramics 23 p3437 A83-48288

High temperature fatigue failure in pressureless sintered silicon nitride 23 p3437 A83-48289

Effect of deformation on the fracture of Si₃N₄ and sialon 23 p3437 A83-48290

Cyclic fatigue behavior of ceramics 23 p3437 A83-48291

The fracture behaviour of hot-pressed silicon nitride between room temperature and 1400 C 23 p3437 A83-48292

Parameter studies on the oxidation and the strength behaviour of silicon nitride 23 p3437 A83-48293

Influence of corrosion and microstructure on mechanical properties of SiYON ceramics 23 p3437 A83-48296

Thermal shock resistance of two nitrogen ceramics 23 p3438 A83-48298

Non-destructive failure prediction in ceramics 23 p3467 A83-48299

Non-destructive evaluation of ceramic gas turbine components by X-rays and other methods 23 p3468 A83-48300

Surface damage in ceramics - Implications for strength degradation, erosion and wear 23 p3438 A83-48301

Contact stresses at ceramic interfaces 23 p3438 A83-48302

Sintering, properties and fabrication of Si3N4 + Y2O3 based ceramics 23 p3438 A83-48303

Lucas Syalons - Composition, structure, properties and uses 23 p3438 A83-48304

The nature of SiC for use in heat engines as compared to Si3N4 - An overview of property differences 23 p3438 A83-48305

Fabrication of complex shaped ceramic articles by slip casting and injection molding 23 p3466 A83-48306

Hot isostatic pressing of ceramics 23 p3438 A83-48307

US national programs in ceramics for energy conversion 23 p3438 A83-48308

Status report 1981 on the German BMFT-sponsored programme 'Ceramic components for vehicular gas turbines' 23 p3438 A83-48309

Nitrogen ceramics in France 23 p3438 A83-48310

Current Japanese research programmes into nitrogen ceramics 23 p3439 A83-48311

The use of ceramics for engines 23 p3439 A83-48636

Factors influencing residual surface stresses due to a stress-induced phase transformation --- in alumina-zirconia ceramics 24 p3567 A83-48960

[ACS PAPER 83-B-82] 24 p3567 A83-48960

Properties of isostatically hot-pressed silicon nitride [ACS PAPER 168-B-83] 24 p3568 A83-48962

New results on hot corrosion of silicon ceramics 24 p3569 A83-49520

Interfacial conduction in lithium iodide containing inert oxides 24 p3558 A83-49947

CEREBRAL CORTEX

An electroencephalographic investigation of the human cerebral cortex during the processing of the solution of visual-motor problems with training 01 p0083 A83-10530

An investigation of the role of deep brain structures in the regulation of intracerebral microcirculation 02 p0219 A83-11518

The reflection of the success of the solving of arithmetic and visual tasks in the spatial-temporal distribution of cerebral cortical biopotentials 02 p0224 A83-12214

The voluntary regulation of alpha and theta EEG rhythms in humans 02 p0224 A83-12215

Spatial-frequency characteristics of receptive fields of the cat visual cortex in cases of homogeneous and inhomogeneous backgrounds 03 p0376 A83-14362

The significance of functional lateralization in the formation of complex motor acts in athletes 04 p0522 A83-15784

Peculiarities of the reaction of cortical pyramidal neurons to the cessation of oxygen supply by the effect of cAMP 04 p0520 A83-15890

The response of the neurons of the visual centers of the rabbit brain to electric stimuli and a combination of the latter with nonvisual stimuli 05 p0672 A83-17638

The cortical evoked negative wave as a reflection of selective attention 06 p0799 A83-18967

Blocking the negative delta waves in the rabbit visual cortex by light flashes 06 p0795 A83-18972

Structural foundations of the reliability of the functioning of cortical neurons 06 p0795 A83-18984

The neuronal receptive fields of the visual cortex of cats during changes in the level of wakefulness 07 p0973 A83-20352

The visual function of the nonprojected sections of the cortex and its reflection in the evoked potentials 07 p0973 A83-20353

The asymmetry of the brain hemispheres from the viewpoint of the identification of visual forms 07 p0977 A83-20355

The role of various cortical regions in visual-motor coordination 07 p0973 A83-20356

The dynamics of oxygen transport from the capillaries to the nerve cells of the brain 08 p1145 A83-22104

The degrees of freedom of a neuron and the cortical neuronal modules 08 p1145 A83-22117

The characteristics, neuronal mechanisms, and functional significance of cortical inhibition 13 p1895 A83-30303

The types of spatial-frequency filters in the visual cortex of cats 13 p1896 A83-30408

The structural differences of the spatial-frequency filters in the visual cortex of cats 13 p1896 A83-30409

The spatial and temporal organization of the receptive fields of the striatal cortex in cats 13 p1896 A83-30427

The mechanisms of the classification of visual images according to spatial signs in normal dogs and after the excision of the parietal and the supertemporal cortices 13 p1896 A83-30439

The role of the inferotemporal and inferoparietal cortices in the description of a visual image in monkeys 13 p1896 A83-30440

The cerebral cortex - The integrator of information of sensory inputs 14 p2065 A83-33315

The phasic neuron reactions of the visual cortex to flashes of light in various conditions of stimulation 14 p2066 A83-33340

The age characteristics of cortical auditory evoked potentials 14 p2071 A83-33341

The effect of spatial-structural stimulus parameters on the evoked potentials in the visual and posterior associative areas of the cortex in humans 14 p2071 A83-33342

Adrenocortical activity in athletes after repeated physical loads during the course of the day 16 p2398 A83-35909

Electron-microscope cytochemical study of ribonucleoprotein particles in cerebral cortex neurons in a posthypoxic period 16 p2395 A83-36812

Age-related changes of interneuronal connections in the cerebral cortex of humans 17 p2560 A83-38193

Differences in the description of a visual image at the level of the posterior parietal and inferotemporal cortices of monkeys 18 p2732 A83-39521

The function of dream sleep 18 p2732 A83-39961

Statistical mechanics of neocortical interactions - Dynamics of synaptic modification 18 p2751 A83-40414

Comparison of the spatial response properties of the human retina and cortex as measured by simultaneously recorded pattern ERGs and VEPs 19 p2880 A83-40750

The effects of the electrical stimulation of the visual cortex of cats on the behavioral model of the placement of a paw on a support 19 p2871 A83-40811

The dependence between spatial and spatial-frequency characteristics of the receptive fields of the visual cortex in cats 19 p2871 A83-40812

Rhythms in the range of 4.5-12 Hz of the background EEG from the visual and sensorimotor cortex in rats under different patterns of locomotor activity 19 p2876 A83-41565

The gravitational field and brain function 19 p2877 A83-42045

The discrimination of amplitude and temporal parameters of the direct electrical stimulation of the visual cortex 19 p2878 A83-42069

The role of inhibition in the formation of a dynamic mosaic of neuronal assemblies in the cerebral cortex 19 p2879 A83-42090

The first cortical implant of a multiplexed multi-electrode semiconductor brain electrode 20 p3035 A83-42553

Specificity of cortico-cortical connections in monkey visual system 20 p3034 A83-43545

Visual motion and cortical velocity 20 p3035 A83-43558

Direct cortical responses and the integrating activity of the brain 21 p3185 A83-45372

The relationship between blood flow, partial pressure, and oxygen demand in the human cortex (A theory of tissue gas exchange) 23 p3497 A83-47113

CEREBRAL VASCULAR ACCIDENTS

Emotional stresses and their role in cerebrovascular disturbances 05 p0672 A83-17598

Pulmonary complications during acute disorders of the cerebral blood circulation 14 p2070 A83-33311

A table for predicting the development of cerebral strokes 15 p2213 A83-34969

CEREBROSPINAL FLUID

The mechanical properties of the brain in the process of the development of postischemic edema 01 p0079 A83-10526

The effect of xenogenous cerebrospinal fluid on the course of experimental hypercholesterolemia 05 p0670 A83-17187

The importance of laboratory data for the differentiation of mild and moderately severe craniocerebral injuries 06 p0798 A83-18977

Light and propranolol suppress the nocturnal elevation of serotonin in the cerebrospinal fluid of rhesus monkeys 18 p2732 A83-39935

CEREBRUM

The local cerebral blood flow and the local vascular reactivity during brain contusions in an experiment under conditions of arterial normal tension and hypertension 06 p0795 A83-18978

The problem of tissue adaptation to hypoxia 09 p1322 A83-25168

Changes in the loco-regional cerebral blood flow /r.C.B.F./ during a simulation of weightlessness 11 p1641 A83-27349

Evoked potentials of the posterior associative regions of the cerebrum during the discrimination and identification of human facial images 12 p1764 A83-29302

The asymmetry of the functional condition of the cerebral hemispheres during the adaptation to new climatic and geographical conditions 12 p1764 A83-29303

An investigation of the microcirculatory bed in flightcrew members with conjunctivitis during the initial appearance of cerebral atherosclerosis 13 p1905 A83-30949

The aminergic control of the cerebral arteries 14 p2063 A83-32099

The role of the cerebral hemispheres in the realization of the adaptive mechanisms in humans (in conditions of sleep deprivation) 14 p2071 A83-33343

Hyperthermic responses to central injections of some peptide and non-peptide opioids in the guinea-pig 16 p2394 A83-36719

Cholinergic and adrenergic innervation of intracerebral arteries during ontogenesis in humans 17 p2560 A83-38194

Local cerebral blood flow increases during auditory and emotional processing in the conscious rat 19 p2873 A83-40906

The central noradrenergic regulation of cerebral blood flow 23 p3496 A83-48565

CERENKOV COUNTERS

Investigation of the spatial distribution function of Cerenkov emission from extensive air showers at the Samarkand University installation 02 p0275 A83-11751

Observations of gamma radiation at 10 to the 12th eV from the X-ray source Cyg X-3 at the Tien-Shan installation in 1977 and 1978 17 p2589 A83-37687

Detectors of ultraheavy cosmic rays 23 p3455 A83-47754

The IMB proton decay detector 23 p3455 A83-47763

CERENKOV EFFECT

U CERENKOV RADIATION

CERENKOV RADIATION

Computer simulations of atmospheric Cerenkov radiation in large cosmic-ray showers 01 p0130 A83-11043

The Samarkand EAS installation and experimental results 02 p0275 A83-11750

Investigation of the spatial distribution function of Cerenkov emission from extensive air showers at the Samarkand University installation 02 p0275 A83-11751

Analysis of the spatial distribution of Cerenkov emission from extensive air showers obtained at the Samarkand University installation 02 p0275 A83-11752

Experimental data on the pulse shape of EAS Cerenkov radiation and the analysis of these data 02 p0275 A83-11753

On the formation of the diffuse component of solar electron streams 03 p0436 A83-13664

Cherenkov parametric optical oscillations in a 'double' Fabry-Perot interferometer 07 p0934 A83-20116

Grains spin-up by inverse Cerenkov effect --- in interstellar gas 10 p1501 A83-25493

Gain and efficiency of a stimulated Cerenkov optical klystron 10 p1428 A83-26020

Pumping of a two-mirror resonator with rippled walls by a relativistic electron beam 10 p1410 A83-26236

Cerenkov-type optical parametric oscillation in a 'double' Fabry-Perot interferometer 11 p1578 A83-27540

The ground state of an atom moving in a medium 11 p1654 A83-28067

Transition radiation and transition scattering 11 p1649 A83-28243

Model of the Cerenkov laser 11 p1586 A83-28713

Measurements of the stimulated Cerenkov interaction at optical wavelengths 13 p1856 A83-31138

Relativistic quasi-optical Cerenkov oscillator with Wood anomalies 14 p2023 A83-32116

Intense electromagnetic radiation from relativistic particles 15 p2228 A83-33786

A search for very high energy gamma-ray transients from Cygnus X-3 and PSR 0531 16 p2441 A83-36639

The results of observations of the X-ray source Cyg X-3 at energies exceeding 10 to the 12th eV made at the Tien Shan installation for detecting Cerenkov flashes in extensive air showers 17 p2589 A83-37661

An exact-time registration system for observations of very-high-energy gamma-quanta 17 p2510 A83-37719

An unguided wave Cerenkov amplifier 17 p2497 A83-37754

The Cherenkov effect and plasma turbulent reactors 17 p2582 A83-37893

Stimulated Cerenkov emission from ultrarelativistic helical electron beams 17 p2499 A83-38492

Comment on the cosmic ray energy spectrum in the light of results from atmospheric Cerenkov studies 19 p2925 A83-41539

A high-energy, laser accelerator for electrons using the inverse Cherenkov effect 20 p2994 A83-42586

- The excitation of microwaves by a relativistic electron beam in a dielectric-lined waveguide
21 p3124 A83-43945
- Cerenkov radiation from periodic electron bunches
22 p3277 A83-45928
- Experimental study of the 'Cerenkov' emission of solitons in two-dimensional LC-lattices
23 p3504 A83-48480

CERES ASTEROID

- Observations of 1 Ceres and 2 Pallas at centimeter wavelengths
02 p0268 A83-12922
- Worldwide photometry and lightcurve observations of 1 Ceres during the 1975-1976 apparition
14 p2097 A83-32603

CERIUM

- The effect of cerium on high temperature tensile and creep behavior of a superalloy
10 p1396 A83-25864
- The maser effect in a paramagnetic crystal caused by the thermal action of the spin system aided by a pulsed magnetic field
19 p2853 A83-41500

CERIUM COMPOUNDS

- NT CERIUM OXIDES
A kinetic model of hydrogen absorption in CeMg12
15 p2193 A83-34868

CERIUM OXIDES

- New identifications of YO and CeO in R Cygni
01 p0126 A83-10966
- Identification of new CeO features in the S star Pi Gruis
11 p1673 A83-27988

CERMETS

- A new diffusion-inhibited oxidation-resistant coating for superalloys
01 p0024 A83-10299
- Fatigue behavior of SiC reinforced Ti/6Al-4V/ at 650 C
02 p0150 A83-12414
- A structural study of detonation-sprayed tungsten carbide-cobalt coatings
02 p0159 A83-13030
- Wear-resistant hard alloys based on titanium-chromium diboride
03 p0293 A83-14816
- Optical properties of gold-magnesia selective cermets --- for solar collectors
04 p0504 A83-15482
- Denitrification of TiN-Ni compacts during sintering
06 p0732 A83-19107
- Effects of metal diboride additives on grain growth and mechanical properties of TiB2-MeB2-CoB systems
06 p0734 A83-19108
- Chemical deposition of coatings with additions of fibrous fillers
07 p0877 A83-20686
- A study of the formation conditions and refractory properties of silicon carbide and boron carbide coatings on GMZ-grade graphite
07 p0900 A83-20706
- The interaction of elements in Ni-Cr-Si-B powder mixtures during heating
07 p0889 A83-20709
- Hot-rolled silicon carbide-aluminum composites
10 p1388 A83-25627
- Static and fatigue testing of 2024 Al-SiC /F-9/ T-4 [ASME PAPER 82-WA/AERO-2]
10 p1388 A83-25677
- Advanced alloys and metal/ceramic composites from lunar source materials
11 p1531 A83-27345
- The structure and certain physicomaterial properties of Fe-Ni-Cr-Mo alloys --- for cermets matrix materials
11 p1547 A83-27923
- The effect of temperature and heat treatment on the fracture toughness of powder-metallurgy tungsten
11 p1549 A83-28482
- A study of the conditions of tongue-and-groove rolling on the structure and properties of VA-grade tungsten rods and wire
13 p1821 A83-30698
- Mechanical properties of SiC fiber reinforced Al composites
18 p2659 A83-40259
- New method for solid-state bonding between ceramics and metals
19 p2818 A83-40911
- Structure and phase composition of nickel-boride composite coatings
21 p3113 A83-44485
- Metallic infiltration of reaction bonded silicon nitride
23 p3436 A83-48285
- A study of the heat resistance and thermal stability of calorized plasma-sprayed coatings on titanium
24 p3560 A83-49085
- Development and characterization of multilayer heat-insulating coatings based on plasma-sprayed thermoreactive metal-ceramic compositions
24 p3568 A83-49086
- Fracture toughness and limiting strength of cermets
24 p3560 A83-49327
- Al2O3 scales on ODS alloys --- oxide dispersion strengthened
24 p3563 A83-49490

CERTIFICATION

- On-line certification for ATE systems
01 p0001 A83-10785
- General conditions of operational and technical utilization of ILS during Category III operations
02 p0134 A83-13008
- Experience with specifications applicable to certification --- of photovoltaic modules for large-scale application
04 p0504 A83-15463

- DC-9 Super 80 digital flight guidance system simulation techniques for certification
05 p0592 A83-17305
- Software aspects in certification of new European civil transport aircraft
05 p0679 A83-17314
- Helicopter icing - Testing and certification
06 p0716 A83-18381
- Additional remarks with respect to the American decree of regarding the suspension of foreign certificates of airworthiness
08 p1171 A83-21899
- Determination of horizontal tail load and hinge moment characteristics from flight data --- on Learjet Model 55 Longhorn
13 p1805 A83-30162
- Flight development and certification - How efficient can it be?
14 p1975 A83-32929
- Use of simulated ice shapes in known icing certification
14 p1973 A83-32936
- A contribution to airworthiness certification of gas turbine disks
16 p2305 A83-35872
- From aerostats to DC-10s - Recognition of certificates of airworthiness
22 p3369 A83-45829
- Interchange of aircraft --- international lease regulations
22 p3369 A83-45832
- The right to be heard - The British practice --- refusal or revocation of licenses in air transport
22 p3370 A83-45841
- Certification of avionic systems; Proceedings of the Symposium, London, England, April 27, 1982
22 p3247 A83-45843
- Military systems acceptance criteria --- for digital avionic systems
22 p3247 A83-45844
- Certification of digital systems for civil aircraft
22 p3252 A83-45848
- Helicopter avionic systems certification
22 p3255 A83-45849
- Certification of the Lockheed 1011-500 active control system
22 p3255 A83-45850
- FAA rotorcraft icing regulations and directions
22 p3251 A83-46927

CESIUM

- NT CESIUM VAPOR
Theoretical determination of the X 1Sigma g + potential of Cs2 using relativistic effective core potentials
07 p0991 A83-21055
- 5s/2/5p/4/-5s5p/5/ transitions in Cs IV, Ba V, and La VI
09 p1342 A83-24095
- The specific heat of liquid cesium at temperatures up to 2000 K and pressures up to 12 MPa
11 p1550 A83-28558
- Evaluation of the light shift in a frequency standard based on Raman induced Ramsey resonance
12 p1729 A83-29192
- Performance of the four NRC long-beam primary cesium clocks Cs V, Cs VIA, Cs VIB, and Cs VIC
13 p1847 A83-31293
- Collisional broadening of intra-Doppler resonances of selective reflection on the D2 line of cesium
14 p2082 A83-32619
- Experimental investigation of absorption coefficient of cesium resonance doublets in a plasma of combustion products
18 p2746 A83-39859
- Stark interference effects in a weak magnetic field on the 6S-7S forbidden transition of cesium
19 p2898 A83-41180
- Rb and Cs broadening of the Na resonance lines
24 p3626 A83-48835

CESIUM COMPOUNDS

- NT CESIUM HYDRIDES
NT CESIUM IODIDES

CESIUM DIODES

- Plasma layers near the electrodes of a cesium diode - Cathode layer
09 p1348 A83-23989
- Plasma layers near the electrodes of a cesium diode - Anode layer
09 p1348 A83-23990

CESIUM HALIDES

- NT CESIUM IODIDES

CESIUM HYDRIDES

- Ab initio calculation of the X 1 Sigma + state of CsH
14 p2083 A83-33106

CESIUM IODIDES

- Quantum efficiency of opaque CsI photocathodes with channel electron multiplier arrays in the extreme and far ultraviolet
03 p0330 A83-14383

CESIUM PLASMA

- Population inversion in copper on transitions with wavelengths of 510.6 and 578.2 nm in a recombining Cu-Cs plasma
24 p3588 A83-49114

CESIUM VAPOR

- Conversion of 3-micron infrared radiation in cesium vapor
05 p0649 A83-17055
- Axial and angular distribution of current density in a thermionic converter with nonisothermal electrodes
10 p1445 A83-25887
- Efficient laser-induced plasma formation in alkali-metal vapors
11 p1658 A83-27587

- Compression filter based on optically oriented cesium-vapor atoms with low diffusion
14 p2084 A83-32121

CESSNA AIRCRAFT

- Autogas flight test in a Cessna 150 airplane [SAE PAPER 830706]
20 p2933 A83-43317

CESSNA MILITARY AIRCRAFT

- U MILITARY AIRCRAFT

CEYLON

- A holistic approach to the monitoring of land cover changes in Sri Lanka using intermediate remote sensing techniques
15 p2181 A83-33565

CF-104 AIRCRAFT

- U CANADAIR AIRCRAFT
U F-104 AIRCRAFT

CFRP

- U CARBON FIBER REINFORCED PLASTICS

CH-53 HELICOPTER

- U H-53 HELICOPTER

CH-113 HELICOPTER

- U CH-46 HELICOPTER

CH-46 HELICOPTER

- Training effectiveness evaluation of device 2F117 - OFT for CH-46 helicopter
10 p1456 A83-26326
- Output feedback pole assignment under system variation --- with CH-46 example
21 p3195 A83-44948

CH-47 HELICOPTER

- Multivariable stability margins for vehicle flight control systems
09 p1210 A83-24815

CHAFF

- Dual Doppler observations of diffusion and rolls --- due to atmospheric circulation patterns
11 p1629 A83-27059
- A radar study of topographic effects
11 p1629 A83-27060

CHAINS

- An approach for the generation of kinematic chains with multiple joints
21 p3147 A83-44030

CHAIRS

- U SEATS

CHALCOGENIDES

- NT ALUMINUM OXIDES
NT ANHYDRIDES
NT BERYLLIUM OXIDES
NT BISMUTH SULFIDES
NT CADMIUM SELENIDES
NT CADMIUM SULFIDES
NT CADMIUM TELLURIDES
NT CALCIUM OXIDES
NT CALCIUM SULFIDES
NT CARBON DIOXIDE
NT CARBON DISULFIDE
NT CARBON MONOXIDE
NT CHLORINE OXIDES
NT CHROMITES
NT CHROMIUM OXIDES
NT COBALT OXIDES
NT COPPER OXIDES
NT COPPER SELENIDES
NT COPPER SULFIDES
NT DISULFIDES
NT ENSTATITE
NT GERMANIUM OXIDES
NT HAFNIUM OXIDES
NT HEAVY WATER
NT HYDROGEN PEROXIDE
NT HYDROGEN SULFIDE
NT ILMENITE
NT INDIUM SULFIDES
NT INDIUM TELLURIDES
NT INORGANIC PEROXIDES
NT INORGANIC SULFIDES
NT IRON OXIDES
NT LEAD OXIDES
NT LEAD SULFIDES
NT LEAD TELLURIDES
NT LITHIUM OXIDES
NT MAGNESIUM OXIDES
NT MAGNETITE
NT MANGANESE OXIDES
NT MERCURY TELLURIDES
NT METAL OXIDES
NT MOLYBDENUM DISULFIDES
NT MOLYBDENUM OXIDES
NT MOLYBDENUM SULFIDES
NT NICKEL OXIDES
NT NIOBIUM OXIDES
NT NITRIC OXIDE
NT NITROGEN DIOXIDE
NT NITROGEN OXIDES
NT NITROGEN TETROXIDE
NT NITROUS OXIDES
NT ORGANIC PEROXIDES
NT OXIDES
NT PEROXIDES

- NT PHOSPHORUS OXIDES
 NT POLYSULFIDES
 NT POTASSIUM OXIDES
 NT PYRITES
 NT PYROXENES
 NT QUARTZ
 NT RUTILE
 NT SAPPHIRE
 NT SELENIDES
 NT SILICON DIOXIDE
 NT SILICON OXIDES
 NT SILVER OXIDES
 NT SODIUM PEROXIDES
 NT SULFIDES
 NT SULFUR DIOXIDES
 NT SULFUR OXIDES
 NT TANTALUM OXIDES
 NT TELLURIDES
 NT TIN OXIDES
 NT TIN TELLURIDES
 NT TITANIUM OXIDES
 NT TROLITE
 NT TUNGSTEN OXIDES
 NT VANADIUM OXIDES
 NT WURTZITE
 NT YTTRIUM OXIDES
 NT ZINC OXIDES
 NT ZINC SELENIDES
 NT ZINC SULFIDES
 NT ZINC TELLURIDES
 NT ZINCBLENDE
 NT ZIRCONIUM OXIDES
 Features of the Raman spectra of noncrystalline semiconductor compounds of the type Hg/Ge/-As/Sb/-S-I 01 p0110 A83-10847
 Paramagnetism in X-irradiated chalcogenide glasses and crystals 04 p0540 A83-15503
 Photoinduced structural transformations in complex chalcogenide glasses 13 p1929 A83-30446
 The peculiarities of current transmission in degenerate semiconductor-semiconductor heterojunctions 14 p2087 A83-32128
 Chalcogenide glasses - Promising materials for quantum electronics. I - The interaction and structure of As-S glasses 14 p2088 A83-32167
 Middle IR As-S and As-Se glass fibres with optical losses lower than 1 dB/m 19 p2900 A83-41280
 Tunable diode lasers and laser systems for the 3 to 30 microns infrared spectral region 22 p3297 A83-46638
- CHANCE-VOUGHT MILITARY AIRCRAFT**
 U MILITARY AIRCRAFT
- CHANDLER MOTION**
 U POLAR WANDERING (GEOLOGY)
- CHANDRASEKHAR EQUATION**
 Emden-Chandrasekhar axisymmetric, solid-body rotating polytropes. II - Power series solutions to EC associated equations of degree 0 and 2 12 p1793 A83-29070
 Asymptotic expansions of singularly perturbed Chandrasekhar type of equations 17 p2571 A83-37146
- CHANNEL CAPACITY**
 Analysis of systems containing multiple, irregular sampling 01 p0095 A83-11131
 A high speed 10MHz multiplex data bus interface 01 p0042 A83-11152
 Components for angular division multiplexing --- for increasing optical fiber information capacity 03 p0394 A83-13775
 Pre-operational tests of high-speed /56 kbps/ transmission over MARISAT 07 p0870 A83-19702
 On information flow in relay networks 07 p0908 A83-19734
 Light route TDMA for business communications 07 p0911 A83-19784
 Advances in Serial MSK modems 07 p0917 A83-19789
 High packing density modulation techniques for satellite links 07 p0912 A83-19799
 Game-theoretical evaluation of capacity in the case of channel parameters that are unknown to the operator 07 p0985 A83-20772
 A method of increasing satellite link capacity 08 p1078 A83-22994
 Coherent optical space communications system architecture and technology issues 09 p1214 A83-23578
 High throughput non-dispersive hard X-ray spectrograph with angular resolution for cosmic bursts, transients, and sources 09 p1268 A83-24108
 Communications and tracking - Light and IR will help carry high traffic 09 p1215 A83-24354
 Distributed hypothesis formation in sensor fusion systems 09 p1334 A83-24811
- One-way multiaddress satellite data communication system 11 p1557 A83-28133
 The use of resource sharing and coding to increase the capacity of digital satellites 11 p1557 A83-28135
 Deep-space laser communications. I - Optical receivers probe the depths of space 11 p1535 A83-28154
 The effect of the limitation of the spectrum of a linear-FM signal with intrapulse phase shift keying on the characteristics of optimal reception 13 p1829 A83-30734
 Capacity limit of the noiseless, energy-efficient optical PPM channel 14 p2001 A83-32870
 Dynamic frame length ALOHA 14 p2001 A83-32871
 Go-back-N ARQ schemes for point-to-multipoint satellite communications --- automatic-repeat-request 14 p2001 A83-32873
 Speech encoding for 6/4 GHz band small capacity omni-use terminal satellite system 15 p2144 A83-33509
 Switching system for 6/4 GHz band small capacity omni-use terminal satellite system 15 p2144 A83-33510
 Information theory and causal information transmission with feedback 15 p2221 A83-35104
 Conflict resolution protocols for random multiple-access channels with binary feedback 15 p2147 A83-35122
 Optical fiber repeatered transmission systems utilizing SAW filters 16 p2345 A83-35648
 Capacity allocation scheme for transmission of packets over satellite links 17 p2493 A83-37792
 Comparative evaluation of the noise immunity and capacity of communication systems with separation of channel according to the form of the signals 18 p2675 A83-40092
 On the capacity of multihop slotted ALOHA networks with regular structure 19 p2825 A83-40893
 On the capacity of single-hop slotted ALOHA networks for various traffic matrices and transmission strategies 19 p2826 A83-40894
 High capacity low delay packet switching via a processing satellite 19 p2828 A83-41337
 Throughput analysis of an asynchronous code division multiple access (CDMA) system 19 p2830 A83-41362
 20 x 20 IF switch matrix for SS-TDMA systems 19 p2839 A83-41369
 Intelsat architectures for the 1990s 19 p2830 A83-41370
 A selective-repeat ARQ scheme and its throughput analysis 19 p2832 A83-41398
 Performance analysis of M-ary code shift keying in code division multiple access systems 19 p2833 A83-41408
 Hybrid frequency-domain coding of speech signals 20 p2965 A83-43685
 Towards the fundamental limits of optical-fiber communications 21 p3204 A83-44215
 Synchronous and channel-sense asynchronous dynamic group-random-access schemes for multiple-access communications 22 p3272 A83-45738
 Increasing the shipborne telemetric systems capacity with the channel frequency division [IAF PAPER 83-89] 23 p3441 A83-47260
 Improved estimate of the channel capacity of the geostationary orbit 23 p3444 A83-48516
- CHANNEL FLOW**
 NT OPEN CHANNEL FLOW
 The development of jets in stratified fluids 02 p0169 A83-11860
 Numerical solutions to natural convection in a channel with porous walls under a transverse magnetic field 02 p0171 A83-12666
 A down-stream boundary procedure for the Euler equations 02 p0174 A83-13021
 Spectral method solutions for some laminar channel flows with separation 03 p0315 A83-13138
 Spectral modeling of linear mechanisms in nonhomogeneous turbulent flows --- French thesis 03 p0317 A83-14104
 Conditionally averaged patterns of coherent events in a wall-bounded turbulent flow 03 p0320 A83-14483
 Transonic shear flow in a three-dimensional channel 03 p0321 A83-14586
 Computation of 3-D internal transonic flows 03 p0280 A83-14609
 Calculation of total-pressure losses in channels with variable cross-section area in the presence of turbulent mixing 04 p0475 A83-15080
 Kinematic, integral, and thermal characteristics of the turbulent flow of a suspension in a gas under the effect of thermal nonstationarity 04 p0476 A83-15446
 Heat transfer in the turbulent flow of dissociating and vibrationally relaxing gas in a channel with rough walls 04 p0477 A83-15862
- The STD/MHD codes - Comparison of analyses with experiments --- MHD generator performance prediction and tests 04 p0538 A83-16105
 Hall effects on MHD flow through a porous straight channel 04 p0539 A83-16434
 Reduction of flow-measurement uncertainties in laser velocimeters with nonorthogonal channels [AIAA PAPER 83-0051] 05 p0642 A83-16486
 Three-dimensional fluid and electrodynamic modeling for MHD DCW channels [AIAA PAPER 83-0464] 05 p0686 A83-16732
 Aerodynamic features of turbulent flames [AIAA PAPER 83-0470] 05 p0636 A83-16737
 On certain aspects of three-dimensional instability of parallel flows 07 p0927 A83-21353
 Idealized model for plasma acceleration in an MHD channel --- current distribution in plasma thruster 08 p1052 A83-22126
 Determination of the cavitation boundary in liquid flows through constricting devices 09 p1258 A83-23432
 Flow in the base region in a channel --- supersonic jet discharge from nozzle 09 p1197 A83-24042
 Calculation of channel flows of gases by the Monte-Carlo method with correction for collisions 09 p1260 A83-24048
 Hydraulics of a channel with a linear jet array --- heat transfer coefficient enhancement by transpiration cooling 09 p1260 A83-24049
 Determination of amplitude-frequency response of thermoacoustic oscillations in a liquid at supercritical pressures 09 p1260 A83-24050
 Measurement and calculation of shock attenuation in a channel with perforated walls 10 p1414 A83-26141
 Propagation of two-dimensional nonsteady detonation in a channel with backward-facing step 10 p1416 A83-26165
 Development of finite-amplitude disturbances in a Poiseuille flow 11 p1566 A83-27706
 The effect of the nonuniformity of supersonic flow with shocks on friction and heat transfer in plane channels 11 p1526 A83-27710
 Motion of a circular cylinder in a rectangular channel 11 p1567 A83-27720
 A numerical simulation of transition in plane channel flow [AIAA PAPER 83-0047] 11 p1568 A83-28347
 Qualitative analysis of equations describing quasi-one-dimensional nonequilibrium flow in channels 11 p1569 A83-28535
 Radiative-convective heat transfer during turbulent flow of carbon dioxide in a plane channel 11 p1570 A83-28793
 A study of flow in a short cavity with one-way fluid inlet and outlet 11 p1570 A83-28794
 An analysis of the thermal state of plane channels with allowance for the mutual influence of the processes in the wall and in the fluid 11 p1570 A83-28796
 Secondary instability of plane channel flow to subharmonic three-dimensional disturbances 13 p1839 A83-30101
 Measurements of the periodic velocity oscillations near the wall in unsteady turbulent channel flow 15 p2154 A83-33652
 Combined free and forced laminar convection in a vertical channel 15 p2160 A83-34257
 Free and induced oscillations in Poiseuille flow 16 p2349 A83-35642
 The two-dimensional character of the instability of an ionizable gas flow in the channel of a plasma accelerator 16 p2415 A83-35724
 Effect of heat transfer augmentation on two-phase flow instabilities in a vertical boiling channel 16 p2350 A83-35800
 Heat and mass transfer and hydrodynamics of swirling flows in axisymmetric channels --- Russian book 16 p2353 A83-36437
 Investigations of particle-grid turbulence 16 p2354 A83-36957
 Experimental study of the flow of a viscous compressible gas through a cylindrical channel and through a porous insert 17 p2447 A83-37265
 Microscales and correlation tensors in the viscous turbulent sublayer 17 p2504 A83-37391
 Experimental study of jet-flap diffusers 17 p2448 A83-37534
 Forced oscillations of a viscous incompressible fluid in a semiinfinite channel 17 p2505 A83-37628
 Turbulence structure in stably stratified open-channel flow 18 p2680 A83-39204
 On unstable oscillations in a viscous-fluid flow through an infinite channel 18 p2684 A83-39480
 Calculation of steady two-dimensional turbulent flow in a curved channel 18 p2684 A83-39481
 Flow in the base region of a channel in non-self-similar regimes 19 p2792 A83-41894

- Buoyancy effect on heat transfer in forced channel flows 20 p2971 A83-42661
- Radiative heat transfer in a model porous body 20 p2974 A83-42695
- Finite analytic numerical solution of heat transfer and flow past a square channel cavity 20 p2975 A83-42703
- Heat transfer in the turbulent swirling flow in a channel of complex shape 20 p2976 A83-42714
- Natural, mixed and forced convection in a vertical channel with asymmetric uniform heating 20 p2979 A83-42750
- Acoustic enhancement of heat transfer in plane channels 20 p2929 A83-42751
- Linear stability analysis of heated parallel channels 20 p2981 A83-42768
- The gasdynamic momentum of flow in axisymmetric channels 20 p2982 A83-42886
- Free convection in hydromagnetic flows in a vertical wavy channel 20 p2982 A83-42971
- Shock diffraction in channels with 90 deg bends 20 p2985 A83-43100
- Flow characteristics in the curved rectangular channels Visualization of secondary flow 21 p3129 A83-44064
- Prediction of curved channel flow with an extended k-epsilon model of turbulence 21 p3134 A83-45578
- Isentropic magnetogasdynamic flow of a perfect plasma 22 p3363 A83-46462
- A summary of developments of the mean-stream-line method in China --- for design and calculation of flow channels [ASME PAPER 83-GT-11] 23 p3393 A83-47883
- Heat transfer experiments in high aspect ratio rectangular channel with epoxied short pin fins [ASME PAPER 83-GT-57] 23 p3447 A83-47913
- Two-dimensional behaviour of MHD fully developed turbulence (Rm much greater than 1) 23 p3510 A83-48045
- Prediction of sudden expansion flows using the boundary-layer equations [ASME PAPER 83-FE-11] 23 p3450 A83-48230
- Mixed boundary value problems of the contouring of supersonic nozzles and channels 23 p3400 A83-48663
- Flow of a gas mixture in a cylindrical channel at intermediate Knudsen numbers 24 p3576 A83-48940
- Experimental study of the effect of pulsations on the development of flow-core velocity oscillations and wall friction in a convergent channel 24 p3576 A83-48950
- Experimental investigation of heat transfer with interaction of a density discontinuity with a turbulent boundary layer on the permeable surface of a rectangular channel 24 p3577 A83-49121
- CHANNEL MULTIPLIERS**
- Quantum efficiency of opaque CsI photocathodes with channel electron multiplier arrays in the extreme and far ultraviolet 03 p0330 A83-14383
- An imaging gas scintillation proportional counter coupled to a channel multiplier array for application in cosmic X-ray spectroscopy 11 p1573 A83-27755
- Differential imaging using charge-coupled device (CCD) imagers with on-chip charge storage 14 p2015 A83-31986
- CHANNEL NOISE**
- Elimination of false-locking in long loop phase-locked receivers 03 p0312 A83-13868
- Performance of coherent M-ary PSK systems in an impulsive and Gaussian noise environment 03 p0304 A83-13871
- Design of stabilizing controller with incomplete state data for linear stochastic system with multiplicative noise 04 p0527 A83-15923
- Mitigation of pulsed RFI via automatic gain control 07 p0905 A83-19696
- Performance of IJF-OQPSK modulation schemes in the presence of noise, interchannel and cochannel interference 07 p0905 A83-19699
- Performance of split-phase signals in an impulsive noise channel 07 p0909 A83-19749
- Space-time distribution of the velocity of tidal motions, with allowance for Coriolis force 07 p0962 A83-20773
- The evaluation of the receiver noise level of a lidar response 08 p1074 A83-21873
- Performance of delta modulation algorithms on noisy channels 09 p1246 A83-23693
- Adjacent channel interference in the case of the precision distance measuring system DME/P 10 p1374 A83-26480
- Noise analysis of a PSK carrier recovery DPLL 11 p1559 A83-26973

- Performance of a direct sequence spread-spectrum system with long period and short period code sequences 13 p1827 A83-30224
- Measurement of the noise of a magnetron oscillator 13 p1833 A83-30708
- Soft decision demodulation and transform coding of images 14 p2076 A83-32872
- Optimal coding for information transmission through a Poisson type channel 15 p2221 A83-35118
- Optimal control of radio-signal power in channels with fading and fluctuation noise 15 p2147 A83-35159
- Performance of narrow-band Manchester coded FSK with discriminator detection 16 p2343 A83-36604
- The effects of noise correlation and power imbalance on terrestrial and satellite DPSK channels 16 p2344 A83-36906
- Statistical characteristics of signals in composite TWT amplifiers in the case of modulating noise 17 p2499 A83-38489
- Theory of multiplicative noise caused by coupling loss and amplitude vector rotation in optical communication channels 19 p2826 A83-40895
- Reception of PSK signals over fading channels via quadrature amplitude estimation 19 p2826 A83-40897
- Signaling performance over a piecewise linear limited channel in the presence of interference and Gaussian noise 19 p2826 A83-40921
- Deep space communication - A one billion mile noisy channel 19 p2813 A83-41343
- Modulation characteristics of constricted double-heterojunction AlGaAs laser diodes 21 p3144 A83-44216

CHANNELS (DATA TRANSMISSION)

- Distributed ATE systems software 01 p0088 A83-10771
- Innovation in inertial ATE interfaces 01 p0017 A83-10782
- Four-channel multiplexed resolver-to-digital converter 01 p0009 A83-11100
- Bus protocols for a digital audio distribution system 01 p0005 A83-11126
- Computer simulation of waveforms on time division command/response multiplex data buses 01 p0042 A83-11150
- A high speed 10MHz multiplex data bus interface 01 p0042 A83-11152
- Description and planned use of a data distribution evaluation system for fiber optic data buses 01 p0006 A83-11183
- Future Navy data bus requirements - Modular approach for flexible evolution 01 p0006 A83-11184
- Single chip Bus Interface Unit eases MIL-STD-1553B remote terminal/bus controller designs 01 p0042 A83-11185
- The design and implementation of the KC-135 Avionics Hot Bench Monitor 01 p0010 A83-11227
- A fast microprocessor communication network design for interprocessor communications for an integrated flight control system 02 p0133 A83-11902
- On implementing self-checking microprocessors 02 p0227 A83-11909
- 3 x 2 channel waveguide gyroscope couplers - Theory 02 p0177 A83-12171
- Error rate bounds for differential PSK 05 p0622 A83-17272
- Data transmission rate in a memoryless discrete channel with data feedback 05 p0623 A83-17686
- The noise immunity of reception of PSK signals in a channel with gamma fading 05 p0623 A83-17687
- Optimization and comparison of binary and multistep digital transmission systems with and without quantified feedback --- German thesis 06 p0751 A83-18498
- Adjacent channel interference degradation with minimum shift keyed modulation 07 p0905 A83-19698
- An experimental study of the concatenated Reed-Solomon/Viterbi channel coding system performance and its impact on space communications 07 p0871 A83-19733
- On information flow in relay networks 07 p0908 A83-19734
- On the performance of a code division multiple access scheme with transmit/receive conflicts 07 p0908 A83-19737
- Performance analysis for an adaptive polling access-control scheme employing a dynamic reservation protocol 07 p0908 A83-19738
- Preferred access in packet-switching radio networks 07 p0908 A83-19739
- New error bounds for modulation and coding under mismatch 07 p0909 A83-19745
- A technique for voice-data integration over packet radio channels 07 p0912 A83-19790
- Bandwidth of crossbar and multiple-bus connections for multiprocessors 07 p0984 A83-20250

- Experimental evaluation of adaptive threshold detection with estimated sequence processor performance 07 p0914 A83-20555
- Summary of Intelsat VI communications performance specifications 07 p0869 A83-20557
- Game-theoretical evaluation of capacity in the case of channel parameters that are unknown to the operator 07 p0985 A83-20772
- Time synchronisation of an HF radio modem 08 p1075 A83-21995
- New fiber optic data bus topology 08 p1152 A83-22493
- Synthesis of optimal signals for single-channel systems of delay search 08 p1078 A83-23155
- Parasitic channels of a superregenerative parametric amplifier 08 p1082 A83-23168
- Methods of investigating data transmission networks --- Russian book 09 p1326 A83-23818
- Data systems - Optical bus will connect distributed system 09 p1215 A83-24352
- Digital-signal transmission in the analog channel of ETMS-A and simultaneous transmission of three parameters in one channel of ETMS-A --- telemetry system satellite 10 p1382 A83-25332
- Simplified tone detector for PCM channel 10 p1402 A83-25634
- Analysis of systems in structurally indefinite conditions --- in communication channels 10 p1407 A83-26953
- A practical approach toward maximum likelihood sequence estimation for band-limited nonlinear channels 11 p1553 A83-26974
- Performance evaluation of an integrated access scheme in a satellite communication channel 11 p1557 A83-28137
- A geostationary satellite platform for future communications services 11 p1534 A83-28219
- The design of adaptive information-transfer systems for automatic control --- Russian book 12 p1769 A83-29333
- Calibration of the VIS-channel of Meteosat-2 12 p1708 A83-29692
- Two-dimensional DPCM image transmission over fading channels 13 p1827 A83-30222
- Circuit and packet integrated switching in a satellite communication channel 13 p1829 A83-30780
- Dynamic frame length ALOHA 14 p2001 A83-32871
- Approximate analytical performance evaluation in bus oriented multicomputer systems 15 p2219 A83-35130
- Propulsion control sensor sharing opportunities [AIAA PAPER 83-0536] 16 p2318 A83-36059
- Analysis of a real-time application [AIAA PAPER 83-1088] 16 p2406 A83-36212
- Delay analysis of a satellite channel reservation system with variable frame format 16 p2343 A83-36581
- The effects of noise correlation and power imbalance on terrestrial and satellite DPSK channels 16 p2344 A83-36906
- An automated multichannel measuring system 17 p2563 A83-37674
- Communications performance specifications of the INTEL SAT V-A 17 p2494 A83-37797
- Noise immunity of selection algorithms in the whole 18 p2674 A83-39426
- On the penetration of an electromagnetic field through circular and annular holes 18 p2677 A83-40096
- Comments on the Neyman and Beall formulas for 'contagious' type-A probability distributions applied to burst processes especially in the field of digital transmission 19 p2827 A83-41313
- Improving stability and delay characteristics of multiple access systems employing ALOHA type channels 19 p2828 A83-41333
- Random TDMA access protocol with application to multi beam satellites 19 p2834 A83-41413
- Wavelength-division multiplexing of channels in fiber-optic communication lines (review) 20 p3048 A83-43776
- Optical fibre sensors - Principles and applications 21 p3140 A83-44824
- The transmission of discrete messages in radio channels (2nd revised and enlarged edition) --- Russian book 21 p3121 A83-45009
- The transmission of analog information over digital communications channels --- Russian book 23 p3443 A83-48425
- The use of Walsh functions to transmit data in channels with short-duration interruptions 23 p3444 A83-48520
- Laser bias effect on the receiver sensitivity of passive fibre optic star bus networks 24 p3627 A83-48746
- TOPPSY - A time overlapped parallel processing system 24 p3620 A83-49197

CHANNELTRONS

U CHANNEL MULTIPLIERS

CHAOTIC CLOUD PATTERNS

U CLOUDS (METEOROLOGY)

CHAPLYGIN EQUATION

Computational method for Chaplygin function

14 p2012 A83-32969

CHAPMAN SHEAR LAYER

U SHEAR LAYERS

CHAPMAN-ENSKOG THEORY

Diffusion processes in Ap stars and white dwarfs

06 p0832 A83-18841

Transport coefficients of ternary gas mixtures

08 p1170 A83-21988

nonequilibrium systems 09 p1350 A83-23599

Hydrodynamic equations for partially ionized

multicomponent gas mixtures with higher approximations

to the transport coefficients 13 p1925 A83-30653

On the kinetic theory of dense gases

13 p1932 A83-30656

Calculation of the kinetic coefficients for a moderately

dense gas 13 p1932 A83-30657

CHAPMAN-JOUGET FLAME

U CHEMICAL EQUILIBRIUM

U DETONATION

U FLAME PROPAGATION

CHARACTER RECOGNITION

Optical matched filtering for character recognition

16 p2412 A83-35885

Curve fitting with conic splines

17 p2571 A83-38060

A distance measure between attributed relational graphs

for pattern recognition 19 p2889 A83-41297

Asymptotically optimal test algorithms in problems of

recognition 24 p3620 A83-49124

CHARACTERISTIC EQUATIONS

U EIGENVALUES

U EIGENVECTORS

CHARACTERISTIC FUNCTIONS

U EIGENVALUES

U EIGENVECTORS

CHARACTERISTIC METHOD

U METHOD OF CHARACTERISTICS

CHARACTERS

U SYMBOLS

CHARGE CARRIERS

NT FREE ELECTRONS

NT HOLES (ELECTRON DEFICIENCIES)

NT MAJORITY CARRIERS

NT MINORITY CARRIERS

Photovoltaic emf in conditions of the heating of charge

carriers by light 04 p0539 A83-15127

Schottky revisited --- model limitations and steps for

extending treatment to solar cell structures

04 p0540 A83-15509

Current-voltage characteristic for bipolar p-n junction

devices with drift fields, including correlation between

carrier lifetimes and shallow-impurity concentration --- with

implications for solar cells 04 p0543 A83-16069

Radiation-induced charge dynamics in dielectrics

05 p0618 A83-17502

Accumulation effects at contacts to n-type

cadmium-mercury-telluride photoconductors

06 p0753 A83-18947

Use of magnetic circular dichroism for nondestructive

measurement of charge carrier concentration in wideband

semiconductors 08 p1113 A83-22406

Influence of diffusion of hot carriers on collection

efficiency of solar cells - a-Si:H 09 p1292 A83-23665

Forces acting on free carriers in semiconductors of

inhomogeneous composition I, II 11 p1663 A83-28449

Spectroscopic search for fractional charge in ultrapure

semiconductors 13 p1929 A83-30595

Photoinduced infrared activity in polyacetylene

16 p2421 A83-36565

The dependence of the polarization and intensity of

recombination radiation on the spin orientation of current

carriers in GaAs semiconductors 19 p2905 A83-41221

Inversion of hot carriers in Landau levels

20 p3051 A83-42279

Electric-field-dependent charge-carrier trapping in a

one-dimensional organic solid 21 p3216 A83-43888

CHARGE COUPLED DEVICES

An enhancement mode Schottky barrier gate

charge-coupled device on a high electron mobility

transistor structure 01 p0039 A83-10994

Physics, technology and applications of junction

charge-coupled devices --- Thesis 02 p0167 A83-11974

Noise reduction techniques for CCD image sensors

02 p0167 A83-12012

Technical issues in focal plane development;

Proceedings of the Meeting, Washington, DC, April 21,

22, 1981 03 p0325 A83-13726

Design requirements for large-scale focal planes

03 p0325 A83-13727

Development of Teal Ruby Experiment radiometric test

requirements 03 p0325 A83-13728

Teal Amber visible focal plane technology

03 p0325 A83-13730

Signal conditioning for infrared staring arrays

03 p0326 A83-13732

Source-coupling for hybrid focal planes

03 p0326 A83-13733

Large time-delay-and-integration /TDI/ arrays and focal

plane structures with intrinsic silicon response

03 p0309 A83-13736

1.0 to 2.5 micrometer short wavelength infrared /SWIR/

linear array technology for low background applications

03 p0326 A83-13739

Signal processing for Time Delay and Integrating

Charge-Coupled Device /TDI-CCD/ in the panoramic scan

mode 03 p0309 A83-13740

CCD observations of radio sources from the 5C6 and

5C7 surveys 03 p0409 A83-13936

Electron bombardment charge-coupled device /CCD/

detectors for the vacuum ultraviolet

03 p0288 A83-13964

Use of charge-coupled device /CCD/ detectors for

imaging in the vacuum ultraviolet

03 p0288 A83-13966

Advances in detectors for astronomical spectroscopy

04 p0547 A83-15806

An adaptive sensitive time control circuit implemented

with a CCD sampled delay line for clutter rejection in a

radar processor 04 p0474 A83-16449

Development of a photon counting hybrid CCD digicon

detector

[AIAA PAPER 83-0103] 05 p0608 A83-16521

Electron-bombarded CCD detectors for ultraviolet

atmospheric remote sensing

[AIAA PAPER 83-0106] 05 p0609 A83-16524

Experimental results on junction charge-coupled

devices 06 p0752 A83-18760

Input devices for CCDs 06 p0754 A83-19351

Evaluation of a virtual phase charge-coupled device

as an imaging X-ray spectrometer

07 p0931 A83-21379

Signal processing for staring infrared imagers

08 p1094 A83-22439

Correction of pixel nonuniformities for solid-state

imagers 08 p1094 A83-22441

Microprocessor-based image processing system for

dedicated applications or interactive image processing

08 p1155 A83-22538

Mosaic focal plane methodologies II; Proceedings of the

Conference, San Diego, CA, August 27, 28, 1981

08 p1100 A83-22598

RDA requirements for optimum hybrid focal plane

performance --- Resistance-Area product for IR detector

arrays 08 p1100 A83-22599

Charge-coupled device /CCD/ visible light sensor for

the Teal Ruby Experiment 08 p1051 A83-22602

Progress in 800 x 800 charge-coupled device /CCD/

imager development and applications

08 p1051 A83-22603

AlGaAs/GaAs heterojunction charge-coupled devices

/CCDs/ for visible/near infrared imaging applications

08 p1080 A83-22604

The Teal Ruby Experiment - A potpourri of advanced

technology 08 p1051 A83-22607

Infrared Schottky barrier focal plane array technology

08 p1081 A83-22610

Noise in time-discrete analog filters

09 p1252 A83-23409

Ring laser gyroscopes - Charge-coupled device /CCD/

readout and signal processing for high resolution

applications 09 p1267 A83-23590

CCD camera observations of nearby rich clusters. I -

R photometry of brightest galaxies

09 p1355 A83-24998

The high resolution imaging detector program for X-ray

astronomy at the Smithsonian Astrophysical Observatory

10 p1496 A83-26250

CCD photometry of the center of M31

10 p1508 A83-26364

Infrared array detectors --- for astronomical

observation - 11 p1537 A83-27734

C.C.D. imaging - Solid state sensor now out performs

vidicon in tracking application; Back cover illustration

contrasts the dimensions of these sensors against the

magnified silicon structure of a C.C.D.

11 p1573 A83-28179

Advances in auroral imaging from space

13 p1814 A83-30768

WAMDI - A wide angle Michelson Doppler imaging

interferometer for Spacelab 13 p1815 A83-30770

Instrumentation in astronomy IV; Proceedings of the

Fourth Conference, Tucson, AZ, March 8-10, 1982

14 p2014 A83-31976

Differential imaging using charge-coupled device (CCD)

imagers with on-chip charge storage

14 p2015 A83-31986

Optimization of charge-coupled device (CCD) imager

performance for astronomy 14 p2015 A83-31987

Royal Greenwich Observatory (RGO) charge-coupled

device (CCD) camera 14 p2015 A83-31988

Galileo Institute for Astronomy (IFA) charge-coupled

device (CCD) system 14 p2015 A83-31989

Software simulations of the detection of rapidly moving

asteroids by a charge-coupled device

14 p2095 A83-31990

Development of a dual microchannel plate intensified

charge-coupled device (CCD) speckle camera

14 p2015 A83-31991

Application of a charge-coupled device (CCD) detector

for coudespectroscopy 14 p2016 A83-31992

Charge-coupled device (CCD)/transit instrument (CTI)

deep photometric and polarimetric survey - A progress

report 14 p2016 A83-31993

Drift scan observations with a charge-coupled device

(CCD) 14 p2016 A83-31994

Texas Instruments' virtual phase charge-coupled device

(CCD) imager operated in the frontside

electron-bombarded mode 14 p2016 A83-31995

Applications of an infrared charge-coupled device

Schottky diode array in astronomical instrumentation

14 p2016 A83-31996

Multiple object fiber optic spectroscopy

14 p2017 A83-32012

Charge-coupled device (CCD) television camera for

NASA's Galileo mission to Jupiter

14 p1983 A83-32024

Starlab detector system - A wide field, high resolution,

photon counting array 14 p2018 A83-32038

A PISO JCCD filter with high-speed linear charge

injection --- serial-in, parallel-out junction charge coupled

devices 15 p2151 A83-33890

CCD photometry of Abell clusters. II - Surface

photometry of 249 cluster galaxies

15 p2255 A83-34077

Covariance analysis of a charge carrier device

processing algorithm for stellar sensors

17 p2474 A83-37062

A high accuracy sun sensor 17 p2481 A83-37461

Multipurpose sun sensor using CCD detector

17 p2481 A83-37462

Star detection and tracking using CCDs

17 p2481 A83-37464

Experimental observation of avalanche multiplication in

charge-coupled devices 18 p2678 A83-40382

CCD photometry of the BL Lacertae object 1400 + 162

and the associated group of galaxies

20 p3059 A83-43040

Analytical noise/performance modeling of detector

charge-coupled device (CCD) hybrid devices

22 p3292 A83-46603

Picosecond transient digitizer for optical pulse analysis

22 p3360 A83-46651

Advanced visible and near-infrared radiometer for earth

observation

[IAF PAPER 83-107] 23 p3424 A83-47270

CCD surface photometry of two southern active galaxies,

NGC 1316 and 1052 24 p3659 A83-49378

CCD astrometry. I - Preliminary results from the KPNO

4-m/CCD parallax program 24 p3646 A83-49886

CHARGE DISTRIBUTION

The residual voltage in fast electrophotography of

a-SiH_x/x/ 04 p0540 A83-15511

Effects of operating mode on electrooptic spatial light

modulator resolution and sensitivity

05 p0684 A83-16832

Nondestructive laser method for measuring charge

profiles in irradiated polymer films

05 p0618 A83-17501

Modeling of ionizing radiation effects in short-channel

MOSFETs 05 p0626 A83-17508

Dosimetric silica films - The influence of fields on the

capture of positive charge 05 p0691 A83-17535

Modeling of charge transfer by surface acoustic waves

in a monolithic metal/ZnO/SiO₂/Si system

06 p0752 A83-18754

Altitude, thickness and charge concentration of charged

regions of four thunderstorms during trip 1981 based upon

in situ balloon electric field measurements

07 p0958 A83-20093

Characteristics of statoliths from rootcaps and

coleoptiles - 11 p1637 A83-27810

A designer's guide to digital filters

11 p1648 A83-28151

Energy and charge distribution of energetic helium ions

in the outer radiation belt of the earth

18 p2787 A83-39954

Measurement of charge composition of primary cosmic

ray using CR-39 plastic track detector

21 p3245 A83-44529

CHARGE EFFICIENCY

- Computerized design of CAD --- Charge Activated Devices 04 p0465 A83-15415
- Self-discharge behavior of engineering-scale LiAl/FeS cells 07 p0952 A83-19879
- Sealed nickel cadmium batteries --- Book 15 p2188 A83-33614
- Defects in nsutite (gamma-MnO₂) and dry-cell battery efficiency 18 p2708 A83-39964
- Collection of charge from alpha-particle tracks in silicon devices 18 p2678 A83-40381
- Effect of photoelectrochemical etching on charge collection efficiency in CdS - An electron beam induced current study 20 p3053 A83-42613
- A long-lasting polyacetylene battery with high energy density 20 p3012 A83-43400
- On the suppression of self discharge of the zinc electrodes of zinc-air cells and other related battery systems 24 p3599 A83-49931
- Electrochemical method for studying the reversibility of the lithium intercalation in secondary batteries 24 p3600 A83-49942
- Behaviour of various cathode materials for nonaqueous lithium cells 24 p3600 A83-49944
- Li-AgBi(CrO₄)₂ - A new highly reliable lithium battery for long service life applications 24 p3600 A83-49945
- Galvanostatic cycling of vanadium oxide (V₆O₁₃) in a nonaqueous secondary lithium cell 24 p3601 A83-49952

CHARGE EXCHANGE

- NT RESONANCE CHARGE EXCHANGE
- A review of studies on ion thruster beam and charge-exchange plasmas [AIAA PAPER 82-1944] 02 p0146 A83-12504
- A comparison of experimental and computer model results on the charge-exchange plasma flow from a 30 cm mercury ion thruster [AIAA PAPER 82-1946] 02 p0146 A83-12505
- Ion thruster charge-exchange plasma flow 02 p0148 A83-13089
- On charge exchange and knock-on processes in the exosphere of Io 03 p0434 A83-14214
- Charge exchange in the Io torus and exosphere 05 p0705 A83-17385
- Charge transfer in H⁺/+H and H⁺/+D collisions within the energy range 0.1-150 eV 06 p0809 A83-19243
- Surface potential relaxation in a biased Hg/1-x/Cd/x/Te metal-insulator-semiconductor capacitor 07 p0918 A83-19993
- Optical orientation of a dense sodium charge-exchange target for producing polarized protons and H⁺/- ions 07 p0992 A83-20604
- Charge-exchange in the magnetosheaths of Venus and Mars - A comparison 07 p0967 A83-21560
- Binary encounter calculations for electron capture from noble gases by He²⁺/+ 08 p1167 A83-21987
- Charge exchange of C⁶⁺/+ and O⁸⁺/+ ions with hydrogen atoms - Strong coupling calculation 10 p1486 A83-25885
- Charge transfer reaction of O³⁺/+H yields O²⁺/+H(+)/+ in low energy collision 12 p1777 A83-29005
- Charge exchange in solar wind-cometary interactions 15 p2259 A83-34115
- Particle charge interchange during acceleration in flare regions 15 p2284 A83-35224
- Solar wind governing the response of Venusian atmosphere and ionosphere 16 p2434 A83-35356
- Charge exchange collision experiments with highly charged ions -status repor 16 p2414 A83-35630
- Studies of collision interactions and kinetic energy distribution of eV recoil ions inside Penning traps 16 p2409 A83-35631
- Charge exchange of highly charged ions at low energy --- in astrophysical plasmas 16 p2427 A83-35637
- Charge exchange between atoms and multiply-charged ions 21 p3213 A83-44655
- Charge exchange reactions in astrophysical plasmas 24 p3651 A83-49139

CHARGE SEPARATION

U POLARIZATION (CHARGE SEPARATION)

CHARGE TRANSFER

- Charge transfer at large scattering angles in asymmetric ion-atom collisions 01 p0105 A83-10195
- Radiation from a charge moving in a lossy waveguide 01 p0036 A83-10419
- The influence of charge transfer on ion probe measurements of laser-produced plasmas 01 p0107 A83-10693
- A two-dimensional analysis of transfer in a charge injection infrared sensor --- French thesis 03 p0310 A83-13801
- Shock-induced color changes in nontronite - Implications for the Martian fines 04 p0567 A83-15579
- Radiation-induced charge dynamics in dielectrics 05 p0618 A83-17502

Oxygen transfer on substituted ZrO₂, Bi₂O₃, and CeO₂ electrolytes with platinum electrodes. I - Electrode resistance by dc polarization 07 p0880 A83-19887

Oxygen transfer on substituted ZrO₂, Bi₂O₃, and CeO₂ electrolytes with platinum electrodes. II - ac impedance study 07 p0880 A83-19888

A high-density effusive target of atomic hydrogen 08 p1162 A83-21981

Intersystem collisional transfer of excitation in low altitude aurora 10 p1448 A83-25553

The effect of photon transfer on the distribution of nonequilibrium charge-carriers in a semiconductor 13 p1832 A83-30269

Charge transfer of doubly charged and trebly charged ions with atomic hydrogen at thermal energies 13 p1916 A83-31352

Charge transfer of O(3+) ions in collisions with atomic hydrogen 13 p1916 A83-31354

Differential imaging using charge-coupled device (CCD) imagers with on-chip charge storage 14 p2015 A83-31986

Degradation of sodium beta-double-prime alumina - Effect of microstructure --- in sodium/sodium and sodium/sulfur cells 14 p1989 A83-32631

An EBIS for atomic physics experiments --- Electron Beam Ion Source 16 p2409 A83-35628

Excited states created in charge transfer collisions between atoms and highly charged ions 16 p2409 A83-35636

Energy disposal in charge transfer reactions producing NH₃(+,) - Dependence of the NH₃(+,) + H₂O reaction on NH₃(+,) internal energy 16 p2327 A83-36520

Enhancement of charge-transfer reaction rate constants by vibrational excitation at kinetic energies below 1 eV 16 p2327 A83-36522

State-selective electron capture by C(2+), C(3+), N(2+), and Ar(2+) ions in rare gases 17 p2579 A83-38365

Charge transfer and ionisation processes involving multiply charged ions in collision with atomic hydrogen 18 p2742 A83-39447

Single collision ion-molecule reactions at thermal energy Rotational and vibrational distributions from N(+) + CO yields N + CO(+) 19 p2897 A83-40771

Effect of molecular rotation upon charge transport between disordered carbazole units 20 p3053 A83-42602

Optical waveguides in LiTaO₃ formed by proton exchange 22 p3356 A83-45969

Lattice dynamics of solid I₂ under high pressure 23 p3511 A83-47634

Line emission from charge transfer with atomic hydrogen at thermal energies 24 p3650 A83-48830

Transient Workman-Reynolds freezing potentials --- at ice-water interfaces causing thunderstorm electrification and aircraft static 24 p3610 A83-49337

CHARGE TRANSFER DEVICES

NT CHARGE COUPLED DEVICES

- Source-coupling for hybrid focal planes 03 p0326 A83-13733
- A two-dimensional analysis of transfer in a charge injection infrared sensor --- French thesis 03 p0310 A83-13801
- Modeling of charge transfer by surface acoustic waves in a monolithic metal/ZnO/SiO₂/Si system 06 p0752 A83-18754
- CTD MTI radar filter with charge-transfer inefficiency compensation 06 p0754 A83-19043
- InSb charge-injection device array performance 14 p2015 A83-31979
- Two-dimensional infrared speckle interferometry with a 32 x 32 InSb charge-injection device (CID) array 14 p2095 A83-31980
- Fluorescent plastic coatings for improving ultraviolet and blue response of cooled silicon charge-injection devices (CIDs) 14 p2015 A83-31984
- An advanced star tracker design using the charge injection device 17 p2481 A83-37465
- New concept for a guide star tracker [AIAA PAPER 83-2288] 19 p2818 A83-41748

CHARGED PARTICLES

- NT ALPHA PARTICLES
- NT ANTIPROTONS
- NT ARGON PLASMA
- NT ARTIFICIAL RADIATION BELTS
- NT BETA PARTICLES
- NT BOUNDARY LAYER PLASMAS
- NT CATIONS
- NT CESIUM PLASMA
- NT COLD PLASMAS
- NT COLLISIONAL PLASMAS
- NT COLLISIONLESS PLASMAS
- NT CONDUCTION ELECTRONS
- NT COSMIC PLASMA
- NT CYLINDRICAL PLASMAS
- NT DENSE PLASMAS

- NT DEUTERIUM PLASMA
- NT DEUTERONS
- NT ELECTRON PLASMA
- NT ELECTRONS
- NT ELLIPTICAL PLASMAS
- NT ENERGETIC PARTICLES
- NT FREE ELECTRONS
- NT HEAVY NUCLEI
- NT HELIUM PLASMA
- NT HIGH ENERGY ELECTRONS
- NT HIGH TEMPERATURE PLASMAS
- NT HOT ELECTRONS
- NT HYDROGEN PLASMA
- NT INNER RADIATION BELT
- NT LASER PLASMAS
- NT MAGNETICALLY TRAPPED PARTICLES
- NT METAL IONS
- NT METALLIC PLASMAS
- NT MICROPLASMAS
- NT NEGATIVE IONS
- NT NITROGEN PLASMA
- NT NONEQUILIBRIUM PLASMAS
- NT NONUNIFORM PLASMAS
- NT NUCLEI (NUCLEAR PHYSICS)
- NT OUTER RADIATION BELT
- NT PHOTOELECTRONS
- NT PLASMA CLOUDS
- NT PLASMA FOCUS
- NT PLASMA LAYERS
- NT PLASMA SHEATHS
- NT PLASMA SLABS
- NT PLASMAS (PHYSICS)
- NT POLARONS
- NT POSITIVE IONS
- NT POSITRONS
- NT PROTON BELTS
- NT PROTONS
- NT RADIATION BELTS
- NT RAREFIED PLASMAS
- NT RELATIVISTIC ELECTRON BEAMS
- NT RELATIVISTIC PLASMAS
- NT ROTATING PLASMAS
- NT SOLAR ELECTRONS
- NT SOLAR PROTONS
- NT SOLAR WIND
- NT SPHERICAL PLASMAS
- NT STELLAR WINDS
- NT STRONGLY COUPLED PLASMAS
- NT THERMAL PLASMAS
- NT TOROIDAL PLASMAS

The kinetics of charged particles in the polar ionosphere 01 p0071 A83-10595

The formation of a universal energy spectrum for charged particles in the shear flow of the cosmic plasma 02 p0272 A83-11703

The propagation characteristics of charged particles in the solar corona 02 p0269 A83-11717

Partial inelasticity coefficients K-gamma in pi-A and pA interactions 02 p0234 A83-11734

Transport of neutrinos, radiation and energetic particles in accretion flows 02 p0276 A83-12031

Modulation of the monoenergetic spectrum of galactic cosmic rays 02 p0276 A83-12417

The emission of electromagnetic waves in the case of a smooth variation of parameters of a radiating system 03 p0390 A83-13427

Findings on rings and inner satellites of Saturn of Pioneer 11 03 p0133 A83-13830

Transition radiation caused by a chiral plate --- electromagnetic field due to charged particle traversing plate 03 p0313 A83-14025

The field of a test body in a flux of charged particles 05 p0687 A83-16894

Nonlinear theory of a positive column in a magnetic field 05 p0688 A83-17361

Transport and propagation of cosmic rays in galaxies. II - The effect of a galactic wind on the mean lifetime and age distribution of non-decaying cosmic rays 06 p0857 A83-18077

The adiabatic motion of charged dust grains in rotating magnetospheres --- and for ring systems of Jupiter and Saturn 06 p0847 A83-18276

Charged particle behavior in low-frequency geomagnetic pulsations. III - Spin phase dependence 06 p0783 A83-18291

Infinity subtraction in a quantum field theory of charges and monopoles 06 p0805 A83-18330

Generalized expressions for momentum and energy losses of charged particle beams in non-Maxwellian multi-species plasmas and spherical symmetry 06 p0812 A83-18915

Electromagnetic instability of a beam of charged particles in a dense plasma 06 p0813 A83-19186

New operation mode of a microchannel plate for the detection of low-energy positive ions 06 p0764 A83-19231

The adiabatic invariant and evolution equations for the motion of a particle in a strongly nonuniform magnetic field 06 p0806 A83-19328

Emission from particles in periodic media 06 p0806 A83-19417

Investigation of the dynamics of charged particles in the dispersion of a reaction jet in conditions of orbital flight 06 p0724 A83-19558

Theory of electrostatic probes under intermediate collisional conditions 07 p0995 A83-20063

The possibility of the acceleration of charged particles by laser radiation 07 p0935 A83-20306

Mathematical modeling of systems for the formation and focusing of intense charged-particle beams 07 p0996 A83-20316

Exact solutions of relativistic wave equations --- Russian book 07 p0989 A83-20378

Drift theory of the motion of a charged particle in a high-frequency wave in the case of finite Larmor radius 07 p0998 A83-20874

On rotating charged dust in general relativity. IV 07 p1027 A83-21356

Interaction of massless scalar field and charged dust in nonrigid rotation 08 p1181 A83-22744

Theoretical proposal of a high-energy experiment fit to reveal a three-dimensional time 08 p1162 A83-22949

Laser acceleration of particles 09 p1270 A83-23380

Computational studies of first-Born scattering cross sections. I - Spectral properties of Bethe surfaces. II - Moment-theory approach 09 p1341 A83-23722

Theory of the motion of a relativistic charged particle in highly nonuniform crossed electric and magnetic fields 09 p1348 A83-23984

Excitation of surface cyclotron waves in a solid-state plasma by charged-particle beams 09 p1348 A83-23985

Inverse problems of the dynamics of dions and magnetic monopoles 09 p1338 A83-24204

Neutral and charged clusters in the atmosphere - Their importance and potential role in heterogeneous catalysis 09 p1297 A83-25179

Relativistic coherent curvature radiation 10 p1500 A83-25376

A note on total cross sections and decay rates in the presence of a laser field 10 p1425 A83-25409

Grains spin-up by inverse Cerenkov effect --- in interstellar gas 10 p1501 A83-25493

The unit gravitational charge $/hc/4/1/2$ the unitor/, the structure of the electron and muon, and their anomalous magnetic moments 11 p1655 A83-27498

Transition radiation and transition scattering 11 p1649 A83-28243

Features of transition radiation from charged particles in a nonstationary magnetoplasma 11 p1660 A83-28568

Geometrical mass of charged particle in Brans-Dicke theory 12 p1774 A83-28875

Closed form for Van Stockum interior solution of Einstein's equations 12 p1794 A83-29164

Particle and optical measurements aboard the Aureol-3 spacecraft (ARCAD 3 project) 13 p1814 A83-30764

Measurements of the energy spectra of charged particles within the Vertical-10 rocket experiment 13 p1814 A83-30767

Deductions concerning accumulations of electrified particles in thunderclouds based on electric field changes associated with lightning 13 p1892 A83-30904

Thin charged shells and the violation of the third law of black hole mechanics 14 p2102 A83-33044

Charged scalar-tensor spheres - General solutions 14 p2103 A83-33048

New general relativistic effect by means of charged-particle interferometry 15 p2224 A83-33792

A proposed observational test of six-dimensional relativity 15 p2225 A83-34137

Charged particle measurements from a rocket-borne electron accelerator experiment 15 p2197 A83-34179

Spontaneous emission of a charged particle beam inside a plasma - Coherent and incoherent aspects 15 p2235 A83-34206

The artificially injected charged particles as a tool for the measurement of the electric field in the magnetosphere 15 p2198 A83-34215

Thermal relaxation and entropy for charged particles in a heat bath with fields 16 p2421 A83-35616

W-shaped occultation signatures - Inference of entwined particle orbits in charged planetary ringlets 16 p2435 A83-35729

Effect of oppositely directed particle streams on the characteristics of an intense relativistic electron beam produced by a magnetically insulated diode 16 p2417 A83-36926

Potential of a charge at rest in a magnetized plasma in an alternating electromagnetic field 16 p2418 A83-36938

The kinetic theory of electromagnetic processes 17 p2575 A83-37165

First order and second order Fermi acceleration of energetic charged particles by shock waves --- cosmic ray transport 17 p2629 A83-37933

Instability of charged-particle fluxes through a statistically inhomogeneous medium 17 p2584 A83-38980

Charged particle motion on and off the equatorial plane of a magnetic star in Rosen's bimetric gravity 18 p2775 A83-39754

General solutions for the field of a charged particle in Brans-Dicke theory of gravitation 18 p2741 A83-40418

Charged particle erosion of frozen volatiles in ice grains and comets 19 p2914 A83-40728

The dynamics of charged-particle fluxes and structural features of the interplanetary magnetic field from December 27, 1981 to January 1, 1982 19 p2924 A83-41246

The Boltzmann equation theory of charged particle transport 19 p2906 A83-41536

On the drift mechanism for energetic charged particles at shocks 19 p2925 A83-41621

Approximate solutions of the equations of motion of a charged particle in the field of a magnetic dipole 20 p3050 A83-43394

Low-pressure pulsed discharge in a transverse axisymmetric magnetic field 21 p3210 A83-44138

Plasma current sheet studied by means of particle motion 21 p3211 A83-44288

The analytical trajectory of the charged particle moving in a neutral magnetic field 21 p3213 A83-44576

Estimation of the height of the region in which charged particles are accelerated on the sun 21 p3244 A83-45285

Whistler induced charged particle precipitation and distortion of geomagnetic field 22 p3337 A83-47074

Radiation from fast particles in a turbulent medium --- cosmic ray showers 23 p3540 A83-48491

Phobis, a photon beam ion source for production of highly-charged ions 24 p3627 A83-49750

Black hole electromagnetic fields and negative energy states for charged particles 24 p3668 A83-50092

An explicit Lagrangian for a system of charged particles to higher-order terms - Quadrupole radiation 24 p3624 A83-50167

CHARGING

A practical SCR model for computer aided analysis of AC resonant charging circuits 01 p0041 A83-11018

Spectroscopic evidence for the formation of polysulfide species during charging of an Li-Al/S couple 11 p1546 A83-28298

CHARON

A photometric study of Pluto near perihelion. I - U,B,V photometry 03 p0408 A83-13895

Digital speckle interferometry of Juno, Amphitrite and Pluto's moon Charon 09 p1367 A83-25301

On the global distribution of Pluto's atmosphere 13 p1962 A83-31438

Speckle interferometry observations of Pluto's moon Charon 23 p3516 A83-47439

CHARPY IMPACT TEST

Fracture behavior of polymers by Charpy impact tests 05 p0618 A83-17100

An analysis of impact failure modes for fiber-reinforced composite laminates by using fault tree 05 p0611 A83-17104

Comparison of impact testing on Charpy V-notch specimens and WOL-1X-specimens 08 p1058 A83-21672

Fracture of nickel-base superalloy single crystals 08 p1065 A83-22018

The influence of inclusions on the J integral value determined by a Charpy test with digital instrumentation 08 p1124 A83-23242

Laser welding of a titanium alloy 15 p2135 A83-33643

The evaluation of tempered martensite embrittlement in 4130 steel by instrumented Charpy V-notch testing 16 p2329 A83-35689

Analysis of Charpy impact failure for unidirectional fiber-reinforced composite laminates by using a computerized fault tree 18 p2655 A83-40212

Impact behaviour of quasi-isotropic CFRP laminate 18 p2656 A83-40220

CHARRING

Thermal analysis of solid rocket motor's heat insulation materials [AIAA PAPER 83-1438] 14 p2010 A83-32710

Charring ablation by finite element 15 p2159 A83-34237

CHARTS

NT BOND GRAPHS

NT GRAPHS (CHARTS)

NT METEOROLOGICAL CHARTS

CHASSIS

Chassis dynamics related to a low-cost magnetically suspended vehicle 12 p1783 A83-29522

CHEBYSHEV APPROXIMATION

Asymptotic error behavior in the Gaussian quadrature procedure --- German thesis 01 p0101 A83-10166

A geometrical construction for Chebyshev Z-plane zeros 01 p0103 A83-11380

A note on a Runge-Kutta-Chebyshev method 03 p0388 A83-14511

Comparison of time integration /finite difference and spectral/ for the non-linear Burgers equation 03 p0389 A83-14603

FFT vs. conjugate gradient method for solution of flow equations by pseudo-spectral methods 03 p0322 A83-14614

The Fourier-Chebyshev approximation for time series with a great many terms --- for describing motions of celestial bodies 06 p0817 A83-17991

The Chebyshev approximation as the solution of the problem of multigoal planning in the case of arbitrarily correlated errors of measurement 06 p0805 A83-18352

A direct Chebyshev approach with practical applicability in optimal control problems --- of orbital transfer 10 p1465 A83-26523

Construction of continuous Chebyshev approximations for planetary coordinates 11 p1673 A83-28037

Representation of planetary coordinates by Chebyshev approximations which are continuous along with their first derivatives 11 p1673 A83-28042

A pseudospectral scheme for the numerical calculation of shocks 12 p1725 A83-29622

Chebyshev series solution of the controlled Duffing oscillator 12 p1776 A83-29630

Computation of Faber series with application to numerical polynomial approximation in the complex plane 13 p1912 A83-31364

The Dufort-Frankel Chebyshev method for parabolic initial boundary value problems 15 p2224 A83-33867

A strange convergence property of the Lobatto-Chebyshev method for the numerical determination of stress intensity factors 15 p2179 A83-34564

An efficient short-arc orbit computation 19 p2814 A83-41559

A Chebyshev expansion of singular integral equations with a logarithmic kernel 21 p3198 A83-45523

CHECKOUT

Requirements for debug capability of HOL-source code during software test in avionics laboratories 01 p0092 A83-11225

Design methods of single-output built-in self-checking circuits for equilibrium codes 10 p1460 A83-25467

Model test and full-scale checkout of dry-cooled jet run sound suppressors 23 p3413 A83-48217

CHECKOUT EQUIPMENT**U TEST EQUIPMENT****CHELATION**

Reversible loss of gravitropic sensitivity in maize roots after tip application of calcium chelators 16 p2394 A83-36017

CHEMICAL ANALYSIS

NT ELECTROPHOTOMETRY

NT GAS ANALYSIS

NT GAS SPECTROSCOPY

NT LASER SPECTROSCOPY

NT MICROANALYSIS

NT NEUTRON ACTIVATION ANALYSIS

NT OZONOMETRY

NT QUALITATIVE ANALYSIS

NT QUANTITATIVE ANALYSIS

NT SPECTROSCOPIC ANALYSIS

NT URINALYSIS

NT VOLUMETRIC ANALYSIS

Analysis of low-pressure chemical vapor deposited silicon nitride by Rutherford backscattering spectrometry 01 p0110 A83-10990

A verification and identification system for the quality control of materials 03 p0338 A83-14824

Determination of trace elements in CuInS₂ 04 p0456 A83-15485

Physicochemical methods for studying organosilicate coatings 07 p0900 A83-20715

Analysis of high temperature materials --- Book 09 p1227 A83-24949

The features of the atomic structure of pure inorganic ferroelastics 13 p1928 A83-30311

Compositional analysis of CuInS₂ chalcopyrite semiconductor 14 p2089 A83-32257

- An alpha particle instrument with alpha, proton, and X-ray modes for planetary chemical analyses 16 p2357 A83-36718
- Chemical and isotopic study of extraterrestrial particles from the ocean floor 24 p3672 A83-49398
- CHEMICAL ATTACK**
- NT INTERGRANULAR CORROSION
- NT TRANSGRANULAR CORROSION
- Chemically driven cavity growth 07 p0887 A83-20632
- Comparison of several accelerated laboratory tests for the determination of localized corrosion resistance of high-performance alloys 08 p1066 A83-22650
- The high-temperature corrosion of aluminum-rich coatings in an atmosphere of sulfur vapor containing oxygen 08 p1068 A83-23243
- A study of the stability of protective coatings against sulfide-oxide corrosion 09 p1229 A83-23512
- Fluoroelastomers --- materials for hostile fluid environments 16 p2336 A83-36066
- Analyses of microstructural and chemical effects on fatigue crack growth 17 p2490 A83-38396
- Corrosion behavior of annealed niobium-tantalum alloys 18 p2665 A83-39173
- Mechanism of low temperature hot corrosion 20 p2953 A83-42250
- Corrosion of pre-oxidized nickel in SO₂ atmospheres 24 p3564 A83-49508
- The kinetics and mechanism of the attack of MCr-type alloys in oxygen-sulphur environments at 700 C 24 p3565 A83-49511
- CHEMICAL BONDS**
- NT COVALENT BONDS
- NT HYDROGEN BONDS
- Electronic correlations and transient effects in disordered systems 04 p0540 A83-15506
- Chemical bonding in amorphous semiconductors 04 p0541 A83-15516
- Defects in amorphous III-V compounds 04 p0542 A83-15531
- Radiation-induced defects in SiO₂ as determined with XPS 05 p0691 A83-17479
- The role of the liquid in environmental stress cracking of polyethylene 05 p0619 A83-17571
- Quantum chemical studies of a model for peptide bond formation Formation of formamide and water from ammonia and formic acid 07 p0976 A83-21052
- Molecular micromechanics of polymer fracture 08 p1070 A83-21800
- A molecular dynamics simulation of the vitreous silica surface 09 p1226 A83-24133
- Evidence for pseudo bridge bonding of c(2 x 2)-O on Ni(100) 13 p1817 A83-30920
- On the nature of the bonding in Cu₂ - An ab initio viewpoint 13 p1818 A83-31809
- Ab initio calculation of the X 1 Sigma + state of CsH 14 p2083 A83-33106
- Diffuse reflectance Fourier transform infrared spectroscopic study of chemical bonding and hydrothermal stability of an aminosilane on metal oxide surfaces 18 p2672 A83-40146
- Coulomb effects on one-dimensional Peierls instability - The Peierls-Hubbard model --- of dimerization 19 p2820 A83-40956
- Quantum chemical studies of a model for peptide bond formation. II - Role of amine catalyst in formation of formamide and water from ammonia and formic acid 19 p2819 A83-41865
- An ab initio study of core-valence correlation --- in atoms 20 p3045 A83-42636
- Molecular geometry of cis- and trans-polyacetylene by nutation NMR spectroscopy 23 p3433 A83-47611
- An XPS study of silicon/noble metal interfaces - Bonding trends and correlations with the Schottky barrier heights 23 p3511 A83-48050
- Silicate structures and atomic substitution 23 p3427 A83-48253
- Theoretical evidence for multiple one-electron 3d bonding in a first row transition metal dimer - The 5 Sigma u-state of Sc₂ 24 p3625 A83-48799
- CHEMICAL CLEANING**
- NT PICKLING (METALLURGY)
- A three-point flexure test configuration for improved sensitivity to metal/adhesive interfacial phenomena 04 p0487 A83-15875
- Cleaning gas turbine compressors - Some service experience with a wet-wash system 07 p0867 A83-21350
- Cleaning chemistry of InSb(100) molecular beam epitaxy substrates 17 p2485 A83-37616
- Nb₃Al/oxide/Pb Josephson tunnel junctions fabricated using a CF₄ cleaning process 22 p3279 A83-46740
- CHEMICAL CLOUDS**
- NT BARIUM ION CLOUDS
- Tracer experiments with turbulently dispersed air ions 23 p3479 A83-48730

- A long-range atmospheric tracer field test 24 p3616 A83-50190
- CHEMICAL COMPOSITION**
- NT CARBON DIOXIDE CONCENTRATION
- On the problem of the chemical composition of Beta Lyrae 01 p0121 A83-10329
- The simultaneous measurement of four functional parameters of blood platelets 01 p0080 A83-10553
- Energy gap versus alloy composition and temperature in Hg/1-x/Cd/x/Te [AD-A125659] 01 p0109 A83-10644
- Tests of blending and correlation of distillate fuel properties 01 p0028 A83-11050
- Evidence for primitive nebular components in chondrules from the Chainpur chondrite 02 p0262 A83-11550
- Investigation of the chemical composition of cosmic-ray nuclei in the 20-1000 GeV/nucleon energy range by means of transition radiation 02 p0272 A83-11705
- The global troposphere - Biogeochemical cycles, chemistry, and remote sensing 02 p0198 A83-11828
- Some properties of r.f.-sputtered hafnium nitride coatings 02 p0160 A83-12653
- Effect of composition and structure on the properties of wrought aluminum alloys of the D16 type 03 p0297 A83-13255
- On the nature of the stellar population in the nucleus of the Sd galaxy NGC 7793 03 p0414 A83-13336
- Chemical composition of cometary nuclei 03 p0415 A83-13379
- Correlation between albedo and polarization properties of the moon /heterogeneity of the relative porosity of the surface of the western part of the visible hemisphere/ 03 p0133 A83-13667
- Model calculations of the molecular composition of interstellar grain mantles 03 p0427 A83-14757
- The Apollo 15 yellow impact glasses - Chemistry, petrology, and exotic origin 04 p0560 A83-15342
- The Apollo 14 regolith - Chemistry of cores 14210/14211 and 14220 and soils 14141, 14148, and 14149 04 p0561 A83-15349
- Lunar regolith - Petrology of the less than 10 micron fraction 04 p0561 A83-15350
- Chemical composition of the Howardite Parent Body deduced from Kapoeta primary 'matic' magmas 04 p0562 A83-15358
- Composition determination of CuInS₂ by a chemical analysis method 04 p0456 A83-15484
- Chemical composition of Martian fines 04 p0567 A83-15576
- Composition of the surfaces of the Galilean satellites 04 p0570 A83-16232
- Petrography, mineral chemistry and origin of Type I enstatite chondrites 04 p0572 A83-16351
- The compositional classification of chondrites. III - Ungrouped carbonaceous chondrites 04 p0572 A83-16354
- Combustion response to compositional fluctuations --- of composite solid propellants [AIAA PAPER 83-0476] 05 p0619 A83-16740
- Chemical composition of the Tsarev meteorite 05 p0705 A83-17456
- Petrography, mineralogy, and chemical composition of the Bakhardok meteorite 05 p0705 A83-17459
- The classification of ordinary chondrites according to chemical composition 05 p0706 A83-17460
- On the nature of isotopic anomalies in meteorites 05 p0706 A83-17462
- Morphology and physical structure of trioxane and styrene copolymers 06 p0734 A83-18025
- The effect of 24, 25-dihydroxycalciferol on the chemical composition of the bone tissue of rats during hypokinesia 06 p0795 A83-18987
- The equivalent-width calibration of the KPNO echelle spectrograph 06 p0822 A83-19076
- The ages and compositions of old clusters 06 p0840 A83-19283
- Activation analysis in the Nuclear Physics Institute of the Academy of Sciences of the Uzbek SSR 06 p0727 A83-19419
- Compositional heterogeneity of tephra from the 1980 eruptions of Mount St. Helens 07 p0961 A83-20237
- The effects of heat treatment and composition on the stress corrosion cracking resistance of Inconel alloy X-750 07 p0884 A83-20255
- A method for spectroscopically detecting chemical anomalies on the surface of an Ap star with a nonvariable spectrum 07 p1006 A83-20659
- Chemical systematics among the moldavite tektites 07 p1035 A83-21328
- Phase composition and phase stability of alloy IN939 07 p0894 A83-21483
- Relations between chemistry, solidification behaviour, and microstructure in IN 100 07 p0894 A83-21485
- The origin of the Crab Nebula and electron capture supernova of 8-10 solar-mass stars 08 p1177 A83-21835

- Optical fiber composition and radiation hardness 08 p1165 A83-22479
- Silicone sealants as adhesives 09 p1237 A83-23624
- The sources of sulfate in precipitation. II - Sensitivities to chemical variables 09 p1296 A83-24266
- Interstellar grain composition and the infrared spectrum of OH26.5+0.6 09 p1362 A83-24985
- High dispersion investigation of CP stars around the H-alpha line 09 p1356 A83-25300
- 100% oxygen breathing during acute heat stress - Effect on sweat composition 10 p1454 A83-25669
- Physical metallurgy of recycling wrought aluminum alloys 10 p1398 A83-26276
- Nickel-base superalloys - Physical metallurgy of recycling 10 p1398 A83-26277
- Effects of a shock on the molecular composition of a diffuse interstellar cloud 10 p1509 A83-26373
- Chemical separation in horizontal-branch stars 10 p1514 A83-26727
- Forces acting on free carriers in semiconductors of inhomogeneous composition I, II 11 p1663 A83-28449
- Element composition of Venus rocks - Preliminary results from Venera 13 and Venera 14 12 p1799 A83-29486
- Investigation of phase stability in the system SiC-AlN 12 p1717 A83-29974
- The effect of the chemical composition on the high-cycle and low-cycle fatigue behavior of D16 and V95 alloy sheets under pulsating tension 13 p1819 A83-30068
- The chemical composition and climatology of the earth's early atmosphere 13 p1878 A83-31156
- Solution of gamma-prime phase in nickel heat-resistant aging alloys 13 p1823 A83-31214
- The element composition of Venus rocks 14 p2111 A83-31970
- The effect of changes of the electrolytic composition of the perilymph on the endocochlear potential 14 p2063 A83-32567
- A technique for the nondestructive detection of voids and composition anomalies in metal matrix composite wires using X-rays [AIAA PAPER 83-843] 14 p2028 A83-32793
- The peculiarities of the xenon isotope composition in the chondrites Saratov (L4), Elenovka (L5), and Zhigailovka (LL6) 14 p2112 A83-32971
- On the nature of Upsilon Sagittarii 14 p2105 A83-33200
- The Wolf-Rayet stars 14 p2108 A83-33263
- Ultraviolet observations of planetary nebulae - NGC 6572, NGC 5315 and BD + 30 deg 3639 14 p2109 A83-33280
- Ultraviolet spectrum of the planetary nebula NGC 7662 14 p2109 A83-33281
- Observations and models 14 p2109 A83-33281
- Source contributions to acid precipitation in Texas 15 p2194 A83-34043
- Density inhomogeneities and the deduced chemical composition of planetary nebulae 15 p2261 A83-34502
- The chemical composition of Algol systems. II - The carbon and nitrogen abundances of the secondaries of U Cep and U Sge 15 p2265 A83-34593
- Studies of proton-irradiated cometary-type ice mixtures 15 p2270 A83-34716
- The determination of circulating immune complexes by a spectrophotometric method 15 p2213 A83-34950
- Emission spectrochemical analysis of main components in superalloys using electrolytic iron dilution-high frequency induction melting and centrifugal cast samples 16 p2329 A83-35603
- Effect of fuel composition on Navy aircraft engine hot section components [AIAA PAPER 83-1147] 16 p2306 A83-36244
- The chemical composition and thermal history of the ice of a cometary nucleus 16 p2425 A83-36679
- The phospholipid composition of various tissues of rats in dehydration conditions 16 p2395 A83-36829
- The cold sterilization of surgical materials and the cleaning of the surgeon's hands on sea vessels during prolonged voyages 16 p2400 A83-36843
- The isotopic composition of primary xenon and the fission of Pu-244 --- on earth 17 p2619 A83-37818
- Development of Al-Li-X alloys using rapidly solidified powders 17 p2489 A83-37851
- The elemental and isotopic composition of galactic cosmic ray nuclei 17 p2630 A83-38283
- The composition, propagation and acceleration of energetic solar particles - A review of United States research 1979-1982 17 p2627 A83-38284
- Mapping of chemical elements on the surfaces of Ap stars. I Solution of the inverse problem of finding local profiles of spectral lines 17 p2611 A83-38558
- Measurement of compositional inhomogeneity of liquid phase epitaxial InGaPAs 20 p3055 A83-43602

Destabilization of a 650 km chemical boundary layer and its bearing on the evolution of the continental crust 21 p3171 A83-44363

The process of the formation and evolution of the Jilin meteorite 21 p3240 A83-44502

Study on the chemical composition of 9 chondrites in China 21 p3241 A83-44504

AES study on the chemical composition of ferroelectric BaTiO3 thin films RF sputter-deposited on silicon 21 p3217 A83-44609

An analytical and experimental study of zoning in plagioclase 22 p3332 A83-46711

The hydrolytic stability of some commercially available polycarbonates 22 p3270 A83-46907

Isotopy of the hydrosphere --- Russian book 23 p3480 A83-47150

The effect of the dispersion medium on the properties of complex Li lubricants 23 p3439 A83-48545

Observations on the chemical composition of rain using short sampling times during a single event 23 p3479 A83-48683

Analysis of nickel- and iron-base heat resisting alloys by spark source mass spectrometry 24 p3554 A83-49326

H II regions --- review of IUE studies 24 p3662 A83-49568

CHEMICAL DEFENSE

Chemical defense, environmental control systems study [SAE PAPER 820866] 13 p1806 A83-30944

CHEMICAL EFFECTS

Relations between chemistry, solidification behaviour, and microstructure in IN 100 07 p0894 A83-21485

Correlation of Fermi-level energy and chemistry at InP /100/ interfaces 08 p1170 A83-22766

A modified chemical-stress crazing test method 20 p2958 A83-42545

Preliminary study of the effects of a reversible chemical reaction on gas bubble dissolution --- for space glass refining 20 p2941 A83-43285

CHEMICAL ELEMENTS

NT ACTINIDE SERIES

NT ALKALI METALS

NT ALUMINUM

NT ALUMINUM 26

NT ANTIMONY

NT ARGON

NT ARGON ISOTOPES

NT ARSENIC

NT BARIUM

NT BARIUM ISOTOPES

NT BERYLLIUM

NT BERYLLIUM 9

NT BERYLLIUM 10

NT BISMUTH

NT BISMUTH ISOTOPES

NT BORON

NT BROMINE

NT CADMIUM

NT CALCIUM

NT CALCIUM ISOTOPES

NT CALIFORNIUM ISOTOPES

NT CARBON

NT CARBON ISOTOPES

NT CARBON 12

NT CARBON 13

NT CARBON 14

NT CERIUM

NT CESIUM

NT CESIUM VAPOR

NT CHLORINE

NT CHROMIUM

NT COBALT

NT COBALT ISOTOPES

NT COBALT 60

NT COPPER

NT DEUTERIUM

NT DEUTERIUM PLASMA

NT ERBIUM

NT EUROPIUM

NT FLUORINE

NT FLUORINE ISOTOPES

NT GADOLINIUM

NT GALLIUM

NT GALLIUM ISOTOPES

NT GERMANIUM

NT GERMANIUM ISOTOPES

NT GOLD

NT GOLD ISOTOPES

NT HAFNIUM ISOTOPES

NT HALOGENS

NT HELIUM

NT HELIUM ATOMS

NT HELIUM ISOTOPES

NT HOLMIUM

NT HOLMIUM ISOTOPES

NT HYDROGEN

NT HYDROGEN ATOMS

NT HYDROGEN IONS

NT HYDROGEN ISOTOPES

NT HYDROGEN PLASMA

NT INDIUM

NT IODINE

NT IODINE ISOTOPES

NT IRIDIUM

NT IRON

NT IRON ISOTOPES

NT IRON 57

NT ISOTOPES

NT KRYPTON

NT LANTHANUM ISOTOPES

NT LEAD (METAL)

NT LEAD ISOTOPES

NT LIGHT ELEMENTS

NT LIQUID HELIUM

NT LIQUID HELIUM 2

NT LIQUID HYDROGEN

NT LIQUID NITROGEN

NT LITHIUM

NT LITHIUM ISOTOPES

NT LUTETIUM ISOTOPES

NT MAGNESIUM

NT MAGNESIUM ISOTOPES

NT MANGANESE

NT MANGANESE ISOTOPES

NT MERCURY (METAL)

NT MERCURY ISOTOPES

NT METALLIC HYDROGEN

NT METALLOIDS

NT MOLYBDENUM

NT NEODYMIUM

NT NEODYMIUM ISOTOPES

NT NEON

NT NEON ISOTOPES

NT NICKEL

NT NICKEL ISOTOPES

NT NIOBIUM

NT NITROGEN

NT NITROGEN ATOMS

NT NITROGEN IONS

NT NITROGEN ISOTOPES

NT NITROGEN 15

NT NUCLIDES

NT OSMIUM ISOTOPES

NT OXYGEN

NT OXYGEN ATOMS

NT OXYGEN IONS

NT OXYGEN ISOTOPES

NT OXYGEN PLASMA

NT OXYGEN 18

NT PALLADIUM

NT PHOSPHORUS

NT PLATINUM

NT PLUTONIUM 238

NT PLUTONIUM 244

NT POLONIUM 210

NT POTASSIUM

NT POTASSIUM ISOTOPES

NT POWDERED ALUMINUM

NT RADIOACTIVE ISOTOPES

NT RADON

NT RADON ISOTOPES

NT RARE EARTH ELEMENTS

NT RARE GASES

NT REFRACTORY METALS

NT RUBIDIUM

NT RUBIDIUM ISOTOPES

NT RUTHENIUM

NT SAMARIUM

NT SCANDIUM

NT SELENIUM

NT SILICON

NT SILICON ISOTOPES

NT SILVER

NT SILVER ISOTOPES

NT SINTERED ALUMINUM POWDER

NT SODIUM

NT SODIUM VAPOR

NT SOLID NITROGEN

NT STRONTIUM

NT STRONTIUM ISOTOPES

NT STRONTIUM 87

NT SULFUR

NT SULFUR ISOTOPES

NT TANTALUM

NT TANTALUM ISOTOPES

NT TECHNETIUM

NT TELLURIUM

NT TERBIUM

NT THALLIUM

NT THALLIUM ISOTOPES

NT THORIUM

NT THORIUM ISOTOPES

NT TIN

NT TITANIUM

NT TITANIUM ISOTOPES

NT TRACE ELEMENTS

NT TRITIUM

NT TUNGSTEN

NT TUNGSTEN ISOTOPES

NT URANIUM

NT URANIUM ISOTOPES

NT VANADIUM

NT XENON

NT XENON ISOTOPES

NT XENON 129

NT XENON 133

NT YTTRIUM

NT ZINC

NT ZIRCONIUM

The distribution of Na, K, Ca, P, and S in the vestibular apparatus and eye of the larvae of the fish Brachydanio rerio 15 p2210 A83-34937

CHEMICAL ENERGY

NT ENERGY OF FORMATION

Stored chemical energy propulsion system for underwater applications [AIAA PAPER 81-1601] 08 p1132 A83-23132

Chemical amplification of optoacoustic signals 08 p1162 A83-23269

Cylindrically converging shock and detonation waves 18 p2687 A83-40502

CHEMICAL ENGINEERING

Radioactive nuclear waste stabilization - Aspects of solid-state molecular engineering and applied geochemistry 14 p2083 A83-33478

CHEMICAL EQUILIBRIUM

NT ACID BASE EQUILIBRIUM

The autonomy of shock waves in a sonic downstream state - The case of detonation 03 p0320 A83-14570

On the question of the mechanism for the thermal decomposition of ammonium perchlorate 05 p0620 A83-17143

Chemical nonequilibrium effects on flowfields for aeroassist orbital transfer vehicles [AIAA PAPER 83-0214] 05 p0602 A83-17913

Thermodynamics of silicon nitridation - Effect of hydrogen [ACS PAPER 33-B-80P] 06 p0734 A83-18052

A stratospheric chemical instability 07 p0960 A83-20213

The equilibrium constant for the reversible reaction $H_2S + 3H_2O + /Li_0.66K_0.34/2 CO_3$ yields $4H_2 + CO_2 + /Li_0.66K_0.34/2 SO_4$ at elevated temperature --- in molten carbonate fuel cells 07 p0954 A83-20590

Investigations concerning the electrochemical equilibrium in the system tin-bismuth-oxygen 09 p1233 A83-24124

Sulfur-dioxide/water equilibria between 0 and 50 C - An examination of data at low concentrations 09 p1298 A83-25195

The principles of the mathematical description and analysis of the composition of equilibrium chemical systems 11 p1546 A83-28198

Toward the formulation of a global local equilibrium kinetics model for laminar hydrocarbon flames 15 p2132 A83-34035

The status of rotational nonequilibrium in HF chemical lasers [AIAA PAPER 83-1699] 17 p2513 A83-37196

Photochemistry of the Venus atmosphere 17 p2617 A83-37415

Sensitivity on nonequilibrium chemical systems to gravitational field 18 p2751 A83-39910

Three-body association reactions of $NO(+)$ and $O_2(+)$ with N_2 21 p3201 A83-43957

Chemical equilibrium laminar or turbulent three-dimensional viscous shock-layer flows 23 p3398 A83-48133

The thermodynamics of evolution. II - Chemical and biological oscillations and instabilities 23 p3513 A83-48600

CHEMICAL EVOLUTION

The appearance of life in the marine environment 01 p0077 A83-10381

Expected frequencies of codon use as a function of mutation rates and codon fitnesses 01 p0081 A83-11033

An evolutionary model for the insect vitellins 01 p0081 A83-11034

Study on the chemical evolution of low molecular weight compounds in a highly oxidized atmosphere using electric discharges 02 p0226 A83-11630

Nucleoside and deoxynucleoside phosphorylation in formamide solutions --- under prebiotic conditions 02 p0226 A83-11631

Formation and catalytic activity of high molecular weight soluble polymers produced by heating amino acids in a modified sea medium 02 p0219 A83-11632

Evolutionary roots of catalysis by nicotinamide and flavins in C-H oxidoreductases and in photosynthesis 02 p0219 A83-11633

Template directed reactions of 2-aminoadenylic acid derivatives 02 p0148 A83-11842

What are comets made of - A model based on interstellar dust 03 p0415 A83-13380

Comets and origin of life 03 p0384 A83-13403

Formation of pyrophosphate on hydroxapatite with thioesters as condensing agents 05 p0613 A83-17234

Globular proteins, GU wobbling, and the evolution of the genetic code 06 p0794 A83-18248

The possible role of soluble salts in chemical evolution 06 p0800 A83-18249

Stages of emerging life - Five principles of early organization 06 p0801 A83-18250

Voyager Mission: Implications for planetary biology; Proceedings of the Sixth Annual Colloquium on Chemical Evolution, University of Maryland, College Park, MD, October 4-6, 1981 06 p0801 A83-19401

The prebiological paleoatmosphere - Stability and composition 06 p0801 A83-19402

Heteropolypeptides on Titan 06 p0801 A83-19405

Criteria for the emergence and evolution of life in the solar system 06 p0801 A83-19406

Formation of amino acids from models of Titan and more oxidized atmospheres 06 p0801 A83-19407

The chemical structure of DNA sequence signals for RNA transcription 06 p0796 A83-19408

The Voyager mission and the origin of life - Selected references 06 p0801 A83-19409

Quantum chemical studies of a model for peptide bond formation Formation of formamide and water from ammonia and formic acid 07 p0976 A83-21052

The Re-187 - Os-187 chronology and chemical evolution of the Galaxy 07 p1024 A83-21214

Importance of the Lu-Hf isotopic system in studies of planetary chronology and chemical evolution 08 p1190 A83-22996

Evolution of chemical abundances in massive stars. I - OB stars, Hubble-Sandage variables and Wolf-Rayet stars - Changes at stellar surfaces and galactic enrichment by stellar winds. II - Abundance anomalies in Wolf-Rayet stars in relation with cosmic rays and ²²Ne in meteorites 12 p1790 A83-28890

A probable prebiotic peptide formation from glycineamide and related compounds in a neutral aqueous medium participation of nucleoside and 5'-mononucleotide 12 p1767 A83-29423

Radiolysis of aqueous solutions of hydrogen cyanide (pH about 6) - Compounds of interest in chemical evolution studies 12 p1767 A83-29424

The instability of the autogen --- theory of chemical evolution 12 p1767 A83-29425

The display of molecular models with the Ames Interactive Modeling System (AIMS) 12 p1768 A83-29548

Interaction of metal ions and amino acids - Possible mechanisms for the adsorption of amino acids on homoionic smectite clays 12 p1712 A83-29556

An investigation of the abiogenic synthesis of peptides in a model open system 13 p1908 A83-30100

Cosmochemistry and the origin of life; Proceedings of the Advanced Study Institute, Maratea, Italy, June 1-12, 1981 13 p1899 A83-31151

Cosmochemistry and the origin of life 13 p1908 A83-31152

Synthesis of the chemical elements --- cosmochemical evolution 13 p1947 A83-31153

The largest molecules in space - Interstellar dust 13 p1947 A83-31154

Impact of solar system exploration on theories of chemical evolution and the origin of life 13 p1908 A83-31155

The chemical composition and climatology of the earth's early atmosphere 13 p1878 A83-31156

Inorganic chemistry of earliest sediments - Bioinorganic chemical aspects of the origin and evolution of life 13 p1899 A83-31158

Organic molecules as chemical fossils - The molecular fossil record 13 p1899 A83-31160

Stochastic effects in the chemical evolution of galaxies 13 p1956 A83-31687

The formation and the evolution process of the Jilin meteorite 14 p2112 A83-32597

Convective mixing length and the galactic carbon to oxygen ratio 14 p2107 A83-33241

Chemical enrichment in halo planetary nebulae 14 p2110 A83-33282

DDO integrated photometry of globular clusters and initial chemical evolution of the galaxy 15 p2262 A83-34536

Chemical evolution of the galactic halo. I - Effects of possible mass segregation mechanisms 15 p2272 A83-34779

The isotopic and chemical evolution of Mount St. Helens 16 p2382 A83-36750

Geochemical evolution of the crust and mantle 17 p2543 A83-38325

Stochastic star formation and chemical evolution of dwarf irregular galaxies 17 p2609 A83-38423

AMP synthesis in aqueous solution of adenosine and phosphorus pentoxide 17 p2563 A83-38891

Formation of amino acids from reactor-irradiated ammonium acetate 17 p2563 A83-38892

Catalytic mechanism of histone in peptide formation from phenylalanyl adenylate 17 p2557 A83-38893

Material cycling and organic evolution 17 p2557 A83-38894

Enantioselective catalysis as a possible path for optical activation of organic compounds in nature 17 p2557 A83-38898

Role of succinic acid in chemical evolution 17 p2563 A83-38900

Chemical evolution of OB associations 18 p2774 A83-39726

Primordial organic chemistry 19 p2886 A83-41510

Self-organization of the protocell was a forward process 19 p2876 A83-41858

Quantum chemical studies of a model for peptide bond formation. II - Role of amine catalyst in formation of formamide and water from ammonia and formic acid 19 p2819 A83-41865

Life sciences and space research XX(2); Proceedings of the Workshop and Topical Meeting, Ottawa, Canada, May 16-June 2, 1982 19 p2877 A83-42029

Amino acids in meteorites 19 p2886 A83-42030

Chemical evolution in space - A source of prebiotic molecules 19 p2886 A83-42031

The escape of molecular hydrogen and the synthesis of organic nitriles in planetary atmospheres 19 p2886 A83-42032

The atmosphere of the primitive earth and the prebiotic synthesis of organic compounds 19 p2886 A83-42033

Prebiotic oligodeoxynucleotide synthesis in a cyclic evaporating system at low temperatures 19 p2887 A83-42034

Prebiotic synthesis and reactions of nucleosides and nucleotides 19 p2887 A83-42035

A novel way for the formation of alpha-amino acids and their derivatives in an aqueous medium 19 p2887 A83-42036

Chemical evolution and the origin of life 19 p2887 A83-42037

Experimental studies related to the origin of the genetic code and the process of protein synthesis - A review 19 p2879 A83-42156

Nonenzymatic phosphorylation of acetate by carbamyl phosphate - A model reaction for prebiotic activation of carboxyl groups 19 p2887 A83-42157

Photochemical synthesis of biomolecules under anoxic conditions 19 p2887 A83-42158

Chemical evolution and the origin of life - Bibliography supplement 1981 19 p2887 A83-42160

Evolution of the amino acid code - Inferences from mitochondrial codes 20 p3033 A83-42397

Thiol-catalyzed formation of lactate and glycerate from glyceraldehyde --- significance in molecular evolution 20 p3036 A83-42398

The evolutionary pattern of aromatic amino acid biosynthesis and the emerging phylogeny of pseudomonad bacteria 20 p3033 A83-42399

Photochemical reactions of water and carbon monoxide in earth's primitive atmosphere 20 p3036 A83-42847

The process of the formation and evolution of the Jilin meteorite 21 p3240 A83-44502

The concentrating of molecules in coacervate droplets and the origin of life 21 p3189 A83-44700

Kinematical and chemical evolution of the galactic disc 21 p3233 A83-44754

Radiogenic isotopes and crustal evolution 22 p3323 A83-45781

Globular clusters and the early chemical history of galactic halos 22 p3378 A83-46409

Prebiotic evolution on a universal scale. I 23 p3500 A83-48054

The efficiency of coupled processes in connection with geochemical and biogeological evolution 23 p3485 A83-48508

The thermodynamics of evolution. II - Chemical and biological oscillations and instabilities 23 p3513 A83-48600

Type I planetary nebulae 24 p3652 A83-49143

Planetary nebulae and the chemical evolution of galaxies 24 p3653 A83-49158

Time-dependent chemistry. I - Modelling of a static cloud --- in interstellar space 24 p3659 A83-49374

Star formation and abundance gradients in the galaxy 24 p3664 A83-49997

Chemical evolution of the galactic halo. II - Enrichment in primary elements 24 p3670 A83-50154

CHEMICAL EXPLOSIONS

NT GAS EXPLOSIONS

Critical characteristics of thermal self-ignition in reacting systems with two-stage reactions 07 p0878 A83-19640

The spectral characteristics and nature of the radiation emitted by explosions in an enclosed region. II - Explosions of mixtures of CS₂/O₂ = 1/4 07 p0880 A83-19962

Structure of a detonation front 07 p0926 A83-20898

Fiber optics as light-detector probes in the accurate measurement of detonation velocities in two-phase fuel-air explosions 08 p1095 A83-22498

Explosion-driven shock tubes /Review/ 10 p1380 A83-26257

A study of the steady-state reaction-zone structure of a homogeneous and a heterogeneous explosive 14 p1991 A83-33383

Cylindrically converging shock and detonation waves 18 p2687 A83-40502

The homogeneous thermal explosion with dissociation and recombination 22 p3267 A83-46762

Characteristics of the initiation of fast chemical reactions in oxidizer-combustible mixtures 24 p3557 A83-49790

Deformation of a cylindrical shell during an explosion in the vicinity of a concentrated explosive charge 24 p3595 A83-49905

CHEMICAL EXTINGUISHERS

U FIRE EXTINGUISHERS

CHEMICAL FRACTIONATION

Are C1 chondrites chemically fractionated - A trace element study 02 p0267 A83-12844

Systematic compositional variations in the Cape York iron meteorite 02 p0267 A83-12848

Variations in the isotopic composition of xenon under the annealing and selective dissolution of material from the Tsarev meteorite 03 p0432 A83-13524

The effects of C, P, and S on trace element partitioning during solidification in Fe-Ni alloys --- iron meteorites 04 p0564 A83-15372

On the siting of noble gases in E-chondrites 04 p0572 A83-16356

Strangways Crater, Northern Territory, Australia - Siderophile element enrichment and lithophile element fractionation 07 p0950 A83-21316

The mass-independent fractionation of oxygen - A novel isotope effect and its possible cosmochemical implications 08 p1188 A83-22688

Radiolysis of aqueous solutions of hydrogen cyanide (pH about 6) - Compounds of interest in chemical evolution studies 12 p1767 A83-29424

Biologically mediated isotope fractionations - Biochemistry, geochemical significance and preservation in the earth's oldest sediments 13 p1899 A83-31159

The formation and the evolution process of the Jilin meteorite 14 p2112 A83-32597

Refractory precursor components of Semarkona chondrules and the fractionation of refractory elements among chondrites 17 p2623 A83-38854

The process of the formation and evolution of the Jilin meteorite 21 p3240 A83-44502

Study of complex coacervation in low concentration by virial expansion method. II - Salt-containing systems 23 p3427 A83-47626

CHEMICAL FUELS

NT AIRCRAFT FUELS

NT AUTOMOBILE FUELS

NT DIESEL FUELS

NT GASOLINE

NT HIGH ENERGY FUELS

NT HYDROCARBON FUELS

NT HYDROGEN FUELS

NT JET ENGINE FUELS

NT JP-4 JET FUEL

NT KEROSENE

NT LIQUID FUELS

NT METAL FUELS

NT SLURRY PROPELLANTS

NT SYNTHETIC FUELS

CHEMICAL KINETICS

U REACTION KINETICS

CHEMICAL LASERS

Kinetic processes in the HgBr/B-X//HgBr₂ dissociation laser 03 p0331 A83-13917

Numerical modeling of processes occurring in the cavity of a CW chemical HF laser on the basis of Navier-Stokes equations 03 p0332 A83-14061

Simple arrangement for spatially scanning gain measurements in CW lasers 03 p0332 A83-14165

Refractive index of HF from 2.5 microns to 2.9 microns 03 p0332 A83-14393

A new numerical method for turbulent mixing of supersonic reacting flows in chemical laser cavities [ONERA, TP NO. 1982-85] 03 p0332 A83-14537

Continuous-wave reaction-product chemical lasers /review/ 05 p0648 A83-17038

Analysis of the energetics of a chemical oxygen-iodine laser 05 p0648 A83-17047

Pulsed high-pressure chemical HF laser with electric-discharge initiation 05 p0650 A83-17084

Iodine monofluoride B 3Pi/0+ / to X 1Sigma+ lasing from collisionally pumped states 05 p0651 A83-17653

Flowfield experiments on a DF chemical laser 07 p0932 A83-19815

Model for pure source flow chemical lasers 07 p0932 A83-19817

Influence of translational and rotational relaxation on the specific energy characteristics of a CW chemical HF laser 07 p0933 A83-20103

A supersonic multikilohertz pulsed HF chemical laser 07 p0936 A83-20729

Continuous-wave HF R-branch laser demonstration 08 p1110 A83-22637

Chemical lasers --- Russian book 09 p1271 A83-23824

Rotational nonequilibrium influences in CW HF/DF chemical lasers 10 p1429 A83-26167

High gain CO chemical laser produced in a shock tunnel 10 p1429 A83-26168

Shock/Ludwig-tube driven HF laser 10 p1429 A83-26169

Pumping of pulsed gas lasers by bulk and sliding spark discharges 10 p1431 A83-26464

Use of unstable resonators in CW chemical lasers with radial flow of a gas mixture 10 p1431 A83-26652

Numerical modeling of a chemical oxygen-iodine laser 10 p1433 A83-26676

Radio frequency pumped infrared lasers 11 p1580 A83-27576

Nascent DF energy distributions for the D + F2 and F + D2 reactions 11 p1580 A83-27578

LIF and chemiluminescence methods for the flow diagnostics of supersonic mixing chemical lasers --- laser induced fluorescence 11 p1580 A83-27581

Laser action during the induction period of photoinitiated F2/H2 chain reactions 11 p1580 A83-27582

On analytical models of gas flow and chemical lasers 11 p1580 A83-27583

Cavity-dumped mercury-bromide laser 11 p1582 A83-27613

Gradually mixing model used to calculate mixing nonequilibrium flow --- in chemical and mixing gasdynamic lasers 11 p1582 A83-27616

Effects of optical irregularities in the active medium on angular divergence of a beam in a CW supersonic DF-CO2 chemical laser 13 p1851 A83-30819

Gain anisotropy in low-pressure chemical lasers 13 p1857 A83-31456

Characteristics of a pulsed chemical laser utilizing an H2-F2 mixture and initiated by radiation from an XeCl excimer laser 14 p2022 A83-31903

HF chemical laser amplification properties in homologous turbulent shear flow 15 p2170 A83-35250

Possibility of operation of a chemical oxygen-iodine laser without a cooled trap 16 p2359 A83-35893

The status of rotational nonequilibrium in HF chemical lasers [AIAA PAPER 83-1699] 17 p2513 A83-37196

Performance characteristics of a transverse-flow, oxygen-iodine chemical laser in a low gas-flow velocity 17 p2513 A83-37609

Simple model for base pressure effects in source flow chemical lasers 19 p2850 A83-40858

Computation of reacting flowfield with radiation interaction in chemical lasers 20 p2995 A83-43445

Formation of free fluorine atoms by laser-collisional initiation of the CH3F + F2 reaction 20 p2997 A83-43789

Energy lost in formation of fluorine atoms in the course of electron-beam dissociation of fluorine and fluoride molecules 20 p2997 A83-43797

Chemical laser amplifier using a photon-branched reaction in an aerosol medium 20 p2998 A83-43808

Continuous wave laser damage on optical components 21 p3142 A83-43865

The use of piecewise-exponential functions in transfer theory --- of chemical laser energy characteristics 21 p3146 A83-45222

Snowing criteria for cold traps --- utilization in chemical oxygen iodine lasers 21 p3147 A83-45593

CHEMICAL MACHINING

NT ELECTROCHEMICAL MACHINING

Physicochemical methods of semiconductor surface treatment --- Russian book 21 p3218 A83-45036

CHEMICAL MILLING

U CHEMICAL MACHINING

CHEMICAL PROPERTIES

NT ACIDITY

NT HEAT OF COMBUSTION

NT HEAT OF FUSION

NT HEAT OF VAPORIZATION

NT SALINITY

NT THERMOCHEMICAL PROPERTIES

The physicochemical basis of the formation of refractory silicide coatings on niobium and its alloys 01 p0024 A83-10388

Immunobiological properties of teichoic acids --- for diagnosing staphylococcal infections 01 p0081 A83-10556

Boundary-layer diffusion on a plate with inhomogeneous chemical properties 03 p0323 A83-14900

Surface and interface characterization of advanced materials 08 p1053 A83-22252

Infrared transmitting germanate glasses 09 p1346 A83-24962

Synthesis and properties of 1,1,1,3,5,5,5-heptanitropentane 09 p1243 A83-25273

Physicochemical properties of Cu(x)S 14 p1989 A83-32300

The stability of oils in aviation systems 15 p2142 A83-34499

The effect of ultrasound on the physical and chemical properties of hydroxyprogesterone capronate (experimental investigation) 18 p2733 A83-40570

The metal chemistry of complex alloying --- Russian book 23 p3431 A83-47098

CHEMICAL PROPULSION

NT HYBRID PROPULSION

Advanced propulsion for future planetary spacecraft 02 p0148 A83-13083

A comparison between advanced chemical and MPD propulsion for geocentric missions [AIAA PAPER 83-1391] 16 p2322 A83-36381

Comparison of electric and chemical thruster systems for secondary propulsion on a large space system [AIAA PAPER 83-1393] 16 p2322 A83-36383

CHEMICAL REACTION CONTROL

Resonance deexcitation and the possibility of controlling chemical reactions 13 p1818 A83-31345

CHEMICAL REACTIONS

NT ALKYLATION

NT ASSOCIATION REACTIONS

NT ATOMIC RECOMBINATION

NT BROMINATION

NT CARBONIZATION

NT COPOLYMERIZATION

NT CRACKING (CHEMICAL ENGINEERING)

NT DENITROGENATION

NT ELECTROCHEMICAL OXIDATION

NT EXOTHERMIC REACTIONS

NT FERMENTATION

NT FLUORINATION

NT GLYCOLYSIS

NT HYDROGENATION

NT HYDROLYSIS

NT ION RECOMBINATION

NT METAL-WATER REACTIONS

NT METHANATION

NT METHYLATION

NT NITRIDING

NT OXIDATION

NT OXIDATION-REDUCTION REACTIONS

NT OXYGEN RECOMBINATION

NT OXYGENATION

NT PHOSPHORYLATION

NT PHOTOCHEMICAL REACTIONS

NT PHOTODECOMPOSITION

NT PHOTOLYSIS

NT PHOTOOXIDATION

NT PHOTOSYNTHESIS

NT PYROLYSIS

NT RADIOLYSIS

NT REDUCTION (CHEMISTRY)

NT SULFATION

NT THERMAL DECOMPOSITION

NT THERMAL DISSOCIATION

Molecular mechanisms for the participation of peptides in the functions of nerve cells 01 p0081 A83-10918

Temperature and third-body dependence of the rate constant for the reaction O + O2 + M yields O3 + M 02 p0151 A83-11839

Discontinuous precipitation reactions in alpha and gamma phases of meteoritic metal 03 p0133 A83-13724

Analogy between the wave motions of chemically active and two-phase media 03 p0323 A83-14896

Chemical modification of amorphous arsenic 04 p0542 A83-15532

Advances in picosecond spectroscopy 04 p0456 A83-15820

Chemically reacting turbulent shear layers [AIAA PAPER 83-0475] 05 p0636 A83-16739

The effect of plasma-chemical processes of the formation of electronegative molecules on the parameters of non-self-sustained discharges 06 p0811 A83-17984

A simple model of mixing and chemical reaction in a turbulent shear layer [AD-A128220] 06 p0758 A83-19021

The structural-chemical role of iron in the reaction processes of the soldering of titanium with iron-containing alkali-free aluminoborosilicate glasses 07 p0873 A83-20685

Chemical deposition of coatings with additions of fibrous fillers 07 p0877 A83-20686

The interaction of elements in Ni-Cr-Si-B powder mixtures during heating 07 p0889 A83-20709

Component interaction in a glass-ceramic layer 07 p0900 A83-20710

Suppression of the solid-state reaction between Ni-base alloys and Si-base ceramics 08 p1053 A83-22253

Formation of silicon carbide and silicon nitride by vapor-phase reaction 08 p1071 A83-22256

The characterization of diaminodiphenyl sulfone /DDS/ cured tetraglycidyl 4, 4'-diaminodiphenyl methane /TGDDM/ epoxies 09 p1221 A83-23610

The role of aging in the modeling of elevated temperature deformation 09 p1232 A83-24064

The interaction between titanium alloys and materials containing carbon 09 p1224 A83-24407

Heterogeneous atmospheric chemistry --- Book 09 p1297 A83-25176

Chemical reactions with aerosols 09 p1297 A83-25182

Atmospheric gases on cold surfaces - Condensation, thermal desorption, and chemical reactions 09 p1298 A83-25191

Reversible chemical reactions for energy storage in a large-scale heat utility 11 p1609 A83-27315

Nascent DF energy distributions for the D + F2 and F + D2 reactions 11 p1580 A83-27578

On reactions between silicon and nitrogen. I - Mechanisms 12 p1712 A83-29501

A statistical model of nonstationary nonequilibrium processes in rarefied multicomponent chemically reacting gases 13 p1933 A83-30673

A flow-system comparison of the reactivities of calcium superoxide and potassium superoxide with carbon dioxide and water vapor [SAE PAPER 820873] 13 p1907 A83-30946

An EPR study of the reaction between poly(p-phenylene sulfide) and electron-acceptor dopants 13 p1825 A83-30951

Ab initio studies of the CO2-HF and N2O-HF complexes 13 p1818 A83-30966

Coherent anti-Stokes Raman scattering as a probe in reactive media 14 p2021 A83-33172

Operator splitting methods for the computation of reacting flows 15 p2157 A83-33866

The effect of Lewis number greater than unity on an unsteady propagation flame with one-step chemistry 15 p2132 A83-34030

Discussion of test problem B --- numerical methods in flame propagation 15 p2132 A83-34031

Calculation of laminar premixed and diffusion flames with fast chemical reaction using a self-consistent method 15 p2132 A83-34269

New trends in combustion research for gas turbine engines 16 p2303 A83-35806

Fogwater chemistry in an urban atmosphere 16 p2372 A83-36128

Relative rate constants for the reactions of atomic oxygen with HO2 and OH radicals 16 p2327 A83-36711

The probability distribution of passive-additive concentration in a mixing layer 17 p2505 A83-37631

Physical and chemical effects induced by energetic ions on comets 17 p2609 A83-38417

Formation of sulfate in a cloud-free environment 18 p2711 A83-39117

A study of the kinetics and mechanisms of the degradation of polybutadiene rubber due to thermal oxidation in vaporized hydrochloric acid 18 p2672 A83-39170

The infrared spectrum of HNO 18 p2742 A83-39857

Single collision ion-molecule reactions at thermal energy Rotational and vibrational distributions from N(+) + CO yields N + CO(+) 19 p2897 A83-40771

The possibility of the formation of aerosol in the chemical reaction between SO₂ and NH₃ in conditions of the Venus atmosphere 19 p2923 A83-41240
Cobalt oxide-SO₂/SO₃ reactions in cobalt-sodium mixed sulfate formation and low temperature hot corrosion 20 p2949 A83-42251
Response of liquid carbon disulfide to shock compression Equation of state at normal and high densities 20 p3055 A83-42638
On the computation of ionization levels in rocket exhaust flames 22 p3261 A83-45716

CHEMICAL REACTORS

Prospects for using titanium alloys in the manufacture of apparatus for the hydrochloric acid hydrolysis of yeast 19 p2821 A83-40805

CHEMICAL RELAXATION

U MOLECULAR RELAXATION

CHEMICAL SHIFT

U CHEMICAL EQUILIBRIUM

CHEMICAL STERILIZATION

The cold sterilization of surgical materials and the cleaning of the surgeon's hands on sea vessels during prolonged voyages 16 p2400 A83-36843

CHEMICAL TESTS

NT CHEMICAL ANALYSIS
NT ELECTROPHOTOMETRY
NT GAS ANALYSIS
NT GAS SPECTROSCOPY
NT MICROANALYSIS
NT NEUTRON ACTIVATION ANALYSIS
NT OZONOMETRY
NT QUALITATIVE ANALYSIS
NT QUANTITATIVE ANALYSIS
NT SALT SPRAY TESTS
NT SPECTROSCOPIC ANALYSIS
NT URINALYSIS
NT VOLUMETRIC ANALYSIS

CHEMICAL WARFARE

Chemical defense, environmental control systems study [SAE PAPER 820866] 13 p1806 A83-30944

CHEMILUMINESCENCE

Modification of a commercial NO_x detector for high sensitivity 03 p0328 A83-14168
The spectral characteristics and nature of the radiation emitted by explosions in an enclosed region. II - Explosions of mixtures of CS₂/O₂ = 1/4 07 p0880 A83-19962
CO + O chemiluminescence - Rate coefficient and spectral distribution 10 p1480 A83-26181
Nascent DF energy distributions for the D + F₂ and F + D₂ reactions 11 p1580 A83-27578
LIF and chemiluminescence methods for the flow diagnostics of supersonic mixing chemical lasers --- laser induced fluorescence 11 p1580 A83-27581
Measurement of the vertical ozone distribution by means of an in situ gas phase chemiluminescence ozonometer during the intercomparison ozone campaign, Gap, France, June 1981 18 p2716 A83-39790
Determination of ethylene and other reactive hydrocarbons in the atmospheric air at Trombay, Bombay by gas chromatography using a chemiluminescent detector 19 p2849 A83-41984
Spectroscopic analysis of the chemiluminescence from lead oxide flames 20 p2950 A83-42579

CHEMISORPTION

Comparison of photon stimulated dissociation of gas phase and chemisorbed CO 10 p1389 A83-25556
Diatomic molecules and metallic adhesion, cohesion, and chemisorption - A single binding-energy relation 13 p1817 A83-30921
Hydrogen vibration on Si(111) 7 x 7 - Evidence for a unique chemisorption site 15 p2131 A83-33897
A kinetic model of hydrogen absorption in CeMg12 15 p2193 A83-34868
Quantum motion of chemisorbed hydrogen on Ni surfaces 21 p3218 A83-45198

CHEMONUCLEAR PROPULSION

U CHEMICAL PROPULSION

U NUCLEAR PROPULSION

CHEMORECEPTORS

The role of Fc-receptors of lymphocytes, macrophages, and other mammalian cells during the immune processes 01 p0082 A83-11406
The role of central and peripheral serotonergic mechanisms 04 p0520 A83-15895
Electrogustometric investigations during manned space flight 06 p0796 A83-18186
Chemoreceptor sensitivity in adaptation to high altitude 07 p0977 A83-20780
The oxygen tension in the skeletal muscles of rats adapted to cold 08 p1145 A83-22112
Opposing actions of dibutyryl cyclic AMP and GMP on temperature in conscious guinea-pigs 12 p1762 A83-29530

Central effects of some peptide and non-peptide opioids and naloxone on thermoregulation in the rabbit 12 p1763 A83-29533
Effect of hypoxia and hypercapnia on catecholamine content in cat carotid body 14 p2064 A83-32822
The internalization and intracellular conversions of biologically active polypeptides and their receptors 14 p2065 A83-33320
Hyperthermic responses to central injections of some peptide and non-peptide opioids in the guinea-pig 16 p2394 A83-36719
Peptide and non-peptide opioid-induced hyperthermia in rabbits 16 p2396 A83-36985
The regulation of the breathing pattern during muscular activity in conditions of normal and altered chemoreceptor stimulation 17 p2558 A83-37244
Effects of chronic hypoxia on pulmonary vascular responses to biogenic amines 20 p3033 A83-43487

CHEMOTHERAPY

Pleurodesis - The results of treatment for spontaneous pneumothorax in the Royal Air Force 07 p0978 A83-20786

CHEST

Role of impact velocity and chest compression in thoracic injury 06 p0794 A83-18189

CHEWING

U MASTICATION

CHILD-LANGMUIR LAW

Space-charge conditions in an intense relativistic particle beam 10 p1486 A83-25889

CHILDREN

Age-related patterns of lateral movement preferences 05 p0673 A83-17156
The effect of external environmental factors on the rhythm of physiological functions of pre-school-age children 14 p2069 A83-32952
The condition of the vestibular apparatus in children with hereditary hearing defects 19 p2884 A83-41843

CHILLING

U COOLING

CHIMES

U AUDITORY SIGNALS

CHIMNEYS

Growth of 'black smoker' bacteria at temperatures of at least 250 C 16 p2394 A83-35992

CHINA

Satellite monitoring of recent desertification in the Yulin region The People's Republic of China 09 p1287 A83-24569
Monitoring arid land changes in the Turpan Depression, People's Republic of China 09 p1288 A83-24569
Remote sensing and mineral exploration in China 17 p2527 A83-38135
Landsat analysis of the Yangjiatan tungsten district, Hunan Province, People's Republic of China 17 p2528 A83-38141
Satellite broadcasting - The best way to meet the needs of television education in China [IAF PAPER 83-308] 23 p3513 A83-47337

CHINA (COMMUNIST) MAINLAND

U CHINA

CHINESE PEOPLES REPUBLIC

U CHINA

CHINESE SPACE PROGRAMS

China's long march to orbit 12 p1705 A83-29674

CHINESE SPACECRAFT

Space flight test of MDT-2A --- pulsed plasma microthruster [AIAA PAPER 82-1874] 02 p0143 A83-12462
China's long march to orbit 12 p1705 A83-29674

CHINOOK HELICOPTER

U CH-47 HELICOPTER

CHIPPING

Titanium - A model material for analysis of the high speed machining process 15 p2171 A83-33647

CHIPS (ELECTRONICS)

Single chip Bus Interface Unit eases MIL-STD-1553B remote terminal/bus controller designs 01 p0042 A83-11185
Test chips for custom ICs - Six kinds of test structures 02 p0167 A83-11824
Multimicroprocessor systems 02 p0227 A83-11916
Integrated sensors - Interfacing electronics to a non-electronic world 02 p0180 A83-12809
Flip-chip BeO technology applied to GaAs active aperture radars 03 p0308 A83-13442
Planar multijunction high voltage solar cell chip 03 p0355 A83-13923
Pin limitations and partitioning of VLSI interconnection networks 05 p0679 A83-17244
A low-power, high-throughput maximum-likelihood convolutional decoder chip for NASA's 30/20 GHz program 07 p0917 A83-19754
A monolithic single-chip X-band four-bit phase shifter 07 p0923 A83-21534

CAD system for VLSI in Japan

07 p0924 A83-21543

Systolic array processor implementation

08 p1153 A83-22798

Programmable systems components - A comprehensive approach to signal processing 08 p1154 A83-22819
Very high speed integrated circuit /VHSIC/ antijam communications chipset and brassboard demonstration 08 p1081 A83-22820

Analysis and test of ceramic substrates for packaging of leadless chip carriers 13 p1834 A83-30861
Test data on leadless chip carriers with ceramic substrates in severe random vibration environments 13 p1835 A83-30866

6-bit 25 MHz NMOS parallel A/D converter 13 p1838 A83-31786

I/O limitations of multi-chip VLSI systems

15 p2218 A83-35116
16 p2346 A83-36021

Yield enhancement of bit level systolic array chips using fault tolerant techniques 18 p2679 A83-40389
A 12 bit monolithic 70 ns DAC --- Digital to Analog Converter 19 p2837 A83-40792

VLSI: Silicon compilation and the art of automatic microchip design --- Book 19 p2841 A83-41873
The first cortical implant of a multiplexed multi-electrode semiconductor brain electrode 20 p3035 A83-42553

A new method of VLSI conform design for MOS cells 20 p2967 A83-43026
Temperature sensitivity in silicon piezoresistive pressure transducers 20 p2991 A83-43352

CHIPS (MEMORY DEVICES)

32K bit MNOS BORAM --- Block Oriented RAM 01 p0089 A83-11211
A 4K NVRAM utilizing n-channel SNOS technology --- Silicon Nitride Oxide Silicon structure for non-volatile RAM 01 p0089 A83-11212

System programmable redundancy in a 64K EEPROM --- Electronically Erasable PROM 01 p0089 A83-11213
Soft error in MOS dynamic RAM 07 p0918 A83-20072

Programmable systems components - A comprehensive approach to signal processing 08 p1154 A83-22819
Comparison of memory chip organizations vs reliability in virtual memories 17 p2517 A83-37290

Chip architecture - A revolution brewing 17 p2497 A83-37739

CHIRAL DYNAMICS

Remarks on origins of biomolecular asymmetry 02 p0219 A83-11635

CHIRP

NT CHIRP SIGNALS

CHIRP SIGNALS

Error-signal response of a phase-locked loop to a coherent chirp signal 03 p0311 A83-13856

CHLORATES

The electrochemistry of molten lithium chlorate and its possible use with lithium in a battery 11 p1546 A83-28296

CHLORELLA

The effect of an intermittent-light frequency on the quantum yield of chlorella photosynthesis 13 p1895 A83-30406

CHLORIDES

NT AMMONIUM CHLORIDES
NT CARBON TETRACHLORIDE
NT COPPER CHLORIDES
NT DICHLORIDES
NT HYDROCHLORIC ACID
NT HYDROGEN CHLORIDES
NT LITHIUM CHLORIDES
NT MAGNESIUM CHLORIDES
NT NITROSYL CHLORIDES
NT NITROXYCHLORIDES
NT POTASSIUM CHLORIDES
NT SILICON TETRACHLORIDE
NT SODIUM CHLORIDES
NT SULFUR CHLORIDES
NT TETRACHLORIDES
NT ZINC CHLORIDES
Spectral study of the D-X system of the diatomic mercury chloride molecule 01 p0105 A83-10204
Picosecond amplification and kinetic studies of XeCl 02 p0184 A83-12272
Calculation of SF₆/SF₆ and Cl-/CFCl₃ electron attachment cross sections in the energy range 0-100 meV 05 p0613 A83-17231
Determination of the minimum X-ray flux for effective preionization of an XeCl laser 06 p0767 A83-19255
Applications of titanium and prospects for the use of AT-series titanium alloys in environments containing chlorides 09 p1235 A83-24404
Electrochemical studies of Cu(I) and Cu(II) in an aluminum chloride-N(n-butyl)pyridinium chloride ionic liquid 15 p2133 A83-34693

Cleaning chemistry of InSb(100) molecular beam epitaxy substrates 17 p2485 A83-37616

Effect of defects on phase transitions in tetraselenotetracene chloride, (TSeT)2Cl 20 p3051 A83-42272

Polarization of the lithium electrode in sulfuril chloride solutions 24 p3558 A83-49939

CHLORINE

Sputtering of Al2O3 and LiNbO3 in the electronic stopping region [BAP-24] 07 p0901 A83-21057

Evidence for aerosol chlorine reactivity during filter sampling 09 p1299 A83-25203

Formation of the Cl I line at 1351 Å in the solar chromosphere 10 p1522 A83-26396

Effects of low concentrations of chlorine on pulmonary function in humans 13 p1905 A83-30509

Nonlinear response of stratospheric ozone column to chlorine injections 13 p1872 A83-30880

CHLORINE COMPOUNDS

NT AMMONIUM CHLORIDES

NT AMMONIUM PERCHLORATES

NT CARBON TETRACHLORIDE

NT CHLORATES

NT CHLORIDES

NT CHLORINE OXIDES

NT CHLOROCARBONS

NT COPPER CHLORIDES

NT DICHLORIDES

NT HYDROCHLORIC ACID

NT LITHIUM CHLORIDES

NT LITHIUM PERCHLORATES

NT MAGNESIUM CHLORIDES

NT NITROSYL CHLORIDES

NT NITROXYCHLORIDES

NT POTASSIUM CHLORIDES

NT SILICON TETRACHLORIDE

NT SODIUM CHLORIDES

NT SULFUR CHLORIDES

NT TETRACHLORIDES

NT ZINC CHLORIDES

Chlorine nitrate - The sole product of the ClO + NO2 + M recombination 16 p2381 A83-36154

On the photodecomposition of ClONO2 in the middle ultraviolet 21 p3109 A83-44486

Background concentration of organochlorine compounds and 3,4-benzopyrene in the environment (according to worldwide data) 24 p3602 A83-49104

CHLORINE OXIDES

Spectroscopic studies of the hazards of Li/SOCI2 batteries during anode-limited cell reversal 02 p0202 A83-12056

The kinetics of the reaction of OH with ClO 08 p1056 A83-22214

Infrared heterodyne spectroscopy of seven gases in the vicinity of chlorine monoxide lines 14 p1990 A83-32915

Is there any chlorine monoxide in the stratosphere? 17 p2546 A83-38625

A re-evaluation of laser heterodyne radiometer ClO measurements --- for stratospheric chemistry studies 20 p3026 A83-43209

CHLOROAROMATICS

Synthesis and characteristics of poly(bisdichloromaleimides/ 05 p0610 A83-17475

CHLOROCARBONS

A statistical analysis of Umkehr measurements of 32-46 km ozone 07 p0957 A83-20803

Chlorocarbon emission scenarios - Potential impact on stratospheric ozone 09 p1296 A83-24270

Photoassisted heterogeneous catalysis - Definition and hydrocarbon and chlorocarbon oxidations 09 p1297 A83-25188

Global distribution and southern hemispheric trends of atmospheric CCl3F 14 p2056 A83-31920

A two-dimensional photochemical model of the atmosphere. I Chlorocarbon emissions and their effect on stratospheric ozone 20 p3013 A83-42845

A two-dimensional photochemical model of the atmosphere. II The tropospheric budgets of the anthropogenic chlorocarbons CO, CH4, CH3Cl and the effect of various NO(x) sources on tropospheric ozone 20 p3013 A83-42846

The Atmospheric Lifetime Experiment. II - Calibration 24 p3606 A83-49329

The atmospheric lifetime experiment. III - Lifetime methodology and application to three years of CFCL3 data 24 p3606 A83-49330

CHLOROETHYLENE

Experimental study of electrochemical fluorination of trichloroethylene 04 p0456 A83-15870

CHLOROFORM

Atmospheric chloroform (CHCl3) - Ocean-air exchange and global mass balance 21 p3169 A83-44378

CHLOROPHYLLS

Effect of particle size distribution and chlorophyll content on beam attenuation spectra 02 p0203 A83-12314

Remotely sensed reflectance and its dependence on vertical structure - A theoretical derivation 02 p0218 A83-12606

Initial analysis of OSTA-1 ocean color experiment imagery 03 p0372 A83-13352

The possibilities of determining chlorophyll content in plants on the basis of their reflection spectra 07 p0951 A83-19912

A kinetic model of the electron and conformational transitions in the photosynthetic reaction centers of purple bacteria 07 p0974 A83-20966

Basis for spectral curvature algorithms in remote sensing of chlorophyll 10 p1453 A83-26644

The relationships between the chlorophyll concentration, LAI and reflectance of a simple vegetation canopy --- leaf area index 15 p2187 A83-35280

The red edge of plant leaf reflectance 15 p2188 A83-35282

Remote sensing of phytoplankton in the sea - Surface-layer chlorophyll as an estimate of water-column chlorophyll and primary production 15 p2209 A83-35286

Delineation of seasonal changes of chlorophyll frontal boundaries in Mediterranean coastal waters with Nimbus-7 coastal zone color scanner data 17 p2554 A83-37623

Red edge measurements for remotely sensing plant chlorophyll content 17 p2529 A83-38161

CHLOROPLASTS

Picosecond fluorescence in spinach chloroplasts 22 p3346 A83-46672

CHOICE

U SELECTION

CHOKES (FUEL SYSTEMS)

The cold locking of the duct of a gas-liquid mixer by burning fuel jets 18 p2663 A83-39168

CHOKES (RESTRICTIONS)

A consideration on dynamic characteristics of pneumatic conduit systems with a cylindrical choke - Influence of the position of a cylindrical choke 02 p0187 A83-13074

Effects of choke-load position on radiation properties in double-choked small horn antennas 13 p1830 A83-31778

Experiments on flow through one to four inlets of the orifice and Borda type 20 p2986 A83-43235

CHOLESKY FACTORIZATION

Rutishauser's modified method for computing the eigenvalues of symmetric matrices 05 p0682 A83-17898

Scattering arrays for matrix computations 08 p1153 A83-22804

CHOLESTEROL

An approach for determining common cholesterol and its structural-functional fractions in erythrocytes on the basis of the digitonin method 03 p0375 A83-14327

Relative content of cholesterol and the microviscosity of serum apo-B-containing lipoproteins of mammals 03 p0376 A83-14372

The effect of xenogenous cerebrospinal fluid on the course of experimental hypercholesterolemia 05 p0670 A83-17187

The lipid balance of technical flight personnel between 50 and 55 years old in commercial and civil aviation 06 p0798 A83-18340

The biosynthesis of cholesterol in the tissues of irradiated rats 18 p2731 A83-39520

The effect of liquid crystals on the lubricating properties of mineral oils 19 p2824 A83-41975

Cholesterol esters increase the permeability of lecithin bilayer membranes 21 p3184 A83-45223

Experimental injury of the aorta of rabbits of various ages by immune complexes 21 p3185 A83-45342

CHOLINERGIC BLOCKING AGENTS

U ANTICHOLINERGICS

CHOLINERGICS

NT ANTICHOLINERGICS

The effect of polymethylene and polyoxyethylene-bis-/2-amino-1,3-diazepinium/ iodides on cell and model membranes 01 p0079 A83-10537

The participation of the dopaminergic system of the brain in the realization of the generalization function 01 p0080 A83-10540

A cholinergic mechanism for the regulation of the cardiac function during acute transitory coronary insufficiency 15 p2210 A83-34961

Environmentally induced cholinergic urticaria and anaphylaxis 15 p2214 A83-34989

Cholinergic and adrenergic innervation of intracerebral arteries during ontogenesis in humans 17 p2560 A83-38194

CHONDRITES

A cholinergic-sensitive channel in the cat visual system tuned to low spatial frequencies 21 p3183 A83-44364

The pattern of the changes in the concentration of catecholamines and acetylcholine in the blood during the prolonged action of a constant magnetic field with a high induction 21 p3186 A83-45379

CHOLINESTERASE

The effect of cholinesterase inhibitors on the electrically excitable membranes of frog muscle fibers 02 p0219 A83-11520

The reaction of chronically irradiated dogs to radiation as evaluated by changes in the activity of cholinesterase 09 p1321 A83-24932

CHONDRITES

NT BRUDERHEIM METEORITE

NT CARBONACEOUS CHONDRITES

NT CARBONACEOUS METEORITES

NT ORGUEIL METEORITE

Fine, nickel-poor Fe-Ni grains in the olivine of unequilibrated ordinary chondrites 02 p0262 A83-11549

Evidence for primitive nebular components in chondrules from the Chainpur chondrite 02 p0262 A83-11550

Fission track studies of xenolithic chondrites - Implications regarding brecciation and metamorphism 02 p0267 A83-12840

The geochemical coherence of Pu and Nd and the Pu-244/U-238 ratio of the early solar system 02 p0267 A83-12843

Are C1 chondrites chemically fractionated - A trace element study 02 p0267 A83-12844

Petrology and shock metamorphism of Pampa del Infierno chondrite 02 p0267 A83-12847

A direct measurement of the distribution in depth of Al-26 in the Estacado meteorite 02 p0267 A83-12849

Comment on 'Thermoluminescence of meteorites and their terrestrial ages' 02 p0267 A83-12850

The variable carbon isotopic composition of type 3 ordinary chondrites 04 p0562 A83-15354

Deuterium enrichments in type 3 ordinary chondrites 04 p0562 A83-15355

Petrography, mineral chemistry and origin of Type I enstatite chondrites 04 p0572 A83-16351

On the siting of noble gases in E-chondrites 04 p0572 A83-16356

Absolute age of formation of chondrites studied by the /Rb-87/-/Sr-87/ method 05 p0703 A83-16846

The Guangrao meteorite - A newly fallen L6-5 chondrite 05 p0703 A83-16949

The Tsarev stony-meteorite rain 05 p0705 A83-17452

Peculiarities of the composition and structure of the Tsarev meteorite 05 p0705 A83-17453

Mineralogy of some fragments of the Tsarev meteorite 05 p0705 A83-17454

The composition and structure of plesite in the Tsarev chondrite 05 p0705 A83-17455

Chemical composition of the Tsarev meteorite 05 p0705 A83-17456

Peculiarities of the magnetic properties of the Tsarev meteorite 05 p0705 A83-17457

Composition, structure, and preatmospheric sizes of the Kutais chondrite 05 p0705 A83-17458

Petrography, mineralogy, and chemical composition of the Bakhardok meteorite 05 p0705 A83-17459

The classification of ordinary chondrites according to chemical composition 05 p0706 A83-17460

Investigation of the Tsarev and Northern Kolchik chondrites by Moessbauer spectroscopy 05 p0706 A83-17467

Magnetic anisotropy and porosity of chondrites 07 p1028 A83-20098

Magnetic properties and paleointensity determination of seven H-group chondrites 07 p1031 A83-20971

Magnetite in Cl chondrites 07 p1034 A83-21307

Nature of the H chondrite parent body regolith - Evidence from the Dimmitt breccia 07 p1034 A83-21308

Nuclear track and compositional studies of olivines in Cl and CM chondrites 07 p1034 A83-21309

The thermoluminescence carrier in the Dhajala chondrite 07 p1034 A83-21311

High magnetic coercivity of meteorites containing the ordered FeNi /tetrataenite/ as the major ferromagnetic constituent 07 p1034 A83-21312

Actinide microdistributions in the enstatite meteorites 07 p1035 A83-21329

Chemical and physical studies of type 3 chondrites. I - Metamorphism related studies of Antarctic and other type 3 ordinary chondrites 07 p1035 A83-21331

Chemical studies of L chondrites. II - Shock-induced trace element mobilization 07 p1035 A83-21333

Mineralogy and petrology of the Abbee enstatite chondrite breccia and its dark inclusions 08 p1187 A83-21640

Ar-40/Ar-39 and U-Th-Pb dating of separated clasts from the Abbee E4 chondrite 08 p1188 A83-21641

- Nuclear track records in the Abee enstatite chondrite 08 p1188 A83-21643
- Nitrogen contents and isotopic ratios of clasts from the enstatite chondrite Abee 08 p1188 A83-21644
- Composition and origin of clasts and inclusions in the Abee enstatite chondrite breccia 08 p1188 A83-21645
- Plessite formation by discontinuous precipitation reaction from gamma-Fe,Ni in Richardton /H5/ ordinary chondrite 08 p1190 A83-23270
- Chemical characteristics and origin of H chondrite regolith breccias 09 p1367 A83-25175
- Distribution of lead and thallium in the matrix of the Allende meteorite and the extent of terrestrial lead contamination in chondrites 12 p1797 A83-29174
- The variations of cosmic rays in the heliosphere according to the results of an investigation of extraterrestrial matter 14 p2117 A83-32970
- The peculiarities of the xenon isotope composition in the chondrites Saratov (L4), Elenovka (L5), and Zhigalovka (LL6) 14 p2112 A83-32971
- Grain-size distribution and morphology of metal in E-chondrites 14 p2112 A83-33069
- An unequilibrated inclusion in the Romero (H3-4) chondrite 14 p2113 A83-33072
- Summary of several recent chondrite finds from the Texas Panhandle 14 p2113 A83-33073
- Early solar system magnetic fields as recorded in meteorites 15 p2276 A83-35007
- U-Th-Pb in chondrites - Evidence of elemental mobilities and the singularity of primordial Pb 16 p2438 A83-36745
- Cooling history of pyroxene chondrules in the Yamato-74191 chondrite (L3) - An electron microscopic study 16 p2438 A83-36748
- Ca-Al-rich chondrules and inclusions in ordinary chondrites 17 p2623 A83-38593
- Alkali differentiation in LL-chondrites 17 p2623 A83-38853
- Refractory precursor components of Semarkona chondrules and the fractionation of refractory elements among chondrites 17 p2623 A83-38854
- Rare earth abundances in chondritic phosphates and their implications for early stage chronologies 18 p2780 A83-40348
- Mossbauer studies on Moci (Romania) meteorite 20 p3077 A83-42316
- Cosmogenic records in Antarctic meteorites 20 p3078 A83-43149
- D/H ratios in meteorites - Some results and implications 21 p3240 A83-44232
- Study on the chemical composition of 9 chondrites in China 21 p3241 A83-44504
- Description, chemical composition and noble gases of the chondrite Nogata 22 p3384 A83-46371
- The Atlanta enstatite chondrite breccia 22 p3385 A83-46373
- Al-Sm-Eu-Sr systematics of eucrites and moon rocks 24 p3672 A83-49348
- Implications for planetary bulk compositions 24 p3672 A83-49349
- Cumberland Falls chondritic inclusions. II - Trace element contents of forsterite chondrites and meteorites of similar redox state 24 p3672 A83-49349
- The Adhi Kot breccia and implications for the origin of chondrules and silica-rich clasts in enstatite chondrites 24 p3673 A83-50174
- CHONDRULE**
- Moessbauer spectroscopy of chondrules and matrix from a stony meteorite /ALHA 77278/ 01 p0128 A83-10200
- Fine, nickel-poor Fe-Ni grains in the olivine of unequilibrated ordinary chondrites 02 p0262 A83-11549
- Evidence for primitive nebular components in chondrules from the Chainpur chondrite 02 p0262 A83-11550
- Microchondrule-bearing clast in the Piancaldoli LL3 meteorite - A new kind of type 3 chondrite and its relevance to the history of chondrules 02 p0267 A83-12841
- I-Xe ages of individual Bjurböle chondrules 04 p0562 A83-15356
- Refractory residues, condensates and chondrules from solar furnace experiments 04 p0563 A83-15371
- Radiation history of lunar microbreccias and lithic chondrules from Weston meteorite by track data 07 p1034 A83-21310
- Cooling history of pyroxene chondrules in the Yamato-74191 chondrite (L3) - An electron microscopic study 16 p2438 A83-36748
- Ca-Al-rich chondrules and inclusions in ordinary chondrites 17 p2623 A83-38593
- Refractory precursor components of Semarkona chondrules and the fractionation of refractory elements among chondrites 17 p2623 A83-38854
- The Adhi Kot breccia and implications for the origin of chondrules and silica-rich clasts in enstatite chondrites 24 p3673 A83-50174

- CHOPPERS (ELECTRIC)**
- U ELECTRIC CHOPPERS
- CHORDS (GEOMETRY)**
- Generalized chord transformation for distortion-invariant optical pattern recognition 19 p2900 A83-41096
- Determination of a chord length from laser and camera observations made on common orbital arc 23 p3421 A83-48068
- CHORUS (DAWN PHENOMENON)**
- U DAWN CHORUS
- CHORUS PHENOMENON**
- U DAWN CHORUS
- CHROMATES**
- Some characteristics of and measurements on dichromated gelatin reflection holograms 21 p3140 A83-44838
- Electrochemical reduction of calcium chromate --- cathode material in Ca/CaCrO₄/Fe thermally activated batteries 22 p3268 A83-46895
- Li-AgBi(CrO₄)₂ - A new highly reliable lithium battery for long service life applications 24 p3600 A83-49945
- CHROMATOGRAPHY**
- NT GAS CHROMATOGRAPHY
- NT LIQUID CHROMATOGRAPHY
- The use of chromatography for determining kallikrein and prekallikrein in canine blood serum 01 p0080 A83-10546
- Structural and functional changes in the hemoglobin of irradiated dogs 06 p0796 A83-19379
- CHROME**
- U CHROMIUM
- CHROMIC ACID**
- Structure in carbon/carbon fibre composites as studied by microscopy and etching with chromic acid 12 p1709 A83-29502
- Improved chromatic acid anodize seal for optimum paint adhesion [SAE PAPER 820603] 22 p3301 A83-45864
- CHROMITES**
- Sorption of noble gases by solids, with reference to meteorites. II - Chromite and carbon. III - Sulfides, spinels, and other substances; on the origin of planetary gases 02 p0262 A83-11547
- On some transport properties of strontium-doped lanthanum chromite ceramics 18 p2671 A83-39057
- CHROMIUM**
- Structure of the coating on a nickel alloy after chromoaluminizing in vacuum 01 p0025 A83-10449
- Mapping of iron and chromium on the surface of the Ap star Epsilon Ursae Majoris 03 p0418 A83-13880
- Two Cr II multiplets around 1430 Å appearing in absorption in the spectrum of a solar active region 03 p0436 A83-13952
- The influence of different deposition parameters on the aluminum content in alloy coatings obtained by cathodic sputtering [ONERA, TP NO. 1982-86] 03 p0300 A83-14538
- Low-temperature refractory metal film deposition 03 p0301 A83-14936
- Study of MIS silicon solar cells by ESCA and AES 04 p0539 A83-15489
- An investigation of deposition parameter dependence of optical properties, microstructure and thermal stability of black chrome selective surfaces 04 p0505 A83-15497
- A study of the deposition conditions and properties of plasma-sprayed nickel-chromium coatings on parts of spherical shape 07 p0888 A83-20697
- The interaction of elements in Ni-Cr-Si-B powder mixtures during heating 07 p0889 A83-20709
- Study of the thermal conversion of semi-insulating GaAs:Cr with cathodoluminescence, photoluminescence, and secondary ion mass spectrometry 07 p1000 A83-20747
- Characterization and corrosion behavior of duplex-chromized steel for the sulfur container in Na-S cells 10 p1394 A83-25537
- Laser-controlled etching of chromium-doped 100 line-type GaAs 10 p1390 A83-25986
- The effect of heat treatment on some properties of electrodeposited nickel and chromium coatings 10 p1399 A83-26896
- A correlation of atomic and electrical measurements of Cr and residual donors in thermally processed semi-insulating GaAs 16 p2419 A83-35672
- Solar absorber material stability under high solar flux 22 p3319 A83-46585
- CHROMIUM ALLOYS**
- NT ASTROLOY (TRADEMARK)
- NT CHROMIUM STEELS
- Sulfidation properties of Fe-Cr alloys at 1073 K in H₂S-H₂ atmospheres of sulfur pressures 0.01 and 0.00001 Pa 01 p0024 A83-10244
- Protection of Fe-Cr-Al alloys in sulfidizing environments by means of an alpha-Al₂O₃ scale 01 p0024 A83-10245

- X-ray powder diffraction evidence for the incorporation of W and Mo into M23C6 extracted from high-temperature alloys 02 p0154 A83-11670
- Pulse plating of chromium-cobalt alloys containing a phase with the A-15 structure 02 p0154 A83-12053
- Formation mechanisms of keying or pegging yttrium oxide and increased plasticity of alumina scale on FeCrAlY 03 p0296 A83-13121
- The influence of superficially applied oxide powders on the high-temperature oxidation behavior of Cr₂O₃-forming alloys 03 p0296 A83-13124
- Influence of structural parameters on oxidation of austenitic Fe-Ni-Cr-Al alloys 05 p0615 A83-17562
- An investigation of heat-affected zone hot cracking in alloy 800 06 p0728 A83-18399
- Factors influencing the creep behaviour of a cast Ni-Cr-base alloy 07 p0893 A83-21474
- Phase composition and phase stability of alloy IN939 07 p0894 A83-21483
- The tribological properties of highly oriented cobalt and Co-Cr ion platings 10 p1395 A83-25550
- The wear resistance of chromium-base alloys during high-temperature friction 10 p1396 A83-25633
- Isothermal oxidation of the COTAC 74 in-situ composite between 800 and 1300 °C 10 p1389 A83-26891
- Effect of tungsten on the properties of austenitic precipitation-hardening Fe-Cr-Ni alloys 13 p1823 A83-31213
- Thermomechanical treatment of the Elvilar alloy 44NKhMT using plain shear 13 p1823 A83-31216
- The effect of oxygen and sulfur on segregation at the surface of a nickel-chromium alloy 13 p1823 A83-31300
- A study of the dissolution and precipitation kinetics of secondary phases in a Cr15Ni70W10MoAlTiB alloy 14 p1991 A83-31944
- The effect of temperature and deformation rate on the dynamic recrystallization of KhN77TiYr alloy single crystals 15 p2138 A83-34018
- Thermodynamic calculation of phase equilibria in Cr-V-N alloys 16 p2335 A83-36897
- Oxide scale induced cleavage fracture in an ODS Fe-Cr-Al alloy 18 p2670 A83-40639
- An investigation of residual stress of oxide scale affected by the addition rare earth elements in Fe-Cr-Al alloys at 1200 °C and 1350 °C 20 p2952 A83-42237
- Electrochemical assessment of MCrAlY coating alloys at 750 and 900 °C in air and CO/CO₂ mixtures 20 p2953 A83-42253
- Structural transformations during the aging of Ni-Cr-Nb alloys 20 p2955 A83-43495
- The effect of the parameters of cyclic loading on the kinetics of deformation and fracture of El826 alloy 21 p3114 A83-45317
- Phase composition and phase stability of a high-chromium nickel-based superalloy, IN939 22 p3269 A83-46395
- Characteristics of the precipitation of the gamma-prime phase in 40KhNy alloy 24 p3560 A83-49068
- The kinetics of metal powder consolidation during hot pressing in porous shells. III - An experimental study 24 p3561 A83-49473
- Effect of oxygen pressure on the high temperature oxidation of Ni-Cr alloys 24 p3562 A83-49489
- High temperature corrosion of pure nickel and nickel-20 percent chromium alloy in the presence of calcium sulfate and graphite 24 p3563 A83-49497
- Hot corrosion of Ni-20Cr base alloys induced by Na₂SO₄-NaCl mixtures 24 p3564 A83-49505
- The kinetics and mechanism of the attack of MCr-type alloys in oxygen-sulphur environments at 700 °C 24 p3565 A83-49511
- The sulfidation behavior of nickel chromium and nickel-aluminum binary alloys with and without yttrium 24 p3565 A83-49514
- Environmental effects on high temperature creep properties of Ni - 20 Cr - W alloys in air, vacuum and helium 24 p3565 A83-49516
- High temperature oxidation of Ni-25Cr-15W alloy 24 p3565 A83-49517

CHROMIUM BORIDES

- Wear-resistant hard alloys based on titanium-chromium diboride 03 p0293 A83-14816
- Thermally stable wear-resistant coatings containing chromium borides 07 p0888 A83-20703

CHROMIUM CARBIDES

- The oxidation of ultrafine powders of boron, vanadium, and chromium carbides 09 p1240 A83-25067
- Plasma- and vacuum-plasma-sprayed Cr₃C₂ composite coatings 10 p1400 A83-25531

CHROMIUM COMPOUNDS

- NT CHROMATES
- NT CHROMIC ACID
- NT CHROMITES

NT CHROMIUM BORIDES
 NT CHROMIUM CARBIDES
 NT CHROMIUM OXIDES

Relative intensity changes of L3MM Auger transitions in maximal-valent V and Cr compounds under ion bombardment 12 p1778 A83-29543

Influence of polarized optical pumping on the ferromagnetism of CdCr₂Se₄ 15 p2237 A83-33798

Temperature-dependent ion mixing and diffusion during sputtering of thin films of CrSi₂ on silicon 19 p2903 A83-40740

Interatomic Auger transitions in maximal valent V and Cr compounds 21 p3109 A83-44618

CHROMIUM OXIDES
 NT CHROMITES

The influence of superficially applied oxide powders on the high-temperature oxidation behavior of Cr₂O₃-forming alloys 03 p0296 A83-13124

Catalytic recombination of nitrogen and oxygen on iron-cobalt-chromia spinel [AIAA PAPER 83-0585] 05 p0612 A83-16804

Determination of chromium in chromium oxide layers synthesized on the surface of carbonaceous solid substances 08 p1057 A83-22626

Microstructure, adhesion and growth kinetics of protective scales on metals and alloys 18 p2666 A83-39731

High temperature oxidation of chromium 20 p2951 A83-42231

Coatings containing chromium, aluminum, and silicon for high temperature alloys 20 p2953 A83-42260

Fabrication of ZrCx/Zr and Cr-CrOx films for practical solar selective absorption systems 22 p3319 A83-46584

Chromium oxides as cathodes for lithium cells 24 p3600 A83-49943

Behaviour of AgBi(Cr₂O₇)₂ as a possible cathode for lithium cells 24 p3601 A83-49953

CHROMIUM STEELS

The thermodynamic principles of calorizing 07 p0887 A83-20679

The propagation of short fatigue cracks in 12% chromium steels 08 p1060 A83-21712

Structural and microstructural changes in the inner races of ball bearings 09 p1276 A83-23346

Creep of rotors under triaxial tension 09 p1276 A83-23361

Cavitation and creep crack growth in low alloy steels 09 p1233 A83-24077

The effect of cycle waveshape on the low cycle fatigue behaviour of 20%Cr-25%Ni-Nb stainless steel at 650 C 11 p1547 A83-27852

The fracture of 15Kh1M1F steel in creep as a function of the type of structure 13 p1819 A83-30067

The effects of tempering reactions on temper embrittlement of alloy steels 16 p2329 A83-35688

Corrosion fatigue behaviour of 13Cr stainless steel and Ti-6Al-4V at ultrasonic frequency 16 p2332 A83-36192

Influence of silicon additions on the oxidation resistance of a stainless steel 18 p2666 A83-39853

Magnetic, electrical, and mechanical properties of 12KhN3A and 12Kh2N4A steels and of case-hardened layers on them 21 p3111 A83-43879

The long-term strength of metals in a complex stressed state 21 p3114 A83-45318

Oxidation of high alloyed steels 24 p3563 A83-49494

CHROMOSOMES

The effect of heavy ions on mammalian cells. I - The cytogenic effects during the irradiation of Chinese hamster cells induced by accelerated ions of helium, carbon, and neon 03 p0377 A83-14884

The mutagenic effect of laser radiation in the visible range on cultured human cells 03 p0377 A83-14890

An evaluation of the carcinogenic effect of radiation at the cellular level 06 p0796 A83-19380

The effect of activators of cAMP accumulation on the separate stages of genome expression in cells during acute radiation injuries of organisms. VI - Peculiarities of the inhibition of RNA synthesis on a template of isolated chromatin by separate fractions of histones from the liver of normal, irradiated and serotonin-treated rats 14 p2061 A83-32051

The changes in the chromosome pattern of mouse lymphosarcoma cells during prolonged irradiation 14 p2061 A83-32054

Some results of the effect of space flight factors on Drosophila melanogaster 19 p2872 A83-40843

The reaction of the human lymphocyte chromosome to graded doses of neutrons during irradiation in vitro 19 p2874 A83-41006

An investigation of the potential radiation damages of chromosomes in the cells of mammals with the aid of chemical modification and premature chromosome condensation 19 p2874 A83-41010

DNA fusion product of phage P2 with plasmid pBR322 - A new phasnid 21 p3183 A83-44860

The effect of a constant magnetic field and gamma-radiation on the hereditary structure of somatic cells - The effect of the combination of a constant magnetic field and ionizing radiation on the blood lymphocytes of humans in vitro 23 p3498 A83-48210

CHROMOSPHERE

Fluid motions the solar chromosphere-corona transition region. II Active region flows in C IV from narrow slit Dopplergrams 02 p0268 A83-11603

Chromospheric evaporation in soft X-ray flares 03 p0436 A83-13157

The 810 MHz solar radio emission in the years 1968-1970 03 p0437 A83-14719

Chromospheres of F, G, K type stars. VIII - Energy balance in transition region 03 p0437 A83-14720

Chromospheric Mg II emission in A5 to K5 main sequence stars from high resolution IUE spectra 04 p0550 A83-15035

Measurements of solar transition zone velocities and line broadening using the ultraviolet spectrometer and polarimeter on the Solar Maximum Mission 04 p0573 A83-15044

Flow of material at the chromosphere-corona transition zone of the sun 04 p0574 A83-15119

Internal gravity waves in the solar atmosphere. II - Effects of radiative damping 04 p0575 A83-15639

Chromospheric evaporation in a well-observed compact flare 04 p0575 A83-15640

The Rayleigh-Taylor instability in filaments and 'spotless' two ribbon flares 05 p0707 A83-16851

Evolution of chromospheres and coronae in solar mass stars - A far-ultraviolet and soft X-ray comparison of Arcturus /K2 III/ and Alpha Centauri A /G2 V/ 05 p0699 A83-17005

Magnetic field-related heating instabilities in the surface layers of the sun and stars 05 p0699 A83-17018

Responses of transition region models to magnetic field geometry and downflow velocities --- in solar atmosphere 05 p0708 A83-17021

Radio emission from the extended chromosphere of Alpha Orionis 05 p0700 A83-17033

On the relationship between the chromospheric flares and type I noise storm 05 p0709 A83-17827

Spectral manifestations of the spatial structure and dynamic processes of chromospheric flares on the sun 05 p0709 A83-17828

Model of the chromosphere over a dark umbral feature 06 p0851 A83-18112

An empirical view of the chromospheric temperature structure above a sunspot umbra 06 p0851 A83-18113

The sunspot chromosphere-corona transition region 06 p0851 A83-18114

The chromospheric evershed flow observed in the EUV spectrum 06 p0852 A83-18122

On the dynamics of the chromosphere above sunspots 06 p0855 A83-19129

High resolution EUV structure of the chromosphere-corona transition region above a sunspot 06 p0855 A83-19130

Hydrodynamic response of the solar chromosphere to an elementary flare burst. II - Thermal model 06 p0855 A83-19131

An attempt to determine stellar Lyman-alpha emission-line fluxes for F stars with different metal abundances 07 p1022 A83-21131

Flare loop radiative hydrodynamics. I - Basic methods 07 p1037 A83-21145

Flare loop radiative hydrodynamics. III - Nonlocal radiative transfer effects 07 p1038 A83-21146

Fluid motions in the solar chromosphere-corona transition region. I - Line widths and Doppler shifts for C IV 07 p1038 A83-21147

The ultraviolet spectra of three N-type carbon stars 08 p1183 A83-23060

Impact linear polarization observed in a UV chromospheric line during a solar flare 08 p1191 A83-23071

Chromospheric activity of late-type giants and supergiants Reappearance of dynamo activity in the interior due to the spin-up of the core in evolution 08 p1185 A83-23105

Physical processes determining the structure of stellar chromospheres. I 09 p1358 A83-24014

Self-consistent models of flare heated solar chromospheres 09 p1368 A83-24470

Brightness oscillations of the sun's chromosphere in K and H-alpha 10 p1521 A83-25494

Einstein observations of three classical Cepheids 10 p1494 A83-25714

Observation of stellar winds and chromospheres in visible and infra-red 10 p1505 A83-25853

Formation of the Cl I line at 1351 A in the solar chromosphere 10 p1522 A83-26396

Rapid rotation and stellar activity in the triple system HD 165590 10 p1514 A83-26725

Flare loop radiative hydrodynamics. IV - Dynamic evolution of unstable semiempirical loop models 10 p1522 A83-26743

The dependence of H-alpha on chromospheric activity in G and K main-sequence stars 10 p1516 A83-26759

Chromospheric jets - Possible extreme-ultraviolet observations of spicules 10 p1522 A83-26760

Seismology of sunspot atmospheres 11 p1690 A83-27655

Conductive flux in flaring solar chromospheres deduced from the linear polarization observations 11 p1691 A83-27685

Physical processes determining the structure of stellar chromospheres. II 12 p1794 A83-29298

Stellar rotation as a controller of coronae and chromospheres of giant stars 12 p1797 A83-29952

The sun as a star 13 p1949 A83-31316

Stellar chromospheres as a random phenomenon 13 p1949 A83-31327

Investigation of the radial velocities of chromospheric spicules 13 p1965 A83-31393

An H-alpha survey of southern hemisphere active chromosphere stars 13 p1951 A83-31419

Dynamical behaviour of surges --- solar prominences 13 p1953 A83-31553

Active chromosphere in the carbon star TW Horologium 13 p1954 A83-31578

A study of shapes of Ca II chromospheric emissions in late type stars 13 p1955 A83-31655

Connection between chromospheric activity of F, G, K type stars and their magnetic field 13 p1955 A83-31658

Low noise spectrometer for the daily measurement of solar chromospheric flux 14 p2017 A83-32007

Resonance scattering of radiation in solar prominences. I Partial redistribution in optically thin subordinate lines 14 p2114 A83-32390

Numerical simulation of nonstationary hydrodynamic phenomena in solar flares 14 p2115 A83-32537

Numerical simulation of the heating of the solar chromosphere by intense heat fluxes 14 p2115 A83-32538

Microwave diagnostics of solar magnetic fields 14 p2115 A83-32540

Wave resonances in the solar atmosphere 14 p2115 A83-32542

The circumstellar envelopes of F- and G-type supergiants in the Large Magellanic Cloud 14 p2107 A83-33244

Observational aspects of chromospheres and coronae in hot stars 15 p2252 A83-33609

Chromospheric emission of W Ursae Majoris-type stars and its relation to the structure of their common envelopes 15 p2258 A83-34106

Chromospheric heating by electron and proton bombardment in the solar flare of June 7, 1980 15 p2280 A83-34297

The photometric variability of solar-type stars. II - Stars selected from Wilson's chromospheric activity survey [AD-A129861] 15 p2262 A83-34506

Stellar chromospheric temperatures 15 p2262 A83-34539

Direct evidence for chromospheric evaporation in a well-observed compact flare 15 p2284 A83-35217

Post-flare coronal arches 16 p2440 A83-36621

Ca II chromospheric emission and rotation of main sequence stars 16 p2429 A83-36633

Solar limb brightening measurements at 3.4 mm wavelength 16 p2440 A83-36686

The structure of the undisturbed chromosphere observed above the solar limb (Review) 16 p2440 A83-36854

Fluid motions in the solar chromosphere-corona transition region. III - Active region flows from wide slit Dopplergrams 17 p2624 A83-37334

Some spectral plasma diagnostics for prominences and structures in the middle chromosphere 17 p2624 A83-37336

Variability of the Lyman alpha flux with solar activity 17 p2625 A83-37601

The distribution of chromospheric flares in relation to the sectoral boundaries of the interplanetary magnetic field extrapolated onto the sun 17 p2625 A83-37668

The structure of the magnetic field and its evolution around sunspots 17 p2626 A83-37678

Certain features of the rotation of sunspots 17 p2626 A83-37713

Closed coronal structures. V - Gasdynamic models of flaring loops and comparison with SMM observations 17 p2627 A83-37928

The narrow ultraviolet emission lines of the red dwarf Au Microscopii (dM1.6e) 17 p2605 A83-37939

- Evidence of high chromospheric activity in Hyades dwarfs from spectroscopic observations 17 p2609 A83-38416
- Solar activity with respect to Ca-phages 17 p2628 A83-38539
- Are plasma satellites present among chromospheric lines? 18 p2780 A83-39019
- Origin of the weakening of EUV emission lines formed in the chromosphere-corona transition zone 18 p2781 A83-39020
- On photospheric and chromospheric penumbral waves 18 p2781 A83-39023
- High-resolution photography of the solar chromosphere. XVI H-alpha contrast profiles of active region loops 18 p2781 A83-39026
- The chromosphere above sunspot umbrae. IV - Frequency analysis of umbral oscillations 19 p2923 A83-40717
- Chromospheric and coronal emissions from the giants in the Hyades 20 p3072 A83-43060
- Outer atmospheres of cool stars. XIII - Capella at critical phases 21 p3237 A83-45553
- High spatial and temporal resolution observations of the solar Ca II H line 21 p3244 A83-45569
- Outer atmospheres of cool stars. XIV - A model for the chromosphere and transition region of Beta Ceti (G9.5 III) 22 p3382 A83-46995
- A static model of chromospheric heating in solar flares 22 p3389 A83-47002
- The distribution of chromospheric emission strengths among red dwarfs 23 p3520 A83-47482
- Quiescent coronae of active chromosphere stars 23 p3521 A83-47484
- Stellar activity and calcium emission variability 23 p3521 A83-47492
- RS CVn stars - Chromospheric phenomena 23 p3522 A83-47512
- Coronal and chromospheric structure in AR Lac. II - Physical characteristics of the atmosphere 23 p3523 A83-47524
- Flares on red dwarf stars as a result of the dynamical response of the chromosphere to the heating 23 p3525 A83-47546
- Observation of chromospheric evaporation during the Solar Maximum Mission 23 p3531 A83-47665
- Conductive flux in the chromosphere derived from line linear polarization observation 23 p3532 A83-47670
- Behavior of transition-region lines during impulsive solar flares 23 p3532 A83-47674
- Heating of chromospheric magnetic features by direct current dissipation 23 p3536 A83-47711
- Transfer of H I Lyman-alpha radiation in optically thick media 24 p3674 A83-49632
- CHRONIC CONDITIONS**
- The effect of chronic alcoholic intoxication on the temporal parameters of the process of "motor command" organization and on the interhemispheric functional relations in humans 01 p0085 A83-10533
- Test with graded physical load on bicycle-ergometer and treadmill in patients with chronic ischemic heart disease 03 p0381 A83-14346
- The adaptation of the heart to chronic high-altitude hypoxia 04 p0522 A83-15780
- The cytokinetics and morphology of hemopoiesis during chronic irradiation --- Russian book 05 p0669 A83-17122
- The dependence of the development of complications in patients with an infarction of the myocardium and chronic ischemic heart disease on the state of the electromagnetic field of the earth 08 p1146 A83-22777
- The reaction of chronically irradiated dogs to radiation as evaluated by changes in the activity of cholinesterase 09 p1321 A83-24932
- Effects of chronic acceleration on body composition 11 p1635 A83-27780
- Enhancement of chronic acceleration tolerance by selection 11 p1637 A83-27804
- The condition of hemodynamics in pulmonary blood circulation in patients with hypertension combined with chronic heart disease 19 p2881 A83-41432
- The content of immunoglobulins in the blood serum of patients with various forms of chronic inflammation of the middle ear 19 p2883 A83-41826
- The effect of microwave radiation on several parameters of cellular immunity in conditions of chronic exposure 23 p3495 A83-48207
- CHRONOGRAPHS**
- U CHRONOMETERS
- CHRONOLOGY**
- NT GEOCHRONOLOGY
- A statistical method for determining ages of globular clusters by fitting isochrones 04 p0547 A83-15619
- The ancient solar activity maxima epochs of various periods 05 p0707 A83-16859
- Nuclear cosmochronology or the age of the elements 06 p0842 A83-19457
- Age and metal abundance of a globular cluster, as derived from Stromgren photometry 09 p1364 A83-25289
- The age of the young large magellanic cloud cluster NGC 1866 10 p1501 A83-25580
- Cl-36 and Mn-53 in Antarctic meteorites and (Be-10)-(Cl-36) dating of Antarctic ice 12 p1797 A83-29175
- New actinide chronometer production ratios and the age of the Galaxy 17 p2610 A83-38429
- Cosmological estimate of the age of stars exploding as Type I supernovae 20 p3075 A83-43537
- The primordial helium abundance and the age of the universe 24 p3665 A83-50034
- CHRONOMETERS**
- Picosecond spectrochronography 14 p2022 A83-33418
- Ultrafast picosecond chronography 22 p3293 A83-46679
- CHRONOPHOTOGRAPHY**
- An exact-time registration system for observations of very-high-energy gamma-quanta 17 p2510 A83-37719
- CHRONOTRONS**
- U PULSE RATE
- U TIME LAG
- CHUCKCHI SEA**
- Atmosphere - Sea ice interactions in the Beaufort/Chukchi Sea and in the European sector of the Arctic 15 p2208 A83-33497
- CHUGGING**
- U COMBUSTION STABILITY
- CINDER CONES**
- U CONES (VOLCANOES)
- CINEFLUOROGRAPHY**
- U MOTION PICTURES
- U RADIOGRAPHY
- CINEMATOGRAPHY**
- Recent development in high speed cinematographic and interferometric studies of high power laser target interaction 01 p0052 A83-11067
- Computer animated representations to optically observe numerical evaluations 01 p0092 A83-11199
- International Symposium of Biomechanics Cinematography and High Speed Photography, 2nd, San Diego, CA, August 24-26, 1981, Proceedings 08 p1102 A83-22790
- Cinematography data systems at the Naval Biodynamics Laboratory 08 p1102 A83-22791
- The use of 16 mm movie cameras for evaluation of the Space Shuttle remote manipulator system 17 p2482 A83-38358
- Vacuum chamber trajectory measurement by high speed cinematography 22 p3287 A83-45975
- CINERADIOGRAPHY**
- U MOTION PICTURES
- U RADIOGRAPHY
- CIRCADIAN RHYTHMS**
- The ensemble of circadian rhythms and the effectiveness of training activities conducted at various times of the day 01 p0083 A83-10518
- Circadian rhythms and fatigue - A discrimination of their effects on performance 02 p0223 A83-12411
- Structure of the sleep-wakefulness cycle during experimental insufficiency of cerebral circulation 03 p0373 A83-13599
- The role of endogenous circadian rhythmicity in Air-Force flight accidents due to pilot error 04 p0521 A83-15402
- The optimal shift schedule of work in industry 04 p0522 A83-15785
- The opioid peptide dynorphin, circadian rhythms, and starvation 05 p0669 A83-16940
- Diurnal biological rhythms and paranoid schizophrenia 05 p0676 A83-17163
- Possible mechanisms for the organization of the structure of the sleep-wakefulness cycle according to the data of factor analysis 06 p0794 A83-18971
- An investigation of the discrimination capability of the vision of a human operator during vestibular influences 07 p0976 A83-20335
- The effect of changes of the regime of work and rest on the psychophysiological efficiency of an operator 07 p0976 A83-20350
- Free-running activity rhythms in the rat - Entrainment by melatonin 08 p1146 A83-22689
- Circadian variations in tolerance to +Gz acceleration 11 p1642 A83-27783
- Daily rhythms of activity and temperature of Macaca nemestrina 11 p1641 A83-27843
- The circadian rhythm of the body temperature, arterial pressure, and heart rate 12 p1765 A83-29311
- Diurnal respiratory rhythms in young healthy people in Siberia and the Far North 12 p1765 A83-29312
- The role of suprachiasmatic nuclei of the anterior hypothalamus in the organization of the circadian rhythms of locomotor activity in rats 14 p2063 A83-32564
- The circadian rhythm of liver phospholipids in normal golden hamsters and in those with opisthorchiasis 15 p2211 A83-34963
- A model for prediction of resynchronization after time-zone flights 15 p2214 A83-34983
- Circadian rhythm amplitude - Is it related to rhythm adjustment and/or worker motivation? 16 p2396 A83-35562
- Physiological shifts in the sleep-wakefulness cycle under the influence of a physical load 16 p2397 A83-35901
- Adrenocortical activity in athletes after repeated physical loads during the course of the day 16 p2398 A83-35909
- The induction of circadian rhythm by light impulses - The dependence on illumination and duration of the impulse 16 p2395 A83-36808
- Task variables determine which biological clock controls circadian rhythms in human performance 20 p3035 A83-43546
- An analysis of the circadian rhythm of physiological functions in sailors performing watch duties 23 p3497 A83-47107
- Circadian clock in Xenopus eye controlling retinal serotonin N-acetyltransferase 23 p3495 A83-48086
- Multi-oscillatory control of circadian rhythms in human performance 24 p3619 A83-50109
- CIRCLES (GEOMETRY)**
- NT GREAT CIRCLES
- CIRCUIT BOARDS**
- Effective electromagnetic shielding in multilayer printed circuit boards 04 p0473 A83-16122
- Systolic array processor implementation 08 p1153 A83-22798
- The thermal management of printed circuit board assemblies 12 p1720 A83-29515
- Computer-aided interactive structural optimization of printed-circuit-board design 13 p1834 A83-30862
- Random vibration effects on piece part applications 13 p1835 A83-30863
- Component lead wire strain relief for random vibration environments 13 p1835 A83-30867
- Random vibration testing and analysis of a large ceramic substrate assembly 13 p1835 A83-30868
- Microelectronic packaging 16 p2346 A83-36021
- CIRCUIT BREAKERS**
- Experimental and theoretical study of a dc arc in an orifice nozzle flow 05 p0636 A83-16692
- [AIAA PAPER 83-0399] Theoretical and experimental study of a dual-flow circuit breaker nozzle flow 17 p2503 A83-37223
- [AIAA PAPER 83-1748] Analysis of cold flow reestablishment time in a circuit breaker nozzle 17 p2503 A83-37224
- [AIAA PAPER 83-1749]
- CIRCUIT DIAGRAMS**
- Preamplifiers and clock drivers for the University of California at Los Angeles Reticon spectrometer 14 p2017 A83-32020
- CIRCUIT PROTECTION**
- A class of codes with unequal protection of symbols, based on balanced incomplete solvable block-schemes 01 p0094 A83-10567
- A compact and comprehensive micro-electronic control system for an unorthodox inverter-converter 01 p0040 A83-11008
- A high voltage, high power pulsed TWT power supply for space application 01 p0021 A83-11022
- AEHP for advanced technology aircraft --- Atmospheric Electricity Hazard Protection 01 p0001 A83-11086
- Methods for minimizing the effects of lightning transients on aircraft electrical systems 01 p0009 A83-11088
- Integration of solid-state microwave control and protection devices /Review/ 01 p0043 A83-11303
- High-power solid-state microwave protection devices 01 p0043 A83-11306
- The limits to hardening electronic boxes to IEMP coupling 05 p0628 A83-17523
- Hardness assurance experience on the DSCS III spacecraft program 05 p0608 A83-17531
- An RF-primed all-halogen gas plasma microwave high-power receiver protector 07 p0922 A83-21530
- A technique for calculating shunt leakage and cell currents in bipolar stacks having divided or undivided cells 14 p2047 A83-32637
- Proton implantation isolation for microwave monolithic circuits 21 p3123 A83-43845
- CIRCUIT RELIABILITY**
- Effects of dV/dt in MOSFET and bipolar junction transistor switches 01 p0041 A83-11020
- Aircraft power management control system designed for fast response and high reliability 01 p0012 A83-11151

Test chips for custom ICs - Six kinds of test structures
02 p0167 A83-11824

A radiation hardened 256 x 4 bulk CMOS RAM
03 p0313 A83-13996

Thermal annealing of radiation damage in CMOS ICs
in the temperature range -140 C to +375 C
05 p0627 A83-17515

Total dose response of STL and I2L logic devices ---
Schottky Transistor Logic 05 p0627 A83-17517

Calculation of cosmic-ray induced soft upsets and
scaling in VLSI devices 05 p0629 A83-17541

A feedback time constant concept
06 p0803 A83-19038

Soft error in MOS dynamic RAM
07 p0918 A83-20072

The effect of materials and processes on package
reliability 07 p0920 A83-20473

Design for testability - A survey --- of integrated circuit
technology 07 p0923 A83-21541

Failure modes induced in TTL-LS bipolar logics by
negative inputs 09 p1253 A83-23696

Radiation effects in microelectronics for space
instruments 09 p1254 A83-24106

Latchup-free Schottky-barrier CMOS
09 p1255 A83-24494

Yield considerations for ion-implanted GaAs MMIC's
09 p1256 A83-24680

Mode-fault diagnosis and a design of testability
09 p1333 A83-24796

Design methods of single-output built-in self-checking
circuits for equilibrium codes 10 p1460 A83-25467

Radiation induced soft fails in space electronics
13 p1812 A83-30185

A new design method for m-out-of-n TSC checkers ---
Totally Self-Checking for codes 13 p1908 A83-30791

The effects of nuclear radiation on integrated circuits
14 p2005 A83-32416

Node-fault diagnosis and a design of testability
15 p2151 A83-33926

Fail safe logic design 16 p2345 A83-35555

Radiation effects on MOS devices - dosimetry,
annealing, irradiation sequence, and sources
16 p2346 A83-36023

Microelectronic system reliability prediction
17 p2517 A83-37288

On some reliability implications of electronic circuit
design 17 p2496 A83-37296

Yield enhancement of bit level systolic array chips using
fault tolerant techniques 18 p2679 A83-40389

Cosmic ray induced soft error rate in VLSI circuits
21 p3123 A83-43844

Main mechanisms for the failures of monolithic
integrated circuits 21 p3125 A83-44591

Robust matched filters 22 p3278 A83-46097

CIRCUITS

NT ADDING CIRCUITS

NT ANALOG CIRCUITS

NT AUTODYNES

NT BISTABLE CIRCUITS

NT CANCELLATION CIRCUITS

NT CIRCULATORS (PHASE SHIFT CIRCUITS)

NT COMPARATOR CIRCUITS

NT COUNTING CIRCUITS

NT COUPLING CIRCUITS

NT DELAY CIRCUITS

NT DIGITAL INTEGRATORS

NT DIPLEXERS

NT DISCRIMINATORS

NT ECHO SUPPRESSORS

NT ELECTRIC BRIDGES

NT EQUIVALENT CIRCUITS

NT FEEDBACK CIRCUITS

NT FLIP-FLOPS

NT FLUID SWITCHING ELEMENTS

NT FLUIDIC CIRCUITS

NT FRAUNHOFER LINE DISCRIMINATORS

NT FREQUENCY DISCRIMINATORS

NT GATES (CIRCUITS)

NT HYBRID CIRCUITS

NT INTEGRATED CIRCUITS

NT LARGE SCALE INTEGRATION

NT LC CIRCUITS

NT LIMITER CIRCUITS

NT LINEAR CIRCUITS

NT LINEAR INTEGRATED CIRCUITS

NT LOGIC CIRCUITS

NT MAGNETIC CIRCUITS

NT MATRICES (CIRCUITS)

NT MICROWAVE CIRCUITS

NT MIXING CIRCUITS

NT MULTIVIBRATORS

NT NEGATIVE RESISTANCE CIRCUITS

NT PHASE DETECTORS

NT PHASE SHIFT CIRCUITS

NT PNEUMATIC CIRCUITS

NT POWER SUPPLY CIRCUITS

NT PRINTED CIRCUITS

NT RC CIRCUITS

NT RLC CIRCUITS

NT SQUELCH CIRCUITS

NT SWITCHING CIRCUITS

NT THRESHOLD GATES

NT TRANSISTOR CIRCUITS

NT TRANSMISSION CIRCUITS

NT TRIGGER CIRCUITS

NT TTL INTEGRATED CIRCUITS

NT VARACTOR DIODE CIRCUITS

NT VERY LARGE SCALE INTEGRATION

NT VHSIC (CIRCUITS)

NT WHEATSTONE BRIDGES

Peltier effect exchanges in contact thermocouples -
Application to the characterization of new thermoelectric
circuits --- French thesis 11 p1612 A83-28636

Macroencapsulation of electronic circuits
12 p1719 A83-29215

Josephson-junction circuit analysis via integral
manifolds 15 p2151 A83-33928

CIRCUIT CONES

Asymmetric vortex formation from cones at incidence
- A simple inviscid model 04 p0442 A83-15148

Aerodynamic drag of a cone in two-phase flow
19 p2792 A83-41899

CIRCUULAR CYLINDERS

Electromagnetic scattering by open circular
waveguides 02 p0165 A83-12630

Deflections of inflated cylindrical cantilever beams
subjected to bending and torsion 02 p0196 A83-12853

Flows in diffusers interfered with wake behind a circular
cylinder 02 p0174 A83-13068

Flow characteristics around a circular cylinder with a
slit. II Effect of boundary layer suction 02 p0175 A83-13069

Flow behavior and heat transfer around a circular
cylinder at high blockage ratios 03 p0315 A83-13344

Potential flow analysis of an arbitrary cascade using a
conformal transformation into a row of circular cylinders
03 p0278 A83-13564

Thermal and optical analysis of an evacuated circular
cylindrical concentrating collector 03 p0354 A83-13697

Electromagnetic transmission through apertures in a
cavity in a thick conductor 03 p0306 A83-14016

Regge poles, natural frequencies, and surface wave
resonance of a circular cylinder with a constant surface
impedance 03 p0307 A83-14034

Scattering of a plane electromagnetic wave by a
conducting circular cylinder of finite length 03 p0307 A83-14134

Torsional stresses and stress intensity factors of circular
cylinder with internal longitudinal crack 03 p0342 A83-14489

The effects of surface roughness on the flow past circular
cylinders at high Reynolds numbers 03 p0321 A83-14584

Nonlinear interaction of longitudinal-transverse acoustic
waves in a circular cylinder 04 p0532 A83-15076

Comparison of elasticity, shell core, and sandwich shell
theories 04 p0496 A83-15291

Axisymmetric vortex breakdown in rotating fluid within
a container 04 p0476 A83-15696

Investigation of wall induced modifications to vortex
shedding from a circular cylinder 04 p0478 A83-16143

The unsteady collision of free-convective boundary
layers 04 p0480 A83-16363

Subsonic potential flow past a circle and the transonic
controversy 04 p0443 A83-16366

Interaction of a pair of curved wall jets after a circular
cylinder [AIAA PAPER 83-0290] 05 p0584 A83-16632

State of the waveguide art 05 p0624 A83-17340

Natural convection from a horizontal cylinder at small
Grashof numbers 05 p0641 A83-17744

Boundary-layer development on circular cylinders
06 p0756 A83-18235

Diffraction from cylindrically truncated planar surfaces
with application to an aperture matched horn design 06 p0742 A83-18666

Characteristics of a wave field in a semiinfinite elastic
cylinder /edge resonance/ 07 p0990 A83-19943

Analytical study of the scattering properties of a structure
consisting of two open cylindrical screens 07 p0915 A83-20870

Concerning the radiation pattern in the problem of the
excitation of an array of circular dielectric cylinders by a
local source 07 p0915 A83-20871

Radiation from a dislocation oscillating in a circular
cylinder 07 p0948 A83-21169

Fluid flow and heat transfer in the separated region of
a circular cylinder with wake control 08 p1084 A83-22238

Magneto-thermo-elastic plane waves in an infinite
circular cylinder 08 p1123 A83-22746

Vortex shedding from a rectangular prism and a circular
cylinder placed vertically in a turbulent boundary layer
08 p1086 A83-23091

Scattering by a rotating circular cylinder with finite
conductivity 09 p1247 A83-23801

Axisymmetric flows in spin-up from rest of a stratified
fluid in a cylinder 10 p1412 A83-25414

Conditional analysis of intermittency in the near wake
of a circular cylinder 10 p1414 A83-25783

Cylindrical eigencurrents --- during electromagnetic
scattering by conducting surfaces 10 p1406 A83-26840

Motion of a circular cylinder in a rectangular channel
11 p1567 A83-27720

Theoretical stress analysis for a non-isotropic body of
cylindrical configuration containing a row of cracks
11 p1596 A83-28447

Certain features of transverse flow past a cylinder with
longitudinal fins 11 p1569 A83-28551

The effects of yaw and finite length upon the vortex
wakes of stationary and vibrating circular cylinders
12 p1722 A83-29228

The vibrating cylinder gyro 12 p1730 A83-29516

Computation of steady laminar flow over a circular
cylinder with third-order boundary conditions 12 p1725 A83-29664

Stability of imperfect laminated cylinders - A comparison
between theory and experiment 12 p1738 A83-29758

[AIAA 83-0874] 12 p1738 A83-29758

Buffeting of a slender circular beam in axial turbulent
flows [AIAA 83-0928] 12 p1744 A83-29854

Transient thermal stress problem for a circumferentially
cracked hollow cylinder 12 p1747 A83-29921

Transient thermal stress problem in a transversely
isotropic finite circular cylinder under three-dimensional
temperature field 12 p1747 A83-29924

Hybrid modes in circular cylindrical optical fibers
13 p1922 A83-31146

The structure of a turbulent wake behind a cruciform
circular cylinder. I - The mean velocity field 14 p2013 A83-33091

Sound diffraction at wall impedance discontinuities in
a circular cylinder - Investigated using Wiener-Hopf
technique [AIAA PAPER 83-0730] 15 p2226 A83-33485

The structure of a turbulent wake behind a cruciform
circular cylinder. II - The streamwise development of
turbulent flow field 15 p2158 A83-34007

Unsteady heat transfer from circular cylinder immersed
in impulsively started flow 15 p2159 A83-34249

Laminar, natural convection heat transfer in a horizontal
gap, bounded by an elliptic and A circular cylinder
15 p2160 A83-34260

Finite extension and torsion of thin elastic strips
15 p2177 A83-34343

Diffraction of an H-polarized electromagnetic wave by
a circular cylinder with an infinite axial slot 15 p2148 A83-35176

Creeping waves and resonances in transient scattering
by smooth convex objects 15 p2148 A83-35177

Mode propagation in nonuniform circular ducts with
potential flow 16 p2351 A83-36082

Planck mean radiation-pressure cross sections for
nonspherical grains. I 17 p2603 A83-37891

An axisymmetric-elastodynamic analysis of a crack in
orthotropic media using a path-independent integral
17 p2523 A83-38393

Compression of an elastic cylinder between two rigid
planes Application of the indirect fictitious-boundary
integral method to a contact problem 18 p2697 A83-39455

The aerodynamic characteristics at the mid-span of a
circular cylinder with tangential blowing 18 p2684 A83-39457

Aerodynamics of pointed forebodies at high angles of
attack [AIAA PAPER 83-2117] 19 p2793 A83-41942

Flat spin of bodies with circular cross-section
[AIAA PAPER 83-2147] 19 p2807 A83-41968

Effects of free stream turbulence intensity and integral
length scale on heat transfer from a circular cylinder in
crossflow 20 p2976 A83-42711

Spanwise mass transfer variations on a cylinder in
'nominally' uniform crossflow 20 p2984 A83-43019

Effect of Rayleigh accelerations applied to an initially
moving fluid --- in circular cylinders under low gravity
associated with space flight 20 p2940 A83-43274

Heat transfer in unsteady flow past a heated impulsively
started circular cylinder 21 p3128 A83-44022

- Fracture toughness measurement of cast magnesium alloy by cylindrical specimen with ring-shaped crack 21 p3111 A83-44107
- Numerical calculation of torsional problem for circular shaft with variable diameters using non-orthogonal curvilinear coordinates 21 p3147 A83-44108
- Plastic buckling of axially compressed circular cylindrical shells 21 p3152 A83-44249
- Natural and forced vortex shedding 22 p3282 A83-46440
- Vortex shedding from a circular cylinder in oscillatory flow 22 p3282 A83-46441
- Some characteristics of the unsteady wake flow past a circular cylinder 22 p3282 A83-46442
- Research in infrared hollow waveguides 22 p3358 A83-46633
- Anomalous wave scattering by a finite number of longitudinally slit cylinders of small wave dimensions 22 p3275 A83-46789
- Three-dimensional structure of the turbulent wake behind an intersecting cruciform circular cylinder 22 p3251 A83-47027
- Creep of thin-walled circular cylinder under axial force, bending, and twisting moments [ASME PAPER 83-GT-154] 23 p3469 A83-47980
- On the force fluctuations acting on a circular cylinder in crossflow from subcritical up to transcritical Reynolds numbers 23 p3398 A83-48118
- Mathematical modeling of unsteady separated flow past a circular cylinder 23 p3452 A83-48667
- Large strain inelastic behaviour of cylindrical tubes 23 p3474 A83-48698
- The periodic normal force on a circular cylinder in cross flow - An unsteady Magnus effect 24 p3544 A83-49022
- Simple formula for the RCS of a finite hollow circular cylinder 24 p3571 A83-49994

CIRCULAR ORBITS**NT STATIONARY ORBITS**

- Improved solution of optimal impulsive fixed-time rendezvous 02 p0139 A83-13081
- Quasi-periodic solutions of the plane three-body problem near Euler's orbits 03 p0404 A83-13416
- A method for constructing explicit solutions to a simplified version of the spatial circular restricted three-body problem 03 p0408 A83-13898
- Linearized transfer between inclined circular orbits using low-thrust blow down propulsion system [AIAA PAPER 83-0194] 05 p0602 A83-16579
- The construction of periodic orbits of satellites in a system of rotating axes. I 06 p0817 A83-17988
- Algorithm for the estimation of the parameters of the relative motion of two satellites given a full complement of measurements 06 p0721 A83-18354
- Equilibrium positions of a satellite gyrostat in a circular orbit 06 p0723 A83-18355
- Preferred orbit planes in the gravitational field of a tumbling spheroidal galaxy 06 p0843 A83-19480
- Cost-efficient transport of loads in geostationary orbit and in near-earth circular orbits [DGLR PAPER 82-077] 09 p1211 A83-24191
- Systems of artificial earth satellites in stable circular diurnal orbits 09 p1212 A83-25027
- Optimal control of the elements of a plane almost-circular orbit 09 p1212 A83-25028
- On the continuous survey of the earth's surface --- with optimized satellite networks 10 p1381 A83-26817
- Ice particles in circular orbits around the sun 14 p2101 A83-33288
- Local regularization of the magnetic-binary problem --- charged particle motion and two body problem with magnetic dipoles 20 p3061 A83-43570
- High and low thrust acceleration 24 p3551 A83-49625
- Near-circular satellite orbits in an oblate, diurnally varying atmosphere 24 p3551 A83-49878

CIRCULAR PLATES

- Natural frequencies of circular plates with partially free, partially clamped edges 01 p0060 A83-11039
- Small transverse vibrations of circular laminate plates 02 p0191 A83-12334
- An averaged Lagrangian-finite element technique for the solution of nonlinear vibration problems 02 p0194 A83-12747
- On the design of containment shields 02 p0195 A83-12766
- Axisymmetric flexure of circular sandwich plate including transverse shear facings 03 p0342 A83-14508
- A mode solution for the finite deflections of a circular plate loaded impulsively 04 p0500 A83-16199
- Transient nonlinear response of impulsively-loaded circular plates 04 p0501 A83-16200
- Axisymmetric vibrations of an isotropic elastic non-homogeneous circular plate of linearly varying thickness 04 p0501 A83-16342

- An elastic-plastic constitutive equation for transversely isotropic materials and its application to the bending of perforated circular plates 05 p0656 A83-17947
- Vibrations of initially imperfect circular plates including the shear and rotatory inertial effects 06 p0773 A83-18394

- A high efficiency splashplate feed --- for satellite terminals 06 p0741 A83-18663
- Large deflections of circular plates of variable thickness 09 p1278 A83-23671
- Note on non-linear dynamic response of a clamped orthotropic circular plate to pulse excitations 09 p1278 A83-23707

- Delamination buckling and growth in laminates [ASME PAPER 83-APM-3] 10 p1441 A83-26445
- The optimum design of a round plastic plate 11 p1596 A83-28459

- Dynamics of delamination buckling [AIAA 83-0873] 12 p1798 A83-29757
- Analysis of progressive damage in thin circular laminates due to static-equivalent impact loads [AIAA 83-0997] 12 p1711 A83-29872
- Nonlinear analysis of composite circular plates [AIAA 83-1036] 12 p1745 A83-29881
- Boundary integral equation solution of the Berger equation 13 p1866 A83-30447
- Finite element analysis of the buckling of variable thickness discs 13 p1867 A83-30845
- Vibrations of Mindlin's circular plates with variable thickness 14 p2033 A83-33094
- Utilization of the method of continuation with respect to the length of the integration segment for calculating circular corrugated plates 15 p2178 A83-34444
- A reinvestigation of post-buckling behaviour of elastic circular plates using a simple finite element formulation 15 p2179 A83-34566

- Geometrically nonlinear formulation for the axis-symmetric transition finite elements 15 p2179 A83-34567
- Postbuckling analysis of moderately thick elastic circular plates 17 p2520 A83-37393
- Investigations of axisymmetric deformation of geometrically nonlinear, rotationally orthotropic, circular plates 18 p2700 A83-39567
- Further applications of the singularity function method to plate problems 18 p2701 A83-40048
- On a method for the investigation of nonlinear periodic vibrations of circular plates 18 p2702 A83-40121
- Stress concentrations in cylindrically orthotropic plates with radial variation of the compliances 18 p2703 A83-40165

- A method for solving problems concerning the bending of a round plate with a crack 19 p2856 A83-40806
- Analysis of symmetrically loaded thin circular plates 20 p3008 A83-43672
- The elastic solution of the dynamic elastic-plastic response of a circular plate 21 p3151 A83-44104
- Multiple mode nonlinear analysis of circular plates 21 p3153 A83-44549
- The bending vibrations of an anisotropic free circular plate of regular symmetry 21 p3159 A83-44933
- The problem of the bending of a circular plate with a supporting rib of varying cross-section 21 p3162 A83-45301

- Flexural vibrations of clamped polygonal and circular plates having rectangular orthotropy 23 p3469 A83-47600
- Optimisation of cylindrically orthotropic annular plates with simply supported edges subjected to a constraint on fundamental frequency 24 p3591 A83-48899
- The vibration of an elastic-plastic plate under the effect of normal impact loads 24 p3592 A83-49030
- Buckling of a heated thin non-homogeneous annular circular plate of variable thickness 24 p3597 A83-50132
- Non-simple quasi-static thermoelastic deflection of a thin clamped circular plate 24 p3597 A83-50136

CIRCULAR POLARIZATION

- The effect of reflections on a circularly polarized radio signal radiated from the sea surface 01 p0031 A83-10811
- A circularly polarized compact flat source 01 p0032 A83-10924
- Characteristics of modified spiral and helical antennas 02 p0164 A83-12003
- Theory of envelope solitons of electromagnetic waves 03 p0396 A83-13188
- A design method of circularly polarized rectangular microstrip antenna by one-point feed 03 p0314 A83-14128
- Radar properties of Europa, Ganymede, and Callisto 04 p0570 A83-16233
- Circular polarization from compact extragalactic radio sources as a result of nonuniform magnetic fields 05 p0697 A83-16986

- A design of back-feed type circularly polarized microstrip disk antennas having symmetrical perturbation element by one-point feed 05 p0622 A83-17279
- A theoretical and experimental investigation of the circularly polarised elliptical printed-circuit antenna 06 p0742 A83-18671
- Measurements of circularly-polarised transmissions from the OTS and SIRIO satellites in the 11 GHz band 06 p0745 A83-18712
- Operational measurements of a 4/6-GHz adaptive polarization compensation network employing up/down-link correlation algorithms 06 p0746 A83-18727

- Investigation of nonlinear absorption in H₂O vapors subjected to strong optical fields with linear and circular polarizations 07 p0991 A83-20128
- Synthesis of circular polarization with nonresonant slots in the narrow wall of a rectangular waveguide 07 p0921 A83-20822
- Electromagnetic fields in twisted coordinate system 08 p1080 A83-22234
- Liquid crystals as large aperture waveplates and circular polarizers 08 p1166 A83-22571
- Symmetrical crossed rectangular horn for a circularly polarized multiple-beam reflector antenna 09 p1248 A83-23811

- Semicircular-waveguide radiator with circular polarization 09 p1257 A83-24925
- Giant Raman optical activity of the 128/cm mode in alpha-quartz 10 p1481 A83-25432
- The broad-band circular polarization of sunspots, 0.37-4.5 microns 10 p1521 A83-25750
- Ice crystal observations at 1.8 cm wavelength using a polarization diversity radar 11 p1629 A83-27066
- Dual-frequency circularly polarised printed antenna composed of strips and slots 11 p1560 A83-27895
- Measurement of the phase difference between fluctuating signals received by orthogonally polarized antennas 13 p1828 A83-30283
- Microwave and hard X-ray imaging of a solar flare on 1980 November 5 15 p2278 A83-34113
- The behavior of the active region McMath 14822 at a wavelength of 13.5 mm 17 p2625 A83-37671
- A catalog of high accuracy circular polarization measurements 17 p2591 A83-37830
- The sun at 1.4 GHz - Intensity and polarization 20 p3080 A83-42390

- Polarization of interstellar molecular radiofrequency absorption lines 22 p3376 A83-45633
- Localization of circularly polarized intense electromagnetic waves in relativistic plasmas 22 p3361 A83-46012

- Microphysical interpretation of multi-parameter radar measurements in rain. I - interpretation of polarization measurements and estimation of raindrop shapes. II Estimation of raindrop distribution parameters by combined dual-wavelength and polarization measurements 22 p3341 A83-46855

- Earth magnetic field fluctuations produced by filamentation instabilities of electromagnetic heater waves 23 p3482 A83-47868

CIRCULAR SHELLS

- Free torsional vibration of thick isotropic incompressible circular cylindrical shell subjected to uniform external pressure 01 p0058 A83-10272
- The forms of the wave motion of circular cylindrical shells 01 p0059 A83-10678
- Post-buckling dynamic behavior of periodically supported imperfect shells 01 p0060 A83-10860
- Nonlinear analysis of axially-loaded laminated cylindrical shells 02 p0194 A83-12743
- Large deformations in a shallow shell that is circular when viewed from above and that has a reinforcing ring 03 p0341 A83-14096
- Cylinder-symmetrical and plane problems 06 p0777 A83-19196
- Shell-core method for the analysis of a long circular cylindrical sandwich shell subjected to axisymmetric loading 08 p1123 A83-22413
- An analysis of intersecting cylindrical shells loaded by internal pressure 10 p1442 A83-26799
- Methods for the synthesis of the stressed state in shell theory 13 p1865 A83-30003
- Dynamic behaviour of a thin-walled circular cylindrical shell 15 p2173 A83-33611
- Buckling and postbuckling of imperfect cylindrical shells under axial compression 15 p2180 A83-34568
- Vibrations of cantilevered circular cylindrical shells 16 p2369 A83-36958
- Shallow versus deep shell theory 17 p2520 A83-37525
- Allowing for the effect of small cross-sectional shape imperfections on the stressed state of nonreinforced thin-walled circular cylindrical shells subjected to pressure gradients 18 p2702 A83-40122
- Deformation of a circular cylindrical shell with a periodic system of holes 18 p2702 A83-40122

Highly non-linear cylindrical deformations of rings and shells 20 p3008 A83-43649

Free vibration of a circular cylindrical shell elastically restrained by axially spaced springs 23 p3468 A83-47594

CIRCULAR TUBES

Selection of molybdenum sheet for deep drawing applications 02 p0154 A83-11786

Boundary layer effects on sound in a circular duct 04 p0532 A83-15066

Circular tube turbulent heat transfer in the downstream of an orifice 04 p0477 A83-16125

Scattering by a conducting tube of finite length 06 p0737 A83-18608

Excess loss of TE₁₁/ modes in curved circular waveguide 06 p0751 A83-18698

Acoustic waves in a Rijke tube with radiation impedance 12 p1777 A83-29382

Flow of highly rarefied gas through a circular tube of finite length 14 p2009 A83-32512

Turbulent heat transfer in the separated reattached and redevelopment regions of a circular tube [AIAA PAPER 83-1520] 14 p2010 A83-32753

Gas flow through a cylindrical tube under free molecular conditions 20 p2985 A83-43105

Large strain inelastic behaviour of cylindrical tubes 23 p3474 A83-48698

Three-component laser-Doppler anemometry measurements in a circular mixing tube 24 p3585 A83-49824

CIRCULATION

NT ATMOSPHERIC CIRCULATION

NT BLOOD CIRCULATION

NT BRAIN CIRCULATION

NT COASTAL CURRENTS

NT CORONARY CIRCULATION

NT ISCHEMIA

NT LOMONOSOV CURRENT

NT OCEAN CURRENTS

NT OCULAR CIRCULATION

NT PERIPHERAL CIRCULATION

NT PULMONARY CIRCULATION

NT WATER CIRCULATION

CIRCULATION CONTROL AIRFOILS

Circulation controlled STOL wing optimization [AIAA PAPER 83-0082] 05 p0579 A83-16509

The performance of a circulation control airfoil at transonic speeds [AIAA PAPER 83-0083] 05 p0579 A83-16510

High-speed characteristics of circulation control airfoils [AIAA PAPER 83-0265] 05 p0583 A83-16621

Analysis of circulation-controlled airfoils in transonic flow 09 p1196 A83-24032

Viscous/inviscid analysis of curved sub- or supersonic wall jets [AIAA PAPER 83-1679] 17 p2452 A83-38086

Aerodynamic characteristics of a circulation controlled elliptical airfoil with blown jets [AIAA PAPER 83-1794] 17 p2453 A83-38633

Development of advanced circulation control wing high lift airfoils [AIAA PAPER 83-1847] 17 p2456 A83-38675

Circulation-controlled elliptical airfoil 20 p2928 A83-42537

CIRCULATION CONTROL ROTORS

Aeroelastic stability of an elastic circulation control rotor blade in hover [AIAA PAPER 83-0985] 14 p1975 A83-32785

Numerical and experimental simulation of circulation control rotor pneumodynamics [AIAA PAPER 83-2551] 23 p3399 A83-48372

CIRCULATION DISTRIBUTION

Local recirculation zones in a supersonic boundary layer on a moving surface 01 p0003 A83-11272

CIRCULATORS (PHASE SHIFT CIRCUITS)

Nonreciprocal devices in open-boundary structures for millimeter-wave integrated circuits 05 p0624 A83-17278

A finite element analysis of planar circulators using arbitrarily shaped resonators 06 p0753 A83-18772

The low-frequency limit of the application of ferrite circulators 10 p1412 A83-26940

Resonant frequencies, Q-factor, and susceptance slope parameter of waveguide circulators using weakly magnetized open resonators 17 p2497 A83-37798

2000 W mean-power X-band waveguide junction circulator using a composite turnstile resonator 20 p2966 A83-42370

Ka-band y-circulators in integrated waveguide technology 21 p3125 A83-44955

CIRCULATORY SYSTEM

NT AORTA

NT ARTERIES

NT BLOOD VESSELS

NT CAPILLARIES (ANATOMY)

NT GLOMERULUS

NT VASCULAR SYSTEM

NT VEINS

A rheological investigation of the circulatory system during high-altitude hypoxia and an orthostatic test 06 p0798 A83-19374

Age-related peculiarities of the functional condition of the vascular system in patients with bronchial asthma in the case of mountain-climate therapy 18 p2735 A83-40569

CIRCUMPOLAR WESTERLIES

Stratospheric sudden coolings and the role of nonlinear wave interactions in preconditioning the circumpolar flow 16 p2386 A83-35483

CIRCUMSTELLAR MATTER

U STELLAR ENVELOPES

CIRROSTRATUS CLOUDS

The variability of the optical characteristics of cirrostratus clouds 09 p1317 A83-25234

CIRRUS CLOUDS

The transfer of 3.7 micrometer radiation through model cirrus clouds 03 p0371 A83-14655

Review of cirrus cloud optical properties and effects on infrared sensors 08 p1135 A83-22544

The use of stereoscopic satellite observation in the determination of the emissivity of cirrus 12 p1761 A83-29700

On the effect of radiative exchange in the 8 to 12 micron spectral region on the diffusional growth of ice crystals 15 p2205 A83-34062

Diurnal variations of satellite-measured black-body temperature areal distribution and eye diameter of mature typhoons 16 p2390 A83-36492

Distribution of high clouds above the Northern Hemisphere 23 p3486 A83-47129

CISLUNAR SPACE

Comparison of advanced propulsion systems in cis-lunar space [IAF PAPER 83-16] 23 p3425 A83-47234

CITIES

NT PHOENIX (AZ)

Urban albedo as a function of the urban structure - A model experiment 01 p0069 A83-10720

Urban albedo as a function of the urban structure - A two-dimensional numerical simulation 01 p0069 A83-10721

An evaluation of Seasat SAR imagery for urban analysis 05 p0656 A83-16904

Intercomparisons of upper air and surface winds in an urban region 06 p0781 A83-18238

The use of contextual information in the classification of remotely sensed data 07 p0951 A83-20147

Space investigations for urban planning --- Russian book 09 p1283 A83-23816

Urban encroachment on agricultural land 09 p1285 A83-24544

The relative importance of various urban sulfate aerosol production mechanisms - A theoretical comparison 09 p1298 A83-25199

Separate determination of the nitrogen oxides NO, NO₂, and NO_x/ in city air by an automatic gas analyzer and a chemical method 11 p1613 A83-28202

Landsat digital enhancements for change detection in urban environments 14 p2035 A83-32614

An approximation method for predicting changes in the level of atmospheric pollution in a city 14 p2048 A83-33042

Urbanization of the Tokyo metropolitan area and its thermal condition using Landsat MSS and NOAA-6/AVHRR data 15 p2182 A83-33571

A study of land transformation processes after the atomic bombing damage in Hiroshima 15 p2182 A83-33572

Metropolitan expansion and population density patterns in third world supercities as indicated by integration of space and ground data 15 p2182 A83-33573

Aircraft survey of the secondary photochemical pollutants covering the Tokyo metropolitan area 15 p2194 A83-34047

Cities and the environment: Studies from space --- Russian book 15 p2241 A83-34167

Urban land use classification using synthetic aperture radar 15 p2184 A83-34808

Urban change detection procedures using Landsat digital data 15 p2241 A83-34815

Urban land use classification using synthetic aperture radar 15 p2187 A83-35279

Fogwater chemistry in an urban atmosphere 16 p2372 A83-36128

A numerical investigation of the transport of coagulating aerosols in the atmosphere of a city 16 p2372 A83-36875

An analysis of thematic mapper simulator data for urban environments 17 p2526 A83-37625

Survey and analysis of present or potential environmental impact sites in Woburn, Massachusetts 17 p2536 A83-38359

The contribution of SPOT to the study of the urban environment 17 p2534 A83-38452

Observations and modeling of downward radiative fluxes /Solar and Infrared/ in urban/rural areas 18 p2712 A83-39114

Stability of the surface layer and its relation to the dispersion of primary pollutants in St. Louis 18 p2711 A83-39122

The numerical modeling of the diurnal variations of meteorological elements in a large city 19 p2868 A83-41584

A dynamic model for the production of H (+), NO₃(-), and SO₄(2-) in urban fog 20 p3013 A83-42844

The mechanism of NO₃ and HONO formation in the nighttime chemistry of the urban atmosphere 20 p3013 A83-42848

Total soluble and insoluble sulfur concentrations in urban snow 22 p3321 A83-45923

Measurements of benzene, toluene and xylenes in urban air 24 p3603 A83-50192

CIVIL AVIATION

General conditions of operational and technical utilization of ILS during Category III operations 02 p0134 A83-13008

Recent developments in aviation case law 03 p0400 A83-13429

Airline economics --- Book 03 p0400 A83-14000

Chicago to spend \$1 billion to expand O'Hare, Midway airports 04 p0450 A83-15825

Highlights of the new national aeronautical research and technology policy 04 p0441 A83-16374

Thunderstorms and aviation - Operational forecasting programs at the National Severe Storms Forecast Center [AIAA PAPER 83-0442] 05 p0666 A83-16716

Center Weather Service Unit - The future of aviation weather services [AIAA PAPER 83-0445] 05 p0666 A83-16718

International civil aviation in the South Pacific: A perspective --- Book 05 p0591 A83-17116

Numerical and psychopathological data bearing upon 700 certifications of civil aviation flight personnel 06 p0799 A83-18333

Fuel savings in air transport 06 p0714 A83-19150

The transport aircraft of tomorrow - A single element of an overall system 06 p0711 A83-19410

Fixed wing and rotary wing flight testing of Navstar GPS as a civilian navigation system 07 p0865 A83-19777

Management of bird problem in Indian airlines 08 p1043 A83-21877

Additional remarks with respect to the American decree of regarding the suspension of foreign certificates of airworthiness 08 p1171 A83-21899

Fiber optic wavelength multiplexing for civil aviation applications 08 p1045 A83-22492

The psychological fitness of the ground personnel in charge of airspace security depending on the civil aviation authority Evaluation at recruiting, disorders observed during the period of employment 08 p1151 A83-22970

Air traffic control for tomorrow - Problems and solutions 09 p1200 A83-23494

Development trend in general aviation [DGLR PAPER 82-026] 09 p1195 A83-24153

Economic conditions and key points of BMFT air transport research requirements in the eighties [DGLR PAPER 82-044] 09 p1196 A83-24168

The maintenance of modern engines in civil aviation [DGLR PAPER 82-070] 09 p1206 A83-24184

Flight, flight duty, and rest times - A comparison between the regulations of different countries 10 p1454 A83-25667

Advances related to the measurement and representation of real multipath propagation --- for radio navigation and instrument landing applications 10 p1374 A83-26485

Reliability of NAVSTAR GPS for civil aviation 11 p1529 A83-28791

Automation of preplanning as a means for improving quality in connection with flight operational control. I 12 p1699 A83-29372

Air traffic control into the 21st century 13 p1805 A83-30275

Current barotraumatic otitis of the commercial flight personnel in civil aviation 14 p2067 A83-32454

Medical problems peculiar to airline pilots 14 p2067 A83-32461

Integration of ground and air services through use of STOLmobiles [AIAA PAPER 83-1587] 14 p2095 A83-33357

Standardized pavement strength reporting system - ACN/PCN --- Aircraft Classification Number/Pavement Classification Number [AIAA PAPER 83-1602] 14 p1978 A83-33365

NASA technology program for future civil air transports
[AIAA PAPER 83-1603] 14 p1973 A83-33366
Airline safety and labor relations law - Balancing rights and responsibility 15 p2240 A83-34475
AISA - Program for automated treatment of aeronautical data --- for civil aviation applications 16 p2311 A83-35598
Concepts for a future joint airlift development program [AIAA PAPER 83-1591] 16 p2297 A83-36951
Worldwide aviation outlook --- for passenger and freight traffic 1982-1992
[AIAA PAPER 83-1597] 16 p2297 A83-36952
Collegiate weather education for pilots 17 p2586 A83-38744
Regional airline turboprop engine technology [AIAA PAPER 83-1158] 18 p2641 A83-39101
Automated systems of control in civil aviation of the USSR 18 p2639 A83-39219
Maintenance according to technical conditions --- for aircraft 18 p2631 A83-39221
Automation of preplanning as a means for enhancing quality in operational flight control. II 18 p2638 A83-39222
Public interest under the Federal Aviation Act of 1958 and the Airline Deregulation Act of 1978 18 p2753 A83-39695
Airport use and access 18 p2753 A83-39698
Airborne reconnaissance in the civilian sector - Agricultural monitoring from high-altitude powered platforms 18 p2706 A83-39939
Experiences in medical coverage of airport disasters at Logan International Airport in Boston 18 p2638 A83-40356
The role of the Air Force in the transfer of general-aviation-traffic control from ITAV to AAAV/TAG 19 p2795 A83-41226
SITELCOM-82 - Telecommunications and data processing in the air transport industry; Proceedings of the Conference, Monte Carlo, Monaco, March 2-4, 1982 21 p3090 A83-45076
ARGHOS - A tool for schedule planning --- for airlines 21 p3090 A83-45077
Impact of new technology on engineering and maintenance systems --- of airlines 21 p3085 A83-45078
SITA - Advanced telecommunications services --- for air transport industry 21 p3090 A83-45079
The role of information systems in airline management functions 21 p3221 A83-45080
Airline common databases and data processing applications 21 p3190 A83-45081
The implications of the United Nations Convention on International Multimodal Transport of Goods (Geneva, 1980) for International Civil Aviation 22 p3367 A83-45804
Security of International Civil Aviation - Role of ICAO 22 p3367 A83-45805
With regards to the Warsaw Convention - A bad process for false problems --- legal liability in air law 22 p3367 A83-45806
Comfort criteria and/or national requirements in the issuance of a license for air service in Canada 22 p3367 A83-45807
Essays in air law 22 p3368 A83-45826
The Warsaw Convention - Past, present and future 22 p3369 A83-45827
Some thoughts on the economic significance of limited liability in air passenger transport 22 p3369 A83-45828
From aerostats to DC-10s - Recognition of certificates of airworthiness 22 p3369 A83-45829
Unlawful interference with civil aviation 22 p3369 A83-45830
Passenger liability in international carriage by air - Lines of development 22 p3369 A83-45831
Interchange of aircraft --- international lease regulations 22 p3369 A83-45832
Airline subsidies --- a historical review 22 p3369 A83-45833
Deregulation of aviation in the United States 22 p3369 A83-45834
Air safety - Enforcement of the Federal Aviation Regulations 22 p3369 A83-45836
International multimodal transport - A legal labyrinth 22 p3369 A83-45837
The 'legislative hearing' on IATA traffic conferences Creative procedure in a high stakes setting 22 p3370 A83-45838
The Freedom of Information Act - Its impact on civil aviation 22 p3370 A83-45839
The right to fly - Review at random 22 p3370 A83-45840
The right to be heard - The British practice --- refusal or revocation of licenses in air transport 22 p3370 A83-45841

Certification of digital systems for civil aircraft 22 p3252 A83-45848
Status of area navigation 22 p3253 A83-46960
Ten years of promoting the development of air transport research 23 p3391 A83-47185
DAS, a DME-supported multifunction system with a wide applications range for distance and angle measurements with data transfer 23 p3401 A83-47199
Development of aerodynamical technology for large civil aviation aircraft 23 p3391 A83-47204
Studies and designs for a new helicopter cockpit 23 p3402 A83-47210
Airplane reliability in a nutshell 23 p3467 A83-47614
Maintenance aspects of modern avionics 23 p3392 A83-47654
Improvements in SSR 23 p3401 A83-47655
Helicopter noise [ONERA, TP NO. 1983-80] 23 p3506 A83-48195
Airline requirements for future civil transport aircraft [AIAA PAPER 83-2501] 23 p3401 A83-48354
International relations in civil aviation --- Russian book 24 p3637 A83-49200
Commonality potential of future public service helicopters and Army light utility helicopters [AIAA PAPER 83-2553] 24 p3546 A83-49593

CIVIL DEFENSE

The use of telecommunications satellites by the air, sea, and land military forces and by civil defense - Project SICRAL AM/136/80 19 p2812 A83-41227

CLADDING

Creep and long-term strength of 5VMTs alloy clad with alloy VN7 02 p0157 A83-12338
Low-loss quadruple-clad single-mode lightguides with dispersion below 2 ps/km nm over the 1.28-1.65 micron wavelength range 04 p0534 A83-15243
The production of clad rolled sheets from secondary aluminum powder 09 p1236 A83-25064
Modal analysis of separate-confinement heterojunction lasers with inhomogeneous cladding layers 13 p1851 A83-30750
Characteristics of the formation of plasma-sprayed coatings based on clad carbide powders 24 p3590 A83-49087

CLAMPS

The trigonometric contour series method applied to clamped plates with arbitrary contours 08 p1115 A83-21635

CLARK Y AIRFOIL

U AIRFOIL PROFILES

CLASSIC AIRCRAFT

U IL-62 AIRCRAFT

CLASSICAL MECHANICS

NT ASTRODYNAMICS
NT CELESTIAL MECHANICS
NT KEPLER LAWS
NT MINIMUM VARIANCE ORBIT DETERMINATION
NT ORBITAL MECHANICS
Conservation laws for a dynamical system in group variables 01 p0104 A83-10122
Investigation of regions of the possibility of motion in mechanical systems 06 p0805 A83-17979
On an analogy to the Steklov case for a balanced gyrost in a Newtonian gravitational force field 07 p0988 A83-20145
Balance laws of continuum physics 07 p0989 A83-20643
Uniform semiclassical quantization of regular and chaotic classical dynamics on the Henon-Heiles surface 09 p1344 A83-25215
Approximate constants of motion for classically chaotic vibrational dynamics - Vague tori, semiclassical quantization, and classical intramolecular energy flow 09 p1344 A83-25216
Equations in Rodrigues-Hamilton parameters for a heavy rigid body rotating about a stationary point 23 p3504 A83-48452
The stability of the stationary motions of a plane body in the field of a central force 23 p3504 A83-48458
Classical statistical mechanics of a lattice model of superradiance 23 p3505 A83-48590

CLASSIFICATIONS

NT BBGKY HIERARCHY
NT HIERARCHIES
NT INDEXES (DOCUMENTATION)
Contextual classification of multispectral image data 01 p0061 A83-10027
Probabilistic cluster labeling of imagery data 01 p0096 A83-11410
Signal classification for automatic industrial inspection 01 p0029 A83-11442
A means for utilizing ancillary information in multispectral classification --- of remotely sensed data 05 p0656 A83-16905

An investigation and classification of the fractures of refractory nickel-base PM alloys 06 p0729 A83-18747
Selection of information features for the classification of multispectral images 07 p0951 A83-19917
The use of contextual information in the classification of remotely sensed data 07 p0951 A83-20147
A physically based classification of supernovae 07 p1015 A83-20667
Photointerpretation - Unsupervised or supervised classification 08 p1124 A83-21902
Picture classification and segmentation by feature combination in multispectral data 08 p1124 A83-21905
Classification of clouds on multispectral images acquired by meteorological satellites 08 p1138 A83-21907
Direction dependant classification of airborne multispectral scanner data 08 p1125 A83-21914
Automatic classification of infrared ship imagery 08 p1095 A83-22443
Eolian sand bodies of the world --- classification techniques for Landsat imagery applications 09 p1284 A83-24533
Soil classification and potentials in Sinai peninsula from Landsat images 09 p1285 A83-24540
Normal modes of Bardeen discs. III - Short wavelength analysis and classification --- of stellar oscillation modes 09 p1362 A83-24980
Principal components analysis of spectral data. I - Methodology for spectral classification --- of A and F type stars 10 p1493 A83-25657
Results of the simulation of an adaptive nonparametric linear classifier of polarization-shift-keyed signals 10 p1407 A83-26939
Resolution classifier --- Bayesian approach for astronomical images 14 p2096 A83-32034
Refining the class boundaries under alternative forecasting --- of weather 14 p2056 A83-32369
Classification of the Allan Hills A77307 meteorite 14 p2112 A83-33066
Nearest neighbors and automatic classification - Applications to industrial data --- French thesis 15 p2220 A83-33696
A proposed new white dwarf spectral classification system 15 p2248 A83-34635
Classification systems for natural resource management 15 p2184 A83-34803
Hierarchical modeling for image classification 15 p2185 A83-34820
The application of local textural transformation to automatic cartography of a tropical vegetation zone (Sumatra) 17 p2533 A83-38439
A hybrid image classification instructional package 21 p3191 A83-43893
Improved landuse classification through principal component analysis based on category statistics and synthetic variables 22 p3308 A83-46119
Classification of agricultural crops in radar images 22 p3315 A83-46239
Neighboring gray level dependence matrix for texture classification 22 p3315 A83-46254
New and misclassified planetary nebulae 24 p3638 A83-49128
The classification of asteroids 24 p3646 A83-49999

CLASSIFIERS
Improved light-scattering cavitation nuclei classifier 08 p1106 A83-23229
Histogram deconvolution - An aid to automated classifiers 22 p3350 A83-46253

CLASSIFYING
Optimal performance limits for detection and classification algorithms 09 p1266 A83-23537
Target classification algorithms for video and forward looking infrared /FLIR/ imagery 09 p1266 A83-23541
Methods for the investigation of rigid-body motions and their application to the classification of motions 09 p1337 A83-23556
A classification of severe squall-line development using WSR-57 radar data 11 p1625 A83-27013
The mechanisms of the classification of visual images according to spatial signs in normal dogs and after the excision of the parietal and the supertemporal cortices 13 p1896 A83-30439

CLAYS
NT MONTMORILLONITE
Clay mineralogy of the Cretaceous-Tertiary boundary clay --- in search for asteroid ejecta 07 p1029 A83-20301
Quantum-chemical modeling of smectite clays 07 p0873 A83-21044
Interaction of metal ions and amino acids - Possible mechanisms for the adsorption of amino acids on homoionic smectite clays 12 p1712 A83-29556

Inter-layered clay stacks in Jurassic shales
21 p3174 A83-45060

CLEAN ENERGY
Solar thermal electricity generation - EURELIOS, the 1
MW/el/ helioelectric power plant of the European
communities 02 p0201 A83-11802
Mathematical model for a noniterative optimization of
each system for exploiting solar energy 02 p0201 A83-11849
Advances in wind energy technology
[DGLR PAPER 82-082] 09 p1293 A83-24194
National project of new energy development in Japan
11 p1607 A83-27243
Photovoltaic Solar Energy Conference; Proceedings of
the Fourth International Conference, Stresa, Italy, May
10-14, 1982 14 p2036 A83-32176
15 kW experimental photovoltaic solar power plant
14 p2037 A83-32187
Modular simulation model for a wind turbine system
17 p2536 A83-38017
Wind power assessments and remote sensing
17 p2525 A83-38345
An assessment of large-scale solar hydrogen production
in Canada 18 p2708 A83-39561
On the evaluation of wind power from short wind
records 22 p3339 A83-45711
Combined solar-wind power plants 24 p3599 A83-48958

CLEAN FUELS
NT FUEL OILS

CLEAN ROOMS
Optical alignment measurements at Goddard Space
Flight Center 02 p0139 A83-12311
The effects of variations in garment protection on clean
room cleanliness levels 05 p0677 A83-16930
Blueprint of a clean room 13 p1864 A83-31506
New technology for improved clean room operations
13 p1865 A83-31520
Particulate fallout predictions for clean rooms
13 p1865 A83-31523
A tumble test for determining the level of detachable
particles associated with clean room garments and clean
room wipers 13 p1865 A83-31524
Features and testing of clean room apparel 13 p1865 A83-31525

CLEANERS
NT AIR FILTERS

CLEANING
NT HOUSEKEEPING (SPACECRAFT)
The cleaning of the exterior of the aircraft
03 p0277 A83-14325
Performance degradation and cleaning of photovoltaic
arrays 11 p1607 A83-27236
Personnel training for precision cleaning of aerospace
hardware to military standard 1246 A levels
13 p1865 A83-31519

CLEANLINESS
NT HOUSEKEEPING (SPACECRAFT)
The effects of variations in garment protection on clean
room cleanliness levels 05 p0677 A83-16930

CLEAR AIR TURBULENCE
Detection of clear air turbulence using a diagnostic
Richardson number tendency formulation 01 p0074 A83-10177
Some characteristics of clear-air turbulence in the middle
stratosphere 04 p0517 A83-15938
Role of gas absorption in formation of fluctuations in
parameters of cleared cloud medium and laser radiation
11 p1631 A83-27606
Poker Flat MST radar observations of shear-induced
turbulence --- Mesosphere-Stratosphere-Troposphere
16 p2389 A83-36142
Grid-scale turbulence coefficients and their connection
with clear air turbulence 16 p2391 A83-36845
Numerical and analytical investigations of
three-dimensional lee waves 17 p2553 A83-38763
Numerical simulation of the atmosphere during a CAT
encounter 17 p2553 A83-38764
CAT detection and forecasting using operational NMC
analysis data 17 p2553 A83-38765
The diagnosis and evaluation of turbulence which
influences the flight of aircraft, according to rawinsonde
network observation data 21 p3181 A83-45326
Clouds and entrainment --- cumulus convective
turbulence in clear air 24 p3612 A83-49694

CLEARANCES
A way to relax the dimensional tolerance requirements
of clearance regenerators --- in small Stirling engine
design 11 p1588 A83-27286
Effects of displacer seal clearance on free-piston Stirling
engine performance 11 p1589 A83-27295
The measurement of turbomachinery stator-to-drum
running clearances
[ASME PAPER 83-GT-204] 23 p3410 A83-48005

CLEARINGS (OPENINGS)

Prospects for multimtemporal studies focusing on a
forested region - Proof of clear-cutting 08 p1127 A83-21939

CLEAVAGE
Mechanisms and criteria for cleavage 08 p1058 A83-21666
Numerical modelling of warm prestress effect using a
damage function for cleavage fracture 08 p1060 A83-21703
The influence of specimen geometry on fracture of
unwelded and welded steel specimens - Comparison of
experimental results with FEM-calculation 08 p1060 A83-21707
Quantitative fractography and dislocation interpretations
of the cyclic cleavage crack growth process 08 p1123 A83-23224
Prediction of failure probabilities for cleavage fracture
from the scatter of crack geometry and of fracture
toughness using the weakest link model 16 p2368 A83-36510
Oxide scale induced cleavage fracture in an ODS
Fe-Cr-Al alloy 18 p2670 A83-40639
An engineering interpretation of pop-in arrest and tearing
arrest in terms of static crack arrest, K(Ia) 21 p3162 A83-45186

CLIMATE

The influence of ground moisture conditions in North
America on summer climate as modeled in the GISS
GCM 02 p0218 A83-13062
Optimal weighting of data to detect climatic change -
Application to the carbon dioxide problem 07 p0969 A83-20216
Direct relations between solar activity and atmospheric
circulation, its effect on changes of weather and climate
12 p1758 A83-29405
Rare earth elements in these sedimentary cycle - A pilot
study of the first leg 12 p1748 A83-29554
Cost effective utilization of environmental design criteria:
MIL-STD-210B updated 13 p1863 A83-31503
Interannual variability and climatic noise in
satellite-observed outgoing longwave radiation 15 p2195 A83-33884
A thermodynamic investigation of climate variability at
high latitudes --- Russian book 15 p2206 A83-34173
The effects of seasonal differences in climatic conditions
on Landsat spectral signatures and associated land cover
classification 15 p2185 A83-34817
The geologic record of climatic change 18 p2730 A83-40327
General circulation model experiments on the climatic
effects due to a doubling and quadrupling of carbon dioxide
concentration 20 p3031 A83-42843
Solar variability, weather and climate - An update 21 p3179 A83-44390
Active measures for reducing the global climatic impacts
of escalating CO2 concentrations
[IAF PAPER 83-106] 23 p3488 A83-47269

CLIMATOLOGY

NT AGROCLIMATOLOGY
NT BIOCLIMATOLOGY
NT MICROCLIMATOLOGY
A radiation scheme for circulation and climate models
01 p0074 A83-10221
Climatic research in the United States 01 p0075 A83-10461
A climatological estimate of the radiative cooling of the
atmosphere 02 p0213 A83-11977
The parameterization of longwave flux in energy balance
climate models 02 p0213 A83-12229
Climate - Multiyear average 02 p0214 A83-12299
Delineation of cold-prone areas using nighttime
SMS/GOES thermal data Effects of soils and water
02 p0216 A83-12961
Computing and mapping Thiessen weighting factors
from digitized district boundaries and climatological station
latitudes and longitudes 02 p0217 A83-12964
Atmospheric ozone and changes in the global climate
--- Russian book 03 p0358 A83-13820
A time-dependent ice sheet model - Preliminary
results 03 p0359 A83-14505
The satellite power system - Assessment of the
environmental impact on middle atmosphere composition
and on climate 03 p0360 A83-14517
Relations between climatic anomalies -
Teleconnections --- global correlation between local
atmospheric phenomena 03 p0370 A83-14575
Comparison between albedo changes and
lidar-measured aerosol changes for a set of aerosol
events 03 p0370 A83-14641
Diurnal radiation budget - Four months assembled into
an annual mean 03 p0370 A83-14646
Time and space spectra of earth-emitted radiation at
large scales 03 p0370 A83-14648
Results from a monex radiation experiment 03 p0370 A83-14649

A one-dimensional model of the atmosphere considered
as a climatic system block comprising the ocean, the
atmosphere, and the ice cover 03 p0371 A83-14826
Seasonal climatic sources of heat in the North Atlantic
03 p0373 A83-14833
Origin, nature and world climate effect of Arctic Ocean
ice-cover [AD-A130919] 03 p0344 A83-14922
A seasonal global climate model with an equivalent
meridional atmospheric circulation 04 p0515 A83-15852
A possible marine mechanism for internally generated
long-peroid climate cycles 04 p0517 A83-15944
Low-cost, focused-science Mars mission
[AIAA PAPER 83-0519] 05 p0600 A83-16764
A Pioneer-class Mars climatology mission
[AIAA PAPER 83-0521] 05 p0600 A83-16766
Measurement of true mean temperature for
determination of climatic trends 05 p0668 A83-17449
Physical climatology 05 p0668 A83-17699
Changes in the solar constant and climatic effects
05 p0668 A83-17796
The diagnostic calculation and analysis of mean climatic
sources for winter conditions in the Northern
Hemisphere 06 p0787 A83-17993
Quasi-biennial cyclicity as a parametric phenomenon in
the climatic system 06 p0788 A83-17994
An empirical investigation of climate sensitivity
06 p0788 A83-17995
Radiative-convective models of climate 06 p0788 A83-17997
Fine-dispersion aerosol and climate 06 p0788 A83-17998
Formulation and testing of a climatonomical simulation
of the microclimate of the dry valleys and of the Little
America V Station in Antarctica 06 p0788 A83-18236
Climate studies with a multi-layer energy balance model.
I - Model description and sensitivity to the solar constant.
II - The role of feedback mechanisms in the CO2
problem 06 p0789 A83-18251
Parameterization of outgoing infrared radiation derived
from detailed radiative calculations 06 p0789 A83-18252
Some features of the climatology of the Northern
Hemisphere stratosphere revealed by NMC upper
atmosphere analyses 06 p0790 A83-18258
A synoptic climatology of northwest flow severe weather
outbreaks. I - Nature and significance 06 p0792 A83-18468
El Chichon climate effect estimated 06 p0786 A83-18815
PUKK - A meso-scale experiment at the German North
Sea coast --- Project for Investigation of Coastal Climate
06 p0793 A83-18995
The climatology of the geopotential of the 500 mb
surface of the northern hemisphere as obtained by natural
orthogonal functions in the wave number region 06 p0793 A83-19249
The faint young sun-climate paradox - Volcanic
influences 07 p0959 A83-20187
Climatic fluctuations due to deep ocean circulation
07 p0969 A83-20299
The stratospheric aerosol and its effect on the earth's
climate 07 p0970 A83-20887
The radiative energetics of the climate system 07 p0970 A83-20888
The pattern of the current climate of the polar regions
07 p0970 A83-20889
Large-scale changes in North Pacific and North
American weather patterns in recent decades 08 p1139 A83-22289
A statistical-climatological tropical cyclone track
prediction technique using an EOF representation of the
synoptic forcing --- Empirical Orthogonal Functions
08 p1139 A83-22294
Global mean sea level - Indicator of climate change
08 p1144 A83-22325
A water vapor-energy balance model designed for
sensitivity testing of climatic feedback processes 08 p1142 A83-23004
The effect of tropospheric aerosols on the earth's
radiation budget - A parameterization for climate models
08 p1142 A83-23009
The dust cloud of the century 08 p1138 A83-23271
Feedback mechanisms in the climate system affecting
future levels of carbon dioxide 09 p1294 A83-24252
A preliminary global oceanic cloud climatology from
satellite albedo observations 09 p1314 A83-24275
Monitoring land use and land use appropriateness in
the central Sudan - A combination of Landsat data and
statistical analysis of climatic data 09 p1290 A83-24608

Global distribution of stratospheric aerosols by satellite measurements 09 p1306 A83-24675
 Fuzzy differential equations and their possible use in meteorology 09 p1316 A83-25145
 Building a balanced model of the climate 09 p1317 A83-25241
 Climate as determined by observations from space 09 p1317 A83-25259
 Diagnostic analysis and spectral energetics of a blocking event in the GLAS climate model simulation 10 p1449 A83-25380
 Empirical orthogonal function analysis of wind vectors over the tropical Pacific region 10 p1451 A83-26098
 The effect of spatial and temporal averaging on sampling strategies for cloud amount data 10 p1451 A83-26100
 An aspect of the use of radar as a climatological tool - The radar bias problem 11 p1627 A83-27037
 Dynamics of the middle atmosphere 11 p1631 A83-27404
 Doppler-SODAR measured variations of mean and turbulent wind field during PUKK --- project for the investigation of the coastal climate 11 p1632 A83-27974
 Marine biological controls on atmospheric CO₂ and climate 11 p1600 A83-28400
 The effect of aerosols on climate and aerosol climatology on the basis of observations from space 12 p1759 A83-29558
 The role of aerosols in the climate system - Results of numerical experiments in climate models 12 p1759 A83-29559
 Passive remote sensing of aerosols from space now and in the future 12 p1754 A83-29560
 Climatic influence of background and volcanic stratosphere aerosol models 12 p1756 A83-29580
 Climate studies from satellite observations - Special problems in the verification of earth radiation balance, cloud climatology, and related climate experiments 12 p1759 A83-29677
 Geomagnetic excursions and climate change 12 p1756 A83-29712
 Investigation of the possibilities of predicting astroclimate 13 p1935 A83-30271
 The modeling of certain long-period atmospheric processes 13 p1884 A83-30292
 A quantitative assessment of the climate-determining effect of topography 13 p1884 A83-30294
 A mesoscale, climatologically-based forecast technique for Colorado 13 p1888 A83-30568
 Radiation-fog intensities associated with surface synoptic patterns at Albany, New York 13 p1890 A83-30592
 Upper level cloud climatology from an orbiting satellite 13 p1893 A83-31040
 The chemical composition and climatology of the earth's early atmosphere 13 p1878 A83-31156
 Climatic effects of atmospheric carbon dioxide 13 p1893 A83-31200
 The cosmic horizons of climatology 13 p1893 A83-31315
 A simple model of the ocean climate 13 p1894 A83-31349
 The dependence of air temperature and the temperature of precipitates on the amount of carbon dioxide in the atmosphere 14 p2056 A83-32365
 Climatology of the southeastern United States continental shelf waters 14 p2061 A83-33088
 Ice and snow feedbacks and the latitudinal and seasonal distribution of climate sensitivity 16 p2386 A83-35489
 Statistical analysis and wavenumber-frequency spectra of the 500 mb geopotential along 50 deg S 16 p2387 A83-35493
 A theory of stochastic resonance in climatic change 16 p2387 A83-35696
 Comments on 'the relative effect of solar altitude on surface temperatures and energy budget components on two contrasting landscapes' 16 p2388 A83-35798
 Efficient three-dimensional global models for climate studies - Models I and II 16 p2388 A83-36026
 Orbital forcing, climatic interactions, and glaciation cycles 16 p2379 A83-36133
 CO₂ radiative parameterization used in climate models Comparison with narrow band models and with laboratory data 16 p2389 A83-36134
 Further studies on single station climatology. III - Time spectral analysis of Halley Bay (Antarctic) rawinsonde data 16 p2391 A83-36585
 The distribution of climatic changes with global warming 16 p2391 A83-36844
 A global model of the ocean-atmosphere system and an investigation of its sensitivity to changes in CO₂ concentration 16 p2392 A83-36864
 Middle atmosphere dynamics 17 p2541 A83-38281

Advances in short term climate prediction 17 p2547 A83-38321
 Some aspects of major dry and wet periods in the contiguous United States, 1895-1981 18 p2721 A83-39109
 A comparison of sea surface temperature climatologies 18 p2723 A83-39138
 Global vegetation and land use - New high-resolution data bases for climate studies 18 p2706 A83-39141
 Extrapolation of solar radiation measurements - Mesoscale analyses from Arizona and Tennessee Valley Authority regions 18 p2723 A83-39142
 Modeling the effect of stratospheric aerosols on climate 18 p2723 A83-39437
 The albedo of the underlying surface-cloudy atmosphere system 18 p2723 A83-39439
 An analysis of the ground temperature and reflectivity pattern about St. Louis, Missouri, using HCMM satellite data 18 p2724 A83-39679
 Orbital forcing of the inception of the Laurentide ice sheet? 18 p2718 A83-39960
 Observations of liquid water in orographic clouds over Elk Mountain 18 p2729 A83-40042
 The International Satellite Cloud Climatology Project (ISCCP) - The first project of the World Climate Research Programme 18 p2730 A83-40320
 Global temperature variations in the troposphere and stratosphere, 1958-1982 20 p3029 A83-42501
 Variability of the Indian summer monsoon and tropical circulation features 20 p3029 A83-42505
 Explosive cyclogenesis over the northeast Pacific Ocean 20 p3030 A83-42516
 The atmosphere --- dynamics and climatology 20 p3020 A83-42821
 The climatological minimum in tropical outgoing infrared radiation - Contributions of humidity and clouds 21 p3179 A83-44395
 A general circulation model study of January climate anomaly patterns associated with interannual variation of equatorial Pacific sea surface temperatures 21 p3180 A83-44702
 The influence of poloidal motions and latent heat release on the equilibrium ice extent in a simple climate model 21 p3180 A83-44703
 An introduction to the theory of climate --- Russian book 21 p3180 A83-45010
 Gaseous contaminants in the atmosphere and changes of the global climate 21 p3169 A83-45334
 Some singularities and irregularities in the seasonal progression of the 700 mb height field 22 p3338 A83-45702
 Global climate space reflector systems - Some legal issues 22 p3368 A83-45815
 Numerical experiments with a stochastic zonal climate model 22 p3340 A83-46846
 Aviation climatology 23 p3486 A83-47126
 Climate theory and numerical weather forecasting 23 p3487 A83-47151
 Calculation of the circulation, heat budget, and moisture cycle of the atmosphere for July on the basis of a model of the general circulation of the atmosphere 23 p3488 A83-47152
 Inclusion of dynamic factors in a thermodynamic model of climate and numerical forecasting of mean monthly air temperature in the troposphere 23 p3488 A83-47153
 Integration of the equations of atmospheric dynamics for long time periods using nested grids 23 p3488 A83-47159
 Global climate variations connected with sea surface temperature anomalies in the eastern equatorial Pacific Ocean for the 1958-73 period 23 p3489 A83-47398
 Short-period atmospheric gravity waves - A study of their statistical properties and source mechanisms 23 p3489 A83-47402
 Synoptic forcing of the planetary boundary layer - A case study from the PUKK experiment --- project for investigation of coastal climate 24 p3609 A83-48815
 Numerical simulation of the effects of changes of the gas composition of the atmosphere on climate 24 p3609 A83-49278
 Mathematical model of the glaciers-ocean-atmosphere system 24 p3610 A83-49556

CLIMBING FLIGHT

Altitude transitions in energy climbs 10 p1379 A83-26604
 Optimal turning climb-out and descent of commercial jet aircraft [SAE PAPER 821468] 17 p2464 A83-37999
 The effect of wind variability on Space Shuttle flight 17 p2553 A83-38768
 Energy state revisited --- for minimum-time aircraft climbs [AIAA PAPER 83-2138] 19 p2799 A83-41960
 Wing extensions for improving climb performance [AIAA PAPER 83-2556] 23 p3405 A83-48375

CLINICAL MEDICINE

Extratympanic electrocochleography in clinical practice 01 p0083 A83-10515
 Liquorrhea via fistula in the area of the cochlear window 01 p0083 A83-10516
 Sport gastroenterology - Some results and prospects of development 01 p0083 A83-10519
 Heterotopic ossifications in regions of the elbow joint and their treatment with ultrasound 01 p0084 A83-11393
 A case report - Unilateral cycloplegia resulting from careless use of Transderm-V 02 p0223 A83-12410
 A stimulating laser therapy for sclerotic and posttraumatic central dystrophies of the retina 03 p0378 A83-13607
 Current aspects of prophylaxis and treatment of hearing disorders in patients with Meniere's disease 05 p0672 A83-16950
 Arterial hypertonia in miners working in deep mines 05 p0673 A83-17167
 Pilots are treated and rest here 05 p0673 A83-17178
 The use of a constant magnetic field in the treatment of dystrophies of the extremities 05 p0673 A83-17197
 Mathematical methods for optimizing treatment and diagnosis in cardiology /current status and future prospects/ 05 p0674 A83-17199
 A rare case of pulmonary hypertension 05 p0674 A83-17206
 Laser treatment of open-angle glaucoma: Randomized comparative studies - Cyclotrabeculospas and trabeculoplasty 05 p0674 A83-17212
 Clinical and EKG criteria for disorders of the cardiac rhythm in the weak sinus node syndrome 05 p0674 A83-17216
 Clinical aviation medicine --- Book 05 p0674 A83-17300
 The determination of the circulating immune complexes in humans 07 p0978 A83-20999
 The metrological possibilities of the tetrapolar transthoracic impedance rheoplethysmography method in clinical conditions 13 p1906 A83-30306
 The patterns of the postirradiation recovery of an organism in conditions of external nonuniform radiation effects. VII - The dependence of the postirradiation radiosensitivity of rats on the dose of preliminary irradiation in the case of an oral form of radiation sickness 14 p2062 A83-32067
 A review of the literature concerning resuscitation from hypothermia. I - The problem and general approaches 14 p2068 A83-32689
 The suppression of blood platelet aggregation with immune complexes. I - Clinical investigations 14 p2070 A83-33331
 The diagnostics, treatment, and prophylactic measures for the initial appearances of brain blood insufficiencies 15 p2212 A83-34927
 The objective measurement of anatomical and optical parameters of emmetropic and ametropic eyes 15 p2212 A83-34939
 The application of ephylline electrophoresis with sinusoidal modulated currents in the treatment of patients with transitory disorders of the brain blood circulation 15 p2213 A83-34972
 Practical aspects of the medical check-up of nonprofessional pilots 16 p2397 A83-35585
 Methods for determining the extent of myocardial infarction 16 p2400 A83-36837
 The cerebral blood circulation of patients with vibration disease during treatment at health resorts 17 p2560 A83-38191
 Successful reversal of presumed carbon monoxide-induced semicoma 18 p2734 A83-40362
 Stereotaxic computer tomography 18 p2737 A83-40576
 The kinetics of hemopoiesis and its clinical significance 19 p2882 A83-41451
 The EKG and physical work capacity in patients with hypertension 19 p2882 A83-41452
 The system of the regulation of the aggregation condition of the blood in patients with ischemic heart disease 19 p2882 A83-41453
 Optoelectronic methods for increasing the information content of ultrasonic ocular scanograms 19 p2882 A83-41459
 The clinical picture of covered perforated gastric and duodenal ulcers in young individuals 19 p2884 A83-42025
 Medical psychology --- Russian book 21 p3188 A83-43915
 Electrophoresis '82; Proceedings of the Fourth International Conference, Athens, Greece, April 21-24, 1982 22 p3265 A83-45757
 A new detailed lipidogram - Methods and clinical applications 22 p3347 A83-45766

- Clinical possibilities in the evaluation of extreme effects --- on humans 23 p3496 A83-47102
 Emergency care for burns --- Russian book 23 p3498 A83-48150
 The direct electrical stimulation of the upper urinary tract in case of ureteroliths in flight crew personnel 24 p3618 A83-49071
 Disorders of the peripheral nervous system in conditions of a hot, humid climate 24 p3618 A83-49072

CLOCK PARADOX

- Questions on universal constants and four-dimensional symmetry from a broad viewpoint. I 12 p1792 A83-29044

CLOCKS

- NT ATOMIC CLOCKS
 NT CHRONOMETERS

- Clocks and gravity 06 p0806 A83-19446
 Automated timekeeping II 13 p1847 A83-31291
 Preamplifiers and clock drivers for the University of California at Los Angeles Reticon spectrometer 14 p2017 A83-32020

CLOSE PACKED LATTICES

- Stacking fault energy and texture changes during the polygonization of alpha titanium alloys 03 p0300 A83-14162
 The deformation and fracture mechanisms of coarse-grained textured alpha-titanium alloys 06 p0729 A83-18748
 Precipitation of T1 phase in α /alpha + T1/ type Al-4.2%Cu-1.3%Li alloy 07 p0885 A83-20294
 A modulus method of determining the type of rolling texture in sheets of hexagonal metals 08 p1066 A83-22627
 Changes in the base dislocation density at the initial stage of the plastic deformation of magnesium single crystals 08 p1068 A83-22785
 Deformation of polycrystalline alpha-SiC 09 p1239 A83-24073
 Effect of alpha phase morphology on mechanical properties of commercial purity titanium 10 p1393 A83-25401
 Alpha-beta interface sliding in Ti-Mn alloys 10 p1398 A83-26285
 Strengthening mechanisms in hot-rolled magnesium and magnesium alloys 16 p2330 A83-36070
 Distribution of aluminum, molybdenum, and zirconium among phases in Ti-Al-Mo-Zr alloys 16 p2335 A83-36898

CLOSED BASINS

- U STRUCTURAL BASINS

CLOSED CYCLES

- Investigation of the active medium in a fast-flow closed-cycle industrial CO2 laser 07 p0933 A83-20105
 Characteristics of a closed Brayton cycle piston engine 08 p1112 A83-23135

CLOSED ECOLOGICAL SYSTEMS

- A theoretical and experimental analysis of the turnover of substances in a closed microecosystem. II - The stable steady states and the limiting factors of turnover 03 p0384 A83-14326
 Stable ecological structures in time-lag models 03 p0376 A83-14361
 Numerical study of the stochastic behavior of a simple biological system 03 p0376 A83-14365
 Microbiological problems of closed ecological systems --- Russian book 13 p1906 A83-30425
 An evaluation of microorganisms for unconventional food regeneration schemes in CELSS - Research recommendations [SAE PAPER 820852] 13 p1899 A83-30940
 SOYCHMBR.I - A model designed for the study of plant growth in a closed chamber 13 p1899 A83-30941
 [SAE PAPER 820853] 13 p1899 A83-30941
 Plant growth and mineral recycle trade-offs in different scenarios for a CELSS --- Closed Ecological Life Support System [SAE PAPER 820855] 13 p1907 A83-30942
 Closed microbial ecosystems as gas exchange units in CELSS --- Controlled Environment Life Support System [SAE PAPER 820857] 13 p1907 A83-30943
 Changes in symbiotic and associative interrelations in a higher plant-bacterial system during space flight 19 p2878 A83-42058

CLOSED FAULTS

- U GEOLOGICAL FAULTS

CLOSED LOOP SYSTEMS

- U FEEDBACK CONTROL

CLOSURE LAW

- The prediction of the intermittency factor for turbulent shear flows [AIAA PAPER 83-0382] 05 p0635 A83-16683
 Operational evaluation of a turbulence closure model forecast system [AD-A125467] 06 p0791 A83-18460

- Towards a unification of the parameters underlying elementary particles and cosmology 06 p0835 A83-18896

- On low-order non-linear stochastic-dynamic systems --- for atmospheric circulation 11 p1632 A83-28079
 On a method for the closure of the energy equation formulated relative to the total enthalpy in the case of turbulent flow in a boundary layer 17 p2505 A83-37530
 Development of a turbulence closure model for geophysical fluid problems 17 p2507 A83-38227
 Variational approach to the closure problem of turbulence theory 21 p3128 A83-43931

CLOTH

- U FABRICS

CLOTHING

- NT FLIGHT CLOTHING
 NT GARMENTS
 NT GLOVES
 NT HELMETS
 NT PRESSURE SUITS
 NT PROTECTIVE CLOTHING
 NT SPACE SUITS
 NT SUITS
 Hygienic evaluation of clothing made of chemical fibers 05 p0677 A83-17191
 Features and testing of clean room apparel 13 p1865 A83-31525

CLOUD COVER

- Grouping of clouds in a numerical cumulus convection model 01 p0074 A83-10222
 Radar studies of clouds in various regions above the world ocean 01 p0076 A83-10831
 The relationship between the cloud amount and the temperature when averaged over a large space 02 p0213 A83-11978
 The parameterization of longwave flux in energy balance climate models 02 p0213 A83-12229
 Microwave noise temperature and attenuation of clouds - Statistics of these effects at various sites in the United States, Alaska, and Hawaii 02 p0164 A83-12618
 A diffusive model of the turbulent mixing of dry and cloudy air 02 p0215 A83-12942
 Horizontal displacement of simulated cloud particles by the propeller of an aeroplane --- particle measurement accuracy 02 p0216 A83-12944
 On the distribution and evolution of clouds and rain over the Vosges and Black Forest mountains - A three-dimensional mesoscale simulation with parameterized microphysics 03 p0368 A83-14437
 The icing of aircraft gas turbine engines 03 p0280 A83-14619
 Evaluation of methods for estimating solar irradiance in Canada 03 p0370 A83-14633
 On short term variations of zenith polarization during twilight 03 p0361 A83-14645
 Infrared emissivity of water clouds 03 p0371 A83-14654
 Effects of cloud shape on cloud field identification 03 p0371 A83-14656
 A climate index indicative of cloudiness derived from satellite infrared sounder data 03 p0371 A83-14658
 An estimate of the effect of the indicatrix of scattering on the mean free path lengths of photons in clouds 03 p0372 A83-14836
 The effect of cloud cover on radio-wave refraction 04 p0515 A83-15769
 The frequency of cloud-free viewing intervals [AIAA PAPER 83-0441] 05 p0666 A83-16715
 High resolution planetary albedos - Values and variability 05 p0660 A83-16906
 The effects of changing solar angles, cloud regimes, and air temperatures on the temperatures of contrasting surfaces 06 p0779 A83-18234
 Cloud-ensemble relations based on the gamma probability distribution for the higher-order models of the planetary boundary layer 06 p0789 A83-18254
 A parameterized model for global insolation under partially cloudy skies 06 p0792 A83-18552
 Contrast transmittance models for cloudy atmospheres 08 p1135 A83-22550
 Infrared remote sensing of the vertical and horizontal distribution of clouds 09 p1312 A83-23954
 A preliminary global oceanic cloud climatology from satellite albedo observations 09 p1314 A83-24275
 Mesoscale mapping of available hourly solar irradiance by use of data collected by 'Meteosat' 09 p1315 A83-24633
 Spectroscopic measurements of the 'additional absorbing mass' in total and partial cloudiness 09 p1316 A83-25055
 Extensive cloudiness and radiation 09 p1316 A83-25227

- The results of aircraft investigations of cloudiness and radiation carried out over the eastern Arctic during the Second Observational Period of the Global Weather Experiment 09 p1316 A83-25228

- A subsatellite experiment in the Arctic --- atmospheric radiation study 09 p1316 A83-25233
 Modeling the optical properties of Venusian clouds 09 p1367 A83-25237

- The effect of spatial and temporal averaging on sampling strategies for cloud amount data 10 p1451 A83-26100

- Modification of raindrop size distributions in subcloud downdrafts 11 p1627 A83-27034

- The statistical characterization of rain areas in terms of fractals 11 p1628 A83-27049
 Dual Doppler observations of diffusion and rolls --- due to atmospheric circulation patterns 11 p1629 A83-27059

- Cumulonimbus mother and daughter cells observed by NOAA7 - And 'The cumulus spore theory' 11 p1632 A83-27975

- A probability density function for the clearness index, with applications 12 p1749 A83-28938

- Climate studies from satellite observations - Special problems in the verification of earth radiation balance, cloud climatology, and related climate experiments 12 p1759 A83-29677

- Comparison of cloud top heights measured by airborne lidar and Tiros-N image data 12 p1759 A83-29678
 Validation of Nimbus-7 temperature-humidity infrared radiometer estimates of cloud type and amount 12 p1759 A83-29679

- Determination of surface global radiation using Meteosat images and ground based visibility measurements 12 p1760 A83-29681

- Satellite measurements of cloud reflectance and optical thickness 12 p1760 A83-29682

- Stereoscopic observations from meteorological satellites 12 p1760 A83-29694

- Applications of stereoscopic height computations from dual geosynchronous satellite data/joint NASA-Japan stereo project 12 p1761 A83-29699

- The use of stereoscopic satellite observation in the determination of the emissivity of cirrus 12 p1761 A83-29700

- An objective diagnostic aid in locating meteorologically significant boundaries 13 p1888 A83-30571

- Upper level cloud climatology from an orbiting satellite 13 p1893 A83-31040

- Mapping of global radiation and cloudiness from Meteosat image data - Theory and ground truth comparisons 14 p2048 A83-31844

- Determination of convective precipitation on the basis of Meteosat infrared data 14 p2055 A83-31846

- An interpretation of weather conditions on the basis of conventional analyses, and of diagnoses utilizing satellite imagery and model parameters 14 p2055 A83-31847

- Measurement of illumination in the cloud layer of Venus by means of small solar arrays 14 p1984 A83-32043

- A cloud formation process contradictory to the classical occlusion development investigated with satellite images and model output parameters 14 p2057 A83-32409

- Raindrop charges, electric field and space charge measurements at a mountain station covered with monsoon clouds 14 p2057 A83-32411

- Observation of wintertime clouds and precipitation in the Arctic Canada (POLEX-north). I - Characteristic features of clouds and precipitation 14 p2057 A83-32435

- Observation of wintertime clouds and precipitation in the Arctic Canada (POLEX-north). II - Characteristic properties of precipitation particles 14 p2057 A83-32436

- Observation of wintertime clouds and precipitation in the Arctic Canada (POLEX-north). III - Radar observation of precipitating clouds 14 p2057 A83-32437

- Identification of snow cover and cloud cover on the basis of the spectral brightness of near infrared radiation measured from space 14 p2058 A83-32495

- Analysis of cloud characteristics derived from archived satellite data 15 p2206 A83-34161

- The prediction of the dissipation of radiation fogs over Sofia airport 15 p2206 A83-34415

- Study of the deep cloud structure in the equatorial region of Jupiter from Voyager infrared and visible data 15 p2275 A83-34719

- An objective boundary layer characterization using satellite photographs 15 p2207 A83-35098

- The mesoscale and microscale structure and organization of clouds and precipitation in midlatitude cyclones. VI Wavelike rainbands associated with a cold-frontal zone 16 p2384 A83-35459

The mesoscale and microscale structure and organization of clouds and precipitation in midlatitude cyclones. VII Formation, development, interaction and dissipation of rainbands 16 p2384 A83-35460

The response of a spectral general circulation model to refinements in radiative processes 16 p2384 A83-35462

Remote determination of cloud liquid water path from bandwidth-limited shortwave measurements [AD-A130447] 16 p2384 A83-35465

Diurnal variations of satellite-measured black-body temperature areal distribution and eye diameter of mature typhoons 16 p2390 A83-36492

Empirical prediction of overcast area in the Northern Hemisphere using a NWP model (8L-NHM) output 16 p2390 A83-36497

A complex vortex-system observed by the AVHRR of NOAA 6 16 p2391 A83-36591

The development and persistence of a cumulo-nimbus-cluster over central Europe observed by Meteosat 2 17 p2547 A83-38513

Measured cloud data obtained in Northwest and Great Lakes United States and northern Canada during icing certification tests 17 p2549 A83-38719

Cloud encounter statistics in the 28.5-43.5 KFT altitude region from four years of GASP observations 17 p2550 A83-38733

Statistical models for meteorological data analysis 17 p2551 A83-38745

Remote sounding of cloud parameters from a combination of infrared and microwave channels 18 p2721 A83-39119

An explanation of uncertainties in point cloudiness/solar energy relationships 18 p2722 A83-39128

Determination of the attenuation of visible, infrared, and millimeter waves in clouds on the basis of meteorological models 18 p2674 A83-39427

The albedo of the underlying surface-cloudy atmosphere system 18 p2723 A83-39439

A model of a cloud ensemble with two zones of mass ejection from clouds 18 p2723 A83-39440

Comparison of parameters of wave storm zones in the Pacific Ocean with cloud information from satellites 18 p2724 A83-39443

A millimeter-wavelength dual-polarization Doppler radar for cloud and precipitation studies 18 p2726 A83-39873

The remote monitoring of cloud cover over the ocean in the infrared spectral band 18 p2731 A83-40596

Filtering of semitransparent cloud cover 18 p2692 A83-40597

Some radiation budget and cloud measurements derived from Meteosat 1 data 18 p2731 A83-40646

Synoptic cloud variations in a low resolution spectral atmospheric model 20 p3030 A83-42840

Backscatter and extinction in water clouds 20 p3031 A83-42859

The effect of the microstructure of clouds on their radio emission 20 p3031 A83-42873

The life cycle of a tornadic cloud as seen from a geosynchronous satellite 20 p3031 A83-43436

Aqueous-phase source of formic acid in clouds 20 p3028 A83-43555

Measurements of the mean, solar-fixed temperature and cloud structure of the middle atmosphere of Venus 21 p3240 A83-44391

The climatological minimum in tropical outgoing infrared radiation - Contributions of humidity and clouds 21 p3179 A83-44395

Method for calculating radio-brightness temperature in problems of satellite meteorology 21 p3181 A83-45294

Multiple scattering of optical pulses in scale model clouds --- impact on optical communications 22 p3274 A83-46081

Determination of the horizontal and vertical distribution of clouds from infrared satellite sounding data 22 p3340 A83-46140

Aviation climatology 23 p3486 A83-47126

Distribution of cumulonimbus cloud cover and thunderstorms above continents of the Northern Hemisphere 23 p3486 A83-47127

Experimental data on the typification of synoptic situations and cloud fields over Europe 23 p3486 A83-47128

Distribution of high clouds above the Northern Hemisphere 23 p3486 A83-47129

Method for investigating the distribution laws of values of meteorological visibility range in the case of a cloud-cover scale of 0 to 8 23 p3486 A83-47131

Features of the spatial-temporal distribution of meteorological visibility range in the case of a cloud-cover scale of 0 to 8 23 p3486 A83-47132

On the mechanism of variations of the height of low cloud cover (an attempt at a mesoanalysis) 23 p3487 A83-47144

Relative frequency and diurnal variation of high cold clouds in the tropical Atlantic and Pacific 23 p3490 A83-47403

Orbital and cloud cover sampling analyses for multisatellite earth radiation budget experiments 23 p3483 A83-48138

Satellite-derived cloud statistics for Great Plains cumulus 24 p3613 A83-49706

Characteristics and evolution of mesoscale cloud vortices occurring in polar airstreams [AD-A126050] 24 p3614 A83-49712

Spatial and temporal variations of cloud liquid water determined by aircraft and microwave radiometer measurements in northern Colorado orographic storms 24 p3615 A83-49724

CLOUD DISPERSAL

Peculiarities of laser radiation refraction in the clearing process of cloud medium 11 p1632 A83-27608

The turbulent dissipation of a cloud of heavy particles settling from a great height 13 p1872 A83-30295

CLOUD GLACIATION

A numerical study on the combined action of droplet coagulation, ice particle riming and the splintering process concerning maritime cumuli 01 p0074 A83-10220

Investigation of the radio characteristics of hailstorm clouds 02 p0212 A83-11691

Scattering by single ice needles and plates at 30 GHz 02 p0141 A83-12624

A numerical study of thunderstorm electrification using a three dimensional model incorporating the ice phase 02 p0215 A83-12938

Criteria for the formation and water content of cumulus clouds 03 p0364 A83-14097

The icing of aircraft gas turbine engines 03 p0280 A83-14619

Lidar identification of drop and crystal clouds 03 p0372 A83-14831

An approach to the radar investigation of the cell structure of hail processes 04 p0515 A83-15722

Influence of multidroplet size distribution on icing collection efficiency [AIAA PAPER 83-0110] 05 p0666 A83-16526

A comparison between the calculated and measured characteristics of an advection fog and a stratus over ice 09 p1316 A83-25229

Comparison of aircraft and dual-polarization radar measurements in convective clouds 11 p1629 A83-27065

On the size, shape, and orientation of noctilucent cloud particles 11 p1616 A83-28094

Meteorological problems of cloud physics and their theoretical and instrumental analysis; WOPHYS '82 Colloquium, Koenigstein im Taunus, May 17-19, 1982, Proceedings 15 p2204 A83-34051

On the effect of an ice particle enhancement process operating in supercooled continental clouds 15 p2205 A83-34063

Production of ice particles in clouds due to aircraft penetrations 18 p2721 A83-39120

The polarization structure of backscattering by water-droplet and ice clouds 18 p2730 A83-40080

The phase realignment of clouds 19 p2868 A83-41583

An application of chemical kinetic theory and methodology to characterize the ice nucleating properties of aerosols used for weather modification 22 p3342 A83-46942

Contact ice nucleation by submicron atmospheric aerosols 24 p3612 A83-49692

Measurements of natural ice nuclei with a continuous flow diffusion chamber 24 p3612 A83-49693

Observation of ice aggregation at temperatures near -50 C 24 p3612 A83-49699

Ice crystal and ice nucleus measurements in cap clouds 24 p3614 A83-49713

Vertical continuity of microphysical processes and updrafts in supercooled portions of Florida cumuli 24 p3614 A83-49716

Glaciating characteristics of Montana and Florida summer cumuli - Comparisons based on observations and modeling 24 p3614 A83-49717

Characteristics of icing conditions in wintertime stratiform clouds 24 p3614 A83-49719

Microphysical growth processes during a rapidly evolving orographic cloud system 24 p3615 A83-49725

CLOUD HEIGHT INDICATORS

Polarization studies of the Venus UV contrasts - Cloud height and haze variability 02 p0266 A83-12567

A climate index indicative of cloudiness derived from satellite infrared sounder data 03 p0371 A83-14658

Stereoscopic imaging from polar orbit and synthetic stereo imaging --- for photogrammetric cloud height determination 12 p1731 A83-29697

DFVLR-remote slant visual range (SVR) and wind vector measuring systems 17 p2552 A83-38750

On the mechanism of variations of the height of low cloud cover (an attempt at a mesoanalysis) 23 p3487 A83-47144

Estimating the temperature and height of overshooting thunderstorm tops from geostationary satellite infrared data 24 p3615 A83-49727

CLOUD PHOTOGRAPHS

Objective analysis of satellite cloud imagery 01 p0074 A83-10046

Cloud-top structure of tornadic storms on 10 April 1979 from rapid scan and stereo satellite observations 02 p0214 A83-12323

Photographic documentation of some distinctive cloud forms observed beneath a large cumulonimbus 16 p2387 A83-35743

Filtering of semitransparent cloud cover 18 p2692 A83-40597

CLOUD PHOTOGRAPHY

Mesoscale convective complexes over the United States during 1981 - Annual summary 02 p0218 A83-13064

Classification of clouds on multispectral images acquired by meteorological satellites 08 p1138 A83-21907

Results from a comparison of ground and satellite observations of cloud shapes 09 p1317 A83-25236

Tropical storm structure revealed by stereoscopic photographs from Skylab 12 p1760 A83-29695

Stereoscopic imaging from polar orbit and synthetic stereo imaging --- for photogrammetric cloud height determination 12 p1731 A83-29697

Stereoscopic observations of hurricanes and tornadic thunderstorms from geosynchronous satellites 12 p1761 A83-29698

Preliminary efforts in developing a technique that uses satellite data for analyzing precipitation from extratropical cyclones 13 p1887 A83-30562

A mesoscale, climatologically-based forecast technique for Colorado 13 p1888 A83-30568

Digital processing of Spacelab imagery 13 p1846 A83-30769

Rope cloud over land 15 p2204 A83-33886

Improvements in cloud photogrammetry using airborne, side-looking, time-lapse cameras 22 p3307 A83-45707

Cloud photogrammetry from aircraft 24 p3613 A83-49710

CLOUD PHYSICS

Remote determination of cloud properties from solar photometric data 01 p0074 A83-10043

Radar studies of clouds in various regions above the world ocean 01 p0076 A83-10831

The physics of clouds and cloud modification --- Russian book 01 p0076 A83-11496

Convective cloud merging and its effect on rainfall 02 p0215 A83-12827

Aircraft observations of marine stratocumulus during JASIN --- Joint Air-Sea Interaction Experiment 02 p0215 A83-12940

Noctilucent clouds - Simulation studies of their genesis, properties and global influences 04 p0509 A83-14973

An approach to the radar investigation of the cell structure of hail processes 04 p0515 A83-15722

Mathematical description of the shape of conical hydrometeors 04 p0517 A83-15941

Numerical study of the effect of CCN on the size distribution of cloud droplets. I - Cloud droplets in the stage of condensation growth --- Cloud Condensation Nuclei 04 p0518 A83-16017

A technique for parameterization of the turbulence associated with precipitation events in a three-dimensional model of cloud convection 06 p0788 A83-18060

Altitude, thickness and charge concentration of charged regions of four thunderstorms during trip 1981 based upon in situ balloon electric field measurements 07 p0958 A83-20093

Cloud height differences on Saturn 08 p1189 A83-22934

A theoretical determination of capture efficiency of small columnar ice crystals by large cloud drops 08 p1142 A83-23010

Measured collection efficiencies for cloud drops --- collision and coalescence mechanisms 08 p1142 A83-23011

Case studies of radiation in the cloud-capped atmospheric boundary layer 09 p1310 A83-23356

The mirror image relation in the vertical distributions of electric field and precipitation charge in winter thunderclouds 09 p1311 A83-23897

Cloud dynamics; Proceedings of the Symposium, Hamburg, West Germany, August 17-28, 1981 09 p1311 A83-23951

An introduction to shallow convective systems --- in clouds 09 p1312 A83-23952

Radiative influence on small scale convection within stratus cloud layers 09 p1312 A83-23953

On the preferred mode of cumulus convection in a conditionally unstable atmosphere

09 p1312 A83-23958

Toward a unified theory of atmospheric convective instability

09 p1312 A83-23959

Cloud bands in the atmosphere

09 p1312 A83-23960

An introduction to deep convective systems --- thunderstorm development

09 p1312 A83-23961

The development of the cumulonimbus clouds which move along a valley

09 p1313 A83-23964

Precipitation in convective storms - An observational and numerical study

09 p1313 A83-23971

Turbulence parameterization in a deep convection model --- for cloud physics

09 p1313 A83-23972

The First GARP Global Experiment, Volume 2 - Polar aerosols, extensive cloudiness, and radiation --- Russian book

09 p1316 A83-25226

The variability of the optical characteristics of cirrostratus clouds

09 p1317 A83-25234

A method of calculating fluxes and the influx of long-wave and solar radiation in a model of low clouds and fogs

09 p1317 A83-25235

Topics in the theory of radiative transfer in horizontally inhomogeneous media --- scattering of sunlight in clouds

09 p1317 A83-25255

Cloud and aerosol effects in radiant heat transfer --- in planetary atmospheres

09 p1367 A83-25260

Cloud liquid water content comparisons in rain using radar differential reflectivity measurements and aircraft measurements

11 p1629 A83-27064

Millimeter wave Doppler radar

11 p1631 A83-27095

Role of gas absorption in formation of fluctuations in parameters of cleared cloud medium and laser radiation

11 p1631 A83-27606

On the size, shape, and orientation of noctilucent cloud particles

11 p1616 A83-28094

Numerical modeling of the influence of thermals on the development of cumulus clouds

13 p1883 A83-30030

The upslope effect

13 p1888 A83-30565

Verification of MOS guidance for cloud amount, ceiling, and visibility --- model output statistics

13 p1889 A83-30581

Deductions concerning accumulations of electrified particles in thunderclouds based on electric field changes associated with lightning

13 p1892 A83-30904

Investigation of the structure of the Venus clouds using the nephelometers on the Venera-13 and Venera-14 probes

14 p2111 A83-31967

Refining a radiation model of a stratiformis cloud

14 p2058 A83-32856

The possible nature of the prethunderstorm electromagnetic radiation of convective clouds

14 p2059 A83-32864

Meteorological problems of cloud physics and their theoretical and instrumental analysis; WOPHYS '82 Colloquium, Koenigstein im Taunus, May 17-19, 1982, Proceedings

15 p2204 A83-34051

The dependence of ice formation on the evolution of the liquid phase

15 p2204 A83-34052

The measurement of cloud droplet concentration with a hot film probe

15 p2204 A83-34053

The airborne Knollenberg cloud droplet spectrometer probes of DFVLR

15 p2164 A83-34054

The measurement of the humidity spectrum and of the concentration of the cloud condensation nuclei

15 p2164 A83-34055

The determination of representative cloud droplet spectra

15 p2204 A83-34056

The measurement of the size distribution of atmospheric ice nuclei, taking into consideration humidity

15 p2204 A83-34057

A model experiment concerning particle scavenging by cloud and rain drops

15 p2205 A83-34058

The influence of aerosol and meteorological parameters on maximum supersaturation and activation of particles in a cloud

15 p2205 A83-34059

Condensation growth of droplet spectra

15 p2205 A83-34060

On the mathematical simulation of non-equilibrium cloud condensation rates

15 p2205 A83-34061

On the effect of radiative exchange in the 8 to 12 micron spectral region on the diffusional growth of ice crystals

15 p2205 A83-34062

Detailed and parameterized modeling of cloud-microphysics in a stationary cloud model

15 p2205 A83-34064

A numerical model of the dynamics and microphysics of warm cumulus convection - Model description and preliminary results

15 p2205 A83-34065

The numerical simulation of the interaction of cloud formation and lee waves

15 p2206 A83-34067

A quasi-one-dimensional, time-dependent and non-precipitating cumulus cloud model - On the bimodal distribution of cumulus cloud height

16 p2384 A83-35464

Comparison of Monte Carlo calculations with observations of light scattering in finite clouds

16 p2387 A83-35491

Comments on 'Skylab near-infrared observations of clouds indicating supercooled liquid water droplets'

16 p2387 A83-35496

Numerical experiments with a one-dimensional higher order turbulence model - Simulation of the Wangarda Day 33 case

16 p2387 A83-35795

The clouds are hazes of Venus

17 p2617 A83-37417

Progress in cloud physics 1979-1982

17 p2547 A83-38314

Cloud electrification --- during thunderstorms

17 p2547 A83-38315

The Fog Project - 1982

17 p2549 A83-38721

Convection model for stratus cloud over a warm water surface

18 p2720 A83-39012

Extrapolation of the Goff-Gratch formula for vapor pressure of liquid water at temperatures below 0 deg C

18 p2723 A83-39143

The mesoscale and microscale structure and organization of clouds and precipitation in midlatitude cyclones. VIII - A model for the 'seeder-feeder' process in warm-frontal rainbands

18 p2729 A83-40035

Theoretical experiments on cumulus dynamics

18 p2729 A83-40039

A numerical simulation of winter cumulus electrification.

18 p2729 A83-40040

Observations of liquid water in orographic clouds over Elk Mountain

18 p2729 A83-40042

The phase realignment of clouds

19 p2868 A83-41583

The effect of the microstructure of clouds on their radio emission

20 p3031 A83-42873

Enhancement and initiation of a cumulus by a heat island

20 p3032 A83-43462

Boundary layer evolution in the region between shore and cloud edge during cold-air outbreaks

21 p3180 A83-44705

The role of cloud top entrainment in cumulus clouds

21 p3180 A83-44706

Characteristics of the precipitation of a cloud of hot particles onto a horizontal surface

21 p3133 A83-45349

Diurnal radiance patterns of finite and semi-infinite clouds in observations of cloud fields

22 p3338 A83-45708

Bulk parameterization of the snow field in a cloud model

22 p3338 A83-45709

The physics of thunderclouds

22 p3339 A83-45877

A cloud physical parameterization method using movable basis functions - Stochastic coalescence parcel calculations

22 p3341 A83-46850

Positive cloud to ground lightning return strokes

24 p3610 A83-49336

Conference on Cloud Physics, Chicago, IL, November 15-18, 1982, Preprints

24 p3610 A83-49676

Boundary layer processes and cloud formation

24 p3610 A83-49677

Mechanisms of radiation fog formation on four consecutive nights

24 p3611 A83-49678

Physical properties of arctic stratus clouds

24 p3611 A83-49679

An investigation of the interaction between developing convective systems and the boundary layer --- for south Florida cumulonimbus

24 p3611 A83-49680

A mechanism for the initiation of convective cumulus clouds in mountainous terrain

24 p3611 A83-49682

Aircraft observations of 'turbulent fluxes' of momentum, heat and moisture in the sub-cloud layer and associated cloud microphysical and electrical characteristics

24 p3611 A83-49683

Interstitial CCN measurements --- Cloud Condensation Nuclei

24 p3611 A83-49687

An experimental study of the ice column habit transitions --- crystal growth in atmosphere

24 p3611 A83-49690

Evidence for the production of ice particles in clouds due to aircraft penetrations

24 p3612 A83-49691

Clouds and entrainment --- cumulus convective turbulence in clear air

24 p3612 A83-49694

Cloud droplet spectra in summertime cumulus clouds

24 p3612 A83-49695

5-cm radar echoes and their microphysical significance in Florida cumuli

24 p3612 A83-49697

Aircraft observations of large scale cloud systems

24 p3612 A83-49698

Merging of moderate-sized convective cells on day 261 of GATE

24 p3613 A83-49701

Ice crystal and ice nucleus measurements in cap clouds

24 p3614 A83-49713

The three-dimensional simulation of Florida convective clouds-sensitivity to cloud microphysical processes

24 p3614 A83-49714

Graupel characteristics in relation to the dynamics of Florida cumuli

24 p3614 A83-49715

Vertical continuity of microphysical processes and updrafts in supercooled portions of Florida cumuli

24 p3614 A83-49716

Glaciating characteristics of Montana and Florida summer cumuli - Comparisons based on observations and modeling

24 p3614 A83-49717

Droplet spectra and liquid water content measurements in aircraft icing environments

24 p3614 A83-49718

5500 miles of liquid water and drops size measurements in supercooled clouds below 10,000 feet agl

24 p3614 A83-49720

Microphysical influences on aircraft icing

24 p3546 A83-49722

Microphysical growth processes during a rapidly evolving orographic cloud system

24 p3615 A83-49725

Retrieval of microphysical and thermal variables in observed convective storms

24 p3616 A83-49731

CLOUD SEEDING

The physics of clouds and cloud modification --- Russian book

01 p0076 A83-11496

Studies of variations of cell parameters to be exceeded to confirm certain seeding hypotheses --- for cumulus clouds

11 p1626 A83-27031

Radar reflectivity seeding signatures

11 p1627 A83-27032

An intercomparison of two radars used in the Montana HIPLEX

11 p1627 A83-27038

On using historical comparisons in evaluating cloud seeding operations

18 p2725 A83-39684

An application of chemical kinetic theory and methodology to characterize the ice nucleating properties of aerosols used for weather modification

22 p3342 A83-46942

The use of model representations and empirical data in the problem of passive-active radar sounding of clouds and precipitation

23 p3487 A83-47138

CLOUDS

NT ANVIL CLOUDS

NT BARIUM ION CLOUDS

NT CAP CLOUDS

NT CHEMICAL CLOUDS

NT CIRROSTRATUS CLOUDS

NT CIRRUS CLOUDS

NT CLOUDS (METEOROLOGY)

NT CONVECTION CLOUDS

NT CUMULONIMBUS CLOUDS

NT CUMULUS CLOUDS

NT ELECTRON CLOUDS

NT HYDROGEN CLOUDS

NT MAGELLANIC CLOUDS

NT MOLECULAR CLOUDS

NT NOCTILUCENT CLOUDS

NT PLASMA CLOUDS

NT STRATOCUMULUS CLOUDS

NT STRATUS CLOUDS

NT VENUS CLOUDS

A search for diffuse band profile variations in the rho Ophiuchi cloud

03 p0423 A83-14194

Magnetic clouds - Voyager observations between 2 and 4 AU

03 p0438 A83-14917

A magnetic cloud and a coronal mass ejection

07 p1037 A83-20189

Thermal infrared constraints on ammonia ice particles as candidates for clouds in the atmosphere of Saturn

11 p1684 A83-27361

Spatially resolved methane band photometry of Saturn. II - Cloud structure models at four latitudes

11 p1684 A83-27362

The state of clouds in a violent interstellar medium

11 p1680 A83-28259

Cometary Globule 1 --- dense interstellar dust cloud

11 p1675 A83-28270

Numerical simulations of collapsing, isothermal, magnetic clouds

13 p1945 A83-30365

Artificial viscosity and the simulation of fragmentation --- of rotating self-gravitating clouds

13 p1945 A83-30368

The dissipation of a sodium cloud

13 p1882 A83-31627

Microphysical properties of the Shuttle exhaust cloud

17 p2536 A83-38707

Experimental comparison of icing cloud instruments

19 p2794 A83-42099

The distribution of absorption lines in QSO spectra

21 p3232 A83-44731

On the fragmentation of differentially rotating clouds --- in stellar formation

21 p3233 A83-44748

- El Chichon eruption cloud - Latitudinal variation of the spectral optical thickness for October 1982 22 p3333 A83-46884
- El Chichon eruption cloud - Comparison of lidar and optical thickness measurements for October 1982 22 p3334 A83-46885

CLOUDS (METEOROLOGY)

- NT ANVIL CLOUDS
- NT BARIUM ION CLOUDS
- NT CAP CLOUDS
- NT CHEMICAL CLOUDS
- NT CIRROSTRATUS CLOUDS
- NT CIRRUS CLOUDS
- NT CONVECTION CLOUDS
- NT CUMULONIMBUS CLOUDS
- NT CUMULUS CLOUDS
- NT NOCTILUCENT CLOUDS
- NT STRATOCUMULUS CLOUDS
- NT STRATUS CLOUDS
- Investigation of the radio characteristics of hailstorm clouds 02 p0212 A83-11691
- Cloud thermodynamic models in saturation point coordinates 02 p0213 A83-12232
- Correlation between surface and cloud base CCN spectra in Montana --- Cloud Condensation Nuclei 02 p0216 A83-12953
- Emission characteristics of earth and cloud surfaces as measured by the ERB scanning channels on the NIMBUS-7 satellite 03 p0370 A83-14647
- Numerical experiments on the role of radiative processes in the development and maintenance of upper level clouds 03 p0371 A83-14653
- Effects of cloud shape on cloud field identification 03 p0371 A83-14656
- Comparison of parallel plate thermal diffusion chambers used for measuring the cloud condensation nuclei concentration in the atmosphere 05 p0668 A83-17450
- Cloud-cluster-scale circulations and the vorticity budget of synoptic-scale waves over the eastern Atlantic intertropical convergence zone 06 p0792 A83-18470
- El Chichon climate effect estimated 06 p0786 A83-18815
- Estimation of sulfate deposition 07 p0957 A83-20811
- Extinction by clouds consisting of polydisperse and randomly oriented nonspherical particles at arbitrary wavelengths 08 p1135 A83-22356
- Estimation of liquid water amount in an extended cloud by Nimbus-5 microwave data 09 p1311 A83-23894
- Cloud bands in the atmosphere 09 p1312 A83-23960
- Complex radar methods of hail cloud structure, evolution dynamics and microstructure 09 p1313 A83-23967
- Kinetics of 'blurring' process accompanying CO₂ laser radiation propagation in cloud medium 11 p1632 A83-27609
- Pollutant transfer in upland regions by occult precipitation 11 p1613 A83-28393
- Theoretical performance of a vortex generator type of cloud droplet sampler 12 p1728 A83-28897
- Operational use of the deformation zone concept in analyzing and forecasting cloud boundaries 13 p1889 A83-30578
- Composite study of comma clouds and their association with severe weather over the Great Plains 13 p1890 A83-30584
- Size distribution of radar echoes as an indicator of growth mechanisms in monsoon clouds around Madras 13 p1893 A83-31039
- Cloud and precipitation chemistry research and Whiteface Mountain 13 p1873 A83-31527
- Method and results of an analysis of comma cloud developments by means of vorticity fields from upper tropospheric satellite wind data 14 p2055 A83-31848
- Numerical modeling of an atmospheric front with a cloud system and precipitation 14 p2056 A83-32367
- Solar-radiation transfer in the atmosphere in the presence of semitransparent clouds --- satellite multispectral photography 14 p2035 A83-32500
- Experiments in shower-top forecasting using an interactive one-dimensional cloud model 16 p2389 A83-36036
- The 1980 eruptions of Mount St. Helens - Physical and chemical processes in the stratospheric clouds 16 p2380 A83-36146
- An investigation of the spectral transmission of a crystalline cloud medium 16 p2392 A83-36869
- Determination of supercooled liquid water content by measuring rime rate 18 p2721 A83-39116
- Improved cloud motion wind vector and altitude assignment using VAS --- Visible Infrared Spin-Scan Radiometer Atmospheric Sounder 18 p2722 A83-39132

- On the bispectral method for cloud parameter determination from satellite VISSR data - Separating broken cloud and semitransparent cloud 18 p2723 A83-39137
- Design and verification of a cloud field optical simulator 18 p2727 A83-39886
- The problem of the scattering of light by a horizontally inhomogeneous cloud 18 p2730 A83-40081
- The International Satellite Cloud Climatology Project (ISCCP) - The first project of the World Climate Research Programme 18 p2730 A83-40320
- Acid clouds and precipitation in eastern Colorado 19 p2863 A83-41982
- A separator for obtaining samples of cloud water in aircraft 19 p2849 A83-41983
- Influence of the precipitations and clouds on the performance of a synthetic aperture radar 22 p3289 A83-46197
- Experimental thermal-microwave radiometric determination of the moisture content of a cloudy atmosphere 23 p3487 A83-47139
- Information content, accuracy, and optimal conditions of indirect ground-based thermal-microwave radiometric measurements of the integral water-vapor content of the atmosphere, and the water content and effective temperature of clouds 23 p3487 A83-47140
- A method for determining water-vapor content in the atmosphere on the basis of joint infrared and microwave radiometric measurements 23 p3487 A83-47141
- Infrared cooling in cloudy atmospheres - Precision of grid point selection for numerical models 23 p3491 A83-47416
- Lidar measurements of clouds 23 p3491 A83-47804
- The pH and ionic composition of stratiform cloud water 23 p3479 A83-48684
- Temperature and humidity spectra in cloud- and cloud-free air and associated cloud electrical and microphysical characteristics 24 p3611 A83-49681
- The broadening of droplet spectra by cloud top entrainment 24 p3612 A83-49696
- A method of determining mesoscale air motions for cloud physical studies and its application to the water budget of a squall line 24 p3613 A83-49702
- Sensitivity of radiative-convective processes to boundary layer clouds 24 p3613 A83-49703
- Cloud particle identification near the melting layer with dual polarization K-band Doppler radar 24 p3614 A83-49721
- Mature thunderstorm cloud top structure - Three-dimensional numerical simulation versus satellite observations 24 p3615 A83-49730
- CLUSTER ANALYSIS**
- A group-linking classifier 01 p0096 A83-11412
- Multidimensional clustering - An application to three-dimensional /3D/ surface extraction 09 p1265 A83-23533
- Discrimination of phosphate, gypsum, limestone, halide and quartz-sand deposits in south-central Tunisia by cluster analysis of Landsat multispectral data 09 p1286 A83-24552
- Cluster studies of CO adsorption. III - CO on small Cu clusters 13 p1817 A83-30965
- Probabilistic cluster labeling of imagery data 15 p2224 A83-33686
- Nearest neighbors and automatic classification - Applications to industrial data --- French thesis 15 p2220 A83-33696
- Cluster analysis of the nonlinear evolution of large-scale structure in an axion/gravitino/photino-dominated universe 21 p3227 A83-44200
- Statistics of binary stars. I - Multivariate analysis of spectroscopic binaries 21 p3223 A83-44427
- Simulation tool supporting the development of sensor signal processing 22 p3278 A83-46595
- CLUTTER**
- A technique to empirically model clutter signals in airborne pulse Doppler radar 01 p0008 A83-11251
- Theoretical limitation of the sea on the detection of low Doppler targets by over-the-horizon radar 01 p0032 A83-11351
- Simulation of mid-infrared clutter rejection. I - One-dimensional LMS spatial filter and adaptive threshold algorithms 02 p0177 A83-12305
- Adaptive spatial/temporal/spectral filters for background clutter suppression and target detection 03 p0386 A83-13874
- An adaptive sensitive time control circuit implemented with a CCD sampled delay line for clutter rejection in a radar processor 04 p0474 A83-16449
- An adaptive MTI for weather clutter suppression 06 p0754 A83-19029
- MTI processing and Weibull-distributed ground clutter 06 p0748 A83-19047

- Design of recursive filters to simulate clutter for the evaluation of radar MTI processors 08 p1079 A83-21973
- Clutter rejection for infrared surveillance sensors 08 p1094 A83-22437
- Simulation of clutter rejection signal processing for mid-infrared surveillance systems 08 p1094 A83-22438
- Spectral discrimination for long range search/track infrared systems 08 p1094 A83-22442
- Recent measurements of earth background spatial radiance variations 08 p1103 A83-22843
- Radiative transfer and 4.3 micron atmospheric clutter observations --- with balloon-borne sensors 08 p1051 A83-22849
- An adaptive scheme for optimal target detection in variable clutter environment 09 p1200 A83-24779
- A real-time Doppler spectrum analyzer --- for radar clutter rejection 11 p1624 A83-27008
- Ground clutter rejection in the frequency domain --- for radar meteorology applications 11 p1625 A83-27019
- Autocorrelation techniques for ground clutter rejection 11 p1626 A83-27021
- Evaluating ground clutter filters for weather radars 11 p1626 A83-27022
- Considerations for the design of ground clutter cancelers for weather radars 11 p1626 A83-27023
- On ambiguity resolution by random phase processing --- of cluttered meteorological radar signals 11 p1626 A83-27024
- Adaptive clutter suppression for airborne phased array radars 11 p1527 A83-27919
- A study on the MTI weather radar system for rejecting ground clutter 13 p1894 A83-31670
- Nonstationary probabilistic target and clutter scattering models 15 p2148 A83-35185
- Maneuvering target tracking in a cluttered environment with variable dimension filter 17 p2567 A83-37125
- Parametric estimation of Doppler spectral moments - An alternative ground clutter rejection technique --- for radar meteorology 18 p2727 A83-39879
- Group-complementary array coding for radar clutter rejection 19 p2826 A83-41144
- The effect of the initial approximation on the convergence speed of processes of the adaptive adjustment of clutter-suppression systems 19 p2835 A83-41775
- Radar performance studies of adaptive lattice clutter-suppression filters 20 p2964 A83-43676
- Weibull-distributed sea clutter 20 p2965 A83-43687
- The detection of unresolved targets using the Hough transform 21 p3120 A83-44276
- Consistency and robustness of PDAF for target tracking in cluttered environments --- Probabilistic Data Association Filter 21 p3194 A83-44370
- Simplified calculation of the effects of jitter on clutter leakage --- performance prediction of mosaic infrared sensor 22 p3294 A83-46830
- False-alarm probabilities for a log-t detector in K-distributed clutter 23 p3444 A83-48716
- CMOS**
- System programmable redundancy in a 64K EEPROM --- Electronically Erasable PROM 01 p0089 A83-11213
- Test chips for custom ICs - Six kinds of test structures 02 p0167 A83-11824
- A radiation hardened 256 x 4 bulk CMOS RAM 03 p0313 A83-13996
- Hot-electron induced excess carriers in MOSFET's 05 p0624 A83-17287
- Self-registered gradually doped source drain extension short channel CMOS/SOS devices 05 p0624 A83-17291
- SOI/CMOS circuits fabricated in zone-melting-recrystallized Si films on SiO₂-coated Si substrates 05 p0624 A83-17292
- Gamma-ray irradiation effects on VLSI geometry MOSFETs fabricated on laser recrystallized SOI wafers 05 p0627 A83-17511
- CMOS/SOS 4K RAMS hardened to 100 Krads/Si/ 05 p0627 A83-17513
- Radiation response of two Harris semiconductor radiation hardened 1K CMOS RAMS 05 p0627 A83-17514
- Thermal annealing of radiation damage in CMOS ICs in the temperature range -140 C to +375 C 05 p0627 A83-17515
- Latchup window tests 05 p0628 A83-17526
- Error analysis and prevention of cosmic ion-induced soft errors in static CMOS RAMs 05 p0629 A83-17537
- Single event error immune CMOS RAM 05 p0629 A83-17538
- Single event upset vulnerability of selected 4K and 16K CMOS static RAM's 05 p0629 A83-17539

Effect of CMOS miniaturization on cosmic-ray-induced error rate 05 p0629 A83-17540

A low-power, high-throughput maximum-likelihood convolutional decoder chip for NASA's 30/20 GHz program 07 p0917 A83-19754

Investigation of aspects of the design of base-crystal matrix computing devices 08 p1152 A83-22182

Latchup-free Schottky-barrier CMOS 09 p1255 A83-24494

Low-power high-drive CMOS operational amplifiers 10 p1410 A83-26125

Portable design rules for bulk CMOS 11 p1562 A83-28150

An LSI adaptive array processor 15 p2216 A83-33887

Use of a Cf-252 source in cosmic ray simulation studies on CMOS memories 15 p2152 A83-34519

On testing stuck-open faults in CMOS combinational circuits 15 p2153 A83-35141

Design and performance of two 1K CMOS/SOS hardened RAMs 16 p2346 A83-36024

NORA - A racefree dynamic CMOS technique for pipelined logic structures 19 p2887 A83-40790

A versatile CMOS rate multiplier/variable divider 19 p2837 A83-40791

High-density and reduced latchup susceptibility CMOS technology for VLSI 19 p2837 A83-41020

Switching conditions for CMOS latch-up path with shunt resistances 21 p3124 A83-43858

Subthreshold currents in CMOS transistors made on oxygen-implanted silicon 21 p3126 A83-44962

CN EMISSION

CN in dark clouds 07 p1020 A83-21119

Determination of the physical parameters of the neutral coma of Comet Bennett /1970 II/ 11 p1679 A83-27889

Certain parameters of the CN atmosphere of Comet Bradfield 1979I 11 p1673 A83-27892

On the contributions of the Orion reflection nebulosity to the continuous UV spectrum of the Herbig-Haro objects HH 1 and HH 2 and of the C-S Star 19 p2921 A83-41650

A theoretical investigation of the radiative properties of the CN red and violet systems 21 p3238 A83-45572

CNOIDAL WAVES

Solitary waves induced by boundary motion 21 p3199 A83-43826

Nonlinear lattice and soliton theory 22 p3353 A83-45696

COAGULATION

NT BLOOD COAGULATION

A numerical investigation of the transport of coagulating aerosols in the atmosphere of a city 16 p2372 A83-36875

COAL DERIVED GASES

Combustion characteristics of hydrogen-carbon monoxide based gaseous fuels 01 p0023 A83-11491

Development and application of advanced diagnostics methods in fossil fuel combustion studies 07 p0902 A83-20436

Coal gas as a feed fuel for phosphoric acid fuel cell power plants 20 p3012 A83-42952

COAL DERIVED LIQUIDS

The properties of fuel fractions obtained by the hydrogenation of Kansk-Achinsk coal 10 p1401 A83-26920

Effect of using emulsions of high nitrogen containing fuels and water in a gas turbine combustor on NOx and other emissions [ASME PAPER 82-GT-224] 18 p2673 A83-39992

COAL GASIFICATION

NOx results from two combustors tested on medium BTU coal gas 01 p0070 A83-11493

Clean-up and processing of coal-derived gas for hydrogen applications 11 p1611 A83-27336

Coal gasification using solar energy 13 p1872 A83-31612

Coal gas as a feed fuel for phosphoric acid fuel cell power plants 20 p3012 A83-42952

COAL UTILIZATION

NOx formation experiments in an MHD simulation facility 04 p0507 A83-16103

Toroidal flow coal-fired MHD combustor design study and tests [AIAA PAPER 83-0467] 05 p0686 A83-16734

Remote sensing of coal-fired MHD by optical diagnostic techniques [AIAA PAPER 83-0469] 05 p0643 A83-16736

Development and application of advanced diagnostics methods in fossil fuel combustion studies 07 p0902 A83-20436

Flames with impinging jets 07 p0882 A83-21423

An isothermal second-order Ringbom-Stirling engine computer program 11 p1587 A83-27281

Polarization and sidewall effects in a coal-fired MHD channel 13 p1924 A83-30188

The atmospheric oxidation of flue gases from a coal-fired power plant - A comparison between smog chamber and airborne plume sampling 15 p2193 A83-33503

Infrared optical properties of a coal-fired power plant plume 16 p2372 A83-36760

Comparison of radiative transfer approximations for a highly forward scattering planar medium 18 p2680 A83-39181

Economic aspects of advanced coal-fired gas turbine locomotives [ASME PAPER 83-GT-241] 23 p3514 A83-48031

The coal-fired gas turbine locomotive - A new look [ASME PAPER 83-GT-242] 23 p3466 A83-48032

COALESCENCE

U COALESCING

COALESCING

Measured collection efficiencies for cloud drops --- collision and coalescence mechanisms 08 p1142 A83-23011

A study of the coalescence process inside the miscibility gap in Zn-Bi alloys 20 p2942 A83-43306

COANDA EFFECT

Interaction of a pair of curved wall jets after a circular cylinder [AIAA PAPER 83-0290] 05 p0584 A83-16632

A study of the momentum loss of a slot jet propagating along a curved surface 17 p2450 A83-37639

The Coanda/refraction concept for gas turbine engine test cell noise suppression [SAE AIR 1813] 17 p2471 A83-38105

Turbulent wall jet issued from a Coanda nozzle 24 p3580 A83-49808

COARSENESS

On particle coarsening during sintering of silicon 04 p0464 A83-16271

COASTAL CURRENTS

Monthly mean sea-level variability along the west coast of North America 05 p0669 A83-17233

A finite element method for the shallow water equations 08 p1089 A83-23201

Norwegian remote sensing experiment in a marginal ice zone 13 p1894 A83-31198

Gulf Stream frontal statistics from Florida Straits to Cape Hatteras derived from satellite and historical data 14 p2060 A83-33077

Subsurface energetics of the Gulf Stream cyclonic frontal zone off Onslow Bay, North Carolina 14 p2060 A83-33083

Initial observations of the subsurface structure and short-term variability of the seaward deflection of the Gulf Stream off Charleston, South Carolina 14 p2060 A83-33085

The influence of a coastal headland on oceanic boundary currents 15 p2208 A83-34325

Analysis of effects after typhoon 8115 in coastal area and fields in Hokkaido, Northern Japan, using Landsat MSS data 17 p2534 A83-38453

An observation of the surface circulation in a Gulf Stream frontal perturbation 19 p2869 A83-41131

Peru coastal currents during El Nino - 1976 and 1982 22 p3344 A83-46802

Large-scale thermal anomalies in the California current during the 1982-1983 El Nino 23 p3493 A83-47857

COASTAL DUNES

U DUNES

COASTAL ECOLOGY

The use of remote sensing in global biosystem studies --- in ecology 19 p2861 A83-42040

Remote sensing for coastal areas 22 p3343 A83-46144

COASTAL MARSHLANDS

U MARSHLANDS

COASTAL PLAINS

The depth of the daytime mixed layer at two coastal sites - A model and its validation 06 p0788 A83-18057

Correlation between the SIR-A radar survey, the Landsat data, and the IR surveys in the Corinth canal zone 17 p2534 A83-38451

COASTAL WATER

Detection of coastal zone environmental conditions using synthetic aperture radar 01 p0076 A83-10068

A comparison data set for the evaluation of remote sensing systems ability for ocean wave data collection 01 p0048 A83-10071

Remote sensing and geographic data bases as applied to the Louisiana coastal zone 01 p0064 A83-10074

Effect of particle size distribution and chlorophyll content on beam attenuation spectra 02 p0203 A83-12314

Application of remote sensing techniques in oceanographic studies of the British Columbia Salmon Fishery 03 p0347 A83-14258

Passive microwave detection of river-plume fronts in the German Bight 05 p0646 A83-17713

Delineation of estuarine fronts in the German Bight using airborne laser-induced water Raman backscatter and fluorescence of water column constituents 05 p0646 A83-17715

Laboratory analysis of techniques for remote sensing of estuarine parameters using laser excitation 06 p0762 A83-18583

Remote sensing /Nimbus-7 CZCS/ analysis of phytoplankton distribution in coastal waters of the Gulf of Lions /northwestern Mediterranean/ 08 p1143 A83-21953

An operational program for monitoring surface temperatures of lakes and coastal-zone waters in Canada from polar-orbiting satellite infrared data 08 p1143 A83-21955

Remote sensing of coastal processes with emphasis on the Nile Delta 09 p1286 A83-24556

The legal regime of the airspace above the exclusive economic zone 09 p1351 A83-25119

Field investigation of techniques for remote laser sensing of oceanographic parameters 10 p1419 A83-25643

Doppler radar measurements of moisture divergence in a coastal cyclone 11 p1630 A83-27075

Kinematics and correlation of the surface wind field in the South Atlantic Bight 14 p2059 A83-33079

Canadian Landsat studies for monitoring hydrologic conditions and coastal environments - A summary 15 p2183 A83-33579

Temporal analysis of suspended solid in Tokyo Bay by Landsat data 15 p2183 A83-33580

'Larus' and 'VP-1' tested in winter 1982 15 p2242 A83-34859

Remote sensing of phytoplankton in the sea - Surface-layer chlorophyll as an estimate of water-column chlorophyll and primary production 15 p2209 A83-35286

Delineation of seasonal changes of chlorophyll frontal boundaries in Mediterranean coastal waters with Nimbus-7 coastal zone color scanner data 17 p2554 A83-37623

Monitoring of water characteristic using the synchronous observation data of Landsat and NOAA 17 p2554 A83-38455

Shallow water bottom topography from radar imagery 17 p2554 A83-38612

Measured aerosol size distributions and calculated EM extinction in air masses moving off the east coast 17 p2550 A83-38730

Remote sensing for coastal areas 22 p3343 A83-46144

Global biology - An interdisciplinary scientific research program at NASA, Ames Research Center [IAF PAPER 83-100] 23 p3474 A83-47264

COASTAL ZONE COLOR SCANNER

Phytoplankton pigment concentrations in the Middle Atlantic Bight - Comparison of ship determinations and CZCS estimates --- Coastal Zone Color Scanner 06 p0793 A83-18580

Remote sensing /Nimbus-7 CZCS/ analysis of phytoplankton distribution in coastal waters of the Gulf of Lions /northwestern Mediterranean/ 08 p1143 A83-21953

Quality of upwelling radiance retrieved from coastal zone colour scanner /CZCS/ data for ocean colour determination 08 p1050 A83-21954

A study of blooms of phytoplankton on the Roscoff-Plymouth radial /western English Channel/ in 1980 and 1981 - The contribution from satellite imagery of the ocean color --- French thesis 11 p1635 A83-28639

Aerosol observations from Nimbus-7 CZCS along the South African West Coast --- Coastal Zone Color Scanner 12 p1755 A83-29569

Delineation of seasonal changes of chlorophyll frontal boundaries in Mediterranean coastal waters with Nimbus-7 coastal zone color scanner data 17 p2554 A83-37623

Satellites for the study of ocean primary productivity 19 p2869 A83-42041

Satellite and ship studies of coccolithophore production along a continental shelf edge 20 p3032 A83-42171

COASTING FLIGHT

The attainability domain of a coasting vehicle 10 p1380 A83-26073

COASTS

Super high altitude photography for coastal geomorphology --- from approximately 20 km altitude 05 p0657 A83-17840

PUKK - A meso-scale experiment at the German North Sea coast --- Project for Investigation of Coastal Climate 06 p0793 A83-18995

Interpretability of linear phenomena on Seasat-1 imagery in the western coastal zone of Belgium in relation to the azimuthal and range resolutions 08 p1125 A83-21919

- Post-Aswan High Dam changes of the Nile Delta coast, east of Ras El Bar, interpreted from aerial photographs 09 p1289 A83-24600
- Inductive coupling between idealized conductors and its significance for the geomagnetic coast effect 10 p1447 A83-25435
- The use of a mesoscale numerical model for evaluations of pollutant transport and diffusion in coastal regions and over irregular terrain 10 p1451 A83-26099
- Doppler-SODAR measured variations of mean and turbulent wind field during PUKK --- project for the investigation of the coastal climate 11 p1632 A83-27974
- An analysis of explosive cyclogenesis over the eastern United States 13 p1888 A83-30569
- Coastal wind forecasts based on Model Output Statistics 13 p1889 A83-30580
- The influence of coastal shape on winter mesoscale air-sea interaction 13 p1891 A83-30801
- Airborne measurements of the free convective internal boundary layer during the sea breeze 14 p2057 A83-32442
- The use of spectral methods in evaluating certain structural characteristics of breezes 14 p2058 A83-32855
- The evolution of the southern coastline of the Vendee (France) according to data from Landsat 1, 2, 3 and Seasat 15 p2182 A83-33578
- Transition zones between the continents and the oceans --- Russian book 15 p2200 A83-34375
- Measurements of katabatic winds between Dome C and Dumont d'Urville 15 p2207 A83-34747
- A framework for analysis of temporal and spatial patterns of land use changes in Michigan's coastal zone 15 p2186 A83-34835
- The application of SPOT simulated data to the remote sensing of an intertidal environment 17 p2534 A83-38457
- COATING**
- NT ANODIZING
- NT ELECTROPLATING
- NT ENCAPSULATING
- NT METALLIZING
- COATINGS**
- NT ALUMINUM COATINGS
- NT ANODIC COATINGS
- NT ANTIREFLECTION COATINGS
- NT BIREFRINGENT COATINGS
- NT CATHODIC COATINGS
- NT CERAMIC COATINGS
- NT ELECTROPLATING
- NT ENAMELS
- NT ENCAPSULATING
- NT GLASS COATINGS
- NT GLAZES
- NT GOLD COATINGS
- NT INORGANIC COATINGS
- NT MAGNETIC FILMS
- NT METAL COATINGS
- NT METALLIZING
- NT NICKEL COATINGS
- NT PAINTS
- NT PLASTIC COATINGS
- NT PRIMERS (COATINGS)
- NT PROTECTIVE COATINGS
- NT REFRACTORY COATINGS
- NT SPRAYED COATINGS
- NT THERMAL CONTROL COATINGS
- Evaluation of fretting corrosion by means of a new device for the control of oscillation amplitude 05 p0652 A83-17255
- Optical properties of narrowband spectral filter coatings related to layer structure and preparation 07 p0993 A83-20157
- Formation of beta-Si₃N₄ coatings by chemical vapor deposition 07 p0898 A83-20172
- Infrared application to the detection of induced surface currents 08 p1103 A83-22845
- Processing modifications for improved propellants - Coated oxidizers 09 p1241 A83-23838
- Thin film transmissive phase retarders --- for reflective coatings 11 p1656 A83-27569
- Structure in carbon/carbon fibre composites as studied by microscopy and etching with chromic acid 12 p1709 A83-29502
- The nonorthogonal-series method in problems of electromagnetic wave diffraction by coated bodies 13 p1827 A83-30096
- Certain contact problems of nonlinear steady state creep in the presence of thin coatings 16 p2364 A83-35546
- The problem of applying new reflective coatings to the mirrors of devices while experiments are being conducted beyond the atmosphere --- for spaceborne reflecting telescopes 17 p2473 A83-37694

- Polymer coating of glass microballoons levitated in a focused acoustic field 20 p2962 A83-43258
- Quantitative measurement of energy deposited in optical coatings 21 p3205 A83-44785
- Applications of interference coatings in optical processing 21 p3206 A83-44791
- Synthesis of optical coatings for the oblique incidence of light 21 p3208 A83-45218
- Optical coatings for energy efficiency and solar applications; Proceedings of the Seminar, Los Angeles, CA, January 28, 29, 1982 22 p3319 A83-46580
- Development of high temperature solar selective absorbers utilizing rare earth, transitional, and group metals 22 p3319 A83-46583
- Solar absorber material stability under high solar flux 22 p3319 A83-46585
- Another method to separate principal strains in photoelastic coatings 22 p3306 A83-46806
- COAXIAL CABLES**
- Video distribution requirements for future tactical aircraft 01 p0006 A83-11182
- A comparison of lightwave, microwave, and coaxial transmission technologies 02 p0164 A83-12165
- Attenuation and localization of an electromagnetic wave on the surface of a cylindrical conductor 04 p0465 A83-15072
- Dyadic Green's functions for a coaxial line 10 p1411 A83-26845
- Analysis and modeling of 'two-gap' coaxial line rectangular waveguide junctions 13 p1831 A83-30233
- Waveguide-to-coax-to-microstrip transitions for millimeter-wave monolithic circuits 17 p2498 A83-37897
- Radiation from circular symmetric sources in warm plasma column --- electromagnetic transmission in plasma media 17 p2495 A83-38537
- Radiation characteristics of coaxial waveguides as a small primary feed 20 p2964 A83-42488
- A 3M-device cavity-type power combiner 24 p3573 A83-48967
- COAXIAL FLOW**
- The effect of transverse injection on steady liquid flows between a rotating and a stationary porous disk 04 p0480 A83-16389
- An energy analysis of the stability of flexible filaments in coaxial flow 07 p0926 A83-20899
- Conventional profile coaxial jet noise prediction 08 p1162 A83-22128
- Prediction of turbulent mixing in confined co-axial reacting jets 08 p1088 A83-23191
- Coaxial supersonic jet-flows, shock structure and related problems with noise-suppression assessment and prediction [AIAA PAPER 83-0707] 11 p1651 A83-28011
- The relationship between the aerodynamic and acoustic characteristics of coaxial jets 16 p2408 A83-35712
- Aerodynamic studies on swirled coaxial jets from nozzles with divergent quarls 17 p2504 A83-37398
- A study of the distribution of the noise source strengths in coaxial double jet 17 p2578 A83-37570
- Pressure measurements of coaxial jet of high mean-velocity ratio 20 p2969 A83-42348
- Turbulent flow between coaxial cylinders with the inner cylinder rotating [ASME PAPER 83-GT-48] 23 p3447 A83-47907
- COAXIAL NOZZLES**
- Effect of excitation on coaxial jet noise 07 p0990 A83-19811
- Comparison of measured and predicted flight effects on high-bypass coaxial jet exhaust noise [AIAA PAPER 83-0749] 10 p1478 A83-26450
- Statistical characteristics of velocity, concentration, mass transport, and momentum transport for coaxial jet mixing in a confined duct [ASME PAPER 83-GT-39] 23 p3447 A83-47899
- COAXIAL PLASMA ACCELERATORS**
- The two-dimensional character of the instability of an ionizable gas flow in the channel of a plasma accelerator 16 p2415 A83-35724
- Production of a high-density fast plasma flow 22 p3363 A83-46490
- COAXIAL TRANSMISSION**
- U COAXIAL CABLES
- COBALT**
- NT COBALT ISOTOPES
- NT COBALT 60
- Morphology of corrosion products formed on cobalt and nickel in argon-oxygen-chlorine mixtures at 1000 K 01 p0024 A83-10247
- An electrochemical study of Ni/2+/, Co/2+/, and Zn/2+/- ions in melts of composition CaMgSi₂O₆ 02 p0152 A83-12845
- A structural study of detonation-sprayed tungsten carbide-cobalt coatings 02 p0159 A83-13030

- Sulfidation-oxidation of nickel and cobalt - Reactions between the metals and their sulfates 03 p0296 A83-13122
- Use and recycling of cobalt. I 06 p0727 A83-17962
- Gas-phase high-temperature photoelectron spectroscopy - An investigation of the transition metals iron, cobalt and nickel 06 p0808 A83-19005
- Cobalt, consumption and recycling. II - Development tasks for a low-loss raw-material cycle 09 p1233 A83-24125
- A deformation map for cobalt 14 p1997 A83-32945
- Investigations of the constitution in the beryllium-rich region of the beryllium-cobalt-nickel system 18 p2665 A83-39174
- Occurrence of the dynamic Jahn-Teller effect in CdTe:Co crystals 19 p2904 A83-40998
- The maser effect in a paramagnetic crystal caused by the thermal action of the spin system aided by a pulsed magnetic field 19 p2853 A83-41500
- The measurement of the cross sections of excitation of several quartet states of the cobalt atom by electron impact 24 p3626 A83-49737
- COBALT ALLOYS**
- NT ASTROLOY (TRADEMARK)
- A comparative study of the physical parameters of steady-state creep in precipitation-hardening and dispersion-strengthened materials 01 p0024 A83-10390
- A model for the formation of subboundaries in the matrix of eutectic alloys of the system M-MeC --- Ni or Co alloyed with Ta, Nb or Hf carbides 01 p0025 A83-10397
- Pulse plating of chromium-cobalt alloys containing a phase with the A-15 structure 02 p0154 A83-12053
- The effect of the stacking fault energy on the characteristics of the high-temperature creep of nickel-cobalt alloys 02 p0157 A83-12331
- Interaction between the components in the ternary system W-Co-P 02 p0158 A83-12948
- Wear of cobalt and a nickel alloy [ASLE PREPRINT 82-LC-4B-2] 03 p0296 A83-13241
- The relationship between the combustion parameters and the phase diagram of the systems Ti-Co and Ti-Ni 03 p0299 A83-14055
- A study of the ordering kinetics of an equiatomic cobalt-platinum alloy using the method of nuclear gamma resonance 03 p0299 A83-14156
- Comparison of the quench rates attained in gas-atomized powders and melt-spun ribbons of Co- and Ni-base superalloys - Influence on resulting microstructures [ONERA, TP NO. 1982-132] 04 p0460 A83-15993
- Equivalence of indentation and compressive creep tests on a WC/Co hardmetal 04 p0460 A83-15997
- Thermodynamic assessment of heat treatments for a Co-Cr-Mo alloy 05 p0615 A83-17565
- Effects of metal boride additives on grain growth and mechanical properties of TiB₂-MeB₂-CoB systems 06 p0734 A83-19108
- Nickel-base alloys as alternatives to cobalt-base alloys for P/M wear and environmental resistant components 06 p0733 A83-19111
- Superalloy technology - Today and tomorrow 07 p0891 A83-21452
- Recent approaches to the development of corrosion resistant coatings 07 p0891 A83-21453
- Effects of cobalt in nickel-base superalloys 07 p0892 A83-21467
- Contiguity and the fracture process of WC-Co alloys 08 p1061 A83-21721
- Wear-resistant cobalt-base alloys 09 p1230 A83-23746
- High temperature low cycle fatigue of MAR-M 509 superalloy. I - The influence of temperature on the low cycle fatigue behaviour from 20 to 1100 C. II - The influence of oxidation at high temperature 10 p1393 A83-25417
- The tribological properties of highly oriented cobalt and Co-Cr ion platings 10 p1395 A83-25550
- The effect of hafnium on the phase composition and the mechanical and corrosion properties of cobalt alloys 10 p1395 A83-25632
- The effect of deformation and temperature on the structure and mechanical properties of a high-cobalt alloy 10 p1399 A83-26794
- The influence of electrode potential on the corrosion of gas turbine alloys in sulfate melts 11 p1550 A83-28672
- Investigations of the precipitation behavior in the binding phase of WC-TiC-(Ta, Nb) C-Co alloys 15 p2138 A83-34425
- Nickel diffusion in the M/MeC phase boundaries 15 p2141 A83-35310

- Diffusion anomalies in cobalt alloys
15 p2141 A83-35313
- Microstructure of in-situ composites
16 p2324 A83-35999
- Fatigue softening in precipitation hardened copper-cobalt single crystals
17 p2490 A83-38381
- Microstructural features of low temperature hot corrosion in nickel and cobalt base MCrAlY coating alloys
20 p2953 A83-42249
- Mechanism of low temperature hot corrosion
20 p2953 A83-42250
- Intermetallic compounds of the micron- and P-phases of Co7Mo6 studied by 1 MV electron microscopy
20 p2956 A83-43616
- X-ray analysis of the crystal structure and thermal expansion of the intermetallic compound (Tb0.8Gd0.2)3Co crystallized in space
[IAF PAPER 83-159] 23 p3414 A83-47295
- Aluminide coatings on superalloys
[ONERA, TP NO. 1983-68] 23 p3432 A83-48189
- On the Co-Ti system
24 p3561 A83-49435
- Studies on the corrosion resistance of MCrAlY alloys at high temperatures
24 p3564 A83-49506
- The study of the effect of cobalt on the hot corrosion resistance of nickel-based high temperature alloys
24 p3564 A83-49507

COBALT COMPOUNDS**NT COBALT OXIDES**

- Investigation of the surface grain refinement for superalloys castings
07 p0895 A83-21499
- Liquid phase growth of epitaxial Ni and Co silicides
21 p3219 A83-45494

COBALT ISOTOPES**NT COBALT 60**

- Moessbauer study of the lattice location of Co-57 implanted in graphite
24 p3636 A83-49756

COBALT OXIDES

- A mechanistic study of oxygen evolution on Li-doped Co3O4 --- by electrolysis
07 p0881 A83-20586
- High temperature degradation in cobalt oxide selective absorber
12 p1716 A83-28942
- Heat loss optimisation of a concentric cylindrical solar collector employing a cobalt oxide selective absorber
15 p2192 A83-34675
- Cobalt oxide-SO2/SO3 reactions in cobalt-sodium mixed sulfate formation and low temperature hot corrosion
20 p2949 A83-42251
- The effects of metal pretreatment and oxide grain size on the oxidation of cobalt
24 p3562 A83-49485

COBALT 60

- Radiation-induced paramagnetic defects in MOS structures
05 p0691 A83-17478
- A study of cosmogenic nuclides on meteorites
21 p3241 A83-44586

COBE**U COSMIC BACKGROUND EXPLORER SATELLITE****COCHLEA**

- The endocochlear potential of the inner ear and its changes under the influence of dihydrostreptomycin and etacrinic acid
01 p0078 A83-10514
- Extratympanic electrocochleography in clinical practice
01 p0083 A83-10515
- Liquorrhea via fistula in the area of the cochlear window
01 p0083 A83-10516
- The use of reflexotherapy for cochleovestibular disorders
03 p0381 A83-14338
- Mathematical models of the hydrodynamics of the cochlea of the inner ear
07 p0972 A83-19927
- The effect of changes of the electrolytic composition of the perilymph on the endocochlear potential
14 p2063 A83-32567

COCKPIT SIMULATORS

- Dot-matrix display light measurement and interpretation techniques --- for qualification tests techniques
01 p0011 A83-11257
- A glimpse into the future of air combat --- via computerized cockpit simulators
[AIAA PAPER 83-0143] 05 p0599 A83-16552
- Multifunction display simulation facility
05 p0596 A83-17302
- An algorithm of flight simulation on a dynamic stand of support type
15 p2123 A83-34429
- An investigation of motion base cueing and G-seat cueing on pilot performance in a simulator
[AIAA PAPER 83-1084] 16 p2401 A83-36209
- Air-to-air combat in a plastic dome
18 p2642 A83-40620
- Studies and designs for a new helicopter cockpit
23 p3402 A83-47210

COCKPITS

- Advanced speech technology in fighter cockpits - A new perspective on issues and applications
01 p0005 A83-11125
- Video stand-alone instrument multi-function cockpit display system
01 p0010 A83-11172

- Evaluating cockpit components with hand displacement time scores
01 p0086 A83-11189

The complete book of cockpits

- 02 p0135 A83-11575
- The 1981 Naval and Marine Corps aviation anthropometry survey and applications
04 p0525 A83-15414
- Advanced P-3 flight station studies
04 p0447 A83-15429
- Negative transfer - A threat to flying safety
04 p0523 A83-15541
- Human engineering in aircraft and system design
04 p0446 A83-16127
- 'Light bar' attitude indicator
04 p0448 A83-16136
- Cockpit visibility and contrail detection
07 p0982 A83-20623

- The automated cockpit
07 p0866 A83-20849
- Multicriterial estimation in the synthesis of means for information interaction in complex systems --- cockpit display optimization
08 p1156 A83-22125
- Ergonomic analysis and evaluation procedures for cockpit operating positions
09 p1324 A83-23496
- Increasing flight safety under shear wind conditions by modifying thrust regulation systems and existing cockpit instrumentation
09 p1209 A83-24159

- [DGLR PAPER 82-033] 09 p1209 A83-24159
- Automatic return in multifunction control logic --- for fighter cockpits
10 p1459 A83-26317
- Flight deck display
11 p1530 A83-27123
- Stresses affecting the cockpit personnel and automation
12 p1767 A83-29373
- Simulation of T-38 aircraft student canopy response to cockpit pressure and thermal loads using MAGMA --- Material and Geometrically Nonlinear Analysis
[AIAA 83-0942] 12 p1701 A83-29772

- Analysis of in-trail following dynamics of CDTI-equipped aircraft --- Cockpit Displays of Traffic Information
13 p1807 A83-30161

Chemical defense, environmental control systems study

- [SAE PAPER 820866] 13 p1806 A83-30944
- Flight operations: A study of flight deck management --- Book
15 p2120 A83-33767
- Human factors approach in certification flight test
[SAE PAPER 821340] 17 p2562 A83-37951
- Aircraft night lighting systems
[SAE PAPER 830713] 20 p2936 A83-43323
- Smoke/fumes in the cockpit
21 p3187 A83-43997
- Man, machine and configuration - Human factors versus hardware in avionic display design
21 p3189 A83-44686

Wide field of view head-up displays

- 21 p3091 A83-44690
- Aircraft keyboard ergonomics - A review
21 p3189 A83-44691
- Space technology - The art and science of ergonomics
21 p3092 A83-45605
- A mathematical model on the thermal behaviour of an aircraft cabin --- Thesis
22 p3254 A83-46691
- Central operating and display unit for avionics systems
23 p3401 A83-47193

CODE DIVISION MULTIPLE ACCESS

- The performance of a sequential acquisition system for PN codes --- in NASA Tracking Data Relay Satellite System
01 p0019 A83-11216
- On initial acquisition of FH/TH Spread Spectrum signal --- Frequency-Hopping/Time-Hopping
07 p0904 A83-19678
- On the performance of a code division multiple access scheme with transmit/receive conflicts
07 p0908 A83-19737
- Considerations for spread spectrum systems design
07 p0909 A83-19744
- Increasing the efficiency of the cyclic phasing of contiguous classes of cyclic codes
13 p1829 A83-30730
- Throughput analysis of an asynchronous code division multiple access (CDMA) system
19 p2830 A83-41362
- Adaptive acquisition of multiple access codes
19 p2833 A83-41407
- Performance analysis of M-ary code shift keying in code division multiple access systems
19 p2833 A83-41408

CODE DIVISION MULTIPLEXING

- Asynchronous multiplexing for an optical-fibre local-area network
15 p2144 A83-34523

CODERS

- Digital transducers
05 p0644 A83-16917
- Switched-capacitor second-order noise-shaping coder
08 p1082 A83-22923
- Increasing the speed of response of multichannel voltage-to-code converters of parallel operation for radio systems
13 p1828 A83-30290

CODES

- Orthogonal sequences on the basis of full code rings and their correlation properties
01 p0094 A83-10410

- The effects of extended practice on the evaluation of visual display codes
10 p1456 A83-26000
- A user oriented design system for Stirling cycle codes
11 p1586 A83-27267

- Generation of codes with good autocorrelation properties
19 p2827 A83-41276

CODING

- NT DECODING
- NT REDUNDANCY ENCODING
- NT SIGNAL ENCODING

- Concerning the optimality of discrete-data compression in a four-letter coding system
01 p0094 A83-10565
- A class of codes with unequal protection of symbols, based on balanced incomplete solvable block-schemes
01 p0094 A83-10567

- An experimental study of the concatenated Reed-Solomon/Viterbi channel coding system performance and its impact on space communications
07 p0871 A83-19733
- New error bounds for modulation and coding under mismatch
07 p0909 A83-19745

- Comparison of transform image coding techniques for compression of tactical imagery
08 p1100 A83-22597

- Noise-immune coding of discrete information --- bibliography 1972-1979
09 p1327 A83-24248
- Anisotropic nonstationary image estimation and its applications. I - Restoration of noisy images. II - Predictive image coding
13 p1845 A83-30223
- The Laplacian pyramid as a compact image code
14 p2075 A83-32868

- Block Truncation Coding on PASM --- reconfigurable microprocessor for image processing
15 p2219 A83-35149

- Symbolic manipulation and computational fluid dynamics
[AIAA PAPER 83-1952] 18 p2738 A83-39396

- Depth-first picture expression viewed from digital picture processing
20 p2989 A83-42646
- An image transform coding scheme based on spatial domain considerations
21 p3135 A83-43954
- Simple coding scheme for modular arithmetic
21 p3190 A83-44969

- Efficient coding and resonance spike identification for topside ionogram processing
22 p3330 A83-46512

COEFFICIENT OF FRICTION

- Effects of amplitude of oscillation on the wear of dry bearings containing PTFE
[ASME PAPER 81-LUB-6] 02 p0186 A83-11942
- Hot wire gauges for skin friction measurement / design, calibration, applications/
02 p0178 A83-12349
- On the mechanism of lubrication by tricesylphosphate /TCP/ - The coefficient of friction as a function of temperature for TCP on M-50 steel
[ASLE PREPRINT 82-LC-4C-1] 03 p0333 A83-13228

- Overall characteristics of bearings lubricated with ferrofluids
[ASME PAPER 82-LUB-14] 03 p0335 A83-13508

- New skin friction and entrainment correlations for turbulent boundary layers
04 p0478 A83-16144
- Friction, metallic transfer and debris analysis of sliding surfaces
04 p0487 A83-16348

- Effect of turbulent viscosity of the external flow on heat transfer in a turbulent boundary layer
06 p0759 A83-19152

- The effect of the nonuniformity of supersonic flow with shocks on friction and heat transfer in plane channels
11 p1526 A83-27710

- Tribological properties of sintered polycrystalline and single-crystal silicon carbide
12 p1716 A83-29397
- Tribological behavior of carbon fiber reinforced metals
18 p2660 A83-40267

- Blade platform friction damping tests on a model blade (methods and results)
20 p3002 A83-42572

- The formation of surface layers during the friction of metal-polymer composite materials
21 p3108 A83-45315

- Refinement of the limiting relative friction law for a permeable plate with gas injection
21 p3133 A83-45345

COEFFICIENTS

- NT ACCOMMODATION COEFFICIENT
- NT AERODYNAMIC COEFFICIENTS
- NT ATTENUATION COEFFICIENTS
- NT COEFFICIENT OF FRICTION
- NT COHERENCE COEFFICIENT
- NT CORRELATION COEFFICIENTS
- NT COUPLING COEFFICIENTS
- NT DIFFUSION COEFFICIENT
- NT DISCHARGE COEFFICIENT
- NT FLOW COEFFICIENTS

NT HEAT TRANSFER COEFFICIENTS
 NT INFLUENCE COEFFICIENT
 NT IONIZATION COEFFICIENTS
 NT NOZZLE THRUST COEFFICIENTS
 NT RECOMBINATION COEFFICIENT
 NT SCATTERING COEFFICIENTS
 NT STRUCTURAL INFLUENCE COEFFICIENTS
 NT WIGNER COEFFICIENT

Averaging of partial differential equations with rapidly oscillating coefficients 07 p0986 A83-20304

COENZYMES

NT CYSTEAMINE
 NT CYTOCHROMES
 NT GLUTATHIONE
 NT THIAMINE

COERCIVITY

Electron-microscope investigation of aluminum steel in a highly coercive state 03 p0298 A83-13267
 High magnetic coercivity of meteorites containing the ordered FeNi /tetrataenite/ as the major ferromagnetic constituent 07 p1034 A83-21312

COFFIN-MANSON LAW

Various criteria for determining the equivalent plastic deformation range in the theory of low-cycle fatigue 06 p0777 A83-19304
 Low cycle fatigue and life prediction methods 07 p0892 A83-21462
 Notch effect on torsional low-cycle fatigue 10 p1399 A83-26893

COGENERATION

A method of evaluating and sizing solar cogeneration systems 08 p1132 A83-23127
 Cogeneration using a thermionic combustor 11 p1608 A83-27300
 Measured effect of wind generation on the fuel consumption of an isolated diesel power system 16 p2371 A83-36410

COGNITION

Psychometric measures of task difficulty under varying levels of information load 10 p1457 A83-26328
 Cognitive task performance time during tracking 10 p1457 A83-26333
 Impaired memory registration and speed of reasoning caused by low body temperature 19 p2880 A83-41133
 Cognitive performance during a heat acclimatization regimen 21 p3187 A83-43992
 The dependence of the functional activity of the heart on mental activity 24 p3618 A83-49547

COGNITIVE PSYCHOLOGY

Individual differences in spatial representations during operator activity 03 p0382 A83-13282
 The model human processor - A model for making engineering calculations of human performance 10 p1459 A83-26323
 Compatibility and resource competition between modalities of input, central processing, and output --- in human task performance in military aircraft 15 p2215 A83-34075
 Reflection and the organization of creative thinking and the self-development of personality 18 p2737 A83-40559
 Attending to different levels of structure in a visual image 22 p3349 A83-45954

COHERENCE

Numerical analysis of nonreciprocity for spatial coherence and spot dancing in random media 02 p0233 A83-12627
 Phenomenal coherence of moving visual patterns 05 p0676 A83-16865
 A new class of optical multistabilities and instabilities induced by atomic coherence 10 p1481 A83-25434

COHERENCE COEFFICIENT

Amplitude coherence in an absorption region --- measurement on millimeter wave transmission loss 03 p0307 A83-14033
 Measurement of coherence of radiation from diffusely illuminated beam splitters 21 p3140 A83-44842

COHERENT ACOUSTIC RADIATION

Acoustic imaging with two dimensional arrays 04 p0493 A83-15229
 High bypass ratio engine noise component separation by coherence technique 08 p1046 A83-22159

COHERENT ANTI-STOKES RAMAN SPECTROSCOPY

U RAMAN SPECTROSCOPY

COHERENT ELECTROMAGNETIC RADIATION

NT COHERENT LIGHT

Effective propagation constants for coherent electromagnetic wave propagation in media embedded with dielectric scatters 03 p0304 A83-13915
 A relativistic-electron-beam klystron 05 p0630 A83-17597
 Coherent emission from electron clusters in free-electron lasers 06 p0765 A83-17981

Investigation of the noise immunity of reception of quantum coherent signals with multilevel PSK 09 p1245 A83-23458

Synthesis of spatial filters for investigation of the transverse mode composition of coherent radiation 10 p1432 A83-26669

Coherent electromagnetic emission from an electron-ion beam 11 p1584 A83-28564

High-power submillimeter gyrotron with a pulsed magnetic field 13 p1851 A83-30911

Experimental results from the HDL orotron - A tunable source of coherent millimeter wave radiation 13 p1855 A83-31126

A model for superradiance and superfluorescence in free-electron lasers 15 p2169 A83-34274

Generation of coherent picosecond pulses using mode-locked semiconductor lasers 16 p2358 A83-35886

Applicability of the Bourret and Kraichnan approximations to solving problems of the propagation of coherent waves in a medium with strong random inhomogeneities 19 p2835 A83-41769
 An increase in laser gain to free electrons by means of laser radiation from an external source 21 p3145 A83-45202

Generation of coherent far-infrared radiation using lasers 22 p3296 A83-46497

COHERENT LIGHT

The nonlinear coherent coupler 02 p0227 A83-12166

Coherent optical methods for applications in robot visual sensing [AD-A110107] 03 p0324 A83-13446

Spatial frequency pseudocolor filters 03 p0328 A83-14094

Optical coherence effects on a fiber-sensing Fabry-Perot interferometer 03 p0330 A83-14390

Coherent transitional processes in the presence of standing waves 04 p0484 A83-15270

Transformation of the spatial statistics of a partially coherent light beam in a nonlinear medium 04 p0485 A83-15902

Holographic aberration compensation with partially coherent light 05 p0643 A83-16834

Review - Progress of coherent optical fibre communication systems 05 p0685 A83-17887

Three-wave mixing and light diffraction by transient light induced gratings for the study of fast relaxation processes 05 p0651 A83-17888

Coherent optical-fibre sensors with modulated laser sources 06 p0762 A83-18568

Fast determination of the extent of spatial and temporal coherence 06 p0767 A83-19191

Closure hypotheses from the method of smoothing for coherent wave propagation in discrete random media 07 p0989 A83-20792

Low-loss LiNbO₃ waveguide bends with coherent coupling 07 p0993 A83-20799

Heterodyne detection of partially coherent optical signal 07 p0993 A83-20824

Optically integrated coherently coupled Al_x/Ga_{1-x}/As lasers 07 p0937 A83-21367

Partially coherent optical processing of images 08 p1093 A83-22427

Influence of semiconductor-laser phase noise on coherent optical communication systems 08 p1077 A83-22638

Recent progress in acoustic processing by coherent optical techniques 08 p1167 A83-22810

Thermal blooming of a partially coherent light beam 09 p1271 A83-23493

Coherent optical space communications system architecture and technology issues 09 p1214 A83-23578

Uncertainty principle for partially coherent light 09 p1344 A83-24082

Coherent-optical processor for two-dimensional antenna arrays with a complex format of signal recording 09 p1345 A83-24920

Coherent large telescopes 10 p1494 A83-25836

Coherence and interferometry through optical fibers --- of stellar interferometers 10 p1482 A83-25847

Measurement of temperatures in a shock tube by coherent anti-Stokes Raman spectroscopy /CARS/ 10 p1421 A83-26136

Application of VanderLugt's operational notation to finite aperture lens systems 10 p1484 A83-26856

Nonlinear local image preprocessing using coherent optical techniques 10 p1484 A83-26863

Coherent optical production of the Hough transform 10 p1484 A83-26866

Modeling propagation of coherent optical pulses through molecular vapor 11 p1577 A83-27535

Cooperative effects and transverse coherence in superfluorescence 11 p1577 A83-27536

Generation and application of coherent radiation at Lyman-alpha 11 p1583 A83-27619

Theory of the coherent interaction of light pulses and resonant multilevel media 11 p1584 A83-28059

New measurement method for polarisation dispersion in single-mode fibres employing frequency-modulated optical signal 12 p1779 A83-29460

Velocity measurements in an axisymmetric laminar flow using an optical technique of visualization in coherent light 12 p1726 A83-29704

Phase modulation of coherent light in long multimode fiber light guides 13 p1919 A83-30815

Phase modulation efficiency of coherent light in fiber light guides 13 p1919 A83-30816

Coherent optical system of modular imaging collectors (COSMIC) telescope array - Astronomical goals and preliminary image reconstruction results 13 p1920 A83-30997

Calculations of the intensity of a partially coherent optical beam in a turbulent atmosphere 14 p2023 A83-31908

Antenna arrays with filtering of interfering spatial radio signals by coherent-optical methods using controlled liquid-crystal transparencies 14 p2000 A83-32118

Digital image processing with coherent light - A method and some applications 14 p2021 A83-33174

Realization of 90- and 180 degree hybrids for optical frequencies 16 p2411 A83-35520

Coherent Anti-Stokes Raman scattering with reflective optics 17 p2485 A83-37742

Energy model of image formation by an optical system 17 p2580 A83-38480

Relationship between spectral properties and spatial coherence properties in one-dimensional free fields 17 p2580 A83-38968

A simple passive technique for generating short pulses 21 p3143 A83-44187

Coherent image amplification and optical phase conjugation with photorefractive materials 21 p3206 A83-44799

Propagation, transverse, diffraction effects, and coherent pump dynamics in three-level superfluorescence and light control by light 21 p3144 A83-44801

Optical image processing in coherent and incoherent light - A short comparative review 21 p3207 A83-44825

Measurement of coherence of radiation from diffusely illuminated beam splitters 21 p3140 A83-44842

Rayleigh backscattering in a fiber gyroscope with limited coherence sources 22 p3287 A83-45730

Application of fiber optics to speckle metrology - A feasibility study 22 p3293 A83-46807

Coherent light scattering from ruby dressed with RF photons 23 p3462 A83-48323

Evolution of spontaneous and coherent radiation in the free-electron-laser oscillator 24 p3586 A83-48838

COHERENT RADAR

Coherent radar signal processing and matched filtering 06 p0748 A83-18936

Bandpass signal sampling and coherent detection 06 p0749 A83-19048

Millimetric wavelength components and coherent radar systems 07 p0918 A83-20176

A simple speckle smoothing algorithm for synthetic aperture radar images 08 p1093 A83-22349

Physics and technology of coherent infrared radar; Proceedings of the Meeting, San Diego, CA, August 25, 26, 1981 08 p1095 A83-22499

Military applications of coherent infrared radar 08 p1095 A83-22500

Overview of technology developments in coherent infrared radar 08 p1109 A83-22501

Feasibility and design considerations of a global wind sensing coherent infrared radar /WINDSAT/ 08 p1051 A83-22503

National Oceanic and Atmospheric Administration's /NOAA/ pulsed, coherent, infrared Doppler lidar - Characteristics and data 08 p1096 A83-22506

Design and calibration of a coherent lidar for measurement of atmospheric backscatter 08 p1096 A83-22507

Detection efficiency for large-aperture coherent laser radars 08 p1096 A83-22508

Atmospheric propagation effects on coherent laser radars 08 p1096 A83-22509

Experimental studies with a coherent CO₂ laser radar 08 p1096 A83-22510

On estimation of image signal-to-noise ratio and centroid of coherent laser radar target images 08 p1096 A83-22512

Relative merit of coherent vs noncoherent laser radars 08 p1096 A83-22513

Transverse velocity measurements using coherent lidar 08 p1096 A83-22514

Frequency-stabilized transversely excited atmospheric /TEA/ CO2 lasers for coherent infrared radar systems 08 p1109 A83-22515

Electronically scanned coherent CO2 laser radar techniques 08 p1096 A83-22516

Programmable transmitters for coherent laser radars 08 p1109 A83-22517

Holographic beam shaping for optical heterodyne arrays in laser radars 08 p1097 A83-22519

Coherent adaptive speckle tracking 08 p1097 A83-22522

Coherent Doppler tomography for microwave imaging 10 p1420 A83-26069

Rain backscattering effects in coherent polarization-diversity radar signals 11 p1630 A83-27078

Measurement of the phase of a coherent-pulsed signal in the presence of correlated noise 17 p2495 A83-38500

Coherent IR radar technology 23 p3442 A83-47805

Tactical and atmospheric coherent laser radar technology 23 p3462 A83-47806

Atmospheric remote sensing using the NOAA coherent lidar system 23 p3458 A83-47807

Coherent CO2 lidar systems for remote atmospheric measurements 23 p3458 A83-47808

COHERENT RADIATION

NT COHERENT ACOUSTIC RADIATION

NT COHERENT ELECTROMAGNETIC RADIATION

NT COHERENT LIGHT

Coherent-optical synthesis of an antenna radiation pattern with a zero in a prescribed direction 02 p0166 A83-11686

Cooperative transients in inter-atomic correlation in the presence of an externally applied coherent field - Relation to intrinsic mirrorless optical bistability 03 p0394 A83-13789

Coherent ultraviolet radiation from accreting neutron stars 03 p0421 A83-13950

Coherent polarization methods of nonlinear gas spectroscopy in a longitudinal magnetic field 04 p0456 A83-15759

Spatial coherence of laser light propagating in an optical fibre 04 p0535 A83-15793

An M-ARY coherent optical receiver for the free-space channel 07 p0905 A83-19708

The effects of transmitter/receiver clock time base instability on coherent communication system performance 07 p0871 A83-19770

Stimulated Raman scattering in a multipass cell filled with CO2 07 p0935 A83-20125

Continuously tunable coherent spectroscopy for the 0.1-1.0-THz region 07 p0931 A83-21357

Coherence effects in laser testing of long wavelength infrared /LWIR/ sensors 08 p1052 A83-22879

Signal detection in a clutter environment in a bistatic system 08 p1078 A83-23156

Gaussian Schell-model sources - An example and some perspectives --- generation of directional light beams 09 p1344 A83-24083

Propagation in correlated distributions of large-spaced scatterers 09 p1338 A83-24089

The polarization characteristics of coherent transient phenomena in two-photon resonance 09 p1346 A83-25091

Relativistic coherent curvature radiation 10 p1500 A83-25376

Coherent versus incoherent detection for interferometry at infrared wavelengths 10 p1495 A83-25846

Statistical radiometry 10 p1471 A83-26035

Generation of 35.5-nm coherent radiation 10 p1429 A83-26115

Coherent emission by relativistic particles interacting with atomic rows during reflection from a crystal surface 10 p1489 A83-26237

Nonperturbative calculations of the indices of refraction of multilevel systems 11 p1577 A83-27537

Coherent gyromagnetic emission --- in astrophysical objects 13 p1944 A83-30362

Free-electron generators of coherent radiation - /Volumes 8 & 9/ 13 p1852 A83-31101

Pulse propagation in the tapered wiggler 13 p1854 A83-31116

The quantum beats of the coherent radiation of atoms in a magnetic field 14 p2082 A83-32138

Radiation friction in the problem of emission from an oscillator in a coherent state 14 p2081 A83-33399

Interaction of a low frequency coherent magneto-acoustic wave with a turbulent spectrum of extra-ordinary waves 18 p2745 A83-39611

The scintillations for weak atmospheric turbulence using a partially coherent source 18 p2676 A83-40653

Diffraction of an atomic beam by standing-wave radiation 19 p2852 A83-40966

Coherent effects in the generation and amplification of ultrashort pulses in YAG:Nd and ruby at low temperatures 20 p2993 A83-42288

Cerenkov radiation from periodic electron bunches 22 p3277 A83-45928

Temporal coherence characteristics of InGaAsP laser diode with single-longitudinal-mode oscillation 22 p3295 A83-45972

Generation of high power, very coherent radiation by interaction of a free electron laser with a molecular (or ionic) medium 23 p3463 A83-48573

COHERENT SCATTERING

Coherent scattering of a surface wave by an electron beam with a spatially modulated velocity 06 p0767 A83-19366

Interaction of a coherent wave with a nonisothermal plasma 07 p0995 A83-20057

New results on coherent scattering from randomly rough conducting surfaces 09 p1246 A83-23776

Coherent scattering of a spherical wave from an irregular surface --- antenna pattern effects 09 p1267 A83-23784

Stimulated scattering of electromagnetic waves by a magnetized relativistic beam of oscillators 10 p1426 A83-25886

Mutual coherence functions and intensities of backscattered signals in a turbulent medium 10 p1403 A83-26036

CARS-spectroscopy of UF6 and SF6 11 p1654 A83-27552

Theory of the stimulated scattering of electromagnetic waves in a waveguide by a relativistic electron beam 11 p1583 A83-27960

Coherent scattering in the solar spectrum - Survey of linear polarization in the range 3165-4230 A 12 p1799 A83-28871

Possibility of detecting relict massive neutrinos 13 p1966 A83-30800

Free-electron coherent relativistic scatterer for UV generation 13 p1856 A83-31137

Coherent anti-Stokes Raman scattering as a probe in reactive media 14 p0201 A83-33172

Resonance-enhanced coherent anti-Stokes Raman scattering in C2 [ONERA, TP NO. 1983-1] 16 p2327 A83-36416

The nonstationary coherent spectroscopy of the Raman scattering of gaseous hydrogen in the region of Dicke narrowing 19 p2898 A83-41496

Detection of hidden diffractors by coherence measurements 21 p3208 A83-44841

COHERENT SOURCES

U COHERENT RADIATION

U RADIATION SOURCES

COHERENT TRANSMISSION

U COHERENT RADIATION

COHESION

A summary of Viking sample-trench analyses for angles of internal friction and cohesions 04 p0567 A83-15574

Diatomic molecules and metallic adhesion, cohesion, and chemisorption - A single binding-energy relation 13 p1817 A83-30921

The cohesive and adhesive strength of ice --- adhering to stainless steel, titanium, and anodized aluminum engineering structures 15 p2130 A83-35069

COILS

Polarisation holding in coiled high-birefringence fibres 24 p3630 A83-49992

COIN AIRCRAFT

NT F-5 AIRCRAFT

COLD ACCLIMATIZATION

The dependence of immunological changes in athletes in polar regions on the intensity of the physical load 01 p0084 A83-11387

Serotonin and the adrenocortical response to cold during the early postnatal development of rats 03 p0375 A83-14328

The mechanisms of the effect of the adaptation to cold on the resistance of an organism to hyperoxia 04 p0520 A83-15897

The effect of hypothermia on the glutamate dehydrogenase activity in the brain 07 p0975 A83-20982

The oxygen tension in the skeletal muscles of rats adapted to cold 08 p1145 A83-22112

The results of an investigation of the intermittent effects of low temperature on the human body 09 p1322 A83-23973

The changes of the protein metabolism characteristics during the acclimatization of humans in the Arctic 09 p1322 A83-23974

The localization of the cold thermoreceptors in various skin layers 10 p1454 A83-26787

Restraint hypothermia in cold-exposed rats at 3 G and 1 G 11 p1637 A83-27806

COLD FRONTS

The hematological changes during the adaptation to polar conditions 11 p1644 A83-28803

The asymmetry of the functional condition of the cerebral hemispheres during the adaptation to new climatic and geographical conditions 12 p1764 A83-29303

Diurnal respiratory rhythms in young healthy people in Siberia and the Far North 12 p1765 A83-29312

The thermal condition and systemic blood circulation of the human body in the case of moderate (physiological) levels of cooling 12 p1765 A83-29313

Sympathoadrenal responses to cold and ketamine anesthesia in the rhesus monkey 13 p1898 A83-30496

Effect of cold exposure on various sites of core temperature measurements [AD-A130437] 13 p1904 A83-30502

The electrophysiological characteristics of the muscle fibers of rats adapted to cold 14 p2063 A83-32566

The problems of health protection in polar expeditions and their importance for space flights 15 p2214 A83-35049

The characteristics of thermoregulation and blood circulation during prolonged exposure to low temperature 16 p2398 A83-35912

Behavioral thermoregulation 16 p2399 A83-35914

Erythropoiesis during adaptation to cold 16 p2399 A83-35916

Changes in the liver of white rats under the influence of low temperatures 17 p2556 A83-38198

Substrates for cold thermogenesis in tyrotoxic dogs 22 p3345 A83-45981

Changes in vascular responsiveness following chronic exposure to cold in the rat 22 p3346 A83-45993

Hypergravic fields and parallel controllers for thermoregulation 22 p3346 A83-45998

The content of gonadotropin hormones and hydrocortisone in women during adaptation to conditions of high latitudes 23 p3497 A83-47104

The morphofunctional reorganization of the vessels of the microcirculatory bed under the influence of local cooling 23 p3497 A83-47114

The action of palmitate on the energy coupling in mitochondria of the skeletal muscles and liver 24 p3617 A83-49546

COLD CATHODE TUBES

NT FREQUENCY MODULATION PHOTOMULTIPLIERS

NT PHOTOMULTIPLIER TUBES

COLD FLOW TESTS

Experimental and theoretical study of a dc arc in an orifice nozzle flow [AIAA PAPER 83-0399] 05 p0636 A83-16692

Investigation of a dual inlet side dump combustor using liquid fuel injection [AIAA PAPER 83-0420] 05 p0609 A83-16703

Pulsing techniques for solid-propellant rocket motors - Modeling and cold-flow testing 09 p1220 A83-24886

Numerical simulation of cold flow in an axisymmetric centerbody combustor [AIAA PAPER 83-1741] 17 p2467 A83-37219

Analysis of cold flow reestablishment time in a circuit breaker nozzle [AIAA PAPER 83-1749] 17 p2503 A83-37224

COLD FORMING

U COLD WORKING

COLD FRONTS

Satellite estimates of ocean-air heat fluxes during cold air outbreaks 02 p0218 A83-13059

Structure of the cold front observed in SESAME-AVE III and its comparison with the Hoskins-Bretherton frontogenesis model --- Severe Environmental Storms And Mesoscale Experiment - Atmospheric Variability Experiment 06 p0790 A83-18261

Two severe freezes in Brazil - Precursors and synoptic evolution 10 p1450 A83-25390

Structure of thunderstorms along a squall line on May 2, 1979 11 p1622 A83-26982

Dual Doppler radar analysis of a convection line 11 p1622 A83-26986

Some characteristics of chemical precipitation 11 p1612 A83-27672

A wintertime mesoscale cold front in the southern plains 13 p1889 A83-30583

The influence of coastal shape on winter mesoscale air-sea interaction 13 p1891 A83-30801

Gravitational character of cold surges during winter MONEX 13 p1891 A83-30802

A cloud formation process contradictory to the classical occlusion development investigated with satellite images and model output parameters 14 p2057 A83-32409

Slow waves near the mesopause 14 p2059 A83-32860

Rope cloud over land 15 p2204 A83-33886

- The mesoscale and microscale structure and organization of clouds and precipitation in midlatitude cyclones. VI Wavelike rainbands associated with a cold-frontal zone 16 p2384 A83-35459
- The mesoscale and microscale structure and organization of clouds and precipitation in midlatitude cyclones. VII Formation, development, interaction and dissipation of rainbands 16 p2384 A83-35460
- Short-term planetary-scale interactions over the tropics and midlatitudes. II - Winter-MONEX period 23 p3490 A83-47406

COLD GAS

- An investigation of energy separation in a vortex tube 11 p1569 A83-28376
- The effect of viscosity on the interaction of an underexpanded jet with an infinite plane barrier perpendicular to its axis 19 p2792 A83-41895
- COLD PLASMAS**
- On the influence of a plasma hot component on whistler propagation beyond the plasmopause 02 p0206 A83-12020
- Study of the energy relaxation of sputtered atoms in a plasma 04 p0536 A83-15701
- Relaxation oscillations in a plasma with an ultrarelativistic electron beam 04 p0537 A83-15907
- The dissociative recombination of an electron and a molecular ion 05 p0686 A83-16887
- Contact discontinuities in a cold collision-free two-beam plasma 05 p0689 A83-17382
- Generation of nonthermal continuum radiation in the magnetosphere 05 p0681 A83-17395
- Potentials on large spacecraft in LEO 05 p0607 A83-17489
- Method of remote sensing of horizontal stratification due to an ionospherically reflected powerful radio wave 06 p0786 A83-18321
- Approximate method of solving problems of radiation transfer in a cold plasma with strong magnetic field 06 p0838 A83-19228
- Appearance of electrodynamic boundary layers during the propagation of sound in a confined low-temperature plasma 07 p0994 A83-19638
- Theory of the double layer --- in hot and cold plasma acceleration 07 p0995 A83-20062
- Certain characteristics of the production of thermally stable coatings by spraying materials with a low-temperature plasma jet 07 p0940 A83-20702
- Radiative damping of waves in a cold magnetized plasma 07 p0998 A83-20858
- Observation of suprathermal electrons produced by stimulated Raman scattering processes 08 p1168 A83-22376
- Nonlinear theory of strata in a low-temperature plasma 08 p1169 A83-23163
- Waves in a cold pure electron plasma of finite length 10 p1485 A83-25785
- Theory of dissociative recombination 10 p1479 A83-25991
- Radiation from a moving point charge in a drifting anisotropic plasma 10 p1486 A83-26041
- General solution of the Clemmow differential equation in a relativistic cold plasma 12 p1780 A83-29028
- Orbit-averaged implicit particle codes --- for studying plasma kinetics 12 p1781 A83-29601
- Possibility of amorphous glassy state in astrophysical dense plasmas 13 p1947 A83-30422
- Accuracy of mass spectrometric low-temperature plasma diagnostics 13 p1925 A83-30812
- The radiative Reynolds number --- for magnetohydrodynamic stability analysis 14 p2086 A83-32552
- Electron beam as a source of electrostatic waves 15 p2228 A83-34205
- General solution of the Clemmow equation in a three-dimensional cold plasma, with a zero-velocity stream 15 p2235 A83-34273
- Some applications of transformation to the space-independent frame in the processes of strong radiation in plasmas 15 p2235 A83-34493
- Reflection and transmission coefficients for local resonances in a cold magnetoplasma 16 p2341 A83-35408
- Instability problems in plasma diagnostics --- Russian book 16 p2416 A83-36434
- The measurements of dynamical parameters of low temperature plasma flows by means of ultrasound 16 p2417 A83-36881
- Emission, absorption, and tunneling of whistler waves in an inhomogeneous magnetic field 17 p2581 A83-37034
- Approximations in magnetoionic theory 17 p2543 A83-38370
- Refractive index surfaces --- for describing EM wave propagation in ionosphere and magnetosphere 17 p2543 A83-38371

- Experimental investigation of absorption coefficient of cesium resonance doublets in a plasma of combustion products 18 p2746 A83-39859
- Oblique incidence of a strong electromagnetic wave on a cold inhomogeneous electron plasma - Relativistic effects 18 p2748 A83-40508
- Eigenfunction analysis of the beam-plasma instability with finite radial dimensions 18 p2749 A83-40515
- Electron temperature measurements using a 12-channel array probe 20 p3049 A83-42292
- Electromagnetic radiation from a dipole source in a homogeneous magnetoplasma 20 p3050 A83-43417
- Radiation properties of a vacuum-insulated infinite flat slotted plate antenna in a cold isotropic homogeneous plasma 22 p3274 A83-46526
- The effect of cold plasmaspheric and ionospheric plasmas on the electron-cyclotron instability of the frontal boundary layer 23 p3484 A83-48384
- Energy distribution functions of electrons in low-temperature helium-neon plasma at low pressures 24 p3632 A83-49113
- Localized waves in a cold inhomogeneous plasma 24 p3632 A83-49535

COLD PRESSING

- Characteristics of the cold compaction of wurtzite-like boron nitride powders at high pressures 02 p0160 A83-13026
- Properties of P/M titanium alloy produced from elemental blends - The current state of development 07 p0883 A83-19831
- The cold pressing of wurtzitic boron nitride powders at high pressures 09 p1239 A83-25065
- Cold pressed cadmium selenide photoanodes for electrochemical solar cells 18 p2708 A83-39929

COLD ROLLING

- Microstructures in cold-rolled polycrystalline aluminum 07 p0897 A83-21608
- The effect of cold deformation during rolling on the mechanical properties of sheets and foil of magnesium-lithium alloys 13 p1821 A83-30699
- The effect of V and Zr on the rolling texture, recrystallization, and Young's modulus anisotropy of Ti-V and Ti-Zr alloys 13 p1821 A83-30738

COLD STRENGTH

- Investigation of the hydrogen-influenced tendency toward cold cracking in high-strength low-alloy fine-grained structural steel, with regard to the implant experiment --- German thesis 01 p0026 A83-10469
- The nature of the cold brittleness of transition metals 03 p0339 A83-13265
- Microstructural aspects of the cold deformation of Nimonic alloy 115 07 p0897 A83-21607
- Causes of cold cracking in multipass welded joints in corrosion-resisting 08Kh15N5d2T type maraging steels 10 p1397 A83-26222
- Low temperature fatigue fracture of metals and alloys 13 p1824 A83-31585
- A study of the short-term strength of structural materials under static loading --- of metal alloys at cryogenic temperatures 14 p1997 A83-33013
- The use of the acoustic emission method for studying the strength and ductility of materials at low temperatures 14 p1997 A83-33014
- A study of the low-cycle fatigue of the structural alloys for cryogenic applications 14 p1998 A83-33018

COLD SURFACES

- Atmospheric gases on cold surfaces - Condensation, thermal desorption, and chemical reactions 09 p1298 A83-25191
- Characteristics of the precipitation of a cloud of hot particles onto a horizontal surface 21 p3133 A83-45349

COLD TOLERANCE

- The effects of rest and exercise in the cold on substrate mobilization and utilization 04 p0521 A83-15534
- The thermoregulatory activity of the intercostal muscles in conditions of a hypercapnic load 10 p1454 A83-26790
- The influence of waterproofing failure on the thermal insulation of sealed flightsuits used in military aviation 14 p2072 A83-32467
- Thermal reaction and manual performance during cold exposure while wearing cold-protective clothing 16 p2401 A83-35559
- The effect of calcium ions on the temperature sensitivity of humans 23 p3498 A83-47118
- COLD TRAPS**
- Possibility of operation of a chemical oxygen-iodine laser without a cooled trap 16 p2359 A83-35893
- Snowing criteria for cold traps --- utilization in chemical oxygen iodine lasers 21 p3147 A83-45593
- COLD WALLS**
- U COLD SURFACES

COLD WATER

- Increasing summer peak power with aquifer storage 11 p1609 A83-27313
- Active diver thermal protection requirements for cold water diving 18 p2737 A83-40363

COLD WEATHER

- The effect of cold on the thermoregulatory reactions of humans in Siberia 02 p0223 A83-12218
- Delineation of cold-prone areas using nighttime SMS/GOES thermal data Effects of soils and water 02 p0216 A83-12961
- Cold stress at high altitudes 21 p3183 A83-44073

COLD WEATHER TESTS

- Effects of exposure to low O₂ or high CO₂ environments on respiration in hibernating hamsters and ground squirrels 04 p0520 A83-16009

COLD WORKING

- NT COLD ROLLING
- Determination of fracture toughness from stretch zone width measurement in predeformed AISI type 4340 steel 01 p0024 A83-10217
- A nucleus-free mechanism of irregular grain growth in metals 01 p0026 A83-10450
- Properties of cold extruded aluminum-Al2O₃ powder materials 06 p0731 A83-19088
- Microstructural analysis of the cold working effect on the fracture toughness of weld metal in HSLA steel welds 08 p1061 A83-21726
- Decomposition of the metastable beta phase in the textured alloy VT19 11 p1550 A83-28545
- Elastic-plastic behavior of coldworked holes [AIAA 83-0865] 12 p1738 A83-29753

COLLAGENS

- Type II collagen-induced autoimmune endolymphatic hydrops in guinea pig 23 p3495 A83-47819

COLLAPSE

- Acoustic fluidization and the scale dependence of impact crater morphology 07 p1034 A83-21317
- Collapse by ponding of shells --- stability analysis 11 p1594 A83-28411
- Collapse analysis of cylindrical composite panels with cutouts [AIAA 83-0875] 12 p1738 A83-29759
- The dynamic collapse of a column impacting a rigid surface 19 p2856 A83-40873
- Damage tolerant design using collapse techniques 21 p3164 A83-45591
- Inelastic buckling of cylindrical shells subjected to axial tension and external pressure 21 p3164 A83-45597
- The collapse of a gas bubble attached to a solid wall by a shock wave and the induced impact pressure [ASME PAPER 83-FE-3] 23 p3450 A83-48228

COLLECTION

- Influence of multidroplet size distribution on icing collection efficiency [AIAA PAPER 83-0110] 05 p0666 A83-16526

COLLECTORS**U ACCUMULATORS****COLLEGES****U UNIVERSITIES****COLLIMATION**

- Adaptive beam forming for radar 01 p0030 A83-10260
- Jitter in SS 433-A clue to the collimation mechanism 01 p0126 A83-10967
- Holographic HUDs de-mystified 01 p0010 A83-11171
- Electronic beam steering of semiconductor injection lasers - A theoretical analysis 07 p0935 A83-20162
- On the collimation phase error computation of a space-fed planar phased array 09 p1247 A83-23797
- Use of a laser in the collimation of the CIDA Schmidt camera 14 p2101 A83-33293
- Beam models for radio sources. IV - Improved jet collimation 19 p2917 A83-41612
- Wide-band acoustooptical spectral analyzer of the autocollimation type 23 p3507 A83-47573
- COLLIMATORS**
- Rotation modulation phoswich: Design for an image-forming system for the hard X-ray region /greater than 20 keV/ --- German thesis 01 p0116 A83-10475
- X-ray imaging techniques - Modulation collimator and coded mask 11 p1657 A83-27752
- Imaging systems using modulation and coded aperture masks --- for gamma ray telescopes 18 p2756 A83-39284
- Autocollimation multibeam interferometer with spatial beam separation and its use in frequency selection of laser radiation 20 p2997 A83-43790
- Fast beam deflectors based on phase matching 21 p3206 A83-44815
- Optical angle marker --- for calibrating inertial guidance test equipment 22 p3291 A83-46591
- Development of a tantalum pentoxide Luneberg lens 22 p3359 A83-46644

Improved X-ray collimation system for diamond-anvil high-pressure cells 23 p3455 A83-47650

COLLINEARITY

Collinear relative equilibria of the planar n-body problem 03 p0404 A83-13407

Collinear-track altimetry in the Gulf of Mexico from Seasat - Measurements, models, and surface truth 09 p1318 A83-24290

Non-singular stresses effects on two interacting equal collinear cracks 18 p2696 A83-39076

COLLISION AVOIDANCE

Terrain following/terrain avoidance for advanced penetrating aircraft 01 p0006 A83-11146

Sensor snap and narrow field-of-view inset for terrain avoidance flight 01 p0010 A83-11188

Collision risk models 02 p0133 A83-13012

Electromagnetic environment simulation for TCAS avionics --- Threat Alert and Collision Avoidance Systems 05 p0592 A83-17304

Space flight and meteoroids 08 p1048 A83-21883

Automated navigation and collision avoidance for high-speed surface craft [AIAA PAPER 83-0631] 08 p1173 A83-22174

Aircraft separation assurance - Systems design 09 p1199 A83-23371

Aircraft separation assurance - Systems design 09 p1201 A83-24863

Viewpoints on selection of collision avoidance systems 09 p1202 A83-24874

Conflict recognition and collision probability in connection with horizontal evasion maneuvers 10 p1373 A83-26481

Advantages of statistically interrogating onboard anticollision systems 10 p1374 A83-26482

Solving the find-path problem by good representation of free space 13 p1910 A83-31070

Man-made debris in low earth orbit - A threat to future space operations 15 p2125 A83-33740

Computer model of a collision-avoidance system for air traffic control 15 p2121 A83-35275

Development of airborne collision avoidance algorithms compatible with the national airspace system 17 p2461 A83-37141

A collision avoidance tool for aircraft pilots 17 p2461 A83-37142

Status of the TCAS program 22 p3255 A83-46959

Classification of orbits with regard to collision hazard in space 23 p3417 A83-48137

COLLISION PARAMETERS

NT COLLISION RATES

Collision between an evaporating drop and a hot wall 04 p0478 A83-16166

The possibility of using electromagnetic accelerators for studying processes occurring during the high-velocity collision of solids 04 p0465 A83-16388

An experimental and theoretical study of the rebound of short rods from a solid obstacle 04 p0501 A83-16396

Electron impact excitation of forbidden transitions in Si IX 06 p0835 A83-19012

Charge transfer in H/ + /-H and H/ + /-D collisions within the energy range 0.1-150 eV 06 p0809 A83-19243

A determination of the collision relaxation constants for a forbidden transition by means of nonlinear polarization spectroscopy for a three-level gas in a magnetic field 06 p0809 A83-19541

Numerical modeling of intraplate deformation - Simple mechanical models of continental collision 07 p0961 A83-20230

Laboratory simulation of planetesimal collision 07 p1029 A83-20239

A possible mechanism for the recurrent activity in galaxy nuclei 07 p1014 A83-20652

Modern exospheric theories and their observational relevance --- kinetic theory 07 p1031 A83-20839

A theoretical determination of capture efficiency of small columnar ice crystals by large cloud drops 08 p1142 A83-23010

Electron collision strengths for transitions within the 1s/2/2s/2l/2p/2l' configuration of Si IX 09 p1347 A83-23653

Density drift instabilities and weak collisions --- in space plasmas 09 p1303 A83-23766

Families of periodic collision orbits in the general three-body problem 12 p1786 A83-29111

Tunable diode laser measurements of the band strength and collision halfwidths of nitric oxide 12 p1778 A83-29149

Laser studies of electronic energy transfer in atomic copper 13 p1851 A83-30957

The critical energy density and the inelasticity coefficient for asteroidal catastrophic collisions 15 p2250 A83-35029

On the definition of collision efficiency of atmospheric particles 16 p2387 A83-35495

Collision strengths for the N = 2 excitation of hydrogenic ions 17 p2583 A83-38960

Some essential details for application of Bleck's method to the collision-breakup equation --- raindrop development model 18 p2725 A83-39691

Collision operator for a strongly magnetized pure electron plasma 21 p3209 A83-43936

COLLISION RATES

A laser-based measurement of electron collision rates for excited states of ionised helium in a plasma 03 p0398 A83-14662

Cratering time scales for the Galilean satellites 04 p0548 A83-16235

Collisional rates for vibrational-rotational transitions in circumstellar SiO masers 07 p1023 A83-21159

Calculation of the rate coefficients for the electron impact excitation of the n = 2 terms of O IV 08 p1179 A83-21989

Flocculent and grand design spiral galaxies in groups - Time scales for the persistence of grand design spiral structures 10 p1512 A83-26705

Collisional forcing of raindrop oscillations 13 p1893 A83-31042

Line radiation from a hot, optically thin plasma - Collision strengths and emissivities --- in stellar atmospheres 16 p2416 A83-35974

Ion-neutral collision frequency variations in the lower thermosphere from incoherent scatter measurements 17 p2545 A83-38538

Cometary impacts with the sun - Physical and dynamical considerations 22 p3376 A83-47087

Electron collisional rate coefficients for low-level transitions in hydrogen 24 p3626 A83-49386

COLLISION WARNING DEVICES

U COLLISION AVOIDANCE

U WARNING SYSTEMS

COLLISIONAL PLASMAS

NT STRONGLY COUPLED PLASMAS

Oscillation of cyclotron-echo signals in a plasma 03 p0396 A83-13182

Electron distribution function in a weakly ionized plasma in an inhomogeneous electric field. II - Strong fields /energy balance determined by inelastic collisions/ 03 p0397 A83-13195

Theoretical features of the radial collisional transport in magnetoplasmas 03 p0398 A83-14507

Rayleigh-Taylor instability of a partially ionized medium in the presence of a variable horizontal magnetic field 04 p0535 A83-14961

Collisional relaxation of a plasma in the field of a plane gravitational wave 04 p0536 A83-15711

An approximate collision operator in the theory of collisional transport for quiescent magnetoplasmas 04 p0536 A83-15818

Lower-hybrid instability in current-carrying plasmas 06 p0812 A83-18920

Theory of electrostatic probes under intermediate collisional conditions 07 p0995 A83-20063

Perturbed bifurcation of stationary striations in a contaminated, nonuniform plasma 08 p1168 A83-22739

Resonant absorption in a self-consistent density profile at moderate intensities --- in inhomogeneous plasmas 10 p1485 A83-25789

Collisional coupling of fluctuations in plasmas 13 p1925 A83-30520

Variational theory of collisional transport for a toroidal axisymmetric plasma in the weakly collisional regime 16 p2416 A83-36552

Kinetic theory of the anomalous electrical conductivity of a turbulent plasma 16 p2417 A83-36937

Temperature effects on the beat heating of a collisional magnetoplasma 18 p2745 A83-39612

Collision operator for a strongly magnetized pure electron plasma 21 p3209 A83-43936

Purely growing thermal instability of an electromagnetic wave in a collisional plasma 21 p3209 A83-43938

Coronal and collisional - Radiative model of the plasma for the case of hydrogen glow discharge 21 p3212 A83-44353

Electromagnetic two-stream and filamentation instabilities for a relativistic beam-plasma system 22 p3362 A83-46020

Relativistic corrections for the conventional, classical Nyquist theorem 23 p3510 A83-47607

The collisional absorption of plasma cyclotron oscillations 23 p3510 A83-48394

COLLISIONLESS PLASMAS

A Schroedinger-Poisson model for the numerical simulation of collisionless plasmas - Some results of a linear analysis 01 p0107 A83-10922

The dissipation of electromagnetic waves in plasmas 01 p0107 A83-11296

An experimental investigation of nonlinear dissipation of electromagnetic waves in inhomogeneous collisionless plasmas 01 p0107 A83-11297

Collisionless absorption of electromagnetic waves in plasmas and 'slow' nonlinear phenomena 01 p0107 A83-11298

Nonlinear effects in the propagation of electron plasma waves in an inhomogeneous plasma layer 01 p0107 A83-11299

Vlasov equation --- for galactic and stellar plasma dynamics 02 p0261 A83-12547

Stability of a thick two-dimensional quasineutral sheet 03 p0396 A83-13120

Analysis of ion solitons in an unmagnetized plasma 03 p0397 A83-13193

The permittivity of an ultrarelativistic plasma 03 p0397 A83-13536

Interaction of waves with an interface moving in a collisionless plasma 04 p0536 A83-15756

Contact discontinuities in a cold collision-free two-beam plasma 05 p0689 A83-17382

Spiky ion acoustic waves in collisionless auroral plasma 06 p0784 A83-18306

Evolution of nonlinear Alfvén waves propagating along the magnetic field in a collisionless plasma 06 p0812 A83-18916

Collisionless electrostatic interchange instabilities 06 p0812 A83-18922

A class of soliton solutions of the hydrodynamic equations of motion for ions in a uniform plasma without external fields 07 p0995 A83-20060

Drift- and lower-hybrid eigenmodes in a plasma cylinder 07 p0997 A83-20539

Ponderomotive force in a warm two-fluid plasma 10 p1485 A83-25788

Superimposed electron and ion beams - Model for an evolving collisionless plasma 10 p1486 A83-25993

Plasma in astrophysics 11 p1680 A83-28242

The self-focusing of whistler waves 11 p1660 A83-28250

General solution of the Clemmow differential equation in a relativistic cold plasma 12 p1780 A83-29028

Collisionless tearing modes in the presence of shear flow 12 p1780 A83-29073

Ion-acoustic waves in finite geometry 13 p1923 A83-30112

Nonlinear Landau damping phenomenon in a strongly turbulent plasma 13 p1924 A83-30414

On the temperature of a collisionless plasma 13 p1926 A83-31338

Total current to cylindrical collectors in collisionless plasma flow 13 p1948 A83-31529

The effect of microscale random Alfvén waves on the propagation of large-scale Alfvén waves 13 p1927 A83-31646

General solution of the Clemmow equation in a three-dimensional cold plasma, with a zero-velocity stream 15 p2235 A83-34273

Collisionless dissipation processes in quasi-parallel shocks --- in solar wind 15 p2202 A83-34735

Buneman instability and Pierce instability in a collisionless bounded plasma 18 p2747 A83-39922

Linear mode conversion in laser plasmas 18 p2748 A83-40511

Ion-acoustic solitary waves in a magnetized plasma with arbitrary electron equation of state 21 p3209 A83-43937

A nonlinear kinetic energy principle for two-dimensional collision-free plasmas 21 p3209 A83-43940

The Knudsen ion layer problem in the theory of the collisionless sheath 21 p3212 A83-44356

Coupling mechanism of boundary sheaths and wave launcher in a collisionless plasma 21 p3214 A83-45189

Structure of perpendicular shocks in collisionless plasma 22 p3362 A83-46023

Anomalous resistivity due to low-frequency turbulence --- of collisionless plasma with limited acceleration of high velocity runaway electrons 22 p3336 A83-47061

On the variation of a pulse envelope with filling in a dispersive medium 23 p3510 A83-48477

High-speed flow of a collisionless plasma past a cylinder with allowance for the electric field 24 p3632 A83-49663

COLLISIONS

NT ATOMIC COLLISIONS

NT BIRD-AIRCRAFT COLLISIONS

NT COULOMB COLLISIONS

NT INELASTIC COLLISIONS

NT IONIC COLLISIONS

NT METEORITE COLLISIONS

NT MIDAIR COLLISIONS

NT MOLECULAR COLLISIONS

NT PARTICLE COLLISIONS

The asteroids as outcomes of catastrophic collisions 08 p1175 A83-22927

Effects of galaxy collisions on the structure and evolution of galaxy clusters. I - Mass and luminosity functions and background light 15 p2255 A83-34078

- Computer simulations of gravitational encounters between pairs of binary star systems 22 p3377 A83-46389
- Motion near quadruple collision in the trapezoidal four-body problem 24 p3643 A83-49392
- COLLOCATION**
- Fundamental solutions for the collocation method in planar elastostatics 01 p0060 A83-10711
- Convergence and stability of a collocation method for the generalized airfoil equation 03 p0278 A83-13844
- Collocation methods for boundary value problems on 'long' intervals 07 p0986 A83-20505
- Collocation methods for weakly singular second-kind Volterra integral equations with non-smooth solution 11 p1648 A83-27996
- A numerical solution of singular integral equations without using special collocation points --- in stress analysis problems 11 p1594 A83-28420
- Numerical experiments involving Galerkin and collocation methods for linear integral equations of the first kind 12 p1771 A83-29098
- Collocations and thirtieth order resonant harmonics --- for determining earth's gravitational field 20 p3023 A83-43153
- COLLOIDS**
- NT AEROSOLS
- NT FOG
- Visible light induced cleavage of water into hydrogen and oxygen in colloidal and microheterogeneous systems 15 p2131 A83-33862
- The concentrating of molecules in concave droplets and the origin of life 21 p3189 A83-44700
- COLUMBIA**
- An analysis of natural features of the Columbian plans by remote sensing 11 p1601 A83-28148
- COLOR**
- NT WATER COLOR
- Color graphics in ATE 01 p0028 A83-10747
- Application and experience of colour CRT flight deck displays 21 p3091 A83-44688
- Color signal correlation detection by matched spatial filtering 23 p3459 A83-48704
- COLOR (PARTICLE PHYSICS)**
- U QUANTUM CHROMODYNAMICS
- COLOR CENTERS**
- Passively Q-switched laser utilizing concentrated Li-Nd-La phosphate glass 07 p0933 A83-20102
- Infrared absorption spectroscopy with color center lasers 11 p1653 A83-27529
- Progress in the development of color centers for stable CW tunable laser operation 11 p1578 A83-27542
- A single mode /F2+/-asterisk color-center laser for application in optical pumping of helium 11 p1578 A83-27543
- Tunable visible lasers using defects in oxides 11 p1578 A83-27545
- Laser action continuously tunable from 1.98 to 3.76 microns using F2+ and lithium /F2+/-A centers in KI 11 p1578 A83-27546
- Investigations on the dynamical occupation behavior of optically excited F-centers in alkali halides by use of picosecond laser spectroscopy 11 p1579 A83-27554
- Tone-burst modulated color-center-laser spectroscopy 15 p2167 A83-33758
- Characteristics of lasers with condensed active media exhibiting linear anisotropy induced by polarized pump radiation 23 p3460 A83-47162
- COLOR CODING**
- Spatial frequency pseudocolor filters 03 p0328 A83-14094
- White-light optical processing of misfocused speckle interferograms 08 p1093 A83-22362
- Spatial carriers with orthogonal subcodes --- signal coding and decoding for optical communication 15 p2230 A83-33810
- A new concept of retinal colour coding 15 p2210 A83-34871
- Dual-beam encoding for color holographic construction 20 p2992 A83-43630
- Multiplexed speckle and holographic interferometry with color encoding by white-light processing 21 p3134 A83-43872
- Color coding in quasi-interferometry 24 p3582 A83-49011
- COLOR INFRARED PHOTOGRAPHY**
- The use of near color infrared photography to assess the impact of the oil and natural gas industry on Louisiana's wetlands 01 p0063 A83-10069
- Evaluation of photographic enhancements of Landsat imagery 02 p0198 A83-12035
- A colorimetric mapping of the moon's surface in the 0.62-0.95-micron spectral region 03 p0432 A83-13368
- Environmental monitoring of the Athabasca Oil Sands Region 03 p0346 A83-14238

- Remote sensing applications for British Columbia wetlands using 35 mm aerial photography 03 p0347 A83-14251
- The application of remote sensing in southern Alberta's mountain pine beetle management 03 p0347 A83-14257
- Predicting permafrost conditions with infrared sensing techniques 03 p0348 A83-14264
- Remote measurement of biomass 03 p0350 A83-14306
- The classification of forest species types using gradient analysis and spectral data 17 p2531 A83-38340

COLOR PERCEPTION

U COLOR VISION

COLOR PHOTOGRAPHY

- Remote sensing applications for British Columbia wetlands using 35 mm aerial photography 03 p0347 A83-14251
- Colour Landsat images and mosaics - Basic tools in areal and ecological differentiation in Canada 03 p0348 A83-14265
- The development of a computer controlled camera system for archiving image data [AIAA PAPER 83-0656] 05 p0643 A83-16820
- Multiple-aperture three-dimensional image construction utilizing fringe-modulated speckle patterns 05 p0643 A83-16835
- Landsat multitemporal color composites 07 p0952 A83-21433
- White-light prefiltering for real-time digital image transmission of still and moving color video images 08 p1076 A83-22430
- Application of the IHS color transform to the processing of multisensor data and image enhancement --- Intensity, Hue and Saturation in satellite remote sensing data 09 p1287 A83-24576
- The first color panoramic pictures of the Venus surface transmitted by the Venera 13, 14 probes 14 p2014 A83-31956
- Broad spectral band color image deblurring 14 p2020 A83-32904
- Method for the production of color synthesized photographs and photoplans using a photorectifier 17 p2510 A83-37725
- Color photography from Mauna Kea 17 p2595 A83-38616
- Dual-beam encoding for color holographic construction 20 p2992 A83-43630
- Restoration of out-of-focused color photographic images 20 p2992 A83-43631

COLOR TELEVISION

- An adaptive DPCM algorithm for predicting contours in NTSC composite video signals 01 p0034 A83-11429
- TV bandwidth compression techniques using time-companded differentials and their applications to satellite transmissions 06 p0749 A83-19597
- An adaptive DPCM encoder for NTSC composite video signals 07 p0907 A83-19731
- TV bandwidth compression techniques using time companded differentials and their applications to satellite transmissions 07 p0909 A83-19743
- Time multiplexed compression - New dimensions in satellite TV 07 p0914 A83-20847
- Trinoscope color displays for simulation 08 p1102 A83-22831
- Uniform color scale applications to computer graphics 21 p3190 A83-44268

COLOR VISION

- Color vision is altered during the suppression phase of binocular rivalry 02 p0222 A83-12067
- Retroactive phenomena in the visual system 03 p0377 A83-13281
- Color-stress as a method for detecting the focal reaction in endogenous uveitis 03 p0377 A83-13293
- Photophysical processes in retinoid molecules, related to visual chromophores 03 p0375 A83-14357
- The time of identification of the shapes of colored stimuli 04 p0523 A83-15779
- Color selection and verification testing for airborne color CRT displays 04 p0524 A83-16128
- The perception of colour on electro-optical displays 04 p0524 A83-16328
- Colour flight deck displays 04 p0448 A83-16336
- Sensitivity to spatiotemporal colour contrast in the peripheral visual field 05 p0675 A83-17746
- Electronic visualizations and means of protection for the visual function - A method of study 06 p0800 A83-18344
- The peculiarities of the optimization of the visual activity of an operator under conditions of a time deficit 07 p0979 A83-20348
- The spatial parameters of color vision in humans 07 p0977 A83-20357
- Electrophysiological investigations of color vision in humans 07 p0977 A83-20358

- Calligraphic/raster color display for simulation 08 p1102 A83-22832
- A presentation of a new protocol for the evaluation of color sense in aeronautics 08 p1147 A83-22956
- The perception of the color of a stimulus equal in brightness to the color of the background - The assimilation of color 13 p1901 A83-30437
- The polyfunctionality of visual rhodopsin 14 p2065 A83-33321
- A new concept of retinal colour coding 15 p2210 A83-34871
- Color vision and vision at low light levels 16 p2396 A83-35577
- The selective sensitivity of color mechanisms of vision to spatial frequency 16 p2398 A83-35903
- Neurophysiological aspects of color vision in primates: Comparative studies on simian retinal ganglion cells and the human visual system --- Book 19 p2875 A83-41517
- Photoreceptors: Their role in vision --- Book 19 p2877 A83-41989
- On seeing reddish green and yellowish blue 21 p3187 A83-44365
- Comparison of color and black-and-white visual displays as indicated by bombing performance in the 2B35 TA-4J flight simulator 21 p3092 A83-44692
- Expedient range enhanced 3-D robot colour vision 21 p3118 A83-44694
- Color segregation and selective attention in a nonsearch task 22 p3349 A83-45955
- Sleep and the McCollough Effect --- orientation-contingent chromatic visual aftereffect 23 p3498 A83-48125

COLORADO

- Acid clouds and precipitation in eastern Colorado 19 p2863 A83-41982

COLORATION

U COLOR

COLORIMETRY

- A colorimetric mapping of the moon's surface in the 0.62-0.95-micron spectral region 03 p0432 A83-13368
- Photometric characteristics of the night sky in the Crimea 03 p0407 A83-13673
- Remote comets and related bodies - VJHK colorimetry and surface materials 08 p1181 A83-22926
- Comparison of the Mt. Stromlo/AAO and Caltech/Tololo infrared photometric systems 18 p2757 A83-39599
- Infrared (JHK) photometry of asteroids. II 18 p2757 A83-39605
- Central distribution of the near-infrared colours in two early-type spirals 22 p3375 A83-46572
- The rotation, color, phase coefficient, and diameter of 1915 Quetzalcoatl 22 p3388 A83-47090

COLUMBIA RIVER BASIN (ID-OR-WA)

- The role of remotely sensed and other spatial data for predictive modeling - The Umatilla, Oregon, example 15 p2186 A83-34832

COLUMBIUM

U NIOBIUM

COLUMNS (SUPPORTS)

- Refined design of self-expanding stayed column for use in space 02 p0142 A83-12753
- Maximum stiffness beam-columns 09 p1282 A83-25103
- Numerical interpretations of creep buckling behavior of columns 09 p1282 A83-25105
- Nonlinear behavior of thin columns under parametrically excited load 12 p1738 A83-29750
- [AIAA 83-0862] Stability of short Beck and Leipholz columns on elastic foundation 16 p2366 A83-36098
- The dynamic collapse of a column impacting a rigid surface 19 p2856 A83-40873
- The ultimate load sensitivity of lipped channel columns to column axis imperfection 21 p3153 A83-44624

COMA

- Successful reversal of presumed carbon monoxide-induced semicoma 18 p2734 A83-40362
- Neutral cometary atmospheres. IV - Brightness profiles in the inner coma of comet Kohoutek 1973 XII 20 p3059 A83-42463

COMBAT

- Combat survivability with advanced aircraft propulsion development 01 p0008 A83-10179
- Computer models for determining countermeasures effectiveness of expendables in air-to-air engagements 01 p0103 A83-11162
- Toward 'combat realistic' tests, evaluations, exercises - and training 01 p0015 A83-11237
- The influence of differential physical conditioning regimens on simulated aerial combat maneuvering tolerance 02 p0223 A83-12406
- [AD-A126486] The Northrop F-20 avionics mission simulator [AIAA PAPER 83-0142] 05 p0599 A83-16551

- A glimpse into the future of air combat --- via computerized cockpit simulators
[AIAA PAPER 83-0143] 05 p0599 A83-16552
- Solution of three dimensional interception by inclined plane using the forced singular perturbations technique
07 p0862 A83-21013
07 p0862 A83-21026
- Dynamics of air combat
Objective summary of U.S. Army electro-optical modeling and field testing in an obscuring environment
08 p1093 A83-22351
- EOSAEL 82 - A library of battlefield obscuration models
08 p1093 A83-22352
- Transmission effects of explosion-produced dust clouds on downward viewing airborne platforms
08 p1132 A83-22543
- Air interdiction mission planning using dynamic programming
09 p1196 A83-24768
- Combat damage - A unique element
15 p2243 A83-34865
- Data base considerations for a tactical environment simulation
[AIAA PAPER 83-1099] 16 p2312 A83-36219
- Dynamics of air combat
16 p2287 A83-36914
- Air-to-air combat in a plastic dome
18 p2642 A83-40620
- Poststall flight in close combat
[AIAA PAPER 83-2120] 19 p2806 A83-41945
- An eccentric two-target differential game model for qualitative air-to-air combat analysis
[AIAA PAPER 83-2122] 19 p2789 A83-41947
- Correlation of flight test and analytic M-on-N air combat exchange ratios --- Many-on-Many
23 p3392 A83-48219
- COMBINATORIAL ANALYSIS**
NT PARTITIONS (MATHEMATICS)
Combinatorial reliability analysis of multiprocessor computers
08 p1152 A83-22711
- A combinatorial limit to the computing power of VLSI circuits
13 p1908 A83-30793
- COMBINED STRESS**
An energy theory for postbuckling of composite plates under combined loading
02 p0195 A83-12758
- The fracture mechanics of microsphere-filled composites
03 p0293 A83-14739
- Deformation characteristics of metal composites with brittle fibers during bending
03 p0293 A83-14817
- Free vibrations and the stability of annular plates under nonuniform tension and compression
04 p0497 A83-15390
- Stability and optimization of viscoelastic composite cylindrical shells under combined loading
06 p0775 A83-18507
- On method of successive approximations in a class of problems of the general theory of plasticity
07 p0945 A83-20142
- The nonlinear problem of the stability of cylindrical sandwich shells under combined loading
08 p1114 A83-21628
- On the maximum-energy-release-rate criterion for fracture under combined loads
08 p1116 A83-21659
- K-determination in mixed-mode crack problems by interferometry
08 p1117 A83-21720
- Twin shear stress yield criterion
08 p1122 A83-21993
- Combined loadings in the theory of plasticity --- Book
08 p1123 A83-23025
- Effects of plastic prestrain on the creep of aluminium under biaxial stress
09 p1233 A83-24078
- Postbuckling of long orthotropic plates in combined shear and compression
12 p1738 A83-29760
- Carbon/epoxy laminates under combined fastener bearing and tension bypass loading
[AIAA 83-0967] 12 p1710 A83-29778
- Buckling of anisotropic laminated cylindrical plates
[AIAA 83-0979] 12 p1740 A83-29786
- Stability analysis of Centaur-in-Shuttle composite corrugated adapters
[AIAA 83-1003] 12 p1707 A83-29791
- Comparison of frequency determination techniques for cantilevered plates with bending-torsion coupling
[AIAA 83-0953] 12 p1745 A83-29885
- A mixed-mode fracture criterion for composite materials
12 p1711 A83-29895
- Stress relaxation characteristics and data utilization
12 p1746 A83-29914
- Deformation of an elastoviscoplastic composite under complex loading
16 p2364 A83-35503
- A machine for the mechanical testing of polymers in a three-dimensional stressed state
16 p2364 A83-35513
- An experimental study of the failure of elastoplastic cylindrical shells under combined loading
16 p2365 A83-35929
- The deterioration of sodium ion conductors under applied stress
16 p2326 A83-35976
- Metal-metal composites loaded at ultrasonic frequencies
16 p2324 A83-36190
- On the description of cyclic hardening under complex loading histories
[ONERA, TP NO. 1983-7] 16 p2333 A83-36420
- Some consequences of the two-parameter model of fatigue-life scatter --- under complex and cyclic loading
17 p2518 A83-37269
- On the stability of a cylindrical shell under torsion and under a combined load with torsion
17 p2520 A83-37537
- Fatigue life prediction for complex load versus time histories
18 p2700 A83-39995
- Quasi-homogeneous states in composite materials with small-scale bends in the structure
18 p2701 A83-40112
- Algorithm for investigating the stability of rings of variable thickness under nonuniform loading
18 p2702 A83-40120
- The effect of the direction of shear on the buckling of laminated plates subjected to combined shear and compressive loading
18 p2704 A83-40188
- Properties of composite box beams under combined impact loading
18 p2705 A83-40222
- Postbuckling behavior of a thick plate
19 p2856 A83-40868
- Elastoplastic double-wall shells under complex nonisothermal loading
19 p2859 A83-41603
- Material performance under combined stresses in the hard space environment of the sunprobe Helios-A
20 p2945 A83-42371
- Fracture toughness of composite adherend adhesive joints under mixed mode I and III loading
21 p3115 A83-44121
- The behaviour of a channel cantilever under combined bending and torsional loads
21 p3153 A83-44623
- An analysis of the energy release rate for non-coplanar crack growth in fiber reinforced composite materials
21 p3107 A83-44913
- The long-term strength of metals in a complex stressed state
21 p3114 A83-45318
- Low-cycle fatigue during symmetric disproportionate deformation
21 p3163 A83-45363
- Characteristics of brittle fracture under general combined modes including those under bi-axial tensile loads
24 p3594 A83-49866
- COMBUSTIBILITY**
U FLAMMABILITY
COMBUSTIBLE FLOW
Three-dimensional model of spray combustion in gas turbine combustors
01 p0011 A83-10652
- Performance predictions for confined swirling flows
01 p0045 A83-10663
- Lewis number effects on the structure and extinction of diffusion flames due to strain
01 p0023 A83-10897
- Coherent structures in turbulent combustion
01 p0023 A83-10899
- Probing of the unsteady reacting muzzle exhaust flow of 20 MM gun
[ASME PAPER 82-HT-34] 02 p0172 A83-12792
- A new numerical method for turbulent mixing of supersonic reacting flows in chemical laser cavities
[ONERA, TP NO. 1982-85] 03 p0332 A83-14537
- Flame quenching by turbulence
03 p0295 A83-14848
- The nonuniqueness and instability of steady-state combustion modes in a boundary layer with intense injection
03 p0296 A83-14898
- The flow field in a suddenly enlarged combustion chamber
04 p0476 A83-15288
- Spectral characteristics of the aerodynamic field of a turbulent diffusion flame at a low Froude number
04 p0480 A83-16443
- Measurements and predictions for nonevaporating sprays in a quiescent environment
[AIAA PAPER 83-0151] 05 p0633 A83-16558
- Nonadiabatic nonisobaric propagation of a planar premixed flame - Constant-volume enclosure
[AIAA PAPER 83-0239] 05 p0612 A83-16605
- On the modeling of turbulent premixed flames
[AIAA PAPER 83-0241] 05 p0612 A83-16607
- Numerical study of a ramjet dump combustor flow field
[AIAA PAPER 83-0421] 05 p0585 A83-16704
- A double reaction zone model and perturbation analysis for finite rate kinetics in hydrocarbon fuel combustors
[AIAA PAPER 83-0599] 05 p0612 A83-16810
- An implicit finite-difference method for chemical nonequilibrium flow through an axisymmetric supersonic nozzle
05 p0589 A83-16928
- Velocity field characteristics of a swirling flow combustor
[AIAA PAPER 83-0314] 06 p0761 A83-19586
- Influence of the vortex shedding process on a bluff-body diffusion flame
[AIAA PAPER 83-0335] 06 p0727 A83-19588
- On the influence of the plate thickness on the boundary layer ignition for large activation energies
07 p0878 A83-19839
- A laser anemometer seeding technique for combustion flows with multiple stream injection
07 p0928 A83-19843
- Structure of a detonation front
07 p0926 A83-20898
- The asymptotic structure of a counterflow premixed flame for large activation energies
07 p0882 A83-21166
- A comparison of techniques for reconstructing axisymmetric reacting flow fields from absorption measurements
08 p1057 A83-22393
- Isothermal models of gas-turbine combustors
08 p1057 A83-23097
- A numerical study of turbulent, confined, swirling jets
08 p1088 A83-23193
- Premixed, turbulent combustion of a sudden-expansion flow
09 p1225 A83-23748
- Premixed combustion in a turbulent boundary layer with injection
09 p1225 A83-23750
- Estimation of pressure fields in combustion of vapour clouds
09 p1262 A83-24419
- Ignition dynamics of fully reactive propellant in stagnation flow
09 p1226 A83-24666
- Using a global hydrogen-air combustion model in turbulent reacting flow calculations
09 p1227 A83-24667
- Acoustic imaging for diagnostics of chemically reacting systems
[AIAA PAPER 83-0761] 10 p1476 A83-25955
- A study on the hydrogen-oxygen diffusion flame in high speed flow
10 p1391 A83-26199
- Experimental investigation of shock initiated methane-combustion near a wall
10 p1391 A83-26200
- Fast motions of a gas in a porous medium
11 p1569 A83-28539
- Filtration combustion of gases
14 p1988 A83-32083
- The propagation of a curved flame front in a specified gas-flow field
14 p1989 A83-32088
- Nonstationary phenomena in flows of a viscous reactive fluid
14 p1989 A83-32091
- The turbulence modelling of variable density flows - A mixed-weighted decomposition
15 p2156 A83-33673
- Operator splitting methods for the computation of reacting flows
15 p2157 A83-33866
- Assessment of two computational procedures for spray combustors
15 p2160 A83-34255
- Fluid flow within reciprocating-engine cylinders
15 p2160 A83-34265
- Numerical study of transient laminar combustion in boundary layer flow
15 p2161 A83-34267
- Effects of chemical modeling on three-dimensional nonequilibrium viscous shock-layer flows
[AIAA PAPER 83-1425] 15 p2120 A83-34902
- Laser tomography for simultaneous concentration and temperature measurement in reacting flows
[AIAA PAPER 83-1553] 15 p2165 A83-34924
- Regular reflection of detonation waves
16 p2350 A83-35723
- Computation of tridimensional gas flow with recirculation and combustion
[ONERA, TP NO. 1983-49] 16 p2350 A83-35807
- The effects of large heat release on a two dimensional mixing layer
[AIAA PAPER 83-0472] 16 p2351 A83-36055
- Importance of inlet boundary conditions for numerical simulation of combustor flows
[AIAA PAPER 83-1263] 16 p2308 A83-36314
- Prediction of an axisymmetric combustor flow
[AIAA PAPER 83-1264] 16 p2326 A83-36315
- Laser applications to combustion research
[AIAA PAPER 83-1360] 16 p2360 A83-36358
- An Eulerian-Lagrangian method for turbulent combustion
[ONERA, TP NO. 1983-16] 16 p2327 A83-36426
- Correlating downward flame spread rates for thick fuel beds
17 p2484 A83-37045
- Aerodynamic studies on swirled coaxial jets from nozzles with divergent quarls
17 p2504 A83-37398
- The probability distribution of passive-additive concentration in a mixing layer
17 p2505 A83-37631
- The effect of pressure-velocity correlation in a premixed, planar, turbulent flame
17 p2485 A83-38029
- Calculation of turbulent diffusion flame using the coherent flame sheet model
[AIAA PAPER 83-1322] 18 p2663 A83-39108
- Use of planar laser-induced fluorescence for the study of combustion flowfields
[AIAA PAPER 83-1361] 18 p2688 A83-39263

- Finite-difference calculations of unsteady premixed flame-flow interactions
[AIAA PAPER 83-1917] 18 p2664 A83-39373
- Structure and extinction of convective diffusion flames with general Lewis numbers 18 p2664 A83-40312
- Stability of the stationary plane-parallel convective motion of a chemically active medium
19 p2842 A83-41261
- Statistical processing of multiplexed data from turbulent flames
20 p2950 A83-42581
- Studies on luminous and non-luminous flames with spray combustor. II - Case of swirl combustor
21 p3109 A83-44067
- A reverse flow chamber for small turbomachines
[ONERA, TP NO. 1983-30] 21 p3092 A83-44309
- Velocity-pressure gradient correlation in reactive turbulent flows
21 p3132 A83-44999
- The influence of stretch on a premixed flame with two-step kinetics
22 p3267 A83-46760
- A calculation of wrinkled flames
22 p3267 A83-46761
- An analysis of nozzle flows for various models of reacting gases --- Russian book
23 p3392 A83-47124
- An investigation of the establishment of a recirculation zone by swirling flows within a conical duct
[ASME PAPER 83-GT-93] 23 p3448 A83-47939
- Effects of external burning on spike-induced separated flow
23 p3398 A83-48132
- On the transformation of planar detonation to cylindrical detonation
23 p3430 A83-48157
- Turbulent premixed combustion - Further discussions on the scales of fluctuations
[ONERA, TP NO. 1983-67] 23 p3430 A83-48188
- Lagrangian models for turbulent combustion
[ONERA, TP NO. 1983-106] 24 p3554 A83-49417
- Precautions that have to be taken in applying LDV to combustion chambers
[ONERA, TP NO. 1983-112] 24 p3583 A83-49423
- Visualization of two-dimensional nonstationary flows of combustible media
24 p3555 A83-49766
- Characteristics of the supersonic combustion of nonmixed gases in ducts
24 p3556 A83-49778
- The use of the techniques of holographic interferometry in qualitative studies of gas-dynamic flows with chemical reactions
24 p3584 A83-49780
- COMBUSTION**
- NT AFTERBURNING
- NT BOUNDARY LAYER COMBUSTION
- NT DEFLAGRATION
- NT EROSION BURNING
- NT FUEL COMBUSTION
- NT HYDROCARBON COMBUSTION
- NT HYPERSONIC COMBUSTION
- NT METAL COMBUSTION
- NT PROPELLANT COMBUSTION
- NT SOLID PROPELLANT COMBUSTION
- NT SOLID PROPELLANT IGNITION
- NT SPONTANEOUS COMBUSTION
- NT SUPERSONIC COMBUSTION
- Multiphase combustion experimentation in microgravity
[IAF PAPER 83-141] 23 p3429 A83-47288
- COMBUSTION CHAMBERS**
- Impacts of broadened-specification fuels on aircraft turbine engine combustors
01 p0028 A83-10655
- Characteristic time ignition model extended to an annular gas turbine combustor
01 p0011 A83-10666
- Combustion characteristics of hydrogen-carbon monoxide based gaseous fuels
01 p0023 A83-11491
- Multifuel evaluation of rich/quench/lean combustor
01 p0023 A83-11492
- NOx results from two combustors tested on medium BTU coal gas
01 p0070 A83-11493
- Centrifugal mixing - A comparison of temperature profiles in nonrecirculating swirling and nonswirling flames
02 p0152 A83-12076
- Measured and predicted soot profiles in a gas turbine combustor
02 p0136 A83-12077
- Nonlinear structural and life analyses of a combustor liner
02 p0195 A83-12764
- Assessment of candidate combustor configurations as test beds for modeling complex flows
[ASME PAPER 82-HT-36] 02 p0172 A83-12793
- Low temperature /650 to 700 C/ burner rig testing
02 p0158 A83-12835
- The influence of equivalence ratio variation on pollutant formation in a gas turbine type combustor
02 p0136 A83-13095
- The flow field in a suddenly enlarged combustion chamber
04 p0476 A83-15288
- Radiative transfer in spectrally dissimilar absorbing-emitting-scattering adjacent mediums
04 p0476 A83-15294
- TF41/Lamilly accelerated mission test
04 p0449 A83-15319

- An experimental study and modeling of heat transfer in boilers of small and medium power --- French thesis
04 p0456 A83-15841
- Gaseous emissions of gas turbine combustors
[AIAA PAPER 83-0242] 05 p0596 A83-16608
- Swirling flow in a research combustor
[AIAA PAPER 83-0313] 05 p0612 A83-16644
- Small gas turbine combustor study - Combustor liner evaluation
[AIAA PAPER 83-0337] 05 p0596 A83-16663
- Investigation of a dual inlet side dump combustor using liquid fuel injection
[AIAA PAPER 83-0420] 05 p0609 A83-16703
- A one-dimensional unsteady model of dual mode scramjet operation
[AIAA PAPER 83-0422] 05 p0597 A83-16705
- Toroidal flow coal-fired MHD combustor design study and tests
[AIAA PAPER 83-0467] 05 p0686 A83-16734
- Dynamic behavior of turbulent flow in a widely-spaced co-axial jet diffusion flame combustor
[AIAA PAPER 83-0575] 05 p0637 A83-16800
- Velocity field characteristics of a swirling flow combustor
[AIAA PAPER 83-0314] 06 p0761 A83-19586
- Instantaneous two-component laser anemometry and temperature measurements in a complex flow model combustor
[AIAA PAPER 83-0334] 06 p0765 A83-19587
- Improved fault detection in the hot section of turbojet engines by individual monitoring procedures
07 p0867 A83-19666
- Measurements of reactive recirculating jet mixing in a combustor
07 p0924 A83-19819
- Effect of broad properties fuel on injector performance in a reverse flow combustor
[AIAA PAPER 83-0154] 07 p0867 A83-21079
- Flames with impinging jets
07 p0882 A83-21423
- Errors in the experimental determination of the parameters of supersonic combustion ramjet engines
08 p1046 A83-22653
- Isothermal models of gas-turbine combustors
08 p1057 A83-23097
- Gas turbine combustor modelling for calculating pollutant emission
08 p1046 A83-23142
- Fast acting hydrogen valve
08 p1112 A83-23295
- Studies of a diffusion flame matrix burner in a combustion chamber with heat exchanger
09 p1225 A83-23334
- An experimental study of an annular film-evaporation combustion chamber in a low-power gas turbine engine
09 p1205 A83-23443
- The relationship between the aerodynamics of a combustion chamber and the dynamics of heat release
09 p1205 A83-23446
- Radiation and smoke from the gas turbine combustor using heavy fuels
09 p1242 A83-23877
- Future fuels for turbojet engines and their impacts on combustion chambers and fuel systems
[DGLR PAPER 82-089] 09 p1242 A83-24201
- Energy and entropy balances in a combustion chamber - Analytical solution
09 p1226 A83-24363
- A model for the transient behavior of catalytic combustors
09 p1226 A83-24364
- A diffusion combustor and methane-air flame propagation in concentration gradient fields
09 p1226 A83-24366
- Experimental study of jet mixing mechanisms in a model secondary combustor
09 p1198 A83-24664
- Mean flowfields in axisymmetric combustor geometries with swirl
09 p1263 A83-24668
- Sensitivity of chamber turbulence to intake flows in axisymmetric reciprocating engines
09 p1207 A83-24677
- NASA clean catalytic combustor program
[ASME PAPER 82-JPGC-GT-11] 09 p1227 A83-25269
- Catalyst durability evaluation for advanced gas turbine engines
[ASME PAPER 82-JPGC-GT-21] 09 p1274 A83-25270
- Cogeneration using a thermionic combustor
11 p1608 A83-27300
- The design and combustion performance of practical swirlers for integral rocket/ramjets
12 p1703 A83-28964
- Some fuel effects on carbon formation in gas turbine combustors
12 p1717 A83-29392
- Solution of burner-stabilized premixed laminar flames by boundary value methods
12 p1712 A83-29642
- Fuel character effects on the TF41 engine combustion system
13 p1807 A83-30190
- Institute of environmental sciences aircraft engine combustor casing life simulation for increased reliability
13 p1807 A83-31493
- The combustion stability of a wedge
14 p1989 A83-32086

- Flow measurement in a model combustion chamber
[AIAA PAPER 83-1550] 14 p1990 A83-32771
- Acoustic modal analysis of a full-scale annular combustor
[AIAA PAPER 83-0760] 15 p2226 A83-33486
- Cross spectra between temperature and pressure in a constant area duct downstream of a combustor
[AIAA PAPER 83-0762] 15 p2227 A83-33487
- Assessment of two computational procedures for spray combustors
15 p2160 A83-34255
- Fluid flow within reciprocating-engine cylinders
15 p2160 A83-34265
- Simultaneous CARS and luminosity measurements in a bluff-body combustor
[AIAA PAPER 83-1481] 15 p2134 A83-34915
- Temperature and composition measurements in a research gas turbine combustion chamber
16 p2302 A83-35790
- The introduction of tangential or perpendicular nonisothermal plane jets into a turbulent crossflow for the purpose of film cooling
16 p2350 A83-35799
- An experimental study on configuration of secondary combustion chamber for ram-rocket
16 p2318 A83-35802
- Solid ducted rocket engine combustor tests
16 p2303 A83-35803
- New trends in combustion research for gas turbine engines
16 p2303 A83-35806
- Combustor modelling by assembly of well-stirred reactors
16 p2325 A83-35808
- The effect of fuel atomization on soot-free combustion in a prevaporizing combustor
16 p2303 A83-35812
- Existence and stability of limit cycles for pressure oscillations in combustion chambers
[AIAA PAPER 83-0576] 16 p2326 A83-36060
- Methanol combustion in a CF6I-80A engine combustor
[AIAA PAPER 83-1138] 16 p2339 A83-36241
- Experiments in dilution jet mixing
[AIAA PAPER 83-1201] 16 p2352 A83-36277
- Liquid fuel cyclone combustors for gas turbine applications
[AIAA PAPER 83-1205] 16 p2361 A83-36280
- Application of 3D aerodynamic/combustion model to combustor primary zone study
[AIAA PAPER 83-1265] 16 p2308 A83-36316
- Unsteady aerodynamics in open cavities applications to rocket propulsion
[AIAA PAPER 83-1314] 16 p2295 A83-36335
- A JT8D low emissions combustor by radial zoning
[AIAA PAPER 83-1324] 16 p2309 A83-36339
- The performance of an annular vane swirler --- to aid in modeling gas turbine combustor flowfields and swirling confined flow turbulence
[AIAA PAPER 83-1326] 16 p2309 A83-36340
- Analytical characterization of flow fields in side-inlet dump combustors
[AIAA PAPER 83-1399] 16 p2322 A83-36389
- Longitudinal pressure oscillations in ramjet combustors
[AIAA PAPER 83-2018] 16 p2310 A83-36404
- An Eulerian-Lagrangian method for turbulent combustion
[ONERA, TP NO. 1983-16] 16 p2327 A83-36426
- Numerical simulation of cold flow in an axisymmetric centerbody combustor
[AIAA PAPER 83-1741] 17 p2467 A83-37219
- Development and operating characteristics of an advanced two-stage combustor
17 p2469 A83-38022
- Longitudinal modes of gas oscillations in the main combustion chamber of gas-turbine engines
18 p2641 A83-39169
- A study of the formation of nitrogen oxides during the combustion of a lean homogeneous mixture in the hybrid combustion chamber of an automotive gas-turbine engine
19 p2821 A83-42134
- A study of the effect of the combustion process on mass transfer in the primary zone of the combustion chamber of a gas-turbine engine
19 p2801 A83-42150
- Increasing the combustion efficiency of fuel in an air-heating chamber operating on a prevaporized fuel
19 p2801 A83-42151
- Mathematical modelling of heat transfer processes with constraints
20 p2974 A83-42693
- The effect of cold air jet injection upon the film cooling effectiveness of combustion chamber walls for different injection geometries
20 p2978 A83-42738
- Study of convective heat transfer in gas turbine combustion chambers
20 p2984 A83-43024
- A reverse flow chamber for small turbomachines
[ONERA, TP NO. 1983-30] 21 p3092 A83-44309
- Velocity measurements in a confined swirl driven recirculating flow
21 p3131 A83-44682
- Velocity and turbulence measurements in combustion systems
21 p3131 A83-44684

- Aerodynamic-wave break-up of liquid sheets in swirling airflows and combustor modules
[AIAA PAPER 83-1204] 21 p3133 A83-45511
- Development of new combustion chamber technologies for future alternative combustion fuels
23 p3406 A83-47183
- Testing of a full-scale staged combustor operating with a synthetic liquid fuel
[ASME PAPER 83-GT-27] 23 p3464 A83-47890
- Combustion experiments with a new burner air distribution concept
[ASME PAPER 83-GT-31] 23 p3406 A83-47893
- A configuration to improve the aerodynamics and scope of can-annular combustors
[ASME PAPER 83-GT-37] 23 p3406 A83-47898
- A compact diffuser system for annular combustors
[ASME PAPER 83-GT-43] 23 p3407 A83-47903
- Full coverage discrete hole wall cooling - Discharge coefficients
[ASME PAPER 83-GT-79] 23 p3447 A83-47932
- Comparison-effects of broadened property jet fuels on older and modern J79 combustors
[ASME PAPER 83-GT-81] 23 p3407 A83-47934
- Flashback in prevaporizing/premixing combustion systems
[ASME PAPER 83-GT-94] 23 p3429 A83-47940
- Modelling of soot formation in spray combustors
[ASME PAPER 83-GT-190] 23 p3429 A83-47996
- Three-dimensional modeling of horseshoe vortex flows
[ASME PAPER 83-GT-191] 23 p3397 A83-47997
- Temperature profile development in turbulent mixing of coolant jets with a confined hot cross flow
[ASME PAPER 83-GT-220] 23 p3448 A83-48019
- Effectiveness measurements for a cooling film disrupted by a single jet
[ASME PAPER 83-GT-250] 23 p3397 A83-48037
- Precautions that have to be taken in applying LDV to combustion chambers
[ONERA, TP NO. 1983-112] 24 p3583 A83-49423
- The effect of the acceleration of the external force on the evolution of a combustion site in a closed vessel
24 p3555 A83-49759
- Methodology for a multiparametric study of the combustion of metal particles in a free-falling chamber
24 p3555 A83-49767
- COMBUSTION CONTROL**
- Influence of confinement on flame acceleration due to repeated obstacles
07 p0878 A83-19836
- Transient processes during the formation of a combustion surface in hydraulically controlled solid-propellant rocket engines
09 p1220 A83-23435
- Raman oxygen detection for combustion control and regulation
10 p1425 A83-26876
- The space transportation system reaction control system
11 p1534 A83-27467
- Flow field description for the reaction control system of the Space Shuttle Orbiter
[AIAA PAPER 83-1548] 14 p1981 A83-32770
- Service life analysis of rocket motors with internal gas generation
15 p2129 A83-33736
- Controlling mechanisms of flame spread
17 p2484 A83-37043
- The detailed processes involved in flame spread over solid fuels
17 p2484 A83-37044
- A study of the effect of certain factors on the linear pyrolysis and combustion of polyamide-6
24 p3569 A83-49781
- COMBUSTION EFFICIENCY**
- Impacts of broadened-specification fuels on aircraft turbine engine combustors
01 p0028 A83-10655
- Transient thermal boundary layer in heating of droplet with internal circulation - Evaluation of assumptions
02 p0175 A83-13098
- The conditions of flame propagation in metal particle suspensions in air
03 p0295 A83-14059
- Some recent developments in the theory of premixed turbulent flames
03 p0319 A83-14472
- Effect of burning rate modifiers on propellant performance - A theoretical study
04 p0464 A83-15474
- Burning rate measurements in solid rocket motors
[AIAA PAPER 83-0481] 09 p1269 A83-24149
- Ignition dynamics of fully reactive propellant in stagnation flow
09 p1226 A83-24666
- Computed and measured turbulence in axisymmetric reciprocating engines
09 p1207 A83-24669
- Catalyst durability evaluation for advanced gas turbine engines
[ASME PAPER 82-JPGC-GT-21] 09 p1274 A83-25270
- Possibilities of improving exhaust emissions and energy consumption in mixed hydrogen-gasoline operation
11 p1589 A83-27334
- The design and combustion performance of practical swirlers for integral rocket/ramjets
12 p1703 A83-28964
- Some experiments on model composite solid propellants
13 p1826 A83-31675
- A model of freely burning pool fires
16 p2325 A83-35789
- An experimental study on configuration of secondary combustion chamber for ram-rocket
16 p2318 A83-35802
- Experimental research of the mechanism of flame stabilization in two phase mixture
16 p2325 A83-35822
- The influence of flame stabiliser pressure loss on mixing, combustion performance and flame stability
16 p2325 A83-35823
- Effect of fuel composition on Navy aircraft engine hot section components
[AIAA PAPER 83-1147] 16 p2306 A83-36244
- Small turbine engine experience with high density fuels
[AIAA PAPER 83-1177] 16 p2339 A83-36262
- Performance of a low thrust LO2/LH2 engine with a 300:1 area ratio nozzle
[AIAA PAPER 83-1313] 16 p2320 A83-36334
- LOX/hydrocarbon injector performance
[AIAA PAPER 83-1390] 16 p2322 A83-36380
- Development and operating characteristics of an advanced two-stage combustor
17 p2469 A83-38022
- Procedure for the calculation of basic emission parameters for aircraft turbine engines
[SAE AIR 1533] 17 p2469 A83-38104
- Losses in the combustion chamber of low-thrust engines
19 p2818 A83-42142
- Increasing the combustion efficiency of fuel in an air-heating chamber operating on a prevaporized fuel
19 p2801 A83-42151
- Performance study using natural gas, hydrogen-supplemented natural gas and hydrogen in AVL research engine
21 p3168 A83-45425
- Mixing and fuel atomisation effects on premixed combustion performance
[ASME PAPER 83-GT-55] 23 p3407 A83-47911
- Emissions from enclosed swirl stabilised premixed flames
[ASME PAPER 83-GT-192] 23 p3410 A83-47998
- Optimum conditions for the acceleration of the flame of gas mixtures at discontinuous obstacles in large volume
24 p3555 A83-49768
- COMBUSTION HEAT**
- U HEAT OF COMBUSTION
- COMBUSTION INSTABILITY**
- U COMBUSTION STABILITY
- COMBUSTION PHYSICS**
- Coherent structures in turbulent combustion
01 p0023 A83-10899
- Spatially precise laser diagnostics for combustion
01 p0055 A83-11060
- Transition from combustion to detonation in solid explosives
02 p0151 A83-11659
- Weak and strong ignition. I - Numerical simulations of shock tube experiments
02 p0152 A83-12078
- Weak and strong ignition. II - Sensitivity of the hydrogen-oxygen system
02 p0152 A83-12079
- Combustion of condensed two-component systems with spatially separated components
03 p0294 A83-14052
- An experimental study of transient combustion in low-gas heterogeneous systems
03 p0294 A83-14053
- Numerical modeling of the development of a combustion nucleus in a closed vessel under the conditions of natural convection
03 p0295 A83-14054
- The effect of mechanical stresses on the combustion velocity of solid fuel mixtures
03 p0295 A83-14057
- Burning to detonation transition in porous beds of a high-energy propellant
03 p0303 A83-14846
- Activation energy asymptotics applied to burning carbon particles
03 p0296 A83-14849
- Flame propagation with a sequential reaction mechanism
04 p0457 A83-16362
- Nonadiabatic nonisobaric propagation of a planar premixed flame - Constant-volume enclosure
[AIAA PAPER 83-0239] 05 p0612 A83-16605
- Ignition of confined gaseous mixtures by hot surfaces and hot wires
[AIAA PAPER 83-0240] 05 p0612 A83-16606
- Trajectory with diffusion method for predicting the fuel distribution in a transverse stream
[AIAA PAPER 83-0336] 05 p0596 A83-16662
- A new kind of spin combustion
07 p0878 A83-19641
- Investigation of slurry fuel performance for use in a ramjet propulsor
07 p0902 A83-21014
- Further studies on the ignition and flame quenching of quiescent dust clouds
07 p0882 A83-21351
- Countercurrent jet combustion of a hydrocarbon fuel in air
07 p0882 A83-21422
- On the numerical accuracy of homogeneous solid propellant combustion models
08 p1073 A83-22346
- The effect of viscosity on hydrodynamic stability of a plane flame front
08 p1057 A83-22395
- Estimation of some correlations in a premixed reactive turbulent flow
08 p1057 A83-22396
- Ignition of a combustible half space
08 p1057 A83-22738
- A model for the transient behavior of catalytic combustors
09 p1226 A83-24364
- Theory of laminar flames --- Book
09 p1227 A83-24946
- Flame spread in an opposed flow with a linear velocity gradient
10 p1390 A83-25897
- Sensitivity analysis for premixed, laminar, steady state flames
10 p1390 A83-25898
- Combustion of carbon particles, initiated by laser radiation
10 p1392 A83-26777
- Fast motions of a gas in a porous medium
11 p1569 A83-28539
- Strained premixed laminar flames under nonadiabatic conditions
11 p1546 A83-28599
- An asymptotic theory of condensed two-phase flame propagation
12 p1712 A83-29000
- The state-selective reactions of vibrationally excited CH (X 2 Pi) with oxygen and nitrogen
13 p1817 A83-30956
- Instabilities, pattern formation, and turbulence in flames
13 p1818 A83-31080
- The effect of natural convection on the concentration limits of ignition for combustible mixtures in a closed container
14 p1988 A83-32081
- Filtration combustion of gases
14 p1988 A83-32083
- Calculation of the characteristics of submerged combustion
14 p1988 A83-32084
- A model equation for the probability distribution of the velocity and concentration during turbulent mixing and diffusive combustion of gases
14 p1988 A83-32085
- 10-Hz coherent anti-Stokes Raman spectroscopy apparatus for turbulent combustion studies
14 p2020 A83-32823
- Polymer ignition - A review
14 p1999 A83-33400
- An asymptotic theory of deflagrations and detonations. I - The steady solutions
16 p2325 A83-35694
- A combustion theory for very high regression-rate solid propellant
[AIAA PAPER 83-1196] 16 p2339 A83-36272
- Effects of AP particle size on combustion response to crossflow
[AIAA PAPER 83-1270] 16 p2340 A83-36317
- Burning rate characterization from one motor firing - An analytical approach
[AIAA PAPER 83-1315] 16 p2340 A83-36336
- Laser applications to combustion research
[AIAA PAPER 83-1360] 16 p2360 A83-36358
- Absorption measurements of H2O at high temperatures using a CO laser
16 p2328 A83-36795
- Modelling the fuel temperature effect on flame spread limits in opposed flow
17 p2484 A83-37046
- A two-dimensional flow model of laser supported combustion waves
[AIAA PAPER 83-1718] 17 p2507 A83-38088
- On the propagation laws of combustion waves in solids (pyrotechnic reactions)
17 p2486 A83-38995
- Degenerate regimes of heterogeneous combustion and extinction of a particle in a gaseous oxidizer
18 p2663 A83-39157
- A theory for the ignition of metal particles
18 p2663 A83-39158
- The ignition of a fuel on contact with an oxidizer
18 p2663 A83-39159
- The effect of pressure on the combustion characteristics of melting heterogeneous systems
18 p2663 A83-39162
- Theory of the combustion of condensed substances with blowing past them
18 p2663 A83-39163
- Calculation of the dispersity of the combustion products of a metal particle
18 p2663 A83-39164
- The detection property of a curved flame front
18 p2663 A83-39167
- Fuel-air explosions; Proceedings of the International Conference, McGill University, Montreal, Canada, November 4-6, 1981
19 p2820 A83-41523
- On an integral method for solving problems of the thermal theory of the ignition of condensed substances
19 p2820 A83-42067
- Optical recording of nonstationary processes of mixture formation and combustion --- atomized jet droplets characteristics
19 p2850 A83-42141
- Fast deflagration waves
21 p3130 A83-44462
- Fire flame radiation
22 p3265 A83-45717
- Turbulent flame propagation and combustion in spark ignition engines
23 p3429 A83-48156

A mathematical model for the dynamics of liquid-propellant rocket engines

24 p3552 A83-48928

All-Union Symposium on Combustion and Explosion, 7th, Chernogolovka, USSR, October 1983, Proceedings

24 p3555 A83-49758

Critical conditions of the combustion of plane layers of polymethyl methacrylate on substrates of various thickness and thermal conductivity

24 p3555 A83-49760

Multidimensional combustion of samples of rectangular cross-section

24 p3555 A83-49761

The mechanism of acoustic emission from a turbulent gas flame

24 p3555 A83-49762

The effect of the pressure and molecular properties of gases on turbulent combustion

24 p3555 A83-49764

The limiting conditions of polymer combustion in the absence of free convection

24 p3555 A83-49765

Thermal self-ignition of a system of hot ignition sites

24 p3555 A83-49771

The ignition of a vapor bubble in a liquid

24 p3556 A83-49774

A universal relationship for heat release in the condensed phase and gas microkinetics during the combustion of ballistite powders

24 p3556 A83-49779

Combustion regimes with laser-induced plasma

24 p3556 A83-49782

Phase transformations in an inverse wave of filtration combustion

24 p3556 A83-49783

Characteristics of the initiation of fast chemical reactions in oxidizer-combustible mixtures

24 p3557 A83-49790

Ignition of crystalline hexogen with adiabatic compression of the adjacent gas pocket

24 p3557 A83-49792

COMBUSTION PRODUCTS

Combustion-related pollutants of polydisperse single-composition aerosols and advection fog formation

01 p0070 A83-10226

Numerical analysis of the dispersion of detonation products

01 p0047 A83-11274

Combustion characteristics of hydrogen-carbon monoxide based gaseous fuels

01 p0023 A83-11491

NOx results from two combustors tested on medium BTU coal gas

01 p0070 A83-11493

Aerosol characterization of a smoldering source

02 p0203 A83-11829

Design considerations for aerodynamically quenching gas sample probes

[ASME PAPER 82-HT-39]

02 p0172 A83-12794

Analysis of combustion in recirculating flow for rocket exhausts in supersonic streams

02 p0148 A83-13087

The influence of equivalence ratio variation on pollutant formation in a gas turbine type combustor

02 p0136 A83-13095

Particle sampling of solid rocket motor /SRM/ exhausts in high-altitude test cells

[AIAA PAPER 83-0245]

05 p0609 A83-16611

Flow visualization in combustion gases using planar laser-induced fluorescence

[AIAA PAPER 83-0405]

05 p0643 A83-16694

Experimental verification of a computational model for a combustion-product CO₂-GDL for high stagnation temperatures

06 p0767 A83-19556

Investigation of the dynamics of charged particles in the dispersion of a reaction jet in conditions of orbital flight

06 p0724 A83-19558

Ignition, propagation, and structure of deflagrations and detonations - Stable species concentration of a turbulent premixed methane-air flame

07 p0878 A83-19835

The total emissivities of high-temperature flames

07 p0879 A83-19840

Effect of molecular structure on incipient soot formation

07 p0879 A83-19847

The composition of the products of the combustion of pyropowder at atmospheric pressure

07 p0880 A83-19954

Numerical simulation of fog formation and liquid water content on polydisperse multi-composition aerosols due to combustion-related pollutants

07 p0963 A83-21038

NO₂ formation in laminar flames

08 p1057 A83-22397

Sooting tendency of fuels containing polycyclic aromatics in a research combustor

08 p1073 A83-23138

Studies of a diffusion flame matrix burner in a combustion chamber with heat exchanger

09 p1225 A83-23334

Laser-saturated fluorescence measurements of OH concentration in flames

09 p1225 A83-23749

Laser fluorescence measurements of the OH concentration in a combustion boundary layer

09 p1226 A83-24367

Combustion toxicology: Principles and test methods --- Book

09 p1227 A83-24903

The effect of fuel injection on NO_x emissions and undesirable combustion for hydrogen-fuelled piston engines

11 p1589 A83-27335

Qualitative analysis of equations describing quasi-one-dimensional nonequilibrium flow in channels

11 p1569 A83-28535

Some fuel effects on carbon formation in gas turbine combustors

12 p1717 A83-29392

RECLAS - Resonant-enhanced CARS from C₂ produced by laser ablation of soot particles

13 p1844 A83-30201

Laser induced fluorescence and absorption measurements of NO in NH₃/O₂ and CH₄/air flames

13 p1818 A83-30969

Gross mechanisms of smoke aerosol production from solids, liquids and gases

13 p1818 A83-31521

The effect of the fuel quality on the degree of combustion product ionization in gas-turbine engines

14 p1988 A83-32078

The formation of nitrogen oxides in a nonequilibrium turbulent diffusion flame

14 p1989 A83-32090

Experimental investigation of bipropellant exhaust plume flowfield, heating, and contamination, and comparison with the CONTAM computer model predictions

[AIAA PAPER 83-1447]

14 p1984 A83-32715

In situ measurement of the complex refractive index of combustion generated particulates

[AIAA PAPER 83-1518]

14 p2020 A83-32751

Fiber-optic absorption/fluorescence probes for combustion measurements

14 p2020 A83-32902

A simple model for carbon monoxide in laminar and turbulent hydrocarbon diffusion flames

14 p1990 A83-32939

Soot carbon and excess fine potassium - Long-range transport of combustion-derived aerosols

15 p2193 A83-34003

The effects of fuel properties upon pollutants present in gas turbine aero-engines

16 p2338 A83-35813

The effects of large heat release on a two dimensional mixing layer

[AIAA PAPER 83-0472]

16 p2351 A83-36055

The formation of NO(x) from nitrogen-containing additives in premixed methane flames

17 p2485 A83-38027

Nitric oxide formation in an ammonia-doped methane-oxygen low pressure flame

17 p2485 A83-38028

Calculation of the dispersity of the combustion products of a metal particle

18 p2663 A83-39164

Comparison of radiative transfer approximations for a highly forward scattering planar medium

18 p2680 A83-39181

Soot formation in pyrolysis of acetylene, allene and 1,3-butadiene

18 p2664 A83-39274

Experimental investigation of absorption coefficient of cesium resonance doublets in a plasma of combustion products

18 p2746 A83-39859

Effect of using emulsions of high nitrogen containing fuels and water in a gas turbine combustor on NO_x and other emissions

[ASME PAPER 82-GT-224]

18 p2673 A83-39992

Hydroxyl concentration measurements in the NH₃-NO-O₂ reaction in postflame gases

18 p2664 A83-40311

A study of the formation of nitrogen oxides during the combustion of a lean homogeneous mixture in the hybrid combustion chamber of an automotive gas-turbine engine

19 p2821 A83-42134

The effect of soot particles on the thermodynamic condition of heated gases at various temperatures

19 p2821 A83-42145

Combustion system processes leading to corrosive deposits

20 p2949 A83-42246

Prediction of gas emissivity for a wide range of process conditions

20 p2974 A83-42691

A gaseous tracer model for air pollution from residential wood burning

22 p3321 A83-45924

Laser-induced fluorescence spectroscopy for combustion diagnostics

23 p3455 A83-47656

The effect of hydrocarbon structure upon fuel sooting tendency in a turbulent spray diffusion flame

[ASME PAPER 83-GT-90]

23 p3440 A83-47937

Modelling of soot formation in spray combustors

[ASME PAPER 83-GT-190]

23 p3429 A83-47996

Dispersion limitations of oxidation in power plant plumes during long-range transport

23 p3479 A83-48085

The formation of carbon monoxide during turbulent diffusion combustion --- for aircraft gas turbine combustion chambers

24 p3569 A83-49769

A theoretical study of the formation of condensed products during the combustion of metal particles

24 p3555 A83-49770

A thermal-fluctuation spectroscopy study of the combustion of ballistite powders

24 p3556 A83-49776

COMBUSTION STABILITY

NT FLAME STABILITY

Transient processes in metal droplet combustion

03 p0295 A83-14123

The nonuniqueness and instability of steady-state combustion modes in a boundary layer with intense injection

03 p0296 A83-14898

Combustion response to compositional fluctuations --- of composite solid propellants

[AIAA PAPER 83-0476]

05 p0619 A83-16740

Experimental investigation of pressure and velocity coupled response functions of aluminized and non-aluminized solid propellants

[AIAA PAPER 83-0478]

05 p0620 A83-16741

Pulsar design criteria for solid propellant rocket motors

[AIAA PAPER 83-0577]

05 p0609 A83-16801

Theoretical and experimental nonlinear dynamics of heterogeneous deflagration waves

06 p0727 A83-19162

A new kind of spin combustion

07 p0878 A83-19641

Effects of chemical reactions in the shocked gas on the propagation characteristics of cylindrical detonation waves

07 p0878 A83-19838

The combustion of substances with a liquid reaction layer

07 p0880 A83-19953

An analysis of transient combustion states of diffusion flame

07 p0881 A83-20280

Liftoff characteristics of turbulent jet diffusion flames

08 p1056 A83-22140

On the changes in the structure of steady plane flames as their speed increases

09 p1225 A83-23747

Processing modifications for improved propellants - Coated oxidizers

09 p1241 A83-23838

Non-steady burning in a randomly layered composite propellant

[AIAA PAPER 83-0477]

09 p1220 A83-24148

A numerical study of nonlinear instability phenomena in solid rocket motors

09 p1220 A83-24663

Pulsing techniques for solid-propellant rocket motors - Modeling and cold-flow testing

09 p1220 A83-24886

Instability of surface combustion on exposure to laser radiation

10 p1433 A83-26680

One-dimensional stability of a combustion process in a magnetic field

12 p1781 A83-29268

On the loss of stability of detonation waves in long heterogeneous-explosive charges

13 p1843 A83-31372

The combustion stability of a wedge

14 p1989 A83-32086

Discontinuation of periodic vortex formation behind a stabilizer in an acoustically damped chamber following mixture ignition

14 p1989 A83-32089

Combustion instability in liquid fuel ramjets

16 p2303 A83-35804

Existence and stability of limit cycles for pressure oscillations in combustion chambers

[AIAA PAPER 83-0576]

16 p2326 A83-36060

The stability of the steady-state combustion of gunpowder under conditions of constant light flux

18 p2663 A83-39165

Nonstationary combustion regimes of porous gunpowders

18 p2663 A83-39166

Incomplete combustion - A possible cause of combustion instability --- in solid propellant rocket engines

19 p2818 A83-40862

Unsteady regimes of the convective combustion of a porous powder fuel

24 p3555 A83-49539

A theoretical study of the nonstationary combustion of a gasifiable solid fuel during a pressure drop

24 p3569 A83-49763

Results of a qualitative analysis of the equation of nonstationary convective combustion for porous systems

24 p3556 A83-49772

Application of the theory of bifurcations to the study of unsteady regimes of combustion

24 p3556 A83-49777

Development of perturbations at the detonation front

24 p3556 A83-49787

A pulsating detonation front

24 p3557 A83-49799

Critical phenomena in detonation associated with an impulse loss

24 p3557 A83-49800

COMBUSTION TEMPERATURE

The relationship between the combustion parameters and the phase diagram of the systems Ti-Co and Ti-Ni

03 p0299 A83-14055

The application of coherent anti-Stokes Raman scattering to turbulent combustion thermometry

07 p0879 A83-19844

The erosion combustion of a solid fuel under various temperatures of the ventilating flow

07 p0901 A83-19951

The rules governing changes in combustion characteristics for competing reactions
14 p1989 A83-32092

Comparison of CARS combustion temperatures with standard techniques
[AIAA PAPER 83-1482] 14 p1990 A83-32731

Coherent anti-Stokes Raman spectroscopic modeling for combustion diagnostics
14 p2021 A83-33173

Critical conditions for the combustion of macroheterogeneous systems of the type fuel-inert material
15 p2134 A83-35318

CARS temperature and species measurements in augmented jet engine exhausts --- Coherent Anti-Stokes Raman Spectroscopy
[AIAA PAPER 83-1294] 16 p2309 A83-36328

Effect of erosive burning on pressure and temperature sensitivity --- of composite propellants
[IAF PAPER 83-368] 23 p3439 A83-47361

The effect of the solid phase and thermophysical characteristics of a central single supersonic jet of an engine on base pressure and temperature
24 p3552 A83-49665

A thermal-fluctuation spectroscopy study of the combustion of ballistite powders
24 p3556 A83-49776

COMBUSTION VIBRATION

Investigations of the excitation mechanism of thermoacoustic vibrations - The Rijke phenomenon --- German thesis
01 p0022 A83-10167

Ejecta pulsing of subscale solid propellant rocket motors
[AIAA PAPER 83-0578] 05 p0610 A83-17930

An analysis of transient combustion states of diffusion flame
07 p0881 A83-20280

Stratification instability of switching front in an active trigger diffusive medium --- oscillations and wave processes during combustion
10 p1471 A83-25893

A matrix of the frequency characteristics of a combustion zone
15 p2133 A83-34898

Existence and stability of limit cycles for pressure oscillations in combustion chambers
[AIAA PAPER 83-0576] 16 p2326 A83-36060

Longitudinal modes of gas oscillations in the main combustion chamber of gas-turbine engines
18 p2641 A83-39169

Fluctuations during the combustion of fuels
24 p3556 A83-49785

COMBUSTION WAVES

U FLAME PROPAGATION

COMBUSTORS

U COMBUSTION CHAMBERS

COMET HEADS

Comet head photometry - Past, present, and future
03 p0403 A83-13392

On two mechanisms of disintegration of interplanetary dust grains in cometary heads
10 p1517 A83-26914

Scientific instrumentation of PLANET-A VUV imaging of the hydrogen coma of Halley
11 p1537 A83-27746

Determination of the physical parameters of the neutral coma of Comet Bennet /1970 II/
11 p1679 A83-27889

Electrodynamics of submicron dust in the cometary coma
13 p1958 A83-31733

COMET NUCLEI

Dynamic coma models for comet Bennett 1970 II
02 p0247 A83-12530

A CO₂-rich coma model applied to the neutral coma of Comet West
02 p0262 A83-12923

Comets --- Book
03 p0415 A83-13376

Overview of comet observations
03 p0415 A83-13377

Chemical composition of cometary nuclei
03 p0415 A83-13379

The infrared spectral properties of frozen volatiles --- in cometary nuclei
03 p0415 A83-13381

Structure and origin of cometary nuclei
03 p0415 A83-13382

The rotation of comet nuclei
03 p0415 A83-13383

Relationships between comets, large meteors, and meteorites
03 p0403 A83-13386

Ultraviolet spectroscopy of comae
03 p0416 A83-13394

Laboratory studies of photochemical and spectroscopic phenomena related to comets
03 p0416 A83-13395

Photochemical processes in the inner coma --- comet nuclei
03 p0416 A83-13396

Brightness of the physical nucleus of a comet
03 p0426 A83-14679

Heat transport in porous cometary nuclei
04 p0551 A83-15369

Cratering time scales for the Galilean satellites
04 p0548 A83-16235

Visual and infrared observations of the distant Comets P/Stephan-Oterma /1980g/, Panther /1980u/, and Bowell /1980b/
06 p0833 A83-18873

A search for frosts in Comet Bowell /1980b/
06 p0833 A83-18874

Observations of the red auroral oxygen lines in nine comets
06 p0822 A83-19074

Ultraviolet spectroscopy and the composition of cometary ice
07 p1013 A83-20296

Ice in Comet Bowell
08 p1186 A83-23275

H₂ production in comets.
10 p1500 A83-25374

The effect of the charge of the surface of ice grains and the nucleus of a comet on the rate of their sublimation
11 p1679 A83-27876

The durability of dust matrices formed during the sublimation of dusty ice --- in comets
11 p1679 A83-27888

Determination of the physical parameters of the neutral coma of Comet Bennet /1970 II/
11 p1679 A83-27889

On the function λ_{max}/r , describing the relative mass loss of a comet nucleus
11 p1679 A83-27891

On the formation of cometary nuclei in dense globules
12 p1793 A83-29062

Reaction deceleration of comet nuclei and their relation to the structure of meteor swarms
13 p1940 A83-31344

P/Halley - First signs of activity? --- nucleus ice vaporization
13 p1943 A83-31729

Electrodynamics of submicron dust in the cometary coma
13 p1958 A83-31733

Quasi-liquefaction in the surface layers of cometary nuclei. I - The static layer at the threshold of quasi-liquefaction
14 p2102 A83-31836

Attitude perturbations of the Giotto spacecraft in the dust cloud of Comet Halley
14 p1979 A83-33472

The derivation of Halley parameters from observations
15 p2273 A83-35018

The infrared synthetic spectrum of comet Halley
15 p2273 A83-35019

Analysis of the nucleus and circumnuclear area of Comet Halley with the 'I.K.S.' infrared sounder from the 'Vega' flyby probes --- Venera satellite-borne IR imaging spectrometer
15 p2249 A83-35026

The chemical composition and thermal history of the ice of a cometary nucleus
16 p2425 A83-36679

Physical and chemical effects induced by energetic ions on comets
17 p2609 A83-38417

Charged particle erosion of frozen volatiles in ice grains and comets
19 p2914 A83-40728

The lifetime of cometary ice nuclei and the secular decrease of the brightness of periodic comets
19 p2915 A83-40820

COMET TAILS

On the flaring of cometary plasma tails
02 p0257 A83-12144

Overview of comet observations
03 p0415 A83-13377

Observations and dynamics of plasma tails --- of comets
03 p0416 A83-13397

Theories of physical processes in the cometary comae and ion tails
03 p0416 A83-13399

The estimates of the magnetic field in Halley's comet
03 p0431 A83-14872

Heat transport in porous cometary nuclei
04 p0551 A83-15369

The structure of cometary dust tails. II - Tail brightness profiles and dust characteristics of comet Arend-Roland, 1957 III
05 p0695 A83-16855

Helical wave and K-H instability in Type I comet tails. I - Waves of infinitesimal amplitude in incompressible plasma
06 p0832 A83-18850

Two dust populations of particle fragments in the striated tail of Comet MRKOS 1957 V
06 p0833 A83-18872

Comet Bradfield 1979 X event on 1980 February 6 - Correlation with an interplanetary solar wind disturbance.
12 p1796 A83-29545

Helical wave and K-H instability in type I comet tails. II
Waves of infinitesimal amplitude in compressible plasma
14 p2102 A83-32924

Dynamic stabilization of hydromagnetic surface waves
Applications to cometary plasma tails
14 p2106 A83-33221

Geometry of the distribution of plasma tail rays in a cometary type I tail
14 p2113 A83-33285

Magnetic field distribution in the tail of Halley's Comet found from the kinematics of a plasma formation
15 p2271 A83-34772

The Halley dust model
15 p2273 A83-35015

Interpretation of the event in the plasma tail of comet Bradfield 1979 X on 1980 February 6
17 p2608 A83-38407

Cryogenic particle collection on a cometary mission
20 p2945 A83-43241

The effect of MHD instabilities on the flaring of cometary plasma tails
21 p3238 A83-45570

COMET TAILS

On the flaring of cometary plasma tails
02 p0257 A83-12144

Overview of comet observations
03 p0415 A83-13377

Observations and dynamics of plasma tails --- of comets
03 p0416 A83-13397

Theories of physical processes in the cometary comae and ion tails
03 p0416 A83-13399

The estimates of the magnetic field in Halley's comet
03 p0431 A83-14872

Heat transport in porous cometary nuclei
04 p0551 A83-15369

The structure of cometary dust tails. II - Tail brightness profiles and dust characteristics of comet Arend-Roland, 1957 III
05 p0695 A83-16855

Helical wave and K-H instability in Type I comet tails. I - Waves of infinitesimal amplitude in incompressible plasma
06 p0832 A83-18850

Two dust populations of particle fragments in the striated tail of Comet MRKOS 1957 V
06 p0833 A83-18872

Comet Bradfield 1979 X event on 1980 February 6 - Correlation with an interplanetary solar wind disturbance.
12 p1796 A83-29545

Helical wave and K-H instability in type I comet tails. II
Waves of infinitesimal amplitude in compressible plasma
14 p2102 A83-32924

Dynamic stabilization of hydromagnetic surface waves
Applications to cometary plasma tails
14 p2106 A83-33221

Geometry of the distribution of plasma tail rays in a cometary type I tail
14 p2113 A83-33285

Magnetic field distribution in the tail of Halley's Comet found from the kinematics of a plasma formation
15 p2271 A83-34772

The Halley dust model
15 p2273 A83-35015

Interpretation of the event in the plasma tail of comet Bradfield 1979 X on 1980 February 6
17 p2608 A83-38407

Cryogenic particle collection on a cometary mission
20 p2945 A83-43241

The effect of MHD instabilities on the flaring of cometary plasma tails
21 p3238 A83-45570

COMETARY ATMOSPHERES

A CO₂-rich coma model applied to the neutral coma of Comet West
02 p0262 A83-12923

Penetration of the solar wind magnetic field into cometary ionospheres
03 p0412 A83-13221

Ultraviolet spectroscopy of comae
03 p0416 A83-13394

Theories of physical processes in the cometary comae and ion tails
03 p0416 A83-13399

The photochemistry and dynamics of a dusty cometary atmosphere
03 p0431 A83-14865

On photochemical heating of cometary comae - The cases of H₂O and CO-rich comets
06 p0845 A83-19518

Laboratory simulation of cometary dust collection and analysis
07 p1010 A83-21577

Experimental investigation of the glow of certain fragments observed in cometary spectra
11 p1679 A83-27887

Determination of the physical parameters of the neutral coma of Comet Bennet /1970 II/
11 p1679 A83-27889

Certain parameters of the CN atmosphere of Comet Bradfield 1979I
11 p1673 A83-27892

A multi-fluid model of an H₂O-dominated dusty cometary atmosphere
11 p1683 A83-28382

L1642 - A dust cloud in a cometary globule?
13 p1946 A83-30388

Fluorescence excitation of CO in comets
13 p1940 A83-31439

Quasi-liquefaction in the surface layers of cometary nuclei. I - The static layer at the threshold of quasi-liquefaction
14 p2102 A83-31836

Charge exchange in solar wind-cometary interactions
15 p2259 A83-34115

Magnetic field distribution in the tail of Halley's Comet found from the kinematics of a plasma formation
15 p2271 A83-34772

Analysis of the nucleus and circumnuclear area of Comet Halley with the 'I.K.S.' infrared sounder from the 'Vega' flyby probes --- Venera satellite-borne IR imaging spectrometer
15 p2249 A83-35026

On the penetration of the solar wind into the cometary ionosphere
17 p2598 A83-37337

The cometary atmosphere and its interaction with the solar wind
17 p2606 A83-38228

Infrared and microwave fluorescence of carbon monoxide in comets
17 p2608 A83-38412

Neutral cometary atmospheres. IV - Brightness profiles in the inner coma of comet Kohoutek 1973 XII
20 p3059 A83-42463

Towards an artificial comet
21 p3227 A83-43977

Radio observations of Comet 1983 d
23 p3515 A83-47430

The effect of gas on dust temperature in comets
24 p3650 A83-48955

COMETS

NT COMET HEADS

NT COMET NUCLEI

NT COMET TAILS

NT ENCKE COMET

NT GIACOBINI-ZINNER COMET

NT HALLEY'S COMET

NT IRAS-ARAKI-ALCOCK COMET

NT KOHOOTEK COMET

NT MRKOS COMET

NT SCHWASSMANN-WACHMANN COMET

NT WEST COMET

Towards the encounter with Halley's comet
01 p0123 A83-10376

NH/+/- A candidate for comets and interstellar space
01 p0125 A83-10934

Giant molecular clouds and the solar system comets
01 p0127 A83-11049

Probing the presently tenuous link between comets and the origin of life
02 p0226 A83-11629

Dynamic coma models for comet Bennett 1970 II
02 p0247 A83-12530

Improved orbital elements for periodic comet Schorr /1918 III/
02 p0247 A83-12536

Comets --- Book
03 p0415 A83-13376

Overview of comet observations
03 p0415 A83-13377

Comet discoveries, statistics, and observational selection
03 p0403 A83-13378

What are comets made of - A model based on interstellar dust
03 p0415 A83-13380

The problem of split comets in review
03 p0403 A83-13384

Radar detectability of comets
03 p0403 A83-13385

Optical and infrared observations of bright comets in the range 0.5 micrometers to 20 micrometers
03 p0415 A83-13387

Interpreting the thermal properties of cometary dust
03 p0415 A83-13388

Dusty gas-dynamics in real comets
03 p0416 A83-13389

Cometary dust in the solar system
03 p0416 A83-13390

Spectrophotometry of comets at optical wavelengths
03 p0416 A83-13393

Laboratory studies of photochemical and spectroscopic phenomena related to comets
03 p0416 A83-13395

Dynamical history of the Oort Cloud
03 p0403 A83-13400

Evolution of long- and short-period orbits --- of comets
03 p0404 A83-13401

Do comets evolve into asteroids - Evidence from physical studies
03 p0404 A83-13402

Comets and origin of life
03 p0384 A83-13403

Basic information and references --- concerning comets
03 p0416 A83-13404

Infrared photometry of periodic comets Encke, Chernykh, Kearns-Kwee, Stephan-Oterma, and Tuttle
03 p0407 A83-13826

Characteristics and origin of the comet family of Uranus
03 p0410 A83-14678

The 27-day periodicity of outbursts of Comet Schwassman-Wachmann I
03 p0410 A83-14680

On the spectrum of Comet Bradfield 1980 t
03 p0428 A83-14774

Coronagraphic observations of two new sungrazing comets
04 p0545 A83-14955

Pre-discovery encounters between short-period comets and Jupiter estimated by a Keplerian approximation
05 p0695 A83-17831

Investigation of the orbit of periodic comet Ashbrook-Jackson
05 p0695 A83-17856

Perturbations by Jupiter of the particles ejected from Comet Lexell
06 p0816 A83-18529

Visual and infrared observations of the distant Comets P/Stephan-Oterma /1980g/, Panther /1980u/, and Bowell /1980b/
06 p0833 A83-18873

Comets - Their evolution and origin
06 p0842 A83-19472

New original and future cometary orbits
07 p1004 A83-19868

Ultraviolet spectroscopy and the composition of cometary ice
07 p1013 A83-20296

Comets produce submicron particles in the solar system
07 p1014 A83-20409

Impact of an asteroid or comet in the ocean and extinction of terrestrial life
07 p0950 A83-21314

Remote comets and related bodies - VJHK colorimetry and surface materials
08 p1181 A83-22926

Lyman-alpha observations of comets West 1976 VI and P d'Arrest 1976 XI with Copernicus
08 p1175 A83-23058

The mass of the Oort cloud
09 p1360 A83-24463

Evolution of cometary perihelion distances in Oort cloud - Another statistical approach
10 p1492 A83-25511

Planets, asteroids and comets at high angular resolution
10 p1495 A83-25849

Numerical theory of the motion of Comet P/Wolf /1884 III/ during 1884-1984
10 p1498 A83-26796

Determination of the mass of Jupiter from perturbations of the orbit of Comet P/Wolf in its sphere of action in 1922
10 p1498 A83-26797

The linking of five apparitions of Comet P/Ashbrook-Jackson during 1948-1979 and the prediction of its apparition during 1985-1986
10 p1498 A83-26798

An image-tube camera for cometary spectrography
10 p1498 A83-26911

Electrification of comets by solar corpuscular fluxes
10 p1517 A83-26912

Cosmogonic characteristics of almost-parabolic orbits
11 p1672 A83-27881

Phase-angle distribution of comet perihelions
11 p1672 A83-27882

Velocity-change distribution in the problem of long-period comets
11 p1672 A83-27885

The possibility of the rediscovery of lost periodic comets
11 p1672 A83-27886

The effect of solar activity on the brightness of Comet Bradfield 1974b
11 p1673 A83-27890

Intermediate orbits approximating the initial part of the perturbed motion
11 p1673 A83-28026

Investigation of encounters of Comet Chernykh /1978 IV/ with Jupiter in 1978-1981 and with Saturn in 1981-1984
11 p1674 A83-28052

The flight trajectories of comet probes
11 p1532 A83-28054

Comets and interstellar travel
12 p1784 A83-29453

Comets, planet X and the orbit of Neptune
12 p1789 A83-29709

The secular variation of cometary magnitude
13 p1939 A83-31205

Comets as indicators of the interplanetary medium
13 p1949 A83-31312

High-resolution spectra of C2 Swan bands from comet West 1976 VI
14 p2099 A83-33222

Light curves of some periodic comets
14 p2101 A83-33287

Ice particles in circular orbits around the sun
14 p2101 A83-33288

Asteroid and comet bombardment of the earth
14 p2095 A83-33483

Emission features in the solar corona after the perihelion passage of Comet 1979 XI
15 p2281 A83-34533

An upper limit to the microwave continuum radiation from Comet Austin (1982g)
15 p2248 A83-34650

A new view on the origin of comets and other minor bodies
15 p2248 A83-34688

On the time evolution of the cometary influx in the region of the terrestrial planets
15 p2274 A83-34715

Studies of proton-irradiated cometary-tye ice mixtures
15 p2270 A83-34716

Comet West 1976 VI - Photopolarimetry by the Helios 2 Zodiacal Light Experiment
15 p2249 A83-35020

A capacitor impact sensor (CIS) on board Giotto for detection of cometary dust particles
15 p2129 A83-35024

A study of the motion of the periodic comet Stephan-Oterma (1980g)
16 p2426 A83-36777

Trajectory corrections for flight to short-period comets in the solar system in 1981-1991
17 p2472 A83-37448

Holetschek's effect revisited --- cometary statistics
17 p2592 A83-38234

Asteroids and comets
17 p2608 A83-38272

Interpretation of the event in the plasma tail of comet Bradfield 1979 X on 1980 February 6
17 p2608 A83-38407

The Oort comet halo and giant molecular clouds
18 p2758 A83-39632

Classification of cometary orbits based on the concept of orbital mean temperature
19 p2915 A83-40786

Cometary globules in the Gum-Vela complex
20 p3069 A83-42783

Satellites of Uranus and the hypothesis of ejection of comets
20 p3079 A83-43412

Capture and eruption hypotheses for comets
20 p3061 A83-43413

Velocities of ejection of comets by Jupiter and Saturn
20 p3061 A83-43414

The disappearance of OH from Comet P/Encke
21 p3227 A83-44086

On the origin of comets
21 p3228 A83-44297

Evolutionary relation between meteorites, meteoroids and asteroids or comets
21 p3240 A83-44298

Statistical analysis of the plasma comets
21 p3231 A83-44525

The structure and evolution of the solar system comet cloud
21 p3224 A83-44739

ISEE-3 - A late entry in the great comet chase
22 p3372 A83-46348

Distribution of cometary binding energies based on the assumption of steady state
22 p3379 A83-46564

Cometary impacts with the sun - Physical and dynamical considerations
22 p3376 A83-47087

Calculations of comet orbits from observations of 1980/81
23 p3517 A83-48064

Cometary matter in the environment
24 p3598 A83-49105

Modern view on Laplace's problem --- of comet orbits
24 p3644 A83-49394

Lectures on the planets: The comets - Halley's Comet
24 p3661 A83-49459

On the first transit of nearly parabolic comets across the inner part of the solar system
24 p3644 A83-49629

The formation of comets by radiation pressure in the outer protosun. II - Dependence on the radiation-grain coupling. III - Dependence on the anisotropy of the radiation field
24 p3664 A83-49889

Infrared fluorescence of molecules in comets - The general synthetic spectrum
24 p3669 A83-50098

COMFORT
A description of an experimental protocol for the study of the seat comfort of an aircraft pilot
16 p2402 A83-35586

Active gust load alleviation and ride comfort improvement
24 p3549 A83-49193

COMMAND AND CONTROL
The development of JTIDS distributed TDMA /DTDMA/ advanced development model /ADM/ terminals --- Joint Tactical Information Distribution System
01 p0004 A83-11094

Adaptive power management - A hierarchical/control system with a central multiplex system --- for aircraft applications
01 p0012 A83-11202

Local command-control networks - Operational reliability --- French thesis
03 p0386 A83-13802

Semantic definitions of spacecraft command and control languages using hierarchical graphs
04 p0527 A83-16117

Effects of control saturation on the command response of statically unstable aircraft
[AIAA PAPER 83-0065]
05 p0598 A83-16497

An overview of the MX Command, Control and Communications system
07 p0903 A83-19657

United States Air Force tactical reconnaissance - An analysis and commentary
08 p1041 A83-22574

Integrating robot manipulator control into PASCAL
09 p1328 A83-24711

Concepts for description and evaluation of military C3 systems
09 p1331 A83-24763

Navy space sensors face tough requirements
13 p1848 A83-31550

A new method of satellite attitude control using a bias-momentum
17 p2478 A83-37457

Impact of spacecraft design on remote control of satellite operations
17 p2479 A83-37490

Elaboration of daily programs and operational control of the ARCAD-3 scientific payload aboard the AUREOL-3 satellite
18 p2647 A83-39584

A global HF telecommand system for long duration balloon flights
18 p2639 A83-39813

A computationally efficient pointing command law
[AIAA PAPER 83-2208]
19 p2815 A83-41692

COMMAND GUIDANCE
Closed-loop eigenvalue selection for reduced autopilot sensitivity to radome errors
[AIAA PAPER 83-0062]
05 p0592 A83-16494

Guidance and control of a balloon-borne X-ray telescope with onboard and ground based computers
18 p2641 A83-39823

COMMAND SYSTEMS
U COMMAND GUIDANCE

COMMAND-CONTROL
U COMMAND AND CONTROL

COMMERCE
Economic and industrial aspects of the conquest of space
01 p0111 A83-10438

Airline economics --- Book
03 p0400 A83-14000

Cooperative development of application specifications, giving particular attention to the realization of software for specific branches of the economy --- German thesis
11 p1647 A83-28661

The Space Transportation Company Inc.
[SAE PAPER 821368]
17 p2586 A83-37961

Spacecraft insurance
22 p3368 A83-45816

COMMERCIAL AIRCRAFT
NT A-300 AIRCRAFT
NT BOEING 727 AIRCRAFT
NT BOEING 737 AIRCRAFT
NT BOEING 747 AIRCRAFT
NT BOEING 757 AIRCRAFT
NT BOEING 767 AIRCRAFT
NT CV-990 AIRCRAFT
NT DC 8 AIRCRAFT
NT DC 9 AIRCRAFT
NT DC 10 AIRCRAFT
NT EUROPEAN AIRBUS
NT F-28 TRANSPORT AIRCRAFT
NT IL-62 AIRCRAFT
NT L-1011 AIRCRAFT
NT LEAR JET AIRCRAFT
NT LIGHT TRANSPORT AIRCRAFT

Economic modeling of fault tolerant flight control systems in commercial applications
01 p0013 A83-11156

The impact of composite technology on commercial transport aircraft
02 p0135 A83-12969

Application of software design standards to commercial aircraft equipment
05 p0592 A83-17312

Demonstration of reparability and repair quality on graphite/epoxy structural subelements
07 p0861 A83-20485

Operator influences on aircraft design
07 p0866 A83-21032

Will technology make the helicopter competitive
07 p0866 A83-21574

Advances in high-speed rolling-element bearings --- for aircraft engine and transmission application
08 p1111 A83-22319

The maintenance of modern engines in civil aviation
[DGLR PAPER 82-070]
09 p1206 A83-24184

Flight management systems and data links
09 p1209 A83-24424

Applications of head-up displays in commercial transport aircraft
09 p1204 A83-24428

ECS schemes for All Electric Airliners
[SAE PAPER 820870]
10 p1375 A83-25769

PW4000 uses JT9D, new technology
10 p1378 A83-26072

Changing the course of U.S. aviation
13 p1803 A83-30830

A review of commuter propulsion technology
[SAE PAPER 820716]
13 p1807 A83-31801

Operator influences on aircraft design
13 p1803 A83-31813

Current barotraumatic otitis of the commercial flight personnel in civil aviation 14 p2067 A83-32454

Impact of stretching wide-bodied aircraft on existing airport facilities

[AIAA PAPER 83-1578] 14 p1978 A83-33351

Identifying aircraft and airport compatibility - A straightforward approach to complexity

[AIAA PAPER 83-1582] 14 p1978 A83-33354

CRAF today - An airline perspective --- Civil Reserve Air Fleet

[AIAA PAPER 83-1589] 14 p1973 A83-33358

Advanced Civil Military Aircraft - Technical feasibility assessment

[AIAA PAPER 83-1592] 14 p1973 A83-33359

Aircraft design trends for cargo compatibility

[AIAA PAPER 83-1609] 14 p1973 A83-33370

Flight operations: A study of flight deck management --- Book 15 p2120 A83-33767

Cruise missile propulsion versus commercial airliner propulsion - Different challenges can produce similar engine cycles

[AIAA PAPER 83-1176] 16 p2307 A83-36261

Development of 4-D time-controlled guidance laws using singular perturbation methodology

17 p2461 A83-37149

New aircraft. II 17 p2464 A83-38329

Avionics analyzed. III - The hidden sensors

17 p2461 A83-38471

Safety in the skies 19 p2794 A83-41467

Interference to satellite earth stations due to scatter of terrestrial transmissions by aircraft

19 p2835 A83-41554

Flight management systems - Where are we today and what have we learned?

[AIAA PAPER 83-2236] 19 p2803 A83-41713

Shot peening for advanced aerospace design; Proceedings of the Aerospace Congress and Exposition, Anaheim, CA, October 25-28, 1982

22 p3302 A83-45872

The application of shot peen forming technology to commercial aircraft wing skins

[SAE PAPER 821456] 22 p3247 A83-45875

Development of aerodynamical technology for large civil aviation aircraft

23 p3391 A83-47204

Commercial aircraft with reduced longitudinal stability and active tail planes, and the unsteady aerodynamics of rapidly adjusted control surfaces

23 p3412 A83-47213

Advanced lightweight, fire retardant floor paneling for aircraft

[AIAA PAPER 83-2442] 23 p3403 A83-48330

Advanced commercial engines for the 1990's

[AIAA PAPER 83-2479] 23 p3411 A83-48342

An airline view of LH2 as a fuel for commercial aircraft

23 p3440 A83-48598

A very large cargo aircraft design project

24 p3547 A83-49436

Civil transport aircraft design methodology

[AIAA PAPER 83-2463] 24 p3547 A83-49579

Material selection for the new-technology commercial transport - The designer's dilemma

[AIAA PAPER 83-2477] 24 p3553 A83-49583

A McDonnell Douglas perspective - Commercial aircraft for the next generation

[AIAA PAPER 83-2502] 24 p3548 A83-49587

Transport aircraft requirements - How much? How soon? How to pay?

[AIAA PAPER 83-2504] 24 p3546 A83-49588

Generalized flight optimization equations for commercial aircraft

24 p3548 A83-50135

COMMERCIAL AVIATION

U CIVIL AVIATION

U COMMERCIAL AIRCRAFT

COMMERCIAL ENERGY

Developing technologies for synthetic fuels

01 p0068 A83-10658

SOLERAS solar active cooling field test operations

11 p1607 A83-27239

An analysis of the cost/performance characteristics of passive solar materials and components

11 p1608 A83-27247

The Mississippi County Community College large-scale demonstration project a success story

14 p2037 A83-32186

Hydrogen fuel for space conditioning of buildings

15 p2193 A83-35305

Technical, economic and legal aspects of wind energy utilization

20 p3012 A83-43370

COMMINUTION

NT CRUSHING

NT GRINDING (COMMINUTION)

COMMITTEE ON SPACE RESEARCH

Progressive development of international space law

08 p1171 A83-22663

Legal problems of space exploration in the framework of the Legal Subcommittee of the U.N. Committee on the Peaceful Uses of Outer Space 08 p1171 A83-22664

Gamma-ray astronomy in perspective of future space experiments; Proceedings of the Symposium, Ottawa, Canada, May 16-June 2, 1982 18 p2755 A83-39275

Life sciences and space research XX(2); Proceedings of the Workshop and Topical Meeting, Ottawa, Canada, May 16-June 2, 1982 19 p2877 A83-42029

COMMONALITY (EQUIPMENT)

Commonality potential of future public service helicopters and Army light utility helicopters

[AIAA PAPER 83-2553] 24 p3546 A83-49593

COMMUNICATING

NT AIRCRAFT COMMUNICATION

NT GROUND-AIR-GROUND COMMUNICATION

NT INFORMATION DISSEMINATION

NT INTERSTELLAR COMMUNICATION

NT POINT TO POINT COMMUNICATION

NT VERBAL COMMUNICATION

COMMUNICATION

NT FACSIMILE COMMUNICATION

NT INFORMATION DISSEMINATION

NT LINE OF SIGHT COMMUNICATION

NT OPTICAL COMMUNICATION

NT SHIP TO SHORE COMMUNICATION

NT VERBAL COMMUNICATION

Annual Allerton Conference on Communication, Control, and Computing, 19th, Monticello, IL, September 30-October 2, 1981, Proceedings

15 p2220 A83-35101

COMMUNICATION CABLES

NT BEAM WAVEGUIDES

NT COAXIAL CABLES

NT OPTICAL WAVEGUIDES

NT PLASMAGUIDES

NT RECTANGULAR GUIDES

NT WAVEGUIDES

Electrical properties of an input-output cable for Josephson applications

02 p0168 A83-12815

Fiber-optic technology takes to the air

05 p0592 A83-16867

SGEMP-induced transfer admittance coupling in cable bundles

05 p0628 A83-17522

Vulnerability of fiber optic cables to thermal pulses

08 p1165 A83-22482

Fiber optic cables for severe environment

08 p1165 A83-22483

Cold-induced losses in loose-sheath fiber-optic cables

08 p1165 A83-22484

Air-deployed, over-ocean, small, ruggedized optical fiber

08 p1074 A83-22486

Geomagnetic induction effects in ground-based systems

11 p1615 A83-27403

COMMUNICATION EQUIPMENT

NT DIGITAL SPACECRAFT TELEVISION

NT DIPLEXERS

NT RADIO RECEIVERS

NT SATELLITE TELEVISION

NT SPACECRAFT TELEVISION

NT STEREOTELEVISION

NT SUPERHETERODYNE RECEIVERS

NT TRANSMITTER RECEIVERS

NT WHISTLER RECORDERS

Intelsat VI SS-TDMA 01 p0043 A83-11277

Millimeter wave integrated circuits for communications and radar applications

03 p0310 A83-13794

PTC '81; Proceedings of the Pacific Telecommunications Conference, Honolulu, HI, January 12-14, 1981

07 p0903 A83-19656

An overview of the MX Command, Control and Communications system

07 p0903 A83-19657

NTC '81; National Telecommunications Conference, New Orleans, LA, November 29-December 3, 1981, Record. Volumes 1, 2, 3 & 4

07 p0903 A83-19676

Results obtained with a digital computer simulator of spread spectrum communications systems

07 p0983 A83-19794

Environmental testing of UV-cured acrylate-coated fibers

08 p1073 A83-22488

Control and communication technology in laser systems; Proceedings of the Twenty-fifth Annual International Technical Symposium, San Diego, CA, August 25, 26, 1981

09 p1214 A83-23576

Concepts for description and evaluation of military C3 systems

09 p1331 A83-24763

FM-SCPC system and equipments for satellite communication --- Single Channel Per Carrier

10 p1404 A83-26084

A spectral analysis of M-ary direct sequence spread-spectrum multiple access communication systems

14 p2001 A83-32869

Recent advances in the performance and reliability of InGaAsP: LED's for lightwave communication systems

15 p2229 A83-33677

Productivity goals drive office automation

18 p2752 A83-40308

Equipment design considerations for Intelsat TDMA traffic terminals

19 p2829 A83-41357

Satellite ranging instrumentation developed at ILR [IAF PAPER 83-461] 23 p3420 A83-47384

COMMUNICATION NETWORKS

Earth stations for satellite telecommunications - State of the art and perspectives

01 p0031 A83-10430

Field calibration of ATE via satellite

01 p0050 A83-10766

Bus protocols for a digital audio distribution system

01 p0005 A83-11126

Computer simulation of waveforms on time division command/response multiplex data buses

01 p0042 A83-11150

A high speed 10MHz multiplex data bus interface

01 p0042 A83-11152

A fast microprocessor communication network design for interprocessor communications for an integrated flight control system

02 p0133 A83-11902

The design of a packet switched network for aeronautical data interchange

03 p0281 A83-14862

Analysis of time fluctuations in synchronous information networks --- German thesis

04 p0467 A83-15839

The SPINE programme and the associated demonstrations at UNISPACE 82 --- satellite data transmission via Space Information Network Experiment

05 p0622 A83-17427

Operational measurements of a 4/6-GHz adaptive polarization compensation network employing up/down-link correlation algorithms

06 p0746 A83-18727

An overview of PANACEA, a software package for analyzing Markovian queueing networks

06 p0802 A83-19596

INTELSAT: The global telecommunications network --- Book

07 p0902 A83-19650

PTC '82; Proceedings of the Pacific Telecommunications Conference, Honolulu, HI, January 17-20, 1982

07 p0903 A83-19651

Case study - Australian national satellite system

07 p0903 A83-19653

Commercial satellite communications for developing areas of the Pacific

07 p0903 A83-19654

One third of the world - A review of Pacific islands telecommunications requirements

07 p1001 A83-19655

PTC '81; Proceedings of the Pacific Telecommunications Conference, Honolulu, HI, January 12-14, 1981

07 p0903 A83-19656

An overview of the MX Command, Control and Communications system

07 p0903 A83-19657

NTC '81; National Telecommunications Conference, New Orleans, LA, November 29-December 3, 1981, Record. Volumes 1, 2, 3 & 4

07 p0903 A83-19676

Detection of M'ARY communication with truncated symbols

07 p0904 A83-19679

The potential role of intersatellite links in future satellite communications

07 p0870 A83-19689

A general analysis of anti-jam communication systems

07 p0904 A83-19694

An analysis of full-duplex data links in SNA networks --- Systems Network Architecture

07 p0907 A83-19724

Communication protocol for a multisatellite communication system

07 p0907 A83-19725

On information flow in relay networks

07 p0908 A83-19734

Performance analysis for an adaptive polling access-control scheme employing a dynamic reservation protocol

07 p0908 A83-19738

Preferred access in packet-switching radio networks

07 p0908 A83-19739

Steady-state performance of an adaptive sequential routing algorithm

07 p0911 A83-19775

TDMA demand assignment operation in Telecom 1 business services network

07 p0911 A83-19783

A technique for voice-data integration over packet radio channels

07 p0912 A83-19790

A microwave approach to fault tolerance in satellite networking

07 p0914 A83-20674

Design of a demand-assignment satellite-switched Space Division Multiple Access Communication network

07 p0915 A83-21030

Controlling the complexity of menu networks

07 p0983 A83-21041

The development of global satellite telecommunications

07 p0916 A83-21618

The development of standards for the common ICAO Data Interchange Network /CIDIN/

08 p1075 A83-22027

Data systems - Optical bus will connect distributed system

09 p1215 A83-24352

Distributed hypothesis formation in sensor fusion systems

09 p1334 A83-24811

Symbiosis between a terrestrial-based integrated services digital network and a digital satellite network 11 p1557 A83-28132

A space-division multiple-access protocol for spot-beam antenna and satellite-switched communication network 11 p1557 A83-28134

International connection of plesiochronous networks via TDMA satellite link 11 p1557 A83-28138

Zones serviced by satellite communications systems --- Russian book 12 p1718 A83-28820

File allocation in a distributed computer communication network 13 p1909 A83-30788

6/4 GHz band small capacity omni-use terminal satellite system 15 p2143 A83-33508

Asynchronous multiplexing for an optical-fibre local-area network 15 p2144 A83-34523

I/O limitations of multi-chip VLSI systems 15 p2218 A83-35116

Analysis of the packet formation process in packet-switched networks 15 p2147 A83-35123

Application of 2-D bin packing algorithms for task scheduling in PASM --- sparse crossbar interconnection network designs for data transmission 15 p2219 A83-35132

Alaska's giant satellite network 17 p2493 A83-37740

Design summary of the Intelsat V spacecraft 18 p2646 A83-40014

Viewpoints on control of military satellite communications 18 p2675 A83-40314

Low probability of intercept --- satellite communication system performance at EHF and SHF 18 p2675 A83-40315

On the capacity of multihop slotted ALOHA networks with regular structure 19 p2825 A83-40893

On the capacity of single-hop slotted ALOHA networks for various traffic matrices and transmission strategies 19 p2826 A83-40894

An overview of a new integrated system for communication, navigation, and identification - The Joint Tactical Information Distribution System 19 p2795 A83-41310

Systems for radiocommunication with ships via satellite - The INMARSAT organization 19 p2813 A83-41311

Using SLAM and SDL to assess Space Shuttle experiments --- programming language and data base management system for simulation of models and analysis of results 19 p2887 A83-41325

Network control system using traffic databases 19 p2828 A83-41338

Deep space communication - A one billion mile noisy channel 19 p2813 A83-41343

A postulated topographical architecture for the Defense Communications System of 2004 19 p2829 A83-41356

Trunk transmission network using K-band SS-TDMA system 19 p2831 A83-41378

Optimum utilization of domestic communication satellites for data and television transmission 19 p2831 A83-41382

A coupled phase-locked loops system for carrier tracking improvement 19 p2814 A83-41395

An iterative scheme for performance modeling of slotted ALOHA packet radio networks 19 p2832 A83-41397

Combined FDMA-TDMA - A cost effective technique for digital satellite communication networks 19 p2834 A83-41414

Need for, and financial feasibility of, satellite-aided land mobile communications 19 p2834 A83-41415

Feasibility of international transport communications system 19 p2834 A83-41418

Space Station information systems [AIAA PAPER 83-7105] 19 p2814 A83-42089

Performance of a random access packet network with time-capture capability 21 p3119 A83-44037

Space telecommunications. III - The ground sector. Satellite telecommunications systems --- French book 21 p3121 A83-45082

The Italsat programme 21 p3122 A83-45431

The recognition of address sequences by the method of fast transforms 22 p3271 A83-45655

PTC '83 - Pacific Telecommunications Conference, Honolulu, HI, January 16-19, 1983, Proceedings 22 p3273 A83-45751

System configurations and applications in domestic/regional satellite communications 22 p3273 A83-45754

Atmospheric noise and its effects on telecommunication systems performance 22 p3273 A83-45883

Beam forming networks for mm-wave satellite communications 22 p3274 A83-46000

The legal and political considerations of the 1985 World Administrative Radio Conference 22 p3371 A83-46316

Single-mode fiber systems for deep space communication network 22 p3360 A83-46657

Traffic control in satellite-aided slotted-ALOHA system using HDLC procedure for an error recovery --- High-Level Data Link Control 22 p3275 A83-46916

The Mexican national satellite system [IAF PAPER 83-79] 23 p3441 A83-47257

Multiple access equipment design for satellite communication systems in the USSR [IAF PAPER 83-84] 23 p3441 A83-47258

A high-speed, time-division multiple-access communication link demonstration 23 p3443 A83-48140

Beyond the global village 23 p3416 A83-48638

COMMUNICATION SATELLITES

NT COMMUNICATIONS TECHNOLOGY SATELLITE

NT COMSTAR SATELLITES

NT EUROPEAN COMMUNICATIONS SATELLITE

NT INTELSAT SATELLITES

NT L-SAT

NT MARECS MARITIME SATELLITES

NT MAROTS (ESA)

NT RCA SATCOM SATELLITES

NT RELAY SATELLITES

NT SYMPHONIE SATELLITES

NT SYNCOM SATELLITES

Earth stations for satellite telecommunications - State of the art and perspectives 01 p0031 A83-10430

Testing of a communications satellite 01 p0018 A83-11066

Space: Mankind's fourth environment; International Astronautical Congress, 32nd, Rome, Italy, September 1981, Selected Papers 01 p0016 A83-11276

Intelsat VI SS-TDMA 01 p0043 A83-11277

Italy in millimeter waves activities for space communication 01 p0032 A83-11278

Estimations of attenuations of earth-satellite links in France 01 p0032 A83-11336

Development of a microwave 20 x 20 switch matrix for 30/20 GHz SS-TDMA application 01 p0044 A83-11484

A multiple beam antenna concept for a 30/20 GHz satellite communications system 01 p0034 A83-11485

A 1 watt GaAs power amplifier for the NASA 30/20 GHz communication system 01 p0044 A83-11489

Apple - Indian experimental geostationary communication satellite --- Ariane Passenger Payload Experiment 02 p0139 A83-11781

OSCAR - Amateur radio satellites and spacecraft 02 p0139 A83-11818

Satellite communications research - The problems of propagation 02 p0163 A83-11820

Insat-1 - India's dual spacecraft 02 p0140 A83-12645

Attitude sensing of apple --- Ariane Passenger Payload Experiment 02 p0142 A83-12967

Systems by satellite - A step toward the integrated services digital network 02 p0165 A83-13018

An optimal switching algorithm for multibeam satellite systems with variable bandwidth beams 03 p0304 A83-13872

Single sideband, amplitude modulated, satellite voice communication system having 6000 channels per transponder 03 p0305 A83-13997

Narrow multibeam satellite ground station antenna employing a linear array with a geosynchronous arc coverage of 60 deg. I - Theory 03 p0305 A83-14004

Experimental and theoretical statistics of microwave amplitude scintillations on satellite down-links 03 p0305 A83-14010

Domestic satellite communications systems - Background and projections 04 p0466 A83-15664

The ESA Large Telecommunications Satellite Programme and its projections into the future 04 p0466 A83-15665

Novel technique for antenna gain measurement in satellite earth stations 04 p0468 A83-16022

Industry looks at military exceptionally high frequency bands 05 p0621 A83-18688

The SPINE programme and the associated demonstrations at UNISPACE 82 --- satellite data transmission via Space Information Network Experiment 05 p0622 A83-17427

The development of satellite communications and its socio-economic implications 06 p0816 A83-18372

A planar array antenna for TV broadcasting communications 06 p0737 A83-18607

The Quad aperture /hoop/column/ antenna for advanced communications missions in the 1990's 06 p0738 A83-18621

Radomes for satellite communication earth-stations 06 p0742 A83-18677

The effect of interference from satellites on digital radio-relay systems operating between 15.4 and 40 GHz 06 p0747 A83-18729

11-GHz MIC QPSK modulator for regenerative satellite repeater 06 p0752 A83-18766

Optimization of coverage pattern for regional communications satellite 06 p0723 A83-19036

Commercial satellite communications for developing areas of the Pacific 07 p0903 A83-19654

One third of the world - A review of Pacific islands telecommunications requirements 07 p1001 A83-19655

Satellite communication in presence of multipath fading 07 p0903 A83-19659

NTC '81; National Telecommunications Conference, New Orleans, LA, November 29-December 3, 1981, Record. Volumes 1, 2, 3 & 4. 07 p0903 A83-19676

Broadcasting satellites and the system of the United States Satellite Broadcasting Company 07 p0904 A83-19680

Packet-switched data communication over a multibeam satellite with on-board processing 07 p0870 A83-19684

30/20 GHz experimental communications satellite system 07 p0904 A83-19688

The potential role of intersatellite links in future satellite communications 07 p0870 A83-19689

Satellite clusters and frequency reuse 07 p0904 A83-19690

Digital satellites with time and frequency divided channels 07 p0904 A83-19691

Systems and technology aspects of a direct broadcast satellite service for the United States 07 p0904 A83-19692

Maximizing satellite transponder utilization for video teleconferencing 07 p0904 A83-19693

Fault tolerant techniques for a multiple microprocessor-based space borne packet switch 07 p0906 A83-19714

Microcomputer-based improvements to the AFSATCOM System 07 p0906 A83-19716

The 1985/87 Space Planning Conference --- on use of geostationary satellite orbits for satellite services 07 p0906 A83-19718

Communication protocol for a multisatellite communication system 07 p0907 A83-19725

Demand Assignment Multiple Access /DAMA/ techniques for satellite communications 07 p0907 A83-19727

Evaluation of a 14/12 GHz digital satellite link as the facility between digital switches 07 p0908 A83-19742

Conservation of the geostationary spectrum 07 p0910 A83-19760

Geostationary communications satellite orbit utilization strategies for the 1980s 07 p0910 A83-19761

Future satellite systems - Market demand assessment 07 p0910 A83-19762

On-board process - An overview 07 p0910 A83-19771

Maximizing performance in a multibeam satellite system 07 p0910 A83-19773

A high capacity satellite switched TDMA microwave switch matrix 07 p0911 A83-19776

A cost effective TDMA terminal for Intelsat/Eutelsat applications 07 p0911 A83-19782

Light route TDMA for business communications 07 p0911 A83-19784

Mitelnet - A private network using TDMA 07 p0911 A83-19787

The practical tradeoff among bandwidth efficiency, modulation schemes, availability, and cost in satellite communication system design considerations 07 p0912 A83-19798

High packing density modulation techniques for satellite links 07 p0912 A83-19799

Optimum orbital location of a communications satellite 07 p0913 A83-20553

Experimental evaluation of adaptive threshold detection with estimated sequence processor performance 07 p0914 A83-20555

Design and performance of interference cancellation circuit --- for radio communications 07 p0914 A83-20821

Rain attenuation considerations for satellite paths in Australia 07 p0915 A83-21029

Intermodulation spectra for 2-carrier-level SPC system 07 p0916 A83-21575

Orbital error analysis of time synchronization via geostationary broadcast satellite 08 p1048 A83-22039

Satellite systems for the acquisition and processing of geomagnetic data 08 p1133 A83-22082

A unifying concept for future fixed satellite service payloads for Europe 08 p1076 A83-22369

A method of increasing satellite link capacity 08 p1078 A83-22994

A 14 GHz DCPK direct demodulator for satellite applications 08 p1082 A83-23244

GaAs laser beacon for satellite communications 09 p1214 A83-23582

An application of unsupported film adhesive to fabricate spacecraft structures 09 p1238 A83-23629

MMIC technology for microwave radar and communication systems 09 p1255 A83-24349

A review of satellite communication and propagation experiments for frequencies above 10 GHz 09 p1249 A83-24646

The 'Oribita-RV' satellite sound broadcasting and newspaper column transmission system 10 p1402 A83-25876

Satellite television broadcasting systems in the USSR 10 p1402 A83-25877

Precision phase comparison via communication satellites using loop-back tones 10 p1403 A83-26042

Experimental system for computer network via satellite /CS/. I - Summary of the system 10 p1403 A83-26077

Experimental system for computer network via satellite /CS/. II - Communication protocols 10 p1403 A83-26078

Experimental system for computer network via satellite /CS/. III - Network control processor 10 p1403 A83-26079

Experimental system for computer network via satellite /CS/. V - Data collecting and processing system 10 p1403 A83-26081

The invariant imbedding - Stochastic approximation algorithm with application to communications satellites 10 p1382 A83-26594

Comparison of computer-predicted and in-orbit solar array performance for geosynchronous communications satellites 11 p1541 A83-27251

Parametric study of intersatellite CO2 laser data links 11 p1535 A83-27605

A survey of modem design and performance in digital satellite communications 11 p1556 A83-28126

Impact of a new TWTA linearizer upon QPSK/TDMA transmission performance 11 p1556 A83-28129

Symbiosis between a terrestrial-based integrated services digital network and a digital satellite network 11 p1557 A83-28132

One-way multiaddress satellite data communication system 11 p1557 A83-28133

A space-division multiple-access protocol for spot-beam antenna and satellite-switched communication network 11 p1557 A83-28134

The use of resource sharing and coding to increase the capacity of digital satellites 11 p1557 A83-28135

An experiment in integrated digital satellite communications 11 p1557 A83-28136

Performance evaluation of an integrated access scheme in a satellite communication channel 11 p1557 A83-28137

SS/TDMA steady-state synchronization - Analysis and operation during deep signal fades 11 p1557 A83-28139

Optimal on-board clock control 11 p1573 A83-28140

A wide-band satellite microwave switch matrix for SS/TDMA communications 11 p1562 A83-28142

OTS - The lynchpin of the European space telecommunications programme 11 p1534 A83-28182

High stability communications hardware for spacecraft 11 p1562 A83-28184

A geostationary satellite platform for future communications services 11 p1534 A83-28219

Satellite handling for the Shuttle 11 p1535 A83-28416

A low-noise GaAs FET preamplifier for 21 GHz satellite earth terminals 11 p1563 A83-28591

Zones serviced by satellite communications systems --- Russian book 12 p1718 A83-28820

Orbital perturbations due to radiation pressure for a spacecraft of complex shape 12 p1705 A83-29102

Comparative analysis of large antenna spacecraft using the ideas system 12 p1707 A83-29731

[AIAA 83-0798] The space race - Here comes Japan --- scientific and communication satellite technology 13 p1808 A83-29999

United States space law: National and international regulation. I --- Book 13 p1934 A83-30137

Diversity ALOHA - A random access scheme for satellite communications 13 p1827 A83-30225

Circuit and packet integrated switching in a satellite communication channel 13 p1829 A83-30780

RCA Satcom test planning 13 p1810 A83-31186

The challenge of the 80's: Some environment-sensitive technologies - Status and problems 13 p1827 A83-31477

Thermal modeling and design considerations for large communications spacecraft [AIAA PAPER 83-1463] 14 p1982 A83-32722

Go-back-N ARQ schemes for point-to-multipoint satellite communications --- automatic-repeat-request 14 p2001 A83-32873

Orbital efficiency through satellite digital switching 14 p2002 A83-33158

Speech encoding for 6/4 GHz band small capacity omni-use terminal satellite system 15 p2144 A83-33509

Switching system for 6/4 GHz band small capacity omni-use terminal satellite system 15 p2144 A83-33510

Earth-oriented space activities and their legal implications; Proceedings of the Symposium, McGill University, Montreal, Canada, October 15, 16, 1981 15 p2240 A83-34651

Direct broadcasting satellites - International policy issues 15 p2240 A83-34653

A new service at the starting line - Direct broadcasting from satellites 15 p2144 A83-34654

Video teleconference by satellite 16 p2341 A83-35425

Space 2000; International Astronautical Congress, 33rd, Paris, France, September 27-October 2, 1982, Selection of Papers 16 p2313 A83-35951

Delay analysis of a satellite channel reservation system with variable frame format 16 p2343 A83-36581

The effects of noise correlation and power imbalance on terrestrial and satellite DPSK channels 16 p2344 A83-36906

Space: The high frontier in perspective --- Book 17 p2471 A83-37174

Digital control loops for TELECOM 1 AOCSS --- Altitude and Orbit Control System 17 p2477 A83-37440

Development of a 60-channel FDM-TDM transmultiplexer 17 p2497 A83-37789

Capacity allocation scheme for transmission of packets over satellite links 17 p2493 A83-37792

Third-order distortion of television and sound multiplexed signals in satellite FM systems 17 p2493 A83-37793

Design summary of the Insat lightweight, deployable solar array [SAE PAPER 821397] 17 p2482 A83-37971

Alternative techniques to GPS/NAVSTAR 17 p2462 A83-38937

Non-linear distortion analysis in frequency division multi-access satellite communication systems 18 p2674 A83-39093

A critical look at space technology and the developing world 18 p2752 A83-39827

The evolution of space technology and its economic impact Reflection on the transposition of the European model in the countries of the Third World 18 p2752 A83-39828

Near term perspectives of LSI implementation of on-board switching units for SS-TDMA systems 18 p2677 A83-39998

Considerations on the redundancy structures of on-board processors for SS-TDMA satellites 18 p2674 A83-39999

Reliability performance evaluation of an on-board processor for SS-TDMA satellites 18 p2675 A83-40000

Communication satellite for future military aircraft 19 p2812 A83-40885

Signaling performance over a piecewise linear limited channel in the presence of interference and Gaussian noise 19 p2826 A83-40921

Beam area determination for multiple-beam satellite communication applications 19 p2827 A83-41147

Orbital inclination effects on communications satellite system design 19 p2815 A83-41149

The use of telecommunications satellites by the air, sea, and land military forces and by civil defense - Project SICRAL AM/136/80 19 p2812 A83-41227

ICC '82 - The digital revolution; International Conference on Communications, Philadelphia, PA, June 13-17, 1982, Conference Record. Volumes 1, 2 & 3 19 p2827 A83-41326

The effects of rain on system performance for the NASA 30/20 GHz Experimental Satellite 19 p2827 A83-41327

The enhancement of propagation reliability for millimeter wave satellite communication systems 19 p2827 A83-41329

Impact of monolithic microwave integrated circuit development on communications satellites 19 p2828 A83-41334

High efficiency broadband FET power amplifier for C-band TWTA replacement 19 p2839 A83-41335

Packet communication system for a multi-beam beam switched satellite repeater 19 p2828 A83-41336

High capacity low delay packet switching via a processing satellite 19 p2828 A83-41337

Network control system using traffic databases 19 p2828 A83-41338

A one kilowatt class direct broadcast satellite 19 p2829 A83-41352

12 GHz band satellite broadcasting receiver with direct converting system 19 p2829 A83-41353

Optimum frequency assignment for satellite SSCP systems 19 p2829 A83-41358

Computer modeling of spectral efficiency and sidelobe buildup effects in nonlinear satellite links 19 p2830 A83-41366

Advanced 30/20 GHz multiple beam antenna for future communications satellites 19 p2830 A83-41367

20 GHz GaAs FET transmitter 19 p2839 A83-41368

20 x 20 IF switch matrix for SS-TDMA systems 19 p2839 A83-41369

Launch vehicles for communications satellites 19 p2812 A83-41374

A network control concept for the 30/20 GHz communication system baseband processor 19 p2813 A83-41389

Comparative study of FDMA, TDMA and hybrid 30/20 GHz satellite communications systems for small users 19 p2832 A83-41390

Onboard processing for a 30/20 GHz communications satellite 19 p2813 A83-41391

On-board clock correction by drift prediction 19 p2832 A83-41392

FLTSATCOM - Current and future 19 p2833 A83-41401

The LEASAT communication satellite 19 p2812 A83-41402

Advanced DOD military satellite communications 19 p2833 A83-41403

Demand-assignment schemes for SSCP FDMA satellite systems with contiguous spot beams 19 p2835 A83-41553

Manned space station relevance to commercial telecommunication satellites - A prospectus to year 2000 [AIAA PAPER 83-7091] 19 p2808 A83-42079

Weight and structural analysis of four structural concepts for a land mobile satellite system [SAWE PAPER 1456] 20 p2945 A83-43737

25 years of NASA - Reflections and projections-applications [AAS PAPER 83-153] 20 p2943 A83-43761

Application of a space station to communications satellites [AAS PAPER 83-197] 20 p2945 A83-43773

New telecommunications for the developing world 21 p3220 A83-44530

Future configurations of communication and broadcast satellites 21 p3096 A83-44531

Intelsat - Making the future happen 21 p3120 A83-44532

A figure of merit for competing communications satellite designs 21 p3221 A83-44533

High power and pointing accuracy from body-spun spacecraft 21 p3100 A83-44534

Aussat - A milestone in Australia's communication history 21 p3120 A83-44535

Major developments in space law from 1957 to 1982 - A general survey 21 p3221 A83-44536

Satellites and switching 21 p3120 A83-44537

A primer on communications satellite design 21 p3101 A83-44873

Space telecommunications. III - The ground sector. Satellite telecommunications systems --- French book 21 p3121 A83-45082

Electrothermal decomposition of monomethylhydrazine 21 p3117 A83-45089

The future for communication satellites of the PAM-D/half Ariane class 21 p3096 A83-45427

Design evolution and economics of future communication satellite platforms 21 p3103 A83-45428

Trends in propulsion systems for communications satellites 21 p3104 A83-45429

Reliability of space systems - Need for new tools 21 p3149 A83-45430

Broadcasting aspects of a projected African regional satellite telecommunications system 21 p3122 A83-45432

Space technology - Telecommunications: Clarke's legacy 21 p3122 A83-45603

Commercial launch vehicle services 22 p3258 A83-45720

Space communications in Japan 22 p3273 A83-45752

The layer model and error control for satellite communications 22 p3273 A83-45756

The international politics of the orbit-spectrum issue --- concerning communication satellites 22 p3367 A83-45809

The genesis of the 1985/87 ITU world administrative radio conference on the use of the geostationary-satellite orbit and the planning (1) of space services utilizing it 22 p3367 A83-45811

An economic assessment of CCIR's five methods for assuring guaranteed access to the orbit-spectrum resource 22 p3368 A83-45819

Teleinformatics, the protection of privacy and the law 22 p3368 A83-45820

Communications spacecraft payload testing 22 p3257 A83-45824

System functional testing of a communication satellite 22 p3257 A83-45825

Communication satellites in the geostationary orbit --- Book 22 p3274 A83-45911

World atlas of satellites --- Book on communication satellite services 22 p3258 A83-45912

Beam forming networks for mm-wave satellite communications 22 p3274 A83-46000

Commercial Atlas/Centaur program [IAF PAPER 83-21] 23 p3419 A83-47235

Athos, an experimental telecommunication program to promote new platform and payload technologies [IAF PAPER 83-59] 23 p3419 A83-47246

Power conditioning system of an international amateur radio satellite [IAF PAPER 83-61] 23 p3425 A83-47247

A control method of antenna pointing error due to orbital inclination for a spin-stabilized satellite [IAF PAPER 83-67] 23 p3416 A83-47249

The terrestrial coverage of the geostationary satellite beam [IAF PAPER 83-73] 23 p3441 A83-47252

The high power section of the TV-SAT-TDF-1 repeaters [IAF PAPER 83-74] 23 p3445 A83-47253

On board and ground equipment for TV broadcast applications State of the art and evolution [IAF PAPER 83-75] 23 p3441 A83-47254

Transmitting antenna for direct broadcasting satellites with radio frequency beam fine pointing capability [IAF PAPER 83-76] 23 p3441 A83-47255

Multiple access equipment design for satellite communication systems in the USSR [IAF PAPER 83-84] 23 p3441 A83-47258

The commercial Centaur family [IAF PAPER 83-233] 23 p3514 A83-47316

Economics of telecommunications space segments [IAF PAPER 83-234] 23 p3514 A83-47317

Cost reduction trends in space communications by larger satellites/platforms [IAF PAPER 83-235] 23 p3514 A83-47318

Communications satellites - The experimental years [IAF PAPER 83-302] 23 p3419 A83-47335

Education and communication satellites - Opportunities for outreach [IAF PAPER 83-307] 23 p3513 A83-47336

A semi-passive procedure for librational control of communications and earth sensing satellites [IAF PAPER 83-337] 23 p3421 A83-47347

Operating model satellite for space education [IAF PAPER 83-440] 23 p3513 A83-47382

A transportable satellite earth station for television outside broadcast contributions 23 p3442 A83-47652

A high-speed, time-division multiple-access communication link demonstration 23 p3443 A83-48140

Beyond the global village 23 p3416 A83-48638

Advanced communications satellite systems 24 p3551 A83-49855

30 GHz band low noise receiver for 30/20 GHz single-conversion transponder 24 p3570 A83-49857

A 20 GHz band 0.5 W GaAs FET amplifier for satellite communications 24 p3574 A83-49858

COMMUNICATION SYSTEMS

U TELECOMMUNICATION

COMMUNICATION THEORY

NT WORDS (LANGUAGE)

Detection and reception of complex signals masked by noise and lumped interference 01 p0031 A83-10409

Choice of parameters of a multistage detector of binary-quantized pulsed signals, minimizing time expenditures on detection 01 p0031 A83-10808

Estimation of the parameters of disturbances on long-range radio-communication paths 01 p0031 A83-10810

Detection of a signal on a background of non-Gaussian noise with unknown nonstationarity characteristics 02 p0162 A83-11531

The efficiency of an adaptive algorithm with regularization of the sampled correlation matrix --- for filter optimization 02 p0162 A83-11532

Notes on the theory of linear, time-discrete signal processing with a rational sampling rate conversion. I 02 p0165 A83-12989

Discrete-analog signal processing --- Russian book 03 p0311 A83-13815

Radiation from aperture antennas radiating in the presence of a dielectric sphere 03 p0307 A83-14031

The noise immunity of group transmissions of binary data given constraints on the composite signal 04 p0465 A83-15142

Conditions of the transformation of a binary signal under the effect of noise of random pulsed sequence type 04 p0466 A83-15716

Quantization of signals on a background of noise 04 p0467 A83-15736

Nonequidistant discrete frequency modulated signals of complex form 04 p0467 A83-15749

Notes on the theory of linear, time-discrete signal processing with a rational sampling rate conversion. II 04 p0472 A83-16038

The application of game theory to the synthesis of an optimal system of symbol data transmission 05 p0623 A83-17689

Interference field analysis with superimposed noise --- German thesis 06 p0736 A83-18500

Excitation of an infinite periodic structure by a local harmonic source with an imprecisely specified frequency 06 p0749 A83-19333

Capacity and coding in the presence of fading and jamming 07 p0905 A83-19697

International Union of Radio Science and Nachrichtentechnische Gesellschaft, General Meeting, Kleinheubach, West Germany, October 4-8, 1982, Lectures and Reports 09 p1243 A83-23376

Simple algorithms for calculating optical communication performance through turbulence 09 p1245 A83-23581

Evaluation of the efficiency of a two-position reception system using discrete algorithms in the frequency domain 10 p1407 A83-26927

Effectiveness of the frequency-adaptive parallel transmission of discrete signals 10 p1407 A83-26936

Error statistics in delta modulation and differential pulse code modulation communication systems 10 p1407 A83-26938

Analysis of systems in structurally indefinite conditions --- in communication channels 10 p1407 A83-26953

Power gain of complex signals of parallel structure 10 p1470 A83-26957

Nonperiodic electromagnetic fields in a sectoral horn 11 p1555 A83-27932

Optimal nonlinear estimation of signals with jumpwise variations of their parameters 11 p1648 A83-27958

Statistical radio communication /2nd revised and enlarged edition/ --- Russian book 12 p1718 A83-28829

The use of elements of the theory of R-functions to analyze receivers of composite signals with redundancy 13 p1828 A83-30288

Probabilistic models of radio-signal phase 14 p2001 A83-32484

Analysis of the accuracy and sensitivity of algorithms for the processing of multidimensional signals and noise 14 p2001 A83-32488

Carrier-tracking loop performance for quaternary and binary PSK signals 14 p2002 A83-33126

Test results with an experimental direction-finding system 14 p2002 A83-33128

Accuracy of the linear filtering of a narrow-band Gaussian signal from a mixture with Markovian Gaussian correlation noise and white noise 17 p2494 A83-38498

The energy characteristics of N-position sequences in the case of relative methods of transmission 18 p2675 A83-40088

Comparative evaluation of the noise immunity and capacity of communication systems with separation of channel according to the form of the signals 18 p2675 A83-40092

Noise immunity of the transmission of messages via Walsh signals 20 p2964 A83-42902

Noise immunity of the reception of discrete signals in transmission systems with a nonlinear group link 20 p2964 A83-42909

Three-position shift-keying in communication systems 21 p3120 A83-44770

The transmission of discrete messages in radio channels (2nd revised and enlarged edition) --- Russian book 21 p3121 A83-45009

Removing the polymodality of an a posteriori distribution by using information redundancy 22 p3271 A83-45660

Evaluating the effectiveness of using adaptive algorithms in communication lines with fading 22 p3271 A83-45662

Signal sets with optimal correlation properties 22 p3272 A83-45740

Signal representation in the time-frequency plane 22 p3274 A83-45973

First application of the mathematical theory of cooperative games of two persons in problems of communications theory 23 p3444 A83-48521

Regularization of algorithms for the processing of signals and noise in adaptive antenna arrays 23 p3444 A83-48522

COMMUNICATIONS TECHNOLOGY SATELLITE

Results of 11.7-GHz CTS rain attenuation measurements at Waltham, Massachusetts 02 p0140 A83-12617

COMMUNITIES

NT MOUNTAIN INHABITANTS

COMMUTATORS

Estimated power quality for line commutated photovoltaic residential system 24 p3599 A83-49324

COMPACTING

Characteristics of the cold compaction of wurtzite-like boron nitride powders at high pressures 02 p0160 A83-13026

The cold pressing of wurtzitic boron nitride powders at high pressures 09 p1239 A83-25065

Porous metal hydride compacts - Preparation, properties and use 11 p1545 A83-27338

A dilatometric study of the growth of Ti-Al compacts during liquid-phase sintering 11 p1547 A83-27922

The effect of the stress pattern on the ductility of aluminum-alloy powder compacts 16 p2334 A83-36886

COMPANDING

TV bandwidth compression techniques using time-companded differentials and their applications to satellite transmissions 06 p0749 A83-19597

TV bandwidth compression techniques using time companded differentials and their applications to satellite transmissions 07 p0909 A83-19743

Adaptive companded pulse-code-modulation 15 p2146 A83-35103

Adaptive companded pulse code modulation 16 p2344 A83-36609

COMPANION STARS

X-ray observations of Be stars 01 p0122 A83-10341

The hot component of KS Persei /HD 30353/ 01 p0117 A83-10931

The light curve of the eclipsing binary system CX Cephei and the properties of the Wolf-Rayet component 03 p0418 A83-13661

Observations of 12-200 keV X-rays from GX 339-4 03 p0425 A83-14207

Influence of rotation and a binary companion on the frequency of the radial pulsations of a homogeneous star 06 p0837 A83-19216

HD 191765 - A Wolf-Rayet binary with a low-mass companion 07 p1014 A83-20657

B and V photometry of HR 8752 11 p1675 A83-28287

Emission-line profiles for selected planetary nebulae and symbiotic stars, V1016 Cygni, and HM Sagittae 12 p1797 A83-29959

An observational study of the influence of close companions on the pulsations of Beta Cephei stars 13 p1943 A83-31740

The X-ray absorption spectrum of 4U 1700-37 and its implications for the stellar wind of the companion HD 153919 15 p2268 A83-34637

Do all barium stars have a white dwarf companion? 17 p2604 A83-37917

The astrometric position of T Tauri and the nature of its companion 17 p2592 A83-37941

HD 187282 - A possible Wolf-Rayet binary with a low-mass companion 17 p2614 A83-38844

Astrometry of the low-luminosity stars VB8 and VB10 18 p2757 A83-39602

The search for invisible companions of binary stars 19 p2910 A83-40754

Confirmation among visual multiples of an increase of Ap stars with age 21 p3237 A83-45546

Symbiotic stars - Spectrophotometry at 3-4 and 8-13 microns 22 p3375 A83-46550

The pulsar P/P distribution and the postulated solar companion 22 p3379 A83-46569

A failed search for black dwarfs as companions to nearby stars 24 p3643 A83-49390

The runaway Wolf-Rayet star HD 143414 - Evidence for a low-mass companion 24 p3649 A83-50099

COMPARATOR CIRCUITS

Optical comparator - A new application for avalanche phototransistors 15 p2229 A83-33684

COMPARATORS

Motion-error immunity in photo coordinate determination - A novel approach to the absolute comparator 08 p1100 A83-22594

COMPARTMENTS

NT AIRCRAFT COMPARTMENTS
NT ANECHOIC CHAMBERS
NT HYPERBARIC CHAMBERS
NT PRESSURE CHAMBERS
NT PRESSURIZED CABINS
NT TEST CHAMBERS
NT VACUUM CHAMBERS

COMPASSES

NT GYROCOMPASSES

COMPATIBILITY

NT ELECTROMAGNETIC COMPATIBILITY
NT SYSTEMS COMPATIBILITY

Identifying aircraft and airport compatibility - A straightforward approach to complexity
[AIAA PAPER 83-1582] 14 p1978 A83-33354
Aerodynamic performance of a fan stage utilizing variable inlet guide vanes (VIGV's) for thrust modulation --- subsonic V/STOL aircraft
[AIAA PAPER 83-1162] 21 p3088 A83-45508
A survey of inlet/engine distortion compatibility
[AIAA PAPER 83-1166] 21 p3088 A83-45509

COMPENSATION

Mutual coupling compensation for small, circularly symmetric planar antenna arrays
02 p0164 A83-12006
A novel feedforward compensation canceling input filter-regulator interaction
14 p2007 A83-33133
The structural and functional bases of the compensation of functions in the case of spinal cord trauma --- Russian book
23 p3494 A83-47099

COMPENSATORS

Digital stochastic iterative procedures for the adaptive adjustment of noise compensation systems - Analysis of convergence and convergence rate
01 p0031 A83-10412
An analysis of the efficiency of a noise self-compensator with correlation feedback with respect to the suppression coefficient
04 p0470 A83-15143
Feedback representation of precompensators
06 p0803 A83-19387
Pole assignment and minimal feedback design
06 p0803 A83-19388
Dynamic output feedback controller
08 p1158 A83-23019
Optimal control of flexible structures
09 p1217 A83-24755
Simultaneous design of control systems
09 p1332 A83-24781
Multivariable system compensation
[ASME PAPER 82-WA/DSC-19] 10 p1462 A83-25682
On the compensation in linear feedback control systems - Transfer functions attainable by realizable linear compensation
10 p1464 A83-26519
Minimum variance control harnessed for non-minimum-phase plants
10 p1467 A83-26553
Compensation for the static and dynamic thermal effects on quartz oscillators
13 p1836 A83-31174
Design of unity feedback systems to achieve arbitrary denominator matrix
14 p2077 A83-33449
Generic pole assignment using dynamic output feedback
15 p2221 A83-35112
Design and adjustment of polarization compensators for coudoptics of stellar telescopes
16 p2423 A83-35686
A synthesis theory for a class of saturating systems --- in feedback control
17 p2570 A83-38821
The design of automatic compensators
18 p2677 A83-40091
Output feedback pole assignment under system variation --- with CH-46 example
21 p3195 A83-44948
An alternative view of the optimal output feedback compensator problem
21 p3195 A83-45106
Suboptimal stochastic control with compensators of reduced size for discrete-time non-stationary systems [ONERA, TP NO. 1983-57] 23 p3501 A83-48179

COMPENSATION TRACKING

Nonlinear filter for pilot's remnant attenuation
09 p1209 A83-24436
Cognitive task performance time during tracking
10 p1457 A83-26333
The identification of subjective evaluations of the interaction of a human operator and technical facilities
14 p2072 A83-32954
Digital homing guidance - Stability vs. performance trade-offs
[AIAA PAPER 83-2167] 19 p2795 A83-41663
On the problem of manual control. I
20 p3036 A83-43504

COMPILATION (COMPUTERS)

U COMPILERS

COMPILER PROGRAMS

U COMPILERS

COMPILERS

An Atlas implementation for the '80s
01 p0091 A83-10740
An Automated Verification System for JOVIAL J73
01 p0089 A83-11166
Compiler validations - A tutorial and some observations
01 p0089 A83-11167
HOML compiler - High Order Microcode Language
01 p0092 A83-11194
A general precompiler for algebraic manipulation
12 p1768 A83-29110
VLSI: Silicon compilation and the art of automatic microchip design --- Book
19 p2841 A83-41873
COMPLEMENTARY METAL OXIDE SEMICONDUCTORS
U CMOS
COMPLEMENTS (MATHEMATICS)
Elastic-plastic boundary element analysis as a linear complementarity problem
11 p1593 A83-27774
Sets of complementary sequences
23 p3502 A83-48711

COMPLETENESS

Completeness of derivatives of squared Schroedinger eigenfunctions and explicit solutions of the linearized KdV equation
17 p2572 A83-38464

COMPLEX COMPOUNDS

Electrochemically modified electrodes - Poly(2-methyl-8-quinolinol/ and poly(8-quinolinol/ complexing films obtained by electropolymerizing substituted phenols: Their voltammetric and electrical properties in relation to their geometric structure
07 p0881 A83-20583

COMPLEX NUMBERS

A simple approach to the error analysis of division-free numerical algorithms
15 p2217 A83-33904
The use of hypercomplex numbers in the algorithms for the operation of a strapdown inertial navigation system
21 p3097 A83-44637

COMPLEX SYSTEMS

Gigabit logic - A review
01 p0035 A83-10293
Testing of complex ECM systems
01 p0057 A83-10746
Feedback control of linear multivariable systems with uncertain description in the frequency domain
02 p0230 A83-12550
Matrix analysis of mildly nonlinear, multiple-input, multiple-output systems with memory
04 p0474 A83-16322
A one-dimensional logarithmic criterion for the evaluation of multiparametric systems
06 p0803 A83-19176
Irreducible divisors of lambda-matrices and their applications to multivariable control systems
06 p0803 A83-19386
An algorithm for identifying multi-input, multi-output linear dynamical systems based on the maximum likelihood method
06 p0804 A83-19568
Determination of the probability of the disruption of tracking in multidimensional radio tracking systems
07 p0915 A83-20878
Controlling the complexity of menu networks
07 p0983 A83-21041
Optimization and filtering of linear systems of finite dimension by hierarchical calculation --- French thesis
08 p1156 A83-22089
Multicriterial estimation in the synthesis of means for information interaction in complex systems --- cockpit display optimization
08 p1156 A83-22125
Method of designing a program module for the simulation of complex dynamic systems on a hybrid computer --- for flight simulation
08 p1154 A83-22184
An analytic method for uncertainty analysis of nonlinear output functions, with applications to fault-tree analysis
08 p1160 A83-22710
Application of multivariable systems theory; Symposium, Plymouth, England, October 26-28, 1982, Collected Papers
08 p1158 A83-23171
Separability and estimation of parameters in identification of complex static systems
09 p1326 A83-23977
Systems and operations - Living with complexity and growth
09 p1213 A83-24357
Model reference adaptive control of large structural systems
09 p1327 A83-24433
Adaptive parameter estimation of large-scale systems by reduced-order modeling
09 p1327 A83-24710
Minimal Padé model reduction of multivariable systems
09 p1330 A83-24748
The Total Synthesis Problem of linear multivariable control. II - Unity feedback and the design morphism
09 p1332 A83-24782
A new design for decentralized control with output feedbacks
09 p1334 A83-24802
An algorithm for computing singular values of large matrices for use in the analysis of large systems
09 p1335 A83-24816
Identification of high dimensional system by the general parameter method
10 p1466 A83-26534

Control science and technology for the progress of society; Proceedings of the Eighth Triennial World Congress, Kyoto, Japan, August 24-28, 1981. Volume 2 - Stochastic and large systems
10 p1466 A83-26539

Fuzzy-probabilistic algorithms in identification of fuzzy systems
10 p1466 A83-26541
Two approaches for adaptive observer in multi-output systems
10 p1468 A83-26563
Scalar output feedback in linear multivariable systems
10 p1469 A83-26568
Perfect and subperfect regulation in linear multivariable control systems
10 p1469 A83-26569
Chained aggregation - A geometric analysis --- of large scale systems
10 p1469 A83-26576
Model of a process of the design of complex systems and a method for its paralleling
12 p1769 A83-29349

Scientific foundations of advanced technology --- Russian book on production engineering techniques
13 p1826 A83-30525

Suboptimal control of large-scale mechanical systems
13 p1910 A83-30650

A graph-theoretic algorithm for hierarchical decomposition of dynamic systems with applications to estimation and control
13 p1911 A83-31071
Tradeoffs in level of automation in large-scale computerized test systems
13 p1861 A83-31190
Reliability of redundant systems
13 p1863 A83-31498

Dynamic modeling of structures from measured complex modes
14 p2033 A83-32988
New computer architectures tackle bottleneck --- processor-memory link bypass
14 p2073 A83-33141
Control of locally testable duplex system for large-scale implementation
15 p2218 A83-34524

A new method for failure detection and location in complex dynamic systems
17 p2565 A83-37094
I-O stability analysis of multiple nonlinear-multivariable systems
17 p2567 A83-37119
Quadratic weight adjustment for the enhancement of feedback properties
17 p2568 A83-37138
Fuzzy set theory for improving and evaluating reliability of complex systems
17 p2518 A83-37767

The immersion under feedback of a multidimensional discrete-time non-linear system into a linear system
17 p2570 A83-38823
Estimation of the life cycle costs of complex technical systems
18 p2752 A83-39990
Priority setting in complex problems
19 p2907 A83-41302

Sensitivity synthesis of systems subject to large parameter variations
19 p2890 A83-41480
Identification of submodels of multi-input, multi-output systems
19 p2890 A83-41485
A square-root algorithm for the adaptive control of multivariate systems
19 p2891 A83-41573

Sufficient conditions for the decomposability of control problems
19 p2893 A83-42006
Experimental analysis of methods for determining psychological factors of the complexity of solution of control problems
20 p3035 A83-43507
Infinite-valued logic in problems of cybernetics --- Russian book
21 p3192 A83-43910

On the status of stability of interconnected systems
21 p3198 A83-44098
Principles for synthesizing the structure of complex systems --- Russian book
21 p3195 A83-45021
Multivariable feedback: A quasi-classical approach --- Book
21 p3195 A83-45100
Modelling of a multivariable system on the basis of frequency data
22 p3351 A83-45979

State-feedback decomposition of multivariable systems via block-pole placement
22 p3351 A83-46367
The use of structural properties in linear multivariable control system design --- Thesis
22 p3352 A83-46690
What is synergetics? --- self-organization in multicomponent systems
23 p3505 A83-48548

Extended discrete-time multivariable adaptive control using long-term predictor
23 p3502 A83-48644
Multiplex control systems - Stochastic stability and dynamic reliability
23 p3502 A83-48645
The absolute stability of systems with several nonlinearities
24 p3620 A83-49549
Block decompositions and block modal controls of multivariable control systems
24 p3621 A83-49920

COMPLEX VARIABLES

NT ANALYTIC FUNCTIONS

NT BESSEL FUNCTIONS

NT CAUCHY INTEGRAL FORMULA

NT CONFORMAL MAPPING

NT CONJUGATES

NT ELLIPTIC FUNCTIONS

NT ENTIRE FUNCTIONS

NT EXPONENTIAL FUNCTIONS

NT GAMMA FUNCTION
 NT HANKEL FUNCTIONS
 NT HARMONIC FUNCTIONS
 NT HYPERBOLIC FUNCTIONS
 NT HYPERGEOMETRIC FUNCTIONS
 NT LAGUERRE FUNCTIONS
 NT LEGENDRE FUNCTIONS
 NT LIOUVILLE THEOREM
 NT LOGARITHMS
 NT MATHIEU FUNCTION
 NT MEROMORPHIC FUNCTIONS
 NT NAKED SINGULARITIES
 NT ORTHOGONAL FUNCTIONS
 NT RATIONAL FUNCTIONS
 NT SCHWARZ-CHRISTOFFEL TRANSFORMATION
 NT SINGULARITY (MATHEMATICS)
 NT SPHERICAL HARMONICS

A new method for simultaneous complex addition and subtraction --- of two input optical signals with holographic grating 05 p0646 A83-17890
 Generalised root iterations for the simultaneous determination of multiple complex zeros 06 p0804 A83-18072

Calculation of complex Fourier coefficients using natural splines 06 p0804 A83-18898
 Enforcing irreducibility for phase retrieval in two dimensions 07 p0930 A83-20795

Complex eigenfrequencies of axisymmetric perfectly conducting bodies - Radar spectroscopy 07 p0916 A83-21544
 Complex-frequency poles and creeping-wave transients in electromagnetic-wave scattering 07 p0916 A83-21545

Complex eigenvalue bounds in magnetoatmospheric shear flow. II 09 p1359 A83-24128
 A complex gradient operator and its application in adaptive array theory 11 p1554 A83-27902

The KS-transformation in hypercomplex form 12 p1786 A83-29103
 Frequency-domain identification of transmission-zero locations of linear multivariable plants 12 p1769 A83-29469

Computation of Faber series with application to numerical polynomial approximation in the complex plane 13 p1912 A83-31364

On the complex resonant frequency of open dielectric resonators 14 p2008 A83-33458
 Painleve property of anharmonic systems with an external periodic field 15 p2225 A83-34135

A complex amplitude detector for radiofrequency signals analysis 21 p3127 A83-45418
 Sets of complementary sequences 23 p3502 A83-48711

COMPLEXITY

NT TASK COMPLEXITY

A stable solution to the Wiener-Hopf equation in the frequency domain on the basis of the complexity principle 05 p0681 A83-17659

The evaluation of the complexity of digital filters 08 p1156 A83-21647

COMPLIANCE (ELASTICITY)

U MODULUS OF ELASTICITY

COMPLICATION

U COMPLEXITY

COMPONENT RELIABILITY

The reliability and testing of radio components and parts --- Russian book 01 p0037 A83-10671

High voltage equipment parts evaluation tests --- for airborne power supplies 01 p0042 A83-11204
 Maintenance policies for equipments with planned interrupted operation 02 p0188 A83-12655

Reliability assessment and techniques 02 p0188 A83-12656
 Life development of components/systems of aircraft 02 p0188 A83-12657

Reliability model for planetary gear trains [ASME PAPER 82-DET-81] 02 p0187 A83-12777

The effect of electronically active defects on the characteristics and the reliability of MOS structures --- French thesis 03 p0311 A83-13804

Cast transage 175 titanium alloy for durability critical structural components 04 p0458 A83-15318

Allowance for the mutual influence of factors in the analysis of reliability 04 p0494 A83-15918

Preventing the strength failure of machines by vibrodiagnostic techniques. I 06 p0770 A83-19313

Preventing the strength failure of machines by vibrodiagnostic methods. II - The use of vibrodiagnostics for preventing the failure of certain parts and assemblies of gas-turbine engines 06 p0770 A83-19314

Moisture induced stress in potted magnetic components 07 p0920 A83-20472

Techniques for assessing product reliability in polymeric materials used in aerospace electronic circuitry 09 p1236 A83-23604

Component identification using ultrasonic signature analysis 09 p1275 A83-23923

Radiation effects in microelectronics for space instruments 09 p1254 A83-24106

Radiation induced soft fails in space electronics 13 p1812 A83-30185

Random vibration effects on piece part applications 13 p1835 A83-30863

GPS test experience under MIL-STD-1540 guidelines 13 p1810 A83-31181

Card level acceptance testing 13 p1861 A83-31183

An in-depth evaluation of mission profile testing: Environmental engineering aspects - Reliability engineering aspects 13 p1864 A83-31510

Temperature readjustment factors for application to MIL-HDBK-217C failure rates --- electronic equipment reliability prediction 13 p1837 A83-31516

Production sequence screening - A candidate for EVOP? --- Evolutionary Operations for electronic component quality control 13 p1864 A83-31517

Reliability testing for GW systems 16 p2363 A83-35500

Component life reduction due to use of AVGAS in gas turbine engines 16 p2305 A83-35869

Life estimation methods of gas turbine rotating components 16 p2305 A83-35870

An experimental investigation of fatigue reliability laws 17 p2523 A83-38398

Method for a reliability study on photovoltaic modules Application for the qualification of cells and modules 18 p2710 A83-40528

Photovoltaic module control test specifications Specification 501 18 p2696 A83-40539

LHX system design for improved performance and affordability --- Light Helicopter 19 p2797 A83-41080

Reliability considerations in the placement of control system components [AIAA PAPER 83-2260] 19 p2816 A83-41730

Availability as a function of usage profile [AIAA PAPER 83-2287] 19 p2855 A83-41747

Autonomy and fault tolerant design --- for satellite system and components [AAS PAPER 83-044] 21 p3104 A83-44171

PAVE PILLAR - A new road to avionics reliability 23 p3401 A83-48643

COMPOSITE FUNCTIONS

Vector quantiser of video signals 04 p0527 A83-15238

A sequence of E-type composite analytical solutions of the Lane-Emden equation --- for polytropic stellar models 13 p1945 A83-30367

COMPOSITE MATERIALS

NT ALUMINUM BORON COMPOSITES

NT ALUMINUM GRAPHITE COMPOSITES

NT BORON REINFORCED MATERIALS

NT BORON-EPOXY COMPOUNDS

NT CARBON FIBER REINFORCED PLASTICS

NT CARBON-CARBON COMPOSITES

NT CERAMIC MATRIX COMPOSITES

NT CERMETS

NT COMPOSITE PROPELLANTS

NT EPOXY MATRIX COMPOSITES

NT EUTECTIC COMPOSITES

NT FIBER COMPOSITES

NT FIBER REINFORCED COMPOSITES

NT GLASS FIBER REINFORCED PLASTICS

NT GLASSY CARBON

NT GRAPHITE-EPOXY COMPOSITES

NT GRAPHITE-POLYIMIDE COMPOSITES

NT LAMINATES

NT METAL MATRIX COMPOSITES

NT POLYMER MATRIX COMPOSITES

NT REINFORCED PLASTICS

NT RESIN MATRIX COMPOSITES

NT THREE DIMENSIONAL COMPOSITES

NT WHISKER COMPOSITES

The viscoelastic constitutive modelling of adhesives 01 p0027 A83-10242

On composites with periodic structure 01 p0058 A83-10283

Approximate analysis of postbuckled through-width delaminations 02 p0191 A83-12061

Fatigue life prediction on the basis of the characteristic parameters of the loading process 02 p0156 A83-12328

Long-term strength of composite compacts under programmed uniaxial tension-compression. I - A comparative analysis of some accumulated damage hypotheses. II - Modification of a hereditary long-term strength criterion 02 p0192 A83-12355

Multicriterion design of thin-walled structural elements of composite materials 02 p0192 A83-12362

A study of the stress-strain state of composites with disperse reinforcement using speckle holographic interferometry 02 p0178 A83-12370

Composites with periodic microstructure 02 p0150 A83-12734

Boundary value problems of composite media 02 p0233 A83-12763

Mass transport of molten metals in sintered composites based on titanium carbide 02 p0150 A83-12947

The impact of composite technology on commercial transport aircraft 02 p0135 A83-12969

The Canadair challenger advanced composite material program 02 p0151 A83-12971

Composite fan exit guide vanes for high bypass ratio gas turbine engines 03 p0282 A83-13159

Wear and friction of high-temperature self-lubricating composites [ASLE PREPRINT 82-LC-2B-2] 03 p0334 A83-13234

Stiffness and strength behaviour of woven fabric composites 03 p0291 A83-13685

Microstructure of Si3N4-TiN composites prepared by chemical-vapour deposition 03 p0291 A83-13687

Pressure enhancement by conically convergent shocks in composite cylinders and its application to shock recovery experiments 03 p0304 A83-13913

The fracture mechanics of composite materials under axial compression - Brittle fracture 03 p0291 A83-14064

A simple approach to determination of stiffness characteristics of unidirectional composites 03 p0291 A83-14491

Damage in composite materials: Basic mechanisms, accumulation, tolerance, and characterization --- Book 03 p0292 A83-14551

Toward the nondestructive characterization of fatigue damage in composite materials 03 p0292 A83-14552

What is fatigue damage 03 p0342 A83-14565

Thermoelastic moduli of fiber-reinforced composites by differential scheme 04 p0494 A83-14975

One-dimensional finite element analysis of thermal ablation with pyrolysis 04 p0475 A83-15014

Comparison of elasticity, shell core, and sandwich shell theories 04 p0496 A83-15291

Design for global damage tolerance and associated mass penalties 04 p0496 A83-15321

Stress function interface and boundary conditions in anisotropic materials [ASME PAPER 82-WA/APM-4] 04 p0498 A83-15685

A bimodulus elasticity theory --- Russian book 04 p0499 A83-15833

Reinforced plastics/composites adhesives and thermosets; Proceedings of the Sixth Annual Pacific Technical Conference and Displays, Los Angeles, CA, August 25-27, 1981 04 p0454 A83-16176

EMI shielding today with conductive plastics 04 p0464 A83-16179

Helicopter technology for the 1990s 04 p0446 A83-16372

The thermal-stress state of a two-temperature half-space with a periodically varying surface-temperature 04 p0502 A83-16403

The asymptotics of the averaged characteristics of periodic elastic media with strongly varying properties 04 p0456 A83-16411

Material effects on the dynamic stability of a flexible skirted air cushion [AIAA PAPER 83-0369] 05 p0692 A83-16675

The construction of ten-foot long composite space tubes [AIAA PAPER 83-0644] 05 p0653 A83-16811

Japan Congress on Materials Research, 25th, Tokyo, Japan, October 1981, Proceedings 05 p0610 A83-17086

Effects of hole curvature on transient hygrothermal stresses in plates with a hole / moisture and temperature coupling effects/ 05 p0611 A83-17107

Studies of aerofoils and blade tips for helicopters 05 p0589 A83-17317

Wave propagation in linear viscoelastic composites modelled as interpenetrating solid continua 05 p0654 A83-17323

Piezoelectric composites with 3-1 connectivity and a foamed polyurethane matrix 06 p0734 A83-17956

Evolution of the application of composite materials to helicopters 06 p0716 A83-18376

Composite technology in the UK helicopter industry 06 p0716 A83-18377

A study of the deformation and fracture of structural elements of composite materials by speckle-holographic interferometry 06 p0775 A83-18513

A resonance-type machine for studying the fatigue properties of composite materials 06 p0762 A83-18518

On one-dimensional acceleration waves in composite materials modeled as interpenetrating solid continua
06 p0776 A83-19000

The compaction characteristics of solid-lubricant composites
07 p0874 A83-19965

Computer simulation of the fracture of composite materials with various degrees of physicochemical interaction between the components
07 p0874 A83-19971

Averaging of a system of elasticity theory with almost-periodic coefficients
07 p0945 A83-20141

National SAMPE Symposium and Exhibition, 27th, San Diego, CA, May 4-6, 1982, Proceedings
07 p0874 A83-20426

Composite drapability - A too often ignored impacting cost characteristic
07 p0875 A83-20438

The development of advanced composite front fuselage technology
07 p0865 A83-20464

High performance, low viscosity resin systems
07 p0899 A83-20465

Polyimide composites - Grumman application case histories
07 p0876 A83-20475

Mold treatments and part removal methods for composites
07 p0876 A83-20482

Progress report - Large sprayed metal composite tooling
07 p0876 A83-20483

Advanced composite materials in aerobatic aircraft
07 p0865 A83-20496

A study of the structural strength and ductility of nickel screens --- for aircraft hydraulic system filters
07 p0940 A83-20910

An instrument for studying the thermophysical properties of solids at low temperatures
07 p0931 A83-20961

The relationship of compliance changes during fatigue loading to the fracture of composite materials
08 p1054 A83-21682

Central ductile crack in an orthotropic strip of finite width
08 p1120 A83-21818

Discussion on criteria for crack initiation in the immediate vicinity of the sharp edges of dispersed inclusions
08 p1121 A83-21824

Design, analyses, and model tests of an aeroelastically tailored lifting surface
08 p1044 A83-22155

Annual Conference on Composites and Advanced Ceramic Materials, 6th, Cocoa Beach, FL, January 17-21, 1982, Proceedings
08 p1071 A83-22251

Solar receiver cavity insulation evaluation
08 p1130 A83-22275

Dynamic /transient/ analysis of layered anisotropic composite-material plates
08 p1123 A83-22944

Material and process advances '82; Proceedings of the Fourteenth National SAMPE Technical Conference, Atlanta, GA, October 12-14, 1982
09 p1220 A83-23601

Fabrication of aircraft components using prepried broadgoods layed-up in the flat and subsequently formed - Cost benefits and resource utilization enhancements
09 p1195 A83-23602

Penthrite in castable composite explosives
09 p1242 A83-23847

Fracture of composite materials; Proceedings of the Second USA-USSR Symposium, Lehigh University, Bethlehem, PA, March 9-12, 1981
09 p1222 A83-23926

Tight bounds for the probability distribution of the strength of composites
09 p1222 A83-23928

Two approaches in fracture mechanics of composites
09 p1222 A83-23929

Some peculiarities of fracture in heterogeneous materials
09 p1223 A83-23932

Physical principles of prediction of heterogeneous material fracture
09 p1279 A83-23933

Influence of stress interaction on the behavior of off-axis unidirectional composites
09 p1223 A83-23934

A theory of viscoelastic composites modeled as interpenetrating solid continua with memory
09 p1280 A83-24136

Determination of the temperature dependence of the heat conductivity coefficient of a composite material from the data of a nonstationary experiment
09 p1224 A83-24233

Optimally discretized finite elements for boundary-layer stresses in composite laminates
09 p1281 A83-24671

Geometrically nonlinear transient analysis of laminated composite plates
09 p1281 A83-24672

Composite engine inlet particle separator swirl frame --- CAD for T700 helicopter engine centrifugal filter
09 p1208 A83-24841

Plasma- and vacuum-plasma-sprayed Cr3C2 composite coatings
10 p1400 A83-25531

Impact-resistant transparencies for marine service --- windscreens for aircraft
[ASME PAPER 82-WA/OCE-4]
10 p1400 A83-25686

Noise transmission characteristics of advanced composite structural materials
[AIAA PAPER 83-0694]
10 p1473 A83-25915

Composite materials - Some recent developments
10 p1389 A83-26122

Axisymmetric problem of a flat interface annular crack between an elastic layer and a half-space
10 p1440 A83-26424

The interface crack behavior in dissimilar anisotropic composites under mixed-mode loading
[ASME PAPER 83-APM-7]
10 p1441 A83-26444

Deformation work density fracture criterion for composite materials
10 p1442 A83-26771

A Monte Carlo simulation of the strength of laminated hybrid composites
10 p1389 A83-26965

Recent advances in composite flywheel containment design technology
11 p1589 A83-27302

Twin disk composite flywheel
11 p1609 A83-27304

Composite salt/ceramic media for thermal energy storage applications
11 p1610 A83-27319

On the nature of stress singularities in anisotropic layered composites
11 p1592 A83-27437

Nonlinear viscoelastic material behavior including void and tear generation
11 p1592 A83-27440

In-plane thermal expansion and thermal bending coefficients of fabric composites
11 p1592 A83-27444

On linear thermoelasticity of composite materials
11 p1595 A83-28422

The theoretical principles underlying composite materials with a disordered structure
11 p1544 A83-28451

Thermoelastic stress analysis of anisotropic composite sandwich plates by finite element method
11 p1599 A83-28721

The manufacture of sintered products --- Russian book
12 p1732 A83-28812

Digital nondestructive evaluation of composite materials
12 p1710 A83-29592

Delamination-based compression residual-strength prediction model for composites
[AIAA 83-0872]
12 p1738 A83-29756

A building block approach to design verification testing of primary composite structure
[AIAA 83-0947]
12 p1739 A83-29775

Statistical modeling of ballistic damage and residual strength in composite structures
[AIAA 83-1002]
12 p1711 A83-29790

Use of composite materials in NASTRAN
[AIAA 83-1004]
12 p1740 A83-29792

Design, analysis and test of composite curved frames for helicopter fuselage structure
[AIAA 83-1005]
12 p1741 A83-29805

Nonlinear analysis of composite circular plates
[AIAA 83-1036]
12 p1745 A83-29881

Comparison of frequency determination techniques for cantilevered plates with bending-torsion coupling
[AIAA 83-0953]
12 p1745 A83-29885

The elastic characteristics of unidirectionally reinforced hybrid composites
13 p1815 A83-30052

Allowing for temperature in descriptions of the delayed fracture of inelastic materials
13 p1865 A83-30056

The finite-element method in solutions of boundary value problems for anisotropic plates of composite materials. I
Refined theories for anisotropic plates and finite-element approximations
13 p1866 A83-30059

Nondestructive testing of composites
13 p1862 A83-31192

Evolution of new materials for space applications
[AIAA PAPER 83-0792]
14 p1985 A83-32794

Influence of quality control variables on failure of graphite/epoxy under extreme moisture conditions
14 p1987 A83-33125

Charring ablation by finite element
15 p2159 A83-34237

The determination of hygrothermal stress development in anisotropic composites
15 p2175 A83-34239

A variable power singular element for analysis of fracture mechanics problems
15 p2176 A83-34321

Elastic composites
16 p2364 A83-35505

The topological aspects of the statistical theory of composite strength
16 p2364 A83-35507

An analysis of the load-bearing capacity of thin-walled tubular rods of composite materials
16 p2364 A83-35511

Standard failure criteria needed for advanced composites
16 p2324 A83-35771

Microstructure of in-situ composites
16 p2324 A83-35999

Creep-fatigue-effects in composites
16 p2324 A83-36172

Demonstration of the feasibility of an all-composite space motor
[AIAA PAPER 83-1185]
16 p2318 A83-36264

Effective macroscopic description for heat conduction in periodic composites
16 p2353 A83-36593

Encyclopedia of composite materials and components --- Book
17 p2483 A83-37166

Percentiles of pooled estimates of Weibull parameters
17 p2517 A83-37294

Composite materials and deployable boom technology [SAE PAPER 821395]
17 p2480 A83-37970

Stress intensity factors for radial cracks in bimaterial media
17 p2523 A83-38391

Sudden twisting of partially bonded cylindrical rods
17 p2523 A83-38392

Energy criteria for the brittle fracture of composite materials with initial stresses
17 p2523 A83-38503

Optical properties of oxide glasses containing nickel microgranules
18 p2649 A83-39060

Diffusion in composite layers with automatic solution of the eigenvalue problem
18 p2684 A83-39848

Resonance effects and the ultrasonic effective properties of particulate composites
18 p2741 A83-39974

Secondary loading of I-spar caps due to shear deformation of the web
18 p2700 A83-39991

An experimental study of the thermal cycling of composite materials with disperse reinforcement
18 p2649 A83-40104

Estimation of the dimensions of growing cracks and relaxation regions from acoustic signal parameters
18 p2701 A83-40109

The effect of proton-electron irradiation on the properties of composites with disperse reinforcement
18 p2650 A83-40111

Quasi-homogeneous states in composite materials with small-scale bends in the structure
18 p2701 A83-40112

Love surface waves in regularly layered isotropic composites
18 p2701 A83-40113

Progress in science and engineering of composites; Proceedings of the Fourth International Conference on Composite Materials, Tokyo, Japan, October 25-28, 1982, Volumes 1 & 2
18 p2650 A83-40126

Composites in Japan
18 p2650 A83-40127

Composite materials in aircraft structures
18 p2650 A83-40130

ACM reinforcement fiber production and its application in Japan
18 p2650 A83-40132

Three-dimensional interlaminar stress distribution in symmetric composite laminate
18 p2702 A83-40148

Fracture analysis of composite materials
18 p2704 A83-40195

On the thermoviscoelastic characterization of adhesives and composites
18 p2705 A83-40207

Application of the finite element method to determine the moisture content of composites under transient conditions
18 p2656 A83-40226

Statistical aspects of heterogeneous materials
18 p2657 A83-40235

Hybrid composite application to the Boeing 767 wing/body fairing
18 p2640 A83-40244

The next step in getting the composite story right
Industrialisation of manufacturing systems
18 p2752 A83-40277

Composites molding - Separation and removal of parts from molds
18 p2661 A83-40279

Flow state of composite materials in the forging die during the molding process
18 p2661 A83-40281

From outer space to the great ocean's depths - An adventure in high performance composite materials
18 p2661 A83-40288

Composite flywheel rotor containment
18 p2709 A83-40294

'82 update - Composite manufacturing technology
18 p2662 A83-40298

Titanium-steel interaction under production and operation temperatures
18 p2667 A83-40299

Advanced composites for advanced aircraft
18 p2662 A83-40342

Silicon carbide yarn stimulates development of new composites
19 p2819 A83-41034

A singular approximation in the theory of elastoplastic media with microstructures
19 p2858 A83-41218

Service life characteristics of the composite material KAS-1A
19 p2820 A83-41601

Theory of the vibrations of composite materials with small-scale distortions in the structure
19 p2860 A83-42060

Crack deceleration and arrest phenomena at an oblique bimaterial interface
20 p3001 A83-42518

Design, fabrication, and qualification of composite carbon/epoxy horizontal stabilizer components
20 p2927 A83-42546

Battle damage and repair of an advanced composite A-7 outer wing
20 p2927 A83-42547

On the application of an integral equation method for the solution of heat transfer problems in heterogeneous and cellular media
20 p2971 A83-42664

Surface integral numerical solution for general steady heat conduction in composite media 20 p2971 A83-42666

A differential scheme for multiphase composites. I - Overall elastic moduli. II - Thermal expansion coefficients and conductivities 20 p3002 A83-42800

A comparison of exact and model solutions for the initiation of debond fracture 20 p3004 A83-42973

Boundary integral equations applied in the characterization of elastic materials 20 p3006 A83-42995

Interfacial matrix stresses in composites due to misfitting cylindrical constituents 20 p3007 A83-43144

Energy absorption of composite materials 20 p2948 A83-43148

Matrix alloys for composite materials based on aluminum, magnesium, and titanium 20 p2948 A83-43498

Appliance for fatigue tests of materials with symmetrical and asymmetrical loading 20 p2992 A83-43624

Design-to-cost in the application of advanced composite technology [SAWE PAPER 1480] 20 p3056 A83-43749

Advanced material application on the European wide body transport aircraft Airbus [SAWE PAPER 1484] 20 p2935 A83-43751

Application of finite element analysis techniques to the derivation of advanced composite structure weight [SAWE PAPER 1490] 20 p3009 A83-43757

A differential scheme for multiphase composites 21 p3105 A83-44044

Pin joints in composites 21 p3151 A83-44053

Nondestructive evaluation of composite materials - A philosophy, an approach, and an example 21 p3149 A83-45069

Improved moire interferometry and applications in fracture mechanics, residual stress and damaged composites 21 p3160 A83-45144

Moire interferometry for damage analysis of composites 21 p3108 A83-45148

A strain-gage transducer for measuring strains in composite materials 21 p3141 A83-45150

The Iosipescu shear test as applied to composite materials 21 p3108 A83-45170

Torsional impact response of a penny-shaped crack lying on a bimaterial interface 21 p3162 A83-45188

An elasticity relationship for an anisotropic body whose deformation characteristics depend on the type of stressed state --- for composite materials 21 p3108 A83-45360

The role of the polymeric matrix in the processing and structural properties of composite materials; Proceedings of the Joint U.S.-Italy Symposium on Composite Materials, Capri, Italy, June 15-19, 1981 22 p3262 A83-46279

Control of composite cure processes 22 p3262 A83-46284

A preliminary study of composite reaction injection molding 22 p3263 A83-46287

Reinforced polyester structural foam 22 p3264 A83-46300

In situ analysis of the interface --- of composites 22 p3264 A83-46303

Design impact of composites on fighter aircraft. I - They force a fresh look at the design process 22 p3254 A83-46347

Safe structures for future aircraft 22 p3254 A83-46350

Analysis of composite materials - A survey 23 p3427 A83-47589

Stress analysis of stepped-lap joints with bondline flaws 23 p3471 A83-48214

Depot level repairability, maintainability, and supportability of advanced composites [AIAA PAPER 83-2516] 23 p3404 A83-48360

An experimental study of the stress-strain state of three-layer shells made of high-modulus anisotropic composite materials 23 p3428 A83-48437

Delamination of composites under compression 23 p3472 A83-48467

Crack transient torsional wave interaction in an elastic bi-material 24 p3591 A83-48870

Impact of composites on fighter aircraft. II - Composites New look to the aircraft production line 24 p3543 A83-48889

The electroconductivity of composites with binary fillers containing high-conductivity components 24 p3553 A83-49054

Developments in UK rotor blade technology [AIAA PAPER 83-2525] 24 p3579 A83-49589

Thermochemical ablation of the glass-graphite surface of a blunt cone at the spreading line in a three-dimensional boundary layer 24 p3579 A83-49662

A study of the deformation properties of an isotropic carbon material at elevated temperatures 24 p3554 A83-49666

A photoelectric scanning system, OSS-50-1300, for measuring thermal deformations in specimens of degradable composites 24 p3585 A83-49918

SH waves in composite media under initial stresses 24 p3597 A83-50134

Applications of mass spectrometry techniques to autoclave curing of materials 24 p3559 A83-50143

COMPOSITE PROPELLANTS

Parametric study of acceleration effects on burning rates of metallized solid propellants 02 p0161 A83-13084

An improved model for the combustion of AP composite propellants 03 p0303 A83-13142

Combustion of condensed two-component systems with spatially separated components 03 p0294 A83-14052

Burning to detonation transition in porous beds of a high-energy propellant 03 p0303 A83-14846

The cook-off phenomenon of solid propellants 04 p0464 A83-15475

Effect of oxidizer particle size on burning rate and thermal decomposition of composite solid propellants 04 p0465 A83-16430

Combustion response to compositional fluctuations --- of composite solid propellants [AIAA PAPER 83-0476] 05 p0619 A83-16740

Theoretical and experimental nonlinear dynamics of heterogeneous deflagration waves 06 p0727 A83-19162

Erosive burning of composite solid propellants - Mechanism, correlation, and grain design applications [AIAA PAPER 81-1581] 07 p0902 A83-20418

Fine ammonium perchlorate manufacture by the use of the vibro-energy mill wet grinding process 09 p1240 A83-23830

Characterisation of NC/NG propellant pastes 09 p1241 A83-23835

Processing modifications for improved propellants - Coated oxidizers 09 p1241 A83-23838

Base-bleed solid propellants with thermoplastic elastomers as binders 09 p1241 A83-23839

A simple insulation method of end-burning composite propellant and its application to the motors loaded with high burning rate propellants 09 p1242 A83-23842

Phenomena of static electricity in fabrication and processing of solid propellants 09 p1242 A83-23843

Techniques in the formulation and handling of composite and very-low-density explosives 09 p1242 A83-23845

Non-steady burning in a randomly layered composite propellant [AIAA PAPER 83-0477] 09 p1220 A83-24148

Gas phase ignition of a composite solid propellant subjected to radiant heating 09 p1243 A83-24369

A pocket model for aluminum agglomeration in composite propellants 12 p1717 A83-28962

Some experiments on model composite solid propellants 13 p1826 A83-31675

Ignition of nitramine propellants under rapid pressurization [AIAA PAPER 83-1194] 16 p2339 A83-36270

Bonding agents for AP and nitramine/HTPB composite propellants [AIAA PAPER 83-1199] 16 p2340 A83-36275

Extruded composite propellant technology development [AIAA PAPER 83-1272] 16 p2340 A83-36318

The laser ignition of compact mixed compositions 18 p2663 A83-39171

Calculation of transient thermal stresses in solid rocket propellants [AIAA PAPER 82-1098] 18 p2673 A83-40020

Ignition of composite solid propellant at subatmospheric pressures 18 p2673 A83-40313

Projectile impact ignition characteristics of propellants. III - Effect of particle size and porosity 21 p3117 A83-44998

Experimental and theoretical burning of solid rocket propellants near the pressure deflagration limit [IAF PAPER 83-367] 23 p3439 A83-47360

Effect of erosive burning on pressure and temperature sensitivity --- of composite propellants [IAF PAPER 83-368] 23 p3439 A83-47361

Tetrachlorophthalocyanhydride based chloropolyesters for inhibition of double rocket propellants [IAF PAPER 83-370] 23 p3439 A83-47362

COMPOSITE STRUCTURES

NT LAMINATES

Sweep composite wing aeroelastic divergence experiments 01 p0009 A83-10193

Fracture of fatigue-loaded composite laminates 02 p0149 A83-12013

Survey of recent research in the analysis of composite plates 02 p0191 A83-12065

Fracture of thermoelectric reinforced shells from a probabilistic viewpoint 02 p0191 A83-12335

Dimensional information through industrial computerized tomography 03 p0337 A83-13435

Optimization procedure for material composition of composite material structures 06 p0724 A83-18231

Fatigue sensitivity of composite structure for fighter aircraft 06 p0717 A83-18402

The vibration of a multilayer cylindrical panel with anisotropic layers at large deflections 06 p0775 A83-18506

Stability and optimization of viscoelastic composite cylindrical shells under combined loading 06 p0775 A83-18507

The development of a precision composite spacecraft antenna reflector 07 p0920 A83-20463

Damage tolerance and reparability of advanced composite structures 07 p0876 A83-20484

Composites fabrication cost estimating technique /FACET/ - An automated estimating system 07 p0877 A83-20494

Computer-aided design of complex composite material systems and structures 07 p0877 A83-20498

Elevated temperature repairs of advanced composite structures 07 p0877 A83-20499

Instability of short stiffened composite cylindrical shells under bending with prebuckling displacements 08 p1121 A83-21891

Composite flywheels with rim and hub 08 p1073 A83-21992

Fabrication of bonded graphite/polyimide structures for advanced aerospace applications 09 p1210 A83-23636

Advanced composites structures at Hughes Helicopters, Inc 09 p1202 A83-23645

Accelerated aging studies of low density /hydrocarbon/ resin systems 09 p1222 A83-23646

Strength of layered composite cylindrical shells under dynamic loading 09 p1224 A83-23946

Strength of mechanically fastened composite joints 10 p1439 A83-25880

Energy absorption in composite tubes 10 p1439 A83-25883

Scattering cross sections for composite surfaces that cannot be treated as perturbed-physical optics problems 10 p1403 A83-26032

Stacbeam - An efficient, low-mass, sequentially deployable structure --- for satellite solar power 11 p1536 A83-27248

1982 advances in aerospace structures and materials; Proceedings of the Winter Annual Meeting, Phoenix, AZ, November 14-19, 1982 11 p1591 A83-27426

Geometrically nonlinear analysis of layered composite shells 11 p1591 A83-27431

Three-dimensional finite-element analysis of layered composite plates 11 p1591 A83-27432

General relations for exact and inexact involute bodies of revolution 11 p1592 A83-27446

Characterization of two nitrile-epoxy structural adhesives 12 p1716 A83-29550

Collapse analysis of cylindrical composite panels with cutouts [AIAA 83-0875] 12 p1738 A83-29759

Buckling behavior and imperfection sensitivity of composite panels [AIAA 83-0877] 12 p1739 A83-29761

Effect of stitching on the strength of bonded composite single lap joints [AIAA 83-0969] 12 p1739 A83-29779

The effect of acoustic-thermal environments on advanced composite fuselage panels [AIAA 83-0955] 12 p1744 A83-29857

A shell structure under the effect of pulsed loading 13 p1866 A83-30072

Repairing composite structures 13 p1803 A83-30074

Composite thin-foil bandpass filter for EUV astronomy Titanium-antimony-titanium 13 p1918 A83-30209

Optical properties of codeposited aluminum-silicon composite films 13 p1918 A83-30211

The stability of the plane bending mode of a composite rod with allowance for the initial irregularities 14 p2030 A83-32381

Certain relationships for operators constructed on the basis of the Green tensor of the equilibrium equation and their use in the theory of composites 15 p2178 A83-34442

An analytic description of the kinetics of fatigue cracks in laminated composites 15 p2180 A83-35041

Investigation of the load-carrying capacity and efficiency of thin-walled shells made of epoxy composites 17 p2521 A83-37560

The stability of composite sandwich shells with load-carrying layers of different stiffness under axial compression and external pressure 17 p2521 A83-37561

Interaction between a bonded stiffening rib and a composite plate 18 p2701 A83-40108

Adhesive bonding and composites 18 p2650 A83-40131

Tubular lap joints in composite cylindrical shells under external bending and shear 18 p2703 A83-40154

Unsymmetrically laminated composites
18 p2703 A83-40163

In-plane tensile strength of multidirectional composite laminates
18 p2653 A83-40173

Buckling of continuous filament composite isogrid panels
Theory and experiment
18 p2704 A83-40183

Compressive buckling of graphite-epoxy composite circular cylindrical shells
18 p2704 A83-40184

Stability optimization of laminated composite plates under in-plane loads
18 p2704 A83-40185

Coupling effect on axial compressive buckling of laminated composite cylindrical shells
18 p2704 A83-40187

Damage and fracture of tridirectional composites
18 p2704 A83-40194

Development of advanced composite fabrication for aerospace structures
18 p2661 A83-40278

Warping, a nightmare for composite parts producers
18 p2661 A83-40283

Design, analysis and testing of two concepts for a dimensional stable structure --- composite antenna tower for communication satellites
18 p2662 A83-40289

Fabrication and spin tests of composite flywheels
18 p2709 A83-40295

Computer assisted dielectric cure monitoring in material quality and cure process control
19 p2823 A83-41029

Undetectable critical defects in safety-of-flight structure
20 p2999 A83-42544

Application of logic-algebraic and numerical methods to multidimensional heat exchange problems in regions of complex geometry filled with uniform or composite media
20 p2971 A83-42668

Analysis of moisture gradients in service and in the laboratory --- in composite materials
20 p2947 A83-42803

Observations of severe in-flight environments on airplane composite structural components
20 p2933 A83-43330

Design, fabrication and test of a composite elevator
21 p3151 A83-44046

Approximate solution of problems concerning the deformation of nearly cylindrical composite bodies
21 p3154 A83-44721

Preparation of materials for composite photoelastic models
21 p3107 A83-45146

Composites in commercial aircraft
22 p3262 A83-46281

Design of continuous fiber composite structures
22 p3264 A83-46306

Consideration on the fatigue damage of specimens used for composite critical components qualification
22 p3305 A83-46307

Unresolved stress analysis problems in Kevlar composite pressure vessels --- helically wound solid rocket motor cases
22 p3305 A83-46308

A jointless and bearingless tail rotor of fiber-reinforced-composite construction
23 p3402 A83-47215

Application of composites and computer graphics in the design of the MH-53E fuel sponson
[AIAA PAPER 83-2441]
23 p3403 A83-48329

Design concepts for low cost composite engine frames
[AIAA PAPER 83-2445]
23 p3411 A83-48331

Frequency domain analysis of entropy generation through heat flow
24 p3575 A83-48908

COMPOSITE WRAPPING

A generalized model for the winding mechanics of polymer composite shells
02 p0187 A83-12363

A study of the stressed state of a helically reinforced composite in shear
03 p0343 A83-14740

Optimal cooling of cross-ply composite laminates and adhesive joints
[ASME PAPER 82-WA/APM-24]
04 p0455 A83-15679

Design and manufacture of composite tubes for compression applications
07 p0874 A83-20427

Reliability analysis of circumferentially wound FRP flywheels
07 p0950 A83-21625

Modeling the fracture of thin-walled structural elements of multidirectional layered composites
13 p1865 A83-30054

Tapewrapped phenolic composites reinforced with advanced carbon fabrics
18 p2657 A83-40231

COMPOSITES

U COMPOSITE MATERIALS

COMPOSITION (PROPERTY)

NT ATMOSPHERIC COMPOSITION

NT ATMOSPHERIC MOISTURE

NT ATOM CONCENTRATION

NT BODY COMPOSITION (BIOLOGY)

NT CARBON DIOXIDE CONCENTRATION

NT CHEMICAL COMPOSITION

NT CONCENTRATION (COMPOSITION)

NT GAS COMPOSITION

NT IONOSPHERIC COMPOSITION

NT LUNAR COMPOSITION

NT METEORITIC COMPOSITION

NT METEOROID CONCENTRATION

NT MOISTURE CONTENT

NT PLANETARY COMPOSITION

NT PLASMA COMPOSITION

The principles of the mathematical description and analysis of the composition of equilibrium chemical systems
11 p1546 A83-28198

A differential scheme for multiphase composites. I - Overall elastic moduli. II - Thermal expansion coefficients and conductivities
20 p3002 A83-42800

COMPRESSED AIR

Factors affecting storage of compressed air in solution mined salt cavities
11 p1609 A83-27311

Thermal energy storage media for advanced compressed air energy storage systems
11 p1609 A83-27312

Influence of atomizer design features on mean drop size
19 p2800 A83-40865

Air Storage System Energy Transfer (ASSET) plants
22 p3320 A83-46778

COMPRESSED GAS

NT HIGH PRESSURE OXYGEN

Dynamic equation of state of a gas with evaporating drops
04 p0544 A83-15445

The effect of forced and free convection in the discharge of a pressurized gas
08 p1090 A83-23210

Energy balance of solar absorption and vapor compression cooling systems
14 p2046 A83-32350

Three-dimensional turbulent boundary layers on bielliptic bodies in flows of a compressible gas at angle of attack
16 p2289 A83-35704

A numerical study of the instability of a tangential velocity discontinuity in compressible gases
16 p2350 A83-35716

Compression of spin-polarized hydrogen to high density
19 p2897 A83-40974

COMPRESSIBILITY

Processes in periodic media that cannot be described in terms of average characteristics
09 p1338 A83-24216

Finite difference modeling of rotor flows including wake effects
[ONERA, TP NO. 1982-114]
09 p1197 A83-24326

COMPRESSIBILITY EFFECTS

Compressibility effects on hydromagnetic surface waves --- in solar atmosphere
03 p0437 A83-14903

Effect of compressibility on the Rayleigh-Taylor instability
08 p1085 A83-22386

The development of intermittent turbulence on a swept attachment line including the effects of compressibility
11 p1567 A83-27872

Compressible Rayleigh-Taylor instability
13 p1840 A83-30111

Compressibility effects in turbulence modeling
13 p1841 A83-30637

Compressibility effects in turbulent shear layers
14 p2012 A83-32998

Radiation from circular symmetric sources in warm plasma column --- electromagnetic transmission in plasma media
17 p2495 A83-38537

A note on compressibility and energy cascade in turbulent molecular clouds
22 p3383 A83-47007

COMPRESSIBLE BOUNDARY LAYER

Performance of LDI in predicting density profiles of compressible boundary layers --- laser differential interferometry
01 p0053 A83-11078

Numerical simulation of turbulent flows in three-dimensional boundary layers
02 p0170 A83-11873

Compressible second-order boundary layers for three-dimensional stagnation point flows with mass transfer
02 p0170 A83-12049

Compressible boundary-layer flow at a three-dimensional stagnation point with massive blowing
03 p0322 A83-14672

Direct/inverse, compressible turbulent boundary-layer computations using a two-equation turbulence model
[AIAA PAPER 83-0453]
05 p0636 A83-16724

On the stability of boundary-layer flow over a spring-mounted piston
06 p0757 A83-19017

Compressible turbulent boundary layer in strong adverse pressure gradient
09 p1198 A83-24674

Influence of finite slot size on boundary layer with suction or injection
09 p1263 A83-24676

Numerical calculation of local convective heat transfer coefficients over air-cooled vane surfaces
10 p1418 A83-26772

Reduced first order differential equation with optimal control finite element penalty functions --- applied to convection-radiation heat transfer and boundary layer problems
12 p1721 A83-28853

Numerical simulation of a compressible turbulent boundary layer over a conductive wall with line heat source
15 p2157 A83-33865

Prediction of stagnation flow heat transfer on turbomachinery airfoils
[AIAA PAPER 83-1173]
16 p2294 A83-36259

An experimental study of surface curvature effects on a supersonic turbulent boundary layer
[AIAA PAPER 83-1672]
17 p2444 A83-37182

Numerical solutions of three-dimensional time-dependent compressible turbulent integral boundary-layer equations in general curvilinear coordinates
[AIAA PAPER 83-1674]
17 p2501 A83-37183

Self-similar solutions of the equations of a boundary layer on a moving surface
17 p2506 A83-37635

Similar velocity profiles of the compressible boundary layer over a rotating cylinder in an axial flow
18 p2681 A83-39349

The uniqueness of polynomials representing the integral quantities of a compressible boundary layer on a cylinder rotating in a flow
21 p3129 A83-44323

An inverse integral computational method for compressible turbulent boundary layers
22 p3250 A83-46479

Three-dimensional boundary-layer calculations in design aerodynamics
22 p3251 A83-47034

Turbulent boundary layers on three-dimensional configurations
22 p3286 A83-47035

The asymptotic solutions of compressible, nonsteady boundary layer
24 p3581 A83-50129

COMPRESSIBLE FLOW

NT TRANSONIC FLOW

Fundamentals of compressible flow --- Book
01 p0045 A83-10883

Models of solar differential rotation
02 p0271 A83-12977

Density measurement in compressible flows using off-resonant laser-induced fluorescence
02 p0183 A83-13075

Numerical treatment of boundaries in compressible flow problems
03 p0322 A83-14616

Finite element formulations for convection dominated flows with particular emphasis on the compressible Euler equations
[AIAA PAPER 83-0125]
05 p0633 A83-16538

Compressible flow analysis about three-dimensional wing surfaces using a combination technique
[AIAA PAPER 83-0183]
05 p0581 A83-16575

A hybrid explicit-implicit numerical algorithm for the three-dimensional compressible Navier-Stokes equations
[AIAA PAPER 83-0223]
05 p0582 A83-16593

Solution procedures for accurate numerical simulations of flow in turbomachinery cascades
[AIAA PAPER 83-0257]
05 p0583 A83-16615

Instability and atomization of a liquid layer adjacent to a gas stream
[AIAA PAPER 83-0339]
05 p0635 A83-16665

Preliminary measurements of velocity, density and total temperature fluctuations in compressible subsonic flow
[AIAA PAPER 83-0384]
05 p0635 A83-16684

A computational method for subsonic compressible flow in diffusers
[AIAA PAPER 83-0505]
05 p0587 A83-16753

On a finite-difference method for solving transient viscous flow problems
[AIAA PAPER 83-0560]
05 p0637 A83-16788

Quantitative measurement of density and velocity in compressible flows using laser-induced iodine fluorescence
[AIAA PAPER 83-0049]
05 p0646 A83-17903

Turbulence measurements in a compressible reattaching shear layer
[AIAA PAPER 83-0299]
05 p0591 A83-17917

Effects of Mach number on the development of a subsonic rectangular jet
07 p0863 A83-19805

Two-dimensional subsonic flow of a compressible medium
08 p1083 A83-22047

Correlation of Preston tube data with laminar skin friction
08 p1084 A83-22134

Rayleigh-Taylor instabilities of an accelerating compressible, perfectly conducting plane layer
08 p1168 A83-22385

A new type of boundary layer in a rapidly rotating gas
08 p1086 A83-23098

A finite element solution of compressible flow through cascades of turbomachines
08 p1089 A83-23203

Semi-elliptic computation of axi-symmetric transonic flows
08 p1089 A83-23204

Flow characteristics and methods of flow calculation of high-speed compressible flow through pipe orifices
09 p1257 A83-23332

Application of the modified Lax-Wendroff method to the solution of unsteady self-similar problems of boundary layer theory
09 p1258 A83-23572

An analysis of the two-dimensional acoustic field in a nonuniform duct carrying compressible flow
[AIAA PAPER 83-0669] 10 p1473 A83-25906

ADI on staggered mesh - A method for the calculation of compressible convection 12 p1724 A83-29621

Far field boundary conditions for compressible flows 12 p1725 A83-29649

Numerical solution of the equations of compressible viscous flow 12 p1698 A83-29933

Notes on the stationary vortex motions of a continuum 14 p2009 A83-32363

A numerical study of the Burgers turbulence at extremely large Reynolds numbers 14 p2009 A83-32520

Direct simulation of homogeneous turbulent shear flows on the Illiac IV computer - Applications to compressible and incompressible modeling 15 p2156 A83-33674

Laminar compressible flow between close rotating disks - An asymptotic and numerical study 15 p2157 A83-33869

Theory of waves in the shear flows of an inhomogeneous compressible fluid 16 p2349 A83-35530

The aerodynamics of hypersonic velocities (On flows with low Mach numbers) 16 p2288 A83-35535

Calculation of a laminar flow of a compressible gas in plane curvilinear ducts with heat transfer 16 p2349 A83-35701

A time dependent numerical scheme for three-dimensional inviscid compressible flows in curvilinear coordinates 16 p2290 A83-35815

Turbulence modeling for computational aerodynamics 16 p2293 A83-36079

A variation on MacCormack's method for axisymmetric viscous compressible flows 16 p2352 A83-36093

Three-dimensional compressible viscous analysis of mixer nozzles 16 p2295 A83-36391

[AIAA PAPER 83-1401] 16 p2295 A83-36391

Turbulence modeling methods for the compressible Navier-Stokes equations 17 p2502 A83-37192

[AIAA PAPER 83-1693] 17 p2502 A83-37192

Evaluation of the Baldwin-Lomax turbulence model for two-dimensional shock wave boundary layer interactions [AIAA PAPER 83-1697] 17 p2445 A83-37195

Measurements of compressible secondary flow in a circular S-duct 17 p2446 A83-37218

[AIAA PAPER 83-1739] 17 p2446 A83-37218

Experimental study of the flow of a viscous compressible gas through a cylindrical channel and through a porous insert 17 p2447 A83-37265

Subsonic compressible-gas separated flow past a low-aspect-ratio wing 17 p2450 A83-37626

On a self-similar problem of magnetohydrodynamics 17 p2582 A83-37648

k-epsilon equation for compressible reciprocating engine flows 17 p2507 A83-38021

The aerodynamics of propellers and rotors using an acoustic formulation in the time domain 17 p2455 A83-38653

[AIAA PAPER 83-1821] 17 p2455 A83-38653

Test problems, coordinate transformations, and technique for nonsteady compressible flow analysis 17 p2508 A83-38797

Conformal grid generation for multielement airfoils 17 p2458 A83-38800

The hybrid model and its application for studying free expansion --- of hot gas cylinders into vacuum 18 p2681 A83-39218

Wall-function boundary conditions in the solution of the Navier-Stokes equations for complex compressible flows [AIAA PAPER 83-1694] 18 p2633 A83-39268

The treatment of vortex sheets in compressible potential flow 18 p2634 A83-39352

[AIAA PAPER 83-1881] 18 p2634 A83-39352

Numerical solution of the Navier-Stokes equations for compressible turbulent two/three dimensional flows in the terminal shock region of an inlet/diffuser [AIAA PAPER 83-1892] 18 p2634 A83-39358

The prediction of compressible, laminar viscous flows using a time-marching control volume and multigrid technique [AIAA PAPER 83-1896] 18 p2682 A83-39360

A semi-direct solver for compressible three-dimensional rotational flow 18 p2682 A83-39367

[AIAA PAPER 83-1909] 18 p2682 A83-39367

Comparison between the integro-differential technique and the finite - difference method in solving unsteady compressible viscous flow over airfoils [AIAA PAPER 83-1912] 18 p2635 A83-39370

A time-split finite-volume algorithm for three-dimensional flow-field simulation [AIAA PAPER 83-1957] 18 p2636 A83-39400

Implicit upwind methods for the compressible Navier-Stokes equations [AIAA PAPER 83-1958] 18 p2682 A83-39401

New diagonal implicit scheme for the compressible Navier-Stokes equations [AIAA PAPER 83-1891] 18 p2683 A83-39407

Multi-dimensional formulation of CSCM - An upwind flux difference eigenvector split method for the compressible Navier-Stokes equations --- Conservative 18 p2683 A83-39414

[AIAA PAPER 83-1895] 18 p2683 A83-39414

Spectral methods for the Euler equations [AIAA PAPER 83-1942] 18 p2683 A83-39420

Compressible, conductive, steady MHD flow in a gravitational field --- applied to mass flow in sunspots 18 p2784 A83-39733

Two-point implicit scheme for the Euler equations --- for computational fluid dynamics 18 p2686 A83-39917

A vortex sheet method for calculating separated two-dimensional flows 19 p2789 A83-40855

The motion of compressible fluids and inhomogeneous media 19 p2845 A83-41877

Computational technique for three-dimensional compressible flow past wings at high angles of attack [AIAA PAPER 83-2078] 19 p2792 A83-41912

Factorization method for calculating the three-dimensional flows of a viscous compressible gas 19 p2845 A83-42008

Turbulent solutions of the compressible Navier-Stokes equations using a composite velocity procedure 20 p2970 A83-42556

Strict error estimation of numerical solution of compressible flow in two-dimensional space 20 p2985 A83-43171

Finite element methods in aerodynamics 21 p3086 A83-44551

ISOMS - A implicit difference scheme for solving complete compressible Navier-Stokes equations --- Implicit Second-Order Monotone Scheme 21 p3130 A83-44553

Weakly contracting systems and attractors of the Galerkin approximations of the Navier-Stokes equations on the two-dimensional toroid 21 p3130 A83-44657

Numerical method for the study of the planar unsteady-state flow of compressible viscous liquids 21 p3132 A83-45000

Rotating compressible flow over an infinite disk 23 p3446 A83-47590

Matrix solution of compressible flow on S1 surface through a turbomachine blade row with splitter vanes or tandem blades [ASME PAPER 83-GT-10] 23 p3393 A83-47882

A simple method for designing optimum annular diffusers [ASME PAPER 83-GT-42] 23 p3407 A83-47902

COMPRESSIBLE FLUIDS

A numerical simulation of three-dimensional transonic flows of compressible perfect fluids around aircraft by use of the finite element and least squares methods [AAAF PAPER NT 81-23] 02 p0169 A83-11779

Hydrodynamic gravitational instability of an infinite cylinder of a compressible fluid --- in relation to the dynamics of spiral arms of galaxies 04 p0549 A83-14984

Obtaining axisymmetric flows from plane-parallel ones 04 p0475 A83-15087

Turbulent compressible convection in a deep atmosphere. I - Preliminary two-dimensional results --- of stars 05 p0699 A83-17017

On the theory of compressible fluids 06 p0756 A83-18071

Fast magnetic field-line reconnection in a compressible fluid. II - Skewed field lines 06 p0812 A83-18914

Kelvin-Helmholtz instability at the magnetopause. I - Solution for compressible plasmas. II - Energy flux into the magnetosphere 07 p0966 A83-21511

The rotational motions of compressible fluids. II 09 p1262 A83-24501

The effect of initial stresses on the back wave in the system prestressed compressible cylinder-liquid 11 p1596 A83-28457

The propagation of small perturbations in a system consisting of a prestressed compressed solid body and a viscous compressible fluid 11 p1597 A83-28474

Finite-sized fluid particle in a nonuniform moving grid 12 p1725 A83-29627

Normal oscillations of an ideal compressible fluid in rotating elastic vessels 13 p1838 A83-30012

The impact of compressible liquids 13 p1843 A83-31078

Theoretical studies of boundary layers --- Russian book 15 p2158 A83-34163

Submersion of a disk into a compressible fluid at an angle to the free surface 16 p2350 A83-35714

On waves of general type propagating at the interface between an elastic half-space and a liquid 16 p2369 A83-36549

On a method for the closure of the energy equation formulated relative to the total enthalpy in the case of turbulent flow in a boundary layer 17 p2505 A83-37530

Transonic Euler simulations by means of finite element explicit schemes [AIAA PAPER 83-1924] 18 p2635 A83-39378

Determination of transfer functions in the problem of the unsteady interaction of a fluid with an elastic elliptical shell 18 p2702 A83-40119

Response of liquid carbon disulfide to shock compression Equation of state at normal and high densities 20 p3055 A83-42638

Thrust augmenting ejectors. I 21 p3089 A83-45586

COMPRESSING

NT PLASMA COMPRESSION

NT SPEECH BASEBAND COMPRESSION

Squeeze effects in misaligned radial face seals with coning 14 p2027 A83-32622

Compression of an elastic cylinder between two rigid planes Application of the indirect fictitious-boundary integral method to a contact problem 18 p2697 A83-39455

Helium liquefier cycles with saturated vapor compression 20 p2960 A83-43225

COMPRESSION LOADS

NT AXIAL COMPRESSION LOADS

NT IMPACT LOADS

A study of the stability of compressed cylindrical shells with thin eccentric ribs using a polynomial approximation of deflections 01 p0059 A83-10682

Application of finite-part integrals to the singular integral equations of crack problems in plane and three-dimensional elasticity 02 p0190 A83-12001

The deformation and fracture of Beta HMX 02 p0161 A83-12030

One-dimensional isentropic compression measurements of multiply loaded polymethylmethacrylate 02 p0191 A83-12280

A study of the mechanism of the steady-state creep of aluminum under compression 03 p0300 A83-14161

Compression fatigue behavior of composites in the presence of delaminations 03 p0293 A83-14562

Free vibrations and the stability of annular plates under nonuniform tension and compression 04 p0497 A83-15390

Surface instability and splitting in compressed brittle elastic solids containing crack arrays [ASME PAPER 82-WA/APM-16] 04 p0498 A83-15682

Flutter of a buckled plate as an example of chaotic motion of a deterministic autonomous system 04 p0501 A83-16339

The discrete interaction of a plate and a compressed and stretched rod 04 p0502 A83-16407

Influence of compressive residual stress on the crack-opening behavior of part-through fatigue cracks 05 p0615 A83-17265

The standoff distance of a compression shock upon impingement of an underexpanded jet onto a spherical baffle 05 p0590 A83-17419

Compression of ice VII to 500 kbar --- possible solid modifications of planetary water 05 p0707 A83-17844

The fracture of a unidirectional fiber composite with an elastoplastic matrix under compression 06 p0725 A83-18503

A continuum theory for the fracture of metal-matrix composites under compression 06 p0726 A83-19542

Stability and postbuckling behavior of simply supported trapezoidal plates under compression 07 p0947 A83-21088

Initial postbifurcation behavior of a ring subjected to the simultaneous action of normal and constant-directional pressures 08 p1121 A83-21868

On failure modes of unidirectional composites under compressive loading 09 p1223 A83-23937

The stressed state of an elastic ring fitted into a circular hole in a tensioned plate 09 p1282 A83-25017

Contact between a rigid cylinder and an orthotropic beam under initial stress 11 p1591 A83-27433

Curved crack growth in brittle solids under farfield compression 11 p1592 A83-27439

Smooth contact between a rigid indenter and an initially stressed orthotropic beam 11 p1592 A83-27441

On the Liapounov-Movchan stability of equilibrium of elastic orthotropic plates 11 p1593 A83-27860

The optimum design of a round plastic plate 11 p1596 A83-28459

Eigenfunctions of an integral operator generated by a logarithmic kernel on two intervals and their application to contact problems 11 p1596 A83-28462

Numerical solution of an elastic boundary layer problem using a multiple shooting technique 12 p1736 A83-29614

Delamination-based compression residual-strength prediction model for composites [AIAA 83-0872] 12 p1738 A83-29756

- Dynamics of delamination buckling
[AIAA 83-0873] 12 p1738 A83-29757
- Postbuckling of long orthotropic plates in combined shear and compression
[AIAA 83-0876] 12 p1738 A83-29760
- Finite element analysis of the buckling of variable thickness discs 13 p1867 A83-30845
- A case of quasi-isentropic compression of a medium 14 p2027 A83-32094
- A study on the transmission and reflection of an ultrasonic beam at machined surfaces pressed against each other 15 p2172 A83-33499
- Simultaneous multimode pressure-induced frequency-shift measurements in shock-compressed organic liquid mixtures by use of reflected broadband coherent anti-Stokes Raman scattering 15 p2131 A83-33800
- Stability loss of compressed longitudinally reinforced cylindrical shells in the case of finite displacements with allowance for local buckling of rib-plates 15 p2178 A83-34439
- Contact problems concerning the discrete interaction of a plate and a rod 15 p2178 A83-34441
- Certain problems of the contact interaction of an elastic infinite plane having a round hole with ring-shaped patches 15 p2180 A83-35150
- Localization of deformation and recrystallization in molybdenum crystals deformed by compression 15 p2141 A83-35309
- On the evaporation of shock-compressed metals during expansion 16 p2328 A83-35539
- Energy losses due to plastic deformation during the radial compression of a cylindrical shell 16 p2364 A83-35544
- The opening of a natural macrocrack 16 p2365 A83-35551
- Smooth contact between a rigid indenter and an initially stressed orthotropic beam 16 p2366 A83-36092
- Rectangular plates compressed by a series of in-plane loads Stability and stress distribution 16 p2369 A83-36614
- Compressive creep and oxidation resistance of an Si3N4 material fabricated in the system Si3N4-Si2N2O-Y2Si2O7 16 p2337 A83-36950
- Elastic stability of plane laminates 18 p2697 A83-39422
- Dynamic contact problem of flexible orthotropic plates and shells with allowance for transverse shear 18 p2702 A83-40123
- Compressive buckling of graphite-epoxy composite circular cylindrical shells 18 p2704 A83-40184
- The effect of the direction of shear on the buckling of laminated plates subjected to combined shear and compressive loading 18 p2704 A83-40188
- The problem of the compression of two elastic bodies in the presence of bonding and slipping segments 19 p2858 A83-41220
- A crack growth fatigue life under spectrum loading 20 p3009 A83-43692
- Compression fatigue behaviour of notched composite laminates 21 p3106 A83-44334
- A class of contact problems for a cylindrical shell 21 p3154 A83-44716
- An approximate solution to a plane contact elasticity problem 21 p3162 A83-45302
- An experimental study of the behavior of cylindrical shells with concentrated masses under dynamic external pressure 21 p3164 A83-45370
- Conditions for a phase transition in solids under nonhydrostatic compression 22 p3364 A83-45620
- Shot peening - Control and measurement [SAE PAPER 821453] 22 p3302 A83-45874
- Observation of damage growth in compressively loaded laminates 22 p3264 A83-46810
- The effect of plastic deformation on phase transformations during the aging of VT3-1 titanium alloy 23 p3431 A83-47179
- Contact stresses at ceramic interfaces 23 p3438 A83-48302
- Delamination of composites under compression 23 p3472 A83-48467
- Numerical optimum design of elastic annular plates with respect to buckling 24 p3594 A83-49443
- COMPRESSION RATIO**
- Numerical studies of the formation and destruction of vortices in a motored four-stroke piston-cylinder configuration [AIAA PAPER 83-0497] 05 p0652 A83-16749
- COMPRESSION TESTERS**
- U COMPRESSION TESTS**
- COMPRESSION TESTS**
- Present state of methods for static testing of composites /Review/ 01 p0022 A83-10297
- Compressive creep of Si3N4/MgO alloys 04 p0463 A83-15992
- Compressive failure and kinking in uniaxially aligned glass-resin composite under superposed hydrostatic pressure 04 p0455 A83-15994
- Equivalence of indentation and compressive creep tests on a WC/Co hardmetal 04 p0460 A83-15997
- Mechanical behavior of thick filament-wound composites tested in transverse compression 09 p1221 A83-23606
- On the origin of the first peak of acoustic emission in 7075 aluminium alloy 12 p1714 A83-29507
- Compressive fatigue behaviour of a glass fibre-reinforced polyester composite at 300 K and 77 K 12 p1710 A83-29720
- Effects of MoS2 concentration on friction 15 p2143 A83-35244
- An analysis of the load-bearing capacity of thin-walled tubular rods of composite materials 16 p2364 A83-35511
- The compressive behaviour of carbon fibre reinforced plastic 18 p2653 A83-40171
- Analysis of compression failures in fibre composite laminates 18 p2653 A83-40172
- Tensile and compressive deformation and fracture behavior of the Al-Al3Ni eutectic composites at elevated temperatures 18 p2667 A83-40255
- Strain aging of Ti-6242 at hot-working temperatures 18 p2670 A83-40638
- The environmental degradation of notched CFRP in compression 20 p2947 A83-42806
- Energy absorption of composite materials 20 p2948 A83-43148
- Experimental study on compressive properties of sheets and plates and shapes 20 p2957 A83-43693
- Review of experimental techniques for thin-walled structures liable to buckling. I - Neutral and unstable buckling 22 p3306 A83-46423
- COMPRESSION WAVES**
- Ground-Satellite correlative study of a giant pulsation event 03 p0357 A83-13299
- Shock development from compression waves due to confined burning in porous solid propellants/explosives [AIAA PAPER 83-0480] 05 p0620 A83-16742
- Point source radiation of a solid-fluid interface - Numerical solution using a Fourier-Bessel transformation [ONERA, TP NO. 1982-110] 06 p0807 A83-18436
- The inhomogeneous development of the decomposition reaction of shock-compressed homogeneous explosives 07 p0880 A83-19960
- Propagation of plane waves of a two-component strain state in a nonlinear-elastic compressible medium 07 p0945 A83-20146
- P/n/ velocity and cooling of the continental lithosphere --- upper mantle compression waves in North America 07 p0961 A83-20227
- Centred compression-wave in polytropic gas, and its disintegration 07 p0927 A83-21449
- An asymptotic theory of deflagrations and detonations. I - The steady solutions 16 p2325 A83-35694
- ADINA modeling of elastoplastic shear/compression waves in tubes 20 p3004 A83-42936
- COMPRESSIVE STRENGTH**
- The effect of defects on the strength of composite sandwich assemblies 07 p0876 A83-20461
- On failure modes of unidirectional composites under compressive loading 09 p1223 A83-23937
- An estimation of the compressive strength of a fibrous composite 09 p1224 A83-23944
- Bending of orthotropic beams which are nonlinear in shear and compression 11 p1593 A83-27465
- Compressive fatigue behaviour of a glass fibre-reinforced polyester composite at 300 K and 77 K 12 p1710 A83-29720
- Effects of extreme aircraft storage and flight environments on graphite/epoxy 14 p1987 A83-33122
- Comparative study of the temperature dependence of hardness and compressive strength in ceramics 16 p2336 A83-35979
- Deformation and strength of ring-stiffened orthotropic cylindrical shells under dynamic compressive loads 18 p2701 A83-40107
- The effect of fibre surface treatment on the compressive strength of CFRP laminates 18 p2651 A83-40145
- Experimental study on compressive properties of sheets and plates and shapes 20 p2957 A83-43693
- A plasticity criterion and basic relationships for an anisotropic shell with different strengths in tension and compression 21 p3162 A83-45303
- Fatigue crack initiation from a notch tip under a cyclic compressive load 22 p3304 A83-45622
- Compressive strength of fiber-reinforced materials 24 p3597 A83-50147
- COMPRESSOR BLADES**
- Study of fan noise sources through thin film pressure transducers 02 p0136 A83-12350
- Preliminary results on the abrasability of porous, sintered seal material [ASME PAPER 82-LUB-7] 03 p0298 A83-13504
- Experimental evaluation of shockless supercritical airfoils in cascade [AIAA PAPER 83-0003] 05 p0577 A83-16455
- Numerical prediction of choking flutter of axial compressor blades [AIAA PAPER 83-0006] 05 p0596 A83-16458
- A method of predicting the performance deterioration of a compressor cascade due to sand erosion [AIAA PAPER 83-0178] 05 p0596 A83-16572
- The computation of the compressor cascade boundary layer 06 p0712 A83-18153
- A finite element solution of compressible flow through cascades of turbomachines 08 p1089 A83-23203
- A solution to inverse problem of quasi three-dimensional flow in centrifugal impeller 09 p1257 A83-23331
- Analytical and experimental investigation of bird impact on fan and compressor blading [AIAA 83-0954] 12 p1704 A83-29856
- Minimum contact magnetic sensing of turbine blade speed 13 p1807 A83-30175
- The fatigue strength of compressor disks 14 p2030 A83-32387
- A sensor for flow measurements near the surface of a compressor blade 14 p2019 A83-32400
- Investigation of flow through high cambered supersonic compressor cascade 16 p2291 A83-35845
- Optimization of the plane compressor blade aerodynamic design 16 p2291 A83-35857
- High angle-of-attack cascade measurements and analysis 16 p2292 A83-35875
- Stress analysis of critical areas of low-pressure compressor-disc assembly of a developmental aero-engine 16 p2305 A83-35880
- Transient blade response due to surge induced structural loads [SAE PAPER 821438] 17 p2468 A83-37986
- Freestream turbulence effects on compressor cascade wake 19 p2789 A83-41051
- The rule of forbidden signals and apparent Mach numbers in supersonic compressor cascades 20 p2928 A83-42560
- Analytical method for predicting compressor stage performance 20 p2928 A83-42561
- Calculations for a three-dimensional boundary layer in a compressor [ONERA, TP NO. 1983-47] 21 p3086 A83-44321
- A study of the damping capacity of rods in a centrifugal force field 21 p3148 A83-45322
- Effect of particle presence on the incompressible inviscid flow through a two dimensional compressor cascade [ASME PAPER 83-GT-95] 23 p3395 A83-47941
- Modifications of the Ives-liutermozza conformal-mapping procedure for turbomachinery cascades [ASME PAPER 83-GT-116] 23 p3395 A83-47947
- Theory of blade design for large deflections. I Two-dimensional cascade [ASME PAPER 83-GT-124] 23 p3396 A83-47953
- Theory of blade design for large deflections. II - Annular cascades [ASME PAPER 83-GT-125] 23 p3396 A83-47954
- Analysis of an axial compressor blade vibration based on wave reflection theory [ASME PAPER 83-GT-151] 23 p3409 A83-47970
- Redesign and performance analysis of a transonic axial compressor stator and equivalent plane cascades with subsonic controlled diffusion blades [ASME PAPER 83-GT-208] 23 p3397 A83-48009
- Experimental cascade analysis of a transonic compressor rotor blade section [ASME PAPER 83-GT-209] 23 p3397 A83-48010
- A three-dimensional model for the prediction of shock losses in compressor blade rows [ASME PAPER 83-GT-216] 23 p3410 A83-48016
- COMPRESSOR EFFICIENCY**
- The entropy efficiency of blade machines 05 p0597 A83-16953
- On the question of calculating the pressurization start-up regimes of a gas-turbine plant 14 p2027 A83-32651
- Experimental study of a high-through-flow transonic axial compressor stage 16 p2291 A83-35853
- Effect of humidity on jet engine axial-flow compressor performance 16 p2304 A83-35856
- Design and performance of a low aspect ratio, high tip speed multi-stage compressor [AIAA PAPER 83-1161] 16 p2306 A83-36253
- Analytical method for predicting compressor stage performance 20 p2928 A83-42561
- Effect of particle presence on the incompressible inviscid flow through a two dimensional compressor cascade 20 p2928 A83-42562
- Gas turbine engine cascade wind tunnel with automatic data acquisition and control 20 p2938 A83-42563

- On the influence of the diffuser inlet shape on the performance of a centrifugal compressor stage
[ASME PAPER 83-GT-9] 23 p3406 A83-47881
- Effect of relative velocity distribution on efficiency and exit flow of centrifugal impellers
[ASME PAPER 83-GT-74] 23 p3447 A83-47927
- Gas turbine compressor interstage cooling using methanol
[ASME PAPER 83-GT-230] 23 p3466 A83-48026

COMPRESSOR ROTORS

- Numerical calculation of the laminar flow in the inlet of the axial sealing gap of radial-flow compressors
07 p0864 A83-21339
- Flow measurements using a laser-2-focus velocimeter in a high-pressure ratio centrifugal impeller
12 p1695 A83-28836
- Investigation of the tip clearance flow inside and at the exit of a compressor rotor passage. II - Turbulence properties
12 p1695 A83-28843
- 18:1 pressure ratio axial/centrifugal compressor demonstration program
12 p1732 A83-29013
- An analysis of the natural vibrations of the rotors of centrifugal compressor machines
13 p1859 A83-30310
- Development of process models to produce a dual-property titanium alloy compressor disk
15 p2134 A83-33634
- Experience in the development of computer-controlled high response probe diagnostics for turbomachines
16 p2355 A83-35851
- Tip clearance flow in a compressor rotor passage at design and off-design conditions
16 p2291 A83-35855
- Characteristics of the occurrence and elimination of a stall in an axial-flow compressor in the presence of a rotating irregularity at the inlet
19 p2800 A83-42132
- The role of forbidden signals and apparent Mach numbers in supersonic compressor cascades
20 p2928 A83-42560
- Analytical method for predicting compressor stage performance
20 p2928 A83-42561
- Substructuring and wave propagation - An efficient technique for impeller dynamic analysis
[ASME PAPER 83-GT-150] 23 p3409 A83-47969
- Experimental cascade analysis of a transonic compressor rotor blade section
[ASME PAPER 83-GT-209] 23 p3397 A83-48010
- COMPRESSORS**
- NT CENTRIFUGAL COMPRESSORS
- NT SUPERCHARGERS
- NT SUPERSONIC COMPRESSORS
- NT TRANSONIC COMPRESSORS
- NT TURBOCOMPRESSORS
- Evaluating Scroll refrigerant compressors for reducing size and weight of military aircraft ECS
[SAE PAPER 820877] 10 p1375 A83-25771
- Three dimensional holographic flow visualization
10 p1422 A83-26420
- Study of a hypetrochoidal compressor with paddles --- French thesis
11 p1590 A83-28634
- The performance of single-shaft gas turbine load compressor auxiliary power units
[AIAA PAPER 83-1159] 16 p2306 A83-36251
- A computer-aided system for interactive geometric modeling, structural/dynamics analysis and N/C manufacturing/inspection of radial flow compressors
[SAE PAPER 821440] 17 p2493 A83-37988
- Large scale aeroengine compressor test facility
19 p2807 A83-41534
- Miniature J-T refrigerators using adsorption compressors
20 p2960 A83-43231
- The response of a compressor to a periodic pressure variation in the output region
[ONERA, TP NO. 1983-29] 21 p3092 A83-44308
- COMPTON EFFECT**
- Kinetics of the isotropic expansion of an optically transparent plasma in the Compton stage
04 p0536 A83-15710
- Second-order scattering approximation to X-ray photon transport at balloon altitudes
05 p0665 A83-17803
- Accurate formula for the self-Compton X-ray flux density from a uniform, spherical, compact radio source
06 p0841 A83-19293
- Inverse Compton gamma-ray from pulsars. I - The Vela pulsar
07 p1017 A83-20932
- A feature in the X-ray spectrum of Cygnus X-1 - A possible positron annihilation line
07 p1022 A83-21136
- Electron kinetic equations for Comptonization by isotropic photons --- in stellar magnetic fields
08 p1184 A83-23067
- Gamma ray detection with long NaI/Tl scintillator bars
09 p1268 A83-24104
- Comptonization effects in spherical accretion onto black holes
10 p1515 A83-26739

- Inverse Compton scattering in a strong magnetic field
12 p1795 A83-29358
- Design considerations of a Compton scattering free-electron laser with an axial electrical field
13 p1855 A83-31131
- Nonlinear saturation mechanisms and improvement in free-electron lasers
13 p1855 A83-31132
- Comptonization in a radiation-dominated shock, and the spectra of X-ray pulsars
15 p2254 A83-33718
- Parametric interaction and backward wave oscillation in stimulated Compton scattering
15 p2169 A83-34372
- High-energy gravitational antennas - A theoretical approach
15 p2261 A83-34405
- Correlations between synchrotron and self-Compton spectra
18 p2764 A83-39004
- The intensity and spectrum of galactic center beta (+) annihilation protons after Compton scattering
19 p2913 A83-40696
- Compton heated winds and coronae above accretion disks. II Radiative transfer and observable consequences
20 p3067 A83-42438
- Nonlinear theory of stimulated scattering of electromagnetic waves by a magnetized beam of electrons in a waveguide
23 p3445 A83-47572

COMPUTATION**NT MINIMUM VARIANCE ORBIT DETERMINATION****NT ORBIT CALCULATION**

- Concerning the calculation of geodetic heights
01 p0072 A83-10852
- Computational methods in control - A survey and introduction to the literature
10 p1460 A83-26529
- Error free computation - A direct method to convert finite-segment p-adic numbers into rational numbers
15 p2217 A83-33903
- International Symposium on Geodetic Networks and Computations, Munich, West Germany, August 31-September 5, 1981, Proceedings. Volume 7 - Combination of horizontal, vertical and gravity networks
22 p3316 A83-46351

COMPUTATIONAL CHEMISTRY

- On the computation of ionization levels in rocket exhaust flames
22 p3261 A83-45716

COMPUTATIONAL FLUID DYNAMICS

- Free convection fluctuating boundary layer on a horizontal plate
01 p0044 A83-10124
- Comparison of computational and experimental jet effects
01 p0002 A83-10185
- Finite element analysis of ideal flow over axisymmetric solid body /sphere/
01 p0045 A83-10277
- Numerical investigation of a turbulent boundary layer for the case of a positive pressure gradient
01 p0045 A83-10457
- Some exact solutions describing unsteady plane gas flows with shocks
01 p0045 A83-10493
- On a geophysical inviscid vortex
01 p0075 A83-10496
- Certain numerical methods for solving problems of gas dynamics in Euler coordinates
01 p0045 A83-10566
- Nonstationary flow in gas lines
01 p0045 A83-10582
- Solution of Burgers' equation with a large Reynolds number
01 p0045 A83-10710
- An iteration method and solvability conditions for Navier-Stokes-type equations
01 p0045 A83-10822
- Fundamentals of compressible flow --- Book
01 p0045 A83-10883
- The role of coherent structures in modelling turbulence and mixing; Proceedings of the International Conference, Madrid, Spain, June 25-27, 1980
01 p0045 A83-10884
- Coherent structures in turbulent flow
01 p0046 A83-10885
- The deterministic description of the coherent structure of free shear layers
01 p0046 A83-10886
- Theoretical investigation of interaction and coalescence of large scale structures in the turbulent mixing layer
01 p0046 A83-10888
- Coherent structures and studies of perturbed and unperturbed jets
01 p0046 A83-10894
- Coherent structures in turbulent combustion
01 p0023 A83-10899
- Inertial forces on an expanding bubble in motion in a fluid
01 p0047 A83-10921
- Conservative difference schemes for equations of a viscous incompressible fluid in curvilinear orthogonal coordinates
01 p0047 A83-11267
- Asymptotic solutions for the motion of a viscous incompressible fluid filling the cavity of a rotating body
01 p0047 A83-11268
- Shock fitting in the numerical analysis of supersonic conical flows
01 p0003 A83-11269
- Local recirculation zones in a supersonic boundary layer on a moving surface
01 p0003 A83-11272
- Asymptotic expansions for the problem of boundary layer formation
01 p0047 A83-11273

- Numerical analysis of the dispersion of detonation products
01 p0047 A83-11274
- Analysis of flows of an equilibrium dissociated, ionized, and radiating gas by the method of large particles
01 p0003 A83-11275
- On the total axial-symmetric expansion of a supersonic stream
01 p0003 A83-11329
- The transport equation for the strain rate tensor and the description of an ideal incompressible fluid by a set of dynamic equations
02 p0169 A83-11642
- Modeling of three-dimensional turbulent structures around missiles
02 p0131 A83-11769
- [AAAF PAPER NT 81-02] 02 p0131 A83-11769
- Three-dimensional or unsteady boundary layers
[AAAF PAPER NT 81-16] 02 p0169 A83-11776
- A numerical simulation of three-dimensional transonic flows of compressible perfect fluids around aircraft by use of the finite element and least squares methods
[AAAF PAPER NT 81-23] 02 p0169 A83-11779
- Higher order boundary layer approximations for some flows of a power law fluid - Related solutions
02 p0169 A83-11858
- The development of jets in stratified fluids
02 p0169 A83-11860
- Numerical simulation of turbulent flows in three-dimensional boundary layers
02 p0170 A83-11873
- Friction and heat transfer from plates to normally-incident axisymmetric turbulent jets
02 p0170 A83-11874
- Multiple grid methods for equations of the second kind with applications in fluid mechanics --- Thesis
02 p0170 A83-11899
- Theory of lubrication with ferrofluids - Application to short bearings
[ASME PAPER 81-LUB-39] 02 p0186 A83-11940
- An exact solution to the problem of diffusion in a periodic velocity field and turbulent diffusion
02 p0170 A83-11954
- Partial regularity of suitable weak solutions of the Navier-Stokes equations
02 p0170 A83-12100
- Flow of a non-Newtonian second-order fluid under an enclosed rotating disc with uniform suction and injection
02 p0171 A83-12663
- Numerical solutions to natural convection in a channel with porous walls under a transverse magnetic field
02 p0171 A83-12666
- A two-dimensional isoparametric Galerkin finite element for acoustic-flow problems
[ASME PAPER 82-DET-97] 02 p0234 A83-12778
- Analysis and computation of heat transfer around a cylinder in argon plasma cross flow
[ASME PAPER 82-HT-30] 02 p0171 A83-12789
- Finite analytic numerical solution of axisymmetric Navier-Stokes and energy equations
[ASME PAPER 82-HT-42] 02 p0172 A83-12795
- Numerical solutions of radiative heat transfer with convection
[ASME PAPER 82-HT-45] 02 p0172 A83-12798
- Fluid injection to a laminar boundary layer with variable wall mass and heat flux
[ASME PAPER 82-HT-61] 02 p0173 A83-12801
- Finite-element simulation of natural convection in three-dimensional enclosures
[ASME PAPER 82-HT-71] 02 p0173 A83-12803
- Mixed convection over a horizontal heated flat plate
[ASME PAPER 82-HT-75] 02 p0173 A83-12804
- Slow rotating stratified flow past obstacles of large height
02 p0173 A83-12856
- Numerical solution of subsonic and transonic cascade flows
02 p0132 A83-12901
- The simulation of secondary flow effects in turbulent non-circular passage flows
02 p0173 A83-12902
- Finite element, stream function-vorticity solution of steady laminar natural convection
02 p0173 A83-12903
- General hyperbolic difference formulas for linear and quasilinear hyperbolic equations
02 p0231 A83-12905
- Time-dependent convection under reduced gravity
02 p0174 A83-12993
- Thermal Marangoni convection in a floating zone. Microgravity experiment during the TEXUS IIIB rocket flight
02 p0138 A83-12995
- On the stability of almost parallel boundary layer flows
02 p0174 A83-13019
- A numerical analysis of two-dimensional flow past a rectangular prism by a discrete vortex model
02 p0174 A83-13020
- A down-stream boundary procedure for the Euler equations
02 p0174 A83-13021
- Comparison of different integration schemes based on the concept of characteristics as applied to the ablated blunt body problem
02 p0132 A83-13022
- Pressure distribution on a simple delta wing
02 p0132 A83-13023

Analysis of combustion in recirculating flow for rocket exhausts in supersonic streams 02 p0148 A83-13087

The velocity field induced by a helical vortex filament 03 p0277 A83-13113

Elementary derivation of Poisson structures for fluid dynamics and electrodynamics 03 p0396 A83-13119

Large-scale vortex-lattice model for the locally separated flow over wings 03 p0277 A83-13127

Numerical experiments on the leading-edge flowfield 03 p0277 A83-13131

Modeling the curved turbulent wall jet 03 p0315 A83-13137

Spectral method solutions for some laminar channel flows with separation 03 p0315 A83-13138

Numerical simulation of steady supersonic flow over spinning bodies of revolution 03 p0277 A83-13140

Laminar and turbulent natural convection in the annulus between horizontal concentric cylinders 03 p0315 A83-13485

An improved method for calculating isentropic transonic flows in two-dimensional turbine cascades of arbitrary smooth profiles 03 p0278 A83-13492

Comments on the radial turbulent jet 03 p0316 A83-13493

Transient lubricating films with inertia [ASME PAPER 82-LUB-12] 03 p0335 A83-13507

Surface roughness effects in hydrodynamic lubrication - The flow factor method [ASME PAPER 82-LUB-45] 03 p0337 A83-13523

Self-consistent extrapolation of the results of numerical experiments for fluid structures 03 p0389 A83-13537

Potential flow analysis of an arbitrary cascade using a conformal transformation into a row of circular cylinders 03 p0278 A83-13564

On a higher order accurate fully discrete Galerkin approximation to the Navier-Stokes equations 03 p0316 A83-13568

The first boundary value problem for the linearized Navier-Stokes equations 03 p0316 A83-13694

Convergence and stability of a collocation method for the generalized airfoil equation 03 p0278 A83-13844

An analytical study of the flow of a two-phase mixture in a nozzle with allowance for gas-dynamic division 03 p0316 A83-14060

Co-energy methods for elliptic flow and related problems 03 p0384 A83-14080

Spectral modeling of linear mechanisms in nonhomogeneous turbulent flows --- French thesis 03 p0317 A83-14104

Finite-difference techniques for vectorized fluid dynamics calculations --- Book 03 p0317 A83-14225

A study of the intermittent phases in the wall region of a turbulent flow 03 p0317 A83-14460

Buoyancy flow limited mixed layer depth in oscillating grid turbulence 03 p0319 A83-14477

A theoretical model for coherent structures in wall turbulence 03 p0319 A83-14478

A phenomenological model of the organized vortex in the two-dimensional mixing layer 03 p0319 A83-14479

Some problems of second order modelling of mass transfer in a turbulent gas mixture 03 p0319 A83-14480

Approximation of extremal surface elements /hyperbolic type/ by means of characteristic three-dimensional quadrilateral elements 03 p0388 A83-14493

The existence and uniqueness of a solution for a boundary-value problem for an equation of mixed type in a rectangular domain 03 p0388 A83-14495

Vibration-induced change of flow in the annular space between two concentric pipes 03 p0320 A83-14506

Calculation method for transonic separated flows over airfoils including spoiler effects [ONERA, TP NO. 1982-66] 03 p0279 A83-14526

Inhomogeneous flow calculations by spectral methods - Mono-domain and multi-domain techniques [ONERA, TP NO. 1982-67] 03 p0320 A83-14527

Experimental and theoretical investigations on the turbulence in transonic shock boundary layer interactions [ONERA, TP NO. 1982-77] 03 p0279 A83-14531

A new numerical method for turbulent mixing of supersonic reacting flows in chemical laser cavities [ONERA, TP NO. 1982-85] 03 p0332 A83-14537

A numerical study of a moderate Reynolds number flow in a nozzle 03 p0320 A83-14568

The autonomy of shock waves in a sonic downstream state - The case of detonation 03 p0320 A83-14570

Solution of the transonic integral equation using a polar coordinate formulation 03 p0279 A83-14572

Experiments on the role of amplitude and phase modulations during transition to turbulence 03 p0321 A83-14576

Path-integral methods for turbulent diffusion 03 p0321 A83-14577

On the spreading of a turbulent spot in the absence of a pressure gradient 03 p0321 A83-14578

The forced mixing layer between parallel streams 03 p0321 A83-14579

Transonic shear flow in a three-dimensional channel 03 p0321 A83-14586

Numerical solution for fully developed flow in heated curved tubes 03 p0322 A83-14587

Conference on Numerical Methods in Fluid Mechanics, 4th, Ecole Nationale Supérieure de Techniques Avancées, Paris, France, October 7-9, 1981, Proceedings 03 p0322 A83-14601

Comparison of time integration /finite difference and spectral/ for the non-linear Burgers equation 03 p0389 A83-14603

Methods for solving Euler's equations for airfoil and intake flow 03 p0279 A83-14604

Computation of vortex flow around wings using the Euler equations 03 p0279 A83-14605

Explicit and implicit corrected viscosity schemes for the computation of steady transonic flows 03 p0279 A83-14606

A posteriori numerical techniques for enforcing simultaneous conservation of integral invariants upon finite-difference shallow-water equation models 03 p0322 A83-14607

A family of flux-correction methods to avoid overshoot occurring with solutions of unsteady flow problems 03 p0322 A83-14608

Computation of 3-D internal transonic flows 03 p0280 A83-14609

Algorithms for advection and shock problems 03 p0322 A83-14611

Boundary layer on finite wings and related bodies with consideration of the attachment line region 03 p0280 A83-14612

On a multi-time step procedure to accelerate time-asymptotic flow calculations 03 p0322 A83-14613

FFT vs. conjugate gradient method for solution of flow equations by pseudo-spectral methods 03 p0322 A83-14614

Solution of the Navier-Stokes equations using the finite-difference method of Hermitian type 03 p0322 A83-14615

Numerical treatment of boundaries in compressible flow problems 03 p0322 A83-14616

Numerical comparison of radiative heat transfer models 03 p0322 A83-14670

Compressible boundary-layer flow at a three-dimensional stagnation point with massive blowing 03 p0322 A83-14672

Numerical computations of wall-jet flows 03 p0323 A83-14674

Approximate analytical methods for calculating the motion of shock waves in stellar envelopes 03 p0426 A83-14692

Stability of nonparallel developing flow in an annulus 03 p0323 A83-14698

Penalty-finite-element analysis of 3-D Navier-Stokes equations 03 p0323 A83-14699

Flow of a conducting rotating fluid above a disc under uniform suction 03 p0323 A83-14724

Analogy between the wave motions of chemically active and two-phase media 03 p0323 A83-14896

Statistical extreme-value problems and unique solvability of a three-dimensional Navier-Stokes system under almost any initial conditions 03 p0323 A83-14897

Oscillating stagnation point flow 04 p0474 A83-14949

Fenomech '81; Proceedings of the Second International Conference on Finite Elements in Nonlinear Mechanics, Stuttgart, West Germany, August 25-28, 1981. Parts 1, 2 & 3 04 p0465 A83-15001

Streamline upwind/Petrov-Galerkin formulations for convection dominated flows with particular emphasis on the incompressible Navier-Stokes equations 04 p0475 A83-15005

On current aspects of finite element computational fluid mechanics for turbulent flows 04 p0475 A83-15006

A fast pseudo-time integration scheme for the solution of the steady transonic flow problem 04 p0441 A83-15015

Numerical investigation of the problem of viscous reacting gas flow past blunt bodies 04 p0441 A83-15078

Calculation of total-pressure losses in channels with variable cross-section area in the presence of turbulent mixing 04 p0475 A83-15080

Calculation of a three-dimensional boundary layer on a triangular plate of finite length in a hypersonic flow 04 p0441 A83-15081

Flow past a profile at angle of attack to a transonic flow 04 p0441 A83-15083

Approximate integration of the nonstationary equations of a diffusion or thermal boundary layer 04 p0475 A83-15084

Applicability of the Boussinesq approximation to solve problems of nonstationary concentrational natural convection 04 p0475 A83-15093

Flow of a rarefied gas past a sphere under the conditions of surface injection 04 p0442 A83-15099

Asymmetric vortex formation from cones at incidence - A simple inviscid model 04 p0442 A83-15148

Concerning dynamic stall --- of laminar flow near leading edges of airfoils 04 p0442 A83-15150

Shock-fitting bicharacteristic algorithm for three-dimensional scarfed nozzle flowfields 04 p0442 A83-15278

Streamwise corner flow with wall suction 04 p0442 A83-15279

The use of an error index to improve numerical solutions for unsteady lifting airfoils 04 p0442 A83-15281

A fast algorithm for the calculation of transonic flow over wing/body combinations 04 p0442 A83-15283

Correlation of the detachment of two-dimensional turbulent boundary layers 04 p0442 A83-15284

Nonlinear aerodynamic modeling of flap oscillations in transonic flow - A numerical validation [AIAA PAPER 81-0073] 04 p0442 A83-15290

A comparative study of time-marching and space-marching numerical methods --- for flowfield codes 04 p0476 A83-15297

Numerical evaluation of principal value integral by Gauss-Laguerre quadrature 04 p0530 A83-15299

Some recent applications of high-lift computational methods at Boeing 04 p0443 A83-15313

A new approach to optimization for aerodynamic applications 04 p0443 A83-15325

Relaxation computation of transonic flows around wings with blunt leading-edge and discussion on its stability and convergence 04 p0443 A83-15543

Axisymmetric vortex breakdown in rotating fluid within a container 04 p0476 A83-15696

Properties of parallel-surfaces coordinate systems --- for balance equations in computational fluid dynamics 04 p0530 A83-15817

Heat transfer for flows past non-isothermal bodies --- Russian book 04 p0476 A83-15830

Simulation of laboratory vortex flow by axisymmetric similarity solutions 04 p0477 A83-15858

Approximate equation of state for multicomponent gaseous mixtures 04 p0544 A83-15861

Laminar flow of vapor flux in the condensation region of heat tubes 04 p0477 A83-15864

Momentum theory, dynamic inflow, and the vortex-ring state 04 p0443 A83-16026

Mathematical model for the analysis of wind-turbine wakes 04 p0507 A83-16108

Numerical study of wall heat transfer in the recirculating flow region of a confined jet 04 p0477 A83-16124

Development of secondary flow and vorticity in curved ducts, cascades, and rotors, including effects of viscosity and rotation 04 p0478 A83-16141

Unidirectional unsteady flow of an instantaneously heated gas out of a cylinder with various locations of the heating zones 04 p0479 A83-16172

Dynamics and thermodynamics of volcanic eruptions - Implications for the plumes on lo 04 p0571 A83-16243

The unsteady collision of free-convective boundary layers 04 p0480 A83-16363

Rotational plane flows of a viscous fluid 04 p0480 A83-16364

The use of the method of generalized self-similarity for computing turbulent boundary layers 04 p0480 A83-16392

Calculation method for three dimensional turbulent boundary layers 04 p0480 A83-16431

An integral method applied to the solution of fluid mechanics problems 04 p0480 A83-16445

PAN AIR applications to complex configurations --- computer program for predicting subsonic and supersonic linear potential flows [AIAA PAPER 83-0007] 05 p0577 A83-16459

Calculation of supersonic flow over realistic configurations by an updated low-order panel method [AIAA PAPER 83-0010] 05 p0578 A83-16461

Computation of supersonic viscous flows around pointed bodies at large incidence [AIAA PAPER 83-0034] 05 p0578 A83-16474

High angle-of-attack calculations of the subsonic vortex flow on slender bodies [AIAA PAPER 83-0035] 05 p0578 A83-16475

A perspective of theoretical and applied computational fluid dynamics [AIAA PAPER 83-0037] 05 p0632 A83-16477

A shock-fitting solution of the supersonic flowfield in a rounded internal corner [AIAA PAPER 83-0038] 05 p0578 A83-16478

Computation of shock wave/target interaction
[AIAA PAPER 83-0039] 05 p0632 A83-16479

A characteristic flux difference splitting for the hyperbolic conservation laws of inviscid gasdynamics
[AIAA PAPER 83-0040] 05 p0632 A83-16480

Computations of two-phase supersonic nozzle flows by a space-marching method
[AIAA PAPER 83-0041] 05 p0578 A83-16481

Computational wing design for an advanced trainer
[AIAA PAPER 83-0093] 05 p0594 A83-16517

SAMID, an interactive system for the analysis and constrained minimization of induced drag of aircraft configurations
[AIAA PAPER 83-0095] 05 p0594 A83-16519

A contribution to the numerical prediction of unsteady flows
[AIAA PAPER 83-0121] 05 p0632 A83-16534

New implicit boundary procedures - Theory and applications
[AIAA PAPER 83-0123] 05 p0579 A83-16536

A multigrid method for the Euler equations
[AIAA PAPER 83-0124] 05 p0580 A83-16537

Finite element formulations for convection dominated flows with particular emphasis on the compressible Euler equations
[AIAA PAPER 83-0125] 05 p0633 A83-16538

A class of central bidiagonal schemes with implicit boundary conditions for the solution of Euler's equations
[AIAA PAPER 83-0126] 05 p0633 A83-16539

Unsteady flows about a Joukowski airfoil in the presence of moving vortices
[AIAA PAPER 83-0129] 05 p0580 A83-16542

Autrotation of an elliptic airfoil
[AIAA PAPER 83-0130] 05 p0580 A83-16543

The role of CFD in aeropropulsion ground testing --- Computational Fluid Dynamics
[AIAA PAPER 83-0149] 05 p0599 A83-16557

Numerical simulation of near-critical and unsteady subcritical inlet flow fields
[AIAA PAPER 83-0175] 05 p0580 A83-16570

A method of predicting the performance deterioration of a compressor cascade due to sand erosion
[AIAA PAPER 83-0178] 05 p0596 A83-16572

Laminar viscous flow-field prediction of Shuttle-like vehicle aerodynamics
[AIAA PAPER 83-0211] 05 p0581 A83-16586

An efficient method for supersonic viscous flow field calculations
[AIAA PAPER 83-0222] 05 p0582 A83-16592

A hybrid explicit-implicit numerical algorithm for the three-dimensional compressible Navier-Stokes equations
[AIAA PAPER 83-0223] 05 p0582 A83-16593

Navier-Stokes computations of the projectile base flow with and without base injection
[AIAA PAPER 83-0224] 05 p0582 A83-16594

Calculation of viscous hypersonic flow over a severely indented nosetip
[AIAA PAPER 83-0226] 05 p0582 A83-16596

Calculation of steady and unsteady transonic flows using parametric differentiation and an extended integral equation method
[AIAA PAPER 83-0232] 05 p0582 A83-16600

Numerical simulation of 2-D unsteady transonic flows using the full-potential equation
[AIAA PAPER 83-0233] 05 p0582 A83-16601

A multi-grid method for the computation of viscid/inviscid interactions on airfoils
[AIAA PAPER 83-0234] 05 p0582 A83-16602

Three-dimensional Euler equation simulation of propeller-wing interaction in transonic flow
[AIAA PAPER 83-0236] 05 p0582 A83-16603

Computations of projectile Magnus effect at transonic velocities
[AIAA PAPER 83-0237] 05 p0583 A83-16604

A viscous-inviscid interactive procedure for rotational flow in cascades of two-dimensional airfoils of arbitrary shape
[AIAA PAPER 83-0256] 05 p0583 A83-16614

Solution procedures for accurate numerical simulations of flow in turbomachinery cascades
[AIAA PAPER 83-0257] 05 p0583 A83-16615

Basic calibration of a partially-parabolic procedure aimed at centrifugal impeller analysis
[AIAA PAPER 83-0260] 05 p0583 A83-16616

Computational Transonic Equivalent Strip method for applications to unsteady three-dimensional aerodynamics
[AIAA PAPER 83-0261] 05 p0583 A83-16617

A multi-grid method for transonic wing analysis and design
[AIAA PAPER 83-0262] 05 p0583 A83-16618

Jet wing vortex lattice theory with nonlinear wake and tip flows
[AIAA PAPER 83-0263] 05 p0583 A83-16619

A fast viscous correction method for unsteady transonic flow about airfoils
[AIAA PAPER 83-0264] 05 p0583 A83-16620

A study with sensitivity analysis of the k-epsilon turbulence model applied to jet flows
[AIAA PAPER 83-0285] 05 p0633 A83-16630

Calculations of a plane turbulent jet
[AIAA PAPER 83-0286] 05 p0634 A83-16631

A separation model for two-dimensional airfoils in transonic flow
[AIAA PAPER 83-0298] 05 p0584 A83-16638

A finite difference method for inverse solutions of 3-D turbulent boundary-layer flow
[AIAA PAPER 83-0301] 05 p0634 A83-16639

Confined swirling flow predictions
[AIAA PAPER 83-0316] 05 p0634 A83-16646

Instability and atomization of a liquid layer adjacent to a gas stream
[AIAA PAPER 83-0339] 05 p0635 A83-16665

Subsonic surface panel method for airframe analysis and wing design
[AIAA PAPER 83-0341] 05 p0584 A83-16667

Hypersonic Mach number and real gas effects on Space Shuttle Orbiter aerodynamics
[AIAA PAPER 83-0343] 05 p0584 A83-16668

An enhanced version of an implicit code for the Euler equations
[AIAA PAPER 83-0344] 05 p0584 A83-16669

Prediction of line sail during lines-first deployment --- parachute suspension simulation
[AIAA PAPER 83-0370] 05 p0584 A83-16676

Monotone implicit algorithms for the small-disturbance and full potential equations applied to transonic flows
[AIAA PAPER 83-0371] 05 p0585 A83-16677

A new consistent spatial differencing scheme for the transonic full-potential equation
[AIAA PAPER 83-0373] 05 p0585 A83-16678

Multi-grid calculation of three-dimensional transonic potential flows
[AIAA PAPER 83-0374] 05 p0585 A83-16679

Non-isentropic potential formulation for transonic flows
[AIAA PAPER 83-0375] 05 p0635 A83-16680

The prediction of the intermittency factor for turbulent shear flows
[AIAA PAPER 83-0382] 05 p0635 A83-16683

Transient flow analysis of the AEDC/HPDE MHD generator
[AIAA PAPER 83-0395] 05 p0686 A83-16691

Numerical study of a ramjet dump combustor flow field
[AIAA PAPER 83-0421] 05 p0585 A83-16704

A survey of grid generation techniques in computational fluid dynamics
[AIAA PAPER 83-0447] 05 p0636 A83-16719

Three-dimensional grid generation using elliptic equations with direct grid distribution control
[AIAA PAPER 83-0448] 05 p0636 A83-16720

Grid adaption for problems with separation, cell Reynolds number, shock-boundary layer interaction, and accuracy
[AIAA PAPER 83-0449] 05 p0636 A83-16721

A new approach to truly adaptive grid generation
[AIAA PAPER 83-0450] 05 p0681 A83-16722

Adaptive grids generated by elliptic systems --- for computational fluid dynamics
[AIAA PAPER 83-0451] 05 p0636 A83-16723

Direct/inverse, compressible turbulent boundary-layer computations using a two-equation turbulence model
[AIAA PAPER 83-0453] 05 p0636 A83-16724

Computation of three-dimensional boundary layers at fuselages
[AIAA PAPER 83-0455] 05 p0586 A83-16725

Conical, noncircular, second-order, small disturbance potential theory of supersonic flow
[AIAA PAPER 83-0459] 05 p0586 A83-16728

A computational investigation of supersonic axisymmetric flow over boattails containing a centered propulsive jet
[AIAA PAPER 83-0462] 05 p0586 A83-16730

Performance prediction of high inlet blockage diffusers
[AIAA PAPER 83-0466] 05 p0636 A83-16733

Numerical simulation of transonic flow about isolated afterbodies
[AIAA PAPER 83-0498] 05 p0586 A83-16750

Numerical computation of transonic flow about wing-fuselage configurations on a vector computer
[AIAA PAPER 83-0499] 05 p0587 A83-16751

An exploratory study of finite difference grids for transonic unsteady aerodynamics
[AIAA PAPER 83-0503] 05 p0587 A83-16752

A computational method for subsonic compressible flow in diffusers
[AIAA PAPER 83-0505] 05 p0587 A83-16753

An implicit, transonic, full-potential code for cascade flow on H-grid topology
[AIAA PAPER 83-0506] 05 p0587 A83-16754

A fast finite element method for transonic potential flow calculations
[AIAA PAPER 83-0507] 05 p0587 A83-16755

Flow simulations for general nacelle configurations using Euler equations
[AIAA PAPER 83-0539] 05 p0587 A83-16775

Some applications of a generalized aerodynamic forces and moments theory
[AIAA PAPER 83-0543] 05 p0587 A83-16778

Viscous primary/secondary flow analysis for use with nonorthogonal coordinate systems
[AIAA PAPER 83-0556] 05 p0588 A83-16785

Multi-grid solution of Neumann pressure problem for viscous flows using primitive variables
[AIAA PAPER 83-0557] 05 p0637 A83-16786

On a finite-difference method for solving transient viscous flow problems
[AIAA PAPER 83-0560] 05 p0637 A83-16788

An implicit numerical analysis for two-dimensional, two-phase turbulent interior ballistic flows
[AIAA PAPER 83-0561] 05 p0637 A83-16789

Calculation of the pressure distribution and streamline pattern around a ring wing using finite difference methods
[AIAA PAPER 83-0645] 05 p0588 A83-16812

Numerical solution to the glancing sidewall oblique shock wave/turbulent boundary layer interaction in three-dimension
[AIAA PAPER 83-0136] 05 p0588 A83-16823

Aerodynamic performance of an annular classical airfoil cascade
[AIAA PAPER 83-0179] 05 p0588 A83-16824

Interactive phenomena in supersonic jet mixing problems
[AIAA PAPER 83-0288] 05 p0588 A83-16826

Transonic wing-body calculations using Euler equations
[AIAA PAPER 83-0501] 05 p0589 A83-16828

Calculation of three-dimensional transonic flow past a slender body /a wing/
05 p0589 A83-16877

Calculation of fundamental aerodynamic derivatives of aircraft
05 p0589 A83-16882

An implicit finite-difference method for chemical nonequilibrium flow through an axisymmetric supersonic nozzle
05 p0589 A83-16928

A numerical study of the effects of ambipolar diffusion on the collapse of magnetic gas clouds
05 p0698 A83-16997

Numerical investigation of the nozzle flow of a vibrationally nonequilibrium medium of a CO₂ gasdynamic laser
05 p0649 A83-17050

An asymptotic analysis of free convection boundary layer on a horizontal flat plate due to small fluctuations in surface temperature
05 p0638 A83-17321

Conical vortices - A class of exact solutions of the Navier-Stokes equations
05 p0638 A83-17353

A modulated point-vortex model for geostrophic, beta-plane dynamics
[AD-A126704] 05 p0639 A83-17355

Point vortex motions with a center of symmetry
05 p0639 A83-17356

Strained spiral vortex model for turbulent fine structure
05 p0639 A83-17357

Calculation of the flow of a dust-laden gas over a disk and the flat end of a cylinder
05 p0639 A83-17406

Calculation of the dispersal of a layer of granular material by a supersonic gas jet
05 p0639 A83-17407

Motion of a droplet in a nonisothermal flow
05 p0639 A83-17411

A three-dimensional hypersonic gas flow over a slender wing
05 p0589 A83-17412

Flow over flat and axisymmetric bodies moving at high variable velocities
05 p0589 A83-17413

Diagnostics of a discontinuity in a self-similar gas flow
05 p0639 A83-17415

An approach to calculating the flow following impingement of an underexpanded jet onto an infinite planar baffle
05 p0590 A83-17420

Use of limiting solutions of Falkner-Skan-Type equations in the integral method of evaluation of near wakes
05 p0590 A83-17422

Construction of pointwise bounds for solutions of the problem of flow on a uniformly heated moving continuous flat surface
05 p0640 A83-17552

Derivation and solution of the transonic integral equation for lifting flows
05 p0590 A83-17553

An implicit scheme for determining temperature in the presence of radiative-conductive heat transfer
05 p0691 A83-17644

Construction and investigation of schemes for the calculation of radiative transfer
05 p0640 A83-17645

The use of substantially nonuniform grids in the numerical solution of the Navier-Stokes equations
05 p0640 A83-17646

Instability of a convergent spherical shock wave
05 p0640 A83-17647

A high-order difference method for the computation of viscous-gas flows
05 p0590 A83-17648

The stability of positive solutions of inverse problems of heat conduction
05 p0640 A83-17649

Geophysical fluid dynamics --- Book
05 p0640 A83-17650

On the thermal and hydrodynamic stability of a fluid in a vertical slot
05 p0641 A83-17722

A method of limiting intermediate values of volume fraction in iterative two-fluid computations
05 p0641 A83-17725

Numerical calculation of two-dimensional natural convection in isothermal open cavities
05 p0641 A83-17742

Finite-element solution of the incompressible Navier-Stokes equations
05 p0641 A83-17743

Natural convection from a horizontal cylinder at small Grashof numbers
05 p0641 A83-17744

Discussion of 'On the calculation of turbulent heat transport downstream from an abrupt pipe expansion'
05 p0641 A83-17745

Far field conditions in unsteady subsonic flow
05 p0590 A83-17834

The hydromagnetic viscous boundary layer at the free surface of a rotating baroclinic fluid
05 p0641 A83-17835

The calculation of some laminar flows using various discretisation schemes
05 p0642 A83-17900

Modeling rotating stall by vortex dynamics
[AIAA PAPER 83-0002] 05 p0590 A83-17901

Prediction of secondary vortex flowfields induced by multiple free-jets issuing in close proximity
[AIAA PAPER 83-0289] 05 p0642 A83-17916

Approximate factorization schemes for 3D nonlinear supersonic potential flow
[AIAA PAPER 83-0376] 05 p0591 A83-17923

Real gas flow fields about three dimensional configurations
[AIAA PAPER 83-0581] 05 p0591 A83-17931

Branching of the Falkner-Skan solutions for gamma less than zero
05 p0642 A83-17942

The Oseen model for internal separated flows
05 p0642 A83-17943

A solution to the problem of multiparameter optimization in calculating flow around bodies with injection
06 p0712 A83-18143

A new transformation and method of solution of laminar boundary layer equations
06 p0756 A83-18152

The computation of the compressor cascade boundary layer
06 p0712 A83-18153

Testing subroutines solving advection-diffusion equations in atmospheric environments
06 p0756 A83-18374

Rotor blade flap-lag stability in turbulent flows
06 p0716 A83-18380

Finite-volume solutions to the Euler equations in transonic flow
[AIAA PAPER 81-1265] 06 p0712 A83-18405

Comparison of subsonic/transonic airbody flow prediction methods
06 p0712 A83-18408

An implicit time marching method for the calculation of transonic flows using Euler equations
[ONERA, TP NO. 1982-111] 06 p0712 A83-18437

Computer-aided analysis of three dimensional confined vortex flow
06 p0757 A83-18453

A comparison of two explicit time integration schemes applied to the transient heat equation
06 p0757 A83-18467

Boundary-layer pressures and the Corcos model - A development to incorporate low-wavenumber constraints
06 p0757 A83-19013

The generalized Lagrangian-mean equations and hydrodynamic stability
06 p0757 A83-19014

Wave-induced longitudinal-vortex instability in shear flows
06 p0757 A83-19015

Longitudinal-dispersion calculations in laminar flows by statistical analysis of molecular motions
06 p0758 A83-19019

A simple model of mixing and chemical reaction in a turbulent shear layer
[AD-A128220] 06 p0758 A83-19021

Local isotropy and anisotropy in a high-Reynolds-number turbulent boundary layer
06 p0758 A83-19023

The behavior of two-dimensional nonplane-parallel vortex flows of inviscid gas
06 p0758 A83-19118

The behavior of small perturbations of one-dimensional stationary transonic flows
06 p0758 A83-19119

Deformation of a drop in a viscous flow and conditions for the existence of the equilibrium form of the drop
06 p0758 A83-19122

Fully developed turbulent flow in a pipe - An intermediate layer
06 p0759 A83-19321

Application of Gyarmati's variational principle to laminar stagnation flow problem
06 p0760 A83-19400

Parietal jets, II - A problem of hypersustentation --- upper surface blowing
06 p0713 A83-19412

A two-scale semiempirical theory for turbulent boundary layers and jets
06 p0760 A83-19428

A numerical study of the lateral interaction between an axisymmetric jet issuing into vacuum and an obstacle
06 p0760 A83-19431

The stability of a preseparation boundary layer at the leading edge of a thin profile
06 p0713 A83-19432

Computing three-dimensional transonic gas flow through an axial-turbine stage
06 p0713 A83-19437

The far nonlinear field in transonic flows past nonlifting profiles
06 p0713 A83-19442

Spectral methods for flows in complex geometries
[AIAA PAPER 83-0229] 06 p0761 A83-19583

Boundary layer calculations in the inverse mode for incompressible flows over infinite swept wings
[AIAA PAPER 83-0454] 06 p0714 A83-19590

Critical angle of incidence for the flow around spheroids
07 p0862 A83-19668

Numerical prediction of dynamic forces on arbitrarily pitched airfoils
07 p0862 A83-19801

Computation of high Reynolds number internal/external flows
07 p0863 A83-19803

Measurements of reactive recirculating jet mixing in a combustor
07 p0924 A83-19819

Transonic airfoil calculations using solution-adaptive grids
07 p0863 A83-19824

Algorithms and methods for computer simulation of transonic flow
07 p0863 A83-19999

A numerical analysis of flow using streamline coordinates - The case of two-dimensional steady incompressible flow
07 p0925 A83-20277

A new multifold series general solution of the steady, laminar boundary layers. I - Theory of the multifold series expansion. II - Application theory of the Euler transformation
07 p0925 A83-20278

Response of parallel-flow and counterflow heat exchangers to sinusoidal flow rate changes of large amplitude
07 p0925 A83-20290

Current problems of mathematical physics and computational mathematics --- Russian book
07 p0988 A83-20302

Application of the small-parameter method to the numerical solution of differential equations
07 p0986 A83-20309

Methods of the numerical modeling of turbulent flows of an incompressible viscous fluid
07 p0925 A83-20314

The stability of flows near an infinite wedge or cone situated in supersonic gas flow
07 p0863 A83-20315

Solution of two-dimensional problems of radiating-gas dynamics
07 p0925 A83-20319

Optimization of the supersonic drag of a smooth wing by use of linearized potential theory --- French thesis
07 p0863 A83-20400

Analysis of secondary flows for tube-launched rocket configurations
07 p0863 A83-20417

The shape of low Reynolds number jets
07 p0926 A83-20527

Numerical calculation of the translational forced oscillations of a sloshing liquid in axially symmetric tanks
07 p0926 A83-21003

About a turbulence model to predict heat transfer correlations
07 p0926 A83-21008

On numerical methods of subsonic lifting surface theory
07 p0864 A83-21012

Transonic flow calculations by a finite element method
07 p0864 A83-21023

A class of exact solutions of the Navier-Stokes equations - Plane unsteady flow
07 p0927 A83-21171

Numerical calculation of the laminar flow in the inlet of the axial sealing gap of radial-flow compressors
07 p0864 A83-21339

Formation of turbulence around flow singularities
07 p0927 A83-21341

On spatial and temporal stability in three dimensional fluid flows
07 p0927 A83-21343

A finite boundary method for fluid flow field computations
07 p0927 A83-21436

Steady supersonic flow of a viscous heat-conducting gas past a cylinder with a flat end-face
08 p1041 A83-21630

Combination rotational fields in real flows
08 p1083 A83-21861

Two-dimensional flow impinging obliquely on a moving plane wall
08 p1083 A83-21867

An integral method in laminar film condensation of plane and axisymmetric bodies
08 p1083 A83-21893

Two-dimensional subsonic flow of a compressible medium
08 p1083 A83-22047

Self-preservation for a turbulent boundary layer over a d-type rough surface
08 p1083 A83-22066

Numerical calculations for performances of propellers in a static-state by vortex theory accounting of slipstream deformation and their comparisons with experiments
08 p1041 A83-22072

Fuselage-lifting surfaces interaction in unsteady subsonic flow --- French thesis
08 p1041 A83-22093

Numerical solution of transonic stream function equation
08 p1084 A83-22127

A finite element formulation for steady transonic Euler equations
08 p1042 A83-22129

Inviscid axisymmetric jet impingement with recirculating stagnation regions
08 p1042 A83-22130

An unsteady interactive separation process --- from downstream moving wall
08 p1042 A83-22131

Unsteady transonic flow over wings including inviscid/viscous interaction
08 p1042 A83-22132

Space basis for weakly solenoidal functions --- incompressible fluid dynamics
08 p1084 A83-22277

Nonlinear hydrodynamic pressure on an accelerating plate
08 p1084 A83-22377

Consistent modeling of scalars in turbulent flows
08 p1084 A83-22380

Two models of truncated Navier-Stokes equations on a two-dimensional torus
08 p1085 A83-22384

Analysis of aero-optic interface phenomena
08 p1042 A83-22588

A transonic quasi-3D analysis for gas turbine engines including split-flow capability for turbfans
08 p1042 A83-22647

Investigation of solution of Navier-Stokes equations using a variational formulation
08 p1085 A83-22648

Numerical solution of viscous flows using integral equation methods
08 p1085 A83-22649

Numerical calculation of the separation and connection of two-dimensional supersonic flows in channels with discontinuous boundaries
08 p1046 A83-22658

A sub-boundary layer with a two dimensional turbulent boundary layer - An intermediate layer
08 p1085 A83-22771

Modern methods of numerical investigation of rarefied gas phenomena
08 p1085 A83-22992

Some aspects of the fluid dynamics of laser welding
08 p1112 A83-23090

An experimental and theoretical investigation of the onset of convection in rotating spherical shells
08 p1086 A83-23094

On the nonlinear stability of slowly varying time-dependent viscous flows
08 p1086 A83-23096

Isothermal models of gas-turbine combustors
08 p1057 A83-23097

Numerical study of the performance of tornado-type wind energy systems
08 p1132 A83-23133

Numerical methods in laminar and turbulent flow; Proceedings of the Second International Conference, Venice, Italy, July 13-16, 1981
08 p1087 A83-23176

On the marching solution of elliptic equations in viscous fluid mechanics
08 p1087 A83-23177

On the numerical solution of some types of unsteady incompressible viscous flow
08 p1087 A83-23178

Numerical solution of the Navier-Stokes equations by multi-grid techniques
08 p1088 A83-23183

Numerical simulation of three dimensional flows in duct
08 p1088 A83-23184

Different finite element formulations for the Navier-Stokes equations
08 p1088 A83-23185

On the finite element simulation of incompressible turbulent flow in general two-dimensional geometries
08 p1088 A83-23187

A refined PUMPIN / Pressure Update by Multiple Path INtegration/ method for updating pressures in the numerical solution of the incompressible fluid equations
08 p1088 A83-23188

Prediction of developing turbulent flow by the finite element method
08 p1088 A83-23189

Improvements of the optimal control method to solve turbulent flows
08 p1088 A83-23190

Prediction of turbulent mixing in confined co-axial reacting jets
08 p1088 A83-23191

Computer modelling of turbulent recirculating flows in engineering applications
08 p1088 A83-23192

A numerical study of turbulent, confined, swirling jets
08 p1088 A83-23193

Accurate solutions for laminar and turbulent boundary layers at very large pressure gradient parameters
08 p1089 A83-23195

The numerical simulation of the turbulent boundary layers at a rough, air-water interface
08 p1089 A83-23196

Numerical prediction of turbulent boundary layer development on a two-dimensional curved wall
08 p1089 A83-23198

Numerical calculations of turbulent heat transfer downstream of a rearward-facing step
08 p1089 A83-23199

Momentum and heat transfer characteristics in turbulent flow 08 p1089 A83-23200

A finite element method for the shallow water equations 08 p1089 A83-23201

Current and density structure in shelf waters due to fresh water discharge - A numerical study 08 p1089 A83-23202

A finite element solution of compressible flow through cascades of turbomachines 08 p1089 A83-23203

Semi-elliptic computation of axis-symmetric transonic flows 08 p1089 A83-23204

Hypersonic viscous flows in a streamline coordinate system 08 p1090 A83-23205

Numerical study on flow behaviour and heat transfer in the vicinity of starting point of transpiration 08 p1090 A83-23206

Numerical solution of the momentum equations in unsteady incompressible flow 08 p1090 A83-23207

Natural convection in a rotating annulus 08 p1090 A83-23209

The effect of forced and free convection in the discharge of a pressurized gas 08 p1090 A83-23210

Numerical calculation of the heat transfer by natural convection in a cubical enclosure 08 p1090 A83-23212

A semi analytic method for viscous flows in the vicinity of singular corners 08 p1090 A83-23213

On a deferred-correction procedure for determination of central-difference solutions to the Navier-Stokes equations 08 p1090 A83-23214

An experimental investigation of the dispersion of a gas jet in a coflowing stream of air 08 p1042 A83-23215

Error and stability analysis of the finite element solution for the transport equation 08 p1090 A83-23216

Symmetric marching technique /SMT/ for the efficient solution of discretized Poisson equation on non-rectangular regions 08 p1091 A83-23218

Finite element analysis of mixed convection applied to the storage of solar energy 08 p1091 A83-23219

A solution to inverse problem of quasi three-dimensional flow in centrifugal impeller 09 p1257 A83-23331

Flow characteristics and methods of flow calculation of high-speed compressible flow through pipe orifices 09 p1257 A83-23332

Influence of gas inertia forces generated within the stabilizing restrictor on dynamic characteristics of externally pressurized thrust gas bearings. II - Case of turbulent flow at the capillary restriction 09 p1273 A83-23336

The modeling of heat transfer in a boundary layer 09 p1257 A83-23427

An evaluation of the thermal two-phase-state parameter given the nonstationary turbulence of a two-phase flow in a tube 09 p1258 A83-23441

A study of the processes involved in the filling of pipelines with liquid 09 p1258 A83-23444

The calculation of the coefficient-optimal total pressure of a system of plane shock waves 09 p1258 A83-23447

A difference scheme of second-order accuracy with a minimal pattern for hyperbolic equations 09 p1335 A83-23567

Numerical method for solving radiative-transfer equations in one-dimensional problems of radiative gas-dynamics 09 p1258 A83-23568

Calculation of three-dimensional transonic flow past elongated bodies 09 p1196 A83-23570

Application of the modified Lax-Wendroff method to the solution of unsteady self-similar problems of boundary layer theory 09 p1258 A83-23572

The influence of mathematical viscosity on the difference solution in problems of two-temperature gas dynamics 09 p1347 A83-23573

Helicopter-rotor aeroelastic equilibrium under nonlinear aerodynamic forces 09 p1202 A83-23679

Quasi-Lagrangian rezoning of fluid codes maintaining an orthogonal mesh 09 p1259 A83-23721

On the symmetric form of systems of conservation laws with entropy 09 p1350 A83-23724

Spurious solutions in driven cavity calculations 09 p1259 A83-23725

Diffusion slipping of a binary gas mixture of moderate density along a flat surface 09 p1259 A83-23983

Classification and stability criteria of separated flows 09 p1259 A83-24010

Analysis of circulation-controlled airfoils in transonic flow 09 p1196 A83-24032

Modifying a general aviation airfoil for supercritical flight 09 p1196 A83-24039

Calculation of channel flows of gases by the Monte-Carlo method with correction for collisions 09 p1260 A83-24048

Boundary value problems of mathematical physics and related questions in the theory of functions. 14 --- Russian book 09 p1339 A83-24316

Attractors of the Navier-Stokes system and of parabolic equations, and the estimation of their dimensionality 09 p1260 A83-24317

The finite-dimensionality of bounded invariant sets for the Navier-Stokes system and other dissipative systems 09 p1261 A83-24321

Theoretical justification of the method of successive approximations for stationary problems of the mechanics of viscous fluids with free boundaries 09 p1261 A83-24323

Solutions of a stationary system of Navier-Stokes equations having an infinite Dirichlet integral 09 p1261 A83-24324

Calculation of the average slipstream of a propeller and its effect on the performance of an aircraft [ONERA, TP NO. 1982-120] 09 p1197 A83-24331

Vortex sheets and concentrated vorticity - A variation on the theme of asymptotic modelling in fluid mechanics 09 p1261 A83-24335

Numerical solutions for spin-up from rest in a cylinder 09 p1261 A83-24415

On the application of the integral invariants and decay laws of vorticity distributions [AD-A128456] 09 p1262 A83-24421

An asymptotic solution near the separation point of a shock layer in the case of hypersonic flow around pointed bodies 09 p1197 A83-24483

The rotational motions of compressible fluids. II 09 p1262 A83-24501

The supersonic combustion around a truncated cone 09 p1198 A83-24504

Moment coefficient of the NACA 65 profile in delay cascades 09 p1198 A83-24509

Nonlinear truncation error analysis of finite difference schemes for the Euler equations [AIAA PAPER 81-0193] 09 p1336 A83-24654

Wall pressure fluctuations in attached boundary-layer flow 09 p1198 A83-24655

A higher order panel method applied to vortex sheet roll-up 09 p1198 A83-24658

An interaction algorithm for three-dimensional turbulent subsonic aerodynamic juncture region flow 09 p1198 A83-24659

A method of predicting unsteady turbulent flows and its application to diffusers with unsteady inlet conditions [AIAA PAPER 82-0349] 09 p1198 A83-24660

Using a global hydrogen-air combustion model in turbulent reacting flow calculations 09 p1227 A83-24667

Computed and measured turbulence in axisymmetric reciprocating engines 09 p1207 A83-24669

On heat transfer modelling for turbulent shear flows on curved surfaces 09 p1263 A83-24822

Computation of hypersonic viscous flow over a body with mass transfer and/or spin 09 p1198 A83-24878

Pulsing techniques for solid-propellant rocket motors - Modeling and cold-flow testing 09 p1220 A83-24886

On the calculation of the velocity induced by a vortex-source cone 09 p1198 A83-25024

Kinematic compatibility in the stream function-vorticity formulation 09 p1263 A83-25111

Equations for the general two-dimensional supersonic flow 09 p1198 A83-25112

A study of thermal convection and heat transfer --- Russian book 09 p1264 A83-25246

Axisymmetric flows in spin-up from rest of a stratified fluid in a cylinder 10 p1412 A83-25414

Finite-element method for time-dependent Euler equation --- of inviscid incompressible flow 10 p1413 A83-25462

Multiprocessor computer modeling of transonic flow 10 p1460 A83-25468

A time efficient finite differences algorithm for the solution of the meridional flow in turbo compressor impellers [ASME PAPER 82-WA/FE-3] 10 p1413 A83-25683

A stall margin design method for planar and axisymmetric diffusers [ASME PAPER 82-WA/FE-8] 10 p1413 A83-25685

A numerical and experimental investigation of turbulent heat transport of an axisymmetric jet impinging on a flat plate [ASME PAPER 82-WA/HT-55] 10 p1413 A83-25695

Comments on the dynamical effects of radiative viscosity --- in astrophysics 10 p1503 A83-25719

Flow through rotating straight pipes of a circular cross section 10 p1413 A83-25780

A model of the excitation of large scale fluctuations in a shear layer [AIAA PAPER 83-0724] 10 p1475 A83-25935

Aeroacoustic computation of cylinder wake flow [AIAA PAPER 83-0736] 10 p1476 A83-25940

Amplification of non-linear standing waves in a cylindrical cavity with varying cross section 10 p1414 A83-26143

Shock induced unsteady flat plate boundary layers and transitions 10 p1414 A83-26147

Shock capturing using flux-corrected transport algorithms with adaptive gridding 10 p1415 A83-26161

Shock wave diffraction at a sharp edge and the effect of baffles in a shock tube 10 p1416 A83-26164

Propagation of two-dimensional nonsteady detonation in a channel with backward-facing step 10 p1416 A83-26165

Shock diffraction computations over complex structures 10 p1417 A83-26196

Number of modes governing two-dimensional viscous, incompressible flows 10 p1417 A83-26272

Loss measurements using a fast traverse in an ILPT transient cascade --- Isentropic Light Piston Cascade Tunnel 10 p1372 A83-26423

Numerical calculation of local convective heat transfer coefficients over air-cooled vane surfaces 10 p1418 A83-26772

Shock-capturing parabolized Navier-Stokes model /SCIPVIS/ for the analysis of turbulent underexpanded jets [AIAA PAPER 83-0704] 10 p1418 A83-26916

Prediction of the surge line of axial multistage compressor 10 p1373 A83-26924

Fluctuating flow induced by a rotating disc 11 p1564 A83-27101

Computer simulation of transient energy storage in a packed-bed of iron spheres with liquid-metal through-flow by numerical inversion of Laplace transforms 11 p1610 A83-27320

A basic code for the prediction of transient three-dimensional turbulent flowfields 11 p1565 A83-27412

Near-wall similarity in three-dimensional turbulent boundary layers. I - Model review. II - Pressure-driven flow results 11 p1565 A83-27414

Solution of particulate viscous flow over a two dimensional cylinder 11 p1566 A83-27424

Solid particle dynamic behavior through twisted blade rows 11 p1525 A83-27478

Concentration of vorticity and spiral vortices 11 p1566 A83-27703

Use of an equation for the transport of the energy of turbulent pulsations to calculate two-phase jets 11 p1567 A83-27707

Theoretical and experimental study of the flow of a viscous fluid near the line of intersection of cylindrical and plane surfaces 11 p1525 A83-27709

A scheme for the analysis of a developed cavitation flow past a wedge 11 p1567 A83-27719

Motion of a circular cylinder in a rectangular channel 11 p1567 A83-27720

Regular intersection of two weak shock waves 11 p1567 A83-27772

Semi-elliptic computation of an axis-symmetric transonic nozzle flow 11 p1526 A83-27775

Hypersonic slender-wedge analysis with gradual change in angle of attack 11 p1526 A83-27864

Effect of initial conditions on constant pressure mixing between two turbulent streams 11 p1567 A83-27875

Blockage effect on vortex shedding from bluff bodies 11 p1567 A83-28000

Generalized dynamics of three-dimensional vortex singularities /vortons/ 11 p1568 A83-28065

Spatial Fourier modes controlling Navier-Stokes flow 11 p1568 A83-28236

A numerical simulation of transition in plane channel flow [AIAA PAPER 83-0047] 11 p1568 A83-28347

Methods for solving nonstationary problems of the theory of radiative-convective heat transfer 11 p1568 A83-28369

A short look at nonlinear hydrodynamic stability theory 11 p1569 A83-28404

Asymptotic solution of the Navier-Stokes equations for the problems of the radial flow of a fluid in a gap formed by two rotating disks 11 p1569 A83-28532

On the self-excited circumferential nonuniformity of a potential fluid flow near a circular cascade of profiles 11 p1569 A83-28534

Estimation of the vortex ratio and Karman constant for vortices 11 p1570 A83-28553

Single-mode theory of diffusive layers in thermohaline convection 11 p1570 A83-28755

An analysis of the thermal state of plane channels with allowance for the mutual influence of the processes in the wall and in the fluid 11 p1570 A83-28796

A radial temperature gradient in swirling gas flow 11 p1570 A83-28797

Mixed laminar convection on a vertical surface under conditions of strong injection 11 p1571 A83-28799

The penalty function method in mechanics - A review of recent advances 12 p1717 A83-28852

A penalty finite element algorithm for parabolic flow problems 12 p1721 A83-28855

Standard and asymptotic finite element methods for incompressible viscous flows 12 p1721 A83-28856

The penalty function method and its applications to the numerical solution of boundary value problems 12 p1770 A83-28857

Three-dimensional, two-phase supersonic nozzle flows 12 p1695 A83-28955

Euler equations - Implicit schemes and boundary conditions 12 p1695 A83-28959

A fuzzy algorithm to compute transonic profile flow 12 p1696 A83-28973

Computations of unsteady transonic cascade flows 12 p1696 A83-28975

MHD free-convection flow in the Stokes problem for a porous vertical plate by finite difference method 12 p1779 A83-28984

Three-dimensional viscous analysis of ducts and flow splitters 12 p1696 A83-29010

Computational treatment of three-dimensional transonic canard-wing interactions 12 p1696 A83-29021

Computation of nonlinear supersonic potential flow over three-dimensional surfaces 12 p1696 A83-29022

Wave interaction in radiative gas dynamics 12 p1775 A83-29032

High resolution schemes for hyperbolic conservation laws 12 p1771 A83-29095

Compact finite difference schemes for the Euler and Navier-Stokes equations 12 p1722 A83-29096

Steady viscous flows by compact differences in boundary-fitted coordinates 12 p1722 A83-29099

A comparison of experimental and numerical results obtained for the secondary flow in a large turbine cascade 12 p1696 A83-29157

Simplified multilayer insulation pumpdown calculation approach 12 p1722 A83-29217

The flow between two finite rotating disks enclosed by a cylinder 12 p1723 A83-29229

Calculation of fully developed turbulent flows in ducts of arbitrary cross-section 12 p1723 A83-29231

Secondary instability of wall-bounded shear flows 12 p1723 A83-29234

Flow of a thin fluid layer covered by a magnetizable surfactant 12 p1781 A83-29263

The conjugate heat-transfer problem of a controlled laminar boundary layer in a magnetic field 12 p1781 A83-29265

Hierarchical model of two-dimensional turbulence 12 p1781 A83-29266

Investigation of rotating flow in a longitudinal magnetic field 12 p1781 A83-29267

The method of successive approximations in the problem of a boundary layer with longitudinal and transverse pressure differentials 12 p1723 A83-29284

A finite element method for high Reynolds number viscous fluid flow using two step explicit scheme 12 p1724 A83-29442

Wave processes in solids-laden gas flows 12 p1724 A83-29443

Implicit time integration for plasma simulation 12 p1781 A83-29608

Elliptic-vortex method for incompressible flow at high Reynolds number 12 p1724 A83-29609

Adaptive zoning for singular problems in two dimensions 12 p1771 A83-29613

Numerical estimates of Hausdorff dimensions --- for problems in turbulence theory 12 p1724 A83-29615

Three-dimensional steady stratified flows - A numerical approach 12 p1724 A83-29616

Relationship between the truncation errors of centered finite-difference approximations on uniform and nonuniform meshes 12 p1771 A83-29619

ADI on staggered mesh - A method for the calculation of compressible convection 12 p1724 A83-29621

Finite-sized fluid particle in a nonuniform moving grid 12 p1725 A83-29627

Computational techniques for spherical boundary conditions --- thermodynamic systems 12 p1783 A83-29629

A numerical study of the two-dimensional Navier-Stokes equations in vorticity-velocity variables 12 p1725 A83-29639

On local relaxation methods and their application to convection-diffusion equations 12 p1725 A83-29644

Numerical boundary condition procedures and multigrid methods; Proceedings of the Symposium, NASA Ames Research Center, Moffett Field, CA, October 19-22, 1981 12 p1772 A83-29646

Fully implicit shock tracking 12 p1725 A83-29651

High-Re solutions for incompressible flow using the Navier-Stokes equations and a multigrid method 12 p1725 A83-29659

Application of multigrid methods for integral equations to two problems from fluid dynamics 12 p1725 A83-29661

Computation of steady laminar flow over a circular cylinder with third-order boundary conditions 12 p1725 A83-29664

Spatial resolution requirements for direct numerical simulation of the Rayleigh-Benard convection 12 p1725 A83-29666

An open boundary condition for incompressible stratified flows 12 p1725 A83-29667

An overrelaxation method for Euler equations in steady transonic flow 12 p1726 A83-29668

Driven cavity flows by efficient numerical techniques 12 p1726 A83-29669

Calculation of unsteady small disturbance transonic flow at arbitrary reduced frequency using an extended integral equation method. 12 p1697 A83-29832

[AIAA 83-0884] Calculation of unsteady aerodynamic coefficients using transonic time domain methods 12 p1697 A83-29833

[AIAA 83-0885] A Harmonic Gradient method for unsteady supersonic flow calculations 12 p1697 A83-29834

[AIAA 83-0887] Effects of viscosity on transonic-aerodynamic and aeroelastic characteristics of oscillating airfoils 12 p1697 A83-29835

[AIAA 83-0888] Flutter analysis of a transport wing using XTRAN3S 12 p1743 A83-29848

[AIAA 83-0922] Describing function flutter analysis for transonic flow Extension and comparison with time marching analysis 12 p1744 A83-29859

[AIAA 83-0958] Airfoil shape and thickness effects on transonic airloads and flutter 12 p1702 A83-29860

[AIAA 83-0959] A discretized asymptotic method for unsteady helicopter rotor airloads 12 p1697 A83-29867

[AIAA 83-0989] Fast iterative solution of Poisson equation with Neumann boundary conditions in nonorthogonal curvilinear coordinate systems by a multiple grid method 12 p1726 A83-29898

Use of the finite-element method for natural convection in a horizontally confined infinite layer of fluid 12 p1726 A83-29899

On partial spectral expansions with natural convection in spherical annulus enclosures as an example 12 p1726 A83-29900

Transonic, shock, and multidimensional flows: Advances in scientific computing; Proceedings of the Symposium, University of Wisconsin, Madison, WI, May 13-15, 1981 12 p1726 A83-29926

Computational fluid dynamics of airfoils and wings 12 p1698 A83-29927

Steady-state solution of the Euler equations for transonic flow 12 p1698 A83-29929

Computational study of the asymptotic flow structure of a high-aspect-ratio swept wing in transonic flow [AD-A129934] 12 p1698 A83-29931

Numerical solution of the equations of compressible viscous flow 12 p1698 A83-29933

Implicit finite difference simulation of inviscid and viscous compressible flow 12 p1726 A83-29934

Towards a closer cooperation between theoretical and numerical analysis in gas dynamics 12 p1698 A83-29936

Tracking of interfaces for fluid flow: Accurate methods for piecewise smooth problems. 12 p1726 A83-29937

Shock calculations and the numerical solution of singular perturbation problems 12 p1726 A83-29938

The design and numerical analysis of vortex methods 12 p1727 A83-29940

Relaxation of Reynolds shear stress in a nonequilibrium turbulent boundary layer 13 p1838 A83-30040

On an iterative method with fictitious unknowns 13 p1912 A83-30076

The small-parameter method in problems involving unsteady two-phase flows with shock waves 13 p1839 A83-30080

On the maximal invariance group and the general solution of the one-dimensional equations of gas dynamics 13 p1839 A83-30083

Asymptotics of solutions of the Orr-Sommerfeld equation describing unstable oscillations at large Reynolds numbers 13 p1839 A83-30091

On the motion of a spherical fluid film 13 p1839 A83-30092

Equation of motion for a small rigid sphere in a nonuniform flow 13 p1839 A83-30104

Effect of rotation on the stability of a bounded cylindrical layer of fluid heated from below 13 p1839 A83-30105

Nonlinear interfacial progressive waves near a boundary in a Boussinesq fluid 13 p1839 A83-30106

A two-equation turbulence model for two-phase flows 13 p1839 A83-30109

Asymmetries in evaporation and condensation Knudsen layer problems 13 p1840 A83-30110

Computational hydraulics --- Book 13 p1840 A83-30132

Calculation of fundamental aerodynamic derivatives of aircraft. II 13 p1804 A83-30516

Conference on Complex Turbulent Flows: Comparison of Computation and Experiment, Stanford University, Stanford, CA, September 3-6, 1980, Proceedings. Volume 1 - Objectives, evaluation of data, specifications of test cases, discussion and position papers 13 p1840 A83-30626

Experimental data needs for computational fluid dynamics - A position paper 13 p1840 A83-30627

Conference on Complex Turbulent Flows: Comparison of Computation and Experiment, Stanford University, Stanford, CA, September 14-18, 1981, Proceedings. Volume 2 - Taxonomies, reporters' summaries, evaluation, and conclusions 13 p1840 A83-30630

Overview of taxonomy - Morphology of the flows and computational methods 13 p1841 A83-30631

Integral techniques --- for turbulence modeling 13 p1841 A83-30632

Turbulence modeling in the vicinity of a wall 13 p1841 A83-30635

Compressibility effects in turbulence modeling 13 p1841 A83-30637

Influence of numerics and computer variance in the computation of complex turbulent flows 13 p1841 A83-30639

A user's viewpoint on computational fluid dynamics 13 p1842 A83-30642

Prediction of turbulent flows - A Boeing view 13 p1804 A83-30643

Conference on Complex Turbulent Flows: Comparison of Computation and Experiment, Stanford University, Stanford, CA, September 14-18, 1981, Proceedings. Volume 3 - Comparison of computation with experiment, and computers' summary reports 13 p1842 A83-30644

Ways to improve the effectiveness of methods of the direct statistical computerized simulation of rarefied-gas flows 13 p1932 A83-30659

Long eddies in sheared flows 13 p1842 A83-30915

Annual review of fluid mechanics, Volume 15 --- Book 13 p1842 A83-31076

Homogeneous turbulence 13 p1843 A83-31081

Low-Reynolds-number airfoils 13 p1804 A83-31082

The turbulent wall jet - Measurements and modeling 13 p1843 A83-31085

Flow in curved pipes 13 p1843 A83-31086

Numerical optimization studies of axisymmetric unsteady sprays 13 p1843 A83-31368

Tracing complex singularities with spectral methods 13 p1914 A83-31370

Two-dimensional plasma model for the arc-driven rail gun 13 p1926 A83-31381

Classification of difference schemes of gas dynamics by the method of differential approximation. I - One-dimensional case 13 p1844 A83-31592

On the construction of K-consistent difference schemes of gas dynamics 13 p1913 A83-31594

Application of contour-conformal mapping to the flow along an S2 current sheet 13 p1805 A83-31798

A calculation of the gas flow in a zone of energy release during a cylindrical explosion 14 p2008 A83-31896

A numerical solution to the equations for the dynamics of a viscous incompressible fluid containing dispersed particles 14 p2008 A83-31897

Applying the method of flows to a problem concerning the dynamics of a viscous, stratified fluid 14 p2008 A83-31898

The propagation of a curved flame front in a specified gas-flow field 14 p1989 A83-32088

Nonstationary phenomena in flows of a viscous reactive fluid 14 p1989 A83-32091

The homogeneous property and flux splitting in gas dynamics 14 p2094 A83-32124

Conservation form, in general non steady coordinates, of the Navier-Stokes equations and boundary conditions for a moving boundary problem 14 p2008 A83-32149

Thin axisymmetric cavities in flow past a body in a longitudinal gravitational field 14 p2008 A83-32158

Negative viscosity effect in large-scale turbulence Long-wave instability of a periodic system of eddies 14 p2009 A83-32422

The unsteady flow around an oscillating sphere in a viscous fluid 14 p2009 A83-32515

A numerical study of the Burgers turbulence at extremely large Reynolds numbers 14 p2009 A83-32520

Low Reynolds number shear flow along an elliptic hole in a wall 14 p2009 A83-32522

Disadvantages of thin airfoil formulations for closely coupled airfoils 14 p1970 A83-32591

The large-particle method in gas dynamics - A computational experiment --- Russian book 14 p2009 A83-32600

Viscous shock-layer flowfield analysis by an explicit-implicit method [AIAA PAPER 83-1423] 14 p1970 A83-32702

Knudsen layer characteristics for a highly cooled blunt body in hypersonic rarefied flow [AIAA PAPER 83-1424] 14 p1970 A83-32703

Viscous real gas flowfields about three dimensional configurations [AIAA PAPER 83-1511] 14 p1970 A83-32748

Investigation of the simultaneous variable solution for velocity and pressure in incompressible fluid flow problems [AIAA PAPER 83-1519] 14 p2010 A83-32752

An inviscid three-dimensional analysis of the Space Shuttle main engine hot-gas manifold [AIAA PAPER 83-1523] 14 p1984 A83-32754

An implicit solution procedure for finite difference modeling of the Stefan problem [AIAA PAPER 83-1527] 14 p2011 A83-32758

Computation of two-dimensional jet interaction flow field [AIAA PAPER 83-1546] 14 p1971 A83-32769

Analysis of aerothermal loads on spherical dome protuberances [AIAA PAPER 83-1557] 14 p1971 A83-32775

A strongly implicit simultaneous variable solution procedure for velocity and pressure in fluid flow problems [AIAA PAPER 83-1569] 14 p2012 A83-32781

Computational method for Chaplygin function 14 p2012 A83-32969

Aerodynamic theory for wing with side edge passing subsonically through a gust 14 p1971 A83-32977

A finite element algorithm for computational fluid dynamics 14 p2078 A83-32978

An implicit, bidiagonal numerical method for solving the Navier-Stokes equations 14 p2012 A83-32979

Transonic flow calculations using the Euler equations 14 p1971 A83-32981

A more accurate transonic computational method for wing-body configurations 14 p1971 A83-32982

Decay of streamwise vorticity downstream of a three-dimensional protuberance 14 p1971 A83-32983

Numerical solution of transonic wing flowfields 14 p1971 A83-32984

A split-coefficient/locally monotonic scheme for multishocked supersonic flow 14 p1971 A83-32985

Force and moment in incompressible flows 14 p2012 A83-32991

Efficient computation of volume in flow predictions 14 p2012 A83-32994

Unsteady transonic small disturbance approximation with strong shock waves 14 p1972 A83-32995

Analytical approximation of two-dimensional separated turbulent boundary-layer velocity profiles 14 p2012 A83-32997

Numerical analysis of an axisymmetric viscous flow 14 p2013 A83-33375

Analysis of self-similar problems of imploding shock waves by the method of characteristics 14 p2013 A83-33386

Turbulent shear flows 3; International Symposium, 3rd, University of California, Davis, CA, September 9-11, 1981, Selected Papers 15 p2154 A83-33651

Dynamics of an unsteady turbulent boundary layer 15 p2154 A83-33654

The assessment of numerical diffusion in upwind difference calculations of turbulent recirculating flows 15 p2155 A83-33667

A model of three-dimensional transfer in non-isotropic homogeneous turbulence 15 p2156 A83-33670

Second order closure for variable density free shear layer 15 p2156 A83-33672

The turbulence modelling of variable density flows - A mixed-weighted decomposition 15 p2156 A83-33673

Direct simulation of homogeneous turbulent shear flows on the Illiac IV computer - Applications to compressible and incompressible modeling 15 p2156 A83-33674

Impingement of an oblique shock wave on a cylinder 15 p2156 A83-33727

Hypersonic viscous flows past general bodies at angle of attack and yaw 15 p2119 A83-33728

Variational principles and free-boundary problems --- Book 15 p2223 A83-33749

Viscous-inviscid interactions in cascades 15 p2120 A83-33790

Technical improvements for direct numerical simulation of homogeneous three-dimensional turbulence 15 p2156 A83-33820

On one-dimensional stretching functions for finite-difference calculations --- computational fluid dynamics 15 p2224 A83-33821

Application of the multigrid method to Poisson's equation in boundary-fitted coordinates 15 p2157 A83-33824

Generation of boundary-fitted curvilinear coordinate systems for a two-dimensional axisymmetric flow problem 15 p2157 A83-33825

Finite elements and characteristics applied to advection-diffusion equations 15 p2157 A83-33864

Numerical simulation of a compressible turbulent boundary layer over a conductive wall with line heat source 15 p2157 A83-33865

Operator splitting methods for the computation of reacting flows 15 p2157 A83-33866

Progress in computational physics 15 p2216 A83-33868

Laminar compressible flow between close rotating disks - An asymptotic and numerical study 15 p2157 A83-33869

The two-dimensional, viscous boundary-value problem for fluctuations in boundary layers [AIAA PAPER 83-0044] 15 p2158 A83-33998

Thermal model of a cylindrically symmetric solar pond 15 p2190 A83-34073

The fictitious domain method for the numerical solution of nonstationary thermal problems 15 p2158 A83-34227

Unsteady non-linear heat conduction in complex geometries 15 p2159 A83-34233

Computation of the three-dimensional unsteady thermal field in a cooled mirror by a finite difference explicit method 15 p2159 A83-34247

Stable spline methods for parabolic partial differential equations --- of relevance to heat transfer and fluid mechanics 15 p2159 A83-34251

The consistent method for computing derived boundary quantities when the Galerkin FEM is used to solve thermal and/or fluids problems 15 p2159 A83-34252

A quasi-three dimensional analysis of thermal ablation from a hypersonic missile 15 p2159 A83-34254

Assessment of two computational procedures for spray combustors 15 p2160 A83-34255

Accuracy aspects of the finite element method in free convection heat transfer problems 15 p2160 A83-34256

An effective numerical technique for entry length laminar convective heat transfer in vertical and horizontal ducts of any cross section 15 p2160 A83-34258

A coupled conduction-convection study in the slip-flow regime 15 p2160 A83-34261

Laminar flow heat transfer with axial conduction in a circular tube - A finite difference solution 15 p2160 A83-34262

Method to solve some coupled convection and conduction problems 15 p2160 A83-34264

Fluid flow within reciprocating-engine cylinders 15 p2160 A83-34265

Numerical study of transient laminar combustion in boundary layer flow 15 p2161 A83-34267

Nonlinear convection in a rotating layer - Amplitude expansions and normal forms 15 p2161 A83-34324

Axisymmetric vortex flow in a turbine stage under variable operating conditions 15 p2120 A83-34899

A theoretical and experimental study of non-adiabatic wall effects on transonic shock/boundary layer interaction [AIAA PAPER 83-1421] 15 p2120 A83-34901

Effects of chemical modeling on three-dimensional nonequilibrium viscous shock-layer flows [AIAA PAPER 83-1425] 15 p2120 A83-34902

Improvements in rocket engine nozzle and high altitude plume computations [AIAA PAPER 83-1547] 15 p2130 A83-34922

Numerical integration of the unsteady-flow equations for a two-dimensional supersonic free jet 15 p2162 A83-34977

Laminar natural convection from a horizontal plate and the influence of plate-edge extensions 16 p2348 A83-35337

A statistical model of fluid-element motions and vertical diffusion in a homogeneous stratified turbulent flow 16 p2371 A83-35340

Numerical processing of flow-visualization pictures Measurement of two-dimensional vortex flow 16 p2348 A83-35341

Self-consistent calculation of the alpha-effect and turbulent magnetic diffusion 16 p2414 A83-35342

Experiments on solitary internal Kelvin waves 16 p2348 A83-35343

A viscous vortex pair in ground effect 16 p2348 A83-35344

The evolution of Tollmien-Schlichting waves near a leading edge. II - Numerical determination of amplitudes 16 p2348 A83-35346

Generating exact solutions of the two-dimensional Burgers' equations 16 p2349 A83-35524

Optimum design for potential flows 16 p2288 A83-35525

Unsteady gas flow into vacuum through a perforated barrier 16 p2349 A83-35536

Free convection about a sphere at small Grashof number 16 p2349 A83-35558

Calculation of a laminar flow of a compressible gas in plane curvilinear ducts with heat transfer 16 p2349 A83-35701

A study of the distribution of static pressure and tangential stresses on the walls of a curved duct 16 p2350 A83-35719

A solution to the direct problem of a Laval nozzle for a two-phase medium 16 p2289 A83-35720

Compact reversal of a plane supersonic flow 16 p2289 A83-35721

A study of supersonic nonstationary flow past conical bodies 16 p2289 A83-35722

A finite hybrid numerical analysis of the internal and external transonic flow fields of inlets 16 p2289 A83-35814

A time dependent numerical scheme for three-dimensional inviscid compressible flows in curvilinear coordinates 16 p2290 A83-35815

Development of a short computation time implicit method for computing transonic flows with strong shock waves [ONERA, TP NO. 1983-50] 16 p2290 A83-35816

Experiments and mathematical simulation of plate distortion simulators 16 p2351 A83-35817

Semi implicit calculation method of the flow field in a duct with the flame stabilized by a step --- for aircraft engine combustion chamber design [ONERA, TP NO. 1983-52] 16 p2303 A83-35820

Applications of computational techniques in the design of ramjet engines 16 p2290 A83-35828

Investigation of flow field in a turbocompressor by the finite element method 16 p2290 A83-35834

Axisymmetric flow in front of a transonic compressor with unique incidence condition [ONERA, TP NO. 1983-51] 16 p2290 A83-35835

Application of streamline iteration and relative flow field methods to the calculation of the subsonic flow field of S1 stream surface of turbomachinery 16 p2290 A83-35836

Blade-to-blade transonic flow calculation in axial turbomachines 16 p2290 A83-35837

Numerical computation of turbulent flow around the spinner of a turbofan engine 16 p2291 A83-35838

Computation of blade cascade aerodynamic losses due to detached shock waves [ONERA, TP NO. 1983-53] 16 p2291 A83-35844

A contribution to the calculation of secondary flows in an axial flow compressor 16 p2291 A83-35852

Prediction of cascade performance in the presence of a separating boundary layer 16 p2292 A83-35876

Evaluation of a surface panel method coupled with several boundary layer analyses [AIAA PAPER 83-0011] 16 p2351 A83-36039

Improved relaxation schemes for transonic potential calculations [AIAA PAPER 83-0372] 16 p2292 A83-36053

Three-dimensional nonequilibrium viscous shock-layer flow over the Space Shuttle Orbiter [AIAA PAPER 83-0487] 16 p2293 A83-36056

Parabolized Navier-Stokes solutions for hypersonic flow fields [AIAA PAPER 83-0580] 16 p2293 A83-36061

Turbulence modeling for computational aerodynamics 16 p2293 A83-36079

Mode propagation in nonuniform circular ducts with potential flow 16 p2351 A83-36082

A variation on McCormack's method for axisymmetric viscous compressible flows 16 p2352 A83-36093

Calculation of a simulated 3-D high speed inlet using the Navier-Stokes equations [AIAA PAPER 83-1165] 16 p2293 A83-36255

Numerical calculations of time dependent three-dimensional viscous flows in a blade passage with tip clearance [AIAA PAPER 83-1171] 16 p2294 A83-36258

Similarity considerations of isothermal turbulent recirculating flowfields in axisymmetric bluff-body near wakes [AIAA PAPER 83-1203] 16 p2294 A83-36279

Aerodynamic design of propan powered transports [AIAA PAPER 83-1213] 16 p2300 A83-36285

Method for calculating effects of a propan on aircraft aerodynamics at subsonic speeds [AIAA PAPER 83-1216] 16 p2294 A83-36287

- Importance of inlet boundary conditions for numerical simulation of combustor flows
[AIAA PAPER 83-1263] 16 p2308 A83-36314
- Prediction of an axisymmetric combustor flow
[AIAA PAPER 83-1264] 16 p2326 A83-36315
- The analysis of thrust reversal performance --- of solid propellant rocket motors
[AIAA PAPER 83-1316] 16 p2320 A83-36337
- Analysis of viscous transonic flow over aircraft forebodies and afterbodies
[AIAA PAPER 83-1366] 16 p2295 A83-36362
- Progress toward the analysis of complex propulsion installation flow phenomenon
[AIAA PAPER 83-1367] 16 p2295 A83-36363
- PAN AIR applications to aero-propulsion integration
[AIAA PAPER 83-1368] 16 p2295 A83-36364
- PANAIR Pilot Code application to subsonic nacelle type interior flows
[AIAA PAPER 83-1369] 16 p2295 A83-36365
- Analytical characterization of flow fields in side-inlet dump combustors
[AIAA PAPER 83-1399] 16 p2322 A83-36389
- Computational and experimental study of the effect of mass transfer on liquid jet break-up
[AIAA PAPER 83-1400] 16 p2353 A83-36390
- Three-dimensional compressible viscous analysis of mixer nozzles
[AIAA PAPER 83-1401] 16 p2295 A83-36391
- An integral analysis of transonic normal shock wave/turbulent boundary layer interactions in internal flow
[AIAA PAPER 83-1402] 16 p2295 A83-36392
- Three-dimensional transonic nacelle/inlet flowfield computations using an efficient approximate factorization algorithm
[AIAA PAPER 83-1417] 16 p2295 A83-36401
- Finite element methods for internal flow calculations
[AIAA PAPER 83-1404] 16 p2296 A83-36415
- A multigrid finite element method for the calculation of transonic potential flows
[ONERA, TP NO. 1983-18] 16 p2296 A83-36427
- Solution of the Navier-Stokes equations by a spectral method of subdomains
[ONERA, TP NO. 1983-19] 16 p2353 A83-36428
- Numerical simulation of turbulence on a multiprocessor system
[ONERA, TP NO. 1983-23] 16 p2404 A83-36432
- Effects of mass transfer on the hydromagnetic flow past a vertical limiting surface
16 p2416 A83-36534
- Improved numerical method for unsteady lifting surfaces in incompressible flow
16 p2296 A83-36917
- Correction to the wing source velocity error in Woodward's USSAERO code
16 p2297 A83-36920
- Analysis of externally pressurized gas-lubricated conical bearings
16 p2363 A83-36941
- Calculation of curved shear layers with two-equation turbulence models
17 p2501 A83-37030
- Formation and damping of relativistic strong shocks
17 p2595 A83-37033
- Hypersonic flows over biconics using a variable-effective-gamma, Parabolized-Navier-Stokes code
[AIAA PAPER 83-1666] 17 p2443 A83-37177
- Calculation of viscous supersonic flows over finned bodies
[AIAA PAPER 83-1667] 17 p2443 A83-37178
- Flow over a biconic configuration with an afterbody compression flap - A comparative numerical study
[AIAA PAPER 83-1668] 17 p2444 A83-37179
- Numerical simulation of hypersonic viscous flow over cones at very high incidence
[AIAA PAPER 83-1669] 17 p2444 A83-37180
- Numerical solutions of three-dimensional time-dependent compressible turbulent integral boundary-layer equations in general curvilinear coordinates
[AIAA PAPER 83-1674] 17 p2501 A83-37183
- Navier-Stokes calculations for the vortex wake of a rotor in hover
[AIAA PAPER 83-1676] 17 p2444 A83-37184
- Finite-difference simulation of transonic separated flow using a full potential boundary layer interaction approach
[AIAA PAPER 83-1689] 17 p2502 A83-37189
- A hybrid field panel/finite difference method for 3-D potential unsteady transonic flow calculations
[AIAA PAPER 83-1690] 17 p2444 A83-37190
- Evaluation of simple subgrid-scale models for the numerical simulation of homogeneous isotropic and anisotropic turbulence
[AIAA PAPER 83-1692] 17 p2502 A83-37191
- Turbulence modeling methods for the compressible Navier-Stokes equations
[AIAA PAPER 83-1693] 17 p2502 A83-37192
- Scaling and modeling of three-dimensional, pressure-driven, turbulent boundary layers
[AIAA PAPER 83-1695] 17 p2502 A83-37193
- Near-wake computations with Reynolds stress models
[AIAA PAPER 83-1696] 17 p2445 A83-37194
- Evaluation of the Baldwin-Lomax turbulence model for two-dimensional shock wave boundary layer interactions
[AIAA PAPER 83-1697] 17 p2445 A83-37195
- Droplet heating and vaporization at high Reynolds and Peclet numbers
[AIAA PAPER 83-1706] 17 p2502 A83-37203
- Calculation of afterbody flows with a composite velocity formulation
[AIAA PAPER 83-1736] 17 p2445 A83-37215
- Effect of suction on the wake structure of a three-dimensional turret
[AIAA PAPER 83-1738] 17 p2445 A83-37217
- Theoretical and experimental study of a dual-flow circuit breaker nozzle flow
[AIAA PAPER 83-1748] 17 p2503 A83-37223
- Numerical study of the effect of an embedded surface-heat source on the separation bubble of supersonic flow
[AIAA PAPER 83-1753] 17 p2446 A83-37226
- Experimental and computational investigation of the flow in the leading edge region of a swept wing
[AIAA PAPER 83-1762] 17 p2446 A83-37233
- The impact of CFD on development test facilities - A National Research Council projection --- computational fluid dynamics
[AIAA PAPER 83-1764] 17 p2503 A83-37234
- Self-similar problem concerning the separated flow of an ideal fluid from a diffuser
17 p2446 A83-37258
- Computer in analysis and design --- for heat transfer analysis
17 p2504 A83-37275
- A numerical investigation for curved pipe flow at high Reynolds number
[ASME PAPER 83-APM-18] 17 p2504 A83-37376
- The effect of stochastic modulations on the stability characteristics of hydrodynamic flows --- German thesis
17 p2504 A83-37501
- Boundary layer separation from the moving surface of a body in a supersonic gas flow
17 p2448 A83-37509
- The stability of a laminar boundary layer on an elastic surface
17 p2505 A83-37510
- Theory of vortex interaction on a blunt cone
17 p2448 A83-37511
- Supersonic flow field analysis for a twin-engine aircraft model
17 p2448 A83-37521
- Transonic flow at the break point of a profile with a free streamline
17 p2448 A83-37527
- Three-dimensional hypersonic flow past a body of finite thickness
17 p2448 A83-37528
- Application of numerical methods to the calculation of the characteristics of supersonic and hypersonic jet-engine air intakes
17 p2448 A83-37532
- Calculation of transonic noncirculatory flow past a highly oblate ellipsoid
17 p2449 A83-37538
- Calculation of three-dimensional supersonic flows with allowance for the real properties of the gas
17 p2449 A83-37539
- Flow in a three-dimensional corner with large entropy differences
17 p2449 A83-37540
- Comparison of computational and experimental data concerning flow past axisymmetric air intakes in regimes with an expelled shock wave
17 p2449 A83-37541
- Calculation of transonic axisymmetric flow past bodies of revolution
17 p2450 A83-37627
- The application of splines to the numerical solution of the Navier-Stokes equations at high Reynolds numbers
17 p2505 A83-37629
- Transformation of the equations of a three-dimensional boundary layer for numerical calculation
17 p2506 A83-37633
- The effect of a sudden change in the motion of a plate surface on flow in a laminar boundary layer in supersonic flow
17 p2450 A83-37634
- Singular matrix inversion in fluid dynamics computations
17 p2571 A83-37735
- A numerical study of slow nonisothermal flows past axisymmetrical bodies
17 p2506 A83-37805
- Allowing for the effect of a weak inhomogeneity in a boundary-layer flow on its stability characteristics
17 p2506 A83-37812
- A solution to the direct problem of a plane Laval nozzle
17 p2451 A83-37813
- Aerodynamic simulation - A key technology not only for aviation
17 p2451 A83-37860
- Numerical model for dynamic and thermal developments of a pulsed laminar ducted flow
17 p2506 A83-37867
- Similarity solutions of free shear flows with mean Reynolds stress turbulence models
17 p2506 A83-37868
- A few applications of the Nec-Kovaszny model for shear flow turbulence
17 p2506 A83-37876
- Three-dimensional flow development in MHD generators at part load
17 p2582 A83-38012
- k-epsilon equation for compressible reciprocating engine flows
17 p2507 A83-38021
- Simulation of starting transients in the UTSI MHD generator
17 p2582 A83-38024
- Sound scattering by a vortex wake behind a cylinder
17 p2578 A83-38049
- On conforming mixed finite element methods for incompressible viscous flow problems
17 p2507 A83-38057
- Calculation of incompressible turbulent boundary layers over moving wavy surfaces
[AIAA PAPER 83-1670] 17 p2507 A83-38083
- The spiral singularity in the supersonic inviscid flow over a cone
[AIAA PAPER 83-1665] 17 p2451 A83-38084
- Viscous/inviscid analysis of curved sub- or supersonic wall jets
[AIAA PAPER 83-1679] 17 p2452 A83-38086
- Numerical investigation of unsteady flow development in a nozzle-duct configuration
[AIAA PAPER 83-1714] 17 p2452 A83-38087
- Modeling of turbulent flow fields through cascade of airfoils at stall conditions
[AIAA PAPER 83-1743] 17 p2452 A83-38091
- Computation of three-dimensional turbulent shear flows in corners
[AIAA PAPER 83-1733] 17 p2507 A83-38092
- A survey of numerical methods developed by ONERA, applicable to calculations of flows inside turbomachinery [ONERA, TP NO. 1983-96] 17 p2452 A83-38332
- Convar 990 transonic flow-field simulation about the forward fuselage
[AIAA PAPER 83-1785] 17 p2452 A83-38626
- Assessment of NASA and RAE viscous-inviscid interaction methods for predicting transonic flow over nozzle afterbodies
[AIAA PAPER 83-1789] 17 p2453 A83-38629
- Advanced airfoil design for general aviation propellers
[AIAA PAPER 83-1791] 17 p2453 A83-38631
- Design and true Reynolds number 2-D testing of an advanced technology airfoil
[AIAA PAPER 83-1792] 17 p2453 A83-38632
- High angle of attack inviscid flow calculations over a Shuttle-like vehicle with comparisons to flight data
[AIAA PAPER 83-1798] 17 p2453 A83-38636
- Application of a full potential method for predicting supersonic flow fields and aerodynamic characteristics
[AIAA PAPER 83-1802] 17 p2453 A83-38637
- An extension of a transonic wing/body code to include underwing pylon/nacelle effects
[AIAA PAPER 83-1805] 17 p2454 A83-38639
- Coupled Euler/Integral Boundary Layer analysis in transonic flow
[AIAA PAPER 83-1806] 17 p2508 A83-38640
- An algebraic grid generation method coupled with an Euler solver for simulating three-dimensional flows
[AIAA PAPER 83-1807] 17 p2454 A83-38641
- Some recent applications of XTRAN3S --- time marching finite difference code for solution of three-dimensional transonic small perturbation flow
[AIAA PAPER 83-1811] 17 p2454 A83-38644
- A flow analysis procedure based on velocity potentials
[AIAA PAPER 83-1818] 17 p2508 A83-38650
- Experience with hybrid aerodynamic methods
[AIAA PAPER 83-1819] 17 p2455 A83-38651
- Quasi-three-dimensional turbomachinery flow calculations on multiple hub-to-shroud stream surfaces
[AIAA PAPER 83-1820] 17 p2455 A83-38652
- The aerodynamics of propellers and rotors using an acoustic formulation in the time domain
[AIAA PAPER 83-1821] 17 p2455 A83-38653
- Evaluation of factors determining the accuracy of linearized subsonic panel methods
[AIAA PAPER 83-1826] 17 p2455 A83-38658
- Analysis of complex inlet configurations using a higher-order panel method
[AIAA PAPER 83-1828] 17 p2455 A83-38659
- Analysis of surface pressure distributions on two elliptic missile configurations
[AIAA PAPER 83-1841] 17 p2456 A83-38670
- A method for predicting low-speed aerodynamic characteristics of transport aircraft
[AIAA PAPER 83-1845] 17 p2456 A83-38673
- A three-dimensional solution of flows over arbitrary jet-flapped configurations using a higher-order panel method
[AIAA PAPER 83-1846] 17 p2456 A83-38674
- An assessment of PANDORA using a Canard/Wing/Body configuration --- Preliminary Automated Numerical Design of Realistic Aircraft
[AIAA PAPER 83-1850] 17 p2456 A83-38678
- Computational analysis for an advanced transport configuration with engine nacelle
[AIAA PAPER 83-1851] 17 p2465 A83-38679

Computation of transonic flow field over Wing-Body-Pylon-Store combinations [AIAA PAPER 83-1852] 17 p2456 A83-38680

Calculation of axisymmetric inlet flowfield using the Euler equations [AIAA PAPER 83-1853] 17 p2457 A83-38681

Numerical investigation of three-dimensional transonic flow through air intakes disturbed by a missile plume [AIAA PAPER 83-1854] 17 p2457 A83-38682

Computational aerodynamic design methodology [AIAA PAPER 83-1865] 17 p2457 A83-38692

Supercritical inlet design [AIAA PAPER 83-1866] 17 p2457 A83-38693

Computational and experimental study of trailing vortices [AIAA PAPER 83-1868] 17 p2458 A83-38694

Numerical and analytical investigations of three-dimensional lee waves 17 p2553 A83-38763

Numerical grid generation; Proceedings of the Symposium on Numerical Generation of Curvilinear Coordinate Systems and Their Use in the Numerical Solution of Partial Differential Equations, Nashville, TN, April 13-16, 1982 17 p2572 A83-38776

Coordinate system control - Adaptive meshes 17 p2573 A83-38787

On application of body conforming curvilinear grids for finite difference solution of external flow 17 p2458 A83-38788

Application of curvilinear coordinate generation techniques to the computation of internal flows 17 p2458 A83-38791

Solution of viscous internal flows on curvilinear grids generated by the Schwarz-Christoffel transformation 17 p2508 A83-38796

Test problems, coordinate transformations, and technique for nonsteady compressible flow analysis 17 p2508 A83-38797

An experience in mesh generation for three-dimensional calculation of potential flow around a rotating propeller 17 p2458 A83-38798

Fast generation of three-dimensional computational boundary-conforming periodic grids of C-type --- for turbine blades and propellers 17 p2573 A83-38799

Conformal grid generation for multielement airfoils 17 p2458 A83-38800

Conformal mappings onto multiply connected regions with specified boundary shapes 17 p2573 A83-38801

Generation of boundary-fitted coordinate systems using segmented computational regions 17 p2574 A83-38802

Grid generation by elliptic partial differential equations for a tri-element Augmentor-Wing airfoil 17 p2458 A83-38803

Numerical generation of composite three dimensional grids by quasilinear elliptic systems 17 p2574 A83-38804

Three-dimensional grid generation using Poisson equations 17 p2574 A83-38805

2-D elliptic grid generation using a singularity method and its application to transonic interference flows 17 p2458 A83-38808

Marching grid generation using parabolic partial differential equations 17 p2574 A83-38810

An implicit scheme for water wave problems 17 p2508 A83-38812

Equidistant mesh for gas dynamic calculations 17 p2508 A83-38814

Method of fundamental solutions in plane steady linear aerodynamics 17 p2458 A83-38850

Application of the panel method to airships [AIAA PAPER 83-1978] 17 p2458 A83-38909

Airfoil generation with a desktop computer using Lighthill's exact inverse method [AIAA PAPER 83-1867] 18 p2632 A83-39096

Comparison of panel method formulations and its influence on the development of QUADPAN, an advanced low-order method [AIAA PAPER 83-1827] 18 p2632 A83-39097

The LANN program - An experimental and theoretical study of steady and unsteady transonic airloads on a supercritical wing [AIAA PAPER 83-1686] 18 p2632 A83-39099

On boundary value problems for the domain exterior to a thin or slender region 18 p2680 A83-39146

Features of the numerical solution of gasdynamic problems with many interacting discontinuities 18 p2680 A83-39152

The detection property of a curved flame front 18 p2663 A83-39167

Small-scale structure of the Taylor-Green vortex 18 p2681 A83-39210

On the modelling of effects of negative production of temperature-fluctuation intensity in the turbulent mixing layer 18 p2681 A83-39211

Flow development in the vicinity of the sharp trailing edge on bodies impulsively set into motion. II 18 p2632 A83-39213

Viscosity renormalization based on direct-interaction closure 18 p2681 A83-39215

An error estimate for a finite-element approximation of an elliptic variational inequality formulation of a Hele-Shaw moving-boundary problem 18 p2739 A83-39254

Wall-function boundary conditions in the solution of the Navier-Stokes equations for complex compressible flows [AIAA PAPER 83-1694] 18 p2633 A83-39268

Free convection flow on a nonisothermal flat plate under nonuniform gravity 18 p2681 A83-39347

Computational Fluid Dynamics Conference, 6th, Danvers, MA, July 13-15, 1983, Collection of Technical Papers 18 p2633 A83-39351

The treatment of vortex sheets in compressible potential flow [AIAA PAPER 83-1881] 18 p2634 A83-39352

Numerical solution of the Reynolds stress equations in a developing duct flow [AIAA PAPER 83-1883] 18 p2634 A83-39353

Shock correction and trailing edge pressure jump in two-dimensional transonic potential flows at subsonic uniform Mach numbers [AIAA PAPER 83-1884] 18 p2634 A83-39354

Calculations of transonic potential flows by a parameter free procedure [AIAA PAPER 83-1886] 18 p2634 A83-39355

A conservative type-dependent full potential method for the treatment of supersonic flows with embedded subsonic regions [AIAA PAPER 83-1887] 18 p2634 A83-39356

A comparative study of the nonuniqueness problem of the potential equation --- for transonic flow past airfoils [AIAA PAPER 83-1888] 18 p2634 A83-39357

Numerical solution of the Navier-Stokes equations for compressible turbulent two/three dimensional flows in the terminal shock region of an inlet/diffuser [AIAA PAPER 83-1892] 18 p2634 A83-39358

Efficient solution of the Euler and Navier-Stokes equations with a vectorized multiple-grid algorithm [AIAA PAPER 83-1893] 18 p2634 A83-39359

The prediction of compressible, laminar viscous flows using a time-marching control volume and multigrid technique [AIAA PAPER 83-1896] 18 p2682 A83-39360

Improving the convergence rate of parabolic ADI methods [AIAA PAPER 83-1897] 18 p2739 A83-39361

Three-dimensional algebraic grid generation [AIAA PAPER 83-1904] 18 p2739 A83-39363

Quasi three-dimensional grid generation using conformal mapping [AIAA PAPER 83-1906] 18 p2739 A83-39365

Computation of leading edge vortices [AIAA PAPER 83-1907] 18 p2634 A83-39366

A semi-direct solver for compressible three-dimensional rotational flow [AIAA PAPER 83-1909] 18 p2682 A83-39367

Three-dimensional viscous-flow computations using a directionally hybrid implicit-explicit procedure [AIAA PAPER 83-1910] 18 p2682 A83-39368

Global PNS solutions for laminar and turbulent flow --- Parabolized Navier-Stokes equations around boattail, flat plate and NACA 0012 airfoil geometries [AIAA PAPER 83-1911] 18 p2635 A83-39369

Comparison between the integro-differential technique and the finite - difference method in solving unsteady compressible viscous flow over airfoils [AIAA PAPER 83-1912] 18 p2635 A83-39370

The effect of strong heat addition on the convergence of implicit schemes [AIAA PAPER 83-1914] 18 p2635 A83-39371

An interacting boundary layer model for cascades [AIAA PAPER 83-1915] 18 p2635 A83-39372

Finite-difference calculations of unsteady premixed flame-flow interactions [AIAA PAPER 83-1917] 18 p2664 A83-39373

Finite element analysis in computational fluid dynamics [AIAA PAPER 83-1918] 18 p2682 A83-39374

Progress in finite element techniques for transonic flows [AIAA PAPER 83-1919] 18 p2635 A83-39375

Transonic flow calculations using triangular finite elements [AIAA PAPER 83-1922] 18 p2635 A83-39376

Conjugate gradients methods for solution of finite element and finite difference flow problems [AIAA PAPER 83-1923] 18 p2682 A83-39377

Transonic Euler simulations by means of finite element explicit schemes [AIAA PAPER 83-1924] 18 p2635 A83-39378

Implicit methods of second-order accuracy for the Euler equations [AIAA PAPER 83-1925] 18 p2682 A83-39379

Solution of the Euler equations for complex configurations [AIAA PAPER 83-1929] 18 p2635 A83-39381

Implicit upwind methods for the Euler equations [AIAA PAPER 83-1930] 18 p2682 A83-39382

Adaptive mesh schemes based on grid speeds [AIAA PAPER 83-1931] 18 p2739 A83-39383

A discussion of some criteria for the use of adaptive gridding [AIAA PAPER 83-1932] 18 p2740 A83-39384

Alternating direction adaptive grid generation [AIAA PAPER 83-1937] 18 p2740 A83-39387

A fast Euler solver for steady flows [AIAA PAPER 83-1940] 18 p2682 A83-39389

High resolution applications of the Osher upwind scheme for the Euler equations [AIAA PAPER 83-1943] 18 p2636 A83-39390

A flexible grid embedding technique with application to the Euler equations [AIAA PAPER 83-1944] 18 p2636 A83-39391

Multiple-gridding of the Euler equations with an implicit scheme [AIAA PAPER 83-1945] 18 p2636 A83-39392

A new stream function formulation for the Euler equations [AIAA PAPER 83-1947] 18 p2636 A83-39393

Computation of three dimensional transonic flows using two stream functions [AIAA PAPER 83-1948] 18 p2636 A83-39394

Analysis by computer of the convergence to steady state of discrete approximations to the Euler equations [AIAA PAPER 83-1951] 18 p2636 A83-39395

Symbolic manipulation and computational fluid dynamics [AIAA PAPER 83-1952] 18 p2738 A83-39396

Prediction of laminar separated flows using the partially parabolized Navier-Stokes equations [AIAA PAPER 83-1954] 18 p2682 A83-39397

Iterative PNS method for attached flows with upstream influence --- Parabolic Navier-Stokes [AIAA PAPER 83-1955] 18 p2636 A83-39398

Application of the implicit MacCormack scheme to the PNS equations [AIAA PAPER 83-1956] 18 p2636 A83-39399

A time-split finite-volume algorithm for three-dimensional flow-field simulation [AIAA PAPER 83-1957] 18 p2636 A83-39400

Implicit upwind methods for the compressible Navier-Stokes equations [AIAA PAPER 83-1958] 18 p2682 A83-39401

A method for solving the transonic full-potential equation for general configurations [AIAA PAPER 83-1889] 18 p2637 A83-39402

Stability analysis of intermediate boundary conditions in approximate factorization schemes [AIAA PAPER 83-1898] 18 p2740 A83-39403

Flux vector splitting and approximate Newton methods --- for solution of steady Euler equations [AIAA PAPER 83-1899] 18 p2683 A83-39404

The computation of inviscid rotational gasdynamic flows using an alternate velocity decomposition [AIAA PAPER 83-1900] 18 p2637 A83-39405

A spectral method for the solution of transonic potential flow about an arbitrary two-dimensional airfoil [AIAA PAPER 83-1949] 18 p2637 A83-39406

New diagonal implicit scheme for the compressible Navier-Stokes equations [AIAA PAPER 83-1891] 18 p2683 A83-39407

Numerical simulation of the leading-edge separation vortex for a wing and strake-wing configuration [AIAA PAPER 83-1908] 18 p2637 A83-39408

Robust calculation of 3D transonic potential flow based on the nonlinear FAS multi-grid method and incomplete LU decomposition [AIAA PAPER 83-1950] 18 p2637 A83-39409

Large eddy simulation by spectral method or by multi level particle method [AIAA PAPER 83-1880] 18 p2683 A83-39410

A general perturbation approach for the equations of fluid dynamics [AIAA PAPER 83-1903] 18 p2637 A83-39411

3-D calculation of transonic viscous flows by an implicit method [AIAA PAPER 83-1953] 18 p2637 A83-39412

Entropy and vorticity corrections for transonic flows [AIAA PAPER 83-1926] 18 p2637 A83-39413

Multi-dimensional formulation of CSCM - An upwind flux difference eigenvector split method for the compressible Navier-Stokes equations --- Conservative Supra-Characteristics Method [AIAA PAPER 83-1895] 18 p2683 A83-39414

New discretization and solution techniques for incompressible viscous flow problems
[AIAA PAPER 83-1921] 18 p2683 A83-39415

Implicit conservative characteristic modeling schemes for the Euler equations - A new approach
[AIAA PAPER 83-1939] 18 p2683 A83-39416

Study of incompressible separated flow using an implicit time-dependent technique
[AIAA PAPER 83-1894] 18 p2683 A83-39417

A nonstationary relaxation method for the Cauchy-Riemann and 1-D Euler equations
[AIAA PAPER 83-1901] 18 p2683 A83-39418

A zonal approach for the steady transonic simulation of inviscid rotational flow
[AIAA PAPER 83-1927] 18 p2637 A83-39419

Numerical analysis of 3-D potential flow in axial flow turbomachines 18 p2684 A83-39458

On unstable oscillations in a viscous-fluid flow through an infinite channel 18 p2684 A83-39480

Calculation of steady two-dimensional turbulent flow in a curved channel 18 p2684 A83-39481

The effect of temperature gradient on the motion of a bubble in reduced gravity 18 p2686 A83-39906

Two-point implicit scheme for the Euler equations --- for computational fluid dynamics 18 p2686 A83-39917

Analysis of the Couette flow by means of the new direct-simulation method 18 p2686 A83-39920

Calculation of two-dimensional diffusers 18 p2686 A83-39989

Non-linear systems of a fluid mechanical type and an algebraic model of stability of a stationary flow. I - Theory, II Application 18 p2687 A83-40002

Real gas flows over complex geometries at moderate angles of attack 18 p2638 A83-40004

Nonequilibrium viscous shock-layer flows over blunt sphere-cones at angle of attack 18 p2638 A83-40006

Ignition and flame propagation studies with adaptive numerical grids 18 p2664 A83-40310

Structure and extinction of convective diffusion flames with general Lewis numbers 18 p2664 A83-40312

Comparison of supercritical airfoil flow calculations with wind-tunnel results
[AIAA PAPER 83-1688] 18 p2638 A83-40472

Applications of exponential splines in computational fluid dynamics 19 p2893 A83-40852

Finite element methods for transonic flow analysis 19 p2789 A83-40854

A vortex sheet method for calculating separated two-dimensional flows 19 p2789 A83-40855

Simple model for base pressure effects in source flow chemical lasers 19 p2850 A83-40858

Pseudospectral approximation in a three-dimensional Navier-Stokes code 19 p2841 A83-40876

Reynolds stresses for unsteady turbulent flows 19 p2842 A83-40877

Stagnation point heat transfer for jet impingement to a plane surface 19 p2842 A83-40879

Acoustic excitation of Tollmien-Schlichting waves in a supersonic boundary layer 19 p2790 A83-41256

Computing methods in applied sciences and engineering, V; Proceedings of the Fifth International Symposium, Versailles, France, December 14-18, 1981 19 p2896 A83-41526

Flow distribution in parallel connected manifolds for evacuated tubular solar collectors 19 p2862 A83-41538

Nonsimilar laminar incompressible boundary layer flow over a rotating sphere 19 p2843 A83-41542

Drag on a sphere oscillating in a dusty gas 19 p2843 A83-41543

A numerical study of the effect of free convection on the development of a vertical semifinite turbulent gas jet 19 p2844 A83-41568

A numerical analysis of the development of a system of jets in the mixing region of counterrotated annular flows 19 p2844 A83-41569

The calculation of planar inlet flows --- German thesis 19 p2844 A83-41809

The application of the matched-asymptotic-expansion method to two-dimensional laminar flows with finite separated regions --- German thesis 19 p2844 A83-41810

Explicit finite difference predictor and convex corrector with applications to hyperbolic partial differential equations 19 p2893 A83-41852

Finite element computational fluid mechanics --- Book 19 p2844 A83-41874

Allowance for finite Mach numbers in hypersonic asymptotics for blunt axisymmetric bodies 19 p2791 A83-41880

Calculation of shock-layer parameters for the hypersonic flow of equilibrium-dissociated air around bodies with bends of the generatrix 19 p2791 A83-41881

On the behavior of a body with a frontal circulation zone in unsteady flow (the computational model) 19 p2791 A83-41885

On an approximate solution to the problem of unsteady flow around two-dimensional and axisymmetric bodies moving at high variable velocity 19 p2792 A83-41886

Mathematical description of the flow of a gas and suspended particles around a body with allowance for the effect of reflected particles 19 p2845 A83-41897

Calculation of dusty-gas flow around a sphere with allowance for the effect of reflected particles 19 p2845 A83-41898

The impact of computational aerodynamics on aircraft design
[AIAA PAPER 83-2060] 19 p2798 A83-41901

Computational aerodynamics applications to transport aircraft design
[AIAA PAPER 83-2061] 19 p2792 A83-41902

Computational aerodynamic design of fighter aircraft Progress and pitfalls
[AIAA PAPER 83-2063] 19 p2798 A83-41903

Computational technique for three-dimensional compressible flow past wings at high angles of attack
[AIAA PAPER 83-2078] 19 p2792 A83-41912

Computational method of the drag of axisymmetric afterbodies in subsonic flow
[AIAA PAPER 83-2079] 19 p2792 A83-41913

Aerodynamic characteristics of missile control fins in nonlinear flow fields
[AIAA PAPER 83-2083] 19 p2792 A83-41917

Factorization method for calculating the three-dimensional flows of a viscous compressible gas 19 p2845 A83-42008

Modeling of turbulent transport processes in a supersonic boundary layer 19 p2794 A83-42137

On the calculation of ducted propeller performance in axisymmetric flows --- Book 20 p2969 A83-42201

A convergence analysis of a numerical method for solving the balance equation --- of atmospheric circulation 20 p3029 A83-42507

Computational interferometric description of nested flow fields 20 p2988 A83-42527

Numerical calculations of a confined two-dimensional turbulent isothermal mixing layer 20 p2969 A83-42528

The development of a comprehensive two-dimensional linearized airfoil theory 20 p2928 A83-42529

Study of 2-D laminar separated flow using unsteady incompressible Navier-Stokes equations 20 p2969 A83-42530

Analysis of viscous flows using multi-grid solution of Neumann pressure problem 20 p2969 A83-42531

Study of asymptotic incompressible flow in curved ducts using a multi-grid technique 20 p2969 A83-42532

Theoretical gust response prediction of a Joukowski airfoil 20 p2928 A83-42536

Development of compatible numerical software for application to aircraft dynamic analysis 20 p3038 A83-42538

Flutter investigation of a repaired T-38 horizontal stabilizer using NASTRAN 20 p3002 A83-42541

Global PNS solutions for subsonic strong interaction flows over a cone-cylinder-boattail geometry --- Parabolized Navier-Stokes equation 20 p2928 A83-42554

Global pressure relaxation procedure for flows with strong viscous-inviscid interaction 20 p2969 A83-42555

Turbulent solutions of the compressible Navier-Stokes equations using a composite velocity procedure 20 p2970 A83-42556

Two-dimensional numerical simulation of an inductively driven imploding foil plasma 20 p3049 A83-42590

New representation of Navier-Stokes equations governing self-similar homogeneous turbulence 20 p2970 A83-42648

Numerical methods in heat transfer 20 p2970 A83-42653

Surface integral numerical solution for general steady heat conduction in composite media 20 p2971 A83-42666

A finite difference study of natural convection in complex enclosures 20 p2972 A83-42678

Numerical simulation of laminar natural convection in shallow inclined enclosures 20 p2973 A83-42680

Overshooting and damped oscillations of transient natural convection flows in cavities 20 p2973 A83-42683

Theoretical and experimental investigation of three-dimensional buoyant turbulent jets 20 p2973 A83-42687

Finite analytic numerical solution of heat transfer and flow past a square channel cavity 20 p2975 A83-42703

Heat transfer in a vertical rotating annulus - A numerical study 20 p2975 A83-42705

Turbulent heat transfer in a swirl flow downstream of an abrupt pipe expansion 20 p2976 A83-42712

Flow and heat transfer past a semi-infinite vertical plate with oscillating plate temperature 20 p2977 A83-42720

A new approach for calculating heat transfer characteristics of turbulent wall flows 20 p2977 A83-42725

Calculation of heat transfer in turbulent transpired boundary layers 20 p2978 A83-42730

Modeling of mass transport in turbulent shear flows 20 p2978 A83-42734

A turbulent burst model for boundary layer flows with pressure gradient 20 p2978 A83-42736

Cross flow influence upon impingement convective heat transfer in circular arrays of jets - A general correlation 20 p2978 A83-42741

Combined natural and forced convection in vertical ducts 20 p2979 A83-42749

Wake interference for a heated oscillating cylinder 20 p2980 A83-42753

Problems of mechanics and heat transfer in space technology 20 p2939 A83-42876

Viscous interaction of an underexpanded jet with a supersonic wake 20 p2982 A83-42885

Free convection in hydromagnetic flows in a vertical wavy channel 20 p2982 A83-42971

Exact unsteady solutions of the Navier-Stokes equation 20 p2983 A83-43008

Floating shock fitting in transonic flow 20 p2929 A83-43009

Laminar flow in the interior of a rotating hollow sphere as it is set in motion 20 p2983 A83-43010

Thermal instability of two-dimensional stagnation-point boundary layers 20 p2984 A83-43095

Tests of subgrid models in the near-wall region using represented velocity fields 20 p2985 A83-43101

The laminar unsteady flow of a viscous fluid away from a plane stagnation point 20 p2985 A83-43102

Strict error estimation of numerical solution of compressible flow in two-dimensional space 20 p2985 A83-43171

The calculation of two-dimensional transonic flow over aerofoils including boundary layer and wake effects
[SAE PAPER 830708] 20 p2930 A83-43318

Numerical experiments with the Osher upwind scheme for the Euler equations 20 p2930 A83-43439

A finite-volume, adaptive grid algorithm applied to planetary entry flowfields 20 p2930 A83-43440

Prediction of separated asymmetric trailing-edge flows at transonic Mach numbers 20 p2930 A83-43441

An efficient, full-potential implicit method based on characteristics for supersonic flows 20 p2930 A83-43442

A grid overlapping scheme for flowfield computations about multicomponent configurations 20 p2930 A83-43443

Computation of reacting flowfield with radiation interaction in chemical lasers 20 p2995 A83-43445

Design of supercritical cascades with high solidity 20 p2930 A83-43446

Numerical solution of natural convection in eccentric annuli 20 p2987 A83-43451

A discrete vortex simulation of Kelvin-Helmholtz instability 20 p2987 A83-43453

A numerical method for weakening shock wave strength in transonic cascade flow fields 20 p2931 A83-43695

Nonparametric solution of the Euler equations for steady flow 21 p3127 A83-43827

Computation of turbulent flow over a moving wavy boundary 21 p3128 A83-43927

Kinematics of velocity and vorticity correlations in turbulent flow 21 p3128 A83-43929

Vortex flow over delta and double-delta wings 21 p3085 A83-43975

Numerical analysis of moving boundary problem in matrix with a thin alternate matrix 21 p3197 A83-44012

A Meksyn series method for the Falkner-Skan equation with mass transfer 21 p3128 A83-44023

New computers will aid advanced designs 21 p3190 A83-44102

Numerical computations of non-linear waves in solar atmosphere 21 p3243 A83-44303

ONERA research on afterbody viscid/inviscid interaction with special emphasis on base flows
[ONERA, TP NO. 1983-26] 21 p3085 A83-44305

Simulation of turbulent flows by a method of point vortices
[ONERA, TP NO. 1983-35] 21 p3129 A83-44313

Calculations for a three-dimensional boundary layer in a compressor
[ONERA, TP NO. 1983-47] 21 p3086 A83-44321

A method for experimental analysis of the shock-boundary layer interaction in cascades [ONERA, TP NO. 1983-48] 21 p3086 A83-44322

Small-disturbance stability of a non-isothermal tube flow of power law fluids. I - Derivation of the Orr-Sommerfeld equation extended. II - Numerical solution of the problem 21 p3129 A83-44349

Similarity solutions of the boundary-layer equations for a stretching wall 21 p3129 A83-44459

Unified unsteady supersonic/hypersonic theory of flow past double wedge airfoils 21 p3086 A83-44465

Energy stability in the Benard problem for a fluid of second grade 21 p3130 A83-44467

Evolution scheme to compute periodic solutions of first-order nonlinear equations containing translation operators 21 p3197 A83-44468

Finite element methods in aerodynamics 21 p3086 A83-44551

Families of variation principle for the semi-inverse problem and the A-type hybrid problem on the S2-stream sheet in radial turbomachines and the extensions and applications of semi-inverse problem to the mixed-type turbomachines 21 p3130 A83-44552

ISOMS - A implicit difference scheme for solving complete compressible Navier-Stokes equations --- Implicit Second-Order Monotone Scheme 21 p3130 A83-44553

Numerical solution for 2-D turbulent separated flow at supersonic speed 21 p3086 A83-44554

Calculation of three-dimensional turbulent boundary layer on an infinite swept wing 21 p3086 A83-44555

On the numerical solution of head-on vehicle shock-planar incident shock interaction flow 21 p3086 A83-44556

A method of streamline curvature for calculating transonic velocities in turbomachinery 21 p3087 A83-44557

Influence of asymmetric transition on static stability of blunt cones 21 p3087 A83-44562

3-D shock-boundary layer solution from Navier-Stokes equations 21 p3087 A83-44563

An investigation of the effect of the nonuniform field feature around a delta-wing on the separated vortex breakdown 21 p3087 A83-44566

A simplified calculation method for the nonequilibrium wake of the blunt-cone body 21 p3087 A83-44568

Design of transonic shock-free airfoil 21 p3087 A83-44572

Calculations of the one-dimensional nonequilibrium nozzle flow 21 p3130 A83-44573

Computation of turbulent flow through constrictions 21 p3130 A83-44588

Statistical solutions to Navier-Stokes system and Euler's systems 21 p3131 A83-44658

Hydrodynamics and heat transfer in sphere assemblages Cylindrical cell models 21 p3131 A83-44928

Rayleigh-Taylor instability and the use of conformal maps for ideal fluid flow 21 p3132 A83-44986

A comparison of finite element and finite difference solutions of the one- and two-dimensional Burgers' equations 21 p3132 A83-44989

Numerical method for the study of the planar unsteady-state flow of compressible viscous liquids 21 p3132 A83-45000

Monotonic second-order difference scheme for hyperbolic systems with two independent variables --- in unsteady gas dynamics 21 p3133 A83-45213

Analysis of some low-order finite element schemes for the Navier-Stokes equations 21 p3133 A83-45521

Finite volume calculation of three-dimensional potential flow around a propeller 21 p3089 A83-45577

Prediction of curved channel flow with an extended k-epsilon model of turbulence 21 p3134 A83-45578

An implicit lambda scheme --- for transonic inviscid flow simulation 21 p3089 A83-45581

A study of turbulent flow downstream of an abrupt pipe expansion 21 p3134 A83-45582

Thrust augmenting ejectors. I 21 p3089 A83-45586

A low Mach number Euler formulation and application to time-iterative LBI schemes --- Linearized Block Implicit 21 p3134 A83-45592

Evolution of weak discontinuities in the unsteady flow of thermally conducting dissociating gases 21 p3134 A83-45598

Structure and stability of streets of finite vortices 22 p3280 A83-45909

The representation of planar separated flow by regions of uniform vorticity 22 p3280 A83-45910

Zigzag instability and axisymmetric rolls in Rayleigh-Benard convection - The effects of curvature 22 p3280 A83-45939

Performing literal calculation with a micro-computer --- symbolic calculations applied to aeroelasticity problem 22 p3350 A83-45980

Axial coherence functions of circular turbulent jets based on an inviscid calculation of damped modes 22 p3281 A83-46002

Experimental and numerical investigation of a turbulent boundary layer subjected to a sudden transverse strain 22 p3247 A83-46004

Turbulent time scales and the dissipation rate of temperature variance in the thermal mixing layer 22 p3281 A83-46006

The turbulence problem - A survey 22 p3281 A83-46425

Response of a turbulent boundary layer to a pulsation of the external flow with and without adverse pressure gradient 22 p3248 A83-46434

Numerical experiments on transition triggering off in a two-dimensional shear flow 22 p3282 A83-46439

Some characteristics of the unsteady wake flow past a circular cylinder 22 p3282 A83-46442

An oscillatory approach to turbulence 22 p3282 A83-46447

Recent contributions to fluid mechanics 22 p3283 A83-46454

Topological analysis of computed three-dimensional viscous flow fields 22 p3248 A83-46457

Finite-difference solutions for laminar boundary layer flows with separation 22 p3249 A83-46459

Turbulent flow simulation - A large eddy simulator's viewpoint 22 p3283 A83-46460

Investigation of the three-dimensional transonic flow around an air intake by a finite-volume method for the Euler equations 22 p3249 A83-46463

Calculation of a laminar-turbulent two-dimensional turbine blade boundary layer including surface curvature effects 22 p3249 A83-46464

Considerations of the vorticity fields on wings 22 p3249 A83-46465

Turbulent heat transfer 22 p3283 A83-46467

Random walk and diffusion in two-dimensional Lagrangian systems --- calculations of vortex motion 22 p3284 A83-46470

Mesh influence on vortex shedding in inviscid flow computations 22 p3249 A83-46471

A numerical method to solve the steady-state Navier-Stokes equations for natural convection in enclosures 22 p3284 A83-46472

Computational study of the Magnus effect on boattailed shell at supersonic speeds 22 p3249 A83-46473

Viscid-inviscid interaction analysis on airfoils with an inverse boundary layer approach 22 p3249 A83-46474

An inverse integral computational method for compressible turbulent boundary layers 22 p3250 A83-46479

Numerical aerodynamics - Replacement of analytical solutions and/or the experiment by the supercomputer? 22 p3250 A83-46485

Numerical computation of three-dimensional convective flows in horizontal and tilted containers 22 p3284 A83-46488

Numerical computation of laminar steady-state inlet-aperture flow and the evolving flow after an embankment 22 p3284 A83-46493

Calculation of three-dimensional transonic flow over thin body (wing) 22 p3250 A83-46499

Navier-Stokes equations and nonlinear functional analysis --- Book 22 p3284 A83-46692

A contribution to the numerical description of rotating two-phase flow --- Thesis 22 p3285 A83-46693

Three-dimensional turbulent boundary layers; Proceedings of the Symposium, Berlin, West Germany, March 29-April 1, 1982 22 p3285 A83-47011

An investigation of surface flow pattern and pressure distribution for viscous, sonic flow over hemisphere-cylinder at incidence 22 p3286 A83-47029

A method for three-dimensional boundary layer calculations on arbitrary bodies - Some results on aircraft wings and engine cowls 22 p3251 A83-47031

Comparison of three-dimensional turbulent boundary-layer calculations with experiment 22 p3251 A83-47032

Three-dimensional boundary-layer calculations in design aerodynamics 22 p3251 A83-47034

Turbulent boundary layers on three-dimensional configurations 22 p3286 A83-47035

An evaluation of the final discussion of the IUTAM Symposium on three-dimensional boundary layers 22 p3286 A83-47036

An analysis of nozzle flows for various models of reacting gases --- Russian book 23 p3392 A83-47124

Combined penalty multiplier optimization methods to enforce integral invariants conservation --- for shallow water equations 23 p3489 A83-47397

Some additional reflections on the viscous flow in a vortex chamber 23 p3446 A83-47576

Rotating compressible flow over an infinite disk 23 p3446 A83-47590

Matrix solution of compressible flow on S1 surface through a turbomachine blade row with splitter vanes or tandem blades [ASME PAPER 83-GT-10] 23 p3393 A83-47882

A summary of developments of the mean-stream-line method in China --- for design and calculation of flow channels [ASME PAPER 83-GT-11] 23 p3393 A83-47883

An experimental and computational study of transonic three-dimensional flow in a turbine cascade [ASME PAPER 83-GT-12] 23 p3393 A83-47884

Experience with the development of an Euler code for rotor rows [ASME PAPER 83-GT-36] 23 p3394 A83-47897

A Navier-Stokes analysis of three-dimensional turbulent flows inside turbine blade rows at design and off-design conditions [ASME PAPER 83-GT-40] 23 p3394 A83-47900

Inlet-fan flow field computation [ASME PAPER 83-GT-41] 23 p3394 A83-47901

A theory of rotating stall of multistage axial compressors. II - Finite disturbances [ASME PAPER 83-GT-45] 23 p3394 A83-47905

Turbulent flow between coaxial cylinders with the inner cylinder rotating [ASME PAPER 83-GT-48] 23 p3447 A83-47907

Effect of particle presence on the incompressible inviscid flow through a two dimensional compressor cascade [ASME PAPER 83-GT-95] 23 p3395 A83-47941

Calculation of three-dimensional, inviscid, rotational flow in axial turbine blade rows [ASME PAPER 83-GT-119] 23 p3395 A83-47948

Design of shock-free compressor cascades including viscous boundary layer effects [ASME PAPER 83-GT-134] 23 p3396 A83-47961

Boundary conditions for the potential equation in transonic internal flow calculation [ASME PAPER 83-GT-135] 23 p3396 A83-47962

Three dimensional inviscid computation of an impeller flow [ASME PAPER 83-GT-210] 23 p3397 A83-48011

The prevalence of two-dimensional motion in the turbulent mixing layer 23 p3449 A83-48044

The dynamics of two-dimensional ideal MHD 23 p3510 A83-48046

Modelling subgrid scales in numerical simulation of two-dimensional turbulent flows 23 p3449 A83-48048

On the calculation of separation bubbles 23 p3449 A83-48119

Chemical equilibrium laminar or turbulent three-dimensional viscous shock-layer flows 23 p3398 A83-48133

Calculation of potential flow about arbitrary three dimensional wings using internal singularity distributions 23 p3398 A83-48143

Progress in calculation of the interaction between a perfect fluid and a viscous fluid [ONERA, TP NO. 1983-61] 23 p3398 A83-48182

A coupling method for the inverse mode calculation of transonic internal flows with a shock wave [ONERA, TP NO. 1983-62] 23 p3398 A83-48183

PAN AIR applications to complex configurations --- computer program for predicting subsonic and supersonic linear potential flows 23 p3399 A83-48221

Numerical prediction of turbulent flow over surface mounted ribs [ASME PAPER 83-FE-13] 23 p3450 A83-48231

Calculation of deflected-walled backward-facing step flows Effects of angle of deflection on the performance of four models of turbulence [ASME PAPER 83-FE-16] 23 p3450 A83-48233

Generation of Taylor-Goertler vortices in decaying swirl flow [ASME PAPER 83-FE-17] 23 p3450 A83-48234

Approximate unsteady fluid jet properties from one-dimensional theory [ASME PAPER 83-FE-25] 23 p3450 A83-48236

Unified approach to the solution of problems of unsteady laminar flow in long pipes [ASME PAPER 83-APM-2] 23 p3451 A83-48240

Numerical and experimental simulation of circulation control rotor aerodynamics [AIAA PAPER 83-2551] 23 p3399 A83-48372

Evolution of axisymmetric distributions of vorticity in an ideal incompressible stratified fluid (the linear description) 23 p3451 A83-48530

Nonlinear resonant interaction of acoustic waves with Tollmein-Schlichting waves 23 p3451 A83-48652

Asymptotic theory of turbulent separation 23 p3452 A83-48655

Computational-experimental study of the gas dynamics of two-dimensional symmetric nozzles having a region of constant height and two contour bend points in the critical section 23 p3400 A83-48661

Calculation of stellar-wind flow past an x-ray source 23 p3528 A83-48662

Mixed boundary value problems of the contouring of supersonic nozzles and channels 23 p3400 A83-48663

A method for calculating the regime of strong viscous interaction on a delta wing 23 p3400 A83-48664

Unsteady thermal convection in a cylindrical vessel in the case of lateral heat injection 23 p3452 A83-48668

Non-uniform flows in axial compressors due to tip clearance variation 24 p3548 A83-48824

Fluid turbulence and the renormalization group - A preliminary calculation of the eddy viscosity 24 p3575 A83-48848

A numerical method for potential flows with a free surface 24 p3575 A83-48871

A least squares finite element scheme for transonic flow around harmonically oscillating airfoils 24 p3543 A83-48872

The turbulence problem - A survey 24 p3576 A83-48925

Alternating-triangular difference scheme for solving the Navier-Stokes equations 24 p3576 A83-48946

Study of turbulence modeling in transonic shock wave-boundary layer interaction [ONERA, TP NO. 1983-84] 24 p3544 A83-49403

Classes of splitting-up schemes for solving two and three-dimensional Navier-Stokes equations [ONERA, TP NO. 1983-85] 24 p3577 A83-49404

Effects of rotation on isotropic turbulence [ONERA, TP NO. 1983-108] 24 p3577 A83-49419

The standing vortex behind a disk normal to uniform flow at small Reynolds number 24 p3577 A83-49468

Spinning modes on axisymmetric jets. I 24 p3578 A83-49469

The occurrence of separation in oscillatory flow 24 p3578 A83-49470

Boundary layer with self-induced pressure during the transonic flow past the corner point of an airfoil 24 p3545 A83-49526

Supersonic turbulent boundary-layers in the presence of a pressure gradient - Computation using a k-epsilon model 24 p3545 A83-49644

Numerical calculation of mixed flows in plate nozzles --- for spacecraft engines 24 p3552 A83-49656

The effect of the intensity of pressure pulses on the splashing of a liquid in a vessel 24 p3579 A83-49673

Mature thunderstorm cloud top structure - Three-dimensional numerical simulation versus satellite observations 24 p3615 A83-49730

Simulation of turbulent shear flows at Stanford and NASA-Ames - What can we do and what have we learned? 24 p3579 A83-49802

Transition prediction based on a differential field theory of turbulence 24 p3580 A83-49830

Propagation of finite amplitude disturbances in the weakly non-parallel boundary layer 24 p3580 A83-49832

A time-dependent approach for calculating steady inverse boundary-layer flows with separation 24 p3580 A83-49879

The asymptotic solutions of compressible, nonsteady boundary layer 24 p3581 A83-50129

An extension of the pressure unitary formula, valid both for compression and expansion, over the whole transonic regime (freestream M greater than 1) 24 p3546 A83-50130

COMPUTATIONAL GRIDS

Steady viscous flows by compact differences in boundary-fitted coordinates 12 p1722 A83-29099

The detection of shape discrepancies between a material surface and a reference model using a moirebeginning from a specific grid 12 p1729 A83-29377

Adaptive zoning for singular problems in two dimensions 12 p1771 A83-29613

Relationship between the truncation errors of centered finite-difference approximations on uniform and nonuniform meshes 12 p1771 A83-29619

A segmentation approach to grid generation using biharmonics 12 p1772 A83-29635

High-Re solutions for incompressible flow using the Navier-Stokes equations and a multigrid method 12 p1725 A83-29659

Spatial resolution requirements for direct numerical simulation of the Rayleigh-Benard convection 12 p1725 A83-29666

Shape optimization of two-dimensional structures with geometric problem description and adaptive mesh refinement [AIAA 83-0941] 12 p1739 A83-29771

Assessment of equivalent monocoque isogrid shell modeling technique for dynamic response to impulsive loads [AIAA 83-0926] 12 p1744 A83-29852

Special mesh for determining aerodynamic interference between casing walls and rotating blade rows of subsonic and transonic turbines and compressors 13 p1804 A83-30512

Two-dimensional deforming finite element methods for surface ablation [AIAA PAPER 83-1555] 14 p2012 A83-32773

An arbitrary-mesh computer program with applications to astrophysics 15 p2254 A83-33817

Application of the multigrid method to Poisson's equation in boundary-fitted coordinates 15 p2157 A83-33824

On the use of adaptive grids in numerically calculating adiabatic flame speeds 15 p2132 A83-34032

Solving fully 3-D nonlinear anisotropic multi-material heat conduction problems on a microcomputer 15 p2158 A83-34232

Conditions of the construction and accuracy characteristics of reference grids on planets and satellites 16 p2435 A83-35502

Evaluation of simple subgrid-scale models for the numerical simulation of homogeneous isotropic and anisotropic turbulence [AIAA PAPER 83-1692] 17 p2502 A83-37191

A note on the mathematical formulation of the problem of numerical coordinate generation 17 p2571 A83-37768

A discretized-intensity method proposed for two-dimensional systems enclosing radiative and conductive media 17 p2506 A83-37865

Finite element triangular meshing optimization for pure torsion 17 p2525 A83-38576

An algebraic grid generation method coupled with an Euler solver for simulating three-dimensional flows [AIAA PAPER 83-1807] 17 p2454 A83-38641

Numerical grid generation; Proceedings of the Symposium on Numerical Generation of Curvilinear Coordinate Systems and Their Use in the Numerical Solution of Partial Differential Equations, Nashville, TN, April 13-16, 1982 17 p2572 A83-38776

General curvilinear coordinate systems 17 p2572 A83-38777

Error induced by coordinate systems 17 p2572 A83-38778

Elliptic grid generation 17 p2572 A83-38780

Conformal grid generation 17 p2508 A83-38781

Algebraic grid generation 17 p2573 A83-38782

Transfinite mappings and their application to grid generation 17 p2573 A83-38783

Orthogonal grid generation 17 p2573 A83-38784

Patched coordinate systems --- numerical body-fitted grid generation for surface boundary treatment of aerodynamic structures 17 p2573 A83-38785

Solid mechanics applications of boundary fitted coordinate systems 17 p2525 A83-38786

Coordinate system control - Adaptive meshes 17 p2573 A83-38787

On application of body conforming curvilinear grids for finite difference solution of external flow 17 p2458 A83-38788

The use of solution adaptive grids in solving partial differential equations 17 p2573 A83-38789

Adaptive gridding for finite difference solutions to heat and mass transfer problems 17 p2508 A83-38790

Application of curvilinear coordinate generation techniques to the computation of internal flows 17 p2458 A83-38791

Automated three-dimensional grid refinement on a minicomputer 17 p2573 A83-38792

Automatic algebraic coordinate generation 17 p2564 A83-38793

Automatic topology generation and generalised B spline mapping 17 p2564 A83-38794

Conformal grid generation for multielement airfoils 17 p2458 A83-38800

Conformal mappings onto multiply connected regions with specified boundary shapes 17 p2573 A83-38801

Generation of boundary-fitted coordinate systems using segmented computational regions 17 p2574 A83-38802

Grid generation by elliptic partial differential equations for a tri-element Augmentor-Wing airfoil 17 p2458 A83-38803

Numerical generation of composite three dimensional grids by quasilinear elliptic systems 17 p2574 A83-38804

Three-dimensional grid generation using Poisson equations 17 p2574 A83-38805

Numerical generation of three-dimensional coordinates between bodies of arbitrary shapes 17 p2574 A83-38806

Semidirect/marching solutions and elliptic grid generation 17 p2574 A83-38807

2-D elliptic grid generation using a singularity method and its application to transonic interference flows 17 p2458 A83-38808

Three dimensional grid generation using biharmonics 17 p2574 A83-38809

Marching grid generation using parabolic partial differential equations 17 p2574 A83-38810

Assessing the quality of curvilinear coordinate meshes by decomposing the Jacobian matrix 17 p2574 A83-38811

Idealized dynamic grid computation of physical systems 17 p2574 A83-38813

Equidistant mesh for gas dynamic calculations 17 p2508 A83-38814

Orthogonal coordinate meshes with manageable Jacobian 17 p2574 A83-38815

Comparison of fast iterative methods for symmetric systems 18 p2739 A83-39255

Efficient solution of the Euler and Navier-Stokes equations with a vectorized multiple-grid algorithm [AIAA PAPER 83-1893] 18 p2634 A83-39359

The prediction of compressible, laminar viscous flows using a time-marching control volume and multigrid technique [AIAA PAPER 83-1896] 18 p2682 A83-39360

Three-dimensional algebraic grid generation [AIAA PAPER 83-1904] 18 p2739 A83-39363

Three-dimensional grid generation from elliptic systems [AIAA PAPER 83-1905] 18 p2739 A83-39364

Quasi three-dimensional grid generation using conformal mapping [AIAA PAPER 83-1906] 18 p2739 A83-39365

Adaptive mesh schemes based on grid speeds [AIAA PAPER 83-1931] 18 p2739 A83-39383

A discussion of some criteria for the use of adaptive gridding [AIAA PAPER 83-1932] 18 p2740 A83-39384

A new self-adaptive grid method [AIAA PAPER 83-1934] 18 p2740 A83-39385

Fast body-fitted grid generation around 3-D configurations [AIAA PAPER 83-1936] 18 p2635 A83-39386

Alternating direction adaptive grid generation [AIAA PAPER 83-1937] 18 p2740 A83-39387

Computational errors of difference schemes for calculating discontinuous solutions [AIAA PAPER 83-1938] 18 p2740 A83-39388

A fast Euler solver for steady flows [AIAA PAPER 83-1940] 18 p2682 A83-39389

A flexible grid embedding technique with application to the Euler equations [AIAA PAPER 83-1944] 18 p2636 A83-39391

Multiple-gridding of the Euler equations with an implicit scheme [AIAA PAPER 83-1945] 18 p2636 A83-39392

Robust calculation of 3D transonic potential flow based on the nonlinear FAS multi-grid method and incomplete LU decomposition [AIAA PAPER 83-1950] 18 p2637 A83-39409

Convergence characteristics of nonlinear vortex-lattice methods for configuration aerodynamics [AIAA PAPER 83-1882] 18 p2637 A83-39421

Some essential details for application of Bleck's method to the collision-breakup equation --- raindrop development model 18 p2725 A83-39691

Ignition and flame propagation studies with adaptive numerical grids 18 p2664 A83-40310

Analysis of the error associated with grid representation of point sources --- for pollutant dispersion 19 p2863 A83-41969

Unigrid for multigrid simulation 20 p3041 A83-42496

On smooth multivariate spline functions 20 p3041 A83-42499

Analysis of viscous flows using multi-grid solution of Neumann pressure problem 20 p2969 A83-42531

Study of asymptotic incompressible flow in curved ducts using a multi-grid technique 20 p2969 A83-42532

A finite-volume, adaptive grid algorithm applied to planetary entry flowfields 20 p2930 A83-43440

A grid overlapping scheme for flowfield computations about multicomponent configurations 20 p2930 A83-43443

An explicit Lagrangian scheme for solving plane and axisymmetric aerodynamic problems, and the mesh rezoning 21 p3130 A83-44558

Introduction to multi-grid methods for the numerical solution of boundary value problems 22 p3352 A83-45767

Mesh influence on vortex shedding in inviscid flow computations 22 p3249 A83-46471
 Integration of the equations of atmospheric dynamics for long time periods using nested grids 23 p3488 A83-47159
 Infrared cooling in cloudy atmospheres - Precision of grid point selection for numerical models 23 p3491 A83-47416
 Improved stress simulation with simple finite element meshes [ASME PAPER 83-GT-89] 23 p3469 A83-47936
 Modelling subgrid scales in numerical simulation of two-dimensional turbulent flows 23 p3449 A83-48048
 Efficient computational grid generation for three-dimensional aircraft configurations [AIAA PAPER 83-2557] 23 p3405 A83-48376
 The multigrid method for accelerated solution of the discretized Schroedinger equation 24 p3622 A83-48873
 Numerical generation of boundary-fitted coordinate systems with optimal control of orthogonality [ONERA, TP NO. 1983-82] 24 p3622 A83-49401
 The use of the method of dividing grids for studying plastic deformations in the stress concentration region 24 p3596 A83-49917

COMPUTER AIDED DESIGN
 Rapid solidification --- for alloy design and process control 01 p0023 A83-10213
 Analytical design of thin-wall wings at the drafting stage 01 p0058 A83-10453
 Demonstration of a figure of merit for inherent testability 01 p0050 A83-10790
 Computation of the zeros and zero directions of linear multivariable systems 01 p0095 A83-10961
 Parametric study of minimum reactor mass in energy-storage dc-to-dc converters 01 p0040 A83-11011
 Nonlinear program based optimization of boost and buck-boost converter designs 01 p0040 A83-11016
 A practical SCR model for computer aided analysis of AC resonant charging circuits 01 p0041 A83-11018
 Software optimization of a Kalman filter for an AP-120B array processor 01 p0091 A83-11111
 Design and application of a multivariable, digital controller to the A-7D Digita II aircraft model 01 p0013 A83-11148
 AEDCS - A computer-aided system design tool for integrated avionics 01 p0089 A83-11176
 Testability using Logmod --- Logic Model method for functional analysis of system design 01 p0029 A83-11232
 EASYCADC - A VAX implementation of a universal user interface for a system of computer aided circuit design /CADC/ programs 01 p0093 A83-11247
 On an index for array optimization and the discrete prolate spheroidal functions 01 p0034 A83-11379
 Some modifications of Newton's method for the determination of the steady-state response of nonlinear oscillatory circuits 02 p0166 A83-11796
 ROMAPT - A new link between CAD and CAM 02 p0228 A83-11816
 Interactive smoothing of digitized point data 02 p0226 A83-11817
 Computer-aided control of sheet metal forming processes 02 p0161 A83-12086
 Approximating shapes using parameterized curves 02 p0231 A83-12174
 The design and technology development for A 150 mlb resistor for H2 or NH3 [AIAA PAPER 82-1949] 02 p0146 A83-12506
 Grazing incidence relay optics 02 p0240 A83-12723
 PANDA - Interactive program for minimum weight design of stiffened cylindrical panels and shells 02 p0194 A83-12745
 Data management in FEM-based optimization software 02 p0228 A83-12751
 Further developments in the controlled growth approach for optimal structural synthesis [ASME PAPER 82-DET-82] 02 p0232 A83-12773
 On the evaluation of manipulator workspace [ASME PAPER 82-DET-126] 02 p0187 A83-12780
 Block-indexed solution of very large linear equation systems with symmetric DBBF coefficient matrix --- Double Bounded Band Form 02 p0228 A83-12839
 Second-order sensitivity derivatives in structural analysis 03 p0338 A83-13149
 Space-invariant composite matched filters for space-variant processors 03 p0394 A83-13774
 Dual-mode realisations for asymmetric filter characteristics 03 p0311 A83-13849
 Beam scanning and focal surfaces for parabolic cylinder reflectors 03 p0305 A83-14006
 A wide-band electrically small superdirective array 03 p0306 A83-14018

Planar array synthesis with prescribed pattern nulls 03 p0306 A83-14019
 The multilevel substructure and the local analysis of structure 03 p0341 A83-14485
 Evaluation procedures to be used during the development of CAD systems 04 p0465 A83-15146
 A fast algorithm for the calculation of transonic flow over wing/body combinations 04 p0442 A83-15283
 Computerized design of CAD --- Charge Activated Devices 04 p0465 A83-15415
 Electronic Circuit Analysis Language /ECAL/ 04 p0470 A83-15550
 Computer-aided design within the framework of the algorithmic selection procedure for the design with catalogs --- German thesis 04 p0487 A83-15844
 The dynamics of plane supporting structures - A computer-aided experimental analysis of structure dynamic problems with interactive method of test --- German thesis 04 p0499 A83-15847
 Contoured-beam synthesis for array-fed reflector antennas by field correlation 04 p0468 A83-16202
 Pan Air versus S/HABP - An evaluation of two diverse approaches to supersonic missile aerodynamic analysis --- Advanced Panel Pilot Code and Supersonic/Hypersonic Arbitrary Body Program 05 p0578 A83-16460
 [AIAA PAPER 83-0008] Iterative optimal subcritical aerodynamic design code including profile drag 05 p0578 A83-16462
 [AIAA PAPER 83-0012] GASAP - A general aviation airplane analysis and synthesis program 05 p0594 A83-16488
 [AIAA PAPER 83-0054] Development of a flight test maneuver autopilot for a highly maneuverable aircraft 05 p0597 A83-16493
 [AIAA PAPER 83-0061] Computational wing design for an advanced trainer 05 p0594 A83-16517
 [AIAA PAPER 83-0093] Missile Datcom status report - Body and fin alone methodology 05 p0581 A83-16574
 [AIAA PAPER 83-0181] CAD/CAM and analysis - A production tool for spacecraft design 05 p0620 A83-16589
 [AIAA PAPER 83-0218] Interactive systems analysis of four structural concepts for a Land Mobile Satellite System 05 p0606 A83-16590
 [AIAA PAPER 83-0219] An interactive method for surface fitting three-dimensional bodies 05 p0581 A83-16591
 [AIAA PAPER 83-0220] The optimal projection approach to fixed-order compensation - Numerical methods and illustrative results --- for large flexible spacecraft design 05 p0680 A83-16641
 [AIAA PAPER 83-0303] Aerodynamic heating and surface temperatures on vehicles for computer-aided design studies 05 p0585 A83-16699
 [AIAA PAPER 83-0411] A supersonic maneuver wing designed for nonlinear attached flow 05 p0585 A83-16707
 [AIAA PAPER 83-0425] Evaluation of finite-element software packages for stress analysis of laminated composites 05 p0678 A83-16936
 CAD/CAM improves productivity in nonaerospace job shops 05 p0621 A83-17283
 Design and testing of low-temperature intense electron beam diodes 05 p0625 A83-17365
 Rapid annealing in advanced bipolar microcircuits 05 p0627 A83-17516
 Isogeometric approximation of functions of one variable --- explicit spline method for CAD of curves and surfaces 05 p0682 A83-17641
 Optimality criterion approach using tapered finite elements with nodal averaging technique for two-dimensional problems 05 p0655 A83-17736
 Diffraction models of slot and strip elements of microwave integrated circuits with suspended substrates for the purpose of computer-aided design 06 p0750 A83-17986
 Application of optimization to aircraft engine disk synthesis 06 p0718 A83-18213
 Optimal shape design to minimize stress concentration factors in pressure vessel components 06 p0772 A83-18214
 PANDA - Interactive computer program for preliminary minimum weight design of composite or elastic-plastic, stiffened cylindrical panels and shells under combined in-plane loads 06 p0773 A83-18227
 Interactive optimum design system --- for two dimensional elastic structures 06 p0773 A83-18228
 Derivation and convergence of power series in structural design 06 p0773 A83-18233
 Adaptive null steering by reflector antennas 06 p0739 A83-18631
 Diffraction from cylindrically truncated planar surfaces with application to an aperture matched horn design 06 p0742 A83-18666

A novel technique for the computation of secondary patterns of reflector antennas 06 p0743 A83-18687
 A comparison between the Craig-Cox and the Kacker-Okapuu methods of turbine performance prediction 06 p0718 A83-19025
 Computer simulations of optimum boost and buck-boost converters 06 p0754 A83-19032
 An overview of PANACEA, a software package for analyzing Markovian queueing networks 06 p0802 A83-19596
 New developments regarding traveling-wave tubes and backward-wave oscillators in the millimeter-wavelength region. II - Electron optics and experimental results 06 p0755 A83-19614
 Digital image processing - A systems approach --- Book 07 p0928 A83-19925
 An analysis of coplanar waveguides with finite conductor thickness-computation and measurement of characteristic impedance 07 p0918 A83-20070
 Optimized low-insertion-loss millimetre-wave fin-line and metal insert filters 07 p0919 A83-20178
 Curvature transitions of composite curves and surfaces - Questions regarding details of computer-aided design --- German thesis 07 p0982 A83-20398
 Optimization using sensitivity analysis --- of inertial upper stage design 07 p0872 A83-20411
 Computer-aided design of complex composite material systems and structures 07 p0877 A83-20498
 4-GHz high-efficiency broadband FET power amplifiers 07 p0920 A83-20556
 An optimization technique for lumped-distributed two ports 07 p0922 A83-21528
 Closed-form expressions for the parameters of finned and ridged waveguides 07 p0923 A83-21532
 A simplified 'real frequency' technique applied to broad-band multistage microwave amplifiers 07 p0923 A83-21537
 Device modeling --- computer aided design of semiconductor devices for VLSI applications 07 p0923 A83-21538
 Circuit analysis, logic simulation, and design verification for VLSI 07 p0923 A83-21539
 Automatic hardware synthesis 07 p0923 A83-21540
 CAD system for VLSI in Japan 07 p0924 A83-21543
 Intermodulation spectra for 2-carrier-level SPC system 07 p0916 A83-21575
 ESABASE - A computer-aided engineering framework facilitating integrated systems design 08 p1171 A83-22372
 Minimax optimization of two-dimensional Cartesian and Fresnel lens phased arrays 08 p1161 A83-22474
 Robust computer-aided control systems design for nonlinear plants 08 p1159 A83-23173
 A mathematical model for a turboshaft gas-turbine engine with an optimum control program for high-level computer-aided design 09 p1205 A83-23436
 A system of criteria for evaluating the energy efficiency of an engine at the state of technical proposals 09 p1205 A83-23437
 Selection of the optimal output parameters for the starting device of a double-shaft turbofan engine 09 p1205 A83-23442
 Diffraction of electromagnetic waves by a two-dimensional periodic waveguide-dielectric array 09 p1244 A83-23451
 The application of mathematical programming to problems of the diffraction synthesis of antennas 09 p1245 A83-23455
 The automation of control system design. Number 4 --- Russian book 09 p1326 A83-24225
 Systems and operations - Living with complexity and growth 09 p1213 A83-24357
 An integral method theorem for heat conduction --- computer aided design of reentry vehicles 09 p1216 A83-24673
 Illustration of the applicability of computer aided design packages 09 p1243 A83-24719
 Composite engine inlet particle separator swirl filter --- CAD for T700 helicopter engine centrifugal filter 09 p1208 A83-24841
 File structures and data bases for CAD; Proceedings of the Working Conference, Seeheim, West Germany, September 14-16, 1981 09 p1325 A83-25095
 On automatic recognition of 3D structures from 2D representations 10 p1461 A83-25474
 Semi-automatic system for defining free-form curves and surfaces 10 p1461 A83-25475
 Design of dielectric ridge waveguides for millimeter-wave integrated circuits 10 p1408 A83-25804
 Computer-aided design of millimeter-wave E-plane filters 10 p1409 A83-25805
 ADAM - An axisymmetric duct aeroacoustic modeling system [AIAA PAPER 83-0666] 10 p1473 A83-25903

Design and operation of a collective millimeter-wave free-electron laser 10 p1427 A83-26014

GG-pseudo-band method for the design of multivariable control systems 10 p1464 A83-26520

The manipulation of interaction effects in multivariable feedback systems 10 p1465 A83-26525

A design method for nonlinear control systems based upon partial knowledge about controlled objects 10 p1465 A83-26528

On a problem of Optimal Model Reference Adaptive System 10 p1468 A83-26560

A design procedure for linear multi-variable feedback systems 10 p1468 A83-26564

Wheelchair analysis - A CAD/CAM application 10 p1401 A83-26578

Results of a world survey of computer-aided manufacture 10 p1460 A83-26579

Analysis of the performance of adaptive beam forming system for perturbation sequences 10 p1405 A83-26833

A new minimum blocking condition including subreflector and quadropud shadow for the design of dual reflector systems 10 p1406 A83-26842

The development of a central electrical generating system for transport vehicles 10 p1411 A83-26885

Algorithms for the design of integrated circuits 10 p1412 A83-26926

A new regenerator theory --- Stirling engine design 11 p1664 A83-27263

A user oriented design system for Stirling cycle codes 11 p1586 A83-27267

Computation techniques and computer programs to analyze Stirling cycle engines using characteristic dynamic energy equations 11 p1665 A83-27272

An isothermal second-order Ringbom-Stirling engine computer program 11 p1587 A83-27281

An approach to the design of Stirling engine regenerator matrix using packs of wire gauzes 11 p1588 A83-27287

Optimization of manipulator workspace 11 p1552 A83-27486

Interactive graphical programming and control of robotic systems 11 p1645 A83-27488

Simple expressions model antenna radiation patterns 11 p1558 A83-28153

Integrating computer programs for engineering analysis and design [AIAA PAPER 83-0597] 11 p1647 A83-28350

Data base organization in computer-aided design systems 11 p1646 A83-28622

Interactive computer graphics - Why's, wherefore's and examples 11 p1553 A83-28690

Interactive graphical preprocessing of three-dimensional framed structures 11 p1646 A83-28718

Formation of a library of mathematical models of complex surfaces of special form 12 p1768 A83-29293

Comparative analysis of large antenna spacecraft using the ideas system [AIAA 83-0798] 12 p1707 A83-29731

Structural tailoring of engine blades (STAEBL) [AIAA 83-0828] 12 p1703 A83-29737

ADS-1 - A new general-purpose optimization program [AIAA 83-0831] 12 p1768 A83-29740

Structural optimization by multilevel decomposition [AIAA 83-0832] 12 p1737 A83-29741

Approximate aerodynamic analysis for horizontal axis wind turbines 13 p1870 A83-30194

Design and performance of W-band broad-band integrated circuit mixers 13 p1831 A83-30230

System for the computer-aided design of robot devices 13 p1906 A83-30619

A user's viewpoint on computational fluid dynamics 13 p1842 A83-30642

Computer-aided interactive structural optimization of printed-circuit-board design 13 p1834 A83-30862

High-technology factory of the future 13 p1827 A83-31052

Development history of the Hybrid Test Vehicle 13 p1934 A83-31088

The role of computer modeling and simulation in electric and hybrid vehicle research and development 13 p1935 A83-31095

Design automation for integrated circuits 13 p1836 A83-31161

An algorithm for constructing shape functions for a rectangular finite element 13 p1867 A83-31322

The selection of optimum parameters for stiffened cylindrical shells loaded by internal pressure and an axial compressive force 13 p1867 A83-31324

Development of two airfoil sections for helicopter rotor blades 13 p1805 A83-31623

The concept of force and moment as a computational quantity in continuum mechanics 13 p1915 A83-31799

Structural optimization - Challenges and opportunities 13 p1869 A83-31814

A detailed package of digital codes specially developed for the array design 14 p2074 A83-32210

A small geometry MOSFET model for CAD applications 14 p2006 A83-32672

Thermal modeling and analysis of structurally complex spacecraft using the IDEAS system [AIAA PAPER 83-1459] 14 p1981 A83-32719

Numerical method for spacecraft radiator mass minimization [AIAA PAPER 83-1490] 14 p1982 A83-32735

Surfaces in computer aided geometric design; Proceedings of the Conference, Oberwolfach, West Germany, April 25-30, 1982 15 p2216 A83-33613

CAD 82; Proceedings of the Fifth International Conference and Exhibition on Computers in Design Engineering, Brighton, England, March 30-April 1, 1982 15 p2216 A83-33615

A basis for the quantitative comparison of computer number systems 15 p2217 A83-33906

CADAC - A controlled-precision decimal arithmetic unit 15 p2217 A83-33907

Optimum design of n(+) - n-n(-) InP devices in the millimeter-range frequency limitation - RF performances 15 p2151 A83-33917

Mathematical methods for the optimization of automatic-control-system devices and algorithms --- Russian book 15 p2220 A83-34175

A network formulation for phased arrays - Application to log-periodic arrays of monopoles on curved surfaces 15 p2121 A83-35090

Alternate formulas for near-field computation 15 p2146 A83-35091

Modelling polyhedral solids bounded by multi-curved parametric surfaces 16 p2402 A83-35322

INTFIS - An interactive package for electronic filter synthesis 16 p2403 A83-35323

Nonlinear programming on a microcomputer 16 p2403 A83-35647

Broad-band compensation for diffraction in surface acoustic wave filters 16 p2345 A83-35649

Booster and orbiter configurations 16 p2316 A83-35768

Computer aided preliminary design of solid rocket motors [AIAA PAPER 83-1254] 16 p2319 A83-36310

Monte Carlo simulation of the engine development process [AIAA PAPER 83-1405] 16 p2310 A83-36394

Comparison of design techniques for pumps with skewed blades [AIAA PAPER 83-1282] 16 p2362 A83-36411

Computer aided multivariable control system design package 17 p2564 A83-37089

Controller design for uncertain nonlinear systems 17 p2566 A83-37110

Maximum entropy stochastic approach to control design for uncertain structural systems 17 p2567 A83-37114

A fluidic/pneumatic interface amplifier 17 p2501 A83-37117

The handbook of antenna design. Volumes 1 & 2 17 p2493 A83-37158

The impact of CFD on development test facilities - A National Research Council projection --- computational fluid dynamics [AIAA PAPER 83-1764] 17 p2503 A83-37234

Method for the formation of design schemes for calculating load-bearing structures 17 p2518 A83-37254

Computer in analysis and design --- for heat transfer analysis 17 p2504 A83-37275

Damping-augmentation mechanism for flexible spacecraft 17 p2478 A83-37469

Analysis of natural waves of planar lines --- German thesis 17 p2496 A83-37503

Method of calculating radiative heat transfer for computer-aided analysis systems --- in flight vehicle structures 17 p2505 A83-37524

Simulate airborne radar environments 17 p2461 A83-37821

Utilization of computer aided design for the development of advanced turbomachinery components [SAE PAPER 821423] 17 p2468 A83-37980

A unified approach to turbine blade life prediction [SAE PAPER 821439] 17 p2468 A83-37987

A computer-aided system for interactive geometric modeling, structural/dynamics analysis and N/C manufacturing/inspection of radial flow compressors [SAE PAPER 821440] 17 p2493 A83-37988

Interactive analysis of a large aperture Earth Observations Satellite [SAWE PAPER 1556] 17 p2480 A83-38053

An algorithm for engineering design optimization 17 p2575 A83-38573

PAN AIR modeling studies --- higher order panel method for aircraft design [AIAA PAPER 83-1830] 17 p2455 A83-38660

An assessment of PANDORA using a Canard/Wing/Body configuration --- Preliminary Automated Numerical Design of Realistic Aircraft [AIAA PAPER 83-1850] 17 p2456 A83-38678

The combination of a geometry generator with transonic design and analysis algorithms [AIAA PAPER 83-1862] 17 p2457 A83-38689

Improved method for transonic airfoil design-by-optimization [AIAA PAPER 83-1864] 17 p2457 A83-38691

Computer-aided design of structurally constrained multivariable regulators. I - Problem statement, analysis and solution 18 p2738 A83-40070

Computer-aided engineering - The AI connection 18 p2738 A83-40307

Computational topology - A study of topological manipulations and interrogations in computer graphics and geometric modeling 18 p2740 A83-40339

The role and application of data base management in integrated computer-aided design 19 p2887 A83-41049

Analysis of slow-wave coplanar waveguide for monolithic integrated circuits 19 p2838 A83-41089

Dominance optimisation in multivariable design 19 p2890 A83-41479

Sensitivity synthesis of systems subject to large parameter variations 19 p2890 A83-41480

Computer aided design in real-time adaptive control 19 p2890 A83-41481

Design of feedback controllers for nonlinear systems 19 p2891 A83-41491

Tradeoff studies in multiobjective insensitive design of airplane control systems [AIAA PAPER 83-2273] 19 p2804 A83-41739

VLSI: Silicon compilation and the art of automatic microchip design --- Book 19 p2841 A83-41873

Simplified computation of coplanar waveguide with finite conductor thickness 20 p2966 A83-42363

Studies on certain modified Luneberg lenses 20 p2963 A83-42369

A computer program for system dynamic synthesis of flexible structures from component data 20 p3002 A83-42543

Future CAD systems 20 p3038 A83-42799

Development of a mathematical model of a flight vehicle and the experimental verification of its reliability 20 p2933 A83-42888

Variational geometry - A new method for modifying part geometry for finite element analysis 20 p3041 A83-42935

A strategy for optimization of wind energy systems 20 p3012 A83-43371

Nonlinear inverse perturbation method in dynamic analysis 20 p3007 A83-43449

Complex combined curve design and fitting - A B-spline multiple knot method 20 p3042 A83-43699

Algorithmic mass-factoring of finite element model analyses [SAWE PAPER 1451] 20 p3009 A83-43733

An interactive weight estimating program for maneuverable reentry vehicles [SAWE PAPER 1458] 20 p2945 A83-43739

Weight control program for a graphite/epoxy aircraft [SAWE PAPER 1485] 20 p2948 A83-43752

LEONARDO - A computer-aided engineering system [SAWE PAPER 1488] 20 p3037 A83-43755

Optimum design of 3-dB branch-line couplers using microstrip lines 21 p3123 A83-43839

The automation of the design of optical systems --- Russian book 21 p3203 A83-43921

Design Optimization Codes for Structures - DOCS computer program 21 p3124 A83-43974

A methodology for custom VLSI layout 21 p3124 A83-44099

New computers will aid advanced designs 21 p3190 A83-44102

A new method of boundary layer correction in the design of supersonic wind tunnel nozzle 21 p3087 A83-44561

Synthesised design of optical filters assisted by microcomputer 21 p3206 A83-44790

Electronic power devices - An introduction to automated design --- Russian book 21 p3126 A83-45044

Multivariable feedback: A quasi-classical approach --- Book 21 p3195 A83-45100

Discrete nonlinear systems --- Russian book 21 p3197 A83-45201

The Jacobi-Bessel and the pseudo-sampling techniques in the analysis of reflector antennas 21 p3121 A83-45410

A computer-assisted study of forced relaxation oscillations 22 p3353 A83-45695

- Computer-aided SAR system design
22 p3350 A83-46177
- Sensor design using computer tools; Proceedings of the Conference, Los Angeles, CA, January 28, 29, 1982
22 p3291 A83-46593
- Detailed computer modeling of an infrared tracker using simulation of passive infrared equipment (SPIRE) techniques
22 p3292 A83-46594
- Computer-aided infrared sensor thermal design
22 p3292 A83-46602
- Computer-aided design of infrared detector preamplifiers having switched feedback resistors
22 p3292 A83-46604
- Integration of electro-optical sensor computing systems
22 p3350 A83-46605
- The use of structural properties in linear multivariable control system design --- Thesis
22 p3352 A83-46690
- Application of advanced CAD/CAM procedures in areas other than air transport technology
23 p3440 A83-47189
- The increase in the cost effectiveness of the construction of and preparation of manufacturing processes for flight equipment through integrated and graphic data processing-CAD/CAM
23 p3440 A83-47191
- Design of skewed reaction wheels controller for three-axis stabilized satellite
[IAF PAPER 83-ST-13]
23 p3423 A83-47389
- Interval reliability for initiating and enabling events
23 p3467 A83-47615
- An algorithm for the empirical optimization of antenna arrays
23 p3443 A83-47845
- A summary of developments of the mean-stream-line method in China --- for design and calculation of flow channels
[ASME PAPER 83-GT-11]
23 p3393 A83-47883
- A CAD method for centrifugal compressor impellers
[ASME PAPER 83-GT-65]
23 p3395 A83-47920
- Advancing electronic technology impact on integrated propulsion/airframe controls design and development
[ASME PAPER 83-GT-161]
23 p3402 A83-47985
- Three-dimensional modeling of horseshoe vortex flows
[ASME PAPER 83-GT-191]
23 p3397 A83-47997
- Squeeze-film damper technology. I - Prediction of finite length damper performance
[ASME PAPER 83-GT-247]
23 p3466 A83-48035
- Application of composites and computer graphics in the design of the MH-53E fuel sponson
[AIAA PAPER 83-2441]
23 p3403 A83-48329
- Aircraft synthesis using numerical optimization methodology
[AIAA PAPER 83-2458]
23 p3500 A83-48336
- Conceptual kinematic design using homogeneous coordinate transformations
[AIAA PAPER 83-2460]
23 p3500 A83-48337
- Computer-aided design of radiating systems of antenna-radome type
23 p3444 A83-48523
- A relational database for nonmanipulative representation of solid objects
23 p3500 A83-48726
- Database systems - Their applications to CAD software design
23 p3500 A83-48727
- Smoothing of bicubic parametric surfaces
23 p3502 A83-48728
- An offset spline approximation for plane cubic splines
23 p3502 A83-48729
- A general-purpose program for nonlinear microwave circuit design
24 p3573 A83-48971
- Aeroelastic considerations for automatic structural design procedures
24 p3547 A83-49189
- Numerical optimum design of elastic annular plates with respect to buckling
24 p3594 A83-49443
- Conceptual design of transport aircraft
24 p3547 A83-49475
- The development of a generalized advanced propeller analysis system
[AIAA PAPER 83-2466]
24 p3549 A83-49581
- Three-dimensional CAD/CAM methodology for determining Space Shuttle small payload volumes
[AIAA PAPER 83-2548]
24 p3552 A83-49591
- Real-time parameter identification in a class of distributed systems using Lyapunov design method. I - Theory
24 p3620 A83-49895
- Design of digital two- and three-term controllers for discrete-time multivariable systems
24 p3620 A83-49897
- COMPUTER AIDED MANUFACTURING**
Improving T700 nozzle manufacture
01 p0056 A83-10974
- ROMAPT - A new link between CAD and CAM
02 p0228 A83-11816
- Computer-aided control of sheet metal forming processes
02 p0161 A83-12086
- CAM networks for the factory of the future
[AIAA PAPER 83-0217]
05 p0679 A83-16588
- CAD/CAM and analysis - A production tool for spacecraft design
[AIAA PAPER 83-0218]
05 p0620 A83-16589
- CAD/CAM improves productivity in nonaerospace job shops
05 p0621 A83-17283
- USAF's design guide coming out next month
07 p1001 A83-20647
- Automated machining of turbine blades by Rolls-Royce
07 p0941 A83-21348
- An anatomy of industrial robots and their controls
08 p1074 A83-22415
- Optimizing the cutting of stock with the aid of computers --- Russian book
09 p1274 A83-23826
- World survey of CAM --- Book
09 p1243 A83-25097
- Wheelchair analysis - A CAD/CAM application
10 p1401 A83-26578
- Results of a world survey of computer-aided manufacture
10 p1460 A83-26579
- AML - A manufacturing language
11 p1646 A83-28100
- High-technology factory of the future
13 p1827 A83-31052
- Surfaces in computer aided geometric design; Proceedings of the Conference, Oberwolfach, West Germany, April 25-30, 1982
15 p2216 A83-33613
- Development of process models to produce a dual-property titanium alloy compressor disk
15 p2134 A83-33634
- Nonstationary temperature fields during the heat treatment of titanium disks of complex configurations
16 p2361 A83-35589
- Utilization of computer aided design for the development of advanced turbomachinery components
[SAE PAPER 821423]
17 p2468 A83-37980
- Implementation and integration of process planning
[SAE PAPER 821424]
17 p2493 A83-37981
- A computer-aided system for interactive geometric modeling, structural/dynamics analysis and N/C manufacturing/inspection of radial flow compressors
[SAE PAPER 821440]
17 p2493 A83-37988
- Computer assisted dielectric cure monitoring in material quality and cure process control
19 p2823 A83-41029
- Conventional controller design for industrial robots - A tutorial
19 p2824 A83-41295
- Future CAD systems
20 p3038 A83-42799
- Planning in time - Windows and durations for activities and goals
21 p3198 A83-43951
- Sensor-based robotic assembly systems - Research and applications in electronic manufacturing
21 p3118 A83-44070
- Current status and future of intelligent industrial robots
21 p3118 A83-44079
- Automatix Incorporated in aerospace applications
[SME PAPER MS83-230]
21 p3119 A83-44862
- Process planning at Sikorsky
21 p3119 A83-44872
- Integration of electro-optical sensor computing systems
22 p3350 A83-46605
- Construction of a computer-supported flexible production chain for metal components
23 p3440 A83-47184
- Application of advanced CAD/CAM procedures in areas other than air transport technology
23 p3440 A83-47189
- The increase in the cost effectiveness of the construction of and preparation of manufacturing processes for flight equipment through integrated and graphic data processing-CAD/CAM
23 p3440 A83-47191
- CIM at GE's factory of the future
23 p3441 A83-48700
- Three-dimensional CAD/CAM methodology for determining Space Shuttle small payload volumes
[AIAA PAPER 83-2548]
24 p3552 A83-49591
- COMPUTER AIDED MAPPING**
Cartographic modeling - Procedures for extending the utility of remotely sensed data
15 p2186 A83-34830
- Application of computers for the mapping of photogrammetric parameters --- for planet and satellite surfaces
17 p2615 A83-37019
- Heat flux display and heat transmission coefficient calculation with the finite element method
20 p2971 A83-42669
- The system of physical spatial units ('Naturraumliche Gliederung') as an aid in the evaluation of satellite data
22 p3311 A83-46165
- COMPUTER ASSISTED INSTRUCTION**
Computer-based pre-simulator training
05 p0676 A83-17308
- COMPUTER COMPATIBLE TAPES**
Standardization of computer compatible tape formats for remote sensing data
01 p0064 A83-10075
- A practical attempt at correlation of rock units from CCT print out --- Computer Compatible Tapes
09 p1291 A83-24627
- Landsat standard family of CCT formats Europe specific problems --- Computer Compatible Tapes
22 p3311 A83-46172
- COMPUTER COMPONENTS**
Programmable systems components - A comprehensive approach to signal processing
08 p1154 A83-22819
- A parallel computation of connected components
15 p2218 A83-35114
- COMPUTER DESIGN**
Marconi avionics standard central air data computer
01 p0009 A83-11119
- A study of an arbiter function in the structures of a shared bus --- French thesis
02 p0166 A83-11700
- PICCOLO logic for a picture database computer and its implementation
02 p0228 A83-12248
- Fundamentals handbook of electrical and computer engineering. Volume 1 Circuits fields and electronics
03 p0314 A83-14047
- The optical computer
06 p0810 A83-19240
- On a method of designing processors for searching for the roots of algebraic equations
08 p1151 A83-22181
- Investigation of aspects of the design of base-crystal matrix computing devices
08 p1152 A83-22182
- A 200 million operations per second /MOPS/ systolic processor
08 p1155 A83-22796
- The software-implemented fault tolerance /SIFT/ approach to fault tolerant computing
08 p1155 A83-22825
- Design methods of single-output built-in self-checking circuits for equilibrium codes
10 p1460 A83-25467
- The NYU ultracomputer - Designing an MIMD shared memory parallel computer --- Multiple Instruction Multiple Data stream
10 p1461 A83-26258
- Vector computations on a parallel-pipelined processor
11 p1646 A83-28623
- Buffering of optoelectronic memory and its effect on computer efficiency
11 p1646 A83-28624
- Design and implementation of the Delft Image Processor DIP-1 --- Thesis
11 p1575 A83-28641
- Nanocomputers from organic molecules? --- molecular electronic nanocircuits for computers
15 p2149 A83-33504
- On the conversion of Hensel codes to Farey rationals --- algorithms based on p-adic computer arithmetic
15 p2216 A83-33902
- A basis for the quantitative comparison of computer number systems
15 p2217 A83-33906
- Finite precision rational arithmetic - An arithmetic unit
15 p2217 A83-33908
- The design of error checkers for self-checking residue number arithmetic
15 p2217 A83-33909
- A parallel computation of connected components
15 p2218 A83-35114
- Operational fault-tolerant microcomputer for very high reliability
16 p2403 A83-36963
- NORA - A racefree dynamic CMOS technique for pipelined logic structures
19 p2887 A83-40790
- Space technology - Computers: Learning from dinosaurs
21 p3191 A83-45602
- COMPUTER GRAPHICS**
Color graphics in ATE
01 p0028 A83-10747
- Demonstration of a figure of merit for inherent testability
01 p0050 A83-10790
- Color, pictorial display formats for future fighters
01 p0010 A83-11134
- Video stand-alone instrument multi-function cockpit display system
01 p0010 A83-11172
- Computer animated representations to optically observe numerical evaluations
01 p0092 A83-11199
- Representation of a region as a forest of quad trees --- describing pixels in image processing analysis
01 p0097 A83-11415
- Normalized quadrees with respect to translations --- in image processing
01 p0097 A83-11416
- Approaches to recursive image decomposition
01 p0097 A83-11417
- On the statistical image segmentation techniques
01 p0098 A83-11432
- A facet model region growing algorithm --- for image processing
[AD-A125 566]
01 p0098 A83-11435
- Description of two hardware convolvers as a part of a general image computer
01 p0089 A83-11437
- Texture simulation using a best-fit model
01 p0101 A83-11479
- Automatic feature extraction system - Test bed
01 p0090 A83-11481
- A language for bitmap manipulation
02 p0228 A83-11782
- A generalization of algebraic surface drawing
02 p0226 A83-11783
- Computer-assisted photo interpretation system
02 p0180 A83-12684

Interactive computer graphic preprocessing for three-dimensional boundary-integral element analysis 02 p0228 A83-12744

Model-based three-dimensional interpretations of two-dimensional image5 02 p0182 A83-12896

Flight simulator display capability significantly advanced 02 p0135 A83-12935

Computerized tomography inspection of trident rocket motors - A capability demonstration 03 p0337 A83-13436

Holographic display of 3D digital data 03 p0324 A83-13437

Perception of position by the pilot in the case of computer-generated external visual scene displays for a landing approach --- German book 03 p0383 A83-14111

Results of stereoscopic image simulations for the SPOT HRV carried out at the Gun Lake site in British Columbia 03 p0350 A83-14292

Computer graphics displays of nonlinear calculations 04 p0526 A83-15019

Enhancement of a graph drawing package 04 p0527 A83-15147

Computer-aided design within the framework of the algorithmic selection procedure for the design with catalogs --- German thesis 04 p0487 A83-15844

Semantic definitions of spacecraft command and control languages using hierarchical graphs 04 p0527 A83-16117

Pilot judgements of distance, height and glide slope angle from computer generated landing scenes 04 p0524 A83-16327

Putting texture in perspective --- flight simulation by application of computer generated imagery techniques 04 p0524 A83-16330

Characteristics of flight simulator visual systems 04 p0450 A83-16331

Simple CIG - An approach to visual simulation for procedure training --- Computer Image Generation 04 p0450 A83-16335

AOI displays in simulation --- Area Of Interest 04 p0448 A83-16337

GASAP - A general aviation airplane analysis and synthesis program [AIAA PAPER 83-0054] 05 p0594 A83-16488

Critical evaluation of eight semiempirical aerodynamic coefficient prediction programs for missiles and stores [AIAA PAPER 83-0185] 05 p0581 A83-16576

CAD/CAM and analysis - A production tool for spacecraft design [AIAA PAPER 83-0218] 05 p0620 A83-16589

An interactive method for surface fitting three-dimensional bodies [AIAA PAPER 83-0220] 05 p0581 A83-16591

The development of a computer controlled camera system for archiving image data [AIAA PAPER 83-0656] 05 p0643 A83-16820

A method of rotating areas on a raster scan graphic display 05 p0644 A83-16871

Computer tomography applied to the study of inflammatory diseases of the brain /a survey of the literature/ 05 p0673 A83-17179

CAD/CAM improves productivity in nonaerospace job shops 05 p0621 A83-17283

Multifunction display simulation facility 05 p0596 A83-17302

Computer graphics applications in electromagnetic computer modeling --- treatment of wire objects by method of moments 06 p0802 A83-18667

Computer-aided speckle pattern interferometry 07 p0928 A83-20155

Real-time image computer configuration 08 p1152 A83-22528

Advanced architecture for graphics and image processing 08 p1152 A83-22530

System architecture of Vicom digital image processor 08 p1097 A83-22533

Advances in electro-optic shutter stereoscopic displays 08 p1098 A83-22566

A method of automatic image reconstruction from holograms by a homomorphic system of logarithmic transform type 08 p1101 A83-22625

Calligraphic/raster color display for simulation 08 p1102 A83-22832

Computer-generated images in visual simulation and avionic technologies 08 p1047 A83-22835

Pilot task profiles, human factors, and image realism 08 p1047 A83-22836

Multidimensional clustering - An application to three-dimensional /3D/ surface extraction 09 p1265 A83-23533

Electromagnetic radiation emissions from visual display units - A review 09 p1324 A83-23885

New displays for the next generation of civil aircraft - Airbus A 310 and A 300/600 color cathode tubes 09 p1204 A83-24374

Computer mapping of shoreline fluctuations by satellite Great Salt Lake, Utah, U.S.A. 09 p1287 A83-24571

Illustration of the applicability of computer aided design packages 09 p1243 A83-24719

Selection and experimental comparison of computer input devices --- Book 09 p1325 A83-24902

Semi-automatic system for defining free-form curves and surfaces 10 p1461 A83-25475

Computer generated cockpit engine displays 10 p1376 A83-26309

The manipulation of interaction effects in multivariable feedback systems 10 p1465 A83-26525

D-decomposition in the space of feedback gains for arbitrary pole regions 10 p1465 A83-26526

Interactive Doppler editing software 11 p1646 A83-27084

An interactive software package for the rectification of radar data to three-dimensional Cartesian coordinates 11 p1646 A83-27085

Using program transformations to derive lind-drawing algorithms 11 p1646 A83-27121

Hidden line elimination in projected grid surfaces 11 p1646 A83-27122

Interactive graphical programming and control of robotic systems 11 p1645 A83-27488

Computer graphics robot simulation programs - A comparison 11 p1646 A83-27489

Interactive computer graphics - Why's, wherefore's and examples 11 p1553 A83-28690

Getting the picture through computer graphics 11 p1525 A83-28691

Interactive graphical preprocessing of three-dimensional framed structures 11 p1646 A83-28718

Single-polarisation operation of highly birefringent bow-tie optical fibres 12 p1779 A83-29462

Mode analysis of optical fibres using computer-generated matched filters 12 p1779 A83-29463

The display of molecular models with the Ames Interactive Modeling System (AIMS) 12 p1768 A83-29548

An automated finite element procedure for fatigue crack propagation analyses [AIAA 83-0841] 12 p1737 A83-29748

Methods of reconstruction and visualization of three-dimensional images in X-ray computed tomography --- French thesis 13 p1844 A83-30128

Anisotropic nonstationary image estimation and its applications. I - Restoration of noisy images. II - Predictive image coding 13 p1845 A83-30223

ARAP (AFOS Radar Processor) 13 p1909 A83-30531

A method of analyzing height and vorticity fields using AFOS 13 p1885 A83-30534

A general purpose meteorological analysis and graphical display computer program 13 p1909 A83-30542

Computer constructed imagery of distant plasma interaction boundaries 13 p1876 A83-30777

Interactive analysis of magnetic field data --- using BANAL and TANAL computer programs 13 p1876 A83-30779

New console design - An example --- for telescope control 13 p1938 A83-31004

Histogram concavity analysis as an aid in threshold selection --- in image processing 13 p1911 A83-31073

Fresnel detour-phase circular computer generated holograms 14 p2083 A83-31948

Thermal modeling and analysis of structurally complex spacecraft using the IDEAS system [AIAA PAPER 83-1459] 14 p1981 A83-32719

A parallel algorithm for determining convex hulls of sets of points in two dimensions 15 p2218 A83-35115

Modelling polyhedral solids bounded by multi-curved parametric surfaces 16 p2402 A83-35322

Simulator performance definition by cue synchronization analysis [AIAA PAPER 83-1092] 16 p2312 A83-36216

Design of a real-time CGSI system [AIAA PAPER 83-1101] 16 p2341 A83-36221

Curve fitting with conic splines 17 p2571 A83-38060

The 8 by 8 display 17 p2564 A83-38061

Quantitative analysis of vector graphics system performance 17 p2564 A83-38062

The GEMPAK Barnes interactive objective map analysis scheme --- General Meteorological Software Package 17 p2548 A83-38709

An evaluation of interactive computer display systems for short-range terminal forecasting applications [AD-A129839] 17 p2548 A83-38711

An interactive meteorological display and analysis system 17 p2549 A83-38713

Advances in systems for interactive processing and display of meteorological data 17 p2549 A83-38714

An operational interactive graphics system --- for weather forecasting and analysis 17 p2549 A83-38715

McIDAS III - A modern interactive data access and analysis system --- Man computer Interactive Data Access System 18 p2726 A83-39874

Computational topology - A study of topological manipulations and interrogations in computer graphics and geometric modeling 18 p2740 A83-40339

Computer-aided graphic visualization of wave propagation 19 p2887 A83-40796

Image processing in automatic systems for scientific investigations --- Russian book 19 p2889 A83-40986

Computational interferometric description of nested flow fields 20 p2988 A83-42527

A hidden line elimination method for curved surfaces 20 p3036 A83-42797

Three-space hidden surface removal using boundary traversal logic 20 p3036 A83-42798

Variational geometry - A new method for modifying part geometry for finite element analysis 20 p3041 A83-42935

Complex combined curve design and fitting - A B-spline multiple knot method 20 p3042 A83-43699

LEONARDO - A computer-aided engineering system [SAWE PAPER 1488] 20 p3037 A83-43755

Sensitivity of X-ray computer tomography in the inspection of thin layers, glued joints, cracks, laminations, and coatings 21 p3149 A83-43877

Segmentation of digital curves using linguistic techniques 21 p3194 A83-44259

Uniform color scale applications to computer graphics 21 p3190 A83-44268

Environmental data display 21 p3142 A83-45615

Technology for large digital mosaics of Landsat data 22 p3318 A83-46766

The increase in the cost effectiveness of the construction of and preparation of manufacturing processes for flight equipment through integrated and graphic data processing-CAD/CAM 23 p3440 A83-47191

The large-scale structure of the universe 23 p3526 A83-47825

Application of composites and computer graphics in the design of the MH-53E fuel sponson [AIAA PAPER 83-2441] 23 p3403 A83-48329

The application of a graphic display for the analysis of scientific telemetry data in experiments involving the search for gamma-ray transients on Prognoz 6 and 7 23 p3500 A83-48417

A relational database for nonmanipulative representation of solid objects 23 p3500 A83-48726

Smoothing of bicubic parametric surfaces 23 p3502 A83-48728

An offset spline approximation for plane cubic splines 23 p3502 A83-48729

The software of an interactive image-processing system 24 p3620 A83-49043

Image enhancement in a dithered picture 24 p3583 A83-49198

COMPUTER METHODS

U COMPUTER PROGRAMS

COMPUTER NETWORKS

The U.K. StarLink computer network 01 p0093 A83-10134

ASTRONET - The network for analysis and retrieval of astronomical data in Italy 01 p0113 A83-10135

Star - A local network system for real-time management of imagery data 02 p0228 A83-12242

SIMD image resampling 02 p0228 A83-12243

Local command-control networks - Operational reliability --- French thesis 03 p0386 A83-13802

A file management system for a network of dissimilar computers --- French thesis 04 p0545 A83-15849

CAM networks for the factory of the future [AIAA PAPER 83-0217] 05 p0679 A83-16588

A practical algorithm for the solution of triangular systems on a parallel processing system 05 p0678 A83-17241

Pin limitations and partitioning of VLSI interconnection networks 05 p0679 A83-17244

From state machines to temporal logic - Specification methods for protocol standards --- of computer communication networks 05 p0621 A83-17270

Communication structures in multicmicrocomputer systems 07 p0983 A83-19715

Performance models of distributed databases 07 p0982 A83-19797

Routing schemes for the augmented data manipulator network in an MIMD system 07 p0984 A83-20248

Bandwidth of crossbar and multiple-bus connections for multiprocessors 07 p0984 A83-20250

New York University /NYU/ ultracomputer - A general-purpose parallel processor 08 p1155 A83-22803

Multicomputer systems in real-time sensor data processing - A look at the problems of throughput and reliability 08 p1155 A83-22826
Cooperative Highly Available Multiprocessor /CHAMP/ networks have great potential for signal processing 08 p1155 A83-22829
Simulation of computer network reliability 09 p1326 A83-23979
Experimental system for computer network via satellite /CS/. I - Summary of the system 10 p1403 A83-26077
Experimental system for computer network via satellite /CS/. II - Communication protocols 10 p1403 A83-26078
Experimental system for computer network via satellite /CS/. III - Network control processor 10 p1403 A83-26079
Experimental system for computer network via satellite /CS/. IV - Packet transmission controller 10 p1403 A83-26080
Experimental system for computer network via satellite /CS/. V - Data collecting and processing system 10 p1403 A83-26081
File allocation in a distributed computer communication network 13 p1909 A83-30788
Asynchronous and clocked control structures for VSLI based interconnection networks 13 p1909 A83-30792
Sub-regional information system formation using multi-resolution remote sensing products 15 p2239 A83-34807
Some properties of the binary n-cube as a network interconnection structure 15 p2219 A83-35133
On graph theoretic approach to n- and (2n-1) stage interconnection networks 15 p2219 A83-35134
On the capacity of multihop slotted ALOHA networks with regular structure 19 p2825 A83-40893
On the capacity of single-hop slotted ALOHA networks for various traffic matrices and transmission strategies 19 p2826 A83-40894
Ad Hoc modeling, expert problem solving, and R&T program evaluation 19 p2907 A83-41304
Optimum utilization of domestic communication satellites for data and television transmission 19 p2831 A83-41382
Distribution design of logical database schemas 20 p3038 A83-43117
Plastic optical passive devices and their application to a local computer network 21 p3205 A83-44219
The layer model and error control for satellite communications 22 p3273 A83-45756

COMPUTER PROGRAM INTEGRITY
Design for safe software [AIAA PAPER 83-0323] 05 p0678 A83-16652
Using fault trees to find design errors in real time software [AIAA PAPER 83-0325] 05 p0678 A83-16654
Applying existing safety design techniques to software safety [AIAA PAPER 83-0327] 05 p0678 A83-16656
Software correctness and reliability 09 p1326 A83-24247
Theory of the computer code RET 1 for the calculation of space-time dependent temperature and composition properties of metal hydride hydrogen storage beds 11 p1545 A83-27337
A method of designing fault tolerant software 22 p3350 A83-45847
Consolidated TPS implementation today and tomorrow --- quality Test Program Sets for aircraft industry [AIAA PAPER 83-2495] 23 p3468 A83-48350

COMPUTER PROGRAMMING
NT LANGUAGE PROGRAMMING
NT MICROPROGRAMMING
NT MULTIPROGRAMMING
NT PARALLEL PROGRAMMING
NT SYMBOLIC PROGRAMMING
ADATLAS - The test language of the future 01 p0091 A83-10741
Increasing test programmer productivity 01 p0091 A83-10788
Independent verification & validation /IV & V/ 01 p0103 A83-11112
Signal processing /SP/ language 01 p0092 A83-11197
Jovial language control procedures with a view toward Ada 01 p0092 A83-11198
Reusable software engineering 01 p0092 A83-11244
A software integration and test facility - Components and test philosophy 01 p0093 A83-11246
Recursive generation of hierarchical data structures for multidimensional digital images 01 p0097 A83-11414
ADA, an introduction: ADA reference manual, /July 1980/ --- Book 01 p0093 A83-11503

DARTS - A software manufacturing technology [AIAA PAPER 83-0324] 05 p0678 A83-16653
Interactive graphical programming and control of robotic systems 11 p1645 A83-27488
A linguistic concept for the advancement of structured programming --- German thesis 11 p1647 A83-28662
An efficient implementation of Batchers' odd-even merge algorithm and its application in parallel sorting schemes 13 p1908 A83-30789
Binary trees and parallel scheduling algorithms 13 p1909 A83-30795
Robot motion: Planning and control --- Book 15 p2172 A83-33695
Developments in test software philosophy and techniques 16 p2363 A83-35499
An algorithm for engineering design optimization 17 p2575 A83-38573
Processes, tasks, and monitors - A comparative study of concurrent programming primitives 20 p3038 A83-43115
Robot programming 21 p3191 A83-44069
An attribute grammar for the semantic analysis of Ada --- Book 21 p3191 A83-45140
Design and implementation of SPIDER - A transportable image processing software package 22 p3350 A83-46251

COMPUTER PROGRAMS

NT APPLICATIONS PROGRAMS (COMPUTERS)
NT COMPILERS
NT COMPUTER SYSTEMS PROGRAMS
NT EDITING ROUTINES (COMPUTERS)
NT INPUT/OUTPUT ROUTINES
NT MERGING ROUTINES
NT NASTRAN
NT OPERATING SYSTEMS (COMPUTERS)
NT SOURCE PROGRAMS
NT SUBROUTINES
System software approaches to the analysis of multidimensional data structures 01 p0090 A83-10137
International standards for software structures in astronomy 01 p0113 A83-10140
A data analysis facility for the Faint Object Camera 01 p0114 A83-10143
The system SPORA --- software package oriented to research in astronomy 01 p0114 A83-10145
Human factors and intelligent products 01 p0085 A83-10254
Some management views on test program set /TPS/ salvageability 01 p0088 A83-10729
A systematic approach to comprehensive TPS diagnostics for electronic modules --- Test Program Set 01 p0037 A83-10730
Consolidated TPS implementation today and tomorrow 01 p0090 A83-10731
ATE support of RF line replaceable units 01 p0013 A83-10732
Automatic selection of switching paths 01 p0037 A83-10734
Distributed system architectures --- modular approach to ATE 01 p0088 A83-10736
An Atlas implementation for the '80s 01 p0091 A83-10740
Voice ATLAS 01 p0091 A83-10742
The first implementation of ATLAS for testing gas turbine engines 01 p0001 A83-10750
PETTS /Programmable Engine Trim Test Set/ 01 p0014 A83-10752
The rationale for a standard unit-under-test-interface 01 p0037 A83-10754
Cost-effective approaches for extending the useful life of ATE and test program sets 01 p0088 A83-10762
Emulation, a cost effective alternative for replacing obsolete ATE 01 p0088 A83-10763
Software quality assurance for automated calibration laboratories 01 p0091 A83-10768
A demonstration of microprogramming for increased ATE throughput 01 p0091 A83-10772
Application of static Automatic Test Program Generators /ATPG/ to dynamic circuitry 01 p0038 A83-10775
Operator test control and interface evaluation 01 p0086 A83-10783
The solution of 'real-world' aircraft EMC problems using the AAPG computer program 01 p0041 A83-11085
A software lifecycle case study using the PRICE model 01 p0112 A83-11105
A top down software cost estimating technique 01 p0112 A83-11106
A software implementation of the cordic technique as applied to trigonometric functions 01 p0091 A83-11110
Software optimization of a Kalman filter for an AP-120B array processor 01 p0091 A83-11111

Software reliability enhancement techniques and assessment method for embedded computer systems 01 p0091 A83-11113
On the certification of digital computer programs for flight safety 01 p0002 A83-11115
Large-scale software development - Management techniques 01 p0087 A83-11143
A survey of avionics software support environments 01 p0087 A83-11163
Software development support system for advanced avionics applications incorporating a parallel machine architecture 01 p0087 A83-11164
An experiment in assessment of flight control software development techniques 01 p0092 A83-11177
A digital flight control system verification laboratory 01 p0015 A83-11178
HOML compiler - High Order Microcode Language 01 p0092 A83-11194
Requirements for debug capability of HOL-source code during software test in avionics laboratories 01 p0092 A83-11225
A ray tracing computer analysis program /RAYCAP/ for airborne surveillance radar applications 01 p0007 A83-11243
Reusable software engineering 01 p0092 A83-11244
EASYCADC - A VAX implementation of a universal user interface for a system of computer aided circuit design /CADC/ programs 01 p0093 A83-11247
Operational software evaluation for the Air Launched Cruise Missile fly-off 01 p0093 A83-11248
An operational software simulator for passive ECM processing 01 p0093 A83-11250
Life Cycle Cost analysis of standard avionics hardware and software 01 p0112 A83-11256
ROMAPT - A new link between CAD and CAM 02 p0228 A83-11816
Nodal crossing changes for sun synchronous satellites with solar electric propulsion 02 p0138 A83-12461
[AIAA PAPER 82-1873] Software and system level tests of a test flight mercury ion thruster subsystem 02 p0145 A83-12485
[AIAA PAPER 82-1912] PANDA - Interactive program for minimum weight design of stiffened cylindrical panels and shells 02 p0194 A83-12745
Calculated and experimental stress distributions in a ribbon parachute canopy 03 p0280 A83-13168
Transient performance of evacuated tubular solar collectors 03 p0352 A83-13478
ESACAP - A minicomputer-oriented network-analysis program 03 p0385 A83-13847
Power-system simulation for low-orbit spacecraft - The EBLOS computer program 03 p0290 A83-13848
Atmospheric transmittance and radiance - The LOWTRAN 5 code 03 p0358 A83-13988
REALTRAN - Real-time implementation of atmospheric-transmittance codes 03 p0359 A83-13989
Atmospheric spectral transmittance and radiance - FASCOD1B 03 p0359 A83-13992
Elliptic problem solvers --- Book 03 p0384 A83-14076
Ellpack - Progress and plans 03 p0384 A83-14081
The ltpack package for large sparse linear systems 03 p0385 A83-14082
Sparse vectorized direct solution of elliptic problems 03 p0385 A83-14083
Adapting iterative algorithms developed for symmetric systems to nonsymmetric systems 03 p0388 A83-14088
Survey of engineering computational methods and experimental programs for estimating supersonic missile aerodynamic characteristics 03 p0278 A83-14124
Remote sensing software for airborne image analysis 03 p0349 A83-14273
The digital image processing system MOBI-DIVAH 03 p0352 A83-14944
Studies on plastic structures - Stability, anisotropic hardening, cyclic loads 04 p0495 A83-15012
Numerical analysis of shielded dielectric resonators including substrate, support disc and tuning post 04 p0470 A83-15237
Easiest ejection seat stability and control analysis capability 04 p0446 A83-15428
Algorithm 49 - Fast Fourier transforms with recursively generated trigonometric functions 04 p0530 A83-15700
A comparison between predicted and measured data from wind turbine wakes 04 p0506 A83-15799
An interactive procedure to solve the background subtraction problems in IUE high resolution spectra - Application to the image SWP 4616 04 p0547 A83-15972

Close binary systems before and after mass transfer.
 III - Spectroscopic binaries 04 p0557 A83-15980
 PAN AIR applications to complex configurations ---
 computer program for predicting subsonic and supersonic
 linear potential flows
 [AIAA PAPER 83-0007] 05 p0577 A83-16459
 Iterative optimal subcritical aerodynamic design code
 including profile drag
 [AIAA PAPER 83-0012] 05 p0578 A83-16462
 SYMBOL - A computer program for the automatic
 generation of symbolic equations of motion for systems
 of hinge-connected rigid bodies
 [AIAA PAPER 83-0013] 05 p0678 A83-16463
 GASAP - A general aviation airplane analysis and
 synthesis program
 [AIAA PAPER 83-0054] 05 p0594 A83-16488
 Improving the data base generation process for flight
 simulator data bases
 [AIAA PAPER 83-0138] 05 p0598 A83-16547
 Critical evaluation of eight semiempirical aerodynamic
 coefficient prediction programs for missiles and stores
 [AIAA PAPER 83-0185] 05 p0581 A83-16576
 A multi-grid method for transonic wing analysis and
 design
 [AIAA PAPER 83-0262] 05 p0583 A83-16618
 DARTS - A software manufacturing technology
 [AIAA PAPER 83-0324] 05 p0678 A83-16653
 Fast algorithms for linear prediction and system
 identification filters with linear phase
 05 p0680 A83-16914
 Direct form expansion of the transfer function for a digital
 Butterworth low-pass filter 05 p0623 A83-16916
 Evaluation of finite-element software packages for stress
 analysis of laminated composites
 05 p0678 A83-16936
 Numerical simulation of GaAs/GaAlAs heterojunction
 bipolar transistors 05 p0624 A83-17294
 Use of emulation in fault analyses of digital systems
 05 p0678 A83-17303
 Software design for the Douglas DC-9 Super 80 digital
 flight guidance system 05 p0592 A83-17311
 Application of software design standards to commercial
 aircraft equipment 05 p0592 A83-17312
 Hardware and software configuration control - History
 and current status 05 p0621 A83-17313
 Software aspects in certification of new European civil
 transport aircraft 05 p0679 A83-17314
 Treatment of late time instabilities in finite-difference
 EMP scattering codes 05 p0628 A83-17532
 Application of the PANAIR production code to a complex
 canard/wing configuration
 [AIAA PAPER 83-0009] 05 p0590 A83-17902
 ACCESS computer program for the synthesis of large
 structural systems 06 p0772 A83-18225
 Large scale structural optimization by finite elements
 06 p0772 A83-18226
 Some aspects of multimicroprocessor systems
 06 p0802 A83-18347
 Priming considerations of heat pipes in zero-G
 06 p0757 A83-18454
 Application of the rectilinear impact pseudostate method
 to modeling of third-body effects on interplanetary
 trajectories
 [AIAA PAPER 83-0015] 06 p0721 A83-19576
 An overview of PANACEA, a software package for
 analyzing Markovian queueing networks
 06 p0802 A83-19596
 Computation of high Reynolds number internal/external
 flows 07 p0863 A83-19803
 Numerical calculations of ultrasonic fields. I - Transducer
 near fields 07 p0942 A83-20269
 HP-41C programs for Bayesian binomial and exponential
 interval estimation with a uniform prior on the reliability
 07 p0942 A83-20513
 Multispectral image classification by the separating
 hyperplanes method - A computer program
 08 p1124 A83-21906
 A program pack for constructing a dynamic model for
 use in the hybrid control system of a manipulator robot
 08 p1154 A83-22179
 Thermoelastohydrodynamic analysis of an oil pumping
 ring seal 08 p1111 A83-22322
 EOSAEL 82 - A library of battlefield obscuration
 models 08 p1093 A83-22352
 Study on the elastic-plastic buckling strength of plate
 structures 08 p1123 A83-22422
 Interactive algorithm development system for tactical
 image exploitation 08 p1097 A83-22527
 Programmable image processing element
 08 p1097 A83-22532
 Numerical calculation of mean mission duration
 08 p1114 A83-22706
 Parameterization of VLF natural modes in a curved
 waveguide 09 p1244 A83-23404

Evaluation of characteristic parameters for
 Schwarzschild, extreme Kerr, and Hawking black holes
 09 p1356 A83-23683
 Radial multi-slit coding for X-ray imaging of laser
 microplasmas 09 p1267 A83-23709
 Basic conceptions of the external software system for
 programmable logic controllers
 09 p1325 A83-24244
 Automated observations of the sun. II - Methods of
 observation 09 p1369 A83-24488
 Linear cascade codes --- Russian book
 09 p1335 A83-25099
 The modular structure of algorithms and programs in
 problems involving continuous medium mechanics and
 computer structure 09 p1326 A83-25239
 Development of symbolic testing methods for computer
 programs 10 p1461 A83-25466
 Algebraic programming of Hamiltonian formalism in
 general relativity - Application to inhomogeneous
 space-times 10 p1506 A83-26093
 Computational methods in control - A survey and
 introduction to the literature 10 p1460 A83-26529
 Software for automatic control of spacecraft
 instruments 10 p1382 A83-26598
 Complex of programs for the astrometric reduction of
 photographic observations 10 p1498 A83-26915
 A field-programmable integrator for weather radar
 signals 11 p1624 A83-27005
 An interactive software package for the rectification of
 radar data to three-dimensional Cartesian coordinates
 11 p1646 A83-27085
 Modular radar analysis software system /MRASS/
 11 p1646 A83-27086
 Using program transformations to derive lind-drawing
 algorithms 11 p1646 A83-27121
 Optimization of manipulator workspace
 11 p1552 A83-27486
 Computer graphics robot simulation programs - A
 comparison 11 p1646 A83-27489
 Finite-element solution of three-dimensional
 electromagnetic problems 11 p1560 A83-27893
 Convergence time of sidelobe cancellation systems
 11 p1554 A83-27908
 Polarisation-vector translation in radar systems
 11 p1555 A83-27920
 Symbolic error analysis and robot planning
 11 p1648 A83-28103
 Calculate waveguide aperture susceptance
 11 p1562 A83-28152
 Computer assisted information retrieval
 11 p1666 A83-28168
 Ground operations software at the IRAS Operations
 Control Centre --- IR Astronomical Satellite
 11 p1533 A83-28215
 Integrating computer programs for engineering analysis
 and design
 [AIAA PAPER 83-0597] 11 p1647 A83-28350
 A software package for computing the three-dimensional
 stressed state of the blades of gas-turbine engines
 11 p1598 A83-28507
 Cooperative development of application specifications,
 giving particular attention to the realization of software
 for specific branches of the economy --- German thesis
 11 p1647 A83-28661
 Research on the thermomechanical stress in turbine
 disks under thermal manipulations --- German thesis
 11 p1531 A83-28667
 Inertial Upper Stage navigation algorithms evaluation
 11 p1536 A83-28778
 NASA aerial applications wake interaction research ---
 particle trajectories in aircraft induced wakes
 12 p1699 A83-28899
 On the use of spectral radiance models to obtain
 irradiances on surfaces of arbitrary orientation
 12 p1752 A83-28945
 A general precompiler for algebraic manipulation
 12 p1768 A83-29110
 Program implementation in the application software
 package NOLINEAR 12 p1768 A83-29541
 ADS-1 - A new general-purpose optimization program
 [AIAA 83-0831] 12 p1768 A83-29740
 Flutter analysis of a transport wing using XTRAN3S
 [AIAA 83-0922] 12 p1743 A83-29848
 On the propagation and control of geosynchronous
 orbits 13 p1809 A83-29996
 A core software concept for integrated control
 13 p1909 A83-30170
 Meteorological data assimilation using AFOS
 13 p1885 A83-30530
 ARAP (AFOS Radar Processor)
 13 p1909 A83-30531
 AFOS objective analysis - A meteorological tool
 13 p1885 A83-30532
 AFOS era automated forecast verification
 13 p1885 A83-30533

A method of analyzing height and vorticity fields using
 AFOS 13 p1885 A83-30534
 The centralized storm information system at the NOAA
 Kansas City complex 13 p1885 A83-30535
 The Navy SPADS - A second generation environmental
 display system --- Satellite Processing And Display
 System 13 p1909 A83-30541
 A general purpose meteorological analysis and graphical
 display computer program 13 p1909 A83-30542
 A verification program for severe convective storm
 forecasts 13 p1886 A83-30547
 An efficient implementation of Batchers' odd-even
 merge algorithm and its application in parallel sorting
 schemes 13 p1908 A83-30789
 An efficient parallel algorithm for the solution of large
 sparse linear matrix equations 13 p1908 A83-30790
 An objective procedure for detecting and correcting
 errors in geophysical data. II - Multidimensional
 applications 13 p1877 A83-30897
 Geometric configuration factors for polygonal zones
 using Nusselt's unit sphere --- in structural design of solar
 receivers 13 p1872 A83-31609
 Charge-coupled device (CCD)/transit instrument (CTI)
 deep photometric and polarimetric survey - A progress
 report 14 p2016 A83-31993
 Supporting flight data analysis for Space Shuttle Orbiter
 Experiments at NASA Ames Research Center
 [AIAA PAPER 83-1532] 14 p1981 A83-32762
 A three degree-of-freedom, typical section flutter
 analysis using harmonic transonic air forces
 [AIAA PAPER 83-0960] 14 p2032 A83-32797
 Surface roughness effects on the stress analysis of
 adhesive joints 14 p2032 A83-32843
 Pseudo-updated constrained solution algorithm for
 nonlinear heat conduction 14 p2012 A83-32989
 An arbitrary-mesh computer program with applications
 to astrophysics 15 p2254 A83-33817
 Integrated verification and testing system (IVTS) for
 HAL/S programs 15 p2219 A83-33971
 Light-curve analysis of eclipsing variables - The
 interpretation of photometric observations
 15 p2264 A83-34570
 Computer approximation of the spectrograms of radio
 sources 15 p2249 A83-34774
 A 'user friendly' geographic information system in a color
 interactive digital image processing system environment
 15 p2186 A83-34829
 INTFIS - An interactive package for electronic filter
 synthesis 16 p2403 A83-35323
 Testability - A military users point of view
 16 p2363 A83-35497
 Fortran computer program for inextensional bending of
 a doubly curved shell triangular element
 16 p2365 A83-35643
 An inlet system installed performance prediction
 program using simplified modeling
 [AIAA PAPER 83-1167] 16 p2293 A83-36256
 Perspectives on the mixing of a row of jets with a confined
 crossflow
 [AIAA PAPER 83-1200] 16 p2352 A83-36276
 PANAIR Pilot Code application to subsonic nacelle type
 interior flows
 [AIAA PAPER 83-1369] 16 p2295 A83-36365
 Progress toward the analysis of supersonic inlet flows
 [AIAA PAPER 83-1371] 16 p2295 A83-36366
 Correction to the wing source velocity error in
 Woodward's USSAERO code 16 p2297 A83-36920
 Computer performance monitoring during the Centaur
 launch countdown 17 p2472 A83-37060
 Analysis of cold flow reestablishment time in a circuit
 breaker nozzle
 [AIAA PAPER 83-1749] 17 p2503 A83-37224
 Photoelectric photometry of 2 Pallas
 17 p2589 A83-37369
 Software for the closed loop control of experiments on
 the GEOS spacecraft 17 p2472 A83-37483
 Boundary-element program realization for the solution
 of two or three-dimensional thermoelastic problems with
 volume forces --- German thesis
 17 p2520 A83-37500
 Evaluating concave and convex aspherical mirrors with
 a T-shaped spherometer 17 p2580 A83-37691
 Robotic testing for digital systems --- for software in
 avionics and flight control systems
 [SAE PAPER 821422] 17 p2563 A83-37979
 The expanded PDCS digital image processing system
 (EPDCS) 17 p2532 A83-38438
 Some recent applications of XTRAN3S --- time marching
 finite difference code for solution of three-dimensional
 transonic small perturbation flow
 [AIAA PAPER 83-1811] 17 p2454 A83-38644
 AFOS terminal forecast monitoring system - Operational
 aspects --- Automation of Field Operations and Services
 17 p2548 A83-38702
 An interactive meteorological display and analysis
 system 17 p2549 A83-38713

Automatic algebraic coordinate generation
17 p2564 A83-38793

The numerical differentiation of discrete functions using polynomial interpolation methods
17 p2564 A83-38795

Generation of boundary-fitted coordinate systems using segmented computational regions
17 p2574 A83-38802

Grid generation by elliptic partial differential equations for a tri-element Augmentor-Wing airfoil
17 p2458 A83-38803

Comparison of panel method formulations and its influence on the development of QUADPAN, an advanced low-order method
[AIAA PAPER 83-1827] 18 p2632 A83-39097

Design and development of a radar control program for the NOAA/WPL pulse-Doppler radars --- Wave Propagation Laboratory
18 p2727 A83-39880

Comprehensive missile aerodynamics programs for preliminary design
18 p2638 A83-40025

An overview of the general programme - Finite element analysis of structures (FEAST)
19 p2857 A83-40887

The role and application of data base management in integrated computer-aided design
19 p2887 A83-41049

Flight software for optimal trajectories in transport aircraft
[AIAA PAPER 83-2241] 19 p2796 A83-41718

Utilization of path length fuzing in the Peacekeeper Weapon System
[AIAA PAPER 83-2251] 19 p2810 A83-41763

On the theory of program synthesis
19 p2888 A83-41992

Conjugate duality and the exponential Fourier spectrum --- Book
20 p3040 A83-42204

Development of compatible numerical software for application to aircraft dynamic analysis
20 p3038 A83-42538

Residual strength predictions for ballistically damaged aircraft
20 p3001 A83-42540

A computer program for system dynamic synthesis of flexible structures from component data
20 p3002 A83-42543

A method for the computation of inertial properties for general areas
20 p3038 A83-42796

Determination and simulation of stable crack growth in ADINA
20 p3003 A83-42927

The use of NONSAP to compare the Von Mises and a modified Von Mises yield criteria
20 p3003 A83-42928

Three-dimensional J-integral calculations of part-through surface crack problems
20 p3003 A83-42930

ADINA modeling of elastoplastic shear/compression waves in tubes
20 p3004 A83-42936

The solution of three-dimensional elasticity problems using the boundary-element method
20 p3006 A83-42999

Praxis-oriented results processing in the calculation of electromagnetic fields by discretization methods
20 p2967 A83-43027

Simulating motion elements of general-purpose robot arms
20 p3039 A83-43108

NASA wake interactions research and applications [SAE PAPER 830764]
20 p2930 A83-43329

An interactive weight estimating program for maneuverable reentry vehicles
[SAWE PAPER 1458] 20 p2945 A83-43739

Metrication of aerospace engineering computer programs
[SAWE PAPER 1475] 20 p3037 A83-43745

Weight control program for a graphite/epoxy aircraft [SAWE PAPER 1485]
20 p2948 A83-43752

Minimum-fuel aeroassisted coplanar orbit transfer using lift-modulation
[AIAA PAPER 83-2094] 20 p2944 A83-43812

Design Optimization Codes for Structures - DOCS computer program
21 p3150 A83-43974

An operating system interface for transportable image processing software
21 p3191 A83-44264

Robust penalty method for structural synthesis
21 p3153 A83-44546

A technique for evaluation of three-dimensional behavior in turbulent boundary layers using computer augmented hydrogen bubble-wire flow visualization
21 p3131 A83-44679

Process planning at Sikorsky
21 p3119 A83-44872

A personal computer approach to automating stress corrosion studies
21 p3158 A83-44915

Digital signal processing --- German book
21 p3126 A83-45092

Core resource management for large real-time computer program development
21 p3191 A83-45472

Design and implementation of SPIDER - A transportable image processing software package
22 p3350 A83-46251

Experience with the development of an Euler code for rotor rows
[ASME PAPER 83-GT-36] 23 p3394 A83-47897

A brief note on the 'local least squares' stress smoothing technique
23 p3471 A83-48172

PAN AIR applications to complex configurations --- computer program for predicting subsonic and supersonic linear potential flows
23 p3399 A83-48221

Wave drag prediction using a simplified supersonic area rule
23 p3399 A83-48222

A conceptual design program for educational purposes
[AIAA PAPER 83-2473] 23 p3403 A83-48339

Consolidated TPS implementation today and tomorrow --- quality Test Program Sets for aircraft industry
[AIAA PAPER 83-2495] 23 p3468 A83-48350

Time-dependent chemistry. I - Modelling of a static cloud --- in interstellar space
24 p3659 A83-49374

Solution of linear equations with a symmetrically skyline-stored nonsymmetric matrix
24 p3620 A83-49438

Conceptual design of transport aircraft
24 p3547 A83-49475

The development of a generalized advanced propeller analysis system
[AIAA PAPER 83-2466] 24 p3549 A83-49581

COMPUTER SIMULATION

U. COMPUTERIZED SIMULATION

COMPUTER STORAGE DEVICES

NT BUBBLE MEMORY DEVICES

NT BUFFER STORAGE

NT COMPUTER COMPATIBLE TAPES

NT CORE STORAGE

NT FLIP-FLOPS

NT MAGNETIC DISKS

NT MAGNETIC TAPES

NT RANDOM ACCESS MEMORY

NT READ-ONLY MEMORY DEVICES

Stellar bibliography retrieving system in Japan
01 p0114 A83-10147

Content-addressable read/write memories for image analysis
02 p0227 A83-12246

PICAP - A system approach to image processing
02 p0229 A83-12249

Target design of an archival electron beam memory
04 p0526 A83-16051

Effects of cache coherency in multiprocessors
05 p0679 A83-17242

Memory interference in synchronous multiprocessor systems
05 p0680 A83-17245

The use of scanning control loops in magnetic disk memory --- German thesis
06 p0802 A83-18525

Analysis of the effect of dispersion errors of memories on the precision of discrete spectral analysis
06 p0802 A83-19180

Pseudo-associative store with hardware hashing --- data-flow approach in parallel computing systems
07 p0982 A83-19624

Comparison of the efficiency of the paralleling of sequential programs for computing systems with local and common memory
08 p1154 A83-22183

Cryogenic frequency domain optical mass memory
08 p1166 A83-22808

Buffering of optoelectronic memory and its effect on computer efficiency
11 p1646 A83-28624

Investigation of the characteristics of programmed devices of pulsed-signal search
20 p2964 A83-42907

An iterative approach to region growing using associative memories
21 p3191 A83-43956

Core resource management for large real-time computer program development
21 p3191 A83-45472

A system of active data-storage for experiments on gamma-ray transients
23 p3500 A83-48416

A conditional algorithm for setting a discrete device with memory to a definite state
24 p3622 A83-50206

COMPUTER SYSTEMS DESIGN

Use of multifunctional computers with decentralized control for digital signal processing with floating point decimal representation --- German thesis
01 p0031 A83-10476

System performance ramifications of ATS architectures
01 p0088 A83-10735

The modular ATE/UUT interface
01 p0037 A83-10753

The microprocessor controlled ATE - A cost effective approach to dedicated automatic test equipment
01 p0088 A83-10760

Computer support system
01 p0088 A83-10787

Embedded microprocessors for avionic applications
01 p0088 A83-11104

On the certification of digital computer programs for flight safety
01 p0002 A83-11115

The U.S. Air Force and U.S. Navy Standard Central Air Data Computer
01 p0009 A83-11120

A predictive tracking EW preprocessor using standard computer instruction set architectures
01 p0088 A83-11133

Terrain following/terrain avoidance for advanced penetrating aircraft
01 p0006 A83-11146

A prototype parallel computer architecture for advanced avionics applications
01 p0088 A83-11153

Software development support system for advanced avionics applications incorporating a parallel machine architecture
01 p0087 A83-11164

An integrated support software system for the VHSC era
01 p0089 A83-11165

Compiler validations - A tutorial and some observations
01 p0089 A83-11167

AEDCS - A computer-aided system design tool for integrated avionics
01 p0089 A83-11176

Incorporating IPS into a commercial CAD system
01 p0092 A83-11195

A cost effective approach to design evaluation of advanced system display switchology
01 p0093 A83-11200

Use of the onboard simulation concept for the integrated flight and fire control program
01 p0007 A83-11201

Adaptive power management - A hierarchical/control system with a central multiplex system --- for aircraft applications
01 p0012 A83-11202

A closed loop test facility for validating flight control software
01 p0015 A83-11226

Reusable software engineering
01 p0092 A83-11244

A software integration and test facility - Components and test philosophy
01 p0093 A83-11246

Contextual classification on PASM --- multimicroprocessor system for image processing and pattern recognition
01 p0090 A83-11441

Architectures for neighborhood processing --- of images by computer serial array processors
01 p0090 A83-11446

PUMPS architecture for pattern analysis and image database management --- shared resource multiprocessor computer
01 p0090 A83-11448

ZMOB - Hardware from a user's viewpoint --- multiprocessor with architecture including 256 autonomous microprocessors
01 p0090 A83-11449

Some thoughts on the development of computer-based systems --- airborne equipment design to cost
02 p0135 A83-11807

A fast microprocessor communication network design for interprocessor communications for an integrated flight control system
02 p0133 A83-11902

Data acquisition/reduction system for flight testing general aviation aircraft
02 p0135 A83-11903

A simulation-aided multiple processor architecture design for BMD underlay terminal defense
02 p0226 A83-11904

A mixed distributed/parallel processing experiment for real-time radar control
02 p0226 A83-11905

A microprocessor-based fault-tolerant computer system
02 p0227 A83-11907

Implementation of the DAST ARW II control laws using an 8086 microprocessor and an 8087 floating-point coprocessor --- drones for aeroelasticity research
02 p0227 A83-11910

Multimicroprocessor systems
02 p0227 A83-11916

PICAP - A system approach to image processing
02 p0229 A83-12249

Infrared astronomical data base and catalog of infrared observations
03 p0406 A83-13467

Application of a parallel processor to the solution of finite difference problems
03 p0385 A83-14086

Evaluation procedures to be used during the development of CAD systems
04 p0465 A83-15146

A file management system for a network of dissimilar computers --- French thesis
04 p0545 A83-15849

CAM networks for the factory of the future
[AIAA PAPER 83-0217] 05 p0679 A83-16588

The ETH-Multiprocessor EMPRESS - A dynamically configurable MIMD system
05 p0679 A83-17237

Design of HM2p - A hierarchical multimicroprocessor for general-purpose applications
05 p0679 A83-17238

Wavefront array processor - Language, architecture, and applications
05 p0679 A83-17239

Effects of cache coherency in multiprocessors
05 p0679 A83-17242

Some aspects of multimicroprocessor systems
06 p0802 A83-18347

Development environment for the design and test of applications software for a distributed multiprocessor computer system
07 p0983 A83-19625

Communication structures in multimicrocomputer systems
07 p0983 A83-19715

Optical data-transmission equipment for computer systems - Optical data mux 07 p0983 A83-19780
 Message delays using prioritized packet switching 07 p0912 A83-19792
 Partitioned matrix algorithms for VLSI arithmetic systems 07 p0982 A83-20249
 Controlling the complexity of menu networks 07 p0983 A83-21041
 Automatic hardware synthesis 07 p0923 A83-21540
 On the design of algorithms for VLSI systolic arrays 07 p0923 A83-21542
 The influence of software errors on the reliability of data processing systems --- French thesis 08 p1154 A83-22084
 Design of digital image processing systems: Proceedings of the Meeting, San Diego, CA, August 27, 28, 1981 08 p1097 A83-22524
 Use of array processors in image processing 08 p1152 A83-22529
 PAR image processing system /PARIPS/ - A testbed for automating image interpretation 08 p1154 A83-22536
 Powerful hardware/software architecture for a minicomputer-based interactive image processing system 08 p1097 A83-22537
 Microprocessor-based image processing system for dedicated applications or interactive image processing 08 p1155 A83-22538
 Large scale multipurpose interactive image processing facility at ETH-Zurich 08 p1098 A83-22539
 New York University /NYU/ ultracomputer - A general-purpose parallel processor 08 p1155 A83-22803
 A large scale integration based, signal processor - Its application and possible evolution 08 p1155 A83-22811
 Advanced onboard signal processors for satellite communication systems 08 p1050 A83-22822
 Architecture and applications of the HEP multiprocessor computer system 08 p1155 A83-22823
 Multicomputer systems in real-time sensor data processing - A look at the problems of throughput and reliability 08 p1155 A83-22826
 Motivation for a combined data flow-control flow processor 08 p1155 A83-22827
 Cooperative Highly Available Multiprocessor /CHAMP/ networks have great potential for signal processing 08 p1155 A83-22829
 The theory and practice of reliable system design --- Book 09 p1325 A83-24947
 AML - A manufacturing language 11 p1646 A83-28100
 On board computing - Intelligent modules add a new dimension to satellite control systems 11 p1645 A83-28169
 Integrating computer programs for engineering analysis and design [AIAA PAPER 83-0597] 11 p1647 A83-28350
 Comparison of various data allocation schemes in the memory of a multiprocessor computing system 11 p1647 A83-28625
 The display of molecular models with the Ames Interactive Modeling System (AIMS) 12 p1768 A83-29548
 Black box multigrid 12 p1773 A83-29658
 Development and use of an integrated analysis capability [AIAA 83-1017] 12 p1773 A83-29799
 ARAP (AFOS Radar Processor) 13 p1909 A83-30531
 The centralized storm information system at the NOAA Kansas City complex 13 p1885 A83-30535
 Interactive data processing for mesoscale forecasting applications 13 p1885 A83-30539
 Prototype workstation for mesoscale forecasting - A look to the 1990's 13 p1885 A83-30540
 The Navy SPADS - A second generation environmental display system --- Satellite Processing And Display System 13 p1909 A83-30541
 Computational systems and methods in the automation of investigations and control --- Russian book 13 p1910 A83-30616
 Tradeoffs in level of automation in large-scale computerized test systems 13 p1861 A83-31190
 MIDAS - ESO's new image processing system 13 p1942 A83-31581
 Reducing the cost for airborne instrumentation hardware testing 14 p1978 A83-32928
 Analysis of timed Petri nets and application to distributed systems --- French thesis 15 p2219 A83-33697
 Approximate analytical performance evaluation in bus oriented multicomputer systems 15 p2219 A83-35130
 On graph theoretic approach to n- and (2n-1) stage interconnection networks 15 p2219 A83-35134

Analysis of a real-time application [AIAA PAPER 83-1088] 16 p2406 A83-36212
 Benchmarks for a computer system for NASA's Shuttle procedures simulator [AIAA PAPER 83-1089] 16 p2314 A83-36213
 Implementing parallel applications on a multi-array processor architecture [ONERA, TP NO. 1983-13] 16 p2404 A83-36423
 The HEAO experience - design through operations 17 p2473 A83-37482
 Quantitative analysis of vector graphics system performance 17 p2564 A83-38062
 Experiments in automatic microcode generation 19 p2888 A83-41037
 Divide-and-conquer for parallel processing 19 p2887 A83-41038
 The role and application of data base management in integrated computer-aided design 19 p2887 A83-41049
 Normative predicates of next-generation management support systems 19 p2906 A83-41294
 Space Station information systems [AIAA PAPER 83-7105] 19 p2814 A83-42089
 The enchanted loom --- Book on evolution of intelligence 20 p3033 A83-42174
 Development of a totally computer-controlled triple quadrupole mass spectrometer system 20 p2988 A83-42298
 Scientific and defense shops - The computers 20 p3036 A83-43032
 A flight control and navigation system for small RPVs 20 p2932 A83-43723
 A method of designing fault tolerant software 22 p3350 A83-45847
 Modern digital air-data computer 23 p3405 A83-47186
 A development of a high speed image processing system - TIAS 3000 [IAF PAPER 83-125] 23 p3454 A83-47281
 New approaches to planetary exploration - Spacecraft and information systems design [IAF PAPER 83-348] 23 p3415 A83-47354
 Method for choosing the required complex configuration of a multiprocessor computing complex 24 p3620 A83-50210

COMPUTER SYSTEMS PERFORMANCE

Increasing test programmer productivity 01 p0091 A83-10788
 Operational software evaluation for the Air Launched Cruise Missile fly-off 01 p0093 A83-11248
 Image processing on ZMOB 02 p0228 A83-12244
 CPU coverage evaluation using automatic fault injection 03 p0385 A83-14842
 Design of HM2p - A hierarchical multimicroprocessor for general-purpose applications 05 p0679 A83-17238
 Minimization of interprocessor communication for parallel computation 05 p0679 A83-17240
 Effects of cache coherency in multiprocessors 05 p0679 A83-17242
 Queueing network models for parallel processing with asynchronous tasks 05 p0679 A83-17243
 Memory interference in synchronous multiprocessor systems 05 p0680 A83-17245
 The influence of software errors on the reliability of data processing systems --- French thesis 08 p1154 A83-22084
 Combinatorial reliability analysis of multiprocessor computers 08 p1152 A83-22711
 Architecture and applications of the HEP multiprocessor computer system 08 p1155 A83-22823
 The modular structure of algorithms and programs in problems involving continuous medium mechanics and computer structure 09 p1326 A83-25239
 Experimental system for computer network via satellite /CS/. II - Communication protocols 10 p1403 A83-26078
 The organization of circuit analysis on array architectures --- Thesis 11 p1564 A83-28648
 Quantitative analysis of vector graphics system performance 17 p2564 A83-38062
 Dialog with a computer - Psychological aspects 18 p2737 A83-40560
 Abstractions for node level passive fault detection in distributed systems 19 p2889 A83-41036
 Optical systolic array processor using residue arithmetic 22 p3350 A83-46834

COMPUTER SYSTEMS PROGRAMS

NT INPUT/OUTPUT ROUTINES
 NT OPERATING SYSTEMS (COMPUTERS)
 Distributed ATE systems software 01 p0088 A83-10771
 Calibration of third-generation ATE systems 01 p0091 A83-10784
 Increasing productivity in software engineering projects 01 p0087 A83-11142

Software configuration control in a real-time flight test environment 01 p0009 A83-11144
 F-4F fire control system software support - An integrated approach to ground and flight testing 01 p0015 A83-11228
 Systems programming aids /SPA/ methodology 01 p0092 A83-11245
 A language for bitmap manipulation 02 p0228 A83-11782
 Architecture for scientific software. I - Data centralization 02 p0229 A83-12348
 Spacelab software for science applications 03 p0285 A83-13710
 SAMID, an interactive system for the analysis and constrained minimization of induced drag of aircraft configurations [AIAA PAPER 83-0095] 05 p0594 A83-16519
 Design for safe software [AIAA PAPER 83-0323] 05 p0678 A83-16652
 Architecture for scientific software. II - Analysis of a quadratic programming algorithm 05 p0680 A83-17319
 Software correctness and reliability 09 p1326 A83-24247
 On the optimal structuring of program resources for the organization of parallel computations 11 p1647 A83-28523
 Space Shuttle primary onboard software - STS-1 to operational use 13 p1909 A83-30157
 A framework for software fault tolerance in real-time systems 16 p2403 A83-35325
 Ground support software for the Exosat onboard computer 17 p2472 A83-37489
 An automated system for processing information in radio astronomy on the M-6000 computer during observations 17 p2564 A83-37675
 Software for hybrid computing systems. I - Systems of analog and hybrid programming automations 19 p2888 A83-41421
 A method of designing fault tolerant software 22 p3350 A83-45847
 Software for hybrid systems. II - Systems software 24 p3620 A83-50202

COMPUTER SYSTEMS SIMULATION

An operational software simulator for passive ECM processing 01 p0093 A83-11250
 Cellular array processing simulation 02 p0228 A83-12881
 An improved model for isolated word recognition 04 p0529 A83-16324
 The ETH-Multiprocessor EMPRESS - A dynamically configurable MIMD system 05 p0679 A83-17237
 Queueing network models for parallel processing with asynchronous tasks 05 p0679 A83-17243
 Memory interference in synchronous multiprocessor systems 05 p0680 A83-17245
 Combinatorial reliability analysis of multiprocessor computers 08 p1152 A83-22711
 Simulation of computer network reliability 09 p1326 A83-23979

COMPUTER TECHNIQUES

Application of computer axial tomography /CAT/ to measuring crop canopy geometry --- corn and soybeans 01 p0065 A83-10096
 Automated data retrieval in astronomy; Proceedings of the Sixty-fourth Colloquium, Universite de Strasbourg I, Strasbourg, France, July 7-10, 1981 01 p0113 A83-10126
 The system SPORA --- software package oriented to research in astronomy 01 p0114 A83-10145
 The use of computers at hospitals in the Ukrainian SSR 01 p0086 A83-10562
 The organization of computational work --- Russian book 01 p0090 A83-10667
 Innovation in inertial ATE interfaces 01 p0017 A83-10782
 Simplification of digital control systems by adjusting zeros 01 p0095 A83-11174
 An automatic test generation system for complex digital logic 01 p0042 A83-11230
 Computer tracking of moving objects using a Fourier-domain filter based on a model of the human visual system 01 p0097 A83-11420
 Textural anisotropy features for texture analysis 01 p0101 A83-11475
 A generalization of algebraic surface drawing 02 p0226 A83-11783
 A method of automated processing of flaw inspection results 02 p0188 A83-12164
 Advances and trends in structural and solid mechanics; Proceedings of the Symposium, Washington, DC, October 4-7, 1982 02 p0193 A83-12732
 The hierarchical concept in finite element analysis 02 p0193 A83-12737
 A Newton-Lanczos method for solution of nonlinear finite element equations 02 p0194 A83-12748

Lanczos eigenvalue algorithm for large structures on a minicomputer 02 p0194 A83-12749

A sparse matrix finite element technique for iterative structural optimization 02 p0194 A83-12750

The diagnostic significance of the integral assessment of myocardial ischemia in patients with ischemic heart disease for the computerized monitoring of the EKG during the treadmill test 03 p0379 A83-13624

Celestial navigation in the computer age --- Book 03 p0280 A83-14116

Finite-difference techniques for vectorized fluid dynamics calculations --- Book 03 p0317 A83-14225

An experimental Landsat Quicklook System for Alaska 03 p0348 A83-14271

Statistical synthesis of an algorithm for the computer-aided processing of cardiac signals 03 p0384 A83-14329

Forecast results from the Navy operational regional atmospheric prediction system 03 p0367 A83-14430

A family of flux-correction methods to avoid overshoot occurring with solutions of unsteady flow problems 03 p0322 A83-14608

Derivative calculation from finite element solutions 03 p0389 A83-14696

An iteration procedure for reducing the expenses of static, elastoplastic and eigenvalue problems in finite element analysis 03 p0389 A83-14697

Penalty-finite-element analysis of 3-D Navier-Stokes equations 03 p0323 A83-14699

Quantitative evaluation of real-time synthetic aperture acoustic images [AD-A130062] 04 p0493 A83-15228

A new method of finite element structure discretization 04 p0498 A83-15549

A computational method for performing the multiblade coordinate transformation 04 p0446 A83-16029

Limits of stability for an area-preserving polynomial mapping 04 p0532 A83-16360

An implicit, transonic, full-potential code for cascade flow on H-grid topology [AIAA PAPER 83-0506] 05 p0587 A83-16754

Comparison of plasma focus calculations 05 p0689 A83-17372

A method for the operational calculation of the expected number of stars in a given region of the celestial sphere 05 p0694 A83-17677

Computer-controlled high-speed photometry, taking into account the example of the occultation of 57 Orionis by the moon. I 05 p0695 A83-17855

Automatic determination of frequency response parameters and distortion in resonant microwave cavities 06 p0750 A83-17970

The recursive-iterative algorithm for solving the characteristic equation for stabilized spacecraft. II 06 p0723 A83-18353

Experience with the parallel solution of partial differential equations on a distributed computing system 07 p0983 A83-20247

Interactive system for scanning tracks in nuclear research emulsions 07 p0931 A83-21378

Application of a direct procedure for numerical handling of self-adjoint, positive definite eigenvalue problems for linear normal differential equations with piecewise continuous coefficient functions 08 p1159 A83-21864

Some problems of computer-assisted mapping of land use from Landsat data - The Hong Kong case 08 p1128 A83-21965

Organization of a computational process for solving systems of difference equations in a parallel grid processor 08 p1154 A83-22180

ARMA time series modeling - An effective method 08 p1158 A83-22730

Testing diamond turned aspheric optics using computer-generated holographic /CGH/ interferometry 08 p1103 A83-22869

A computer-controlled broadband system for measuring scattered fields and for locating scattering centers 09 p1244 A83-23382

Computational studies of first-Born scattering cross sections. I - Spectral properties of Bethe surfaces. II - Moment-theory approach 09 p1341 A83-23722

Spurious solutions in driven cavity calculations 09 p1259 A83-23725

Applied control theory --- Book 09 p1335 A83-24894

Coherent optical production of the Hough transform 10 p1484 A83-26866

Certain parallel iterative methods for solving nonlinear equations 10 p1470 A83-26943

Coefficient perturbation adaptive HF array 11 p1555 A83-27914

Computable finite element error bounds for Poisson's equation 11 p1649 A83-27998

The identification of the variation of atherosclerosis plaques by invasive and non-invasive methods 11 p1643 A83-28760

Matrix formulation of the Picard method for parallel computation 12 p1771 A83-29107

On the choice of the equatorial coordinates of celestial bodies from computer printouts during the calculation of their azimuths 12 p1706 A83-29322

A method for the organization of matrix computational structures 12 p1767 A83-29342

The use of the method of multisegment argument-transformation for the high-precision hardware implementation of elementary functions 12 p1768 A83-29348

Chebyshev series solution of the controlled Duffing oscillator 12 p1776 A83-29630

Equivalence and singularities - An application of computer algebra --- metric calculation in general relativity 12 p1776 A83-29645

An automated technique for improving model matrices by means of experimentally obtained dynamic data [AIAA 83-0881] 12 p1746 A83-29890

Numerical solutions for unsteady aeroflows using internal singularity distributions 12 p1698 A83-29971

A fast computational technique for accurate permittivity determination using transmission line methods 13 p1831 A83-30226

Effect of exercise on QRS duration in healthy men - A computer ECG analysis 13 p1905 A83-30506

Binary trees and parallel scheduling algorithms 13 p1909 A83-30795

Current progress and prospects in numerical techniques for weather prediction models 13 p1893 A83-31365

On life time predictions with the strain range partitioning method 13 p1824 A83-31543

Viscous shock-layer flowfield analysis by an explicit-implicit method [AIAA PAPER 83-1423] 14 p1970 A83-32702

On the machine computation of the orbits of eclipsing binaries 14 p2099 A83-33249

Error free computation - A direct method to convert finite-segment p-adic numbers into rational numbers 15 p2217 A83-33903

Unconditionally stable implicit-explicit algorithms for coupled thermal stress waves 15 p2176 A83-34317

Annual Allerton Conference on Communication, Control, and Computing, 19th, Monticello, IL, September 30-October 2, 1981, Proceedings 15 p2220 A83-35101

Systolic and SIMD algorithms for digital filtering 15 p2219 A83-35148

An algorithm of fast Kotel'nikov interpolation --- for optical image simulation 15 p2223 A83-35262

A framework for software fault tolerance in real-time systems 16 p2403 A83-35325

Generating exact solutions of the two-dimensional Burgers' equations 16 p2349 A83-35524

Ordering of Walsh functions 16 p2404 A83-35782

Computer tomography in the diagnosis of cranio-cerebral injuries 16 p2400 A83-36832

Prospects of the development of planimetric and topographic bases for lunar maps 17 p2614 A83-37006

Method of random image synthesis by means of computer 17 p2563 A83-38032

Forecasting upslope stratus and fog in the central plains 17 p2550 A83-38725

The Air Force Global Weather Central computer flight planning system 17 p2552 A83-38761

CAT detection and forecasting using operational NMC analysis data 17 p2553 A83-38765

Automated three-dimensional grid refinement on a minicomputer 17 p2573 A83-38792

Conformal mappings onto multiply connected regions with specified boundary shapes 17 p2573 A83-38801

Numerical generation of three-dimensional coordinates between bodies of arbitrary shapes 17 p2574 A83-38806

Semidirect/marching solutions and elliptic grid generation 17 p2574 A83-38807

The employment of a miniature calculating device for the determination of the center of gravity 18 p2642 A83-39220

Implicit methods of second-order accuracy for the Euler equations [AIAA PAPER 83-1925] 18 p2682 A83-39379

Fast body-fitted grid generation around 3-D configurations [AIAA PAPER 83-1936] 18 p2635 A83-39386

A flexible grid embedding technique with application to the Euler equations [AIAA PAPER 83-1944] 18 p2636 A83-39391

Analysis by computer of the convergence to steady state of discrete approximations to the Euler equations [AIAA PAPER 83-1951] 18 p2636 A83-39395

A new computer approach to the modeling of close binary stars 18 p2775 A83-39746

Organization of a microprocessor computing system for the numerical integration of linear differential equations 18 p2738 A83-40094

Effects of complicated deformation history on inelastic deformation behaviour of metals 18 p2705 A83-40334

The elevation of the ST segment during physical loading

Computer analysis, comparison with angiographic data, and clinical significance 18 p2735 A83-40547

Stereotaxic computer tomography 18 p2737 A83-40576

Computer tomography for tumors of the posterior regions of the third ventricle and the pineal body 18 p2733 A83-40577

Computer tomography of organs of the abdominal cavity 18 p2736 A83-40579

Filtering of semitransparent cloud cover 18 p2692 A83-40597

Computer-aided graphic visualization of wave propagation 19 p2887 A83-40796

Holographic laser scanners for multidirectional scanning 19 p2847 A83-41100

X-ray imaging of extended objects using nonoverlapping redundant array 19 p2847 A83-41104

A distance measure between attributed relational graphs for pattern recognition 19 p2889 A83-41297

Necessary and sufficient conditions of the convergence asynchronous iterative computational processes when solving systems of linear algebraic equations 19 p2888 A83-41420

Computer tomography of the brain during migraine (Review) 19 p2883 A83-41463

Computing methods in applied sciences and engineering, V; Proceedings of the Fifth International Symposium, Versailles, France, December 14-18, 1981 19 p2896 A83-41526

Computer measurement of line strengths with application to the methane spectrum 19 p2820 A83-41868

Characterization of grain boundaries in polycrystalline solar cells using a computerized electron beam induced current system 20 p2988 A83-42299

Algorithm for the fast computation of the two-dimensional discrete Fourier transformation 20 p3041 A83-42903

On the automatic solution of nonlinear finite element equations --- for structural analysis 20 p3003 A83-42933

A paradigm for the design of parallel algorithms with applications 20 p3038 A83-43114

Performance analysis of FFT algorithms on multiprocessor systems 20 p3036 A83-43118

Hardware-based Fourier transforms - Algorithms and architectures 20 p3037 A83-43681

Digital image processing using the Apple II microcomputer 21 p3190 A83-43892

A personal computer approach to automating stress corrosion studies 21 p3158 A83-44915

Computer controlled decreasing Delta-K fatigue threshold test 21 p3162 A83-45184

Contour-based motion estimation 22 p3350 A83-46252

Neighboring gray level dependence matrix for texture classification 22 p3315 A83-46254

Hybrid experimental-numerical stress analysis 22 p3307 A83-46811

Non destructive testing of honeycomb structures by computerized thermographic systems --- for spacecraft applications [IAF PAPER 83-419] 23 p3415 A83-47378

In situ balancing of flexible rotors using influence coefficient balancing and the unified balancing approach [ASME PAPER 83-GT-178] 23 p3465 A83-47989

The impact of computers on the test cell of tomorrow --- for gas turbine engine tests [ASME PAPER 83-GT-187] 23 p3409 A83-47993

A simple algorithm for the nonlinear dynamic analysis of networks 23 p3470 A83-48160

Systolic array for recursive least-squares minimization 23 p3500 A83-48718

Iconics: Theory and methods of image processing 24 p3582 A83-49042

COMPUTER VISION

Dot-matrix display light measurement and interpretation techniques --- for qualification tests techniques 01 p0011 A83-11257

Motion detection using Hough techniques 01 p0097 A83-11418

Motion and image differencing --- computer analysis of dynamic scenes 01 p0097 A83-11425

The GLGS image representation and its application to preliminary segmentation and pre-attentive visual search --- Gray Level Geographic Structure 01 p0098 A83-11431

Systolic cellular logic - Inexpensive parallel image processors 01 p0089 A83-11438
'Bilevel' processing of 'multilevel' pictures 01 p0099 A83-11439

A fast technique for segmentation and recognition of binary patterns --- image processing algorithms 01 p0099 A83-11444
Relaxation labeling using staged updating --- in image processing 01 p0099 A83-11456
Robots and image processing 02 p0161 A83-11795

A pipelined pseudoparallel system architecture for real-time dynamic scene analysis 02 p0227 A83-12245
Summary of the DARPA Image Understanding Research Program 02 p0181 A83-12876

Fast adaptive algorithms for low-level scene analysis - Applications of polar exponential grid /PEG/ representation to high-speed, scale-and-rotation invariant target segmentation 02 p0181 A83-12880
Computational models for texture analysis and synthesis 02 p0230 A83-12893
3-D machine perception; Proceedings of the Conference, Washington, DC, April 23, 24, 1981 03 p0324 A83-13444
Coherent optical methods for applications in robot visual sensing [AD-A110107] 03 p0324 A83-13446
Toward the robot eye - Isomorphic representation for machine vision 03 p0384 A83-13447
Noncontact visual three-dimensional ranging devices 03 p0324 A83-13448
Perceptual capabilities, ambiguities, and artifacts in man and machine [AD-A109864] 03 p0383 A83-13450
A mathematical model for computer image tracking 04 p0528 A83-16030

Some accuracy and resolution aspects of computer vision distance measurements 04 p0528 A83-16032
Studies of object recognition using three-dimensional information 08 p1156 A83-22063
Dynamic-automaton models in the visualization of three-dimensional scenes 08 p1157 A83-22177
Application of a digital-analog computer structure to the simulation of visual-scene problems 08 p1151 A83-22178
Surface location in scene content analysis 08 p1157 A83-22435
PAR image processing system /PARIPS/ - A testbed for automating image interpretation 08 p1154 A83-22536
On automatic recognition of 3D structures from 2D representations 10 p1461 A83-25474
Use of computer vision techniques in estimating echo motion 11 p1571 A83-27039
Information theory analysis of sensor-array imaging systems for computer vision 12 p1728 A83-28898
A perspective on range finding techniques for computer vision 12 p1767 A83-28946
Model-based three-dimensional interpretations of two-dimensional images 12 p1728 A83-28947
Volumetric descriptions of objects from multiple views 12 p1769 A83-28948
Multiframe image point matching and 3-D surface reconstruction 12 p1728 A83-28949
Detection of edges using range information 12 p1769 A83-28950
Calculation of the parameters of the optical system of the image converter of an adaptive industrial robot 12 p1767 A83-29325
On a method for the representation of images in the process of their arrival 13 p1910 A83-30617
Solving the find-path problem by good representation of free space 13 p1910 A83-31070
Elimination of redundant operations for a fast Sobel operator --- in automatic image segmentation by edge detection 13 p1911 A83-31074
Object recognition using three-dimensional information 20 p3039 A83-42644
Pseudodistance measures for recognition of curved objects 20 p3039 A83-42645
A wide-field scanning triangulation rangefinder for machine vision 20 p2991 A83-43111
Multiple-window parallel adaptive boundary finding in computer vision 21 p3192 A83-43952
Applications of vector fields to image processing 21 p3135 A83-43953
Geometrical aspects of interpreting images as a three-dimensional scene 21 p3135 A83-44068
Sensor-based robotic assembly systems - Research and applications in electronic manufacturing 21 p3118 A83-44070
Machine vision for robotics 21 p3135 A83-44078
Ridges and valleys on digital images 21 p3193 A83-44251

An implementation of a computational theory of visual surface interpolation 21 p3136 A83-44252
Rotationally symmetric operators for surface interpolation 21 p3193 A83-44253
Rigid body motion from depth and optical flow --- for computer vision 21 p3194 A83-44254
3-D shape from contour and selective confirmation 21 p3137 A83-44257
On the information in optical flows --- computer vision 21 p3194 A83-44258
Detection of moving edges 21 p3190 A83-44269
Fast algorithms for estimating local image properties 21 p3137 A83-44270
Approximating point-set images by line segments using a variation of the Hough transform 21 p3190 A83-44271
Determining 3-D motion and structure of a rigid body using the spherical projection 21 p3118 A83-44273
A discrete spatial representation for lateral motion stereo 21 p3118 A83-44274
Representation of three-dimensional motion in dynamic scenes 21 p3118 A83-44275
An approach to the segmentation of textured dynamic scenes 21 p3137 A83-44277
Expedient range enhanced 3-D robot colour vision 21 p3118 A83-44694
A curvilinear snake arm robot with gripper-axis fibre-optic image processor feedback 21 p3119 A83-44695
Dynamic sensing for robots - An analysis and implementation 23 p3501 A83-48635
The computer-aided matching and geometric alignment of images 24 p3582 A83-49045
Multilevel computational processes for visual surface reconstruction 24 p3619 A83-49196
Normalisation of Fourier descriptors of planar shapes 24 p3621 A83-49984

COMPUTERIZED CONTROL

U NUMERICAL CONTROL

COMPUTERIZED DESIGN

U COMPUTER AIDED DESIGN

COMPUTERIZED SIMULATION

NT ANALOG SIMULATION

NT DIGITAL SIMULATION

A model for simulation and processing of radar images 01 p0061 A83-10026
Numerical simulation of soil brightness temperatures at wavelength of 21 cm 01 p0062 A83-10038
Resolution requirements for a soil moisture imaging radar 01 p0020 A83-10039
Using radar image simulation to assess relative geometric distortions inherent in radar imagery 01 p0030 A83-10054
Geological terrain models 01 p0064 A83-10080
Thermal activation analysis of the structural stability of refractory alloys and computer simulation of the fracture process 01 p0024 A83-10391
Training systems --- Russian book 01 p0094 A83-10467
A time dependent theory of crazing behavior in polymers 01 p0027 A83-10608
Perfect mode locking of solid-state lasers by a double passive modulation 01 p0054 A83-10616
The organization of computational work --- Russian book 01 p0090 A83-10667
Turbulent structures in wall-bonded shear flows observed via three-dimensional numerical simulations --- using the Iliac 4 computer 01 p0046 A83-10890
A multiprocessor for power electronic circuit simulation 01 p0041 A83-11026
Microprocessor control for automated guideway transit vehicles 01 p0112 A83-11035
Intelligence allocation and digital control for automated guideway transit systems 01 p0112 A83-11036
The solution of 'real-world' aircraft EMC problems using the AAPG computer program 01 p0041 A83-11085
Computer simulation of waveforms on time division command/response multiplex data buses 01 p0042 A83-11150
Computer models for determining countermeasures effectiveness of expendables in air-to-air engagements 01 p0103 A83-11162
The design and implementation of the KC-135 Avionics Hot Bench Monitor 01 p0010 A83-11227
Dynamic infrared missile evaluator /DIME/ 01 p0015 A83-11236
An operational software simulator for passive ECM processing 01 p0093 A83-11250
A technique to empirically model clutter signals in airborne pulse Doppler radar 01 p0008 A83-11251
Dot-matrix display light measurement and interpretation techniques --- for qualification tests techniques 01 p0011 A83-11257
Texture simulation using a best-fit model 01 p0101 A83-11479
A generalization of algebraic surface drawing 02 p0226 A83-11783

The structure of electron avalanches at high E/P --- electric field - pressure relations 02 p0241 A83-11956
Weak and strong ignition. I - Numerical simulations of shock tube experiments 02 p0152 A83-12078
Development of dynamics and control simulation of large flexible space systems 02 p0141 A83-12456
A comparison of experimental and computer model results on the charge-exchange plasma flow from a 30 cm mercury ion thruster [AIAA PAPER 82-1946] 02 p0146 A83-12505
An efficient triangular plate bending finite element for crash simulation 02 p0194 A83-12755
Human performance can drastically affect critical systems operation 02 p0225 A83-12975
Development of analytical and experimental techniques for determining store airload distributions 02 p0132 A83-13077
Preliminary assessment of SIRE's potential for contamination --- Space Infrared Experiment 03 p0284 A83-13470
Controlling the motion of a moving robot using a neuroid network 03 p0385 A83-13475
Numerical simulation of natural convection in concentric and eccentric horizontal cylindrical annuli 03 p0315 A83-13484
A pitting model for rolling contact fatigue [ASME PAPER 82-LUB-10] 03 p0335 A83-13506
A design method for closed loop solar energy systems with concentrating collectors 03 p0353 A83-13583
Shuttle/payload contamination evaluation /SPACE/ program improvements 03 p0286 A83-13750
Power conditioning in an autonomous system controlled by a microprocessor Simulation of use with a photovoltaic generator --- French thesis 03 p0386 A83-13807
ESACAP - A minicomputer-oriented network-analysis program 03 p0385 A83-13847
Power-system simulation for low-orbit spacecraft - The EBLOS computer program 03 p0290 A83-13848
Whatever happened to band models --- for calculating atmospheric IR spectral transmittance 03 p0358 A83-13987
Atmospheric model for laser transmission in the infrared 03 p0359 A83-13990
High-resolution lower atmospheric transmission predictions over long paths 03 p0359 A83-13991
Atmospheric spectral transmittance and radiance - FASCOD1B 03 p0359 A83-13992
An optimum inversion method for the remote probing of defective phase shifters in phased arrays 03 p0328 A83-14020
Winter simulation of standing and travelling waves with the UCLA general circulation model 03 p0366 A83-14412
Numerical simulation of air flow over and around a long mountain range 03 p0367 A83-14421
Recent improvements to the nested grid model of the national meteorological center 03 p0367 A83-14431
On the distribution and evolution of clouds and rain over the Vosges and Black Forest mountains - A three-dimensional mesoscale simulation with parameterized microphysics 03 p0368 A83-14437
Numerical simulation of the airflow over Lake Michigan for a major lake-affected snow event 03 p0368 A83-14438
Lake-effect disturbances over Lake Michigan - Some numerical results 03 p0368 A83-14439
An analysis of the LFM-11 simulations of the Presidents' Day Cyclone, February 18-19, 1979 03 p0368 A83-14442
A numerical simulation of a stratocumulus-topped mixed layer 03 p0369 A83-14450
An operational turbulence closure model forecast system 03 p0369 A83-14451
The comparative performance of selected solar global models 03 p0370 A83-14634
Non-LTE atmospheric radiance and transmittance 03 p0360 A83-14638
A simple model for relative air mass 03 p0370 A83-14644
Rapid crack propagation and arrest in the DCB specimen - An improved numerical analysis --- Double Cantilever Beam 03 p0343 A83-14711
Numerical simulation of radiative transfer in circumstellar dust shells. I - Spherical shells 03 p0428 A83-14768
Coronal response to a solar event in a corona evacuated by a prior transient 03 p0437 A83-14789
Numerical simulation of crystal fractionation in shergottite meteorites 04 p0563 A83-15363
Easiest ejection seat stability and control analysis capability 04 p0446 A83-15428
A program system for dynamic analysis of aeronautical structures /HAJIF-II/ 04 p0497 A83-15545
Electronic Circuit Analysis Language /ECAL/ 04 p0470 A83-15550

Numerical simulation of electrostatic waves in plasmas
 --- German thesis 04 p0537 A83-15845
 The diagnostics of disturbances in components of turbojet engines with gasdynamics parameter monitoring 04 p0449 A83-15850
 The effects of moisture on trapped mountain lee waves 04 p0517 A83-15934
 Current-waveform dependence of punchthrough probability in a Josephson tunnel junction 04 p0473 A83-16072
 The STD/MHD codes - Comparison of analyses with experiments --- MHD generator performance prediction and tests 04 p0538 A83-16105
 An analytical evaluation of the icing properties of several low and medium speed airfoils [AIAA PAPER 83-0109] 05 p0579 A83-16525
 A glimpse into the future of air combat --- via computerized cockpit simulators [AIAA PAPER 83-0143] 05 p0599 A83-16552
 Solution procedures for accurate numerical simulations of flow in turbomachinery cascades [AIAA PAPER 83-0257] 05 p0583 A83-16615
 A Differential Dynamic Programming approach to nonlinear parameter identification [AIAA PAPER 83-0284] 05 p0678 A83-16629
 Measurement of the frequency response of a digital autopilot [AIAA PAPER 83-0326] 05 p0605 A83-16655
 A dynamic model for aircraft poststall departure [AIAA PAPER 83-0367] 05 p0595 A83-16674
 Evaluation of the perceptual attributes of emissive and non-emissive display designs using computer simulation 05 p0677 A83-16870
 Turbulent compressible convection in a deep atmosphere. I - Preliminary two-dimensional results --- of stars 05 p0699 A83-17017
 Radio Technical Commission for Aeronautics, Technical Symposium and Annual Assembly Meeting, Washington, DC, November 18-20, 1981, Proceedings 05 p0577 A83-17301
 Effect of CMOS miniaturization on cosmic-ray-induced error rate 05 p0629 A83-17540
 A process simulation model for multilayer structures involving polycrystalline silicon 05 p0630 A83-17752
 A re-extrapolation technique in Newton-SOR computer simulation of semiconductor devices --- Successive Over Relaxation 05 p0631 A83-17765
 Power MOSFET characteristics with modified SPICE modeling 05 p0631 A83-17772
 Recombination of small ions in the troposphere and lower stratosphere 05 p0665 A83-17784
 An experimental investigation of control surface effectiveness and real-gas simulation for bionics [AIAA PAPER 83-0213] 05 p0591 A83-17912
 A parametric analysis of the performances of a linear collectors' network of a solar power plant 06 p0779 A83-18139
 Boeing gains real-time flight data 06 p0719 A83-18270
 Rockwell B-1B design to be studied in new cab 06 p0719 A83-18271
 Real-time scenarios aid McDonnell weapons work 06 p0719 A83-18272
 Ames expands rotorcraft capability 06 p0719 A83-18273
 Computer models cut USAF test costs 06 p0719 A83-18274
 Rotational discontinuities and the structure of the magnetopause 06 p0782 A83-18286
 A two-dimensional simulation of the interaction of the plasma sheet with the lobes of the earth's magnetotail 06 p0782 A83-18287
 Global dynamo simulation of ionospheric currents and their connection with the equatorial electrojet and counter electrojet - A case study 06 p0783 A83-18296
 Convection electric fields and ionospheric currents derived from model field-aligned currents at high latitudes [AD-A125082] 06 p0783 A83-18297
 Computer-aided analysis of three dimensional confined vortex flow 06 p0757 A83-18453
 Priming considerations of heat pipes in zero-G 06 p0757 A83-18454
 An assessment of wind energy resource for northwestern California 06 p0779 A83-18456
 Experimental comparison of simulation methods of aeronautic type loading [ONERA, TP NO. 1982-130] 06 p0775 A83-18598
 Computer simulations of inaccuracies in spherical near-field testing 06 p0741 A83-18653
 Computer graphics applications in electromagnetic computer modeling --- treatment of wire objects by method of moments 06 p0802 A83-18667

Computer analysis of the significance of surface boundary conditions on the collection of alpha-induced charge --- carrier transport simulation 06 p0753 A83-18960
 Computer simulations of optimum boost and buck-boost converters 06 p0754 A83-19032
 Effects of finite wire scatterers in the field of VOR 06 p0716 A83-19039
 Fast algorithms for time domain broadband adaptive array processing 06 p0748 A83-19041
 Self-noise produced by quadrupling of QPSK signals 06 p0748 A83-19042
 The process view of simulation in ADA 07 p0983 A83-19647
 Application of simulation and zero-one programming for analysis of numerically controlled machining operations in the aerospace industry 07 p0902 A83-19648
 Tactical air war - A SIMSCRIPT model 07 p0987 A83-19649
 Improvements of antijam performance of spread spectrum systems 07 p0906 A83-19720
 Simulation study of DQPSK Intelsat V regenerative/non-regenerative satellite systems --- Differential Quaternary PSK 07 p0912 A83-19800
 A three-dimensional modified strongly implicit procedure for heat conduction 07 p0924 A83-19823
 Computer simulation of the fracture of composite materials with various degrees of physicochemical interaction between the components 07 p0874 A83-19971
 Algorithms and methods for computer simulation of transonic flow 07 p0863 A83-19999
 The analysis of performance of Stirling engines. I - Computer simulation model 07 p0939 A83-20287
 Hardware simulation facility for 120-Mbit/s QPSK/TDMA system 07 p0914 A83-20554
 Two-dimensional simulation of the gravitational superclustering of collisionless particles 07 p0108 A83-20940
 Bias in observed nearby clusters of galaxies 07 p1008 A83-21206
 Microporosity formation in investment castings of nickel-base superalloys Metallurgical effects, thermal modelling and foundry assessment 07 p0895 A83-21497
 Device modeling --- computer aided design of semiconductor devices for VLSI applications 07 p0923 A83-21538
 Circuit analysis, logic simulation, and design verification for VLSI 07 p0923 A83-21539
 Computer simulation of micro and macromechanisms of fibre reinforced composite fracture 08 p1054 A83-21801
 Computer simulations of stellar collapse and supernovae explosions - Non-rotating and rotating models 08 p1177 A83-21833
 CTOL, STOAL, V/STOL - An operational comparison for forward deployed CVNs 08 p1043 A83-22157
 Application of a digital-analog computer structure to the simulation of visual-scene problems 08 p1151 A83-22178
 Method of designing a program module for the simulation of complex dynamic systems on a hybrid computer --- for flight simulation 08 p1154 A83-22184
 Numerical simulation of a disk-shaped electron accelerating electrostatic probe 08 p1093 A83-22336
 Computer simulation of fluid-physics-module operations on the first Spacelab flight 08 p1049 A83-22373
 Effects of atmospheric and man-made obscuration on visual contrast 08 p1135 A83-22541
 Validation of a digital simulation of an optical matched filter correlator applied to aerial reconnaissance 08 p1100 A83-22589
 ARMA time series modeling - An effective method 08 p1158 A83-22730
 Computer simulation of carrier transport in planar doped barrier diodes 08 p1081 A83-22762
 Neural analog information processing 08 p1158 A83-22812
 Real-time multiradar simulation with a multiprocessor 08 p1044 A83-22824
 Pitch control system for large-scale wind turbines 08 p1132 A83-23140
 Computer modelling of turbulent recirculating flows in engineering applications 08 p1088 A83-23192
 Realistic 'feel' in flight simulators is based on precise control loading 08 p1048 A83-23240
 Comparison between two-dimensional short-channel MOSFET models 09 p1252 A83-23350
 Computer experiments related to the plasma microfield 09 p1347 A83-23393
 Quasi-Lagrangian rezoning of fluid codes maintaining an orthogonal mesh 09 p1259 A83-23721
 Time domain modeling of nonlinear loads --- for wire antennas 09 p1253 A83-23792

f-Chart - Predictions and measurements --- of solar heating systems 09 p1293 A83-23880
 Ground contamination by fuel jettisoned from aircraft in flight [AD-A128451] 09 p1294 A83-24041
 Calculation of thermal radiation from jets by the Monte-Carlo method 09 p1260 A83-24047
 A molecular dynamics simulation of the vitreous silica surface 09 p1226 A83-24133
 Optimal design of a baro/radio supported inertial altitude system [DGLR PAPER 82-041] 09 p1204 A83-24165
 Vortex sheets and concentrated vorticity - A variation on the theme of asymptotic modelling in fluid mechanics 09 p1261 A83-24335
 Computer simulation of negative-differential-conductivity effects, including trapping --- Gunn effect 09 p1255 A83-24499
 A numerical study of nonlinear instability phenomena in solid rocket motors 09 p1220 A83-24663
 Using a global hydrogen-air combustion model in turbulent reacting flow calculations 09 p1227 A83-24667
 High-voltage two-dimensional simulations of permeable base transistors 09 p1256 A83-24684
 Numerical comparison of DMOS, VMOS, and UMOS power transistors 09 p1256 A83-24686
 Concepts for description and evaluation of military C3 systems 09 p1331 A83-24763
 Numerical plasma simulation of the interaction between a space probe emitting photoelectrons and the solar wind --- German thesis 09 p1348 A83-24847
 A computer model for gas turbine blade cooling analysis [ASME PAPER 82-JPGC-GT-6] 09 p1208 A83-25267
 Multiprocessor computer modeling of transonic flow 10 p1460 A83-25468
 A heat pipe simulation technique for spacecraft thermal testing under variable orientation [SAE PAPER 820860] 10 p1383 A83-25760
 A hybrid facility for the simulation, development, and validation of ECS microprocessor based controls [SAE PAPER 820867] 10 p1379 A83-25766
 Melting transition of near-monolayer xenon films on graphite - A computer simulation study 10 p1390 A83-25798
 Three-dimensional propagation in free-electron laser amplifiers 10 p1427 A83-26006
 Reconstruction of objects from coded images by simulated annealing 10 p1420 A83-26110
 Propagation of shock waves through nonuniform and random media 10 p1416 A83-26163
 Three-dimensional computer simulations of star formation in dwarf galaxies 10 p1508 A83-26362
 Study on longitudinal dynamic characteristics of pilot-airplane system - Approach to the method for studying PIO problem --- Pilot-Induced Oscillation 10 p1379 A83-26762
 A Monte Carlo simulation of the strength of laminated hybrid composites 10 p1389 A83-26965
 Simulations of airborne Doppler radar 11 p1629 A83-27069
 Reliability modeling of high voltage batteries 11 p1540 A83-27200
 Computer modeling of thermoelectric generator performance 11 p1540 A83-27218
 Dimensional analysis of pumping losses in a Stirling cycle machine 11 p1587 A83-27269
 AQUASTOR - A computer model for cost analysis of aquifer thermal energy storage coupled with district heating or cooling systems 11 p1609 A83-27314
 Computer simulation of transient energy storage in a packed-bed of iron spheres with liquid-metal through-flow by numerical inversion of Laplace transforms 11 p1610 A83-27320
 Modeling and evaluation of designs for solid hydrogen storage beds 11 p1610 A83-27333
 A basic code for the prediction of transient three-dimensional turbulent flowfields 11 p1565 A83-27412
 Near wall region behavior of unsteady layers with favorable and adverse pressure gradients 11 p1565 A83-27413
 Computer graphics robot simulation programs - A comparison 11 p1646 A83-27489
 Interpulse kinetics in copper and copper halide lasers 11 p1583 A83-27624
 Comparison of cardiovascular effects of space flight and its analogs using computer simulations 11 p1642 A83-27792
 Computer simulation analysis of the behavior of renal-regulating hormones during hypogravic stress 11 p1642 A83-27794
 Computer simulation of the optical behaviour of amorphous silicon solar cells 11 p1611 A83-27979

- New GaAs Impatt theory explains mm-wave operation 11 p1562 A83-28158
- The extended Kalman filter and its use in estimating aerodynamic derivatives 11 p1531 A83-28183
- Waves and instabilities in a magnetized plasma 11 p1659 A83-28228
- Effects of trapped particles on strongly nonlinear electron plasma waves 11 p1659 A83-28229
- Recent development in the statistical theory of high-density plasmas 11 p1659 A83-28244
- A review of double layer simulations 11 p1660 A83-28249
- Gravitational collapse of pressureless inhomogeneous spheroids 11 p1681 A83-28275
- Monte Carlo simulations of the initial stellar mass function 11 p1682 A83-28279
- Computer simulation of whistler mode wave-particle interactions using a free-boundary encounter model 11 p1617 A83-28310
- Numerically simulated two-dimensional auroral double layers 11 p1618 A83-28314
- Theoretical simulation of a pulsed HF optical resonance transfer laser 11 p1585 A83-28703
- Computer simulation of a differential GPS for civil applications 11 p1529 A83-28790
- NASA aerial applications wake interaction research --- particle trajectories in aircraft induced wakes 12 p1699 A83-28899
- Computational treatment of three-dimensional transonic canard-wing interactions 12 p1696 A83-29021
- Computer-controlled polishing of telescope mirror segments 12 p1778 A83-29145
- VOR area navigation - Techniques and results 12 p1700 A83-29205
- Numerical results on the simulation of microstrip elements and units of microwave integrated circuits 12 p1719 A83-29343
- Orbit-averaged implicit particle codes --- for studying plasma kinetics 12 p1781 A83-29601
- Stability and application of an orbit-averaged magneto-inductive particle code 12 p1781 A83-29602
- Implicit time integration for plasma simulation 12 p1781 A83-29608
- The implementation of lattice calculations on the DAP --- Distributd Array Processor 12 p1768 A83-29623
- Electron sub-cycling in particle simulation of plasma 12 p1782 A83-29625
- Computational techniques for spherical boundary conditions --- thermodynamic systems 12 p1783 A83-29629
- Quasineutral hybrid simulation of macroscopic plasma phenomena 12 p1782 A83-29634
- Conjugate gradient method for the solution of linear equations - Application to molecular electronic structure calculations 12 p1778 A83-29640
- Spatial resolution requirements for direct numerical simulation of the Rayleigh-Benard convection 12 p1725 A83-29666
- Simulation of T-38 aircraft student canopy response to cockpit pressure and thermal loads using MAGMA --- Materially and Geometrically Nonlinear Analysis [AIAA 83-0942] 12 p1701 A83-29772
- DYSCO - An executive control system for dynamic analysis of synthesized structures [AIAA 83-0944] 12 p1768 A83-29773
- A survey of advanced continuous simulation language (ACSL) applications [AIAA 83-0945] 12 p1769 A83-29774
- Numerical simulation of material fatigue by a thermodynamic approach [AIAA 83-0977] 12 p1740 A83-29784
- Time domain response envelope for structural dynamic systems [AIAA 83-0818] 12 p1707 A83-29817
- Control design and performance analysis of a 6 MW wind turbine-generator 12 p1750 A83-29897
- Transonic, shock, and multidimensional flows: Advances in scientific computing; Proceedings of the Symposium, University of Wisconsin, Madison, WI, May 13-15, 1981 12 p1726 A83-29926
- Tracking of interfaces for fluid flow: Accurate methods for piecewise smooth boundaries 12 p1726 A83-29937
- Turbulent relaxation of counterstreaming plasma beams Results of numerical simulation on the M-10 computer 13 p1923 A83-30097
- Electromagnetic radiation from beam-plasma instabilities 13 p1923 A83-30122
- Sensing relative attitudes for automatic docking 13 p1809 A83-30169
- Direct simulation of homogeneous turbulence at low Reynolds numbers 13 p1841 A83-30640
- Ways to improve the effectiveness of methods of the direct statistical computerized simulation of rarefied-gas flows 13 p1932 A83-30659
- Modified signals. I - Basic properties of modified signals. II - Results of computerized simulation 13 p1829 A83-30728
- SOYCHMBR.I - A model designed for the study of plant growth in a closed chamber [SAE PAPER 820853] 13 p1899 A83-30941
- The role of computer modeling and simulation in electric and hybrid vehicle research and development 13 p1935 A83-31095
- A two-dimensional numerical model of the tapered wiggler free-electron laser 13 p1856 A83-31142
- The rotationally resolved 3400- to 3800-A terrestrial nightglow 13 p1879 A83-31247
- Damping of large-amplitude plasma waves propagating perpendicular to the magnetic field 13 p1926 A83-31358
- Institute of environmental sciences aircraft engine combustor casing life simulation for increased reliability 13 p1807 A83-31493
- Geometric configuration factors for polygonal zones using Nusselt's unit sphere --- in structural design of solar receivers 13 p1872 A83-31609
- Numerical simulation of radiative transfer in circumstellar dust shells. II - Ellipsoidal shells 13 p1959 A83-31741
- Software simulations of the detection of rapidly moving asteroids by a charge-coupled device 14 p2095 A83-31990
- Fluorescent planar concentrator (FPC) Monte-Carlo Computer model limit efficiency and latest experimental results 14 p2043 A83-32274
- Optical optimization of amorphous silicon solar cells 14 p2044 A83-32288
- Singular-value decomposition approach to time series modelling 14 p2075 A83-32429
- New thermal and trajectory model for high-altitude balloons 14 p1974 A83-32579
- Computer simulation and controlled growth of large diameter Czochralski silicon crystals 14 p2092 A83-32641
- Computation of two-dimensional jet interaction flow field [AIAA PAPER 83-1546] 14 p1971 A83-32769
- The possibilities of the investigation of nonlinear connections using digital simulation --- heliogeophysical effects on human physiological parameters 14 p2069 A83-32960
- Diagnostic and prognostic numerical circulation studies of the South Atlantic Bight 14 p2060 A83-33078
- Zero-frequency cyclotron wave on an intense relativistic-electron beam 14 p2087 A83-33389
- Turbulent flow induced by a jet in a cavity-measurements and 3D numerical simulation 15 p2155 A83-33666
- Direct simulation of homogeneous turbulent shear flows on the Iliac IV computer - Applications to compressible and incompressible modeling 15 p2156 A83-33674
- Impingement of an oblique shock wave on a cylinder 15 p2156 A83-33727
- An empirical method for computing leeside centerline heating on the Space Shuttle Orbiter 15 p2120 A83-33731
- Methods for validating computer simulation models of missile systems 15 p2219 A83-33739
- Modeling sources of gravitational radiation 15 p2254 A83-33816
- A numerical algorithm for solving inverse problems of two-dimensional wave equations 15 p2223 A83-33819
- Compact dc model of GaAs FET's for large-signal computer calculation 15 p2151 A83-33892
- Error analysis of certain floating-point on-line algorithms 15 p2217 A83-33905
- Computer simulation of amorphous silicon based alloy p-i-n solar cells 15 p2189 A83-33919
- On the effect of an ice particle enhancement process operating in supercooled continental clouds 15 p2205 A83-34063
- The numerical simulation of the interaction of cloud formation and lee waves 15 p2206 A83-34067
- Source reliability in a combined wind-solar-hydro system 15 p2190 A83-34147
- The operating experiences and performance characteristics during the first year of operation of the Crotched Mt. New Hampshire windfarm 15 p2190 A83-34148
- Methods of reducing wind power changes from large wind turbine arrays 15 p2190 A83-34149
- A dynamic simulation of a flat-plate collector system 15 p2191 A83-34409
- On the evolution of interacting, magnetized, galactic plasmas 15 p2262 A83-34528
- On the Monte Carlo methodology for cumulative damage 15 p2179 A83-34563
- Computer simulation of auroral kilometric radiation 15 p2202 A83-34738
- Use of Landsat data to develop a fuels database for a wildland fire simulation model 15 p2187 A83-34847
- Computer studies of ACV heave performance as a function of vent valve control parameters 15 p2123 A83-34854
- Dust modelling of fast flyby missions - Implications of in situ measurements 15 p2128 A83-35022
- Computer studies of ACV heave dynamics stabilization 15 p2243 A83-35055
- Analysis of the packet formation process in packet-switched networks 15 p2147 A83-35123
- Approximate analytical performance evaluation in bus oriented multicomputer systems 15 p2219 A83-35130
- A deductive method for the simulation of faults in Programmable Logic Arrays 15 p2218 A83-35142
- Distributed real-time simulation of multibody systems 15 p2223 A83-35143
- VHF propagation over hilly, forested terrain 15 p2148 A83-35184
- Computer simulation complex for the investigation of systems for the control of the manipulators of autonomous robots 15 p2223 A83-35261
- Computer model of a collision-avoidance system for air traffic control 15 p2121 A83-35275
- Modelling polyhedral solids bounded by multi-curved parametric surfaces 16 p2402 A83-35322
- F-region ion composition modeling 16 p2376 A83-35398
- Effects of detector coil size and configuration on measurements of the magnetoencephalogram 16 p2401 A83-35452
- January and July simulations with a spectral general circulation model 16 p2384 A83-35461
- An optical residue processor for computing inner products 16 p2411 A83-35516
- Numerical and experimental study of a GaAs transferred electron device without transit-time limitation 16 p2345 A83-35523
- Propagation of intense relativistic electron beams through drift tubes with perturbed walls 16 p2345 A83-35747
- Combustor modelling by assembly of well-stirred reactors 16 p2325 A83-35808
- Numerical simulation of airfoil ice accretion [AIAA PAPER 83-0112] 16 p2297 A83-36042
- Numerical simulation of electrothermal de-icing systems [AIAA PAPER 83-0114] 16 p2297 A83-36043
- Simulator fidelity and flight test data - Improving the flight performance of the B-52H WST production unit flight station simulator [AIAA PAPER 83-1075] 16 p2299 A83-36204
- Sinusoidal integration for simulation of second-order systems [AIAA PAPER 83-1086] 16 p2406 A83-36210
- Error sources in hybrid computer based flight simulation [AIAA PAPER 83-1090] 16 p2299 A83-36214
- Compensation for time delay in flight simulator visual-display systems [AIAA PAPER 83-1080] 16 p2312 A83-36222
- Calculation of a simulated 3-D high speed inlet using the Navier-Stokes equations [AIAA PAPER 83-1165] 16 p2293 A83-36255
- Importance of inlet boundary conditions for numerical simulation of combustor flows [AIAA PAPER 83-1263] 16 p2308 A83-36314
- Performance capability of a Compact Multimission Aircraft Propulsion Simulator [AIAA PAPER 83-1358] 16 p2312 A83-36356
- Numerical simulation of pulsed inductive thruster plasma [AIAA PAPER 83-1396] 16 p2416 A83-36386
- Monte Carlo simulation of the engine development process [AIAA PAPER 83-1405] 16 p2310 A83-36394
- Numerical calculations and wind tunnel experiments on gas diffusion in thermally stratified flow over a ridge 16 p2390 A83-36495
- Computer simulation for the intergranular corrosion of Alloy 800 16 p2335 A83-36899
- Formation of ion-acoustic double layers 17 p2581 A83-37037
- A new method for failure detection and location in complex dynamic systems 17 p2565 A83-37094
- Flow over a biconic configuration with an afterbody compression flap - A comparative numerical study [AIAA PAPER 83-1668] 17 p2444 A83-37179
- Simulation of compression molding for fiber reinforced thermosetting polymers 17 p2516 A83-37365
- Validation of the in-orbit checkout of the IRAS gyroscopes using computer simulations 17 p2481 A83-37475

Voyager 2 observations of energetic particle variations in the Ganymede wake region - A possible acceleration mechanism 17 p2618 A83-37581

Aerodynamic simulation - A key technology not only for aviation 17 p2451 A83-37860

Closed-loop engine fuel system simulation [SAE PAPER 821374] 17 p2468 A83-37964

Validation of the KC-10 refueling boom digital control system [SAE PAPER 821421] 17 p2463 A83-37978

Modular simulation model for a wind turbine system 17 p2536 A83-38017

Dynamic analysis of the Magnus Aerospace Corporation LTA 20-1 heavy-lift aircraft [AIAA PAPER 83-1977] 17 p2466 A83-38908

Computer simulation of formation of terrestrial planets from planetesimals 18 p2764 A83-38999

The parallel implementation of a nonlinear real-time simulation technique 18 p2738 A83-39150

A directional gamma-ray telescope using coded aperture techniques 18 p2756 A83-39289

Computer simulation study of multiple germanium gamma-ray sensor arrays 18 p2756 A83-39295

A system for load isolation and precision pointing 18 p2648 A83-39938

Procedure for generating ground wind environments for Shuttle liftoff studies 18 p2687 A83-40024

Simulated fan-beam radar imagery --- use in assessing aircraft approach-to-landing paths 18 p2675 A83-40302

Monte Carlo simulation of methanol masers 18 p2778 A83-40478

Validation of simulation models of solar heating systems with data from the solar pilot test facilities 18 p2710 A83-40535

Development of a minicomputer atmospheric noise model 18 p2720 A83-40661

Quiet starts for galaxy simulations 19 p2910 A83-40751

Modeling of interaction of artificially released lithium with the earth's bow shock 19 p2864 A83-41114

Numerical modelling of the ionospheric filtration of an ULF micropulsation signal 19 p2866 A83-41318

Using SLAM and SDL to assess Space Shuttle experiments --- programming language and data base management system for simulation of models and analysis of results 19 p2887 A83-41325

A nonparametric detector for signal detection and time delay estimation 19 p2828 A83-41347

Computer modeling of spectral efficiency and sidelobe buildup effects in nonlinear satellite links 19 p2830 A83-41366

The paralleling of algorithms for the simulation of nonlinear systems of large dimensionality 19 p2888 A83-41422

Problems in the optimization of computer-simulation methods for flaw detection in phased arrays 19 p2834 A83-41424

Stability analysis of multirate nonlinear sampled-data control systems 19 p2890 A83-41488

A numerical method for the analysis of harmonic balance conditions in multiloop non-linear feedback systems 19 p2891 A83-41489

Use of the ACSL language to integrate multiple disciplines for system engineering applications [AIAA PAPER 83-2200] 19 p2888 A83-41685

Hovering limit cycles - A man-in-the-loop approach [AIAA PAPER 83-2232] 19 p2803 A83-41710

Mixing 4D equipped and unequipped aircraft in the terminal area [AIAA PAPER 83-2240] 19 p2796 A83-41717

Adaptive control for large space structures [AIAA PAPER 83-2246] 19 p2816 A83-41722

A new measure of ICBM effectiveness that accounts for optimal fuzing [AIAA PAPER 83-2250] 19 p2894 A83-41726

New results in fault latency modelling [AIAA PAPER 83-2303] 19 p2888 A83-41760

A simulation study of the low-speed characteristics of a light twin with an engine-out [AIAA PAPER 83-2128] 19 p2806 A83-41951

Numerical stimulation of photochemical air pollution over the Ise Bay District 20 p3013 A83-42202

Mie scattering subroutines (DBMIE and MIEV0) - A comparison of computational times 20 p3037 A83-42205

Friction damping studies in multiple turbine blade systems by lumped mass method 20 p3002 A83-42571

Computer simulation of the main gel-fluid phase transition of lipid bilayers 20 p3033 A83-42639

Determination and simulation of stable crack growth in ADINA 20 p3003 A83-42927

On elastic-plastic analysis of I-beams in bending and torsion 20 p3003 A83-42929

Analysis of surface cracks in plates and shells using the line-spring model and ADINA 20 p3003 A83-42934

ADINA modeling of elastoplastic shear/compression waves in tubes 20 p3004 A83-42936

Computer simulation studies of VLF triggered emissions deformation of distribution function by trapping and detrapping --- of resonant electrons in inhomogeneous geomagnetic field 20 p3024 A83-43186

Theoretical studies in isoelectric focusing --- mathematical modeling and computer simulation for biological purification process 20 p2951 A83-43280

Trends in interactive finite element modeling [SAWE PAPER 1489] 20 p3037 A83-43756

Embedding impedance of a millimeter wave Schottky mixer Scaled model measurements and computer simulations 21 p3125 A83-44384

Distortional hardening rules for metal plasticity 21 p3113 A83-44547

Finite element methods in aerodynamics 21 p3086 A83-44551

Opto-optical light deflection 21 p3207 A83-44834

Direct implicit large time-step particle simulation of plasmas 21 p3213 A83-44988

Computer modeling of membrane structures and the distribution of admixture particles in a lipid bilayer 21 p3184 A83-45224

Numerical experiments in the analysis of mathematical models of the ionosphere 21 p3174 A83-45233

Three-dimensional flow over a conical afterbody containing a centered propulsive jet - A numerical simulation [AIAA PAPER 83-1709] 21 p3088 A83-45518

Computer simulation of model isoelectric focusing experiments 22 p3266 A83-45760

A remark on viscosity and convection in the mantle 22 p3325 A83-45801

Electric microfield distributions in strongly coupled plasmas 22 p3361 A83-45935

Observation of self-binding turbulent fluctuations in simulation plasma and their relevance to plasma kinetic theories 22 p3361 A83-46009

Structure of perpendicular shocks in collisionless plasma 22 p3362 A83-46023

Structure of the quasi-parallel bow shock - Results of numerical simulations 22 p3325 A83-46031

Computer simulation of speckle in a synthetic aperture radar image pixel 22 p3290 A83-46243

Computer simulations of gravitational encounters between pairs of binary star systems 22 p3377 A83-46389

Adaptive manipulator control (movement learning algorithms) 22 p3352 A83-46399

Sensor design using computer tools; Proceedings of the Conference, Los Angeles, CA, January 28, 29, 1982 22 p3291 A83-46593

Detailed computer modeling of an infrared tracker using simulation of passive infrared equipment (SPIRE) techniques 22 p3292 A83-46594

Facility for brassboard infrared sensor simulations 22 p3292 A83-46596

Aircraft contrast signatures in the infrared spectral region 22 p3292 A83-46598

Modeling of the atmosphere for analysis of horizon sensor performance 22 p3261 A83-46599

Horizon sensor errors calculated by computer models compared with errors measured in orbit 22 p3261 A83-46600

Analytical noise/performance modeling of detector charge-coupled device (CCD) hybrid devices 22 p3292 A83-46603

Numerical experiments with a stochastic zonal climate model 22 p3340 A83-46846

A cloud physical parameterization method using movable basis functions - Stochastic coalescence parcel calculations 22 p3341 A83-46850

Recent advances in lunar base simulation [IAF PAPER 83-237] 23 p3414 A83-47319

The mathematical model for space flight visual simulation by computer generated image [IAF PAPER 83-350] 23 p3418 A83-47355

Future research directions - Theoretical approach and perspective 23 p3525 A83-47551

Solar flares and shock waves 23 p3531 A83-47575

Control of reflector vibrations in large spaceborne antennas by means of movable dampers 23 p3423 A83-47598

Selection of Weibull shape parameter, based on adaptive estimation 23 p3467 A83-47618

Improved stress simulation with simple finite element meshes [ASME PAPER 83-GT-89] 23 p3469 A83-47936

Orbital and cloud cover sampling analyses for multisatellite earth radiation budget experiments 23 p3483 A83-48138

Simulations used in the development and flight test of the HIMAT vehicle [AIAA PAPER 83-2505] 23 p3404 A83-48355

Calculation of macroparameters in the Monte Carlo method of direct statistical simulation --- of molecular gas dynamics 23 p3513 A83-48501

A computer-aided simulation model for the I-V characteristic of M-n-p silicon Schottky-barrier diodes produced by use of low-energy arsenic-ion implantation 23 p3446 A83-48608

A time-dependent and two-dimensional numerical model for MOSFET device operation 23 p3446 A83-48610

AlGaAs/GaAs cascade solar cell computer modeling under high solar concentration 23 p3478 A83-48616

First-passage-time distributions and switching statistics in a bistable two-mode laser 24 p3587 A83-48840

Inhomogeneity effects in a gas laser 24 p3587 A83-48842

Theoretical modeling of amorphous silicon-based alloy p-n solar cells 24 p3634 A83-48914

On the transient analysis of circuits containing multiple diodes 24 p3573 A83-48972

Generation of radar echo images from a contour map 24 p3619 A83-49199

Models of ellipticals and bulges 24 p3641 A83-49247

Simulations of galaxy mergers 24 p3642 A83-49259

The three-dimensional simulation of Florida convective clouds-sensitivity to cloud microphysical processes 24 p3614 A83-49714

Three-dimensional simulation of large-scale structure in the universe 24 p3669 A83-50106

Investigation of a two-dimensional model of an MOS structure 24 p3575 A83-50203

Application of the statistical simulation method to determine the electromagnetic-compatibility factors of radio systems 24 p3571 A83-50209

Computer analysis of the operation of a pendulum accelerometer 24 p3586 A83-50211

COMPUTERS

NT AIRBORNE/SPACEBORNE COMPUTERS

NT ANALOG COMPUTERS

NT DIGITAL COMPUTERS

NT EMBEDDED COMPUTER SYSTEMS

NT HYBRID COMPUTERS

NT ICL COMPUTERS

NT ILLIAC 4 COMPUTER

NT MICROCOMPUTERS

NT MINICOMPUTERS

NT PARALLEL COMPUTERS

NT SEQUENTIAL COMPUTERS

NT VAX-11/780 COMPUTER

Scientific and defense shops - The computers 20 p3036 A83-43032

COMSTAR SATELLITES

Measurements of ice depolarization at 28.56 GHz using the COMSTAR beacon simultaneously with a 16.5 GHz polarization diversity radar 01 p0032 A83-11354

Correlation of slant path ice depolarization events at 28.56 GHz with radar reflectivity structure and the determination of ice depolarization statistics for Wallops Island, Virginia 06 p0744 A83-18700

Melting layer attenuation at 28.56 GHz from simultaneous Comstar beacon and 16.5 GHz polarization diversity radar observations --- below ice crystals or snow 06 p0744 A83-18701

Depolarization of 19-GHz signals --- from satellite beacons 07 p0871 A83-20552

Bootstrapping adaptive cross pol cancelers for satellite communications 19 p2831 A83-41386

CONCATENATED CODES

Concatenated error correcting system 07 p0984 A83-19685

A new design method for m-out-of-n TSC checkers --- Totally Self-Checking for codes 13 p1908 A83-30791

CONCAVITY

Characteristics of a turbulent boundary layer on the concave surface of a 90-degree bend 04 p0475 A83-15094

Histogram concavity analysis as an aid in threshold selection --- in image processing 13 p1911 A83-31073

CONCENTRATION (COMPOSITION)

NT ATMOSPHERIC MOISTURE

NT ATOM CONCENTRATION

NT CARBON DIOXIDE CONCENTRATION

NT METEOROID CONCENTRATION

NT MOISTURE CONTENT

A method for calculating the threshold filler concentration for polytetrafluorethylene-matrix composites 02 p0160 A83-12369

Aerosol minima --- in Arctic 03 p0357 A83-13546

Rayleigh scattering measurements of the gas concentration field in turbulent jets 04 p0481 A83-15286

Temperature and concentration measurements in an internal combustion engine using laser Raman spectroscopy [AIAA PAPER 83-1551] 14 p1990 A83-32772

The dependence of the fluorescence and absorption spectra of anthracene vapor on concentration 14 p2082 A83-32828

Laser tomography for simultaneous concentration and temperature measurement in reacting flows [AIAA PAPER 83-1553] 15 p2165 A83-34924

The probability distribution of passive-additive concentration in a mixing layer 17 p2505 A83-37631

Time-resolved two-dimensional concentration measurements in an acoustically driven flow 19 p2841 A83-40856

CONCENTRATORS

A methodology of evaluation and design of fields of focusing heliostats --- French thesis 02 p0201 A83-11768

Generalized conic concentrators 02 p0236 A83-12310

Thermal response of solar receiver aperture plates during sun walk-off [ASME PAPER 82-HT-33] 02 p0202 A83-12791

A design method for closed loop solar energy systems with concentrating collectors 03 p0353 A83-13583

A study of different techniques for cooling solar cells in centralized concentrator photovoltaic power plants --- French thesis 03 p0355 A83-14109

Automatic methods for the adjustment of faceted solar-energy concentrators and heliostats 04 p0503 A83-15131

Studies on radiation intensity distribution in the focus of compound parabolic concentrators 06 p0781 A83-18565

Prospects for the construction of solar furnaces for industry 06 p0781 A83-19236

Area utilization efficiency of a sloping heliostat system for solar concentration 08 p1130 A83-22618

EA study of solar concentrator panels with fluorescent compounds 08 p1131 A83-22911

Simplified calculational procedure for determining the amount of intercepted sunlight in an imaging solar concentrator 09 p1293 A83-23884

Comparison of advanced thermal and electrical storage for parabolic dish solar thermal power systems 11 p1606 A83-27232

Cassegrainian concentrator solar array exploratory development module 11 p1541 A83-27250

Design of large, low-concentration-ratio solar arrays for low earth orbit applications 11 p1541 A83-27254

Concentrator systems in photovoltaic conversion - Assessment and perspectives --- French thesis 11 p1612 A83-28653

Efficiency of luminescence in luminescent solar concentrators 13 p1870 A83-30205

A regenerable solid amine CO2 concentrator for space station [SAE PAPER 820847] 13 p1907 A83-30938

Multisection planar focusing lenses as concentrators of solar radiation 14 p2036 A83-32047

The combination of hollow focusing concentrators with fiber-optic waveguides --- for solar energy transmission 14 p2036 A83-32048

Photovoltaic concentrator module characterization 14 p2039 A83-32202

Series resistance analysis of concentrator cells under high injection conditions 14 p2004 A83-32246

High efficiency GaAs solar cells for concentrator and flat plate arrays 14 p2042 A83-32260

Photovoltaic concentrator technology in the USA 14 p2042 A83-32261

Lambertian analysis of mirrors and Fresnel lenses for solar concentration 14 p2043 A83-32271

750 suns concentrator modules using GaAs solar cells 14 p2043 A83-32272

A 500 Wpk photovoltaic concentrator using a glass laminated metal membrane reflector 14 p2043 A83-32273

Fluorescent planar concentrator (FPC) Monte-Carlo Computer model limit efficiency and latest experimental results 14 p2043 A83-32274

Luminescent solar concentrators for energy conversion 15 p2189 A83-33861

Solar flux distributions from circular cylindrical concentrators 15 p2189 A83-34068

The design and performance of ideal solar concentrators based on the prism-assisted cylindrical reflector 15 p2190 A83-34070

Stationary nonimaging concentrator as a second stage element in tracking systems 15 p2190 A83-34074

Measurements of the distribution of the flux of energy in the focus of a solar concentrator with visualization techniques 15 p2191 A83-34406

Static concentrators theory for non-homogeneous extended sources 15 p2192 A83-34666

Luminescent solar concentrators as bifacial captors 15 p2192 A83-34669

Application of 2-D bin packing algorithms for task scheduling in PASM --- sparse crossbar interconnection network designs for data transmission 15 p2219 A83-35132

Dish concentrators for solar thermal energy 17 p2536 A83-38015

Low cost process for ohmic contacts on GaAs/Ga(1-x)Al(x)As concentrator solar cells based on palladium and gold deposition 20 p2965 A83-42353

A thermoelectric detector for high radiant flux densities 21 p3135 A83-43900

Limit of concentration for cylindrical concentrators under extended light sources --- parabolic solar collectors 21 p3167 A83-44149

Mathematical analysis of the performance of cylindrical-parabolic solar concentrators 21 p3167 A83-44361

Sun tracking by peak power positioning for photovoltaic concentrator arrays 21 p3167 A83-44625

Analysis of a combined thermal-photovoltaic solar system based on the spherical reflector/tracking absorber concentrator 21 p3168 A83-45062

High-efficiency (21.4 pct) Ga0.75In0.25As/GaAs (Eg = 1.15 eV) concentrator solar cells and the influence of lattice mismatch on performance 21 p3169 A83-45493

Directional intercept factor of truncated CPCs --- compound parabolic concentrators 22 p3318 A83-46089

Limit of concentration under extended nonhomogeneous light sources 22 p3318 A83-46090

Neodymium laser glasses as optical media for luminescent solar concentrators 23 p3476 A83-47169

Modular energy installations with quasi-paraboloidal solar-energy concentrators 23 p3477 A83-48399

CONCENTRIC CYLINDERS

Optical analysis of solar energy tubular absorbers 02 p0202 A83-12596

Natural convection heat transfer between eccentric horizontal cylinders [ASME PAPER 82-HT-43] 02 p0172 A83-12796

Numerical simulation of natural convection in concentric and eccentric horizontal cylindrical annuli 03 p0315 A83-13484

Laminar and turbulent natural convection in the annulus between horizontal concentric cylinders 03 p0315 A83-13485

New flows in a circular Couette system with co-rotating cylinders 17 p2501 A83-37028

Sudden twisting of partially bonded cylindrical rods 17 p2523 A83-38392

Effect of curvature on the thermal stability of a fluid between two long vertical coaxial cylinders 20 p2973 A83-42682

Rarefied gas flow in a cylindrical annulus 24 p3575 A83-48738

Thermophysical characteristics of coaxial high-power laser chambers 24 p3588 A83-49123

CONCENTRIC SPHERES

Natural convection in a spherical annulus filled with heat generating fluid 20 p2972 A83-42677

CONCRETE STRUCTURES

Airfield coatings incorporating polymer materials - Repair and maintenance --- Russian book 21 p3093 A83-45029

CONCRETES

Reflective properties of asphalt and concrete surfaces 08 p1126 A83-21925

Thermal properties of some asphaltic concrete mixes [AIAA PAPER 83-1598] 14 p1978 A83-33361

Evaluation of properties of recycled asphalt concrete hot mix [AIAA PAPER 83-1599] 14 p1978 A83-33362

CONDENSATES

Refractory residues, condensates and chondrules from solar furnace experiments 04 p0563 A83-15371

A study of the corrosion activity of the fuselage condensate of passenger aircraft 04 p0445 A83-15398

An asymptotic theory of condensed two-phase flame propagation 12 p1712 A83-29000

The formation of solid solutions in vacuum condensates of the system Al2O3-ZrO2 17 p2492 A83-37575

Theory of the combustion of condensed substances with blowing past them 18 p2663 A83-39163

On an integral method for solving problems of the thermal theory of the ignition of condensed substances 19 p2820 A83-42067

Ignition of a thin plate of condensed matter by a heated block 24 p3555 A83-49543

A theoretical study of the formation of condensed products during the combustion of metal particles 24 p3555 A83-49770

CONDENSATION

Kinetic analysis of evaporation and condensation in a vapor-gas mixture 03 p0315 A83-13118

The dynamics of the moist atmosphere 07 p0970 A83-20885

Laboratory studies of the condensation and properties of amorphous silicate smokes 07 p1027 A83-21319

Atmospheric gases on cold surfaces - Condensation, thermal desorption, and chemical reactions 09 p1298 A83-25191

Investigations of homogeneous nucleation in Fe, Si, Fe/Si, FeO/x/, and SiO/x/ vapors and their subsequent condensation 10 p1490 A83-26191

Condensation kinetics of iron and silicon in the vapor phase 10 p1490 A83-26192

The formation and the evolution process of the Jilin meteorite 14 p2112 A83-32597

Evaporation and condensation on two parallel plates at finite Reynolds numbers 14 p2094 A83-33379

The chemical composition and thermal history of the ice of a cometary nucleus 16 p2425 A83-36679

An accurate theoretical approximation for adiabatic condensation temperature 20 p3030 A83-42514

Heat and mass transfer in a low speed turbulent boundary layer with condensation 20 p2984 A83-43018

The process of the formation and evolution of the Jilin meteorite 21 p3240 A83-44502

Study of complex coacervation in low concentration by viral expansion method. II - Salt-containing systems 23 p3427 A83-47626

CONDENSATION NUCLEI

NT AITKEN NUCLEI

Diffusion mechanism of the interaction of aerosol drops and the possibility of controlling this mechanism by means of electromagnetic radiation 13 p1874 A83-30043

Condensation nuclei events at 30 km and possible influences of solar cosmic rays 13 p1874 A83-30219

Unusual behavior in the condensation nuclei concentration at 30 km 13 p1877 A83-30885

Effects of CCN concentrations on stratus clouds 13 p1893 A83-31044

Meteorological problems of cloud physics and their theoretical and instrumental analysis; WOPHYS '82 Colloquium, Koenigstein im Taunus, May 17-19, 1982, Proceedings 15 p2204 A83-34051

The dependence of ice formation on the evolution of the liquid phase 15 p2204 A83-34052

The measurement of the humidity spectrum and of the concentration of the cloud condensation nuclei 15 p2164 A83-34055

The influence of aerosol and meteorological parameters on maximum supersaturation and activation of particles in a cloud 15 p2205 A83-34059

On the mathematical simulation of non-equilibrium cloud condensation rates 15 p2205 A83-34061

Modeling the effect of temperature changes in the stratosphere on the growth of drops of a sulfate aerosol 16 p2382 A83-36870

The function and response of an improved stratospheric condensation nucleus counter 20 p2990 A83-42858

A new method to measure homogeneous nucleation rates in shock tubes 21 p3132 A83-44972

Calculated droplet size distributions and opacities of condensed sulfuric acid aerosols 22 p3321 A83-46898

Interstitial CCN measurements --- Cloud Condensation Nuclei 24 p3611 A83-49687

The broadening of droplet spectra by cloud top entrainment 24 p3612 A83-49696

CONDENSATION TRAILS

U CONTRAILS

CONDENSER RADIATORS

U CONDENSERS (LIQUEFIERS)

U HEAT RADIATORS

CONDENSERS (LIQUEFIERS)

Surface tension effects in a space radiator condenser with capillary liquid drainage [AIAA PAPER 83-1525] 14 p2011 A83-32756

Heat transfer in the evaporation and condensation zones of heat pipes intensely heated at the end 15 p2161 A83-34471

CONDENSING

NT FILM CONDENSATION

Laminar flow of vapor flux in the condensation region of heat tubes 04 p0477 A83-15864

- Numerical study of the effect of CCN on the size distribution of cloud droplets. I - Cloud droplets in the stage of condensation growth --- Cloud Condensation Nuclei
04 p0518 A83-16017
- Formation of pyrophosphate on hydroxyapatite with thioesters as condensing agents
05 p0613 A83-17234
- The growth of filaments by the condensation of coronal arches
06 p0855 A83-19134
- Balloon-borne observations of stratospheric aerosol and condensation nuclei during the year following the Mt. St. Helens eruption
07 p0959 A83-20205
- Kinetic theory of evaporation and condensation for a cylindrical condensed phase
10 p1490 A83-25784
- Shock-tube simulation experiment of supersonic condensation flow accompanying a shock wave
10 p1417 A83-26193
- Analysis of moisture condensation in engine inlet ducts
11 p1566 A83-27482
- Vapor flow through a porous membrane - A throttling process with condensation and evaporation
11 p1567 A83-27859
- Asymmetries in evaporation and condensation Knudsen layer problems
13 p1840 A83-30110
- The similarity of condensation processes in expanding CO₂ jets
16 p2349 A83-35527
- Heat and mass transfer through condensation, in an incompressible turbulent boundary layer, on a flat plate with low level exchange
18 p2681 A83-39350
- A two-dimensional model of the electrocoagulation-hygroscopic dissipation of warm fogs
18 p2724 A83-39442
- Condensation in the annulus of a double-walled cryogenic storage tank
20 p2961 A83-43237
- The heterogeneous condensation of interstellar ice grains
20 p3077 A83-43665
- A cloud physical parameterization method using movable basis functions - Stochastic coalescence parcel calculations
22 p3341 A83-46850

CONDITIONED REFLEXES

- The effect of amphetamine and amizyl on the interaction of the delayed reaction and the conditioned reflex differentiation in rhesus monkeys and capuchins
01 p0079 A83-10532
- Disturbances of conditioned reflex activity during hypokinesia in rats and the normalizing effect of motor loads
01 p0079 A83-10534
- The peculiarities of DNA metabolism in rat brains in the process of the elaboration of a conditioned reflex
01 p0080 A83-10552
- A comparative analysis of several behavioral, neurochemical, and vegetropic effects of meprobamate and diazepam
03 p0374 A83-13626
- Further studies and the comparative characteristics of potential stimulants of higher nervous activity
03 p0374 A83-13634
- The participation of the pallidum in the mechanisms of memory
06 p0794 A83-18968
- The features of the behavior and the delayed reactions to visual and auditory conditioned stimuli during various time intervals between signals
07 p0980 A83-20842
- An electronic model of the conditioned reflex
14 p2072 A83-32571
- Induction and deduction as the function of different hemispheres --- of brain
19 p2870 A83-40810
- The discrimination of amplitude and temporal parameters of the direct electrical stimulation of the visual cortex
19 p2878 A83-42069
- The interaction of the dominant and the conditioned reflex as the functional unity of the organization of behavior
21 p3189 A83-45371

CONDITIONED RESPONSES

U CONDITIONING (LEARNING)

CONDITIONING (LEARNING)

- The systemic determination of the activity of neurons in behavior
08 p1145 A83-22118
- Changes in diastolic coronary resistance during submaximal exercise in conditioned dogs
13 p1898 A83-30504

CONDITIONS

- NT ADIABATIC CONDITIONS
- NT CHRONIC CONDITIONS
- NT FLIGHT CONDITIONS
- NT KUTTA-JOUKOWSKI CONDITION
- NT NONADIABATIC CONDITIONS
- NT NONEQUILIBRIUM CONDITIONS
- NT RUNWAY CONDITIONS

- Numerical boundary condition procedures and multigrid methods; Proceedings of the Symposium, NASA Ames Research Center, Moffett Field, CA, October 19-22, 1981
12 p1772 A83-29646
- Fully implicit shock tracking
12 p1725 A83-29651
- Three-dimensional boundary conditions in supersonic flow
12 p1697 A83-29654

CONDUCTANCE

U RESISTANCE

CONDUCTING FLUIDS

- Magnetohydrodynamic stratified flow past a sphere
01 p0106 A83-10275
- The role of the helicity spectrum function in turbulent dynamo theory
02 p0242 A83-12985
- Antennas in conducting media /Review/
04 p0466 A83-15726
- An isothermal shock wave in a perfectly-conducting and non-homogeneous stellar interior
05 p0702 A83-17811
- Nonlinear breaking of waves in an electrically conducting and radiating gas
05 p0642 A83-17836
- The rapid dissipation of magnetic fields in highly conducting fluids --- in solar or stellar atmospheres
06 p0835 A83-18930
- The excitation of waves of finite amplitude on the surface of an ideally conducting fluid by a variable magnetic field
06 p0813 A83-19553
- Holtzmark electric field distribution in a two-dimensional electron fluid
08 p1168 A83-22950
- Rayleigh-Taylor instability at the interface of conducting and nonconducting fluids in a variable magnetic field
11 p1658 A83-27704
- Linear and nonlinear waves in liquid dielectrics
11 p1658 A83-27711
- Investigation of rotating flow in a longitudinal magnetic field
12 p1781 A83-29267
- Heat and mass transfer of an oscillatory flow with Hall current
15 p2236 A83-34557
- On a self-similar problem of magnetohydrodynamics
17 p2582 A83-37648
- Strict exceptionality for a heat-conducting relativistic fluid
18 p2742 A83-40649
- The dynamics of a rigid body having an ellipsoidal cavity filled with a magnetic fluid --- in theory of neutron stars
19 p2916 A83-41209
- Heat and mass transfer of an oscillatory flow with Hall current. II
24 p3633 A83-50164
- Variational formulation for the equilibrium condition of a conducting fluid in an electric field
24 p3624 A83-50195

CONDUCTING MEDIA

U CONDUCTORS

CONDUCTION BANDS

- Bulk unipolar diodes in MBE GaAs
16 p2347 A83-36486
- Thickness dependence of kink temperature and band bending in amorphous silicon
17 p2585 A83-38954
- Solid-state superlattices
24 p3635 A83-49445

CONDUCTION ELECTRONS

- Valency control of glow discharge produced a-SiC:H and its application to heterojunction solar cells
03 p0354 A83-13649

CONDUCTIVE HEAT TRANSFER

- Theory of thermal conductivity, heat conduction and convective heat transfer in fiber filled polymer composites
02 p0149 A83-11804
- A multiple step random walk Monte Carlo method for heat conduction involving distributed heat sources [ASME PAPER 82-HT-25]
02 p0171 A83-12788
- A transient one-dimensional inverse heat conduction problem with overspecified data at one boundary
02 p0174 A83-12932
- Mechanisms for lithospheric heat transport on Venus
Implications for tectonic style and volcanism
02 p0268 A83-13102
- Boundary integral equation method calculations of surface regression effects in flame spreading
03 p0294 A83-13488
- Finite element thermal analysis of an icing protective system [AIAA PAPER 83-0113]
05 p0632 A83-16528
- Simplified Laplace transform inversion for unsteady surface element method [AIAA PAPER 83-0527]
05 p0638 A83-16830
- On invariant solutions of the equation of nonlinear heat conduction with a source
05 p0640 A83-17643
- An implicit scheme for determining temperature in the presence of radiative-conductive heat transfer
05 p0691 A83-17644
- The stability of positive solutions of inverse problems of heat conduction
05 p0640 A83-17649
- Energy transfer in magnetized plasmas
06 p0812 A83-18923
- Experimental investigation of radiative-conductive heat transfer between a thermal plasma and a solid
06 p0759 A83-19159
- Estimate of the transient conduction of heat in materials with linear thermal properties based on the solution for constant properties
06 p0760 A83-19399
- A three-dimensional modified strongly implicit procedure for heat conduction
07 p0924 A83-19823
- Concerning the utilization of variational principles in numerical modeling
07 p0986 A83-20318
- Pointwise bounds for the solution of a nonlinear problem in heat conduction
08 p1083 A83-21866

- Application of variational embedding technique to nonlinear heat transfer problems
08 p1084 A83-22149

- Signal and systems analysis for unsteady heat conduction problems
08 p1170 A83-22334
- Some comments on Beck's solution of the inverse problem of heat conduction through the use of Duhamel's theorem
08 p1087 A83-23144
- The influence of mathematical viscosity on the difference solution in problems of two-temperature gas dynamics
09 p1347 A83-23573
- Determination of the temperature dependence of the heat conductivity coefficient of a composite material from the data of a nonstationary experiment
09 p1224 A83-24233
- An integral method theorem for heat conduction --- computer aided design of reentry vehicles
09 p1216 A83-24673
- One-dimensional problem of the identification of temperature distribution in an infinite plate
09 p1263 A83-25101
- Analysis of transient thermal responses in a carbon-carbon composite
11 p1543 A83-27459
- Conductive flux in flaring solar chromospheres deduced from the linear polarization observations
11 p1691 A83-27685
- A temperature problem for a half-plane with a crack
11 p1598 A83-28489
- Thermal diffusion in gases --- Russian book
12 p1723 A83-29341
- The thermal management of printed circuit board assemblies
12 p1720 A83-29515
- The temperature field of plates and infinite prismatic bodies of complex cross section in the case of a heat transfer coefficient that varies in time
13 p1838 A83-30047
- Approximate solution of the heat-conduction equation with nonlinear boundary conditions
13 p1843 A83-31469
- Pseudo-updated constrained solution algorithm for nonlinear heat conduction
14 p2012 A83-32989
- Non-linear potential problems
15 p2225 A83-33853
- Numerical simulation of a compressible turbulent boundary layer over a conductive wall with line heat source
15 p2157 A83-33865
- Thermal model of a cylindrically symmetric solar pond
15 p2190 A83-34073
- The fictitious domain method for the numerical solution of nonstationary thermal problems
15 p2158 A83-34227
- Discontinuous boundary elements for heat conduction
15 p2158 A83-34228
- On the accuracy of the boundary element method for three-dimensional conduction problems
15 p2158 A83-34229
- Three-dimensional non-linear variational analysis of a non homogeneous heat conduction problem - Finite element results
15 p2158 A83-34230
- On the comparison of finite difference and finite element time integration schemes for the heat conduction equation
15 p2158 A83-34231
- Solving fully 3-D nonlinear anisotropic multi-material heat conduction problems on a microcomputer
15 p2158 A83-34232
- Unsteady non-linear heat conduction in complex geometries
15 p2159 A83-34233
- ADI methods for solution of the transient heat conduction problems in spherical geometry
15 p2159 A83-34234
- Heat transfer accompanied with melting and freezing for solar heat storage
15 p2190 A83-34235
- A coupled conduction-convection study in the slip-flow regime
15 p2160 A83-34261
- Laminar flow heat transfer with axial conduction in a circular tube - A finite difference solution
15 p2160 A83-34262
- Exact finite elements for conduction and convection
15 p2160 A83-34263
- Method to solve some coupled convection and conduction problems
15 p2160 A83-34264
- A local equilibrium axiom on the flows in relativistic thermodynamics
15 p2239 A83-34410
- Exact analytic solutions to three-dimensional thermoelasticity problems
15 p2180 A83-35037
- Elastic composites
16 p2364 A83-35505
- Thermoelasticity, heat conduction, and strength of laminated composites
16 p2323 A83-35510
- The effects of conductive, convective and radiative heat transfer on rocket motor service life [AIAA PAPER 83-1120]
16 p2318 A83-36231
- Effective macroscopic description for heat conduction in periodic composites
16 p2353 A83-36593

Numerical study of the effect of an embedded surface-heat source on the separation bubble of supersonic flow
[AIAA PAPER 83-1753] 17 p2446 A83-37226

On the formulation of the finite-element method in heat-conduction problems for aircraft structures
17 p2520 A83-37515

A discretized-intensity method proposed for two-dimensional systems enclosing radiative and conductive media
17 p2506 A83-37865

Diffusion in composite layers with automatic solution of the eigenvalue problem
18 p2684 A83-39848

The modeling of inverse problems of heat conduction with movable phase transition boundaries
19 p2844 A83-41571

Results of an experimental study of the thermal state of blades in turbines with partial root cooling
19 p2801 A83-42138

Numerical methods in heat transfer
20 p2970 A83-42653

Radiation heat transfer - Interaction with conduction and convection and appropriate methods in radiation
20 p2970 A83-42655

On the application of an integral equation method for the solution of heat transfer problems in heterogeneous and cellular media
20 p2971 A83-42664

A perturbation method for nonlinear, one-dimensional conduction with heat generation
20 p2971 A83-42665

Surface integral numerical solution for general steady heat conduction in composite media
20 p2971 A83-42666

An approximate transformation for nonlinear transient heat conduction problems
20 p2971 A83-42667

Application of logic-algebraic and numerical methods to multidimensional heat exchange problems in regions of complex geometry filled with uniform or composite media
20 p2971 A83-42668

Heat flux display and heat transmission coefficient calculation with the finite element method
20 p2971 A83-42669

Measurements of the conduction of heat in water vapor, nitrogen and mixtures of these gases in an extended temperature range
20 p2972 A83-42671

Two-dimensional energy transfer in radiatively participating media with conduction by the P-N approximation
20 p2974 A83-42697

Convective, conductive and radiative heat transfer in a tube submitted to a non uniform circumferential flux
20 p2975 A83-42702

Subcooled film boiling and the behavior of vapor film on a horizontal wire and a sphere
20 p2981 A83-42764

On the numerical solution of nonlinear problems of transient heat conduction
20 p3003 A83-42895

Variational embedding solutions of radiative heat transfer upon a semi-infinite body with variable thermal properties
21 p3128 A83-44020

On a scheme for solving the equations of a viscous heat-conducting gas
21 p3133 A83-45216

Method for solving equations of radiative-conductive heat transfer
21 p3214 A83-45217

Conductive flux in the chromosphere derived from line linear polarization observation
23 p3532 A83-47670

Heat conduction anisotropy and the texture of VT1-0 alloy sheets
24 p3560 A83-48944

Mixed and hybrid non-linear variational analysis of a three dimensional heat conduction problem - Finite element results
24 p3577 A83-49402

[ONERA, TP NO. 1983-83] 24 p3577 A83-49402

A class of similarity solutions for the nonlinear thermal conduction problem
24 p3581 A83-50201

Simulators for solving internal inverse heat-conduction problems
24 p3620 A83-50205

CONDUCTIVITY

EMI shielding today with conductive plastics
04 p0464 A83-16179

CONDUCTIVITY METERS

NT ELECTRICAL CONDUCTIVITY METERS

CONDUCTORS

NT ELECTRIC CONDUCTORS

NT ELECTRIC WIRE

NT ELECTROLYTES

NT ION EXCHANGE MEMBRANE ELECTROLYTES

NT JUMPERS

NT MOLTEN SALT ELECTROLYTES

NT NONAQUEOUS ELECTROLYTES

NT PHOTOCONDUCTORS

NT SOLID ELECTROLYTES

NT SUPERCONDUCTORS

NT THERMAL CONDUCTORS

Antennas in conducting media /Review/
04 p0466 A83-15726

The reason for high-temperature strain gauge drift, especially in those with PtW conductors
06 p0763 A83-19123

On the mutually unique correspondence between an ideally conducting body and the field scattered by it
08 p1078 A83-23153

SCATHA conductive spacecraft materials development
09 p1218 A83-24891

The excitation of a perfectly conducting multihedral body
09 p1251 A83-25083

Magnetic anisotropy of the organic conductors /TMTTF/2X
11 p1662 A83-28075

The nonorthogonal-series method in problems of electromagnetic wave diffraction by coated bodies
13 p1827 A83-30096

CONES

NT ABLATIVE NOSE CONES

NT CIRCULAR CONES

NT CONICAL BODIES

NT NOSE CONES

NT ROCKET NOSE CONES

NT SLENDER CONES

The turbulence transport properties of a supersonic boundary layer on a sharp cone at angle-of-attack
[AIAA PAPER 83-0456] 05 p0591 A83-17927

A three-dimensional problem for a deformable cone with an asymmetrically perturbed surface
11 p1596 A83-28452

Electromagnetic excitation of a finite cone by an annular magnetic flux
16 p2346 A83-35942

Numerical simulation of hypersonic viscous flow over cones at very high incidence
[AIAA PAPER 83-1669] 17 p2444 A83-37180

Theory of vortex interaction on a blunt cone
17 p2448 A83-37511

The effect of an increase in the temperature factor of a cone on the parameters of the base region
17 p2451 A83-37811

The stressed state of an inhomogeneous orthotropic hollow cone
21 p3154 A83-44712

A three-dimensional problem for a deformable cone with a symmetrically perturbed surface
23 p3468 A83-47173

The effect of injection in the boundary layer on supersonic flow past an oscillating cone
23 p3400 A83-48654

CONES (VOLCANOES)

Absence of silicic volcanism on Mars - Implications for crustal composition and volatile abundance
04 p0566 A83-15563

SIR-A radar images of sand dunes and volcanic fields
22 p3314 A83-46225

CONFERENCES

International Geoscience and Remote Sensing Symposium, Washington, DC, June 8-10, 1981, Digest. Volumes 1 & 2
01 p0061 A83-10001

Be stars; Proceedings of the Symposium, Munich, West Germany, April 6-10, 1981
01 p0119 A83-10301

AUTOTESTCON '81; Proceedings of the Conference, Orlando, FL, October 19-21, 1981
01 p0087 A83-10726

Investigations of the Arctic, the Antarctic and the world ocean; Conference-Seminar, Moscow, USSR, February 9-13, 1981, Reports
01 p0077 A83-10826

The role of coherent structures in modelling turbulence and mixing; Proceedings of the International Conference, Madrid, Spain, June 25-27, 1980
01 p0045 A83-10884

PESC '81; Power Electronics Specialists Conference, University of Colorado, Boulder, CO, June 29-July 3, 1981, Record
01 p0039 A83-11001

ICIASF '81; International Congress on Instrumentation in Aerospace Simulation Facilities, Dayton, OH, September 30, 1981, Record
01 p0051 A83-11051

NAECON 1982; Proceedings of the National Aerospace and Electronics Conference, Dayton, OH, May 18-20, 1982, Volumes 1, 2 & 3
01 p0001 A83-11083

Space: Mankind's fourth environment; International Astronautical Congress, 32nd, Rome, Italy, September 1981, Selected Papers
01 p0016 A83-11276

Origin and evolution of galaxies; Proceedings of the International School of Cosmology and Gravitation, Course, 7th, Erice, Italy, May 11-23, 1981
01 p0127 A83-11287

Space: Mankind's fourth environment; Proceedings of the Thirty-second International Astronautical Congress, Rome, Italy, September 6-12, 1981
01 p0016 A83-11330

Conference on Pattern Recognition and Image Processing, Dallas, TX, August 3-5, 1981, Proceedings
01 p0096 A83-11409

All-Union Conference on Cosmic Rays, Samarkand, Uzbek SSR, October 27-29, 1981, Proceedings
02 p0272 A83-11701

Mini and microcomputers in control and measurement; Proceedings of the International Symposium, San Francisco, CA, May 20-22, 1981
02 p0226 A83-11901

Spacelab, space platforms and the future; Proceedings of the Fourth Joint AAS/DGLR Symposium and Twentieth Goddard Memorial Symposium, Washington, DC, March 17-19, 1982
02 p0137 A83-11926

The Venus environment; Proceedings of the International Conference, Palo Alto, CA, November 1-6, 1981
02 p0265 A83-12555

Electro-optical instrumentation for resources evaluation; Proceedings of the Meeting, Washington, DC, April 21, 22, 1981
02 p0199 A83-12669

Thermal infrared sensing applied to energy conservation in building envelopes /Thermosense IV/; Proceedings of the Meeting, Ottawa, Ontario, Canada, September 1-4, 1981
02 p0180 A83-12686

Reflecting optics for synchrotron radiation; Proceedings of the Meeting, Upton, NY, November 16-18, 1981
02 p0236 A83-12690

High resolution soft X-ray optics; Proceedings of the Meeting, Brookhaven, NY, November 18-20, 1981
02 p0239 A83-12721

Advances and trends in structural and solid mechanics; Proceedings of the Symposium, Washington, DC, October 4-7, 1982
02 p0193 A83-12732

Solid State Transducer Symposium, Boston, MA, November 18, 19, 1981, Proceedings
02 p0180 A83-12807

Techniques and applications of image understanding; Proceedings of the Meeting, Washington, DC, April 21-23, 1981
02 p0181 A83-12875

Conference on Mathematical Methods in Celestial Mechanics, 7th, Oberwolfach, West Germany, August 24-28, 1981, Proceedings
03 p0404 A83-13405

3-D machine perception; Proceedings of the Conference, Washington, DC, April 23, 24, 1981
03 p0324 A83-13444

Infrared astronomy - Scientific/military thrusts and instrumentation; Proceedings of the Meeting, Washington, DC, April 21, 22, 1981
03 p0405 A83-13451

NASA-ESA Spacelab systems and programs; Proceedings of the Seminar, Washington, DC, April 23, 24, 1981
03 p0284 A83-13703

Technical issues in focal plane development; Proceedings of the Meeting, Washington, DC, April 21, 22, 1981
03 p0325 A83-13726

Shuttle optical environment; Proceedings of the Meeting, Washington, DC, April 23, 24, 1981
03 p0286 A83-13741

Integrated optics and millimeter and microwave integrated circuits; Proceedings of the Conference, Huntsville, AL, November 16-19, 1981
03 p0309 A83-13753

Ultraviolet and vacuum ultraviolet systems; Proceedings of the Meeting, Washington, DC, April 21, 22, 1981
03 p0327 A83-13954

Atmospheric transmission; Proceedings of the Meeting, Washington, DC, April 21, 22, 1981
03 p0344 A83-13976

International Conference on Energy Storage, Brighton, Sussex, England, April 29-May 1, 1981, Proceedings
03 p0355 A83-14045

Canadian Symposium on Remote Sensing, 7th, Winnipeg, Canada, September 8-11, 1981, Proceedings
03 p0345 A83-14226

Conference on Numerical Weather Prediction, 5th, Monterey, CA, November 2-6, 1981, Preprints [AD-A125468]
03 p0365 A83-14401

Conference on Numerical Methods in Fluid Mechanics, 4th, Ecole Nationale Supérieure de Techniques Avancées, Paris, France, October 7-9, 1981, Proceedings
03 p0322 A83-14601

Conference on Atmospheric Radiation, 4th, Toronto, Canada, June 16-18, 1981, Preprints
03 p0360 A83-14626

Fenomech '81; Proceedings of the Second International Conference on Finite Elements in Nonlinear Mechanics, Stuttgart, West Germany, August 25-28, 1981, Parts 1, 2 & 3
04 p0465 A83-15001

The source region of the solar wind; Proceedings of the Ninth Lindau Workshop, Lindau, West Germany, November 1981
04 p0573 A83-15112

Review of progress in quantitative nondestructive evaluation. Volume 1 - Proceedings of the Eighth USAF/Defense Advanced Research Projects Agency Symposium on Quantitative Nondestructive Evaluation, University of Colorado, Boulder, CO, August 2-7, 1981
04 p0487 A83-15151

All-Union Conference on Laser Optics, 3rd, Leningrad, USSR, January 4-8, 1982, Proceedings
04 p0483 A83-15253

Lunar and Planetary Science Conference, 13th, Houston, TX, March 15-19, 1982, Proceedings. Part 1
04 p0559 A83-15326

SAFE Association, Annual Symposium, 19th, Las Vegas, NV, December 6-10, 1981, Proceedings
04 p0524 A83-15401

Commercial Photovoltaics Measurements Workshop, Vail, CO, July 27-29, 1981, Proceedings
04 p0503 A83-15452

International Colloquium on Mars, 3rd: Dedicated to Thomas A. Mutch / 1931-1980/, Pasadena, CA, August 30-September 2, 1982, Proceedings
04 p0564 A83-15551

International Scientific Conference on Space, 22nd, Rome, Italy, March 25, 26, 1982, Proceedings
04 p0450 A83-15655

Advanced Aircrew Display Symposium, 5th, Patuxent River, MD, September 15, 16, 1981, Proceedings
04 p0447 A83-16126

Weather predictions by fine mesh models; Proceedings of the Third Course of the International School of Meteorology of the Mediterranean, Erice, Italy, October 17-30, 1981
04 p0518 A83-16151

Reinforced plastics/composites adhesives and thermosets; Proceedings of the Sixth Annual Pacific Technical Conference and Displays, Los Angeles, CA, August 25-27, 1981
04 p0454 A83-16176

Flight simulation - Avionic systems and aero medical aspects; Proceedings of the International Conference, London, England, April 6, 7, 1982
04 p0441 A83-16326

Japan Congress on Materials Research, 25th, Tokyo, Japan, October 1981, Proceedings
05 p0610 A83-17086

Intense atmospheric vortices; Proceedings of the Joint Symposium, Reading, Berks., England, July 14-17, 1981
05 p0667 A83-17113

Advances in energy technology; Proceedings of the Eighth Annual UMR-DNR Conference on Energy, University of Missouri-Rolla, Rolla, MO, November 4-7, 1981
05 p0658 A83-17115

Materials evaluation under fretting conditions; Proceedings of the Symposium, Warminster, PA, June 3, 1981
05 p0652 A83-17251

Residual stress effects in fatigue; Proceedings of the Symposium, Phoenix, AZ, May 11, 1981
05 p0615 A83-17260

Radio Technical Commission for Aeronautics, Technical Symposium and Annual Assembly Meeting, Washington, DC, November 18-20, 1981, Proceedings
05 p0577 A83-17301

Global implications of space activities; Proceedings of the Conference, Aspen, CO, August 30-September 4, 1981
05 p0710 A83-17349

Annual Conference on Nuclear and Space Radiation Effects, 19th, Las Vegas, NV, July 20-22, 1982, Proceedings
05 p0625 A83-17476

Air traffic management - Current problems and future concepts; Proceedings of the Spring Convention, London, England, May 12, 13, 1982
05 p0593 A83-17726

Fluid mechanics of mechanical seals; Proceedings of the Winter Annual Meeting, Phoenix, AZ, November 14-19, 1982
06 p0768 A83-18046

The physics of sunspots; Proceedings of the Conference, Sunspot, NM, July 14-17, 1981
06 p0850 A83-18101

International Symposium on Optimum Structural Design and ONR Naval Structural Mechanics Symposium, 11th, University of Arizona, Tucson, AZ, October 19-22, 1981
06 p0771 A83-18201

Heat Transfer and Fluid Mechanics Institute, Meeting, 28th, California State University, Sacramento, CA, June 28, 29, 1982, Proceedings
06 p0757 A83-18451

International Conference on Antennas and Propagation, 2nd, University of York, York, England, April 13-16, 1981, Proceedings. Part 1 - Antennas. Part 2 - Propagation
06 p0736 A83-18601

Voyager Mission: Implications for planetary biology; Proceedings of the Sixth Annual Colloquium on Chemical Evolution, University of Maryland, College Park, MD, October 4-6, 1981
06 p0801 A83-19401

1982 Winter Simulation Conference, San Diego, CA, December 6-8, 1982, Proceedings. Volumes 1 & 2
07 p0987 A83-19646

PTC '82; Proceedings of the Pacific Telecommunications Conference, Honolulu, HI, January 17-20, 1982
07 p0903 A83-19651

PTC '81; Proceedings of the Pacific Telecommunications Conference, Honolulu, HI, January 12-14, 1981
07 p0903 A83-19656

NTC '81; National Telecommunications Conference, New Orleans, LA, November 29-December 3, 1981, Record. Volumes 1, 2, 3 & 4
07 p0903 A83-19676

1981 National Powder Metallurgy Conference, Philadelphia, PA, May 3-6, 1981, Proceedings
07 p0883 A83-19830

Gamma ray transients and related astrophysical phenomena; Proceedings of the Workshop, La Jolla, CA, August 5-8, 1981
07 p1010 A83-20001

National SAMPE Symposium and Exhibition, 27th, San Diego, CA, May 4-6, 1982, Proceedings
07 p0874 A83-20426

The origin and evolution of galaxies; Proceedings of the International School of Cosmology and Gravitation, Course, 7th, Erice, Italy, May 11-23, 1981
07 p1015 A83-20757

Israel Annual Conference on Aviation and Astronautics, 24th, Tel Aviv and Haifa, Israel, February 17, 18, 1982, Collection of Papers
07 p0862 A83-21001

Lunar and Planetary Science Conference, 13th, Houston, TX, March 15-19, 1982, Proceedings. Part 2
07 p1031 A83-21281

High temperature alloys for gas turbines 1982; Proceedings of the Conference, Liege, Belgium, October 4-6, 1982
07 p0891 A83-21451

Deformation of polycrystals: Mechanisms and microstructures; Proceedings of the Second Riso International Symposium on Metallurgy and Materials Science, Roskilde, Denmark, September 14-18, 1981
07 p0896 A83-21601

Advances in fracture research; Proceedings of the Fifth International Conference on Fracture, Cannes, France, March 29-April 3, 1981. Volumes 1, 2, 3, 4, 5, & 6
08 p1115 A83-21651

Supernovae: A survey of current research; Proceedings of the Advanced Study Institute, Cambridge University, Cambridge, England, June 29-July 10, 1981
08 p1176 A83-21826

International Society for Photogrammetry and Remote Sensing, International Symposium, Toulouse, France, September 13-17, 1982, Transactions. Volume 1
08 p1124 A83-21901

International Conference on Metrology and Properties of Engineering Surfaces, 2nd, Leicester Polytechnic, Leicester, England, April 14-16, 1982, Proceedings
08 p1073 A83-22001

Annual Conference on Composites and Advanced Ceramic Materials, 6th, Cocoa Beach, FL, January 17-21, 1982, Proceedings
08 p1071 A83-22251

Israel Conference on Mechanical Engineering, 16th, Technion - Israel Institute of Technology, Haifa, Israel, July 13, 14, 1982, Proceedings
08 p1111 A83-22318

Processing of images and data from optical sensors; Proceedings of the Meeting, San Diego, CA, August 25, 26, 1981
08 p1093 A83-22426

Wavefront distortions in power optics; Proceedings of the Meeting, San Diego, CA, August 27, 28, 1981
08 p1107 A83-22449

New methods for optical, quasi-optical, acoustic and electromagnetic synthesis; Proceedings of the Meeting, San Diego, CA, August 25, 26, 1981
08 p1161 A83-22468

Fiber optics in adverse environments; Proceedings of the Seminar, San Diego, CA, August 25-27, 1981
08 p1164 A83-22475

Physics and technology of coherent infrared radar; Proceedings of the Meeting, San Diego, CA, August 25, 26, 1981
08 p1095 A83-22499

Design of digital image processing systems; Proceedings of the Meeting, San Diego, CA, August 27, 28, 1981
08 p1097 A83-22524

Atmospheric effects on electro-optical, infrared, and millimeter wave systems performance; Proceedings of the Meeting, San Diego, CA, August 27, 28, 1981
08 p1098 A83-22540

Polarizers and applications; Proceedings of the Meeting, San Diego, CA, August 27, 28, 1981
08 p1098 A83-22563

Airborne reconnaissance V; Proceedings of the Seminar, San Diego, CA, August 27, 28, 1981
08 p1099 A83-22573

Mosaic focal plane methodologies II; Proceedings of the Conference, San Diego, CA, August 27, 28, 1981
08 p1100 A83-22598

International Symposium of Biomechanics Cinematography and High Speed Photography, 2nd, San Diego, CA, August 24-26, 1981, Proceedings
08 p1102 A83-22790

Real-time signal processing IV; Proceedings of the Meeting, San Diego, CA, August 25-28, 1981
08 p1152 A83-22794

Visual simulation and image realism II; Proceedings of the Conference, San Diego, CA, August 27, 28, 1981
08 p1102 A83-22830

Modern utilization of infrared technology VII; Proceedings of the Seventh Annual Seminar, San Diego, CA, August 27, 28, 1981
08 p1102 A83-22838

Contemporary methods of optical fabrication; Proceedings of the Meeting, San Diego, CA, August 25, 26, 1981
08 p1111 A83-22863

Contemporary infrared standards and calibration; Proceedings of the Meeting, San Diego, CA, August 25, 26, 1981
08 p1104 A83-22873

Image quality; Proceedings of the Seminar, San Diego, CA, August 27, 28, 1981
08 p1105 A83-22890

International Congress on Aerospace Medicine, 29th, Nancy, France, September 7-11, 1981, Scientific Reports
08 p1147 A83-22951

Application of multivariable systems theory; Symposium, Plymouth, England, October 26-28, 1982, Collected Papers
08 p1158 A83-23171

Numerical methods in laminar and turbulent flow; Proceedings of the Second International Conference, Venice, Italy, July 13-16, 1981
08 p1087 A83-23176

Ionospheric modification; General Assembly of the International Union of Radio Science, 20th, Washington, DC, August 10-19, 1981, Papers
09 p1299 A83-23301

Royal Society, Discussion on the Joint Air-Sea Interaction Project /JASIN/, London, England, June 2, 3, 1982, Proceedings
09 p1309 A83-23351

Measurements in hostile environments; Proceedings of the International Conference, University of Edinburgh, Edinburgh, Scotland, August 31-September 4, 1981
09 p1264 A83-23358

International Union of Radio Science and Nachrichtentechnische Gesellschaft, General Meeting, Kleinheubach, West Germany, October 4-8, 1982, Lectures and Reports
09 p1243 A83-23376

Fatigue Conference and Exposition, Dearborn, MI, April 14-16, 1982, Proceedings
09 p1276 A83-23416

Infrared technology for target detection and classification; Proceedings of the Meeting, San Diego, CA, August 25, 26, 1981
09 p1265 A83-23526

Control and communication technology in laser systems; Proceedings of the Twenty-fifth Annual International Technical Symposium, San Diego, CA, August 25, 26, 1981
09 p1214 A83-23576

Material and process advances '82; Proceedings of the Fourteenth National SAMPE Technical Conference, Atlanta, GA, October 12-14, 1982
09 p1220 A83-23601

Chemical and mechanical technology of propellants and explosives; International Annual Meeting, 12th, Karlsruhe, West Germany, July 1-3, 1981, Reports
09 p1240 A83-23829

Fracture of composite materials; Proceedings of the Second USA-USSR Symposium, Lehigh University, Bethlehem, PA, March 9-12, 1981
09 p1222 A83-23926

Cloud dynamics; Proceedings of the Symposium, Hamburg, West Germany, August 17-28, 1981
09 p1311 A83-23951

Creep and fracture of engineering materials and structures; Proceedings of the International Conference, University College of Swansea, Swansea, Wales, March 24-27, 1981
09 p1279 A83-24051

Nuclear Science Symposium, 29th, and Symposium on Nuclear Power, 14th, Washington, DC, October 20-22, 1982, Proceedings
09 p1268 A83-24103

Conference on Atomic and Molecular Reactions and Structure, Flinders University of South Australia, Bedford Park, Australia, February 1982, Proceedings
09 p1342 A83-24142

Remote sensing of arid and semi-arid lands; Proceedings of the International Symposium on Remote Sensing of Environment, Cairo, Egypt, January 19-25, 1982. Volumes 1 & 2
09 p1284 A83-24526

Conference on Decision and Control, 20th, and Symposium on Adaptive Processes, San Diego, CA, December 16-18, 1981, Proceedings. Volumes 1, 2 & 3
09 p1327 A83-24701

Integrated navigation: Actual and potential - Sea-air-space; Proceedings of the International Congress, Paris, France, September 21-24, 1982. Volumes 1 & 2
09 p1200 A83-24851

Emerging optical materials; Proceedings of the Conference, San Diego, CA, August 25, 26, 1981
09 p1345 A83-24951

International Conference on Future Energy Concepts, 3rd, London, England, January 27-30, 1981, Proceedings
09 p1294 A83-24975

File structures and data bases for CAD; Proceedings of the Working Conference, Seeheim, West Germany, September 14-16, 1981
09 p1325 A83-25095

Metallurgical coatings 1981; Proceedings of the Eighth International Conference, San Francisco, CA, April 6-10, 1981. Volumes 1 & 2
10 p1388 A83-25526

Miami International Conference on Alternative Energy Sources, 5th, Miami Beach, FL, December 13-15, 1982, Proceedings of Condensed Papers
10 p1445 A83-25575

Scientific importance of high angular resolution at infrared and optical wavelengths; Proceedings of the Conference, Garching, West Germany, March 24-27, 1981
10 p1494 A83-25826

Shock tubes and waves; Proceedings of the Thirteenth International Symposium, Niagara Falls, NY, July 6-9, 1981
10 p1414 A83-26126

Active nuclei of galaxies; Goutelas Spring School, 5th, Goutelas, France, April 6-10, 1981, Proceedings 10 p1506 A83-26226

Human Factors Society, Annual Meeting, 25th, Rochester, NY, October 12-16, 1981, Proceedings 10 p1456 A83-26301

Measuring techniques in transonic and supersonic flows in cascades and turbomachines; Proceedings of the Symposium, Ecole Centrale de Lyon, Ecully, Rhone, France, October 15, 16, 1981 10 p1421 A83-26409

The Special Research Area of Flight Control, Colloquium, Brunswick, West Germany, September 9, 10, 1981, Reports 10 p1374 A83-26476

Control science and technology for the progress of society; Proceedings of the Eighth Triennial World Congress, Kyoto, Japan, August 24-28, 1981. Volume 1 - Control theory 10 p1463 A83-26501

Control science and technology for the progress of society; Proceedings of the Eighth Triennial World Congress, Kyoto, Japan, August 24-28, 1981. Volume 2 - Stochastic and large systems 10 p1466 A83-26539

Control science and technology for the progress of society; Proceedings of the Eighth Triennial World Congress, Kyoto, Japan, August 24-28, 1981. Volume 4. Part A - Mechanical systems and robots. Part B - Aerospace and transportation 10 p1380 A83-26577

Conference on Radar Meteorology, 20th, Boston, MA, November 30-December 3, 1981, Preprints 11 p1621 A83-26976

IECEC '82; Proceedings of the Seventeenth Intersociety Energy Conversion Engineering Conference, Los Angeles, CA, August 8-12, 1982. Volumes 1, 2, 3, 4 & 5 11 p1601 A83-27126

Progress in solar-terrestrial physics; Proceedings of the Fifth International Symposium, Ottawa, Canada, May 17-22, 1982. Parts 1-7 11 p1686 A83-27376

Three dimensional turbulent shear flows; Proceedings of the Joint Fluids, Plasma, Thermophysics and Heat Transfer Conference, St. Louis, MO, June 7-11, 1982 11 p1565 A83-27409

Cavitation and Polyphase Flow Forum-1982; Proceedings of the Third Joint Thermophysics, Fluids, Plasma, and Heat Transfer Conference, St. Louis, Mo, June 7-11, 1982 11 p1566 A83-27420

1982 advances in aerospace structures and materials; Proceedings of the Winter Annual Meeting, Phoenix, AZ, November 14-19, 1982 11 p1591 A83-27426

Thermomechanical behavior of high-temperature composites; Proceedings of the Symposium, Phoenix, AZ, November 14-19, 1982 11 p1543 A83-27457

Shuttle propulsion systems; Proceedings of the Winter Annual Meeting, Phoenix, AZ, November 14-19, 1982 11 p1532 A83-27466

Particulate laden flows in turbomachinery; Proceedings of the Joint Fluids, Plasma, Thermophysics and Heat Transfer Conference, St. Louis, MO, June 7-11, 1982 11 p1525 A83-27476

Robotics research and advanced applications; Proceedings of the Winter Annual Meeting, Phoenix, AZ, November 14-19, 1982 11 p1552 A83-27484

Lasers '81; Proceedings of the International Conference, New Orleans, LA, December 14-18, 1981 11 p1576 A83-27501

Problems of solar and stellar oscillations; Proceedings of the Sixty-sixth Colloquium, Nauchny, Ukrainian SSR, September 1-5, 1981 11 p1687 A83-27626

Advanced space instrumentation in astronomy; Proceedings of the Fourth Symposium, Ottawa, Canada, May 20-22, 1982 11 p1669 A83-27726

International Union of Physiological Sciences, Annual Meeting, 4th, San Diego, CA, October 10-15, 1982, Proceedings 11 p1635 A83-27776

Remote sensing and regional land management; Conference, Universite de Picardie, Amiens, France, October 26, 27, 1981, Reports 11 p1600 A83-28144

International Conference on Plasma Physics, Goteborg, Sweden, June 9-15, 1982, Proceedings, Part 1 11 p1658 A83-28226

The characterization of carbon dioxide absorbing agents for life support equipment; Proceedings of the Winter Annual Meeting, Phoenix, AZ, November 14-19, 1982 11 p1644 A83-28329

Conference on the Fabrication of Profiled Crystals and Products using Stepanov's Method and Their Applications in National Economy, Leningrad, USSR, March 10-12, 1982, Proceedings 11 p1662 A83-28351

National Aerospace Meeting, Moffett Field, CA, March 24, 25, 1982, Proceedings 11 p1528 A83-28776

Engineering applications of laser velocimetry; Proceedings of the Symposium, Phoenix, AZ, November 14-19, 1982 12 p1727 A83-28830

Penalty-finite element methods in mechanics; Proceedings of the Winter Annual Meeting, Phoenix, AZ, November 14-19, 1982 12 p1717 A83-28851

Institute of Navigation, Annual Meeting, 38th, U.S. Air Force Academy, Colorado Springs, CO, June 14-17, 1982, Proceedings 12 p1700 A83-29201

Space observations of aerosols and ozone; Proceedings of the Topical Meeting, Ottawa, Canada, May 16-June 2, 1982 12 p1754 A83-29557

Numerical boundary condition procedures and multigrad methods; Proceedings of the Symposium, NASA Ames Research Center, Moffett Field, CA, October 19-22, 1981 12 p1772 A83-29646

Weather satellites: Stereoscropy and Sounding; Proceedings of the Topical Meeting, Ottawa, Canada, May 16-June 2, 1982 12 p1759 A83-29676

Structures, Structural Dynamics and Materials Conference, 24th, Lake Tahoe, NV, May 2-4, 1983, Collection of Technical Papers, Part 1 - Structures and materials. Part 2 - Structural dynamics 12 p1736 A83-29729

Transonic, shock, and multidimensional flows: Advances in scientific computing; Proceedings of the Symposium, University of Wisconsin, Madison, WI, May 13-15, 1981 12 p1726 A83-29926

International Conference on Results of Tests and Experiments with the European OTS Satellite, London, England, April 8-10, 1981, Proceedings 13 p1811 A83-30139

Conference on the Application of Accelerators in Research and Industry, 7th, North Texas State University, Denton, TX, November 8-10, 1982, Proceedings 13 p1917 A83-30176

International Conference on Plasma Physics, Goteborg, Sweden, June 9-15, 1982, Proceedings, Part 2 13 p1924 A83-30412

Conference on Weather Forecasting and Analysis, 9th, Seattle, WA, June 28-July 1, 1982, Preprints 13 p1884 A83-30526

Conference on Complex Turbulent Flows: Comparison of Computation and Experiment, Stanford University, Stanford, CA, September 3-6, 1980, Proceedings, Volume 1 - Objectives, evaluation of data, specifications of test cases, discussion and position papers 13 p1840 A83-30626

Conference on Complex Turbulent Flows: Comparison of Computation and Experiment, Stanford University, Stanford, CA, September 14-18, 1981, Proceedings, Volume 2 - Taxonomies, reporters' summaries, evaluation, and conclusions 13 p1840 A83-30630

Conference on Complex Turbulent Flows: Comparison of Computation and Experiment, Stanford University, Stanford, CA, September 14-18, 1981, Proceedings, Volume 3 - Comparison of computation with experiment, and computers' summary reports 13 p1842 A83-30644

Instruments and analysis techniques for space physics; Proceedings of the Workshop, Ottawa, Canada, May 16-June 2, 1982 13 p1813 A83-30751

Fifth All-Union Symposium on High and Superhigh Resolution Molecular Spectroscopy 13 p1915 A83-30848

Designing electronic equipment for random vibration environments; Proceedings of the Meeting, Los Angeles, CA, March 25, 26, 1982 13 p1834 A83-30851

International Conference on Advanced Technology Optical Telescopes, Tucson, AZ, March 11-13, 1982, Proceedings 13 p1936 A83-30976

Cosmochemistry and the origin of life; Proceedings of the Advanced Study Institute, Maratea, Italy, June 1-12, 1981 13 p1899 A83-31151

Aerospace Testing Seminar, 6th, Los Angeles, CA, March 11-13, 1981, Proceedings 13 p1809 A83-31176

Conference on Precision Electromagnetic Measurements, University of Colorado, Boulder, CO, June 28-July 1, 1982, Proceedings 13 p1836 A83-31276

All-Union Conference on Ferroelectricity, 10th, Minsk, Belorussian SSR, September 19-23, 1982, Proceedings 13 p1930 A83-31301

Environmental stress impact and environmental engineering methods; Proceedings of the Twenty-seventh Annual Technical Meeting on Emerging Environmental Solutions for the Eighties, Los Angeles, CA, May 5-7, 1981. Volume 1 13 p1862 A83-31476

Enhancement of quality through environmental technology; Proceedings of the Twenty-eighth Annual Technical Meeting, Atlanta, GA, April 21-23, 1982 13 p1864 A83-31507

Instrumentation in astronomy IV; Proceedings of the Fourth Conference, Tucson, AZ, March 8-10, 1982 14 p2014 A83-31976

Photovoltaic Solar Energy Conference; Proceedings of the Fourth International Conference, Stresa, Italy, May 10-14, 1982 14 p2036 A83-32176

Mechanical properties of BCC metals; Proceedings of the U.S.-Japan Seminar, Honolulu, HI, March 23-27, 1981 14 p1995 A83-32874

Society of Flight Test Engineers, Annual Symposium, 12th, Dayton, OH, September 16-18, 1981, Proceedings 14 p1969 A83-32926

Composites for extreme environments --- Book 14 p1986 A83-33114

Regional Latin American Conference on Astronomy, 2nd, Merida, Venezuela, January 19-23, 1981, Proceedings 14 p2107 A83-33235

Short fiber reinforced composite materials 14 p1988 A83-33294

Study of land transformation processes from space and ground observations; Proceedings of the Symposium, Ottawa, Canada, May 16-June 2, 1982 15 p2181 A83-33551

Advanced processing methods for titanium; Proceedings of the Symposium, Louisville, KY, October 13-15, 1981 15 p2134 A83-33632

Turbulent shear flows 3; International Symposium, 3rd, University of California, Davis, CA, September 9-11, 1981, Selected Papers 15 p2154 A83-33651

Numerical methods in laminar flame propagation; Proceedings of the Workshop, Aachen, West Germany, October 12-14, 1981 15 p2131 A83-34026

Meteorological problems of cloud physics and their theoretical and instrumental analysis; WOPHYS '82 Colloquium, Koenigstein im Taunus, May 17-19, 1982, Proceedings 15 p2204 A83-34051

Numerical methods in thermal problems. Volume 2 - Proceedings of the Second International Conference, Venice, Italy, July 7-10, 1981 15 p2158 A83-34226

Micro and macro mechanics of crack growth; Proceedings of the Symposium, Louisville, KY, October 13-15, 1981 15 p2179 A83-34476

Earth-oriented space activities and their legal implications; Proceedings of the Symposium, McGill University, Montreal, Canada, October 15, 16, 1981 15 p2240 A83-34651

Remote sensing: An input to geographic information systems in the 1980's; Proceedings of the Seventh Pecora Symposium, Sioux Falls, SD, October 18-21, 1981 15 p2184 A83-34801

Canadian Symposium on Air Cushion Technology, 16th, Charlottetown, Prince Edward Island, Canada, October 19-21, 1982, Preprints 15 p2241 A83-34851

Recent researches into solid bodies and magnetic fields in the solar system; Proceedings of the Topical Meeting and Symposium, Ottawa, Canada, May 16-June 2, 1982 15 p2124 A83-35001

Canadian Symposium on Air Cushion Technology, 15th, Toronto, Canada, September 29, 30, 1981, Proceedings 15 p2243 A83-35051

Antenna Applications Symposium, Monticello, IL, September 23-25, 1981, Proceedings 15 p2145 A83-35076

Annual Allerton Conference on Communication, Control, and Computing, 19th, Monticello, IL, September 30-October 2, 1981, Proceedings 15 p2220 A83-35101

Solar Maximum Year; Proceedings of the Symposium, Ottawa, Canada, May 16-June 2, 1982 15 p2282 A83-35201

Hydrogen energy in Canada - I Proceedings of the First Hydrogen Energy Symposium, University of Western Ontario, London, Canada, May 1, 1981 15 p2193 A83-35301

The upper atmospheres of the earth and planets; Proceedings of the Topical Meeting, Ottawa, Canada, May 16-June 2, 1982 16 p2434 A83-35351

Production and physics of highly charged ions; Proceedings of the International Symposium, Stockholm, Sweden, June 1-5, 1982 16 p2409 A83-35626

Saturn Conference, Tucson, AZ, May 11-15, 1982, Proceedings 16 p2435 A83-35726

International Symposium on Air Breathing Engines, 6th, Paris, France, June 6-10, 1983, Symposium Papers 16 p2302 A83-35801

Space 2000; International Astronautical Congress, 33rd, Paris, France, September 27-October 2, 1982, Selection of Papers 16 p2313 A83-35951

The terrestrial upper atmosphere; Proceedings of the Workshop, Ottawa, Canada, May 16-June 2, 1982 16 p2377 A83-36101

Ultrasonic fatigue; Proceedings of the First International Conference on Fatigue and Corrosion Fatigue up to Ultrasonic Frequencies, Champion, PA, October 25-30, 1981 16 p2367 A83-36176

Flight Simulation Technologies Conference, Niagara Falls, NY, June 13-15, 1983, Collection of Technical Papers 16 p2287 A83-36203

Aircraft Prototype and Technology Demonstrator Symposium, Dayton, OH, March 23, 24, 1983, Proceedings 16 p2287 A83-36457

International Astronomical Union, General Assembly, 18th, Patras, Greece, August 17-26, 1982, Proceedings 16 p2422 A83-36725

Symposium on High Temperature Gas Dynamics, Liblice, Czechoslovakia, September 15-19, 1981, Proceedings 16 p2354 A83-36876

American Control Conference, 1st, Arlington, VA, June 14-16, 1982, Proceedings. Volumes 1, 2 & 3 17 p2564 A83-37076

Gallium arsenide and related compounds 1982; International Symposium, 10th, Albuquerque, NM, September 19-22, 1982, Contributed Papers --- Book 17 p2584 A83-37160

Polymer processing: Analysis and innovation; Proceedings of the Design Conference, Washington, DC, September 13-15, 1982 17 p2516 A83-37364

Automatic control in space 1982; Proceedings of the Ninth Symposium, Noordwijkerhout, Netherlands, July 5-9, 1982 17 p2476 A83-37432

High-strength powder metallurgy aluminum alloys; Proceedings of the Symposium, Dallas, TX, February 17, 18, 1982 17 p2487 A83-37832

The giant planets and their satellites; Proceedings of the Symposium, Ottawa, Canada, May 16-June 2, 1982 17 p2620 A83-38106

Remote sensing and mineral exploration - 1982; Proceedings of the Symposium and Workshop, Ottawa, Canada, May 16-June 2, 1982 17 p2526 A83-38126

Meeting on Tribology - In Theory and Practice: Wear - Lifetime - Economics, Essen, West Germany, September 28, 29, 1982, Reports 17 p2517 A83-38223

American Congress on Surveying and Mapping and American Society of Photogrammetry Convention; APS Annual Meeting, 48th, Denver, CO, March 14-20, 1982, Technical Papers 17 p2530 A83-38336

Defects, fracture and fatigue; Proceedings of the Second International Symposium, Mont Gabriel, Quebec, Canada, May 30-June 5, 1982 17 p2489 A83-38376

International Society for Photogrammetry and Remote Sensing, International Symposium, Toulouse, France, September 13-17, 1982, Transactions. Volume 2 17 p2532 A83-38434

Conference on Aerospace and Aeronautical Meteorology, 9th, Omaha, NE, June 6-9, 1983, Preprints 17 p2548 A83-38701

Numerical grid generation; Proceedings of the Symposium on Numerical Generation of Curvilinear Coordinate Systems and Their Use in the Numerical Solution of Partial Differential Equations, Nashville, TN, April 13-16, 1982 17 p2572 A83-38776

Lighter-Than-Air Systems Conference, Anaheim, CA, July 25-27, 1983, Collection of Technical Papers 17 p2443 A83-38901

Cosmic magnetic fields; Proceedings of the Workshop, Florence, Italy, October 21-23, 1982 18 p2765 A83-39226

Gamma-ray astronomy in perspective of future space experiments; Proceedings of the Symposium, Ottawa, Canada, May 16-June 2, 1982 18 p2755 A83-39275

Computational Fluid Dynamics Conference, 6th, Danvers, MA, July 13-15, 1983, Collection of Technical Papers 18 p2633 A83-39351

Workshop on Light-induced Change in a-si:H and its Effect on Solar Cell Stability, San Diego, CA, September 24, 25, 1982 18 p2707 A83-39461

Kinematics, dynamics and structure of the Milky Way; Proceedings of the Workshop on the Milky Way, Vancouver, British Columbia, Canada, May 17-19, 1982 18 p2767 A83-39626

Symposium on the Orion Nebula to Honor Henry Draper, New York University, New York, NY, December 4, 5, 1981, Proceedings 18 p2771 A83-39699

Astronomische Gesellschaft, Scientific Meeting on Cosmology and Relativistic Astrophysics, Constance, West Germany, March 22-25, 1983, Reports 18 p2776 A83-39770

Scientific ballooning - III; Proceedings of the Workshop, Ottawa, Canada, May 16-June 2, 1982 18 p2631 A83-39801

Role and impact of space research in developing countries; Proceedings of the Workshop, Ottawa, Canada, May 16-June 2, 1982 18 p2787 A83-39825

Fundamental aspects of materials science in space; Proceedings of the Symposium, Ottawa, Canada, May 16-June 2, 1982 18 p2643 A83-39889

Progress in science and engineering of composites; Proceedings of the Fourth International Conference on Composite Materials, Tokyo, Japan, October 25-28, 1982, Volumes 1 & 2 18 p2650 A83-40126

ESO Infrared Workshop, 2nd, Garching, West Germany, April 20-23, 1982, Proceedings 18 p2760 A83-40419

The galactic center; Proceedings of the Workshop, California Institute of Technology, Pasadena, CA, January 7, 8, 1982 19 p2911 A83-40676

Life sciences and Space Research XX(1); Proceedings of the Workshops and Topical Meeting, Ottawa, Canada, May 16-June 2, 1982 19 p2871 A83-40826

Metal-hydrogen systems; Proceedings of the Miami International Symposium, Miami Beach, FL, April 13-15, 1981 19 p2818 A83-40850

ICC '82 - The digital revolution; International Conference on Communications, Philadelphia, PA, June 13-17, 1982, Conference Record. Volumes 1, 2 & 3 19 p2827 A83-41326

Lasers in metallurgy; Proceedings of the Symposium, Chicago, IL, February 22-26, 1981 19 p2854 A83-41468

Continuum models of discrete systems 4; Proceedings of the Fourth International Conference, Stockholm, Sweden, June 29-July 3, 1981 19 p2896 A83-41469

Numerical solutions of partial differential equations; Proceedings of the Conference, University of Melbourne, Parkville, Victoria, Australia, August 23-27, 1981 19 p2893 A83-41471

International Conference on Small and Special Electrical Machines, 2nd, London, England, September 22-24, 1981, Proceedings 19 p2839 A83-41472

Digital processing of signals in communications; Proceedings of the International Conference, Loughborough, England, April 7-10, 1981 19 p2834 A83-41473

Control and its applications; Proceedings of the International Conference, Warwick, England, March 23-25, 1981 19 p2890 A83-41476

Boundary element methods; Proceedings of the Third International Seminar, Irvine, CA, July 7-9, 1981 19 p2896 A83-41516

Fuel-air explosions; Proceedings of the International Conference, McGill University, Montreal, Canada, November 4-6, 1981 19 p2820 A83-41523

Mechanical and thermal behaviour of metallic materials; Proceedings of the International School of Physics, Course, 82nd, Varenna, Italy, June 30-July 10, 1981 19 p2822 A83-41525

Computing methods in applied sciences and engineering, V; Proceedings of the Fifth International Symposium, Versailles, France, December 14-18, 1981 19 p2896 A83-41526

Guidance and Control Conference, Gatlinburg, TN, August 15-17, 1983, Collection of Technical Papers 19 p2891 A83-41659

Solar radiation data; Proceedings of the Contractor's Meeting, Brussels, Belgium, November 20, 1981 19 p2862 A83-41990

Life sciences and space research XX(2); Proceedings of the Workshop and Topical Meeting, Ottawa, Canada, May 16-June 2, 1982 19 p2877 A83-42029

High temperature corrosion; Proceedings of the International Conference, San Diego, CA, March 2-6, 1981 20 p2951 A83-42226

Annual Mini-Symposium on Aerospace Science and Technology, 9th, USAF, Institute of Technology, Wright-Patterson AFB, OH, March 22, 1983, Proceedings 20 p2927 A83-42526

Heat transfer 1982; Proceedings of the Seventh International Conference, Technische Universitaet Muenchen, Munich, West Germany, September 6-10, 1982. Volume 1 - Review and keynote papers 20 p2970 A83-42651

Heat transfer 1982; Proceedings of the Seventh International Conference, Technische Universitaet Muenchen, Munich, West Germany, September 6-10, 1982. Volume 2 - General papers: Conduction, natural convection, environmental heat transfer, radiation 20 p2971 A83-42663

Heat transfer 1982; Proceedings of the Seventh International Conference, Technische Universitaet Muenchen, Munich, West Germany, September 6-10, 1982. Volume 3 - General papers: Forced convection, mixed convection 20 p2975 A83-42700

Heat transfer 1982; Proceedings of the Seventh International Conference, Technische Universitaet Muenchen, Munich, West Germany, September 6-10, 1982. Volume 4 - General papers: Pool boiling, flow boiling, measuring techniques 20 p2980 A83-42757

Environmental effects on fibre-reinforced plastics; Proceedings of the Symposium, Imperial College of Science and Technology, London, England, July 12, 13, 1983 20 p2946 A83-42801

Gesellschaft fuer angewandte Mathematik und Mechanik, Annual Scientific Meeting, Budapest, Hungary, April 13-16, 1982, Reports. Part 1 20 p3004 A83-42979

Heat transfer 1982; Proceedings of the Seventh International Conference, Technische Universitaet Muenchen, Munich, West Germany, September 6-10, 1982. Volume 6 - General papers: Combined heat and mass transfer, particle heat transfer, heat exchangers, industrial heat transfer, heat transfer in energy utilization 20 p2993 A83-43013

Materials processing in the reduced gravity environment of space; Proceedings of the Annual Meeting, Boston, MA, November 16-18, 1981 20 p2939 A83-43251

Remotely piloted vehicles; International Conference, 3rd, Bristol, England, September 13-15, 1982, Proceedings and Supplementary Papers 20 p2933 A83-43700

Integrated optics, fiber optics and holography; International School on Coherent Optics and Holography, 2nd, Varna, Bulgaria, September 28-October 3, 1981, Proceedings 20 p3048 A83-43774

Engineering science and mechanics; Proceedings of the International Symposium, Tainan, Republic of China, December 29-31, 1981. Parts 1 & 2 21 p3117 A83-44001

Guidance and control 1983; Proceedings of the Annual Rocky Mountain Conference, Keystone, CO, February 5-9, 1983 21 p3099 A83-44160

American Vacuum Society, National Symposium, 29th, Baltimore, MD, November 16-19, 1982, Proceedings. Part 1 21 p3109 A83-44601

The Max Born Centenary Conference, University of Edinburgh, Edinburgh, Scotland, September 7-10, 1982, Proceedings 21 p3205 A83-44780

Energy technology X - A decade of progress; Proceedings of the Tenth Conference, Washington, DC, February 28-March 2, 1983 21 p3168 A83-45064

Composite materials: Quality assurance and processing; Proceedings of the Symposium, St. Louis, MO, October 20, 1981 21 p3107 A83-45065

SITELCOM-82 - Telecommunications and data processing in the air transport industry; Proceedings of the Conference, Monte Carlo, Monaco, March 2-4, 1982 21 p3090 A83-45076

Atmospheric chemistry; Dahlem Workshop, Berlin, West Germany, May 2-7, 1982, Report 21 p3165 A83-45094

Dynamics and control of large flexible spacecraft; Proceedings of the Third Symposium, Blacksburg, VA, June 15-17, 1981 21 p3101 A83-45101

Advances in dynamic analysis and testing; Proceedings of the Aerospace Congress and Exposition, Anaheim, CA, October 25-28, 1982 22 p3303 A83-45746

Photogrammetric Week, 38th, University of Stuttgart, Stuttgart, West Germany, October 5-10, 1981, Reports 22 p3307 A83-45750

PTC '83 - Pacific Telecommunications Conference, Honolulu, HI, January 16-19, 1983, Proceedings 22 p3273 A83-45751

Electrophoresis '82; Proceedings of the Fourth International Conference, Athens, Greece, April 21-24, 1982 22 p3265 A83-45757

Testing for space and weapon products; Proceedings of the Symposium, London, England, January 18, 1983 22 p3303 A83-45821

Certification of avionics systems; Proceedings of the Symposium, London, England, April 27, 1982 22 p3247 A83-45843

Annual Airline Plating and Metal Finishing Forum, 18th, Orlando, FL, March 16-18, 1982, Proceedings 22 p3301 A83-45863

Shot peening for advanced aerospace design; Proceedings of the Aerospace Congress and Exposition, Anaheim, CA, October 25-28, 1982 22 p3302 A83-45872

International Forum for Air Cargo, 11th, New York, NY, September 27-30, 1982, Proceedings 22 p3251 A83-45900

Vortex motion; Proceedings of the Colloquium, Goettingen, West Germany, November 1982 22 p3279 A83-45901

1982 International Geoscience and Remote Sensing Symposium, Munich, West Germany, June 1-4, 1982, Digest. Volumes 1 & 2 22 p3307 A83-46101

International Geoscience and Remote Sensing Symposium, Universitaet Muenchen, Munich, West Germany, June 1-4, 1982, Proceedings 22 p3314 A83-46227

Law and security in outer space; Proceedings of the Workshop, University of Mississippi, University, MS, May 21, 22, 1982 22 p3370 A83-46309

International Symposium on Geodetic Networks and Computations, Munich, West Germany, August 31-September 5, 1981, Proceedings. Volume 4 - Modern observation techniques for terrestrial networks 22 p3315 A83-46336

- International Symposium on Geodetic Networks and Computations, Munich, West Germany, August 31-September 5, 1981, Proceedings. Volume 7 - Combination of horizontal, vertical and gravity networks 22 p3316 A83-46351
- International Symposium on Geodetic Networks and Computations, Munich, West Germany, August 31-September 5, 1981, Proceedings. Volume 5 - Network analysis models 22 p3317 A83-46359
- Unsteady turbulent shear flows; Proceedings of the Symposium, Toulouse, France, May 5-8, 1981 22 p3281 A83-46426
- Publication on the occasion of the 65th birthday of Prof. Dr.-Ing. Erich Truckenbrodt; Scientific Colloquium, Technische Universitaet Muenchen, Munich, West Germany, February 1, 1982, Reports 22 p3284 A83-46482
- Symposium on Coordinated Observations of the Ionosphere and the Magnetosphere in the Polar Regions, 4th, Tokyo, Japan, February 23-25, 1981, Proceedings 22 p3329 A83-46501
- Optical coatings for energy efficiency and solar applications; Proceedings of the Seminar, Los Angeles, CA, January 28, 1982 22 p3319 A83-46580
- Optical systems engineering II; Proceedings of the Second Conference, Los Angeles, CA, January 26, 27, 1982 22 p3357 A83-46587
- Sensor design using computer tools; Proceedings of the Conference, Los Angeles, CA, January 28, 29, 1982 22 p3291 A83-46593
- Laser and laser systems reliability; Proceedings of the Conference, Los Angeles, CA, January 28, 29, 1982 22 p3296 A83-46611
- Advances in infrared fibers II; Proceedings of the Second Meeting, Los Angeles, CA, January 26-28, 1982 22 p3357 A83-46621
- Integrated optics II; Proceedings of the Meeting, Los Angeles, CA, January 28, 29, 1982 22 p3359 A83-46643
- Picosecond lasers and applications; Proceedings of the Conference, Los Angeles, CA, January 26, 27, 1982 22 p3297 A83-46663
- National Aerospace Meeting, Arlington, VA, March 22-25, 1983, Proceedings 22 p3252 A83-46952
- Three-dimensional turbulent boundary layers; Proceedings of the Symposium, Berlin, West Germany, March 29-April 1, 1982 22 p3285 A83-47011
- Activity in red-dwarf stars; Proceedings of the Seventy-first Colloquium, Catania, Italy, August 10-13, 1982 23 p3520 A83-47476
- U.S.-Japan Seminar on the Recent Advances in the Understanding of Solar Flares, Tokyo, Japan, October 5-8, 1982, Proceedings 23 p3531 A83-47658
- Composition and origin of cosmic rays; Proceedings of the Advanced Study Institute, Erice, Italy, June 20-30, 1982 23 p3538 A83-47735
- Structure of the upper and middle atmosphere; Proceedings of the Meeting, Leeds, England, August 23-27, 1982 24 p3603 A83-48751
- Anticorrosion coatings; All-Soviet Conference on Refractory Coatings, 10th, Leningrad, USSR, May 12-14, 1981, Proceedings 24 p3553 A83-49076
- Planetary nebulae; Proceedings of the Symposium, University College, London, England, August 9-13, 1982 24 p3638 A83-49126
- International Symposium on Aeroelasticity, Nuremberg, West Germany, October 5-7, 1981, Collected Papers [DGLR BERICHT 82-01] 24 p3543 A83-49176
- Internal kinematics and dynamics of galaxies; Proceedings of the Symposium, Universitede Franche-Comte, Besancon, France, August 9-13, 1982 24 p3654 A83-49201
- High temperature corrosion of metals and alloys; Proceedings of the Third International Symposium, Mount Fuji, Japan, November 17-20, 1982 24 p3561 A83-49476
- Conference on Cloud Physics, Chicago, IL, November 15-18, 1982, Preprints 24 p3610 A83-49676
- All-Union Symposium on Combustion and Explosion, 7th, Chernogolovka, USSR, October 1983, Proceedings 24 p3555 A83-49758
- Symposium on Turbulence, 7th, University of Missouri-Rolla, Rolla, MO, September 21-23, 1983, Proceedings 24 p3584 A83-49801
- International Meeting on Lithium Batteries, Rome, Italy, April 27-29, 1982 24 p3600 A83-49932
- Workshop on Astronomical Measuring Machines, Edinburgh, Scotland, September 28-30, 1982, Proceedings 24 p3647 A83-50001
- CONFIDENCE**
- Performance uncertainty analysis 01 p0103 A83-11173
- CONFIDENCE LIMITS**
- Confidence intervals for the percent nonconforming based on variables data 02 p0232 A83-12093
- Maximum precision of the measurement of gravity gradients 07 p0989 A83-20854
- Accuracy of univariate, bivariate, and a "modified double Monte Carlo" technique for finding lower confidence limits of system reliability 08 p1114 A83-22712
- Statistical determination of a flaw detection probability curve 10 p1437 A83-26763
- Percentiles of pooled estimates of Weibull parameters 17 p2517 A83-37294
- Planning and statistical processing of the results of tests for plotting quantile fatigue curves 19 p2824 A83-40762
- Confidence limits for availability of maintained systems Exact and Monte Carlo method 20 p2999 A83-42551
- CONFIGURATION INTERACTION**
- Wavefunctions and oscillator strengths for Si II 06 p0827 A83-18164
- A kinetic model of the electron and conformational transitions in the photosynthetic reaction centers of purple bacteria 07 p0974 A83-20966
- Multiconfiguration Hartree-Fock Breit-Pauli results for 2P1/2-2P3/2 transitions in the boron sequence 08 p1162 A83-21985
- Transition probabilities for forbidden lines in the 3p4 configuration. III --- in astrophysics 09 p1362 A83-24986
- The low-lying 2-sigma-minus states of OH 11 p1655 A83-28528
- CASSCF/CI calculations for first row transition metal hydrides - The TiH(4-phi), VH(5-delta), CrH(6-sigma-plus), MnH(7-sigma-plus), FeH(4,6-delta) and NiH(2-delta) states 11 p1655 A83-28530
- On the nature of the bonding in Cu2 - An ab initio viewpoint 13 p1818 A83-31809
- Energy levels of atomic nitrogen calculated in a multiconfiguration optimized potential model 15 p2228 A83-35297
- Correlation energy in triplet states - Comparison of many-body perturbation theory and configuration interaction for CH2 and O2 19 p2899 A83-41862
- The dissociation energy of Cu2 - Do we want to perform multi-reference singles and doubles CIs on many-electron systems? 19 p2898 A83-41864
- Correlation and the 3s2 3p5 2P0 to 3s 3p6 2S, 3s2 3p5 2P0 to 3s2 3p4 3d2S transitions in Fe X 21 p3202 A83-44749
- A theoretical investigation of the radiative properties of the CN red and violet systems 21 p3238 A83-45572
- CONFIGURATION MANAGEMENT**
- Software configuration control in a real-time flight test environment 01 p0009 A83-11144
- Hardware and software configuration control - History and current status 05 p0621 A83-17313
- Choice of the initial configuration for a solid body which assures the fulfillment of a prescribed ablation law 24 p3579 A83-49668
- CONFINEMENT**
- Effect of confinement in small space flight size cages on insulin sensitivity of exercise-trained rats 24 p3617 A83-48881
- CONFLUENCE**
- U CONVERGENCE
- CONFORMAL MAPPING**
- Extension of the Carafoli tracer method to profiles cascades 01 p0002 A83-10578
- Relativistic kinematics for motions faster than light 01 p0124 A83-10705
- Conformal-plane gravitational fields of a viscous fluid 03 p0390 A83-13526
- Potential flow analysis of an arbitrary cascade using a conformal transformation into a row of circular cylinders 03 p0278 A83-13564
- Mesh generation by conformal and quasiconformal mappings 03 p0388 A83-14089
- On the analytic treatment of non-integrable difference equations 06 p0805 A83-18327
- Conformal Minkowski space-time. I - Relative infinity and proper time 08 p1160 A83-22012
- Cascade of period doublings of tori 08 p1162 A83-22948
- Minimal-order realizations for continuous-time 2-power input-output maps 09 p1329 A83-24730
- Numerical conformal mapping and analytic continuation 10 p1470 A83-25875
- A one-dimensional-map model for noise-induced transitions between bistable states 11 p1649 A83-28066
- Branched cracks at small angles /An addendum/ 11 p1595 A83-28438
- Some difficulties generated by small sinks in the numerical study of dynamical systems - Two examples 12 p1775 A83-29163
- The value distribution of holomorphic maps --- Russian book 12 p1774 A83-29336
- Orthogonal mapping 13 p1912 A83-31367
- Application of contour-conformal mapping to the flow along an S2 current sheet 13 p1805 A83-31798
- Analytical tools for nonlinear image restoration 14 p2076 A83-32901
- Large thermal deflections of elastic plates by conformal transformation 15 p2175 A83-34246
- Blade-to-blade transonic flow calculation in axial turbomachines 16 p2290 A83-35837
- Conformal grid generation 17 p2508 A83-38781
- Conformal grid generation for multielement airfoils 17 p2458 A83-38800
- Conformal mappings onto multiply connected regions with specified boundary shapes 17 p2573 A83-38801
- Generation of boundary-fitted coordinate systems using segmented computational regions 17 p2574 A83-38802
- Orthogonal coordinate meshes with manageable Jacobian 17 p2574 A83-38815
- Elimination of the standard big bang singularity and particle horizon through quantum conformal fluctuations 17 p2614 A83-38962
- Airfoil generation with a desktop computer using Lighthill's exact inverse method [AIAA PAPER 83-1867] 18 p2632 A83-39096
- Quasi three-dimensional grid generation using conformal mapping [AIAA PAPER 83-1906] 18 p2739 A83-39365
- Fast body-fitted grid generation around 3-D configurations [AIAA PAPER 83-1936] 18 p2635 A83-39386
- The development of a comprehensive two-dimensional linearized airfoil theory 20 p2928 A83-42529
- Lyapunov exponents for multidimensional orbits 20 p3043 A83-43566
- Characteristic impedance of an oval located symmetrically between the ground planes of finite width --- for transmission lines 21 p3123 A83-43840
- Theorems of stability in geometry and analysis --- Russian book 21 p3199 A83-43905
- Rayleigh-Taylor instability and the use of conformal maps for ideal fluid flow 21 p3132 A83-44986
- Modifications of the lives-liutermoza conformal-mapping procedure for turbomachinery cascades [ASME PAPER 83-GT-116] 23 p3395 A83-47947
- CONFORMAL TRANSFORMATIONS**
- U CONFORMAL MAPPING
- CONGENITAL ANOMALIES**
- The condition of the vestibular apparatus in children with hereditary hearing defects 19 p2884 A83-41843
- CONGENITAL CONDITIONS**
- U CONGENITAL ANOMALIES
- CONGRESSIONAL REPORTS**
- Law and security in outer space - The role of Congress in space law and policy 22 p3371 A83-46314
- CONICAL BODIES**
- NT SLENDER CONES
- Supersonic flow around a conical fuselage of arbitrary section isolated or equipped with a delta wing with subsonic leading edges 01 p0002 A83-10579
- Generalized conic concentrators 02 p0236 A83-12310
- Experimental forces and moments on cone-derived waveriders for freestream M = 3 to 5 02 p0132 A83-13092
- A formulation of radiation view factors from conical surfaces [AIAA PAPER 83-0156] 05 p0633 A83-16560
- A phased horn with a main lobe of elliptical cross section 05 p0623 A83-17690
- Electromagnetic excitation of a truncated cone by a plane wave 07 p0914 A83-20775
- The effect of an axial force on a conical body 08 p1122 A83-22056
- Evaluation of total body heat transfer in hypersonic flow 08 p1042 A83-22150
- Boundary-layer transition on a rotating cone in still fluid 09 p1262 A83-24417
- The supersonic combustion around a truncated cone 09 p1198 A83-24504
- The conical antenna as a sensor or probe 10 p1404 A83-26488
- Experimental investigation on a method of lowering the silhouette of conical log-spiral antenna 10 p1406 A83-26843
- Computation of nonequilibrium, supersonic three-dimensional inviscid flow over blunt-nosed bodies 14 p1971 A83-32980
- A common-aperture X- and S-band four-function feedcone --- hornfeed design for antennas of Deep Space Network 15 p1226 A83-35086
- Separated flows on a concave conical wing 16 p2289 A83-35707
- A study of supersonic nonstationary flow past conical bodies 16 p2289 A83-35722

- The wake drag of bodies with a conical tail section
17 p2452 A83-38093
- A shock-on-shock interaction model for multiconic interceptors
[AIAA PAPER 83-1843] 17 p2456 A83-38671
- Measurements of the three-dimensional boundary layers on conical bodies at Mach 3 and Mach 5
[AIAA PAPER 83-1675] 18 p2633 A83-39266
- The maximum aerodynamic efficiency of conical wing-body combinations at high supersonic speeds
19 p2790 A83-41266
- Aerodynamics of pointed forebodies at high angles of attack
[AIAA PAPER 83-2117] 19 p2793 A83-41942
- Coupling between two conical horns placed side by side
20 p2963 A83-42368
- Influence of asymmetric transition on static stability of blunted cones
21 p3087 A83-44562
- A simplified calculation method for the nonequilibrium wake of the blunt-cone body
21 p3087 A83-44568
- Elastoplastic state of a conical tube
21 p3164 A83-45393
- Three-dimensional flow over a conical afterbody containing a centered propulsive jet - A numerical simulation
[AIAA PAPER 83-1709] 21 p3088 A83-45518
- CONICAL CAMBER**
SC3 - A wing concept for supersonic maneuvering
[AIAA PAPER 83-1858] 17 p2457 A83-38685
- CONICAL FLARE**
- U CONES**
- CONICAL FLOW**
Shock fitting in the numerical analysis of supersonic conical flows
01 p0003 A83-11269
- Numerical study of flowfields about asymmetric external conical corners
03 p0277 A83-13130
- Numerical computations of wall-jet flows
03 p0323 A83-14674
- A shock-fitting solution of the supersonic flowfield in a rounded internal corner
[AIAA PAPER 83-0038] 05 p0578 A83-16478
- New implicit boundary procedures - Theory and applications
[AIAA PAPER 83-0123] 05 p0579 A83-16536
- Conical, noncircular, second-order, small disturbance potential theory of supersonic flow
[AIAA PAPER 83-0459] 05 p0586 A83-16728
- Conical vortices - A class of exact solutions of the Navier-Stokes equations
05 p0638 A83-17353
- An experimental investigation of control surface effectiveness and real-gas simulation for biconics
[AIAA PAPER 83-0213] 05 p0591 A83-17912
- Approximate factorization schemes for 3D nonlinear supersonic potential flow
[AIAA PAPER 83-0376] 05 p0591 A83-17923
- The stability of flows near an infinite wedge or cone situated in supersonic gas flow
07 p0863 A83-20315
- Pressure measurements of a rotating liquid for impulsive coning motion
09 p1263 A83-24877
- Nonsimilar boundary layers on the leeside of cones at incidence
13 p1804 A83-31591
- A study of supersonic nonstationary flow past conical bodies
16 p2289 A83-35722
- Three-dimensional nonequilibrium viscous shock-layer flows over complex geometries
[AIAA PAPER 83-0212] 16 p2292 A83-36048
- Topology of vortices in conical flow
[AIAA PAPER 83-1664] 17 p2443 A83-37176
- Hypersonic flows over biconics using a variable-effective-gamma, Parabolized-Navier-Stokes code
[AIAA PAPER 83-1666] 17 p2443 A83-37177
- Conical similarity of shock/boundary layer interactions generated by swept fins
[AIAA PAPER 83-1756] 17 p2446 A83-37229
- Characteristics of supersonic gas flow and heat transfer in the shadow region of a sharp cone
17 p2447 A83-37261
- Flow in a three-dimensional corner with large entropy differences
17 p2449 A83-37540
- Pressure distribution on a wedge and cone in a hypersonic nonequilibrium gas flow
17 p2449 A83-37555
- The spiral singularity in the supersonic inviscid flow over a cone
[AIAA PAPER 83-1665] 17 p2451 A83-38084
- Application of a full potential method for predicting supersonic flow fields and aerodynamic characteristics
[AIAA PAPER 83-1802] 17 p2453 A83-38637
- Viscous effects on the performance of cone-derived waveriders
[AIAA PAPER 83-2084] 19 p2792 A83-41918
- Numerical experiments with the Osher upwind scheme for the Euler equations
20 p2930 A83-43439

- An investigation of the establishment of a recirculation zone by swirling flows within a conical duct
[ASME PAPER 83-GT-93] 23 p3448 A83-47939
- Optimization of waverider configurations generated from axisymmetric conical flows
23 p3398 A83-48134
- Second-order boundary-layer flow past sharp cones
23 p3399 A83-48625
- Turbulent kinetic energy balance in a conical diffuser
24 p3579 A83-49805

CONICAL INLETS

- Characteristics of the regular reflection of a shock wave from the walls of a conical funnel
17 p2507 A83-38072

CONICAL NOZZLES

- Effects of approaching flow types on the performances of straight conical diffusers
03 p0316 A83-13565
- Ion extraction from a plasma through a conical orifice
05 p0687 A83-16920
- Theoretical and experimental study of a dual-flow circuit breaker nozzle flow
[AIAA PAPER 83-1748] 17 p2503 A83-37223
- Analysis of flow in a conical nozzle with an oblique exit section and in the jet issuing from it
17 p2450 A83-37566

CONICAL SCANNING

- Transverse beam scanning for an offset dual-reflector system with symmetric main reflector
06 p0740 A83-18638
- Determination of the coordinates of sources of solar radio bursts in the conical scanning mode
17 p2628 A83-38976
- Beam area determination for multiple-beam satellite communication applications
19 p2827 A83-41147
- Off-axis scanning of cylindrical lenses
23 p3442 A83-47831

CONICAL SHELLS

- An averaged Lagrangian-finite element technique for the solution of nonlinear vibration problems
02 p0194 A83-12747
- Vibrations of conical shells with variable thickness
02 p0197 A83-13073
- Investigation of the effect of initial deflection on the natural-vibration frequencies of rib-stiffened conical shells
04 p0502 A83-16409
- Axisymmetric vibrations of conical shells with variable thickness
07 p0945 A83-20281
- Buckling of a thin-walled conical shell under axisymmetric loads beyond the elastic limit
07 p0947 A83-21087
- Dynamic analysis of thin elastic noncircular conical shells
07 p0948 A83-21346
- Buckling of a conical sandwich shell beyond the elastic limit under combined load
08 p1115 A83-21637
- Dynamic characteristics of conical shell with variable modulus of elasticity
09 p1280 A83-24506
- Solution of the problem of the stressed state of an inhomogeneous hollow cone
10 p1439 A83-25592
- Optimum cone angles in aeroelastic flutter
11 p1599 A83-28720
- Numerical solution of two-dimensional boundary value problems of the statics of flexible conical shells
13 p1866 A83-30071
- The use of orthogonal-matrix filtering in solving shell stability equations
14 p2029 A83-32154
- The nonaxisymmetric deformation of flexible conical shells of variable thickness
16 p2365 A83-35926
- The stability of thin-walled ribbed conical shells
17 p2524 A83-38508
- Buckling loads in the case of imperfect truncated conical shells under axial pressure
20 p3005 A83-42983
- Dynamics and stability of open conical shells
20 p3005 A83-42993
- Finite element analysis of 3-ply laminated conical shell for flutter
21 p3160 A83-45052
- Two-dimensional problems of the stability and vibrations of shells of zero Gaussian curvature
21 p3164 A83-45395

CONICS

- NT PARABOLAS**
Properties of conic state transition matrices
[AIAA PAPER 83-0014] 05 p0681 A83-16464
- Curve fitting with conic splines
17 p2571 A83-38060

CONIFERS

- Assessment of spruce budworm defoliation using digital airborne MSS data
03 p0347 A83-14248
- The application of remote sensing in southern Alberta's mountain pine beetle management
03 p0347 A83-14257
- Radar scattering from a solitary fir tree
22 p3312 A83-46189
- The use of the Monte Carlo method in investigating the influence of the dimensions of a conifer on the angular dependence of its coefficient of spectral brightness
23 p3476 A83-48114

CONJUGATES

- An iterative method for the Helmholtz equation
12 p1771 A83-29097
- The basic types of conjugate problems of heat and mass transfer
13 p1838 A83-30048
- Conjugate gradients methods for solution of finite element and finite difference flow problems
[AIAA PAPER 83-1923] 18 p2682 A83-39377

CONJUGATION**NT PHASE CONJUGATION****CONJUNCTIVA**

- An investigation of the microcirculatory bed in flightcrew members with conjunctivitis during the initial appearance of cerebral atherosclerosis
13 p1905 A83-30949
- A device for the biomicroscopic study of the blood vessel bed in the eyeball conjunctiva
16 p2402 A83-36811

CONJUNCTIVITIS

- The effect of maximum physical work on the cardiodynamics and microcirculatory bed of young athletes and of individuals not pursuing athletic activities
16 p2398 A83-35907

CONNECTIONS**U JOINTS (JUNCTIONS)****CONNECTIVE TISSUE****NT COLLAGENS**

- The treatment of trauma of the locomotor system in athletes /Study of the work of the athletic clinic for trauma in Austria/
01 p0084 A83-11385
- Laser treatment of open-angle glaucoma: Randomized comparative studies - Cyclotrabeulospas and trabeculoplasty
05 p0674 A83-17212

CONNECTORS**NT ELECTRIC CONNECTORS****NT UNIONS (CONNECTORS)****CONNECTORS (ELECTRIC)****U ELECTRIC CONNECTORS****CONOIDS****U CONICAL BODIES****CONSERVATION****NT ENERGY CONSERVATION****CONSERVATION EQUATIONS**

- A posteriori numerical techniques for enforcing simultaneous conservation of integral invariants upon finite-difference shallow-water equation models
03 p0322 A83-14607
- A hemispheric barotropic quasi-geostrophic model of the atmosphere with conservation of the degrees of potential vorticity
09 p1315 A83-24934
- An explicit finite-difference scheme with exact conservation properties
12 p1772 A83-29624
- Implicit finite difference simulation of inviscid and viscous compressible flow
12 p1726 A83-29934
- Tracking of interfaces for fluid flow: Accurate methods for piecewise smooth problems.
12 p1726 A83-29937
- Conservation form, in general non steady coordinates, of the Navier-Stokes equations and boundary conditions for a moving boundary problem
14 p2008 A83-32149
- Model field flux conservation and the Beard magnetotail model - Two corrections
17 p2539 A83-37607
- A conservative type-dependent full potential method for the treatment of supersonic flows with embedded subsonic regions
[AIAA PAPER 83-1887] 18 p2634 A83-39356
- The effect of coupling between the heat equation and the equations of motion in case of shock-like temperature stresses
20 p3005 A83-42985
- Discrete mechanics - Some remarks --- numerical method in celestial mechanics
20 p3062 A83-43573

CONSERVATION LAWS

- Conservation laws for a dynamical system in group variables
01 p0104 A83-10122
- Conservation laws and material momentum in thermoelasticity
[ASME PAPER 82-WA/APM-26] 04 p0498 A83-15677
- A characteristic flux difference splitting for the hyperbolic conservation laws of inviscid gasdynamics
[AIAA PAPER 83-0040] 05 p0632 A83-16480
- The conservation laws of a viscoelastoplastic medium with finite strains
07 p0945 A83-19945
- A conservation law for small-amplitude quasi-geostrophic disturbances on a zonally asymmetric basic flow
08 p1142 A83-23007
- On the symmetric form of systems of conservation laws with entropy
09 p1350 A83-23724
- High resolution schemes for hyperbolic conservation laws
12 p1771 A83-29095
- Compact finite difference schemes for the Euler and Navier-Stokes equations
12 p1722 A83-29096
- Convergence of approximate solutions to conservation laws --- in parabolic systems and finite difference schemes
12 p1727 A83-29939

Experimental test of baryon conservation - A new limit on neutron-antineutron oscillations in oxygen 13 p1917 A83-30916

Self-adjusting grid methods for one-dimensional hyperbolic conservation laws 15 p2224 A83-33822

On physical and material conservation laws 15 p2177 A83-34335

Shock waves and reaction-diffusion equations --- Book 17 p2575 A83-37162

High resolution applications of the Osher upwind scheme for the Euler equations [AIAA PAPER 83-1943] 18 p2636 A83-39390

Implicit conservative characteristic modeling schemes for the Euler equations - A new approach [AIAA PAPER 83-1939] 18 p2683 A83-39416

Coordinate-invariant conservation laws in Schwarzschild geometry 20 p3075 A83-43389

Numerical experiments with the Osher upwind scheme for the Euler equations 20 p2930 A83-43439

Conservation laws for some separable gyroscopic dynamical systems 24 p3624 A83-50125

CONSOLES

NT REMOTE CONSOLES

New console design - An example --- for telescope control 13 p1938 A83-31004

Central operating and display unit for avionics systems 23 p3401 A83-47193

CONSTANT VOLUME BALLOONS

U SUPERPRESSURE BALLOONS

CONSTANTS

NT GRAVITATIONAL CONSTANT

NT GRUNEISEN CONSTANT

NT HUBBLE CONSTANT

NT PERCEPTUAL TIME CONSTANT

NT PLANCKS CONSTANT

NT SOLAR CONSTANT

NT TIME CONSTANT

Numerical values of fundamental constants and the anthropocentric principle --- universe models 01 p0113 A83-10824

Corrections to fundamental constants from photoelectric observations of lunar occultations 03 p0409 A83-13939

Precision measurements and fundamental constants 08 p1092 A83-22323

Questions on universal constants and four-dimensional symmetry from a broad viewpoint. I 12 p1792 A83-29044

Thermal constants of materials. Number 10 - Li, Na, K, Rb, Cs, Fr. Part 3 - Tables of literature references, appendices, bibliography, index --- Russian book 18 p2672 A83-40602

The angular momentum of celestial bodies and the fundamental dimensionless constants of nature 23 p3518 A83-47423

The cosmological constant and classical tests of general relativity 23 p3528 A83-48591

CONSTELLATIONS

NT CENTAURUS CONSTELLATION

NT CORONA BOREALIS CONSTELLATION

NT CYGNUS CONSTELLATION

NT LYRAE CONSTELLATION

NT ORION CONSTELLATION

NT SCORPIUS CONSTELLATION

NT TAURUS CONSTELLATION

CONSTITUTIONAL DIAGRAMS

U PHASE DIAGRAMS

CONSTITUTIVE EQUATIONS

Nonlinear structural and life analyses of a combustor liner 02 p0195 A83-12764

Multiaxial nonproportional cyclic deformation 03 p0340 A83-13911

Role of the strain history on the flow law for high temperature creep 04 p0457 A83-14998

Finite endochronic theory for ratcheting and cyclic plasticity 04 p0500 A83-16096

Numerical solution and development of a transient temperature rate dependent constitutive equation --- model for crystalline solids [AIAA PAPER 83-0648] 05 p0653 A83-16815

An elastic-plastic constitutive equation for transversely isotropic materials and its application to the bending of perforated circular plates 05 p0656 A83-17947

Three-dimensional constitutive relations and ductile fracture --- Book 06 p0774 A83-18477

On constitutive relations in thermoplasticity 06 p0774 A83-18488

Finite deformation constitutive relations including ductile fracture damage 06 p0774 A83-18490

Constitutive equations and global criteria for ductile fracture 06 p0774 A83-18491

Net-stress analysis in creep mechanics 06 p0778 A83-19324

Parametric representation of crack growth rate under creep, fatigue and creep-fatigue interaction at high temperatures 07 p0883 A83-19671

Comments on anisotropic plastic flow and incompressibility 07 p0946 A83-20638

Requirements of constitutive models for two nickel-base superalloys 07 p0891 A83-21071

A constitutive theory for transversely isotropic bimodulus materials with a class of steady wave solutions 07 p0948 A83-21344

Constitutive relations including ductile fracture damage - Application to cracked bodies 08 p1117 A83-21700

A Saint-Venant principle for nonlinear elasticity 09 p1279 A83-24134

A theory of viscoelastic composites modeled as interpenetrating solid continua with memory 09 p1280 A83-24136

Study of the constitutive creep laws using biaxial relaxation tests 10 p1393 A83-25416

Effective constitutive relations for the microstructure of periodic frames [AIAA 83-1006] 12 p1740 A83-29793

An uncoupled viscoplastic constitutive model for metals at elevated temperature [AIAA 83-1016] 12 p1740 A83-29798

On non-universal finite elastic deformations 15 p2176 A83-34331

Thermoelasticity of ideal fibre-reinforced materials 16 p2324 A83-35775

Bounds on stress concentration factors in finite anti-plane shear 16 p2368 A83-36548

A viscoelastic-viscoplastic constitutive equation and its finite element implementation 16 p2369 A83-36557

Constitutive equations for damaging materials [ASME PAPER 83-APM-12] 17 p2519 A83-37384

Plastic materials with continuous transition between loading and unloading states 19 p2859 A83-41544

Some aspects of thermoplasticity 20 p3004 A83-42980

On inverse problem in elasticity and plasticity 20 p3006 A83-42994

A simple algorithm for the nonlinear dynamic analysis of networks 23 p3470 A83-48160

CONSTRAINTS

NT BRUNT-VAISALA FREQUENCY

NT METEOROLOGICAL PARAMETERS

On the definity of quadratic forms subject to linear constraints 01 p0101 A83-10252

Additional necessary conditions for optimal control with state-variable inequality constraints 04 p0527 A83-15945

Structural optimization on geometrical configuration and element sizing with statical and dynamical constraints 06 p0771 A83-18205

A new method for optimal design of structures 06 p0773 A83-18229

Operational considerations on the moon-day project 06 p0720 A83-19148

Constraint equations from rigid elements including initial strains 07 p0949 A83-21447

A linear programming approach for multivariable feedback control with inequality constraints 09 p1328 A83-24720

Projected Newton methods for optimization problems with wimple constraints 09 p1331 A83-24767

Comparison of directional and derivative constraints for beamformers subject to multiple linear constraints 11 p1554 A83-27907

Novel concepts for constraint treatments and approximations in efficient structural synthesis [AIAA 83-0940] 12 p1739 A83-29770

Constraints on the invariant functions of axisymmetric turbulence 16 p2351 A83-36083

Design of minimum-mass panels with allowance for constraints on fatigue life, and residual and static strength 17 p2520 A83-37536

Constraints on evolution of earth's mantle from rare gas systematics 17 p2545 A83-38598

High-order necessary optimality conditions for control problems with terminal constraints 19 p2888 A83-40673

Mathematical modelling of heat transfer processes with constraints 20 p2974 A83-42693

CONSTRICTIONS

Computation of turbulent flow through constrictions 21 p3130 A83-44588

CONSTRUCTION

Construction of a 1-3 micron infrared photometer and its test observations 01 p0049 A83-10233

CONSTRUCTION IN SPACE

U ORBITAL ASSEMBLY

CONSTRUCTION MATERIALS

The combined action of physical factors of gases released from polymers used on ships 01 p0081 A83-11398

Figures of merit for dispersive birefringent filter materials 02 p0236 A83-12303

Matching materials and structures in vertical axis wind turbines 07 p0953 A83-20434

Use of the phase method for evaluating defects in the form of developing microcracks 07 p0944 A83-21414

Experimental studies of stable crack growth 08 p1060 A83-21705

Creep and fracture of engineering materials and structures; Proceedings of the International Conference, University College of Swansea, Swansea, Wales, March 24-27, 1981 09 p1279 A83-24051

Development of a new family of improved infrared /IR/ dome ceramics 09 p1239 A83-24952

Application of fracture mechanics for selection of metallic structural materials --- Book 10 p1392 A83-25317

Equipment for the electrochemical machining of specimens of structural materials 13 p1859 A83-31222

Mechanical tests of structural alloys at cryogenic temperatures 14 p1997 A83-33012

Silicon carbide (SiSiC), a new material for apparatus construction 16 p2336 A83-36000

A model of a material with internal friction 17 p2521 A83-37542

The development of structural materials on the basis of new processes 20 p2956 A83-43497

The components of gas turbines: Materials and strength (2nd revised and enlarged edition) --- Russian book 21 p3147 A83-43912

CONSUMABLES (SPACECRAFT)

NT PROPELLANT STORAGE

NT SOAPS

NT SPACE LOGISTICS

NT WORKING FLUIDS

CONSUMABLES (SPACECREW SUPPLIES)

NT SOAPS

CONSUMPTION

NT ENERGY CONSUMPTION

NT FUEL CONSUMPTION

NT OXYGEN CONSUMPTION

NT WATER CONSUMPTION

CONTACT LENSES

Measurement of ocular counterrolling /OCR/ by polarized light 08 p1151 A83-22568

CONTACT POTENTIALS

Solution of gamma-prime phase in nickel heat-resistant aging alloys 13 p1823 A83-31214

High-precision test of the universality of the Josephson voltage-frequency relation 19 p2837 A83-40959

Fermi levels in electrolytes and the absolute scale of redox potentials 20 p2951 A83-43608

CONTACT RESISTANCE

Can standards be set for reliable measurements of thermal contact conductance [AIAA PAPER 83-0533] 05 p0621 A83-16771

Evaluation of a process for achieving low between-metal contact resistance in plasma etched polyimide vias --- for integrated circuits 07 p0917 A83-19898

The characteristics of Au-Ge-based ohmic contacts to n-GaAs including the effects of aging 14 p2006 A83-32671

Electrical characteristics of amorphous iron-tungsten contacts on silicon 15 p2238 A83-33851

Laser annealing of submicrometer NMOS test structures and devices 15 p2152 A83-34696

A light load model combining surface roughness and waviness to predict thermal contact conductance [AIAA PAPER 83-1435] 15 p2143 A83-34905

Ohmic contacts for laser diodes 16 p2346 A83-35988

Contact resistivity of TiN on p(-)-Si and n(+)-Si --- measurement for metal contact diffusion barrier in solar cell 20 p2965 A83-42354

Prediction of interfacial filler thickness for minimum thermal contact resistance 20 p2987 A83-43450

CONTACTS (ELECTRIC)

U ELECTRIC CONTACTS

CONTAINERLESS MELTS

Crystallization of copper under zero-g conditions 09 p1229 A83-23520

The effect of electromagnetic forces on the hydrodynamics of a melt in the process of high-frequency floating zone melting 12 p1782 A83-29269

On the solidification of melts in weightlessness 20 p2939 A83-42892

Atomic fluorescence study of high temperature aerodynamic levitation 20 p2939 A83-43256

Crystal nucleation in Pd-Si alloys --- in containerless environment 20 p2939 A83-43260

Solidification studies of Nb-Ge alloys at large degrees of supercooling 20 p2940 A83-43261

Application of microgravity and containerless environments to the investigation of fusion target fabrication technology 20 p2962 A83-43262

- Development of electrostatic levitator at JPL
20 p2940 A83-43264
- Gels and gel-derived glasses in the Na₂O-B₂O₃-SiO₂ system --- containerless melting in space
20 p2941 A83-43288
- Solidification of undercooled monotectic alloys
20 p2942 A83-43300

CONTAINMENT

- On the design of containment shields
02 p0195 A83-12766
- The performance of containment facilities
06 p0800 A83-19613
- Recent advances in composite flywheel containment design technology
11 p1589 A83-27302

CONTAMINANTS

- NT RADIOACTIVE CONTAMINANTS
- NT TRACE CONTAMINANTS
- A statistical plume model with first-order decay
05 p0659 A83-17438
- Effects of fine airborne particles on equipment reliability
13 p1863 A83-31500
- Isolation and molecular identification of ultramicro contaminants by Fourier transform infrared spectroscopy
13 p1848 A83-31522
- Particulate fallout predictions for clean rooms
13 p1865 A83-31523
- Kriometric determination of purity of materials forming solid solutions with their contaminants
[AIAA PAPER 83-1473] 14 p1985 A83-32727
- Potential for cross-contamination for payloads in the STS bay
[AIAA PAPER 83-1562] 14 p1981 A83-32779
- The effect of contamination of the probe surface and coating on the accuracy of the measurement of electron temperature using the Langmuir probe --- in satellite and rocket experiments
15 p2128 A83-34420
- Emissions variability and traversing on production RB211 engines
[ASME PAPER 83-GT-141] 23 p3409 A83-47966
- Monitoring the contamination of jet fuels by corrosion inhibitors
23 p3440 A83-48544
- Internal and external sulphidation of Ni77Cr16Fe7 alloys
24 p3565 A83-49510

CONTAMINATION

- NT FUEL CONTAMINATION
- NT SPACECRAFT CONTAMINATION
- The effect of fluoride contamination on the durability of PAA surfaces --- preparation of aluminum alloy surfaces for adhesive bonding by phosphoric acid anodize solution
09 p1230 A83-23625
- Distribution of lead and thallium in the matrix of the Allende meteorite and the extent of terrestrial lead contamination in chondrites
12 p1797 A83-29174
- A tumble test for determining the level of detachable particles associated with clean room garments and clean room wipers
13 p1865 A83-31524
- Analysis of contamination degradation of thermal control surfaces on operational satellites
[AIAA PAPER 83-1449] 15 p2127 A83-34908
- Abatement of gaseous and particulate contamination in a space instrument
[AIAA PAPER 83-1567] 16 p2318 A83-36407
- Determination of the sensitivity of U.S. Air Force aircraft hydraulic system components to particulate contamination
16 p2362 A83-36910
- U.S. planetary protection program - Implementation highlights
19 p2807 A83-40827

CONTENT**NT BONE MINERAL CONTENT****CONTINENTAL DRIFT**

- The expanding and pulsating earth
01 p0071 A83-10378
- Continental rifting and the implications for plate tectonic reconstructions
07 p0961 A83-20228
- Landst and the southward drift of Madagascar
09 p1287 A83-24562
- The Newfoundland basin - Ocean-continent boundary and Mesozoic seafloor spreading history
12 p1752 A83-29173
- Fragmentation and assembly of the continents, mid-carboniferous to present
12 p1753 A83-29247
- Transition zones between the continents and the oceans --- Russian book
15 p2200 A83-34375
- Palaeocontinental configurations and geoid anomalies
16 p2376 A83-35997
- Acquisition of long wavelength magnetic anomalies pre-dates continental drift
21 p3171 A83-44362
- Back arc thrusting in the eastern Sunda arc, Indonesia - A consequence of arc-continent collision
22 p3322 A83-45742
- Analytic comparison of apparent polar wander paths
24 p3608 A83-50175

CONTINENTAL SHELVES

- Current and density structure in shelf waters due to fresh water discharge - A numerical study
08 p1089 A83-23202

- Multimode Rayleigh wave attenuation and Q beta in the crust of the Barents Shelf --- shear wave internal friction
12 p1757 A83-29961
- Low-frequency current and temperature variability from Gulf Stream frontal eddies and atmospheric forcing along the southeast U.S. outer continental shelf
14 p2059 A83-33076
- Climatology of the southeastern United States continental shelf waters
14 p2061 A83-33088
- Satellite and ship studies of coccolithophore production along a continental shelf edge
20 p3032 A83-42171
- Peru coastal currents during El Nino - 1976 and 1982
22 p3344 A83-46802

CONTINENTS

- NT AFRICA
- NT AUSTRALIA
- NT EUROPE
- NT NORTH AMERICA
- NT SOUTH AMERICA
- Convective thinning of the lithosphere - A mechanism for the initiation of continental rifting
02 p0212 A83-12871
- P/n/ velocity and cooling of the continental lithosphere --- upper mantle compression waves in North America
07 p0961 A83-20227
- Numerical modeling of intraplate deformation - Simple mechanical models of continental collision
07 p0961 A83-20230
- Continental lithospheric thickness and deglaciation induced true polar wander
09 p1305 A83-24337
- Fragmentation and assembly of the continents, mid-carboniferous to present
12 p1753 A83-29247
- Evolution of the oceans and continents
18 p2715 A83-39495
- The continental crust
20 p3020 A83-42819
- Simple energy balance model resolving the seasons and the continents - Application to the astronomical theory of the ice ages
20 p3021 A83-42841
- Deep crustal structure - Implications for continental evolution
22 p3323 A83-45779
- Radiogenic isotopes and crustal evolution
22 p3323 A83-45781
- Geosphere interactions and earth chemistry
22 p3323 A83-45784

CONTINUITY (MATHEMATICS)

- Uniqueness and continuous data dependence in dynamical problems of nonlinear thermoelasticity
06 p0775 A83-18806
- High level continuity for coordinate generation with precise controls
12 p1772 A83-29632
- CONTINUITY EQUATION**
- An approximate analytical solution for self-similar flow behind a radiation driven shockwave
20 p2987 A83-43658

CONTINUOUS RADIATION

- NT MODULATED CONTINUOUS RADIATION
- Theoretical surface brightness distributions and continuum polarization of rapidly rotating B stars
01 p0123 A83-10355
- Terrestrial continuum radiation observations with GEOS-1 and ISEE-1
03 p0357 A83-13543
- 1 millimeter continuum observations of quasars
03 p0422 A83-14182
- Observations of Jupiter's distant magnetotail and wake
[AD-A123812] 05 p0704 A83-17384
- Generation of nonthermal continuum radiation in the magnetosphere
05 p0661 A83-17395
- High frequency radio continuum observations of bright spiral galaxies
06 p0817 A83-18095
- Radio continuum emission - A tracer for star formation
06 p0826 A83-18096
- A high power gyrotron operating in the TE₀₄₁/ mode
06 p0752 A83-18758
- The radio continuum morphology of NGC 4631 at 2.7 and 8.1 GHz
06 p0833 A83-18858
- Improvements of antijam performance of spread spectrum systems
07 p0906 A83-19720
- The mathematical modeling of problems of continuous media with nonequilibrium transfer
07 p0989 A83-20307
- A radio continuum survey of M31 at 4850 MHz I - Observations - List of sources
07 p1008 A83-21220
- Radioastronomy measurement and reduction procedures for the detection of extensive continuum emission
09 p1352 A83-23390
- Anomalous radio continuum features in edge-on spiral galaxies
10 p1516 A83-26748
- Propagation of intense CW-light through a strongly absorbing medium - Self-focusing and spatial ringings
11 p1576 A83-27514
- Multiple-frequency measurements of a flare continuum event
13 p1964 A83-30372
- A radio continuum survey of southern E and SO galaxies at 2.7 GHz and 5.0 GHz
13 p1947 A83-30393

- Rejection of CW interference in QPSK systems using decision-feedback filters
14 p2001 A83-32865
- Secondary peaks in solar microwave outbursts
[AD-A129962] 15 p2281 A83-34305
- An upper limit to the microwave continuum radiation from Comet Austin (1982g)
15 p2248 A83-34650
- Continuum emission from classical nova winds
17 p2606 A83-38236
- Calculation of heating of metals by continuous laser radiation in an oxidizing atmosphere
20 p2996 A83-43780
- Picosecond continuum generation and spectroscopy
21 p3145 A83-44819
- The origin of line-free XUV continuum emission from laser-produced plasmas of the elements Z = 62-74
23 p3511 A83-48586

CONTINUOUS SPECTRA

- The ultraviolet continuous and emission-line spectra of the Herbig-Haro objects HH 2 and HH 1
02 p0256 A83-12125
- Irregularities of the limb of the solar disk in white light
03 p0436 A83-13676
- The visible and ultraviolet continuum from a Herbig-Haro object in the core of M 16 /NGC 6611/
03 p0428 A83-14773
- IUE observations of Markarian 3 and 6 - Reddening and the nonstellar continuum
07 p1019 A83-21109
- The continuous spectrum of supernovae
07 p1026 A83-21254
- The Monte Carlo method for multilevel problems of radiation transfer with allowance for processes in the continuum --- for astronomical models
07 p1027 A83-21279
- Some improvements and complements to the infrared emissivity algorithm including a parameterization of the absorption in the continuum region --- for atmospheric radiation transfer
08 p1143 A83-23015
- H II regions in M33. I - Radio and H-alpha observations of the H II complex NGC595
11 p1669 A83-27679
- Inclusion of discrete-to-continuum coupling in multiphoton excitation and dissociation calculations
11 p1546 A83-28758
- Development of a numerical model of a cosmic radio source with a continuous mission spectrum
13 p1944 A83-30273
- Visible continuum emission and gravity waves
13 p1881 A83-31536
- On the Baldwin effect in optically-selected quasars
13 p1943 A83-31711
- Observations of the interacting galaxy pair NGC 4490/85
13 p1959 A83-31754
- Ultraviolet continuum and H2 fluorescent emission in Herbig-Haro objects 43 and 47
14 p2107 A83-33231
- Spectral evidence of type II shock influence on Razin-cutoff frequency in the decametric type IV continuum
15 p2280 A83-34299
- Zebra pattern flux density observation during the type IV burst on October 12, 1981
15 p2280 A83-34304
- Photometric investigations of the short-period brightness variability in Nova Cygni 1975 (V1500 Cyg) in a continuum
17 p2590 A83-37707
- A determination of the physical conditions of continuous-emission grains --- in solar spectra
17 p2626 A83-37715
- A helium-3 cooled bolometer system for one millimeter continuum observations
17 p2510 A83-37751
- The broad-band X-ray spectrum of Cygnus X-2
17 p2605 A83-37923
- Continuum reddening of Seyfert 1 nuclei
17 p2607 A83-38260
- The variability of the spectrum of Arakelian 120
18 p2757 A83-39590
- Radio observations of compact H II regions
18 p2757 A83-39594
- On the contributions of the Orion reflection nebulosity to the continuous UV spectrum of the Herbig-Haro objects HH 1 and HH 2 and of the C-S Star
19 p2921 A83-41650
- Evidence for a highly polarized continuum in the nucleus of NGC 1068
20 p3069 A83-42469
- Extended near-infrared emission from visual reflection nebulae
20 p3069 A83-42470
- The timescales of variations in continuum and hydrogen lines during stellar flares
23 p3521 A83-47498
- Absolute measurements of the flux in the continuum of galactic Wolf-Rayet stars - Comparison with main sequence OB stars
24 p3663 A83-49849
- CONTINUOUS WAVE LASERS**
- CW-laser annealed solar cells
01 p0068 A83-10638
- Room-temperature CW operation in the visible spectral range of 680-700 nm by AlGaAs double heterojunction lasers
01 p0055 A83-10983
- Multikilowatt electron beams for pumping CW ion lasers
01 p0039 A83-10987

- Dispersion-induced instability in CW laser oscillators
02 p0184 A83-12270
- Optical bistability in nematic films utilizing self-focusing of light
02 p0236 A83-12278
- Continuous-wave garnet ring laser emitting single-mode linearly polarized radiation and intracavity second harmonic generation in LiIO₃
03 p0330 A83-13584
- High-power single-mode AlGaAs laser diodes
03 p0331 A83-13875
- Nozzle design yielding interferometrically flat fluid jets for use in single-mode dye lasers
03 p0332 A83-14164
- Simple arrangement for spatially scanning gain measurements in CW lasers
03 p0332 A83-14165
- Continuous wave high-power, high-temperature semiconductor laser phase-locked arrays
03 p0333 A83-14932
- High-pressure tunable CW waveguide CO₂ lasers
04 p0483 A83-15255
- Thermal self-defocusing of a CW CO₂-laser beam during the interaction with water aerosol
04 p0484 A83-15734
- Effects of cavity length on 20 micron stripe laser waveguiding
04 p0486 A83-16221
- Continuous-wave reaction-product chemical lasers /review/
05 p0648 A83-17038
- Analysis of the energetics of a chemical oxygen-iodine laser
05 p0648 A83-17047
- Technological CW CO₂ laser with a nonself-sustained discharge
05 p0649 A83-17067
- Quasi-CW lasing of a Ne-Xe-HCl mixture excited by an electric discharge
05 p0650 A83-17083
- High-temperature selective gasdynamic continuous CO₂ laser
06 p0765 A83-18450
- High-performance single-mode AlGaAs Gaussian channel substrate planar laser diodes
06 p0765 A83-18566
- Small signal gain measurements for the 00/0/1-02/0/0 and 00/0/1-10/0/0 bands in a flowing-gas CW CO₂ laser
06 p0766 A83-18945
- Single longitudinal mode operation of high power multiple-stripe injection lasers
06 p0767 A83-19256
- Influence of translational and rotational relaxation on the specific energy characteristics of a CW chemical HF laser
07 p0933 A83-20103
- Rapid-flow combined-action industrial CO₂ laser
07 p0933 A83-20104
- New heartbeat phenomenon, and the concept of 2-D optical turbulence
07 p0935 A83-20160
- Studies of a glow discharge electron beam
07 p0997 A83-20733
- Generation of continuous-wave 194-nm radiation by sum-frequency mixing in an external ring cavity
07 p0936 A83-20789
- Influence of transient absorber gratings on the pulse parameters of passively mode-locked CW dye ring lasers
07 p0937 A83-21362
- CW recombination laser action in a cadmium vapor arc
07 p0938 A83-21370
- Cull laser with a helical hollow cathode discharge
08 p1106 A83-21978
- Medium induced phase aberrations in continuous wave /CW/ hydrogen fluoride chemical lasers
08 p1109 A83-22460
- Mode-medium interactions --- high power CO₂ laser output instability
08 p1109 A83-22461
- Rapid extended range tuning of single-mode ring dye lasers
08 p1110 A83-22613
- Continuous-wave HF R-branch laser demonstration
08 p1110 A83-22637
- High optical power CW operation in visible spectral range by window V-channeled substrate inner stripe lasers
08 p1110 A83-22753
- A rangefinder for coherent detection with a CW CO₂ laser - Study and design
09 p1272 A83-24643
- High power operation of a CW 28-micron water vapor laser
10 p1425 A83-25428
- Operating conditions of a CW water-vapour laser at 28, 47, 78, 79 and 119 microns
10 p1425 A83-25454
- Continuous 300-K laser operation of strained superlattices
10 p1426 A83-25977
- Statistical analysis of aging-induced degradation /or lifetime/ variations in /Al, Ga/As/GaAs double-heterostructure lasers
10 p1429 A83-26028
- Rotational nonequilibrium influences in CW HF/DF chemical lasers
10 p1429 A83-26167
- Shock/Ludwig-tube driven HF laser
10 p1429 A83-26169
- Fluid-dynamical aspects of laser-metal interaction
10 p1416 A83-26172
- CW electro-optical characteristics of graded-index waveguide separate-confinement heterostructure lasers with proton-delineated stripe
10 p1430 A83-26202
- Photodissociation CW laser using condensation and evaporation for a closed cycle
10 p1430 A83-26235
- Use of unstable resonators in CW chemical lasers with radial flow of a gas mixture
10 p1431 A83-26652
- Numerical modeling of a chemical oxygen-iodine laser
10 p1433 A83-26676
- Electric-discharge CW industrial CO₂ laser
10 p1433 A83-26687
- Thermal action of laser radiation on imidization
10 p1392 A83-26690
- Continuous-wave YAG:Nd/3+ /laser with mode locking and intracavity frequency doubling
10 p1434 A83-26695
- Thermal distortions of focused laser beams in the atmosphere
10 p1434 A83-26782
- Progress in the development of color centers for stable CW tunable laser operation
11 p1578 A83-27542
- Spectral diversity crystalline fluoride lasers
11 p1581 A83-27588
- Pulse formation and amplification in an absorbing medium by optical phase switching
11 p1582 A83-27600
- Optical multistability in silicon observed with a CW laser at 1.06 microns
11 p1657 A83-27849
- CW operation of 1.5 micron GaInAsP/InP buried heterostructure laser with a reactive ion-etched facet
11 p1585 A83-28606
- CW operation of an injection ring laser
11 p1585 A83-28673
- Real time monitoring of CW mode-locked dye laser pulses using a rapid-scanning autocorrelator
12 p1729 A83-29194
- Runaway self-absorption in multikilowatt CO₂ lasers
13 p1850 A83-30328
- Phase-locked (GaAl)As laser emitting 1.5 W CW per mirror
13 p1850 A83-30330
- Effects of optical irregularities in the active medium on angular divergence of a beam in a CW supersonic DF-CO₂ chemical laser
13 p1851 A83-30819
- Two-cavity klystron uses single-cavity tuning
13 p1835 A83-30913
- Continuous-wave laser radiation simulation
13 p1810 A83-31193
- Gain anisotropy in low-pressure chemical lasers
13 p1857 A83-31456
- Radio-frequency-excited carbon dioxide metal waveguide laser
13 p1857 A83-31457
- Random modulation CW lidar
13 p1857 A83-31464
- Investigation of CW operation of a GaAs laser pumped by an electron beam
14 p2022 A83-31906
- Tunable sealed-off CW CO laser at room temperature
14 p2023 A83-31950
- Influences of thermal effects on high power CW outputs of b-axis Nd:YAP lasers
14 p2024 A83-32596
- Dynamics of the colliding pulse mode locking in CW dye ring lasers
14 p2026 A83-33406
- Compression mechanism of subpicosecond pulses by malachite green dye in passively mode-locked rhodamine 6G/DODCI CW dye lasers
14 p2026 A83-33407
- Dynamics of the CO₂ upper laser level as measured with a tunable diode laser
14 p2027 A83-33435
- Laser welding of a titanium alloy
15 p2135 A83-33643
- Continuous-wave industrial electron-beam-controlled CO laser of 10 kW output power
15 p2168 A83-33976
- Modeling study of a CW HF optical resonance transfer laser model
17 p2513 A83-37197
- [AIAA PAPER 83-1700] Performance characteristics of a transverse-flow, oxygen-iodine chemical laser in a low gas-flow velocity
17 p2513 A83-37609
- A new stabilization system for optically pumped CW far infrared lasers
17 p2514 A83-37752
- Optically pumped CW semiconductor ring laser
17 p2514 A83-38044
- 1-W CW Zn ion laser
17 p2514 A83-38045
- Breathing, spiking and chaos in a laser with injected signal
17 p2515 A83-38975
- Calculation of optimal lasing regimes for CW supersonic electroionization CO lasers
18 p2692 A83-39516
- High-efficiency and high-power AlGaAs/GaAs laser
19 p2851 A83-40935
- A compact CW HCN gas laser with RF-excited discharge
19 p2852 A83-40946
- Multi-mode CW dye laser
19 p2853 A83-41187
- Experimental study of launched ion-acoustic waves in a plasma using continuous wave CO₂ laser scattering
19 p2902 A83-41309
- Increasing the transillumination capacity of a laser beam in the atmosphere
19 p2854 A83-41768
- Lithium niobate laser with frequency-degenerate pumping
20 p2993 A83-42290
- Efficient backward and forward pumping CW Raman amplification for InGaAsP laser light in silica fibres
20 p2993 A83-42486
- High pressure measurements on photopumped low threshold Al(x)Ga(1-x)As quantum well lasers
20 p2994 A83-42595
- CW laser-annealing behavior of Se(+)-implanted InP investigated by ellipsometry
20 p3055 A83-43603
- Investigation of the power stability of a CW carbon monoxide laser
20 p2997 A83-43793
- Continuous wave laser damage on optical components
21 p3142 A83-43865
- Broad band electro-optic tuning of a CW dye laser
21 p3143 A83-44188
- A 28 micron water-vapor laser interferometer for plasma diagnostics
21 p3144 A83-44381
- Distortions of a CW light beam propagating through gas Self-lensing and spatial ringings
21 p3144 A83-44804
- Operation and performance of the CW visible atomic mercury laser
21 p3145 A83-44813
- Continuous wave (CW) Doppler free two-photon frequency modulated (FM) spectroscopy
21 p3139 A83-44816
- Broadly tunable mode-locked HgCdTe lasers
21 p3146 A83-45478
- Associative ionization in collisions between two Na(3P) atoms
22 p3361 A83-45926
- Nonlinear optics with a diode-laser light source
22 p3356 A83-45963
- Storage and time reversal of light pulses using photon echoes
22 p3356 A83-45965
- Continuous laser amplification in a monomode fiber longitudinally pumped by evanescent field coupling
22 p3295 A83-45971
- Continuous-wave HF optical resonance transfer laser model
22 p3296 A83-46087
- Forward CW CO₂-laser scattering on a high density plasma column
22 p3362 A83-46267
- Tunable diode lasers and laser systems for the 3 to 30 microns infrared spectral region
22 p3297 A83-46638
- Synchronously mode-locked continuous wave dye lasers - Recent advances and applications
22 p3297 A83-46664
- Comparisons of traveling-wave and standing-wave operations of mode-locked continuous-wave dye lasers
22 p3297 A83-46666
- Continuous-wave mode locked Nd:YAG laser - A picosecond pump source for the future
22 p3298 A83-46669
- Reliability of InGaAsP/InP buried heterostructure 1.3 micron lasers
22 p3301 A83-46824
- Vernier fringe-counting device for laser wavelength measurements
23 p3454 A83-47645
- A 1.5 W CW optically pumped 12.08 microns NH₃ laser
23 p3462 A83-48317
- Generation of continuous-wave 243-nm radiation by sum-frequency mixing
23 p3462 A83-48321
- Bistable operation of a dual-wavelength synchronously mode-locked CW dye laser
23 p3463 A83-48705
- Generation of tunable single-frequency continuous-wave coherent vacuum-ultraviolet radiation
24 p3587 A83-48852
- CONTINUOUS WAVE RADAR**
The effect of reference's phase on radio-frequency holographic imaging
03 p0328 A83-14026
- Dual-polarization radar observations of Mars - Tharsis and environs
05 p0704 A83-16968
- Random modulation CW lidar
13 p1857 A83-31464
- CONTINUOUS WAVES**
U CONTINUOUS RADIATION
CONTINUUM FLOW
A continuous-flow microcalorimeter
11 p1576 A83-28800
- The freezing of the translational degrees of freedom of molecules in multiphase flows
13 p1933 A83-30672
- CONTINUUM MECHANICS**
The relationship between the solutions to mixed dynamic problems for a continuous elastic medium and a lattice
02 p0189 A83-11655
- A continuum theory of nonlinear thermodynamics
02 p0244 A83-12372
- An experimental and analytical study of the dynamic response of a linkage fabricated from a unidirectional fiber-reinforced composite laminate
02 p0187 A83-12775
- Basic properties of elastic-plastic boundaries in stress wave propagation in a bar
03 p0341 A83-14484
- Thermomechanical response of solids at high strains - natural approach
04 p0494 A83-15002
- A bimodulus elasticity theory --- Russian book
04 p0499 A83-15833
- On a thermodynamic theory of fiber-reinforced thermoelastic materials with thermo-kinematic constraints
04 p0455 A83-16098

- A mathematical theory of wave propagation in media with memory --- Russian book 05 p0654 A83-17130
- Adhesion of solids 06 p0805 A83-18144
- Three-dimensional constitutive relations and ductile fracture --- Book 06 p0774 A83-18477
- On constitutive relations in thermoplasticity 06 p0774 A83-18488
- On one-dimensional acceleration waves in composite materials modeled as interpenetrating solid continua 06 p0776 A83-19000
- Solution of bifurcation problems and limit load problems in certain nonlinear boundary-value problems of continuum mechanics 06 p0777 A83-19322
- Some theoretical considerations and experimental results concerning elastic-plastic stress-strain relations 06 p0778 A83-19323
- Net-stress analysis in creep mechanics 06 p0778 A83-19324
- On method of successive approximations in a class of problems of the general theory of plasticity 07 p0945 A83-20142
- Some questions of the theory of modular analysis and parallel programming for problems of mathematical physics and continuum mechanics 07 p0983 A83-20313
- Balance laws of continuum physics 07 p0989 A83-20643
- Analytical and experimental fracture mechanics --- Book 07 p0948 A83-21098
- A thermodynamic description of inelastic fracture 08 p1118 A83-21775
- Resonantly interacting waves 08 p1161 A83-22741
- A theory of viscoelastic composites modeled as interpenetrating solid continua with memory 09 p1280 A83-24136
- Processes in periodic media that cannot be described in terms of average characteristics 09 p1338 A83-24216
- New physical trends in experimental mechanics --- Book 09 p1243 A83-25096
- The modular structure of algorithms and programs in problems involving continuous medium mechanics and computer structure 09 p1326 A83-25239
- Aspects of the theory of dislocations 10 p1437 A83-25307
- On a micromechanical fracture model for cracked reinforced composites 10 p1438 A83-25470
- Thermodynamic inequalities in continuum mechanics 11 p1665 A83-27994
- Post-instability in continuous systems. I - Failure of differentiability of solutions in continuum mechanics 11 p1649 A83-28089
- Damage tensors in continuum mechanics 11 p1595 A83-28432
- Approximate methods for the calculation of Cauchy integrals of a special form --- Russian book 12 p1770 A83-28816
- Continuum theory of dilatant transformation toughening in ceramics 12 p1716 A83-29025
- An equivalent continuum representation of structures composed of repeated elements [AIAA 83-1007] 12 p1740 A83-29794
- Residual stress and stress relaxation; Proceedings of the Twenty-eighth Sagamore Army Materials Research Conference, Lake Placid, NY, July 13-17, 1981 12 p1746 A83-29901
- System identification of large flexible structures by using simple continuum models 13 p1812 A83-29995
- Notion of continuum damage mechanics and its application to anisotropic creep damage theory 13 p1866 A83-30241
- The concept of force and moment as a computational quantity in continuum mechanics 13 p1915 A83-31799
- A calculation of the asymptotic behavior of 'intensity coefficients' in approaching corner and conical points 14 p2077 A83-31895
- Statically permissible stress fields in incompressible media 14 p2030 A83-32353
- Structural parameters in a continuum model of ductile fracture 14 p1992 A83-32382
- Dynamics of gyro-elastic continua [AIAA PAPER 83-0826] 14 p2032 A83-32795
- A variational approach to finite elasticity 15 p2177 A83-34333
- On physical and material conservation laws 15 p2177 A83-34335
- A continuum mechanical approach to the ultrasonic relaxation of ferroelectric materials 15 p2238 A83-34348
- Digitization of a video signal and stress analyses using IR thermography 15 p2178 A83-34401
- The solution of the equations of the applied theory of elasticity by the method of variational iterations 15 p2178 A83-34433

- Dislocation shielding of a crack in a quasi-continuum approximation 15 p2179 A83-34479
- The relaxation of submicrosecond pressure pulses in a solid body 16 p2364 A83-35543
- Dynamic analysis of geometrically nonlinear truss structures 16 p2369 A83-36556
- Post instability in continuous systems. II - Post-instability models of continua 16 p2408 A83-36984
- On the acoustoelastic effect 17 p2576 A83-37728
- Dislocation kinetics and the formation of deformation bands 17 p2522 A83-38383
- Motion of the crack under constant loading and at high constant temperature 17 p2523 A83-38389
- Solid mechanics applications of boundary fitted coordinate systems 17 p2525 A83-38786
- A linear model of ductile plastic damage 19 p2858 A83-41321
- Continuum models of discrete systems 4; Proceedings of the Fourth International Conference, Stockholm, Sweden, June 29-July 3, 1981 19 p2896 A83-41469
- Elastic media with microstructure. I - One-dimensional models 19 p2897 A83-41875
- A differential scheme for multiphase composites. I - Overall elastic moduli. II - Thermal expansion coefficients and conductivities 20 p3002 A83-42800
- The effect of coupling between the heat equation and the equations of motion in case of shock-like temperature stresses 20 p3005 A83-42985
- On inverse problem in elasticity and plasticity 20 p3006 A83-42994
- A dissipation postulate for discrete and continuous plastic systems 21 p3155 A83-44849
- Large increments technique in the elastic-plastic analysis 21 p3159 A83-44932
- Physical equations of thermoviscoplasticity --- Russian book 21 p3160 A83-45007
- Theory of spinors and its application in physics and mechanics --- Russian book 21 p3200 A83-45031
- Some recent advances in boundary element methods 22 p3352 A83-46419
- Equivalent linearization for continuous dynamical systems [ASME PAPER 83-APM-30] 23 p3503 A83-48241
- On dynamics and stability of continuous systems subjected to a distributed moving load 23 p3473 A83-48496
- The effective moduli of short-fiber composites 23 p3474 A83-48697
- Anisotropic creep damage in the framework of continuum damage mechanics [ONERA, TP NO. 1983-90] 24 p3593 A83-49409
- CONTINUUMS**
- The electrodynamics of continuous media (2nd revised and enlarged edition) --- Russian book 12 p1774 A83-28821
- CONTOUR SENSORS**
- The GLGS image representation and its application to preliminary segmentation and pre-attentive visual search --- Gray Level Geographic Structure 01 p0098 A83-11431
- The digital edge --- in images 01 p0099 A83-11436
- 'Bilevel' processing of 'multilevel' pictures 01 p0099 A83-11439
- A simple contour matching algorithm 01 p0100 A83-11471
- Interpretation of geometric structure from image boundaries 02 p0182 A83-12891
- Projection moire for remote contour analysis 09 p1268 A83-24098
- Detection of edges using range information 12 p1769 A83-28950
- Automated laser speckle interferometry displacement contour analyzer 12 p1730 A83-29587
- The identification of orientation at the threshold of line detectors 13 p1900 A83-30429
- The interaction between detectors of line orientations 13 p1900 A83-30430
- Spatial adaptation and line detectors 13 p1900 A83-30431
- Optical-correlation quasi-interferometry - A new viewpoint on spatial frequency filtering 24 p3582 A83-49012
- Generation of radar echo images from a contour map 24 p3619 A83-49199

CONTOURS

- Microscopic contour changes of tribological surfaces by chemical and mechanical action [ASLE PREPRINT 82-LC-3B-3] 03 p0334 A83-13237
- A turbulence model for three dimensional turbulent shear flows over curved rotating bodies [AIAA PAPER 83-0559] 05 p0637 A83-16787
- One form of apodization of telescopes 07 p1009 A83-21275

- The trigonometric contour series method applied to clamped plates with arbitrary contours 08 p1115 A83-21635
- A method of calculating the surface contour that accurately corrects the spherical aberration on the axis in a centered optical system 17 p2590 A83-37692
- Object recognition using three-dimensional information 20 p3039 A83-42644
- 3-D shape from contour and selective conformation 21 p3137 A83-44257
- The roles of contour and luminance distribution in determining perceived centers within shapes 22 p3349 A83-45956
- Stimulus determinants of brightness and distinctness of subjective contours 22 p3349 A83-46756
- Mixed boundary value problems of the contouring of supersonic nozzles and channels 23 p3400 A83-48663

CONTRACT MANAGEMENT

- The significant elements of the reliability and maintainability programs for the modernized Cobra helicopter weapons/weapons control systems 13 p1863 A83-31499
- Durability and damage tolerance control plans for U.S. Air Force aircraft 19 p2797 A83-41045

CONTRACTION

- Static and dynamic components of the heterometric regulation of myocardial contractions of the auricle and ventricle 04 p0520 A83-15893
- The problem of the contractility of the myocardium 14 p2063 A83-32098

CONTRACTORS

- Prime contractor/subcontractor product liability exposure under government contracts 18 p2753 A83-39693

CONTRAILS

- Cockpit visibility and contrail detection 07 p0982 A83-20623

CONTRAST

- NT IMAGE CONTRAST
- NT PHASE CONTRAST
- Acoustooptical device with extremely high contrast ratio 10 p1424 A83-26872

CONTROL

- System identification - On the variety and coherence in parameter- and other estimation methods --- Thesis 13 p1913 A83-30146
- Annual Allerton Conference on Communication, Control, and Computing, 19th, Monticello, IL, September 30-October 2, 1981, Proceedings 15 p2220 A83-35101
- Determination of physically achievable accelerations in the problem of the spatial convergence of a material point --- for ergatic control system synthesis 20 p3035 A83-43502

CONTROL BOARDS

- Ergonomic evaluation of two-hand control location 02 p0225 A83-12088
- Ergonomic aspects of aircraft keyboard design - The effects of gloves and sensory feedback on keying performance 04 p0526 A83-15900
- Integrated control/display unit vs. dedicated control heads for radio tuning in a KC-135 flight simulator 10 p1459 A83-26318
- Humanscale 4/5/6 --- Book on human factors engineering information 13 p1906 A83-30155
- New console design - An example --- for telescope control 13 p1938 A83-31004
- CONTROL CONFIGURED VEHICLES**
- Experiment control in problems of minimax estimation --- for aircraft longitudinal control 01 p0094 A83-10455
- F-104 CCV research flight test program 07 p0867 A83-20074
- Design and implementation of an active load alleviation system, taking into account the example of a modern transport aircraft [DGLR PAPER 82-045] 09 p1209 A83-24170
- Solution of the fundamental control problem /FCP/ --- for aircraft 12 p1704 A83-29291
- Design of the flutter suppression system for DAST ARW-1R - A status report [AIAA 83-0990] 12 p1702 A83-29868
- Active suppression of aeroelastic instabilities on a forward swept wing [AIAA 83-0991] 12 p1704 A83-29869
- Certain aspects of the optimum design of hydrodynamic lifting complexes 14 p1972 A83-33002
- Equations of the necessary extremum condition for a class of incorrect extreme-value problems --- for optimization of aerodynamic configurations 14 p1972 A83-33011
- A comparison of minimizing strategies for maximum likelihood identification --- stability and control derivatives of wide body aircraft 17 p2565 A83-37085

- Control configured vehicle as a new generation aircraft 19 p2801 A83-40884
- Rigid-body structural mode coupling on a forward swept wing aircraft 19 p2797 A83-41046
- Aeroelastic interactions with flight control (A survey paper) 19 p2803 A83-41700
- [AIAA PAPER 83-2219] 19 p2803 A83-41700
- Vectoring exhaust systems for STOL tactical aircraft [ASME PAPER 83-GT-212] 23 p3410 A83-48013
- STOL fighter technology program [ASME PAPER 83-GT-243] 23 p3403 A83-48033
- Effect of aircraft configuration and control integration on surface actuation [AIAA PAPER 83-2487] 23 p3404 A83-48347
- Aerodynamics propulsion and longitudinal control requirements for a tilt-nacelle V/STOL with control vanes submerged in the nacelle slipstream [AIAA PAPER 83-2513] 23 p3404 A83-48357

CONTROL DEVICES**U. CONTROL EQUIPMENT****CONTROL EQUIPMENT**

- NT CONTROL STICKS
- NT CRYOSTATS
- NT PRESSURE REGULATORS
- NT TELEOPERATORS
- NT THERMOSTATS
- Attempt to determine the power demand of a helicopter control system on the basis of flight tests 01 p0012 A83-10439
- Phase-locked-loop control systems using pulse frequency modulation 01 p0095 A83-10958
- Evaluating cockpit components with hand displacement time scores 01 p0086 A83-11189
- An operational software simulator for passive ECM processing 01 p0093 A83-11250
- A microprocessor-based fault-tolerant computer system 02 p0227 A83-11907
- Assembling, setting up, and tuning the instruments of automatic control systems --- Russian book 02 p0230 A83-11972
- Device technology for control systems and problems of its reliability --- Russian book 02 p0161 A83-12196
- An aggregate complex of fluidic integrated modules 02 p0171 A83-12200
- Synthesis of control systems using coordinate-parametric and parametric feedback 03 p0386 A83-13591
- Investigation of the nonlinear control signal amplification in the case of a continuous tracking problem --- German book 03 p0384 A83-14112
- Aircraft electrical equipment --- Russian book 05 p0597 A83-17125
- A program pack for constructing a dynamic model for use in the hybrid control system of a manipulator robot 08 p1154 A83-22179
- Robust computer-aided control systems design for nonlinear plants 08 p1159 A83-23173
- Control and communication technology in laser systems; Proceedings of the Twenty-fifth Annual International Technical Symposium, San Diego, CA, August 25, 26, 1981 09 p1214 A83-23576
- An end effector for robotic drilling 09 p1273 A83-23639
- Abstract and structural theory of relay devices --- Russian book 09 p1327 A83-24243
- Control - Demands mushroom as station grows 09 p1216 A83-24355
- Generic faults and architecture design considerations in flight-critical systems 09 p1203 A83-24426
- Illustration of the applicability of computer aided design packages 09 p1243 A83-24719
- Regulation of a system with variable structure --- for boilers of solar powered central receivers 09 p1293 A83-24761
- Equipment for monitoring the electromagnetic-compatibility parameters of scientific instruments in spacecraft 10 p1386 A83-25330
- Electronic devices in automatic systems --- Russian book on flight vehicle control 10 p1408 A83-25624
- Evolutionary spacecraft control 10 p1384 A83-26580
- Computer control of the Infra-Red Astronomical Satellite /IRAS/ 10 p1384 A83-26583
- Control and design aspects of magnetically suspended vehicles 10 p1491 A83-26605
- CONEX gyroscope 11 p1575 A83-28782
- The vibro-mass gyroscope 12 p1728 A83-28844
- Synthesis of control systems with quasi-continuous generation of the control signal 13 p1910 A83-30077
- Thermal control subsystem for free flying satellites [SAE PAPER 820844] 13 p1812 A83-30936
- A novel feedforward compensation canceling input filter-regulator interaction 14 p2007 A83-33133

- Mathematical methods for the optimization of automatic-control-system devices and algorithms --- Russian book 15 p2220 A83-34175
- Method for calculating the orientation angle of the workpiece for the control systems of adaptive industrial robots 15 p2143 A83-35265
- System design approaches to integrated controls 17 p2460 A83-37103
- TALIS - A proposed system for taxiway control --- Taxiing Aircraft Location and Identification System 17 p2462 A83-38934
- Conventional controller design for industrial robots - A tutorial 19 p2824 A83-41295
- Restructurable controls for aircraft [AIAA PAPER 83-2255] 19 p2804 A83-41728
- Reliability considerations in the placement of control system components [AIAA PAPER 83-2260] 19 p2816 A83-41730
- Control system of TT-500A sounding rocket for materials processing in space 21 p3103 A83-45599
- Electronic control of aircraft turbine engine 21 p3093 A83-45600
- Tradeoff between laser diodes and light-emitting diodes (LEDs) for the common weapon control system 22 p3278 A83-46616
- The use of production hardware for the development of control laws --- LSI for engine control [ASME PAPER 83-GT-6] 23 p3406 A83-47879
- CONTROL MOMENT GYROSCOPES**
- An investigation of the properties of systems of two-degrees-of-freedom force gyroscopes 04 p0453 A83-15377
- NAPC gyroscopic moment test facility 06 p0720 A83-18407
- Instability of a gyroscopic compass under resonance due to variable moments on the rotor 06 p0764 A83-19549
- A scheme of feedback compensation for CMG gimbal compliance, using multiple rate sensors --- Control Moment Gyroscope [ASME PAPER 82-WA/DSC-10] 10 p1419 A83-25681
- Number and placement of control system actuators considering possible failures --- for large space structures 17 p2476 A83-37078
- Choice of the optimal correcting moment of a gyrovertical on the basis of an applications program 21 p3141 A83-45309

CONTROL PANELS**U. CONTROL BOARDS****CONTROL ROCKETS**

- Hierarchy of mathematical models of engines for spacecraft control 08 p1053 A83-22661

CONTROL SIMULATION

- Simulated mission endurance control system 01 p0014 A83-10751
- Continuous time adaptive identification and control algorithms via newly developed adaptive laws 01 p0095 A83-10960
- Design and application of a multivariable, digital controller to the A-7D Digitaic II aircraft model 01 p0013 A83-11148
- Use of the onboard simulation concept for the integrated flight and fire control program 01 p0007 A83-11201
- Implementation of the DAST ARW II control laws using an 8086 microprocessor and an 8087 floating-point coprocessor --- drones for aeroelasticity research 02 p0227 A83-11910
- Development of dynamics and control simulation of large flexible space systems 02 p0141 A83-12456
- Integration function and modeling of the central nervous system in forearm movement control 03 p0384 A83-14126
- An analytical pilot rating method for highly elastic aircraft 03 p0282 A83-14843
- Stimulation versus simulation --- as illustrated with Mission System Avionics for Airborne Early Warning Nimrod 04 p0445 A83-16332
- Simulation of a terrain following system 04 p0445 A83-16333
- Assessment of advanced fighter powered approach simulations [AIAA PAPER 83-0141] 05 p0598 A83-16550
- Identification of certain dynamic characteristics of a helicopter-autopilot system by means of simulation 08 p1047 A83-23222
- Multipulse control of saccadic eye movements 09 p1325 A83-24706
- Control of robotic manipulator with adaptive controller 09 p1328 A83-24713
- A linear programming approach for multivariable feedback control with inequality constraints 09 p1328 A83-24720
- Static shape determination and control for a large space antenna 09 p1328 A83-24722

- A function space approach to smoothing with applications to model error estimation for flexible spacecraft control 09 p1217 A83-24759
- Multivariable self-tuning regulators 09 p1333 A83-24791
- Analytical verification of undesirable properties of direct model reference adaptive control algorithms 09 p1334 A83-24806
- Automatic return in multifunction control logic --- for fighter cockpits 10 p1459 A83-26317
- State-space aeroelastic modeling and its application in flutter calculation 10 p1442 A83-26761
- On the propagation and control of geosynchronous orbits 13 p1809 A83-29996
- Experimental demonstration of static shape control --- for large space structure development 13 p1812 A83-30165
- A fast and efficient digital simulation technique for control systems 16 p2404 A83-35348
- Model reference adaptive control with inexact model matching. I 17 p2568 A83-37126
- Adaptive control of nonlinear self-oscillating systems using MRAS technique 17 p2568 A83-37127
- Model reference adaptive control in the presence of measurement noise 17 p2568 A83-37128
- A model following algorithm for polynomial inputs 17 p2568 A83-37129
- An adaptive attitude control system for large-angle slew manoeuvres 17 p2477 A83-37449
- Development of a compact real-time turbofan engine dynamic simulation [SAE PAPER 821401] 17 p2468 A83-37974
- Helicopter IFR approaches into major terminals using RNAV, MLS, and CDTI 19 p2794 A83-41042
- Stability analysis of multirate nonlinear sampled-data control systems 19 p2890 A83-41488
- Design of feedback controllers for nonlinear systems 19 p2891 A83-41491
- Robust fault detection, isolation, and accommodation to support integrated aircraft control [AIAA PAPER 83-2161] 19 p2802 A83-41661
- Simulation evaluation of flight controls and display concepts for VTOL shipboard operations [AIAA PAPER 83-2173] 19 p2789 A83-41668
- Robustness of flexible spacecraft control to actuator and sensor model errors 19 p2815 A83-41676
- Application of Monte-Carlo techniques to the 757/767 autoland dispersion analysis by simulation [AIAA PAPER 83-2193] 19 p2802 A83-41678
- Adaptive control of variable flow ducted rockets [AIAA PAPER 83-2202] 19 p2797 A83-41686
- Development of the functional simulator for the Galileo attitude and articulation control system [AIAA PAPER 83-2299] 19 p2817 A83-41757
- Informational evaluation of operator activity in an ergatic system with a learning model 20 p3035 A83-43503
- Digital simulation and control of the Machan UMA 20 p2932 A83-43718
- Simulation of hot spot tracking loops [AAS PAPER 83-007] 21 p3104 A83-44166
- A model-based investigation of manipulator characteristics and pilot/vehicle performance 21 p3189 A83-45463
- Modelling of a multivariable system on the basis of frequency data 22 p3351 A83-45979
- Flight simulation for an inertial navigation system 23 p3420 A83-47178
- Air traffic control simulation in the airport area 23 p3401 A83-47200
- Dynamic modeling of flexible spacecraft - A general program for simulation and control [IAF PAPER 83-339] 23 p3421 A83-47348
- A new approach to fault-tolerant helicopter swashplate control [AIAA PAPER 83-2485] 23 p3412 A83-48345
- Tuning of a multivariable discrete time PI controller for unknown systems 24 p3620 A83-49894
- A method for the identification of nonlinear inertial systems 24 p3622 A83-50204
- CONTROL STABILITY**
- Relative stability test for continuous and sampled-data control systems using the generalised sign matrix 01 p0094 A83-10291
- Phase-locked-loop control systems using pulse frequency modulation 01 p0095 A83-10958
- Decentralized stabilization of a class of non-linear interconnected systems 01 p0095 A83-10959
- A note on the generalized inverse Nyquist stability criterion 01 p0095 A83-10962
- Investigations of stability and dynamic performances of switching regulators employing current-injected control 01 p0039 A83-11002
- Instabilities in current-mode controlled switching voltage regulators 01 p0039 A83-11003

On the maximum regulation range in boost and buck-boost converters 01 p0040 A83-11013
 Large signal design of a buck converter for high power dc/ac conversion 01 p0041 A83-11028
 The use of modal control to minimize errors in the analytical reconstruction of flight control sensor signals 01 p0013 A83-11210
 Digital servo/filter analysis using the phase plane 02 p0230 A83-11911
 Dynamic stabilization methods for bilateral control of remote manipulation 02 p0230 A83-11913
 Feedback control of linear multivariable systems with uncertain description in the frequency domain 02 p0230 A83-12550
 Bounded error adaptive control 03 p0386 A83-14589
 Stable model reference adaptive control in the presence of bounded disturbances 03 p0386 A83-14590
 A plant parameter identifier for an adaptive system of nonsearching self-adjusting class 04 p0527 A83-15925
 Robustness of the independent modal-space control method 04 p0528 A83-16116
 A model reference adaptive control system for discrete multivariable systems with time delays 04 p0528 A83-16147
 Principal gains and phases - Insensitive robustness measures for assessing the closed-loop stability property 04 p0529 A83-16186
 Analysis of feedback systems with structured uncertainties 04 p0529 A83-16187
 Stability margins of diagonally perturbed multivariable feedback systems 04 p0529 A83-16188
 Frequency-response design of robust optimal controllers 04 p0529 A83-16189
 Multivariable stability-margin optimisation with decoupling and output regulation 04 p0529 A83-16191
 Robust control strategy for a linear time-invariant multivariable sampled-data servomechanism problem 04 p0529 A83-16192
 Robustness properties of model-reference adaptive control systems 04 p0529 A83-16193
 Properties of min-max controllers in uncertain dynamical systems 04 p0529 A83-16195
 Effects of control saturation on the command response of statically unstable aircraft [AIAA PAPER 83-0065] 05 p0598 A83-16497
 Model following and pole-placement self-tuners 05 p0680 A83-17579
 Discrete adaptive control of a manipulator arm 05 p0681 A83-17585
 A feedback time constant concept 06 p0803 A83-19038
 Feedback representation of precompensators 06 p0803 A83-19387
 A geometric approach to stabilization by output feedback 06 p0804 A83-19390
 Absolute stability and absolute instability of control systems with two nonlinear nonstationary elements. II 07 p0984 A83-19997
 Design of adaptive controllers using the method of Lyapunov functions 07 p0984 A83-19998
 Convergence in distribution of LMS-type adaptive parameter estimates 07 p0984 A83-20721
 Design of linear systems with saturating linear control and bounded states 07 p0985 A83-20725
 Joint torque control by a direct feedback for industrial robots 08 p1074 A83-22416
 Stabilization of a class of plants with possible loss of outputs or actuator failures 08 p1157 A83-22418
 The stability of non-linear multivariable systems - Review of frequency domain methods 08 p1158 A83-23172
 The stability of linear multivariable systems 09 p1326 A83-23690
 The control of angular momentum for asymmetric rigid bodies 09 p1327 A83-24705
 Stability and stabilization of delay systems with sampled feedback 09 p1328 A83-24714
 Robust Lyapunov stability results and adaptive systems 09 p1328 A83-24724
 Direct adaptive pole placement with application to nonminimum phase systems 09 p1329 A83-24728
 Filtering for piecewise linear drift and observation 09 p1330 A83-24740
 Singular perturbation, state aggregation and nonlinear filtering 09 p1330 A83-24741
 Explicit weighted minimum variance self-tuning controllers 09 p1330 A83-24745
 Qualitative stability of large space structures with noncollocated actuators and sensors 09 p1217 A83-24756
 Global parameterization of feedback systems 09 p1332 A83-24780
 Simultaneous design of control systems 09 p1332 A83-24781

Decentralized stabilization and stability region estimation for a class of non linear dynamic systems 09 p1333 A83-24800
 Analytical verification of undesirable properties of direct model reference adaptive control algorithms 09 p1334 A83-24806
 Nonoptimality of one-dimensional singular controls of first order of degeneration 10 p1461 A83-25616
 Continuous time relay-controlled model reference adaptive system 10 p1462 A83-26070
 Modified Smith predictor control for multivariable systems with multiple delays subject to unmeasurable disturbances 10 p1463 A83-26509
 On the bifurcation phenomena and the problem of the loss of stability in the nonlinear control systems 10 p1464 A83-26510
 A variational method for investigating absolute stability and absolute instability of nonlinear control systems 10 p1464 A83-26511
 Extension of V. M. Popov's hyperstability theory of its application in adaptive system design 10 p1464 A83-26513
 On the compensation in linear feedback control systems - Transfer functions attainable by realizable linear compensation 10 p1464 A83-26519
 Invariance and identifiability in adaptive coordinate-parametric control 10 p1465 A83-26533
 On a problem of Optimal Model Reference Adaptive System 10 p1468 A83-26560
 A design procedure for linear multi-variable feedback systems 10 p1468 A83-26564
 Robust control of tracking problem with internal stability for linear structured system 10 p1469 A83-26575
 Principles of the synthesis of a magnetic multistable element in the steady-state regime 12 p1719 A83-29324
 Frequency-domain identification of transmission-zero locations of linear multivariable plants 12 p1769 A83-29469
 Robust controller design for linear dynamic systems using approximate models 12 p1770 A83-29521
 Control design and performance analysis of a 6 MW wind turbine-generator 12 p1750 A83-29897
 Stability of override control systems 14 p2074 A83-31928
 An algebraic algorithm for determining the desired gain of multivariable feedback systems 14 p2074 A83-31930
 Stabilization of the stationary motions of mechanical systems 14 p2079 A83-32358
 On the stability of discrete quadratic systems with periodic coefficients [ONERA, TP NO. 1983-22] 16 p2405 A83-36431
 Multivariable sensitivity reduction and decentralized control 17 p2567 A83-37118
 I-O stability analysis of multiple nonlinear-multivariable systems 17 p2567 A83-37119
 Model reference adaptive control with inexact model matching. I 17 p2568 A83-37126
 Adaptive control of nonlinear self-oscillating systems using MRAS technique 17 p2568 A83-37127
 Model reference adaptive control in the presence of measurement noise 17 p2568 A83-37128
 The design of decentralized controllers for the robust servomechanism problem using parameter optimization methods 17 p2568 A83-37130
 Fundamental issues in guidance and control of uncertain systems 17 p2568 A83-37132
 Structural information in robustness analysis 17 p2568 A83-37144
 Asymptotic expansions of singularly perturbed Chandrasekhar type of equations 17 p2571 A83-37146
 Sampled control stability of the ESA instrument pointing system 17 p2480 A83-37438
 Coordinate-parametric control system for spacecraft Functioning algorithms 17 p2569 A83-37442
 Attitude control system with quantization elements 17 p2478 A83-37456
 Frequency responses to minimize output disturbances caused by parameter variations and noise 17 p2570 A83-38817
 An optimal design approach for the robust controller problem 17 p2570 A83-38818
 Robust stability - Parameter-dependent perturbations 17 p2570 A83-38819
 Stability of systems - A survey 19 p2891 A83-41490
 Robust fault detection, isolation, and accommodation to support integrated aircraft control [AIAA PAPER 83-2161] 19 p2802 A83-41661
 Digital homing guidance - Stability vs. performance trade-offs [AIAA PAPER 83-2167] 19 p2795 A83-41663
 Line of sight reconstruction for faster homing guidance [AIAA PAPER 83-2170] 19 p2796 A83-41666

Stability of the Shuttle on-orbit flight control system for a class of flexible payloads [AIAA PAPER 83-2178] 19 p2815 A83-41672
 Robustness analysis of a multiloop flight control system [AIAA PAPER 83-2189] 19 p2802 A83-41675
 Robustness of flexible spacecraft control to actuator and sensor model errors [AIAA PAPER 83-2190] 19 p2815 A83-41676
 The use of singular value gradients and optimization techniques to design robust controllers for multiloop systems [AIAA PAPER 83-2191] 19 p2891 A83-41677
 Coulomb damper describing function analysis of shuttle entry with IUS/TDRS payload [AIAA PAPER 83-2197] 19 p2812 A83-41682
 Tradeoff studies in multiobjective insensitive design of airplane control systems [AIAA PAPER 83-2273] 19 p2804 A83-41739
 Time domain analysis for Stability Robustness of large scale LQG regulators [AIAA PAPER 83-2293] 19 p2892 A83-41752
 Flight test experience with pilot-induced-oscillation suppressor filters [AIAA PAPER 83-2107] 19 p2806 A83-41936
 Tracking control of non-linear systems using sliding surfaces, with application to robot manipulators 20 p3040 A83-43621
 Finite-dimensional discrete-time control of linear distributed parameter systems 21 p3192 A83-44009
 On the status of stability of interconnected systems 21 p3198 A83-44098
 Suboptimality and stability of linear distributed parameter systems with finite-dimensional controllers 21 p3196 A83-45136
 Closed-loop control performance sensitivity to parameter variations --- applied to orbiting large space structures 21 p3103 A83-45471
 Stabilization and structural assignment of Dirichlet boundary feedback parabolic equations 22 p3351 A83-46093
 Global adaptive pole placement - Detailed analysis of a first-order system 22 p3351 A83-46368
 On asymptotically stabilizing feedback control of bilinear systems 22 p3352 A83-46370

CONTROL STICKS

Plans and the structure of target acquisition behavior 10 p1457 A83-26332
 Sidestick controller design requirements 14 p1977 A83-32934
 Simulator performance definition by cue synchronization analysis [AIAA PAPER 83-1092] 16 p2312 A83-36216

CONTROL SURFACES

NT AERIAL RUDDERS
 NTAILERONS
 NTELEVATORS (CONTROL SURFACES)
 NTELEVONS
 NTEXTERNALLY BLOWN FLAPS
 NTFLAPS (CONTROL SURFACES)
 NTGUIDE VANES
 NTHORIZONTAL TAIL SURFACES
 NTJET FLAPS
 NTJET VANES
 NTLEADING EDGE FLAPS
 NTLEADING EDGE SLATS
 NTSPOILERS
 NTTABS (CONTROL SURFACES)
 NTTRAILING-EDGE FLAPS
 NTWING FLAPS
 Remotely driven model control surfaces for efficient wind-tunnel operations [AIAA PAPER 83-0148] 05 p0599 A83-16556
 An experimental investigation of control surface effectiveness and real-gas simulation for biconics [AIAA PAPER 83-0213] 05 p0591 A83-17912
 Realistic 'feel' in flight simulators is based on precise control loading 08 p1048 A83-23240
 Development and testing of Skyship 500 11 p1530 A83-28191
 On the routes - Boeing 757 with British Airways 12 p1701 A83-29241
 Aerothermal environment in control surface gaps in hypersonic flow - An overview [AIAA PAPER 83-1483] 14 p1970 A83-32732
 The effect of a sudden change in the motion of a plate surface on flow in a laminar boundary layer in supersonic flow 17 p2450 A83-37634
 Self-similar solutions of the equations of a boundary layer on a moving surface 17 p2506 A83-37635
 Equivalent angle-of-attack method for estimating nonlinear aerodynamics of missile fins 18 p2638 A83-40010

- Commercial aircraft with reduced longitudinal stability and active tail planes, and the unsteady aerodynamics of rapidly adjusted control surfaces 23 p3412 A83-47213
- CONTROL SYSTEMS**
- U CONTROL**
- CONTROL THEORY**
- Numerical solution of minimax problems of optimal control. I. II 01 p0093 A83-10251
- Adaptive control of certain systems with the aid of the Liapunov function 01 p0094 A83-10454
- The design of robust feedback controllers for partly unknown systems by optimal control procedures 01 p0094 A83-10799
- A discrete model reference adaptive control system for a plant with input amplitude constraints 01 p0095 A83-10956
- Stability multipliers and multivariable circle criteria 01 p0095 A83-10957
- The MCP-100 - A turnkey system for implementing multivariable flight control laws 01 p0009 A83-11101
- Simplification of digital control systems by adjusting zeros 01 p0095 A83-11174
- Model reference adaptive control of bilinear systems 02 p0229 A83-11789
- Pole placement and order reduction in two-time-scale control systems through Riccati iteration 02 p0229 A83-11838
- Mini and microcomputers in control and measurement; Proceedings of the International Symposium, San Francisco, CA, May 20-22, 1981 02 p0226 A83-11901
- Nondifferentiable optimization --- Russian book 02 p0231 A83-11975
- Synthesis of control systems using coordinate-parametric and parametric feedback 03 p0386 A83-13591
- Control, identification, and input optimization --- Book 03 p0386 A83-14039
- Transfer function matrix description of decentralized fixed modes 03 p0386 A83-14591
- Multivariable and optimal systems --- Book 04 p0527 A83-15838
- Estimation of the accuracy of synthesis of approximately optimal control for a nonlinear plant 04 p0527 A83-15915
- Additional necessary conditions for optimal control with state-variable inequality constraints 04 p0527 A83-15945
- Robust model following systems 04 p0528 A83-16146
- Improved design technique for uncertain multiple-input-multiple-output feedback systems 04 p0528 A83-16148
- Uncertain multiple-input-multiple-output systems with internal variable feedback 04 p0528 A83-16149
- Quantitative feedback theory 04 p0528 A83-16185
- An approximation theory for nonlinear partial differential equations with applications to identification and control 04 p0530 A83-16194
- Boundary stabilization of hyperbolic systems with no dissipative conditions 04 p0530 A83-16196
- Active control of a relaxed-static-stability airplane using a discrete model following technique [AIAA PAPER 83-0279] 05 p0598 A83-16624
- Parametric correction of control systems --- Russian book 05 p0653 A83-17121
- Stochastic control in structural design 06 p0771 A83-18208
- Concerning a method of extremal control 06 p0803 A83-19114
- Irreducible divisors of lambda-matrices and their applications to multivariable control systems 06 p0803 A83-19386
- Feedback representation of precompensators 06 p0803 A83-19387
- Pole assignment and minimal feedback design 06 p0803 A83-19388
- Time suboptimal feedback control of high order linear systems 06 p0803 A83-19389
- A geometric approach to stabilization by output feedback 06 p0804 A83-19390
- Generic pole assignment using dynamic output feedback 06 p0804 A83-19391
- On the minimality of feedback realizations 06 p0804 A83-19392
- The learning behaviour of trainee pilots during aircraft-landing - A simulator study 07 p0981 A83-19662
- Optimization of the Eulerian turn of a nonlinear flexible object --- for spacecraft with appendages 07 p0872 A83-19936
- Optimal control of periodic vibrations of a vibroimpact system 07 p0988 A83-19939
- Extended perfect model following --- control system synthesis technique 07 p0984 A83-20289
- Constrained eigenvalue/eigenvector assignment - Application to flight control systems 07 p0867 A83-21006
- The problem of guaranteeing robust disturbance rejection in linear multivariable feedback systems 07 p0985 A83-21161
- Pole placement in multi-input systems via elementary transformations 07 p0985 A83-21162
- Weak global controllability of nonlinear systems 08 p1156 A83-22043
- On the problem of observation spillover in self-adjoint distributed-parameter systems 08 p1156 A83-22044
- Distributed control of a system governed by Dirichlet and Neumann problems for a self-adjoint elliptic operator with an infinite number of variables 08 p1156 A83-22045
- Optimization and filtering of linear systems of finite dimension by hierarchical calculation --- French thesis 08 p1156 A83-22089
- Control of wave processes with distributed controls supported on a subregion 08 p1157 A83-22243
- Dynamic programming, fuzzy sets, and the modeling of R&D management control Systems 08 p1159 A83-22348
- Stabilization of a class of plants with possible loss of outputs or actuator failures 08 p1157 A83-22418
- Variable-structure systems and system zeros 08 p1158 A83-23018
- Dynamic output feedback controller 08 p1158 A83-23019
- Application of multivariable systems theory; Symposium, Plymouth, England, October 26-28, 1982, Collected Papers 08 p1158 A83-23171
- The construction of augmented tracking regulators for piloting highly maneuverable aircraft [ONERA, TP NO. 1982-118] 09 p1209 A83-24329
- Conference on Decision and Control, 20th, and Symposium on Adaptive Processes, San Diego, CA, December 16-18, 1981, Proceedings. Volumes 1, 2 & 3 09 p1327 A83-24701
- Rate of convergence in model reference adaptive control 09 p1328 A83-24725
- On order overspecification for a direct adaptive pole placer 09 p1329 A83-24729
- Minimal-order realizations for continuous-time 2-power input-output maps 09 p1329 A83-24730
- A group-theoretic approach to discrete-time non-linear controllability 09 p1329 A83-24732
- Control of nonlinear time-varying systems 09 p1329 A83-24733
- Controllability conditions and effective controls for nonlinear systems 09 p1329 A83-24734
- A Lie algebraic decomposition of nonlinear systems 09 p1329 A83-24735
- Some methods of integration in function space for use in control and filtering 09 p1329 A83-24738
- Suboptimal LQG-design via balanced realizations --- Linear Quadratic Gaussian regulators 09 p1331 A83-24752
- An eigenstructure approach to noninteracting control synthesis 09 p1331 A83-24753
- Fast-sampling tracking systems incorporating Lur'e plants with multiple switching nonlinearities 09 p1331 A83-24762
- Control problems in Autonomous Life Support Systems 09 p1325 A83-24764
- Iterative procedures for constrained and unilateral optimization problems 09 p1331 A83-24765
- A new nonlinear filtering approximation 09 p1331 A83-24772
- Adaptive digital control implemented using residue number systems 09 p1332 A83-24774
- Adaptive control algorithm design for high-speed cameras 09 p1269 A83-24778
- The Total Synthesis Problem of linear multivariable control. II - Unity feedback and the design morphism 09 p1332 A83-24782
- The decentralized control of large flexible space structures 09 p1217 A83-24786
- Controller design for asymptotic stability of flexible spacecraft 09 p1217 A83-24788
- A globally stable adaptive controller for multivariable systems 09 p1332 A83-24789
- Robustness tests utilizing the structure of modelling error 09 p1333 A83-24798
- Internal model adaptive control 09 p1334 A83-24804
- Modeling and representation of dynamical systems defined in terms of external variables 09 p1334 A83-24809
- Stability and controllability in systems with quasicyclic coordinates --- German thesis 09 p1212 A83-24849
- Applied control theory --- Book 09 p1335 A83-24894
- The design of optimal output regulators for linear multivariable systems with constant disturbances 10 p1461 A83-25400
- Nonoptimality of one-dimensional singular controls of first order of degeneration 10 p1461 A83-25616
- Multivariable system compensation [ASME PAPER 82-WA/DSC-19] 10 p1462 A83-25682
- Optimal adaptive control of linear-quadratic-Gaussian systems 10 p1462 A83-25996
- Control science and technology for the progress of society; Proceedings of the Eighth Triennial World Congress, Kyoto, Japan, August 24-28, 1981. Volume 1 - Control theory 10 p1463 A83-26501
- A discrete tracking control law for nonlinear plants --- applied to F-8 aircraft stall recovery 10 p1378 A83-26503
- Self-tuning control of nonlinear systems characterized by Hammerstein models 10 p1463 A83-26507
- On the bifurcation phenomena and the problem of the loss of stability in the nonlinear control systems 10 p1464 A83-26510
- Inverse systems of nonlinear plant represented by discrete volterra functional series 10 p1464 A83-26516
- The internal model principle of regulator theory on differentiable manifolds 10 p1464 A83-26517
- GG-pseudo-band method for the design of multivariable control systems 10 p1464 A83-26520
- Suboptimal feedback control with inaccessible state variables via moving model 10 p1464 A83-26521
- A new approach to pulse frequency modulated control --- mathematical models for analysis and design of control systems 10 p1465 A83-26522
- A design method for nonlinear control systems based upon partial knowledge about controlled objects 10 p1465 A83-26528
- Computational methods in control - A survey and introduction to the literature 10 p1460 A83-26529
- An approach to optimal control problems via exact penalty functions 10 p1465 A83-26530
- A new method for synthesis of nonlinear parameter and state estimators for noisily disturbed processes 10 p1465 A83-26532
- Invariance and identifiability in adaptive coordinate-parametric control 10 p1465 A83-26533
- Unbiased identification of state space models 10 p1466 A83-26535
- Control science and technology for the progress of society; Proceedings of the Eighth Triennial World Congress, Kyoto, Japan, August 24-28, 1981. Volume 2 - Stochastic and large systems 10 p1466 A83-26539
- Theory and applications of adaptive control 10 p1466 A83-26540
- New results on stationary stochastic feedback processes 10 p1466 A83-26542
- Control of coupled bilinear stochastic systems 10 p1466 A83-26543
- Generalized observations control in problems of stochastic optimization 10 p1466 A83-26545
- Optimal cyclostationary control - A parameter-optimization frequency-domain approach 10 p1467 A83-26546
- Adaptive control with forgetting factor 10 p1467 A83-26554
- Combining model reference adaptive controllers and stochastic self-tuning regulators 10 p1468 A83-26556
- Synthesis of C(asterisk)-model reference adaptive flight controller 10 p1379 A83-26559
- An adaptive observer with exponential rate of convergence for single-input single-output linear systems 10 p1468 A83-26562
- Scalar output feedback in linear multivariable systems 10 p1469 A83-26568
- Perfect and subperfect regulation in linear multivariable control systems 10 p1469 A83-26569
- Structural optimality of linear optimal control 10 p1469 A83-26573
- Control science and technology for the progress of society; Proceedings of the Eighth Triennial World Congress, Kyoto, Japan, August 24-28, 1981. Volume 4. Part A - Mechanical systems and robots. Part B - Aerospace and transportation 10 p1380 A83-26577
- Zero PID control for bias momentum satellites --- Proportional Integral Derivative 10 p1385 A83-26584
- Dynamics and control of Maglev vehicles with parameter uncertainties 10 p1491 A83-26607
- Supervisory control of a multilegged robot 11 p1648 A83-28098
- Determination of the optimal characteristic polynomial in automatic control systems --- of autopilots 12 p1769 A83-29289

- Multivariable system theory and design --- Book
12 p1770 A83-29536
- Hierarchical robot control system synthesis
12 p1770 A83-29542
- A preliminary look at control augmented dynamic response of structures
[AIAA 83-0850] 12 p1708 A83-29825
- Block-independent control of distributed structures
[AIAA 83-0852] 12 p1742 A83-29826
- State control of distributed parameter systems
13 p1909 A83-30001
- Method of Liapunov functions in the theory of the analytical design of nonlinear controllers
13 p1910 A83-30013
- Control of distributed parameter systems
13 p1910 A83-30078
- Symbolic representation of translatory motion in multivarying-link mechanisms --- application to multidegree-of-freedom manipulators and robots
13 p1858 A83-30166
- An engineering concept of adaptive control for manipulation robots via parametric sensitivity analysis
13 p1907 A83-30972
- Stochastic independent modal-space control of distributed-parameter systems
13 p1911 A83-31249
- Differential-geometric methods in control theory
13 p1911 A83-31723
- Game systems of adaptive control
14 p2076 A83-32962
- Mathematical models of discrete systems of automatic control with indeterminate parameters
14 p2076 A83-32963
- On a numerical method for the synthesis of optimal control for nonlinear dynamic systems
14 p2076 A83-32965
- On an algorithm for the simulation of a vector random process
14 p2076 A83-32966
- Control of stochastic systems with Markov interrupted observations
14 p2076 A83-33131
- Optimal-control of nonlinear systems
15 p2220 A83-33525
- Mathematical methods for the optimization of automatic-control-system devices and algorithms --- Russian book
15 p2220 A83-34175
- On the decoupling of linear systems into single input-multiple output subsystems
15 p2221 A83-35110
- On decoupling of multivariable square plants
15 p2221 A83-35111
- Generic pole assignment using dynamic output feedback
15 p2221 A83-35112
- The Riccati equation, imprimitive actions and symplectic forms --- with application to decentralized optimal control problem
15 p2222 A83-35124
- Optimal quantized control
15 p2222 A83-35125
- A z-transform theory for distributed sensing and control
15 p2222 A83-35128
- Interactive fine-tuning of linear-quadratic governors by selective and direct action on the poles of the control system
[ONERA, TP NO. 1983-21] 16 p2404 A83-36430
- On the stability of discrete quadratic systems with periodic coefficients
[ONERA, TP NO. 1983-22] 16 p2405 A83-36431
- Time-optimization of automatic control systems --- Russian book
16 p2405 A83-36441
- A singular perturbation canonical form of invertible systems Determination of multivariable root-loci
16 p2405 A83-36452
- A new approach for the design of multivariable feedback systems
16 p2405 A83-36453
- Symmetric linear systems - An application of algebraic systems theory
16 p2405 A83-36454
- A modified algorithm for determining structural controllability
16 p2405 A83-36455
- Reconstructable states of linear multivariable systems with unknown inputs
16 p2405 A83-36456
- American Control Conference, 1st, Arlington, VA, June 14-16, 1982, Proceedings. Volumes 1, 2 & 3
17 p2564 A83-37076
- An algebraically derived nonlinear control theory
17 p2566 A83-37098
- Proportional + integral + double integral adaptive laws for Liapunov MRAC --- Model Reference Adaptive Control
17 p2566 A83-37100
- Integrated control techniques
17 p2566 A83-37102
- On tracking domains of continuous-time non-linear control systems
17 p2566 A83-37113
- Control-theoretic approach to optimal search for a class of Markovian targets
17 p2567 A83-37116
- Multivariable sensitivity reduction and decentralized control
17 p2567 A83-37118
- I-O stability analysis of multiple nonlinear-multivariable systems
17 p2567 A83-37119
- Model reference adaptive control with inexact model matching. I
17 p2568 A83-37126
- A model following algorithm for polynomial inputs
17 p2568 A83-37129
- Fundamental issues in guidance and control of uncertain systems
17 p2568 A83-37132
- Quadratic weight adjustment for the enhancement of feedback properties
17 p2568 A83-37138
- Frequency-shaped penalty functions for robust control design
17 p2568 A83-37143
- Asymptotic expansions of singularly perturbed Chandrasekhar type of equations
17 p2571 A83-37146
- Microprocessor controlled optimal helicopter turret control system
17 p2462 A83-37148
- Modal synthesis of missile autopilot control law
17 p2476 A83-37152
- Optimal guidance for accelerating missiles
17 p2474 A83-37153
- Applying stochastic control theory to robot sensing, teaching, and long term control
17 p2568 A83-37154
- Synthesis of terminal control sequence algorithms with the use of moving-point guidance --- in hypersonic spacecraft reentry
17 p2477 A83-37446
- One new method of dynamic flight control
17 p2569 A83-37447
- Recent advances in the control of large flexible spacecraft
17 p2478 A83-37468
- Adaptive systems with reduced models --- Book
17 p2569 A83-37494
- Design of modern control systems --- Book
17 p2569 A83-37495
- Synthesis of adaptive tracking systems
17 p2570 A83-38483
- Robust stability - Parameter-dependent perturbations
17 p2570 A83-38819
- On model-following using measured output feedback
17 p2570 A83-38820
- A synthesis theory for a class of saturating systems --- in feedback control
17 p2570 A83-38821
- The immersion under feedback of a multidimensional discrete-time non-linear system into a linear system
17 p2570 A83-38823
- Fast suboptimal state-space self-tuner for linear stochastic multivariable systems
18 p2738 A83-40069
- Computer-aided design of structurally constrained multivariable regulators. I - Problem statement, analysis and solution
18 p2738 A83-40070
- Structure detection and model validity tests in the identification of nonlinear systems
18 p2739 A83-40071
- High-order necessary optimality conditions for control problems with terminal constraints
19 p2888 A83-40673
- Linear models in nonlinear control systems --- Russian book
19 p2889 A83-40990
- Control and its applications; Proceedings of the International Conference, Warwick, England, March 23-25, 1981
19 p2890 A83-41476
- Stability of systems - A survey
19 p2891 A83-41490
- Regulator design for the F100 turbofan engine
19 p2800 A83-41492
- A square-root algorithm for the adaptive control of multivariate systems
19 p2891 A83-41573
- Classical vs. modern control system design for terminal guidance of bank-to-turn intercept missiles
[AIAA PAPER 83-2203] 19 p2802 A83-41687
- Control law design for ejection seats
[AIAA PAPER 83-2204] 19 p2797 A83-41688
- Integrated task-tailored control augmentation synthesis --- for multi-axis air-to-air tracking
[AIAA PAPER 83-2215] 19 p2803 A83-41697
- Reduced order control design benefits and costs of frequency-shaped LQG methodology --- Linear-Quadratic-Gaussian
[AIAA PAPER 83-2229] 19 p2891 A83-41708
- Applications on nonlinear programming for automated optimum multivariable control system design
[AIAA PAPER 83-2275] 19 p2892 A83-41741
- Decentralization of the identification or control laws of adaptive systems with a large dimension reference model --- French thesis
19 p2892 A83-41812
- Optimal control of orbital transfer vehicles
[AIAA PAPER 83-2092] 19 p2811 A83-41927
- Sufficient conditions for the decomposability of control problems
19 p2893 A83-42006
- The abstract theory of systems (ATS) and applied studies
20 p3039 A83-42915
- Bilinear logico-dynamic model for a controlled process
20 p3039 A83-42917
- Observed realization of nonlinear controlled dynamic systems
20 p3039 A83-42918
- Analysis of the controllability property in linear control systems with parameters
20 p3039 A83-42920
- Limit-optimal control of linear stochastic plants
20 p3039 A83-42921
- The field of expanded extremals of a controlled process
20 p3039 A83-42922
- Numerical synthesis of time-optimal control for the electric motor of an electromechanical system
20 p2967 A83-42925
- Experimental analysis of methods for determining psychological factors of the complexity of solution of control problems
20 p3035 A83-43507
- Application of factor-analysis methods to evaluate the quality of ergatic control systems --- of aircraft landing by human operator
20 p3036 A83-43508
- On the design of ergatic systems for the solution of a two-goal game-theoretical problem of control
20 p3036 A83-43509
- Discrete models for linear multivariable systems
20 p3040 A83-43619
- Deadbeat control in multivariable non-linear time-varying systems with constraints of control inputs
20 p3040 A83-43620
- Engineering science and mechanics; Proceedings of the International Symposium, Tainan, Republic of China, December 29-31, 1981. Parts 1 & 2
21 p3117 A83-44001
- Principles of sensor and actuator location in distributed systems
21 p3192 A83-44002
- Modal cost analysis as an aid in control system design for large space structures
21 p3098 A83-44005
- Limit cycle analysis of control system with complex nonlinearities
21 p3192 A83-44010
- Control of distributed hyperbolic systems - 'What does a tokamak and a large spacecraft have in common?'
21 p3192 A83-44011
- Solution methods for the enhanced modal control Riccati equation
21 p3193 A83-44018
- The determination of the degree of controllability for dynamic systems with repeated eigenvalues
21 p3193 A83-44039
- Guidance and control 1983; Proceedings of the Annual Rocky Mountain Conference, Keystone, CO, February 5-9, 1983
21 p3099 A83-44160
- Navigation, guidance and control curriculum at the Air Force Academy
[AAS PAPER 83-021] 21 p3220 A83-44167
- The differential-topological structure of the varieties of motion of vibration-resistant dynamical systems
21 p3200 A83-44647
- Problems in the control of relativistic and quantum dynamic systems (physical and informational aspects) --- Russian book
21 p3195 A83-45033
- Nonsmooth problems in optimization and control theory --- Russian book
21 p3195 A83-45045
- Multivariable feedback: A quasi-classical approach --- Book
21 p3195 A83-45100
- Spillover and model error bounding techniques for large scale systems
21 p3195 A83-45104
- Minimum information approach to regulator design - Numerical methods and illustrative results
21 p3195 A83-45108
- Application of classical techniques to control of continuous systems
21 p3196 A83-45109
- Finite-dimensional controllers for hyperbolic systems
21 p3196 A83-45118
- An integrated approach to optimal reduced order control theory
21 p3196 A83-45131
- Partitioning control of Large Space Structures
21 p3103 A83-45132
- Active control of large flexible spacecraft - A new design approach based on minimum information modelling of parameter uncertainties
21 p3196 A83-45133
- Exact pole assignment using direct or dynamic output feedback
21 p3196 A83-45135
- Suboptimality and stability of linear distributed parameter systems with finite-dimensional controllers
21 p3196 A83-45136
- Optimal regulator design using minimum information modelling of parameter uncertainties - Ramifications of the new design approach
21 p3196 A83-45137
- Feedback strategies for partially observable stochastic systems --- Book
21 p3197 A83-45142
- Discrete nonlinear systems --- Russian book
21 p3197 A83-45201
- An optimal control approach to pilot/vehicle analysis and the Neal-Smith criteria
21 p3093 A83-45462
- Structural properties of the linear-quadratic stochastic control problem
22 p3351 A83-46091
- Optimal control problems involving second boundary value problems of parabolic type
22 p3351 A83-46092
- The use of structural properties in linear multivariable control system design --- Thesis
22 p3352 A83-46690

On the controllability and control law design for an orbiting large flexible antenna system
[IAF PAPER 83-340] 23 p3422 A83-47349

Angular points of the boundaries of domains of attainability --- for dynamic control of linear systems
23 p3501 A83-48528

Extended discrete-time multivariable adaptive control using long-term predictor
23 p3502 A83-48644

Multiplex control systems - Stochastic stability and dynamic reliability
23 p3502 A83-48645

Stability analysis of non-linear dynamical systems
23 p3502 A83-48647

Block decompositions and block modal controls of multivariable control systems
24 p3621 A83-49920

Stability analysis of adaptively controlled systems subject to bounded disturbances
24 p3621 A83-49921

Convergence analysis of recursive identification algorithms with forgetting factor
24 p3621 A83-49922

An adaptive robustizing approach to Kalman filtering
24 p3621 A83-49924

CONTROL VALVES

Optical-to-optical image conversion with the liquid crystal light valve
03 p0394 A83-13776

Silicon liquid crystal light valves for optical-data processing
03 p0394 A83-13778

Computer-aided design within the framework of the algorithmic selection procedure for the design with catalogs --- German thesis
04 p0487 A83-15844

Use of thermocapillary migration in a controllable heat valve
04 p0477 A83-16093

Computer studies of ACV heave performance as a function of vent valve proportional control parameters
15 p2241 A83-33547

Computer studies of ACV heave performance as a function of vent valve control parameters
15 p2123 A83-34854

An analytical design of electrohydraulic position servo systems with variable structure
21 p3118 A83-44038

CONTROLLABILITY

Controllability and observability of nonlinear systems and the synthesis of terminal control
02 p0230 A83-11951

In-flight deflection measurement of the HiMAT aeroelastically tailored wing
03 p0281 A83-13167

An analytical pilot rating method for highly elastic aircraft
03 p0282 A83-14843

Computation of a degree of controllability via system discretization --- with application to flexible spacecraft control
03 p0287 A83-14844

Global transformations of nonlinear systems
07 p0984 A83-20719

Weak global controllability of nonlinear systems
08 p1156 A83-22043

A unifying framework for longitudinal flying qualities criteria
09 p1209 A83-24429

On local controllability
09 p1329 A83-24731

A group-theoretic approach to discrete-time non-linear controllability
09 p1329 A83-24732

Controllability conditions and effective controls for nonlinear systems
09 p1329 A83-24734

A Lie algebraic decomposition of nonlinear systems
09 p1329 A83-24735

An eigenstructure approach to noninteracting control synthesis
09 p1331 A83-24753

Multivariable adaptive pole placement
09 p1333 A83-24790

Stability and controllability in systems with quasicyclic coordinates --- German thesis
09 p1212 A83-24849

Cylindrical piezoelectric transducer with controllable characteristics
10 p1421 A83-26291

Applications of Laurent expansions in multivariable control systems
10 p1469 A83-26571

Optimal-control of nonlinear systems
15 p2220 A83-33525

Performance of the advanced twin gimbal fan aeromobile
16 on varied terrain in 1982 15 p2242 A83-34857

Bring cohesion to handling-qualities engineering
16 p2298 A83-35772

A modified algorithm for determining structural controllability
16 p2405 A83-36455

The effects of engine and height-control characteristics on helicopter handling qualities
19 p2802 A83-41078

Simulator applications and technology
[AIAA PAPER 83-2172] 19 p2807 A83-41667

Status of the development of handling criteria for VSTOL transition
[AIAA PAPER 83-2103] 19 p2806 A83-41932

Comparison of fixed-base and in-flight simulation results for lateral high order systems
[AIAA PAPER 83-2105] 19 p2806 A83-41934

Handling qualities criteria for STOL flight path control for approach and landing
[AIAA PAPER 83-2106] 19 p2806 A83-41935

Analysis of the controllability property in linear control systems with parameters
20 p3039 A83-42920

The determination of the degree of controllability for dynamic systems with repeated eigenvalues
21 p3193 A83-44039

A definition of the degree of controllability for fuel-optimal systems
21 p3195 A83-45102

On the controllability and control law design for an orbiting large flexible antenna system
[IAF PAPER 83-340] 23 p3422 A83-47349

Controllabilization and observabilization of the attitude control system with flywheel
[IAF PAPER 83-341] 23 p3422 A83-47350

NOTAR - The viable alternative to a tail rotor
[AIAA PAPER 83-2527] 23 p3404 A83-48365

CONTROLLED ATMOSPHERES

NT CABIN ATMOSPHERES

NT HELIUM-OXYGEN ATMOSPHERES

NT SPACECRAFT CABIN ATMOSPHERES

An atmospheric exposure chamber for small animals
01 p0086 A83-11108

Certain biochemical indices in healthy humans under the effect of high concentrations of carbon monoxide and carbon dioxide in a sealed chamber
01 p0085 A83-11403

Two methods for absolute calibration of dynamic pressure transducers
03 p0329 A83-14170

Applications of permeable membranes as carbon dioxide scrubbers
11 p1645 A83-28339

SOYCHMBR.I - A model designed for the study of plant growth in a closed chamber
[SAE PAPER 820853] 13 p1899 A83-30941

Meteorology in a space colony
20 p2938 A83-42336

The corrosion of nickel in SO₂ atmospheres
24 p3564 A83-49509

CONTROLLED FUSION

International Conference on Plasma Physics, Goteborg, Sweden, June 9-15, 1982, Proceedings. Part 2
13 p1924 A83-30412

Mathematical modeling of plasmas --- Russian book
15 p2233 A83-34164

CONTROLLED STABILITY

U. CONTROL

CONTROLLERS

NT SERVOMECHANISMS

Properties of min-max controllers in uncertain dynamical systems
04 p0529 A83-16195

Self-tuning controller with integral action
05 p0681 A83-17581

Design of error-actuated controllers for multivariable plants with unknown dynamics and unmeasurable outputs --- for automatic control of industrial processes and gas turbine engines
06 p0718 A83-19385

Feedback representation of precompensators
06 p0803 A83-19387

Adaptive linear controller for robotic manipulators
08 p1157 A83-22417

Pitch control system for large-scale wind turbines
08 p1132 A83-23140

The automation of control system design. Number 4 --- Russian book
09 p1326 A83-24225

Basic conceptions of the external software system for programmable logic controllers
09 p1325 A83-24244

Controller design for asymptotic stability of flexible spacecraft
09 p1217 A83-24788

Closed-loop asymptotic stability and robustness conditions for large space systems with reduced-order controllers
09 p1218 A83-24819

A new class of stabilizing controllers for uncertain dynamical systems
10 p1462 A83-25997

Experimental system for computer network via satellite /CS/. IV - Packet transmission controller
10 p1403 A83-26080

Selection of remotely labeled switch functions during dual task performance
10 p1459 A83-26315

On stabilization of classes of nonlinear systems with state observers
10 p1463 A83-26505

High-gain tracking systems incorporating Lur'e plants with multiple switching nonlinearities
10 p1463 A83-26506

Modified Smith predictor control for multivariable systems with multiple delays subject to unmeasurable disturbances
10 p1463 A83-26509

On receding horizon feedback control
10 p1464 A83-26518

A new approach to pulse frequency modulated control --- mathematical models for analysis and design of control systems
10 p1465 A83-26522

Synthesis of C(asterisk)-model reference adaptive flight controller
10 p1379 A83-26559

A samarium cobalt motor-controller for mini-RPV propulsion
11 p1530 A83-27187

Controller design for flexible, distributed parameter mechanical arms via combined state space and frequency domain techniques
11 p1647 A83-27487

On a method of frozen coefficients in the synthesis of linear controllers
13 p1910 A83-30079

Number and placement of control system actuators considering possible failures --- for large space structures
17 p2476 A83-37078

A Z-domain controller design method for sampled-data systems having feedback dynamics
17 p2565 A83-37083

Computer aided multivariable control system design package
17 p2564 A83-37089

Displacement control of elastic structures - Integral control with a robustness property
17 p2565 A83-37090

Controller scheduling - A possible algebraic viewpoint
17 p2565 A83-37093

The design of decentralized controllers for the robust servomechanism problem using parameter optimization methods
17 p2568 A83-37130

A delayed pulse roll/yaw controller for a momentum biased spacecraft
17 p2478 A83-37458

An optimal design approach for the robust controller problem
17 p2570 A83-38818

Active flutter suppression using eigenspace and linear quadratic design techniques
[AIAA PAPER 82-2222] 19 p2803 A83-41702

Synthesis of insensitive regulators with comparative evaluations in aerospace applications
[AIAA PAPER 83-2224] 19 p2891 A83-41704

MIMO controller design for longitudinal decoupled aircraft motion --- Multi-Input/Multi-Output
[AIAA PAPER 83-2274] 19 p2804 A83-41740

Direct design of multivariable control systems through singular value decomposition
[AIAA PAPER 83-2276] 19 p2892 A83-41742

Robust active vibration damping of flexible spacecraft
[AIAA PAPER 83-2289] 19 p2816 A83-41749

Robust control system design techniques for large flexible space structures having non-co-located sensors and actuators
[AIAA PAPER 83-2294] 19 p2817 A83-41753

Carrier landing simulation results of precision flight path controllers in manual and automatic approach
[AIAA PAPER 83-2072] 19 p2796 A83-41909

First order solution of the optimal control problem for distributed parameter elastic system
21 p3193 A83-44040

Control of a flexible satellite via elimination of observation spillover
21 p3101 A83-45103

Spillover and model error bounding techniques for large scale systems
21 p3195 A83-45104

Numerical implementation of suboptimal output feedback control for large space structures
21 p3195 A83-45105

Application of classical techniques to control of continuous systems
21 p3196 A83-45109

Optimal positive real controllers for large space structures
21 p3102 A83-45117

Finite-dimensional controllers for hyperbolic systems
21 p3196 A83-45118

An integrated approach to optimal reduced order control theory
21 p3196 A83-45131

Exact pole assignment using direct or dynamic output feedback
21 p3196 A83-45135

Suboptimality and stability of linear distributed parameter systems with finite-dimensional controllers
21 p3196 A83-45136

Optimal controller design for a helicopter using its lower order dynamic model
[AIAA PAPER 83-2550] 23 p3412 A83-48371

Tuning of a multivariable discrete time PI controller for unknown systems
24 p3620 A83-49894

Design of digital two- and three-term controllers for discrete-time multivariable systems
24 p3620 A83-49897

CONVAIR MILITARY AIRCRAFT

U MILITARY AIRCRAFT

CONVAIR 990 AIRCRAFT

U CV-990 AIRCRAFT

CONVECTION

NT BENARD CELLS

NT FORCED CONVECTION

NT FREE CONVECTION

NT MARANGONI CONVECTION

NT RAYLEIGH-BENARD CONVECTION

Solutions to the equations for corotating magnetospheric convection
02 p0263 A83-11602

Magnetospheric convection at a low level power epsilon
02 p0204 A83-11968

Convection in pulsating stars. I - Nonlinear hydrodynamics. II - RR Lyrae convection and stability
02 p0257 A83-12137

SUBJECT INDEX

A mechanism for the initiation of convective cumulus clouds in mountainous terrain			
[AD-A122033]	24	p3611	A83-49682
Distribution of acidity in convective clouds due to the aqueous phase oxidation of sulfur dioxide by ozone - A numerical simulation	24	p3602	A83-49685
Cloud-base statistics from aircraft observations of early storms in COPE --- Cooperative Convective Precipitation Experiment	24	p3613	A83-49700
Merging of moderate-sized convective cells on day 261 of GATE	24	p3613	A83-49701
Indirect effects of cumulus convection on large-scale radiative heating rates	24	p3613	A83-49704
Zonally asymmetric aspects of large-scale thermodynamic forcing by cumulus convection	24	p3613	A83-49705
The three-dimensional simulation of Florida convective clouds-sensitivity to cloud microphysical processes	24	p3614	A83-49714
Cumulus convection as observed from an airborne infrared radiometer	24	p3615	A83-49726
Retrieval of microphysical and thermal variables in observed convective storms	24	p3616	A83-49731
Characteristics of downdrafts and turbulence within thunderstorms	24	p3616	A83-49734
CONVECTION CURRENTS			
Two-dimensional convection in non-constant shear - A model of mid-latitude squall lines	02	p0215	A83-12936
Effects of mesoscale atmospheric convection cells on the waters of the East China Sea	03	p0363	A83-13270
Investigation of clear air convective structures in the PBL using a dual Doppler radar and a Doppler sodar	07	p0969	A83-20808
The nonlinear spectral dynamics of large-scale atmospheric motions	08	p1140	A83-22419
A convection parameterization scheme based on a direct algorithm of dry convective adjustment --- for atmospheric models	09	p1315	A83-24939
Helicity and alpha-effect of simple convection cells --- in solar envelope	10	p1520	A83-25378
On the measurement of hail cells by radar and hailpads	11	p1624	A83-27002
Life cycles of convective cells in organized mesoscale systems in gate	11	p1626	A83-27026
Studies of variations of cell parameters to be exceeded to confirm certain seeding hypotheses --- for cumulus clouds	11	p1626	A83-27031
A study of the tornadic region with a supercell thunderstorm	13	p1892	A83-31036
A note on the criteria for the onset of stationary parallel-plate convection subject to mean vertical motion	16	p2348	A83-35494
On the rotation of the polar cap potential pattern and associated polar phenomena	17	p2539	A83-37605
Ground based CO2 Doppler lidar wind measurements of winds in the vicinity of cumulus convection	17	p2552	A83-38752
Sloping convection in the laboratory and in the atmospheres of Jupiter and Saturn	21	p3240	A83-44233
The effect of magnetospheric convection on the concentration of H(+) ions in the plasmasphere	21	p3175	A83-45244
Parametric excitation and suppression of convective plasma instabilities in the high-latitude F region ionosphere	22	p3328	A83-46060
An analytic solution for the response of the neutral atmosphere to the high-latitude convection pattern	22	p3337	A83-47069
CONVECTIVE FLOW			
NT BENARD CELLS			
NT RAYLEIGH-BENARD CONVECTION			
Flow visualization in natural convection	01	p0052	A83-11070
A theory of the limits of flame propagation on the surface of a combustible material	02	p0151	A83-11958
On the convective mechanism for formation of the plasma sheet in the magnetospheric tail	02	p0204	A83-11963
A scale analysis of deep moist convection and some related numerical calculations	02	p0213	A83-12233
Numerical solutions to natural convection in a channel with porous walls under a transverse magnetic field	02	p0171	A83-12666
Surface tension driven flows in micro-gravity conditions	02	p0174	A83-12904
Models of solar differential rotation	02	p0271	A83-12977
Nonlinear dynamo oscillations	02	p0242	A83-12981
Time-dependent convection under reduced gravity	02	p0174	A83-12993

A-332

Thermal Marangoni convection in a floating zone. Microgravity experiment during the TEXUS IIIB rocket flight 02 p0138 A83-12995

The inclusion of moist downdraft effects in the Arakawa-Schubert cumulus parameterization 03 p0368 A83-14445

Turbulent transport in the mixed convection over a heated horizontal plane 03 p0319 A83-14474

Streamline upwind/Petrov-Galerkin formulations for convection dominated flows with particular emphasis on the incompressible Navier-Stokes equations 04 p0475 A83-15005

Applicability of the Boussinesq approximation to solve problems of nonstationary concentrational natural convection 04 p0475 A83-15093

The dynamics of a rotating mesometeorological convective turbulent vortex in an unstably stratified atmosphere 04 p0509 A83-15720

Finite-amplitude convective motions in a solute layer with solid boundaries 04 p0477 A83-15878

MHD free-convection flow in the Stokes problem for a porous vertical plate 04 p0538 A83-15985

The existence of Hadley convective regimes of atmospheric motion 04 p0519 A83-16367

Orthogonal decomposition techniques to identify convected flow structures [AIAA PAPER 83-0048] 05 p0632 A83-16484

Finite element formulations for convection dominated flows with particular emphasis on the compressible Euler equations [AIAA PAPER 83-0125] 05 p0633 A83-16538

Motion in the interiors and atmospheres of Jupiter and Saturn - Scale analysis, anelastic equations, barotropic stability criterion 05 p0703 A83-16960

Turbulent compressible convection in a deep atmosphere. I - Preliminary two-dimensional results --- of stars 05 p0699 A83-17017

Buoyancy-induced two-dimensional vertical flows in a thermally stratified environment 06 p0756 A83-18375

Convection and gravity waves in two layer models. I - Overstable modes driven in conducting boundary layers --- of solar and stellar models 06 p0835 A83-18934

Convection in degenerate shells of neutron stars 06 p0837 A83-19214

An asymptotic theory of natural convection --- French thesis 08 p1084 A83-22091

An experimental and theoretical investigation of the onset of convection in rotating spherical shells 08 p1086 A83-23094

Natural convection in a rotating annulus 08 p1090 A83-23209

Magnetoconvection --- interaction between convection and imposed magnetic field in Boussinesq fluid 09 p1357 A83-23861

Cloud dynamics; Proceedings of the Symposium, Hamburg, West Germany, August 17-28, 1981 09 p1311 A83-23951

An introduction to shallow convective systems --- in clouds 09 p1312 A83-23952

Radiative influence on small scale convection within stratus cloud layers 09 p1312 A83-23953

Lake-effect snow storms on Lake Michigan, USA 09 p1312 A83-23956

On the preferred mode of cumulus convection in a conditionally unstable atmosphere 09 p1312 A83-23958

Toward a unified theory of atmospheric convective instability 09 p1312 A83-23959

Cloud bands in the atmosphere 09 p1312 A83-23960

An introduction to deep convective systems --- thunderstorm development 09 p1312 A83-23961

Use of the radar differential reflectivity radar technique for observing convective systems 09 p1313 A83-23966

Detection of convective storms based on penetrative cloud top from satellite infrared and rawinsonde data, and gravity waves from Doppler sounder 09 p1313 A83-23970

Precipitation in convective storms - An observational and numerical study 09 p1313 A83-23971

Turbulence parameterization in a deep convection model --- for cloud physics 09 p1313 A83-23972

Steady three-dimensional convection at high Prandtl numbers 09 p1261 A83-24412

The stability and disturbance-amplification characteristics of vertical mixed convection flow 09 p1261 A83-24413

Two comments of the sun's differential rotation 09 p1368 A83-24452

An investigation of the convergence of a moist convective adjustment scheme 09 p1315 A83-24938

Fluid mechanics instabilities 09 p1264 A83-25150

A study of thermal convection and heat transfer --- Russian book 09 p1264 A83-25246

The relationship between convective adjustment, Hadley circulation and normal modes of the ANMRC spectral model 10 p1450 A83-25381

The stratification of magnetospheric convection and its manifestations in the high-latitude ionosphere 10 p1448 A83-25605

Buoyant plane jets in thermally stratified media [ASME PAPER 82-WA/HT-57] 10 p1413 A83-25696

The magnetosphere of Uranus - Plasma sources, convection, and field configuration 10 p1518 A83-25734

Convection induced by insulated boundaries in a square 10 p1413 A83-25781

Recurrent spatial structures in convective systems --- automated weather radar data analysis 11 p1622 A83-26981

Evolution of a mid-latitude mesoscale convective system 11 p1625 A83-27012

Magnetic structure of the boundary layer --- explaining magnetospheric convection 11 p1614 A83-27391

Adiabatic oscillations of solar models with a high-Z convective core 11 p1689 A83-27644

Nonlinear anelastic modal theory for solar convection 11 p1690 A83-27658

Noise generation by a finite span swept airfoil [AIAA PAPER 83-0768] 11 p1652 A83-28023

Mixed laminar convection on a vertical surface under conditions of strong injection 11 p1571 A83-28799

Flatness change in the transition to turbulent convection 12 p1721 A83-29003

Experimental study of the boundary layer over a gentle terrain near a mountain range. III - Turbulence structure in the boundary layer near the ground analyzed by acoustic sounding 12 p1758 A83-29130

Turbulent characteristics of a shallow convective internal boundary layer 12 p1758 A83-29138

ADI on staggered mesh - A method for the calculation of compressible convection 12 p1724 A83-29621

On local relaxation methods and their application to convection-diffusion equations 12 p1725 A83-29644

An examination of natural convection between two horizontal walls --- French thesis 12 p1727 A83-29945

A verification program for severe convective storm forecasts 13 p1886 A83-30547

Thermodynamic analysis procedures at the National Severe Storms Forecast Center 13 p1888 A83-30573

Effect of an electron beam on the current-convective instability --- in diffuse auroral plasmas 13 p1926 A83-31244

Periodic and irregular convective self-oscillations in an ellipsoid 13 p1843 A83-31343

Multiscale model equations for turbulent convection and convective overshoot --- relevant to study of solar or stellar evolution 13 p1952 A83-31432

Accretion in cataclysmic binaries. I - Modified alpha-disks with convection. II - Observational data 13 p1955 A83-31654

Generation of magnetohydrodynamic waves in white dwarfs 13 p1955 A83-31656

Stability criteria for convection at small Prandtl numbers 14 p2009 A83-32516

Numerical simulation of the heating of the solar chromosphere by intense heat fluxes 14 p2115 A83-32538

The seasonal variation of the thermal structure of the atmosphere of Uranus 14 p2112 A83-32608

Differential rotation in F stars - A comparison between theory and observation 14 p2105 A83-33202

Investigation of a laboratory model of a developing convective vortex 14 p2059 A83-33398

On the constancy of spectral-line bisectors --- for cool stars 14 p2110 A83-33463

Pressure effects on triple correlations in turbulent convective flows 15 p2156 A83-33669

Sunspot bright rings and the thermal diffusivity of solar convection 15 p2278 A83-34278

Nonlinear convection in a rotating layer - Amplitude expansions and normal forms 15 p2161 A83-34324

Transport effects associated with turbulence with particular attention to the influence of helicity 15 p2161 A83-34400

Heat transfer and horizontally averaged temperature of convection with large viscosity variations 16 p2348 A83-35339

Free convection about a sphere at small Grashof number 16 p2349 A83-35558

On the temperature profile at the surface of a rotating convection zone 16 p2353 A83-36547

Analysis of transient natural convection flow at high Prandtl number using a matched asymptotic expansion technique 16 p2354 A83-36596

Rise times of horizontal magnetic flux tubes in the convection zone of the sun 16 p2440 A83-36690

On the large-scale dynamics of rapidly rotating convection zones --- in solar and stellar interiors 17 p2597 A83-37329

Quasi-periodic oscillations in the solar atmosphere 17 p2626 A83-37677

A numerical study of slow nonisothermal flows past axisymmetrical bodies 17 p2506 A83-37805

Existence of a steady state of a natural convective flow in a confined medium 17 p2507 A83-38066

The kinematics of hexagonal magnetoconvection --- in solar photosphere 17 p2583 A83-38530

Period doubling and chaos in partial differential equations for thermosolutal convection 17 p2576 A83-38606

On the influence of the vertical wind structure on convective precipitation 18 p2723 A83-39145

Theory of magnetic activity of late type stars 18 p2765 A83-39241

Free convection flow on a nonisothermal flat plate under nonuniform gravity 18 p2681 A83-39347

Experimental studies of the turbulence structure parameters of the convective boundary layer 18 p2725 A83-39682

Hall effects on MHD free-convection flow in the Stokes problem for a vertical porous plate 18 p2746 A83-39765

Correlations concerning turbulent natural convection Influence of pressure and nature of the gas 18 p2685 A83-39851

Two-component Benard convection - Interfacial deformation, oscillatory instabilities and the onset of turbulence 18 p2685 A83-39892

Convective-diffusive transport in vapor growth ampoules 18 p2685 A83-39897

Morphological and convective instabilities during solidification 18 p2686 A83-39902

The kinematics of orographic airflow during Sierra storms 18 p2729 A83-40037

Structure and extinction of convective diffusion flames with general Lewis numbers 18 p2664 A83-40312

Regimes of mixed convection in a vertical layer whose boundaries undergo unsteady deformation 19 p2842 A83-41205

Stability of the stationary plane-parallel convective motion of a chemically active medium 19 p2842 A83-41261

On the thermal state of the earth's mantle 20 p3017 A83-42373

Natural convection in a spherical annulus filled with heat generating fluid 20 p2972 A83-42677

Overshooting and damped oscillations of transient natural convection flows in cavities 20 p2973 A83-42683

Flow reversal in turbulent mixed convection 20 p2980 A83-42756

Magnetic-flux transport by a convecting layer - Topological, geometrical and compressible phenomena --- in solar magnetic field 20 p3081 A83-43094

Liquid materials and flow processes in reduced gravity 20 p2940 A83-43268

The calculation of transport phenomena in electromagnetically levitated metal droplets 20 p2963 A83-43273

Effect of Rayleigh accelerations applied to an initially moving fluid --- in circular cylinders under low gravity associated with space flight 20 p2940 A83-43274

Convective and interfacial instabilities during solidification of succinonitrile containing ethanol 20 p2946 A83-43299

An interferometric investigation of separated forced convection in laminar flow past cavities 20 p2986 A83-43360

Numerical solution of natural convection in eccentric annuli 20 p2987 A83-43451

A theoretical study of the development of an axisymmetric thermal plume - The influence of the thermophysical properties of the gas 21 p3169 A83-44852

Mass transfer and free convection through a porous medium by the presence of a rotating fluid 21 p3131 A83-44853

Features of the energetic regime of the plasmasphere in the zone of magnetospheric convection 21 p3177 A83-45283

The relationship between the surface wind field and convective precipitation over the St. Louis area 22 p3338 A83-45703

Surface plates and thermal plumes - Separate scales of the mantle convective circulation 22 p3324 A83-45796

A remark on viscosity and convection in the mantle 22 p3325 A83-45801

- Zigzag instability and axisymmetric rolls in Rayleigh-Benard convection - The effects of curvature 22 p3280 A83-45939
- The characteristics of salt fingers in a variety of fluid systems, including stellar interiors, liquid metals, oceans, and magmas 22 p3281 A83-46003
- Self-consistent theory of three-dimensional convection in the geomagnetic tail 22 p3326 A83-46036
- Numerical computation of three-dimensional convective flows in horizontal and tilted containers 22 p3284 A83-46488
- Influence of turbulent pressure on solar convective modes 22 p3388 A83-46537
- Comparison of model high-latitude electron densities with Millstone Hill observations 22 p3335 A83-47042
- Recent developments in surface-tension driven instabilities [IAF PAPER 83-144] 23 p3446 A83-47289
- Ergodic stream-lines in steady convection 23 p3449 A83-48199
- The convective mechanism of the formation of the plasma sheet in the magnetospheric tail 23 p3484 A83-48380
- Mechanism for transition to turbulence in buoyant plume flow 23 p3451 A83-48623
- Stability of convection rolls in the presence of a horizontal magnetic field 24 p3632 A83-49643
- An investigation of the interaction between developing convective systems and the boundary layer --- for south Florida cumulonimbus 24 p3611 A83-49680
- ### CONVECTIVE HEAT TRANSFER
- A hypothesis on the hydromagnetic activity of T Tau type stars and related objects 01 p0119 A83-10267
- Verification of the oscillatory state of thermocapillary convection in a floating zone under low gravity 01 p0047 A83-11327
- Theory of thermal conductivity, heat conduction and convective heat transfer in fiber filled polymer composites 02 p0149 A83-11804
- Consistency of the mixing length theory --- for solar convection zone 02 p0257 A83-12140
- Finite analytic numerical solution of axisymmetric Navier-Stokes and energy equations [ASME PAPER 82-HT-42] 02 p0172 A83-12795
- Natural convection heat transfer between eccentric horizontal cylinders [ASME PAPER 82-HT-43] 02 p0172 A83-12796
- Effect of aspect ratio on heat transfer in shallow enclosures [ASME PAPER 82-HT-44] 02 p0172 A83-12797
- Numerical solutions of radiative heat transfer with convection [ASME PAPER 82-HT-45] 02 p0172 A83-12798
- Mixed convection over a horizontal heated flat plate [ASME PAPER 82-HT-75] 02 p0173 A83-12804
- Convective thinning of the lithosphere - A mechanism for the initiation of continental rifting 02 p0212 A83-12871
- Modes of mantle convection and the removal of heat from the earth's interior 02 p0212 A83-12872
- Differential rotation driven by convection in a rapidly rotating annulus 02 p0174 A83-12978
- Heat transfer on cylinder covered with close-fitting fabrics. I - Wind penetration through fabrics 02 p0226 A83-13070
- Heat transfer in a parallelogram shaped enclosure. II Free convection in infinitely stacked parallelogram shaped enclosure. III - Combined free convection and radiation heat transfer 02 p0175 A83-13071
- A kinematic thermal history of the earth's mantle 02 p0212 A83-13101
- Fin geometry for minimum entropy generation in forced convection 03 p0315 A83-13483
- Numerical simulation of natural convection in concentric and eccentric horizontal cylindrical annuli 03 p0315 A83-13484
- Large Prandtl number finite-amplitude thermal convection with Maxwell viscoelasticity --- earth mantle rheological model 03 p0304 A83-14521
- Nonlinear modal analysis of penetrative convection --- in stratified fluids under astrophysical and geophysical conditions 03 p0320 A83-14523
- Chromospheres of F, G, K type stars. VIII - Energy balance in transition region 03 p0437 A83-14720
- Improved formulations for the analysis of convecting and radiating finned surfaces 04 p0476 A83-15292
- Finite element thermal analysis of an icing protective system [AIAA PAPER 83-0113] 05 p0632 A83-16528
- Base heating on an aerobraking orbital transfer vehicle [AIAA PAPER 83-0408] 05 p0607 A83-16697
- Integral method to thermally developing laminar flow in a duct subjected to external radiation and convection [AIAA PAPER 83-0529] 05 p0637 A83-16768
- Transient nonlinear heating and cooling of a plate with heat generation 05 p0640 A83-17556
- On turbulent heat transport in rotating convective zones --- in stellar hydrodynamics 05 p0709 A83-17854
- Radiative-convective models of climate 06 p0788 A83-17997
- Heat conduction in an undulating heating wire 06 p0756 A83-18063
- Time-dependent solutions of multimode convection equations 06 p0757 A83-19018
- Combined /radiative-convective/ heat transfer from laminar and turbulent radiating flows in cooled ducts 06 p0759 A83-19160
- Experiments on natural convection heat transfer in low aspect ratio enclosures 07 p0924 A83-19822
- Numerical calculation of pressure loss and forced convective heat transfer in rotating channels of arbitrary rectangular cross section 08 p1083 A83-21634
- Effect of vibration on natural convection heat transfer from vertical fin arrays 08 p1083 A83-21894
- Evaluation of total body heat transfer in hypersonic flow 08 p1042 A83-22150
- An experimental study of unsteady heat transfer from a flat plate to an oscillating air flow 08 p1084 A83-22239
- The relationship between surface topography, gravity anomalies, and temperature structure of convection 08 p1135 A83-22365
- Analysis of viscous dissipation effect on thermal entrance heat transfer in laminar pipe flows with convective boundary conditions 08 p1086 A83-23123
- Numerical calculations of turbulent heat transfer downstream of a rearward-facing step 08 p1089 A83-23199
- Laminar natural convection along vertical corners and rectangular channels 08 p1090 A83-23208
- Thermoconvective heat transfer in a rectangular cavity with constant wall cooling rate 08 p1090 A83-23211
- Finite element analysis of mixed convection applied to the storage of solar energy 08 p1091 A83-23219
- The use of the theory of thermal regularity in investigating the effect of radiation on free convection 09 p1258 A83-23448
- Free convection flow of water at 4 C past an infinite porous plate with constant suction and free stream velocity 09 p1258 A83-23600
- Influence of free-stream turbulence on turbulent boundary layer heat transfer and mean profile development. I - Experimental data. II - Analysis of results 09 p1259 A83-23876
- Heat transfer from interrupted plates 09 p1259 A83-23879
- Convective losses from cavity solar receivers - Comparisons between analytical predictions and experimental results 09 p1293 A83-23881
- Convective heat losses from flat-plate solar collectors in turbulent winds 09 p1293 A83-23883
- Character and stability of axisymmetric thermal convection in spheres and spherical shells --- model for heat transfer in planetary interiors 09 p1365 A83-24126
- The effect of multiple exposures to radiative heat on the resistance of the body to convective heating and total cooling 09 p1321 A83-25157
- A computer model for gas turbine blade cooling analysis [ASME PAPER 82-JPGC-GT-6] 09 p1208 A83-25267
- A model of mean zonal flows in the major planets 10 p1517 A83-25415
- Heating-rate measurements over 30 deg and 40 deg /half-angle/ blunt cones in air and helium in the Langley expansion tube facility 10 p1371 A83-26146
- Numerical calculation of local convective heat transfer coefficients over air-cooled vane surfaces 10 p1418 A83-26772
- Methods for solving nonstationary problems of the theory of radiative-convective heat transfer 11 p1568 A83-28369
- Thermal stresses in a semiinfinite orthotropic plate heated by a heating region moving along the end face 11 p1596 A83-28463
- Radiative-convective heat transfer during turbulent flow of carbon dioxide in a plane channel 11 p1570 A83-28793
- Reduced first order differential equation with optimal control finite element penalty functions --- applied to convection-radiation heat transfer and boundary layer problems 12 p1721 A83-28853
- Thermal convection instability of liquid metals of magneto-hydrodynamics 12 p1780 A83-29053
- Convective plumes in the atmospheric boundary layer as observed with an acoustic Doppler sodar 12 p1758 A83-29132
- Energy estimates for latent-heat driven convection in the earth's core 12 p1753 A83-29238
- Thermal diffusion in gases --- Russian book 12 p1723 A83-29341
- The thermal management of printed circuit board assemblies 12 p1720 A83-29515
- Thermal stresses in partially absorbing flat plate due to sudden interruption of steady-state asymmetric radiation. I Convective cooling at rear surface. II - Convective cooling at front surface 12 p1747 A83-29922
- Parametric method for solving problems of heat transfer for the film flow of a fluid 13 p1838 A83-30045
- Convective heat transfer in rotating cylindrical cavity [ASME PAPER 82-GT-151] 13 p1840 A83-30239
- Thermally indirect motions in the convective atmospheric boundary layer 13 p1892 A83-31035
- The influence of heat-transfer factors on results of the thermal optimization of solar power plants 14 p2036 A83-32050
- The effect of natural convection on the concentration limits of ignition for combustible mixtures in a closed container 14 p1988 A83-32081
- Thermal stresses in a semiinfinite cylindrical shell locally heated by convective heat transfer 14 p2030 A83-32377
- Parameterization of the surface fluxes of heat and momentum for the convective atmospheric boundary layer 14 p2056 A83-32402
- Measurement of thermoacoustic convection heat transfer phenomenon [AIAA PAPER 83-1422] 14 p2009 A83-32701
- Prediction of density and constant pressure specific heat for several fluids in the near-critical region [AIAA PAPER 83-1476] 14 p2094 A83-32730
- Turbulent heat transfer in the separated reattached and redevelopment regions of a circular tube [AIAA PAPER 83-1520] 14 p2010 A83-32753
- Scaling analysis of thermoacoustic convection in a zero-gravity environment 15 p2156 A83-33745
- A numerical model of the dynamics and microphysics of warm cumulus convection - Model description and preliminary results 15 p2205 A83-34065
- Accuracy aspects of the finite element method in free convection heat transfer problems 15 p2160 A83-34256
- Combined free and forced laminar convection in a vertical channel 15 p2160 A83-34257
- An effective numerical technique for entry length laminar convective heat transfer in vertical and horizontal ducts of any cross section 15 p2160 A83-34258
- Combined convection in an annulus applied to a thermal storage problem 15 p2191 A83-34259
- Laminar, natural convection heat transfer in a horizontal gap, bounded by an elliptic and A circular cylinder 15 p2160 A83-34260
- A coupled conduction-convection study in the slip-flow regime 15 p2160 A83-34261
- Exact finite elements for conduction and convection 15 p2160 A83-34263
- Method to solve some coupled convection and conduction problems 15 p2160 A83-34264
- A balloon and its basket in the Venus' atmosphere 15 p2124 A83-34271
- Laminar natural convection from a horizontal plate and the influence of plate-edge extensions 16 p2348 A83-35337
- Heat transfer and horizontally averaged temperature of convection with large viscosity variations 16 p2348 A83-35339
- On the mechanism for the development of polar lows 16 p2386 A83-35480
- The effect of thermal boundary conditions on the heat transport in vertical channels heated from below 16 p2349 A83-35557
- Profile losses during the release of air onto the surface of nozzle vanes 16 p2288 A83-35590
- The effects of conductive, convective and radiative heat transfer on rocket motor service life [AIAA PAPER 83-1120] 16 p2318 A83-36231
- Analysis of transient natural convection flow at high Prandtl number using a matched asymptotic expansion technique 16 p2354 A83-36596
- Thermal theory of convectively cooled mirrors, windows for CW and repetitively pulsed lasers [AIAA PAPER 83-1720] 17 p2503 A83-37209
- A survey of the core helium flash with dynamic convection 17 p2597 A83-37330
- A statistical theory of thermally-driven turbulent shear flows, with the derivation of a subgrid model 17 p2507 A83-37877
- Unsteady forced convective heat transfer from a hot film in non-reversing and reversing shear flow 18 p2681 A83-39348

A discussion of some criteria for the use of adaptive gridding
[AIAA PAPER 83-1932] 18 p2740 A83-39384

The effect of a porous coating on the convective heat transfer during boiling 18 p2684 A83-39475

Thermal instabilities --- convective heat transfer in materials science 18 p2685 A83-39890

Numerical methods in heat transfer
20 p2970 A83-42653

Visualization of heat transfer 20 p2970 A83-42654

Radiation heat transfer - Interaction with conduction and convection and appropriate methods in radiation
20 p2970 A83-42655

Advanced boundary-layer theory in heat transfer
20 p2970 A83-42657

Heat transfer in the atmosphere
20 p3030 A83-42658

Enhancement of heat transfer
20 p2970 A83-42659

Natural convection heat transfer in cavities and cells
20 p2971 A83-42662

Convection in a horizontal fluid layer having a shear-free upper surface and uniform volumetric energy sources
20 p2972 A83-42672

Numerical study of the interaction of natural convection with radiation in nongray gases in a narrow vertical cavity
20 p2972 A83-42674

Aspects of Galerkin approximations for hydrodynamic simulations
20 p2972 A83-42675

Natural convection with volumetric energy sources in a fluid bounded by a spherical segment
20 p2972 A83-42676

A finite difference study of natural convection in complex enclosures
20 p2972 A83-42678

Numerical simulation of laminar natural convection in shallow inclined enclosures
20 p2973 A83-42680

Natural convection in an open cavity
20 p2973 A83-42681

Heat transfer 1982; Proceedings of the Seventh International Conference, Technische Universitaet Muenchen, Munich, West Germany, September 6-10, 1982. Volume 3 - General papers: Forced convection, mixed convection
20 p2975 A83-42700

Convective, conductive and radiative heat transfer in a tube submitted to a non uniform circumferential flux
20 p2975 A83-42702

Heat transfer in a vertical rotating annulus - A numerical study
20 p2975 A83-42705

Numerical study of unsteady convective heat transfer in pulsating duct flows
20 p2975 A83-42708

Pressure loss and heat transfer through multiple rows of short pin fins
20 p2975 A83-42709

A turbulent burst model for energy transfer in the wall region
20 p2978 A83-42735

Cross flow influence upon impingement convective heat transfer in circular arrays of jets - A general correlation
20 p2978 A83-42741

Convective heat transfer from laminar and turbulent premixed flames
20 p2979 A83-42748

Combined forced and free convection between parallel plates
20 p2979 A83-42752

Experimental mixed convection from a large, vertical plate in a horizontal flow
20 p2980 A83-42754

Nucleate pool boiling in microgravity environment
20 p2980 A83-42759

Holographic interferometry studies of temperature profiles in thermal boundary layer in free convection and bubble boiling
20 p2980 A83-42760

Forced convection film boiling on a sphere immersed in (a) subcooled or (b) superheated liquid
20 p2981 A83-42770

Radiative-convective heat transfer and heat shielding for spacecraft descending to the earth's surface and to the surfaces of other solar-system planets
20 p2945 A83-42881

Heat transfer at hyperbolic flight velocities - Physical model and theoretical and experimental studies
20 p2929 A83-42882

Convective heat transfer in vertical layers of an anisotropic porous material --- thermal insulation
20 p2982 A83-42894

The effect of ordered structure of turbulence on momentum, heat and mass transfer of impinging round jets
20 p2984 A83-43020

Study of convective heat transfer in gas turbine combustion chambers
20 p2984 A83-43024

Influence of diffusion and convective transport on dendritic growth in dilute alloys
20 p3054 A83-43298

The effect of the natural convection on the transition from columnar to equiaxed crystals
20 p3054 A83-43311

Towards consistency in simple prescriptions for stellar convection
21 p3232 A83-44727

Effects of variable fluid properties and boundary conditions on thermal convection
21 p3131 A83-44854

Low Reynolds number flow heat exchangers; Proceedings of the Fourth Advanced Study Institute, Ankara, Turkey, July 13-24, 1981
21 p3133 A83-45099

Calculation of the heating of layered bodies
21 p3163 A83-45351

The parametric excitation of internal waves and convective instabilities in a fluid layer heated from above
22 p3322 A83-45639

Terrestrial heat flow history and temperature profiles
22 p3324 A83-45795

Surface plates and thermal plumes - Separate scales of the mantle convective circulation
22 p3324 A83-45796

A mixing-length model for the prediction of convex curvature effects on turbulent boundary layers --- for turbine blade convective heat transfer prediction
23 p3447 A83-47933

Convective heat transfer on flat plate at very high temperature and pressure gradient
23 p3448 A83-47946

Unsteady thermal convection in a cylindrical vessel in the case of lateral heat injection
23 p3452 A83-48668

Unsteady regimes of the convective combustion of a porous powder fuel
24 p3555 A83-49539

Results of a qualitative analysis of the equation of nonstationary convective combustion for porous systems
24 p3556 A83-49772

CONVENTIONS

The United Nations Convention on International Multimodal Transport of Goods /1980/- Discussion of the operations of pick-up and delivery with particular attention to the air mode
06 p0816 A83-18100

The interpretation of international conventions supporting a uniform law in international relations
22 p3367 A83-45803

The implications of the United Nations Convention on International Multimodal Transport of Goods (Geneva, 1980) for International Civil Aviation
22 p3367 A83-45804

The Warsaw Convention - Past, present and future
22 p3369 A83-45827

CONVERGENCE

Formal convergence characteristics of elliptically constrained incremental Newton-Raphson algorithms
01 p0101 A83-10273

Digital stochastic iterative procedures for the adaptive adjustment of noise compensation systems - Analysis of convergence and convergence rate
01 p0031 A83-10412

The superconvergence of finite element method solutions in mesh norms
01 p0102 A83-11266

Galerkin methods for second kind integral equations with singularities
03 p0387 A83-13573

Convergence and stability of a collocation method for the generalized airfoil equation
03 p0278 A83-13844

Global convergence of output error recursions in colored noise
03 p0386 A83-14592

Relaxation computation of transonic flows around wings with blunt leading-edge and discussion on its stability and convergence
04 p0443 A83-15543

Limiting behavior of bang-bang controls for Sobolev problems
04 p0528 A83-15947

Estimation of convergence speed in the second uniform limit theorem of Kolmogoroff
04 p0530 A83-16410

An iterative method for solving an eigenvalue problem
05 p0682 A83-17639

The convergence speed of projection methods in eigenvalue problems
05 p0682 A83-17640

Instability of a convergent spherical shock wave
05 p0640 A83-17647

Questions of convergence, duality, and averaging for a class of functionals of the calculus of variations
06 p0804 A83-17976

Derivation and convergence of power series in structural design
06 p0773 A83-18233

Uniform convergence of interpolation by cubic splines
06 p0804 A83-18900

On the convergent solution in Kopal's iterative method of solving eclipsing binary orbits
06 p0822 A83-19164

Convergence of interpolational cubic splines on nonuniform grids
06 p0804 A83-19599

Convergence in distribution of LMS-type adaptive parameter estimates
07 p0984 A83-20721

Second-order convergence analysis of stochastic adaptive linear filtering
07 p0985 A83-20723

Extension of the region of convergence of an iterative method for solving the inverse refraction problem
07 p0989 A83-20853

On the convergence of the finite element approximation of eigentrequencies and eigenvectors to Maxwell's boundary value problem
08 p1159 A83-22077

The convergence of the Richardson method in problems concerning the nonlinear theory of elasticity
09 p1280 A83-24242

Convergence properties of LMS adaptive estimators with unbounded dependent inputs
09 p1330 A83-24743

The characterization of Q-superlinear convergence of methods for constrained optimization
09 p1331 A83-24766

An investigation of the convergence of a moist convective adjustment scheme
09 p1315 A83-24938

Solution of large sparse nonlinear systems by monotone convergent iterations and applications
09 p1336 A83-25109

A block-by-block method for the numerical solution of Volterra delay integro-differential equations
10 p1470 A83-25590

On approximation by the interpolating series of G. Valiron
10 p1470 A83-26475

Exponential convergence of adaptive identification and control algorithms
10 p1467 A83-26548

Adaptive control with forgetting factor
10 p1467 A83-26554

An adaptive observer with exponential rate of convergence for single-input single-output linear systems
10 p1468 A83-26562

Two approaches for adaptive observer in multi-output systems
10 p1468 A83-26563

Concentration of vorticity and spiral vortices
11 p1566 A83-27703

Rapid interference suppression using a Kalman filter technique
11 p1554 A83-27906

Convergence time of sidelobe cancellation systems
11 p1554 A83-27908

Collocation methods for weakly singular second-kind Volterra integral equations with non-smooth solution
11 p1648 A83-27996

Application of generalized Padeapproximants to the special function evaluation problem
12 p1772 A83-29637

An overrelaxation method for Euler equations in steady transonic flow
12 p1726 A83-29668

Auxiliary convergence criteria for Mindlin plate elements and their application to the four-node quadrilateral
12 p1737 A83-29743

On partial spectral expansions with natural convection in spherical annulus enclosures as an example
12 p1726 A83-29900

Convergence of approximate solutions to conservation laws --- in parabolic systems and finite difference schemes
12 p1727 A83-29939

Volterra-like expansions for solutions of nonlinear integral equations and nonlinear differential equations
13 p1912 A83-30872

Convergence of Galerkin approximations for the Korteweg-de Vries equation
13 p1912 A83-31360

A computational study of finite element methods for second order linear two-point boundary value problems
13 p1912 A83-31362

New results on the vibrating string with a continuous obstacle
14 p2080 A83-32837

Progress in computational physics
15 p2216 A83-33868

Fast iterative division of p-adic numbers
15 p2217 A83-33910

Convergence of vector quantizers with application to the design of optimal quantizers
15 p2221 A83-35105

Convergence of partitioned adaptive filters for systems with unknown biases
17 p2569 A83-37550

Piecewise polynomial Galerkin approximation to invariant densities of one-dimensional difference equations
17 p2571 A83-38037

Improving the convergence rate of parabolic ADI methods
18 p2739 A83-39361

The effect of strong heat addition on the convergence of implicit schemes
18 p2635 A83-39371

Implicit upwind methods for the Euler equations
18 p2682 A83-39382

Approximation of solutions of strongly nonstationary stochastic extremal problems in continuous time. II
19 p2889 A83-40899

Convergence of algorithms
19 p2889 A83-40899

A survey of methods for iterative signal restoration
19 p2830 A83-41376

Necessary and sufficient conditions of the convergence asynchronous iterative computational processes when solving systems of linear algebraic equations
19 p2888 A83-41420

A convergence analysis of a numerical method for solving the balance equation --- of atmospheric circulation
20 p3029 A83-42507

- Cubic spline approximation techniques for parameter estimation in distributed systems 20 p3040 A83-43405
- Determination of physically achievable accelerations in the problem of the spatial convergence of a material point --- for ergatic control system synthesis 20 p3035 A83-43502
- Generalized f and g series and convergence of the power series solution of the n-body problem 20 p3062 A83-43575
- Economical solution technique for boundary integral matrices 20 p3042 A83-43648
- Approximate-factorization scheme of transonic small-disturbance potential equation 21 p3088 A83-44574
- On the convergence of numerical results in modal analysis --- of parallel plate waveguides 23 p3445 A83-47840
- Convergence analysis of recursive identification algorithms with forgetting factor 24 p3621 A83-49922

CONVERGENT NOZZLES

- Film flow of a liquid on a convergent-nozzle surface 11 p1568 A83-28372
- A model for the film flow of a fluid along the surface of a convergent nozzle 20 p2987 A83-43516

CONVERGENT-DIVERGENT NOZZLES

- A numerical study of a moderate Reynolds number flow in a nozzle 03 p0320 A83-14568
- Internal performance prediction for advanced exhaust systems --- for tactical aircraft 08 p1046 A83-22156
- Mechanism of pseudo-shock wave in supersonic jet 10 p1373 A83-26425
- Some remarks on the numerical solution of tricom-type equations 12 p1726 A83-29932
- Analytical method for determining the nonequilibrium parameters of an air plasma in a Laval nozzle 13 p1922 A83-30044
- Critical flashing flows in nozzles with subcooled inlet conditions 15 p2157 A83-33996
- A solution to the direct problem of a Laval nozzle for a two-phase medium 16 p2289 A83-35720
- A static investigation of yaw vectoring concepts on two-dimensional convergent-divergent nozzles [AIAA PAPER 83-1288] 16 p2294 A83-36324
- Analysis of cold flow reestablishment time in a circuit breaker nozzle [AIAA PAPER 83-1749] 17 p2503 A83-37224
- A solution to the direct problem of a plane Laval nozzle 17 p2451 A83-37813
- The effect of strong heat addition on the convergence of implicit schemes [AIAA PAPER 83-1914] 18 p2635 A83-39371
- Characteristic frequencies of transonic diffuser flow oscillations 20 p2930 A83-43438
- Subsonic/supersonic aeropropulsive characteristics of nonaxisymmetric nozzles installed on an F-18 model 23 p3411 A83-48215
- Computational-experimental study of the gas dynamics of two-dimensional symmetric nozzles having a region of constant height and two contour bend points in the critical section 23 p3400 A83-48661

CONVERTAPLANES**U V/STOL AIRCRAFT****CONVERTERS**

- A magnetically controlled electrovacuum converter of displacement into pulsed signals 04 p0472 A83-15913
- Analysis of the magnetic circuit of a magnetic-modulation converter 04 p0472 A83-15914
- Synthesis of a waveguide field-converter 06 p0755 A83-19361
- New magnetic structures for switching converters 08 p1082 A83-23100
- Structural method for the synthesis of magnetic elements 12 p1719 A83-29323
- Converters of the levels of logical elements --- Russian book 15 p2152 A83-34174
- Active microwave filters on the basis of transistorized impedance converters 15 p2153 A83-35151
- Synthesis and analysis of pulsed measuring converters of information and measuring systems --- Russian book 18 p2679 A83-40606

CONVEXITY

- Measurements in the heated turbulent boundary layer on a mildly curved convex surface 15 p2155 A83-33657

CONVOLUTION INTEGRALS

- Description of two hardware convolvers as a part of a general image computer 01 p0089 A83-11437
- Wiener estimator for inversion of linear operators and superresolution 01 p0099 A83-11454
- Two-dimensional convolute integrals for analytical instrumentation 02 p0183 A83-13110
- A bulk-acoustic-wave device for the convolution of microwave signals 04 p0469 A83-15140

- Convolution equations in multidimensional spaces --- Russian book 05 p0681 A83-17120
- The application of acoustoelectronic convolvers in phase-locked systems 06 p0750 A83-18035
- Remote determination of the structure constant profile from amplitude scintillation data using Tikhonov's regularized inverse method --- Fourier transform for solving convolution equations 09 p1311 A83-23795
- An integral equation connected with the Jacobi polynomials 09 p1336 A83-24371
- On the deconvolution of brightness profiles of galaxies from seeing - Application to NGC 3379 10 p1494 A83-25834

- Features of the search for pseudorandom signals according to delay using acoustoelectronic convolvers 10 p1412 A83-26958
- Fast digital convolution using p-adic transforms 12 p1770 A83-29473

- A parallel-pipeline architecture of the fast polynomial transform for computing a two-dimensional cyclic convolution 13 p1908 A83-30794
- Estimation of the free distance of convolutional codes with rate 1/2 14 p2075 A83-32486
- Objective procedures for lineament enhancement and extraction --- digital convolution enhanced images 14 p2035 A83-33346

- Fast convolution methods for hexagonally sampled two-dimensional signals 15 p2220 A83-33518
- Inversion of synchrotron spectra 16 p2428 A83-36532

- A method of stabilizing the clean algorithm --- for deconvolution of Fourier synthesis point spread functions from radio astronomy images 16 p2425 A83-36646
- Contribution to the reduction of photoelectric occultation observations using an integrated deconvolution method 16 p2425 A83-36651

- Fast Fourier transform and convolution algorithms / 2nd revised edition/ 17 p2571 A83-37175
- Parallel architectures for computing cyclic convolutions 20 p3037 A83-43679
- The quick convolution of galaxy profiles, with application to power-law intensity distributions 21 p3234 A83-44764

- Simple coding scheme for modular arithmetic 21 p3190 A83-44969
- Modeling and deconvolution for reconstruction of airborne gamma ray radiometer data 22 p3288 A83-46125

- Image reconstruction by parametric cubic convolution 22 p3350 A83-46250
- Histogram deconvolution - An aid to automated classifiers 22 p3350 A83-46253
- Real-time image deblurring using four-wave mixing 24 p3628 A83-48750

CONVOLUTIONS (MATHEMATICS)**U CONVOLUTION INTEGRALS****CONVULSIONS**

- Effect of age on benzodiazepine-induced behavioural convulsions in rats 12 p1763 A83-29711

COOLANTS**NT ENGINE COOLANTS****NT ORGANIC COOLANTS**

- Back-to-back test for determining the pumping losses in a Stirling cycle machine 11 p1588 A83-27290

COOLERS

- Preliminary investigation on the performance of regenerative turbofan with inter-cooled compressor and its influence to aircraft 16 p2303 A83-35830

COOLING**NT ABSORPTION COOLING****NT AIR COOLING****NT CRYOGENIC COOLING****NT EVAPORATIVE COOLING****NT FILM COOLING****NT GAS COOLING****NT LIQUID COOLING****NT MAGNETIC COOLING****NT PLASMA COOLING****NT PRECOOLING****NT QUENCHING (COOLING)****NT RADIANT COOLING****NT REGENERATIVE COOLING****NT SOLAR COOLING****NT SPACE COOLING (BUILDINGS)****NT SUPERCOOLING****NT SURFACE COOLING****NT SWEAT COOLING****NT THERMOELECTRIC COOLING**

- An experimental study of single medium thermocline thermal energy storage [ASME PAPER 82-HT-53] 02 p0173 A83-12800
- Restoration of thermoregulatory response to body cooling by cooling hands and feet 03 p0378 A83-13578

- Effect of cooling rate on the microstructure of a 90W-7Ni-3Fe heavy alloy 06 p0732 A83-19105

- P/n/ velocity and cooling of the continental lithosphere --- upper mantle compression waves in North America 07 p0961 A83-20227

- Cooling rates for glass containing lunar compositions 07 p1035 A83-21324

- Glass formation - A contemporary view 08 p1070 A83-22190

- Determination of the cooling rates and nucleation histories of eight group IVA iron meteorites using local bulk Ni and P variation 08 p1189 A83-22929

- The effect of the cooling rate on the temperature of the beta-alpha transformation and the structure of titanium 09 p1234 A83-24384

- The effect of multiple exposures to radiative heat on the resistance of the body to convective heating and total cooling 09 p1321 A83-25157

- The characteristics of the thermoregulation in rats adapted to heat during the effect of cold 09 p1321 A83-25158

- On-site production of electrolytic hydrogen for generator cooling 11 p1605 A83-27209
- On the response of ocean currents to atmospheric cooling 11 p1635 A83-28084

- The growth of profiled silicon crystals by Stepanov's method using various heating schedules 11 p1663 A83-28362

- Thermal stresses in partially absorbing flat plate due to sudden interruption of steady-state asymmetric radiation. I Convective cooling at rear surface. II - Convective cooling at front surface 12 p1747 A83-29922

- Temperature readjustment factors for application to MIL-HDBK-217C failure rates --- electronic equipment reliability prediction 13 p1837 A83-31516

- Calorimetry with heat flux transducers - Comparison with a suit calorimeter 14 p2072 A83-32819
- Thermal analysis and control of electronic equipment --- Book 15 p2143 A83-33747

- Head and/or torso cooling during simulated cockpit heat stress 15 p2216 A83-34979
- Cooling history of pyroxene chondrules in the Yamato-74191 chondrite (L3) - An electron microscopic study 16 p2438 A83-36748

- Thermal theory of convectively cooled mirrors, windows for CW and repetitively pulsed lasers [AIAA PAPER 83-1720] 17 p2503 A83-37209

- A technique for the evaluation of the temperature profile during local cooling of the medulla oblongata 19 p2876 A83-41846

- Radiative heat transfer in a cylindrical chamber in the presence of an attenuating medium 19 p2846 A83-42143

- Cooling of the earth - A constraint on paleotectonic hypotheses 22 p3325 A83-45800
- Hot spot heat transfer - Its application to Venus and implications to Venus and earth 23 p3528 A83-47812

- An experimental investigation of endwall heat transfer and aerodynamics in a linear vane cascade [ASME PAPER 83-GT-52] 23 p3394 A83-47909

- A comparative study of the influence of different means of turbine cooling on gas turbine performance [ASME PAPER 83-GT-180] 23 p3465 A83-47991

COOLING FINNS

- Analysis and evaluation of extended surface thermal systems --- Book 03 p0317 A83-14114

- Improved formulations for the analysis of convecting and radiating finned surfaces 04 p0476 A83-15292

- Nodal averaging technique in the optimality criterion approach using tapered finite elements 08 p1121 A83-21889

- Effect of vibration on natural convection heat transfer from vertical fin arrays 08 p1083 A83-21894

- Recent developments in the analysis and design of extended surface 15 p2157 A83-33994

- Pressure loss and heat transfer through multiple rows of short pin fins 20 p2975 A83-42709

- Heat transfer experiments in high aspect ratio rectangular channel with epoxied short pin fins [ASME PAPER 83-GT-57] 23 p3447 A83-47913

- Heat transfer and friction loss characteristics of pin fin cooling configuration [ASME PAPER 83-GT-123] 23 p3448 A83-47952

COOLING SYSTEMS

- Cryo-cooler development for space flight applications 03 p0303 A83-13460

- A study of different techniques for cooling solar cells in centralized concentrator photovoltaic power plants --- French thesis 03 p0355 A83-14109

- Two years orbital performance summary of Stirling cycle mechanical refrigerators 08 p1053 A83-22847

- Hydraulics of a channel with a linear jet array --- heat transfer coefficient enhancement by transpiration cooling 09 p1260 A83-24049

- Actively cooled silicon mirrors --- for high energy cw lasers 09 p1346 A83-24972

- Shuttle Water Spray Boiler flight performance --- lubricant cooling for Orbiter Hydraulic System and APU [SAE PAPER 820885] 10 p1383 A83-25751
- SOLERAS solar active cooling field test operations 11 p1607 A83-27239
- Use of parabolic trough collectors for residential/light commercial solar cooling systems 11 p1608 A83-27245
- Steady flow examination of a cryocooler 11 p1564 A83-27289
- A method for producing heat pipes for cooling semiconductor photovoltaic cells and the heat pipe characteristics 11 p1553 A83-28366
- The thermal management of printed circuit board assemblies 12 p1720 A83-29515
- Thermal control system for a Manned Space Station [SAE PAPER 820836] 13 p1906 A83-30933
- Development and production of advanced cooling techniques for hybrid microcircuits 13 p1837 A83-31518
- Energy balance of solar absorption and vapor compression cooling systems 14 p2046 A83-32350
- Aluminum/ammonia heat pipe gas generation and long term system impact for the Space Telescope's Wide Field Planetary Camera [AIAA PAPER 83-1428] 14 p2009 A83-32704
- Microelectronic packaging 16 p2346 A83-36021
- Optimization of the jet cooling of a rotating disk 19 p2844 A83-41567
- A method for ensuring the proper operation of an optical instrument for measuring the temperature of the blades of a high-temperature turbine 19 p2799 A83-42152
- Cooling of a rotating disk by means of an impinging jet 20 p2978 A83-42739
- Superfluid-supercritical helium tradeoff analysis for the Shuttle Infrared Telescope Facility (SIRTF) 20 p2962 A83-43245
- Improved active phase separator for He II space cooling systems 20 p2962 A83-43246
- Analysis of coolant entrance boundary shape of porous region to control cooling along exit boundary 20 p2986 A83-43361
- The one-dimensional analysis of fin assembly heat transfer 20 p2986 A83-43365
- Techniques for obtaining detailed heat transfer coefficient measurements within gas turbine blade and vane cooling passages [ASME PAPER 83-GT-58] 23 p3447 A83-47914
- An experimental investigation of a gas turbine disk cooling system [ASME PAPER 83-GT-78] 23 p3447 A83-47931
- Full coverage discrete hole wall cooling - Discharge coefficients [ASME PAPER 83-GT-79] 23 p3447 A83-47932
- Absolute cavity pyrheliometer with two-stage cooling of the detector 24 p3583 A83-49289
- COORDINATE SYSTEMS**
U COORDINATES
- COORDINATE TRANSFORMATIONS**
- Determination of the transformation parameters of spatial rectangular coordinates --- for space geodesy and photogrammetry 01 p0072 A83-10851
- A software implementation of the cordic technique as applied to trigonometric functions 01 p0091 A83-11110
- Fermi normal co-ordinate system and electromagnetic detectors of gravitational waves. I - Calculation of the metric 02 p0254 A83-12028
- Approximating shapes using parameterized curves 02 p0231 A83-12174
- Coordinate transformation during the geometric correction of the space scanner imagery of the earth 03 p0350 A83-14313
- Properties of parallel-surfaces coordinate systems --- for balance equations in computational fluid dynamics 04 p0530 A83-15817
- Toroidal solutions of the Gegenbauer equation --- for space gravitational and plasma problems 04 p0532 A83-15961
- A computational method for performing the multiblade coordinate transformation 04 p0446 A83-16029
- The use of stereopairs with unknown orientation elements for the solution of the direct and inverse problems of photogrammetry and for the identification of objects 04 p0482 A83-16386
- State variable representation of a class of linear shift-variant systems 05 p0680 A83-16911
- Quality of trial functions in quadratic isoparametric representation of an arc 07 p0949 A83-21441
- Block overrelaxation methods for non-rectangular co-ordinates 07 p0949 A83-21442
- Electromagnetic fields in twisted coordinate system 08 p1080 A83-22234
- Time suboptimal feedback control design through coordinate transformation 10 p1461 A83-25396
- Map transformations by optical anamorphic processing 10 p1484 A83-26859
- On often used gauge transformations in gravitational radiation-reaction calculations. 12 p1791 A83-29027
- The use of multiple coordinate systems to form stiffness matrices of thin-walled structures on the basis of hybrid computational schemes 12 p1735 A83-29283
- Relationship between the truncation errors of centered finite-difference approximations on uniform and nonuniform meshes 12 p1771 A83-29619
- Coordinate generation with precise controls over mesh properties 12 p1772 A83-29631
- High level continuity for coordinate generation with precise controls 12 p1772 A83-29632
- Equivalence and singularities - An application of computer algebra --- metric calculation in general relativity 12 p1776 A83-29645
- Symbolic representation of translatory motion in multivarying-link mechanisms --- application to multidegree-of-freedom manipulators and robots 13 p1858 A83-30166
- Expansion of the coordinates of elliptical motion with respect to the Levi-Civita parameter 13 p1940 A83-31271
- Orthogonal mapping 13 p1912 A83-31367
- Block adjustment in photographic astrometry 14 p2100 A83-33253
- An analysis of coordinate transformation in Schmidt telescope photographic plates 14 p2100 A83-33256
- Generation of boundary-fitted curvilinear coordinate systems for a two-dimensional axisymmetric flow problem 15 p2157 A83-33825
- Large thermal deflections of elastic plates by conformal transformation 15 p2175 A83-34246
- Transformation of the equations of a three-dimensional boundary layer for numerical calculation 17 p2506 A83-37633
- A note on the mathematical formulation of the problem of numerical coordinate generation 17 p2571 A83-37768
- Algebraic grid generation 17 p2573 A83-38782
- Orthogonal grid generation 17 p2573 A83-38784
- Automatic algebraic coordinate generation 17 p2564 A83-38793
- Solution of viscous internal flows on curvilinear grids generated by the Schwarz-Christoffel transformation 17 p2508 A83-38796
- Test problems, coordinate transformations, and technique for nonsteady compressible flow analysis 17 p2508 A83-38797
- Generation of boundary-fitted coordinate systems using segmented computational regions 17 p2574 A83-38802
- The dependence of the Kolmogorov entropy of mappings on coordinate systems 18 p2740 A83-39001
- A streamline coordinate system for distorted two-dimensional shear flows 18 p2680 A83-39208
- A method for the computation of inertial properties for general areas 20 p3038 A83-42796
- Coordinate-invariant conservation laws in Schwarzschild geometry 20 p3075 A83-43389
- Coordinate transformations via multifacet holographic optical elements 21 p3134 A83-43871
- Model reduction by cost decomposition - Implications of coordinate selection 21 p3192 A83-44003
- Local similarity solution of the Tricomi equation in the elliptic coordinates 21 p3197 A83-44021
- New coordinates for three-body problems 21 p3224 A83-44648
- Product decompositions for certain types of coordinate transformation 23 p3502 A83-48141
- Conceptual kinematic design using homogeneous coordinate transformations [AIAA PAPER 83-2460] 23 p3500 A83-48337
- COORDINATES**
- NT ASTRONOMICAL COORDINATES
- NT CARTESIAN COORDINATES
- NT GEOCENTRIC COORDINATES
- NT GEODETIC COORDINATES
- NT HYPERBOLIC COORDINATES
- NT LAGRANGE COORDINATES
- NT PLANETOCENTRIC COORDINATES
- NT POLAR COORDINATES
- NT SPHERICAL COORDINATES
- Accuracy of the estimation of point-target coordinates and their derivatives 01 p0030 A83-10407
- Instantaneous determination of the locations of acoustic-emission signal sources in three coordinates 02 p0188 A83-12157
- Accuracy of the measurement of the angular coordinate in the case of discrete antenna-beam scanning 04 p0466 A83-15713
- The method of moving coordinates as a technique for comparing various electrodynamic problems in systems having cylindrical conductors 04 p0467 A83-15746
- The accuracy of measuring angular coordinates by means of antenna arrays 04 p0467 A83-15751
- A survey of grid generation techniques in computational fluid dynamics [AIAA PAPER 83-0447] 05 p0636 A83-16719
- A method for the approximate calculation of the current errors of mismatch in two-coordinate pursuit tracking 07 p0981 A83-20328
- 2-D coordinate grid generation by a vortex singularity method 07 p0864 A83-21018
- Synthesis of a quasi-optimal meter of the angular coordinates of a point source of signals 10 p1407 A83-26931
- Application of multigrid methods for integral equations to two problems from fluid dynamics 12 p1725 A83-29661
- Spectral multigrid methods for elliptic equations 12 p1773 A83-29663
- Application of the multigrid method to Poisson's equation in boundary-fitted coordinates 15 p2157 A83-33824
- Basic differential models for coordinate generation 17 p2572 A83-38779
- Elliptic grid generation 17 p2572 A83-38780
- Patched coordinate systems --- numerical body-fitted grid generation for surface boundary treatment of aerodynamic structures 17 p2573 A83-38785
- Solid mechanics applications of boundary fitted coordinate systems 17 p2525 A83-38786
- The use of complex normal coordinates during an investigation of nonlinear systems by the averaging method --- equations of motion for vibration 21 p3199 A83-44638
- The 1982 control network of Mars 22 p3384 A83-45744
- Assigning coordinates to objects on aerospace photographs 23 p3476 A83-48116
- COORDINATION**
- Uniformity of coordinated time scales 05 p0646 A83-17832
- COPERNICUS SPACECRAFT**
U CAO 3
- COPILOTS**
U AIRCRAFT PILOTS
- COPOLYMERIZATION**
- Morphology and physical structure of trioxane and styrene copolymers 06 p0734 A83-18025
- COPOLYMERS**
NT VITON
- Morphology and physical structure of trioxane and styrene copolymers 06 p0734 A83-18025
- Filtration coefficient and hydraulic permeability of Nafion 125 membranes in metal alkali solutions 10 p1390 A83-26056
- Photooxidative degradation of clear ultraviolet absorbing acrylic copolymer surfaces 11 p1552 A83-28753
- COPPER**
- Applications of remote sensing to porphyry copper exploration with emphasis on the proposed Landsat-D thematic mapper 01 p0062 A83-10034
- Diffusion welding for water-cooled gas turbine applications 02 p0187 A83-12071
- Electromigration transport mobility associated with pulsed direct current in fine-grained evaporated Al-0.5%Cu thin films 07 p0921 A83-20744
- Cull laser with a helical hollow cathode discharge 08 p1106 A83-21978
- Crystallization of copper under zero-g conditions 09 p1229 A83-23520
- Characterization of copper in phosphoric-acid-anodized 2024-T3 aluminum by Auger electron spectroscopy and Rutherford backscattering 10 p1395 A83-25547
- Thermal physics of transverse-discharge copper vapor lasers 10 p1433 A83-26682
- The initial stages of cavitation damage and erosion on copper and brass tested in a rotating disk device 11 p1547 A83-27421
- Optical properties of metal surfaces during laser irradiation 11 p1656 A83-27562
- Seasonal variations of Cd, Pb, Cu and Ni levels in snow from the eastern Arctic Ocean 11 p1613 A83-27673
- On the structure of tilt grain boundaries in cubic metals. I - Symmetrical tilt boundaries. II - Asymmetrical tilt boundaries. III - Generalizations of the structural study and implications for the properties of grain boundaries 11 p1551 A83-28807
- The geometrical factor during the extrusion of complex metal materials 13 p1859 A83-30688
- Laser studies of electronic energy transfer in atomic copper 13 p1851 A83-30957
- Cluster studies of CO adsorption. III - CO on small Cu clusters 13 p1817 A83-30965
- On the nature of the bonding in Cu₂ - An ab initio viewpoint 13 p1818 A83-31809
- Large-bore copper-vapor lasers - Kinetics and scaling issues 16 p2358 A83-35429

- Thermoelectricity, heat conduction, and strength of laminated composites 16 p2323 A83-35510
- Load and material flow in hot extrusion of aluminium and copper powder compacts 16 p2329 A83-35607
- Fatigue limits of Cu and Al up to 10 to the 10th loading cycles 16 p2332 A83-36189
- The effect of microstructure on the fatigue crack growth behavior near threshold in Cu and Al 16 p2333 A83-36198
- Effects of triaxial stressing on creep cavitation of grain boundaries 16 p2335 A83-36961
- High neon pressure longitudinal copper vapour laser 19 p2853 A83-41185
- The dissociation energy of Cu₂ - Do we want to perform multi-reference singles and doubles CIS on many-electron systems? 19 p2898 A83-41864
- Single and multiple pulse catastrophic damage in diamond-turned Cu and Ag mirrors at 10.6, 1.06, and 0.532 microns 21 p3203 A83-43863
- Landsat-D TM application to porphyry copper exploration 22 p3309 A83-46132
- Thermodynamics of a highly compressed plasma in the megabar range 22 p3363 A83-46791
- Population inversion in copper on transitions with wavelengths of 510.6 and 578.2 nm in a recombining Cu-Cs plasma 24 p3588 A83-49114
- COPPER ALLOYS**
- NT BRASSES**
- NT MANGANIN (TRADEMARK)**
- Effect of nickel plating on Fe-B-Cu-Mo and -W 02 p0155 A83-12074
- Determination of stress relaxation by damping measurements 07 p0946 A83-20522
- Recovery and work hardening during high temperature creep of fcc alloys of low stacking fault energy 09 p1231 A83-24055
- Study of the constitutive creep laws using biaxial relaxation tests 10 p1393 A83-25416
- The structure of electrodeposited alloys based on the metals of the iron subgroup 13 p1819 A83-30064
- Problems arising with fatigue-testing at ultrasonic frequencies in single and double transducer systems 16 p2331 A83-36180
- Practical applications 16 p2331 A83-36180
- Fatigue softening in precipitation hardened copper-cobalt single crystals 17 p2490 A83-38381
- Observations of grain boundary sliding during superplastic deformation 18 p2669 A83-40635
- High temperature oxidation of hafnium and its alloys 20 p2952 A83-42233
- The effect of structural transformations on the properties of the aluminum alloy VAD23 20 p2955 A83-43494
- High resolution electron microscopy studies on the precipitation in an Al-4 percent Cu alloy 20 p2956 A83-43614
- The long-term strength of metals in a complex stressed state 21 p3114 A83-45318
- Visualization of fatigue defects by an electrodischarge high-frequency method 22 p3269 A83-46330
- Effect of Cu addition on intergranular corrosion of Al-5.5 percent Zn-2.5 percent Mg alloy 24 p3566 A83-49860
- COPPER CHLORIDES**
- Metallic conductivity and air stability in copper chloride intercalated carbon fibers 04 p0473 A83-16095
- High-resolution line-shape analyses of the pulsed cuprous chloride-laser oscillator and amplifier 10 p1435 A83-26878
- Temporal measurement of the gain of a CuCl laser 11 p1585 A83-28702
- Low frequency dielectric relaxation in boracites 12 p1709 A83-29555
- COPPER COMPOUNDS**
- NT COPPER CHLORIDES**
- NT COPPER FLUORIDES**
- NT COPPER OXIDES**
- NT COPPER SELENIDES**
- NT COPPER SULFIDES**
- EXAFS investigation of dilute Cu impurities in amorphous As₂Se₃ 04 p0540 A83-15502
- Fe/II/, Co/II/, Ni/II/, Cu/II/, Zn/II/, Cd/II/ and Hg/II/ complexes of 4'-nitrobenzylidene-2-hydroxy-3,5-dinitroaniline 04 p0454 A83-16427
- Influence of electron heating during recombination of copper atoms in copper halide vapor lasers on their output parameters 05 p0650 A83-17068
- Service life of a copper bromide vapor laser 10 p1432 A83-26674
- Pressure-induced disproportionation in CuBr 12 p1782 A83-29168
- Changes in the reactivity of a solid substance at the interface of the reagent and the product of the topochemical reaction --- thermal decomposition of ammonium perchlorate 23 p3430 A83-48506

- Surface modification of polycrystalline p-CuInS₂ and p-CuInSe₂ electrodes for improved solar cell performance 24 p3601 A83-50177
- COPPER FLUORIDES**
- Advances in divalent transition-metal lasers 11 p1578 A83-27541
- COPPER OXIDES**
- Experimental and theoretical studies of Cu₂O solar cells 08 p1131 A83-22907
- Properties of oxidized copper surfaces for solar applications. I 12 p1716 A83-29512
- Properties of oxidized copper surfaces for solar applications. II 12 p1716 A83-29513
- Selective surfaces of anodic copper oxide for solar collectors 16 p2371 A83-35457
- The total anodization of copper films on platinum - Use as selective surface absorbers at high temperature 20 p3012 A83-42615
- Investigation of copper oxide coatings for solar selective applications 24 p3601 A83-50176
- COPPER SELENIDES**
- Optical properties and grain boundary effects in CuInSe₂ 21 p3167 A83-44606
- COPPER SULFIDES**
- Use of test structures in the production of CdS/Cu₂S photovoltaic devices 04 p0504 A83-15455
- Composition determination of CuInS₂ by a chemical analysis method 04 p0456 A83-15484
- Determination of trace elements in CuInS₂ 04 p0456 A83-15485
- The effects of heat treatments on the transport properties of Cu/x/S thin films 04 p0543 A83-16083
- Heat-treatment studies on thin-film CdS/Cu/x/S solar cells 04 p0507 A83-16084
- Compositional depth profiles of chemiplated Cu₂S/Zn,Cd/S heterojunction solar cells 08 p1130 A83-22339
- Role of impurities in sintered CdS/Cu₂S solar cells 09 p1292 A83-23666
- X-ray diffraction study of the dry formation of Cu₂S-CdS solar cells 10 p1444 A83-25448
- Fabrication of large area Cu₂S/CdS thin film solar modules 14 p2041 A83-32230
- Front contacts for large area high efficiency Cu₂S-CdS solar cells 14 p2041 A83-32231
- The assessment of thin film Cu(x)S-CdS solar cells using cathodoluminescence techniques 14 p2041 A83-32254
- Compositional analysis of CuInS₂ chalcopyrite semiconductor 14 p2089 A83-32257
- Large area CdS/Cu(x)S thin film solar cells produced by electrophoretic deposition 14 p2044 A83-32282
- Sprayed zinc-cadmium sulfide films for backwall Cu₂S/(ZnCd)S cells 14 p2044 A83-32283
- Temperature dependence of the IV-characteristic of Cu₂S-CdS thin film solar cells and related phenomena 14 p2044 A83-32294
- Thin film Cu₂S/CdS junctions produced by evaporation and sputtering - Effect of thermal treatments in vacuum 14 p2089 A83-32297
- Electrochemical preparation and conditioning of Cu₂S for Cu₂S-CdS solar cells 14 p2045 A83-32299
- Physicochemical properties of Cu(x)S 14 p1989 A83-32300
- An XPS study of Cu(x)S formed on Zn(0.15)Cd(0.85)S --- for solar cells 14 p2092 A83-32639
- Technology of all electroplated CdS:Cu(x)S solar cells 14 p2047 A83-32847
- Sprayed CdS-Cu₂S solar cells. I - Formation of cuprous sulphide 14 p2047 A83-32848
- The growth of Cu₂S on polished or etched single crystal CdS substrates 16 p2419 A83-35573
- Single crystal Cu₂S/CdS photovoltaic devices with optimum performance before a post barrier air bake 18 p2708 A83-39930
- Degradation of the performance of Cu₂S/CdS solar cells due to a two-way solid state diffusion process 20 p3052 A83-42358
- Sprayed CdS-Cu₂S solar cells. II - preparation of CdS by aerosol spray 21 p3167 A83-44328
- The electrical characteristics of thin film Cu(x)S-CdS solar cells and their dependence on the ambient atmosphere during annealing 23 p3477 A83-48198
- Structural and optical studies of topotaxially-grown Cu₂S from sprayed CdS thin films 24 p3636 A83-50181
- CORDITE**
- U DOUBLE BASE PROPELLANTS**
- CORE FLOW**
- Effect of swirl on the potential core in two-dimensional ejector nozzles 06 p0712 A83-18416
- Uniform asymptotic approximations for duct eigenfunctions in a thin boundary layer flow [AIAA PAPER 83-0668] 10 p1473 A83-25905
- MHD pseudoshock and qualitative model in the performance of supersonic generators 13 p1924 A83-30189

- Natural convection heat transfer in cavities and cells 20 p2971 A83-42662
- Experimental and theoretical investigation of the stability of a linear vortex with a deformed core 20 p2987 A83-43517
- Experimental study of the effect of pulsations on the development of flow-core velocity oscillations and wall friction in a convergent channel 24 p3576 A83-48950
- CORE SAMPLING**
- Methane - The record in polar ice cores 03 p0357 A83-13539
- Modal petrology of six soils from Apollo 16 double drive tube core 64002 04 p0561 A83-15346
- The Apennine Front core 15007/8 - Irradiational and depositional history 04 p0561 A83-15347
- The Apollo 14 regolith - Petrology of cores 14210/14211 and 14220 and soils 14141, 14148, and 14149 04 p0561 A83-15348
- The Apollo 14 regolith - Chemistry of cores 14210/14211 and 14220 and soils 14141, 14148, and 14149 04 p0561 A83-15349
- Sulphur content and sulphur isotope composition of orange and black glasses in Apollo 17 drive tube 74002/1 15 p2274 A83-34497
- CORE STORAGE**
- Core resource management for large real-time computer program development 21 p3191 A83-45472
- CORES**
- NT EARTH CORE**
- NT HONEYCOMB CORES**
- NT LUNAR CORE**
- NT PLANETARY CORES**
- NT REACTOR CORES**
- The 5-min oscillations of the sun are incompatible with a rapidly-rotating core 05 p0709 A83-17797
- The luminosity-core mass relation - Why and how 14 p2105 A83-33211
- CORIOLIS EFFECT**
- Quasistatic approximation of atmospheric dynamics. VI - Rossby waves over orographically modified terrain 04 p0510 A83-16035
- An investigation of the effectiveness of motion sickness drugs by the method of dispersion analysis 06 p0798 A83-18975
- Space-time distribution of the velocity of tidal motions, with allowance for Coriolis force 07 p0962 A83-20773
- Adiabatic oscillations of a differentially-rotating star - Second-order perturbation theory 11 p1677 A83-27656
- The effect of vision on the endurance by humans of the continuous action of Coriolis acceleration 12 p1764 A83-29273
- The effect of perturbations in Coriolis and centrifugal forces on the nonlinear stability of equilibrium points in the restricted problem of three bodies 15 p2246 A83-34395
- Transport effects associated with turbulence with particular attention to the influence of helicity 15 p2161 A83-34400
- The problem of the origin of the centrifugal force according to Mach's principle 15 p2262 A83-34526
- Effect of the Coriolis force and slowly varying flow on the Kelvin-Helmholtz instability 15 p2161 A83-34783
- A conception of normal mode expansion procedure applied to a limited-area model. II - Linear aspects. III - Derivation and theoretical discussion of a nonlinear approach --- of geostrophic balance 15 p2207 A83-35096
- The stability of the elliptically deformed rotation of an ideal incompressible fluid in a Coriolis force field 18 p2687 A83-40079
- Flows and pressure recovery in a rotating diffuser - Effects of inlet velocity distributions 21 p3129 A83-44065
- Supersonic stabilization of a tangential shear in a thin atmosphere 22 p3285 A83-46938
- On the importance of shear deformation, rotatory inertia and Coriolis forces in turbine blade vibrations [ASME PAPER 83-GT-167] 23 p3469 A83-47987
- CORN**
- Application of computer axial tomography /CAT/ to measuring crop canopy geometry --- corn and soybeans 01 p0065 A83-10096
- Microwave radiometric signatures of corn 08 p1126 A83-21923
- Identification of corn fields using multirate radar data 17 p2526 A83-37624
- CORNEA**
- An experiment on oxygen permeability through corneal tissue 03 p0373 A83-13291
- Stimulation laser therapy for diseases of the cornea with the irradiation of a ruby laser 03 p0378 A83-13604

An experimental study of the possibility of using a CO2 laser for changing the cornea refraction /A preliminary report/ 05 p0671 A83-17211

CORNER FLOW

Numerical study of flowfields about asymmetric external conical corners 03 p0277 A83-13130

Streamwise corner flow with wall suction 04 p0442 A83-15279

A shock-fitting solution of the supersonic flowfield in a rounded internal corner [AIAA PAPER 83-0038] 05 p0578 A83-16478

Aerosound from corner flow and flap flow [AIAA PAPER 81-2039] 07 p0990 A83-19813

Instantaneous pressure fields at a corner associated with vortex impingement 08 p1086 A83-23092

Laminar natural convection along vertical corners and rectangular channels 08 p1090 A83-23208

A semi analytic method for viscous flows in the vicinity of singular corners 08 p1090 A83-23213

Formation of streamwise vortices in the flow past a corner 10 p1371 A83-25569

Flow in a rectangular diffuser with local flow detachment in the corner region 11 p1565 A83-27410

Theoretical and experimental study of the flow of a viscous fluid near the line of intersection of cylindrical and plane surfaces 11 p1525 A83-27709

Asymmetric flows in corner configurations 16 p2288 A83-35532

Evaluation of the Baldwin-Lomax turbulence model for two-dimensional shock wave boundary layer interactions [AIAA PAPER 83-1697] 17 p2445 A83-37195

Flow in a three-dimensional corner with large entropy differences 17 p2449 A83-37540

Computation of three-dimensional turbulent shear flows in corners [AIAA PAPER 83-1733] 17 p2507 A83-38092

The shape of a shock wave diffracted by a rounded corner 19 p2843 A83-41267

Shock diffraction in channels with 90 deg bends 20 p2985 A83-43100

Some measurements in the intermittent region of a turbulent boundary layer along a corner 22 p3286 A83-47025

Boundary layer with self-induced pressure during the transonic flow past the corner point of an airfoil 24 p3545 A83-49526

CORNERS

Growth of physically short corner cracks at circular notches 03 p0340 A83-13909

CORONA BOREALIS CONSTELLATION

The normal color indices and absolute stellar magnitudes of selected Coronae Borealis variables 14 p2101 A83-31828

CORONA DISCHARGES

U ELECTRIC CORONA

CORONAGRAPHS

Simultaneous radio scattering and white light observations of a coronal transient 02 p0271 A83-12830

Shuttle contamination effects on ultraviolet coronagraphic observations 03 p0288 A83-13745

Calculation of illuminance in the shadow of the external occulting screen of a coronagraph. VI - Theory of tolerances 03 p0330 A83-14695

Coronagraphic observations of two new sungrazing comets 04 p0545 A83-14955

Optical observations of the solar corona 04 p0573 A83-15113

The analysis of Fe XIV 5303 coronal emission-line polarization measurements 06 p0854 A83-18535

The solar corona on 31 July, 1981 13 p1963 A83-29982

Broad-band, high-resolution photograph of the solar corona February 16, 1980 18 p2782 A83-39033

A space-telescope able to see the planets and even the satellites around the nearest stars [IAF PAPER 83-222] 23 p3515 A83-47313

Solar instruments on the P78-1 spacecraft 23 p3424 A83-47660

Calculation of coronal line intensities for boron-like ions 23 p3536 A83-47721

CORONAL HOLES

Transient response of the solar wind to changes in flow geometry 02 p0271 A83-12588

The influence of divergent geometries on stellar winds 03 p0428 A83-14764

Acceleration of the solar wind 04 p0574 A83-15120

Observations of coronal structure during sunspot maximum 04 p0574 A83-15122

Change in the radio radius of the sun upon the emergence of a coronal hole at the limb 06 p0854 A83-18844

The quiet sun brightness temperature at 127 MHz 06 p0854 A83-19126

Cosmic ray intensity variations and two types of high speed solar streams 06 p0858 A83-19139

The dissipation of shock waves in the outer solar atmosphere - A reappraisal 11 p1691 A83-27702

Self-consistent magnetohydrodynamic coronal hole flows 11 p1692 A83-28580

The properties of coronal voids 11 p1692 A83-28582

An observation of prominence condensation out of a coronal void 11 p1692 A83-28583

The solar corona on 31 July, 1981 13 p1963 A83-29982

A simple model of a coronal hole 13 p1964 A83-30369

Thirty-five years of patrol measurements of the intensity of the corona outside eclipses 15 p2278 A83-34283

Coronal hole dynamics 15 p2281 A83-34494

Flow-tube dynamics and coronal holes 18 p2781 A83-39022

Temperature profile and Alfvén fluctuation energy flux in coronal hole 21 p3243 A83-44578

Comparison of coronal holes observed in soft X-ray and HE I 10830 A spectroheliograms 23 p3535 A83-47707

CORONAL LOOPS

The thermal stability of solar coronal loops in hydrostatic equilibrium 01 p0129 A83-10944

Resonant electrodynamic heating and the thermal stability of coronal loops 01 p0129 A83-10950

Fluid motions the solar chromosphere-corona transition region. II Active region flows in C IV from narrow slit Dopplergrams 02 p0268 A83-11603

Dynamics of the eruptive prominence of 6 May 1980 and its relationship to the coronal transient 02 p0269 A83-12543

Properties of coronal arches 02 p0270 A83-12578

Thermally isolated coronal loops in hydrostatic equilibrium 02 p0270 A83-12579

Simultaneous radio scattering and white light observations of a coronal transient 02 p0271 A83-12830

The structure, stability and flaring of solar coronal loops 03 p0435 A83-13155

Coronal loop transients in streamer configurations 03 p0437 A83-14788

EUV arcades - Signatures of filament instability 03 p0438 A83-14911

The study of toroidal magnetic configurations in a spherically symmetric gravitational field with applications to coronal loops and transients 04 p0573 A83-14988

Coronal transient phenomena 04 p0574 A83-15123

Solar eclipse observations of a magnetic loop structure at 2, 3.2, 8.2 and 21 cm 04 p0574 A83-15599

Theories for simple-loop and two-ribbon solar flares 04 p0575 A83-16224

Magnetostatic atmospheres with variations in three dimensions --- static equilibrium of coronal loops 05 p0708 A83-17019

Ballooning instability driven by fast magnetosonic waves and its application to coronal loop transients associated with a flare 05 p0708 A83-17020

Numerical study of line-tied magnetic reconnection 06 p0855 A83-19133

The growth of filaments by the condensation of coronal arches 06 p0855 A83-19134

MHD stability of incompressible coronal loops with radiative energy loss 06 p0856 A83-19295

Flare loop radiative hydrodynamics. I - Basic methods 07 p1037 A83-21145

Observations of H-alpha and microwave brightening caused by a distant solar flare 08 p1192 A83-23073

Numerical simulations of loops heated to solar flare temperatures. I - Gasdynamics. II - X-ray and UV spectroscopy 08 p1192 A83-23074

The heating of postflare loops 10 p1521 A83-25733

Dynamics and spectroscopy of asymmetrically heated coronal loops 10 p1522 A83-26742

Flare loop radiative hydrodynamics. IV - Dynamic evolution of unstable semiempirical loop models 10 p1522 A83-26743

Thermal and nonthermal phenomena in solar flare loops at 20 cm wavelength and in X-rays 11 p1692 A83-28576

Electric fields in coronal magnetic loops 11 p1692 A83-28581

Coronal transients - Loop or bubble 11 p1693 A83-28586

High-resolution observations of solar radio bursts at 2, 6, and 20 cm wavelength 13 p1963 A83-29986

On the theory of type IV solar radio bursts 13 p1965 A83-31266

First observations of stellar coronal structure - The coronae of AR Lacertae 13 p1951 A83-31421

Microwave and hard X-ray imaging of a solar flare on 1980 November 5 15 p2278 A83-34113

A relaxation law for evaporating and draining coronal plasma 15 p2279 A83-34286

MHD equilibrium and stability properties of a bipolar current loop --- in solar atmosphere 15 p2279 A83-34288

Evolution of electron and proton temperatures in a flaring loop. I - A case of thermal heating of electrons 15 p2280 A83-34298

Self studies of mass motions arising in flares --- Study of Energy Release in Flares 15 p2285 A83-35226

Diamagnetic aspects of the coronal transient phenomenon 15 p2285 A83-35230

The 1980 April 12 flare and transient - Report on progress in interpretation 15 p2285 A83-35233

Post-flare coronal arches 16 p2440 A83-36621

Turbulent resistive heating of solar coronal arches 17 p2624 A83-37332

VLA observations of a solar active region and coronal loops 17 p2624 A83-37333

Fluid motions in the solar chromosphere-corona transition region. III - Active region flows from wide slit Dopplergrams 17 p2624 A83-37334

X-ray and microwave observations of active regions 18 p2782 A83-39036

Magnetic heating of solar and stellar coronae 18 p2785 A83-39232

Recent developments in flare dynamics 18 p2783 A83-39233

Relationship between the characteristics of solar cosmic rays and the structure of the coronal magnetic field 18 p2784 A83-39306

Magnetic reconnection as a mechanism for heating the persistent coronal loops 18 p2785 A83-40483

The thermal evolution of resonantly heated coronal loops 19 p2923 A83-40711

Solar-type U bursts and coronal transients 19 p2924 A83-40723

Electrodynamic coupling in magnetically confined X-ray plasmas of astrophysical origin 20 p3073 A83-43070

On the stability of coronal magnetic loops 21 p3242 A83-44281

The equilibrium configuration of the corona loop and the corona archide 21 p3242 A83-44287

Observations of high-energy jets in the corona above the quiet sun, the heating of the corona, and the acceleration of the solar wind 21 p3244 A83-45567

A dynamical model of coronal loops 22 p3389 A83-47000

Development of flare morphology in X-rays, and the flare scenario 23 p3531 A83-47661

Hydrodynamics of flaring loops - SMM observations and numerical simulations 23 p3532 A83-47673

Behavior of transition-region lines during impulsive solar flares 23 p3532 A83-47674

Observation of the flare of 12 June 1982 by Norikura coronagraph and Hinotori 23 p3533 A83-47676

Positional measurements on the eruptive loop prominence of 27 April 1981 and comparison with the X-ray sources 23 p3533 A83-47677

Spatial characteristics of microwave bursts --- from solar flares 23 p3533 A83-47678

Vertical structure of hard X-ray flare 23 p3534 A83-47689

Dynamical interpretation of the very hot region appearing at the top of the loop 23 p3534 A83-47693

Heating of chromospheric magnetic features by direct current dissipation 23 p3536 A83-47711

The H-alpha cyclonic spectra of a flare loop system on 1981 April 27 23 p3536 A83-47714

Transient brightenings of interconnecting loops. III Interpretation --- solar corona 23 p3537 A83-47725

Magnetic stability of coronal arcades relevant to two-ribbon flares 23 p3537 A83-47726

Magnetic equilibrium in coronal arcades 23 p3537 A83-47727

The emerging magnetic flux and the elementary eruptive phenomenon --- for solar flares 23 p3537 A83-47728

On the storage of high-energy protons in the solar corona The cyclotron instability 23 p3537 A83-47730

The relationships between disappearing solar filaments, coronal mass ejections, and geomagnetic activity 23 p3481 A83-47734

CORONARY ARTERY DISEASE

Morphological and functional peculiarities of the myocardium during extreme coronary insufficiency 05 p0671 A83-17219

Discordance of exercise thallium testing with coronary arteriography in patients with atypical presentations 07 p0978 A83-21053

High density lipoprotein /HDL/ finding in young airline patients 08 p1147 A83-22953

A histopathological study on hearts in ischaemic heart disease fatalities 09 p1323 A83-24009
The measurement of risk indicators for coronary heart disease in Air Traffic Control Officers - A screening study in a healthy population 10 p1454 A83-25672
The problem of sudden coronary death in the light of mathematical catastrophe theory 13 p1900 A83-30093

Social stress and atherosclerosis in normcholesterolemic monkeys 13 p1899 A83-31166

A cholinergic mechanism for the regulation of the cardiac function during acute transitory coronary insufficiency 15 p2210 A83-34961

Minimal coronary artery disease and continuation of flying status 15 p2214 A83-34988

The phospholipid content of subfractions of high-density lipoproteins in women with angiographically documented atherosclerosis of the coronary arteries 18 p2735 A83-40543

The neural apparatus of the coronary arteries in normal conditions and in patients with ischemic heart disease 18 p2736 A83-40585

Coronary artery spasm induced in atherosclerotic miniature swine 19 p2873 A83-40904

CORONARY CIRCULATION

The effect of dopamine on coronary circulation 05 p0671 A83-17220

Changes in diastolic coronary resistance during submaximal exercise in conditioned dogs 13 p1898 A83-30504

The effect of insulin on the reaction of the coronary and systemic blood circulation during the inspiration of hypoxic mixtures 17 p2555 A83-37239

The role of collateral coronary blood flow in the compensation of regional disorders of the energy metabolism of heart muscle during experimental myocardial ischemia 18 p2732 A83-40544

The adrenoreactivity of the contractile myocardium and coronary arteries in the case of chronic overload and acute ischemic injuries of the heart 18 p2733 A83-40556

Coronary artery spasm induced in atherosclerotic miniature swine 19 p2873 A83-40904

Alteration of ischemic cardiac function in normal heart by daily exercise 19 p2875 A83-41134

CORONAS

NT CORONAL HOLES

NT CORONAL LOOPS

NT ELECTRIC CORONA

NT SOLAR CORONA

NT STELLAR CORONAS

X-ray observations to detect hot coronae around galaxies 05 p0697 A83-16983

Hydromagnetic wave heating of the galactic corona 11 p1681 A83-28262

Time-dependent aureole about a source in a multiple-scattering medium --- for solar blind UV communication and warning systems 15 p2201 A83-34458

Local temperature of a plasma corona 20 p3049 A83-42270

Properties of the corona generated by the incidence of intense CO₂ laser pulses on spherical targets 24 p3631 A83-48820

CORPUSCULAR RADIATION

NT BETA PARTICLES

NT CYCLOTRON RADIATION

NT ELECTRON BEAMS

NT ELECTRON PRECIPITATION

NT ELECTRON RADIATION

NT ENERGETIC PARTICLES

NT ION CYCLOTRON RADIATION

NT PRIMARY COSMIC RAYS

NT RADIATION BELTS

NT RELATIVISTIC ELECTRON BEAMS

NT SOLAR CORPUSCULAR RADIATION

NT SOLAR COSMIC RAYS

NT SOLAR ELECTRONS

NT SOLAR PROTONS

CORRECTION

NT OPTICAL CORRECTION PROCEDURE

On the correction of stellar proper motions for random error 03 p0408 A83-13892

The effect of some systematic errors on the determination of time and latitude, and group corrections 05 p0693 A83-16858

The problem of correction in inertial navigation --- Russian book 12 p1706 A83-29330

Time-of-day corrections in measures of aircraft noise exposure 14 p2081 A83-33024

CORRELATION

NT ANGULAR CORRELATION

NT AUTOCORRELATION

NT CORRELATION COEFFICIENTS

NT CORRELATION DETECTION

NT CROSS CORRELATION

NT DATA CORRELATION

NT SIGNAL ANALYSIS

NT SPECTRAL CORRELATION

NT STATISTICAL CORRELATION

Orthogonal sequences on the basis of full code rings and their correlation properties 01 p0094 A83-10410

Optical biasing on quasi-interferometry with coded correlation filtering 02 p0177 A83-12306

The estimation of galaxy angular correlation functions 03 p0408 A83-13930

Nondestructive evaluation of materials by optical correlation 04 p0492 A83-15219

On the question of correlation in satellite geodesy networks 04 p0514 A83-16382

An experimental study of the correlation between the root-mean-square thermal displacements of atoms and the resistance to creep --- of nickel and aluminum alloys 06 p0729 A83-18750

Correlation methods of the analysis of the reaction of individual neurons of the auditory system. I - The correlation of an auditory signal with impulse activity 07 p0972 A83-19930

Tracking of obscured targets via generalized correlation measures 09 p1266 A83-23542

Correlation analysis of the optical fields in optoacoustic interaction 09 p1344 A83-24001

The existence of teleconnections in the geopotential field of the Northern Hemisphere 09 p1315 A83-24942

Utilization of the decorrelation properties of discrete spectral transformations for the multialternative recognition of signals on a background of correlated noise 10 p1470 A83-26955

The use of splines for correlation-function estimation 11 p1649 A83-28494

The relationship of acquisition systems to automated stereo correlation 12 p1731 A83-29919

Estimation of the correlation function of incoherent-scatter signals in multiposition radar systems 13 p1829 A83-30726

A new evaluation of the four-point galaxy correlation function amplitudes 13 p1949 A83-31402

The suppression of blood platelet aggregation with immune complexes. I - Clinical investigations 14 p2070 A83-33331

Systems of orthogonal signals with optimal correlation functions 18 p2675 A83-40087

Pair correlations in an expanding universe for a multicomponent system 21 p3235 A83-45526

Exact solution of some discrete stochastic models with chaos 22 p3354 A83-45936

CORRELATION COEFFICIENTS

Concerning the nonstationarity of the correlation of solar-wind parameters with the AE and a sub p indices of magnetic activity 02 p0211 A83-12448

The four-point function in the BBGKY hierarchy --- galaxy correlation in clustering pattern 03 p0422 A83-14178

Measurement of turbulence correlations in a two-dimensional supersonic wake 03 p0278 A83-14470

Measurement of the pressure-velocity correlation in turbulent reactive flows [AIAA PAPER 83-0400] 05 p0612 A83-16693

Geomagnetic westward drift using the correlation coefficient 08 p1138 A83-23258

Statistical properties of geomagnetic pulsations at the Furstenfeldbruck Observatory determined by means of pulsation indices. I - Method and cross-correlation 11 p1617 A83-28117

Performance of Karhunen-Loeve and discrete cosine transforms for data having widely varying values of intersample correlation coefficient 12 p1769 A83-29465

Behaviour of a generalised covariance model in picture coding 12 p1769 A83-29470

A correlation-regression analysis of the relationship between the properties of VA-grade tungsten and the characteristics of the initial powder 13 p1821 A83-30692

Microscales and correlation tensors in the viscous turbulent sublayer 17 p2504 A83-37391

Processing of microwave radiometry data for earth scientific purposes 22 p3311 A83-46174

Space-correlation measurement of attaching jets by the new scanning laser Doppler velocimeter using a diffraction grating 24 p3585 A83-49827

Dependence of MHD turbulence spectra on the velocity field-magnetic field correlation --- of solar wind 24 p3675 A83-50083

CORRELATION DETECTION

Identification of optimally correlated subsets --- algorithm to allow robust tracking methodology 01 p0096 A83-11220

On the correlation structure of random field models of images and textures 01 p0100 A83-11473

X-ray illumination of globular cluster puzzles --- globular cluster X ray sources as clues to Milky Way Galaxy age and evolution 02 p0255 A83-12117

Method of main components in nondestructive testing. II Signal detection and estimation 02 p0188 A83-12160

Measurement correlation for multiple sensor tracking in a dense target environment 03 p0387 A83-14594

An evaluation of ultrasound NDE correlation flow detection systems 04 p0494 A83-16180

The effect of noise on pulsed rate-tracking systems with correlation discriminators 05 p0623 A83-17683

Rapid acquisition techniques for Direct-Sequence Spread Spectrum Systems using an analog detector 07 p0903 A83-19677

Detection of M'ARY communication with truncated symbols 07 p0904 A83-19679

Effect of transparency fluctuations on the accuracy of lidar correlation measurements of statistically unhomogeneous atmosphere 08 p1133 A83-21874

Intensity correlation techniques for passive optical device detection 09 p1266 A83-23534

Optimal performance limits for detection and classification algorithms 09 p1266 A83-23537

Correlation-extremal methods of navigation --- Russian book 10 p1462 A83-25620

Simplified tone detector for PCM channel 10 p1402 A83-25634

Combination of the dependent channels of the detection of a random signal on a background of noise with an unknown correlation matrix 11 p1555 A83-27937

Associated geomagnetic and ionospheric variations 15 p2199 A83-34363

Some remarks on the selection of sensors for correlation velocity measurement systems 17 p2512 A83-38534

High-speed digital Golay code flow detection system 18 p2695 A83-39564

On the performance of video band complex correlators --- for radio astronomy receivers 19 p2838 A83-41151

A nonparametric detector for signal detection and time delay estimation 19 p2828 A83-41347

Optimal properties of a system of single interperiod compensation --- target detection in correlated noise 21 p3120 A83-44776

Single mode laser spectral spread repulsion in single-mode optical fiber coherent detection systems 21 p3145 A83-44832

Instrumental correlation analysis using delta-modulation 22 p3271 A83-45656

An analysis of the efficiency of adaptive systems utilizing correlation feedback for passive-noise suppression 22 p3271 A83-45659

Color signal correlation detection by matched spatial filtering 23 p3459 A83-48704

CORRELATION FUNCTIONS

U CORRELATION

CORRELATORS

NT IMAGE CORRELATORS

Fine delay estimation with time integrating correlators 02 p0168 A83-12308

Simple distortion-free real-time optical pulse correlator 02 p0178 A83-12599

Fiber optic pulse compression concept for processing wide bandwidth radar signals 03 p0304 A83-13790

An integral-optic correlator with temporal integration 04 p0535 A83-15272

Process correlators in the simplest systems with strange attractors 05 p0683 A83-17634

Digital processor for coherent CO₂ systems 08 p1097 A83-22520

Processing of optical data using a two-beam interferometer 13 p1846 A83-30622

On the performance of video band complex correlators --- for radio astronomy receivers 19 p2838 A83-41151

Optical differential-modulation correlometer for the detection of linear-FM signals in noise 19 p2900 A83-41780

Design and performance of an integrated optical digital correlator 21 p3205 A83-44225

Highly sensitive correlation receiver for radio interferometry 23 p3517 A83-48476

VLSI digital polarity correlator based on an overloading counter technique 24 p3574 A83-49964

CORRIDORS

NT GREAT PLAINS CORRIDOR (NORTH AMERICA)

CORROSION

NT CAVITATION CORROSION

NT ELECTROCHEMICAL CORROSION

NT FRETTLING CORROSION

NT FUEL CORROSION

NT HOT CORROSION

NT INTERGRANULAR CORROSION

NT SCALE (CORROSION)
 NT STRESS CORROSION
 NT TRANSGRANULAR CORROSION

Influence of corrosion deposits on near-threshold fatigue crack growth behavior in 2XXX and 7XXX series aluminum alloys 04 p0460 A83-16005

Growth behavior of small cracks and variation of statistical crack-length distribution in corrosion fatigue 05 p0653 A83-17091

Corrosion processes --- Book 05 p0616 A83-17823

Corrosion of 310 stainless steel in H₂O-H₂S gas mixtures Studies at constant temperature and fixed oxygen potential 07 p0885 A83-20265

Mechanism of corrosion fatigue crack propagation in high strength steels 11 p1548 A83-28446

Corrosion: Aqueous processes and passive films --- Book 17 p2486 A83-37170

Pitting corrosion 17 p2486 A83-37171

Anodic films on aluminium 17 p2486 A83-37173

The effect of the transport properties of epoxy based coatings on metallic substrate corrosion 18 p2671 A83-39052

Reconsideration of the superposition model for environmentally assisted fatigue crack growth 18 p2668 A83-40617

First stages of gas-metal interactions 20 p2948 A83-42227

Combustion system processes leading to corrosive deposits 20 p2949 A83-42246

Influence of corrosion and microstructure on mechanical properties of SiYON ceramics 23 p3437 A83-48296

Friction and wear of iron and nickel in sodium hydroxide solutions 24 p3559 A83-48922

Corrosion of pre-oxidized nickel in SO₂ atmospheres 24 p3564 A83-49508

Demonstration of mobile accelerator neutron radiography for in situ detection of moisture and corrosion in aircraft structures [AIAA PAPER 83-2449] 24 p3591 A83-50073

CORROSION PREVENTION

Sulfidation properties of Fe-Cr alloys at 1073 K in H₂S-H₂ atmospheres of sulfur pressures 0.01 and 0.00001 Pa 01 p0024 A83-10244

Protection of Fe-Cr-Al alloys in sulfidizing environments by means of an alpha-Al₂O₃ scale 01 p0024 A83-10245

Corrosion protection with titanium, zirconium, and tantalum 01 p0026 A83-10568

Water-displacing organic corrosion inhibitors - Their effect on the fatigue characteristics of aluminium alloy bolted joints 02 p0148 A83-12014

The cleaning of the exterior of the aircraft 03 p0277 A83-14325

Materials evaluation under fretting conditions; Proceedings of the Symposium, Warminster, PA, June 3, 1981 05 p0652 A83-17251

The structure of aluminum oxides used for corrosion resistance and primer adhesion 07 p0899 A83-20492

Effect of coatings on the mechanical properties of superalloys 07 p0893 A83-21469

Surface magic - Making metals tougher 08 p1068 A83-22775

Corrosion and fretting effects on fatigue 09 p1277 A83-23419

Sealants - Uses in composite structures 09 p1236 A83-23615

Microanalytical investigations of plasma-sprayed coatings providing protection against corrosion by hot gases 12 p1713 A83-29370

The electrochemical aspect of the corrosion inhibitor action and ways of increasing the effectiveness of inhibitors 14 p1988 A83-32070

High temperature corrosion and use of coatings for protection 14 p1995 A83-32810

Protective coatings against hot corrosion 24 p3590 A83-49479

CORROSION RESISTANCE

NT OXIDATION RESISTANCE

Phase equilibria and certain properties of Ti-TiPd-TiNi alloys at 400 C 01 p0024 A83-10385

Oxidation-resistant materials for hot gas turbines and jet power plants. II 02 p0148 A83-12298

Increasing the corrosion resistance of alloy AK8 03 p0297 A83-13257

Heat resistant and corrosion resistant aluminum alloys hardened with oxide phase 03 p0297 A83-13262

Ion implanting bearing surfaces for corrosion resistance [ASME PAPER 82-LUB-23] 03 p0298 A83-13512

A study of the corrosion activity of the fuselage condensate of passenger aircraft 04 p0445 A83-15398

Review of factors that influence fretting wear 05 p0652 A83-17259

Recent approaches to the development of corrosion resistant coatings --- for Nickel and Cobalt based superalloys used for gas turbines [ONERA, TP NO. 1982-106] 06 p0769 A83-18433

Recent approaches to the development of corrosion resistant coatings 07 p0891 A83-21453

The corrosion resistance of protective coatings 07 p0891 A83-21454

IN939 - Metallurgy, properties and performance 07 p0892 A83-21465

Alloy design for nickel-base superalloys 07 p0894 A83-21484

The effects of section size, coating and environment on creep rupture behaviour of superalloys 07 p0894 A83-21487

The influence of applied coatings on the creep fracture of IN 738 LC 07 p0894 A83-21488

Influence of environment on fracture 08 p1065 A83-21798

Comparison of several accelerated laboratory tests for the determination of localized corrosion resistance of high-performance alloys 08 p1066 A83-22650

The high-temperature corrosion of aluminum-rich coatings in an atmosphere of sulfur vapor containing oxygen 08 p1068 A83-23243

A study of the stability of protective coatings against sulfide-oxide corrosion 09 p1229 A83-23512

The corrosion resistance of titanium-ruthenium alloys in a salt-acid medium 09 p1235 A83-24401

The effect of a gas-saturated layer on the corrosion stability and mechanical strength of titanium alloys 09 p1235 A83-24403

Applications of titanium and prospects for the use of AT-series titanium alloys in environments containing chlorides 09 p1235 A83-24404

The production of clad rolled sheets from secondary aluminum powder 09 p1236 A83-25064

Low-pressure-plasma-deposited coatings formed from mechanically alloyed powders 10 p1394 A83-25532

The use of coatings in high temperature battery systems 10 p1445 A83-25536

Characterization and corrosion behavior of duplex-chromized steel for the sulfur container in Na-S cells 10 p1394 A83-25537

Coatings in industrial gas turbines - Experience and further requirements 10 p1388 A83-25539

Thermal barrier coatings for thermal insulation and corrosion resistance in industrial gas turbine engines 10 p1400 A83-25542

New results on the oxidation and hot corrosion of silicide overlay coatings on nickel-based alloys 10 p1388 A83-25545

Erosion resistance of Co-Cr-Al coatings containing active element additions 10 p1395 A83-25551

The effect of hafnium on the phase composition and the mechanical and corrosion properties of cobalt alloys 10 p1395 A83-25632

Causes of cold cracking in multipass welded joints in corrosion-resisting 08Kh15N5d2T type maraging steels 10 p1397 A83-26222

Effect of local heating on corrosion fatigue strength of a titanium alloy 10 p1398 A83-26225

The effect of heat treatment on some properties of electrodeposited nickel and chromium coatings 10 p1399 A83-26896

Environmental cracking - A review of the role of residual stresses and their measurement 11 p1548 A83-27999

The role of alloying elements in the formation of oxide films on VT14 alloy at a temperature of 1100 C 11 p1549 A83-28487

Damage accumulation in the matrix of an Al-B composite under cyclic deformation 11 p1544 A83-28493

Macroencapsulation of electronic circuits 12 p1719 A83-29215

The anodic dissolution of a Ni-base superalloy 12 p1713 A83-29401

The effect of nitrogen- and hydrogen-containing media on the refractory properties of nickel-base alloys 14 p1993 A83-32388

Microstructure and hot corrosion resistance of aluminide coating on a nickel-base superalloy in 738LC 15 p2137 A83-33973

The effectiveness of the artificial aging of low-alloy duralumin 16 p2335 A83-36889

High-performance of Ni-Cr-Mo-W alloys 17 p2489 A83-38031

Temperature requirements and corrosion rates in combustion driven hydrogen fluoride supersonic diffusion lasers 19 p2850 A83-40857

Dynamic fatigue of a machinable glass-ceramic 19 p2823 A83-40908

The role of ion implantation in high temperature oxidation studies 20 p2946 A83-42230

The development and growth of protective alpha-Al₂O₃ scales on alloys 20 p2952 A83-42235

Kinetics of interfacial reactions of gases on metals and oxides 20 p2949 A83-42239

Coatings containing chromium, aluminum, and silicon for high temperature alloys 20 p2953 A83-42260

High temperature corrosion resistance of ceramic thermal barrier coatings 20 p2957 A83-42262

Influence of the microstructure on the corrosion behavior of magnetron sputter-quenched amorphous metallic alloys 21 p3217 A83-44611

Improved chromatic acid anodize seal for optimum paint adhesion [SAE PAPER 820603] 22 p3301 A83-45864

Effect of zirconium content on properties of type D16 alloy plates 24 p3559 A83-48804

Properties of maraging steels VNS-2 and EP817 after aging 24 p3559 A83-48807

Anticorrosion coatings; All-Soviet Conference on Refractory Coatings, 10th, Leningrad, USSR, May 12-14, 1981, Proceedings 24 p3553 A83-49076

High temperature corrosion of metals and alloys; Proceedings of the Third International Symposium, Mount Fuji, Japan, November 17-20, 1982 24 p3561 A83-49476

Alloy design for hot corrosion resistance 24 p3562 A83-49482

Oxidation and corrosion of a gamma/gamma-prime-NbC unidirectionally solidified pseudo-eutectic alloy 24 p3563 A83-49492

Electrochemical studies of corrosion of iron, nickel and nickel alloys in alkali sulfate melt 24 p3563 A83-49496

Hot corrosion of iron- and nickel-base superalloys caused by deposit of calcium sulfate 24 p3563 A83-49498

A fundamental basis for using the platinum group elements as alloying additions in nickel-base alloys to improve high temperature corrosion 24 p3564 A83-49501

The role of silicon in protection of Ni-base alloys against hot corrosion 24 p3564 A83-49502

Hot corrosion resistance of nickel-base superalloys and aluminide coatings to molten Na₂SO₄-NiSO₄-NaCl salt 24 p3564 A83-49503

Hot corrosion behaviour of a cobalt-free, nickel-base superalloy 24 p3564 A83-49504

Studies on the corrosion resistance of MCrAlY alloys at high temperatures 24 p3564 A83-49506

The study of the effect of cobalt on the hot corrosion resistance of nickel-based high temperature alloys 24 p3564 A83-49507

Reaction mechanism of Ni-20Cr in mixtures of SO₂+O₂ 24 p3565 A83-49513

Corrosion resistance of some composite coatings on Ni-base superalloy 24 p3566 A83-49521

Materials for photothermal solar energy conversion 24 p3601 A83-50063

CORROSION TESTS

NT SALT SPRAY TESTS

Investigation of the tribochemical influence of air pollution on the rolling friction of various materials being used in a newly developed railroad measuring post --- German thesis 01 p0056 A83-10175

Morphology of corrosion products formed on cobalt and nickel in argon-oxygen-chlorine mixtures at 1000 K 01 p0024 A83-10247

Gas corrosion characteristics of nickel-base alloys 01 p0025 A83-10392

Corrosion fatigue of nickel and nickel-base alloys 02 p0156 A83-12223

Heat resistant and corrosion resistant aluminum alloys hardened with oxide phase 03 p0297 A83-13262

The effect of liquid media on the strength of an aluminum-matrix composite 04 p0455 A83-15394

Occurrence of fretting in practice and its simulation in the laboratory 05 p0652 A83-17252

An electrochemical method for investigating corrosion in rubbing surfaces 05 p0652 A83-17256

Comparison of hot-salt corrosion test procedures 07 p0892 A83-21457

A study of stress corrosion cracking in high strength steels using acoustic emission techniques 08 p1064 A83-21770

The high-temperature corrosion of aluminum-rich coatings in an atmosphere of sulfur vapor containing oxygen 08 p1068 A83-23243

A study of the stability of protective coatings against sulfide-oxide corrosion 09 p1229 A83-23512

Nondestructive corrosion detection under organic films using infrared thermography 09 p1275 A83-23630

The corrosion resistance of titanium-ruthenium alloys in a salt-acid medium 09 p1235 A83-24401

The effect of temperature on the kinetics of high-temperature salt corrosion in ZrSi₂ alloy 10 p1395 A83-25631

- Environmental cracking - A review of the role of residual stresses and their measurement 11 p1548 A83-27999
- Unit for corrosion-fatigue testing of samples with stationary and cyclic heating 11 p1550 A83-28620
- The identification of the sulfide NaCrS₂ in nickel-base superalloys during corrosion in sulfate melts 11 p1550 A83-28671
- Localized corrosion of aluminum vacuum brazing T-joints 13 p1822 A83-30844
- The role of the environment on the corrosion cracking of Al-Mg and Al-Li-Mg alloys 14 p1992 A83-32072
- Processing of fatigue test results for corrosion-affected structural materials 14 p1992 A83-32074
- A comparison of procedures used in assessing the anodic corrosion of metal matrix composites and lead alloys for use in lead-acid batteries 14 p1989 A83-32626
- Dissolved metal species mechanism for initiation of crevice corrosion of aluminum. I - Experimental investigations in chloride solutions. II - Mathematical model 14 p1993 A83-32628
- Microstructure, deformation, and corrosion-fatigue behavior of a rapidly solidified Al-Li-Cu-Mn alloy 14 p1996 A83-32890
- The influence of microstructure on the corrosion of Al-Li, Al-Li-Mn, Al-Li-Mg and Al-Li-Cu alloys in 3.5 percent NaCl solution 14 p1997 A83-32892
- Creep/corrosion of two nickel alloys in combustion gas 16 p2329 A83-35692
- Corrosion fatigue crack propagation 16 p2330 A83-36162
- Determination of prefracture damage and failure prediction in corrosion-fatigued Al-2024-T4 by X-ray diffraction methods 16 p2331 A83-36163
- Corrosion fatigue behaviour of 13Cr stainless steel and Ti-6Al-4V at ultrasonic frequency 16 p2332 A83-36192
- Corrosion fatigue testing of implant materials (Nb, Ta, stainless steel) at transonic frequencies 16 p2332 A83-36193
- Hot corrosion of aluminate coatings on nickel-base superalloys in oxidizing and reducing conditions [ONERA, TP NO. 1983-12] 16 p2333 A83-36422
- A fractographic study of corrosion-fatigue crack propagation in a duplex stainless steel 17 p2490 A83-38397
- Corrosion behavior of annealed niobium-tantalum alloys 18 p2665 A83-39173
- Effects of corrosive environments on graphite/epoxy composites 18 p2656 A83-40227
- Facilities for the study of behaviour in corrosive atmospheres and their application to thermal and photovoltaic converters 18 p2673 A83-40532
- Corrosion of nickel in SO₂ atmospheres at elevated temperatures 20 p2952 A83-42240
- Hot corrosion of Sialons 20 p2957 A83-42247
- Various forms of silicon carbide and their effects on seal performance [ASLE PREPRINT 83-AM-4B-1] 20 p2958 A83-43338
- An active dummy cell for use in corrosion studies 22 p3267 A83-46701
- Corrosion behavior of SiC/Al metal matrix composites 22 p3265 A83-46894
- Effect of sensitization on the hot corrosion behaviour of stainless steels in the temperature range of 600-900 C 24 p3563 A83-49500
- Hot corrosion of Ni-20Cr base alloys induced by Na₂SO₄-NaCl mixtures 24 p3564 A83-49505
- The corrosion of nickel in SO₂ atmospheres 24 p3564 A83-49509
- The kinetics and mechanism of the attack of MCr-type alloys in oxygen-sulphur environments at 700 C 24 p3565 A83-49511
- The effect of Hf additions on oxidation behaviour of Ni3Al 24 p3565 A83-49515
- Effect of Cu addition on intergranular corrosion of Al-5.5 percent Zn-2.5 percent Mg alloy 24 p3566 A83-49860
- Stress corrosion cracking and intergranular corrosion of 2017 aluminum alloy 24 p3566 A83-49861
- CORRUGATED PLATES**
- A corrugated core theory of sandwich plates 09 p1280 A83-24512
- Stability analysis of Centaur-in-Shuttle composite corrugated adapters [AIAA 83-1003] 12 p1707 A83-29791
- Utilization of the method of continuation with respect to the length of the integration segment for calculating circular corrugated plates 15 p2178 A83-34444
- Recent developments in zeta-sandwich/plate structures 18 p2703 A83-40168
- Buckling of sinusoidally corrugated plates under axial compression 19 p2856 A83-40878

CORRUGATING

- A direct projection method for calculating the natural modes of a two-dimensional corrugated waveguide 02 p0166 A83-11687
- Perturbation analysis of corrugated dielectric waveguide with application to millimeter-wave filters 05 p0624 A83-17280
- Guided-wave experiments with dielectric waveguides having finite periodic corrugation 13 p1836 A83-31145
- Performance of small primary feeds with trapezoidal and sinusoidal corrugations --- for reflector antennas 13 p1837 A83-31766
- Propagation and radiation properties of corrugated cylindrical coaxial waveguides 15 p2148 A83-35183
- Helically corrugated circular waveguides as antenna feeders 18 p2676 A83-40398
- Three-dimensional stressed state of longitudinally corrugated elastic cylinders 21 p3163 A83-45359
- CORSAIR AIRCRAFT**
- U A-7 AIRCRAFT
- CORTICOSTEROIDS**
- NT ALDOSTERONE
- NT CORTISONE
- Is suppression of bone formation during simulated weightlessness related to glucocorticoid levels 11 p1640 A83-27833

CORTISONE

- The changes in the content of corticosterone in the blood plasma of inbred mice after exposure to stress 01 p0080 A83-10541
- The effect of T-activin and hydrocortisone on transplantation immunity 01 p0080 A83-10549
- The effect of hydrocortisone and dexamethasone on the metabolism of muscle proteins in rats 06 p0795 A83-18986
- The effect of adrenalectomy and hydrocortisone on the carbohydrate metabolism in the lungs and myocardium during chronic hypoxia 07 p0972 A83-19922

CORUNDUM**U ALUMINUM OXIDES****COS-B SATELLITE**

- The diffuse gamma radiation from the local spiral arm 10 p1523 A83-25483
- 'Whatever happened to ...' - A scientific review of three astronomy satellites in which BAe has been involved 11 p1533 A83-28177
- Current wisdom and future possibilities for gamma-ray sources within high-energy astronomy 18 p2755 A83-39277
- Gamma radiation as a tracer of the local interstellar gas 18 p2768 A83-39631
- COS-B gamma-ray measurements and the large-scale distribution of interstellar matter 18 p2786 A83-39658

COSINE SERIES

- Signal reconstruction from cosine transform magnitude [AD-A124945] 05 p0680 A83-17249

COSMIC BACKGROUND EXPLORER SATELLITE

- Optical design of the Diffuse Infrared Background Experiment for NASA's Cosmic Background Explorer 14 p2084 A83-32037

COSMIC DUST

- NT INTERPLANETARY DUST
- NT METEOROID DUST CLOUDS
- NT ZODIACAL DUST
- On the widths of dust layers in galaxies 01 p0119 A83-10266
- Polarization in peculiar emission-line objects 01 p0116 A83-10316
- The scattering phase function of interstellar grains - The case of the reflection nebula NGC 7023 02 p0250 A83-11584
- What are comets made of - A model based on interstellar dust 03 p0415 A83-13380
- Structure and origin of cometary nuclei 03 p0415 A83-13382
- The cosmological term and the torsion of space-time 03 p0417 A83-13530
- A photometric map of interstellar reddening within 300 parsecs 03 p0406 A83-13552
- Infrared photometry of HM Sagittae 03 p0408 A83-13891
- Numerical simulation of radiative transfer in circumstellar dust shells. I - Spherical shells 03 p0428 A83-14768
- The infrared spectrum of interstellar dust --- noting spectroscopic similarity to transmittance of diatomaceous organisms 04 p0526 A83-14981
- Cosmic ray origin above 10 to the 18th eV - Galactic or extragalactic 04 p0575 A83-14983
- An inventory of particles from stratospheric collectors - Extraterrestrial and otherwise 04 p0563 A83-15366
- The heating of dust in the broad-line regions of active galaxies and quasars 04 p0551 A83-15605
- Ultraviolet extinction towards far OB associations 04 p0557 A83-15986

- The infrared emission from the elliptical galaxy NGC 1052 05 p0697 A83-16990
- Distances of galaxies from the apparent size distribution of Dark Clouds. II - NGC 224, NGC 2841 and NGC 7331 05 p0695 A83-17861
- Kinematics of elliptical-like galaxies with dust lanes 06 p0826 A83-18157
- A 3.4-mm HCN and continuum survey of dark clouds 06 p0819 A83-18834
- Condensation of grains --- relevance to astrophysical problems 06 p0842 A83-19455
- Abnormal extinction and dust properties in M 16, M 17, NGC 6357 and the Ophiuchus dark cloud 07 p1025 A83-21241
- Charged dust in Saturn's magnetosphere 07 p1035 A83-21326
- Laboratory simulation of cometary dust collection and analysis 07 p1010 A83-21577
- On the nature of the high-temperature component of the interstellar plasma 08 p1179 A83-22053
- The interstellar medium and star formation 09 p1358 A83-23913
- Evidence for the detection of X-ray scattering from interstellar dust grains 09 p1355 A83-24699
- Interstellar grain composition and the infrared spectrum of OH26.5+0.6 09 p1362 A83-24985
- The fate of dust grains in a shock wave originated by a SN explosion 09 p1365 A83-25295
- Grains spin-up by inverse Cerenkov effect --- in interstellar gas 10 p1501 A83-25493
- Gamma-ray astronomy and the local interstellar medium 10 p1504 A83-25724
- The rotation of small particles from space in the earth's atmosphere 10 p1449 A83-26909
- The durability of dust matrices formed during the sublimation of dusty ice --- in comets 11 p1679 A83-27888
- Mass scales in a universe of dust and blackbody radiation 11 p1679 A83-27989
- Cometary Globule 1 --- dense interstellar dust cloud 11 p1675 A83-28270
- Gravitational collapse of pressureless inhomogeneous spheroids 11 p1681 A83-28275
- Time-dependence of the infrared spectra of nova dust shells 11 p1681 A83-28277
- Magnetic alignment of interstellar dust grains for dominating magnetic effects 12 p1790 A83-28896
- The dust distribution in some small H II regions 12 p1794 A83-29084
- The largest molecules in space - Interstellar dust 13 p1947 A83-31154
- Dustlike stages in the early universe, and constraints on the primordial black hole spectrum 13 p1948 A83-31254
- The dust around the carbon star IRC + 10216 13 p1951 A83-31418
- A dust lane in NGC 6251 13 p1958 A83-31714
- Electrodynamics of submicron dust in the cometary coma 13 p1958 A83-31733
- Numerical simulation of radiative transfer in circumstellar dust shells. II - Ellipsoidal shells 13 p1959 A83-31741
- Quasi-liquefaction in the surface layers of cometary nuclei. I - The static layer at the threshold of quasi-liquefaction 14 p2102 A83-31836
- Thin charged shells and the violation of the third law of black hole mechanics 14 p2102 A83-33044
- The variation of dust temperatures in Maffei 2 14 p2106 A83-33225
- Observation of ice mantles toward HD 29647 14 p2107 A83-33232
- Fragmentation of prestellar clouds by molecule formation 14 p2109 A83-33278
- Grain alignment in the intergalactic magnetic field 15 p2263 A83-34552
- A capacitor impact sensor (CIS) on board Giotto for detection of cometary dust particles 15 p2129 A83-35024
- CO adsorption and the optical properties of interstellar grains 16 p2428 A83-36529
- Status of laboratory experiments on ice mixtures and on the 12 micron H₂O ice feature --- suggesting interstellar IR absorption 16 p2431 A83-36670
- Lorentz forces on the dust in Jupiter's ring 17 p2619 A83-37586
- Planck mean radiation-pressure cross sections for nonspherical grains. I 17 p2603 A83-37891
- Interstellar photoelectric absorption cross sections, 0.03-10 keV 17 p2604 A83-37910
- The conspicuous absence of normal graphite grains in the small Magellanic Cloud 17 p2608 A83-38263
- Polarization of stars in R-associations - Observational data 17 p2611 A83-38555
- The large scale dust distribution in the inner galaxy 18 p2770 A83-39654

- A balloon-borne cooled telescope for far IR astronomy
18 p2762 A83-40460
- Does CO condense on dust in molecular clouds?
19 p2914 A83-40718
- Optical polarimetry of broad-line radio galaxies
20 p3059 A83-42435
- Structure of molecular clouds. VII - Energy balance in clouds with star formation (Type I Ib)
21 p3229 A83-44417
- Discovery of an IR echo from a supernova dust cloud
21 p3234 A83-44993
- 8-13-micron spectral observations of eight moderately extended planetary nebulae
22 p3375 A83-46551
- Diffuse light near Zeta Orionis and the Horsehead nebula, and anomalous extinction of HD 37903, as measured with the ANS
23 p3516 A83-47441
- The dust envelope of the Herbig Ae star, AB Aur
23 p3519 A83-47449
- The effect of gas on dust temperature in comets
24 p3650 A83-48955
- Observations of dust in planetary nebulae
24 p3639 A83-49135
- Effects of dust formation on chemical abundances --- in planetary nebulae
24 p3652 A83-49145
- Polarization observations of the nebula M 20 with filters
24 p3640 A83-49171
- Dust and gas in triaxial galaxies
24 p3657 A83-49255
- Multiple scattering in the reflection nebula NGC 1999 and the nature of interstellar dust
24 p3659 A83-49376
- The fraction of the sky screened by local diffuse dust clouds
24 p3668 A83-50089
- Observationally-based infrared efficiencies and Planck means for circumstellar dust grains
24 p3670 A83-50160
- COSMIC GAMMA RAY BURSTS**
U GAMMA RAY BURSTS
- COSMIC GASES**
NT INTERPLANETARY GAS
NT INTERSTELLAR GAS
NT NEUTRAL GASES
- Gas in the galactic halo
02 p0258 A83-12184
- Spectra of cosmic X-ray sources
02 p0246 A83-12187
- On gaseous disks in Seyfert 1 nuclei
03 p0423 A83-14187
- How well is gas mixed in clusters of galaxies
03 p0428 A83-14767
- X-ray observations to detect hot coronae around galaxies
05 p0697 A83-16983
- New observations of a region of the Magellanic Stream
07 p1010 A83-19857
- The maximum density in heavy-neutrino clouds
07 p1014 A83-20651
- Intergalactic gas in galaxy clusters - Scattering and polarization of the radio emission of a central source
07 p1014 A83-20663
- Galactic spiral structure and the gas motion near and beyond the corotation resonance
07 p1026 A83-21261
- The nature of the ionizing source of the nuclear gas in NGC 1052
10 p1511 A83-26402
- Parastatistics and the equation of state for the early universe
12 p1791 A83-28994
- Neutral hydrogen in X-ray cluster galaxies - A1367
13 p1949 A83-31404
- The incidence of 21 centimeter absorption in QSO redshift systems selected for Mg II absorption - Evidence for a two-phase nature of the absorbing gas
14 p2104 A83-33185
- Why high-latitude clouds in our Galaxy and the highly redshifted clouds observed in front of QSOs do not belong to the same parent population
14 p2106 A83-33224
- Dissipative effects in the gaseous subsystems of flat galaxies
15 p2271 A83-34754
- Optical observations of the interstellar absorption lines towards the M8 nebula
15 p2272 A83-34790
- High-redshift objects as probes of nearby cosmic voids
15 p2272 A83-34792
- Shocks in spiral galaxies
17 p2612 A83-38828
- Distribution of CO in the southern Milky Way
18 p2769 A83-39651
- Special perturbations of rotating isothermal gas clouds with constant rotational velocity
23 p3519 A83-47451
- Dust and gas in triaxial galaxies
24 p3657 A83-49255
- Galactic helium and stellar population colors
24 p3666 A83-50051
- COSMIC NOISE**
An electric noise component with density 1/f identified on ISEE 3
02 p0207 A83-12376
- Autumn and winter anomalies in ionospheric absorption as measured by riometers
17 p2543 A83-38369
- Cosmic noise observations at high radio frequencies
21 p3226 A83-45452
- Analysis of spaceborne VHF incidental noise over the Western Hemisphere
22 p3276 A83-46931
- Massive neutrinos and the anisotropy of the cosmic microwave background radiation
24 p3675 A83-49357
- COSMIC PLASMA**
The ground state of superdense quark-lepton matter
01 p0124 A83-10813
- The formation of a universal energy spectrum for charged particles in the shear flow of the cosmic plasma
02 p0272 A83-11703
- X-ray spectroscopy of the galaxy M87 - Radiative accretion of the hot plasma halo
02 p0254 A83-12105
- Vlasov equation --- for galactic and stellar plasma dynamics
02 p0261 A83-12547
- Particle acceleration during the development of tearing-mode discontinuity --- in cosmic plasma
03 p0356 A83-13209
- High energy gamma-rays from black holes
03 p0439 A83-14721
- Shifts of spectral lines emitted from stars
03 p0431 A83-14947
- Rayleigh-Taylor instability of a partially ionized medium in the presence of a variable horizontal magnetic field
04 p0535 A83-14961
- Dynamo action in cosmic bodies
04 p0556 A83-15959
- Visible light observations of a dense plasmoid associated with a moving Type IV solar radio burst
06 p0853 A83-18531
- The role of turbulence of the relativistic electron-positron plasma in generating in the prepulses of the Crab radio pulsar
06 p0830 A83-18781
- Two-body relaxation in relativistic thermal plasmas
07 p1017 A83-20930
- A turbulent radio jet
07 p1017 A83-20936
- The magnetic and fluid environment of an ellipsoidal circumstellar plasma cavity
07 p1018 A83-20951
- The equivalence of perfect fluid space-times and magnetohydrodynamic space-times in general relativity
08 p1180 A83-22206
- Electronic equipment for spacecraft instruments with probe sensors /classification and methods of study/
10 p1386 A83-25333
- A wind and shock model for active galactic nuclei
10 p1511 A83-26401
- International Conference on Plasma Physics, Goteborg, Sweden, June 9-15, 1982, Proceedings. Part 1
11 p1658 A83-28226
- Paradigm transition in cosmic plasma physics
11 p1658 A83-28227
- Plasma in astrophysics
11 p1680 A83-28242
- Ambipolarity in the motion of ionospheric plasma
11 p1620 A83-28745
- Dissipation of MHD waves in an inhomogeneous streaming plasma
12 p1790 A83-28979
- The state equation of superdense degenerate plasma
12 p1793 A83-29067
- On hierarchical cosmology
12 p1793 A83-29074
- Possibility of amorphous glassy state in astrophysical dense plasmas
13 p1947 A83-30422
- Theory of cosmic ray spectra
13 p1966 A83-30423
- Influence of large-scale inhomogeneities of the interplanetary plasma on the form of temporal scintillation spectra
13 p1948 A83-31265
- Stability of an astrophysical plasma near the onset of electron runaway
13 p1954 A83-31648
- Device for adaptive sweep in probe appliance for direct determination of electron temperature --- of cosmic plasma
14 p1982 A83-31817
- Configuration and structure of the interplanetary magnetoplasma stream from the intense isolated flare of November 22, 1977
14 p2114 A83-31852
- The retardation of ions in a degenerate electron gas
14 p2086 A83-32141
- The hypothesis of the preferential acceleration of heavy elements in the cosmic plasma
14 p2116 A83-32544
- Nonlinear propagation of hydromagnetic waves in high-beta plasmas
14 p2106 A83-33217
- Prediction of the optical properties of ruby and leucosapphire under the effect of the cosmic plasma
14 p2085 A83-33393
- On the evolution of interacting, magnetized, galactic plasmas
15 p2262 A83-34528
- Electric-probe potential in the space plasma
16 p2416 A83-35943
- The thermal pair annihilation spectrum - A detailed balance approach --- for cosmic plasma study
17 p2605 A83-37930
- On the origin of the low-energy cosmic-ray antiprotons
18 p2787 A83-40491
- X-ray pulsar beam patterns for emission by magnetized plasma with vacuum polarization
18 p2778 A83-40492
- Measurement of variations of integral electron density in channels of communication with the Venera 13 and 14 probes
19 p2916 A83-41244
- A search for the Sunyaev-Zel'dovich effect at millimeter wavelengths --- cosmic background photon energy increase due to Compton scattering by high temperature galactic cluster plasma electrons
20 p3082 A83-42467
- The macroscopic magnetohydrodynamics of inhomogeneously turbulent cosmic plasmas
20 p3076 A83-43626
- An electron cyclotron maser instability for astrophysical plasmas
21 p3227 A83-43944
- Effect of rotation on magnetogravitational instability of finite conducting gas in presence of suspended particles
24 p3671 A83-50169
- COSMIC RADIATION**
U COSMIC RAYS
- COSMIC RADIO WAVES**
U EXTRATERRESTRIAL RADIO WAVES
- COSMIC RAY ALBEDO**
Nuclear cascades in Saturn's rings - Cosmic ray albedo neutron decay and origins of trapped protons in the inner magnetosphere
13 p1966 A83-31228
- Ground albedo neutrons produced by cosmic radiations
18 p2786 A83-39915
- COSMIC RAY SHOWERS**
Computer simulations of atmospheric Cerenkov radiation in large cosmic-ray showers
01 p0130 A83-11043
- Deformation of the absorption curves of cosmic rays in the atmosphere and the polarity of the solar magnetic field
02 p0273 A83-11722
- Anisotropy of small atmospheric showers /with E sub 0 of approximately 10 to the 13th eV/
02 p0273 A83-11725
- The modulation characteristics of the Forbush effect
02 p0273 A83-11727
- Quasi-periodic variations of cosmic-ray anisotropy
02 p0274 A83-11729
- Cosmic rays at the maximum of the 21st solar cycle according to Meteor-satellite measurements
02 p0274 A83-11733
- Multiple-nucleon interactions of relativistic heavy nuclei of cosmic rays with Ag and Br nuclei, and characteristics of interactions with a high multiplicity of shower particles in the energy range of 4-400 GeV/nucleon
02 p0274 A83-11739
- Investigation of azimuth effects in gamma families with total energies of 30-1000 TeV
02 p0274 A83-11740
- Experimental studies of superfamily halos. IV --- in cosmic ray showers
02 p0274 A83-11744
- Statistical solution of the inverse problems with application to cosmic-ray experiments
02 p0275 A83-11749
- The Samarkand EAS installation and experimental results
02 p0275 A83-11750
- Investigation of the spatial distribution function of Cerenkov emission from extensive air showers at the Samarkand University installation
02 p0275 A83-11751
- Analysis of the spatial distribution of Cerenkov emission from extensive air showers obtained at the Samarkand University installation
02 p0275 A83-11752
- Experimental data on the pulse shape of EAS Cerenkov radiation and the analysis of these data
02 p0275 A83-11753
- Muons with energies greater than 1 GeV in the composition of extensive air showers
02 p0275 A83-11754
- The interaction of hadrons and the nuclear composition of primary cosmic rays with energies of 200-2000 TeV according to the energy spectrum of hadrons in showers
02 p0275 A83-11755
- The energy spectrum of primary cosmic rays in the range 10 to the 13th-10 to the 16th eV
02 p0275 A83-11756
- Shower curves in the atmosphere and the composition of primary cosmic radiation with an energy greater than 10 to the 15th eV
02 p0275 A83-11757
- Dependence of the mean characteristics of EAS components on the parameters of the elementary-act model
02 p0275 A83-11758
- Using small extensive air showers where the number of electrons is greater than about 10,000 on mountains for calibrating an interaction model
02 p0276 A83-11759
- The relative number of hadrons in an extensive air shower with the number of particles N = 10 to the 4th to 10 to the 6th
02 p0276 A83-11760
- A possibility of detecting optical radiation from superhigh-energy extensive air showers
02 p0276 A83-11761

Unusual characteristics of the cosmic ray intensity increase of September 17-18, 1979

02 p0276 A83-12393

The possibility of detecting electrons with an energy greater than 20 MeV in the region of the Brazilian magnetic anomaly

02 p0210 A83-12444

Dependence on declination of the intensity of cosmic ray showers with primary energies of about 10 to the 16th eV

05 p0709 A83-17268

Investigation of processes of the interaction of cosmic-ray muons at an underground depth of 150 mwe

06 p0858 A83-19342

Ultrahigh-energy cosmic rays

07 p1039 A83-20851

Energy spectrum of cosmic ray primaries at super high energies estimated from the recent balloon-borne calorimeter measurements

09 p1369 A83-24700

The difference coupling coefficients of complex muon-neutron detectors

10 p1420 A83-26105

A determination of coupling coefficients on the basis of latitude measurements made during the 28th voyage of the research vessel Akademik Kurchatov --- cosmic ray neutron intensity analysis

10 p1523 A83-26106

Quasi-periodic variations of cosmic-ray intensity and anisotropy --- Russian book

12 p1800 A83-28814

Heavy particle with long life in cosmic rays above 10 to the 17th eV

12 p1801 A83-29036

Possibility of studying cosmic rays with energies

13 p1966 A83-30799

Periodicity of about 13 days in the cosmic-ray intensity in the solar cycles no. 18, 19 and 20

13 p1967 A83-31583

Detection of 2 x 10 to the 15th to 2 x 10 to the 16th eV gamma-rays from Cygnus X-3

14 p2117 A83-33227

Evidence for a new stable particle with heavy mass around 10 to the 17th eV. --- elementary particle produced in earth atmosphere

15 p2286 A83-34272

The halo effect in a nuclear-electromagnetic cascade

17 p2629 A83-37647

The results of observations of the X-ray source Cyg X-3 at energies exceeding 10 to the 12th eV made at the Tien Shan installation for detecting Cerenkov flashes in extensive air showers

17 p2589 A83-37661

Observations of gamma radiation at 10 to the 12th eV from the X-ray source Cyg X-3 at the Tien-Shan installation in 1977 and 1978

17 p2589 A83-37687

Inelastic p-air cross section at energies between 10,000-1,000,000 TeV estimated from air-shower experiments

17 p2629 A83-37736

Possible observation of a burst of cosmic-ray events in the form of extensive air showers

17 p2629 A83-37738

Thermal neutrons could be a cause of biological extinctions 65 Myr ago

17 p2557 A83-38605

Correlation of cosmic-ray intensity with geomagnetic Kp index and solar-magnetic-field reversal

17 p2630 A83-38868

Cosmic rays and high-energy interactions - Is there a necessity for a new phenomenon?

17 p2630 A83-38942

Determination of absolute fluxes of solar protons with E greater than 100 MeV according to stratospheric and neutron-monitor data

18 p2784 A83-39307

Geomagnetic-cutoff distribution functions for use in estimating detector response to neutrinos of atmospheric origin

19 p2925 A83-40960

Comment on the cosmic ray energy spectrum in the light of results from atmospheric Cerenkov studies

19 p2925 A83-41539

Possible explanation for scaling violation in hadron interactions above 1000 TeV

20 p3082 A83-42291

Interaction mean-free-path of cosmic-ray Fe in air

20 p3083 A83-43667

Radiation from fast particles in a turbulent medium --- cosmic ray showers

23 p3540 A83-48491

Cosmic ray showers at 10 to the 16th eV

24 p3675 A83-48983

Heavy-lepton model for the delayed particles in cosmic rays with (10 to the 15th - 10 to the 18th) eV

24 p3675 A83-49525

Measurement of the relative composition of the cosmic-ray iron group with lexan polycarbonate

24 p3676 A83-50163

COSMIC RAYS

NT COSMIC RAY SHOWERS

NT GALACTIC COSMIC RAYS

NT GAMMA RAY BURSTS

NT PRIMARY COSMIC RAYS

NT SECONDARY COSMIC RAYS

NT SOLAR COSMIC RAYS

Radiation shields for ships and settlements

01 p0019 A83-10706

Investigation of cosmic gamma-ray bursts

01 p0130 A83-10844

Study of diffuse cosmic and atmospheric gamma radiation using a spark chamber in the energy range 4 MeV-100 MeV

02 p0271 A83-11606

The abundance of the actinides in the cosmic radiation as measured on HEAO 3

02 p0272 A83-11619

All-Union Conference on Cosmic Rays, Samarkand, Uzbek SSR, October 27-29, 1981, Proceedings

02 p0272 A83-11701

Comments on the origin of cosmic rays

02 p0272 A83-11702

Interstellar turbulence and the kinetics of cosmic rays

02 p0272 A83-11704

Investigation of the chemical composition of cosmic-ray nuclei in the 20-1000 GeV/nucleon energy range by means of transition radiation

02 p0272 A83-11705

Investigation of fluxes of electrons and gamma quanta with energies exceeding 30 MeV at heights of 300-350 km

02 p0272 A83-11709

Some results of stratospheric studies of cosmic rays in cycles 19-21 of solar activity

02 p0272 A83-11711

Experimental studies of geomagnetic effects in cosmic rays and the spectrum of the increase effect before magnetic storms

02 p0273 A83-11713

Effects of the polarity change of the solar magnetic field in variations of cosmic rays

02 p0273 A83-11720

Variations of solar activity and cosmic rays with periods close to a week

02 p0273 A83-11721

The spectrographic method with allowance for interference of the effects of various classes of cosmic-ray variations

02 p0273 A83-11723

The effect of the large-scale structure of the general magnetic field of the sun on the intensity and anisotropy distribution of cosmic rays in interplanetary space

02 p0273 A83-11724

The 11-year variation of the isotropic and anisotropic flux of galactic cosmic rays

02 p0273 A83-11726

Frequency spectra and dynamics of long-period variations of isotropic and anisotropic fluxes --- of cosmic rays

02 p0273 A83-11728

A spectrograph of cosmic-ray intensity variations for the global network of stations

02 p0176 A83-11730

Installation for the investigation of sporadic radio emission of the earth's ionosphere

02 p0176 A83-11731

Acceleration of cosmic rays by pulsar X-rays

02 p0274 A83-11732

Differences in partial inelasticity coefficients Kpi/0/ for pFe, pFe interactions at energies of 0.5-5 TeV

02 p0235 A83-11735

Interaction of the aluminum nucleus with an energy of approximately 1 TeV per nucleon in a photoemulsion

02 p0274 A83-11737

The structure of gamma families and its relation to the formation of jets. II

02 p0274 A83-11742

The PAMIR-ANI experiments and quantum chromodynamics

02 p0274 A83-11745

Neutral pions from the fragmentation region of an impinging hadron at E sub 0 approximately equal to 10 to the 13th eV

02 p0274 A83-11748

The upper boundary of the energy spectrum of cosmic rays and possible methods for detecting cascades of superhigh energies /10 to the 20th-10 to the 28th eV/

02 p0276 A83-11762

An investigation of the energy spectrum and interactions of cosmic-ray muons with energies up to 10 to the 13th eV at a depth of 550 mwe

02 p0276 A83-11763

Modulation of the monoenergetic spectrum of galactic cosmic rays

02 p0276 A83-12417

Absorption of fluxes of galactic cosmic rays in the atmosphere during 1961-1980

02 p0208 A83-12418

Experimental verification of theoretical calculations of geomagnetic cutoff rigidity

02 p0210 A83-12443

High-energy astrophysics

02 p0245 A83-13103

Electrons with energies of hundreds of MeV in near-earth space

03 p0438 A83-13208

Airglow at a height below 40 km in the vacuum ultraviolet

03 p0356 A83-13216

The interrelation of cosmic gamma-rays and interstellar gas in the range 165-180 deg

03 p0414 A83-13329

Cosmic radiobiology --- Russian book

03 p0380 A83-13818

On the transport and propagation of cosmic rays in galaxies. I - Solution of the steady-state transport equation for cosmic ray nucleons, momentum spectra and heating of the interstellar medium

03 p0439 A83-13943

Samples of the Milky Way --- isotopic abundances in Galactic cosmic rays

03 p0426 A83-14599

Cosmic-ray 13 day oscillation and two-sector interplanetary magnetic field

03 p0439 A83-14874

The effect of adeturon on the survival and the blood system of mice under the effect of various types of ionizing radiation

03 p0376 A83-14880

The neutrino in the universe

03 p0431 A83-14926

Cosmic ray origin above 10 to the 18th eV - Galactic or extragalactic

04 p0575 A83-14983

A general upper limit on the mass and entropy production of a cluster of supermassive objects

04 p0549 A83-14994

The local interstellar medium as traced by gamma rays

04 p0550 A83-15048

Investigations of cosmic-ray-produced nuclides in iron meteorites. IV Identification of noble gas abundance anomalies

04 p0559 A83-15304

Radiobiological research in space

04 p0519 A83-15675

A measurement of the antiproton flux in the cosmic rays

04 p0575 A83-16350

Single event upsets in space --- radiation effects on spacecraft microelectronic circuits

[AIAA PAPER 83-0164]

05 p0606 A83-16564

Cosmic ray north-south anisotropy - The role of the interplanetary magnetic field

05 p0709 A83-17378

Single event error immune CMOS RAM

05 p0629 A83-17538

Single event upset vulnerability of selected 4K and 16K CMOS static RAM's

05 p0629 A83-17539

Effect of CMOS miniaturization on cosmic-ray-induced error rate

05 p0629 A83-17540

Calculation of cosmic-ray induced soft upsets and scaling in VLSI devices

05 p0629 A83-17541

Single event upset sensitivity of low power Schottky devices

05 p0629 A83-17542

Dynamics of the frequency spectrum of fluctuations of the interplanetary magnetic field and cosmic rays

05 p0710 A83-17620

Transport and propagation of cosmic rays in galaxies. II - The effect of a galactic wind on the mean lifetime and age distribution of non-decaying cosmic rays

06 p0857 A83-18077

Discrete sources of cosmic gamma rays

06 p0857 A83-18087

Direction of semi-diurnal anisotropy in relation to interplanetary magnetic fields

06 p0828 A83-18424

Non-linear theory of cosmic ray shocks including self-generated Alfvén waves

06 p0829 A83-18528

Cosmic-ray record in solar system matter

06 p0857 A83-18814

Cosmic ray intensity variations and two types of high speed solar streams

06 p0858 A83-19139

Does gravitation reveal its secret

06 p0816 A83-19246

The propagation of ultraheavy cosmic ray nuclei

06 p0858 A83-19297

Processes of the generation of high-energy muons in cosmic rays

06 p0858 A83-19341

Gamma ray transients and related astrophysical phenomena: Proceedings of the Workshop, La Jolla, CA, August 5-8, 1981

07 p1010 A83-20001

Cosmic rays from active galactic nuclei and in metagalactic space

07 p1040 A83-21152

Effects of drift on the transport of cosmic rays. VI - A three-dimensional model including diffusion

07 p1040 A83-21153

The neutrino background in the early universe, and temperature fluctuations in the cosmic microwave radiation

07 p1026 A83-21257

Numerical modeling of the energy spectrum of the cosmic ray Forbush decrease

07 p1040 A83-21504

The origin of cosmic radiation - Status after 70 years of research

09 p1369 A83-23497

High throughput non-dispersive hard X-ray spectrograph with angular resolution for cosmic bursts, transients, and sources

09 p1268 A83-24108

The contribution of quasi-stellar objects to the cosmic X-ray background

09 p1361 A83-24472

The gamma-ray colour of the Milky Way and the cosmic-ray electron density

09 p1363 A83-24997

Cosmological density fluctuations produced by sources of radiation at z greater than 100

09 p1363 A83-24997

A cosmic-ray dosimeter with a semiconductor detector

10 p1387 A83-25344

Cosmic-ray shock acceleration in the presence of self-excited waves

10 p1523 A83-25356

Investigations of cosmic-ray-produced nuclides in iron meteorites. V - More data on the nuclides of potassium and noble gases, on exposure ages and meteoroid sizes

10 p1518 A83-25452

Evidence for the stochastic acceleration of cosmic rays in supernova remnants

10 p1504 A83-25723

An investigation of cosmic ray fluctuations during Forbush decreases

10 p1523 A83-26101

A model description of fluxes of high-energy protons trapped by the geomagnetic field

10 p1523 A83-26103

An algorithm for detecting hardware errors in the data of supermonitors --- of cosmic ray parameters

Solar cycle variations of cosmic ray intensity and large-scale structure of the heliosphere 11 p1693 A83-27386

Modification of scattering waves and its importance for shock acceleration 11 p1678 A83-27692

Cosmic ray modulations related to the interplanetary magnetic field intensity 11 p1694 A83-28301

Rigidity responses of ionization chambers derived from cosmic-ray time variations 11 p1574 A83-28427

Cosmic rays from binary neutron stars 12 p1800 A83-28983

How stable is our vacuum? 13 p1944 A83-30217

A new installation for studying the sidereal anisotropy of cosmic rays 13 p1846 A83-30394

Theory of cosmic ray spectra 13 p1966 A83-30423

The effects of energetic particle precipitation on the atmospheric electric circuit 13 p1878 A83-30898

Space radiation interaction mechanisms in materials [AIAA PAPER 80-0588] 13 p1918 A83-31299

Cosmic-ray abundances of Sn, Te, Xe, and Ba nuclei measured on HEAO 3 13 p1953 A83-31446

The possible effect of atmospheric wind regimes on results of sonde measurements of cosmic rays 14 p2055 A83-31853

The possibility of using a neutron monitor without lead for the investigation of variations of cosmic-ray intensity 14 p2014 A83-31854

The hypothesis of the preferential acceleration of heavy elements in the cosmic plasma 14 p2116 A83-32544

Acceleration of cosmic rays in interplanetary space as a consequence of solar activity 14 p2116 A83-32545

The interaction of fast particles with long-wave MHD turbulence 14 p2116 A83-32546

Spectrographic method for the study of cosmic-ray variations 14 p2116 A83-32548

A method for determining the age of cosmic rays in the Galaxy 14 p2116 A83-32598

The variations of cosmic rays in the heliosphere according to the results of an investigation of extraterrestrial matter 14 p2117 A83-32970

The galactic gamma-ray source population 14 p2104 A83-33189

Isotopic anomalies among solar energetic particles Contribution of preacceleration in collapsing magnetic neutral sheets 14 p2115 A83-33216

Nonlinear propagation of hydromagnetic waves in high-beta plasmas 14 p2106 A83-33217

Search for short-term increases of the flux of heavy cosmic-ray nuclei according to Prognos-satellite data 14 p2117 A83-33392

Neutron high-energy spectra at seven different depths in the atmosphere from 0 to 40 mbar near the geomagnetic equator 15 p2196 A83-33948

Use of a Cf-252 source in cosmic ray simulation studies on CMOS memories 15 p2152 A83-34519

Decay of long-lived particles in the early universe 15 p2286 A83-34612

The retention of spallation products in interstellar grains 15 p2270 A83-34717

The role of cosmic rays in hydrostatic equilibrium of the galactic halo 16 p2441 A83-36528

Onion-shell model of cosmic ray acceleration in supernova remnants 16 p2441 A83-36674

Cosmic ray density gradients perpendicular to the solar equatorial plane 16 p2441 A83-36732

Prediction of interstellar antiproton flux using a nonuniform galactic disk model 17 p2629 A83-37338

The stages of the irradiation of protoplanetary matter by cosmic rays 17 p2619 A83-37815

Measurements of galactic plane gamma-ray emission in the energy range 10-80 MeV 17 p2629 A83-37931

First order and second order Fermi acceleration of energetic charged particles by shock waves --- cosmic ray transport 17 p2629 A83-37933

Radio-astronomy antennas for 3 deg K cosmic radiation measurements 17 p2494 A83-38059

The acceleration of cosmic rays by a shock wave in a diffusive medium - Research at high energies --- French thesis 17 p2629 A83-38222

International Union of Geodesy and Geophysics, General Assembly, 18th, Hamburg, West Germany, August 15-27, 1983, U.S. National Committee Report 17 p2586 A83-38265

Overview of cosmic ray studies and associated topics (1979-1982) 17 p2629 A83-38282

The elemental and isotopic composition of galactic cosmic ray nuclei 17 p2630 A83-38283

Cosmic-ray modulation and the anomalous component 17 p2630 A83-38285

Physical and chemical effects induced by energetic ions on comets 17 p2609 A83-38417

The role of non-linear Landau damping in cosmic ray shock acceleration 17 p2609 A83-38421

Status and future of high energy diffuse gamma-ray astronomy 18 p2785 A83-39276

Gamma rays from giant-molecular clouds 18 p2785 A83-39278

The effect of the anisotropy of the random component of the interplanetary magnetic field on the density distribution of cosmic rays 18 p2784 A83-39309

Visual sensations evoked by single electrons and muons 18 p2733 A83-39519

Cosmic rays and magnetic fields in the galaxy 18 p2786 A83-39655

Cosmic-ray anisotropy in interplanetary space 18 p2786 A83-39760

Flux of atmospheric neutrinos 18 p2786 A83-39926

Atmospheric neutrinos, astrophysical neutrinos, and proton-decay experiments 18 p2787 A83-39927

Hydrostatic-equilibrium distribution of cosmic rays and the magnetic field in the galactic halo 18 p2778 A83-40489

On the origin of the low-energy cosmic-ray antiprotons 18 p2787 A83-40491

Charged particle erosion of frozen volatiles in ice grains and comets 19 p2914 A83-40728

Preliminary results of the study of gamma-ray bursts by the SNEG-2MZ device on Venera 13 and 14 19 p2925 A83-41250

Some recent developments in the study of the elements and isotopes of the cosmic radiation 19 p2926 A83-42161

New mechanism for acceleration of cosmic particles in the presence of reflectively noninvariant turbulence 20 p3082 A83-42267

Interaction of solar neutrinos with the cosmic background 20 p3082 A83-42276

Stability of the equilibrium distributions of interstellar gas, cosmic rays, and magnetic field in an external gravitational field 20 p3076 A83-43652

Variations of cosmic-ray energy in interplanetary space 20 p3083 A83-43655

Release of protons with energy higher than 10 to the 18th eV from intergalactic magnetic field into interstellar magnetic field 20 p3077 A83-43664

Design and fabrication of the Indian cosmic ray payload on board Spacelab-3 - A case study 21 p3095 A83-43822

Cosmic ray induced soft error rate in VLSI circuits 21 p3123 A83-43844

Measurements of cosmic-radiation absolute ionization in the atmosphere 21 p3244 A83-44304

Boundary conditions for energetic particle transport at shocks 21 p3244 A83-44405

A method for determining the age of cosmic rays in the galaxy 21 p3245 A83-44506

The propagation of extra-relativistic cosmic ray electron in the interstellar medium 21 p3245 A83-44577

Particle acceleration in shocks - The effect of finite cosmic-ray pressure on the energy distribution 21 p3233 A83-44746

Polymerization induced on interstellar grains by low-energy cosmic rays 21 p3234 A83-44765

Cosmic rays in the upper atmosphere --- Russian book 21 p3174 A83-45019

Short-period variations of the rate of change of solar activity as a possible geoefficient parameter 21 p3174 A83-45227

Determination of variations of the north-south asymmetry of cosmic rays using the method of crossed telescopes 21 p3245 A83-45228

Characteristics of an anomalous component of cosmic rays in the stratosphere 21 p3245 A83-45229

The effect of local perturbations of the geomagnetic field on cosmic ray cutoff rigidities at Jungfraujoch and Kiel 22 p3390 A83-46035

Recent cosmic ray exposure history of ALHA 81005 22 p3386 A83-46868

A unified theory of cosmic ray diurnal variations 22 p3390 A83-46893

Implications of HEAO 3 data for the acceleration and propagation of galactic cosmic rays 22 p3390 A83-47003

Earth's magnetic field as a radiator to detect cosmic ray electrons of energy greater than 10 to the 12th eV 22 p3390 A83-47043

Cosmic ray acceleration in supernova blast waves 23 p3518 A83-47436

The maximum energy of cosmic rays accelerated by supernova shocks 23 p3518 A83-47440

Distributed acceleration of cosmic rays 23 p3538 A83-47613

Composition and origin of cosmic rays; Proceedings of the Advanced Study Institute, Erice, Italy, June 20-30, 1982 23 p3538 A83-47735

The spectra of cosmic ray nuclei greater than 1 GeV/nuc Implications for acceleration and propagation 23 p3539 A83-47737

Significance of ultraheavy cosmic rays 23 p3539 A83-47738

Cosmic-ray isotopic composition 23 p3539 A83-47739

Cosmic ray electrons and positrons - A review of current measurements and some implications 23 p3539 A83-47740

Cosmic ray composition at 10 to the 12th - 10 to the 15th eV derived from muon measurements 23 p3539 A83-47741

Antiprotons in the cosmic radiation 23 p3539 A83-47742

Ultra high energy cosmic rays 23 p3539 A83-47743

Cosmic ray acceleration mechanisms 23 p3539 A83-47746

Galactic propagation of cosmic rays 23 p3539 A83-47748

Sources of extragalactic cosmic rays - Photons and neutrinos as probes 23 p3540 A83-47750

Extragalactic cosmic rays, active galaxies and quasi-stellar objects 23 p3540 A83-47751

Deep Underwater Muon and Neutrino Detection (DUMAND) 23 p3540 A83-47752

Future muon and neutrino experiments 23 p3540 A83-47753

Detectors of ultraheavy cosmic rays 23 p3455 A83-47754

The BUGS 4 cosmic ray detector 23 p3455 A83-47755

A detector to investigate the anomalous component of cosmic rays and its rarer constituents including a possible molecular ion component 23 p3540 A83-47756

Complete fragment yields from spallation reactions via a combined time-of-flight and delta-E-E technique 23 p3455 A83-47757

Improvement of calculations of cross sections and cosmic-ray propagation 23 p3540 A83-47758

Matrix methods of cosmic ray propagation 23 p3540 A83-47759

The effect of cross-section uncertainties on the derivation of source abundances from cosmic-ray composition observations 23 p3540 A83-47760

The IMB proton decay detector 23 p3455 A83-47763

The decay of 'mesotrons' (1939-1943), experimental particle physics in the age of innocence 23 p3540 A83-47765

Positrons in cosmic rays and the galactic gamma radiation associated with them 24 p3675 A83-49173

Structure of the cosmic microwave background 24 p3670 A83-50110

COSMIC X RAYS

The origin of the cosmic X-ray background 04 p0575 A83-16047

Studies with the Pinhole/Occulter Facility [AIAA PAPER 83-0513] 05 p0692 A83-16759

X-80 - A spectroscopy, transient and timing mission for X-ray astrophysics 05 p0601 A83-17432

Second-order scattering approximation to X-ray photon transport at balloon altitudes 05 p0665 A83-17803

An imaging gas scintillation proportional counter coupled to a channel multiplier array for application in cosmic X-ray spectroscopy 11 p1573 A83-27755

Stigmatic Bragg crystal spectrometers for cosmic X-rays 11 p1573 A83-27758

Relative contribution of various secondary X-ray components below 100 keV at balloon altitudes 17 p2512 A83-38545

Exosat/Delta - Demonstrated short-term backup launcher capability through international cooperation [IAF PAPER 83-01] 23 p3418 A83-47227

COSMOCHEMISTRY

Tracks of heavy and superheavy cosmic nuclei in olivines of extraterrestrial origin 01 p0130 A83-11339

Sorption of noble gases by solids, with reference to meteorites. I - Magnetite and carbon 02 p0262 A83-11546

Sorption of noble gases by solids, with reference to meteorites. II - Chromite and carbon. III - Sulfides, spinels, and other substances; on the origin of planetary gases 02 p0262 A83-11547

Physical conditions and carbon monoxide abundance in the dark cloud B5 02 p0251 A83-11586

The chemical composition of R Coronae Borealis and XX Camelopardalis 02 p0252 A83-11594

Processes affecting abundances in the solar wind 04 p0574 A83-15121

Chemical weathering and the Viking biology experiments on Mars 04 p0567 A83-15577

On the formation of carbon star characteristics and the production of neutron-rich isotopes in asymptotic giant branch stars of small core mass

- 04 p0555 A83-15651
Nitrogen overabundances in Population II dwarfs
04 p0555 A83-15652
Warm CNO nucleosynthesis as a possible enrichment mechanism for oxygen and fluorine isotopes --- stellar burning
05 p0699 A83-17014
Spectroscopic analysis of alpha Andromedae
05 p0702 A83-17812
The galactic abundance of deuterium - A test for cosmological models
06 p0837 A83-19215
Formation of planetary systems --- Book
06 p0849 A83-19451
A few relevant facts on the problem of the origin of the solar system
06 p0842 A83-19454
Condensation of grains --- relevance to astrophysical problems
06 p0842 A83-19455
Cosmochemistry and primitive evolution of planets
06 p0842 A83-19456
Nuclear cosmochronology or the age of the elements
06 p0842 A83-19457
A brief survey of the solar system
06 p0849 A83-19463
The hydrogen to helium ratio in Jupiter and Saturn
06 p0849 A83-19465
Comets - Their evolution and origin
06 p0842 A83-19472
The sp-process and Allende isotope anomalies in calcium and titanium
06 p0850 A83-19506
The chemical evolution of galaxies
07 p1016 A83-20766
Primordial retention of nitrogen by terrestrial planets and meteorites
07 p1034 A83-21320
The role of S in the evolution of the parental cores of the iron meteorites
07 p1035 A83-21327
The mass-independent fractionation of oxygen - A novel isotope effect and its possible cosmochemical implications
08 p1188 A83-22688
Accelerator mass spectrometry measurement of cosmogenic Al-26 in terrestrial and extraterrestrial matter
08 p1187 A83-23293
Re-187 - Os-187 systematics in meteorites and cosmochemical consequences
10 p1517 A83-25445
Some cosmochemical consequences of a turbulent protoplanetary cloud
10 p1501 A83-25509
The chemical inhomogeneity of M22
10 p1502 A83-25711
The hydrogen-depleted planetary nebulae Abell 30 and Abell 78
10 p1504 A83-25726
Interstellar abundances of oxygen and nitrogen
10 p1505 A83-25747
Analysis of estimates of the influx of meteor matter to the earth
11 p1685 A83-27877
The distribution of atomic and molecular hydrogen in the Galactic plane
11 p1681 A83-28260
Circumstellar silicon chemistry and the SiO maser
11 p1681 A83-28263
The matter of the universe --- Russian book
12 p1789 A83-28817
Cosmochemistry and the origin of life; Proceedings of the Advanced Study Institute, Maratea, Italy, June 1-12, 1981
13 p1899 A83-31151
Cosmochemistry and the origin of life
13 p1908 A83-31152
Synthesis of the chemical elements --- cosmochemical evolution
13 p1947 A83-31153
Cosmic-ray abundances of Sn, Te, Xe, and Ba nuclei measured on HEAO 3
13 p1953 A83-31446
The Crab Nebula
13 p1953 A83-31563
Note on technetium in stars
16 p2433 A83-36703
Nickel isotopic studies in meteorites
16 p2438 A83-36746
Nitrogen and oxygen as indicators of primordial enrichment
17 p2608 A83-38402
The chemical inhomogeneity of the Sculptor dwarf spheroidal galaxy
20 p3067 A83-42439
Handbook of isotope geochemistry --- in Russian
21 p3239 A83-43909
A method for determining the age of cosmic rays in the galaxy
21 p3245 A83-44506
Abundance gradients in galaxies in the Sculptor and Centaurus groups
21 p3233 A83-44750
Cosmic-ray isotopic composition
23 p3539 A83-47739
Cosmic ray sources
23 p3539 A83-47749
Prebiotic evolution on a universal scale. I
23 p3500 A83-48054
Cometary matter in the environment
24 p3598 A83-49105
Effects of dust formation on chemical abundances --- in planetary nebulae
24 p3652 A83-49145
Al-Sm-Eu-Sr systematics of eucrites and moon rocks
Implications for planetary bulk compositions
24 p3672 A83-49348

- ESO Workshop on Primordial Helium, Garching, West Germany, February 2, 3, 1983, Proceedings
24 p3664 A83-50030
The origin of the light elements - A quite complex problem --- primordial abundances in universe
24 p3664 A83-50031
Neutrinos, the He-4 abundance, and stellar evolution
24 p3665 A83-50033
Pregalactic synthesis of deuterium
24 p3665 A83-50037
Evolution of zero metal stars and early chemical enrichment of the Galaxy
24 p3665 A83-50038
Abundance of lithium in old dwarf stars
24 p3667 A83-50060

COSMOGONY

U COSMOLOGY

COSMOLOGY

NT BIG BANG COSMOLOGY

NT HUBBLE DIAGRAM

- On the neutrino mass and the Lemaitre model
01 p0119 A83-10235
Matter and antimatter in the universe
01 p0123 A83-10377
Astrophysics and cosmic physics --- Russian book
01 p0124 A83-10838
Intergalactic gas in galactic clusters, the microwave background radiation and cosmology
01 p0124 A83-10839
Topology of cosmological models near critical points
01 p0125 A83-10907
The cosmic density wave and its observable vestige
01 p0125 A83-10933
Implications of gravitational interactions for the angular momenta of galaxies
01 p0126 A83-10965
Mach's principle and the microwave background --- in homogeneous cosmology
01 p0126 A83-10971
Generalized theory of gravitation and its physical consequences
01 p0127 A83-11292
The primeval magnetic field --- magnetic moment/intrinsic angular momentum relation
01 p0127 A83-11293
Formation of galaxies in G-variable cosmologies
01 p0127 A83-11294
Some aspects of gravitational waves in an isotropic background universe
01 p0127 A83-11295
The lepton Brusselator - Creation of structure in the early Universe
02 p0254 A83-12091
Asymptotic breaking and restoration of symmetry in a statistical system of particles with short-range vector interaction and isotropic cosmological models
03 p0417 A83-13533
On the large-scale variations of M/L --- mass to light ratio in universe
03 p0422 A83-14176
An approximately 300 Mpc void of rich clusters of galaxies
03 p0422 A83-14177
The four-point function in the BBGKY hierarchy --- galaxy correlation in clustering pattern
03 p0422 A83-14178
Heat death and oscillation in model universes containing interacting matter and radiation
03 p0422 A83-14179
Lu-176 - Cosmic clock and stellar thermometer
03 p0425 A83-14209
On the cosmological evolution of the X-ray emission from quasars
03 p0425 A83-14215
Galactic neutrino models
03 p0429 A83-14778
Shifts of spectral lines emitted from stars
03 p0431 A83-14947
Steady wave model of spiral galaxies and its application in cosmogony
04 p0549 A83-14995
Null influence of possible local extragalactic perturbations on tests of redshift-distance laws
04 p0550 A83-15047
Large-scale background temperature and mass fluctuations due to scale-invariant primeval perturbations
04 p0554 A83-15646
Space-time curvature and cosmology
04 p0555 A83-15707
Multisheet models of the universe
04 p0555 A83-15901
Dynamo action in cosmic bodies
04 p0556 A83-15959
Post-Newtonian approximations in scale covariant gravitation
04 p0556 A83-15960
Nucleosynthesis in bouncing cosmologies
04 p0557 A83-15977
Steady-state versus viscous cosmology
04 p0557 A83-15983
Cosmology and unified gauge theory
04 p0558 A83-16441
Luminosity evolution of QSOs
05 p0695 A83-16856
Dynamical models and our Virgo-centric deviation from Hubble flow
05 p0696 A83-16976
Grand unified reactions and dissipation in anisotropic cosmologies
05 p0696 A83-16977

- Manifestations of a cosmological density of compact objects in quasar light
05 p0696 A83-16978
Relaxation terms and entropy production in a cosmological model
05 p0701 A83-17225
Cosmological molecular hydrogen and the distortion of the relic radiation spectrum
05 p0710 A83-17804
Inhomogeneous cosmological models with flat slices generated from the Einstein-de Sitter universe
05 p0702 A83-17852
Cosmological testing of Mach's principle
05 p0703 A83-17859
Chaos in the mixmaster universe
05 p0703 A83-17937
On the gravitational radius - Velocity dispersion correlation for clusters of galaxies
06 p0827 A83-18172
Gowdy three-handle and S/3/ inhomogeneous cosmological models
06 p0828 A83-18324
Containment of a diffuse ionized mass orbiting around a magnetized central body --- for solar system development
06 p0828 A83-18475
The 'black' regions of the Universe
06 p0830 A83-18776
The origin of large-scale cell structure in the universe
06 p0831 A83-18789
On the existence of cosmological evolutionary effects.
I - A morphological selection effect in the counts of quasars
06 p0834 A83-18880
Towards a unification of the parameters underlying elementary particles and cosmology
06 p0835 A83-18896
The galactic abundance of deuterium - A test for cosmological models
06 p0837 A83-19215
Inhomogeneity of the early Universe and formation of primordial black holes
06 p0837 A83-19217
Effect of variable obscuration on the clustering of galaxies
06 p0839 A83-19265
The ages and compositions of old clusters
06 p0840 A83-19283
The evolution of large-scale structures in the Universe.
II
06 p0841 A83-19395
Electric charge in the Kruskal space-time and the Jeans conjecture
06 p0841 A83-19447
Theories of the origin of the solar system - Some historical remarks
06 p0842 A83-19452
CCD photometry of Abell clusters. I - Magnitudes and redshifts for 84 brightest cluster galaxies
06 p0842 A83-19476
Superclusters as nondissipative pancakes - Flattening
06 p0843 A83-19479
The peculiar velocity field in flattened superclusters
06 p0845 A83-19521
An introduction to tensor calculus, relativity and cosmology /3rd edition/ --- Book
07 p0988 A83-19675
Cosmology and astrophysics - Essays in honor of Thomas Gold --- Book
07 p1013 A83-20401
Steady state cosmology revisited
07 p1013 A83-20402
Grand unification and cosmology
07 p1015 A83-20759
Theory and evidence about the origin of cosmological structure
07 p1015 A83-20760
Evolution of potential perturbations after decoupling /The adiabatic scenario/ --- in early Universe
07 p1016 A83-20763
Primordial stars - The precursors to galaxy formation
07 p1016 A83-20764
Cosmological evolution of QSOs and radio galaxies
07 p1016 A83-20770
Epilogue - Do we understand how galaxies formed
07 p1017 A83-20771
Upper bound on gauge-fermion masses
07 p0992 A83-20814
Analysis of the large-scale structure of the universe
07 p1017 A83-20935
Tidal distension in protostructures - The shapes of galaxies and systems of galaxies
07 p1017 A83-20937
The nonuniqueness of the limit transition from Brans-Dicke theory to Einstein theory
07 p0990 A83-20970
Perfect fluids in the Einstein-Cartan theory
07 p0990 A83-21065
Bias in observed nearby clusters of galaxies
07 p1008 A83-21206
The Re-187 - Os-187 chronology and chemical evolution of the Galaxy
07 p1024 A83-21214
Holes in cosmology
07 p1026 A83-21253
The influence of a nonzero rest mass upon the growth of perturbations in an isotropic universe
07 p1026 A83-21256
The neutrino background in the early universe, and temperature fluctuations in the cosmic microwave radiation
07 p1026 A83-21257

- Pregalactic very massive objects and their cosmological consequences ... 08 p1178 A83-21843
- Perfect fluid spheres in general relativity 08 p1180 A83-22207
- The Inflationary Universe lives 08 p1181 A83-22398
- Interaction of massless scalar field and charged dust in nonrigid rotation 08 p1181 A83-22744
- The structure and expansion law of a shock wave in an expanding universe 08 p1181 A83-23026
- An upper limit on the stochastic background of ultralow-frequency gravitational waves 08 p1184 A83-23076
- Upper limits on the isotropic gravitational radiation background from pulsar timing analysis 08 p1184 A83-23077
- Inflation and time asymmetry in the universe 08 p1186 A83-23272
- How galaxies acquire their neutrino haloes 08 p1187 A83-23285
- VLA source counts at 6-cm wavelength 08 p1187 A83-23291
- Is there evidence for universal rotation 08 p1187 A83-23294
- A 10.7-GHz source survey of 0.0016 steradians --- for studying cosmological evolution 09 p1353 A83-23732
- On linear perturbations in generalized Einstein space 09 p1359 A83-24203
- Perturbation of the magnitude-redshift relation in an inhomogeneous relativistic model. III - Redshift effect intrinsic to clusters of galaxies 09 p1360 A83-24462
- Astronomy and astrophysics for the 1980's. Volume 1 - Report of the Astronomy Survey Committee. Volume 2 - Reports of the Panels --- Book 09 p1351 A83-24950
- Cosmological density fluctuations produced by sources of radiation at z greater than 100 09 p1363 A83-24997
- Small-angle anisotropy of the microwave background radiation in the adiabatic theory --- concerning structure of Universe 09 p1364 A83-25002
- Age and metal abundance of a globular cluster, as derived from Stromgren photometry 09 p1364 A83-25289
- On semi-degenerate equilibrium configurations of a collisionless self-gravitating Fermi gas 10 p1500 A83-25482
- A new approach to scale-invariant gravity /or: A variable-mass embedding for general relativity/ 10 p1501 A83-25497
- Inner ring structures in galaxies as distance indicators. IV - Distances to several groups, clusters, the Hercules supercluster, and the value of the Hubble constant 10 p1502 A83-25701
- Is there nonluminous matter in dwarf spheroidal galaxies 10 p1504 A83-25740
- Some implications of nonluminous matter in dwarf spheroidal galaxies 10 p1504 A83-25741
- Cosmological constant and absence of particle creation 10 p1505 A83-25799
- Gravitational lenses 10 p1505 A83-25899
- Algebraic programming of Hamiltonian formalism in general relativity - Application to inhomogeneous space-times 10 p1506 A83-26093
- Can galactic halos be made of axions 10 p1507 A83-26270
- Markarian galaxies and voids in the galaxy distribution 10 p1507 A83-26352
- Paired quasars near NGC 2639 - Evidence for quasars in superclusters 10 p1507 A83-26353
- The cosmological evolution and luminosity function of X-ray selected active galactic nuclei 10 p1510 A83-26399
- Quasar evolution - Not a deficit at 'low' redshifts 10 p1511 A83-26701
- The distribution of quasars from a small area survey 10 p1512 A83-26702
- Why weakly non-linear effects are small in a zero-pressure cosmology 11 p1682 A83-28283
- Limits on the neutrino number and baryon density of a realistic universe 11 p1694 A83-28286
- Classical and quantum models of strong cosmic censorship 12 p1774 A83-28873
- The evolution of shear and gravitational wave perturbations of Friedmann models and the isotropy of the universe 12 p1790 A83-28889
- Robertson-Walker cosmologies with a trace anomaly effect in their dynamical description 12 p1791 A83-28985
- The quark-hadron phase transition and the temperature of the MW background radiation 12 p1792 A83-29030
- On the origin of the solar system and the exceptional position of the sun in the galaxy 12 p1792 A83-29055
- Gravitational Debye-Hueckel theory for a Newtonian cosmology 12 p1793 A83-29061
- On hierarchical cosmology 12 p1793 A83-29074
- Asymptotic freedom and entropy in a perpetually oscillating universe 12 p1794 A83-29166
- The redshift distribution of quasar absorption lines and its origin 12 p1795 A83-29353
- A search for large-scale lineations in the apparent distribution of galaxies 12 p1788 A83-29490
- The impossibility of a bouncing Universe 13 p1944 A83-30216
- How stable is our vacuum? 13 p1944 A83-30217
- Five crucial tests of the cosmic distance scale using the Galaxy as fundamental standard 13 p1935 A83-30356
- Limiting density of matter as a universal law of nature 13 p1947 A83-30798
- Possibility of detecting relic massive neutrinos 13 p1966 A83-30800
- Supersymmetry and supergravity 13 p1914 A83-31163
- Dustlike stages in the early universe, and constraints on the primordial black hole spectrum 13 p1948 A83-31254
- The structure of the inhomogeneity field and the formation of primordial black holes 13 p1948 A83-31255
- Constraint on the photino mass from cosmology 13 p1949 A83-31357
- A survey of galaxy redshifts. V - The two-point position and velocity correlations 13 p1949 A83-31401
- A new evaluation of the four-point galaxy correlation function amplitudes 13 p1949 A83-31402
- The formation of disc galaxies 13 p1953 A83-31552
- Fermion-induced monopole-antimonopole annihilation 13 p1954 A83-31606
- The renormalized coupling constant in an open static Einstein universe 13 p1954 A83-31607
- Adiabatic density perturbations in a cosmological model with massive neutrinos 13 p1955 A83-31652
- Core radii determination for eleven southern clusters of galaxies 13 p1955 A83-31665
- The geometry of two superclusters Coma-A1367 and Perseus-Pisces 13 p1958 A83-31732
- The opacity of the universe and the strong equivalence principle 14 p2102 A83-32421
- A scalar field with self-interaction leads to the absence of a singularity in cosmology 14 p2102 A83-32424
- Quantum cosmology and stationary states 14 p2102 A83-33046
- Exact solutions for the early universe in general scalar-tensor theories 14 p2102 A83-33047
- Search for neutral hydrogen in the early universe 14 p2107 A83-33236
- Towards a study of southern distant clusters of galaxies 14 p2099 A83-33240
- Are dominant central galaxies the proto-nuclei of rich clusters? 14 p2101 A83-33468
- Cosmological models with a quasistable de Sitter stage 15 p2253 A83-33705
- How can we approach the study of cosmology? 15 p2254 A83-33753
- The galaxy as fundamental calibrator of the extragalactic distance scale. I - The basic scale factors of the galaxy and two kinematic tests of the long and short distance scales 15 p2255 A83-34076
- CCD photometry of Abell clusters. II - Surface photometry of 249 cluster galaxies 15 p2255 A83-34077
- Numerical solutions of high-frequency perturbations in Bianchi type IX models --- for formation of galaxies in homogeneous isotropic universe 15 p2255 A83-34079
- Spherical simulations of holes and honeycombs in Friedmann universes 15 p2256 A83-34080
- Physical properties of the intergalactic medium and the Lyman-alpha absorbing clouds 15 p2259 A83-34118
- A new test of the cosmological interpretation of QSO redshifts 15 p2260 A83-34378
- A special law of variation for Hubble's parameter 15 p2261 A83-34411
- An exact viscous fluid FRW cosmology --- Friedmann-Robertson-Walker 15 p2261 A83-34491
- Limits from the timing of pulsars on the cosmic gravitational wave background 15 p2264 A83-34583
- A new view on the origin of comets and other minor bodies 15 p2248 A83-34688
- Evolution of a homogeneous universe with a posthydrodynamic stress-energy tensor for the ultrarelativistic medium 15 p2270 A83-34751
- High-redshift objects as probes of nearby cosmic voids 15 p2272 A83-34792
- Large-scale anisotropy of the 3 K background radiation in density wave models 16 p2441 A83-36677
- Large numbers hypothesis. IV - The cosmological constant and quantum physics 16 p2408 A83-36987
- Spinning fluids in the Einstein-Cartan theory 16 p2408 A83-36989
- Quasar evolution derived from the Palomar bright quasar survey and other complete quasar surveys 17 p2596 A83-37302
- The V/V(max) test for QSOs - Comments on the paper by Hawkins and Stewart 17 p2604 A83-37904
- Bright radio sources at 178 MHz - Flux densities, optical identifications and the cosmological evolution of powerful radio galaxies 17 p2606 A83-38241
- Ionization curves and last scattering surfaces in neutrino-dominated universes 17 p2609 A83-38422
- Distance and model dependence of observational galaxy cluster concepts 17 p2610 A83-38427
- The dynamical role of a primordial electromagnetic field in spatially homogeneous, diagonal Bianchi type I-IX cosmologies 17 p2610 A83-38546
- Inflation can solve the rotation problem --- of universe 17 p2612 A83-38608
- The infrared luminosity-H I profile width-surface brightness relation, and the cosmological expansion 17 p2612 A83-38826
- Cosmological models with S3 topology 17 p2614 A83-38951
- Magnetic fields in the cosmos 18 p2764 A83-39087
- Posterior probability of the deceleration parameter q sub 0 from quasars provided with a luminosity indicator 18 p2764 A83-39194
- Primordial nucleosynthesis and scale-covariant cosmology 18 p2774 A83-39736
- Spatially self-similar cosmological model of Bianchi type-I(l) 18 p2775 A83-39749
- On dissipational processes in the cosmological GUT era 18 p2775 A83-39761
- Astronomische Gesellschaft, Scientific Meeting on Cosmology and Relativistic Astrophysics, Constance, West Germany, March 22-25, 1983, Reports 18 p2776 A83-39770
- Quantum gravity - A unified model of existence? 18 p2776 A83-39773
- Renormalizability of quantum gravity with cosmological constant 18 p2777 A83-39923
- Gravitational scintillation, anisotropies of background radiation and density inhomogeneities of cosmic matter 18 p2777 A83-40364
- General solutions for the field of a charged particle in Brans-Dicke theory of gravitation 18 p2741 A83-40418
- Mechanism of generating isothermal perturbation by a strong CP nonconservation --- in early universe 19 p2915 A83-40972
- Compactification of Friedmann's hyperbolic model 19 p2915 A83-40978
- On the global geometry of the Stephani universe 19 p2916 A83-41284
- A bimetric Machian approach to gravitation 19 p2916 A83-41285
- Frame dragging in Einstein and Einstein zero mass scalar cosmologies 19 p2916 A83-41307
- Cosmology and life in the universe 19 p2908 A83-41512
- The evolution of voids in the expanding universe 19 p2917 A83-41604
- A modification of the Newtonian dynamics as a possible alternative to the hidden mass hypothesis 19 p2917 A83-41606
- Numerical experiments on the clustering of galaxies 19 p2917 A83-41608
- The ultimate fate of the universe --- Book 20 p3063 A83-42173
- Isotropization of arbitrary cosmological expansion given an effective cosmological constant 20 p3064 A83-42269
- Zero-curvature Friedmann-Robertson-Walker models as exact viscous magnetohydrodynamic cosmologies 20 p3066 A83-42428
- Limits on the accuracy of determining $q(0)$ from supernovae 20 p3070 A83-42786
- Primordial quantum fluctuations and the origin of galaxies 20 p3070 A83-42787
- The quadrupole component of the relic radiation in a quasi-hyperbolic cosmological model 20 p3070 A83-42789
- Certain scientific problems relating to planetary missions 20 p3078 A83-42890
- Vacuum field, modified cosmical term and non-singular cosmology 20 p3070 A83-42940
- Nonlinear evolution of large-scale structure in the universe 20 p3070 A83-43035
- Alignment of faint galaxy images - Cosmological distortion and rotation 20 p3070 A83-43036
- Principles, problems, and paradoxes of cosmogony 20 p3074 A83-43130

On the behaviour of test matter in the neighbourhood of caustics of homogeneous cosmological models 20 p3074 A83-43377

Stress-energy density tensor of isotropic homogeneous universe 20 p3075 A83-43388

Magnitude-redshift relation in clusters, groups and pairs of galaxies 20 p3075 A83-43393

Capture and eruption hypotheses for comets 20 p3061 A83-43413

Can population III stars generate primordial helium? 20 p3075 A83-43538

Hf chronometer for the early solar system 20 p3076 A83-43539

Cluster analysis of the nonlinear evolution of large-scale structure in an axion/gravitino/photino-dominated universe 21 p3227 A83-44200

On the origin of comets 21 p3228 A83-44297

Evolutionary relation between meteorites, meteoroids and asteroids or comets 21 p3240 A83-44298

The stability of general relativistic cosmological theory 21 p3231 A83-44475

Exact rotating and expanding radiation-filled universe 21 p3231 A83-44496

A study of cosmogenic nuclides on meteorites 21 p3241 A83-44586

Bifurcations and phase transitions of self-gravitating and uniformly rotating fluid 21 p3232 A83-44737

Particle physics meets cosmology - The search for decaying neutrinos 21 p3245 A83-44859

A deep survey of galaxies 22 p3372 A83-46377

Three-dimensional numerical model of the formation of large-scale structure in the Universe 22 p3378 A83-46539

Very large spiral galaxies 22 p3374 A83-46540

Non-Einsteinian gravitational Lagrangians assuring cosmological solutions without collapse 22 p3380 A83-46753

On the statistical distribution of massive fermions and bosons in a Friedmann universe 23 p3518 A83-47442

The problem of the Grand Unification Theory --- in cosmology 23 p3503 A83-48058

The cosmological problem as initial value problem on the observer's past light cone - Observations 23 p3526 A83-48059

Bianchi type-I universes of the Brans-Dicke vacuum theory 23 p3526 A83-48060

The influence of quantum effects on the structure of space-time near singularities in general relativity 23 p3504 A83-48445

Hydrodynamics, fields, and constants in gravitation theory --- Russian book 23 p3527 A83-48450

The cosmological constant and classical tests of general relativity 23 p3528 A83-48591

The breakdown of the connectedness of physical space --- in cosmology and during gravitational collapse 24 p3651 A83-49060

New solutions to the Einstein equations, allowing for vacuum effects of quantized fields 24 p3651 A83-49064

Cosmological term in a nonsingular cosmological model of the Einstein-Cartan gravitation theory 24 p3651 A83-49067

Scalar-tensor theories of gravitation - Foundations and prospects 24 p3651 A83-49100

Mass distribution and dark halos 24 p3654 A83-49215

The formation of galaxies 24 p3657 A83-49266

Galaxy formation - Some comparisons between theory and observation 24 p3657 A83-49267

Experimental tests of the 'invisible' axion --- elementary particles in cosmology 24 p3658 A83-49292

Magnetohydrodynamic effects of a first-order cosmological phase transition 24 p3658 A83-49299

Proto-galactic perturbations 24 p3658 A83-49365

The anthropic principle and the actual size of the universe 24 p3661 A83-49523

Non-equilibrium relativistic cosmology 24 p3663 A83-49650

Photometric studies of faint galaxies on deep UKST plates with COSMOS 24 p3648 A83-50021

Clustering and alignment of quasars 24 p3649 A83-50026

Clustering of QSO's and galaxies 24 p3649 A83-50027

ESO Workshop on Primordial Helium, Garching, West Germany, February 2, 3, 1983, Proceedings 24 p3664 A83-50030

On the mass range of the first stars 24 p3665 A83-50036

Three-dimensional simulation of large-scale structure in the universe 24 p3669 A83-50106

Structure of the cosmic microwave background 24 p3670 A83-50110

Plane symmetric vacuum Bianchi type I cosmological model in Brans-Dicke theory 24 p3670 A83-50157

Apparent superluminal velocities due to the curvature of space 24 p3670 A83-50159

COSMONAUTS

Salyut-7 from June to August 05 p0601 A83-17775

Features of cosmonaut training 15 p2215 A83-34945

A unique laboratory - Interview with the pilot-cosmonaut A. A. Serebrov --- of Salyut 6 and 7 flights 19 p2807 A83-41462

The Soviet cosmonaut team, 1960-1971 23 p3416 A83-48631

The Soviet cosmonaut team, 1971-1983 23 p3416 A83-48632

COSMOS SATELLITES

NT COSMOS 1129 SATELLITE

NT INTERCOSMOS SATELLITES

Experimental study of the effect of solar radiation reflected from the earth and its cloud cover on the thermal regime of solar arrays mounted on one of the Cosmos satellites 04 p0454 A83-15126

Reentry of the Soviet satellite Cosmos 1402 predicted for the end of January 06 p0720 A83-19175

Artificial satellite break-ups. I - Soviet ocean surveillance satellites 07 p0869 A83-21616

Reflection characteristics of certain classes of Soviet space objects 07 p0871 A83-21621

Sarsat-Kospas - Satellite search-and-rescue trials presage new international system 09 p1211 A83-25138

Status of joint US/USSR experiments planned for the Cosmos '83 biosatellite mission 11 p1636 A83-27791

Ion sensor signal fluctuations during spacecraft jet engine operation 17 p2481 A83-37467

Hydrophysical analysis of remote measurements of the ocean from space [IAF PAPER 83-103] 23 p3493 A83-47266

COSMOS 1129 SATELLITE

Results on artemia cysts, lettuce and tobacco seeds in the Biobloc 4 experiment flown aboard the Soviet biosatellite Cosmos 1129 19 p2872 A83-40842

COSPAR (COMMITTEE)

U COMMITTEE ON SPACE RESEARCH

COST ANALYSIS

Approach to Nitinol power plant cost analysis 01 p0111 A83-10656

Life Cycle Cost analysis of standard avionics hardware and software 01 p0112 A83-11256

Some thoughts on the development of computer-based systems --- airborne equipment design to cost 02 p0135 A83-11807

Building a small format, in-house aerial photography system 03 p0329 A83-14274

Determination of minimum cost interference between services sharing the same frequency bands 04 p0465 A83-15074

Aerodynamic platform comparison for jet-stream electricity generation 04 p0507 A83-16102

Mitnet - A private network using TDMA 07 p0911 A83-19787

Composite drapability - A too often ignored impacting cost characteristic 07 p0875 A83-20438

The Fokker F28 and a four-engined newcomer 07 p0886 A83-21349

Size effects in DAWT innovative wind energy system design [ASME PAPER 82-WA/SOL-20] 10 p1445 A83-25688

A viable process for producing hydrogen synfuel using nuclear fusion heat 11 p1605 A83-27210

Is LH2 the high cost option for aircraft fuel 11 p1552 A83-27215

An analysis of the cost/performance characteristics of passive solar materials and components 11 p1608 A83-27247

AQUASTOR - A computer model for cost analysis of aquifer thermal energy storage coupled with district heating or cooling systems 11 p1609 A83-27314

Cost and performance of thermal storage concepts in solar thermal systems, Phase 2-liquid metal receivers 11 p1609 A83-27316

Satellite assembly, integration, and test and analysis 13 p1810 A83-31189

On the certainty of synergistic effects --- in environmental reliability testing 13 p1862 A83-31480

The helicopter preliminary design process 13 p1806 A83-31812

Spaced out: Satellite remote sensing - The costs and benefits 15 p2286 A83-34655

The space transportation system mixed fleet economics [SAE PAPER 821370] 17 p2586 A83-37962

Availability as a function of usage profile [AIAA PAPER 83-2287] 19 p2855 A83-41747

Economic evaluation of wind energy applications for remote location power supply 20 p3056 A83-43367

Modal cost analysis as an aid in control system design for large space structures 21 p3098 A83-44005

Economics of telecommunications space segments [IAF PAPER 83-234] 23 p3514 A83-47317

The economics of space development - The cost of space development [IAF PAPER 83-239] 23 p3514 A83-47320

Competition in space - Government vs. industry 23 p3514 A83-47322

A comparison of Navy and contractor gas turbine acquisition cost [ASME PAPER 83-GT-198] 23 p3410 A83-48001

Comparative cost of military aircraft - Fiction versus fact [AIAA PAPER 83-2565] 23 p3392 A83-48378

COST EFFECTIVENESS

Some management views on test program set /TPS/ salvageability 01 p0088 A83-10729

ADATLAS - The test language of the future 01 p0091 A83-10741

Cost-effective approaches for extending the useful life of ATE and test program sets 01 p0088 A83-10762

More efficient and effective defense system acquisition through unified system effectiveness analysis and control /SEAC/ 01 p0111 A83-1117

The Aquila - A versatile, cost-effective military tool shows its potential 04 p0447 A83-16399

The dynamic inducer as a cost-effective wind turbine system 06 p0779 A83-18457

A cost effective TDMA terminal for Intelsat/Eutelsat applications 07 p0911 A83-19782

The practical tradeoff among bandwidth efficiency, modulation schemes, availability, and cost in satellite communication system design considerations 07 p0912 A83-19798

Goal programming for preliminary design and critical technology identification - Application to infrared step-stare moving target detection 08 p1051 A83-22842

Cost control of aircraft manufacture - A modern approach 08 p1171 A83-23148

Cost-efficient transport of loads in geostationary orbit and in near-earth circular orbits [DGLR PAPER 82-077] 09 p1211 A83-24191

The application of a sub-scale flight demonstrator as a cost effective approach to aircraft development 12 p1701 A83-29395

A summary of EHV propulsion technology --- Electric and Hybrid Vehicle 13 p1934 A83-31087

Zinc-bromine battery design for electric vehicles 13 p1871 A83-31091

Fuel cell power plants for automotive applications 13 p1871 A83-31092

Systems environmental testing and redundancy vs Shuttle on-orbit repair/satellite retrieval 13 p1810 A83-31180

Effective low cost testing - A laboratory perspective 13 p1863 A83-31490

Cost effective development of a Shuttle-based astronomical instrument control system 14 p1984 A83-32040

Performance testing and module monitoring at the EC Necessary steps to develop cost-effective PV modules 14 p2038 A83-32194

On the economic efficiency of using satellite data to assess the condition of crops 14 p2034 A83-32497

A cost effective quick-response test station 14 p1977 A83-32927

Flight development and certification - How efficient can it be? 14 p1975 A83-32929

Recent advancements in titanium near-net-shape technology 15 p2171 A83-33633

Cost-effective methods for hydrogen production 15 p2193 A83-35304

Cost effective performance restoration of high by-pass engines 16 p2303 A83-35833

NGT sub-scale flight demonstrator - A cost-effective approach to aircraft development --- Next Generation Trainer [SAE PAPER 821341] 17 p2462 A83-37952

Advanced DOD military satellite communications 19 p2833 A83-41403

Combined FDMA-TDMA - A cost effective technique for digital satellite communication networks 19 p2834 A83-41414

The cost-effectiveness of modular and single-purpose rocket boosters and worldwide trends 20 p2944 A83-42566

The entropy of affordability 20 p3042 A83-42569

A figure of merit for competing communications satellite designs 21 p3221 A83-44533

The cost-effectiveness of modular and single-purpose rocket boosters and worldwide trends [IAF PAPER 83-06] 23 p3418 A83-47230

Designing for supportability and cost effectiveness
[AIAA PAPER 83-2499] 24 p3543 A83-49586

COST ESTIMATES

A software lifecycle case study using the PRICE model 01 p0112 A83-11105

A top down software cost estimating technique 01 p0112 A83-11106

Independent verification & validation /IV & V/ 01 p0103 A83-11112

How parametric cost estimating models can be used by the program manager 01 p0112 A83-11145

Activity distribution analysis --- for life cycle budgeting and program management 01 p0112 A83-11154

The TRANSCOSTTM - Model for estimation of launch vehicle development, fabrication and operations cost [AAS 82-139] 02 p0244 A83-11935

Future satellite systems - Market demand assessment 07 p0910 A83-19762

Composites fabrication cost estimating technique /FACET/ - An automated estimating system 07 p0877 A83-20494

The cost definition phase of a new commercial aircraft programme 09 p1196 A83-24425

Can industry afford solar energy 09 p1294 A83-25144

ESA procedures to account for inflation 11 p1666 A83-27372

University of Texas 7.6 meter telescope project 13 p1937 A83-30989

Estimation of the life cycle costs of complex technical systems 18 p2752 A83-39990

A critical look at the development and application of airframe cost models 20 p2935 A83-43747

[SAWE PAPER 1478] 20 p2935 A83-43747

An integrated model for production cost estimation and design-to-cost control of small missiles 20 p3056 A83-43750

[SAWE PAPER 1481] 20 p3056 A83-43750

Commercial launch vehicle services 22 p3258 A83-45720

COST REDUCTION

Fuel-optimal aircraft trajectories with fixed arrival times 04 p0446 A83-16115

Optimization of multiple safety factors in structural designs --- for weight and test cost reduction 06 p0723 A83-18223

Light route TDMA for business communications 07 p0911 A83-19784

USAF's design guide coming out next month 07 p1001 A83-20647

Will technology make the helicopter competitive 07 p0866 A83-21574

The British Hovercraft Corporation's Ap.1-88 hovercraft 08 p1173 A83-22424

[AIAA PAPER 83-0634] 08 p1173 A83-22424

Fabrication of aircraft components using prepried broadgoods layed-up in the flat and subsequently formed - Cost benefits and resource utilization enhancements 09 p1195 A83-23602

How to reduce the drilling cost for the aerospace industry 09 p1273 A83-23638

Environmental control and life support - Partially closed system will save big money 09 p1324 A83-24356

Structural optimality of linear optimal control 10 p1469 A83-26573

Cassegrainian concentrator solar array exploratory development module 11 p1541 A83-27250

Cost factors and approach methodology in selecting structural materials and manufacturing technologies [AIAA 83-0791] 12 p1783 A83-29730

Benefits of mission profile testing 13 p1862 A83-31481

Standardization of environmental requirements and related test methods 13 p1863 A83-31501

Subsystem engineering and development of grid-connected photovoltaic systems 14 p2039 A83-32205

Array structures for fixed flat-plate photovoltaic power generators 14 p2039 A83-32206

The photovoltaic solar system - Analysis and basic design rules 14 p2039 A83-32209

Minimum cost of photovoltaic energy for a utility grid and general features of a generating plant using costless solar cells. 14 p2040 A83-32214

Simple transformerless inverter with automatic grid-tracking and negligible harmonic content for utility interactive photovoltaic systems 14 p2004 A83-32216

Flat plate module technology - Overview 14 p2040 A83-32222

Method of raw material continuous feeding on silicon ribbon growth 14 p2090 A83-32319

Reducing the cost for airborne instrumentation hardware testing 14 p1978 A83-32928

EHF planar module for spatial combining 14 p2007 A83-33074

Vacuum hot pressing of large near net shape spar fittings 15 p2171 A83-33635

Structural members made of high-strength cast aluminum and their properties --- and reduction of aircraft production costs 15 p2136 A83-33954

Minimizing the average cost of testing coherent systems Complexity and approximate algorithms 17 p2517 A83-37292

Optimal number of failures before replacement time 17 p2518 A83-37297

B-1B manufacturing - Rockwell management plan saving costs, time 18 p2632 A83-40331

Reengining the key to aircraft renewal [AIAA PAPER 83-1372] 21 p3091 A83-45514

MATE institutionalization --- Management of Automatic Test Equipment for weapon systems 22 p3303 A83-45823

Cost reduction trends in space communications by larger satellites/platforms [IAF PAPER 83-235] 23 p3514 A83-47318

Thermal spraying for cost reduction and efficiency 23 p3467 A83-48637

COSTS

NT AIRCRAFT PRODUCTION COSTS

NT LIFE CYCLE COSTS

NT LOW COST

NT OPERATING COSTS

The Memorandum of Understanding between the United States and Certain ECAC Member States on Pricing Regime between U.S. and Europe 20 p3057 A83-43127

The costs and benefits of sulphur oxide control 22 p3321 A83-46774

COTTON

Reflectance measurement of artificially induced ultraviolet radiation stress on cotton leaves 05 p0657 A83-16907

Reflectance differences between untreated and Mepiquat Chloride-treated, field-grown cotton through a growing season 05 p0657 A83-16909

Visible light reflectance, transmittance, and absorbance of differently pigmented cotton leaves 17 p2526 A83-37622

COUETTE FLOW

End effects on the transition to time-dependent motion in the Taylor experiment 07 p0926 A83-20528

Experiments on wave number selection in rotating Couette-Taylor flow 13 p1842 A83-30918

An implicit, bidiagonal numerical method for solving the Navier-Stokes equations 14 p2012 A83-32979

New flows in a circular Couette system with co-rotating cylinders 17 p2501 A83-37028

Analysis of the Couette flow by means of the new direct-simulation method 18 p2686 A83-39920

Unsteady Couette flow and heat transfer in a dusty gas 21 p3131 A83-44855

Unsteady magnetohydrodynamic Couette flow 23 p3510 A83-48153

Characteristic lengths in the wavy vortex state of Taylor-Couette flow 24 p3576 A83-48920

Low-dimensional chaos in a hydrodynamic system 24 p3577 A83-49295

COUGH

The functional condition of the respiratory center during the coughing reflex in normoxic and hypoxic conditions 17 p2556 A83-37249

COULOMB COLLISIONS

Coulomb interactions in Anderson localized disordered systems 04 p0540 A83-15508

Collisions in spherical stellar systems 06 p0831 A83-18829

The superradiance of a polyatomic system with allowance for the Coulomb interaction 09 p1273 A83-25090

Accreting X-ray pulsar atmospheres heated by Coulomb deceleration of protons 10 p1505 A83-25743

The threshold laws for electron-atom and positron-atom impact ionization 13 p1915 A83-30177

The bremsstrahlung of a slow electron at a Coulomb center in an external electromagnetic field 14 p2079 A83-32139

Electrons in an ultrastrong magnetic field 16 p2411 A83-35595

Coulomb effects on one-dimensional Peierls instability - The Peierls-Hubbard model --- of dimerization 19 p2820 A83-40956

Effect of Coulomb interactions on the Peierls instability --- in one dimensional solids 19 p2903 A83-40957

The generalized Hubbard model in the theory of trimerizable molecular crystals --- such as Cs(2)(TCNQ)(3)-organic charge transfer salt 21 p3220 A83-45505

The collisional absorption of plasma cyclotron oscillations 23 p3510 A83-48394

COULOMB POTENTIAL

Formation of electrostatic potential barrier between different plasmas 12 p1780 A83-29100

Potential of a charge at rest in a magnetized plasma in an alternating electromagnetic field 16 p2418 A83-36938

Measurement of potential aboard spacecrafts [IAF PAPER 83-220] 23 p3424 A83-47312

COUNTDOWN

Computer performance monitoring during the Centaur launch countdown 17 p2472 A83-37060

COUNTER ROTATION

Development of counter-rotating intershaft support bearing technology --- for aircraft gas turbine engines 14 p1976 A83-32587

Design analysis of a self-acting spiral-groove ring seal for counter-rotating shafts --- o ring seals [AIAA PAPER 83-1134] 16 p2361 A83-36239

Super choppers --- helicopters with counter rotating rotors 17 p2465 A83-38700

Counter-rotation propellers - A feasibility study 21 p3092 A83-44874

The dynamics of a rigid body on an absolutely rough plane 23 p3505 A83-48529

COUNTERFLOW

Transient extinction of counter flow diffusion flame 01 p0022 A83-10497

An experimental study of fuel combustion in a high-temperature air counterflow 03 p0295 A83-14056

Response of parallel-flow and counterflow heat exchangers to sinusoidal flow rate changes of large amplitude 07 p0925 A83-20290

The asymptotic structure of a counterflow premixed flame for large activation energies 07 p0882 A83-21166

Countercurrent jet combustion of a hydrocarbon fuel in air 07 p0882 A83-21422

Experimental study on inhibited diffusion and premixed flames in a counterflow system 08 p1057 A83-22347

Formation of a counter current region near a gravitating sphere in a steady Stokes flow of a viscous ideal gas 18 p2680 A83-39010

A numerical analysis of the development of a system of jets in the mixing region of countertwisted annular flows 19 p2844 A83-41569

Film condensation in a tube with counter current vapor flow 20 p2969 A83-42535

Stabilization of tangential shear instability in shallow water with 'supersonic' fluid flow 22 p3285 A83-46939

Interaction of a jet issuing from a body with a supersonic rarefied-gas counterflow 23 p3400 A83-48666

COUNTERMEASURES

NT CHAFF

NT ELECTRONIC COUNTERMEASURES

NT JAMMING

Conflict radar /A systems analysis/ --- Russian book 04 p0527 A83-15827

Development of countermeasures against adverse effects of weightlessness on the human body 08 p1149 A83-22987

COUNTERS

NT CERENKOV COUNTERS

NT ELECTRON COUNTERS

NT NEUTRON COUNTERS

NT PARTICLE TELESCOPES

NT PROPORTIONAL COUNTERS

NT QUANTUM COUNTERS

NT RADIATION COUNTERS

NT SCINTILLATION COUNTERS

COUNTING CIRCUITS

Trends in microwave counter technology 13 p1836 A83-30975

VLSI digital polarity correlator based on an overloading counter technique 24 p3574 A83-49964

COUPLED MODES

High-power multiple-stripe injection lasers with channel guides 02 p0184 A83-12269

Single-mode fiber-to-channel waveguide coupling 03 p0393 A83-13758

Nonlinear astrophysical dynamo - Three-mode interaction 04 p0557 A83-15981

On radiation modes in the time-dependent coupled power theory for optical waveguides 05 p0686 A83-17891

Coupling and imaging of Gaussian beams in parallel dielectric slab waveguides 06 p0749 A83-17967

Theory and design of a Ku-band TE/21/-mode coupler 06 p0752 A83-18763

The effect of the quantum current on the relaxation of paired modes of the CO2 molecule 06 p0809 A83-19557

The use of natural modes to describe the forced vibrations of asymmetric shafts on flexible supports
07 p0947 A83-21091

Analysis of distributed-feedback diode lasers with gain-induced waveguiding
08 p1110 A83-22671

Resonantly interacting waves
08 p1161 A83-22741

Hydromagnetic waves in inhomogeneous plasmas
09 p1347 A83-23394

Optical strip waveguide - A detailed analysis including leaky modes
09 p1344 A83-24096

Saturation of the lower-hybrid-drift instability by mode coupling
10 p1485 A83-25777

Shock/Ludwig-tube driven HF laser
10 p1429 A83-26169

New configurations for high-efficiency prism couplers with application to GeO₂ optical waveguides
10 p1483 A83-26638

Bandwidth of a low sidelobe level multimode radiating coupled waveguide array
10 p1405 A83-26834

Mechanism for chaos in the Duffing equation
10 p1472 A83-26969

Resonant coupling between solar gravity modes
11 p1689 A83-27648

Nonlinear dynamical models of plasma turbulence
11 p1659 A83-28230

The nonlinear three-wave system - Strange attractors and asymptotic solutions
11 p1659 A83-28237

Shielded dielectric resonators
12 p1720 A83-29461

Creation and checking of load transformation matrices for modally coupled systems using the acceleration method with recursive equations
12 p1742 A83-29815

[AIAA 83-0816]
State vector formulation of substructure coupling for damped systems
12 p1744 A83-29863

[AIAA 83-0965]
Nonlinear optical coupling between radiation and confined modes
13 p1918 A83-30329

Theoretical study of processes in a system with 'conjugate' M-type interaction
13 p1833 A83-30705

Coupled vibrations of beams - An exact dynamic element stiffness matrix
13 p1868 A83-31637

Nonlinear mode coupling in oscillating stars. I - Second order theory of the coherent mode coupling
13 p1954 A83-31651

The local resonance interaction of normal waves in coupled waveguides
14 p2080 A83-33000

Dynamic qualification of spacecraft by means of modal synthesis. II
14 p1982 A83-33474

Electrooptic interaction in oversized waveguide modulators
16 p2315 A83-35521

Coupled multiple waveguide systems
16 p2412 A83-35965

Nonlinear mixing of surface acoustic waves propagating in opposite directions
17 p2578 A83-37727

Stable single-longitudinal-mode operation under high-speed direct modulation in cleaved-coupled-cavity GaInAsP semiconductor lasers
17 p2515 A83-38885

Mode coupling phenomena of Tonks-Dattner resonances in an asymmetrically inhomogeneous plasma column
18 p2747 A83-40072

Bragg reflection characteristics of millimeter waves in a corrugated H-guide
19 p2838 A83-41090

Graphical representation of prism coupling into thin films
20 p3047 A83-42223

Depolarization in a single-mode optical fiber
21 p3204 A83-44204

Fiber-optic gyroscopes with broad-band sources
21 p3136 A83-44210

Coupled-mode analysis of anisotropic dielectric planar branching waveguides
21 p3205 A83-44227

The wave equations for the coupling of propagation in inhomogeneous and bi-fluids plasmas
21 p3211 A83-44299

Coupled-mode equations for nonresonant interaction of high-frequency surface waves
21 p3211 A83-44345

Method for improving incomplete modal coupling
21 p3152 A83-44545

Transient effects, transverse mode coupling, and diffraction in swept-gain superradiance in the nonlinear regime Evolution from the superradiant state
21 p3144 A83-44793

Mode coupling analysis of bending losses in hollow infrared waveguides
22 p3358 A83-46634

Three-dimensional vector coupled-wave analysis of planar-grating diffraction
23 p3507 A83-47577

Field-theoretical analysis and synthesis of mode couplers --- for synchronous communication satellites
23 p3421 A83-47977

A two-mode waveguide-dielectric resonator below cutoff
23 p3445 A83-48489

Transition to chaos for ballooning modes stabilized by finite Larmor radius effects
23 p3511 A83-48575

Measurement of polarization mode coupling along a polarization-maintaining optical fiber using a backscattering technique
24 p3628 A83-48858

Phase conjugation during a nonlinear interaction of lightguide modes with external radiation
24 p3628 A83-48867

On the problem of applying mode-matching techniques in analyzing conical waveguide discontinuities
24 p3570 A83-48965

The electron-acoustic-drift instability
24 p3633 A83-49753

COUPLERS

NT ANTENNA COUPLERS
NT COUPLING CIRCUITS
NT DIPLEXERS
3 x 2 channel waveguide gyroscope couplers - Theory
02 p0177 A83-12171

Polarisation preserving single-mode-fibre coupler
06 p0809 A83-18570

A fail-safe node for lightguide digital networks
07 p0992 A83-19712

New fiber optic data bus topology
08 p1152 A83-22493

Analysis of an H-plane slotted directional coupler based on uniformly curved waveguides
11 p1561 A83-27929

Analysis of a directional coupler based on fused single-mode optical fibers
16 p2413 A83-36767

Polarisation-holding directional coupler made from elliptically cored fibre having a D section
20 p3047 A83-42477

Optimum design of 3-dB branch-line couplers using microstrip lines
21 p3123 A83-43839

Polarization characteristics of LiNbO₃ channel waveguide directional couplers
21 p3205 A83-44221

Three-guide optical couplers in GaAs
22 p3356 A83-45734

Expressions for the coupling coefficient of a rectangular-waveguide directional coupler
22 p3357 A83-45970

16 x 16 optical star coupler using a mixing block with two perfect mirrors
22 p3292 A83-46610

Field-theoretical analysis and synthesis of mode couplers --- for synchronous communication satellites
23 p3421 A83-47977

COUPLES

A concentrated couple acting on an elastic half-plane
17 p2522 A83-38100

COUPLING

NT COUPLES
NT CROSS COUPLING
NT GYROSCOPIC COUPLING
NT MICROWAVE COUPLING
NT OPTICAL COUPLING
NT THERMODYNAMIC COUPLING

Theoretical and experimental analysis of cylindrical dipoles with minimal mutual coupling
06 p0744 A83-18694

Coupling of Love waves with the bulk elastic waves in the substrate --- for microwave applications
16 p2344 A83-35433

Rotational excitation of OH by H₂ - Calculations in intermediate coupling
17 p2579 A83-38364

A coupling method for the inverse mode calculation of transonic internal flows with a shock wave
[ONERA, TP NO. 1983-62] 23 p3398 A83-48183

COUPLING CIRCUITS

Fluxon propagation in Josephson junction transmission lines coupled by resistive networks
01 p0036 A83-10639

Optical-waveguide hybrid coupler
02 p0235 A83-11567

Nonreciprocal circuit for laser-diode-to-single-mode-fibre coupling employing a YIG sphere
04 p0534 A83-15245

Measurement of 2-port devices by a reflectometer system
04 p0473 A83-16207

Analysis of the general nonsymmetrical directional coupler with arbitrary terminations
04 p0474 A83-16211

Single-mode-fiber 1 x N directional coupler
05 p0685 A83-17886

Switchable coaxial optical coupler using a liquid crystal mixture
07 p0994 A83-21361

Generalized network representations for small-aperture coupling between dissimilar regions
09 p1254 A83-23804

Monolithic GaAs interdigitated couplers
09 p1256 A83-24683

Electromagnetic coupling to an infinite wire through a slot in a conducting plane
10 p1411 A83-26838

Analysis of an H-plane slotted directional coupler based on uniformly curved waveguides
11 p1561 A83-27929

Ultra-wideband quadrature coupler
11 p1563 A83-28602

Direct-coupled Josephson exclusively or gate with a high gain and a wide margin
11 p1563 A83-28615

An ideal six-port network consisting of a matched reciprocal lossless five-port and a perfect directional coupler
13 p1831 A83-30231

Experimental study of orthonode couplers for use in power combining and distribution
20 p2965 A83-42362

Unidirectional waveguide couplers with strong coupling in the millimeter band
22 p3277 A83-45677

Wide-band chain-type divider-summaters based on quarter-wave lossy couplers
22 p3277 A83-45679

Second-order averaging of forced and coupled nonlinear oscillators
22 p3354 A83-45698

Quantum nondemolition measurements via quadratic coupling --- for gravitational radiation detection
24 p3623 A83-48827

Monomode-polarization-maintaining fiber directional couplers
24 p3628 A83-48857

New properties of double-layer coupled slot lines configuration
24 p3574 A83-49990

COUPLING COEFFICIENTS

Single-mode-fiber 1 x N directional coupler
05 p0685 A83-17886

Restrictions imposed on light scalar particles by measurements of van der Waals forces
07 p0989 A83-20610

The difference coupling coefficients of complex muon-neutron detectors
10 p1420 A83-26105

A determination of coupling coefficients on the basis of latitude measurements made during the 28th voyage of the research vessel Akademik Kurchatov --- cosmic ray neutron intensity analysis
10 p1523 A83-26106

Rigidity responses of ionization chambers derived from cosmic-ray time variations
11 p1574 A83-28427

Theoretical and experimental study of the coupling of two waveguides by a large aperture
13 p1833 A83-30712

Coupling between microstrip line and image guide through small apertures in the common ground plane [AD-A129977]
13 p1836 A83-31150

Nonlinear mode coupling in oscillating stars. I - Second order theory of the coherent mode coupling
13 p1954 A83-31651

Method for determining the coupling coefficient of a SQUID magnetic-flux sensor with an inductance coil
16 p2356 A83-35934

Expressions for the coupling coefficient of a rectangular-waveguide directional coupler
22 p3357 A83-45970

COUPLINGS

A study of the engineering stability of a system of coupled bodies with damping elements
16 p2316 A83-35931

COVALENT BONDS

EXAFS investigation of dilute Cu impurities in amorphous As₂Se₃
04 p0540 A83-15502

COVARIANCE

Performance uncertainty analysis
01 p0103 A83-11173

Covariational analysis of the correlation between lunar relief and the acceleration due to gravity
03 p0432 A83-13369

Conformal-plane gravitational fields of a viscous fluid
03 p0390 A83-13526

Post-Newtonian approximations in scale covariant gravitation
04 p0556 A83-15960

Generation of a random sequence having a jointly specified marginal distribution and autocovariance
05 p0680 A83-16915

Covariance analysis of oscillatory systems under combined periodic and random forced vibrations
08 p1160 A83-21862

Analytical properties of a covariance noise matrix in the theory of receiving antenna arrays
11 p1558 A83-28681

Behaviour of a generalised covariance model in picture coding
12 p1769 A83-29470

Covariance analysis of a charge carrier device processing algorithm for stellar sensors
17 p2474 A83-37062

Real-time solution of linear least-squares estimation problem with semi-degenerate covariance
17 p2566 A83-37105

Gain optimization with nonlinear controls
17 p2566 A83-37109

Adjustment problems in inertial positioning
22 p3316 A83-46343

COVERINGS

Heat loss coefficients and effective tau-alpha products for flat-plate collectors with diathermanous covers
12 p1749 A83-28939

COVES

U BAYS (TOPOGRAPHIC FEATURES)

COWELL METHOD

U NUMERICAL INTEGRATION

COWLINGS

- A method for three-dimensional boundary layer calculations on arbitrary bodies - Some results on aircraft wings and engine cowls 22 p3251 A83-47031

CRAB NEBULA

- The Crab Nebula's progenitor 02 p0253 A83-11623
- Limits on a radio shell around the Crab Nebula 02 p0248 A83-12829
- An optical emission mechanism for the Crab pulsar 03 p0419 A83-13888
- Absolute photometry of the Crab Nebula 03 p0411 A83-14793
- Gamma-ray emission from the galactic anticenter at MeV energies 05 p0698 A83-16995
- The role of turbulence of the relativistic electron-positron plasma in generating in the prepulses of the Crab radio pulsar 06 p0830 A83-18781
- Timing of the Crab pulsar - Consequences of the large glitch of 1975 07 p1017 A83-20928
- 4C21.53 - A possible supernova remnant in Vulpecula 07 p1018 A83-20941
- The origin of the Crab Nebula and electron capture supernova of 8-10 solar-mass stars 08 p1177 A83-21835
- Trail of the Crab progenitor star 08 p1187 A83-23286
- Theory of NP 0532 pulsar radiation and the nature of the activity of the Crab Nebula 12 p1790 A83-28980
- The Crab Nebula 13 p1953 A83-31563
- The pulse profile of the Crab pulsar in the energy range 45 keV-1.2 MeV 15 p2268 A83-34638
- Supernova shell structure and the spur of the Crab 16 p2429 A83-36626
- A model of the Crab nebula - The emission spectrum and the distribution of brightness 17 p2600 A83-37660
- Hard X-ray observations of the Crab Nebula and A0535+26 with a high energy resolution spectrometer 17 p2604 A83-37913
- Three-dimensional structure of the Crab Nebula 17 p2607 A83-38257
- The observation of the galactic anticenter region by the balloon borne gamma-ray telescope Natallya-1 18 p2785 A83-39282
- May 1980 low energy gamma-ray observations with the 'MISO' telescope 18 p2756 A83-39292
- Discovery of large radial velocities in the supernova remnant 3C 58 19 p2920 A83-41649
- High-resolution polarization images of Crab Nebula with a charge-coupled device camera 20 p3059 A83-42330
- Gamma-ray line features from the Crab Nebula in the energy range 50-2000 keV 24 p3659 A83-49370
- Do filaments form at the time of supernova explosions 24 p3667 A83-50077

CRACK ARREST

- Crack propagation and arrest in plastic medium 11 p1593 A83-27771
- Overload induced crack growth rate attenuation behavior in aluminum alloys 11 p1548 A83-28223
- Arrest of fast Mode-I fracture in an elastic-viscoplastic transition zone 14 p2031 A83-32657
- Brittle fracture of plates in tension - Relative significance of boundary reflected body and Rayleigh waves 16 p2368 A83-36516
- Microfracture model for hydrogen embrittlement of austenitic steels 18 p2670 A83-40643
- Crack deceleration and arrest phenomena at an oblique bimaterial interface 20 p3001 A83-42518
- A FEM analysis of crack arrest experiments 21 p3157 A83-44905
- An engineering interpretation of pop-in arrest and tearing arrest in terms of static crack arrest, K(Ia) 21 p3162 A83-45186

CRACK CLOSURE

- Key curve analysis of crack-growth-resistance curves 02 p0190 A83-12041
- Effects of closure on the detection probability of fatigue cracks 04 p0490 A83-15186
- Crack closure effects in ultrasonic NDE for real part-through fatigue cracks in Al-alloy 04 p0458 A83-15206
- Evaluation of the effect of fatigue crack closure 04 p0459 A83-15399
- Decrease in closure and delay of fatigue crack growth in plane strain 04 p0501 A83-16258
- Influence of tensile pre-strain on fatigue crack closure in aluminum alloy 2017-T3 05 p0614 A83-17095
- On the controlling parameters for fatigue-crack threshold at low homologous temperatures 07 p0887 A83-20636
- General solution of a certain mixed boundary value crack problem 07 p0948 A83-21167

Numerical modelling of warm prestress effect using a damage function for cleavage fracture

- 08 p1060 A83-21703
- The effect of overloads upon fatigue crack tip opening displacement and crack tip opening/closing loads in aluminum alloys 08 p1060 A83-21709
- Threshold Delta-K values and non-closure of fatigue cracks 08 p1061 A83-21733
- Analysis of closure behavior of small fatigue cracks 09 p1275 A83-23299
- The interface crack between dissimilar anisotropic composite materials [ASME PAPER 83-APM-6] 10 p1441 A83-26443
- Influence of flaw bridging on the stress concentration in composites 11 p1592 A83-27445
- Influence of crack closure on the stress intensity factor for plates subjected to bending - A 3-D finite element analysis 11 p1595 A83-28436
- Allowing for the coalescence of microcracks in a statistical kinetic model for the fracture of materials under uniaxial tension 13 p1866 A83-30057
- The healing of cracks in metals by means of crossed electric and magnetic fields 14 p1993 A83-32383
- Fatigue crack closure after overload 14 p2031 A83-32660
- Partial closure of cracks at the interface between a layer and a half space 16 p2368 A83-36506
- Crack closure studies under constant amplitude loading 16 p2333 A83-36508
- A simple model of stress intensity range threshold and crack closure stress 18 p2665 A83-39081
- The effect of crack closure and estimation of the cyclic fracture toughness of structural alloys 19 p2856 A83-40803
- Critical loading conditions and stress intensity factors for partial or entire closure of a Griffith crack under thermo-mechanical loading 21 p3157 A83-44909
- Surface microcrack closure in fatigue - A comparison of compliance and crack sectioning data 21 p3158 A83-44922
- The effect of hydrogen induced surface asperities of fatigue crack closure in ultrahigh strength steel 23 p3431 A83-47850

CRACK FORMATION

U CRACK INITIATION

CRACK GEOMETRY

NT CRACK TIPS

- Ultrasonic mode-converted wave flaw quantification method for measuring depth of open cracks 01 p0057 A83-10281
- On crack kinking and curving 01 p0058 A83-10282
- Electrothermal inspection of conducting materials 01 p0057 A83-10364
- Stability of the elastic equilibrium of an infinite plate in the vicinity of a randomly oriented rectilinear crack under plane-stressed state 01 p0059 A83-10684
- Penny-shaped crack in a transversely isotropic plate of finite thickness 02 p0190 A83-12039
- Bounds for the dislocation densities and the stress intensity factors in elastic crack problems 02 p0190 A83-12042
- Some axially symmetric thermal stress distributions in an elastic solid containing an annular crack 02 p0191 A83-12050
- Special analytical solution for use in debond stress analysis 02 p0191 A83-12172
- The effect of the shape and size of a fatigue crack on the cyclic fracture toughness of titanium alloy VT9 02 p0156 A83-12330
- On the concentrated loading of an external elliptical crack 02 p0196 A83-12854
- Quantitative evaluation of fatigue strength of metals containing various small defects or cracks 03 p0338 A83-13197
- Digitized measurements of the shape of corner cracks at fastener holes 03 p0339 A83-13202
- A closed-form solution of a slant crack under biaxial loading 03 p0339 A83-13337
- A comparison of the geometry dependence of several nonlinear fracture toughness parameters 03 p0298 A83-13339
- Variations of various fracture parameters during the process of subcritical crack growth 03 p0298 A83-13341
- Dimensional information through industrial computerized tomography 03 p0337 A83-13435
- Solution of the axisymmetric problem for an elastic body with a cylindrical crack 03 p0339 A83-13692
- Indentation microfracture in the Palmqvist crack regime - Implications for fracture toughness evaluation by the indentation method 03 p0290 A83-13725
- Bending of a semiinfinite anisotropic plate with curvilinear cracks 03 p0340 A83-14070

Torsional stresses and stress intensity factors of circular cylinder with internal longitudinal crack

- 03 p0342 A83-14489
- A simple yet accurate finite element procedure for computing stress intensity factors 03 p0342 A83-14707
- Computing the static path of crack propagation 03 p0343 A83-14727
- Use of finite element method for determining stress intensity factors with a conic-section simulation model of crack surface 03 p0343 A83-14818
- A hollow oblate spheroid subjected to internal or external pressure and an oblate spheroid with a penny-shaped crack 03 p0343 A83-14819
- An investigation of stress intensity factors for plates with equal and unequal parallel edge cracks 03 p0343 A83-14821
- An optimization process for evaluating complex stress intensity factors in cracked plates from isopachics 03 p0343 A83-14823
- Crack-tip measurements in photoelastic models 03 p0344 A83-14939
- Growth and stability of interacting surface flaws of arbitrary shape 04 p0495 A83-15060
- Analytical solution for embedded elliptical cracks, and finite element alternating method for elliptical surface cracks, subjected to arbitrary loadings 04 p0496 A83-15063
- An enhancement for the ultrasonic test bed to inspect engine disk bolt holes 04 p0488 A83-15160
- Crack characterization by the combined use of time-domain and frequency-domain scattering data 04 p0491 A83-15199
- The scattering of elastic waves by isolated cracks using a new integral equation model 04 p0491 A83-15201
- Test bed for quantitative NDE - Imaging results 04 p0493 A83-15230
- Estimates and asymptotics of the stress-strain state of a three-dimensional body with a crack in the theory of elasticity and the theory of creep 04 p0500 A83-15884
- Crack height measurement - An evaluation of the accuracy of ultrasonic timing methods 05 p0653 A83-16875
- A study on threshold of macro-crack growth in a soft epoxy resin 05 p0618 A83-17101
- Defects and crack shape development in fillet welded joints 05 p0656 A83-17895
- Stress intensity factors in a hollow cylinder containing a radial crack 06 p0776 A83-18910
- A unified description of micro and macroscopic fatigue crack behaviour 06 p0776 A83-18938
- Change in impedance of a single-turn coil due to a flaw in a conducting half space 07 p0942 A83-20270
- Fatigue crack front shape and its effect on fracture toughness measurements 07 p0886 A83-20519
- Boundary element method in fracture mechanics 07 p0947 A83-20925
- Elastic wave scattering by a circular crack 07 p0947 A83-21081
- On the problem of two coplanar cracks inside an infinite isotropic elastic solid 07 p0949 A83-21440
- An empirical approach to determining K for surface cracks 08 p1115 A83-21653
- Analysis and repair of flaws in thick structures 08 p1115 A83-21654
- The fracture toughness of high strength engineering alloys containing short cracks 08 p1058 A83-21655
- Analytic asymptotic solution of the kinked crack problem 08 p1116 A83-21657
- An integral equations method for resolution, in opening mode, of the problem of plane cracks at free surface 08 p1116 A83-21661
- Application of the equivalent initial damage method to fretting fatigue 08 p1059 A83-21691
- A.C. field measurements - A new method for detecting and measuring fatigue cracks 08 p1112 A83-21761
- A technique for measuring crack length and load in compact fracture mechanics specimens using strain gauges 08 p1118 A83-21763
- Analysis of closure behavior of small fatigue cracks 09 p1275 A83-23299
- Transient hygrothermal and mechanical stress intensities around cracks 09 p1223 A83-23930
- Experimental determination of flaw shapes and stress intensity distributions - Conditions for application to composite materials 09 p1224 A83-23949
- Change in geometry of surface cracks during alternating tension and bending 09 p1280 A83-24137
- The boundary integral method for the solution of planar multicrack problems of linear elastostatics --- German thesis 09 p1281 A83-24846
- The effect of the crack geometry on the test result in surface defect testing 09 p1281 A83-24945
- Accuracy and precision of crack length measurements using a compliance technique 10 p1438 A83-25424

Thermal stress in a transversely isotropic medium containing a penny-shaped crack
[ASME PAPER 83-APM-8] 10 p1440 A83-26427

The penny-shaped interface crack with heat flow. I - Perfect contact
[ASME PAPER 83-APM-10] 10 p1440 A83-26428

Stress intensity factor variation with loading and crack depth for long flaws of quasi-semielliptical shape
11 p1591 A83-27434

Curved crack growth in brittle solids under farfield compression
11 p1592 A83-27439

Crack shape evolution studies in threaded connections using A.C.F.M. --- Alternating Current Field Measurement
11 p1590 A83-27858

Crack deflection processes. I - Theory
11 p1595 A83-28424

Branched cracks at small angles / An addendum/
11 p1595 A83-28438

Experimental study of the T-criterion in ductile fractures
11 p1596 A83-28445

Theoretical stress analysis for a non-isotropic body of cylindrical configuration containing a row of cracks
11 p1596 A83-28447

An alternating method for analysis of surface-flawed aircraft structural components
12 p1734 A83-28966

The influence of skin depth on crack measurement by the ac field technique
12 p1733 A83-29140

Problem of a crack in a transversely isotropic sandwich plate
12 p1735 A83-29410

Stress intensity factor calculation for designing with fiber reinforced composite materials
[AIAA 83-0835] 12 p1737 A83-29744

Effect of indenter geometry on controlled-surface-flaw fracture toughness
12 p1717 A83-29975

Crack size distribution in crystalline bodies
13 p1928 A83-30319

Dynamic stress intensity factors around a rectangular crack in an infinite plate under impact load
14 p2031 A83-32659

The influence of crack length on stress corrosion crack velocity
14 p1994 A83-32683

Quarter-point elements for curved crack fronts
15 p2179 A83-34565

Determination of stresses in an infinite plate with a kinked or branched crack
16 p2365 A83-35550

A fracture mechanics analysis of indentation-induced Palmqvist crack in ceramics
16 p2336 A83-35572

Prediction of failure probabilities for cleavage fracture from the scatter of crack geometry and of fracture toughness using the weakest link model
16 p2368 A83-36510

Sudden twisting of an external circular crack in an infinite medium with a cylindrical inclusion
16 p2368 A83-36513

Measurement of crack profile of semi-elliptical surface cracks using the ac potential technique
16 p2363 A83-36726

Unstable growth of branched cracks
17 p2523 A83-38394

The nonstationary thermoelasticity problem for a cylinder weakened by a periodic system of penny-shaped cracks
17 p2524 A83-38510

The crack tip opening angle (CTOA) of the plane stress moving crack
18 p2696 A83-39079

Singular stresses in an infinite solid with a flat annular crack around a spherical cavity under tension
18 p2696 A83-39080

The general solutions of the doubly periodic cracks
18 p2696 A83-39083

Periodic problem of the plane theory of elasticity for an infinite plane with cracks and holes
18 p2698 A83-39505

Determination of zones of crack distribution in flexible specimens --- of aluminum alloys
18 p2666 A83-39509

Estimation of the dimensions of growing cracks and relaxation regions from acoustic signal parameters
18 p2701 A83-40109

The wedging of a square specimen with a lateral crack
19 p2856 A83-40808

A theoretical analysis of the effect of short cracks on the endurance limit of materials
19 p2859 A83-41597

Photoelastic determination of complex stress intensity factors for slant cracks under biaxial loading with higher-order term effects
19 p2860 A83-41998

Infinite row of parallel cracks in an orthotropic strip
20 p3004 A83-42938

A note on the problem of an annular crack subjected to an arbitrary normal pressure
20 p3004 A83-42975

Elastic-plastic interaction of Dugdale type cracks and plastified matrix material in self-stressed fibre-reinforced composites
20 p3006 A83-42996

Thermal conductivities of a cracked solid
20 p3007 A83-43145

Nondestructive inspection by the method of magnetic leakage fields - Theoretical and experimental foundations of the detection of surface cracks of finite and infinite depth
20 p3000 A83-43178

The behaviour of short cracks in the sub-critical crack growth regime
[ASME PAPER 83-PVP-98] 20 p3009 A83-43732

Fracture toughness measurement of cast magnesium alloy by cylindrical specimen with ring-shaped crack
21 p3111 A83-44107

Crack-front shape effects in the double torsion test
21 p3152 A83-44329

Some geometrical observations on crack front profiles in PMMA double torsion specimens
21 p3152 A83-44330

On crack branching and curving in a finite body
21 p3156 A83-44887

Elastic moduli of a cracked body
21 p3156 A83-44896

On the small crack fracture mechanics
21 p3159 A83-44924

Ray methods for waves in elastic solids with applications to scattering by cracks --- Book
21 p3160 A83-45139

Dynamic crack curving - A photoelastic evaluation
21 p3161 A83-45164

A method for estimating the stress intensity factor
21 p3163 A83-45361

Relation between the actual and nominal boundaries of an extended defect in ultrasonic examination of a thick sheet
22 p3303 A83-46326

Torsion of an elastic rod of circular cross section weakened by an arbitrary number of radial cracks emerging at the surface
23 p3473 A83-48502

A thermoelasticity problem for a half-plane with a partially contacting crack
23 p3473 A83-48543

The elastostatic axisymmetric problem of a sphere containing a penny-shaped crack in a nonequatorial plane
24 p3591 A83-48869

A remark on the solution of the integral equation of planar cracks in three-dimensional elasticity
24 p3595 A83-49869

Statistical properties of hybrid composites. I - Recursion analysis
24 p3554 A83-49876

CRACK INITIATION

A comparison of theoretical and experimental methods of calibrating the electric potential drop technique for crack length determination
02 p0190 A83-12040

Derivation of Wells' COD estimation formula and re-calculation of gamma values
02 p0190 A83-12047

Special analytical solution for use in debond stress analysis
02 p0191 A83-12172

Designing composites for maximum toughness
02 p0151 A83-12970

Indentation microfracture in the Palmqvist crack regime - Implications for fracture toughness evaluation by the indentation method
03 p0290 A83-13725

Low-cycle fatigue damage accumulation of aluminum alloys
03 p0299 A83-13903

J-integral analysis for initiation of notch fatigue crack
03 p0342 A83-14490

Rapid crack propagation and arrest in the DCB specimen - An improved numerical analysis --- Double Cantilever Beam
03 p0343 A83-14711

A mechanical model to predict elastic-plastic fracture toughness in high strength materials
04 p0458 A83-15061

Crack opening displacement as a fracture mechanics parameter in eddy current NDE
04 p0496 A83-15185

Surface instability and splitting in compressed brittle elastic solids containing crack arrays
[ASME PAPER 82-WA/APM-16] 04 p0498 A83-15682

Conditions for spontaneous cracking of a brittle matrix due to the presence of thermoelastic stresses
04 p0464 A83-16274

Influence of compressive residual stress on the crack-opening behavior of part-through fatigue cracks
05 p0615 A83-17265

Experimental and numerical study of the different stages in ductile rupture - Application to crack initiation and stable crack growth
06 p0774 A83-18484

Experimental comparison of simulation methods of aeronautic type loading
[ONERA, TP NO. 1982-130] 06 p0775 A83-18598

The formation of microcracks under developed plastic deformation
06 p0777 A83-19305

Review of the effects of fatigue cracking loads on plane strain fracture toughness
07 p0886 A83-20518

Introduction to the viewpoint set on creep cavitation
07 p0886 A83-20626

Mechanisms of intergranular cavity nucleation and growth during creep
07 p0887 A83-20630

Continuous cavity nucleation and creep fracture
07 p0887 A83-20631

On the exterior crack with contact zones
07 p0946 A83-20640

A study of the cracking of oxide films on MoSi2 using the method of acoustic emission
07 p0899 A83-20680

The effect of the structure factor on the formation of the fracture surface in molybdenum alloys
07 p0889 A83-20900

The fatigue fracture of metals from the standpoint of physics and fracture mechanics
07 p0890 A83-20914

Boundary element method in fracture mechanics
07 p0947 A83-20925

Requirements of constitutive models for two nickel-base superalloys
07 p0891 A83-21071

Characteristics of the amplitude distribution of acoustic emission in the nucleation and propagation of fatigue cracks
07 p0943 A83-21405

Use of the phase method for evaluating defects in the form of developing microcracks
07 p0944 A83-21414

An operational definition of life to crack initiation in high temperature fatigue
07 p0893 A83-21477

Crack initiation and propagation in a forged nickel-base alloy under high mechanical and thermal loading
07 p0894 A83-21480

Fatigue-crack initiation in IMI 829 caused by high-temperature fretting
07 p0896 A83-21566

An integral equations method for resolution, in opening mode, of the problem of plane cracks at free surface
08 p1116 A83-21661

Mechanical model and mathematical analysis for ductile fracture
08 p1116 A83-21665

Fatigue crack initiation after different surface treatments in precipitation hardening alloys
08 p1058 A83-21668

Examination of several mechanical parameters to analyse the plastic fatigue crack initiation in geometrical concentration zones and mechanical notches
08 p1116 A83-21670

Fatigue crack initiation and propagation in Ti-6Al and Ti-6Al-4V
08 p1058 A83-21671

Prediction of crack formation life in notched specimens
08 p1117 A83-21686

Deriving a design fatigue resistance curve for analysing crack initiation
08 p1059 A83-21687

Mechanism of SCC and hydrogen-induced delayed cracking
08 p1061 A83-21718

On the relation between the creep mechanism and creep fracture
08 p1118 A83-21748

On fatigue crack initiation and propagation at elevated temperature
08 p1064 A83-21784

In-situ study of deformation and initiation of ductile fracture at a notch-root
08 p1119 A83-21789

Discussion on criteria for crack initiation in the immediate vicinity of the sharp edges of dispersed inclusions
08 p1121 A83-21824

Use of vacuum metallography methods for evaluating the effectiveness of materials with protective coatings
08 p1066 A83-22629

New method of determining the onset of ring cracking
08 p1106 A83-23233

Some peculiarities of fracture in heterogeneous materials
09 p1223 A83-23932

Development of a microfracture model for high rate tensile damage
09 p1279 A83-24071

Post-weld heat-treatment cracking in superalloys
10 p1393 A83-25407

Fatigue crack evolution in overaged Ni-14.4at.% alloy with coherent precipitates
10 p1394 A83-25423

Micromechanical predictions of crack initiation, propagation and crack growth resistance in boron/aluminum composites
10 p1389 A83-25879

Experimental study of the T-criterion in ductile fractures
11 p1596 A83-28445

Determination of the stress intensity factors for short cracks initiated by stress raisers
11 p1598 A83-28485

An alternating method for analysis of surface-flawed aircraft structural components
12 p1734 A83-28966

Turbine blade nonlinear structural and life analysis
12 p1703 A83-29024

Ion implantation effect on fatigue crack initiation in Ti-24V
12 p1714 A83-29724

A brittle to ductile transition in NiAl of a critical grain size
12 p1714 A83-29726

Numerical simulation of material fatigue by a thermodynamic approach
[AIAA 83-0977] 12 p1740 A83-29784

The conditions for the adhesion of freshly generated metal surfaces under load
13 p1819 A83-30018

The multiplicity of factors causing intergranular fracture
13 p1822 A83-30742

- Observation of voids and cracks on ductile fracture process in tensile test of 5083 aluminum alloy plate
13 p1822 A83-30842
- Residual stress craze and crack formation in poly(methyl methacrylate)
13 p1825 A83-31049
- Microinitiation, micropropagation and damage
13 p1823 A83-31171
- A comment on the multispecimen R curve approach to crack initiation toughness testing
14 p2031 A83-32664
- Metallography of fatigue crack initiation in an overaged high-strength aluminum alloy
14 p1994 A83-32681
- Cyclic deformation, fatigue crack nucleation and propagation in metals and alloys
14 p1995 A83-32806
- Subsurface crack initiation in high cycle fatigue in Ti6Al4V and in a typical Martensitic stainless steel
14 p1997 A83-32944
- Crack nucleation in tungsten on crystallographic planes and on grain boundaries of twist misorientation
14 p1997 A83-32946
- SEM observations of the initiation and propagation of cracks in a short fibre-reinforced thermoplastic composite under stress
16 p2323 A83-35568
- Fatigue crack initiation and microcrack propagation in X7091 type aluminum P/M alloys
16 p2329 A83-35691
- A review of the role of frequency on fatigue crack initiation and growth at elevated temperatures
16 p2332 A83-36194
- Initial strain field and fatigue crack initiation mechanics [ASME PAPER 83-APM-20]
17 p2519 A83-37385
- Fatigue crack initiation and microcrack propagation in X7091 type aluminum P/M alloys
17 p2487 A83-37834
- Statistical mechanics of early growth of fatigue cracks
17 p2490 A83-38384
- The effect of homo- and heterogeneous mechanisms coupling on microcrack nucleation in metals
17 p2490 A83-38385
- A model of high-cycle fatigue-crack initiation at grain boundaries by persistent slip bands
17 p2490 A83-38386
- Fracture of an aluminum alloy at the prespalling stage
18 p2666 A83-39504
- Fracture initiation under gross yielding - Strain energy density criterion
18 p2666 A83-39546
- The initiation of fracture in fiber-composites at elevated loading rates
18 p2656 A83-40217
- Fatigue crack initiation and propagation in several nickel-base superalloys at 650 C
19 p2821 A83-41199
- A comparison of exact and model solutions for the initiation of debond fracture
20 p3004 A83-42973
- Consideration of short cracks in high stress fatigue design
20 p3009 A83-43730
- [ASME PAPER 83-PVP-90]
20 p3009 A83-43730
- Micro-crack initiation, propagation and threshold in elevated temperature inelastic fatigue
20 p3009 A83-43731
- [ASME PAPER 83-PVP-97]
20 p3009 A83-43731
- A critical commentary on magnetic particle inspection
21 p3148 A83-43829
- Fracture mechanics approach to fatigue crack initiation from deep notches
21 p3162 A83-45187
- A theory for the Bilby-Cottrell mechanism of crack nucleation in metals
21 p3115 A83-45364
- Fatigue crack initiation from a notch tip under a cyclic compressive load
22 p3304 A83-45622
- Creep and fracture initiation in fibre reinforced plastics
22 p3264 A83-46296
- Detection of cracks under installed fasteners in aircraft structures
22 p3304 A83-46769
- Estimating initiation times of secondary fatigue cracks in damage tolerance analysis
23 p3470 A83-48148
- Characteristics of brittle fracture under general combined modes including those under bi-axial tensile loads
24 p3594 A83-49866
- Mixed-mode crack opening in fatigue
24 p3567 A83-49874
- CRACK PROPAGATION**
- Fatigue behaviour of two nickel-base alloys. I - Experimental results on low cycle fatigue, fatigue crack propagation and substructures. II - Physical modelling of the fatigue crack propagation process
01 p0023 A83-10215
- The viscoelastic constitutive modelling of adhesives
01 p0027 A83-10242
- Study of plastic zones in fatigue - A photogrid technique
01 p0058 A83-10276
- Stress intensity factor for crack-line loaded specimens
01 p0058 A83-10278
- On crack kinking and curving
01 p0058 A83-10282
- Effect of stress frequency on fatigue crack propagation in titanium
01 p0026 A83-10647
- Recommendations for the measurement of R-curves using centre-cracked panels
01 p0026 A83-11029
- The relationship between the solutions to mixed dynamic problems for a continuous elastic medium and a lattice
02 p0189 A83-11655
- On the Markovian models for fatigue accumulation
02 p0190 A83-11863
- Application of finite-part integrals to the singular integral equations of crack problems in plane and three-dimensional elasticity
02 p0190 A83-12001
- The deformation and fracture of Beta HMX
02 p0161 A83-12030
- A comparison of theoretical and experimental methods of calibrating the electric potential drop technique for crack length determination
02 p0190 A83-12040
- Key curve analysis of crack-growth-resistance curves
02 p0190 A83-12041
- Some observations on creep crack growth
02 p0190 A83-12043
- The extension of the J-integral concept to fatigue cracks
02 p0190 A83-12044
- On the J-integral blunting line for soft materials
02 p0190 A83-12045
- Slip-bands emanating from a crack tip under anti-plane deformation
02 p0190 A83-12046
- Moving cracks in layered composites
02 p0190 A83-12048
- Improving the weldability of Ni-base superalloy 713C
02 p0155 A83-12073
- Research of hydrogen-induced cracking and stress corrosion cracking in an aluminum alloy
02 p0156 A83-12222
- Fracture diagrams for the case of monotonic loading at elevated temperatures --- in aluminum alloys
02 p0156 A83-12326
- Fracture modes of inelastic materials as a function of loading rate and temperature, and associated fracture criteria
02 p0192 A83-12354
- Environmental fatigue crack growth analysis based on elastic-plastic fracture mechanics
02 p0196 A83-12769
- [ASME PAPER 82-PVP-23]
02 p0196 A83-12769
- Tentative test procedure for determining the plane strain JI-R curve
02 p0158 A83-12831
- The use of composite patches for repair of aircraft structural parts
02 p0131 A83-12968
- Modeling of the frequency effect on fatigue crack propagation in PMMA
03 p0301 A83-13198
- An experimental investigation of dynamic crack propagation --- for PMMA
03 p0302 A83-13199
- Digitized measurements of the shape of corner cracks at fastener holes
03 p0339 A83-13202
- On prediction of wear coefficients in sliding wear
03 p0333 A83-13231
- Effect of particles of the insoluble phase Al9FeNi on the kinetics of fatigue crack propagation in alloy AK4-1
03 p0297 A83-13256
- Dynamic fracture of a beam or plate under tensile loading
03 p0339 A83-13338
- Variations of various fracture parameters during the process of subcritical crack growth
03 p0298 A83-13341
- The effect of load ratio on fatigue crack growth in Ti8-Al-1Mo-1V
03 p0298 A83-13342
- A description of fatigue crack growth in terms of plastic work
03 p0339 A83-13343
- A pitting model for rolling contact fatigue
03 p0335 A83-13506
- [ASME PAPER 82-LUB-10]
03 p0335 A83-13506
- TEM observations of dislocation emission at crack tips in aluminium
03 p0298 A83-13679
- Time-of-flight measurements of the mass-to-charge ratio of positive ion emission accompanying fracture --- related to crack propagation in materials
03 p0302 A83-13681
- Growth of short cracks during high strain fatigue and thermal cycling
03 p0340 A83-13908
- Growth of physically short corner cracks at circular notches
03 p0340 A83-13909
- Two decades of progress in the assessment of multiaxial low-cycle fatigue life
03 p0340 A83-13910
- The dependence of transverse cracking and delamination on ply thickness in graphite/epoxy laminates
03 p0292 A83-14559
- Characterizing delamination growth in graphite-epoxy
03 p0293 A83-14561
- Crack propagation in bending thin plates
03 p0342 A83-14567
- Influence of the gaseous environment on fatigue crack propagation in an austenitic steel
03 p0300 A83-14701
- A combination of statistics and subcritical crack extension
03 p0342 A83-14703
- Rapid crack propagation and arrest in the DCB specimen
03 p0343 A83-14711
- An improved numerical analysis --- Double Cantilever Beam
- Computing the static path of crack propagation
03 p0343 A83-14727
- The J contour integral in the plastic region
03 p0343 A83-14729
- Dynamic crack-tip stresses under stress wave loading - A comparison of theory and experiment
03 p0343 A83-14820
- A compendium of sources of fracture toughness and fatigue crack growth data for metallic alloys. II
03 p0301 A83-14822
- Microstructure and fracture of fiber reinforced thermoplastic polyethylene terephthalate /P.E.T./
03 p0293 A83-14825
- Interfacial fracture of Space-Shuttle thermal-protection system
03 p0303 A83-14940
- The effect of microstructure and environment on the crack growth behavior of Inconel 718 alloy at 650 C under fatigue, creep and combined loading
04 p0458 A83-14999
- Growth and stability of interacting surface flaws of arbitrary shape
04 p0495 A83-15060
- A mechanical model to predict elastic-plastic fracture toughness in high strength materials
04 p0458 A83-15061
- Elastic-plastic finite element analysis of dynamic fracture
04 p0495 A83-15062
- Path dependent nature of fatigue crack growth
04 p0496 A83-15064
- The fatigue behavior of SiSiC
04 p0462 A83-15125
- Mechanisms which influence the applicability of fracture mechanics for short cracks
04 p0496 A83-15184
- Crack opening displacement as a fracture mechanics parameter in eddy current NDE
04 p0496 A83-15185
- Acoustic emission during plastic deformation and crack growth in 2024 and 2124 aluminium alloys
04 p0458 A83-15196
- Develop in-flight acoustic emission monitoring of aircraft to detect fatigue crack growth
04 p0447 A83-15197
- Establishing signal processing and pattern recognition techniques for inflight discrimination between crack-growth acoustic emission and other acoustic waveforms
04 p0491 A83-15198
- Characterization of NDE reliability
04 p0492 A83-15211
- Nondestructive evaluation of ceramics
04 p0463 A83-15213
- An antiplane problem concerning crack propagation in a lattice
04 p0497 A83-15388
- Methods for determining the crack growth rate during the testing of materials for cyclic fracture toughness
04 p0497 A83-15395
- Effect of shear and rotary inertia on dynamic fracture of a beam or plate in pure bending
04 p0498 A83-15683
- [ASME PAPER 82-WA/APM-9]
04 p0498 A83-15683
- Fracture toughness - A rationalization of the role of microstructure in an alpha-beta titanium alloy
04 p0460 A83-16003
- Influence of corrosion deposits on near-threshold fatigue crack growth behavior in 2XXX and 7XXX series aluminum alloys
04 p0460 A83-16005
- Investigation of the electron-beam weldability of a heat-resistant iron-based superalloy /A286/
04 p0461 A83-16175
- Microstructural influence on fatigue crack growth near threshold in 7075 Al alloy
04 p0461 A83-16251
- The effect of aluminum oxide particles and precipitate type on near-threshold fatigue crack propagation rate in P/M 7XXX aluminum alloys
04 p0461 A83-16255
- Decrease in closure and delay of fatigue crack growth in plane strain
04 p0501 A83-16258
- Growth behavior of small cracks and variation of statistical crack-length distribution in corrosion fatigue
05 p0653 A83-17091
- SIF of surface cracks and fatigue crack propagation behaviour in a cylindrical bar
05 p0614 A83-17092
- Statistical aspect of fatigue crack propagation from surface defects
05 p0614 A83-17093
- A simple method for evaluating the subcritical crack growth of brittle materials
05 p0618 A83-17099
- Fracture behavior of polymers by Charpy impact tests
05 p0618 A83-17100
- A study on threshold of macro-crack growth in a soft epoxy resin
05 p0618 A83-17101
- Effect of transverse direction strain on fracture of notched 0 deg/90 deg GRP laminate under biaxial fatigue
05 p0611 A83-17105
- The effect of glass fibers filled in polyester on fatigue crack arrest
05 p0611 A83-17106
- The use of fractography and fracture mechanics in analysing fatigue cracks
05 p0654 A83-17229
- Stress intensity factors, crack profiles, and fatigue crack growth rates in residual stress fields
05 p0654 A83-17261

- Effect of residual stresses on fatigue crack growth rates in weldments of aluminum alloy 5456 plate
05 p0615 A83-17262
- Effects of residual stress on fatigue crack propagation
05 p0654 A83-17263
- The fracture of particulate-filled epoxide resins. I
05 p0611 A83-17563
- Increase of crack resistance during slow crack growth in Al2O3 bend specimens
05 p0619 A83-17566
- Fatigue initiation in a short glass fibre composite
05 p0612 A83-17569
- Introduction to the fundamentals of fracture mechanics. III - Fatigue crack growth in fracture mechanics representation
05 p0654 A83-17573
- Damage to structures by high-cycle fatigue
05 p0655 A83-17672
- The short crack problem
05 p0655 A83-17673
- The growth of small fatigue cracks in 7075-T6 aluminum
05 p0616 A83-17674
- An elastic-plastic finite element analysis of a compact tension specimen
05 p0655 A83-17721
- The effect of environment on fatigue crack growth behavior of 2021 aluminum alloy
05 p0616 A83-17894
- An evaluation of overload loads on the retardation behavior in a Ti-6Al-4V alloy
05 p0616 A83-17896
- Surface damage and near-threshold fatigue crack growth in a Ni-base superalloy in vacuum
05 p0616 A83-17897
- Effect of water on the interlaminar fracture behaviour of glass fibre-reinforced polyester composite
06 p0724 A83-17966
- Dependence of fracture toughness of alumina on grain size and test technique
06 p0734 A83-18051
- Slow growth of microcracks - Evidence for one type of ZrO2 toughening
06 p0734 A83-18054
- Stress-induced transformation during subcritical crack growth in partially stabilized zirconia
06 p0734 A83-18055
- Crack separation energy rates for inclined cracks in an elastic-plastic material
06 p0774 A83-18479
- Fatigue crack growth theory for ductile material
06 p0774 A83-18480
- Problems in environmentally-affected creep crack growth
06 p0728 A83-18481
- Experimental and numerical study of the different stages in ductile rupture - Application to crack initiation and stable crack growth
06 p0774 A83-18484
- A quantitative description of fracture toughness under plane stress conditions by the R-curve method
06 p0774 A83-18487
- A thermodynamic description of the running crack problem
06 p0774 A83-18489
- Constitutive equations and global criteria for ductile fracture
06 p0774 A83-18491
- Elastic-plastic fields in steady crack growth
06 p0774 A83-18492
- Experimental comparison of simulation methods of aeronautic type loading
[ONERA, TP NO. 1982-130] 06 p0775 A83-18598
- Mixed mode plane stress ductile fracture
06 p0775 A83-18909
- A unified description of micro and macroscopic fatigue crack behaviour
06 p0776 A83-18938
- On the influence of rubbing fracture surfaces on fatigue crack propagation in Mode III
06 p0776 A83-18940
- Stable and unstable crack growth in sintered and infiltrated P/M steels
06 p0730 A83-19084
- Application of the double slip plane crack model to temperature and strain rate sensitive BCC metals
06 p0733 A83-19146
- The problem of a crack in an orthotropic strip
06 p0778 A83-19546
- Parametric representation of crack growth rate under creep, fatigue and creep-fatigue interaction at high temperatures
07 p0883 A83-19671
- Stationary subsonic motion of a crack in an elastic strip
07 p0944 A83-19944
- Surface deformation of Westerly granite during creep
07 p0959 A83-20097
- Effect of fracture surface roughness on growth of short fatigue cracks
07 p0884 A83-20257
- A summary of fracture mechanics concepts
07 p0945 A83-20520
- Fracture mechanics analysis of the effects of residual stress on fatigue life
07 p0946 A83-20521
- On the exterior crack with contact zones
07 p0946 A83-20640
- Evidence of microscopic crack jumping in an epoxy resin
07 p0901 A83-21085
- Characteristics of the amplitude distribution of acoustic emission in the nucleation and propagation of fatigue cracks
07 p0943 A83-21405
- A relaxation technique for evaluating stress intensity factors by the finite element method
07 p0949 A83-21439
- On the problem of two coplanar cracks inside an infinite isotropic elastic solid
07 p0949 A83-21440
- Fracture mechanics and crack growth in fatigue
07 p0892 A83-21464
- Fatigue crack propagation at elevated temperature in MAR-M002 single crystals
07 p0893 A83-21476
- Crack initiation and propagation in a forged nickel-base alloy under high mechanical and thermal loading
07 p0894 A83-21480
- The influence of applied coatings on the creep fracture of IN 738 LC
07 p0894 A83-21488
- Fracture behaviour of a single-fibre graphite/epoxy model composite containing a broken fibre or cracked matrix
07 p0877 A83-21565
- Observations on prediction of non-self-similar subcritical crack growth and stress intensity distributions
08 p1115 A83-21652
- An empirical approach to determining K for surface cracks
08 p1115 A83-21653
- Defect forces, defect couples and path integrals --- J integral study of crack propagation stability
08 p1115 A83-21656
- Analytic asymptotic solution of the kinked crack problem
08 p1116 A83-21657
- On the maximum-energy-release-rate criterion for fracture under combined loads
08 p1116 A83-21659
- Mechanical model and mathematical analysis for ductile fracture
08 p1116 A83-21665
- Mechanisms and criteria for cleavage
08 p1058 A83-21666
- Slip plane facets in fatigued aluminum alloys
08 p1058 A83-21667
- The influence of dispersoids on fatigue crack propagation in Al-Mg-Si alloys
08 p1058 A83-21669
- Fatigue crack initiation and propagation in Ti-6Al and Ti-6Al-4V
08 p1058 A83-21671
- Criterion for crack instability under short pulse loads
08 p1116 A83-21674
- The effect of a time-dependent craze stress on crack growth in a linear viscoelastic material
08 p1116 A83-21675
- Modelling R ratio effects in fatigue crack growth in polymers
08 p1068 A83-21676
- Normalization of fatigue crack propagation behavior in polymers
08 p1068 A83-21677
- Hygrothermal aging effects on the micromechanisms of crack extension in glass fibre and carbon fibre composites
08 p1053 A83-21679
- Analysis of thermal cracking of unidirectionally reinforced composite structures in the micromechanical range
08 p1054 A83-21680
- Propagation of damage in elastic and plastic solids
08 p1116 A83-21684
- Geometry and size requirements for fatigue life similitude among notched members
08 p1059 A83-21685
- Fatigue crack propagation from crack arrays
08 p1059 A83-21688
- Fracture and fatigue crack propagation in bearing steels
08 p1059 A83-21689
- Elastic-plastic fields in steady crack growth in a strain-hardening material
08 p1117 A83-21692
- The growth of macroscopic cracks in creeping materials
08 p1117 A83-21693
- A finite element analysis of creep deformation in a specimen containing a macroscopic crack
08 p1117 A83-21694
- An incremental crack growth model for high temperature rupture in metals
08 p1059 A83-21695
- Shear bands and fracture in crystalline polymers
08 p1069 A83-21697
- The effect of specimen thickness and morphology on fracture toughness of thermoplastic polymers
08 p1069 A83-21698
- The relation between microstructural fracture processes and macroscopic crack tip characterizing parameters during the stable growth of cracks
08 p1117 A83-21699
- Constitutive relations including ductile fracture damage - Application to cracked bodies
08 p1117 A83-21700
- The influence of specimen geometry on stable crack growth for a high strength steel
08 p1060 A83-21704
- Experimental studies of stable crack growth
08 p1060 A83-21705
- An analysis of fatigue crack growth under yielding conditions
08 p1060 A83-21708
- Fatigue crack propagation response in extruded and cast aluminum alloys
08 p1060 A83-21710
- The metallography of fatigue in the high strength aluminium alloy 7010
08 p1060 A83-21711
- The propagation of short fatigue cracks in 12% chromium steels
08 p1060 A83-21712
- The use of the plastic crack tip opening displacement to correlate fatigue crack growth data for a structural steel
08 p1060 A83-21713
- R ratio influence and overload effects on fatigue crack mechanisms
08 p1060 A83-21714
- Low rates of fatigue crack growth in beta heat treated titanium alloy
08 p1061 A83-21715
- The influence of prior austenite grain size and stress ratio on near threshold fatigue crack growth behavior in high strength steel
08 p1061 A83-21716
- Mechanism of SCC and hydrogen-induced delayed cracking
08 p1061 A83-21718
- The implications of recent developments in elastic plastic fracture mechanics on the growth of stress corrosion cracks
08 p1061 A83-21719
- K-determination in mixed-mode crack problems by interferometry
08 p1117 A83-21720
- Stress biaxiality effects on slow crack growth in polymethylmethacrylate
08 p1069 A83-21723
- A J based engineering usage of fracture mechanics
08 p1117 A83-21725
- Fracture mechanisms in the peeling failure of adhesive joints
08 p1069 A83-21730
- Crack growth mechanism maps
08 p1117 A83-21731
- Creep crack growth characterization of austenitic stainless steel
08 p1061 A83-21732
- Experimental procedure for fast measurement of threshold in fatigue crack propagation
08 p1062 A83-21734
- On the mechanisms of threshold behaviour --- in fatigue crack propagation
08 p1062 A83-21735
- High strain fracture analysis
08 p1062 A83-21739
- The mechanism and mechanics of subcritical crack propagation in hot-pressed SiC above 1000 C
08 p1069 A83-21740
- Fractographic identification of subcritical to critical crack growth transition mechanisms in ceramics
08 p1069 A83-21743
- Plane stress fracture under biaxial loading
08 p1062 A83-21749
- Fracture assessment in ductile tearing situations
08 p1063 A83-21751
- Instability problems in ductile fracture
08 p1063 A83-21752
- Development of the nonlinear energy method for fracture toughness determination
08 p1063 A83-21753
- The effect of overloading on fatigue crack propagation in two aluminum alloys and an austenitic stainless steel
08 p1063 A83-21754
- Influence of specimen geometry on delayed retardation phenomena of fatigue crack growth in HT80 steel and A5083 aluminum alloy
08 p1063 A83-21755
- An estimation method of fatigue crack propagation rate under varying loading conditions of low stress intensity level
08 p1063 A83-21756
- Practical application of a model for fatigue damage with irregular cyclic loading
08 p1063 A83-21757
- Fatigue crack propagation behavior under complex mode loading
08 p1063 A83-21758
- Mode II fatigue crack growth in aluminum alloys and mild steel
08 p1063 A83-21759
- Measurements and mechanisms of crack growth at elevated temperatures up to 1273 K
08 p1063 A83-21762
- Bidirectional coupling of a cracking test machine to a calculator
08 p1112 A83-21764
- Fatigue crack growth under controlled K
08 p1118 A83-21765
- Analysis of steady state crack growth by discrete dislocation theory
08 p1118 A83-21774
- A thermodynamic description of inelastic fracture
08 p1118 A83-21775
- Plastic effects in dynamic crack propagation
08 p1118 A83-21776
- Crack-tip plasticity for rapid crack propagation
08 p1118 A83-21777
- The crack tip stress intensification associated with crack propagation and arrest
08 p1118 A83-21778
- Dynamic steady antiplane shear crack growth in an elastic-plastic material
08 p1119 A83-21779
- The suppression of creep cavitation and slow crack growth in Si-Al-O-N ceramics
08 p1070 A83-21781
- Effect of hold times on the elevated temperature fatigue crack growth behavior of Inconel 718 alloy
08 p1064 A83-21782
- Fatigue of cast nickelbase superalloys at 850 C
08 p1064 A83-21783
- On fatigue crack initiation and propagation at elevated temperature
08 p1064 A83-21784
- Growth of small fatigue cracks at high temperature - Applicability of conventional fracture mechanics
08 p1064 A83-21785
- Recrystallization methods for quantitative analysis of strain in plastic zones
08 p1119 A83-21788
- A comparative study on different methods to measure the crack opening displacement
08 p1064 A83-21790

- Some effects of inelastic constitutive models on crack tip fields in steady quasistatic growth 08 p1119 A83-21793
- An improved methodology for predicting random spectrum load interaction effects on fatigue crack growth 08 p1064 A83-21794
- Influence of environment on fracture 08 p1065 A83-21798
- An improved methodology for predicting random spectrum load interaction effects on fatigue crack growth 08 p1065 A83-21802
- A generalization of the concept of Cauchy-type principal value integrals for plane elasticity crack problems 08 p1121 A83-21865
- Fracture of nickel-base superalloy single crystals 08 p1065 A83-22018
- The experimental evaluation on the brittle fracture characterization under the mixed mode 08 p1122 A83-22069
- Evaluation of creep crack growth criteria for IN-100 at elevated temperature 08 p1066 A83-22142
- Physics of fracture /The Sosman Lecture/ --- crack propagation and crack-tip phenomena in structural ceramics 08 p1070 A83-22188
- Controlled flaws in ceramics - A comparison of Knoop and Vickers indentation 08 p1070 A83-22193
- An automated measuring system for analyzing the development of fatigue cracks in the case of nonstationary loading 08 p1113 A83-22404
- Failure mechanism for alloy KhN67VM under the action of a copper-silver solder 08 p1067 A83-22698
- Fatigue crack propagation in composites with spherical fillers. I 08 p1055 A83-22715
- Moving Griffith crack in an orthotropic material 08 p1123 A83-22722
- The effect of structural components on the energy of intergranular fracture --- in Mo and W alloys 08 p1068 A83-22784
- Quantitative fractography and dislocation interpretations of the cyclic cleavage crack growth process 08 p1123 A83-23224
- J-integral analysis for cracks emanated from elliptical holes 09 p1275 A83-23298
- Analysis of closure behavior of small fatigue cracks 09 p1275 A83-23299
- The role of plastic deformation in plane strain crack propagation 09 p1279 A83-23870
- Stable crack growth during fracture toughness testing in Ti-6Al-4V alloy 09 p1230 A83-23916
- Physical principles of prediction of heterogeneous material fracture 09 p1279 A83-23933
- Determination of fracture toughness of unidirectionally fiber-reinforced composites 09 p1223 A83-23936
- The relationship of stiffness changes in composite laminates to fracture-related damage mechanisms 09 p1223 A83-23940
- Experimental determination of flaw shapes and stress intensity distributions - Conditions for application to composite materials 09 p1224 A83-23949
- Models for intergranular creep crack growth by diffusion 09 p1279 A83-24069
- Creep crack extension by grain-boundary cavitation 09 p1279 A83-24070
- Cavitation and creep crack growth in low alloy steels 09 p1233 A83-24077
- The lateral buckling-fracture stability of thin-sheet structural components with deep cracks 09 p1280 A83-24648
- Measurement of fatigue crack propagation at -70 C with the direct-current potential probe method 09 p1281 A83-24944
- The effect of the crack geometry on the test result in surface defect testing 09 p1281 A83-24945
- On a certain dynamic crack problem in elastic and elastic-plastic media 09 p1282 A83-25104
- Flaws responsible for slow cracking in the delayed fracture of alumina 09 p1240 A83-25205
- Effect of cavities on creep 09 p1283 A83-25206
- Static fatigue of silica in hermetic environments 09 p1240 A83-25207
- Void growth and collapse in viscous solids 10 p1437 A83-25303
- Elastic-plastic crack growth 10 p1438 A83-25314
- Concepts of fracture mechanics 10 p1392 A83-25318
- Fracture properties of aluminum alloys 10 p1393 A83-25322
- Fracture properties of titanium alloys 10 p1393 A83-25323
- Effect of alpha phase morphology on mechanical properties of commercial purity titanium 10 p1393 A83-25401
- Cavity growth and failure in superplastic alloys 10 p1393 A83-25402
- Accuracy and precision of crack length measurements using a compliance technique 10 p1438 A83-25424
- On path-independent integrals and fracture criteria in non-linear fracture dynamics 10 p1438 A83-25471
- Dynamic in situ high voltage electron microscopy studies of tensile cracks in thin stainless steel films 10 p1395 A83-25546
- The study of dynamic fracture propagation using a special finite element technique [ASME PAPER 82-WA/DE-13] 10 p1439 A83-25680
- Crack and cavity nucleation at interfaces during creep 10 p1396 A83-25861
- Effects of hydrogen on near-threshold crack propagation in niobium 10 p1396 A83-25867
- Micromechanical predictions of crack initiation, propagation and crack growth resistance in boron/aluminum composites 10 p1389 A83-25879
- On the estimation of energy release rates [ASME PAPER 83-APM-11] 10 p1440 A83-26426
- Deformations of anisotropic layered materials 10 p1442 A83-26818
- A theoretical study on the running crack path by energy balance method 10 p1442 A83-26968
- Fracture control and its application within the agency's programmes 11 p1536 A83-27374
- A theory for transverse cracks in composite laminates 11 p1591 A83-27435
- Curved crack growth in brittle solids under farfield compression 11 p1592 A83-27439
- Effects of matrix viscoelasticity and cracking on fiber composite response during thermal cycling 11 p1592 A83-27461
- Stresses during fabrication of cylindrically woven carbon-carbon composites 11 p1543 A83-27462
- Crack propagation and arrest in plastic medium 11 p1593 A83-27771
- On the nature of boundary conditions for crack tip stress 11 p1593 A83-27773
- Propagation of fatigue cracks under polymodal loading 11 p1547 A83-27853
- EUROMECH colloquium on short fatigue cracks 11 p1547 A83-27854
- The formulation of a crack growth equation for short cracks 11 p1547 A83-27855
- A comparison of the strain intensity and cyclic J approaches to crack growth 11 p1593 A83-27856
- The behaviour of short cracks 11 p1593 A83-27857
- Crack shape evolution studies in threaded connections using A.C.F.M. --- Alternating Current Field Measurement 11 p1590 A83-27858
- Overload induced crack growth rate attenuation behavior in aluminum alloys 11 p1548 A83-28223
- Fatigue crack advance presumably detected by acoustic emission signals 11 p1590 A83-28225
- Crack deflection processes. I - Theory 11 p1595 A83-28424
- An experimental and theoretical study of crack propagation in crossply fiber composites 11 p1544 A83-28437
- Branched cracks at small angles /An addendum/ 11 p1595 A83-28438
- Resonance controlled fatigue crack propagation 11 p1595 A83-28440
- A new method of determining J_{IC} of steel by means of single specimen 11 p1548 A83-28442
- Experimental study of the T-criterion in ductile fractures 11 p1596 A83-28445
- Mechanism of corrosion fatigue crack propagation in high strength steels 11 p1548 A83-28446
- Estimates and approximation formulas in the problem of elasticity theory concerning a plane normal crack 11 p1597 A83-28472
- The effect of anisotropy, thickness, and operating time on the crack growth in pressed and rolled products of D16chT and V95pchT1 alloys 11 p1549 A83-28478
- A diagram for the discrete growth of a fatigue crack under self-similarity conditions 11 p1597 A83-28480
- Calculation of the durability distribution functions for structural elements with cracks 11 p1598 A83-28484
- Correlation between the energy characteristics of fracture - Crack propagation and spalling 11 p1598 A83-28503
- Further considerations on the development of surface cracks under stable crack extension 11 p1599 A83-28571
- Characterization of the behaviour of part-through cracks under stable crack extension 11 p1599 A83-28572
- Theoretical and experimental investigations regarding crack propagation in sheet metal --- German thesis 11 p1599 A83-28658
- Continuum theory of dilatant transformation toughening in ceramics 12 p1716 A83-29025
- A study of the effect of notches and cracks on creep rupture life 12 p1713 A83-29225
- The effect of dispersoids on the micromechanisms of crack extension in Al-Mg-Si alloys 12 p1714 A83-29509
- Effect of multiple crack propagation on the high temperature low cycle fatigue of a cast nickel-base alloy 12 p1714 A83-29725
- A crack-tip strain model for the growth of small fatigue cracks --- in engineering alloys 12 p1715 A83-29727
- Dynamic crack propagation analysis using a new path-independent integral and moving isoparametric elements [AIAA 83-0838] 12 p1737 A83-29746
- On the effect of residual stresses on crack growth from a hole [AIAA 83-0840] 12 p1737 A83-29747
- An automated finite element procedure for fatigue crack propagation analyses [AIAA 83-0841] 12 p1737 A83-29748
- Improved damage-tolerance analysis methodology [AIAA 83-0863] 12 p1738 A83-29751
- Elastic-plastic behavior of coldworked holes [AIAA 83-0865] 12 p1738 A83-29753
- A stochastic theory of fatigue crack propagation [AIAA 83-0978] 12 p1740 A83-29785
- Statistical crack propagation in fastener holes under spectrum loading [AIAA 83-0808] 12 p1741 A83-29808
- A mixed-mode fracture criterion for composite materials 12 p1711 A83-29895
- Linear elastic fracture mechanics and fatigue crack growth Residual stress effects 12 p1746 A83-29905
- Stress corrosion crack growth in the presence of residual stresses 12 p1746 A83-29906
- Finite element analysis of slow crack growth 12 p1747 A83-29942
- The effect of specimen size on J(R) resistance curve in limited amounts of crack growth 12 p1715 A83-29943
- Stress corrosion and hydrogen induced cracking behaviour in an Al alloy 13 p1820 A83-30325
- Observation of voids and cracks on ductile fracture process in tensile test of 5083 aluminum alloy plate 13 p1822 A83-30842
- Fatigue crack propagation behaviors of AZ31 magnesium alloy at temperatures from room temperature (17 + or - 2 C) to 50 C 13 p1822 A83-30843
- Influence of external environments on fatigue crack growth in epoxy resin 13 p1825 A83-31047
- Microinitiation, micropropagation and damage 13 p1823 A83-31171
- Method of examining subcritical crack growth in ceramics during the double twisting of specimens 13 p1825 A83-31220
- Investigation of thermal effects on weapon system components 13 p1859 A83-31298
- The effect of environment on the growth of small fatigue cracks 13 p1824 A83-31539
- On the relation between stable crack growth and fatigue 13 p1867 A83-31540
- Slow fatigue crack growth and threshold behaviour in IMI 685 --- in titanium alloys 13 p1824 A83-31541
- A study of short fatigue crack growth behaviour in titanium alloy IMI 685 13 p1824 A83-31542
- The role of the environment on the corrosion cracking of Al-Mg and Al-Li-Mg alloys 14 p1992 A83-32072
- The residual strength of prefabricated structures made of pressed panels of D16chT alloy and its modifications 14 p2029 A83-32075
- The development of the foundations of fracture mechanics for materials with initial stresses 14 p2029 A83-32151
- On the cyclic behavior of cast and extruded aluminum alloys. I - Fatigue crack propagation 14 p1992 A83-32342
- On the cyclic behavior of cast and extruded aluminum alloys. B - Fractography 14 p1992 A83-32343
- A Dugdale problem for a finite internally cracked plate 14 p2029 A83-32346
- Degradation of sodium beta-double-prime alumina - Effect of microstructure --- in sodium/sodium and sodium/sulfur cells 14 p1989 A83-32631
- Creep-fatigue-environment interactions --- Book 14 p1993 A83-32650
- Path-independent integrals, energy release rates, and general solutions of near-tip fields in mixed-mode dynamic fracture mechanics 14 p2031 A83-32652
- Effect of bending moment on the dynamic fracture of a beam or plate under tensile loading 14 p2031 A83-32653
- Plastic rotational factor and J-COD relationship of three point bend specimen 14 p1993 A83-32655
- A mixed-mode crack analysis of rotating disk using finite element method 14 p2031 A83-32658
- Fatigue crack closure after overload 14 p2031 A83-32660

Discrete dislocation analysis and path dependent plasticity 14 p2031 A83-32662
 Hydrogen-induced cracking in 4340-type steel - Effects of composition, yield strength, and H₂ pressure 14 p1994 A83-32678
 The effects of B and Zr on the creep and fatigue crack growth behavior of a Ni-base superalloy 14 p1994 A83-32679
 The influence of crack length on stress corrosion crack velocity 14 p1994 A83-32683
 Cyclic deformation, fatigue crack nucleation and propagation in metals and alloys 14 p1995 A83-32806
 Infrared measurement of specimen temperature profiles during fatigue crack propagation tests 14 p2020 A83-32825
 The effect of microstructure and moisture on the low cycle fatigue and fatigue crack propagation of two Al-Li-X alloys 14 p1996 A83-32889
 Microstructure, deformation, and corrosion-fatigue behavior of a rapidly solidified Al-Li-Cu-Mn alloy 14 p1996 A83-32890
 Theory of fatigue for brittle flaws originating from residual stress concentrations 14 p2032 A83-32974
 Determination of threshold stress intensity for crack growth at high temperature in silicon carbide ceramics 14 p1999 A83-32975
 Local buckling of thin tensioned plate with a crack 14 p2033 A83-33374
 A new transducer to monitor fatigue crack propagation 15 p2162 A83-33513
 Development of technical cracks on Al-2024-T3 in the case of one-stage and non-one-stage vibratory stresses 15 p2136 A83-33957
 Residual life prediction for jet engine rotor disks at elevated temperature 15 p2174 A83-33974
 Interaction of cracks in elastic media 15 p2177 A83-34349
 The calculation of the crack propagation forces while taking account of the unilateral contact between the edges of the crack 15 p2178 A83-34402
 Behavior of solutions of dynamic problems near the edge of a crack propagating at transonic velocity in an elastic medium 15 p2178 A83-34436
 Micro and macro mechanics of crack growth; Proceedings of the Symposium, Louisville, KY, October 13-15, 1981 15 p2179 A83-34476
 Micro and macro mechanics aspects of time-dependent crack growth 15 p2138 A83-34477
 Thermodynamics of crack growth 15 p2179 A83-34478
 Dislocation shielding of a crack in a quasi continuum approximation 15 p2179 A83-34479
 Micromechanics of crack propagation in Ti-6Al and Ti-6Al-4V 15 p2139 A83-34480
 Hydrogen-assisted crack-growth in titanium alloys 15 p2139 A83-34481
 Effects of environment and internal hydrogen on the sustained load cracking of Ti-6211 15 p2139 A83-34482
 Stability of crack extension rates in ductile materials 15 p2179 A83-34483
 Mechanisms of creep crack growth 15 p2179 A83-34484
 High temperature time-dependent crack growth 15 p2139 A83-34485
 Micromechanisms of creep crack growth in nickel based superalloys 15 p2139 A83-34486
 Temperature dependence of creep crack growth in aluminum alloy RR58 15 p2139 A83-34487
 Effects of environment on intermediate temperature crack growth in superalloys 15 p2139 A83-34488
 Cavity nucleation during fatigue crack growth caused by linkage of grain boundary cavities 15 p2139 A83-34489
 Microstructural basis and crack growth theories for post irradiation ductility loss in Nimonic PE16 15 p2139 A83-34490
 Temperature effects on fatigue thresholds and structure sensitive crack growth in a nickel-base superalloy 15 p2139 A83-34740
 The plastic zone and growth of fatigue cracks in magnesium MA12 alloy at room and low temperatures 15 p2140 A83-34741
 An analytic description of the kinetics of fatigue cracks in laminated composites 15 p2180 A83-35041
 Dynamic fatigue of brittle materials containing indentation line flaws 15 p2180 A83-35064
 The kinetics of surface craze growth in polycarbonate exposed to normal hydrocarbons 15 p2142 A83-35070
 Some aspects of crack growth and failure in fibre reinforced composites 15 p2130 A83-35075
 The opening of a natural macrocrack 16 p2365 A83-35551

SEM observations of the initiation and propagation of cracks in a short fibre-reinforced thermoplastic composite under stress 16 p2323 A83-35568
 The role of microcracking during crack growth in brittle materials 16 p2365 A83-35571
 Fatigue crack initiation and microcrack propagation in X7091 type aluminum P/M alloys 16 p2329 A83-35691
 Heat evolution investigated by a liquid crystal film technique during fracture in metals 16 p2330 A83-35978
 Fatigue crack growth rates for very short cracks developing at fastener holes in 7075 and 7010 aluminium alloys 16 p2330 A83-35982
 Overview of temperature and environmental effects on fatigue of structural metals 16 p2330 A83-36161
 Corrosion fatigue crack propagation 16 p2330 A83-36162
 Delta K thresholds in titanium alloys - The role of microstructure, temperature and environment 16 p2331 A83-36164
 The effect of microstructure on the fatigue behavior of Ni base superalloys 16 p2331 A83-36166
 Creep crack growth 16 p2331 A83-36167
 Environment, frequency and temperature effects on fatigue in engineering plastics 16 p2337 A83-36170
 Thermal fatigue analysis --- of turbine components 16 p2366 A83-36173
 Life prediction for turbine engine components 16 p2366 A83-36174
 A kinetic model of high temperature fatigue crack growth 16 p2331 A83-36175
 Review of the application of ultrasonic fatigue test methods for the determination of crack growth and threshold behavior of metallic materials 16 p2332 A83-36186
 A review of the role of frequency on fatigue crack initiation and growth at elevated temperatures 16 p2332 A83-36194
 A comparison of environmentally-influenced near-threshold fatigue crack growth behavior in high and lower strength steels at conventional frequencies 16 p2332 A83-36195
 The influence of frequency on fatigue crack propagation of some heat resisting alloys using ultrasonic fatigue 16 p2332 A83-36196
 Near-threshold fatigue crack growth determination at ultrasonic frequencies 16 p2333 A83-36197
 The effect of microstructure on the fatigue crack growth behavior near threshold in Cu and Al 16 p2333 A83-36198
 Evaluation of fatigue limits and crack growth properties of PM-Mo alloys tested at cyclic frequencies of 200 Hz and 20 kHz 16 p2333 A83-36199
 LCC evaluation of advanced engine damage tolerance goals for a hot-section disk --- in aircraft engines [AIAA PAPER 83-1407] 16 p2310 A83-36396
 On statistical moments of fatigue crack propagation 16 p2368 A83-36501
 Statistical modeling of fatigue-crack growth in a nickel-base superalloy 16 p2333 A83-36502
 Estimating the statistical properties of crack growth for small cracks 16 p2333 A83-36504
 On the electrical potential analysis of a cracked fracture mechanics test specimen using the finite element method 16 p2368 A83-36509
 Near-threshold fatigue crack propagation of several high strength steels 16 p2334 A83-36512
 Brittle fracture of plates in tension - Relative significance of boundary reflected body and Rayleigh waves 16 p2368 A83-36516
 Reliability theory of stochastic fracture processes in sustained loading. I 16 p2369 A83-36623
 Measurement of crack profile of semi-elliptical surface cracks using the ac potential technique 16 p2363 A83-36726
 Intergranular crack-deflection toughening in silicon carbide 16 p2337 A83-36948
 Isoparametric finite element analysis of large elasto-plastic strain problems and its applications in fracture mechanics 17 p2518 A83-37272
 Low cycle fatigue of tubular specimens 17 p2519 A83-37299
 Acoustoelastic determination of forces on a crack in mixed-mode loading 17 p2518 A83-37387
 A model for determining the reliability of an aircraft wing structure 17 p2521 A83-37638
 Fatigue crack initiation and microcrack propagation in X7091 type aluminum P/M alloys 17 p2487 A83-37834
 Investigation of the fatigue and crack propagation properties of X7091-T7E69 extrusion 17 p2487 A83-37836
 Effects of microstructure and aging treatment on the fatigue crack growth behavior of high strength P/M aluminum alloy X7091 17 p2487 A83-37837

Fatigue crack tip plasticity and crack growth mechanics in powder metallurgy and wrought aluminum alloys 17 p2488 A83-37840
 Microstructure/strength/fatigue crack growth relations in high temperature P/M aluminum alloys 17 p2488 A83-37844
 Dynamic crack growth during pop-in fracture in 7075 aluminum alloy 17 p2489 A83-38123
 Direct observations of crack tip dislocation behavior during tensile and cyclic deformation 17 p2489 A83-38377
 Statistical mechanics of early growth of fatigue cracks 17 p2490 A83-38384
 A pseudo-linear analysis of yielding and crack growth - Strain energy density criterion 17 p2522 A83-38388
 Motion of the crack under constant loading and at high constant temperature 17 p2523 A83-38389
 Unstable growth of branched cracks 17 p2523 A83-38394
 Analyses of microstructural and chemical effects on fatigue crack growth 17 p2490 A83-38396
 A fractographic study of corrosion-fatigue crack propagation in a duplex stainless steel 17 p2490 A83-38397
 An experimental investigation of fatigue reliability laws 17 p2523 A83-38398
 On cracking instability in plates containing circular holes 17 p2523 A83-38399
 Energy criteria for the brittle fracture of composite materials with initial stresses 17 p2523 A83-38503
 A partially contacting crack in a plate with an elliptic hole 17 p2524 A83-38509
 Effect of rigid grains separation on the diffusive growth of crack-like cavities on grain boundaries 17 p2491 A83-38526
 Dynamic fields near a crack tip growing in an elastic-perfectly-plastic solid 17 p2524 A83-38528
 On the nature of craze development and breakdown during fatigue 18 p2671 A83-39059
 Influence of overloads and block loading sequences on mode III fatigue crack propagation in A469 rotor steel 18 p2665 A83-39075
 Non-singular stresses effects on two interacting equal collinear cracks 18 p2696 A83-39076
 A synergistic fracture mechanics approach to fatigue life evaluation 18 p2665 A83-39077
 The effects of load ratio on environmentally assisted fatigue crack growth 18 p2665 A83-39078
 Condition for stable growth of branched cracks 18 p2696 A83-39082
 Fatigue crack growth rate under full yielding condition for 15CDV6 steel 18 p2665 A83-39084
 Growth of ring-shaped edge cracks under reversed torsional fatigue 18 p2697 A83-39452
 On the crack energy density and energy release rate for an elasto-plastic crack 18 p2697 A83-39456
 Micromechanisms of fatigue crack growth retardation following overloads 18 p2699 A83-39540
 The transition between stress corrosion crack growth and plastic fracture 18 p2699 A83-39541
 On the probabilistic modeling of fatigue crack growth 18 p2699 A83-39544
 Further remarks on an exact solution for crack problems 18 p2699 A83-39551
 An analysis of free-edge delamination in laminated composite under uniform axial strain 18 p2702 A83-40150
 On fracture behavior during crack propagation in carbon-fiber composites 18 p2654 A83-40192
 Prediction of fracture toughness of unidirectional metal matrix composites 18 p2654 A83-40196
 Fatigue crack growth behavior in the vicinity of interface of dissimilar materials 18 p2705 A83-40204
 Fracture mechanism of short glass fiber reinforced polyamide thermoplastics 18 p2657 A83-40232
 Thermal cycling of W-wire reinforced metal matrix composites 18 p2667 A83-40260
 Reconsideration of the superposition model for environmentally assisted fatigue crack growth 18 p2668 A83-40617
 Creep crack growth behavior of several structural alloys --- superalloys 18 p2669 A83-40636
 Low cycle fatigue of Ti-Mn alloys - Microstructural aspects of fatigue crack growth 18 p2670 A83-40637
 Fatigue crack growth rate of Ti-6Al-4V prealloyed powder compacts 18 p2670 A83-40642
 The effect of hydrogen on the fracture toughness and subcritical crack growth behavior of alpha+beta titanium alloys 19 p2821 A83-40801
 A method for solving problems concerning the bending of a round plate with a crack 19 p2856 A83-40806
 The bending of a laterally cracked beam clamped at its ends 19 p2856 A83-40807
 Slow crack growth behavior in transformation-toughened Al₂O₃-ZrO₂(Y₂O₃) ceramics 19 p2823 A83-40907

Fatigue crack initiation and propagation in several nickel-base superalloys at 650 C 19 p2821 A83-41199

Some effects of material property data selection on crack propagation analyses 19 p2821 A83-41200

Subsonic motion of the edge of a shear shift with friction along an interface between elastic materials 19 p2858 A83-41214

Contour invariants of the fracture theory for thermoelastic bodies 19 p2858 A83-41215

Service life characteristics of the composite material KAS-1A 19 p2820 A83-41601

Diffraction of SH waves by a moving crack 19 p2860 A83-41999

Fatigue crack micromechanisms in ingot and powder metallurgy 7XXX aluminum alloys in air and vacuum 19 p2822 A83-42028

Determination of stable crack growth resistance of ductile material using an RDCB specimen --- Reinforced Double Cantilever Beam 20 p2954 A83-42830

Determination and simulation of stable crack growth in ADINA 20 p3003 A83-42927

Thermal stresses in an orthotropic elastic half-plane weakened by a Griffith crack 20 p3004 A83-42937

An integral equation approach for simultaneous solution of rectangular hole and rectangular block problems 20 p3004 A83-42972

A note on the problem of an annular crack subjected to an arbitrary normal pressure 20 p3004 A83-42975

Elastic-plastic interaction of Dugdale type cracks and plastified matrix material in self-stressed fibre-reinforced composites 20 p3006 A83-42996

Fatigue crack propagation in random short-fiber SMC composite --- Sheet Molding Compound 20 p2948 A83-43147

The effect of grain size on fatigue growth of short cracks 20 p2954 A83-43346

Predicting stress corrosion crack growth rates at high stress levels. II - The general yield situation 20 p2955 A83-43472

The opening of a crack in the elastic region under the effect of a moving load 20 p3008 A83-43524

The effect of the unsteadiness of a stress field on crack growth in creep 20 p3008 A83-43525

Reliability theory of stochastic fracture processes in sustained loading. II - Stochastic loading 20 p3008 A83-43582

An energy approach to evaluating the crack resistance of materials 20 p3008 A83-43622

A crack growth fatigue life under spectrum loading 20 p3009 A83-43692

Structural stability considerations in elastic-plastic fracture mechanics [ASME PAPER 83-PVP-40] 20 p3009 A83-43728

Consideration of short cracks in high stress fatigue design [ASME PAPER 83-PVP-90] 20 p3009 A83-43730

The behaviour of short cracks in the sub-critical crack growth regime [ASME PAPER 83-PVP-98] 20 p3009 A83-43732

On subcritical crack growth in ceramics as influenced by grain size and energy-dissipative mechanisms 21 p3116 A83-44122

Microstructures and subcritical crack growth in oxidized hot-pressed Si3N4 21 p3116 A83-44331

On crack branching and curving in a finite body 21 p3156 A83-44887

A new singular integral equation for the classical crack problem in plane and antiplane elasticity 21 p3156 A83-44890

On the modelling of the process region at crack growth 21 p3156 A83-44891

Numerical analysis of fast mode-I fracture of a strip of viscoplastic work-hardening material 21 p3156 A83-44892

A mechanism of void growth in the region of the plastic zone ahead of a crack-tip 21 p3156 A83-44895

Steady interface crack propagation between two viscoelastic standard solids 21 p3157 A83-44901

Localization of deformation in rate sensitive porous plastic solids 21 p3157 A83-44902

Statistical approach to time-dependent failure of brittle material 21 p3157 A83-44903

The asymptotic near-tip solution for mode-III crack in steady growth in power hardening media 21 p3157 A83-44904

The effect of work-hardening on plane strain crack growth under small scale yielding conditions 21 p3157 A83-44907

The cyclic J-integral as a criterion for fatigue crack growth 21 p3158 A83-44910

Some comments on the geometry dependence of the J versus c relation for plane strain crack growth 21 p3158 A83-44912

An analysis of the energy release rate for non-coplanar crack growth in fiber reinforced composite materials 21 p3107 A83-44913

A personal computer approach to automating stress corrosion studies 21 p3158 A83-44915

A simple velocity gauge for measuring crack growth 21 p3158 A83-44917

Fatigue crack growth of a corner crack in an attachment lug 21 p3158 A83-44920

Load-shedding techniques for fatigue-threshold determination 21 p3161 A83-45149

Simultaneous measurements of stress intensity and toughness for fast-running cracks in steel 21 p3114 A83-45154

A hybrid technique for improved K determination from photoelastic data 21 p3161 A83-45156

Dynamic crack curving - A photoelastic evaluation 21 p3161 A83-45164

Three-dimensional elastic-plastic finite element analysis of small surface cracks 21 p3162 A83-45182

Model of fatigue crack propagation by damage accumulation at the crack tip 21 p3162 A83-45183

Computer controlled decreasing Delta-K fatigue threshold test 21 p3162 A83-45184

Quasistatic thermal crack growth in unidirectionally fiber reinforced composite materials 21 p3108 A83-45185

The stressed state of a plate weakened by two circular holes and a crack 21 p3163 A83-45366

Dynamics of a rupture-shear crack at the interface of two elastic materials 21 p3164 A83-45394

Fracture mechanics of plates and shells 22 p3305 A83-45773

Elastoplastic crack propagation (fatigue and failure) 22 p3305 A83-45977

A new method for the determination of the critical value of crack tip opening displacement at the initiation of crack growth using a single three-point bend specimen 22 p3305 A83-46025

Definition of interphase in composites 22 p3264 A83-46302

Detection of cracks under installed fasteners in aircraft structures 22 p3304 A83-46769

Influence of late-breaking ligaments on crack propagation in compact specimens - A photoelastic study 22 p3306 A83-46808

Observation of damage growth in compressively loaded laminates 22 p3264 A83-46810

Fatigue fracture of polycarbonate 22 p3270 A83-46902

On the influence of internal hydrogen on fatigue thresholds of HSLA steel 23 p3432 A83-47851

Extremum principles for the energy-release problem of elastic-perfectly plastic body subjected to prescribed change of material properties 23 p3470 A83-48093

A note on the dynamic stress field near a propagating crack 23 p3470 A83-48099

The behaviour of fatigue cracks subject to applied biaxial stress - A review of experimental evidence 23 p3470 A83-48146

The effect of water vapor on fatigue crack tip mechanics in 7075-T651 aluminum alloy 23 p3432 A83-48147

On the transition from near-threshold to intermediate growth rates in fatigue 23 p3432 A83-48149

Equations of fatigue crack growth 23 p3472 A83-48465

Fatigue crack growth in vacuum and a gaseous environment 23 p3433 A83-48540

Development of fatigue cracks in polymethyl methacrylate 23 p3439 A83-48541

Stiffness changes in unidirectional composites caused by crack systems. 23 p3428 A83-48602

Stress activated Raman scattering and microcrack detection 24 p3581 A83-48868

Crack transient torsional wave interaction in an elastic bi-material 24 p3591 A83-48870

Propagation of crazing in viscoelastic media 24 p3567 A83-48902

The stress-strain state at the point of accumulation of collinear cracks 24 p3591 A83-48927

Mechanical parameters applied to the propagation of creep cracks 24 p3591 A83-48995

The transformation ratio of acoustic emission during irreversible deformation of crystals 24 p3590 A83-49058

Green's function solution and applications for cracks emanating from a circular hole in an infinite sheet 24 p3594 A83-49599

Strain energy density fracture criterion in elastodynamic mixed mode crack propagation 24 p3594 A83-49863

Effects of crack growth on the load-displacement characteristics of precracked specimens under bending 24 p3594 A83-49864

Crack growth resistance characterized by the strain energy density function 24 p3595 A83-49867

The microstructure of an aluminum alloy at early stages of spall damage 24 p3567 A83-49913

Analytical determination of the crack path and elastic energy release rate under cyclic loading with allowance for welding stresses 24 p3596 A83-49915

Enlargement and accumulation of submicrocracks in oriented crystalline polymers 24 p3596 A83-49916

The disentanglement time of the craze fibrils in polymethylmethacrylate 24 p3569 A83-50068

CRACK TIPS

Evaluation of process zone by using Jext integral under large scale yielding - Structure of J integral 08 p1116 A83-21658

Near-crack tip finite strain analysis 08 p1116 A83-21662

The growth of macroscopic cracks in creeping materials 08 p1117 A83-21693

The relation between microstructural fracture processes and macroscopic crack tip characterizing parameters during the stable growth of cracks 08 p1117 A83-21699

An analysis of fatigue crack growth under yielding conditions 08 p1060 A83-21708

The effect of overloads upon fatigue crack tip opening displacement and crack tip opening/closing loads in aluminum alloys 08 p1060 A83-21709

The use of the plastic crack tip opening displacement to correlate fatigue crack growth data for a structural steel 08 p1060 A83-21713

K-determination in mixed-mode crack problems by interferometry 08 p1117 A83-21720

Simplified determination of J-integral and its availability as a strain intensity parameter at notch tip 08 p1118 A83-21750

Analysis of steady state crack growth by discrete dislocation theory 08 p1118 A83-21774

A thermodynamic description of inelastic fracture 08 p1118 A83-21775

Crack-tip plasticity for rapid crack propagation 08 p1118 A83-21777

A survey of recent developments in the evaluation of stress intensity factors from isochromatic crack-tip fringe patterns 08 p1119 A83-21786

An experimental study of the Dugdale model --- relation between crack tip displacement and applied load 08 p1119 A83-21787

Recrystallization methods for quantitative analysis of strain in plastic zones 08 p1119 A83-21788

A comparative study on different methods to measure the crack opening displacement 08 p1064 A83-21790

Some effects of inelastic constitutive models on crack tip fields in steady quasistatic growth 08 p1119 A83-21793

Crack-tip singularity fields in nonlinear fracture mechanics - A survey of current status 08 p1064 A83-21797

Central ductile crack in an orthotropic strip of finite width 08 p1120 A83-21818

On the accuracy of J-integral value evaluated by finite element method for mixed mode 08 p1122 A83-22068

Physics of fracture /The Sosman Lecture/ --- crack propagation and crack-tip phenomena in structural ceramics 08 p1070 A83-22188

A thermoelastic problem for a crack between dissimilar anisotropic media 09 p1278 A83-23669

The topography of the core-region around cracks under modes I, II and III of fracture 09 p1282 A83-25050

Acousto-elastic measurement of stress and stress intensity factors around crack tips 09 p1283 A83-25116

On a micromechanical fracture model for cracked reinforced composites 10 p1438 A83-25470

On the nature of boundary conditions for crack tip stress 11 p1593 A83-27773

Appearance aspects of isochromatic mode-I crack tip fringe loops 11 p1593 A83-27862

Double slip plane crack model 11 p1595 A83-28423

On the fundamental basis of fracture mechanics 11 p1596 A83-28444

The stress-strain state of a plate weakened by a through defect having a small radius of curvature at the tip 11 p1598 A83-28492

Laser microspeckle technique in displacement measurement near a crack tip 11 p1575 A83-28701

Estimating singularity powers with finite elements 11 p1599 A83-28723

A crack-tip strain model for the growth of small fatigue cracks --- in engineering alloys 12 p1715 A83-29727

A Dugdale problem for a finite internally cracked plate 14 p2029 A83-32346

The asymptotic behavior of the stress-strain state of inhomogeneously aging bodies near the tip of a crack 14 p2030 A83-32352

Path-independent integrals, energy release rates, and general solutions of near-tip fields in mixed-mode dynamic fracture mechanics 14 p2031 A83-32652

Plastic rotational factor and J-COD relationship of three point bend specimen 14 p1993 A83-32655

Limitations of the crack tip blunting line used in the J-sub-IC test procedure 14 p2031 A83-32665

On the criteria for hydrogen assisted fracture at the threshold stress intensity 14 p1997 A83-32947

A variable power singular element for analysis of fracture mechanics problems 15 p2176 A83-34321

Plane plastic strain in close proximity to a crack tip 15 p2178 A83-34437

Dislocation shielding of a crack in a quasi continuum approximation 15 p2179 A83-34479

Stability of crack extension rates in ductile materials 15 p2179 A83-34483

A strange convergence property of the Lobatto-Chebyshev method for the numerical determination of stress intensity factors 15 p2179 A83-34564

The plastic zone and growth of fatigue cracks in magnesium MA12 alloy at room and low temperatures 15 p2140 A83-34741

Wear debris due to mode II opening of mode I fatigue cracks in an aluminum alloy 16 p2330 A83-35693

Fatigue crack tip plasticity and crack growth mechanics in powder metallurgy and wrought aluminum alloys 17 p2488 A83-37840

Direct observations of crack tip dislocation behavior during tensile and cyclic deformation 17 p2489 A83-38377

Stress intensity factors for radial cracks in bimaterial media 17 p2523 A83-38391

An axisymmetric-elastodynamic analysis of a crack in orthotropic media using a path-independent integral 17 p2523 A83-38393

Dynamic fields near a crack tip growing in an elastic-perfectly-plastic solid 17 p2524 A83-38528

Constitutive behavior and crack tip fields for materials undergoing creep-constrained grain boundary cavitation 17 p2492 A83-38860

Non-singular stresses effects on two interacting equal collinear cracks 18 p2696 A83-39076

The crack tip opening angle (CTOA) of the plane stress moving crack 18 p2696 A83-39079

The fracture toughness of structural alloys under cyclic loading, I, II 18 p2665 A83-39498

The effect of biaxiality of loading in the orientation of caustics 18 p2699 A83-39538

Comparison of static and dynamic energy release rates for different fracture specimens --- of nonmetallic materials 18 p2671 A83-39549

Further remarks on an exact solution for crack problems 18 p2699 A83-39551

A method for determining the critical strain, δ_{IIc} , at the tip of a longitudinal shear crack 19 p2856 A83-40809

Steady state vacancy concentration around a plastic crack 20 p3007 A83-43345

The influence of the crack tip stress field on the nucleation and growth of voids 20 p3008 A83-43467

On the validity of the singular integral equations of crack problems at the crack tips 21 p3152 A83-44350

Effect of thickness on plastic zone size in BCS theory of fracture --- Bilby, Cottrell and Swinden 21 p3155 A83-44882

Analysis of crack-tip moiré fringe patterns 21 p3156 A83-44888

A mechanism of void growth in the region of the plastic zone ahead of a crack-tip 21 p3156 A83-44895

Effect of non-uniform pressure on the extension of an external crack 21 p3157 A83-44898

The inclined crack under biaxial and uniaxial loading 21 p3157 A83-44900

A Griffith crack shielded by a dislocation pile-up 21 p3157 A83-44908

The use of the method of lines in 3-D fracture mechanics analyses with application to compact tension specimens 21 p3158 A83-44911

The stress intensity factor for the double cantilever beam 21 p3158 A83-44914

Engineering formulae for fatigue strength reduction due to crack-like notches 21 p3158 A83-44916

The accuracy of COD values calculated according to BS 5762 21 p3158 A83-44918

Analysis of cracks with multiple branches 21 p3159 A83-44927

Fine-grid method for large-strain analysis near a notch tip 21 p3161 A83-45155

Crack-tip stresses as computed from strains determined by stereomaging 21 p3161 A83-45163

Transient response of a central crack to a tensile pulse 21 p3161 A83-45168

Model of fatigue crack propagation by damage accumulation at the crack tip 21 p3162 A83-45183

Finite element procedures in fracture mechanics 22 p3305 A83-45771

Structures with cracks in the case of superimposed normal and shear stresses 22 p3305 A83-45772

A new method for the determination of the critical value of crack tip opening displacement at the initiation of crack growth using a single three-point bend specimen 22 p3305 A83-46025

An equivalent procedure for the evaluation of the stress intensity factors of a radial crack in a disc 22 p3306 A83-46392

The effect of water vapor on fatigue crack tip mechanics in 7075-T651 aluminum alloy 23 p3432 A83-48147

Longitudinal shear in a body with an acute-angled inclusion and an interface crack 23 p3473 A83-48542

The effect of biaxial loading on the size of a plastic zone near a crack 24 p3593 A83-49038

Bending vibration of a simply supported rectangular plate with a crack parallel to one edge 24 p3594 A83-49865

Simple bounds for the stress intensity factors by the method of singular integral equations 24 p3595 A83-49868

Mixed-mode crack opening in fatigue 24 p3567 A83-49874

CRACKING (CHEMICAL ENGINEERING)

NT PYROLYSIS

Improved combustion turbine efficiency with reformed alcohol fuels [ASME PAPER 83-GT-60] 23 p3464 A83-47916

CRACKING (FRACTURING)

NT STRESS CORROSION CRACKING

Effect of resin flexibility on the properties of filament wound tubes 01 p0022 A83-10241

Bursting and bulging of carbon fibre composite discs 01 p0022 A83-10243

Investigation of the hydrogen-influenced tendency toward cold cracking in high-strength low-alloy fine-grained structural steel, with regard to the implant experiment --- German thesis 01 p0026 A83-10469

Fracture toughness test by impact-fatigue method 02 p0154 A83-11851

An analysis of cracking and the reliability of thin walled tubes under fatigue using the Weibull law 02 p0189 A83-11861

A new approach to the weldability of nickel-base as-cast and powder metallurgy superalloys 02 p0155 A83-12069

High-temperature electron beam welding of the nickel-base superalloy IN-738 LC 02 p0155 A83-12072

An analytical and experimental study of the plate tearing mode of fracture 03 p0339 A83-13201

An asymptotic analysis on the cracked plates including transverse shear deformation 03 p0341 A83-14488

An investigation of cumulative damage development in quasi-isotropic graphite/epoxy laminates 03 p0292 A83-14555

Stiffness-reduction mechanisms in composite laminates 03 p0292 A83-14558

Double torsion fracture toughness test for evaluating transverse cracking in composites 04 p0455 A83-15996

The role of the liquid in environmental stress cracking of polyethylene 05 p0619 A83-17571

An investigation of heat-affected zone hot cracking in alloy 800 06 p0728 A83-18399

Crack testing with endoscope and eddy current probe 06 p0770 A83-19125

Practical application of fracture mechanics 08 p1119 A83-21799

Comparative evaluation of the effect of titanium and aluminum on properties of creep-resisting metal deposited by the argon-arc method 10 p1397 A83-26223

Axisymmetric problem of a flat interface annular crack between an elastic layer and a half-space 10 p1440 A83-26424

Discontinuity sources in manufacturing processes --- for metals 17 p2523 A83-38400

The use of acoustic emission techniques to monitor fracture processes in high strength precipitation hardened aluminum alloys 17 p2491 A83-38525

Effects of antimony additions on the fracture of nickel at 600 C 17 p2491 A83-38858

The crack problem in a specially orthotropic shell with double curvature 18 p2699 A83-39536

3-D elastic-plastic investigation of fracture parameters in side-grooved compact specimen 21 p3157 A83-44906

Evaluation of dynamic crack instability criteria 21 p3159 A83-44925

On the approximate evaluation of interaction of cracks in elastic media 21 p3159 A83-44935

Determination of stress-intensity factors for cracks in tubes under torsion 22 p3306 A83-46805

A note on the cracked plates reinforced by a line stiffener 24 p3595 A83-49872

CRACKS

NT CRACK TIPS

NT MICROCRACKS

NT SURFACE CRACKS

On the behaviour of a cracked elastic body with /or without/ friction 02 p0189 A83-11856

Magnetic field at the tip of a crack around which current flows 02 p0188 A83-12159

Cracked shells under skew-symmetric loading --- Reissner theory 03 p0338 A83-13125

Analysis of bonded repairs to damaged fibre composite structures 03 p0291 A83-13200

Computerized tomography inspection of trident rocket motors - A capability demonstration 03 p0337 A83-13436

Stability of thin plates with cracks under biaxial tension 03 p0340 A83-14071

Stress intensity factors for two cracks emanating from two holes and approaching each other 04 p0496 A83-15065

Inversion of ultrasonic scattering data 04 p0489 A83-15168

NDE of fastener hole cracks by the electric current perturbation method 04 p0491 A83-15192

Inversion algorithms for crack-like flaws 04 p0492 A83-15204

Role of cracks in the creep deformation of brittle polycrystalline ceramics 05 p0619 A83-17560

Elastic-plastic finite element analyses of short cracks 05 p0655 A83-17675

Thermoelastic fracture solutions using distributions of singular influence functions. I - Determining crack stress fields from dislocation distributions 05 p0656 A83-17875

Gel electrode imaging of fatigue cracks in aluminum alloys 06 p0730 A83-18941

Peripheral edge crack around a spherical cavity under uniaxial tension field 07 p0946 A83-20642

Detection and measurement of cracks in threaded bolts with an a.c. potential difference method 07 p0943 A83-21355

Effect of fatigue damage in members of a sectional structure on its damping 07 p0948 A83-21416

Vibration and bending of a cracked plate 08 p1115 A83-21632

Two stress intensity factor calculation methods and solutions for various three-dimensional crack problems 08 p1116 A83-21660

Regularities of similarity and fatigue damage accumulation under irregular loading 08 p1118 A83-21737

Crack detection by ultrasonic methods - Theory and experiment 08 p1112 A83-21766

Official liability for insufficient airworthiness - Comments in connection with a supreme-court decision 08 p1171 A83-21898

Inverse ray tracing in elastic solids with unknown anisotropy 08 p1160 A83-22226

Crack depth measurements using AC potential drop 08 p1113 A83-22408

SH-wave scattering by a cylinder with an interfacial crack 09 p1276 A83-23375

New Challenger engine cracks found 09 p1220 A83-23500

The frictionless contact of cracked elastic bodies 09 p1283 A83-25108

Causes of cold cracking in multipass welded joints in corrosion-resisting 08Kh15N5d2T type maraging steels 10 p1397 A83-26222

Stress distributions for a quarter plane containing an arbitrarily oriented crack 10 p1440 A83-26429

The interface crack behavior in dissimilar anisotropic composites under mixed-mode loading [ASME PAPER 83-APM-7] 10 p1441 A83-26444

An investigation of the stress intensity factor for a finite internally cracked plate by using variational method 11 p1595 A83-28441

Bounding theorems for Stress Intensity Factors 11 p1596 A83-28443

A Mohr-circle graphical method for stress intensity factors in cracked plates under different loadings 14 p2031 A83-32656

Automatic eddy current bolt-hole scanning system 16 p2363 A83-35760

Tabulated stress intensity factor solutions for flawed fastener holes 16 p2368 A83-36514

Processing-related fracture origins. II - Agglomerate motion and cracklike internal surfaces caused by differential sintering 16 p2337 A83-36946

Sanders' energy-release rate integral for a circumferentially cracked cylindrical shell [ASME PAPER 83-APM-32] 17 p2519 A83-37386

- The effect of stringers on the stress-strain state near a hole or crack in an anisotropic plate
17 p2520 A83-37516
- A method for obtaining stress intensity factor by F.E.M. and its application to dynamic problem. II - A treatment for mixed mode cracks
18 p2697 A83-39451
- Stress intensity factors in two bonded elastic layers containing cracks perpendicular to and on the interface. I Analysis. II - Solution and results
18 p2698 A83-39535
- A new method for calculating the elastic component of the Crack Opening Displacement (COD)
18 p2699 A83-39548
- Three-dimensional curved crack in an elastic body
18 p2700 A83-39558
- Stability loss and fracture of plates with cracks under biaxial tension
18 p2702 A83-40124
- Sensitivity of X-ray computer tomography in the inspection of thin layers, glued joints, cracks, laminations, and coatings
21 p3149 A83-43877
- Antiplane vibration of an elastic layer with a midplane crack
21 p3155 A83-44884
- Comparison of finite element solutions with analytical and experimental data for elastic-plastic cracked problems
21 p3156 A83-44894
- Analysis of cracks with multiple branches
21 p3159 A83-44927
- Concentration of elastic stresses near dies, cracks, thin inclusions, and reinforcements --- Russian book
21 p3160 A83-45025
- Plane-stress fracture testing of finite sheets under biaxial loads
21 p3161 A83-45161
- Torsional impact response of a penny-shaped crack lying on a bimaterial interface
21 p3162 A83-45188
- Surface waves due to scattering by a near-surface parallel crack
22 p3302 A83-45700
- An axisymmetric problem for an elastic medium with a spherical inclusion weakened by an interface crack
23 p3468 A83-47172
- Internal and edge cracks in a plate of finite width under bending
23 p3469 A83-47596
- Impact response of a cracked orthotropic medium
23 p3469 A83-47597
- The crack problem for a nonhomogeneous plane [ASME PAPER 83-APM-35]
23 p3471 A83-48243
- Integral-equation solution for half planes bonded together or in contact and containing internal cracks or holes
23 p3473 A83-48495
- CRANIUM**
- NT INTRACRANIAL CAVITY
- Gradations of severity in the condition of patients with craniocerebral injuries and unified criteria for their determination
06 p0798 A83-18976
- The importance of laboratory data for the differentiation of mild and moderately severe craniocerebral injuries
06 p0798 A83-18977
- Otoneurological symptoms in the differential diagnosis of mild and moderately severe craniocerebral injuries
06 p0798 A83-18979
- Scintigraphy with (Tc-99)-pyrophosphate and computer tomography in the diagnosis of tumors of the cranial bone
19 p2881 A83-41440
- CRANK-NICHOLSON METHOD**
- New diagonal implicit scheme for the compressible Navier-Stokes equations [AIAA PAPER 83-1891]
18 p2683 A83-39407
- Numerical analysis of moving boundary problem in matrix with a thin alternate matrix
21 p3197 A83-44012
- CRASH INJURIES**
- An analysis of spinal injuries after ejections and crash landings in the IAF
02 p0223 A83-12254
- Vertebral lesions after the aircraft crashes
16 p2396 A83-35579
- Basilar skull fracture in U.S. Army aircraft accidents --- helmet design for pilot protection
18 p2737 A83-40359
- CRASH LANDING**
- An analysis of spinal injuries after ejections and crash landings in the IAF
02 p0223 A83-12254
- Studies on an acceleration platform and at the time of a simulated crash of helicopter anticrash seats
08 p1043 A83-22976
- Crashing for safety
13 p1805 A83-31588
- Status of FAA crash dynamics program - Transport category aircraft [SAE PAPER 821483]
17 p2459 A83-38002
- The Jetstar overrun at Luton
21 p3089 A83-44880
- CRASHES**
- NT CRASH LANDING
- Energy absorption of composite materials under crash conditions
18 p2705 A83-40216
- CRASHWORTHINESS**
- An efficient triangular plate bending finite element for crash simulation
02 p0194 A83-12755
- Application of the nonlinear finite element method to crashworthiness analysis of aircraft seats [AIAA 83-0929]
12 p1699 A83-29855
- Crashing for safety
13 p1805 A83-31588
- Status of FAA crash dynamics program - Transport category aircraft [SAE PAPER 821483]
17 p2459 A83-38002
- Aircraft crashworthiness in the United States - Some legal and technical parameters
18 p2752 A83-39044
- Analysis of aircraft dynamic behavior in a crash environment
21 p3091 A83-43966
- Composite helicopter structure tested for crashworthiness
21 p3091 A83-44875
- Aircraft crashworthiness and the manufacturer's tort liability in the United States
22 p3367 A83-45808
- Safe structures for future aircraft
22 p3254 A83-46350
- CRATERING**
- NT PROJECTILE CRATERING
- Impact events at the Cretaceous-Paleogene boundary
01 p0129 A83-11325
- Interpreting the cratering record - Mercury to Ganymede and Callisto
04 p0570 A83-16234
- Cratering time scales for the Galilean satellites
04 p0548 A83-16235
- Experimental simulation of impact cratering on icy satellites
04 p0570 A83-16236
- Diaplectic labradorite glass from the Manicouagan impact crater. I - Physical properties, crystallization, structural and genetic implications
07 p0950 A83-21046
- Crater ejecta scaling laws - Fundamental forms based on dimensional analysis
09 p1366 A83-25074
- Asteroid and comet bombardment of the earth
14 p2095 A83-33483
- Impact experiments on ice --- for understanding cratering on Callisto and Mimas
18 p2779 A83-40322
- Asteroids and meteorites - Parent bodies and delivered samples
22 p3388 A83-47088
- CRATERS**
- NT LUNAR CRATERS
- NT MARS CRATERS
- NT METEORITE CRATERS
- NT PLANETARY CRATERS
- The geology of Ganymede
04 p0571 A83-16238
- The geology of Europa
04 p0571 A83-16239
- Cratering experiments in sands and a trial for general scaling law
07 p0950 A83-21318
- Comment on 'A schematic model of crater modification by gravity' by H. J. Melosh
09 p1367 A83-25075
- Giant volcanic calderas
14 p2054 A83-33099
- Escape of ejecta from cratered solar system satellites
21 p3224 A83-44740
- CRAZING**
- U SURFACE CRACKS
- CREATINE**
- Estimation of skeletal muscle mass from body creatine content
11 p1637 A83-27803
- CREATION**
- U CREATIVITY
- CREATIVITY**
- Reflection and the organization of creative thinking and the self-development of personality
18 p2737 A83-40559
- CREEP ANALYSIS**
- Analysis of test system misalignment in the creep test
01 p0026 A83-10648
- A study of the creep of thin-walled shells under nonstationary loading
01 p0059 A83-10681
- Calculating the limiting state of refractory alloys under high-cycle loading
01 p0026 A83-10687
- The stress factor in metal-creep equations
01 p0026 A83-11347
- Enhancement of the diffusional creep of polycrystalline Al₂O₃ by simultaneous doping with manganese and titanium
02 p0159 A83-11668
- Particle-coarsening, sigma-0 and tertiary creep
04 p0462 A83-16268
- Creep of ceramics. I - Mechanical characteristics
05 p0619 A83-17557
- Mechanical description of creep damage state and its experimental verification
07 p0945 A83-20365
- Introduction to the viewpoint set on creep cavitation
07 p0886 A83-20626
- Analysis of creep rupture data of Nimocast alloy 739
07 p0893 A83-21473
- The suppression of creep cavitation and slow crack growth in Si-Al-O-N ceramics
08 p1070 A83-21781
- Modeling the creep and fracture of the directionally solidified gamma/gamma-prime-McC eutectic
08 p1068 A83-22786
- Beryllium microdeformation mechanisms
09 p1231 A83-24058
- On the power-law breakdown during high temperature creep of fcc metals
09 p1231 A83-24059
- Creep crack extension by grain-boundary cavitation
09 p1279 A83-24070
- Criteria for prolonging the safe operation of structures through the assessment of the onset of creep damage using nondestructive metallographic measurements
09 p1275 A83-24081
- Effect of cavities on creep
09 p1283 A83-25206
- Study of the constitutive creep laws using biaxial relaxation tests
10 p1393 A83-25416
- A unified analysis of high-temperature creep rates from a point of view of recovery
12 p1712 A83-29224
- Notion of continuum damage mechanics and its application to anisotropic creep damage theory
13 p1866 A83-30241
- A study of the creep behavior of turbomachine components
13 p1867 A83-31320
- Diffusive relaxation of stress concentrations at grain boundary cavities in elevated temperature creep
14 p2033 A83-33452
- Viscoplasticity and creep using boundary elements
15 p2174 A83-33859
- Boundary element methods in creep and fracture --- Book
17 p2518 A83-37159
- A model based on nonlinear oscillations to explain jumps on creep curves. II - Approximate solutions
18 p2699 A83-39553
- A criterion for predicting creep fracture mechanisms
19 p2858 A83-41290
- Microstructural contributions to friction stress and recovery kinetics during creep of the nickel-base superalloy IN738LC
19 p2822 A83-42026
- Uniaxial and biaxial transient creep behavior of aluminum alloy
21 p3111 A83-44057
- Stress analysis for creep --- Book
21 p3160 A83-45097
- A creep theory for hardenable materials
21 p3163 A83-45362
- Creep of thin-walled circular cylinder under axial force, bending, and twisting moments [ASME PAPER 83-GT-154]
23 p3469 A83-47980
- Nonlinear creep problems for variable-boundary aging bodies
23 p3472 A83-48464
- Mechanical parameters applied to the propagation of creep cracks
24 p3591 A83-48995
- Anisotropic creep damage in the framework of continuum damage mechanics [ONERA, TP NO. 1983-90]
24 p3593 A83-49409
- Steady state and transient creep of Al at 400 K - An analysis in terms of recovery controlled by thermally activated glide
24 p3566 A83-49600
- CREEP BUCKLING**
- A finite element analysis of creep deformation in a specimen containing a macroscopic crack
08 p1117 A83-21694
- Numerical interpretations of creep buckling behavior of columns
09 p1282 A83-25105
- Creep buckling of structures [AIAA 83-0864]
12 p1738 A83-29752
- The creep of three-layer reinforced cylindrical panels
13 p1866 A83-30308
- On the analysis of creep stability and rupture
20 p3003 A83-42932
- Creep and stability of shallow elastic shells of revolution --- Russian book
21 p3150 A83-43916
- CREEP DIAGRAMS**
- A study of the mechanism of the steady-state creep of aluminum under compression
03 p0300 A83-14161
- Experimental examination of several material hypotheses on the basis of mutual predetermination of stress-strain and creep curves --- German thesis
07 p0873 A83-20393
- Creep damage and fracture --- in wrought and cast precipitation-hardened superalloys
07 p0892 A83-21468
- Some interactions of creep and fatigue in IN 738 LC at 850 C
07 p0893 A83-21472
- Deformation of polycrystalline materials at high temperatures
07 p0874 A83-21604
- A model based on nonlinear oscillations to explain jumps on creep curves. II - Approximate solutions
18 p2699 A83-39553
- CREEP PROPERTIES**
- NT SHEAR CREEP
- NT STEADY STATE CREEP
- NT TENSILE CREEP
- Thermal activation analysis of the structural stability of refractory alloys and computer simulation of the fracture process
01 p0024 A83-10391
- Predicting the thermal ratcheting and creep behaviour of a component with a stress concentration
01 p0060 A83-11032
- Induced creep and creep/fatigue of a nickel-base superalloy at ambient temperatures
02 p0157 A83-12415
- An evaluation of four creep-fatigue models for a nickel-base superalloy
03 p0299 A83-13904

Damage accumulation and fracture life in high-temperature low-cycle fatigue 03 p0339 A83-13905

Investigation of the thermoelastoplastic state of shells of revolution with allowance for creep deformations 03 p0340 A83-14067

A creep type strategy used for tracing the load path in elastoplastic post buckling analysis 04 p0494 A83-15009

Analysis of ductile deformation processes on the basis of a mixed variational principle 04 p0497 A83-15387

A unified, self-consistent theory for the plastic-creep deformation of metals 04 p0498 A83-15678

A bimodulus elasticity theory --- Russian book 04 p0499 A83-15833

A theory of plasticity and creep with allowance for microcracking 04 p0499 A83-15880

Estimates and asymptotics of the stress-strain state of a three-dimensional body with a crack in the theory of elasticity and the theory of creep 04 p0500 A83-15884

Compressive creep of Si₃N₄/MgO alloys 04 p0463 A83-15992

On dislocation-incoherent particle interactions at high temperatures 04 p0461 A83-16254

Correlations between cavitation, creep and dilation for multiaxial loading 04 p0501 A83-16269

The influence of fatigue stress on the creep behaviour of metals 04 p0462 A83-16275

Cyclic creep behavior of pure aluminum 05 p0614 A83-17089

Creep of ceramics. I - Mechanical characteristics 05 p0619 A83-17557

Role of cracks in the creep deformation of brittle polycrystalline ceramics 05 p0619 A83-17560

The creep behavior of inhomogeneously aging bodies 05 p0656 A83-17774

Problems in environmentally-affected creep crack growth 06 p0728 A83-18481

Creep cavitation of grain interfaces 06 p0728 A83-18483

Predicting the creep behavior of a unidirectionally reinforced composite with thermorheologically simple structural components 06 p0725 A83-18511

The relationship between the time to failure and the minimum creep rate during long-term loading under plane stressed state 06 p0733 A83-19309

Net-stress analysis in creep mechanics 06 p0778 A83-19324

A study of the elastic-plastic state of bodies of revolution under variable nonisothermal loading with allowance for creep 06 p0778 A83-19543

Parametric representation of crack growth rate under creep, fatigue and creep-fatigue interaction at high temperatures 07 p0883 A83-19671

Mixed variational principle of creep theory in problems of long-term strength 07 p0945 A83-19946

Anelastic relaxation controlled cyclic creep and cyclic stress rupture behavior of an oxide dispersion strengthened alloy 07 p0885 A83-20263

Intergranular cavitation in creeping alloys 07 p0887 A83-20627

Models of creep cavitation and their interrelationships 07 p0887 A83-20628

Mechanisms of cavity growth in creep 07 p0887 A83-20629

Determination of the stress-strain state and time to fracture of structural elements with allowance for material damage in the process of creep 07 p0946 A83-20907

Creep strengthening mechanisms 07 p0892 A83-21466

The effect of hot corrosion on creep and fracture behaviour of cast nickel-based superalloy IN738LC 07 p0895 A83-21490

The creep of silicon carbide fibres 07 p0901 A83-21572

The growth of macroscopic cracks in creeping materials 08 p1117 A83-21693

High strain fracture analysis 08 p1062 A83-21739

Metallographic aspects of creep fracture in a cast Ni-Cr-base alloy 08 p1062 A83-21745

On the relation between the creep mechanism and creep fracture 08 p1118 A83-21748

Effect of hold times on the elevated temperature fatigue crack growth behavior of Inconel 718 alloy 08 p1064 A83-21782

Influence of environment on fracture 08 p1065 A83-21798

Evaluation of creep crack growth criteria for IN-100 at elevated temperature 08 p1066 A83-22142

Creep of rotors under triaxial tension 09 p1276 A83-23361

Creep and fracture of engineering materials and structures; Proceedings of the International Conference, University College of Swansea, Swansea, Wales, March 24-27, 1981 09 p1279 A83-24051

Recovery and work hardening during high temperature creep of fcc alloys of low stacking fault energy 09 p1231 A83-24055

Creep of directionally solidified superalloys and eutectic composites 09 p1232 A83-24062

A theoretical consideration of the microstructural origins of friction stress in a cast gamma prime-strengthened superalloy 09 p1232 A83-24063

Factors controlling the creep behavior of a nickel-base superalloy 09 p1232 A83-24065

A unifying view of the kinetics of creep cavity growth 09 p1279 A83-24066

Cavitation in nickel during oxidation and creep 09 p1232 A83-24067

Models for intergranular creep crack growth by diffusion 09 p1279 A83-24069

Mechanisms of creep deformation and fracture in single and two-phase Si-Al-O-N ceramics 09 p1238 A83-24072

Deformation of polycrystalline alpha-SiC 09 p1239 A83-24073

Microstructural aspects of the creep of alloys based on Nimonic 80A 09 p1232 A83-24075

Role of grain boundary segregation in diffusional creep 10 p1396 A83-25859

Crack and cavity nucleation at interfaces during creep 10 p1396 A83-25861

The effects of segregation on the kinetics of intergranular cavity growth under creep conditions 10 p1396 A83-25862

High temperature embrittlement of Ni and Ni-Cr alloys by trace elements 10 p1396 A83-25863

The effect of cerium on high temperature tensile and creep behavior of a superalloy 10 p1396 A83-25864

Improving the quality of diffusion bonded joints in QT-4 alloy workpieces containing argon-arc welded joints 10 p1436 A83-26218

On the question of damage and fracture criteria in creep 11 p1549 A83-28501

An approach to the analysis of the compliance of threaded connections in creep 11 p1598 A83-28502

Effect of ion implantation on creep of molybdenum 11 p1551 A83-28806

The fracture of 15Kh1M1F steel in creep as a function of the type of structure 13 p1819 A83-30067

A study on the notch effect on the low cycle fatigue of metals in creep-fatigue interacting conditions at elevated temperature 13 p1820 A83-30240

The asymptotic behavior of the stress-strain state of inhomogeneously aging bodies near the tip of a crack 14 p2030 A83-32352

Creep-fatigue-environment interactions --- Book 14 p1993 A83-32650

Creep and high temperature deformation of simple metals and superalloys 14 p1995 A83-32807

A study of the low-cycle fatigue of the structural alloys for cryogenic applications 14 p1998 A83-33018

Viscoelastic characterization of a random fiber composite material employing micromechanics 14 p1988 A83-33297

The influence of creep and transformation plasticity in the analysis of stresses due to heat-treatment 15 p2175 A83-34240

Stability of crack extension rates in ductile materials 15 p2179 A83-34483

Mechanisms of creep crack growth 15 p2179 A83-34484

Micromechanisms of creep crack growth in nickel based superalloys 15 p2139 A83-34486

Temperature dependence of creep crack growth in aluminum alloy RR58 15 p2139 A83-34487

The effect of creep on the magnitude of elastic deformation in a laminated composite 16 p2323 A83-35506

Creep crack growth 16 p2331 A83-36167

A study relating slip steps and substructure produced during creep of an Al-Zn alloy 17 p2486 A83-37298

Creep behavior of aluminum-nickel alloys 17 p2491 A83-38475

Constitutive behavior and crack tip fields for materials undergoing creep-constrained grain boundary cavitation 17 p2492 A83-38860

Annealing of Hg₂Cl₂ crystals - Project of the experiment --- in space and terrestrial conditions 18 p2644 A83-39913

Creep behaviour of carbon-epoxy (+ or - 45 deg)2s laminates 18 p2655 A83-40209

High temperature creep properties of alpha Ti-Ti₅Ge₃ 18 p2667 A83-40256

Creep crack growth behavior of several structural alloys --- superalloys 18 p2669 A83-40636

Viscosity and conductivity of the lower mantle - An experimental study on a MgSiO₃ perovskite analogue, KZnF₃ 19 p2865 A83-41175

Elastic-plastic-creep behaviour of a compact-tension specimen 20 p3002 A83-42831

Creep behaviour of hot isostatically pressed niobium alloy powder compacts 21 p3111 A83-44332

Creep and fracture initiation in fibre reinforced plastics 22 p3264 A83-46296

Evaluation of a uniaxial nonlinear, second-order differential overstress model for rate-dependence, creep and relaxation 23 p3470 A83-48092

Creep and internal oxidation of reaction bonded silicon nitride 23 p3437 A83-48295

Environmental effects on high temperature creep properties of Ni - 20 Cr - W alloys in air, vacuum and helium 24 p3565 A83-49516

Work-hardening rates during the high temperature creep of aluminium determined from the instantaneous strain on sudden stress changes 24 p3567 A83-49875

CREEP RESISTANCE

U CREEP STRENGTH

CREEP RUPTURE STRENGTH

Creep fracture by coupled power-law creep and diffusion under multiaxial stress 02 p0197 A83-12930

Micromechanism-dependent model of the high-temperature strength and lifetime of particle-hardened alloys 04 p0461 A83-16174

Anelastic relaxation controlled cyclic creep and cyclic stress rupture behavior of an oxide dispersion strengthened alloy 07 p0885 A83-20263

Mechanisms of intergranular cavity nucleation and growth during creep 07 p0887 A83-20630

Continuous cavity nucleation and creep fracture 07 p0887 A83-20631

A description of the long-term strength under stepped loading 07 p0946 A83-20902

Creep damage and fracture --- in wrought and cast precipitation-hardened superalloys 07 p0892 A83-21468

Analysis of creep rupture data of Nimocast alloy 739 07 p0893 A83-21473

Alloy design for nickel-base superalloys 07 p0894 A83-21484

The effects of section size, coating and environment on creep rupture behaviour of superalloys 07 p0894 A83-21487

The influence of applied coatings on the creep fracture of IN 738 LC 07 p0894 A83-21488

A finite element analysis of creep deformation in a specimen containing a macroscopic crack 08 p1117 A83-21694

An incremental crack growth model for high temperature rupture in metals 08 p1059 A83-21695

Study of fracture criteria for ductile rupture of A508 steel 08 p1059 A83-21701

Creep fracture behavior of austenitic stainless steels from 550 to 800 C 08 p1062 A83-21746

Static fatigue of preoxidized hot-pressed silicon nitride 08 p1071 A83-22201

Anelastic relaxation, cyclic creep and stress rupture of gamma prime and oxide dispersion strengthened superalloys 09 p1232 A83-24074

Analysis of the causes of scatter in stress rupture properties of a nickel-base superalloy 09 p1233 A83-24076

Effect of grain flow on creep properties of heat-resistant aluminium-alloy forgings 10 p1394 A83-25473

A study of the effect of notches and cracks on creep rupture life 12 p1713 A83-29225

Effect of boride stress rupture properties of an FeNiCr-base alloy 13 p1820 A83-30323

The effects of B and Zr on the creep and fatigue crack growth behavior of a Ni-base superalloy 14 p1994 A83-32679

Effect of cyclic stress on creep rupture strength of a cast superalloy with high Al and Ti contents 15 p2137 A83-34002

High-temperature static fatigue in ceramics 16 p2337 A83-36169

Effect of rigid grains separation on the diffusive growth of crack-like cavities on grain boundaries 17 p2491 A83-38526

High temperature uniaxial tensile stress rupture strength of sintered alpha SiC 18 p2671 A83-39051

Disaggregation and a fracture criterion under creep 18 p2698 A83-39484

The prediction of long term viscoelastic properties of fiber reinforced plastics 18 p2655 A83-40210

Long term strength of glass reinforced plastics 18 p2656 A83-40224

The high temperature creep of dispersion strengthened Ni-Al₂O₃ alloy 18 p2667 A83-40258

Cyclic creep and stress rupture of a mechanically alloyed oxide dispersion and precipitation strengthened nickel-base superalloy 18 p2669 A83-40633

- The effect of titanium on creep strength in 2.25 pct Cr-1 pct Mo steels 18 p2669 A83-40634
- Thermal stability in microstructure and rupture strength of directionally solidified Ni-Al-Ti eutectic alloys 19 p2819 A83-40775
- On the analysis of creep stability and rupture 20 p3003 A83-42932
- Creep fracture in polymers - Technique and data handling for a statistical characterization 20 p2958 A83-43470
- The effect of the unsteadiness of a stress field on crack growth in creep 20 p3008 A83-43525
- A simplified approach for evaluating secondary stresses in elevated temperature design [ASME PAPER 83-PVP-51] 20 p3009 A83-43727
- Time-temperature effects in nitride and carbide ceramics 23 p3437 A83-48288
- Properties of isostatically hot-pressed silicon nitride [ACS PAPER 168-B-83] 24 p3568 A83-48962
- Effect of hot corrosion on strength and fracture of a nickel-base superalloy subjected to creep-fatigue interaction 24 p3563 A83-49499
- CREEP STRENGTH**
- Threshold stresses in materials containing dispersed particles 02 p0149 A83-11864
- The effect of the stacking fault energy on the characteristics of the high-temperature creep of nickel-cobalt alloys 02 p0157 A83-12331
- Creep and long-term strength of 5VMTs alloy clad with alloy VN7 02 p0157 A83-12338
- Structural changes in tungsten single crystals during creep in the medium-temperature range 04 p0459 A83-15470
- Mechanisms and mechanisms of intergranular cavitation in creeping alloys 06 p0728 A83-18478
- Microdamage distribution in the volume of a polymer material under long-term creep 06 p0734 A83-18515
- Characteristics of the formation of the structure and properties of refractory niobium-base high alloys 06 p0729 A83-18746
- An experimental study of the correlation between the root-mean-square thermal displacements of atoms and the resistance to creep --- of nickel and aluminum alloys 06 p0729 A83-18750
- A study of the principles underlying the deformation and fracture of a polycrystalline molybdenum alloy under high-temperature cyclic creep. I - The long-term strength and creep 06 p0733 A83-19307
- A study of the principles underlying the deformation and fracture of a polycrystalline molybdenum alloy under high-temperature cyclic creep. II - Structural changes during creep 06 p0733 A83-19308
- A study of the high-temperature creep and long-term strength of a niobium alloy with a complex coating in an oxidizing medium 07 p0887 A83-20683
- Fatigue and creep considerations in the design of turbine components 07 p0949 A83-21461
- Creep strengthening mechanisms 07 p0892 A83-21466
- The interaction of high temperature corrosion and mechanical properties of alloys 07 p0893 A83-21470
- Fatigue-crack initiation in IMI 829 caused by high-temperature fretting 07 p0896 A83-21566
- The effect of instantaneous strain on creep measurements at apparent constant structure 09 p1231 A83-24057
- Prestrain-induced particle microcracking and creep cavitation in IN597 09 p1236 A83-25139
- Grain boundary sliding and stress concentration during creep 10 p1396 A83-25860
- Comparative evaluation of the effect of titanium and aluminum on properties of creep-resisting metal deposited by the argon-arc method 10 p1397 A83-26223
- The effect of environment and temperature on the fatigue behavior of titanium alloys 16 p2331 A83-36171
- Influence of stress cycling on creep behaviour of an Al-Mg alloy under strain ageing conditions 16 p2334 A83-36727
- Compressive creep and oxidation resistance of an Si3N4 material fabricated in the system Si3N4-Si2N2O-Y2Si2O7 16 p2337 A83-36950
- Characteristics of the viscoelastic behavior of heat-resistant polymers in creep (with reference to polyoxadiazole) 19 p2824 A83-41600
- Creep of structures - A continuous damage mechanics approach 20 p3001 A83-42520
- Structure and short-term creep resistance of alloy TsM2A after nitriding 21 p3112 A83-44479
- A study of the creep of cylindrical shells weakened by a hole 21 p3154 A83-44717
- Orientation dependence of creep behavior of single crystal gamma-prime (Ni3Al) 22 p3268 A83-45623
- Notch sensitivity of high-alloy nickel alloys 24 p3559 A83-48803
- Effect of heat treatments on the creep behaviour of a Ni-base single crystal superalloy [ONERA, TP NO. 1983-102] 24 p3561 A83-49413
- CREEP TESTS**
- Analysis of test system misalignment in the creep test 01 p0026 A83-10648
- The temperature and force dependence of the activation energy of cyclic creep for refractory alloys 03 p0301 A83-14730
- Creep response of strip-cast Al-1wt.%Mn-1wt.%Mg alloy to thermomechanical treatment 04 p0457 A83-14996
- Role of the strain history on the flow law for high temperature creep 04 p0457 A83-14998
- The effect of microstructure and environment on the crack growth behavior of Inconel 718 alloy at 650 C under fatigue, creep and combined loading 04 p0458 A83-14999
- Equivalence of indentation and compressive creep tests on a WC/Co hardmetal 04 p0460 A83-15997
- Particle-coarsening, sigma-0 and tertiary creep 04 p0462 A83-16268
- Surface deformation of Westerly granite during creep 07 p0959 A83-20097
- Mechanical description of creep damage state and its experimental verification 07 p0945 A83-20365
- High-temperature creep of unalloyed niobium in vacuum 07 p0889 A83-20903
- Factors influencing the creep behaviour of a cast Ni-Cr-base alloy 07 p0893 A83-21474
- Microstructural changes and deformation mechanisms during creep of an unidirectionally solidified gamma/delta and gamma/gamma'-alpha eutectic alloy at elevated temperature 07 p0897 A83-21610
- Creep deformation induced substructure in polycrystalline molybdenum 07 p0897 A83-21612
- Creep crack growth characterization of austenitic stainless steel 08 p1061 A83-21732
- Effect of doping simultaneously with iron and titanium on the diffusional creep of polycrystalline Al2O3 08 p1071 A83-22195
- Creep of plasma-sprayed-ZrO2 thermal-barrier coatings 08 p1072 A83-22273
- A microscopic approach of the aluminum creep rate at intermediate temperature 09 p1231 A83-24053
- Deformation and dislocation behaviour in metals and single-phase alloys at elevated temperatures 09 p1231 A83-24054
- Cavitation and creep crack growth in low alloy steels 09 p1233 A83-24077
- Effects of plastic prestrain on the creep of aluminium under biaxial stress 09 p1233 A83-24078
- Creep damage concepts and applications to design life prediction 09 p1233 A83-24080
- A study of the effect of notches and cracks on creep rupture life 12 p1713 A83-29225
- On the description of cyclic hardening under complex loading histories 13 p1822 A83-31170
- Microinitiation, micropropagation and damage 13 p1823 A83-31171
- Thermal stability of titanium alloys '685' and '5524S' 13 p1823 A83-31173
- Microstructure of aluminium during creep at intermediate temperatures. III - The rate controlling process 13 p1825 A83-31650
- The effects of extensional creep and creep recovery on the dynamic properties of an unfilled and filled crosslinked polyester resin 15 p2142 A83-35071
- A high temperature straining stage (300-1000 K) for a 200 kV microscope 15 p2166 A83-35253
- Creep/corrosion of two nickel alloys in combustion gas 16 p2329 A83-35692
- Creep-fatigue-effects in composites 16 p2324 A83-36172
- Effects of triaxial stressing on creep cavitation of grain boundaries 16 p2335 A83-36961
- Creep cavitation and fracture due to a stress concentration in 2-1/4 Cr-1 Mo 17 p2490 A83-38390
- The high temperature creep of dispersion strengthened Ni-Al2O3 alloy 18 p2667 A83-40258
- The influence of pack aluminized coatings on the creep behavior of Nimonic 105 20 p2953 A83-42256
- The effect of the parameters of cyclic loading on the kinetics of deformation and fracture of El826 alloy 21 p3114 A83-45317
- Time dependent properties of injection moulded composites 22 p3263 A83-46293
- On feasibility of accelerated creep measurements in some polymeric materials 22 p3263 A83-46295
- Gamma prime shape changes during creep of a nickel-base superalloy 23 p3432 A83-47855
- The stability of a stiffened cylindrical shell in creep 23 p3472 A83-48470
- Effect of hot corrosion on strength and fracture of a nickel-base superalloy subjected to creep-fatigue interaction 24 p3563 A83-49499
- Environmental effects on high temperature creep properties of Ni - 20 Cr - W alloys in air, vacuum and helium 24 p3565 A83-49516
- Influence of stress cycling on creep behaviour of an Al-Mg alloy under strain ageing conditions 24 p3566 A83-49598
- Creep of Kevlar 49 fibre and a Kevlar 49-cement composite 24 p3554 A83-50066
- CRESTATIONS**
- U TRAVELING WAVE TUBES
- CREAVASSES**
- NT GLACIERS
- CREVICES**
- U CRACKS
- CREW PROCEDURES (INFLIGHT)**
- Evaluation of the sensitivity and intrusion of workload estimation techniques in piloting tasks emphasizing mediational activity 07 p0980 A83-21075
- Application of advanced speech technology /AST/ in manned penetration bombers 10 p1459 A83-26302
- Space Station crew operations impact on ECLSS design [SAE PAPER 820839] 13 p1906 A83-30934
- Benchmarks for a computer system for NASA's Shuttle procedures simulator [AIAA PAPER 83-1089] 16 p2314 A83-36213
- CREW STATIONS**
- NT CREW WORK STATIONS
- Space-station crew-safety requirements 16 p2315 A83-36408
- CREW WORK STATIONS**
- Space Telescope neutral buoyancy mockup - A test bed for evaluating man/system interfaces 10 p1459 A83-26304
- Human factors in equipment development for the Space Shuttle - A study of the general purpose work station 10 p1459 A83-26310
- CREWS**
- NT FLIGHT CREWS
- NT SPACECREWS
- Astronauts and seamen - A legal comparison 07 p1002 A83-21389
- CRICKETS**
- NT BEETLES
- CRITERIA**
- NT STRUCTURAL DESIGN CRITERIA
- Evaluation of solar reflective surfaces for dish concentrators 11 p1607 A83-27237
- A new look at commonly used failure theories in composite laminates [AIAA 83-0837] 12 p1710 A83-29745
- The information content of tests employed for characterizing the physical preparation of humans 15 p2212 A83-34946
- Criteria for optimizing starting cycles for high performance fighter engines [AIAA PAPER 83-1127] 16 p2306 A83-36236
- CRITICAL EXPERIMENTS**
- Effect of the number density of heterogeneities on the critical diameter of condensed explosives 22 p3266 A83-46007
- CRITICAL FLICKER FUSION**
- A method for the quantitative integral evaluation of fatigue 01 p0085 A83-11400
- CRITICAL FLOW**
- Critical angle of incidence for the flow around spheroids 07 p0862 A83-19668
- Critical flashing flows in nozzles with subcooled inlet conditions 15 p2157 A83-33996
- Amplitude-dependent stability of boundary-layer flow with a strongly non-linear critical layer 17 p2509 A83-38924
- Initial-value problems for Rossby waves in a shear flow with critical level 23 p3449 A83-48122
- Heat transfer and flow resistance in the turbulent pipe flow of a fluid with near-critical state parameters 24 p3576 A83-49120
- CRITICAL FREQUENCIES**
- The correlation of f0F2 disturbances with variations in solar radio emission 01 p0129 A83-10592
- The stability of the diurnal variation of the degree of disturbance of f0F2 during the cycle of solar activity 01 p0071 A83-10593
- Calculation of electromagnetic fields and critical frequencies of waveguides of complex cross section 04 p0471 A83-15764
- Improving ionospheric maps using theoretically derived values of f(0)F/2/ 07 p0961 A83-20372
- Design of waveguide dielectric filters based on beyond-the-cutoff waveguides 09 p1257 A83-25164
- The statistical model of the F2-layer critical frequency 18 p2713 A83-39316

- Correlations between cyclic increments of F2-layer critical frequencies 18 p2713 A83-39317
- A model for the variations of the critical frequency of F2 layer during the negative phases of ionospheric storms 20 p3024 A83-43173
- The correlations between the typhoon and the (F)F(2) of ionosphere 21 p3172 A83-44518
- Estimation of the critical frequency of the F2-layer from the difference of the reflection heights of magnetoionic components 21 p3174 A83-45235
- Global distribution of the ionospheric F-layer critical frequency f0F2 21 p3177 A83-45446
- Short-term prediction of HF propagation 21 p3122 A83-45450

CRITICAL LOADING

- The effect of oscillations on the stability of cylindrical shells under axial compression 01 p0059 A83-10690
- An experimental method for determining the maximum stress during spalling 02 p0191 A83-12333
- Stability of composite plates in plane shear under mixed edge conditions 02 p0192 A83-12359
- The effect of a longitudinal delamination in a laminate cylindrical shell on the critical external pressure 02 p0192 A83-12360
- The role of the generalized fracture toughness in fracture mechanics [ASME PAPER 82-PVP-21] 02 p0157 A83-12768
- A study on threshold of macro-crack growth in a soft epoxy resin 05 p0618 A83-17101
- A solution to the three-dimensional stability problem for a rectangular plate given an inhomogeneous subcritical state 06 p0770 A83-18140
- Curve-plotting methods for peak load statistics 06 p0777 A83-19195
- Solution of bifurcation problems and limit load problems in certain nonlinear boundary-value problems of continuum mechanics 06 p0777 A83-19322
- On exactness of the kinematical approach in the structural shakedown and limit analysis 06 p0778 A83-19325
- Buckling of a thin-walled conical shell under axisymmetric loads beyond the elastic limit 07 p0947 A83-21087
- Buckling of a conical sandwich shell beyond the elastic limit under combined load 08 p1115 A83-21637
- Study of fracture criteria for ductile rupture of A508 steel 08 p1059 A83-21701
- The effect of overloads upon fatigue crack tip opening displacement and crack tip opening/closing loads in aluminum alloys 08 p1060 A83-21709
- Fractographic identification of subcritical to critical crack growth transition mechanisms in ceramics 08 p1069 A83-21743
- A criterion for hydrogen-induced fracture 08 p1063 A83-21760
- Dynamic stability boundaries for a sinusoidal shallow arch under pulse loads 08 p1122 A83-22148
- Combined loadings in the theory of plasticity --- Book 08 p1123 A83-23025
- A study of the effect of stresses below the fatigue limit on the life of D16T alloy under programmed loading 09 p1228 A83-23501
- An existence theorem for a non linear shell model in large displacements analysis 10 p1438 A83-25463
- On the geometrical theory of shell stability 11 p1597 A83-28473
- Uniform strengthening of plates with holes 11 p1600 A83-28773
- An analysis of the stress-strain state in the internal deformation zone during hot forming 12 p1733 A83-29280
- Stability analysis of a spherical shell of imperfect shape on the basis of an improved buckling pattern 12 p1735 A83-29292
- Finite element analysis of the buckling of variable thickness discs 13 p1867 A83-30845
- Statically permissible stress fields in incompressible media 14 p2030 A83-32353
- Stability of a thick neo-Hookean plate 15 p2177 A83-34342
- The temperature dependence of the ultimate stress for eutectic tungsten alloys with titanium, zirconium, and hafnium carbides 15 p2141 A83-35311
- The load-bearing behavior of shear-stressed square plates of fiber-reinforced composite materials under large deformations --- German thesis 17 p2520 A83-37499
- The stability of composite sandwich shells with load-carrying layers of different stiffness under axial compression and external pressure 17 p2521 A83-37561
- A model for determining the reliability of an aircraft wing structure 17 p2521 A83-37638
- Variational-difference method of calculating critical loads for shells of revolution 18 p2698 A83-39506

- Determination of critical dynamic axial compression stresses for rib-stiffened layered cylindrical shells 18 p2702 A83-40115
- Algorithm for investigating the stability of rings of variable thickness under nonuniform loading 18 p2702 A83-40120
- A method for determining the critical strain, delta IIIc, at the tip of a longitudinal shear crack 19 p2856 A83-40809
- On buckling paradox 20 p3001 A83-42349
- Residual strength predictions for ballistically damaged aircraft 20 p3001 A83-42540
- Buckling loads in the case of imperfect truncated conical shells under axial pressure 20 p3005 A83-42983
- Critical loading conditions and stress intensity factors for partial or entire closure of a Griffith crack under thermo-mechanical loading 21 p3157 A83-44909
- Load-shedding techniques for fatigue-threshold determination 21 p3161 A83-45149
- Review of experimental techniques for thin-walled structures liable to buckling. I - Neutral and unstable buckling 22 p3306 A83-46423
- Review of experimental techniques for thin-walled structures liable to buckling. II - Stable buckling 24 p3592 A83-48997

CRITICAL MACH NUMBER**U CRITICAL VELOCITY****U MACH NUMBER****CRITICAL MASS**

- The influence of a net charge on the critical mass of a neutron star 05 p0702 A83-17807
- The boundary between explosion and collapse in very massive objects 08 p1178 A83-21842

CRITICAL POINT

- Topology of cosmological models near critical points 01 p0125 A83-10907
- Measurement of temperature conductivity of pure fluids and binary mixtures with the aid of dynamic light scattering in the general region of the critical point --- German thesis 06 p0757 A83-18521
- Rarefaction shock wave near the critical liquid-vapour point 08 p1086 A83-23089
- Prediction of thermal conductivity and viscosity for some fluids in the near-critical region [AIAA PAPER 83-1475] 14 p2094 A83-32729
- Prediction of density and constant pressure specific heat for several fluids in the near-critical region [AIAA PAPER 83-1476] 14 p2094 A83-32730
- Diffusion across characteristic boundaries with critical points 20 p3043 A83-43121

CRITICAL PRESSURE

- The critical pressure of initiation of powdered explosives 06 p0726 A83-18003
- The effect of supercritical pressure gradients on heat transfer in turbine nozzle cascades 19 p2801 A83-42140
- Nonaxisymmetric buckling and supercritical behavior of elastic spherical shells in the case of a double critical value of load 23 p3473 A83-48537

CRITICAL REYNOLDS NUMBER**U CRITICAL VELOCITY****U REYNOLDS NUMBER****CRITICAL SPEED****U CRITICAL VELOCITY****CRITICAL STRESS****U CRITICAL LOADING****CRITICAL TEMPERATURE**

- High-temperature superconductivity --- Book 01 p0110 A83-10878
- Critical heat flux in a closed two-phase thermosyphon 18 p2684 A83-39849
- Theory of the Leidenfrost phenomenon 18 p2685 A83-39866
- Impurity scattering in partially dielectricized superconductors 19 p2904 A83-41000

CRITICAL VELOCITY

- Nonlinear forced oscillations of a rotating shaft carrying an unsymmetrical rotor at the major critical speed 07 p0939 A83-20288
- Unstable vibrations of an unsymmetrical shaft at the secondary critical speed due to ball bearings 07 p0939 A83-20291
- Low Reynolds number flow between interrupted flat plates 09 p1259 A83-23878
- On experimental methods for determining critical speeds --- of rotor systems 10 p1436 A83-26766
- On the critical speed of empennage flutter with allowance for the rudder 12 p1704 A83-29286
- Response in passing through critical speed of arbitrarily distributed flexible rotor system. I - Case without gyroscopic effect. II - Case with gyroscopic effect 21 p3148 A83-45475

CROCCO METHOD

- Non-isentropic potential formulation for transonic flows [AIAA PAPER 83-0375] 05 p0635 A83-16680

- A mathematical model for the dynamics of liquid-propellant rocket engines 24 p3552 A83-48928

CROP DUSTING

- Putting the microlight to work 09 p1195 A83-23686
- NASA wake interactions research and applications [SAE PAPER 830764] 20 p2930 A83-43329

CROP GROWTH

- Action plan for remote sensing applications for rice production --- Book [IFAORS-207] 03 p0345 A83-14121
- Investigation of the relationship between the seasonal dynamics of the spectral brightness coefficients of certain sorts of wheat and plant physiological parameters 07 p0951 A83-19911
- Monitoring the growth of crops using digital Landsat MSS data 09 p1288 A83-24588
- Role of auxin and protons in plant shoot gravitropism 11 p1638 A83-27813
- Effect of cultural conditions on the seed-to-seed growth of Arabidopsis and Cardamine - A study of growth rates and reproductive development as affected by test tube seals 11 p1639 A83-27825
- A comparative study of monocot and dicot root development in normal /earth/ and hypogravity /space/ environments 11 p1639 A83-27827
- Mechanical stress regulation of growth and photosynthetic productivity of Glycine max /L./ Merr. cv Wells II under different environmental regimes --- soybean plant growth retardation by shaking and rubbing 11 p1639 A83-27829
- Estimation of sugar beet productivity from reflection in the red and infrared spectral bands 15 p2188 A83-35285
- Discrimination of growth and water stress in wheat by various vegetation indices through clear and turbid atmospheres 17 p2526 A83-37620

CROP IDENTIFICATION

- Satellite orbital dynamics and observation strategies in support of agricultural applications 01 p0066 A83-10717
- Satellite remote sensing for domestic crop reporting in the United States and Canada - A look to the future 03 p0345 A83-14229
- Vegetation change detection in an agricultural area - A simple approach for use with geo-data base 03 p0345 A83-14236
- Potentials of Landsat-D and SPOT-1 for crop identification in the maritimes 03 p0346 A83-14240
- Classification of SAR imagery from an agricultural region using digital textural analysis 08 p1125 A83-21917
- Microwave radiometric signatures of corn 08 p1126 A83-21923
- Effects of vegetation cover on the microwave radiometric sensitivity to soil moisture 08 p1129 A83-22681
- Seasat synthetic aperture radar /SAR/ response to lowland vegetation types in eastern Maryland and Virginia 09 p1283 A83-24315
- Use of vegetation indicators for crop group stratification and efficient full frame analysis 09 p1288 A83-24587
- Remote sensing of row crop structure and component temperatures using directional radiometric temperatures and inversion techniques 10 p1443 A83-25644
- Discrimination of growth and water stress in wheat by various vegetation indices through clear and turbid atmospheres 17 p2526 A83-37620
- Visible light reflectance, transmittance, and absorbance of differently pigmented cotton leaves 17 p2526 A83-37622
- Identification of corn fields using multirate radar data 17 p2526 A83-37624
- The use of reflection spectra in recognition of crops 17 p2529 A83-38157
- Enhanced crop discrimination using the mid-IR (1.55-1.75 microns) 17 p2530 A83-38165
- The relationship between spectrometric and photographic methods for the remote sensing of earth resources 18 p2707 A83-40593
- An experiment in multispectral, multitemporal crop classification using relaxation techniques 21 p3165 A83-44267
- Microwave radiometric features of vegetated surfaces 21 p3166 A83-45419
- Active microwave signatures of soil and crops - Significant results of three years of experiments 22 p3308 A83-46104
- Ground truth measurements and results from the interpretation of multispectral data during the Convoir project at the Straubing test site (D9) 22 p3310 A83-46137
- Qualitative and quantitative evaluation of airborne scanner imagery for pedological and agricultural purposes in north Germany 22 p3310 A83-46162

On the design and operation of a SLAR system with digital recording 22 p3289 A83-46181

Wind influence on the backscattering coefficient from crops 22 p3312 A83-46186

A statistical model for radar images of agricultural scenes 22 p3312 A83-46191

Comparison of multifrequency band radars for crop classification 22 p3314 A83-46234

Classification of agricultural crops in radar images 22 p3315 A83-46239

Radar backscattering properties of corn and soybeans at frequencies of 1.6, 4.75, and 13.3. GHz 22 p3315 A83-46248

Remote sensing estimators of potential and actual crop yield 23 p3474 A83-47220

CROP INVENTORIES

AgRISTARS - Plans and first-year achievements --- Agriculture and Resources Inventory Surveys Through Aerospace Remote Sensing 01 p0065 A83-10095

Visual analysis of 1:250,000 Landsat data for forage assessment during the 1980 drought in western Manitoba 03 p0345 A83-14235

Aerial survey of crop losses due to grasshoppers /Orthoptera - Acrididae/ in Saskatchewan 03 p0347 A83-14255

The use of large-area spectral data in wheat yield estimation 05 p0657 A83-16910

A Canadian approach to large region crop area estimation with Landsat 08 p1126 A83-21932

Analysis of man-induced and natural resources of an arid region in California 09 p1285 A83-24543

Multispectral radiometer to measure crop canopy characteristics 13 p1845 A83-30259

The role of remotely sensed and other spatial data for predictive modeling - The Umatilla, Oregon, example 15 p2186 A83-34832

Estimation of shelter temperatures from operational satellite sounder data --- for farm crop monitoring 18 p2706 A83-39131

Large-area relation of Landsat MSS and NOAA-6 AVHRR spectral data to wheat yields 23 p3474 A83-47218

An effort to determine the weed content of agricultural fields in springtime 24 p3598 A83-49283

CROP INVENTORIES BY REMOTE SENSING

U AGRISTARS PROJECT

CROP VIGOR

Application of computer axial tomography /CAT/ to measuring crop canopy geometry --- corn and soybeans 01 p0065 A83-10096

Atmospheric effects on radiation reflected from soil and vegetation as measured by orbital sensors using various scanning directions 02 p0198 A83-12315

Computing and mapping Thiessen weighting factors from digitized district boundaries and climatological station latitudes and longitudes 02 p0217 A83-12964

A concept for global crop forecasting --- using microwave radiometer satellites 07 p0872 A83-21617

On the economic efficiency of using satellite data to assess the condition of crops 14 p2034 A83-32497

An investigation of the strength of action and the interaction of genes determining the differences in the stem length of Arabidopsis thaliana (L.) Heynh. (three hybrid cross) 18 p2733 A83-40573

The effect of irradiation and reflectance variability on vegetation condition assessment 20 p3011 A83-42965

CROPLANDS

U FARMLANDS

CROSS CORRELATION

The cross-correlation of the Zwicky and Shane-Wirtanen catalogs of galaxies 02 p0245 A83-11610

Effects of partial correlation on the multiple-access capability of direct-sequence spread spectrum 07 p0908 A83-19735

Determination of velocity gradients with scattered light cross-correlation measurements 07 p0928 A83-20165

Application of correlation technology to radio observation problems 09 p1244 A83-23413

A study of a correlation tracking method to improve imaging quality of ground-based solar telescopes 10 p1492 A83-25489

Cross spectral-correlation processing of signals in various orthogonal bases 10 p1470 A83-26951

Cross-correlation of velocity and temperature in a premixed turbulent flame 14 p1990 A83-32941

XP3K - A new cross-correlated phase-shift keying modulation technique 16 p2343 A83-36607

Dynamic optical cross-correlator using a liquid crystal light valve for real time data input 21 p3207 A83-44827

Signal sets with optimal correlation properties 22 p3272 A83-45740

CROSS COUPLING

SGEMP-induced transfer admittance coupling in cable bundles 05 p0628 A83-17522

The limits to hardening electronic boxes to IEMP coupling 05 p0628 A83-17523

Effects of finite wire scatterers in the field of VOR 06 p0716 A83-19039

Theory and design of narrow-passband stripline filters with finite transmission zeros realized with extra cross couplings 07 p0922 A83-21084

Dielectric and width effect on H-plane and E-plane coupling between rectangular microstrip antennas 09 p1246 A83-23780

Multivariable approach to the problem of structural cross coupling of force feedback electrohydraulic actuators --- for structural testing of aircraft and their components 10 p1379 A83-26601

Analysis and modeling of 'two-gap' coaxial line rectangular waveguide junctions 13 p1831 A83-30233

Mutual coupling and radiation patterns of two slots asymmetrically located on a square plate 15 p2149 A83-35197

Cancellation performance degradation of a fully adaptive Yagi array due to inner-element coupling 16 p2342 A83-36483

Mutual coupling between short-circuited microstrip antennas 16 p2342 A83-36484

Theory of multiplicative noise caused by coupling loss and amplitude vector rotation in optical communication channels 19 p2826 A83-40895

Coupling between two conical horns placed side by side 20 p2963 A83-42368

A theoretical study and an experimental evaluation of the mutual coupling effects in MIC array antennas 21 p3127 A83-45411

CROSS FAULTS

U GEOLOGICAL FAULTS

CROSS FLOW

Analysis and computation of heat transfer around a cylinder in argon plasma cross flow [ASME PAPER 82-HT-30] 02 p0171 A83-12789

Mass transfer in the neighborhood of jets entering a crossflow 02 p0173 A83-12802

A study of transverse turbulent jets in a cross flow --- for gas turbine combustion process modelling 02 p0136 A83-13100

A simple tandem disk model for a cross-wind machine 04 p0506 A83-15800

Analysis of multiple jets in a cross-flow [ASME PAPER 82-WA/FE-4] 04 p0478 A83-16140

Jet trajectories and surface pressures induced on a body of revolution with various dual jet configurations [AIAA PAPER 83-0080] 05 p0579 A83-16508

Prediction of liquid fuel spray capture by v-gutter downstream of plain orifice injector under uniform cross air-flow [AIAA PAPER 83-0153] 05 p0596 A83-16559

Some observations on the aerodynamics of an airfoil with a jet exhausting from the lower surface [AIAA PAPER 83-0173] 05 p0580 A83-16569

Maximum vortex-induced side force revisited --- for aerodynamic design [AIAA PAPER 83-0458] 05 p0586 A83-16727

Flow visualization studies of bodies with square cross sections [AIAA PAPER 83-0563] 05 p0637 A83-16791

Aerodynamic estimation techniques for aerostats and airships 06 p0712 A83-18404

Atomization of impinging liquid jets in a supersonic crossflow [AD-A130714] 07 p0924 A83-19806

Dynamic wind tunnel tests of the simulated Shuttle external cable trays 07 p0869 A83-20412

Prediction of the trajectory of triple jets in a uniform crossflow 10 p1418 A83-26629

The effect of a passive cross-stream temperature gradient on the evolution of temperature variance and heat flux in grid turbulence 12 p1723 A83-29233

Experimental investigation of multiple jets in a cross-flow [AIAA PAPER 83-1545] 14 p1971 A83-32768

Swirl characteristics of an S-shaped air intake with both horizontal and vertical offsets 16 p2289 A83-35621

The introduction of tangential or perpendicular nonisothermic plane jets into a turbulent crossflow for the purpose of film cooling 16 p2350 A83-35799

Perspectives on the mixing of a row of jets with a confined crossflow [AIAA PAPER 83-1200] 16 p2352 A83-36276

Effects of AP particle size on combustion response to crossflow [AIAA PAPER 83-1270] 16 p2340 A83-36317

CROSS POLARIZATION

Effects of Reynolds number and corner radius on two-dimensional flow around hexadecagonal cylinders [AIAA PAPER 83-1705] 17 p2502 A83-37202

Surface pressures induced on a flat plate with in-line and side-by-side dual jet configurations [AIAA PAPER 83-1849] 17 p2456 A83-38677

The effect of the wave injection of a fluid jet into a gas cross-stream 19 p2794 A83-42155

Effects of free stream turbulence intensity and integral length scale on heat transfer from a circular cylinder in crossflow 20 p2976 A83-42711

Theoretical and experimental study of turbulence effects on heat transfer around the stagnation point of a cylinder 20 p2976 A83-42713

Cross flow influence upon impingement convective heat transfer in circular arrays of jets - A general correlation 20 p2978 A83-42741

Spanwise mass transfer variations on a cylinder in 'nominally' uniform crossflow 20 p2984 A83-43019

Experiments on a crossflow heat exchanger with tubes of lenticular shape 20 p2986 A83-43364

An efficient, full-potential implicit method based on characteristics for supersonic flows 20 p2930 A83-43442

Effect of crossflow on the vortex-layer-type three-dimensional flow separation 22 p3250 A83-47018

Cross-hatching - An interaction between shock and turbulent boundary layer 22 p3286 A83-47030

Heat transfer characteristics for jet array impingement with initial crossflow [ASME PAPER 83-GT-28] 23 p3393 A83-47891

Penetration and break-up behaviour of a discrete liquid jet in a cross flowing airstream - A further study [ASME PAPER 83-GT-170] 23 p3448 A83-47971

On the force fluctuations acting on a circular cylinder in crossflow from subcritical up to transcritical Reynolds numbers 23 p3398 A83-48118

Local heat transfer rates from two adjacent spheres in turbulent flow 23 p3451 A83-48624

The periodic normal force on a circular cylinder in cross flow - An unsteady Magnus effect 24 p3544 A83-49022

A 3-D laser Doppler velocimeter for use in high-speed flows 24 p3585 A83-49825

CROSS POLARIZATION

Microwave propagation in sand and dust storms 02 p0162 A83-11551

Crosspolarisation in scattering at low frequencies 02 p0163 A83-11553

Ground station antenna crosspolarisation measurements with an imperfectly polarised ancillary antenna 02 p0164 A83-11986

A curved-aperture corrugated horn having very low cross-polar performance 03 p0305 A83-14005

Crosspolar levels of ring arrays in reflection at 45 deg incidence - Influence of lattice spacing 04 p0466 A83-15252

Characteristics of the cross-polarized radiation of dielectric rod lenses 04 p0466 A83-15718

Dual offset reflectors shaped for zero crosspolarisation with asymmetric feed pattern 04 p0468 A83-16204

Effects of element cross-polarisation in adaptive antennas 06 p0739 A83-18626

OTS propagation experiments with radar, electric field and thunder location data 06 p0744 A83-18699

Correlation of slant path ice depolarization events at 28.56 GHz with radar reflectivity structure and the determination of ice depolarization statistics for Wallops Island, Virginia 06 p0744 A83-18700

Attenuation and crosspolarisation on satellite-earth paths observed with O.T.S. beacons 06 p0745 A83-18709

Measurements of tropospheric fading and crosspolarisation in the Arctic using orbital test satellite 06 p0745 A83-18711

RF methods for adaptive cancellation of cross polarisation in microwave satellite systems 06 p0746 A83-18728

Crosspolarisation properties of reflector antennas with random surface errors 08 p1074 A83-21974

Direct- and cross-polarized scatter from a turbulent laboratory plasma 10 p1486 A83-26050

Calculation of the cross-polarization in the far field of waveguide radiators 10 p1412 A83-26888

Difference-channel cross-polarization patterns of parabolic antennas 11 p1559 A83-28687

Effects of choke-load position on radiation properties in double-choked small horn antennas 13 p1830 A83-31778

Experimental study of edge effects in open resonators in the millimeter-wave range 14 p2003 A83-32108

Cross-polarized radar image anomalies as sensitive measures of L-band vegetation penetration capability 15 p2187 A83-34846

- Theoretical model for calculating rain-induced crosspolarisation 17 p2495 A83-38878
 Cross polarization discrimination during multipath fading activity 19 p2829 A83-41355
 Bootstrapping adaptive cross pol cancelers for satellite communications 19 p2831 A83-41386
 Effect of ice-induced cross-polarization on digital earth-space links 19 p2833 A83-41400
 Axial cross polarization in reflector antennas with surface errors of large correlation diameter 23 p3443 A83-47841

CROSS SECTIONS

- Electron loss from fast one-electron ions colliding with He, N₂, and Ar 01 p0105 A83-10194
 Investigation of regular waveguides of arbitrary cross section by the method of equivalent sources 04 p0470 A83-15729
 A note on total cross sections and decay rates in the presence of a laser field 10 p1425 A83-25409
 Direct radiative recombination of electrons with atomic ions Cross sections and rate coefficients 16 p2415 A83-35655
 Improvement of calculations of cross sections and cosmic-ray propagation 23 p3540 A83-47758

CROSSED FIELD AMPLIFIERS

- Investigation of nonperiodic crossed-field systems using a model of particles of variable charge 13 p1832 A83-30701
 Theoretical study of processes in a system with 'conjugate' M-type interaction 13 p1833 A83-30705

CROSSED FIELDS

- Additional noise sources in cross-field microwave devices 01 p0044 A83-11310
 Theory of the motion of a relativistic charged particle in highly nonuniform crossed electric and magnetic fields 09 p1348 A83-23984
 Finite parallel wavelengths and ionospheric structuring 13 p1879 A83-31239
 The healing of cracks in metals by means of crossed electric and magnetic fields 14 p1993 A83-32383
 A kinetic cross-field streaming instability 14 p2087 A83-33387
 Stability of relativistic laminar flow equilibria for electrons drifting in crossed fields 17 p2496 A83-37042
 Rotating electron beam in crossed fields - Space charge, nonlinear effects 17 p2500 A83-38987

CROSSEFFECTS

- The effects of extensional creep and creep recovery on the dynamic properties of an unfilled and filled crosslinked polyester resin 15 p2142 A83-35071
 Crosslinking of fluorocarbon elastomers - Characterization of crosslinking system to obtain transparent, tough materials 22 p3270 A83-46906

CROSSTALK

- NT IONOSPHERIC CROSS MODULATION
 Electrical and acoustical crosstalk in integrated optical strip waveguide devices 02 p0168 A83-13044
 Cross-talk fiber-optic temperature sensor 07 p0930 A83-20833
 Crosstalk and loss of information in holography 16 p2355 A83-35890
 X-ray imaging of extended objects using nonoverlapping redundant array 19 p2847 A83-41104
 Splicing of single polarization-maintaining fibers 21 p3204 A83-44205
 8 km-long polarisation-maintaining fibre with highly stable polarisation state 24 p3630 A83-49974

CRUCIFORM WINGS

- Application of the Carafoli method to the supersonic flow around a cruciform wing 01 p0003 A83-10581
 Subsonic rolling moments for wing roll control of a cruciform missile model 09 p1210 A83-24876
 Experimental investigation of rolling moment for a body-wing-tail missile configuration with wrap around wings and straight tails at supersonic speeds [AIAA PAPER 83-2081] 19 p2805 A83-41915

CRUDE OIL

- Applications of remote sensing to petroleum exploration 01 p0062 A83-10030
 Exploration for fractured petroleum reservoirs using radar/Landsat merge combinations 01 p0062 A83-10031
 The effect of the melt heat treatment time on the properties of lithium lubricants with additives 10 p1401 A83-26921
 Jet fuels based on West Siberian oils 14 p1999 A83-32077

CRUISE MISSILES

- NT TOMAHAWK MISSILES
 Strapdown inertial performance needed for the 1990s 01 p0005 A83-11127
 Operational software evaluation for the Air Launched Cruise Missile fly-off 01 p0093 A83-11248
 The Magnuswirl turbine wheel - The unique solution for the high temperature cruise missile 09 p1274 A83-23647

- U.S. cruise missile programs: Development, deployment and implications for arms control --- Book 15 p2119 A83-33769
 Cruise flight of a tail mounted ramjet 16 p2303 A83-35805
 Cruise missile propulsion versus commercial airliner propulsion - Different challenges can produce similar engine cycles [AIAA PAPER 83-1176] 16 p2307 A83-36261
 Small turbine engine experience with high density fuels [AIAA PAPER 83-1177] 16 p2339 A83-36262

CRUISING FLIGHT

- Fuel-optimal aircraft trajectories with fixed arrival times 04 p0446 A83-16115
 A comparison of trim drag for conventional and supercritical wings [AIAA PAPER 83-0094] 05 p0579 A83-16518
 Supercritical airfoil boundary-layer and near-wake measurements 09 p1196 A83-24027
 Measurements and predictions of turboprop noise at high cruise speed [AIAA PAPER 83-0689] 11 p1651 A83-28008
 Transonic flows with viscous effects 12 p1698 A83-29935
 Application of maximum likelihood estimation to the identification of the stability derivatives of a wide body transport aircraft 15 p2123 A83-35121
 Optimal mass distribution between the stages of a two-stage aircraft for maximization of the flight cruise range 17 p2462 A83-37267
 Effects of nacelle position and shape on performance of subsonic cruise aircraft [AIAA PAPER 83-1124] 17 p2464 A83-38079
 Intensity of focused sonic booms in straight flight at constant altitude 18 p2742 A83-39424

CRUSADER AIRCRAFT**U F-8 AIRCRAFT****CRUSHING**

- Crushing analysis of rotationally symmetric plastic shells 01 p0060 A83-11031
 Adsorption and excess fission Xe - Adsorption of Xe on vacuum crushed minerals 04 p0564 A83-15376
 Simplified crushing analysis of thin-walled columns and beams 04 p0500 A83-16197

CRUSTAL FRACTURES

- Airborne laser ranging system for monitoring regional crustal deformation 01 p0047 A83-10024
 Variations in the earth's rotation and crustal deformations 02 p0205 A83-11997
 Lithospheric flexure at fracture zones 02 p0212 A83-12870
 Convective thinning of the lithosphere - A mechanism for the initiation of continental rifting 02 p0212 A83-12871
 Relative lateration across the Los Angeles basin using a satellite laser ranging system 07 p0952 A83-21524
 Thermal parameters of the oceanic lithosphere estimated from geoid height data 08 p1144 A83-22363
 On the size distribution of solid jointings --- in rocks formed by geological fracture processes 13 p1873 A83-30005
 Patterns of fracture and tidal stresses on Europa 13 p1961 A83-31203
 The internal structure of the earth and its concentric faults 13 p1880 A83-31348
 How continents break up 16 p2377 A83-36020
 Fractures of the earth's crust according to space remote sensing data and their connection with mineral resources (using the example of the Urals) 17 p2526 A83-37697
 Global tectonics and metallogeny - Deep roots of some ore-controlling fracture zones: A possible relation to small-scale convective cells at the base of the lithosphere? 17 p2529 A83-38153
 Deep crustal structure - Implications for continental evolution 22 p3323 A83-45779
 Transregional faults in the northeastern part of the USSR appearing in space photographs 23 p3483 A83-48107

CRUSTS

- NT EARTH CRUST
 NT LUNAR CRUST
 Craters and basins on Ganymede and Callisto - Morphological indicators of crustal evolution 04 p0570 A83-16237
 Investigation of the isostatic state of the Elysium dome on Mars by gravity models 17 p2623 A83-38696
 The oceanic crust 20 p3020 A83-42818

CRYODEPOSIT

- Cryodeposit mass transfer at near vacuum in nonisothermal enclosures 20 p2973 A83-42689
 Cryolithogenesis --- Russian book 21 p3169 A83-43919

CRYOGENIC COOLING

- Application of JFets to low background focal planes in space 03 p0308 A83-13456
 Cryo-cooler development for space flight applications 03 p0303 A83-13460
 Practical problems of design and manufacture of a 2-D model and of the device for its cooling and introduction into the T2 pressurized cryogenic intermittent tunnel [ONERA, TP NO. 1982-88] 03 p0282 A83-14540
 IR optical properties of thin CO, NO, CH₄, HCl, N₂O, O₂, N₂ and Ar cryofilms [AIAA PAPER 83-0244] 05 p0684 A83-16610
 Calculation of the energy characteristics of a pulse-periodic electron-beam-controlled CO₂ laser with a cooled active mixture 07 p0935 A83-20131
 Helium purge flow prevention of atmospheric contamination of cryogenically cooled optics on orbiting infrared telescopes 08 p1074 A83-22723
 Fabrication of cryogenic mirrors 08 p1112 A83-22870
 Control of cryogenic Fourier transform spectrometer scanning mirrors 09 p1267 A83-23591
 A near omnidirectional sunshade for cryogenic instruments [SAE PAPER 820842] 10 p1383 A83-25754
 Rocketborne cryogenic /10 K/ high-resolution interferometer spectrometer flight HIRIS - Auroral and atmospheric IR emission spectra [AD-A128358] 10 p1423 A83-26642
 The effect of parasitic refrigeration on the efficiency of magnetic liquefiers 11 p1552 A83-27212
 Steady flow examination of a cryocooler 11 p1564 A83-27289
 Space adapted cryogenics 11 p1553 A83-27737
 Heat transfer during the film boiling of liquids under conditions of free convection 11 p1570 A83-28555
 LOX/LH₂ propulsion system for launch vehicle upper stage. I System study 12 p1708 A83-29416
 Cryogenic testing of mirrors for infrared space telescopes 13 p1939 A83-31026
 Cryogenic testing of stepper motors 14 p1999 A83-31982
 Infrared optical properties of solid mixtures of molecular species at 20K [AIAA PAPER 83-1452] 14 p2084 A83-32717
 The resistance of structural materials to fracture during impact bending 14 p2033 A83-33015
 Cryogenic heat transfer - He-4 Kapitza conductances including phase change effects 20 p2971 A83-42660
 Advances in cryogenic engineering. Volume 27 - Proceedings of the Cryogenic Engineering Conference, San Diego, CA, August 11-14, 1981 20 p2960 A83-43220
 Thermodynamic aspects of small 4.2-K cryocoolers 20 p2960 A83-43224
 Semimetal cascades - Solid state precursors to spacecraft slush hydrogen refrigerators 20 p2961 A83-43233
 History, status and future applications of spaceborne cryogenic systems 20 p2961 A83-43240
 Progress report on the infrared astronomical satellite cryogenic system 20 p2961 A83-43242
 Performance of a superfluid helium facility for Spacelab payloads 20 p2961 A83-43243
 Integrating and testing the thermal model of the German Infrared Laboratory (GIRL) 20 p2961 A83-43244
 Development of gas gap cryogenic thermal switch 20 p2962 A83-43249
 Computer-aided infrared sensor thermal design 22 p3292 A83-46602
 Superconducting magnetic energy storage 22 p3320 A83-46780

CRYOGENIC EQUIPMENT

- Heat and mass transfer apparatuses in cryogenics --- Russian book 01 p0028 A83-10672
 CIRRIIS - A cryogenic infrared /IR/ radiance instrument for Shuttle 03 p0324 A83-13455
 Cryogenic infrared /IR/ spectral measurements on board the Space Shuttle - CIRRIIS 03 p0288 A83-13752
 Cryogenic X-band ferrite phase shifter/attenuator 08 p1079 A83-21977
 Cryogenic engineering --- Russian book 10 p1401 A83-25595
 Space adapted cryogenics 11 p1553 A83-27737
 Development and test at T equals 4.2 K of a capacitive resonant transducer for cryogenic gravitational-wave antennas 11 p1574 A83-28426
 Optimum design of dewar supports --- for launching and maintaining in long term orbit [AIAA 83-0829] 12 p1707 A83-29738
 Cryogenic infrared radiance instrument for Shuttle (CIRRIIS) telescope 14 p1983 A83-32004

Thermal conductance of pressed contacts at liquid helium temperatures 14 p2010 A83-32708

[AIAA PAPER 83-1436]

Mechanical tests of structural alloys at cryogenic temperatures 14 p1997 A83-33012

A study of the low-cycle fatigue of the structural alloys for cryogenic applications 14 p1998 A83-33018

A study of the high-cycle fatigue of materials under plane cantilever bending 14 p1998 A83-33020

Filament wound composite thermal isolator structures for cryogenic dewars and instruments --- glass fiber reinforced epoxy laminates for spaceborne equipment 14 p1982 A83-33120

A cryogenic Fabry-Perot for far infrared astronomy 18 p2692 A83-40461

230-271 GHz cryogenic radiometer 19 p2848 A83-41279

Pulsed ion beam generation with cryogenic-anode diode 20 p2959 A83-42584

Radiative properties of metals at cryogenic temperatures 20 p2974 A83-42694

Magnetically suspended Stirling cryogenic space refrigerator Status report 20 p2960 A83-43228

Novel titanium-aluminum joints for cryogenic cold finger structures 20 p2960 A83-43229

Single shot demountable self-contained He-3 refrigerator 20 p2960 A83-43230

Damping of thermoacoustic oscillations 20 p2961 A83-43234

Orbital performance of a one-year lifetime superfluid helium dewar based on ground testing and computer modelling 20 p2962 A83-43247

Development of gas gap cryogenic thermal switch 20 p2962 A83-43249

Instrumentation, data acquisition and reduction for a large spaceborne helium dewar 20 p2962 A83-43250

Cryogenic gas engines --- Russian book 21 p3117 A83-43925

30-MJ superconducting magnetic energy storage system for electric utility transmission stabilization 22 p3320 A83-46781

Dewar design for optically pumped semiconductor ring laser 23 p3461 A83-47646

CRYOGENIC FLUID STORAGE

Long term storage of cryogens in space 01 p0029 A83-11487

Leak-before-break characterization and demonstration of a high-pressurant helium storage vessel 08 p1118 A83-21773

Application of the turbo-refrigerator to long-term cryogenic storage 13 p1812 A83-30935

[SAE PAPER 820841]

Debris from spallation of foam insulation of cryogenic fuel tanks in space launch systems 14 p1980 A83-32718

[AIAA PAPER 83-1457]

Cryogenic fluid management experiment trunnion fatigue verification 14 p1982 A83-32782

[AIAA PAPER 83-0911]

Experimental study of flash boiling in liquid nitrogen 16 p2341 A83-36369

[AIAA PAPER 83-1378]

Condensation in the annulus of a double-walled cryogenic storage tank 20 p2961 A83-43237

Potential for catastrophic rupture of large liquid oxygen storage tanks 20 p2961 A83-43238

CRYOGENIC FLUIDS

NT FERMI LIQUIDS

NT LIQUID HELIUM

NT LIQUID HELIUM 2

NT LIQUID HYDROGEN

NT LIQUID NITROGEN

NT LIQUID OXYGEN

NT SOLIDIFIED GASES

Heat and mass transfer apparatuses in cryogenics --- Russian book 01 p0028 A83-10672

High resolution acoustic microscopy in superfluid helium 14 p2022 A83-33443

Suction performance of high speed cryogenic inducers [AIAA PAPER 83-1387] 16 p2321 A83-36377

The effect of a porous coating on the convective heat transfer during boiling 18 p2684 A83-39475

Acoustic velocities of two-phase mixtures of cryogenic fluids 20 p2983 A83-43012

Cryogenic liquids and aviation --- biological effects and safety hazards 23 p3499 A83-48695

The unexpectedly high solubility of water in cryogenic liquids 24 p3570 A83-50114

CRYOGENIC GYROSCOPES

Analysis of the force characteristics of the suspension of a cryogenic gyroscope 11 p1574 A83-28466

CRYOGENIC ROCKET PROPELLANTS

LO2/LH2 propulsion for outer planet orbiter spacecraft [AIAA PAPER 83-1305] 16 p2320 A83-36330

Vapor flow into a capillary propellant-acquisition device [AIAA PAPER 83-1380] 16 p2321 A83-36371

Small cryogenic propulsion unit for upper stage application [IAF PAPER 83-388] 23 p3426 A83-47368

Dynamic response of a centrifugal liquid oxygen rocket pump [ASME PAPER 83-FE-24] 23 p3426 A83-48235

CRYOGENIC WIND TUNNELS

Feasibility study on strain gauge balances for cryogenic wind tunnels at ONERA [ONERA, TP NO. 1982-87] 03 p0282 A83-14539

Practical problems of design and manufacture of a 2-D model and of the device for its cooling and introduction into the T2 pressurized cryogenic intermittent tunnel [ONERA, TP NO. 1982-88] 03 p0282 A83-14540

Thermal behavior and insulation of a cryogenic wind tunnel [ONERA, TP NO. 1982-89] 06 p0720 A83-18427

Cryogenic wind tunnels for high Reynolds number testing 14 p1977 A83-32175

The effect of the real properties of a carrier vapor on the evaporation time of a drop 17 p2506 A83-37814

Boundary layer calculations for cryogenic wind tunnel flows 22 p3250 A83-46478

Cryogenic-wind-tunnel technology - A way to measurement at higher Reynolds numbers 22 p3256 A83-46484

Status report on the European Transonic Wind Tunnel and on the Cologne Cryotunnel 23 p3412 A83-47207

Development of a six-component weighing device for cryogenic applications 23 p3412 A83-47208

CRYOGENICS

Statistical mechanics of dilute liquid mixtures of He3 in He4 05 p0691 A83-17228

Significance of pop-in fracture in high nickel cryogenic steel weldments 08 p1061 A83-21727

The optical constants of indium antimonide at 1.5 K in the near millimeter wavelength region 08 p1164 A83-22250

Cryogenic frequency domain optical mass memory 08 p1166 A83-22808

Cryogenic engineering --- Russian book 10 p1401 A83-25595

A cryogenic millimeter-wave Schottky-diode mixer 10 p1409 A83-25819

Cryocrystals 20 p3053 A83-42897

Materials at low temperatures --- Book 21 p3114 A83-45098

Infrared optical properties of solid monomethyl hydrazine, N2O4, and N2H4 at cryogenic temperatures 23 p3508 A83-47585

CRYOPUMPING

Suction performance of high speed cryogenic inducers [AIAA PAPER 83-1387] 16 p2321 A83-36377

Emissivity measurements of metallic surfaces used in cryogenic applications 20 p2954 A83-43221

CRYOSORPTION

U SORPTION

CRYOSTATS

Low-temperature studies of plasticity and strength /instruments, techniques, and methods/ --- Russian book 12 p1729 A83-29328

Proposal for advanced infrared spectrophotometers 14 p2016 A83-31997

A study of the short-term strength of structural materials under static loading --- of metal alloys at cryogenic temperatures 14 p1997 A83-33013

He-3 bolometers for MM- and SUBMM-photometry 18 p2691 A83-40444

Performance of a superfluid helium facility for Spacelab payloads 20 p2961 A83-43243

Top-off procedure for space-bound superfluid helium cryostats 20 p2962 A83-43248

CRYSTAL DEFECTS

NT CRYSTAL DISLOCATIONS

NT EDGE DISLOCATIONS

NT FRENKEL DEFECTS

NT POINT DEFECTS

NT SCREW DISLOCATIONS

NT VACANCIES (CRYSTAL DEFECTS)

Propagation and interaction of stacking faults in crystals under shock loading 02 p0153 A83-11648

Mechanisms of defect formation and migration in semiconductors --- Russian book 02 p0242 A83-11924

Defects and disorder in the fast-ion electrode lithium-aluminum 02 p0154 A83-12057

The effect of electronically active defects on the characteristics and the reliability of MOS structures --- French thesis 03 p0311 A83-13804

The evolution of a defect structure and its relation to the deformation parameters in Ti-Al-Nb-Zr alloy at 4.2 K 04 p0457 A83-14997

Electronic correlations and transient effects in disordered systems 04 p0540 A83-15506

Effect of defect structure upon the mechanical behavior of beta-LiAl through dislocation damping and hardness studies 04 p0460 A83-16002

Radiation-induced paramagnetic defects in MOS structures 05 p0691 A83-17478

Radiation-induced defects in SiO2 as determined with XPS 05 p0691 A83-17479

Anti-phase domain boundary tubes in Ni3Al --- crystal defect structures 05 p0616 A83-17792

Localized macroscopic shear in compressed molybdenum crystals 06 p0728 A83-18135

On the mechanism of carrier transport in metal-thin-oxide semiconductor diodes on polycrystalline silicon 06 p0751 A83-18752

Short time annealing --- in silicon processing 07 p0999 A83-20592

A study of defects in amorphous silicon films 07 p0999 A83-20735

Fracture mechanics and crack growth in fatigue 07 p0892 A83-21464

Dynamics of microstructural changes in a superplastic aluminum alloy 07 p0897 A83-21611

Effect of doping simultaneously with iron and titanium on the diffusional creep of polycrystalline Al2O3 08 p1071 A83-22195

High-sensitivity resistivity technique for studies of defect behavior 08 p1106 A83-23234

Radiation processes in corundum crystals 09 p1349 A83-23450

Shearing in inhomogeneous media --- Russian book on fracture mechanics 09 p1278 A83-23823

Defects in silicon 09 p1349 A83-23860

A study of impurities and traps in liquid phase epitaxial InP in relation to melt rebaking 10 p1488 A83-26063

Hydrogen passivation of defects in silicon ribbon grown by the edge-defined film-fed growth process 10 p1489 A83-26215

Tunable visible lasers using defects in oxides 11 p1578 A83-27545

Influence of stacking defects with low probability on X-ray diffraction patterns /Survey/ 11 p1664 A83-28617

The development of a system for characterization of deep traps by transient capacity --- French thesis 11 p1563 A83-28628

Photoemission and population depletion in MOS structures - Characterization of defects in the oxide --- French thesis 11 p1563 A83-28629

Kinetic equations and an analysis of the stability of irradiated matter 13 p1927 A83-30008

Study of electronically active defects in GaAlAs:Sn devices and their role in degradation --- French thesis 13 p1830 A83-30129

The influence of defects on the switching of the pure ferroelastic KH3(SeO3)2 13 p1928 A83-30314

Evidence that the gold donor and acceptor in silicon are two levels of the same defect 13 p1928 A83-30340

Observation of defects in mercury cadmium telluride crystals grown by chemical vapor transport 13 p1929 A83-30348

Effects of very low growth rates on GaAs grown by molecular beam epitaxy at low substrate temperatures 13 p1929 A83-31064

Defect nature of the 0.4-eV center in O-doped GaAs [AD-A129932] 13 p1930 A83-31068

The effect of various types of defects on the physical properties of crystals of the triglycine sulfate group 13 p1930 A83-31308

A model for photovoltaic centers in ferroelectrics 14 p2088 A83-32169

Positive feedback model of defect formation in gradually degraded GaAlAs light emitting devices 15 p2237 A83-33678

Electroplastic deformation of metals (Review) 15 p2140 A83-35046

Photovoltaic and structural properties of CuInSe2/CdS solar cells 16 p2371 A83-36744

A study of the inhomogeneity of deformation in AD1-M aluminum alloy 16 p2335 A83-36894

Defects, fracture and fatigue; Proceedings of the Second International Symposium, Mont Gabriel, Quebec, Canada, May 30-June 5, 1982 17 p2489 A83-38376

Discontinuity sources in manufacturing processes --- for metals 17 p2523 A83-38400

The design and manufacture of an experimental device for irradiation at low temperature and a study of the effects of electron irradiation on type n InAs --- French thesis 17 p2585 A83-38433

Defects in nsutite (gamma-MnO2) and dry-cell battery efficiency 18 p2708 A83-39964

Thickness and stacking sequence effect on the acoustic emission of CFRP 18 p2660 A83-40271

- Determination of the inhomogeneities of semiconductor materials in the infrared 18 p2744 A83-40405
 Muon trapping and Knight shift at a dilute structural defect in zinc --- around hydrogenlike interstitial impurity 19 p2904 A83-40977
 An electron microscopy study of alpha-planar defects formed by boron in alloys of bcc refractory metals 19 p2822 A83-41978
 A study of radiation defects in V3Si compound 19 p2906 A83-42074
 Effect of radiation-induced lattice defects in silicon single crystals on the characteristic states of an interstitial muonium atom 20 p3051 A83-42266
 Effect of defects on phase transitions in tetraselenotetracene chloride, (TSeT)2Cl 20 p3051 A83-42272
 Annealing behaviour of gamma-ray-induced electron traps in LEC n-InP 20 p3052 A83-42482
 Defect and impurity states in silicon nitride 20 p3053 A83-42603
 Semiconductor crystal growth and segregation problems on earth and in space 20 p2941 A83-43291
 New trend of atom resolution electron microscopy - Direct observations of atoms, vacancies and impurity atoms in crystal and on-line image analysis 20 p2992 A83-43609
 Intermetallic compounds of the micron- and P-phases of Co7Mo6 studied by 1 MV electron microscopy 20 p2956 A83-43616
 Electric-field-dependent charge-carrier trapping in a one-dimensional organic solid 21 p3216 A83-43888
 Electron-beam-induced current measurements in silicon-on-insulator films prepared by zone-melting recrystallization 21 p3219 A83-45496
 Correlation among secondary ion mass spectrometry, cross-section transmission electron microscopy, and Rutherford backscattering analyses for defect density and depth distribution determination 22 p3365 A83-46728
 Study of deep-level defects and annealing effects in undoped and Sn-doped GaAs solar cells irradiated by one-MeV electrons 23 p3427 A83-48605
 On the relation between Young's modulus and orientation in carbon fibres 24 p3553 A83-48898
 The transformation ratio of acoustic emission during irreversible deformation of crystals 24 p3590 A83-49058
 Defects and transport properties in oxides and sulfides 24 p3554 A83-49477

CRYSTAL DISLOCATIONS

NT EDGE DISLOCATIONS

NT SCREW DISLOCATIONS

- A model for the formation of subboundaries in the matrix of eutectic alloys of the system M-MeC --- Ni or Co alloyed with Ta, Nb or Hf carbides 01 p0025 A83-10397
 A nucleus-free mechanism of irregular grain growth in metals 01 p0026 A83-10450
 Characteristics of the amplitude dependence of internal friction and Young's modulus defect in solids at low deformation amplitudes 02 p0155 A83-12206
 Susceptibility of a pseudo-alpha titanium alloy to cyclic damage in the frequency range from 33 Hz to 10 KHz 02 p0156 A83-12329
 The effect of the stacking fault energy on the characteristics of the high-temperature creep of nickel-cobalt alloys 02 p0157 A83-12331
 Liquid encapsulated Czochralski growth of low dislocation GaAs 03 p0399 A83-13784
 A study of the mechanism of the steady-state creep of aluminum under compression 03 p0300 A83-14161
 A study of polygonization in aluminum deformed by cyclic bending using low-angle X-ray scattering 03 p0300 A83-14163
 Adiabatic heating at a dislocation pile-up avalanche 03 p0291 A83-14497
 Prismatic slip in the plastic deformation of alpha-Ti single crystals below 700 K [ONERA, TP NO. 1982-127] 03 p0300 A83-14702
 Creep response of strip-cast Al-1wt.%Mn-1wt.%Mg alloy to thermomechanical treatment 04 p0457 A83-14996
 Mechanical instability of a cellular dislocation structure 04 p0459 A83-15469
 Structural changes in tungsten single crystals during creep in the medium-temperature range 04 p0459 A83-15470
 Nature of subsurface damage in an aluminium-22 wt% silicon during dry sliding wear 04 p0460 A83-15995
 On dislocation-incoherent particle interactions at high temperatures 04 p0461 A83-16254
 A new instrument for acoustic emission activity, with an application to the thermoelastic instability 05 p0644 A83-16922
 The topographic characteristics of the thermal decomposition of ammonium perchlorate 05 p0620 A83-17141

- Internal stress measurements during the saturation fatigue of polycrystalline aluminum 05 p0616 A83-17865
 An experimental study of the correlation between the root-mean-square thermal displacements of atoms and the resistance to creep --- of nickel and aluminum alloys 06 p0729 A83-18750
 The formation of microcracks under developed plastic deformation 06 p0777 A83-19305
 A quantitative study of the relationship between interfacial carbon and line dislocation density in silicon molecular beam epitaxy 07 p0998 A83-19896
 Microstructure of fiber and particulate SiC in 6061 Al composites 07 p0877 A83-20634
 The fatigue fracture of metals from the standpoint of physics and fracture mechanics 07 p0890 A83-20914
 Characteristics of the oxide phase formation during the low-temperature oxygenation of niobium alloys 07 p0891 A83-20923
 Creep strengthening mechanisms 07 p0892 A83-21466
 Creep damage and fracture --- in wrought and cast precipitation-hardened superalloys 07 p0892 A83-21468
 Flow in polycrystals and the scaling of mechanical properties 07 p0896 A83-21602
 Microstructures and strengthening of aluminium alloys 07 p0896 A83-21605
 The structure of grain boundaries and their effect on mechanical properties 07 p0896 A83-21606
 Microstructural aspects of the cold deformation of Nimonic alloy 115 07 p0897 A83-21607
 Microstructures in cold-rolled polycrystalline aluminium 07 p0897 A83-21608
 Microstructural changes and deformation mechanisms during creep of an unidirectionally solidified gamma/delta and gamma/gamma'-alpha eutectic alloy at elevated temperature 07 p0897 A83-21610
 Creep deformation induced substructure in polycrystalline molybdenum 07 p0897 A83-21612
 Stress-strain behaviour and microstructure of polycrystalline alpha-titanium 07 p0897 A83-21614
 The effects of very high cumulative deformation on structure and mechanical properties of aluminium 07 p0897 A83-21615
 The orientation and temperature dependence of the 0.2% proof stress of single crystal Ni3/Al/Ti 08 p1067 A83-22750
 Generation of holes during the disintegration of dislocations and mechanoluminescence of metals 08 p1170 A83-22781
 Short-range stratification in Ti-Zr, Ti-Hf, and Zr-Hf alloys and lattice instability 08 p1068 A83-22783
 Changes in the base dislocation density at the initial stage of the plastic deformation of magnesium single crystals 08 p1068 A83-22785
 Quantitative fractography and dislocation interpretations of the cyclic cleavage crack growth process 08 p1123 A83-23224
 Defects and dislocations in the upper mantle /asthenosphere/ and attenuation of shear waves 09 p1301 A83-23674
 Dislocation creep in subgrain-forming pure metals and alloys 09 p1231 A83-24052
 Deformation and dislocation behaviour in metals and single-phase alloys at elevated temperatures 09 p1231 A83-24054
 Dislocation dynamics and viscosity effects associated with a plane stress wave in metals 09 p1233 A83-24208
 Aspects of the theory of dislocations 10 p1437 A83-25307
 Superplasticity --- and relation to grain size 10 p1392 A83-25308
 Grain boundary sliding and stress concentration during creep 10 p1396 A83-25860
 A method for calculating the dislocation density in pure crystals grown from melts by the methods of Czochralski and Stepanov and by crucibleless zone melting 11 p1662 A83-28359
 Double slip plane crack model 11 p1595 A83-28423
 An electron microscopy study of the interaction between dislocations and grain boundaries during deformation 11 p1550 A83-28547
 Transmission electron spectroscopic observation of tungsten hemicarbon - A study of dislocation structures after high temperature plastic deformation --- French thesis 11 p1551 A83-28626
 Grain-boundary diffusion in metals 12 p1713 A83-29240
 Stress fluctuations accompanying strain rate change in an aluminium alloy 2017 12 p1714 A83-29414
 Strain localization and hydrogen embrittlement 12 p1714 A83-29722

- Micromechanics of solid solution effects in BCC alloys [AIAA 83-0976] 12 p1715 A83-29783
 Recombination enhanced dislocation glide in InP single crystals 13 p1928 A83-30336
 Change of characteristic parameters of polycrystalline titanium during its deformation 13 p1822 A83-30971
 Microstructure of aluminium during creep at intermediate temperatures. III - The rate controlling process 13 p1825 A83-31650
 Mechanical properties of BCC metals; Proceedings of the U.S.-Japan Seminar, Honolulu, HI, March 23-27, 1981 14 p1995 A83-32874
 Cyclic stress relaxation of polycrystalline metals at elevated temperature 15 p2138 A83-34145
 Deformation martensite in VT22 titanium alloy 15 p2141 A83-35307
 Determination of prefracture damage and failure prediction in corrosion-fatigued Al-2024-T4 by X-ray diffraction methods 16 p2331 A83-36163
 Dislocation distribution in plastically deformed metals 16 p2331 A83-36165
 The behavior of molybdenum single crystals in the deformation zone during rolling between grooved rolls 16 p2335 A83-36891
 Superplasticity - A review of data 16 p2335 A83-36959
 Direct observations of crack tip dislocation behavior during tensile and cyclic deformation 17 p2489 A83-38377
 Dislocation dynamics in aluminum and in aluminum-based alloys investigated by TEM and NMR techniques 17 p2490 A83-38379
 The elastic strain energy of dislocation structures in fatigued metals 17 p2490 A83-38382
 Dislocation kinetics and the formation of deformation bands 17 p2522 A83-38383
 Analyses of microstructural and chemical effects on fatigue crack growth 17 p2490 A83-38396
 Viscosity and conductivity of the lower mantle - An experimental study on a MgSiO3 perovskite analogue, KZnF3 19 p2865 A83-41175
 The influence of the crack tip stress field on the nucleation and growth of voids 20 p3008 A83-43467
 High-efficiency (21.4 pct) Ga0.75 In0.25 As/GaAs (Eg = 1.15 eV) concentrator solar cells and the influence of lattice mismatch on performance 21 p3169 A83-45493
 The use of the internal friction method for studying laser-irradiated materials 21 p3115 A83-45502
 Solitons in solids 22 p3354 A83-45894
 Positron investigations of titanium-based alloys irradiated by neutrons 23 p3433 A83-48396
 Theory for saturation stress difference in torsion versus other types of deformation at low temperatures 23 p3473 A83-48601
 Strains in the oxide scales and the substrate metals during oxidation 24 p3562 A83-49487
 Elastic properties (the stiffness constants, the shear modulus and the dislocation line energy and tension) of Ni-Al solid solutions and of the nimonic alloy PE 16 24 p3567 A83-49873

CRYSTAL FILTERS

- Dynamic spatial filter for optical signal processing using a liquid crystal light valve 08 p1166 A83-22809
 Antenna arrays with filtering of interfering spatial radio signals by coherent-optical methods using controlled liquid-crystal transparencies 14 p2000 A83-32118

CRYSTAL GROWTH

- NT CZOCHRALSKI METHOD
 NT DIRECTIONAL SOLIDIFICATION (CRYSTALS)
 NT ELECTROEPITAXY
 NT EPITAXY
 NT HYDROTHERMAL CRYSTAL GROWTH
 NT LIQUID PHASE EPITAXY
 NT MOLECULAR BEAM EPITAXY
 NT VAPOR PHASE EPITAXY
 Structure and growth of thin films 01 p0108 A83-10214
 A nucleus-free mechanism of irregular grain growth in metals 01 p0026 A83-10450
 Crystal size and orientation in ice grown by droplet accretion in wet and spongy regimes 02 p0214 A83-12238
 Effect of annealing conditions on grain growth in the complex Ti/1-x/Nb/x/C/0.5/N/0.5/ solid solutions 02 p0158 A83-12949
 Protein single crystal growth in a microgravity field 02 p0138 A83-12996
 A simplified method of generating layer sequences for SiC polytypes 03 p0399 A83-13683
 Recent developments in infrared acousto-optic tunable filters 03 p0393 A83-13770
 The growth and structure of niobium bicrystals 03 p0300 A83-14159

Composition determination of CuInS₂ by a chemical analysis method 04 p0456 A83-15484

Thin germanium nitride films grown by thermal reaction process 04 p0543 A83-16077

Effects of annealing on the electrical properties of Cd/x/Hg/1-x/Te 04 p0543 A83-16085

Directional grain growth in the activated sintering of 0.5% Ni doped W-powder 04 p0461 A83-16253

The topographic characteristics of the thermal decomposition of ammonium perchlorate 05 p0620 A83-17141

The nucleation mechanism during the low-temperature decomposition of ammonium perchlorate 05 p0620 A83-17142

An analytical approach to thermal modeling of Bridgman-type crystal growth. I - One-dimensional analysis 05 p0638 A83-17235

Effect of nitrogen content on grain growth in Ti/C,N/-Ni-Mo sintered alloy 05 p0615 A83-17549

Case study of a hailstorm in Colorado. II - Particle growth processes at mid-levels deduced from in-situ measurements 06 p0790 A83-18264

A comparative study of the rates of development of potential graupel and hail embryos in high plains storms 06 p0790 A83-18265

Observation of ice crystal formation in lower Arctic atmosphere 06 p0790 A83-18266

Initiation of ZrC dendritic growth on the surface of spark machined zirconium 07 p0884 A83-20251

C-axis inclined ZnO piezoelectric shear wave films 07 p0922 A83-21371

Production of large-area single-crystal wafers of cubic SiC for semiconductor devices 08 p1170 A83-22767

Beryllium optical mirrors by vapor deposition 08 p1112 A83-22865

X-ray diffraction study of the dry formation of Cu₂S-CdS solar cells 10 p1444 A83-25448

Continuous 300-K laser operation of strained superlattices 10 p1426 A83-25977

Silicon melt, regrowth, and amorphization velocities during pulsed laser irradiation 10 p1490 A83-26269

Fluid mechanics in crystal growth - The 1982 Freeman scholar lecture 10 p1401 A83-26626

Nucleation during solidification of aluminum-titanium alloys 10 p1399 A83-26890

Energy transfer in stoichiometric rare-earth crystals --- laser materials 11 p1581 A83-27589

The effect of gravity on freely growing crystals 11 p1662 A83-28171

Conference on the Fabrication of Profiled Crystals and Products using Stepanov's Method and Their Applications in National Economy, Leningrad, USSR, March 10-12, 1982, Proceedings 11 p1662 A83-28351

The dynamics of crystal formation during growth by Stepanov's method 11 p1662 A83-28353

The stability of the crystallization process during the growth of tubular sections by Stepanov's method 11 p1662 A83-28355

The effect of radiant heat transfer on the shape of the solidification front and temperature distribution in refractory semitransparent crystals pulled from a melt 11 p1662 A83-28357

The formation of slip bands under the effect of thermal stresses during the growth of profiled semiconductor crystals 11 p1663 A83-28360

The growth of profiled silicon crystals, investigation of their electronic properties and defect structures, manufacture of solar cells, and determination of their parameters 11 p1663 A83-28361

The growth of profiled silicon crystals by Stepanov's method using various heating schedules 11 p1663 A83-28362

The growth and structural characteristics of silicon single-crystal ribbons 11 p1663 A83-28364

The growth of lithium niobate ribbons using Stepanov's method 11 p1663 A83-28365

Growth of thin ribbons of aluminum-base regular eutectic compositions and a study of their microstructures 11 p1548 A83-28367

Thermal convection instability of liquid metals of magneto-hydrodynamics 12 p1780 A83-29053

Observation of defects in mercury cadmium telluride crystals grown by chemical vapor transport 13 p1929 A83-30348

Effects of very low growth rates on GaAs grown by molecular beam epitaxy at low substrate temperatures 13 p1929 A83-31064

The effect of growth conditions on the polarization of triglycine sulfate doped with L-alpha-alanine 13 p1930 A83-31306

Epsilon nonlinearly of doped triglycine sulfate crystals depending on conditions of growth 13 p1930 A83-31307

Transient thermal Marangoni convection in a liquid bridge 13 p1844 A83-31625

High efficiency tandem type solar cells consisting of a-Si:H and a-SiGe:H 14 p2042 A83-32263

All thin film n-CdTe/ITO solar cell 14 p2090 A83-32302

Progress in unconventional crystallization of silicon 14 p2090 A83-32307

Solar grade floating-zone silicon 14 p2045 A83-32316

Method of raw material continuous feeding on silicon ribbon growth 14 p2090 A83-32319

Impurity incorporation in R.A.D. polysilicon layers and consequences on their electrical properties --- Ribbon Against Drop 14 p2091 A83-32320

Fast silicon-sheet growth with the supported-web method 14 p2091 A83-32321

Computer simulation and controlled growth of large diameter Czochralski silicon crystals 14 p2092 A83-32641

Growth and characterization of Ga(0.47)In(0.53)As films on InP substrates using triethylgallium, triethylindium, and arsine 14 p2092 A83-32643

Effect of heat treatment on the bulk diffusion length of EFG ribbon silicon --- Edge-defined Film-fed Growth 14 p2092 A83-32670

Segregation and structure in rapidly solidified cast metals 14 p1994 A83-32802

An investigation of the formation of texture in ZnO films during growth --- Russian book 14 p2093 A83-33298

New opportunities in space - Research in microgravity 15 p2123 A83-33544

Single crystal growth of SiC substrate material for blue light emitting diodes 15 p2237 A83-33676

On the effect of radiative exchange in the 8 to 12 micron spectral region on the diffusional growth of ice crystals 15 p2205 A83-34062

The growth of Cu₂S on polished or etched single crystal CdS substrates 16 p2419 A83-35573

Crystal growth of mode-stabilized semiconductor diode lasers by liquid-phase epitaxy 16 p2420 A83-35987

High-pressure growth of polycrystalline molybdenum disulphide 16 p2337 A83-36071

Nitridation of Si(111) by nitrogen atoms. II 16 p2328 A83-36723

Gallium arsenide and related compounds 1982; International Symposium, 10th, Albuquerque, NM, September 19-22, 1982, Contributed Papers --- Book 17 p2584 A83-37160

Thermal instabilities --- convective heat transfer in materials science 18 p2685 A83-39890

Conditions for the onset of temperature oscillations in a simulated floating-zone configuration 18 p2643 A83-39894

Convective-diffusive transport in vapor growth ampoules 18 p2685 A83-39897

Two-dimensional convection in liquid layer related to crystal growth techniques in space 18 p2643 A83-39900

Solid/liquid interface instability - Limits and morphological aspects in microgravity conditions 18 p2643 A83-39904

A sounding rocket experiment on the Marangoni convection 18 p2644 A83-39912

Annealing of Hg₂Cl₂ crystals - Project of the experiment --- in space and terrestrial conditions 18 p2644 A83-39913

Effects of growth temperatures and surface roughness on crystal orientation of ice accreted in a dry regime 18 p2729 A83-40041

Statistical analysis of a holographic system intended for the Space Shuttle 19 p2817 A83-41099

Analytical methods: High-melting metals --- Book 19 p2905 A83-41848

Semiconductor crystal growth and segregation problems on earth and in space 20 p2941 A83-43291

Modelling of TGS growth in space --- triglycine sulfate 20 p2941 A83-43293

Growth of triglycine sulfate (TGS) crystals by solution technique 20 p2941 A83-43294

Directional solidification and characterization of Hg(1-x)Cd(x)Te alloys 20 p3054 A83-43295

Gravity-driven convection studies in compound semiconductor crystal growth by physical vapor transport 20 p3054 A83-43297

Influence of diffusion and convective transport on dendritic growth in dilute alloys 20 p3054 A83-43298

The effect of the natural convection on the transition from columnar to equiaxed crystals 20 p3054 A83-43311

Shape of growing crystals of primary phases in eutectic alloys of the systems Fe-Fe₂B and Ni-Ni₃B 21 p3112 A83-44476

Growth and characterization of single crystal refractory oxide fibers 22 p3358 A83-46629

Effect of variable thermal conductivity on isotherms in Bridgman growth 22 p3285 A83-46707

The influence of radiative transfer on the mass and heat budgets of ice crystals falling in the atmosphere 22 p3341 A83-46851

Crystal growth of GaSb under microgravity conditions [IAF PAPER 83-153] 23 p3413 A83-47292

Experimental system to produce artificial snow on the STS-6 [IAF PAPER 83-162] 23 p3414 A83-47297

An experimental study of the ice column habit transitions --- crystal growth in atmosphere 24 p3611 A83-49690

Observation of ice aggregation at temperatures near -50 C 24 p3612 A83-49699

GaAlAs buried-heterostructure lasers grown by a two-step MOCVD process 24 p3590 A83-49963

CRYSTAL LATTICES

NT BODY CENTERED CUBIC LATTICES

NT CLOSE PACKED LATTICES

NT CUBIC LATTICES

NT FACE CENTERED CUBIC LATTICES

Photosensitive gate structures based on epitaxial layers of Fe-doped GaP 01 p0108 A83-10373

The equilibrium of inhomogeneously alloyed single-crystal plates. I - Equilibrium conditions. II - Cubic lattice 01 p0060 A83-10825

Tunable electroluminescence from GaAs doping superlattices 01 p0110 A83-10991

Pulse plating of chromium-cobalt alloys containing a phase with the A-15 structure 02 p0154 A83-12053

Crystal size and orientation in ice grown by droplet accretion in wet and spongy regimes 02 p0214 A83-12238

Micromechanics 02 p0193 A83-12733

A study of the ordering kinetics of an equiatomic cobalt-platinum alloy using the method of nuclear gamma resonance 03 p0299 A83-14156

The effect of the initial structure on the characteristics of beta solid solution decomposition in high-strength titanium alloy VT22 03 p0300 A83-14157

The growth and structure of niobium bicrystals 03 p0300 A83-14159

Numerical simulation of crystal fractionation in shergottite meteorites 04 p0563 A83-15363

An antiplane problem concerning crack propagation in a lattice 04 p0497 A83-15388

Grain boundary diffusion mechanisms in metals 04 p0460 A83-16001

Dipole-field sums and Lorentz factors for orthorhombic lattices, and implications for polarizable molecules 05 p0690 A83-17226

The Bloch-FET - A lateral surface superlattice device 05 p0690 A83-17289

Transmission electron microscopy studies on the oxidation of aluminum 05 p0617 A83-17952

Phonons in Group II B-Group VI A semiconductors /Review/ 06 p0815 A83-19573

Spectroscopic study of the mechanism of the linear electrooptic effect 06 p0810 A83-19575

On the prediction of lattice parameter vs. concentration for solid solutions extended by rapid quenching from the melt 07 p0887 A83-20635

Nuclear gamma resonance of Fe-57 impurity atoms in Ti₃Al 07 p0890 A83-20920

Unit cell parameters for a new crystalline polymorph of lead phthalocyanine and for two polymorphs of magnesium phthalocyanine 07 p1000 A83-21573

The structure of grain boundaries and their effect on mechanical properties 07 p0896 A83-21606

The effect of alloying on the physical properties, electron structure, and phase stability of titanium alloys 09 p1234 A83-24378

A hydrogen molecular crystal in a multiparticle approximation 09 p1350 A83-25094

Crystal elasticity --- mechanical behavior under loading 10 p1392 A83-25311

Estimation of the high-temperature strength of a nickel alloy on the basis of the degree of misorientation of the lattices of the matrix and strengthening phases during alloying with niobium and chromium 10 p1395 A83-25630

Continuous 300-K laser operation of strained superlattices 10 p1426 A83-25977

Use of a superlattice to enhance the interface properties between two bulk heterolayers 10 p1489 A83-26214

Energy transfer in stoichiometric rare-earth crystals --- laser materials 11 p1581 A83-27589

Theory of silicon superlattices - Electronic structure and enhanced mobility 11 p1664 A83-28710

Grain-boundary diffusion in metals 12 p1713 A83-29240

On reactions between silicon and nitrogen. I - Mechanisms 12 p1712 A83-29501

- Piezoelectricity and pyroelectricity in polyvinylidene fluoride - Influence of the lattice structure
12 p1782 A83-29531
- Low frequency dielectric relaxation in boracites
12 p1709 A83-29555
- The implementation of lattice calculations on the DAP --- Distributed Array Processor
12 p1768 A83-29623
- Oriented crystallization of metals in the presence of electric current
13 p1822 A83-30906
- Thermal stability of titanium alloys '685' and '5524S'
13 p1823 A83-31173
- Solution of gamma-prime phase in nickel heat-resistant aging alloys
13 p1823 A83-31214
- The polymerization reaction as a method of studying the characteristics of the state of molecules in a crystal lattice under shock-wave loading
14 p1985 A83-32093
- Microstructural characteristics of Al-Li alloys
14 p1996 A83-32882
- The Raman scattering of light and crystal-lattice dynamics
14 p2092 A83-33037
- Group-theory properties of crystal vibrations with allowance for spatial symmetry
14 p2092 A83-33040
- Specific site location of S and Si in ion-implanted GaAs
14 p2093 A83-33445
- Lattice images of amorphous-like Ni-B films prepared by the electroless plating method
16 p2328 A83-35601
- Diatom polymers, mixed-stack compounds, and the soliton lattice
16 p2420 A83-35749
- Will diamond transform under Megabar pressures?
16 p2421 A83-36563
- Nitridation of Si(111) by nitrogen atoms. II
16 p2328 A83-36723
- Quantum-chemical modeling of boron and noble gas dopants in silicon
17 p2584 A83-38211
- Positron and electron channeling radiation from germanium
17 p2585 A83-38955
- Classical magnetoresistance of a two-dimensional electron gas in a one-dimensional superlattice
20 p3051 A83-42283
- Absorption spectra, energy levels and crystal-field analysis of trivalent neodymium in the gamma phase of neodymium sesquisulfide (gamma-Nd₂S₃)
20 p3053 A83-42627
- Internal photoemission from quantum well heterojunction superlattices by phononless free-carrier absorption
20 p3054 A83-43593
- High resolution lattice images of G.P. zones in an Al-3.97 wt pct Cu alloy --- Guinier-Preston
20 p2956 A83-43613
- The lattice images of amorphous-like Ni-B alloy films prepared by electroless plating method
20 p2956 A83-43615
- The generalized Hubbard model in the theory of trimerizable molecular crystals --- such as Cs₂(TCNQ)(3)-organic charge transfer salt
21 p3220 A83-45505
- Solitons in solids
22 p3354 A83-45894
- An analytical and experimental study of zoning in plagioclase
22 p3332 A83-46711
- Modification of optical properties of GaAs-Ga(1-x)Al(x)As superlattices due to band mixing
22 p3365 A83-46725
- Analysis of the spin-Hamiltonian parameters for Cr(3+) in mirror and inversion symmetry sites of alexandrite (Al₂-x/3Cr_x/BeO/4) - Determination of the relative site occupancy by EPR
23 p3461 A83-47630
- The effect of foil preparation technique on interface phase formation in Ti alloys
23 p3432 A83-47854
- Ordered structures in Ti Al alloys in the composition range from AB to AB₃
23 p3432 A83-48186
- [ONERA, TP NO. 1983-65]
23 p3635 A83-49445
- Solid-state superlattices
24 p3635 A83-49445
- Moessbauer study of the lattice location of Co-57 implanted in graphite
24 p3636 A83-49756
- CRYSTAL OPTICS**
- Crystal rocking-diffraction of backscattered and transmitted electrons as an alternative method to conventional electron diffraction, especially for obtaining energy-filtered diffraction pictures --- German thesis
01 p0048 A83-10174
- Optical bistability in nematic films utilizing self-focusing of light
02 p0236 A83-12278
- Gyrotropic isoindex filter
02 p0178 A83-12597
- Control of the spatial characteristics of laser radiation based on the electro-optical effect in crystals
04 p0483 A83-15259
- The creation on nonlinear dispersion in crystals and its application to signal compression
04 p0484 A83-15269
- Opto-optical modulation in N-/p-methoxybenzylidene-/p-butylaniline
05 p0647 A83-16833
- Optical inhomogeneity of nonlinear crystals and maximum efficiencies of parametric frequency amplifiers pumped by beams with inhomogeneous transverse intensity distributions
05 p0648 A83-17042
- Amplification of light in inhomogeneous waveguides with an adjacent active medium
05 p0685 A83-17076
- Harmonic generation with noncollinear laser beams - Application to pulse stacking
06 p0766 A83-18958
- Lasers with distributed feedback and reflection on the basis of cholesteric liquid crystals /CLC/
06 p0768 A83-19572
- Spectroscopic study of the mechanism of the linear electrooptic effect
06 p0810 A83-19575
- Induced dichroism in passive laser switches
07 p0934 A83-20111
- Influence of aperture effects on the spectral structure of stimulated Raman scattering by optical phonons and polaritons in a resonator
07 p0992 A83-20119
- Time-resolved reflectivity measurements of femtosecond-optical-pulse-induced phase transitions in silicon
07 p1000 A83-20819
- Optical pulse compression using polarizing techniques
08 p1166 A83-22570
- Liquid crystals as large aperture waveplates and circular polarizers
08 p1166 A83-22571
- Versatile curved crystal spectrometer for laboratory extended X-ray absorption fine structure measurements
08 p1105 A83-23227
- Radiation processes in corundum crystals
09 p1349 A83-23450
- Ferroelectric crystals for the control of laser radiation --- Russian book
09 p1271 A83-23815
- Light scattering in polycrystalline materials
09 p1346 A83-24969
- Giant Raman optical activity of the 128/cm mode in alpha-quartz
10 p1481 A83-25432
- Submillimeter emission of CdS crystals pumped by intense light
10 p1430 A83-26234
- Investigation of an electrooptic modulator formed from coupled channel diffused waveguides in LiNbO₃
10 p1483 A83-26656
- Spectral composition of the radiation emitted from a concentrated LiNdLa phosphate glass laser with a Q switch made of an LiF crystal with F²/- centers
10 p1432 A83-26662
- Generation of light in optical fibers made of glasses formed from rare-earth ultraphosphate crystals
10 p1432 A83-26670
- Tuning characteristics of multistage stimulated Raman scattering by polaritons in a layer of an LiIO₃ crystal
10 p1432 A83-26671
- Acoustooptical device with extremely high contrast ratio
10 p1424 A83-26872
- Progress in the development of color centers for stable CW tunable laser operation
11 p1578 A83-27542
- A Bragg crystal spectrometer for the soft X-ray diffuse background
11 p1573 A83-27757
- Stigmatic Bragg crystal spectrometers for cosmic X-rays
11 p1573 A83-27758
- Optical multistability in silicon observed with a CW laser at 1.06 microns
11 p1657 A83-27849
- Raman scattering of light in crystals with the participation of the Bose-Einstein condensate of excitons
11 p1663 A83-28561
- Excitation of surface polaritons by nondegenerate four-wave mixing of evanescent waves
12 p1782 A83-29200
- Fabrication of optical waveguides in LiNbO₃ and LiTaO₃ crystals by ion irradiation
13 p1919 A83-30824
- Correlation of the electron spectra and temperatures of phase transformations in solid solutions based on barium titanate
13 p1930 A83-31305
- Dispersion and luminescence measurements of optical waveguides
13 p1922 A83-31388
- The nature of temperature anomalies of the piezooptical coefficient in crystals of the triglycine sulfate group
14 p2087 A83-32127
- Diffraction gyration and reversal of the wavefront of laser beams in electrooptical crystals
14 p2084 A83-32134
- The lasing mechanism, active layer thickness, natural resonator effects, and the nature of the M and P bands of the emission spectrum of CdS pumped by a nitrogen laser - T - 4.2-420 K
14 p2023 A83-32163
- Dynamic free-carrier holograms in semiconductors
14 p2084 A83-32164
- Time-dependent oscillations of the gain factor during the stimulated Raman scattering of light by polaritons under nonstationary conditions
14 p2024 A83-32166
- Chalcogenide glasses - Promising materials for quantum electronics. I - The interaction and structure of As-S glasses
14 p2088 A83-32167
- Real-time edge enhancement in four-wave mixing with photorefractive BGO crystals
14 p2084 A83-32450
- Raman scattering of light during phase transitions in crystals
14 p2092 A83-33038
- Theory of a self-pumped phase conjugator with two coupled interaction regions
15 p2228 A83-33528
- Autocorrelation of ultrashort optical pulses using polarization interferometry
15 p2230 A83-33764
- Fiber-optic waveguides in the medium infrared range
15 p2231 A83-34879
- The properties of holographic gratings in silicon crystals recorded by means of ultrashort light pulses
16 p2412 A83-35944
- Synthetic nonlinear semiconductors
16 p2420 A83-35957
- Infrared specular reflectance of pressed crystal powders and mixtures
16 p2413 A83-36759
- Relative contribution of various secondary X-ray components below 100 keV at balloon altitudes
17 p2512 A83-38545
- X-ray crystal-optics --- Russian book
18 p2750 A83-40604
- The Brillouin-scattering method in quantum electronics and laser-induced damage
18 p2694 A83-40608
- Investigation of Brillouin light scattering in crystals and glasses with application to problems of quantum electronics and fiber optics
18 p2694 A83-40609
- Investigation of mechanisms of damage induced in ionic crystals by pulsed nanosecond laser radiation
18 p2694 A83-40610
- Nearly noncritically phase-matched UV generation at 3547 Å in NaCHO₂
19 p2851 A83-40929
- Self-diffraction of light waves in gyrotropic crystals
19 p2899 A83-40997
- Occurrence of the dynamic Jahn-Teller effect in CdTe:Co crystals
19 p2904 A83-40998
- Image transmission through a turbulent medium using a point reflector and four-wave mixing in BSO crystal --- Bismuth Silicon Oxide
19 p2847 A83-41107
- Freedericksz transition in a nematic liquid crystal under the action of the field of the standing light wave --- in nonlinear Fabry-Perot resonator
19 p2900 A83-41190
- Phase-conjugate wavefront generation in four-wave mixing with photorefractive Bi₁₂GeO₂₀ (BGO) crystals
19 p2900 A83-41555
- Investigation of a probe sensor of electric field strength with a Pockels-effect cell
19 p2849 A83-41816
- Peripheral photoresponse of a p-n junction
20 p3053 A83-42612
- Vacuum-ultraviolet refractive index of LiF and MgF₂ in the temperature range 80-300 K
21 p3203 A83-43875
- Dynamic holograms in semiconductors
21 p3138 A83-44698
- Fast beam deflectors based on phase matching
21 p3206 A83-44815
- Dynamic optical cross-correlator using a liquid crystal light valve for real time data input
21 p3207 A83-44827
- Luminescence of strong exciton transitions
21 p3219 A83-45336
- Resonance Raman scattering of light and characteristics of the formation of low-temperature luminescence in anthracene crystals
21 p3219 A83-45337
- Superradiation in molecular impurity crystals
21 p3146 A83-45338
- Ultrasonic modulation of persistent spectral holes in crystals
21 p3219 A83-45486
- Continuous-wave self-pumped phase conjugator with wide field of view
22 p3356 A83-45964
- Material dispersion considerations for infrared fibers
22 p3358 A83-46628
- Setting up the Sagnac experiment in a gamma-ray ring interferometer --- Russian book
23 p3453 A83-47122
- Investigation of the effect of uniform compression on the angle of the optical axes of olivine single crystals
23 p3485 A83-48509
- Optically induced Freedericksz transition and bistability in a nematic liquid crystal
24 p3628 A83-48843
- Attenuation at 10.6 microns in loaded and unloaded polycrystalline KRS-5 fibers
24 p3629 A83-49017
- Optical bistability in GaSe
24 p3629 A83-49530
- CRYSTAL OSCILLATORS**
- NT PIEZOELECTRIC CRYSTALS**
- Application to variable-frequency transducers of ONERA studies on the stability of crystal oscillators
02 p0178 A83-12344
- The anomalously small dissipation of electromagnetic waves in an ionic crystal
04 p0474 A83-16413
- Frequency control of high-frequency quartz resonators
05 p0630 A83-17685
- Optical bistability in InSb at room temperature with two-photon excitation
07 p0994 A83-21365
- Crystal structure of the microwave dielectric resonator Ba₂Ti₉O₂₀
12 p1717 A83-29973
- A new type of laser probe --- for surface acoustic wave beam measurement
13 p1846 A83-30334

- Compensation for the static and dynamic thermal effects on quartz oscillators 13 p1836 A83-31174
- A study of the coupled and continuous vibrational states of dielectric crystals by Raman spectroscopy 14 p2092 A83-33039
- Intense electromagnetic radiation from relativistic particles 15 p2228 A83-33786
- Superemission (collective spontaneous emission) of photons by atoms moving in a substance 16 p2361 A83-36966

CRYSTAL STRUCTURE

- The kinetics and mechanism of tungsten-vanadium alloy oxidation 01 p0025 A83-10399
- Ferroelectricity and coherent phonon generation in piezoelectric composition-modulated structures 01 p0108 A83-10622
- Properties of Al/x/Ga/1-x/N films prepared by reactive molecular beam epitaxy 01 p0109 A83-10624
- Morphological and frictional behavior of sputtered MoS₂ films 02 p0160 A83-12652
- Crystal structure and electrical resistance of MoS₂-NbS₂ alloys obtained by the method of self-propagating high-temperature synthesis 02 p0161 A83-13036
- Effect of composition and structure on the properties of wrought aluminum alloys of the D16 type 03 p0297 A83-13255
- A simplified method of generating layer sequences for SiC polytypes. II - Application to the determination of new polytypes 20H/a/ and 20H/b/ 03 p0399 A83-13684
- Hexagonal ferrites for millimeter wave applications 03 p0399 A83-13786
- Single-crystal elastic constants in nondestructive evaluation of welds 04 p0492 A83-15215
- Comparison of thermal history of orthopyroxenes between lunar norites 78236, 72255, and diogenites 04 p0560 A83-15339
- A study of textures by modeling pole figures --- crystal structure computerized simulation for metal microstructure study 04 p0459 A83-15472
- Optical properties of disordered silicon in the range 1-10 eV 04 p0541 A83-15521
- Structure refinement of yttrium alpha-sialon from X-ray powder profile data 04 p0464 A83-15999
- Crystal chemistry of RT5H/D/x, RT2H/D/x and RT3H/D/x hydrides based on intermetallic compounds of CaCu₅, MgCu₂, MgZn₂ and PuNi₃ structure types 04 p0457 A83-16043
- Crystal structure of several SiC polytypes belonging to special structure family 05 p0690 A83-17146
- Semiconductor structures for repeated velocity overshoot 05 p0690 A83-17295
- 7 x 7 reconstruction on Si(111) resolved in real space 05 p0691 A83-17936
- Morphology and physical structure of trioxane and styrene copolymers 06 p0734 A83-18025
- Anharmonic properties - Ionic model of the effects of compression and coordination change --- thermodynamic properties in planetary interior minerals 07 p1029 A83-20233
- Investigation of the surface grain refinement for superalloys castings 07 p0895 A83-21499
- Characterization of AlN ceramics containing long-period polytypes 07 p0901 A83-21569
- Flow in polycrystals and the scaling of mechanical properties 07 p0896 A83-21602
- Shear bands and fracture in crystalline polymers 08 p1069 A83-21697
- Directional acoustic microscopy for observation of elastic anisotropy 08 p1101 A83-22755
- Structural studies of isolated small particles using molecular beam techniques --- atmospheric aerosols 09 p1308 A83-25181
- Structure and spectra of H₂O in hydrated beta-alumina 09 p1227 A83-25212
- The theory of finite plastic deformation of crystalline solids 10 p1437 A83-25309
- Investigation of the features of formation of crystalline structures grown in conditions of microgravity 11 p1661 A83-27447
- Spectroscopic and luminescent investigation of third group metal oxides 11 p1581 A83-27596
- A semiempirical self-consistent field Hartree-Fock crystal orbital approach to the infinite tetraza porphyrin nickel(II) system 11 p1661 A83-28072
- The crystalline structure of gas-saturated beta titanium alloys 11 p1550 A83-28546
- Piezoelectricity and pyroelectricity in polyvinylidene fluoride - Influence of the lattice structure 12 p1782 A83-29531
- Crystal structure of the microwave dielectric resonator Ba₂Ti₉O₂₀ 12 p1717 A83-29973
- Structural features of two-phase clinopyroxene from the Luna-24 regolith 13 p1960 A83-30088
- The Barkhausen effect and viscous phenomena in gadolinium molybdate single crystals 13 p1928 A83-30315

- Structural studies of new series of crystals 13 p1928 A83-30316
- Oriented crystallization of metals in the presence of electric current 13 p1822 A83-30906
- Evidence for pseudo bridge bonding of c(2 x 2)-O on Ni(100) 13 p1817 A83-30920
- Photogalvanic currents in reduced crystals of lithium tantalate 13 p1930 A83-31303
- The mechanism of fatigue in metals and alloys during thermal cycling 14 p1993 A83-32366
- Dry ice II, a new polymorph of CO₂ 16 p2437 A83-35996
- New class of materials - Half-metallic ferromagnets 16 p2421 A83-36564
- Reaction of Si(100) single crystals with nitrogen atoms 16 p2327 A83-36722
- Structural features of solid solutions in magnesium-yttrium alloys 16 p2334 A83-36888
- A study of the hardening of cast aluminum containing refractory tungsten compounds 16 p2335 A83-36893
- Defects in nsutite (gamma-MnO₂) and dry-cell battery efficiency 18 p2708 A83-39964
- Analytical methods: High-melting metals --- Book 19 p2905 A83-41848
- The electron structure and properties of solids --- Russian book 19 p2905 A83-41995
- Molecular dynamical studies of the dissociation of a diatomic molecular crystal. I - Energy exchange in rapid exothermic reactions 20 p2950 A83-42628
- The influence of gravity on the solidification of monotectic and near monotectic Cu-Pb alloys 20 p2942 A83-43307
- Many-beam imaging studies of crystal structure of ordered alloys 20 p2992 A83-43610
- High resolution electron microscopy studies on the precipitation in an Al-4 percent Cu alloy 20 p2956 A83-43614
- Structural phase transitions --- Russian book on metals and oxides 21 p3218 A83-45012
- Growth of single crystals by the pulling method --- Russian book 21 p3218 A83-45039
- Channeling, radiation, and reactions in crystals at high energies --- Russian book 21 p3218 A83-45048
- Characterization of some solvent-resistant thermoplastic matrix composites 21 p3107 A83-45072
- Pressure-induced phase transition of HgS 22 p3364 A83-46278
- Structural instability of the Laves phases Hf(x)Zr(1-x)V₂ 23 p3431 A83-47180
- X-ray analysis of the crystal structure and thermal expansion of the intermetallic compound (Tb_{0.8}Gd_{0.2})₃Co crystallized in space [IAF PAPER 83-159] 23 p3414 A83-47295
- Ordered structures on the bcc lattice with first, second, third and fifth neighbour interactions [ONERA, TP NO. 1983-63] 23 p3512 A83-48184
- Ordered structures in Ti Al alloys in the composition range from AB to AB₃ [ONERA, TP NO. 1983-65] 23 p3432 A83-48186
- Silicate structures and atomic substitution 23 p3427 A83-48253
- The characterization of alpha-prime-sialons and the alpha-beta relationships in sialons and silicon nitrides 23 p3434 A83-48254
- The structural characterisation of sialon polytypoids 23 p3434 A83-48255
- Sialon X-phase --- crystal structure 23 p3436 A83-48278
- Mechanistic studies of oxide electrodes reversibly incorporating Li(+) ions 24 p3558 A83-49941
- Structural and optical studies of topotaxially-grown Cu₂S from sprayed CdS thin films 24 p3636 A83-50181

CRYSTAL SURFACES

- Photoconductivity kinetics in Cd/x/Hg/1-x/Te crystals under surface excitation 01 p0108 A83-10374
- 7 x 7 reconstruction on Si(111) resolved in real space 05 p0691 A83-17936
- Diamond /111/ studied by electron energy loss spectroscopy in the characteristic loss region 10 p1390 A83-25675
- Coherent emission by relativistic particles interacting with atomic rows during reflection from a crystal surface 10 p1489 A83-26237
- The faceting of crystals pulled from a melt 11 p1662 A83-28352
- Reaction of Si(100) single crystals with nitrogen atoms 16 p2327 A83-36722
- Photovoltaic and structural properties of CuInSe₂/CdS solar cells 16 p2371 A83-36744
- XPS, AES and friction studies of single-crystal silicon carbide 16 p2338 A83-36973
- Drastic reduction of adsorption of CO and H₂ on (111)-type Pd layers 16 p2328 A83-36990
- SAW convolvers using the transverse-horizontal bilinear field 17 p2500 A83-38877

- Monatom-high level electron microscopy of metal surfaces 20 p2992 A83-43611
- Temperature stability of surface-generated bulk waves 23 p3446 A83-48722

CRYSTALLINITY

- Dispersed crystalline powders - An analysis of the scientific-technical literature 14 p1992 A83-32144
- Solar system ice - Amorphous or crystalline? 24 p3671 A83-48809

CRYSTALLIZATION

- NT DIRECTIONAL SOLIDIFICATION (CRYSTALS)
- NT MELT SPINNING
- NT RECRYSTALLIZATION
- Structural features and the stimulated crystallization of amorphous films of chalcogenide semiconductors 01 p0110 A83-10849
- Direct conversion from amorphous to beta-Si₃N₄ under high pressure 02 p0160 A83-11677
- Automatic apparatus for nucleation investigations --- crystalline phase detection 03 p0329 A83-14171
- Effects of fractional crystallization and cumulus processes on mineral composition trends of some lunar and terrestrial rock series 04 p0559 A83-15332
- SNC meteorites - Evidence against an asteroidal origin 04 p0563 A83-15364
- Hydrothermally altered impact melt rock and breccia - Contributions to the soil of Mars 04 p0567 A83-15578
- Crystallization sequences of Ca-Al-rich inclusions from Allende - An experimental study 04 p0572 A83-16352
- Pulsed radio emission during the crystallization of water and certain dielectrics --- for remote sensing 05 p0645 A83-17633
- Characterization and crystallization of Y-Si-Al-O-N glass 06 p0734 A83-18053
- Cooling rates for glass containing lunar compositions 07 p1035 A83-21324
- The creep of silicon carbide fibres 07 p0901 A83-21572
- Glass formation - A contemporary view 08 p1070 A83-22190
- Crystallization of copper under zero-g conditions 09 p1229 A83-23520
- The effect of the melt pressure on the stability of crystal growth by Stepanov's method 11 p1662 A83-28354
- Kinetics of crystallization of ZrF₄-BaF₂-LaF₃ glass by differential scanning calorimetry 12 p1717 A83-29972
- Heat of crystallization and melting point of amorphous silicon 13 p1825 A83-30344
- Super strong polymers in planar directions 13 p1826 A83-31250
- Ge-seeded crystallisation on SiO₂ by using a slider system with RF heated strip heater 13 p1931 A83-31758
- Epitaxial crystallization of nylon 6 cast from solution on the surface of poly(p-phenylene terephthalamide) filament 13 p1817 A83-31796
- Interfacial interaction between poly(p-phenylene terephthalamide) filament and nylon 6 matrix crystallized from the melt 13 p1817 A83-31797
- Progress in unconventional crystallization of silicon 14 p2090 A83-32307
- Segregation of impurities at grain boundaries and other compositional inhomogeneities in chill-casted silicon ingots 14 p2090 A83-32309
- Current aspects of the C.G.E. semicrystalline silicon ingots elaboration method 14 p2090 A83-32317
- Fast silicon-sheet growth with the supported-web method 14 p2091 A83-32321
- Critical technology limits to silicon material and sheet production 14 p2091 A83-32323
- Economic viability of the UCP semicrystalline silicon sheet technology --- Ubiquitous Crystallization Process 14 p2091 A83-32324
- Correlation of solar cell electrical properties with material characteristics of silicon cast by the ubiquitous crystallization process 15 p2192 A83-34695
- Microstructure of semi-crystalline thermoplastics structural foams 16 p2336 A83-35569
- Crystallization of amorphous Si₃N₄ prepared by the thermal decomposition of Si(NH)₂ 16 p2336 A83-35985
- The effect of the crystallization conditions of diamonds under high-temperature shock compression on their optical properties 18 p2750 A83-39531
- Crystallization of germanium-silicon solid solution from the vapour phase in microgravity conditions 18 p2644 A83-39914
- The effect of solute on the homogeneous crystal nucleation frequency in metallic melts 20 p2946 A83-43309
- Electrodeposition of zinc on glassy carbon from ZnCl₂ and ZnBr₂ electrolytes 20 p2951 A83-43420

- X-ray diffraction analysis at high temperature on two ceramic systems 21 p3116 A83-44127
- Structure and mechanical properties of Al-Si alloys obtained by crystallization under pressure 21 p3112 A83-44481
- Influence of zero-gravity state on crystallization of metallic materials [IAF PAPER 83-160] 23 p3414 A83-47296
- CRYSTALLOGRAPHY**
- Coherent bremsstrahlung from relativistic electrons axially channeled in crystals 01 p0054 A83-10815
- The magnetization of a single nickel crystal under intense magnetic fields and the Holstein-Primakoff test 01 p0110 A83-10923
- Radiation characteristics of channeled particles 03 p0313 A83-13960
- Magnetic and crystallographic characteristics of R2Ni2Ga and R2Ni2Al compounds --- rare earth compounds 03 p0299 A83-14153
- Thermal annealing of experimentally shocked feldspar crystals 04 p0564 A83-15375
- Asymmetry of conductivity along the polarization axis in ferroelectric crystals 04 p0542 A83-15885
- Structure refinement of yttrium alpha-sialon from X-ray powder profile data 04 p0464 A83-15999
- Grain boundary diffusion mechanisms in metals 04 p0460 A83-16001
- Theoretical strength of a perfect nickel crystal under simple stresses 04 p0461 A83-16063
- Transformation toughening of beta double prime-alumina by incorporation of zirconia 05 p0619 A83-17558
- Supercooled beta phase decomposition in titanium alloy VT23 06 p0728 A83-18134
- Growth of CdTe films on sapphire by molecular beam epitaxy 07 p0998 A83-19985
- Effect of structure, substructure, and crystallographic texture on the mechanical properties of titanium alloys 08 p1067 A83-22692
- Role of crystallites in the performance of polycrystalline solar cells 08 p1131 A83-22906
- Radiation processes in corundum crystals 09 p1349 A83-23450
- Analysis of high temperature materials --- Book 09 p1227 A83-24949
- Orientation relationships between bcc Mo and fcc gamma in a Ni-Al-Mo-W superalloy 10 p1398 A83-26284
- The crystallographic aspects of the decomposition of supersaturated solid solutions based on aluminum 10 p1399 A83-26792
- Conference on the Fabrication of Profiled Crystals and Products using Stepanov's Method and Their Applications in National Economy, Leningrad, USSR, March 10-12, 1982, Proceedings 11 p1662 A83-28351
- The dynamics of crystal formation during growth by Stepanov's method 11 p1662 A83-28353
- The physicochemical fundamentals of semiconductor materials technology --- Russian book 12 p1782 A83-28822
- The features of the atomic structure of pure inorganic ferroelastics 13 p1928 A83-30311
- The dielectric permittivity tensor and its spontaneous rotation in the submillimeter range for the ferroelastics KH3(SeO3)2 and KD3(SeO3)2 13 p1928 A83-30313
- The influence of defects on the switching of the pure ferroelastic KH3(SeO3)2 13 p1928 A83-30314
- Crystallographic features of subgranular structure and their relationship to the deformation texture 13 p1822 A83-30741
- A Mossbauer study of commercial beryllium 13 p1822 A83-30743
- Crack nucleation in tungsten on crystallographic planes and on grain boundaries of twist misorientation 14 p1997 A83-32946
- An investigation of the spectral transmission of a crystalline cloud medium 16 p2392 A83-36869
- Phase transformations and structure of metals and alloys --- Russian book 19 p2822 A83-41993
- Optical and crystallographic properties and impurity incorporation of Ga(x)In(1-x)As (with x between 0.44 and 0.49) grown by liquid phase epitaxy, vapor phase epitaxy, and metal organic chemical vapor deposition 20 p3053 A83-42606
- Paraelectric resonance --- Russian book on microwave spectroscopy of tunneling dipole centers in crystals 21 p3216 A83-43917
- Enlargement and accumulation of submicrocracks in oriented crystalline polymers 24 p3596 A83-49916
- CRYSTALS**
- NT BICRYSTALS
- NT BOULES
- NT CREATINE
- NT CRYSTAL OSCILLATORS
- NT DENDRITIC CRYSTALS
- NT DOPED CRYSTALS

- NT IONIC CRYSTALS
- NT LIQUID CRYSTALS
- NT METAL CRYSTALS
- NT MIXED CRYSTALS
- NT PIEZOELECTRIC CRYSTALS
- NT POLYCRYSTALS
- NT QUARTZ CRYSTALS
- NT SINGLE CRYSTALS
- NT WHISKERS (CRYSTALS)
- Andalusite traveling-wave masers for the middle part of the millimeter wave band 01 p0054 A83-10413
- Numerical solution and development of a transient temperature rate dependent constitutive equation --- model for crystalline solids [AIAA PAPER 83-0648] 05 p0653 A83-16815
- Investigation of aspects of the design of base-crystal matrix computing devices 08 p1152 A83-22182
- Density-functional theory for solid nitrogen and carbon dioxide at high pressure 13 p1929 A83-30958
- Acoustic crystals --- Russian book 15 p2238 A83-34165
- Cryocrystals 20 p3053 A83-42897
- Determination of the parameters of the equivalent circuit of the active region of an FET crystal 20 p2967 A83-42914
- Ice crystal and ice nucleus measurements in cap clouds 24 p3614 A83-49713
- CTD**
- U CHARGE TRANSFER DEVICES
- CUBA**
- Investigating the possibility of producing a land-use map for Cuba on the basis of space imagery 03 p0350 A83-14305
- CUBIC EQUATIONS**
- Factors for cubics and quartics 03 p0389 A83-14841
- Uniform convergence of interpolation by cubic splines 06 p0804 A83-18900
- Convergence of interpolational cubic splines on nonuniform grids 06 p0804 A83-19599
- Smoothing with periodic cubic splines 09 p1335 A83-23873
- A study of the effects of a cubic nonlinearity on a modern modal identification technique [AIAA 83-0810] 12 p1773 A83-29810
- Method of multiple scales and identification of nonlinear structural dynamic systems [AIAA 83-0813] 12 p1774 A83-29813
- The cubic spline numerical solution of the albatron problem [AIAA PAPER 83-1556] 14 p2012 A83-32774
- Smoothing of cubic parametric splines 16 p2406 A83-35324
- Image reconstruction by parametric cubic convolution 22 p3350 A83-46250
- CUBIC LATTICES**
- NT BODY CENTERED CUBIC LATTICES
- NT FACE CENTERED CUBIC LATTICES
- Surface waves in cubic elastic materials 10 p1437 A83-25304
- CUES**
- Improved g-cueing system --- for motion simulation in combat pilot training simulators 01 p0013 A83-10178
- Old problem/new solutions - Motion cueing algorithms revisited [AIAA PAPER 83-1082] 16 p2404 A83-36223
- CUESTAS**
- U RIDGES
- CULTURAL RESOURCES**
- Using remote sensing in a predictive archaeological model - The Jackson purchase region, Kentucky 15 p2186 A83-34837
- CULTURE TECHNIQUES**
- The significance of cellular contacts for the differentiation of precursor cells of hemopoietic stroma in long-term bone marrow cultures 01 p0080 A83-10548
- Cloning higher plants from aseptically cultured tissues and cells 02 p0219 A83-11823
- Effect of cultural conditions on the seed-to-seed growth of Arabidopsis and Cardamine - A study of growth rates and reproductive development as affected by test tube seals 11 p1639 A83-27825
- Growth of 'black smoker' bacteria at temperatures of at least 250 C 16 p2394 A83-35992
- Oxygen toxicity in cultured aortic endothelium Selenium-induced partial protective effect 20 p3033 A83-43478
- CUMULATIVE DAMAGE**
- Analysis of accumulated damage in accelerated fatigue testing by the increasing load methods 01 p0059 A83-10686
- The morphology of surface damage caused by friction [ASME PAPER 81-LUB-14] 02 p0186 A83-11943

- Fatigue life prediction on the basis of the characteristic parameters of the loading process 02 p0156 A83-12328
- Susceptibility of a pseudo-alpha titanium alloy to cyclic damage in the frequency range from 33 Hz to 10 KHz 02 p0156 A83-12329
- Cumulative damage and life-estimations in fatigue 02 p0193 A83-12660
- An anisotropic plasticity model for inelastic multi-axial cyclic deformation 02 p0193 A83-12736
- Low-cycle fatigue damage accumulation of aluminum alloys 03 p0299 A83-13903
- Damage accumulation and fracture life in high-temperature low-cycle fatigue 03 p0339 A83-13905
- Cumulation of high-temperature low-cycle fatigue damage in two-temperature tests 03 p0299 A83-13906
- Damage in composite materials: Basic mechanisms, accumulation, tolerance, and characterization --- Book 03 p0292 A83-14551
- An investigation of cumulative damage development in quasi-isotropic graphite/epoxy laminates 03 p0292 A83-14555
- Effect of stacking sequence on damage propagation and failure modes in composite laminates 03 p0293 A83-14563
- What is fatigue damage 03 p0342 A83-14565
- Application of fatigue-strength analysis to the evaluation of the consequences of local damage and the effects of wing-shell repairs. III - An example of the application of fatigue-strength analysis using a specific fatigue wear 03 p0342 A83-14620
- Analysis of accumulated damage in gas-turbine blade material during thermal cycling and vibration in a gas stream 03 p0301 A83-14732
- A study of cumulative fatigue damage in aluminum alloy 2011-T3 05 p0616 A83-17864
- Microdamage distribution in the volume of a polymer material under long-term creep 06 p0734 A83-18515
- The effects of very high cumulative deformation on structure and mechanical properties of aluminium 07 p0897 A83-21615
- Propagation of damage in elastic and plastic solids 08 p1116 A83-21684
- Application of the equivalent initial damage method to fretting fatigue 08 p1059 A83-21691
- The relation between microstructural fracture processes and macroscopic crack tip characterizing parameters during the stable growth of cracks 08 p1117 A83-21699
- Constitutive relations including ductile fracture damage - Application to cracked bodies 08 p1117 A83-21700
- Numerical modelling of warm prestress effect using a damage function for cleavage fracture 08 p1060 A83-21703
- Regularities of similarity and fatigue damage accumulation under irregular loading 08 p1118 A83-21737
- A unit for investigating microplastic deformations 08 p1101 A83-22630
- Analysis of progressive plastic buckling in cylindrical shell as contact problem 08 p1123 A83-22772
- Cumulative damage analysis 09 p1276 A83-23418
- Theoretical fatigue life prediction using the cumulative damage approach 09 p1277 A83-23423
- A study of the effect of stresses below the fatigue limit on the life of D16T alloy under programmed loading 09 p1228 A83-23501
- Physical principles of prediction of heterogeneous material fracture 09 p1279 A83-23933
- Equation of state for reinforced plastic materials subjected to mechanical and thermal loading with the account taken of damage and physical-chemical transformations 09 p1224 A83-23945
- A damage law for predicting the elevated temperature low cycle fatigue life of a martensitic stainless steel 10 p1393 A83-25418
- Experimental determination of stresses in damaged composites using an electric analogue 10 p1441 A83-26446
- Measurement of local stress distributions in damaged composites using an electric analogue 11 p1592 A83-27438
- Damage accumulation in the matrix of an Al-B composite under cyclic deformation 11 p1544 A83-28493
- On the question of damage and fracture criteria in creep 11 p1549 A83-28501
- Fatigue tests on fillet welded joints to assess the validity of Miner's cumulative damage rule 12 p1736 A83-29596
- Improved damage-tolerance analysis methodology [AIAA 83-0863] 12 p1738 A83-29751

- Reliability-based fatigue damage predictions under random vibration environments
[AIAA 83-0809] 12 p1741 A83-29809
- An accumulated-damage fracture criterion for a three-component layered composite 13 p1865 A83-30055
- Notion of continuum damage mechanics and its application to anisotropic creep damage theory 13 p1866 A83-30241
- Mathematical modeling of damage in unidirectional composites 14 p1986 A83-32344
- An experimental study of the progressive deformation and adaptability of thin-walled cylindrical shells under thermal cycling 14 p2030 A83-32380
- Morphology of ductile metals eroded by a jet of spherical particles impinging at normal incidence 14 p1993 A83-32624
- An approach to accelerated testing 15 p2173 A83-33549
- On the Monte Carlo methodology for cumulative damage 15 p2179 A83-34563
- Fatigue damage and degradation in random short-fiber SMC composite --- sheet molding compound 15 p2130 A83-34794
- On life behavior under spectrum loading --- effects of cumulative damage in structures 16 p2368 A83-36503
- Titanium fan disc Structural Life Prediction/Correlation program [SAE PAPER 821437] 17 p2522 A83-37985
- A partially contacting crack in a plate with an elliptic hole 17 p2524 A83-38509
- Disaggregation and a fracture criterion under creep 18 p2698 A83-39484
- Analysis of mechanical damage growth in notched carbon-epoxy (+ or - 45 deg) laminates 18 p2654 A83-40191
- Damage and fracture of tridirectional composites 18 p2704 A83-40194
- Compressive fatigue damage accumulation near holes in graphite/epoxy laminates 18 p2655 A83-40203
- The modelling of failure processes and the role of the matrix in the failure of carbon fibre reinforced epoxy resin 18 p2655 A83-40208
- Use of S/N-sensors for measuring the fatigue damage of materials 20 p2992 A83-43563
- On the nature of the accumulation effect in laser-induced damage to optical materials 21 p3203 A83-43862
- Buckling by cumulative plastic deformations under cyclic additional loading 21 p3152 A83-44458
- On some recent developments in the shakedown theory 21 p3154 A83-44660
- Model of fatigue crack propagation by damage accumulation at the crack tip 21 p3162 A83-45183
- Estimation of the extent of damage in reinforced composites under mechanical loading 21 p3163 A83-45320
- Low-cycle fatigue during symmetric disproportionate deformation 21 p3163 A83-45363
- Examination of the development of fatigue damage in metals by the eddy-current method 22 p3303 A83-46325
- Statistical cumulative damage theory for fatigue life prediction 23 p3468 A83-47595
- Surface damage in ceramics - Implications for strength degradation, erosion and wear 23 p3438 A83-48301
- Enhanced aircraft structural maintenance using organic depot damage tolerance analysis [AIAA PAPER 83-2450] 23 p3392 A83-48333
- Self-similarity of fatigue fracture - Cumulative damage 23 p3472 A83-48466
- Anisotropic creep damage in the framework of continuum damage mechanics [ONERA, TP NO. 1983-90] 24 p3593 A83-49409
- CUMULONIMBUS CLOUDS**
NT ANVIL CLOUDS
- Convective cloud merging and its effect on rainfall 02 p0215 A83-12827
- A numerical study of thunderstorm electrification using a three dimensional model incorporating the ice phase 02 p0215 A83-12938
- Vertical mass transport in cumulonimbus clouds on day 261 of GATE 08 p1140 A83-22297
- The development of the cumulonimbus clouds which move along a valley 09 p1313 A83-23964
- Cumulonimbus mother and daughter cells observed by NOAA7 - And 'The cumulus spore theory' 11 p1632 A83-27975
- Photographic documentation of some distinctive cloud forms observed beneath a large cumulonimbus 16 p2387 A83-35743
- The development and persistence of a cumulo-nimbus-cluster over central Europe observed by Meteosat 2 17 p2547 A83-38513
- A radar investigation of the wind field divergence in convective clouds 18 p2730 A83-40078
- Momentum transport by a line of cumulonimbus 22 p3341 A83-46856
- Aviation climatology 23 p3486 A83-47126
- Distribution of cumulonimbus cloud cover and thunderstorms above continents of the Northern Hemisphere 23 p3486 A83-47127
- CUMULUS CLOUDS**
NT ANVIL CLOUDS
- A numerical study on the combined action of droplet coagulation, ice particle riming and the splintering process concerning maritime cumuli 01 p0074 A83-10220
- Grouping of clouds in a numerical cumulus convection model 01 p0074 A83-10222
- The significance of thermodynamic forcing by cumulus convection in a general circulation model 02 p0213 A83-12231
- Entrainment and the droplet spectrum in cumulus clouds 02 p0215 A83-12941
- On the droplet distribution near the base of cumulus clouds 02 p0215 A83-12943
- Criteria for the formation and water content of cumulus clouds 03 p0364 A83-14097
- Numerical simulation of the tropical cyclone life cycle using a spectral cumulus parameterization 03 p0367 A83-14434
- NORAPS - The Navy Operational Regional Atmospheric Prediction System 03 p0368 A83-14441
- The inclusion of moist downdraft effects in the Arakawa-Schubert cumulus parameterization 03 p0368 A83-14445
- A lateral boundary condition for cumulus models which simulates the mesoscale response to convection 03 p0369 A83-14448
- Entrainment and detrainment in a simple cumulus cloud model 06 p0790 A83-18262
- A method for calculating the effects of deep cumulus convection in numerical models 06 p0791 A83-18459
- Attempt to directly simulate cloud-radiation interaction in the case of small cumuli 09 p1312 A83-23957
- On the preferred mode of cumulus convection in a conditionally unstable atmosphere 09 p1312 A83-23958
- Influence of sea roughness and atmospheric inhomogeneities on microwave radiation of the atmosphere-ocean system 10 p1422 A83-26494
- Studies of variations of cell parameters to be exceeded to confirm certain seeding hypotheses --- for cumulus clouds 11 p1626 A83-27031
- Numerical modeling of the influence of thermals on the development of cumulus clouds 13 p1883 A83-30030
- On the effect of an ice particle enhancement process operating in supercooled continental clouds 15 p2205 A83-34063
- A numerical model of the dynamics and microphysics of warm cumulus convection - Model description and preliminary results 15 p2205 A83-34065
- A quasi-one-dimensional, time-dependent and non-precipitating cumulus cloud model - On the bimodal distribution of cumulus cloud height 16 p2384 A83-35464
- Cumulus parameterization and rainfall rates. II 16 p2389 A83-36035
- Intercomparison of instruments used for measurement of cloud drop concentration and size distribution 18 p2688 A83-39136
- Theoretical experiments on cumulus dynamics 18 p2729 A83-40039
- A numerical simulation of winter cumulus electrification. I Shallow cloud 18 p2729 A83-40040
- Duration of convective events related to visible cloud, convergence, radar and rain gage parameters in south Florida 20 p3030 A83-42509
- Cumulus cloud transport of transient tracers 20 p3021 A83-42842
- Enhancement and initiation of a cumulus by a heat island 20 p3032 A83-43462
- The role of cloud top entrainment in cumulus clouds 21 p3180 A83-44706
- Visual cloud histories related to first radar echo formation in northeast Colorado cumulus 22 p3338 A83-45705
- A mechanism for the initiation of convective cumulus clouds in mountainous terrain [AD-A122033] 24 p3611 A83-49682
- Clouds and entrainment --- cumulus convective turbulence in clear air 24 p3612 A83-49694
- Cloud droplet spectra in summertime cumulus clouds 24 p3612 A83-49695
- 5-cm radar echoes and their microphysical significance in Florida cumuli 24 p3612 A83-49697
- Indirect effects of cumulus convection on large-scale radiative heating rates 24 p3613 A83-49704
- Zonally asymmetric aspects of large-scale thermodynamic forcing by cumulus convection 24 p3613 A83-49705
- Satellite-derived cloud statistics for Great Plains cumulus 24 p3613 A83-49706
- Graupel characteristics in relation to the dynamics of Florida cumuli 24 p3614 A83-49715
- Vertical continuity of microphysical processes and updrafts in supercooled portions of Florida cumuli 24 p3614 A83-49716
- Glaciating characteristics of Montana and Florida summer cumuli - Comparisons based on observations and modeling 24 p3614 A83-49717
- Radar and aircraft observations of generating cells --- tropospheric cumulus-like clouds generating ice crystals 24 p3615 A83-49723
- Cumulus convection as observed from an airborne infrared radiometer 24 p3615 A83-49726
- CURING**
- Synthesis and characterization of bisimide amines and bisimide amine-cured epoxy resins 01 p0027 A83-11486
- Effects of moisture, residual thermal curing stresses, and mechanical load on the damage development in quasi-isotropic laminates 03 p0292 A83-14556
- Photoelastic stress analysis of epoxy resin having an inserted metal. I - Residual stress caused by curing 05 p0611 A83-17096
- VOC compliant aircraft and transportation primers --- Volatile Organic Compound 07 p0898 A83-20430
- Material characterization and specification development for 350 F curing epoxy-graphite materials 07 p0875 A83-20443
- The effects of humidity on the processing and performance of a structural adhesive 07 p0899 A83-20453
- The effect of cure temperature on stresses in encapsulated electronic assemblies 07 p0919 A83-20457
- The dielectric properties of anhydride-cured epoxy potting compounds 07 p0899 A83-20458
- Resin flow during the cure of fiber reinforced composites 08 p1054 A83-21822
- Bisimide amine cured epoxy /IME/ resins and composites. II - Ten-degree off-axis tensile and shear properties of Celion 6000/IME composites 09 p1221 A83-23608
- The characterization of diaminodiphenyl sulfone /DDS/ cured tetraglycidyl 4, 4'-diaminodiphenyl methane /TGDDM/ epoxies 09 p1221 A83-23610
- Characterization of room temperature curing adhesives 09 p1237 A83-23622
- Heat of reaction, degree of cure, and viscosity of Hercules 3501-6 resin 10 p1400 A83-25882
- Assessment of chemical cure-shrinkage stresses in two technical resins 12 p1716 A83-29732
- [AIAA 83-0799] 12 p1716 A83-29732
- Evaluation of the curing of structural adhesives by ultrasonic interface waves - Correlation with strength 13 p1826 A83-31617
- Dynamic mechanical characterization of cure of a polyimide-graphite fiber composite (PMR 15/Celion 6000) 13 p1816 A83-31793
- Curing of epoxy matrix composites 15 p2130 A83-34795
- The effects of extensional creep and creep recovery on the dynamic properties of an unfilled and filled crosslinked polyester resin 15 p2142 A83-35071
- A model of the curing process of epoxy matrix composites 18 p2650 A83-40128
- Lower-curing-temperature PMR polyimides 19 p2823 A83-40923
- Computer assisted dielectric cure monitoring in material quality and cure process control 19 p2823 A83-41029
- Dynamic dielectric characterization of the cure process LARC-160 19 p2823 A83-41030
- Cure monitoring and control with combined dielectric/temperature probes 19 p2823 A83-41031
- Control of composite cure processes 21 p3119 A83-45067
- Calculation of cure process variables during cure of graphite/epoxy composites 21 p3107 A83-45071
- Characterization of quick-cure and vacuum-bag cure composites 21 p3119 A83-45073
- Network structure description and analysis of amine-cured epoxy matrices 22 p3262 A83-46283
- Control of composite cure processes 22 p3262 A83-46284
- Internal stresses in fibre reinforced plastics 22 p3264 A83-46304
- The curing of a bisphenol A-type epoxy resin with 1,8 diamino-p-menthane 22 p3270 A83-46905
- Applications of mass spectrometry techniques to autoclave curing of materials 24 p3559 A83-50143
- CURL (VECTORS)**
NT VORTICITY

CURRENT AMPLIFIERS

NT FREQUENCY MODULATION

PHOTOMULTIPLIERS

NT PHOTOMULTIPLIER TUBES

Highly sensitive temperature-stable DC amplifier for space probe experiment 08 p1080 A83-22279
Use of voltage and current amplifiers in ultrasonic apparatus 08 p1080 A83-22403
A low-noise low input impedance amplifier for magnetic measurements of nerve action currents 14 p2020 A83-32798

Double heterojunction Al(x)Ga(1-x)As/GaAs bipolar transistors (DHBJT's) by MBE with a current gain of 1650 15 p2151 A83-33916
Voltage and current amplifiers in ultrasonic equipment 22 p3290 A83-46327

CURRENT CONVERTERS (AC TO DC)

The physics of power rectifiers at very high current levels - Electric and thermal aspects --- French thesis 02 p0166 A83-11699

An operational description for static converters - Application to rectifier circuits 08 p1079 A83-22058
Application of microprocessor-based controls in an ac/dc power conversion system 11 p1559 A83-27151

CURRENT DENSITY

Loading schemes for a 50 MWth diagonally connected MHD generator 01 p0106 A83-10659
Corrosion fatigue of nickel and nickel-base alloys 02 p0156 A83-12223
Determination of the value of the field-aligned current density in the daytime polar cusp 02 p0211 A83-12449

Current distribution in a quasi-steady MPD arcjet [AIAA PAPER 82-1917] 02 p0145 A83-12489

Dipolar field propulsion - Principles and concepts [AIAA PAPER 82-1933] 02 p0146 A83-12499

Ion extraction capabilities of closely spaced grids [AIAA PAPER 82-1894] 02 p0147 A83-12551

Electron transverse velocity measurements in an intense relativistic electron beam diode 03 p0398 A83-13916

Computer analysis of dc field and current-density profiles of DAR IMPATT diode --- Double Avalanche Region 05 p0631 A83-17764

Morphological studies on the Li-Al electrode in fused salt electrolytes --- in Li-Al/FeS cells 07 p0879 A83-19877

The molten carbonate carbon dioxide concentrator - Cathode performance at high CO₂ utilization --- in manned space station cabin atmospheres 07 p0879 A83-19880

Simple porous electrode models for molten carbonate fuel cells 07 p0953 A83-19891

Regional variations of equatorial electrojet parameters 08 p1134 A83-22308

An investigation of the equatorial electrojet by means of ground-based magnetic measurements in Brazil 08 p1134 A83-22309

Diode laser threshold current density and lasing wavelength as functions of active region thickness 08 p1110 A83-22751

High efficiency p+/+n-n/+ back-surface field silicon solar cells with very large short-circuit current densities 08 p1131 A83-22913

Axial and angular distribution of current density in a thermionic converter with nonisothermal electrodes 10 p1445 A83-25887

Electric field enhanced diffusion in trans/CH/x --- battery cells 10 p1446 A83-26053

Rotational symmetries of electromagnetic radiation fields 10 p1406 A83-26853

Optimal design of Pb/1-x/Sn/x/Te double heterostructure injection lasers 11 p1583 A83-27622

Open-circuit voltages across two junctions in n/+/-p-p/+/- solar cells under high illumination levels 11 p1611 A83-27976

A two-dimensional numerical model of the tapered wiggler free-electron laser 13 p1856 A83-31142

Laboratory simulation and investigation of flare processes in plasmas 14 p2086 A83-32529

Imaging of spatial structures in superconducting tunnel junctions by electron-beam scanning 15 p2164 A83-34141

Electrodeposition of Ni-B4 C dispersion coatings 17 p2483 A83-38051

Explosive-emission mechanism for producing a cathode spot and extreme energy characteristics of a nanosecond volume discharge in nitrogen 21 p3210 A83-44141

Field-aligned current density versus electric potential characteristics for magnetospheric flux tubes 21 p3173 A83-44672

A decaying volt-ampere characteristic in the longitudinal current region 21 p3176 A83-45266

Comparison of height-integrated current densities derived from ground-based magnetometer and rocket-borne observations during the Porcupine F3 and F4 flights 22 p3337 A83-47068

The dependence of the characteristics of the slow phase of the galvanic nystagmus on the electrical stimulation parameters 23 p3497 A83-47109

The effective lifetime in semicrystalline silicon --- for solar cells 23 p3512 A83-48618

CURRENT DISTRIBUTION

On the optimization of magnetic field sources in electromechanical energy conversion 01 p0037 A83-10641

A study of secondary-emission microwave discharges with large electron transit angles 01 p0104 A83-11300

Polarization phenomena in the transition layer of SOS films 01 p0111 A83-11348

Current oscillations in semi-insulating GaAs associated with field-enhanced capture of electrons by the major deep donor EL2 02 p0243 A83-12294

Current distribution in a quasi-steady MPD arcjet [AIAA PAPER 82-1917] 02 p0145 A83-12489

Current distribution in MPD arcjets with applied magnetic fields [AIAA PAPER 82-1918] 03 p0289 A83-13600

Scattering by wires near a material half-space 03 p0306 A83-14017

Balanced helical antenna with tapered open ends 03 p0307 A83-14130

Effect of the near-wall layer on current oscillations in a plasma emitter 04 p0537 A83-15860

The excitation of a metal-bar grating by a current passing across one of the gaps 05 p0630 A83-17594

Numerical methods for current analysis in microstrip planar antennas 06 p0751 A83-18670

Idealized model for plasma acceleration in an MHD channel --- current distribution in plasma thruster 08 p1052 A83-22126

Edge effects in dipole phased arrays 08 p1076 A83-22236

Cross-sectional current distribution in coal fired diagonal conducting wall MHD generator 08 p1168 A83-23130

MHD channel electrical boundary-layer theory and applications 08 p1168 A83-23131

Investigation of a slow-wave structure of ring-bar type --- for high power traveling wave tubes in linear accelerators 09 p1252 A83-23453

The eigenfunction solution for scattered fields and surface currents of a vertex 09 p1248 A83-23812

Cylindrical eigencurrents --- during electromagnetic scattering by conducting surfaces 10 p1406 A83-26840

Algorithm for the calculation of the current distribution of electrically long curvilinear conductors 10 p1412 A83-26961

Current distribution within sulfur electrodes of cylindrical sodium-sulfur cells 11 p1603 A83-27172

Analytical and numerical techniques in the Green's function treatment of microstrip antennas and scatterers 11 p1553 A83-27896

Transformation of the matrix of generalized impedances in the case of frequency variation --- for antenna radiation pattern calculations 11 p1556 A83-27945

Modes of resonance of the Jerusalem cross in frequency-selective surfaces 12 p1718 A83-29438

Two-dimensional analysis of hot-electron emission current in MOS FET 13 p1834 A83-30783

A technique for calculating shunt leakage and cell currents in bipolar stacks having divided or undivided cells 14 p2047 A83-32637

Ionospheric and Birkeland current distributions inferred from the MAGSAT magnetometer data 15 p2196 A83-33940

Efficient numerical evaluation of electromagnetic fields due to rectangular patches of electric current 15 p2146 A83-35092

The singular integral problem in surfaces 15 p2148 A83-35187

On the current distribution for open surfaces 15 p2154 A83-35190

The electromagnetic field in a layered earth induced by an arbitrary stationary current distribution 16 p2341 A83-35410

Choice of optimal geometric parameters for conical spiral antennas comprising a conductor with additional bends 18 p2674 A83-39433

Finite-width currents, magnetic shear, and the current-driven ion-cyclotron instability 18 p2748 A83-40509

The role of current fluctuations in the control circuit of the active element in a Thompson oscillator 19 p2840 A83-41777

First-order equivalent current and corner diffraction scattering from flat plate structures 23 p3442 A83-47829

CURRENT REGULATORS

Loading schemes for a 50 MWth diagonally connected MHD generator 01 p0106 A83-10659

Large-signal dynamic-stability analysis of synchronised current-controlled modulators - Application to sine-wave high-power inverters 14 p2008 A83-33475

CURRENT SHEETS

Explosive destruction of current sheets and solar flares 01 p0129 A83-10384

Determination of the magnetospheric current system parameters and development of experimental geomagnetic field models based on data from IMP and HEOS satellites 02 p0204 A83-11961

Energetic particle losses and trapping boundaries as deduced from calculations with a realistic magnetic field model 02 p0204 A83-11962

Diagnostics of preflare current sheets in solar active regions 03 p0436 A83-13665

The energy of electric current sheets. I - Models with moving magnetic dipoles 03 p0438 A83-14912

Structure of the heliospheric current sheet in the early portion of sunspot cycle 21 05 p0708 A83-17379

Quadrupole distortions of the heliospheric current sheet in 1976 and 1977 05 p0708 A83-17380

Contact discontinuities in a cold collision-free two-beam plasma 05 p0689 A83-17382

Convection electric fields and ionospheric currents derived from model field-aligned currents at high latitudes [AD-A125082] 06 p0783 A83-18297

The origins of Birkeland currents 07 p0962 A83-20840

Current sheet acceleration of ions in the geomagnetic tail and the properties of ion bursts observed at the lunar distance 08 p1137 A83-23119

Neutral sheet current interruption and field-aligned current generation by three-dimensional driven reconnection 09 p1306 A83-24343

Observations of small-scale auroral vortices by the S3-2 satellite [AD-A127796] 11 p1618 A83-28315

Collisionless tearing modes in the presence of shear flow 12 p1780 A83-29073

Excitation of an electrostatic wave by a cold electron current sheet of finite thickness 13 p1881 A83-31530

Application of contour-conformal mapping to the flow along an S2 current sheet 13 p1805 A83-31798

The dynamics of current sheets and the physics of solar activity --- Russian book 14 p2114 A83-32526

The formation of current sheets in spatially nonuniform magnetic fields and plasma flows --- and solar flare theory 14 p2114 A83-32528

Laboratory simulation and investigation of flare processes in plasmas 14 p2086 A83-32529

Numerical simulation of a current sheet in the vicinity of the magnetic zero line 14 p2086 A83-32530

Neutral current sheets in the formation of reversed magnetic configurations 14 p2086 A83-32531

Magnetic-field configuration and plasma flow in the vicinity of a current sheet --- with reference to solar physics 14 p2114 A83-32532

Current sheets at the boundary of the magnetosphere 14 p2052 A83-32533

Nonhydrodynamic problems of a plasma focus 14 p2086 A83-32549

Magnetic field line reconnection experiments. V - Current disruptions and double layers 15 p2233 A83-33933

Ionospheric and Birkeland current distributions inferred from the MAGSAT magnetometer data 15 p2196 A83-33940

The energy of electric current sheets. II - The magnetic free energy and the photosphere magnetic flux 15 p2278 A83-34284

Tearing mode in a neutral current sheet in a plasma flow 16 p2417 A83-36934

Dependence of fast magnetic reconnection on electrical resistivity in an isolated current-sheet system 17 p2581 A83-37035

Current sheet models for solar prominences. I Magnetohydrostatics of support and evolution through quasi-static models 17 p2628 A83-38415

Magnetic reconnection as a mechanism for heating the persistent coronal loops 18 p2785 A83-40483

Electron distribution functions in a current sheet 18 p2749 A83-40518

Shape of the magnetosphere 19 p2865 A83-41119

Fast annihilation of oppositely directed magnetic fields in plasma 20 p3049 A83-42271

Generation of auroral arc elements in an inverted-V arc due to ion cyclotron turbulence 20 p3019 A83-42426

- Simulation of auroral current sheet equilibria and associated V-shaped potential structures
20 p3026 A83-43213
- Geomagnetic implications of a simple IMF model
21 p3170 A83-44246
- A static structural model of the outer magnetosphere of Jupiter
21 p3240 A83-44286
- Plasma current sheet studied by means of particle motion
21 p3211 A83-44288
- Kelvin-Helmholtz instability in boundary layer regions of the plasma sheet during magnetospheric substorm recovery
21 p3171 A83-44291
- Forced reconnection by fast magnetosonic waves in a current sheet with stagnation-point flows
21 p3214 A83-45193
- Plasma regimes in the deep geomagnetic tail - ISEE 3
22 p3334 A83-46891
- A comparison of coronal and interplanetary current sheet inclinations
22 p3389 A83-47046
- Comparison of heliospheric current sheet structure obtained from potential magnetic field computations and from observed polarization coronal brightness
22 p3389 A83-47071
- The dynamics of two-dimensional ideal MHD
23 p3510 A83-48046
- CURRENT STABILIZERS**
U CURRENT REGULATORS
- CURTISS-WRIGHT MILITARY AIRCRAFT**
U MILITARY AIRCRAFT
- CURVATURE**
On the non-linear evolution of Goertler vortices in non-parallel boundary layers
02 p0170 A83-12173
- Modeling the curved turbulent wall jet
03 p0315 A83-13137
- Interferometric determination of curvatures of flexed plate
[ASME PAPER 82-WA/APM-27]
04 p0499 A83-15688
- Space-time curvature and cosmology
04 p0555 A83-15707
- Structure of turbulence in curved wall boundary layers
[AIAA PAPER 83-0457]
05 p0636 A83-16726
- Measurement of scoliosis by orthopedic surgeons and radiologists
06 p0797 A83-18198
- Curvature transitions of composite curves and surfaces
- Questions regarding details of computer-aided design
--- German thesis
07 p0982 A83-20398
- Quality of trial functions in quadratic isoparametric representation of an arc
07 p0949 A83-21441
- On heat transfer modelling for turbulent shear flows on curved surfaces
09 p1263 A83-24822
- Stability properties of cylindrically curved mean flows
--- in atmosphere
14 p2058 A83-32469
- Transonic shock/turbulent boundary-layer interaction on curved surfaces
14 p1970 A83-32590
- Calculation of curved shear layers with two-equation turbulence models
17 p2501 A83-37030
- An experimental study of surface curvature effects on a supersonic turbulent boundary layer
[AIAA PAPER 83-1672]
17 p2444 A83-37182
- The wavefront curvature of an optically pumped waveguide laser
17 p2514 A83-37762
- Alternating direction adaptive grid generation
[AIAA PAPER 83-1937]
18 p2740 A83-39387
- The crack problem in a specially orthotropic shell with double curvature
18 p2699 A83-39536
- An offset spline approximation for plane cubic splines
23 p3502 A83-48729
- Apparent superluminal velocities due to the curvature of space
24 p3670 A83-50159
- CURVE FITTING**
Algorithms for smoothing data with periodic and parametric splines
01 p0102 A83-10284
- Shock fitting in the numerical analysis of supersonic conical flows
01 p0003 A83-11269
- A two-stage method of fitting conic arcs and straight-line segments to digitized contours
01 p0098 A83-11427
- Goodness-of-fit of the Ramberg-Osgood analytic stress-strain curve to tensile test data
02 p0158 A83-12833
- Stresses in rotating disc with eccentric hole
02 p0196 A83-12873
- An interactive method for surface fitting three-dimensional bodies
[AIAA PAPER 83-0220]
05 p0581 A83-16591
- Abel inversion with a simple analytic representation for experimental data
07 p0988 A83-19984
- Smoothing with periodic cubic splines
09 p1335 A83-23873
- Processing of 2-dimensional lidar-derived windfields
11 p1630 A83-27070
- A reanalysis of the data of three classical Cepheids - V381 Cen, V500 Sco, and SV Vel
12 p1791 A83-28991
- Boundary-fitted coordinate systems for numerical solution of partial differential equations - A review
12 p1772 A83-29620
- Analysis of forced vibration by reduced impedance method. III - Damped vibration
15 p2174 A83-34008
- An adaptive filter using polynomial least squares methods
15 p2221 A83-35108
- Smoothing of cubic parametric splines
16 p2406 A83-35324
- Curve fitting with conic splines
17 p2571 A83-38060
- Period determination of the Delta Scuti star HR 5005
19 p2910 A83-41063
- Complex combined curve design and fitting - A B-spline multiple knot method
20 p3042 A83-43699
- Approximating point-set images by line segments using a variation of the Hough transform
21 p3190 A83-44271
- CURVED BEAMS**
Thermal stresses in anisotropic noncylindrical beams
09 p1280 A83-24511
- Geometrically non-linear formulation for two dimensional curved beam elements
11 p1600 A83-28725
- Creep buckling of structures
[AIAA 83-0864]
12 p1738 A83-29752
- Design, analysis and test of composite curved frames for helicopter fuselage structure
[AIAA 83-1005]
12 p1741 A83-29805
- Galerkin method as a tool to investigate the planar and non-planar behavior of curved beams
23 p3471 A83-48171
- CURVED PANELS**
PANDA - Interactive program for minimum weight design of stiffened cylindrical panels and shells
02 p0194 A83-12745
- Noise transmission into semicylindrical enclosures through discretely stiffened curved panels
04 p0532 A83-15069
- PANDA - Interactive computer program for preliminary minimum weight design of composite or elastic-plastic, stiffened cylindrical panels and shells under combined in-plane loads
06 p0773 A83-18227
- The stability of elastoplastic arches and cylindrical panels
10 p1442 A83-26821
- Dynamic stability of cylindrical sandwich panel subjected to axial compression
11 p1593 A83-27770
- Interaction of a surface wave with a crack situated on a curved surface
11 p1597 A83-28475
- Further comparison of the numerical and experimental buckling behaviors of composite panels
11 p1599 A83-28722
- Collapse analysis of cylindrical composite panels with cutouts
[AIAA 83-0875]
12 p1738 A83-29759
- Buckling behavior and imperfection sensitivity of composite panels
[AIAA 83-0877]
12 p1739 A83-29761
- The creep of three-layer reinforced cylindrical panels
13 p1866 A83-30308
- The stability of stiffened toroidal panels under external radial pressure
13 p1867 A83-31399
- Free vibrations of antisymmetric angle-ply laminated circular cylindrical panels
16 p2365 A83-35641
- Moisture and temperature effects on the instability of cylindrical composite panels
21 p3105 A83-43968
- CURVED SURFACES**
U CONTOURS
U SHAPES
U SURFACES
- CURVES (GEOMETRY)**
Approximating shapes using parameterized curves
02 p0231 A83-12174
- Low-loss LiNbO3 waveguide bends with coherent coupling
07 p0993 A83-20799
- Semi-automatic system for defining free-form curves and surfaces
10 p1461 A83-25475
- Flow in curved pipes
13 p1843 A83-31086
- Determination of quadric surfaces from two projective views
14 p2021 A83-33344
- Multi-segments approximation to a three-dimensional curved line using the least-squares locating method.
14 p2022 A83-33345
- Segmentation of digital curves using linguistic techniques
21 p3194 A83-44259
- CURVILINEAR COORDINATES**
U SPHERICAL COORDINATES
- CUSHIONCRAFT GROUND EFFECT MACHINE**
A review and assessment of methods for prediction of the dynamic stability of air cushions
01 p0112 A83-11038
- CUSHIONS**
Material effects on the dynamic stability of a flexible skirted air cushion
[AIAA PAPER 83-0369]
05 p0692 A83-16675
- Effectiveness of seat cushion blocking layer materials against cabin fires
[SAE PAPER 821484]
17 p2459 A83-38003
- CUSPS**
NT CUSPS (MATHEMATICS)
- CUSPS (MATHEMATICS)**
Does IMF B(y) induce the cusp field-aligned currents?
13 p1882 A83-31626
- CUT-OUTS**
U OPENINGS
- CUTTERS**
Two-stage personnel parachute delay cutter development
04 p0526 A83-15431
- CUTTING**
NT BLANKING (CUTTING)
NT LASER CUTTING
NT METAL CUTTING
NT MILLING (MACHINING)
NT PLANING
NT SLICING
NT SPARK MACHINING
- Optimizing the cutting of stock with the aid of computers --- Russian book
09 p1274 A83-23826
- Recognition of cutting states for difficult-to-cut materials
Application of pattern recognition technique
20 p3040 A83-43698
- The effects of cut and edge on the ultimate tensile strength of planar randomly-distributed short fiber composites
21 p3106 A83-44052
- CV-2 AIRCRAFT**
U DHC 4 AIRCRAFT
- CV-990 AIRCRAFT**
Convair 990 transonic flow-field simulation about the forward fuselage
[AIAA PAPER 83-1785]
17 p2452 A83-38626
- CW RADAR**
U CONTINUOUS WAVE RADAR
- CYANATES**
Effect of increased blood oxygen affinity on skeletal muscle surface oxygen pressure fields
13 p1897 A83-30457
- CYANIDE EMISSION**
U CN EMISSION
- CYANIDES**
NT CYANOGEN
- The kinetic temperature and density of the Sagittarius B2 molecular cloud from observations of methyl cyanide
10 p1504 A83-25729
- Detection of the J = 1 - 0 transition of CH3CN
10 p1516 A83-26757
- Positive ion composition measurements and acetonitrile in the upper stratosphere
15 p2199 A83-34223
- Kr(+) and Ar(+) laser-excited fluorescence of CN in a flame
17 p2485 A83-37746
- CYANO COMPOUNDS**
Cyano-bacterial symbiosis - A well into the past --- Y
13 p1895 A83-30320
- Dense cores in dark clouds. IV - HC5N observations
19 p2919 A83-41626
- Cyanoacetylene as a density probe of molecular clouds
20 p3067 A83-42443
- A possible mechanism for the reduction of voltage delay in the Li/SOCI2 system via cyanoacrylate coatings on lithium
24 p3599 A83-49929
- CYANOGEN**
Supplements to the identification of CN lines in the solar spectrum in the wavelength range of 4145-4190 A - Weak lines not listed in Rowland's Tables of 1966
06 p0854 A83-18846
- The Cyanogen distribution of the red giants in M5
06 p0840 A83-19284
- The cyanogen inhomogeneity of NGC 362
11 p1669 A83-27114
- On the CN(0,0) spectrum of comet Kohoutek 1973 XII
14 p2101 A83-33286
- The C2H, C2, and CN electronic absorption bands in the carbon star HD 19557
17 p2605 A83-37918
- The Al I-cyanogen correlation in the spectra of globular cluster red giants and the origin of intracluster heavy element variations
22 p3382 A83-46992
- CYBERNETICS**
Semantic questions pertaining to artificial intelligence
01 p0094 A83-10508
- Cybernetics, applied mathematics --- Russian book
01 p0094 A83-10563
- Neural analog information processing
08 p1158 A83-22812
- Abstract and structural theory of relay devices --- Russian book
09 p1327 A83-24243
- The modelling of hierarchical systems of spatial-temporal synchronous connections of the human brain
10 p1462 A83-25625
- The formation of nonlinear binary sequences
14 p2075 A83-32477
- Estimation of the free distance of convolutional codes with rate 1/2
14 p2075 A83-32486

Adaptation and learning in systems of control and decision making --- Russian book

- 14 p2076 A83-33025
Linear ill-posed problems with random errors in the data 19 p2889 A83-40987
The abstract theory of systems (ATS) and applied studies 20 p3039 A83-42915
Infinite-valued logic in problems of cybernetics --- Russian book 21 p3192 A83-43910
Principles for synthesizing the structure of complex systems --- Russian book 21 p3195 A83-45021
Stability and stabilization of discrete processes --- Russian book 21 p3195 A83-45038
Nonsmooth problems in optimization and control theory --- Russian book 21 p3195 A83-45045
A solution of the problem of nonlinear filtering in conditions of ambiguous measurements 22 p3350 A83-45658

CYCLES

NT ACTIVITY CYCLES (BIOLOGY)

NT BRAYTON CYCLE

NT CARBON CYCLE

NT CARNOT CYCLE

NT OTTO CYCLE

NT RANKINE CYCLE

NT SOLAR CYCLES

NT STIRLING CYCLE

NT STRESS CYCLES

NT SUNSPOT CYCLE

NT THERMODYNAMIC CYCLES

NT WORK-REST CYCLE

Lithium cycling behavior in 2-methyltetrahydrofuran with alcohol additives --- in lithium batteries

- 07 p0880 A83-19890
The seasonal cycle over the United States and Mexico 10 p1450 A83-25389
Cyclic oxidation of superalloys 20 p2952 A83-42234

Complete cycle of the individual development of *Arabidopsis thaliana* (L.) Heynh. plants aboard Salyut-7 23 p3496 A83-48515

CYCLIC ACCELERATORS

NT STORAGE RINGS (PARTICLE ACCELERATORS)

NT SYNCHROCYCLOTRONS

CYCLIC ADENOSINE MONOPHOSPHATE

U CYCLIC AMP

CYCLIC AMP

The content of endogenous serotonin in the lymph organs of rats during the adaptation to high-altitudes and the pattern of radiation sickness

- 11 p1641 A83-28763
Opposing actions of dibutylryl cyclic AMP and GMP on temperature in conscious guinea-pigs 12 p1762 A83-29530
Regulation of glycogenolysis in human muscle in response to epinephrine infusion 13 p1902 A83-30455

The effect of activators of cAMP accumulation on the separate stages of genome expression in cells during acute radiation injuries of organisms. VI - Peculiarities of the inhibition of RNA synthesis on a template of isolated chromatin by separate fractions of histones from the liver of normal, irradiated and serotonin-treated rats

- 14 p2061 A83-32051
AMP synthesis in aqueous solution of adenosine and phosphorus pentoxide 17 p2563 A83-38891

CYCLIC COMPOUNDS

NT CYCLIC AMP

NT CYCLIC HYDROCARBONS

An investigation of DNA synthesis in the liver of irradiated and serotonin-treated rats following the removal of the cycloheximide block 14 p2061 A83-32053

CYCLIC HYDROCARBONS

NT ANTHRACENE

- Radiation-induced loss of unsaturation in 1,2-polybutadiene 07 p0874 A83-21077
Background concentration of organochlorine compounds and 3,4-benzopyrene in the environment (according to worldwide data) 24 p3602 A83-49104

CYCLIC LOADS

Calculating the limiting state of refractory alloys under high-cycle loading 01 p0026 A83-10687

- Fracture of fatigue-loaded composite laminates 02 p0149 A83-12013
Determination of the degree of defectiveness in structural components 02 p0191 A83-12156

Life determination under dual-frequency loading. II - Proposed method --- for metals and welded joints 02 p0156 A83-12327

Susceptibility of a pseudo-alpha titanium alloy to cyclic damage in the frequency range from 33 Hz to 10 KHz 02 p0156 A83-12329

- The effect of the shape and size of a fatigue crack on the cyclic fracture toughness of titanium alloy VT9 02 p0156 A83-12330

DSO-series devices for fatigue testing under repeated impact and harmonic loading with various cycle ratios

- 02 p0191 A83-12342
An anisotropic plasticity model for inelastic multi-axial cyclic deformation 02 p0193 A83-12736
The cyclic strength of reinforced magnesium-matrix composites 02 p0151 A83-13038

Low-cycle fatigue and life prediction --- Book

- 03 p0339 A83-13901
Low-cycle fatigue damage accumulation of aluminum alloys 03 p0299 A83-13903
Cumulation of high-temperature low-cycle fatigue damage in two-temperature tests 03 p0299 A83-13906

Multiaxial nonproportional cyclic deformation 03 p0340 A83-13911

A study of polygonization in aluminum deformed by cyclic bending using low-angle X-ray scattering 03 p0300 A83-14163

The temperature and force dependence of the activation energy of cyclic creep for refractory alloys 03 p0301 A83-14730

Studies on plastic structures - Stability, anisotropic hardening, cyclic loads 04 p0495 A83-15012
Path dependent nature of fatigue crack growth 04 p0496 A83-15064

Methods for determining the crack growth rate during the testing of materials for cyclic fracture toughness 04 p0497 A83-15395

Finite endochronic theory for ratcheting and cyclic plasticity 04 p0500 A83-16096

Transient nonlinear response of impulsively-loaded circular plates 04 p0501 A83-16200
The influence of fatigue stress on the creep behaviour of metals 04 p0462 A83-16275

Cyclic creep behavior of pure aluminum 05 p0614 A83-17089
Damage to structures by high-cycle fatigue 05 p0655 A83-17672

The interlayer strength criteria for carbon composites under cyclic loads 06 p0725 A83-18502
A study of the effect of low-cycle loading on the mechanical characteristics and structure of a unidirectional organic-fiber-reinforced composite 06 p0725 A83-18505

The effect of the deformation history and loading cycle ratio on the cyclic fracture toughness characteristics of VT9 alloy 06 p0733 A83-19303

Various criteria for determining the equivalent plastic deformation range in the theory of low-cycle fatigue 06 p0777 A83-19304

A study of the effect of cyclic block loading on the deformation characteristics and strength of structural materials under plane stressed state. I - Resistance to elastic-plastic deformation 06 p0733 A83-19306

A study of the principles underlying the deformation and fracture of a polycrystalline molybdenum alloy under high-temperature cyclic creep. I - The long-term strength and creep 06 p0733 A83-19307

A study of the principles underlying the deformation and fracture of a polycrystalline molybdenum alloy under high-temperature cyclic creep. II - Structural changes during creep 06 p0733 A83-19308

Anelastic relaxation controlled cyclic creep and cyclic stress rupture behavior of an oxide dispersion strengthened alloy 07 p0885 A83-20263

The effect of cyclic mechanical loads on the endurance of wedge-shaped structures during thermal cycling in a gas flow --- for Ni superalloy gas turbine blades 07 p0946 A83-20904

Deformation characteristics of shape-memory alloys under nonstationary cyclic loading 07 p0890 A83-20908

Characteristics of the plastic deformation of titanium alloys under impulsive loading 07 p0890 A83-20909
Tensile fatigue of carbon fiber reinforced plastics 07 p0877 A83-20924

Requirements of constitutive models for two nickel-base superalloys 07 p0891 A83-21071
High cycle fatigue properties of cast nickel base superalloys IN 738LC and IN 939 07 p0892 A83-21463

The influence of creep on the high temperature cyclic life of IN738LC 07 p0893 A83-21471
Some interactions of creep and fatigue in IN 738 LC at 850 C 07 p0893 A83-21472

Time dependent low cycle fatigue of PM Astroloy at 1003 K 07 p0893 A83-21475
Fatigue of high-temperature materials at ultrasonic frequencies 07 p0894 A83-21479

Crack initiation and propagation in a forged nickel-base alloy under high mechanical and thermal loading 07 p0894 A83-21480

Mechanisms of high cycle fatigue of cast nickel base alloys 07 p0894 A83-21482

The effects of very high cumulative deformation on structure and mechanical properties of aluminum

- 07 p0897 A83-21615
Near-crack tip finite strain analysis 08 p1116 A83-21662

The relationship of compliance changes during fatigue loading to the fracture of composite materials 08 p1054 A83-21682

On the interaction of hardening and fatigue damage in the 316 stainless steel 08 p1062 A83-21736

The low-cycle fatigue and cyclic behaviour of zirconium 08 p1062 A83-21738
Practical application of a model for fatigue damage with irregular cyclic loading 08 p1063 A83-21757

Fatigue crack propagation behavior under complex mode loading 08 p1063 A83-21758
Fatigue crack growth under controlled K 08 p1118 A83-21765

Deflections of elastic-plastic hyperstatic beams under cyclic loading 08 p1120 A83-21810
Low-cycle fatigue of base metals and welded joints at elevated temperature - Life prediction, application, transferability 08 p1065 A83-22029

Comparison of static, cyclic, and thermal-shock fatigue in ceramic composites 08 p1055 A83-22268
Variable amplitude fatigue life estimation models 09 p1277 A83-23421

Estimation of the cyclic fatigue life of parts subjected to complex loading patterns --- for compressor disks and turbine wheels in aircraft engines 09 p1228 A83-23502

A study of the effect of the cycle ratio on the fatigue of titanium alloys under high-frequency loading 09 p1228 A83-23503

The relationship of stiffness changes in composite laminates to fracture-related damage mechanisms 09 p1223 A83-23940
Fatigue crack evolution in overaged Ni-14.4at.% alloy with coherent precipitates 10 p1394 A83-25423

The effect of an elastic wall on the boundary layer 10 p1413 A83-25593
Effects of hydrogen on near-threshold crack propagation in niobium 10 p1396 A83-25867

High temperature low cycle fatigue of IN 738 and application of strain range partitioning 10 p1398 A83-26282

The effect of cycle waveshape on the low cycle fatigue behaviour of 20%Cr-25%Ni-Nb stainless steel at 650 C 11 p1547 A83-27852

Overload induced crack growth rate attenuation behavior in aluminum alloys 11 p1548 A83-28223
Mechanism of corrosion fatigue crack propagation in high strength steels 11 p1548 A83-28446

The effect of anisotropy, thickness, and operating time on the crack growth in pressed and rolled products of D16chT and V95pchT1 alloys 11 p1549 A83-28478

The effect of the annealing conditions on the cyclic fracture toughness of the magnesium alloy VMD-10 11 p1549 A83-28488

Damage accumulation in the matrix of an Al-B composite under cyclic deformation 11 p1544 A83-28493

The effect of block cyclic loading on the deformability and strength of structural materials under conditions of plane stressed state. II - The limiting states /yield and strength/ 11 p1549 A83-28504

Method for low-cycle fatigue testing of isothermal and nonisothermal loading 11 p1550 A83-28618
Observations of cyclic grain boundary migration in aluminum after large numbers of fatigue cycles 12 p1714 A83-29510

A recommended procedure for determining the strain rate sensitivity in superplasticity --- of metal alloys 12 p1714 A83-29721

Ion implantation effect on fatigue crack initiation in Ti-24V 12 p1714 A83-29724
On the effect of residual stresses on crack growth from a hole [AIAA 83-0840] 12 p1737 A83-29747

Delamination-based compression residual-strength prediction model for composites [AIAA 83-0872] 12 p1738 A83-29756

Low cycle fatigue behavior of aluminum/stainless steel composites [AIAA 83-0806] 12 p1711 A83-29886

The effect of the chemical composition on the high-cycle and low-cycle fatigue behavior of D16 and V95 alloy sheets under pulsating tension 13 p1819 A83-30068

On the description of cyclic hardening under complex loading histories 13 p1822 A83-31170

On the relation between stable crack growth and fatigue 13 p1867 A83-31540

Slow fatigue crack growth and threshold behaviour in IMI 685 --- in titanium alloys 13 p1824 A83-31541

A study of short fatigue crack growth behaviour in titanium alloy IMI 685 13 p1824 A83-31542

On life time predictions with the strain range partitioning method 13 p1824 A83-31543

Anisotropic yield surfaces in cyclic plasticity 13 p1867 A83-31544

Factors leading to the formation of surface oxide layer on metal during cyclic loading under conditions of fretting corrosion 14 p1992 A83-32071

On the cyclic behavior of cast and extruded aluminum alloys. B - Fractography 14 p1992 A83-32343

Metallography of fatigue crack initiation in an overaged high-strength aluminum alloy 14 p1994 A83-32681

The effects of radiation on vibrational heating of polymers-heat explosion theory [AIAA PAPER 83-1505] 14 p2010 A83-32743

Cyclic deformation, fatigue crack nucleation and propagation in metals and alloys 14 p1995 A83-32806

Subsurface crack initiation in high cycle fatigue in Ti6Al4V and in a typical Martensitic stainless steel 14 p1997 A83-32944

A study of the low-cycle fatigue of the structural alloys for cryogenic applications 14 p1998 A83-33018

A study of the fatigue of structural alloys under repeated static loading with superposed vibration 14 p1998 A83-33019

A study of the high-cycle fatigue of materials under plane cantilever bending 14 p1998 A83-33020

Low cycle fatigue of aluminum at elevated temperatures 15 p2138 A83-34133

Prediction of constant amplitude fatigue lives of precracked specimens from accelerated fatigue data 15 p2140 A83-34743

The use of a structural model for determining the adaptability curve for turbine disks in stress concentration zones 15 p2123 A83-35039

Life estimation methods of gas turbine rotating components 16 p2305 A83-35870

Overview of temperature and environmental effects on fatigue of structural metals 16 p2330 A83-36161

Temperature dependent deformation mechanisms of Alloy 718 in low cycle fatigue 16 p2331 A83-36168

Environment, frequency and temperature effects on fatigue in engineering plastics 16 p2337 A83-36170

Strain rate sensitivity effects in cyclic deformation and fatigue fracture 16 p2332 A83-36188

Fatigue limits of Cu and Al up to 10 to the 10th loading cycles 16 p2332 A83-36189

A review of the role of frequency on fatigue crack initiation and growth at elevated temperatures 16 p2332 A83-36194

Evaluation of fatigue limits and crack growth properties of PM-Mo alloys tested at cyclic frequencies of 200 Hz and 20 kHz 16 p2333 A83-36199

On the description of cyclic hardening under complex loading histories [ONERA, TP NO. 1983-7] 16 p2333 A83-36420

Influence of stress cycling on creep behaviour of an Al-Mg alloy under strain ageing conditions 16 p2334 A83-36727

The relationship between the structure and cyclic fracture toughness of alpha titanium alloys 16 p2335 A83-36890

Some consequences of the two-parameter model of fatigue-life scatter --- under complex and cyclic loading 17 p2518 A83-37269

Low cycle fatigue of tubular specimens 17 p2519 A83-37299

Direct observations of crack tip dislocation behavior during tensile and cyclic deformation 17 p2489 A83-38377

Influence of overloads and block loading sequences on mode III fatigue crack propagation in A469 rotor steel 18 p2665 A83-39075

The fracture toughness of structural alloys under cyclic loading. I, II 18 p2665 A83-39498

Prediction of the fatigue life of Duralumin specimens 18 p2665 A83-39499

Separate processing of the results of low-cycle and high-cycle fatigue tests --- of aluminum alloys 18 p2665 A83-39500

Fatigue life prediction for complex load versus time histories 18 p2700 A83-39995

Deformation of a circular cylindrical shell with a periodic system of holes 18 p2702 A83-40122

Fatigue behaviour of carbon fiber reinforced epoxy composite materials with edge notch 18 p2655 A83-40202

Cyclic creep and stress rupture of a mechanically alloyed oxide dispersion and precipitation strengthened nickel-base superalloy 18 p2669 A83-40633

Method of investigating the rules of deformation and failure under conditions of low-cycle nonisothermal loading 19 p2855 A83-40763

The cyclic fracture toughness, K_{IC}, of aluminum alloys 19 p2821 A83-40802

The effect of crack closure and estimation of the cyclic fracture toughness of structural alloys 19 p2856 A83-40803

Generic aspects of three-dimensional internal-damage development in fatigue-loaded composite laminates 19 p2819 A83-41035

Plastic materials with continuous transition between loading and unloading states 19 p2859 A83-41544

A theoretical analysis of the effect of short cracks on the endurance limit of materials 19 p2859 A83-41597

The strength of GTE structural elements under low-cycle loading 20 p2936 A83-42877

The cyclic stress-strain response of polycrystalline Al-Zn-Mg alloy and commercial alloys based on this system 20 p2955 A83-43469

Investigation of the mechanism of failure under low-cycle nonisothermal load --- for structural steels 20 p2956 A83-43562

Use of S/N-sensors for measuring the fatigue damage of materials 20 p2992 A83-43563

Appliance for fatigue tests of materials with symmetrical and asymmetrical loading 20 p2992 A83-43624

Cyclic thermal shock [ASME PAPER 83-PVP-56] 20 p3009 A83-43729

Buckling by cumulative plastic deformations under cyclic additional loading 21 p3152 A83-44458

The cyclic J-integral as a criterion for fatigue crack growth 21 p3158 A83-44910

Fatigue crack growth of a corner crack in an attachment lug 21 p3158 A83-44920

The effect of the parameters of cyclic loading on the kinetics of deformation and fracture of El826 alloy 21 p3114 A83-45317

Low-cycle fatigue during symmetric disproportionate deformation 21 p3163 A83-45363

Fatigue crack initiation from a notch tip under a cyclic compressive load 22 p3304 A83-45622

A technique for cyclic-plastic notch-strain measurement 22 p3307 A83-46812

Statistical cumulative damage theory for fatigue life prediction 23 p3468 A83-47595

Cyclic fatigue behavior of ceramics 23 p3437 A83-48291

Self-similarity of fatigue fracture - Cumulative damage 23 p3472 A83-48466

Influence of stress cycling on creep behaviour of an Al-Mg alloy under strain ageing conditions 24 p3566 A83-49598

Analytical determination of the crack path and elastic energy release rate under cyclic loading with allowance for welding stresses 24 p3596 A83-49915

CYCLING
U CYCLES

CYCLOGENESIS
The effect of initial divergence on prediction of extratropical cyclogenesis 03 p0367 A83-14426

An analysis of the LFM-11 simulations of the Presidents' Day Cyclone, February 18-19, 1979 03 p0368 A83-14442

Numerical modelling of the mesoscale airflow downwind of the Alps - Two case studies under cyclogenetic conditions 04 p0518 A83-16153

Cyclone development in polar air streams over the wintertime continent 06 p0792 A83-18469

Precipitation distribution and implications for cyclonic storm development 11 p1630 A83-27072

An analysis of explosive cyclogenesis over the eastern United States 13 p1888 A83-30569

Explosive cyclogenesis in the northeast Pacific Ocean 13 p1889 A83-30576

Disturbances and eddy fluxes in Northern Hemisphere flows Instability of three-dimensional January and July flows 16 p2385 A83-35478

The impact of model moist processes on the energetics of extratropical cyclones 16 p2388 A83-36032

A moist baroclinic model for monsoonal mid-tropospheric cyclogenesis 18 p2728 A83-40032

Explosive cyclogenesis over the northeast Pacific Ocean 20 p3030 A83-42516

Angular momentum transports in tropical cyclones 21 p3179 A83-44396

Numerical simulations of a case of explosive marine cyclogenesis 23 p3489 A83-47393

CYCLONES

NT CYCLOGENESIS
NT HURRICANES
NT TYPHOONS

The isotopic composition of cyclonic precipitation 02 p0216 A83-12952

Tropical cyclone movement and surrounding flow relationships 02 p0217 A83-13054

The role of cross-equatorial tropical cyclone pairs in the southern oscillation 02 p0218 A83-13057

CYCLOTRIMETHYLENE TRINITRAMINE

The impact of TIROS N soundings on the analysis of a cyclone in the Gulf of Alaska, Oct. 21-22, 1979 03 p0365 A83-14406

The impact of model moist processes on baroclinic wave energetics 03 p0367 A83-14427

On the question of tropopause resolution for midlatitude cyclone forecasts 03 p0367 A83-14429

Numerical simulation of the tropical cyclone life cycle using a spectral cumulus parameterization 03 p0367 A83-14434

On the predictability of tropical cyclone motion [AD-125566] 03 p0368 A83-14435

The effects of latent heat release on the May 20 Sesame '77 wave cyclone 03 p0368 A83-14443

A study of the adequacy of quasi-geostrophic dynamics for modeling the effect of cyclone waves on the larger scale flow 04 p0516 A83-15929

Intense atmospheric vortices; Proceedings of the Joint Symposium, Reading, Berks., England, July 14-17, 1981 05 p0667 A83-17113

Observation of atmospheric waves generated by cyclone centres 06 p0791 A83-18422

A statistical-climatological tropical cyclone track prediction technique using an EOF representation of the synoptic forcing --- Empirical Orthogonal Functions 08 p1139 A83-22294

Seasat scatterometer detection of gale force winds near tropical cyclones 09 p1314 A83-24295

Experimental investigations of small-scale turbulence and turbulent exchange in cyclones and anticyclones at middle latitudes 09 p1315 A83-25053

Conference on Radar Meteorology, 20th, Boston, MA, November 30-December 3, 1981, Preprints 11 p1621 A83-26976

Wintertime cyclonic storms over the north east Pacific Ocean 11 p1630 A83-27073

Origins, behaviors, and interactions of mesoscale rainbands in extratropical cyclones 11 p1630 A83-27074

Doppler radar measurements of moisture divergence in a coastal cyclone 11 p1630 A83-27075

Automatic recognition of mesocyclones from single Doppler radar data 11 p1630 A83-27088

Analysis of the field of motion of a cyclone in mid geographic latitudes 11 p1633 A83-28120

Preliminary efforts in developing a technique that uses satellite data for analyzing precipitation from extratropical cyclones 13 p1887 A83-30562

Tropical cyclone motion - Environmental interaction plus a beta effect 13 p1892 A83-31034

Investigation of a laboratory model of a developing convective vortex 14 p2059 A83-33398

The mesoscale and microscale structure and organization of clouds and precipitation in midlatitude cyclones. VI Wavelike rainbands associated with a cold-frontal zone 16 p2384 A83-35459

The mesoscale and microscale structure and organization of clouds and precipitation in midlatitude cyclones. VII Formation, development, interaction and dissipation of rainbands 16 p2384 A83-35460

Monitoring tropical cyclone evolution with NOAA satellite microwave observations 18 p2726 A83-39870

The mesoscale and microscale structure and organization of clouds and precipitation in midlatitude cyclones. VIII - A model for the 'seeder-feeder' process in warm-frontal rainbands 18 p2729 A83-40035

Easterly waves in the Intertropical Convergence Zone 19 p2868 A83-42118

On the relative motion of binary tropical cyclones 20 p3029 A83-42503

Monitoring tropical-cyclone intensity using environmental wind fields derived from short-interval satellite images 20 p3029 A83-42506

Eastern North Pacific tropical cyclones of 1982 20 p3030 A83-42513

The energy budgets for the eye and eye wall of a numerically simulated tropical cyclone 20 p3031 A83-43461

Angular momentum transports in tropical cyclones 21 p3179 A83-44396

Transformed Eliassen balanced vortex model 21 p3180 A83-44709

On the evolution of the QE II storm. I - Synoptic aspects. II - Dynamic and thermodynamic structure 23 p3488 A83-47392

The Vorticity Area Index --- cyclonic activity measure 24 p3610 A83-49619

CYCLONES (EQUIPMENT)

U CENTRIFUGES

CYCLOTETRAMETHYLENE TETRANITRAMINE

U HMX

CYCLOTRIMETHYLENE TRINITRAMINE

U RDX

CYCLOTRON FREQUENCY

- Helium resonance and dispersion effects on geostationary Alfvén/ion cyclotron waves
02 p0207 A83-12384
- Oscillation of cyclotron-echo signals in a plasma
03 p0396 A83-13182
- Electromagnetic cyclotron-loss-cone instability associated with weakly relativistic electrons
06 p0812 A83-18919
- Observations of LHR noise with banded structure by the sounding rocket S29 barium-GEOS
13 p1879 A83-31246
- Zero-frequency cyclotron wave on an intense relativistic-electron beam
14 p2087 A83-33389
- Frequency gap formation in electromagnetic cyclotron wave distributions --- in magnetosphere
20 p3025 A83-43193
- An electron cyclotron maser instability for astrophysical plasmas
21 p3227 A83-43944
- Weakly relativistic dielectric tensor and dispersion functions of a Maxwellian plasma
21 p3214 A83-45194

CYCLOTRON RADIATION

NT ION CYCLOTRON RADIATION

- On the formation of the diffuse component of solar electron streams
03 p0436 A83-13664
- Cyclotron emission in strongly magnetized plasmas
03 p0429 A83-14795
- Cyclotron lines in the hard X-ray spectrum of Hercules X-1
05 p0699 A83-17006
- The loss-cone driven electron-cyclotron maser
05 p0650 A83-17269
- The motion and radiation of electrons in a neutral sheet
05 p0689 A83-17813
- On the interpretation of gamma-ray burst continua and possible cyclotron absorption lines
07 p1011 A83-20019
- Induced electron-cyclotron emission from inhomogeneous, anisotropic plasmas with electron population inversion
07 p0996 A83-20532
- Excitation of surface cyclotron waves in a solid-state plasma by charged-particle beams
09 p1348 A83-23985
- Coulomb bremsstrahlung and cyclotron emissivity in hot magnetized plasmas --- of magnetic X-ray pulsar
09 p1360 A83-24460
- A free electron laser oscillator based on a cyclotron-undulator interaction
10 p1427 A83-26012
- Radiated electromagnetic waves in an inhomogeneous magnetoplasma near the upper hybrid frequency
10 p1487 A83-26697
- The kinematics of cyclotron emission for quantized electrons --- in super-strong stellar magnetic fields
13 p1944 A83-30361
- Helium cyclotron emission from accreting magnetized neutron stars
13 p1958 A83-31726
- Zero-frequency cyclotron wave on an intense relativistic-electron beam
14 p2087 A83-33389
- Excitation of whistler waves by reflected auroral electrons
15 p2199 A83-34359
- Absorption coefficient of electron cyclotron radiation in a plasma in the temperature range 5-20 keV
16 p2416 A83-35891
- The role of proton cyclotron emission near accreting magnetic neutron stars
18 p2765 A83-39199
- Heating of heavy ions on auroral field lines
19 p2865 A83-41121
- The excitation of a cyclotron potential instability in the magnetospheres of pulsars
19 p2916 A83-41223
- Selective nonresonant acceleration of He-3(2+) and heavy ions by H(+) cyclotron waves --- in solar flares
19 p2925 A83-41657
- Observations of odd-half cyclotron harmonic emissions in a shell-Maxwellian laboratory plasma
22 p3362 A83-46047
- Observation of the backward cyclotron wave in a spiral electron beam-plasma system
23 p3510 A83-47623
- The collisional absorption of plasma cyclotron oscillations
23 p3510 A83-48394
- Drift motion of a charged particle in a uniform magnetic field and in the electric field of an azimuthally traveling potential wave
16 p2416 A83-35945
- Discrete chorus emissions recorded at Nainital
16 p2381 A83-36617
- Cyclotron instability in the plasmasphere in the presence of the transport of energetic particles across L-shells
18 p2714 A83-39337
- Quantum cyclotron resonance in silicon
21 p3216 A83-44383
- Excitation of slow cyclotron waves by an ion beam in a polyhelical relativistic electron beam
21 p3215 A83-45388
- Narrow spectral peaks in electrons precipitating from the slot region
22 p3337 A83-47073
- Ion neutralization in helical electron beams
23 p3460 A83-47556
- On the storage of high-energy protons in the solar corona
23 p3537 A83-47730
- The cyclotron instability
23 p3537 A83-47730
- Stochastic behavior in presence of an electrostatic wave due to the crossing of multiple cyclotron resonances in an inhomogeneous magnetic field
23 p3510 A83-48200
- Bistable cyclotron resonance in semiconductors
24 p3635 A83-49743

CYCLOTRON RESONANCE DEVICES

- Experimental investigation of the electrodynamic system of a semiconductor cyclotron-resonance maser
04 p0484 A83-15765
- A submillimeter gyrotron with a pulsed magnetic field
04 p0471 A83-15809
- A high power gyrotron operating in the TE/041/ mode
06 p0752 A83-18758
- Loaded Q's and field profiles of tapered axisymmetric gyrotron cavities
06 p0752 A83-18759
- Application of advanced millimeter/far-infrared sources to collective Thomson scattering plasma diagnostics
10 p1487 A83-26647
- The gyrotron energy transfer equation
10 p1411 A83-26649
- High-power submillimeter gyrotron with a pulsed magnetic field
13 p1851 A83-30911
- Bernstein mode quasi-optical gyrokystron [AD-A130124]
17 p2497 A83-37760
- Excitation of TM waves and mode selection in relativistic cyclotron-resonance masers
17 p2516 A83-38988
- Small-signal theory of a large-orbit electron-cyclotron harmonic maser
18 p2694 A83-40516
- Low-frequency fluctuations of oscillations in a gyrotron caused by thermal noise
19 p2840 A83-41779
- Submillimeter-wave gyrotrons - Theory and experiment
21 p3125 A83-44385
- Operation of a millimeter-wave harmonic gyrotron
21 p3125 A83-44386
- Theory of gyrotron amplifier in a tape helix loaded waveguide
22 p3278 A83-46272
- Enhancement of high-harmonic gyrotron gain by a dielectric rod
22 p3279 A83-46750
- Cyclotron-autoresonance maser with a wavelength of 2.4 mm
22 p3300 A83-46792
- Diffractional Q-factor of weakly conical resonators of gyrotrons
23 p3445 A83-48492

CYCLOTRONS

NT MICROTRONS

NT SYNCHROCYCLOTRONS

- Relativistic cyclotron accelerator exploiting the anomalous Doppler effect
09 p1271 A83-23999

CYGNUS CONSTELLATION

- Spectrophotometry of the Cygnus Loop
02 p0255 A83-12120
- A model of the Cygnus Loop
03 p0413 A83-13322
- CI Cyg - The stage of case C mass transfer
06 p0829 A83-18530
- The X-ray flux variations of Cygnus X-2
06 p0818 A83-18533
- The nature of NML Cygnus
10 p1513 A83-26719
- Detection of 2×10 to the 15th to 2×10 to the 16th eV gamma-rays from Cygnus X-3
14 p2117 A83-33227
- A 300-day periodicity of CYG X-1
15 p2247 A83-34558
- The Cygnus Superbubble as the remnant of a peculiar supernova
17 p2613 A83-38831
- Isophotes of a field in the Cygnus Loop photographed in the forbidden O III and forbidden N II + H-alpha lines
17 p2613 A83-38832
- The Cygnus X region. XIV - The radio continuum of the North America-Pelican nebulae
20 p3065 A83-42392
- Cygnus X-1 - Optical variation on the 294 day X-ray period
20 p3073 A83-43085
- Similarity solutions and experiment for turbulent wakes
03 p0315 A83-13116

CYLINDERS

- Pressure enhancement by conically convergent shocks in composite cylinders and its application to shock recovery experiments
03 p0304 A83-13913
- Measurement of bursting period and test of surface renewal model in a turbulent boundary layer disturbed by a cylinder
03 p0318 A83-14462
- Light scattering by arbitrarily oriented cylinders
03 p0395 A83-14636
- The method of moving coordinates as a technique for comparing various electrodynamic problems in systems having cylindrical conductors
04 p0467 A83-15746
- A study of internal waves generated by the rapid horizontal motion of cylinders and spheres
06 p0760 A83-19433
- Steady supersonic flow of a viscous heat-conducting gas past a cylinder with a flat end-face
08 p1041 A83-21630
- Contact between a rigid cylinder and an orthotropic beam under initial stress
11 p1591 A83-27433
- Stresses during fabrication of cylindrically woven carbon-carbon composites
11 p1543 A83-27462
- Radiation pressure and 360 deg scattering diagrams for infinite cylinders
13 p1829 A83-30748
- On a method of the asymptotic theory of diffraction
14 p2079 A83-32104
- Scattering phase matrix comparison for randomly hexagonal cylinders and spheroids
15 p2226 A83-34463
- A study of residual stresses in the blades of the last stage of the low-pressure cylinder of a 500-MW turbine
15 p2172 A83-35038
- Two-dimensional Rayleigh scattering in a semi-infinite cylindrical medium exposed to a laser beam
23 p3463 A83-48650

CYLINDRICAL AFTERBODIES

U AFTERBODIES

U CYLINDRICAL BODIES

CYLINDRICAL ANTENNAS

- VHF parabolic cylinder antenna for incoherent scatter radar research
02 p0168 A83-12636
- Analytic determination of the transient response of a thin-wire antenna based upon an SEM representation --- Singular Expansion Method
03 p0306 A83-14015
- Attenuation and localization of an electromagnetic wave on the surface of a cylindrical conductor
04 p0465 A83-15072
- Characteristics and design of high-gain dielectric circular antennas operated in X-band
06 p0736 A83-18425
- Scattering by a conducting tube of finite length
06 p0737 A83-18608
- Limits of VSWR for optimal broadband capacitively loaded cylindrical antennas versus their length
06 p0741 A83-18661
- Theoretical and experimental analysis of cylindrical dipoles with minimal mutual coupling
06 p0744 A83-18694
- Analytical study of the scattering properties of a structure consisting of two open cylindrical screens
07 p0915 A83-20870
- Concerning the radiation pattern in the problem of the excitation of an array of circular dielectric cylinders by a local source
07 p0915 A83-20871
- Transient response of an infinite cylindrical antenna
09 p1247 A83-23802
- Cylindrical-rectangular microstrip antenna
09 p1248 A83-23809
- Diffraction of a wave beam by a closed cylindrical screen
09 p1251 A83-25086
- The loop antenna with a cylindrical core - Theory and experiment
10 p1405 A83-26826
- Driving-point impedance of a linear cylindrical antenna
11 p1558 A83-28607
- A numerical analysis of the diffraction of radio waves --- Russian book
12 p1718 A83-28827
- Wave resistance and energy losses in a cylindrical slotted line
14 p2003 A83-32106
- The resonant cylindrical dielectric cavity antenna
15 p2148 A83-35175
- Numerical calculations of low-frequency TE fields in arbitrarily shaped inhomogeneous lossy dielectric cylinders
16 p2407 A83-35407
- Experimental study of the electrodynamic properties of an open cylinder in a rectangular waveguide
17 p2498 A83-38478
- Measurements and calculations of the impedance of a cylindrical antenna in an isotropic plasma
21 p3211 A83-44300
- Anomalous wave scattering by a finite number of longitudinally slit cylinders of small wave dimensions
22 p3275 A83-46789
- Inverse scattering for an exterior Dirichlet problem --- due to metallic cylinder
01 p0104 A83-10494

Radar waveform synthesis for single-mode scattering by a thin cylinder and application for target discrimination 01 p0032 A83-11355

A new expression for the scattering of a Gaussian beam by a conducting cylinder 01 p0033 A83-11356

Noise measurement at an obstacle in a wind tunnel [AAAF PAPER NT 81-10] 02 p0234 A83-11771

Receiving analysis of the shaped cylindrical reflector antenna 02 p0164 A83-12004

Analysis and computation of heat transfer around a cylinder in argon plasma cross flow [ASME PAPER 82-HT-30] 02 p0171 A83-12789

Measurement of thermophysical properties of solids by arbitrary heating. III - Measurement of thermal diffusivity and thermal conductivity of cylindrical or hollow cylindrical specimen 02 p0175 A83-13072

Concerning the formulation of the problem of calculating the stress-strain state in shell-reinforced cylinders by the finite element method 03 p0341 A83-14073

Crack propagation in bending thin plates 03 p0342 A83-14567

Strouhal numbers of rectangular cylinders 03 p0321 A83-14585

Hydromagnetic gravitational instability of an infinite cylinder of a compressible fluid --- in relation to the dynamics of spiral arms of galaxies 04 p0549 A83-14984

The diffraction of a nonstationary transverse wave by a cylindrical cavity 04 p0497 A83-15385

Unidirectional unsteady flow of an instantaneously heated gas out of a cylinder with various locations of the heating zones 04 p0479 A83-16172

Scattering of acoustic waves by rigid cylindrical objects with sharp corners 04 p0533 A83-16318

Computation of shock wave/target interaction [AIAA PAPER 83-0039] 05 p0632 A83-16479

Maximum vortex-induced side force revisited --- for aerodynamic design [AIAA PAPER 83-0458] 05 p0586 A83-16727

Transient ablation of blunt bodies at the angle of attack [AIAA PAPER 83-0583] 05 p0637 A83-16803

SIF of surface cracks and fatigue crack propagation behaviour in a cylindrical bar 05 p0614 A83-17092

Calculation of the flow of a dust-laden gas over a disk and the flat end of a cylinder 05 p0639 A83-17406

Concerning the reflection of a shock wave by a cylinder and a sphere 05 p0589 A83-17417

A solution to the problem of H-polarized electromagnetic wave diffraction by piecewise linear cylindrical surfaces 05 p0623 A83-17593

Stress intensity factors in a hollow cylinder containing a radial crack 06 p0776 A83-18910

A study of the short-term strength of boron-composite-reinforced tubular specimens at room and cryogenic temperatures 06 p0725 A83-19310

Integral photoelasticity of cylindrical bodies with measurement of light-ray deflection 07 p0944 A83-19634

A new kind of spin combustion 07 p0878 A83-19641

The stressed state of cylindrical specimens during thermal-stability testing 07 p0897 A83-19969

Calculation of symmetric vortex separation affecting subsonic bodies at high incidence 08 p1042 A83-22137

Third-order conditional transport correlations in the two-dimensional turbulent wake 08 p1085 A83-22382

Numerical solution of the momentum equations in unsteady incompressible flow 08 p1090 A83-23207

The use of Bessel function and Jacobi polynomial in radial vibrations of a gas in an infinite cylindrical tube 08 p1091 A83-23217

Scattering by a rotating circular cylinder with finite conductivity 09 p1247 A83-23801

Variational calculations of electromagnetic scattering from two randomly separated Rayleigh dielectric cylinders 09 p1249 A83-24102

The applicability of the theory of small elastoplastic deformations in the case of simple loading 09 p1280 A83-24237

A study of the characteristics of a cylindrical resonator with a two-layer filler 09 p1256 A83-24918

Aeroacoustic computation of cylinder wake flow [AIAA PAPER 83-0736] 10 p1476 A83-25940

Sound radiation from a vibrating cylinder in flow [AIAA PAPER 83-0737] 10 p1476 A83-25941

Cylindrical piezoelectric transducer with controllable characteristics 10 p1421 A83-26291

Solution of particulate viscous flow over a two dimensional cylinder 11 p1566 A83-27424

Free-surface oscillations of a liquid in a cylindrical container under longitudinal vibrations 11 p1569 A83-28458

Single- and double-wall cylinder noise reduction 12 p1777 A83-29017

Calculation of the depth and hardness of the carburization layer of cylindrical parts --- for aircraft engines 12 p1713 A83-29282

Approximate calculation of the aerodynamic characteristics of a cylindrical body of small aspect ratio in an incompressible flow 12 p1696 A83-29287

Cross-sectional distortion of an elastic hollow cylinder subjected to shear deformation - Theory and experiment 12 p1735 A83-29360

Investigation of cylindrical resonators containing annular inhomogeneities 13 p1832 A83-30276

Total current to cylindrical collectors in collisionless plasma flow 13 p1948 A83-31529

Impingement of an oblique shock wave on a cylinder 15 p2156 A83-33727

A spectral-iteration technique for analyzing scattering from arbitrary bodies. I - Cylindrical scatterers with E-wave incidence 15 p2148 A83-35186

A spectral-iteration technique for analyzing scattering from arbitrary bodies. II - Conducting cylinders with H-wave incidence 15 p2149 A83-35198

Sudden twisting of an external circular crack in an infinite medium with a cylindrical inclusion 16 p2368 A83-36513

Effects of Reynolds number and corner radius on two-dimensional flow around hexagonal cylinders [AIAA PAPER 83-1705] 17 p2502 A83-37202

Active flow control effects on boundary layer development around a protuberance at high subsonic speed [AIAA PAPER 83-1737] 17 p2445 A83-37216

Sound scattering by a vortex wake behind a cylinder 17 p2578 A83-38049

Three dimensional stress state in an internally-pressurized hollow cylinder with a reinforcing ring 18 p2697 A83-39453

Reduced stiffness axial load buckling of cylinders 18 p2700 A83-39559

Tensile stability of cylindrical membranes 18 p2700 A83-39569

Normal vibrations of a finite-length cylinder with a restrained lateral surface 18 p2701 A83-40114

The hydrodynamic forces acting on a cylinder set in motion in an impulsive manner 19 p2843 A83-41264

Turbulent boundary layers on moving, nonisothermal continuous cylinders 20 p2976 A83-42717

LDA measurements of separated flows and a simple calculation method for the drag of a sharp-edged cylinder 20 p2929 A83-43006

Low-Reynolds-number flow past a cylindrical body 20 p2985 A83-43103

Analysis of the elastic field of ultrasonic waves scattered by a cylindrical cavity 21 p3148 A83-43876

Approximate solution of problems concerning the deformation of nearly cylindrical composite bodies 21 p3154 A83-44721

Computation of aerodynamic forces on bodies with non-circular cross-section in supersonic viscous flow [AIAA PAPER 83-2077] 21 p3089 A83-45519

Scattering and mode conversion of guided modes by an arbitrary cross-sectional cylindrical object in an optical slab waveguide 22 p3355 A83-45729

Off-axis scanning of cylindrical lenses 23 p3442 A83-47831

Self-similarity of fatigue fracture - Cumulative damage 23 p3472 A83-48466

Nonlinear antiplane strain of a body weakened by a luse-shaped recess 24 p3594 A83-49527

Choice of the initial configuration for a solid body which assures the fulfillment of a prescribed ablation law 24 p3579 A83-49668

CYLINDRICAL CHAMBERS

Swirl flow in cylindrical chamber. II - Energy loss in chamber and its effect on flow characteristics 07 p0925 A83-20283

Experimental investigation of the scattering effects of a sphere in a cylindrical resonant chamber 10 p1472 A83-25822

Radiation characteristics of nonisothermal cavities --- for temperature and radiation measuring instruments 16 p2355 A83-35588

Radiative heat transfer in a cylindrical chamber in the presence of an attenuating medium 19 p2846 A83-42143

CYLINDRICAL COORDINATES
U CARTESIAN COORDINATES

CYLINDRICAL PLASMAS

A theoretical investigation of the distribution of electron concentration in the positive column of a glow discharge with a longitudinal flow of gas 02 p0240 A83-11514

The field of a test body in a flux of charged particles 05 p0687 A83-16894

Theory of cylindrical and spherical Langmuir probes in the limit of vanishing Debye number 05 p0688 A83-17370

Dispersion of a plasma cloud on a less dense plasma background 06 p0814 A83-19560

Perturbed bifurcation of stationary striations in a contaminated, nonuniform plasma 08 p1168 A83-22739

Gravitational collapse and fragmentation of isothermal, non-rotating, cylindrical clouds 10 p1500 A83-25492

Solitary surface waves on a plasma cylinder 10 p1485 A83-25778

Waves in a cold pure electron plasma of finite length 10 p1485 A83-25785

Plasma column formed by a traveling ionizing electromagnetic wave 10 p1486 A83-25990

Drift-resistive interchange and tearing modes in cylindrical geometry 13 p1923 A83-30114

Tonks-Dattner diagnostics of electron density profiles 15 p2237 A83-35299

Dipole resonance of a plasma ellipsoid in a dielectric shell with allowance for radiation damping 17 p2584 A83-38985

Ionizational instability due to a surface wave and its effect on the structure of a steady microwave discharge 21 p3210 A83-44139

CYLINDRICAL SHELLS

Free torsional vibration of thick isotropic incompressible circular cylindrical shell subjected to uniform external pressure 01 p0058 A83-10272

Optimization of the regimes of intense heating of a cylindrical shell 01 p0058 A83-10451

An extension of classical shell theory - The influence of thickness strains and cross-sectional warping 01 p0059 A83-10575

The forms of the wave motion of circular cylindrical shells 01 p0059 A83-10678

A study of the stressed state of inhomogeneous cylindrical shells 01 p0059 A83-10679

A study of the creep of thin-walled shells under nonstationary loading 01 p0059 A83-10681

A study of the stability of compressed cylindrical shells with thin eccentric ribs using a polynomial approximation of deflections 01 p0059 A83-10682

The critical equilibrium of a simply supported cylindrical glass-reinforced plastic shell 01 p0059 A83-10689

The effect of oscillations on the stability of cylindrical shells under axial compression 01 p0059 A83-10690

Post-buckling dynamic behavior of periodically supported imperfect shells 01 p0060 A83-10860

A new class of solutions for buckling of a short cylindrical shell in pure bending 02 p0191 A83-12075

Efficient reinforcement of orthotropic viscoelastic cylindrical shells under axial compression 02 p0192 A83-12357

A numerical study of the buckling process and strength analysis of layered cylindrical shells under axial impact 02 p0192 A83-12358

The effect of a longitudinal delamination in a laminate cylindrical shell on the critical external pressure 02 p0192 A83-12360

Dynamic instability of suddenly heated angle-ply laminated composite cylindrical shells 02 p0194 A83-12742

Nonlinear analysis of axially-loaded laminated cylindrical shells 02 p0194 A83-12743

PANDA - Interactive program for minimum weight design of stiffened cylindrical panels and shells 02 p0194 A83-12745

The effect of filler stiffness on the thermoplastic stressed state of cylindrical sandwich shells 03 p0340 A83-14066

Determination of optimal reinforcement-parameters for cylindrical shells under axial compression that increases rapidly with time 03 p0341 A83-14074

Stability and vibrations of compressed, aeolotropic, composite cylindrical shells 04 p0499 A83-15689

Free vibrations of a composite shell system 04 p0500 A83-16050

Elastic-plastic analysis of thermally loaded cylindrical shells 05 p0655 A83-17719

Experimental and theoretical correlations for elastic buckling of axially compressed stringer stiffened cylinders 05 p0655 A83-17720

Vibration of waffle cylinders 06 p0770 A83-18069

Stability and optimization of viscoelastic composite cylindrical shells under combined loading 06 p0775 A83-18507

Cylinder-symmetrical and plane problems 06 p0777 A83-19196

Jet flow of an ideal liquid past a flexible shell 06 p0760 A83-19430

Optimization of stiffened cylindrical shells under local loads on the basis of strength conditions 06 p0778 A83-19544

Vibration effects in bodies containing a gas-liquid medium 06 p0760 A83-19547

A variant of the theory of plastic flow, based on the shear mechanism of deformation 06 p0778 A83-19567

Theoretical and experimental evaluation of transmission loss of cylinders --- as idealized aircraft fuselages 07 p0990 A83-19808

On the buckling and vibration of antisymmetric angle-ply laminated circular cylindrical shells 07 p0946 A83-20639

The nonlinear problem of the stability of cylindrical sandwich shells under combined loading 08 p1114 A83-21628

Vibrations of layered shells with transverse shear and rotatory inertia effects 08 p1120 A83-21808

Instability of short stiffened composite cylindrical shells under bending with prebuckling displacements 08 p1121 A83-21891

Shell-core method for the analysis of a long circular cylindrical sandwich shell subjected to axisymmetric loading 08 p1123 A83-22413

Analysis of progressive plastic buckling in cylindrical shell as contact problem 08 p1123 A83-22772

Strength of layered composite cylindrical shells under dynamic loading 09 p1224 A83-23946

Natural vibrations of a ribbed cylindrical shell with intermediate supports and an ideal solid 09 p1281 A83-25009

Natural vibrations of a prestressed cylindrical shell with varying thickness 09 p1281 A83-25010

The quasi-static stability loss in a rotating cylindrical shell containing a liquid 09 p1281 A83-25013

Evaluation of the assumptions of the semimomentless theory of cylindrical shells 10 p1439 A83-25615

Plastic buckling of initially imperfect stiffened cylinders in axial compression 10 p1440 A83-26433

An analysis of intersecting cylindrical shells loaded by internal pressure 10 p1442 A83-26789

Influence of tangential displacements on the dynamic buckling of viscoplastic cylindrical shells 10 p1442 A83-26820

Dynamic stability of cylindrical sandwich panel subjected to axial compression 11 p1593 A83-27770

Impulsive loading of a cylindrical shell with transverse shear and rotatory inertia 11 p1594 A83-28412

Stability of three-layer cylindrical shells with a discrete filler under axial compression 11 p1596 A83-28455

Solution of an asymmetric problem for a two-layer hollow cylinder of finite length by the finite element method 11 p1597 A83-28465

The stability of inhomogeneous cylindrical shells --- Russian book 12 p1735 A83-29339

Experimental and theoretical correlations for elastic buckling of axially compressed ring stiffened cylinders 12 p1736 A83-29445

Stability of imperfect laminated cylinders - A comparison between theory and experiment [AIAA 83-0874] 12 p1738 A83-29758

Buckling of anisotropic laminated cylindrical plates [AIAA 83-0979] 12 p1740 A83-29786

Methods for the synthesis of the stressed state in shell theory 13 p1865 A83-30003

The selection of optimum parameters for stiffened cylindrical shells loaded by internal pressure and an axial compressive force 13 p1867 A83-31324

A solution to the bending problem for a layered inhomogeneous hollow cylinder 14 p2029 A83-32152

Periodic and bi-periodic solutions to the equations of an engineering theory for an elastic cylindrical shell 14 p2029 A83-32153

Thermal stresses in a semi-infinite cylindrical shell locally heated by convective heat transfer 14 p2030 A83-32377

The design of flywheels made of fibrous materials 14 p2046 A83-32378

An experimental study of the progressive deformation and adaptability of thin-walled cylindrical shells under thermal cycling 14 p2030 A83-32380

Stability loss of compressed longitudinally reinforced cylindrical shells in the case of finite displacements with allowance for local buckling of rib-plates 15 p2178 A83-34439

Determination of boundary-layer width from the minimum-energy condition --- for edge damped cylindrical shells 15 p2178 A83-34443

Buckling and postbuckling of imperfect cylindrical shells under axial compression 15 p2180 A83-34568

Stability loss during the plastic deformation of shells 15 p2180 A83-35034

Energy losses due to plastic deformation during the radial compression of a cylindrical shell 16 p2364 A83-35544

On the stability of thin shallow shells of negative Gaussian curvature 16 p2365 A83-35548

Existence of solutions for dynamic problems of one-dimensional plastic structures 16 p2365 A83-35552

An experimental study of the failure of elastoplastic cylindrical shells under combined loading 16 p2365 A83-35929

Free vibrations of simply supported cylindrical shells of oval cross section 16 p2366 A83-36090

Vibrations of cantilevered circular cylindrical shells Shallow versus deep shell theory 16 p2369 A83-36958

Sanders' energy-release rate integral for a circumferentially cracked cylindrical shell [ASME PAPER 83-APM-32] 17 p2519 A83-37386

Allowing for the effect of small cross-sectional shape imperfections on the stressed state of nonreinforced thin-walled circular cylindrical shells subjected to pressure gradients 17 p2520 A83-37525

On the stability of a cylindrical shell under torsion and under a combined load with torsion 17 p2520 A83-37537

Solution of problems in the dynamics of noncircular cylindrical shells in a liquid 17 p2521 A83-37573

Plane flow past an air-supported soft cylindrical shell 17 p2522 A83-38099

Shrinkage stresses in products of high-modulus composites 17 p2524 A83-38512

Vibrations of noncircular cylindrical shells 18 p2697 A83-39460

Stress concentration in a circular cylindrical shell weakened by a large hole 18 p2697 A83-39482

Stability of asymmetric three-layer cylindrical shells with a low-rigidity core under axial compression 18 p2701 A83-40106

Deformation and strength of ring-stiffened orthotropic cylindrical shells under dynamic compressive loads 18 p2701 A83-40107

Determination of critical dynamic axial compression stresses for rib-stiffened layered cylindrical shells 18 p2702 A83-40115

Natural vibrations of a rib-stiffened cylindrical shell 18 p2702 A83-40116

Calculation of transfer functions in internal problems of the unsteady hydroelasticity of cylindrical and spherical shells 18 p2702 A83-40117

Experimental and theoretical study of the elastoplastic buckling of cylindrical shells under axial impact 18 p2702 A83-40118

Deformation of a circular cylindrical shell with a periodic system of holes 18 p2702 A83-40122

Tubular lap joints in composite cylindrical shells under external bending and shear 18 p2703 A83-40154

Compressive buckling of graphite-epoxy composite circular cylindrical shells 18 p2704 A83-40184

Coupling effect on axial compressive buckling of laminated composite cylindrical shells 18 p2704 A83-40187

Stress concentration around circular cutouts in laminated composite cylindrical shells - Experimental investigation and finite element analysis 19 p2857 A83-40883

The stress-strain state of rib-stiffened cylindrical shells 19 p2859 A83-41602

Determination of the initial loss of stability of shells by the shadow moiré method 20 p3008 A83-43623

Highly non-linear cylindrical deformations of rings and shells 20 p3008 A83-43649

Plastic buckling of axially compressed circular cylindrical shells 21 p3152 A83-44249

A class of contact problems for a cylindrical shell 21 p3154 A83-44716

A study of the creep of cylindrical shells weakened by a hole 21 p3154 A83-44717

Analysis of random response of a shallow cylindrical shell 21 p3159 A83-44934

An asymptotic integration method in problems concerning wave propagation in shells of revolution 21 p3163 A83-45368

An experimental study of the behavior of cylindrical shells with concentrated masses under dynamic external pressure 21 p3164 A83-45370

Inelastic buckling of cylindrical shells subjected to axial tension and external pressure 21 p3164 A83-45597

Free vibration of a circular cylindrical shell elastically restrained by axially spaced springs 23 p3468 A83-47594

Optimal plastic design of stiffened shells 23 p3470 A83-48094

Contact stiffness of layered cylindrical shells. I - An analytical solution to the problem in the axisymmetric case 23 p3472 A83-48439

The stability of a stiffened cylindrical shell in creep 23 p3472 A83-48470

On some treatment of the equations of motion for cylindrical shells based on an improved theory 23 p3473 A83-48497

Calculation of the oscillation-damping decrement of a low-viscosity fluid rotating in a cylindrical vessel --- in weightlessness conditions 23 p3452 A83-48659

Resonant acoustic scattering from elastic cylindrical shells 24 p3624 A83-48974

A modification of Potter's method for diagonal matrices with common unknown 24 p3593 A83-49440

An analysis of nonstationary processes resulting from the nonaxisymmetric loading of multiple-layer finite cylinders 24 p3595 A83-49901

Deformation of a cylindrical shell during an explosion in the vicinity of a concentrated explosive charge 24 p3595 A83-49905

CYLINDRICAL TANKS

Turbulence and waves in a rotating tank [AD-A128174] 06 p0758 A83-19024

Performance of a cylindrical phase-change thermal energy storage unit 12 p1749 A83-28969

Unsteady thermal convection in a cylindrical vessel in the case of lateral heat injection 23 p3452 A83-48668

CYLINDRICAL WAVES

The interaction of a cylindrical convergent shock wave with a transverse magnetic field given significant magnetic Reynolds numbers 06 p0813 A83-19554

Cylindrical resonators --- shock wave production in jet nozzles 10 p1380 A83-26162

A calculation of the gas flow in a zone of energy release during a cylindrical explosion 14 p2008 A83-31896

Self-similar flows behind cylindrical shock waves in magnetogasdynamics 18 p2746 A83-39750

Cylindrically converging shock and detonation waves 18 p2687 A83-40502

On the transformation of planar detonation to cylindrical detonation 23 p3430 A83-48157

Behavior of singularities of solutions of diffraction problems and the Rayleigh hypothesis 24 p3623 A83-49274

Simulation of detonation cell kinematics using two-dimensional reactive blast waves 24 p3580 A83-49836

CYLINDROIDS

U CYLINDRICAL BODIES

CYSTEAMINE

The mechanisms of the potentiation and the prolongation of the radioprotective effect of multicomponent preparations 19 p2874 A83-41014

CYSTS

Results on arteria cysts, lettuce and tobacco seeds in the Biobloc 4 experiment flown aboard the Soviet biosatellite Cosmos 1129 19 p2872 A83-40842

CYTOCHROMES

A study of the protective properties of nicotinamide and cytochrome C during aminoglycoside ototoxicosis 09 p1321 A83-25155

Nocardiosis antarcticus - A new species of actinomycetes isolated from the ice sheet of the Central Antarctica glacier 21 p3185 A83-45377

CYTOGENESIS

The regulation of erythropoiesis /Status of the problem/ 01 p0081 A83-10916

The molecular mechanisms of the interphase death of lymphoid cells. VI - A low molecular weight DNA fraction in the products of the degradation of the chromatin of irradiated rat thymus 03 p0377 A83-14883

The effect of heavy ions on mammalian cells. I - The cytogenic effects during the irradiation of Chinese hamster cells induced by accelerated ions of helium, carbon, and neon 03 p0377 A83-14884

The mutagenic effect of laser radiation in the visible range on cultured human cells 03 p0377 A83-14890

The cytogenetics and morphology of hemopoiesis during chronic irradiation --- Russian book 05 p0669 A83-17122

Growth and aging of the lens 05 p0670 A83-17196

The effect of heavy ions on mammalian cells. II - The evaluation of the relative biological effectiveness of accelerated ions of helium, carbon, and neon according to cytogenetic parameters 06 p0796 A83-19381

Timing of neuron development in the rodent vestibular system 11 p1638 A83-27819

CYTOLOGY

The simultaneous measurement of four functional parameters of blood platelets 01 p0080 A83-10553

Disturbance of cell differentiation during microsporogenesis in *Tradescantia paludosa* due to the change in orientation of the mitotic spindle in the first postmeiotic mitosis under the effect of space flight factors 02 p0219 A83-11650

Cytochemical labeling and morphological characterization of lymphocyte subpopulations in health and disease 03 p0381 A83-14332

The relationship between peroxide oxidation and cell respiration 03 p0376 A83-14368

The regulation of the defense functions of organisms --- Russian book 04 p0520 A83-15826

Microbiochemical criteria for adaptive reactions in certain barrier systems of the organism 05 p0670 A83-17204

The ultracytochemical analysis of nuclear ribonucleoproteins /RNP/ 06 p0795 A83-18981

A cytochemical investigation of the hearing system during acoustic stimulation 07 p0972 A83-19935

DNA damage during the action of ionizing radiation with different physical characteristics 09 p1321 A83-24926

The histochemical and ultrastructural characteristics of the neuron reactions of mammillary nuclei in old animals to injections of adrenaline 09 p1321 A83-25154

Characteristics of statoliths from rootcaps and coleoptiles 11 p1637 A83-27810

Microbodies in the living cell 12 p1762 A83-29249

The structural differences of the spatial-frequency filters in the visual cortex of cats 13 p1896 A83-30409

Polymerization of brain tubulin in and around the area of application of an electric field 14 p2061 A83-31818

Influence of magnetic field on the process of self-assembly of tubulin 14 p2061 A83-31819

The dependence of wound healing on the condition of the immune system 14 p2065 A83-33302

The structure of the microtubule organizational centers in a comparative evolutionary aspect 14 p2065 A83-33318

The effect of preparations acting mainly in the region of the peripheral M-choline reactive systems on bone marrow eosinophils 14 p2066 A83-33332

The content of bioelements in the tissues during the aging of an organism (Review of the literature) 15 p2210 A83-34942

A threshold molecular quantum regulator 16 p2394 A83-36802

Electron-microscope cytochemical study of ribonucleoprotein particles in cerebral cortex neurons in a posthypoxic period 16 p2395 A83-36812

The secretory activity of acinar cells of the pancreas at various times of the day and the sequence of the maturation process of secretory granules 16 p2395 A83-36814

The functional activity and metabolism of neutrophils of the blood under the effect of low-intensity microwaves 16 p2395 A83-36834

The relation between the degree of cardiodynamic disorders and the volume of myocardial injuries during cytotoxic actions on the heart 17 p2555 A83-37236

The structural-functional organization of the fibrous framework of the Achilles tendon in humans 17 p2560 A83-38199

The protective effect of extracellular K(+) in the myocardium during disorders of energy generation 18 p2732 A83-40552

The effect of decimeter waves on the physical and chemical condition of membranes, the chromatin of thymocytes, and the immunological reactivity of an organism 18 p2733 A83-40567

The role of changes in the concentration of oxygen in the case of the reproductive death of cells in vitro. III - The modification of the radiosensitivity by oxygen-reducing compounds 19 p2874 A83-41005

The kinetics of hemopoiesis and its clinical significance 19 p2882 A83-41451

The development of several ideas of V. V. Parin in the physiology and the pathophysiology of blood circulation 19 p2875 A83-41461

A technique for obtaining isolated smooth muscle cells 19 p2876 A83-41847

Functional state of chromatin and proliferative activity of meristematic cells in pea seedlings under various clinostatic conditions 19 p2878 A83-42053

Biological effects of weightlessness and clinostatic conditions registered in cells of root meristem and cap of higher plants 19 p2878 A83-42056

Specificity of cortico-cortical connections in monkey visual system 20 p3034 A83-43545

Cytological aspects of higher plant ontogenesis under microgravity [IAF PAPER 83-190] 23 p3494 A83-47306

Age-related characteristics of the postirradiation regeneration of the blood system 23 p3495 A83-48206

The walls of vessels in atherosclerosis and thrombogenesis (Investigations in the USSR) --- Russian book 24 p3617 A83-49073

CYTOPLASM

The cytokinetics and morphology of hemopoiesis during chronic irradiation --- Russian book 05 p0669 A83-17122

The participation of an insulin-dependent cytoplasmic regulator in carbohydrate metabolism during immobilization 19 p2871 A83-40818

CZECHOSLOVAKIA

Orographic trough or low in the Alpine region /and their effect on weather in the CSR/ 11 p1633 A83-28114

CZECHOSLOVAKIAN SPACECRAFT

Review of the scientific usage of Interkosmos satellite observations at the Astronomical Institute of the Czechoslovak Academy of Sciences 04 p0546 A83-15101

Space research activities in Czechoslovakia in 1981 --- Book 07 p1003 A83-21070

CZOCCHRALSKI METHOD

Liquid encapsulated Czochralski growth of low dislocation GaAs 03 p0399 A83-13784

A quantitative model for carbon incorporation in Czochralski silicon melts 07 p0880 A83-19894

Residual double acceptors in bulk GaAs 07 p0998 A83-19989

EL2 distributions in doped and undoped liquid encapsulated Czochralski GaAs --- deep donor concentration 08 p1169 A83-22756

Defects in silicon 09 p1349 A83-23860

A method for calculating the dislocation density in pure crystals grown from melts by the methods of Czochralsky and Stepanov and by crucibleless zone melting 11 p1662 A83-28359

Computer simulation and controlled growth of large diameter Czochralski silicon crystals 14 p2092 A83-32641

Characterization of electron traps in ion-implanted GaAs MESFET's on undoped and Cr-doped LEC semi-insulating substrates 18 p2750 A83-40372

Oxygen-induced recombination centers in as-grown Czochralski silicon crystals 19 p2903 A83-40739

The role of fluid flow phenomena in the Czochralski growth of oxides 20 p3053 A83-43292

Growth of single crystals by the pulling method --- Russian book 21 p3218 A83-45039

D

D LAYER

U D REGION

D LINES

Na I D brightening phenomena in quiescent prominences 02 p0270 A83-12576

Collisional broadening of intra-Doppler resonances of selective reflection on the D2 line of cesium 14 p2082 A83-32619

An instrument for absolute or relative measurement of wavenumbers of a continuous or pulsed laser - The sigmometer. Application to the spectroscopic study of the D lines of a series of alkaline radioactive isotopes --- French thesis 17 p2912 A83-38432

Nightglow intensity variations in the O2(0-1) atmospheric band, the NaD lines, the OH(6-2) band, the yellow-green continuum at 5750 Å and the oxygen green line 20 p3016 A83-42308

D REGION

The possibility of calculating and deterministic method of predicting ionospheric parameters at the heights of the E and F1 regions for particular heliogeophysical conditions 01 p0071 A83-10599

The role of photochemistry and dynamics in the D region of the ionosphere 01 p0071 A83-10601

Temperature and solar zenith angle control of D-region positive ion chemistry 02 p0204 A83-11970

[AD-A126882] A comparison between HF partial reflection profiles from the D-region and simultaneous Langmuir probe electron density measurements 02 p0205 A83-12017

Meteorological effects in the variations of ionospheric parameters. I - The lower thermosphere 03 p0361 A83-14741

An observational study of the D-region winter anomaly and sudden stratospheric warmings 03 p0362 A83-14746

Results inferred from electron density measurements at Saskatoon, Canada /L = 4.4/ by a partial reflection technique. I - Variations of nitric oxide in the D-region during quiet periods 03 p0362 A83-14747

Combined mass spectrometric composition measurements of positive and negative ions in the lower ionosphere. II - Negative ions 05 p0665 A83-17787

Ion kinetics, minor neutral and excited constituents in the D region with a high level of ionization. I - Formulation of the problem and a general scheme for the processes 06 p0786 A83-18360

Models of the ionospheric D region at noon 06 p0786 A83-18730

A method of estimating the electron density profile of the D layer from a knowledge of the VLF reflection coefficients 07 p0962 A83-20374

Ionospheric modification experiments in northern Scandinavia 09 p1299 A83-23304

Meteorological control of the D region - /Tutorial Lecture/ 11 p1615 A83-27407

NO and temperature control of the D region 11 p1615 A83-27408

An investigation of the mid-latitude ionospheric D-region under twilight conditions in summer 12 p1753 A83-29237

On the role of solar Lyman alpha radiation in radio-wave absorption in the D-region 12 p1753 A83-29406

High-latitude plasma densities and their relation to riometer absorption 12 p1754 A83-29431

An analysis of several ionospheric parametric anomalies associated with the South Atlantic Geomagnetic Anomaly by means of VLF waves 13 p1880 A83-31471

Propagation of VLF atmospherics on 27 kHz 13 p1882 A83-31548

Estimation of effective recombination coefficient and its variation with height for D-region 13 p1882 A83-31549

The solar X-rays and the sudden phase anomalies (SPA) 13 p1883 A83-31721

Errors in the determination of electron density in the D-region of the ionosphere by the method of partial reflections 14 p2049 A83-31856

Variations of electron density in the D-region 14 p2050 A83-31875

The effect of the winter anomaly of the D-region according to measurements on the Kerguelen Islands 14 p2050 A83-31876

Seasonal differences of the effects of sudden ionospheric disturbances in the D region 14 p2050 A83-31877

The D region under the conditions of nighttime PCA - The rate of transformation of positive ion clusters and negative ions 14 p2054 A83-33034

Synopsis of D- and E-region electron densities during the energy budget campaign 16 p2373 A83-35364

D-region IRI profiles in relation to radio observations 16 p2375 A83-35389

Latitudinal influences on the quiet daytime D-region [AD-A128591] 16 p2375 A83-35391

Collision frequencies in the high-latitude D-region 17 p2544 A83-38375

Diffusion of a multi-component plasma 17 p2583 A83-38514

Results inferred from electron density measurements at Saskatoon, Canada (L = 4.4) by a partial reflection technique. II - Ion production rates and nitric oxide in the D-region during post-storm periods 18 p2712 A83-39067

Tests of an ion-chemical model of the D- and lower E-region 18 p2712 A83-39072

Laboratory measurements of the association rate coefficients of NO(+), O2(+), N(+), and N2(+) ions with N2 and CO2 at temperatures between 100 K and 400 K 20 p3024 A83-43165

Modelling of the ion composition of the middle atmosphere 21 p3173 A83-44669

Cross modulation of VLF and LF waves by gravity waves --- in nocturnal D region 22 p3332 A83-46533

Electron density and energetic particle precipitation observed during the eclipse of 26 February 1979 23 p3480 A83-47466

A model of the lower ionosphere above Red Lake, Canada, during the 26 February 1979 solar eclipse 23 p3480 A83-47467

Positive and negative ion composition measurements in the Dand E-regions during the 26 February 1979 solar eclipse 23 p3480 A83-47470

Steady-state model of the D-region during the February 1979 eclipse 23 p3481 A83-47472

D-region positive and negative ion concentration and mobilities during the February 1979 eclipse 23 p3481 A83-47473

A possible cause of the winter disturbance of the ionospheric D-region 24 p3608 A83-49540

DAEMO (DATA ANALYSIS)

U DATA PROCESSING

U DATA REDUCTION

U DATA TRANSMISSION

DAMA

U DEMAND ASSIGNMENT MULTIPLE ACCESS

DAMAGE

NT CUMULATIVE DAMAGE

NT FIRE DAMAGE

NT IMPACT DAMAGE

NT LASER DAMAGE

NT METEORITIC DAMAGE

NT RADIATION DAMAGE

NT RAIN IMPACT DAMAGE

NT STORM DAMAGE

DAMAGE ASSESSMENT

- Effects of moisture, residual thermal curing stresses, and mechanical load on the damage development in quasi-isotropic laminates 03 p0292 A83-14556
- Mechanisms of fatigue damage in boron/aluminum composites 03 p0292 A83-14557
- Mechanical description of creep damage state and its experimental verification 07 p0945 A83-20365
- Defining three-dimensional damage effects in polymers 08 p1068 A83-21683
- On the interaction of hardening and fatigue damage in the 316 stainless steel 08 p1062 A83-21736
- Damage tensors in continuum mechanics 11 p1595 A83-28432
- Combat damage - A unique element 15 p2243 A83-34865
- Constitutive equations for damaging materials [ASME PAPER 83-APM-12] 17 p2519 A83-37384
- A linear model of ductile plastic damage 19 p2858 A83-41321
- Damage tolerant design using collapse techniques 21 p3164 A83-45591
- DAMAGE ASSESSMENT**
- Overview of Mount St. Helens volcanic eruption 02 p0211 A83-12670
- Landsat observations of Mount St. Helens 02 p0199 A83-12671
- Mount St. Helens quick response damage assessment using high-altitude infrared photography 02 p0199 A83-12672
- Damage in composite materials: Basic mechanisms, accumulation, tolerance, and characterization --- Book 03 p0292 A83-14551
- Toward the nondestructive characterization of fatigue damage in composite materials 03 p0292 A83-14552
- Damage documentation in composites by stereo radiography 03 p0292 A83-14553
- The dependence of transverse cracking and delamination on ply thickness in graphite/epoxy laminates 03 p0292 A83-14559
- Damage mechanism and life prediction of graphite/epoxy composites 03 p0293 A83-14564
- What is fatigue damage 03 p0342 A83-14565
- New method for monitoring and correlating cavitation noise to erosion capability 04 p0478 A83-16138
- Improved fault detection in the hot section of turbojet engines by individual monitoring procedures 07 p0867 A83-19666
- Analysis of target coverage for an unstabilized 35 mm panoramic strike camera 08 p1100 A83-22596
- Cumulative damage analysis 09 p1276 A83-23418
- Damage and repair of the APS graphite/epoxy composite skins due to Columbia first flight April 12-14, 1981 --- Aft Propulsion System 09 p1210 A83-23633
- Advanced methods for damage analysis in graphite-epoxy composites 09 p1222 A83-23648
- Some peculiarities of fracture in heterogeneous materials 09 p1223 A83-23932
- Equation of state for reinforced plastic materials subjected to mechanical and thermal loading with the account taken of damage and physical-chemical transformations 09 p1224 A83-23945
- Damageability evaluation of organic and carbon fiber plastics by nondestructive technique 09 p1224 A83-23947
- Criteria for prolonging the safe operation of structures through the assessment of the onset of creep damage using nondestructive metallographic measurements 09 p1275 A83-24081
- A damage law for predicting the elevated temperature low cycle fatigue life of a martensitic stainless steel 10 p1393 A83-25418
- Improved fatigue life tracking procedures for Navy aircraft structures [AIAA 83-0805] 12 p1703 A83-29807
- Microinitiation, micropropagation and damage 13 p1823 A83-31171
- A study of land transformation processes after the atomic bombing damage in Hiroshima 15 p2182 A83-33572
- LCC evaluation of advanced engine damage tolerance goals for a hot-section disk --- in aircraft engines [AIAA PAPER 83-1407] 16 p2310 A83-36396
- Generic aspects of three-dimensional internal-damage development in fatigue-loaded composite laminates 19 p2819 A83-41035
- Method of thermodynamic function control and of damage analysis regarding aircraft engines with the aid of flight data recording systems --- German thesis 19 p2800 A83-41850
- Battle damage and repair of an advanced composite A-7 outer wing 20 p2927 A83-42547
- EAGLE/DTA - A life cycle cost model for damage tolerance assessment --- Engine/Aircraft Generalized Life cycle cost Evaluator [ASME PAPER 83-GT-76] 23 p3407 A83-47929

The effect of damage in structural elements on the ground resonance of a helicopter 24 p3547 A83-49446

DAMAGE THRESHOLD

U YIELD POINT

DAMPERS

- Design of dry-friction dampers for turbine blades 16 p2306 A83-35883
- A study of the characteristics of short hydrodynamic dampers of aircraft engine motors with allowance for turbulization of the working fluid in the damper clearance 19 p2800 A83-42129
- The dynamic analysis of a structure having discrete dampers 21 p3151 A83-44106
- An investigation into the effect of side-plate clearance in an uncentralized squeeze-film damper [ASME PAPER 83-GT-176] 23 p3464 A83-47975
- The effect of fluid inertia in squeeze film damper bearings: A heuristic and physical description [ASME PAPER 83-GT-177] 23 p3465 A83-47976
- Squeeze-film damper technology. I - Prediction of finite length damper performance [ASME PAPER 83-GT-247] 23 p3466 A83-48035

DAMPING

- NT ELASTIC DAMPING
- NT LANDAU DAMPING
- NT VIBRATION DAMPING
- NT VISCOELASTIC DAMPING
- NT VISCOUS DAMPING
- Implementation of a laboratory model Yaw Damper digital filter 02 p0230 A83-11908
- A proposed new method for damping relaxation oscillations in laser diodes 03 p0330 A83-13560
- Damping of large-amplitude plasma waves propagating perpendicular to the magnetic field 13 p1926 A83-31358
- A simple model for radiation damping 14 p2102 A83-33045
- On the damping of type III solar radio bursts 15 p2277 A83-33711
- Optimum wire screens for control of turbulence in wind tunnels 15 p2120 A83-33772
- A study of the engineering stability of a system of coupled bodies with damping elements 16 p2316 A83-35931
- Dynamic analysis of a hydrodynamic seal with helical grooves 16 p2363 A83-36944
- Formation and damping of relativistic strong shocks 17 p2595 A83-37033
- Damping mechanisms for ion plasma waves excited by a fast ion beam 21 p3210 A83-44128
- Axial coherence functions of circular turbulent jets based on an inviscid calculation of damped modes 22 p3281 A83-46002
- Application of the quadratic functional to nonconservative problems of elastic stability 23 p3471 A83-48170
- Identification of the dynamic characteristics of a simple system with quadratic damping 24 p3597 A83-50137

DAMPING FACTOR

U DAMPING

DAMPING IN PITCH

U DAMPING

U PITCH (INCLINATION)

DAMPING IN ROLL

U DAMPING

U ROLL

DAMPING IN YAW

U DAMPING

U YAW

DAMPING TESTS

- On the damping effect of sloshing fluid on flexible rotor systems [ASME PAPER 82-DET-140] 02 p0196 A83-12783
- Determination of stress relaxation by damping measurements 07 p0946 A83-20522

DAMPNESS

U MOISTURE CONTENT

DAMS

- Monitoring of water quality and environmental changes in the Aswan High Dam reservoir from Landsat imagery 09 p1286 A83-24555

DANGER

U HAZARDS

DARK ADAPTATION

- The accuracy of binocular vergence for peripheral stimuli 05 p0675 A83-17747
- Effects of hypoxia on the luminance threshold for target detection 07 p0977 A83-20778
- Inhibitory influence of unstimulated rods in the human retina - Evidence provided by examining cone flicker 17 p2558 A83-37771

DARKENING

NT LIMB DARKENING

DART TURBOPROP ENGINES

U TURBOPROP ENGINES

DASSAULT AIRCRAFT

- Long-range Falcon - Flight-test Dassault Falcon 50 06 p0716 A83-18074

DATA ACQUISITION

- Combining land use data acquired from Landsat with soil map data 01 p0066 A83-10117
- Fundamental data for FK4/FK4Sup stars 01 p0115 A83-10161
- Application of pulse code modulation technology to aircraft dynamics data acquisition 01 p0008 A83-10182
- High speed signal acquisition and processing in EW ATE 01 p0031 A83-10745
- Acquisition and analysis of the EMG power spectra - A reproducible technique for assessment of muscle fatigue --- electromyogram 01 p0086 A83-11107
- The performance of a sequential acquisition system for PN codes --- in NASA Tracking Data Relay Satellite System 01 p0019 A83-11216
- Data acquisition/reduction system for flight testing general aviation aircraft 02 p0135 A83-11903
- Analytical plotter for data input into geo-based information systems 02 p0180 A83-12683
- Interpretation of aerial thermographic data 02 p0200 A83-12687
- Material-testing machine concepts for the integration of material testing into central in-service data acquisition 02 p0189 A83-12987
- Applications of digital image acquisition in anthropometry 03 p0384 A83-13449
- Reference quicklook images for monitor of Landsat image data acquisition 03 p0349 A83-14286
- Water survey of Canada's experience with data acquisition and telemetry systems 03 p0349 A83-14287
- Preliminary overview analyses of U.S. Navy Aircrew Automated Escape Systems /AAES/ in-service usage data 04 p0444 A83-15405
- U.S. Navy Aircrew Automated Escape Systems /AAES/ In-Service Data Analysis program 04 p0444 A83-15408
- New method for monitoring and correlating cavitation noise to erosion capability 04 p0478 A83-16138
- Dual-wavelength correlation measurements with an airborne pulsed carbon dioxide laser system 05 p0643 A83-16831
- A means for utilizing ancillary information in multispectral classification --- of remotely sensed data 05 p0656 A83-16905
- Results of the First GARP Global Experiment 06 p0787 A83-17992
- The impact of data processing on wind tunnel testing [ONERA, TP NO. 1982-92] 06 p0720 A83-18429
- New pulsed laser data-acquisition system 06 p0764 A83-19233
- Rapid acquisition techniques for Direct-Sequence Spread Spectrum Systems using an analog detector 07 p0903 A83-19677
- The Russian surface temperature data set 07 p0969 A83-20801
- A simple and accurate on-line data acquisition program --- for astronomical photometry 07 p1007 A83-21039
- Reception, preparation, and geometric processing of imagery of meteorological satellites --- German thesis 07 p0951 A83-21069
- Satellite systems for the acquisition and processing of geomagnetic data 08 p1133 A83-22082
- Thermal infrared pushbroom imagery acquisition and processing --- of NASA's Advanced Land Observing System 08 p1045 A83-22841
- Hydrologic data collection using satellite systems 09 p1286 A83-24554
- Statistics and the analysis of hydrometeorological data --- Russian book 10 p1451 A83-25623
- Experimental system for computer network via satellite /CS/. V - Data collecting and processing system 10 p1403 A83-26081
- Structure of thunderstorms along a squall line on May 2, 1979 11 p1622 A83-26982
- An intercomparison of two radars used in the Montana HIPLEX 11 p1627 A83-27038
- A multifunction integrated approach to providing aircraft inertial data 11 p1528 A83-28595
- Solar rotation results at Mount Wilson 13 p1963 A83-29988
- Application of numerical Fourier transformation on measurements made on board rotating spacecraft 13 p1812 A83-30778
- Test data on leadless chip carriers with ceramic substrates in severe random vibration environments 13 p1835 A83-30866
- Additional experimental results from the Stanford 3 micron FEL 13 p1852 A83-31103
- Data on total and spectral solar irradiance 13 p1880 A83-31461

- Digital data acquisition and analysis in structural dynamic testing 13 p1867 A83-31494
- European Southern Observatory (ESO) coudeechelle spectrometer 14 p2084 A83-32005
- Processing of fatigue test results for corrosion-affected structural materials 14 p1992 A83-32074
- A microprocessor-based instrument for automatic solar cell characterization 14 p2004 A83-32204
- Disequilibria in series connected solar cells - An approach to the protection by parallel diodes 14 p2004 A83-32213
- A computational system for the automatic and simultaneous acquisition of radio telescope data from four different directions 14 p2101 A83-33292
- The development and application of a county-level geographic data base 15 p2186 A83-34828
- Conversion of raster coded images to polygonal data structures 15 p2165 A83-34838
- Controlling the IES013 spectrometer for spacelab and its data retrieval 16 p2317 A83-35786
- Experience in the development of computer-controlled high response probe diagnostics for turbomachines 16 p2355 A83-35851
- The GOES operational support system (GOSS) 17 p2548 A83-38710
- Preliminary results of the AFGL icing study [AD-A129843] 17 p2549 A83-38718
- Design of a fiber-optic data-acquisition network 18 p2743 A83-39435
- Measuring laser flow fields with a 64-channel heterodyne interferometer 19 p2847 A83-41102
- Satellite relayed tracking and data acquisition for the 1990's 19 p2813 A83-41340
- Applications of state estimation in aircraft flight-data analysis 19 p2798 A83-41919
- Solar radiation data; Proceedings of the Contractor's Meeting, Brussels, Belgium, November 20, 1981 19 p2862 A83-41990
- Gas turbine engine cascade wind tunnel with automatic data acquisition and control 20 p2938 A83-42563
- The time-space relationships among data points from multispectral spatial scanners 20 p2990 A83-42962
- Something about to improve the accuracy of testing in low speed wind tunnel 21 p3093 A83-44571
- Acquisition and manipulation of image statistics 21 p3139 A83-44787
- Methodological requirements in information gathered by an extensive network of ground-based meteorological and specialized stations 21 p3181 A83-45023
- A data acquisition system for a fast X ray directional detector - Application to time-resolved studies --- French thesis 21 p3141 A83-45083
- On the application of housekeeping data to ISS-b operations 21 p3096 A83-45444
- Earth feature classification developments for remote sensing 22 p3308 A83-46116
- Comparative study of data acquired by various types of remote sensors 22 p3308 A83-46120
- Modeling and deconvolution for reconstruction of airborne gamma ray radiometer data 22 p3288 A83-46125
- Defining system requirements for acquiring and processing land remote sensing data 22 p3310 A83-46150
- The Swedish SPOT data acquisition and processing system 23 p3475 A83-47283
- [IAF PAPER 83-128] 23 p3475 A83-47283
- Internationally supported data acquisition for solar system exploration in the 1990's 23 p3420 A83-47309
- [IAF PAPER 83-209] 23 p3420 A83-47309
- A microprocessor controlled data acquisition and processing system for hot-wire anemometry 24 p3584 A83-49810
- DATA ADAPTIVE EVALUATOR/MONITOR**
- U DATA PROCESSING
- U DATA REDUCTION
- U DATA TRANSMISSION
- DATA ANALYSIS**
- U DATA PROCESSING
- U DATA REDUCTION
- DATA BASE MANAGEMENT SYSTEMS**
- The National Space Science Data Center /NSSDC/ and the World Data Center A for Rockets and Satellites /WDC-A-R&S/ - Their role in X-ray astronomy data 01 p0113 A83-10132
- System software approaches to the analysis of multidimensional data structures 01 p0090 A83-10137
- Archiving and retrieval of data from the International Ultraviolet Explorer /IUE/ mission 01 p0113 A83-10141
- PUMPS architecture for pattern analysis and image database management --- shared resource multiprocessor computer 01 p0090 A83-11448
- A relational image data base system for remote sensing /LAND DBMS/ 01 p0067 A83-11462
- Data management in FEM-based optimization software 02 p0228 A83-12751
- A file management system for a network of dissimilar computers --- French thesis 04 p0545 A83-15849
- Organization of relational models for scene analysis 04 p0528 A83-16031
- Improving the data base generation process for flight simulator data bases 05 p0598 A83-16547
- [AIAA PAPER 83-0138] 05 p0598 A83-16547
- Geology and image processing 08 p1129 A83-22525
- File structures and data bases for CAD; Proceedings of the Working Conference, Seeheim, West Germany, September 14-16, 1981 09 p1325 A83-25095
- DYSCO - An executive control system for dynamic analysis of synthesized structures 12 p1768 A83-29773
- [AIAA 83-0944] 12 p1768 A83-29773
- File allocation in a distributed computer communication network 13 p1909 A83-30788
- Sub-regional information system formation using multi-resolution remote sensing products 15 p2239 A83-34807
- Compressing interpreted satellite imagery for geographic information systems applications over extensive regions 15 p2185 A83-34824
- Generalized balanced ternary - An approach to handling spatial data 15 p2165 A83-34841
- Development of an occupational health data base system 15 p2239 A83-34990
- The role and application of data base management in integrated computer-aided design 19 p2887 A83-41049
- Using SLAM and SDL to assess Space Shuttle experiments --- programming language and data base management system for simulation of models and analysis of results 19 p2887 A83-41325
- A causal model for analyzing distributed concurrency control algorithms 20 p3038 A83-43116
- A data structure and algorithm based on a linear key for a rectangle retrieval problem 24 p3619 A83-49194
- DATA BASES**
- Remote sensing and geographic data bases as applied to the Louisiana coastal zone 01 p0064 A83-10074
- The astronomical data base and retrieval system at NASA 01 p0113 A83-10127
- Infrared astronomical data base and catalog of infrared observations 01 p0113 A83-10130
- A data base solution to ATE resource management 01 p0087 A83-10728
- Embedded microprocessors for avionics applications 01 p0088 A83-11104
- An Automated Verification System for JOVIAL J73 01 p0089 A83-11166
- PUMPS architecture for pattern analysis and image database management 02 p0227 A83-12247
- PICCOLO logic for a picture database computer and its implementation 02 p0228 A83-12248
- Registration of a synthetic aperture radar /SAR/ reconnaissance image with a map reference data base 02 p0200 A83-12885
- Data base support for automated photo interpretation 02 p0200 A83-12888
- Infrared astronomical data base and catalog of infrared observations 03 p0406 A83-13467
- SIRE - Transition from free-flyer to Shuttle sortie --- space infrared sensor 03 p0287 A83-13469
- Definition and potential of geocoded satellite imagery products 03 p0349 A83-14272
- On the flight derived/aerodynamic data base performance comparisons for the NASA Space Shuttle entries during the hypersonic regime 05 p0606 A83-16529
- [AIAA PAPER 83-0115] 05 p0606 A83-16529
- Improving the data base generation process for flight simulator data bases 05 p0598 A83-16547
- [AIAA PAPER 83-0138] 05 p0598 A83-16547
- A means for utilizing ancillary information in multispectral classification --- of remotely sensed data 05 p0656 A83-16905
- Methodology for thematic image processing using thematic and topographic data bases and base-integrated multi-sensor imagery 08 p1124 A83-21903
- Renewal of land use data base with the aid of remote sensing 08 p1128 A83-21952
- Numerical weather prediction studies from the FGGE Southern Hemisphere data base 08 p1138 A83-22285
- Objective summary of U.S. Army electro-optical modeling and field testing in an obscuring environment 08 p1093 A83-22351
- ESABASE - A computer-aided engineering framework facilitating integrated systems design 08 p1171 A83-22372
- Spatial calibration of a multispectral data base --- of airborne scanner systems 08 p1045 A83-22882
- File structures and data bases for CAD; Proceedings of the Working Conference, Seeheim, West Germany, September 14-16, 1981 09 p1325 A83-25095
- The Earthnet LEDA-2 image catalogue system 11 p1666 A83-27375
- Data base organization in computer-aided design systems 11 p1646 A83-28622
- Integrated GPS, DLMS, and radar altimeter measurements for improved terrain determination 12 p1700 A83-29212
- Experimental data needs for computational fluid dynamics - A position paper 13 p1840 A83-30627
- The data library --- for flow data storage 13 p1934 A83-30629
- Analysis of cloud characteristics derived from archived satellite data 15 p2206 A83-34161
- Employing Landsat MSS data in land use mapping - Observations and considerations 15 p2184 A83-34804
- Forest management applications of Landsat data in a geographic information system 15 p2185 A83-34823
- The development and application of a county-level geographic data base 15 p2186 A83-34828
- A geographic data base for Texas pecan 16 p2370 A83-35740
- Data base considerations for a tactical environment simulation 16 p2312 A83-36219
- [AIAA PAPER 83-1099] 16 p2312 A83-36219
- A strategy for mineral and energy resource independence 17 p2529 A83-38155
- Global vegetation and land use - New high-resolution data bases for climate studies 18 p2706 A83-39141
- Network control system using traffic databases 19 p2828 A83-41338
- Prediction of transport properties related to heat transfer 20 p2970 A83-42656
- Distribution design of logical database schemas 20 p3038 A83-43117
- Data from remote sensing in the geographical information system - The construction of territorial data banks 20 p3011 A83-43137
- A focused bibliography on robotics 21 p3118 A83-44076
- Airline common databases and data processing applications 21 p3190 A83-45081
- Environmental data display 21 p3142 A83-45615
- A relational database for nonmanipulative representation of solid objects 23 p3500 A83-48726
- Database systems - Their applications to CAD software design 23 p3500 A83-48727
- A hybrid structure for the storage and manipulation of very large spatial data sets 24 p3619 A83-49195
- 5500 miles of liquid water and dropsize measurements in supercooled clouds below 10,000 feet agl 24 p3614 A83-49720
- DATA BUSSES**
- U CHANNELS (DATA TRANSMISSION)
- DATA COLLECTION PLATFORMS**
- Performance assessment of future European remote sensing systems 01 p0021 A83-10109
- Water survey of Canada's experience with data acquisition and telemetry systems 03 p0349 A83-14287
- DATA COMPACTION**
- U DATA COMPRESSION
- DATA COMPRESSION**
- Concerning the optimality of discrete-data compression in a four-letter coding system 01 p0094 A83-10565
- Image data compression with the Laplacian pyramid 01 p0098 A83-11426
- An adaptive transform image data compression scheme incorporating pattern recognition procedures 01 p0098 A83-11428
- Residual recursive displacement estimation --- for motion detection 01 p0100 A83-11464
- The problem of the maximum data compression in an information system with large data flows 05 p0623 A83-17657
- TV bandwidth compression techniques using time-companded differentials and their applications to satellite transmissions 06 p0749 A83-19597
- Spectral properties and bandlimiting effects of time compressed television signals 07 p0907 A83-19728
- A new architecture for adaptive transform compression of NTSC composite video signal 07 p0908 A83-19732
- An experimental study of the concatenated Reed-Solomon/Viterbi channel coding system performance and its impact on space communications 07 p0871 A83-19733
- TV bandwidth compression techniques using time companded differentials and their applications to satellite transmissions 07 p0909 A83-19743

Two types of speech compression systems using inverse filter codebook 07 p0912 A83-20068
Image bandwidth compression by pre-compensative interpolation 08 p1075 A83-22235
Hardware systems design of an airborne video bandwidth compressor 08 p1099 A83-22585
Comparison of transform image coding techniques for compression of tactical imagery 08 p1100 A83-22597

Hardware-constrained hybrid coding of video imagery 08 p1077 A83-22731
Video compression using sampled data analog devices 08 p1078 A83-22813
Image quality experiments for TV reconnaissance at reduced transmission bandwidth 08 p1105 A83-22902

Method and device for the compression of spectrometric data 10 p1423 A83-26814
The autocorrelation function and Doppler spectral moments - Geometric and asymptotic interpretations --- of meteorological radar data 11 p1625 A83-27020
The Laplacian pyramid as a compact image code 14 p2075 A83-32868

Compressing interpreted satellite imagery for geographic information systems applications over extensive regions 15 p2185 A83-34824

An efficient source coding technique for data compression of multilevel digitized images 15 p2223 A83-35146

Image source coding using median filter roots 15 p2223 A83-35147

Block Truncation Coding on PASM --- reconfigurable multimicroprocessor for image processing 15 p2219 A83-35149

The effect of data reduction on image interpretation 17 p2532 A83-38435

Stationary transform processing of digital images for data compression 19 p2847 A83-41105

Compressed quantum states of a harmonic oscillator in the problem of detecting gravitational waves 19 p2896 A83-41495

On filtering and compressing LAGEOS laser range data 19 p2860 A83-41558

Generalized ambiguity function of signals with compression in the case of the scattering of waves by bodies of complex shape 19 p2835 A83-41776

Depth-first picture expression viewed from digital picture processing 20 p2989 A83-42646

Nonlinear image processing for optimum composite source coding 20 p3040 A83-43683

DATA CONVERSION ROUTINES

NT SUBROUTINES

DATA CONVERTERS

NT ANALOG TO DIGITAL CONVERTERS

NT DIGITAL TO ANALOG CONVERTERS

Four-channel multiplexed resolver-to-digital converter 01 p0009 A83-11100

Increasing the speed of response of multichannel voltage-to-code converters of parallel operation for radio systems 13 p1828 A83-30290

DATA CORRELATION

NT SIGNAL ANALYSIS

Horizontal correlation of satellite temperature errors 01 p0074 A83-10045

Correlations between BCD parameters of the continuous spectrum and the Balmer decrement of Be stars 01 p0120 A83-10310

Data correlation of measurements made by automatic test systems 01 p0057 A83-10744

Lift-off ignition overpressure - A correlation --- full-scale measurements on Titan vehicle launch conditions 02 p0140 A83-13086

Correlation between albedo and polarization properties of the moon /heterogeneity of the relative porosity of the surface of the western part of the visible hemisphere/ 03 p0133 A83-13667

The relationships between morphological type and quantitative measures in the cluster environment 03 p0421 A83-14140

Optimal interpolation and the Kalman filter --- for analysis of numerical weather predictions 03 p0365 A83-14409

A practical correlation test for cooperative passive optical sensors 04 p0482 A83-16123

Dual-wavelength correlation measurements with an airborne pulsed carbon dioxide lidar system 05 p0643 A83-16831

On the methods for determining galaxy velocity dispersions 07 p1009 A83-21236

Are there correlations between radio and optical axes of radio galaxies 12 p1785 A83-28996

Performance of Karhunen-Loeve and discrete cosine transforms for data having widely varying values of intersample correlation coefficient 12 p1769 A83-29465

On possible correlations in the photospheric magnetic field 13 p1963 A83-29978

Kinematics and correlation of the surface wind field in the South Atlantic Bight 14 p2059 A83-33079

Correlations of solar insolation and wind data for SOLMET stations 15 p2197 A83-33991

Correlation analysis of Doppler radar data and retrieval of the horizontal wind 18 p2722 A83-39125

The correlations between the typhoon and the $f_0(F_2)$ of ionosphere 21 p3172 A83-44518

The relationship between indices AE and Dst --- reflecting intensities of equatorial ring current and auroral electrojet due to geomagnetic disturbances 21 p3173 A83-44583

Galaxy groups - Correlations between luminosities, velocity dispersions, and virial radii 23 p3519 A83-47456

Experiments on digital image data comparison --- for Landsat satellite photos 24 p3598 A83-48990

DATA HANDLING SYSTEMS

U DATA SYSTEMS

DATA INTEGRATION

A technique for voice-data integration over packet radio channels 07 p0912 A83-19790

Self-adaptive filters for the integration of navigation data 09 p1204 A83-23374

Integration of Landsat RBV and MSS imagery to produce land use maps of Soviet cities --- Return Beam Vidicon 15 p2241 A83-34805

Remote sensing data integration into a geographic information system for the creation of a biogenic hydrocarbon inventory of the San Francisco Bay area 15 p2185 A83-34819

Integration and manipulation of remotely sensed and other data in geographic information systems 15 p2185 A83-34821

Combining land use data acquired from Landsat with soil map data using an information system 15 p2186 A83-34833

An interactive meteorological display and analysis system 17 p2549 A83-38713

DATA LINKS

A high speed 10MHz multiplex data bus interface 01 p0042 A83-11152

AEDCS - A computer-aided system design tool for integrated avionics 01 p0089 A83-11176

High speed data link concepts for military aircraft 01 p0010 A83-11233

ROMAPT - A new link between CAD and CAM 02 p0228 A83-11816

A note on some common diffraction link loss models 02 p0165 A83-12628

On the choice of discretization for solving P.D.E.'s on a multi-processor 03 p0385 A83-14090

System testing of communications and tracking links for first orbital flight of the Space Transportation System - An update 07 p0870 A83-19701

An analysis of full-duplex data links in SNA networks --- Systems Network Architecture 07 p0907 A83-19724

Communication protocol for a multisatellite communication system 07 p0907 A83-19725

Performance evaluation of multideestination /broadcast/ protocols for satellite transmission 07 p0907 A83-19726

Evaluation of a 14/12 GHz digital satellite link as the facility between digital switches 07 p0908 A83-19742

The integrated transfer subsystem /ITS/ - A GPS-to-GPS data link 07 p0871 A83-19765

Efficiency in an ARQ system with a constraining number of outstanding blocks 07 p0912 A83-19791

Summary of Intelsat VI communications performance specifications 07 p0869 A83-20557

X-ray induced transient attenuation at low temperatures in polymer clad silica /PCS/ fibers 08 p1165 A83-22478

Deep space optical communication via relay satellite 09 p1214 A83-23579

Flight management systems and data links 09 p1209 A83-24424

Precision phase comparison via communication satellites using loop-back tones 10 p1403 A83-26042

Experimental system for computer network via satellite /CS/. II - Communication protocols 10 p1403 A83-26078

Experimental system for computer network via satellite /CS/. III - Network control processor 10 p1403 A83-26079

Parametric study of intersatellite CO2 laser data links 11 p1535 A83-27605

Transmission code for high-speed fibre-optic data networks 11 p1558 A83-28604

Remote observing experiments at Kitt Peak National Observatory 13 p1939 A83-31005

Remote operation of telescopes - Long-distance observation 13 p1939 A83-31006

Relay balloon --- data terminal for long duration synoptic earth observations 18 p2640 A83-39811

A high-speed, time-division multiple-access communication link demonstration 23 p3443 A83-48140

DATA MANAGEMENT

Management of astronomical data at Kanazawa Data Center 01 p0113 A83-10129

The UK Schmidt Telescope Plate Catalogue and problems associated with increasing numbers of plates and users 01 p0114 A83-10153

Star - A local network system for real-time management of imagery data 02 p0228 A83-12242

PUMPS architecture for pattern analysis and image database management 02 p0227 A83-12247

Architecture for scientific software. I - Data centralization 02 p0229 A83-12348

Spacelab data management 03 p0286 A83-13709

The satellite situation center 04 p0502 A83-16290

The origin and evolution of the coordinated data analysis workshop process --- for International Magnetospheric Study 04 p0513 A83-16303

Status of IMS workshops - CDAAW 1: December 1977 events --- Coordinated Data Analysis Workshop 04 p0513 A83-16304

Pseudo-associative store with hardware hashing --- data-flow approach in parallel computing systems 07 p0982 A83-19624

Performance models of distributed databases 07 p0982 A83-19797

Digital image processing - A systems approach --- Book 07 p0928 A83-19925

Development and use of an integrated analysis capability 12 p1773 A83-29799

Application of data management to thermal/structural analysis of space trusses 12 p1741 A83-29802

The wetlands inventory of the Northern Great Plains - An example of operational remote sensing and data management 15 p2185 A83-34827

Controlling the 1ES013 spectrometer for spacelab and its data retrieval 16 p2317 A83-35786

Ad Hoc modeling, expert problem solving, and R-T program evaluation 19 p2907 A83-41304

Space Station information systems 19 p2814 A83-42089

Organizing Space Shuttle parametric data for maintainability 21 p3097 A83-45473

NASA/NOAA implementation of the USAID-sponsored satellite ground station and data processing facility for Bangladesh 23 p3475 A83-47282

[IAF PAPER 83-127] 23 p3475 A83-47282

Data management scheme for Japanese experiments of FMPT --- First Material Processing Test 23 p3424 A83-47299

[IAF PAPER 83-164] 23 p3424 A83-47299

Particle-sampling statistics in laser anemometers Sample-and-hold systems and saturable systems 23 p3458 A83-48120

High speed read/write techniques for advanced printing and data handling; Proceedings of the Meeting, Los Angeles, CA, January 20, 21, 1983 24 p3637 A83-48996

DATA PROCESSING

NT ASSOCIATIVE PROCESSING (COMPUTERS)

NT BATCH PROCESSING

NT CENSORED DATA (MATHEMATICS)

NT CENTRAL ELECTRONIC MANAGEMENT SYSTEM

NT DATA CORRELATION

NT DATA REDUCTION

NT DATA RETRIEVAL

NT DATA SMOOTHING

NT DATA STORAGE

NT DATA STRUCTURES

NT DISTRIBUTED PROCESSING

NT KARHUNEN-LOEVE EXPANSION

NT MULTIPROCESSING (COMPUTERS)

NT OPTICAL DATA PROCESSING

NT PARALLEL PROCESSING (COMPUTERS)

NT PIPELINING (COMPUTERS)

NT SCENE ANALYSIS

NT SIGNAL ANALYSIS

NT SIGNAL PROCESSING

NT VOICE DATA PROCESSING

Use of reflectance spectra of native plant species for interpreting airborne multispectral scanner data in the East Tintic Mountains, Utah 01 p0063 A83-10060

Standardization of computer compatible tape formats for remote sensing data 01 p0064 A83-10075

Automated data retrieval in astronomy; Proceedings of the Sixty-fourth Colloquium, Universite de Strasbourg I, Strasbourg, France, July 7-10, 1981 01 p0113 A83-10126

The Soviet Center of Astronomical Data
01 p0113 A83-10128

ASTRONET - The network for analysis and retrieval of astronomical data in Italy
01 p0113 A83-10135

International standards for software structures in astronomy
01 p0113 A83-10140

Data in astronomy --- and its management
01 p0114 A83-10152

Shear layer models and computer analysis of data
01 p0046 A83-10887

Future Navy data bus requirements - Modular approach for flexible evolution
01 p0006 A83-11184

Low cost word recognition using programmable VLSI
01 p0096 A83-11217

A simulation-aided multiple processor architecture design for BMD underlay terminal defense
02 p0226 A83-11904

A method of automated processing of flaw inspection results
02 p0188 A83-12164

Discrete Fourier transforms of nonuniformly spaced data
02 p0231 A83-12925

Pattern-recognition analysis of experimental data --- Russian book
03 p0327 A83-13811

Visual analysis of 1:250,000 Landsat data for forage assessment during the 1980 drought in western Manitoba
03 p0345 A83-14235

NOGAPS - Navy Operational Global Atmospheric Prediction System
03 p0366 A83-14414

Status of IMS workshops - CDAW 1: December 1977 events --- Coordinated Data Analysis Workshop
04 p0513 A83-16304

The impact of data processing on wind tunnel testing [ONERA, TP NO. 1982-92]
06 p0720 A83-18429

Satellite data assimilation using NASA Data Systems Test 6 observations --- for numerical weather forecasting
06 p0792 A83-18466

Discussion on the maximum likelihood method for determination of membership in open clusters
06 p0822 A83-19163

Optimal processing of the correction data of an aircraft fuel-measurement system
06 p0718 A83-19177

The use of a two-dimensional fast Fourier transformation algorithm for processing information from a linear antenna array
06 p0749 A83-19359

Generalized synthetic aperture, focused transducer, pulse-echo, ultrasonic scan data processing for non-destructive inspection
06 p0770 A83-19474

Innovative air data system for the Space Shuttle Orbiter
07 p0872 A83-20421

Optimal processing of satellite-derived magnetic anomaly data
07 p0963 A83-20972

Consideration of the local shape of the terrain in height interpolation with the aid of finite elements
08 p1129 A83-22031

Incremental linear normal mode initialization in four-dimensional data assimilation --- for numerical weather forecasting
08 p1138 A83-22284

Challenges in processing data from mosaic sensors
08 p1100 A83-22608

The relation of the quality of information processing with the level of the work activity of a human operator
09 p1323 A83-25156

An algorithm for detecting hardware errors in the data of supermonitors --- of cosmic ray parameters
10 p1420 A83-26104

SPOT communication and data handling concept
10 p1382 A83-26599

A triple-Doppler case study of a small multi-cell convective storm
11 p1623 A83-26995

IRAS preliminary science analysis at the OCC
11 p1533 A83-28216

U.S. data processing for the IRAS project --- by Jet Propulsion Laboratory Scientific Data Analysis System
11 p1674 A83-28217

Computational systems and methods in the automation of investigations and control --- Russian book
13 p1910 A83-30616

Interactive analysis of magnetic field data --- using BANAL and TANAL computer programs
13 p1876 A83-30779

Objective analysis and assimilation of observational data from FGGE --- First GARP Global experiment
13 p1891 A83-30804

Digital data acquisition and analysis in structural dynamic testing
13 p1867 A83-31494

Digital processing and analysis of satellite multispectral scanner data
14 p2035 A83-32504

Supporting flight data analysis for Space Shuttle Orbiter Experiments at NASA Ames Research Center [AIAA PAPER 83-1532]
14 p1981 A83-32762

Nearest neighbors and automatic classification - Applications to industrial data --- French thesis
15 p2220 A83-33696

Urban land use classification using synthetic aperture radar
15 p2184 A83-34808

The role of change data in a land use and land cover map updating program
15 p2184 A83-34811

An overview of remote sensing input to geographic information systems
15 p2185 A83-34822

GIS information layers derived from Landsat classification --- Geographic Information Systems
15 p2185 A83-34826

AISA - Program for automated treatment of aeronautical data --- for civil aviation applications
16 p2311 A83-35598

The influence of seeing on the observation of short period fluctuations in the solar atmosphere
16 p2440 A83-36648

Human thinking and the computer processing of information
16 p2402 A83-36825

Synthesis of geophysical data with space-acquired imagery - A review
17 p2540 A83-38147

Comparison of simulated data of SPOT and Landsat-D sensors Application to an agricultural region
17 p2529 A83-38162

Comparing digital data processing techniques for surface mine and reclamation monitoring
17 p2530 A83-38337

The GOES operational support system (GOSS)
17 p2548 A83-38710

Lessons learned from the CSIS --- Centralized Storm Information System
17 p2549 A83-38717

Processing of scientific telemetry data using a real-time operating system for the flights of Venera 13 and 14
19 p2813 A83-41234

Processing of scientific data from the Venera 13 and 14 descent modules in real time
19 p2813 A83-41235

Statistical processing of multiplexed data from turbulent flames
20 p2950 A83-42581

Scientific and defense shops - The computers
20 p3036 A83-43032

Impact of metrication on data processing [SAWE PAPER 1476]
20 p3037 A83-43746

Performance of concurrent tasks - A psychophysiological analysis of the reciprocity of information-processing resources
21 p3189 A83-44366

SITELCOM-82 - Telecommunications and data processing in the air transport industry; Proceedings of the Conference, Monte Carlo, Monaco, March 2-4, 1982
21 p3090 A83-45076

SITA - Advanced telecommunications services --- for air transport industry
21 p3090 A83-45079

Airline common databases and data processing applications
21 p3190 A83-45081

The four-dimensional assimilation of asymptotic information on the basis of a nonlinear filtration scheme --- for numerical weather forecasting
21 p3181 A83-45331

Teleinformatics, the protection of privacy and the law
22 p3368 A83-45820

Processing of microwave radiometry data for earth scientific purposes
22 p3311 A83-46174

Principles of organization of the on-ground data processing for remote sensing purposes using finite rings and fields
23 p3501 A83-47285

[IAF PAPER 83-130]
23 p3489 A83-47395

DATA PROCESSING EQUIPMENT

NT AIRBORNE/SPACEBORNE COMPUTERS

NT ANALOG COMPUTERS

NT COMPUTERS

NT DATA PROCESSING TERMINALS

NT DIGITAL COMPUTERS

NT EMBEDDED COMPUTER SYSTEMS

NT HYBRID COMPUTERS

NT ICL COMPUTERS

NT ILLIAC 4 COMPUTER

NT MICROCOMPUTERS

NT MICROPROCESSORS

NT MINICOMPUTERS

NT PARALLEL COMPUTERS

NT PRINTERS (DATA PROCESSING)

NT SEQUENTIAL COMPUTERS

NT VAX-11/780 COMPUTER

Photoconductor-liquid crystal photosensitive structures --- for optoelectronic information processing
02 p0235 A83-12197

Adaptive optical processor
02 p0178 A83-12592

Frequency-multiplexed and pipelined iterative optical systolic array processors
06 p0802 A83-18588

Model of the task-execution process in a pipeline processing unit
09 p1325 A83-23978

Interfacing Spacelab payloads for the first mission and the development of the processor interface adaptor (PIA)
17 p2482 A83-37873

Considerations on the redundancy structures of on-board processors for SS-TDMA satellites
18 p2674 A83-39999

Reliability performance evaluation of an on-board processor for SS-TDMA satellites
18 p2675 A83-40000

Comparison of photon correlation laser Doppler anemometry data processing techniques
21 p3139 A83-44798

Multiple access equipment design for satellite communication systems in the USSR [IAF PAPER 83-84]
23 p3441 A83-47258

The application of a graphic display for the analysis of scientific telemetry data in experiments involving the search for gamma-ray transients on Prognoz 6 and 7
23 p3500 A83-48417

DATA PROCESSING TERMINALS

Human factors and the design of display terminals
01 p0085 A83-10253

The development of JTIDS distributed TDMA /DTDMA/ advanced development model /ADM/ terminals --- Joint Tactical Information Distribution System
01 p0004 A83-11094

SCPC terminal and signal strength measuring apparatus for 30/20 GHz frequency band
10 p1403 A83-26082

The 8 by 8 display
17 p2564 A83-38061

Data broadcast to microterminals via satellite using spread-spectrum techniques
21 p3122 A83-45433

DATA PROCESSORS

U DATA PROCESSING EQUIPMENT

DATA READOUT SYSTEMS

U DATA SYSTEMS
U DISPLAY DEVICES

DATA RECORDERS

The widening of the dynamic range of data measuring systems of a five-channel spectrophotometer
17 p2510 A83-37721

Method of thermodynamic function control and of damage analysis regarding aircraft engines with the aid of flight data recording systems --- German thesis
19 p2800 A83-41850

Flight data recorders - An investigator's tool
21 p3092 A83-44877

DATA RECORDING

The compiled catalogue of galaxies in machine-readable form and its statistical investigation
01 p0115 A83-10158

Advanced signal processing of turbine rotor bore waveforms
04 p0488 A83-15156

Quasi-real-time antenna near-field/far-field transformation without phase and amplitude recording
06 p0741 A83-18652

High-speed television camera and video tape recording system for motion analysis
08 p1097 A83-22531

Cryogenic frequency domain optical mass memory
08 p1166 A83-22808

Recording and reproduction of microwave holograms according to the scanning procedure and their optical subsequent treatment
09 p1265 A83-23379

Holographic recording on board the Salyut-6 space station
13 p1815 A83-30813

Method of improving image quality in holographic interferometers
15 p2164 A83-34424

Oscillating bipolar electric field changes due to close lightning return strokes
16 p2383 A83-35413

Scheduling of ISS-b operations --- ground station computer algorithm and onboard data recording Ionosphere Sounding Satellite
21 p3098 A83-45440

DATA REDUCTION

NT DATA SMOOTHING

Combining satellite, radar, and conventional data to observe mesoscale features pertinent to thunderstorm development
01 p0074 A83-10042

On the surface radiation budget
01 p0065 A83-10100

The U.K. StarLink computer network
01 p0093 A83-10134

System software approaches to the analysis of multidimensional data structures
01 p0090 A83-10137

Acquisition and analysis of the EMG power spectra - A reproducible technique for assessment of muscle fatigue --- electromyogram
01 p0086 A83-11107

A high order language for the analysis of experimental data
01 p0089 A83-11196

Scene classification of Landsat multispectral scanner data by means of the Adaptive Learning Network methodology
01 p0067 A83-11458

Data acquisition/reduction system for flight testing general aviation aircraft
02 p0135 A83-11903

Preliminary results of an assessment of FGGE 'special effort' data and its impact on GLAS model analyses and forecasts
03 p0365 A83-14402

Global data assimilation experiments with scatterometer winds from Seasat-A
03 p0365 A83-14403

The impact of starting ECMWF medium-range forecasts from 00Z analyses with short data cutoff times

03 p0365 A83-14405

Towards the optimum control of gravity waves and ageostrophic circulations for data assimilation

03 p0366 A83-14411

Orbiter entry leeside heat-transfer data analysis

[AIAA PAPER 83-0484] 05 p0586 A83-16745

A means for utilizing ancillary information in multispectral classification --- of remotely sensed data

05 p0656 A83-16905

A note on errors and uncertainties in NCAR aircraft pyrgeometer data from MONEX

05 p0644 A83-17275

Intermediate band filter spectrophotometry of bright galaxies. II - Data reductions

05 p0694 A83-17663

Analysis of pulsations --- of geomagnetic fields

05 p0664 A83-17781

Abel inversion with a simple analytical representation for experimental data

07 p0988 A83-19984

Photographic surface photometry of the Milky Way. I - Data and reduction methods

07 p1005 A83-20559

Research advances in satellite-aided crop forecasting

08 p1126 A83-21930

Development of real-time VLB and measurements of scintillation

08 p1075 A83-22038

Radioastronomy measurement and reduction procedures for the detection of extensive continuum emission

09 p1352 A83-23390

Uncertainty of flyover noise data

[AIAA PAPER 83-0701] 10 p1474 A83-25921

Recurrent spatial structures in convective systems --- automated weather radar data analysis

11 p1622 A83-26981

An attenuation-correction technique for dual-wavelength analyses --- of meteorological radar signals

11 p1571 A83-27081

IRAS preliminary science analysis at the OCC

11 p1533 A83-28216

U.S. data processing for the IRAS project --- by Jet Propulsion Laboratory Scientific Data Analysis System

11 p1674 A83-28217

A study of the effects of a cubic nonlinearity on a modern modal identification technique

[AIAA 83-0810] 12 p1773 A83-29810

Contributions to the theory of uncertainty analysis for single-sample experiments

13 p1913 A83-30628

A generalized algorithm for efficient photometric reductions

13 p1941 A83-31569

Cape Romain and the Charleston Bump - Historical and recent hydrographic observations

14 p2060 A83-33086

A period-finding method for sparse randomly spaced observations of 'How long is a piece of string?' --- for variable stars

15 p2248 A83-34580

Automatic calculation of electron density profiles from digital ionograms. III - Processing of bottomside ionograms

16 p2376 A83-35421

Contribution to the reduction of photoelectric occultation observations using an integrated deconvolution method

16 p2425 A83-36651

Ray-trace analysis and data reduction methods for the Ritchey-Common test --- for optically flat surfaces

16 p2413 A83-36763

Improvements of the performance of triple hot wire probes

17 p2509 A83-36999

The widening of the dynamic range of data measuring systems of a five-channel spectrophotometer

17 p2510 A83-37721

Application of sine transform in image processing

17 p2570 A83-38886

Design of algorithms to extract data from capacitance sensors to measure fastener hole profiles

19 p2855 A83-41026

On the extraction of tidal information from measurements covering a fraction of a day --- for upper atmosphere meteorology

19 p2865 A83-41128

Analysis of solar-radiation characteristics at the EURELIOS power plant of Adrano

19 p2862 A83-41165

The spectral matrix, eigenvalues, and principal components in the analysis of multichannel geophysical data

21 p3119 A83-44230

Something about to improve the accuracy of testing in low speed wind tunnel

21 p3093 A83-44571

Spacecraft model verification using swept sine data analysis

[SAE PAPER 821479] 22 p3303 A83-45748

Efficient coding and resonance spike identification for topside ionogram processing

22 p3330 A83-46512

Information extraction from thematic mapper data

[IAF PAPER 83-114] 23 p3475 A83-47275

Solar rotation 1947-1981 - Determined from sunspot data

23 p3530 A83-47454

Measurement and analyses of heat flux data in a turbine stage. I - Description of experimental apparatus and data analysis

[ASME PAPER 83-GT-121] 23 p3408 A83-47950

Variational approach to problems of the interpolation of physical fields --- Russian book on oceanography

24 p3622 A83-49041

IUE data reduction

24 p3644 A83-49558

Crowded-field stellar photometry

24 p3647 A83-50003

Evaluation of optimal parameters for photographic plate measurement and data reduction --- in astronomical photography

24 p3647 A83-50011

DATA RETRIEVAL

Automated data retrieval in astronomy; Proceedings of the Sixty-fourth Colloquium, Universite de Strasbourg I, Strasbourg, France, July 7-10, 1981

01 p0113 A83-10126

The astronomical data base and retrieval system at NASA

01 p0113 A83-10127

Data on time and polar motion - Immediate accessibility

01 p0111 A83-10131

A fast method to retrieve data from a large star catalogue file

01 p0113 A83-10138

Archiving and retrieval of data from the International Ultraviolet Explorer (IUE) mission

01 p0113 A83-10141

A process for retrieval of data from a compiled star catalogue

01 p0114 A83-10142

Stellar bibliography retrieving system in Japan

01 p0114 A83-10147

The Bibliographical Star Index

01 p0114 A83-10148

Aids to the retrieval and evaluation of astronomical data

01 p0114 A83-10149

Data and data retrieval in space astronomy

01 p0114 A83-10156

Data retrieval in the metacatalogue of galaxies

01 p0115 A83-10157

Geneva photometric boxes. IV - A refined method for direct access --- to stellar color data

01 p0115 A83-10159

Remarks about the cataloguing of open cluster data

01 p0115 A83-10162

Binary multiplexing and the phase-retrieval problem

05 p0643 A83-16836

Information search and retrieval in the areas of astronomy and geodesy --- Russian book

07 p1001 A83-20375

Enforcing irreducibility for phase retrieval in two dimensions

07 p0930 A83-20795

A two step linear statistical technique using leaps and bounds procedure for retrieval of geophysical parameters from microwave radiometric data

15 p2194 A83-33692

Controlling the 1ESO13 spectrometer for spacelab and its data retrieval

16 p2317 A83-35786

A review of geostationary satellite alternatives for retrieving data from long duration balloon flights

18 p2639 A83-39812

Retrieval of the optical properties of aerosols from aureole and extinction data

24 p3604 A83-49002

A data structure and algorithm based on a linear key for a rectangle retrieval problem

24 p3619 A83-49194

DATA SAMPLING

Relative stability test for continuous and sampled-data control systems using the generalised sign matrix

01 p0094 A83-10291

Sampled-data modeling of switching regulators

01 p0041 A83-11025

Analysis of systems containing multiple, irregular sampling

01 p0095 A83-11131

Transmission matrix approach to variable-rate sampled-data systems

01 p0095 A83-11132

Confidence intervals for the percent nonconforming based on variables data

02 p0232 A83-12093

Optimum sampling for digital terrain models - A trend towards automation

03 p0345 A83-14092

Optimum angular and spatial sampling of reflected radiance fields

03 p0361 A83-14650

To mix or match - On choosing matched samples in comparative aerial surveys

03 p0351 A83-14664

Sampling theory for synoptic satellite observations. I Space-time spectra, resolution, and aliasing. II - Fast Fourier synoptic mapping

04 p0517 A83-15940

Robust control strategy for a linear time-invariant multivariable sampled-data servomechanism problem

04 p0529 A83-16192

Measurement of true mean temperature for determination of climatic trends

05 p0668 A83-17449

Techniques of self-tuning

05 p0680 A83-17578

Model following and pole-placement self-tuners

05 p0680 A83-17579

Sampling approach for fast computation of scattered fields

06 p0736 A83-18569

A generalized sampling and sampling-like technique for fast analysis of reflector antennas

06 p0743 A83-18688

The effect of undersampling and finite truncation of the antenna near-field data on the predicted far-field pattern

06 p0743 A83-18689

Multichannel recovery of quadrature components of bandpass signals

06 p0748 A83-19046

Bandpass signal sampling and coherent detection

06 p0749 A83-19048

Quadrature sampling with high dynamic range

06 p0749 A83-19049

The effect of sampling offset on the Pe performance of partial response systems --- probability of error in signal processing

07 p0909 A83-19750

The development of a sampling procedure for urban land use mapping from aerial photographs - A study in Calabar, Nigeria

08 p1172 A83-21960

Synthesis of sliding discrete Fourier transform and sliding Hadamard transform circuits

08 p1157 A83-22232

Effect of sampling, optical transfer function shape, and anisotropy on subjective image quality

08 p1167 A83-22894

Analysis of spatially correlated images with implications for independent sampling and linear correlator image detection

08 p1105 A83-22901

Practical comparison of optoelectronic sampling systems and devices

09 p1251 A83-23347

Selection of CO2 concentration data from whole-air sampling at three locations between 1968 and 1974

09 p1295 A83-24263

Simplified tone detector for PCM channel

10 p1402 A83-25634

Large sample identification and spectral estimation of noisy multivariate autoregressive processes

10 p1462 A83-25637

The processing of periodically sampled multidimensional signals

10 p1402 A83-25641

The effect of spatial and temporal averaging on sampling strategies for cloud amount data

10 p1451 A83-26100

Approximation of multivariable linear systems with impulse response and autocorrelation sequences

10 p1463 A83-26502

An experimental verification of laser-velocimeter sampling bias and its correction

12 p1727 A83-28840

Contributions to the theory of uncertainty analysis for single-sample experiments

13 p1913 A83-30628

A method of calculating the natural components of meteorological fields

14 p2058 A83-32852

Subpicosecond electrical sampling

14 p2008 A83-33423

Fast convolution methods for hexagonally sampled two-dimensional signals

15 p2220 A83-33518

A z-transform theory for distributed sensing and control

15 p2222 A83-35128

Modeling, analysis, and control of dynamic systems --- Book

17 p2569 A83-37400

Sampled control stability of the ESA instrument pointing system

17 p2480 A83-37438

Conditional sampling of turbulence in the atmospheric surface layer

18 p2721 A83-39110

Identification of submodels of multi-input, multi-output systems

19 p2890 A83-41485

Stability analysis of multirate nonlinear sampled-data control systems

19 p2890 A83-41488

Digital complex sampling

20 p2963 A83-42481

Picosecond signal sampling and multiplication by using integrated tandem light modulators

21 p3205 A83-44229

Choice of sampling period and secondary optimization of digital Wiener filters

21 p3197 A83-45307

The Jacobi-Bessel and the pseudo-sampling techniques in the analysis of reflector antennas

21 p3121 A83-45410

On the sampling problem in radiation budget studies

22 p3329 A83-46232

Probe correction in near field measurements by pseudo sampling technique

24 p3571 A83-49995

DATA SIMULATION

Statistically dependent normal places in orbit calculations --- using synthetic satellite tracking data

11 p1535 A83-28027

Comparison of simulated data of SPOT and Landsat-D sensors Application to an agricultural region

17 p2529 A83-38162

The application of SPOT simulated data to the remote sensing of an intertidal environment

17 p2534 A83-38457

The use of the SPOT satellite for remote sensing of land use in the Mediterranean region - A first assessment of simulated images of Corsica

17 p2534 A83-38459

DATA SMOOTHING

Selective image enhancement and restoration
 01 p0061 A83-10028
 Algorithms for smoothing data with periodic and
 parametric splines 01 p0102 A83-10284
 Interactive smoothing of digitized point data
 02 p0226 A83-11817
 A program for satellite-orbit determination - An
 application to the case of earth-observation satellites
 [IAF PAPER 82-301] 03 p0283 A83-14400
 The impact of manually derived bogus data on the
 analysis and forecast models at the Air Force Global
 Weather Central 03 p0365 A83-14404
 Variational normal mode balancing in the Navy
 operational data assimilation system --- for numerical
 weather prediction 03 p0366 A83-14410
 A nonlinear smoothing procedure for the reconstruction
 of flight trajectories on the basis of radar data
 03 p0280 A83-14494
 Smoothing of output-signal fading for a fiber ring
 interferometer, determined by instabilities of the
 parameters of a one-mode fiber-optic waveguide
 04 p0482 A83-15747
 State description for the root-signal set of median
 filters 05 p0680 A83-16912
 Optimal adaptive smoothing in correlated noise
 conditions 07 p0984 A83-20000
 Closure hypotheses from the method of smoothing for
 coherent wave propagation in discrete random media
 07 p0989 A83-20792
 Bootstrap algorithms for parameter and smoothing state
 estimation 08 p1158 A83-22732
 Smoothing with periodic cubic splines
 09 p1335 A83-23873
 Recursive algorithms for two-dimensional smoothing
 using bicubic hermite polynomial 09 p1336 A83-24717
 Estimating planetary terrain slopes from range
 measurements using a two dimensional spline smoothing
 technique 10 p1381 A83-26595
 Processing of 2-dimensional lidar-derived windfields
 11 p1630 A83-27070
 A stable smoothing algorithm --- for digital processing
 of radar signals 11 p1556 A83-27948
 Smooth extremal problems in spectra of constant
 matrices 13 p1910 A83-30620
 An objective procedure for detecting and correcting
 errors in geophysical data. II - Multidimensional
 applications 13 p1877 A83-30897
 Some results on the median filtering of signals and
 additive white noise 15 p2221 A83-35107
 Optimal smoothing of 'noisy' data by fast Fourier
 transform 15 p2223 A83-35257
 Smoothing of cubic parametric splines
 16 p2406 A83-35324
 Quantitative evaluation of some edge-preserving
 noise-smoothing techniques 21 p3191 A83-44265
 Fringe pattern recognition and interpolation using
 nonlinear regression analysis 22 p3352 A83-46838
 Three-dimensional wind field analysis from dual-Doppler
 radar data. I - Filtering, interpolating and differentiating
 the raw data 22 p3342 A83-46943
 Smoothing of bicubic parametric surfaces
 23 p3502 A83-48728

DATA STORAGE

New developments in data storage
 01 p0087 A83-10136
 Data and data retrieval in space astronomy
 01 p0114 A83-10156
 Efficient local searching in sparse images
 01 p0100 A83-11469
 Minimization of interprocessor communication for
 parallel computation 05 p0679 A83-17240
 Effects of cache coherency in multiprocessors
 05 p0679 A83-17242
 A note on word length and memory requirements in
 digital control 09 p1332 A83-24775
 Comparison of various data allocation schemes in the
 memory of a multiprocessor computing system
 11 p1647 A83-28625
 Principles of a three-dimensional molecular electronic
 memory 12 p1720 A83-29458
 New computer architectures tackle bottleneck ---
 processor-memory link bypass 14 p2073 A83-33141
 Developments in scientific information systems
 19 p2907 A83-41291
 A system of active data-storage for experiments on
 gamma-ray transients 23 p3500 A83-48416
 A hybrid structure for the storage and manipulation of
 very large spatial data sets 24 p3619 A83-49195

DATA STRUCTURES

Content-addressable read/write memories for image
 analysis 02 p0227 A83-12246
 A method of rotating areas on a raster scan graphic
 display 05 p0644 A83-16871

Conversion of raster coded images to polygonal data
 structures 15 p2165 A83-34838
 Generalized balanced ternary - An approach to handling
 spatial data 15 p2165 A83-34841
 A paradigm for the design of parallel algorithms with
 applications 20 p3038 A83-43114
 A data structure and algorithm based on a linear key
 for a rectangle retrieval problem 24 p3619 A83-49194
 TOPPSY - A time overlapped parallel processing
 system 24 p3620 A83-49197
 Method for choosing the required complete configuration
 of a multiprocessor computing complex 24 p3620 A83-50210

DATA SYSTEMS

NT NEEDS (DATA SYSTEM)
 Responsibilities and practical limitations in the operation
 of an astronomical data center 01 p0114 A83-10144
 Advanced facility for processing aircraft dynamic test
 data 01 p0013 A83-10189
 Instrumentation applications to Space Shuttle models
 and thermal protection system tiles tested in NASA-AMES
 wind tunnels 01 p0017 A83-11065
 Air data systems for airplanes of the 1990's
 01 p0004 A83-11099
 Future Navy data bus requirements - Modular approach
 for flexible evolution 01 p0006 A83-11184
 A high order language for the analysis of experimental
 data 01 p0089 A83-11196
 Visible and infrared spin scanning radiometer /VISSR/
 atmospheric sounder /VAS/ ground data system
 02 p0142 A83-12679
 Analytical plotter for data input into geo-based
 information systems 02 p0180 A83-12683
 Evolution of the NMC data assimilation system -
 September 1978-January 1982 02 p0217 A83-13052
 Motivation for a combined data flow-control flow
 processor 08 p1155 A83-22827
 Data systems - Optical bus will connect distributed
 system 09 p1215 A83-24352
 A multifunction integrated approach to providing aircraft
 inertial data 09 p1200 A83-24853
 The Integrated Inertial Navigation System -
 AN/ASN-132 09 p1201 A83-24855
 IRAS preliminary science analysis at the OCC
 11 p1533 A83-28216
 Semantic representative languages in document
 retrieval systems - Effects of a representation of meaning
 involving differences in depth on the system
 characteristics --- German thesis 11 p1666 A83-28660
 Cooperative development of application specifications,
 giving particular attention to the realization of software
 for specific branches of the economy --- German thesis
 11 p1647 A83-28661
 Synergistic integration of JTIDS/GPS technology ---
 Joint Tactical Information Distribution System
 11 p1529 A83-28789
 PMUX - The interface for engine data to AIDS ---
 propulsion multiplexer Aircraft Integrated Data System
 13 p1807 A83-30158
 Development and test of an integrated sensory system
 for advanced aircraft 13 p1807 A83-30159
 Meteorological data assimilation using AFOS
 13 p1885 A83-30530
 Medium-range objective predictions of thunderstorms on
 the McIDAS/CSIS interactive computer system ---
 Computer Interactive Data Access System/Centralized
 Storm Information System 13 p1885 A83-30536
 Interactive data processing for mesoscale forecasting
 applications 13 p1885 A83-30539
 The Navy SPADS - A second generation environmental
 display system --- Satellite Processing And Display
 System 13 p1909 A83-30541
 Application of a charge-coupled device (CCD) detector
 for codespectroscopy 14 p2016 A83-31992
 Certain characteristics of the use of photothermoplastic
 materials in remote-sensing imaging systems
 14 p2019 A83-32503
 A Z-domain controller design method for sampled-data
 systems having feedback dynamics 17 p2565 A83-37083
 Project Skywater environmental data network --- for
 weather modification and forecasting 17 p2548 A83-38712
 An interactive meteorological display and analysis
 system 17 p2549 A83-38713
 Automation of preplanning as a means for enhancing
 quality in operational flight control. II 18 p2638 A83-39222
 McIDAS III - A modern interactive data access and
 analysis system --- Man computer Interactive Data Access
 System 18 p2726 A83-39874

Synthesis and analysis of pulsed measuring converters
 of information and measuring systems --- Russian book
 18 p2679 A83-40606
 Ad Hoc modeling, expert problem solving, and R&T
 program evaluation 19 p2907 A83-41304
 Landsat-D - An end-to-end data system 19 p2813 A83-41339
 Development of a totally computer-controlled triple
 quadrupole mass spectrometer system 20 p2988 A83-42298
 Production and analysis of output data products for
 Landsat-4 in the engineering check-out phase
 [AAS PAPER 83-158] 20 p3011 A83-43762
 Multisensor satellites and data systems for earth
 observations [AAS PAPER 83-195] 20 p3011 A83-43772
 Modern digital air-data computer 23 p3405 A83-47186

DATA TRANSMISSION

NT CODE DIVISION MULTIPLE ACCESS
 NT FREQUENCY DIVISION MULTIPLE ACCESS
 NT MULTIPLE ACCESS
 NT SINGLE CHANNEL PER CARRIER
 TRANSMISSION
 Euronet-DIANE, the first European network for data
 transmission 01 p0111 A83-10133
 Approximation techniques of a selective ARQ protocol
 01 p0032 A83-11093
 Fiber optic aircraft multiplex systems - Planning for the
 1990s 01 p0006 A83-11180
 Bit error rate performance of Image Processing Facility
 high density tape recorders 02 p0179 A83-12681
 The design of a packet switched network for aeronautical
 data interchange 03 p0281 A83-14862
 Optoelectronic digital/analogue converter-emitter
 04 p0534 A83-15241
 From state machines to temporal logic - Specification
 methods for protocol standards --- of computer
 communication networks 05 p0621 A83-17270
 The SPINE programme and the associated
 demonstrations at UNISPACE 82 --- satellite data
 transmission via Space Information Network Experiment
 05 p0622 A83-17427
 Data transmission rate in a memoryless discrete channel
 with data feedback 05 p0623 A83-17686
 The application of game theory to the synthesis of an
 optimal system of symbol data transmission 05 p0623 A83-17689
 Transmission of two-dimensional images through a
 single optical fiber by wavelength-time encoding
 05 p0685 A83-17885
 The characteristics of HF propagation paths and their
 implications in digital communication system design
 06 p0747 A83-18736
 Self-noise produced by quadrupling of QPSK signals
 06 p0748 A83-19042
 Detection of M'ARY communication with truncated
 symbols 07 p0904 A83-19679
 Pre-operational tests of high-speed /56 kbps/
 transmission over MARISAT 07 p0870 A83-19702
 Error probabilities in lasercom PPM systems
 07 p0905 A83-19705
 Considerations for spread spectrum systems design
 07 p0909 A83-19744
 Error rates for narrowband Manchester coded digital
 FM 07 p0909 A83-19748
 Viterbi decoder VLSI integrated circuit for bit error
 correction 07 p0917 A83-19755
 Discrimination of speech and high-speed data using an
 adaptive predictor for DSI application --- Digital Speech
 Interpolation 07 p0910 A83-19756
 Optical data-transmission equipment for computer
 systems - Optical data mux 07 p0983 A83-19780
 Mitelnet - A private network using TDMA
 07 p0911 A83-19787
 Advances in Serial MSK modems 07 p0917 A83-19789
 Efficiency in an ARQ system with a constraining number
 of outstanding blocks 07 p0912 A83-19791
 Message delays using prioritized packet switching
 07 p0912 A83-19792
 Spread-spectrum multiple access data loop
 07 p0912 A83-19795
 Routing schemes for the augmented data manipulator
 network in an MIMD system 07 p0984 A83-20248
 A line-scanning system with fiber-optic elements
 07 p0929 A83-20776
 Experimental results on constant envelope signaling with
 reduced spectral sidelobes 07 p0916 A83-21200
 The development of standards for the common ICAO
 Data Interchange Network /CIDIN/ 08 p1075 A83-22027
 Air-deployed, over-ocean, small, ruggedized optical
 fiber 08 p1074 A83-22486
 Fiber optics for electro-magnetic pulse /EMP/
 simulators 08 p1047 A83-22495

Processing display system architectures
08 p1152 A83-22534

Comparison of transform image coding techniques for compression of tactical imagery
08 p1100 A83-22597

Noise sources affecting the transmission of data with the aid of lightguides
09 p1243 A83-23377

Thoughts on the design of a duplex modem with echo extinction
09 p1244 A83-23411

Methods of investigating data transmission networks --- Russian book
09 p1326 A83-23818

High-speed decoding technique for slip detection in data transmission systems using modified cyclic block codes
09 p1249 A83-24115

ARINC 429 digital data communications for commercial aircraft
09 p1200 A83-24435

The 'Oribita-RV' satellite sound broadcasting and newspaper column transmission system
10 p1402 A83-25876

Experimental system for computer network via satellite /CS/. I - Summary of the system
10 p1403 A83-26077

The NYU ultracomputer - Designing an MIMD shared memory parallel computer --- Multiple Instruction Multiple Data stream
10 p1461 A83-26258

Data transmission in the case of secondary radar /Mode S/
11 p1527 A83-27124

Performance of IJF-OQPSK and Partial Response /PR/ IJF-OQPSK modems in a nonlinearly amplified and adjacent-channel interference satellite environment
11 p1556 A83-28128

One-way multiaddress satellite data communication system
11 p1557 A83-28133

On the synthesis of a class of self-synchronizing signals
13 p1828 A83-30289

New syndrome decoder for (n, 1) convolutional codes
13 p1912 A83-31785

Noise immunity of data transmission systems using pulse code modulation (Review)
14 p2000 A83-32476

Strategies for weather-dependent data acquisition
14 p1981 A83-32867

Performance analysis of some ARQ protocols
15 p2144 A83-33521

Bit error rate evaluation of GSTDN/TDRSS communication links
15 p2125 A83-33734

Spatial carriers with orthogonal subcodes --- signal coding and decoding for optical communication
15 p2230 A83-33810

Synthesis of holographic components for optical data storage and transmission systems allowing for characteristics of semiconductor laser radiation
15 p2163 A83-33983

The transmission of two-dimensional and color images through a single fiber by the spectral scanning technique
15 p2232 A83-34889

Information theory and causal information transmission with feedback
15 p2221 A83-35104

Optimal coding for information transmission through a Poisson type channel
15 p2221 A83-35118

Application of 2-D bin packing algorithms for task scheduling in PASM --- sparse crossbar interconnection network designs for data transmission
15 p2219 A83-35132

Optimal reception of a pseudorandom PSK signal, carrier-frequency-modulated by the information message
15 p2148 A83-35170

Spread-spectrum systems with surface-acoustic-wave components
16 p2345 A83-35518

Application of catastrophe theory to a slotted ALOHA communication system
16 p2343 A83-36580

A modified selective-repeat type-II hybrid ARQ system and its performance analysis --- Automatic Repeat reQuest
16 p2343 A83-36601

Multiple dwell serial search - Performance and application to direct sequence code acquisition
16 p2343 A83-36603

Analysis and stability considerations in a reservation multiaccess system
16 p2343 A83-36606

Electrooptical imaging system using wavelength coding
17 p2510 A83-37748

Fiber-optic image transmission system with high resolution
17 p2580 A83-37749

Capacity allocation scheme for transmission of packets over satellite links
17 p2493 A83-37792

Control systems for European satellites
17 p2475 A83-37854

Biased Gaussian noise source for digital-transmission-system simulations
18 p2675 A83-40395

Acknowledgement based random access transmission control - An equilibrium analysis
19 p2828 A83-41332

Scientific satellite data communications
19 p2813 A83-41341

Noise models for detection
19 p2828 A83-41345

Optimum utilization of domestic communication satellites for data and television transmission
19 p2831 A83-41382

A selective-repeat ARQ scheme and its throughput analysis
19 p2832 A83-41398

Performance analysis of M-ary code shift keying in code division multiple access systems
19 p2833 A83-41408

Hybrid diversities in a spread spectrum mobile communication system
19 p2833 A83-41409

Quantum measurements and the reliability of information transfer
19 p2896 A83-41494

The limitation of radiation directivity in the case of image transmission
19 p2835 A83-41781

Class of linear cyclic block codes for burst errors occurring in one-, two- and three-dimensional channels
20 p3040 A83-43686

Plastic optical passive devices and their application to a local computer network
21 p3205 A83-44219

Three-position shift-keying in communication systems
21 p3120 A83-44770

Data broadcast to microterminals via satellite using spread-spectrum techniques
21 p3122 A83-45433

Optimal symbol-by-symbol detection for duobinary signaling
22 p3272 A83-45739

Landsat standard family of CCT formats Europe specific problems --- Computer Compatible Tapes
22 p3311 A83-46172

The transmission of analog information over digital communications channels --- Russian book
23 p3443 A83-48425

DATING

U CHRONOLOGY
U TIME MEASUREMENT

DAWN CHORUS

Latitudinal variation of chorus frequency observed in the topside ionosphere
08 p1133 A83-22035

Discrete chorus emissions recorded at Nainital
16 p2381 A83-36617

Terrestrial versus Jovian VLF chorus - A comparative study
20 p3078 A83-42409

Spatial distribution of the polar chorus at high latitudes
21 p3176 A83-45265

DAYGLOW

Atomic oxygen density deduced from limb-scans of the UV dayglow
[AIAA PAPER 83-0021]
05 p0659 A83-16469

Bulgaria-1300 UV day glow spectra, related to the ozone problem
12 p1756 A83-29693

Multiple fluorescent scattering of N2 ultraviolet emissions in the atmospheres of the earth and Titan
15 p2274 A83-33932

Satellite measurements of earth's night and dayglow upper atmosphere spectra in the vacuum U. V. region
15 p2201 A83-34446

An imaging spectrometric observatory for Spacelab
17 p2482 A83-38577

DAYTIME

Determination of the value of the field-aligned current density in the daytime polar cusp
02 p0211 A83-12449

Characteristics of gaps in discrete dayside auroras
07 p0965 A83-21186

Possible enhancement of previously unobserved /NII/ emissions in the mid-day aurora associated with nighttime substorm activity
07 p0967 A83-21561

Dual Fabry-Perot spectrometer measurements of daytime thermospheric temperature and wind velocity - Data analysis procedures
09 p1306 A83-24449

Daytime mesospheric temperatures over the low-latitude station Thumba derived from rocket-borne solar Lyman-alpha absorption measurements
09 p1307 A83-24691

On the formation of daytime troughs in the F-region within the plasmasphere
14 p2053 A83-32697

Latitudinal influences on the quiet daytime D-region [AD-A128591]
16 p2375 A83-35391

Atmospheric angular momentum fluctuations, length-of-day changes and polar motion
16 p2376 A83-35638

A simple scheme for daytime estimates of the surface fluxes from routine weather data
18 p2724 A83-39675

The rate of occurrence of dayside Pc 3.4 pulsations - The L-value dependence of the IMF cone angle effect
20 p3025 A83-43200

Daytime high-latitude profile of solar-cosmic-ray protons with Ep not less than about 1 MeV
21 p3244 A83-45286

Interaction of the solar wind with the dayside magnetosphere
23 p3485 A83-48553

DC (CURRENT)

U DIRECT CURRENT

DC 8 AIRCRAFT

The recipe for re-engining jet transports
[SAE PAPER 821441]
17 p2463 A83-37989

DC 9 AIRCRAFT

DC-9 Super 80 digital flight guidance system simulation techniques for certification
05 p0592 A83-17305

Software design for the Douglas DC-9 Super 80 digital flight guidance system
05 p0592 A83-17311

DC-9 Super 80 Digital Flight Guidance System integrated system testing
[SAE PAPER 821364]
17 p2467 A83-37959

DC 10 AIRCRAFT

The KC-10A - USAF's newest range extender
03 p0281 A83-14700

Validation of the KC-10 refueling boom digital control system
[SAE PAPER 821421]
17 p2463 A83-37978

Testing of antimisting kerosene in the DC-10/KC-10 fuel system simulator
[SAE PAPER 821485]
17 p2492 A83-38004

DE HAVILLAND AIRCRAFT

NT DHC 4 AIRCRAFT

Development of a structural, bird impact resistant, de-iced wing leading edge for the de Havilland Dash 8 aircraft using fibre-reinforced composites
06 p0717 A83-18823

Dash 8 - Canada's new commuter
12 p1701 A83-29675

The Dash 8 development program
15 p2121 A83-33546

Dashing ahead in commuterliners
17 p2464 A83-38470

DE HAVILLAND DHC 4 AIRCRAFT

U DHC 4 AIRCRAFT

DE LAVAL NOZZLES

U CONVERGENT-DIVERGENT NOZZLES

DEAD RECKONING

Intelligent control of tactical target cueing --- by subsonic flight vehicles
02 p0133 A83-12879

Flight tests of integrated navigation by least squares adjustment
09 p1202 A83-24871

Multiconfiguration Kalman filter design for high-performance GPS navigation
10 p1373 A83-26262

DEADWEIGHT

U STATIC LOADS

DEAFNESS

U AUDITORY DEFECTS

DEBRIS

NT SPACE DEBRIS

The nature of wear debris generated during lubricated wear-in
[ASLE PREPRINT 82-LC-3B-1]
03 p0334 A83-13235

Effects of the El Chichon volcanic cloud in the stratosphere on the intensity of light from the sky
20 p3028 A83-42209

FOD hazard from tire-lofted debris --- Foreign Object Damage
20 p2931 A83-42557

DEBUGGING

U CHECKOUT

DEBYE LENGTH

Statistical thermodynamics of nonideal plasma
05 p0687 A83-17267

Transition from single to multiple double layers --- of plasma
05 p0688 A83-17351

Theory of cylindrical and spherical Langmuir probes in the limit of vanishing Debye number
05 p0688 A83-17370

DEBYE TEMPERATURE

U SPECIFIC HEAT

DEBYE-HUCKEL THEORY

Gravitational Debye-Hueckel theory for a Newtonian cosmology
12 p1793 A83-29061

DECAMETRIC WAVES

Synthesis of an adaptive analyzer of levels of nonstationary radio interference --- for decametric wave band
01 p0031 A83-10809

Decametric emission of Jupiter and solar activity
02 p0268 A83-12860

Formation of Jovian decametric S bursts by modulated electron streams
05 p0705 A83-17387

The quiet sun brightness temperature at 127 MHz
06 p0854 A83-19126

A theory of Jovian decameter radiation
07 p1036 A83-21505

Influence of interplanetary magnetic field sector boundary passages on Jovian decametric radio bursts
07 p1036 A83-21587

Non-linear interaction of decametric radio waves at close frequencies in oblique propagation --- in ionosphere
09 p1300 A83-23313

A theory of the Io phase asymmetry of the Jovian decametric radiation
09 p1365 A83-23756

Theories of radio emissions and plasma waves --- in Jupiter magnetosphere
10 p1520 A83-26620

Absorption bursts in the radio emission from the sun at decameter wavelengths
11 p1691 A83-27991

Spectral evidence of type II shock influence on Razin-cutoff frequency in the decametric type IV continuum 15 p2280 A83-34299

Secondary peaks in solar microwave outbursts [AD-A129962] 15 p2281 A83-34305

The Io-control of Jupiter's decametric radiation - The Alfven wave model 17 p2620 A83-38115

Diffuse radio emission from the Coma cluster of galaxies at decametre wavelengths 18 p2764 A83-39191

The source location of certain Jovian decametric radio emissions 20 p3078 A83-42408

Observations on the slowly varying component of solar radio emission at decameter wavelengths 23 p3538 A83-47733

A catalogue of Jovian radio observations from January 1980 to December 1981 24 p3672 A83-49318

A new type of decametric radio emission from Jupiter 24 p3673 A83-49631

Sounding of the supercorona by decametric emission from 3C144 24 p3675 A83-49634

DECAY

NT ACOUSTIC EMISSION

NT ALPHA DECAY

NT CATHODE GLOW

NT CATHODOLUMINESCENCE

NT CHEMILUMINESCENCE

NT CN EMISSION

NT ELECTROLUMINESCENCE

NT ELECTRON EMISSION

NT EXHAUST EMISSION

NT FIELD EMISSION

NT FLUORESCENCE

NT HYDROXYL EMISSION

NT ION EMISSION

NT LIGHT EMISSION

NT LUMINESCENCE

NT MICROWAVE EMISSION

NT NEUTRON DECAY

NT NEUTRON EMISSION

NT NUCLEAR FISSION

NT OPTICAL RESONANCE

NT PARTICLE EMISSION

NT PHOSPHORESCENCE

NT PHOTOELECTRIC EFFECT

NT PHOTOELECTRIC EMISSION

NT PHOTOIONIZATION

NT PHOTOLUMINESCENCE

NT PHOTOPRODUCTION

NT PLASMA DECAY

NT RADIO EMISSION

NT RADIOACTIVE DECAY

NT RESONANCE FLUORESCENCE

NT SECONDARY EMISSION

NT SELF SUSTAINED EMISSION

NT SHOCK WAVE LUMINESCENCE

NT SOLAR RADIO BURSTS

NT SOLAR RADIO EMISSION

NT SPECTRAL EMISSION

NT SPONTANEOUS EMISSION

NT STIMULATED EMISSION

NT THERMAL EMISSION

NT THERMIONIC EMISSION

NT THERMOLUMINESCENCE

NT TRIBOLUMINESCENCE

NT TYPE 2 BURSTS

NT TYPE 3 BURSTS

NT TYPE 4 BURSTS

NT WATER MASERS

NT WEAK ENERGY INTERACTIONS

NT X RAY FLUORESCENCE

DECAY RATES

Comment on 'Thermoluminescence of meteorites and their terrestrial ages' 02 p0267 A83-12850

Decay of a plasma created between negatively biased walls 05 p0688 A83-17369

Theoretical decay rates of cataclysmic variable eruptions 06 p0827 A83-18165

A note on total cross sections and decay rates in the presence of a laser field 10 p1425 A83-25409

An electrostatic charge decay technique for nondestructive evaluation of nonmetallic materials 12 p1734 A83-29591

Dispersion characteristics for decaying or amplifying waves. I - An observational approach. II - Analysis of a beam-plasma system 16 p2414 A83-35422

Measurement of the lifetime of the c 3 Pi u state of molecular nitrogen by the delayed coincidence method 16 p2410 A83-36797

Experimental limits on magnetic monopole catalysis of nucleon decay 19 p2925 A83-40952

Seasonal averages of net decay rate of SO₂ over northern Europe 19 p2864 A83-41988

Classical derivation of the laser rate equation 22 p3300 A83-46814

The effect of fluorescence decay time on echo-signal kinetics in the case of remote laser sounding of water bodies 23 p3493 A83-48505

DECCELERATION

NT SPIN REDUCTION

The structure and parameters of the deceleration region of a pulsed supersonic jet of metallic plasma incident on a plane barrier 02 p0241 A83-11694

Measurement of the high-frequency parameters of slow-wave systems in O-type microwave devices 10 p1412 A83-26962

Reaction deceleration of comet nuclei and their relation to the structure of meteor swarms 13 p1940 A83-31344

Limiting payload deceleration during ground impact 15 p2122 A83-33726

Computational study of an unregulated air intake of a hypersonic ramjet engine with three-dimensional deceleration of the flow at freestream Mach numbers of 5-7 17 p2449 A83-37559

Posterior probability of the deceleration parameter q sub 0 from quasars provided with a luminosity indicator 18 p2764 A83-39194

Recovery system for the Lockheed Aquila R.P.V. 20 p2938 A83-43724

DECCELERATORS

U BRAKES (FOR ARRESTING MOTION)

DECIDUOUS TREES

The changes in leaf reflectance of sugar maple (Acer saccharum Marsh) seedlings in response to heavy metal stress 15 p2209 A83-34156

Mapping of deciduous forest cover using simulated Landsat-D TM data 22 p3311 A83-46166

DECIMETER WAVES

An interpretation of the decimeter flux variability of extragalactic radio sources 06 p0831 A83-18831

Coherence time for 430-MHz VLBI 09 p1352 A83-23326

A non-linear wave-wave interaction mechanism for the solar Type-IV decimetric bursts 12 p1800 A83-29356

Solar EUV and decimetric indices and thermospheric models 16 p2378 A83-36112

The effect of decimeter waves on the physical and chemical condition of membranes, the chromatin of thymocytes, and the immunological reactivity of an organism 18 p2733 A83-40567

Narrow-band decimeter bursts and X-ray emissions - Possible evidence of negative absorption or maser effect --- of sun 23 p3535 A83-47700

DECISION ELEMENTS

U LOGICAL ELEMENTS

DECISION MAKING

The complete ATE decision system - A demonstration report 01 p0103 A83-10761

Operator test control and interface evaluation 01 p0086 A83-10783

A study of an arbiter function in the structures of a shared bus --- French thesis 02 p0166 A83-11700

VLSI and intelligent transducers 02 p0168 A83-12810

Controlling the motion of a moving robot using a neuroid network 03 p0385 A83-13475

Overview of probabilistic failure prediction and accept-reject decisions 04 p0488 A83-15155

Conflict radar /A systems analysis/ --- Russian book 04 p0527 A83-15827

How decisions are made - Major considerations for aircraft programs 06 p0717 A83-18398

Test of a fuzzy set based decision model as an aid in solving human factors design problems 10 p1470 A83-26324

An experience-judgement approach to tactical flight training 10 p1458 A83-26337

Fleet planning models --- in airline operations 12 p1699 A83-29967

A dynamic decision model of human task selection performance 13 p1907 A83-31069

Adaptation and learning in systems of control and decision making --- Russian book 14 p2076 A83-33025

Planning intra-airport transportation - A framework for decision making 14 p1978 A83-33356

[AIAA PAPER 83-1585] 14 p1978 A83-33356

Stability of decision rules in pattern recognition problems 15 p2220 A83-33901

Minimizing the average cost of testing coherent systems 17 p2517 A83-37292

Complexity and approximate algorithms 17 p2517 A83-37292

Pilot judgment - Current developments in evaluation and training and future issues in aviation cases 18 p2736 A83-39042

Normative predicates of next-generation management support systems 19 p2906 A83-41294

Risk/dispersion index method 19 p2894 A83-41296

A participative approach to program evaluation 19 p2906 A83-41299

Priority setting in complex problems 19 p2907 A83-41302

Control of a heterogeneous two-server exponential queueing system 20 p3038 A83-43119

Information induced multimodel solutions in multiple decisionmaker problems 21 p3198 A83-44100

DECISION THEORY

NT STATISTICAL DECISION THEORY

Investigation of the noise immunity of reception of quantum coherent signals with multilevel PSK 09 p1245 A83-23458

Minimax filtering problems for observed Poisson processes with uncertain rate functions 09 p1330 A83-24742

Sample sizes for variables sampling plans based on a decision theoretic approach [AD-A130452] 12 p1734 A83-29523

The role of decision trees in weather forecasting 13 p1884 A83-30528

DECKS (FLOORS)

U FLOORS

DECLINATION

Dependence on declination of the intensity of cosmic ray showers with primary energies of about 10 to the 16th eV 05 p0709 A83-17268

Santiago 67 Catalogue - Catalogue of 7610 stars declination zone -25 deg to -47 deg equinox 1950.0 09 p1353 A83-23900

Improved parameters for 40 pulsars 21 p3225 A83-44769

DECODERS

A low-power, high-throughput maximum-likelihood convolutional decoder chip for NASA's 30/20 GHz program 07 p0917 A83-19754

Viterbi decoder VLSI integrated circuit for bit error correction 07 p0917 A83-19755

New syndrome decoder for (n, 1) convolutional codes 13 p1912 A83-31785

Class of linear cyclic block codes for burst errors occurring in one-, two- and three-dimensional channels 20 p3040 A83-43686

DECODING

Influence of LSI and VLSI technology on the design of error-correction coding systems 02 p0163 A83-11552

Pulse decoding in stretched pulse laser PMM systems 07 p0905 A83-19706

Error rates for narrowband Manchester coded digital FM 07 p0909 A83-19748

The impact of mismatch on the performance of coded narrow-band FM with limiter/discriminator detection 07 p0916 A83-21198

High-speed decoding technique for slip detection in data transmission systems using modified cyclic block codes 09 p1249 A83-24115

Spatial carriers with orthogonal subcodes --- signal coding and decoding for optical communication 15 p2230 A83-33810

Optimal coding for information transmission through a Poisson type channel 15 p2221 A83-35118

A modified selective-repeat type-II hybrid ARQ system and its performance analysis --- Automatic Repeat reQuest 16 p2343 A83-36601

DECOMPOSITION

NT CRACKING (CHEMICAL ENGINEERING)

NT GLYCOLYSIS

NT PHOTODECOMPOSITION

NT PHOTODISSOCIATION

NT PHOTOLYSIS

NT PROPELLANT DECOMPOSITION

NT RADIOLYSIS

NT THERMAL DECOMPOSITION

The effect of the characteristics of interstitial solid solution decomposition on the fine structure and properties of cast alloys of molybdenum 01 p0025 A83-10393

Mechanisms of the isothermal decomposition of beta-solid solution in two-phase martensitic titanium alloys 01 p0025 A83-10446

A Lie algebraic decomposition of nonlinear systems 09 p1329 A83-24735

A study of coalescence processes in Al - 2.8 pct Li alloy 13 p1821 A83-30739

Sufficient conditions for the decomposability of control problems 19 p2893 A83-42006

LU and Cholesky decomposition on an optical systolic array processor 20 p3037 A83-43629

Decomposition processes in Al-Zn-Mg alloys 21 p3111 A83-44119

Product decompositions for certain types of coordinate transformation 23 p3502 A83-48141

Block decompositions and block modal controls of multivariable control systems 24 p3621 A83-49920

DECOMPRESSION

U PRESSURE REDUCTION

DECOMPRESSION SICKNESS

- The peculiarities of the pathogenesis of decompression barotrauma of the lungs 03 p0382 A83-14547
- Survival following accidental decompression to an altitude greater than 74,000 feet /22,555 m/ 04 p0522 A83-15538
- Role of lung surfactant in cerebral decompression sickness 06 p0793 A83-18188
- The effects of various gases on cortical and spinal somatosensory evoked potentials at pressures up to 10 bar 07 p0974 A83-20777
- An evaluation of plasma volume expanders in the treatment of decompression sickness 10 p1453 A83-25668
- Decompression sickness - USAF experience 1970-80 10 p1455 A83-25674
- The reaction of the central blood circulation of healthy individuals to the decompression of various areas of the body 12 p1764 A83-29306

DECONTAMINATION

NT SPACECRAFT STERILIZATION

- Approach to payload contamination integration 03 p0286 A83-13748
- Insights into contamination control for the Shuttle Payload Integration Facility /SPIF/ at the Eastern Launch Site /ELIS/ 03 p0284 A83-13749
- A statistical plume model with first-order decay 05 p0659 A83-17438
- Personnel training for precision cleaning of aerospace hardware to military standard 1246 A levels 13 p1865 A83-31519
- Spectral decontamination of a real-time helicopter simulation [AIAA PAPER 83-1087] 16 p2299 A83-36211
- A method for the identification and elimination of contamination during carbon isotopic analyses of extraterrestrial samples 22 p3385 A83-46375

DECOUPLING

- Decoupling the structural modes estimated using recursive lattice filters 03 p0386 A83-14174
- Multivariable stability-margin optimisation with decoupling and output regulation 04 p0529 A83-16191
- Decoupling of antennas by means of plane elements 07 p0915 A83-20880
- Disturbance decoupling, decentralized control and the Riccati equation 09 p1334 A83-24801
- Decoupling of antennas with the aid of underlying surfaces 11 p1559 A83-28685
- Control of large spaceborne antenna systems with flexible booms by mechanical decoupling 18 p2646 A83-39095
- Linear feedback decoupling - Transfer function analysis 22 p3351 A83-46365

DECOYS

- Computer models for determining countermeasures effectiveness of expendables in air-to-air engagements 01 p0103 A83-11162

DEDUCTION

- Induction and deduction as the function of different hemispheres --- of brain 19 p2870 A83-40810

DEEP SCATTERING LAYERS

- The most probable trajectories of rays in a plane-stratified scattering medium. I - A linear layer --- in ionosphere 05 p0663 A83-17612
- Plane wave scattering by a thick lossy dielectric half-plane 06 p0805 A83-18714
- Approximate solution of the problem of the coefficient of reflection from a layer of a one-dimensional, randomly inhomogeneous medium 06 p0806 A83-19332
- Solar scattered radiation measurements by Venus probes 17 p2617 A83-37420

DEEP SPACE

NT INTERPLANETARY SPACE

NT INTERSTELLAR SPACE

- Deep space optical communication via relay satellite 09 p1214 A83-23579
- Antimatter and distant space flight 12 p1705 A83-29673

DEEP SPACE INSTRUMENTATION FACILITY

- Teal Amber visible focal plane technology 03 p0325 A83-13730

DEEP SPACE NETWORK

- MERLIN observations of superluminal radio sources --- Multi Element Radio Linked Interferometer Network 02 p0245 A83-11621
- A high performance, continuously variable data rate, digitally implemented BPSK modem for deep space network 07 p0917 A83-19687
- Deep-space laser communications. I - Optical receivers probe the depths of space 11 p1535 A83-28154
- Design considerations for deep-space transmitters. II - Deep-space laser communications 11 p1535 A83-28156

- A common-aperture X- and S-band four-function feedcone --- hornfeed design for antennas of Deep Space Network 15 p2126 A83-35086

- Processing of scientific telemetry data using a real-time operating system for the flights of Venera 13 and 14 19 p2813 A83-41234

- Processing of scientific data from the Venera 13 and 14 descent modules in real time 19 p2813 A83-41235

- Deep space communication - A one billion mile noisy channel 19 p2813 A83-41343
- Single-mode fiber systems for deep space communication network 22 p3360 A83-46657

DEER

NT CARIBOUS

- Integration of Landsat imagery into a program for aerial surveying of deer populations in Alberta 03 p0347 A83-14252
- A multispectral approach to remote detection of deer 03 p0351 A83-14666

DEFECTS

NT AUDITORY DEFECTS

NT CRYSTAL DEFECTS

NT CRYSTAL DISLOCATIONS

NT EDGE DISLOCATIONS

NT FRENKEL DEFECTS

NT INCLUSIONS

NT POINT DEFECTS

NT SCREW DISLOCATIONS

NT SURFACE DEFECTS

NT VACANCIES (CRYSTAL DEFECTS)

- Stability problems for inelastic solids with defects and imperfections 04 p0500 A83-16099

- Effects of defects on fatigue properties of P/M disk alloys 06 p0732 A83-19098

- The deformation of materials with defects 07 p0945 A83-19947

- The effect of defects on the strength of composite sandwich assemblies 07 p0876 A83-20461

- Flaws and defects of structural carbon fibers 09 p1238 A83-23950

- On three-dimensional fibrous flaws in unidirectional fibre reinforced elastic composites 09 p1281 A83-24821

- Plastic buckling of initially imperfect stiffened cylinders in axial compression 10 p1440 A83-26433

- Identification and resolution of a material defect in high strength beryllium 12 p1715 A83-29755

- [AIAA 83-0871] Determination of electromagnetic field scattered by small defects and influence of boundary between media 13 p1860 A83-30838

- Influence of quality control variables on failure of graphite/epoxy under extreme moisture conditions 14 p1987 A83-33125

- Safety assessments in fracture-mechanics defect evaluation for biaxial stresses 18 p2696 A83-39256

- Properties of the defect causing solar cell degradation 18 p2749 A83-39468

- Effect of defect on the behaviour of composites 18 p2656 A83-40215

- Kinks and polarons in polyacetylene 20 p3053 A83-42640

- Algorithm for determining the dimensions of flaws in the theory of eddy-current flaw detection by superposed transducers 20 p3000 A83-43179

- Flaw classification by a spectral division of ultrasonic echoes 20 p3000 A83-43559

- A standard photometric method of determining beam sizes of defects 20 p3000 A83-43642

- Self-excitation of subharmonic of orthotropic plate with initial imperfection 21 p3150 A83-44029

- Concentrated body force loading of an elastically bridged penny shaped flaw in a unidirectional fibre reinforced composite 21 p3156 A83-44893

- Estimation of a particle size distribution when detection probability depends on particle size 22 p3304 A83-46768

- Stress analysis of stepped-lap joints with bondline flaws 23 p3471 A83-48214

DEFENSE COMMUNICATIONS SATELLITE SYSTEM

NT FLEET SATELLITE COMMUNICATION SYSTEM

- Hardness assurance experience on the DSCS III spacecraft program 05 p0608 A83-17531

- DSCS III A-1 ACS flight experience --- evaluation and testing of Attitude Control System [AAS PAPER 83-085] 21 p3100 A83-44185

DEFENSE COMMUNICATIONS SYSTEM (DCS)

- Steady-state performance of an adaptive sequential routing algorithm 07 p0911 A83-19775

- A postulated topographical architecture for the Defense Communications System of 2004 19 p2829 A83-41356

- The role of satellite communications in the future DCS 19 p2832 A83-41399

- A fault tolerant design for autonomous attitude control of the DSCS-III communication satellite [AIAA PAPER 83-2264] 19 p2816 A83-41734

DEFENSE INDUSTRY

NT WEAPONS INDUSTRY

- Defense Mapping Agency /DMA/ overview of mapping, charting, and geodesy /MC&G/ applications of digital image pattern recognition 02 p0200 A83-12877

DEFENSE METEOROLOGICAL SATELLITE PROGRAM

U DMSP SATELLITES

DEFENSE PROGRAM

NT DMSP SATELLITES

- Rationalizing Tacair force development in the next decade 01 p0002 A83-11116

- More efficient and effective defense system acquisition through unified system effectiveness analysis and control /SEAC/ 01 p0111 A83-11117

- DOD payload interface verification in the Shuttle era 13 p1810 A83-31179

- U.S. cruise missile programs: Development, deployment and implications for arms control --- Book 15 p2119 A83-33769

- Concepts for a future joint airlift development program [AIAA PAPER 83-1591] 16 p2297 A83-36951

- The entropy of affordability 20 p3042 A83-42569

- The fruits of space exploration - Cornucopia or Armageddon --- prospects for prevention of space militarization 23 p3414 A83-47321

- Challenges for military airlift in the 1990's [AIAA PAPER 83-2437] 23 p3400 A83-48327

DEFLAGRATION

- The structure of the carbon-burning deflagration front in a degenerate stellar core 03 p0418 A83-13878

- Theoretical and experimental nonlinear dynamics of heterogeneous deflagration waves 06 p0727 A83-19162

- CO2-laser-induced deflagration of fuel/oxygen mixtures 07 p0882 A83-20732

- A pocket model for aluminum agglomeration in composite propellants 12 p1717 A83-28962

- An asymptotic theory of deflagrations and detonations. I - The steady solutions 16 p2325 A83-35694

- Fast deflagration waves 21 p3130 A83-44462

DEFLATING

U INFLATABLE STRUCTURES

U PRESSURE REDUCTION

DEFLECTION

- A study of the stability of compressed cylindrical shells with thin eccentric ribs using a polynomial approximation of deflections 01 p0059 A83-10682

- An integral equation approach to finite deflection of elastic plates 01 p0060 A83-10861

- Investigation of the effect of initial deflection on the natural-vibration frequencies of rib-stiffened conical shells 04 p0502 A83-16409

- The vibration of a multilayer cylindrical panel with anisotropic layers at large deflections 06 p0775 A83-18506

- Large deflections of point loaded cantilevers with nonlinear behaviour 09 p1281 A83-24823

- A second order theory for large deflections of slender beams 12 p1736 A83-29706

- Telescope mirror supports - Plate deflections on point supports 13 p1859 A83-31003

- On the nonlinear aberrations with self-deflection of a light beam in a moving medium 14 p2025 A83-33397

- Effects of spherically-symmetric gravitational lenses produced by galaxies and clusters 15 p2262 A83-34538

- Large deflection analysis of clamped skew sandwich plates by parametric differentiation 16 p2369 A83-36561

- Minimum slope/deflection design of rectangular cantilever beams 19 p2857 A83-40886

- Experimental results of a deflected thrust V/STOL nozzle research program [AIAA PAPER 83-0170] 19 p2794 A83-42100

- Measurement of curvature and bending stiffness of thin carbon composite plates using holographic interferometry 21 p3155 A83-44829

- Opto-optical light deflection 21 p3207 A83-44834

- Deflection of a phase-conjugate wave in nondegenerate four-wave mixing 23 p3509 A83-48322

- The asymptotic form of the deflection of a plate partly supported by an elastic base under hydrostatic tension 24 p3592 A83-49028

- Deflection from the incidence plane of a light beam refracted in an absorbing (amplifying) isotropic medium 24 p3629 A83-49552

- Non-simple quasi-static thermoelastic deflection of a thin clamped circular plate 24 p3597 A83-50136

DEFLECTORS

- Calculation of an electrooptic diffraction deflector with allowance for edge effects 02 p0235 A83-11536

Flow measurements of an airfoil with deflected spoiler
[AIAA PAPER 83-0365] 05 p0584 A83-16672

DEFOCUSING

Waveguide-type solutions for light beams with nonlocal self-defocusing in the geometric-optics approximation
01 p0054 A83-10816

Analysis of the output signal of devices for measuring the defocusing of lenses under coherent illumination
11 p1574 A83-28498

The identification of clear and defocused images during short periods of the presentation of visual objects
13 p1901 A83-30433

Restoration of out-of-focused color photographic images
20 p2992 A83-43631

Image restoration for a defocused optical system
22 p3294 A83-46827

Optical-correlation quasi-interferometry - A new viewpoint on spatial frequency filtering
24 p3582 A83-49012

Thermal defocusing (LIMP) in stable CO₂ resonators
24 p3589 A83-49835

DEFOLIATION

Assessment of spruce budworm defoliation using digital airborne MSS data
03 p0347 A83-14248

DEFORESTATION

Utilization of Landsat data to monitor deforestation of Kenya's Mau Forest
17 p2534 A83-38461

DEFORMATION

NT AXIAL STRAIN

NT ELASTIC BENDING

NT ELASTIC BUCKLING

NT ELASTIC DEFORMATION

NT PLASTIC DEFORMATION

NT STATIC DEFORMATION

NT TENSILE DEFORMATION

NT WAVE FRONT DEFORMATION

A note on two-dimensional finite-deformation theories of shells
01 p0060 A83-10862

The deformation and fracture of Beta HMX
02 p0161 A83-12030

The relation between the network structure, deformation and failure processes, and mechanical properties of epoxies
02 p0160 A83-12063

Development of complex textures during deformation of bcc metals
02 p0155 A83-12201

Certain characteristics of the flexural deformation and subsequent annealing of molybdenum single crystals
02 p0155 A83-12202

Characteristics of the amplitude dependence of internal friction and Young's modulus defect in solids at low deformation amplitudes
02 p0155 A83-12206

The forming limit diagram of sheet metals and effects of strain path changes on formability - A dislocation treatment
03 p0301 A83-14704

A simple finite element for elastic-plastic deformations of shells
04 p0495 A83-15020

Contribution to the determination of forming limit curves for titanium and aluminum - Proposal of an intrinsic criterion --- French thesis
04 p0459 A83-15840

Deformation maps for titanium and zirconium
04 p0462 A83-16256

Role of cracks in the creep deformation of brittle polycrystalline ceramics
05 p0619 A83-17560

A study of the deformation and fracture of structural elements of composite materials by speckle-holographic interferometry
06 p0775 A83-18513

The deformation and fracture mechanisms of coarse-grained textured alpha-titanium alloys
06 p0729 A83-18748

Path dependence of acoustic velocity and attenuation in experimentally deformed Westerly granite
07 p0959 A83-20096

Surface deformation of Westerly granite during creep
07 p0959 A83-20097

Numerical modeling of intraplate deformation - Simple mechanical models of continental collision
07 p0961 A83-20230

Deformation, gravity, and potential changes due to volcanic loading of the crust
07 p0961 A83-20231

Applications of deformation analysis in geodesy and geodynamics
07 p0962 A83-20837

Deformation of polycrystals: Mechanisms and microstructures; Proceedings of the Second Riso International Symposium on Metallurgy and Materials Science, Roskilde, Denmark, September 14-18, 1981
07 p0896 A83-21601

Anisotropy of bulk-formability in 2024-T351 aluminum plates and bars
08 p1058 A83-21664

Variational equations of thermal diffusion for deformable thin-walled shells of finite shear stiffness
09 p1282 A83-25016

Structural deformation model of spatially reinforced composites
09 p1282 A83-25107

The influence of inplane deformation on the buckling loads of isotropic elastic plates
09 p1283 A83-25218

Study of deformed samples using an interferometer attached to the sample
10 p1422 A83-26469

A three-dimensional problem for a deformable cone with an asymmetrically perturbed surface
11 p1596 A83-28452

Numerical solution of large deformation problems involving surface contact and impact
12 p1734 A83-28854

Cross-sectional distortion of an elastic hollow cylinder subjected to shear deformation - Theory and experiment
12 p1735 A83-29360

Speckle interferometry, a simple method for deformation analysis
12 p1735 A83-29362

Finite deformation analysis of shells - A hybrid finite element method based on assumed stress-function vector and rotation tensor
12 p1738 A83-29749

[AIAA 83-0861] X-ray measurements of long-range strains - A bridge between micromechanics and macromechanics
12 p1715 A83-29913

The inverse problem of elastic-plastic deformation for a shallow shell
13 p1866 A83-30307

HVEM in situ deformation of Al-Li-X alloys --- High Voltage Electron Microscope
14 p1997 A83-32948

Cold deformation of a nickel-base superalloy
15 p2138 A83-34134

Operator split methods in the numerical solution of the finite deformation elastoplastic dynamic problem
15 p2176 A83-34314

A method for deriving deformation characteristics in the nonlinear theory of shells
16 p2365 A83-35927

Theoretical and experimental investigation of the nonlinear torsion and extension of initially twisted bars
17 p2519 A83-37383

The load-bearing behavior of shear-stressed square plates of fiber-reinforced composite materials under large deformations --- German thesis
17 p2520 A83-37499

The cyclic deformation of titanium - Dislocation substructures and effective and internal stresses
17 p2490 A83-38380

A method for obtaining stress intensity factor by F.E.M. and its application to dynamic problem. II - A treatment for mixed mode cracks
18 p2697 A83-39451

Deformation of a circular cylindrical shell with a periodic system of holes
18 p2702 A83-40122

Design of an experiment to determine deformations using holographic interferometry
23 p3454 A83-47560

High temperature deformation and fracture phenomena of polypphase Si₃N₄ materials
23 p3437 A83-48287

Finite element analysis of steadily moving contact fields
24 p3593 A83-49437

A study of the deformation properties of an isotropic carbon material at elevated temperatures
24 p3554 A83-49666

Elasto-plastic analysis of an anisotropic rotating disc
24 p3597 A83-50146

DEGASSING

NT DEOXYGENATION

The effect of hydrogen gas on high-grade iron and steel at high and medium pressure --- German thesis
01 p0026 A83-10471

Hydrogen in pure aluminum solidified unidirectionally
13 p1824 A83-31601

Eruption age of a Pleistocene basalt from Ar-40-Ar-39 analysis of partially degassed xenoliths
16 p2381 A83-36599

Gas emissions and the eruptions of Mount S. Helens through 1982
22 p3333 A83-46798

DEGENERATIVE FEEDBACK

U NEGATIVE FEEDBACK

DEGRADATION

NT THERMAL DEGRADATION

Mechanisms of degradation of graphite composites in a simulated space environment
[AIAA PAPER 83-0590] 05 p0610 A83-16807

Effects of 140 Mbit/s operation on degradation of GaAlAs DH lasers
09 p1272 A83-24113

FLTSATCOM solar array degradation
11 p1541 A83-27253

Physical nature of the degradation of light emitting diodes and semiconductors lasers
13 p1849 A83-30261

Properties of the defect causing solar cell degradation
18 p2749 A83-39468

On the processes responsible for the degradation of the aluminium-lithium electrode used as anode material in lithium aprotic electrolyte batteries
24 p3600 A83-49933

DEGREES OF FREEDOM

Analysis of some degenerate quadruple collisions
03 p0389 A83-13410

A theory of substructure modal synthesis
[ASME PAPER 82-WA/APM-29] 04 p0499 A83-15693

Numerical study of periodic orbit properties in a dynamical system with three degrees of freedom
04 p0548 A83-16361

Parametrically excited non-linear multidegree-of-freedom systems with repeated natural frequencies
06 p0773 A83-18392

The degrees of freedom of a neuron and the cortical neuronal modules
08 p1145 A83-22117

Dynamic response analysis of structures with large degrees of freedom by step-by-step transfer matrix method
09 p1276 A83-23335

Cooperative solution in the synthesis of multidegree-of-freedom shock isolation systems
11 p1553 A83-28122

Progressive phase trends in multi-degree-of-freedom systems
12 p1774 A83-28850

Orthogonal polynomials as variable-order finite element shape functions
12 p1770 A83-28977

The freezing of the translational degrees of freedom of molecules in multiphase flows
13 p1933 A83-30672

A resonance problem of two degrees of freedom --- for artificial earth satellite orbits
15 p2124 A83-34390

A two-degree-of-freedom gyrocompass
16 p2356 A83-35936

Coupled flap-lag-torsional dynamics of hingeless rotor blades in forward flight
16 p2298 A83-35948

Hypersonic dynamic testing of ablating models with three-degree-of-freedom gas bearings
23 p3412 A83-48135

DEHYDRATION

Impact induced dehydration of serpentine and the evolution of planetary atmospheres
04 p0564 A83-15374

The phospholipid composition of various tissues of rats in dehydration conditions
16 p2395 A83-36829

The diagnostic informativity of drugs used for revealing intralabyrinthine hydrops according to data of audiological and biochemical investigations
19 p2883 A83-41828

DEICERS

Finite element thermal analysis of an icing protective system
[AIAA PAPER 83-0113] 05 p0632 A83-16528

NASA Lewis Research Center's program on icing research
[AIAA PAPER 83-0204] 05 p0577 A83-16582

Helicopter icing - Testing and certification
06 p0716 A83-18381

Development of a structural, bird impact resistant, de-iced wing leading edge for the de Havilland Dash 8 aircraft using fibre-reinforced composites
06 p0717 A83-18823

Anti-icing system design and test optimization --- for shipboard or ground missile launcher components
[SAE PAPER 820879] 13 p1809 A83-30948

Numerical simulation of electrothermal de-icing systems
[AIAA PAPER 83-0114] 16 p2297 A83-36043

Pneumatic rotor blade deicing
22 p3254 A83-46926

DEICING

Wind tunnel study of icing and de-icing on oscillating rotor blades
[ONERA, TP NO. 1982-116] 09 p1199 A83-24327

U.S. Army helicopter icing developments
[SAE PAPER 821504] 17 p2459 A83-38011

Review of helicopter icing protection systems
[AIAA PAPER 83-2529] 23 p3401 A83-48367

DEICING SYSTEMS

U DEICERS

DEIMOS

Infrared observations of Phobos and Deimos from Viking
04 p0569 A83-15594

Phobos and Deimos
06 p0823 A83-19469

The Martian satellites
06 p0823 A83-19470

Interpretation of whole-disk photometry of Phobos and Deimos
09 p1366 A83-25073

Mars and its satellites: A detailed commentary on the nomenclature / 2nd revised edition/ --- Book
13 p1960 A83-30049

Orbital evolution and origin of the Martian satellites
19 p2910 A83-40785

DELAMINATING

Approximate analysis of postbuckled through-width delaminations
02 p0191 A83-12061

Special analytical solution for use in debond stress analysis
02 p0191 A83-12172

The effect of a longitudinal delamination in a laminate cylindrical shell on the critical external pressure
02 p0192 A83-12360

Dimensional information through industrial computerized tomography
03 p0337 A83-13435

Damage documentation in composites by stereo radiography
03 p0292 A83-14553

- The dependence of transverse cracking and delamination on ply thickness in graphite/epoxy laminates 03 p0292 A83-14559
- Characterization of delamination onset and growth in a composite laminate 03 p0293 A83-14560
- Characterizing delamination growth in graphite-epoxy 03 p0293 A83-14561
- Compression fatigue behavior of composites in the presence of delaminations 03 p0293 A83-14562
- NDE of simulated Space Shuttle tile disbands 04 p0452 A83-15183
- Mechanism of interfacial bond failure 04 p0463 A83-15873
- A three-point flexure test configuration for improved sensitivity to metal/adhesive interfacial phenomena 04 p0487 A83-15875
- Delamination in graphite/epoxy laminates 07 p0875 A83-20437
- An analysis of delamination in drilling composite materials 09 p1273 A83-23640
- Delamination of T300/5208 graphite/epoxy laminates 09 p1223 A83-23938
- Delamination buckling and growth in laminates [ASME PAPER 83-APM-3] 10 p1441 A83-26445
- Redistribution of stresses in a fractured fiber during its delamination from the viscoelastic matrix of a composite material 11 p1597 A83-28471
- Delamination-based compression residual-strength prediction model for composites [AIAA 83-0872] 12 p1738 A83-29756
- Dynamics of delamination buckling [AIAA 83-0873] 12 p1738 A83-29757
- The effect of friction on the delamination of heterogeneous materials 13 p1865 A83-30053
- Lamination and microlamination in parts made of Tsm2A alloy sheet --- molybdenum alloy 13 p1823 A83-31215
- Calculation of stresses on the free edge in composite plates undergoing mechanical and thermal loading [ONERA, TP NO. 1983-20] 16 p2368 A83-36429
- Stress intensity factors in two bonded elastic layers containing cracks perpendicular to and on the interface. I Analysis. II - Solution and results 18 p2698 A83-39535
- Stress and strength analysis of composite laminates at delamination 18 p2651 A83-40149
- An analysis of free-edge delamination in laminated composite under uniform axial strain 18 p2702 A83-40150
- Fracture mechanics for delamination problems in composite materials 18 p2652 A83-40153
- Analysis and evaluation of interfacial delamination energy of notched laminated composites 18 p2660 A83-40272
- Fracture mechanics for delamination problems in composite materials 20 p3007 A83-43143
- Interlaminar stresses at a hole in a composite member subjected to in-plane loading 20 p3007 A83-43146
- Acoustic emission from graphite/epoxy composite laminates with special reference to delamination 21 p3106 A83-44126
- Delamination of composites under compression 23 p3472 A83-48467

DELAY CIRCUITS

- The complex dynamics of delayed-feedback oscillators /Review/ 09 p1257 A83-25077
- Conditions of amplitude self-modulation in a delay oscillator 11 p1561 A83-27943
- A cascaded echo canceller 19 p2832 A83-41393
- Modification of phase-locked-loop performance using a sample-and-hold circuit 21 p3121 A83-44961

DELAY LINES

- NT ACOUSTIC DELAY LINES
- Transmission of pulsed signals with linearly changing frequency through a delay system with a dielectric 02 p0166 A83-11693
- Fibre-optic variable delay lines 04 p0534 A83-15236
- An evaluation of ultrasound NDE correlation flaw detection systems 04 p0494 A83-16180
- Characteristics of wave propagation in coupled slow-wave structures of finite length 06 p0750 A83-18032
- Temperature dependence of SAW dispersive delay lines 07 p0918 A83-20073
- Interferometric connection of the Canada-France-Hawaii 3.6 metre telescope and the United Kingdom 3.8 metre telescope on Mauna Kea 10 p1495 A83-25843
- 1-Gbit/s code generator and matched filter using an optical fiber tapped delay line 10 p1483 A83-26204
- A comb-shaped slow-wave structure in waveguides of complex cross section 13 p1832 A83-30286
- Autocorrelation compression filter for radio pulses with linear frequency modulation 13 p1829 A83-30729

- Observations on the spectral response of a driven unlocked SAW delay line oscillator 16 p2345 A83-35650
- Optical fiber V-groove transversal filter 18 p2744 A83-40056
- Linearly dispersive time-delay control of magnetostatic surface wave by variable ground-plane spacing 18 p2679 A83-40394
- High-speed pulse-train generation using single-mode-fibre recirculating delay lines 24 p3589 A83-49962

DELFT CAMERA

- Design and implementation of the Delft Image Processor DIP-1 --- Thesis 11 p1575 A83-28641

DELINEATION

- Landsat for delineation and mapping of saline soils in dryland areas in southern Alberta 03 p0348 A83-14261

DELIVERY

- NT PAYLOAD DELIVERY (STS)
- NT WEAPONS DELIVERY

DELTA ANTENNAS

- High gain and broad band Yagi-Uda array antenna composed of twin-delta loops 06 p0743 A83-18680

DELTA LAUNCH VEHICLE

- Launch vehicles for communication satellites 19 p2812 A83-41374
- The future for communication satellites of the PAM-D/half Ariane class 21 p3096 A83-45427
- Exosat/Delta - Demonstrated short-term backup launcher capability through international cooperation [IAF PAPER 83-01] 23 p3418 A83-47227

DELTA MODULATION

- Tri-state delta modulation system for Space Shuttle digital TV downlink 07 p0870 A83-19730
- Performance of delta modulation algorithms on noisy channels 09 p1246 A83-23693
- Error statistics in delta modulation and differential pulse code modulation communication systems 10 p1407 A83-26938
- Instrumental correlation analysis using delta-modulation 22 p3271 A83-45656

DELTA WINGS

- Supersonic flow around a conical fuselage of arbitrary section isolated or equipped with a delta wing with subsonic leading edges 01 p0002 A83-10579
- Pressure distribution on a simple delta wing 02 p0132 A83-13023
- Nonequilibrium flow over delta wings with detached shock waves 03 p0277 A83-13126
- Numerical simulation of wing-fuselage interference 03 p0277 A83-13129
- Numerical study of flowfields about asymmetric external conical corners 03 p0277 A83-13130
- Calculation of a three-dimensional boundary layer on a triangular plate of finite length in a hypersonic flow 04 p0441 A83-15081
- A study of the effect of the transverse sweep of delta wings on their vortex structures and aerodynamic characteristics in separated flows at low subsonic velocities 04 p0442 A83-15096
- Segmented vortex flaps [AIAA PAPER 83-0424] 05 p0585 A83-16706
- Evolution of aircraft trailing vortices in a stratified fluid [AIAA PAPER 83-0564] 05 p0588 A83-16792
- Aerodynamic characteristics of polygonal lifting bodies at supersonic speeds 06 p0713 A83-19571
- Leading edge vortex flap aerodynamics 07 p0863 A83-21004
- Theoretical stiffness matrix correction by using static test results 07 p0947 A83-21007
- Delta canard configuration at high angle of attack 09 p1210 A83-24650
- Alleviation of the subsonic pitch-up of delta wings 14 p1969 A83-32583
- Investigation of the parameters of a boundary layer before the inlet of a supersonic air intake mounted under the surface of a triangular plate 17 p2448 A83-37533

- The effect of the blunting of the leading edges on the characteristics of separated flow past delta wings of low aspect ratio 17 p2449 A83-37551
- Separated flows at the leeward side of a delta wing and body of revolution in supersonic flow 17 p2449 A83-37553
- The fluid mechanics of slender wing rock --- vortex shedding of delta configurations [AIAA PAPER 83-1810] 17 p2454 A83-38643
- The impact of strakes on a vortex-flapped delta wing [AIAA PAPER 83-1814] 17 p2454 A83-38647
- An investigation of wing leading-edge vortices at supersonic speeds 17 p2454 A83-38648
- Computation of leading edge vortices [AIAA PAPER 83-1907] 18 p2634 A83-39366

- Numerical simulation of the leading-edge separation vortex for a wing and strake-wing configuration [AIAA PAPER 83-1908] 18 p2637 A83-39408
- Supersonic three-dimensional oscillatory piecewise continuous kernel function method --- for planar supersonic wing study 19 p2789 A83-41043
- The maximum aerodynamic efficiency of conical wing-body combinations at high supersonic speeds 19 p2790 A83-41266
- Interference during flow around a wing and an axisymmetric nacelle 19 p2791 A83-41879
- Computational technique for three-dimensional compressible flow past wings at high angles of attack [AIAA PAPER 83-2078] 19 p2792 A83-41912
- Experimental and analytical investigation of the subsonic aerodynamics of slender wings with leading-edge vortex flaps [AIAA PAPER 83-2113] 19 p2793 A83-41940
- An investigation of the breakdown of the leading edge vortices on a delta wing at high angles of attack [AIAA PAPER 83-2114] 19 p2793 A83-41941
- Flow in a hypersonic boundary layer on a delta wing of finite length at angle of attack 20 p2931 A83-43522

- Vortex flow over delta and double-delta wings 21 p3085 A83-43975

- An investigation of the effect of the nonuniform field feature around a delta-wing on the separated vortex breakdown 21 p3087 A83-44566
- Large-scale wind-tunnel investigation of a close-coupled canard-delta-wing fighter model through high angles of attack [AIAA PAPER 83-2554] 23 p3399 A83-48373
- Wing loading on a 60 degree delta wing with vortex flaps [AIAA PAPER 83-2555] 23 p3399 A83-48374
- A method for calculating the regime of strong viscous interaction on a delta wing 23 p3400 A83-48664
- Vortex sheet shortening in the Smith model for slender delta wings with leading-edge separation 24 p3544 A83-49025

- Experimental investigation of the turbulent structure of vortex wakes [ONERA, TP NO. 1983-107] 24 p3544 A83-49418

DELTA S

- NT MISSISSIPPI DELTA (LA)
- Post-Aswan High Dam changes of the Nile Delta coast, east of Ras El Bar, interpreted from aerial photographs 09 p1289 A83-24600
- Monitoring vegetation in the Nile Delta with NOAA-6 and NOAA-7 AVHRR imagery 09 p1290 A83-24609
- The use of space photographs for analyzing recent tectonic movements /using the Amu Darya as an example/ 23 p3483 A83-48108

DEMAGNETIZATION

- Magnetic properties and paleointensity determination of seven H-group chondrites 07 p1031 A83-20971
- Sub-Kelvin temperatures in space 20 p2961 A83-43232

DEMAND ASSIGNMENT MULTIPLE ACCESS

- Demand Assignment Multiple Access /DAMA/ techniques for satellite communications 07 p0907 A83-19727
- TDMA demand assignment operation in Telecom 1 business services network 07 p0911 A83-19783
- Design of a demand-assignment satellite-switched Space Division Multiple Access Communication network 07 p0915 A83-21030
- A space-division multiple-access protocol for spot-beam antenna and satellite-switched communication network 11 p1557 A83-28134
- An experiment in integrated digital satellite communications 11 p1557 A83-28136
- Demand-assignment schemes for SPCF FDMA satellite systems with contiguous spot beams 19 p2835 A83-41553
- Satellites and switching 21 p3120 A83-44537

DEMINERALIZING

- NT BONE DEMINERALIZATION

DEMULATION

- Ionospheric demodulation of signals of radio-broadcasting stations and magnetospheric ELF noise 14 p1999 A83-31880
- Soft decision demodulation and transform coding of images 14 p2076 A83-32872

DEMULATORS

- NT MODEMS
- NT PHASE DEMODULATORS
- NT PHASE LOCK DEMODULATORS

DEMULPLEXING

- Fiber optics for the future - Wavelength division multiplexing 03 p0395 A83-14122
- Large symmetric pi transformations for Hadamard transforms 10 p1406 A83-26865
- Wavelength-discriminating photodetector for lightwave systems 21 p3208 A83-44957

- Practical two-wavelength multi-demultiplexer - Design and performance 24 p3629 A83-49018
- DENDRITIC CRYSTALS**
- Initiation of ZrC dendritic growth on the surface of spark machined zirconium 07 p0884 A83-20251
- Metallographic features of the subdendritic structure of aluminum alloy ingots 13 p1819 A83-30065
- Kinetic aspects of the solidification of aluminium-zinc alloys 18 p2665 A83-39048
- Influence of diffusion and convective transport on dendritic growth in dilute alloys 20 p3054 A83-43298
- The effect of the natural convection on the transition from columnar to equiaxed crystals 20 p3054 A83-43311
- Order of magnitude analysis of convective effects in dendritic solidification --- of alloys [IAF PAPER 83-150] 23 p3413 A83-47290
- DENDRITIC DRAINAGE**
- U DRAINAGE PATTERNS
- DENITROGENATION**
- Denitrification of TiN-Ni compacts during sintering 06 p0732 A83-19107
- DENSE PLASMAS**
- NT PLASMA FOCUS
- NT STRONGLY COUPLED PLASMAS
- The ground state of superdense quark-lepton matter 01 p0124 A83-10813
- Generation of surface waves in a solid-state plasma --- in vicinity of solid body 01 p0039 A83-10908
- Propagation of an electromagnetic beam in an inhomogeneous plasma formed during the interaction of this beam with a thin dense-gas layer 02 p0240 A83-11681
- Relaxation kinetics of a high-pressure inert-gas plasma 03 p0397 A83-13194
- Visible light observations of a dense plasmoid associated with a moving Type IV solar radio burst 06 p0853 A83-18531
- Electromagnetic instability of a beam of charged particles in a dense plasma 06 p0813 A83-19186
- Temperature minimum in the electrical conductivity and viscosity of a dense degenerate hydrogen plasma 07 p0995 A83-20066
- The role of acceleration processes in the formation of nanosecond volume discharges in dense gases 07 p0998 A83-20867
- A microfield in a dense plasma and calculation of the Stark profiles emitted by highly charged ions --- French thesis 08 p1167 A83-22090
- Amorphous glassy plasma in dense stellar matter 08 p1185 A83-23085
- A model for the formation of spokes in Saturn's rings 11 p1684 A83-27355
- Recent development in the statistical theory of high-density plasmas 11 p1659 A83-28244
- The state equation of superdense degenerate plasma 12 p1793 A83-29067
- Space-charge effects in high-density plasmas 12 p1781 A83-29618
- Broadening of Lyman lines of hydrogen and hydrogenic ions by low-frequency fields in dense plasmas 16 p2415 A83-35662
- Calculation of free-free Gaunt factors in hot dense plasmas 16 p2415 A83-35664
- Density-functional theory of correlations in dense plasmas Improvement on the hypernetted-chain scheme 16 p2415 A83-35665
- Enhancement of thermonuclear reaction rate due to screening by relativistic degenerate electrons 17 p2579 A83-37348
- Perpendicular distribution of electrostatic electron-cyclotron radiation under dense plasma conditions 18 p2748 A83-40506
- Laser diagnostics of a nonuniform dense plasma 21 p3211 A83-44147
- Shifts of hydrogen lines from electron collisions in dense plasmas 22 p3361 A83-45931
- Production of a high-density fast plasma flow 22 p3363 A83-46490
- Theoretical possibility of confining a dense adiabatic plasma using a self-consistent electrostatic field of subsonic solitons 23 p3509 A83-47568
- Nonlinearly induced radiation from an overdense plasma region 24 p3631 A83-48821
- DENSIFICATION**
- Necklace structure obtained by forging astroloy supersolidus-sintered preforms 02 p0154 A83-11666
- Workability of low temperature sintered tungsten compacts 06 p0732 A83-19103
- Densification of calcia-stabilized zirconia with borates 08 p1071 A83-22200
- On the use of powder beds in the nitridation and subsequent densification of RBSN --- Reaction-Bonded Silicon Nitrides 16 p2336 A83-35574

- The effect of process variables on the density of titanium ingots cast under electromagnetic pressure 19 p2822 A83-42005
- Liquid phase sintering 23 p3435 A83-48265
- Densification and transformation mechanisms in nitrogen ceramics 23 p3435 A83-48269
- Microstructure of densified reaction bonded silicon nitride 23 p3435 A83-48271
- Sintering of aluminium nitride with low oxide addition 23 p3435 A83-48272
- Sintering, properties and fabrication of Si3N4 + Y2O3 based ceramics 23 p3438 A83-48303
- Properties of isostatically hot-pressed silicon nitride [ACS PAPER 168-B-83] 24 p3568 A83-48962
- Sintering of submicron tungsten-based heavy alloys 24 p3560 A83-48982

DENSIMETERS

- Electric pulse-time densimeters --- Russian book 10 p1419 A83-25617

DENSITOMETERS

NT MICRODENSITOMETERS

- A comparison of several image processing techniques applied to photographically recorded astronomical spectra 19 p2909 A83-40715

DENSITY (MASS/VOLUME)

NT ATMOSPHERIC DENSITY

NT GAS DENSITY

NT SPACE DENSITY

- Limiting density of matter as a universal law of nature 13 p1947 A83-30798
- Prediction of density and constant pressure specific heat for several fluids in the near-critical region [AIAA PAPER 83-1476] 14 p2094 A83-32730
- Critical fields of liquid superconducting metallic hydrogen 16 p2421 A83-36991
- Developing lake sampling strategies with existing Landsat data 17 p2531 A83-38353
- Inertia coefficient considerations and the structure of Jovian planets 24 p3672 A83-49396

DENSITY (NUMBER/VOLUME)

NT CARRIER DENSITY (SOLID STATE)

NT ELECTRON DENSITY (CONCENTRATION)

NT ELECTRON DENSITY PROFILES

NT ELECTRON DISTRIBUTION

NT ION DENSITY (CONCENTRATION)

NT IONOSPHERIC ELECTRON DENSITY

NT IONOSPHERIC ION DENSITY

NT MAGNETOSPHERIC ELECTRON DENSITY

NT MAGNETOSPHERIC ION DENSITY

NT MAGNETOSPHERIC PROTON DENSITY

NT METEOROID CONCENTRATION

NT PACKING DENSITY

NT PARTICLE DENSITY (CONCENTRATION)

NT PLASMA DENSITY

NT PROTON DENSITY (CONCENTRATION)

NT SPACE DENSITY

- Geocoronal imaging with Dynamics Explorer - A first look 19 p2864 A83-41116
- Effect of the number density of heterogeneities on the critical diameter of condensed explosives 22 p3266 A83-46007

DENSITY (RATE/AREA)

U FLUX DENSITY

DENSITY DISTRIBUTION

- Inversion of gravity gradients for density information 01 p0070 A83-10067
- Variability of satellite refraction in the Northern Hemisphere atmosphere 01 p0072 A83-10855
- Formation of galaxies in G-variable cosmologies 01 p0127 A83-11294
- Turbulent momentum and heat transfer in thermally-stratified flows 02 p0170 A83-11870
- Nonequilibrium flow over delta wings with detached shock waves 03 p0277 A83-13126
- The space density distribution of late-type giants in the solar neighbourhood 04 p0547 A83-15969
- A unified instability criterion for heterogeneous shear flows 05 p0640 A83-17551
- Massive configurations with constant densities --- of neutron stars 06 p0834 A83-18891
- Profile steepening by resonance absorption in spherically-expanding plasmas --- density analysis 07 p0997 A83-20542
- Modeling of G333.6-0.2 as a spherical H II region 07 p1021 A83-21122
- Noble gas components in clasts and separates of the Abee meteorite 08 p1188 A83-21642
- Diagnostics of shock tube flows by laser interferometry 08 p1083 A83-22062
- Core radii determination for eleven southern clusters of galaxies 13 p1955 A83-31665
- Periodic orbits and warps --- of spiral galaxies 13 p1959 A83-31746
- An investigation of the star cluster NGC 6913 (M 29) 14 p2095 A83-31835

- Geometry of the distribution of plasma tail rays in a cometary type 1 tail 14 p2113 A83-33285
- Statistical genesis of a lognormal distribution as a source of properties observed in the clumping of galaxies 15 p2253 A83-33703
- Infrared observations of OB star formation in NGC 6334 17 p2597 A83-37322
- The gravitational field and density distribution inside Mars 17 p2619 A83-37696
- The large-scale structure of atomic hydrogen --- in Galaxy 18 p2768 A83-39641
- The spatial structure of air density variations according to scintillation observations 18 p2719 A83-40085
- Gravitational scintillation, anisotropies of background radiation and density inhomogeneities of cosmic matter 18 p2777 A83-40364
- Distribution of QSOs around NGC 1097 18 p2760 A83-40365
- A planetary density model and the normal gravitational field of the earth 19 p2866 A83-41475
- Empirical indicators of the evolution of clusters of galaxies 20 p3074 A83-43131
- H2 densities and masses of the molecular clouds close to the galactic center 21 p3231 A83-44452
- Time evolution of density perturbations in accelerating stratified fluids 22 p3280 A83-45932
- The quadrupole oscillations of neutron stars 22 p3377 A83-46260
- Geometrical analysis of catalogs of galaxies 24 p3640 A83-49168
- Gas at large radii --- in spiral galaxies 24 p3654 A83-49210
- Theory of spiral structure --- of Milky Way Galaxy 24 p3655 A83-49221

DENSITY MEASUREMENT

NT X RAY DENSITY MEASUREMENT

- Performance of LDI in predicting density profiles of compressible boundary layers --- laser differential interferometry 01 p0053 A83-11078
- Density measurement in compressible flows using off-resonant laser-induced fluorescence 02 p0183 A83-13075
- Electric pulse-time densimeters --- Russian book 10 p1419 A83-25617
- Minority species concentration measurements in flames using the photoacoustic and photothermal deflection technique 11 p1572 A83-27617
- Ionization curves, masses, and densities of 276 meteor bodies according to radar observations from five points 11 p1685 A83-27878
- Cyanoacetylene as a density probe of molecular clouds 20 p3067 A83-42443
- Equatorial ozone characteristics as measured at Natal (5.9 deg S, 35.2 deg W) 20 p3021 A83-42863
- New approach for analysis and prediction of liquid-vapor coexistence densities including the critical region 20 p3055 A83-43236
- Laser optical measurements of density and temperature in flowing gases 22 p3291 A83-46487
- CARS - The only tool for the diagnostics of reactive media? [ONERA, TP NO. 1983-77] 23 p3430 A83-48192
- Density of liquid Hg(1-x)Cd(x)Te 24 p3636 A83-48741

DENSITY WAVE MODEL

- The cosmic density wave and its observable vestige 01 p0125 A83-10933
- Optical study of the morphology and velocity field of the galaxy NGC 6946 02 p0259 A83-12518
- On the history of the wave theory of spiral structure 03 p0418 A83-13675
- Steady wave model of spiral galaxies and its application in cosmogony 04 p0549 A83-14995
- Cosmic density wave and its observable vestiges - Maximum scale of inhomogeneities in the distribution of galaxies and features in the distribution of absorption-line redshifts of quasars 05 p0702 A83-17850
- Lifetime of spurs in galaxies 06 p0825 A83-18090
- The 'black' regions of the Universe 06 p0830 A83-18776
- On the global density waves in self-gravitating flat disks 06 p0843 A83-19482
- Gravitationally induced spurs in spiral galaxies - An example in M31 06 p0843 A83-19488
- The shape of cooling filaments in old supernova remnants 07 p1021 A83-21125
- Galactic spiral structure and the gas motion near and beyond the corotation resonance 07 p1026 A83-21261
- Cosmological density fluctuations produced by sources of radiation at z greater than 100 09 p1363 A83-24997
- Spiral motions in projective relativity 10 p1506 A83-26097

- One-dimensional periodic flows with a shock transition
- Application to the density wave theory of spiral structure 10 p1512 A83-26711
Bending waves in Saturn's rings 11 p1683 A83-27353
Global shearing modes of galactic disks 12 p1794 A83-29079
Sectoral density waves in a stellar disk model 14 p2102 A83-32972
Can graininess in the early universe make galaxies? 14 p2103 A83-33178
Density inhomogeneities and the deduced chemical composition of planetary nebulae 15 p2261 A83-34502
Large-scale anisotropy of the 3 K background radiation in density wave models 16 p2441 A83-36677
The energy and momentum of slow drift spiral density waves 17 p2600 A83-37645
Spiral structure and gas motion in M81 17 p2610 A83-38547
On the local standard of rest --- comoving with young objects in gravitational field of spiral galaxies 18 p2768 A83-39633
Local galactic structure and velocity field 18 p2768 A83-39635
Spiral modes and the Milky Way 18 p2770 A83-39663
Self-modulation and envelope solitons of spiral density waves --- in approximation of galactic structure 20 p3075 A83-43386
Tunneling between conductors with a charge-density wave 22 p3366 A83-46936
Spiral structure - Density waves or material arms? 24 p3656 A83-49231
Numerical experiments on the response mechanism of barred spirals 24 p3656 A83-49237
Proto-galactic perturbations 24 p3658 A83-49365
- DENTISTRY**
Prevention of tooth decay among seamen 05 p0673 A83-17176
- DEOXYGENATION**
Cooperative deoxygenation of haemoglobin - Asymmetry of binding and subunit differences 05 p0676 A83-17795
Blood osmolality in vitro - Dependence on P(CO₂), lactic acid concentration, and O₂ saturation 13 p1902 A83-30459
- DEOXYRIBONUCLEIC ACID**
Molecular structure of r(GCG/d/TATACGC/ - A DNA-RNA hybrid helix joined to double helical DNA 01 p0077 A83-10209
Hybridization of the DNA of purple phototrophic bacteria 01 p0078 A83-10423
The peculiarities of DNA metabolism in rat brains in the process of the elaboration of a conditioned reflex 01 p0080 A83-10552
Is cell aging caused by respiration-dependent injury to the mitochondrial genome 02 p0220 A83-11834
The activity of AP-endonuclease in thymocytes of normal and irradiated rats 03 p0376 A83-14877
The molecular mechanisms of the interphase death of lymphoid cells. VI - A low molecular weight DNA fraction in the products of the degradation of the chromatin of irradiated rat thymus 03 p0377 A83-14883
Photobiological aspects of the damage of cells by radiation 03 p0377 A83-14927
The structure of DNA and the transformation of cells 06 p0795 A83-18980
Free radicals induced by UV light in aqueous solutions of DNA with various amounts of protein at 77 K 06 p0796 A83-19377
The chemical structure of DNA sequence signals for RNA transcription 06 p0796 A83-19408
DNA damage during the action of ionizing radiation with different physical characteristics 09 p1321 A83-24926
A comparative analysis of the effect of alkylating agents, ionizing radiation, and ultraviolet radiation on the progression of mammalian cells through the mitotic cycle. II - The effect of gamma-radiation and N-methyl-N'-nitro-N-nitrosoguanidine on DNA synthesis in HeLa cells 09 p1321 A83-24928
An investigation of DNA synthesis in the liver of irradiated and serotonin-treated rats following the removal of the cycloheximide block 14 p2061 A83-32053
The effect of the radiation dose rate on the formation of double-strand DNA breaks 14 p2062 A83-32063
An investigation of the biological activity during irradiation of calf spleen extracts containing an inhibitor of DNase I 14 p2062 A83-32066
Strongly acidic polypeptides as inhibitors of the repair of single-strand DNA breaks caused by gamma-irradiation 16 p2393 A83-35919
Negatively supercoiled simian virus 40 DNA contains Z-DNA segments within transcriptional enhancer sequences 17 p2557 A83-38607

- The mechanism of the radiation damage of the secondary structure of DNA 19 p2873 A83-41002
The mechanism of the secondary postirradiation degradation of DNA in thymocytes of irradiated rats. I - The substrate specificity of alkaline endonuclease 19 p2874 A83-41003
Atmospheric evolution, the Drake equation, and DNA - Sparse life in an infinite universe 19 p2886 A83-41515
The effect of electrostimulation of the hypothalamus on the methylation of DNA from the livers of rats 19 p2876 A83-41844
Role of metabolic rate and DNA-repair in *Drosophila* aging. Implications for the mitochondrial mutation theory of aging 19 p2877 A83-41861
DNA fusion product of phage P2 with plasmid pBR322 - A new phasmid 21 p3183 A83-44860
Damages of the superhelical structures of nuclear DNA by gamma-rays and heavy ions 23 p3495 A83-48201
The effect of beta-mercaptopethylamine on the accumulation of DNA strand breaks in *Bac. stearothermophilus* exposed to gamma-radiation, UV radiation, and nitrosomethylurea treatment --- Mercapto Ethyl Amine 23 p3495 A83-48204
- DEPENDENCE**
NT SPATIAL DEPENDENCIES
NT TEMPERATURE DEPENDENCE
NT TIME DEPENDENCE
The detection of drug addiction among flight personnel 08 p1148 A83-22965
- DEPENDENCY**
U DEPENDENCE
- DEPLOYMENT**
How parametric cost estimating models can be used by the program manager 01 p0112 A83-11145
An overview of the potential threat as related to missile requirements [AIAA PAPER 83-0568] 05 p0710 A83-16795
Tether deployment dynamics 07 p0869 A83-21426
Air-deployed, over-ocean, small, ruggedized optical fiber 08 p1074 A83-22486
U.S. cruise missile programs: Development, deployment and implications for arms control --- Book 15 p2119 A83-33769
Operational deployment of the air cushion vehicle 15 p2242 A83-34864
Damped response of spacecraft with flexible deploying appendages 21 p3101 A83-45113
- DEPOLARIZATION**
Polarization phenomena in the transition layer of SOS films 01 p0111 A83-11348
Measurements of ice depolarization at 28.56 GHz using the COMSTAR beacon simultaneously with a 16.5 GHz polarization diversity radar 01 p0032 A83-11354
Using site-diversity reception to overcome rain depolarization in millimeter wave satellite communications systems 01 p0033 A83-11370
The Hanle effect and the diagnostics of turbulent magnetic fields in the solar atmosphere 02 p0269 A83-12572
Results of the VPI&SU Comstar experiment --- depolarization and attenuation due to rain 02 p0140 A83-12610
A semi-empirical formula for microwave depolarization versus rain attenuation on earth-space paths 05 p0622 A83-12723
Correlation of slant path ice depolarization events at 28.56 GHz with radar reflectivity structure and the determination of ice depolarization statistics for Wallops Island, Virginia 06 p0744 A83-18700
Slant-path depolarisation measurements at 12 and 14GHz carried out at Martlesham Heath using the OTS satellite 06 p0745 A83-18708
De-polarisation due to non-symmetry in raindrops 06 p0746 A83-18718
Correlation effects in collisional depolarisation and redistribution of radiation 06 p0808 A83-19010
Polarized fluorescence line narrowing measurements of Nd laser glasses - Evidence of stimulated emission cross section anisotropy 06 p0767 A83-19258
Depolarization of 19-GHz signals --- from satellite beacons 07 p0871 A83-20552
Scattering and depolarization of electromagnetic waves in irregular stratified spheroidal structures of finite conductivity - Full wave analysis 08 p1161 A83-22282
Antenna effects in depolarization measurements 08 p1077 A83-22683
An S band radar for studying the effects of weather on the Sirio and Comstar satellite downlink signals 11 p1628 A83-27053
A statistical study of abnormal depolarization 14 p2000 A83-32419

- Uplink depolarisation control in TV feeder link earth stations 15 p2144 A83-34520
Polarization noise in single mode fibres and its reduction by depolarizers 18 p2744 A83-40349
Measurement-based estimates of outage on earth-space RF links from attenuation and depolarization 19 p2830 A83-41371
Assessment of principal planes orientation in a terrestrial link at 18 GHz during intense rainfall 20 p2964 A83-42484
A rigorous analysis for the study of rain attenuation and depolarization statistics for terrestrial and earth-space links 22 p3275 A83-46530
The impact of ice along satellite-to-earth paths on 11-GHz depolarization statistics 22 p3275 A83-46531
Technological aspects of sulfur dioxide depolarized electrolysis for hydrogen production 23 p3430 A83-48596

DEPOLARIZERS**U DEPOLARIZATION****DEPOSITION**

- NT ANODIZING
NT ELECTRODEPOSITION
NT ELECTROLESS DEPOSITION
NT ELECTROPLATING
NT VACUUM DEPOSITION
NT VAPOR DEPOSITION
Competing processes of Si molecular beam reactive etching and simultaneous deposition on film and bulk SiO₂ 01 p0108 A83-10623
Spectra of cosmic X-ray sources 02 p0246 A83-12187
Structural and thermal analysis studies of magnetron sputter-deposited amorphous metallic /Mo0.6Ru0.4/82B18 films 02 p0243 A83-12649
Low-temperature refractory metal film deposition 03 p0301 A83-14936
Effect of temperature on the performance of the PEC cells formed with chemically deposited CdS films --- photoelectrochemical cells 04 p0505 A83-15491
Effect of discharge conditions on characteristics of hydrogenated amorphous silicon deposited by DC glow discharge decomposition 04 p0539 A83-15498
Late stage of planet growth in accretion theory 06 p0849 A83-19462
Chemical bath deposition of thin film cadmium selenide for photoelectrochemical cells 07 p0954 A83-20594
Deposition and blade fouling of gas turbines by fuel impurities and additives 07 p0941 A83-21456
Reversible and irreversible wet deposition processes involving atmospheric admixtures 09 p1294 A83-23547
Laboratory measurements of dry deposition of acetone over adobe clay soil 09 p1297 A83-25186
A study of irregular-shaped particle deposition in turbulent flows and application to gas turbines 11 p1525 A83-27480
Correlation and prediction of thermophoretic and inertial effects on particle deposition from non-isothermal turbulent boundary layers 11 p1566 A83-27481
Deposition and properties of zinc phosphide films 11 p1664 A83-28715
Laser induced deposition of zinc oxide 13 p1928 A83-30335
Power-law asymptotic mass distributions for systems of accreting or fragmenting bodies 15 p2264 A83-34587
High performance hydrogenated amorphous silicon solar cells made at a high deposition rate by glow discharge of disilane 16 p2371 A83-36774
Combustion system processes leading to corrosive deposits 20 p2949 A83-42246
Effect of deposition rate and substrate temperature on properties of CdTe film 20 p3054 A83-43396
Catalytically deposited carbon solar selective absorber 22 p3319 A83-46582
Recent progress on LADA growth of HgCdTe and CdTe epitaxial layers --- laser assisted deposition 24 p3633 A83-48739
Chemical deposition of Cd(1-x)Hg(x)S thin film electrodes for liquid-junction solar cells 24 p3602 A83-50186

DEPOSITS**NT CRYODEPOSITS****DEPRESSANTS****NT CENTRAL NERVOUS SYSTEM DEPRESSANTS****DEPRESSIONS (TOPOGRAPHY)****U STRUCTURAL BASINS****DEPRESSURIZATION****U PRESSURE REDUCTION****DEPRIVATION**

- NT SENSORY DEPRIVATION
NT SLEEP DEPRIVATION
NT WATER DEPRIVATION

DEPTH

- Depth separation and the Ponzo illusion
22 p3348 A83-45949

DEPTH MEASUREMENT

- Evaluating depth to shallow groundwater using heat capacity mapping mission /HCMM/ data
03 p0351 A83-14668
- Junction depth measurement for VLSI structures
07 p0998 A83-19895
- Compositional depth profile of a native oxide LPCVD MNOS structure using X-ray photoelectron spectroscopy and chemical etching
10 p1391 A83-26062
- Determination of aerosol optical depth from ground measurements
12 p1730 A83-29576
- Relative performances of central and dipole frequency soundings over a layered earth
15 p2202 A83-34748

DEPTH PERCEPTION

- U SPACE PERCEPTION

DERIVATION CALCULUS

- U DIFFERENTIAL CALCULUS

DESALINATION

- Universal solar energy desalination system
11 p1607 A83-27241
- Performance of solar multiflash desalination plants
11 p1607 A83-27242
- The photovoltaic-powered water desalination plant 'SORO' design, start up, operating experience
14 p2037 A83-32184

DESATURATION

- Desaturation of H₂ quadrupole lines in the atmospheres of the outer planets
20 p3078 A83-43077

DESCENT

- NT PARACHUTE DESCENT

- Dynamics of the Venera 13 and 14 descent modules
19 p2809 A83-41239

DESCENT TRAJECTORIES

- NT REENTRY TRAJECTORIES

- Controllability conditions and effective controls for nonlinear systems
09 p1329 A83-24734
- Method of the complex postflight ballistic analysis of the descent trajectories of Venera-type descent modules
09 p1212 A83-25032
- Ballistics and navigation of the automatic interplanetary probes Venera-13 and Venera-14
14 p1981 A83-31952
- Analysis of the descent trajectories of the Venera-13 and Venera-14 descent modules in the atmosphere of the planet
14 p1979 A83-31953
- Investigation of the characteristics of the Venus stratosphere from acceleration measurements during the braking of the Venera-13 and Venera-14 probes
14 p2110 A83-31959
- Optimal turning climb-out and descent of commercial jet aircraft
[SAE PAPER 821468]
17 p2464 A83-37999
- Instantaneous, predictable balloon system descent from high altitude
18 p2640 A83-39808
- Analysis of results of aerodynamic studies on the Venera 13 and 14 descent modules
19 p2809 A83-41237
- Accelerated calculation of the descent trajectories in an atmosphere of ballistic reentry vehicles with allowance for their motion with respect to the center of the mass
21 p3094 A83-45277

DESCRIPTIVE GEOMETRY

- Isogeometric approximation of functions of one variable --- explicit spline method for CAD of curves and surfaces
05 p0682 A83-17641
- Chained aggregation - A geometric analysis --- of large scale systems
10 p1469 A83-26576

DESSERTLINE

- Remote sensing in the global monitoring of environment
09 p1284 A83-24527
- Joint U.S.-Mexican activities in arid land management and desertification control
09 p1284 A83-24531
- Dynamic modeling of vegetation change in arid lands
09 p1285 A83-24537
- Use of aerial photographs in land reclamation
09 p1285 A83-24541
- Quantifying agricultural indicators of desert encroachment
09 p1285 A83-24542
- Approaches to desertification monitoring in the Sudan using Landsat data: A test of a geographical data base approach - Preliminary results
09 p1286 A83-24558
- Sand distribution in the Kharga depression of Egypt - Observations from Landsat images
09 p1289 A83-24590

DESERTS

- NT GOBI DESERT
- NT LIBYAN DESERT
- NT SAHARA DESERT (AFRICA)
- A parameter review and assessment of attenuation and backscatter properties associated with dust storms over desert regions in the frequency range of 1 to 10 GHz
03 p0306 A83-14012

- Application of remote sensing for preparation of nature conservation maps and natural processes dynamics study
08 p1128 A83-21951
- Soil classification and potentials in Sinai peninsula from Landsat images
09 p1285 A83-24540
- Landsat data for monitoring rural settlement and population A test in the Umm Ruwaba region, the Sudan
09 p1286 A83-24559
- Desert construction siting utilizing remote sensing technology
09 p1287 A83-24564
- Desert terrain elevations from satellite radar altimetry
09 p1287 A83-24568
- Satellite monitoring of recent desertification in the Yulin region The People's Republic of China
09 p1287 A83-24569
- Further studies on the mineral potentials of Berenice area based on Landsat imagery
09 p1289 A83-24597

- Application of visual interpretation and digital processing of Landsat data for the preparation of a geological interpretation map of southwestern Egypt at a scale of 1:500,000
09 p1289 A83-24598
- Landsat investigation and tectonic interpretation of the lineaments of the Central Eastern Desert, Egypt
09 p1290 A83-24612
- Structural geomorphology of Rajasthan basin, India-interpreted through Landsat imagery and aerial photos
09 p1291 A83-24626
- Particle size and spacing variations in desert surface sediments - Importance for remote sensing of arid regions
09 p1291 A83-24632
- The T700-GE-700 engine experience in sand environment
09 p1208 A83-24842
- Some aspects of land transformation in the western Mediterranean desert of Egypt
15 p2181 A83-33553
- Landsat monitoring of desert vegetation growth, 1972-1979 using a plant-shadowing model
15 p2181 A83-33556
- Utilization of remote-sensing methods for the mapping of tree and bush vegetation in the southern Kysyl-Kum
18 p2706 A83-40588
- Desertification in Kaokoland (northern South West Africa/Namibia) - Field evidence, recognition in satellite imagery, mapping of spatial distribution by satellite image interpretation (Landsat 1)
22 p3309 A83-46135
- Certain results of a comparison of airborne data with satellite measurements --- spectral brightness and albedo of deserts and agricultural regions
24 p3598 A83-49280

DESICCANTS

- Performance and operational analysis of a liquid desiccant open-flow solar collector
11 p1608 A83-27246

DESIGN

- The technical 'productivity gap'
13 p1933 A83-30831

DESIGN ANALYSIS

- Human factors and the design of display terminals
01 p0085 A83-10253
- Analytical design of thin-wall wings at the drafting stage
01 p0058 A83-10453
- End region effects upon the performance of a magnetohydrodynamic channel
01 p0107 A83-10665
- Design for testability /DFT/
01 p0058 A83-10757
- A cost effective approach to design evaluation of advanced system display switchology
01 p0093 A83-11200
- A methodology of evaluation and design of fields of focusing heliostats --- French thesis
02 p0201 A83-11768
- Optimal design of the lateral feed of a turbomachine [AAAF PAPER NT 81-04]
02 p0169 A83-11770
- Design of FIR digital filters using tapped cascaded FIR subfilters
02 p0167 A83-11822
- Galvanometric devices --- Russian book
02 p0176 A83-11947
- Extra-solar astronomy with a 2.4 m normal incidence X-ray telescope at 0.1 arcsec resolution
02 p0247 A83-12726
- High repetition rate mini TEA CO₂ laser using a semiconductor preionizer
02 p0185 A83-12816
- Second-order sensitivity derivatives in structural analysis
03 p0338 A83-13149
- An experimental investigation of a stationary reflector/tracking absorber solar collector at intermediate temperatures
03 p0353 A83-13479
- Hybrid thermoelectric solar collector design and analysis
03 p0353 A83-13482
- Fail-safe optimal design of complex structures with substructures
03 p0339 A83-13490
- Optimum design of metallic reciprocating seals [ASME PAPER 82-LUB-44]
03 p0336 A83-13522
- A design method for closed loop solar energy systems with concentrating collectors
03 p0353 A83-13583

- Optimization of parabolic trough solar collectors
03 p0354 A83-13699
- Design requirements for large-scale focal planes
03 p0325 A83-13727
- Conceptual design and requirements of a pushroom focal plane
03 p0325 A83-13729
- Recent developments in infrared acousto-optic tunable filters
03 p0393 A83-13770
- Design and implementation of a broadband infrared atmospheric transmissometer
03 p0327 A83-13993
- Batteries and fuel cells: Design, employment, chemistry --- German book
03 p0355 A83-14041
- A novel radar reflector with variable RCS
03 p0307 A83-14133
- Optical figuring process, Dupont 2.6-m telescope
03 p0410 A83-14381
- Tentative principles of the evaluation of the airworthiness of aircraft of one-of-a-kind design
03 p0280 A83-14623
- Investigation of ultrasonic transducers as used for non-destructive testing
04 p0493 A83-15222
- Design and development of Cartridge Actuated Device /CAD/ primer
04 p0464 A83-15433
- A look at the Russell 'Lobe' parachute - The first ultrastable parachute design
04 p0444 A83-15434
- Computer-aided design within the framework of the algorithmic selection procedure for the design with catalogs --- German thesis
04 p0487 A83-15844
- Extremal MHD generator
04 p0538 A83-16110
- A description of the Bell Laboratories scanned acoustic microscope
04 p0482 A83-16321
- GASAP - A general aviation airplane analysis and synthesis program
05 p0594 A83-16488
- [AIAA PAPER 83-0054]
Acoustic capabilities of the German-Dutch wind tunnel DNW
05 p0599 A83-16554
- [AIAA PAPER 83-0146]
Design of optimum propellers
05 p0581 A83-16578
- [AIAA PAPER 83-0190]
CAD/CAM and analysis - A production tool for spacecraft design
05 p0620 A83-16589
- [AIAA PAPER 83-0218]
Evaluation of the perceptual attributes of emissive and non-emissive display designs using computer simulation
05 p0677 A83-16870
- Software design for the Douglas DC-9 Super 80 digital flight guidance system
05 p0592 A83-17311
- Techniques for the solution of MHD generator flows [AIAA PAPER 83-0465]
05 p0689 A83-17928
- The management of engineering change procedure
06 p0816 A83-17957
- Geometric Programming for continuous design problems
06 p0801 A83-18221
- Interactive optimum design system --- for two dimensional elastic structures
06 p0773 A83-18228
- Derivation and convergence of power series in structural design
06 p0773 A83-18233
- The dynamic inducer as a cost-effective wind turbine system
06 p0779 A83-18457
- The Pratt & Whitney PW100 - Evolution of the design concept
06 p0718 A83-18821
- A wind tunnel for unsteady turbulent shear flows - Design and flow calculation
07 p0867 A83-19664
- Unbalance response analysis of a complete turbomachine
07 p0938 A83-19674
- Curvature transitions of composite curves and surfaces - Questions regarding details of computer-aided design --- German thesis
07 p0982 A83-20398
- The future for fighter aircraft
07 p0862 A83-20597
- Technology and modern fighter aircraft - The evolutionary F-16
07 p0865 A83-20598
- NGT - The Next Generation Trainer
07 p0866 A83-20599
- Studies on a versatile handling system having multijointed fingers
08 p1151 A83-22064
- Setting design goals for advanced propulsion systems [AIAA PAPER 81-1505]
08 p1045 A83-22154
- A lightweight, low-cost, magnetic-bearing reaction wheel for satellite attitude-control applications
08 p1050 A83-22370
- LCAC - from test craft to production design --- air cushion vehicles for amphibious assault landing operations [AIAA PAPER 83-0622]
08 p1173 A83-22423
- Errors in the experimental determination of the parameters of supersonic combustion ramjet engines
08 p1046 A83-22653
- Optimal design of a minimum weight thermal diffuser with constraint on the output thermal power flux
08 p1085 A83-22773
- Spectral characterization methodology of thin-film optical filters
08 p1104 A83-22880
- MHD channel performance for potential early commercial MHD power plants
08 p1169 A83-23134
- Pitch control system for large-scale wind turbines
08 p1132 A83-23140

A system of criteria for evaluating the energy efficiency of an engine at the state of technical proposals
 09 p1205 A83-23437

Optimal design of elastic plates with a constraint on the slope of the thickness function
 09 p1278 A83-23670

Analysis, design and construction of rare-gas halide discharge lasers
 09 p1271 A83-23695

The theoretical principles underlying the design of solid-propellant rocket engines --- Russian book
 09 p1220 A83-23821

Maneuver load control for reducing the design loads of modern combat aircraft
 [DGLR PAPER 82-046] 09 p1209 A83-24169

Design and implementation of an active load alleviation system, taking into account the example of a modern transport aircraft
 [DGLR PAPER 82-045] 09 p1209 A83-24170

Some aspects of the engine design of future fighter planes
 [DGLR PAPER 82-071] 09 p1206 A83-24185

On the design philosophy of fighter aircraft engines
 [DGLR PAPER 82-073] 09 p1206 A83-24187

The automation of control system design. Number 4 --- Russian book
 09 p1326 A83-24225

Design, fabrication, and evaluation of 2- and 3-bit GaAs MESFET analog-to-digital converter IC's
 09 p1256 A83-24678

Design of multivariable optimal control systems using asymptotic root loci
 09 p1335 A83-24814

Mathematical method for the design of the intake branch in the case of centrifugal blade machines --- Book
 09 p1263 A83-24850

Assessment of future solid rocket motor flight instrumentation/data needs
 09 p1219 A83-24888

The use of piezoceramic vibrators in vibrating mounts for spacecraft scientific instrumentation
 10 p1387 A83-25348

A stall margin design method for planar and axisymmetric diffusers
 [ASME PAPER 82-WA/FE-8] 10 p1413 A83-25685

Size effects in DAWT innovative wind energy system design
 [ASME PAPER 82-WA/SOL-20] 10 p1445 A83-25688

Coherent large telescopes
 10 p1494 A83-25836

FM-SCPC system and equipments for satellite communication --- Single Channel Per Carrier
 10 p1404 A83-26084

Design of interdigitated capacitors and their application to gallium arsenide monolithic filters
 10 p1410 A83-26341

Design considerations for a lithium-aluminum/iron sulfide electric vehicle battery
 11 p1603 A83-27173

Design flexibility of redox flow systems --- for energy storage applications
 11 p1604 A83-27177

Optimization of PM machines due to advancements in containment structure
 11 p1560 A83-27188

Accelerated cycle life tests of Ni/Cd cells with ED nickel electrodes - Comparison of three separators
 11 p1605 A83-27192

Design of large, low-concentration-ratio solar arrays for low earth orbit applications
 11 p1541 A83-27254

Design and experiences with a laboratory Stirling cycle machine
 11 p1588 A83-27284

Program overview and diesel/flywheel hybrid power train design - Fibre composite flywheel development program for road vehicle applications
 11 p1667 A83-27306

Fibre composite rotor selection and design / Fibre composite flywheel development program for road vehicle applications/
 11 p1667 A83-27307

The use of mechanical energy storage in an unconventional, rough terrain vehicle
 11 p1667 A83-27309

Increasing summer peak power with aquifer storage
 11 p1609 A83-27313

On aerodynamic design of the Savonius windmill rotor
 11 p1610 A83-27325

Design options for the SP-100 thermoelectric Nuclear Space Power Plant
 11 p1542 A83-27327

Space Shuttle - Reaction control systems tanks
 11 p1535 A83-27468

STS Manned Maneuvering Unit propulsion system
 11 p1644 A83-27469

STS Orbital Maneuvering Systems tanks
 11 p1535 A83-27473

Optimal design of Pb/1-x/Sn/x/Te double heterostructure injection lasers
 11 p1583 A83-27622

Mathematical programming models for the economic design and assessment of wind energy conversion systems
 11 p1611 A83-27870

Proposal for a new design of wind power generator
 11 p1611 A83-27871

Construction of the reflector radio telescope TNA-1500
 11 p1675 A83-28677

Chassis dynamics related to a low-cost magnetically suspended vehicle
 12 p1783 A83-29522

Optimum design of dewar supports --- for launching and maintaining in long term orbit
 [AIAA 83-0829] 12 p1707 A83-29738

A robust Feasible Directions algorithm for design synthesis
 [AIAA 83-0938] 12 p1773 A83-29768

Shape optimization of two-dimensional structures with geometric problem description and adaptive mesh refinement
 [AIAA 83-0941] 12 p1739 A83-29771

Design methods for viscoelastically damped plates
 [AIAA 83-0904] 12 p1743 A83-29843

Generalized modal shock spectra within indeterminate interface --- for spacecraft design
 [AIAA 83-0996] 12 p1708 A83-29871

Landing gear design handbook
 13 p1805 A83-30143

Approximate aerodynamic analysis for horizontal axis wind turbines
 13 p1870 A83-30194

Modular method for centrifugal compressor performance prediction
 13 p1804 A83-31169

The development of STS payload environmental engineering standards
 13 p1811 A83-31197

An indicator of the reliability of analytical design and initial manufacturing process
 13 p1863 A83-31491

Design features of a new commuter turboprop engine
 [SAE PAPER 820717] 13 p1807 A83-31802

The CAC-100 - Design features --- passenger commuter transport aircraft
 [SAE PAPER 820730] 13 p1806 A83-31806

The helicopter preliminary design process
 13 p1806 A83-31812

Structural optimization - Challenges and opportunities
 13 p1869 A83-31814

Space telescope low scattered light camera - A model
 14 p2096 A83-32026

Alicudi project --- photovoltaic solar energy system for electric power supplying
 14 p2038 A83-32190

Photovoltaic power for walk-in coolers
 14 p2038 A83-32192

Monogroove heat pipe development for the space constructible radiator system
 [AIAA PAPER 83-1431] 14 p2010 A83-32706

An automated on-orbit thermal acquisition device --- reusable heat rejectors for space platforms
 [AIAA PAPER 83-1465] 14 p1982 A83-32723

Ceramic tube development for solar receiver applications
 [AIAA PAPER 83-1501] 14 p2047 A83-32740

Impact of stretching wide-bodied aircraft on existing airport facilities
 [AIAA PAPER 83-1578] 14 p1978 A83-33351

A new approach to FIR digital filters with fewer multipliers and reduced sensitivity
 15 p2151 A83-33927

Exergy analysis for the performance of solar collectors
 15 p2189 A83-33990

An innovative type of icebreaker for the arctic environment
 15 p2242 A83-34856

New concept in hovercraft design diesel versus gas turbines
 15 p2242 A83-34860

ACV lift air systems - More puff for less power
 15 p2242 A83-34861

AP-1-88 craft 001 prototype clearance trials
 15 p2242 A83-34862

Developments in air cushion vehicle spray suppression
 15 p2243 A83-35056

A design synthesis model for ACV/SES lift systems
 15 p2243 A83-35057

A servo compensator design approach for variable structure systems
 15 p2222 A83-35126

Optimum design for potential flows
 16 p2288 A83-35525

Combustor modelling by assembly of well-stirred reactors
 16 p2325 A83-35808

Application of the separation singularity difference method to inlet aerodynamic design
 16 p2290 A83-35827

Experimental study of a high-through-flow transonic axial compressor stage
 16 p2291 A83-35853

Tip clearance flow in a compressor rotor passage at design and off-design conditions
 16 p2291 A83-35855

Optimization of the plane compressor blade aerodynamic design
 16 p2291 A83-35857

Contribution to centrifugal compressor impeller design
 16 p2305 A83-35865

Analytical design and experimental verification of S-duct diffusers for turboprop installations with an offset gearbox
 [AIAA PAPER 83-1211] 16 p2294 A83-36283

A comprehensive method for preliminary design optimization of axial gas turbine stages. II - Code verification
 [AIAA PAPER 83-1403] 16 p2309 A83-36393

Monte Carlo simulation of the engine development process
 [AIAA PAPER 83-1405] 16 p2310 A83-36394

Comparison of design techniques for pumps with skewed blades
 [AIAA PAPER 83-1282] 16 p2362 A83-36411

Design of modern control systems --- Book
 17 p2569 A83-37495

A two-mirror stigmatic system in which the figure of one of the mirrors is known
 17 p2580 A83-37672

Interactive analysis of a large aperture Earth Observations Satellite
 [SAWE PAPER 1556] 17 p2480 A83-38053

Aircraft flexible tanks general design and installation recommendations
 [SAE ARP 1664] 17 p2464 A83-38102

An algorithm for engineering design optimization
 17 p2575 A83-38573

Smart aerodynamic optimization
 [AIAA PAPER 83-1863] 17 p2457 A83-38690

Super choppers --- helicopters with counter rotating rotors
 17 p2465 A83-38700

Design and development of advanced-composite shrouds
 18 p2662 A83-40297

Vertical seeking ejection seat boosts pilots odds
 18 p2641 A83-40305

Constraint on design parameters and twist of S1 surfaces in turbomachines
 18 p2638 A83-40367

An improved chopping secondary design --- of infrared telescopes
 18 p2691 A83-40439

Performance test procedures for thermal collectors - Solar simulators
 18 p2709 A83-40524

Performance of a hybrid solar heating system of the solar laboratory at the JRC-ISPR
 18 p2710 A83-40533

A new approach for the design and analysis of On-Off reaction control systems --- for satellite launch vehicle upper stages
 19 p2815 A83-40882

Blade design for reduced helicopter vibration
 19 p2797 A83-41076

Active flutter suppression using eigenspace and linear quadratic design techniques
 [AIAA PAPER 82-2222] 19 p2803 A83-41702

Synthesis of insensitive regulators with comparative evaluations in aerospace applications
 [AIAA PAPER 83-2224] 19 p2891 A83-41704

Attitude stabilization of flexible spacecraft during stationkeeping maneuvers
 [AIAA PAPER 83-2226] 19 p2815 A83-41706

Optimal design of a passive vibration absorber for a truss beam
 [AIAA PAPER 83-2291] 19 p2816 A83-41750

Photovoltaic energy systems: Design and installation --- Book
 20 p3011 A83-42175

Universities - Have they a role in aeronautical research? Aerodynamics
 20 p2928 A83-42621

Design of shell-and-tube heat exchangers to avoid flow-induced vibration
 20 p2984 A83-43021

Phoenix GCS - Some considerations which influence the design of computer assisted ground control stations for RPV
 20 p2932 A83-43714

determination of the rate constants used in design calculations relating to low-temperature CO₂-D₂ gasdynamic lasers
 20 p2998 A83-43801

Design and fabrication of payload for OH emission experiment onboard Spacelab - A case study
 21 p3095 A83-43821

Design and fabrication of the Indian cosmic ray payload on board Spacelab-3 - A case study
 21 p3095 A83-43822

An analytic approach to optimum oscillator design using S-parameters
 21 p3122 A83-43832

Aircraft-borne lightning sensor
 21 p3134 A83-43867

Flaw detector DVT-24 for the inspection of axial holes in deep drilling
 21 p3135 A83-43880

Optical design and aeroelastic investigation of segmented windmill rotor blades
 21 p3166 A83-44028

A new technique for high voltage power transistor
 21 p3124 A83-44055

Wide field of view head-up displays
 21 p3091 A83-44690

Optimal positive real controllers for large space structures
 21 p3102 A83-45117

Damage tolerant design using collapse techniques
 21 p3164 A83-45591

A review of large wind turbine systems
 22 p3318 A83-45919

Design and implementation of SPIDER - A transportable image processing software package
 22 p3350 A83-46251

Design of continuous fiber composite structures
 22 p3264 A83-46306

Optical systems engineering II; Proceedings of the Second Conference, Los Angeles, CA, January 26, 27, 1982 22 p3357 A83-46587

Design and fabrication of the NASA 2.4-meter space telescope 22 p3357 A83-46592

The features of the space structures dynamic design [IAF PAPER 83-409] 23 p3423 A83-47377

Simplified inverse design of a straight vaneless diffuser of radial stage [ASME PAPER 83-GT-2] 23 p3392 A83-47877

The impact of three-dimensional analysis on fan design --- for turbine engines [ASME PAPER 83-GT-136] 23 p3408 A83-47963

Aerodynamic tests on centrifugal process compressors Influence of diffuser diameter ratio, axial stage pitch and impeller cut-back [ASME PAPER 83-GT-172] 23 p3396 A83-47973

A design study of a reaction control system for a V/STOL fighter/attack aircraft [ASME PAPER 83-GT-199] 23 p3410 A83-48002

Aircraft design (3rd revised and enlarged edition) --- Russian book 23 p3403 A83-48100

Design and technology influences - 'Maturity' at introduction of the 214ST [AIAA PAPER 83-2528] 23 p3404 A83-48366

Bucking the current --- electric actuators for V/STOL aircraft 24 p3547 A83-48887

Methods for teaching aerospace vehicle design [AIAA PAPER 83-2475] 24 p3637 A83-49582

Servo-system design technique utilising sensitivity as a design parameter 24 p3621 A83-50198

DESIGN OF EXPERIMENTS
U EXPERIMENT DESIGN

DESIGN TO COST
Some thoughts on the development of computer-based systems --- airborne equipment design to cost 02 p0135 A83-11807

USAF's design guide coming out next month 07 p1001 A83-20647

Goal programming for preliminary design and critical technology identification - Application to infrared step-stare moving target detection 08 p1051 A83-22842

Cost engineering --- programs in aerospace industry 11 p1666 A83-28181

Cost factors and approach methodology in selecting structural materials and manufacturing technologies [AIAA 83-0791] 12 p1783 A83-29730

The loss of power supply probability as a technique for designing stand-alone solar electrical (photovoltaic) systems 12 p1749 A83-29896

Performance testing and module monitoring at the EC Necessary steps to develop cost-effective PV modules 14 p2038 A83-32194

Reliability and performance experience with flat-plate photovoltaic modules 14 p2038 A83-32195

Cost optimization of the dimensions of the antennas of a solar power satellite system 15 p2193 A83-35167

Life cycle cost applications to conceptual designs [SAWE PAPER 1479] 20 p3056 A83-43748

Design-to-cost in the application of advanced composite technology [SAWE PAPER 1480] 20 p3056 A83-43749

An integrated model for production cost estimation and design-to-cost control of small missiles [SAWE PAPER 1481] 20 p3056 A83-43750

The cost-effectiveness of modular and single-purpose rocket boosters and worldwide trends [IAF PAPER 83-06] 23 p3418 A83-47230

Designing for supportability and cost effectiveness [AIAA PAPER 83-2499] 24 p3543 A83-49586

Army family of light rotorcraft (LHX) concept formulation [AIAA PAPER 83-2552] 24 p3548 A83-49592

DESORPTION
Simple analysis of a forced flow solar regeneration system 01 p0068 A83-10664

Atmospheric gases on cold surfaces - Condensation, thermal desorption, and chemical reactions 09 p1298 A83-25191

Comparison of photon stimulated dissociation of gas phase and chemisorbed CO 10 p1389 A83-25556

Cf-252 plasma desorption in ion implanted mica 15 p2133 A83-34381

DESPINNING
U SPIN REDUCTION

DESTRUCTIVE TESTS
Tentative test procedure for determining the plane strain JI-R curve 02 p0158 A83-12831

Evaluation of the tentative JI-R curve testing procedure by round robin tests of HY130 steel 02 p0158 A83-12832

Experimental mechanics of fiber reinforced composite materials --- Book 03 p0341 A83-14117

Double torsion fracture toughness test for evaluating transverse cracking in composites 04 p0455 A83-15996

Simplified crushing analysis of thin-walled columns and beams 04 p0500 A83-16197

Engineering safety analysis via destructive numerical experiments 04 p0500 A83-16198

The possibility of using electromagnetic accelerators for studying processes occurring during the high-velocity collision of solids 04 p0465 A83-16388

Dependence of fracture toughness of alumina on grain size and test technique 06 p0734 A83-18051

The fracture toughness of high strength engineering alloys containing short cracks 08 p1058 A83-21655

Fracture test methods 10 p1392 A83-25319

DESYNCHRONIZED SLEEP
U RAPID EYE MOVEMENT STATE

DETECTION
NT AIRCRAFT DETECTION
NT CORRELATION DETECTION
NT FOREST FIRE DETECTION
NT HAZE DETECTION
NT MISSILE DETECTION
NT RADAR DETECTION
NT REMOTE SENSING
NT SIGNAL DETECTION
NT TARGET RECOGNITION
NT ULTRASONIC FLAW DETECTION

DETECTORS
A 4-quadrant lightning detector 11 p1571 A83-27009

Low light level detectors in astronomy --- Book 21 p3226 A83-45095

DETERIORATION
A method of predicting the performance deterioration of a compressor cascade due to sand erosion [AIAA PAPER 83-0178] 05 p0596 A83-16572

Performance deterioration on turbomachinery with presence of solid particles 11 p1525 A83-27477

DETERMINATION
U MEASUREMENT

DETONABLE GAS MIXTURES
Weak and strong ignition. I - Numerical simulations of shock tube experiments 02 p0152 A83-12078

Weak and strong ignition. II - Sensitivity of the hydrogen-oxygen system 02 p0152 A83-12079

Hydrogen oxidation kinetics in gaseous detonations 02 p0153 A83-13097

Numerical modeling of the development of a combustion nucleus in a closed vessel under the conditions of natural convection 03 p0295 A83-14054

The surface temperature and the concentration of alumina particles in the detonation products of a gas mixture 03 p0295 A83-14063

The propagation of powerful blast waves in a gas-particle mixture 07 p0878 A83-19633

Ignition, propagation, and structure of deflagrations and detonations - Stable species concentration of a turbulent premixed methane-air flame 07 p0878 A83-19835

Effects of chemical reactions in the shocked gas on the propagation characteristics of cylindrical detonation waves 07 p0878 A83-19838

The spectral characteristics and nature of the radiation emitted by explosions in an enclosed region. II - Explosions of mixtures of CS₂/O₂ = 1/4 07 p0880 A83-19962

The dependence of the permeability of detonation-sprayed aluminum oxide coatings on the composition of the detonation gas mixture 07 p0900 A83-20693

CO₂-laser-induced deflagration of fuel/oxygen mixtures 07 p0882 A83-20732

Energy and entropy balances in a combustion chamber - Analytical solution 09 p1226 A83-24363

Estimation of pressure fields in combustion of vapour clouds 09 p1262 A83-24419

Temperature measurement of detonation using UV-absorption of O₂ 10 p1421 A83-26137

Generation of the patterns in gaseous detonations 10 p1415 A83-26158

A study on the hydrogen-oxygen diffusion flame in high speed flow 10 p1391 A83-26199

Regular reflection of detonation waves 16 p2350 A83-35723

Laminar boundary layers behind detonation waves 18 p2684 A83-39450

DETONATION
Transition from combustion to detonation in solid explosives 02 p0151 A83-11659

Burning to detonation transition in porous beds of a high-energy propellant 03 p0303 A83-14846

Detonation properties of 1,3,5-triamino-2,4,6-trinitrobenzene when impacted by hypervelocity projectiles 04 p0464 A83-15473

Detonation driven induction generators with parallel and antiparallel external and induced magnetic fields 05 p0689 A83-17371

Detonation --- Russian book 06 p0726 A83-18001

The critical pressure of initiation of powdered explosives 06 p0726 A83-18003

Some aspects of the detonation of explosive mixtures 06 p0726 A83-18005

Detonation characteristics of retarded explosives 06 p0726 A83-18006

The methods and results of the diagnosis of the detonation spraying of coatings 07 p0940 A83-20692

Phase transformations during detonation spraying and their effect on the wear resistance of aluminum oxide coatings 07 p0900 A83-20694

Shock initiation of high explosives 13 p1826 A83-31722

Detonation propulsion experiments and theory --- for spacecraft in high pressure planetary atmospheres 21 p3105 A83-45585

The detonation-spraying method of coating deposition, its current status and prospects for further development 24 p3590 A83-49083

The effect of additives on the critical diameter of detonation of nitroesters 24 p3557 A83-49791

DETONATION WAVES
A quasi-steady divergent detonation wave 01 p0047 A83-10920

Instrumentation for the measurement of blast waves attenuated by water sheets 01 p0052 A83-11062

Numerical analysis of the dispersion of detonation products 01 p0047 A83-11274

Hydrogen oxidation kinetics in gaseous detonations 02 p0153 A83-13097

Numerical simulation of a light-absorbing plasma at a shock front 03 p0396 A83-13177

The autonomy of shock waves in a sonic downstream state - The case of detonation 03 p0320 A83-14570

On the existence of a second detonation front for two-phase mixtures of hydrogen-oxygen-nitrogen and aluminum particles 04 p0457 A83-16444

A study of detonation initiation in TNT and TH 50/50 by shock waves of short duration 06 p0726 A83-18004

The effect of aluminum on the detonation wave profile of greatly diluted Hexogen 06 p0726 A83-18007

Estimating the propelling action of explosives 06 p0726 A83-18009

Effects of chemical reactions in the shocked gas on the propagation characteristics of cylindrical detonation waves 07 p0878 A83-19838

The distribution of the state variables in the products of spherical detonation 07 p0880 A83-19963

Structure of a detonation front 07 p0926 A83-20898

Fiber optics as light-detector probes in the accurate measurement of detonation velocities in two-phase fuel-air explosions 08 p1095 A83-22498

Techniques in the formulation and handling of composite and very-low-density explosives 09 p1242 A83-23845

The occurrence of detonation in the case of the incidence of a shock wave on a wall 09 p1226 A83-24236

Blast waves in free air 09 p1264 A83-25272

Generation of the patterns in gaseous detonations 10 p1415 A83-26158

Propagation of two-dimensional nonsteady detonation in a channel with backward-facing step 10 p1416 A83-26165

On the loss of stability of detonation waves in long heterogeneous-explosive charges 13 p1843 A83-31372

A case of quasi-isentropic compression of a medium 14 p2027 A83-32094

A study of the steady-state reaction-zone structure of a homogeneous and a heterogeneous explosive 14 p1991 A83-33383

An asymptotic theory of deflagrations and detonations. I - The steady solutions 16 p2325 A83-35694

Regular reflection of detonation waves 16 p2350 A83-35723

A non-similar solution for blast waves driven by an asymptotic piston expansion [AIAA PAPER 83-0496] 16 p2351 A83-36057

Interaction of oblique shock and detonatin waves 16 p2352 A83-36088

Magnetogasdynamic effects on the growth of transverse acoustic waves in a reacting gas 18 p2744 A83-39149

High-speed laser visualization of detonation-sprayed particles 18 p2688 A83-39172

Laminar boundary layers behind detonation waves 18 p2684 A83-39450

A self-similar flow behind a spherical shock wave with thermal radiation. I 18 p2745 A83-39737

Self-similar flows behind cylindrical shock waves in magnetogasdynamics 18 p2746 A83-39750

- Cylindrically converging shock and detonation waves
18 p2687 A83-40502
- Flame velocity for the onset of detonation
19 p2820 A83-40861
- Gasdynamic approach to solving the problem of the fracture of a brittle rod by an intense shock wave
19 p2845 A83-41888
- The blast wave propagating in a moving medium with variable density
21 p3227 A83-44293
- Fast deflagration waves
21 p3130 A83-44462
- Effect of the number density of heterogeneities on the critical diameter of condensed explosives
22 p3266 A83-46007
- Detonic research infrared radiometer with nanosecond response
23 p3454 A83-47648
- On the transformation of planar detonation to cylindrical detonation
23 p3430 A83-48157
- Process of the transition from none-dimensional explosion-induced flows to one-dimensional ones
23 p3452 A83-48660
- Development of perturbations at the detonation front
24 p3556 A83-49787
- Critical diameter of the steady detonation of highly dense explosives - The effect of the shell
24 p3557 A83-49789
- Ignition of crystalline hexogen with adiabatic compression of the adjacent gas pocket
24 p3557 A83-49792
- A study of the acceleration and heating dynamics of metal particles behind a detonation wave
24 p3557 A83-49793
- Possibility of the steady detonation of condensed explosives in charges without shells in connection with the properties of shock polars
24 p3557 A83-49797
- Parameters and regimes of the detonation of condensed explosives
24 p3557 A83-49798
- A pulsating detonation front
24 p3557 A83-49799
- Critical phenomena in detonation associated with an impulse loss
24 p3557 A83-49800
- Simulation of detonation cell kinematics using two-dimensional reactive blast waves
24 p3580 A83-49836
- Deformation of a cylindrical shell during an explosion in the vicinity of a concentrated explosive charge
24 p3595 A83-49905
- DEUTERIDES**
- Surface chemistry of deuterated molecules --- of interstellar molecular clouds
11 p1677 A83-27678
- The nuclear hyperfine structure of deuterated ammonia
13 p1958 A83-31730
- DEUTERIUM**
- The isotopic composition of cyclonic precipitation
02 p0216 A83-12952
- Radial ion acceleration at a virtual cathode formed in a neutral gas by a relativistic electron beam
03 p0392 A83-13178
- Deuterium enrichments in type 3 ordinary chondrites
04 p0562 A83-15355
- The galactic abundance of deuterium - A test for cosmological models
06 p0837 A83-19215
- A few relevant facts on the problem of the origin of the solar system
06 p0842 A83-19454
- FM spectroscopy detection of stimulated Raman gain
07 p0937 A83-20798
- Resonance absorption measurements of atom concentrations in reacting gas mixtures. IX - Measurements of O atoms in oxidation of H₂ and D₂
10 p1480 A83-26182
- High-resolution spectroscopy of selected absorption lines toward quasi-stellar objects. I - Lyman-alpha toward PHL 957
10 p1512 A83-26703
- High orbital angular momentum states in H₂ and D₂
11 p1653 A83-27491
- Cosmological implications of helium and deuterium abundances on Jupiter and Saturn
11 p1686 A83-28388
- The ratio of deuterium to hydrogen in interstellar space.
V The line of sight to Epsilon Persei
12 p1790 A83-28882
- Observation of autoionising states in H₂ and D₂ above 30 eV by electron impact
18 p2743 A83-40317
- Deuterium transport and trapping in aluminum alloys
18 p2669 A83-40629
- Evidence of hourly variations in the deuterium Lyman line profiles toward Epsilon Persei
20 p3065 A83-42389
- Energy barrier height variations of Pd-Si Schottky diodes induced by deuterium
21 p3123 A83-43849
- D/H ratios in meteorites - Some results and implications
21 p3240 A83-44232
- Stellar deuterium abundance - A new upper limit in Canopus
21 p3228 A83-44406
- Nonthermal escape of hydrogen and deuterium from Venus and implications for loss of water
22 p3387 A83-47081
- The reaction H₂ + D₂ - 2HD - A long history of erroneous interpretation of shock tube results
23 p3429 A83-47633
- Laboratory measurements of D/H ratios in interplanetary dust
23 p3529 A83-48084
- Pregalactic synthesis of deuterium
24 p3665 A83-50037
- Helium and deuterium in the outer solar system
24 p3665 A83-50042
- Observations of interstellar deuterium
24 p3667 A83-50059
- DEUTERIUM COMPOUNDS**
- NT DEUTERIDES**
- NT DEUTERIUM FLUORIDES**
- NT HEAVY WATER**
- Some H/D exchange reactions involved in the deuteration of interstellar molecules
04 p0552 A83-15614
- High-resolution rotation-vibration spectra of HDO in the region of the nu₁ and 2nu₂ bands
06 p0835 A83-19006
- High power pulsed FIR laser lines from CD₃OH
10 p1425 A83-25429
- Line positions and strengths in the /001/, /110/, and /030/ bands of HDO
10 p1481 A83-26877
- Time-resolved infrared-ultraviolet double resonance spectroscopy of formaldehyde
11 p1653 A83-27528
- A statistical analysis of Na I D1 profile fluctuations at the center of the solar disk. I - Data reduction and resolvable velocities
13 p1963 A83-29981
- The absorption spectrum of (C-12)D₂ in the 1.06-micron region
14 p2048 A83-32833
- Preparation of nanogram quantities of deuteromethane for stable carbon isotope analysis --- using mass spectrometer
15 p2166 A83-35256
- Measurement of the J = 0-1 rotational transitions of three isotopes of ArD(+)
20 p3045 A83-42642
- A long-range atmospheric tracer field test
24 p3616 A83-50190
- DEUTERIUM FLUORIDE LASERS**
- U DF LASERS**
- DEUTERIUM FLUORIDES**
- A shock tube study of DF dissociation
10 p1389 A83-25561
- DEUTERIUM OXIDES**
- U HEAVY WATER**
- DEUTERIUM PLASMA**
- Anode-plasma parameters of a high-voltage glow discharge of about 150 kV
18 p2746 A83-39863
- Effects of ion-acoustic instability on light ion beam transport in deuterium channels
22 p3362 A83-46019
- DEUTERONS**
- Identification of deuterium ions in the ionosphere of Venus
23 p3529 A83-47864
- DEVELOPERS (PHOTOGRAPHY)**
- U PHOTOGRAPHIC DEVELOPERS**
- DEVELOPING NATIONS**
- Photointerpretation, remote sensing, and photogrammetric elements applied to road-planning studies
02 p0198 A83-11866
- One third of the world - A review of Pacific islands telecommunications requirements
07 p1001 A83-19655
- The development of a sampling procedure for urban land use mapping from aerial photographs - A study in Calabar, Nigeria
08 p1172 A83-21960
- Low cost monitoring of land use and soil erosion in the humid tropics - An application of aerial photography
08 p1129 A83-21967
- Remote sensing of arid and semi-arid lands; Proceedings of the International Symposium on Remote Sensing of Environment, Cairo, Egypt, January 19-25, 1982. Volumes 1 & 2
09 p1284 A83-24526
- Remote sensing in the global monitoring of environment
09 p1284 A83-24527
- Resource inventories of arid and semi-arid lands using Landsat
09 p1284 A83-24534
- Landsat as an aid in consulting projects in the Middle East and Africa some examples of applications on VBB/SWECO projects
09 p1289 A83-24592
- Solar photovoltaic systems in the development of Papua New Guinea
14 p2038 A83-32198
- Field trial of rural solar photovoltaic system
14 p2039 A83-32199
- Satellite data as a basis for planning studies of infrastructure and related rural development in Atacora Province, Benin, West Africa
15 p2181 A83-33560
- Metropolitan expansion and population density patterns in third world supercities as indicated by integration of space and ground data
15 p2182 A83-33573
- Assessing the user environment for Landsat in developing countries
15 p2187 A83-35277
- Satellite remote sensing needs and applications in Less Developed Countries
16 p2370 A83-35424
- Land resources inventory assessment by Landsat image processing case study - Kano State, Nigeria (Africa)
17 p2532 A83-38354
- Barriers and possibilities for the use of airships in developing countries
17 p2460 A83-38905
- Role and impact of space research in developing countries; Proceedings of the Workshop, Ottawa, Canada, May 16-June 2, 1982
18 p2787 A83-39825
- Transfer of space science and technology - A Third World point of view
18 p2751 A83-39826
- A critical look at space technology and the developing world
18 p2752 A83-39827
- The evolution of space technology and its economic impact Reflection on the transposition of the European model in the countries of the Third World
18 p2752 A83-39828
- Space sciences in developing countries - The Indian experience
18 p2787 A83-39829
- The status of space science and technology in developed countries - The European experience
18 p2643 A83-39830
- Impact of space research and technology on small countries --- developing nations
18 p2705 A83-39831
- Status of space science and technology - An Australian perspective
18 p2787 A83-39832
- Basic space sciences - The Latin American experience
18 p2787 A83-39833
- Basic space sciences in Africa
18 p2788 A83-39835
- Impact of space research and technology on small countries
18 p2788 A83-39836
- Balloon research and cooperative programmes
18 p2631 A83-39838
- Establishing satellite data bases in developing countries - A critical view
18 p2706 A83-39839
- Meteorological satellites and cooperative programmes
18 p2725 A83-39840
- The role of space communication in promoting national development with specific reference to experiments conducted in India
18 p2752 A83-39841
- Earth survey satellites and cooperative programmes
18 p2706 A83-39843
- New telecommunications for the developing world
21 p3220 A83-44530
- Status of flat-plate photovoltaic systems for applications in developing countries
22 p3318 A83-46096
- DEVITRIFICATION**
- U CRYSTALLIZATION**
- DEW POINT**
- Short-term prediction of convective development using dew point convergence
13 p1887 A83-30557
- DEWAR SYSTEMS**
- U CRYOGENIC EQUIPMENT**
- DEXTRANS**
- Hemodynamic effects of Dextran 40 on hemorrhagic shock during hyperbaria and hyperbaric hyperoxia
14 p2064 A83-32687
- DF**
- U DEUTERIUM FLUORIDES**
- DF LASERS**
- Absorption spectra of deuterated water at DF laser wavelengths
02 p0211 A83-12601
- Flowfield experiments on a DF chemical laser
07 p0932 A83-19815
- Rotational nonequilibrium influences in CW HF/DF chemical lasers
10 p1429 A83-26167
- Shock/Ludwig-tube driven HF laser
10 p1429 A83-26169
- High performance DF-CO₂ chain-reaction laser
11 p1579 A83-27572
- Nascent DF energy distributions for the D + F₂ and F + D₂ reactions
11 p1580 A83-27578
- Effects of optical irregularities in the active medium on angular divergence of a beam in a CW supersonic DF-CO₂ chemical laser
13 p1851 A83-30819
- The status of rotational nonequilibrium in HF chemical lasers
17 p2513 A83-37196
- [AIAA PAPER 83-1699]
Absorption of H₂S at DF laser wavelengths
19 p2852 A83-41108
- Formation of free fluorine atoms by laser-collisional initiation of the CH₃F + F₂ reaction
20 p2997 A83-43789
- Narrow output line from a distributed-feedback dye laser with broad-spectrum pumping
22 p3299 A83-46784
- DHC 4 AIRCRAFT**
- Spatial calibration of a multispectral data base --- of airborne scanner systems
08 p1045 A83-22882
- DIABETES MELLITUS**
- The phospholipid composition of blood platelets in healthy individuals and in individuals with diabetes mellitus
05 p0674 A83-17205

DIAGNOSIS

The electrical position of the heart and variants of a normal cartogram of 35 leads 01 p0083 A83-10511

The integral EKG, the ventricular gradient, the differential EKG, and their diagnostic possibilities 03 p0379 A83-13621

The diagnostic significance of the integral assessment of myocardial ischemia in patients with ischemic heart disease for the computerized monitoring of the EKG during the treadmill test 03 p0379 A83-13624

The diagnostic possibilities of ultrasonic sector scanning of the heart 03 p0380 A83-13625

An approach for determining common cholesterol and its structural-functional fractions in erythrocytes on the basis of the digitonin method 03 p0375 A83-14327

Mathematical methods for optimizing treatment and diagnosis in cardiology /current status and future prospects/ 05 p0674 A83-17199

The importance of laboratory data for the differentiation of mild and moderately severe craniocerebral injuries 06 p0798 A83-18977

Otoneurological symptoms in the differential diagnosis of mild and moderately severe craniocerebral injuries 06 p0798 A83-18979

The diagnosis of latent vestibular disorders in patients with otosclerosis 07 p0978 A83-20877

Discordance of exercise thallium testing with coronary arteriography in patients with atypical presentations 07 p0978 A83-21053

Determination of the mean time of the absence of defects in objects with a variable period of utilization and diagnostics 08 p1113 A83-22122

An investigation of human blood, erythrocytes, and plasma using the method of ESR at 77 K 08 p1150 A83-23022

Echocardiography in assessment of cardiovascular problems of Air Force personnel 09 p1323 A83-24006

The identification of the variation of atherosclerosis plaques by invasive and non-invasive methods 11 p1643 A83-28760

The value of echocardiography in diagnosing diseases of the cardiovascular system 11 p1643 A83-28801

The formalization of the choice of the acoustic stimulus parameters in a small automatic device for the examination and diagnosis of the functional condition of the auditory analyzer 14 p2073 A83-33312

The use of the sound loading test in comprehensive audiological diagnosis 15 p2213 A83-34973

Methods for determining the extent of myocardial infarction 16 p2400 A83-36837

The application of noninvasive methods for the study of patients with ischemic heart disease 16 p2400 A83-36838

Subjective and objective methods in the diagnosis of fatigue 17 p2559 A83-38184

The diagnosis of changes in the vessels and membranes of eyes using fluorescent angiography 17 p2560 A83-38202

The diagnostics of the subclinical stage of vibration sickness 17 p2561 A83-38926

The differential diagnosis of functional murmurs and defects of the heart using ultrasonic pulse Doppler detection 18 p2734 A83-40541

The diagnostic possibilities of myocardial scintigraphy using TI-201 in the case of acute myocardial infarction 18 p2735 A83-40545

Stereotaxic computer tomography 18 p2737 A83-40576

Computer tomography for tumors of the posterior regions of the third ventricle and the pineal body 18 p2733 A83-40577

Scintigraphy with (Tc-99)-pyrophosphate and computer tomography in the diagnosis of tumors of the cranial bone 19 p2881 A83-41140

A test of the lateralization of ultrasound in the diagnosis of early forms of neurosensory amblycusia 19 p2881 A83-41444

The diagnostic value of ambulatory electrocardiographic monitoring 19 p2882 A83-41450

Optoelectronic methods for increasing the information content of ultrasonic ocular scanograms 19 p2882 A83-41459

The classification of positional nystagmus and the positional vestibular syndrome 19 p2883 A83-41834

The clinical picture of covered perforated gastric and duodenal ulcers in young individuals 19 p2884 A83-42025

DIAGRAMS

NT BENDING DIAGRAMS

NT BLOCK DIAGRAMS

NT CIRCUIT DIAGRAMS

NT CREEP DIAGRAMS

NT HERTZSPRUNG-RUSSELL DIAGRAM

NT NYQUIST DIAGRAM

NT PHASE DIAGRAMS

NT S-N DIAGRAMS

NT STRESS-STRAIN DIAGRAMS

A diagram technique in the theory of relaxation processes 04 p0544 A83-15912

DIALYSIS

NT ELECTRODIALYSIS

DIAMAGNETISM

Diamagnetic force on a flux tube 06 p0856 A83-19509

Ejection of magnetic fields from the sun - Acceleration of a solar wind containing diamagnetic plasmoids 07 p1037 A83-21144

Diamagnetic aspects of the coronal transient phenomenon 15 p2285 A83-35230

DIAMETERS

The diameter of 88 Thisbe from its occultation of SAO 187124 09 p1352 A83-23324

Free rotation of a circular ring about a diameter 09 p1339 A83-24820

Diameter distribution and Sigma-D relation of SNRs in M31 and M33 12 p1785 A83-28894

Stellar interferometry - Diameters and effective temperatures of five giant stars 13 p1941 A83-31564

Stellar diameter measurements by two-aperture interferometry in the infrared 14 p2099 A83-33208

Standard photometric diameters of galaxies 24 p3645 A83-49842

DIAMINES

Network structure description and analysis of amine-cured epoxy matrices 22 p3262 A83-46283

The curing of a bisphenol A-type epoxy resin with 1,8 diamino-p-menthane 22 p3270 A83-46905

DIAMOND WINGS

U LOW ASPECT RATIO WINGS

U SWEPT WINGS

DIAMONDS

Bipolar transistor action in ion implanted diamond 02 p0168 A83-12286

Polishing and testing of aspheric diamond-turned surfaces 02 p0239 A83-12720

Primitive helium in diamonds 08 p1136 A83-22687

Subnanosecond time-resolved photoconductive response of semiconducting diamond 08 p1169 A83-22761

Diamond machining of infrared refractors utilizing two-axis machine tool technology 08 p1112 A83-22868

Testing diamond turned aspheric optics using computer-generated holographic /CGH/ interferometry 08 p1103 A83-22869

Diamond /111/ studied by electron energy loss spectroscopy in the characteristic loss region 10 p1390 A83-25675

Archean diamond-bearing mantle in the expanding-earth model 13 p1873 A83-30020

Will diamond transform under Megabar pressures? 16 p2421 A83-36563

Carbon isotopic variation in spectral type II diamonds 17 p2545 A83-38603

Carbon isotopic variation within individual diamonds 17 p2545 A83-38604

Evaluation of the efficiency of the diamond burnishing of gas-turbine-engine parts 18 p2695 A83-39511

The effect of the crystallization conditions of diamonds under high-temperature shock compression on their optical properties 18 p2750 A83-39531

High voltage optoelectronic switching in diamond 18 p2677 A83-40066

A diamond opto-electronic switch 19 p2838 A83-41182

DIAPHRAGMS (MECHANICS)

Electromagnetic-wave scattering by a finite system of ideally conducting rods with dielectric diaphragms 01 p0030 A83-10405

A special silicon diaphragm pressure sensor with high output and high accuracy 02 p0180 A83-12811

A shock tube driver with a 'cyclone' separator 10 p1380 A83-26130

Radially pleated diaphragms for Stirling engines 11 p1588 A83-27283

Speckle-shear interferometry with double Dove prisms 21 p3136 A83-44189

Experimental study of the dynamic loading of metal disks 21 p3161 A83-45152

DIASTOLE

Changes in diastolic coronary resistance during submaximal exercise in conditioned dogs 13 p1898 A83-30504

The effect of calcium on the diastolic phases in healthy individuals and in patients with heart failure 18 p2735 A83-40549

The mechanism of the heart diastole 19 p2871 A83-40815

Effect of exercise on left ventricular diastolic filling in athletes and nonathletes 20 p3034 A83-43477

DIASTOLIC PRESSURE

The circadian rhythm of the body temperature, arterial pressure, and heart rate 12 p1765 A83-29311

DIATOMIC GASES

Asymptotic solution of the diatomic Boltzmann equation 07 p0926 A83-20531

Vibrational relaxation in gas systems containing sources of vibrationally excited molecules --- Russian book 10 p1490 A83-25600

On the viscosity of monatomic and diatomic gases at intermediate temperatures 13 p1931 A83-30098

Characteristics of the vibrational relaxation of a system of anharmonic oscillators 21 p3202 A83-45384

DIATOMIC MOLECULES

Spectral study of the D-X system of the diatomic mercury chloride molecule 01 p0105 A83-10204

The asymptotic theory of resonance charge exchange between diatomics 06 p0807 A83-18044

A semiclassical study of laser-induced atomic fluorescence from Na2, K2 and NaK [AD-A127849] 07 p0991 A83-21051

Theoretical determination of the X 1Sigma g + potential of Cs2 using relativistic effective core potentials 07 p0991 A83-21055

Doppler-free polarization spectroscopy of diatomic molecules in flame reactions 08 p1056 A83-21884

Semiclassical vibrational spectra for diatomic molecules - Application to HF, CO, and NO 09 p1342 A83-24131

Electron thermalization in gases. V - Diatomic molecules H2, N2, and CO 09 p1342 A83-24132

An approximate method for calculating the ultraviolet radiation of diatomic molecules at low pressures 09 p1342 A83-24231

The properties of dimers and their role in the atmosphere 10 p1448 A83-25522

Elastic scattering of electrons by N2, O2, and CO in the energy range 0.1-3 keV 10 p1479 A83-25557

Studies of the vibrational relaxation of diatomic molecules in a shock heated molecular beam and its application to ionization by electron impact 10 p1479 A83-26179

The thermodynamic properties of diatomic molecules at elevated temperatures - Role of continuum and metastable states 11 p1665 A83-27495

Pulsed optical-optical double resonance spectroscopy of the gerade excited states of 7Li2 11 p1653 A83-27524

Diatomic molecules as storage media for high energy lasers 11 p1580 A83-27573

Diatomic molecules and metallic adhesion, cohesion, and chemisorption - A single binding-energy relation 13 p1817 A83-30921

On the nature of the bonding in Cu2 - An ab initio viewpoint 13 p1818 A83-31809

Resonance-enhanced coherent anti-Stokes Raman scattering in C2 [ONERA, TP NO. 1983-1] 16 p2327 A83-36416

Astrophysical molecules of A1H and CaH - RKR potential and dissociation energies --- Rydberg-Klein-Rees 18 p2764 A83-39192

Molecular dynamical studies of the dissociation of a diatomic molecular crystal. I - Energy exchange in rapid exothermic reactions 20 p2950 A83-42628

Electron affinities of the alkali dimers - Na2, K2, and Rb2 20 p3045 A83-42635

Low temperature operation of an S2 laser using radio frequency simmer discharges 20 p2994 A83-42794

A unified molecular force field via a model theory of isoelectronic diatomic molecules 21 p3202 A83-43961

Abundances of carbon-bearing diatomic molecules in diffuse interstellar clouds 22 p3377 A83-46259

Expectation values for Morse oscillators 23 p3506 A83-47629

DICHLORIDES

Annealing of Hg2Cl2 crystals - Project of the experiment --- in space and terrestrial conditions 18 p2644 A83-39913

The Atmospheric Lifetime Experiment. IV - Results for CF2Cl2 based on three years data 24 p3606 A83-49331

DICHROISM

A study of silicon and GaAs solar cells, and their optical coupling by means of a dichroic mirror --- French thesis 02 p0200 A83-11764

Induced dichroism in passive laser switches 07 p0934 A83-20111

Use of magnetic circular dichroism for nondestructive measurement of charge carrier concentration in wideband semiconductors 08 p1113 A83-22406

Double-square frequency-selective surfaces and their equivalent circuit 21 p3121 A83-44958

- Performance of two tripole arrays as frequency-selective surfaces 23 p3444 A83-48710
- DICHROMATES**
U CHROMATES
- DICKE RADIOMETERS**
The theory of Dicke superradiation - An exact solution of the quasi-one-dimensional quantum model 05 p0682 A83-16890
- DICKE TYPE RADIOMETERS**
U DICKE RADIOMETERS
- DICTIONARIES**
Dictionary of the nomenclature of celestial objects 01 p0114 A83-10151
- DIELECTRIC CONSTANT**
U PERMITTIVITY
- DIELECTRIC MATERIALS**
U DIELECTRICS
- DIELECTRIC PERMEABILITY**
Epsilon nonlinearity of doped triglycine sulfate crystals depending on conditions of growth 13 p1930 A83-31307
- DIELECTRIC POLARIZATION**
Phenomenological theory of shock-induced polarization. I 13 p1915 A83-31383
- DIELECTRIC PROPERTIES**
NT PERMITTIVITY
Dielectric and optical measurements from 30 to 1000 GHz 07 p0929 A83-20185
The dielectric properties of anhydride-cured epoxy potting compounds 07 p0899 A83-20458
The dielectric properties of liquids in the submillimeter range 08 p1082 A83-23151
Dielectric lens shaping and coma-correction zoning. I - Analysis 09 p1248 A83-23813
Ferromagnetics --- Russian book 09 p1349 A83-23817
Average dielectric properties of discrete random media using multiple scattering theory 10 p1411 A83-26851
Viscosity phenomena in ferroelectrics and ferroelastics 13 p1930 A83-31309
Dielectric currents in the low-latitude boundary layer and geomagnetic tail 15 p2202 A83-34734
Electrical response of relaxing dielectrics compressed by arbitrary stress pulses 16 p2418 A83-35440
Dielectric relaxation in insulators slightly damaged by stress pulses 16 p2418 A83-35441
On the dielectric properties of semiconducting materials as obtained from impedance measurements on Schottky barriers 16 p2419 A83-35618
An electrogasdynamic boundary layer on a dielectric plate 17 p2505 A83-37523
Thermal dielectric breakdown with cylindrical electrodes 17 p2498 A83-38216
Dynamic dielectric characterization of the cure process LARC-160 19 p2823 A83-41030
Cure monitoring and control with combined dielectric/temperature probes 19 p2823 A83-41031
Capacitance transducers for nondestructive testing (2nd revised and enlarged edition) 21 p3135 A83-43920
High- ϵ dielectric disk resonators 22 p3276 A83-45669
Dielectric surface discharges - Effects of combined low-energy and high-energy incident electrons 24 p3572 A83-48900
- DIELECTRICS**
NT LOSSLESS MATERIALS
NT RADOME MATERIALS
Remote sensing of dielectric media with periodic rough surfaces --- microwave scattering from farmlands 01 p0055 A83-10106
Fundamental relations for radiowave ellipsometry of 'thin metal film on dielectric substrate' system 01 p0049 A83-10362
Electromagnetic-wave scattering by a finite system of ideally conducting rods with dielectric diaphragms 01 p0030 A83-10405
Calculation of axisymmetric H-modes in dielectric resonators by the integral-equation method 01 p0035 A83-10406
Radar resonance reflection from sets of plane dielectric layers --- and possible applications 01 p0031 A83-10614
Self-focusing of ion cyclotron waves in a plasma 01 p0106 A83-10618
Ferroelectricity and coherent phonon generation in piezoelectric composition-modulated structures 01 p0108 A83-10622
Practical problems in the time-domain probing of lossy dielectric media 01 p0034 A83-11372
Crosspolarisation in scattering at low frequencies 02 p0163 A83-11553
Transmission of pulsed signals with linearly changing frequency through a delay system with a dielectric 02 p0166 A83-11693

- Ellipsometric study of silicon nitride on gallium arsenide 02 p0242 A83-11812
Mechanisms of defect formation and migration in semiconductors --- Russian book 02 p0242 A83-11924
Curved dielectric optical waveguides with reduced transition losses 02 p0235 A83-12005
Thin film pressure transducers and their applications 02 p0178 A83-12346
Radiation patterns of interfacial dipole antennas 02 p0165 A83-12631
Physically motivated approximations in some inverse scattering problems 02 p0233 A83-12632
Dielectrophoretic, thermal instability in a spherical shell of fluid 02 p0174 A83-12983
Mode selection with a three-layer dielectric rib waveguide 03 p0393 A83-13762
Integrated-optical techniques for near-millimeter-wave technology 03 p0309 A83-13779
Recent advances in dielectric millimeter wave integrated circuits 03 p0309 A83-13781
Effective propagation constants for coherent electromagnetic wave propagation in media embedded with dielectric scatters 03 p0304 A83-13915
Input impedance and mutual coupling of rectangular microstrip antennas 03 p0313 A83-14021
Transition radiation caused by a chiral plate --- electromagnetic field due to charged particle traversing plate 03 p0313 A83-14025
Radiation pattern computation of a spherical lens using Mie series 03 p0306 A83-14027
Radiation from aperture antennas radiating in the presence of a dielectric sphere 03 p0307 A83-14031
Bipolar transistor oscillators for measurements of material parameters 03 p0338 A83-14300
A novel method to analyze electromagnetic scattering of complex objects 03 p0308 A83-14548
Attenuation and localization of an electromagnetic wave on the surface of a cylindrical conductor 04 p0465 A83-15072
Numerical analysis of shielded dielectric resonators including substrate, support disc and tuning post 04 p0470 A83-15237
Characteristics of the cross-polarized radiation of dielectric radio lenses 04 p0466 A83-15718
Simultaneous diffraction of two waves at a reflection volume hologram 04 p0535 A83-15795
Focussing of submillimeter radiation guided by a dielectric sheet 04 p0535 A83-15810
Investigations of optically pumped submillimeter wave laser modes 04 p0485 A83-15814
Spectroscopic measurements on discharges along a dielectric surface 04 p0538 A83-16061
Amplification of light in inhomogeneous waveguides with an adjacent active medium 05 p0685 A83-17076
Propagation and conversion of light waves in corrugated waveguide structures 05 p0685 A83-17081
Perturbation analysis of corrugated dielectric waveguide with application to millimeter-wave filters 05 p0624 A83-17280
Analysis, design and characteristics of X-band dielectric wedge waveguide antennas 05 p0622 A83-17341
Electrical conductivity and discharge in spacecraft thermal control dielectrics 05 p0618 A83-17491
Characteristics of RF resulting from dielectric discharges 05 p0626 A83-17494
Optical measurement of the velocity of dielectric surface arcs 05 p0618 A83-17495
Effect of laser produced pinholes upon the charging characteristics of spacecraft thermal control surfaces 05 p0608 A83-17499
Charging and discharging characteristics of dielectric materials exposed to low- and mid-energy electrons 05 p0618 A83-17500
Radiation-induced charge dynamics in dielectrics 05 p0618 A83-17502
A radiation-hardened 1K-bit dielectrically isolated random access memory 05 p0628 A83-17518
Ionization-induced breakdown and conductivity of satellite dielectrics 05 p0618 A83-17520
Pulsed radio emission during the crystallization of water and certain dielectrics --- for remote sensing 05 p0645 A83-17633
Electromagnetic scattering from two dielectric spheres - Comparison between theory and experiment 05 p0683 A83-17883
Coupling and imaging of Gaussian beams in parallel dielectric slab waveguides 06 p0749 A83-17967
Characteristics and design of high-gain dielectric circular antennas operated in X-band 06 p0736 A83-18425
High frequency scattering by a thin dielectric slab 06 p0737 A83-18611
Dielectric image line groove antennas for millimeterwaves 06 p0738 A83-18613

- Q-band dielectric-loaded short backfire antenna arrays 06 p0738 A83-18615
A family of two-reflector antennas with identical dielectric primary feeds 06 p0742 A83-18664
A modified rhombic dielectric plate antenna 06 p0742 A83-18665
Aberrative properties of a planar dielectric sheet --- effects on antenna radiation patterns 06 p0742 A83-18675
Plane wave scattering by a thick lossy dielectric half-plane 06 p0805 A83-18714
Scattering of a plane wave by a rotating dielectric sphere 06 p0805 A83-18741
The influence of losses of hollow dielectric waveguides on the mode shape 06 p0810 A83-18906
Propagation of submillimeter radiation from the output of a hollow dielectric waveguide 06 p0767 A83-19362
Fixation of bubbles and drops of specified shapes in a liquid dielectric by an electric field 06 p0813 A83-19434
The use of a dielectric sensor to record pressure pulses 06 p0764 A83-19566
Power flux distribution of the guided modes of an asymmetric dielectric slab waveguide 06 p0811 A83-19600
Three-dimensional nonlinear quasi-monochromatic waves in piezodielectrics with allowance for linear viscosity and heat conduction 06 p0807 A83-19603
Artificial microburst dielectrics produced in laser-sol interactions 07 p0994 A83-20050
Optical properties of narrowband spectral filter coatings related to layer structure and preparation 07 p0993 A83-20157
Dielectric waveguide - A low-cost technology for millimetre wave integrated circuits 07 p0919 A83-20179
An integral equation method for electromagnetic scattering of guided modes by boundary deformations of dielectric slab waveguides 07 p0913 A83-20367
High-energy solid-state electronics --- Russian book 07 p0919 A83-20388
Materials characterization and fracture mechanics of a space grade dielectric silicone insulation 07 p0899 A83-20456
Concerning the radiation pattern in the problem of the excitation of an array of circular dielectric cylinders by a local source 07 p0915 A83-20871
Improved equivalent network analysis of a dielectric waveguide placed on a ground plane 07 p0922 A83-21173
Bends in nonradiative dielectric waveguides 07 p0922 A83-21526
Modal solutions of active dielectric waveguides by approximate methods 07 p0924 A83-21626
Scattering of surface waves in semi-infinite slab dielectric waveguide 08 p1160 A83-22052
Electromagnetic treatment of discontinuities in dielectric waveguides - Application to dielectric resonators --- French thesis 08 p1079 A83-22085
Thin double layer approximation for electrophoresis and dielectric response 08 p1056 A83-22221
Propagation constants for linearly polarized modes of arbitrarily shaped optical fibers or dielectric waveguides 08 p1166 A83-22639
Mode selection with a three-layer dielectric rib waveguide 08 p1077 A83-22669
Diffraction of an electric polarized wave by a dielectric wedge 08 p1161 A83-22742
Stripline dipole with dielectric covering 09 p1243 A83-23381
Diffraction of electromagnetic waves by a two-dimensional periodic waveguide-dielectric array 09 p1244 A83-23451
Experimental study of junctions of dielectric strip waveguides in the millimeter-wave range 09 p1253 A83-23471
The propagation of a surface wave along a dielectric waveguide with a jump-like change of the parameters. I - A solution by the method of factorization 09 p1253 A83-23488
Matching properties of arbitrarily large dielectric covered phased arrays 09 p1246 A83-23782
High frequency scattering by a thin lossless dielectric slab 09 p1247 A83-23790
Scattering and absorption characteristics of lossy dielectric objects exposed to the near fields of aperture sources --- of electromagnetic radiation 09 p1324 A83-23791
Variational calculations of electromagnetic scattering from two randomly separated Rayleigh dielectric cylinders 09 p1249 A83-24102
Dielectronic satellite spectra of Mg XI with inner-shell and helium-like excitation rates - Application to solar observations 09 p1368 A83-24471

Wave diffraction by an open waveguide structure with a homogeneous laminar filler 09 p1250 A83-24912

Surface wave scattering at the junction of two dielectric waveguides 09 p1256 A83-24917

The propagation of a surface wave along a dielectric waveguide with a jump-like change of the parameters. II - Solution by the variational method 09 p1257 A83-25084

Design of waveguide dielectric filters based on beyond-the-cutoff waveguides 09 p1257 A83-25164

On the spectrum of complex waves of a circular dielectric waveguide 09 p1257 A83-25165

Design of dielectric ridge waveguides for millimeter-wave integrated circuits 10 p1408 A83-25804

Design of dielectric grating antennas for millimeter-wave applications 10 p1402 A83-25816

Submicrometer periodicity gratings as artificial anisotropic dielectrics 10 p1482 A83-25978

Sharp bends with low losses in dielectric optical waveguides 10 p1483 A83-26637

Comparison of the methods used to describe the process of scattering of a guided mode by an inhomogeneous part of a dielectric waveguide 10 p1484 A83-26672

A new procedure for improving the solution stability and extending the frequency range of the EBCM --- Extended Boundary Condition Method for EM absorption and scattering in biological dielectric objects 10 p1460 A83-26839

Linear and nonlinear waves in liquid dielectrics 11 p1658 A83-27711

Analysis of waveguides of complex cross section with inhomogeneous dielectric-slab loading 11 p1560 A83-27928

Electromagnetic-wave diffraction by a doubly periodic array of semiinfinite dielectric rods 11 p1556 A83-27961

Induction method for the continuous registration of the velocity of condensed media in shock-wave processes 11 p1574 A83-28542

Rectangular dielectric resonator antenna [AD-A129976] 11 p1558 A83-28608

Measurement of the indices of refraction and the absorption coefficients of dielectric materials in the millimeter wave region 11 p1664 A83-28717

The generation of electric currents by the turbulent flow of dielectric liquids. I - Long pipes 12 p1722 A83-29089

The generation of electric currents by the turbulent flow of dielectric liquids. II - Pipes of finite length 12 p1722 A83-29158

Diffraction of electromagnetic waves by a thick dielectric comb and a grating made of rectangular bars 12 p1718 A83-29262

Temperature distribution in uniform and layered microwave absorbers in waveguide 12 p1720 A83-29441

Shielded dielectric resonators 12 p1720 A83-29461

New dielectric waveguide structure for millimetre-wave optical control 12 p1720 A83-29466

Travelling waves in a dielectric slab with an abrupt change in thickness 12 p1775 A83-29597

Crystal structure of the microwave dielectric resonator Ba₂Ti₉O₂₀ 12 p1717 A83-29973

The nonorthogonal-series method in problems of electromagnetic wave diffraction by coated bodies 13 p1827 A83-30096

Nondestructive measurement of a dielectric layer using surface electromagnetic waves 13 p1831 A83-30227

Determination of loaded, unloaded, and external quality factors of a dielectric resonator coupled to a microstrip line 13 p1831 A83-30228

Optimization of an electrodynamic basis for determination of the resonant frequencies of microwave cavities partially filled with a dielectric 13 p1831 A83-30234

A note concerning modes in dielectric waveguide gratings for filter applications 13 p1831 A83-30237

Electrodynamic characteristics of the natural modes of a circular waveguide with a dielectric rod 13 p1833 A83-30713

Determination of the effect of losses in the dielectric substrate on the radiation of a plane logarithmic spiral with a screen 13 p1828 A83-30715

Investigation of the band characteristics of waveguide radiators coupled with dielectric-cylinder filters 13 p1834 A83-30732

Radiation pressure and 360 deg scattering diagrams for infinite cylinders 13 p1829 A83-30748

Guided-wave experiments with dielectric waveguides having finite periodic corrugation 13 p1836 A83-31145

Large signal design of GaAs FET oscillators using input dielectric resonators 13 p1836 A83-31149

Three-dimensional higher-order mode analysis of transition from waveguide to shielded dielectric image line 13 p1837 A83-31771

Loss reduction in curved dielectric optical slab waveguide 13 p1922 A83-31775

An investigation of the effect of polarizing radiation, scattered by an optically inhomogeneous layer, on the quality of its holographic image 14 p2019 A83-32126

Characterization of planar discontinuities in open dielectric waveguides - Application to the study of passive microwave components 14 p2006 A83-32418

Low pressure nitrided-oxide as a thin gate dielectric for MOSFET's 14 p2006 A83-32640

A study of the coupled and continuous vibrational states of dielectric crystals by Raman spectroscopy 14 p2092 A83-33039

Short cavity InGaAsP/InP lasers with dielectric mirrors 14 p2027 A83-33436

On the complex resonant frequency of open dielectric resonators 14 p2008 A83-33458

Wave scattering and guidance by dielectric waveguides with periodic surfaces 15 p2229 A83-33537

Orthogonality and nonnormalization of radiation modes in dielectric waveguides - An alternative derivation 15 p2229 A83-33538

Microwave nondestructive testing methods --- Book 15 p2173 A83-33624

Coherent anti-Stokes Raman scattering in thin-film dielectric waveguides 15 p2230 A83-33756

Diffraction by an ideally conducting wedge with a dielectric coating on one edge 15 p2145 A83-34710

Change formulas in the theory of dielectric waveguides 15 p2153 A83-34877

Shaped lens antennas 15 p2146 A83-35081

Radiation efficiency of a slot in a conducting screen coated with a dielectric layer 15 p2147 A83-35155

Radiation from a dielectric-filled flange waveguide 15 p2153 A83-35156

The resonant cylindrical dielectric cavity antenna 15 p2148 A83-35175

The synthesis of surface reactance using an artificial dielectric 15 p2154 A83-35182

Multiple scattering theory for waves in discrete random media and comparison with experiments 16 p2406 A83-35406

Numerical calculations of low-frequency TE fields in arbitrarily shaped inhomogeneous lossy dielectric cylinders 16 p2407 A83-35407

Simultaneously tunable two-wavelength dye laser using two dielectric multilayer filters 16 p2361 A83-36754

Coherence properties and cutoff wavelength determination in dielectric waveguides 16 p2413 A83-36766

High-power, long-pulse CO₂ laser transversely excited by a damped oscillating discharge through dielectric electrodes 17 p2513 A83-36998

Dielectric resonator stabilization of a Gunn diode oscillator 17 p2495 A83-37021

Nonradiative dielectric waveguide circuit components 17 p2497 A83-37761

Experimental study of submillimeter radiation patterns produced by HCN waveguide laser and HCN laser-excited oversized hollow dielectric waveguide 17 p2514 A83-37763

Grating diplexer using dielectric waveguides for millimeter wavelengths 17 p2498 A83-38038

Electric discharge pulses in irradiated solid dielectrics in space 17 p2480 A83-38040

Numerical method for the analysis of an inhomogeneous multiconductor line 17 p2499 A83-38481

General boundary conditions for the wave equation around non-homogeneous scatterers 17 p2576 A83-38618

Instability of charged-particle fluxes through a statistically inhomogeneous medium 17 p2584 A83-38980

Hybrid guided HE-modes of a symmetric dielectric slab waveguide 17 p2500 A83-38984

Dipole resonance of a plasma ellipsoid in a dielectric shell with allowance for radiation damping 17 p2584 A83-38985

Natural and forced oscillations of open resonance systems based on dielectric disk resonators 17 p2500 A83-38986

Bandpass filters based on multilayer dielectric structures 18 p2676 A83-39432

Computation of the dielectric tensor of a Maxwellian plasma 18 p2747 A83-40075

Solid-state microwave oscillator with a multilayer dielectric structure 18 p2677 A83-40090

A millimeter-wave oscillator, stabilized by a disk-shaped dielectric resonator 18 p2677 A83-40095

Low insertion-loss, temperature-compensated dielectric filters for microwave integrated circuits 18 p2679 A83-40393

Complex waves on shielded lossless rectangular dielectric image guide 18 p2679 A83-40399

Impurity scattering in partially dielectricized superconductors 19 p2904 A83-41000

Computer assisted dielectric cure monitoring in material quality and cure process control 19 p2823 A83-41029

Dielectrically loaded corrugated waveguide - Variational analysis of a nonstandard eigenproblem 19 p2838 A83-41084

A proposal of a new dielectric resonator construction for MIC's 19 p2838 A83-41085

Investigation of anisotropic films by a resonance method 19 p2840 A83-41802

Investigation of a probe sensor of electric field strength with a Pockels-effect cell 19 p2849 A83-41816

The dispersion properties of artificial anisotropic dielectrics 19 p2841 A83-41818

Acoustoelectric oscillations in a bounded active stratified-periodic medium 19 p2841 A83-41820

Gyromagnetic perturbation of a slow-wave structure partially loaded by a dielectric 19 p2841 A83-41824

A technique for analyzing planar dielectric waveguides for millimeter wave integrated circuits 19 p2841 A83-42164

Nonreciprocal phaseshift in ferrite loaded rectangular waveguides 19 p2841 A83-42165

Simultaneous determination of refractive index and size of spherical dielectric particles from light scattering data 20 p3046 A83-42214

Dielectric image line leaky wave antenna for broadside radiation 20 p2964 A83-42491

Reactively RF magnetron sputtered AlN films as gate dielectric 20 p2967 A83-42609

Parametric excitation of electrohydrodynamic surface waves 20 p3051 A83-43671

An iterative extended boundary condition method for solving the absorption characteristics of lossy dielectric objects of large aspect ratios --- under exposure to incident plane wave radiation 21 p3189 A83-43833

Coupling characteristics of nonradiative dielectric waveguides 21 p3122 A83-43834

The excitation of microwaves by a relativistic electron beam in a dielectric-lined waveguide 21 p3124 A83-43945

A simple passive technique for generating short pulses 21 p3143 A83-44187

Dielectric multilayer thin-film filters for WDM transmission systems --- Wavelength Division Multiplexing in optical fiber communication 21 p3204 A83-44213

Coupled-mode analysis of anisotropic dielectric planar branching waveguides 21 p3205 A83-44227

Nature of radiation effects in layered MOS structures (review) 21 p3217 A83-44592

Optical extinction theorem in the nonlinear theory of optical multistability 21 p3206 A83-44803

A numerical study of the interaction of a plane electromagnetic wave with a closed dielectric screen 22 p3271 A83-45649

A theory of the diffraction of light by shear waves in an isotropic solid dielectric 22 p3355 A83-45651

Resonance phenomena in multiple-boundary periodic metal-dielectric systems 22 p3277 A83-45676

A below-cutoff resonator partially filled with a ferrite dielectric 22 p3277 A83-45678

A millimeter-band waveguide-dielectric filter with increased sensitivity 22 p3277 A83-45684

Cerenkov radiation from periodic electron bunches 22 p3277 A83-45928

Enhanced Raman scattering from silicon microstructure 22 p3356 A83-45968

Effects of gaps on long range surface plasmon polaritons 22 p3363 A83-46271

Radiation effects in dielectrically enhanced reflectance mirrors 22 p3357 A83-46620

Enhancement of high-harmonic gyrotron gain by a dielectric rod 22 p3279 A83-46750

A bistable hybrid optical device using an integrated modulator with an induced dielectric channel 23 p3507 A83-47561

Scattering of electromagnetic waves by the edge of a semiinfinite dielectric slab imbedded in an ideally conducting half-space 23 p3445 A83-48486

A two-mode waveguide-dielectric resonator below cutoff 23 p3445 A83-48489

Highly stable FET DROs using new linear dielectric resonator material --- Dielectric Resonator Oscillators 23 p3446 A83-48723

Simple expressions for predicting substrate, volume, and interface absorption and reflective phase shifts in high-reflectance quarter-wave stacks at oblique angles of incidence 24 p3623 A83-48977

The metal-insulator transition in transition-metal compounds 24 p3635 A83-49074

The metal-insulator transition in oxides and sulfides of 3d metals 24 p3635 A83-49075

- Direct methods for calculating irregular waveguides with inhomogeneous dielectric filler 24 p3573 A83-49268
On the effect of the correlation in phonon motion on the viscosity of impure dielectrics 24 p3636 A83-49755
Behaviour of guided modes in systems of parallelly located transmission lines on dielectric substrates 24 p3574 A83-49969

DIELECTRONIC SATELLITE LINES**U RESONANCE LINES****DIENES****NT BUTADIENE****DIES**

- An analysis of the stress-strain state in the internal deformation zone during hot forming 12 p1733 A83-29280
Flow state of composite materials in the forging die during the molding process 18 p2661 A83-40281
Concentration of elastic stresses near dies, cracks, thin inclusions, and reinforcements --- Russian book 21 p3160 A83-45025

DIESEL ENGINES

- Powder selection for plasma sprayed coatings in diesel engine applications 06 p0733 A83-19109
Hot-film anemometer measurements in a starting turbulent jet 07 p0924 A83-19826
A wind-isolated energy system for Grimsey, Iceland 08 p1130 A83-22021
U.S. Army/Detroit Diesel Allison Advanced Technology Demonstrator Engine 09 p1208 A83-24836
A systems analysis comparing conventional and hydrogen powered rail locomotives 11 p1667 A83-27213
Program overview and diesel/flywheel hybrid power train design - Fibre composite flywheel development program for road vehicle applications 11 p1667 A83-27306
Progressive phase trends in multi-degree-of-freedom systems 12 p1774 A83-28850
A new approach to soot control in Diesel engines by fuel-drop charging 13 p1859 A83-31225
New concept in hovercraft design diesel versus gas turbines 15 p2242 A83-34860
US Army Tank-Automotive Command (TACOM) adiabatic engine program [AIAA PAPER 83-1283] 16 p2362 A83-36321
An update on high output lightweight diesel engines for aircraft applications [AIAA PAPER 83-1339] 16 p2311 A83-36925
Hydrogen aspiration in a direct injection type diesel engine its effects on smoke and other engine performance parameters 20 p2998 A83-42956
Hovercraft auxiliary power units (APUs) 21 p3147 A83-44372
Wind turbine generator interaction with diesel generators on an isolated power system 21 p3167 A83-44673
Use of flight engine technology in stationary industrial gas turbines and diesel motors 23 p3464 A83-47203

DIESEL FUELS

- Catalytic combustion with steam injection [ASME PAPER 82-JPGC-GT-23] 09 p1294 A83-25271
Propagation at 10 microns through smoke produced by atmospheric combustion of diesel fuel 10 p1447 A83-26641
The properties of fuel fractions obtained by the hydrogenation of Kansk-Achinsk coal 10 p1401 A83-26920
Measured effect of wind generation on the fuel consumption of an isolated diesel power system 16 p2371 A83-36410

DIETS

- The lipidic balance of technical flight personnel between 50 and 55 years old in commercial and civil aviation 06 p0798 A83-18340
Potentiation of oxygen toxicity in rats by dietary protein or amino acid deficiency 13 p1897 A83-30461
Chronic low-sodium diet in rats - Hormonal and physiological effects during exercise in the heat 22 p3346 A83-45994

DIFFERENCE EQUATIONS

- Conservative difference schemes for equations of a viscous incompressible fluid in curvilinear orthogonal coordinates 01 p0047 A83-11267
Difference approximations of derivatives and polynomial splines 01 p1012 A83-11270
General hyperbolic difference formulas for linear and quasilinear hyperbolic equations 02 p0231 A83-12905
Methods for solving Euler's equations for airfoil and intake flow 03 p0279 A83-14604
A new automatic mesh selection strategy for the solution of boundary value problems with selfadaptive difference methods 03 p0389 A83-14610
Algorithms for advection and shock problems 03 p0322 A83-14611

- State description for the root-signal set of median filters 05 p0680 A83-16912
On the analytic treatment of non-integrable difference equations 06 p0805 A83-18327
Stability theory of difference approximations for multidimensional initial-boundary value problems 07 p0986 A83-20504
Organization of a computational process for solving systems of difference equations in a parallel grid processor 08 p1154 A83-22180
Frequency limitations and optimal step size for the two-point central difference derivative algorithm with applications to human eye movement data 10 p1460 A83-26650

- An implicit scheme for nonlinear evolution equations 12 p1776 A83-29641

- Classification of difference schemes of gas dynamics by the method of differential approximation. I - One-dimensional case 13 p1844 A83-31592

- On the construction of K-consistent difference schemes of gas dynamics 13 p1913 A83-31594

- On a numerical method for the synthesis of optimal control for nonlinear dynamic systems 14 p2076 A83-32965

- The assessment of numerical diffusion in upwind difference calculations of turbulent recirculating flows 15 p2155 A83-33667

- Application of the separation singularity difference method to inlet aerodynamic design 16 p2290 A83-35827

- Method of random image synthesis by means of computer 17 p2563 A83-38032

- Piecewise polynomial Galerkin approximation to invariant densities of one-dimensional difference equations 17 p2571 A83-38037

- Computational errors of difference schemes for calculating discontinuous solutions [AIAA PAPER 83-1938] 18 p2740 A83-39388

- New diagonal implicit scheme for the compressible Navier-Stokes equations [AIAA PAPER 83-1891] 18 p2683 A83-39407

- Variational-difference method of calculating critical loads for shells of revolution 18 p2698 A83-39506

- Relaxation method for solving a difference biharmonic equation 21 p3198 A83-45214

- On an efficient algorithm for the Dirichlet variational-difference problem 21 p3198 A83-45215

- Application of the method of parallel chords to solve implicit difference equations of magnetohydrodynamics 21 p3215 A83-45219

- Quaternion algebra applied to polygon theory in three dimensional space --- Thesis 22 p3353 A83-46697

DIFFERENCES

- Stability of an economical difference scheme for the solution of a boundary value problem of diffraction 01 p0104 A83-11271

DIFFERENTIAL ALGEBRA

- U DIFFERENTIAL CALCULUS
U MATRICES (MATHEMATICS)

DIFFERENTIAL AMPLIFIERS

- Partial processing of information aboard a satellite via double differentiation of the volt-ampere characteristics by electronic means 10 p1386 A83-25338
Topological synthesis of RC active circuits using the root-hodograph method 15 p2154 A83-35266

DIFFERENTIAL ANALYZERS**U ANALOG COMPUTERS****DIFFERENTIAL CALCULUS**

- Derivative calculation from finite element solutions 03 p0389 A83-14696
Thermoelastic moduli of fiber-reinforced composites by differential scheme 04 p0494 A83-14975
Post-instability in continuous systems. I - Failure of differentiability of solutions in continuum mechanics 11 p1649 A83-28089
Calculation of critical branching points in two-parameter bifurcation problems 13 p1913 A83-31371

DIFFERENTIAL EQUATIONS

- NT BIHARMONIC EQUATIONS
NT BURGER EQUATION
NT CAUCHY-RIEMANN EQUATIONS
NT CHANDRASEKHAR EQUATION
NT COSINE SERIES
NT DUFFING DIFFERENTIAL EQUATION
NT ELLIPTIC DIFFERENTIAL EQUATIONS
NT FALKNER-SKAN EQUATION
NT FOKKER-PLANCK EQUATION
NT GAUSS EQUATION
NT HELMHOLTZ VORTICITY EQUATION
NT HYPERBOLIC DIFFERENTIAL EQUATIONS
NT LAME WAVE EQUATIONS
NT LIOUVILLE EQUATIONS
NT MONGE-AMPERE EQUATION
NT PARABOLIC DIFFERENTIAL EQUATIONS
NT PARTIAL DIFFERENTIAL EQUATIONS

- NT POISSON EQUATION
NT VLASOV EQUATIONS
NT VORTICITY EQUATIONS

- The method of differential amplitude approximation for solving dynamic viscoelasticity problems 01 p0059 A83-10683

- Approximation of an integral exponent by means of quadrature formulas 01 p0102 A83-11263

- Boundary value problems for a class of equations containing a derivative with respect to time 01 p0102 A83-11315

- Concerning a method for solving boundary value problems for third-order equations 01 p0103 A83-11316

- Linear systems of ordinary differential equations 02 p0231 A83-11640

- Second-order sensitivity derivatives in structural analysis 03 p0338 A83-13149

- Eigenvalue problems on infinite intervals 03 p0387 A83-13569

- Inclusions and separation of the zeros of exponential trinomials with constant coefficients 03 p0389 A83-14510

- Computation of eigenvalues using two-point boundary value problem codes 03 p0389 A83-14712

- The reduction of a system of differential equations for the motion of a satellite that is dynamically compressed relative to the center of mass to a special form 04 p0451 A83-15771

- On a modified differential approximation method in radiative gas dynamics 04 p0544 A83-15819

- Two person zero sum differential games and singular surfaces [AIAA PAPER 83-0572] 05 p0682 A83-16798

- Deterministic and stochastic differential games [AIAA PAPER 83-0573] 05 p0682 A83-16799

- Asymptotics of the solution of the Cauchy problem for a class of singularly perturbed systems of integro-differential equations 05 p0682 A83-17833

- Numerical analysis of the behavior of a quasi-periodic solution to a periodic differential equation by means of a method of sections 06 p0804 A83-17974

- Application of the small-parameter method to the numerical solution of differential equations 07 p0986 A83-20309

- Analytical methods of nonlinear mechanics --- Russian book 07 p0989 A83-20377

- Block Runge-Kutta methods for the numerical integration of initial value problems in ordinary differential equations. I - The nonstiff case. II - The stiff case 07 p0986 A83-20506

- Additive Runge-Kutta methods for stiff ordinary differential equations 07 p0986 A83-20507

- Numerical solution of multiparameter eigenvalue problems 08 p1159 A83-21863

- Application of a direct procedure for numerical handling of self-adjoint, positive definite eigenvalue problems for linear normal differential equations with piecewise continuous coefficient functions 08 p1159 A83-21864

- Pointwise bounds for the solution of a nonlinear problem in heat conduction 08 p1083 A83-21866

- Linear functional differential equations as semigroups on product spaces 08 p1156 A83-22025

- The maximum principle for a system of equations of energy and nonstationary radiative transfer 09 p1338 A83-23569

- The representation of a matricant of a linearized system of differential equations of motion in a field of forces possessing potential 09 p1338 A83-23865

- Fuzzy differential equations and their possible use in meteorology 09 p1316 A83-25145

- Qualitative methods of investigating nonlinear differential equations and nonlinear oscillations --- Russian book 09 p1340 A83-25262

- Closed geodesics 09 p1340 A83-25263

- A block-by-block method for the numerical solution of Volterra delay integro-differential equations 10 p1470 A83-25590

- Reduced first order differential equation with optimal control finite element penalty functions --- applied to convection-radiation heat transfer and boundary layer problems 12 p1721 A83-28853

- General solution of the Clemmow differential equation in a relativistic cold plasma 12 p1780 A83-29028

- Solution of the fundamental control problem /FCP/ --- for aircraft 12 p1704 A83-29291

- The use of the Walsh transformation to solve systems of linear differential equations with variable coefficients 12 p1771 A83-29344

- Stability of periodic solutions under stochastic perturbations 12 p1771 A83-29599

- Stability analysis of numerical boundary conditions and implicit difference approximations for hyperbolic equations 12 p1772 A83-29650

- Boundary treatments for implicit solutions to Euler and Navier-Stokes equations 12 p1725 A83-29655
- Numerical calculations of discontinuities by shape preserving splines 12 p1773 A83-29670
- Nonclassical thermoelasticity equations for piecewise homogeneous media 13 p1865 A83-30051
- Interpolational and extremal properties of L-spline functions --- Thesis 13 p1912 A83-30148
- Volterra-like expansions for solutions of nonlinear integral equations and nonlinear differential equations 13 p1912 A83-30872
- On the Benjamin-Ono equation-method for exact solution 14 p2077 A83-32513
- The use of the asymptotic method of short-time space for solving systems of differential and algebraic equations 14 p2078 A83-33010
- Equations of the necessary extremum condition for a class of incorrect extreme-value problems --- for optimization of aerodynamic configurations 14 p1972 A83-33011
- Exact finite elements for conduction and convection 15 p2160 A83-34263
- Integro-differential equations of the dynamics of elastic systems in nonstationary flows --- flight vehicle dynamics in turbulent nonseparated flow 16 p2366 A83-35933
- Estimation of the value of the small parameter in a linear singularly perturbed system of differential equations 17 p2571 A83-38074
- Basic differential models for coordinate generation 17 p2572 A83-38779
- On a multipoint boundary value problem for integrodifferential-extremal equations with deviating argument of ultraneutral type 17 p2575 A83-38866
- Monotonicity methods for nonlinear singular integral and integro-differential equations 18 p2740 A83-39987
- Organization of a microprocessor computing system for the numerical integration of linear differential equations 18 p2738 A83-40094
- Boundary conditions of the second-order differential equation and the Riccati equation 20 p3041 A83-42525
- Reduction of the number of variables in a differential system --- of Pfaff equations 20 p3041 A83-42916
- Generation of a countable set of homoclinic flows through bifurcation 20 p3043 A83-43564
- On the integrability of some generalized Lotka-Volterra systems 20 p3043 A83-43567
- The method of equivalent systems in the theory of wave propagation --- Russian book 21 p3199 A83-43906
- Subspace iteration for the eigenvalue problems of self-adjoint differential equations and its applications in the vibration analysis of structures 21 p3151 A83-44109
- Accelerated method for the computer calculation of a nonlinear oscillatory system 21 p3200 A83-45212
- Toolkit for nonlinear dynamics 22 p3354 A83-45697
- On closed form solutions for the differential matrix Riccati equation problem 22 p3352 A83-46366
- Systems of singular perturbation problems with a first order turning point 22 p3353 A83-46922
- Singular perturbation problems with a singularity of the second kind 22 p3307 A83-46923
- Matrix methods of cosmic ray propagation 23 p3540 A83-47759
- DIFFERENTIAL GEOMETRY**
- NT LIE GROUPS
- NT RIEMANN MANIFOLD
- NT SPINOR GROUPS
- NT TENSOR ANALYSIS
- Geometrically derived difference formulae for the numerical integration of trajectory problems 02 p0231 A83-12928
- Moving frames and prolongation algebras 07 p0988 A83-21043
- One pursuer and two evaders on the line - A stochastic pursuit-evasion differential game 12 p1773 A83-29245
- A geometric model of space-time and matter 14 p2083 A83-33043
- Theorems of stability in geometry and analysis --- Russian book 21 p3199 A83-43905
- Existence of the solution of Szebehely's equation in three dimensions using a two-parametric family of orbits 24 p3638 A83-48767
- DIFFERENTIAL INTERFEROMETRY**
- Performance of LDI in predicting density profiles of compressible boundary layers --- laser differential interferometry 01 p0053 A83-11078
- Application of optical fibers to wide-band differential interferometry 07 p0993 A83-20175
- Cross-talk fiber-optic temperature sensor 07 p0930 A83-20833
- Tracking geosynchronous satellites by very-long-baseline interferometry 21 p3098 A83-45468
- Analysis of two-beam interferometry for bulk wave measurements 22 p3294 A83-46839
- DIFFERENTIAL OPERATORS**
- U DIFFERENTIAL EQUATIONS
- U OPERATORS (MATHEMATICS)
- DIFFERENTIAL PULSE CODE MODULATION**
- An adaptive DPCM algorithm for predicting contours in NTSC composite video signals 01 p0034 A83-11429
- An adaptive DPCM encoder for NTSC composite video signals 07 p0907 A83-19731
- Design of Pel Adaptive DPCM coding based upon image partition 08 p1077 A83-22623
- Hardware-constrained hybrid coding of video imagery 08 p1077 A83-22731
- Image quality experiments for TV reconnaissance at reduced transmission bandwidth 08 p1105 A83-22902
- Error statistics in delta modulation and differential pulse code modulation communication systems 10 p1407 A83-26938
- Two-dimensional DPCM image transmission over fading channels 13 p1827 A83-30222
- DPCM encoding of regenerative composite sources 15 p2221 A83-35102
- An efficient source coding technique for data compression of multilevel digitized images 15 p2223 A83-35146
- Constrained transform coding and surface fitting 16 p2405 A83-36610
- Stationary transform processing of digital images for data compression 19 p2847 A83-41105
- Effects of mismatch and low rate for coding of autoregressive data by tree-searched DPCM 19 p2832 A83-41387
- Two-dimensional hybrid block transform/DPCM coding of images 19 p2832 A83-41388
- DIFFERENTIAL THERMAL ANALYSIS**
- Thermal characterization of polymeric materials --- Book 01 p0027 A83-11502
- Structural and thermal analysis studies of magnetron sputter-deposited amorphous metallic /Mo0.6Ru0.4/82B18 films 02 p0243 A83-12649
- Studies on thermal decomposition of double-base propellants 09 p1243 A83-24884
- Thermal radiation effects in thermal conductivity measurements - Analysis and remedies 12 p1722 A83-29153
- DIFFERENTIATION (BIOLOGY)**
- The functional differentiation of the vascular smooth muscle cells and the basal tonus of the vessels 01 p0078 A83-10486
- The significance of cellular contacts for the differentiation of precursor cells of hemopoietic stroma in long-term bone marrow cultures 01 p0080 A83-10548
- Disturbance of cell differentiation during microsporangogenesis in Tradescantia paludosa due to the change in orientation of the mitotic spindle in the first postmeiotic mitosis under the effect of space flight factors 02 p0219 A83-11650
- The hair cell's of the inner ear 04 p0521 A83-16046
- The structure of DNA and the transformation of cells 06 p0795 A83-18980
- The genetics of immunoglobulins - Successes and problems 06 p0795 A83-18982
- Peculiarities of genital organ formation in Arabidopsis thaliana (L) heyhn. under spaceflight conditions 19 p2878 A83-42055
- DIFFRACTION**
- NT ELECTRON DIFFRACTION
- NT FRESNEL DIFFRACTION
- NT NEUTRON DIFFRACTION
- NT PULSE DIFFRACTION
- NT WAVE DIFFRACTION
- NT X RAY DIFFRACTION
- Diffraction models of slot and strip elements of microwave integrated circuits with suspended substrates for the purpose of computer-aided design 06 p0750 A83-17986
- Diffraction on a segmented telescope mirror 17 p2580 A83-38567
- Diffraction of an atomic beam by standing-wave radiation 19 p2852 A83-40966
- Wide field of view head-up displays 21 p3091 A83-44690
- DIFFRACTION GRATINGS**
- U GRATINGS (SPECTRA)
- DIFFRACTION LIMITED CAMERAS**
- Probabilistic diffraction limited imaging through turbulence 08 p1164 A83-22361
- Probability of diffraction-limited images in infrared through turbulence experimental results 10 p1420 A83-25839
- Interferometry with the multiple mirror telescope and conventional telescopes 10 p1495 A83-25845

- How to achieve diffraction limited resolution with large space telescopes 11 p1656 A83-27727
- IR-camera for GIRL --- German Infrared Laboratory 18 p2691 A83-40449

DIFFRACTION PATHS

- Determining basic parameters of radio meteors based on amplitude characteristics with weakened diffraction 03 p0403 A83-13374
- Nonlinear analysis of a diffraction-radiation generator with two field spots 09 p1270 A83-23472
- Acoustooptical device with extremely high contrast ratio 10 p1424 A83-26872

DIFFRACTION PATTERNS**NT RAINBOWS**

- Crystal rocking-diffraction of backscattered and transmitted electrons as an alternative method to conventional electron diffraction, especially for obtaining energy-filtered diffraction pictures --- German thesis 01 p0048 A83-10174
- Coherent image fringe contrast measurement with sensing arrays 01 p0051 A83-10863
- Surface recession measurements using a projected fringe technique 01 p0053 A83-11077
- Quantitative deformation measurement with virtual-image holographic interferometry --- Dutch thesis 02 p0176 A83-11897
- Optical biasing on quasi-interferometry with coded correlation filtering 02 p0177 A83-12306
- Extension of oblique-incidence method to photo-orthotropic elasticity 03 p0344 A83-14941
- Second-harmonic diffraction field in nonlinear propagation of transversely limited surface acoustic wave beams 04 p0473 A83-16058
- The intricate patterns of stress 05 p0654 A83-17282

- Diffraction-field structure in the Fraunhofer zone 06 p0809 A83-17983

- A method for calculating the surface displacement field of a solid body from double-exposure holographic interferometry data 06 p0764 A83-19315
- A study on the measurement of particle size distribution with laser diffraction systems 07 p0929 A83-20286
- Electromagnetic-field diffraction by a system of curvilinear screens 07 p0914 A83-20774
- One form of apodization of telescopes 07 p1009 A83-21275

- K-determination in mixed-mode crack problems by interferometry 08 p1117 A83-21720
- A survey of recent developments in the evaluation of stress intensity factors from isochromatic crack-tip fringe patterns 08 p1119 A83-21786
- Assessment of surface texture from analysis of the signal visibility of a laser Doppler anemometer 08 p1091 A83-22003

- Orthogonal in-plane and out-of-plane fringe maps in holographic interferometry 08 p1101 A83-22635
- The dependence of the sharpness of an interference pattern on the quantum state of the electromagnetic field 09 p1346 A83-25092

- Enhancement of fringe visibility in a fibre interferometer 10 p1481 A83-25405
- Imaging by dilute apertures in the presence of atmospheric turbulence 10 p1482 A83-25840
- Diffraction coupled phase-locked semiconductor laser array 10 p1430 A83-26203

- Contributions of amplitude and phase modulation to diffraction efficiency in three-dimensional reflective holograms 10 p1422 A83-26470
- Appearance aspects of isochromatic mode-1 crack tip fringe loops 11 p1593 A83-27862
- Influence of stacking defects with low probability on X-ray diffraction patterns /Survey/ 11 p1664 A83-28617
- Automated digital processing of interferograms --- Thesis 11 p1575 A83-28650
- Complex interferometry 14 p2021 A83-32911
- Real-time fringe-pattern analysis 14 p2021 A83-32912

- The radiation of charges moving in the vicinity of individual localized inhomogeneities 14 p2007 A83-33299
- Lensless Fourier holography applied to nondestructive testing - Experimental results 15 p2163 A83-33754
- Fabry-Perot interferograms for amplitude and phase modulated light 15 p2163 A83-33755
- Polarization effects in the diffraction of electromagnetic waves - The role of disclinations 16 p2407 A83-35639

- The properties of holographic gratings in silicon crystals recorded by means of ultrashort light pulses 16 p2412 A83-35944

- Analysis of photoelastic fringes in wave propagation problems 17 p2519 A83-37392
- Phenomenon of interference between two light beams propagating in optical fibers having a large path difference 17 p2580 A83-37744

- Measurement of movements in the ionosphere using radio reflections 18 p2712 A83-39070
- Automatic fringe analysis with a computer image-processing system 19 p2847 A83-41106
- Temporal and interference fringe analysis of excimer TEM01 zone laser modes 21 p3142 A83-43874
- Recent high-resolution resonant refractivity studies of a sodium-seeded flame 21 p3110 A83-44680
- Detection of hidden diffractors by coherence measurements 21 p3208 A83-44841
- Application of Winograd's fast Fourier transform (FFT) to the calculation of diffraction optical transfer function (OTF) 21 p3208 A83-44843
- Toward a pure shear specimen for K11c determination 21 p3156 A83-44897
- Estimation of the angular position of an optical source whose emission is received by a photodetector array 22 p3355 A83-45691
- Fringe pattern recognition and interpolation using nonlinear regression analysis 22 p3352 A83-46838
- Volume vector holograms with opposed reference beams 23 p3453 A83-47168
- Holographic plasma interferometry in the infrared spectrum. II - Using nonlinear effects to increase the sensitivity 23 p3454 A83-47554
- Design of an experiment to determine deformations using holographic interferometry 23 p3454 A83-47560
- Vernier fringe-counting device for laser wavelength measurements 23 p3454 A83-47645
- On-line calibration technique for laser diffraction droplet sizing instruments [ASME PAPER 83-GT-232] 23 p3458 A83-48028
- Applications of the Fraunhofer-diffraction method for plasma-wave measurements 24 p3633 A83-49900
- DIFFRACTION PROPAGATION**
- An attenuation function for multiple knife-edge diffraction --- of electromagnetic waves in communication systems 02 p0165 A83-12629
- Multiple diffraction effects in VHF propagation 06 p0746 A83-18725
- Experimental study of hysteresis phenomena in a diffraction-radiation generator 06 p0754 A83-19335
- Formation of a non-Gaussian intensity profile in a laser with inhomogeneous mirrors 07 p0934 A83-20110
- A millimeter-wave amplifier based on a diffraction-radiation generator electrodynamic system 10 p1435 A83-26963
- On a method of the asymptotic theory of diffraction 14 p2079 A83-32104
- Theory of acoustooptic interaction in active resonators 19 p2854 A83-41774
- Diffracting optics 21 p3207 A83-44837
- Characteristics of diffraction radiation generators with multiple electron drift 22 p3294 A83-45664
- DIFFRACTION TELESCOPES**
- U SPECTROSCOPIC TELESCOPES**
- DIFFRACTOMETERS**
- An optical technique for measuring fiber orientation in short fiber composites 22 p3290 A83-46298
- DIFFUSE RADIATION**
- Study of diffuse cosmic and atmospheric gamma radiation using a spark chamber in the energy range 4 MeV-100 MeV 02 p0271 A83-11606
- Diffuse galactic gamma-ray line emission from nucleosynthetic Fe-60, Al-26, and Na-22 - Preliminary limits from HEAO 3 03 p0439 A83-14210
- Application of Monte Carlo techniques to transient thermal modeling of cavity radiometers having diffuse-specular surfaces 03 p0289 A83-14652
- Transmittance of reflected diffuse radiation --- for solar collectors 06 p0780 A83-18564
- Identification of some diffuse interstellar features 06 p0835 A83-18895
- A point method for three-dimensional photoelasticity - Application 06 p0777 A83-19200
- Diffusion of a light wave in a polarized state propagating through the atmosphere 07 p0993 A83-21083
- Optical and radio structure of the quasar PKS 0812 + 02 07 p1019 A83-21105
- The diffuse radio aurora and field-aligned currents 07 p0964 A83-21182
- The diffuse gamma radiation from the local spiral arm 10 p1523 A83-25483
- Far-ultraviolet diffuse emission lines from the interstellar medium 10 p1511 A83-26406
- The diffuse interstellar feature at 4430 A and interstellar extinction in the far-ultraviolet 10 p1516 A83-26756
- Anomalous diffuse features in dust-embedded stars 11 p1682 A83-28289
- Automated processing of holographic interferograms in determining the deformations of diffusely reflecting objects 11 p1574 A83-28499
- Diffuse reflection and transmission of radiation for Rayleigh phase function 12 p1775 A83-29077

- Investigation of the atmospheric aerosols by the visible and IR channels of the AVHRR radiometer on NOAA-6 12 p1755 A83-29568
- A multi-dimensional differential approximation for absorbing/emitting and anisotropically scattering media with collimated irradiation [ASME PAPER 82-WA/HT-49] 14 p2008 A83-31937
- Optical design of the Diffuse Infrared Background Experiment for NASA's Cosmic Background Explorer 14 p2084 A83-32037
- Kosmos 856 and Kosmos 914 measurements of high-energy diffuse gamma rays 15 p2286 A83-33706
- 2-165 keV observations of active galaxies and the diffuse background 17 p2596 A83-37307
- Diffuse radio emission from the Coma cluster of galaxies at decametre wavelengths 18 p2764 A83-39191
- Status and future of high energy diffuse gamma-ray astronomy 18 p2785 A83-39276
- Positron annihilation radiation from Seyfert nuclei and the cosmic diffuse gamma-ray background 18 p2775 A83-39762
- Effectiveness of the model of volume backscattering in the theory of radiation transfer in media with axisymmetric scattering indices 18 p2685 A83-39865
- Evaluation of effective emissivities of nonisothermal cavities 20 p2988 A83-42217
- Measurement of coherence of radiation from diffusely illuminated beam splitters 21 p3140 A83-44842
- A theoretical approach to the morphology and the dynamics of diffuse auroral zones 22 p3327 A83-46054
- Diffuse ultraviolet radiation in the intergalactic medium 22 p3378 A83-46549
- DIFFUSERS**
- Flows in diffusers interfered with wake behind a circular cylinder 02 p0174 A83-13068
- Effects of approaching flow types on the performances of straight conical diffusers 03 p0316 A83-13565
- Performance prediction of high inlet blockage diffusers [AIAA PAPER 83-0466] 05 p0636 A83-16733
- A computational method for subsonic compressible flow in diffusers [AIAA PAPER 83-0505] 05 p0587 A83-16753
- Development of a radial diffuser with boundary layer control 07 p0863 A83-21009
- Optimal design of a minimum weight thermal diffuser with constraint on the output thermal power flux 08 p1085 A83-22773
- A stall margin design method for planar and axisymmetric diffusers [ASME PAPER 82-WA/FE-8] 10 p1413 A83-25685
- Flow in a rectangular diffuser with local flow detachment in the corner region 11 p1565 A83-27410
- Effect of outlet diffusers on vortex amplifier characteristics 11 p1568 A83-28174
- Investigation of the combined regulation of the intermediate stage of a centrifugal compressor by an axial regulating apparatus and a two-row diffuser 14 p2028 A83-33149
- Keeled rotors for diffusion by a captive vortex [AAAF PAPER NT 82-17] 14 p1972 A83-33168
- The effect of variation of diffuser design on the performance of centrifugal compressors 16 p2305 A83-35866
- Effects of interstage diffuser flow distortion on the performance of a 15.41-centimeter tip diameter axial power turbine [AIAA PAPER 83-1179] 16 p2307 A83-36263
- Analytical design and experimental verification of S-duct diffusers for turboprop installations with an offset gearbox [AIAA PAPER 83-1211] 16 p2294 A83-36283
- Experimental investigation of the effects of wall suction and blowing on the performance of highly offset diffusers [AIAA PAPER 83-1169] 16 p2297 A83-36922
- Self-similar problem concerning the separated flow of an ideal fluid from a diffuser 17 p2446 A83-37258
- Calculation of two-dimensional diffusers 18 p2686 A83-39989
- Calculation of various diffuser flows with inlet swirl and inlet distortion effects 19 p2789 A83-40863
- Determination of full pressure losses in stepped annular diffusers with rectilinear outer walls and a uniform velocity field at the inlet 19 p2800 A83-42130
- Flows and pressure recovery in a rotating diffuser - Effects of inlet velocity distributions 21 p3129 A83-44065
- Measurements of some features of turbulence in wall-proximity 21 p3132 A83-44973
- The design of optimum diffusers for incompressible flow 22 p3250 A83-46480

- On the influence of the diffuser inlet shape on the performance of a centrifugal compressor stage [ASME PAPER 83-GT-9] 23 p3406 A83-47881
- Pressure recovery of collectors with annular curved diffusers [ASME PAPER 83-GT-35] 23 p3394 A83-47896
- A configuration to improve the aerodynamics and scope of can-annular combustors [ASME PAPER 83-GT-37] 23 p3406 A83-47898
- A simple method for designing optimum annular diffusers [ASME PAPER 83-GT-42] 23 p3407 A83-47902
- A preliminary study of annular diffusers with constant diameter outer walls (suitable for turbine exits) [ASME PAPER 83-GT-218] 23 p3411 A83-48018
- Subsonic diffuser development of advanced tactical aircraft [AIAA PAPER 83-1168] 24 p3544 A83-49300
- Numerical analysis of turbulent separated flow in a cascade of airfoils 24 p3545 A83-49531
- Turbulent kinetic energy balance in a conical diffuser 24 p3579 A83-49805
- DIFFUSION**
- NT AMBIPOLAR DIFFUSION**
- NT ATMOSPHERIC DIFFUSION**
- NT ELECTRON DIFFUSION**
- NT GASEOUS DIFFUSION**
- NT IONIC DIFFUSION**
- NT MAGNETIC DIFFUSION**
- NT MOLECULAR DIFFUSION**
- NT PARTICLE DIFFUSION**
- NT PLASMA DIFFUSION**
- NT SELF DIFFUSION (SOLID STATE)**
- NT SELF PROPAGATION**
- NT SURFACE DIFFUSION**
- NT THERMAL DIFFUSION**
- NT TURBULENT DIFFUSION**
- Diffusion processes in the sintering of nickel alloy powders with spherical particles under pressure 02 p0158 A83-12946
- A-posteriori error analysis and adaptive finite element methods for singularly perturbed convection-diffusion equations 03 p0388 A83-14496
- Grain boundary diffusion mechanisms in metals 04 p0460 A83-16001
- A study of the effectiveness of certain refractory diffusion coatings on nickel alloys 07 p0888 A83-20690
- Finite elements and characteristics applied to advection-diffusion equations 15 p2157 A83-33864
- GaAs/(GaAl)As deep Zn-diffused channelled-substrate laser 16 p2358 A83-35454
- Abatement of gaseous and particulate contamination in a space instrument [AIAA PAPER 83-1567] 16 p2318 A83-36407
- Semiconvective diffusion and energy transport --- in stellar interiors 24 p3669 A83-50102
- DIFFUSION BONDING**
- U DIFFUSION WELDING**
- DIFFUSION COEFFICIENT**
- Diffusion of carbon in beryllium 01 p0027 A83-11350
- Transport properties of Nafion membranes for use in three-electrode photoelectrochemical storage cells 02 p0202 A83-12055
- Concerning the wavelength dependence of the effective diffusion coefficient determined from radar meteor data 02 p0210 A83-12447
- Measurement of the concentration-dependence of interdiffusion coefficients in fused salts --- in microgravity environments 02 p0138 A83-12997
- Transport and propagation of cosmic rays in galaxies. II - The effect of a galactic wind on the mean lifetime and age distribution of non-decaying cosmic rays 06 p0857 A83-18077
- Pioneer 11 observations of trapped particle absorption by Amalthea 06 p0847 A83-18279
- Tungsten diffusion in molybdenum 06 p0729 A83-18744
- Role of the conductivity of the confining layers in DH-laser spatial hole burning effects 06 p0766 A83-18903
- Propagation effects in the hydrogen-to-helium ratio in the solar cosmic rays 06 p0856 A83-19170
- The temperature dependence of the coefficients of mutual diffusion in the system Ti-Ni-Co 07 p0890 A83-20918
- Fracture mechanical studies of the strength resulting from polymer interdiffusion 08 p1068 A83-21696
- An approximate method for calculating the transfer coefficients of multicomponent mixtures --- transport properties of gases 09 p1350 A83-24232
- Diffusion of nitrogen in alpha-Ti 10 p1397 A83-25980
- Grain-boundary diffusion in metals 12 p1713 A83-29240

- Physicochemical properties of Cu(x)S
14 p1989 A83-32300
- Impurity diffusion in amorphous silicon and its implications for solar cells
14 p2005 A83-32336
- Modeling the carbon cycle using the method of fractional-order derivatives
14 p2051 A83-32366
- A model calculation of the coefficients of turbulent diffusion in a nonstratified atmospheric surface layer
14 p2058 A83-32854
- Plasmapause diffusion
15 p2196 A83-33949
- A study of the diffusion of oxygen in alpha-titanium oxidized in the temperature range 460-700 C
15 p2133 A83-34699
- Diffusion anomalies in cobalt alloys
15 p2141 A83-35313
- Eddy diffusion coefficients in the lower thermosphere
17 p2539 A83-37603
- Atomic diffusion coefficients calculated for transition metals in olivine
17 p2623 A83-38596
- A note on estimating the vertical eddy diffusion coefficient from Landsat imagery
18 p2721 A83-39016
- Diffusion induced grain boundary migration in Ni-C alloys
18 p2668 A83-40615
- Cross field diffusion of a hollow magnetoplasma
18 p2749 A83-40650
- Carbon diffusion in Ti-Nb alloys
19 p2822 A83-42071
- Superdiffusion of 4 T-hydrogen in vanadium
21 p3111 A83-43887
- Electron-beam-induced current measurements in silicon-on-insulator films prepared by zone-melting recrystallization
21 p3219 A83-45496
- Diffusion of chromium and silicon in nickel solid-solution alloys of the Ni-Cr-Si system
22 p3269 A83-46702
- Some results of the space metallurgy program 'BEALUCA'
23 p3414 A83-47293
- [IAF PAPER 83-154]
23 p3414 A83-47293
- Electron transport coefficients in weakly ionized nonequilibrium plasma of CO₂:N₂ mixtures
24 p3632 A83-49112
- DIFFUSION EFFECT**
U DIFFUSION
- DIFFUSION FLAMES**
Transient extinction of counter flow diffusion flame
01 p0022 A83-10497
- Lewis number effects on the structure and extinction of diffusion flames due to strain
01 p0023 A83-10897
- Combustion of a layer of fuel in a flow of oxidizer over its surface
03 p0295 A83-14058
- Turbulent flow structure effect on diffusion and premixed flame propagation
03 p0295 A83-14602
- Instantaneous CARS thermometry in turbulent flames
03 p0295 A83-14847
- Spectral characteristics of the aerodynamic field of a turbulent diffusion flame at a low Froude number
04 p0480 A83-16443
- Turbulent properties of a flat plate boundary layer with mass addition and diffusion flame
05 p0636 A83-16738
- [AIAA PAPER 83-0471]
05 p0636 A83-16738
- Dynamic behavior of turbulent flow in a widely-spaced co-axial jet diffusion flame combustor
05 p0637 A83-16800
- [AIAA PAPER 83-0575]
05 p0637 A83-16800
- A double reaction zone model and perturbation analysis for finite rate kinetics in hydrocarbon fuel combustors
05 p0612 A83-16810
- [AIAA PAPER 83-0599]
05 p0612 A83-16810
- The effect of turbulence on the formation of large superequilibrium concentrations of atoms and free radicals in diffusion flames
06 p0727 A83-19426
- Influence of the vortex shedding process on a bluff-body diffusion flame
06 p0727 A83-19588
- [AIAA PAPER 83-0335]
06 p0727 A83-19588
- Effects of envelope flames on drop gasification rates in turbulent diffusion flames
07 p0879 A83-19846
- Effect of molecular structure on incipient soot formation
07 p0879 A83-19847
- The combustion of substances with a liquid reaction layer
07 p0880 A83-19953
- An analysis of transient combustion states of diffusion flame
07 p0881 A83-20280
- Lift-off characteristics of turbulent jet diffusion flames
08 p1056 A83-22140
- Temperature and optimum ionization in the micro diffusion flame
08 p1056 A83-22343
- Experimental study on inhibited diffusion and premixed flames in a counterflow system
08 p1057 A83-22347
- Steady state diffusion flame structure with Lewis number variations
08 p1057 A83-22392
- Prediction of turbulent mixing in confined co-axial reacting jets
08 p1088 A83-23191
- Studies of a diffusion flame matrix burner in a combustion chamber with heat exchanger
09 p1225 A83-23334
- A model for calculating the probabilistic behavior gasdynamic variables of a jet undergoing physical and chemical transformation
09 p1259 A83-24043
- Local quenching due to flame stretch and non-premixed turbulent combustion
09 p1226 A83-24362
- Joint measurements of radial velocity and scalars in a turbulent diffusion flame
09 p1226 A83-24365
- A diffusion combustor and methane-air flame propagation in concentration gradient fields
09 p1226 A83-24366
- A study on the hydrogen-oxygen diffusion flame in high speed flow
10 p1391 A83-26199
- Instantaneous Ramanography of a turbulent diffusion flame
13 p1817 A83-30747
- Calculation of the characteristics of submerged combustion
14 p1988 A83-32084
- The formation of nitrogen oxides in a nonequilibrium turbulent diffusion flame
14 p1989 A83-32090
- The influence of the temperature dependence of diffusivities on the dynamics of flame fronts
14 p1989 A83-32125
- 10-Hz coherent anti-Stokes Raman spectroscopy apparatus for turbulent combustion studies
14 p2020 A83-32823
- A simple model for carbon monoxide in laminar and turbulent hydrocarbon diffusion flames
14 p1990 A83-32939
- In-situ optical measurement of additive effects on particulates in a sooting diffusion flame
14 p1991 A83-32943
- Thermal structure of a flat plate turbulent boundary layer diffusion flame
14 p2013 A83-33092
- Investigations on a reaction model for turbulent diffusion flames
15 p2155 A83-33662
- Calculation of laminar premixed and diffusion flames with fast chemical reaction using a self-consistent method
15 p2132 A83-34269
- CARS thermometry and N₂ number density measurements in a turbulent diffusion flame
15 p2134 A83-34914
- [AIAA PAPER 83-1480]
15 p2134 A83-34914
- Simultaneous CARS and luminosity measurements in a bluff-body combustor
15 p2134 A83-34915
- [AIAA PAPER 83-1481]
15 p2134 A83-34915
- Interpretation of optical measurements of soot in flames
15 p2134 A83-34926
- [AIAA PAPER 83-1516]
15 p2134 A83-34926
- Numerical solution of the problem of flame propagation by the use of the random element method
16 p2326 A83-36062
- [AIAA PAPER 83-0600]
16 p2326 A83-36062
- Analysis of turbulent diffusion flames using unique relationships from laminar flame calculations
16 p2326 A83-36360
- [AIAA PAPER 83-1364]
16 p2326 A83-36360
- Controlling mechanisms of flame spread
17 p2484 A83-37043
- Calculation of turbulent diffusion flame using the coherent flame sheet model
18 p2663 A83-39108
- [AIAA PAPER 83-1322]
18 p2663 A83-39108
- Structure and extinction of convective diffusion flames with general Lewis numbers
18 p2664 A83-40312
- Dynamic behavior of a bluff-body diffusion flame
21 p3110 A83-45584
- Instability and coherent structures in jet flames
22 p3266 A83-46458
- Comments on rates of creeping spread of flames over thermally thin fuels
22 p3267 A83-46764
- High-temperature physical-chemical processes in the atmosphere during thunderstorms
23 p3485 A83-48504
- Combustion regimes with laser-induced plasma
24 p3556 A83-49782
- Combustion-wave propagation along a thin layer of a material during a gas-phase reaction between fuel and oxidizer
24 p3556 A83-49786
- DIFFUSION THEORY**
An exact solution to the problem of diffusion in a periodic velocity field and turbulent diffusion
02 p0170 A83-11954
- An empirical investigation of methods for nonsymmetric linear systems
03 p0385 A83-14091
- Approximate integration of the nonstationary equations of a diffusion or thermal boundary layer
04 p0475 A83-15084
- A diffusion equation illustrating spectral theory for boundary layer stability
04 p0479 A83-16182
- [AD-A123209]
04 p0479 A83-16182
- Helium radiation diffusion in prominences
06 p0855 A83-19135
- Iron and magnesium in the white dwarf GD 40 - A test of diffusion theory
10 p1509 A83-26384
- Flux-limited diffusion with relativistic corrections --- in radiative transfer
10 p1490 A83-26393
- On the theory of stress-assisted diffusion, II
11 p1593 A83-27865
- An interpolation method of randomly distributed atmospheric data in the height-time domain
12 p1758 A83-29133
- Thermal diffusion in gases --- Russian book
12 p1723 A83-29341
- On local relaxation methods and their application to convection-diffusion equations
12 p1725 A83-29644
- A simulation of the carbon cycle in the system atmosphere-ocean-biosphere in the framework of linear and diffusion models
13 p1874 A83-30296
- Asymptotic analysis of radiative transfer problems
14 p2093 A83-31934
- Diffusion-convection function of cosmic rays
14 p2117 A83-32925
- Diffusion across characteristic boundaries with critical points
20 p3043 A83-43121
- The characteristics of salt fingers in a variety of fluid systems, including stellar interiors, liquid metals, oceans, and magmas
22 p3281 A83-46003
- Oxidation theory of alloys
24 p3561 A83-49478
- DIFFUSION WELDING**
Diffusion welding for water-cooled gas turbine applications
02 p0187 A83-12071
- Hot isostatic pressing technology. III - Diffusional bonding
02 p0156 A83-12296
- Ultrasonic test samples
04 p0490 A83-15182
- Diffusion bonding of superalloys for gas turbines
07 p0941 A83-21503
- Effect of diffusion welding thermal cycle on the strength of alloy VT20
08 p1067 A83-22696
- Improving the quality of diffusion bonded joints in OT4-1 alloy workpieces containing argon-arc welded joints
10 p1436 A83-26218
- Special features of the formation of the joint between platinum and titanium during vacuum diffusion bonding
10 p1397 A83-26219
- Superplastic forming and diffusion bonding
11 p1589 A83-28176
- Forming SPF/DB structure --- Superplastic Forming/Diffusion Bonding of metal sheets
15 p2171 A83-33638
- Metal honeycomb to porous wireform substrate diffusion bond evaluation
18 p2695 A83-39620
- Fabrication of carbon fiber reinforced aluminum composites by roll diffusion bonding method
18 p2659 A83-40262
- Non-destructive testing and acoustic microscopy of diffusion bonds
21 p3149 A83-44123
- The potential drop across an imperfect diffusion bond
21 p3149 A83-44124
- The construction and testing of pilot installations for making diffusion connections and for depositing layers on high-alloy engine components
23 p3440 A83-47206
- DIFFUSIVITY**
A new diffusion-inhibited oxidation-resistant coating for superalloys
01 p0024 A83-10299
- Evidence for low diffusivity and mobility of minority carriers in highly doped Si and interpretation
06 p0814 A83-19261
- Hydrogen permeation and diffusion in niobium
07 p0884 A83-20259
- Diffusivity in zinc chloride-potassium chloride electrolyte
07 p0954 A83-20582
- Hydrogen permeability and diffusivity in nickel and Ni-base alloys
14 p1997 A83-32950
- The effect of Lewis number greater than unity on an unsteady propagation flame with one-step chemistry
15 p2132 A83-34030
- Measurement of boron diffusivity in hydrogenated amorphous silicon by using nuclear reaction B-10(n, alpha)Li-7
16 p2418 A83-35437
- Modeling of diffusion processes during carburization of alloys --- surface precipitation reactions
20 p2954 A83-42523
- DIFFLUORIDES**
NT CALCIUM FLUORIDES
- DIFFLUORO COMPOUNDS**
NT POLYTETRAFLUOROETHYLENE
- The Atmospheric Lifetime Experiment. IV - Results for CF₂Cl₂ based on three years data
24 p3606 A83-49331
- DIGESTIVE SYSTEM**
NT GASTROINTESTINAL SYSTEM
- NT INTESTINES
- NT PANCREAS
- NT STOMACH
- NT TEETH
- Analgesic intestinal peptides - New agents of bodily defense
07 p0975 A83-21000
- DIGITAL COMMUNICATION**
U PULSE COMMUNICATION
- DIGITAL COMPUTERS**
NT ICL COMPUTERS
- NT ILLIAC 4 COMPUTER
- NT MICROCOMPUTERS
- NT MINICOMPUTERS
- NT PARALLEL COMPUTERS
- NT SEQUENTIAL COMPUTERS
- NT VAX-11/780 COMPUTER

- Computer support system 01 p0088 A83-10787
The MCP-100 - A turnkey system for implementing multivariable flight control laws 01 p0009 A83-11101
A software implementation of the cordic technique as applied to trigonometric functions 01 p0091 A83-11110
Marconi avionics standard central air data computer 01 p0009 A83-11119
Application of a digital-analog computer structure to the simulation of visual-scene problems 08 p1151 A83-22178
Microelectronic packaging 16 p2346 A83-36021
Multi-body dynamics analysis on small computers 21 p3190 A83-45123
A new binary logarithm-based computing system 24 p3619 A83-48999

DIGITAL DATA

- Water resources management and remote sensing 01 p0061 A83-10010
Selective image enhancement and restoration 01 p0061 A83-10028
A digital Seasat SAR correlation-simulation program 01 p0062 A83-10052
Analyzing and mapping regional land use trends by combining Landsat and topographic data 01 p0066 A83-10119
Shape analysis of segmented objects using moments 01 p0097 A83-11422
Pattern recognition and digital image processing as applied to remote sensing in India 01 p0067 A83-11450
Adaptive optical processor 02 p0178 A83-12592
Defense Mapping Agency /DMA/ overview of mapping, charting, and geodesy /MC&G/ applications of digital image pattern recognition 02 p0200 A83-12877
Line finding with subpixel precision 02 p0182 A83-12890
Holographic display of 3D digital data 03 p0324 A83-13437
Discrete-analog signal processing --- Russian book 03 p0311 A83-13815
Quality assessment of remote-sensing data - The SAR case 03 p0344 A83-13845
Assessment of spruce budworm defoliation using digital airborne MSS data 03 p0347 A83-14248
Surficial geology mapping from Landsat-Kaminak Lake, N.W.T. 03 p0348 A83-14268
Quantization of signals on a background of noise 04 p0467 A83-15736
Digital transducers 05 p0644 A83-16917
The SPINE programme and the associated demonstrations at UNISPACE 82 --- satellite data transmission via Space Information Network Experiment 05 p0622 A83-17427
Time synchronisation of an HF radio modem 08 p1075 A83-21995
Photogrammetry and digital elevation models - Current status of development and application 08 p1129 A83-22032
Information density and efficiency of two-dimensional /2-D/ sampled imagery 08 p1105 A83-22895
Receivers for modulated digital signals 09 p1244 A83-23410
Monitoring the growth of crops using digital Landsat MSS data 09 p1288 A83-24588
Monitoring arid land changes in the Turpan Depression, People's Republic of China 09 p1288 A83-24589
Digital data acquisition and analysis in structural dynamic testing 13 p1867 A83-31494
Some technical considerations on the evolution of the IBIS system --- Image Based Information System 15 p2186 A83-34834
Comparing digital data processing techniques for surface mine and reclamation monitoring 17 p2530 A83-38337
An interactive system for compositing digital radar and satellite data 18 p2726 A83-39869
Comments on the Neyman and Beall formulas for 'contagious' type-A probability distributions applied to burst processes especially in the field of digital transmission 19 p2827 A83-41313
Ridges and valleys on digital images 21 p3193 A83-44251
The influence of the image scale on the precision of morphotopo analysis from aerial photographs performed by a digital shape recognition analysis 22 p3308 A83-46117
Effect of differences in categories dispersion patterns on digital image classification results 22 p3308 A83-46118
Image enhancement for determination of agricultural fields using Digital-SLAR data 22 p3313 A83-46211
Principles of organization of the on-ground data processing for remote sensing purposes using finite rings and fields [IAF PAPER 83-130] 23 p3501 A83-47285

DIGITAL FILTERS

NT FIR FILTERS

- Analysis of digital adaptive rejection filters 01 p0038 A83-10806
Digital adaptive methods of signal processing 02 p0162 A83-11529
Eigenvalue sensitivity of digital filters based on the expanded state model 02 p0229 A83-11792
Implementation of a laboratory model Yaw Damper digital filter 02 p0230 A83-11908
Digital servo/filter analysis using the phase plane 02 p0230 A83-11911
Two-dimensional convolute integers for analytical instrumentation 02 p0183 A83-13110
Enhancement of astronomical images using digital filtration methods 03 p0407 A83-13672
Decoupling the structural modes estimated using recursive lattice filters 03 p0386 A83-14174
State description for the root-signal set of median filters 05 p0680 A83-16912
FIR filter structures having low sensitivity and roundoff noise 05 p0623 A83-16913
Generation of a random sequence having a jointly specified marginal distribution and autocovariance 05 p0680 A83-16915
Direct form expansion of the transfer function for a digital Butterworth low-pass filter 05 p0623 A83-16916
The parametric discrete Fourier transformation 06 p0802 A83-18028
Signal processing for recovery of cardiac conducting system activity 07 p0980 A83-19628
An adaptive digital filter as a sinusoidal noise canceller 07 p0921 A83-20820
An analysis of a real-time transform domain filtering digital communication system. II - Wide-band interference rejection 07 p0915 A83-21197
Experimental study of digital nonrecursive inverse signal filtration in nondestructive monitoring 07 p0932 A83-21409
Synthesis of digital inverse filters by nonlinear programming --- for flaw detectors 07 p0985 A83-21410
The evaluation of the complexity of digital filters 08 p1156 A83-21647
Digital image enhancement of noisy scanner imagery 08 p1091 A83-21911
Design of recursive filters to simulate clutter for the evaluation of radar MTI processors 08 p1079 A83-21973
A new realization of a digital filter using a number theory transform 08 p1157 A83-22233
White-light prefiltering for real-time digital image transmission of still and moving color video images 08 p1076 A83-22430
Digital pipelined hardware median filter design for real-time image processing 08 p1153 A83-22817
Analysis of the effect of finite register length on the efficiency of digital filters for the detection of signals on a noise background 08 p1082 A83-23159
Conditions of the existence of periodic and stationary distributions of phase error in first-order digital phase-locked loops with a discrete averaging device 08 p1082 A83-23161
Adaptive digital control implemented using residue number systems 09 p1332 A83-24774
The design of digital filters using interactive optimization 09 p1332 A83-24776
Digital filter structures for canonic signed-digit code implementation by microprocessor 10 p1460 A83-25500
Simplified tone detector for PCM channel 10 p1402 A83-25634
Recursive maximum likelihood estimation of autoregressive processes 10 p1462 A83-25636
The real-time signal processor 10 p1408 A83-25638
The design of wind shear filters 10 p1378 A83-26483
Approximation of multivariable linear systems with impulse response and autocorrelation sequences 10 p1463 A83-26502
Generation of two normal random signals by filters with binary random weighting function 10 p1464 A83-26514
Design of two-dimensional digital filters for blurred image restoration 10 p1464 A83-26515
Hybrid optical-digital signal processing applied to an optimal nonlinear phase estimator 10 p1406 A83-26861
A method of designing 2-D digital filters with quadrantal symmetry 10 p1412 A83-26887
Ground clutter rejection in the frequency domain --- for radar meteorology applications 11 p1625 A83-27019
A designer's guide to digital filters 11 p1648 A83-28151

Fast digital convolution using p-adic transforms

- 12 p1770 A83-29473
Diagnostic analysis of vibration signals using adaptive digital filtering techniques [AIAA 83-0883] 12 p1770 A83-29831
Approximation of 2-D separable in denominator filters 13 p1910 A83-30873
Sampling rate and peak detection requirements for digital shock response spectra calculations 13 p1848 A83-31497
Efficient positive coefficient algorithm for image processing 13 p1911 A83-31776
System matrices of wave-digital filter related by similarity transformations 13 p1838 A83-31781
Spatial lattice filter for high-resolution spectral analysis of array data 14 p2075 A83-32434
Algorithms for processing a stream of binarily quantized signals with a known beginning and end of the envelope 14 p2001 A83-32489
Rejection of CW interference in QPSK systems using decision-feedback filters 14 p2001 A83-32865
Performance of digital implementations of an adaptive processor 14 p2007 A83-33127
A circuit that changes the word rate of pulse code modulated signals 15 p2143 A83-33501
Epsilon-separating nonlinear digital filter and its applications 15 p2220 A83-33519
Memory requirements for the hardware implementation of decimators 15 p2218 A83-33924
Noise rejection in array data 15 p2223 A83-35144
Image source coding using median filter roots 15 p2223 A83-35147
Accuracy and resolution of Earth Radiation Budget Estimates 16 p2376 A83-35488
Optical fiber repeatered transmission systems utilizing SAW filters 16 p2345 A83-35648
Fast realisation of 2-D digital filters using logarithmic number systems 16 p2404 A83-36012
Signal selection for robust matched filtering 16 p2347 A83-36605
Digital signal processing --- Book 17 p2496 A83-37163
Fast Fourier transform and convolution algorithms /2nd revised edition/ 17 p2571 A83-37175
Digital simulation of devices of simultaneous detection and filtering 18 p2674 A83-39430
On the possibility of reducing the number of quantization levels in MTI digital filters by using randomized algorithms 18 p2677 A83-40093
Spatial-domain design of separable-denominator two-dimensional digital filters 18 p2678 A83-40383
Generation of codes with good autocorrelation properties 19 p2827 A83-41276
Mechanisms of high-frequency-signal interference in time-multiplex transmission and switching systems 19 p2827 A83-41312
Orthogonal-mixing adaptive detection in incompletely specified noise 19 p2828 A83-41346
Digital processing of signals in communications; Proceedings of the International Conference, Loughborough, England, April 7-10, 1981 19 p2834 A83-41473
On filtering and compressing LAGEOS laser range data 19 p2860 A83-41558
Parameter testing for lattice filter based adaptive modal control systems [AIAA PAPER 83-2245] 19 p2892 A83-41721
Digital complex sampling 20 p2963 A83-42481
Fast realization of nonrecursive digital filters with limits on signal delay 20 p2967 A83-42908
Discrete Fourier transform processor based on the prime-factor algorithm 20 p3037 A83-43169
Parallel architectures for computing cyclic convolutions 20 p3037 A83-43679
Digital line-artifact removal --- image processing 21 p3134 A83-43868
Devices for the discrimination of radar signals from noise --- Russian book 21 p3119 A83-43904
Optimum recursive filtering of noisy two-dimensional data with sequential parameter identification 21 p3192 A83-43955
Digital signal processing --- German book 21 p3126 A83-45092
Choice of sampling period and secondary optimization of digital Wiener filters 21 p3197 A83-45307
Instrumental correlation analysis using delta-modulation 22 p3271 A83-45656
Sequential detection of abrupt changes in spectral characteristics of digital signals 22 p3274 A83-46098
Adaptive control of a flexible beam using least square lattice filters 22 p3351 A83-46099
Technology for large digital mosaics of Landsat data 22 p3318 A83-46766

- Statistical performance of the circular harmonic filter for rotation-invariant pattern recognition 22 p3352 A83-46832
- General form for representing the Fourier transform 24 p3621 A83-49966
- Analytical expressions of 2-D complex cepstrum 24 p3621 A83-49986
- Design and optimization of digital filters without multipliers 24 p3575 A83-50119
- Self-error feedback in recursive digital filters 24 p3621 A83-50197
- DIGITAL INTEGRATORS**
- Linear digital phase-locked loops using integrators in a pulse frequency-modulation system 02 p0166 A83-11556
- Simple distortion-free real-time optical pulse correlator 02 p0178 A83-12599
- Self-tuning controller with integral action 05 p0681 A83-17581
- A field-programmable integrator for weather radar signals 11 p1624 A83-27005
- DIGITAL NAVIGATION**
- Software optimization of a Kalman filter for an AP-120B array processor 01 p0091 A83-11111
- Design and application of a multivariable, digital controller to the A-7D Digitaic II aircraft model 01 p0013 A83-11148
- Measurement of the frequency response of a digital autopilot [AIAA PAPER 83-0326] 05 p0605 A83-16655
- CINNA - A system for preparing reconnaissance missions 08 p1044 A83-22591
- Synergistic integration of JTIDS/GPS technology --- Joint Tactical Information Distribution System 11 p1529 A83-28789
- An advanced single-channel NAVSTAR GPS multiplex receiver with up to eight pseudochannels 12 p1700 A83-29213
- An onboard navigator for the extremely low-altitude satellite utilizing accelerometers 13 p1812 A83-30167
- An overview of a new integrated system for communication, navigation, and identification - The Joint Tactical Information Distribution System 19 p2795 A83-41310
- Robustness of a decoupled multivariable digital flight control system [AIAA PAPER 83-2272] 19 p2804 A83-41738
- A Kalman filter algorithm for terminal-area navigation with sensors of moderate accuracy 21 p3090 A83-45460
- Post-flight compensation for a master navigator error 22 p3253 A83-46966
- Comparison of simple position resets and Kalman filter position updates for correcting inertial navigation system errors 22 p3253 A83-46967
- Collins avionics NAVSTAR GPS advanced digital receiver 22 p3253 A83-46969
- A new generation of navigation and landing aids for aviation 23 p3401 A83-47188
- MACS - The ESA standard for guidance/control and robotics --- Modular Attitude Control Systems [IAF PAPER 83-346] 23 p3422 A83-47352
- Integrated navigation systems for aircraft 23 p3402 A83-48735
- DIGITAL RADAR SYSTEMS**
- A model for simulation and processing of radar images 01 p0061 A83-10026
- Using radar image simulation to assess relative geometric distortions inherent in radar imagery 01 p0030 A83-10054
- Terrain following/terrain avoidance for advanced penetrating aircraft 01 p0006 A83-11146
- Integrated and transferable hardware/software checkout --- of digitally controlled flight systems 01 p0093 A83-11249
- Synthetic aperture radar signal processing for airborne applications 02 p0162 A83-11524
- A mixed distributed/parallel processing experiment for real-time radar control 02 p0226 A83-11905
- Trends in radar signal processing 02 p0163 A83-11917
- The CCRS SAR processing system 03 p0349 A83-14289
- An adaptive MTI for weather clutter suppression 06 p0754 A83-19029
- Modeling and a correlation algorithm for spaceborne SAR signals 06 p0763 A83-19030
- Rainfall patterns observed by digitized radar during the landfall of Hurricane Frederic /1979/ 08 p1139 A83-22293
- Digital radar information in the Swiss Meteorological Institute 11 p1624 A83-27003
- A general interactive system for compositing digital radar and satellite data 11 p1647 A83-27089
- The COMPAS system for more efficient approach traffic --- for aircraft 18 p2639 A83-39345
- Design and development of a radar control program for the NOAA/WPL pulse-Doppler radars --- Wave Propagation Laboratory 18 p2727 A83-39880
- Digital homing guidance - Stability vs. performance trade-offs [AIAA PAPER 83-2167] 19 p2795 A83-41663
- On the design and operation of a SLAR system with digital recording 22 p3289 A83-46181
- A comparative study of real-time spaceborne synthetic aperture radar processing techniques 22 p3289 A83-46208
- Automated preprocessing of spaceborne SAR data 22 p3290 A83-46210
- Generation of radar echo images from a contour map 24 p3619 A83-49199
- DIGITAL SIMULATION**
- Suggestions regarding the use of microprogrammable multiple computer systems for the digital simulation of dynamic systems --- German thesis 01 p0090 A83-10470
- On missiles modelling, simulation and evaluation in presence of noise and multi-source environment 01 p0004 A83-10707
- Urban albedo as a function of the urban structure - A two-dimensional numerical simulation 01 p0069 A83-10721
- Application of static Automatic Test Program Generators /ATPG/ to dynamic circuitry 01 p0038 A83-10775
- Shear layer models and computer analysis of data 01 p0046 A83-10887
- Digital computer simulation of 3-phase full-wave SCR bridge regulator 01 p0043 A83-11252
- A two-stage method of fitting conic arcs and straight-line segments to digitized contours 01 p0098 A83-11427
- Simulation of mid-infrared clutter rejection. I. - One-dimensional LMS spatial filter and adaptive threshold algorithms 02 p0177 A83-12305
- Numerical simulation of the tropical cyclone life cycle using a spectral cumulus parameterization 03 p0367 A83-14434
- Numerical simulation of GaAs/GaAlAs heterojunction bipolar transistors 05 p0624 A83-17294
- Results obtained with a digital computer simulator of spread spectrum communications systems 07 p0983 A83-19794
- Analysis of a linear array taking into account satellite-sensor performances and a digital terrain model 08 p1124 A83-21904
- Simulation of panchromatic SPOT-data at the National Land Survey of Sweden 08 p1125 A83-21912
- Launch-vehicle simulation for uniaxial transient vibration testing of satellites 08 p1050 A83-22374
- Validation of a digital simulation of an optical matched filter correlator applied to aerial reconnaissance 08 p1100 A83-22589
- Design of a multivariable model following adaptive control system 09 p1333 A83-24793
- Self-tuning control of nonlinear systems characterized by Hammerstein models 10 p1463 A83-26507
- Features of the digital-computer simulation of a dynamically tunable gyroscope 11 p1574 A83-28497
- Simulation of nonlinear processes in an O-type TWT by an iterative method 13 p1832 A83-30287
- Digital simulation of the operation of an O-type traveling wave tube with two beams of different velocities in the beam-current-modulation mode. II 13 p1834 A83-30736
- Numerical modeling of power MOSFETs 14 p2007 A83-32673
- Transforming images into block stationary behavior 14 p2020 A83-32907
- A fast and efficient digital simulation technique for control systems 16 p2404 A83-35348
- Digital simulation of devices of simultaneous detection and filtering 18 p2674 A83-39430
- Digital simulation of counterspun nutation damper operation under non-ideal operating conditions 23 p3417 A83-48175
- Digital model of a radio-astronomical measuring complex 24 p3638 A83-48957
- DIGITAL SPACECRAFT TELEVISION**
- Tri-state delta modulation system for Space Shuttle digital TV downlink 07 p0870 A83-19730
- DIGITAL SYSTEMS**
- NT DIGITAL NAVIGATION
- NT DIGITAL RADAR SYSTEMS
- Low-sensitivity observer-compensator design for two-dimensional digital systems 01 p0094 A83-10292
- Gigabit logic - A review 01 p0035 A83-10293
- A test pattern generation technique for detection of digital circuits 01 p0038 A83-10773
- Microprocessor controlled digital test subsystem tailored to automatic test program generator output 01 p0038 A83-10776
- Digital engine control for V/STOL and V/TOL aircraft 01 p0012 A83-10871
- Bus protocols for a digital audio distribution system 01 p0005 A83-11126
- Analysis of systems containing multiple, irregular sampling 01 p0095 A83-11131
- Simplification of digital control systems by adjusting zeros 01 p0095 A83-11174
- An experiment in assessment of flight control software development techniques 01 p0092 A83-11177
- A digital flight control system verification laboratory 01 p0015 A83-11178
- Design of direct digital adaptive flight-mode control systems for high-performance aircraft 01 p0013 A83-11179
- Wideband spread spectrum testbed 01 p0032 A83-11215
- An automatic test generation system for complex digital logic 01 p0042 A83-11230
- Interactive smoothing of digitized point data 02 p0226 A83-11817
- Improved acquisition in phase-locked loops with sawtooth phase detectors 03 p0312 A83-13866
- Performance analysis of digital tanlock loop 03 p0312 A83-13869
- CPU coverage evaluation using automatic fault injection 03 p0385 A83-14842
- Digital computational synthesizers of two-level signals with compensation of phase errors 04 p0470 A83-15712
- Outage prediction of digital radio systems 04 p0467 A83-16020
- Advanced fighter technology integrator /AFTI/ F-16 display mechanization 04 p0448 A83-16132
- An evaluation of ultrasound NDE correlation flaw detection systems 04 p0494 A83-16180
- Qualification of the flight-critical AFTI/F-16 digital flight control system --- Advanced Fighter Technology Integration [AIAA PAPER 83-0060] 05 p0597 A83-16492
- Assessment of advanced fighter powered approach simulations [AIAA PAPER 83-0141] 05 p0598 A83-16550
- Error rate bounds for differential PSK 05 p0622 A83-17272
- Use of emulation in fault analyses of digital systems 05 p0678 A83-17303
- DC-9 Super 80 digital flight guidance system simulation techniques for certification 05 p0592 A83-17305
- Software design for the Douglas DC-9 Super 80 digital flight guidance system 05 p0592 A83-17311
- Application of software design standards to commercial aircraft equipment 05 p0592 A83-17312
- Software aspects in certification of new European civil transport aircraft 05 p0679 A83-17314
- Techniques of self-tuning 05 p0680 A83-17578
- Optimization and comparison of binary and multistep digital transmission systems with and without quantified feedback --- German thesis 06 p0751 A83-18498
- The effect of interference from satellites on digital radio-relay systems operating between 15.4 and 40 GHz 06 p0747 A83-18729
- The characteristics of HF propagation paths and their implications in digital communication system design 06 p0747 A83-18736
- The digital multi-channel radiospectrograph in Nancy --- for solar radio burst observation 06 p0763 A83-19140
- Digital satellites with time and frequency divided channels 07 p0904 A83-19691
- A fail-safe node for lightguide digital networks 07 p0992 A83-19712
- Evaluation of a 14/12 GHz 90 Mbit digital satellite link 07 p0908 A83-19741
- Numerical calculation of spectra for digital FM signals 07 p0909 A83-19747
- Discrimination of speech and high-speed data using an adaptive predictor for DSL application --- Digital Speech Interpolation 07 p0910 A83-19756
- Digital processor for coherent CO2 systems 08 p1097 A83-22520
- Design of digital image processing systems; Proceedings of the Meeting, San Diego, CA, August 27, 28, 1981 08 p1097 A83-22524
- Digital cartographic systems at the Defense Mapping Agency Aerospace Center 08 p1129 A83-22526
- Use of array processors in image processing 08 p1152 A83-22529
- Programmable image processing element 08 p1097 A83-22532
- System architecture of Vicom digital image processor 08 p1097 A83-22533

Multi-imagery exploitation system /MIES/ tactical scenario analysis 08 p1099 A83-22586
 Design of Pel Adaptive DPCM coding based upon image partition 08 p1077 A83-22623
 Quality metrics of digitally derived imagery and their relation to interpreter performance 08 p1150 A83-22893
 A method for the representation of a discrete signal in a complex form on the basis of its Hilbert transformation 08 p1078 A83-23160
 The influence of inclusions on the J integral value determined by a Charpy test with digital instrumentation 08 p1124 A83-23242
 Facilities of the formal description of the semantics of input languages for the automated logic design of digital systems 09 p1325 A83-24245
 Future applications and limitations for digital GaAs IC technology 09 p1255 A83-24347
 Flight management systems and data links 09 p1209 A83-24424
 Fault isolation methodology for the L-1011 digital avionics flight control system 09 p1209 A83-24427
 Fast-sampling tracking systems incorporating Lur'e plants with multiple switching nonlinearities 09 p1331 A83-24762
 A note on word length and memory requirements in digital control 09 p1332 A83-24775
 A family of special purpose microprogrammable digital signal processor IC's in an LPC vocoder system 10 p1410 A83-26124
 Effects of blur and noise on digital imagery interpretability 10 p1456 A83-26322
 Development of adaptation and identification algorithms in adaptive digital aircraft control systems 10 p1379 A83-26600
 A new method of quantized feedback for the regeneration of digital signals 10 p1412 A83-26899
 Flight deck display 11 p1530 A83-27123
 A survey of modern design and performance in digital satellite communications 11 p1556 A83-28126
 Symbiosis between a terrestrial-based integrated services digital network and a digital satellite network 11 p1557 A83-28132
 An experiment in integrated digital satellite communications 11 p1557 A83-28136
 US Navy begins shift to digital telemetry 11 p1558 A83-28159
 Analysis of high-order digital servo systems on a phase plane 11 p1648 A83-28495
 Automated digital processing of interferograms --- Thesis 11 p1575 A83-28650
 AFTI/F-16 aeroservoelastic analyses and ground test with a digital flight control system 12 p1704 A83-29888
 A core software concept for integrated control 13 p1909 A83-30170
 Orbital efficiency through satellite digital switching 14 p2002 A83-33158
 Comments on 'Silicon MESFET digital circuit techniques' 15 p2151 A83-33895
 A 'user friendly' geographic information system in a color interactive digital image processing system environment 15 p2186 A83-34829
 Generalized balanced ternary - An approach to handling spatial data 15 p2165 A83-34841
 Some properties of the binary n-cube as a network interconnection structure 15 p2219 A83-35133
 An efficient source coding technique for data compression of multilevel digitized images 15 p2223 A83-35146
 Flight/propulsion control system integration [AIAA PAPER 83-1238] 16 p2308 A83-36301
 Comparison of an experience with full authority digital engine controls in rotary wing and jet-lift VSTOL aircraft [AIAA PAPER 83-1241] 16 p2308 A83-36304
 Receiver design for digital fiber optic transmission systems using Manchester (biphase) coding 16 p2343 A83-36602
 XPSK - A new cross-correlated phase-shift keying modulation technique 16 p2343 A83-36607
 Implementation of a multirate speech digitizer 16 p2344 A83-36908
 Design and analysis of a digitally controlled integrated flight/fire control system 17 p2460 A83-37063
 An algebraically derived nonlinear control theory 17 p2566 A83-37098
 State synthesiser - A digital observer for spacecraft attitude control systems 17 p2569 A83-37452
 A new method of satellite attitude control using a bias-momentum 17 p2478 A83-37457
 The choice of an astatic system for the regulation of the rotational velocity of a dc electric motor for azimuthal mountings of a gamma-telescope 17 p2496 A83-37720

Microcomputer brings digital power to the small aircraft gas turbine [SAE PAPER 821402] 17 p2468 A83-37975
 Validation of the KC-10 refueling boom digital control system [SAE PAPER 821421] 17 p2463 A83-37978
 Robotic testing for digital systems --- for software in avionics and flight control systems [SAE PAPER 821422] 17 p2563 A83-37979
 High-speed digital Golay code flaw detection system 18 p2695 A83-39564
 GaAs digital dynamic IC's for applications up to 10 GHz 19 p2837 A83-40793
 Phototransistors in digital optical communication systems 19 p2899 A83-40949
 Stationary transform processing of digital images for data compression 19 p2847 A83-41105
 Optimal linear receiver filters for binary digital signals 19 p2839 A83-41348
 A postulated topographical architecture for the Defense Communications System of 2004 19 p2829 A83-41356
 Estimated performance of a QPR digital microwave radio in the presence of frequency selective fading --- Quadrature Partial Response 19 p2833 A83-41406
 Digital PLL frequency synthesizers: Theory and design 19 p2839 A83-41529
 The Air Force ejection seat as a vehicle for digital flight control [AIAA PAPER 83-2205] 19 p2798 A83-41689
 Flight management systems - Where are we today and what have we learned? [AIAA PAPER 83-2236] 19 p2803 A83-41713
 Flight Management Systems III - Where are we going and will it be worth it? [AIAA PAPER 82-2237] 19 p2804 A83-41714
 A generalized stage-state method for centralized fault-tolerant flight control system [AIAA PAPER 83-2301] 19 p2892 A83-41759
 Functional development of the 757/767 digital cat. IIIB Autoland System [AIAA PAPER 83-2192] 19 p2796 A83-41762
 Sensitivity of digital flight control design to parameter estimation error [AIAA PAPER 83-2089] 19 p2805 A83-41921
 Flight test experience with pilot-induced-oscillation suppressor filters [AIAA PAPER 83-2107] 19 p2806 A83-41936
 Investigation of transient processes in a digital phase locked loop by the state-space method 20 p2967 A83-42906
 Investigation of the characteristics of programmed devices of pulsed-signal search 20 p2964 A83-42907
 Digital simulation and control of the Machan UMA 20 p2932 A83-43718
 Digital control system design for a precision pointing system [AAS PAPER 83-003] 21 p3103 A83-44163
 Avionics analysed. IV - Aircraft grey matter 21 p3090 A83-44494
 Intelsat - Making the future happen 21 p3120 A83-44532
 Aircraft keyboard ergonomics - A review 21 p3189 A83-44691
 Design of broadband (fast) systems of digital signals processing 21 p3190 A83-44773
 Hybrid optical-digital image processing system for pattern recognition 21 p3194 A83-44826
 Measurement of the parameters of digital integrated microcircuits --- Russian book 21 p3126 A83-45040
 Discrete nonlinear systems --- Russian book 21 p3197 A83-45201
 Electronic control of aircraft turbine engine 21 p3093 A83-45600
 Processing signals the optical way 23 p3508 A83-47821
 The transmission of analog information over digital communications channels --- Russian book 23 p3443 A83-48425
 General aviation goes digital - Many advantages, but some problems 23 p3406 A83-48640
 Integrated digital avionics systems - Promise and threats 24 p3572 A83-48890
 Flight-control designer becomes metalogician 24 p3619 A83-48892
 Spectral channel of a digital radio spectrometer with an analysis band of 180 kHz 24 p3581 A83-48959
 Design of digital two- and three-term controllers for discrete-time multivariable systems 24 p3620 A83-49897
 VLSI digital polarity correlator based on an overloading counter technique 24 p3574 A83-49964
 A generator of test sequences for probabilistic systems of the fault diagnostics of digital devices 24 p3575 A83-50207

DIGITAL TECHNIQUES

Realization and switching behavior of digital phase modulators for millimeter waves --- German thesis 01 p0035 A83-10168
 Application of pulse code modulation technology to aircraft dynamics data acquisition 01 p0008 A83-10182
 Adaptive beam forming for radar 01 p0030 A83-10260
 A preliminary digital analysis of the spectrum of Beta Lyrae 01 p0121 A83-10334
 Digital stochastic iterative procedures for the adaptive adjustment of noise compensation systems - Analysis of convergence and convergence rate 01 p0031 A83-10412
 Use of multifunctional computers with decentralized control for digital signal processing with floating point decimal representation --- German thesis 01 p0031 A83-10476
 On the certification of digital computer programs for flight safety 01 p0002 A83-11115
 High accuracy digital sensor 01 p0053 A83-11118
 The real-time image processing problem 01 p0053 A83-11218
 Recursive generation of hierarchical data structures for multidimensional digital images 01 p0097 A83-11414
 Rotation-invariant digital pattern recognition using circular harmonic expansion 02 p0230 A83-12593
 The employment of digital signal processing in radar devices - Advantages and disadvantages for the practice 02 p0134 A83-13014
 Digitized measurements of the shape of corner cracks at fastener holes 03 p0339 A83-13202
 Real-time NDE of flaws using a digital acoustic imaging system 03 p0337 A83-13434
 Optimum sampling for digital terrain models - A trend towards automation 03 p0345 A83-14092
 Digital colour enhancement of Landsat data for mapping vegetation of bareground caribou winter range in northern Manitoba 03 p0347 A83-14249
 Applications of Robert's gradient operator for the digital enhancement of icebergs from SAR imagery 03 p0349 A83-14278
 A method for the digital processing of contour imagery 03 p0329 A83-14312
 The digital image processing system MOBI-DIVAH 03 p0352 A83-14944
 Digital controlled time-gate of the Ondrejov laser radar --- for satellite distance measurement 04 p0546 A83-15111
 Digital transducers 05 p0644 A83-16917
 A four-element VHF adaptive array processor 06 p0739 A83-18634
 Generation of random processes on the basis of simple digital circuits --- for vibration testing systems 06 p0763 A83-19179
 On initial acquisition of FH/TH Spread Spectrum signal --- Frequency-Hopping/Time-Hopping 07 p0904 A83-19678
 Digital image processing - A systems approach --- Book 07 p0928 A83-19925
 Computer-aided speckle pattern interferometry 07 p0928 A83-20155
 Reception, preparation, and geometric processing of imagery of meteorological satellites --- German thesis 07 p0951 A83-21069
 Methodology for thematic image processing using thematic and topographic data bases and base-integrated multi-sensor imagery 08 p1124 A83-21903
 Seasat/SIR-A digital registration over Algeria 08 p1126 A83-21922
 Digital image processing in Europe - Some highlights 08 p1093 A83-22431
 Real-time nonuniformity correction for focal plane arrays using 12-bit digital electronics 08 p1094 A83-22440
 On-line processing of high resolution imagery from meteorological satellites 08 p1140 A83-22535
 Digital reconnaissance imagery processing system for real-time and near-real-time imagery exploitation 08 p1099 A83-22579
 Modified FFT algorithms with a reduced number of multiplication operations 08 p1154 A83-23169
 Optimal digital algorithms of data reception by symbol estimation 09 p1245 A83-23457
 Digital control system for the Lasercom Space Measurement Unit 09 p1215 A83-23589
 Digital engine control unit - Future employment possibilities [DGLR PAPER 82-085] 09 p1206 A83-24197
 Recent developments in digital control for helicopter powerplants 09 p1207 A83-24829
 Digital speckle interferometry of Juno, Amphitrite and Pluto's moon Charon 09 p1367 A83-25301

Application of digital image analysis techniques to antimisting fuel spray characterization
[ASME PAPER 82-WA/HT-23]

- 10 p1401 A83-25690
- Digital enhancement of SAR imagery as an aid in geologic data extraction 10 p1443 A83-25970
- Digital image reconstruction of microwave holograms 10 p1424 A83-26855
- Spectral analysis algorithms for the laser velocimeter - A comparative study 12 p1728 A83-28961
- Digital nondestructive evaluation of composite materials 12 p1710 A83-29592
- Digital processing of Spacelab imagery 13 p1846 A83-30769
- Applications of optimal control concepts to digital shaker control systems 13 p1911 A83-31496
- Digital processing and analysis of satellite multispectral scanner data 14 p2035 A83-32504
- Digital image processing of flow visualization photographs 14 p2020 A83-32906
- In-flight simulation of a digitally implemented direct force mode --- for flight control 14 p1977 A83-32933
- Digital image processing with coherent light - A method and some applications 14 p2021 A83-33174
- Spatially variant contrast enhancement using local range modification 14 p2021 A83-33177
- Objective procedures for lineament enhancement and extraction --- digital convolution enhanced images 14 p2035 A83-33346
- Techniques to reduce the inherent limitations of fully digit on-line arithmetic 15 p2217 A83-33913
- Digital image processing systems and remote sensing 15 p2183 A83-34159
- The problem of the visualization of information and digital image processing 15 p2165 A83-34968
- Numerical separation of overlapping ordinary and extraordinary echoes in digital ionograms 16 p2341 A83-35416
- A system of orthogonal functions for the fast spectral analysis of signals 16 p2404 A83-35935
- Efficient algorithm for image enhancement 16 p2405 A83-36964
- Digital picture processing. Volumes 1 & 2 /2nd edition/ --- Book 17 p2509 A83-37167
- Image reconstruction by the speckle-masking method 17 p2592 A83-37949
- Depth-first picture expression viewed from digital picture processing 20 p2989 A83-42646
- Digital image processing - Overview and areas of application 20 p2990 A83-43028
- Fail-operational DAFCS for business/commuter aircraft --- Digital Automatic Flight Control System [SAE PAPER 830714] 20 p2937 A83-43324
- Amplitude calibration of spaceborne synthetic aperture radars --- Synthetic Aperture Radar 21 p3103 A83-43979
- Segmentation of digital curves using linguistic techniques 21 p3194 A83-44259
- Digital techniques for enhancing and processing dynamic stress-analysis data 21 p3141 A83-45145
- Efficient coding and resonance spike identification for topside ionogram processing 22 p3330 A83-46512
- Image restoration for a defocused optical system 22 p3294 A83-46827
- A digital technique for the simultaneous measurement of streamwise and lateral velocities in turbulent flows 23 p3458 A83-48117
- Experiments on digital image data comparison --- for Landsat satellite photos 24 p3598 A83-48990
- Digital thermal anemometry 24 p3585 A83-49818
- Digital processing of objective prism-stellar spectrograms 24 p3648 A83-50022
- DIGITAL TELEVISION**
- NT DIGITAL SPACECRAFT TELEVISION
- Image quality experiments for TV reconnaissance at reduced transmission bandwidth 08 p1105 A83-22902
- DIGITAL TO ANALOG CONVERTERS**
- Microprocessor control for automated guideway transit vehicles 01 p0112 A83-11035
- Optoelectronic digital/analogue converter-emitter 04 p0534 A83-15241
- GaAs integrated digital-to-analogue convertor for control of power dual-gate FETs 16 p2347 A83-36479
- A 12 bit monolithic 70 ns DAC --- Digital to Analog Converter 19 p2837 A83-40792
- DIGITAL TRANSDUCERS**
- Digital transducers 05 p0644 A83-16917
- A simplified approach to the design of apodised SAW filters 10 p1408 A83-25503
- The effect of losses on the characteristics of a surface-acoustic-wave resonator with distributed feedback 11 p1561 A83-27964
- DIGITIZERS**
- U ANALOG TO DIGITAL CONVERTERS

DIGITS

NT BINARY DIGITS

DIHEDRAL EFFECT

U LATERAL STABILITY

DIHYDROXYPHENYLALANINE

U DOPA

DILATATION

U STRETCHING

DILATOMETERS

U EXTENSOMETERS

DILATOMETRY

A dilatometric study of the growth of Ti-Al compacts during liquid-phase sintering 11 p1547 A83-27922

DILUTION

NT GEOMETRIC DILUTION OF PRECISION

DIMENSIONAL ANALYSIS

Attractors of the Navier-Stokes system and of parabolic equations, and the estimation of their dimensionality 09 p1260 A83-24317

Crater ejecta scaling laws - Fundamental forms based on dimensional analysis 09 p1366 A83-25074

Dimensional analysis of pumping losses in a Stirling cycle machine 11 p1587 A83-27269

Numerical estimates of Hausdorff dimensions --- for problems in turbulence theory 12 p1724 A83-29615

Humanscale 7/8/9 --- Book on human factors engineering information 13 p1906 A83-30154

The correct use of dimensional analysis

[ONERA, TP NO. 1983-2] 16 p2402 A83-36417

On the dimensionality of turbulent-motion attractors 18 p2741 A83-39514

What can be achieved by similarity laws? --- for fluid dynamics 22 p3284 A83-46481

On the fractal dimension of the Henon attractor 23 p3505 A83-48588

DIMENSIONAL MEASUREMENT

Two-parameter gap independence in eddy-current thickness gauging on conducting plates, strips, films, and coatings 01 p0057 A83-10368

Dimensional information through industrial computerized tomography 03 p0337 A83-13435

Electromagnetic excitation of a finite cone by an annular magnetic flux 16 p2346 A83-35942

Thin-film thickness measurements with thermal waves 18 p2689 A83-40060

The measurement of turbomachinery stator-to-drum running clearances [ASME PAPER 83-GT-204] 23 p3410 A83-48005

DIMENSIONAL STABILITY

NT SHELL STABILITY

NT STRUCTURAL STABILITY

Space environmental effects on materials 03 p0291 A83-14125

Microstructural and dimensional stabilities of a potential gamma/gamma prime-alpha/Mo/ directionally solidified eutectic superalloy under cyclic thermal exposure to 1000 C 04 p0460 A83-15987

Dimensional stability of Superinvar 16 p2334 A83-36751

Design, analysis and testing of two concepts for a dimensional stable structure --- composite antenna tower for communication satellites 18 p2662 A83-40289

Dimensional stability of reinforced matrices 22 p3264 A83-46301

DIMENSIONLESS NUMBERS

NT GRASHOF NUMBER

NT LEWIS NUMBERS

NT MACH NUMBER

NT NUSSELT NUMBER

NT PRANDTL NUMBER

NT RAYLEIGH NUMBER

NT REYNOLDS NUMBER

NT RICHARDSON NUMBER

NT STROUHAL NUMBER

The significance of the dimensionless constant in the rate equation for superplastic flow 02 p0157 A83-12416

The angular momentum of celestial bodies and the fundamental dimensionless constants of nature 23 p3518 A83-47423

DIMENSIONS

NT DEPTH

NT DIAMETERS

NT FILM THICKNESS

NT HEIGHT

NT LARMOR RADIUS

NT LENGTH

NT RADII

Morphometric consistency with the Hausdorff-Besicovich dimension 02 p0203 A83-11844

DIMERIZATION

Diatonic polymers, mixed-stack compounds, and the soliton lattice 16 p2420 A83-35749

Coulomb effects on one-dimensional Peierls instability

- The Peierls-Hubbard model --- of dimerization 19 p2820 A83-40956

DIMERS

3.508 micron-HeXe-laser line absorption by formaldehyde monomer and dimer and by nitrogen dioxide monomer and dimer without and in the presence of argon 05 p0684 A83-17871

Optically pumped sodium-dimer supersonic-beam laser 07 p0933 A83-19981

The properties of dimers and their role in the atmosphere 10 p1448 A83-25522

Quantum dynamics of the van der Waals molecule /N₂/2 - An ab initio treatment 10 p1480 A83-26460

New optically pumped alkali metal dimer lasers 11 p1579 A83-27555

Gain lineshapes studies in optically pumped dimer lasers 12 p1731 A83-29193

Electron affinities of the alkali dimers - Na₂, K₂, and Rb₂ 20 p3045 A83-42635

An ab initio study of core-valence correlation --- in atoms 20 p3045 A83-42636

The rotational spectrum of water dimers (H₂O)₂ in atmospheric conditions 22 p3322 A83-45637

Theoretical evidence for multiple one-electron 3d bonding in a first row transition metal dimer - The 5 Sigma u -state of Sc₂ 24 p3625 A83-48799

DIODES

NT AVALANCHE DIODES

NT BARRITT DIODES

NT CESIUM DIODES

NT GUNN DIODES

NT JUNCTION DIODES

NT LIGHT EMITTING DIODES

NT MIM DIODES

NT PHOTODIODES

NT PLASMA DIODES

NT SCHOTTKY DIODES

NT SEMICONDUCTOR DIODES

NT THERMIONIC DIODES

NT TUNNEL DIODES

NT VARACTOR DIODES

The physics of power rectifiers at very high current levels - Electric and thermal aspects --- French thesis 02 p0166 A83-11699

Electron transverse velocity measurements in an intense relativistic electron beam diode 03 p0398 A83-13916

A study of the characteristics of a thermal diode heat pipe in the direct and reverse modes of operation 04 p0478 A83-16165

Design and testing of low-temperature intense electron beam diodes 05 p0625 A83-17365

Transient shutdown of an axial-groove liquid trap heat pipe thermal diode 06 p0759 A83-19161

Characteristics of a new class of diode-switched integrated antenna phase shifter 09 p1247 A83-23798

Nuclear radiation effects on linear circuits (Reference diode, operational amplifier) 14 p2006 A83-32417

Modulation detuning characteristics of actively mode-locked diode lasers 19 p2852 A83-40939

Pulsed ion beam generation with cryogenic-anode diode 20 p2959 A83-42584

DIONE

Saturn's magnetosphere - Observations of ion cyclotron waves near the Dione L shell 22 p3387 A83-47045

DIOPHANTINE EQUATION

Classical Diophantine equations in two unknowns --- Russian book 10 p1471 A83-25596

Diophantine approximations and transcendental numbers --- Russian book 10 p1471 A83-25597

DIOXIDES

NT CARBON DIOXIDE

NT HYDROGEN PEROXIDE

NT QUARTZ

NT SILICON DIOXIDE

NT SULFUR DIOXIDES

DIPHENYL COMPOUNDS

Superradiation in molecular impurity crystals 21 p3146 A83-45338

DIPHOSPHATES

NT ADENOSINE DIPHOSPHATE

A spatio-temporal light modulator with a DKDP crystal in an adaptive optical system 04 p0534 A83-15262

DIPLEXERS

Grating diplexer using dielectric waveguides for millimeter wavelengths 17 p2498 A83-38038

DIPOLE ANTENNAS

Characteristics of receiving antennas consisting of independently loaded dipoles --- rectennas 01 p0039 A83-10911

Error analysis of image representations for sources near to a dissipative earth 01 p0073 A83-11374

An electric noise component with density 1/f identified on ISEE 3 02 p0207 A83-12376

- Radiation patterns of interfacial dipole antennas
02 p0165 A83-12631
- The emission of electromagnetic waves in the case of a smooth variation of parameters of a radiating system
03 p0390 A83-13427
- Analytic determination of the transient response of a thin-wire antenna based upon an SEM representation --- Singular Expansion Method
03 p0306 A83-14015
- New formulas for the electromagnetic field of a vertical electric dipole in a dielectric or conducting half-space near its horizontal interface
[AD-A125370]
04 p0468 A83-16054
- Mechanics of the flexible dipole antenna of WISP --- Waves in Space Plasma
[AIAA PAPER 83-0433]
05 p0607 A83-16712
- A wideband UHF circular array
06 p0743 A83-18681
- A printed array of symmetrical dipoles with a novel feeding configuration
06 p0751 A83-18693
- Theoretical and experimental analysis of cylindrical dipoles with minimal mutual coupling
06 p0744 A83-18694
- Modeling of simple antennas near to and penetrating an interface
07 p0916 A83-21546
- Edge effects in dipole phased arrays
08 p1076 A83-22236
- On the effect of substrate thickness and permittivity on printed circuit dipole properties
09 p1246 A83-23779
- External and internal mutual impedance effects on the radiation patterns of circularly disposed arrays using antennafiers or passive monopoles
09 p1246 A83-23786
- Time domain modeling of nonlinear loads --- for wire antennas
09 p1253 A83-23792
- Analysis of the loop-coupled log-periodic dipole array
10 p1405 A83-26831
- The broad-band scattering response of periodic arrays
10 p1405 A83-26832
- Pulse response of linear dipole antenna
10 p1411 A83-26850
- Experimental study of the efficiency of rectenna elements
11 p1561 A83-27950
- Horizontal dipole antenna above an imperfectly conducting ground fed by a two-wire line
13 p1828 A83-30648
- Waveguide slot antenna with a coupled dipole above the slot
13 p1830 A83-31760
- Directivity optimization for Yagi-Uda arrays of shaped dipoles
15 p2149 A83-35193
- Antennas for nonsinusoidal waves. II - Sensors
16 p2342 A83-35781
- A comparative study of feed impedances of a circular and three different spiral antenna arrays
16 p2344 A83-36731
- An analysis of radiation patterns of corrugated corner reflector antenna systems
16 p2344 A83-36734
- Antennas for nonsinusoidal waves. III - Arrays
22 p3276 A83-46933
- The optimum feed voltage for a dipole antenna for pulse radiation
23 p3442 A83-47827
- A simple power series for the radiation resistance of center-fed dipoles
23 p3443 A83-47837
- DIPOLE MOMENTS**
- NT MAGNETIC MOMENTS**
- The decrease in the earth's magnetic dipole moment
09 p1302 A83-23675
- Determination of electromagnetic field scattered by small defects and influence of boundary between media
13 p1860 A83-30838
- The electromagnetic field in a layered earth induced by an arbitrary stationary current distribution
16 p2341 A83-35410
- Determination of the third derivatives of the dipole moment function for CO₂
21 p3203 A83-45385
- Electrooptical investigations of the effect of the humidification processes of various types of aerosols on the dipole characteristics of the particles
22 p3321 A83-45636
- DIPOLES**
- Minimization of a field scattered by thin dipoles
22 p3272 A83-45683
- DIRAC EQUATION**
- Formation of galaxies in G-variable cosmologies
01 p0127 A83-11294
- Exact solutions of relativistic wave equations --- Russian book
07 p0989 A83-20378
- Comment on 'Dirac states for unit position and momentum Phase consistency of their angular momentum representations'
12 p1775 A83-29532
- The fine-structure constant, magnetic monopoles and dirac charge quantization condition
15 p2225 A83-34275
- Dirac's large numbers hypothesis and continuous creation --- of universe
20 p3066 A83-42429

DIRECT CURRENT

- Numerical simulation of the excitation of a direct current in a plasma through electron acceleration in a plasma-resonance region
03 p0396 A83-13184
- Experimental and theoretical study of a dc arc in an orifice nozzle flow
[AIAA PAPER 83-0399]
05 p0636 A83-16692
- Computer analysis of dc field and current-density profiles of DAR IMPATT diode --- Double Avalanche Region
05 p0631 A83-17764
- Electromigration transport mobility associated with pulsed direct current in fine-grained evaporated Al-0.5%Cu thin films
07 p0921 A83-20744
- Numerical modeling of nonisothermal transient processes in semiconductor power devices under the effect of a high-power dc pulse
08 p1080 A83-22124
- An ultra-low-drift dc amplifier for use with photomultipliers
09 p1267 A83-23743
- Measurement of fatigue crack propagation at -70 C with the direct-current potential probe method
09 p1281 A83-24944
- The effects of direct-current magnetic fields on turtle retinas in vitro
13 p1899 A83-31165
- Josephson-junction circuit analysis via integral manifolds
15 p2151 A83-33928
- Direct-current power supply units GVG 800/350
24 p3549 A83-50115

DIRECT POWER GENERATORS

- NT ALKALINE BATTERIES**
- NT DRY CELLS**
- NT ELECTROSTATIC GENERATORS**
- NT FUEL CELLS**
- NT HOMOJUNCTIONS**
- NT HYDROGEN OXYGEN FUEL CELLS**
- NT MAGNETOHYDRODYNAMIC GENERATORS**
- NT METAL AIR BATTERIES**
- NT NICKEL ZINC BATTERIES**
- NT PHOSPHORIC ACID FUEL CELLS**
- NT PRIMARY BATTERIES**
- NT RADIOISOTOPE BATTERIES**
- NT REGENERATIVE FUEL CELLS**
- NT SOLAR CELLS**
- NT SOLAR SEA POWER PLANTS**
- NT THERMAL BATTERIES**
- NT THERMIONIC CONVERTERS**
- NT THERMOELECTRIC GENERATORS**
- NT ZINC-OXYGEN BATTERIES**
- The calculation of energy storage flywheels of fiber composites with electric energy converter --- German thesis
11 p1590 A83-28666
- Special electrical machines: Sources and converters of energy --- Russian book
21 p3126 A83-45018

DIRECTION FINDERS (RADIO)**U RADIO DIRECTION FINDERS****DIRECTION FINDING**

- Interference field analysis with superimposed noise --- German thesis
06 p0736 A83-18500
- Cyclical, broadband economical scanning procedure for determining the direction of incidence of electromagnetic waves --- German thesis
06 p0736 A83-18522
- Interferometric acoustooptic signal processor for simultaneous direction finding and spectrum analysis
10 p1424 A83-26871
- Direction finding using an adaptive null tracker
11 p1555 A83-27912
- Test results with an experimental direction-finding system
14 p2002 A83-33128
- Multimode planar spiral for DF applications
15 p2121 A83-35089
- Variations of the direction-finding characteristics in the case of the direction finding of the source of a signal with unmatched polarization
15 p2147 A83-35158
- The LLP lightning locating system --- Lightning Location and Protection
17 p2549 A83-38720
- Instrumentation --- for atmospheric analysis
22 p3287 A83-45890
- Comparison between the arrival direction of auroral hiss and the location of aurora observed at Syowa Station
22 p3329 A83-46504

DIRECTIONAL ANTENNAS

- NT DIPOLE ANTENNAS**
- NT HELICAL ANTENNAS**
- NT HORN ANTENNAS**
- NT LENS ANTENNAS**
- NT LOG PERIODIC ANTENNAS**
- NT LOOP ANTENNAS**
- NT PARABOLIC ANTENNAS**
- NT RADAR ANTENNAS**
- NT RHOMBIC ANTENNAS**
- NT SLOT ANTENNAS**
- NT STEERABLE ANTENNAS**
- NT TWO REFLECTOR ANTENNAS**
- NT YAGI ANTENNAS**

Coherent-optical synthesis of an antenna radiation pattern with a zero in a prescribed direction

- 02 p0166 A83-11686
- A wide-band electrically small superdirective array**
03 p0306 A83-14018
- Effects of phase and amplitude quantization errors on hybrid phased-array reflector antennas**
03 p0306 A83-14030
- Circular arrays - Their properties and potential applications**
06 p0737 A83-18602
- Beam-forming in the nearfield of small spherical reflectors**
06 p0740 A83-18637
- A directional antenna element for use in a phase array with H-plane scanning - Requirements, realisation, nearfields**
06 p0751 A83-18674
- Synthesis of conformal HF and VHF directional arrays on spherical bodies using surface resonator techniques**
06 p0743 A83-18679
- The potential possibilities of antennas in terms of directional properties and field attenuation in the shadow zone**
06 p0749 A83-19357
- Synthesis of directional couplers with a fixed phase difference of output signals**
11 p1564 A83-28689
- Phase synthesis of highly directional antenna arrays with a low sidelobe level on one side of the main lobe**
13 p1827 A83-30278
- The effect of errors in the amplitude-phase distribution of a linear antenna on its scattering coefficient**
13 p1828 A83-30282
- Laser-plasma antennas, concentrators, and directional couplers for the rf range**
13 p1851 A83-30910
- Analysis of threshold effects in estimating the location of a random-signal source**
14 p2000 A83-32479
- Small array illuminations for pattern nulling with sidelobe level control**
15 p2146 A83-35083
- On the quality factor and energy center of antennas**
17 p2494 A83-38476
- Spectral domain analysis of interacting microstrip resonant structures**
21 p3123 A83-43841
- Optimization of director antennas**
21 p3121 A83-44778
- Broadband microstrip directional coupler**
24 p3574 A83-49977

DIRECTIONAL CONTROL**NT THRUST VECTOR CONTROL**

- Space Shuttle third flight /STS-3/ entry RCS analysis --- Reaction Control System
[AIAA PAPER 83-0116]
05 p0604 A83-16530
- A summary of NASA/FAA experiments concerning helicopter IFR airworthiness criteria**
19 p2794 A83-41079

DIRECTIONAL SOLIDIFICATION (CRYSTALS)

- Microstructural and dimensional stabilities of a potential gamma/gamma prime-alpha/Mo/ directionally solidified eutectic superalloy under cyclic thermal exposure to 1000 C**
04 p0460 A83-15987
- Thermal expansion of the directionally solidified Ni3Al-Ni3Nb eutectic alloy and its constituent phases**
04 p0461 A83-16006
- An analytical approach to thermal modeling of Bridgman-type crystal growth. I - One-dimensional analysis**
05 p0638 A83-17235
- The effect of heating on the structure of Zh56F alloy in the directionally solidified blades of gas-turbine engines**
07 p0889 A83-20905
- Relations between chemistry, solidification behaviour, and microstructure in IN 100**
07 p0894 A83-21485
- Formation of micropores in a D.S. Ni-Ti-C alloy --- Directionally Solidified**
07 p0895 A83-21498
- Microstructural changes and deformation mechanisms during creep of an unidirectionally solidified gamma/delta and gamma/gamma'-alpha eutectic alloy at elevated temperature**
07 p0897 A83-21610
- Modeling the creep and fracture of the directionally solidified gamma/gamma'-prime-MeC eutectic**
08 p1068 A83-22786
- Structure formation in binary refractory carbide eutectics based on niobium and molybdenum**
09 p1229 A83-23522
- Creep of directionally solidified superalloys and eutectic composites**
09 p1232 A83-24062
- Features observed in the alloying of refractory nickel alloys in the case of directional solidification**
09 p1233 A83-24222
- Some physical aspects of unidirectional crystallization in microgravity**
11 p1531 A83-27343
- Tensile properties of directionally solidified Ni-Al-Ti-(Ta) gamma/gamma prime eutectic alloys**
12 p1714 A83-29415
- Hydrogen in pure aluminum solidified unidirectionally**
13 p1824 A83-31601
- The growth and characterization of epitaxial solar cells on resolidified metallurgical-grade silicon**
16 p2420 A83-35986

- Influence of freezing rate changes of MnBi-Bi eutectic microstructure --- effects of space processing
18 p2643 A83-39899
- The formation of aligned spheres in miscibility gap systems --- during directional solidification of monotectics
19 p2822 A83-42027
- Numerical analysis of heat and mass transfer processes during directional solidification in weightlessness
20 p2939 A83-42893
- Directional solidification and characterization of Hg(1-x)Cd(x)Te alloys
20 p3054 A83-43295
- Convective and interfacial instabilities during solidification of succinonitrile containing ethanol
20 p2946 A83-43299
- Influence of gravity driven convection on the directional solidification of Bi/MnBi eutectic composites
20 p2942 A83-43302
- Directional solidification of alloys in systems containing a liquid miscibility gap
20 p2942 A83-43305
- The influence of gravity on the solidification of monotectic and near monotectic Cu-Pb alloys
20 p2942 A83-43307
- Gravitationally induced convection during directional solidification of off-eutectic Mn-Bi alloys
20 p2942 A83-43308
- The effect of the natural convection on the transition from columnar to equiaxed crystals
20 p3054 A83-43311
- Finite element analysis of the effect of a non-planar solid-liquid interface on the lateral solute segregation during unidirectional solidification
20 p2943 A83-43312
- Ni-base MC-carbide reinforced eutectic alloys for jet engine application
21 p3111 A83-44061
- Effect of swaging on the 1000 C compressive slow plastic flow characteristics of the directionally solidified eutectic alloy gamma/gamma prime-alpha
21 p3111 A83-44340
- Growth of single crystals by the pulling method --- Russian book
21 p3218 A83-45039
- A study of the structure and physicomechanical properties of magnesium alloys under various conditions of solidification by the Stepanov method
21 p3114 A83-45340
- Effect of variable thermal conductivity on isotherms in Bridgman growth
22 p3285 A83-46707
- Order of magnitude analysis of convective effects in dendritic solidification --- of alloys
23 p3413 A83-47290
- [IAF PAPER 83-150]
23 p3413 A83-47290
- Unidirectional solidification behaviors at high cooling rates in Al-Fe-Mn ternary eutectic alloys
23 p3431 A83-47651
- Oxidation and corrosion of a gamma/gamma-prime-NbC unidirectionally solidified pseudo-eutectic alloy
24 p3563 A83-49492
- DIRECTIONAL STABILITY**
NT GYROSCOPIC STABILITY
F/A-18 high angle of attack departure resistant criteria for control law development
[AIAA PAPER 83-2126]
19 p2806 A83-41950
- An improved method for predicting lateral-directional dynamic stability characteristics
[SAE PAPER 830711]
20 p2937 A83-43321
- DIRECTIVITY**
On an index for array optimization and the discrete prolate spheroidal functions
01 p0034 A83-11379
- The gain/directive gain ratio of phased-array antennas with a spread of parameters
02 p0162 A83-11538
- Antenna synthesis on the basis of maximum directive gain
04 p0466 A83-15727
- Electronic beam steering of semiconductor injection lasers - A theoretical analysis
07 p0935 A83-20162
- Electromagnetic-radiation directivity and the mutual intensity function
11 p1555 A83-27926
- Optimization of the directivity of a parabolic reflector antenna
15 p2146 A83-35094
- Directivity of planar array feeds for satellite reflector applications
15 p2126 A83-35181
- Studies on certain modified Luneberg lenses
20 p2963 A83-42369
- On the sampling problem in radiation budget studies
22 p3329 A83-46232
- Loop antennas for directive transmission into a material half space
22 p3274 A83-46527
- DIRECTORS (ANTENNA ELEMENTS)**
Cyclical, broadband economical scanning procedure for determining the direction of incidence of electromagnetic waves --- German thesis
06 p0736 A83-18522
- Calculation of multislot directional couplers, with allowance for the thickness of the common wall between waveguides of different width
08 p1082 A83-23154
- Directivity optimization for Yagi-Uda arrays of shaped dipoles
15 p2149 A83-35193
- Electromagnetic waves in a doubly periodic array of circular longitudinally magnetized ferrite rods
17 p2494 A83-38477
- Analysis of the element pattern shape for circular arrays
24 p3571 A83-49989
- DIRICHLET PROBLEM**
Inverse scattering for an exterior Dirichlet problem --- due to metallic cylinder
01 p0104 A83-10494
- General hyperbolic difference formulas for linear and quasilinear hyperbolic equations
02 p0231 A83-12905
- The behavior of generalized solutions of second-order elliptic equations and of the system of elasticity theory in the neighborhood of a boundary point
05 p0654 A83-17137
- On the shear center of a prismatic bar with T- and channel-cross-section
06 p0771 A83-18150
- Vacuum polarization near the horizon of a black hole in the presence of boundaries
06 p0847 A83-19610
- Distributed control of a system governed by Dirichlet and Neumann problems for a self-adjoint elliptic operator with an infinite number of variables
08 p1156 A83-22045
- Dirichlet boundary control problem for parabolic equations with quadratic cost - Analyticity and Riccati's feedback synthesis
08 p1157 A83-22242
- Behavior of generalized solutions of the Dirichlet problem for high-order elliptic equations near a boundary
09 p1339 A83-24320
- Solutions of a stationary system of Navier-Stokes equations having an infinite Dirichlet integral
09 p1261 A83-24324
- Regional Monte Carlo solution of elliptic partial differential equations
12 p1773 A83-29626
- Spectral multigrid methods for elliptic equations
12 p1773 A83-29663
- On torsion of prismatical beams with longitudinal cavities
17 p2525 A83-38775
- On an efficient algorithm for the Dirichlet variational-difference problem
21 p3198 A83-45215
- Stabilization and structural assignment of Dirichlet boundary feedback parabolic equations
22 p3351 A83-46093
- DIRIGIBLES**
U AIRSHIPS
- DISCHARGE COEFFICIENT**
Experimental study of the air flow through labyrinth seal
16 p2361 A83-35860
- Full coverage discrete hole wall cooling - Discharge coefficients
[ASME PAPER 83-GT-79]
23 p3447 A83-47932
- DISCHARGE TUBES**
U GAS DISCHARGE TUBES
- DISCHARGERS**
NT STATIC DISCHARGERS
- DISCONTINUITY**
NT SHOCK DISCONTINUITY
Instability of an extended tangential discontinuity - The first term of the wave-vector expansion
02 p0169 A83-11641
- Stability of flows with discontinuity surfaces
04 p0475 A83-15077
- Large-scale structure of the core of a spiral discontinuity in a fluid
04 p0475 A83-15082
- Uniqueness of the coupling of fields of a nonlinear ionizing electromagnetic wave at a discontinuity at the point of plasma resonance
06 p0813 A83-19189
- Balance laws of continuum physics
07 p0989 A83-20643
- Electromagnetic treatment of discontinuities in dielectric waveguides - Application to dielectric resonators --- French thesis
08 p1079 A83-22085
- A numerical study of the instability of a tangential velocity discontinuity in compressible gases
16 p2350 A83-35716
- Features of the numerical solution of gasdynamic problems with many interacting discontinuities
18 p2680 A83-39152
- Monotonic second-order difference scheme for hyperbolic systems with two independent variables --- in unsteady gas dynamics
21 p3133 A83-45213
- Reflection properties of phase transition and compositional change models of the 670-km discontinuity --- in earth mantle
23 p3481 A83-47810
- Growth and decay of sonic discontinuities in non-equilibrium magnetogasdynamics
24 p3633 A83-50162
- DISCOS (SATELLITE ATTITUDE CONTROL)**
NOVA-1 - The 'drag-free' navigation satellite
11 p1534 A83-28780
- DISCOVERER SATELLITES**
American photoreconnaissance satellites
06 p0722 A83-19413
- DISCRETE ADDRESS BEACON SYSTEM**
Performance analysis of a dwell-time processor for monopulse beacon radars
08 p1044 A83-22726

DISCRETE FUNCTIONS

- Generalized formulas for the computation of the discrete Fourier transformation
01 p0102 A83-10285
- Concerning the optimality of discrete-data compression in a four-letter coding system
01 p0094 A83-10565
- Further developments in the controlled growth approach for optimal structural synthesis
[ASME PAPER 82-DET-62]
02 p0232 A83-12773
- Discrete Fourier transforms of nonuniformly spaced data
02 p0231 A83-12925
- Analysis of a multilevel iterative method for nonlinear finite element equations
03 p0387 A83-13571
- Solar irradiance calculations in the UV and visible using the adjoint discrete ordinates method
03 p0360 A83-14637
- Computation of a degree of controllability via system discretization --- with application to flexible spacecraft control
03 p0287 A83-14844
- The parametric discrete Fourier transformation
06 p0802 A83-18028
- The use of the intraperiod symmetry of harmonic basis functions to compute the discrete Fourier transformation
06 p0802 A83-18039
- Numerical solution of the Navier-Stokes equations by multi-grid techniques
08 p1088 A83-23183
- Adaptive Nystroem-Runge-Kutta methods for systems of second-order ordinary differential equations
10 p1470 A83-25589
- Geometrical criterion for the stability of discrete stationary systems with one nonlinearity
13 p1910 A83-30090
- Method for generating discrete soliton equations. I, II
14 p2080 A83-32517
- Mathematical models of discrete systems of automatic control with indeterminate parameters
14 p2076 A83-32963
- Stabilizability of multidimensional discrete systems in cases of complete and incomplete information
14 p2076 A83-32964
- A system of orthogonal functions for the fast spectral analysis of signals
16 p2404 A83-35935
- Discrete variable theory of triatomic photodissociation
16 p2327 A83-36519
- An adaptive identifier for discrete-time linear systems
17 p2565 A83-37088
- Fast Fourier transform and convolution algorithms /2nd revised edition/
17 p2571 A83-37175
- A discretized-intensity method proposed for two-dimensional systems enclosing radiative and conductive media
17 p2506 A83-37865
- The numerical differentiation of discrete functions using polynomial interpolation methods
17 p2564 A83-38795
- The immersion under feedback of a multidimensional discrete-time non-linear system into a linear system
17 p2570 A83-38823
- Continuum models of discrete systems 4; Proceedings of the Fourth International Conference, Stockholm, Sweden, June 29-July 3, 1981
19 p2896 A83-41469
- Numerical methods in heat transfer
20 p2970 A83-42653
- Algorithm for the fast computation of the two-dimensional discrete Fourier transformation
20 p3041 A83-42903
- Discrete mechanics - Some remarks --- numerical method in celestial mechanics
20 p3062 A83-43573
- Discrete models for linear multivariable systems
20 p3040 A83-43619
- The transmission of discrete messages in radio channels (2nd revised and enlarged edition) --- Russian book
21 p3121 A83-45009
- Stability and stabilization of discrete processes --- Russian book
21 p3195 A83-45038
- Stability of vertical discretization schemes for semi-implicit primitive equation models - Theory and application
23 p3489 A83-47394
- DISCRIMINANT ANALYSIS (STATISTICS)**
Inter-class discrimination using synthetic discriminant functions /SDFs/
09 p1266 A83-23539
- An application of discriminant analysis to variable and nonvariable stars
09 p1353 A83-23742
- DISCRIMINANT FUNCTIONS**
U DISCRIMINANT ANALYSIS (STATISTICS)
- DISCRIMINATION**
NT BRIGHTNESS DISCRIMINATION
NT SENSORY DISCRIMINATION
NT TACTILE DISCRIMINATION
NT VISUAL DISCRIMINATION
- DISCRIMINATORS**
NT FRAUNHOFER LINE DISCRIMINATORS
NT FREQUENCY DISCRIMINATORS
Discrimination of speech and high-speed data using an adaptive predictor for DSI application --- Digital Speech Interpolation
07 p0910 A83-19756

DISEASES

- NT AIRBORNE INFECTION
 NT ANEMIAS
 NT ARTERIOSCLEROSIS
 NT ASTHMA
 NT ASTIGMATISM
 NT BONE DEMINERALIZATION
 NT CANCER
 NT CARBON MONOXIDE POISONING
 NT CATARACTS
 NT CONJUNCTIVITIS
 NT CORONARY ARTERY DISEASE
 NT DIABETES MELLITUS
 NT EDEMA
 NT EMPHYSEMA
 NT ENCEPHALITIS
 NT EYE DISEASES
 NT GLAUCOMA
 NT HEADACHE
 NT HEART DISEASES
 NT INFECTIOUS DISEASES
 NT KERATITIS
 NT KIDNEY DISEASES
 NT LEAD POISONING
 NT MENINGITIS
 NT MYOCARDIAL INFARCTION
 NT NEURITIS
 NT OSTEOPOROSIS
 NT PARALYSIS
 NT PARASITIC DISEASES
 NT PULMONARY LESIONS
 NT RADIATION SICKNESS
 NT RESPIRATORY DISEASES
 NT TACHYCARDIA
 NT THROMBOSIS
 NT TOXIC DISEASES
 NT TUMORS
 NT ULCERS

Treatment of degenerative-dystrophic diseases of the vertebral column by a helium-neon laser

03 p0381 A83-14341
 Ultrasonic study of the gall bladder

03 p0381 A83-14342
 Prevalence of selected pathology among currently certified active airmen 04 p0521 A83-15535
 Current aspects of prophylaxis and treatment of hearing disorders in patients with Meniere's disease 05 p0672 A83-16950

Clinical aviation medicine --- Book

05 p0674 A83-17300
 Pointers to diagnosis of psychiatric illness in aircrew 18 p2737 A83-40354

Type II collagen-induced autoimmune endolymphatic hydrops in guinea pig 23 p3495 A83-47819

DISHES

U PARABOLIC REFLECTORS

DISILICIDES

A study of the cracking of oxide films on MoSi₂ using the method of acoustic emission 07 p0899 A83-20680

Temperature-dependent ion mixing and diffusion during sputtering of thin films of CrSi₂ on silicon 19 p2903 A83-40740

Liquid phase growth of epitaxial Ni and Co silicides 21 p3219 A83-45494

The effect of the thickness of a protective molybdenum disilicide coating on the maximum operating temperature of heaters 24 p3568 A83-49078

Thermal stability of compositions consisting of molybdenum disilicide, quartz, and glass 24 p3568 A83-49080

The use of the acoustic emission method for analyzing the quality of protective coatings --- molybdenum disilicide coatings on Mo 24 p3568 A83-49082

DISINFECTANTS

U ANTISEPTICS

DISK GALAXIES

Mapping the Local Supercluster 01 p0115 A83-10206

A nuclear spectroscopic survey of disk galaxies. II - Galaxies with emission lines not excited by stellar photoionization 02 p0254 A83-12109

A nuclear spectroscopic survey of field disk galaxies 03 p0406 A83-13553

A mass estimate for the companion to the 'Cartwheel' galaxy 03 p0421 A83-13953

Photographic photometry of galaxies using the INMP. I - The lenticulars NGC404 and NGC524 --- Interactive Numerical Mapping Package 04 p0546 A83-15046

The warping of disk galaxies. I - Theory 05 p0697 A83-16992

Stable polar gas disks in triaxial S0 galaxies 05 p0700 A83-17026

Statistics of structure and rotation parameters of disk galaxies 06 p0836 A83-19172

On the global density waves in self-gravitating flat disks 06 p0843 A83-19482

Inner ring structures in galaxies as distance indicators. III - Distances to 453 spiral and lenticular galaxies 07 p1013 A83-20080

Disc stability and halo mass 07 p1016 A83-20768

The NGC 1961 group of galaxies 07 p1018 A83-20954

Time evolution of disk galaxies undergoing stochastic self-propagating star formation 07 p1020 A83-21112

The effects of induced star formation on the evolution of the galaxy. II - The galactic ecosystem 07 p1020 A83-21117

The L varies as sigma to the n power relation for the bulge components of disk galaxies 08 p1181 A83-23032

Rotational velocities and central velocity dispersions for a sample of S0 galaxies 08 p1182 A83-23035

Effects of environment on neutral hydrogen distribution for disk galaxies in the Virgo Cluster area 10 p1512 A83-26706

Dynamic effects of the angular asymmetry of stellar motions in galaxies 10 p1516 A83-26901

The formation of disc galaxies 13 p1953 A83-31552

The origin of the nonthermal radio emission in normal disk galaxies 13 p1953 A83-31559

Rotation curve of the edge-on spiral galaxy NGC 5907: disc and halo masses 13 p1957 A83-31698

The ages of the disks of S0 galaxies 14 p2098 A83-33186

Nonlinear effects in a gravitating plasma disk subject to a poloidal magnetic field 15 p2254 A83-33721

Very red, yet H I rich galaxies 15 p2255 A83-33826

Mass model of spiral galaxies disk 15 p2262 A83-34535

Tidal interactions of disc galaxies 15 p2266 A83-34607

Dissipative effects in the gaseous subsystems of flat galaxies 15 p2271 A83-34754

Surface photometry of edge-on galaxies. III - Luminosity distributions in eight galaxies 16 p2422 A83-35676

Bulge-halo effects in barred galaxies 16 p2426 A83-36688

The energy and momentum of slow drift spiral density waves 17 p2600 A83-37645

Numerical investigation of the generation of global spiral structure in interacting galaxies 17 p2603 A83-37889

Stochastic self-propagating star formation in three-dimensional disk galaxy simulations 17 p2604 A83-37907

The stability of a differentially rotating disk of stars 17 p2610 A83-38551

On the nonlinear theory for the stability of a rotating gravitating disk 17 p2614 A83-38848

On a general fluid dynamical theory of discrete unstable spiral modes in disk-shaped galaxies 18 p2764 A83-39008

Colliding and merging galaxies. II - S0 galaxies with polar rings 18 p2767 A83-39589

Quiet starts for galaxy simulations 19 p2910 A83-40751

Scalloped disk galaxies - A Kelvin-Helmholtz instability? 19 p2918 A83-41618

The Riemann disks. I - Equilibrium and secular evolution 20 p3071 A83-43051

The Riemann disks. II - Stability 20 p3071 A83-43052

Resonant effects during the tidal encounter of disc galaxies 21 p3232 A83-44732

Kinematical and chemical evolution of the galactic disc 21 p3233 A83-44754

The rate of star formation in normal disk galaxies 21 p3235 A83-45531

Rotation, mass and physical conditions in nucleus of spiral galaxy NGC 7537 23 p3527 A83-48444

Transfer of angular momentum in a galactic disk by the interaction of clouds of interstellar gas 24 p3653 A83-49166

Rotation curve and mass model for the edge-on galaxy NGC 5907 24 p3641 A83-49211

Vertical motion and the thickness of H I disks - Implications for galactic mass models 24 p3654 A83-49213

Do spiral galaxies have a variable disk thickness? 24 p3654 A83-49214

NGC 3992 - A galaxy without a massive halo 24 p3654 A83-49217

On the evolution of perturbed gas disks 24 p3655 A83-49224

Conflicts and directions in spiral structure --- in disk galaxies 24 p3656 A83-49232

Theories of warps --- in disk galaxies 24 p3656 A83-49233

Disk stability --- and barred galaxies

24 p3641 A83-49234

Instabilities of hot stellar discs

24 p3656 A83-49235

Stabilizing a cold disk with a 1/r force law

24 p3656 A83-49236

The barred galaxy NGC 7741

24 p3656 A83-49243

Formation of rings and lenses --- in disk galaxies

24 p3657 A83-49245

Collisions and merging of disk galaxies

24 p3642 A83-49261

Is the Hubble type of a disk system essentially determined by one parameter - Total mass?

24 p3657 A83-49264

Environmental effects on the flattening distribution of galaxies

24 p3664 A83-49880

DISKS (SHAPES)

NT ACTUATOR DISKS

NT INTERVERTEBRAL DISKS

NT ROTATING DISKS

Excitation of elastic wave in a layer by disk-shape radiator of finite dimensions 01 p0057 A83-10371

Determination of thermal stresses in disks with the Boundary Element Method 01 p0058 A83-10574

Effects of friction in tensile and compressive stress problems for a rigid circular disk in an infinite plate 02 p0197 A83-13066

Analysis of process stresses in SiC-Si two-layer disks 03 p0302 A83-14735

Calculation of the flow of a dust-laden gas over a disk and the flat end of a cylinder 05 p0639 A83-17406

Evolution of the regular precession of a rigid body carrying a viscoelastic disk 06 p0806 A83-19121

Pulsed laser excitation of normal modes in a metal disk 08 p1107 A83-22405

Estimation of residual stresses in heterogeneous disks 09 p1277 A83-23514

The boundary integral method for the solution of planar multicrack problems of linear elastostatics --- German thesis 09 p1281 A83-24846

Analysis of the puncture of a bisphenol-A polycarbonate disc 10 p1400 A83-26075

Nonstationary temperature fields during the heat treatment of titanium disks of complex configurations 16 p2361 A83-35589

Submersion of a disk into a compressible fluid at an angle to the free surface 16 p2350 A83-35714

High-frequency nonaxisymmetric vibrations of elastic disks 17 p2521 A83-37574

Dynamic notch-stress problem in a perforated circular disk 20 p3006 A83-43001

High-q dielectric disk resonators 22 p3276 A83-45669

An equivalent procedure for the evaluation of the stress intensity factors of a radial crack in a disc 22 p3306 A83-46392

Diffraction of a plane wave by a structure consisting of an ideally rigid disk and a spherical mirror 23 p3503 A83-47174

Fast pulsars with disks 23 p3526 A83-47873

A new approach to fault-tolerant helicopter swashplate control [AIAA PAPER 83-2485] 23 p3412 A83-48345

The standing vortex behind a disk normal to uniform flow at small Reynolds number 24 p3577 A83-49468

DISLOCATIONS (MATERIALS)

NT CRYSTAL DISLOCATIONS

NT EDGE DISLOCATIONS

NT SCREW DISLOCATIONS

Bounds for the dislocation densities and the stress intensity factors in elastic crack problems 02 p0190 A83-12042

The forming limit diagram of sheet metals and effects of strain path changes on formability - A dislocation treatment 03 p0301 A83-14704

Thermoelastic fracture solutions using distributions of singular influence functions. I - Determining crack stress fields from dislocation distributions 05 p0656 A83-17875

Analysis of steady state crack growth by discrete dislocation theory 08 p1118 A83-21774

Kinetic enrichment of hydrogen at interfaces and voids by dislocation sweep-in of hydrogen 10 p1398 A83-26279

On the origin of the first peak of acoustic emission in 7075 aluminium alloy 12 p1714 A83-29507

Discrete dislocation analysis and path dependent plasticity 14 p2031 A83-32662

Dislocation shielding of a crack in a quasi continuum approximation 15 p2179 A83-34479

The relaxation of submicrosecond pressure pulses in a solid body 16 p2364 A83-35543

Stress field related to dislocation arrangements observed in the phase boundary of a lamellar in-situ composite 18 p2667 A83-40257

Diffusion induced grain boundary migration in Ni-C alloys 18 p2668 A83-40615

A Griffith crack shielded by a dislocation pile-up 21 p3157 A83-44908

DISORIENTATION

NT JET LAG

Spatial disorientation in the naval aviation environment 08 p1149 A83-22979

DISPENSERS

Aerodynamic development of a spinning submunition dispenser [AIAA PAPER 83-2082] 19 p2805 A83-41916

DISPERSING

Numerical analysis of the dispersion of detonation products 01 p0047 A83-11274

Dispersed crystalline powders - An analysis of the scientific-technical literature 14 p1992 A83-32144

Stability of the surface layer and its relation to the dispersion of primary pollutants in St. Louis 18 p2711 A83-39122

Geography of trace elements: Global dispersion --- Russian book 23 p3483 A83-48250

Correlation of pulsational velocities of the dispersed phase in jet flows 23 p3452 A83-48657

DISPERSION

Fine-dispersion aerosol and climate 06 p0788 A83-17998

Analysis of the effect of dispersion errors of memories on the precision of discrete spectral analysis 06 p0802 A83-19180

The medium dispersion prism of the UK Schmidt Telescope 13 p1936 A83-30398

Energy characteristics of an electromagnetic field and an extraneous particle in a dispersive medium 14 p2079 A83-32168

Calculation of the dispersy of the combustion products of a metal particle 18 p2663 A83-39164

DISPERSION PRECIPITATION HARDENING

U PRECIPITATION HARDENING

DISPERSIONS

NT AEROSOLS

NT COLLOIDS

NT EMULSIONS

NT FOG

NT LIQUID-GAS MIXTURES

NT NUCLEAR EMULSIONS

NT PHOTOGRAPHIC EMULSIONS

NT SMOKE

The effect of dispersoids on the ductile fracture toughness of Al-Mg-Si alloys 08 p1065 A83-22015

The use of kinetic theory for describing disperse media 13 p1933 A83-30670

Aluminum-lithium dispersion alloys 14 p1995 A83-32877

Meteorological tracer techniques for parameterizing atmospheric dispersion 18 p2727 A83-39885

DISPLACEMENT

A note on two-dimensional finite-deformation theories of shells 01 p0060 A83-10862

Key curve analysis of crack-growth-resistance curves 02 p0190 A83-12041

A formulation and solution procedure for post-buckling of thin-walled structures 04 p0494 A83-15007

A theory of substructure modal synthesis [ASME PAPER 82-WA/APM-29] 04 p0499 A83-15693

An improved dislocation approach in solving three-dimensional boundary value problems 05 p0681 A83-17324

The design and control of linear bidirectional stepping motors - Application to machine tools --- French thesis 06 p0750 A83-18495

The use of the plastic crack tip opening displacement to correlate fatigue crack growth data for a structural steel 08 p1060 A83-21713

Notes on the relationship between symmetric plane strain and torsion-free axis-symmetric problems 08 p1123 A83-22725

A Saint-Venant principle for nonlinear elasticity 09 p1279 A83-24134

St. Venant formulae for generalized St. Venant problems 09 p1279 A83-24135

An algorithm for kinetoelastodynamic analysis of plane mechanisms with rectilinear elements 09 p1280 A83-24505

On minimum-principles for the initial-boundary-value problem of elastic-plastic plates with moderate rotations 09 p1283 A83-25217

Influence of tangential displacements on the dynamic buckling of viscoplastic cylindrical shells 10 p1442 A83-26820

Auxiliary convergence criteria for Mindlin plate elements and their application to the four-node quadrilateral [AIAA 83-0834] 12 p1737 A83-29743

Displacement effects in transonic airflow flows 13 p1804 A83-30638

Stability loss of compressed longitudinally reinforced cylindrical shells in the case of finite displacements with allowance for local buckling of rib-plates 15 p2178 A83-34439

Exact analytic solutions to three-dimensional thermoelasticity problems 15 p2180 A83-35037

Displacement control of elastic structures - Integral control with a robustness property 17 p2565 A83-37090

Calculation of stresses, strains and displacements in an n-layer elastic-continuous system under the action of two complex loads uniformly distributed on circular areas 17 p2519 A83-37273

A displacement formulation for the finite element elastic-plastic problem 19 p2857 A83-41153

The accuracy of COD values calculated according to BS 5762 21 p3158 A83-44918

Determination of nodal forces in elements under surface and bulk loads for axisymmetric and plane elasticity problems 21 p3163 A83-45323

A curvilinear triangular finite element for plate bending by a hybrid method of assumed displacements supplemented with assumed stresses 24 p3593 A83-49442

Effects of crack growth on the load-displacement characteristics of precracked specimens under bending 24 p3594 A83-49864

DISPLACEMENT MEASUREMENT

Quantitative deformation measurement with virtual-image holographic interferometry --- Dutch thesis 02 p0176 A83-11897

Derivation of Wells' COD estimation formula and re-calculation of gamma values 02 p0190 A83-12047

Horizontal wind vector determination from the displacement of aerosol distribution patterns observed by a scanning lidar 02 p0216 A83-12959

In-flight deflection measurement of the HiMAT aeroleastically tailored wing 03 p0281 A83-13167

On-line acquisition and analysis for holographic nondestructive evaluation 03 p0337 A83-13873

Large deformation whole-field measurements of isotropic plates by sandwich hologram interferometry 03 p0341 A83-14399

Crack opening displacement as a fracture mechanics parameter in eddy current NDE 04 p0496 A83-15185

Effects of closure on the detection probability of fatigue cracks 04 p0490 A83-15186

Applications of the white light speckle method to interior displacement measurement 05 p0646 A83-17717

The application of fibre optics to remote speckle metrology using incoherent light 05 p0647 A83-17939

Microwave interferometer for measurements of small displacements 07 p0929 A83-20546

Towards displacement measurement in remote locations by holographic fiber optics probes 09 p1264 A83-23362

In-plane interferometric strain/displacement measurement at high temperatures 09 p1264 A83-23363

Transient measurements in hostile environments 09 p1265 A83-23367

Precision optical encoder 09 p1267 A83-23588

Deformations of anisotropic layered materials 10 p1442 A83-26818

Real-time holographic interferometry - A microcomputer system for the measurement of vector displacements 10 p1424 A83-26873

Laser microspeckle technique in displacement measurement near a crack tip 11 p1575 A83-28701

Electromagnetic acoustic transducer for in-plane and plane-normal velocity measurements 12 p1728 A83-29142

Acoustical speckle interferometry 12 p1730 A83-29586

Automated laser speckle interferometry displacement contour analyzer 12 p1730 A83-29587

A review of holographic nondestructive evaluation at Lawrence Livermore National Laboratory 12 p1734 A83-29589

Lensless Fourier holography applied to nondestructive testing - Experimental results 15 p2163 A83-33754

Linear capacitive microdisplacement transduction using phase read-out 17 p2512 A83-38533

Measurement of an object's displacements along six coordinates by a differential laser method 18 p2690 A83-40402

On the off-axis tension test for unidirectional composites 19 p2819 A83-41033

Holographic technique for simultaneous measurement of displacement and tilt 19 p2847 A83-41101

Interferometric displacement sensing in the open atmosphere 19 p2848 A83-41177

Calculation of electromagnetic fields in displacement transducers 19 p2841 A83-42016

Analysis of crack-tip moiré fringe patterns 21 p3156 A83-44888

X-ray interferometer calibration of microdisplacement transducers 21 p3140 A83-44949

Transient response of a central crack to a tensile pulse 21 p3161 A83-45168

Design of an experiment to determine deformations using holographic interferometry 23 p3454 A83-47560

DISPLAY DEVICES

NT ANEMOMETERS

NT APPROACH INDICATORS

NT FLOW DIRECTION INDICATORS

NT HEAD-UP DISPLAYS

NT HELMET MOUNTED DISPLAYS

NT HOT-FILM ANEMOMETERS

NT HOT-WIRE ANEMOMETERS

NT KINFOFORM

NT PLASMA DISPLAY DEVICES

NT POSITION INDICATORS

NT RADARSCOPES

NT RADIO DIRECTION FINDERS

NT SONIC ANEMOMETERS

NT SPACECRAFT POSITION INDICATORS

NT SPEED INDICATORS

NT TACHOMETERS

NT WIND VANES

Human factors and the design of display terminals 01 p0085 A83-10253

Color graphics in ATE 01 p0028 A83-10747

Color, pictorial display formats for future fighters 01 p0010 A83-11134

Airborne electronic terrain map display - An update 01 p0010 A83-11135

Integrated perceptual information for designers 01 p0029 A83-11136

Investigating the correlation between reading errors and degraded numerics - Or, do missing dots call the shots 01 p0085 A83-11168

Flat-panel video resolution LED display system 01 p0029 A83-11170

Video stand-alone instrument multi-function cockpit display system 01 p0010 A83-11172

A cost effective approach to design evaluation of advanced system display switchology 01 p0093 A83-11200

Dot-matrix display light measurement and interpretation techniques --- for qualification tests techniques 01 p0011 A83-11257

The complete book of cockpits 02 p0135 A83-11575

Interactive smoothing of digitized point data 02 p0226 A83-11817

Evaluation of alternative alphanumeric keying logics 02 p0225 A83-12087

Flight simulator display capability significantly advanced 02 p0135 A83-12935

Trend analysis concerning the displays and the keyboard of GPS navigation receivers for different applications 02 p0135 A83-13010

The employment of digital signal processing in radar devices - Advantages and disadvantages for the practice 02 p0134 A83-13014

Compensation electronics for staring focal plane arrays 03 p0326 A83-13734

Perception of position by the pilot in the case of computer-generated external visual scene displays for a landing approach --- German book 03 p0383 A83-14111

The display capacity of alphanumeric information on visual display units with restrictions in the electrical or visual channel --- Dutch book 03 p0383 A83-14113

Display methods of laser radar data using a computer system 03 p0328 A83-14132

The effect of two types of induced-motion displays on perceived location of the induced target 03 p0383 A83-14525

Computer graphics displays of nonlinear calculations 04 p0526 A83-15019

Advanced Aircrew Display Symposium, 5th, Patuxent River, MD, September 15, 16, 1981, Proceedings 04 p0447 A83-16126

Color selection and verification testing for airborne color CRT displays 04 p0524 A83-16128

Information requirements for pilot supervision of automatic landing in low visibility conditions 04 p0524 A83-16129

The maneuvering flight path display - An update 04 p0447 A83-16130

Advanced fighter technology integrator /AFTI/ F-16 display mechanization 04 p0448 A83-16132
Airborne electronic colour displays 04 p0448 A83-16133
'Light bar' attitude indicator 04 p0448 A83-16136
The perception of colour on electro-optical displays 04 p0524 A83-16328
Characteristics of flight simulator visual systems 04 p0450 A83-16331
Simulator studies to develop and improve flight attitude information 04 p0448 A83-16334
Simple CIG - An approach to visual simulation for procedure training --- Computer Image Generation 04 p0450 A83-16335
AOI displays in simulation --- Area Of Interest 04 p0448 A83-16337
Evaluation of the perceptual attributes of emissive and non-emissive display designs using computer simulation 05 p0677 A83-16870
A method of rotating areas on a raster scan graphic display 05 p0644 A83-16871
Improving simulation training through research 05 p0676 A83-17309
Digital image processing - A systems approach --- Book 07 p0928 A83-19925
The automated cockpit 07 p0866 A83-20849
Multicriterial estimation in the synthesis of means for information interaction in complex systems --- cockpit display optimization 08 p1156 A83-22125
System architecture of Vicom digital image processor 08 p1097 A83-22533
Processing display system architectures 08 p1152 A83-22534
Advances in electro-optic shutter stereoscopic displays 08 p1098 A83-22566
Visual simulation and image realism II: Proceedings of the Conference, San Diego, CA, August 27, 28, 1981 08 p1102 A83-22830
Trinoscope color displays for simulation 08 p1102 A83-22831
Calligraphic/raster color display for simulation 08 p1102 A83-22832
Two years of training with the first true three-dimensional simulator 08 p1047 A83-22833
Computer-generated images in visual simulation and avionic technologies 08 p1047 A83-22835
Pilot task profiles, human factors, and image realism 08 p1047 A83-22836
Image quality and observer performance 08 p1150 A83-22891
Electromagnetic radiation emissions from visual display units - A review 09 p1324 A83-23885
Selection and experimental comparison of computer input devices --- Book 09 p1325 A83-24902
Multifunction screens for cathode ray tubes 09 p1257 A83-25114
The effects of extended practice on the evaluation of visual display codes 10 p1456 A83-26000
A study on airborne integrated display system and human information processing 10 p1456 A83-26086
Computer generated cockpit engine displays 10 p1376 A83-26309
Human factors in the application of large screen electronic displays to transport flight station design 10 p1376 A83-26312
A comparison of color versus black and white visual display as indicated by bombing performance in the 2B35 TA-4J flight simulator 10 p1376 A83-26313
Potential uses of two types of stereographic display systems in the airborne fire control environment 10 p1376 A83-26314
Selection of remotely labeled switch functions during dual task performance 10 p1459 A83-26315
Integrated control/display unit vs. dedicated control heads for radio tuning in a KC-135 flight simulator 10 p1459 A83-26318
The manipulation of interaction effects in multivariable feedback systems 10 p1465 A83-26525
A C-band weather radar system with spherics to serve multiple diverse users in the Canadian climate 11 p1631 A83-27096
Using program transformations to derive lind-drawing algorithms 11 p1646 A83-27121
Flight deck display 11 p1530 A83-27123
The display of molecular models with the Ames Interactive Modeling System (AIMS) 12 p1768 A83-29548
Humanscale 4/5/6 --- Book on human factors engineering information 13 p1906 A83-30155
Analysis of in-trail following dynamics of CDTI-equipped aircraft --- Cockpit Displays of Traffic Information 13 p1807 A83-30161
Information theory and visual displays 13 p1911 A83-31584
The optical-waveguide readout of signals in surface acoustic wave devices 15 p2153 A83-35168

Operator's activities at CRT terminals - A behavioural approach 16 p2400 A83-35564
Advanced display techniques for training the multi-member tactical air crew 16 p2302 A83-36207
[AIAA PAPER 83-1079]
Compensation for time delay in flight simulator visual-display systems 16 p2312 A83-36222
[AIAA PAPER 83-1080]
The 8 by 8 display 17 p2564 A83-38061
Lessons learned from the CSIS --- Centralized Storm Information System 17 p2549 A83-38717
Temporal integration following intensification of long-lasting visual displays 19 p2884 A83-40749
Simulation evaluation of flight controls and display concepts for VTOL shipboard operations 19 p2789 A83-41668
[AIAA PAPER 83-2173]
Uniform color scale applications to computer graphics 21 p3190 A83-44268
Man, machine and configuration - Human factors versus hardware in avionic display design 21 p3189 A83-44686
Development of terrain-following displays for the tornado aircraft 21 p3091 A83-44687
Application and experience of colour CRT flight deck displays 21 p3091 A83-44688
Four-dimensional flight management using colour CRT displays 21 p3091 A83-44689
Comparison of color and black-and-white visual displays as indicated by bombing performance in the 2B35 TA-4J flight simulator 21 p3092 A83-44692
Biocular magnifiers for use with cathode ray tube (CRT) displays 21 p3139 A83-44786
Evolution of map display optical systems 21 p3092 A83-44830
Space technology - The art and science of ergonomics 21 p3092 A83-45605
Judgments of relative motion in tactical displays [AD-A129722] 22 p3349 A83-46699
Experimental evaluation of the visual efficiency of candidate devices for the display of meteorological radar data 23 p3453 A83-47146
Central operating and display unit for avionics systems 23 p3401 A83-47193
Stereotelevision display devices --- Russian book 23 p3459 A83-48249
Operational and control display concepts for flight management systems in new generation transport aircraft [AIAA PAPER 83-2489] 23 p3405 A83-48348
The application of a graphic display for the analysis of scientific telemetry data in experiments involving the search for gamma-ray transients on Prognost 6 and 7 23 p3500 A83-48417

DISPLAY SYSTEMS

U DISPLAY DEVICES

DISPOSAL

NT WASTE DISPOSAL

DISSIPATION

NT ENERGY DISSIPATION

NT OHMIC DISSIPATION

Dissipationless galaxy formation and the r to the

1/4-power law 03 p0420 A83-13935

The dissipation of a sodium cloud

13 p1882 A83-31627

Anisotropy in MHD turbulence due to a mean magnetic field 18 p2745 A83-39618

A dissipation postulate for discrete and continuous plastic systems 21 p3155 A83-44849

DISSIPATORS

U DISSIPATION

DISSOCIATION

NT AUTOIONIZATION

NT GAS DISSOCIATION

NT PHOTODISSOCIATION

NT THERMAL DISSOCIATION

Determination of the activation energies of

monomolecular dissociation reactions by means of IR

spectroscopy-N-nitrodimethylamine 01 p0023 A83-11323

Supersonic nozzle beam source of atomic oxygen

produced by electric discharge heating [AD-A122032] 02 p0234 A83-12819

Kinetic processes in the HgBr/B-X//HgBr2 dissociation

laser 03 p0331 A83-13917

Electron-sulphur dioxide total ionisation and electron

attachment cross-sections 10 p1479 A83-25649

Analysis of multistage dissociation of polyatomic

molecules 10 p1480 A83-26679

Inclusion of discrete-to-continuum coupling in

multiphoton excitation and dissociation calculations 11 p1546 A83-28758

The relation between the molecular emissivity and the

molecular absorptivity of the surfaces of bodies 13 p1817 A83-30665

Dissociative recombination of electrons with NO(+) ions 17 p2579 A83-38521

Astrophysical molecules of A1H and CaH - RKR potential

and dissociation energies --- Rydberg-Klein-Rees 18 p2764 A83-39192

The dissociation energy of Cu2 - Do we want to perform

multi-reference singles and doubles CIs on many-electron

systems? 19 p2898 A83-41864

Energy lost in formation of fluorine atoms in the course

of electron-beam dissociation of fluorine and fluoride

molecules 20 p2997 A83-43797

Merged electron-ion beam experiments. V - Dissociative

recombination of OH(+), H2O(+), H3O(+) and D3O(+) 23 p3511 A83-48583

Integrated navigation by supplementing MLS with DAS
--- DME-based Azimuth System 09 p1202 A83-24872

Simple integrated navigation systems 09 p1202 A83-24873

Adjacent channel interference in the case of the precision distance measuring system DME/P 10 p1374 A83-26480

Estimation regarding the feasibility of using larger distances in measurements with L2F systems in flight tests --- Laser-two-Focus 10 p1431 A83-26487

Development of an optical distance sensor for robots 11 p1573 A83-28101

VOR/DME automated station selection algorithm 11 p1528 A83-28597

Self-calibrating surface measuring machine --- for fabrication of aspheric optical elements 13 p1847 A83-31016

Telescope alignment with the absolute distance interferometer 13 p1921 A83-31023

An interference technique of distance measurement using a fiber-optic waveguide 18 p2688 A83-39436

The potential accuracy of distance measurements in passive detection and ranging 22 p3272 A83-45670

DAS, a DME-supported multifunction system with a wide applications range for distance and angle measurements with data transfer 23 p3401 A83-47199

The measurement of turbomachinery stator-to-drum running clearances [ASME PAPER 83-GT-204] 23 p3410 A83-48005

Improvement of a captive trajectory system by using optical distance sensors --- store separation from aircraft [ONERA, TP NO. 1983-115] 24 p3550 A83-49426

DISTANCE PERCEPTION
U SPACE PERCEPTION

DISTILLATION
Tests of blending and correlation of distillate fuel properties 01 p0028 A83-11050

DISTORTION
NT FLOW DISTORTION
NT SIGNAL DISTORTION
NT SURFACE DISTORTION

Stability of compensation regimes for nonlinear distortions of beams with any polarization 05 p0650 A83-17077

Restoration of bilinearly distorted images. I - Finite impulse response linear digital filtering 08 p1101 A83-22672

Residual stresses and distortion in weldments - A review of the present state-of-the-art 12 p1746 A83-29903

Distortions of a CW light beam propagating through gas Self-lensing and spatial ringings 21 p3144 A83-44804

A survey of inlet/engine distortion compatibility [AIAA PAPER 83-1166] 21 p3088 A83-45509

Dynamic distortion in a short s-shaped subsonic diffuser with flow separation --- Lewis 8 by 6 foot Supersonic Wind Tunnel [AIAA PAPER 83-1412] 21' p3092 A83-45515

DISTRIBUTED AMPLIFIERS
A compact broad-band multifunction ECM MIC module 07 p0923 A83-21533

Analysis of distributed-feedback diode lasers with gain-induced waveguiding 08 p1110 A83-22671

On theory and performance of solid-state microwave distributed amplifiers 17 p2497 A83-37799

On noise in distributed amplifiers at microwave frequencies 21 p3122 A83-43836

DISTRIBUTED PARAMETER SYSTEMS
Distributed-parameter microwave active devices /Review/ 01 p0035 A83-10401

The gain/directive gain ratio of phased-array antennas with a spread of parameters 02 p0162 A83-11538

Complex wave regimes in distributed dynamic systems /Review/ 02 p0232 A83-11678

The nature of the temporal solutions of damped distributed systems with classical normal modes [ASME PAPER 82-WA/APM-14] 04 p0531 A83-15692

Systematic occurrence of repeated eigenvalues in structural optimization 04 p0500 A83-15946

Robustness of the independent modal-space control method 04 p0528 A83-16116

Estimation of convergence speed in the second uniform limit theorem of Kolmogoroff 04 p0530 A83-16410

An optimization technique for lumped-distributed two ports 07 p0922 A83-21528

On the problem of observation spillover in self-adjoint distributed-parameter systems 08 p1156 A83-22044

Distributed control of a system governed by Dirichlet and Neumann problems for a self-adjoint elliptic operator with an infinite number of variables 08 p1156 A83-22045

A new multiple-model adaptive filter for continuous-time stochastic distributed parameter systems 08 p1156 A83-22073

Control of wave processes with distributed controls supported on a subregion 08 p1157 A83-22243

Parameter estimation of nonlinear nonautonomous distributed systems 09 p1327 A83-24709

Optimal control and controller location for distributed parameter elastic systems 09 p1328 A83-24723

Digital stochastic control of distributed-parameter systems --- large flexible space structures 09 p1216 A83-24754

Problems in the application of multivariable adaptive control to flexible spacecraft 09 p1217 A83-24792

Stability of a class of stochastic distributed parameter systems with random boundary conditions 09 p1334 A83-24807

Parametric identification of multiple scattering systems via the quasilinearization 10 p1466 A83-26536

Certain parallel iterative methods for solving nonlinear equations 10 p1470 A83-26943

Controller design for flexible, distributed parameter mechanical arms via combined state space and frequency domain techniques 11 p1647 A83-27487

Theory on distributed feedback /DFB/ lasers including strong modulations 11 p1578 A83-27548

Block-independent control of distributed structures [AIAA 83-0852] 12 p1742 A83-29826

State control of distributed parameter systems 13 p1909 A83-30001

Control of distributed parameter systems 13 p1910 A83-30078

Stochastic independent modal-space control of distributed-parameter systems 13 p1911 A83-31249

Finite-dimensional servomechanism design for parabolic distributed-parameter systems 14 p2074 A83-31927

A z-transform theory for distributed sensing and control 15 p2222 A83-35128

Parameter estimation and control of distributed systems with application to large deployable antennae 17 p2475 A83-37077

Least-squares sequential parameter and state estimation for large space structures 17 p2476 A83-37079

Identification of distributed parameter systems using finite element approximation 17 p2565 A83-37095

Methods in optimal estimation theory for problems involving the vibration of dynamic distributed-parameter systems 17 p2570 A83-38925

Sensitivity synthesis of systems subject to large parameter variations 19 p2890 A83-41480

Adaptive parameter estimation for a flexible structure Effects of spillover [AIAA PAPER 83-2244] 19 p2891 A83-41720

Control of nonconservative distributed-parameter systems [AIAA PAPER 83-2247] 19 p2892 A83-41723

Cubic spline approximation techniques for parameter estimation in distributed systems 20 p3040 A83-43405

Principles of sensor and actuator location in distributed systems 21 p3192 A83-44002

Finite-dimensional discrete-time control of linear distributed parameter systems 21 p3192 A83-44009

Control of distributed hyperbolic systems - 'What does a tokamak and a large spacecraft have in common?' 21 p3192 A83-44011

General conditions on reduced-order control for ensuring full-order closed-loop asymptotic stability --- of large space structures 21 p3099 A83-44033

First order solution of the optimal control problem for distributed parameter elastic system 21 p3193 A83-44040

On adaptive regulation of flexible spacecraft 21 p3101 A83-45114

Finite-dimensional controllers for hyperbolic systems 21 p3196 A83-45118

Suboptimality and stability of linear distributed parameter systems with finite-dimensional controllers 21 p3196 A83-45136

Response in passing through critical speed of arbitrarily distributed flexible rotor system. I - Case without gyroscopic effect. II - Case with gyroscopic effect 21 p3148 A83-45475

Distributed-parameter solar cells - Volt-ampere characteristics under uniform and nonuniform illumination 23 p3477 A83-48397

Real-time parameter identification in a class of distributed systems using Lyapunov design method. I - Theory 24 p3620 A83-49895

DISTRIBUTED PROCESSING
Distributed system architectures --- modular approach to ATE 01 p0088 A83-10736

Distributed ATE systems software 01 p0088 A83-10771

A study of an arbiter function in the structures of a shared bus --- French thesis 02 p0166 A83-11700

A mixed distributed/parallel processing experiment for real-time radar control 02 p0226 A83-11905

DISTRIBUTION FUNCTIONS
Local command-control networks - Operational reliability --- French thesis 03 p0386 A83-13802

Automated ultrasonic dimensional and defect inspection of complex geometry gas turbine airfoil shapes 04 p0488 A83-15158

A file management system for a network of dissimilar computers --- French thesis 04 p0545 A83-15849

Development environment for the design and test of applications software for a distributed multiprocessor computer system 07 p0983 A83-19625

Performance models of distributed databases 07 p0982 A83-19797

Experience with the parallel solution of partial differential equations on a distributed computing system 07 p0983 A83-20247

Routing schemes for the augmented data manipulator network in an MIMD system 07 p0984 A83-20248

Distributed microprocessor application for marine systems monitor and control [AIAA PAPER 83-0630] 08 p1173 A83-22173

Advanced onboard signal processors for satellite communication systems 08 p1050 A83-22822

Real-time modular distributed signal processing --- sensors for ballistic missile defense systems 08 p1051 A83-22828

Distributed dynamic programming --- for multiprocessor problem solving 09 p1326 A83-24769

The implementation of lattice calculations on the DAP --- Distributd Array Processor 12 p1768 A83-29623

File allocation in a distributed computer communication network 13 p1909 A83-30788

Analysis of timed Petri nets and application to distributed systems --- French thesis 15 p2219 A83-33697

Distributed detection with waveform observations - Correlated observation processes 17 p2567 A83-37124

Microcomputer control of a robotic arm in a distributed computing environment 17 p2568 A83-37155

The parallel implementation of a nonlinear real-time simulation technique 18 p2738 A83-39150

Abstractions for node level passive fault detection in distributed systems 19 p2889 A83-41036

Experiments in automatic microcode generation 19 p2888 A83-41037

Processes, tasks, and monitors - A comparative study of concurrent programming primitives 20 p3038 A83-43115

A causal model for analyzing distributed concurrency control algorithms 20 p3038 A83-43116

Distribution design of logical database schemas 20 p3038 A83-43117

DISTRIBUTION (PROPERTY)
NT ANGULAR DISTRIBUTION
NT ANTENNA RADIATION PATTERNS
NT BOLTZMANN DISTRIBUTION
NT BRIGHTNESS DISTRIBUTION
NT CHARGE DISTRIBUTION
NT CURRENT DISTRIBUTION
NT DIFFRACTION PATTERNS
NT ELECTRON DENSITY PROFILES
NT ELECTRON DISTRIBUTION
NT ENERGY DISTRIBUTION
NT FLOW DISTRIBUTION
NT FORCE DISTRIBUTION
NT FREQUENCY DISTRIBUTION
NT HOLE DISTRIBUTION (ELECTRONICS)
NT HOLE DISTRIBUTION (MECHANICS)
NT ION DISTRIBUTION
NT LOAD DISTRIBUTION (FORCES)
NT MASS DISTRIBUTION
NT MOMENT DISTRIBUTION
NT NEUTRON DISTRIBUTION
NT PRESSURE DISTRIBUTION
NT RADIAL DISTRIBUTION
NT RADIATION DISTRIBUTION
NT RAINBOWS
NT SIDELOBES
NT SPATIAL DISTRIBUTION
NT SPECTRAL ENERGY DISTRIBUTION
NT STAR DISTRIBUTION
NT STRESS CONCENTRATION
NT TEMPERATURE DISTRIBUTION
NT VELOCITY DISTRIBUTION
NT VERTICAL DISTRIBUTION

Dislocation distribution in plastically deformed metals 16 p2331 A83-36165

DISTRIBUTION FUNCTIONS
Analysis of maximum-likelihood estimation on a randomly censored sample with a small fraction of failures in the example of exponential distributions 01 p0103 A83-10296

Approximation of the distribution functions of the phase and phase cosine of the sum of a harmonic signal and noise 01 p0031 A83-10411

Particle correlation in a relativistic plasma 01 p0107 A83-10906

- Recognizing random signals described by a beta distribution 04 p0527 A83-15750
- Computing the distribution of a random variable via Gaussian quadrature rules 04 p0530 A83-16323
- Estimation of convergence speed in the second uniform limit theorem of Kolmogoroff 04 p0530 A83-16410
- The stability of one-dimensional stellar systems 04 p0558 A83-16446
- Electron velocity distributions near the earth's bow shock 06 p0782 A83-18285
- A new approach to pitch angle scattering in the magnetosphere 06 p0783 A83-18294
- Distribution functions of the number of cascade electrons at various stages of the development of a shower in lead at high energies 06 p0858 A83-19347
- Plasma instabilities and their role in the dynamics of the solar wind 06 p0856 A83-19420
- A measure of the incompleteness of a statistical description and irreversibility Fluctuation-dissipation relation /FDR/ for multiparticle distribution functions 07 p1001 A83-20607
- Auroral ion velocity distribution function - Generalized polynomial solution of Boltzmann's equation 07 p0968 A83-21586
- Electron beam energy branching in a gas mixture 09 p1343 A83-23678
- Uncertainty principle for partially coherent light 09 p1344 A83-24082
- Invalidity of local thermodynamic equilibrium for electrons in the solar transition region. I - Fokker-Planck results 10 p1521 A83-25730
- An instrument for rapidly measuring plasma distribution functions with high resolution 13 p1814 A83-30761
- Electron distribution function in a laser plasma 16 p2415 A83-35888
- On the self-similar solution for the distribution function of particles accelerated by Alfvén waves 17 p2583 A83-38825
- Method of estimating Langmuir's turbulence in a solar flare 18 p2785 A83-39980
- The Boltzmann equation theory of charged particle transport 19 p2906 A83-41536
- Estimation of the parameters of the phase distribution function of a radio signal 20 p2964 A83-42904
- Computer simulation studies of VLF triggered emissions deformation of distribution function by trapping and detrapping --- of resonant electrons in inhomogeneous geomagnetic field 20 p3024 A83-43186
- Noise generators with an arbitrary distribution law 21 p3125 A83-44772
- Weakly relativistic dielectric tensor and dispersion functions of a Maxwellian plasma 21 p3214 A83-45194
- A cloud physical parameterization method using movable basis functions - Stochastic coalescence parcel calculations 22 p3341 A83-46850
- Energy distribution functions of electrons in low-temperature helium-neon plasma at low pressures 24 p3632 A83-49113

DISTRIBUTION MOMENTS

- NT MEAN
- NT ORTHOGONALITY
- NT STANDARD DEVIATION
- Investigation of the statistical moments of a field of short waves propagating in a medium with strong Gaussian random inhomogeneities - The system of moment equations 02 p0162 A83-11526

DISTURBANCE THEORY

U PERTURBATION THEORY

DISTURBING FUNCTIONS

- Near insensitivity of linear feedback systems 09 p1335 A83-24817
- Possible evolution of feedback types and their applications in control of nonstationary plants 10 p1467 A83-26555
- Model reference adaptive control of system having purely deterministic disturbances 22 p3351 A83-46369

DISULFIDES

NT CARBON DISULFIDE

- Reactions of FeS₂, CoS₂, and NiS₂ electrodes in molten LiCl-KCl electrolytes 07 p0881 A83-20578

DITHERS

- Resolution improvement in an analog-to-digital converter by the superposed dither signal 08 p1080 A83-22231
- Application of a method of averaging to the study of dithers in non-linear systems 23 p3502 A83-48646
- Image enhancement in a dithered picture 24 p3583 A83-49198

DITHIOLS

U THIOLS

DIURESIS

- The relative contributions of gravity, buoyancy, and cold to the changes of human plasma volume during simulated weightlessness 11 p1643 A83-27802
- Effects of water immersion on plasma catecholamines in normal humans 13 p1902 A83-30465

DIURETICS

- The effect of several diuretics on the renal excretion of glycine in dogs 07 p0975 A83-20988

DIURNAL RHYTHMS

U CIRCADIAN RHYTHMS

DIURNAL VARIATIONS

- The stability of the diurnal variation of the degree of disturbance of f0F2 during the cycle of solar activity 01 p0071 A83-10593
- Effects of the polarity change of the solar magnetic field in variations of cosmic rays 02 p0273 A83-11720
- A numerical simulation of soil temperature and moisture variations for a bare field 02 p0198 A83-11843
- Further developments of a general method for deducing average hourly insulations from average daily insulations 02 p0203 A83-11845
- Fluctuations on OTS-earth copolar link against diurnal and seasonal variations 02 p0163 A83-11983
- A finite-element model of the atmospheric boundary layer suitable for use with numerical weather prediction models 02 p0214 A83-12236
- The correlation of parameters of the F2 and F1 layers of the ionosphere in the case of day-to-day variations 02 p0210 A83-12445
- Average diurnal variations of the intensity of geomagnetic pulsations in the period ranges of pc 2-pc 5 observed at Fuerstenfeldbruck during the years 1960-1971 03 p0357 A83-13300
- Diurnal radiation budget - Four months assembled into an annual mean 03 p0370 A83-14646
- Effects of cloud shape on cloud field identification 03 p0371 A83-14656
- Regulation of the diurnal variation of the cold productivity of an adsorption-type solar refrigeration system 04 p0503 A83-15135
- Geographical and seasonal distribution of critical frequencies in the F2-layer during a period of high solar activity 04 p0509 A83-15724
- Analysis of the diurnal oscillation of surface geostrophic wind over Western Europe 04 p0516 A83-15855
- On the variability of the solar diameter 06 p0853 A83-18129
- Global dynamo simulation of ionospheric currents and their connection with the equatorial electrojet and counter electrojet - A case study 06 p0783 A83-18296
- The atmospheric neutral sodium layer. II - Diurnal variations 06 p0785 A83-18313
- Variations in ion and neutral composition at Venus - Evidence of solar control of the formation of the predawn bulges in H/ +/ and He I 07 p1029 A83-20611
- Periodogram of nearly diurnal variations in the latitude of Gorkii 07 p1027 A83-21273
- A correlation between measured E-region current and geomagnetic daily variation at equatorial latitude 07 p0966 A83-21429
- Solar and lunar daily magnetic variations at Hyderabad, 1965-77 08 p1133 A83-22301
- A study of quiet day magnetic field variations in East Asia at sunspot minimum 08 p1134 A83-22304
- On the position of the Sq /H/ focus in years of sunspot minimum --- solar quiet day geomagnetic variations 08 p1134 A83-22306
- Effect of the equatorial counter-electrojet in the Indian region on the geomagnetic solar and lunar daily variations 08 p1134 A83-22310
- Bi-diurnal geomagnetic variations 08 p1134 A83-22311
- The variation of the magnetic field and its interaction with the equatorial electrojet in eastern Senegal 08 p1135 A83-22314
- A study of the post-sunset increase in the F2-region electron density at low and middle latitudes in the Asian zone during sunspot maximum and minimum periods 08 p1135 A83-22315
- Recent measurements of earth background spatial radiance variations 08 p1103 A83-22843
- Preliminary study of CO₂ variations at Amsterdam Island /Territoire des Terres Australes et Antarctiques Françaises/ 09 p1295 A83-24259
- The lunar semi-diurnal tide observed by stratospheric sounding units on the TIROS-N series of satellites 09 p1307 A83-24689
- The relative importance of geomagnetic effects in the observed secular, eleven-year, and solar-diurnal variations of cosmic rays 10 p1523 A83-26102
- The influence of optical water type on the diurnal response of the upper ocean 11 p1634 A83-27674
- Circadian variations in tolerance to +Gz acceleration 11 p1642 A83-27783

- Circadian rhythms of work capacity, the activity of the sympathoadrenal system and myocardial infarction 12 p1765 A83-29308

- A mesospheric ozone profile at sunset 12 p1756 A83-29582
- Features of the relationship between the spatial-temporal behavior of pulsations of decreasing period with magnetic activity 13 p1876 A83-30614
- An analysis of several ionospheric parameters associated with the South Atlantic Geomagnetic Anomaly by means of VLF waves 13 p1880 A83-31471
- Intensity variations and ratios of (9-4) and (7-3) hydroxyl bands in nightglow at Poona 13 p1882 A83-31632
- Longitudinal and latitudinal abnormalities in the daily variation of f0F2 in the South-American region 13 p1883 A83-31719
- Variations of electron density in the D-region 14 p2050 A83-31875
- Possible effects of distant field sources in Sq variations 14 p2051 A83-31889
- Radar meteor rates and solar activity 14 p2051 A83-32395
- Diurnal patterns of wheat spectral reflectances 15 p1883 A83-33687
- Investigation of atmospheric processes of different scale in the POLYMODE experiment 15 p2206 A83-34352
- Seasonal variations of harmonic constants of diurnal and semidiurnal waves of atmospheric pressure according to POLYMODE data 15 p2206 A83-34354
- The circadian rhythm of liver phospholipids in normal golden hamsters and in those with opisthorchiasis 15 p2211 A83-34963
- Diurnal variations of vegetation canopy structure 15 p2188 A83-35281
- Characteristics of low-latitude whistlers and their relation with f0F2 and magnetic activity 16 p2375 A83-35393
- The semi-diurnal tide at the equinoxes - MF radar observations for 1978-1982 at Saskatoon (52 deg N, 107 deg W) 16 p2386 A83-35487
- The secretory activity of acinar cells of the pancreas at various times of the day and the sequence of the maturation process of secretory granules 16 p2395 A83-36814
- Some results of ionospheric slab thickness observations at Lunping 17 p2537 A83-37577
- Depth of the nonconducting layer at the Nigerian dip equator 17 p2537 A83-37578
- Equatorial radio scintillations of ATS-6 radio beacons. Phase II - Ootacamund 1975-76 17 p2545 A83-38542
- Nonuniformity of the earth's rotation within a day 17 p2545 A83-38562
- The Fog Project - 1982 17 p2549 A83-38721
- Light and propranolol suppress the nocturnal elevation of serotonin in the cerebrospinal fluid of rhesus monkeys 18 p2732 A83-39935
- Lunar-solar periodicities of large earthquakes in southern California 18 p2718 A83-39956
- On the extraction of tidal information from measurements covering a fraction of a day --- for upper atmosphere meteorology 19 p2865 A83-41128
- The numerical modeling of the diurnal variations of meteorological elements in a large city 19 p2868 A83-41584
- Variability of meteorological fields in the equatorial Atlantic 19 p2868 A83-42115
- The diurnal behaviour of the auroral current system 20 p3016 A83-42302
- Scattering and precipitation of particles of the magnetotail under the action of the dawn-dusk electric field 21 p3172 A83-44522
- The relation between the onset times of the negative phase of ionospheric storms and the main phase of magnetic storms and a theoretical model 21 p3172 A83-44524
- Analysis of the periodic variations of atmospheric pressure over Greece 21 p3181 A83-45408
- Diurnal radiance patterns of finite and semi-infinite clouds in observations of cloud fields 22 p3338 A83-45708
- Equivalent ionospheric current systems representing lunar daily variations of the polar geomagnetic field 22 p3327 A83-46052
- Lower thermospheric structure from Millstone Hill incoherent scatter radar measurements. I - Daily mean temperature. II Semidiurnal temperature component 22 p3328 A83-46057
- Latitudinal (seasonal) variations in the thermospheric midnight temperature maximum - A tidal analysis 22 p3328 A83-46058
- A unified theory of cosmic ray diurnal variations 22 p3390 A83-46893
- Comparison of model high-latitude electron densities with Millstone Hill observations 22 p3335 A83-47042

Modeling the total electron content observations above Ascension Island 22 p3337 A83-47064
Relative frequency and diurnal variation of high cold clouds in the tropical Atlantic and Pacific 23 p3490 A83-47403
A comparative study of scintillation analysis over two line-of-sight paths at 6.7 GHz and 7.6 GHz 23 p3443 A83-47834

DIVERGENCE

NT MAGNETIC CHARGE DENSITY
Swept composite wing aeroelastic divergence experiments 01 p0009 A83-10193
Influence of mean divergence, mean vorticity and height-dependent eddy viscosity on thermal instability 16 p2391 A83-36583
Optimization of structures subjected to aeroelastic instability phenomena 19 p2859 A83-41541

DIVERGENT NOZZLES

An experimental study of the vortex tube - Where the vortex chamber includes a divergent tube 05 p0639 A83-17375
Prediction of sudden expansion flows using the boundary-layer equations [ASME PAPER 83-FE-11] 23 p3450 A83-48230

DIVERSITY

Passive planar multibranch optical power divider - Some design considerations 20 p3047 A83-42224
Wide-band chain-type divider-summatrors based on quarter-wave lossy couplers 22 p3277 A83-45679

DIVIDING (MATHEMATICS)

Fast iterative division of p-adic numbers 15 p2217 A83-33910
The use of floating-point and interval arithmetic in the computation of error bounds 15 p2218 A83-33914
Concurrent error detection in multiply and divide arrays 15 p2218 A83-33915

DIVING (UNDERWATER)

A theoretical model of CO2 absorption in a mixed alkali bed under hyperbaric conditions 11 p1645 A83-28336
Liquid ventilation in dogs - An apparatus for normobaric and hyperbaric studies 13 p1898 A83-30510
A Trimix saturation dive to 660 m studies of cognitive performance, mood and sleep quality 16 p2400 A83-35565
Active diver thermal protection requirements for cold water diving 18 p2737 A83-40363

DMSP SATELLITES

The use of satellite visible and infrared data in detecting local regions of strong winds in coastal zones 13 p1886 A83-30550
Response of nightside auroral-oval boundaries to the interplanetary magnetic field 13 p1947 A83-31233

DNA

U DEOXYRIBONUCLEIC ACID

DO-28 AIRCRAFT

Optimal design of a baro/radio supported inertial altitude system [DGLR PAPER 82-041] 09 p1204 A83-24165
The consideration of operational aspects for utility-/commuter aircraft, taking into account the example of the Dornier 228 [DGLR PAPER 82-047] 09 p1199 A83-24171
The research aircraft of the Special Research Area 'Flight Control' as scientific test stand 10 p1376 A83-26484

DOCKING

U SPACECRAFT DOCKING

DOCUMENT STORAGE

Computer assisted information retrieval 11 p1666 A83-28168
The data library --- for flow data storage 13 p1934 A83-30629
Developments in scientific information systems 19 p2907 A83-41291

DOCUMENTATION

Tornados, dark days, anomalous precipitation, and related weather phenomena - A catalog of geophysical anomalies --- Book 22 p3339 A83-45914

DOCUMENTS

NT ABSTRACTS
NT ASTRONOMICAL CATALOGS
NT BIBLIOGRAPHIES
NT ENGINEERING DRAWINGS
NT HANDBOOKS
NT MANUALS
NT PERIODICALS
NT POSTLAUNCH REPORTS
NT TEXTBOOKS
NT USER MANUALS (COMPUTER PROGRAMS)
NT VIDEO DISKS
NASA educational briefs 02 p0244 A83-11819

Semantic representative languages in document retrieval systems - Effects of a representation of meaning involving differences in depth on the system characteristics --- German thesis 11 p1666 A83-28660

DOLOMITE (MINERAL)

Amino acids from the Late Precambrian Thule Group, Greenland 02 p0219 A83-11636

DOMAINS

NT MAGNETIC DOMAINS

Finite element iterative techniques for determining the interface boundary between Laplace and Poisson domains - Characteristic analysis of a field effect transistor 11 p1563 A83-28417
Solution of the Navier-Stokes equations by a spectral method of subdomains [ONERA, TP NO. 1983-19] 16 p2353 A83-36428
Histogram deconvolution - An aid to automated classifiers 22 p3350 A83-46253

DOMES (STRUCTURAL FORMS)

NT RADOMES

Acceptance testing of graphite/epoxy composite parts using an acoustic emission monitoring technique 05 p0653 A83-16874
Target TV projector with dynamic raster shaping for use in dome simulators 08 p1102 A83-22834
Development of a new family of improved infrared /IR/ dome ceramics 09 p1239 A83-24952
Progress in the development of ternary sulfides for use from 8 to 14 microns 09 p1345 A83-24955
Thermostructural evaluation of spinel infrared /IR/ domes 09 p1239 A83-24966
Dome induced image motion --- in astronomical telescopes 13 p1920 A83-30999
Air-to-air combat in a plastic dome 18 p2642 A83-40620
Deformation and stability studies of thin-walled domes under uniform external pressure 20 p3002 A83-42832
A model for radial flow in a tube-dome junction of a telescope 23 p3508 A83-47846

DOMESTIC ENERGY

Preliminary test results for the small community solar power system [ASME PAPER 82-WA/SOL-30] 10 p1445 A83-25687
An analysis of the cost/performance characteristics of passive solar materials and components 11 p1608 A83-27247
Thermal energy storage - Air Force user considerations in various modes of operation 11 p1609 A83-27305

DOMESTIC SATELLITE COMMUNICATIONS SYSTEMS

DBS platforms - A viable solution 03 p0284 A83-13899
Three is not enough - Why the U.S. specified four DBS service areas 03 p0304 A83-13900
The Swedish space programme - Particularly the Viking and Tele-X projects 04 p0450 A83-15658
Domestic satellite communications systems - Background and projections 04 p0466 A83-15664
Japan's BSE program --- Broadcasting Satellite for Experimental purpose 04 p0468 A83-16415
Aspects of the satellite broadcasting experiments using the BSE and its in-orbit performance 04 p0468 A83-16416
Transmission characteristics of transponders --- onboard Japanese experimental broadcasting satellite 04 p0468 A83-16418
The attitude control performance of the BSE and its influence on the received television signal strengths on the ground 04 p0453 A83-16420
Up-link power control experiment --- of Japanese Medium-scale Broadcasting Satellite 04 p0468 A83-16421
Switching control system for access to a broadcast satellite from multiple earth stations 04 p0468 A83-16422
High definition television broadcasting by satellite 04 p0469 A83-16423
Transmission system for the television broadcasting satellite 04 p0469 A83-16424
Operational broadcasting satellite in Japan 04 p0469 A83-16425
The development of satellite communications and its socio-economic implications 06 p0816 A83-18372
Optimization of coverage pattern for regional communications satellite 06 p0723 A83-19036
Case study - Australian national satellite system 07 p0903 A83-19653
Broadcasting satellites and the system of the United States Satellite Broadcasting Company 07 p0904 A83-19680
Systems and technology aspects of a direct broadcast satellite service for the United States 07 p0904 A83-19692

Compelled inter-register signalling via satellite - A novel approach 07 p0905 A83-19704
New TDMA terminal design for domestic satellite applications 07 p0908 A83-19740
Evaluation of a 14/12 GHz 90 Mbit digital satellite link 07 p0908 A83-19741
Orbit utilization - Current regulations 07 p0910 A83-19759
TDMA demand assignment operation in Telecom 1 business services network 07 p0911 A83-19783
Japanese domestic TDMA system 07 p0911 A83-19786
30-20 GHz domestic satellite communication system experiments 08 p1075 A83-21997
Satellite television broadcasting systems in the USSR 10 p1402 A83-25877
Measurement of relative propagation delay between C- and K-band satellite loops 10 p1403 A83-26076
SCPC terminal and signal strength measuring apparatus for 30/20 GHz frequency band 10 p1403 A83-26082
Small earth stations at 20/30 GHz 10 p1404 A83-26083
FM-SCPC system and equipments for satellite communication --- Single Channel Per Carrier 10 p1404 A83-26084
MCPC system and terminal equipment for satellite communication --- Multi-Channel Per Carrier 10 p1404 A83-26085
Zones serviced by satellite communications systems --- Russian book 12 p1718 A83-28820
6/4 GHz band small capacity omni-use terminal satellite system 15 p2143 A83-33508
Status of space science and technology - An Australian perspective 18 p2787 A83-39832
The role of space communication in promoting national development with specific reference to experiments conducted in India 18 p2752 A83-39841
Beam area determination for multiple-beam satellite communication applications 19 p2827 A83-41147
Implication of a color multibeam communications satellite in the 30/20 GHz bands 19 p2827 A83-41328
Domestic broadcasting-satellite systems - The need for a common standard and the case for block allotment planning 19 p2829 A83-41349
Orbit utilization in the US Broadcast Satellite Service 19 p2829 A83-41350
Spacecraft technology for direct broadcast missions 19 p2812 A83-41351
Trunk transmission network using K-band SS-TDMA system 19 p2831 A83-41378
India's domestic satellite communication system - INSAT 19 p2831 A83-41379
TDMA site diversity switching experiments with Japanese CS 19 p2831 A83-41380
Low elevation angle site diversity satellite communications for the Canadian Arctic 19 p2831 A83-41381
Optimum utilization of domestic communication satellites for data and television transmission 19 p2831 A83-41382
Concepts of 2.6/2.5 GHz mobile satellite communication system 19 p2834 A83-41419
Aussat - A milestone in Australia's communication history 21 p3120 A83-44535
The Italsat programme 21 p3122 A83-45431
System configurations and applications in domestic/regional satellite communications 22 p3273 A83-45754
L-band transistor HPA with adaptive bias [IAF PAPER 83-62] 23 p3444 A83-47248
The Mexican national satellite system [IAF PAPER 83-79] 23 p3441 A83-47257
Satellite broadcasting - The best way to meet the needs of television education in China [IAF PAPER 83-308] 23 p3513 A83-47337
Advanced communications satellite systems 24 p3551 A83-49855

DOMINANCE
NT EYE DOMINANCE
Dominance optimisation in multivariable design 19 p2890 A83-41479

DONNELL EQUATIONS
On the buckling and vibration of antisymmetric angle-ply laminated circular cylindrical shells 07 p0946 A83-20639
Dynamic characteristics of conical shell with variable modulus of elasticity 09 p1280 A83-24506

DONOR MATERIALS

Current oscillations in semi-insulating GaAs associated with field-enhanced capture of electrons by the major deep donor EL2 02 p0243 A83-12294
Donor discrimination and bound exciton spectra in InP 07 p1000 A83-20746

- EL2 distributions in doped and undoped liquid encapsulated Czochralski GaAs --- deep donor concentration 08 p1169 A83-22756
- Evidence for effective-mass states of a gold-related doubly charged donor in silicon 11 p1661 A83-28071
- Evidence that the gold donor and acceptor in silicon are two levels of the same defect 13 p1928 A83-30340
- Direct measurement of the melt depth of silicon during laser irradiation 13 p1929 A83-30351
- A correlation of atomic and electrical measurements of Cr and residual donors in thermally processed semi-insulating GaAs 16 p2419 A83-35672
- ### DOORS
- Serviceability evaluation of advanced composite F-14A main-landing-gear-strut doors and overwing fairings 07 p0861 A83-20480
- ### DOPA
- The participation of the dopaminergic system of the brain in the realization of the generalization function 01 p0080 A83-10540
- Intracerebroventricular injections of cholecystokinin decreases the activity of the dopaminergic and serotonergic systems in the brain 02 p0219 A83-11519
- ### DOPED CRYSTALS
- Photosensitive gate structures based on epitaxial layers of Fe-doped GaP 01 p0108 A83-10373
- Tunable electroluminescence from GaAs doping superlattices 01 p0110 A83-10991
- Deep photoluminescence band related to oxygen in gallium arsenide 01 p0110 A83-10993
- Enhancement of the diffusional creep of polycrystalline Al₂O₃ by simultaneous doping with manganese and titanium 02 p0159 A83-11668
- Iron metal production in silicate melts through the direct reduction of Fe/II/ by Ti/III/, Cr/II/, and Eu/II/ --- in lunar basalts 02 p0267 A83-12846
- Application of molecular beam epitaxy to microwave and millimeter wave devices 03 p0310 A83-13796
- Preparation and characteristics of a-Si:Cl:H films 04 p0539 A83-15478
- Oxygen evolution improvement at a Cr-doped SrTiO₃ photoanode by a Ru-oxide coating 04 p0505 A83-15493
- Dependence of hydrogen evolution from a-Si:H on boron doping and substrate potential 04 p0541 A83-15518
- Electronic properties of doped glow-discharge amorphous germanium 04 p0542 A83-15530
- Optical and electrical characterization of multiply doped silicon - A study of the Si:/In,Al/ system 04 p0542 A83-16065
- Resistivity, superconductivity, and order-disorder transformations in transition metal carbides and hydrogen-doped carbides 04 p0543 A83-16075
- Selenium doping of molecular beam epitaxial GaAs using SnSe₂ 04 p0544 A83-16094
- Influence of tantalum alloying additives on the solid solubility limit of carbon in molybdenum 04 p0461 A83-16173
- Thin film polycrystalline Si p-n junction solar cells with preferential doping 05 p0691 A83-17766
- Evidence for low diffusivity and mobility of minority carriers in highly doped Si and interpretation 06 p0814 A83-19261
- Radiation effects on modulation-doped GaAs-Al_x/x/Ga/1-x/As heterostructures 06 p0815 A83-19263
- Ceramic SrTiO₃ photoanodes - Enhancement of photoactivity through donor doping 07 p0954 A83-20579
- A mechanistic study of oxygen evolution on Li-doped Co₃O₄ --- by electrolysis 07 p0881 A83-20586
- Long wavelength Pb/1-x/Sn/x/Te homostructure diode lasers having a gallium-doped cladding layer 07 p0937 A83-21369
- Effect of doping simultaneously with iron and titanium on the diffusional creep of polycrystalline Al₂O₃ 08 p1071 A83-22195
- Photoconductivity and photovoltaic effect in indium selenide 08 p1169 A83-22337
- EL2 distributions in doped and undoped liquid encapsulated Czochralski GaAs --- deep donor concentration 08 p1169 A83-22756
- Computer simulation of carrier transport in planar doped barrier diodes 08 p1081 A83-22762
- Laser-controlled etching of chromium-doped 100 line-type GaAs 10 p1390 A83-25986
- Lattice parameter changes in Al/0.39/Ga/0.61/As due to O, Ge, Si, and S doping 10 p1488 A83-26059
- Defects in electron-irradiated, gallium-doped silicon --- in solar cells 10 p1489 A83-26213
- Optical transitions of RbMgF₃:Eu²⁺/+ and RbMgF₃:Mn²⁺/+,Eu²⁺/+ 11 p1581 A83-27590

- Some surprising results in studies of transition-metal-doped crystals --- materials for tunable lasers 11 p1581 A83-27595
- Light sensitivity of Al/0.25/Ga/0.75/As/GaAs modulation-doped structures grown by molecular beam epitaxy - Effect of substrate temperature 11 p1664 A83-28603
- Optical fibres with an Al₂O₃-doped silicate core composition 12 p1779 A83-29471
- Synthesis and investigation of GdScO₃ single crystals, activated by Nd(3+) ions 13 p1849 A83-30263
- Defect nature of the 0.4-eV center in O-doped GaAs [AD-A129932] 13 p1930 A83-31068
- Piezooptical properties of crystals of triglycine sulfate doped with L-alpha-alanine 13 p1930 A83-31304
- The effect of growth conditions on the polarization of triglycine sulfate doped with L-alpha-alanine 13 p1930 A83-31306
- Epsilon nonlinearity of doped triglycine sulfate crystals depending on conditions of growth 13 p1930 A83-31307
- The effect of various types of defects on the physical properties of crystals of the triglycine sulfate group 13 p1930 A83-31308
- Highly conductive boron doped Si-layers prepared by plasma decomposition of SiH₄ 14 p2089 A83-32252
- A model for analysis of optical measurements carried on a-Si:H films for photovoltaic applications 14 p2041 A83-32253
- Antimony doping in vacuum deposited thin film silicon photovoltaic cells 14 p2089 A83-32292
- The vibronic spectra of neodymium-doped crystals 14 p2025 A83-32830
- InP:Fe photoconductors as photodetectors 15 p2150 A83-33685
- Minority carrier recombination in heavily-doped silicon 16 p2419 A83-35673
- Growth rate dependence of the interface distribution coefficient in the system Ge-Ga 16 p2421 A83-36714
- Effect of heat transfer of melt/solid interface shape and solute segregation in Edge-Defined Film-Fed growth - Finite element analysis 16 p2354 A83-36715
- Density of the gap states in undoped and doped glow discharge a-Si:H 16 p2421 A83-36740
- Effect of boron doping and its profile on characteristics of p-i-n a-Si:H solar cells 16 p2371 A83-36742
- Mode of incorporation of phosphorus in Hg(0.8)Cd(0.2)Te 17 p2584 A83-37615
- Quantum-chemical modeling of boron and noble gas dopants in silicon 17 p2584 A83-38211
- The effect of the crystallization conditions of diamonds under high-temperature shock compression on their optical properties 18 p2750 A83-39531
- Ideal FET doping profile 18 p2678 A83-40376
- Energy-band distortion in highly doped silicon 18 p2750 A83-40377
- Moessbauer spectroscopic study of iodine-doped polyacetylene 20 p2949 A83-42341
- Amplified spontaneous emission in doped alkali-halides 21 p3145 A83-44814
- Ultraviolet (UV) photochemical doping of silicon 21 p3218 A83-44817
- Three holes bound to a double acceptor - Be(+) in germanium 21 p3218 A83-45199
- Ultrasonic modulation of persistent spectral holes in crystals 21 p3219 A83-45486
- Tunneling in the reverse dark current characteristic of Be-implanted GaAlAsSb avalanche photodetectors 22 p3365 A83-46656
- Incoherent light-induced diffusion of arsenic into silicon from a spin-on source 22 p3365 A83-46736
- Analysis of the spin-Hamiltonian parameters for Cr(3+) in mirror and inversion symmetry sites of alexandrite (Al/2-x/Cr/x/BeO/4/) - Determination of the relative site occupancy by EPR 23 p3461 A83-47630
- Study of deep-level defects and annealing effects in undoped and Sn-doped GaAs solar cells irradiated by one-MeV electrons 23 p3427 A83-48605
- Effect of grain size on the resistivity of polycrystalline material 23 p3512 A83-48611
- Moessbauer study of the lattice location of Co-57 implanted in graphite 24 p3636 A83-49756

DOPES

- Improved performance and rotational spectral characteristics of a doped helical TEA CO₂ laser 11 p1583 A83-27623

DOPING (ADDITIVES)

U ADDITIVES

DOPPLER EFFECT

- Jitter in SS 433-A clue to the collimation mechanism 01 p0126 A83-10967
- Theoretical limitation of the sea on the detection of low Doppler targets by over-the-horizon radar 01 p0032 A83-11351

- Estimating wind speed from HF skywave radar sea backscatter 01 p0076 A83-11352
- The equivalence of the short periods measured in the spectrum of SS 433 03 p0424 A83-14205
- The antenna phase center in satellite radio-Doppler geodetic systems 03 p0287 A83-14860
- Shifts of spectral lines emitted from stars 03 p0431 A83-14947
- Positron annihilation in non-destructive testing 04 p0492 A83-15218
- The accuracy, stability, and filtering properties of a linear pulsed phase-locked loop system for tracking the rate of Doppler shift changes 04 p0467 A83-15752
- Critique of tunable infrared lasers 04 p0485 A83-15803
- Interaction of three coherent fields with Doppler broadened serial four-level systems - Application to four-level FIR lasers 06 p0766 A83-18907
- Doppler measurements applied to the location of emergency radio beacons 07 p0870 A83-19703
- A demonstration of relative positioning using conventional GPS Doppler receivers 07 p0865 A83-19779
- On reducing the inherent noise in the double-pulse Doppler technique 07 p0913 A83-20371
- A new millimeter free electron laser using a relativistic beam with spiraling electrons 07 p0936 A83-20544
- Compatibility of Doppler measurements of the drift of auroral scattering at different frequencies 07 p0964 A83-21180
- Relativistic cyclotron accelerator exploiting the anomalous Doppler effect 09 p1271 A83-23999
- The anomalous Doppler effect and the radiation instability of oscillator motion in hydrodynamics 09 p1260 A83-24214
- Influence of Doppler broadening on the stability of monomode ring lasers 10 p1425 A83-25430
- Doppler frequency effects due to source, medium, and receiver motions of constant velocity [AIAA PAPER 83-0702] 10 p1474 A83-25922
- Noninvasive echo-Doppler duplex measurements of common femoral artery blood flow variables during supine exercise and post-occlusive reactive hyperemia 10 p1455 A83-26120
- Doppler imaging system: An optical device for measuring vector winds. I - General principles 10 p1423 A83-26643
- Estimation of turbulence severity in precipitation environments by radar 11 p1627 A83-27044
- Analysis of Doppler spectrum broadening mechanisms in thunderstorms 11 p1628 A83-27045
- Full-disk observations of solar oscillations from the geographic South Pole - Latest results 11 p1688 A83-27631
- Doppler-SODAR measured variations of mean and turbulent wind field during PUKK --- project for the investigation of the coastal climate 11 p1632 A83-27974
- Wind velocities estimated from Venera 13 and Venera 14 Doppler measurements - Initial results 12 p1798 A83-29481
- Solar rotation results at Mount Wilson 13 p1963 A83-29988
- Radio aurora magnetic and streaming aspect sensitivities on 6 simultaneous links at 50 MHz 13 p1876 A83-30775
- Solar atmospheric temperature inhomogeneities induce a 13-day oscillation in full-disk Doppler measurements 13 p1966 A83-31792
- High-velocity, asymmetric Doppler shifts of the X-ray emission lines of Cassiopeia A 14 p2104 A83-33193
- Single-mode operation of Doppler-broadened lasers by injection locking 15 p2167 A83-33761
- On the mechanism for imaging ocean waves by synthetic aperture radar 15 p2166 A83-35200
- A differential-Doppler study of traveling ionospheric disturbances from Millstone Hill 16 p2376 A83-35418
- Plasma effects on Doppler measurements of interplanetary spacecraft. I - Discontinuities and waves 16 p2429 A83-36635
- A matrix photodiode array to measure Doppler shifts of solar spectral lines 16 p2425 A83-36664
- Determination of the mass flow and electron content of the coma of Halley's comet using Doppler measurements of signals from the Giotto probe 18 p2777 A83-39784
- The differential diagnosis of functional murmurs and defects of the heart using ultrasonic pulse Doppler detection 18 p2734 A83-40541
- Ambiguities in spaceborne synthetic aperture radar systems 19 p2861 A83-41146
- Measurement of ocean surface currents by synthetic aperture radar 22 p3343 A83-46128
- Doppler imaging of starspots 23 p3516 A83-47513

DOPPLER NAVIGATION

A review of geodetic and geodynamic satellite Doppler positioning 07 p0871 A83-20836

DOPPLER RADAR**NT MULTISTATIC RADAR**

Doppler weather radar for forecasting and warning 01 p0073 A83-10014

Errors in fixed and moving frame of references - Applications for conventional and Doppler radar analysis 02 p0214 A83-12237

A simplified model for interpreting the Doppler spectrum of forward-scatter radar signals 03 p0307 A83-14032

Applications of Doppler radar to aviation operations - JAWS experiences [AIAA PAPER 83-0205] 05 p0666 A83-16583

Phase instability of ionospheric propagation and its influence on HF Doppler radar remote sensing 06 p0747 A83-18735

Effects of volume averaging on the line spectra of vertical velocity from multiple-Doppler radar observations 07 p0969 A83-20807

Investigation of clear air convective structures in the PBL using a dual Doppler radar and a Doppler sodar 07 p0969 A83-20808

Doppler weather radar for profiling and mapping winds in the prestorm environment 08 p1141 A83-22678

Passive noise in Doppler systems for measuring the velocity of motion 08 p1078 A83-23167

A diagnostic study of the tornadic storm based on dual-Doppler wind measurements 09 p1313 A83-23968

Coherent Doppler tomography for microwave imaging 10 p1420 A83-26069

Conference on Radar Meteorology, 20th, Boston, MA, November 30-December 3, 1981, Preprints 11 p1621 A83-26976

Modifications to the Sunset radar to provide antenna beam steering 11 p1621 A83-26978

Combined radar and aircraft analysis of a Doppler radar 'black hole' region in an Oklahoma squall line 11 p1622 A83-26985

Dual Doppler radar analysis of a convection line 11 p1622 A83-26986

Exponential size distributions of raindrops and vertical air motions deduced from zenith-pointing Doppler radar in a frontal precipitation 11 p1622 A83-26989

A mechanism of gravity wave excitation observable with atmospheric radars 11 p1623 A83-26992

A triple-Doppler case study of a small multi-cell convective storm 11 p1623 A83-26995

Vertical air mass flux properties in the northeast Colorado hailstorm of 22 July 1976 11 p1623 A83-26996

Supercell flow inferred from single-Doppler radar and environmental data 11 p1623 A83-26997

A comparison of meteorological Doppler radars with magnetron and klystron transmitters 11 p1624 A83-27006

A real-time Doppler spectrum analyzer --- for radar clutter rejection 11 p1624 A83-27008

Ground clutter rejection in the frequency domain --- for radar meteorology applications 11 p1625 A83-27019

The autocorrelation function and Doppler spectral moments - Geometric and asymptotic interpretations --- of meteorological radar data 11 p1625 A83-27020

Autocorrelation techniques for ground clutter rejection 11 p1626 A83-27021

Doppler signal processing using IF limiting 11 p1626 A83-27025

Doppler radar study of a region of widespread precipitation trailing a mid-latitude squall line 11 p1626 A83-27028

Radar measurement of tropospheric wind profiles 11 p1627 A83-27041

Evidence and characteristics of wave-like motions deduced from single Doppler radar measurements 11 p1627 A83-27042

Doppler radar and aircraft measurements of thunderstorm turbulence 11 p1627 A83-27043

Precipitation and precipitation efficiencies derived from single Doppler radar 11 p1628 A83-27047

Selected comment on multiple Doppler analysis --- of radar scanned storm with advection error correction 11 p1628 A83-27051

Dual Doppler observations of diffusion and rolls --- due to atmospheric circulation patterns 11 p1629 A83-27059

Prestorm boundary layer observations with Doppler radar 11 p1629 A83-27061

Simulated radar sampling of a realistically-scaled analytical model of the planetary boundary layer 11 p1629 A83-27062

Three-dimensional wind field from dual-Doppler radar - Application of variational concept for integrating the continuity equation 11 p1629 A83-27068

Simulations of airborne Doppler radar 11 p1629 A83-27069

Doppler radar measurements of moisture divergence in a coastal cyclone 11 p1630 A83-27075

Doppler radar observations of upslope snowstorms 11 p1630 A83-27076

A 35 GHz meteorological Doppler radar with polarization diversity capability 11 p1630 A83-27077

Utilization of the optimal polarization concept in radar meteorology 11 p1630 A83-27079

Interactive Doppler editing software 11 p1646 A83-27084

An interactive software package for the rectification of radar data to three-dimensional Cartesian coordinates 11 p1646 A83-27085

Modular radar analysis software system /MRASS/ 11 p1646 A83-27086

Automatic recognition of mesocyclones from single Doppler radar data 11 p1630 A83-27088

A dual frequency 10 cm Doppler weather radar 11 p1559 A83-27094

Millimeter wave Doppler radar 11 p1631 A83-27095

The NEXRAD program - An overview --- Next Generation Weather Radar 11 p1631 A83-27097

Convective plumes in the atmospheric boundary layer as observed with an acoustic Doppler sodar 12 p1758 A83-29132

On the extraction of atmospheric turbulence parameters from radar backscatter Doppler spectra. I - Theory 12 p1758 A83-29427

Fine Doppler resolution observations of thin turbulence structures in the tropostratosphere at Millstone Hill 13 p1892 A83-30896

Vertical profiles of wind velocity in the Venus atmosphere according to Doppler measurements of the Venera-13 and Venera-14 probes 14 p2111 A83-31960

Optimization of the autodyne mode of operation of Gunn-diodes 15 p2153 A83-34892

Case study of a hailstorm in Colorado. III - Airflow from triple-Doppler measurements 16 p2384 A83-35466

Radar detection of wingtip vortices 17 p2458 A83-38748

Ground based CO2 Doppler lidar wind measurements of winds in the vicinity of cumulus convection 17 p2552 A83-38752

Measurement of movements in the ionosphere using radio reflections 18 p2712 A83-39070

Correlation analysis of Doppler radar data and retrieval of the horizontal wind 18 p2722 A83-39125

Exponential size distributions of raindrops and vertical air motions deduced from vertically pointing Doppler radar data using a new method 18 p2722 A83-39135

A millimeter-wavelength dual-polarization Doppler radar for cloud and precipitation studies 18 p2726 A83-39873

Parametric estimation of Doppler spectral moments - An alternative ground clutter rejection technique --- for radar meteorology 18 p2727 A83-39879

The measurement of the velocity of small-caliber projectiles with Doppler radar --- German thesis 19 p2849 A83-41808

A multi-function radar system for RPVs 20 p2932 A83-43722

Weather radar research at the USA's storm laboratory 22 p3340 A83-46167

A new VHF Doppler radar experiment at Syowa Station, Antarctica 22 p3332 A83-46523

HF Doppler measurement in the auroral ionosphere 22 p3332 A83-46524

A comparison of techniques to estimate vertical velocities and drop size spectra 24 p3613 A83-49711

Dual-Doppler radar and surface network observations of a west-African squall line during the COPT 81 experiment 24 p3616 A83-49735

DORNIER AIRCRAFT

NT DO-28 AIRCRAFT

Development and testing of a high-technology amphibious flying vehicle 23 p3402 A83-47192

DORNIER DO-28 AIRCRAFT

U DO-28 AIRCRAFT

DOSAGE

NT RADIATION DOSAGE

The endocochlear potential of the inner ear and its changes under the influence of dihydrostreptomycin and etacrinic acid 01 p0078 A83-10514

An investigation of the effect of local vibration at fragmented doses for the substantiation of a model of a sparing regime --- for human body 01 p0083 A83-10528

An experimental study of the dose dependence of the effect of noise 01 p0084 A83-11397

The application of methods of the mathematical theory of experiment in the development of multicomponent radioprotective preparations 23 p3495 A83-48202

DOSE**U DOSAGE****DOSIMETERS****NT THRESHOLD DETECTORS (DOSIMETERS)**

Automation of a Crawford-cell exposure system 01 p0051 A83-10865

Dosimetric silica films - The influence of fields on the capture of positive charge 05 p0691 A83-17535

An MOS dosimeter for use in space 09 p1219 A83-24110

A general-purpose device for the measurement of thermoluminescent materials 10 p1418 A83-25350

Measurement of multiple differential electron distributions in an electron beam in nitrogen --- German thesis 11 p1575 A83-28659

Radiation effects on MOS devices - dosimetry, annealing, irradiation sequence, and sources 16 p2346 A83-36023

Radiation dosimetry --- Russian book 19 p2849 A83-41994

DOSIMETRY**U DOSIMETERS****DOUBLE BASE PROPELLANTS****NT DOUBLE BASE ROCKET PROPELLANTS**

Burning to detonation transition in porous beds of a high-energy propellant 03 p0303 A83-14846

Screw extrusion of double base propellants 09 p1241 A83-23833

New procedure for incorporating burning moderators in double-base solid propellants 09 p1241 A83-23834

Characterisation of NC/NG propellant pastes 09 p1241 A83-23835

Investigations of the extrusion process 09 p1241 A83-23836

Studies on thermal decomposition of double-base propellants 09 p1243 A83-24884

A universal relationship for heat release in the condensed phase and gas microkinetics during the combustion of ballistite powders 24 p3556 A83-49779

DOUBLE BASE ROCKET PROPELLANTS

Model for double-base propellants combustion, without and with additives 16 p2339 A83-36273

[AIAA PAPER 83-1197] Assessment of the thermal decomposition and combustion behavior of double-base propellants 18 p2673 A83-40017

Tetrachlorophthalicanhydride based chloropolyesters for inhibition of double rocket propellants [IAF PAPER 83-370] 23 p3439 A83-47362

DOUBLE SIDEBAND TRANSMISSION

A coupled mode approach to modulation instability and envelope solitons 24 p3623 A83-48904

DOUBLE STARS**U BINARY STARS****DOUGLAS AIRCRAFT****NT DC 8 AIRCRAFT****NT DC 9 AIRCRAFT****NT DC 10 AIRCRAFT****DOUGLAS DC-8 AIRCRAFT****U DC 8 AIRCRAFT****DOUGLAS DC-9 AIRCRAFT****U DC 9 AIRCRAFT****DOUGLAS MILITARY AIRCRAFT****U MILITARY AIRCRAFT****DOVAP****U DOPPLER EFFECT****DOWN-CONVERTERS**

Wideband millimeter-wave impedance measurements 13 p1836 A83-30974

Trends in microwave counter technology 13 p1836 A83-30975

Subharmonic sampling for the measurement of short-term stability of microwave oscillators 13 p1837 A83-31290

Efficient parametric decay in dissipative media 19 p2895 A83-40973

A 12 GHz Downconverter for direct broadcast satellite ground station 19 p2829 A83-41354

High efficiency mid-IR generation by Raman down conversion in liquid nitrogen 24 p3587 A83-48907

DOWNLINKING

Fluctuations on OTS-earth copolar link against diurnal and seasonal variations 02 p0163 A83-11983

Diversity reception of Comstar satellite 19/29-GHz beacons with the Tampa Triad, 1978-1981 02 p0141 A83-12621

Experimental and theoretical statistics of microwave amplitude scintillations on satellite down-links 03 p0305 A83-14010

Statistics of rain attenuation and other environmental effects associated with the BSE satellite down-link at 12 GHz in Japan 04 p0468 A83-16417

- Measurement of microwave scintillations on a satellite down-link at X-band 06 p0746 A83-18720
- Operational measurements of a 4/6-GHz adaptive polarization compensation network employing up/down-link correlation algorithms 06 p0746 A83-18727
- Tri-state delta modulation system for Space Shuttle digital TV downlink 07 p0870 A83-19730
- Injection locking performance of a 41-GHz 10-W power combining amplifier 10 p1409 A83-25811
- An S band radar for studying the effects of weather on the Sirio and Comstar satellite downlink signals 11 p1628 A83-27053
- Maritime communications satellite in-orbit measurements 17 p2475 A83-37794
- Reception and recording facilities of the French wide-band telemetry from the AUREOL-3 satellite for the Soviet ground stations 18 p2646 A83-39585
- Onboard processing for a 30/20 GHz communications satellite 19 p2813 A83-41391
- DOWNWASH**
- Obscuration by helicopter-produced snow clouds 08 p1043 A83-22357
- DPCM (MODULATION)**
- U DIFFERENTIAL PULSE CODE MODULATION
- DRAFTING (DRAWING)**
- ROMAPT - A new link between CAD and CAM 02 p0228 A83-11816
- DRAG**
- NT AERODYNAMIC DRAG
- NT FRICTION DRAG
- NT INTERFERENCE DRAG
- NT PRESSURE DRAG
- NT SATELLITE DRAG
- NT SUPERSONIC DRAG
- NT VISCOUS DRAG
- NT WAVE DRAG
- An analytic solution to the classical two-body problem with drag 06 p0720 A83-17990
- The boundary element method applied to the creeping motion of a sphere 08 p1087 A83-23182
- The prediction of the drag on structural beams 08 p1088 A83-23194
- A scheme for the analysis of a developed cavitation flow past a wedge 11 p1567 A83-27719
- Integrals of motion for the classical two-body problem with drag 18 p2644 A83-39568
- DRAG BALANCE**
- U AERODYNAMIC BALANCE
- U LIFT DRAG RATIO
- DRAG COEFFICIENTS**
- The effect of the geometrical parameters of an air intake with a central body on drag relative to the fluid streamline in the case when there is an incompressible-gas flow around it 17 p2448 A83-37531
- The wake drag of bodies with a conical tail section 17 p2452 A83-38093
- DRAG DEVICES**
- NT AERODYNAMIC BRAKES
- NT LEADING EDGE SLATS
- NT SPOILERS
- NT TRAILING-EDGE FLAPS
- NT WING FLAPS
- DRAG EFFECT**
- U DRAG
- DRAG MEASUREMENT**
- Determination of satellite drag coefficient from the orbital analysis of the ANS satellite /1974-70A/ 02 p0138 A83-12867
- A comparison of trim drag for conventional and supercritical wings [AIAA PAPER 83-0094] 05 p0579 A83-16518
- Influence of wall permeability on turbulent boundary-layer properties [AIAA PAPER 83-0294] 05 p0634 A83-16634
- Friction drag measurements of acoustic surfaces [AIAA PAPER 83-1356] 16 p2296 A83-36414
- An airbody drag prediction technique for military airlifters [AIAA PAPER 83-1787] 17 p2452 A83-38627
- The flow around an oscillating sphere. II - The measurement of unsteady drag 21 p3129 A83-44066
- A method for measuring the integral characteristics of boundary layers 24 p3581 A83-48949
- DRAG REDUCTION**
- Reductions in parachute drag due to forebody wake effects 04 p0443 A83-15315
- Propulsion installation characteristics for turbofan transports [AIAA PAPER 83-0087] 05 p0579 A83-16513
- Developments in the NASA transport aircraft laminar flow program [AIAA PAPER 83-0090] 05 p0579 A83-16514

- A comparison of trim drag for conventional and supercritical wings [AIAA PAPER 83-0094] 05 p0579 A83-16518
- SAM/D, an interactive system for the analysis and constrained minimization of induced drag of aircraft configurations [AIAA PAPER 83-0095] 05 p0594 A83-16519
- Passive shock wave/boundary layer control for transonic airfoil drag reduction [AIAA PAPER 83-0137] 05 p0580 A83-16546
- Turbulent drag reduction for external flows [AIAA PAPER 83-0227] 05 p0582 A83-16597
- Turbulent drag characteristic of small amplitude rigid surface waves [AIAA PAPER 83-0228] 05 p0633 A83-16598
- An experimental study of changes in the structure of a turbulent boundary layer due to surface geometry changes [AIAA PAPER 83-0230] 05 p0633 A83-16599
- Alteration of outer flow structures for turbulent drag reduction [AIAA PAPER 83-0293] 05 p0584 A83-16633
- New results, a review and synthesis of the mechanism of turbulence production in boundary layers and its modification [AIAA PAPER 83-0377] 05 p0635 A83-16681
- The design of a human-powered vehicle [AIAA PAPER 83-0649] 05 p0621 A83-16816
- Ion wind drag reduction [AIAA PAPER 83-0231] 05 p0689 A83-17914
- Trim Tank system for optimizing drag at the center of gravity [DGLR PAPER 82-030] 09 p1209 A83-24156
- Riblets as a viscous drag reduction technique 09 p1263 A83-24653
- An overview of two nonlinear supersonic wing design studies [AIAA PAPER 83-0182] 11 p1527 A83-28349
- Investigation of the possibility of reducing aerodynamic drag by a mechanism of initial vortex formations 13 p1804 A83-30723
- Research on non-planar wall geometries for turbulence control and skin-friction reduction 14 p1969 A83-31975
- Calculation of the aerodynamic efficiency of winglets 17 p2446 A83-37257
- Optimal form of the middle surface of a wing with supersonic leading edge, assuring minimum drag for a prescribed lift force and pitching moment 17 p2448 A83-37518
- Effects of nacelle position and shape on performance of subsonic cruise aircraft [AIAA PAPER 83-1124] 17 p2464 A83-38079
- Calculation of incompressible turbulent boundary layers over moving wavy surfaces [AIAA PAPER 83-1670] 17 p2507 A83-38083
- Axisymmetric bluff-body drag reduction using circumferential grooves [AIAA PAPER 83-1788] 17 p2453 A83-38628
- Flight investigation of natural laminar flow on the Bellanca Skyrocket II [SAE PAPER 830717] 20 p2933 A83-43326
- Grumman's forward swept wing feasibility studies and X-29A technology demonstrator [SAE PAPER 1454] 20 p2935 A83-43736
- Wing tip devices for energy conservation and other purposes Experimental and analytical work in progress at the Lockheed-Georgia Company 21 p3086 A83-44358
- Effects of external burning on spike-induced separated flow 23 p3398 A83-48132
- Design integration of laminar flow control for transport aircraft [AIAA PAPER 83-2440] 24 p3547 A83-49577
- DREGULATORS**
- U BRAKES (FOR ARRESTING MOTION)
- DRAINAGE**
- Surface tension effects in a space radiator condenser with capillary liquid drainage [AIAA PAPER 83-1525] 14 p2011 A83-32756
- DRAINAGE PATTERNS**
- Relict drainages, conical hills, and the eolian veneer in southwest Egypt - Applications to Mars 04 p0566 A83-15567
- New geological, structural lineaments and drainage maps of Egypt based on Landsat imagery interpretation and field investigations 09 p1292 A83-24635
- DRAINING**
- U DRAINAGE
- DRAWING**
- Enhancement of a graph drawing package 04 p0527 A83-15147
- DRAWINGS**
- NT ENGINEERING DRAWINGS

DREAMS

- A window on the sleeping brain --- paralysis inhibition during REM state 10 p1454 A83-26300
- The function of dream sleep 18 p2732 A83-39961

DREDGED MATERIALS

- The use of near color infrared photography to assess the impact of the oil and natural gas industry on Louisiana's wetlands 01 p0063 A83-10069

DRIFT

- A split delta-V technique for drift control of geosynchronous spacecraft [AIAA PAPER 83-0017] 05 p0601 A83-16466

DRIFT (INSTRUMENTATION)

- Mechanically dithered RLQ at the quantum limit --- Ring-Laser Gyro 01 p0053 A83-11130
- Design of a microprocessor-based A/D converter with drift and offset correction 03 p0385 A83-13499
- The reason for high-temperature strain gauge drift, especially in those with PtW conductors 06 p0763 A83-19123
- A technique for reducing low-frequency, time-dependent errors present in network-type surveys --- magnetic and gravity drift corrections 07 p0957 A83-19872
- Drift compensation in a mosaic sensor 08 p1103 A83-22839
- Beryllium microdeformation mechanisms 09 p1231 A83-24058
- Filtering for piecewise linear drift and observation 09 p1330 A83-24740
- The effect of certain fabrication factors on the errors of a dynamically tuned gyroscope with a displaced center of mass 15 p2167 A83-35264
- Minimization of a class of temperature errors of float-type gyroinstruments 15 p2167 A83-35268
- Development of methods for calibration and testing gyroscopic instruments for GW applications 16 p2354 A83-35498
- On-board clock correction by drift prediction 19 p2832 A83-41392
- The efficiency of compact damping systems for gyroscopes under conditions of angular vibration of the base 21 p3138 A83-44643
- Measuring strain gages directly without signal conditioning 22 p3291 A83-46424

DRIFT RATE

- Poisson series solution of geosynchronous drift [AIAA PAPER 83-0016] 05 p0601 A83-16465
- On the variability of the solar diameter 06 p0853 A83-18129
- Vertical ionization drift velocities and range type spread F in the evening equatorial ionosphere 06 p0785 A83-18308
- Geomagnetic westward drift using the correlation coefficient 08 p1138 A83-23258
- An azimuth rate inertial navigation system 10 p1382 A83-26768
- Electron drift velocities in gas mixtures of He, N₂, and CO₂ 11 p1655 A83-28707
- Measurement of high electron drift velocity in a submicron, heavily doped graded gap Al(x)Ga(1-x)As layer 13 p1929 A83-31056
- The drift behavior of PSR 0809+74 13 p1948 A83-31263
- The drift of barium ion clouds and the electric field over Volgograd 14 p2051 A83-31886
- Rosby solitons - Stability, collisions, asymmetry, and generation by flows with a velocity shear --- for planetary atmospheres 14 p2111 A83-32142
- Drift velocity measurements in relativistic electron beams --- for free electron laser experiments 15 p2168 A83-33843
- A first comparison of STARE and EISCAT electron drift velocity measurements --- Scandinavian twin auroral radar experiment and European incoherent scatter facility 17 p2539 A83-37600
- The energy and momentum of slow drift spiral density waves 17 p2600 A83-37645
- Dependence of ionospheric drift speed on geomagnetic activity 17 p2495 A83-38544
- Electron drift velocity in molecular gas rare gas mixtures 20 p3049 A83-42577
- Modeling of spaced-receiver scintillation measurements --- of drift velocity in ionosphere 22 p3275 A83-46534

DRILLING

- NT LASER DRILLING
- How to reduce the drilling cost for the aerospace industry 09 p1273 A83-23638
- An end effector for robotic drilling 09 p1273 A83-23639
- An analysis of delamination in drilling composite materials 09 p1273 A83-23640
- Manufacturing methods for composite graphite hole generation [SAE PAPER 821418] 17 p2516 A83-37976

DRINKING

Drinking and water balance during exercise and heat acclimation 13 p1903 A83-30471

DROGUES

U TOWED BODIES

DRONE AIRCRAFT

NT TARGET DRONE AIRCRAFT

Analysis and flight data for a drone aircraft with active flutter suppression 01 p0008 A83-10192

Implementation of the DAST ARW II control laws using an 8086 microprocessor and an 8087 floating-point coprocessor --- drones for aeroelasticity research 02 p0227 A83-11910

Application of matrix singular value properties for evaluating gain and phase margins of multiloop systems --- stability margins for wing flutter suppression and drone lateral attitude control 02 p0230 A83-12457

Robustness analysis of a multiloop flight control system [AIAA PAPER 83-2189] 19 p2802 A83-41675

The use of singular value gradients and optimization techniques to design robust controllers for multiloop systems [AIAA PAPER 83-2191] 19 p2891 A83-41677

AN/USD-502 (CL 289) reconnaissance drone system 20 p2934 A83-43704

Design of a candidate flutter suppression control law for DAST ARW-2 --- Drones for Aerodynamic and Structural Testing Aeroelastic Research Wing [AIAA PAPER 83-2221] 23 p3402 A83-47125

DRONE HELICOPTERS

U DRONE AIRCRAFT

U HELICOPTERS

DRONE VEHICLES

NT DRONE AIRCRAFT

NT TARGET DRONE AIRCRAFT

DROP SIZE

Characteristic time ignition model extended to an annular gas turbine combustor 01 p0011 A83-10666

Entrainment and the droplet spectrum in cumulus clouds 02 p0215 A83-12941

On the droplet distribution near the base of cumulus clouds 02 p0215 A83-12943

Drop-size distribution of fog droplets determined from transmission measurements in the 0.53-10.1-microns wavelength range 03 p0365 A83-14378

Raindrop size distribution from microwave scattering measurements in equatorial and tropical climates 04 p0466 A83-15239

Numerical study of the effect of CCN on the size distribution of cloud droplets. I - Cloud droplets in the stage of condensation growth --- Cloud Condensation Nuclei 04 p0518 A83-16017

The role of the heat-up period in fuel drop evaporation [AIAA PAPER 83-0068] 05 p0632 A83-16500

Effect of liquid phase decomposition on fuel droplet distribution function [AIAA PAPER 83-0069] 05 p0632 A83-16501

Influence of multidroplet size distribution on icing collection efficiency [AIAA PAPER 83-0110] 05 p0666 A83-16526

Self-excitation of surface oscillations of droplets in an electromagnetic wave field 05 p0649 A83-17063

Deformation of a drop in a viscous flow and conditions for the existence of the equilibrium form of the drop 06 p0758 A83-19122

Fixation of bubbles and drops of specified shapes in a liquid dielectric by an electric field 06 p0813 A83-19434

A performance test of a raindrop sizer of microphonic type by artificial waterdrops and photographing of the drop shapes 08 p1075 A83-22037

Bistatic radar reflectivities of Pruppacher-and-Pitter form raindrops at 14.3 and 5.33 GHz 08 p1075 A83-22041

Remote sensing of precipitation parameters using K-band dual polarization radar 09 p1310 A83-23407

Droplet size effects on NO/x/ formation in a one-dimensional monodisperse spray combustion system [ASME PAPER 82-JPGG-GT-10] 09 p1227 A83-25268

Effect of size distribution variations on precipitation parameters determined by dual-measurement techniques 11 p1625 A83-27016

Comparison of raindrop size distributions observed in New England and Switzerland 11 p1625 A83-27017

Axis ratios of oscillating raindrops 11 p1628 A83-27046

Complications in deducing rain parameters from polarization measurements 11 p1629 A83-27067

Collisional forcing of raindrop oscillations 13 p1893 A83-31042

The determination of representative cloud droplet spectra 15 p2204 A83-34056

On the mathematical simulation of non-equilibrium cloud condensation rates 15 p2205 A83-34061

Effect of air, liquid and injector geometry variables upon the performance of a plain-jet airblast atomizer 16 p2351 A83-35809

Further studies on the prediction of spray evaporation rates --- for aircraft fuels 16 p2338 A83-35811

The effect of fuel atomization on soot-free combustion in a prevaporizing combustor 16 p2303 A83-35812

Effects of properties and location in the plume on droplet diameter for injection in a supersonic stream 16 p2351 A83-36080

Slurry fuel droplet breakup by irradiation at discrete frequencies [AIAA PAPER 83-1142] 16 p2339 A83-36242

Modeling the effect of temperature changes in the stratosphere on the growth of drops of a sulfate aerosol 16 p2382 A83-36870

Exponential size distributions of raindrops and vertical air motions deduced from vertically pointing Doppler radar data using a new method 18 p2722 A83-39135

Intercomparison of instruments used for measurement of cloud drop concentration and size distribution 18 p2688 A83-39136

Influence of atomizer design features on mean drop size 19 p2800 A83-40865

Experimental comparison of icing cloud instruments [AIAA PAPER 83-0026] 19 p2794 A83-42099

The effect of the microstructure of clouds on their radio emission 20 p3031 A83-42873

Settling of fixed erythrocyte suspension droplets 21 p3183 A83-44649

Aspects of light scattering by spherical particles 21 p3207 A83-44836

Microphysical interpretation of multi-parameter radar measurements in rain. I - Interpretation of polarization measurements and estimation of raindrop shapes. II Estimation of raindrop distribution parameters by combined dual-wavelength and polarization measurements 22 p3341 A83-46855

The interdependence of spray characteristics and evaporation history of fuel sprays in stagnant air [ASME PAPER 83-GT-7] 23 p3440 A83-47880

Spray characteristics of plain-jet airblast atomizers [ASME PAPER 83-GT-138] 23 p3448 A83-47965

Drop size measurements in evaporating realistic sprays of emulsified and neat fuels [ASME PAPER 83-GT-231] 23 p3440 A83-48027

On-line calibration technique for laser diffraction droplet sizing instruments [ASME PAPER 83-GT-232] 23 p3458 A83-48028

Generation and size distribution of droplet in annular two-phase flow [ASME PAPER 83-FE-2] 23 p3450 A83-48227

A comparison of techniques to estimate vertical velocities and drop size spectra 24 p3613 A83-49711

Graupel characteristics in relation to the dynamics of Florida cumuli 24 p3614 A83-49715

Droplet spectra and liquid water content measurements in aircraft icing environments [AD-A122516] 24 p3614 A83-49718

5500 miles of liquid water and drops size measurements in supercooled clouds below 10,000 feet agl 24 p3614 A83-49720

Microphysical influences on aircraft icing 24 p3546 A83-49722

DROP TESTS

Post-impact fatigue performance of carbon fibre laminates with non-woven and mixed-woven layers 20 p2948 A83-42814

Composite helicopter structure tested for crashworthiness 21 p3091 A83-44875

DROP TOWERS

7A simple drop table for fractional gravity - Design and instrumentation 18 p2673 A83-39847

DROP TRANSFER

Deformation of a drop in a viscous flow and conditions for the existence of the equilibrium form of the drop 06 p0758 A83-19122

Heat transfer between two-phase flow and a nozzle wall under conditions of entrainment of droplets from the surface of a condensed film 09 p1258 A83-23431

The calculation of transport phenomena in electromagnetically levitated metal droplets 20 p2963 A83-43273

DROP TUBES

U DROP TOWERS

DROP WEIGHT TESTS

U DROP TESTS

DROPOUTS

Space Shuttle siphon dropout prediction [AIAA PAPER 83-1383] 16 p2321 A83-36374

DROPS (LIQUIDS)

NT RAINDROPS

Transient thermal boundary layer in heating of droplet with internal circulation - Evaluation of assumptions 02 p0175 A83-13098

Dynamic equation of state of a gas with evaporating drops 04 p0544 A83-15445

Collision between an evaporating drop and a hot wall 04 p0478 A83-16166

An analytical evaluation of the icing properties of several low and medium speed airfoils [AIAA PAPER 83-0109] 05 p0579 A83-16525

Trajectory with diffusion method for predicting the fuel distribution in a transverse stream [AIAA PAPER 83-0336] 05 p0596 A83-16662

Self-excitation of surface oscillations of droplets in an electromagnetic wave field 05 p0649 A83-17063

Motion of a droplet in a nonisothermal flow 05 p0639 A83-17411

A comparative study of the rates of development of potential graupel and hail embryos in high plains storms 06 p0790 A83-18265

Coherent echo spectroscopy of small liquid particles 07 p0881 A83-20112

Growth of aqueous solution droplets of HNO₃ and HCl in the atmosphere 08 p1133 A83-23008

A theoretical determination of capture efficiency of small columnar ice crystals by large cloud drops 08 p1142 A83-23010

Measured collection efficiencies for cloud drops --- collision and coalescence mechanisms 08 p1142 A83-23011

Flow in a differentially rotated cylindrical drop at low Reynolds number 08 p1086 A83-23093

Ground contamination by fuel jettisoned from aircraft in flight [AD-A128451] 09 p1294 A83-24041

The heating and vaporization of water drops under the effect of radiation in the case of inhomogeneous internal heat-evolution 10 p1434 A83-26779

Drop explosion under the effect of intense laser radiation 10 p1434 A83-26780

Analysis of moisture condensation in engine inlet ducts 11 p1566 A83-27482

A theory of nondilute spray evaporation based upon multiple drop interactions 13 p1843 A83-31223

Vapor/droplet coupling and the mist flow (OTEC) cycle 15 p2189 A83-33992

The measurement of cloud droplet concentration with a hot film probe 15 p2204 A83-34053

The airborne Knollenberg cloud droplet spectrometer probes of DFVLR 15 p2164 A83-34054

The determination of representative cloud droplet spectra 15 p2204 A83-34056

A model experiment concerning particle scavenging by cloud and rain drops 15 p2205 A83-34058

Condensation growth of droplet spectra 15 p2205 A83-34060

Comments on 'Skylab near-infrared observations of clouds indicating supercooled liquid water droplets' 16 p2387 A83-35496

Effects of properties and location in the plume on droplet diameter for injection in a supersonic stream 16 p2351 A83-36080

Droplet heating and vaporization at high Reynolds and Peclet numbers [AIAA PAPER 83-1706] 17 p2502 A83-37203

The effect of the real properties of a carrier vapor on the evaporation time of a drop 17 p2506 A83-37814

The dependence of the shape and stability of captive rotating drops on multiple parameters 17 p2507 A83-38615

Theory of the Leidenfrost phenomenon 18 p2685 A83-39866

Thermocapillary migration of bubbles and droplets 18 p2686 A83-39907

Influence of acoustic fields on drop dynamics in an acoustic resonator 18 p2686 A83-39908

Drop motion in a rotating immiscible liquid body 18 p2686 A83-39909

The phase realignment of clouds 19 p2868 A83-41583

Optical recording of nonstationary processes of mixture formation and combustion --- atomized jet droplets characteristics 19 p2850 A83-42141

A theory of electrophoresis of emulsion drops in aqueous two-phase polymer systems 20 p2951 A83-43278

Thermocapillary motion of bubbles inside drops --- in free fall environment with axisymmetric surface temperature field 20 p2940 A83-43279

Search for fractional charges in water 21 p3203 A83-43884

Heat and mass exchange of a droplet in a polyatomic gas 21 p3220 A83-43933

Settling of fixed erythrocyte suspension droplets 21 p3183 A83-44649

The concentrating of molecules in coacervate droplets and the origin of life 21 p3189 A83-44700

- Aerodynamic-wave break-up of liquid sheets in swirling airflows and combustor modules
 [AIAA PAPER 83-1204] 21 p3133 A83-45511
 Stability of rotating liquid drops. I - Uncharged drops
 22 p3280 A83-46001
 Nonaxisymmetric equilibrium shapes of a drop on a plane
 23 p3452 A83-48670
 Theory of thermophoresis of nonvolatile liquid aerosol particles
 24 p3575 A83-48861
 Water droplet growth at precritical radii
 24 p3611 A83-49686
 Cloud droplet spectra in summertime cumulus clouds
 24 p3612 A83-49695
 Shape and stability of electrostatically levitated drops
 24 p3580 A83-49877
 Variational formulation for the equilibrium condition of a conducting fluid in an electric field
 24 p3624 A83-50195

DROSOPHILA

- The induction of circadian rhythm by light impulses - The dependence on illumination and duration of the impulse
 16 p2395 A83-36808
 Some results of the effect of space flight factors on *Drosophila melanogaster*
 19 p2872 A83-40843
 Antioxidants, metabolic rate and aging in *Drosophila*
 21 p3183 A83-44600

DROUGHT

- Visual analysis of 1:250,000 Landsat data for forage assessment during the 1980 drought in western Manitoba
 03 p0345 A83-14235
 Influence of solar wind variability of the recurrence of droughts
 03 p0363 A83-14918
 Drought-induced wind erosion in southwestern Kansas, U.S.A. - Integration of Landsat, Seasat, and airborne multispectral data
 09 p1290 A83-24606
 Some aspects of major dry and wet periods in the contiguous United States, 1895-1981
 18 p2721 A83-39109

DROUGHT CONDITIONS**U DROUGHT****DROWSINESS****U SLEEP****DRUG THERAPY****U CHEMOTHERAPY****DRUGS**

- NT ADRENERGICS
 NT ANESTHETICS
 NT ANTIADRENERGICS
 NT ANTIBIOTICS
 NT ANTICHOLINERGICS
 NT ANTICONSULSANTS
 NT ANTIDIURETICS
 NT ANTIHYPERTENSIVE AGENTS
 NT ANTIRADIATION DRUGS
 NT ATROPINE
 NT CAFFEINE
 NT CENTRAL NERVOUS SYSTEM DEPRESSANTS
 NT CENTRAL NERVOUS SYSTEM STIMULANTS
 NT CHLOROFORM
 NT CHOLINERGICS
 NT CORTISONE
 NT EPINEPHRINE
 NT HEMOSTATICS
 NT INSULIN
 NT METHYL CHLORIDE
 NT MORPHINE
 NT MOTION SICKNESS DRUGS
 NT MUSCLE RELAXANTS
 NT NARCOTICS
 NT NORADRENALINE
 NT NOREPINEPHRINE
 NT PSYCHOTROPIC DRUGS
 NT STREPTOMYCIN
 NT TRANQUILIZERS
 NT VASOCONSTRICTOR DRUGS
 The effect of emotional and pain stress on the activity of Na,K-ATPase in the heart muscle
 01 p0079 A83-10535
 The effect of trapidil on the formation of prostacycline in rabbit cardiac tissue --- triazolo-pyrimidine derivative
 01 p0079 A83-10539
 The distribution of functionally different cells in immunocompetent organs after an injection of haloperidol
 01 p0080 A83-10550
 The effects of nonachlazine on the energy supply of the heart contractile activity during experimental myocardial infarction
 03 p0374 A83-13628
 The effect of cordinamine and mesatone on the EKG under conditions of acute microwave irradiation
 03 p0374 A83-13629
 The effects of hypotensive drugs on the humoral factors of the regulation of blood circulation
 03 p0380 A83-13631
 A quantitative determination of the hemodepressive effect of some alkylating agents
 03 p0374 A83-13633

- A method for the assessment of enzyme activity in drug metabolism
 03 p0381 A83-14335
 The effect of succinic acid on work capacity and recovery during muscle activity in conditions of various ambient temperatures
 03 p0382 A83-14351
 The effect of 8-methoxypsoralen and UV radiation on the electric stability of liposome membranes
 03 p0375 A83-14360
 Refractoriness of heart tissues during a decrease of fast sodium current - A comparison of the atrium and the ventricle
 03 p0376 A83-14370
 The use of cordarone during acute myocardial infarctions
 05 p0674 A83-17221
 The characteristics of the mechanism of action of cyproheptadine /peritol/ on the activity of the hypothalamo-hypophysial-adrenal system
 07 p0974 A83-20979
 The role of the kidneys in the pharmacokinetics of novocainamide
 07 p0975 A83-20989
 The detection of drug addiction among flight personnel
 08 p1148 A83-22965
 An evaluation of plasma volume expanders in the treatment of decompression sickness
 10 p1453 A83-25668
 Prostacyclin-induced hyperthermia - Implication of a protein mediator
 11 p1641 A83-28756
 Timolol maleate - Side effects on healthy nonglaucomatous volunteers
 12 p1764 A83-28937
 Central effects of some peptide and non-peptide opioids and naloxone on thermoregulation in the rabbit
 12 p1763 A83-29533
 The energy balance of the myocardium and its correction by antiarrhythmics
 13 p1895 A83-30407
 Several problems of the chemical protection of golden hamsters from ionizing radiation
 14 p2062 A83-32056
 The chemoprophylaxis of malaria in flight personnel
 14 p2067 A83-32452
 The intensity of kininergic reactions of the cardiovascular system for various levels of the activity of the kallikrein-kinin system in blood plasma
 14 p2064 A83-32569
 Drug disposition under hyperbaric and hyperbaric hyperoxic conditions - Meperidine in the dog
 14 p2064 A83-32686
 Site of pulmonary hypoxic vasoconstriction studied with arterial and venous occlusion
 14 p2064 A83-32814
 The dependence of wound healing on the condition of the immune system
 14 p2065 A83-33302
 The use of a combined pressure and medication treatment for the rehabilitation and recovery of the functions of the locomotor system
 14 p2070 A83-33307
 Heart function and certain mechanisms for its regulation when simulating the adaptation to hypoxia by administering 2,4-dinitrophenol
 15 p2210 A83-34958
 Methazolamide and acetazolamide in acute mountain sickness
 18 p2734 A83-40357
 The condition of peripheral hemodynamics and the effect on it of several drugs in patients with chronic ischemic heart disease and left ventricular insufficiency
 18 p2735 A83-40546
 The effect of seduxen on hemodynamic reactions in patients with hypertension during emotional stress
 18 p2735 A83-40550
 The effect of ultrasound on the physical and chemical properties of hydroxyprogesterone capronate (experimental investigation)
 18 p2733 A83-40570
 The significance of the strength of the central nervous system in the variability of the reaction in sick persons to acebutolol
 18 p2736 A83-40578
 The change in the reaction of systemic and regional blood circulation to immobilization stress in rats in the case of pharmacological desympathization
 19 p2871 A83-40816
 The prevention of early forms of medication-induced ototoxicosis in experimental studies
 19 p2875 A83-41442
 Hemodynamic effects of lactated ringer's solution on hemorrhagic shock during exposure to hyperbaric air and hyperbaric hyperoxia
 21 p3182 A83-43991
 The effect of an antioxidant on the recovery of hemopoiesis and the aggregation of thrombocytes
 21 p3186 A83-45380
 Effect of ethanol and naloxone on control of ventilation and load perception
 22 p3348 A83-45996
- DRUMLINS**
U GLACIAL DRIFT
- DRUMS (CONTAINERS)**
 Transfiling and maintenance of oxygen cylinders [SAE AIR 1059A]
 17 p2471 A83-38103
- DRY CELLS**
 NT NICKEL ZINC BATTERIES
 Defects in insulite (gamma-MnO₂) and dry-cell battery efficiency
 18 p2708 A83-39964

DRY FRICTION

- Morphological and frictional behavior of sputtered MoS₂ films
 02 p0160 A83-12652
 Analytical experimental heat transfer in dry sliding of polymeric composites
 [ASLE PREPRINT 82-LC-2B-1]
 03 p0333 A83-13233
 Nature of subsurface damage in an aluminium-22 wt% silicon during dry sliding wear
 04 p0460 A83-15995
 The effect of friction on the delamination of heterogeneous materials
 13 p1865 A83-30053
 The motion of an ellipsoid along a rough plane with slip
 14 p2079 A83-32359
 Subsurface damage during dry sliding wear of Al-Al₃Ni eutectic alloy
 14 p1993 A83-32623
 Effects of friction dampers on aerodynamically unstable rotor stages
 [AIAA PAPER 83-0848]
 14 p1976 A83-32791
 Design of dry-friction dampers for turbine blades
 16 p2306 A83-35883
 The dryout region in frictionally heated sliding contacts
 20 p2980 A83-42762
 A method for determining the inertial-dissipative parameters of an astatic gyroscope
 21 p3138 A83-44641
 Dry wear studies on glass-fibre-reinforced epoxy composites
 23 p3428 A83-48154
- DRY HEAT**
 Sweating efficiency in acclimated men and women exercising in humid and dry heat
 13 p1904 A83-30499
 The daily food ration and the ascorbic acid supply of the human body during work in an arid zone
 23 p3496 A83-47103

DRYING**NT DEHYDRATION****DSIF (INSTRUMENTATION FACILITY)****U DEEP SPACE INSTRUMENTATION FACILITY****DTA (ANALYSIS)****U DIFFERENTIAL THERMAL ANALYSIS****DTMB-111 GROUND EFFECT MACHINE****U GROUND EFFECT MACHINES****DTMB-430 GROUND EFFECT MACHINE****U GROUND EFFECT MACHINES****DUAL MODE PROPULSION****U HYBRID PROPULSION****DUAL SPIN SPACECRAFT**

- Certain classes of exact solutions of the problem of the motion of two coupled bodies --- dual-spin satellite model
 13 p1812 A83-31373
 The attitude and orbit control system for GIOTTO, ESA's Halley encounter mission
 17 p2476 A83-37435
 Attitude stability of flexible asymmetric dual spin spacecraft
 [AIAA PAPER 83-2177]
 19 p2815 A83-41671
 Effects of energy addition and dissipation on dual-spin spacecraft attitude motion
 21 p3103 A83-45466

DUAL THRUST NOZZLES

- Jet trajectories and surface pressures induced on a body of revolution with various dual jet configurations
 [AIAA PAPER 83-0080]
 05 p0579 A83-16508

DUALITY PRINCIPLE

- A duality principle for state estimation with partially noise corrupted measurements
 09 p1330 A83-24746
 A duality principle for state estimation with partially noise-corrupted measurements
 14 p2074 A83-31929
 Conjugate duality and the exponential Fourier spectrum --- Book
 20 p3040 A83-42204

DUALITY THEOREM

- A penalty duality method for the Budiansky-Sanders shell model
 04 p0501 A83-16310
 Questions of convergence, duality, and averaging for a class of functionals of the calculus of variations
 06 p0804 A83-17976
 Geometric Programming for continuous design problems
 06 p0801 A83-18221
 Duality for multidimensional MEM spectral analysis --- Maximum-Entropy Method
 [AD-A130045]
 14 p2075 A83-32431

DUCT GEOMETRY

- Laminar natural convection along vertical corners and rectangular channels
 08 p1090 A83-23208
 Analytical design and experimental verification of S-duct diffusers for turboprop installations with an offset gearbox
 [AIAA PAPER 83-1211]
 16 p2294 A83-36283
 Heat transfer performance of ceramic regenerator matrices with sine-duct shaped passages
 16 p2353 A83-36592
 Performance study of shock tubes with area change at the diaphragm section - Effects on the shock tube performance of diaphragm location, area ratio and convergent angle
 21 p3129 A83-44063

DUCTED BODIES

On the calculation of ducted propeller performance in axisymmetric flows --- Book 20 p2969 A83-42201

DUCTED FANS

Sound propagation in segmented exhaust ducts - Theoretical predictions and comparison with measurements [AIAA PAPER 83-0734] 11 p1651 A83-28016
ACV lift air systems - More puff for less power 15 p2242 A83-34861

DUCTED FLOW**NT KNUDSEN FLOW**

The simulation of secondary flow effects in turbulent non-circular passage flows 02 p0173 A83-12902
Characteristics of a turbulent boundary layer on the concave surface of a 90-degree bend 04 p0475 A83-15094

Development of secondary flow and vorticity in curved ducts, cascades, and rotors, including effects of viscosity and rotation 04 p0478 A83-16141
Integral method to thermally developing laminar flow in a duct subjected to external radiation and convection [AIAA PAPER 83-0529] 05 p0637 A83-16768

Multi-grid solution of Neumann pressure problem for viscous flows using primitive variables [AIAA PAPER 83-0557] 05 p0637 A83-16786
The Oseen model for internal separated flows 05 p0642 A83-17943

Combined /radiative-convective/ heat transfer from laminar and turbulent radiating flows in cooled ducts 06 p0759 A83-19160
An observation on the origin of secondary flow in straight noncircular ducts 08 p1086 A83-23122

The application of boundary value techniques in the solution of the Navier-Stokes equation 08 p1087 A83-23179
Numerical solution of the Navier-Stokes equations by multi-grid techniques 08 p1088 A83-23183

Numerical simulation of three dimensional flows in duct 08 p1088 A83-23184
Prediction of developing turbulent flow by the finite element method 08 p1088 A83-23189
Semi-elliptic computation of axi-symmetric transonic flows 08 p1089 A83-23204

Laminar natural convection along vertical corners and rectangular channels 08 p1090 A83-23208
Thermoconvective heat transfer in a rectangular cavity with constant wall cooling rate 08 p1090 A83-23211
A nonstationary approach to the investigation of heat transfer in the cooling ducts of turbine blades 09 p1258 A83-23429

An analysis of the two-dimensional acoustic field in a nonuniform duct carrying compressible flow [AIAA PAPER 83-0669] 10 p1473 A83-25906
Experimental method for determining the dynamic properties of gas flows 10 p1417 A83-26293

Analysis of moisture condensation in engine inlet ducts 11 p1566 A83-27482
Experimental investigation of geometry and flow effects on acoustic radiation from duct inlets [AIAA PAPER 83-0713] 11 p1651 A83-28012

Three-dimensional viscous analysis of ducts and flow splitters 12 p1696 A83-29010
A 2D model of turbulent solar induced flows in passive air collectors 12 p1749 A83-29039
Calculation of fully developed turbulent flows in ducts of arbitrary cross-section 12 p1723 A83-29231

Towards a closer cooperation between theoretical and numerical analysis in gas dynamics 12 p1698 A83-29936
Turbulent flow induced by a jet in a cavity-measurements and 3D numerical simulation 15 p2155 A83-33666

An effective numerical technique for entry length laminar convective heat transfer in vertical and horizontal ducts of any cross section 15 p2160 A83-34258
Laminar flow heat transfer with axial conduction in a circular tube - A finite difference solution 15 p2160 A83-34262

The swirl in an S-duct of typical air intake proportions 16 p2289 A83-35620
Swirl characteristics of an S-shaped air intake with both horizontal and vertical offsets 16 p2289 A83-35621
Calculation of a laminar flow of a compressible gas in plane curvilinear ducts with heat transfer 16 p2349 A83-35701

A study of a supersonic three-dimensional jet flow in a duct 16 p2289 A83-35718
A study of the distribution of static pressure and tangential stresses on the walls of a curved duct 16 p2350 A83-35719

Compact reversal of a plane supersonic flow 16 p2289 A83-35721
Semi implicit calculation method of the flow field in a duct with the flame stabilized by a step --- for aircraft engine combustion chamber design [ONERA, TP NO. 1983-52] 16 p2303 A83-35820

Mode propagation in nonuniform circular ducts with potential flow 16 p2351 A83-36082

Analytical understanding of WTR ignition/duct overpressure induced by Space Shuttle solid rocket motor ignition transient --- Western Test Range [AIAA PAPER 83-1113] 16 p2315 A83-36227

Heat transfer performance of ceramic regenerator matrices with sine-duct shaped passages 16 p2353 A83-36592

Measurements of compressible secondary flow in a circular S-duct [AIAA PAPER 83-1739] 17 p2446 A83-37218

An experimental investigation of multiple shock wave/turbulent boundary layer interactions in a circular duct [AIAA PAPER 83-1744] 17 p2446 A83-37220

Sound propagation in ducts with impedance walls in the presence of an air flow. II - Optimization of acoustic attenuation in ducts 17 p2577 A83-37512

Numerical model for dynamic and thermal developments of a pulsed laminar ducted flow 17 p2506 A83-37867

Numerical investigation of unsteady flow development in a nozzle-duct configuration [AIAA PAPER 83-1714] 17 p2452 A83-38087

Numerical solution of the Reynolds stress equations in a developing duct flow [AIAA PAPER 83-1883] 18 p2634 A83-39353

The effect of duct walls on the vortex formation in the wake of a bluff body 19 p2842 A83-41253
Calculation of heat transfer from polydisperse flows of gas suspensions in straight ducts and pipes 19 p2846 A83-42135

Study of asymptotic incompressible flow in curved ducts using a multi-grid technique 20 p2969 A83-42532
Numerical study of unsteady convective heat transfer in pulsating duct flows 20 p2975 A83-42708

A new approach for calculating heat transfer characteristics of turbulent wall flows 20 p2977 A83-42725
Combined natural and forced convection in vertical ducts 20 p2979 A83-42749

Acoustic enhancement of heat transfer in plane channels 20 p2929 A83-42751
Maldistributed inlet flow effects on turbulent heat transfer and pressure drop in a flat rectangular duct 20 p2986 A83-43363

Some recent progress in the analysis of transonic internal flows 21 p3085 A83-44019
Peripheral temperature variation in the walls of noncircular ducts 21 p3129 A83-44247

Statistical characteristics of velocity, concentration, mass transport, and momentum transport for coaxial jet mixing in a confined duct [ASME PAPER 83-GT-39] 23 p3447 A83-47899

Turbulent flow between coaxial cylinders with the inner cylinder rotating [ASME PAPER 83-GT-48] 23 p3447 A83-47907
Entropy production rates from viscous flow calculations. II Flow in a rectangular elbow [ASME PAPER 83-GT-71] 23 p3512 A83-47924

Laminar flow in the entrance region of elliptical ducts [ASME PAPER 83-FE-1] 23 p3449 A83-48226

Multiple jet mixing in a rectangular duct - Centre-plane behaviour [ASME PAPER 83-FE-35] 23 p3399 A83-48238

Characteristics of the supersonic combustion of nonmixed gases in ducts 24 p3556 A83-49778

DUCTED ROCKET ENGINES

Solid ducted rocket engine combustor tests 16 p2303 A83-35803

DUCTILITY

Determination of fracture toughness of ductile materials using a reinforced double cantilever beam specimen 01 p0026 A83-11030

Selection of molybdenum sheet for deep drawing applications 02 p0154 A83-11786
The effect of heat treatment conditions on the fine structure and mechanical properties of titanium alloy VT3-1 03 p0300 A83-14158

Analysis of ductile deformation processes on the basis of a mixed variational principle 04 p0497 A83-15387
The influence of grain structure on the ductility of the Al-Cu-Li-Mn-Cd alloy 2020 04 p0460 A83-16004

Mechanical properties of ductile Fe-Ni-Zr and Fe-Ni-Zr /Nb or Ta/ amorphous alloys containing fine crystalline particles 05 p0615 A83-17559

Three-dimensional constitutive relations and ductile fracture --- Book 06 p0774 A83-18477

Fatigue crack growth theory for ductile material 06 p0774 A83-18480

On certain macroscopic and microscopic aspects of plastic flow of ductile materials 06 p0728 A83-18482

Experimental and numerical study of the different stages in ductile rupture - Application to crack initiation and stable crack growth 06 p0774 A83-18484

The plastic work spent in ductile fracture 06 p0774 A83-18485

A quantitative description of fracture toughness under plane stress conditions by the R-curve method 06 p0774 A83-18487

Finite deformation constitutive relations including ductile fracture damage 06 p0774 A83-18490

Constitutive equations and global criteria for ductile fracture 06 p0774 A83-18491

Mixed mode plane stress ductile fracture 06 p0775 A83-18909

Why ductile fracture mechanics 07 p0944 A83-19669

Models of creep cavitation and their interrelationships 07 p0887 A83-20628

Hole nucleation and ductile failure in multiaxial states of stress 08 p1116 A83-21663

Mechanical model and mathematical analysis for ductile fracture 08 p1116 A83-21665

Mechanisms and criteria for cleavage 08 p1058 A83-21666

Fracture assessment in ductile tearing situations 08 p1063 A83-21751

Instability problems in ductile fracture 08 p1063 A83-21752

In-situ study of deformation and initiation of ductile fracture at a notch-root 08 p1119 A83-21789

Some effects of inelastic constitutive models on crack tip fields in steady quasistatic growth 08 p1119 A83-21793

Central ductile crack in an orthotropic strip of finite width 08 p1120 A83-21818

The effect of dispersoids on the ductile fracture toughness of Al-Mg-Si alloys 08 p1065 A83-22015

Effects of morphology and hardness of inclusions on ductile fracture 08 p1066 A83-22078

Effect of structure on the ductile-brittle transition temperature of molybdenum alloy Tsm-6 08 p1067 A83-22695

The application of the J-integral to small specimens of ductile material to be exposed to high temperatures and high levels of irradiation 09 p1233 A83-24079

Microstructure and tensile ductility in a beta heat treated titanium alloy 10 p1398 A83-26280

A study of the ductility of TiTi intermetallics 13 p1821 A83-30690

The workability of alloys 13 p1821 A83-30694

The effect of cold deformation during rolling on the mechanical properties of sheets and foil of magnesium-lithium alloys 13 p1821 A83-30699

Effect of tungsten on the properties of austenitic precipitation-hardening Fe-Cr-Ni alloys 13 p1823 A83-31213

Structural parameters in a continuum model of ductile fracture 14 p1992 A83-32382

A study of the short-term strength of structural materials under static loading --- of metal alloys at cryogenic temperatures 14 p1997 A83-33013

The use of the acoustic emission method for studying the strength and ductility of materials at low temperatures 14 p1997 A83-33014

The ductile fracture of metals - A microstructural viewpoint 15 p2138 A83-34131

Microstructural basis and crack growth theories for post irradiation ductility loss in Nimonic PE16 15 p2139 A83-34490

Ductility and the abrasive wear of an ultrahigh strength steel 15 p2141 A83-35242

Variations in ductility produced by strain rate changes in tensile testing 16 p2334 A83-36568

Effects of antimony additions on the fracture of nickel at 600 C 17 p2491 A83-38858

The structure and mechanical properties of the high-strength powder metallurgy steel 60Kh2 following thermomechanical treatment 17 p2492 A83-38872

A map of fracture mechanisms for tungsten 17 p2492 A83-38874

On the knee-point of cross-ply composite 18 p2653 A83-40175

The strength, ductility and failure of thermoplastics reinforced with short-glass fibres 18 p2657 A83-40233

A linear model of ductile plastic damage 19 p2858 A83-41321

Creep of structures - A continuous damage mechanics approach 20 p3001 A83-42520

Characteristics of the hydrogen plasticizing of titanium alloys 20 p2956 A83-43499

Effect of modification on the ductility of alloy Zhs6K 21 p3113 A83-44484

The effect of molybdenum on the ductility of a niobium alloy precipitation-hardened by zirconium nitrides 21 p3113 A83-44846

DUCTS

- Recovery behavior of hydrogen charged 7075-T6 aluminum 22 p3268 A83-45625
- DUCTS**
- NT ACOUSTIC DUCTS
- NT AIR DUCTS
- NT ANNULAR DUCTS
- Cross spectra between temperature and pressure in a constant area duct downstream of a combustor [AIAA PAPER 83-0762] 15 p2227 A83-33487
- Instantaneous, predictable balloon system descent from high altitude 18 p2640 A83-39808
- Composite engine duct fabrication 18 p2631 A83-39941
- DUFFING DIFFERENTIAL EQUATION**
- Analog computer simulation of a Duffing oscillator and comparison with statistical linearization 02 p0233 A83-12869
- Peculiarities of the appearance of subharmonic and subultraharmonic resonances in systems which are described by Duffing's equation 04 p0531 A83-15379
- Mechanism for chaos in the Duffing equation 10 p1472 A83-26969
- Chebyshev series solution of the controlled Duffing oscillator 12 p1776 A83-29630
- Universal scaling property in bifurcation structure of Duffing's and of generalized Duffing's equations 22 p3354 A83-45933
- Radiation balance and the stochastic Van der Pol-Duffing equation 22 p3354 A83-46771
- DUMMY LOADS**
- U IMPEDANCE
- U OUTPUT
- DUNES**
- Use of satellite images for detecting wind dynamics - Sand deposits, fixed dunes, wind erosion and desertification in the Sahel, south of Sahara 09 p1287 A83-24570
- Radar scatterometry of sand dunes and lava flows 22 p3313 A83-46218
- SIR-A radar images of sand dunes and volcanic fields 22 p3314 A83-46225
- Speculation on Martian north polar wind circulation and the resultant orientations of polar sand dunes 22 p3388 A83-47084
- DUNGEYS WIND SHEAR MECHANISM**
- U WIND SHEAR
- DUPLEX OPERATION**
- Investigation and design of a highly integrable echo cancellation procedure for duplex transmission 04 p0472 A83-16039
- An analysis of full-duplex data links in SNA networks --- Systems Network Architecture 07 p0907 A83-19724
- Multichannel duplex fiber-optic communication line operating at the wavelength in the region of 1.3 micron 07 p0993 A83-20122
- DUPLEXERS**
- Near-millimeter wave polarizing duplexer/isolator 10 p1483 A83-26646
- Folded Fabry-Perot quasi-optical ring resonator duplexer Theory and experiment 14 p2027 A83-33457
- DURABILITY**
- Particulate laden flows in turbomachinery; Proceedings of the Joint Fluids, Plasma, Thermophysics and Heat Transfer Conference, St. Louis, MO, June 7-11, 1982 11 p1525 A83-27476
- An analysis of the durability characteristics of aircraft structures on the basis of fracture mechanics 11 p1597 A83-28477
- An overview of turbine engine structural design - Development trends in the Air Force [AIAA 83-0952] 12 p1703 A83-29777
- Deterioration trending enhances jet engine hardware durability assessment and part management [AIAA PAPER 83-1234] 16 p2308 A83-36297
- Development trends in engine durability --- for USAF aircraft gas turbines [AIAA PAPER 83-1297] 16 p2309 A83-36329
- Durability and damage tolerance control plans for U.S. Air Force aircraft 19 p2797 A83-41045
- The durability of aircraft tyres 21 p3116 A83-44879
- DURATION**
- U TIME
- DUST**
- NT COSMIC DUST
- NT INTERPLANETARY DUST
- NT LUNAR DUST
- NT METEOROID DUST CLOUDS
- NT ZODIACAL DUST
- Solar-band radiative characteristics of the Mt. St. Helens dust cloud, determined by remote sensing 03 p0370 A83-14640
- Spectral evidence for the mineralogy of high-albedo soils and dust on Mars 04 p0568 A83-15583

- Hydromagnetic unsteady flow of a dusty viscous fluid between a flat wall and a long wavy wall 04 p0539 A83-16435
- Physical and optical properties of dust particles [AIAA PAPER 83-0549] 05 p0659 A83-16784
- Automatic laser radar systems for measurement of atmospheric pollutants 05 p0651 A83-17281
- Attenuation due to accretion of dust and sand on reflector antennas at microwave frequencies 06 p0744 A83-18696
- Environmental effects of an impact-generated dust cloud - Implications for the Cretaceous-Tertiary extinctions 06 p0779 A83-18816
- Lidar observations of dust layers' transience in the stratosphere following the El Chichon volcanic eruption 07 p0958 A83-20090
- Further studies on the ignition and flame quenching of quiescent dust clouds 07 p0882 A83-21351
- Flame propagation through dust clouds of carbon, coal, aluminium and magnesium in an environment of zero gravity 07 p0882 A83-21352
- On the passage of a shock wave through a dusty-gas layer 07 p0927 A83-21354
- On rotating charged dust in general relativity. IV 07 p1027 A83-21356
- Optical characteristics of windblown dust 08 p1135 A83-22542
- Features in using lidars for measuring the dust content of air 11 p1573 A83-28203
- The effect of aerosols on climate and aerosol climatology on the basis of observations from space 12 p1759 A83-29558
- Most suitable conditions for aerosol monitoring from space 12 p1754 A83-29561
- The effect of the stratospheric aerosol layer on the total radiation 14 p2051 A83-32372
- Shock waves in dusty gas with radiation effects 15 p2157 A83-33873
- High temperature erosion study of INCO 600 metal 15 p2141 A83-35247
- Formation of fine dust on Saturn's rings as suggested by the presence of spokes 16 p2436 A83-35732
- Radiative properties of the stratospheric dust cloud from the May 18, 1980, eruption of Mount St. Helens 16 p2380 A83-36145
- Circumglobal transport of the El Chichon volcanic dust cloud 17 p2540 A83-37773
- Simulation of transport and removal processes of the Saharan dust 18 p2725 A83-39685
- Calculation of dusty-gas flow around a sphere with allowance for the effect of reflected particles 19 p2845 A83-41898
- On some radiative features of the El Chichon volcanic stratospheric dust cloud and a cloud of unknown origin observed at Mauna Loa 20 p3021 A83-42856
- The force effect of a supersonic flow of a dust-filled gas on a blunt body 21 p3088 A83-45347
- Background concentration of ozone, dust, and nitrogen and sulfur compounds in the atmosphere (according to worldwide data) 24 p3602 A83-49102
- Certain characteristics of the radiation balance in the cloudless atmosphere and at the ocean surface depending on the dustiness of the atmosphere 24 p3605 A83-49281
- DUST COLLECTORS**
- Laboratory simulation of cometary dust collection and analysis 07 p1010 A83-21577
- Separation characteristics of the T700 engine inlet particle separator 11 p1530 A83-27479
- A proposal to use an upper atmosphere satellite tethered to the Space Shuttle for the collection of micro-meteoritic material 20 p2938 A83-42828
- DUST STORMS**
- Microwave propagation in sand and dust storms 02 p0162 A83-11551
- A parameter review and assessment of attenuation and backscatter properties associated with dust storms over desert regions in the frequency range of 1 to 10 GHz 03 p0306 A83-14012
- Martian dust mantling and surface composition - Interpretation of thermophysical properties 04 p0566 A83-15570
- Rate of wind abrasion on Mars 04 p0567 A83-15572
- Wind streaks in Tharsis and Elysium - Implications for sediment transport by slope winds 04 p0567 A83-15573
- Two Mars years of surface changes seen at the Viking Landing sites 04 p0567 A83-15575
- Band-pass filtering of one year of daily mean pressures on Mars 04 p0568 A83-15586
- Remote sensing evidence for regolith water vapor sources on Mars 04 p0569 A83-15589
- Dust loading of the normal atmosphere [AIAA PAPER 81-0548] 05 p0659 A83-16783

- Monitoring of Saharan dust over the Atlantic using Meteosat-VIS-data 12 p1759 A83-29571
- Transport of mineral aerosol from Asia over the North Pacific Ocean 16 p2380 A83-36148
- The thermal structure of the atmospheric surface boundary layer on Mars as modified by the radiative effect of aeolian dust 16 p2437 A83-36158
- Martian great dust storms - Interpretive axially symmetric models 21 p3239 A83-44090
- Dust storm simulation for accelerated life testing of solar collector mirrors 21 p3168 A83-45063
- DWARF GALAXIES**
- Dwarf galaxies in the M81/82 group - New photometric data 05 p0695 A83-17853
- The color and surface brightness of the Leo II dwarf galaxy 06 p0820 A83-18857
- A survey of the distribution of wavelength 2.8 cm radio continuum in nearby galaxies. III - A small sample of irregular and blue compact galaxies 07 p1025 A83-21246
- The H I distribution in an extremely faint dwarf irregular galaxy M81 dwA 08 p1182 A83-23038
- From dwarfs to giants - Signposts of galaxy formation 08 p1187 A83-23284
- A comment on the colors of globular clusters in elliptical galaxies 09 p1357 A83-23728
- 21-cm line observations of 59 lenticular and spiral galaxies 09 p1355 A83-24523
- Discovery of an S star in the Fornax dwarf elliptical galaxy 10 p1491 A83-25353
- Accurate radial velocities for carbon stars in Draco and Ursa Minor - The first hint of a dwarf spheroidal mass-to-light ratio 10 p1504 A83-25739
- Is there nonluminous matter in dwarf spheroidal galaxies 10 p1504 A83-25740
- Some implications of nonluminous matter in dwarf spheroidal galaxies 10 p1504 A83-25741
- Three-dimensional computer simulations of star formation in dwarf galaxies 10 p1508 A83-26362
- X-ray and ultraviolet observations of extragalactic H II regions 10 p1508 A83-26365
- Carbon stars and the seven dwarfs --- stellar evolution in dwarf spheroidal galaxies 10 p1514 A83-26728
- A color-magnitude diagram for Leo II 11 p1668 A83-27108
- Blue compact dwarf galaxies. II - Near-infrared studies and stellar populations 15 p2257 A83-34092
- Dwarf elliptical galaxies 15 p2259 A83-34120
- An example of the performance of the space telescope planetary camera 15 p2247 A83-34511
- A multifrequency study of star formation in the blue compact dwarf galaxy I Zw 36 17 p2596 A83-37310
- Integrated magnitudes and mean colors of DDO dwarf galaxies in the UBV system. II - Distances, luminosities, and H I properties 17 p2602 A83-37779
- Structure and stellar content of dwarf elliptical galaxies 17 p2602 A83-37781
- Stochastic star formation and chemical evolution of dwarf irregular galaxies 17 p2609 A83-38423
- The local group irregular galaxies LGS 3 and Pegasus 18 p2757 A83-39591
- Stellar populations in local group dwarf elliptical galaxies. I - NGC 147 19 p2918 A83-41616
- The velocity dispersion of the globular clusters in the Fornax dwarf galaxy 19 p2920 A83-41646
- The structure of the Carina dwarf elliptical galaxy 20 p3064 A83-42319
- The chemical inhomogeneity of the Sculptor dwarf spheroidal galaxy 20 p3067 A83-42439
- The magellanic irregular galaxy DDO 155 20 p3067 A83-42440
- Slippery evidence on the Galaxy's invisible heavy halo 22 p3380 A83-46577
- The origin of dwarf spheroidal galaxies 24 p3654 A83-49216
- Neutral hydrogen observations of the dwarf elliptical galaxies NGC 185 and NGC 205 24 p3642 A83-49254
- DWARF NOVAE**
- Localized thermonuclear runaways and volcanoes on degenerate dwarf stars 02 p0252 A83-11600
- Ultraviolet light curves of the dwarf novae U Geminorum and VW Hydri 02 p0256 A83-12127
- PS 74 - The discovery of a new SU UMa type dwarf nova with high orbital inclination 03 p0410 A83-14753
- Photometric observations of CN Orionis 03 p0411 A83-14807
- A time-resolved spectroscopic study and modeling of the dwarf nova BV Centauri 04 p0554 A83-15631
- Theoretical decay rates of cataclysmic variable eruptions 06 p0827 A83-18165
- Dwarf-novae outbursts 06 p0823 A83-19422
- The structure and outburst mechanisms of dwarf novae and their evolutionary status among cataclysmic variables 06 p0846 A83-19531

Constraints on the system parameters of the dwarf nova
 AH Herculis 07 p1009 A83-21240
 Eclipse timings in U Geminorum 09 p1353 A83-23737
 VW Hydris revisited - Conclusions on dwarf nova outburst models 09 p1360 A83-24464
 First detection of radio emission from a dwarf nova 09 p1361 A83-24698
 EX Hydrae - A coordinated campaign of photoelectric photometry from four observatories 10 p1499 A83-25371
 Dwarf novae: Observational results and their interpretation. I - Light variations; basic model of a cataclysmic binary; outburst models 11 p1676 A83-27125
 Time-resolved spectrophotometry of the emission lines in the galactic X-ray source H2252-035 13 p1940 A83-31427
 A model for the standstill of the Z Camelopardalis variables 13 p1959 A83-31737
 Angular momentum loss and the evolution of cataclysmic binaries 14 p2106 A83-33212
 IUE observations of cataclysmic variables 15 p2251 A83-33592
 Einstein X-ray observations of cataclysmic variables 15 p2251 A83-33593
 Ultraviolet and optical observations of the dwarf novae VW and WX Hydris during outburst 15 p2264 A83-34576
 High speed photometry of the dwarf nova V2051 Ophiuchi 15 p2264 A83-34579
 The correlated X-ray and optical time variability of TT Arietis 17 p2605 A83-37920
 Dwarf novae - Observational results and their interpretation. II - Orbital periods, masses, inherent colors, absolute magnitude 18 p2765 A83-39223
 Photoelectric UVB photometry of southern and equatorial dwarf novae 19 p2910 A83-41055
 The breakdown of nuclear quasi-equilibrium in highly compact binaries and the origin of the 2-3 hour gap in the orbital period distribution of cataclysmic variables 19 p2921 A83-41653
 Magnetism in the AM Herculis variable CW 1103 + 254 20 p3072 A83-43066
 Ultraviolet photometry of dwarf novae in outburst 20 p3060 A83-43068
 BD Pavonis - A unique cataclysmic variable 21 p3229 A83-44423
 Dwarf novae: Observational results and their interpretation. III - What separates dwarf novae from novae, and what characteristics do they share? 21 p3234 A83-44929
 On the nature of dwarf novae 21 p3237 A83-45554
 Photoionization models for the winds from cataclysmic variables 21 p3237 A83-45555
 An infrared study of the eclipsing dwarf nova U Geminorum 22 p3375 A83-46557
 Superoutbursts - A general phenomenon in dwarf novae 23 p3518 A83-47429
 Transient X-ray rings around dwarf novae 23 p3526 A83-47874
 Outburst period-energy relations in cataclysmic novae 23 p3527 A83-48072
 On the evolution of accretion disc flow in cataclysmic variables. I - The prospect of a limit cycle in dwarf nova systems 24 p3659 A83-49377

DWARF STARS
 NT DWARF NOVAE
 NT FLARE STARS
 NT RED DWARF STARS
 NT SUBDWARF STARS
 NT WHITE DWARF STARS
 Evolution of low mass stars through mass loss - Transition from the main sequence to the degenerate phase 01 p0126 A83-10947
 A possible CH subdwarf 01 p0118 A83-11498
 Infrared photometry of Hyades dwarfs 02 p0249 A83-12916
 The ellipsoidal light curve of VV Puppis 03 p0413 A83-13312
 Observations of nearby M dwarf stars in VRI colors 03 p0421 A83-14146
 Abundance of lithium in unevolved halo stars and old disk stars - Interpretation and consequences 04 p0550 A83-15043
 Nitrogen overabundances in Population II dwarfs 04 p0555 A83-15652
 An unusual microwave flare with 56 second oscillations on the M dwarf L726-8 A 05 p0700 A83-17032
 Starspots - A review of observations and theory 06 p0826 A83-18132
 The evolution of dwarf binaries 07 p1015 A83-20671
 Evolution of very low-mass stars 10 p1499 A83-25364

Studies of late-type dwarfs. V - Theoretical models for lower main-sequence stars 10 p1509 A83-26382
 Emissions from the transition regions and coronae of three cool dwarf stars 11 p1678 A83-27686
 HR 6522 - A previously unknown multiperiodic Delta Scuti star 12 p1784 A83-28859
 The spectra of late type dwarfs and sub-dwarfs in the near ultraviolet. II - Limits to variability in MgII emission from IUE spectrophotometry 12 p1789 A83-28869
 ANS ultraviolet observations of dwarf Cepheids 12 p1797 A83-29958
 The metallic hydride dwarfs 13 p1946 A83-30381
 Detection of flare like events and their relationship to presumed spot regions on V471 Tau - A solar-stellar connection 13 p1951 A83-31420
 HR 7578 - A K dwarf double-lined spectroscopic binary with peculiar abundances 13 p1951 A83-31422
 On the constancy of spectral-line bisectors --- for cool stars 14 p2110 A83-33463
 Rotational velocities for a new sample of F-K dwarfs with X-ray emission 14 p2110 A83-33466
 Solar and late-type dwarfs 15 p2252 A83-33602
 A photometric search for halo binaries. I - New observational data. II - Results 15 p2245 A83-33830
 The minimum period and the gap in periods of cataclysmic binaries 15 p2258 A83-34108
 Revised list of pulsating stars with ultra-short periods 15 p2247 A83-34530
 Rotational studies of late-type stars. III - Rotation among BY Draconis stars 15 p2268 A83-34634
 Spectroscopic analysis of dwarf and subgiant stars in 47 Tucanae 17 p2597 A83-37318
 Brightness variations of the star HD 29697 17 p2590 A83-37705
 Evidence of high chromospheric activity in Hyades dwarfs from spectroscopic observations 17 p2609 A83-38416
 The radial pulsation modes of the Delta Scuti stars, and their nonuniform period distribution 17 p2610 A83-38554
 Outer atmospheres of late stars 17 p2611 A83-38556
 A lambda 10830 vs X-ray correlation among late-type stars 18 p2767 A83-39600
 A photometric study of the lower main sequences of the Hyades and the field stars 18 p2758 A83-39628
 Dependence of the velocity ellipsoid for nearby stars upon metallicity and spectral type 18 p2778 A83-40482
 Secondaries of eclipsing binaries. V - Ek Cephei 20 p3060 A83-43064
 Bright, rapid, highly polarized radio spikes from the M dwarf AD Leonis 22 p3376 A83-45629
 A photometric and spectrographic study of YZ Bootis 22 p3374 A83-46415
 The multiple system Beta Sco and the age of the Upper Scorpius complex 23 p3519 A83-47447
 Activity in red-dwarf stars; Proceedings of the Seventy-first Colloquium, Catania, Italy, August 10-13, 1982 23 p3520 A83-47476
 Mean colors and effective temperatures of K and M dwarfs 23 p3520 A83-47479
 The quiescent chromospheres and transition regions of active dwarf stars - What are we learning from recent observations and models? 23 p3520 A83-47480
 Quiescent coronae of active chromosphere stars 23 p3521 A83-47484
 Spots, spot-cycles, and magnetic fields of late-type dwarfs 23 p3521 A83-47487
 Stellar activity and calcium emission variability 23 p3521 A83-47492
 Results from optical and UV stellar flare spectroscopy 23 p3521 A83-47496
 Contact binary stars 23 p3523 A83-47525
 Theory and observations of negative preflares in UV Cet stars 23 p3525 A83-47545
 Three-colour electrophotometry of Dy Peg 23 p3517 A83-48442
 Second Byurakan spectral sky survey. I - Quasistellar and Seyfert objects 24 p3640 A83-49162
 A failed search for black dwarfs as companions to nearby stars 24 p3643 A83-49390
 The helium abundance of halo dwarfs 24 p3666 A83-50044
 The helium abundances of G-K main sequence halo and disk stars, the helium galactic abundance evolution and the astrometric satellite Hipparcos 24 p3666 A83-50046
 Abundance of lithium in old dwarf stars 24 p3667 A83-50060

DYADICS
 A computational alternative for variational expressions that involve dyadic Green functions --- for electromagnetic scattering 01 p1013 A83-11373
 Radiation from a dipole in the presence of a grounded gyromagnetic slab 03 p0312 A83-13914

Analysis of microstrip wraparound antennas using dyadic Green's function 10 p1374 A83-26830
 Dyadic Green's functions for a coaxial line 10 p1411 A83-26845

DYE LASERS
 Photon-counting statistics of pulsed light sources [AD-A124141] 02 p0175 A83-11563
 Frequency locking to absorption lines by wave competition in a tunable ring dye laser 02 p0185 A83-12302
 Two-line atomic fluorescence temperature measurement in flames - An experimental study 02 p0179 A83-12608
 Nozzle design yielding interferometrically flat fluid jets for use in single-mode dye lasers 03 p0332 A83-14164
 A laser-based measurement of electron collision rates for excited states of ionised helium in a plasma 03 p0398 A83-14662
 Survey of lasers for spectroscopic use - Optical and ultraviolet 04 p0485 A83-15802
 A distributed-feedback tunable laser with dye-activated polymer matrices 04 p0486 A83-16325
 Higher-order distributed feedback and generation of light 05 p0648 A83-17049
 Dye lasers --- in tunable high-power modes 05 p0650 A83-17224
 Velocity-specific atomic-state selection in an atomic beam by continuous-wave optical pumping [AD-A127187] 05 p0651 A83-17881
 The violet emissions produced by laser excitation of Na vapor in the 570-595 nm region 06 p0808 A83-18952
 Injection-locked dye laser pumped and injected by a pulsed xenon-ion laser 06 p0767 A83-19144
 Lasers with distributed feedback and reflection on the basis of cholesteric liquid crystals /CLC/ 06 p0768 A83-19572
 Laser-induced photoelectrochemical transients at a dye solution-SnO2 interface 07 p0953 A83-19901
 Generation of continuous-wave 194-nm radiation by sum-frequency mixing in an external ring cavity 07 p0936 A83-20789
 Influence of transient absorber gratings on the pulse parameters of passively mode-locked CW dye ring lasers 07 p0937 A83-21362
 Measurement of picosecond ultraviolet laser pulsewidths using an electrical autocorrelator 07 p0937 A83-21368
 Rapid extended range tuning of single-mode ring dye lasers 08 p1110 A83-22613
 Measurement of the 1s2p2p-prime 4Pe resonance in He/-/ photodetachment 08 p1163 A83-22644
 Single frequency scanning laser as a plasma diagnostic 08 p1111 A83-23230
 Shock-tube absorption measurements of OH using a remotely located dye laser 09 p1269 A83-24438
 Multiphoton ionization and third-harmonic generation in atoms and molecules 11 p1579 A83-27556
 Real time monitoring of CW mode-locked dye laser pulses using a rapid-scanning autocorrelator 12 p1729 A83-29194
 Intracavity dye-laser photothermal deflection spectroscopy 13 p1845 A83-30253
 A passive film gate for mode-locked infrared lasers 13 p1850 A83-30267
 Frequency-angular diffusion of intense quasinonresonant radiation 14 p0204 A83-32617
 An investigation of the possibilities for lowering the detection limits of elements in a graphite laser torch using the intracavity method for the registration of atomic absorption 14 p0200 A83-32826
 Passive mode lockers for lasers generating at a wavelength of 1.06 micron 14 p0205 A83-32832
 Synchronous amplification of subpicosecond pulses 14 p0205 A83-33403
 Pulse shaping in passively mode-locked ring dye lasers 14 p0205 A83-33405
 Calculation of the colliding pulse mode locking in CW dye ring lasers 14 p0206 A83-33406
 Compression mechanism of subpicosecond pulses by malachite green dye in passively mode-locked rhodamine 6G/DODCI CW dye lasers 14 p0206 A83-33407
 Single and double mode-locked ring dye lasers - Theory and experiment 14 p0206 A83-33408
 Simultaneous determination of the spectral and temporal properties of tunable, single, picosecond pulses from a short cavity dye laser 14 p0206 A83-33409
 Pulse shortening in dye laser side-pumped by TEA N2 laser 14 p0206 A83-33410
 Passive mode locking of flashlamp-pumped dye lasers in the 508-583 nm range 14 p0206 A83-33411
 Measurement conditions for continuously recording picosecond pump-and-probe spectrometers 14 p0202 A83-33419

Amplitude and phase nonlinear response of bleachable dyes using picosecond excitation

14 p2026 A83-33431
Metal plasma induced by the bombardment of 308 nm excimer and 585 nm dye laser pulses at low pressure

15 p2235 A83-34368
Dye laser spectrum narrowing by 'double pulse' flashlamp pumping

15 p2169 A83-34369
Experimental and theoretical investigations of the influence of a saturation grating in an absorber on pulse generation in a passively mode-locked dye laser

16 p2359 A83-35887
Third order autocorrelation study of amplified subpicosecond laser pulses

16 p2359 A83-35953
Time-resolved study of the laser optogalvanic effect in I2

16 p2360 A83-36716
Simultaneously tunable two-wavelength dye laser using two dielectric multilayer filters

16 p2361 A83-36754
Passive mode locking in the blue spectral region

17 p2515 A83-38969
Optical bistability in four-level nonradiative dyes

17 p2515 A83-38974
Multi-mode CW dye laser

19 p2853 A83-41187
Long pulse DCM dye laser

20 p2994 A83-42793
High-power rhodamine 6G laser with an extended service life

20 p2996 A83-43778
Plastics for high-power laser applications - A review

21 p3115 A83-43861
Broad band electro-optic tuning of a CW dye laser

21 p3143 A83-44188
Lasing and fluorescent characteristics of nine, new, flashlamp-pumpable, coumarin dyes in ethanol and ethano:water

21 p3143 A83-44193
Tunable infrared difference-frequency generation in lithium iodate

21 p3143 A83-44194
Recent high-resolution resonant refractivity studies of a sodium-seeded flame

21 p3110 A83-44680
High resolution spectroscopy using picosecond pulse trains

21 p3140 A83-44818
Picosecond continuum generation and spectroscopy

21 p3145 A83-44819
Storage and time reversal of light pulses using photon echoes

22 p3356 A83-45965
Synchronously mode-locked continuous wave dye lasers - Recent advances and applications

22 p3297 A83-46664
Subpicosecond pulses from a synchronously mode-locked traveling-wave ring dye laser

22 p3297 A83-46665
Comparisons of traveling-wave and standing-wave operations of mode-locked continuous-wave dye lasers

22 p3297 A83-46666
Optical switches for generation and pulse shaping of ultrashort electrical pulses

22 p3278 A83-46677
Accurate range gating technique with mode-locked dye lasers

22 p3298 A83-46680
Narrow output line from a distributed-feedback dye laser with broad-spectrum pumping

22 p3299 A83-46784
Generation of extreme ultraviolet radiation at 79 nm by sum frequency mixing

22 p3300 A83-46821
Characteristics of lasers with condensed active media exhibiting linear anisotropy induced by polarized pump radiation

23 p3460 A83-47162
Progress in dye and excimer laser sources for remote sensing

23 p3462 A83-47800
Bistable operation of a dual-wavelength synchronously mode-locked CW dye laser

23 p3463 A83-48705
Transient stimulated Raman scattering of femtosecond laser pulses

24 p3586 A83-48782
Generation of tunable single-frequency continuous-wave coherent vacuum-ultraviolet radiation

24 p3587 A83-48852
Generation of single longitudinal mode pulses in passively Q-switched lasers via passive pre-lasing

24 p3589 A83-49614

DYES

Optimal ring lasers with coupled resonators and a homogeneously broadened active medium

03 p0330 A83-13587
Studies on photogalvanic effect in systems containing toluidine blue

06 p0780 A83-18561
EA study of solar concentrator panels with fluorescent compounds

08 p1131 A83-22911
Passive mode locking in iodine photodissociation laser

14 p2023 A83-31913
Passive mode locking of a long pulse XeCl laser

22 p3299 A83-46724

DYNAMIC CHARACTERISTICS

NT AERODYNAMIC DRAG

NT AERODYNAMIC STABILITY

NT AIRCRAFT STABILITY

NT ATTITUDE STABILITY

NT BOUNDARY LAYER STABILITY

NT COMBUSTION STABILITY

NT CONTROL STABILITY

NT DIRECTIONAL STABILITY

NT DRAG

NT DYNAMIC PRESSURE

NT DYNAMIC STABILITY

NT FLAME STABILITY

NT FLOW CHARACTERISTICS

NT FLOW DISTRIBUTION

NT FLOW STABILITY

NT FLOW VELOCITY

NT FREQUENCY STABILITY

NT FRICTION DRAG

NT GYROSCOPIC STABILITY

NT HOVERING STABILITY

NT INTERFERENCE DRAG

NT LATERAL STABILITY

NT LIFT

NT LONGITUDINAL STABILITY

NT MAGNETOHYDRODYNAMIC STABILITY

NT MOTION STABILITY

NT PRESSURE DRAG

NT ROTARY STABILITY

NT SATELLITE DRAG

NT SPACECRAFT STABILITY

NT SUPERSONIC DRAG

NT TRANSIENT RESPONSE

NT VISCOS DRAG

NT WAVE DRAG

NT WEIBEL INSTABILITY

The motion of planar rod systems --- for dynamic automata

01 p0086 A83-10452
Meteorological effects in ionospheric processes /Survey/

01 p0071 A83-10589
Investigations of stability and dynamic performances of switching regulators employing current-injected control

01 p0039 A83-11002
On the extraction of features from slowly wandering patterns

01 p0096 A83-11411
Residual recursive displacement estimation --- for motion detection

01 p0100 A83-11464
Determination of the dynamic characteristics of nonlinear oscillatory systems from motion measurements

02 p0191 A83-12336
Determining optical flow --- distribution of apparent movement velocities of image brightness patterns

02 p0182 A83-12897
Finite-length solutions for rotodynamic coefficients of turbulent annular seals

03 p0336 A83-13521
Investigation of dynamic characteristics of an elastic wing due to correction of mass and stiffness matrices [AIAA PAPER 83-0653]

05 p0595 A83-16818
The dynamic structure of the turbopause

05 p0666 A83-17948
Certain classes of exact solutions to the problem of motion of a system of Lagrangian gyroscopes

06 p0807 A83-19606
Determination of the orientation of a sensor trihedron using angular information

07 p0988 A83-19938
Matching materials and structures in vertical axis wind turbines

07 p0953 A83-20434
The dynamic braking of a linear induction motor at a variable speed

08 p1080 A83-22224
Model studies of the dynamic characteristics of the pumps and turbines of liquid propellant rocket engines in transition regimes

08 p1052 A83-22660
Load following impacts of a large wind farm on an interconnected electric utility system

08 p1131 A83-22675
Identification of certain dynamic characteristics of a helicopter-autopilot system by means of simulation

08 p1047 A83-23222
Influence of gas inertia forces generated within the stabilizing restrictor on dynamic characteristics of externally pressurized thrust gas bearings. II - Case of turbulent flow at the capillary restriction

09 p1273 A83-23336
Catastrophe theory in physics

09 p1338 A83-23852
The motion of a top along a plane in the presence of friction

09 p1338 A83-24240
Study on longitudinal dynamic characteristics of pilot-airplane system - Approach to the method for studying PIO problem --- Pilot-Induced Oscillation

10 p1379 A83-26762
Investigation of types of root loci of Fourth-order linear and linearized systems --- automatic pilot control system

11 p1647 A83-27448
Dynamic characteristics of the 40-by 80-/80-by 120-foot wind tunnel drive fan blades

12 p1704 A83-29846
Dynamic mechanical characterization of cure of a polyimide-graphite fiber composite (PMR 15/Celion 6000)

13 p1816 A83-31793
Determination of the transfer functions of a dynamically tunable gyroscope

14 p2019 A83-32159
A probability of logical-dynamical systems with random structural changes

14 p2075 A83-32573

Application of system identification flight analysis techniques to the pitch-heave dynamics of an air cushion vehicle

15 p2241 A83-34852
Microwave cineholography

15 p2165 A83-35166
Dynamic properties of linear vibration-isolation systems --- Russian book

16 p2362 A83-36440
Forced and self-excited vibrations of gas-turbine assemblies with perfect and perturbed symmetry

16 p2311 A83-36791
Equations of a dynamic object when its properties are represented by a response to a prescribed action

16 p2405 A83-36901
Dynamics of space cable systems

17 p2472 A83-37473
The dynamics of spatial linked quadrangle chains

20 p2999 A83-42986
Gas bearings. I - Dynamic analysis and solution method

21 p3147 A83-44374
Certain properties of gyroscopic systems in relation to the Hertzian concept in mechanics

21 p3199 A83-44627
The dynamics of an elastic body --- rotary gyroscopes

21 p3199 A83-44629
Local structures of manifolds of motion of vibration-protected dynamic systems

21 p3200 A83-44646
Identification of structural dynamics systems using least-square lattice filters --- large space structures

21 p3103 A83-45467
Dynamic behavior of an unsteady turbulent boundary layer

22 p3281 A83-46428
State-space analysis of the dynamic characteristics of a variable thrust liquid propellant rocket engine [IAF PAPER 83-ST-06]

23 p3426 A83-47385
The direct method of solving the problem concerning the combined three-dimensional motions of the system solid-liquid

23 p3504 A83-48473
What is synergetics? --- self-organization in multicomponent systems

23 p3505 A83-48548
A mathematical model for the dynamics of liquid-propellant rocket engines

24 p3552 A83-48928
Dynamical mechanisms for discrete unstable spiral modes in galaxies

24 p3655 A83-49223

DYNAMIC CONTROL

Dynamic characteristics of an integrated flight and fire control system

01 p0013 A83-11208
On the dynamic analysis and behavior of industrial robotic manipulators with elastic members

02 p0187 A83-12771
Controlling the translational-rotational motion of a solid body

03 p0391 A83-14891
The necessary and sufficient conditions for stability in the large

03 p0391 A83-14892
The programming level of a walking machine moving at a specified speed

04 p0524 A83-15381
Properties of min-max controllers in uncertain dynamical systems

04 p0529 A83-16195
Pole assignment and minimal feedback design

06 p0803 A83-19388
A system for programming and controlling sensor-based robot manipulators

07 p0985 A83-21424
Dynamic spatial filter for optical signal processing using a liquid crystal light valve

08 p1166 A83-22809
Dynamic output feedback controller

08 p1158 A83-23019
Locomotion in anthropomorphic mechanisms --- Russian book

09 p1324 A83-23825
Simplified robot arm dynamics for control

09 p1328 A83-24712
Stability and stabilization of delay systems with sampled feedback

09 p1328 A83-24714
Control of nonlinear time-varying systems

09 p1329 A83-24733
Necessary and sufficient conditions for regulation of linear systems

09 p1333 A83-24794
Decentralized stabilization and stability region estimation for a class of non linear dynamic systems

09 p1333 A83-24800
A new design for decentralized control with output feedbacks

09 p1334 A83-24802
Control of the constrained planar simple inverted pendulum

10 p1461 A83-25397
The design of optimal output regulators for linear multivariable systems with constant disturbances

10 p1461 A83-25400
Static properties of dynamic systems that have controllers using a prediction model

10 p1461 A83-25465
A new class of stabilizing controllers for uncertain dynamical systems

10 p1462 A83-25997
Asymptotic behavior of the input-output cross-variance function of nonlinear dynamic systems

10 p1462 A83-26067
An economical algorithm of adaptive control of a multidimensional static plant

10 p1462 A83-26068

- On the compensation in linear feedback control systems
- Transfer functions attainable by realizable linear compensation 10 p1464 A83-26519
Invariance and identifiability in adaptive coordinate-parametric control 10 p1465 A83-26533
Possible evolution of feedback types and their applications in control of nonstationary plants 10 p1467 A83-26555
- One robust, dynamic control algorithm for manipulation systems 11 p1648 A83-28102
On the kinematic control of the motion of a vessel with an ideal heavy fluid 11 p1649 A83-28468
Robust controller design for linear dynamic systems using approximate models 12 p1770 A83-29521
Hierarchical robot control system synthesis 12 p1770 A83-29542
Synthesis of control systems with quasi-continuous generation of the control signal 13 p1910 A83-30077
Control of distributed parameter systems 13 p1910 A83-30078
Smooth extremal problems in spectra of constant matrices 13 p1910 A83-30620
Game systems of adaptive control 14 p2076 A83-32962
Stabilizability of multidimensional discrete systems in cases of complete and incomplete information 14 p2076 A83-32964
On a numerical method for the synthesis of optimal control for nonlinear dynamic systems 14 p2076 A83-32965
Stabilization of linear dynamic systems 14 p2076 A83-33007
Linear dynamic output feedback - Invariants and stability [AD-A129968] 14 p2077 A83-33447
Computer simulation complex for the investigation of systems for the control of the manipulators of autonomous robots 15 p2223 A83-35261
Controller design for uncertain nonlinear systems 17 p2566 A83-37110
Modeling, analysis, and control of dynamic systems --- Book 17 p2569 A83-37400
One new method of dynamic flight control 17 p2569 A83-37447
The choice of an astatic system for the regulation of the rotational velocity of a dc electric motor for azimuthal mountings of a gamma-telescope 17 p2496 A83-37720
Synthesis of dynamic algorithms for the motion control of manipulator robots 18 p2737 A83-39527
Linear models in nonlinear control systems --- Russian book 19 p2889 A83-40990
A new approach to exact model-matching with applications to aircraft systems 19 p2890 A83-41477
Observed realization of nonlinear controlled dynamic systems 20 p3039 A83-42918
Analysis of the controllability property in linear control systems with parameters 20 p3039 A83-42920
The field of expanded extremals of a controlled process 20 p3039 A83-42922
The programmed motion of a solid controlled by paired gyroscopes 21 p3100 A83-44630
The differential-topological structure of the varieties of motion of vibration-resistant dynamical systems 21 p3200 A83-44647
Dynamics and control of large flexible spacecraft; Proceedings of the Third Symposium, Blacksburg, VA, June 15-17, 1981 21 p3101 A83-45101
Exact pole assignment using direct or dynamic output feedback 21 p3196 A83-45135
Flight simulation for an inertial navigation system 23 p3420 A83-47178
Technical issues in dynamics and control of large space structures [IAF PAPER 83-403] 23 p3422 A83-47375
The dynamics of systems with elastic elements of high rigidity 23 p3504 A83-48461
Angular points of the boundaries of domains of attainability --- for dynamic control of linear systems 23 p3501 A83-48528
Is dynamic control needed in robotic systems, and, if so, to what extent? 23 p3501 A83-48633
Dynamic sensing for robots - An analysis and implementation 23 p3501 A83-48635
Multiplex control systems - Stochastic stability and dynamic reliability 23 p3502 A83-48645
Stability analysis of non-linear dynamical systems 23 p3502 A83-48647
- DYNAMIC LOADS**
NT AERODYNAMIC LOADS
NT BLAST LOADS
NT CYCLIC LOADS
NT GUST LOADS
NT IMPACT LOADS
- NT LANDING LOADS
NT ROLLING CONTACT LOADS
NT SHOCK LOADS
NT THRUST LOADS
NT TRANSIENT LOADS
NT VIBRATORY LOADS
NT WING LOADING
Post-buckling dynamic behavior of periodically supported imperfect shells 01 p0060 A83-10860
Basic properties of elastic-plastic boundaries in stress wave propagation in a bar 03 p0341 A83-14484
Axisymmetric elastic waves excited by a point source in a plate [ASME PAPER 82-WA/APM-15] 04 p0498 A83-15687
Toroidal shells - Delayed catastrophes under dynamic loading 04 p0499 A83-15881
A review of aero-generator fatigue problems 06 p0781 A83-18939
Criterion for crack instability under short pulse loads 08 p1116 A83-21674
Pulse load of annular plastic plates supported on both edges 08 p1120 A83-21812
Dynamic stability boundaries for a sinusoidal shallow arch under pulse loads 08 p1122 A83-22148
Time-dependent small-angle X-ray scattering from stress-induced crazes in polymers 08 p1073 A83-22757
Nonuniform loading of shells by ponderomotive forces 09 p1277 A83-23505
Strength of layered composite cylindrical shells under dynamic loading 09 p1224 A83-23946
On a certain dynamic crack problem in elastic and elastic-plastic media 09 p1282 A83-25104
The study of dynamic fracture propagation using a special finite element technique [ASME PAPER 82-WA/DE-13] 10 p1439 A83-25680
The excitation of a fluid-loaded plate stiffened by a semi-infinite array of beams 11 p1594 A83-27995
Lower bounds to large displacements of impulsively loaded plastically orthotropic structures 11 p1594 A83-28408
Assessment of equivalent monocoque isogrid shell modeling technique for dynamic response to impulsive loads 12 p1744 A83-29852
[AIAA 83-0926] Wind loading of large astronomical telescopes 13 p1938 A83-31001
Method of high-speed loading in determining fracture 13 p1823 A83-31218
Special features of the measurement of adhesion of steel fibers to a polymer matrix in a wide range of loading rates 13 p1816 A83-31221
Diffusive relaxation of stress concentrations at grain boundary cavities in elevated temperature creep 14 p2033 A83-33452
Dynamic fatigue of brittle materials containing indentation line flaws 15 p2180 A83-35064
On the question of hardening during plastic deformation 17 p2521 A83-37544
The dynamic bending load on a satellite launcher due to inclined lift-off 17 p2480 A83-37572
A technique for measuring the large elastoplastic deformations of dynamically loaded plates and shells 18 p2698 A83-39501
Deformation and strength of ring-stiffened orthotropic cylindrical shells under dynamic compressive loads 18 p2701 A83-40107
Determination of critical dynamic axial compression stresses for rib-stiffened layered cylindrical shells 18 p2702 A83-40115
Stress damping in viscoelastic composite laminates under uniform harmonic loading 19 p2820 A83-41599
The opening of a crack in the elastic region under the effect of a moving load 20 p3008 A83-43524
Experimental study of the dynamic loading of metal disks 21 p3161 A83-45152
On dynamics and stability of continuous systems subjected to a distributed moving load 23 p3473 A83-48496
- DYNAMIC MODELS**
Conservation laws for a dynamical system in group variables 01 p0104 A83-10122
Suggestions regarding the use of microprogrammable multiple computer systems for the digital simulation of dynamic systems --- German thesis 01 p0090 A83-10470
Dynamic model of the principal types of convection, field-aligned currents, and volumetric structure of the polar ionosphere 02 p0209 A83-12422
Dynamic finite element model for laminated structures 02 p0195 A83-12761
A vortex-street model of the flow in the similarity region of a two-dimensional free turbulent jet 03 p0322 A83-14588
Attitude control of a satellite with a rotating solar array 03 p0287 A83-14845
A dynamic model for aircraft poststall departure [AIAA PAPER 83-0367] 05 p0595 A83-16674
Dynamical models and our Virgocentric deviation from Hubble flow 05 p0696 A83-16976
Investigation of regions of the possibility of motion in mechanical systems 06 p0805 A83-17979
Inverse dynamic problems for an anisotropic elastic medium 07 p0944 A83-19632
On the analysis of Hopf bifurcations 07 p0989 A83-20641
Tether deployment dynamics 07 p0869 A83-21426
Dynamic-automaton models in the visualization of three-dimensional scenes 08 p1157 A83-22177
A program pack for constructing a dynamic model for use in the hybrid control system of a manipulator robot 08 p1154 A83-22179
Method of designing a program module for the simulation of complex dynamic systems on a hybrid computer --- for flight simulation 08 p1154 A83-22184
A simulation model for the analysis of the dynamic behavior of a helicopter rotor under nonstationary limit flight conditions 08 p1044 A83-23220
Dynamic modeling of vegetation change in arid lands 09 p1285 A83-24537
Modeling and representation of dynamical systems defined in terms of external variables 09 p1334 A83-24809
A scheme of feedback compensation for CMG gimbal compliance, using multiple rate sensors --- Control Moment Gyroscope [ASME PAPER 82-WA/DSC-10] 10 p1419 A83-25681
Dynamics of the middle atmosphere 11 p1631 A83-27404
Nonlinear dynamical models of plasma turbulence 11 p1659 A83-28230
The dynamics of crystal formation during growth by Stepanov's method 11 p1662 A83-28353
Study of dynamical effects using phase conjugation of light waves 12 p1729 A83-29167
Power MOSFET dynamic large-signal model 12 p1719 A83-29419
Time-domain quasi-linear identification of nonlinear dynamic systems 12 p1773 A83-29811
[AIAA 83-0811] Identification of helicopter rotor dynamic models 12 p1702 A83-29866
[AIAA 83-0988] Anti-flutter control concept using a reduced non-linear dynamic model of elastic structure aircraft 12 p1704 A83-29870
[AIAA 83-0993] On an algorithm for the simplified integration of dynamic systems --- for flight trajectory analysis 13 p1914 A83-30724
A graph-theoretic algorithm for hierarchical decomposition of dynamic systems with applications to estimation and control 13 p1911 A83-31071
Concerning the correctness on the whole of boundary value problems for models of the dynamics of the atmosphere and the ocean 13 p1880 A83-31326
Uniform ultimate boundedness of the solutions of uncertain dynamic delay systems with state-dependent and memoryless feedback control 14 p2074 A83-31933
The synthesis of dynamic systems identical with respect to the output process 14 p2079 A83-32160
Dynamic modeling of structures from measured complex modes 14 p2033 A83-32988
An algorithm of flight simulation on a dynamic stand of support type 15 p2123 A83-34429
Dynamic modeling of an air cushion vehicle 15 p2243 A83-35054
Distributed real-time simulation of multibody systems 15 p2223 A83-35143
A dynamic model of turbojet in starting at high altitude 16 p2304 A83-35846
A mechanistic model of Eulerian, Lagrangian mean, and Lagrangian ozone transport by steady planetary waves 16 p2379 A83-36136
Modeling rotational dynamics of a flexible space platform for application of multilevel attitude control 17 p2476 A83-37108
Modeling, analysis, and control of dynamic systems --- Book 17 p2569 A83-37400
The atmospheric dynamics of Venus according to Doppler measurements by the Venera entry probes 17 p2617 A83-37423
Lumped parameter dynamic models for large space structures with flexible and rigid parts 17 p2477 A83-37444

Alternative bond graph causal patterns and equation formulations for dynamic systems

17 p2569 A83-37545

On model-following using measured output feedback

17 p2570 A83-38820

An atmospheric sounding balloon with ballast - An automatic numerical model for its manufacture and simulation of its evolution

18 p2640 A83-39804

Improvement of a large analytical model using test data

19 p2856 A83-40870

Diagnostics of the conditions of gas-turbine engines using models reflecting the dynamics of changes in the controlled parameters

19 p2801 A83-42133

New perspectives on hot corrosion mechanisms

20 p2949 A83-42248

A nonparametric method of identification of vibration damping in non-linear dynamic systems

20 p3001 A83-42517

A dynamic model for the production of $H(+) , NO_3(-)$, and $SO_4(2-)$ in urban fog

20 p3013 A83-42844

Bilinear logico-dynamic model for a controlled process

20 p3039 A83-42917

Conditions of the generalized similarity of simulators to aircraft

20 p3036 A83-43505

On the integrability of some generalized Lotka-Volterra systems

20 p3043 A83-43567

Discrete models for linear multivariable systems

20 p3040 A83-43619

Origin-of long-time tails in strongly chaotic systems

21 p3199 A83-43883

Analysis of aircraft dynamic behavior in a crash environment

21 p3091 A83-43966

On stabilizing uncertain systems

21 p3192 A83-44008

Finite element approximations in transient analysis --- of flexible structures

21 p3150 A83-44024

Martian great dust storms - Interpretive axially symmetric models

21 p3239 A83-44090

Dynamical processes in the atmosphere and the use of models

21 p3179 A83-44389

Problems in the control of relativistic and quantum dynamic systems (physical and informational aspects) --- Russian book

21 p3195 A83-45033

Active control of large flexible spacecraft - A new design approach based on minimum information modelling of parameter uncertainties

21 p3196 A83-45133

The dynamic parameters of an autooscillatory model of geomagnetic pulsations

21 p3175 A83-45248

The formation of a stable layer of atoms and ions of metals in the upper atmosphere

21 p3176 A83-45262

A plain man's guide to bifurcations

22 p3353 A83-45694

Toolkit for nonlinear dynamics

22 p3354 A83-45697

A dynamical model of coronal loops

22 p3389 A83-47000

Dynamic modeling of flexible spacecraft - A general program for simulation and control

[IAF PAPER 83-339]

23 p3421 A83-47348

Dynamical interpretation of the very hot region appearing at the top of the loop

23 p3534 A83-47693

Optimal controller design for a helicopter using its lower order dynamic model

[AIAA PAPER 83-2550]

23 p3412 A83-48371

On the structure of quasi-hyperbolic stochasticity in an inertial autooscillator

23 p3504 A83-48483

DYNAMIC MODULUS OF ELASTICITY

Dynamic characteristics of conical shell with variable modulus of elasticity

09 p1280 A83-24506

Elastic and viscoelastic properties of fibre-reinforced composite materials

24 p3553 A83-48895

The mechanism of elastic energy absorption in boron fibers

24 p3553 A83-49474

DYNAMIC PRESSURE

The dynamics of the Venus ionosphere. II - The effects of the time scale of the solar wind dynamic pressure variations

02 p0265 A83-12562

Two methods for absolute calibration of dynamic pressure transducers

03 p0329 A83-14170

Sting line feasibility for force measurements in the European wind tunnel

[ONERA, TP NO. 1982-90]

03 p0283 A83-14541

Open seat ejection at high dynamic pressure - A radical approach

04 p0445 A83-15308

The reduction of a system of differential equations for the motion of a satellite that is dynamically compressed relative to the center of mass to a special form

04 p0451 A83-15771

Experimental study of the shock generation at the collapse of cavitation bubble

07 p0925 A83-20284

Nonlinear hydrodynamic pressure on an accelerating plate

08 p1084 A83-22377

Measurement of dynamic pressure in shock tube by streak photography

10 p1421 A83-26135

The effects of tower shadow on the dynamics of a horizontal-axis wind turbine

11 p1611 A83-27869

Parameters and regimes of the detonation of condensed explosives

24 p3557 A83-49798

DYNAMIC PROGRAMMING

Nonnegative matrices in dynamic programming --- Thesis

02 p0229 A83-11898

The programming level of a walking machine moving at a specified speed

04 p0524 A83-15381

A Differential Dynamic Programming approach to nonlinear parameter identification

[AIAA PAPER 83-0284]

05 p0678 A83-16629

Optimal finite element discretization - A dynamic programming approach --- for structural analysis of linear elastic systems

06 p0773 A83-18230

Dynamic programming in problems of the synthesis of multichannel phasing devices

07 p0921 A83-20881

Dynamic programming, fuzzy sets, and the modeling of R&D management control Systems

08 p1159 A83-22348

Air interdiction mission planning using dynamic programming

09 p1196 A83-24768

Distributed dynamic programming --- for multiprocessor problem solving

09 p1326 A83-24769

Model adaptive dual control of MIMO stochastic systems

09 p1332 A83-24777

Algorithm for the optimal planning of spacecraft operation

09 p1211 A83-25030

A variational method for investigating absolute stability and absolute instability of nonlinear control systems

10 p1464 A83-26511

Dynamic programming algorithm for optimal estimation of speech parameter contours

13 p1911 A83-31072

State estimation/parameter identification - Guaranteed error approach

21 p3193 A83-44036

DYNAMIC PROPERTIES

U DYNAMIC CHARACTERISTICS

DYNAMIC RESPONSE

NT TRANSIENT RESPONSE

Analysis of the static characteristics and dynamic response of push-pull switching converters operating in the current programmed mode

01 p0040 A83-11004

Time-varying feedback gains for power circuits with active waveshaping

01 p0040 A83-11006

Complex wave regimes in distributed dynamic systems /Review/

02 p0232 A83-11678

A study of the dynamic behavior of flexible rotors --- French thesis

03 p0337 A83-14103

Dynamic analysis of multirigid-body system based on the Gauss principle

03 p0391 A83-14509

Solution to the backward-Kolmogorov equation for a nonstationary oscillation problem

04 p0531 A83-15697

Hidden supersymmetry in stochastic dissipative dynamics

04 p0532 A83-15911

An experimental study of the unsteady response of the rotor blades of an axial flow compressor operating in the rotating stall regime

[AIAA PAPER 83-0001]

05 p0577 A83-16454

Optimum structural designs in dynamic response

06 p0771 A83-18204

Parameterization in finite element analysis --- in optimal structural design

06 p0772 A83-18216

Dynamics of electrooptic bistable devices with delayed feedback

06 p0810 A83-18904

Unbalance response analysis of a complete turbomachine

07 p0938 A83-19674

On tuned bladed disk dynamics - Some aspects of friction related mistuning

08 p1120 A83-21807

Rain-induced vibration --- of space vehicle

08 p1050 A83-22145

Note on non-linear dynamic response of a clamped orthotropic circular plate to pulse excitations

09 p1278 A83-23707

A theory of viscoelastic composites modeled as interpenetrating solid continua with memory

09 p1280 A83-24136

Characterization of the dynamical response of receivers to fading

10 p1404 A83-26471

The dynamic response of the high-latitude thermosphere and geostrophic adjustment

11 p1618 A83-28318

Impulsive loading of a cylindrical shell with transverse shear and rotatory inertia

11 p1594 A83-28412

Dynamic behavior of fluid bearings - Linear and nonlinear study --- French thesis

11 p1589 A83-28631

Some difficulties generated by small sinks in the numerical study of dynamical systems - Two examples

12 p1775 A83-29163

A short cut integration scheme to determine the dynamic response of a launch vehicle with several payloads

[AIAA 83-0817]

12 p1707 A83-29816

Flutter and forced response of mistuned rotors using standing wave analysis

[AIAA 83-0845]

12 p1742 A83-29823

A preliminary look at control augmented dynamic response of structures

[AIAA 83-0850]

12 p1708 A83-29825

Assessment of equivalent monocoque isograd shell modeling technique for dynamic response to impulsive loads

[AIAA 83-0926]

12 p1744 A83-29852

Nonlinear response of double wall sandwich panels

[AIAA 83-1037]

12 p1745 A83-29882

Response spectrum analysis for random vibration

13 p1860 A83-30854

Dynamic-mechanical response of graphite/epoxy composite laminates and neat resin

13 p1817 A83-31795

Dynamic taxi response (have bounce) testing of the C-5A aircraft

[AIAA PAPER 83-1024]

14 p1975 A83-32783

Vibration analysis of rotor-bearing system by quasi-modal transformation - Analyses of complex eigenvalue and response history

14 p2028 A83-33093

Thermomechanical characterization of graphite/polyimide composites

14 p1987 A83-33117

Coupled flap-lag-torsional dynamics of hingeless rotor blades in forward flight

15 p2121 A83-33506

Impact damping and airplane towing

15 p2120 A83-33625

The response of aircraft to pulse excitation

15 p2122 A83-34312

On the dynamic atmospheric response to the Chandler wobble forcing

16 p2386 A83-35484

Measurement of high gas-stream temperature using dynamic thermocouples

16 p2355 A83-35556

Coupled flap-lag-torsional dynamics of hingeless rotor blades in forward flight

16 p2298 A83-35948

Dynamic response of the LE-5 rocket engine liquid oxygen pump

[AIAA PAPER 83-1385]

16 p2321 A83-36375

Dynamic behaviour of a GaAs-AlGaAs MQW laser diodes --- Multi-Quantum-Well

16 p2360 A83-36485

Dynamic elasto-plastic response of shells in an acoustic medium - EPSA code

17 p2524 A83-38570

X-ray crystal-optics --- Russian book

18 p2750 A83-40604

Models of the static and dynamic behavior of stripe geometry lasers

19 p2851 A83-40931

The calculation of robot dynamics using articulated-body inertias

20 p2959 A83-43109

Formulation and solution of rotary-wing aeroelastic stability and response problems

20 p2933 A83-43673

Reanalysis and design in structural dynamics

21 p3151 A83-44031

The elastic solution of the dynamic elastic-plastic response of a circular plate

21 p3151 A83-44104

The dynamics of a two-gimbal elastically suspended gyroscope

21 p3137 A83-44632

Dynamic holograms in semiconductors

21 p3138 A83-44698

Response in passing through critical speed of arbitrarily distributed flexible rotor system. I - Case without gyroscopic effect. II - Case with gyroscopic effect

21 p3148 A83-45475

Evaluation of four subcritical response methods for on-line prediction of flutter onset in wind tunnel tests

23 p3413 A83-48212

Dynamic response of a centrifugal liquid oxygen rocket pump

[ASME PAPER 83-FE-24]

23 p3426 A83-48235

Equivalent linearization for continuous dynamical systems

[ASME PAPER 83-APM-30]

23 p3503 A83-48241

Practical applications of system identification in flutter testing

24 p3550 A83-49182

DYNAMIC STABILITY

NT AERODYNAMIC STABILITY

NT AIRCRAFT STABILITY

NT ATTITUDE STABILITY

NT BOUNDARY LAYER STABILITY

NT COMBUSTION STABILITY

NT CONTROL STABILITY

NT DIRECTIONAL STABILITY

A review and assessment of methods for prediction of the dynamic stability of air cushions
01 p0112 A83-11038

Dynamic stabilization methods for bilateral control of remote manipulation
02 p0230 A83-11913

On the instability of thick accretion disks
02 p0257 A83-12136

Dynamic instability of suddenly heated angle-ply laminated composite cylindrical shells
02 p0194 A83-12742

Global sensitivity to velocity errors at the libration points
03 p0405 A83-13420

The dynamic stability of a liquid-gas oscillatory system under the effect of vibration
03 p0341 A83-14075

Nonlinear diffusive instabilities in differentially rotating stars
03 p0425 A83-14522

Static and dynamic stability of nonlinear elastic systems under nonconservative forces - Natural approach
04 p0494 A83-15003

The possibility of parametric resonance in a fourth-order system in the presence of dissipation and gyroscopic terms
04 p0531 A83-15770

The non-linear response of hydrodynamic seals
04 p0487 A83-16346

Material effects on the dynamic stability of a flexible skirted air cushion
[AIAA PAPER 83-0369]
05 p0692 A83-16675

Instability and confined chaos in a nonlinear dispersive wave system --- application to gravity waves in deep water
05 p0638 A83-17354

Dynamic stabilisation of Rayleigh-Taylor instability
05 p0641 A83-17821

Concepts of stochastic stability in rotor dynamics
06 p0717 A83-18382

Stability of tearing fracture in structural steels
06 p0728 A83-18486

Stability of a stationary Rossby wave embedded in the monsoon zonal flow
06 p0792 A83-18992

Diocotron instability of magnetized tubular electron beams
06 p0754 A83-19336

Stability limits for 'isothermal' cores in globular cluster models - Two-component systems
06 p0844 A83-19490

Optimization of solutions of the equations of motion of shells of revolution to enhance the dynamic-stability parameters
07 p0946 A83-20897

An energy analysis of the stability of flexible filaments in coaxial flow
07 p0926 A83-20899

Normal modes of Bardeen discs. I - Uniformly rotating incompressible discs --- perturbation and stability of stellar models
09 p1362 A83-24978

Normal modes of Bardeen discs. II - A sequence of $n = 2$ polytropes --- of rotating stars
09 p1362 A83-24979

Chaotic and stochastic self-oscillations
09 p1340 A83-25265

Integrable Hamiltonian systems. I - Methods for the integration of Hamiltonian systems. II - Series of integrable systems
09 p1340 A83-25266

Dynamic analysis of a precision servosystem for the stabilization of astrophysical instrumentation
10 p1383 A83-25329

On the stability of toroidal flux tubes in differentially rotating stars
10 p1499 A83-25363

On axisymmetric perturbations of some rotating stars
10 p1503 A83-25720

New algorithms for quasi-periodic solutions --- of oscillating systems in celestial mechanics
11 p1673 A83-28040

Stability criteria in many-body systems. V - On the totality of possible hierarchical general four-body systems
12 p1787 A83-29117

On the stability of the solar system
12 p1794 A83-29297

Methods for the study of 'pendulum'-type dynamic systems --- Russian book
12 p1775 A83-29340

Vibration characteristics and dynamic stability of stiffened plates
[AIAA 83-0890]
12 p1743 A83-29837

Method of Liapounov functions in the theory of the analytical design of nonlinear controllers
13 p1910 A83-30013

Perturbation methods in mechanics
14 p1972 A83-33001

Dynamic stability of a flight vehicle near a perturbed surface
14 p1977 A83-33008

A study of the statistical dynamics of flight vehicles
14 p1977 A83-33009

Nonlinear evolution of the transverse instability of plane-envelope solitons
14 p2080 A83-33388

Large-signal dynamic-stability analysis of synchronised current-controlled modulators - Application to sine-wave high-power inverters
14 p2008 A83-33475

Instability of finite amplitude elastic waves
15 p2177 A83-34337

Stability in the restricted problem of three bodies with Liapounov Characteristic Numbers
15 p2246 A83-34394

The effect of perturbations in Coriolis and centrifugal forces on the nonlinear stability of equilibrium points in the restricted problem of three bodies
15 p2246 A83-34395

The stability of stationary motions of systems of a certain type
15 p2226 A83-34431

An over-view of UTIAS research on the dynamic stability of air cushion vehicles
15 p2242 A83-34853

Technical aspects of the AEROBAC AB-7
15 p2242 A83-34858

Computer studies of ACV heave dynamics stabilization
15 p2243 A83-35055

Shear-driven instabilities of annular relativistic electron beams in vacuum
17 p2496 A83-37041

Stability of aircraft motion in critical cases
17 p2470 A83-37066

Investigation of the stability of satellite large angle attitude manoeuvres using nonlinear optimization methods
17 p2477 A83-37443

Dynamic instabilities in magnetically levitated models
17 p2586 A83-37619

Dynamic behaviour and stability of thermistor air flowmeters
17 p2512 A83-38531

Effect of static preloading on the dynamic stability of structures
19 p2856 A83-40871

Resonances in dynamic systems under parametric excitation
20 p3043 A83-42887

The Riemann disks. II - Stability
20 p3071 A83-43052

Dynamic behavior of a bluff-body diffusion flame
21 p3110 A83-45584

Stability of rotating liquid drops. I - Uncharged drops
22 p3280 A83-46001

Further studies on criteria for the onset of dynamical instability in general three-body systems
22 p3373 A83-46388

The method of pole displacement in the artificial stabilization of dynamic systems
22 p3352 A83-46500

The features of the space structures dynamic design [IAF PAPER 83-409]
23 p3423 A83-47377

The dynamics of a rigid body suspended by a string
23 p3504 A83-48451

A study of nonsymmetrical periodic motions of symmetrical dynamic systems
23 p3501 A83-48460

The dynamics of systems with elastic elements of high rigidity
23 p3504 A83-48461

On the structure of quasi-hyperbolic stochasticity in an inertial autooscillator
23 p3504 A83-48483

On dynamics and stability of continuous systems subjected to a distributed moving load
23 p3473 A83-48496

Conservation laws for some separable gyroscopic dynamical systems
24 p3624 A83-50125

The dynamic stability of slender, thrust-vector-guided flight vehicles
[MBB-VA-733-83-DE]
24 p3552 A83-50139

DYNAMIC STRUCTURAL ANALYSIS

In-flight structural dynamic characteristics of the XV-15 tilt-rotor research aircraft
01 p0008 A83-10191

Free vibrations of plates in fluid using finite and infinite elements
01 p0058 A83-10279

The method of differential amplitude approximation for solving dynamic viscoelasticity problems
01 p0059 A83-10683

Introduction to the vibration of mechanical systems with internal impacts --- Czech book
01 p0060 A83-10877

On the two frequency spectra of Timoshenko beams
01 p0060 A83-11037

Determination of the degree of defectiveness in structural components
02 p0191 A83-12156

Determination of the dynamic characteristics of nonlinear oscillatory systems from motion measurements
02 p0191 A83-12336

Dynamic homogeneous solutions for plates of the orthorhombic class
02 p0192 A83-12371

Development of dynamics and control simulation of large flexible space systems
02 p0141 A83-12456

An averaged Lagrangian-finite element technique for the solution of nonlinear vibration problems
02 p0194 A83-12747

Nonlinear equations of dynamics for spinning paraboloidal antennas
02 p0142 A83-12754

An efficient triangular plate bending finite element for crash simulation
02 p0194 A83-12755

An experimental and analytical study of the dynamic response of a linkage fabricated from a unidirectional fibre-reinforced composite laminate
[ASME PAPER 82-DET-67]
02 p0187 A83-12775

A linear finite element approach to the solution of the variational inequalities arising in contact problems of structural dynamics
02 p0196 A83-12838

DYNAMIC STRUCTURAL ANALYSIS

Bending waves in strongly anisotropic elastic plates
02 p0196 A83-12855

Improved numerical computation of uniform beam characteristic values and characteristic functions
02 p0197 A83-13001

Vibrations of split beams
02 p0197 A83-13002

Modal cross-spectral terms may be important and an alternative method of analysis be preferable
02 p0197 A83-13003

Nonlinear flapping vibrations of rotating blades
02 p0197 A83-13004

Dynamic fracture of a beam or plate under tensile loading
03 p0339 A83-13338

A minimum strain energy approach for obtaining optimal unbalance distribution in flexible rotors
03 p0335 A83-13491

Dynamic analysis of turbulent annular seals based on Hirs' lubrication equation
[ASME PAPER 82-LUB-41]
03 p0336 A83-13520

Generalized dynamic problem of thermoelasticity and thermoviscoelasticity for an infinite cylindrically anisotropic plate
03 p0339 A83-13691

A method for investigating the modes of motion of a nonlinear system with limited excitation
03 p0337 A83-14069

A study of the dynamic behavior of flexible rotors --- French thesis
03 p0337 A83-14103

Application of fatigue-strength analysis to the evaluation of the consequences of local damage and the effects of wing-shell repairs. III - An example of the application of fatigue-strength analysis using a specific fatigue wear
03 p0342 A83-14620

On some unconditionally stable, higher order methods for the numerical solution of the structural dynamics equations
03 p0342 A83-14708

Elastic-plastic finite element analysis of dynamic fracture
04 p0495 A83-15062

Noise transmission into semicylindrical enclosures through discretely stiffened curved panels
04 p0532 A83-15069

The diffraction of a nonstationary transverse wave by a cylindrical cavity
04 p0497 A83-15385

A program system for dynamic analysis of aeronautical structures /HAJIF-II/
04 p0497 A83-15545

System identification and aircraft flutter
04 p0497 A83-15546

Application of multiple dynamic absorbers to reducing the vibration level of a complex cantilever structure
04 p0497 A83-15547

A spectral approach for analyzing the vibration of a periodic structure with random parameters
04 p0497 A83-15548

A theory of substructure modal synthesis
[ASME PAPER 82-WA/APM-29]
04 p0499 A83-15693

Natural frequencies of out-of-plane vibration of arcs
04 p0499 A83-15694

The dynamics of plane supporting structures - A computer-aided experimental analysis of structure dynamic problems with interactive method of test --- German thesis
04 p0499 A83-15847

A mode solution for the finite deflections of a circular plate loaded impulsively
04 p0500 A83-16199

Transient nonlinear response of impulsively-loaded circular plates
04 p0501 A83-16200

An approach to the numerical study of the free vibrations of thin-wall structures
04 p0502 A83-16404

Numerical analysis of wave processes in a shell-rod system
04 p0502 A83-16405

Solution of the dynamic problem of viscoelastic shells
04 p0502 A83-16412

Transient dynamics during the Space Shuttle based manufacture of structural components - General formulation of the problem
[AIAA PAPER 83-0432]
05 p0600 A83-16711

Parametric instability of tapered beams by finite element method
05 p0655 A83-17723

Parametric vibrations of a horizontal beam with a concentrated mass at one end
05 p0656 A83-17946

Vibration of waffle cylinders
06 p0770 A83-18069

Impact of a body on a mass attached to an elastically restrained beam
06 p0770 A83-18070

Dynamic analysis of constant-lift and free-tip rotors
06 p0773 A83-18386

A general dynamic synthesis for structures with discrete substructures
06 p0773 A83-18391

Dynamic coefficient of a two-layered thick beam with imperfect bonding
06 p0774 A83-18396

Bracketing of the eigenfrequencies of spatial skeletons. I, II
06 p0777 A83-19198

Application of Trefftz-Fichera's method for improvable bracketing of the natural angular eigenfrequencies of a beam subject to bending vibration
06 p0777 A83-19199

Calculation of exact vibration modes for plane grillages by the dynamic stiffness method

07 p0947 A83-21073
Dynamic analysis of thin elastic noncircular conical shells 07 p0948 A83-21346
Numerical operational methods for time-dependent linear problems 07 p0948 A83-21437
Analysis of membranes stretched over a unilateral support 08 p1115 A83-21638
Dynamic steady antiplane shear crack growth in an elastic-plastic material 08 p1119 A83-21779
Lagrange-type formulation for finite element analysis of non-linear beam vibrations 08 p1120 A83-21805
Hydroelastic effects of separated flow 08 p1084 A83-22144

Dynamic qualification of spacecraft by means of modal synthesis. I 08 p1050 A83-22375
Dynamic /transient/ analysis of layered anisotropic composite-material plates 08 p1123 A83-22944
On the inclusion principle for the hierarchical finite element method 08 p1159 A83-22946
Dynamic response analysis of structures with large degrees of freedom by step-by-step transfer matrix method 09 p1276 A83-23335

Fundamental frequency of an elastically restrained beam with discontinuous moment of inertia and an intermediate support 09 p1276 A83-23342

The Green function of an infinite, fluid loaded membrane 09 p1278 A83-23705

A numerical solution to problems relating to the vibrations of thin plates acted upon by impact loads 09 p1280 A83-24489

An algorithm for kinetoelastodynamic analysis of plane mechanisms with rectilinear elements 09 p1280 A83-24505

Dynamic characteristics of conical shell with variable modulus of elasticity 09 p1280 A83-24506
Aggregation of large space structure dynamics with respect to actuator and sensor influences 09 p1217 A83-24784

A study of the dynamic characteristics of thin-walled structures with attached loads 09 p1281 A83-25014
Sensitivity of the solutions of the equation of the linear vibrations of a membrane to changes of the coefficients of the equation 09 p1282 A83-25021

Practical stress analysis in engineering design --- Book 10 p1438 A83-25425
Vibration of a plate of arbitrary shape with free and simply supported mixed edges 10 p1439 A83-25824

Dynamic stress concentration around a circular hole in an infinite elastic strip 10 p1440 A83-26430
Theory of viscoplastic shells for dynamic response 10 p1441 A83-26438

Multi-level substructural analysis in modal synthesis - Two improved substructural assembling techniques 10 p1442 A83-26764

Linear analysis by the finite element method of the dynamics of axisymmetric structures subjected to arbitrary loads 10 p1442 A83-26819

Influence of tangential displacements on the dynamic buckling of viscoplastic cylindrical shells 10 p1442 A83-26820
Projection moire interferometer for vibration analysis 10 p1424 A83-26869

Dynamic stability of cylindrical sandwich panel subjected to axial compression 11 p1593 A83-27770
A stabilization procedure for the quadrilateral plate element with one-point quadrature 11 p1594 A83-28419

Damped second-order Rayleigh-Timoshenko beam vibration in space - An exact complex dynamic member stiffness matrix 11 p1595 A83-28421

Dynamic behavior of fluid bearings - Linear and nonlinear study --- French thesis 11 p1589 A83-28631
Fractional calculus - A different approach to the analysis of viscoelastically damped structures 12 p1734 A83-28965

Finite element modeling techniques for constrained layer damping 12 p1735 A83-28976
Frequency effects in tilting-pad journal bearing dynamic coefficients 12 p1732 A83-29125

Electronic housing design for a random vibration environment 12 p1732 A83-29216
Vibrations of a shallow shell with an attached mass distributed on part of its surface 12 p1735 A83-29276

Numerical solution of an elastic boundary layer problem using a multiple shooting technique 12 p1736 A83-29614

Structures, Structural Dynamics and Materials Conference, 24th, Lake Tahoe, NV, May 2-4, 1983, Collection of Technical Papers. Part 1 - Structures and materials. Part 2 - Structural dynamics 12 p1736 A83-29729

Nonlinear behavior of thin columns under parametrically excited load 12 p1738 A83-29750

DYSCO - An executive control system for dynamic analysis of synthesized structures 12 p1768 A83-29773

Statistical crack propagation in fastener holes under spectrum loading 12 p1741 A83-29808

Time-domain quasi-linear identification of nonlinear dynamic systems 12 p1773 A83-29811

Direct structural parameter identification by modal test results 12 p1741 A83-29812

Method of multiple scales and identification of nonlinear structural dynamic systems 12 p1774 A83-29813

Near-real-time flutter boundary prediction from turbulence excited response 12 p1741 A83-29814

Creation and checking of load transformation matrices for modally coupled systems using the acceleration method with recursive equations 12 p1742 A83-29815

Time domain response envelope for structural dynamic systems 12 p1707 A83-29817

On the dynamic response and collapse of slender guyed booms for space application 12 p1742 A83-29818

Vibration characteristics of hexagonal radial rib and hoop platforms 12 p1742 A83-29819

Nonlinear structural dynamics analysis using a modified modal method 12 p1742 A83-29820

A revised version of the transfer matrix method to analyze one-dimensional structures 12 p1742 A83-29821

The coupled aeroelastic response of turbomachinery blading to aerodynamic excitations 12 p1742 A83-29822

A preliminary look at control augmented dynamic response of structures 12 p1708 A83-29825

Block-independent control of distributed structures 12 p1742 A83-29826

Close-mode identification performance of the ITD algorithm 12 p1774 A83-29829

Experiments using least square lattice filters for the identification of structural dynamics 12 p1742 A83-29830

Vibration characteristics and dynamic stability of stiffened plates 12 p1743 A83-29837

The influence of an internal resonance on nonlinear structural vibrations under subharmonic resonance conditions 12 p1743 A83-29838

Nonlinear incremental inverse perturbation method for structural redesign 12 p1743 A83-29839

Transient response of damped space systems 12 p1743 A83-29840

Fractional calculus in the transient analysis of viscoelastically damped structures 12 p1743 A83-29841

A refined finite element for vibration analysis of twisted blades based on beam theory 12 p1743 A83-29845

Substructuring concepts for transient response of slender shell structures 12 p1744 A83-29851

Space Shuttle solid rocket booster initial water impact loads and dynamics - Analysis, tests, and flight experience 12 p1706 A83-29858

A travelling wave approach to the dynamic analysis of large space structures 12 p1744 A83-29862

State vector formulation of substructure coupling for damped systems 12 p1744 A83-29863

Generalized modal shock spectra within indeterminate interface --- for spacecraft design 12 p1708 A83-29871

Bending effects on structural dynamic instabilities of transonic wings 12 p1745 A83-29887

An automated technique for improving model matrices by means of experimentally obtained dynamic data 12 p1746 A83-29890

On normal mode vibrations of nonlinear conservative systems --- Book 13 p1914 A83-30147

Mirror control system for the University of California technical demonstration prototype 13 p1921 A83-31021

Method of high-speed loading in determining fracture 13 p1823 A83-31218

Digital data acquisition and analysis in structural dynamic testing 13 p1867 A83-31494

On dynamical description of fiber reinforced composites 13 p1868 A83-31622

Coupled vibrations of beams - An exact dynamic element stiffness matrix 13 p1868 A83-31637

Structural dynamics studies of rotating bladed-disk assemblies coupled with flexible shaft motions [AIAA PAPER 83-0919] 14 p1976 A83-32787

Dynamics of gyro-elastic continua [AIAA PAPER 83-0826] 14 p2032 A83-32795

Optimum sensitivity derivatives of objective functions in nonlinear programming 14 p2076 A83-32992

Vibration analysis of rotor-bearing system by quasi-modal transformation - Analyses of complex eigenvalue and response history 14 p2028 A83-33093

Dynamic tests of graphite/epoxy composites in hydrothermal environments 14 p1987 A83-33124

Dynamic qualification of spacecraft by means of modal synthesis. II 14 p1982 A83-33474

Dynamic behaviour of a thin-walled circular cylindrical shell 15 p2173 A83-33611

Effective widths in plate buckling 15 p2173 A83-33612

Gears and their vibration: A basic approach to understanding gear noise --- Book 15 p2171 A83-33616

Structural control research and experiments at NASA/LaRC 15 p2220 A83-33968

Analysis of forced vibration by reduced impedance method. IV Proposition and application of multiple reduced impedance method 15 p2174 A83-34009

A study of shear factors in reduced-selective integration Mindlin beam elements 15 p2175 A83-34313

Operator split methods in the numerical solution of the finite deformation elastoplastic dynamic problem 15 p2176 A83-34314

Deformation and vibration of rotating elastic cylinders 15 p2177 A83-34340

Nonlinear statics and dynamics of thin axisymmetric shells by high precision finite elements 15 p2177 A83-34347

The calculation of the crack propagation forces while taking account of the unilateral contact between the edges of the crack 15 p2178 A83-34402

Numerical determination of the parameters of Krupkowski's function for a torsion test taking into consideration the strain hardening ranges 15 p2140 A83-35066

Existence of solutions for dynamic problems of one-dimensional plastic structures 16 p2365 A83-35552

Free vibrations of simply supported cylindrical shells of oval cross section 16 p2366 A83-36090

Methods of static and dynamic calculations of structures with cyclic symmetries [ONERA, TP NO. 1983-14] 16 p2367 A83-36424

The mean transverse shear in stratified anisotropic plates [ONERA, TP NO. 1983-15] 16 p2368 A83-36425

Partial closure of cracks at the interface between a layer and a half space 16 p2368 A83-36506

Sudden twisting of an external circular crack in an infinite medium with a cylindrical inclusion 16 p2368 A83-36513

Dynamic analysis of geometrically nonlinear truss structures 16 p2369 A83-36556

Large deflection analysis of clamped skew sandwich plates by parametric differentiation 16 p2369 A83-36561

Dynamic analysis of the electrostatically controlled membrane mirror using multiple scales 17 p2476 A83-37081

A new higher order dynamic theory for thermoelastic bars. I General theory. II - Application to thermoelastic circular and rectangular bars 17 p2521 A83-37726

Free vibration of circular-segment-shaped membranes and plates of rectangular orthotropy 17 p2522 A83-37730

Transient blade response due to surge induced structural loads [SAE PAPER 821438] 17 p2468 A83-37986

A computer-aided system for interactive geometric modeling, structural/dynamics analysis and N/C manufacturing/inspection of radial flow compressors [SAE PAPER 821440] 17 p2493 A83-37988

Status of FAA crash dynamics program - Transport category aircraft [SAE PAPER 821483] 17 p2459 A83-38002

Unstable growth of branched cracks
17 p2523 A83-38394

Numerical solution of axisymmetric problems in the dynamics of thin-walled orthotropic shells of revolution
17 p2524 A83-38507

Dynamic elasto-plastic response of shells in an acoustic medium - EPSA code
17 p2524 A83-38570

An iterative algorithm for solving inverse problems in structural dynamics
17 p2525 A83-38571

Utilization of the dynamic characteristics of a structure to evaluate its technological state --- dynamic structural analysis of caissons
18 p2698 A83-39510

Reduced stiffness axial load buckling of cylinders
18 p2700 A83-39559

Investigations of axisymmetric deformation of geometrically nonlinear, rotationally orthotropic, circular plates
18 p2700 A83-39567

Dynamic contact problem of flexible orthotropic plates and shells with allowance for transverse shear
18 p2702 A83-40123

Mechanical behaviours in high velocity tension of composites
18 p2656 A83-40213

On the stress wave velocity of fiber reinforced rectangular bar by means of finite prism method
18 p2705 A83-40218

Dynamic stress concentrations in some composite strips with a circular hole under high-velocity tension
18 p2705 A83-40221

Blade loss transient dynamic analysis of turbomachinery
19 p2800 A83-40864

Improvement of a large analytical model using test data
19 p2856 A83-40870

The dynamic collapse of a column impacting a rigid surface
19 p2856 A83-40873

Rigid-body structural mode coupling on a forward swept wing aircraft
19 p2797 A83-41046

The reaction of a piezoceramic shell to concentrated actions
19 p2858 A83-41212

Subsonic motion of the edge of a shear shift with friction along an interface between elastic materials
19 p2858 A83-41214

Identification of vibrating structures
19 p2858 A83-41530

Optimization of structures subjected to aeroelastic instability phenomena
19 p2859 A83-41541

Impact of aircraft structural dynamics on integrated control design
[AIAA PAPER 83-2216] 19 p2798 A83-41698

Prediction of the dynamic behavior of bladed disk assemblies --- French thesis
19 p2860 A83-41811

Doubly symmetric interactive buckling of plate structures
20 p3001 A83-42519

A computer program for system dynamic synthesis of flexible structures from component data
20 p3002 A83-42543

Comparison of damping material properties from various characterization tests
20 p3002 A83-42573

Mechanical random vibrations
20 p3004 A83-42981

A fast Fourier method for the dynamic analysis of linear structures with frequency dependent properties
20 p3005 A83-42989

Dynamics and stability of open conical shells
20 p3005 A83-42993

Dynamic notch-stress problem in a perforated circular disk
20 p3006 A83-43001

Nonlinear inverse perturbation method in dynamic analysis
20 p3007 A83-43449

Implementation of an improved bisection algorithm in buckling problems
20 p3008 A83-43647

Analysis of aircraft dynamic behavior in a crash environment
21 p3091 A83-43966

Dynamic analysis of viscoelastic structures using incremental finite element method
21 p3150 A83-44026

Reanalysis and design in structural dynamics
21 p3151 A83-44031

The dynamic analysis of a structure having discrete dampers
21 p3151 A83-44106

Subspace iteration for the eigenvalue problems of self-adjoint differential equations and its applications in the vibration analysis of structures
21 p3151 A83-44109

Effective widths of plates loaded uniaxially
21 p3152 A83-44250

Time integration of the motion equations of a damped structure
21 p3152 A83-44359

On axial and lateral buckling of end-loaded anisotropic cantilever beams
21 p3152 A83-44464

Method for improving incomplete modal coupling
21 p3152 A83-44545

Multiple mode nonlinear analysis of circular plates
21 p3153 A83-44549

Markov approximation to transient vibration
21 p3153 A83-44550

The behaviour of a channel cantilever under combined bending and torsional loads
21 p3153 A83-44623

On some recent developments in the shakedown theory
21 p3154 A83-44660

A comparative analysis of certain versions of shear models in problems regarding the equilibrium and vibration of multilayer plates
21 p3155 A83-44723

Antiplane vibration of an elastic layer with a midplane crack
21 p3155 A83-44884

A theory of shells with small strain accompanied by moderate rotation
21 p3159 A83-44939

A new approach to the dynamic analysis of structures using fixed frequency dynamic stiffness matrices
21 p3160 A83-45051

Finite element models and system identification of large space structures
21 p3196 A83-45115

Multi-body dynamics analysis on small computers
21 p3190 A83-45123

A variational perturbation method for problems in nonlinear structural dynamics
21 p3160 A83-45127

Low-velocity impact response of laminated plates
21 p3164 A83-45589

Advances in dynamic analysis and testing; Proceedings of the Aerospace Congress and Exposition, Anaheim, CA, October 25-28, 1982
22 p3303 A83-45746

Conceptual support design of the high resolution mirror assembly for the Advanced X-ray Astrophysics Facility (AXAF)
22 p3302 A83-46589

Practical stress analysis in engineering design --- Book
22 p3306 A83-46687

Nonlinear shell dynamics - Intrinsic and semi-intrinsic approaches
23 p3468 A83-47592

Structural response due to blade vane interaction
[ASME PAPER 83-GT-133] 23 p3408 A83-47960

Substructuring and wave propagation - An efficient technique for impeller dynamic analysis
[ASME PAPER 83-GT-150] 23 p3409 A83-47969

Vibrations of blades with variable thickness and curvature by shell theory
[ASME PAPER 83-GT-152] 23 p3469 A83-47978

Effects of static friction on the forced response of frictionally damped turbine blades
[ASME PAPER 83-GT-155] 23 p3409 A83-47981

Vibration analysis of radial compressor impellers
[ASME PAPER 83-GT-156] 23 p3469 A83-47982

A simple algorithm for the nonlinear dynamic analysis of networks
23 p3470 A83-48160

Dynamic finite element analysis of nonaxisymmetric structures
23 p3471 A83-48163

Harmonic acceleration method for dynamic structural analysis
23 p3471 A83-48165

A partitioned finite element method for dynamical systems
23 p3471 A83-48166

The effect of viscosity on the forced vibrations of a fluid-filled elastic shell
[ASME PAPER 83-APM-34] 23 p3471 A83-48242

Bimodal solutions in problems of the optimization of eigenvalues --- in structural design and stability analysis
23 p3473 A83-48526

Nonlinear flexural vibrations of initially deflected cross-ply laminated plates with elastically restrained edges
24 p3591 A83-48894

International Symposium on Aeroelasticity, Nuremberg, West Germany, October 5-7, 1981, Collected Papers [DGLR BERICHT 82-01] 24 p3543 A83-49176

Finite element analysis of steadily moving contact fields
24 p3593 A83-49437

A three-dimensional nonlinear analysis of cross-ply rectangular composite plates
24 p3593 A83-49439

A modification of Potter's method for diagonal matrices with common unknown
24 p3593 A83-49440

Boundary methods for calculating the natural frequencies of elastic structures
24 p3594 A83-49454

Dynamic problem of elasticity theory for a region with curved slits (plane strain)
24 p3594 A83-49534

A numerical study of the plastic adaptation of plates and shells of revolution by equilibrium finite elements
24 p3594 A83-49645

Effects of uni-directional geometric imperfections on vibrations of pressurized shallow spherical shells
24 p3595 A83-49899

The asymptotic method in the problem of the nonlinear vibration of shells
24 p3596 A83-49907

Deliberations on the improvement of the computational model with measured eigenmagnitudes --- for linear elastomechanic systems
24 p3596 A83-50128

Identification of the dynamic characteristics of a simple system with quadratic damping
24 p3597 A83-50137

Compressive strength of fiber-reinforced materials
24 p3597 A83-50147

DYNAMO TESTS

Advanced facility for processing aircraft dynamic test data
01 p0013 A83-10189

The effect of test system misalignment in the dynamic tension test
01 p0026 A83-10649

Support interference in static and dynamic tests --- of wind tunnel models at high angles of attack
01 p0014 A83-11074

A tensile technique for materials testing at high strain rates
02 p0154 A83-12007

The use of dynamic impact experiments in the determination of the strain rate sensitivity of metals and alloys
04 p0462 A83-16272

Analytical and experimental fracture mechanics --- Book
07 p0948 A83-21098

Plastic effects in dynamic crack propagation
08 p1118 A83-21776

Protection of radio electronic and other precision equipment against dynamic effects --- Russian book
09 p1254 A83-23820

Static and damage tolerance tests of an advanced composite vertical fin for L-1011 aircraft
[AIAA 83-0970] 12 p1701 A83-29780

An automatic test set for the dynamic characterization of A/D converters
13 p1836 A83-31288

Control of the material properties and structural application of carbon fibre reinforced plastics
[AIAA PAPER 83-0859] 14 p1986 A83-32790

Zero gravity simulator for dynamic testing of pointing mounts
[AIAA PAPER 83-2300] 19 p2811 A83-41758

Design and experimentation within the Mobility Development Laboratory (MDL) utilizing the Static and Dynamic Test Machines
20 p2938 A83-42549

Dynamic measurements in gas flowfields using rotational Raman spectroscopy
20 p2950 A83-42580

A dynamic technique for measurements of thermophysical properties at high temperatures
20 p2991 A83-43257

Advances in dynamic analysis and testing; Proceedings of the Aerospace Congress and Exposition, Anaheim, CA, October 25-28, 1982
22 p3303 A83-45746

Variation of dynamic mechanical properties of polycarbonate as a result of deformation
22 p3270 A83-46903

Hypersonic dynamic testing of ablating models with three-degree-of-freedom gas bearings
23 p3412 A83-48135

DYNAMICS

Dynamic properties of gravitational fields
14 p2079 A83-32351

Analytical methods in rotor dynamics
19 p2854 A83-41519

The dynamics of a rigid body on an absolutely rough plane
23 p3505 A83-48529

DYNAMICS EXPLORER SATELLITES
NT DYNAMICS EXPLORER 1 SATELLITE
NT DYNAMICS EXPLORER 2 SATELLITE

Stable and rugged etalon for the Dynamics Explorer Fabry-Perot interferometer. I - Design and construction
02 p0142 A83-12312

Stable and rugged etalon for the Dynamics Explorer Fabry-Perot interferometer. II - Performance
02 p0142 A83-12313

Upward electron beams measured by DE-1 - A primary source of dayside region-1 Birkeland currents
20 p3026 A83-43215

DYNAMICS EXPLORER 1 SATELLITE

Geocoronal imaging with Dynamics Explorer - A first look
19 p2864 A83-41116

Characteristics of thermal and suprathermal ions associated with the dayside plasma trough as measured by the dynamics explorer retarding ion mass spectrometer
22 p3335 A83-47053

DYNAMICS EXPLORER 2 SATELLITE

Neutral winds in the polar magnetosphere as measured from Dynamics Explorer
16 p2374 A83-35376

Some dynamical design considerations for momentum biased spacecraft
[IAF PAPER 83-358] 23 p3422 A83-47357

DYNAMO THEORY

Magnetospheric convection at a low level power epsilon
02 p0204 A83-11968

Reducing the non-axisymmetry of a planetary dynamo and an application to Saturn
02 p0268 A83-12980

Nonlinear dynamo oscillations
02 p0242 A83-12981

The role of the helicity spectrum function in turbulent dynamo theory
02 p0242 A83-12985

Stationary magnetic field in a periodic flow
04 p0537 A83-15883

Dynamo action in cosmic bodies
04 p0556 A83-15959

Nonlinear astrophysical dynamo - Three-mode interaction
04 p0557 A83-15981

An idea of flare dynamo mechanism
05 p0707 A83-16854

Dynamo action in a supermassive rotator and the active galactic nuclei
05 p0697 A83-16988

- Mechanism of the stationary biaxial dynamo 05 p0664 A83-17629
- Constraints on the size of the moon's core 06 p0847 A83-18176
- Global dynamo simulation of ionospheric currents and their connection with the equatorial electrojet and counter electrojet - A case study 06 p0783 A83-18296
- Convective dynamos with intermediate and strong fields 06 p0813 A83-18932
- Analysis of geodynamo equations by means of perturbation theory 06 p0787 A83-18933
- Some remarks on the antidynamo theorem 07 p0996 A83-20140
- The nonzero-flow-rate /accretion/ semidynamo - Two simple examples 07 p1027 A83-21277
- Magnetic dipole moment estimates for an ancient lunar dynamo 07 p1032 A83-21293
- A comprehensive view of solar-terrestrial relationships in terms of a chain of four dynamo-powered plasma acceleration processes 07 p0968 A83-21578
- [AD-A126953] 07 p0968 A83-21578
- Dynamics of the global Sq-field --- current distribution and geomagnetic variations 08 p1134 A83-22305
- VLF/ELF radiation from the ionospheric dynamo current system modulated by powerful HF signals 09 p1300 A83-23311
- The Hall effect in a unipolar inductor - A possible mechanism for a dynamo and an antidynamo --- pulsar model 09 p1364 A83-25088
- On the stability of toroidal flux tubes in differentially rotating stars 10 p1499 A83-25363
- Topological semi-dynamos 10 p1485 A83-25413
- Solar-wind disturbances and the solar wind-magnetosphere energy coupling function 11 p1687 A83-27389
- Evidence for the phi-dependent rotation-oscillation of the sun /and for the driving mechanism of the asymmetric dynamo/ 11 p1690 A83-27662
- Hydromagnetic waves in a differentially rotating sphere --- applied to geomagnetic secular variations 12 p1752 A83-29226
- Energy estimates for latent-heat driven convection in the earth's core 12 p1753 A83-29238
- An example of an almost-toroidal dynamo in a fluid sphere 12 p1781 A83-29264
- On the first-order smoothing expression for the alpha-effect in dynamo theory 13 p1952 A83-31433
- Problems of the solar dynamo 14 p2115 A83-32543
- Recent developments in the dynamo theory of planetary magnetism 14 p2113 A83-33479
- A dynamo theory of solar flares 15 p2279 A83-34292
- On the depth dependence of the solar rotation velocity determined from Fraunhofer lines 15 p2281 A83-34307
- Planetary magnetic fields 15 p2274 A83-34399
- Transport effects associated with turbulence with particular attention to the influence of helicity 15 p2161 A83-34400
- MHD turbulence via extended Burgers' equation 15 p2235 A83-34544
- The Janet/Busch oscillator - A multivibratory dissipative structure relevant to dynamic theories of geomagnetic flux reversals 17 p2537 A83-37082
- Dynamo region and the equatorial electrojet in the Jovian atmosphere 17 p2623 A83-38517
- F-region dynamo in the evening - Interpretation of equatorial Delta D anomaly found by MAGSAT 18 p2712 A83-39074
- Magnetic fields in the cosmos 18 p2764 A83-39087
- The solar dynamo 18 p2783 A83-39229
- The solar dynamo and the concentration of magnetic fields in the photosphere 18 p2783 A83-39230
- Observations of rotation and velocity fields of cool stars 18 p2765 A83-39237
- Theory of magnetic activity of late type stars 18 p2765 A83-39241
- The central powerhouse of active galactic nuclei 18 p2766 A83-39249
- Equatorial disturbance dynamo electric fields 19 p2864 A83-41117
- Choice of dimensions for devices simulating the MHD dynamo and self-excitation of magnetic fields in them 19 p2903 A83-42003
- The earth's core 20 p3020 A83-42816
- Dynamo generation of magnetic fields in three-dimensional space - Solar cycle main flux tube formation and reversals 21 p3242 A83-44111
- The mechanism of acceleration of ring current during a substorm of magnetosphere 21 p3171 A83-44302
- Dynamics of the earth's core and the geodynamo 22 p3323 A83-45780
- Planetary magnetism and the thermal evolution of planetary cores 22 p3384 A83-45787

- A new interpretation of the alpha effect --- turbulently generated emf in magnetized plasma 22 p3362 A83-46014
- Dynamo theory in the sun and stars 23 p3525 A83-47541
- Solar cycle dynamo wave origin of sunspot intensity and X-ray bright point number variation 23 p3537 A83-47723
- Magnetohydrodynamic effects of a first-order cosmological phase transition 24 p3658 A83-49299

DYNAMOMETERS

- A method for measuring the integral characteristics of boundary layers 24 p3581 A83-48949

E

E GLASS

- NT S GLASS

E LAYERS

- U E REGION

E REGION

- NT E-2 LAYER
NT SPORADIC E LAYER

- Vertical displacements of stratification in the E-layer during sunrise 02 p0205 A83-11996
- A neutral vortex induced by an auroral arc 02 p0209 A83-12429
- Gradient-drift instability of nighttime mid-latitude Es-layers 03 p0361 A83-14745
- A correlation between measured E-region current and geomagnetic daily variation at equatorial latitude 07 p0966 A83-21429
- A test of the cosine relationship using three-radar velocity measurements --- of electron drift in ionospheric E layer 10 p1449 A83-26044
- Ionospheric observations at Pruhonice during the solar eclipse of April 29, 1976 11 p1616 A83-28111
- Influence of the E region dynamo on equatorial spread F 11 p1618 A83-28319
- High-latitude plasma densities and their relation to riometer absorption 12 p1754 A83-29431
- A theory of coherent radar spectra in the auroral E region 13 p1879 A83-31240
- Ionospheric E-region drifts at Sibirsk during 1970-75 13 p1882 A83-31547
- Synopsis of D- and E-region electron densities during the energy budget campaign 16 p2373 A83-35364
- Energy distribution of thermal electrons at the height of lower-E-region 16 p2373 A83-35366
- Electric field and electron density measurements in the equatorial E-region 16 p2373 A83-35367
- Neutral temperatures from Thomson scatter measurements Comparisons with the CIRAP(1972) [AD-A130290] 16 p2378 A83-36120
- Tests of an ion-chemical model of the D- and lower E-region 18 p2712 A83-39072
- The effect of the conductivity of the E-region on the growth increment of the Rayleigh-Taylor instability in the ionospheric plasma of the equatorial F-region 18 p2714 A83-39331
- Ground-based observations of subauroral energetic-electron arcs 19 p2865 A83-41122
- Ionospheric characteristics of a detached arc in the evening-sector trough 19 p2865 A83-41123
- Production of auroral zone E region irregularities by powerful HF heating 20 p3020 A83-42427
- Short wavelength gradient-drift waves at high latitudes 21 p3170 A83-44243
- Modelling of the ion composition of the middle atmosphere 21 p3173 A83-44669
- A new radar auroral backscatter experiment 21 p3173 A83-44995
- Possible mechanism for a synapse variation of electron density in the E and F2 regions of the ionosphere 21 p3174 A83-45234
- Ionospheric absorption of radio waves on reflection by the E layer and by the shielding Es layer 21 p3177 A83-45275
- VHF radar observation of auroral E-region irregularities associated with moving-arcs 22 p3330 A83-46511
- Polar cleft structure and SEC associated plasma irregularities observed by Greenland rocket experiment, 1976 --- Slant E Condition 22 p3331 A83-46519
- A new VHF Doppler radar experiment at Syowa Station, Antarctica 22 p3332 A83-46523
- Electron density and energetic particle precipitation observed during the eclipse of 26 February 1979 23 p3480 A83-47466
- A model of the lower ionosphere above Red Lake, Canada, during the 26 February 1979 solar eclipse 23 p3480 A83-47467
- E-region nitric oxide concentrations inferred from the 26 February 1979 eclipse expedition 23 p3480 A83-47469

- Positive and negative ion composition measurements in the D and E-regions during the 26 February 1979 solar eclipse 23 p3480 A83-47470
- Simultaneous geomagnetic and radio auroral observations 24 p3605 A83-49302

E-2 LAYER

- Vertical displacements of stratification in the E-layer during sunrise 02 p0205 A83-11996

EAR

- NT COCHLEA
NT LABYRINTH
NT MIDDLE EAR
NT VESTIBULES

The hair cells of the inner ear

04 p0521 A83-16046

The evolution of the structural-functional organization of the organ of hearing of vertebrates

07 p0972 A83-19933

The role of the sections of the hearing system in the localization of the source of sound

07 p0972 A83-19934

The impairment of the defensive and adaptive mechanisms of the ear as a result of the exposure to noise

07 p0978 A83-20876

The diagnostic value of the otolithic reflex in patients with chronic suppurative inflammation of the middle ear

19 p2881 A83-41441

The distribution of streptomycin in the structures of the inner ear following its parenteral administration (a histoautoradiographic investigation)

19 p2875 A83-41443

EARLY STARS

- NT PROTOSTARS
NT T TAURI STARS

Application of a computer controlled intensity registering procedure to the spectral region at 4430 A

01 p0116 A83-10268

Luminosity classification of Be stars by Balmer line narrow band photometry

01 p0120 A83-10307

Optical variations of the Be star HDE 245770/A 0535+26

01 p0120 A83-10313

Hydrodynamical models of rotating magnetic winds

01 p0123 A83-10354

Analysis of the ultraviolet spectrum of RWT 152 - A subluminescent O star with a main-sequence visual spectrum

02 p0256 A83-12126

Membership of the Rosette Nebula cluster, NGC 2244

02 p0248 A83-12913

Spectral types in the direction of the Magellanic Stream

03 p0401 A83-13307

Complex ionized structure in the theta-2 Orionis region

03 p0413 A83-13315

On C3 molecules in diffuse interstellar clouds

03 p0414 A83-13327

UBV-/H-beta/ photometry of luminous stars between l equals 335 deg and l equals 6 deg

03 p0402 A83-13365

IUE high dispersion spectra of luminous stars in symmetric nebulae

03 p0417 A83-13555

Optical observations of ultraviolet objects. II - Classification and photometry /I = 0 to 145 deg/

03 p0409 A83-13932

Is NGC 1851-UV5 a binary star in a globular cluster

03 p0421 A83-14139

Berkeley 87, a heavily-obscured young cluster associated with the ON2 star-formation complex and containing the WO star Stephenson 3

03 p0409 A83-14141

Ultraviolet emission in the Mg II h and k lines in Be stars

03 p0424 A83-14201

The optical spectrum of R136a - The central object of the 30 Doradus nebula

04 p0552 A83-15612

Star formation and pre-main-sequence stellar evolution

04 p0557 A83-16223

The return of mass and energy to the interstellar medium by winds from early-type stars

05 p0698 A83-17000

Angular diameters, effective temperatures, radii, and luminosities of O3, O4, and O5 stars

05 p0698 A83-17002

The helium 10830 A line in early-type stars - An atlas of Fabry-Perot scans

05 p0698 A83-17003

Determination of mass-loss rates from the first order moment W1 of unsaturated Cygni line profiles

05 p0702 A83-17805

Polarization of early-type stars in Norma

06 p0820 A83-18861

Meridional circulation in rotating stars. IV - The approach to the mean steady state in early-type stars

06 p0841 A83-19294

A study of visual double stars with early type primaries. I - Spectroscopic results

07 p1006 A83-20574

A study of visual double stars with early type primaries. II - Photometric results

07 p1006 A83-20575

An X-ray emitting bubble in the Cep OB3 association

07 p1018 A83-20948

Infrared photometry of O stars

07 p1021 A83-21129

Abnormal extinction and dust properties in M 16, M 17, NGC 6357 and the Ophiuchus dark cloud
07 p1025 A83-21241

NGC 2447 and the reddening and luminosity of normal red giants
09 p1351 A83-23319

A photometric study of early-type stars
09 p1353 A83-23736
09 p1358 A83-23910

Young star groups
09 p1358 A83-23910

Observations of diffuse interstellar lines toward stars with low column densities of H2
10 p1505 A83-25746

Spectrophotometry B, A, and F stars. III
10 p1497 A83-26380

Comment on 'A comparative study of rotational properties of high-velocity and low-velocity early-type stars'
10 p1516 A83-26758

HD 129929 - A multiperiodic pulsating early-type star at intermediate galactic latitude
11 p1678 A83-27693

The neutral gas toward HD 93206
11 p1679 A83-27992

Anomalous diffuse features in dust-embedded stars
11 p1682 A83-28289

On the variability of the two brightest stars in the galactic cluster IC 2391
12 p1789 A83-28861

A re-analysis of the eclipsing binary system VV Orionis --- for UVB and uvby observations
12 p1792 A83-29052

UBV photometry for southern OB stars
12 p1786 A83-29090

High-density gas associated with 'molecular jets' - NGC 1333 and NGC 2071
13 p1953 A83-31449

The early B-type eclipsing binary FZ CMa (HD 52942)
13 p1941 A83-31566

- A massive triple system
13 p1941 A83-31566

Ultraviolet spectroscopy of LSI + 61 303
13 p1957 A83-31706

An observational study of the influence of close companions on the pulsations of Beta Cephei stars
13 p1943 A83-31740

Massive eclipsing binary candidates
14 p2098 A83-33151

Simultaneous X-ray and ultraviolet observations of Epsilon Orionis and Kappa Orionis
14 p2105 A83-33198

Infall and outflow of S(+3) ions in 15 Monocerotis, Tau Canis Majoris and Iota Orionis
14 p2105 A83-33199

Mass loss from hot stars
14 p2108 A83-33262

Episodic mass loss and narrow lines in gamma Cassiopeiae and in other early-type stars
15 p2258 A83-34107

Zinc as a tracer of metallicity in the interstellar medium
15 p2266 A83-34604

On the structure of intermediate- and high-velocity clouds
15 p2266 A83-34605

Optical observations of the interstellar absorption lines towards the M8 nebula
15 p2272 A83-34790

Intrinsic UV colour indices of early-type stars
16 p2432 A83-36684

Ultraviolet flux distributions of stars in the Orion Nebula cluster
17 p2604 A83-37916

The spectra of 12 new subliminous O stars
17 p2605 A83-37938

Intrinsic polarization and extinction features of early-type stars with emission lines due to X-ray irradiation
18 p2774 A83-39738

Bipolar gas jets in star-forming regions
18 p2777 A83-40343

Biconical nebulae and early-type stars - A model for S 106
20 p3065 A83-42386

Einstein Observations of X-ray emission from A stars
20 p3068 A83-42452

Meridional circulation in rotating stars. VI - The effects of anisotropic eddy viscosity
20 p3068 A83-42457

Studies of extremely young clusters. VII - Spectroscopic observations of faint stars in the Orion Nebula
20 p3060 A83-43058

A search for rapid spectroscopic variability in the early-type supergiants Gamma and Theta Ara
21 p3222 A83-44412

Relaxation oscillations and double temperature structures in stellar coronae
21 p3230 A83-44441

Determination of effective temperatures for hot stars from integrated fluxes
21 p3231 A83-44455

The discovery of a hot stellar wind
22 p3376 A83-45630

The magnetic fields of the helium-weak B stars
22 p3377 A83-46265

Early-type high-velocity stars in the solar neighborhood. III - Radial velocities, rotation indices, and line-strength indices for southern candidates
22 p3373 A83-46383

Photometric variability of B- and A-type supergiants
22 p3373 A83-46405

IUE observations of stars in the M8 nebula
22 p3379 A83-46566

Properties of young clusters near reflection nebulae
23 p3516 A83-47464

On the origin of H2 in T Tau stars
23 p3524 A83-47537

Magnetic accretion model for the activities of very young stars
23 p3525 A83-47548

Visible and UV observations of the giant early-type members of the Large Magellanic Cloud
24 p3658 A83-49366

On the nature of early-type stars in the galactic halo
24 p3660 A83-49383

Some aspects of the velocity fields in early-type stars
24 p3662 A83-49569

Radial velocities for early type stars in six galactic regions
24 p3664 A83-49854

Helium abundances from young stars and open clusters
24 p3666 A83-50043

EARLY WARNING SYSTEMS

Stimulation versus simulation --- as illustrated with Mission System Avionics for Airborne Early Warning Nimrod
04 p0445 A83-16332

Beyond the far horizon - USAF's ionosphere-bouncing radar finally set to go
04 p0469 A83-16453

U.S. and Soviet early warning satellites
14 p1980 A83-31823

Infrared fiber early warning receiver
22 p3255 A83-46640

EARTH (PLANET)

Planetary magnetospheres
02 p0264 A83-12181

Current investigations at TsNIIGAiK in the area of physical geodesy
08 p1136 A83-22788

Earth and Mars - Early thermal profiles
09 p1365 A83-24140

Entropy productions on the earth and other planets of the solar system
14 p2111 A83-32523

Relative performances of central and dipole frequency soundings over a layered earth
15 p2202 A83-34748

A synoptic earth vegetation atlas from satellite imagery for the biological and geographical sciences
15 p2185 A83-34818

Evolution of the earth
22 p3322 A83-45776

Inferences from other bodies for the earth's composition and evolution
22 p3384 A83-45790

Initial state of the earth and its early evolution
22 p3324 A83-45797

EARTH ALBEDO

Urban albedo as a function of the urban structure - A model experiment
01 p0069 A83-10720

Urban albedo as a function of the urban structure - A two-dimensional numerical simulation
01 p0069 A83-10721

Investigation of albedo neutrons by the Intercompos-17 satellite
02 p0272 A83-11710

Experimental study of the effect of solar radiation reflected from the earth and its cloud cover on the thermal regime of solar arrays mounted on one of the Cosmos satellites
04 p0454 A83-15126

A simple method to compute the change in earth-atmosphere radiative balance due to a stratospheric aerosol layer
04 p0510 A83-15939

High resolution planetary albedos - Values and variability
05 p0660 A83-16906

The formation of albedo-electron fluxes in the geomagnetic field
05 p0662 A83-17603

The effect of troposphere aerosol on the integral albedo of the system consisting of the atmosphere and the underlying surface
06 p0782 A83-17999

Radiation budget parameters at the top of the earth's atmosphere derived from Meteosat data
07 p0962 A83-20809

Effects of the earth-reflected sunlight on the orbit of the LAGEOS satellite
07 p0868 A83-21204

Determination of disturbing components of the pressure force of solar radiation reflected from the earth, with allowance for the shadow effect in the case of intermediate satellite-motion
08 p1048 A83-22094

Power series for determining satellite motion perturbations caused by solar radiation reflected from the earth, with allowance for the shadow effect
08 p1048 A83-22095

Measurement of changes in Sahelian surface cover using Landsat albedo images
15 p2181 A83-33555

Atmospheric effects in satellite imaging of mountainous terrain
15 p2183 A83-34466

The albedo of the underlying surface-cloudy atmosphere system
18 p2723 A83-39439

Direct determination of surface albedos from satellite imagery
18 p2715 A83-39676

Remotely sensed characteristics of snow covered lands
22 p3309 A83-46123

Reconstructing the components of the radiation balance of the earth's surface on the basis of satellite data
23 p3483 A83-48101

Vertical variations of the albedo of the system including the underlying surface and the atmosphere
24 p3605 A83-49279

Certain results of a comparison of airborne data with satellite measurements --- spectral brightness and albedo of deserts and agricultural regions
24 p3598 A83-49280

EARTH ATMOSPHERE

NT ARTIFICIAL RADIATION BELTS

NT BIOSPHERE

NT D REGION

NT E REGION

NT E-2 LAYER

NT EXOSPHERE

NT F REGION

NT F 1 REGION

NT F 2 REGION

NT FREE ATMOSPHERE

NT GEOMAGNETIC TAIL

NT INNER RADIATION BELT

NT IONOSPHERE

NT LOWER ATMOSPHERE

NT LOWER IONOSPHERE

NT MAGNETOPAUSE

NT MAGNETOSPHERE

NT MESOPAUSE

NT MESOSPHERE

NT MIDDLE ATMOSPHERE

NT MIDLITUDE ATMOSPHERE

NT OUTER RADIATION BELT

NT OZONOSPHERE

NT PRIMITIVE EARTH ATMOSPHERE

NT PROTON BELTS

NT RADIATION BELTS

NT SPORADIC E LAYER

NT STRATOSPHERE

NT THERMOSPHERE

NT TROPOPAUSE

NT TROPOSPHERE

NT TURBOPAUSE

NT UPPER ATMOSPHERE

NT UPPER IONOSPHERE

Advanced sensors for spaceborne measurements of the earth's atmosphere
01 p0053 A83-11279

Heavy element fission products on earth --- Russian book
02 p0204 A83-11923

Ionospheric disturbances over Japan due to the 18 May 1980 eruption of Mount St. Helens
02 p0206 A83-12019

Correlations of magnetospheric ion composition with geomagnetic and solar activity
02 p0207 A83-12382

Investigation of meteor ablation in the atmospheres of the earth, Mars, and Venus
03 p0432 A83-13211

Diurnal and seasonal variations in the atmospheric structure parameter /C/n/-squared/ that affect the atmospheric modulation transfer function /MTF/
03 p0364 A83-13978

Atmospheric spectral transmittance and radiance - FASCOD1B
03 p0359 A83-13992

Capabilities and limitations of atmospheric transmission field measurement systems
03 p0359 A83-13995

Available potential energy in the northern hemisphere during the FGGE year
04 p0515 A83-15853

The existence of Hadley convective regimes of atmospheric motion
04 p0519 A83-16367

Spectroscopic detection of acetylene and ethane in the terrestrial atmosphere using ground-based solar IR observations
04 p0508 A83-16447

Atmospheric diffusion of a passive contaminant in a spatially homogeneous flow with transverse velocity [AIAA PAPER 83-0272]
05 p0633 A83-16623

Radiation enhancement by nonequilibrium in earth's atmosphere --- for aero-assisted OTV [AIAA PAPER 83-0410]
05 p0607 A83-16698

Optical refraction in the earth's atmosphere /Horizontal paths/ --- Russian book
05 p0660 A83-17127

The isotopic composition of primordial xenon
05 p0706 A83-17461

Thermal and suprathreshold protons and alpha particles in the earth's plasma sheet
06 p0782 A83-18289

Radio occultation of the atmosphere by means of sources of artificial and natural origin
06 p0787 A83-19352

Satellite methods for detecting and investigating the aerosols in the earth's atmosphere
06 p0787 A83-19372

A large-scale explosion in an inhomogeneous terrestrial atmosphere with allowance for spectral radiation --- simulating Tunguska event
06 p0849 A83-19435

Radiation budget parameters at the top of the earth's atmosphere derived from Meteosat data
07 p0962 A83-20809

Experimental and mathematical modeling of the conditions of the seeing of objects through a turbid-medium layer --- earth atmosphere
07 p0963 A83-20893

- Short-period geomagnetic, atmospheric and earth-rotation variations 09 p1306 A83-24455
- The rotation of small particles from space in the earth's atmosphere 10 p1449 A83-26909
- Interaction between large cosmic bodies and atmosphere 11 p1600 A83-27346
- On the origin of oscillations in a solar diameter observed through the earth's atmosphere - A terrestrial atmospheric or a solar phenomenon 11 p1688 A83-27637
- Effects of planetary wave propagation and finite depth on the predictability of atmospheres 13 p1892 A83-31033
- The generation of Rossby waves during the disintegration of internal gravity waves 13 p1880 A83-31394
- Neutron high-energy spectra at seven different depths in the atmosphere from 0 to 40 mbar near the geomagnetic equator 15 p2196 A83-33948
- The upper atmospheres of the earth and planets; Proceedings of the Topical Meeting, Ottawa, Canada, May 16-June 2, 1982 16 p2434 A83-35351
- Comparative neutral composition instrumentation and new results --- for measurement of planetary atmospheres 16 p2317 A83-35399
- On the relevance of the MHD approach to study the Kelvin-Helmholtz instability of the terrestrial magnetopause 16 p2376 A83-35785
- Infrared limb-darkening effects for the earth-atmosphere system [AIAA PAPER 83-0161] 16 p2377 A83-36045
- Modeling planetary magnetospheres 17 p2542 A83-38299
- Planetary lightning - Earth, Jupiter, and Venus 18 p2780 A83-40328
- Increase and seasonal cycles of nitrous oxide in the earth's atmosphere 18 p2720 A83-40644
- Terrestrial versus Jovian VLF chorus - A comparative study 20 p3078 A83-42409
- Heat transfer during ionized-gas flow past bodies 20 p2929 A83-42880
- Radiative-convective heat transfer and heat shielding for spacecraft descending to the earth's surface and to the surfaces of other solar-system planets 20 p2945 A83-42881
- Origin of the moon - Capture by gas drag of the earth's primordial atmosphere 20 p3079 A83-43590
- CRC handbook of atmospheres. Volumes 1 & 2 22 p3307 A83-45876
- Analytical yield spectrum approach to electron energy degradation in earth's atmosphere 22 p3327 A83-46055
- Oxygen and ozone in the early earth's atmosphere 22 p3332 A83-46698
- BAS - The project of an earth-atmosphere-spectrophotometer for basic research [IAF PAPER 83-113] 23 p3453 A83-47274
- The young sun and the atmosphere and photochemistry of the early earth 23 p3483 A83-48075
- Interaction of the solar wind with the dayside magnetosphere 23 p3485 A83-48553
- The turbulent electrode effect as influenced by interfacial ion transfer --- between atmosphere and aerodynamically rough earth surface 24 p3607 A83-49334
- Glutathione reductase in evolution 24 p3617 A83-49620
- EARTH AXIS**
- The choice of axis for the ephemeris nutation of the earth 17 p2546 A83-38846
- Directions of axes of the earth's ellipsoid of inertia derived from satellite orbit dynamics 19 p2860 A83-41317
- EARTH CORE**
- Could the earth's core and moon have formed at the same time 03 p0432 A83-13548
- A model for the formation of the earth's core 07 p0965 A83-21284
- Energy estimates for latent-heat driven convection in the earth's core 12 p1753 A83-29238
- Electrical conductivity deep inside the earth --- Russian book 12 p1753 A83-29335
- Geomagnetism of earth's core 17 p2542 A83-38309
- The earth's core 20 p3020 A83-42816
- The component of 29.8 years in polar motion and Delta I.o.d. and oscillation of earth's inner core --- Length Of Day 20 p3010 A83-43172
- A moving source of the secular variations in the geomagnetic field at the boundary between the core and the mantle 21 p3175 A83-45251
- The structure, density, and homogeneity of the earth's core 22 p3323 A83-45778
- Dynamics of the earth's core and the geodynamo 22 p3323 A83-45780
- On the mechanism of the gravitational differentiation in the inner earth 22 p3324 A83-45792
- The role of oxidation-reduction reactions in the earth's early history 22 p3324 A83-45793
- Terrestrial heat flow history and temperature profiles 22 p3324 A83-45795
- A thermodynamic approach to equations of state and melting at mantle and core pressures 22 p3324 A83-45799
- Possible heterogeneity of the earth's core deduced from PKIKP travel times --- seismic wave phase 24 p3608 A83-50108
- EARTH CRUST**
- Ultrabases of the early stages in the development of the earth's crust 01 p0073 A83-11324
- Variations in the earth's rotation and crustal deformations 02 p0205 A83-11997
- Oscillatory spreading explanation of anomalously old uplifted crust near oceanic transforms 03 p0363 A83-14925
- The law governing the variation of the anomalous gravitational field with the survey altitude 04 p0510 A83-16037
- Deformation, gravity, and potential changes due to volcanic loading of the crust 07 p0961 A83-20231
- Siderophile trace elements in the earth's oceanic crust and upper mantle 07 p0965 A83-21285
- Crustal geomagnetic field - Two-dimensional intermediate-wavelength spatial power spectra 09 p1305 A83-24139
- The physical geography of the world's oceans --- Russian book 10 p1452 A83-25598
- Multimode Rayleigh wave attenuation and Q beta in the crust of the Barents Shelf --- shear wave internal friction 12 p1757 A83-29961
- Tectonic zonality in early Precambrian formations in southern Siberia 13 p1880 A83-31340
- The electromagnetic field in a layered earth induced by an arbitrary stationary current distribution 16 p2341 A83-35410
- Space techniques to monitor movements in the earth's crust 16 p2370 A83-35423
- How continents break up 16 p2377 A83-36020
- Investigations of the internal geomagnetic field by means of a global model of the earth's crust 16 p2381 A83-36616
- Fractures of the earth's crust according to space remote sensing data and their connection with mineral resources (using the example of the Urals) 17 p2526 A83-37697
- Induced geomagnetic variation and crustal evolution of the southern peninsula of India 17 p2528 A83-38144
- Geochemical evolution of the crust and mantle 17 p2543 A83-38325
- Petrological evolution of the crust and mantle 17 p2543 A83-38326
- Crustal processes at spreading centers 17 p2543 A83-38327
- Models of crustal deformation 17 p2543 A83-38328
- A dynamical basis for crustal deformation and seismotectonic block movements in central Europe 17 p2546 A83-38697
- Evolution of the oceans and continents 18 p2715 A83-39495
- Geological features of the present-day and ancient oceans 18 p2715 A83-39532
- On a new type of rotation-tectonic lines in the earth's lithosphere 18 p2715 A83-39533
- The Airborne Laser Ranging System - Its capabilities and applications 19 p2848 A83-41560
- The continental crust 20 p3020 A83-42819
- Destabilization of a 650 km chemical boundary layer and its bearing on the evolution of the continental crust 21 p3171 A83-44363
- Deep crustal structure - Implications for continental evolution 22 p3323 A83-45779
- Radiogenic isotopes and crustal evolution 22 p3323 A83-45781
- Geosphere interactions and earth chemistry 22 p3323 A83-45784
- Intraplate stress orientations from Alberta oil-wells 22 p3323 A83-45786
- Mineral deposits as guides to supracrustal evolution 22 p3323 A83-45789
- Combination of leveling and gravity data for detecting real crustal movements 22 p3316 A83-46353
- Orientation information of levelling and gravity measurements in threedimensional regional networks 22 p3317 A83-46355
- International Symposium on Geodetic Networks and Computations, Munich, West Germany, August 31-September 5, 1981, Proceedings. Volume 5 - Network analysis models 22 p3317 A83-46359
- Precise leveling across active faults in California 22 p3329 A83-46362
- Constraints on the structure of the Himalaya from an analysis of gravity anomalies and a flexural model of the lithosphere 23 p3482 A83-47811
- The efficiency of coupled processes in connection with geochemical and biogeological evolution 23 p3485 A83-48508
- EARTH CURRENTS**
- U TELLURIC CURRENTS**
- EARTH ENVIRONMENT**
- Electrons with energies of hundreds of MeV in near-earth space 03 p0438 A83-13208
- The ionizing particle environment near earth --- effects on spacecraft microelectronics [AIAA PAPER 83-0163] 05 p0606 A83-16563
- On the possibility for a fourth test of general relativity in earth's gravitational field 05 p0683 A83-17148
- The propagation of radio waves in the terrestrial environment --- French book 17 p2493 A83-37496
- EARTH FIGURE**
- U GEODESY**
- EARTH HYDROSPHERE**
- Impact induced dehydration of serpentine and the evolution of planetary atmospheres 04 p0564 A83-15374
- The physical geography of the world's oceans --- Russian book 10 p1452 A83-25598
- The chemical composition and climatology of the earth's early atmosphere 13 p1878 A83-31156
- Isotopy of the hydrosphere --- Russian book 23 p3480 A83-47150
- EARTH LIMB**
- Satellite-borne limb scanning UV spectrometer for thermospheric remote sensing 02 p0177 A83-12317
- Earth limb altitude determination for the Solar Mesosphere Explorer [AIAA PAPER 83-0429] 05 p0603 A83-17926
- Earth limb emission analysis of Spectral Infrared Rocket Experiment /SPIRE/ data at 2.7 micrometers 08 p1051 A83-22851
- Ozone densities in the lower mesosphere measured by a limb scanning ultraviolet spectrometer 12 p1750 A83-28902
- Sensitivity of ozone retrievals in limb-viewing experiments to errors in line-width parameters 18 p2664 A83-39183
- Tests of an inversion algorithm for spectrally resolved limb emission 22 p3328 A83-46080
- Microwave atmospheric sounder for earth limb observations from space 22 p3261 A83-46170
- EARTH MANTLE**
- Modes of mantle convection and the removal of heat from the earth's interior 02 p0212 A83-12872
- A kinematic thermal history of the earth's mantle 02 p0212 A83-13101
- Large Prandtl number finite-amplitude thermal convection with Maxwell viscoelasticity --- earth mantle rheological model 03 p0304 A83-14521
- The relationship between the statistical characteristics of the anomalous magnetic field and the upper, magnetically active mantle of the earth 04 p0510 A83-16036
- P/n/ velocity and cooling of the continental lithosphere --- upper mantle compression waves in North America 07 p0961 A83-20227
- Viscosity of the lower mantle as inferred from rotational data 07 p0961 A83-20232
- Phase transformations in the transition zone of the mantle and possible changes in the earth's radius 07 p0961 A83-20273
- Phase transitions and mantle discontinuities 07 p0962 A83-20838
- Siderophile trace elements in the earth's oceanic crust and upper mantle 07 p0965 A83-21285
- The relationship between surface topography, gravity anomalies, and temperature structure of convection 08 p1135 A83-22365
- Primitive helium in diamonds 08 p1136 A83-22687
- Defects and dislocations in the upper mantle /asthenosphere/ and attenuation of shear waves 09 p1301 A83-23674
- Shock temperatures of SiO2 and their geophysical implications 09 p1292 A83-25070
- Present seismic evidence for a boundary layer at the base of the mantle 12 p1757 A83-29962
- Archean diamond-bearing mantle in the expanding-earth model 13 p1873 A83-30020
- Noble gas constraints on the layered structure of the mantle 14 p2051 A83-31922
- Terrestrial inert gases - Isotope tracer studies and clues to primordial components in the mantle 14 p2055 A83-33481
- Redox state of earth's upper mantle from kimberlitic ilmenites 15 p2198 A83-34218
- The Indian Ocean gravity low - Evidence for an isostatically uncompensated depression in the upper mantle 15 p2202 A83-34726

Molecular refraction in the earth's mantle	15	p2203	A83-34749
Phase transformations in the mantle and expansion of the earth	16	p2376	A83-35594
Effect of a Hadean terrestrial magma ocean on crust and mantle evolution	16	p2381	A83-36598
Effects of pressure and temperature on the physical behavior of mantle-relevant olivine, orthopyroxene and garnet. I Compressibility, thermal properties and macroscopic Gruenisen parameters	16	p2383	A83-36975
Electromagnetic induction studies --- of earth lithosphere and asthenosphere	17	p2543	A83-38311
Geochemical evolution of the crust and mantle	17	p2543	A83-38325
Petrological evolution of the crust and mantle	17	p2543	A83-38326
Constraints on evolution of earth's mantle from rare gas systematics	17	p2545	A83-38598
Dynamic effects from mantle phase transitions on true polar wander during ice ages	17	p2546	A83-38613
Solidus and liquidus temperatures and mineralogies for anhydrous garnet-ilmenite to 15 GPa	17	p2546	A83-38698
Dynamic compression of diopside and salite to 200 GPa --- in earth's mantle	19	p2864	A83-41109
Viscosity and conductivity of the lower mantle - An experimental study on a MgSiO ₃ perovskite analogue, KZnF ₃	19	p2865	A83-41175
On the thermal state of the earth's mantle	20	p3017	A83-42373
The earth's mantle	20	p3020	A83-42817
Constraint on deep mantle viscosity from Lagesos acceleration data	20	p3028	A83-43557
Destabilization of a 650 km chemical boundary layer and its bearing on the evolution of the continental crust	21	p3171	A83-44363
A moving source of the secular variations in the geomagnetic field at the boundary between the core and the mantle	21	p3175	A83-45251
Thermal conductivity of minerals at high pressure - The effect of phase transitions	22	p3322	A83-45741
Magnetometer arrays and geodynamics	22	p3323	A83-45785
The role of oxidation-reduction reactions in the earth's early history	22	p3324	A83-45793
A two-layer convective mantle with an internal boundary layer	22	p3324	A83-45794
Terrestrial heat flow history and temperature profiles	22	p3324	A83-45795
Surface plates and thermal plumes - Separate scales of the mantle convective circulation	22	p3324	A83-45796
Electrical conduction in mantle materials	22	p3324	A83-45798
A thermodynamic approach to equations of state and melting at mantle and core pressures	22	p3324	A83-45799
Cooling of the earth - A constraint on paleotectonic hypotheses	22	p3325	A83-45800
A remark on viscosity and convection in the mantle	22	p3325	A83-45801
Upper mantle anisotropy and the oceanic lithosphere	22	p3333	A83-46878
Reflection properties of phase transition and compositional change models of the 670-km discontinuity --- in earth mantle	23	p3481	A83-47810
The minimum mantle viscosity of an accreting earth	23	p3529	A83-47856
Rare gases from the undepleted mantle?	23	p3483	A83-48080
Phase relations in the MgO-SiO ₂ system under the P-T parameters of the mantle's transition region	24	p3604	A83-48951
Mantle plume noble gas component in glassy basalts from Reykjanes Ridge	24	p3608	A83-50111
EARTH MOTION			
Data on time and polar motion - Immediate accessibility	01	p0111	A83-10131
Excitation of the earth's eigenvibrations by gravitational radiation from astrophysical sources	19	p2915	A83-41164
The component of 29.8 years in polar motion and Delta I.o.d. and oscillation of earth's inner core --- Length Of Day	20	p3010	A83-43172
EARTH MOVEMENTS			
NT EARTHQUAKES			
NT LANDSLIDES			
The expanding and pulsating earth	01	p0071	A83-10378
The tides of the planet earth /2nd edition/ --- Book	09	p1307	A83-24948
The driving mechanism of plate tectonics - Relation to age of the lithosphere at trenches	12	p1748	A83-28910

Fragmentation and assembly of the continents, mid-carboniferous to present	12	p1753	A83-29247
On the size distribution of solid jointings --- in rocks formed by geological fracture processes	13	p1873	A83-30005
Space techniques to monitor movements in the earth's crust	16	p2370	A83-35423
Toward a mathematical theory of paleotectonic analysis	18	p2715	A83-39488
International Symposium on Geodetic Networks and Computations, Munich, West Germany, August 31-September 5, 1981, Proceedings. Volume 5 - Network analysis models	22	p3317	A83-46359
Precise leveling across active faults in California	22	p3329	A83-46362
Deformation of the Australian plate - Preliminary findings from laser ranging to the LAGEOS satellite	22	p3317	A83-46363
Information from space and the prediction of exogenous processes --- in tectonics	23	p3483	A83-48106
The use of space photographs for analyzing recent tectonic movements /using the Amu Darya as an example/	23	p3483	A83-48108
Reconstruction of the strike-slip faults of the Adycha-Taryn region	23	p3483	A83-48110
EARTH OBSERVATIONS (FROM SPACE)			
NT PHOTOCONNAISSANCE			
NT SATELLITE OBSERVATION			
NT SPOT (FRENCH SATELLITE)			
NOAA/NESS satellite snowmapping techniques	01	p0061	A83-10012
Passive microwave remote sensing for meteorology	01	p0073	A83-10015
Earth observation - Evolution of requirements and systems	01	p0066	A83-10429
The GDTA - Remote sensing at the service of users	02	p0198	A83-11867
ATLAS C - A cartographic free-flyer system --- satellite-borne metric camera for photomapping	02	p0139	A83-11929
[AAS 82-115]	02	p0139	A83-11929
Modifications of SL-1 microwave equipment for reflights on Shuttle	02	p0142	A83-11931
[AAS 82-124]	02	p0142	A83-11931
Delineation of cold-prone areas using nighttime SMS/GOES thermal data Effects of soils and water	02	p0216	A83-12961
Matched and optimal filters for the creation of a local-vertical reference --- for spaceborne infrared scanning	03	p0287	A83-13205
Shuttle imaging radar experiment	03	p0344	A83-13348
Canadian Symposium on Remote Sensing, 7th, Winnipeg, Canada, September 8-11, 1981, Proceedings	03	p0345	A83-14226
Measurements of the characteristic reflectance spectra of surficial deposits	03	p0348	A83-14266
Solar radiation estimation using GOES satellite data	03	p0364	A83-14267
Operational planning of the process of earth survey by satellites	03	p0350	A83-14314
Radar images of the earth from space	03	p0351	A83-14598
Attitude control of a satellite with a rotating solar array	03	p0287	A83-14845
The night sky from Salyut	04	p0514	A83-16370
Multi-anode microchannel arrays - New detectors for imaging and spectroscopy in space	05	p0608	A83-16523
[AIAA PAPER 83-0105]	05	p0608	A83-16523
Flight path design issues for the TOPEX mission --- Ocean Topography Experiment	05	p0599	A83-16581
[AIAA PAPER 83-0197]	05	p0599	A83-16581
Use of the Space Shuttle for remote sensing experimentation during the 1980's	05	p0609	A83-16762
[AIAA PAPER 83-0517]	05	p0609	A83-16762
Global implications of space activities; Proceedings of the Conference, Aspen, CO, August 30-September 4, 1981	05	p0710	A83-17349
Basic principles underlying the application of space images to small-scale geological mapping	07	p0950	A83-19907
Current plate motions based on Doppler satellite observations	07	p0958	A83-20095
Southern Hemisphere western boundary current variability revealed by GEOS 3 altimeter	07	p0971	A83-20545
Classification by thresholding --- analysis of remotely sensed earth observations data	07	p0986	A83-21425
Main advances and needs on the study of geothermal resources in Chile by using remote sensing techniques	08	p1127	A83-21946
Overcoming urban monitoring problems with the new generation satellite sensors	08	p1172	A83-21964
Problems of international cooperation in the area of the remote sensing of the earth	08	p1172	A83-22667

Some scientific objectives of a satellite-borne lightning mapper	08	p1141	A83-22702
Photographs of lightning from the Space Shuttle	08	p1141	A83-22705
Absolute measurement by satellite altimetry of dynamic topography of the Pacific Ocean	08	p1144	A83-23277
Smear compensation for a pushbroom scan --- in satellite observations of earth	09	p1218	A83-23545
Collinear-track altimetry in the Gulf of Mexico from Seasat - Measurements, models, and surface truth	09	p1318	A83-24290
M2 ocean tide at Cobb seamount from Seasat altimeter data	09	p1318	A83-24291
Calculations of atmospheric refraction for spacecraft remote-sensing applications	09	p1306	A83-24448
A practical attempt at correlation of rock units from CCT print out --- Computer Compatible Tapes	09	p1291	A83-24627
Methods for constructing a local-vertical reference and the evaluation of their effectiveness --- in IR satellite scanning of earth	09	p1219	A83-25045
Climate as determined by observations from space	09	p1317	A83-25259
Optimization of the spectral sensitivity of survey systems for the remote sensing of the earth	10	p1444	A83-26813
On the continuous survey of the earth's surface --- with optimized satellite networks	10	p1381	A83-26817
Thematic mapping on the basis of the application of space information	10	p1444	A83-26824
The Earthnet LEDA-2 image catalogue system	11	p1666	A83-27375
An orbiting micro-wave imager	11	p1537	A83-28165
The characterization of atmospheric spread functions affecting satellite remote sensing of the earth's surface	12	p1748	A83-29578
A method for estimating cross radiance	12	p1748	A83-29579
Sea surface temperature measurement from satellites	12	p1761	A83-29683
Validation and accuracy	12	p1761	A83-29683
Issues surrounding the commercialization of civil land remote sensing from space	12	p1783	A83-29915
Instruments and analysis techniques for space physics; Proceedings of the Workshop, Ottawa, Canada, May 16-June 2, 1982	13	p1813	A83-30751
Advances in auroral imaging from space	13	p1814	A83-30768
Digital processing of Spacelab imagery	13	p1846	A83-30769
The efficiency of using space imagery in hydrogeological studies	14	p2034	A83-32493
Identification of snow cover and cloud cover on the basis of the spectral brightness of near infrared radiation measured from space	14	p2058	A83-32495
On the efficiency and basic design parameters of satellites for continuous observations of elemental natural phenomena	14	p2035	A83-32505
Statistical evaluation of the ground coverage by a satellite and of the station visibility	14	p1980	A83-33476
Cities and the environment: Studies from space --- Russian book	15	p2241	A83-34361
Space techniques to monitor movements in the earth's crust	16	p2370	A83-35423
Satellite remote sensing needs and applications in Less Developed Countries	16	p2370	A83-35424
Autonomous earth feature classification - Shuttle and aircraft flight test results	16	p2370	A83-36054
[AIAA PAPER 83-0417]	16	p2370	A83-36054
Space: The high frontier in perspective --- Book	17	p2471	A83-37174
New developments in infra-red sensors for three-axis stabilized satellites	17	p2481	A83-37463
Preliminary analysis of Shuttle multispectral radiometer data for southern Egypt	17	p2528	A83-38142
The NOAA satellites - A largely neglected tool in the land sciences	17	p2529	A83-38154
Correlation between the SIR-A radar survey, the Landsat data, and the IR surveys in the Corinth canal zone	17	p2534	A83-38451
An imaging spectrometric observatory for Spacelab	17	p2482	A83-38577
Sensitivity study of orbital atmospheric density models	17	p2546	A83-38755
Earth survey satellites and cooperative programmes	18	p2706	A83-39843
Evaluation of the influence of illumination conditions on results of the spaceborne spectrophotometry of the earth	18	p2719	A83-40594
Exploration of the nocturnal sky by photography from the Salyut space station	19	p2864	A83-40753
Methodological problems in the development of space systems for the remote sensing of earth resources	20	p3010	A83-42889

- The economic benefits of operational environmental satellites
[AAS PAPER 83-188] 20 p3010 A83-43770
- Multisensor satellites and data systems for earth observations
[AAS PAPER 83-195] 20 p3011 A83-43772
- Remote sensing --- of earth resources
21 p3165 A83-43820
- Signature extension versus retraining for multispectral classification of surface mines in arid regions
21 p3165 A83-43894
- If they are here, where are they? Observational and search considerations --- extraterrestrial artifacts in solar system
21 p3222 A83-44092
- Lightning detection from space
22 p3259 A83-45887
- Manual of remote sensing. Volume 2 - Theory, instruments and techniques / 2nd edition/
22 p3307 A83-45921
- Remote sensing of stratospheric and mesospheric winds by gas correlation electrooptic phase-modulation spectroscopy
22 p3328 A83-46063
- Earth feature classification developments for remote sensing
22 p3308 A83-46116
- United States remote sensing policy - A perspective
22 p3310 A83-46145
- The use of the Space Shuttle for land remote sensing
22 p3259 A83-46146
- Application of remote sensing techniques to study environmental conditions and natural resources in Antarctic Peninsula
22 p3313 A83-46206
- Shuttle Multispectral Infrared Radiometer - Preliminary results from the second flight of Columbia
22 p3261 A83-46220
- The Shuttle Imaging Radar (SIR-A) sensor and experiment
22 p3313 A83-46221
- Comparative analysis of co-registered SIR-A, Seasat and Landsat images
22 p3314 A83-46224
- International Geoscience and Remote Sensing Symposium, Universitaet Muenchen, Munich, West Germany, June 1-4, 1982, Proceedings
22 p3314 A83-46227
- The thematic mapper - An overview --- Landsat-borne earth resources sensor performance
22 p3261 A83-46230
- Synthetic aperture radar imaging from an inclined geosynchronous orbit
22 p3315 A83-46238
- The ocean color experiment (OCE) on the second orbital flight test of the Space Shuttle (OSTA-1)
22 p3344 A83-46242
- Test computations of threedimensional geodetic networks with observables in geometry and gravity space
22 p3317 A83-46357
- Mission 8 completes multiple objectives
22 p3259 A83-46400
- Comparison of winter-nocturnal geostationary satellite infrared-surface temperature with shelter-height temperature in Florida
23 p3474 A83-47221
- Tracking and data relay satellite system (TDRSS) - A worldwide view from space
[IAF PAPER 83-78] 23 p3420 A83-47256
- Research and development of synthetic aperture radar
[IAF PAPER 83-94] 23 p3424 A83-47263
- Method of determining optical atmospheric parameters based on space-imagery earth-surface
[IAF PAPER 83-102] 23 p3480 A83-47265
- Advanced visible and near-infrared radiometer for earth observation
[IAF PAPER 83-107] 23 p3424 A83-47270
- The hot spot effect of a homogeneous vegetative cover
23 p3476 A83-48113
- Information about the environment from spaceborne observations and the national-economic significance and cost effectiveness of this information
24 p3598 A83-49291
- EARTH ORBITING SPACE STATIONS**
U EOSS
- EARTH ORBITS**
NT PERIGEEES
- Optimal sun-alignment techniques of large solar arrays in electric propulsion spacecraft
[AIAA PAPER 82-1898] 02 p0141 A83-12475
- On the history of the lunar orbit
03 p0407 A83-13837
- Power-system simulation for low-orbit spacecraft - The EBLOS computer program
03 p0290 A83-13848
- Evaluation of 15th-order harmonics in the geopotential from analysis of resonant orbits
04 p0509 A83-15451
- Linearized transfer between inclined circular orbits using low-thrust blow down propulsion system
[AIAA PAPER 83-0194] 05 p0602 A83-16579
- A three-dimensional wake model for low earth orbit
[AIAA PAPER 83-0309] 05 p0607 A83-16642

- Configuration design of a closed-loop, pseudogravitational, environmental research facility in low earth orbit
[AIAA PAPER 83-0651] 05 p0607 A83-16817
- Expansion of the coordinates of the elliptical motion of an artificial earth satellite in series of multiples of the eccentric anomaly
05 p0602 A83-17678
- Algorithm for computing the first- and second-order partial derivatives of geopotential on the basis of artificial-earth-satellite coordinates
05 p0664 A83-17680
- Analytical theory of the libration of the moon
08 p1190 A83-23125
- Systems of artificial earth satellites in stable circular diurnal orbits
09 p1212 A83-25027
- An efficient system for transportation to and from earth orbit
11 p1536 A83-27347
- Motion of an earth satellite. II - Nonlinear perturbations
11 p1532 A83-28034
- Formulas free of singularities at zero inclinations and eccentricities for improving the orbits of low earth satellites
11 p1532 A83-28036
- The effect of resonance perturbations from a planet's gravitational field on the motion of a satellite
11 p1532 A83-28041
- Linear perturbations of the coordinates of satellites in ellipsoidal orbits due to the effect of atmospheric drag in the standard gravitational field of the earth
11 p1532 A83-28053
- Man-made debris in low earth orbit - A threat to future space operations
15 p2125 A83-33740
- The motion of a stationary satellite in the neighbourhood of the equilibrium points of a central potential perturbed by the J(22) term
17 p2472 A83-38941
- The optimum selection of an artificial earth satellite orbit in polar motion studies
19 p2810 A83-41551
- A linear solution of the equations of motion of an earth-orbiting satellite based on a Lie-series
20 p2944 A83-43578
- Optimal aeroassisted return from high earth orbit with plane change
[IAF PAPER 83-330] 23 p3417 A83-47344
- Classification of orbits with regard to collision hazard in space
23 p3417 A83-48137
- Orbital rates of earth satellites at resonances to test the accuracy of earth gravity field models
24 p3550 A83-48768
- EARTH PLANETARY STRUCTURE**
Concerning the problem of the relationship between geoid undulations and tectonic structures
04 p0514 A83-16379
- Phase transformations in the transition zone of the mantle and possible changes in the earth's radius
07 p0961 A83-20273
- Phase transitions and mantle discontinuities
07 p0962 A83-20838
- The Manicouagan impact structure - An analysis of its original dimensions and form
07 p0950 A83-21315
- Sm-Nd studies of Archaean metasediments and metavolcanics from West Greenland and their implications for the earth's early history
09 p1304 A83-23886
- The Newfoundland basin - Ocean-continent boundary and Mesozoic seafloor spreading history
12 p1752 A83-29173
- The global stress field in the lithosphere obtained from the satellite gravitational harmonics
12 p1752 A83-29222
- On the stability of gravitating liquid bodies containing small solid cores
13 p1962 A83-31272
- Tectonic zonality in early Precambrian formations in southern Siberia
13 p1880 A83-31340
- The internal structure of the earth and its concentric faults
13 p1880 A83-31348
- Results from the Magsat mission
15 p2195 A83-33773
- Palaeocontinental configurations and geoid anomalies
16 p2376 A83-35997
- On a new type of rotation-tectonic lines in the earth's lithosphere
18 p2715 A83-39533
- A planetary density model and the normal gravitational field of the earth
19 p2866 A83-41475
- The dynamic earth
20 p3020 A83-42815
- The component of 29.8 years in polar motion and Delta I.o.d. and oscillation of earth's inner core --- Length Of Day
20 p3010 A83-43172
- Geological development of the earth during the Precambrian --- Russian book
21 p3174 A83-45035
- Temperature profiles in the earth
22 p3323 A83-45777
- The structure, density, and homogeneity of the earth's core
22 p3323 A83-45778
- Plate tectonic patterns and convection in the Phanerozoic
22 p3324 A83-45791
- On the mechanism of the gravitational differentiation in the inner earth
22 p3324 A83-45792

- A two-layer convective mantle with an internal boundary layer
22 p3324 A83-45794
- Terrestrial heat flow history and temperature profiles
22 p3324 A83-45795
- Surface plates and thermal plumes - Separate scales of the mantle convective circulation
22 p3324 A83-45796
- Reflection properties of phase transition and compositional change models of the 670-km discontinuity --- in earth mantle
23 p3481 A83-47810
- Possible heterogeneity of the earth's core deduced from PKIKP travel times --- seismic wave phase
24 p3608 A83-50108

EARTH RADIATION

U TERRESTRIAL RADIATION

EARTH RADIATION BUDGET EXPERIMENT

- Emission characteristics of earth and cloud surfaces as measured by the ERB scanning channels on the NIMBUS-7 satellite
03 p0370 A83-14647
- Time and space spectra of earth-emitted radiation at large scales
03 p0370 A83-14648
- Calibration of spaceborne thermal detectors
08 p1052 A83-22881
- Experimental evaluation of self-calibrating cavity radiometers for use in earth flux radiation balance measurements from satellites
08 p1052 A83-22887
- Radiometric calibration for the Earth Radiation Budget Experiment instruments
08 p1049 A83-22888
- Accuracy and resolution of Earth Radiation Budget Estimates
16 p2376 A83-35488
- Annual cycle and spatial spectra of earth emitted radiation at large scales
16 p2386 A83-35490
- A radiative transfer model for surface radiation budget studies
18 p2751 A83-39184
- A spacecraft design for Shuttle --- Earth Radiation Budget Experiment
[IAF PAPER 83-347] 23 p3422 A83-47353
- Orbital and cloud cover sampling analyses for multisatellite earth radiation budget experiments
23 p3483 A83-48138
- Satellite observation of the Earth Radiation Budget
24 p3609 A83-48811

EARTH RESOURCES

- NT AQUIFERS
- NT CRUDE OIL
- NT FORESTS
- NT FOSSIL FUELS
- NT GEOTHERMAL RESOURCES
- NT GLACIERS
- NT ICEBERGS
- NT LAND ICE
- NT OIL FIELDS
- NT PEAT
- NT RAIN FORESTS
- NT SPRINGS (WATER)
- NT TAR SANDS
- NT UNDERWATER RESOURCES
- NT WATER RESOURCES
- Advanced operational earth resources satellite systems
[AAS 82-128] 02 p0137 A83-11932
- Electro-optical instrumentation for resources evaluation; Proceedings of the Meeting, Washington, DC, April 21, 22, 1981
02 p0199 A83-12669
- Image enhancement through film recorder response contouring
02 p0199 A83-12685
- The importance of remote sensing for Canada - Past achievements, future needs
03 p0345 A83-14227
- A position-based resource mapping study of the Kananaskis Valley using Landsat
03 p0345 A83-14232
- Ecological land classification in the Yukon
03 p0347 A83-14250
- The accuracy of a component analysis in space studies of natural environments --- for thematic mapping of earth resources and photointerpretation
03 p0350 A83-14304
- Remote sensing in the global monitoring of environment
09 p1284 A83-24527
- Resource inventories of arid and semi-arid lands using Landsat
09 p1284 A83-24534
- Analysis of man-induced and natural resources of an arid region in California
09 p1285 A83-24543
- Agricultural resource assessment in tropical arid Djibouti
09 p1290 A83-24605
- Contrast enhancement applied to Guayule distribution in Mexico for commercial rubber production
09 p1290 A83-24617
- Natural resources investigation in West Kharga Oasis Plain, Western Desert, Egypt using Landsat imagery interpretation
09 p1292 A83-24637
- Classification of Landsat data for hydrologic application, Everglades National Park
12 p1748 A83-29916
- A multiple beam synthetic aperture radar design concept for geoscience applications
15 p2128 A83-33691

Integration and manipulation of remotely sensed and other data in geographic information systems 15 p2185 A83-34821

Cartographic modeling - Procedures for extending the utility of remotely sensed data 15 p2186 A83-34830

A geographic information system for New Mexico 15 p2187 A83-34843

Assessing the user environment for Landsat in developing countries 15 p2187 A83-35277

Photointerpretation for agricultural purposes --- Russian book 16 p2370 A83-36445

Tectonics and metallogenic provinces 17 p2526 A83-38127

Mineral and energy exploration in Yugoslavia - Activity of the IGCP Project 143 Working Group 17 p2527 A83-38129

Application of remote sensing techniques in mineral resources survey - A case study pertaining to Singbhum Shear Zone, Bihar, India 17 p2527 A83-38133

Landsat analysis of the Yangjiantan tungsten district, Hunan Province, People's Republic of China 17 p2528 A83-38141

Synthesis of geophysical data with space-acquired imagery - A review 17 p2540 A83-38147

Techniques for the selection of spectral intervals for multispectral survey of the earth's resources from space 17 p2529 A83-38158

American Congress on Surveying and Mapping and American Society of Photogrammetry Convention; APS Annual Meeting, 48th, Denver, CO, March 14-20, 1982, Technical Papers 17 p2530 A83-38336

Aerial photograph interpretation to update and refine LUNR forest land classifications --- New York State Land Use and Natural Resource Inventory 17 p2530 A83-38338

Land resources inventory assessment by Landsat image processing case study - Kano State, Nigeria (Africa) 17 p2532 A83-38354

The role of aerial photography in multiresource inventories Techniques and tests in applications research 17 p2532 A83-38362

International Society for Photogrammetry and Remote Sensing, International Symposium, Toulouse, France, September 13-17, 1982, Transactions, Volume 2 17 p2532 A83-38434

Establishing satellite data bases in developing countries - A critical view 18 p2706 A83-39839

The relationship between spectrometric and photographic methods for the remote sensing of earth resources 18 p2707 A83-40593

Methodological problems in the development of space systems for the remote sensing of earth resources 20 p3010 A83-42889

The importance of remote sensing from space to the Indian subcontinent 20 p3010 A83-42959

Data from remote sensing in the geographical information system - The construction of territorial data banks 20 p3011 A83-43137

Remote sensing --- of earth resources 21 p3165 A83-43820

Aerial photography and scanning aerial methods in engineering geological investigations --- Russian book 21 p3166 A83-45013

Manual of remote sensing, Volume 2 - Interpretation and applications (2nd edition) 22 p3307 A83-45920

1982 International Geoscience and Remote Sensing Symposium, Munich, West Germany, June 1-4, 1982, Digest, Volumes 1 & 2 22 p3307 A83-46101

Landsat-D, about to be reality 22 p3258 A83-46147

Trends in solid state image sensors for remote sensing 22 p3260 A83-46152

Application possibilities of active microwave systems for remote sensing - A survey of respective DFVLR activities 22 p3311 A83-46175

Application of remote sensing techniques to study environmental conditions and natural resources in Antarctic Peninsula 22 p3313 A83-46206

Remote sensing as a tool for resource development 22 p3313 A83-46214

The thematic mapper - An overview --- Landsat-borne earth resources sensor performance 22 p3261 A83-46230

Studies on Japan's earth resource satellite-1 [IAF PAPER 83-120] 23 p3421 A83-47277

Some results of the Salyut-6 phenological experiment 23 p3476 A83-48514

EARTH RESOURCES INFORMATION SYSTEM

Water resources management and remote sensing 01 p0061 A83-10010

Some technical considerations on the evolution of the IBIS system --- Image Based Information System 15 p2186 A83-34834

EARTH RESOURCES PROGRAM

NT SEASAT PROGRAM

Technical issues in focal plane development for terrestrial resource observations 03 p0326 A83-13735

Radar signatures of terrain - Useful monitors of renewable resources 05 p0657 A83-17248

Earth resources techniques applied to planetary exploration 14 p1984 A83-32036

Earth survey satellites and cooperative programmes 18 p2706 A83-39843

Advanced visible and near-infrared radiometer for earth observation [IAF PAPER 83-107] 23 p3424 A83-47270

Tropical Earth Resources Satellite (TERS) [IAF PAPER 83-121] 23 p3419 A83-47278

EARTH RESOURCES SHUTTLE IMAGING RADAR

Shuttle imaging radar - Research sensor for earth resources observation 01 p0020 A83-10003

Earth resources observation with the Shuttle imaging radar 02 p0179 A83-12676

Shuttle Imaging Radar-A information and data availability 07 p0951 A83-20148

EARTH RESOURCES SURVEY PROGRAM

NT SEASAT PROGRAM

AgRISTARS - Plans and first-year achievements --- Agriculture and Resources Inventory Surveys Through Aerospace Remote Sensing 01 p0065 A83-10095

EARTH RESOURCES TECHNOLOGY SATELLITE B

U LANDSAT 2

EARTH RESOURCES TECHNOLOGY SATELLITE C

U LANDSAT 3

EARTH RESOURCES TECHNOLOGY SATELLITE D

U LANDSAT 4

EARTH RESOURCES TECHNOLOGY SATELLITES

U LANDSAT SATELLITES

EARTH ROTATION

Variations in the earth's rotation and crustal deformations 02 p0205 A83-11997

A comparative spectral analysis of the earth's rotation and the solar activity 03 p0435 A83-14775

Concerning the processing and the accuracy estimation of results of very long baseline interferometry in a single system of coordinates --- for geodesy 04 p0514 A83-16380

From the pendulum to the laser gyroscope 05 p0644 A83-16899

Viscosity of the lower mantle as inferred from rotational data 07 p0961 A83-20232

Geomagnetic westward drift using the correlation coefficient 08 p1138 A83-23258

Short-period geomagnetic, atmospheric and earth-rotation variations 09 p1306 A83-24455

On the theory of the rotational motion of a deformable earth 11 p1674 A83-28105

Comparison of earth rotation as inferred from radio interferometric, laser ranging and astrometric observations 13 p1874 A83-30218

A search for objects near the earth-moon Lagrangian points 13 p1939 A83-31206

Choosing artificial satellites for studies of the earth's rotation on the basis of optical detection and ranging data 14 p2048 A83-31838

The solution for seasonal variations in the earth's rate of rotation 15 p2246 A83-34393

Thermally driven flow in a rotating spherical shell Axisymmetric states 16 p2385 A83-35479

On the dynamic atmospheric response to the Chandler wobble forcing 16 p2386 A83-35484

Atmospheric angular momentum fluctuations, length-of-day changes and polar motion 16 p2376 A83-35638

On the variations of the earth's rotation rate on short time scale during 1973-1976 16 p2376 A83-35687

Variations in atmospheric angular momentum on global and regional scales and the length of day 16 p2381 A83-36157

Ocean tides and periodic variations of the earth's rotation 16 p2382 A83-36619

Polar motion and earth rotation 17 p2525 A83-38305

Regimes of flow in a planet's atmosphere - A numerical study 17 p2547 A83-38463

Nonuniformity of the earth's rotation within a day 17 p2545 A83-38562

Secular variation of earth's gravitational harmonic J2 coefficient from Lageos and nontidal acceleration of earth rotation 17 p2545 A83-38597

The choice of axis for the ephemeris nutation of the earth 17 p2546 A83-38846

The motion of a solid body along the smooth surface of the earth --- with reference to hurricane motion theory 18 p2724 A83-39441

On a new type of rotation-tectonic lines in the earth's lithosphere 18 p2715 A83-39533

The introduction of the IAU 1980 nutation theory in the computation of the Earth Rotation Parameters by the Bureau International de l'Heure 19 p2860 A83-41561

The contributions of the Zentralinstitut fuer Physik der Erde to the MERIT project --- Monitor Earth-Rotation and Intercompare the Techniques of observation and analysis 20 p3022 A83-43132

Investigations on an active satellite system for earth kinematics and positioning 22 p3258 A83-46112

Characteristics of the rhythm of solar, geomagnetic, and atmospheric phenomena and their relation to the earth rotation 23 p3484 A83-48387

EARTH SATELLITES

NT AEROS SATELLITE

NT ANIK 2

NT ANIK 3

NT ARIEL SATELLITES

NT ARIEL 3 SATELLITE

NT ARIEL 5 SATELLITE

NT ASTRONOMICAL NETHERLANDS SATELLITE

NT ATS 1

NT ATS 6

NT BEACON SATELLITES

NT BIOSATELLITES

NT COMMUNICATION SATELLITES

NT COMMUNICATIONS TECHNOLOGY SATELLITE

NT COMSTAR SATELLITES

NT COS-B SATELLITE

NT COSMIC BACKGROUND EXPLORER SATELLITE

NT COSMOS SATELLITES

NT COSMOS 1129 SATELLITE

NT DISCOVERER SATELLITES

NT DYNAMICS EXPLORER SATELLITES

NT DYNAMICS EXPLORER 1 SATELLITE

NT DYNAMICS EXPLORER 2 SATELLITE

NT ENVIRONMENTAL RESEARCH SATELLITES

NT EOSS

NT ERS-1 (ESA SATELLITE)

NT ESA SATELLITES

NT EUROPEAN COMMUNICATIONS SATELLITE

NT EXOSAT SATELLITE

NT EXPLORER 1 SATELLITE

NT EXPLORER 12 SATELLITE

NT EXPLORER 47 SATELLITE

NT EXPLORER 50 SATELLITE

NT EXPLORER 51 SATELLITE

NT EXPLORER 54 SATELLITE

NT EXPLORER 55 SATELLITE

NT FRENCH SATELLITES

NT GEODETIC SATELLITES

NT GEOPHYSICAL SATELLITES

NT GEOS SATELLITES (ESA)

NT GEOS 1 SATELLITE

NT GEOS 2 SATELLITE

NT GEOS 3 SATELLITE

NT GOES SATELLITES

NT GRAVSAT SATELLITE

NT HAWKEYE SATELLITES

NT HEAO 1

NT HEAO 2

NT HEAO 3

NT HELIOS A

NT HELIOS SATELLITES

NT HELIOS 1

NT HELIOS 2

NT HEOS SATELLITES

NT HIPPARCOS SATELLITE

NT INFRARED ASTRONOMY SATELLITE

NT INTELSAT SATELLITES

NT INTERCOSMOS SATELLITES

NT INTERNATIONAL SUN EARTH EXPLORER 1

NT INTERNATIONAL SUN EARTH EXPLORER 2

NT INTERNATIONAL SUN EARTH EXPLORER 3

NT INTERNATIONAL SUN EARTH EXPLORERS

NT IRIS SATELLITES

NT IUE

NT L-SAT

NT LAGEOS (SATELLITE)

NT LANDSAT D PRIME

NT LANDSAT SATELLITES

NT LANDSAT 2

NT LANDSAT 3

NT LANDSAT 4

NT MAGELLAN MISSION

NT MAGSAT SATELLITES

NT MAPSAT

NT MARECS MARITIME SATELLITES

NT MARISAT SATELLITES

NT MARITIME SATELLITES

NT MAROTS (ESA)

NT METEOROLOGICAL SATELLITES

NT METEOSAT SATELLITE

NT MOON

NT MULTISPECTRAL RESOURCE SAMPLER

NT NAVIGATION SATELLITES

NT NAVSTAR SATELLITES
 NT NIMBUS SATELLITES
 NT NIMBUS 4 SATELLITE
 NT NIMBUS 5 SATELLITE
 NT NIMBUS 6 SATELLITE
 NT NIMBUS 7 SATELLITE
 NT NOAA SATELLITES
 NT NOAA 6 SATELLITE
 NT NOVA SATELLITES
 NT OAO 3
 NT OSO-8
 NT OTS (ESA)
 NT POGO
 NT PROGNOZ SATELLITES
 NT RCA SATCOM SATELLITES
 NT RELAY SATELLITES
 NT ROSAT MISSION
 NT SAGE SATELLITE
 NT SARSAT
 NT SAS-2
 NT SCATHA SATELLITE
 NT SEASAT SATELLITES
 NT SEASAT 1
 NT SIRIO SATELLITE
 NT SOLAR POWER SATELLITES
 NT SYMPHONIE SATELLITES
 NT SYNCHRONOUS METEOROLOGICAL SATELLITE
 NT SYNCHRONOUS SATELLITES
 NT SYNCOM SATELLITES
 NT TD SATELLITES
 NT TD-1 SATELLITE
 NT TETHERED SATELLITES
 NT TIROS N SERIES SATELLITES
 NT TIROS SATELLITES
 NT TRANSIT SATELLITES
 NT VENERA SATELLITES
 NT VENERA 8 SATELLITE
 NT VENERA 9 SATELLITE
 NT VENERA 11 SATELLITE
 NT VENERA 12 SATELLITE

The artificial earth satellite motion in an oblate, rotating atmosphere with symmetrical diurnal effect

01 p0017 A83-10269
 A program for satellite-orbit determination - An application to the case of earth-observation satellites [IAF PAPER 82-301] 03 p0283 A83-14400

Flight path design issues for the TOPEX mission --- Ocean Topography Experiment [AIAA PAPER 83-0197] 05 p0599 A83-16581

Expansion of the coordinates of the elliptical motion of an artificial earth satellite in series of multiples of the eccentric anomaly 05 p0602 A83-17678

Algorithm for computing the first- and second-order partial derivatives of geopotential on the basis of artificial-earth-satellite coordinates 05 p0664 A83-17680

Propagation effects on microwave and millimetre-wave earth-satellite links 06 p0745 A83-18703

Photography of orbiting satellites 06 p0723 A83-18966

Comments on 'Rosette constellations of earth satellites' 06 p0721 A83-19045

Maximization of the accuracy of autonomous navigation in the case of the measurement of angles between directions from an artificial earth satellite to a known star and an unspecified ground reference point 09 p1215 A83-25043

Thermal control subsystem for free flying satellites [SAE PAPER 820844] 13 p1812 A83-30936

On the attitude estimation of earth observation satellites 17 p2478 A83-37454

A determination of gravitational perturbations in the intermediate motion of artificial earth satellites 19 p2809 A83-41546

Power series for perturbations in the intermediate motion of artificial earth satellites caused by the tidal deformation of the earth 19 p2809 A83-41547

A determination of the intermediate orbit of artificial earth polar satellites 19 p2810 A83-41549

Series summation under recurrent relations in problems involving the motion of artificial earth satellites 19 p2810 A83-41550

The critical inclination problem with small eccentricity. II Application to earth satellites 20 p2944 A83-43577

Nodal period of a satellite perturbed by the earth's oblateness 21 p3094 A83-43981

EARTH SHAPE

U GEODESY

EARTH SURFACE

An approximate model for backscattering and emission from land and sea 01 p0063 A83-10062

Mean dyadic Green's function for remote sensing of a two layer random medium 01 p0063 A83-10066

On the surface radiation budget 01 p0065 A83-10100

Variations of the refractive index in the atmospheric surface layer 01 p0072 A83-10854

The screen effect of the earth in the TETG - Theory of a screening experiment of a sample body at the equator, using the earth as a screen --- electrothermodynamic theory of gravitation 01 p0127 A83-11044

Error analysis of image representations for sources near to a dissipative earth 01 p0073 A83-11374

The relationship between the cloud amount and the temperature when averaged over a large space 02 p0213 A83-11978

The effect of ordered vertical velocities and of the earth's surface on the trajectories of particles of polluted air in the atmosphere 02 p0205 A83-12000

Beryllium-10 in Australasian tektites - Evidence for a sedimentary precursor 02 p0264 A83-12066

The relative effect of solar altitude on surface temperatures and energy budget components on two contrasting landscapes 03 p0363 A83-13272

Construction and interpretation of a thermal inertia image using airborne data 03 p0348 A83-14260

Measurements of the characteristic reflectance spectra of surficial deposits 03 p0348 A83-14266

Coordinate transformation during the geometric correction of the space scanner imagery of the earth 03 p0350 A83-14313

A simple relation between active and passive microwave remote sensing measurements of earth terrain 03 p0352 A83-14857

A backscatter model for a randomly perturbed periodic surface --- radar imagery of earth soil with row structure 03 p0352 A83-14859

The origin of tektites - settled at last 04 p0558 A83-14953

Comparison between the hot spot and geomagnetic field reference frames 04 p0508 A83-14957

Adsorption and excess fission Xe - Adsorption of Xe on vacuum crushed minerals 04 p0564 A83-15376

Reflected solar radiances from regional scale scenes 05 p0662 A83-17446

The bilateral symmetry of circular impact structures --- of astroblemes 05 p0706 A83-17473

Active and passive microwave remote sensing of earth terrain 06 p0779 A83-18715

Operational considerations on the moon-day project 06 p0720 A83-19148

Anelastic response of the earth to a dip slip earthquake 07 p0957 A83-19869

Cartometric aspects of the use of space scanner images of the earth 07 p0950 A83-19908

Determination of the temperature of the earth's surface on the basis of the angular structure of radiation in atmospheric windows 07 p0958 A83-19913

Evaluation of nonlinear distortions of the optical image of the earth's surface in the horizontally inhomogeneous atmosphere 07 p0951 A83-19914

A global system of spiraling geosutures --- large scale geological structures on earth and Mars 07 p1028 A83-20229

Digital image enhancement of noisy scanner imagery 08 p1091 A83-21911

Effects of increased CO2 concentrations on surface temperature of the early earth 08 p1138 A83-23256

Terrain effect in monostatic, multistatic, and network radar 09 p1244 A83-23412

Optimal signal discrimination and problems of monitoring --- Russian book 09 p1283 A83-23819

Estimates of regional evapotranspiration in South-Eastern France using thermal and albedo data from the heat capacity mapping mission satellite 09 p1291 A83-24631

Inductive coupling between idealized conductors and its significance for the geomagnetic coast effect 10 p1447 A83-25435

Potentialities of electric and magnetic wave tilt measurements --- for airborne survey of earth surface and subsurface propagation features 10 p1449 A83-26040

Structural interpretation of space photographs based on a comparison of photographic images with the relief of the earth's surface 10 p1444 A83-26808

A model for calculating the brightness-field contrast of homogeneous objects 10 p1423 A83-26811

The use of mechanical energy storage in an unconventional, rough terrain vehicle 11 p1667 A83-27309

Wind profiles over complex terrain 12 p1758 A83-29135

Different atmospheric effects in remote sensing of uniform and nonuniform surfaces 12 p1748 A83-29577

Data on total and spectral solar irradiance 13 p1880 A83-31461

Monitoring of the location of the magnetospheric ring current by means of synchronous magnetic-field measurements in geostationary orbit and on the earth's surface 14 p2051 A83-31890

A numerical study of the divergence of spherical harmonic series of the gravity and height anomalies at the earth's surface 14 p2051 A83-31899

Airflow resistivity instrument for in situ measurement on the earth's ground surface 14 p2020 A83-32824

Statistical evaluation of the ground coverage by a satellite and of the station visibility 14 p1980 A83-33476

Asteroid and comet bombardment of the earth 14 p2095 A83-33483

Satellite monitoring of surface temperatures in semi-desert - Differences between anthropogenically impacted terrain and protected natural vegetation 15 p2181 A83-33557

Assessment of modified surface temperatures and solar reflectance using meteorological satellite and aircraft data 15 p2194 A83-33558

Method for the production of color synthesized photographs and photoplans using a photorectifier 17 p2510 A83-37725

The motion of a solid body along the smooth surface of the earth --- with reference to hurricane motion theory 18 p2724 A83-39441

Measurement and analysis of solar radiation data 18 p2719 A83-40521

Causes of the relative stability of the mean temperature of the earth's surface in the geological past 19 p2867 A83-42068

Interpreting electromagnetic anomalies with the method of moments 21 p3175 A83-45252

An evaluation of the contribution of natural and anthropogenic factors to the variability of solar radiation at the surface of the earth 21 p3181 A83-45332

International Symposium on Geodetic Networks and Computations, Munich, West Germany, August 31-September 5, 1981, Proceedings. Volume 7 - Combination of horizontal, vertical and gravity networks 22 p3316 A83-46351

Combination of horizontal, vertical and gravity networks - A review 22 p3316 A83-46352

Three-dimensional adjustment of geodetic networks using gravity field data 22 p3317 A83-46358

The possibility of deducing ionospheric and field-aligned currents from ground magnetic perturbations 22 p3331 A83-46514

Comparison of winter-nocturnal geostationary satellite infrared-surface temperature with shelter-height temperature in Florida 23 p3474 A83-47221

Reconstructing the components of the radiation balance of the earth's surface on the basis of satellite data 23 p3483 A83-48101

An investigation of the possibility of determining the geometrical characteristics of surfaces having large irregularities on the basis of microwave-radiometric measurements 23 p3476 A83-48112

Vertical variations of the albedo of the system including the underlying surface and the atmosphere 24 p3605 A83-49279

Some results of the use of data on the angular anisotropy of surface reflection to calculate the flux of outgoing short-wave radiation --- for earth radiation balance 24 p3605 A83-49282

The turbulent electrode effect as influenced by interfacial ion transfer --- between atmosphere and aerodynamically rough earth surface 24 p3607 A83-49334

EARTH TERMINAL MEASUREMENT SYSTEM

SCPC terminal and signal strength measuring apparatus for 30/20 GHz frequency band 10 p1403 A83-26082

FM-SCPC system and equipments for satellite communication --- Single Channel Per Carrier 10 p1404 A83-26084

MCPC system and terminal equipment for satellite communication --- Multi-Channel Per Carrier 10 p1404 A83-26085

EARTH TERMINALS

120 Mbps TDMA terminal equipment 07 p0903 A83-19658

New TDMA terminal design for domestic satellite applications 07 p0908 A83-19740

A cost effective TDMA terminal for Intelsat/Eutelsat applications 07 p0911 A83-19782

Digital modulation techniques for new earth stations 07 p0914 A83-20848

Acquisition and tracking system for a ground-based laser communications receiver terminal 09 p1245 A83-23594

Small earth stations at 20/30 GHz 10 p1404 A83-26083

Performance evaluation of an integrated access scheme in a satellite communication channel 11 p1557 A83-28137

- 6/4 GHz band small capacity omni-use terminal satellite system 15 p2143 A83-33508
- Speech encoding for 6/4 GHz band small capacity omni-use terminal satellite system 15 p2144 A83-33509
- Switching system for 6/4 GHz band small capacity omni-use terminal satellite system 15 p2144 A83-33510
- Equipment design considerations for Intelsat TDMA traffic terminals 19 p2829 A83-41357
- Feasibility of international transport communications system 19 p2834 A83-41418
- Space telecommunications. III - The ground sector. Satellite telecommunications systems --- French book 21 p3121 A83-45082
- Madley - Growth of a large earth station 23 p3442 A83-47653

EARTH TIDES

- A discussion of world-wide measurements of tidal gravity with respect to oceanic interactions, lithosphere heterogeneities, earth's flattening and inertial forces 07 p0963 A83-20973
- The tides of the planet earth /2nd edition/ --- Book 09 p1307 A83-24948
- Earth's flattening effect on the tidal forcing field 16 p2381 A83-36618
- Power series for perturbations in the intermediate motion of artificial earth satellites caused by the tidal deformation of the earth 19 p2809 A83-41547
- Tidal evolution of the earth-moon system during the resonant excitation of tides in the world ocean 24 p3608 A83-49528
- Radiation tides in the ocean and atmosphere 24 p3608 A83-49545

EARTH-MOON SYSTEM

- The moon and the ecosphere 01 p0129 A83-10704
- Could the earth's core and moon have formed at the same time 03 p0432 A83-13548
- On the history of the lunar orbit 03 p0407 A83-13837
- On the stability of the inner planets, satellites and close binaries 04 p0547 A83-15600
- Relativistic perturbations of the moon in ELP 2000 06 p0817 A83-18084
- The origin of the moon - A reappraisal 06 p0849 A83-19467
- Experimental investigation of the partitioning of phosphorus between metal and silicate phases - Implications for the earth, moon and eucrite parent body 08 p1190 A83-22997
- The fourth test of General Relativity 09 p1357 A83-23855
- Calculation of ephemerides for libration points 09 p1355 A83-25282
- The evolution of the earth-moon system 12 p1788 A83-29296
- A search for objects near the earth-moon Lagrangian points 13 p1939 A83-31206
- Autonomous navigation using lunar beacons [AIAA PAPER 83-0351] 16 p2315 A83-36052
- The earth-moon tidal force function 16 p2426 A83-36783
- Accuracy of the external orientation of a selenodetic coordinate system 16 p2439 A83-36860
- Determination of the orientation angles of a selenodetic coordinate system on the basis of photographic positional observations of the moon 16 p2439 A83-36861
- Kepler and two-body problems in bimetric Machian gravitation 18 p2763 A83-40625
- The lunar ephemeris ELP 2000 20 p3059 A83-42383
- Lunar magnetism, polar displacements and primeval satellites in the earth-moon system 21 p3241 A83-45055
- Compact space power station - Building up scenario --- for solar energy transfer to lunar bases [IAF PAPER 83-429] 23 p3415 A83-47380
- Tidal evolution of the earth-moon system during the resonant excitation of tides in the world ocean 24 p3608 A83-49528

EARTH-MOON TRAJECTORIES

- Lunar utilization --- materials resources and cislunar transportation considerations for space industrialization 22 p3257 A83-45857
- Space transportation 22 p3258 A83-45859

EARTH-VENUS TRAJECTORIES

- Method of the complex postflight ballistic analysis of the descent trajectories of Venera-type descent modules 09 p1212 A83-25032
- Ballistics and navigation of the automatic interplanetary probes Venera-13 and Venera-14 14 p1981 A83-31952
- Analysis of the descent trajectories of the Venera-13 and Venera-14 descent modules in the atmosphere of the planet 14 p1979 A83-31953

EARTHQUAKES

- Overview of Mount St. Helens volcanic eruption 02 p0211 A83-12670
 - Anelastic response of the earth to a dip slip earthquake 07 p0957 A83-19869
 - Vertical movements following a dip-slip earthquake 07 p0958 A83-20094
 - Focal depths and fault plane solutions of earthquakes under the Tibetan plateau 08 p1135 A83-22366
 - A mechanism to explain the generation of earthquake lights 09 p1307 A83-24696
 - The rupture process and asperity distribution of three great earthquakes from long-period diffracted P-waves 12 p1752 A83-29220
 - An integrated study of reservoir-induced seismicity and Landsat imagery at Lake Kariba, Africa 12 p1748 A83-29917
 - An experiment in systematic study of global seismicity Centroid-moment tensor solutions for 201 moderate and large earthquakes of 1981 12 p1757 A83-29960
 - Models of crustal deformation 17 p2543 A83-38328
 - Lunar-solar periodicities of large earthquakes in southern California 18 p2718 A83-39956
 - Age dependence of oceanic intraplate seismicity and implications for lithospheric evolution 21 p3169 A83-43824
 - Deep earthquakes beneath Mount St. Helens - Evidence for magmatic gas transport 22 p3333 A83-46801
- ## EAST GERMANY
- Experiences of the GDR in space sciences and technology 18 p2788 A83-39837
- ## EBERT SPECTROMETERS
- Temperature measurements in the earth's stratosphere using a limb scanning visible light spectrometer --- onboard Solar Mesosphere Explorer 12 p1751 A83-28907
 - Measurements of NO2 in the earth's stratosphere using a limb scanning visible light spectrometer 12 p1751 A83-28908

EBF

- U EXTERNALLY BLOWN FLAPS

EBR-2 REACTOR

- U EXPERIMENTAL BREEDER REACTOR 2

EBULLITION

- U BOILING

ECCENTRIC ORBITS

- Orbital ring systems and Jacob's ladders. I 01 p0016 A83-10702
- The stability of eccentric polar orbits around the moon 01 p0017 A83-11333
- Orbital eccentricity in a logarithmic potential 02 p0249 A83-12924
- Numerical determination of proper inclinations of Hilda-type asteroids 03 p0404 A83-13419
- Statistics of the complete set of bright and faint asteroids 03 p0133 A83-13668
- Self-gravitation in Saturn's rings 03 p0435 A83-14863
- Variation of the mean and median inclinations in the numbered minor planet sample 04 p0546 A83-15104
- The distribution of orbital eccentricities of minor planets 04 p0548 A83-16440
- The air drag perturbation of satellite in an orbit with small-eccentricity 05 p0602 A83-16857
- Expansion of the coordinates of the elliptical motion of an artificial earth satellite in series of multiples of the eccentric anomaly 05 p0602 A83-17678
- Periodic perturbations in close binary systems due to rotational distortion 06 p0821 A83-18885
- The two-body problem in regularized time 08 p1049 A83-22098
- Nature of the Kirkwood gaps in the asteroid belt 08 p1176 A83-23259
- Orbital evolution of the Galilean satellites - Capture into resonance 10 p1492 A83-25510
- The variations in eccentricity and apse precession rate of a narrow ring perturbed by a close satellite 10 p1492 A83-25512
- The effects of sudden mass loss and a random kick velocity produced in a supernova explosion on the dynamics of a binary star of arbitrary orbital eccentricity - Applications to X-ray binaries and to the binary pulsars 10 p1515 A83-26734
- On the double averaged three-body problem 12 p1787 A83-29118
- Hyperion - Collisional disruption of a resonant satellite 16 p2436 A83-35739
- A new method for the analysis of apsidal motions in eclipsing binaries 16 p2424 A83-36544
- Spectroscopic binaries near the north galactic pole. VI - BD 33.2206 deg 18 p2754 A83-39196
- The critical inclination problem with small eccentricity. II Application to earth satellites 20 p2944 A83-43577

ECLIPSING BINARY STARS

- New nonsingular forms of perturbed satellite equations of motion 21 p3095 A83-45469
 - On the first transit of nearly parabolic comets across the inner part of the solar system 24 p3644 A83-49629
 - The gravitational escape/capture of planetary satellites 24 p3646 A83-49891
- ## ECCENTRICITY
- Natural convection heat transfer between eccentric horizontal cylinders [ASME PAPER 82-HT-43] 02 p0172 A83-12796
 - Oscillations of a satellite with compensating devices in an elliptical orbit 03 p0287 A83-13204
 - Numerical simulation of natural convection in concentric and eccentric horizontal cylindrical annuli 03 p0315 A83-13484
 - Oblique instream streamline intersections 17 p2501 A83-37026

ECHOLON FAULTS

- U GEOLOGICAL FAULTS

ECHO SOUNDING

- The use of radar methods of optimum detection for ultrasonic echo monitoring 01 p0049 A83-10370
- A new method for the laser sounding of the atmosphere based on the reception of an echo signal by the laser 05 p0645 A83-17632
- Echosonde - Design and development 06 p0762 A83-18420
- Acoustic remote sensing of the boundary layer 08 p1141 A83-22991
- Some problems of designing the system of time control of the sensitivity of pulse-echo flaw detectors 22 p3303 A83-46324
- The effect of fluorescence decay time on echo-signal kinetics in the case of remote laser sounding of water bodies 23 p3493 A83-48505

ECHO SUPPRESSORS

- An adaptive MTI for weather clutter suppression 06 p0754 A83-19029
- Echo Cancellers - How to improve satellite circuit performance 07 p0914 A83-20846
- Thoughts on the design of a duplex modem with echo extinction 09 p1244 A83-23411
- Polarisation-vector translation in radar systems 11 p1555 A83-27920
- A cascaded echo canceller 19 p2832 A83-41393

ECHOCARDIOGRAPHY

- Indices of hemodynamics in patients with hypertension according to echocardiography data 03 p0381 A83-14345
- The results of focused and projector ultrasonic Doppler cardiovalvulography /a study of patients with pulmonary normotension and hypertension/ 05 p0674 A83-17215
- Echocardiography in assessment of cardiovascular problems of Air Force personnel 09 p1323 A83-24006
- The value of echocardiography in diagnosing diseases of the cardiovascular system 11 p1643 A83-28801
- The condition of the contractile function of the myocardium and the hemodynamics in patients with heart diseases according to echocardiography 11 p1644 A83-28802
- Asymmetrical hypertrophy of the myocardium in patients with hypertension (According to echocardiographic data) 17 p2559 A83-38180

ECHOES

- NT AURORAL ECHOES
- NT CLUTTER
- NT LUNAR ECHOES
- NT RADAR ECHOES
- NT RADIO ECHOES
- NT SIGNAL REFLECTION
- NT VENUS RADAR ECHOES
- Investigation and design of a highly integrable echo cancellation procedure for duplex transmission 04 p0472 A83-16039
- Billiard ball echo model --- atomic recoil model of photo. Raman and grating echoes in gases 11 p1654 A83-27615

ECLIPSES

- NT LUNAR ECLIPSES
- NT SOLAR ECLIPSES
- Analysis of additional absorption components of MgII lines in Algol in terms of a model of gas stream 13 p1955 A83-31668

ECLIPSING BINARY STARS

- NT DWARF NOVAE
- Photoelectric light-curves of the eclipsing binary XY Leonis 01 p0116 A83-10236
- The 1975 eclipse of AZ Cassiopeiae 01 p0116 A83-10238
- A preliminary digital analysis of the spectrum of Beta Lyrae 01 p0121 A83-10334

Absolute dimensions and masses of eclipsing binaries.
 III - CW Canis Majoris 02 p0252 A83-11595
 Evidence for accretion activity and obscured hot component stars in W Serpenteis type binaries
 02 p0256 A83-12130
 A search for magnetic fields in the symbiotic and VV Cephei variables 02 p0246 A83-12131
 AN And - A detached eclipsing binary system with an Am primary member 02 p0260 A83-12526
 A spectroscopic investigation of the eclipsing variable ER Vulpeculae 03 p0412 A83-13303
 The mid-ultraviolet spectrum of Epsilon Aurigae
 03 p0415 A83-13362
 The light curve of the eclipsing binary system CX Cephei and the properties of the Wolf-Rayet component
 03 p0418 A83-13661
 LY Aurigae, NY Cephei, and the mass-luminosity anomaly within O type binaries 03 p0424 A83-14197
 X-ray observations of AM Herculis in its low state
 03 p0424 A83-14204
 A light curve of BX Pegasi 03 p0410 A83-14722
 A study of ultraviolet spectra of Zeta Aur/VV Cep systems. I - Resonance line formation
 03 p0430 A83-14800
 SS 433 - New results 03 p0431 A83-14929
 Properties of Wolf-Rayet stars in eclipsing binary systems 04 p0548 A83-14978
 A photometric study of the eclipsing binary V 889 Aql - An example of relativistic apsidal motion
 04 p0546 A83-15039
 Secondaries of eclipsing binaries. IV - The triple system Lambda Tauri 04 p0554 A83-15630
 Photoelectric photometry of Z Herculis
 04 p0547 A83-15955
 Theory of the light curves of eclipsing systems with oscillating components. I 04 p0556 A83-15963
 The light curve variations in AR Lacertae
 04 p0547 A83-15970
 Photoelectric observations of the eclipsing binary U Pegasi 04 p0548 A83-15973
 A photometric study of the short-period eclipsing binary BW Eridani 05 p0695 A83-17817
 A new light curve analysis of the eclipsing binary SX Aur 05 p0703 A83-17857
 The eclipsing binary CV Serpenteis - U, B, V, R photometry and properties of the Wolf-Rayet component
 06 p0831 A83-18800
 Theory of the light curves of eclipsing systems with oscillating components. II 06 p0834 A83-18884
 IUE observations of certain short period RS CVn-like stars 06 p0834 A83-18890
 AF Geminorum - An eclipsing triple star
 06 p0821 A83-19059
 Spectrographic material for RS Canum Venaticorum and Algol binaries 06 p0836 A83-19061
 Detection of the secondary star in the eclipsing cataclysmic variable AC Cancr
 06 p0821 A83-19063
 Notes on ten Southern Hemisphere eclipsing binaries
 06 p0821 A83-19069
 Photoelectric observations of CN Andromedae
 06 p0821 A83-19072
 On the convergent solution in Kopal's iterative method of solving eclipsing binary orbits
 06 p0822 A83-19164
 Photographic photometry of the eclipsing binary AD Bootes 06 p0822 A83-19173
 Four-color photometry of RZ Ophiuchi and its accretion disk
 06 p0841 A83-19288
 HD 207739 - A strange composite star
 06 p0823 A83-19301
 WY Sagittae/Nova 1783/ - Spectroscopic confirmation of Weaver's candidate and discovery of deep eclipses
 06 p0824 A83-19498
 The distance, space motions, and revised absolute parameters of R Canis Majoris 07 p1004 A83-19866
 Photoelectric photometry of the eclipsing binary NN Cephei 07 p1006 A83-20561
 Seasonal light curves of TY UMa - Observations and solutions
 07 p1006 A83-20568
 A multicolour photometric analysis of the eclipsing binary VV Ori 07 p1006 A83-20569
 HD 191765 - A Wolf-Rayet binary with a low-mass companion
 07 p1014 A83-20657
 Orbital variability and the white dwarf spectrum of BD + 16 516 /V471 Tau/
 07 p1017 A83-20939
 Optical eclipses and precession effects in the X-ray binary system HD 77581=4U 0900-40
 07 p1009 A83-21265
 Spectroscopic and photometric analysis of the WN7 eclipsing binary CQ Cephei 08 p1183 A83-23061
 The eclipsing binary V 836 Cygni - Photometric evidence for an early evolutionary status
 08 p1185 A83-23101
 Eclipsing star systems with extended atmospheres and disk-shaped envelopes
 09 p1358 A83-23903

Spectroscopic observations of eclipsing binaries. V - Accurate mass determination for the B-type systems V539 Arae and Zeta Phoenicis 10 p1491 A83-25360
 EX Hydrae - A coordinated campaign of photoelectric photometry from four observatories
 10 p1499 A83-25371
 Short-period components in the relativistic radial velocities of SS 433 equals V 1343 Aql
 10 p1501 A83-25498
 IUE studies of the Wolf-Rayet binaries HD 186943 and HD 211853 during eclipse 10 p1492 A83-25586
 Determination of parameters of W UMa systems. IV - BV Dra, BW Dra, EM Lac, SW Lac
 10 p1493 A83-25656
 Binary stars - Remarks on the determination of stellar masses
 10 p1495 A83-25855
 International Ultraviolet Explorer observations of the peculiar variable spectrum of the eclipsing binary R Arae
 10 p1497 A83-26383
 High-energy X-ray observations of Vela X-1
 10 p1497 A83-26388
 A two-component X-ray spectrum from SMC X-1
 10 p1510 A83-26390
 Time-resolved spectrophotometry of the nova-like variable RW Trianguli
 10 p1514 A83-26726
 The period distribution of eclipsing binary systems
 11 p1677 A83-27683
 VBLUW photometry of the high-latitude, eclipsing system BL Tel
 11 p1678 A83-27691
 V388 Cygni - A binary system in the rapid phase of mass exchange
 11 p1681 A83-28272
 Light curves of four southern bright hitherto unknown eclipsing binaries
 12 p1784 A83-28860
 Infrared photometry of the RS CVn binaries. I - TY Pyxidis
 12 p1785 A83-28885
 U, B, V light curves of CO Lacertae
 12 p1792 A83-29051
 A re-analysis of the eclipsing binary system VV Orionis --- for UVB and uvby observations
 12 p1792 A83-29052
 A quest for initial parameters of the semi-detached eclipsing binary Mu(1)Sco
 12 p1793 A83-29078
 Three colour photoelectric observations of the symbiotic eclipsing binary CI Cyg
 12 p1786 A83-29081
 The short-period eclipsing system XY UMa - 1982 UVB light curves and a flare-like event
 12 p1794 A83-29182
 A UVB photoelectric investigation of the eclipsing binary system DM Virginis
 12 p1788 A83-29183
 IUE looks at the Algol paradox
 13 p1935 A83-30025
 Changing depth of minima of SV Cen
 13 p1945 A83-30376
 Period variations of the eclipsing system DI Pegasi
 13 p1945 A83-30377
 The light variation of the eclipsing variable UX Eridani
 13 p1945 A83-30378
 Changes in the period of the eclipsing system AH Virginis
 13 p1945 A83-30379
 The CQ Cephei system - U, B, V, R photometry, period variation, and mass loss by the Wolf-Rayet component
 13 p1940 A83-31261
 Detection of flare like events and their relationship to presumed spot regions on V471 Tau - A solar-stellar connection
 13 p1951 A83-31420
 First observations of stellar coronal structure - The coronae of AR Lacertae
 13 p1951 A83-31421
 The early B-type eclipsing binary FZ Cma (HD 52942)
 - A massive triple system 13 p1941 A83-31566
 The low mass main sequence stars
 13 p1955 A83-31659
 Statistics of binary stars - Eclipse depths
 13 p1959 A83-31739
 An observational study of the influence of close companions on the pulsations of Beta Cephei stars
 13 p1943 A83-31740
 TV Cassiopeiae in the Utrecht photometric system
 14 p2097 A83-33053
 Lightcurve synthesis of the semi-detached binaries LT Her, WX Eri, AW Cam
 14 p2103 A83-33062
 Four-colour photometry of eclipsing binaries. XV B - Light curves of V Puppi
 14 p2098 A83-33064
 Massive eclipsing binary candidates
 14 p2098 A83-33151
 General properties of Algol binaries
 14 p2103 A83-33154
 On the machine computation of the orbits of eclipsing binaries
 14 p2099 A83-33249
 Preliminary report on the IUE spectra of Mu(1) Scorpii
 14 p2108 A83-33265
 Einstein observations of high luminosity X-ray binaries
 15 p2251 A83-33590
 Orbital periods of novae before eruption
 15 p2257 A83-34096
 Orbital period changes in Centaurus X-3
 15 p2258 A83-34105

Chromospheric emission of W Ursae Majoris-type stars and its relation to the structure of their common envelopes
 15 p2258 A83-34106
 ANS spectrophotometry - Delta Pictoris as an upper-main-sequence algol system
 15 p2247 A83-34508
 Computation of the elements of eclipsing binaries from a part of their light curve. I - Spherical model
 15 p2263 A83-34553
 The early-contact system BH Centauri - UVB photometry
 15 p2247 A83-34555
 Light-curve analysis of eclipsing variables - The interpretation of photometric observations
 15 p2264 A83-34570
 High speed photometry of the dwarf nova V2051 Ophiuchi
 15 p2264 A83-34579
 X-ray emission from RS CVn binaries
 15 p2265 A83-34590
 The X-ray absorption spectrum of 4U 1700-37 and its implications for the stellar wind of the companion HD 153919
 15 p2268 A83-34637
 The partial phase of the eclipse of epsilon Aurigae
 15 p2269 A83-34649
 U,B,V photometry of the X-ray binary HD 153919 = 4U 1700-37
 15 p2249 A83-34761
 Characteristics of the Wolf-Rayet star in the eclipsing system CQ Cep
 15 p2271 A83-34764
 MM Herculis - An eclipsing binary of the RS CVn
 15 p2272 A83-34789
 Notes on the associated alpha-functions and related integrals --- for variable eclipsing binary star studies
 15 p2249 A83-34791
 Light curve variation and period changes of VW Cep
 16 p2428 A83-36530
 The geometrical elements of 10 totally-eclipsing systems of the type of W Ursae Majoris
 16 p2424 A83-36531
 A study of the eclipsing binary XX Cas
 16 p2424 A83-36536
 An estimate of the effects of light travel times in the optical jets of SS433
 16 p2428 A83-36537
 A new method for the analysis of apsidal motions in eclipsing binaries
 16 p2424 A83-36544
 Absolute dimensions of eclipsing binaries. I - The early-type detached system QX Carinae
 16 p2430 A83-36645
 The Beta Cephei eclipsing binary system 16 Lacertae
 16 p2432 A83-36682
 Photometric observations of AC Boo
 17 p2587 A83-37286
 Narrow-band photometric periods in SS 433
 17 p2588 A83-37321
 Light curve and pulse profile of the X-ray pulsar Vela X-1
 17 p2599 A83-37355
 Short-period noncontact close binary systems. I - UU Lyncis
 17 p2588 A83-37362
 Polarimetric observations of Polar AN UMa
 17 p2590 A83-37706
 A spectral investigation of the eclipsing binary V822 Aql
 17 p2601 A83-37709
 IUE observations of the perplexing bipolar planetary nebula NGC 2346
 17 p2592 A83-37914
 Stellar images derived from rotation broadening - AW Ursae Majoris
 17 p2605 A83-37919
 Differential photometry of the metallic-line eclipsing binary AN Andromedae
 17 p2592 A83-38052
 Ultraviolet observations of AR Lacertae
 17 p2594 A83-38405
 WBVR photometry of SS 433 - Spectra of the 'normal' star and the accretion disk
 17 p2611 A83-38559
 Temperature distribution in the atmosphere of the Wolf-Rayet component of V444 Cygni, based on infrared data
 17 p2614 A83-38842
 Photoelectric and spectral observations of Vela X-1 during the time of sudden changes in its X-ray pulse period
 18 p2754 A83-38997
 Reflection effect in close binaries. I - Distribution of radiation from a point source
 18 p2765 A83-39203
 Intrinsic polarization in Beta Lyrae and Nova T-Pyxidis due to irradiation of silicate glassy grains
 18 p2775 A83-39745
 A new computer approach to the modeling of close binary stars
 18 p2775 A83-39746
 Extensive photometric study of RT Lacertae
 18 p2759 A83-39751
 A photometric and spectroscopic study of the short-period eclipsing binary BV Eridani
 18 p2775 A83-39757
 Photometric variability of SS 433 in 1979-1981
 18 p2763 A83-40475
 Light curves and elements of AH Virginis
 19 p2910 A83-41054
 YZ Cassiopeiae and the Utrecht photometric system
 19 p2911 A83-41071
 Discovery of eclipses in the X-ray source HD 155638
 19 p2911 A83-41654

The F-type eclipsing binaries ZZ Bootis, CW Eridani, and BK Pegasi	20	p3058	A83-42197
SS Bootis - A totally eclipsing binary of the RS CVn type	20	p3064	A83-42198
A photometric orbit for the eclipsing binary AG Phoenicis	20	p3058	A83-42318
Narrow- and intermediate-band H-alpha and O I 7774 A photometry and reticon spectroscopy of SX Cassiopeiae	20	p3058	A83-42322
Secondaries of eclipsing binaries. V - Ek Cephei	20	p3060	A83-43064
New light curve analyses for the eclipsing binaries u Her and UV Leo	20	p3074	A83-43380
HD 134518 - A main-sequence detached or a semi-detached eclipsing binary?	20	p3075	A83-43395
Apsidal motion in the eclipsing binary AS Cam	20	p3062	A83-43657
The angular momentum of eclipsing binaries	20	p3062	A83-43663
A uvby, beta photometric survey of southern hemisphere	21	p3222	A83-44115
A study of UV spectra of Zeta Aur/UV Cep stars. IV - System parameters and mass-loss of Delta Sge	21	p3228	A83-44416
BD Pavonis - A unique cataclysmic variable	21	p3229	A83-44423
On the orbital periods of the eclipsing binaries CM Lacertae, AB Andromedae and YY Eridani	21	p3224	A83-44650
SW Lacertae - A quadruple system --- W UMA-type eclipsing binary	21	p3225	A83-44869
A study of the period of U Ophiuchi	21	p3225	A83-44871
Electrophotometry of variable stars	21	p3225	A83-44930
A new look at BE Ursae Majoris	21	p3237	A83-45549
RW Tauri as a weak W Serpentis star	21	p3237	A83-45550
An infrared study of the eclipsing dwarf nova U Geminorum	22	p3375	A83-46557
Recent photometry of the central star of NGC 2346	22	p3375	A83-46578
The possible long-period eclipsing binary BM Eri	23	p3520	A83-47462
RS CVn stars - Chromospheric phenomena	23	p3522	A83-47512
Recent photometry of AR Lacertae	23	p3517	A83-47516
Coronal and chromospheric structure in AR Lac. II - Physical characteristics of the atmosphere	23	p3523	A83-47524
Contact binary stars	23	p3523	A83-47525
The evolutionary status of short-period RS CVn and related W UMA eclipsing binaries	23	p3523	A83-47526
The VW Cephei system	23	p3524	A83-47530
A bright spot and a serendipitous stellar flare on the contact-binary VW Cep	23	p3524	A83-47531
The light curve changes of VW Cephei	23	p3527	A83-48063
Gamma-ray line emission from SS433	23	p3527	A83-48073
Four-colour photometry of eclipsing binaries. XVI - Light curves of VV Pyxidis	24	p3642	A83-49319
Four-colour photometry of eclipsing binaries. XVII - Light curves of DM Virginis	24	p3642	A83-49320
The evolution of viscous disks. IV - Stream penetration effects --- dwarf novae accretion disks	24	p3658	A83-49362
Optical and X-ray observations of 2S 0921-630	24	p3660	A83-49381
A nebula around Nova BT Monocerotis	24	p3643	A83-49389
Infrared photometry of the RS CVn binaries. III - JHK light curves of UV Psc	24	p3645	A83-49841
A photometric study of the eclipsing binary V478 Cygni	24	p3645	A83-49844
Photometric observations and elements of the eclipsing binary TT Herculis	24	p3649	A83-50090
The BUSS spectrum of Beta Lyrae --- Balloon-borne Ultraviolet Stellar Spectrograph	24	p3669	A83-50093

ECLIPTIC

Observations of hard X-rays along the ecliptic by the Sneg-2MP instrument	23	p3425	A83-48420
---	----	-------	-----------

ECOLOGICAL SYSTEMS

U ECOLOGY

ECOLOGY

NT COASTAL ECOLOGY

Ecological land classification in the Yukon	03	p0347	A83-14250
Colour Landsat images and mosaics - Basic tools in areal and ecological differentiation in Canada	03	p0348	A83-14265

Mathematical modeling of global biospheric processes --- Russian book	12	p1747	A83-29338
Application of remotely sensed data for the assessment of landscape ecology	22	p3311	A83-46164
Global biology - An interdisciplinary scientific research program at NASA, Ames Research Center [IAF PAPER 83-100]	23	p3474	A83-47264
Ecological monitoring and regulation of the state of the environment	24	p3598	A83-49275

ECONOMETRICS

Cooperative development of application specifications, giving particular attention to the realization of software for specific branches of the economy --- German thesis	11	p1647	A83-28661
--	----	-------	-----------

ECONOMIC ANALYSIS

Developing technologies for synthetic fuels	01	p0068	A83-10658
Economic modeling of fault tolerant flight control systems in commercial applications	01	p0013	A83-11156
Airline economics --- Book	03	p0400	A83-14000
The development of satellite communications and its socio-economic implications	06	p0816	A83-18372
Coal gasification using solar energy	13	p1872	A83-31612
Economic viability of the UCP semicrystalline silicon sheet technology --- Ubiquitous Crystallization Process	14	p2091	A83-32324
Dry process for economic cell manufacturing	14	p2046	A83-32333
The new space transportation begins today	16	p2315	A83-35767
Should we make products on the moon?	16	p2313	A83-35774
The economical utilization of geothermal energy --- German thesis	17	p2535	A83-37505
The space transportation system mixed fleet economics [SAE PAPER 821370]	17	p2586	A83-37962
Economic feasibility of retrofit solar hot water systems	17	p2536	A83-38018
Economic evaluation of a standard product of fiber-reinforced composite material in comparison with steel	17	p2483	A83-38875
Satellite-aided land mobile communications system implementation considerations	19	p2834	A83-41417
The economic benefits of operational environmental satellites [AAS PAPER 83-188]	20	p3010	A83-43770
Design evolution and economics of future communication satellite platforms	21	p3103	A83-45428
An economic assessment of CCIR's five methods for assuring guaranteed access to the orbit-spectrum resource	22	p3368	A83-45819
Systems analysis and economics --- of space industrialization	22	p3257	A83-45860
The economics of space development - The cost of space development [IAF PAPER 83-239]	23	p3514	A83-47320
Economic aspects of advanced coal-fired gas turbine locomotives [ASME PAPER 83-GT-241]	23	p3514	A83-48031

ECONOMIC DEVELOPMENT

Future land remote sensing data and services - A commercial perspective [AAS 82-129]	02	p0244	A83-11933
Space Phase III - The commercial era dawns	13	p1808	A83-31807
Legal framework of economic activity in space --- Book	14	p2094	A83-32951

ECONOMIC FACTORS

Economic and industrial aspects of the conquest of space	01	p0111	A83-10438
Wind power for the electric-utility industry: Policy incentives for fuel conservation --- Book	02	p0201	A83-11896
Air traffic and requirements for future passenger aircraft [DGLR PAPER 82-024]	09	p1195	A83-24151
Economic conditions and key points of BMFT air transport research requirements in the eighties [DGLR PAPER 82-044]	09	p1196	A83-24168
Mathematical programming models for the economic design and assessment of wind energy conversion systems	11	p1611	A83-27870
Why billions can and should be spent on space	13	p1934	A83-30832
Legal framework of economic activity in space --- Book	14	p2094	A83-32951
Aircraft noise and the airport community [AIAA PAPER 83-1580]	14	p2048	A83-33352
Economics of spectrum allocation	22	p3273	A83-45755
Economics of telecommunications space segments [IAF PAPER 83-234]	23	p3514	A83-47317

Push to commercialize space runs into budget cutbacks, boondoggle charges, and fear of high risks	23	p3514	A83-47820
---	----	-------	-----------

ECONOMIC IMPACT

Semiconductors - The key to computational plenty --- technological advances and impacts on society	05	p0624	A83-17247
Role and impact of space research in developing countries; Proceedings of the Workshop, Ottawa, Canada, May 16-June 2, 1982	18	p2787	A83-39825
The evolution of space technology and its economic impact Reflection on the transposition of the European model in the countries of the Third World	18	p2752	A83-39828
Impact of space research and technology on small countries --- developing nations	18	p2705	A83-39831
Basic space sciences in Africa	18	p2788	A83-39835
Impact of space research and technology on small countries	18	p2788	A83-39836

ECOSYSTEMS

The moon and the ecosphere	01	p0129	A83-10704
Use of Landsat data to predict the trophic state of Minnesota lakes	07	p0952	A83-21432
Control problems in Autonomous Life Support Systems	09	p1325	A83-24764
Air pollutants and forest decline	16	p2372	A83-35764
The use of remote sensing in global biosystem studies --- in ecology	19	p2861	A83-42040

ECS

U EUROPEAN COMMUNICATIONS SATELLITE

ECUADOR

Origin of Espanola Island and the age of terrestrial life on the Galapagos Islands	19	p2864	A83-40902
--	----	-------	-----------

EDDIES

U VORTICES

EDDINGTON APPROXIMATION

The Eddington limit and supercritical accretion. II - Time-dependent calculations	07	p1022	A83-21137
Fragmentation of prestellar clouds by molecule formation	14	p2109	A83-33278
Super-Eddington luminosity characteristics of active galactic nuclei	21	p3230	A83-44439

EDDY CURRENTS

Theoretical questions of eddy-current flaw detection with superposed transducers - Rigorous mathematical solution of two-dimensional problems	01	p0057	A83-10365
Two-parameter gap independence in eddy-current thickness gauging on conducting plates, strips, films, and coatings	01	p0057	A83-10368
Calculation of the signal created in a superposed eddy-current transducer by a crack	02	p0188	A83-12158
Interaction of cylindrical eddy-current transducers with a multilayered spherical product	03	p0338	A83-14294
Numerical analysis of two-dimensional fields in the theory of eddy-current flaw detection by superposed transducers	03	p0338	A83-14295
Crack opening displacement as a fracture mechanics parameter in eddy current NDE	04	p0496	A83-15185
A theory of eddy current NDE for cracks in nonmagnetic materials	04	p0490	A83-15187
Analytical methods in eddy current NDE	04	p0490	A83-15188
Impedance changes produced by a crack in a plane surface	04	p0490	A83-15189
System analysis of eddy-current measurements	04	p0491	A83-15190
Multisegment eddy current probe	04	p0481	A83-15191
Crack testing with endoscope and eddy current probe	06	p0770	A83-19125
The ac field around a plane crack in a metal surface when the skin depth is large	07	p0929	A83-20268
Change in impedance of a single-turn coil due to a flaw in a conducting half space	07	p0942	A83-20270
Approximate calculations of two-dimensional models in the theory of eddy-current inspection with superposed transducers	07	p0944	A83-21417
Calculated electromagnetic fields of transfer and superposed eddy-current transducers when spherical conducting bodies with flaws are present	07	p0944	A83-21418
Control of the mechanical properties of alloy D16 sheets by the eddy-current method taking the kinetics of aging into account	07	p0891	A83-21419
Eddy current impedance plane analysis	08	p1114	A83-22410
A method of reducing the effect of the gap in eddy-current measurements of conductivity	13	p1860	A83-30839

- Approximate calculation of three-dimensional models in the theory of eddy current inspection with attached transducers 13 p1860 A83-30840
- Automatic eddy current bolt-hole scanning system 16 p2363 A83-35760
- Algorithm for determining the dimensions of flaws in the theory of eddy-current flaw detection by superposed transducers 20 p3000 A83-43179
- Automatic devices for the electromagnetic inspection of the thickness of the coating on small components 20 p2991 A83-43180
- Nondestructive inspection of the quality of materials and components using multitransducer eddy-current devices 20 p3000 A83-43643
- Flaw detector DVT-24 for the inspection of axial holes in deep drilling 21 p3135 A83-43880
- Examination of the development of fatigue damage in metals by the eddy-current method 22 p3303 A83-46325
- Microwave eddy-current transducers for monitoring metals 22 p3304 A83-46332

EDDY DIFFUSION

U TURBULENT DIFFUSION

EDDY VISCOSITY

- Subgrid scale model for isotropic turbulence [ONERA, TP NO. 1982-80] 03 p0320 A83-14532
- Simple subgrid scale stresses models for homogeneous isotropic turbulence 05 p0638 A83-17315
- Parameters for the simulation of high temperature blown shock layers 07 p0924 A83-19829
- Eddy viscosity in axisymmetric swirling jets 09 p1263 A83-25025
- Stress/strain relations in differential methods for turbulent flows 13 p1841 A83-30634
- Influence of mean divergence, mean vorticity and height-dependent eddy viscosity on thermal instability 16 p2391 A83-36583
- Turbulence modeling methods for the compressible Navier-Stokes equations [AIAA PAPER 83-1693] 17 p2502 A83-37192
- Viscosity renormalization based on direct-interaction closure 18 p2681 A83-39215
- Dissipation of thick accretion disks 18 p2774 A83-39742
- Meridional circulation in rotating stars. VI - The effects of anisotropic eddy viscosity 20 p3068 A83-42457
- Turbulent solutions of the compressible Navier-Stokes equations using a composite velocity procedure 20 p2970 A83-42556
- Viscous dissipation effects on heat transfer from turbulent flow with high Prandtl number fluids 20 p2977 A83-42723
- Fluid turbulence and the renormalization group - A preliminary calculation of the eddy viscosity 24 p3575 A83-48848

EDEMA

- The mechanical properties of the brain in the process of the development of postischemic edema 01 p0079 A83-10526
- The pulmonary circulation and the right ventricular function in experimental models of high-altitude acute edema of the lungs 01 p0080 A83-10543
- Significance of the measurement of colloidal-oncotic and hydrostatic pressures in lung capillaries for the diagnosis of edema of the lungs 05 p0673 A83-17177
- The effect of the pharmacological blocking of the alpha and beta adrenoreceptors on the development of experimental high-altitude acute pulmonary edema 09 p1322 A83-25171
- Pulmonary complications during acute disorders of the cerebral blood circulation 14 p2070 A83-33311
- The ultrastructural bases of pulmonary edema in patients with myocardial infarction 15 p2213 A83-34956

EDGE DISLOCATIONS

- Slip-bands emanating from a crack tip under anti-plane deformation 02 p0190 A83-12046
- TEM observations of dislocation emission at crack tips in aluminium 03 p0298 A83-13679
- The mode of plastic deformation of beta Ti-V alloys 03 p0298 A83-13850
- Damage mechanics approach to the orientations of slip bands and related cracking in polycrystalline metals 05 p0614 A83-17090
- Application of the double slip plane crack model to temperature and strain rate sensitive BCC metals 06 p0733 A83-19146
- Electromigration-induced failure by edge displacement in fine-line aluminum-0.5% copper thin film conductors 07 p0921 A83-20743
- Superplastic deformation of an oxide-dispersion strengthened superalloy 07 p0897 A83-21613
- Slip plane facets in fatigued aluminum alloys 08 p1058 A83-21667
- Fatigue crack initiation after different surface treatments in precipitation hardening alloys 08 p1058 A83-21668

- The influence of dispersoids on fatigue crack propagation in Al-Mg-Si alloys 08 p1058 A83-21669
- The formation of slip bands under the effect of thermal stresses during the growth of profiled semiconductor crystals 11 p1663 A83-28360
- The mechanism of fatigue in metals and alloys during thermal cycling 14 p1993 A83-32386
- A study relating slip steps and substructure produced during creep of an Al-Zn alloy 17 p2486 A83-37298
- The behavior of dislocations and the formation of wall structures observed by in situ high voltage electron microscopy 17 p2489 A83-38378
- The elastic strain energy of dislocation structures in fatigued metals 17 p2490 A83-38382
- Dislocation kinetics and the formation of deformation bands 17 p2522 A83-38383
- A model of high-cycle fatigue-crack initiation at grain boundaries by persistent slip bands 17 p2490 A83-38386
- Steady state vacancy concentration around a plastic crack 20 p3007 A83-43345
- Cross-slip on the first order pyramidal plane (10 -11) of a-type dislocations /1 -210/ in the plastic deformation of alpha-titanium single crystals 21 p3216 A83-44341
- Dislocation wall and cell structures and long-range internal stresses in deformed metal crystals 21 p3113 A83-44492
- A theory for the Bilby-Cottrell mechanism of crack nucleation in metals 21 p3115 A83-45364
- Orientation dependence of creep behavior of single crystal gamma-prime (Ni3Al) 22 p3268 A83-45623
- ## EDGE LOADING
- Calculation of the stresses on the free edges in symmetric composite plates with or without a hole - Comparison with experiment [ONERA, TP NO. 1982-97] 03 p0342 A83-14544
- An investigation of stress intensity factors for plates with equal and unequal parallel edge cracks 03 p0343 A83-14821
- Solution of the dynamic problem of viscoelastic shells 04 p0502 A83-16412
- Theoretical and experimental evaluation of edge stresses under severe edge loads --- for nearly cylindrical rollers 06 p0768 A83-18199
- A novel approach to the solution of a problem concerning contact interaction between a semiinfinite stringer and a half-plane 06 p0778 A83-19601
- Peripheral edge crack around a spherical cavity under uniaxial tension field 07 p0946 A83-20642
- A new method for solving three-dimensional problems of the nonlinear theory of elastic rods 09 p1278 A83-23565
- Deformation of a rod by end moments 09 p1278 A83-23566
- St. Venant formulae for generalized St. Venant problems 09 p1279 A83-24135
- Optimally discretized finite elements for boundary-layer stresses in composite laminates 09 p1281 A83-24671
- Vibration of a plate of arbitrary shape with free and simply supported mixed edges 10 p1439 A83-25824
- Edge effects in composites by moire interferometry 11 p1594 A83-28076
- Saint-Venant's principle in elasticity 14 p2029 A83-32123
- Determination of boundary-layer width from the minimum-energy condition --- for edge damped cylindrical shells 15 p2178 A83-34443
- Calculation of stresses on the free edge in composite plates undergoing mechanical and thermal loading [ONERA, TP NO. 1983-20] 16 p2368 A83-36429
- Analysis of shells of revolution subjected to axisymmetric deformation 17 p2524 A83-38506
- Analysis of symmetrically loaded thin circular plates 20 p3008 A83-43672
- Peculiarities in stress solutions in laminated composites 21 p3105 A83-44047
- Nonlinear vibrations of a clamped rectangular plate with initial deflection and initial edge displacement. II Experiment 21 p3151 A83-44248
- On axial and lateral buckling of end-loaded anisotropic cantilever beams 21 p3152 A83-44464
- ## EDGES
- NT BLUNT LEADING EDGES
- NT LEADING EDGES
- NT SHARP LEADING EDGES
- NT TRAILING EDGES
- Calculation of an electrooptic diffraction deflector with allowance for edge effects 02 p0235 A83-11536
- The singular edge in problems of diffraction by inhomogeneities with a gyrotropic medium 06 p0754 A83-19356
- Noise effects for edge operators 08 p1158 A83-22447

- Detection of edges using range information 12 p1769 A83-28950
- Edge and line detection in multidimensional noisy imagery data 15 p2183 A83-33688
- A comparative study of linear and nonlinear edge finding techniques for Landsat multispectral data 15 p2187 A83-34840
- Detection of moving edges 21 p3190 A83-44269
- Edge detection for synthetic aperture radar and other noisy images 22 p3278 A83-46212
- ## EDITING ROUTINES (COMPUTERS)
- Interactive Doppler editing software 11 p1646 A83-27084

EDUCATION

- NT ASTRONAUT TRAINING
- NT FLIGHT TRAINING
- NT PILOT TRAINING
- NT SPACE FLIGHT TRAINING
- The dynamics of the growth of the results of heavy athletes in connection with psychomotor peculiarities of personality 01 p0085 A83-10522
- An electroencephalographic investigation of the human cerebral cortex during the processing of the solution of visual-motor problems with training 01 p0083 A83-10530
- NASA educational briefs 02 p0244 A83-11819
- Biofeedback as an important mechanism in the success of teaching humans to control the skin-galvanic reaction 07 p0979 A83-20330
- The changes of several parameters of the quality of the activity and the functional condition of an operator during the process of forming control habits in a tracking regime 07 p0979 A83-20337
- Aviation medicine training for aircrew in the 1980's 14 p2067 A83-32463
- Education in aerospace medicine at the German Air Force Institute of Aviation Medicine 14 p2063 A83-32464
- The use of biochemical indicators in a controlled training process for highly-trained biathlon participants 14 p2070 A83-33308
- Navigation, guidance and control curriculum at the Air Force Academy [AAS PAPER 83-021] 21 p3220 A83-44167
- Education and training in remote sensing 22 p3366 A83-46215
- Education and communication satellites - Opportunities for outreach 23 p3513 A83-47336
- [IAF PAPER 83-307]
- A cooperative educational program in aerospace science and technology for the high school and middle school - Model for international implementation [IAF PAPER 83-439] 23 p3513 A83-47381
- Operating model satellite for space education [IAF PAPER 83-440] 23 p3513 A83-47382
- A conceptual design program for educational purposes [AIAA PAPER 83-2473] 23 p3403 A83-48339
- Aeronautics - A coop aerospace education program at University of Sherbrooke, Canada [AIAA PAPER 83-2474] 23 p3513 A83-48340
- Scientific and technical training in the Soviet Union [AIAA PAPER 83-2520] 23 p3513 A83-48362
- Formulation of a helicopter preliminary design course [AIAA PAPER 83-2521] 23 p3404 A83-48363
- Methods for teaching aerospace vehicle design [AIAA PAPER 83-2475] 24 p3637 A83-49582
- ## EDUCATIONAL TELEVISION
- A critical look at space technology and the developing world 18 p2752 A83-39827
- Satellite broadcasting - The best way to meet the needs of television education in China [IAF PAPER 83-308] 23 p3513 A83-47337

EKG (ELECTROENCEPHALOGRAMS)

U ELECTROENCEPHALOGRAPHY

- ## EFFECTIVENESS
- NT COST EFFECTIVENESS
- NT SYSTEM EFFECTIVENESS
- ## EFFECTORS
- U CONTROL EQUIPMENT
- ## EFFERENT NERVOUS SYSTEMS
- A comparative analysis of several behavioral, neurochemical, and vegetropic effects of mebicar and diazepam 03 p0374 A83-13626
- The significance of functional lateralization in the formation of complex motor acts in athletes 04 p0522 A83-15784
- Evolutionary and experimental principles of muscle hygiene 05 p0673 A83-17168
- The role of various cortical regions in visual-motor coordination 07 p0973 A83-20356
- Experimental analysis of motor effects of weightlessness 11 p1642 A83-27789
- Weightlessness hypokinesia - Significance of motor unit studies 11 p1640 A83-27839

- Rhythms in the range of 4.5-12 Hz of the background EEG from the visual and sensorimotor cortex in rats under different patterns of locomotor activity 19 p2876 A83-41565
- EFFICIENCY**
- NT CHARGE EFFICIENCY
- NT COMBUSTION EFFICIENCY
- NT COMPRESSOR EFFICIENCY
- NT ENERGY CONVERSION EFFICIENCY
- NT NOZZLE EFFICIENCY
- NT POWER EFFICIENCY
- NT PROPELLER EFFICIENCY
- NT PROPULSIVE EFFICIENCY
- NT THERMODYNAMIC EFFICIENCY
- NT TRANSMISSION EFFICIENCY
- EFFUSIVES**
- NT LAVA
- EGGS**
- Reversal of early pattern formation in inverted amphibian eggs 11 p1638 A83-27821
- EGYPT**
- Relict drainages, conical hills, and the eolian veneer in southwest Egypt - Applications to Mars 04 p0566 A83-15567
- Sand distribution in the Kharga depression of Egypt - Observations from Landsat images 09 p1289 A83-24590
- An example of the application of a procedure for determining the extent of erosional and depositional features and rock and soil units in the Kharga Oasis Region, Egypt, using remote sensing 09 p1290 A83-24603
- EIGENFUNCTIONS**
- U EIGENVECTORS
- EIGENSTATES**
- U EIGENVECTORS
- EIGENVALUES**
- Asymptotic rates of convergence for the symmetric successive overrelaxation /SSOR/ iterative method by means of an associated eigenvalue problem 01 p0101 A83-10201
- Determination of two dominant eigenvalues 01 p0102 A83-10713
- Upper and lower bounds for the solution to the discrete Lyapunov matrix equation 01 p0102 A83-10964
- A direct projection method for calculating the natural modes of a two-dimensional corrugated waveguide 02 p0166 A83-11687
- Eigenvalue sensitivity of digital filters based on the expanded state model 02 p0229 A83-11792
- Solvability and eigenvalues of a system of Grigolyuk-Chulkov nonlinear equations 02 p0192 A83-12361
- Lanczos eigenvalue algorithm for large structures on a minicomputer 02 p0194 A83-12749
- Continuous temporal eigenvalue spectrum of an Ekman boundary layer 03 p0315 A83-13115
- Eigenvalue problems on infinite intervals 03 p0387 A83-13569
- A note on a Runge-Kutta-Chebyshev method 03 p0388 A83-14511
- An iteration procedure for reducing the expenses of static, elastoplastic and eigenvalue problems in finite element analysis 03 p0389 A83-14697
- Computation of eigenvalues using two-point boundary value problem codes 03 p0389 A83-14712
- New computation method for characteristic modes --- eigenvalue equation solution for perfectly conducting object 04 p0466 A83-15234
- A new theory of rectangular optical waveguides 04 p0535 A83-15794
- Systematic occurrence of repeated eigenvalues in structural optimization 04 p0500 A83-15946
- Closed-loop eigenvalue selection for reduced autopilot sensitivity to radome errors [AIAA PAPER 83-0062] 05 p0592 A83-16494
- An iterative method for solving an eigenvalue problem 05 p0682 A83-17639
- The convergence speed of projection methods in eigenvalue problems 05 p0682 A83-17640
- Rutishauser's modified method for computing the eigenvalues of symmetric matrices 05 p0682 A83-17898
- Optimal design of a structure for system stability for a specified eigenvalue distribution 06 p0771 A83-18202
- An iterative eigenvector technique for optimization analysis 06 p0804 A83-18206
- Application of perturbation method to optimal design of structures 06 p0771 A83-18209
- A general dynamic synthesis for structures with discrete substructures 06 p0773 A83-18391
- Bracketing of the eigenfrequencies of spatial skeletons. I, II 06 p0777 A83-19198

- Application of Trefftz-Fichera's method for improvable bracketing of the natural angular eigenfrequencies of a beam subject to bending vibration 06 p0777 A83-19199
- On the global density waves in self-gravitating flat disks 06 p0843 A83-19482
- Eigensolutions for liners in uniform mean flow ducts 07 p0990 A83-19810
- Drift- and lower-hybrid eigenmodes in a plasma cylinder 07 p0997 A83-20539
- Constrained eigenvalue/eigenvector assignment - Application to flight control systems 07 p0867 A83-21006
- An iterative method for finite dimensional structural optimization problems with repeated eigenvalues 07 p0949 A83-21444
- Numerical solution of multiparameter eigenvalue problems 08 p1159 A83-21863
- Application of a direct procedure for numerical handling of self-adjoint, positive definite eigenvalue problems for linear normal differential equations with piecewise continuous coefficient functions 08 p1159 A83-21864
- Normal and anomalous geomagnetic fields separated by solving the eigenvalue problem 08 p1134 A83-22312
- Design with several eigenvalue constraints by finite elements and linear programming 08 p1122 A83-22411
- Computation of minimum eigenvalue of Toeplitz matrix by Levinson algorithm 08 p1154 A83-22800
- On the inclusion principle for the hierarchical finite element method 08 p1159 A83-22946
- On the existence of branch points in the eigenvalues of the electric field integral equation operator in the complex frequency plane 09 p1253 A83-23787
- Complex eigenvalue bounds in magnetospheric shear flow. I 09 p1359 A83-24127
- Complex eigenvalue bounds in magnetospheric shear flow. II 09 p1359 A83-24128
- A shooting method for the numerical solution of optimal periodic control problems 09 p1327 A83-24707
- An eigenstructure approach to noninteracting control synthesis 09 p1331 A83-24753
- An algorithm for computing singular values of large matrices for use in the analysis of large systems 09 p1335 A83-24816
- On the unsymmetric eigenproblem for the buckling of shells under pressure loading 10 p1440 A83-26434
- D-decomposition in the space of feedback gains for arbitrary pole regions 10 p1465 A83-26526
- Cylindrical eigencurrents --- during electromagnetic scattering by conducting surfaces 10 p1406 A83-26840
- A convenient method to obtain stellar eigenfrequencies 11 p1677 A83-27652
- On the influence of nonlinearities on the eigenfrequencies of five-minute oscillations of the sun 11 p1689 A83-27653
- Bounds for the singular values of a matrix 11 p1649 A83-27997
- Finite element interpolation error bounds with applications to eigenvalue problems 12 p1773 A83-29705
- Close-mode identification performance of the ITD algorithm [AIAA 83-0878] 12 p1774 A83-29829
- Eigenvalue approach to thermoelasticity 12 p1747 A83-29923
- Calculation of critical branching points in two-parameter bifurcation problems 13 p1913 A83-31371
- System matrices of wave-digital filter related by similarity transformations 13 p1838 A83-31781
- Nonlinear eigenvalue problems on infinite intervals 14 p2077 A83-32834
- Observability, eigenvalues, and Kalman filtering 14 p2076 A83-33134
- The calculation of electromagnetic fields by numerical methods 16 p2406 A83-35517
- Splitting of steady multiple eigenvalues may lead to periodic cascading bifurcation 16 p2407 A83-35699
- On the question of using the method of false perturbations in astronomical practice 16 p2427 A83-36862
- Asymptotic unbounded root loci - Formulas and computation 17 p2571 A83-37548
- Diffusion in composite layers with automatic solution of the eigenvalue problem 18 p2684 A83-39848
- Dielectrically loaded corrugated waveguide - Variational analysis of a nonstandard eigenproblem 19 p2838 A83-41084
- Algorithm improvements for optical eigenfunction computers 19 p2893 A83-41095
- Implementation of an improved bisection algorithm in buckling problems 20 p3008 A83-43647

- The determination of the degree of controllability for dynamic systems with repeated eigenvalues 21 p3193 A83-44039
- Subspace iteration for the eigenvalue problems of self-adjoint differential equations and its applications in the vibration analysis of structures 21 p3151 A83-44109
- The spectral matrix, eigenvalues, and principal components in the analysis of multichannel geophysical data 21 p3119 A83-44230
- Method for improving incomplete modal coupling 21 p3152 A83-44545
- Eigenvalues of the Orr-Sommerfeld equation in an unbounded domain 21 p3132 A83-44938
- Polyspheroidal periodic functions 21 p3198 A83-45211
- Matrix method for determining propagation characteristics of optical waveguides 22 p3361 A83-46815
- Application of the quadratic functional to nonconservative problems of elastic stability 23 p3471 A83-48170
- Bimodal solutions in problems of the optimization of eigenvalues --- in structural design and stability analysis 23 p3473 A83-48526
- Transversely anisotropic optical fibers - Variational analysis of a nonstandard eigenproblem 24 p3628 A83-48968
- Boundary methods for calculating the natural frequencies of elastic structures 24 p3594 A83-49454
- EIGENVECTORS**
- Determination of two dominant eigenvalues 01 p0102 A83-10713
- Improved numerical computation of uniform beam characteristic values and characteristic functions 02 p0197 A83-13001
- New computation method for characteristic modes --- eigenvalue equation solution for perfectly conducting object 04 p0466 A83-15234
- An iterative eigenvector technique for optimization analysis 06 p0804 A83-18206
- Constrained eigenvalue/eigenvector assignment - Application to flight control systems 07 p0867 A83-21006
- On the convergence of the finite element approximation of eigenfrequencies and eigenvectors to Maxwell's boundary value problem 08 p1159 A83-22077
- The eigenfunction solution for scattered fields and surface currents of a vertex 09 p1248 A83-23812
- A shooting method for the numerical solution of optimal periodic control problems 09 p1327 A83-24707
- An eigenstructure approach to noninteracting control synthesis 09 p1331 A83-24753
- On the spectral expansion of the electric and magnetic dyadic Green's functions in cylindrical harmonics 10 p1472 A83-26037
- Eigenfilter approaches to adaptive array processing 11 p1554 A83-27904
- Eigenfunctions of an integral operator generated by a logarithmic kernel on two intervals and their application to contact problems 11 p1596 A83-28462
- A recursive algorithm by using eigenvector method for identifying multivariable linear time-invariant systems 17 p2565 A83-37086
- Completeness of derivatives of squared Schroedinger eigenfunctions and explicit solutions of the linearized KdV equation 17 p2572 A83-38464
- Waves in scale-invariant systems 17 p2577 A83-38979
- Eigenfunction analysis of the beam-plasma instability with finite radial dimensions 18 p2749 A83-40515
- Active flutter suppression using eigenspace and linear quadratic design techniques [AIAA PAPER 82-2222] 19 p2803 A83-41702
- An automatic orthonormalization method for solving stiff boundary-value problems 21 p3198 A83-45524
- Deliberations on the improvement of the computational model with measured eigenmagnitudes --- for linear elastomechanic systems 24 p3596 A83-50128
- EIKONAL EQUATION**
- The Eikonal approximation in elastic wave scattering theory 04 p0489 A83-15162
- Elastic scattering of electrons by N₂, O₂, and CO in the energy range 0.1-3 keV 10 p1479 A83-25557
- Application of the eikonal approximation in the theory of transition X-radiation 20 p3046 A83-43530
- EINSTEIN EQUATIONS**
- Certain exact vacuum solutions of the Einstein equations 03 p0390 A83-13529
- Charged relativistic spheres 05 p0683 A83-16901
- Inhomogeneous cosmological models with flat slices generated from the Einstein-de Sitter universe 05 p0702 A83-17852
- On equations of motion for cross term modified gravitational field equations 05 p0703 A83-17860

- Self-similar collision of plane neutrino waves in general relativity 07 p1013 A83-20143
- Perfect fluids in the Einstein-Cartan theory 07 p0990 A83-21065
- Interaction of massless scalar field and charged dust in nonrigid rotation 08 p1181 A83-22744
- Exact relativistic model for a superdense star 08 p1185 A83-23108
- On linear perturbations in generalized Einstein space 09 p1359 A83-24203
- Uniform semiclassical quantization of regular and chaotic classical dynamics on the Henon-Heiles surface 09 p1344 A83-25215
- Approximate constants of motion for classically chaotic vibrational dynamics - Vague tori, semiclassical quantization, and classical intramolecular energy flow 09 p1344 A83-25216
- New solutions of Einstein equations from analytic mappings 10 p1471 A83-25408
- The absorber theory for the Einstein equations in the first approximation 11 p1677 A83-27455
- Space-time ordered electromagnetic radiation outside a massive plane 12 p1774 A83-28874
- Geometrical mass of charged particle in Brans-Dicke theory 12 p1774 A83-28875
- Closed form for Van Stockum interior solution of Einstein's equations 12 p1794 A83-29164
- Chronometrically invariant variations in the Einstein gravitation theory 13 p1944 A83-30099
- Limiting density of matter as a universal law of nature 13 p1947 A83-30798
- Einstein relations for gain-guided semiconductor lasers 13 p1858 A83-31782
- Quantum cosmology and stationary states 14 p2102 A83-33046
- A note on the formation of clusters of galaxies 15 p2256 A83-34083
- An exact viscous fluid FRW cosmology --- Friedmann-Robertson-Walker 15 p2261 A83-34491
- The universal solution of Einstein's equations of general relativity. I - Gravitation 15 p2226 A83-34550
- Solutions of Einstein-Maxwell field equations for a static charged perfect fluid sphere 16 p2407 A83-36538
- Cosmological models with S3 topology 17 p2614 A83-38951
- The black hole formed by electromagnetic radiation 17 p2614 A83-38958
- Black holes in neutrino fields 18 p2767 A83-39529
- Local toroidal black holes that are static and axisymmetric 19 p2916 A83-41292
- Frame dragging in Einstein and Einstein zero mass scalar cosmologies 19 p2916 A83-41307
- Coordinate-invariant conservation laws in Schwarzschild geometry 20 p3075 A83-43389
- Cylindrically symmetric Einstein-Maxwell-massless scalar field equations 21 p3199 A83-44367
- The stability of general relativistic cosmological theory 21 p3231 A83-44475
- On calculation of magnetic-type gravitation and experiments 22 p3354 A83-46751
- Einstein equation solutions related to the Weyl metric through Ehlers method 23 p3503 A83-47601
- The complete integration of the Einstein vacuum and the Maxwell-Einstein equations, of type D 23 p3503 A83-48051
- On a class of non-static perfect fluid spheres in general relativity 23 p3527 A83-48572
- Soliton collision in general relativity 24 p3650 A83-48918
- New solutions to the Einstein equations, allowing for vacuum effects of quantized fields 24 p3651 A83-49064
- Cosmological term in a nonsingular cosmological model of the Einstein-Cartan gravitation theory 24 p3651 A83-49067
- Some exact models for nonspherical collapse. I 24 p3651 A83-49096
- Some exact models for nonspherical collapse. II 24 p3651 A83-49097
- EINSTEIN OBSERVATORY**
U HEAO 2
- EISCAT RADAR SYSTEM (EUROPE)**
VHF parabolic cylinder antenna for incoherent scatter radar research 02 p0168 A83-12636
- First results with Eiscat --- for ionospheric plasma diagnostics 09 p1301 A83-23388
- Measurement of autocorrelation functions in a bi-static incoherent scatter radar 09 p1249 A83-24694
- Eiscat first plasma line experiment 13 p1883 A83-31715
- On the possibility to measure the high altitude light ion concentrations with Eiscat 13 p1883 A83-31716

A first comparison of STARE and EISCAT electron drift velocity measurements --- Scandinavian twin auroral radar experiment and European incoherent scatter facility 17 p2539 A83-37600

EJECTA

- The bilateral symmetry of circular impact structures --- of astroblemes 05 p0706 A83-17473
- Ejecta pulsing of subscale solid propellant rocket motors [AIAA PAPER 83-0578] 05 p0610 A83-17930
- Phobos and Deimos 06 p0823 A83-19469
- Compositional heterogeneity of tephra from the 1980 eruptions of Mount St. Helens 07 p0961 A83-20237
- Clay mineralogy of the Cretaceous-Tertiary boundary clay --- in search for asteroid ejecta 07 p1029 A83-20301
- Geochemical studies of feldspathic fragmental breccias and the nature of North Ray Crater ejecta 07 p1033 A83-21300
- Do oblique impacts produce Martian meteorites 07 p1034 A83-21313
- Crater ejecta scaling laws - Fundamental forms based on dimensional analysis 09 p1366 A83-25074
- The Halley dust model 15 p2273 A83-35015
- Meteorites from Mars? 16 p2437 A83-36571
- Escape of ejecta from cratered solar system satellites 21 p3224 A83-44740
- Ferromagnetic resonance and magnetic properties of ALHA 81005 22 p3386 A83-46869
- Thermoluminescence and nuclear particle tracks in ALHA-81005 Evidence for a brief transit time 22 p3386 A83-46870
- Possible lunar source areas of meteorite ALHA 81005 Geochemical remote sensing information 22 p3386 A83-46871
- Antarctic meteorite ALHA 81005 - A piece from the ancient lunar crust 22 p3386 A83-46872
- Compositional implications regarding the lunar origin of the ALHA 81005 meteorite 22 p3386 A83-46876
- Plasma ion-induced molecular ejection on the Galilean satellites - Energies of ejected molecules 22 p3387 A83-46886
- Asteroids and meteorites - Parent bodies and delivered samples 22 p3388 A83-47088
- Rb-Sr, Sm-Nd, K-Ca, O, and H isotopic study of Cretaceous-Tertiary boundary sediments, Caravaca, Spain Evidence for an oceanic impact site 24 p3672 A83-49399

EJECTION

- NT STELLAR MASS EJECTION**
Calculation of the flow rate characteristic of a jet-throttling hydraulic distributor with allowance for the ejection properties of a tube-plate system 19 p2799 A83-42128

EJECTION INJURIES

- An analysis of spinal injuries after ejections and crash landings in the IAF 02 p0223 A83-12254
- An analysis of the fatality rate data from 'jettison-canopy' and 'through-the-canopy' ejections from automated airborne escape systems 04 p0443 A83-15403
- Preliminary generalized thoughts concerning ejection flail phenomena 04 p0443 A83-15404
- Preliminary overview analyses of U.S. Navy Aircrew Automated Escape Systems /AAES/ in-service usage data 04 p0444 A83-15405
- Preliminary generalized thoughts concerning jettisoned vs through-the-canopy ejection escape systems 04 p0444 A83-15406
- Preliminary analyses of flail, windblast and tumble problems and injuries associated with usage of U.S. Navy Aircrew Automated Escape Systems /AAES/ 04 p0444 A83-15407
- A standardized instrumentation methodology for assessing ejection seat performance 04 p0525 A83-15412
- The United States Navy's injury experience in aircraft mishaps 04 p0445 A83-15411
- Some observations on bail out injuries 08 p1148 A83-22975
- Unusual ejection injury - A case report 09 p1323 A83-24008
- Vertebral lesions after pilot ejection from fighter aircraft 16 p2397 A83-35580
- Hazards of loose harness during flying 23 p3499 A83-48693

EJECTION SEATS

- NT FLYING EJECTION SEATS**
Open seat ejection at high dynamic pressure - A radical approach 04 p0445 A83-15308
- Preliminary overview analyses of U.S. Navy Aircrew Automated Escape Systems /AAES/ in-service usage data 04 p0444 A83-15405
- Investigation of the motion of the center of mass of an occupant under ejection accelerations 04 p0525 A83-15411

A standardized instrumentation methodology for assessing ejection seat performance 04 p0525 A83-15412

- Computerized design of CAD --- Charge Activated Devices 04 p0465 A83-15415
- First stage propulsion for the maximum performance ejection system 04 p0445 A83-15421
- MPES update 1981 --- Navy Maximum Performance Ejection System program 04 p0445 A83-15425
- Easiest ejection seat stability and control analysis capability 04 p0446 A83-15428
- Design and development of Cartridge Actuated Device /CAD/ primer 04 p0464 A83-15433
- Advanced escape system design for future combat aircraft 04 p0446 A83-15436
- Development and testing of a microwave radiometric vertical sensor for application to a vertical seeking aircrew escape system 04 p0447 A83-15437
- The next generation - The Stencil S45 ejection seat development program 04 p0446 A83-15440
- Design considerations for a electrical signal transmission subsystem /STS/ for the maximum performance ejection system /MPES/ 04 p0446 A83-15442
- Assessment of advanced ejection seat concepts /A progress report/ 04 p0446 A83-15444
- Performance assessment of a reclined ejection seat 17 p2462 A83-37879
- Control law design for ejection seats [AIAA PAPER 83-2204] 19 p2797 A83-41688
- The Air Force ejection seat as a vehicle for digital flight control [AIAA PAPER 83-2205] 19 p2798 A83-41689
- EJECTORS**
Investigation of supersonic air ejectors. II - Effects of throat-area-ratio on ejector performance 07 p0863 A83-20285
- Upgrading vortex amplifier performance by matched ejectors 11 p1568 A83-28175
- Entrainment and mixing in thrust augmenting ejectors [AIAA PAPER 83-0172] 16 p2292 A83-36046
- Ejector nozzle test results at simulated flight conditions for an advanced supersonic transport propulsion system [AIAA PAPER 83-1287] 16 p2309 A83-36323
- Thrust augmenting ejectors. I 21 p3089 A83-45586
- A new ejector concept for V/STOL aircraft [AIAA PAPER 83-2514] 23 p3411 A83-48358
- EKMAN LAYER**
The Charney stability problem with a lower Ekman layer 02 p0213 A83-12227
- Slow rotating stratified flow past obstacles of large height 02 p0173 A83-12856
- Continuous temporal eigenvalue spectrum of an Ekman boundary layer 03 p0315 A83-13115
- The structure of the turbulent atmospheric boundary layer 09 p1309 A83-23354
- Hall effects on non-linear Hartmann-Ekman layers 14 p2087 A83-33455
- Bounds on the growth of perturbations to non-parallel steady flow on the barotropic beta plane 18 p2729 A83-40036
- ELASTIC ANISOTROPY**
Anisotropic beam theory and applications 02 p0195 A83-12756
- The asymptotics of the averaged characteristics of periodic elastic media with strongly varying properties 04 p0455 A83-16411
- Averaging of a system of elasticity theory with almost-periodic coefficients 07 p0945 A83-20141
- An anisotropic strip weakened by an array of cracks 07 p0946 A83-20637
- A modulus method of determining the type of rolling texture in sheets of hexagonal metals 08 p1066 A83-22627
- Directional acoustic microscopy for observation of elastic anisotropy 08 p1101 A83-22755
- Estimation of residual stresses in heterogeneous disks 09 p1277 A83-23514
- Medium frequency linear vibrations of anisotropic elastic structures 09 p1278 A83-23680
- The effect of friction on the delamination of heterogeneous materials 13 p1865 A83-30053
- Saint-Venant's principle in elasticity 14 p2029 A83-32123
- Vibrational characteristics of a nonlinear system associated with asymmetry in the elastic response 14 p2029 A83-32157
- The fracture toughness of interlayers in joints with layers of different moduli under static tension 14 p2030 A83-32384
- Asymptotic methods in the elasticity theory for an orthotropic body --- Russian book 15 p2180 A83-34575
- Analysis of elastic anisotropy in CFRP laminate beam 18 p2652 A83-40164

Boundary integral equations applied in the characterization of elastic materials 20 p3006 A83-42995

The structural dependence of the anisotropy of the elastic properties of fiber composites 21 p3107 A83-44850

An elasticity relationship for an anisotropic body whose deformation characteristics depend on the type of stressed state --- for composite materials 21 p3108 A83-45360

Uppermantle anisotropy and the oceanic lithosphere 22 p3333 A83-46878

Correlation function of a stress field in an elastic medium with point defects 23 p3473 A83-48536

Anisotropic creep damage in the framework of continuum damage mechanics [ONERA, TP NO. 1983-90] 24 p3593 A83-49409

The effect of anisotropy and viscosity on wave propagation in multilayer cylinders 24 p3596 A83-49910

Determination of anisotropy during the analysis of the long-term strength under conditions of plane stressed state 24 p3596 A83-49912

ELASTIC BARS

Shear force effect on the static deformations of straight bars 01 p0059 A83-10587

Extension and torsion of elastic bars with initial twist 04 p0498 A83-15684

Stability problems for inelastic solids with defects and imperfections 04 p0500 A83-16099

Numerical analysis of wave processes in a shell-rod system 04 p0502 A83-16405

The discrete interaction of a plate and a compressed and stretched rod 04 p0502 A83-16407

Optimization of the shapes of elastic bodies --- Russian book 05 p0654 A83-17131

A study of the radiation characteristics of a vibrating elastic bar in contact with a plate covering a liquid layer 05 p0654 A83-17222

Upper and lower bounds for the torsional stiffness of a prismatic bar strengthened by a thin shell at its edges 06 p0777 A83-19197

Post-yield deflections of elastic-plastic beams under uniformly increasing loads 08 p1114 A83-21631

Investigation of shock wave structure in elasto-visco-plastic bars using the asymptotic method 08 p1120 A83-21815

Nonlinear micropolar continuum model of a composite reinforced by elements of finite rigidity. I - Equations of motion and constitutive relations 08 p1120 A83-21816

Optimum elastic design of a reinforced beam 08 p1121 A83-21825

A new method for solving three-dimensional problems of the nonlinear theory of elastic rods 09 p1278 A83-23565

Deformation of a rod by end moments 09 p1278 A83-23566

Maximum stiffness beam-columns 09 p1282 A83-25103

Minimax estimation of the torsion of thin-walled rods 10 p1439 A83-25613

Analysis of elastic torsion in a bar with circular holes by a special boundary integral method [ASME PAPER 83-APM-15] 10 p1440 A83-26435

Generation of shock waves in one-dimensional systems by a moving source 11 p1599 A83-28544

A longitudinal impact of a slender viscoelastic bar 13 p1866 A83-30449

Finite extension and torsion of thin elastic strips 15 p2177 A83-34343

Contact problems concerning the discrete interaction of a plate and a rod 15 p2178 A83-34441

A new higher order dynamic theory for thermoelastic bars. I General theory. II - Application to thermoelastic circular and rectangular bars 17 p2521 A83-37726

Resonances in dynamic systems under parametric excitation 20 p3043 A83-42887

Instability of thin walled bars 21 p3152 A83-44540

Torsion of an elastic rod of circular cross section weakened by an arbitrary number of radial cracks emerging at the surface 23 p3473 A83-48502

Formulation of the resolving relationships of the finite element method for elasticity problems. II 24 p3595 A83-49902

ELASTIC BENDING

Derivation of Wells' COD estimation formula and re-calculation of gamma values 02 p0190 A83-12047

Large deformations in a shallow shell that is circular when viewed from above and that has a reinforcing ring 03 p0341 A83-14096

Axisymmetric flexure of circular sandwich plate including transverse shear facings 03 p0342 A83-14508

Concerning a refined theory of plates in the case of finite deflections 04 p0502 A83-16406

Bending of orthotropic beams which are nonlinear in shear and compression 11 p1593 A83-27465

Influence of crack closure on the stress intensity factor for plates subjected to bending - A 3-D finite element analysis 11 p1595 A83-28436

A simple mixed formulation for elastica problems 11 p1600 A83-28724

The second-order asymptotic solution for the shell of zero Gaussian curvature with closed cross sections 12 p1747 A83-29941

On thermal bending of layered composite plates and shells of biomodulus materials 15 p2175 A83-34242

A solution to the bending problem for an elastic-plastic shell 16 p2366 A83-35930

Generalization of the results of calculations of the stressed state of structures with cutouts --- such as wing and fuselage combinations 17 p2518 A83-37268

The dynamic bending load on a satellite launcher due to inclined lift-off 17 p2480 A83-37572

Thick plate flexure --- for lithospheric models of Mars and earth 17 p2540 A83-38055

Nonsymmetric bending of a plate reinforced by a symmetric system of radial ribs 19 p2857 A83-41211

A thermoelastic contact problem concerning the bending of a band with allowance for its deformability in the thickness direction 19 p2859 A83-41572

A three-dimensional nonlinear analysis of cross-ply rectangular composite plates 24 p3593 A83-49439

Formulation of the resolving relationships of the finite element method for elasticity problems. II 24 p3595 A83-49902

ELASTIC BODIES

Instrumentation for the measurement of mobility and mechanical impedance 01 p0057 A83-10588

Energy criteria of the brittle fracture of materials with initial stresses 01 p0059 A83-10676

Wave propagation in a medium with nonuniform initial state deformation 01 p0060 A83-10823

The relationship between the solutions to mixed dynamic problems for a continuous elastic medium and a lattice 02 p0189 A83-11655

On the behaviour of a cracked elastic body with /or without/ friction 02 p0189 A83-11856

Some axially symmetric thermal stress distributions in an elastic solid containing an annular crack 02 p0191 A83-12050

Composites with periodic microstructure 02 p0150 A83-12734

On the concentrated loading of an external elliptical crack 02 p0196 A83-12854

Solution of the axisymmetric problem for an elastic body with a cylindrical crack 03 p0339 A83-13692

Stability and postbuckling analysis of nonlinear structures 04 p0494 A83-15008

Determination of three-dimensional temperature fields and stresses in an infinite body with cracks 04 p0497 A83-15384

Investigation of dynamic characteristics of an elastic wing due to correction of mass and stiffness matrices [AIAA PAPER 83-0653] 05 p0595 A83-16818

The torsion-extension coupling in pretwisted elastic beams 05 p0656 A83-17874

Impact of a body on a mass attached to an elastically restrained beam 06 p0770 A83-18070

Calculation of the lift distribution and aerodynamic derivatives of quasi-static elastic aircraft 06 p0712 A83-18151

Connectedness criterion and the unique optimum of the izo-static trusses 06 p0772 A83-18215

Interactive optimum design system --- for two dimensional elastic structures 06 p0773 A83-18228

Influence of load biaxiality on the fracture load of center cracked sheets 06 p0776 A83-18911

The use of the method of elementary cells for the numerical solution of elasticity problems. I - General principles of the elementary-cell method 06 p0777 A83-19316

Optimization of the Eulerian turn of a nonlinear flexible object --- for spacecraft with appendages 07 p0872 A83-19936

Stationary subsonic motion of a crack in an elastic strip 07 p0944 A83-19944

The aeroelastic behavior of curved helicopter blades in hovering and axial flight 07 p0866 A83-21017

Variational principles of mechanics for variable domains and their use for structural optimization 07 p0947 A83-21089

On the problem of two coplanar cracks inside an infinite isotropic elastic solid 07 p0949 A83-21440

Propagation of damage in elastic and plastic solids 08 p1116 A83-21684

Castigliano's theorem and its limits 08 p1121 A83-21859

Inverse ray tracing in elastic solids with unknown anisotropy 08 p1160 A83-22226

Weak and short waves in inhomogeneous isotropic elastic materials. I 08 p1160 A83-22227

Design with several eigenvale constraints by finite elements and linear programming 08 p1122 A83-22411

Design sensitivity analysis in structural mechanics. III - Effects of shape variation 08 p1122 A83-22412

The use of the unit cell method for the numerical solution of elasticity problems. II - A network model for an elastic body 09 p1277 A83-23507

Medium frequency linear vibrations of anisotropic elastic structures 09 p1278 A83-23680

Thermal stresses in anisotropic noncylindrical beams 09 p1280 A83-24511

On three-dimensional fibrous flaws in unidirectional fibre reinforced elastic composites 09 p1281 A83-24821

The existence of a solution to a class of elasticity problems 09 p1282 A83-25020

On a certain dynamic crack problem in elastic and elastic-plastic media 09 p1282 A83-25104

The frictionless contact of cracked elastic bodies 09 p1283 A83-25108

The theory of elastic ideally plastic systems --- Russian book 09 p1283 A83-25222

A fracture criterion for edge-bonded bimaterial bodies 10 p1439 A83-25878

On the estimation of energy release rates [ASME PAPER 83-APM-11] 10 p1440 A83-26426

A linear theory for pretwisted elastic beams [ASME PAPER 83-APM-9] 10 p1441 A83-26439

Instabilities of a finitely deformed fiber-reinforced elastic material 10 p1441 A83-26440

An effective dispersion theory for layered composites 10 p1441 A83-26441

Steady-state point-source excitation of a laminated composite 10 p1441 A83-26442

Linear analysis by the finite element method of the dynamics of axisymmetric structures subjected to arbitrary loads 10 p1442 A83-26819

An analysis of the transient processes of the interaction between elastic bodies of revolution and a fluid 11 p1596 A83-28456

Cross-sectional distortion of an elastic hollow cylinder subjected to shear deformation - Theory and experiment 12 p1735 A83-29360

Variational methods in elasticity and in elastoplasticity for multilayered structures --- French thesis 12 p1747 A83-29947

Saint-Venant's principle in elasticity 14 p2029 A83-32123

The accuracy of plane strain models for the elastic contact of three-dimensional rough surfaces 14 p2027 A83-32625

Arrest of fast Mode-I fracture in an elastic-viscoplastic transition zone 14 p2031 A83-32657

Diffraction of plane harmonic waves by cracks 15 p2174 A83-34006

Hetenyi's elastic quarter space problem revisited 15 p2174 A83-34143

Bimodal optimization of vibrating shallow arches 15 p2174 A83-34146

Existence of solutions in finite elasticity 15 p2176 A83-34327

Elastic stability, buckling and post-buckling behaviour 15 p2176 A83-34328

A variational approach to finite elasticity 15 p2177 A83-34333

Reflections on the computational approximation of elastic incompressibility 15 p2179 A83-34562

Asymptotic methods in the elasticity theory for an orthotropic body --- Russian book 15 p2180 A83-34575

Modification of the finite element method for solving two-dimensional elastic and plastic contact problems 15 p2180 A83-35036

Investigation of a combined rotor vibratory gyroscope with a common elastic rotor suspension 15 p2166 A83-35263

Two methods for the stress analysis of a rotating disk with cuts 16 p2366 A83-35932

Integro-differential equations of the dynamics of elastic systems in nonstationary flows --- flight vehicle dynamics in turbulent nonseparated flow 16 p2366 A83-35933

On waves of general type propagating at the interface between an elastic half-space and a liquid 16 p2369 A83-36549

Stress concentration coefficient around a three dimensional inclusion in an infinite elastic body 17 p2518 A83-37025

Displacement control of elastic structures - Integral control with a robustness property 17 p2565 A83-37090

Calculation of stresses, strains and displacements in an n-layer elastic-continuous system under the action of two complex loads uniformly distributed on circular areas 17 p2519 A83-37273

- High-frequency nonaxisymmetric vibrations of elastic disks 17 p2521 A83-37574
- Three-dimensional curved crack in an elastic body 18 p2700 A83-39558
- Subsonic motion of the edge of a shear shift with friction along an interface between elastic materials 19 p2858 A83-41214
- Contour invariants of the fracture theory for thermoelastic bodies 19 p2858 A83-41215
- Similarity in the contact problem for elastic bodies 19 p2858 A83-41217
- Integral equations in the theory of elasticity for bodies bounded by piecewise Liapunov surfaces 19 p2858 A83-41219
- The problem of the compression of two elastic bodies in the presence of bonding and slipping segments 19 p2858 A83-41220
- Annular punch on a transversely isotropic layer bonded to a half-space 19 p2859 A83-41540
- Evaluation of the effect of certain factors on the accuracy of acoustoelastic measurements of stresses in solids 19 p2855 A83-41976
- Optimal modification of shape for two-dimensional elastic bodies 20 p3001 A83-42521
- A note on the problem of an annular crack subjected to an arbitrary normal pressure 20 p3004 A83-42975
- Vibrations of an elastic beam with a flexible support 20 p3005 A83-42992
- Brittle fracture near holes --- Russian book 21 p3150 A83-43911
- Design Optimization Codes for Structures - DOCS computer program 21 p3150 A83-43974
- Finite element approximations in transient analysis --- of flexible structures 21 p3150 A83-44024
- The dynamics of an elastic body --- rotary gyroscopes 21 p3199 A83-44629
- A version of a model of a viscoelastic body subjected to large deformations 21 p3154 A83-44719
- Axisymmetric torsion of an elastic half-space with an elastic washer 21 p3154 A83-44720
- Approximate solution of problems concerning the deformation of nearly cylindrical composite bodies 21 p3154 A83-44721
- Antiplane vibration of an elastic layer with a midplane crack 21 p3155 A83-44884
- Interaction of shear waves with a Griffith crack situated in an infinitely long elastic strip 21 p3155 A83-44885
- Elastic moduli of a cracked body 21 p3156 A83-44896
- Critical loading conditions and stress intensity factors for partial or entire closure of a Griffith crack under thermo-mechanical loading 21 p3157 A83-44909
- On the approximate evaluation of interaction of cracks in elastic media 21 p3159 A83-44935
- Ray methods for waves in elastic solids with applications to scattering by cracks --- Book 21 p3160 A83-45139
- A method for estimating the stress intensity factor 21 p3163 A83-45361
- An axisymmetric problem for an elastic medium with a spherical inclusion weakened by an interface crack 23 p3468 A83-47172
- The stability of the stationary motions of a plane body in the field of a central force 23 p3504 A83-48458
- Boundary methods for calculating the natural frequencies of elastic structures 24 p3594 A83-49454
- Mathematical model of a moving system with low-stiffness elastic elements 24 p3624 A83-49670
- ELASTIC BUCKLING**
- A new class of solutions for buckling of a short cylindrical shell in pure bending 02 p0191 A83-12075
- Experimental and theoretical correlations for elastic buckling of axially compressed stringer stiffened cylinders 05 p0655 A83-17720
- Nonaxisymmetric buckling of nonshallow elastic shells of revolution 09 p1281 A83-25011
- Experimental and theoretical correlations for elastic buckling of axially compressed ring stiffened cylinders 12 p1736 A83-29445
- Creep buckling of structures [AIAA 83-0864] 12 p1738 A83-29752
- Finite element analysis of the buckling of variable thickness discs 13 p1867 A83-30845
- Postbuckling analysis of moderately thick elastic circular plates 17 p2520 A83-37393
- Reduced stiffness axial load buckling of cylinders 18 p2700 A83-39559
- Postbuckling behavior of rectangular orthotropic plates with two free side edges 18 p2701 A83-40049
- Experimental and theoretical study of the elastoplastic buckling of cylindrical shells under axial impact 18 p2702 A83-40118
- Generic buckling curves for specially orthotropic rectangular plates 19 p2856 A83-40867
- Postbuckling behavior of a thick plate 19 p2856 A83-40868
- On the post-buckling analysis of thin elastic shells 20 p3005 A83-42991
- Buckling finite element analysis of flat plates with a rectangular hole 21 p3150 A83-44025
- Effective widths of plates loaded uniaxially 21 p3152 A83-44250
- The behaviour of a channel cantilever under combined bending and torsional loads 21 p3153 A83-44623
- The ultimate load sensitivity of lipped channel columns to column axis imperfection 21 p3153 A83-44624
- Review of experimental techniques for thin-walled structures liable to buckling. I - Neutral and unstable buckling 22 p3306 A83-46423
- ELASTIC COLLISIONS**
- U ELASTIC SCATTERING**
- ELASTIC CONSTANTS**
- U ELASTIC PROPERTIES**
- ELASTIC CYLINDERS**
- The vibration of a multilayer cylindrical panel with anisotropic layers at large deflections 06 p0775 A83-18506
- Quasi-static coupled problems of thermoelasticity for cylindrical regions 06 p0775 A83-18805
- Stress intensity factors in a hollow cylinder containing a radial crack 06 p0776 A83-18910
- Characteristics of a wave field in a semifinite elastic cylinder /edge resonance/ 07 p0990 A83-19943
- Magneto-thermo-elastic plane waves in an infinite circular cylinder 08 p1123 A83-22746
- Statistical flow-oscillator modeling of vortex-shedding 09 p1196 A83-23337
- Calculation of the surface stresses of an elastic body 09 p1278 A83-23516
- A Saint-Venant principle for nonlinear elasticity 09 p1279 A83-24134
- St. Venant formulae for generalized St. Venant problems 09 p1279 A83-24135
- The effect of initial stresses on the back wave in the system prestressed compressible cylinder-liquid 11 p1596 A83-28457
- The propagation of small perturbations in a system consisting of a prestressed compressed solid body and a viscous compressible fluid 11 p1597 A83-28474
- Transient thermal stress problem for a circumferentially cracked hollow cylinder 12 p1747 A83-29921
- A general method for solving problems of elastic-wave diffraction by deformable obstacles 13 p1866 A83-30081
- Deformation and vibration of rotating elastic cylinders 15 p2177 A83-34340
- The nonstationary thermoelasticity problem for a cylinder weakened by a periodic system of penny-shaped cracks 17 p2524 A83-38510
- Compression of an elastic cylinder between two rigid planes Application of the indirect fictitious-boundary integral method to a contact problem 18 p2697 A83-39455
- Propagation of flexural waves in noncircular cylinders with initial stresses 19 p2860 A83-42007
- Three-dimensional stressed state of longitudinally corrugated elastic cylinders 21 p3163 A83-45359
- Dynamic finite element analysis of nonaxisymmetric structures 23 p3471 A83-48163
- A numerical solution to boundary-value thermoelasticity problems for multilayer hollow cylinders 23 p3471 A83-48247
- Longitudinal shear in a body with an acute-angled inclusion and an interface crack 23 p3473 A83-48542
- ELASTIC DAMPING**
- NT VISCOELASTIC DAMPING**
- On the damping effect of sloshing fluid on flexible rotor systems [ASME PAPER 82-DET-140] 02 p0196 A83-12783
- Comments on 'On the use of simply supported plate functions in the Rayleigh-Ritz method applied to the flexural vibration of rectangular plates' 02 p0197 A83-13005
- The damping of the elastic vibrations of structures with liquids 04 p0487 A83-15391
- Free out-of-plane vibration of a ring elastically supported at several points 04 p0499 A83-15690
- Vibration and stability of sandwich beams with elastic bonding 06 p0774 A83-18395
- Bending vibrational behavior of laminated rotors --- German thesis 06 p0769 A83-19620
- Dynamic qualification of spacecraft by means of modal synthesis. I 08 p1050 A83-22375
- Numerical analysis of flexural vibrations of rotors resting on elastic supports 11 p1589 A83-27724
- Large-amplitude vibration of laminated composite plates of arbitrary shape [AIAA 83-1035] 12 p1745 A83-29880
- Nonlinear analysis of composite circular plates [AIAA 83-1036] 12 p1745 A83-29881
- A method for the mathematical description and solution of boundary value problems in the deformation mechanics of shells on continuous or discrete elastic supports 13 p1867 A83-31321
- Elastic stability, buckling and post-buckling behaviour 15 p2176 A83-34328
- On certain properties of the second energy variation in problems of the elastic stability of discrete conservative systems 15 p2178 A83-34440
- Stability of the stationary motions of the axis of a rotating rotor mounted in nonlinear bearings 19 p2895 A83-41203
- Time integration of the motion equations of a damped structure 21 p3152 A83-44359
- Optimum characteristics of vibration protection systems 21 p3153 A83-44628
- The dynamics of a two-gimbal elastically suspended gyroscope 21 p3137 A83-44632
- ELASTIC DEFORMATION**
- NT ELASTIC BENDING**
- NT ELASTIC BUCKLING**
- In-flight deflection measurement of the HIMAT aeroelastically tailored wing 03 p0281 A83-13167
- Quasi-periodic boundary-value problems and their application to elasticity theory 03 p0343 A83-14899
- The effect of plastic deformation on the acoustoelastic response of metals 04 p0458 A83-15221
- A study of the relationship between the acoustic emission parameters and the processes of elastic-plastic deformation and fracture of EI-602 alloy 04 p0459 A83-15466
- The perturbation method in boundary value problems of the mechanics of deformable bodies 04 p0501 A83-16401
- Holography and the deformation of metals --- Russian book 05 p0644 A83-17119
- Symmetry and bifurcation in three-dimensional elasticity. I 06 p0776 A83-18928
- A study of the effect of cyclic block loading on the deformation characteristics and strength of structural materials under plane stressed state. I - Resistance to elastic-plastic deformation 06 p0733 A83-19306
- A constitutive theory for transversely isotropic bimodulus materials with a class of steady wave solutions 07 p0948 A83-21344
- General form of the acoustoelasticity equations for the principal stresses 07 p0948 A83-21411
- Elastic-plastic fields in steady crack growth in a strain-hardening material 08 p1117 A83-21692
- Deformation of a rod by end moments 09 p1278 A83-23566
- An estimation of the compressive strength of a fibrous composite 09 p1224 A83-23944
- Free rotation of a circular ring about a diameter 09 p1339 A83-24820
- The elastic interaction between a tensioned strip and a loaded insert 09 p1282 A83-25018
- A 'periodic' solution for an axisymmetric deformable elastic paraboloid of revolution 09 p1282 A83-25019
- Instability and the ill-posed Cauchy problem in elasticity 10 p1437 A83-25310
- Crystal elasticity --- mechanical behavior under loading 10 p1392 A83-25311
- Elastic deformations of rubberlike solids 10 p1438 A83-25313
- The method of R-functions in problems of the theory of small elastoplastic deformations 10 p1439 A83-25594
- A linear theory for pretwisted elastic beams [ASME PAPER 83-APM-9] 10 p1441 A83-26439
- Global-local laminate variational model 11 p1544 A83-28409
- The solution of nonlinear boundary value problems in the statics of flexible layered shells in the supercritical region 11 p1596 A83-28454
- Solution of an asymmetric problem for a two-layer hollow cylinder of finite length by the finite element method 11 p1597 A83-28465
- A second order theory for large deflections of slender beams 12 p1736 A83-29706
- Linear elastic fracture mechanics and fatigue crack growth Residual stress effects 12 p1746 A83-29905
- The elastic distortion of rollers under combined radial and thrust loads 13 p1858 A83-30245
- Viscosity phenomena in ferroelectrics and ferroelastics 13 p1930 A83-31309
- The regularity of one-dimensional elastic waves in an incompressible isotropic material 14 p2030 A83-32356
- The accuracy of plane strain models for the elastic contact of three-dimensional rough surfaces 14 p2027 A83-32625
- Dynamics of gyro-elastic continua [AIAA PAPER 83-0826] 14 p2032 A83-32795

Linear isotropic elasticity with body forces	15	p2173	A83-33856
Nonlinear supersonic flutter of panels considering shear deformation and rotary inertia	15	p2176	A83-34315
On non-universal finite elastic deformations	15	p2176	A83-34331
On uniqueness in finite elasticity	15	p2177	A83-34334
Deformation and vibration of rotating elastic cylinders	15	p2177	A83-34340
Stress concentration layers in finite deformation of fibre-reinforced elastic materials	15	p2130	A83-34344
Local theorems of existence and uniqueness in finite elastostatics	15	p2177	A83-34345
The strain-energy function for rubber-like materials	15	p2142	A83-34346
Description of finite deformations of thin shells by means of the coordinates of reference and actual configurations	15	p2178	A83-34438
Asymptotic methods in the elasticity theory for an orthotropic body --- Russian book	15	p2180	A83-34575
The effect of creep on the magnitude of elastic deformation in a laminated composite	16	p2323	A83-35506
Thermoelasticity of ideal fibre-reinforced materials	16	p2324	A83-35775
Monitoring of high power ultrasonic fatigue systems	16	p2367	A83-36178
A viscoelastic-viscoplastic constitutive equation and its finite element implementation	16	p2369	A83-36557
The stability of a laminar boundary layer on an elastic surface	17	p2505	A83-37510
A model of a material with internal friction	17	p2521	A83-37542
A study of the resistance of rectangular panels during shear in an elastic frame	17	p2521	A83-37543
The elastic strain energy of dislocation structures in fatigued metals	17	p2490	A83-38382
Theory of the torsion of prismatic bars in the case of finite deformations	18	p2698	A83-39483
Periodic problem of the plane theory of elasticity for an infinite plane with cracks and holes	18	p2698	A83-39505
Investigations of axisymmetric deformation of geometrically nonlinear, rotationally orthotropic, circular plates	18	p2700	A83-39567
A thermoelastic contact problem concerning the bending of a band with allowance for its deformability in the thickness direction	19	p2859	A83-41572
Prestrained elastic laminates - Deformations, stability and vibrations	19	p2860	A83-41996
Vibrations of an elastic beam with a flexible support	20	p3005	A83-42992
Highly non-linear cylindrical deformations of rings and shells	20	p3008	A83-43649
The elastic solution of the dynamic elastic-plastic response of a circular plate	21	p3151	A83-44104
Shape design sensitivity of a membrane	21	p3152	A83-44327
The stressed state of an inhomogeneous orthotropic hollow cone	21	p3154	A83-44712
3-D elastic-plastic investigation of fracture parameters in side-grooved compact specimen	21	p3157	A83-44906
Concentration of elastic stresses near dies, cracks, thin inclusions, and reinforcements --- Russian book	21	p3160	A83-45025
An approximate solution to a plane contact elasticity problem	21	p3162	A83-45302
Determination of nodal forces in elements under surface and bulk loads for axisymmetric and plane elasticity problems	21	p3163	A83-45323
Free motions of a nearly spherical deformable solid	21	p3200	A83-45357
A class of integral equations for solving three-dimensional axisymmetric elasticity problems	21	p3163	A83-45358
Three-dimensional stressed state of longitudinally corrugated elastic cylinders	21	p3163	A83-45359
An elasticity relationship for an anisotropic body whose deformation characteristics depend on the type of stressed state --- for composite materials	21	p3108	A83-45360
Variation of dynamic mechanical properties of polycarbonate as a result of deformation	22	p3270	A83-46903
Numerical solution of problems in the mechanics of a deformable inhomogeneous solid	23	p3468	A83-47177
Flexural vibrations of clamped polygonal and circular plates having rectangular orthotropy	23	p3469	A83-47600
Effect of deformation on the fracture of Si3N4 and sialon	23	p3437	A83-48290
A representation of elasticity and plasticity laws in plane problems	23	p3472	A83-48462
Correlation function of a stress field in an elastic medium with point defects	23	p3473	A83-48536
Allowance for the principal types of elastic deformation nonlinearities in axisymmetric problems of the statics of shells of revolution	24	p3592	A83-49032
Solution of certain equilibrium problems for an elastic parallelepiped in stresses	24	p3593	A83-49051
Nonlinear antiplane strain of a body weakened by a lune-shaped recess	24	p3594	A83-49527
ELASTIC MEDIA			
The plane nonlinear problem of stress distribution around holes	01	p0059	A83-10691
Application of finite-part integrals to the singular integral equations of crack problems in plane and three-dimensional elasticity	02	p0190	A83-12001
Bounds for the dislocation densities and the stress intensity factors in elastic crack problems	02	p0190	A83-12042
Special analytical solution for use in debond stress analysis	02	p0191	A83-12172
A simple yet accurate finite element procedure for computing stress intensity factors	03	p0342	A83-14707
The asymptotics of the averaged characteristics of periodic elastic media with strongly varying properties	04	p0456	A83-16411
An improved dislocation approach in solving three-dimensional boundary value problems	05	p0681	A83-17324
Inverse dynamic problems for an anisotropic elastic medium	07	p0944	A83-19632
Averaging of partial differential equations with rapidly oscillating coefficients	07	p0986	A83-20304
Boundary element method in fracture mechanics	07	p0947	A83-20925
Elastic wave scattering by a circular crack	07	p0947	A83-21081
Magneto-thermo-elastic plane waves in rotating media	07	p0948	A83-21168
Nonlinear micropolar continuum model of a composite reinforced by elements of finite rigidity. I - Equations of motion and constitutive relations	08	p1120	A83-21816
SH-wave scattering by a cylinder with an interfacial crack	09	p1276	A83-23375
The Green function of an infinite, fluid loaded membrane	09	p1278	A83-23705
Surface waves in cubic elastic materials	10	p1437	A83-25304
Aspects of the theory of dislocations	10	p1437	A83-25307
Axisymmetric problem of a flat interface annular crack between an elastic layer and a half-space	10	p1440	A83-26424
Stress distributions for a quarter plane containing an arbitrarily oriented crack	10	p1440	A83-26429
Dynamic stress concentration around a circular hole in an infinite elastic strip	10	p1440	A83-26430
Interaction of a P-wave with a laterally stiffened slot	10	p1440	A83-26431
Some remarks on elastic fracture mechanics	11	p1595	A83-28434
On the fundamental basis of fracture mechanics	11	p1596	A83-28444
Theoretical stress analysis for a non-isotropic body of cylindrical configuration containing a row of cracks	11	p1596	A83-28447
Waves in stratified homogeneous elastic media - The method of boundary integrals in nonstationary problems of dynamics --- Russian book	12	p1774	A83-28826
Propagation of sound in highly porous open-cell elastic foams	12	p1776	A83-28848
Surface acoustic admittance of highly porous open-cell, elastic foams	12	p1776	A83-28849
Structural optimization with dynamic behavior constraints [AIAA 83-0936]	12	p1739	A83-29766
The features of the atomic structure of pure inorganic ferroelastics	13	p1928	A83-30311
Applications of ferroelastics	13	p1832	A83-30312
Giant resonances as oscillations of two elastically coupled fluids	15	p2228	A83-33794
Finite strain J2 deformation theory	15	p2177	A83-34336
Interaction of cracks in elastic media	15	p2177	A83-34349
Behavior of solutions of dynamic problems near the edge of a crack propagating at transonic velocity in an elastic medium	15	p2178	A83-34436
Partial closure of cracks at the interface between a layer and a half space	16	p2368	A83-36506
Homogeneity conditions for elastic membranes	17	p2525	A83-38849
Non-singular stresses effects on two interacting equal collinear cracks	18	p2696	A83-39076
Stress intensity factors in two bonded elastic layers containing cracks perpendicular to and on the interface. I Analysis. II - Solution and results	18	p2698	A83-39535
Resonance effects and the ultrasonic effective properties of particulate composites	18	p2741	A83-39974
Elastic media with microstructure. I - One-dimensional models	19	p2897	A83-41875
A theory for gyroscopic compasses in the light of analogies with elastic systems	21	p3137	A83-44626
A new singular integral equation for the classical crack problem in plane and antiplane elasticity	21	p3156	A83-44890
Concentrated body force loading of an elastically bridged penny shaped flaw in a unidirectional fibre reinforced composite	21	p3156	A83-44893
The diffusion of a fluid through a highly elastic spherical membrane	22	p3281	A83-46390
An annular crack in microelasticity	22	p3306	A83-46394
Crack transient torsional wave interaction in an elastic bi-material	24	p3591	A83-48870
A remark on the solution of the integral equation of planar cracks in three-dimensional elasticity	24	p3595	A83-49869
ELASTIC MODULUS			
U MODULUS OF ELASTICITY			
ELASTIC PLATES			
Stability of the elastic equilibrium of an infinite plate in the vicinity of a randomly oriented rectilinear crack under plane-stressed state	01	p0059	A83-10684
An integral equation approach to finite deflection of elastic plates	01	p0060	A83-10861
The response of a fluid-loaded, beam-stiffened plate	01	p0105	A83-11040
Bending waves in strongly anisotropic elastic plates	02	p0196	A83-12855
The effect of shear modulus on the elastic behavior of strongly anisotropic plates	03	p0343	A83-14736
Use of finite element method for determining stress intensity factors with a conic-section simulation model of crack surface	03	p0343	A83-14818
On the energy criterion in the context of plate stability	04	p0495	A83-15011
An approximation method for the stability analysis of plates in the flow of an incompressible fluid	04	p0497	A83-15392
Axisymmetric elastic waves excited by a point source in a plate [ASME PAPER 82-WA/APM-15]	04	p0498	A83-15687
Optimization of reinforcement for a class of openings in plate structures	04	p0499	A83-15695
Application of convex analysis to the calculation of stress-state in elastic-plastic plates	04	p0500	A83-16097
Sampling statistics for vibrating rectangular plates	04	p0501	A83-16314
Axisymmetric vibrations of an isotropic elastic non-homogeneous circular plate of linearly varying thickness	04	p0501	A83-16342
Concerning a refined theory of plates in the case of finite deflections	04	p0502	A83-16406
Optimization of the shapes of elastic bodies --- Russian book	05	p0654	A83-17131
A solution to the three-dimensional stability problem for a rectangular plate given an inhomogeneous subcritical state	06	p0770	A83-18140
Vibrations of initially imperfect circular plates including the shear and rotatory inertial effects	06	p0773	A83-18394
A novel approach to the solution of a problem concerning contact interaction between a semiinfinite stringer and a half-plane	06	p0778	A83-19601
Stationary motions of a gyrostat with deformable plates and their stability in a Newtonian central force field	07	p0872	A83-19937
Inelastic analysis of surface flaws using the line-spring model	08	p1119	A83-21792
Castiglione's theorem and its limits	08	p1121	A83-21859
Integral equation formulation for nonlinear bending of plates - Formulation by weighted residual method	08	p1121	A83-21860
Elliptic plate with clamped edge	08	p1122	A83-22046
Optimal design of elastic plates with a constraint on the slope of the thickness function	09	p1278	A83-23670
The influence of inplane deformation on the buckling loads of isotropic elastic plates	09	p1283	A83-25218

- The effect of an elastic wall on the boundary layer
10 p1413 A83-25593
- A theoretical study on the running crack path by energy balance method
10 p1442 A83-26968
- A finite element method for construction of dynamical theories of layered plates
11 p1591 A83-27429
- On the Liapunov-Movchan stability of equilibrium of elastic orthotropic plates
11 p1593 A83-27860
- Influence of surface compliance on boundary layer noise
[AIAA PAPER 83-0738] 11 p1652 A83-28018
- The problem of the intersection of two half-planes with reinforced edges
11 p1597 A83-28470
- Stress distribution in a strongly anisotropic elastic plane with a parabolic cutout
11 p1598 A83-28486
- Uniform strengthening of plates with holes
11 p1600 A83-28773
- Creep buckling of structures
[AIAA 83-0864] 12 p1738 A83-29752
- Nonlinear response of double wall sandwich panels
[AIAA 83-1037] 12 p1745 A83-29882
- Buckle pattern of biaxially compressed simply supported orthotropic rectangular plates
13 p1868 A83-31619
- Two coplanar Griffith cracks in an orthotropic semi-infinite medium
14 p2032 A83-32921
- Local buckling of thin tensioned plate with a crack
14 p2033 A83-33374
- Large vibrations of elastic plates due to thermal gradient
15 p2175 A83-34245
- Large thermal deflections of elastic plates by conformal transformation
15 p2175 A83-34246
- Two-dimensional approximations of three-dimensional models in nonlinear plate theory
15 p2176 A83-34330
- On a method for solving the plane-stress problem of elasticity for perforated plates
15 p2178 A83-34435
- A reinvestigation of post-buckling behaviour of elastic circular plates using a simple finite element formulation
15 p2179 A83-34566
- Certain problems of the contact interaction of an elastic infinite plane having a round hole with ring-shaped patches
15 p2180 A83-35150
- A solution to the bending problem for an elastic-plastic shell
16 p2366 A83-35930
- Transverse vibrations of nonuniform rectangular orthotropic plates
16 p2366 A83-36097
- Brittle fracture of plates in tension - Relative significance of boundary reflected body and Rayleigh waves
16 p2368 A83-36516
- Postbuckling analysis of moderately thick elastic circular plates
17 p2520 A83-37393
- The load-bearing behavior of shear-stressed square plates of fiber-reinforced composite materials under large deformations --- German thesis
17 p2520 A83-37499
- Interaction between a bonded stiffening rib and a composite plate
18 p2701 A83-40108
- Nonsymmetric bending of a plate reinforced by a symmetric system of radial ribs
19 p2857 A83-41211
- Photoelastic determination of complex stress intensity factors for slant cracks under biaxial loading with higher-order term effects
19 p2860 A83-41998
- Further investigations on the postbuckling behaviour of regularly multilayered rectangular elastic plates
20 p3005 A83-42990
- Nonlinear aeroelasticity
21 p3150 A83-44027
- Analysis of crack-tip moiré patterns
21 p3156 A83-44888
- The control of a flexible square plate in space
21 p3101 A83-45110
- The stressed state of a plate weakened by two circular holes and a crack
21 p3163 A83-45366
- Selection of the optimum orientations of the axes of elastic symmetry of an orthotropic plate
21 p3163 A83-45367
- Shear-elastic plates with built-in edge support
21 p3164 A83-45400
- Numerical optimum design of elastic annular plates with respect to buckling
24 p3594 A83-49443
- An extension of classical shell theory - The influence of thickness strains and cross-sectional warping
01 p0059 A83-10575
- The scale effect in the elastic properties of polycrystalline materials
01 p0026 A83-10677
- The mechanism of the dissipation of elastic energy by a lubricant layer
02 p0186 A83-11647
- The construction of a computational model that uses the finite-element method to solve spatial problems in the theory of elasticity
02 p0191 A83-12341
- Evaluation of the tentative JI-R curve testing procedure by round robin tests of HY130 steel
02 p0158 A83-12832
- The adaptive properties of the major arterial vessels
03 p0379 A83-13620
- Single-crystal elastic constants in nondestructive evaluation of welds
04 p0492 A83-15215
- Comparison of elasticity, shell core, and sandwich shell theories
04 p0496 A83-15291
- Estimates and asymptotics of the stress-strain state of a three-dimensional body with a crack in the theory of elasticity and the theory of creep
04 p0500 A83-15884
- A mathematical theory of wave propagation in media with memory --- Russian book
05 p0654 A83-17130
- The behavior of generalized solutions of second-order elliptic equations and of the system of elasticity theory in the neighborhood of a boundary point
05 p0654 A83-17137
- Temperature dependence of elastic constants of CFRP
06 p0724 A83-17965
- Questions of convergence, duality, and averaging for a class of functionals of the calculus of variations
06 p0804 A83-17976
- Calculating the elastic characteristics of a unidirectional fiber composite by the method of sections
06 p0725 A83-18501
- Love waves in orthotropic periodically layered composites
06 p0725 A83-18510
- Acoustoelastic response of polycrystalline aggregates exhibiting transverse isotropy
07 p0945 A83-20266
- On the exterior crack with contact zones
07 p0946 A83-20640
- A simplified model of the influence of elastic pitch variations on the rotor flapping dynamics
07 p0866 A83-21025
- Variation of in-plane elastic constants in material design of composite laminates
07 p0949 A83-21623
- The crack tip stress intensification associated with crack propagation and arrest
08 p1118 A83-21778
- A quest for micropolar elastic constants. II
08 p1120 A83-21814
- Saint-Venant end effects in composites
08 p1054 A83-21823
- A generalization of the concept of Cauchy-type principal value integrals for plane elasticity crack problems
08 p1121 A83-21865
- Two approaches in fracture mechanics of composites
09 p1222 A83-23929
- The convergence of the Richardson method in problems concerning the nonlinear theory of elasticity
09 p1280 A83-24242
- The stressed state of an elastic ring fitted into a circular hole in a tensioned plate
09 p1282 A83-25017
- Elastic properties of hafnium and zirconium oxides stabilized with praseodymium or terbium oxide
09 p1240 A83-25209
- Vibration of a free rectangular parallelepiped
10 p1441 A83-26437
- Solution of some boundary value problems of elasticity theory in bipolar coordinates
11 p1594 A83-28196
- The effect of the anisotropy of thermophysical and elastic properties on the thermal stresses in profiled sapphire and lithium niobate single crystals
11 p1662 A83-28358
- Bounding theorems for Stress Intensity Factors
11 p1596 A83-28443
- Estimates and approximation formulas in the problem of elasticity theory concerning a plane normal crack
11 p1597 A83-28472
- An approach to the analysis of the compliance of threaded connections in creep
11 p1598 A83-28502
- Measurement of acoustoelastic coefficients of Rayleigh waves in steel alloys
12 p1712 A83-29144
- Optimization of the calculation of the elastic constants from velocity measurements with an ultrasonic wave
12 p1735 A83-29387
- The elastic characteristics of unidirectionally reinforced hybrid composites
13 p1815 A83-30052
- A study of the acoustic properties of a ceramic material
13 p1825 A83-30062
- An iteration method for solving stochastic boundary value elasticity problems
14 p2029 A83-32155
- Control of the material properties and structural application of carbon fibre reinforced plastics
[AIAA PAPER 83-0859] 14 p1986 A83-32790
- A study of the elastic characteristics of structural alloys over a wide temperature range
14 p1998 A83-33017
- Minimum-weight design with displacements constraints in 2-dimensional elasticity
15 p2176 A83-34316
- Finite elasticity
15 p2176 A83-34326
- On uniqueness in finite elasticity
15 p2177 A83-34334
- Penalty methods for constrained problems in nonlinear elasticity
15 p2177 A83-34339
- Fundamentals of the stability theory for shells beyond the elasticity limit --- Russian book
15 p2177 A83-34373
- The solution of the equations of the applied theory of elasticity by the method of variational iterations
15 p2178 A83-34433
- Inverse problem of three-dimensional elasticity
15 p2178 A83-34434
- Elastic composites
16 p2364 A83-35505
- Investigation of anisotropic problems in the mechanics of deformable bodies by the holographic moiré method
16 p2355 A83-35512
- Bounds on stress concentration factors in finite anti-plane shear
16 p2368 A83-36548
- Variational methods in elasticity and plasticity / 3rd edition/ --- Book
17 p2518 A83-37169
- A model of a material with internal friction
17 p2521 A83-37542
- High-frequency nonaxisymmetric vibrations of elastic disks
17 p2521 A83-37574
- On the acoustoelastic effect
17 p2576 A83-37728
- A concentrated couple acting on an elastic half-plane
17 p2522 A83-38100
- Stress intensity factors for radial cracks in bimaterial media
17 p2523 A83-38391
- The solution of elasticity problems for the half-space by the method of Green and Collins
17 p2525 A83-38619
- Elastic stability of plane laminates
18 p2697 A83-39422
- Three dimensional stress state in an internally-pressurized hollow cylinder with a reinforcing ring
18 p2697 A83-39453
- The effect of adhesion on the elastic properties of a composite with a disperse filler
18 p2649 A83-39478
- A new method for calculating the elastic component of the Crack Opening Displacement (COD)
18 p2699 A83-39548
- A boundary-layer theory for the orthotropic plate
18 p2700 A83-39986
- Predicted elastic constants of transversely isotropic composites containing anisotropic fibers
18 p2652 A83-40160
- Material design of composite laminates with required in-plane elastic properties
18 p2662 A83-40292
- On the off-axis tension test for unidirectional composites
19 p2819 A83-41033
- Solution of external boundary-value elasticity problems using the method of boundary integral equations
19 p2857 A83-41210
- Boundary element methods; Proceedings of the Third International Seminar, Irvine, CA, July 7-9, 1981
19 p2896 A83-41516
- Temperature dependence of mechanical and thermal expansion properties of T300/5208 graphite/epoxy
20 p2947 A83-42811
- Fracture mechanics for delamination problems in composite materials
20 p3007 A83-43143
- Experiments on highly-nonlinear elastic composites
21 p3106 A83-44048
- A nonlinear effect in rolling bearings
21 p3148 A83-44639
- A study of the moment of elastic unbalance in a gyroscopic instrument in the case of the main resonance
21 p3138 A83-44640
- Application of electrical analog technique in fracture mechanics
21 p3155 A83-44883
- An analysis of the energy release rate for non-coplanar crack growth in fiber reinforced composite materials
21 p3107 A83-44913
- The crack problem for a nonhomogeneous plane
[ASME PAPER 83-APM-35] 23 p3471 A83-48243
- Variational approach by means of adjoint systems to structural optimization and sensitivity analysis. I - Variation of material parameters within fixed domain
23 p3474 A83-48696
- Solution of two-dimensional elasticity problems in regions with a remote external boundary
24 p3592 A83-49036
- The formulation of plane contact problems of elasticity theory for the wear of interacting bodies
24 p3594 A83-49533
- Dynamic problem of elasticity theory for a region with curved slits (plane strain)
24 p3594 A83-49534

Wrinkling phenomenon in structures. I - Model formulations 24 p3596 A83-50123

ELASTIC SCATTERING

Time resolved study of superelastic collisions in laser excited strontium vapor 02 p0241 A83-12399
Elastic wave scattering calculations, the Born Series and the matrix variational Pade approximant method --- for prediction of spherical voids and inclusions in NDT 04 p0488 A83-15161

The theory of flaw centroids and low-frequency phase shifts - A review 04 p0489 A83-15169
The dissociative recombination of an electron and a molecular ion 05 p0686 A83-16887
The entropy of a gas of hard spheres with respect to the group of space-time translations 05 p0691 A83-17138

Modified-independent-atom-model /MIAM/ calculations for e-CO2 elastic scattering at 50-500 eV 06 p0807 A83-18040

Elastic and inelastic scattering of electrons by atomic hydrogen at intermediate energies in a coupled-channel second-order potential model 06 p0808 A83-19008
Time domain Born approximation --- for ultrasonic nondestructive tests 07 p0942 A83-20271
An augmented technique for backscattering amplitude inversion in the study of cavities and plane defects 09 p1275 A83-23474

Electron thermalization in gases. V - Diatomic molecules H2, N2, and CO 09 p1342 A83-24132
Elastic scattering of electrons by N2, O2, and CO in the energy range 0.1-3 keV 10 p1479 A83-25557
The thermodynamic properties of diatomic molecules at elevated temperatures - Role of continuum and metastable states 11 p1665 A83-27495
Elastic light-scattering Mueller-matrix photopolarimetry 11 p1572 A83-27566

Relation between the free-free and scattering cross sections and 'two-state resonances' in bremsstrahlung 16 p2408 A83-35329

Elastic and inelastic scattering of high-energy electrons and X-rays by NH3, CH4 and H2O molecules 16 p2409 A83-35333

Thermal relaxation and entropy for charged particles in a heat bath with fields 16 p2421 A83-35616
Elastic scattering of electrons by hydrogen atoms in the 2S state 16 p2410 A83-35654

Investigation of superelastic electron scattering by laser-excited Ba - Experimental procedures and results 18 p2743 A83-40407

Elastic and rotational excitation of the oxygen molecule by intermediate-energy electrons 19 p2898 A83-41196

Elastic scattering of heavy ions and the compressibility of nuclear matter 19 p2899 A83-41535
Elastic and inelastic scattering of gamma rays from V3Si 19 p2905 A83-41537

Photometer for quasielastic and classical light scattering 20 p2988 A83-42295
Angular distribution of electrons elastically scattered from O2 at 40-500 eV - A two-potential coherent approach 22 p3355 A83-45941

Nonequilibrium electron velocity distribution and temperature in thermalization of low-energy electrons in molecular hydrogen 24 p3625 A83-48798
Elastic scattering of electrons by the 2s state of atomic hydrogen at intermediate energies 24 p3626 A83-48846

Elastic scattering of electrons by hydrogen atoms in a laser field 24 p3626 A83-49432

Measurement of differential cross sections of low-energy electrons elastically scattered by gaseous molecules. IV Effect of intramolecular double scattering as observed in the scattering of 100 and 500 eV electrons by As4 24 p3626 A83-49433

Elastic scattering of electrons by the 2s state of atomic hydrogen at intermediate energies 24 p3626 A83-48846

ELASTIC SHEETS

A thermoelectric contact problem concerning the bending of a band with allowance for its deformability in the thickness direction 19 p2859 A83-41572

Green's function solution and applications for cracks emanating from a circular hole in an infinite sheet 24 p3594 A83-49599

ELASTIC SHELLS

Optimization of the regimes of intense heating of a cylindrical shell 01 p0058 A83-10451
A study of the stressed state of inhomogeneous cylindrical shells 01 p0059 A83-10679

Axisymmetric thermoplastic state of layered shells on the basis of the theory of small-curvature processes 01 p0059 A83-10680

A new class of solutions for buckling of a short cylindrical shell in pure bending 02 p0191 A83-12075

Concerning the formulation of the problem of calculating the stress-strain state in shell-reinforced cylinders by the finite element method 03 p0341 A83-14073

On nonlinear membrane theory 04 p0495 A83-15010

Nonlinear analysis of elasto-plastic shells by hybrid stress finite elements 04 p0495 A83-15017

A simple finite element for elastic-plastic deformations of shells 04 p0495 A83-15020

An approach to the numerical study of the free vibrations of thin-wall structures 04 p0502 A83-16404

Numerical analysis of wave processes in a shell-rod system 04 p0502 A83-16405
Solution of the dynamic problem of viscoelastic shells 04 p0502 A83-16412

Some general methods for constructing different versions of the shell theory --- Russian book 05 p0654 A83-17128

Optimization of the shapes of elastic bodies --- Russian book 05 p0654 A83-17131

High-frequency vibrations of shells 06 p0770 A83-17980

Jet flow of an ideal liquid past a flexible shell 06 p0760 A83-19430

Optimization of solutions of the equations of motion of shells of revolution to enhance the dynamic-stability parameters 07 p0946 A83-20897

The nonlinear problem of the stability of cylindrical sandwich shells under combined loading 08 p1114 A83-21628

Equations of linear shell theory with allowance for transverse shear strains 08 p1115 A83-21633
Inelastic analysis of surface flaws using the line-spring model 08 p1119 A83-21792

A geometrically nonlinear half-membrane theory of elastic shells 09 p1279 A83-24011
Nonaxisymmetric buckling of nonshallow elastic shells of revolution 09 p1281 A83-25011

The solution of nonlinear boundary value problems in the statics of flexible layered shells in the supercritical region 11 p1596 A83-28454

On the geometrical theory of shell stability 11 p1597 A83-28473

The theory and analysis of shells of revolution --- Russian book 12 p1735 A83-29327

Creep buckling of structures [AIAA 83-0864] 12 p1738 A83-29752
Normal oscillations of an ideal compressible fluid in rotating elastic vessels 13 p1838 A83-30012

A solution to the bending problem for a layered inhomogeneous hollow cylinder 14 p2029 A83-32152

Periodic and biperiodic solutions to the equations of an engineering theory for an elastic cylindrical shell 14 p2029 A83-32153

An analysis of thin-walled electroelastic toroidal shells 14 p2029 A83-32161

Boundary conditions in the theory of piezoceramic shells polarized along the coordinate lines 14 p2030 A83-32355

Dynamic behaviour of a thin-walled circular cylindrical shell 15 p2173 A83-33611

Thermal stress analysis of spherical shells supported on elastic foundation by the residual method 15 p2175 A83-34241

The nonaxisymmetric deformation of flexible conical shells of variable thickness 16 p2365 A83-35926

The stability of flexible shallow shells in a temperature field 17 p2524 A83-38505

Shrinkage stresses in products of high-modulus composites 17 p2524 A83-38512

On some variational principles of shells 18 p2700 A83-40001

Variational theorem of a theory for shells that are inhomogeneous in the thickness direction 18 p2701 A83-40110

Determination of transfer functions in the problem of the unsteady interaction of a fluid with an elastic elliptical shell 18 p2702 A83-40119

Stability equations of the general geometrically non-linear first approximation theory of thin elastic shells 20 p3005 A83-42988

On the post-buckling analysis of thin elastic shells 20 p3005 A83-42991

A simplest consistent version of the geometrically non-linear theory of elastic shells undergoing large/small rotations 20 p3006 A83-43000

Creep and stability of shallow elastic shells of revolution --- Russian book 21 p3150 A83-43916

Nonlinear aeroelasticity 21 p3150 A83-44027

An asymptotic method for the theory of shells 21 p3153 A83-44659

A class of contact problems for a cylindrical shell 21 p3154 A83-44716

Two-dimensional problems of the stability and vibrations of shells of zero Gaussian curvature 21 p3164 A83-45395

The effect of viscosity on the forced vibrations of a fluid-filled elastic shell [ASME PAPER 83-APM-34] 23 p3471 A83-48242

Nonaxisymmetric buckling and supercritical behavior of elastic spherical shells in the case of a double critical value of load 23 p3473 A83-48537

Resonant acoustic scattering from elastic cylindrical shells 24 p3624 A83-48974

ELASTIC STABILITY

U DAMPING

ELASTIC STRENGTH

U PROPORTIONAL LIMIT

ELASTIC SYSTEMS

Universal characteristic equations in problems involving the vibrations and stability of elastic systems 07 p0945 A83-19948

Optimal control and controller location for distributed parameter elastic systems 09 p1328 A83-24723

Component mode analysis of nonlinear, nonconservative systems [ASME PAPER 83-APM-1] 10 p1472 A83-26447

Numerical problems of nonlinear stability analysis of elastic structures 11 p1599 A83-28719

Stability of short Beck and Leipholz columns on elastic foundation 16 p2366 A83-36098

'Non-linear normal modes' and the generalized Ritz method in the problems of vibrations of non-linear elastic continuous systems 18 p2700 A83-39570

First order solution of the optimal control problem for distributed parameter elastic system 21 p3193 A83-44040

ELASTIC WAVES

NT AERODYNAMIC NOISE

NT AIRCRAFT NOISE

NT BAROCLINIC WAVES

NT CAPILLARY WAVES

NT COHERENT ACOUSTIC RADIATION

NT COMPRESSION WAVES

NT DETONATION WAVES

NT ELECTROACOUSTIC WAVES

NT ELECTROSTATIC WAVES

NT ENGINE NOISE

NT GRAVITY WAVES

NT ION ACOUSTIC WAVES

NT IONIC WAVES

NT JET AIRCRAFT NOISE

NT LAMB WAVES

NT LOVE WAVES

NT MACH CONES

NT MAGNETOACOUSTIC WAVES

NT MAGNETOELASTIC WAVES

NT MAGNETOHYDRODYNAMIC WAVES

NT MICROSEISMS

NT NOISE (SOUND)

NT NORMAL SHOCK WAVES

NT OBLIQUE SHOCK WAVES

NT P WAVES

NT PHONONS

NT PLASMA WAVES

NT POLARIZED ELASTIC WAVES

NT RAYLEIGH WAVES

NT RIEMANN WAVES

NT S WAVES

NT SEISMIC WAVES

NT SHOCK WAVES

NT SONIC BOOMS

NT SOUND WAVES

NT STRESS WAVES

NT THERMAL NOISE

NT TOLLMEIN-SCHLICHTING WAVES

NT ULTRASONIC RADIATION

Theoretical and experimental research on the formation, propagation, and use of laser-induced pressure waves --- German thesis 01 p0048 A83-10165

Excitation of elastic wave in a layer by disk-shape radiator of finite dimensions 01 p0057 A83-10371

The forms of the wave motion of circular cylindrical shells 01 p0059 A83-10678

A consideration on dynamic characteristics of pneumatic conduit systems with a cylindrical choke - Influence of the position of a cylindrical choke 02 p0187 A83-13074

Dynamic spalling in rarefaction waves 03 p0339 A83-13596

Interaction between a shock wave and a rarefaction wave in a problem concerning an angular piston 03 p0323 A83-14895

Elastic wave scattering calculations, the Born Series and the matrix variational Pade approximant method --- for prediction of spherical voids and inclusions in NDT 04 p0488 A83-15161

The Eikonal approximation in elastic wave scattering theory 04 p0489 A83-15162

Inverse scattering at long wavelength - Delta mu = 0 04 p0489 A83-15163

The unimoment method for elastic wave scattering problems 04 p0489 A83-15164

Advances in numerical studies of elastic wave propagation and scattering 04 p0489 A83-15165

- Multiple scattering formalism - Application to scattering by two spheres 04 p0489 A83-15166
Inversion of ultrasonic scattering data 04 p0489 A83-15168
The theory of flaw centroids and low-frequency phase shifts - A review 04 p0489 A83-15169
The scattering of elastic waves by isolated cracks using a new integral equation model 04 p0491 A83-15201
A global local finite element analysis of axisymmetric scattering of elastic waves [ASME PAPER 82-WA/APM-3] 04 p0498 A83-15686
Axisymmetric elastic waves excited by a point source in a plate [ASME PAPER 82-WA/APM-15] 04 p0498 A83-15687
On one-dimensional acceleration waves in composite materials modeled as interpenetrating solid continua 06 p0776 A83-19000
Longitudinal elastic wave propagation in laminated composites with bonds 06 p0776 A83-19147
Magnetoacoustic rarefaction solitons and the generation of HF oscillations during the dynamic development of a Z-pinch 06 p0813 A83-19187
Three-dimensional nonlinear quasi-monochromatic waves in piezoelectrics with allowance for linear viscosity and heat conduction 06 p0807 A83-19603
Elastic wave scattering by a circular crack 07 p0947 A83-21081
Coupled magnetothermoelastic problem in elastic half-space 07 p0948 A83-21170
Surface waves in cubic elastic materials 10 p1437 A83-25304
Waves in stratified homogeneous elastic media - The method of boundary integrals in nonstationary problems of dynamics --- Russian book 12 p1774 A83-28826
Electromagnetic acoustic transducer for in-plane and plane-normal velocity measurements 12 p1728 A83-29142
A general method for solving problems of elastic-wave diffraction by deformable obstacles 13 p1866 A83-30081
The regularity of one-dimensional elastic waves in an incompressible isotropic material 14 p2030 A83-32356
Measurement of thermoacoustic convection heat transfer phenomenon [AIAA PAPER 83-1422] 14 p2009 A83-32701
Microwave-induced pressure waves in mammalian brains 14 p2065 A83-33109
Instability of finite amplitude elastic waves 15 p2177 A83-34337
Coupling of Love waves with the bulk elastic waves in the substrate --- for microwave applications 16 p2344 A83-35433
On the excitation of elastic waves in a half-space containing a horizontal elastic cylindrical inclusion 16 p2365 A83-35549
Electrostrictive limit and focusing effects in pulsed photoacoustic detection 18 p2692 A83-39261
Application of a modified scheme of the method of characteristics to calculate the propagation of a plane loading-wave 18 p2698 A83-39503
Critical-cone channeling of thermal phonons at a sapphire-metal interface 19 p2903 A83-40954
Propagation of flexural waves in noncircular cylinders with initial stresses 19 p2860 A83-42007
Corotating pressure waves without fast streams in the solar wind 20 p3080 A83-42401
A comparison of two theories of acoustoelasticity 21 p3152 A83-44493
Shear waves in fiber composites 23 p3427 A83-47171
Strong pressure waves in air-breathing engines 23 p3398 A83-48216
Channeled acoustic waves - Elastic waves of a new type of polydomain ferroelectrics 24 p3634 A83-48866
Determination of changes in the sound velocity in shock loaded Ti-6Al-4V with in-material manganin gauges 24 p3566 A83-49833

ELASTICITY

U ELASTIC PROPERTIES

ELASTICIZERS

U PLASTICIZERS

ELASTIN

- Circulating antibodies to aortic elastin and their significance in atherosclerosis in humans 23 p3499 A83-48674

ELASTODYNAMICS

NT ELASTIC DAMPING

NT ELASTOHYDRODYNAMICS

- On the dynamic analysis and behavior of industrial robotic manipulators with elastic members [ASME PAPER 82-DET-45] 02 p0187 A83-12771

- A linear finite element approach to the solution of the variational inequalities arising in contact problems of structural dynamics 02 p0196 A83-12838
An experimental investigation of dynamic crack propagation --- for PMMA 03 p0302 A83-13199
Elastic-plastic finite element analysis of dynamic fracture 04 p0495 A83-15062
The diffraction of a nonstationary transverse wave by a cylindrical cavity 04 p0497 A83-15385
An antplane problem concerning crack propagation in a lattice 04 p0497 A83-15388
The damping of the elastic vibrations of structures with liquids 04 p0487 A83-15391
Axisymmetric elastic waves excited by a point source in a plate [ASME PAPER 82-WA/APM-15] 04 p0498 A83-15687
Concerning the dynamic bending of plastic plates 04 p0499 A83-15877
Flutter of a buckled plate as an example of chaotic motion of a deterministic autonomous system 04 p0501 A83-16339
An experimental and theoretical study of the rebound of short rods from a solid obstacle 04 p0501 A83-16396
Wave propagation in a unidirectional composite in comparison with that in a layered elastic body 04 p0455 A83-16397
A mathematical theory of wave propagation in media with memory --- Russian book 05 p0654 A83-17130
Higher order flexural transients in a beam 05 p0654 A83-17322
On the resonant nonlinear traveling waves in a thin rotating ring 06 p0770 A83-17975
Optimal finite element discretization - A dynamic programming approach --- for structural analysis of linear elastic systems 06 p0773 A83-18230
Uniqueness and continuous data dependence in dynamical problems of nonlinear thermoelasticity 06 p0775 A83-18806
Inverse dynamic problems for an anisotropic elastic medium 07 p0944 A83-19632
Averaging of a system of elasticity theory with almost-periodic coefficients 07 p0945 A83-20141
Propagation of plane waves of a two-component strain state in a nonlinear-elastic compressible medium 07 p0945 A83-20146
Stationary shock-wave propagation in multi-component medium and its reflection from contact discontinuity 07 p0927 A83-21450
A numerical method for the solution of static and dynamic three-dimensional elasticity problems 08 p1122 A83-21892
The effect of an axial force on a conical body 08 p1122 A83-22056
Moving Griffith crack in an orthotropic material 08 p1123 A83-22722
A theory of viscoelastic composites modeled as interpenetrating solid continua with memory 09 p1280 A83-24136
An algorithm for kinetoelastodynamic analysis of plane mechanisms with rectilinear elements 09 p1280 A83-24505
On a certain dynamic crack problem in elastic and elastic-plastic media 09 p1282 A83-25104
Minimax estimation of the torsion of thin-walled rods 10 p1439 A83-25613
A finite element method for construction of dynamical theories of layered plates 11 p1591 A83-27429
Crack propagation and arrest in plastic medium 11 p1593 A83-27771
A simple mixed formulation for elastica problems 11 p1600 A83-28724
A preliminary look at control augmented dynamic response of structures [AIAA 83-0850] 12 p1708 A83-29825
Vibrational characteristics of a nonlinear system associated with asymmetry in the elastic response 14 p2029 A83-32157
The diffraction of longitudinal shear waves by a rigid tunnel inclusion in an elastic half-space 14 p2030 A83-32379
A mixed-mode crack analysis of rotating disk using finite element method 14 p2031 A83-32658
Quasi-dynamical systems and the stabilization of elastic vibrations with controls whose range is restricted to a finite number of values 15 p2220 A83-33875
Operator split methods in the numerical solution of the finite deformation elastoplastic dynamic problem 15 p2176 A83-34314
On physical and material conservation laws 15 p2177 A83-34335
Behavior of solutions of dynamic problems near the edge of a crack propagating at transonic velocity in an elastic medium 15 p2178 A83-34436

- On certain properties of the second energy variation in problems of the elastic stability of discrete conservative systems 15 p2178 A83-34440
Elastic composites 16 p2364 A83-35505
Brittle fracture of plates in tension - Relative significance of boundary reflected body and Rayleigh waves 16 p2368 A83-36516
The determination of the elastodynamic fields of an ellipsoidal inhomogeneity [ASME PAPER 83-APM-19] 17 p2519 A83-37388
The effect of flexible satellite elasticity on orientation accuracy 17 p2479 A83-37470
Simple waves in a nonlinear-elastic medium 17 p2522 A83-38071
An axisymmetric-elastodynamic analysis of a crack in orthotropic media using a path-independent integral 17 p2523 A83-38393
Change in vibrations of an flexible rotor due to a change in bearings 18 p2695 A83-39423
Determination of zones of crack distribution in flexible specimens --- of aluminum alloys 18 p2666 A83-39509
Analytical methods in rotor dynamics 19 p2854 A83-41519
Diffraction of SH waves by a moving crack 19 p2860 A83-41999
The opening of a crack in the elastic region under the effect of a moving load 20 p3008 A83-43524
Transient response of a central crack to a tensile pulse 21 p3161 A83-45168
An approximate solution to a plane contact elasticity problem 21 p3162 A83-45302
The asymptotic behavior of singular perturbations in the problem of the dynamics of a rigid body with elastic and dissipative elements 21 p3200 A83-45356
Free motions of a nearly spherical deformable solid 21 p3200 A83-45357
Electroelasticity relationships for multilayer piezoceramic shells with layer polarization in the thickness direction 21 p3163 A83-45365
Dynamics of a rupture-shear crack at the interface of two elastic materials 21 p3164 A83-45394
Impact response of a cracked orthotropic medium 23 p3469 A83-47597
On wave propagation in random particulate composites 23 p3428 A83-48095
A note on the dynamic stress field near a propagating crack 23 p3470 A83-48099
A partitioned finite element method for dynamical systems 23 p3471 A83-48166
Application of the quadratic functional to nonconservative problems of elastic stability 23 p3471 A83-48170
The dynamics of systems with elastic elements of high rigidity 23 p3504 A83-48461
On dynamics and stability of continuous systems subjected to a distributed moving load 23 p3473 A83-48496
Analysis of the elastic vibrations of manipulators by the finite element method 24 p3594 A83-49447
Dynamic problem of elasticity theory for a region with curved slits (plane strain) 24 p3594 A83-49534
Strain energy density fracture criterion in elastodynamic mixed mode crack propagation 24 p3594 A83-49863
Analytical determination of the crack path and elastic energy release rate under cyclic loading with allowance for welding stresses 24 p3596 A83-49915
Deliberations on the improvement of the computational model with measured eigenmagnitudes --- for linear elastomechanic systems 24 p3596 A83-50128
- ELASTOHYDRODYNAMICS**
The lubrication of roller bearing ribs - Hydrodynamic approach 01 p0056 A83-10225
Analysis of the squeeze film under elastohydrodynamic conditions 01 p0056 A83-10584
Infrared emission spectrophotometric study of the changes produced by TiN coating of metal surfaces in an operating EHD contact [ASLE PREPRINT 82-LC-3C-3] 03 p0333 A83-13229
The lubrication of the roller-rib contacts of a radial cylindrical roller bearing carrying thrust load [ASLE PREPRINT 82-LC-3C-1] 03 p0334 A83-13238
Elastohydrodynamic lubrication of finite line contacts [ASME PAPER 82-LUB-4] 03 p0335 A83-13503
Analysis of gas lubricated compliant thrust bearings [ASME PAPER 82-LUB-39] 03 p0336 A83-13518
Jet flow of an ideal liquid past a flexible shell 06 p0760 A83-19430
An energy analysis of the stability of flexible filaments in coaxial flow 07 p0926 A83-20899
Surface roughness effects in point contact elastohydrodynamic lubrication 08 p1111 A83-22008

Thermoelastohydrodynamic analysis of an oil pumping ring seal 08 p1111 A83-22322

The anomalous Doppler effect and the radiation instability of oscillator motion in hydrodynamics 09 p1260 A83-24214

Hydrodynamic added-mass identification from resonance tests --- vibrations of structure immersed in fluid 09 p1280 A83-24670

The effect of an elastic wall on the boundary layer 10 p1413 A83-25593

Slip measurement in an angular contact ball bearing [ASME PAPER 81-LUB-33] 13 p1858 A83-30243

Effect of inlet shear heating due to sliding on elastohydrodynamic film thickness 13 p1858 A83-30244

The influence of surface dents and grooves on traction in sliding EHD point contacts 17 p2516 A83-37823

Annular squeeze films with inertial effects 18 p2695 A83-39942

Determination of transfer functions in the problem of the unsteady interaction of a fluid with an elastic elliptical shell 18 p2702 A83-40119

Analysis of multirecess conical hydrostatic thrust bearings under rotation 21 p3147 A83-44373

An investigation into the effect of coolant flow on the vibration characteristics of hollow blades conveying fluid [ASME PAPER 83-GT-217] 23 p3470 A83-48017

Gas bearings. II - Design data for centrally loaded partial arc journal bearings 23 p3466 A83-48155

Inverse problem of the two-dimensional theory of elasticity in the hydrodynamic formulation 23 p3473 A83-48535

ELASTOMERS

NT VITON

NT VULCANIZED ELASTOMERS

Polysulfide sealants for aerospace. I - Theory and background 03 p0302 A83-13562

Elastomermodified epoxy resins for composite applications 07 p0876 A83-20476

Dynamic impact tests of radiated and temperature conditioned elastomers 09 p1238 A83-23628

Base-bleed solid propellants with thermoplastic elastomers as binders 09 p1241 A83-23839

Penthrine in castable composite explosives 09 p1242 A83-23847

Elastomeric binders for electrodes --- in secondary lithium cells 14 p1998 A83-32638

Thermal response characterization of a microballoon-loaded silicone rubber [AIAA PAPER 83-1472] 14 p1998 A83-32726

Expanded uses of infrared scanning data in aerodynamic heating materials tests [AIAA-PAPER 83-1542] 14 p1979 A83-32766

Experimental evaluation of ablative elastomeric insulators --- for thermal protection of liquid fueled propulsion system combustors 16 p2336 A83-35861

Fluoroelastomers --- materials for hostile fluid environments 16 p2336 A83-36066

The development of flame retarded thermoplastic polyurethane elastomers 21 p3116 A83-44665

Crosslinking of fluorocarbon elastomers - Characterization of crosslinking system to obtain transparent, tough materials 22 p3270 A83-46906

Power turbine dynamics - An evaluation of a shear-mounted elastomeric damper [ASME PAPER 83-GT-228] 23 p3466 A83-48025

ELASTOPLASTICITY

Concerning models of thin plates in elastoplasticity 02 p0189 A83-11854

Derivation of Wells' COD estimation formula and re-calculation of gamma values 02 p0190 A83-12047

Elastoplastic behavior of a fiber laminate 02 p0150 A83-12340

Our discrete-Kirchhoff and isoparametric shell elements for nonlinear analysis - An assessment 02 p0193 A83-12740

On the solution of elastic-plastic static and dynamic postbuckling collapse of general structure 02 p0194 A83-12746

Environmental fatigue crack growth analysis based on elastic-plastic fracture mechanics [ASME PAPER 82-PVP-23] 02 p0196 A83-12769

Investigation of the thermoelastoplastic state of shells of revolution with allowance for creep deformations 03 p0340 A83-14067

Basic properties of elastic-plastic boundaries in stress wave propagation in a bar 03 p0341 A83-14484

Plane stress problems of the elastic perfectly-plastic medium 03 p0341 A83-14486

An iteration procedure for reducing the expenses of static, elastoplastic and eigenvalue problems in finite element analysis 03 p0389 A83-14697

System identification for yield limits and hardening moduli in discrete elastic-plastic structures by nonlinear programming 04 p0494 A83-14959

A creep type strategy used for tracing the load path in elastoplastic post buckling analysis 04 p0494 A83-15009

Studies on plastic structures - Stability, anisotropic hardening, cyclic loads 04 p0495 A83-15012

Nonlinear analysis of elasto-plastic shells by hybrid stress finite elements 04 p0495 A83-15017

Finite element analysis of plates with nonlinear properties 04 p0495 A83-15018

Computer graphics displays of nonlinear calculations 04 p0526 A83-15019

A simple finite element for elastic-plastic deformations of shells 04 p0495 A83-15020

A mechanical model to predict elastic-plastic fracture toughness in high strength materials 04 p0458 A83-15061

Elastic-plastic finite element analysis of dynamic fracture 04 p0495 A83-15062

Plasticity analysis of laminated composite plates [ASME PAPER 82-WA/APM-11] 04 p0498 A83-15680

Application of convex analysis to the calculation of stress-state in elastic-plastic plates 04 p0500 A83-16097

Elastic-plastic finite element analyses of short cracks 05 p0655 A83-17675

Elastic-plastic analysis of thermally loaded cylindrical shells 05 p0655 A83-17719

An elastic-plastic finite element analysis of a compact tension specimen 05 p0655 A83-17721

An elastic-plastic constitutive equation for transversely isotropic materials and its application to the bending of perforated circular plates 05 p0656 A83-17947

PANDA - Interactive computer program for preliminary minimum weight design of composite or elastic-plastic, stiffened cylindrical panels and shells under combined in-plane loads 06 p0773 A83-18227

Crack separation energy rates for inclined cracks in an elastic-plastic material 06 p0774 A83-18479

A thermodynamic description of the running crack problem 06 p0774 A83-18489

Elastic-plastic fields in steady crack growth 06 p0774 A83-18492

The fracture of a unidirectional fiber composite with an elastoplastic matrix under compression 06 p0725 A83-18503

Some theoretical considerations and experimental results concerning elastic-plastic stress-strain relations 06 p0778 A83-19323

A study of the elastic-plastic state of bodies of revolution under variable nonisothermal loading with allowance for creep 06 p0778 A83-19543

Why ductile fracture mechanics 07 p0944 A83-19669

Evaluation of fracture toughness J sub Ic/ using single specimen fracture test augmented by finite element analysis 07 p0883 A83-19670

The conservation laws of a viscoelastoplastic medium with finite strains 07 p0945 A83-19945

On method of successive approximations in a class of problems of the general theory of plasticity 07 p0945 A83-20142

Long term elastoplastic behavior of solar boiler tubes 07 p0945 A83-20366

Buckling of a thin-walled conical shell under axisymmetric loads beyond the elastic limit 07 p0947 A83-21087

Stress state for the off-axis tension of perforated materials 07 p0947 A83-21090

A finite element model for thin-walled members 07 p0949 A83-21443

Nonlinear analysis of the statics of thin axisymmetric shells by the finite element method 08 p1114 A83-21629

Buckling of a conical sandwich shell beyond the elastic limit under combined load 08 p1115 A83-21637

Defect forces, defect couples and path integrals --- J integral study of crack propagation stability 08 p1115 A83-21656

Near-crack tip finite strain analysis 08 p1116 A83-21662

The influence of specimen geometry on stable crack growth for a high strength steel 08 p1060 A83-21704

The implications of recent developments in elastic plastic fracture mechanics on the growth of stress corrosion cracks 08 p1061 A83-21719

A J based engineering usage of fracture mechanics 08 p1117 A83-21725

High strain fracture analysis 08 p1062 A83-21739

Simplified determination of J-integral and its availability as a strain intensity parameter at notch tip 08 p1118 A83-21750

Plastic effects in dynamic crack propagation 08 p1118 A83-21776

Crack-tip plasticity for rapid crack propagation 08 p1118 A83-21777

Dynamic steady antiplane shear crack growth in an elastic-plastic material 08 p1119 A83-21779

Inelastic analysis of surface flaws using the line-spring model 08 p1119 A83-21792

Deflections of elastic-plastic hyperstatic beams under cyclic loading 08 p1120 A83-21810

Investigation of shock wave structure in elasto-visco-plastic bars using the asymptotic method 08 p1120 A83-21815

Application of the initial value method to analysis of elastic-plastic plates and shells of revolution 08 p1121 A83-21890

Effects of morphology and hardness of inclusions on ductile fracture 08 p1066 A83-22078

Study on the elastic-plastic buckling strength of plate structures 08 p1123 A83-22422

J-integral analysis for cracks emanated from elliptical holes 09 p1275 A83-23298

The load-carrying capacity of shells with softened regions 09 p1277 A83-23506

A solution technique for indirect boundary integral equation in planar elasto-plastic problems 09 p1278 A83-23668

The applicability of the theory of small elastoplastic deformations in the case of simple loading 09 p1280 A83-24237

The existence of a solution to a class of elasticity problems 09 p1282 A83-25020

On a certain dynamic crack problem in elastic and elastic-plastic media 09 p1282 A83-25104

On minimum-principles for the initial-boundary-value problem of elastic-plastic plates with moderate rotations 09 p1283 A83-25217

The theory of elastic ideally plastic systems --- Russian book 09 p1283 A83-25222

The theory of finite plastic deformation of crystalline solids 10 p1437 A83-25309

Aspects of plastic postbuckling behavior 10 p1437 A83-25312

Elastic-plastic crack growth 10 p1438 A83-25314

The method of R-functions in problems of the theory of small elastoplastic deformations 10 p1439 A83-25594

Three-dimensional elastoplastic finite element analysis 10 p1442 A83-26767

The stability of elastoplastic arches and cylindrical panels 10 p1442 A83-26821

Crack propagation and arrest in plastic medium 11 p1593 A83-27771

Elastic-plastic boundary element analysis as a linear complementarity problem 11 p1593 A83-27774

The effect of prior elastic-plastic cyclic deformation on the mechanical characteristics of 1201 alloy at cryogenic temperatures 11 p1550 A83-28517

Method for low-cycle fatigue testing of isothermal and nonisothermal loading 11 p1550 A83-28618

Elastic-plastic behavior of coldworked holes [AIAA 83-0865] 12 p1738 A83-29753

The generation of residual stresses in metal-forming processes 12 p1715 A83-29908

Finite element analysis of slow crack growth 12 p1747 A83-29942

Variational methods in elasticity and in elastoplasticity for multilayered structures --- French thesis 12 p1747 A83-29947

The inverse problem of elastic-plastic deformation for a shallow shell 13 p1866 A83-30307

Elasto-plastic analysis of anisotropic plates and shells by the Semiloof element 13 p1868 A83-31639

Anisotropic elasto-plastic finite element analysis of thick and thin plates and shells 13 p1868 A83-31640

Simple methods of estimating the stress and strain at the notch root 14 p2033 A83-33089

Bounds on displacements for elastoplastic structures by the application of energy methods 14 p2033 A83-33113

Numerical analysis of ductile fracture experiments using single-edge notched tension specimens 15 p2134 A83-33511

J(Ic) measurement point determination for HY130, CMS-9, and Inconel Alloy 718 15 p2134 A83-33514

The structure of stress-strain relations in finite elasto-plasticity 15 p2174 A83-34144

Operator split methods in the numerical solution of the finite deformation elastoplastic dynamic problem 15 p2176 A83-34314

Stress-strain-temperature curves in pseudoelastic bodies 15 p2177 A83-34338

Plane plastic strain in close proximity to a crack tip 15 p2178 A83-34437

Existence of solutions for dynamic problems of one-dimensional plastic structures 16 p2365 A83-35552

An experimental study of the failure of elastoplastic cylindrical shells under combined loading 16 p2365 A83-35929

A solution to the bending problem for an elastic-plastic shell 16 p2366 A83-35930

Evaluation of J-integral value by using finite element method 16 p2369 A83-36968

Isoparametric finite element analysis of large elasto-plastic strain problems and its applications in fracture mechanics 17 p2518 A83-37272

Tensile loading of a plate with a crack near a reinforced hole filled with an elastic disk 17 p2521 A83-37643

Dynamic fields near a crack tip growing in an elastic-perfectly-plastic solid 17 p2524 A83-38528

Dynamic elasto-plastic response of shells in an acoustic medium - EPSA code 17 p2524 A83-38570

On the crack energy density and energy release rate for an elasto-plastic crack 18 p2697 A83-39456

Mathematical modeling of the elastic-plastic deformation of composite materials with disperse fillers 18 p2649 A83-39479

A technique for measuring the large elastoplastic deformations of dynamically loaded plates and shells 18 p2698 A83-39501

On the applicability of the Kirchhoff-Love hypothesis to the elastoplastic calculation of nonuniformly heated shells 18 p2698 A83-39507

A singular element for a new experimental method of fracture toughness determination 18 p2699 A83-39539

Fatigue life prediction of notched members based on local strain and elastic-plastic fracture mechanics concepts 18 p2699 A83-39543

Discussion - 'The Mises elastic-plastic boundary as the core region in fracture criteria' by P. S. Theocaris and N. P. Andrianopoulos 18 p2699 A83-39550

Further remarks on an exact solution for crack problems 18 p2699 A83-39551

Experimental and theoretical study of the elastoplastic buckling of cylindrical shells under axial impact 18 p2702 A83-40118

Analysis of the elastoplastic behavior of (0 deg/90 deg) and + Theta/-Theta) bidirectionally fiber-reinforced ductile matrix composites in uniaxial loading 18 p2653 A83-40174

Study on elasto-plastic fracture toughness of composite materials 18 p2654 A83-40197

A displacement formulation for the finite element elastic-plastic problem 19 p2857 A83-41153

A singular approximation in the theory of elastoplastic media with microstructures 19 p2858 A83-41218

Elastoplastic double-wall shells under complex nonisothermal loading 19 p2859 A83-41603

A remark on the definition of hardening, softening and perfectly plastic behavior 19 p2860 A83-42000

Elastic-plastic-creep behaviour of a compact-tension specimen 20 p3002 A83-42831

On elastic-plastic analysis of I-beams in bending and torsion 20 p3003 A83-42929

Fracture mechanics J-integral calculations in thermo-elasto-plasticity 20 p3003 A83-42931

ADINA modeling of elastoplastic shear/compression waves in tubes 20 p3004 A83-42936

Effective constitutive equations for fiber-reinforced viscoplastic composites exhibiting anisotropic hardening 20 p3004 A83-42974

On inverse problem in elasticity and plasticity 20 p3006 A83-42994

Elastic-plastic interaction of Dugdale type cracks and plastified matrix material in self-stressed fibre-reinforced composites 20 p3006 A83-42996

On the initial boundary-value problem of elastic-plastic plates with finite deformations 20 p3006 A83-43002

Structural stability considerations in elastic-plastic fracture mechanics [ASME PAPER 83-PVP-40] 20 p3009 A83-43728

Estimation of stress and strain at the notch root in the elastic-plastic range using the J-integral 21 p3151 A83-44062

The elastic solution of the dynamic elastic-plastic response of a circular plate 21 p3151 A83-44104

On some recent developments in the shakedown theory 21 p3154 A83-44660

A dissipation postulate for discrete and continuous plastic systems 21 p3155 A83-44849

On the modelling of the process region at crack growth 21 p3156 A83-44891

Comparison of finite element solutions with analytical and experimental data for elastic-plastic cracked problems 21 p3156 A83-44894

3-D elastic-plastic investigation of fracture parameters in side-grooved compact specimen 21 p3157 A83-44906

The effect of work-hardening on plane strain crack growth under small scale yielding conditions 21 p3157 A83-44907

Large increments technique in the elastic-plastic analysis 21 p3159 A83-44932

A boundary element solution to elasto-plastic torsion of solids of revolution 21 p3160 A83-45053

An experimental determination of the fields of strains and stresses in the elastoplastic range 21 p3162 A83-45169

Three-dimensional elastic-plastic finite element analysis of small surface cracks 21 p3162 A83-45182

Combined experimental and numerical method for determining stress concentrations 21 p3163 A83-45316

Elastoplastic state of a conical tube 21 p3164 A83-45393

Elastoplastic crack propagation (fatigue and failure) 22 p3305 A83-45977

A new method for the determination of the critical value of crack tip opening displacement at the initiation of crack growth using a single three-point bend specimen 22 p3305 A83-46025

Numerical solution of problems in the mechanics of a deformable inhomogeneous solid 23 p3468 A83-47177

The effect of plastic deformation on the acoustoelastic response of metals 23 p3469 A83-47599

Extremum principles for the energy-release problem of elastic-perfectly plastic body subjected to prescribed change of material properties 23 p3470 A83-48093

Dynamic finite element analysis of nonaxisymmetric structures 23 p3471 A83-48163

A representation of elasticity and plasticity laws in plane problems 23 p3472 A83-48462

Analysis of plane elastic-plastic shock-waves from the fourth-order anharmonic theory 23 p3474 A83-48603

The vibration of an elastic-plastic plate under the effect of normal impact loads 24 p3592 A83-49030

A method for solving problems of localized plastic flow 24 p3592 A83-49031

A numerical study of the plastic adaptation of plates and shells of revolution by equilibrium finite elements 24 p3594 A83-49645

Crack growth resistance characterized by the strain energy density function 24 p3595 A83-49867

Elasto-plastic analysis of an anisotropic rotating disc 24 p3597 A83-50146

ELASTOSTATICS

Three dimensional crack analysis for an anisotropic body 01 p0059 A83-10709

Fundamental solutions for the collocation method in planar elastostatics 01 p0060 A83-10711

Interactive computer graphic preprocessing for three-dimensional boundary-integral element analysis 02 p0228 A83-12744

Elastohydrodynamic lubrication of finite line contacts [ASME PAPER 82-LUB-4] 03 p0335 A83-13503

A numerical method for the solution of static and dynamic three-dimensional elasticity problems 08 p1122 A83-21892

The boundary integral method for the solution of planar multicrock problems of linear elastostatics --- German thesis 09 p1281 A83-24846

A boundary integral equation for the solution of a class of problems in anisotropic inhomogeneous thermostatics and elastostatics 10 p1470 A83-25874

Smooth contact between a rigid indenter and an initially stressed orthotropic beam 11 p1592 A83-27441

A method of determining structural flexibility matrix from static experiment data 12 p1747 A83-29944

The elastic distortion of rollers under combined radial and thrust loads 13 p1858 A83-30245

Finite element, boundary element and coupled analysis of unbounded problems in elastostatics 13 p1868 A83-31641

Existence of solutions in finite elasticity 15 p2176 A83-34327

Local theorems of existence and uniqueness in finite elastostatics 15 p2177 A83-34345

Elastic composites 16 p2364 A83-35505

Smooth contact between a rigid indenter and an initially stressed orthotropic beam 16 p2366 A83-36092

Some observations on Kelvin's solution in classical elastostatics as a double tensor field with implications for Somigliana's integral 16 p2369 A83-36550

An integral equation approach for simultaneous solution of rectangular hole and rectangular block problems 20 p3004 A83-42972

Solutions of plates on a heterogeneous elastic foundation 23 p3471 A83-48164

The elastostatic axisymmetric problem of a sphere containing a penny-shaped crack in a nonequatorial plane 24 p3591 A83-48869

ELBOW (ANATOMY)

Heterotopic ossifications in regions of the elbow joint and their treatment with ultrasound 01 p0084 A83-11393

ELECTRIC APPLIANCES

U ELECTRIC EQUIPMENT

ELECTRIC ARCS

NT MERCURY ARCS

Current distribution in MPD arcjets with applied magnetic fields [AIAA PAPER 82-1918] 03 p0289 A83-13600

An examination of instabilities of an electric arc at atmospheric pressure --- French thesis on relation to cathodic material properties 03 p0294 A83-13805

Study of electrical faults in magnetohydrodynamic Faraday generators 04 p0538 A83-16106

Experimental and theoretical study of a dc arc in an orifice nozzle flow [AIAA PAPER 83-0399] 05 p0636 A83-16692

A comparative study of the properties of refractory coatings obtained by electric-arc metallization and plasma spraying 07 p0889 A83-20704

CW recombination laser action in a cadmium vapor arc 07 p0938 A83-21370

Effects of arc current on the life in burner-rig thermal cycling of plasma-sprayed ZrO₂-O₃ 08 p1072 A83-22270

Arc damage of interelectrode insulators in MHD generators 13 p1924 A83-30198

Chemical preparation of ultra-fine aluminium nitride by electric-arc plasma 18 p2671 A83-39054

ELECTRIC AUTOMOBILES

Status cells - A demonstration of performance reproducibility, capacity retention, and cycle life for LiAl/FeS cells 04 p0506 A83-15868

Lithium/metal sulfide cells and battery development progress at Eagle-Picher Industries 11 p1602 A83-27165

Comparison of Na/S and LiAl/FeS batteries 11 p1603 A83-27169

Design considerations for a lithium-aluminum/iron sulfide electric vehicle battery 11 p1603 A83-27173

Acid fuel cell technologies for vehicular power plants 11 p1604 A83-27185

Status of solid polymer electrolyte fuel cell technology and potential for transportation applications 11 p1604 A83-27186

Laboratory facility for testing electric-vehicle batteries Test rig for simulating duty cycles with different discharge modes 16 p2371 A83-35554

Aluminum-air battery development - Toward an electric car 20 p3057 A83-42976

The energetic optimization of propulsion systems for electric vehicles --- Dutch thesis 21 p3221 A83-45075

ELECTRIC BATTERIES

NT ALKALINE BATTERIES

NT DRY CELLS

NT LEAD ACID BATTERIES

NT METAL AIR BATTERIES

NT NICKEL CADMIUM BATTERIES

NT NICKEL HYDROGEN BATTERIES

NT NICKEL ZINC BATTERIES

NT PRIMARY BATTERIES

NT REDOX CELLS

NT SODIUM SULFUR BATTERIES

NT STORAGE BATTERIES

NT THERMAL BATTERIES

NT ZINC-BROMIDE BATTERIES

NT ZINC-CHLORINE BATTERIES

NT ZINC-OXYGEN BATTERIES

Investigation and production control of Li/SO₂ cells by the galvanostatic pulse method 01 p0068 A83-10796

Batteries and fuel cells: Design, employment, chemistry --- German book 03 p0355 A83-14041

Status cells - A demonstration of performance reproducibility, capacity retention, and cycle life for LiAl/FeS cells 04 p0506 A83-15868

Conductive polymers imitate metals 05 p0617 A83-16873

Self-discharge behavior of engineering-scale LiAl/FeS cells 07 p0952 A83-19879

Lithium cycling in polymethoxymethane solvents --- for use in batteries 10 p1390 A83-26058

Integration of large electrical space power systems 11 p1602 A83-27153

Lithium/metal sulfide cells and battery development progress at Eagle-Picher Industries 11 p1602 A83-27165

Development of a tubular LiAl/FeS cell battery 11 p1603 A83-27166

Relaxation-phenomena in LiAl/FeS-cells 11 p1603 A83-27167

Flexible ceramic powder separators for molten salt electrolyte galvanic cells 11 p1603 A83-27168

Comparison of Na/S and LiAl/FeS batteries 11 p1603 A83-27169

Design considerations for a lithium-aluminum/iron sulfide electric vehicle battery 11 p1603 A83-27173

Performance of a 10-cell LiAl/metal sulfide battery 11 p1603 A83-27174

Large nickel alkaline batteries 11 p1604 A83-27176

Reliability modeling of high voltage batteries 11 p1540 A83-27200

The electrochemistry of molten lithium chlorate and its possible use with lithium in a battery 11 p1546 A83-28296

Expected cycle life vs. depth of discharge relationships of well-behaved single cells and cell strings 14 p2046 A83-32627

Voltammetric study of the anodic oxidation of sulfide ions in molten fluorides 14 p1989 A83-32630

Laboratory facility for testing electric-vehicle batteries Test rig for simulating duty cycles with different discharge modes 16 p2371 A83-35554

Statistical analysis of lithium iron sulfide status cell cycle life and failure mode 20 p3013 A83-43419

Battery storage in residential applications of energy from photovoltaic sources 24 p3599 A83-49622

Heat loss measurements on an enclosure for high temperature batteries 24 p3599 A83-49926

A possible mechanism for the reduction of voltage delay in the Li/SOCl₂ system via cyanoacrylate coatings on lithium 24 p3599 A83-49929

International Meeting on Lithium Batteries, Rome, Italy, April 27-29, 1982 24 p3600 A83-49932

The reactivity of organic electrolytes with lithium Mechanistic aspects 24 p3558 A83-49934

Film forming reaction at the lithium/electrolyte interface 24 p3558 A83-49935

Raman spectroscopic studies of the structure of electrolytes used in the Li/SOCl₂ battery 24 p3558 A83-49936

Polarization of the lithium electrode in sulfonyl chloride solutions 24 p3558 A83-49939

Mechanistic studies of oxide electrodes reversibly incorporating Li(+) ions 24 p3558 A83-49941

Li-AgBi(CrO₄)₂ - A new highly reliable lithium battery for long service life applications 24 p3600 A83-49945

Characterization of the chemistry at the anode and cathode in the Li/SO₂ battery system 24 p3600 A83-49948

Behaviour of AgBi(Cr₂O₇)₂ as a possible cathode for lithium cells 24 p3601 A83-49953

The anodic passivation of lithium 24 p3558 A83-49956

ELECTRIC BRIDGES

NT WHEATSTONE BRIDGES

Digital computer simulation of 3-phase full-wave SCR bridge regulator 01 p0043 A83-11252

High-sensitivity resistivity technique for studies of defect behavior 08 p1106 A83-23234

Microwave contactless technique for photoconductivity measurements 11 p1573 A83-27980

A superconducting flip-flop using two interacting weak links 20 p2966 A83-42604

Unbalanced-bridge computational techniques and accuracy for automated multichannel strain-measuring systems 21 p3141 A83-45147

A proposed back action evading read-out for a gravitational wave detector 23 p3459 A83-48593

ELECTRIC CHARGE

NT ELECTRIC DIPOLES

NT ELECTROSTATIC CHARGE

NT ION CHARGE

NT ORBITING DIPOLES

NT SPACE CHARGE

NT TRAVELING CHARGE

Corona type sensor for aircraft electrical potential measurement [ONERA, TP NO. 1982-73] 03 p0282 A83-14530

The influence of a net charge on the critical mass of a neutron star 05 p0702 A83-17807

Infinity subtraction in a quantum field theory of charges and monopoles 06 p0805 A83-18330

Electric charge in the Kruskal space-time and the Jeans conjecture 06 p0841 A83-19447

Variation of e/m in the five-dimensional theory of gravitation, electromagnetism, and scalar field 07 p0989 A83-20852

A new approach to soot control in Diesel engines by fuel-drop charging 13 p1859 A83-31225

Electrodynamics of submicron dust in the cometary coma 13 p1958 A83-31733

The radiation of charges moving in the vicinity of individual localized inhomogeneities 14 p2007 A83-33299

The fine-structure constant, magnetic monopoles and dirac charge quantization condition 15 p2225 A83-34275

Determination of the charging current of a plate in an aerosol flow when a liquid film is separated from its surface 17 p2503 A83-37266

A two-dimensional model of the electrocoagulation-hygroscopic dissipation of warm fogs 18 p2724 A83-39442

Emission from a moving charge during the instantaneous appearance of gyration in the medium 20 p3043 A83-42874

ELECTRIC CHOPPERS

Exact and approximated analysis of voltage-commutated dc-to-dc converters 01 p0041 A83-11024

Results of chopper-controlled discharge life cycling studies on lead-acid batteries 11 p1604 A83-27183

ac characteristics in ac/dc/dc conversion 14 p2006 A83-32427

ELECTRIC CIRCUITS

U CIRCUITS

ELECTRIC COILS

NT MAGNETIC COILS

Advances in cryogenic engineering, Volume 27 - Proceedings of the Cryogenic Engineering Conference, San Diego, CA, August 11-14, 1981 20 p2960 A83-43220

ELECTRIC CONDUCTORS

Electrothermal inspection of conducting materials 01 p0057 A83-10364

Two-parameter gap independence in eddy-current thickness gauging on conducting plates, strips, films, and coatings 01 p0057 A83-10368

A new expression for the scattering of a Gaussian beam by a conducting cylinder 01 p0033 A83-11356

A hybrid diffraction technique - General theory and applications 01 p0104 A83-11357

Electroconducting glass fibres produced by ion-exchange and reduction treatments 02 p0159 A83-11674

Physically motivated approximations in some inverse scattering problems 02 p0233 A83-12632

A stochastic Fourier transform approach to scattering from perfectly conducting randomly rough surfaces 03 p0306 A83-14014

Electromagnetic transmission through apertures in a cavity in a thick conductor 03 p0306 A83-14016

A simple technique for solving E-field integral equations for conducting bodies at internal resonances 03 p0307 A83-14035

Scattering of a plane electromagnetic wave by a conducting circular cylinder of finite length 03 p0307 A83-14134

New computation method for characteristic modes --- eigenvalue equation solution for perfectly conducting object 04 p0466 A83-15234

The method of moving coordinates as a technique for comparing various electrodynamic problems in systems having cylindrical conductors 04 p0467 A83-15746

The shape factor of the capacitance of a conductor 04 p0472 A83-16053

Conductive polymers imitate metals 05 p0617 A83-16873

The excitation of a metal-bar grating by a current passing across one of the gaps 05 p0630 A83-17594

Generation of field scattered by imperfectly conducting objects from the solution of a perfectly conducting object 06 p0736 A83-18575

Scattering by a conducting tube of finite length 06 p0737 A83-18608

The thermal limitation of the velocity of annular conductors under inductive axial acceleration 06 p0755 A83-19561

An analysis of coplanar waveguides with finite conductor thickness-computation and measurement of characteristic impedance 07 p0918 A83-20070

Change in impedance of a single-turn coil due to a flaw in a conducting half space 07 p0942 A83-20270

Complex eigenfrequencies of axisymmetric perfectly conducting bodies - Radar spectroscopy 07 p0916 A83-21544

Complex-frequency poles and creeping-wave transients in electromagnetic-wave scattering 07 p0916 A83-21545

New results on coherent scattering from randomly rough conducting surfaces 09 p1246 A83-23776

The loop antenna with a cylindrical core - Theory and experiment 10 p1405 A83-26826

Electromagnetic plane wave scattering by a system of two parallel conducting prolate spheroids 10 p1405 A83-26836

Cylindrical eigencurrents --- during electromagnetic scattering by conducting surfaces 10 p1406 A83-26840

Algorithm for the calculation of the current distribution of electrically long curvilinear conductors 10 p1412 A83-26961

Electrical characteristics of a probe in a subsonic plasma flow 11 p1658 A83-27717

An admittance solution for electromagnetic coupling through a small aperture 12 p1718 A83-29402

Calculation of electromagnetic scattering by a perfect conductor 12 p1776 A83-29605

Diffraction of an H-polarized electromagnetic wave by a circular cylinder with an infinite axial slot 15 p2148 A83-35176

Creeping waves and resonances in transient scattering by smooth convex objects 15 p2148 A83-35177

A spectral-iteration technique for analyzing scattering from arbitrary bodies. I - Cylindrical scatterers with E-wave incidence 15 p2148 A83-35186

A spectral-iteration technique for analyzing scattering from arbitrary bodies. II - Conducting cylinders with H-wave incidence 15 p2149 A83-35198

Investigation of the efficiency of the acceleration of conductors in the pulsed magnetic field of a solenoid 16 p2340 A83-35540

The effect of a gravitational wave at the contact of conductors 17 p2585 A83-38952

On a classification of one-dimensional conductors 17 p2585 A83-38966

Simplified computation of coplanar waveguide with finite conductor thickness 20 p2966 A83-42363

A dynamic technique for measurements of thermophysical properties at high temperatures 20 p2991 A83-43257

Characteristic impedance of an oval located symmetrically between the ground planes of finite width --- for transmission lines 21 p3123 A83-43840

Electrically conducting polymers 21 p3216 A83-43947

Microstructure and properties of injection molded conductive plastics 21 p3106 A83-44059

Conducting shells in a pulsed electromagnetic field --- Russian book 21 p3126 A83-45047

Hybrid solutions for scattering from perfectly conducting bodies of revolution 23 p3442 A83-47828

Certain characteristics of the vibration of plates in a magnetic field 23 p3472 A83-48469

First indication of Ampere tension in solid electric conductors 23 p3445 A83-48592

Numerical methods for problems of electromagnetic-wave diffraction by ideally conducting screens 24 p3573 A83-49272

ELECTRIC CONNECTORS

High voltage distribution and grounding in high power spacecraft 11 p1539 A83-27156

Laser-formed connections using polyimide --- on integrated circuits 13 p1832 A83-30346

Wear of connector contacts exposed to relative motion 13 p1835 A83-30865

Disequilibria in series connected solar cells - An approach to the protection by parallel diodes 14 p2004 A83-32213

ELECTRIC CONTACTS

Wear of connector contacts exposed to relative motion 13 p1835 A83-30865

The characteristics of Au-Ge-based ohmic contacts to n-GaAs including the effects of aging 14 p2006 A83-32671

Electrical characteristics of amorphous iron-tungsten contacts on silicon 15 p2238 A83-33851

Schottky barrier height variation with metallurgical reactions in aluminum-titanium-gallium arsenide contacts 16 p2419 A83-35671

Low cost process for ohmic contacts on GaAs/Ga(1-x)Al(x)As concentrator solar cells based on palladium and gold deposition 20 p2965 A83-42353

A superconducting flip-flop using two interacting weak links 20 p2966 A83-42604

Internal contacts to photovoltaic structures using ion beam milling 21 p3167 A83-44604

Interfacial chemistry of electrical contacts on GaAs and Al_{0.3}Ga_{0.7}As 21 p3109 A83-44614

Far-field distributions of semiconductor phase-locked arrays with multiple contacts 21 p3145 A83-44953

Phase-locked semiconductor laser array with separate contacts 22 p3299 A83-46721

Characterization of WS_i(x)/GaAs Schottky contacts 22 p3278 A83-46739

ELECTRIC CONTROL

Instabilities in current-mode controlled switching voltage regulators 01 p0039 A83-11003

The use of piezoceramic vibrators in vibrating mounts for spacecraft scientific instrumentation 10 p1387 A83-25348

A scanned antenna with an electrically controlled lens 11 p1559 A83-28684

All-electric vs conventional aircraft - The production/operational aspects 14 p1974 A83-32576

Electrohydraulic fuel-flow regulator for gas-turbine-engine control systems 16 p2311 A83-36793

The all electric airplane-benefits and challenges [SAE PAPER 821434] 17 p2463 A83-37982

- Mode-locked semiconductor lasers with gateable output and electrically controllable optical absorber 20 p2995 A83-43595
- An analytical design of electrohydraulic position servo systems with variable structure 21 p3118 A83-44038

ELECTRIC CORONA

- Altitude, thickness and charge concentration of charged regions of four thunderstorms during trip 1981 based upon in situ balloon electric field measurements 07 p0958 A83-20093
- A mechanism to explain the generation of earthquake lights 09 p1307 A83-24696
- Space charge measurement using a small sphere as a probe 10 p1423 A83-26500
- Recent advances in interpretation of corona test results 11 p1602 A83-27154
- Corona preionization technique for CO₂ TEA lasers 11 p1580 A83-27580
- Corona point measurements in a thundercloud at Langmuir Laboratory 13 p1892 A83-30903
- Radio noise fields generated by corona streamers on a power line 16 p2341 A83-35414
- Corona discharge in a moving gas 19 p2902 A83-41262
- Laboratory and in flight passive dischargers characterization --- for elimination of electrostatic radiation interference [ONERA, TP NO. 1983-54] 23 p3400 A83-48176
- ELECTRIC CURRENT**
- NT ALTERNATING CURRENT
- NT ARC DISCHARGES
- NT AURORAL ELECTROJETS
- NT BALL LIGHTNING
- NT BEAM CURRENTS
- NT DIRECT CURRENT
- NT EDDY CURRENTS
- NT ELECTRIC ARCS
- NT ELECTRIC CORONA
- NT ELECTRIC DISCHARGES
- NT ELECTRIC SPARKS
- NT ELECTRODELESS DISCHARGES
- NT ELECTROJETS
- NT EQUATORIAL ELECTROJET
- NT GAS DISCHARGES
- NT GLOW DISCHARGES
- NT HIGH CURRENT
- NT IONOSPHERIC CURRENTS
- NT LIGHTNING
- NT MERCURY ARCS
- NT PENNING DISCHARGE
- NT PLASMA CURRENTS
- NT RADIO FREQUENCY DISCHARGE
- NT RING CURRENTS
- NT SHORT CIRCUIT CURRENTS
- NT TELLURIC CURRENTS
- NT THRESHOLD CURRENTS
- Loading schemes for a 50 MWth diagonally connected MHD generator 01 p0106 A83-10659
- Determination of the integral currents of solar cells using an improved method of spectral sensitivity measurement 02 p0200 A83-11696
- Magnetic field at the tip of a crack around which current flows 02 p0188 A83-12159
- Experimental investigation of a Hall-current accelerator [AIAA PAPER 82-1920] 02 p0241 A83-12491
- Thinning of field-aligned currents 03 p0357 A83-13544
- NDE of fastener hole cracks by the electric current perturbation method 04 p0491 A83-15192
- Correlation between substrate and gate currents in MOSFET's 05 p0630 A83-17754
- Generation of field scattered by imperfectly conducting objects from the solution of a perfectly conducting object 06 p0736 A83-18575
- Maxwell currents under thunderstorms 07 p0960 A83-20217
- Determination of surface recombination velocity at a grain boundary using electron-beam-induced current 07 p0999 A83-20736
- The diffuse radio aurora and field-aligned currents 07 p0964 A83-21182
- Infrared application to the detection of induced surface currents 08 p1103 A83-22845
- The generation of electric currents by the turbulent flow of dielectric liquids. II - Pipes of finite length 12 p1722 A83-29158
- Oriented crystallization of metals in the presence of electric current 13 p1822 A83-30906
- Does IMF B(y) induce the cusp field-aligned currents? 13 p1882 A83-31626
- Heating of the polar ionosphere by electric currents at various substorm phases 14 p2049 A83-31865

- Electric currents and magnetic fields of a plasma inhomogeneity in the inner magnetosphere 14 p2050 A83-31867
- Grain boundary photocurrent enhancement in solar cells made by laser diffusion 14 p2046 A83-32332
- The healing of cracks in metals by means of crossed electric and magnetic fields 14 p1993 A83-32383
- Induction in power transmission lines during geomagnetic disturbances 14 p2053 A83-32898
- Electroplastic deformation of metals (Review) 15 p2140 A83-35046
- On the temperature rise associated with the electroplastic effect in titanium 17 p2486 A83-37300
- Theory of beam induced current characterization of grain boundaries in polycrystalline solar cells 17 p2535 A83-37614
- The effect of a gravitational wave at the contact of conductors 17 p2585 A83-38952
- The appearance of nonuniform electric fields and currents associated with auroral arcs 18 p2713 A83-39321
- Experiment of artificial lightning triggered with rocket 18 p2731 A83-40335
- A solar cell with enhanced photocurrent 19 p2861 A83-40667
- Gating currents in the membrane of the nerve fiber Pharmacological analysis 21 p3185 A83-45374
- The lightning current 22 p3339 A83-45878
- The boundary layer of the magnetosphere and longitudinal electric currents 23 p3484 A83-48383
- The stability of a longitudinal electric current in a viscous-fluid cylinder in a longitudinal magnetic field 23 p3510 A83-48395

ELECTRIC DIPOLES

- NT ORBITING DIPOLES
- Radiation patterns of interfacial dipole antennas 02 p0165 A83-12631
- The emission of electromagnetic waves in the case of a smooth variation of parameters of a radiating system 03 p0390 A83-13427
- New formulas for the electromagnetic field of a vertical electric dipole in a dielectric or conducting half-space near its horizontal interface [AD-A125370] 04 p0468 A83-16054
- Dipole-field sums and Lorentz factors for orthorhombic lattices, and implications for polarizable molecules 05 p0690 A83-17226
- Stripline dipole with dielectric covering 09 p1243 A83-23381
- On the possibility of microwave generation in the case of avalanche processes in dipole domains 09 p1252 A83-23468
- The excitation of a perfectly conducting multihedral body 09 p1251 A83-25083
- Antennas for nonsinusoidal waves. I - Radiators 10 p1404 A83-26489
- Experimental verification of the breakdown of the electric dipole rotational selection rule in electron impact ionization-excitation of N₂ 11 p1653 A83-27493
- The threshold laws for electron-atom and positron-atom impact ionization 13 p1915 A83-30177
- A method for the calculation of the spatial position of the dipole generators of multidipole model of the equivalent generator of the heart 14 p2073 A83-32958
- Diffraction of an electric-dipole field by an ideally conducting sphere loaded on a rectangular slot 15 p2145 A83-34709
- Relative performances of central and dipole frequency soundings over a layered earth 15 p2202 A83-34748
- Radio noise fields generated by corona streamers on a power line 16 p2341 A83-35414
- Antennas for nonsinusoidal waves. II - Sensors 16 p2342 A83-35781
- Analysis of electromagnetic propulsion of nonionized dipole gases [AIAA PAPER 83-1395] 16 p2322 A83-36385
- Electromagnetic radiation from a dipole source in a homogeneous magnetoplasma 20 p3050 A83-43417
- Paraelectric resonance --- Russian book on microwave spectroscopy of tunneling dipole centers in crystals 21 p3216 A83-43917
- The effects experienced by a point electric dipole in a gravity field 24 p3623 A83-49455

ELECTRIC DISCHARGES

- NT ARC DISCHARGES
- NT BALL LIGHTNING
- NT ELECTRIC ARCS
- NT ELECTRIC CORONA
- NT ELECTRIC SPARKS
- NT ELECTRODELESS DISCHARGES
- NT GAS DISCHARGES
- NT GLOW DISCHARGES
- NT LIGHTNING

- NT MERCURY ARCS
- NT PENNING DISCHARGE
- NT RADIO FREQUENCY DISCHARGE
- Plastic-bonded electrodes for nickel-cadmium accumulators. X - The nature of the second discharge step of nickel oxide electrodes 01 p0068 A83-10793
- Sources of photoionization in transversely excited atmospheric CO₂ lasers 01 p0055 A83-10978
- A study of secondary-emission microwave discharges with large electron transit angles 01 p0104 A83-11300
- Study on the chemical evolution of low molecular weight compounds in a highly oxidized atmosphere using electric discharges 02 p0226 A83-11630
- Experimental investigation of an argon hollow cathode [AIAA PAPER 82-1890] 02 p0241 A83-12472
- Supersonic nozzle beam source of atomic oxygen produced by electric discharge heating [AD-A122032] 02 p0234 A83-12819
- Current distribution in MPD arcjets with applied magnetic fields [AIAA PAPER 82-1918] 03 p0289 A83-13600
- Spectroscopic measurements on discharges along a dielectric surface 04 p0538 A83-16061
- Carbon monoxide laser with selective and nonselective resonators 05 p0648 A83-17048
- High-brightness ultraviolet radiation source based on a cumulative plasmadynamic discharge 05 p0687 A83-17079
- Quasi-CW lasing of a Ne-Xe-HCl mixture excited by an electric discharge 05 p0650 A83-17083
- Pulsed high-pressure chemical HF laser with electric-discharge initiation 05 p0650 A83-17084
- Enhanced electron emission from positive dielectric/negative metal configurations on spacecraft 05 p0607 A83-17490
- Electrical conductivity and discharge in spacecraft thermal control dielectrics 05 p0618 A83-17491
- Environmentally induced discharges in a solar array 05 p0610 A83-17493
- Characteristics of RF resulting from dielectric discharges 05 p0626 A83-17494
- Charging and discharging characteristics of dielectric materials exposed to low- and mid-energy electrons 05 p0618 A83-17500
- Self-discharge behavior of engineering-scale LiAl/FeS cells 07 p0952 A83-19879
- Divergence of radiation from an electric-discharge CO₂ laser having an unstable resonator 07 p0934 A83-20108
- Problems associated with electrodischarge machined, electrochemically machined and ultrasonically machined surfaces 08 p1111 A83-22007
- Analysis, design and construction of rare-gas halide discharge lasers 09 p1271 A83-23695
- Experimental study of an axial discharge in a turbulent gas flow 10 p1430 A83-26252
- Electric-discharge CW industrial CO₂ laser 10 p1433 A83-26687
- Relaxation-phenomena in LiAl/FeS-cells 11 p1603 A83-27167
- Discharge rate capability of nickel-cadmium aircraft batteries 11 p1530 A83-27190
- Diatom molecules as storage media for high energy lasers 11 p1580 A83-27573
- Experimental investigation of the optimum specific input energy on a subsonic CO EDL --- Electric Discharge Laser 11 p1580 A83-27577
- UV-preionized rare gas halide lasers with plasma electrodes 11 p1582 A83-27612
- Breakdown of dynamic equilibrium between the symmetric and deformation mode levels in CO₂ caused by excitation in an electrical discharge 13 p1915 A83-30828
- Expected cycle life vs. depth of discharge relationships of well-behaved single cells and cell strings 14 p2046 A83-32627
- Quasi-continuous excitation regime of electric-discharge exciplex lasers 15 p2168 A83-33980
- Plasma waves and electrical discharges stimulated by beam operations on a high altitude satellite 15 p2233 A83-34183
- Laboratory facility for testing electric-vehicle batteries Test rig for simulating duty cycles with different discharge modes 16 p2371 A83-35554
- Saturn's electrostatic discharges - Properties and theoretical considerations 16 p2436 A83-35733
- Saturn's electrostatic discharges - Could lightning be the cause? 16 p2436 A83-35734
- Plasma pump sources for lasers 16 p2416 A83-35892
- The electrostatic-discharge phenomena on Marecs-A 17 p2480 A83-37871
- Electric discharge pulses in irradiated solid dielectrics in space 17 p2480 A83-38040

- Electrostatic discharges in Saturn's B-ring
17 p2621 A83-38121
- Excitation of violent discharge of charged bodies ---
planetary rings or interplanetary medium
17 p2609 A83-38414
- Characteristics of two types of Beam Plasma Discharge
in a laboratory experiment
19 p2901 A83-41124
- Discharge with electrostatic containment in order to
obtain high performance ion sources
19 p2902 A83-41323
- Mechanism of pulse emission from high-pressure
electric-discharge He-Ar, He-Kr, and He-Xe infrared
lasers
20 p2986 A83-43783
- Maximum input energy for an externally sustained CO2
laser discharge
21 p3143 A83-44144
- The auroral arc as an electrical discharge between the
ionosphere and magnetosphere
21 p3175 A83-45242
- Summary of environmentally induced electrical
discharges on the P78-2 (SCATHA) satellite
23 p3423 A83-48127
- Relative efficiency of Hg-200Br-79, HgBr-79, and HgBr
electric discharge lasers
24 p3586 A83-43781
- Dielectric surface discharges - Effects of combined
low-energy and high-energy incident electrons
24 p3572 A83-48900
- Electric-discharge CO2-laser based on products of the
reaction of oxygen and carbon
24 p3588 A83-49055
- Holographic device for rectilinear surface discharge
visualization
[ONERA, TP NO. 1983-104]
24 p3583 A83-49415
- Li/SOCl2 cells for high temperature applications
24 p3600 A83-49940
- ELECTRIC ENERGY STORAGE**
- Pelletized lithium-metal sulphide cells. II - Some
operating characteristics of pelletized LiAl-FeS cells
01 p0068 A83-10792
- A design for zinc-chlorine batteries
01 p0068 A83-10794
- A failure model for sealed nickel-cadmium batteries
01 p0068 A83-10795
- On the anomalous behaviour of deeply discharged,
sealed Ni-Cd cells
01 p0068 A83-10797
- Parametric study of minimum reactor mass in
energy-storage dc-to-dc converters
01 p0040 A83-11011
- Energy storage and power conditioning for electric
propulsion
[AIAA PAPER 82-1953]
02 p0147 A83-12510
- The energy of electric current sheets. I - Models with
moving magnetic dipoles
03 p0438 A83-14912
- Development of the spherical silicon solar cell
05 p0658 A83-17347
- Electricity from wind - A survey of the state of the art
and future prospects for research and development
[DGLR PAPER 82-081]
09 p1293 A83-24202
- A zinc paste primary battery --- for electric vehicles
10 p1445 A83-26052
- Application of microprocessor-based controls in an
ac/dc power conversion system
11 p1559 A83-27151
- Application of electrochemical energy storage in solar
thermal electric generation systems
11 p1604 A83-27179
- Analysis of fixed-base flywheel systems for electric utility
applications
11 p1609 A83-27310
- The calculation of energy storage flywheels of fiber
composites with electric energy converter --- German
thesis
11 p1590 A83-28666
- The photovoltaic solar system - Analysis and basic
design rules
14 p2039 A83-32209
- Optimization of the energy-storage inductors for dc-to-dc
converters
14 p2007 A83-33130
- Air Storage System Energy Transfer (ASSET) plants
22 p3320 A83-46778
- Advanced electrolysis development for hydrogen-cycle
peak shaving for electric utilities
22 p3320 A83-46779
- Superconducting magnetic energy storage
22 p3320 A83-46780
- 30-MJ superconducting magnetic energy storage system
for electric utility transmission stabilization
22 p3320 A83-46781
- Battery storage in residential applications of energy from
photovoltaic sources
24 p3599 A83-49622
- ELECTRIC EQUIPMENT**
- Methods for minimizing the effects of lightning transients
on aircraft electrical systems
01 p0009 A83-11088
- ECS schemes for All Electric Airliners
[SAE PAPER 820870]
10 p1375 A83-25769
- All-electric vs conventional aircraft - The
production/operational aspects
14 p1974 A83-32576
- Design aspects of systems in all-electric aircraft
[SAE PAPER 821436]
17 p2463 A83-37984
- Regenerative electric heater of gas for a gasdynamic
laser
24 p3588 A83-48937
- ELECTRIC EQUIPMENT TESTS**
- High voltage equipment parts evaluation tests --- for
airborne power supplies
01 p0042 A83-11204
- Distance criteria in near-field and far-field antenna
measurements
06 p0740 A83-18640
- Computer simulations of inaccuracies in spherical
near-field testing
06 p0741 A83-18653
- Contemporary electric vehicle testing and evaluation
11 p1667 A83-27160
- Design for random - An example --- vibration testing
power supply for drone aircraft
13 p1861 A83-30856
- Power supplies designed for random vibration
13 p1835 A83-30864
- ELECTRIC FIELD STRENGTH**
- Electron distribution function in a weakly ionized plasma
in an inhomogeneous electric field. II - Strong fields / energy
balance determined by inelastic collisions/
03 p0397 A83-13195
- Assessment of the error in measuring the strength of
a constant electric field by the double-Langmuir-probe
method
03 p0397 A83-13206
- Electric field and space charge density distributions in
the processes of ambipolar plasma diffusion with volume
recombination
05 p0687 A83-16902
- The effect of an electric field of industrial frequency on
parameters of natural immunity
05 p0669 A83-17164
- The nature of the vertical component of the geoelectric
field during magnetic disturbances
05 p0664 A83-17626
- Extremely linear electrically tunable active receiving
antenna
06 p0751 A83-18616
- Persistence of two-state resonances in a hydrogen atom
under the influence of a periodic impulsive field
08 p1162 A83-21984
- Temperature and field dependence of the generation
of interface states in the Si-SiO2 system after high-field
stress
10 p1489 A83-26208
- Photoionisation of krypton atoms in 'strong' electric
fields
11 p1653 A83-27512
- Linear and nonlinear waves in liquid dielectrics
11 p1658 A83-27711
- Electrical characteristics of a probe in a subsonic plasma
flow
11 p1658 A83-27717
- Measurements of the electric field over the Atlantic and
Indian Oceans
11 p1619 A83-28728
- Hollow probe for measuring ion density in a slightly
ionized plasma flow
12 p1728 A83-29008
- Electron transport in InP at high electric fields
13 p1929 A83-30353
- Electric field in the polar cap
14 p2050 A83-31871
- Raindrop charges, electric field and space charge
measurements at a mountain station covered with
monsoon clouds
14 p2057 A83-32411
- Radar observations of tornadoes and the field intensity
of atmospherics
14 p2057 A83-32414
- The artificially injected charged particles as a tool for
the measurement of the electric field in the
magnetosphere
15 p2198 A83-34215
- Calculation of the electrostatic field strength above the
lunar surface covered by a hydrogen monolayer
15 p2276 A83-34770
- A critical analysis of the results of treatment of
heliometric observations of the moon
15 p2276 A83-34771
- Electric field and electron density measurements in the
equatorial E-region
16 p2373 A83-35367
- Oscillating bipolar electric field changes due to close
lightning return strokes
16 p2383 A83-35413
- The biological effect of the electric component of an
electromagnetic field in the VLF range
16 p2393 A83-35921
- Stimulated emission of oscillators in the case of the
application of a weak longitudinal electrostatic field
17 p2515 A83-38493
- Electric conductivities, electric fields and auroral particle
energy injection rate in the auroral ionosphere and their
empirical relations to the horizontal magnetic
disturbances
17 p2544 A83-38518
- Distribution of electric-field potential near a satellite
injecting electrons in the steady-state regime in the initial
stage of active experiments in the ionosphere
18 p2713 A83-39319
- Investigation of a probe sensor of electric field strength
with a Pockels-effect cell
19 p2849 A83-41816
- Large amplitude middle atmospheric electric fields - Fact
or fiction?
20 p3026 A83-43210
- Comparison of spherical double probe electric field
measurements with plasma bulk flows in plasmas having
densities less than 1 cm-3 --- magnetosphere
parameters
20 p3026 A83-43211
- Parametric excitation of electrohydrodynamic surface
waves
20 p3051 A83-43671
- Compact uniform field electrode profiles --- for use in
TEA laser
21 p3143 A83-44191
- On the anomaly of the electrical field strength in the
magnetized positive column of glow discharges at small
currents
21 p3212 A83-44351
- Calculation of the electric fields due to the azimuthal
component of the interplanetary magnetic field for the
conditions of solstice
21 p3175 A83-45249
- ELECTRIC FIELDS**
- NT EXTERNAL SURFACE CURRENTS**
- Calculation of axisymmetric H-modes in dielectric
resonators by the integral-equation method
01 p0035 A83-10406
- The screen effect of the earth in the TETG - Theory
of a screening experiment of a sample body at the equator,
using the earth as a screen --- electrothermodynamic
theory of gravitation
01 p0127 A83-11044
- Single-particle problem concerning the motion of a
relativistic particle in a static electric field
01 p0104 A83-11349
- Impedance of a radiating slot in the ground plane of a
microstripline
01 p0033 A83-11362
- The structure of electron avalanches at high E/P ---
electric field - pressure relations
02 p0241 A83-11956
- Generation of a longitudinal electric field during the
heating of the magnetospheric plasma
02 p0211 A83-12450
- Dipolar field propulsion - Principles and concepts
[AIAA PAPER 82-1933]
02 p0146 A83-12499
- A simple technique for solving E-field integral equations
for conducting bodies at internal resonances
03 p0307 A83-14035
- A formulation of the finite-length narrow slot or strip
equation
03 p0313 A83-14036
- Electric field detection with a piezoelectric
polymer-jacketed single-mode optical fiber
03 p0330 A83-14384
- The principle of electrostatic stationarity and the electric
field of the sun and planets
03 p0426 A83-14688
- Fracture mechanics in the presence of electric fields
--- for piezoelectrics
04 p0539 A83-15393
- Resonance structure of the photoionization cross
section of atomic hydrogen in an electric field
04 p0534 A83-15903
- Coupled three-dimensional flow and electrical
calculations for Faraday MHD generators
04 p0538 A83-16107
- Relationship between field-aligned currents, diffuse
auroral precipitation and the westward electrojet in the
early morning sector
05 p0661 A83-17397
- Convection electric fields and ionospheric currents
derived from model field-aligned currents at high
latitudes
06 p0783 A83-18297
- Linear theory of the E x B instability with an
inhomogeneous electric field --- of ionospheric plasmas
06 p0785 A83-18311
- Loaded Q's and field profiles of tapered axisymmetric
gyrotron cavities
06 p0752 A83-18759
- A multiple-device cavity oscillator using both magnetic
and electric coupling mechanisms
06 p0753 A83-18769
- Fixation of bubbles and drops of specified shapes in a
liquid dielectric by an electric field
06 p0813 A83-19434
- Characteristics of Schottky diodes at 10.6 microns
07 p0918 A83-19988
- Investigation of the operation of dispersive optical
components
07 p0995 A83-20115
- A one-dimensional model of the atmospheric electric
field near the Venusian surface
07 p1030 A83-20619
- Visualization of the electric field around a moving animal
by numerical calculation
07 p0976 A83-21172
- Solitary waves and double layers on auroral field lines
07 p0966 A83-21517
- A sounding rocket observation of an apparent wake
generated parallel electric field
07 p0967 A83-21521
- An empirical electric field model derived from Chatanika
radar data
07 p0967 A83-21522
- Crack depth measurements using AC potential drop
08 p1113 A83-22408
- Holtmark electric field distribution in a two-dimensional
electron fluid
08 p1168 A83-22950
- Electric field effects in the thermal decomposition of
solids
08 p1057 A83-23254
- Experiences with two new lightning localization
devices
09 p1310 A83-23405
- Ionospheric electric field pulsations - A comparison
between VLF results from an ionospheric heating
experiment and STARE
09 p1304 A83-23770
- On the existence of branch points in the eigenvalues
of the electric field integral equation operator in the
complex frequency plane
09 p1253 A83-23787

The mirror image relation in the vertical distributions of electric field and precipitation charge in winter thunderclouds 09 p1311 A83-23897

Theory of the motion of a relativistic charged particle in highly nonuniform crossed electric and magnetic fields 09 p1348 A83-23984

Dawn-dusk electric field asymmetry of the Io plasma torus 09 p1366 A83-24340

Direct inversion of one-dimensional magnetotelluric data 09 p1308 A83-25069

On the spectral expansion of the electric and magnetic dyadic Green's functions in cylindrical harmonics 10 p1472 A83-26037

Electric field enhanced diffusion in trans/CH/x --- battery cells 10 p1446 A83-26053

Theoretical analysis of the rhombic simulator under pulse excitation 10 p1411 A83-26493

Optical-fiber copolymer-film electric-field sensor 10 p1423 A83-26636

Whistler observations of magnetospheric electric field in the night side plasma-sphere at low latitude 11 p1619 A83-28383

Electric fields in coronal magnetic loops 11 p1692 A83-28581

Annual variations in the gradient of the electric field potential in the atmosphere and their relationship with the forms of atmospheric circulation 11 p1634 A83-28727

Cyclical processes in the atmospheric electric field 11 p1620 A83-28734

The effects of meridional electric fields in the high-latitude ionosphere 11 p1620 A83-28746

Changes in the ionosphere caused by longitudinal electric fields 11 p1620 A83-28748

Fluctuations of the parameters of the longitudinal waves of an electric field in a turbulent-plasma flow 12 p1780 A83-29259

Hydrogen and lithium atoms in a strong electric field 13 p1915 A83-30266

Observation and quasistatic analysis of structure in microwave ionization of highly excited helium atoms 13 p1915 A83-30597

The electrostatic potential of a two-layer three-element symmetric array 13 p1833 A83-30718

Axial expansion of the electron pulse in a free-electron laser 13 p1854 A83-31118

The effect of space charge fields due to finite length electron beams in the free-electron laser 13 p1854 A83-31119

Design considerations of a Compton scattering free-electron laser with an axial electrical field 13 p1855 A83-31131

Observations of large magnetospheric electric fields during the onset phase of a substorm 13 p1878 A83-31231

The plasmaspheric electric field as measured by ISEE 13 p1878 A83-31232

Evidence for electrostatic shocks as the source of discrete auroral arcs 13 p1879 A83-31242

Effect of electric fields on long-wavelength response of infra-red detectors 13 p1931 A83-31762

Polymerization of brain tubulin in and around the area of application of an electric field 14 p2061 A83-31818

The reaction of the ionosphere to variations of electric fields during nighttime baylike disturbances 14 p2049 A83-31866

The hydrogen atom in weak electric and magnetic fields 14 p2082 A83-32140

On the quantitative analysis of fields of active regions --- of sun 14 p2115 A83-32539

On the possibility to determine integral characteristics of the cardiac electric generator from extracardiac electric and magnetic measurements 14 p2072 A83-32799

Induction in power transmission lines during geomagnetic disturbances 14 p2053 A83-32898

Space-time and space-averaged equations for a two-mirror laser - Theory and numerical results 14 p2025 A83-32917

Parallel electric fields and shear instabilities --- in magnetosphere 15 p2195 A83-33934

Joule heating at high latitudes 15 p2196 A83-33941

On the use of artificially injected energetic electrons as indicators of magnetospheric electric fields parallel to the magnetic lines of force 15 p2197 A83-34180

Plasma diagnostics by electron guns and electric field probes on ISEE-1 15 p2233 A83-34184

On the averaged forces in bounded plasma in parallel electric and magnetic fields 15 p2236 A83-35236

Nonlinear electrohydrodynamic Rayleigh-Taylor instability. I. A perpendicular field in the absence of surface charges 16 p2414 A83-35347

Numerical calculations of low-frequency TE fields in arbitrarily shaped inhomogeneous lossy dielectric cylinders 16 p2407 A83-35407

The stability of plane-parallel electrohydrodynamic flows in a longitudinal electric field 16 p2414 A83-35528

Electron current disruption and parallel electric fields associated with electrostatic ion cyclotron waves 17 p2538 A83-37582

Conjugate observations of Pc 5 electric fields with a geostationary satellite and a ground radar facility 17 p2538 A83-37596

An unguided wave Cerenkov amplifier 17 p2497 A83-37754

Semidirect/marching solutions and elliptic grid generation 17 p2574 A83-38807

SAW convolvers using the transverse-horizontal bilinear field 17 p2500 A83-38877

The effect of a gravitational wave at the contact of conductors 17 p2585 A83-38952

Particle acceleration during the explosive phase of a solar flare 18 p2780 A83-39003

Drift wave in the presence of a time varying inhomogeneous electric field 18 p2746 A83-39856

Marangoni effects under electric fields 18 p2686 A83-39911

Experiment of artificial lightning triggered with rocket 18 p2731 A83-40335

Nonlinear electrohydrodynamic Rayleigh-Taylor instability. II - A perpendicular field producing surface charge 18 p2747 A83-40498

Equatorial disturbance dynamo electric fields 19 p2864 A83-41117

Anomalous electric-field-induced damping of ultrasound in superionic crystals 20 p3051 A83-42265

Behavior of the interplanetary and magnetospheric electric fields during very intense storms 20 p3016 A83-42301

Polarization electric fields in the nighttime F layer at Arecibo 20 p3019 A83-42418

Analysis of space charge in photonic tubes 20 p2966 A83-42588

On the ring current energy injection rate --- effect of geomagnetic storms 20 p3023 A83-43162

Electric-field-dependent charge-carrier trapping in a one-dimensional organic solid 21 p3216 A83-43888

Externally sustained RF discharges in electronegative gases 21 p3211 A83-44143

General form for the electron distribution function for an inhomogeneous fully ionized and magnetized plasma interacting with an alternating electric field 21 p3212 A83-44355

Scattering and precipitation of particles of the magnetotail under the action of the dawn-dusk electric field 21 p3172 A83-44522

A simple velocity gauge for measuring crack growth 21 p3158 A83-44917

Quasi-electrostatic fields within the atmosphere 22 p3325 A83-45879

Electric microfield distributions in strongly coupled plasmas 22 p3361 A83-45935

Ion-Pedersen drift and parallel electric field effects on plasma jetting 22 p3327 A83-46048

Electric field induced effects at the Si-SiO₂ interface 22 p3364 A83-46276

Theory and experiment 22 p3364 A83-46276

A statistical study of large electric field events in the earth's magnetotail 22 p3335 A83-47040

Relative contribution of ionospheric conductivity and electric field to the auroral electrojets 22 p3336 A83-47060

Theoretical possibility of confining a dense adiabatic plasma using a self-consistent electrostatic field of subsonic solitons 23 p3509 A83-47568

Nonlinear theory of type I irregularities in the equatorial electrojet 23 p3482 A83-47869

The interpretation of protons and electrons observations from ATS 6 satellite within the frame of McIlwain's electric field model 23 p3482 A83-48055

PIC magnetic pulsations and variations of the ionospheric electric field and conductivity 24 p3606 A83-49307

ELECTRIC FILTERS

NT CRYSTAL FILTERS

NT DIGITAL FILTERS

NT FIR FILTERS

NT MICROWAVE FILTERS

NT RADAR FILTERS

NT RADIO FILTERS

NT TRACKING FILTERS

NT WAVEGUIDE FILTERS

A novel input filter compensation scheme for switching regulators 01 p0044 A83-11494

Evaluating and lessening the effect of the diffraction of surface acoustic waves on the characteristics of frequency filters 04 p0469 A83-15141

Noise in time-discrete analog filters 09 p1252 A83-23409

A novel feedforward compensation canceling input filter-regulator interaction 14 p2007 A83-33133

ELECTRIC GENERATORS

NT AC GENERATORS

NT ALKALINE BATTERIES

NT DIRECT POWER GENERATORS

NT DRY CELLS

NT DYNAMOMETERS

NT ELECTROSTATIC GENERATORS

NT FUEL CELLS

NT HOMOJUNCTIONS

NT HYDROGEN OXYGEN FUEL CELLS

NT MAGNETOHYDRODYNAMIC GENERATORS

NT METAL AIR BATTERIES

NT NICKEL ZINC BATTERIES

NT PHOSPHORIC ACID FUEL CELLS

NT PRIMARY BATTERIES

NT RADIOISOTOPE BATTERIES

NT REGENERATIVE FUEL CELLS

NT SOLAR CELLS

NT SOLAR GENERATORS

NT SOLAR SEA POWER PLANTS

NT THERMAL BATTERIES

NT THERMIONIC CONVERTERS

NT THERMOELECTRIC GENERATORS

NT TURBOGENERATORS

NT ZINC-OXYGEN BATTERIES

On the design and test of an advanced containment structure for PM machines --- in aircraft electrical power systems 01 p0012 A83-11206

A 400 Hz starter/generator system --- for aircraft engines 01 p0012 A83-11207

High-voltage source of constant voltage 10 p1408 A83-25349

The development of a central electrical generating system for transport vehicles 10 p1411 A83-26885

Optimization of PM machines due to advancements in containment structure 11 p1560 A83-27188

Linear moving magnet motor/generator for Stirling engines 11 p1560 A83-27291

The generation of electric currents by the turbulent flow of dielectric liquids. I - Long pipes 12 p1722 A83-29089

Solar salt pond potential site survey for electrical power generation 13 p1871 A83-31526

Experiments on combined photovoltaic-aeolian electric generation in a residential stand-alone system 14 p2038 A83-32189

Study of a photovoltaic concentrating system like 'Sophocle' in fluctuating mode 14 p2039 A83-32200

Microprogrammed coupling system for photovoltaic generators with multiple receptors 14 p2046 A83-32339

Space or terrestrial energy? 15 p2191 A83-34660

International Conference on Small and Special Electrical Machines, 2nd, London, England, September 22-24, 1981, Proceedings 19 p2839 A83-41472

Brushless generators for remote piloted vehicles 20 p2937 A83-43709

Wind turbine generator interaction with diesel generators on an isolated power system 21 p3167 A83-44673

ELECTRIC HYBRID VEHICLES

A summary of EHV propulsion technology --- Electric and Hybrid Vehicle 13 p1934 A83-31087

EHV systems technology - A look at the principles and current status --- Electric and Hybrid Vehicle 13 p1934 A83-31093

Advanced Vehicle system concepts --- nonpetroleum passenger transportation 13 p1935 A83-31094

The role of computer modeling and simulation in electric and hybrid vehicle research and development 13 p1935 A83-31095

ELECTRIC IMPULSES

U ELECTRIC PULSES

ELECTRIC MOTOR VEHICLES

Transistorized PWM inverter-induction motor drive system 01 p0044 A83-11488

Boriding of nickel and other metals at temperatures below 670 C --- for electric vehicle batteries 07 p0880 A83-19892

A zinc paste primary battery --- for electric vehicles 10 p1445 A83-26052

A mission analysis of 'second' cars to determine electric vehicle suitability 11 p1667 A83-27158

The relative attractiveness of electric and hybrid passenger cars 11 p1667 A83-27159

Contemporary electric vehicle testing and evaluation 11 p1667 A83-27160

An advanced electric vehicle powertrain 11 p1667 A83-27161

Energy utilization of electric and hybrid vehicles 11 p1667 A83-27164

A systems analysis comparing conventional and hydrogen powered rail locomotives 11 p1667 A83-27213

Development history of the Hybrid Test Vehicle 13 p1934 A83-31088

Summary of electric vehicle energy source technologies 13 p1871 A83-31089

The lead-acid battery - Demonstrating the systems design approach to a practical electric vehicle power source 13 p1871 A83-31090

Zinc-bromine battery design for electric vehicles 13 p1871 A83-31091

Fuel cell power plants for automotive applications 13 p1871 A83-31092

Advanced Vehicle system concepts --- nonpetroleum passenger transportation 13 p1935 A83-31094

Electric Vehicle Test and Evaluation Program - Site operators' experience 13 p1935 A83-31096

Electric vehicle field test experience 13 p1935 A83-31097

The timing of EV recharging and its effect on utilities --- Electric Vehicles 13 p1871 A83-31098

Longitudinal control and a new spacing policy for automated transit vehicles 17 p2586 A83-37101

Heat loss measurements on an enclosure for high temperature batteries 24 p3599 A83-49926

ELECTRIC MOTORS

NT ASYNCHRONOUS MOTORS

NT INDUCTION MOTORS

NT MICROMOTORS

NT STEPPING MOTORS

NT SYNCHRONOUS MOTORS

The choice of an astatic system for the regulation of the rotational velocity of a dc electric motor for azimuthal mountings of a gamma-telescope 17 p2496 A83-37720

International Conference on Small and Special Electrical Machines, 2nd, London, England, September 22-24, 1981, Proceedings 19 p2839 A83-41472

Numerical synthesis of time-optimal control for the electric motor of an electromechanical system 20 p2967 A83-42925

Special electrical machines: Sources and converters of energy --- Russian book 21 p3126 A83-45018

Gyromotors --- Russian book 23 p3441 A83-48475

ELECTRIC NETWORKS

Investigation of network tree technology as a tool for developing effective fault isolation procedures 01 p0043 A83-11231

EASYCADC - A VAX implementation of a universal user interface for a system of computer aided circuit design /CADC/ programs 01 p0093 A83-11247

Fundamentals handbook of electrical and computer engineering. Volume 1 Circuits fields and electronics 03 p0314 A83-14047

Electronic Circuit Analysis Language /ECAL/ 04 p0470 A83-15550

A Lagrangian approach to the analysis of nonlinear electromagnetic circuits 07 p0922 A83-20969

The use of the unit cell method for the numerical solution of elasticity problems. II - A network model for an elastic body 09 p1277 A83-23507

High voltage distribution and grounding in high power spacecraft 11 p1539 A83-27156

A simulator of satellite power supply 15 p2129 A83-34422

The synthesis of linear electric and electronic networks (the method of state variables) --- Russian book 21 p3126 A83-45046

Experimental study of the 'Cerenkov' emission of solitons in two-dimensional LC-lattices 23 p3504 A83-48480

ELECTRIC POTENTIAL

NT BIOELECTRIC POTENTIAL

NT CONTACT POTENTIALS

NT COULOMB POTENTIAL

NT LOW VOLTAGE

NT OPEN CIRCUIT VOLTAGE

NT PHOTOVOLTAGES

Polarization phenomena in the transition layer of SOS films 01 p0111 A83-11348

A comparison of theoretical and experimental methods of calibrating the electric potential drop technique for crack length determination 02 p0190 A83-12040

The omega-potential - A quantitative indicator of the condition of the structure of the brain and the organism. II - The possibilities and limitations of the use of the omega-potential for rapid evaluations of the condition of the human body 02 p0222 A83-12212

Effect of cathode keeper potential on the discharge characteristics and stability in a 5 cm diameter ion thruster [AIAA PAPER 82-1914] 02 p0145 A83-12486

Corona type sensor for aircraft electrical potential measurement [ONERA, TP NO. 1982-73] 03 p0282 A83-14530

Influence of interface states on field effect and capacitance-voltage characteristics of metal/oxide/a-Si:H structures 04 p0541 A83-15526

Potentials on large spacecraft in LEO 05 p0607 A83-17489

Electrochemical studies of photocorrosion of n-CdSe 07 p0952 A83-19881

Formation of isobaric discontinuities in large-scale flute drift motions 07 p0995 A83-20055

Crack depth measurements using AC potential drop 08 p1113 A83-22408

Coherent behavior of 2N-Josephson junction closed loop 08 p1081 A83-22769

Measurement of fatigue crack propagation at -70 C with the direct-current potential probe method 09 p1281 A83-24944

High-voltage source of constant voltage 10 p1408 A83-25349

The electrostatic potential of a two-layer three-element symmetric array 13 p1833 A83-30718

Auroral electron interaction with the atmosphere in the presence of conjugate field-aligned electrostatic potentials 13 p1879 A83-31245

Phenomenological theory of shock-induced polarization. I 13 p1915 A83-31383

The electrical behavior of GaAs-insulator interfaces - A discrete energy interface state model 13 p1931 A83-31386

Efficiency of the sequential search for a signal using sign processing of the received voltage 14 p2001 A83-32485

Electric-probe potential in the space plasma 16 p2416 A83-35943

On the electrical potential analysis of a cracked fracture mechanics test specimen using the finite element method 16 p2368 A83-36509

The mechanism of explosive emission excitation in thermionic energy conversion processes 16 p2371 A83-36967

Comparison of S3-3 polar cap potential drops with the interplanetary magnetic field and models of magnetopause reconnection 17 p2538 A83-37598

The capacitance-voltage characteristics of m-i-n GaN light emitting diodes --- metal-insulator-n-type semiconductor 17 p2496 A83-37649

Further observations on resonance cones in non-Maxwellian plasmas 18 p2749 A83-40660

Constant voltage scaling of FETs for high frequency and high power applications 19 p2836 A83-40668

Longitudinal voltage distribution in transverse RF discharge waveguide lasers 20 p2994 A83-42592

Field-aligned current density versus electric potential characteristics for magnetospheric flux tubes 21 p3173 A83-44672

Application of electrical analog technique in fracture mechanics 21 p3155 A83-44883

Analytical solutions for threshold voltage calculations in ion-implanted IGFETs 21 p3127 A83-45177

A decaying volt-ampere characteristic in the longitudinal current region 21 p3176 A83-45266

Drain-voltage effects on the threshold voltage of a small-geometry MOSFET 23 p3446 A83-48606

Transient Workman-Reynolds freezing potentials --- at ice-water interfaces causing thunderstorm electrification and aircraft static 24 p3610 A83-49337

A method for the simulation of the transfer of charge carriers and the distribution of electrostatic potential in semiconductor structures 24 p3575 A83-50208

ELECTRIC POWER

The potential for photovoltaics in Europe 14 p2037 A83-32181

Solar thermal technologies - Potential benefits to U.S. utilities and industry 17 p2536 A83-38023

An approach for the application of generic technologies to solar power satellites [IAF PAPER 83-428] 23 p3477 A83-47379

Emergency power for the F-16 aircraft [ASME PAPER 83-GT-189] 23 p3410 A83-47995

ELECTRIC POWER CONVERSION

U. ELECTRIC GENERATORS

ELECTRIC POWER PLANTS

NT FUEL CELL POWER PLANTS

NT NUCLEAR POWER PLANTS

NT SOLAR THERMAL ELECTRIC POWER PLANTS

Approach to Nitinol power plant cost analysis 01 p0111 A83-10656

Wind power for the electric-utility industry: Policy incentives for fuel conservation --- Book 02 p0201 A83-11896

Investigation of the equations of motion of the heliostats of a tower-type solar electric power plant 04 p0503 A83-15133

Hydrogen as a vector for central receiver solar utilities 04 p0506 A83-16044

Transformation of wind energy by a high-altitude power plant 04 p0507 A83-16112

Methods of reducing energy consumption of the oxidant supply system for MHD/steam power plants [AIAA PAPER 83-0468] 05 p0686 A83-16735

Load following impacts of a large wind farm on an interconnected electric utility system 08 p1131 A83-22675

MHD channel performance for potential early commercial MHD power plants 08 p1169 A83-23134

Electric power - Looking at regenerative systems 09 p1220 A83-24353

Ocean thermal-energy conversion 09 p1294 A83-25125

Assessment of phosphoric acid and trifluoromethane sulfonic acid fuel cells for vehicular powerplants 11 p1602 A83-27162

OTEC plants for today's island market 11 p1606 A83-27227

Research and development on ocean thermal energy conversion in Japan 11 p1606 A83-27228

Design, fabrication, and initial testing of solar one receiver 11 p1606 A83-27229

Design and construction of the 'Solar One' thermal storage subsystem 11 p1606 A83-27230

Cogeneration using a thermionic combustor 11 p1608 A83-27300

Solar thermionic energy converter experiment 11 p1608 A83-27301

The behaviour of large solar power stations in the Swiss Alps 14 p2037 A83-32182

Design, installation, and initial performance of 350-kW photovoltaic power system for Saudi Arabian villages 14 p2037 A83-32183

Advanced system design for solar power plants 14 p2037 A83-32185

15 kW experimental photovoltaic solar power plant 14 p2037 A83-32187

Alicudi project --- photovoltaic solar energy system for electric power supplying 14 p2038 A83-32190

A support structure for intermediate PV solar plant 14 p2039 A83-32207

Minimum cost of photovoltaic energy for a utility grid and general features of a generating plant using costless solar cells. 14 p2040 A83-32214

The atmospheric oxidation of flue gases from a coal-fired power plant - A comparison between smog chamber and airborne plume sampling 15 p2193 A83-33503

Thermal energy storage development for solar electrical power and process heat applications 15 p2189 A83-33987

Source reliability in a combined wind-solar-hydro system 15 p2190 A83-34147

The operating experiences and performance characteristics during the first year of operation of the Crochet Mt. New Hampshire windfarm 15 p2190 A83-34148

Engineering design for a Central Station Photovoltaic Power Plant 15 p2190 A83-34150

Measured effect of wind generation on the fuel consumption of an isolated diesel power system 16 p2371 A83-36410

Infrared optical properties of a coal-fired power plant plume 16 p2372 A83-36760

Magnetohydrodynamic generator scaling analysis for baseload commercial powerplants 17 p2582 A83-38020

Analysis of solar-radiation characteristics at the EURELIOS power plant of Adrano 19 p2862 A83-41165

Economic evaluation of wind energy applications for remote location power supply 20 p3056 A83-43367

Development of a point focusing collector farm system 21 p3166 A83-43898

Conceptual design of A 50 MW central station photovoltaic power plant 22 p3320 A83-46773

Air Storage System Energy Transfer (ASSET) plants 22 p3320 A83-46778

Advanced electrolysis development for hydrogen-cycle peak shaving for electric utilities 22 p3320 A83-46779

Superconducting magnetic energy storage 22 p3320 A83-46780

Combined solar-wind power plants 24 p3599 A83-48958

Operation and control of a 2 GW wave-energy scheme 24 p3599 A83-49000

ELECTRIC POWER SUPPLIES

NT SPACECRAFT POWER SUPPLIES

PESC '81; Power Electronics Specialists Conference, University of Colorado, Boulder, CO, June 29-July 3, 1981, Record 01 p0039 A83-11001

DC-to-dc converter power-train optimization for maximum efficiency 01 p0040 A83-11015

Application of transistor emitter-open turn-off scheme to high voltage power inverters 01 p0041 A83-11019

Power conditioning unit development for MAG-TRANSIT 01 p0041 A83-11021

- A multiprocessor for power electronic circuit simulation
01 p0041 A83-11026
- Large signal design of a buck converter for high power
dc/ac conversion 01 p0041 A83-11028
- Aircraft power management control system designed for
fast response and high reliability 01 p0012 A83-11151
- High voltage equipment parts evaluation tests --- for
airborne power supplies 01 p0042 A83-11204
- Integrated electrical power and avionics control
system 01 p0012 A83-11205
- On the design and test of an advanced containment
structure for PM machines --- in aircraft electrical power
systems 01 p0012 A83-11206
- Electric power supply of aircraft --- Russian book
03 p0282 A83-14115
- Investigation of the operation of a two-stage accelerator
with an anode layer with one power source 06 p0755 A83-19562
- High-voltage power supply materials evaluation
07 p0920 A83-20487
- Configuration selection study for isolated loads --- using
parabolic dish modules to supply power for MX shelters
08 p1132 A83-23137
- The development of a central electrical generating
system for transport vehicles 10 p1411 A83-26885
- High voltage power electronics packaging on NASA's
Space Telescope 11 p1539 A83-27155
- Spacecraft power technology 11 p1539 A83-27157
- Optimization of PM machines due to advancements in
containment structure 11 p1560 A83-27188
- Low power, air-cooled DC-Link aircraft generation
systems 11 p1530 A83-27324
- The loss of power supply probability as a technique for
designing stand-alone solar electrical (photovoltaic)
systems 12 p1749 A83-29896
- Design for random - An example --- vibration testing
power supply for drone aircraft 13 p1861 A83-30856
- Power supplies designed for random vibration
13 p1835 A83-30864
- Residential applications of photovoltaics in the United
States 14 p2038 A83-32193
- Operational experience with intermediate flat-plate
photovoltaic systems 14 p2038 A83-32196
- Solar photovoltaic systems in the development of Papua
New Guinea 14 p2038 A83-32198
- A dc/ac modular interface for photovoltaic systems
14 p2004 A83-32215
- Regulated converter circuit for direct photovoltaic energy
feedback into the power grid 14 p2004 A83-32217
- ac characteristics in ac/dc/dc conversion
14 p2006 A83-32427
- Power supplies for long duration balloon flights
18 p2642 A83-39815
- Brushless generators for remote piloted vehicles
20 p2937 A83-43709
- Special electrical machines: Sources and converters of
energy --- Russian book 21 p3126 A83-45018
- Electronic power devices - An introduction to automated
design --- Russian book 21 p3126 A83-45044
- The prospects and potential of all electric aircraft
[AIAA PAPER 83-2478] 23 p3411 A83-48341
- Direct-current power supply units GVG 800/350
24 p3549 A83-50115

ELECTRIC POWER TRANSMISSION

- Recent advances in interpretation of corona test
results 11 p1602 A83-27154
- High voltage distribution and grounding in high power
spacecraft 11 p1539 A83-27156
- Geomagnetic induction effects in ground-based
systems 11 p1615 A83-27403
- A computing model and its experimental testing for an
evaluation of electromagnetic interferences created by
interfering circuits on transmission or high-voltage lines
above a dissipative ground 14 p2002 A83-32894
- Ground observations of power line radiation coupled to
the ionosphere and magnetosphere 14 p2053 A83-32895
- Induction in power transmission lines during
geomagnetic disturbances 14 p2053 A83-32898
- Maximum power transfer for full-wave rectifier circuits
19 p2838 A83-41150
- Electrical transmission lines as models for soliton
propagation in infrared fibers 22 p3358 A83-46632
- Estimated power quality for line commutated
photovoltaic residential system 24 p3599 A83-49324

ELECTRIC PROPULSION

- NT ELECTROMAGNETIC PROPULSION
- NT ELECTROSTATIC PROPULSION
- NT ION PROPULSION
- NT LASER PROPULSION
- NT PLASMA PROPULSION
- NT SOLAR ELECTRIC PROPULSION

- Space flight test of MDT-2A --- pulsed plasma
microthruster [AIAA PAPER 82-1874] 02 p0143 A83-12462
- Advances in series resonant inverter technology and
its effect on spacecraft employing electric propulsion
[AIAA PAPER 82-1881] 02 p0143 A83-12466
- Operational summary of an electric propulsion long term
test facility [AIAA PAPER 82-1903] 02 p0139 A83-12478
- Dipolar field propulsion - Principles and concepts
[AIAA PAPER 82-1933] 02 p0146 A83-12499
- Electric rail gun projectile acceleration to high velocity
[AIAA PAPER 82-1939] 02 p0146 A83-12501
- Theory of the pulsed electrothermal thruster
[AIAA PAPER 82-1952] 02 p0147 A83-12509
- Energy storage and power conditioning for electric
propulsion [AIAA PAPER 82-1953] 02 p0147 A83-12510
- Free radical propulsion concept 03 p0289 A83-13141
- A comparison of potential electric propulsion systems
for orbit transfer [AIAA PAPER 82-1871] 03 p0283 A83-14375
- Electric propulsion research and technology in the
United States [AIAA PAPER 82-1867] 05 p0609 A83-16925
- A samarium cobalt motor-controller for mini-RPV
propulsion 11 p1530 A83-27187
- A summary of EHV propulsion technology --- Electric
and Hybrid Vehicle 13 p1934 A83-31087
- EHV systems technology - A look at the principles and
current status --- Electric and Hybrid Vehicle 13 p1934 A83-31093
- Characterization of advanced electric propulsion
systems 15 p2129 A83-33744
- Procedures to integrate electric secondary propulsion
systems to large deployable space systems
[AIAA PAPER 83-1392] 16 p2322 A83-36382
- Recent developments in electric propulsion in the
USSR [AIAA PAPER 83-1397] 16 p2322 A83-36387
- Combined orbit and attitude control of geostationary
satellites using electric propulsion 17 p2479 A83-37480
- A low signature RPV 20 p2934 A83-43703
- The energetic optimization of propulsion systems for
electric vehicles --- Dutch thesis 21 p3221 A83-45075

ELECTRIC PULSES

- A magnetically controlled electrovacuum converter of
displacement into pulsed signals 04 p0472 A83-15913
- Analysis of electrophysical processes in the power diode
of a transistorized pulsed dc converter 04 p0472 A83-15916
- The processing of signals of neural ensembles using
modernized analyzers of the pulse-amplitude type
07 p0982 A83-20346
- Numerical modeling of nonisothermal transient
processes in semiconductor power devices under the
effect of a high-power dc pulse 08 p1080 A83-22124
- Electric pulse-time densimeters --- Russian book
10 p1419 A83-25617
- Nonstationary processes during the passage of a current
pulse through a slow-wave system 15 p2153 A83-35165
- The effect of electric current pulses on the tensile
behavior of thin metal wires 16 p2335 A83-36892
- Electric discharge pulses in irradiated solid dielectrics
in space 17 p2480 A83-38040
- Measurement of high-voltage pulses employing a quartz
Pockels cell 20 p2990 A83-42790
- The estimate of probability distribution of the dominant
frequencies for the lightning during an eclipse of the sun
21 p3179 A83-44587
- Widening the energy and technological possibilities of
equipment for light beam welding with the pulsed feed of
arc xenon lamps 22 p3301 A83-45701
- An experimental investigation of the parallel-plate EMP
simulator with single-pulse excitation 22 p3279 A83-46934
- First indication of Ampere tension in solid electric
conductors 23 p3445 A83-48592
- Simultaneous pulses in light and electric field from
stepped leaders near ground level 24 p3610 A83-49346

ELECTRIC REACTORS

- Parametric study of minimum reactor mass in
energy-storage dc-to-dc converters 01 p0040 A83-11011

ELECTRIC ROCKET ENGINES

- NT ARC JET ENGINES
- NT ELECTROSTATIC ENGINES
- NT ELECTROTHERMAL ENGINES
- NT ION ENGINES

- NT MERCURY ION ENGINES
- NT PLASMA ENGINES
- NT RESISTOJET ENGINES

ELECTRIC SPARKS

- High-voltage spark atomic emission detector for gas
chromatography 02 p0153 A83-13108
- Electrical discharge machining of aluminum honeycomb
core 07 p0940 A83-20500
- Pumping of pulsed gas lasers by bulk and sliding spark
discharges 10 p1431 A83-26464
- Explosive-emission mechanism for producing a cathode
spot and extreme energy characteristics of a nanosecond
volume discharge in nitrogen 21 p3210 A83-44141
- Dynamics of the formation of optical striations --- by laser
bombardment of plasma columns 21 p3210 A83-44142

ELECTRIC STIMULI

- Long-term posttetanic potentiation in the hippocampus
01 p0081 A83-10917
- An investigation of the role of deep brain structures in
the regulation of intracerebral microcirculation 02 p0219 A83-11518
- Changes in EMG power spectrum /high-to-low ratio/
with force fatigue in humans 03 p0378 A83-13576
- Mechanism for the appearance of the first extrasystole
during short-lived atrial arrhythmia 03 p0376 A83-14366
- The effect of sinusoidal modulated currents on the
cardiorespiratory system and the physical capacity of
athletes 05 p0673 A83-17170
- The response of the neurons of the visual centers of
the rabbit brain to electric stimuli and a combination of
the latter with nonvisual stimuli 05 p0672 A83-17638
- Goal-directed movements of cat's eyes in response to
electrical stimulation of the lateral geniculate body 07 p0972 A83-19645
- The relationship between isometric and isotonic
contractile responses of the myocardium of mammals
08 p1145 A83-22111
- The eye movements of cats induced by the electrical
stimulation of the lateral geniculate body 10 p1454 A83-26786
- The reaction of neurons to prolonged stimulation
Morphological investigations --- Russian book 12 p1762 A83-28818
- Sudden cardiac death - A problem in topology 12 p1762 A83-29250
- The effects of the electrical stimulation of the visual
cortex of cats on the behavioral model of the placement
of a paw on a support 19 p2871 A83-40811
- Electrostimulation for receptor lesions of the ear
19 p2882 A83-41446
- The effect of electrostimulation of the hypothalamus on
the methylation of DNA from the livers of rats 19 p2876 A83-41844
- The discrimination of amplitude and temporal
parameters of the direct electrical stimulation of the visual
cortex 19 p2878 A83-42069
- Instantaneous cardiac acceleration in the cat elicited
by peripheral nerve stimulation 22 p3345 A83-45985
- The dependence of the characteristics of the slow phase
of the galvanic nystagmus on the electrical stimulation
parameters 23 p3497 A83-47109
- The direct electrical stimulation of the upper urinary tract
in case of ureteroliths in flight crew personnel 24 p3618 A83-49071

ELECTRIC SWITCHES

- NT THERMOSTATS
- Solar array switching power management 11 p1538 A83-27132
- Establishment of the steady state during the switching
on of a high-power high-voltage transistor 17 p2499 A83-38496
- A diamond opto-electronic switch 19 p2838 A83-41182
- A fast optoelectronic switch 21 p3125 A83-44541

ELECTRIC TERMINALS

- Description of a 3-port ATE system required for testing
of electro-optical UUT's 01 p0038 A83-10781
- Physical frequency limitations of 2-terminal devices
12 p1719 A83-29420
- An ideal six-port network consisting of a matched
reciprocal lossless five-port and a perfect directional
coupler 13 p1831 A83-30231
- An investigation of a six-port microwave measurement
system 15 p2153 A83-35084

ELECTRIC WELDING

- NT ARC WELDING
- NT ELECTRON BEAM WELDING
- NT GAS TUNGSTEN ARC WELDING
- NT PLASMA ARC WELDING

ELECTRIC WIRE

- Inverse scattering for an exterior Dirichlet problem ---
due to metallic cylinder 01 p0104 A83-10494

Analytic determination of the transient response of a thin-wire antenna based upon an SEM representation --- Singular Expansion Method 03 p0306 A83-14015

Scattering by wires near a material half-space 03 p0306 A83-14017

Heat conduction in an undulating heating wire 06 p0756 A83-18063

Computer graphics applications in electromagnetic computer modeling --- treatment of wire objects by method of moments 06 p0802 A83-18667

Effects of finite wire scatterers in the field of VOR 06 p0716 A83-19039

Electromagnetic coupling to an infinite wire through a slot in a conducting plane 10 p1411 A83-26838

The effect of electric current pulses on the tensile behavior of thin metal wires 16 p2335 A83-36892

Electron-beam guiding and phase-mix damping by an electrostatically charged wire 21 p3203 A83-43882

ELECTRIC WIRING
U ELECTRIC WIRE

ELECTRICAL BREAKDOWN
U ELECTRICAL FAULTS

ELECTRICAL CONDUCTIVITY
U ELECTRICAL RESISTIVITY

ELECTRICAL CONDUCTIVITY METERS
An investigation of the electrical conductivity of biological systems 14 p2065 A83-33317

Measuring strain gages directly without signal conditioning 22 p3291 A83-46424

Atmospheric-pollution monitoring through conductivity measurements 23 p3454 A83-47419

ELECTRICAL ENERGY
U ELECTRIC POWER

ELECTRICAL ENGINEERING
Fundamentals handbook of electrical and computer engineering. Volume 1 Circuits fields and electronics 03 p0314 A83-14047

Unified production planning for integrated circuits --- French thesis 03 p0314 A83-14110

The development of radio engineering 05 p0621 A83-16898

Digital signal processing --- German book 21 p3126 A83-45092

ELECTRICAL FAULTS
NT SHORT CIRCUITS

Automatic fault diagnosis of a switching regulator 01 p0040 A83-11014

Investigation of network tree technology as a tool for developing effective fault isolation procedures 01 p0043 A83-11231

The use of measurements to detect electrical problems in operational photovoltaic arrays 04 p0504 A83-15462

Study of electrical faults in magnetohydrodynamic Faraday generators 04 p0538 A83-16106

The characterization of transistor electrical overstress failure probability density functions 05 p0625 A83-17477

Silicon solar cell damage from electrical overstress 05 p0658 A83-17481

Ionizing radiation effects on power MOSFETs during high speed switching 05 p0625 A83-17485

A comparison of radiation damage in transistors from cobalt-60 gamma rays and 2.2 MeV electrons 05 p0629 A83-17534

Single event upset vulnerability of selected 4K and 16K CMOS static RAM's 05 p0629 A83-17539

An analytical breakdown model for short-channel MOSFET's 05 p0630 A83-17753

A simple model for short-channel effects of a buried-channel MOSFET on the buried insulator 05 p0630 A83-17755

Short-channel MOS transistors in the avalanche-multiplication regime 05 p0631 A83-17760

Analytical investigation of axial field limitations in MHD generators 08 p1168 A83-23126

Numerical comparison of DMOS, VMOS, and UMOS power transistors 09 p1256 A83-24686

Arc damage of interelectrode insulators in MHD generators 13 p1924 A83-30198

Wide-band device modeling using time-domain reflectometry 13 p1830 A83-31286

Reverse bias power dissipation of shadowed or faulty cells in different array configurations 14 p2040 A83-32212

On testing stuck-open faults in CMOS combinational circuits 15 p2153 A83-35141

Effects of short-duration loading faults on high-interaction Faraday and diagonal type MHD generators with subsonic or supersonic flow [AIAA PAPER 83-1745] 17 p2581 A83-37221

Thermal dielectric breakdown with cylindrical electrodes 17 p2498 A83-38216

A simplified model of short-channel MOSFET characteristics in the breakdown mode 18 p2677 A83-40370

Constant voltage scaling of FETs for high frequency and high power applications 19 p2836 A83-40668

Dissipation and dynamic nonlinear behavior in the quantum Hall regime 24 p3635 A83-48921

ELECTRICAL IMPEDANCE
NT CONTACT RESISTANCE
NT ELECTRICAL RESISTANCE
NT REACTANCE
NT SKIN RESISTANCE

Input admittance of a spheroidal antenna excited by the open end of a coaxial line --- application to microwave plasma probes 01 p0035 A83-10404

Input impedance and mutual coupling of rectangular microstrip antennas 03 p0313 A83-14021

The impedance of an elliptical printed-circuit antenna 03 p0313 A83-14022

Regge poles, natural frequencies, and surface wave resonance of a circular cylinder with a constant surface impedance 03 p0307 A83-14034

A hybrid MM-geometrical optics technique for the treatment of wire antennas mounted on a curved surface 03 p0307 A83-14037

Balanced helical antenna with tapered open ends 03 p0307 A83-14130

Impedance changes produced by a crack in a plane surface 04 p0490 A83-15189

Impedance transformation in fin lines 04 p0474 A83-16209

Analysis of monopole-antenna with rectangular reflector 06 p0744 A83-18695

An analysis of coplanar waveguides with finite conductor thickness-computation and measurement of characteristic impedance 07 p0918 A83-20070

Change in impedance of a single-turn coil due to a flaw in a conducting half space 07 p0942 A83-20270

Semiconductor electrodes. XLVII - A-C impedance technique for evaluating surface state properties of n-Mo Te2 in acetonitrile solutions containing various redox couples 07 p0999 A83-20588

Closed-form expressions for the parameters of finned and ridged waveguides 07 p0923 A83-21532

Surface impedance and wave tilt interpretation over horizontally stratified media 08 p1160 A83-22028

Impedance parameters and radiation pattern of two coupled circular microstrip disk antennas 08 p1076 A83-22329

Eddy current impedance plane analysis 08 p1114 A83-22410

External and internal mutual impedance effects on the radiation patterns of circularly disposed arrays using antennafiers or passive monopoles 09 p1246 A83-23786

Impedance and polarization characteristics of rectangular printed radiators in planar phased-array antennas 09 p1250 A83-24922

High-frequency impedance of proton-bombarded injection lasers 10 p1429 A83-26071

Transformation of the matrix of generalized impedances in the case of frequency variation --- for antenna radiation pattern calculations 11 p1556 A83-27945

Driving-point impedance of a linear cylindrical antenna 11 p1558 A83-28607

Cardiac function monitored by impedance cardiography during changing seatback angles and anti-G suit inflation 12 p1766 A83-28930

Conically depressed microstrip patch antenna 12 p1736 A83-29437

Mathematical representation of microwave oscillators by use of the Rieke diagram 13 p1834 A83-30786

Empirical expressions for fin-line design 13 p1836 A83-31147

The diffraction of electromagnetic waves by surfaces with an admittance operator boundary condition 14 p1999 A83-32103

A low-noise low input impedance amplifier for magnetic measurements of nerve action currents 14 p2020 A83-32798

Multimode planar spiral for DF applications 15 p2121 A83-35089

An analysis of annular, annular sector, and circular sector microstrip antennas 15 p2146 A83-35095

The synthesis of surface reactance using an artificial dielectric 15 p2154 A83-35182

Experimental study of the characteristics of top-loaded microstrip monopoles 15 p2149 A83-35195

A comparative study of feed impedances of a circular and three different spiral antenna arrays 16 p2344 A83-36731

A moment solution for waveguide junction problems 19 p2837 A83-41083

Measurement and modeling of the apparent characteristic impedance of microstrip 21 p3122 A83-48331

Optimum design of 3-dB branch-line couplers using microstrip lines 21 p3123 A83-43839

Characteristic impedance of an oval located symmetrically between the ground planes of finite width --- for transmission lines 21 p3123 A83-43840

Measurements and calculations of the impedance of a cylindrical antenna in an isotropic plasma 21 p3211 A83-44300

High-frequency admittance of high-electron-mobility transistors (HEMTs) 21 p3127 A83-45175

Calculation of the characteristic impedances of waveguide slot lines 22 p3277 A83-45685

High-frequency scattering from the edges of impedance discontinuities on a flat plane 23 p3442 A83-47830

A simple power series for the radiation resistance of center-fed dipoles 23 p3443 A83-47837

Equivalence between circular and rectangular posts in guiding structures 23 p3446 A83-48717

Calculation of a slab waveguide with variable surface impedance 24 p3573 A83-49270

ELECTRICAL INSULATION
Experimental study of embedded insulated antennas 01 p0034 A83-11377

Atmospheric electricity and air transport safety [ONERA, TP NO. 1982-82] 03 p0280 A83-14534

Undoped, semi-insulating GaAs layers grown by molecular beam epitaxy 06 p0815 A83-19262

Materials characterization and fracture mechanics of a space grade dielectric silicone insulation 07 p0899 A83-20456

The dielectric properties of anhydride-cured epoxy potting compounds 07 p0899 A83-20458

Vibration resistance of conformal coated axial-lead components on printed wiring assemblies 09 p1253 A83-23613

Removable foam encapsulants 09 p1237 A83-23617

Moisture resistance of conformal coatings 09 p1237 A83-23620

A negative drain conductance property in a super-thin film buried-channel MOSFET on a buried insulator 09 p1256 A83-24685

Flammability handbook for electrical insulation 09 p1221 A83-24895

Arc damage of interelectrode insulators in MHD generators 13 p1924 A83-30198

ELECTRICAL LEADS
U ELECTRIC CONDUCTORS

ELECTRICAL MEASUREMENT
Application of electric resistance probe method to non-destructive inspection 01 p0057 A83-10280

Electrothermal inspection of conducting materials 01 p0057 A83-10364

ATE calibration by means of dynamic transport standards 01 p0050 A83-10764

Galvanometric devices --- Russian book 02 p0176 A83-11947

Horizontal displacement of simulated cloud particles by the propeller of an aeroplane --- particle measurement accuracy 02 p0216 A83-12944

Assessment of the error in measuring the strength of a constant electric field by the double-Langmuir-probe method 03 p0397 A83-13206

Corona type sensor for aircraft electrical potential measurement [ONERA, TP NO. 1982-73] 03 p0282 A83-14530

A theory for spherical electric probes in a weakly ionized plasma at rest 04 p0536 A83-15092

BSO/fibre-optic voltmeter with excellent temperature stability 04 p0481 A83-15250

The use of measurements to detect electrical problems in operational photovoltaic arrays 04 p0504 A83-15462

Development of a standard test method for measuring photovoltaic cell performance 04 p0504 A83-15464

Some problems in determination of gap-state density in amorphous silicon 04 p0541 A83-15527

Spectroscopic measurements on discharges along a dielectric surface 04 p0538 A83-16061

Measurement of 2-port devices by a reflectometer system 04 p0473 A83-16207

A simple parameter measurement system for solar cells 06 p0763 A83-18825

Resistance measurements by radio telemetric system during film deposition by sputtering 06 p0755 A83-19615

Probe characterization in ac field measurements of surface crack depth 07 p0929 A83-20267

Change in impedance of a single-turn coil due to a flaw in a conducting half space 07 p0942 A83-20270

Semiconductor surface characterization using transverse acoustoelectric voltage versus voltage measurements 07 p0921 A83-20752

Detection and measurement of cracks in threaded bolts with an a.c. potential difference method 07 p0943 A83-21355

- Instrumentation for incremental voltage step electrochemical measurements 07 p0932 A83-21382
- A.C. field measurements - A new method for detecting and measuring fatigue cracks 08 p1112 A83-21761
- Measurement of series resistance in IMPATT diodes 09 p1256 A83-24500
- Instruments for space investigations --- current measuring devices for satellite-borne ionospheric and solar probes 10 p1387 A83-25342
- Experimental determination of stresses in damaged composites using an electric analogue 10 p1441 A83-26446
- Information from bias measurements --- on statistical characteristics of fluctuating radar signal 11 p1629 A83-27057
- Recent advances in interpretation of corona test results 11 p1602 A83-27154
- Elaborating methods for measuring atmospheric electrical quantities 11 p1575 A83-28737
- The influence of skin depth on crack measurement by the ac field technique 12 p1733 A83-29140
- An instrument for DC electric field and AC electric and magnetic field measurements aboard 'INTERCOSMOS-BULGARIA-1300' satellite 13 p1813 A83-30757
- Electrical measurements on n(+)-GaAs-undoped Ga(0.6)Al(0.4)As-n-GaAs 13 p1836 A83-31065
- An automatic test set for the dynamic characterization of A/D converters 13 p1836 A83-31288
- Raindrop charges, electric field and space charge measurements at a mountain station covered with monsoon clouds 14 p2057 A83-32411
- Ohmic contacts for laser diodes 16 p2346 A83-35988
- Measurement of crack profile of semi-elliptical surface cracks using the ac potential technique 16 p2363 A83-36726
- Importance of electric field measurement over low latitudes at stratospheric heights by balloons 18 p2717 A83-39819
- SEM-EBIC and traveling light spot diffusion length measurements - Normally irradiated charge-collecting diode 18 p2678 A83-40371
- Spectroscopic laser scanning analysis of photo-induced current on a-Si solar cells 19 p2862 A83-41286
- A comparison of different devices for phase shift measurement at high frequency 19 p2840 A83-41556
- Investigation of a probe sensor of electric field strength with a Pockels-effect cell 19 p2849 A83-41816
- An electrical balance for aerodynamic investigations 19 p2849 A83-41883
- Measurement of high-voltage pulses employing a quartz Pockels cell 20 p2990 A83-42790
- Measurement and simulation of GaAs FET's under electron-beam irradiation 20 p2968 A83-43357
- Recent measurements of electrical conductivity and ion pair production rate, and the ion-ion recombination coefficient derived from them in the lower stratosphere 20 p3027 A83-43401
- A technique for measuring the effective dielectric constant of a microstrip line 21 p3123 A83-43842
- Capacitance transducers for nondestructive testing (2nd revised and enlarged edition) 21 p3135 A83-43920
- The potential drop across an imperfect diffusion bond 21 p3149 A83-44124
- Techniques for improving the Si-SiO₂ interface characterization 22 p3364 A83-46275
- Carbon dioxide laser-induced fast signals from silicon photodiodes 22 p3301 A83-46826
- Measurement of potential aboard spacecrafts [IAF PAPER 83-220] 23 p3424 A83-47312
- Multiwavelength analyzer for the determination of diffusion lengths --- in solar cell base region 23 p3459 A83-48612
- A study of built-in potential in a-Si solar cells by means of back-surface reflected electroabsorption 23 p3478 A83-48702

ELECTRICAL PROPERTIES

- NT CAPACITANCE
- NT CARRIER MOBILITY
- NT CHARGE DISTRIBUTION
- NT CONTACT RESISTANCE
- NT DIELECTRIC PROPERTIES
- NT ELECTRICAL IMPEDANCE
- NT ELECTRICAL RESISTANCE
- NT ELECTRICAL RESISTIVITY
- NT ELECTRON MOBILITY
- NT ELECTROSTRICTION
- NT FERROELECTRICITY
- NT HOLE MOBILITY
- NT INDUCTANCE
- NT IONOSPHERIC CONDUCTIVITY
- NT MAGNETORESISTIVITY
- NT PERMITTIVITY

- NT PHOTOCONDUCTIVITY
- NT PHOTOVOLTAIC EFFECT
- NT PIEZOELECTRICITY
- NT PLASMA CONDUCTIVITY
- NT POLARIZATION CHARACTERISTICS
- NT PYROELECTRICITY
- NT REACTANCE
- NT SKIN RESISTANCE
- NT SUPERCONDUCTIVITY
- Semiconducting and other major properties of gallium arsenide 01 p0108 A83-10605
- Properties of Al_xGa_{1-x}N films prepared by reactive molecular beam epitaxy 01 p0109 A83-10624
- Electrical properties and their thermal stability for silicon nitride films prepared by plasma-enhanced deposition 01 p0109 A83-10625
- Electrical and optical properties of magnesium-diffused silicon 01 p0109 A83-10635
- Semiconducting polymers --- Book 02 p0242 A83-11925
- Electrical properties of an input-output cable for Josephson applications 02 p0168 A83-12815
- Electrophysical properties of niobium carbide single crystals 02 p0161 A83-13037
- Epitaxial HgCdTe/CdTe photodiodes for the 1 to 3 micron spectral region 03 p0309 A83-13737
- The effect of electronically active defects on the characteristics and the reliability of MOS structures --- French thesis 03 p0311 A83-13804
- Electrical properties of frozen ground at VHF near Point Barrow, Alaska 03 p0352 A83-14858
- Use of test structures in the production of CdS/Cu₂S photovoltaic devices 04 p0504 A83-15455
- UPS and Schottky barrier study of TiO₂ electrochemical anodes --- for solar cells 04 p0504 A83-15481
- Optical and electrical characterization of multiply doped silicon - A study of the Si₃Al₂/In₃Al₂ system 04 p0542 A83-16065
- Effects of annealing on the electrical properties of Cd_xHg_{1-x}Te 04 p0543 A83-16085
- An analysis of multicomponent electroacoustic transducers providing matched control of the acoustic field in Bragg acoustooptic devices in the short-wave portion of the microwave range 05 p0630 A83-17595
- Electrical properties of bulk-barrier diodes 05 p0631 A83-17758
- High-voltage power supply materials evaluation 07 p0920 A83-20487
- Performance properties of conductive PVC composites for EMI shielding applications 07 p0876 A83-20488
- Electrochemically modified electrodes - Poly(2-methyl-8-quinolinol)/ and poly(8-quinolinol)/ complexing films obtained by electropolymerizing substituted phenols: Their voltammetric and electrical properties in relation to their geometric structure 07 p0881 A83-20583
- Boride-thermic synthesis of materials 07 p0873 A83-20682
- Improvements on the electrical and luminescent properties of reactive molecular beam epitaxially grown GaN films by using AlN-coated sapphire substrates 08 p1169 A83-22759
- Electrical properties and ion implantation of epitaxial GaN, grown by low pressure metalorganic chemical vapor deposition 08 p1169 A83-22760
- Photoelectrochemical behaviour of electrodeposited and pressure-sintered Bi₂S₃, Bi₂S₃-PbS and Bi₂S₃-Ag₂S semiconductor electrodes 08 p1131 A83-22905
- Accuracy of analytical expressions for solar cell fill factors 08 p1132 A83-22914
- Analytical model of a magnetron 09 p1252 A83-23461
- The electrical properties and electron structure of niobium-molybdenum alloys 09 p1349 A83-24220
- The effects of hydrogen in stabilizing the electrical properties of n-Pb/0.8/Sn/0.2/Te thin films 10 p1488 A83-25455
- Electrical and optical properties of sputtered amorphous silicon films prepared under a reduced pumping speed 10 p1489 A83-26211
- The growth of profiled silicon crystals, investigation of their electronic properties and defect structures, manufacture of solar cells, and determination of their parameters 11 p1663 A83-28361
- The effect of annealing on the structural and electronic properties of profiled silicon 11 p1663 A83-28363
- A critical generalization of the results of experimental studies of the thermal and electrical characteristics of a glow discharge 11 p1660 A83-28557
- Parameters of the RT-3 radio telescope 12 p1788 A83-29299
- Electrical characteristics of an MHD generator with a transversally shaped configuration of magnetic induction 13 p1924 A83-30199
- The electrical properties of GaP MOS structures 13 p1831 A83-30268

- Optical and electrical properties of amorphous silicon films prepared by photochemical vapor deposition 13 p1870 A83-30339
- Method for determining the electrical properties of the underlying surface on inhomogeneous paths from measurements of the fields of VLF radio stations 14 p2050 A83-31882
- Large area hydrogenated amorphous silicon for photovoltaic application 14 p2044 A83-32289
- Electronic properties of doped amorphous SiO(x) 14 p2089 A83-32291
- Impurity incorporation in R.A.D. polysilicon layers and consequences on their electrical properties --- Ribbon Against Drop 14 p2091 A83-32320
- Sealed nickel cadmium batteries --- Book 15 p2188 A83-33614
- Electrical behaviour of doped-yttria stabilized zirconia ceramic materials 15 p2134 A83-35065
- Cuprous oxide-indium-tin oxide thin film photovoltaic cells 16 p2371 A83-35451
- Spectral and semiconducting properties of tetrabenzoporphins 16 p2420 A83-35917
- Transparent heat-reflecting coatings for solar applications based on highly doped tin oxide and indium oxide 16 p2371 A83-36738
- Electrically triggered multimodule KrF laser system with narrow-linewidth output 18 p2692 A83-39092
- Analytical model and characterization of small geometry MOSFET's 18 p2677 A83-40368
- Hydrogenated amorphous silicon produced by laser induced chemical vapor deposition of silane 19 p2903 A83-40743
- The effect of the thickness of the intermediate oxide layers in the metal-semiconductor contact on the properties of solar cells having a Schottky barrier 19 p2862 A83-42013
- Influence of carbon and hydrogen segregation on the electrical properties of grain boundaries in polycrystalline silicon sheets 20 p3051 A83-42351
- A study of the electrical and luminescence characteristics of a novel Si-based thin film electroluminescent device 20 p2966 A83-42607
- Electrical characterization of Hg(1-x)Cd(x)Te alloys 20 p3054 A83-43296
- Electrical and structural properties of pulse laser-annealed polycrystalline silicon films 20 p3054 A83-43347
- Effect of deposition rate and substrate temperature on properties of CdTe film 20 p3054 A83-43396
- A numerical study of the electrical characteristics of the electrode boundary layer of weakly ionized plasmas of molecular gases 20 p3050 A83-43512
- Energy barrier height variations of Pd-Si Schottky diodes induced by deuterium 21 p3123 A83-43849
- Magnetic, electrical, and mechanical properties of 12KhN3A and 12Kh2N4A steels and of case-hardened layers on them 21 p3111 A83-43879
- Electrophysical properties of niobium and niobium nitride films deposited in a getter magnetron discharge device 21 p3217 A83-44594
- Electrophysical properties of heterogeneous CdS photovaractor structures 21 p3217 A83-44595
- Electrical and optical properties of n-CdS/P-Si and n(Zn(x)-Cd(1-x))S/P-Si heterojunction solar cells 21 p3167 A83-44607
- Effects of laser irradiation on the electrophysical properties of an indium antimonide MIS-structure interface 21 p3219 A83-45390
- Photovoltaic properties of In/Trans-polyacetylene/Electrodag +502 Schottky barrier cells 23 p3477 A83-48613
- Electronic properties of non-crystalline materials 24 p3634 A83-48776
- Semiconducting polymers 24 p3634 A83-48778
- Polymer laminate structures --- electrical properties 24 p3552 A83-48779
- Heterojunction formation in (CdZn)S/CuInSe₂ ternary solar cells 24 p3634 A83-48790
- A numerical study of the effect of anomalously low attenuation of electric waves in a plane comb-shaped waveguide 24 p3573 A83-49046

ELECTRICAL RESISTANCE

- NT CONTACT RESISTANCE
- NT SKIN RESISTANCE
- Application of electric resistance probe method to non-destructive inspection 01 p0057 A83-10280
- Crystal structure and electrical resistance of MoS₂-NbS₂ alloys obtained by the method of self-propagating high-temperature synthesis 02 p0161 A83-13036
- A high temperature GaP MESFET 03 p0309 A83-13561
- Measurement of the specific electrical resistance of the blood 03 p0381 A83-14330
- A new method for experimental determination of the series resistance of a solar cell 03 p0355 A83-14512

Electrical resistance of hot-pressed TiC-SiC-C composites 03 p0302 A83-14815

Resistance measurements by radio telemetric system during film deposition by sputtering 06 p0755 A83-19615

Oxygen transfer on substituted ZrO₂, Bi₂O₃, and CeO₂ electrolytes with platinum electrodes. I - Electrode resistance by dc polarization 07 p0880 A83-19887

Oxygen transfer on substituted ZrO₂, Bi₂O₃, and CeO₂ electrolytes with platinum electrodes. II - ac impedance study 07 p0880 A83-19888

Melt dynamics of silicon-on-sapphire during pulsed laser annealing 08 p1170 A83-22764

Carrier distribution and low-field resistance in short n/+/-n/-n/+/- and n/+/-p/-n/+/- structures 09 p1350 A83-24496

Measurement of series resistance in IMPATT diodes 09 p1256 A83-24500

The COMFET - A new high conductance MOS-gated device 12 p1720 A83-29520

Hydrogen solubility in rhenium at pressure up to 90 kb 13 p1824 A83-31333

Nonselective effect of electromagnetic radiation on a superconducting film in the resistive state 14 p2091 A83-32618

The Q-value and resistance of the heliospheric resonator model for the 22-year solar cycle 17 p2628 A83-38524

Ideal FET doping profile 18 p2878 A83-40376

Submicron GaAs microwave FET's with low parasitic gate and source resistances 21 p3123 A83-43848

A decaying volt-ampere characteristic in the longitudinal current region 21 p3176 A83-45266

Pressure-induced alpha-omega transformation in titanium Features of the kinetics data 24 p3559 A83-48910

A method for the measurement of solar cell series resistance 24 p3599 A83-49834

ELECTRICAL RESISTIVITY

NT IONOSPHERIC CONDUCTIVITY

NT MAGNETORESISTIVITY

NT PHOTOCONDUCTIVITY

NT PLASMA CONDUCTIVITY

NT SUPERCONDUCTIVITY

A simple model for plasma temperature in imploded hollow plasma liners 01 p0106 A83-10619

Structural features of conducting quasi-one-dimensional organic halides and pseudohalides 02 p0148 A83-11815

Calculation of the signal created in a superposed eddy-current transducer by a crack 02 p0188 A83-12158

Predicted electrical conductivity between 0 and 80 km in the Venusian atmosphere 02 p0265 A83-12563

Some properties of r.f.-sputtered hafnium nitride coatings 02 p0160 A83-12653

Automatic capacitance-voltage /C-V/ plotter for solar cells 02 p0181 A83-12821

Further efforts to limit lunar internal temperatures from electrical conductivity determinations 04 p0560 A83-15337

Effect of discharge conditions on characteristics of hydrogenated amorphous silicon deposited by DC glow discharge decomposition 04 p0539 A83-15498

Electronic properties of doped glow-discharge amorphous germanium 04 p0542 A83-15530

Chemical modification of amorphous arsenic 04 p0542 A83-15532

Thermal and electrical conductivities of crystals in neutron stars and degenerate dwarfs 04 p0556 A83-15964

Preparation, tunneling, resistivity, and critical current measurements on homogeneous high T_{sub c} A15 Nb₃Ge thin films [AD-A125657] 04 p0543 A83-16074

Resistivity, superconductivity, and order-disorder transformations in transition metal carbides and hydrogen-doped carbides 04 p0543 A83-16075

The effects of heat treatments on the transport properties of Cu/x/S thin films 04 p0543 A83-16083

Metallic conductivity and air stability in copper chloride intercalated carbon fibers 04 p0473 A83-16095

Fully controllable heat pipe containing a short electro-osmotic pumping section [AIAA PAPER 83-0317] 05 p0634 A83-16647

The Bloch-FET - A lateral surface superlattice device 05 p0690 A83-17289

Electrical conductivity and discharge in spacecraft thermal control dielectrics 05 p0618 A83-17491

Anisotropy of kinetic properties of rhenium at high temperatures 06 p0728 A83-18443

Role of the conductivity of the confining layers in DH-laser spatial hole burning effects 06 p0766 A83-18903

Undoped, semi-insulating GaAs layers grown by molecular beam epitaxy 06 p0815 A83-19262

Conductivity of the mixed organic electrolyte containing propylene carbonate and 1,2-dimethoxyethane --- for lithium cells 07 p0880 A83-19889

Quantum corrections to the galvanomagnetic coefficients of quasi-two-dimensional electrons of InSb/GaAs heteroepitaxial structures 07 p0999 A83-20049

Features of a transparent antistatic resin 07 p0899 A83-20489

Highly conductive and transparent amorphous tin oxide 07 p1000 A83-20754

Control of the mechanical properties of alloy D16 sheets by the eddy-current method taking the kinetics of aging into account 07 p0891 A83-21419

Plastic composites for electromagnetic interference shielding applications 08 p1055 A83-22717

High-sensitivity resistivity technique for studies of defect behavior 08 p1106 A83-23234

The microstructure and resistance properties of titanium alloys following hardening from the liquid state 09 p1234 A83-24383

The pattern of the conductivity and the permeability of cells at short periods following gamma-irradiation 09 p1321 A83-24930

Electronic properties of amorphous silicon selenium films 10 p1488 A83-25984

Microwave contactless technique for photoconductivity measurements 11 p1573 A83-27980

Evaluation of tetrafluoroethane-1,2-disulfonic acid as a fuel cell electrolyte 11 p1546 A83-28300

Linear induction machines - Reflexions on the evaluation of efficiency, and on the choice of secondary resistivity 13 p1832 A83-30448

A method of reducing the effect of the gap in eddy-current measurements of conductivity 13 p1860 A83-30839

Change of characteristic parameters of polycrystalline titanium during its deformation 13 p1822 A83-30971

Effect of anodic growth temperature on native oxides of n-(Hg, Cd)Te 13 p1929 A83-31066

Fractional quantum numbers in solids 13 p1930 A83-31164

Quantum oscillations of the electron thermal and electrical conductivities in a neutron-star magnetic field 13 p1840 A83-31259

Influence of light exposure on the transport properties of a-Si:H films 14 p2088 A83-32238

Series resistance analysis of concentrator cells under high injection conditions 14 p2004 A83-32246

Highly conductive boron doped Si-layers prepared by plasma decomposition of SiH₄ 14 p2089 A83-32252

Physicochemical properties of Cu(x)S 14 p1989 A83-32300

An investigation of the electrical conductivity of biological systems 14 p2065 A83-33317

Electrical conductivity in sunspots and the quiet photosphere 15 p2278 A83-34279

Properties of tin doped indium oxide thin films prepared by magnetron sputtering 16 p2419 A83-35447

Dependence of fast magnetic reconnection on electrical resistivity in an isolated current-sheet system 17 p2581 A83-37035

Temperature dependence of electrical transport properties of n-type solar grade polycrystalline silicon 17 p2584 A83-38210

Thickness dependence of kink temperature and band bending in amorphous silicon 17 p2585 A83-38954

Electrical conductivity of alkali metal vapors in the neighborhood of the critical point 18 p2747 A83-39864

Mechanical, thermal, and microstructural properties of neutron-irradiated SiC [ACS PAPER 66-N-82] 19 p2823 A83-40909

Viscosity and conductivity of the lower mantle - An experimental study on a MgSiO₃ perovskite analogue, KZnF₃ 19 p2865 A83-41175

Electrical conductivity of a low-temperature two-dimensional medium 20 p3051 A83-42273

Conductivity of inversion layers in InSb MIS structures below the 'mobility threshold' 20 p3051 A83-42275

Moessbauer spectroscopic study of iodine-doped polyacetylene 20 p2949 A83-42341

Contact resistivity of TiN on p(+)-Si and n(+)-Si --- measurement for metal contact diffusion barrier in solar cell 20 p2965 A83-42354

Electric conduction of low density polyethylene induced by high dose rate gamma rays 20 p3052 A83-42598

Resistivity and mobility of GaP at 300 K 20 p3054 A83-43358

Recent measurements of electrical conductivity and ion pair production rate, and the ion-ion recombination coefficient derived from them in the lower stratosphere 20 p3027 A83-43401

High-resistivity greater than 10 to the 5th ohm/cm InP layers by liquid phase epitaxy 20 p3055 A83-43604

Characterization of metals and alloys by electrical resistivity measurements 21 p3111 A83-43830

Cholesterol esters increase the permeability of lecithin bilayer membranes 21 p3184 A83-45223

Electrical conduction in mantle materials 22 p3324 A83-45798

Eclipse-related measurements of middle-atmosphere electrical parameters 23 p3481 A83-47474

A summary of spacecraft charging results 23 p3423 A83-48129

Effect of grain size on the resistivity of polycrystalline material 23 p3512 A83-48611

Supermetallic conductivity of graphite intercalated with iodine monochloride 24 p3634 A83-48864

Electrical resistivity of an aluminum-graphite composite between 77 K and 300 K 24 p3553 A83-48897

Electrophysical properties of a series of composites based on disperse molybdenum in a styrene-alpha-methylstyrene matrix 24 p3554 A83-49541

Electrical conductivity of the Li₂SO₄-Li₂CO₃ system 24 p3558 A83-49930

Surface films on lithium in acetonitrile-sulphur dioxide solutions 24 p3558 A83-49937

Interfacial conduction in lithium iodide containing inert oxides 24 p3558 A83-49947

The cycling behaviour and stability of the lithium electrode in propylene carbonate and acetonitrile electrolytes 24 p3600 A83-49950

ELECTRICALLY SUSPENDED GYROSCOPES

U. ELECTROSTATIC GYROSCOPES

ELECTRICITY

NT ALTERNATING CURRENT

NT ATMOSPHERIC ELECTRICITY

NT AURORAL ELECTROJETS

NT ELECTROJETS

NT EQUATORIAL ELECTROJET

NT GEOELECTRICITY

NT IONOSPHERIC CURRENTS

NT STATIC ELECTRICITY

NT TELLURIC CURRENTS

ELECTRIFICATION

A numerical study of thunderstorm electrification using a three dimensional model incorporating the ice phase 02 p0215 A83-12938

Role of various charging mechanisms in thundercloud electrification 08 p1140 A83-22316

Electrification of comets by solar corpuscular fluxes 10 p1517 A83-26912

A numerical simulation of winter cumulus electrification, I Shallow cloud 18 p2729 A83-40040

Electrification of metallic bodies in aerosol flows in the case of the fragmentation of solid disperse particles during collisions with the body 24 p3624 A83-49532

ELECTRO-OPTICAL EFFECT

Effects of operating mode on electrooptic spatial light modulator resolution and sensitivity 05 p0684 A83-16832

Spectroscopic study of the mechanism of the linear electrooptic effect 06 p0810 A83-19575

Switchable coaxial optical coupler using a liquid crystal mixture 07 p0994 A83-21361

Light scattering in the reversible electrical memory effect in smectic liquid crystals 09 p1344 A83-23996

Investigation of an electrooptic modulator formed from coupled channel diffused waveguides in LiNbO₃ 10 p1483 A83-26656

Hybrid optical-digital signal processing applied to an optical nonlinear phase estimator 10 p1406 A83-26861

Performance testing of a Gigahertz modulator for 10 microns --- possible use in spaceborne optical communication 11 p1656 A83-27517

Buffering of optoelectronic memory and its effect on computer efficiency 11 p1646 A83-28624

Broadband guided-wave optical frequency translator using an electro-optical Bragg array 13 p1922 A83-31053

Traveling-wave electrooptic modulator 17 p2580 A83-37750

Broad band electro-optic tuning of a CW dye laser 21 p3143 A83-44188

GaAlAs p-i-n junction waveguide modulator 21 p3205 A83-44224

Progress on electro-optic integrated optic devices 22 p3360 A83-46650

Waveguide light modulators using the Keldysh-Franz effect in gallium arsenide 23 p3507 A83-47570

Electro-optic branching-waveguide switch with low drive voltage 24 p3628 A83-48855

Total-internal-reflection electrooptic thin-film modulator 24 p3628 A83-48859

ELECTRO-OPTICAL PHOTOGRAPHY

The numerical stereo camera 03 p0324 A83-13445

- Photography of orbiting satellites
06 p0723 A83-18966
- Weather and thermal electric-optical sensor performance
08 p1098 A83-22545
- The change of limiting resolution of electro-optical systems due to atmospheric effects
08 p1098 A83-22561
- Electro-optic shutter devices utilizing lead lanthanum zirconate titanate /PLZT/ ceramic wafers
08 p1098 A83-22565
- Advances in electro-optic shutter stereoscopic displays
08 p1098 A83-22566
- Minimum/constant voltage lead lanthanum zirconate titanate /PLZT/ electro-optic shutters
08 p1099 A83-22567
- Parallel signal processing for optical satellite detection
08 p1049 A83-22816
- Effect of sampling, optical transfer function shape, and anisotropy on subjective image quality
08 p1167 A83-22894
- The relationship of acquisition systems to automated stereo correlation
12 p1731 A83-29919
- Integration of electro-optical sensor computing systems
22 p3350 A83-46605
- ELECTRO-OPTICS**
- Bandwidth, field distribution, and optimal electrode design for waveguide modulators
01 p0036 A83-10617
- Description of a 3-port ATE system required for testing of electro-optical UUT's
01 p0038 A83-10781
- Dynamic infrared missile evaluator /DIME/
01 p0015 A83-11236
- Calculation of an electrooptic diffraction deflector with allowance for edge effects
02 p0235 A83-11536
- Electro-optic-waveguide frequency translator in LiNbO₃ fabricated by proton exchange
02 p0235 A83-11566
- Suppressed turn-on laser regenerative optoelectronic amplifier
02 p0185 A83-12301
- Electro-optical instrumentation for resources evaluation; Proceedings of the Meeting, Washington, DC, April 21, 22, 1981
02 p0199 A83-12669
- Dimensional automatic target classification
02 p0182 A83-12886
- Mode stabilized terrace InGaAsP lasers on semi-insulating InP
03 p0332 A83-13919
- All-Union Conference on Laser Optics, 3rd, Leningrad, USSR, January 4-8, 1982, Proceedings
04 p0483 A83-15253
- Control of the spatial characteristics of laser radiation based on the electro-optical effect in crystals
04 p0483 A83-15259
- The problems of physical electronics --- Russian book
04 p0472 A83-15837
- The perception of colour on electro-optical displays
04 p0524 A83-16328
- Accuracy of optical angle estimator operating through the turbulent atmosphere
06 p0736 A83-18584
- Dynamics of electrooptic bistable devices with delayed feedback
06 p0810 A83-18904
- Laser switching of constant and radio-frequency signals
06 p0788 A83-19574
- Minimum angular vibration design of airborne electro-optical packages
07 p0944 A83-19820
- Instabilities and chaotic behavior in a hybrid bistable system with a short delay
08 p1163 A83-21886
- Objective summary of U.S. Army electro-optical modelling and field testing in an obscuring environment
08 p1093 A83-22351
- EOSAEL 82 - A library of battlefield obscuration models
08 p1093 A83-22352
- Millimeter wave propagation measurements at the Ballistic Research Laboratory
08 p1076 A83-22353
- Simultaneous multispectral absolute radiometer and transmissometer system
08 p1093 A83-22358
- Military applications of coherent infrared radar
08 p1095 A83-22500
- Atmospheric effects on electro-optical, infrared, and millimeter wave systems performance; Proceedings of the Meeting, San Diego, CA, August 27, 28, 1981
08 p1098 A83-22540
- Effects of atmospheric and man-made obscuration on visual contrast
08 p1135 A83-22541
- Contrast transmittance models for cloudy atmospheres
08 p1135 A83-22550
- Impact of aerosol modeling on performance calculations of electro-optic /EO/ systems operating in marine environments
08 p1136 A83-22555
- Preliminary shipboard optical turbulence measurements
08 p1166 A83-22556
- Itek model 2KL sensor - The mini-electro-optical imaging system /Mini EOIS/
08 p1099 A83-22581
- Calibration of spaceborne thermal detectors
08 p1052 A83-22881
- Electro-optical calibration considerations at intermediate maintenance levels
08 p1104 A83-22883
- An antitank missile seeker employing an infrared Schottky barrier focal plane array
09 p1253 A83-23544
- Electro-optical processor for optimal control
09 p1267 A83-23596
- Ferroelectric crystals for the control of laser radiation --- Russian book
09 p1271 A83-23815
- Coherent-optical processor for two-dimensional antenna arrays with a complex format of signal recording
09 p1345 A83-24920
- A self-setting attenuator for laser pulse energy stabilization
10 p1425 A83-25431
- Theory of optically controlled millimeter-wave phase shifters
10 p1402 A83-25817
- Optoelectronic enhancement of the Sagnac effect in a ring resonator and related effect of directional bistability
10 p1420 A83-25976
- CW electro-optical characteristics of graded-index waveguide separate-confinement heterostructure lasers with proton-delineated stripe
10 p1430 A83-26202
- Optical injection locking of BARITT oscillators
10 p1411 A83-26344
- Image processing by a spatial light modulator utilizing the Pockels effect
10 p1484 A83-26658
- Transient phenomena in optical bistability
11 p1656 A83-27531
- Laser bonding of dissimilar semiconductors
11 p1560 A83-27564
- Pulse sensor to monitor the loading process during programmed fatigue tests on specimens of materials and structural elements
11 p1575 A83-28621
- Electro-optical light modulation in InGaAsP/InP double heterostructure diodes
13 p1918 A83-30343
- Optoelectronically pulsed slot-line antennas
13 p1837 A83-31773
- 2-bit 1-Gsample/s electro-optic guided-wave analogue-to-digital converter system
13 p1838 A83-31780
- Diffraction gratings and reversal of the wavefront of laser beams in electrooptical crystals
14 p2084 A83-32134
- Actively coupled index-guided lasers
14 p2024 A83-32448
- Methodology for calculating turn-off transient of photoconductive circuit elements in picosecond optoelectronics
14 p2007 A83-33421
- Subpicosecond electrical sampling
14 p2008 A83-33423
- High-speed optical Fourier transformer
14 p2085 A83-33425
- Theory of degenerate four-wave mixing in picosecond excitation-probe experiments
14 p2093 A83-33426
- Temperature dependence of the relaxation decay time and the integrated intensity of the photoluminescence from the magnetic semiconductor CdCr₂Se₄
14 p2085 A83-33429
- A single-block hexagonal electrooptical Q-switch
14 p2085 A83-33433
- Electrooptical Bragg modulator based on the Ag-diffused LiTaO₃ waveguide
15 p2232 A83-34888
- Investigation of the characteristics of an integrated-optic analog-to-digital converter
15 p2232 A83-34890
- An optical residue processor for computing inner products
16 p2411 A83-35516
- Electrooptic interaction in oversized waveguide modulators
16 p2315 A83-35521
- Gallium arsenide and related compounds 1982; International Symposium, 10th, Albuquerque, NM, September 19-22, 1982, Contributed Papers --- Book
17 p2584 A83-37160
- Electrooptical imaging system using wavelength coding
17 p2510 A83-37748
- Energy model of image formation by an optical system
17 p2580 A83-38480
- Electro-optic X-witch using single-mode Ti:LiNbO₃ channel waveguides
18 p2744 A83-40396
- Optoelectronic methods of image processing
19 p2846 A83-40985
- Self-diffraction of light waves in gyrotropic crystals
19 p2899 A83-40997
- Isolation spectra for laser diode optical switch
19 p2900 A83-41278
- Second-harmonic generation on reflection from a monomolecular Langmuir layer
20 p3047 A83-42282
- Imaging sensors for an RPV payload
20 p2936 A83-43721
- Electrooptical branching waveguide switches and their application to 1 x 4 optical switching networks
21 p3205 A83-44220
- Time- and frequency-domain response of directional-coupler traveling-wave optical modulators
21 p3205 A83-44223
- A fast optoelectronic switch
21 p3125 A83-44541
- Optoelectronic devices based on silicon carbide p-n junctions produced by various processes
21 p3125 A83-44597
- Coherent image amplification and optical phase conjugation with photorefractive materials
21 p3206 A83-44799
- Electrooptical investigations of the effect of the humidification processes of various types of aerosols on the dipole characteristics of the particles
22 p3321 A83-45636
- Remote sensing of stratospheric and mesospheric winds by gas correlation electrooptic phase-modulation spectroscopy
22 p3328 A83-46063
- Harmonic response of a tunable Soltz filter
22 p3357 A83-46088
- Sensor design using computer tools; Proceedings of the Conference, Los Angeles, CA, January 28, 29, 1982
22 p3291 A83-46593
- Picosecond photoconductivity and its applications
22 p3298 A83-46674
- Advances in picosecond optoelectronics
22 p3298 A83-46675
- New developments in subpicosecond optoelectronics
22 p3298 A83-46676
- Ultrafast picosecond chronography
22 p3293 A83-46679
- Generation and amplification of ultrashort laser pulses and applications to electron trapping in amorphous media
22 p3299 A83-46683
- Electro-optic and infrared sensors
24 p3581 A83-48772
- Semiconductor optoelectronic devices for free-space optical communications
24 p3573 A83-48993
- High-performance avalanche photodiode with separate absorption 'grading' and multiplication regions
24 p3630 A83-49979
- ELECTROACOUSTIC TRANSDUCERS**
- NT MICROPHONES
- An analysis of multicomponent electroacoustic transducers providing matched control of the acoustic field in Bragg acoustooptic devices in the short-wave portion of the microwave range
05 p0630 A83-17595
- Bulk wave Bragg cells with 1 GHz bandwidth
06 p0753 A83-18935
- Semiconductor surface characterization using transverse acoustoelectric voltage versus voltage measurements
07 p0921 A83-20752
- Correlation analysis of the optical fields in optoacoustic interaction
09 p1344 A83-24001
- Electromagnetic acoustic transducer for in-plane and plane-normal velocity measurements
12 p1728 A83-29142
- Acoustic crystals --- Russian book
15 p2238 A83-34165
- Improved feed network for group-type unidirectional transducers
21 p3126 A83-44960
- Acoustic surface wave band filters with weighted fan transducers
23 p3445 A83-47569
- A Lamb wave voltage sensor
23 p3454 A83-47627
- Long-wave acoustic flowmeter
24 p3586 A83-49925
- ELECTROACOUSTIC WAVES**
- Waves in piezoelectric crystals --- Russian book
12 p1719 A83-28824
- Linear and nonlinear modified electron-acoustic waves
18 p2745 A83-39615
- Acoustoelectric oscillations in a bounded active stratified-periodic medium
19 p2841 A83-41820
- ELECTROCARDIOGRAMS**
- U ELECTROCARDIOGRAPHY
- ELECTROCARDIOGRAPHY**
- A pharmacological evaluation of electrical processes in the myocardium
01 p0078 A83-10510
- The electrical position of the heart and variants of a normal cartogram of 35 leads
01 p0083 A83-10511
- Precordial mapping of ST-T segment in acute myocardial infarction
02 p0223 A83-12251
- The integral EKG, the ventricular gradient, the differential EKG, and their diagnostic possibilities
03 p0379 A83-13621
- The diagnostic significance of the integral assessment of myocardial ischemia in patients with ischemic heart disease for the computerized monitoring of the EKG during the treadmill test
03 p0379 A83-13624
- The effect of cordamine and mesatone on the EKG under conditions of acute microwave irradiation
03 p0374 A83-13629
- An investigation of the relations between EEG and vegetative indicators in stress situations in patients with various types of depression
03 p0383 A83-13641
- Statistical synthesis of an algorithm for the computer-aided processing of cardiac signals
03 p0384 A83-14329
- The dependence of the character of the recovery of pulse on the rhythm of the heart and the lability of the sinusoid nodes in athletes after step loads
03 p0382 A83-14355

Clinical and EKG criteria for disorders of the cardiac rhythm in the weak sinus node syndrome

05 p0674 A83-17216

A method for the quantitative evaluation of the contractile function of the myocardium

05 p0675 A83-17695

An integrated noiseproof system of leads for recording the ECG, EMG, EEG, and respiration of an operator

06 p0800 A83-18973

Use of phase spectral information in assessment of frequency contents of ECG waveforms

07 p0980 A83-19627

The diagnostic accuracy of exercise electrocardiography - A review

07 p0978 A83-20785

Several indicators of the EKG and metabolic processes during an experimental coronary spasm in rats exposed to conditions of hypoxia in combination with hypercapnia

07 p0975 A83-20986

Wolf-Parkinson-White syndrome in young, asymptomatic pilot's applicants

08 p1147 A83-22961

Extrasystoles and the fitness of flight personnel - The contribution of the stress EKG tests

08 p1147 A83-22961

Cardiac localizations of sarcoidosis - The importance of the continuous electrocardiogram

08 p1148 A83-22964

Analysis of continuous electrocardiographic tracing of air traffic controllers recorded during work

08 p1148 A83-22969

An automatic system for the evaluation of the psychophysiological condition of an operator according to EKG parameters

09 p1324 A83-23863

Cardiac function monitored by impedance cardiography during changing seatback angles and anti-G suit inflation

12 p1766 A83-28930

Effect of exercise on QRS duration in healthy men - A computer ECG analysis

13 p1905 A83-30506

The stress ECG and the ambulatory continuous ECG in the selection of French astronauts

14 p2067 A83-32455

On the possibility to determine integral characteristics of the cardiac electric generator from extracardiac electric and magnetic measurements

14 p2072 A83-32799

The elevation of the ST segment during physical loading. Computer analysis, comparison with angiographic data, and clinical significance

18 p2735 A83-40547

The diagnostic value of ambulatory electrocardiographic monitoring

19 p2882 A83-41450

The EKG and physical work capacity in patients with hypertension

19 p2882 A83-41452

The information content of functional tests in the elucidation of the causes of repolarization disorders of the myocardium in flight personnel

21 p3188 A83-45299

The effect of a constant electromagnetic field on the EKG parameters and several indicators of the blood in experimental conditions

21 p3184 A83-45306

The effect of sudden changes of the geomagnetic field on several physiological indicators of healthy humans

23 p3498 A83-47119

ELECTROCATALYSTS

Research on oxidation by air and tempering of Raney nickel electrocatalysts for the H₂ anodes of alkali combustion materials cells --- German thesis

06 p0726 A83-18494

Photoelectrocatalysis on silicon in solar light

16 p2328 A83-36775

ELECTROCHEMICAL CELLS

NT ALKALINE BATTERIES

NT DRY CELLS

NT ELECTRIC BATTERIES

NT FUEL CELLS

NT HYDROGEN OXYGEN FUEL CELLS

NT LEAD ACID BATTERIES

NT LITHIUM SULFUR BATTERIES

NT METAL AIR BATTERIES

NT NICKEL CADMIUM BATTERIES

NT NICKEL HYDROGEN BATTERIES

NT NICKEL ZINC BATTERIES

NT PHOSPHORIC ACID FUEL CELLS

NT PRIMARY BATTERIES

NT REDOX CELLS

NT REGENERATIVE FUEL CELLS

NT SODIUM SULFUR BATTERIES

NT STORAGE BATTERIES

NT THERMAL BATTERIES

NT ZINC-BROMIDE BATTERIES

NT ZINC-CHLORINE BATTERIES

NT ZINC-OXYGEN BATTERIES

Electrochemical physics

02 p0151 A83-11814

Characterization of ether electrolytes for rechargeable lithium cells

02 p0152 A83-12052

Transport properties of Nafion membranes for use in three-electrode photoelectrochemical storage cells

02 p0202 A83-12055

Defects and disorder in the fast-ion electrode lithium-aluminum

02 p0154 A83-12057

Polycrystalline p-WSe₂ as photocathode in an electrochemical solar cell

03 p0354 A83-13702

Experimental study of electrochemical fluorination of trichloroethylene

04 p0456 A83-15870

Development of the spherical silicon solar cell

05 p0658 A83-17347

Electrophoretically deposited CdS and CdSe anodes for photoelectrochemical cells

07 p0000 A83-19883

Conductivity of the mixed organic electrolyte containing propylene carbonate and 1,2-dimethoxyethane --- for lithium cells

07 p0880 A83-19889

Lithium cycling behavior in 2-methyltetrahydrofuran with alcohol additives --- in lithium batteries

07 p0880 A83-19890

Effects of solution mass transport on the ECC ozonesonde background current

07 p0959 A83-20100

Electrochemically modified electrodes - Poly(2-methyl-8-quinolinol/ and poly(8-quinolinol/ complexing films obtained by electropolymerizing substituted phenols: Their voltammetric and electrical properties in relation to their geometric structure

07 p0881 A83-20583

Instrumentation for incremental voltage step electrochemical measurements

07 p0932 A83-21382

Effects of solution mass transport on the ECC ozonesonde background current --- Electrochemical Concentration Cell

07 p0967 A83-21556

Electric field enhanced diffusion in trans/CH₃x --- battery cells

10 p1446 A83-26053

Application of electrochemical energy storage in solar thermal electric generation systems

11 p1604 A83-27179

Pore size engineering applied to starved electrochemical cells and batteries

11 p1605 A83-27201

Interface between solid electrode and solid electrolyte - A study of the Li/Li⁺/Al₂O₃/ solid-electrolyte system

11 p1546 A83-28295

The relation between performance and stability of Cd-Chalcogenide/Polysulfide photoelectrochemical cells. I - Model and the effect of photoetching

11 p1546 A83-28297

A technique for calculating shunt leakage and cell currents in bipolar stacks having divided or undivided cells

14 p2047 A83-32637

Rechargeable Li/Li(1+x)V₃O₈ cells

14 p2047 A83-32645

Sealed nickel cadmium batteries --- Book

15 p2188 A83-33614

Equatorial ozone characteristics as measured at Natal (5.9 deg S, 35.2 deg W)

20 p3021 A83-42863

A one-volt p-InP/n-CdSe regenerative photoelectrochemical cell

20 p3013 A83-43421

Synthesization and properties of solid electrolyte Ag₂B₁₈W₄O₁₆

21 p3109 A83-44054

An active dummy cell for use in corrosion studies

22 p3267 A83-46701

Catalysis in solar energy --- development of photoelectrochemical cells

22 p3320 A83-46794

Electro-generated conducting polypyrrole polymers and applications in photoelectrochemical cells

24 p3598 A83-48777

Chromium oxides as cathodes for lithium cells

24 p3600 A83-49943

A reversible graphite-lithium negative electrode for electrochemical generators

24 p3558 A83-49946

ELECTROCHEMICAL CORROSION

Intergranular corrosion mechanism in Al-Mn alloys

04 p0457 A83-14963

An electrochemical method for investigating corrosion in rubbing surfaces

05 p0652 A83-17256

Zeta corrosion of mechanical seals

06 p0768 A83-18047

The hydrogen evolution process on a Ni-28 percent Mo alloy

06 p0728 A83-18146

Mechanisms of the microbial corrosion of aluminum alloys

06 p0726 A83-18550

Electrochemical studies of photocorrosion of n-CdSe

07 p0952 A83-19881

Mechanisms of hot corrosion

07 p0891 A83-21455

Comparison of hot-salt corrosion test procedures

07 p0892 A83-21457

The use of coatings in high temperature battery systems

10 p1445 A83-25536

The influence of electrode potential on the corrosion of gas turbine alloys in sulfate melts

11 p1550 A83-28672

The anodic dissolution of a Ni-base superalloy

12 p1713 A83-29401

The electrochemical aspect of the corrosion inhibitor action and ways of increasing the effectiveness of inhibitors

14 p1988 A83-32070

A comparison of procedures used in assessing the anodic corrosion of metal matrix composites and lead alloys for use in lead-acid batteries

14 p1989 A83-32626

Dissolved metal species mechanism for initiation of crevice corrosion of aluminum. I - Experimental investigations in chloride solutions. II - Mathematical model

14 p1993 A83-32628

The influence of crack length on stress corrosion crack velocity

14 p1994 A83-32683

The influence of microstructure on the corrosion of Al-Li, Al-Li-Mn, Al-Li-Mg and Al-Li-Cu alloys in 3.5 percent NaCl solution

14 p1997 A83-32892

Electrode corrosion in a compartmented flow cell by diffusion from the counterelectrode

15 p2133 A83-34690

Photoelectrochemical and microprobe laser Raman studies of lead corrosion in sulfuric acid

15 p2133 A83-34691

The deterioration of sodium ion conductors under applied stress

16 p2326 A83-35976

On the processes responsible for the degradation of the aluminium-lithium electrode used as anode material in lithium aprotic electrolyte batteries

24 p3600 A83-49933

ELECTROCHEMICAL MACHINING

The time series modelling of non-Gaussian engineering processes

08 p1073 A83-22006

Problems associated with electrodischarge machined, electrochemically machined and ultrasonically machined surfaces

08 p1111 A83-22007

Equipment for the electrochemical machining of specimens of structural materials

13 p1859 A83-31222

Determination of the theoretical profile of the electrode tool in the electrochemical processing of parts of complex shape

14 p2028 A83-32967

ELECTROCHEMICAL OXIDATION

Methane synthesis on nickel by a solid-state ionic method

08 p1056 A83-22324

Electrochemical impedance diagrams of alloy 600 at active-passive transition potentials

09 p1230 A83-23917

Electrochemical oxidation of the ternary alloys Ti-Ru-Ni and Ti-Ru-Co

09 p1235 A83-24402

Selective electrochemical etching of p-CdTe (for photovoltaic cells)

18 p2750 A83-40065

ELECTROCHEMISTRY

NT ELECTROLYSIS

NT PHOTOELECTROCHEMISTRY

Electrochemical physics

02 p0151 A83-11814

Sources of pressure in lithium thionyl chloride batteries

02 p0202 A83-12054

An electrochemical study of Ni/2+/, Co/2+/, and Zn/2+/, ions in melts of composition CaMgSi₂O₆

02 p0152 A83-12845

Batteries and fuel cells: Design, employment, chemistry --- German book

03 p0355 A83-14041

Conductive polymers imitate metals

05 p0617 A83-16873

Electrochemical behavior of Li₂S in fused LiCl-KCl electrolytes --- in redox cells

07 p0879 A83-19886

Reactions of FeS₂, CoS₂, and NiS₂ electrodes in molten LiCl-KCl electrolytes

07 p0881 A83-20578

Instrumentation for incremental voltage step electrochemical measurements

07 p0932 A83-21382

Investigations concerning the electrochemical equilibrium in the system tin-bismuth-oxygen

09 p1233 A83-24124

The electrochemistry of molten lithium chlorate and its possible use with lithium in a battery

11 p1546 A83-28296

Electrochemical preparation and conditioning of Cu₂S for Cu₂S-CdS solar cells

14 p2045 A83-32299

Voltammetric study of the anodic oxidation of sulfide ions in molten fluorides

14 p1989 A83-32630

Electrochemical utilization of metal hydrides

14 p1990 A83-32647

Hydrogen permeability and diffusivity in nickel and Ni-base alloys

14 p1997 A83-32950

Electrochemical studies of Cu(I) and Cu(II) in an aluminum chloride-N-(n-butyl)pyridinium chloride ionic liquid

15 p2133 A83-34693

Electrochemical assessment of MCrAlY coating alloys at 750 and 900 C in air and CO/CO₂ mixtures

20 p2953 A83-42253

Electrochemical reduction of calcium chromate --- cathode material in Ca/CaCrO₄/Fe thermally activated batteries

22 p3268 A83-46895

Polymer-coated electrodes in ambient temperature molten salts

22 p3268 A83-46896

Increased electrochemical window in ambient temperature neutral ionic liquids

22 p3268 A83-46897

- Protective coatings for carbon-fiber materials
24 p3553 A83-49091
- Electrochemical studies of corrosion of iron, nickel and nickel alloys in alkali sulfate melt
24 p3563 A83-49496
- Study of a lithium-lithium propionate electrode in propylene carbonate
24 p3558 A83-49927
- Solid electrolyte interphase (SEI) electrodes. VI
Calcium-Ca(AlCl₄)₂-sulfuryl chloride system
24 p3558 A83-49928
- International Meeting on Lithium Batteries, Rome, Italy, April 27-29, 1982
24 p3600 A83-49932
- Electrochemistry of a nonaqueous lithium/sulfur cell
24 p3600 A83-49938
- Electrochemical method for studying the reversibility of the lithium intercalation in secondary batteries
24 p3600 A83-49942
- Characterization of the chemistry at the anode and cathode in the Li/SO₂ battery system
24 p3600 A83-49948

ELECTROCONDUCTIVITY

- Electrical permittivity and conductivity of carbon black-polyvinyl chloride composites
01 p0036 A83-10627
- Electroconducting glass fibres produced by ion-exchange and reduction treatments
02 p0159 A83-11674
- Electrical conduction in carbon-polymer composites
02 p0149 A83-11785
- Highly conductive and transparent zinc oxide films prepared by rf magnetron sputtering under an applied external magnetic field
02 p0243 A83-12288
- Antennas in conducting media /Review/
04 p0466 A83-15726
- Ionization-induced breakdown and conductivity of satellite dielectrics
05 p0618 A83-17520
- Electrophysical properties of single crystals of n-Cd/x/Hg/1-x/Te /x ranging from 0.24 to 0.40/
09 p1350 A83-24250
- Inductive coupling between idealized conductors and its significance for the geomagnetic coast effect
10 p1447 A83-25435
- Effective generalized conductivity of three-phase cellular systems --- with kerosene-air-water fuel mixture example
12 p1775 A83-29270
- Electrical conductivity deep inside the earth --- Russian book
12 p1753 A83-29335
- A method of reducing the effect of the gap in eddy-current measurements of conductivity
13 p1860 A83-30839
- The effects of energetic particle precipitation on the atmospheric electric circuit
13 p1878 A83-30898
- On the asteroidal conductivities as inferred from meteorites
16 p2438 A83-36782
- Induced geomagnetic variation and crustal evolution of the southern peninsula of India
17 p2528 A83-38144
- The activation energy of conductivity in organic solids and liquids in relation to the cohesive energy density
21 p3216 A83-43948
- Electrical conduction in mantle materials
22 p3324 A83-45798
- The electroconductivity of composites with binary fillers containing high-conductivity components
24 p3553 A83-49054

ELECTRODE FILM BARRIERS

- Squeezable electron tunneling junctions
20 p3055 A83-43607
- Solid electrolyte interphase (SEI) electrodes. VI
Calcium-Ca(AlCl₄)₂-sulfuryl chloride system
24 p3558 A83-49928
- Surface films on lithium in acetonitrile-sulphur dioxide solutions
24 p3558 A83-49937

ELECTRODELESS DISCHARGES

- Amplification in a waveguide CO₂ laser employing an RF electrodeless discharge
07 p0935 A83-20129

ELECTRODEPOSITION

- NT ELECTROPLATING
- Use of electrodeposition to provide coatings for solid state bonding
02 p0155 A83-12070
- Strengthening parts by applying composite coatings --- Russian book
03 p0294 A83-13817
- Preparation and characteristics of a-Si:Cl:H films
04 p0539 A83-15478
- Black chrome solar selective coatings optimized for high temperature applications
04 p0504 A83-15479
- Influence of deposition rate on the character of electrodeposited CdSe used for photoelectrochemical cells
04 p0505 A83-15499
- Hot-electron luminescence in aged electrodeposited CdSe liquid-junction solar cell
05 p0658 A83-16946
- Electrophoretically deposited CdS and CdSe anodes for photoelectrochemical cells
07 p0000 A83-19883
- Thermal degradation of solar collector surfaces
10 p1445 A83-25535

- Effect of substrate surface conditions on the microstructure of nickel electrodeposits
10 p1395 A83-25548
- Structural and compositional characterization of mixed CdS-CdSe films grown by cathodic electrodeposition
10 p1446 A83-26055
- The effect of heat treatment on some properties of electrodeposited nickel and chromium coatings
10 p1399 A83-26896
- Hydrogen absorption and embrittlement of tantalum at cathodic deposition
10 p1399 A83-26897
- Accelerated cycle life tests of Ni/Cd cells with ED nickel electrodes - Comparison of three separators
11 p1605 A83-27192
- The structure of electrodeposited alloys based on the metals of the iron subgroup
13 p1819 A83-30064
- Electrodeposited CdS/CdTe heterojunction solar cells
14 p2044 A83-32280
- The morphology of silicon electrodeposits on graphite substrates --- in solar cells
14 p2091 A83-32629
- Electrodeposition of Ni-B₄C dispersion coatings
17 p2483 A83-38051
- Electrodeposition of zinc on glassy carbon from ZnCl₂ and ZnBr₂ electrolytes
20 p2951 A83-43420
- Film forming reaction at the lithium/electrolyte interface
24 p3558 A83-49935

ELECTRODERMAL RESPONSE**U GALVANIC SKIN RESPONSE****ELECTRODES**

- NT ANODES
- NT CATHODES
- NT CELL ANODES
- NT CELL CATHODES
- NT HOLLOW CATHODES
- NT PHOTOCATHODES
- NT PLASMA ELECTRODES
- NT SOLID ELECTRODES
- NT THERMIONIC CATHODES
- NT TUBE ANODES
- Bandwidth, field distribution, and optimal electrode design for waveguide modulators
01 p0036 A83-10617
- Photoelectrochemical properties of n-type NiTiO₃
01 p0067 A83-10636
- The influence of the interface state on the properties of solar cell semiconductor electrodes
03 p0352 A83-13473
- An examination of instabilities of an electric arc at atmospheric pressure --- French thesis on relation to cathodic material properties
03 p0294 A83-13805
- Polycrystalline lanthanum rhodate and lutetium rhodate photoelectrodes for liquid junction solar cells
04 p0504 A83-15480
- Layered transition metal thiophosphates /MPX3/ as photoelectrodes in photoelectrochemical cells
04 p0504 A83-15483
- Ionization-induced breakdown and conductivity of satellite dielectrics
05 p0618 A83-17520
- Travelling wave power FET with coplanar slow-wave electrode system, modeling and experimental results
06 p0749 A83-17969
- Effective conductivities of a positive electrode in an Li-Al/FeS cell at different states of charge
07 p0952 A83-19878
- Oxygen transfer on substituted ZrO₂, Bi₂O₃, and CeO₂ electrolytes with platinum electrodes. I - Electrode resistance by dc polarization
07 p0880 A83-19887
- Oxygen transfer on substituted ZrO₂, Bi₂O₃, and CeO₂ electrolytes with platinum electrodes. II - ac impedance study
07 p0880 A83-19888
- Construction of reference electrodes for long-term testing of compact Li-Al/FeS cells
07 p0953 A83-19900
- Photoelectrochemical properties of polycrystalline TiO₂ thin film electrodes on quartz substrates
07 p0954 A83-20584
- Modern multistage depressed collectors - A review
09 p1254 A83-24025
- A lithium electrode with a zinc substrate for secondary batteries
10 p1446 A83-26057
- Simple and efficient preionization system for gaseous lasers
13 p1857 A83-31472
- An electrode for the electronystagmography of experimental animals
16 p2395 A83-36827
- Thermal dielectric breakdown with cylindrical electrodes
17 p2498 A83-38216
- The GEL electrode - A new method of detecting fatigue cracks
18 p2668 A83-40612
- The first cortical implant of a multiplexed multi-electrode semiconductor brain electrode
20 p3035 A83-42553
- The mechanism of the action of small amounts of metals in increasing currents at photo electrodes
21 p3108 A83-43949
- Compact uniform field electrode profiles --- for use in TEA laser
21 p3143 A83-44191

- The turbulent electrode effect as influenced by interfacial ion transfer --- between atmosphere and aerodynamically rough earth surface
24 p3607 A83-49334
- Polarization of the lithium electrode in sulfuryl chloride solutions
24 p3558 A83-49939
- Mechanistic studies of oxide electrodes reversibly incorporating Li(+) ions
24 p3558 A83-49941
- A reversible graphite-lithium negative electrode for electrochemical generators
24 p3558 A83-49946
- Optimization of the vanadium oxide (V₆O₁₃) electrode in a nonaqueous secondary lithium cell
24 p3601 A83-49958

ELECTRODIALYSIS

- Energy Storage in a fuel cell with bipolar membranes burning acid and hydroxide
13 p1872 A83-31599

ELECTRODYNAMICS

- NT ELECTROHYDRODYNAMICS
- NT ELECTROMECHANICS
- NT LIGHT-CONE EXPANSION
- NT QUANTUM ELECTRODYNAMICS
- Theoretical questions of eddy-current flow detection with superposed transducers - Rigorous mathematical solution of two-dimensional problems
01 p0057 A83-10365
- Application of Ampere's force law to railgun accelerators
01 p0036 A83-10613
- The limits of electrodynamics - Paraphotons
01 p0106 A83-10814
- Elementary derivation of Poisson structures for fluid dynamics and electrodynamics
03 p0396 A83-13119
- Interaction of cylindrical eddy-current transducers with a multilayered spherical product
03 p0338 A83-14294
- The estimates of the magnetic field in Halley's comet
03 p0431 A83-14872
- The method of moving coordinates as a technique for comparing various electrodynamic problems in systems having cylindrical conductors
04 p0467 A83-15746
- Experimental investigation of the electrodynamic system of a semiconductor cyclotron-resonance maser
04 p0484 A83-15765
- A new theory about the origin of the earth's magnetic field
06 p0782 A83-18020
- Uniqueness of the coupling of fields of a nonlinear ionizing electromagnetic wave at a discontinuity at the point of plasma resonance
06 p0813 A83-19189
- Mathematical modeling of axisymmetric fields by the method of minimal autonomous blocks
06 p0754 A83-19355
- Appearance of electrodynamic boundary layers during the propagation of sound in a confined low-temperature plasma
07 p0994 A83-19638
- Concerning a modification of the semiinversion method --- for electromagnetic wave propagation
07 p0986 A83-20317
- Compensation technique for force balance devices
07 p0929 A83-20548
- Charged dust in Saturn's magnetosphere
07 p1035 A83-21326
- The complex dynamics of delayed-feedback oscillators /Review/
09 p1257 A83-25077
- A perturbation-theory method in the electrodynamics of inhomogeneous and nonstationary media /Review/
09 p1339 A83-25078
- Helicity and alpha-effect of simple convection cells --- in solar envelope
10 p1520 A83-25378
- Radio pulsar disk electrodynamics
10 p1503 A83-25716
- Radiation from a moving point charge in a drifting anisotropic plasma
10 p1486 A83-26041
- Electrodynamic analysis of a reflector in the form of a system of parallel conductors /the E-wave case/
10 p1407 A83-26952
- A millimeter-wave amplifier based on a diffraction-radiation generator electrodynamic system
10 p1435 A83-26963
- Electrodynamics of the outer solar atmosphere
11 p1687 A83-27379
- The electrodynamics of continuous media (2nd revised and enlarged edition) --- Russian book
12 p1774 A83-28821
- Study of dynamical effects using phase conjugation of light waves
12 p1729 A83-29167
- Optimization of an electrodynamic basis for determination of the resonant frequencies of microwave cavities partially filled with a dielectric
13 p1831 A83-30234
- Investigation of cylindrical resonators containing annular inhomogeneities
13 p1832 A83-30276
- Electrodynamic analysis of a model of a two-reflector antenna with strict allowance for the interaction between reflectors
13 p1828 A83-30280
- A comb-shaped slow-wave structure in waveguides of complex cross section
13 p1832 A83-30286
- A new concept of sources of the electromagnetic field and some applications
13 p1914 A83-30649

Electrodynamic characteristics of the natural modes of a circular waveguide with a dielectric rod 13 p1833 A83-30713

Electrodynamics of submicron dust in the cometary coma 13 p1958 A83-31733

Energy characteristics of an electromagnetic field and an extraneous particle in a dispersive medium 14 p2079 A83-32168

The radiation of charges moving in the vicinity of individual localized inhomogeneities 14 p2007 A83-33299

Radiation from long conducting tethers moving in the near-earth environment 15 p2235 A83-34407

An electrogasdynamic boundary layer on a dielectric plate 17 p2505 A83-37523

Plasma effects in the formation, evolution and present configuration of the Saturnian ring system 17 p2521 A83-38120

Middle atmospheric electrodynamicities 17 p2541 A83-38279

On the quality factor and energy center of antennas 17 p2494 A83-38476

Experimental study of the electrodynamic properties of an open cylinder in a rectangular waveguide 17 p2498 A83-38478

Allowance for the skin effect in a superconductor-semiconductor-superconductor d structure 17 p2499 A83-38487

Electrodynamics of the stratosphere using 5000 cu m superpressure balloons 18 p2640 A83-39818

A method for the numerical solution of three-dimensional problems of electrodynamicities 18 p2676 A83-39945

Nonlinear electrohydrodynamic Rayleigh-Taylor instability. II - A perpendicular field producing surface charge 18 p2747 A83-40498

Achievement of an optimal distribution of the high-frequency field in a coaxial orotron 19 p2854 A83-41790

On the electrodynamicity of semiconductor plasmas. The basic equations 19 p2905 A83-41822

Fields of radiation sources in moving media 21 p3200 A83-45049

Electroelasticity relationships for multilayer piezoceramic shells with layer polarization in the thickness direction 21 p3163 A83-45365

Electrodynamic analysis of the propagation of electromagnetic waves in a thin-film semiconductor structure with negative differential resistance 22 p3276 A83-45667

An electrodynamic analysis of helical dipoles 22 p3277 A83-45680

A method for solving a system of equations encountered in problems of electrodynamicities --- for multi-discrete element antennas 22 p3272 A83-45693

Pulsar electrodynamicity - Cylindrical model and radio and gamma-ray radiation 22 p3379 A83-46559

Radiation balance and the stochastic Van der Pol-Duffing equation 22 p3354 A83-46771

The electrodynamicity of a pulsar magnetosphere 23 p3527 A83-48089

Electrodynamics of anisotropic waveguide structures --- Russian book 23 p3445 A83-48325

First indication of Ampere tension in solid electric conductors 23 p3445 A83-48592

The method of canonical transformations in classical electrodynamicities 24 p3623 A83-49065

Direct methods for calculating irregular waveguides with inhomogeneous dielectric filler 24 p3573 A83-49268

Methods of integral equations for the study of mathematical models of convex antenna arrays 24 p3570 A83-49271

Numerical method for calculating plane semiinfinite structures 24 p3573 A83-49273

ELECTRODYNAMOMETERS

U DYNAMOMETERS

ELECTROENCEPHALOGRAM

U ELECTROENCEPHALOGRAPHY

ELECTROENCEPHALOGRAPHY

A device for recording the spatial synchronization of phases of EEG waves 01 p0050 A83-10502

A method for adaptive biocontrol in the multifaceted treatment of patients with cerebral arachnoiditis 01 p0083 A83-10525

An electroencephalographic investigation of the human cerebral cortex during the processing of the solution of visual-motor problems with training 01 p0083 A83-10530

Electrophysiological analysis of delayed-response behavior --- Russian book 02 p0221 A83-12149

The omega-potential - A quantitative indicator of the condition of the structure of the brain and the organism. II - The possibilities and limitations of the use of the omega-potential for rapid evaluations of the condition of the human body 02 p0222 A83-12212

The possible meaning of the rapidly proceeding processes of the spatial-temporal organization of the EEG in the formation of psychic activity 02 p0224 A83-12213

The voluntary regulation of alpha and theta EEG rhythms in humans 02 p0224 A83-12215

Psychological and electroencephalographic changes with aging in relation to aircrew performance 02 p0225 A83-12253

The significance of functional lateralization in the formation of complex motor acts in athletes 04 p0522 A83-15784

An integrated noiseproof system of leads for recording the ECG, EMG, EEG, and respiration of an operator 06 p0800 A83-18973

The pattern of the energy characteristics of the EEG as an indicator of the effectiveness of the autogenic stimulation of work capacity 07 p0979 A83-20344

Pattern recognition approach to human sleep EEG analysis and determination of sleep stages 08 p1150 A83-22051

The effect of a peptide which induces 'delta sleep' and its analogues on the encephalogram of rabbits under normal conditions and during the deprivation of sleep and its effect on learning processes in rats 08 p1144 A83-22101

Some improvements in the measurement of variable latency acoustically evoked potentials in human EEG 14 p2069 A83-33110

Epsilon-separating nonlinear digital filter and its applications 15 p2220 A83-33519

Electroencephalogram indicators and hypoxic shifts in patients with hypertension with different hemodynamic variations 15 p2213 A83-34951

Effects of detector coil size and configuration on measurements of the magnetencephalogram 16 p2401 A83-35452

Rhythms in the range of 4.5-12 Hz of the background EEG from the visual and sensorimotor cortex in rats under different patterns of locomotor activity 19 p2876 A83-41565

The first cortical implant of a multiplexed multi-electrode semiconductor brain electrode 20 p3035 A83-42553

The characteristics of the asymmetry of the EEG rhythm of healthy individuals at rest and during mental loading in connection with left or right-handedness 21 p3187 A83-44664

The effect of sudden changes of the geomagnetic field on several physiological indicators of healthy humans 23 p3498 A83-47119

ELECTROEPITAXY

Effect of substrate surface conditions on the microstructure of nickel electrodeposits 10 p1395 A83-25548

ELECTROEROSION

U SPARK MACHINING

ELECTROEXPLOSIVE DEVICES

U INITIATORS (EXPLOSIVES)

ELECTROFORMING

Transmission electron microscopy of transverse sections through oxide scales on metals 03 p0296 A83-13123

A waveguide slot array for use at millimetric frequencies 06 p0751 A83-18614

ELECTROGENERATORS

U ELECTRIC GENERATORS

ELECTROHYDRAULIC CONTROL

U ELECTRIC CONTROL

U HYDRAULIC CONTROL

ELECTROHYDRODYNAMICS

Dielectrophoretic, thermal instability in a spherical shell of fluid 02 p0174 A83-12983

Three-dimensional fluid and electrodynamic modeling for MHD DCW channels [AIAA PAPER 83-0464] 05 p0686 A83-16732

Ion wind drag reduction [AIAA PAPER 83-0231] 05 p0689 A83-17914

Fixation of bubbles and drops of specified shapes in a liquid dielectric by an electric field 06 p0813 A83-19434

Multivariable approach to the problem of structural cross coupling of force feedback electrohydraulic actuators --- for structural testing of aircraft and their components 10 p1379 A83-26601

Linear and nonlinear waves in liquid dielectrics 11 p1658 A83-27711

Nonlinear electrohydrodynamic Rayleigh-Taylor instability. I A perpendicular field in the absence of surface charges 16 p2414 A83-35347

The stability of plane-parallel electrohydrodynamic flows in a longitudinal electric field 16 p2414 A83-35528

Corona discharge in a moving gas 19 p2902 A83-41262

Electrodynamic coupling in magnetically confined X-ray plasmas of astrophysical origin 20 p3073 A83-43070

Microscopic derivation of plasma electrohydrodynamicities 20 p3050 A83-43568

Parametric excitation of electrohydrodynamic surface waves 20 p3051 A83-43671

Electrogasdynamic flows --- Russian book 23 p3509 A83-47100

Variational formulation for the equilibrium condition of a conducting fluid in an electric field 24 p3624 A83-50195

ELECTROJETS

NT AURORAL ELECTROJETS

NT EQUATORIAL ELECTROJET

Ionospheric ELF radio signal generation due to LF and/or MF radio transmissions. II - Interpretation 02 p0205 A83-12016

Magnetospheric convection effects at mid-latitudes. I - Saint-Santin observations 06 p0783 A83-18295

Determination of the latitude of Sq focus and its relation to the electrojet variations 24 p3606 A83-49306

ELECTROKINETICS

Photoconductivity kinetics in Cd/x/Hg/1-x/Te crystals under surface excitation 01 p0108 A83-10374

On the electrokinetic energy conversion in liquid mixtures 11 p1612 A83-28069

Auroral plasmas in the evening sector - Satellite observations and theoretical interpretations 16 p2382 A83-36620

ELECTROLESS DEPOSITION

Constitution and properties of nickel-boron coatings 12 p1716 A83-29367

Lattice images of amorphous-like Ni-B films prepared by the electroless plating method 16 p2328 A83-35601

The lattice images of amorphous-like Ni-B alloy films prepared by electroless plating method 20 p2956 A83-43615

Electroless nickel applications in aircraft maintenance [SAE PAPER 820609] 22 p3301 A83-45867

ELECTROLUMINESCENCE

Tunable electroluminescence from GaAs doping superlattices 01 p0110 A83-10991

Infrared to visible up-conversion using GaP light-emitting diodes 07 p0992 A83-19990

The aging of electroluminophors in the presence of moisture 13 p1831 A83-30264

Possible experiments to search for axions 20 p3045 A83-42268

A study of the electrical and luminescence characteristics of a novel Si-based thin film electroluminescent device 20 p2966 A83-42607

Studies of electroluminescence in pAlGaAs-pGaAs-nGaAs heterophotocells with distributed parameters 23 p3477 A83-47565

ELECTROLUMINESCENT LAMPS

U ELECTROLUMINESCENCE

U LUMINAIRES

ELECTROLYSIS

Magnetolysis 02 p0151 A83-11810

Precipitate formation during sea water electrolysis 04 p0506 A83-16040

Operation of a steady-state pH-differential water electrolysis cell 04 p0506 A83-16041

Photoelectrolysis of water under visible light with doped SrTiO3 electrodes 07 p0954 A83-20580

A mechanistic study of oxygen evolution on Li-doped Co3O4 --- by electrolysis 07 p0881 A83-20586

Applications of porous flow-through electrodes. I - An experimental study on the hydrogen evolution reaction on packed bed electrodes 07 p0954 A83-20587

Present status of R&D for hydrogen production from water in Japan 09 p1292 A83-23701

On-site production of electrolytic hydrogen for generator cooling 11 p1605 A83-27209

Current research in advanced water electrolysis in the United States and abroad 11 p1552 A83-27216

Interface between solid electrode and solid electrolyte - A study of the Li/LiI/Al2O3/ solid-electrolyte system 11 p1546 A83-28295

Hydrogen energy creeps forward --- hydrogen fuel production and storage 13 p1869 A83-30000

High temperature solar electrothermal processing - Zinc from zinc oxide 13 p1872 A83-31598

Solar generator performance with load matching to water electrolysis - Longterm averages and range of instantaneous efficiencies 14 p2038 A83-32191

Theoretical and experimental aspects of a two-step short cycle, based on ZnO and CdO intended for storage of solar energy 14 p2046 A83-32348

Photoactivated electrolysis on nonporous chlorogallium phthalocyanine thin film electrodes 14 p1989 A83-32632

Countercurrent electrolysis in a thin porous membrane 16 p2328 A83-36965

Industrial water electrolysis - Present and future 18 p2664 A83-39560

- The effect of gas bubble evolution on the energy efficiency in water electrolysis --- Thesis 22 p3266 A83-46688
- Advanced electrolysis development for hydrogen-cycle peak shaving for electric utilities 22 p3320 A83-46779
- The testing of electrodes for alkaline solution water electrolysis 23 p3430 A83-48594
- Iron oxide electrodes for photoelectrolysis of water 23 p3430 A83-48595
- Technological aspects of sulfur dioxide depolarized electrolysis for hydrogen production 23 p3430 A83-48596
- Resource and energy management of syngas production with hydrogen and oxygen requirements from electrolysis 23 p3477 A83-48597

ELECTROLYTE METABOLISM

- Clinical aspects of the disruption of the water-electrolyte metabolism during essential hypertension 03 p0381 A83-14343
- Plasma electrolyte content and concentration during treadmill exercise in humans 05 p0674 A83-17331
- Hydro-electrolytic and hormonal modifications linked to extended decubitus in an antihypertensive position 08 p1149 A83-22982
- Hydroelectrolytic and hormonal modifications related to prolonged bedrest in antihypertensive position 11 p1641 A83-27344
- Clonidine as a counter measure for metabolic studies during weightlessness simulation 11 p1642 A83-27796
- Psychological stress induces sodium and fluid retention in men at high risk for hypertension 12 p1763 A83-28925
- Correction of changes in fluid-electrolyte metabolism in manned space flights 12 p1763 A83-28928
- Effects of water immersion on plasma catecholamines in normal humans 13 p1902 A83-30465
- Fluid and electrolyte homeostasis in space - A primate model to look at mechanisms [SAE PAPER 820832] 13 p1898 A83-30930
- Ionizing radiation decreases veratridine-stimulated uptake of sodium in rat brain synaptosomes 15 p2209 A83-33776
- The phospholipid composition of various tissues of rats in dehydration conditions 16 p2395 A83-36829
- The changes in the water-electrolyte metabolism in the brain of rats during gamma-irradiation of the head at high doses 19 p2874 A83-41012
- The character of water-sodium changes in the bodies of patients with hypertension under the influence of various types of hypotensive therapies 19 p2881 A83-41427
- Fluid and electrolyte homeostasis during prolonged exercise at altitude 20 p3034 A83-43481

ELECTROLYTES

- NT ION EXCHANGE MEMBRANE ELECTROLYTES
- NT JUMPERS
- NT MOLTEN SALT ELECTROLYTES
- NT NONAQUEOUS ELECTROLYTES
- NT SOLID ELECTROLYTES
- Hydrogenated amorphous silicon/electrolyte contacts; band bending and photoresponse dependence on surface reactions 01 p0067 A83-10630
- Electrolyte electroreflectance study of laser annealing effects of the CdTe/Hg(0.8/Cd/0.2)/Te(111) system 01 p0110 A83-10992
- Bromine reduction in a two-phase electrolyte 02 p0151 A83-12051
- Characterization of ether electrolytes for rechargeable lithium cells 02 p0152 A83-12052
- Sources of pressure in lithium thionyl chloride batteries 02 p0202 A83-12054
- The activity of renin in blood plasma, the indicators of central hemodynamics, and the water-electrolyte balance in patients with hypertension 03 p0379 A83-13622
- Conductivity of the mixed organic electrolyte containing propylene carbonate and 1,2-dimethoxyethane --- for lithium cells 07 p0880 A83-19889
- Electrolyte film structure on battery separator and electrode materials 07 p0954 A83-20577
- Diffusivity in zinc chloride-potassium chloride electrolyte 07 p0954 A83-20582
- Surface and redox reactions at GaAs in various electrolytes --- of photoelectrochemical cells 07 p0955 A83-20595
- Observation of 'intrinsic' surface states at the TiO₂-aqueous-electrolyte interface by sub-band-gap electroreflectance spectroscopy 07 p1000 A83-20818
- Ion clustering and proton transport in Nafion membranes and its applications as solid polymer electrolyte 10 p1390 A83-26051
- Pore size engineering applied to starved electrochemical cells and batteries 11 p1605 A83-27201
- Evaluation of tetrafluoroethane-1,2-disulfonic acid as a fuel cell electrolyte 11 p1546 A83-28300

- Palladium-silicondioxide-silicon structures as hydrogen sensors in electrolytes 12 p1712 A83-29464
- The effect of changes of the electrolytic composition of the perilymph on the endocochlear potential 14 p2063 A83-32567
- The deterioration of sodium ion conductors under applied stress 16 p2326 A83-35976
- Determination of the charging current of a plate in an aerosol flow when a liquid film is separated from its surface 17 p2503 A83-37266
- Electrodeposition of zinc on glassy carbon from ZnCl₂ and ZnBr₂ electrolytes 20 p2951 A83-43420
- Fermi levels in electrolytes and the absolute scale of redox potentials 20 p2951 A83-43608
- Quantitative models for the migration of electrolyte gradients in an electric field 22 p3266 A83-45761
- Changes in the urinary levels of electrolytes, uric acid and 17 OHCS with graded heat stress 23 p3499 A83-48692
- The effect of solution concentrations in sulfate aerosols 24 p3602 A83-49688
- The reactivity of organic electrolytes with lithium Mechanistic aspects 24 p3558 A83-49934
- Raman spectroscopic studies of the structure of electrolytes used in the Li/SOCl₂ battery 24 p3558 A83-49936
- The cycling behaviour and stability of the lithium electrode in propylene carbonate and acetonitrile electrolytes 24 p3600 A83-49950
- Galvanostatic cycling of lithium-titanium disulphide cells in propylene carbonate and propylene carbonate-acetonitrile electrolytes 24 p3558 A83-49951

ELECTROLYTIC CELLS

- UPS and Schottky barrier study of TiO₂ electrochemical anodes --- for solar cells 04 p0504 A83-15481
- Operation of a steady-state pH-differential water electrolysis cell 04 p0506 A83-16041
- Studies on photogalvanic effect in systems containing toluidine blue 06 p0780 A83-18561
- Flowing electrolyte battery testing and evaluation 11 p1604 A83-27184
- Interface between solid electrode and solid electrolyte - A study of the Li/Li/Al₂O₃/solid-electrolyte system 11 p1546 A83-28295
- Surface recombination at n-TiO₂ electrodes in photoelectrolytic solar cells 14 p2047 A83-32634
- The deterioration of sodium ion conductors under applied stress 16 p2326 A83-35976
- International Meeting on Lithium Batteries, Rome, Italy, April 27-29, 1982 24 p3600 A83-49932
- Raman spectroscopic studies of the structure of electrolytes used in the Li/SOCl₂ battery 24 p3558 A83-49936
- Surface films on lithium in acetonitrile-sulphur dioxide solutions 24 p3558 A83-49937
- Polarization of the lithium electrode in sulfolyl chloride solutions 24 p3558 A83-49939
- Behaviour of various cathode materials for nonaqueous lithium cells 24 p3600 A83-49944
- Galvanostatic cycling of vanadium oxide (V₆O₁₃) in a nonaqueous secondary lithium cell 24 p3601 A83-49952
- High-temperature solid oxide fuel cell - Technical status 24 p3601 A83-49954
- The anodic passivation of lithium 24 p3558 A83-49956

ELECTROLYTIC GRINDING

U ELECTROCHEMICAL MACHINING

ELECTROMAGNETIC ABSORPTION

- NT AURORAL ABSORPTION
- NT INFRARED ABSORPTION
- NT MULTIPHOTON ABSORPTION
- NT PHOTOABSORPTION
- NT POLAR CAP ABSORPTION
- NT ULTRAVIOLET ABSORPTION
- NT X RAY ABSORPTION
- Automation of a Crawford-cell exposure system 01 p0051 A83-10865
- Effect of particle size distribution and chlorophyll content on beam attenuation spectra 02 p0203 A83-12314
- The absorption of electromagnetic radiation in an advanced propulsion system [AIAA PAPER 82-1950] 02 p0147 A83-12507
- Two-dimensional radiation in absorbing-emitting-scattering media using the P-N approximation [ASME PAPER 82-HT-19] 02 p0171 A83-12786
- Numerical simulation of a light-absorbing plasma at a shock front 03 p0396 A83-13177
- Optical absorption coefficient and minority carrier diffusion length measurements in low-cost silicon solar cell material 03 p0354 A83-13922
- Amplitude coherence in an absorption region --- measurement on millimeter wave transmission loss 03 p0307 A83-14033

- Meteorological effects in the variations of ionospheric parameters. I - The lower thermosphere 03 p0361 A83-14741
- Stationary large-scale irregularities of the ionosphere 03 p0361 A83-14742
- An observational study of the D-region winter anomaly and sudden stratospheric warmings 03 p0362 A83-14746
- Optical absorption above the optical gap of amorphous silicon hydride 04 p0541 A83-15520
- IMS ground observations on optical aurora and ionospheric absorption made in Northern Europe, with examples of data handling 04 p0512 A83-16291
- Self-excitation of surface oscillations of droplets in an electromagnetic wave field 05 p0649 A83-17063
- Absorption of HCN-laser rays with inverse bremsstrahlung in a krypton atom field --- German thesis 06 p0811 A83-18520
- Results obtained on experimental radio circuits over medium distances 06 p0747 A83-18734
- Multistability at microwave frequencies 08 p1079 A83-22011
- Thermal effects in photothermal spectroscopy and photothermal imaging 08 p1092 A83-22335
- The effect of tropospheric aerosols on the earth's radiation budget - A parameterization for climate models 08 p1142 A83-23009
- Measurements of the absorption and brightness temperatures of the atmosphere in the millimeter wavelength range 09 p1301 A83-23481
- Energetic electron fluxes and ionospheric absorption during the August event 1972 09 p1301 A83-23672
- Scattering and absorption characteristics of lossy dielectric objects exposed to the near fields of aperture sources --- of electromagnetic radiation 09 p1324 A83-23791
- Titanium-containing powder-metallurgy alloys with special physical properties --- microwave absorbers 09 p1235 A83-24405
- Comparison of photon stimulated dissociation of gas phase and chemisorbed CO 10 p1389 A83-25556
- Resonant absorption in a self-consistent density profile at moderate intensities --- in inhomogeneous plasmas 10 p1485 A83-25789
- On the effect of absorbing materials on electromagnetic waves with large relative bandwidth 10 p1405 A83-26491
- A new procedure for improving the solution stability and extending the frequency range of the EBCM --- Extended Boundary Condition Method for EM absorption and scattering in biological dielectric objects 10 p1460 A83-26839
- Propagation of intense CW-light through a strongly absorbing medium - Self-focusing and spatial ringings 11 p1576 A83-27514
- Pulse formation and amplification in an absorbing medium by optical phase switching 11 p1582 A83-27600
- Absorption bursts in the radio emission from the sun at decimeter wavelengths 11 p1691 A83-27991
- Relation of absorption of radio waves to solar X-rays and to Lyman-alpha radiation at the time of low solar and geomagnetic activity 11 p1616 A83-28110
- On the role of solar Lyman alpha radiation in radio-wave absorption in the D-region 12 p1753 A83-29406
- Temperature distribution in uniform and layered microwave absorbers in waveguide 12 p1720 A83-29441
- Anomalous absorption by water vapour in the microwave region 13 p1894 A83-31546
- Refraction and absorption in plasma atmospheres 13 p1927 A83-31573
- Fluctuations of the parameters of an electromagnetic wave in a turbulent light absorbing atmosphere 14 p2052 A83-32559
- The matrix coefficient for the brightness of radiation reflected by a semi-infinite absorptive medium with a greatly extended indicatrix of scattering 14 p2085 A83-32857
- The characteristics of a confined light beam in an absorptive medium having a narrow indicatrix of scattering 14 p2085 A83-32858
- Electroabsorption by Stark effect on room-temperature excitons in GaAs/GaAlAs multiple quantum well structures 14 p2093 A83-33442
- An experimental study of the absorption mechanisms in laser-matter interaction at high energies - The effect of wavelength --- French thesis 15 p2232 A83-33699
- Maximum power penetration through an electrically small aperture 15 p2149 A83-35191
- Comparison of A1-absorption data with theoretically computed values based on the International Reference Ionosphere (IRI) 16 p2375 A83-35390

- Emission, absorption, and tunneling of whistler waves in an inhomogeneous magnetic field
17 p2581 A83-37034
- Redistribution - Why half a collision is better than a whole one --- spectra of scattered light from perturbed atomic system
17 p2484 A83-37075
- Absorption of radiation propagation obliquely in a magnetoplasma
17 p2597 A83-37328
- Latitude dependence of geomagnetic storm after-effects in ionospheric absorption
18 p2712 A83-39064
- Density of gap states of silicon grain boundaries determined by optical absorption
18 p2750 A83-40063
- Linear mode conversion in laser plasmas
18 p2748 A83-40511
- Photovoltaic energy converters
18 p2709 A83-40525
- On mechanisms of anomalous absorption of electromagnetic waves near a critical point of a plasma target
19 p2901 A83-41173
- On the maximum interdependence of absorbed and scattered powers --- by receiving antennas or structures covered with absorbing materials
19 p2835 A83-41770
- An iterative extended boundary condition method for solving the absorption characteristics of lossy dielectric objects of large aspect ratios --- under exposure to incident plane wave radiation
21 p3189 A83-43833
- Nonlinear magneto-optics in semiconductors
21 p3218 A83-44800
- Ionospheric absorption of radio waves on reflection by the E layer and by the shielding Es layer
21 p3177 A83-45275
- The rotational spectrum of water dimers (H₂O)₂ in atmospheric conditions
22 p3322 A83-45637
- The effect of modulated electromagnetic radiation on the temperature regime of a monodisperse aerosol medium
22 p3322 A83-45642
- Antisaturation in stimulated Raman emission
22 p3295 A83-45944
- Maximum statistical increase of optical absorption in textured semiconductor films
22 p3356 A83-45967
- Nonlinear absorption of electromagnetic radiation during collisions of particles in a strong magnetic field
23 p3509 A83-47552
- Spectral density of millimeter wave amplitude scintillations in an absorption region
23 p3443 A83-47842
- Simple expressions for predicting substrate, volume, and interface absorption and reflective phase shifts in high-reflectance quarter-wave stacks at oblique angles of incidence
24 p3623 A83-48977
- Electromagnetic wave damping in a nonequilibrium aerosol plasma
24 p3632 A83-49115
- ELECTROMAGNETIC ACCELERATION**
- Electromagnetic projectile acceleration utilizing distributed energy sources
01 p0036 A83-10620
- Magnetic acceleration of interstellar probes
01 p0016 A83-10703
- The possibility of using electromagnetic accelerators for studying processes occurring during the high-velocity collision of solids
04 p0465 A83-16388
- The thermal limitation of the velocity of annular conductors under inductive axial acceleration
06 p0755 A83-19561
- The possibility of the acceleration of charged particles by laser radiation
07 p0935 A83-20306
- Control and design aspects of magnetically suspended vehicles
10 p1491 A83-26605
- An electromagnetic accelerator
11 p1533 A83-28573
- Gain-enhanced free-electron laser with an electromagnetic pump field
13 p1855 A83-31133
- Hypervelocity acceleration techniques - A review of existing capabilities and prospects for future developments
15 p2125 A83-35032
- Investigation of the efficiency of the acceleration of conductors in the pulsed magnetic field of a solenoid
16 p2340 A83-35540
- Fast electromagnetic launchers
21 p3125 A83-44103
- ELECTROMAGNETIC COMPATIBILITY**
- Testing of a communications satellite
01 p0018 A83-11066
- The solution of 'real-world' aircraft EMC problems using the AAPG computer program
01 p0041 A83-11085
- A technique for predicting antenna-to-antenna isolation and electromagnetic compatibility for aircraft
01 p0007 A83-11235
- The electromagnetic environment for the Space Shuttle orbiter
05 p0604 A83-16661
- Equipment for monitoring the electromagnetic-compatibility parameters of scientific instruments in spacecraft
10 p1386 A83-25330
- The technical diagnostics of radio-electronic and other equipment according to electromagnetic-compatibility parameters
10 p1412 A83-26933
- Algorithms for the optimization of an isolated frequency band for a group of radio-electronic devices of one type according to EMC-assurance conditions
10 p1407 A83-26935
- Improvements to a pulse compression radar matched filter
13 p1836 A83-31175
- Electromagnetic compatibility between scientific instruments in the ARCAD-3 project
18 p2646 A83-39586
- Design strategies aid ELF/VLF receivers
22 p3275 A83-46758
- Application of the statistical simulation method to determine the electromagnetic-compatibility factors of radio systems
24 p3571 A83-50209
- ELECTROMAGNETIC CONTROL**
- U ELECTROMAGNETS
- U REMOTE CONTROL
- ELECTROMAGNETIC DEDUCTION**
- U MAGNETIC INDUCTION
- ELECTROMAGNETIC FIELDS**
- NT FAR FIELDS
- NT NEAR FIELDS
- NT SYSTEM GENERATED ELECTROMAGNETIC PULSES
- Theoretical questions of eddy-current flaw detection with superposed transducers - Rigorous mathematical solution of two-dimensional problems
01 p0057 A83-10365
- Analysis of the electromagnetic field in an open resonator
01 p0035 A83-10372
- Dispersion relation for general anisotropic media
01 p0033 A83-11371
- The changes in the nerve and cardiac activity in animals of various ages during the application of electromagnetic fields of low frequency and low voltage
02 p0220 A83-11884
- The biological effectiveness of a weak electromagnetic field of infralow frequency
02 p0221 A83-11887
- The pathological and anatomical characteristics of experimental myocardial infarction under the effect of electromagnetic fields of low frequencies and low strengths
02 p0221 A83-11888
- The reaction of a biological system to adequate or weak low-frequency electromagnetic fields
02 p0221 A83-11889
- The emission of electromagnetic waves in the case of a smooth variation of parameters of a radiating system
03 p0390 A83-13427
- Cooperative transients in inter-atomic correlation in the presence of an externally applied coherent field - Relation to intrinsic mirrorless optical bistability
03 p0394 A83-13789
- Radiation from a dipole in the presence of a grounded gyromagnetic slab
03 p0312 A83-13914
- Numerical analysis of two-dimensional fields in the theory of eddy-current flaw detection by superposed transducers
03 p0338 A83-14295
- Finite-difference analysis of EM fields inside complex cavities driven by large apertures
03 p0308 A83-14549
- A comparison of lightning electromagnetic fields with the nuclear electromagnetic pulse in the frequency range 10 to the 4th to 10 to the 7th Hz
03 p0344 A83-14550
- Calculation of electromagnetic fields and critical frequencies of waveguides of complex cross section
04 p0471 A83-15764
- New formulas for the electromagnetic field of a vertical electric dipole in a dielectric or conducting half-space near its horizontal interface
04 p0468 A83-16054
- Integral representation of electromagnetic fields in inhomogeneous anisotropic media
04 p0532 A83-16451
- The state of hepatic circulation under the combined effect of lead and electromagnetic fields
05 p0673 A83-17159
- Quick microwave field mapping for large antennas
05 p0622 A83-17346
- Gyrotropic waveguides --- Book
05 p0625 A83-17373
- Modeling surface electromagnetic anomalies using horizontally inhomogeneous layers of finite thickness
05 p0663 A83-17618
- The determination of the fields reflected from a twist reflector following illumination by a plane wave
06 p0737 A83-18609
- Scattering by objects in translational motion
06 p0737 A83-18610
- Computer graphics applications in electromagnetic computer modeling --- treatment of wire objects by method of moments
06 p0802 A83-18667
- Non-linear optimization for field, scattering and SEM problems --- Singularity Expansion Methods
06 p0742 A83-18668
- Conversion of an electromagnetic field when the properties of the medium change with time in a limited region
06 p0813 A83-19334
- The amplitude modulation of the short-period oscillations of the earth's electromagnetic field
06 p0787 A83-19421
- Quantum processes in an electromagnetic wave field
06 p0809 A83-19539
- Schumann resonances at high latitudes
07 p0957 A83-19635
- Electromagnetic-field diffraction by a system of curvilinear screens
07 p0914 A83-20774
- Surface fields excited by a vertical electric point source located on a conducting concave spherical surface
07 p0914 A83-20823
- Polarization backscatter analysis of field distributions using fiber optics
07 p0930 A83-20828
- Variation of e/m in the five-dimensional theory of gravitation, electromagnetism, and scalar field
07 p0989 A83-20852
- Drift theory of the motion of a charged particle in a high-frequency wave in the case of finite Larmor radius
07 p0998 A83-20874
- The nonzero-flow-rate /accretion/ semidynamo - Two simple examples
07 p1027 A83-21277
- Surface impedance and wave tilt interpretation over horizontally stratified media
08 p1160 A83-22028
- Electromagnetic test fields near a Schwarzschild horizon
08 p1180 A83-22210
- Electromagnetic fields in twisted coordinate system
08 p1080 A83-22234
- The theory of irregular waveguides and open resonators
08 p1080 A83-22249
- Methods for analyzing optical guided wave structures
08 p1164 A83-22470
- Angular spectrum representation of scattered electromagnetic fields
08 p1161 A83-22668
- Static plane symmetric disordered radiation in Brans-Dicke theory
08 p1181 A83-22745
- The dependence of the development of complications in patients with an infarction of the myocardium and chronic ischemic heart disease on the state of the electromagnetic field of the earth
08 p1146 A83-22777
- On the mutually unique correspondence between an ideally conducting body and the field scattered by it
08 p1078 A83-23153
- Generalized network representations for small-aperture coupling between dissimilar regions
09 p1254 A83-23804
- Inverse problems of the dynamics of dions and magnetic monopoles
09 p1338 A83-24204
- Local momentum representation of a propagator in external gravitational and electromagnetic fields
09 p1338 A83-24212
- The dependence of the sharpness of an interference pattern on the quantum state of the electromagnetic field
09 p1346 A83-25092
- The spectral theory of a light field
09 p1347 A83-25253
- Methods for practical calculations of light fields under conditions of multiple scattering
09 p1347 A83-25257
- Gravitational radiation in Robertson-Walker backgrounds
10 p1506 A83-26096
- Field theory of planar helix traveling-wave tube
10 p1410 A83-26343
- The loop antenna with a cylindrical core - Theory and experiment
10 p1405 A83-26826
- Electromagnetic plane wave scattering by a system of two parallel conducting prolate spheroids
10 p1405 A83-26836
- Rotational symmetries of electromagnetic radiation fields
10 p1406 A83-26853
- Squeezed states in harmonic generation of a laser beam
10 p1435 A83-26971
- Nonperturbative calculations of the indices of refraction of multilevel systems
11 p1577 A83-27537
- Finite-element solution of three-dimensional electromagnetic problems
11 p1560 A83-27893
- Nonperiodic electromagnetic fields in a sectoral horn
11 p1555 A83-27932
- Return-stroke electromagnetic fields of oblique lightning channels
11 p1632 A83-27970
- Simulated emission from ultrarelativistic electrons in strong electric and magnetic fields
11 p1584 A83-28058
- Radiative processes and mass renormalization in plasma physics theory
11 p1659 A83-28232
- On the resolving power of the VLF method
11 p1558 A83-28346
- Driving-point impedance of a linear cylindrical antenna
11 p1558 A83-28607

The electrodynamics of continuous media (2nd revised and enlarged edition) --- Russian book 12 p1774 A83-28821

Space-time ordered electromagnetic radiation outside a massive plane 12 p1774 A83-28874

Robertson-Walker cosmologies with a trace anomaly effect in their dynamical description 12 p1791 A83-28985

The effect of electromagnetic forces on the hydrodynamics of a melt in the process of high-frequency floating zone melting 12 p1782 A83-29269

An admittance solution for electromagnetic coupling through a small aperture 12 p1718 A83-29402

The low-frequency electromagnetic field in the Venus atmosphere - Evidence from Venera 13 and Venera 14 12 p1798 A83-29483

On the theory of electromagnetic induction in the earth by ocean currents 12 p1757 A83-29963

A new concept of sources of the electromagnetic field and some applications 13 p1914 A83-30649

Investigation of nonperiodic crossed-field systems using a model of particles of variable charge 13 p1832 A83-30701

Determination of electromagnetic field scattered by small defects and influence of boundary between media 13 p1860 A83-30838

Coupling between microstrip line and image guide through small apertures in the common ground plane [AD-A129977] 13 p1836 A83-31150

The macroscopic vacuum effects in an inhomogeneous and nonstationary electromagnetic field 14 p2079 A83-32136

The bremsstrahlung of a slow electron at a Coulomb center in an external electromagnetic field 14 p2079 A83-32139

Energy characteristics of an electromagnetic field and an extraneous particle in a dispersive medium 14 p2079 A83-32168

Relative field strength of VHF/UHF horizontally polarized waves in 5 to 100-meter range of propagation 14 p2002 A83-33147

Statistics of photocounts of modulated radiation and coherence of field in optical waveguides 15 p2230 A83-33982

A proposed observational test of six-dimensional relativity 15 p2225 A83-34137

Efficient numerical evaluation of electromagnetic fields due to rectangular patches of electric current 15 p2146 A83-35092

On the current distribution for open surfaces 15 p2154 A83-35190

The electromagnetic field in a layered earth induced by an arbitrary stationary current distribution 16 p2341 A83-35410

The calculation of electromagnetic fields by numerical methods 16 p2406 A83-35517

Polarization effects in the diffraction of electromagnetic waves - The role of disclinations 16 p2407 A83-35639

Antennas for nonsinusoidal waves. II - Sensors 16 p2342 A83-35781

The biological effect of the electric component of an electromagnetic field in the VLF range 16 p2393 A83-35921

Determination of the electromagnetic field produced by a magnetic oblique-rotator. V - Corotating plasma-disk 16 p2428 A83-36533

Coherence properties and cutoff wavelength determination in dielectric waveguides 16 p2413 A83-36766

The halo effect in a nuclear-electromagnetic cascade 17 p2629 A83-37647

Some comments on the analysis of electromagnetic fields in inhomogeneous media 17 p2576 A83-38034

Electromagnetic effects on planetary rings 17 p2621 A83-38119

The dynamical role of a primordial electromagnetic field in spatially homogeneous, diagonal Bianchi type I-IX cosmologies 17 p2610 A83-38546

The sensitivity by age of animals to electromagnetic fields at microwave frequencies 17 p2557 A83-38928

On the penetration of an electromagnetic field through circular and annular holes 18 p2677 A83-40096

Electromagnetic and magnetic fields in the treatment of ischemic heart disease 18 p2734 A83-40540

Some singularities of electromagnetic sources and fields 19 p2837 A83-40794

The method of complex rays --- extended to antenna electromagnetic fields 19 p2894 A83-40797

Topology-finite-element method for solving electromagnetic field problems 19 p2896 A83-41277

Domain modes of operation of a Gunn diode in an external variable field 19 p2840 A83-41785

Achievement of an optimal distribution of the high-frequency field in a coaxial orotron 19 p2854 A83-41790

Calculation of electromagnetic fields in displacement transducers 19 p2841 A83-42016

Praxis-oriented results processing in the calculation of electromagnetic fields by discretization methods 20 p2967 A83-43027

Excitation of electromagnetic fields by a modulated electron beam entering a plasma waveguide 21 p3210 A83-44135

Cylindrically symmetric Einstein-Maxwell-massless scalar field equations 21 p3199 A83-44367

Techniques for measuring the field intensity of radio waves --- Russian book 21 p3121 A83-45042

Conducting shells in a pulsed electromagnetic field --- Russian book 21 p3126 A83-45047

Fields of radiation sources in moving media 21 p3200 A83-45049

Interpreting electromagnetic anomalies with the method of moments 21 p3175 A83-45252

The effect of a constant electromagnetic field on the EKG parameters and several indicators of the blood in experimental conditions 21 p3184 A83-45306

The electromagnetic field in a randomly inhomogeneous medium Phase-space representation 21 p3201 A83-45391

Nonlinear electromagnetics in vacuo - Gravitational effects 21 p3201 A83-45413

Estimation of the angular position of an optical source whose emission is received by a photodetector array 22 p3355 A83-45691

Quasi-electrostatic fields within the atmosphere 22 p3325 A83-45879

Approximate expressions for field penetration through circular apertures 22 p3276 A83-46932

A note on electromagnetic 'tidal' force 23 p3503 A83-47418

Elastic scattering of electrons by hydrogen atoms in a laser field 24 p3626 A83-49432

Electric-magnetic duality of conformal gravitation 24 p3624 A83-49745

Black hole electromagnetic fields and negative energy states for charged particles 24 p3668 A83-50092

Note on a suggested formation of charge from an electromagnetic wave 24 p3624 A83-50200

ELECTROMAGNETIC INTERACTIONS

NT PLASMA-ELECTROMAGNETIC INTERACTION

Stimulated scattering of whistler waves by ion acoustic waves in the magnetosphere 01 p0070 A83-10199

The limits of electrodynamics - Paraphotons 01 p0106 A83-10814

Optical guided-wave interactions with magnetostatic waves at microwave frequencies 01 p0039 A83-10976

Parametric mixing of electromagnetic waves in superarrays 02 p0166 A83-11688

Heat death and oscillation in model universes containing interacting matter and radiation 03 p0422 A83-14179

Spatial changes in the induced fluctuations of the intensity of radiation used to probe a bleachable aerodisperse medium 07 p0988 A83-20106

Concerning problems of optimization in nonlinear optics --- field characteristics and incident radiation 07 p0936 A83-20312

Exact solutions of relativistic wave equations --- Russian book 07 p0989 A83-20378

Polarization effects in the bremsstrahlung production of massive mesons in a magnetic field 07 p0992 A83-20857

Calculated electromagnetic fields of transfer and superposed eddy-current transducers when spherical conducting bodies with flaws are present 07 p0944 A83-21418

A note on total cross sections and decay rates in the presence of a laser field 10 p1425 A83-25409

Interaction of electromagnetic waves with a moving perturbation in a stationary gas 10 p1471 A83-25648

Chaos in the semiclassical N-atom Jaynes-Cummings model - Failure of the rotating-wave approximation 10 p1481 A83-25797

Parametric conversion of electromagnetic waves in a relativistic electron beam moving in a cylindrical waveguide 10 p1472 A83-26462

Interaction between high-intensity arbitrarily polarized radiation and molecules under collisional relaxation conditions 10 p1480 A83-26684

Electromagnetic coupling to an infinite wire through a slot in a conducting plane 10 p1411 A83-26838

Investigation of the effects of interaction of surface magnetostatic waves with slow electromagnetic waves 11 p1561 A83-27939

Diffusion mechanism of the interaction of aerosol drops and the possibility of controlling this mechanism by means of electromagnetic radiation 13 p1874 A83-30043

Modeling of the interaction of a confined electron beam with an electromagnetic wave in distributed-emission magnetron-type systems 13 p1833 A83-30703

Theoretical study of processes in a system with 'conjugate' M-type interaction 13 p1833 A83-30705

Nonlinear interaction of a modulated electron beam with electromagnetic waves in M-type devices 13 p1833 A83-30707

The theory of phase transitions in certain systems with electromagnetic interaction and its application to ferroelectrics 14 p2092 A83-33041

The kinetic theory of electromagnetic processes 17 p2575 A83-37165

A simple example of a classical gauge transformation 19 p2899 A83-41876

Induced currents at the resonant frequency in the Rocket Triggered Lightning Investigation 20 p3030 A83-42534

Theory and applications of electromagnetic levitation 20 p2962 A83-43259

The calculation of transport phenomena in electromagnetically levitated metal droplets 20 p2963 A83-43273

The excitation of microwaves by a relativistic electron beam in a dielectric-lined waveguide 21 p3124 A83-43945

An interaction between gravitational and electromagnetic waves 21 p3232 A83-44730

A numerical study of the interaction of a plane electromagnetic wave with a closed dielectric screen 22 p3271 A83-45649

A video system to demonstrate interactions of near-infrared radiation with plant leaves 23 p3453 A83-47225

Three-wave parametric processes in electron beams 23 p3445 A83-47566

Forced interaction between an electron beam and superpower electromagnetic radiation at the boundary between two media 23 p3463 A83-48434

The effects experienced by a point electric dipole in a gravity field 24 p3623 A83-49455

Nonlinear phenomena in a bulk semiconductor with a superlattice in the millimeter-wave range 24 p3635 A83-49550

ELECTROMAGNETIC INTERFERENCE

NT ATMOSPHERICS

NT CHIRP SIGNALS

NT COSMIC NOISE

NT CROSSTALK

NT DAWN CHORUS

NT ELECTROMAGNETIC NOISE

NT HISS

NT IONOSPHERIC CROSS MODULATION

NT IONOSPHERIC NOISE

NT IONOSPHERICS

NT JAMMING

NT POLAR RADIO BLACKOUT

NT RADIO FREQUENCY INTERFERENCE

NT SHOT NOISE

NT THERMAL NOISE

NT WHISTLERS

NT WHITE NOISE

Shielding techniques tackle EMI excesses. V - EMI shielding 01 p0035 A83-10271

Detection and reception of complex signals masked by noise and lumped interference 01 p0031 A83-10409

A topological approach to the unification of electromagnetic specifications and standards 01 p0041 A83-11084

AEHP for advanced technology aircraft --- Atmospheric Electricity Hazard Protection 01 p0001 A83-11086

Methods for minimizing the effects of lightning transients on aircraft electrical systems 01 p0009 A83-11088

Effects of thermal noise and interference due to scatterers on VOR system accuracy 01 p0004 A83-11092

Integrated CNI - A new testing challenge --- Communication, Navigation and Identification 01 p0004 A83-11095

A technique for predicting antenna-to-antenna isolation and electromagnetic compatibility for aircraft 01 p0007 A83-11235

Investigation of the multimode interference of surface optical waves in a microwaveguide interferometer 02 p0175 A83-11528

Shuttle contamination and experimentation - DoD implications 03 p0284 A83-13466

Transmission of pulse sequences through monomode fibers 03 p0395 A83-14385

Finite-difference analysis of EM fields inside complex cavities driven by large apertures 03 p0308 A83-14549

SEPAC system test in NASDA space chamber --- space experiment with particle accelerator 03 p0284 A83-14850

Design considerations for a electrical signal transmission subsystem /STS/ for the maximum performance ejection system /MPES/ 04 p0446 A83-15442

The suppression of the interference signal in a band of frequencies by means of an adaptive array 04 p0467 A83-15753

An interference light filter with a profiled substrate 05 p0685 A83-17661

German thesis 06 p0736 A83-18500

A discrete model for the distribution of users and the signal-capture effect in ALOHA networks 06 p0749 A83-19569

Experimental results for the interference between FM television signals 07 p0904 A83-19686

Adjacent channel interference degradation with minimum shift keyed modulation 07 p0905 A83-19698

The use of adaptive filters for narrowband interference rejection 07 p0905 A83-19700

Space-time distribution of the velocity of tidal motions, with allowance for Coriolis force 07 p0962 A83-20773

Statistics of differential rain attenuation on adjacent earth-space propagation paths 08 p1074 A83-21646

Plastic composites for electromagnetic interference shielding applications 08 p1055 A83-22717

Steered beam and LMS interference canceler comparison 08 p1077 A83-22728

Adaptive array processing - A tutorial 11 p1553 A83-27901

Rapid interference suppression using a Kalman filter technique 11 p1554 A83-27906

Adaptive antenna design considerations for satellite communication antennas 11 p1535 A83-27915

Adjacent-channel and quadrature-channel interference in minimum shift keying 11 p1556 A83-28127

Behavior of phase-locked loops in the presence of large interfering signal 13 p1834 A83-30785

Rejection of CW interference in QPSK systems using decision-feedback filters 14 p2001 A83-32865

A computing model and its experimental testing for an evaluation of electromagnetic interferences created by interfering circuits on transmission or high-voltage lines above a dissipative ground 14 p2002 A83-32894

Interference irregularities in complex laser resonators 15 p2169 A83-34024

Canonical and quasi-canonical probability models of class A interference 16 p2342 A83-35780

Comment on 'Calculation of site attenuation from antenna factors' 16 p2342 A83-35783

Calculated transmission profile of an interference filter placed in a convergent beam under various incidence angles --- for nightglow observations 16 p2357 A83-36753

Electroplated carbon/graphite fibers 16 p2325 A83-36900

Interference to satellite earth stations due to scatter of terrestrial transmissions by aircraft 19 p2835 A83-41554

Electronic steering of antenna nulls for interference reduction 20 p2965 A83-43680

Communication satellites in the geostationary orbit --- Book 22 p3274 A83-45911

Coping with impulse interference in an advanced development, low-cost Omega/VLF RNAV system 22 p3252 A83-46957

ELECTROMAGNETIC MEASUREMENT

NT ELECTROMAGNETIC NOISE MEASUREMENT

Fermi normal co-ordinate system and electromagnetic detectors of gravitational waves. I - Calculation of the metric 02 p0254 A83-12028

European OTS satellite transmit antenna patterns 04 p0453 A83-16201

Quick microwave field mapping for large antennas 05 p0622 A83-17346

Distance criteria in near-field and far-field antenna measurements 06 p0740 A83-18640

Spherical near-field measurements from a 'compact-range' viewpoint 06 p0740 A83-18650

Measurability analysis of the linearized gravitational field 06 p0806 A83-19448

Multidetector intensity interferometers 08 p1092 A83-22327

Potentialities of electric and magnetic wave tilt measurements --- for airborne survey of earth surface and subsurface propagation features 10 p1449 A83-26040

Thermal registration of electromagnetic fields by thin conducting films 11 p1561 A83-27941

Computation of electromagnetic flowmeter characteristics from magnetic field data. II - Errors 12 p1729 A83-29152

Nondestructive measurement of a dielectric layer using surface electromagnetic waves 13 p1831 A83-30227

Test of large aperture antennas using near-field techniques 13 p1829 A83-31194

Conference on Precision Electromagnetic Measurements, University of Colorado, Boulder, CO, June 28-July 1, 1982, Proceedings 13 p1836 A83-31276

The design of an automated, high-accuracy antenna test facility 13 p1829 A83-31280

Antenna gain measurements by an extended version of the NBS extrapolation method 13 p1829 A83-31281

A near-field antenna measurement system 13 p1830 A83-31282

A holographic surface measurement of the Texas 4.9-m antenna at 86 GHz 13 p1847 A83-31283

Automated timekeeping II 13 p1847 A83-31291

Time domain sensors for radiated impulsive measurements 15 p2166 A83-35178

Antenna pattern measurement with a geostationary satellite 16 p2342 A83-35553

Finite-element model of two-dimensional problems involving moving objects of inspection 22 p3304 A83-46331

The use of Helmholtz coils in the electromagnetic method --- for shock-initiated detonation measurements 24 p3584 A83-49796

High-precision measurements on a compact antenna test range 24 p3571 A83-49967

Probe correction in near field measurements by pseudo sampling technique 24 p3571 A83-49995

ELECTROMAGNETIC NOISE

NT ATMOSPHERICS

NT COSMIC NOISE

NT DAWN CHORUS

NT HISS

NT IONOSPHERIC NOISE

NT IONOSPHERICS

NT SHOT NOISE

NT THERMAL NOISE

NT WHISTLERS

NT WHITE NOISE

Approximation of the distribution functions of the phase and phase cosine of the sum of a harmonic signal and noise 01 p0031 A83-10411

On missiles modelling, simulation and evaluation in presence of noise and multi-source environment 01 p0004 A83-10707

Propagation effects on radio range and noise in earth-space telecommunications 02 p0140 A83-12615

Quantum noise in adaptive optical systems. I 05 p0685 A83-17589

The effect of noise on pulsed rate-tracking systems with correlation discriminators 05 p0623 A83-17683

Quantum noise in adaptive optical systems. II 06 p0810 A83-19330

Electromagnetic noise from an ion engine system 07 p0873 A83-20424

Influence of semiconductor-laser phase noise on coherent optical communication systems 08 p1077 A83-22638

Theory of FM noise of single-mode injection lasers 08 p1110 A83-22919

Noise of semiconductor lasers with external feedback 09 p1270 A83-23378

Solar radio noise bursts during the 21st cycle - Spectra and source properties 09 p1368 A83-23399

Noise in time-discrete analog filters 09 p1252 A83-23409

NCFSK performance improvements by selection diversity in Gaussian and impulsive noise environments 10 p1401 A83-25501

Computer-controlled noise optimization test set for the mm-wave region 10 p1412 A83-26900

The use of derivative techniques in astronomical spectroscopy 12 p1786 A83-29080

Ionospheric demodulation of signals of radio-broadcasting stations and magnetospheric ELF noise 14 p1999 A83-31880

Mathematical models of pulsed noise 14 p2001 A83-32483

Radio noise fields generated by corona streamers on a power line 16 p2341 A83-35414

Investigation of the high-frequency noise and volt-ampere characteristics of Schottky-barrier diodes at high forward currents 17 p2499 A83-38497

Statistical-physical modeling of electromagnetic noise 19 p2826 A83-40950

Man-made radio noise 22 p3273 A83-45884

Effects of photon noise on speckle image reconstruction with the Knox-Thompson algorithm --- in astronomy 23 p3459 A83-48312

Low-frequency noise in GaAs current limiters 23 p3446 A83-48607

ELECTROMAGNETIC NOISE MEASUREMENT

Airborne measurements of infrared atmospheric radiance and sky noise 03 p0324 A83-13461

Uniform noise in Gunn oscillators 04 p0471 A83-15745

Noise in short $n/-/+n/-/-n/+/-$ GaAs diodes 06 p0751 A83-18751

Two-phase frequency-conversion type spectrum analyzer for low-frequency noise measurement 07 p0929 A83-20547

Recent measurements of earth background spatial radiance variations 08 p1103 A83-22843

Temperatures in the plasmasphere determined from VLF observations 09 p1307 A83-24690

Precision measurement of antenna system noise using radio stars 13 p1940 A83-31284

Comparison of noise characteristics of Fabry-Perot-type and travelling-wave-type semiconductor laser amplifiers 13 p1858 A83-31763

Comment on 'Calculation of site attenuation from antenna factors' 16 p2342 A83-35783

Noise measurements in ion implanted MOSFETs 21 p3127 A83-45174

Characteristics of the radio noise receiving equipment --- onboard Ionosphere Sounding Satellite 21 p3104 A83-45436

Hot-electron noise generation in gallium-arsenide Schottky-barrier diodes 24 p3574 A83-49993

ELECTROMAGNETIC PROPAGATION

U ELECTROMAGNETIC WAVE TRANSMISSION

ELECTROMAGNETIC PROPERTIES

NT ABSORPTANCE

NT ABSORPTIVITY

NT BIREFRINGENCE

NT BRIGHTNESS

NT BRIGHTNESS DISTRIBUTION

NT CAPACITANCE

NT COLOR

NT DICHROISM

NT DIELECTRIC PROPERTIES

NT ELECTRICAL PROPERTIES

NT ELECTROMAGNETIC ABSORPTION

NT FARADAY EFFECT

NT FERROELECTRICITY

NT INDUCTANCE

NT INFRARED ABSORPTION

NT KERR MAGNETOOPTICAL EFFECT

NT LUMINOISITY

NT OPACITY

NT OPTICAL BISTABILITY

NT OPTICAL PROPERTIES

NT OPTICAL REFLECTION

NT PERMITTIVITY

NT PHOSPHORESCENCE

NT PHOTOCONDUCTIVITY

NT PHOTOELASTICITY

NT PHOTOELECTRIC EFFECT

NT PHOTOELECTRIC EMISSION

NT PHOTOIONIZATION

NT PHOTOVOLTAIC EFFECT

NT RADIANCE

NT REFLECTANCE

NT REFRACTIVITY

NT SKY BRIGHTNESS

NT SOLAR GRANULATION

NT STELLAR LUMINOSITY

NT STIGMATISM

NT TRANSMISSIVITY

NT TRANSMITTANCE

NT TRANSPARENCE

NT TURBIDITY

NT WATER COLOR

Effective generalized conductivity of three-phase cellular systems --- with kerosene-air-water fuel mixture example 12 p1775 A83-29270

ELECTROMAGNETIC PROPULSION

NT MASS DRIVERS (PAYLOAD DELIVERY)

Electromagnetic projectile acceleration utilizing distributed energy sources 01 p0036 A83-10620

A lightweight efficient argon electric thruster [AIAA PAPER 82-1921] 02 p0145 A83-12492

The flexible magnetic field thruster [AIAA PAPER 82-1936] 02 p0147 A83-12553

Rail accelerator research at Lewis Research Center [AIAA PAPER 82-1938] 08 p1052 A83-22075

On the theory of an electromagnetic-resonator engine 08 p1052 A83-22659

Laser-driven MHD-fanjet [AIAA PAPER 83-1345] 16 p2321 A83-36350

Analysis of electromagnetic propulsion of nonionized dipole gases [AIAA PAPER 83-1395] 16 p2322 A83-36385

ELECTROMAGNETIC PULSES

NT SYSTEM GENERATED ELECTROMAGNETIC PULSES

- The possibility of laboratory detection of long-period gravitational waves 01 p0125 A83-10904
- Experiments with optical solitons 03 p0390 A83-13428
- A comparison of lightning electromagnetic fields with the nuclear electromagnetic pulse in the frequency range 10 to the 4th to 10 to the 7th Hz 03 p0344 A83-14550
- The angular beaming model of microstructure and the subpulse drifting phenomenon --- in pulsars 04 p0550 A83-15033
- A calculation of the impulse responses of acoustically reflecting targets 04 p0531 A83-15073
- Silicon solar cell damage from electrical overstress 05 p0658 A83-17481
- Transient radiation screening of silicon devices using backside laser irradiation --- for military IC hardness against EMP 05 p0628 A83-17527
- Treatment of late time instabilities in finite-difference EMP scattering codes 05 p0628 A83-17532
- Pulsar timing observations at Tidbinbilla - 1975 to 1981 06 p0818 A83-18175
- Forming of ultrafast light pulses with predetermined temporal shape 06 p0766 A83-18957
- Timing of the Crab pulsar - Consequences of the large glitch of 1975 07 p1017 A83-20928
- Fiber optics for electro-magnetic pulse /EMP/ simulators 08 p1047 A83-22495
- Theory of generation of ULF pulsations by ionospheric modification experiments 09 p1300 A83-23308
- Analysis of the radiation characteristics of an aperture antenna excited by a periodic pulsed signal 09 p1245 A83-23454
- Time-dependent theory of resonant tunnel coupling in optical waveguides 10 p1483 A83-26463
- An experimental investigation of the rhombic EMP simulator under pulse excitation 10 p1411 A83-26492
- Theoretical analysis of the rhombic simulator under pulse excitation 10 p1411 A83-26493
- Pulse response of linear dipole antenna 10 p1411 A83-26850
- Pulse formation and amplification in an absorbing medium by optical phase switching 11 p1582 A83-27600
- Study of dynamical effects using phase conjugation of light waves 12 p1729 A83-29167
- Real time monitoring of CW mode-locked dye laser pulses using a rapid-scanning autocorrelator 12 p1729 A83-29194
- Dynamics of intense short pulses in optical waveguides 13 p1918 A83-30009
- High-power submillimeter gyrotron with a pulsed magnetic field 13 p1851 A83-30911
- Optical pulse evolution in the Stanford free-electron laser and in a tapered wiggler 13 p1854 A83-31117
- Scattering of light by an intense saturating pulse in a resonance medium 14 p2078 A83-31901
- High-efficiency laser-pulse compression by stimulated Brillouin scattering 15 p2167 A83-33759
- Proposed quantum-beats, quantum-eraser experiment 17 p2579 A83-38957
- Quantum measurements and the reliability of information transfer 19 p2896 A83-41494
- Theoretical and experimental studies of the electromagnetic coupling mechanisms between aircraft and consecutive lightning strikes, both direct and nearby [ONERA, TP NO. 1983-44] 21 p3089 A83-44318
- The effect of nulls upon subpulse drift in PSRs 0809 + 74 and 0818-13 21 p3232 A83-44733
- Solitons in single mode optical fibres 21 p3207 A83-44823
- Conducting shells in a pulsed electromagnetic field --- Russian book 21 p3126 A83-45047
- An experimental investigation of the parallel-plate EMP simulator with single-pulse excitation 22 p3279 A83-46934
- Transient pulse monitor data from the P78-2 (SCATHA) spacecraft 23 p3423 A83-48128
- UHF interferometric imaging of lightning [ONERA, TP NO. 1983-55] 23 p3492 A83-48177
- On the variation of a pulse envelope with filling in a dispersive medium 23 p3510 A83-48477
- Simultaneous pulses in light and electric field from stepped leaders near ground level 24 p3610 A83-49346

ELECTROMAGNETIC PUMPS

- Investigation of the solidification of titanium castings by means of a conduction MHD pump 12 p1732 A83-29271
- The effect of process variables on the density of titanium ingots cast under electromagnetic pressure 19 p2822 A83-42005

ELECTROMAGNETIC RADIATION

- NT AIRGLOW
- NT BLACK BODY RADIATION
- NT BREMSSTRAHLUNG
- NT CENTIMETER WAVES
- NT CERENKOV RADIATION
- NT CN EMISSION
- NT COHERENT ELECTROMAGNETIC RADIATION
- NT COHERENT LIGHT
- NT COMET TAILS
- NT COSMIC X RAYS
- NT CYCLOTRON RADIATION
- NT DAYGLOW
- NT DECAMETRIC WAVES
- NT DECIMETER WAVES
- NT ELECTROMAGNETIC PULSES
- NT ELECTROMAGNETIC SURFACE WAVES
- NT EXTRATERRESTRIAL RADIO WAVES
- NT EXTREME ULTRAVIOLET RADIATION
- NT FAR INFRARED RADIATION
- NT FAR ULTRAVIOLET RADIATION
- NT GALACTIC RADIO WAVES
- NT GAMMA RAY BURSTS
- NT GAMMA RAYS
- NT GEOCORONAL EMISSIONS
- NT H WAVES
- NT HYDROXYL EMISSION
- NT INFRARED RADIATION
- NT KILOMETRIC WAVES
- NT LIGHT (VISIBLE RADIATION)
- NT LIGHT BEAMS
- NT LONG WAVE RADIATION
- NT LYMAN ALPHA RADIATION
- NT MICROWAVE EMISSION
- NT MICROWAVES
- NT MILLIMETER WAVES
- NT MODULATED CONTINUOUS RADIATION
- NT MONOCHROMATIC RADIATION
- NT NEAR INFRARED RADIATION
- NT NEAR ULTRAVIOLET RADIATION
- NT NIGHTGLOW
- NT NONEQUILIBRIUM RADIATION
- NT PHOTON BEAMS
- NT PLANETARY RADIATION
- NT POLARIZED ELECTROMAGNETIC RADIATION
- NT POLARIZED LIGHT
- NT RADIO BURSTS
- NT RADIO EMISSION
- NT RADIO WAVES
- NT SHORT WAVE RADIATION
- NT SKY RADIATION
- NT SKY WAVES
- NT SOLAR RADIO BURSTS
- NT SOLAR RADIO EMISSION
- NT SOLAR X-RAYS
- NT SOMMERFELD WAVES
- NT SUBMILLIMETER WAVES
- NT SUNLIGHT
- NT SYNCHROTRON RADIATION
- NT SYSTEM GENERATED ELECTROMAGNETIC PULSES
- NT TERRESTRIAL RADIATION
- NT THERMAL RADIATION
- NT TROPOSPHERIC RADIATION
- NT TWILIGHT GLOW
- NT TYPE 2 BURSTS
- NT TYPE 3 BURSTS
- NT TYPE 4 BURSTS
- NT ULTRAVIOLET RADIATION
- NT X RAYS
- NT ZODIACAL LIGHT
- Self-focusing of ion cyclotron waves in a plasma 01 p0106 A83-10618
- Electromagnetic-wave diffraction by a periodic screen with apertures of arbitrary shape 01 p0031 A83-10804
- Parametric interaction between gravitational and electromagnetic radiations 01 p0124 A83-10901
- Investigation, evaluation and forecast of near-earth space radiation situation 01 p0130 A83-11280
- Nonlinear theory of the amplification of electromagnetic waves by an electron beam passing through a stratified inhomogeneous medium 02 p0241 A83-11690
- Fluxes of electromagnetic radiation, energetic particles, and solar wind from the region of a helium-3-rich flare 02 p0269 A83-11718
- Curved dielectric optical waveguides with reduced transition losses 02 p0235 A83-12005
- A theory for determining the stressed state of composite media using electromagnetic waves of the millimeter range 02 p0188 A83-12365
- Two-dimensional radiation in absorbing-emitting-scattering media using the P-N approximation [ASME PAPER 82-HT-19] 02 p0171 A83-12786

- Theory of envelope solitons of electromagnetic waves 03 p0396 A83-13188
- The emission of electromagnetic waves in the case of a smooth variation of parameters of a radiating system 03 p0390 A83-13427
- Radiation characteristics of channeled particles 03 p0313 A83-13960
- A simple technique for solving E-field integral equations for conducting bodies at internal resonances 03 p0307 A83-14035
- Interaction of waves with an interface moving in a collisionless plasma 04 p0536 A83-15756
- Interaction of electromagnetic waves in a classical supergrating 04 p0471 A83-15766
- Electromagnetic resonances in the equatorial ionosphere 04 p0510 A83-15823
- Electromagnetic environment simulation for TCAS avionics --- Threat Alert and Collision Avoidance Systems 05 p0592 A83-17304
- Generation of nonthermal continuum radiation in the magnetosphere 05 p0661 A83-17395
- Radiation of electromagnetic waves from the open end of a plasma waveguide 05 p0689 A83-17591
- Radiation from two plane waveguides formed by three half-planes 05 p0623 A83-17592
- On crossing the Cauchy horizon of a Reissner-Nordstroem black-hole 06 p0824 A83-17972
- Interaction of electromagnetic radiation and microstructural materials with regard to the production of spectral-selective solar absorbers --- German thesis 06 p0779 A83-18497
- Cyclical, broadband economical scanning procedure for determining the direction of incidence of electromagnetic waves --- German thesis 06 p0736 A83-18522
- Measurement of the wave impedance of low frequency electromagnetic waves in the earth-ionosphere duct 06 p0747 A83-18731
- Radial electron distribution in an electromagnetic cascade in the atmosphere 06 p0858 A83-19348
- Electromagnetic waves in a nonstationary open waveguide 06 p0754 A83-19360
- Spatial changes in the induced fluctuations of the intensity of radiation used to probe a bleachable aerodisperse medium 07 p0988 A83-20106
- Generation of electromagnetic oscillations in metal-barrier-metal-barrier-metal structures 07 p0918 A83-20123
- Electromagnetic excitation of a truncated cone by a plane wave 07 p0914 A83-20775
- Theory of the parametric excitation of electromagnetic radiation in a plasma waveguide with an electron beam 07 p0921 A83-20872
- Fourier transform of a polygonal shape function and its application in electromagnetics 09 p1247 A83-23789
- Electromagnetic radiation emissions from visual display units - A review 09 p1324 A83-23885
- Diffraction of a two-dimensional electromagnetic beam wave by a thick slit pierced in a perfectly conducting screen --- for study of objective incident radiation used to obtain image of star 09 p1268 A83-24091
- Multiple acceleration of electrons in plasma resonance 09 p1348 A83-25093
- Plasma column formed by a traveling ionizing electromagnetic wave 10 p1486 A83-25990
- Radiation exchange and oscillations in a pair of cavities sharing a partial reflector 10 p1482 A83-26002
- Generalized description of harmonic generation in a transverse optical klystron 10 p1427 A83-26007
- Quasi-natural modes in a long groove on a plane mirror of a hemispheric open resonator 10 p1412 A83-26960
- Electromagnetic-radiation directivity and the mutual intensity function 11 p1555 A83-27926
- Electromagnetic-wave diffraction by a doubly periodic array of semiinfinite dielectric rods 11 p1556 A83-27961
- Diffraction of a plane electromagnetic wave by a periodic structure consisting of rectangular metallic plates 11 p1558 A83-28521
- Electromagnetic wave instability in plasma with relativistic particles in a random magnetic field 12 p1780 A83-29069
- The nonorthogonal-series method in problems of electromagnetic wave diffraction by coated bodies 13 p1827 A83-30096
- Electromagnetic radiation from beam-plasma instabilities 13 p1923 A83-30122
- The solution of a class of paired integral equations in problems of diffraction theory 13 p1915 A83-31374
- IRAS and Exosat - Europe maintains its contribution to space science 14 p1978 A83-31942
- The diffraction of electromagnetic waves by surfaces with an admittance operator boundary condition 14 p1999 A83-32103

The chaotic motion of a beam of phased oscillators
14 p2086 A83-32137

Nonselective effect of electromagnetic radiation on a
superconducting film in the resistive state
14 p2091 A83-32618

Intense electromagnetic radiation from relativistic
particles
15 p2228 A83-33786

Electromagnetic radiation from beam-plasma
instabilities
15 p2234 A83-34202

Threshold singularities in the diffraction of
electromagnetic waves by a periodic half-space
15 p2145 A83-34708

Diffraction by an ideally conducting wedge with a
dielectric coating on one edge
15 p2145 A83-34710

Effects of propagation on the rise times and the initial
peaks of radiation fields from return strokes
16 p2341 A83-35415

Electromagnetic excitation of a finite cone by an annular
magnetic flux
16 p2346 A83-35942

Large numbers hypothesis. II - Electromagnetic
radiation
16 p2408 A83-36986

New norms for electromagnetic radiation in the
microwave range
17 p2562 A83-38181

Electromagnetic waves in a doubly periodic array of
circular longitudinally magnetized ferrite rods
17 p2494 A83-38477

The black hole formed by electromagnetic radiation
17 p2614 A83-38958

Approximate approach to the problem of wave diffraction
in multimode waveguides with smoothly varying
parameters
17 p2577 A83-38982

Substantiation of the method of nonorthogonal series
and the solution of certain inverse diffraction problems
18 p2674 A83-39154

A spectral approach to the physical theory of
diffraction
19 p2894 A83-40798

The limitation of radiation directivity in the case of image
transmission
19 p2835 A83-41781

Transformation of modes in the case of double
degeneration in a plane anisotropic impedance
waveguide
19 p2836 A83-41801

Frequency gap formation in electromagnetic cyclotron
wave distributions --- in magnetosphere
20 p3025 A83-43193

Electromagnetic radiation from a dipole source in a
homogeneous magnetoplasma
20 p3050 A83-43417

Identification of electromagnetic sources --- generated
in magnetosphere
21 p3170 A83-44241

Hypotheses on the physical mechanisms of VHF-UHF
radiation from lightning
[ONERA, TP NO. 1983-45]
21 p3178 A83-44319

Reduction of the problem of diffraction by parallel
half-planes to the Riemann boundary value problem
21 p3121 A83-44779

Absorption and stimulated radiation of quanta of an
external inhomogeneous electromagnetic field of free
electrons
21 p3145 A83-45204

Electromagnetic lower hybrid waves in the solar wind
22 p3388 A83-46026

A contribution to the analysis of triggered lightning -
First results obtained during the trip 82 experiment
[ONERA, TP NO. 1983-56]
23 p3492 A83-48178

Radiation of the half-space and layer of a nonequilibrium
plasma with active molecules
23 p3510 A83-48392

Features of the development and energetics of the solar
flare of November 22, 1977
23 p3538 A83-48422

Electromagnetic wave damping in a nonequilibrium
aerosol plasma
24 p3632 A83-49115

Numerical methods for problems of
electromagnetic-wave diffraction by ideally conducting
screens
24 p3573 A83-49272

The peak electromagnetic power radiated by lightning
return strokes
24 p3610 A83-49335

An explicit Lagrangian for a system of charged particles
to higher-order terms - Quadrupole radiation
24 p3624 A83-50167

ELECTROMAGNETIC SCATTERING

NT HALOS

NT IONOSPHERIC F-SCATTER PROPAGATION

NT LIGHT SCATTERING

NT MICROWAVE SCATTERING

NT MIE SCATTERING

NT RAMAN SPECTRA

NT RAYLEIGH SCATTERING

NT THOMSON SCATTERING

NT X RAY SCATTERING

Electromagnetic-wave scattering by a finite system of
ideally conducting rods with dielectric diaphragms
01 p0030 A83-10405

Stimulated electromagnetic-wave scattering by a
relativistic electron beam in a refracting medium
01 p0036 A83-10415

Effects of thermal noise and interference due to
scatterers on VOR system accuracy
01 p0004 A83-11092

A new expression for the scattering of a Gaussian beam
by a conducting cylinder
01 p0033 A83-11356

A hybrid diffraction technique - General theory and
applications
01 p0104 A83-11357

Reflections from linearly vibrating objects - Plane mirror
at oblique incidence
01 p0104 A83-11358

A survey of the physical optics inverse scattering
identity
01 p0104 A83-11369

A computational alternative for variational expressions
that involve dyadic Green functions --- for electromagnetic
scattering
01 p0103 A83-11373

Nonuniqueness in inverse source and scattering
problems
01 p0104 A83-11384

Crosspolarisation in scattering at low frequencies
02 p0163 A83-11553

Multiple scattering of electromagnetic waves by rain
02 p0165 A83-12623

Generalization of the Booker-Gordon formula to include
multiple scattering
02 p0165 A83-12626

Numerical analysis of nonreciprocity for spatial
coherence and spot dancing in random media
02 p0233 A83-12627

Electromagnetic scattering by open circular
waveguides
02 p0165 A83-12630

Physically motivated approximations in some inverse
scattering problems
02 p0233 A83-12632

Two-dimensional radiation in
absorbing-emitting-scattering media using the P-N
approximation
02 p0171 A83-12786

[ASME PAPER 82-HT-19]
Effect of nonlinear phase shifts on stimulated scattering
of electromagnetic waves in plasmas
03 p0397 A83-13190

Effective propagation constants for coherent
electromagnetic wave propagation in media embedded
with dielectric scatterers
03 p0304 A83-13915

Computing scattering amplitudes for arbitrary cylinders
under incident plane waves
03 p0390 A83-14001

Flanged parabolic antennas
03 p0305 A83-14007

A stochastic Fourier transform approach to scattering
from perfectly conducting randomly rough surfaces
03 p0306 A83-14014

Scattering by wires near a material half-space
03 p0306 A83-14017

Transition radiation caused by a chiral plate ---
electromagnetic field due to charged particle traversing
plate
03 p0313 A83-14025

Radiation pattern computation of a spherical lens using
Mie series
03 p0306 A83-14027

A simple technique for solving E-field integral equations
for conducting bodies at internal resonances
03 p0307 A83-14035

Scattering of a plane electromagnetic wave by a
conducting circular cylinder of finite length
03 p0307 A83-14134

A novel method to analyze electromagnetic scattering
of complex objects
03 p0308 A83-14548

Plane-wave scattering by bodies of revolution with
absorbing coatings
04 p0466 A83-15728

Treatment of late time instabilities in finite-difference
EMP scattering codes
05 p0628 A83-17532

Electromagnetic scattering from two dielectric spheres
- Comparison between theory and experiment
05 p0683 A83-17883

Atmospheric visibility from gigahertz to petahertz
[AIAA PAPER 83-0352]
05 p0683 A83-17921

Sampling approach for fast computation of scattered
fields
06 p0736 A83-18569

Generation of field scattered by imperfectly conducting
objects from the solution of a perfectly conducting
object
06 p0736 A83-18575

Scattering by a conducting tube of finite length
06 p0737 A83-18608

Scattering by objects in translational motion
06 p0737 A83-18610

High-frequency scattering from offset reflectors
06 p0740 A83-18648

Non-linear optimization for field, scattering and SEM
problems --- Singularity Expansion Methods
06 p0742 A83-18668

Expansion of Gaussian modes and analysis about the
beam waveguide
06 p0744 A83-18697

Plane wave scattering by a thick lossy dielectric
half-plane
06 p0805 A83-18714

The effects of shape on electromagnetic scattering by
ice crystals
06 p0746 A83-18717

An integral equation method for electromagnetic
scattering of guided modes by boundary deformations of
dielectric slab waveguides
07 p0913 A83-20367

Scattering from randomly rough surfaces and the far
field approximation
07 p0989 A83-20369

Electromagnetic-field diffraction by a system of
curvilinear screens
07 p0914 A83-20774

The space and time dynamics of formation of resonant
scattered waves
07 p0990 A83-20868

Analytical study of the scattering properties of a structure
consisting of two open cylindrical screens
07 p0915 A83-20870

Complex-frequency poles and creeping-wave transients
in electromagnetic-wave scattering
07 p0916 A83-21545

Scattering and depolarization of electromagnetic waves
in irregular stratified spheroidal structures of finite
conductivity - Full wave analysis
08 p1161 A83-22282

Angular spectrum representation of scattered
electromagnetic fields
08 p1161 A83-22668

Electromagnetic backscattering from a layer of
vegetation - A discrete approach
08 p1077 A83-22682

Antenna effects in depolarization measurements
08 p1077 A83-22683

A computer-controlled broadband system for measuring
scattered fields and for locating scattering centers
09 p1244 A83-23382

New results on coherent scattering from randomly rough
conducting surfaces
09 p1246 A83-23776

On the existence of branch points in the eigenvalues
of the electric field integral equation operator in the
complex frequency plane
09 p1253 A83-23787

High frequency scattering by a thin lossless dielectric
slab
09 p1247 A83-23790

Scattering and absorption characteristics of lossy
dielectric objects exposed to the near fields of aperture
sources --- of electromagnetic radiation
09 p1324 A83-23791

The eigenfunction solution for scattered fields and
surface currents of a vertex
09 p1248 A83-23812

Propagation in correlated distributions of large-spaced
scatterers
09 p1338 A83-24089

Variational calculations of electromagnetic scattering
from two randomly separated Rayleigh dielectric
cylinders
09 p1249 A83-24102

Prediction of scattering cross-section reductions due to
plate orthogonality errors in trihedral radar reflectors
09 p1249 A83-24116

Inductive twin-strip gratings in incident TE waves
09 p1254 A83-24117

Scattering of radiation by particles in low-altitude
plumes
09 p1220 A83-24893

Reduction of the field scattered by receiving vibrators
09 p1250 A83-24923

Stimulated scattering of electromagnetic waves by a
magnetized relativistic beam of oscillators
10 p1426 A83-25886

Scattering cross sections for composite surfaces that
cannot be treated as perturbed-physical optics problems
10 p1403 A83-26032

Mutual coherence functions and intensities of
backscattered signals in a turbulent medium
10 p1403 A83-26036

Electromagnetic plane wave scattering by a system of
two parallel conducting prolate spheroids
10 p1405 A83-26836

A new procedure for improving the solution stability and
extending the frequency range of the EBCM --- Extended
Boundary Condition Method for EM absorption and
scattering in biological dielectric objects
10 p1460 A83-26839

Cylindrical eigencurrents --- during electromagnetic
scattering by conducting surfaces
10 p1406 A83-26840

Far field in transient two-dimensional scattering
10 p1406 A83-26849

Average dielectric properties of discrete random media
using multiple scattering theory
10 p1411 A83-26851

Wave scattering from a large sphere with rough
surface
10 p1472 A83-26852

Finite-element solution of three-dimensional
electromagnetic problems
11 p1560 A83-27893

On the far-zone distribution of a scattered field - A
numerical experiment
11 p1556 A83-27946

Theory of the stimulated scattering of electromagnetic
waves in a waveguide by a relativistic electron beam
11 p1583 A83-27960

An antenna system with a passive scatterer
11 p1558 A83-26882

Calculation of electromagnetic scattering by a perfect
conductor
12 p1776 A83-29605

The attenuation and scattering of infrared radiation by
polydisperse systems comprising platelets and cylinders
of ice
13 p1883 A83-30029

The possible nature of the prethunderstorm
electromagnetic radiation of convective clouds
14 p2059 A83-32864

Monte Carlo calculations of resonance-line formation
in a plane layer
15 p2253 A83-33710

Iterative solutions for electromagnetic scattering by
gratings
15 p2224 A83-33804

- Electromagnetic scattering by magnetic spheres
15 p2224 A83-33805
- Effects on partial frequency redistribution $R(l)$ on the level population ratios in a resonance line --- for stellar spectrum analysis
15 p2271 A83-34776
- Creeping waves and resonances in transient scattering by smooth convex objects
15 p2148 A83-35177
- A spectral-iteration technique for analyzing scattering from arbitrary bodies. I - Cylindrical scatterers with E-wave incidence
15 p2148 A83-35186
- On the current distribution for open surfaces
15 p2154 A83-35190
- A spectral-iteration technique for analyzing scattering from arbitrary bodies. II - Conducting cylinders with H-wave incidence
15 p2149 A83-35198
- Multiple scattering theory for waves in discrete random media and comparison with experiments
16 p2406 A83-35406
- Electromagnetic scattering from subterranean obstacles in a stratified ground
16 p2341 A83-35409
- Diffraction of electromagnetic waves by a metallic sphere surrounded by a spherically symmetric layer of homogeneous plasma, with allowance for spatial dispersion
16 p2416 A83-35900
- A general theory of the Raman-type free-electron laser
17 p2514 A83-38039
- The problem of backscattering in three-dimensional randomly inhomogeneous media
17 p2577 A83-38981
- Scattering of high-frequency electromagnetic waves by an impedance elliptical cylinder
17 p2495 A83-38993
- Scattering from randomly oriented circular discs with application to vegetation
18 p2707 A83-40654
- A moment solution for waveguide junction problems
19 p2837 A83-41083
- Stimulated Raman and Brillouin scattering of a Gaussian electromagnetic beam in ordinary mode in a magnetoplasma
19 p2901 A83-41197
- On the maximum interdependence of absorbed and scattered powers --- by receiving antennas or structures covered with absorbing materials
19 p2835 A83-41770
- Theory of acoustooptic interaction in active resonators
19 p2854 A83-41774
- Generalized ambiguity function of signals with compression in the case of the scattering of waves by bodies of complex shape
19 p2835 A83-41776
- Bragg resonator in the ionospheric plasma with an artificial quasi-periodic lattice
19 p2866 A83-41792
- The dispersion properties of artificial anisotropic dielectrics
19 p2841 A83-41818
- Mie scattering subroutines (DBMIE and MIEVO) - A comparison of computational times
20 p3037 A83-42205
- The effect of anisotropic scattering on molecular gas radiation
20 p2974 A83-42690
- Stellar winds driven by multiline scattering
21 p3238 A83-45559
- Minimization of a field scattered by thin dipoles
22 p3272 A83-45683
- Effects of a rough boundary surface on polarization of the scattered field from an inhomogeneous medium
22 p3314 A83-46231
- Nonlinear scattering from a plasma column. I - Theory. II Special cases
22 p3363 A83-46536
- Nonlinear theory of stimulated scattering of electromagnetic waves by a magnetized beam of electrons in a waveguide
23 p3445 A83-47572
- Hybrid solutions for scattering from perfectly conducting bodies of revolution
23 p3442 A83-47828
- First-order equivalent current and corner diffraction scattering from flat plate structures
23 p3442 A83-47829
- High-frequency scattering from the edges of impedance discontinuities on a flat plane
23 p3442 A83-47830
- A comparison between backscattering coefficients using Gaussian and non-Gaussian surface statistics
23 p3443 A83-47836
- Scattering of electromagnetic waves by the edge of a semiinfinite dielectric slab imbedded in an ideally conducting half-space
23 p3445 A83-48486
- Scattering of an H-polarized wave by a screen with narrow slots
23 p3445 A83-48487
- Stimulated scattering of a large amplitude electromagnetic wave by the eigenmodes of a plasma slab
23 p3511 A83-48574
- Specular reflection cancellation in an interferometer with a phase-conjugate mirror
24 p3628 A83-48905
- Behavior of singularities of solutions of diffraction problems and the Rayleigh hypothesis
24 p3623 A83-49274
- Analytic treatment of polarization by arbitrary scattering mechanisms in circumstellar envelopes. II - Binary stars
24 p3658 A83-49361
- Theory of radar detection of solitons during ionospheric heating
24 p3608 A83-49754
- Simple formula for the RCS of a finite hollow circular cylinder
24 p3571 A83-49994
- ### ELECTROMAGNETIC SHIELDING
- Shielding techniques tackle EMI excesses. V - EMI shielding
01 p0035 A83-10271
- A topological approach to the unification of electromagnetic specifications and standards
01 p0041 A83-11084
- Effective electromagnetic shielding in multilayer printed circuit boards
04 p0473 A83-16122
- EMI shielding today with conductive plastics
04 p0464 A83-16179
- SGEMP-induced transfer admittance coupling in cable bundles
05 p0628 A83-17522
- Microwave anechoic chambers --- Russian book
07 p0902 A83-20380
- Performance properties of conductive PVC composites for EMI shielding applications
07 p0876 A83-20488
- Plastic composites for electromagnetic interference shielding applications
08 p1055 A83-22717
- Hybrid-mode, shielded, offset parabolic antenna
09 p1248 A83-23874
- Shielded dielectric resonators
12 p1720 A83-29461
- Electroplated carbon/graphite fibers
16 p2325 A83-36900
- Microstructure and properties of injection molded conductive plastics
21 p3106 A83-44059
- A systematic characterization of the effects of atmospheric electricity on the operational conditions of aircraft
23 p3400 A83-48180
- ### ELECTROMAGNETIC SPECTRA
- NT BALMER SERIES
- NT D LINES
- NT ELECTRONIC SPECTRA
- NT FRAUNHOFER LINES
- NT GAMMA RAY SPECTRA
- NT H ALPHA LINE
- NT H BETA LINE
- NT H LINES
- NT INFRARED SPECTRA
- NT K LINES
- NT LINE SPECTRA
- NT LYMAN SPECTRA
- NT MICROWAVE SPECTRA
- NT PASCHEN SERIES
- NT RADIO SPECTRA
- NT RAMAN SPECTRA
- NT RYDBERG SERIES
- NT SOLAR SPECTRA
- NT STELLAR SPECTRA
- NT UVB SPECTRA
- NT ULTRAVIOLET SPECTRA
- NT VIBRATIONAL SPECTRA
- NT VISIBLE SPECTRUM
- NT X RAY SPECTRA
- Conservation of the geostationary spectrum
07 p0910 A83-19760
- On the spectrum of complex waves of a circular dielectric waveguide
09 p1257 A83-25165
- Questions about the experimental status of black-body radiation
12 p1775 A83-29041
- Inversion of synchrotron spectra
16 p2428 A83-36532
- Missile guidance electromagnetic sensors
24 p3546 A83-48769
- ### ELECTROMAGNETIC SURFACE WAVES
- Regge poles, natural frequencies, and surface wave resonance of a circular cylinder with a constant surface impedance
03 p0307 A83-14034
- The discharge produced by a surface wave - Axial inhomogeneity and wave propagation --- French thesis
03 p0398 A83-14107
- Attenuation and localization of an electromagnetic wave on the surface of a cylindrical conductor
04 p0465 A83-15072
- Diffraction of a surface optical wave in an optical slab waveguide by a surface acoustic wave /SAW/
07 p0993 A83-20856
- Surface impedance and wave tilt interpretation over horizontally stratified media
08 p1160 A83-22028
- The propagation of a surface wave along a dielectric waveguide with a jump-like change of the parameters. II - Solution by the variational method
09 p1257 A83-25084
- Potentialities of electric and magnetic wave tilt measurements --- for airborne survey of earth surface and subsurface propagation features
10 p1449 A83-26040
- Excitation of surface polaritons by nondegenerate four-wave mixing of evanescent waves
12 p1782 A83-29200
- Nondestructive measurement of a dielectric layer using surface electromagnetic waves
13 p1831 A83-30227
- A note concerning modes in dielectric waveguide gratings for filter applications
13 p1831 A83-30237
- Guided-wave experiments with dielectric waveguides having finite periodic corrugation
13 p1836 A83-31145
- Acoustooptic excitation of surface electromagnetic waves by a light beam of finite aperture
14 p2003 A83-32119
- Propagation of a large-amplitude surface wave in a plasma column sustained by the wave
16 p2414 A83-35435
- Experimental observation of the long-range surface-plasmon polariton
17 p2576 A83-37946
- Surface-polaritonlike waves guided by thin, lossy metal films
17 p2576 A83-37947
- Linearly dispersive time-delay control of magnetostatic surface wave by variable ground-plane spacing
18 p2679 A83-40394
- Long-range surface plasmons in electrode structures
19 p2899 A83-40733
- Second harmonic generation by oppositely travelling long range surface polaritons
19 p2853 A83-41191
- ### ELECTROMAGNETIC WAVE FILTERS
- NT BANDPASS FILTERS
- NT BIREFRINGENT FILTERS
- NT CRYSTAL FILTERS
- NT DIGITAL FILTERS
- NT ELECTRIC FILTERS
- NT FIR FILTERS
- NT INFRARED FILTERS
- NT MATCHED FILTERS
- NT MICROWAVE FILTERS
- NT OPTICAL FILTERS
- NT RADAR FILTERS
- NT RADIO FILTERS
- NT TRACKING FILTERS
- NT ULTRAVIOLET FILTERS
- NT WAVEGUIDE FILTERS
- Synthesis of spatial filters for investigation of the transverse mode composition of coherent radiation
10 p1432 A83-26669
- ### ELECTROMAGNETIC WAVE TRANSMISSION
- NT DOUBLE SIDEBAND TRANSMISSION
- NT HALOS
- NT IONOSPHERIC F-SCATTER PROPAGATION
- NT IONOSPHERIC PROPAGATION
- NT LIGHT SCATTERING
- NT LIGHT TRANSMISSION
- NT MICROWAVE ATTENUATION
- NT MICROWAVE TRANSMISSION
- NT MULTIPATH TRANSMISSION
- NT RADAR TRANSMISSION
- NT RADIO TRANSMISSION
- NT SCATTER PROPAGATION
- NT SHORT WAVE RADIO TRANSMISSION
- NT SINGLE SIDEBAND TRANSMISSION
- NT SPREAD SPECTRUM TRANSMISSION
- NT TELEVISION TRANSMISSION
- NT TRANSEQUATORIAL PROPAGATION
- NT TRANSORIZON RADIO PROPAGATION
- Simple formulas for transmission through periodic metal grids or plates
01 p0033 A83-11359
- Dispersion relation for general anisotropic media
01 p0033 A83-11371
- On the influence of a plasma hot component on whistler propagation beyond the plasmopause
02 p0206 A83-12020
- An attenuation function for multiple knife-edge diffraction --- of electromagnetic waves in communication systems
02 p0165 A83-12629
- A finite element method for solving Helmholtz type equations in waveguides and other unbounded domains
03 p0390 A83-13567
- Theoretical analysis of single-mode AlGaAs-GaAs double heterostructure lasers with channel-guide structure
03 p0332 A83-13920
- Electromagnetic transmission through apertures in a cavity in a thick conductor
03 p0306 A83-14016
- Properties of the electromagnetic wave propagation in a helix-loaded waveguide
04 p0473 A83-16055
- Radiation of electromagnetic waves from the open end of a plasma waveguide
05 p0689 A83-17591
- A ray theory of three-dimensional photoelasticity
05 p0683 A83-17848
- International Conference on Antennas and Propagation, 2nd, University of York, York, England, April 13-16, 1981, Proceedings. Part 1 - Antennas. Part 2 - Propagation
06 p0736 A83-18601
- Parametric decay of electromagnetic waves in a magnetized vacuum
07 p0988 A83-20043
- Concerning a modification of the semiinversion method --- for electromagnetic wave propagation
07 p0986 A83-20317

The optical scalar equations in the presence of a refractive medium 07 p1023 A83-21142

Surface impedance and wave tilt interpretation over horizontally stratified media 08 p1160 A83-22028

Reflection of electromagnetic waves at a biaxial-isotropic interface 08 p1161 A83-22330

Objective summary of U.S. Army electro-optical modeling and field testing in an obscuring environment 08 p1093 A83-22351

EOSAEL 82 - A library of battlefield obscuration models 08 p1093 A83-22352

Millimeter wave atmospheric turbulence measurements - Preliminary results and instrumentation for future measurements 08 p1076 A83-22354

Effect of the aerosol on fog microstructure 08 p1140 A83-22355

Extinction by clouds consisting of polydisperse and randomly oriented nonspherical particles at arbitrary wavelengths 08 p1135 A83-22356

New methods for optical, quasi-optical, acoustic and electromagnetic synthesis; Proceedings of the Meeting, San Diego, CA, August 25, 26, 1981 08 p1161 A83-22468

Modes of propagation in slot line with layered substrate containing magnetised ferrite 08 p1081 A83-22918

Structure characteristics of refractive-index fluctuations on an oblique tropospheric path 09 p1245 A83-23452

Remote determination of the structure constant profile from amplitude scintillation data using Tikhonov's regularized inverse method--- Fourier transform for solving convolution equations 09 p1311 A83-23795

Transient response of an infinite cylindrical antenna 09 p1247 A83-23802

The method of multiply reflected waves in the problem of the propagation of electromagnetic waves in regular waveguides /Review/ 09 p1250 A83-25076

A perturbation-theory method in the electrodynamics of inhomogeneous and nonstationary media /Review/ 09 p1339 A83-25078

Diffraction of a wave beam by a closed cylindrical screen 09 p1251 A83-25086

On the spectrum of complex waves of a circular dielectric waveguide 09 p1257 A83-25165

Potentialities of electric and magnetic wave tilt measurements --- for airborne survey of earth surface and subsurface propagation features 10 p1449 A83-26040

Improved simulation of ground reflections --- of radio navigation signals for flight control 10 p1374 A83-26486

Dyadic Green's functions for a coaxial line 10 p1411 A83-26845

Average dielectric properties of discrete random media using multiple scattering theory 10 p1411 A83-26851

Resonance transition scattering in vacuum in the presence of an external gravitational field 11 p1649 A83-27456

Natural modes of a periodic array of rectangular longitudinally magnetized ferrite rods 11 p1561 A83-27966

Waves in piezoelectric crystals --- Russian book 12 p1719 A83-28824

A numerical analysis of the diffraction of radio waves --- Russian book 12 p1718 A83-28827

Method for the numerical solution of problems of electromagnetic-wave diffraction by open surfaces of revolution 13 p1827 A83-30014

Reflection of electromagnetic waves from random irregularities in the ionosphere 13 p1828 A83-30285

Colliding plane gravitational and electromagnetic waves 13 p1947 A83-30519

A coordinate-free approach to wave reflection from a uniaxially anisotropic medium 13 p1914 A83-31144

Resonance nonreciprocal effects during wave propagation in layered gyrotropic media and periodic structures with gyrotropic filling 14 p2003 A83-32114

Fluctuations of the parameters of an electromagnetic wave in a turbulent light absorbing atmosphere 14 p2052 A83-32559

Asymptotic solution for the diffraction of an electromagnetic plane wave by a cylinder-tipped half-plane 15 p2144 A83-33806

Experimental study of the propagation of electromagnetic waves in a cylindrical slotted line 15 p2153 A83-35157

Nonstationary processes during the passage of a current pulse through a slow-wave system 15 p2153 A83-35165

Creeping waves and resonances in transient scattering by smooth convex objects 15 p2148 A83-35177

Propagation and radiation properties of corrugated cylindrical coaxial waveguides 15 p2148 A83-35183

Radio-physical and gasdynamic problems of passage through an atmosphere --- Russian book on spacecraft reentry trajectories and communications 16 p2314 A83-36444

Active flow control effects on boundary layer development around a protuberance at high subsonic speed [AIAA PAPER 83-1737] 17 p2445 A83-37216

Absorption of radiation propagation obliquely in a magnetoplasma 17 p2597 A83-37328

Refractive index surfaces --- for describing EM wave propagation in ionosphere and magnetosphere 17 p2543 A83-38371

The emergence of electromagnetic waves from pulsar magnetospheres 17 p2613 A83-38833

Theoretical model for calculating rain-induced crosspolarisation 17 p2495 A83-38878

Features of the propagation of whistlers in magnetospheric ducts in the equatorial region. I - Ducts with high density 18 p2714 A83-39323

Electromagnetic waves in a relativistic one-dimensional plasma propagating along an external magnetic field 18 p2745 A83-39524

Computer-aided graphic visualization of wave propagation 19 p2887 A83-40796

How to detect the gravitationally induced phase shift of electromagnetic waves by optical-fiber interferometry 19 p2846 A83-40967

Waves guided by conductive strips above a periodically perforated ground plane 19 p2826 A83-41086

Emission from a moving charge during the instantaneous appearance of gyration in the medium 20 p3043 A83-42874

Electromagnetic ion-cyclotron instability in the multi-ion Jovian magnetosphere 20 p3079 A83-43192

Purely growing thermal instability of an electromagnetic wave in a collisional plasma 21 p3209 A83-43938

The reflection and transmission of electromagnetic waves from the lossy plasma moving parallel to the interface 21 p3213 A83-44527

Electrodynamic analysis of the propagation of electromagnetic waves in a thin-film semiconductor structure with negative differential resistance 22 p3276 A83-45667

Theory of low frequency wave propagation 22 p3273 A83-45889

Localization of circularly polarized intense electromagnetic waves in relativistic plasmas 22 p3361 A83-46012

Reflection of a linearly polarized plane wave from a lossless stratified mirror in the presence of a phase-conjugate mirror 23 p3508 A83-47587

Distributed acceleration of cosmic rays 23 p3538 A83-47613

A rigorous method for studying the propagation of electromagnetic waves in periodic waveguides 23 p3441 A83-47622

The Sommerfeld half-plane problem revisited. III - Parallel plate media with mixed boundary conditions 23 p3504 A83-48244

On the variation of a pulse envelope with filling in a dispersive medium 23 p3510 A83-48477

Electromagnetic-wave propagation in a conducting waveguide loaded with a tape helix 24 p3572 A83-48963

Electromagnetic propagation in a photorefractive layered medium 24 p3623 A83-48976

The method of canonical transformations in classical electrodynamics 24 p3623 A83-49065

Note on a suggested formation of charge from an electromagnetic wave 24 p3624 A83-50200

ELECTROMAGNETIC WAVES

U ELECTROMAGNETIC RADIATION

ELECTROMAGNETICS

U ELECTROMAGNETISM

ELECTROMAGNETISM

NT MAGNETOSTATICS

Theory of a superposed linear transducer 01 p0049 A83-10366

Discussion of the relative efficiency in the vacuum ultraviolet of diffraction gratings with laminar sinusoidal and triangular grooves 02 p0238 A83-12709

The unified field theory, combining Kaluza's five-dimensional and Weyl's conformal theories 06 p0806 A83-19449

Influence of magnetic shear on the lower-hybrid drift instability in finite beta plasmas 07 p0997 A83-20536

Some singularities of electromagnetic sources and fields 19 p2837 A83-40794

Phenomenological electromagnetism with magnetic poles 23 p3503 A83-47421

ELECTROMAGNETS

NT HIGH FIELD MAGNETS

NT SUPERCONDUCTING MAGNETS

Optimization of PM machines due to advancements in containment structure 11 p1560 A83-27188

Transient performance of permanent magnet synchronous motors 11 p1560 A83-27189

Calculation of the force characteristics and inductance of a suspension electromagnet 13 p1934 A83-30517

ELECTROMECHANICAL DEVICES

On the optimization of magnetic field sources in electromechanical energy conversion 01 p0037 A83-10641

New drive system for large antennas 06 p0750 A83-18000

Electromechanical device for the support of the oscillating secondary mirror of an infrared telescope 08 p1111 A83-22359

A unit for combined inspection of large multilayer parts of composite polymer materials 08 p1113 A83-22401

The calculation of energy storage flywheels of fiber composites with electric energy converter --- German thesis 11 p1590 A83-28666

Electromechanical primary flight control activation systems for fighter/attack aircraft [SAE PAPER 821435] 17 p2463 A83-37983

An electromechanical primary flight control actuation system for military transport aircraft [AIAA PAPER 83-2195] 19 p2802 A83-41680

Numerical synthesis of time-optimal control for the electric motor of an electromechanical system 20 p2967 A83-42925

Special electrical machines: Sources and converters of energy --- Russian book 21 p3126 A83-45018

Electromechanical control systems 23 p3411 A83-47201

Gyromotors --- Russian book 23 p3441 A83-48475

Bucking the current --- electric actuators for V/STOL aircraft 24 p3547 A83-48887

ELECTROMECHANICS

The relationship between length and force in the cardiac muscle - Electromechanical coupling during deformation of the myocardium 03 p0376 A83-14363

Intracellular feedback in the processes of the electromechanical integration of the myocardium in mammals 14 p2063 A83-32100

An ionic mechanism of the Woodwors staircase --- electromechanical coupling in myocardium cells 16 p2395 A83-36806

ELECTROMIGRATION

Electromigration-induced failure by edge displacement in fine-line aluminum-0.5% copper thin film conductors 07 p0921 A83-20743

Electromigration transport mobility associated with pulsed direct current in fine-grained evaporated Al-0.5%Cu thin films 07 p0921 A83-20744

ELECTROMOTIVE FORCES

NT PONDEROMOTIVE FORCES

Theory of a superposed linear transducer 01 p0049 A83-10366

Photovoltaic emf in conditions of the heating of charge carriers by light 04 p0539 A83-15127

Theory of open circuit photo-voltage in degenerate abrupt p-n junctions 05 p0691 A83-17767

Investigations concerning the electrochemical equilibrium in the system tin-bismuth-oxygen 09 p1233 A83-24124

The thermal-emf mechanism of the oxidation kinetics of laser-irradiated metals 09 p1272 A83-24218

Topological semi-dynamos 10 p1485 A83-25413

Investigation of thermoelectromotive force in Al(x)ln(1-x)Sb solid solutions 13 p1928 A83-30272

Change of characteristic parameters of polycrystalline titanium during its deformation 13 p1822 A83-30971

EMF measurements on the Li-Al/Ni3S2 couple in molten salt electrolytes 14 p1990 A83-32636

The thermoelectromotive force of a one-dimensionally inhomogeneous nondegenerated semiconductor 19 p2905 A83-42012

Gravity-induced emf in superionic conductor RbAg415 22 p3364 A83-45621

A new interpretation of the alpha effect --- turbulently generated emf in magnetized plasma 22 p3362 A83-46014

ELECTROMYOGRAMS

U ELECTROMYOGRAPHY

ELECTROMYOGRAPHS

U ELECTROMYOGRAPHY

ELECTROMYOGRAPHY

Acquisition and analysis of the EMG power spectra - A reproducible technique for assessment of muscle fatigue --- electromyogram 01 p0086 A83-11107

Ergonomic evaluation of two-hand control location 02 p0225 A83-12088

Changes in EMG power spectrum /high-to-low ratio/ with force fatigue in humans 03 p0378 A83-13576

- An integrated noiseproof system of leads for recording the ECG, EMG, EEG, and respiration of an operator
06 p0800 A83-18973
- Spectral analysis and the interference EMG
07 p0980 A83-19626
- A preliminary study using surface electromyography of the behavior of air traffic controllers according to the density of traffic
08 p1148 A83-22971
- Quantitative electromyography - Response of the neck muscles to conventional helmet loading
14 p2072 A83-32693
- A clinical and electroneuromyographic investigation of vegetative neuromuscular syndromes
14 p2070 A83-33309
- The electromyographic characteristics of three forms of myotonia
14 p2070 A83-33310
- The time of the development of an interference electromyogram as an indicator of the speed and strength of an athlete
15 p2212 A83-34948
- Factors determining the frequency content of the electromyogram
20 p3034 A83-43480
- The acquisition and validation of the surface electromyogram signal for evaluating muscle fatigue
21 p3187 A83-43998
- ELECTRON ACCELERATION**
- Numerical simulation of the excitation of a direct current in a plasma through electron acceleration in a plasma-resonance region
03 p0396 A83-13184
- Electron acceleration in impulsive solar flares
04 p0575 A83-15641
- Radiation from longitudinally accelerated electrons
04 p0470 A83-15708
- Experimental evidence for the acceleration of thermal electrons by ion cyclotron waves in the magnetosphere
07 p0966 A83-21515
- Numerical simulation of a disk-shaped electron accelerating electrostatic probe
08 p1093 A83-22336
- Observations of fluxes of suprathermal electrons accelerated by HF excited instabilities
09 p1300 A83-23309
- Multiple acceleration of electrons in plasma resonance
09 p1348 A83-25093
- Electrostatic acceleration of a modulated electron beam
11 p1560 A83-27449
- Axial expansion of the electron pulse in a free-electron laser
13 p1854 A83-31118
- Gain-enhanced free-electron laser with an electromagnet pump field
13 p1855 A83-31133
- Solar type II radio emission and the shock drift acceleration of electrons
13 p1965 A83-31435
- Stability of an astrophysical plasma near the onset of electron runaway
13 p1954 A83-31648
- On the physics and modeling of small semiconductor devices. IV - Generalized, retarded transport in ensemble Monte Carlo techniques
14 p2092 A83-32669
- [AD-A128399]
- Theory of beam plasma discharge
15 p2235 A83-34204
- Creation of high-energy electron tails by means of the modified two-stream instability
18 p2747 A83-40496
- Unlimited electron acceleration in laser-driven plasma waves
19 p2901 A83-40969
- A high-energy, laser accelerator for electrons using the inverse Cherenkov effect
20 p2994 A83-42586
- Electron acceleration by Landau resonance with whistler mode wave packets
20 p3024 A83-43185
- PD 1 pearl-electron interactions on the $L = 4.2$ magnetic shell
20 p3024 A83-43191
- Experimental modelling of satellite wakes in auroral arcs
20 p3050 A83-43205
- The change rate of energy of the test electron caused by plasma turbulence
21 p3213 A83-44521
- Acceleration of nonrelativistic electrons in the interplanetary medium
21 p3245 A83-45226
- Alfven wave collapse and the stability of a relativistic electron beam in a magnetized astrophysical plasma
21 p3238 A83-45560
- Forced interaction between an electron beam and superpower electromagnetic radiation at the boundary between two media
23 p3463 A83-48434
- ELECTRON ACCELERATORS**
- Radiated emission noise of the plasma --- in Space Experiments with Particle Accelerators payloads
[AIAA PAPER 82-1883] 02 p0241 A83-12468
- An optimized multicomponent wiggler design for a free electron laser oscillator
10 p1428 A83-26017
- Free-electron generators of coherent radiation - /Volumes 8 & 9/
13 p1852 A83-31101
- The Stanford Superconducting Linear Accelerator --- for powering free electron laser
13 p1917 A83-31104
- Optical pulse evolution in the Stanford free-electron laser and in a tapered wiggler
13 p1854 A83-31117
- High current, high voltage accelerators as free-electron lasers drivers
13 p1917 A83-31128

- Charged particle measurements from a rocket-borne electron accelerator experiment
15 p2197 A83-34179
- Highlights of the observations in the POLAR 5 electron accelerator rocket experiment
15 p2198 A83-34187
- Observations of plasma heating effects in the ionosphere by a rocket borne electron accelerator
15 p2198 A83-34188
- The Norwegian program using particle accelerators in space
15 p2124 A83-34214
- New tools for magnetospheric research
17 p2541 A83-38295
- Radial isolated Blumlein electron beam generator
20 p3045 A83-42293
- Sources of stimulated radiation using resonance electron accelerator
23 p3460 A83-47557

ELECTRON ATTACHMENT

- Ion aging effects on the dissociative-attachment instability in CO₂ lasers
04 p0484 A83-15792
- Calculation of SF₆/SF₆ and Cl-/CFCl₃ electron attachment cross sections in the energy range 0-100 meV
05 p0613 A83-17231
- Mechanism of thermal electron attachment to O₂ as studied by observing isotope effects of attachment rates for O-18/2 systems
08 p1163 A83-22218
- Production of negative ions by dissociative electron attachment to SO₂
10 p1478 A83-25552
- Electron-sulphur dioxide total ionisation and electron attachment cross-sections
10 p1479 A83-25649
- Attachment of low-energy electrons to O₂ molecules in some gases and liquids - An instrument for measuring concentrations of electronegative impurities in gases
10 p1422 A83-26468
- Production of O(-) from CO₂ by dissociative electron attachment
19 p2898 A83-41863

ELECTRON AVALANCHE

- A study of secondary-emission microwave discharges with large electron transit angles
01 p0104 A83-11300
- The structure of electron avalanches at high E/P --- electric field - pressure relations
02 p0241 A83-11956
- Gate-drain avalanche breakdown in GaAs power MESFET's
03 p0314 A83-14515
- Short-channel MOS transistors in the avalanche-multiplication regime
05 p0631 A83-17760
- Analytical solutions for avalanche-breakdown voltages of single-diffused Gaussian junctions
14 p2006 A83-32667
- Avalanche InP/InGaAs heterojunction phototransistor
19 p2899 A83-40948

ELECTRON BEAM WELDING

- High-temperature electron beam welding of the nickel-base superalloy IN-738 LC
02 p0155 A83-12072
- Investigation of the electron-beam weldability of a heat-resistant iron-based superalloy /A286/
04 p0461 A83-16175
- Application of electron beam welding to hot isostatically pressed nickel-base materials
15 p2137 A83-33966
- Major hot section component salvaged through advanced repair methods
[SAE PAPER 821489] 17 p2469 A83-38007

ELECTRON BEAMS

- NT RELATIVISTIC ELECTRON BEAMS**
- Flame diagnosis with electron beam method. Research on elementary reactions in flames during suppression by electron beam fluorescence --- German thesis
01 p0022 A83-10173
- Additional noise sources in cross-field microwave devices
01 p0044 A83-11310
- Control of beam instability in bounded plasma systems
01 p0108 A83-11346
- Nonlinear theory of the amplification of electromagnetic waves by an electron beam passing through a stratified inhomogeneous medium
02 p0241 A83-11690
- On the gain of the free electron laser /FEL/ amplifier for a nonmonochromatic beam
02 p0184 A83-12271
- Emission spectra of an Xe plasma generated by a beam
03 p0397 A83-13593
- Kinetic processes in the HgBr/B-X//HgBr₂ dissociation laser
03 p0331 A83-13917
- An estimate of the maximum modulation bands of an electron beam by means of systems of noncoupled resonators
04 p0469 A83-15137
- Analysis of the propagation of electron waves inside and outside the passband of periodic structures
04 p0471 A83-15741
- Target design of an archival electron beam memory
04 p0526 A83-16051
- Raman backscattering in an electron beam-plasma system
04 p0538 A83-16091
- 0.15 micron channel-length MOSFET's fabricated using e-beam lithography
05 p0624 A83-17297

- Design and testing of low-temperature intense electron beam diodes
05 p0625 A83-17365
- Formation of Jovian decametric S bursts by modulated electron streams
05 p0705 A83-17387
- A theory for the two-beam instability in a plasma
05 p0689 A83-17587
- FET photodetectors - A combined study using optical and electron-beam stimulation
05 p0631 A83-17762
- Analysis of the modulation possibilities of systems of densely packed resonators --- in traveling wave tubes
06 p0750 A83-18038
- The importance of the excitation volume in determination of surface recombination velocity
06 p0814 A83-18755
- Investigation of TWT amplification near the passband boundary on the basis of the theory of excitation of periodic structures
06 p0755 A83-19365
- Coherent scattering of a surface wave by an electron beam with a spatially modulated velocity
06 p0767 A83-19366
- Nonlinear stationary space-charge waves in beam-plasma systems
07 p0995 A83-20058
- Electron-beam-pumped multicomponent semiconductor laser emitting visible radiation
07 p0935 A83-20130
- Calculation of the energy characteristics of a pulse-periodic electron-beam-controlled CO₂ laser with a cooled active mixture
07 p0935 A83-20131
- The use of electron-beam evaporation for producing refractory coatings
07 p0888 A83-20691
- Studies of a glow discharge electron beam
07 p0997 A83-20733
- Determination of surface recombination velocity at a grain boundary using electron-beam-induced current
07 p0999 A83-20736
- Calculation of the frequency spectrum of an electron beam in a klystron with premodulation
07 p0921 A83-20855
- Theory of the parametric excitation of electromagnetic radiation in a plasma waveguide with an electron beam
07 p0921 A83-20872
- Nonlinear wave and oscillation processes in extended electron beams
09 p1252 A83-23462
- Close-range interactions in intense electron beams
09 p1253 A83-23489
- Electron beam energy branching in a gas mixture
09 p1343 A83-23678
- Temperature fields in metals treated with electron beams
09 p1231 A83-23994
- Superimposed electron and ion beams - Model for an evolving collisionless plasma
10 p1486 A83-25993
- Supersonic flow e-beam stabilized discharge excimer lasers
10 p1430 A83-26171
- Theory of beam-induced currents in semiconductors
10 p1489 A83-26212
- Undulator radiation of charged particles moving above a domain structure
10 p1472 A83-26243
- Holographic intensity correlator with a laser electron beam tube for inputting images for processing
10 p1422 A83-26467
- The gyrotron energy transfer equation
10 p1411 A83-26649
- Electrostatic acceleration of a modulated electron beam
11 p1560 A83-27449
- Kinetics of the triatomic Xe₂Cl/asterisk/-laser
11 p1576 A83-27504
- High efficiency infrared xenon laser excited by a U.V. preionized discharge
11 p1580 A83-27579
- Ralicon anodes fabricated by electron beam lithography for image photon counting detectors
11 p1553 A83-27754
- Generation of lower hybrid waves by inhomogeneous electron streams --- with application to wave turbulence in auroral zone and solar corona
11 p1617 A83-28313
- Coherent electromagnetic emission from an electron-ion beam
11 p1584 A83-28564
- Measurement of multiple differential electron distributions in an electron beam in nitrogen --- German thesis
11 p1575 A83-28659
- Nonlinear energy flow in a beam-plasma system
11 p1660 A83-28696
- Propagation of space-charge waves over a statistically rough surface
12 p1719 A83-29260
- Stratification in the electron beams exciting type III solar radio bursts
12 p1800 A83-29498
- The effect of the transverse dimensions of the electron beam on beam-plasma instability
13 p1922 A83-30007
- Steady-state turbulence with a narrow inertial range
13 p1923 A83-30121
- Electromagnetic radiation from beam-plasma instabilities
13 p1923 A83-30122
- Injection gas electronics --- Russian book
13 p1832 A83-30523

Dynamics of a charged-particle beam --- injected into ionosphere along geomagnetic field lines 13 p1875 A83-30612

Modeling of the interaction of a confined electron beam with an electromagnetic wave in distributed-emission magnetron-type systems 13 p1833 A83-30703

Theoretical study of processes in a system with 'conjugate' M-type interaction 13 p1833 A83-30705

The effect of the velocity distribution function in an electron beam on the characteristics of an M-type TWT 13 p1833 A83-30706

Nonlinear interaction of a modulated electron beam with electromagnetic waves in M-type devices 13 p1833 A83-30707

Axial expansion of the electron pulse in a free-electron laser 13 p1854 A83-31118

The effect of space charge fields due to finite length electron beams in the free-electron laser 13 p1854 A83-31119

Hamiltonian picture of the free-electron laser - Multimode, super mode and all that 13 p1854 A83-31120

A diagnostic device for bunched electron beams --- for free electron lasers 13 p1855 A83-31135

Measurements of the stimulated Cerenkov interaction at optical wavelengths 13 p1856 A83-31138

Effect of an electron beam on the current-convective instability --- in diffuse auroral plasmas 13 p1926 A83-31244

A ruby laser in an electron-beam field 14 p2023 A83-32133

The interaction of surface acoustic waves in piezoelectrics and electron beams 14 p2003 A83-32143

Pulsed electron beam annealing of ion implanted germanium for photovoltaic devices 14 p2088 A83-32239

Diffusion length of minority carriers in scanning electron beam annealed silicon 14 p2089 A83-32248

Optimization of pulsed electron beam annealing process for silicon solar cells 14 p2005 A83-32327

Silicon solar cells by ion implantation - E-beam and self annealing 14 p2005 A83-32328

Evolutionary electron beam and MHD two stream instability in solar radio burst models 14 p2114 A83-32391

Surface treatments using laser, electron and ion beam processing methods 14 p2028 A83-32803

Artificial electron beams as probes of the magnetosphere 15 p2195 A83-33742

Continuous-wave industrial electron-beam-controlled CO laser of 10 kW output power 15 p2168 A83-33976

Stationary waves in an electron beam interacting with a waveguide 15 p2151 A83-34025

Imaging of spatial structures in superconducting tunnel junctions by electron-beam scanning 15 p2164 A83-34141

The use of artificial electron beams as probes of the distant magnetosphere 15 p2197 A83-34177

Recent observations of beam plasma interactions in the ionosphere and a comparison with laboratory studies of the beam plasma discharge 15 p2197 A83-34178

Charged particle measurements from a rocket-borne electron accelerator experiment 15 p2197 A83-34179

On the use of artificially injected energetic electrons as indicators of magnetospheric electric fields parallel to the magnetic lines of force 15 p2197 A83-34180

The French-Soviet experiments ARAKS - Main results --- Artificial Radiation and Aurora between Kerguelen and Soviet Union 15 p2197 A83-34181

Wave excitation in electron beam experiment on Japanese satellite 'JIKIKEN (EXOS-B)' 15 p2197 A83-34182

Onboard radiometric photography of EXCEDE SPECTRAL's ejected-electron beam 15 p2128 A83-34190

Visible signatures of the multi-step transition to a beam-plasma-discharge 15 p2234 A83-34195

Electron energy distribution produced by beam-plasma discharge 15 p2234 A83-34196

Studies of beam plasma interactions in a space simulation chamber using prototype Space Shuttle instruments 15 p2234 A83-34197

Transient effects in beam-plasma interactions in a space simulation chamber stimulated by a fast pulse electron gun 15 p2234 A83-34198

Laboratory beam-plasma interactions - Linear and nonlinear 15 p2234 A83-34201

Electromagnetic radiation from beam-plasma instabilities 15 p2234 A83-34202

Electron beam injection and associated phenomena as observed in a large space simulation chamber 15 p2234 A83-34203

Theory of beam plasma discharge 15 p2235 A83-34204

Electron beam as a source of electrostatic waves 15 p2228 A83-34205

Plasma waves generated by rippled, magnetically focused electron beams surrounded by tenuous plasmas 15 p2235 A83-34208

Experimental studies of the neutralization of a charged vehicle in space and in the laboratory in Japan 15 p2126 A83-34210

Measurement of vehicle potential using a mother-daughter tethered rocket 15 p2127 A83-34212

Radio emission by parallel acceleration mechanism --- applied to solar bursts 15 p2279 A83-34289

Nonstationary processes during the passage of a current pulse through a slow-wave system 15 p2153 A83-35165

On soft electron beams in solar active and flare region 15 p2284 A83-35216

An EBIS for atomic physics experiments --- Electron Beam Ion Source 16 p2409 A83-35628

Stability of relativistic laminar flow equilibria for electrons drifting in crossed fields 17 p2496 A83-37042

An unguided wave Cerenkov amplifier 17 p2497 A83-37754

High space harmonic perturbations in travelling wave tubes 17 p2497 A83-37757

Analysis of the interaction of an electron beam with back surface field solar cells 17 p2536 A83-38212

Microwave generation from rotating electron beams in magnetron-type waveguides 17 p2498 A83-38219

Signal amplification in an O-type TWT with noise in the electron beam 17 p2499 A83-38490

Rotating electron beam in crossed fields - Space charge, nonlinear effects 17 p2500 A83-38987

Distribution of electric-field potential near a satellite injecting electrons in the steady-state regime in the initial stage of active experiments in the ionosphere 18 p2713 A83-39319

Electron whistler mode instability in an inhomogeneous thermal plasma in the presence of an inhomogeneous beam of suprathermal electrons 18 p2745 A83-39616

The instability of an electron beam passing through a resistive medium 18 p2749 A83-40514

Further observations on resonance cones in non-Maxwellian plasmas 18 p2749 A83-40660

Characteristics of two types of Beam Plasma Discharge in a laboratory experiment 19 p2901 A83-41124

Antibunching in the Franck-Hertz experiment --- subpoissonian light generation from space-charge limited electron beams colliding with atoms 19 p2900 A83-41189

Quasi-equilibrium states of a pinched electron-ion beam 19 p2902 A83-41499

Radial isolated Blumein electron beam generator 20 p3045 A83-42293

Characterization of grain boundaries in polycrystalline solar cells using a computerized electron beam induced current system 20 p2988 A83-42299

Auroral beam/plasma interaction observed directly 20 p3023 A83-43159

Plasma drift measurements with the electron beam experiment on GEOS-2 during long period pulsations on April 7, 1979 20 p3025 A83-43201

Upward electron beams measured by DE-1 - A primary source of dayside region-1 Birkeland currents 20 p3026 A83-43215

Fourier analysis of the wave number of unstable waves in a spiral beam-plasma system 20 p3050 A83-43397

Energy lost in formation of fluorine atoms in the course of electron-beam dissociation of fluorine and fluoride molecules 20 p2997 A83-43797

Electron-beam guiding and phase-mix damping by an electrostatically charged wire 21 p3203 A83-43882

Small-radii curved rib waveguides in GaAs/GaAlAs using electron-beam lithography 21 p3205 A83-44222

Brillouin backscattering in an electron beam-plasma system 21 p3212 A83-44348

Nonlinear theory of the instability of a modulated electron beam of low density in a plasma. III - Derivation of nonlinear equations for the time- and space-problems (single wave model) 21 p3212 A83-44354

The change rate of energy of the test electron caused by plasma turbulence 21 p3213 A83-44521

Laboratory simulations of controlled energetic electron-beam-plasma interactions in space 21 p3215 A83-45579

A gyrocon with a longitudinal magnetic field 22 p3276 A83-45666

Enhancement of high-harmonic gyrotron gain by a dielectric rod 22 p3279 A83-46750

Ion neutralization in helical electron beams 23 p3460 A83-47556

Nonlinear theory of stimulated scattering of electromagnetic waves by a magnetized beam of electrons in a waveguide 23 p3445 A83-47572

Observation of the backward cyclotron wave in a spiral electron beam-plasma system 23 p3510 A83-47623

Forced interaction between an electron beam and superpower electromagnetic radiation at the boundary between two media 23 p3463 A83-48434

An EBIC equation for solar cells --- Electron Beam Induced Current 23 p3512 A83-48609

Electron-beam-induced emission of $KrXe(+)$ 24 p3589 A83-49613

The longitudinal excitation of vapors of complex organic compounds by an electron beam 24 p3627 A83-49740

ELECTRON BOMBARDMENT

The flexible magnetic field thruster [AIAA PAPER 82-1936] 02 p0147 A83-12553

Ion thruster charge-exchange plasma flow 02 p0148 A83-13089

The flexible magnetic field thruster [AIAA PAPER 82-1936] 03 p0290 A83-14374

Electron-bombarded CCD detectors for ultraviolet atmospheric remote sensing [AIAA PAPER 83-0106] 05 p0609 A83-16524

Pulse radiolysis of epoxy-based matrix materials [AIAA PAPER 83-0586] 05 p0617 A83-16805

The effect of the charge of the surface of ice grains and the nucleus of a comet on the rate of their sublimation 11 p1679 A83-27876

Optimization of pulling conditions by electronic bombardment of polycrystalline silicon ribbons for solar cells --- French thesis 12 p1750 A83-29946

Texas Instruments' virtual phase charge-coupled device (CCD) imager operated in the frontside electron-bombarded mode 14 p2016 A83-31995

Determination of diffusion length of electron beam induced minority carriers in polycrystalline GaAs 15 p2238 A83-33844

Electron-bombarded semiconductor (EBS) switch 18 p2678 A83-40373

Core level excitation of simple gases 24 p3625 A83-48737

ELECTRON BUNCHING

Small-signal gain of the TOK amplifier --- Transverse Optical Klystron 04 p0535 A83-15949

Resonance conversion of waves in modulated electron beams and in systems with modulated traveling parameters 05 p0624 A83-17043

The production of electron-positron bunches in a pulsar magnetosphere and their thermal radioemission 05 p0702 A83-17814

Coherent emission from electron clusters in free-electron lasers 06 p0765 A83-17981

Nonlinear wave and oscillation processes in extended electron beams 09 p1252 A83-23462

On the allowance for intrinsic magnetic field in the theory of the shaping of helical relativistic electron beams 09 p1257 A83-25087

Laser induced bunch lengthening on the ACO storage ring FEL 10 p1428 A83-26016

Electrostatic acceleration of a modulated electron beam 11 p1560 A83-27449

The effect of the velocity distribution function in an electron beam on the characteristics of an M-type TWT 13 p1833 A83-30706

Theory of a resonance oscillator with relay interaction 13 p1834 A83-30735

Digital simulation of the operation of an O-type traveling wave tube with two beams of different velocities in the beam-current-modulation mode. II 13 p1834 A83-30736

Results of the first phase of the ACO storage ring laser experiment 13 p1852 A83-31105

A diagnostic device for bunched electron beams --- for free electron lasers 13 p1855 A83-31135

TOK-transverse optical klystron and converter physics and figures 13 p1856 A83-31136

Free-electron coherent relativistic scatterer for UV generation 13 p1856 A83-31137

The effect of velocity distribution in a bunch on the efficiency of kinetic-energy extraction in a klystron 14 p2003 A83-32115

Radiation from a random train of electron bunches 16 p2417 A83-36933

Adiabatic motion of an electron bunch in the magnetosphere 17 p2544 A83-38520

Cerenkov radiation from periodic electron bunches 22 p3277 A83-45928

ELECTRON CAPTURE

Effects of gate metals on interface effects in metal oxide semiconductor systems after electron trapping 01 p0109 A83-10645

Current oscillations in semi-insulating GaAs associated with field-enhanced capture of electrons by the major deep donor EL2 02 p0243 A83-12294

- Thermal emission rates and capture cross-section of majority carriers at titanium levels in silicon
06 p0814 A83-18959
- Binary encounter calculations for electron capture from noble gases by He²⁺/
08 p1167 A83-21987
- Electron traps in GaAs/1-x/P/x/ alloys
10 p1488 A83-25985
- A study of impurities and traps in liquid phase epitaxial InP in relation to melt prebaking
10 p1488 A83-26063
- State-selective electron capture by N²⁺/ ions in atomic hydrogen using collision spectroscopy
11 p1654 A83-28220
- Electron capture into excited states of hydrogen
14 p2082 A83-32525
- Reversible photoinduced modification of electron-capture cross section at localized states in Alpha-Si:H
14 p2093 A83-33446
- Charge exchange collision experiments with highly charged ions -status repor
16 p2414 A83-35630
- Energy gain and loss spectroscopy of charge changing collisions between multiply charged ions and neutrals
16 p2409 A83-35632
- Experimental investigation of electron capture by highly charged ions of medium velocities
16 p2409 A83-35633
- State-selective electron capture by C(2+), C(3+), N(2+), and Ar(2+) ions in rare gases
17 p2579 A83-38365
- Properties of the defect causing solar cell degradation
18 p2749 A83-39468
- Characterization of electron traps in ion-implanted GaAs MESFET's on undoped and Cr-doped LEC semi-insulating substrates
18 p2750 A83-40372
- Electron capture during gravitational collapse in type II supernovae
19 p2916 A83-41169
- Annealing behaviour of gamma-ray-induced electron traps in LEC n-InP
20 p3052 A83-42482
- Total and partial cross sections for electron capture in collisions of hydrogen atoms with fully stripped ions
22 p3361 A83-45927
- A study of the parameters of traps in hydrogenated amorphous silicon by the method of volt-farad characteristics
24 p3635 A83-49047

ELECTRON CLOUDS

- Preliminary consideration of the modification of the SGEMP response of a triaxial satellite due to electron clouds
05 p0608 A83-17524
- On the evolution of Saturn's 'Spokes' - Theory
11 p1684 A83-27356
- Electron drift velocities in gas mixtures of He, N₂, and CO₂
11 p1655 A83-28707
- The application of a modified form of the S sub N method to the calculation of swarm parameters of electrons in a weakly ionised equilibrium medium
13 p1926 A83-31369
- Miniature imaging photon detector
14 p2018 A83-32022
- Expulsion of a magnetic field by a hot electron cloud
21 p3214 A83-45209

ELECTRON COLLISIONS**U ELECTRON SCATTERING****ELECTRON COMPOUNDS****U INTERMETALLICS****ELECTRON COUNTERS**

- Characteristics of the operation modes of a 2-mm-band detector with an open periodic-structure resonator --- electron counters
01 p0039 A83-10909
- Texas Instruments' virtual phase charge-coupled device (CCD) imager operated in the frontside electron-bombarded mode
14 p2016 A83-31995
- Practical prototype of a transition-radiation detector
20 p2991 A83-43534
- Earth's magnetic field as a radiator to detect cosmic ray electrons of energy greater than 10 to the 12th eV
22 p3390 A83-47043

ELECTRON CYCLOTRON HEATING

- RFI and ECH plasma generator development for ion thrusters
[AIAA PAPER 82-1941]
02 p0146 A83-12503
- Induced electron-cyclotron emission from inhomogeneous, anisotropic plasmas with electron population inversion
07 p0996 A83-20532
- Nonlinear effects at the upper-hybrid layer --- of plasmas
07 p0996 A83-20533
- Millimeter-wave generation by a single-pass, Compton-regime, variable-parameter free-electron laser
13 p1854 A83-31123
- Beam-plasma discharge in a Kyoto beam-plasma-type ion source
16 p2414 A83-35426
- Cyclotron absorption of finite-amplitude waves
16 p2417 A83-36932
- Perpendicular distribution of electrostatic electron-cyclotron radiation under dense plasma conditions
18 p2748 A83-40506

- Small-signal theory of a large-orbit electron-cyclotron harmonic maser
18 p2694 A83-40516

ELECTRON DENSITY (CONCENTRATION)

- NT CARRIER DENSITY (SOLID STATE)
- NT ELECTRON DENSITY PROFILES
- NT IONOSPHERIC ELECTRON DENSITY
- NT MAGNETOSPHERIC ELECTRON DENSITY
- A theoretical investigation of the distribution of electron concentration in the positive column of a glow discharge with a longitudinal flow of gas
02 p0240 A83-11514
- Complex ionized structure in the theta-2 Orionis region
03 p0413 A83-13315
- Electron densities from the semforbidden O IV lambda 1401 multiplet
03 p0430 A83-14809
- Electronic phase transition of molecular hydrogen in the method of an approximating electron-density functional --- bond charge formation in spin polarized biradical state
04 p0456 A83-15704
- Effect of the near-wall layer on current oscillations in a plasma emitter
04 p0537 A83-15860
- Electric field and space charge density distributions in the processes of ambipolar plasma diffusion with volume recombination
05 p0687 A83-16902
- Physical conditions in interacting galaxies, in components of isolated pairs, and in isolated galaxies
06 p0838 A83-19220
- Microwave absorption during resonance heating of a plasma with a high electron density inside a waveguide
07 p0998 A83-20861
- An upper limit on the electron density in Heiles' dust cloud 2 from decameter-wavelength observations
07 p1026 A83-21263
- Electron and local gas densities in diffuse interstellar clouds from measurements of Ca I absorption
08 p1183 A83-23050
- Measurement of plasma conductivity using Faraday rotation of submillimeter waves
08 p1169 A83-23139
- Temperatures in the plasmasphere determined from VLF observations
09 p1307 A83-24690
- The gamma-ray colour of the Milky Way and the cosmic-ray electron density
09 p1363 A83-24992
- New experimental results upon ionizational relaxation of a shock heated xenon plasma
10 p1487 A83-26175
- Number density of the 5s states during the ionisation relaxation of shock heated krypton
10 p1479 A83-26176
- The electron density of faint prominences observed during the solar eclipse of July 31, 1981
11 p1691 A83-27690
- Diffraction method for determining line electron density in meteor trails
11 p1672 A83-27879
- Density-functional theory for solid nitrogen and carbon dioxide at high pressure
13 p1929 A83-30958
- The dissociative recombination of O₂(+)- The quantum yield of O(1S) and O(1D)
13 p1916 A83-31248
- Laboratory simulation and investigation of flare processes in plasmas
14 p2086 A83-32529
- X-ray line ratios from helium-like ions - Updated theory and SMM flare observations
15 p2282 A83-34644
- Electron density in solar atmosphere from forbidden lines
16 p2440 A83-36545
- The forbidden O III electron temperature and density structure in the nucleus of NGC 1068
17 p2609 A83-38419
- Asymmetry in the diurnal variation of temperature and electron loss coefficient in the mesosphere
18 p2712 A83-39068
- The O IV infrared and ultraviolet flux ratios as temperature and density diagnostics --- of planetary nebulae
21 p3229 A83-44421
- The generalized Hubbard model in the theory of trimerizable molecular crystals --- such as Cs(2)(TCNQ)(3)-organic charge transfer salt
21 p3220 A83-45505
- Plasma regimes in the deep geomagnetic tail - ISEE 3
22 p3334 A83-46891
- Converging shock on laser plasma - Density profiles by holographic interferometry
23 p3510 A83-48316
- Plasma electron density measurements by the laser- and collision-induced fluorescence method
24 p3631 A83-48819

ELECTRON DENSITY PROFILES

- Using small extensive air showers where the number of electrons is greater than about 10,000 on mountains for calibrating an interaction model
02 p0276 A83-11759
- On the influence of a plasma hot component on whistler propagation beyond the plasmopause
02 p0206 A83-12020
- Electron density profiles in the nighttime high-latitude lower ionosphere, artificially disturbed by high-power radio waves
02 p0209 A83-12425
- Characteristics of auroral electrons according to Meteor-satellite observations
02 p0209 A83-12428

- The use of 1356-A emission intensity to determine parameters of the F-region
03 p0356 A83-13212
- The dynamics of energetic electrons according to Intercosmos-19 satellite observations in April 1979
03 p0439 A83-13217
- Interferometric measurement of the electron density in laser-matter interaction --- French thesis
03 p0398 A83-13808
- Statistical model of the mass distribution of meteor bodies
03 p0426 A83-14682
- Structure of the electron density profile in the vicinity of localized inhomogeneities in the case of ambipolar diffusion of magnetized recombining plasma
04 p0537 A83-15859
- Using satellite observed UV intensities to deduce electron density profiles
[AIAA PAPER 83-0023]
05 p0659 A83-16471
- The use of a single coupling function for the correction of model profiles of electron density in the ionosphere
05 p0662 A83-17604
- Electron density changes during solar eclipse of 16 Feb. 1980 at Gauhati
06 p0786 A83-18418
- A possible explanation of the variation of the scattering index parameter --- in interstellar medium
06 p0834 A83-18893
- Method for determining the radial profile of the electron density
07 p0995 A83-20065
- A method of estimating the electron density profile of the D layer from a knowledge of the VLF reflection coefficients
07 p0962 A83-20374
- The determination of electron density profiles from refraction measurements obtained using holographic interferometry
10 p1418 A83-25427
- Limitation to the accuracy of interferometrically measured electron density profiles of laser-produced plasmas
11 p1661 A83-28709
- Electron density profiles according to rocket measurements over Hayes Island during magnetospheric substorms
14 p2049 A83-31859
- Electron kinetics in the atmosphere in conditions of repeated air breakdown
14 p2049 A83-31864
- Tonks-Dattner diagnostics of electron density profiles
15 p2237 A83-35299
- D-region IRI profiles in relation to radio observations
16 p2375 A83-35389
- Mesospheric ionisation over dip equator at sunrise
16 p2375 A83-35392
- Automatic calculation of electron density profiles from digital ionograms. III - Processing of bottomside ionograms
16 p2376 A83-35421
- Results inferred from electron density measurements at Saskatoon, Canada (L = 4.4) by a partial reflection technique. II - Ion production rates and nitric oxide in the D-region during post-storm periods
18 p2712 A83-39067
- Interstellar electron density
18 p2765 A83-39198
- Harmonic generation of radiation in a steep density profile
18 p2748 A83-40512
- Measurement of variations of integral electron density in channels of communication with the Venera 13 and 14 probes
19 p2916 A83-41244
- On the structure function of density fluctuations of ionospheric inhomogeneities
19 p2866 A83-41805
- Modeling of the meridional distribution of the F-region electron concentration over Ashkhabad during the storm of August 1972
21 p3176 A83-45271
- The refraction of radiowaves and the vertical gradients of electron density in the day-side ionosphere of Venus
22 p3384 A83-45644
- Charged particle distributions in Jupiter's magnetosphere
22 p3384 A83-46028

ELECTRON DETECTORS**U ELECTRON COUNTERS****ELECTRON DIFFRACTION**

- Crystal rocking-diffraction of backscattered and transmitted electrons as an alternative method to conventional electron diffraction, especially for obtaining energy-filtered diffraction pictures --- German thesis
01 p0048 A83-10174
- Evidence for pseudo bridge bonding of c(2 x 2)-O on Ni(100)
13 p1817 A83-30920
- Electron-diffraction evidence for threefold coordination in amorphous hydrogenated carbon films
19 p2823 A83-40955
- Electron-diffractonal mode selection in free electron lasers
20 p2995 A83-43632

ELECTRON DIFFUSION

- Electron diffusion lengths in p-type InP involved in indium tin oxide/p-InP solar cells
01 p0109 A83-10637
- Electron and hole diffusion length investigation in CdTe thin films by SPV method --- Surface Photovoltage
04 p0539 A83-15495
- Diffusion length of minority carrier in n-type semiconductors - A photoelectrochemical determination in aqueous solvents
04 p0543 A83-16070

Breakdown wave in the self-consistent field of an electromagnetic wave beam 07 p0995 A83-20061

Influence of diffusion of hot carriers on collection efficiency of solar cells - a-Si:H 09 p1292 A83-23665

Jovian modulation of interplanetary electrons as observed with Voyagers 1 and 2 09 p1365 A83-23754

Diffusion length determination in n/+/-p-p/+/- structure based silicon solar cells from the intensity dependence of the short-circuit current for illumination from the p/+/- side 11 p1612 A83-27982

Minority carrier diffusion length measurements - A review and comparison of techniques 11 p1663 A83-28448

The application of a modified form of the S sub N method to the calculation of swarm parameters of electrons in a weakly ionised equilibrium medium 13 p1926 A83-31369

Ultrashort-wave radio emission of the ionosphere of slowly-varying-component type and soft electrons in the auroral zone 14 p2050 A83-31881

Analytical solutions for avalanche-breakdown voltages of single-diffused Gaussian junctions 14 p2006 A83-32667

Effect of heat treatment on the bulk diffusion length of EFG ribbon silicon --- Edge-defined Film-fed Growth 14 p2092 A83-32670

Technology of closed-drift thrusters [AIAA PAPER 83-1398] 16 p2322 A83-36388

Loss cone fluxes and pitch angle diffusion at the equatorial plane during auroral radio absorption events 17 p2543 A83-38372

A statistical study of the dynamics of the equatorward boundary of the diffuse aurora in the pre-midnight sector 20 p3026 A83-43214

Electrostatic waves and the strong diffusion of magnetospheric electrons 23 p3485 A83-48556

Multiwavelength analyzer for the determination of diffusion lengths --- in solar cell base region 23 p3459 A83-48612

High-field transport properties of In0.765Ga0.235As0.5P0.5 23 p3512 A83-48703

Bulk minority carrier diffusion length and photogenerated carrier profile in silicon photovoltaic cells 24 p3635 A83-48916

Electron transport coefficients in weakly ionized nonequilibrium plasma of CO2:N2 mixtures 24 p3632 A83-49112

ELECTRON DISTRIBUTION

NT ELECTRON DENSITY PROFILES

Electron distribution function in a weakly ionized plasma in an inhomogeneous electric field. II - Strong fields /energy balance determined by inelastic collisions/ 03 p0397 A83-13195

Observations of field-aligned energetic electron and ion distributions near the magnetopause at geosynchronous orbit 05 p0660 A83-17389

Electron velocity distributions near the earth's bow shock 06 p0782 A83-18285

Monte Carlo particle simulation of a GaAs short-channel MESFET 06 p0751 A83-18572

Distribution functions of the number of cascade electrons at various stages of the development of a shower in lead at high energies 06 p0858 A83-19347

Radial electron distribution in an electromagnetic cascade in the atmosphere 06 p0858 A83-19348

Vibrational population distribution in the hydroxyl night airglow 09 p1306 A83-24640

Electron spectrum measurements for a tapered-wiggler free-electron laser 10 p1428 A83-26018

Stability of electron distributions within the earth's bow shock 11 p1617 A83-28307

Measurement of multiple differential electron distributions in an electron beam in nitrogen --- German thesis 11 p1575 A83-28659

Non-Maxwellian electrons in a laser produced sodium plasma 13 p1926 A83-31061

Observations of non-linear processes in the ionosphere 15 p2198 A83-34191

Radial dependence of HF wave field strength in the BPD column --- Beam Plasma Discharge 15 p2234 A83-34200

Intensity distribution of dayside polar soft electron precipitation and the IMF 15 p2199 A83-34358

Excitation of whistler waves by reflected auroral electrons 15 p2199 A83-34359

The electron angular distribution of different rotational branches in the VUV photoelectron spectrum of H2 16 p2408 A83-35328

Electron distribution function in a laser plasma 16 p2415 A83-35888

Application of Wiener-Hermite expansion to strong plasma turbulence 16 p2416 A83-36624

The impulsive phase of solar flares. II - Characteristics of the hard X-rays 17 p2624 A83-37335

An analysis of the asymmetric part of electron-electron Boltzmann integral 17 p2583 A83-38208

Loss cone fluxes and pitch angle diffusion at the equatorial plane during auroral radio absorption events 17 p2543 A83-38372

Anode-plasma parameters of a high-voltage glow discharge of about 150 kV 18 p2746 A83-39863

Monte Carlo simulation of a millimeter-wave Gunn-effect relaxation oscillator 18 p2677 A83-40369

Electron distribution functions in a current sheet 18 p2749 A83-40518

The effect of a non-Maxwellian electron distribution on oxygen and iron ionization balances in the solar corona 19 p2924 A83-41642

Determination of the quadrupole moment of the electron distribution function in a plasma 20 p3049 A83-42277

Particle and wave dynamics during plasma injections 20 p3018 A83-42414

General form for the electron distribution function for an inhomogeneous fully ionized and magnetized plasma interacting with an alternating electric field 21 p3212 A83-44355

Comments on the solar neutrino problem 23 p3530 A83-47427

Onefold photoelectron-counting statistics for non-Gaussian light - Scattering from an arbitrary number of weak scatterers 23 p3508 A83-47582

ELECTRON EMISSION

NT FIELD EMISSION

NT PHOTOELECTRIC EMISSION

NT SECONDARY EMISSION

Coherent bremsstrahlung from relativistic electrons axially channeled in crystals 01 p0054 A83-10815

Emission characteristics of refractory materials --- as electrodes in aerodynamic generators 04 p0506 A83-16019

Enhanced electron emission from positive dielectric/negative metal configurations on spacecraft 05 p0607 A83-17490

Coherent emission from electron clusters in free-electron lasers 06 p0765 A83-17981

Laser-generated electron emission from surfaces - Effect of the pulse shape on temperature and transient phenomena 07 p1000 A83-20749

Shockfronts as model targets in laser-plasma interaction experiments 10 p1487 A83-26173

Above threshold ionisation - Multiphoton ionization involving continuum-continuum transitions 11 p1654 A83-27557

On the nature of explosive electron emission 13 p1830 A83-30016

Two-dimensional analysis of hot-electron emission current in MOS FET 13 p1834 A83-30783

Bremsstrahlung emission in a non LTE plasma 15 p2233 A83-34139

The mechanism of explosive emission excitation in thermionic energy conversion processes 16 p2371 A83-36967

Motion and radiation of electrons in an inhomogeneous magnetic field 18 p2744 A83-39005

Computer simulation studies of VLF triggered emissions deformation of distribution function by trapping and detrapping --- of resonant electrons in inhomogeneous geomagnetic field 20 p3024 A83-43186

Energy fluctuations of transition radiation 20 p3046 A83-43529

Quasi-thermal noise corrections due to particle impacts or emission --- for antenna measurement of space plasmas 22 p3364 A83-47070

Emission of electrons from the collector of a thermionic converter 23 p3477 A83-47567

ELECTRON ENERGY

NT ELECTRON STATES

Investigation of the flux of Jupiter electrons with energy not less than 40 keV by the Mars-7 interplanetary probe 02 p0263 A83-11715

Electron distribution function in a weakly ionized plasma in an inhomogeneous electric field. II - Strong fields /energy balance determined by inelastic collisions/ 03 p0397 A83-13195

Coulomb interactions in Anderson localized disordered systems 04 p0540 A83-15508

Influence of electron heating during recombination of copper atoms in copper halide vapor lasers on their output parameters 05 p0650 A83-17068

Semiconductor structures for repeated velocity overshoot 05 p0690 A83-17295

Direct comparison of the electron-temperature model with the particle-mesh /Monte-Carlo/ model for the GaAs MESFET 06 p0752 A83-18761

Physical conditions in interacting galaxies, in components of isolated pairs, and in isolated galaxies 06 p0838 A83-19220

Electron energy transport in ion waves and its relevance to laser-produced plasmas 07 p0997 A83-20543

The role of acceleration processes in the formation of nanosecond volume discharges in dense gases 07 p0998 A83-20867

Another self-similar blast wave - Early time asymptote with shock-heated electrons and high thermal conductivity --- in astrophysics 07 p1023 A83-21141

Electron thermalization in gases. V - Diatomic molecules H2, N2, and CO 09 p1342 A83-24132

Concerning one feature of energy conversion in diffraction-radiation generator/free-electron laser systems 09 p1272 A83-24219

Ballistic transport and velocity overshoot in semiconductors. I - Uniform field effects 09 p1350 A83-24498

Threshold structures in the cross sections of low-energy electron scattering of methane 09 p1343 A83-24825

An instrument for the direct measurement of electron temperature in the ionosphere 10 p1387 A83-25341

Diamond /111/ studied by electron energy loss spectroscopy in the characteristic loss region 10 p1390 A83-25675

The galactic gradient in electron temperature from observations of low-density H II regions 10 p1503 A83-25722

Electron spectrum measurements for a tapered-wiggler free-electron laser 10 p1428 A83-26018

The differential energy spectra of electrons having energies of 0.3-3 MeV on the basis of data from the satellite Prognoz 4 10 p1523 A83-26109

Effects of electron energy spread on self-excitation of free-electron lasers 10 p1431 A83-26466

Changes in the ionosphere caused by longitudinal electric fields 11 p1620 A83-28748

The height distribution of parameters of the auroral ionosphere during a magnetic storm 11 p1621 A83-28749

Heating of thermal ionospheric electrons by suprathermal electrons 12 p1751 A83-28911

Formation of electrostatic potential barrier between different plasmas 12 p1780 A83-29100

Measurements of the energy spectra of charged particles within the Vertical-10 rocket experiment 13 p1814 A83-30767

Laser studies of electronic energy transfer in atomic copper 13 p1851 A83-30957

Theory of a free-electron laser with gain expansion 13 p1853 A83-31111

A note on the Madey gain-spread theorem --- concerning energy change experienced by electrons in free electron laser 13 p1853 A83-31112

Mirror instability and the origin of morningside auroral structure 13 p1878 A83-31236

The dissociative recombination of O2(+) - The quantum yield of O(1S) and O(1D) 13 p1916 A83-31248

Electron energy distribution produced by beam-plasma discharge 15 p2234 A83-34196

Heat balance for the high-temperature component of a solar flare 15 p2279 A83-34294

Extremely high F-region electron temperatures during the maximum of 21st solar cycle 15 p2200 A83-34417

The effect of contamination of the probe surface and coating on the accuracy of the measurement of electron temperature using the Langmuir probe --- in satellite and rocket experiments 15 p2128 A83-34420

Single-channel energospectrometer of low-energy electron and proton fluxes 15 p2128 A83-34448

Stark shift trends in homologous ions 16 p2414 A83-35327

Energy distribution of thermal electrons at the height of lower-E-region 16 p2373 A83-35366

New descriptive temperature model --- for electrons and ions in ionosphere 16 p2375 A83-35396

Relationship between electron density and electron temperature as a function of solar activity 16 p2375 A83-35397

Effect of electrons produced by ionization on calculated electron-energy distributions 16 p2414 A83-35653

Electron temperature differences and double layers 17 p2581 A83-37038

Electron current disruption and parallel electric fields associated with electrostatic ion cyclotron waves 17 p2538 A83-37582

The forbidden O III electron temperature and density structure in the nucleus of NGC 1068 17 p2609 A83-38419

The energy of thermal electrons in electron beam created helium discharges 17 p2583 A83-38965

Elastic and rotational excitation of the oxygen molecule by intermediate-energy electrons 19 p2898 A83-41196

Electron temperature measurements using a 12-channel array probe 20 p3049 A83-42292

Inelastic scattering effects on photoelectron spectra and ionospheric electron temperature 20 p3019 A83-42422

- Electron drift velocity in molecular gas rare gas mixtures 20 p3049 A83-42577
- An empirical relationship between electron temperature and electron density in the subauroral electron-density trough 20 p3022 A83-43133
- Fermi levels in electrolytes and the absolute scale of redox potentials 20 p2951 A83-43608
- Vibrational excitation of CH₄ by electron impact: 3-20 eV 20 p3045 A83-43675
- Generation of static magnetic fields by a test charge in a plasma with an electron temperature anisotropy 21 p3210 A83-44129
- The observed characteristics of a radio outburst on the solar limb 21 p3242 A83-44290
- The change rate of energy of the test electron caused by plasma turbulence 21 p3213 A83-44521
- Suprathermal electron energy deposition in plasmas with the Fokker-Planck method 21 p3215 A83-45520
- Analytical yield spectrum approach to electron energy degradation in earth's atmosphere 22 p3327 A83-46055
- Time-sharing measurements of ionospheric electron temperature and electron density with the electric field using double probes - An experiment on the Antarctic sounding rocket S-310JA-7 22 p3331 A83-46518
- Comments on the solar neutrino problem 23 p3530 A83-47427
- Electron temperature monitor for laser-produced plasmas 23 p3454 A83-47641
- Relation between hard X-ray spectra and electron energy spectra --- of solar X-ray bursts 23 p3533 A83-47683
- The interpretation of protons and electrons observations from ATS 6 satellite within the frame of McIlwain's electric field model 23 p3482 A83-48055
- Electron energy-loss spectroscopy of carbon monoxide. II - The energy region 11 to 20 eV 23 p3506 A83-48581
- Propagation velocity of an ionization front maintained by a relativistic electron beam 24 p3632 A83-48860
- Dielectric surface discharges - Effects of combined low-energy and high-energy incident electrons 24 p3572 A83-48900
- Energy distribution functions of electrons in low-temperature helium-neon plasma at low pressures 24 p3632 A83-49113
- Energies of radiating electrons and angles between the rotation axis and the magnetic dipole in pulsars 24 p3654 A83-49175
- Electron temperature measurements in a HF plasma source using a 200 J Nd:glass laser 24 p3633 A83-49747
- ELECTRON FLUX**
U ELECTRONS
U FLUX (RATE)
- ELECTRON FLUX DENSITY**
Investigation of high-energy electrons by the Intercosmos-17 satellite 02 p0273 A83-11714
- Investigation of the flux of Jupiter electrons with energy not less than 40 keV by the Mars-7 interplanetary probe 02 p0263 A83-11715
- Shower curves in the atmosphere and the composition of primary cosmic radiation with an energy greater than 10 to the 15th eV 02 p0275 A83-11757
- The possibility of detecting electrons with an energy greater than 20 MeV in the region of the Brazilian magnetic anomaly 02 p0210 A83-12444
- Investigation of electron fluxes with energies of 40-500 keV in quiet periods of solar activity by the methods of correlation and spectral analysis 03 p0438 A83-13207
- 5577-A nightglow and electron fluxes in the nightside atmosphere of Venus 03 p0432 A83-13213
- Observations of inverted-V electron precipitation 04 p0510 A83-15824
- The formation of albedo-electron fluxes in the geomagnetic field 05 p0662 A83-17603
- Comparison of calculated and measured values of electron fluxes for the wide-angle detector in the ARAKS experiment --- on ionospheric electron beam injection 06 p0786 A83-18368
- Investigation of a slow-wave structure of ring-bar type --- for high power traveling wave tubes in linear accelerators 09 p1252 A83-23453
- Suprathermal electron pumping of X-ray lasers 11 p1577 A83-27521
- Spatial, spectral, and angular structures of electron fluxes with energies of 30-210 keV at low altitudes during a magnetically quiet period 21 p3245 A83-45288
- Fluxes of quasi-trapped charged particles according to data from a rocket experiment 21 p3245 A83-45295
- Measurements of high-energy electrons in the radiation belt by the Bulgaria-1300 satellite 21 p3245 A83-45296

- Characteristics of the inverted-V events observed by the Kyokko satellite --- auroral electron precipitation 22 p3330 A83-46510

ELECTRON GAS

- Anomalous quantum Hall effect - An incompressible quantum fluid with fractionally charged excitations 13 p1914 A83-30923
- The retardation of ions in a degenerate electron gas 14 p2086 A83-32141
- Exchange energy of an electron gas of arbitrary dimensionality 16 p2422 A83-35695
- TDEG in In(0.53)Ga(0.47)As-InP heterojunction grown by chloride VPE --- two-dimensional electron gas 17 p2585 A83-38880
- Fractional quantization of the Hall effect - A hierarchy of incompressible quantum fluid states 19 p2895 A83-41160
- Classical magnetoresistance of a two-dimensional electron gas in a one-dimensional superlattice 20 p3051 A83-42283
- Field ionised impurity scattering in an AlGaAs/GaAs two-dimensional electron gas 20 p3052 A83-42485

ELECTRON GUNS

- Improved orotron performance in the 50- to 75-GHz frequency region 03 p0314 A83-14516
- e-guns and depressed collectors for two-stage free electron lasers 10 p1427 A83-26008
- The Stanford Superconducting Linear Accelerator --- for powering free electron laser 13 p1917 A83-31104
- Plasma diagnostics by electron guns and electric field probes on ISEE-1 15 p2233 A83-34184
- Stimulation of plasma waves by electron guns on the ISEE-1 satellite 15 p2233 A83-34185
- Transient effects in beam-plasma interactions in a space simulation chamber stimulated by a fast pulse electron gun 15 p2234 A83-34198
- The development of high-perveance electron-optics on the basis of longitudinal compression 19 p2840 A83-41817

ELECTRON IMPACT

- Electron impact ionisation of N₂+/- including autoionisation 01 p0106 A83-10205
- Electron impact cross sections for the 2,2P state excitation of lithium 03 p0391 A83-13225
- Hot-electron induced excess carriers in MOSFET's 05 p0624 A83-17287
- Single and multiple ionization of sulfur atoms by electron impact --- in lo plasma torus 05 p0707 A83-17783
- Electron impact excitation of forbidden transitions in Si IX 06 p0835 A83-19012
- Measurement of the cross sections for excitation of a singly charged iron ion by electron impact --- stellar spectra 07 p1027 A83-21278
- Calculation of the rate coefficients for the electron impact excitation of the n = 2 terms of O IV 08 p1179 A83-21989
- Cross sections for electron impact excitation of the low-lying electron states of CO₂ 08 p1163 A83-23021
- Dissociative excitation of SO₂ by controlled electron impact --- Jupiter emission 08 p1190 A83-23116
- Inverse distribution of populations of vibrational levels in the A₂Sigma state of the HCl/ + / ion excited by electron impact 09 p1271 A83-24000
- EUV studies of N₂ and O₂ produced by low energy electron impact 09 p1342 A83-24130
- Studies of the vibrational relaxation of diatomic molecules in a shock heated molecular beam and its application to ionization by electron impact 10 p1479 A83-26179
- Electron impact excitation of SO₂ - Differential, integral, and momentum transfer cross sections 10 p1480 A83-26456
- Experimental verification of the breakdown of the electric dipole rotational selection rule in electron impact ionization-excitation of N₂ 11 p1653 A83-27493
- Polarisation correlations following electron impact on N₂ 11 p1655 A83-28221
- Concerning sources of O⁺/1D/ in Aurora - Electron impact and dissociative recombination 11 p1619 A83-28326
- Ionisation and appearance potentials of CH₄ by electron impact 12 p1778 A83-29925
- The threshold laws for electron-atom and positron-atom impact ionization 13 p1915 A83-30177
- Electron impact excitation of methane 13 p1916 A83-30955
- Doubly differential cross sections of secondary electron ejected from gases by electron impact - 50-400 eV on N₂ 13 p1916 A83-31353
- Electron-impact excitation of the Cameron system (a(3)pi yields x(1) Sigma) transition of CO 13 p1917 A83-31534
- Electron impact excitation of positive ions of astrophysical interest. I - Theoretical method 14 p2109 A83-33279

Electron impact ionization of complex ions

- 15 p2236 A83-34608
- On electron impact ionization cross-sections and rates for multiply charged ions 15 p2236 A83-34609
- Electron impact excitation from a 1 Delta g state of molecular oxygen 16 p2408 A83-35330
- Measurement of the lifetime of the c 3 Pi u state of molecular nitrogen by the delayed coincidence method 16 p2410 A83-36797
- Emission cross sections of the second positive and first negative systems of N₂ and N₂(+) excited by electron impact 16 p2411 A83-36799
- Electron impact excitation of forbidden transitions in Ca XV 17 p2579 A83-38367
- Metastable excitation measurements in CO and N₂ by high-resolution electron impact, using a low work function detector 17 p2579 A83-38368
- Collision strengths for the N = 2 excitation of hydrogenic ions 17 p2583 A83-38960
- Vibrational excitation of symmetric and bending modes of H₂O by slow electron impact 18 p2742 A83-39446
- Impact ionization in (100)-, (110)-, and (111)-oriented InP avalanche photodiodes 18 p2750 A83-40064
- Observation of autoionising states in H₂ and D₂ above 30 eV by electron impact 18 p2743 A83-40317
- Measured electron-impact ionization of Be-like ions: B(+), C(2+), N(3+), and O(4+) 18 p2743 A83-40406
- Half-widths of neutral fluorine spectral lines 19 p2897 A83-40714
- Cross sections for electron-impact excitation of the electronic states of N₂ 19 p2898 A83-41195
- Vibrational excitation of CH₄ by electron impact: 3-20 eV 20 p3045 A83-43675
- Electron-induced excitation and ionization of multiply-charged ions 21 p3213 A83-44652
- Double electron excitation in heliumlike ions 22 p3354 A83-45940
- Electron impact excitation of lambda 7990-A multiplet 22 p3355 A83-46061
- Quasi-thermal noise corrections due to particle impacts or emission --- for antenna measurement of space plasmas 22 p3364 A83-47070
- Electron excitation of Ca XVII 23 p3506 A83-48580
- Electron collisional rate coefficients for low-level transitions in hydrogen 24 p3626 A83-49386
- Angular intensity distribution of Balmer-alpha emission excited by electron impact on H₂ 24 p3626 A83-49431
- The measurement of the cross sections of excitation of several quartet states of the cobalt atom by electron impact 24 p3626 A83-49737
- ELECTRON INTENSITY**
U ELECTRON FLUX DENSITY
- ELECTRON INTERACTIONS**
U ELECTRON SCATTERING
- ELECTRON IONIZATION**
U IONIZATION
- ELECTRON IRRADIATION**
Comparative studies of tunnel injection and irradiation on metal oxide semiconductor structures 01 p0109 A83-10633
- Solar cell performance at low illumination and temperature for deep-space applications 01 p0068 A83-10662
- Optical and electrical characterization of multiply doped silicon - A study of the Si/In,Al/ system 04 p0542 A83-16065
- Charging and discharging characteristics of dielectric materials exposed to low- and mid-energy electrons 05 p0618 A83-17500
- The damage equivalence of electrons, protons, and gamma rays in MOS devices 05 p0628 A83-17533
- X-ray photoelectron spectroscopy study of radiation-damaged Si-SiO₂ interfaces 08 p1169 A83-22341
- Defects in electron-irradiated, gallium-doped silicon --- in solar cells 10 p1489 A83-26213
- Status of ion-implanted silicon solar cells 14 p2005 A83-32326
- Optimization of pulsed electron beam annealing process for silicon solar cells 14 p2005 A83-32327
- Silicon solar cells by ion implantation - E-beam and self annealing 14 p2005 A83-32328
- The design and manufacture of an experimental device for irradiation at low temperature and a study of the effects of electron irradiation on type n InAs --- French thesis 17 p2585 A83-38433
- The effect of proton-electron irradiation on the properties of composites with disperse reinforcement 18 p2650 A83-40111
- The effect of electron irradiation on the characteristics of MOS structures based on Hg(1-x)Cd(x)Te 21 p3220 A83-45507

Co-60 gamma-ray and electron irradiation damage of GaAs single crystals and solar cells 22 p3364 A83-46274

Study of deep-level defects and annealing effects in undoped and Sn-doped GaAs solar cells irradiated by one-MeV electrons 23 p3427 A83-48605

Effects of 0.5-MeV electrons on the interlaminar shear and flexural strength properties of graphite fiber composites 24 p3553 A83-48901

ELECTRON MICROSCOPES

Dynamic wear tests in the SEM [ASLE PREPRINT 82-LC-1B-1] 03 p0333 A83-13227

A high temperature straining stage (300-1000 K) for a 200 kV microscope 15 p2166 A83-35253

Characterization of grain boundaries in polycrystalline solar cells using a computerized electron beam induced current system 20 p2988 A83-42299

125 kV field emission electron microscope and its application to lattice imaging 20 p2992 A83-43617

ELECTRON MICROSCOPY

Crystal rocking-diffraction of backscattered and transmitted electrons as an alternative method to conventional electron diffraction, especially for obtaining energy-filtered diffraction pictures --- German thesis 01 p0048 A83-10174

Structural features and the stimulated crystallization of amorphous films of chalcogenide semiconductors 01 p0110 A83-10849

Electron-microscopic aspects of the selection of ultrasound intensity in ultrasonic therapy 01 p0081 A83-11394

Transmission electron microscopy of transverse sections through oxide scales on metals 03 p0296 A83-13123

Combined light and electron microscopic investigations of the connections in the central nervous system - A review of current methodological approaches 03 p0375 A83-13646

TEM observations of dislocation emission at crack tips in aluminum 03 p0298 A83-13679

Fractographic studies of graphite/epoxy fatigue specimens 03 p0292 A83-14554

Anti-phase domain boundary tubes in Ni3Al --- crystal defect structures 05 p0616 A83-17792

Transmission electron microscopy studies on the oxidation of aluminum 05 p0617 A83-17952

Techniques for the correction of topographical effects in scanning Auger electron microscopy 07 p0929 A83-20748

Analytical electron microscope study of eight ataxites 07 p1035 A83-21330

Mudrocks examined by backscattered electron microscopy 08 p1130 A83-23278

A microscopic approach of the aluminium creep rate at intermediate temperature 09 p1231 A83-24053

Microstructural aspects of the creep of alloys based on Nimonic 80A 09 p1232 A83-24075

Procedure for the diagnosis of axial electron-optical image defects --- German thesis on electron microscope resolution 09 p1269 A83-24844

Electron beam studies of individual natural and anthropogenic microparticles - Compositions, structures, and surface reactions 09 p1297 A83-25184

Dynamic in situ high voltage electron microscopy studies of tensile cracks in thin stainless steel films 10 p1395 A83-25546

Observation of defects in mercury cadmium telluride crystals grown by chemical vapor transport 13 p1929 A83-30348

Tunneling current microscopy 13 p1846 A83-30350

An experimental study of the dynamics of interaction between rarefied gas flows and a solid surface using the method of field-emission microscopy 13 p1932 A83-30664

HVEM in situ deformation of Al-Li-X alloys --- High Voltage Electron Microscope 14 p1997 A83-32948

Transmission electron microscopy of GaAs permeable base transistor structures grown by vapor phase epitaxy 16 p2419 A83-35450

Lattice images of amorphous-like Ni-B films prepared by the electrodeless plating method 16 p2328 A83-35601

Transmission electron microscopy studies of structural changes in 13Ni-15Co-10Mo maraging steel as a result of aging 16 p2329 A83-35605

Measurement of laser photoelectron image degradation at high current densities 16 p2356 A83-35969

A TEM investigation of the structure of nitrogen-implanted Ti-6Al-4V 16 p2330 A83-36068

Soft X rays and fast atoms as image generators in photoelectron microscopy 17 p2512 A83-38595

Analytical methods: High-melting metals --- Book 19 p2905 A83-41848

New trend of atom resolution electron microscopy - Direct observations of atoms, vacancies and impurity atoms in crystal and on-line image analysis 20 p2992 A83-43609

Many-beam imaging studies of crystal structure of ordered alloys 20 p2992 A83-43610

Monatom-high level electron microscopy of metal surfaces 20 p2992 A83-43611

High resolution lattice images of G.P. zones in an Al-3.97 wt pct Cu alloy --- Guinier-Preston 20 p2956 A83-43613

High resolution electron microscopy studies on the precipitation in an Al-4 percent Cu alloy 20 p2956 A83-43614

Intermetallic compounds of the micron- and P-phases of Co7Mo6 studied by 1 MV electron microscopy 20 p2956 A83-43616

Removal of histological sections from glass for electron microscopy - Use of Quetol 651 resin and heat 21 p3183 A83-44675

A TEM study of microstructural changes during retrogression and reaging in 7075 aluminum 22 p3269 A83-46397

Removal of histological sections from glass for electron microscopy - Use of Quetol 651 resin and heat 22 p3346 A83-46709

Correlation among secondary ion mass spectrometry, cross-section transmission electron microscopy, and Rutherford backscattering analyses for defect density and depth distribution determination 22 p3365 A83-46728

Electron microscopy of acidic aerosols collected over the northeastern United States 23 p3479 A83-48687

Electron microscopy study of microstructural changes in a Ti-1.6 at. pct N alloy 24 p3559 A83-48850

High temperature in situ experimentation in HVEM instrumentation and application to materials science [ONERA, TP NO. 1983-88] 24 p3583 A83-49407

High-resolution imaging of inhomogeneities in superconducting tunnel junctions by scanning with a modulated electron beam 24 p3636 A83-49757

ELECTRON MOBILITY

An enhancement mode Schottky barrier gate charge-coupled device on a high electron mobility transistor structure 01 p0039 A83-10994

Enhancement of electron velocity in modulation-doped /Al, Ga/As/GaAs FETs at cryogenic temperatures 04 p0470 A83-15251

EXAFS investigation of dilute Cu impurities in amorphous As2Se3 04 p0540 A83-15502

Electronic correlations and transient effects in disordered systems 04 p0540 A83-15506

Dispersion relations for hot electrons 04 p0542 A83-16066

The effects of heat treatments on the transport properties of Cu/x/S thin films 04 p0543 A83-16083

Ballistic transport in semiconductors 05 p0690 A83-17286

The Bloch-FET - A lateral surface superlattice device 05 p0690 A83-17289

Radiation effects on modulation-doped GaAs-Al/x/Ga/1-x/As heterostructures 06 p0815 A83-19263

Ballistic and overshoot electron transport in bulk semiconductors and in submicronic devices 07 p0999 A83-20737

Radiation-induced photoconductivity in polymers - Poly(vinylidene fluoride/ compared with polyethylene terephthalate 07 p0920 A83-20739

Third-order optical nonlinearity induced by effective mass gradient in heterostructures [AD-A130018] 07 p0994 A83-21364

Quantum transport in a single layered structure for impurity scattering 07 p1000 A83-21372

Absence of the Gunn effect in p-In/0.53/Ga/0.47/As 07 p1000 A83-21374

Electron mobility in MOS transistors with short channels 08 p1079 A83-21870

Electrophysical properties of single crystals of n-Cd/x/Hg/1-x/Te /x ranging from 0.24 to 0.40/ 09 p1350 A83-24250

Theory of silicon superlattices - Electronic structure and enhanced mobility 11 p1664 A83-28710

Electron transport in InP at high electric fields 13 p1929 A83-30353

Measurement of high electron drift velocity in a submicron, heavily doped graded gap Al(x)Ga(1-x)As layer 13 p1929 A83-31056

The effect of glow discharge excitation frequency on the performance of microcrystalline Si:H thin films and devices 14 p2043 A83-32279

Numerical simulation of nonstationary processes in semiconductor diode structures in the case of the ballistic motion of electrons 15 p2238 A83-35172

Unsteady quasi-ballistic motion of electrons through semiconducting layers of submicron thickness 17 p2585 A83-38494

Photo-induced changes in the bulk density of gap states in hydrogenated amorphous silicon associated with the Staebler-Wronski effect 18 p2750 A83-39472

High-frequency admittance of high-electron-mobility transistors (HEMTs) 21 p3127 A83-45175

Mismatch and electron mobility in MBE Ga(x)In(1-x)As epitaxial layers on InP substrates 23 p3512 A83-48701

ELECTRON MULTIPLIERS

U PHOTOMULTIPLIER TUBES

ELECTRON OPTICS

The problems of physical electronics --- Russian book 04 p0472 A83-15837

New developments regarding traveling-wave tubes and backward-wave oscillators in the millimeter-wavelength region. II - Electron optics and experimental results 06 p0755 A83-19614

Procedure for the diagnosis of axial electron-optical image defects --- German thesis on electron microscope resolution 09 p1269 A83-24844

Integral representation for geometric optics solutions --- of field autocorrelation functions and diffusion tensors for nonuniform plasmas 10 p1485 A83-25786

An image-tube camera for cometary spectrography 10 p1498 A83-26911

Electron-optical system with a thermionic cathode and centrifugal electrostatic shaping of a high-power axisymmetric beam, intended for use in relativistic microwave oscillators 14 p2003 A83-32117

Is magnetic flux quantized in a toroidal ferromagnet? 19 p2895 A83-40962

The development of high-perveance electron-optics on the basis of longitudinal compression 19 p2840 A83-41817

Polychromatic MTF of electrostatic point symmetric electron lenses 21 p3125 A83-44152

Characteristics of diffraction radiation generators with multiple electron drift 22 p3294 A83-45664

ELECTRON ORBITALS

Chemical bonding in amorphous semiconductors 04 p0541 A83-15516

Methods for spectral selection in the region of the 2P^{1/2}-2P^{3/2} transition in an iodine atom under conditions of lasing in a Zeeman inhomogeneous gain profile 05 p0648 A83-17041

Effective collision strengths for electron excitation of the ground state of O VII to the 2/3/S and 2/3/P states 09 p1347 A83-23652

Dielectronic satellite spectra of Mg XI with inner-shell and helium-like excitation rates - Application to solar observations 09 p1368 A83-24471

K-alpha and K-beta spectra from M-shell-ionized ions produced in a vacuum spark 10 p1485 A83-25410

Conjugate gradient method for the solution of linear equations - Application to molecular electronic structure calculations 12 p1778 A83-29640

On the nature of the bonding in Cu2 - An ab initio viewpoint 13 p1818 A83-31809

Ab initio calculation of the X 1 Sigma + state of CsH 14 p2083 A83-33106

Photoelectron angular distributions of the N2O outer valence orbitals in the 19-31 eV photon energy range 15 p2227 A83-34012

On electron impact ionization cross-sections and rates for multiply charged ions 15 p2236 A83-34609

New class of materials - Half-metallic ferromagnets 16 p2421 A83-36564

Rydberg atoms 18 p2743 A83-40003

Small-signal theory of a large-orbit electron-cyclotron harmonic maser 18 p2694 A83-40516

The dissociation energy of Cu2 - Do we want to perform multi-reference singles and doubles CIs on many-electron systems? 19 p2898 A83-41864

Novel short-pulse photoionization electron source - Li (1s2s2p)4P0 deexcitation measurements in a plasma 21 p3209 A83-43885

An analysis of the processes occurring at the cathode of a magnetron oscillator under orbital resonance 22 p3276 A83-45665

Theoretical evidence for multiple one-electron 3d bonding in a first row transition metal dimer - The 5 Sigma u -state of Sc2 24 p3625 A83-48799

Supplemental basis functions for the second transition row elements 24 p3552 A83-48800

ELECTRON OSCILLATIONS

Measurement of relative oscillator strengths for Fe I: Transitions from levels /b-3/-F/2-4/ /2.61 eV-2.56 eV/ - Use of a multipass optical system 03 p0413 A83-13318

Precision measurement of relative oscillator strengths for Ti II. I - Transitions from levels /a-4/-F/3/2-9/2/ /0.00-0.05 eV/, /b-4/-F/5/2-9/2/ /0.12-0.15 eV/ 03 p0413 A83-13319

- Precision measurement of relative oscillator strengths for Ti I, II - Transitions from levels /a-5/-F/1-4/ /0.81-0.84 eV/, /a-1/-D/2/ /0.90 eV/ and /a-3/-P/0-2/ /1.5-1.07 eV/ 03 p0413 A83-13320
- Wavefunctions and oscillator strengths for Si II 06 p0827 A83-18164
- Electron impact excitation of forbidden transitions in Si IX 06 p0835 A83-19012
- Oscillator strengths and collision strengths for O II and O III 06 p0809 A83-19519
- Indium phosphide transferred electron oscillators for millimetre-wave frequencies 07 p0919 A83-20180
- Quantization rules and instabilities of highly excited hydrogen atom in a strong magnetic field 07 p0991 A83-20605
- On the errors of the Kurucz-Peytremann Fe I oscillator strengths 07 p1024 A83-21226
- Stimulated scattering of electromagnetic waves by a magnetized relativistic beam of oscillators 10 p1426 A83-25886
- Upstream electron oscillations and ion overshoot at an interplanetary shock wave 19 p2864 A83-41115
- Low-frequency fluctuations of oscillations in a gyrotron caused by thermal noise 19 p2840 A83-41779
- Nonlinear oscillations and chaos in electrical breakdown in Ge 21 p3124 A83-43889
- Nonlinear electron oscillation driven by an external wave in a plasma 24 p3632 A83-49427
- ELECTRON PARAMAGNETIC RESONANCE**
- Luminescence fatigue and light-induced electron spin resonance in amorphous silicon-hydrogen alloys 04 p0541 A83-15514
- Radiation-induced paramagnetic defects in MOS structures 05 p0691 A83-17478
- An investigation of human blood, erythrocytes, and plasma using the method of ESR at 77 K 08 p1150 A83-23022
- An EPR study of the reaction between poly(p-phenylene sulfide) and electron-acceptor dopants 13 p1825 A83-30951
- Some consequences of a fracture criterion for oriented polymers based on electron spin resonance spectroscopy 21 p3156 A83-44889
- Analysis of the spin-Hamiltonian parameters for Cr(3+) in mirror and inversion symmetry sites of alexandrite (Al₂x/Cr₂x/BeO₄) - Determination of the relative site occupancy by EPR 23 p3461 A83-47630
- ELECTRON PATHS**
- U ELECTRON TRAJECTORIES**
- ELECTRON PHONON INTERACTIONS**
- Thermal and electrical conductivities of crystals in neutron stars and degenerate dwarfs 04 p0556 A83-15964
- Correlation of the electron spectra and temperatures of phase transformations in solid solutions based on barium titanate 13 p1930 A83-31305
- Diatom polymers, mixed-stack compounds, and the soliton lattice 16 p2420 A83-35749
- Free electron lasers [AIAA PAPER 83-1727] 17 p2513 A83-37213
- Effect of Coulomb interactions on the Peierls instability --- in one dimensional solids 19 p2903 A83-40957
- The bounded states of a one-dimensional relativistic polaron in a single-loop approximation 19 p2904 A83-40989
- ELECTRON PHOTON CASCADES**
- Interaction of the aluminum nucleus with an energy of approximately 1 TeV per nucleon in a photoemulsion 02 p0274 A83-11737
- Experimental studies of superfamily halos. IV --- in cosmic ray showers 02 p0274 A83-11744
- Characteristics of inelastic interactions with high transverse momenta of secondary particles 02 p0274 A83-11747
- The Samarkand EAS installation and experimental results 02 p0275 A83-11750
- Muons with energies greater than 1 GeV in the composition of extensive air showers 02 p0275 A83-11754
- Dependence of the mean characteristics of EAS components on the parameters of the elementary-act model 02 p0275 A83-11758
- The relative number of hadrons in an extensive air shower with the number of particles N = 10 to the 4th to 10 to the 6th 02 p0276 A83-11760
- The upper boundary of the energy spectrum of cosmic rays and possible methods for detecting cascades of superhigh energies /10 to the 20th-10 to the 28th eV/ 02 p0276 A83-11762
- Theory of electron-positron showers in double radio sources 02 p0255 A83-12111
- Distribution functions of the number of cascade electrons at various stages of the development of a shower in lead at high energies 06 p0858 A83-19347

- Radial electron distribution in an electromagnetic cascade in the atmosphere 06 p0858 A83-19348
- Certain features of electron-photon cascades in matter 06 p0858 A83-19349
- On the acoustic registration of cascades and single strongly ionized particles 06 p0764 A83-19350
- Polarisation correlations following electron impact on N₂ 11 p1655 A83-28221
- ELECTRON PLASMA**
- An experimental investigation of nonlinear dissipation of electromagnetic waves in inhomogeneous collisionless plasmas 01 p0107 A83-11297
- Nonlinear effects in the propagation of electron plasma waves in an inhomogeneous plasma layer 01 p0107 A83-11299
- A theoretical investigation of the distribution of electron concentration in the positive column of a glow discharge with a longitudinal flow of gas 02 p0240 A83-11514
- On the relationship of the plasmopause to the equatorward boundary of the auroral oval and to the inner edge of the plasma sheet 02 p0207 A83-12380
- Effect of background electron plasma waves on ion-beam neutralization 03 p0396 A83-13179
- Fast-particle production in a parametrically unstable electron plasma 03 p0397 A83-13191
- Kinetics of the isotropic expansion of a homogeneous electron-photon plasma 03 p0397 A83-13535
- Phenomenological model describing orificed, hollow cathode operation 04 p0454 A83-15276
- On the nature of S II emission from Jupiter's hot plasma torus 04 p0569 A83-45642
- Structure of the electron density profile in the vicinity of localized inhomogeneities in the case of ambipolar diffusion of magnetized recombining plasma 04 p0537 A83-15859
- Plasma fluctuations at critical density in a CO₂ laser plasma interaction 05 p0688 A83-17364
- The role of turbulence of the relativistic electron-positron plasma in generating in the prepulses of the Crab radio pulsar 06 p0830 A83-18781
- Vlasov-Maxwell and Vlasov-Poisson equations as models of a one-dimensional electron plasma 08 p1168 A83-22388
- Gain scaling of short-wavelength plasma-recombination lasers 08 p1110 A83-22636
- Holtzmark electric field distribution in a two-dimensional electron fluid 08 p1168 A83-22950
- Measurement of plasma conductivity using Faraday rotation of submillimeter waves 08 p1169 A83-23139
- Nonlinear wave and oscillation processes in extended electron beams 09 p1252 A83-23462
- Modulation of far-infrared radiation by electron-hole plasma in indium antimonide 10 p1488 A83-25456
- Waves in a cold pure electron plasma of finite length 10 p1485 A83-25785
- Effect of a transition between regular and stochastic electron motion on the evolution of an obliquely propagating Langmuir wave 10 p1485 A83-25787
- Direct- and cross-polarized scatter from a turbulent laboratory plasma 10 p1486 A83-26050
- Effects of trapped particles on strongly nonlinear electron plasma waves 11 p1659 A83-28229
- Some nonlinear mechanisms of pulsar emission 11 p1680 A83-28246
- Topics in strong Langmuir turbulence 11 p1660 A83-28450
- General solution of the Clemmow differential equation in a relativistic cold plasma 12 p1780 A83-29028
- Stability and application of an orbit-averaged magneto-inductive particle code 12 p1781 A83-29602
- Electron sub-cycling in particle simulation of plasma 12 p1782 A83-29625
- Quasineutral hybrid simulation of macroscopic plasma phenomena 12 p1782 A83-29634
- Electromagnetic instability of Langmuir waves in a magnetoplasma 13 p1944 A83-30113
- Magnetized-plasma turbulence 13 p1925 A83-30416
- Whistler-mode propagation at frequencies near the electron gyrofrequency 13 p1927 A83-31645
- Quasilinear evolution of current-driven ion-acoustic instability in a magnetic field 15 p2232 A83-33797
- A numerical method based on the Fourier-Fourier transform approach for modeling 1-D electron plasma evolution --- in earth bow shock region 15 p2233 A83-33823
- X-ray line ratios from helium-like ions - Updated theory and SMM flare observations 15 p2282 A83-34644
- Excitation of vibrational and electronic states in a glow discharge column in flowing N₂ 16 p2414 A83-35335
- Mechanism for the loss of fast electrons from a Penning glow discharge 16 p2418 A83-36940

- Approximations in magnetoionic theory 17 p2543 A83-38370
- Motion and radiation of electrons in an inhomogeneous magnetic field 18 p2744 A83-39005
- New method to measure plasma potential with emissive probes 18 p2688 A83-39091
- Gravitational radiation of plasmas - Bremsstrahlung 18 p2744 A83-39522
- Multiphoton absorption of the momentum of an electromagnetic wave in a plasma 18 p2744 A83-39523
- Electromagnetic waves in a relativistic one-dimensional plasma propagating along an external magnetic field 18 p2745 A83-39524
- Radiation spectrum of optically thin relativistic electron-positron plasma 18 p2774 A83-39734
- Mode coupling phenomena of Tonks-Dattner resonances in an asymmetrically inhomogeneous plasma column 18 p2747 A83-40072
- Strong turbulence of a magnetized plasma. I - The generalized Zakharov equations 18 p2747 A83-40073
- Effective proton-proton potential in hydrogen plasmas 18 p2747 A83-40413
- Creation of high-energy electron tails by means of the modified two-stream instability 18 p2747 A83-40496
- Reflection dissipation of an ion-acoustic soliton 18 p2748 A83-40505
- Oblique incidence of a strong electromagnetic wave on a cold inhomogeneous electron plasma - Relativistic effects 18 p2748 A83-40508
- Harmonic generation of radiation in a steep density profile 18 p2748 A83-40512
- Determination of the quadrupole moment of the electron distribution function in a plasma 20 p3049 A83-42277
- The formation of double-valued sheaths in thermionic converters 20 p3012 A83-42591
- Microscopic derivation of plasma electro-hydrodynamics 20 p3050 A83-43568
- Collision operator for a strongly magnetized pure electron plasma 21 p3209 A83-43936
- An electron cyclotron maser instability for astrophysical plasmas 21 p3227 A83-43944
- Generation of static magnetic fields by a test charge in a plasma with an electron temperature anisotropy 21 p3210 A83-44129
- Bremsstrahlung produced by electrons in a hot plasma 21 p3213 A83-44653
- Parametric and Raman wave processes in a magnetized plasma in the region of lower-hybrid electronic frequencies, excited by a high-frequency electric pumping field. I 23 p3510 A83-48393
- Line emission from charge transfer with atomic hydrogen at thermal energies 24 p3650 A83-48830
- Stark widths and shifts of singly ionized silicon spectral lines 24 p3631 A83-48836
- Propagation of oblique waves in a relativistic electron-positron plasma 24 p3653 A83-49174
- ELECTRON PRECIPITATION**
- Observation of guided ULF-waves correlated with auroral particle precipitation theoretically explained by negative landau damping 03 p0357 A83-13298
- The thermospheric heating efficiency under electron precipitation conditions 04 p0508 A83-14966
- Observations of inverted-V electron precipitation 04 p0510 A83-15824
- Space environment monitoring by low-altitude operational satellites 04 p0512 A83-16287
- Relationship between field-aligned currents, diffuse auroral precipitation and the westward electrojet in the early morning sector 05 p0661 A83-17397
- Quiet-time electron precipitation at L = 4 in the South Atlantic anomaly 06 p0783 A83-18293
- Quasi-relativistic electron precipitation due to interactions with coherent VLF waves in the magnetosphere 06 p0784 A83-18301
- Quantitative study of substorm-associated VLF phase anomalies and precipitating energetic electrons on November 13, 1979 07 p0966 A83-21513
- Characteristics of optical emissions and particle precipitation in polar cap arcs 08 p1137 A83-23112
- Controlled stimulation of magnetospheric electrons by radio waves Experimental model for lightning effects 09 p1309 A83-25288
- A planar energy spectrometer for the study of energy distributions of electron and proton fluxes 10 p1387 A83-25343
- The effect of precipitation on diagnostics for electron trap models of solar hard X-ray bursts 11 p1691 A83-27696
- On the ionization of the mid-latitude lower ionosphere by precipitating hard electrons 11 p1617 A83-28119
- Direct observation of radiation belt electrons precipitated by the controlled injection of VLF signals from a ground-based transmitter 12 p1800 A83-28922

Behavior of the energy spectrum in fast pulsations of
fluxes of precipitating electrons 13 p1875 A83-30613

Satellite and ground observations of a pre-substorm
phase on May 4, 1977 13 p1879 A83-31241

Auroral X-ray and luminosity pulsations and microbursts
measured during February 25, 1974 SAMBO-1 balloon
flight 13 p1883 A83-31718

Dynamic parameters of a magnetized flux of low-energy
electrons in the ionosphere 14 p2049 A83-31862

On the possibility that certain types of geomagnetic
pulsations have an ionospheric origin 14 p2050 A83-31869

Auger electrons in the auroral ionosphere 14 p2051 A83-31883

Power-line harmonic radiation and the electron slot 14 p2053 A83-32896

Satellite observations of power line harmonic radiation 14 p2053 A83-32897

Quantitative study of substorm-associated VLF phase
anomalies and precipitating energetic electrons 14 p2055 A83-33146

The apparent spectral broadening of VLF transmitter
signals during transionospheric propagation 15 p2195 A83-33935

Correlated irregular magnetic pulsations and optical
emissions observed at Siple Station, Antarctica 15 p2195 A83-33936

Evidence for beam-stimulated precipitation of high
energy electrons --- in magnetosphere 15 p2198 A83-34186

Intensity distribution of dayside polar soft electron
precipitation and the IMF 15 p2199 A83-34358

Joule heating and particle precipitation --- in auroral
upper atmosphere 16 p2372 A83-35360

Dynamics of the dayside aurora 16 p2373 A83-35365

Systematics of the equatorward diffuse auroral
boundary 17 p2538 A83-37595

Electron pitch-angle scattering by low frequency waves
at the geomagnetic equator 17 p2545 A83-38602

Pulsing hiss and associated phenomena - A
morphological study 18 p2712 A83-39066

Mechanism of the formation near the earth of a halo
of electrons with energies in the hundreds of MeV 18 p2713 A83-39313

Ground-based observations of subauroral
energetic-electron arcs 19 p2865 A83-41122

Ionospheric characteristics of a detached arc in the
evening-sector trough 19 p2865 A83-41123

Electron precipitation and related aeronomy of the
Jovian thermosphere and ionosphere 20 p3077 A83-42407

Electron energy deposition in the middle atmosphere 20 p3019 A83-42419

Neutral and ion gas heating by auroral electron
precipitation 20 p3019 A83-42421

Electron precipitation equatorward of the auroral oval
and the mantle aurora in the midday sector 20 p3023 A83-43161

Photometric evidence of electron precipitation induced
by first HOP whistlers 20 p3024 A83-43187

The modulated precipitation of radiation belt electrons
by controlled signals from VLF transmitters 20 p3024 A83-43188

Observations of VLF transmitter-induced depletions of
inner zone electrons 20 p3024 A83-43189

Energetic electron precipitation due to gyroresonant
interactions in the magnetosphere involving coherent VLF
waves with slowly varying frequency 22 p3326 A83-46042

Altitude and structure of an auroral arc acceleration
region 22 p3327 A83-46050

Spatial relationship of field-aligned currents, electron
precipitation, and plasma convection in the auroral oval 22 p3327 A83-46051

A quantitative description of the spatial distribution and
dynamics of the energy flux in the continuous aurora 22 p3327 A83-46053

A theoretical approach to the morphology and the
dynamics of diffuse auroral zones 22 p3327 A83-46054

Characteristics of the inverted-V events observed by the
Kyokko satellite --- auroral electron precipitation 22 p3330 A83-46510

Ionization by keV electron precipitation in the auroral
zone 22 p3331 A83-46517

Distribution of energy input due to auroral protons and
electrons 22 p3334 A83-46917

The shift of the auroral electron precipitation boundaries
in the dawn-dusk sector in association with geomagnetic
activity and interplanetary magnetic field 22 p3336 A83-47058

Evidence for the E x B drift of pulsating auroras 22 p3336 A83-47059

Narrow spectral peaks in electrons precipitating from
the slot region 22 p3337 A83-47073

Whistler induced charged particle precipitation and
distortion of geomagnetic field 22 p3337 A83-47074

Electron density and energetic particle precipitation
observed during the eclipse of 26 February 1979 23 p3480 A83-47466

Satellite observations of energetic electron precipitation
during the 1979 solar eclipse and comparisons with rocket
measurements 23 p3480 A83-47468

Steady-state model of the D-region during the February
1979 eclipse 23 p3481 A83-47472

The position of the ring current and variation of the fluxes
of precipitated electrons at mid-latitudes 23 p3484 A83-48388

ELECTRON PROBES

Assessment of the accuracy of electron-temperature
measurements by a high-frequency probe 10 p1386 A83-25340

Device for adaptive sweep in probe appliance for direct
determination of electron temperature --- of cosmic
plasma 14 p1982 A83-31817

Time-sharing measurements of ionospheric electron
temperature and electron density with the electric field
using double probes - An experiment on the Antarctic
sounding rocket S-310JA-7 22 p3331 A83-46518

ELECTRON PUMPING

Multikilowatt electron beams for pumping CW ion
lasers 01 p0039 A83-10987

Improved performance of the microwave-pumped XeCl
laser 02 p0184 A83-12266

The loss-cone driven electron-cyclotron maser 05 p0650 A83-17269

Kinetic studies of Kr2F/asterisk/ in electron-beam
excited mixtures 06 p0766 A83-18953

Electron-beam-pumped multicomponent semiconductor
laser emitting visible radiation 07 p0935 A83-20130

Calculation of the energy characteristics of a
pulse-periodic electron-beam-controlled CO2 laser with a
cooled active mixture 07 p0935 A83-20131

Production of electronically excited bismuth in a
supersonic flow 07 p0936 A83-20726

Studies of a glow discharge electron beam 07 p0997 A83-20733

Powerful electroionization laser on Xe infrared atomic
transitions 07 p0938 A83-21589

Characteristics of the electron beam pumped iodine
monofluoride laser 07 p0938 A83-21590

Theoretical analysis of electron-beam-excited KrF laser
performance - New F2 concentration optimization 07 p0938 A83-21599

Electron beam energy branching in a gas mixture 09 p1343 A83-23678

Stimulated emission of a magnetized intense electron
beam with a large thermal velocity spread 10 p1486 A83-25994

Supersonic flow e-beam stabilized discharge excimer
lasers 10 p1430 A83-26171

Pumping of a two-mirror resonator with rippled walls by
a relativistic electron beam 10 p1410 A83-26236

Pumping of gas lasers by runaway-electron beams 10 p1430 A83-26241

Use of epitaxial ZnSe films, grown from organoelemental
compounds, in electron-beam-pumped lasers 10 p1432 A83-26673

Semiconductor lasers 11 p1576 A83-27502

Tuning characteristics of broadband excimer lasers 11 p1576 A83-27503

XeF laser beam quality impact of pump-induced medium
inhomogeneities 11 p1576 A83-27505

Suprathermal electron pumping of X-ray lasers 11 p1577 A83-27521

High performance DF-CO2 chain-reaction laser 11 p1579 A83-27572

Xe Cl laser pumped by an intense short-pulse electron
beam 11 p1582 A83-27611

High-power-density electron-beam-sustained laser 13 p1849 A83-30256

Theoretical evaluation of the rare-gas diluent effects for
an electron-beam-excited XeCl laser 13 p1852 A83-31055

Kinetic theory of a free-electron laser amplifier with guide
magnetic field 13 p1853 A83-31113

Short wavelength laser calculations for electron pumping
in neon-like krypton (Kr XXVII) 13 p1857 A83-31377

Investigation of CW operation of a GaAs laser pumped
by an electron beam 14 p2022 A83-31906

Laser cathode ray tube with a semiconductor
double-heterostructure screen 15 p2163 A83-33921

Stimulated emission from a magnetized intense electron
beam in conditions of cyclotron resonance of the pumping
wave 15 p2170 A83-35164

Kinetics of formation of krypton-halogen atom exciplexes
in electron beam irradiated gases 16 p2358 A83-35436

Optimization of electrically excited XeF(C yields A) laser
performance 16 p2361 A83-36770

The energy of thermal electrons in electron beam
created helium discharges 17 p2583 A83-38965

A compact CW HCN gas laser with RF-excited
discharge 19 p2852 A83-40946

Xenon laser action in discharge and electron-beam
excited Ar-Xe mixture 19 p2853 A83-41183

XeCl excimer laser excited by longitudinal discharge 20 p2995 A83-43597

A selfsustained discharge multiatmospheric CO2 laser
with electron-beam preionization 20 p2995 A83-43633

Investigation of the optical homogeneity of the active
medium of an atmospheric-pressure
electron-beam-controlled CO2 laser during stimulated
emission 20 p2997 A83-43792

Laser action in xenon pumped by pulsed beams of
runaway electrons 20 p2997 A83-43800

Gain on the green (504 nm) excimer band of I2 22 p3299 A83-46726

Estimated lifetime of an He-Ne microwave-pumped laser
using a spectroscopic method 23 p3460 A83-47558

ELECTRON RADIATION

NT BETA PARTICLES

NT ELECTRON BEAMS

NT RELATIVISTIC ELECTRON BEAMS

Space radiation effects on structural composites
[AIAA PAPER 83-0591] 05 p0610 A83-16808

Total dose susceptibility of the SBP 9989

Microprocessor 05 p0628 A83-17519

The kinematics of cyclotron emission for quantized
electrons --- in super-strong stellar magnetic fields 13 p1944 A83-30361

Optical pulse evolution in the Stanford free-electron laser
and in a tapered wiggler 13 p1854 A83-31117

Absorption coefficient of electron cyclotron radiation in
a plasma in the temperature range 5-20 keV 16 p2416 A83-35891

Radiation from a random train of electron bunches 16 p2417 A83-36933

Measurement and simulation
of GaAs FET's under
electron-beam irradiation 20 p2968 A83-43357

ELECTRON RECOMBINATION

NT RADIATIVE RECOMBINATION

Photoconductivity kinetics in Cd/x/Hg/1-x/Te crystals
under surface excitation 01 p0108 A83-10374

Static and transient behavior of pin-diodes at high
injection levels --- German thesis 01 p0036 A83-10474

The origin of the infrared /C I/ emission - H II or H I
regions 01 p0125 A83-10926

Exactly soluble model for a solar cell with nonlinear
recombination 02 p0201 A83-11811

Dissociative recombination of electrons and molecular
ions 02 p0234 A83-12175

Influence of electron heating during recombination of
copper atoms in copper halide vapor lasers on their output
parameters 05 p0650 A83-17068

Electroabsorption produced mixed injection and its effect
on the determination of ionization coefficients --- in low
noise avalanche photodiodes 05 p0691 A83-17769

The importance of the excitation volume in determination
of surface recombination velocity 06 p0814 A83-18755

Features of the formation of the recombination
properties of InSb-base MOS structures 09 p1349 A83-24210

Theory of dissociative recombination 10 p1479 A83-25991

Metal vapor recombination laser research 11 p1583 A83-27618

Photovoltage decay in p-n junction solar cells including
the effects of recombinations in the emitter 11 p1664 A83-28716

The dissociative recombination of O2(+) - The quantum
yield of O(1S) and O(1D) 13 p1916 A83-31248

Limitations of the open circuit voltage of induced junction
silicon solar cells due to surface recombination 14 p2042 A83-32267

Determination of minority carrier lifetime and effective
back surface recombination velocity in BSF silicon solar
cells from transient measurements 15 p2191 A83-34515

Minority carrier recombination in heavily-doped silicon 16 p2419 A83-35673

Carrier recombination at grain boundaries and the
effective recombination velocity 16 p2419 A83-35674

The interpretation of photoconductivity measurements
in hydrogenated amorphous silicon 18 p2750 A83-39471

InP surface states and reduced surface recombination
velocity 18 p2750 A83-40061

Oxygen-induced recombination centers in as-grown
Czochralski silicon crystals 19 p2903 A83-40739

- Observation of spin-dependent thermal emission from deep levels in semiconductors 19 p2904 A83-40970
 Dielectronic recombination 21 p3213 A83-44654
 The significance of interference effects in thin film Cu2S/CdS solar cells 23 p3478 A83-48619
 Population inversion in copper on transitions with wavelengths of 510.6 and 578.2 nm in a recombining Cu-Cs plasma 24 p3588 A83-49114
 Some recent results from UV observations 24 p3639 A83-49136
 Dielectronic recombination at low temperatures --- in gaseous nebulae 24 p3668 A83-50086

ELECTRON RING ACCELERATORS

U STORAGE RINGS (PARTICLE ACCELERATORS)

ELECTRON RUNAWAY (PLASMA PHYSICS)

- Stability of an astrophysical plasma near the onset of electron runaway 13 p1954 A83-31648
 Electron distribution functions in a current sheet 18 p2749 A83-40518
 Anomalous resistivity due to low-frequency turbulence --- of collisionless plasma with limited acceleration of high velocity runaway electrons 22 p3336 A83-47061

ELECTRON SCATTERING

NT CONFIGURATION INTERACTION

NT ELECTRON RUNAWAY (PLASMA PHYSICS)

- Electron loss from fast one-electron ions colliding with He, N2, and Ar 01 p0105 A83-10194
 Rotational excitation of N2, CO and H2O by low-energy electron collisions 01 p0105 A83-10858
 Using small extensive air showers where the number of electrons is greater than about 10,000 on mountains for calibrating an interaction model 02 p0276 A83-11759

- Investigation of the anisotropy of ionospheric inhomogeneities by the differential-phase method 02 p0209 A83-12426
 Oscillation of cyclotron-echo signals in a plasma 03 p0396 A83-13182

- Electron impact cross sections for the 2,2P state excitation of lithium 03 p0391 A83-13225
 Scattering of a neutrino by an electron in a magnetic field 03 p0392 A83-13531
 Electron collision strengths for the far-infrared lines of O III --- in Milky Way Galaxy 03 p0419 A83-13933
 A laser-based measurement of electron collision rates for excited states of ionised helium in a plasma 03 p0398 A83-14662

- Coulomb interactions in Anderson localized disordered systems 04 p0540 A83-15508
 The dissociative recombination of an electron and a molecular ion 05 p0686 A83-16887

- The stochastic behavior of electrons in free electron lasers with variable parameter wigglers 05 p0650 A83-17145
 Low-energy electron scattering from CO, III - Analytic method for outer region in frame-transformation theory 06 p0808 A83-18045

- A new approach to pitch angle scattering in the magnetosphere [AD-A125207] 06 p0783 A83-18294
 Comparison of calculated and measured values of electron fluxes for the wide-angle detector in the ARAKS experiment --- on ionospheric electron beam injection 06 p0786 A83-18368

- Modulation depth in the scattering spectra for a plasma in a magnetic field 06 p0811 A83-18447
 Elastic and inelastic scattering of electrons by atomic hydrogen at intermediate energies in a coupled-channel second-order potential model 06 p0808 A83-19008

- Stimulated bremsstrahlung effect in multimode laser radiation field 07 p0934 A83-20120
 Diffuse electron scattering in the Ti50Ni46Nb4 alloy in the X-phase preprecipitation stage 07 p0889 A83-20860

- Quantum transport in a single layered structure for impurity scattering 07 p1000 A83-21372
 Electron scattering by nitrogen molecules at intermediate energies 08 p1163 A83-23020

- Electron kinetic equations for Comptonization by isotropic photons --- in stellar magnetic fields 08 p1184 A83-23067
 Collective single-beam effects in electron-positron storage rings 09 p1343 A83-23398

- Nonlinear analysis of a diffraction-radiation generator with two field spots 09 p1270 A83-23472
 The scattering of escaping electrons by helicon oscillations in a weakly magnetized plasma --- in ionosphere and magnetosphere 09 p1301 A83-23479

- Electron collision strengths for transitions within the 1s/2/2s/2/2p/2/ configuration of Si IX 09 p1347 A83-23653
 Conference on Atomic and Molecular Reactions and Structure, Flinders University of South Australia, Bedford Park, Australia, February 1982, Proceedings 09 p1342 A83-24142

- A new class of atomic states - The 'Wannier-ridge' resonances 09 p1342 A83-24143

- Angular and energy distribution of photons of the radiative scattering of a neutrino /antineutrino/ by an electron 09 p1344 A83-24205

- Electron scattering from the nitrogen molecule 09 p1343 A83-24824
 Threshold structures in the cross sections of low-energy electron scattering of methane 09 p1343 A83-24825

- Elastic scattering of electrons by N2, O2, and CO in the energy range 0.1-3 keV 10 p1479 A83-25557
 Efficiency of free-electron lasers with a scattered electron beam 10 p1426 A83-25791

- Electron impact excitation of SO2 - Differential, integral, and momentum transfer cross sections 10 p1480 A83-26456
 Polarisation correlations following electron impact on N2 11 p1655 A83-28221

- Numerically simulated two-dimensional auroral double layers 11 p1618 A83-28314
 Study on the onsets of solar energetic electron events 11 p1692 A83-28579

- Atomic calculations for the Fe XX X-ray lines 12 p1799 A83-28872
 Resonant and nonresonant electron scattering in an inhomogeneous laser field 12 p1732 A83-29246

- Hydrogen and lithium atoms in a strong electric field 13 p1915 A83-30266
 Electron impact excitation of methane 13 p1916 A83-30955

- Non-Maxwellian electrons in a laser produced sodium plasma 13 p1926 A83-31061
 AsF5-doped polyparaphenylene - Evidence for polaron and bipolaron formation 13 p1931 A83-31359

- The bremsstrahlung of a slow electron at a Coulomb center in an external electromagnetic field 14 p2079 A83-32139
 Electron scattering and absorption-line formation in type II supernova atmospheres 15 p2254 A83-33717

- Electron energy distribution produced by beam-plasma discharge 15 p2234 A83-34196
 Generation of ultra-violet oxygen emissions with wavelengths of 1304 and 1356 Å by electron collision and some aeronomic consequences 15 p2200 A83-34416

- Relation between the free-free and scattering cross sections and 'two-state resonances' in bremsstrahlung 16 p2408 A83-35329
 Elastic and inelastic scattering of high-energy electrons and X-rays by NH3, CH4 and H2O molecules 16 p2409 A83-35333

- Electrons in an ultrastrong magnetic field 16 p2411 A83-35595
 Elastic scattering of electrons by hydrogen atoms in the 2S state 16 p2410 A83-35654

- Electron thermalization in gas mixtures 16 p2410 A83-35667
 An analysis of the asymmetric part of electron-electron Boltzmann integral 17 p2583 A83-38208

- Laser-modified electron scattering from a slowly ionising atom 17 p2579 A83-38366
 Collision frequencies in the high-latitude D-region 17 p2544 A83-38375

- Non-linear phenomena in the ionosphere traversed by high power radio wave 17 p2495 A83-38541
 Electron pitch-angle scattering by low frequency waves at the geomagnetic equator 17 p2545 A83-38602

- Multiphoton absorption of the momentum of an electromagnetic wave in a plasma 18 p2744 A83-39523
 Investigation of superelastic electron scattering by laser-excited Ba - Experimental procedures and results 18 p2743 A83-40407

- Intrinsic polarization of a precessing, electron-scattering accretion disk, with applications to SS 433 18 p2777 A83-40476
 Impurity scattering in partially dielectricized superconductors 19 p2904 A83-41000

- Calculation of the polarization potential for e-N2 collisions 19 p2898 A83-41193
 Dissociative recombination in low-energy e-H2(+) collisions 19 p2898 A83-41194

- Elastic and rotational excitation of the oxygen molecule by intermediate-energy electrons 19 p2898 A83-41196
 Momentum transfer cross sections for the low-energy electron scattering by NH3 molecules 19 p2898 A83-41293

- A search for the Sunyaev-Zel'dovich effect at millimeter wavelengths --- cosmic background photon energy increase due to Compton scattering by high temperature galactic cluster plasma electrons 20 p3082 A83-42467

- State-to-state differential and integral cross sections for vibrational-rotational excitation and elastic scattering of electrons by N2 at 5-50 eV - Calculations using extended-basis-set Hartree-Fock wave functions 20 p3045 A83-42634
 Resonant electron scattering by metastable nitrogen --- in earth thermosphere 20 p3023 A83-43154

- PD 1 pearl-electron interactions on the L = 4.2 magnetic shell 20 p3024 A83-43191
 Scattering and precipitation of particles of the magnetotail under the action of the dawn-dusk electric field 21 p3172 A83-44522

- Shifts of hydrogen lines from electron collisions in dense plasmas 22 p3661 A83-45931
 Angular distribution of electrons elastically scattered from O2 at 40-500 eV - A two-potential coherent approach 22 p3355 A83-45941

- Collisional modification to the exospheric theory of solar wind halo electron pitch angle distributions 22 p3388 A83-46027
 Nonlinear absorption of electromagnetic radiation during collisions of particles in a strong magnetic field 23 p3509 A83-47552

- Onefold photoelectron-counting statistics for non-Gaussian light - Scattering from an arbitrary number of weak scatterers 23 p3508 A83-47582
 Rotational excitation of CH4 and H2O by slow electron impact 23 p3506 A83-48582

- Estimation of alloy scattering potential in ternaries from the study of two-dimensional electron transport 24 p3634 A83-48794
 Nonequilibrium electron velocity distribution and temperature in thermalization of low-energy electrons in molecular hydrogen 24 p3625 A83-48798

- Plasma electron density measurements by the laser- and collision-induced fluorescence method 24 p3631 A83-48819
 Resonance and intermediate-coupling effects in electron scattering with highly charged ions. I - Collision strengths for Fe(24+), Se(32+), and Mo(40+). II - Autoionization and dielectronic recombination 24 p3631 A83-48829

- Elastic scattering of electrons by the 2s state of atomic hydrogen at intermediate energies 24 p3626 A83-48846
 Ca XVII line ratios in solar flares 24 p3674 A83-49356

- Scattering and backscattering of 1 MeV electrons [ONERA, TP NO. 1983-87] 24 p3627 A83-49406
 Elastic scattering of electrons by hydrogen atoms in a laser field 24 p3626 A83-49432

- Measurement of differential cross sections of low-energy electrons elastically scattered by gaseous molecules. IV Effect of intramolecular double scattering as observed in the scattering of 100 and 500 eV electrons by As4 24 p3626 A83-49433
 Bound states of electrons in a light field 24 p3589 A83-49744

- Electron SOURCES
 Phenomenological model describing orificed, hollow cathode operation 04 p0454 A83-15276
 Radial isolated Blumlein electron beam generator 20 p3045 A83-42293

- ELECTRON SPECTROSCOPY
 Secondary electron spectra in interstellar clouds, and the bremsstrahlung gamma-ray luminosity 03 p0439 A83-14211
 Study of MIS silicon solar cells by ESCA and AES 04 p0539 A83-15489

- Electron energy-loss studies of molecular oxygen in the region 14.8-20.3 eV using a multidetector electron spectrometer 06 p0808 A83-19009
 Spectrometer for momentum-resolved bremsstrahlung spectroscopy 06 p0764 A83-19232

- Electron coincidence spectroscopy - An introduction to momentum space chemistry 09 p1342 A83-24144
 Diamond /111/ studied by electron energy loss spectroscopy in the characteristic loss region 10 p1390 A83-25675

- Transmission electron spectroscopic observation of tungsten hemiacarbon - A study of dislocation structures after high temperature plastic deformation --- French thesis 11 p1551 A83-28626
 Inelastic electron tunneling spectroscopy 16 p2420 A83-36015

- Observation of a new electronic state of carbon monoxide using LIF on highly vibrationally excited CO(X 1Sigma+) 16 p2410 A83-36517
 Single-particle tunneling in the structures metal-insulator-metal (Review) 19 p2905 A83-42070

- Some consequences of a fracture criterion for oriented polymers based on electron spin resonance spectroscopy 21 p3156 A83-44889
 Dependence of auroral FUV emissions on the incidence electron spectrum and neutral atmosphere 22 p3337 A83-47067

ELECTRON SPIN

Effective collision strengths for electron excitation of the ground state of O VII to the 2/3/S and 2/3/P states
09 p1347 A83-23652
Spin-polarized atomic nitrogen and the 7Sigma + u state of N2
10 p1479 A83-25558
Vacuum annealing effects in lithium niobate
12 p1782 A83-29170
Observation of spin-dependent thermal emission from deep levels in semiconductors
19 p2904 A83-40970
Second order perturbation theory for the hydrogen atom in crossed electric and magnetic fields
21 p3202 A83-45206

ELECTRON SPIN RESONANCE

U ELECTRON PARAMAGNETIC RESONANCE

ELECTRON STATES

Electron impact cross sections for the 2,2P state excitation of lithium
03 p0391 A83-13225
Production of neutrino pairs in a strong magnetic field
03 p0392 A83-13532
A laser-based measurement of electron collision rates for excited states of ionised helium in a plasma
03 p0398 A83-14662
The population of localized states and the photoconductivity of disordered systems
04 p0542 A83-15920
NO2A2B2 state properties from Zeeman quantum beats
05 p0684 A83-17652
Theoretical study of NH2 - Potential curves, transition moments, and photodissociation cross sections
05 p0684 A83-17655
2P/0/- resonances in He/-/
06 p0808 A83-19004
Methanol in Orion A - Simultaneous observations of corresponding rotational transitions in the ground and torsionally excited states
06 p0844 A83-19495
An investigation of the distributions of the equilibrium charge states in carbon, the emission spectroscopy and the mean radiative lifetimes of aluminum ions /Al VI-X/
08 p1163 A83-21986
Measurement of the 1s2p2p-prime 4Pe resonance in He/-/ photodetachment
08 p1163 A83-22644
Unimolecular reaction paths of electronically excited species. IV - The C(tilde) 2Sigma plus g state of CO2/plus/
08 p1163 A83-22999
Cross sections for electron impact excitation of the low-lying electron states of CO2
08 p1163 A83-23021
Intersystem collisional transfer of excitation in low altitude aurora
10 p1448 A83-25553
Excitation of the O2/a 1Delta g/ state by low energy electrons in O2-N2 mixtures
10 p1478 A83-25554
Spin-polarized atomic nitrogen and the 7Sigma + u state of N2
10 p1479 A83-25558
Interactions between neutral dissociation and ionization continua in N2O
10 p1479 A83-25560
The state distribution of OH radicals photodissociated from H2O2 at 193 and 248 nm
10 p1389 A83-25562
Theory of dissociative recombination
10 p1479 A83-25991
The uranyl ion, fluorescent and fluorine-like - A review
10 p1390 A83-26061
Microwave ionization of Na Rydberg levels
10 p1480 A83-26273
State-selective spectroscopy in a molecular nitrogen discharge by use of optogalvanic double-resonance spectroscopy
10 p1487 A83-26274
Quantum dynamics of the van der Waals molecule /N2/2 - An ab initio treatment
10 p1480 A83-26460
Determination of accurate dissociation limits and interatomic interactions at large internuclear distances
11 p1653 A83-27526
State-selective electron capture by N/2+/- ions in atomic hydrogen using collision spectroscopy
11 p1654 A83-28220
The low-lying 2-sigma-minus states of OH
11 p1655 A83-28528
CASSCF/CI calculations for first row transition metal hydrides - The TiH(4-phi), VH(5-delta), CrH(6-sigma-plus), MnH(7-sigma-plus), FeH(4,6-delta) and NiH(2-delta) states
11 p1655 A83-28530
Inclusion of discrete-to-continuum coupling in multiphoton excitation and dissociation calculations
11 p1546 A83-28758
Fractional quantum numbers in solids
13 p1930 A83-31164
Transport properties for the nitrogen system - N2, N, N(+) and E
14 p2094 A83-32728
Photoelectron spectroscopy of HNO(-) and DNO(-)
14 p1991 A83-33101
Role of solitons in nearly metallic polyacetylene
15 p2238 A83-33898
Observation of a new electronic state of carbon monoxide using LIF on highly vibrationally excited CO(X 1Sigma +)
16 p2410 A83-36517

On a classification of one-dimensional conductors
17 p2585 A83-38966
Atomic carbon in Orion
18 p2772 A83-39705
Cross sections for electron-impact excitation of the electronic states of N2
19 p2898 A83-41195
The unitary group and the electron correlation problem
19 p2899 A83-41872
Observation of proton and electron detachment from an anthracene molecule during pronounced IR many-photon superexcitation
20 p3044 A83-42274
Kinks and polarons in polyacetylene
20 p3053 A83-42640
Effect of potential fluctuations in a plasma on the population of highly excited atomic states
21 p3211 A83-44145
Comments on the Planck-Larkin partition function --- for solar model calculations
21 p3244 A83-45573
Double electron excitation in heliumlike ions
22 p3354 A83-45940
OH(X2II) state distribution from HNO3 and H2O2 photodissociation at 193 nm
23 p3429 A83-47639
Theoretical evidence for multiple one-electron 3d bonding in a first row transition metal dimer - The 5 Sigma u -state of Sc2
24 p3625 A83-48799
Approximate solution of the strongly magnetized hydrogenic problem with the use of an asymptotic property --- application to stellar magnetic fields
24 p3650 A83-48828
Occupation of quasi-bound states by electrons in a Schwarzschild field
24 p3651 A83-49066
The metal-insulator transition in transition-metal compounds
24 p3635 A83-49074
ELECTRON SWEEPING
U SWEEP FREQUENCY
ELECTRON TELESCOPES
U PARTICLE TELESCOPES
ELECTRON TEMPERATURE
U ELECTRON ENERGY
ELECTRON TRAJECTORIES
Theory of ion acceleration with closed electron drift [AIAA PAPER 82-1919]
02 p0241 A83-12490
Ballistic transport in semiconductors
05 p0690 A83-17286
The motion and radiation of electrons in a neutral sheet
05 p0689 A83-17813
Stochasticity in plasmas with electromagnetic waves
06 p0812 A83-18918
Modern multistage depressed collectors - A review
09 p1254 A83-24025
Ballistic transport and velocity overshoot in semiconductors. I - Uniform field effects
09 p1350 A83-24498
Three-dimensional propagation in free-electron laser amplifiers
10 p1427 A83-26C06
Three-dimensional theory of free electron lasers with an axial guide field
10 p1427 A83-26B10
Approximate method for calculating the characteristics of a magnetron at frequencies above the higher temporal harmonics
13 p1833 A83-30704
Theoretical analysis of the possibilities of an open-cavity klystron
13 p1833 A83-30710
Relationship of FEL physics to accelerator physics --- Free Electron Laser
13 p1852 A83-31102
Optical klystron spontaneous emission and gain --- as undulator for free electron laser
13 p1852 A83-31106
The effect of an axial guide field on free-electron lasers
13 p1855 A83-31130
Intense electromagnetic radiation from relativistic particles
15 p2228 A83-33786
Spontaneous radiation from relativistic electrons in a tapered undulator
18 p2743 A83-40410
Characteristics of the inverted-V events observed by the Kyokko satellite --- auroral electron precipitation
22 p3330 A83-46510
ELECTRON TRANSFER
Projected temperature dependence of quantum yields for photoreactions involving energy or electron transfer
06 p0780 A83-18559
Nonlinear optical studies of picosecond relaxation times of electrons in n-GaAs and n-GaSb
06 p0814 A83-19260
A kinetic model of the electron and conformational transitions in the photosynthetic reaction centers of purple bacteria
07 p0974 A83-20966
Transferred-electron effect in In/0.53/Ga/0.47/As
11 p1663 A83-28601
Approximate nonlinear theory of an orotron
13 p1833 A83-30711
Visible light induced cleavage of water into hydrogen and oxygen in colloidal and microheterogeneous systems
15 p2131 A83-33862
Photoelectrochemical energy conversion involving transition metal d-states and intercalation of layer compounds
15 p2131 A83-33863

Investigation of the effect of the increase of the maximum generation frequency of Gunn diodes
15 p2154 A83-35174
Controlling the duration of photosynthetic charge separation with microwave radiation
16 p2394 A83-35998

ELECTRON TRANSITIONS

N I isoelectronic sequence - Observations of 2s/m/2p/n/-2s/m-1/2p/n+1/- intersystem transitions and improved measurements for Cl XI, K XIII, Ca XIV, Sc XV, Ti XVI, and V XVII
01 p0105 A83-10196
C I isoelectronic sequence - Observations of 2s/m/2p/n/-2s/m-1/2p/n+1/- intersystem transitions and improved measurements for Cl XII, K XIV, Ca XV, Sc XVI, Ti XVII, and V XVIII
01 p0105 A83-10198
B-X transitions in HgCl and Hgl --- for high power UV-visible lasers
01 p0055 A83-10980
Iron diiodide photodissociation laser
02 p0184 A83-12265
Transitions in highly ionized silicon --- of extreme ultraviolet solar spectrum
02 p0270 A83-12582
Measurement of relative oscillator strengths for Fe I: Transitions from levels /b-3/-F/2-4/ /2.61 eV-2.56 eV/ - Use of a multipass optical system
03 p0413 A83-13318
Precision measurement of relative oscillator strengths for Ti II, I - Transitions from levels /a-4/-F/3/2-9/2/ /0.00-0.05 eV/, /b-4/-F/5/2-9/2/ /0.12-0.15 eV/
03 p0413 A83-13319
Precision measurement of relative oscillator strengths for Ti I, II - Transitions from levels /a-5/-F/1-4/ /0.81-0.84 eV/, /a-1/-D/2/ /0.90 eV/ and /a-3/-P/0-2/ /1.5-1.07 eV/
03 p0413 A83-13320
Cyclotron emission in strongly magnetized plasmas
03 p0429 A83-14795
Electron densities from the semiforbidden O IV lambda 1401 multiplet
03 p0430 A83-14809
Coulomb interactions in Anderson localized disordered systems
04 p0540 A83-15508
On the systematics of line ratios along the helium isoelectronic sequence
04 p0554 A83-15645
Magnetic quadrupole transitions in the beryllium isoelectronic sequence
04 p0537 A83-15954
Gain, saturation, and optimization of the XeF discharge laser
04 p0485 A83-16057
Detection of H/C-17/O plus in Sagittarius B2
05 p0700 A83-17034
Methods for spectral selection in the region of the 2P/1/2-2P/3/2/ transition in an iodine atom under conditions of lasing in a Zeeman inhomogeneous gain profile
05 p0648 A83-17041
CO J = 3 - 2 and submillimetre continuum observations of two molecular outflow sources
06 p0825 A83-18091
A search for the J = 1-0 transition of /C-14/O --- and Galactic abundance ratios for carbon isotopes
06 p0827 A83-18174
Methanol in Orion A - Simultaneous observations of corresponding rotational transitions in the ground and torsionally excited states
06 p0844 A83-19495
SiO isotopic maser emission from VY Canis Majoris
06 p0824 A83-19527
Nonadiabatic transitions in a three-level system subjected to a laser radiation field with a smoothly varying frequency
07 p0934 A83-20109
Curves for analysis of the two lowest rotational transitions of carbon monoxide using the large velocity gradient radiative transfer model
07 p1013 A83-20133
Rotational and vibrational spectra of ethynol from quantum-mechanical calculations
07 p0874 A83-21060
Collisional rates for vibrational-rotational transitions in circumstellar SiO masers
07 p1023 A83-21159
Optically pumped ring laser oscillation to vibrational levels near dissociation and to the continuum in Na2
07 p0937 A83-21366
Doppler-free polarization spectroscopy of diatomic molecules in flame reactions
08 p1056 A83-21884
Carbon monoxide in the Martian atmosphere
08 p1188 A83-22059
Generation of holes during the disintegration of dislocations and mechanoluminescence of metals
08 p1170 A83-22781
Inner-shell transitions in Fe XIX-XXII in the X-ray spectra of solar flares and Tokamaks
08 p1192 A83-23075
Effective collision strengths for electron excitation of the ground state of O VII to the 2/3/S and 2/3/P states
09 p1347 A83-23652
Electron collision strengths for transitions within the 1s/2/2s/2/2p/2/ configuration of Si IX
09 p1347 A83-23653
5s/2/5p/4/-5s5p/5/ transitions in Cs IV, Ba V, and La VI
09 p1342 A83-24095
K-alpha and K-beta spectra from M-shell-ionized ions produced in a vacuum spark
10 p1485 A83-25410

Elastic scattering of electrons by N₂, O₂, and CO in the energy range 0.1-3 keV 10 p1479 A83-25557
 Rydberg-Rydberg transitions of NO using an optical-optical double resonance multiphoton ionization technique 10 p1479 A83-25559
 J = 2-1 CO observations of molecular clouds with high-velocity gas - Evidence for clumpy outflows 10 p1504 A83-25728
 The prospects of an X-ray free electron laser using stimulated resonance transition radiation 10 p1427 A83-26015
 Inversion of lithium-like ions with respect to the 2p state in a recombining plasma 10 p1432 A83-26666
 Detection of the J = 1 - 0 transition of CH₃CN 10 p1516 A83-26757
 High orbital angular momentum states in H₂ and D₂ 11 p1653 A83-27491
 Tuning characteristics of broadband excimer lasers 11 p1576 A83-27503
 Kinetics of the triatomic Xe₂Cl/asterisk/-laser 11 p1576 A83-27504
 Evidence of population inversion in Li-like aluminum ions in a laser produced plasma 11 p1577 A83-27522
 Calculation of radiative transition probabilities and lifetimes 11 p1653 A83-27527
 Advances in divalent transition-metal lasers 11 p1578 A83-27541
 Wigner approach to laser-induced molecular collisions 11 p1579 A83-27551
 S II and S III branching ratios in the 600- to 1200-A interval --- applied to modeling of Io plasma torus 11 p1619 A83-28327
 The low-lying 2-sigma-minus states of OH 11 p1655 A83-28528
 Arc measurements of FeII transition probabilities 12 p1789 A83-28863
 Atomic calculations for Ca XVII - UV and X-ray lines 12 p1799 A83-28866
 CW ultraviolet saturation spectroscopy of the 6p 3P0-9s 3S1 transition in Mercury at 246.5 nm 12 p1778 A83-29191
 Relative intensity changes of L3MM Auger transitions in maximal-valent V and Cr compounds under ion bombardment 12 p1778 A83-29543
 Observations of the 1-0 transition of CO towards southern HII regions 13 p1946 A83-30387
 Angular distribution for electron excitation of the 4(2)S yields 4(2)P transition in Zn II - Comparison of experiment and theory 13 p1926 A83-30917
 Laboratory measurement of the 4(04)-(3)13 70 GHz transition of ground-state methylene (CH₂) 13 p1916 A83-31453
 Anti-Stokes scattering as an XUV radiation source --- for spectroscopy 13 p1818 A83-31810
 Frequency-angular diffusion of intense quasisonant radiation 14 p2024 A83-32617
 Photoionization Raman spectroscopy 14 p2082 A83-32620
 Fine-structure transitions occurring in collisional redistribution of light 15 p2227 A83-33795
 Efficient lasing of a TEA Co₂ laser with ultraviolet preionization and utilizing unconventional transitions 15 p2168 A83-33977
 Multiphoton ionization of nitrogen dioxide - Four photon spectroscopy of the np sigma(u) Rydberg series 15 p2227 A83-34013
 Sidebands in cooperative resonance fluorescence in collections of N three-level atoms in strong excitation laser fields 15 p2169 A83-34371
 Observations of NH₃ and H₂O in the Pelican Nebula hotspot 15 p2265 A83-34595
 Improved Ar(III) transition probabilities 15 p2236 A83-34993
 Stark shift trends in homologous ions 16 p2414 A83-35327
 Electron impact excitation from a 1 Delta g state of molecular oxygen 16 p2408 A83-35330
 Multi-charged ion spectroscopy 16 p2414 A83-35629
 Proton excitation of fine-structure transitions in Fe XIV 16 p2410 A83-35652
 Radiationless transitions to atomic M 1,2,3 shells - Results of relativistic theory 16 p2410 A83-35656
 Transition probability of the Si III 189.2-nm intersystem line 16 p2427 A83-35657
 Photoexcitations in trans-(CH)_x - A Fourier-transform infrared study 16 p2420 A83-35748
 Synthetic nonlinear semiconductors 16 p2420 A83-35957
 Observation of a new electronic state of carbon monoxide using LIF on highly vibrationally excited CO(X 1Sigma +) 16 p2410 A83-36517
 Discrete variable theory of triatomic photodissociation 16 p2327 A83-36519
 Laser-modified electron scattering from a slowly ionising atom 17 p2579 A83-38366

Positron and electron channeling radiation from germanium 17 p2585 A83-38955
 Photovoltaic energy converters 18 p2709 A83-40525
 Proposal for high-power radiative-collisional lasers [AD-A122225] 19 p2850 A83-40671
 Photoionization of atoms near threshold 19 p2898 A83-41179
 Laboratory measurement of the J = 2 goes to 3 rotational transition frequency of H(C-17)O(+) 19 p2898 A83-41658
 Dephasing in steady-state and time-varying spectroscopy 20 p3044 A83-42264
 Laser action in xenon pumped by pulsed beams of runaway electrons 20 p2997 A83-43800
 Nascent NO vibrational distribution from 2485 A NO₂ photodissociation 21 p3201 A83-43959
 Interatomic Auger transitions in maximal valent V and Cr compounds 21 p3109 A83-44618
 Correlation and the 3s2 3p5 2P0 to 3s 3p6 2S, 3s2 3p5 2P0 to 3s2 3p4 3d2S transitions in Fe X 21 p3202 A83-44749
 The detection of vinyl cyanide in TMC-1 21 p3236 A83-45541
 Probabilities for transition processes crucial to Li lasers 22 p3295 A83-45945
 Collisional broadening of nonlinear optical resonances 22 p3355 A83-46713
 Nonequilibrium kinetics of coupled photons and electrons in two-level systems of the laser type 23 p3460 A83-47586
 General consideration of electronic transitions in many-electron atoms and ions 23 p3506 A83-48577
 Electron excitation of Ca XVII 23 p3506 A83-48580
 Nonlinear noise fields and strongly driven atomic transitions 24 p3587 A83-48839
 Black-body radiation shifts in ground and metastable levels of Mg and Ca 24 p3626 A83-49524

ELECTRON TUBES

NT CAMERA TUBES
 NT CARCINOTRONS
 NT CATHODE RAY TUBES
 NT GAS DISCHARGE TUBES
 NT IMAGE ORTHICONS
 NT KLYSTRONS
 NT MAGNETRONS
 NT MICROWAVE OSCILLATORS
 NT MICROWAVE TUBES
 NT RETURN BEAM VIDICONS
 NT THERMIONIC DIODES
 NT THYRATRONS
 NT TRAVELING WAVE TUBES
 NT VIDICONS
 Plasma display panels have come of age 02 p0161 A83-11801
 Propagation of intense relativistic electron beams through drift tubes with perturbed walls 16 p2345 A83-35747

ELECTRON TUNNELING

Resonance tunneling in superconductor-semiconductor-superconductor junctions 01 p0109 A83-10821
 Ac Josephson effect in small-area superconducting tunnel junctions at 604 GHz 01 p0039 A83-10995
 An SIS receiver for the 3 mm wavelength range --- Superconductor Insulator Superconductor 04 p0472 A83-15811
 Transport mechanisms for Mg/Zn3P2 junctions 04 p0543 A83-16071
 Current-waveform dependence of punchthrough probability in a Josephson tunnel junction 04 p0473 A83-16072
 Preparation, tunneling, resistivity, and critical current measurements on homogeneous high T sub c A15 Nb3Ge thin films 04 p0543 A83-16074
 Field ionization of deep levels in semiconductors with applications to Hg/1-x/Cd/x/ Te p-n junctions 04 p0544 A83-16089
 Photon-assisted tunneling at 246 and 604 GHz in small-area superconducting tunnel junctions 07 p0999 A83-19995
 Horizontal tunneling and surface band bending - An external technique for wavelength tuning of surface-emitting light-emitting diodes /LEDs/ 08 p1081 A83-22860
 Negative differential resistance in multilayer metal-barrier-metal tunneling structures 10 p1490 A83-26244
 Electron-tunneling measurements on TSeF-TCNQ 11 p1662 A83-28073
 Tunneling current microscopy 13 p1846 A83-30350

Photoresponse characteristics of thin-film nickel-nickel oxide-nickel tunneling junctions 14 p2093 A83-33434
 Photoinduced macroscopic quantum tunneling in superconducting interference devices 15 p2238 A83-33799
 Imaging of spatial structures in superconducting tunnel junctions by electron-beam scanning 15 p2164 A83-34141
 Current injection in multiquantum well lasers 16 p2359 A83-35958
 Inelastic electron tunneling spectroscopy 16 p2420 A83-36015
 Positron and electron channeling radiation from germanium 17 p2585 A83-38955
 A superconducting tunnel junction receiver for 230 GHz 19 p2838 A83-41091
 Single-particle tunneling in the structures metal-insulator-metal (Review) 19 p2905 A83-42070
 Squeezable electron tunneling junctions 20 p3055 A83-43607
 Paraelectric resonance --- Russian book on microwave spectroscopy of tunneling dipole centers in crystals 21 p3216 A83-43917
 Tunneling in the reverse dark current characteristic os Be-implanted GaAlAsSb avalanche photodetectors 22 p3365 A83-46656
 Surface plasmon emission in metal-insulator-degenerate p-type semiconductor structures 22 p3365 A83-46731
 Resonant tunneling through quantum wells at frequencies up to 2.5 THz 22 p3365 A83-46737
 Tunneling between conductors with a charge-density wave 22 p3366 A83-46936
 Microwave properties of superconducting tunnel junctions during quasiparticle tunneling 24 p3572 A83-48865
 High-resolution imaging of inhomogeneities in superconducting tunnel junctions by scanning with a modulated electron beam 24 p3636 A83-49757

ELECTRON-ION RECOMBINATION
NT RADIATIVE RECOMBINATION

Structure of the electron density profile in the vicinity of localized inhomogeneities in the case of ambipolar diffusion of magnetized recombining plasma 04 p0537 A83-15859
 Terrestrial UV environment and emission mechanisms [AIAA PAPER 83-0022] 05 p0659 A83-16470
 The dissociative recombination of an electron and a molecular ion 05 p0686 A83-16887
 Electric field and space charge density distributions in the processes of ambipolar plasma diffusion with volume recombination 05 p0687 A83-16902
 Transversely excited Sr/+/ recombination laser 06 p0767 A83-19251
 CW recombination laser action in a cadmium vapor arc 07 p0938 A83-21370
 Gain scaling of short-wavelength plasma-recombination lasers 08 p1110 A83-22636
 Dielectronic recombination cross section for C/1+/ 08 p1168 A83-22645
 Effect of recombination on the ion saturation current on a cylindrical probe immersed in an argon plasma 09 p1348 A83-23662
 Measurements of the dissociative recombination coefficients of O₂(+), NO(+) and NH₄(+) in the temperature range 200-600 K 14 p2082 A83-32524
 Numerical study of overpopulation density for laser oscillation in recombining hydrogen plasmas 15 p2170 A83-34998
 Direct radiative recombination of electrons with atomic ions Cross sections and rate coefficients 16 p2415 A83-35655
 Dissociative recombination of electrons with NO(+) ions 17 p2579 A83-38521
 Dissociative recombination in low-energy e-H₂(+) collisions 19 p2898 A83-41194
 Measurement of the branching ratio for the dissociative recombination of H₃(+)+e 21 p3202 A83-44199
 Merged electron-ion beam experiments. V - Dissociative recombination of OH(+), H₂O(+), H₃O(+) and D₃O(+) 23 p3511 A83-48583

ELECTRONIC AIRCRAFT

Color, pictorial display formats for future fighters 01 p0010 A83-11134
 Airborne electronic terrain map display - An update 01 p0010 A83-11135
 A study on airborne integrated display system and human information processing 10 p1456 A83-26086
 The all electric airplane-benefits and challenges [SAE PAPER 821434] 17 p2463 A83-37982
 The prospects and potential of all electric aircraft [AIAA PAPER 83-2478] 23 p3411 A83-48341

ELECTRONIC AMPLIFIERS
U AMPLIFIERS

ELECTRONIC CONTROL

Microprocessor controlled digital test subsystem tailored to automatic test program generator output
01 p0038 A83-10776

PESC '81; Power Electronics Specialists Conference, University of Colorado, Boulder, CO, June 29-July 3, 1981, Record
01 p0039 A83-11001

An automatic protection of spacecraft high power lines - The electronic solid state switch /ELSS/
01 p0021 A83-11005

A compact and comprehensive micro-electronic control system for an unorthodox inverter-converter
01 p0040 A83-11008

A multiprocessor for power electronic circuit simulation
01 p0041 A83-11026

Aircraft power management control system designed for fast response and high reliability
01 p0012 A83-11151

Commutating spot transmissive lens antenna
01 p0042 A83-11158

Single chip Bus Interface Unit eases MIL-STD-1553B remote terminal/bus controller designs
01 p0042 A83-11185

System programmable redundancy in a 64K EEPROM --- Electronically Erasable PROM
01 p0089 A83-11213

An operational software simulator for passive ECM processing
01 p0093 A83-11250

A microprocessor controlled variable phase and amplitude antenna feed network unit
02 p0167 A83-11920

On the dynamic analysis and behavior of industrial robotic manipulators with elastic members
[ASME PAPER 82-DET-45] 02 p0187 A83-12771

Design of a microprocessor-based A/D converter with drift and offset correction
03 p0385 A83-13499

Compensation electronics for staring focal plane arrays
03 p0326 A83-13734

Design of electronic optimizer for solar electric drive system
05 p0658 A83-17150

An analysis of multicomponent electroacoustic transducers providing matched control of the acoustic field in Bragg acoustooptic devices in the short-wave portion of the microwave range
05 p0630 A83-17595

Digital electronic engine control system - F-15 flight test
06 p0718 A83-18406

CIECA - Application to current programmed switching Dc-Dc converters --- Current Injection Equivalent Circuit Approach
06 p0753 A83-19028

Transient shutdown of an axial-groove liquid trap heat pipe thermal diode
06 p0759 A83-19161

Flight evaluation of modifications to a digital electronic engine control system in an F-15 airplane
[AIAA PAPER 83-0537] 06 p0718 A83-19593

Electronic beam steering of semiconductor injection lasers - A theoretical analysis
07 p0935 A83-20162

Electronically scanned coherent CO2 laser radar techniques
08 p1096 A83-22516

Plasma analyzing and controlling system with real-time signal processing --- low-light-level high speed spectrometer
08 p1102 A83-22818

A scheme of feedback compensation for CMG gimbal compliance, using multiple rate sensors --- Control Moment Gyroscope
[ASME PAPER 82-WA/DSC-10] 10 p1419 A83-25681

Theory of optically controlled millimeter-wave phase shifters
10 p1402 A83-25817

Electronically cold microwave artificial resistors
10 p1410 A83-26339

Design concepts and performance characteristics of a high performance linear/digital shunt regulator
11 p1559 A83-27134

An advanced electric vehicle powertrain
11 p1667 A83-27161

Use of a multiprocessor for control of a robotic system
11 p1648 A83-28099

Performance of the Multiple Mirror Telescope (MMT). IV - MMT computer systems
13 p1937 A83-30980

Performance of the Multiple Mirror Telescope (MMT). VI - MMT telescope coalignment system
13 p1919 A83-30982

Development history of the Hybrid Test Vehicle
13 p1934 A83-31088

European Southern Observatory (ESO) coude echelle spectrometer
14 p2084 A83-32005

Cost effective development of a Shuttle-based astronomical instrument control system
14 p1984 A83-32040

Electronic control of the difference frequency between two semiconductor lasers
14 p2024 A83-32420

Characterisation of electrical and optical base controlled switching in the V-groove isolated punch through mode mist --- Metal-Insulator (tunnel)-Silicon Thyristor
14 p2006 A83-32666

Control of locally testable duplex system for large-scale implementation
15 p2218 A83-34524

Small array illuminations for pattern nulling with sidelobe level control
15 p2146 A83-35083

Concepts for improved gun fire control systems
15 p2223 A83-35139

Experience in the development of computer-controlled high response probe diagnostics for turbomachines
16 p2355 A83-35851

Advanced propulsion controls - A total system view
16 p2311 A83-36612

Sputtering of silicon and its compounds in the electronic stopping region
16 p2421 A83-36713

Longitudinal control and a new spacing policy for automated transit vehicles
17 p2586 A83-37101

Reliability analysis of a dual-redundant engine controller
17 p2517 A83-37289

The choice of an astatic system for the regulation of the rotational velocity of a dc electric motor for azimuthal mountings of a gamma-telescope
17 p2496 A83-37720

Full Authority Digital Electronic Control (FADEC) - Augmented fighter engine demonstration
[SAE PAPER 821371] 17 p2467 A83-37963

Full Authority Fault Tolerant Electronic Engine Control systems for advanced high performance engines (FAFTEEC)
[SAE PAPER 821398] 17 p2468 A83-37972

Development of a compact real-time turbofan engine dynamic simulation
[SAE PAPER 821401] 17 p2468 A83-37974

Microcomputer brings digital power to the small aircraft gas turbine
[SAE PAPER 821402] 17 p2468 A83-37975

A method for measuring amplitude and phase of each radiating element of a phased array antenna
17 p2494 A83-38033

IFU - A multi-detector IR spectrometer
18 p2690 A83-40432

Integrated airframe/propulsion control system architectures (IAPSA) study
[AIAA PAPER 83-2158] 19 p2797 A83-41660

Development of a totally computer-controlled triple quadrupole mass spectrometer system
20 p2988 A83-42298

Gas turbine engine cascade wind tunnel with automatic data acquisition and control
20 p2938 A83-42563

Mode-locked semiconductor lasers with gateable output and electrically controllable optical absorber
20 p2995 A83-43595

Electronic steering of antenna nulls for interference reduction
20 p2965 A83-43680

Sensor-based robotic assembly systems - Research and applications in electronic manufacturing
21 p3118 A83-44070

Control system of TT-500A sounding rocket for materials processing in space
21 p3103 A83-45599

Electronic control of aircraft turbine engine
21 p3093 A83-45600

PRESTO - A programmable etalon spectrometer for twilight observations
22 p3288 A83-46066

Electronic wavelength tuning with semiconductor integrated etalon interference lasers
22 p3299 A83-46723

The use of production hardware for the development of control laws --- LSI for engine control
[ASME PAPER 83-GT-6] 23 p3406 A83-47879

Advancing electronic technology impact on integrated propulsion/airframe controls design and development
[ASME PAPER 83-GT-161] 23 p3402 A83-47985

Built-In Test Equipment (BITE) on the Garrett model GTC331 APU digital electronic control unit --- for gas turbine aircraft auxiliary power system
[ASME PAPER 83-GT-186] 23 p3409 A83-47992

F-14 aircraft and propulsion control integration evaluation
[ASME PAPER 83-GT-234] 23 p3411 A83-48029

Operation and control of a 2 GW wave-energy scheme
24 p3599 A83-49000

ELECTRONIC COUNTERMEASURES

NT CHAFF

Adaptive beam forming for radar
01 p0030 A83-10260

Testing of complex ECM systems
01 p0057 A83-10746

Computer models for determining countermeasures effectiveness of expendables in air-to-air engagements
01 p0103 A83-11162

A technique for predicting antenna-to-antenna isolation and electromagnetic compatibility for aircraft
01 p0007 A83-11235

New threat simulator /NETS/ a multi-sensor R & D tool for EW development
01 p0015 A83-11238

Transform receivers for ECM applications
02 p0167 A83-11922

Interference suppression techniques for microwave antennas and transmitters --- Book
03 p0307 A83-14118

A glimpse into the future of air combat --- via computerized cockpit simulators
[AIAA PAPER 83-0143] 05 p0599 A83-16552

ASPJ update counters the changing threat --- Airborne Self-Protection Jammer System
05 p0592 A83-16866

Electronic intelligence: The analysis of radar signals --- Book
05 p0622 A83-17374

Coherent radar signal processing and matched filtering
06 p0748 A83-18936

A general analysis of anti-jam communication systems
07 p0904 A83-19694

Computer simulation of a frequency hop system and a direct sequence-frequency hop hybrid system in a collocated environment
07 p0909 A83-19752

AJ/LPI at millimeter wavelengths --- Anti-Jamming/Low Probability of Intercept
07 p0909 A83-19753

A compact broad-band multifunction ECM MIC module
07 p0923 A83-21533

Very high speed integrated circuit /VHSIC/ antijam communications chipset and brassboard demonstration
08 p1081 A83-22820

Simulate airborne radar environments
17 p2461 A83-37821

Millimeter-wave phased array transmitters for ECM
17 p2498 A83-37896

Broadband sensors for lethal defense suppression
24 p3570 A83-48770

ELECTRONIC EQUIPMENT

NT AVALANCHE DIODES

NT BARRITT DIODES

NT BIPOLAR TRANSISTORS

NT CESIUM DIODES

NT CHARGE COUPLED DEVICES

NT CHARGE TRANSFER DEVICES

NT CMOS

NT DIODES

NT ELECTRONIC FILTERS

NT ELECTRONIC MODULES

NT ELECTRONIC PACKAGING

NT ELECTRONIC TRANSDUCERS

NT FIELD EFFECT TRANSISTORS

NT GALLIUM ARSENIDE LASERS

NT GUNN DIODES

NT HETEROJUNCTION DEVICES

NT JFET

NT JUNCTION DIODES

NT JUNCTION TRANSISTORS

NT LIGHT EMITTING DIODES

NT METAL OXIDE SEMICONDUCTORS

NT METAL-NITRIDE-OXIDE-SEMICONDUCTORS

NT MIM (SEMICONDUCTORS)

NT MIM DIODES

NT MINIATURE ELECTRONIC EQUIPMENT

NT MIS (SEMICONDUCTORS)

NT MOM (SEMICONDUCTORS)

NT MULTISPECTRAL LINEAR ARRAYS

NT PHOTODIODES

NT PHOTOTRANSISTORS

NT PHOTOVOLTAIC CELLS

NT PLASMA DIODES

NT RUBY LASERS

NT SCHOTTKY DIODES

NT SEMICONDUCTOR DEVICES

NT SEMICONDUCTOR DIODES

NT SEMICONDUCTOR LASERS

NT SILICON CONTROLLED RECTIFIERS

NT SILICON TRANSISTORS

NT SIS (SEMICONDUCTORS)

NT SOLID STATE DEVICES

NT SOLID STATE LASERS

NT SOS (SEMICONDUCTORS)

NT SPACECRAFT ELECTRONIC EQUIPMENT

NT THERMISTORS

NT THYRISTORS

NT TRANSFERRED ELECTRON DEVICES

NT TRANSISTOR AMPLIFIERS

NT TRANSISTORS

NT TRAPATT DEVICES

NT TUNNEL DIODES

NT VARACTOR DIODES

NT VARISTORS

NT YAG LASERS

A data base solution to ATE resource management
01 p0087 A83-10728

NAECON 1982; Proceedings of the National Aerospace and Electronics Conference, Dayton, OH, May 18-20, 1982, Volumes 1, 2 & 3
01 p0001 A83-11083

Assembling, setting up, and tuning the instruments of automatic control systems --- Russian book
02 p0230 A83-11972

The coincidence tracker - Electronic equipment for a time-of-flight wind-speed measurement system
02 p0177 A83-12009

Reliability assessment and techniques
02 p0188 A83-12656

The aviation and radioelectronic equipment of the Yak-18T aircraft --- Russian book
03 p0282 A83-13814

The problems of physical electronics --- Russian book
04 p0472 A83-15837

A magnetically controlled electrovacuum converter of displacement into pulsed signals
04 p0472 A83-15913

Allowance for the mutual influence of factors in the analysis of reliability
04 p0494 A83-15918

Airborne electronic colour displays
04 p0448 A83-16133

A device for increasing the feedback and speeding the process of forming occupational habits
07 p0981 A83-20338

ESCAF - A new and cheap system for complex reliability analysis and computation
07 p0942 A83-20514

Simplification of power electronics for ion thruster neutralizers
07 p0873 A83-21099

[AIAA PAPER 82-1880]
Techniques for assessing product reliability in polymeric materials used in aerospace electronic circuitry
09 p1236 A83-23604

Vibration resistance of conformal coated axial-lead components on printed wiring assemblies
09 p1253 A83-23613

Protection of radio electronic and other precision equipment against dynamic effects --- Russian book
09 p1254 A83-23820

Radio-electronic guidance systems --- Russian book
10 p1402 A83-25622

Electronic devices in automatic systems --- Russian book on flight vehicle control
10 p1408 A83-25624

Environmental control of an aircraft pod mounted electronics system
[SAE PAPER 820869]
10 p1375 A83-25768

Estimation of the mutual influence of a group of radio-electronic devices --- for air navigation
10 p1375 A83-26934

Algorithms for the optimization of an isolated frequency band for a group of radio-electronic devices of one type according to EMC-assurance conditions
10 p1407 A83-26935

Features of the microprocessor implementation of algorithms of the space-time processing of signals and noise in radio-electronic systems
10 p1460 A83-26956

Electrostatic acceleration of a modulated electron beam
11 p1560 A83-27449

Electronic housing design for a random vibration environment
12 p1732 A83-29216

Injection gas electronics --- Russian book
13 p1832 A83-30523

Production sequence screening - A candidate for EVOP? --- Evolutionary Operations for electronic component quality control
13 p1864 A83-31517

Selecting the optimal photoelectric unit for a transit instrument
14 p2014 A83-31841

General effects of radiation on electronic components
14 p2005 A83-32415

An electronic model of the conditioned reflex
14 p2072 A83-32571

Thermal analysis and control of electronic equipment --- Book
15 p2143 A83-33747

Developments in test software philosophy and techniques
16 p2363 A83-35499

On some reliability implications of electronic circuit design
17 p2496 A83-37296

An automated multichannel measuring system
17 p2563 A83-37674

Productivity goals drive office automation
18 p2752 A83-40308

Developments in scientific information systems
19 p2907 A83-41291

A history of electronic flight instruments - through tomorrow
19 p2799 A83-41532

Electronic oscillator with open resonator (review of theoretical and experimental studies)
19 p2854 A83-41766

Thermodynamic aspects of small 4.2-K cryocoolers
20 p2960 A83-43224

Electronic power devices - An introduction to automated design --- Russian book
21 p3126 A83-45044

The synthesis of linear electric and electronic networks (the method of state variables) --- Russian book
21 p3126 A83-45046

Multiwavelength analyzer for the determination of diffusion lengths --- in solar cell base region
23 p3459 A83-48612

PAVE PILLAR - A new road to avionics reliability
23 p3401 A83-48643

ELECTRONIC EQUIPMENT TESTS

The reliability and testing of radio components and parts --- Russian book
01 p0037 A83-10671

AUTOTESTCON '81; Proceedings of the Conference, Orlando, FL, October 19-21, 1981
01 p0087 A83-10726

A systematic approach to comprehensive TPS diagnostics for electronic modules --- Test Program Set
01 p0037 A83-10730

ATE support of RF line replaceable units
01 p0013 A83-10732

Antenna couplers - The aircraft interface
01 p0004 A83-10738

The evolution of Navy Flight Line EW testers from AN/ALM-66 to AN/USM-406C
01 p0014 A83-10739

ADATLAS - The test language of the future
01 p0091 A83-10741

UUT modeling
01 p0091 A83-10743

High speed signal acquisition and processing in EW ATE
01 p0031 A83-10745

Testing of complex ECM systems
01 p0057 A83-10746

The modular ATE/UUT interface
01 p0037 A83-10753

The rationale for a standard unit-under-test-interface
01 p0037 A83-10754

Tarps test program set /parallel development of avionics and its support capability/
01 p0014 A83-10755

Testability - A quantitative approach
01 p0057 A83-10756

Design for testability /DFT/
01 p0058 A83-10757

Is multi-port ATE in your future
01 p0028 A83-10758

All devices to all pins - Modular architecture and flexible switching provides this capability even for future upgrades
01 p0037 A83-10759

Conformance testing IEEE standard 488-1978 bus interface
01 p0037 A83-10767

Accuracy enhancement of a broadband A.T.E.
01 p0037 A83-10770

A test pattern generation technique for detection of digital circuits
01 p0038 A83-10773

Test generation using binary decision diagrams
01 p0038 A83-10774

Microprocessor controlled digital test subsystem tailored to automatic test program generator output
01 p0038 A83-10776

Testability assessment of a system design
01 p0029 A83-10777

Description of a 3-port ATE system required for testing of electro-optical UUT's
01 p0038 A83-10781

Calibration of third-generation ATE systems
01 p0091 A83-10784

Demonstration of a figure of merit for inherent testability
01 p0050 A83-10790

A topological approach to the unification of electromagnetic specifications and standards
01 p0041 A83-11084

Testing of voice control device for aircraft avionics applications
01 p0005 A83-11122

VHSIC testability - A comprehensive approach
01 p0042 A83-11229

An automatic test generation system for complex digital logic
01 p0042 A83-11230

Test chips for custom ICs - Six kinds of test structures
02 p0167 A83-11824

Tests against certain ordered multinomial alternatives
02 p0232 A83-11832

Design guidelines for the testability of microprocessor based logic designs
02 p0227 A83-11906

ATE accomplishes receiver specification testing with increased speed and throughput
04 p0474 A83-16398

Vibration isolation system development for the FB-111 tail pod electronics
05 p0595 A83-16932

Total dose test results for the 8086 microprocessor
05 p0626 A83-17504

Latchup window tests
05 p0628 A83-17526

Geometrical considerations in the transient ionization testing of digital logic circuits
05 p0628 A83-17528

Hardness assurance and overtesting
05 p0653 A83-17529

A portable system for upset and transient upset testing of VLSI circuits
05 p0628 A83-17530

Experimental results on junction charge-coupled devices
06 p0752 A83-18760

System testing of communications and tracking links for first orbital flight of the Space Transportation System - An update
07 p0870 A83-19701

Hybrid substrate attach evaluation techniques --- in production of microcircuits
07 p0919 A83-20460

Design for testability - A survey --- of integrated circuit technology
07 p0923 A83-21541

Electro-optical calibration considerations at intermediate maintenance levels
08 p1104 A83-22883

Predictive monitoring of radio electronic equipment --- Russian book
09 p1275 A83-23828

Mode-fault diagnosis and a design of testability
09 p1333 A83-24796

The technical diagnostics of radio-electronic and other equipment according to electromagnetic-compatibility parameters
10 p1412 A83-26933

Recent advances in interpretation of corona test results
11 p1602 A83-27154

Designing electronic equipment for random vibration environments; Proceedings of the Meeting, Los Angeles, CA, March 25, 26, 1982
13 p1834 A83-30851

Speaking in a random fashion --- random vibration testing of electronic equipment
13 p1914 A83-30852

Random vibration basics for electronics packaging design
13 p1860 A83-30853

Response spectrum analysis for random vibration
13 p1860 A83-30854

Design guides for random vibration --- for testing electronic packaging design
13 p1861 A83-30855

Guidelines for random vibration design of electronic equipment
13 p1861 A83-30857

Design for long fatigue life in random vibration environment
13 p1861 A83-30858

Designing electronic equipment for random vibration environments
13 p1861 A83-30860

Analysis and test of ceramic substrates for packaging of leadless chip carriers
13 p1834 A83-30861

Computer-aided interactive structural optimization of printed-circuit-board design
13 p1834 A83-30862

Random vibration effects on piece part applications
13 p1835 A83-30863

Wear of connector contacts exposed to relative motion
13 p1835 A83-30865

Test data on leadless chip carriers with ceramic substrates in severe random vibration environments
13 p1835 A83-30866

Component lead wire strain relief for random vibration environments
13 p1835 A83-30867

Random vibration testing and analysis of a large ceramic substrate assembly
13 p1835 A83-30868

Card level acceptance testing
13 p1861 A83-31183

Test of large aperture antennas using near-field techniques
13 p1829 A83-31194

Wide-band device modeling using time-domain reflectometry
13 p1830 A83-31286

An automatic test set for the dynamic characterization of A/D converters
13 p1836 A83-31288

Outdoor and laboratory testing of photovoltaic modules
13 p1862 A83-31482

Stress screening with random vibration --- testing methods to improve electronic system reliability
13 p1862 A83-31485

An indicator of the reliability of analytical design and initial manufacturing process
13 p1863 A83-31491

Results from a test facility for solar cells in Sweden
14 p2003 A83-32203

Analog multifrequency fault diagnosis
15 p2151 A83-33923

Control of locally testable duplex system for large-scale implementation
15 p2218 A83-34524

On testing stuck-open faults in CMOS combinational circuits
15 p2153 A83-35141

A deductive method for the simulation of faults in Programmable Logic Arrays
15 p2218 A83-35142

Comment on 'Calculation of site attenuation from antenna factors'
16 p2342 A83-35783

Design ATE systems for complex assemblies
16 p2348 A83-36962

High-precision test of the universality of the Josephson voltage-frequency relation
19 p2837 A83-40959

Testing for space and weapon products; Proceedings of the Symposium, London, England, January 18, 1983
22 p3303 A83-45821

On target with confidence automated testing of guided weapons
22 p3303 A83-45822

Communications spacecraft payload testing
22 p3257 A83-45824

System functional testing of a communication satellite
22 p3257 A83-45825

Avionics fault tree analyzer
[AIAA PAPER 83-2452]
23 p3401 A83-48335

New concepts for intermediate level maintenance --- of avionics by ATE
[AIAA PAPER 83-2498]
23 p3468 A83-48353

Avionics built-in-test effectiveness and life cycle cost
[AIAA PAPER 83-2448]
24 p3543 A83-49578

A generator of test sequences for probabilistic systems of the fault diagnostics of digital devices
24 p3575 A83-50207

ELECTRONIC FILTERS

Programmable filter technology for integrated communication, navigation and identification systems
01 p0042 A83-11214

The design of high-order active RC filters --- Russian book 09 p1254 A83-23827

Features of the search for pseudorandom signals according to delay using acoustoelectronic convolvers 10 p1412 A83-26958

A PISO JCCD filter with high-speed linear charge injection --- serial-in, parallel-out junction charge coupled devices 15 p2151 A83-33890

INTFIS - An interactive package for electronic filter synthesis 16 p2403 A83-35323

ELECTRONIC LEVELS

- U ELECTRON ENERGY
- U ENERGY LEVELS

ELECTRONIC MODULES

A systematic approach to comprehensive TPS diagnostics for electronic modules --- Test Program Set 01 p0037 A83-10730

A modular interface switch for ATE applications 01 p0037 A83-10733

The modular ATE/UUT interface 01 p0037 A83-10753

All devices to all pins - Modular architecture and flexible switching provides this capability even for future upgrades 01 p0037 A83-10759

Description of a 3-port ATE system required for testing of electro-optical UUT's 01 p0038 A83-10781

Power conditioning unit development for MAG-TRANSIT 01 p0041 A83-11021

A compact broad-band multifunction ECM MIC module 07 p0923 A83-21533

Questions of the modular design of microprocessor models for problems of mathematical physics 12 p1768 A83-29350

On the performance evaluation of multimicroprocessor systems --- Thesis 13 p1908 A83-30149

Accelerated weathering of photovoltaic modules employing natural sunlight 13 p1862 A83-31484

Low cost modular designs for photovoltaic array fields 14 p2039 A83-32208

A dc/ac modular interface for photovoltaic systems 14 p2004 A83-32215

New progress in the development of a 94-GHz pretuned module silicon IMPATT diode 20 p2968 A83-43348

ELECTRONIC PACKAGING

Integrated sensors - Interfacing electronics to a non-electronic world 02 p0180 A83-12809

The effect of cure temperature on stresses in encapsulated electronic assemblies 07 p0919 A83-20457

Hybrid substrate attach evaluation techniques --- in production of microcircuits 07 p0919 A83-20460

The effect of materials and processes on package reliability 07 p0920 A83-20473

Performance properties of conductive PVC composites for EMI shielding applications 07 p0876 A83-20488

Polyimide adhesives to reduce thermal stresses in LSI ceramic packages 09 p1237 A83-23621

High voltage power electronics packaging on NASA's Space Telescope 11 p1539 A83-27155

Macroencapsulation of electronic circuits 12 p1719 A83-29215

Thermorheological analysis of high voltage electronic module potting [AIAA 83-0903] 12 p1720 A83-29842

Random vibration basics for electronics packaging design 13 p1860 A83-30853

Design guides for random vibration --- for testing electronic packaging design 13 p1861 A83-30855

Designing electronic equipment for random vibration environments 13 p1861 A83-30860

Analysis and test of ceramic substrates for packaging of leadless chip carriers 13 p1834 A83-30861

Test data on leadless chip carriers with ceramic substrates in severe random vibration environments 13 p1835 A83-30866

Random vibration testing and analysis of a large ceramic substrate assembly 13 p1835 A83-30868

Integral packaging for millimetre-wave GaAs IMPATT diodes prepared by molecular beam epitaxy 13 p1838 A83-31777

Hybrid packaging approach to improved low-noise operation of photovoltaic InSb detectors 14 p2015 A83-31981

Microelectronic packaging 16 p2346 A83-36021

Temperature and humidity swings in sealed electronic equipment containers 18 p2676 A83-39258

An experimental investigation of a low heat flux, wickless heat pipe 20 p2969 A83-42350

Combined forced and free convection between parallel plates 20 p2979 A83-42752

ELECTRONIC PHOTOGRAPHY

- U ELECTRO-OPTICAL PHOTOGRAPHY
- ELECTRONIC SIGNAL MEASUREMENT
- U SIGNAL MEASUREMENT

ELECTRONIC SPECTRA

Density-dependent Si XII dielectronic satellite spectra 09 p1347 A83-23655

Fourier spectroscopy of the /C-12/ /C-13/ and /C-13/2 Phillips system 09 p1361 A83-24519

The laser magnetic resonance spectrum of the nu2 band of the methylene radical CH2 10 p1480 A83-26453

Principal and dielectronic satellite line spectra for Ca XIX SMM observations --- Solar Maximum Mission 13 p1965 A83-31713

Calculation of the electronic spectrum of Group III A-Group V A compounds and solid solutions based on these compounds using the model-pseudopotential method 14 p2091 A83-32594

The vibronic spectra of neodymium-doped crystals 14 p2025 A83-32830

Measurement of the lifetime of the c 3 Pi u state of molecular nitrogen by the delayed coincidence method 16 p2410 A83-36797

The C2H, C2, and CN electronic absorption bands in the carbon star HD 19557 17 p2605 A83-37918

Impurity scattering in partially dielectricized superconductors 19 p2904 A83-41000

ELECTRONIC STRUCTURE

- U ATOMIC STRUCTURE

ELECTRONIC SWITCHES

- U SWITCHING CIRCUITS

ELECTRONIC TRANSDUCERS

Wind tunnel measurements with an electronically scanned multiport pressure sensor system 01 p0051 A83-11052

A new electronic scanner of pressure designed for installation in wind-tunnel models 01 p0051 A83-11054

Solid State Transducer Symposium, Boston, MA, November 18, 19, 1981, Proceedings 02 p0180 A83-12807

Signal conversion in solid-state transducers 02 p0180 A83-12808

Integrated sensors - Interfacing electronics to a non-electronic world 02 p0180 A83-12809

VLSI and intelligent transducers 02 p0168 A83-12810

Ferroelectric transducers and sensors 19 p2848 A83-41527

Algorithm for determining the dimensions of flaws in the theory of eddy-current flaw detection by superposed transducers 20 p3000 A83-43179

Automatic devices for the electromagnetic inspection of the thickness of the coating on small components 20 p2991 A83-43180

Nondestructive inspection of the quality of materials and components using multitransducer eddy-current devices 20 p3000 A83-43643

Flaw detector DVT-24 for the inspection of axial holes in deep drilling 21 p3135 A83-43880

ELECTRONIC WARFARE

The evolution of Navy Flight Line EW testers from AN/ALM-66 to AN/USM-406C 01 p0014 A83-10739

High speed signal acquisition and processing in EW ATE 01 p0031 A83-10745

Accuracy enhancement of a broadband A.T.E. 01 p0037 A83-10770

The coming weapons 01 p0016 A83-10999

High speed data link concepts for military aircraft 01 p0010 A83-11233

Operational sensitivity of EW receivers 01 p0007 A83-11234

Toward 'combat realistic' tests, evaluations, exercises - and training 01 p0015 A83-11237

New threat simulator /NETS/ a multi-sensor R & D tool for EW development 01 p0015 A83-11238

Sensitivity of EW receivers 03 p0304 A83-13443

ASPJ update counters the changing threat --- Airborne Self-Protection Jammer System 05 p0592 A83-16866

New advances in wide band dual polarization antenna elements for EW applications 15 p2121 A83-35087

ELECTRONICS

Fundamentals handbook of electrical and computer engineering. Volume 1 Circuits fields and electronics 03 p0314 A83-14047

Electronic Circuit Analysis Language /ECAL/ 04 p0470 A83-15550

High-energy solid-state electronics --- Russian book 07 p0919 A83-20388

International Union of Radio Science and Nachrichtentechnische Gesellschaft, General Meeting, Kleinheubach, West Germany, October 4-8, 1982, Lectures and Reports 09 p1243 A83-23376

ELECTRONOGRAPHY

Electronographic photometry in the galactic cluster M 37 03 p0402 A83-13364

The residual voltage in fast electrophotography of a-SiH/x/ 04 p0540 A83-15511

An electronic camera with a remotely controlled shutter at the primary focus of the 3.60 m C.F.H. telescope 06 p0822 A83-19192

Electronographic polarimetry - The Durham polarimeter 22 p3291 A83-46562

Point spread functions from electronographic emulsions --- for astronomical photography 24 p3648 A83-50012

ELECTRONS

NT CONDUCTION ELECTRONS

NT FREE ELECTRONS

NT HIGH ENERGY ELECTRONS

NT HOT ELECTRONS

NT PHOTOELECTRONS

NT POLARONS

NT RELATIVISTIC ELECTRON BEAMS

NT SOLAR ELECTRONS

Radiation characteristics of channeled particles 03 p0313 A83-13960

Invalidity of local thermodynamic equilibrium for electrons in the solar transition region. I - Fokker-Planck results 10 p1521 A83-25730

The unit gravitational charge /hc/4/ 1/2 /the uniton/, the structure of the electron and muon, and their anomalous magnetic moments 11 p1655 A83-27498

Electrostatic bursts generated by electrons in Landau resonance with whistler mode chorus 11 p1617 A83-28311

Auroral electron interaction with the atmosphere in the presence of conjugate field-aligned electrostatic potentials 13 p1879 A83-31245

Pair creation in a strong magnetic field 15 p2270 A83-34687

Electrojet boundaries and electron injection boundaries 17 p2546 A83-36899

Visual sensations evoked by single electrons and muons 18 p2733 A83-39519

Cosmic ray electrons and positrons - A review of current measurements and some implications 23 p3539 A83-47740

ELECTRONYSTAGMOGRAPHY

The diagnosis of latent vestibular disorders in patients with otosclerosis 07 p0978 A83-20877

Electronystagmography in space 08 p1149 A83-22985

An electrode for the electronystagmography of experimental animals 16 p2395 A83-36827

ELECTROPHORESIS

Bioprocessing in space 05 p0600 A83-17284

Fractionation of mineral species by electrophoresis 07 p1029 A83-20235

Thin double layer approximation for electrophoresis and dielectric response 08 p1056 A83-22221

Large area CdS/Cu(x)S thin film solar cells produced by electrophoretic deposition 14 p2044 A83-32282

The application of euphylline electrophoresis with sinusoidal modulated currents in the treatment of patients with transitory disorders of the brain blood circulation 15 p2213 A83-34972

Phenibut electrophoresis as a method of treating muscular spasticity of central genesis 18 p2735 A83-40568

Flow structure in continuous flow electrophoresis chambers 20 p2950 A83-43275

The effect of small temperature gradients on flow in a continuous flow electrophoresis chamber 20 p2951 A83-43276

A theory of electrophoresis of emulsion drops in aqueous two-phase polymer systems 20 p2951 A83-43278

Theoretical studies in isoelectric focusing --- mathematical modeling and computer simulation for biologicals purification process 20 p2951 A83-43280

Isoelectric focusing in space 20 p2940 A83-43281

A micro-computer system for cell electrophoresis measurements 21 p3108 A83-43825

Electrophoresis '82; Proceedings of the Fourth International Conference, Athens, Greece, April 21-24, 1982 22 p3265 A83-45757

Evolution of ideas in electrophoretic developments - Selected highlights 22 p3265 A83-45758

A unified mathematical theory of electrophoretic processes 22 p3265 A83-45759

Computer simulation of model isoelectric focusing experiments 22 p3266 A83-45760

Quantitative models for the migration of electrolyte gradients in an electric field 22 p3266 A83-45761

Free flow field step focusing - A new method for preparative protein isolation 22 p3266 A83-45762

ASECS - Antigen-Specific Electrophoretic Cell Separation 22 p3266 A83-45763

Preparative density gradient electrophoresis of cells and cell organelles - A new separation chamber 22 p3266 A83-45764

Electrophoretic measurements on purple membrane particles 22 p3345 A83-45765

- A new detailed lipidogram - Methods and clinical applications 22 p3347 A83-45766
- ELECTROPHOTOMETERS**
- Corrections to fundamental constants from photoelectric observations of lunar occultations 03 p0409 A83-13939
- Photon-counting array detectors for space and ground-based studies at ultraviolet and vacuum ultraviolet /VUV/ wavelengths 03 p0327 A83-13965
- Search for rapid variability of 53 Cam 04 p0546 A83-15110
- A microprocessor-controlled, integrating photometer 04 p0548 A83-16378
- A photoelectric radial-velocity spectrometer on the 1.2-m telescope of the Dominion Astrophysical Observatory 06 p0822 A83-19075
- Photometry of possible members of the Hyades cluster. V 09 p1353 A83-23731
- An investigation of the narrow-band photometric system. I - Spectral classification 10 p1498 A83-26906
- Star transits with a photoelectric micrometer applied to the transit instrument of Torino Observatory 13 p1943 A83-31752
- Texas Instruments' virtual phase charge-coupled device (CCD) imager operated in the frontside electron-bombarded mode 14 p2016 A83-31995
- Miniature imaging photon detector 14 p2018 A83-32022
- Solar corona photoelectric photometer using mica etalons 14 p2096 A83-32031
- Methods of photoelectric astrometry 14 p2096 A83-32032
- A portable high-speed photometer. I - Photometer controller 15 p2164 A83-34510
- Photoelectric catalogue of globular clusters in the Andromeda Nebula M31 and its companions NGC 147, NGC 185, and NGC 205 15 p2249 A83-34785
- PMC 190 - A new Photoelectric Meridian Circle of Tokyo Astronomical Observatory. I - Determination of instrumental errors. II - Pinhole system for solar and lunar observations. 16 p2422 A83-35677
- ELECTROPHOTOMETRY**
- Photoelectric observations of lunar occultations. XIII 02 p0249 A83-12920
- Physical studies of asteroids. VIII - Photoelectric photometry of the asteroids 42, 48, 93, 105, 145 and 245 03 p0403 A83-13366
- Comet head photometry - Past, present, and future 03 p0403 A83-13392
- Photometry of symbiotic stars in the UBVRJHKLMN system. III - AX Per, AG Dra, BF Cyg, V 443 Her, and YY Her 03 p0407 A83-13663
- Observations of nearby M dwarf stars in VRI colors 03 p0421 A83-14146
- UBVRI photoelectric sequences for M 83 and NGC 5128 03 p0409 A83-14147
- Classification of the results of the electrophotometry of artificial celestial bodies 03 p0286 A83-14684
- Physical studies of asteroids. IX - The light curve of the M asteroid 77 Frigga 03 p0411 A83-14870
- A photoelectric investigation of Ap-stars in open clusters. III - NGC 2362, NGC 2546, and NGC 3228 04 p0546 A83-15034
- Frequency analyses of light and radial velocity observations of Alpha Lupi 04 p0546 A83-15049
- Photoelectric observations of the eclipsing binary U Pegasi 04 p0548 A83-15973
- Photoelectric photometry of asteroids 33 Polyhymnia and 386 Siegena 05 p0693 A83-16970
- Magnetic field development in an isolated active region /McMath No. 13 736/ 05 p0709 A83-17826
- Photoelectric standard stars near V1343 Aquilae /S 433/ 06 p0821 A83-19067
- Notes on ten Southern Hemisphere eclipsing binaries 06 p0821 A83-19069
- Photoelectric observations of CN Andromedae 06 p0821 A83-19072
- Astronomical photometry --- Book 07 p1004 A83-19924
- Photoelectric photometry of the eclipsing binary NN Cephei 07 p1006 A83-20561
- Photoelectric photometry of HD 5303 07 p1017 A83-20927
- Remarkable light changes of the active RSCvN system V 711 Tau /equals HR 1099/ during 1979-1981 07 p1009 A83-21222
- Empirical calibration of the RGU-system. I - Photoelectric realization of the system and definition of standard stars 07 p1009 A83-21248
- Rotation periods and lightcurves of the asteroids 136 Austria and 238 Hypatia 07 p1009 A83-21252
- Color gradients in galactic spheroids. II - Gradient as a function of luminosity and morphology 09 p1356 A83-23317
- The open cluster Tombaugh 1 and its neighbouring Cepheid XZ Canis Majoris 09 p1354 A83-24023

- Study of the open cluster IC 1805 09 p1354 A83-24024
- VW Hydri revisited - Conclusions on dwarf nova outburst models 09 p1360 A83-24464
- EX Hydrae - A coordinated campaign of photoelectric photometry from four observatories 10 p1499 A83-25371
- Photoelectric UBVR-photometry of Wolf-Rayet stars in the Large Magellanic Cloud 10 p1493 A83-25660
- Photoelectric observations of four classical cepheids 10 p1498 A83-26905
- A color-magnitude diagram for Leo II 11 p1668 A83-27108
- UBVRI photometric standard stars around the celestial equator [AD-A130228] 11 p1669 A83-27118
- Certain parameters of the CN atmosphere of Comet Bradfield 1979I 11 p1673 A83-27892
- Physical studies of asteroids. X - Photoelectric light curves of the asteroids 219 and 512 11 p1686 A83-28384
- Five years of photometry of Lambda Andromedae 12 p1785 A83-28995
- Photoelectric photometry of star clusters in M31. VIII 12 p1788 A83-29488
- Photoelectric analysis of asteroid 216 Kleopatra Implications for its shape 13 p1961 A83-31207
- AQ Leonis revisited --- electrophotometry of double-mode RR Lyrae variable 13 p1942 A83-31666
- Simultaneous spectroscopic and photoelectric observations of Beta Cephei stars. I - nu and Beta Centauri 13 p1942 A83-31667
- Microchannel intensified electrophotography 14 p2018 A83-32028
- Photometric properties of the Texas MkII electrophotographic camera 14 p2018 A83-32033
- Asteroid rotation. IV 14 p2097 A83-32607
- New UBVRI photometry for 900 supergiants 14 p2098 A83-33152
- Light curves of some periodic comets 14 p2101 A83-33287
- Photography and photographic-photometry of the solar aureole 15 p2281 A83-34460
- Discovery of a flare star near Sirius 15 p2247 A83-34560
- 2 Pallas pole revisited 16 p2426 A83-36778
- Covariance analysis of a charge carrier device processing algorithm for stellar sensors 17 p2474 A83-37062
- Photoelectric photometry of 2 Pallas 17 p2589 A83-37369
- UBVRI photometry of stars useful for checking equipment orientation stability 17 p2591 A83-37786
- WBVR photometry of SS 433 - Spectra of the 'normal' star and the accretion disk 17 p2611 A83-38559
- Spectroscopic binaries near the north galactic pole. VI - BD 33,2206 deg 18 p2754 A83-39196
- Photometry of magnetic stars 18 p2755 A83-39240
- A photometric study of the lower main sequences of the Hyades and the field stars 18 p2758 A83-39628
- The photometric period of 39 AY Ceti 18 p2759 A83-39739
- Five years of photometry of Sigma Geminorum 18 p2759 A83-39743
- Photoelectric photometry of asteroids 45, 120, 776, 804, 814, and 1982DV 21 p3222 A83-44084
- Electrophotometry of variable stars 21 p3225 A83-44930
- Meridian observations made with the Carlsberg Automatic Meridian Circle at Brorfelde (Copenhagen University Observatory) 1981-1982 21 p3225 A83-44979
- Photoelectric comparison sequences in the fields of four BL Lacertae objects 22 p3372 A83-46378
- New observations of six RV Tauri and SRd variable stars 22 p3374 A83-46414
- BD + 43 deg 1894, a mono-periodic Delta Scuti star 22 p3374 A83-46417
- Analysis of Mount St. Helens ash from optical photoelectric photometry 22 p3329 A83-46418
- The light curve changes of VW Cephei 23 p3527 A83-48063
- Narrow-band photometry of normal and Seyfert galaxies 24 p3653 A83-49160
- A photoelectric UBVR catalogue of 610 stars in Puppis 24 p3643 A83-49367
- A photometric study of the eclipsing binary V478 Cygni 24 p3645 A83-49844
- Study of the variability of the Delta Scuti stars. VI Pulsational behaviour of HR 1392 (69 Tau). VII - The problem of stability and monop periodicity in 20 CVn 24 p3663 A83-49847

- The Rosette nebula. I - An absolutely calibrated photoelectric H-alpha surface photometry 24 p3645 A83-49848
- Narrow-band photometry of G and K stars near the North Galactic Pole 24 p3645 A83-49851
- ELECTROPHYSICS**
- NT ELECTRO-OPTICS
- NT MOLECULAR ELECTRONICS
- Analysis of electrophysical processes in the power diode of a transistorized pulsed dc converter 04 p0472 A83-15916
- Investigation of the electrophysical characteristics of SIS structures based on polycrystalline cadmium telluride 14 p2087 A83-32045
- ELECTROPHYSIOLOGY**
- A pharmacological evaluation of electrical processes in the myocardium 01 p0078 A83-10510
- The endocochlear potential of the inner ear and its changes under the influence of dihydrostreptomycin and etacrinic acid 01 p0078 A83-10514
- Extratympanic electrocochleography in clinical practice 01 p0083 A83-10515
- Several contemporary paths of the analytical investigation of the human neuromotor units 04 p0523 A83-15789
- The effect of sinusoidal modulated currents on the cardiorespiratory system and the physical capacity of athletes 05 p0673 A83-17170
- The electric reactions of the cat brain to light following the section of the optic tracts 05 p0672 A83-17636
- Electrogustometric investigations during manned space flight 06 p0796 A83-18186
- Blocking the negative delta waves in the rabbit visual cortex by light flashes 06 p0795 A83-18972
- The electrophysiological characteristics of the muscle fibers of rats adapted to cold 14 p2063 A83-32566
- Automatic activity and workload during learning of a simulated aircraft carrier landing task 14 p2071 A83-32690
- An investigation of the electrical conductivity of biological systems 14 p2065 A83-33317
- Naloxone augments electrophysiological signs of selective attention in man 21 p3189 A83-44996
- ELECTROPLATING**
- Pulse plating of chromium-cobalt alloys containing a phase with the A-15 structure 02 p0154 A83-12053
- Use of electrodeposition to provide coatings for solid state bonding 02 p0155 A83-12070
- Guide to the selection and use of electroplated and related finishes --- Book 03 p0337 A83-14119
- Electrochemical preparation and conditioning of Cu2S for Cu2S-CdS solar cells 14 p2045 A83-32299
- Technology of all electroplated CdS:Cu(x)S solar cells 14 p2047 A83-32847
- The processing of metallic structures by electroplating methods 15 p2137 A83-33967
- Electroplated carbon/graphite fibers 16 p2325 A83-36900
- Brush plating in aerospace applications [SAE PAPER 820612] 22 p3302 A83-45870
- ELECTROPLETHYSMOGRAPHY**
- Measurement of the specific electrical resistance of the blood 03 p0381 A83-14330
- The effect of low frequency vibrations on the human cardio-circulatory system - A measurement technique and results for an 18 Hz sinusoidal vibration 08 p1149 A83-22978
- ELECTRORETINOGRAPHY**
- Electrophysiological investigations of color vision in humans 07 p0977 A83-20358
- Comparison of the spatial response properties of the human retina and cortex as measured by simultaneously recorded pattern ERGs and VEPs 19 p2880 A83-40750
- ELECTROSEISMIC EFFECT**
- U ELECTRIC CURRENT
- U SEISMIC WAVES
- ELECTROSTATIC CHARGE**
- Charged relativistic spheres 05 p0683 A83-16901
- Features of a transparent antistatic resin 07 p0899 A83-20489
- Electrostatic acceleration of a modulated electron beam 11 p1560 A83-27449
- Electrostatic bursts generated by electrons in Landau resonance with whistler mode chorus 11 p1617 A83-28311
- An electrostatic charge decay technique for nondestructive evaluation of nonmetallic materials 12 p1734 A83-29591
- Formation of fine dust on Saturn's rings as suggested by the presence of spokes 16 p2436 A83-35732
- Saturn's electrostatic discharges - Could lightning be the cause? 16 p2436 A83-35734
- Observations of charging dynamics --- of spacecraft 17 p2480 A83-37591

Electron-beam guiding and phase-mix damping by an electrostatically charged wire 21 p3203 A83-43882

Electrostatic charging and radiation shielding design philosophy for a synchronous satellite 23 p3423 A83-48126

Note on a suggested formation of charge from an electromagnetic wave 24 p3624 A83-50200

ELECTROSTATIC ENGINES

Ion extraction capabilities of closely spaced grids [AIAA PAPER 82-1894] 02 p0147 A83-12551

Ion beamlet vectoring by grid translation [AIAA PAPER 82-1895] 02 p0241 A83-12552

Simplified power processing for ion-thruster subsystems 18 p2648 A83-39271

ELECTROSTATIC EROSION

U SPARK MACHINING

ELECTROSTATIC FIELDS

U ELECTRIC FIELDS

ELECTROSTATIC GENERATORS

Electron-optical system with a thermionic cathode and centrifugal electrostatic shaping of a high-power axisymmetric beam, intended for use in relativistic microwave oscillators 14 p2003 A83-32117

ELECTROSTATIC GYROSCOPES

Trapped flux readout for an electrostatically supported superconducting gyroscope 11 p1576 A83-28786

Determination of the probability characteristics of perturbation moments in gyroscopes with an electrostatic suspension 21 p3142 A83-45352

ELECTROSTATIC PLASMA

U PLASMAS (PHYSICS)

ELECTROSTATIC PROBES

A comparison between HF partial reflection profiles from the D-region and simultaneous Langmuir probe electron density measurements 02 p0205 A83-12017

Phase-locked heterodyne receiver and its application to lower hybrid wave detection by microwave scattering 02 p0242 A83-12820

Ion thruster charge-exchange plasma flow 02 p0148 A83-13089

Assessment of the error in measuring the strength of a constant electric field by the double-Langmuir-probe method 03 p0397 A83-13206

Experimental measurements of the plasma sheath around pinhole defects in a simulated high-voltage solar array [AIAA PAPER 83-0311] 05 p0657 A83-16643

Theory of cylindrical and spherical Langmuir probes in the limit of vanishing Debye number 05 p0688 A83-17370

Theory of electrostatic probes under intermediate collisional conditions 07 p0995 A83-20063

Equivalent circuit for an electrostatic probe 07 p0928 A83-20064

Numerical simulation of a disk-shaped electron accelerating electrostatic probe 08 p1093 A83-22336

Symmetrical theory of the plasma environment of a probe --- German thesis 09 p1307 A83-24843

Equipment for measuring ionospheric parameters by means of a cylindrical Langmuir probe and a planar retarding-potential analyzer on the Cosmos-900 satellite 10 p1386 A83-25335

An instrument for the direct measurement of electron temperature in the ionosphere 10 p1387 A83-25341

The investigation of ionization phenomena in a 800 mm shock-tube 10 p1487 A83-26178

Determination of plasma potential from the ionic part of the volt-ampere characteristics of an electric probe 11 p1658 A83-27450

Langmuir probe characteristic modulated with random fluctuations 11 p1661 A83-28708

Negative-resistance characteristics of a Langmuir probe in a turbulent plasma 12 p1780 A83-29033

Measurement of vehicle potential using a mother-daughter tethered rocket 15 p2127 A83-34212

The effect of contamination of the probe surface and coating on the accuracy of the measurement of electron temperature using the Langmuir probe --- in satellite and rocket experiments 15 p2128 A83-34420

Electric-probe potential in the space plasma 16 p2416 A83-35943

Unipolar currents and electrostatic probe characteristics in a gas discharge plasma 17 p2582 A83-37613

Measurements of turbulent waves by means of microwave scattering and correlation techniques 18 p2688 A83-39090

Plasma diagnostics by Langmuir probes and UV absorption 18 p2745 A83-39552

Determining the concentration of two dominant types of ions with the aid of a cylindrical Langmuir probe --- in aerospace environments 19 p2817 A83-41593

Electron temperature measurements using a 12-channel array probe 20 p3049 A83-42292

Coupling mechanism of boundary sheaths and wave launcher in a collisionless plasma 21 p3214 A83-45189

ELECTROSTATIC PROPULSION

NT ION PROPULSION

Hypervelocity acceleration techniques - A review of existing capabilities and prospects for future developments 15 p2125 A83-35032

Technology of closed-drift thrusters [AIAA PAPER 83-1398] 16 p2322 A83-36388

ELECTROSTATIC SHIELDING

The effect of displacing the center of a protective sphere on the oscillations of a body acted upon by Lorentz forces under conditions of resonance --- stability of rotating electrostatically protected satellite under resonant vibration 04 p0452 A83-15772

ELECTROSTATIC WAVES

An optical emission mechanism for the Crab pulsar 03 p0419 A83-13888

Numerical simulation of electrostatic waves in plasmas --- German thesis 04 p0537 A83-15845

The nonlinear relaxation of a beam of relativistic electrons in a plasma - Nonlinear sound attenuation 05 p0686 A83-16891

Upgoing ion beams. I - Microscopic analysis --- of auroral plasma 05 p0661 A83-17399

A perpendicular ion beam instability - Solutions to the linear dispersion relation --- for F region ionosphere 06 p0784 A83-18304

Particle simulations of electrostatic emissions near the lower hybrid frequency 06 p0785 A83-18320

SABRE - A U.K.-German auroral radar 06 p0747 A83-18738

Collisionless electrostatic interchange instabilities 06 p0812 A83-18922

Drift- and lower-hybrid eigenmodes in a plasma cylinder 07 p0997 A83-20539

A theory of Jovian decameter radiation 07 p1036 A83-21505

Acceleration of hydrogen ions and conic formation along auroral field lines 07 p0966 A83-21516

The nonlocal theory of periodic density drift instabilities 07 p0967 A83-21519

Quasilinear theory of inhomogeneous magnetized plasmas 08 p1168 A83-22387

Solitons and ionospheric modification 09 p1300 A83-23305

Density drift instabilities and weak collisions --- in space plasmas 09 p1303 A83-23766

Solitary surface waves on a plasma cylinder 10 p1485 A83-25778

Waves in a cold pure electron plasma of finite length 10 p1485 A83-25785

A search for Saturn electrostatic discharges in the Voyager plasma wave data 11 p1684 A83-27358

Topics in strong Langmuir turbulence 11 p1660 A83-28450

Drift waves in sheet plasmas 12 p1780 A83-29009

Orbit-averaged implicit particle codes --- for studying plasma kinetics 12 p1781 A83-29601

Narrowband electromagnetic emissions from Jupiter's magnetosphere 12 p1799 A83-29707

Limitation imposed by strong Langmuir turbulence on the self-consistency of the quasi-linear dynamics 13 p1963 A83-29980

On a possibility of the linear kinetic transillumination of an inhomogeneous plasma 13 p1922 A83-30085

Electromagnetic instability of Langmuir waves in a magnetoplasma 13 p1944 A83-30113

Steady-state turbulence with a narrow inertial range 13 p1923 A83-30121

Magnetized-plasma turbulence 13 p1925 A83-30416

Interaction of Langmuir solitons with resonant particles 13 p1925 A83-30417

Thermal cavitons --- Langmuir waves in plasma density depressions 13 p1925 A83-30421

Preferential perpendicular acceleration of heavy ionospheric ions by interactions with electrostatic hydrogen cyclotron waves 13 p1966 A83-31237

Observations of LHR noise with banded structure by the sounding rocket S29 barium-GEOS 13 p1879 A83-31246

Damping of large-amplitude plasma waves propagating perpendicular to the magnetic field 13 p1926 A83-31358

Excitation of an electrostatic wave by a cold electron current sheet of finite thickness 13 p1881 A83-31530

Electrostatic modes in a magnetized plasma with a longitudinal density gradient 13 p1927 A83-31644

Nonlinear phenomena in the plasma-resonance region in an inhomogeneous plasma 14 p2086 A83-32551

The problem of the spectra of developed Langmuir turbulence in a region of plasma resonance 14 p2087 A83-32973

Growth and saturation of the two-plasmon decay instability 14 p2087 A83-33390

Plasmapause diffusion 15 p2196 A83-33949

Electromagnetic radiation from beam-plasma instabilities 15 p2234 A83-34202

Electron beam as a source of electrostatic waves 15 p2228 A83-34205

Parametric excitation of 'cold' ion-Bernstein waves by whistler waves 15 p2235 A83-34492

Method of estimating Langmuir's turbulence in a solar flare 18 p2785 A83-39980

Perpendicular distribution of electrostatic electron-cyclotron radiation under dense plasma conditions 18 p2748 A83-40506

Unified theory of parametric excitations in magnetized plasma produced by the action of nonmonochromatic driver pump. I Modulated driver pump 18 p2748 A83-40507

Finite-width currents, magnetic shear, and the current-driven ion-cyclotron instability 18 p2748 A83-40509

Linear mode conversion in laser plasmas 18 p2748 A83-40511

Stimulated Raman and Brillouin scattering of a Gaussian electromagnetic beam in ordinary mode in a magnetoplasma 19 p2901 A83-41197

Numerical modeling of a Langmuir collapse 19 p2902 A83-41498

Particle and wave dynamics during plasma injections 20 p3018 A83-42414

Apparent electrostatic ion cyclotron waves in the diffuse aurora 20 p3025 A83-43196

Emission of myriametric radiation by coalescence of upper hybrid waves with low-frequency waves --- in magnetosphere 21 p3170 A83-44239

Influences of the ion temperature on the nonlinear electrostatic waves in magnetized plasma 21 p3212 A83-44514

Scattering of waves by Langmuir solitons 21 p3214 A83-45190

Linear density drift instabilities in very low beta plasmas A different approach 21 p3214 A83-45191

Transport by weak electrostatic density drift fluctuations 21 p3214 A83-45196

Nonlinear evolution of an obliquely propagating Langmuir wave - Boundary-value problem 22 p3361 A83-46011

Backscattering cascade of beam modes off ambient density fluctuations 22 p3362 A83-46021

The distribution of auroral electrostatic shocks below 8000-km altitude 22 p3327 A83-46049

Stochastic behavior in presence of an electrostatic wave due to the crossing of multiple cyclotron resonances in an inhomogeneous magnetic field 23 p3510 A83-48200

Electrostatic waves and the strong diffusion of magnetospheric electrons 23 p3485 A83-48556

Selective destabilization of ion cyclotron modes 24 p3631 A83-48822

ELECTROSTATICS

Theoretical calculation of conformational energies of polytetrafluoroethylene 01 p0027 A83-10606

On the physics of relativistic double layers 04 p0537 A83-15953

Electrostatic flow field of satellites moving in ionosphere 08 p1050 A83-21881

Numerically simulated two-dimensional auroral double layers 11 p1618 A83-28314

Evidence for electrostatic shocks as the source of discrete auroral arcs 13 p1879 A83-31242

Plasma waves generated by rippled, magnetically focused electron beams surrounded by tenuous plasmas 15 p2235 A83-34208

Dynamic analysis of the electrostatically controlled membrane mirror using multiple scales 17 p2476 A83-37081

Electron current disruption and parallel electric fields associated with electrostatic ion cyclotron waves 17 p2538 A83-37582

Electrostatic discharges in Saturn's B-ring 17 p2621 A83-38121

A method for the numerical solution of three-dimensional problems of electrodynamics 18 p2676 A83-39945

Influence of the equations of state and of the Z value on the solar five-minute oscillation 19 p2923 A83-40720

Discharge with electrostatic containment in order to obtain high performance ion sources 19 p2902 A83-41323

Electro-static surface control of a large radiometer spacecraft [AIAA PAPER 83-2248] 19 p2816 A83-41724

- Amplification of a two-frequency signal by an electrostatic amplifier 20 p2967 A83-42905
 Development of electrostatic levitator at JPL 20 p2940 A83-43264
 Polychromatic MTF of electrostatic point symmetric electron lenses 21 p3125 A83-44152
 Quasi-electrostatic fields within the atmosphere 22 p3325 A83-45879
 Unstable electrostatic beam modes in free-electron-laser systems 22 p3295 A83-45942
 Atmospheric storm explanation of saturnian electrostatic discharges 23 p3529 A83-47875
 Shape and stability of electrostatically levitated drops 24 p3580 A83-49877
 A method for the simulation of the transfer of charge carriers and the distribution of electrostatic potential in semiconductor structures 24 p3575 A83-50208

ELECTROSTRICTION

- Electrostrictive limit and focusing effects in pulsed photoacoustic detection 18 p2692 A83-39261

ELECTROTHERMAL ENGINES

- NT ARC JET ENGINES
 NT PLASMA ENGINES
 NT RESISTOJET ENGINES
 Augmented electrothermal hydrazine thruster development 09 p1220 A83-24890
 Electrothermal decomposition of monomethylhydrazine 21 p3117 A83-45089

ELEMENT ABUNDANCE**U ABUNDANCE****ELEMENTARY EXCITATIONS**

- NT EXCITONS
 NT MAGNONS
 NT PHONONS
 NT PLASMONS
 NT POLARONS
 Radiation generation by collective phenomena in semiconductors 16 p2358 A83-35522
ELEMENTARY PARTICLE INTERACTIONS
 NT ELECTRON CAPTURE
 NT MESON-NUCLEON INTERACTIONS
 NT NUCLEAR CAPTURE
 NT NUCLEON-NUCLEON INTERACTIONS
 Matter and antimatter in the universe 01 p0123 A83-10377
 Adiabatic vs. isothermal - Two pictures of galaxy origin 01 p0127 A83-11291
 Differences in partial inelasticity coefficients Kpi/0/ for piFe, pFe interactions at energies of 0.5-5 TeV 02 p0235 A83-11735
 Interpretations of changes in the character of the interaction of hadrons at an energy greater than 10 to the 14th eV 02 p0235 A83-11736
 Investigation of azimuth effects in gamma families with total energies of 30-1000 TeV 02 p0274 A83-11740
 Experimental studies of superfamily halos. IV --- in cosmic ray showers 02 p0274 A83-11744
 Neutral pions from the fragmentation region of an impinging hadron at E sub 0 approximately equal to 10 to the 13th eV 02 p0274 A83-11748
 An investigation of the energy spectrum and interactions of cosmic-ray muons with energies up to 10 to the 13th eV at a depth of 550 mwe 02 p0276 A83-11763
 Scattering of a neutrino by an electron in a magnetic field 03 p0392 A83-13531
 Asymptotic breaking and restoration of symmetry in a statistical system of particles with short-range vector interaction and isotropic cosmological models 03 p0417 A83-13533
 Astrophysical consequences of neutron-antineutron oscillations 04 p0556 A83-15965
 Grand unified reactions and dissipation in anisotropic cosmologies 05 p0696 A83-16977
 Cosmic-ray record in solar system matter 06 p0857 A83-18814
 Towards a unification of the parameters underlying elementary particles and cosmology 06 p0835 A83-18896
 Possible new long-range interaction and methods for detecting it 07 p0989 A83-20609
 Restrictions imposed on light scalar particles by measurements of van der Waals forces 07 p0989 A83-20610
 Polarization effects in the bremsstrahlung production of massive mesons in a magnetic field 07 p0992 A83-20857
 Results from a new search for proton decay 08 p1192 A83-22641
 Angular and energy distribution of photons of the radiative scattering of a neutrino /antineutrino/ by an electron 09 p1344 A83-24205
 Characteristics of a detector of tagged neutrinos 10 p1481 A83-25566
 Equilibrium composition and neutrino emissivity of interacting quark matter in neutron stars 10 p1515 A83-26738

- The unit gravitational charge /hc/4/ 1/2 /the uniton/, the structure of the electron and muon, and their anomalous magnetic moments 11 p1655 A83-27498
 Lepton loss and entropy generation in stellar collapse 12 p1791 A83-28987

Cosmology and elementary particles

- 13 p1944 A83-30250

Theory of cosmic ray spectra

- 13 p1966 A83-30423

Possibility of detecting relict massive neutrinos

- 13 p1966 A83-30800

Supergravity '81; Proceedings of the First School, Trieste, Italy, April 22-May 6, 1981

- 13 p1915 A83-31400

Fermion-induced monopole-antimonopole annihilation

- 13 p1954 A83-31606

Monopole heat --- generated by elementary particle interactions

- 13 p1960 A83-31789

Can graininess in the early universe make galaxies?

- 14 p2103 A83-33178

Scattering and absorption of slow particles by a black hole

- 14 p2110 A83-33391

Magnetic monopoles and evaporating black holes

- 15 p2254 A83-33793

Particles with naked beauty --- quarks produced by meson decay

- 16 p2411 A83-36022

Inelastic p-air cross section at energies between 10,000-1,000,000 TeV estimated from air-shower experiments

- 17 p2629 A83-37736

Cosmic rays and high-energy interactions - Is there a necessity for a new phenomenon?

- 17 p2630 A83-38942

Status and future of high energy diffuse gamma-ray astronomy

- 18 p2785 A83-39276

Gamma rays from giant-molecular clouds

- 18 p2785 A83-39278

Black holes in neutrino fields

- 18 p2767 A83-39529

Variable gravity theories

- 18 p2741 A83-39776

Flux of atmospheric neutrinos

- 18 p2786 A83-39926

Ordered pairing in liquid metallic hydrogen

- 19 p2899 A83-41867

Interaction of solar neutrinos with the cosmic background

- 20 p3082 A83-42276

Possible explanation for scaling violation in hadron interactions above 1000 TeV

- 20 p3082 A83-42291

Transport properties of neutrinos in stellar collapse. I Bulk viscosity of collapsing stellar cores

- 21 p3230 A83-44444

Occupation of quasi-bound states by electrons in a Schwarzschild field

- 24 p3651 A83-49066

ELEMENTARY PARTICLES

- NT ALPHA PARTICLES
 NT ANTINEUTRINOS
 NT ANTIPARTICLES
 NT ANTIPROTONS
 NT BARYONS
 NT BETA PARTICLES
 NT BOSONS
 NT CONDUCTION ELECTRONS
 NT DEUTERONS
 NT ELECTRONS
 NT FAST NEUTRONS
 NT FERMIONS
 NT FREE ELECTRONS
 NT GLUONS
 NT GRAVITONS
 NT HADRONS
 NT HIGH ENERGY ELECTRONS
 NT HOT ELECTRONS
 NT LEPTONS
 NT LIGHT BEAMS
 NT MAGNETIC MONOPOLES
 NT MESONS
 NT MUONS
 NT NEUTRINOS
 NT NEUTRON BEAMS
 NT NEUTRONS
 NT NUCLEONS
 NT PHOTOELECTRONS
 NT PHOTONS
 NT PIONS
 NT POLARONS
 NT POSITRONS
 NT PROTONS
 NT QUARKS
 NT SOLAR ELECTRONS
 NT SOLAR NEUTRINOS
 NT SOLAR PROTONS
 NT TACHYONS
 NT THERMAL NEUTRONS
 NT VECTOR MESONS

The era of superheavy-particle dominance and big bang nucleosynthesis

- 03 p0439 A83-13653

- A note on total cross sections and decay rates in the presence of a laser field 10 p1425 A83-25409
 Evidence for a new stable particle with heavy mass around 10 to the 17th eV. --- elementary particle produced in earth atmosphere 15 p2286 A83-34272
 Decay of long-lived particles in the early universe 15 p2286 A83-34612

The thermal pair annihilation spectrum - A detailed balance approach --- for cosmic plasma study

- 17 p2605 A83-37930

Galaxy formation

- 18 p2776 A83-39774

Mechanism of generating isothermal perturbation by a strong CP nonconservation --- in early universe

- 19 p2915 A83-40972

Possible experiments to search for axions

- 20 p3045 A83-42268

Experimental tests of the 'invisible' axion --- elementary particles in cosmology

- 24 p3658 A83-49292

ELEVATION**Photogrammetry and digital elevation models - Current status of development and application**

- 08 p1129 A83-22032

ELEVATION ANGLE**Solar altitude frequency tables**

- 08 p1136 A83-22617

Improved three subaperture method for elevation angle estimation --- of radar targets

- 08 p1077 A83-22734

Estimating the angles of arrival of multiple plane waves

- 08 p1158 A83-22736

Adaptive canceller for elevation angle estimation in the presence of multipath

- 16 p2343 A83-36577

Low elevation angle site diversity satellite communications for the Canadian Arctic

- 19 p2831 A83-41381

ELEVATORS (CONTROL SURFACES)**Cross-coupling between longitudinal and lateral aircraft dynamics in a spiral dive**

- 04 p0449 A83-15312

Design, fabrication and test of a composite elevator

- 21 p3151 A83-44046

ELEVONS**Heating measurements on Space Shuttle Orbiter models with differentially deflected elevons**

- [AIAA PAPER 83-1534] 14 p2011 A83-32763

ELIMINATION**A study of self-initiated eliminating from the flight training. VI - Personality traits of flying students related to self-initiated elimination.**

- 15 p2214 A83-33543

ELLIPSOIDS**Bifurcation and stability of the permanent rotations of a heavy solid whose center of mass is located near the principal plane of the inertia ellipsoid**

- 03 p0391 A83-14893

Inverse scattering at long wavelength - Delta mu = 0

- 04 p0489 A83-15163

The Newtonian potentials and dynamics of a stratified ellipsoid --- study of elliptical galaxies

- 07 p1026 A83-21258

On the nature of orbits in realistic bar potentials

- 10 p1492 A83-25480

The stability of certain Riemann ellipsoids --- rotating liquids

- 11 p1569 A83-28461

Volume integrals of ellipsoids associated with the inhomogeneous Helmholtz equation

- 12 p1775 A83-29528

Numerical simulation of radiative transfer in circumstellar dust shells. II - Ellipsoidal shells

- 13 p1959 A83-31741

The motion of an ellipsoid along a rough plane with slip

- 14 p2079 A83-32359

The rolling of an ellipsoid on a horizontal plane

- 15 p2226 A83-34432

An ellipsoidal frequency selective surface

- 15 p2146 A83-35080

The determination of the elastodynamic fields of an ellipsoidal inhomogeneity

- [ASME PAPER 83-APM-19] 17 p2519 A83-37388

Calculation of transonic noncircular flow past a highly oblate ellipsoid

- 17 p2449 A83-37538

Observable properties of non-axisymmetric galaxies. I Geometrical parameters

- 17 p2595 A83-38581

Dipole resonance of a plasma ellipsoid in a dielectric shell with allowance for radiation damping

- 17 p2584 A83-38985

The gradients of the velocity ellipsoid for nearby stars

- 19 p2909 A83-40713

Directions of axes of the earth's ellipsoid of inertia derived from satellite orbit dynamics

- 19 p2860 A83-41317

A differential scheme for multiphase composites. I - Overall elastic moduli. II - Thermal expansion coefficients and conductivities

- 20 p3002 A83-42800

Effect of surface roughness on the delayed transition on 9:1 heated ellipsoids

- 21 p3134 A83-45583

Turbulent boundary layers on three-dimensional configurations

- 22 p3286 A83-47035

Equations for the small oscillations of an inertial navigation system with allowance for the ellipsoidality of the earth 23 p3421 A83-48456

ELLIPTOMETERS

Fundamental relations for radiowave ellipsometry of 'thin metal film on dielectric substrate' system 01 p0049 A83-10362

Ellipsometric study of silicon nitride on gallium arsenide 02 p0242 A83-11812

Equi-intensity spectroscopic ellipsometry with imperfect optical components 10 p1418 A83-25453

An enhanced sensitivity null ellipsometry technique for studying films on substrates - Application to silicon nitride on gallium arsenide 17 p2584 A83-37618

CW laser-annealing behavior of Se(+)-implanted InP investigated by ellipsometry 20 p3055 A83-43603

ELLIPTIC DIFFERENTIAL EQUATIONS

NT MONGE-AMPERE EQUATION

Solution of a free-boundary problem for elliptic equations 01 p0102 A83-11264

The superconvergence of finite element method solutions in mesh norms 01 p0102 A83-11266

Solvability of boundary value problems for linear and quasi-linear B-elliptic equations 02 p0231 A83-11637

A convergent method for solving the balance equation --- for atmospheric circulation analysis 02 p0217 A83-13053

Plane resonance rotations of a dynamically symmetric satellite in the three-body problem 03 p0407 A83-13670

Elliptic problem solvers --- Book 03 p0384 A83-14076

A multi-level iterative method for nonlinear elliptic equations 03 p0388 A83-14077

Solving elliptic problems - 1930-1980 03 p0388 A83-14078

Co-energy methods for elliptic flow and related problems 03 p0384 A83-14080

Ellpack - Progress and plans 03 p0384 A83-14081

Sparse vectorized direct solution of elliptic problems 03 p0385 A83-14083

On preconditioned iterative methods for elliptic partial differential equations 03 p0388 A83-14084

Applications of transfinite 'blending-function' / interpolation to the approximate solution of elliptic problems 03 p0388 A83-14085

Vector algorithms for elliptic partial differential equations based on the Jacobi method 03 p0388 A83-14087

Mesh generation by conformal and quasiconformal mappings 03 p0388 A83-14089

An empirical investigation of methods for nonsymmetric linear systems 03 p0385 A83-14091

Plane stress problems of the elastic perfectly-plastic medium 03 p0341 A83-14486

Three-dimensional grid generation using elliptic equations with direct grid distribution control [AIAA PAPER 83-0448] 05 p0636 A83-16720

Adaptive grids generated by elliptic systems --- for computational fluid dynamics [AIAA PAPER 83-0451] 05 p0636 A83-16723

The behavior of generalized solutions of second-order elliptic equations and of the system of elasticity theory in the neighborhood of a boundary point 05 p0654 A83-17137

Iterative solution of the global element equations 05 p0682 A83-17899

Projection methods in non-self-adjoint problems of mathematical physics 07 p0986 A83-20310

A finite boundary method for fluid flow field computations 07 p0927 A83-21436

On the marching solution of elliptic equations in viscous fluid mechanics 08 p1087 A83-23177

Boundary value problem of Bitsadze-Samarskii type for a second-order elliptic equation with operator coefficients 09 p1335 A83-24249

Behavior of generalized solutions of the Dirichlet problem for high-order elliptic equations near a boundary 09 p1339 A83-24320

Some methods of integration in function space for use in control and filtering 09 p1329 A83-24738

Regional Monte Carlo solution of elliptic partial differential equations 12 p1773 A83-29626

Spectral multigrid methods for elliptic equations 12 p1773 A83-29663

Finite element interpolation error bounds with applications to eigenvalue problems 12 p1773 A83-29705

Quasi-linear degenerate and nonuniformly elliptic and parabolic equations of second order --- Russian book 13 p1912 A83-30450

The application of iterated defect correction to variational methods for elliptic boundary value problems 14 p2078 A83-32842

Oblique derivative boundary value problems for nonlinear elliptic systems of second order 14 p2078 A83-33155

Performance evaluation of algorithms for mildly nonlinear elliptic problems 16 p2406 A83-35644

Oscillation properties of solutions of second order elliptic equations 17 p2572 A83-38466

Elliptic grid generation 17 p2572 A83-38780

Grid generation by elliptic partial differential equations for a tri-element Augmentor-Wing airfoil 17 p2458 A83-38803

Numerical generation of composite three dimensional grids by quasilinear elliptic systems 17 p2574 A83-38804

Numerical generation of three-dimensional coordinates between bodies of arbitrary shapes 17 p2574 A83-38806

Semidirect/marching solutions and elliptic grid generation 17 p2574 A83-38807

Three-dimensional grid generation from elliptic systems [AIAA PAPER 83-1905] 18 p2739 A83-39364

Analytical methods in the theory of elliptic equations --- Russian book 19 p2893 A83-40984

On the simplified hybrid-combined method --- for solving boundary value problems of elliptic equations 20 p3041 A83-42495

ELLIPTIC FUNCTIONS

Formal convergence characteristics of elliptically constrained incremental Newton-Raphson algorithms 01 p0101 A83-10273

On the numerical construction of ellipsoidal wave functions 07 p0987 A83-20512

Distributed control of a system governed by Dirichlet and Neumann problems for a self-adjoint elliptic operator with an infinite number of variables 08 p1156 A83-22045

An exact solution of the classical Boussinesq equation 14 p2077 A83-32507

The general solutions of the doubly periodic cracks 18 p2696 A83-39083

ELLIPTIC INTEGRALS

U ELLIPTIC FUNCTIONS

ELLIPTIC CYLINDERS

The unsteady boundary layer on an elliptic cylinder following the impulsive onset of translational and rotational motion [AIAA PAPER 83-0128] 05 p0580 A83-16541

Laminar, natural convection heat transfer in a horizontal gap, bounded by an elliptic and A circular cylinder 15 p2160 A83-34260

Unsteady flow field, lift and drag measurements of impulsively started elliptic cylinder and circular-arc airfoil [AIAA PAPER 83-1711] 17 p2502 A83-37205

Scattering of high-frequency electromagnetic waves by an impedance elliptical cylinder 17 p2495 A83-38993

ELLIPTICAL GALAXIES

Dynamics of elliptical galaxies and other spheroidal components 02 p0246 A83-12189

On the origin of the globular cluster system of M87 02 p0261 A83-12909

Absolute ultraviolet fluxes of elliptical galaxies as observed with the Astronomical Netherlands Satellite /ANS/ 03 p0415 A83-13363

Dissipationless galaxy formation and the r to the 1/4-power law 03 p0420 A83-13935

Further observations of the elliptical galaxy NGC 5813 03 p0420 A83-13937

V Zw 311 - The once and future cD 04 p0551 A83-15602

Spectroscopy of galaxies in distant clusters. I - First results for 3C 295 and 0024 + 1654 05 p0696 A83-16980

Triaxial equilibrium models for elliptical galaxies with slow figure rotation 05 p0697 A83-16987

VLBI observations of the nucleus and jet of M87 05 p0697 A83-16989

The infrared emission from the elliptical galaxy NGC 1052 05 p0697 A83-16990

Kinematics of elliptical-like galaxies with dust lanes 06 p0826 A83-18157

H I observations of high-luminosity elliptical galaxies 06 p0819 A83-18853

A study of the two-dimensional luminosity distribution of NGC 3379 06 p0833 A83-18855

Some properties of the centers of cD galaxies 06 p0821 A83-19052

Preferred orbit planes in the gravitational field of a tumbling spheroidal galaxy 06 p0843 A83-19480

The rotation of elliptical galaxies - An application of the theory of tidal torques 06 p0843 A83-19481

Tidal distension in protostructures - The shapes of galaxies and systems of galaxies 07 p1017 A83-20937

On the methods for determining galaxy velocity dispersions 07 p1009 A83-21236

The Newtonian potentials and dynamics of a stratified ellipsoid --- study of elliptical galaxies 07 p1026 A83-21258

Hierarchical merging and the structure of elliptical galaxies 08 p1181 A83-23027

The long term evolution of rotating stellar bars 08 p1182 A83-23037

Infrared photometry of the halo of M87 08 p1176 A83-23080

A radio galaxy at high redshift undergoing strong stellar evolution 08 p1191 A83-23280

Color gradients in galactic spheroids. II - Gradient as a function of luminosity and morphology 09 p1356 A83-23317

A comment on the colors of globular clusters in elliptical galaxies 09 p1357 A83-23728

Velocity field and physical conditions in the active lenticular galaxy NGC 3998 09 p1363 A83-24989

A quasi-stable stellar system with prolate inner and oblate outer parts 09 p1363 A83-25001

Models for elliptical galaxies. I - Oblate spheroids with anisotropy. II - Oblate spheroids with realistic rotation curves 09 p1364 A83-25004

A search for neutral hydrogen in radio galaxies 10 p1492 A83-25477

The arc second radio structure of 12 BL Lacertae objects 10 p1493 A83-25702

The kinematic properties of faint elliptical galaxies 10 p1493 A83-25704

Infrared observations of the jet in M87 10 p1493 A83-25706

Dynamics of yet more ellipticals and bulges 10 p1508 A83-26360

The nature of the ionizing source of the nuclear gas in NGC 1052 10 p1511 A83-26402

NGC 315 - High-velocity H I in an active elliptical galaxy 10 p1511 A83-26404

Millimeter-wavelength outbursts in the elliptical galaxy NGC 1052 10 p1516 A83-26749

Orbital configurations for gas in elliptical galaxies 10 p1497 A83-26751

Sensitive mapping of E and SO galaxies in search of H I content differences between supernovae and non-supernovae producing galaxies 11 p1668 A83-27104

Intrinsic principal axes twists in N-body models of elliptical galaxies 11 p1675 A83-28294

Spectroscopy of three ultraviolet-excess galaxies 12 p1796 A83-29489

Further evidence for M87's massive, dark halo 13 p1950 A83-31407

Thermal conduction and heating by nonthermal electrons in the X-ray halo of M87 13 p1950 A83-31408

Stellar orbits in a triaxial galaxy. I - Orbits in the plane of rotation 13 p1950 A83-31411

The Horologium-Reticulum supercluster of galaxies 13 p1956 A83-31682

Design of a four-channel simultaneous visual infrared photometer 14 p2096 A83-32030

On the equilibrium configurations of prolate, axisymmetric stellar systems 15 p2257 A83-34091

Detection of 10 to the 10th solar masses of hot gas in the normal elliptical galaxy NGC 5846 with the Einstein satellite 15 p2259 A83-34119

Dwarf elliptical galaxies 15 p2259 A83-34120

DDO photometry and metallic abundances of E and SO galaxies and globular clusters of the LMC and SMC 15 p2262 A83-34534

The virial mass of the nucleus of M32 15 p2263 A83-34559

A narrow-line radio galaxy behind the Fornax cluster 15 p2266 A83-34610

NGC 1275 - A burgeoning elliptical galaxy 15 p2267 A83-34622

Synthesized colors and spectra for galaxies of normal chemical composition 15 p2270 A83-34753

The elliptical galaxy NGC 4696 - CCD observations of an absorbing lane 16 p2433 A83-36698

Surface brightness and effective radius for elliptical galaxies 17 p2602 A83-37780

Structure and stellar content of dwarf elliptical galaxies 17 p2602 A83-37781

Simulations of galaxy mergers. II 17 p2593 A83-38244

Is it possible to turn an elliptical radio galaxy into a BL Lac object? 17 p2607 A83-38262

The distribution of violently relaxed matter in galaxies 17 p2609 A83-38418

Why is M87 jet one sided in appearance? 17 p2612 A83-38599

Elliptical galaxies - Can rotation be effective in determining their shapes? 18 p2775 A83-39748

Stellar populations in local group dwarf elliptical galaxies.
I - NGC 147 19 p2918 A83-41616
The structure of the Carina dwarf elliptical galaxy
20 p3064 A83-42319
Simulations of galaxy mergers - Cannibalism and dynamical friction
20 p3066 A83-42431
The Riemann disks. I - Equilibrium and secular evolution
20 p3071 A83-43051
Position angle variation of the major axis of some galaxies
20 p3061 A83-43378
Periodic orbits in elliptical galaxies
21 p3223 A83-44445
High-resolution optical observations of NGC 3379. I - An analysis of previous data
21 p3225 A83-44980
Globular clusters and the early chemical history of galactic halos
22 p3378 A83-46409
Detectability of globular cluster systems in distant galaxies
22 p3378 A83-46410
The reddening of radio elliptical galaxies
22 p3378 A83-46553
Globular cluster systems in the Hydra I elliptical galaxies.
II 22 p3381 A83-46979
The tensor virial theorem for subsystems --- with application to elliptical galaxies
23 p3519 A83-47452
Elliptic stellar disks - Equilibrium solutions in the presence of a halo and in binary systems
24 p3653 A83-49165
Dynamics of early-type galaxies
24 p3657 A83-49246
Scale-free models of elliptical galaxies
24 p3641 A83-49249
Kinematic modelling of NGC 3379
24 p3641 A83-49251
Interstellar matter in elliptical galaxies
24 p3657 A83-49252
Sensitive search for HI in E and SO galaxies
24 p3657 A83-49253
Neutral hydrogen observations of the dwarf elliptical galaxies NGC 185 and NGC 205
24 p3642 A83-49254
Taurus observations of the emission-line velocity field of Centaurus A (NGC 5128)
24 p3642 A83-49257
On the formation and dynamics of shells around elliptical galaxies
24 p3657 A83-49260
The manifold of elliptical galaxies
24 p3657 A83-49265
CCD surface photometry of two southern active galaxies, NGC 1316 and 1052
24 p3659 A83-49378
A high resolution study of the optical jet of M 87
24 p3661 A83-49456
The UV spectrum of elliptical galaxies
24 p3662 A83-49561

ELLIPTICAL ORBITS

NT INTERPLANETARY TRANSFER ORBITS
NT PERIGEEES
NT PERIHELIONS
NT TRANSFER ORBITS
Oscillations of a satellite with compensating devices in an elliptical orbit
03 p0287 A83-13204
Orbit manoeuvres with finite thrust - A study and presentation of results
03 p0283 A83-13846
Expansion of the coordinates of the elliptical motion of an artificial earth satellite in series of multiples of the eccentric anomaly
05 p0602 A83-17678
An empirical initial estimate for the solution of Kepler's equation
07 p0868 A83-21427
Deployment of a long-tethered connection between two bodies in orbit
09 p1212 A83-25042
Criteria of hyperbolic and hyperbolic-elliptical motion in capture theory
11 p1673 A83-28032
Formulas free of singularities at zero inclinations and eccentricities for improving the orbits of low earth satellites
11 p1532 A83-28036
On the integration of functions of elliptical motion
11 p1673 A83-28043
The rotation number of bounded orbits in a central field
12 p1787 A83-29116
On the double averaged three-body problem
12 p1787 A83-29118
Expansion of the coordinates of elliptical motion with respect to the Levi-Civita parameter
13 p1940 A83-31271
Numerical results in the three-body problem
14 p2100 A83-33251
W-shaped occultation signatures - Inference of entwined particle orbits in charged planetary ringlets
16 p2435 A83-35729
Some mechanical invariants of elliptical orbits
16 p2423 A83-35757
A second order Jupiter-Saturn planetary theory
16 p2439 A83-36787
Active attitude control of a spinning symmetrical satellite in an elliptic orbit
17 p2475 A83-37073

Entwined and parallel bundled orbits as alternative models for narrow planetary ringlets
17 p2624 A83-38947
Hill's stability in the elliptic restricted three-body model including body shape
18 p2754 A83-39007
Expansion theory for the elliptic motion of arbitrary eccentricity and semi-major axis. V - Elliptic expansions in terms of the sectorial variables for the first four categories
18 p2759 A83-39747
Stability of the periodic oscillations of a nearly axisymmetrical satellite in the plane of an elliptical orbit.
23 p3418 A83-48455

ELLIPTICAL PLASMAS

Rotating, post-Newtonian near-ellipsoidal configurations of a magnetized homogeneous fluid
07 p1026 A83-21260

ELLIPTICAL POLARIZATION

Analysis of the electromagnetic field in an open resonator
01 p0035 A83-10372
The scattering of an E-polarized plane wave by a finite number of coplanar strips
02 p0162 A83-11540
Some possibilities of identifying the effect of geoelectric inhomogeneities on the polarization of geomagnetic pulsations at midlatitudes
02 p0210 A83-12440
Nonlinear interaction between elliptically polarized waves in a ring gas laser in a magnetic field
03 p0316 A83-13586
Elliptically polarized natural modes in pulsar magnetospheres
13 p1945 A83-30363
Polarimetric techniques in radar signal processing
19 p2825 A83-40758

ELLIPTICITY

Autorotation of an elliptic airfoil
[AIAA PAPER 83-0130] 05 p0580 A83-16543
Significance of non-elliptic regions in balanced flows of the tropical atmosphere
08 p1139 A83-22295
Earth's flattening effect on the tidal forcing field
16 p2381 A83-36618
Determination of transfer functions in the problem of the unsteady interaction of a fluid with an elastic elliptical shell
18 p2702 A83-40119
Ellipticity variations within some globular clusters of the Galaxy and the Magellanic Clouds
23 p3516 A83-47455
Dynamics of an elliptical vortex
23 p3452 A83-48656

ELONGATION

Current problems in superplasticity
09 p1232 A83-24061
The geometrical factor during the extrusion of complex metal materials
13 p1859 A83-30688

ELUTION

Wet classification in the centrifugal force field --- German thesis
07 p0925 A83-20395

ELUTRIATION

U ELUTION

EMBEDDED COMPUTER SYSTEMS

NT AIRBORNE/SPACEBORNE COMPUTERS
Automatic selection of switching paths
01 p0037 A83-10734
An Atlas implementation for the '80s
01 p0091 A83-10740
Software reliability enhancement techniques and assessment method for embedded computer systems
01 p0091 A83-11113
Integrated and transferable hardware/software checkout --- of digitally controlled flight systems
01 p0093 A83-11249
Celestial navigation in the computer age --- Book
03 p0280 A83-14116
Display methods of laser radar data using a computer system
03 p0328 A83-14132
ATE accomplishes receiver specification testing with increased speed and throughput
04 p0474 A83-16398
An anatomy of industrial robots and their controls
08 p1074 A83-22415
A 200 million operations per second /MOPS/ systolic processor
08 p1155 A83-22796
AML - A manufacturing language
11 p1646 A83-28100
Performance of the Multiple Mirror Telescope (MMT).
IV - MMT computer systems
13 p1937 A83-30980
A near-field antenna measurement system
13 p1830 A83-31282
Application of a charge-coupled device (CCD) detector for coudespectroscopy
14 p2016 A83-31992
A computational system for the automatic and simultaneous acquisition of radio telescope data from four different directions
14 p2101 A83-33292
Reflective field optics for IR spectrophotometers
18 p2744 A83-40429
Operation and control of a 2 GW wave-energy scheme
24 p3599 A83-49000

EMBEDDING

Embedded flow characteristics of sharp-edged rectangular wings
08 p1042 A83-22152

EMBOLISMS

NT AEROEMBOLISM
Survival following accidental decompression to an altitude greater than 74,000 feet /22,555 m/
04 p0522 A83-15538

EMBRITTLMENT

Recrystallization and embrittlement of sintered tungsten
02 p0158 A83-12950
The relation between surface energy and effective fracture energy for grain boundary fracture
09 p1279 A83-23869
Post-weld heat-treatment cracking in superalloys
10 p1393 A83-25407
High temperature embrittlement of Ni and Ni-Cr alloys by trace elements
10 p1396 A83-25863
The multiplicity of factors causing intergranular fracture
13 p1822 A83-30742
High-temperature embrittlement of tungsten
15 p2140 A83-35042
The effects of tempering reactions on temper embrittlement of alloy steels
16 p2329 A83-35688
The evaluation of tempered martensite embrittlement in 4130 steel by instrumented Charpy V-notch testing
16 p2329 A83-35689
Embrittlement of P/M X7091 and I/M 7175 aluminium alloys by mercury solutions
16 p2330 A83-35983
Structure and properties of vanadium maraging steels
24 p3559 A83-48805

EMBRYOLOGY

The formation of the vascular-receptor relations in the forearm muscles of humans
07 p0978 A83-20993
The effect of weightlessness on the reproductive function of mammals
11 p1635 A83-27779

EMBRYOS

Experimental data from a study of the toxic effect on embryos exerted by hexachlorophene - A component of antimicrobial fabrics and synthetic articles of everyday use
05 p0677 A83-17203
Reversal of early pattern formation in inverted amphibian eggs
11 p1638 A83-27821

EMERALD

U BERYL

EMERGENCIES

An approach to helicopter power selection
09 p1207 A83-24828
The psychological bases of the training of a human operator for readiness to act in extreme conditions
16 p2401 A83-36823
An FAA analysis of aircraft emergency evacuation demonstrations
17 p2459 A83-38005
The activity of the Italian Air Rescue Service in the transport of high-risk patients in emergency situations
17 p2557 A83-38943
Emergency care for burns --- Russian book
23 p3498 A83-48150

EMERGENCY LOCATOR TRANSMITTERS

Doppler measurements applied to the location of emergency radio beacons
07 p0870 A83-19703
Sarsat-Kospas - Satellite search-and-rescue trials presage new international system
09 p1211 A83-25138
The planned satellite-based maritime distress call system
17 p2494 A83-37853

EMISSION

NT ACOUSTIC EMISSION
NT CATHODE GLOW
NT CATHODOLUMINESCENCE
NT CHEMILUMINESCENCE
NT CN EMISSION
NT ELECTROLUMINESCENCE
NT ELECTRON EMISSION
NT EXHAUST EMISSION
NT FIELD EMISSION
NT FLUORESCENCE
NT HYDROXYL EMISSION
NT ION EMISSION
NT LIGHT EMISSION
NT LUMINESCENCE
NT MICROWAVE EMISSION
NT NEUTRON EMISSION
NT OPTICAL RESONANCE
NT PARTICLE EMISSION
NT PHOSPHORESCENCE
NT PHOTOELECTRIC EFFECT
NT PHOTOELECTRIC EMISSION
NT PHOTOIONIZATION
NT PHOTOLUMINESCENCE
NT RADIO BURSTS
NT RADIO EMISSION
NT RESONANCE FLUORESCENCE
NT SECONDARY EMISSION
NT SELF SUSTAINED EMISSION

NT SHOCK WAVE LUMINESCENCE
NT SOLAR RADIO BURSTS
NT SOLAR RADIO EMISSION
NT SPECTRAL EMISSION
NT SPONTANEOUS EMISSION
NT STIMULATED EMISSION
NT THERMAL EMISSION
NT THERMIONIC EMISSION
NT THERMOLUMINESCENCE
NT TRIBOLUMINESCENCE
NT TYPE 2 BURSTS
NT TYPE 3 BURSTS
NT TYPE 4 BURSTS
NT WATER MASERS
NT X RAY FLUORESCENCE

EMISSION SPECTRA
Optical polarization position angle versus radio source axis in radio galaxies 01 p0115 A83-10210
A radiation scheme for circulation and climate models 01 p0074 A83-10221
Intrinsic reddening of Be stars and its relation with H-alpha emission intensities 01 p0120 A83-10311
Polarization in peculiar emission-line objects 01 p0116 A83-10316
Statistical properties of Be stars 01 p0120 A83-10318
Search for long-period radial velocity variations in some Be stars 01 p0116 A83-10323
A preliminary report on simultaneous ultraviolet and optical observations of Lambda Eridani 01 p0121 A83-10326
Recent changes of the Be star HD 58050 01 p0121 A83-10328
Far-ultraviolet colors of B stars with and without emission lines 01 p0123 A83-10349
Spectroscopic investigations of Herbig-Ae-Be-Stars 01 p0123 A83-10356
The origin of the infrared /C I/ emission - H II or H I regions 01 p0125 A83-10926
Extended and anisotropic high-velocity gas flows in the Orion-KL region 01 p0125 A83-10930
Markarian 914 is a galactic object, lick H-alpha 233 01 p0118 A83-10969
Bound-free emission in HgBr 01 p0055 A83-10979
Detection of bipolar CO outflow in Orion 02 p0253 A83-11617
Luminescence spectra of stripe-geometry laser heterostructures in GaAs-Al/x/Ga/1-x/As 02 p0183 A83-11695
The ultraviolet continuous and emission-line spectra of the Herbig-Haro objects HH 2 and HH 1 02 p0256 A83-12125
HEAO 1 observations of quiescent X-ray emission from flare stars 02 p0256 A83-12129
Copernicus measurement of the Jovian Lyman-alpha emission and its aeronomical significance 02 p0264 A83-12142
2-4 micrometer spectroscopy of the compact H II region G 45.13 + 0.14 A 02 p0260 A83-12520
Na I D brightening phenomena in quiescent prominences 02 p0270 A83-12576
Evidence for starspots on single solar-like stars 02 p0262 A83-12918
Radio and infrared emission from extended stellar envelopes 03 p0412 A83-13152
The Lyman-alpha emission-line profiles in high-redshift QSOs 03 p0413 A83-13323
TAURUS: A wide-field imaging Fabry-Perot spectrometer for astronomy 03 p0401 A83-13324
GX 1-4: pulse period measurement and detection of phase-variable iron line emission 03 p0402 A83-13330
Emission spectra of an Xe plasma generated by a beam 03 p0397 A83-13593
Io - A volcanic flow model for the hot spot emission spectrum and a thermostatic mechanism 03 p0133 A83-13833
Kinematics of gas clouds in Seyfert nuclei and quasars 03 p0418 A83-13876
Wolf-Rayet stars and an extraordinary star-forming region in the barred spiral galaxy NGC 5430 deg 03 p0421 A83-14138
A thermal wind model for the broad emission line region of quasars 03 p0423 A83-14184
Ultraviolet emission in the Mg II h and k lines in Be stars 03 p0424 A83-14201
Diffuse galactic gamma-ray line emission from nucleosynthetic Fe-60, Al-26, and Na-22 - Preliminary limits from HEAO 3 03 p0439 A83-14210
Cyclotron emission in strongly magnetized plasmas 03 p0429 A83-14795
The detection of extranuclear emission lines in the Seyfert galaxies Mkn10 and Mkn79 03 p0430 A83-14811

An emission measure analysis of two sunspots observed by the UVSP instrument on the SMM spacecraft --- ultraviolet spectrometer and Polarimeter on Solar Maximum Mission 03 p0437 A83-14906
Measurements of the magnetic field in solar prominences with a spectrally scanning magnetograph 03 p0438 A83-14910
Asymmetric emission-line regions with out-flowing mass in QSOs and the z/ab/ at least equal to z/em/ systems 04 p0549 A83-15028
Coma quasars 04 p0551 A83-15603
Further examples of companion galaxies with discordant redshifts and their spectral peculiarities 04 p0552 A83-15606
A redshift difference between high and low ionization emission-line regions in QSOs - Evidence for radial motions 04 p0552 A83-15608
The H II regions of Messier 8 04 p0552 A83-15615
Are QSOs local objects. I - A new interpretation of the emission and absorption spectra of a few QSOs 04 p0556 A83-15967
Forbidden line emission from highly ionized atoms in tokamak plasmas 04 p0538 A83-16060
Detection of H/C-17/O plus in Sagittarius B2 05 p0700 A83-17034
Carbon monoxide laser with selective and nonselective resonators 05 p0648 A83-17048
Synthetic spectra for auroral studies - The N2 Vegard-Kaplan band system 05 p0662 A83-17405
Delineation of estuarine fronts in the German Bight using airborne laser-induced water Raman backscatter and fluorescence of water column constituents 05 p0646 A83-17715
Regular and chaotic behaviour of multimode gas lasers 05 p0651 A83-17893
NGC 6503 - Rotation, mass and physical conditions in galaxy nucleus 06 p0824 A83-18017
The chromospheric evershed flow observed in the EUV spectrum 06 p0852 A83-18122
The Seyfert 1 galaxy NGC 4593. I - Variability of the UV spectrum and physical conditions in the broad line emitting region 06 p0826 A83-18161
Detection of molecular hydrogen emission from G 333.6-0.2 06 p0827 A83-18162
Interpretation of line profiles of the symbiotic star V 1016 Cyg 06 p0818 A83-18538
The H-alpha emission line in the star HDE 245770 = A0535 + 26 06 p0830 A83-18786
Neutrino emission spectra of collapsing degenerate stellar cores - Calculations by the Monte Carlo method 06 p0832 A83-18843
Spatial observations of dust emission in NGC 7027 06 p0833 A83-18869
The violet emissions produced by laser excitation of Na vapor in the 570-595 nm region 06 p0808 A83-18952
A search for resonance polarization in stars with enhanced Ca II H and K emission 06 p0821 A83-19062
New H-alpha emission stars in galactic dark clouds 06 p0823 A83-19207
HD 207739 - A strange composite star 06 p0823 A83-19301
The near-infrared spectrum of the Herbig Ae-Be stars 06 p0844 A83-19497
Transient emission events in the early Be star 59 Cygni 07 p1010 A83-19859
Searches for far-infrared emission from dark clouds - Rho Ophiuchi, Heiles 2, L1529, and L183 07 p1010 A83-19860
CO observations of the supernova remnant G78.2+2.1 07 p1010 A83-19862
Rare-earth converters of the emission spectrum of neodymium lasers 07 p0933 A83-19975
New heartbeat phenomenon, and the concept of 2-D optical turbulence 07 p0935 A83-20160
Spectrophotometry of four galaxies of high surface brightness 07 p1007 A83-20665
Observations of the new OH maser source G43.2-0.1 07 p1007 A83-20670
Experimental evidence for collision-induced superradiance 07 p0937 A83-20797
Theoretical quasar emission-line profiles. I - Curve-of-growth effects on observed profiles 07 p1019 A83-21104
Spectrophotometry of the broad absorption-line QSO PHL 5200 07 p1019 A83-21106
Observations of the 145.5 micron O I forbidden emission line in the Orion Nebula 07 p1023 A83-21155
Rocket measurements of the vertical profile of H-beta emission and the background at 4600 A at high latitudes 07 p0964 A83-21179
Ratio of the intensities of 5577-A and 4278-A auroral emissions in proton and electron polar-auroras 07 p0964 A83-21183

Observations of emission line galaxies. I - The Seyfert-1 galaxies Mkn 1040, Mkn 1044 07 p1008 A83-21216
High density molecular gas in the Rho Ophiuchi cloud 07 p1024 A83-21221
On the origin of relativistic particles and gamma-rays in quasars 08 p1181 A83-23030
An optical study of IC 1470 08 p1183 A83-23048
Molecular emission bands in the ultraviolet spectrum of the red rectangle star HD 44179 08 p1183 A83-23053
H I observations of active and interacting galaxies 09 p1356 A83-23316
Slope of the solar radio emission spectrum in the 6.3-8.6 mm range 09 p1368 A83-23490
Atomic nitrogen emissions from photodissociation of N2 09 p1304 A83-23773
EUV studies of N2 and O2 produced by low energy electron impact 09 p1342 A83-24130
On the nature of the /intermittent/ emission line star LKH-alpha 324 09 p1361 A83-24478
Emission-line spectra of H II regions - Dependence on metal abundances in the atmosphere of the ionizing star and in the nebular gas 09 p1361 A83-24482
Velocity and spectrum of the supernova remnant 30 Dor B 09 p1362 A83-24981
Can C IV emission be used as a luminosity indicator --- of quasars 09 p1362 A83-24987
Velocity field and physical conditions in the active lenticular galaxy NGC 3998 09 p1363 A83-24989
The kinematics of the Ori A SO emission zone 09 p1363 A83-24996
IUE observations of variable Seyfert 1 galaxies 09 p1356 A83-25297
The composite UV emission spectrum of Seyfert 1 galaxies 10 p1500 A83-25486
Nuclear activity in the barred spiral galaxy NGC 3660 from radio, optical, and X-ray observations 10 p1500 A83-25488
H1340 no. 10 - A high-redshift QSO with very narrow emission lines 10 p1501 A83-25579
Simultaneous spectroscopy and photometry of the AM Herculis-like star H0139-68 10 p1502 A83-25584
On the presence of O I lambda32 emission in Be stars 10 p1502 A83-25585
Prominent ultraviolet emission lines from Type 1 Seyfert galaxies 10 p1493 A83-25703
IUE observations of E1405-451 - A new AM Herculis type cataclysmic variable 10 p1505 A83-25744
A large-amplitude photometric periodicity on a T Tauri star 10 p1494 A83-25745
Highly compact structures in galactic nuclei and quasars 10 p1496 A83-25858
Shock-excited emission spectrum of tungsten oxide 10 p1479 A83-26166
Physical conditions in the emission regions of active galactic nuclei 10 p1506 A83-26230
The formation of permitted and forbidden lines in quasars 10 p1507 A83-26233
Far-ultraviolet diffuse emission lines from the interstellar medium 10 p1511 A83-26406
Rocketborne cryogenic /10 K/ high-resolution interferometer spectrometer flight HIRIS - Auroral and atmospheric IR emission spectra [AD-A128358] 10 p1423 A83-26642
Characteristics of the laser emission spectrum of a thallium photodissociation laser 10 p1431 A83-26654
Spectral composition of the radiation emitted from a concentrated LiNdLa phosphate glass laser with a Q switch made of an LiF crystal with F2/-/ centers 10 p1432 A83-26662
The polarization of millimeter-wave emission lines in dense interstellar clouds 10 p1513 A83-26713
Time-resolved spectrophotometry of the nova-like variable RW Trianguli 10 p1514 A83-26726
CO emission in the outer Galaxy between longitudes 50 deg and 72 deg 10 p1516 A83-26753
X-ray and optical studies of emission-line Markarian galaxies 11 p1668 A83-27103
A search for weak H-alpha emission line pre-main-sequence stars 11 p1669 A83-27117
Intensity and extinction irregularities in the H2 emission from Orion 11 p1676 A83-27120
Spectral diversity crystalline fluoride lasers 11 p1581 A83-27588
The relationship between soft X-rays and the 1640 A feature fluxes in late-type stars 11 p1678 A83-27684
Emissions from the transition regions and coronae of three cool dwarf stars 11 p1678 A83-27686
IUE observations of the high velocity symbiotic star AG Draconis during active phase 11 p1678 A83-27694
Measurements of metastable N/+/-/D-1 6584 A emission in the twilight thermosphere 11 p1618 A83-28322

Thermospheric odd nitrogen. I - NO, N/4S/, and O/3P/
densities from rocket measurements of the NO delta and
gamma bands and the O2 Herzberg I bands
11 p1618 A83-28323

A white-light /Fe X/H-alpha coronal transient
observation to 10 solar radii
11 p1693 A83-28587

A high-latitude H I-cloud with optical emission
12 p1785 A83-28883

A concentration of quasars in the Sculptor region of
the sky
12 p1788 A83-29708

The optical emission from the supernova remnant HB
3
12 p1797 A83-29955

Identification of Lanning 90 as a previously uncatalogued
cataclysmic variable
12 p1789 A83-29957

On the possibility of discovering flare stars in their quiet
state
13 p1943 A83-30004

Atomic emission spectral analysis using lasers in the
monopulse regime
13 p1817 A83-30260

H76-alpha recombination line emission near Sgr A
13 p1947 A83-30392

Spontaneous spectrum and small-signal gain for a
tapered wiggler free-electron laser
13 p1853 A83-31115

The rotationally resolved 3400- to 3800-A terrestrial
nightglow
13 p1949 A83-31247

Time-resolved spectrophotometry of the emission lines
in the galactic X-ray source H2252-035
13 p1940 A83-31427

R 66(Aeq) - An LMC B supergiant with a massive cool
and dusty wind
13 p1954 A83-31567

Active chromosphere in the carbon star TW
Horologium
13 p1954 A83-31578

A study of shapes of Ca II chromospheric emissions in
late type stars
13 p1955 A83-31655

Remarkable kinematics of the ionized gas in the nucleus
of NGC 1365
13 p1957 A83-31700

Detection of H2 emission in Herbig-Haro object No.
101
13 p1957 A83-31703

On the Baldwin effect in optically-selected quasars
13 p1943 A83-31711

The Cygnus X region. XIII - The dark cloud between
IC 1318b and c
13 p1959 A83-31743

Fluorescence branching ratios from the A2Sigma +
(v-prime = 0) state of NO
14 p2081 A83-31936

On the observability of forbidden lines
14 p2086 A83-31938

The lasing mechanism, active layer thickness, natural
resonator effects, and the nature of the M and P bands
of the emission spectrum of CdS pumped by a nitrogen
laser - T = 4.2-420 K
14 p2023 A83-32163

High-velocity, asymmetric Doppler shifts of the X-ray
emission lines of Cassiopeia A
14 p2104 A83-33193

Survey of H-alpha emission in globular cluster red
giants
14 p2105 A83-33196

Variations in the ultraviolet spectrum of the symbiotic
star Z Andromedae
14 p2108 A83-33264

The spectrum of the star AP Hd 3473
14 p2108 A83-33269

H-alpha emission in F-K high luminosity stars
14 p2108 A83-33271

The spectroscopic orbit of KR Aurigae
14 p2101 A83-33465

Wavelength tuning of GaAs LEDs's through surface
effects
15 p2149 A83-33679

Spectrophotometry of three peculiar emission-line
stars
15 p2253 A83-33708

Catalog of H-alpha emission stars in the region of the
Orion Nebula
15 p2244 A83-33752

The extreme ultraviolet day airglow
15 p2196 A83-33942

The extreme ultraviolet spectrum of dayside and
nightside aurorae - 800-1400 A
15 p2196 A83-33943

O I (7990 A) emission and radiative entrapment of auroral
EUV
15 p2196 A83-33944

Distribution of forbidden neutral carbon emission in the
ring nebula (NGC 6720)
15 p2257 A83-34093

Tentative confirmation of an aurora on Uranus
15 p2274 A83-34221

A new method for the multitemperature analysis of solar
X-ray line emission
15 p2279 A83-34290

Discovery of DHM0054-284 - A quasar of redshift 3.61
15 p2246 A83-34379

Emission features in the solar corona after the perihelion
passage of Comet 1979 XI
15 p2281 A83-34533

Planetary nebulae. II
15 p2247 A83-34569

Near-infrared spectroscopy and monochromatic
isophotometry of NGC 6302
15 p2248 A83-34586

A narrow-line radio galaxy behind the Fornax cluster
15 p2266 A83-34610

Bright emission lines in new Seyfert galaxies
15 p2269 A83-34676

Absorption and emission line profile coefficients of
multilevel atoms. I - Atomic profile coefficients. II
Velocity-averaged profile coefficients
15 p2227 A83-34991

Emission spectrochemical analysis of main components
in superalloys using electrolytic iron dilution-high frequency
induction melting and centrifugal cast samples
16 p2329 A83-35603

Natural fluctuations of the emission frequency of an
He-Ne/CH4 3.39 micron laser
16 p2359 A83-35895

Cathode materials for sealed CO2 waveguide lasers
16 p2360 A83-35962

Parameterization of carbon dioxide 15-micron band
absorption and emission
16 p2379 A83-36135

On the spiral structure in the galactic distribution of CO
clouds
16 p2428 A83-36541

Observations of the iron emission lines in the X-ray
spectrum of the supernova remnant Cassiopeia A
16 p2431 A83-36673

Profiles and intensity ratios of the C IV lambda 1548,
1550 emission lines in planetary nebulae
16 p2433 A83-36706

HM Sge and V 1016 Cyg - Spectroscopic changes in
1981-1982
16 p2433 A83-36708

The expansion velocity field within the planetary nebula
NGC 7008
17 p2587 A83-37280

Spectroscopic evidence for activity in the nuclei of
normal spiral galaxies
17 p2596 A83-37311

Narrow-band photometric periods in SS 433
17 p2588 A83-37321

Rapid X-ray variability from the Seyfert 1 galaxy NGC
4051
17 p2598 A83-37344

Radio continuum observations of the bar of NGC 1097
17 p2588 A83-37347

Solar emission lines near 12 microns
17 p2624 A83-37350

The origin of anomalous Balmer decrements in the
spectra of eruptive stars
17 p2600 A83-37657

The relative intensities of hydrogen lines in moving
media --- stellar spectra
17 p2600 A83-37659

A model of the Crab nebula - The emission spectrum
and the distribution of brightness
17 p2600 A83-37660

Spectrophotometric investigation of the T Tauri type star
AS 353
17 p2589 A83-37682

The behavior of emissions in the spectrum of Gamma
Cassiopeia from September to November 1977 and in
September and October 1979
17 p2601 A83-37708

A determination of the physical conditions of
continuous-emission grains --- in solar spectra
17 p2626 A83-37715

Kr(+) and Ar(+) laser-excited fluorescence of CN in a
flame
17 p2485 A83-37746

Submillimeter detection of stratospheric OH and further
line assignments in the stratospheric emission spectrum
17 p2540 A83-37764

Evidence for inhomogeneous thermal sources of two
similar solar spike events of 1978 May 5 and December
4
17 p2627 A83-37926

Measurements of galactic plane gamma-ray emission
in the energy range 10-80 MeV
17 p2629 A83-37931

Spectrophotometry in the galactic supernova remnants
RCW 86, 103 and Kepler
17 p2593 A83-38248

Optically-selected quasar candidates in a field containing
the South Galactic Pole
17 p2593 A83-38254

Spectrophotometry of the recently discovered
cataclysmic variable CPD-48 deg 1577
17 p2593 A83-38264

Differential inversion --- for thermal emission spectrum
of atmosphere
17 p2572 A83-38743

[AD-A130984]
17 p2613 A83-38834

Infrared variability of the X-ray binary AO535 + 262
17 p2613 A83-38834

Positron and electron channeling radiation from
germanium
17 p2585 A83-38955

Origin of the weakening of EUV emission lines formed
in the chromosphere-corona transition zone
18 p2781 A83-39020

Direct measurements of the gradual extreme ultraviolet
emission from large solar flares
18 p2782 A83-39038

Diffuse radio emission from the Coma cluster of galaxies
at decimeter wavelengths
18 p2764 A83-39191

Advances in gamma-ray line astronomy
18 p2756 A83-39293

Relationship between the intensification of the 6300-A
emission at midlatitudes and geomagnetic pulsations
18 p2714 A83-39336

The variability of the spectrum of Arakelian 120
18 p2757 A83-39590

CO(J = 2-1) observations of galactic HII-regions
18 p2769 A83-39650

Distribution of CO in the southern Milky Way
18 p2769 A83-39651

The Orion Nebula - Large-scale distribution of
far-infrared and submillimeter line emission
18 p2772 A83-39706

Millimeter-wavelength lines from the Orion plateau
source
18 p2772 A83-39709

Recent progress on molecular hydrogen in Orion
18 p2772 A83-39710

Far-infrared CO line emission from Orion-KL
18 p2772 A83-39712

Maser sources in the Orion-KL region
18 p2772 A83-39713

A model for the emission spectrum of active galactic
nuclei
18 p2774 A83-39740

Coronal index of solar activity. IV - Years 1964-1970
18 p2785 A83-39978

Intense laser self-focusing in plasmas
18 p2693 A83-40366

Balmer-alpha and Balmer-beta emission cross sections
for low-energy H collisions with He and H2
18 p2743 A83-40408

Depression of molecular emission in the line of sight
of Sgr A West
19 p2912 A83-40680

Observations of gamma-ray line emission from the
galactic center region
19 p2913 A83-40692

Emission in the 0.3 to 1.0 MeV range from the galactic
center region
19 p2913 A83-40694

Three-micron emission features in Herbig Be/Ae stars
and related objects
19 p2909 A83-40722

Effect of temporal nonstationarity on the spectrum of
injection lasers
19 p2852 A83-40940

Three-dimensional energy band in graphite and
lithium-intercalated graphite
19 p2904 A83-40971

Theory of spontaneous-emission line shape in an ideal
cavity
19 p2898 A83-41155

Variations in atomic oxygen in the region of the
turbopause on the basis of observations of night sky
emissions at 5577 A
19 p2866 A83-41224

Measurement of coronal X-ray emission lines from
Capella
19 p2919 A83-41632

On the contributions of the Orion reflection nebulaosity
to the continuous UV spectrum of the Herbig-Haro objects
HH 1 and HH 2 and of the C-S Star
19 p2921 A83-41650

A survey of H-alpha emission in normal galaxies
20 p3063 A83-42181

The Ca II K emission from the sun as a star. II - The
plage emission profile
20 p3080 A83-42382

Comparison of C(+) distributions with new interstellar
sources of HCO emission
20 p3067 A83-42444

Extended near-infrared emission from visual reflection
nebulae
20 p3069 A83-42470

The evidence for shell formation in V1016 Cygni
20 p3069 A83-42471

Detection of radio emission from the
Becklin-Neugebauer object
20 p3069 A83-42474

Stellar radio emission (Review)
20 p3070 A83-42870

Carbon monoxide emission from planetary nebulae and
their possible precursors
20 p3071 A83-43054

Chromospheric and coronal emissions from the giants
in the Hyades
20 p3072 A83-43060

X-ray emission and spin-up evolution of the 6.1-ms
pulsar
20 p3076 A83-43553

On the dynamical structure of QSOs and the origin of
emission clouds
20 p3076 A83-43654

VLBI observations of NGC 4151, Mk 231 and other
galaxies with broad emission line nuclei
21 p3224 A83-44753

Influence of an external cavity on semiconductor laser
phase noise
21 p3146 A83-45479

The use of thermal infrared images in geologic
mapping
22 p3309 A83-46131

Second-harmonic emission from laser-plasma
interactions
22 p3363 A83-46273

A multiwavelength study of the short-period cataclysmic
variable V442 Ophiuchi
22 p3373 A83-46407

Observations of red variable stars in globular clusters
22 p3378 A83-46546

Symbiotic stars - Spectrophotometry at 3-4 and 8-13
microns
22 p3375 A83-46550

8-13-micron spectral observations of eight moderately
extended planetary nebulae
22 p3375 A83-46551

HZ Her - The nature and origin of the emission lines
22 p3379 A83-46556

Stimulated emission and the flat Balmer decrements of
cataclysmic variable stars
22 p3383 A83-47009

Dependence of auroral FUV emissions on the incidence
electron spectrum and neutral atmosphere
22 p3337 A83-47067

The distribution of chromospheric emission strengths
among red dwarfs
23 p3520 A83-47482

Light curves and Ca II emissions of V711 Tauri during
1981-82
23 p3522 A83-47518

Fine tuning lasers by means of an intracavity
interferometer enclosing an absorbing gas
23 p3461 A83-47620

On the mass motions and the atmospheric states of
moustaches --- in solar atmosphere
23 p3536 A83-47713

Relativistic particles and gamma-rays in quasars and
active galactic nuclei
23 p3540 A83-47761

Gamma-ray line emission from SS433 23 p3527 A83-48073

The origin of line-free XUV continuum emission from laser-produced plasmas of the elements Z = 62-74 23 p3511 A83-48586

Longitudinal mode spectrum of GaAs injection lasers under high-frequency microwave modulation 24 p3586 A83-48780

Fundamental linewidth in solitary, ultranarrow output PbS(1-x)Se(x) diode lasers 24 p3586 A83-48784

Infrared emission lines in planetary nebulae 24 p3639 A83-49133

Physical processes in nebular shells and the interpretation of nebular spectra 24 p3639 A83-49142

Planetary nebulae and Seyfert galaxies - Similarities and differences 24 p3640 A83-49159

Taurus observations of the emission-line velocity field of Centaurus A (NGC 5128) 24 p3642 A83-49257

Is emission line strength a predictor of youth for Orion population stars? 24 p3659 A83-49379

A new type of decametric radio emission from Jupiter 24 p3673 A83-49631

Sounding of the supercorona by decametric emission from 3C144 24 p3675 A83-49634

Broad emission lines of QSOs are consistent with rotating supermassive stars 24 p3670 A83-50112

EMISSIONIVITY

Microwave radiance of early fall sea ice at 1.55 cm 01 p0076 A83-10091

Multispectral radiation detection of small changes in target emissivity --- ice measurements on space shuttle external tank 03 p0327 A83-13795

Some improvements to the infrared emissivity algorithm including a parameterization of the absorption by water vapor polymers 03 p0371 A83-14659

A simple relation between active and passive microwave remote sensing measurements of earth terrain 03 p0352 A83-14857

The effect of the nature of the substrate on the emission properties and thermal stability of the adsorption systems cesium-oxygen film-metal 05 p0690 A83-16903

The total emissivities of high-temperature flames 07 p0879 A83-19840

An improved portable thermoradiometer /TRM/ for measuring the relative emissivity of solids at room temperature 07 p0930 A83-20959

Some improvements and complements to the infrared emissivity algorithm including a parameterization of the absorption in the continuum region --- for atmospheric radiation transfer 08 p1143 A83-23015

Emission properties of titanium alloys under heating in air 11 p1548 A83-28370

A theoretical examination of thermal radiation from rough surfaces - The development of a device for measuring emissivity and application to AISI 316 stainless steel --- French thesis 11 p1650 A83-28633

Interpretation of the results of thermal inspection with changes in the emitting capacity of the surface of objects of inspection 13 p1860 A83-30836

Radiation characteristics of nonisothermal cavities --- for temperature and radiation measuring instruments 16 p2355 A83-35588

Line radiation from a hot, optically thin plasma - Collision strengths and emissivities --- in stellar atmospheres 16 p2416 A83-35974

The measurement of the integral hemispherical emissivity of thermal insulating materials 19 p2848 A83-41575

Evaluation of effective emissivities of nonisothermal cavities 20 p2988 A83-42217

Prediction of gas emissivity for a wide range of process conditions 20 p2974 A83-42691

Non luminous gas radiation - Approximate emissivity models 20 p2974 A83-42692

Improvement in spectral directional emissivity measurement technics by direct methods 20 p2989 A83-42776

Measurement of emissivity and complex refractive index of a solid or a liquid material - Application to the heat transfer by radiation 20 p2982 A83-42777

Emissivity measurements of metallic surfaces used in cryogenic applications 20 p2954 A83-43221

The effect of the emissivity of a surface on the IR measurements of its temperature 21 p3177 A83-45333

Emissivity of the sea surface 22 p3342 A83-45643

Sea ice effective microwave emissivities from satellite passive microwave and infrared observations 22 p3345 A83-46914

An investigation of the possibility of determining the geometrical characteristics of surfaces having large irregularities on the basis of microwave-radiometric measurements 23 p3476 A83-48112

Radiation from a rough surface and its polarization properties. I - Method of calculation 24 p3623 A83-49118

EMISSOGRAPHS

U ACTINOMETERS

U RECORDING INSTRUMENTS

EMITTANCE

Emission characteristics of earth and cloud surfaces as measured by the ERB scanning channels on the NIMBUS-7 satellite 03 p0370 A83-14647

Alpha-s/epsilonin-H measurements of thermal control coatings over four years at geosynchronous altitude --- ratio of solar absorptance to infrared hemispherical emittance [AIAA PAPER 83-1450] 15 p2127 A83-34909

Measurement of the integral hemispherical emissive power of heat-insulating materials 24 p3581 A83-48932

EMITTERS

NT THERMIONIC CATHODES

NT THERMIONIC EMITTERS

Theory and experiments on open circuit voltage decay of p-n junction diodes with arbitrary base width, including the effects of built-in drift field in the base and recombinations in the emitter 04 p0473 A83-16088

The characterization of transistor electrical overstress failure probability density functions 05 p0625 A83-17477

Superradiation in a two-dimensional model 11 p1583 A83-28057

Importance of the emitter in thin back-surface field solar cells 15 p2192 A83-34668

EMOTIONAL FACTORS

The activity of tyrosine hydroxylase in the ganglia of the vegetative nervous system in rabbits during acute experimental emotional stress 01 p0080 A83-10542

The peptide DSIP as a factor for raising the resistance of animals to emotional stress 04 p0521 A83-16414

The structure of qualitative individual peculiarities of emotionality 05 p0676 A83-17181

The reaction of the hypophyseal-adrenal system to emotional stress in patients with hypertension 05 p0674 A83-17200

Respiratory rhythm as one of the indicators of the intensity of motivational-emotional reactions in rabbits 06 p0794 A83-18969

The objective evaluation of the motivational and emotional aspects of the activity of a human operator 07 p0979 A83-20345

The hemodynamic reactions of animals to episodic stimulations of the ventromedial hypothalamus during acute emotional stress 09 p1321 A83-25151

The effect of stress on the tensility, Starling's mechanism, and resistance of the myocardium to hypoxia 14 p2066 A83-33335

Emotional excitation and parameters of cardiac activity during muscular work 17 p2558 A83-37238

Emotional components of self-reports and interpersonal judgments 18 p2737 A83-40558

Local cerebral blood flow increases during auditory and emotional processing in the conscious rat 19 p2873 A83-40906

The nature of 'congestive' excitation during emotional stress as a basis for cardiovascular disorders 19 p2875 A83-41438

The dependence of the pattern of emotional condition on the characteristics of the training load of heavy athletes 19 p2884 A83-41448

EMOTIONS

The brain organization of emotional reactions and states 02 p0224 A83-12209

The so-called 'information theory of emotions' 19 p2885 A83-41839

EMPENNAGE

U TAIL ASSEMBLIES

EMPHYSEMA

The surfactant system of the lungs in experimental papain-induced emphysema 05 p0670 A83-17188

EMPLOYEE RELATIONS

Airline safety and labor relations law - Balancing rights and responsibility 15 p2240 A83-34475

EMULSIONS

NT NUCLEAR EMULSIONS

NT PHOTOGRAPHIC EMULSIONS

Overremoval propensities of the prewash hydrophilic emulsifier fluorescent penetrant process 09 p1275 A83-23921

Effective generalized conductivity of three-phase cellular systems --- with kerosene-air-water fuel mixture example 12 p1775 A83-29270

Emulsification of thermal energy storage materials in an immiscible fluid 14 p2046 A83-32347

Drop size measurements in evaporating realistic sprays of emulsified and neat fuels [ASME PAPER 83-GT-231] 23 p3440 A83-48027

ENAMELS

The use of experimental design during the synthesis of refractory enamel coatings 07 p0899 A83-20681

ENCAPSULATION

The effect of cure temperature on stresses in encapsulated electronic assemblies 07 p0919 A83-20457

Characterization of a polyurethane as a space approved encapsulant for electronic components 07 p0920 A83-20486

EL2 distributions in doped and undoped liquid encapsulated Czochralski GaAs --- deep donor concentration 08 p1169 A83-22756

Removable foam encapsulants 09 p1237 A83-23617

Macroencapsulation of electronic circuits 12 p1719 A83-29215

Evaluation of microencapsulated penetrant inspection 12 p1734 A83-29594

Thermorheological analysis of high voltage electronic module potting [AIAA 83-0903] 12 p1720 A83-29842

Analysis of hot-spot-effects in encapsulated photovoltaic generators by laser scan and partial shadowing 14 p2039 A83-32211

Welding iridium heat source capsules for space missions 20 p2998 A83-42300

ENCELADUS

Crater numbers and geological histories of Iapetus, Enceladus, Tethys and Hyperion 08 p1191 A83-23290

Viscosity of the lithosphere of Enceladus 10 p1518 A83-25514

The evolution of Enceladus 11 p1684 A83-27364

The control networks of Mimas and Enceladus 11 p1684 A83-27365

Tidal dissipation in small viscoelastic ice moons - The case of Enceladus 21 p3239 A83-44082

ENCEPHALITIS

Computer tomography applied to the study of inflammatory diseases of the brain /a survey of the literature/ 05 p0673 A83-17179

ENCKE COMET

Genetic relationship between the Taurid meteor swarm and comet Encke-Baklund 16 p2423 A83-35754

ENCKE METHOD

The modified Encke method --- for orbit calculation 11 p1672 A83-27884

ENCLOSURES

Effect of aspect ratio on heat transfer in shallow enclosures [ASME PAPER 82-HT-44] 02 p0172 A83-12797

Heat transfer in a parallelogram shaped enclosure. II Free convection in infinitely stacked parallelogram shaped enclosure. III - Combined free convection and radiation heat transfer 02 p0175 A83-13071

Experiments on natural convection heat transfer in low aspect ratio enclosures 07 p0924 A83-19822

Thermal design of standard avionic enclosures [SAE PAPER 820878] 10 p1373 A83-25772

A finite difference study of natural convection in complex enclosures 20 p2972 A83-42678

Numerical simulation of laminar natural convection in shallow inclined enclosures 20 p2973 A83-42680

A numerical method to solve the steady-state Navier-Stokes equations for natural convection in enclosures 22 p3284 A83-46472

ENCODERS

U CODERS

ENCODING

U CODING

ENCOUNTERS

Pre-discovery encounters between short-period comets and Jupiter estimated by a Keplerian approximation 05 p0695 A83-17831

END MORAINES

U GLACIAL DRIFT

END-TO-END DATA SYSTEMS

NT NEEDS (DATA SYSTEM)

U.S. data processing for the IRAS project --- by Jet Propulsion Laboratory Scientific Data Analysis System 11 p1674 A83-28217

ENDFIRE ARRAYS

NT YAGI ANTENNAS

ENDOCRINE GLANDS

NT ADRENAL GLAND

NT PANCREAS

NT PINEAL GLAND

NT PITUITARY GLAND

NT THYMUS GLAND

NT THYROID GLAND

Temperature and adrenocortical responses in rhesus monkeys exposed to microwaves 05 p0671 A83-17334

ENDOCRINE SECRETIONS

NT ADRENOCORTICOTROPIN (ACTH) 01 p0080 A83-10546
NT ALDOSTERONE 03 p0380 A83-13636
NT ESTROGENS 05 p0673 A83-17160
NT HORMONES 13 p1903 A83-30476
NT INSULIN 20 p3033 A83-43478
NT PITUITARY HORMONES 23 p3495 A83-47819
NT PROSTAGLANDINS 26 p0770 A83-19125
NT THYROXINE 06 p0770 A83-19125

The use of chromatography for determining kallikrein and prekallikrein in canine blood serum

Compensatory and pathogenetic functions of the kallikrein-kinin system in health and in certain diseases

The functional morphology of the submaxillary salivary glands of rats during age-related disorders of endocrine regulation

ENDOCRINOLOGY

The relationship between the patient's age, the function of certain of his regulatory systems, and myocardial infarction

Plasma volume, renin, and vasopressin responses to graded exercise after training

ENDOLYMPH

Type II collagen-induced autoimmune endolymphatic hydrops in guinea pig

ENDOSCOPES

Crack testing with endoscope and eddy current probe

ENDOTHELIUM

The changes in the venous endothelium after acute hemodynamic disorders

Endotoxin protects against hyperoxic alterations in lung endothelial cell metabolism

Oxygen toxicity in cultured aortic endothelium
Selenium-induced partial protective effect

ENDOTOXINS

Endotoxin protects against hyperoxic alterations in lung endothelial cell metabolism

Role of bacterial endotoxins of intestinal origin in rat heat stress mortality

ENERGETIC PARTICLE EXPLORER A

U EXPLORER 12 SATELLITE

ENERGETIC PARTICLES

NT ARGON PLASMA 01 p0080 A83-10546
NT BETA PARTICLES 03 p0380 A83-13636
NT BOUNDARY LAYER PLASMAS 05 p0673 A83-17160
NT CESIUM PLASMA 13 p1903 A83-30476
NT COLD PLASMAS 20 p3033 A83-43478
NT COLLISIONAL PLASMAS 23 p3495 A83-47819
NT COLLISIONLESS PLASMAS 26 p0770 A83-19125
NT CONDUCTION ELECTRONS 06 p0770 A83-19125
NT COSMIC PLASMA 01 p0080 A83-10546
NT CYLINDRICAL PLASMAS 03 p0380 A83-13636
NT DENSE PLASMAS 05 p0673 A83-17160
NT DEUTERIUM PLASMA 13 p1903 A83-30476
NT ELECTRON PLASMA 20 p3033 A83-43478
NT ELECTRONS 23 p3495 A83-47819
NT ELLIPTICAL PLASMAS 26 p0770 A83-19125
NT HELIUM PLASMA 01 p0080 A83-10546
NT HIGH ENERGY ELECTRONS 03 p0380 A83-13636
NT HIGH TEMPERATURE PLASMAS 05 p0673 A83-17160
NT HOT ELECTRONS 13 p1903 A83-30476
NT LASER PLASMAS 20 p3033 A83-43478
NT METALLIC PLASMAS 23 p3495 A83-47819
NT MICROPLASMAS 26 p0770 A83-19125
NT NITROGEN PLASMA 01 p0080 A83-10546
NT NONEQUILIBRIUM PLASMAS 03 p0380 A83-13636
NT NONUNIFORM PLASMAS 05 p0673 A83-17160
NT NUCLEI (NUCLEAR PHYSICS) 13 p1903 A83-30476
NT OXYGEN PLASMA 20 p3033 A83-43478
NT PLASMA FOCUS 23 p3495 A83-47819
NT PLASMAS (PHYSICS) 26 p0770 A83-19125
NT RAREFIED PLASMAS 01 p0080 A83-10546
NT RELATIVISTIC PLASMAS 03 p0380 A83-13636
NT ROTATING PLASMAS 05 p0673 A83-17160
NT SOLAR WIND 13 p1903 A83-30476
NT SPHERICAL PLASMAS 20 p3033 A83-43478
NT STELLAR WINDS 23 p3495 A83-47819
NT STRONGLY COUPLED PLASMAS 26 p0770 A83-19125
NT THERMAL PLASMAS 01 p0080 A83-10546

Results of multiyear observations of fluxes of superhigh-energy gamma-ray quanta from Cyg X-3

Results of spectrum studies of energetic flare particles by the Venera 11 and 12, and Prognos 5 and 6 spacecraft

Fluxes of electromagnetic radiation, energetic particles, and solar wind from the region of a helium-3-rich flare

Anisotropy of small atmospheric showers /with E sub 0 of approximately 10 to the 13th eV/

Investigation of azimuth effects in gamma families with total energies of 30-1000 TeV

Experimental studies of superfamily halos. IV --- in cosmic ray showers

The PAMIR-ANI experiments and quantum chromodynamics

Absolute calibration of X-ray film by means of spaced X-ray emulsion chambers

Shower curves in the atmosphere and the composition of primary cosmic radiation with an energy greater than 10 to the 15th eV

A possibility of detecting optical radiation from superhigh-energy extensive air showers

The upper boundary of the energy spectrum of cosmic rays and possible methods for detecting cascades of superhigh energies /10 to the 20th-10 to the 28th eV/

Energetic particle losses and trapping boundaries as deduced from calculations with a realistic magnetic field model

Transport of neutrinos, radiation and energetic particles in accretion flows

High-energy astrophysics

The dynamics of energetic electrons according to Intercosmos-19 satellite observations in April 1979

Findings on rings and inner satellites of Saturn of Pioneer 11

Observations of energetic ions near the Venus ionopause

Cosmic ray origin above 10 to the 18th eV - Galactic or extragalactic

Problem of detecting quantum-gravity effects

The dynamics of the intergalactic medium

In situ observations of Io torus plasma

The July 29, 1977 magnetic storm - Observations and modeling of energetic particles at synchronous orbit

Dependence on declination of the intensity of cosmic ray showers with primary energies of about 10 to the 16th eV

Observations of field-aligned energetic electron and ion distributions near the magnetopause at geosynchronous orbit

On ion harmonic structure in auroral zone waves - The effect of ion conic damping of auroral hiss

High-energy tail distributions and resonant wave particle interaction

Boundaries of the trapping and loss of outer-radiation-belt particles, conditioned by the magnetospheric magnetic field

Cosmic-ray record in solar system matter

Processes of the generation of high-energy muons in cosmic rays

Characteristics of multiple muons with energies exceeding 35 and 85 GeV

Investigation of groups and nuclear interactions of muons by the spark-calorimeter method

Solar flare energetics

Energetic ion beam in the earth's magnetotail lobe

Remote sensing of energetic particle boundaries --- in magnetopause

Space Shuttle Orbiter charging

Ultrahigh-energy cosmic rays

Theoretical proposal of a high-energy experiment fit to reveal a three-dimensional time

On the origin of the hot ions in the disturbed dayside magnetosphere

Collective single-beam effects in electron-positron storage rings

Gamma-ray astronomy and the local interstellar medium

A model description of fluxes of high-energy protons trapped by the geomagnetic field

High-energy particles --- in Jovian magnetosphere

Kinoform filter for an incoherent optical processor

Theoretical studies of interplanetary propagation and acceleration

Cosmic rays from binary neutron stars

Some recent advances in energetic ion mass spectrometry

Possibility of studying cosmic rays with energies

The effects of energetic particle precipitation on the atmospheric electric circuit

Remote sensing of a flux transfer event with energetic particles

Satellite and ground observations of a pre-substorm phase on May 4, 1977

Temporal variations of nucleonic abundances in solar flare energetic particle events. I - Well-connected events

On the confinement of high-energy protons in the solar corona

The galactic gamma-ray source population

Detection of 2 x 10 to the 15th to 2 x 10 to the 16th eV gamma-rays from Cygnus X-3

On the use of artificially injected energetic electrons as indicators of magnetospheric electric fields parallel to the magnetic lines of force

Evidence for a new stable particle with heavy mass around 10 to the 17th eV. --- elementary particle produced in earth atmosphere

The detection of energetic cometary and solar particles by the EPONA instrument on the Giotto mission --- Energetic Particle Onset Admonitor

Propagation of energetic particles in the solar wind

Energetic oxygen and sulfur ions in the Jovian magnetosphere and their contribution to the auroral excitation

Voyager 2 observations of energetic particle variations in the Ganymede wake region - A possible acceleration mechanism

ISEE/IMP observations of simultaneous upstream ion events

Energetic ions upstream of the earth's bow shock during an energetic storm particle event

Observations of gamma radiation at 10 to the 12th eV from the X-ray source Cyg X-3 at the Tien-Shan installation in 1977 and 1978

On the variation of the 4.8-hour period of Cyg X-3

Extremely high multiplicities in high-energy nucleus-nucleus collisions

First order and second order Fermi acceleration of energetic charged particles by shock waves --- cosmic ray transport

Energetic ion acceleration and transport in the upstream region of Jupiter - Voyager 1 and 2

The acceleration of cosmic rays by a shock wave in a diffusive medium - Research at high energies --- French thesis

The composition, propagation and acceleration of energetic solar particles - A review of United States research 1979-1982

The association of energetic particles and shocks in the heliosphere

The magnetosphere of Saturn

Dominant acceleration processes of ambient energetic protons (E greater than or equal to 50 keV) at the bow shock Conditions and limitations

Cosmic rays and high-energy interactions - Is there a necessity for a new phenomenon?

Particle acceleration during the explosive phase of a solar flare

An imaging telescope for high energy gamma-ray astronomy

The stochastic instability of high-energy protons of the inner radiation belt at low altitudes

Cyclotron instability in the plasmasphere in the presence of the transport of energetic particles across L-shells

Suprathermal plasma and energetic particle measurements aboard the AUREOL-3 satellite

Energetic particle signatures near magnetospheric boundaries

Motion of flux transfer events on 10 November 1977 determined by energetic particles on ISEE 2

Energy and charge distribution of energetic helium ions in the outer radiation belt of the earth

Stopping of 200-GeV gold nuclei in nuclear emulsions

Energetics of particles accelerated in solar flares

Effect of HZE particles and space hadrons on bacteriophages 19 p2871 A83-40834
Radiation exposures during space flight and their measurement 19 p2880 A83-40846
Unique biological aspects of radiation hazards - An overview 19 p2873 A83-40847
On the drift mechanism for energetic charged particles at shocks 19 p2925 A83-41621
Observations of optical emissions from precipitation of energetic neutral atoms and ions from the ring current 20 p3019 A83-42424
The mass dependence of wave particle interactions as observed with the ISEE-1 energetic ion mass spectrometer 20 p3025 A83-43197
Ionization effects and transition radiation of relativistic charged particles 20 p3045 A83-43526
Ionization effects in real detectors of relativistic charged particles 20 p3045 A83-43527
The path of formation and its role in radiation from moving charges 20 p3045 A83-43528
Application of the eikonal approximation in the theory of transition X-radiation 20 p3046 A83-43530
Particle identification using the angular distribution of transition X-radiation quanta 20 p3046 A83-43532
Particle identification with the use of transition radiation by counting the clusters on the particle track 20 p3046 A83-43533
Practical prototype of a transition-radiation detector 20 p2991 A83-43534
Registration of transition X-radiation at gamma = 1000-10,000 by the photon-counting method 20 p2991 A83-43535
Angular and energy distributions of transition X-radiation 20 p3046 A83-43536
Boundary conditions for energetic particle transport at shocks 21 p3244 A83-44405
Equilibrium functions of the pitch-angle distribution of energetic particles in the case of nonadiabatic scattering by the magnetotail current sheet 21 p3177 A83-45282
Absorption of energetic protons by Saturn's Ring G 22 p3384 A83-46030
Development of substorm activity in multiple-onset substorms at synchronous orbit 22 p3326 A83-46038
Energetic particles in the vicinity of a possible neutral line in the plasma sheet 22 p3334 A83-47038
Electron density and energetic particle precipitation observed during the eclipse of 26 February 1979 23 p3480 A83-47466
The interaction of fast particles with frozen gases in T Tau nebulae - The physical background 23 p3524 A83-47536
Spatial structure of high energy photon sources in solar flares 23 p3534 A83-47694
High energy particle acceleration in solar flares 23 p3535 A83-47697
Observational evidence 23 p3535 A83-47697
Ultra high energy cosmic rays 23 p3539 A83-47743
Solar energetic particle studies 23 p3538 A83-47745
The Desertron - Colliding beams at 20 TeV 23 p3507 A83-47815
An introduction to the theory of diffusive shock acceleration of energetic particles in tenuous plasmas 24 p3630 A83-48802
Cosmic ray showers at 10 to the 16th eV 24 p3675 A83-48983

ENERGY ABSORPTION

NT AURORAL ABSORPTION
NT ELECTROMAGNETIC ABSORPTION
NT INFRARED ABSORPTION
NT MOLECULAR ABSORPTION
NT MULTIPHOTON ABSORPTION
NT PHOTOABSORPTION
NT POLAR CAP ABSORPTION
NT SELF ABSORPTION
NT THERMAL ABSORPTION
NT THERMALIZATION (ENERGY ABSORPTION)
NT ULTRAVIOLET ABSORPTION
NT X RAY ABSORPTION
Optical analysis of solar energy tubular absorbers 02 p2022 A83-12596
Energy absorption in composite tubes 10 p1439 A83-25883
Development of a variable-load energy absorber --- for helicopter seats 10 p1373 A83-25896
A model of a material with internal friction 17 p2521 A83-37542
Energy absorption of composite materials under crash conditions 18 p2705 A83-40216
A technique for measuring energy absorption from high energy laser radiation 20 p2989 A83-42781
Energy absorption of composite materials 20 p2948 A83-43148

Transport of a relativistic electron beam in a dense gas 21 p3143 A83-44134
Quantitative measurement of energy deposited in optical coatings 21 p3205 A83-44785
The mechanism of elastic energy absorption in boron fibers 24 p3553 A83-49474
On the effect of the correlation in phonon motion on the viscosity of impure dielectrics 24 p3636 A83-49755

ENERGY ABSORPTION FILMS

Thermal and optical analysis of an evacuated circular cylindrical concentrating collector 03 p0354 A83-13697
Black chrome solar selective coatings optimized for high temperature applications 04 p0504 A83-15479
Stability of SnO2 thin films used for photovoltaic devices 06 p0780 A83-18563
Hard carbon coatings with low optical absorption 13 p1825 A83-30326
Experimental study of the performance of transparent film temperature sensors under the effects of solar-radiation fluxes of different concentrations 14 p2018 A83-32049
Preparation and characterization of iron oxide thin film electrodes 16 p2347 A83-36743
Optical constants of amorphous hydrogenated carbon and silicon-carbon alloy films and their application in high temperature solar selective surfaces 18 p2708 A83-39931
Surface photoacoustic wave spectroscopy of thin films 18 p2689 A83-40058
Methods of determining optical constants of thin semiconductor films using normal incidence reflectance and transmittance data 21 p3206 A83-44789
Properties and ion implantation of Al(x)Ga(1-x)N epitaxial single crystal films prepared by low pressure metalorganic chemical vapor deposition 21 p3220 A83-45499
Optical coatings for energy efficiency and solar applications; Proceedings of the Seminar, Los Angeles, CA, January 28, 29, 1982 22 p3319 A83-46580
Catalytically deposited carbon solar selective absorber 22 p3319 A83-46582
Fabrication of ZrCx/Zr and Cr-CrOx films for practical solar selective absorption systems 22 p3319 A83-46584
An experimental study of the generation parameters of a laser with a thin absorption layer in the cavity 23 p3460 A83-47163
Photostimulated exoemission and photoconductivity of hydrogenated amorphous silicon 24 p3635 A83-49069

ENERGY BANDS

NT BLOCH BAND
NT CONDUCTION BANDS
NT FORBIDDEN BANDS
Semiconductor structures for repeated velocity overshoot 05 p0690 A83-17295
A new strategy for efficient solar energy conversion - Parallel-processing with surface plasmons 11 p1602 A83-27140
Three-dimensional energy band in graphite and lithium-intercalated graphite 19 p2904 A83-40971

ENERGY BUDGETS

NT ATMOSPHERIC HEAT BUDGET
NT HEAT BUDGET
An evaluation of four thermal models used in thermal inertia analysis --- for thermal mapping from remotely sensed data 01 p0065 A83-10098
On the surface radiation budget 01 p0065 A83-10100
A comparison of model generated radiation fields with satellite measurements 01 p0075 A83-10223
The problem of energetics in the physics of the ionosphere and approaches to its solution 01 p0071 A83-10596
The relative effect of solar altitude on surface temperatures and energy budget components on two contrasting landscapes 03 p0363 A83-13272
The impact of model moist processes on baroclinic wave energetics 03 p0367 A83-14427
The comparative performance of selected solar global models 03 p0370 A83-14634
Comparison between albedo changes and lidar-measured aerosol changes for a set of aerosol events 03 p0370 A83-14641
Diurnal radiation budget - Four months assembled into an annual mean 03 p0370 A83-14646
Time and space spectra of earth-emitted radiation at large scales 03 p0370 A83-14648
Responses of transition region models to magnetic field geometry and downflow velocities --- in solar atmosphere 05 p0708 A83-17021
The effects of changing solar angles, cloud regimes, and air temperatures on the temperatures of contrasting surfaces 06 p0779 A83-18234

ENERGY CONSERVATION

Climate studies with a multi-layer energy balance model. I - Model description and sensitivity to the solar constant. II - The role of feedback mechanisms in the CO2 problem 06 p0789 A83-18251
Environmental effects of an impact-generated dust cloud - Implications for the Cretaceous-Tertiary extinctions 06 p0779 A83-18816
Gold's hypothesis and the energetics of the Jovian magnetosphere 07 p1029 A83-20410
The radiative energetics of the climate system 07 p0970 A83-20888
An attempt to determine stellar Lyman-alpha emission-line fluxes for F stars with different metal abundances 07 p1022 A83-21131
A water vapor-energy balance model designed for sensitivity testing of climatic feedback processes 08 p1142 A83-23004
The effect of tropospheric aerosols on the earth's radiation budget - A parameterization for climate models 08 p1142 A83-23009
Certain topics in the energetics of solar-terrestrial relationships 10 p1448 A83-25603
The albedo of Uranus 10 p1494 A83-25735
Albedo, internal heat flux, and energy balance of Saturn 11 p1684 A83-27359
The atmospheric energy budgets over North America, the North Atlantic and Europe based on ECMWF analyses and forecasts 11 p1633 A83-28082
The analysis and kinetic energy balance of an upper-level wind maximum during intense convection 13 p1890 A83-30588
Basic state energy budget analysis for phases 1, 2 and 3 of GATE 13 p1891 A83-30806
Energy balance and stability --- in stellar coronae 15 p2252 A83-33606
Energy deposition rates by charged particles measured during the energy budget campaign 16 p2372 A83-35363
Energy deposition in the polar ionosphere as determined by measurements aboard 'Intercosmos-Bulgaria-1300' satellite 16 p2373 A83-35368
Vertical density and temperature structure over northern Europe 16 p2373 A83-35373
Wind structure and small-scale wind variability in the stratosphere and mesosphere during the November 1980 Energy Budget Campaign 16 p2383 A83-35374
In situ and remote sensing of thermospheric winds during the Energy Budget Campaign 16 p2374 A83-35375
A theory of stochastic resonance in climatic change 16 p2387 A83-35696
Comments on 'the relative effect of solar altitude on surface temperatures and energy budget components on two contrasting landscapes' 16 p2388 A83-35798
The impact of model moist processes on the energetics of extratropical cyclones 16 p2388 A83-36032
Satellite-derived surface energy balance estimates in the Alaskan sub-Arctic 18 p2721 A83-39112
On the mechanism of the effect of solar corpuscular radiation on the circulation of the lower atmosphere 18 p2724 A83-39489
An intercomparison between radiation budget estimates from Meteosat 1, Nimbus 7 and TIROS-N satellites 18 p2716 A83-39678
The energy budgets for the eye and eye wall of a numerically simulated tropical cyclone 20 p3031 A83-43461
Binaries as a heat source in stellar dynamics - Release of binding energy 22 p3376 A83-45632
On the sampling problem in radiation budget studies 22 p3329 A83-46232
Reconstructing the components of the radiation balance of the earth's surface on the basis of satellite data 23 p3483 A83-48101

ESTIMATION OF AIRCRAFT FUEL CONSUMPTION 01 p0008 A83-10186

ECONOMIC MODELING OF FAULT TOLERANT FLIGHT CONTROL SYSTEMS IN COMMERCIAL APPLICATIONS 01 p0013 A83-11156

Thermal infrared sensing applied to energy conservation in building envelopes /Thermosense IV/; Proceedings of the Meeting, Ottawa, Ontario, Canada, September 1-4, 1981 02 p0180 A83-12686
Field evaluation of aerial infrared surveys for residential applications 02 p0200 A83-12688
Performance of the coned-face end seal with regard to energy conservation [ASLE PREPRINT 82-LC-5C-2] 03 p0335 A83-13245
The application of energy saving concepts to future fighter/attack aircraft design [AIAA PAPER 83-0092] 05 p0594 A83-16516
Advances in energy technology; Proceedings of the Eighth Annual UMR-DNR Conference on Energy, University of Missouri-Rolla, Rolla, MO, November 4-7, 1981 05 p0658 A83-17115

Twenty years of experience with organic Rankine cycle turbines - Their applicability and use in energy conservation and alternative energy systems

11 p1605 A83-27207

R and D of energy saving and new energy utilization in Japanese marine engineering

11 p1606 A83-27225

Energy conservation in air transportation - The Canadian Air Traffic Control Effort

12 p1699 A83-29393

The constraints of energy-conserving vertical finite difference on the hydrostatic equations in a NWP model --- Numerical Weather Prediction

13 p1891 A83-30805

Flight management concepts development for fuel conservation

16 p2304 A83-35843

Solar thermal technologies - Potential benefits to U.S. utilities and industry

17 p2536 A83-38023

An advanced control system for a next generation transport aircraft

19 p2802 A83-41679

Wing tip devices for energy conservation and other purposes Experimental and analytical work in progress at the Lockheed-Georgia Company

21 p3086 A83-44358

Saving fuel with the wide-chord fan

23 p3411 A83-48174

ENERGY CONSUMPTION

Methods of reducing energy consumption of the oxidant supply system for MHD/steam power plants

[AIAA PAPER 83-0468] 05 p0686 A83-16735

Optimal guidance laws for missiles with second order characteristics

10 p1383 A83-26769

Contemporary electric vehicle testing and evaluation

11 p1667 A83-27160

R and D of energy saving and new energy utilization in Japanese marine engineering

11 p1606 A83-27225

The energy balance of the myocardium and its correction by antiarrhythmics

13 p1895 A83-30407

Solar thermal technologies - Potential benefits to U.S. utilities and industry

17 p2536 A83-38023

Energy state revisited --- for minimum-time aircraft climbs

[AIAA PAPER 83-2138] 19 p2799 A83-41960

ENERGY CONVERSION

NT BIOMASS ENERGY PRODUCTION

NT GEOTHERMAL ENERGY CONVERSION

NT OCEAN THERMAL ENERGY CONVERSION

NT PHOTOTHERMAL CONVERSION

NT SATELLITE SOLAR ENERGY CONVERSION

NT SOLAR ENERGY CONVERSION

NT SOLAR TOTAL ENERGY SYSTEMS

NT WATERWAVE ENERGY CONVERSION

Transport theory of semiconductor energy conversion

04 p0544 A83-16087

Rare-earth converters of the emission spectrum of neodymium lasers

07 p0933 A83-19975

Concerning one feature of energy conversion in diffraction-radiation generator/free-electron laser systems

09 p1272 A83-24219

IECEC '82; Proceedings of the Seventeenth Intersociety Energy Conversion Engineering Conference, Los Angeles, CA, August 8-12, 1982. Volumes 1, 2, 3, 4 & 5

11 p1601 A83-27126

A study of energy conversion in the wave number domain

11 p1619 A83-28341

A study of energy, generation and conversion over North America

11 p1619 A83-28342

Joule heating effects in MHD generator boundary layers

12 p1779 A83-28956

The application of free-electron lasers to the transmission of energy in space

13 p1856 A83-31141

ac characteristics in ac/dc/dc conversion

14 p2006 A83-32427

Difficulties in using power laws for wind energy assessment

19 p2861 A83-40767

Special electrical machines: Sources and converters of energy --- Russian book

21 p3126 A83-45018

A new look at the energy cycle --- in atmosphere

22 p3341 A83-46848

US national programs in ceramics for energy conversion

23 p3438 A83-48308

ENERGY CONVERSION EFFICIENCY

Electromagnetic projectile acceleration utilizing distributed energy sources

01 p0036 A83-10620

On the optimization of magnetic field sources in electromechanical energy conversion

01 p0037 A83-10641

Performance of the Wells turbine at starting

01 p0068 A83-10661

On the formula for the upper limit of photovoltaic solar energy conversion efficiency

01 p0068 A83-10699

Multikilowatt electron beams for pumping CW ion lasers

01 p0039 A83-10987

Photoelectrochemical cells based on GaAs/0.6/P/0.4/epilayers - Stabilization and luminescent properties

01 p0069 A83-10997

DC-to-dc converter power-train optimization for maximum efficiency

01 p0040 A83-11015

A study of silicon and GaAs solar cells, and their optical coupling by means of a dichroic mirror --- French thesis

02 p0200 A83-11764

Reflections on solar collectors at elevated temperatures /260-1000 C/ --- French thesis

02 p0201 A83-11766

Determination of the interference between the elements of a central-receiver solar system

02 p0201 A83-11848

Research on the characteristic parameters of thermophotovoltaic /TPV/ converter performance

02 p0202 A83-12029

Improved performance of the microwave-pumped XeCl laser

02 p0184 A83-12266

Advances in series resonant inverter technology and its effect on spacecraft employing electric propulsion [AIAA PAPER 82-1881]

02 p0143 A83-12466

Thermal storage performance calculations by closed form and finite difference solutions

[ASME PAPER 82-HT-52] 02 p0172 A83-12799

The influence of the interface state on the properties of solar cell semiconductor electrodes

03 p0352 A83-13473

Transient performance of evacuated tubular solar collectors

03 p0352 A83-13478

An experimental investigation of a stationary reflector/tracking absorber solar collector at intermediate temperatures

03 p0353 A83-13479

Incident angle modifiers for flat-plate solar collectors - Analysis of measurement and calculation procedures

03 p0353 A83-13480

Analysis of two-phase flow solar collectors with application to heat pumps

03 p0353 A83-13481

Luminescent solar concentrators - A review

03 p0353 A83-13581

Collection of solar energy at specified output temperature

03 p0353 A83-13582

Thermal and optical analysis of an evacuated circular cylindrical concentrating collector

03 p0354 A83-13697

Optimization of parabolic trough solar collectors

03 p0354 A83-13699

A method of rating solar collectors

03 p0354 A83-13701

Planar multijunction high voltage solar cell chip

03 p0355 A83-13923

A p-i-n heterojunction model for the thin-film CuInSe₂/CdS solar cell

03 p0355 A83-14513

Effect of off-south orientation on the performance of collector reflector system in India

03 p0355 A83-14671

Testing of the energy module of a parabolocylindrical solar installation

04 p0503 A83-15130

Role of impurities in silicon solar cell performance

04 p0504 A83-15457

Spectroradiometer measurements in support of photovoltaic device testing

04 p0481 A83-15458

Effect of temperature on the performance of the PEC cells formed with chemically deposited CdS films --- photoelectrochemical cells

04 p0505 A83-15491

Characteristics of a Savonius windmill power system with a synchronous generator

04 p0505 A83-15797

Hydrogenated a-Si/x/Ge/1-x/- A potential solar cell material

04 p0542 A83-15871

Operation of a steady-state pH-differential water electrolysis cell

04 p0506 A83-16041

Hydrogen as a vector for central receiver solar utilities

04 p0506 A83-16044

Evaluation of thermophotovoltaic conversion efficiency

04 p0507 A83-16086

Inflow disk generator for open-cycle MHD power generation

04 p0538 A83-16104

The STD/MHD codes - Comparison of analyses with experiments --- MHD generator performance prediction and tests

04 p0538 A83-16105

The properties and production of solar cells

04 p0507 A83-16183

The dependence of the resonator efficiency of a CO₂ gasdynamic laser on the laser mixture parameters

04 p0486 A83-16387

Performance results of a 300 MWth generator at high magnetic field

[AIAA PAPER 83-0394] 05 p0686 A83-16690

Steady-state pulses in a laser amplifier with a delayed swept gain

05 p0647 A83-16837

Alexandrite-laser performance at high temperature

05 p0647 A83-16838

Continuous-wave reaction-product chemical lasers /review/

05 p0648 A83-17038

Efficient frequency doubling of radiation emitted by a multistage neodymium laser

05 p0648 A83-17040

Optical inhomogeneity of nonlinear crystals and maximum efficiencies of parametric frequency amplifiers pumped by beams with inhomogeneous transverse intensity distributions

05 p0648 A83-17042

Spectral characteristics of the extraction of excitation energy from neodymium glass amplifiers

05 p0649 A83-17051

Conversion of 3-micron infrared radiation in cesium vapor

05 p0649 A83-17055

Influence of radiative losses on the hydrodynamics of a laser plasma corona

05 p0687 A83-17072

Quasi-CW lasing of a Ne-Xe-HCl mixture excited by an electric discharge

05 p0650 A83-17083

Pulsed high-pressure chemical HF laser with electric-discharge initiation

05 p0650 A83-17084

The stochastic behavior of electrons in free electron lasers with variable parameter wigglers

05 p0650 A83-17145

Design of a 13% efficient n-GaAs/1-x/P/x/semiconductor-liquid junction solar cell

05 p0658 A83-17801

Third-harmonic generation in a pulsed supersonic jet of xenon

05 p0651 A83-17879

Coherent emission from electron clusters in free-electron lasers

06 p0765 A83-17981

A parametric analysis of the performances of a linear collectors' network of a solar power plant

06 p0779 A83-18139

Axisymmetric reflectors of the stepped spherical type

06 p0781 A83-19194

Photovoltaic properties of cadmium sulfide/trivalent-metal phthalocyanine heterojunction devices

06 p0754 A83-19259

Regenerative photoelectrochemical cells using polymer-coated n-GaAs photoanodes in contact with aqueous electrolytes

07 p0952 A83-19882

Electrochemical solar cells using CdSe thin film electrodes

07 p0953 A83-19885

Practical limiting efficiencies for crystalline silicon solar cells

07 p0953 A83-19893

Origin of the difference in the open circuit voltage between p-i-n type and n-i-p type hydrogenated amorphous silicon solar cells

07 p0953 A83-19991

Cherenkov parametric optical oscillations in a 'double' Fabry-Perot interferometer

07 p0934 A83-20116

Radiation heat exchange in a solar cavity-type receiver at various times

07 p0953 A83-20138

Study of the thermal conversion of semi-insulating GaAs:Cr with cathodoluminescence, photoluminescence, and secondary ion mass spectrometry

07 p1000 A83-20747

Characteristics of the electron beam pumped iodine monofluoride laser

07 p0938 A83-21590

Theoretical analysis of electron-beam-excited KrF laser performance - New F2 concentration optimization

07 p0938 A83-21599

Amorphous silicon - A new semiconductor material for solar cells

07 p0955 A83-21627

Photoconductivity and photovoltaic effect in indium selenide

08 p1169 A83-22337

Area utilization efficiency of a sloping heliostat system for solar concentration

08 p1130 A83-22618

Photoelectrochemical behaviour of electrodeposited and pressure-sintered Bi₂S₃, Bi₂S₃-PbS and Bi₂S₃-Ag₂S semiconductor electrodes

08 p1131 A83-22905

Effect of an SiC layer on p-i-n amorphous silicon solar cells

08 p1131 A83-22909

A semiconductor-insulator-semiconductor CdO-SiO₂-Si solar cell

08 p1131 A83-22912

High efficiency p/+/-n-n/+/- back-surface field silicon solar cells with very large short-circuit current densities

08 p1131 A83-22913

Accuracy of analytical expressions for solar cell fill factors

08 p1132 A83-22914

MHD channel performance for potential early commercial MHD power plants

08 p1169 A83-23134

Influence of diffusion of hot carriers on collection efficiency of solar cells - a-Si:H

09 p1292 A83-23665

Constant flow solar pond collector/storage system

09 p1292 A83-23702

Convective losses from cavity solar receivers - Comparisons between analytical predictions and experimental results

09 p1293 A83-23881

Organic solar cells - A review

10 p1445 A83-25449

Preliminary test results for the small community solar power system

[ASME PAPER 82-WA/SOL-30] 10 p1445 A83-25687

Regional thermal and electric energy output of salt-gradient solar ponds in the U.S.

[ASME PAPER 82-WA/SOL-27] 10 p1445 A83-25689

- Efficiency of free-electron lasers with a scattered electron beam 10 p1426 A83-25791
- Hyperabrupt junction varactor diodes for millimeter-wavelength harmonic generators 10 p1409 A83-25820
- Spectroscopy and efficiency of the $^1\text{Hg-200/Br-81}$ and $^1\text{Zn-64/I}$ photodissociation lasers 10 p1426 A83-26003
- An optimized multicomponent wiggler design for a free electron laser oscillator 10 p1428 A83-26017
- Gain and efficiency of a stimulated Cherenkov optical klystron 10 p1428 A83-26020
- Results of the Los Alamos Free-Electron Laser Experiment 10 p1428 A83-26021
- A lithium electrode with a zinc substrate for secondary batteries 10 p1446 A83-26057
- Amorphous silicon photovoltaic modules 10 p1446 A83-26064
- Observation of resonantly enhanced sum-frequency generation involving sodium Rydberg states 10 p1429 A83-26113
- Use of unstable resonators in CW chemical lasers with radial flow of a gas mixture 10 p1431 A83-26652
- Thermal physics of transverse-discharge copper vapor lasers 10 p1433 A83-26682
- Electric-discharge CW industrial CO₂ laser 10 p1433 A83-26687
- Radiative energy receiver for high performance energy conversion cycles 11 p1602 A83-27138
- The relative attractiveness of electric and hybrid passenger cars 11 p1667 A83-27159
- Assessment of phosphoric acid and trifluoromethane sulfonic acid fuel cells for vehicular powerplants 11 p1602 A83-27162
- On insulation measurements using pyranometers and solar cell devices 11 p1607 A83-27238
- Development of solar total energy system for industrial sectors 11 p1608 A83-27244
- Space solar cell technology development - A perspective 11 p1541 A83-27255
- Current developments in silicon space cells 11 p1541 A83-27256
- Single and multijunction space solar cells grown by organometallic vapor phase epitaxy /OM-VPE/ 11 p1608 A83-27260
- Stirling engines for solar power generation in the 50 to 500 kW range 11 p1608 A83-27274
- Performance characteristics of wet and dry fluidynes --- Stirling cycle engines 11 p1587 A83-27276
- A new, versatile Stirling energy conversion unit 11 p1587 A83-27280
- A way to relax the dimensional tolerance requirements of clearance regenerators --- in small Stirling engine design 11 p1588 A83-27286
- Direct-energy-conversion implications of space nuclear reactors 11 p1542 A83-27297
- Thermionic converters for terrestrial applications 11 p1608 A83-27299
- Large parabolic dish collectors with small gas-turbine, Stirling engine or photovoltaic power conversion systems 11 p1610 A83-27329
- Performance of parallel-driven flashlamps suitable for photoinitiated lasers 11 p1579 A83-27571
- Experimental investigation of the optimum specific input energy on a subsonic CO EDL --- Electric Discharge Laser 11 p1580 A83-27577
- Experimental study of the efficiency of rectenna elements 11 p1581 A83-27950
- On the electrokinetic energy conversion in liquid mixtures 11 p1612 A83-28069
- Si Impatts exhibit low noise at mm-waves 11 p1562 A83-28157
- New GaAs Impatt theory explains mm-wave operation 11 p1562 A83-28158
- High-efficiency Q-to-W-band MIC frequency doubler 11 p1563 A83-28609
- Factors affecting the efficiency of chemically deposited CdSe based photoelectrochemical cells 12 p1749 A83-29514
- Aerodynamic performance of a Wells air turbine 13 p1869 A83-30191
- Utility operating strategy and requirements for wind power forecast 13 p1869 A83-30192
- Efficiency of luminescence in luminescent solar concentrators 13 p1870 A83-30205
- The efficiency of a graded-band-gap solar cell 13 p1870 A83-30270
- High performance collectors 13 p1870 A83-30847
- Testing the efficiency of solar collectors at the Technical University of Denmark 13 p1871 A83-30850
- Theoretical evaluation of the rare-gas diluent effects for an electron-beam-excited XeCl laser 13 p1852 A83-31055
- Enhanced HgBr(B₂Sigma⁺ - X₂Sigma⁺) emission at low pressures --- blue-green laser 13 p1852 A83-31062
- Zinc-bromine battery design for electric vehicles 13 p1871 A83-31091
- An experiment on FEL efficiency enhancement with a variable wiggler 13 p1853 A83-31114
- Spontaneous spectrum and small-signal gain for a tapered wiggler free-electron laser 13 p1853 A83-31115
- Saturation of side-band instabilities in a free-electron laser 13 p1855 A83-31134
- The solar radiation resource 13 p1872 A83-31600
- Geometric configuration factors for polygonal zones using Nusselt's unit sphere --- in structural design of solar receivers 13 p1872 A83-31609
- On the possibility of solar-radiation storage in organic photoisomers 14 p2036 A83-32046
- Solar generator performance with load matching to water electrolysis - Longterm averages and range of instantaneous efficiencies 14 p2038 A83-32191
- Operational experience with intermediate flat-plate photovoltaic systems 14 p2038 A83-32196
- Study of a photovoltaic concentrating system like 'Sophoche' in fluctuating mode 14 p2039 A83-32200
- Performance of 1 kw peak concentrating photovoltaic array 14 p2039 A83-32201
- Photovoltaic concentrator module characterization 14 p2039 A83-32202
- Subsystem engineering and development of grid-connected photovoltaic systems 14 p2039 A83-32205
- Low cost modular designs for photovoltaic array fields 14 p2039 A83-32208
- Minimum cost of photovoltaic energy for a utility grid and general features of a generating plant using costless solar cells. 14 p2040 A83-32214
- A dc/ac modular interface for photovoltaic systems 14 p2004 A83-32215
- Simple transformerless inverter with automatic grid-tracking and negligible harmonic content for utility interactive photovoltaic systems 14 p2004 A83-32216
- Power conditioning in solar photovoltaic array applications 14 p2040 A83-32218
- Calculation to improve power conversion efficiency in photovoltaic systems 14 p2040 A83-32221
- AM/PM - The rating system for photovoltaic modules --- standard based on whole day insolation 14 p2040 A83-32223
- Organic photovoltaic materials - Polyacetylene 14 p2005 A83-32256
- Studies on CdS/n-InP PEC solar cells 14 p2042 A83-32258
- Advanced photovoltaic devices 14 p2042 A83-32259
- High efficiency GaAs solar cells for concentrator and flat plate arrays 14 p2042 A83-32260
- Photovoltaic concentrator technology in the USA 14 p2042 A83-32261
- High efficiency tandem type solar cells consisting of a-Si:H and a-SiGe:H 14 p2042 A83-32263
- High efficiency shallow p-(---)nn(+) cadmium telluride solar cells 14 p2042 A83-32264
- Role of photoluminescence in the efficiency of a Ga(1-x)Al(x)As-GaAs solar cell 14 p2043 A83-32269
- 750 suns concentrator modules using GaAs solar cells 14 p2043 A83-32272
- Fluorescent planar concentrator (FPC) Monte-Carlo Computer model limit efficiency and latest experimental results 14 p2043 A83-32274
- Physical limitations of present thin film solar cells 14 p2043 A83-32275
- 8 percent efficiency a-SiC:H/a-Si:H heterojunction solar cells 14 p2043 A83-32276
- Amorphous silicon solar cells produced by a consecutive, separated reaction chamber method 14 p2043 A83-32277
- Charge collection in a-Si:H solar cells 14 p2043 A83-32278
- Electrodeposited CdS/CdTe heterojunction solar cells 14 p2044 A83-32280
- Large area and high efficiency A-Si:H solar cell 14 p2044 A83-32284
- Optical optimization of amorphous silicon solar cells 14 p2044 A83-32288
- Photovoltaic performance of CdS heterojunctions on polycrystalline silicon 14 p2044 A83-32293
- Continuous deposition of photovoltaic grade CdS sheet at the unit operations scale 14 p2044 A83-32295
- Cu(x)S(p)-CdZnS(n)-CdS(n+) evaporated thin film solar cells 14 p2045 A83-32296
- Airless sprayed CdS solar cells 14 p2045 A83-32298
- Photovoltaic behaviour of CdSe thin film solar cells 14 p2089 A83-32301
- Cadmium sulfide polyacetylene photovoltaic heterojunction 14 p2090 A83-32305
- Continuous growth of thin polysilicon sheets on a temporary carbon shaper by the R.A.D. process 14 p2090 A83-32311
- Solar grade floating-zone silicon 14 p2045 A83-32316
- Current aspects of the C.G.E. semicrystalline silicon ingots elaboration method 14 p2090 A83-32317
- Laser processing in the preparation of high efficiency polycrystalline silicon solar cells 14 p2005 A83-32329
- An improved derivation of solar cell parameters in terms of transition probabilities 14 p2046 A83-32335
- The world's largest 12volt single string photovoltaic module 14 p2046 A83-32337
- Influences of thermal effects on high power CW outputs of b-axis Nd:YAP lasers 14 p2024 A83-32596
- Analysis of a non-uniformly doped MPN silicon Schottky barrier solar cell 14 p2047 A83-32675
- 8.5 percent efficient screen-printed CdS/CdTe solar cell produced on a 5-cm x 10-cm glass substrate 14 p2047 A83-32838
- Solar collector testing in the European community 14 p2047 A83-32846
- High-efficiency laser-pulse compression by stimulated Brillouin scattering 15 p2167 A83-33759
- Luminiscent solar concentrators for energy conversion 15 p2189 A83-33861
- Optimum design of n(+)---n-n(+) InP devices in the millimeter-range frequency limitation - RF performances 15 p2151 A83-33917
- Efficiency of the a-Si:H solar cell and grain size of SnO₂ transparent conductive film 15 p2189 A83-33922
- Efficient lasing of a TEA Co₂ laser with ultraviolet preionization and utilizing unconventional transitions 15 p2168 A83-33977
- Performance benefits of the direct generation of steam in line-focus solar collectors 15 p2189 A83-33989
- A parametric study on solar ponds 15 p2190 A83-34072
- Importance of the emitter in thin back-surface field solar cells 15 p2192 A83-34668
- Heat loss optimisation of a concentric cylindrical solar collector employing a cobalt oxide selective absorber 15 p2192 A83-34675
- Investigation of the efficiency of the acceleration of conductors in the pulsed magnetic field of a solenoid 16 p2340 A83-35540
- Future development of high-power solid-state laser systems 16 p2358 A83-35884
- New pulsed far infrared laser lines in D₂O 16 p2359 A83-35959
- The growth and characterization of epitaxial solar cells on resolidified metallurgical-grade silicon 16 p2420 A83-35986
- Effect of boron doping and its profile on characteristics of p-i-n a-Si:H solar cells 16 p2371 A83-36742
- Photovoltaic and structural properties of CuInSe₂/CdS solar cells 16 p2371 A83-36744
- Relativistic electron beam diagnostics and microwave emission in a carcinotron 16 p2347 A83-36927
- Limitations on solar cell open-circuit voltage and efficiency 17 p2535 A83-37790
- High-frequency doubler operation of GaAs field-effect transistors 17 p2497 A83-37800
- Magnetohydrodynamic generator scaling analysis for baseload commercial powerplants 17 p2582 A83-38020
- Stability of P-I-N hydrogenated amorphous silicon solar cells to light exposure 18 p2707 A83-39462
- Light-induced effects in indium tin oxide/n-i-p hydrogenated amorphous silicon solar cells 18 p2707 A83-39463
- Effects of optical stress on the properties of sputtered amorphous silicon solar cells and thin films 18 p2707 A83-39466
- Cold pressed cadmium selenide photoanodes for electrochemical solar cells 18 p2708 A83-39929
- Single crystal Cu₂S/CdS photovoltaic devices with optimum performance before a post barrier air bake 18 p2708 A83-39930
- New promise for photovoltaics 18 p2709 A83-40337
- Performance test procedures for thermal collectors - Outdoor testing 18 p2709 A83-40523
- Performance test procedures for thermal collectors - Solar simulators 18 p2709 A83-40524
- Photovoltaic energy converters 18 p2709 A83-40525
- Performance test procedures for solar cells and modules 18 p2710 A83-40526
- Solar cell and module performance assessment based on indoor calibration methods 18 p2710 A83-40527
- Performance of a hybrid solar heating system of the solar laboratory at the JRC-ISPRA 18 p2710 A83-40533

- A solar cell with enhanced photocurrent 19 p2861 A83-40667
- High-efficiency and high-power AlGaAs/GaAs laser 19 p2851 A83-40935
- High-efficiency infrared xenon laser excited by a UV preionized discharge 19 p2852 A83-40947
- Xenon laser action in discharge and electron-beam excited Ar-Xe mixture 19 p2853 A83-41183
- High neon pressure longitudinal copper vapour laser 19 p2853 A83-41185
- Stimulated emission from a relativistic electron beam in a variable-parameter longitudinal magnetic wiggler 19 p2853 A83-41192
- Photovoltaic energy systems: Design and installation --- Book 20 p3011 A83-42175
- Degradation of the performance of Cu₂S/CdS solar cells due to a two-way solid state diffusion process 20 p3052 A83-42358
- Optimization of substrate thickness for interdigitated back contact silicon solar cells 20 p3052 A83-42360
- Efficient backward and forward pumping CW Raman amplification for InGaAsP laser light in silica fibres 20 p2993 A83-42486
- New progress in the development of a 94-GHz pretuned module silicon IMPATT diode 20 p2968 A83-43348
- High efficiency GaInAs/Inp heterojunction IMPATT diodes 20 p2968 A83-43350
- Two-dimensional modeling of the MIS grating solar cell 20 p3054 A83-43356
- An analytic approach to optimum oscillator design using S-parameters 21 p3122 A83-43832
- Fast electromagnetic launchers 21 p3125 A83-44103
- Limit of concentration for cylindrical concentrators under extended light sources --- parabolic solar collectors 21 p3167 A83-44149
- Dynamic single-mode semiconductor lasers with a distributed reflector 21 p3144 A83-44217
- Process control of vacuum-deposited CdS for the fabrication of reproducible 8 percent efficient solar cells 21 p3167 A83-44605
- Fabrication of optically enhanced thin film a-SiH(x) solar cells 21 p3167 A83-44612
- Isentropic magnetogasdynamic flow of a perfect plasma 22 p3363 A83-46462
- Optical coatings for energy efficiency and solar applications; Proceedings of the Seminar, Los Angeles, CA, January 28, 29, 1982 22 p3319 A83-46580
- Low cost and high performance antireflective (AR) coatings for solar cells 22 p3319 A83-46586
- Cascade AlGaAs-GaAs solar cell research using molecular beam epitaxy 22 p3319 A83-46606
- High efficiency GaAs(1-x)P(x) solar cells fabricated by vacuum metalorganic chemical vapor deposition 22 p3319 A83-46607
- The effect of gas bubble evolution on the energy efficiency in water electrolysis --- Thesis 22 p3266 A83-46688
- Dynamic behavior of a class of photovoltaic power systems 22 p3320 A83-46772
- Catalysis in solar energy --- development of photoelectrochemical cells 22 p3320 A83-46794
- Generation of short laser pulses during coherent amplification 22 p3301 A83-46937
- Radiation-proof satellite technology [IAF PAPER 83-69] 23 p3421 A83-47251
- Investigation of complementary p-n-p and n-p-n solar cell stages 23 p3477 A83-47563
- A 1.5 W CW optically pumped 12.08 microns NH₃ laser 23 p3462 A83-48317
- AlGaAs/GaAs cascade solar cell computer modeling under high solar concentration 23 p3478 A83-48616
- Grating solar cells - An experimental comparison of alternative structures 23 p3478 A83-48617
- A study of built-in potential in a-Si solar cells by means of back-surface reflected electroabsorption 23 p3478 A83-48702
- Relative efficiency of Hg-200Br-79, HgBr-79, and HgBr electric discharge lasers 23 p3586 A83-48781
- New types of high efficiency solar cells based on a-Si 24 p3598 A83-48787
- Surface modification of polycrystalline p-CuInS₂ and p-CuInSe₂ electrodes for improved solar cell performance 24 p3601 A83-50177
- Fluorescent window as wavelength shifter for a polysulfide containing photoelectrochemical cell 24 p3601 A83-50183

ENERGY CONVERTERS

U DIRECT POWER GENERATORS

ENERGY DENSITY

U FLUX DENSITY

ENERGY DISSIPATION

- The mechanism of the dissipation of elastic energy by a lubricant layer 02 p0186 A83-11647
- Curved dielectric optical waveguides with reduced transition losses 02 p0235 A83-12005

- A comparison of theoretical and experimental methods of calibrating the electric potential drop technique for crack length determination 02 p0190 A83-12040
- Inhibition of baroclinic instability in low-resolution models 02 p0213 A83-12228
- Field evaluation of aerial infrared surveys for residential applications 02 p0200 A83-12688
- Lower-hybrid drift instability as a dissipation mechanism in the magnetospheric plasma 03 p0356 A83-13187
- Infrared lines from shocked galactic gases 03 p0417 A83-13465
- In situ acceleration in extragalactic radio jets 03 p0423 A83-14185
- Chromospheres of F, G, K type stars. VIII - Energy balance in transition region 03 p0437 A83-14720
- Hidden supersymmetry in stochastic dissipative dynamics 04 p0532 A83-15911
- Investigation of a high-efficiency photodissociation laser operating in the free-lasing regime 05 p0649 A83-17054
- Influence of radiative losses on the hydrodynamics of a laser plasma corona 05 p0687 A83-17072
- The mechanism of dissipation of turbulence energy in the solar wind 05 p0709 A83-17601
- Generalized expressions for momentum and energy losses of charged particle beams in non-Maxwellian multi-species plasmas and spherical symmetry 06 p0812 A83-18915
- Electron energy-loss studies of molecular oxygen in the region 14.8-20.3 eV using a multidetector electron spectrometer 06 p0808 A83-19009
- MHD stability of incompressible coronal loops with radiative energy loss 06 p0856 A83-19295
- Determination of stress relaxation by damping measurements 07 p0946 A83-20522
- Comparison of Venusian lightning observations 07 p1030 A83-20620
- Radiation from a dislocation oscillating in a circular cylinder 07 p0948 A83-21169
- On the maximum-energy-release-rate criterion for fracture under combined loads 08 p1116 A83-21659
- Shock stagnation and neutrino losses in stellar collapse 08 p1177 A83-21832
- Energy loss of slowly moving magnetic monopoles in matter 08 p1192 A83-22640
- Lightning activity on Jupiter 08 p1189 A83-22933
- Analysis of viscous dissipation effect on thermal entrance heat transfer in laminar pipe flows with convective boundary conditions 08 p1086 A83-23123
- Free energy loss during the breakdown of liquid films 08 p1087 A83-23141
- On the orientation precision of satellite solar power stations 08 p1050 A83-23164
- Analytical model of a magnetron 09 p1252 A83-23461
- Convective losses from cavity solar receivers - Comparisons between analytical predictions and experimental results 09 p1293 A83-23881
- Diamond /111/ studied by electron energy loss spectroscopy in the characteristic loss region 10 p1390 A83-25675
- Adiabatic shearing of incompressible fluids with temperature-dependent viscosity 10 p1414 A83-25873
- Nonlinear energy attenuation of pulsed CO₂ laser radiation in the atmospheric surface layer 10 p1434 A83-26776
- The role of dissipation in shepherding of ring particles 11 p1683 A83-27354
- On waves in non-isothermal, compressible, ionized and viscous atmospheres 11 p1677 A83-27654
- The dissipation of shock waves in the outer solar atmosphere - A reappraisal 11 p1691 A83-27702
- Correlation between the energy characteristics of fracture - Crack propagation and spalling 11 p1598 A83-28503
- Certain effects of the dissipation of the auroral electrojet during magnetospheric substorms 11 p1621 A83-28751
- Dissipation length in stable layers --- atmospheric boundary layer energy parameterization 12 p1758 A83-29136
- Improved system for energy-dispersive X-ray diffraction with synchrotron radiation --- phase transition kinetics in KBr 13 p1826 A83-30251
- Energetic ion losses near Io's orbit 13 p1962 A83-31227
- Monopole heat --- generated by elementary particle interactions 13 p1960 A83-31789
- Energy dissipation during the vibration of multilayer shells 14 p2031 A83-32389
- Asymptotic near-wall stress dissipation rates in a turbulent flow 14 p2013 A83-33376
- Low-noise, low power dissipation GaAs monolithic broad-band amplifiers 14 p2008 A83-33459

- A theoretical study of radiative cooling in homogeneous and isotropic turbulence 15 p2156 A83-33671
- Where does the O(1D) energy go? --- in lower thermosphere budget 15 p2196 A83-33945
- The effect of dissipative magnetic moment on the rotation of a satellite relative to its center of mass 15 p2127 A83-34426
- Structurally stable approximations to Friedmann-Lemaître world models --- as dynamic cosmological systems 15 p2272 A83-34781
- Tolman's cosmological models 15 p2272 A83-34782
- Flow-loss, efficiency, and change-of-state calculations for fluid-flow engines and heat exchangers 15 p2162 A83-34976
- Electron impact excitation from a 1 Delta g state of molecular oxygen 16 p2408 A83-35330
- Low-resolution numerical simulation of decaying two-dimensional turbulence 16 p2385 A83-35470
- Energy losses due to plastic deformation during the radial compression of a cylindrical shell 16 p2364 A83-35544
- Solar wind energy dissipation in the upper atmosphere 16 p2377 A83-36110
- Energetics and optimum motion of oscillating lifting surfaces --- energy losses of rigid wings [AIAA PAPER 83-1710] 17 p2445 A83-37204
- Optimization of a heat engine based on a dissipative system 17 p2585 A83-38204
- On the crack energy density and energy release rate for an elasto-plastic crack 18 p2697 A83-39456
- Dissipation of thick accretion disks 18 p2774 A83-39742
- On dissipational processes in the cosmological GUT era 18 p2775 A83-39761
- Formation of saturated solitons in a nonlinear dispersive system with instability and dissipation 19 p2895 A83-40968
- Efficient parametric decay in dissipative media 19 p2895 A83-40973
- Channels of energy losses in erbium laser glasses in the stimulated emission process 19 p2853 A83-41186
- Viscous dissipation effects on heat transfer from turbulent flow with high Prandtl number fluids 20 p2977 A83-42723
- A quantitative comparison between calculated and measured conversion losses of a novel beam-lead GaAs Schottky-barrier mixer diode with minimized parasitics 20 p2968 A83-43359
- Energy lost in formation of fluorine atoms in the course of electron-beam dissociation of fluorine and fluoride molecules 20 p2997 A83-43797
- Tidal dissipation in small viscoelastic ice moons - The case of Enceladus 21 p3239 A83-44082
- On subcritical crack growth in ceramics as influenced by grain size and energy-dissipative mechanisms 21 p3116 A83-44122
- Formation and evolution of the micropinch region in a vacuum spark 21 p3210 A83-44137
- An analysis of the energy release rate for non-coplanar crack growth in fiber reinforced composite materials 21 p3107 A83-44913
- Energy dissipation due to liquid slosh in spinning spacecraft 21 p3102 A83-45124
- Effects of energy addition and dissipation on dual-spin spacecraft attitude motion 21 p3103 A83-45466
- Suprathermal electron energy deposition in plasmas with the Fokker-Planck method 21 p3215 A83-45520
- The dynamics of dissipatively heated spherical accretion --- onto black holes 21 p3238 A83-45561
- Nonlinear effects on dissipative MHD modes 22 p3364 A83-47093
- Optimisation of homogeneous thermal insulation layers 23 p3449 A83-48097
- The thermodynamics of evolution. I - The thermodynamics of the dissipative structures 23 p3513 A83-48599
- Effects of rotation on isotropic turbulence [ONERA, TP NO. 1983-108] 24 p3577 A83-49419
- Heat loss measurements on an enclosure for high temperature batteries 24 p3599 A83-49926

ENERGY DISTRIBUTION

NT SPECTRAL ENERGY DISTRIBUTION

- Measurements of energy distribution and thrust for microwave plasma coupling of electrical energy to hydrogen for propulsion [AIAA PAPER 82-1951] 02 p0147 A83-12508
- The energy problem in Einstein's theory of gravitation /Dedicated to the memory of V. A. Fock/ 03 p0416 A83-13426
- The UV spectrum of the old nova HR Del at different orbital phases 03 p0428 A83-14770
- States in the gap of amorphous hydrogenated silicon 04 p0541 A83-15524

- The seasonal CO₂ cycle on Mars - An application of an energy balance climate model 04 p0569 A83-15592
- Observations of inverted-V electron precipitation 04 p0510 A83-15824
- The energetics of the general circulation of the atmosphere in southern hemisphere during the IGY. I - The distribution of atmospheric energy 04 p0517 A83-16011
- Energy balance in a contracted glow discharge in a longitudinal gas flow 06 p0811 A83-18441
- Electron beam energy branching in a gas mixture 09 p1343 A83-23678
- Angular and energy distribution of photons of the radiative scattering of a neutrino /antineutrino/ by an electron 09 p1344 A83-24205
- The galactic gradient in electron temperature from observations of low-density H II regions 10 p1503 A83-25722
- Electron spectrum measurements for a tapered-wiggler free-electron laser 10 p1428 A83-26018
- Nascent DF energy distributions for the D + F₂ and F + D₂ reactions 11 p1580 A83-27578
- On the energy distribution function for a one-dimensional gravitational system 11 p1682 A83-28293
- Approximate solutions for isothermal flows behind strong spherical shocks with variable energy 12 p1722 A83-29056
- Energy and polarization characteristics of radiation from the open end of a circular waveguide 13 p1828 A83-30714
- Energy characteristics of an electromagnetic field and an extraneous particle in a dispersive medium 14 p2079 A83-32168
- Energy redistribution among internal states of nitric oxide molecules upon scattering from Pt(111) crystal surface 14 p1991 A83-33107
- Ultraviolet continuum of a sample of Be stars 14 p2108 A83-33267
- Dependence of the continuum energy distribution of T Tauri stars on the location of the temperature minimum 14 p2108 A83-33270
- Neutron high-energy spectra at seven different depths in the atmosphere from 0 to 40 mbar near the geomagnetic equator 15 p2196 A83-33948
- Measurements of the distribution of the flux of energy in the focus of a solar concentrator with visualization techniques 15 p2191 A83-34406
- The critical energy density and the inelasticity coefficient for asteroidal catastrophic collisions 15 p2250 A83-35029
- Energy distribution of thermal electrons at the height of lower-E-region 16 p2373 A83-35366
- Studies of collision interactions and kinetic energy distribution of eV recoil ions inside Penning traps 16 p2409 A83-35631
- Effect of electrons produced by ionization on calculated electron-energy distributions 16 p2414 A83-35653
- Vibrational energy distribution in molecules excited by infrared radiation in the collisionless regime 16 p2410 A83-35894
- On the crack energy density and energy release rate for an elasto-plastic crack 18 p2697 A83-39456
- Energy and charge distribution of energetic helium ions in the outer radiation belt of the earth 18 p2787 A83-39954
- Large-scale energy transformations in the high latitudes of the Northern Hemisphere 18 p2728 A83-40026
- Energy fluctuations of transition radiation 20 p3046 A83-43529
- Angular and energy distributions of transition X-radiation 20 p3046 A83-43536
- Particle acceleration in shocks - The effect of finite cosmic-ray pressure on the energy distribution 21 p3233 A83-44746
- A quantitative description of the spatial distribution and dynamics of the energy flux in the continuous aurora 22 p3327 A83-46053
- The non-Maxwellian energy distribution of ions in the warm lo torus 22 p3387 A83-47072
- Energy distribution functions of electrons in low-temperature helium-neon plasma at low pressures 24 p3632 A83-49113
- Energetic distributions of interface states Di(phi sub s) of MOS transistors in extension of Kuhn's quasistatic C(V)-method 24 p3575 A83-50118
- ENERGY EFFICIENCY TRANSPORT PROGRAM**
U ACEE PROGRAM
- ENERGY EQUIPARTITION**
U EQUIPARTITION THEOREM
- ENERGY EXCHANGE**
U ENERGY TRANSFER
- ENERGY GAPS (SOLID STATE)**
Direct-gap group IV semiconductors based on tin 01 p0108 A83-10294
- Energy gap versus alloy composition and temperature in Hg_{1-x}/Cd_x/Te [AD-A125659] 01 p0109 A83-10644
- Dependence of barrier height on energy gap in Au n-type GaAs_{1-x}/P_x/Schottky diodes 02 p0242 A83-11784
- Meaning of the photovoltaic band gap for amorphous semiconductors 02 p0243 A83-12287
- Bulk and interface gap states in a-Si:H - A comparative study of field effect and capacitance measurements on codeposited samples 04 p0539 A83-15487
- Paramagnetism in X-irradiated chalcogenide glasses and crystals 04 p0540 A83-15503
- Electronic correlations and transient effects in disordered systems 04 p0540 A83-15506
- Effects of prolonged illumination on the properties of hydrogenated amorphous silicon 04 p0540 A83-15512
- Optical absorption above the optical gap of amorphous silicon hydride 04 p0541 A83-15520
- Studies of the band tails in a-Si:H by photomodulation spectroscopy 04 p0541 A83-15523
- States in the gap of amorphous hydrogenated silicon 04 p0541 A83-15524
- PAS study of gap-state profiles of P-doped and undoped a-Si:H --- photoacoustic spectroscopy 04 p0541 A83-15525
- Influence of interface states on field effect and capacitance-voltage characteristics of metal/oxide/a-Si:H structures 04 p0541 A83-15526
- Some problems in determination of gap-state density in amorphous silicon 04 p0541 A83-15527
- Semiconductor structures for repeated velocity overshoot 05 p0690 A83-17295
- Theory for nonequilibrium behavior of anisotropy graded heterojunctions 06 p0814 A83-18961
- Donor discrimination and bound exciton spectra in InP 07 p1000 A83-20746
- Direct bandgap, ionizing-radiation insensitive, photodiode structures 08 p1165 A83-22487
- Enhanced bandgap resonant nonlinear susceptibility in quantum-well heterostructures 08 p1167 A83-22917
- Diamond /111/ studied by electron energy loss spectroscopy in the characteristic loss region 10 p1390 A83-25675
- Electronic properties of amorphous silicon selenium films 10 p1488 A83-25984
- Estimation of the band gap of InPO₄ 10 p1489 A83-26210
- The efficiency of a graded-band-gap solar cell 13 p1870 A83-30270
- Studies of the gap states density in undoped and doped amorphous hydrogenated silicon 14 p2088 A83-32237
- Study of gap states in a-Si:H by transient current spectroscopy 14 p2089 A83-32251
- (GaAl)As/GaAs heterojunction bipolar transistors with graded composition in the base 15 p2152 A83-34516
- Dispersion of the refractive index of GaAs and Al(x)Ga(1-x)As 16 p2420 A83-35970
- Density of the gap states in undoped and doped glow discharge a-Si:H 16 p2421 A83-36740
- Staebl-Wronski effects in hydrogenated amorphous Si(1-x)Ge(x) 18 p2749 A83-39469
- The interpretation of photoconductivity measurements in hydrogenated amorphous silicon 18 p2750 A83-39471
- Photo-induced changes in the bulk density of gap states in hydrogenated amorphous silicon associated with the Staebl-Wronski effect 18 p2750 A83-39472
- Density of gap states of silicon grain boundaries determined by optical absorption 18 p2750 A83-40063
- Energy-band distortion in highly doped silicon 18 p2750 A83-40377
- Observation of spin-dependent thermal emission from deep levels in semiconductors 19 p2904 A83-40970
- Density-functional theory of excitation spectra of semiconductors - Application to Si 19 p2905 A83-41159
- Squeezable electron tunneling junctions 20 p3055 A83-43607
- The activation energy of conductivity in organic solids and liquids in relation to the cohesive energy density 21 p3216 A83-43948
- Methods of determining optical constants of thin semiconductor films using normal incidence reflectance and transmittance data 21 p3206 A83-44789
- Theoretical analysis of solar cells based on graded band-gap structures 22 p3318 A83-46277
- Transient response of nonlinear ring resonators using GaAs with photon energy below band gap 22 p3360 A83-46652
- Kinetic phenomena in nondegenerate narrow-gap semiconductors --- Russian book 23 p3511 A83-47121
- HgCdTe heterojunctions 24 p3571 A83-48742
- Reduction in the localized band-gap states in amorphous silicon by annealing and hydrogen implantation 24 p3634 A83-48793
- ENERGY LEVELS**
NT ATOMIC ENERGY LEVELS
NT ELECTRON STATES
NT GROUND STATE
NT INTERMOLECULAR FORCES
NT MOLECULAR ENERGY LEVELS
- Nonadiabatic transitions in a three-level system subjected to a laser radiation field with a smoothly varying frequency 07 p0934 A83-20109
- An optimized weighting algorithm for variations in PCM energy levels 10 p1402 A83-25640
- Radiationless processes and their implications for new laser materials 11 p1581 A83-27593
- New temperature fluctuation method for direct determination of thermal activation energy of deep levels in semiconductors 12 p1782 A83-29475
- Evidence that the gold donor and acceptor in silicon are two levels of the same defect 13 p1928 A83-30340
- Excitation of the rotational levels of interstellar HCN 13 p1948 A83-31258
- Photoinduced angular motion of states and field splitting of levels 20 p3044 A83-42284
- Energy levels and alloy scattering in InP-In(Ga)As heterojunctions 22 p3365 A83-46738
- ENERGY LOSSES**
U ENERGY DISSIPATION
- ENERGY METHODS**
NT STRAIN ENERGY METHODS
- Energy criteria of the brittle fracture of materials with initial stresses 01 p0059 A83-10676
- An energy theory for postbuckling of composite plates under combined loading 02 p0195 A83-12758
- Boundary manifolds for energy surfaces in celestial mechanics 03 p0404 A83-13409
- Co-energy methods for elliptic flow and related problems 03 p0384 A83-14080
- An energy analysis of the stability of flexible filaments in coaxial flow 07 p0926 A83-20899
- Development of the nonlinear energy method for fracture toughness determination 08 p1063 A83-21753
- The experimental evaluation on the brittle fracture characterization under the mixed mode 08 p1122 A83-22069
- Determination of the fracture toughness of polycarbonate using an energy approach 09 p1239 A83-25049
- Numerical interpretations of creep buckling behavior of columns 09 p1282 A83-25105
- Some remarks on elastic fracture mechanics 11 p1595 A83-28434
- Path-independent integrals, energy release rates, and general solutions of near-tip fields in mixed-mode dynamic fracture mechanics 14 p2031 A83-32652
- Virtual work in structural analysis --- Book 15 p2173 A83-33748
- Isoparametric finite difference energy method for plate bending problems 15 p2176 A83-34322
- A nonlinear energy analysis for mixed mode fracture 17 p2518 A83-37271
- Sanders' energy-release rate integral for a circumferentially cracked cylindrical shell [ASME PAPER 83-APM-32] 17 p2519 A83-37386
- Energy criteria for the brittle fracture of composite materials with initial stresses 17 p2523 A83-38503
- Instability of thin walled bars 21 p3152 A83-44540
- The effect of blade discretization on resonant turbine blade response 23 p3469 A83-47983
- [ASME PAPER 83-GT-158] 23 p3469 A83-47983
- Extremum principles for the energy-release problem of elastic-perfectly plastic body subjected to prescribed change of material properties 23 p3470 A83-48093
- Delamination of composites under compression 23 p3472 A83-48467
- ENERGY OF FORMATION**
Standard free energy of formation of iron iodide 11 p1546 A83-28299
- A calculation of the gas flow in a zone of energy release during a cylindrical explosion 14 p2008 A83-31896
- ENERGY POLICY**
Current topics of SPS realization from a European viewpoint 01 p0069 A83-11283
- Wind power for the electric-utility industry: Policy incentives for fuel conservation --- Book 02 p0201 A83-11896
- Evaluation of solar reflective surfaces for dish concentrators 11 p1607 A83-27237
- Summary assessment of the satellite power system 13 p1869 A83-30186

- Technical, economic and legal aspects of wind energy utilization 20 p3012 A83-43370
- Solar power satellites and security considerations - The case for multilateral agreements 22 p3371 A83-46318
- US national programs in ceramics for energy conversion 23 p3438 A83-48308

ENERGY REQUIREMENTS

- Attempt to determine the power demand of a helicopter control system on the basis of flight tests 01 p0012 A83-10439
- Low power challenge to signal processing for space-based mosaic sensors 08 p1049 A83-22609
- Propulsion and fluid management - Station keeping will eat energy on a new scale 09 p1220 A83-24360
- The timing of EV recharging and its effect on utilities --- Electric Vehicles 13 p1871 A83-31098
- Energy balance of solar absorption and vapor compression cooling systems 14 p2046 A83-32350
- A strategy for mineral and energy resource independence 17 p2529 A83-38155
- Economic evaluation of a standard product of fiber-reinforced composite material in comparison with steel 17 p2483 A83-38875
- Wind-load correlation and estimates of the capacity credit of wind power - An empirical investigation 20 p3012 A83-43368

ENERGY SOURCES

- Electromagnetic projectile acceleration utilizing distributed energy sources 01 p0036 A83-10620
- Primary energy: Present status and future perspectives --- Book 03 p0355 A83-14120
- Main advances and needs on the study of geothermal resources in Chile by using remote sensing techniques 08 p1127 A83-21946
- Ocean thermal-energy conversion 09 p1294 A83-25125
- Miami International Conference on Alternative Energy Sources, 5th, Miami Beach, FL, December 13-15, 1982, Proceedings of Condensed Papers 10 p1445 A83-25575
- Summary of electric vehicle energy source technologies 13 p1871 A83-31089
- The lead-acid battery - Demonstrating the systems design approach to a practical electric vehicle power source 13 p1871 A83-31090

ENERGY SPECTRA

- NT ELECTRONIC SPECTRA
- NT NEUTRON SPECTRA
- The formation of a universal energy spectrum for charged particles in the shear flow of the cosmic plasma 02 p0272 A83-11703
- Investigation of the chemical composition of cosmic-ray nuclei in the 20-1000 GeV/nucleon energy range by means of transition radiation 02 p0272 A83-11705
- Concerning a new component of the radiation belts 02 p0272 A83-11708
- Investigation of fluxes of electrons and gamma quanta with energies exceeding 30 MeV at heights of 300-350 km 02 p0272 A83-11709
- Experimental studies of geomagnetic effects in cosmic rays and the spectrum of the increase effect before magnetic storms 02 p0273 A83-11713
- Results of spectrum studies of energetic flare particles by the Venera 11 and 12, and Prognoz 5 and 6 spacecraft 02 p0269 A83-11716
- The interaction of hadrons and the nuclear composition of primary cosmic rays with energies of 200-2000 TeV according to the energy spectrum of hadrons in showers 02 p0275 A83-11755
- The energy spectrum of primary cosmic rays in the range 10 to the 13th-10 to the 16th eV 02 p0275 A83-11756
- The upper boundary of the energy spectrum of cosmic rays and possible methods for detecting cascades of superhigh energies /10 to the 20th-10 to the 28th eV/ 02 p0276 A83-11762
- An investigation of the energy spectrum and interactions of cosmic-ray muons with energies up to 10 to the 13th eV at a depth of 550 mwe 02 p0276 A83-11763
- Modulation of the monoenergetic spectrum of galactic cosmic rays 02 p0276 A83-12417
- Analysis of cataclysmic variable star energy distributions 02 p0262 A83-12919
- Electrons with energies of hundreds of MeV in near-earth space 03 p0438 A83-13208
- Particle acceleration during the development of tearing-mode discontinuity --- in cosmic plasma 03 p0356 A83-13209
- High energy gamma-rays from black holes 03 p0439 A83-14721
- The turbulence spectrum and velocity of the solar wind at elongations of 90-150 degrees 04 p0575 A83-15754
- A new theory of the energy spectrum --- in viscous boundary layer shear flow 06 p0756 A83-18056

- Derivation of vertical muon spectra at superhigh energies from our predicted primary cosmic-ray spectrum using machine interaction parameters and Feynman scaling hypothesis 06 p0857 A83-18136
- Energy spectra of hadrons and leptons in the atmosphere 06 p0858 A83-19346
- Gamma-ray burst spectra 07 p1039 A83-20013
- The low energy spectra of gamma-ray bursts 07 p1039 A83-20018
- Ultrahigh-energy cosmic rays 07 p1039 A83-20851
- Numerical modeling of the energy spectrum of the cosmic ray Forbush decrease 07 p1040 A83-21504
- A simple theoretical model for calculating and parameterizing the ionospheric photoelectron flux 09 p1304 A83-23772
- Energy spectrum of cosmic ray primaries at super high energies estimated from the recent balloon-borne calorimeter measurements 09 p1369 A83-24700
- Threshold structures in the cross sections of low-energy electron scattering of methane 09 p1343 A83-24825
- A planar energy spectrometer for the study of energy distributions of electron and proton fluxes 10 p1387 A83-25343
- GX 339-4 - X-ray spectra of high and low states 10 p1498 A83-25352
- Sources of methodological errors in calculations of the solar cosmic ray spectrum 10 p1521 A83-26107
- The differential energy spectra of electrons having energies of 0.3-3 MeV on the basis of data from the satellite Prognoz 4 10 p1523 A83-26109
- State-selective electron capture by N/2+/- ions in atomic hydrogen using collision spectroscopy 11 p1654 A83-28220
- The use of splines for correlation-function estimation 11 p1649 A83-28494
- An application of the modified zero-fourth-cumulant approximation to homogeneous axisymmetric Boussinesq turbulence 12 p1722 A83-29006
- Turbulence with a spectral gap --- plasma dynamics in astro- and geophysical flows 13 p1839 A83-30103
- Theory of cosmic ray spectra 13 p1966 A83-30423
- Behavior of the energy spectrum in fast pulsations of fluxes of precipitating electrons 13 p1875 A83-30613
- Measurements of the energy spectra of charged particles within the Vertical-10 rocket experiment 13 p1814 A83-30767
- A photoelectron spectroscopic study of (3 + 1) resonant multiphoton ionization of NO and NH3 13 p1916 A83-30964
- Transformation of the spectrum of energetic protons during the motion through the atmosphere 14 p2054 A83-33033
- A model for the turbulent energy spectrum 14 p2013 A83-33385
- Kosmos 856 and Kosmos 914 measurements of high-energy diffuse gamma rays 15 p2286 A83-33706
- Neutron high-energy spectra at seven different depths in the atmosphere from 0 to 40 mbar near the geomagnetic equator 15 p2196 A83-33948
- Electron energy distribution produced by beam-plasma discharge 15 p2234 A83-34196
- The pulse profile of the Crab pulsar in the energy range 45 keV-1.2 MeV 15 p2268 A83-34638
- Low-resolution numerical simulation of decaying two-dimensional turbulence 16 p2385 A83-35470
- The energy spectrum of cosmic fireballs 16 p2431 A83-36672
- Energetic oxygen and sulfur ions in the Jovian magnetosphere and their contribution to the auroral excitation 17 p2618 A83-37580
- Acoustic interaction with a turbulent plane jet - Some effects on turbulent structure 19 p2897 A83-40851
- A method for measuring the spectral power density 19 p2846 A83-40993
- Maximum energy spectral window with frequency domain constraints 19 p2839 A83-41344
- Comment on the cosmic ray energy spectrum in the light of results from atmospheric Cerenkov studies 19 p2925 A83-41539
- Acoustic pulses excited by impacts on objects - Their analytical representation and spectra 20 p3000 A83-43645
- The observed characteristics of a radio outburst on the solar limb 21 p3242 A83-44290
- Neutrino energy production spectra in a relativistic plasma 21 p3231 A83-44449
- Multiple scales for modelling turbulent flows. I - A multiple scales model for the kinetic energy of the turbulence and variance of a passive scalar 21 p3129 A83-44460
- Propagation effects of solar cosmic rays. II - Propagation correction of peak spectrum 21 p3243 A83-44579

- Spectrum of a pulse sequence with a period modulated by a narrow-band random process 21 p3120 A83-44775
- A method of obtaining three-dimensional spectra in a homogeneous turbulence --- French thesis 21 p3133 A83-45084
- Photon and helium energy spectra above 1 TeV for primary cosmic rays 21 p3246 A83-45575
- The stochastic properties of the parametric discrete Fourier transform 22 p3353 A83-45661
- Analytical yield spectrum approach to electron energy degradation in earth's atmosphere 22 p3327 A83-46055
- Narrow spectral peaks in electrons precipitating from the slot region 22 p3337 A83-47073
- Gamma-ray lines and neutrons from solar flares 23 p3535 A83-47698
- The spectra of cosmic ray nuclei greater than 1 GeV/nuc Implications for acceleration and propagation 23 p3539 A83-47737
- Cosmic ray electrons and positrons - A review of current measurements and some implications 23 p3539 A83-47740
- Cosmic ray composition at 10 to the 12th - 10 to the 15th eV derived from muon measurements 23 p3539 A83-47741
- Electron energy-loss spectroscopy of carbon monoxide II - The energy region 11 to 20 eV 23 p3506 A83-48581
- The metal-insulator transition in transition-metal compounds 24 p3635 A83-49074
- Positrons in cosmic rays and the galactic gamma radiation associated with them 24 p3675 A83-49173
- Dependence of MHD turbulence spectra on the velocity field-magnetic field correlation --- of solar wind 24 p3675 A83-50083

ENERGY STORAGE

- NT ELECTRIC ENERGY STORAGE
- NT HEAT STORAGE
- Metallurgy of rechargeable hydrides 02 p0153 A83-11509
- Particle size distribution of Ni microprecipitates in LaNi5 used for hydrogen storage 02 p0202 A83-12295
- International Conference on Energy Storage, Brighton, Sussex, England, April 29-May 1, 1981, Proceedings 03 p0355 A83-14045
- A numerical study of phase change energy transport in two-dimensional rectangular enclosures [AIAA PAPER 83-0321] 05 p0635 A83-16650
- An experimental facility for the investigation of the two-dimensional Stefan problem [AIAA PAPER 83-0322] 05 p0635 A83-16651
- The effect of crystal size on the thermal energy storage capacity of thickened Glauber's salt 06 p0780 A83-18562
- Storing energy in metal hydrides - A review of the physical metallurgy 07 p0955 A83-21562
- Study on composite flywheels for energy storage 08 p1131 A83-22701
- Stored chemical energy propulsion system for underwater applications [AIAA PAPER 81-1601] 08 p1132 A83-23132
- Configuration selection study for isolated loads --- using parabolic dish modules to supply power for MX shelters 08 p1132 A83-23137
- Design flexibility of redox flow systems --- for energy storage applications 11 p1604 A83-27177
- Initial operating characteristics of the Battery Energy Storage /BEST/ Facility 11 p1604 A83-27182
- Alkaline regenerative fuel cell energy storage system for manned orbital satellites 11 p1540 A83-27206
- Evaluation of solar reflective surfaces for dish concentrators 11 p1607 A83-27237
- Compression molded energy storage flywheels 11 p1608 A83-27303
- The use of mechanical energy storage in an unconventional, rough terrain vehicle 11 p1667 A83-27309
- Factors affecting storage of compressed air in solution mined salt cavities 11 p1609 A83-27311
- Increasing summer peak power with aquifer storage 11 p1609 A83-27313
- Reversible chemical reactions for energy storage in a large-scale heat utility 11 p1609 A83-27315
- Hydriding and dehydriding kinetics of Mg2Ni above and below the structural phase transition 11 p1545 A83-27332
- Modeling and evaluation of designs for solid hydrogen storage beds 11 p1610 A83-27333
- Theory of the computer code RET 1 for the calculation of space-time dependent temperature and composition properties of metal hydride hydrogen storage beds 11 p1545 A83-27337
- Porous metal hydride compacts - Preparation, properties and use 11 p1545 A83-27338

- Magnesium for hydrogen storage
11 p1545 A83-27339
- A system of hydrogen-powered vehicles with liquid organic hydrides
11 p1668 A83-27340
- Dynamics of the preflare magnetic field
11 p1687 A83-27380
- Photochemical storage potential of azobenzenes
12 p1709 A83-28941
- Redox ion flow cell for solar energy storage
12 p1749 A83-29407
- Energy Storage in a fuel cell with bipolar membranes burning acid and hydroxide
13 p1872 A83-31599
- On the possibility of solar-radiation storage in organic photoisomers
14 p2036 A83-32046
- Theoretical and experimental aspects of a two-step short cycle, based on ZnO and CdO intended for storage of solar energy
14 p2046 A83-32348
- The design of flywheels made of fibrous materials
14 p2046 A83-32378
- Electrochemical utilization of metal hydrides
14 p1990 A83-32647
- The question of the hydrogen infrastructure for motor vehicles
15 p2243 A83-34869
- Innovative energy storage for ground-based launch systems
16 p2314 A83-36352
- [AIAA PAPER 83-1348]
Minimization of energy storage requirements for internal combustion engine hybrid vehicles
17 p2516 A83-37547
- Composite flywheel rotor containment
18 p2709 A83-40294
- The storage processes of magnetic energy in solar flares
21 p3242 A83-44301
- On the energy storage in the solar atmosphere by twisting magnetic field
21 p3243 A83-44584
- Effects of Ca additions on some Mg-alloy hydrides
21 p3110 A83-45422
- The Mg₂Ni_{0.75}Mg_{0.25} alloys (M = 3d element) - Their application to hydrogen storage
21 p3168 A83-45423
- Low cost energy storage flywheels from structural sheet molding compound
22 p3318 A83-46299
- Choice of parameters for a flywheel energy storage system --- for spacecraft
24 p3552 A83-49674
- ENERGY STORAGE DEVICES**
U ENERGY STORAGE
- ENERGY TECHNOLOGY**
NT GEOTHERMAL TECHNOLOGY
- Developing technologies for synthetic fuels
01 p0068 A83-10658
- Status of new thin-film photovoltaic technologies
02 p0200 A83-11510
- Solar thermal electricity generation - EURELIQS, the 1 MW/el/ helioelectric power plant of the European communities
02 p0201 A83-11802
- Mathematical model for a noniterative optimization of each system for exploiting solar energy
02 p0201 A83-11849
- The rebirth of the Rankine cycle - Energy production on the basis of low- and medium-temperature heat sources
02 p0244 A83-11868
- Performance characteristics of 350 kW photovoltaic power system for Saudi Arabian villages
03 p0353 A83-13647
- A review of UK wind energy activities
03 p0354 A83-13650
- International Conference on Energy Storage, Brighton, Sussex, England, April 29-May 1, 1981, Proceedings
03 p0355 A83-14045
- Primary energy: Present status and future perspectives --- Book
03 p0355 A83-14120
- Regulation of the diurnal variation of the cold productivity of an adsorption-type solar refrigeration system
04 p0503 A83-15135
- Concerning the improvement of solar heating and cooling systems
04 p0503 A83-15136
- Recent advances in amorphous silicon solar cells
04 p0505 A83-15510
- Photovoltaic prospects in Europe
04 p0507 A83-16184
- Advances in energy technology; Proceedings of the Eighth Annual UMR-DNR Conference on Energy, University of Missouri-Rolla, Rolla, MO, November 4-7, 1981
05 p0658 A83-17115
- Biomass energy
06 p0780 A83-18560
- Sunshine project solar photovoltaic program and recent activities in Japan
07 p0953 A83-20137
- Status of photovoltaic materials and process technologies
07 p0953 A83-20435
- Load following impacts of a large wind farm on an interconnected electric utility system
08 p1131 A83-22675
- Present status of R&D for hydrogen production from water in Japan
09 p1292 A83-23701
- Progress in photovoltaic energy conversion
09 p1293 A83-23859
- Advances in wind energy technology
[DGLR PAPER 82-082]
09 p1293 A83-24194
- Electricity from wind - A survey of the state of the art and future prospects for research and development
[DGLR PAPER 82-081]
09 p1293 A83-24202
- International Conference on Future Energy Concepts, 3rd, London, England, January 27-30, 1981, Proceedings
09 p1294 A83-24975
- Solar technology - A whether report
09 p1294 A83-25124
- Ocean thermal-energy conversion
09 p1294 A83-25125
- Can industry afford solar energy
09 p1294 A83-25144
- Metal-insulator-semiconductor silicon solar cells
10 p1444 A83-25447
- Miami International Conference on Alternative Energy Sources, 5th, Miami Beach, FL, December 13-15, 1982, Proceedings of Condensed Papers
10 p1445 A83-25575
- Size effects in DAWT innovative wind energy system design
[ASME PAPER 82-WA/SOL-20]
10 p1445 A83-25688
- New materials for solar cells - Tandem cells
10 p1446 A83-26882
- IECEC '82; Proceedings of the Seventeenth Intersociety Energy Conversion Engineering Conference, Los Angeles, CA, August 8-12, 1982. Volumes 1, 2, 3, 4 & 5
11 p1601 A83-27126
- Energy utilization of electric and hybrid vehicles
11 p1667 A83-27164
- Sodium-sulfur battery program in Japan
11 p1603 A83-27175
- Acid fuel cell technologies for vehicular power plants
11 p1604 A83-27185
- Metal hydride heat pump
11 p1605 A83-27211
- Thermoelectric conversion for space nuclear power
11 p1541 A83-27222
- Marine power - Accomplishments of the 1970s
11 p1606 A83-27223
- Some ocean engineering considerations in the design of OTEC plants
11 p1606 A83-27224
- Developments in tidal power
11 p1606 A83-27226
- OTEC plants for today's island market
11 p1606 A83-27227
- Advanced component research in the solar thermal program
11 p1607 A83-27233
- National project of new energy development in Japan
11 p1607 A83-27243
- Development of solar total energy system for industrial sectors
11 p1608 A83-27244
- Stirling engines for solar power generation in the 50 to 500 kW range
11 p1608 A83-27274
- Further development of the fluidyne liquid-piston engine
11 p1587 A83-27275
- Design of hydraulic output unit for 15 kW free-piston Stirling engine
11 p1587 A83-27277
- Increasing summer peak power with aquifer storage
11 p1609 A83-27313
- High-temperature molten salt solar thermal systems
11 p1609 A83-27317
- The NASA program in Space Energy Conversion Research and Technology
11 p1610 A83-27326
- Augmentation of power in slow-running vertical-axis wind rotors using multiple vanes
11 p1611 A83-27868
- Optimization of pulling conditions by electronic bombardment of polycrystalline silicon ribbons for solar cells --- French thesis
12 p1750 A83-29946
- Hydrogen energy creeps forward --- hydrogen fuel production and storage
13 p1869 A83-30000
- Fundamentals of solar energy conversion --- Textbook
13 p1869 A83-30153
- High performance collectors
13 p1870 A83-30847
- Recent developments in central receiver systems
13 p1870 A83-30849
- Summary of electric vehicle energy source technologies
13 p1871 A83-31089
- Metal-hydride energy-technological processing of hydrogen
13 p1871 A83-31375
- Hydrogen fuel - Universal energy
13 p1871 A83-31504
- Enhancement of quality through environmental technology; Proceedings of the Twenty-eighth Annual Technical Meeting, Atlanta, GA, April 21-23, 1982
13 p1864 A83-31507
- Solar salt pond potential site survey for electrical power generation
13 p1871 A83-31526
- Use of polymeric materials in the assembly of solar cells
13 p1872 A83-31610
- Coal gasification using solar energy
13 p1872 A83-31612
- The use of METEOSAT for solar radiation mapping
14 p2049 A83-31845
- Photovoltaic Solar Energy Conference; Proceedings of the Fourth International Conference, Stresa, Italy, May 10-14, 1982
14 p2036 A83-32176
- Overview of the European community's activities in photovoltaics
14 p2036 A83-32177
- The Italian programme in photovoltaic solar energy
14 p2037 A83-32178
- Application trends for photovoltaics
14 p2037 A83-32180
- The potential for photovoltaics in Europe
14 p2037 A83-32181
- Advanced system design for solar power plants
14 p2037 A83-32185
- Photovoltaic power for walk-in coolers
14 p2038 A83-32192
- Solar photovoltaic systems in the development of Papua New Guinea
14 p2038 A83-32198
- Field trial of rural solar photovoltaic system
14 p2039 A83-32199
- Module design for EC pilot projects --- European Community
14 p2040 A83-32228
- Low cost processes for cast silicon solar cells
14 p2045 A83-32313
- Engineering design for a Central Station Photovoltaic Power Plant
15 p2190 A83-34150
- The solar power satellite - An overview
15 p2191 A83-34657
- Solar power satellites - Technical, social and political implications
15 p2191 A83-34658
- Space or terrestrial energy?
15 p2191 A83-34660
- A solar-hydrogen economy for U.S.A.
15 p2192 A83-34866
- Hydrogen energy in Canada - I Proceedings of the First Hydrogen Energy Symposium, University of Western Ontario, London, Canada, May 1, 1981
15 p2193 A83-35301
- Cost-effective methods for hydrogen production
15 p2193 A83-35304
- Thermal behavior of laboratory models of honeycomb-covered solar ponds
17 p2535 A83-37050
- Ocean thermal energy conversion - Historical highlights, status, and forecast
17 p2535 A83-38014
- Dish concentrators for solar thermal energy
17 p2536 A83-38015
- Operational experience with flat-plate photovoltaic systems
17 p2536 A83-38019
- Solar thermal technologies - Potential benefits to U.S. utilities and industry
17 p2536 A83-38023
- Industrial water electrolysis - Present and future
18 p2664 A83-39560
- Status of hydrogen development for aircraft in five countries - A Canadian perspective
18 p2708 A83-39562
- New promise for photovoltaics
18 p2709 A83-40337
- The photovoltaic pilot projects of the European Community
18 p2710 A83-40536
- Introduction to solar technology --- Book
19 p2862 A83-41518
- Heat transfer in energy problems --- Book
19 p2843 A83-41524
- Solar radiation data; Proceedings of the Contractor's Meeting, Brussels, Belgium, November 20, 1981
19 p2862 A83-41990
- The case for solar/hydrogen energy
20 p3012 A83-42951
- Thermochemical hydrogen production based on magnetic fusion
20 p3049 A83-42954
- Energy technology X - A decade of progress; Proceedings of the Tenth Conference, Washington, DC, February 28-March 2, 1983
21 p3168 A83-45064
- Advances in solar energy. Volume 1
22 p3318 A83-45915
- Crystalline silicon as a material for solar cells
22 p3269 A83-45918
- A review of large wind turbine systems
22 p3318 A83-45919
- Status of flat-plate photovoltaic systems for applications in developing countries
22 p3318 A83-46096
- Conceptual design of A 50 MW central station photovoltaic power plant
22 p3320 A83-46773
- Compact space power station - Building up scenario --- for solar energy transfer to lunar bases
23 p3415 A83-47380
- [IAF PAPER 83-429]
Technological aspects of sulfur dioxide depolarized electrolysis for hydrogen production
23 p3430 A83-48596
- Resource and energy management of synfuels production with hydrogen and oxygen requirements from electrolysis
23 p3477 A83-48597
- Quality factors of solar cell arrays
23 p3478 A83-48615
- Fuels from solar energy - How soon?
24 p3599 A83-48808

- Combined solar-wind power plants
24 p3599 A83-48958
A method for the measurement of solar cell series resistance
24 p3599 A83-48934
Design and performance of a sodium/sulphur multibeta cell
24 p3601 A83-49957

ENGINE TRANSFER

- NT LINEAR ENERGY TRANSFER (LET)
Reversible nonradiative transfer of excitation energy in a system of strongly interacting particles --- in laser materials
01 p0055 A83-10817
An experimental investigation of nonlinear dissipation of electromagnetic waves in inhomogeneous collisionless plasmas
01 p0107 A83-11297
Correlation between the number and energy flux of hadrons and gamma quanta. III
02 p0274 A83-11743
Measurements of energy distribution and thrust for microwave plasma coupling of electrical energy to hydrogen for propulsion
[AIAA PAPER 82-1951]
02 p0147 A83-12508
Two-dimensional radiation in absorbing-emitting-scattering media using the P-N approximation
[ASME PAPER 82-HT-19]
02 p0171 A83-12786
An interpretation of OH maser observations in W3/OH/
03 p0413 A83-13313
Energy transfer and lasing in phosphate glasses activated with chromium, ytterbium, and erbium
03 p0331 A83-13594
Transport of solar energy with optical fibres
03 p0354 A83-13698
Effects of excitation mechanism on linewidth parameters of conventional vacuum ultraviolet /VUV/ discharge line sources
[AD-A112052]
03 p0392 A83-13957
Quantum formalism in gravitation quantitative application to the Titius-Bode law
03 p0411 A83-14867
Thermal gasdynamic laser utilizing rotational transitions in hydrogen halides with energy transfer from H₂ molecules
05 p0649 A83-17065
Exchange of energy and momentum between gases at different temperatures
05 p0691 A83-17359
Test of Sigmund scaling for low collision energies
06 p0807 A83-18043
Projected temperature dependence of quantum yields for photoreactions involving energy or electron transfer
06 p0780 A83-18559
Energy transfer in magnetized plasmas
06 p0812 A83-18923
Electron energy transport in ion waves and its relevance to laser-produced plasmas
07 p0997 A83-20543
A subsynoptic-scale kinetic energy analysis of the Red River Valley tornado outbreak /AVE-SESAME I/ --- Atmospheric Variability Experiment - Severe Environmental Storms and Mesoscale Experiment
08 p1140 A83-22298
Light transport in planar luminescent solar concentrators - The role of DCM self-absorption --- 4-dicyano-methylene-2-methyl-6-p-dimethyl H-pyran
08 p1130 A83-22619
Energy and momentum flow in electromagnetic fields and plasma --- solar wind-magnetospheric interaction
08 p1137 A83-23120
Concerning one feature of energy conversion in diffraction-radiation generator/free-electron laser systems
09 p1272 A83-24219
Energy and entropy balances in a combustion chamber - Analytical solution
09 p1226 A83-24363
A shock tube study of DF dissociation
10 p1389 A83-25561
Collision dynamical information from pressure broadening measurements - Application to carbon monoxide
10 p1479 A83-25564
Saturation of the lower-hybrid-drift instability by mode coupling
10 p1485 A83-25777
Radiation exchange and oscillations in a pair of cavities sharing a partial reflector
10 p1482 A83-26002
A comparison of measured and computed energy exchanger performance
10 p1417 A83-26195
Vibrational energy transfer from OH to other gaseous hydrides
10 p1480 A83-26457
The gyrotron energy transfer equation
10 p1411 A83-26649
Finite element analysis of dynamic energy transfer in a Stirling engine regenerator
11 p1665 A83-27271
Wave particle interactions as an energy transfer mechanism between different particle species --- in magnetosphere
11 p1614 A83-27397
Energy transfer in stoichiometric rare-earth crystals --- laser materials
11 p1581 A83-27589
A theoretical study on the mechanism of electronic to vibrational energy transfer in Hg/3P₁ + CO
11 p1655 A83-28529
Nonlinear energy flow in a beam-plasma system
11 p1660 A83-28696

- Profile measurements in the atmospheric near-surface layer and the use of suitable universal functions for the determination of the turbulent energy exchange
12 p1758 A83-29128
Excimer laser photolysis studies of translational-to-vibrational energy transfer in collisions of H and D atoms with CO
[AD-A129931]
13 p1916 A83-30952
Laser studies of electronic energy transfer in atomic copper
13 p1851 A83-30957
A note on the Maday gain-spread theorem --- concerning energy change experienced by electrons in free electron laser
13 p1853 A83-31112
On the influence of the 'alpha-turbulence' on the energy transport in accretion disks
13 p1960 A83-31755
The combination of hollow focusing concentrators with fiber-optic waveguides --- for solar energy transmission
14 p2036 A83-32048
Subsurface energetics of the Gulf Stream cyclonic frontal zone off Onslow Bay, North Carolina
14 p2060 A83-33083
Rotational energy transfer in HF
15 p2227 A83-34014
A balloon and its basket in the Venus' atmosphere
15 p2124 A83-34271
On certain properties of the second energy variation in problems of the elastic stability of discrete conservative systems
15 p2178 A83-34440
Distribution of brightness over apparent discs of distorted stars
15 p2263 A83-34547
Encounters of binaries. I - Equal energies
15 p2265 A83-34596
Energy transfer in solar flares
15 p2283 A83-35214
Stratified turbulence and the mesoscale variability of the atmosphere
16 p2385 A83-35471
Transient planetary waves simulated by GFDL spectral general circulation models. I - Effects of mountains. II - Effects of nonlinear energy transfer
16 p2386 A83-35485
A nonequilibrium system consisting of a gas, a surface, and a solid body in problems of relaxational gas dynamics
16 p2349 A83-35526
Energy gain and loss spectroscopy of charge changing collisions between multiply charged ions and neutrals
16 p2409 A83-35632
Exchange energy of an electron gas of arbitrary dimensionality
16 p2422 A83-35695
Electron temperature differences and double layers
17 p2581 A83-37038
Beat Cepheids. IV - AX Velorum and mode energy transfer
17 p2606 A83-38232
Energy transfer in the quiet and disturbed magnetosphere
17 p2542 A83-38297
Stimulated emission of oscillators in the case of the application of a weak longitudinal electrostatic field
17 p2515 A83-38493
Relativistic thermodynamics of irreversible processes in a static gravitational field; a theory of phenomenological heat conduction
18 p2777 A83-39780
Maximum power transfer for full-wave rectifier circuits
19 p2838 A83-41150
Possible MHD phenomena in flare processes on the sun
19 p2926 A83-42002
Molecular dynamical studies of the dissociation of a diatomic molecular crystal. I - Energy exchange in rapid exothermic reactions
20 p2950 A83-42628
Interaction of high-velocity rarefied flow with the surface of a solid body
20 p2950 A83-42883
Resonant effects during the tidal encounter of disc galaxies
21 p3232 A83-44732
Binaries as a heat source in stellar dynamics - Release of binding energy
22 p3376 A83-45632
Horizontal energy propagation in a barotropic atmosphere with meridional and zonal structure
22 p3341 A83-46849
Distribution of energy input due to auroral protons and electrons
22 p3334 A83-46917
The structure and energy balance in main sequence stars
23 p3520 A83-47481
Development of flare morphology in X-rays, and the flare scenario
23 p3531 A83-47661
Energetic electrons as an energy transport mechanism in solar flares
23 p3532 A83-47672
On the energy characteristics of the aerodynamic matrix and the relationship to possible flutter
23 p3398 A83-48144
Non-LTE model atmosphere analysis of central stars
24 p3652 A83-49151
An approach to estimating spectral energy transfer due to nonlinear interactions --- during transition to turbulence of two-dimensional wake
24 p3580 A83-49829
Semiconvective diffusion and energy transport --- in stellar interiors
24 p3669 A83-50102

ENGINE AIRFRAME INTEGRATION

- Effects of various empennage parameters on the aerodynamic characteristics of a twin-engine afterbody model
[AIAA PAPER 83-0085]
05 p0579 A83-16511
Propulsion installation characteristics for turbofan transports
[AIAA PAPER 83-0087]
05 p0579 A83-16513
On the aerodynamics of over-the-wing nacelles supported on 'stub-wings'
[AIAA PAPER 83-0538]
05 p0595 A83-16774
Generalities on the problems in integration for a propeller on an airframe - The particular case of a high-powered twin turboprop
[AAAF PAPER NT 82-02]
14 p1975 A83-33160
Progress in propulsion system/airframe structural integration
[AIAA PAPER 83-1123]
16 p2300 A83-36234
Empennage/afterbody integration for single and twin-engine fighter aircraft
[AIAA PAPER 83-1126]
16 p2293 A83-36235
Integrated propulsion-aircraft control evaluation for a current Navy fighter
[AIAA PAPER 83-1236]
16 p2308 A83-36299
PAN AIR applications to aero-propulsion integration
[AIAA PAPER 83-1368]
16 p2295 A83-36364
Wind tunnel tests of over-the-wing nacelles --- supported on 'stub-wings'
16 p2296 A83-36916
Effects of nacelle position and shape on performance of subsonic cruise aircraft
[AIAA PAPER 83-1124]
17 p2464 A83-38079
Integrated airframe/propulsion control system architectures (IAPSA) study
[AIAA PAPER 83-2158]
19 p2797 A83-41660
Propulsion system integration as applied to business jet aircraft
[ASME PAPER 83-GT-227]
23 p3403 A83-48024
- ENGINE CONTROL
NT ROCKET ENGINE CONTROL
NT TURBOJET ENGINE CONTROL
Simulated mission endurance control system
01 p0014 A83-10751
Digital engine control for V/STOL and V/TOL aircraft
01 p0012 A83-10871
Integrated airframe/propulsion controls technology
01 p0013 A83-11175
Adaptive power management - A hierarchical/control system with a central multiplex system --- for aircraft applications
01 p0012 A83-11202
Fiberoptics technology and its application to propulsion control systems
[AIAA PAPER 83-0534]
05 p0595 A83-16772
Digital electronic engine control system - F-15 flight test
06 p0718 A83-18406
Flight evaluation of modifications to a digital electronic engine control system in an F-15 airplane
[AIAA PAPER 83-0537]
06 p0718 A83-19593
Influence coefficients of variable geometry free gas turbine engines
08 p1111 A83-22321
Design of an integrated control system for a supersonic aircraft power plant
08 p1046 A83-23175
Digital engine control unit - Future employment possibilities
[DGLR PAPER 82-085]
09 p1206 A83-24197
Recent developments in digital control for helicopter powerplants
09 p1207 A83-24829
Asynchronous induction micromotors for automatic systems --- Russian book
10 p1408 A83-25618
An economical algorithm of adaptive control of a multidimensional static plant
10 p1462 A83-26068
A samarium cobalt motor-controller for mini-RPV propulsion
11 p1530 A83-27187
Development history of the Hybrid Test Vehicle
13 p1934 A83-31088
Investigation of the combined regulation of the intermediate stage of a centrifugal compressor by an axial regulating apparatus and a two-row diffuser
14 p2028 A83-33149
Some aspects of development of power plant optimum control to increase aircraft fuel efficiency
16 p2303 A83-35841
Inlet, engine, airframe controls integration development for supercruising aircraft
16 p2304 A83-35842
Propulsion control sensor sharing opportunities
[AIAA PAPER 83-0536]
16 p2318 A83-36059
F/A-18A Inflight Engine Condition Monitoring System (IECMS)
[AIAA PAPER 83-1237]
16 p2308 A83-36300
Flight/propulsion control system integration
[AIAA PAPER 83-1238]
16 p2308 A83-36301
United Kingdom military engine usage, condition and maintenance systems experience
[AIAA PAPER 83-1239]
16 p2308 A83-36302
Comparison of an experience with full authority digital engine controls in rotary wing and jet-lift VSTOL aircraft
[AIAA PAPER 83-1241]
16 p2308 A83-36304

Advanced propulsion controls - A total system view
16 p2311 A83-36612

Nonlinear multivariable design by total synthesis --- of gas turbine engine control systems
17 p2467 A83-37092

Reliability analysis of a dual-redundant engine controller
17 p2517 A83-37289

Full Authority Digital Electronic Control (FADEC) - Augmented fighter engine demonstration
[SAE PAPER 821371] 17 p2467 A83-37963

Closed-loop engine fuel system simulation
[SAE PAPER 821374] 17 p2468 A83-37964

Full Authority Fault Tolerant Electronic Engine Control systems for advanced high performance engines (FAFTEEC)
[SAE PAPER 821398] 17 p2468 A83-37972

Microcomputer brings digital power to the small aircraft gas turbine
[SAE PAPER 821402] 17 p2468 A83-37975

The parallel implementation of a nonlinear real-time simulation technique
18 p2738 A83-39150

The effects of engine and height-control characteristics on helicopter handling qualities
19 p2802 A83-41078

Method of thermodynamic function control and of damage analysis regarding aircraft engines with the aid of flight data recording systems --- German thesis
19 p2800 A83-41850

Diagnostics of the conditions of gas-turbine engines using models reflecting the dynamics of changes in the controlled parameters
19 p2801 A83-42133

Parallel induction - A simple fuel control method for hydrogen engines
21 p3148 A83-45426

Electronic control of aircraft turbine engine
21 p3093 A83-45600

The use of production hardware for the development of control laws --- LSI for engine control
[ASME PAPER 83-GT-6] 23 p3406 A83-47879

Built-In Test Equipment (BITE) on the Garrett model GTPC331 APU digital electronic control unit --- for gas turbine aircraft auxiliary power system
[ASME PAPER 83-GT-186] 23 p3409 A83-47992

F-14 aircraft and propulsion control integration evaluation
[ASME PAPER 83-GT-234] 23 p3411 A83-48029

Integrated flight/propulsion control system architectures for a high speed aircraft
[AIAA PAPER 83-2563] 24 p3549 A83-49595

Integrated control system concept for high-speed aircraft
[AIAA PAPER 83-2564] 24 p3549 A83-50074

ENGINE COOLANTS

Experimental investigation on film cooling of a gas turbine blade
03 p0282 A83-13346

TF41/Lamilly accelerated mission test
04 p0449 A83-15319

Radiant heating tests of several liquid metal heat-pipe sandwich panels
[AIAA PAPER 83-0319] 05 p0635 A83-16649

Small gas turbine combustor study - Combustor liner evaluation
[AIAA PAPER 83-0337] 05 p0596 A83-16663

A computer model for gas turbine blade cooling analysis
[ASME PAPER 82-JPGC-GT-6] 09 p1208 A83-25267

A comparative study of the influence of different means of turbine cooling on gas turbine performance
[ASME PAPER 83-GT-180] 23 p3465 A83-47991

An investigation into the effect of coolant flow on the vibration characteristics of hollow blades conveying fluid
[ASME PAPER 83-GT-217] 23 p3470 A83-48017

Gas turbine compressor interstage cooling using methanol
[ASME PAPER 83-GT-230] 23 p3466 A83-48026

ENGINE DESIGN

NT ROCKET ENGINE DESIGN

The theory of aircraft engines --- Russian book
01 p0011 A83-10675

Thunder power for executive and ag-aircraft
01 p0011 A83-10866

Engines for future combat aircraft
01 p0011 A83-10867

Multifuel evaluation of rich/quench/lean combustor
01 p0023 A83-11492

Rotaries for GA - NASA gets serious
02 p0136 A83-11627

Engine technology for the next decade
02 p0136 A83-12098

Ion beamlet vectoring by grid translation
[AIAA PAPER 82-1895] 02 p0241 A83-12552

One millipound pulsed plasma thruster development
[AIAA PAPER 82-1877] 02 p0147 A83-12836

Rolls-Royce engine status report
02 p0136 A83-12933

Composite fan exit guide vanes for high bypass ratio gas turbine engines
03 p0282 A83-13159

Assessment of inflow control structure effectiveness and design system development
03 p0281 A83-13161

Powerplants. I --- turbofan engine design for aircraft
04 p0449 A83-14951

Rolls-Royce RB 211-535 power plant
04 p0449 A83-15311

TF41/Lamilly accelerated mission test
04 p0449 A83-15319

The diagnostics of disturbances in components of turbojet engines with gasdynamics parameter monitoring
04 p0449 A83-15850

Gain and efficiency of a traveling wave heat engine
04 p0480 A83-16312

Supersonic Harrier - One step closer
04 p0449 A83-16371

Radiant heating tests of several liquid metal heat-pipe sandwich panels
[AIAA PAPER 83-0319] 05 p0635 A83-16649

Design of a low emission combustor for an automotive gas turbine
[AIAA PAPER 83-0338] 05 p0652 A83-16664

Transverse jet break-up and atomization with rapid vaporization along the trajectory
[AIAA PAPER 83-0419] 05 p0597 A83-16702

The module concept in a mathematical model of a turboprop engine
05 p0597 A83-16878

New thrusts in engine design
05 p0597 A83-17236

Powerplants. II --- review of current aircraft turbofan engines
06 p0718 A83-18147

Application of optimization to aircraft engine disk synthesis
06 p0718 A83-18213

The Pratt & Whitney PW100 - Evolution of the design concept
06 p0718 A83-18821

Military propulsion technology. I - Fighter power - The need for tomorrow
06 p0718 A83-18948

Military propulsion technology. III - Materials are the key --- for fighter aircraft engines
06 p0730 A83-18950

A comparison between the Craig-Cox and the Kacker-Okapuu methods of turbine performance prediction
06 p0718 A83-19025

Design of multistep turbines using characteristic numbers
06 p0769 A83-19248

Experimental and theoretical studies on the relationship between engine exhaust and the surrounding flow field --- German thesis
06 p0714 A83-19618

The analysis of performance of Stirling engines. I - Computer simulation model
07 p0939 A83-20287

Extended performance 8-cm mercury ion thruster
[AIAA PAPER 82-1913] 07 p0873 A83-21078

Finite element strength analysis of rotating shell-plate structures
07 p0949 A83-21448

Setting design goals for advanced propulsion systems
[AIAA PAPER 81-1505] 08 p1045 A83-22154

Influence coefficients of variable geometry free gas turbine engines
08 p1111 A83-22321

Theory and design of flight-vehicle engines --- Russian book
08 p1046 A83-22651

Errors in the experimental determination of the parameters of supersonic combustion ramjet engines
08 p1046 A83-22653

Features of the selection of the basic parameters of cooled GTE turbines
08 p1046 A83-22655

On the choice of the optimal total wedge angle for the air intake of a hypersonic ramjet engine
08 p1046 A83-22656

The ideas of F. A. Tsander and an assessment of the application of jet engines for the acceleration of aerospace vehicles
08 p1052 A83-22657

Stored chemical energy propulsion system for underwater applications
[AIAA PAPER 81-1601] 08 p1132 A83-23132

Characteristics of a closed Brayton cycle piston engine
08 p1112 A83-23135

Design of an integrated control system for a supersonic aircraft power plant
08 p1046 A83-23175

Choice of the optimal system of shock waves in the inlet part of the diffuser of a supersonic centrifugal compressor
08 p1043 A83-23223

PW 4000 - A radically new jet engine being developed in the USA
08 p1046 A83-23239

A method for calculating the parameters of a turbojet engine in the autorotation regime
09 p1205 A83-23434

A mathematical model for a turboshaft gas-turbine engine with an optimum control program for high-level computer-aided design
09 p1205 A83-23436

A system of criteria for evaluating the energy efficiency of an engine at the state of technical proposals
09 p1205 A83-23437

Determination of the region of efficient use for microturbines with working medium recirculation
09 p1205 A83-23440

The relationship between the aerodynamics of a combustion chamber and the dynamics of heat release
09 p1205 A83-23446

Design and development of a mixer compound exhaust system --- in aircraft turbofan engines
09 p1206 A83-24029

Tactical aircraft engine usage - A statistical study
09 p1206 A83-24033

Jet engines for airliners of the next generation
[DGLR PAPER 82-069] 09 p1206 A83-24183

Some aspects of the engine design of future fighter planes
[DGLR PAPER 82-071] 09 p1206 A83-24185

Development trends regarding jet engines for future combat aircraft
[DGLR PAPER 82-072] 09 p1206 A83-24186

On the design philosophy of fighter aircraft engines
[DGLR PAPER 82-073] 09 p1206 A83-24187

Propulsion systems of flight vehicles and drones - Conditions, requirements, and current and future propulsion systems
[DGLR PAPER 82-086] 09 p1206 A83-24198

Regenerative shaft engines for helicopters, multipurpose and feeder service aircraft
[DGLR PAPER 82-087] 09 p1207 A83-24199

Prospects for the use of heat exchangers in aircraft gas turbines
[DGLR PAPER 82-088] 09 p1207 A83-24200

Future fuels for turbojet engines and their impacts on combustion chambers and fuel systems
[DGLR PAPER 82-089] 09 p1242 A83-24201

Control design for a wind turbine-generator using output feedback
09 p1293 A83-24721

Pre-planned product improvement /P3I/ the T64-GE-418 derivative engine
09 p1207 A83-24826

Propulsion systems for rotary wing aircraft with auxiliary propulsors
09 p1207 A83-24827

An approach to helicopter power selection
09 p1207 A83-24828

U.S. Army/Detroit Diesel Allison Advanced Technology Demonstrator Engine
09 p1208 A83-24836

Helicopter engine development - New standards for the '80s
09 p1208 A83-24837

Technical qualities for combat helicopter powerplants
09 p1208 A83-24839

Warm cycle propulsion for the 1990's heavy lift helicopters
09 p1208 A83-24840

Mathematical method for the design of the intake branch in the case of centrifugal blade machines --- Book
09 p1263 A83-24850

Rotary engines
09 p1369 A83-25140

NASA clean catalytic combustor program
[ASME PAPER 82-JPGC-GT-11] 09 p1227 A83-25269

Asynchronous induction micromotors for automatic systems --- Russian book
10 p1408 A83-25618

Specification, design, and test of aircraft engine isolators for reduced interior noise
[AIAA PAPER 83-0718] 10 p1377 A83-25932

Friction drag and other design parameters for acoustic face sheets --- for aircraft noise reduction
[AIAA PAPER 83-0780] 10 p1477 A83-25962

PW4000 uses JT9D, new technology
10 p1378 A83-26072

A comparison of measured and computed energy exchanger performance
10 p1417 A83-26195

Design of ion thruster system for satellite position control
10 p1388 A83-26592

A concept of heat pipe engine
11 p1605 A83-27208

Simple models for analysis and design of practical Stirling engines
11 p1586 A83-27261

A new regenerator theory --- Stirling engine design
11 p1664 A83-27263

Whence Stirling engines --- auto and air applications
11 p1586 A83-27265

A user oriented design system for Stirling cycle codes
11 p1586 A83-27267

General method for optimization of Stirling engines
11 p1586 A83-27268

Computation techniques and computer programs to analyze Stirling cycle engines using characteristic dynamic energy equations
11 p1665 A83-27272

Further development of the fluidyne liquid-piston engine
11 p1587 A83-27275

Design of hydraulic output unit for 15 kW free-piston Stirling engine
11 p1587 A83-27277

Design of a hydraulic output Stirling engine
11 p1587 A83-27278

Experiences in the commissioning of a prototype, 20 kW, helium charged Stirling engine
11 p1587 A83-27279

A new, versatile Stirling energy conversion unit
11 p1587 A83-27280

An isothermal second-order Ringbom-Stirling engine computer program
11 p1587 A83-27281

50 kW Stirling engine 11 p1588 A83-27282
 Radially pleated diaphragms for Stirling engines 11 p1588 A83-27283
 Design and experiences with a laboratory Stirling cycle machine 11 p1588 A83-27284
 U.K. Consortium Stirling engine programme 11 p1588 A83-27285
 A way to relax the dimensional tolerance requirements of clearance regenerators --- in small Stirling engine design 11 p1588 A83-27286
 An approach to the design of Stirling engine regenerator matrix using packs of wire gauzes 11 p1588 A83-27287
 Improved Stirling engine performance using jet impingement 11 p1588 A83-27288
 Back-to-back test for determining the pumping losses in a Stirling cycle machine 11 p1588 A83-27290
 Linear moving magnet motor/generator for Stirling engines 11 p1560 A83-27291
 Effects of displacer seal clearance on free-piston Stirling engine performance 11 p1589 A83-27295
 A study on two-phase, two-component Stirling engine 11 p1665 A83-27328
 The effect of fuel injection on NOx emissions and undesirable combustion for hydrogen-fuelled piston engines 11 p1589 A83-27335
 The influence of inlet design on the aeroacoustic performance of a JT15D turbofan engine as measured in the NASA-Ames 40 x 80 foot wind tunnel [AIAA PAPER 83-0681] 11 p1531 A83-28006
 The design and combustion performance of practical swirlers for integral rocket/ramjets 12 p1703 A83-28964
 Analysis of engine usage data for tactical systems [AIAA PAPER 81-1370] 12 p1703 A83-29011
 Zero-length inlets for subsonic V/STOL aircraft 12 p1696 A83-29012
 18:1 pressure ratio axial/centrifugal compressor demonstration program 12 p1732 A83-29013
 An overview of turbine engine structural design - Development trends in the Air Force [AIAA 83-0952] 12 p1703 A83-29777
 A review of commuter propulsion technology [SAE PAPER 820716] 13 p1807 A83-31801
 Design features of a new commuter turboprop engine [SAE PAPER 820717] 13 p1807 A83-31802
 AR.318 - Italy's low-cost GA turboprop 16 p2302 A83-35675
 Temperature and composition measurements in a research gas turbine combustion chamber 16 p2302 A83-35790
 Applications of computational techniques in the design of ramjet engines 16 p2290 A83-35828
 Design and development of a small gasturbine engine: Results today - A basis for design criteria of a next generation 16 p2303 A83-35829
 The effect of variation of diffuser design on the performance of centrifugal compressors 16 p2305 A83-35866
 The performance of single-shaft gas turbine load compressor auxiliary power units [AIAA PAPER 83-1159] 16 p2306 A83-36251
 The aerodynamic design and performance of the General Electric/NASA EEE fan --- Energy Efficient Engine [AIAA PAPER 83-1160] 16 p2306 A83-36252
 Integrating engine performance and trajectory analysis in designing future Shuttle systems [AIAA PAPER 83-1189] 16 p2316 A83-36267
 Analytical design and experimental verification of S-duct diffusers for turboprop installations with an offset gearbox [AIAA PAPER 83-1211] 16 p2294 A83-36283
 Advanced turboprop and dual cycle engine performance benefits and installation options on a Mach 0.7 short-haul transport aircraft [AIAA PAPER 83-1212] 16 p2307 A83-36284
 A Monte Carlo simulation of the engine development process [AIAA PAPER 83-1230] 16 p2307 A83-36294
 Nondestructive evaluation methods for implementation of damage-tolerant designed gas turbine engine components [AIAA PAPER 83-1232] 16 p2307 A83-36295
 Optimized high-energy propulsion for multimission applications [AIAA PAPER 83-1247] 16 p2319 A83-36305
 Benefits and costs of low thrust propulsion systems [AIAA PAPER 83-1248] 16 p2316 A83-36306
 Application of 3D aerodynamic/combustion model to combustor primary zone study [AIAA PAPER 83-1265] 16 p2308 A83-36316
 US Army Tank-Automotive Command (TACOM) adiabatic engine program [AIAA PAPER 83-1283] 16 p2362 A83-36321

Instrumental problems in small gas turbine engines [AIAA PAPER 83-1293] 16 p2302 A83-36327
 Development trends in engine durability --- for USAF aircraft gas turbines [AIAA PAPER 83-1297] 16 p2309 A83-36329
 Expander cycle engines for Shuttle cryogenic upper stages [AIAA PAPER 83-1311] 16 p2320 A83-36332
 Advanced LOX/H2 engine technologies for future OTVs [AIAA PAPER 83-1312] 16 p2320 A83-36333
 A JT8D low emissions combustor by radial zoning [AIAA PAPER 83-1324] 16 p2309 A83-36339
 Compound cycle turbofan engine [AIAA PAPER 83-1338] 16 p2309 A83-36346
 Development and application of a liquid-cooled V-8 piston engine for general aviation aircraft [AIAA PAPER 83-1342] 16 p2309 A83-36347
 KC-135/CFM56 re-engine - The best solution [AIAA PAPER 83-1374] 16 p2309 A83-36367
 Introducing the Rolls-Royce Tay [AIAA PAPER 83-1377] 16 p2309 A83-36368
 Monte Carlo simulation of the engine development process [AIAA PAPER 83-1405] 16 p2310 A83-36394
 Design and development of a nozzle extendible exit cone [AIAA PAPER 83-1410] 16 p2323 A83-36399
 Configuration selection and technology transition in 5000 SHP class engines [AIAA PAPER 83-1411] 16 p2310 A83-36400
 Longitudinal pressure oscillations in ramjet combustors [AIAA PAPER 83-2018] 16 p2310 A83-36404
 Fighter engine cycle selection [AIAA PAPER 83-1300] 16 p2310 A83-36412
 Propulsion prototypes at General Electric [AIAA PAPER 83-1053] 16 p2310 A83-36463
 Technology and engine demonstrator programs [AIAA PAPER 83-1064] 16 p2310 A83-36464
 V/STOL status from the engine technology viewpoint 16 p2311 A83-36912
 An update on high output lightweight diesel engines for aircraft applications [AIAA PAPER 83-1339] 16 p2311 A83-36925
 Gas turbine engines 17 p2467 A83-37274
 Experimental research on the design of highly loaded axial fans --- German thesis 17 p2447 A83-37498
 Inlet design for high-speed propfans [SAE PAPER 821359] 17 p2451 A83-37957
 Utilization of computer aided design for the development of advanced turbomachinery components [SAE PAPER 821423] 17 p2468 A83-37980
 727, B-52 retrofit with PW2037 meeting today's requirements [SAE PAPER 821443] 17 p2463 A83-37991
 Re-engineing studies on the P-3 aircraft [SAE PAPER 821445] 17 p2464 A83-37993
 The application of a liquid-cooled V-8 piston engine to general aviation aircraft [SAE PAPER 821446] 17 p2468 A83-37994
 Development and operating characteristics of an advanced two-stage combustor 17 p2469 A83-38022
 Propulsion system integration configurations for future prop-fan powered aircraft [AIAA PAPER 83-1157] 17 p2469 A83-38081
 V/STOL from the propulsion viewpoint (7th Sir Sydney Camm Memorial Lecture) 17 p2470 A83-38869
 Regional airline turboprop engine technology [AIAA PAPER 83-1158] 18 p2641 A83-39101
 Analytical methods in rotor dynamics 19 p2854 A83-41519
 An analysis of the parameters determining the maximum thrust of ramjet engines 19 p2800 A83-42127
 Mathematical modeling of gas-turbine engines with heat regeneration 19 p2801 A83-42154
 PW100 - Canada's commuter turboprop 20 p2936 A83-42524
 A family of small low cost gas turbines for unmanned vehicle systems 20 p2936 A83-42616
 Low cost expendable turbojet engines 20 p2937 A83-43711
 A range of lightweight engines for RPV's 20 p2937 A83-43719
 Optimal design of the blading of axial turbines --- Russian book 21 p3147 A83-43924
 Cryogenic gas engines --- Russian book 21 p3117 A83-43925
 Hovercraft auxiliary power units (APUs) 21 p3147 A83-44372
 The energetic optimization of propulsion systems for electric vehicles --- Dutch thesis 21 p3221 A83-45075
 Demands on the air system of modern aircraft engines 22 p3255 A83-46491

Development of new combustion chamber technologies for future alternative combustion fuels 23 p3406 A83-47183
 Increased energy exploitation in cooled high-temperature turbines 23 p3406 A83-47202
 A new-technology gas generator for medium-power shaft-turbine engines 23 p3406 A83-47217
 Development of the thrust augmented Viking engine and first stage DRAKKAR propulsion systems for the Ariane 3 launcher [IAF PAPER 83-04] 23 p3425 A83-47229
 Simplified inverse design of a straight vaneless diffuser of radial stage [ASME PAPER 83-GT-2] 23 p3392 A83-47877
 The Rolls-Royce annular vaporizer combustor [ASME PAPER 83-GT-49] 23 p3407 A83-47908
 A small engine high temperature core research programme [ASME PAPER 83-GT-56] 23 p3407 A83-47912
 The purpose, the principles and the problems of fault tolerant systems --- for aircraft gas turbine engines [ASME PAPER 83-GT-59] 23 p3407 A83-47915
 A CAD method for centrifugal compressor impellers [ASME PAPER 83-GT-65] 23 p3395 A83-47920
 The impact of three-dimensional analysis on fan design --- for turbine engines [ASME PAPER 83-GT-136] 23 p3408 A83-47963
 Developments in air cooling of gas turbine vanes and blades [ASME PAPER 83-GT-160] 23 p3409 A83-47984
 The GTC331, a 600 hp auxiliary power unit program --- for advanced transport aircraft [ASME PAPER 83-GT-188] 23 p3409 A83-47994
 Status report - DARPA/NASA convertible turbofan/turboshaft engine program [ASME PAPER 83-GT-196] 23 p3410 A83-48000
 Propulsion system screening for survivability and effectiveness [ASME PAPER 83-GT-200] 23 p3410 A83-48003
 A three-dimensional model for the prediction of shock losses in compressor blade rows [ASME PAPER 83-GT-216] 23 p3410 A83-48016
 Gas turbine performance improvement by retrofit of advanced technology [ASME PAPER 83-GT-222] 23 p3465 A83-48020
 An historical review of propeller developments 23 p3411 A83-48173
 Saving fuel with the wide-chord fan 23 p3411 A83-48174
 Design concepts for low cost composite engine frames [AIAA PAPER 83-2445] 23 p3411 A83-48331
 Preliminary design engine thermodynamic cycle selection for advanced fighters [AIAA PAPER 83-2480] 23 p3411 A83-48343
 Calculation of the parameters of a symmetric rhombic drive for a one-cylinder Stirling engine 23 p3466 A83-48400
 Optimum linear synchronous motor design for high speed ground transportation 24 p3573 A83-49325
 Supersonic V/STOL - Tandem fan concepts [AIAA PAPER 83-2567] 24 p3549 A83-49597

ENGINE FAILURE

The effects of firing a weapon on the air intake in a subsonic flow [AAAF PAPER NT 81-11] 02 p0132 A83-11772
 Existing time limit for overwater operations - Its validity 03 p0281 A83-13170
 The icing of aircraft gas turbine engines 03 p0280 A83-14619
 Statistical estimation of the mean time-to-failure of an aircraft engine as a function of the cause of failure 09 p1205 A83-23433
 Full-flow debris monitoring and fine filtration for helicopter propulsion systems 09 p1208 A83-24838
 Computer generated cockpit engine displays 10 p1376 A83-26309
 An overview of turbine engine structural design - Development trends in the Air Force [AIAA 83-0952] 12 p1703 A83-29777
 The influence of defects on the operational strength of disks and wheels in engines 15 p2174 A83-33964
 Statistical study of TBO and estimation of acceleration factors of ASMT for aircraft turbo-engine --- Accelerated Simulated Mission Endurance Testing 16 p2304 A83-35858
 Life estimation methods of gas turbine rotating components 16 p2305 A83-35870
 A contribution to airworthiness certification of gas turbine disks 16 p2305 A83-35872
 A Monte Carlo simulation of the engine development process [AIAA PAPER 83-1230] 16 p2307 A83-36294

- Development trends in engine durability --- for USAF aircraft gas turbines
[AIAA PAPER 83-1297] 16 p2309 A83-36329
- Development of simulated mission endurance test acceleration factors in determining engine component serviceability and failure mode criticality
[AIAA PAPER 83-1409] 16 p2310 A83-36398
- Super integrated power unit (SIPU) for the F-16 engine start system
[SAE PAPER 821462] 17 p2469 A83-37996
- A simulation study of the low-speed characteristics of a light twin with an engine-out
[AIAA PAPER 83-2128] 19 p2806 A83-41951
- Aircraft usage and effects on engine life
[ASME PAPER 83-GT-143] 23 p3409 A83-47967
- ### ENGINE INLETS
- The effects of firing a weapon on the air intake in a subsonic flow
[AAAF PAPER NT 81-11] 02 p0132 A83-11772
- An iterative method for predicting turbofan inlet acoustics
03 p0391 A83-13135
- Airframe effects on a top-mounted fighter inlet system
03 p0278 A83-13166
- Mechanisms of inlet-vortex formation
04 p0479 A83-16260
- Experimental study of flows in a two-dimensional inlet model
[AIAA PAPER 83-0176] 05 p0581 A83-16571
- Viscous primary/secondary flow analysis for use with nonorthogonal coordinate systems
[AIAA PAPER 83-0556] 05 p0588 A83-16785
- Fiber optics for aircraft engine/inlet control
08 p1046 A83-22494
- Calculation of pressure losses in the diffusers of mixing afterburners
09 p1205 A83-23445
- Effect of variable guide vanes on the performance of a high-bypass turbofan engine
09 p1205 A83-24028
- Composite engine inlet particle separator swirl frame --- CAD for T700 helicopter engine centrifugal filter
09 p1208 A83-24841
- In-flight acoustic measurements in the engine intake of a Fokker F28 aircraft
[AIAA PAPER 83-0677] 10 p1376 A83-25909
- Wave envelope and infinite element schemes for fan noise radiation from turbofan inlets
[AIAA PAPER 83-0709] 10 p1474 A83-25925
- A theoretical investigation of the sound radiation fields associated with a Bellmouth inlet
[AIAA PAPER 83-0710] 10 p1474 A83-25926
- Ray-theory and mode-theory predictions of intake-liner performance - A comparison with engine measurements
[AIAA PAPER 83-0711] 10 p1475 A83-25927
- The design and flight test of an engine inlet bulk acoustic liner
[AIAA PAPER 83-0781] 10 p1378 A83-25963
- Optimization of acoustic liners by the hybrid finite element-integral approach
[AIAA PAPER 83-0670] 10 p1478 A83-26917
- Separation characteristics of the T700 engine inlet particle separator
11 p1530 A83-27479
- Analysis of moisture condensation in engine inlet ducts
11 p1566 A83-27482
- The influence of inlet design on the aeroacoustic performance of a JT15D turbofan engine as measured in the NASA-Ames 40 x 80 foot wind tunnel
[AIAA PAPER 83-0681] 11 p1531 A83-28006
- Zero-length inlets for subsonic V/STOL aircraft
12 p1696 A83-29012
- Propulsion system installation design for high-speed prop-fans
12 p1703 A83-29014
- Air intakes for an experimental rocket ramjet
[ONERA, TP NO. 1983-100] 14 p1969 A83-31824
- The integration of internal combustion engines of the General Aviation - Problems raised by ventilation and exhaust
[AAAF PAPER NT 82-16] 14 p1976 A83-33167
- Cruise flight of a tail mounted ramjet
16 p2303 A83-35805
- Application of the separation singularity difference method to inlet aerodynamic design
16 p2290 A83-35827
- Variation of rotor blade vibration due to interaction of inlet and outlet distortion
16 p2305 A83-35882
- Analytical design and experimental verification of S-duct diffusers for turboprop installations with an offset gearbox
[AIAA PAPER 83-1211] 16 p2294 A83-36283
- Aircraft engine inlet pressure distortion testing in a ground test facility
[AIAA PAPER 83-1233] 16 p2307 A83-36296
- Progress toward the analysis of supersonic inlet flows
[AIAA PAPER 83-1371] 16 p2295 A83-36366
- Response of a supersonic inlet to downstream perturbations
[AIAA PAPER 83-2017] 16 p2296 A83-36403
- Inlet design for high-speed propfans
[SAE PAPER 821359] 17 p2451 A83-37957
- Calculation of axisymmetric inlet flowfield using the Euler equations
[AIAA PAPER 83-1853] 17 p2457 A83-38681
- Survey of inlet development for supersonic aircraft
[AIAA PAPER 83-1164] 18 p2638 A83-40473
- F/A-18 inlet/engine compatibility flight test results
19 p2796 A83-41039
- Flow visualization investigation of choking cascade turns
20 p2989 A83-42564
- Dynamic distortion in a short s-shaped subsonic diffuser with flow separation --- Lewis 8 by 6 foot Supersonic Wind Tunnel
[AIAA PAPER 83-1412] 21 p3092 A83-45515
- The response of normal shocks in diffusers
[AIAA PAPER 81-1431] 21 p3089 A83-45580
- On the influence of the diffuser inlet shape on the performance of a centrifugal compressor stage
[ASME PAPER 83-GT-9] 23 p3406 A83-47881
- Inlet-fan flow field computation
[ASME PAPER 83-GT-41] 23 p3394 A83-47901
- Three-dimensional flow measurements in a turbine scroll
[ASME PAPER 83-GT-128] 23 p3396 A83-47957
- ### ENGINE MONITORING INSTRUMENTS
- ASTF test instrumentation system detail design --- Aero propulsion System Test Facility
01 p0014 A83-11059
- Effectiveness of turbine engine diagnostic systems
[AIAA PAPER 83-0535] 05 p0597 A83-16773
- Improved fault detection in the hot section of turbojet engines by individual monitoring procedures
07 p0867 A83-19666
- Helicopter engine development - New standards for the '80s
09 p1208 A83-24837
- PMUX - The interface for engine data to AIDS --- propulsion multiplexer Aircraft Integrated Data System
13 p1807 A83-30158
- Rotorshaft torquemeter --- to increase helicopter performance
13 p1807 A83-30174
- Minimum contact magnetic sensing of turbine blade speed
13 p1807 A83-30175
- F/A-18A Inflight Engine Condition Monitoring System (IECMS)
[AIAA PAPER 83-1237] 16 p2308 A83-36300
- United Kingdom military engine usage, condition and maintenance systems experience
[AIAA PAPER 83-1239] 16 p2308 A83-36302
- Modern technology and airborne engine vibration monitoring systems
[AIAA PAPER 83-1240] 16 p2302 A83-36303
- Comparison of an experience with full authority digital engine controls in rotary wing and jet-lift VSTOL aircraft
[AIAA PAPER 83-1241] 16 p2308 A83-36304
- Instrumental problems in small gas turbine engines
[AIAA PAPER 83-1293] 16 p2302 A83-36327
- Advanced techniques for measurement of strain and temperature in a turbine engine
[AIAA PAPER 83-1296] 18 p2688 A83-39106
- Method of thermodynamic function control and of damage analysis regarding aircraft engines with the aid of flight data recording systems --- German thesis
19 p2800 A83-41850
- Thrust chamber health monitoring for reusable rocket engines
[IAF PAPER 83-389] 23 p3426 A83-47369
- A7E/TF41 Engine Monitoring System (EMS)
[ASME PAPER 83-GT-91] 23 p3408 A83-47938
- Automated diagnostic system for engine maintenance --- vibration data extraction from gas turbine engines
[ASME PAPER 83-GT-103] 23 p3408 A83-47943
- ### ENGINE NOISE
- Tests of a thermal acoustic shield with a supersonic jet
01 p0105 A83-10183
- Rotor wake characteristics relevant to rotor-stator interaction noise generation
01 p0011 A83-10184
- Assessment of inflow control structure effectiveness and design system development
03 p0281 A83-13161
- Generation of desired signals from acoustic drivers --- for aircraft engine internal noise propagation experiment
04 p0449 A83-15068
- Propeller noise at model- and full-scale
04 p0533 A83-15314
- Wind tunnel measurements of blade/vane ratio and spacing effects on fan noise
04 p0533 A83-15317
- Procedure for evaluation of engine isolators for reduced structure-borne noise transmission
04 p0449 A83-15320
- Pressure transfer function of a JT15D nozzle due to acoustic and convected entropy fluctuations
04 p0533 A83-16319
- Eigensolutions for liners in uniform mean flow ducts
07 p0990 A83-19810
- Effect of excitation on coaxial jet noise
07 p0990 A83-19811
- Electromagnetic noise from an ion engine system
07 p0873 A83-20424
- High bypass ratio engine noise component separation by coherence technique
08 p1046 A83-22159
- Turbofan engine blade pressure and acoustic radiation at simulated forward speed
09 p1205 A83-24026
- Design and development of a mixer compound exhaust system --- in aircraft turbofan engines
09 p1206 A83-24029
- ADAM - An axisymmetric duct aeroacoustic modeling system
[AIAA PAPER 83-0666] 10 p1473 A83-25903
- Transient difference solutions of the inhomogeneous wave equation - Simulation of the Green's function
[AIAA PAPER 83-0667] 10 p1473 A83-25904
- An analysis of the two-dimensional acoustic field in a nonuniform duct carrying compressible flow
[AIAA PAPER 83-0669] 10 p1473 A83-25906
- Flight effects on fan noise with static and wind tunnel comparisons
[AIAA PAPER 83-0678] 10 p1377 A83-25910
- Noise transmission through sidewall treatments applicable to twin-engine turboprop aircraft
[AIAA PAPER 83-0695] 10 p1473 A83-25916
- Wave envelope and infinite element schemes for fan noise radiation from turbofan inlets
[AIAA PAPER 83-0709] 10 p1474 A83-25925
- A theoretical investigation of the sound radiation fields associated with a Bellmouth inlet
[AIAA PAPER 83-0710] 10 p1474 A83-25926
- Ray-theory and mode-theory predictions of intake-liner performance - A comparison with engine measurements
[AIAA PAPER 83-0711] 10 p1475 A83-25927
- Simulation of propfan noise impact on a fuselage --- by newly developed siren
[AIAA PAPER 83-0715] 10 p1475 A83-25930
- Specification, design, and test of aircraft engine isolators for reduced interior noise
[AIAA PAPER 83-0718] 10 p1377 A83-25932
- Sources of installed turboprop noise
[AIAA PAPER 83-0744] 10 p1377 A83-25946
- Vane camber and angle of incidence effects in fan noise generation
[AIAA PAPER 83-0766] 10 p1377 A83-25956
- Tone generation by rotor-downstream strut interaction
[AIAA PAPER 83-0767] 10 p1378 A83-25957
- Prediction of high bypass ratio engine static and flyover jet noise
[AIAA PAPER 83-0773] 10 p1378 A83-25958
- Modified jet noise source model for twin-jet shielding analysis
[AIAA PAPER 83-0776] 10 p1477 A83-25960
- The design and flight test of an engine inlet bulk acoustic liner
[AIAA PAPER 83-0781] 10 p1378 A83-25963
- Comparison of measured and predicted flight effects on high-bypass coaxial jet exhaust noise
[AIAA PAPER 83-0749] 10 p1478 A83-26450
- Acoustic measurements on aerofoils moving in a circle at high speed
[AIAA PAPER 83-0674] 11 p1650 A83-28003
- A compact inflow control device for simulating flight fan noise
[AIAA PAPER 83-0680] 11 p1651 A83-28005
- Sound propagation in segmented exhaust ducts - Theoretical predictions and comparison with measurements
[AIAA PAPER 83-0734] 11 p1651 A83-28016
- Model and full-scale studies of the exhaust noise from a bypass engine in flight
[AIAA PAPER 83-0751] 11 p1531 A83-28019
- Application of 3-signal coherence to core noise transmission
[AIAA PAPER 83-0759] 11 p1652 A83-28021
- Laboratory study of add-on treatments for interior noise control in light aircraft
14 p1974 A83-32581
- Compressibility effects in turbulent shear layers
14 p2012 A83-32998
- Effect of sound absorbing wall linings on aerodynamic forces of a subsonic vibrating cascade
14 p2081 A83-33372
- Acoustic modal analysis of a full-scale annular combustor
[AIAA PAPER 83-0760] 15 p2226 A83-33486
- Cross spectra between temperature and pressure in a constant area duct downstream of a combustor
[AIAA PAPER 83-0762] 15 p2227 A83-33487
- Introducing the Rolls-Royce Tay
[AIAA PAPER 83-1377] 16 p2309 A83-36368
- Cabin noise weight penalty requirements for a high-speed propfan-powered aircraft - A progress report
[SAE PAPER 821360] 17 p2463 A83-37958
- The Coanda/refraction concept for gas turbine engine test cell noise suppression
[SAE AIR 1813] 17 p2471 A83-38105

- Interior noise considerations for advanced high-speed turboprop aircraft 21 p0301 A83-43970
- Experimental methods in compressor noise studies [ONERA, TP NO. 1983-79] 23 p3505 A83-48194
- ### ENGINE PARTS
- Retirement for cause inspection system design 04 p0488 A83-15159
- Preventing the strength failure of machines by vibrodiagnostic methods. II - The use of vibrodiagnostics for preventing the failure of certain parts and assemblies of gas-turbine engines 06 p0770 A83-19314
- P/M dual-property wheels for small engines 07 p0938 A83-19834
- Fabrication technology for aircraft engines --- Russian book 07 p0861 A83-20381
- Precision casting for gas turbine engines 07 p0941 A83-21347
- Fatigue and creep considerations in the design of turbine components 07 p0949 A83-21461
- Fatigue failure under fretting conditions 07 p0894 A83-21481
- Blade repair and recovery --- in gas turbines 07 p0941 A83-21496
- Cyclic rig and engine testing of ceramic turbine components 08 p1072 A83-22262
- Estimation of the cyclic fatigue life of parts subjected to complex loading patterns --- for compressor disks and turbine wheels in aircraft engines 09 p1228 A83-23502
- A finite-element study of the stress-strain state of the turbofan rotor of an aircraft gas-turbine engine 09 p1205 A83-23515
- The maintenance of modern engines in civil aviation [DGLR PAPER 82-070] 09 p1206 A83-24184
- Test results of high efficiency Stirling machine components 11 p1588 A83-27292
- Manufacture and testing of fibre composite rotor components /Fibre composite flywheel development program for road vehicle applications/ 11 p1667 A83-27308
- The reusable Space Shuttle Main Engine prepares for long life 11 p1542 A83-27470
- The interaction between a separated blade and the armor ring 11 p1531 A83-28510
- Calculation of the depth and hardness of the carburization layer of cylindrical parts --- for aircraft engines 12 p1713 A83-29282
- Development of counter-rotating intershaft support bearing technology --- for aircraft gas turbine engines 14 p1976 A83-32587
- Determination of the theoretical profile of the electrode tool in the electrochemical processing of parts of complex shape 14 p2028 A83-32967
- Fluid flow within reciprocating-engine cylinders 15 p2160 A83-34265
- Investigation methods on residual stresses in aero engines components 16 p2305 A83-35879
- Life prediction for turbine engine components 16 p2366 A83-36174
- Demonstration of the feasibility of an all-composite space motor [AIAA PAPER 83-1185] 16 p2318 A83-36264
- Nondestructive evaluation methods for implementation of damage-tolerant designed gas turbine engine components [AIAA PAPER 83-1232] 16 p2307 A83-36295
- Deterioration trending enhances jet engine hardware durability assessment and part management [AIAA PAPER 83-1234] 16 p2308 A83-36297
- Advanced techniques for gas and metal temperature measurements in gas turbine engines [AIAA PAPER 83-1291] 16 p2302 A83-36325
- Development of simulated mission endurance test acceleration factors in determining engine component serviceability and failure mode criticality [AIAA PAPER 83-1409] 16 p2310 A83-36398
- Utilization of computer aided design for the development of advanced turbomachinery components [SAE PAPER 821423] 17 p2468 A83-37980
- Implementation and integration of process planning [SAE PAPER 821424] 17 p2493 A83-37981
- Repairing gas turbine hot section airfoils today [SAE PAPER 821487] 17 p2469 A83-38006
- Major hot section component salvaged through advanced repair methods [SAE PAPER 821489] 17 p2469 A83-38007
- Experiences in repair of hot section gas turbine components [SAE PAPER 821490] 17 p2469 A83-38008
- Evaluation of the efficiency of the diamond burnishing of gas-turbine-engine parts 18 p2695 A83-39511
- Composite engine duct fabrication 18 p2631 A83-39941
- B-1B manufacturing - General Electric F101 production nears 18 p2632 A83-40332

- An experimental study of ball bearings in the combined supports of the rotors of gas-turbine engines 19 p2855 A83-42144
- A study of the gas-dynamic efficiency of the labyrinth seals of gas-turbine engines with a profiled stator wall 19 p2801 A83-42153
- The strength of GTE structural elements under low-cycle loading 20 p2936 A83-42877
- The components of gas turbines: Materials and strength (2nd revised and enlarged edition) --- Russian book 21 p3147 A83-43912
- Automotive gas turbine ceramic component testing [ASME PAPER 83-GT-112] 23 p3464 A83-47945
- Effect of particle rebound characteristics on erosion of turbomachinery components [ASME PAPER 83-GT-169] 23 p3397 A83-47988
- Ceramic components for high-temperature vehicular gas turbines - State of the art of the German ceramic program [ASME PAPER 83-GT-205] 23 p3465 A83-48006
- Component qualification and initial build of the AGT 100 advanced automotive gas turbine [ASME PAPER 83-GT-225] 23 p3465 A83-48023
- Progress in net shape fabrication of alpha SiC turbine components [ASME PAPER 83-GT-238] 23 p3466 A83-48030
- Sintering of Si3N4-based materials using the powder bed technique 23 p3435 A83-48268
- The nature of SiC for use in heat engines as compared to Si3N4 - An overview of property differences 23 p3438 A83-48305
- Status report 1981 on the German BMFT-sponsored programme 'Ceramic components for vehicular gas turbines' 23 p3438 A83-48309

ENGINE STARTERS

- A 400 Hz starter/generator system --- for aircraft engines 01 p0012 A83-11207
- Selection of the optimal output parameters for the starting device of a double-shaft turbofan engine 09 p1205 A83-23442
- On the question of calculating the pressurization start-up regimes of a gas-turbine plant 14 p2027 A83-32651
- Criteria for optimizing starting cycles for high performance fighter engines [AIAA PAPER 83-1127] 16 p2306 A83-36236
- Super integrated power unit (SIU) for the F-16 engine start system [SAE PAPER 821462] 17 p2469 A83-37996
- Application of a hot gas high pressure rotary vane motor to aircraft APU starting [SAE PAPER 821464] 17 p2469 A83-37997

ENGINE TESTING LABORATORIES

- Operational summary of an electric propulsion long term test facility [AIAA PAPER 82-1903] 02 p0139 A83-12478

ENGINE TESTS

- NT COLD FLOW TESTS
- NT STATIC FIRING
- Automatic plotting of the results of bench tests of turbine engines 01 p0011 A83-10444
- Fuel property effects on Air Force gas turbine engines - Program genesis 01 p0028 A83-10653
- Effect of oxygen addition on ignition of aero-gas turbine at simulated altitude facility 01 p0011 A83-10660
- The first implementation of ATLAS for testing gas turbine engines 01 p0001 A83-10750
- Simulated mission endurance control system 01 p0014 A83-10751
- PETTS /Programmable Engine Trim Test Set/ 01 p0014 A83-10752
- ASTF test instrumentation system detail design --- Aeropropulsion System Test Facility 01 p0014 A83-11059
- Space flight test of MDT-2A --- pulsed plasma microthruster [AIAA PAPER 82-1874] 02 p0143 A83-12462
- Impulse measurement of a pulsed plasma engine on Engineering Test Satellite-IV [AIAA PAPER 82-1875] 02 p0143 A83-12463
- Status of the J-series 30-cm mercury ion thruster [AIAA PAPER 82-1904] 02 p0144 A83-12479
- Results of the mission profile life test --- for J-series mercury ion engines [AIAA PAPER 82-1905] 02 p0144 A83-12480
- J series thruster thermal test results [AIAA PAPER 82-1906] 02 p0144 A83-12481
- J series thruster isolator failure analysis [AIAA PAPER 82-1907] 02 p0144 A83-12482
- A direct-measurement technique for estimating discharge-chamber lifetime --- for ion thrusters [AIAA PAPER 82-1908] 02 p0144 A83-12483
- Current distribution in a quasi-steady MPD arcjet [AIAA PAPER 82-1917] 02 p0145 A83-12489
- Inert gas test of two 12-cm magnetostatic thrusters [AIAA PAPER 82-1925] 02 p0145 A83-12494

- Plasma characteristics of a 17 cm diameter line-cusp ion thruster [AIAA PAPER 82-1926] 02 p0145 A83-12495
- Low temperature /650 to 700 C/ burner rig testing 02 p0158 A83-12835
- Test stand for fatigue life studies involving superposed mechanical and thermal cyclic stresses 02 p0197 A83-12986
- Parametric study of acceleration effects on burning rates of metallized solid propellants 02 p0161 A83-13084
- Structural service life estimate for a reduced smoke rocket motor 02 p0148 A83-13088
- Assessment of inflow control structure effectiveness and design system development 03 p0281 A83-13161
- The reliability of the engines of flying vehicles --- Russian book 03 p0289 A83-13813
- An enhancement for the ultrasonic test bed to inspect engine disk bolt holes 04 p0488 A83-15160
- TF41/Lamilly accelerated mission test 04 p0449 A83-15319
- Test results of a medium temperature solar engine 04 p0506 A83-16000
- Supersonic Harrier - One step closer 04 p0449 A83-16371
- The role of CFD in aeropropulsion ground testing --- Computational Fluid Dynamics [AIAA PAPER 83-0149] 05 p0599 A83-16557
- Radiant heating tests of several liquid metal heat-pipe sandwich panels [AIAA PAPER 83-0319] 05 p0635 A83-16649
- Effectiveness of turbine engine diagnostic systems [AIAA PAPER 83-0535] 05 p0597 A83-16773
- Ejecta pulsing of subscale solid propellant rocket motors [AIAA PAPER 83-0578] 05 p0610 A83-17930
- NAPC gyroscopic moment test facility 06 p0720 A83-18407
- Compact installation for testing vectored-thrust engines 08 p1047 A83-22158
- Shuttle engine problems spark broad review 08 p1052 A83-22176
- Cyclic rig and engine testing of ceramic turbine components 08 p1072 A83-22262
- Theory and design of flight-vehicle engines --- Russian book 08 p1046 A83-22651
- Current problems in the testing of aircraft engines 08 p1046 A83-22652
- Model studies of the dynamic characteristics of the pumps and turbines of liquid propellant rocket engines in transition regimes 08 p1052 A83-22660
- Evaluation of the technical state of aircraft gas-turbine engines from thermogasdynamic parameters with allowance for the natural scatter of state parameters 09 p1205 A83-23430
- Castable-sprayable insulations for rocket motors 09 p1241 A83-23841
- Burning rate measurements in solid rocket motors [AIAA PAPER 83-0481] 09 p1269 A83-24149
- U.S. Army/Detroit Diesel Allison Advanced Technology Demonstrator Engine 09 p1208 A83-24836
- The T700-GE-700 engine experience in sand environment 09 p1208 A83-24842
- New instrumentation for advanced turbine research 09 p1270 A83-25142
- Performance characteristics of wet and dry fluidynes --- Stirling cycle engines 11 p1587 A83-27276
- 50 kW Stirling engine 11 p1588 A83-27282
- Design and experiences with a laboratory Stirling cycle machine 11 p1588 A83-27284
- U.K. Consortium Stirling engine programme 11 p1588 A83-27285
- An approach to the design of Stirling engine regenerator matrix using packs of wire gauzes 11 p1588 A83-27287
- Test results of high efficiency Stirling machine components 11 p1588 A83-27292
- Fast response thermometry in Stirling engines 11 p1571 A83-27293
- Development of a Stirling engine rod seal 11 p1588 A83-27294
- Effects of displacer seal clearance on free-piston Stirling engine performance 11 p1589 A83-27295
- Separation characteristics of the T700 engine inlet particle separator 11 p1530 A83-27479
- Shaft vibration measurements on turbomachines, taking into consideration the phase angle --- German thesis 11 p1590 A83-28655
- 18:1 pressure ratio axial/centrifugal compressor demonstration program 12 p1732 A83-29013
- Evaluation of the productivity of an automated system for the testing of aircraft engines 12 p1703 A83-29277
- Maintenance of large engines CF6s for the Airbus A310 13 p1807 A83-30073

Special mesh for determining aerodynamic interference between casing walls and rotating blade rows of subsonic and transonic turbines and compressors
13 p1804 A83-30512

The effect of the fuel quality on the degree of combustion product ionization in gas-turbine engines
14 p1988 A83-32078

Development of a turbojet engine simulator for scale model wind tunnel testing of multi-mission aircraft
16 p2304 A83-35848

Ground simulation of engine operation at altitude
16 p2312 A83-35863

Simulation of advanced engine lubrication and rotor dynamics systems - Rig design and fabrication
[AIAA PAPER 83-1133] 16 p2306 A83-36238

Methanol combustion in a CF6I-80A engine combustor
[AIAA PAPER 83-1138] 16 p2339 A83-36241

The aerodynamic design and performance of the General Electric/NASA EEE fan --- Energy Efficient Engine
[AIAA PAPER 83-1160] 16 p2306 A83-36252

A Monte Carlo simulation of the engine development process
[AIAA PAPER 83-1230] 16 p2307 A83-36294

Aircraft engine inlet pressure distortion testing in a ground test facility
[AIAA PAPER 83-1233] 16 p2307 A83-36296

Accelerated Mission Testing of the F110 Engine
[AIAA PAPER 83-1235] 16 p2308 A83-36298

Monomethylhydrazine versus hydrazine fuels - Test results using flight qualified 100 LBF and 5 LBF bipropellant engine configurations
[AIAA PAPER 83-1257] 16 p2340 A83-36311

Results of tests of a rectangular vectoring/reversing nozzle on an F100 engine
[AIAA PAPER 83-1285] 16 p2308 A83-36322

Application of thin film strain gages and thermocouples for measurement on aircraft engine parts
[AIAA PAPER 83-1292] 16 p2302 A83-36326

Performance of a low thrust LO2/LH2 engine with a 300:1 area ratio nozzle
[AIAA PAPER 83-1313] 16 p2320 A83-36334

Accelerated simulated mission endurance test of a turboshaft engine for military attack helicopter application
[AIAA PAPER 83-1359] 16 p2309 A83-36357

Development of simulated mission endurance test acceleration factors in determining engine component serviceability and failure mode criticality
[AIAA PAPER 83-1409] 16 p2310 A83-36398

New transformations of S4 Modane hypersonic wind tunnel for ramjet missiles tests
[ONERA, TP NO. 1983-24] 16 p2313 A83-36433

Full Authority Digital Electronic Control (FADEC) - Augmented fighter engine demonstration
[SAE PAPER 821371] 17 p2467 A83-37963

Closed-loop engine fuel system simulation
[SAE PAPER 821374] 17 p2468 A83-37964

Developments in performance monitoring and diagnostics in aircraft turbine engines
[SAE PAPER 821400] 17 p2468 A83-37973

Development and operating characteristics of an advanced two-stage combustor
17 p2469 A83-38022

The Coanda/refraction concept for gas turbine engine test cell noise suppression
[SAE AIR 1813] 17 p2471 A83-38105

Advanced techniques for measurement of strain and temperature in a turbine engine
[AIAA PAPER 83-1296] 18 p2688 A83-39106

Computerized ultrasonic tomography for testing solid propellant rocket motors
18 p2695 A83-39565

F/A-18 inlet/engine compatibility flight test results
19 p2796 A83-41039

JT9D performance deterioration results from a simulated aerodynamic load test
19 p2800 A83-41040

Large scale aeroengine compressor test facility
19 p2807 A83-41534

An experimental investigation of a low-power Stirling engine
19 p2855 A83-42014

Tapered roller bearings for turbine engines
20 p2998 A83-42559

Hydrogen aspiration in a direct injection type diesel engine Its effects on smoke and other engine performance parameters
20 p2998 A83-42956

Nonsynchronous whirls of the turbine rotor in aerojet engines
20 p2937 A83-43694

A survey of inlet/engine distortion compatibility
[AIAA PAPER 83-1166] 21 p3088 A83-45509

Development of Indonesian sounding rockets
[IAF PAPER 83-379] 23 p3420 A83-47366

Ariane 3 third stage propulsion systems and HM7 B engine development
[IAF PAPER 83-387] 23 p3426 A83-47367

Small cryogenic propulsion unit for upper stage application
[IAF PAPER 83-388] 23 p3426 A83-47368

Five milli Newtons field emission thruster testing
[IAF PAPER 83-394] 23 p3426 A83-47371

Investigation of F/A-18A engine throttle usage and parametric sensitivities
[ASME PAPER 83-GT-64] 23 p3407 A83-47919

Investigation of fixed-rake sampling system for the assessment of emission characteristics of gas turbine engines
[ASME PAPER 83-GT-72] 23 p3407 A83-47925

Test experience with turbine-end foil bearing equipped gas turbine engines
[ASME PAPER 83-GT-73] 23 p3407 A83-47926

Automated diagnostic system for engine maintenance --- vibration data extraction from gas turbine engines
[ASME PAPER 83-GT-103] 23 p3408 A83-47943

The Navy PATE program - A status report --- Propulsion Automatic Test Equipment
[ASME PAPER 83-GT-109] 23 p3408 A83-47944

Automotive gas turbine ceramic component testing
[ASME PAPER 83-GT-112] 23 p3464 A83-47945

Measurement and analyses of heat flux data in a turbine stage. I - Description of experimental apparatus and data analysis
[ASME PAPER 83-GT-121] 23 p3408 A83-47950

Structural response due to blade vane interaction
[ASME PAPER 83-GT-133] 23 p3408 A83-47960

Ceramic Applications in Turbine Engines (CATE) development testing
[ASME PAPER 83-GT-179] 23 p3465 A83-47990

Built-In Test Equipment (BITE) on the Garrett model GTCP331 APU digital electronic control unit --- for gas turbine aircraft auxiliary power system
[ASME PAPER 83-GT-186] 23 p3409 A83-47992

The impact of computers on the test cell of tomorrow --- for gas turbine engine tests
[ASME PAPER 83-GT-187] 23 p3409 A83-47993

Strong pressure waves in air-breathing engines
23 p3398 A83-48216

Dynamic response of a centrifugal liquid oxygen rocket pump
[ASME PAPER 83-FE-24] 23 p3426 A83-48235

ENGINEERING
Computing methods in applied sciences and engineering, V; Proceedings of the Fifth International Symposium, Versailles, France, December 14-18, 1981
19 p2896 A83-41526

ENGINEERING DEVELOPMENT
U PRODUCT DEVELOPMENT

ENGINEERING DRAWINGS
Evaluation procedures to be used during the development of CAD systems
04 p0465 A83-15146

On automatic recognition of 3D structures from 2D representations
10 p1461 A83-25474

Using program transformations to derive lind-drawing algorithms
11 p1646 A83-27121

ENGINEERING MANAGEMENT
The management of engineering change procedure
06 p0816 A83-17957

An investigation of motivational factors among base-level Air Force civil engineers
06 p0798 A83-17958

Handbook on engineering psychology --- in Russian
07 p0982 A83-20389

The technical 'productivity gap'
13 p1933 A83-30831

Airport pavement management - A total system
[AIAA PAPER 83-1600] 14 p1978 A83-33363

Functional management in matrix organizations
15 p2239 A83-33524

Progress measurement during project execution
20 p3056 A83-43399

ENGINES
NT AIR BREATHING ENGINES
NT APOGEE BOOST MOTORS
NT ARC JET ENGINES
NT BOOSTER ROCKET ENGINES
NT BRISTOL-SIDDELEY BS 53 ENGINE
NT CONTROL ROCKETS
NT DIESEL ENGINES
NT DUCTED ROCKET ENGINES
NT ELECTROSTATIC ENGINES
NT ELECTROTHERMAL ENGINES
NT GAS TURBINE ENGINES
NT HELICOPTER ENGINES
NT HYDRAZINE ENGINES
NT HYDROGEN ENGINES
NT HYDROGEN OXYGEN ENGINES
NT INTERNAL COMBUSTION ENGINES
NT ION ENGINES
NT J-79 ENGINE
NT JET ENGINES
NT LIQUID PROPELLANT ROCKET ENGINES
NT MERCURY ION ENGINES

NT MICROROCKET ENGINES
NT NOZZLELESS ROCKET ENGINES
NT NUCLEAR ROCKET ENGINES
NT ORBIT MANEUVERING ENGINE (SPACE SHUTTLE)
NT PISTON ENGINES
NT PLASMA ENGINES
NT PULSED JET ENGINES
NT PULSEJET ENGINES
NT RAMJET ENGINES
NT RESISTOJET ENGINES
NT REUSABLE ROCKET ENGINES
NT RL-10 ENGINES
NT ROCKET ENGINES
NT SOLID PROPELLANT ROCKET ENGINES
NT SPACE SHUTTLE MAIN ENGINE
NT SUPERSONIC COMBUSTION RAMJET ENGINES
NT T-56 ENGINE
NT T-64 ENGINE
NT TF-34 ENGINE
NT TF-41 ENGINE
NT TURBINE ENGINES
NT TURBOFAN ENGINES
NT TURBOJET ENGINES
NT TURBOPROP ENGINES
NT UPPER STAGE ROCKET ENGINES
NT VARIABLE CYCLE ENGINES
NT WANKEL ENGINES

A simple derivation of the generalized Beale number --- for Stirling engines
11 p1664 A83-27262

Whither Stirling engines --- principles and applications
11 p1586 A83-27266

Dimensional analysis of pumping losses in a Stirling cycle machine
11 p1587 A83-27269

Perturbation analysis of the Stirling cycle
11 p1665 A83-27270

ENGLISH CHANNEL
An analysis of Seasat altimeter measurements over a coastal area The English Channel
09 p1318 A83-24292

A study of blooms of phytoplankton on the Roscoff-Plymouth radial /western English Channel/ in 1980 and 1981 - The contribution from satellite imagery of the ocean color --- French thesis
11 p1635 A83-28639

ENGLISH LANGUAGE
Using English as a high-level robot command language
21 p3191 A83-44080

ENHANCEMENT
U AUGMENTATION

ENLARGING
U EXPANSION

ENRICHMENT
NT ISOTOPIC ENRICHMENT
Kinetic enrichment of hydrogen at interfaces and voids by dislocation sweep-in of hydrogen
10 p1398 A83-26279

ENSKOG-CHAPMAN THEORY
U CHAPMAN-ENSKOG THEORY

ENSTATITE
The Tucson iron and its relationship to enstatite meteorites
04 p0563 A83-15361

Petrography, mineral chemistry and origin of Type I enstatite chondrites
04 p0572 A83-16351

Actinide microdistributions in the enstatite meteorites
07 p1035 A83-21329

Mineralogy and petrology of the Abbee enstatite chondrite breccia and its dark inclusions
08 p1187 A83-21640

Nuclear track records in the Abbee enstatite chondrite
08 p1188 A83-21643

Nitrogen contents and isotopic ratios of clasts from the enstatite chondrite Abbee
08 p1188 A83-21644

Composition and origin of clasts and inclusions in the Abbee enstatite chondrite breccia
08 p1188 A83-21645

Pyroxene whiskers and platelets in interplanetary dust - Evidence of vapour phase growth
08 p1191 A83-23279

The Atlanta enstatite chondrite breccia
22 p3385 A83-46373

The Adhi Kot breccia and implications for the origin of chondrules and silica-rich clasts in enstatite chondrites
24 p3673 A83-50174

ENTHALPY
The saturated vapor pressure of nickel
01 p0024 A83-10387

Exergie /4th revised and enlarged edition/ --- German book
02 p0244 A83-12325

Frozen specific heat and heat of phase transition - Titanium
06 p0728 A83-18442

Enthalpies of formation of liquid aluminum-silicon alloys
09 p1229 A83-23518

Developing mass spectrometric techniques for boundary layer measurement in hypersonic high enthalpy test facilities
18 p2689 A83-39937

- The regulation of the heat content of the body
23 p3497 A83-47106
- Enthalpy of formation and transformation in binary and ternary systems of the metals iron, cobalt, nickel, and molybdenum
24 p3561 A83-49434
- ENTIRE FUNCTIONS**
- Enforcing irreducibility for phase retrieval in two dimensions
07 p0930 A83-20795
- Polynomial approximations and white noise integrals
09 p1331 A83-24771
- More on the calculation of oscillatory integrals
12 p1772 A83-29636
- A useful integral function and its application in thermal radiation calculations
24 p3578 A83-49575
- ENTRAINMENT**
- The effects of Reynolds number and pressure gradient on the transitional spot in a laminar boundary layer
01 p0047 A83-10896
- Entrainment and the droplet spectrum in cumulus clouds
02 p0215 A83-12941
- Resonant entrainment of a confined pulsed jet
04 p0478 A83-16139
- New skin friction and entrainment correlations for turbulent boundary layers
04 p0478 A83-16144
- Chemically reacting turbulent shear layers
[AIAA PAPER 83-0475] 05 p0636 A83-16739
- Entrainment and detrainment in a simple cumulus cloud model
06 p0790 A83-18262
- An analysis of the thermal entrainment effect on jet impingement heat transfer
[ASME PAPER 82-WA/HT-54] 10 p1413 A83-25694
- An experimental study of entraining, stress-driven, stratified flow in an annulus
14 p2013 A83-33382
- The shape-factor relationship for turbulent boundary layers
16 p2289 A83-35622
- A study of lean extinction limit for pilot flame holder
16 p2325 A83-35821
- Entrainment and mixing in thrust augmenting ejectors
[AIAA PAPER 83-0172] 16 p2292 A83-36046
- Clouds and entrainment --- cumulus convective turbulence in clear air
24 p3612 A83-49694
- ENTROPY**
- A comparison of the entropies of collapsing stars and black holes
01 p0119 A83-10234
- Concerning certain analogies in physics and information theory
01 p0111 A83-10564
- Exergie /4th revised and enlarged edition/ --- German book
02 p0244 A83-12325
- Fin geometry for minimum entropy generation in forced convection
03 p0315 A83-13483
- Inner structure and entropy production
04 p0544 A83-14960
- A general upper limit on the mass and entropy production of a cluster of supermassive objects
04 p0549 A83-14994
- Pressure transfer function of a JT15D nozzle due to acoustic and convected entropy fluctuations
04 p0533 A83-16319
- The entropy efficiency of blade machines
05 p0597 A83-16953
- The entropy of a gas of hard spheres with respect to the group of space-time translations
05 p0691 A83-17138
- Relaxation terms and entropy production in a cosmological model
05 p0701 A83-17225
- Alternation of derivatives is no criterion for choosing an entropy function --- during free thermal relaxation of gas
06 p0815 A83-18325
- The application of energy and entropy balances for treatment of flow and temperature data at a real wall in an unsteady state
06 p0759 A83-19237
- Estimate of shock thickness based on entropy production
07 p0926 A83-20530
- Thermodynamic fluctuations and gravitational instabilities
07 p1018 A83-20950
- Inflation and time asymmetry in the universe
08 p1186 A83-23272
- On the symmetric form of systems of conservation laws with entropy
09 p1350 A83-23724
- Energy and entropy balances in a combustion chamber - Analytical solution
09 p1226 A83-24363
- Reconstruction of a polarized brightness distribution by the maximum entropy method --- for astronomical maps
09 p1354 A83-24479
- Thermodynamic inequalities in continuum mechanics
11 p1665 A83-27994
- Lepton loss and entropy generation in stellar collapse
12 p1791 A83-28987
- Asymptotic freedom and entropy in a perpetually oscillating universe
12 p1794 A83-29166
- Entropy productions on the earth and other planets of the solar system
14 p2111 A83-32523
- Temperature fluctuations in the background radiation in the entropy theory of galaxy formation
15 p2269 A83-34680

- Tolman's cosmological models
15 p2272 A83-34782
- The effect of an entropy layer on the propagation of unsteady perturbations in a boundary layer --- of hypersonic viscous gas
16 p2288 A83-35534
- On the evaporation of shock-compressed metals during expansion
16 p2328 A83-35539
- Thermal relaxation and entropy for charged particles in a heat bath with fields
16 p2421 A83-35616
- Flow in a three-dimensional corner with large entropy differences
17 p2449 A83-37540
- The dependence of the Kolmogorov entropy of mappings on coordinate systems
18 p2740 A83-39001
- Entropy and vorticity corrections for transonic flows [AIAA PAPER 83-1926] 18 p2637 A83-39413
- A neutrino-dominated universe?
18 p2777 A83-39782
- The effects of nonlinearities on radial and nonradial oscillations
19 p2914 A83-40727
- The effect of trapped lepton number and entropy on the outcome of stellar collapse
19 p2920 A83-41638
- Principles, problems, and paradoxes of cosmogony
20 p3074 A83-43130
- Numerical determination of the parameters in high-entropy layers on slightly blunt bodies in supersonic flow
21 p3088 A83-45220
- The H-theorem and the Onsager principle for the steady Boltzmann equation
21 p3220 A83-45221
- On a variational approach to conservative hyperbolic systems
22 p3352 A83-45978
- Entropy production rates from viscous flow calculations. I - A turbulent boundary layer flow
[ASME PAPER 83-GT-70] 23 p3512 A83-47923
- Entropy production rates from viscous flow calculations. II Flow in a rectangular elbow
[ASME PAPER 83-GT-71] 23 p3512 A83-47924
- Optimal thermodynamics of thermal exchanges
[ONERA, TP NO. 1983-78] 23 p3512 A83-48193
- The thermodynamics of evolution. I - The thermodynamics of the dissipative structures
23 p3513 A83-48599
- Estimation of the Kolmogorov entropy from a chaotic signal
24 p3623 A83-48849
- Frequency domain analysis of entropy generation through heat flow
24 p3575 A83-48908
- Two hidden symmetries of the equations of ideal gasdynamics, and the general solution in a case of non-uniform entropy distribution
24 p3577 A83-49467
- Quantum dissipative processes and gravitational entropy of the universe
24 p3663 A83-49749
- ENTROPY (STATISTICS)**
- NT MAXIMUM ENTROPY METHOD
- Stability and integrability in the planar general three-body problem
18 p2757 A83-39606
- ENVELOPES**
- On the formation and dynamics of shells around elliptical galaxies
24 p3657 A83-49260
- ENVIRONMENT EFFECTS**
- Ice distribution and winter surface circulation patterns, Kachemak Bay, Alaska
02 p0198 A83-12038
- Effects of aerosols on photosynthesis
05 p0659 A83-16850
- El Chichon climate effect estimated
06 p0786 A83-18815
- Environmental effects of an impact-generated dust cloud - Implications for the Cretaceous-Tertiary extinctions
06 p0779 A83-18816
- The dust cloud of the century
08 p1138 A83-23271
- The environmental impact of the use of large wind turbines
11 p1611 A83-27867
- The role of aerosols in the climate system - Results of numerical experiments in climate models
12 p1759 A83-29559
- Systems environmental testing and redundancy vs Shuttle on-orbit repair/satellite retrieval
13 p1810 A83-31180
- Climatic effects of atmospheric carbon dioxide
13 p1893 A83-31200
- The interaction of the cretaceous-tertiary extinction bolide with the atmosphere, ocean, and solid earth
13 p1880 A83-31475
- Effects of fine airborne particles on equipment reliability
13 p1863 A83-31500
- The effect of external environmental factors on the rhythm of physiological functions of pre-school-age children
14 p2069 A83-32952
- Land use systems and their impact on environment - An attempt at a classification
15 p2182 A83-33576
- Air pollutants and forest decline
16 p2372 A83-35764

- Survey and analysis of present or potential environmental impact sites in Woburn, Massachusetts
17 p2536 A83-38359
- A megastructural end to Geologic Time
18 p2754 A83-39607
- Some effects of environment on high temperature mechanical behavior of alloys
20 p2953 A83-42245
- Some environmental effects of forest fires in interior Alaska
20 p3015 A83-43430
- ENVIRONMENT MANAGEMENT**
- Remote sensing in the global monitoring of environment
09 p1284 A83-24527
- Inferring non-point pollution from land cover analysis
15 p2182 A83-33575
- Use of remote sensing inputs in geographic information systems for watershed management
15 p2186 A83-34836
- ENVIRONMENT MODELS**
- Urban albedo as a function of the urban structure - A two-dimensional numerical simulation
01 p0069 A83-10721
- Space diversity performance prediction for earth-satellite paths using radar modeling techniques
02 p0140 A83-12614
- A framework for evaluating air quality models
06 p0781 A83-18240
- Atmospheric balance of sulphur above an equatorial forest
11 p1615 A83-27671
- Models in remote sensing - An approach to mapping vegetation in arid lands
15 p2186 A83-34831
- Using remote sensig in a predictive archaeological model - The Jackson purchase region, Kentucky
15 p2186 A83-34837
- Catch a falling star - Meteorites and old ice
23 p3528 A83-47817
- ENVIRONMENT POLLUTION**
- NT AIR POLLUTION
- NT GLOBAL AIR POLLUTION
- NT INDOOR AIR POLLUTION
- NT OIL POLLUTION
- NT WATER POLLUTION
- The use of model experiments performed in natural conditions to study the interaction of petroleum products with the ocean and atmosphere
01 p0069 A83-10834
- Environmental contamination in light of space law
05 p0692 A83-16973
- The nuclear question and liability in space law
05 p0692 A83-16974
- Heavy metal pollution. VII - Emissions from Mount Etna volcano
07 p0956 A83-20091
- Ground contamination by fuel jettisoned from aircraft in flight
[AD-A128451] 09 p1294 A83-24041
- Laboratory measurements of dry deposition of acetone over adobe clay soil
09 p1297 A83-25186
- PIXE analysis of aerosol in the workplace
13 p1872 A83-30181
- Evaluation of human exposure to the noise from large wind turbine generators
20 p3015 A83-43639
- Atmospheric chloroform (CHCl3) - Ocean-air exchange and global mass balance
21 p3169 A83-44378
- Polymer materials - Toxic properties /Handbook/ --- in Russian
21 p3117 A83-45006
- Total soluble and insoluble sulfur concentrations in urban snow
22 p3321 A83-45923
- Application of space imagery for the study of anthropogenic pollution and its impact on the environment
[IAF PAPER 83-134] 23 p3478 A83-47286
- Optical remote sensing of environmental pollution and danger by molecular species using low-loss optical fiber network system
23 p3508 A83-47802
- Observations on the chemical composition of rain using short sampling times during a single event
23 p3479 A83-48683
- Monitoring of the background pollution of the environment. Number 1 --- Russian book
24 p3602 A83-49101
- Background concentration of lead, mercury, arsenic, and cadmium in the environment (according to worldwide data)
24 p3602 A83-49103
- Background concentration of organochlorine compounds and 3,4-benzopyrene in the environment (according to worldwide data)
24 p3602 A83-49104
- Cometary matter in the environment
24 p3598 A83-49105
- ENVIRONMENT PROTECTION**
- NT CENTRAL ATLANTIC REGIONAL ECOL TEST SITE
- Microwave remote sensing measurements of oil pollution on the ocean
01 p0069 A83-10104
- U.S. program assessing nuclear waste disposal in space - A 1981 status report
01 p0016 A83-11282

The equivalence of the criteria for normative SO2 limit values in the urban region recommended by the Austrian Academy of Sciences Commission on protecting air purity 04 p0508 A83-16225

Environmental protection system for the Shuttle External Tank Air Cargo Carrier [SAE PAPER 820880] 10 p1384 A83-25773

Effects of past and present surface mining observed through remote sensing techniques 17 p2531 A83-38343

Mapping on the basis of space photographs and environment protection --- Russian book 21 p3166 A83-45032

ENVIRONMENT SIMULATION

NT ACOUSTIC SIMULATION

NT ALTITUDE SIMULATION

NT SPACE ENVIRONMENT SIMULATION

NT THERMAL SIMULATION

NT WEIGHTLESSNESS SIMULATION

ICIASF '81; International Congress on Instrumentation in Aerospace Simulation Facilities, Dayton, OH, September 30, 1981, Record 01 p0051 A83-11051

Toward 'combat realistic' tests, evaluations, exercises - and training 01 p0015 A83-11237

Results of stereoscopic image simulations for the SPOT HRV carried out at the Gun Lake site in British Columbia 03 p0350 A83-14292

A conception of a normal-mode expansion procedure applied to a limited-area model. I - The derivation of dynamic equations in normal mode form --- in numerical weather forecasting 04 p0514 A83-15023

Rate of wind abrasion on Mars 04 p0567 A83-15572

'A total G-force environment dynamic flight simulator' - A new dimension in flight simulation [AIAA PAPER 83-0139] 05 p0599 A83-16548

Electromagnetic environment simulation for TCAS avionics --- Threat Alert and Collision Avoidance Systems 05 p0592 A83-17304

Formulation and testing of a climatonic simulation of the microclimate of the dry valleys and of the Little America V Station in Antarctica 06 p0788 A83-18236

Computer graphics applications in electromagnetic computer modeling --- treatment of wire objects by method of moments 06 p0802 A83-18667

Numerical simulation of ice/frost formation on the external tank of the Space Shuttle in varying environments [AIAA PAPER 83-0524] 06 p0722 A83-19592

The simulation of global radiation 07 p0953 A83-20139

Computer-generated images in visual simulation and avionic technologies 08 p1047 A83-22835

An experimental investigation of the factors governing the dynamic structure and intensity of atmospheric vortices 09 p1313 A83-23969

Numerical simulation of the Weddell Sea pack ice 10 p1453 A83-26349

A simulated method of transient environment - The fast swept sine method 13 p1862 A83-31487

MIL-STD-810D - A climatic testing update --- environment simulation 13 p1864 A83-31515

Use of a Cf-252 source in cosmic ray simulation studies on CMOS memories 15 p2152 A83-35419

A simulation model supporting HCMC investigation on geological objectives --- heat capacity mapping mission 15 p2188 A83-35287

A Trimix saturation dive to 660 m studies of cognitive performance, mood and sleep quality 16 p2400 A83-35565

An investigation of the spectral transmission of a crystalline cloud medium 16 p2392 A83-36869

Simulate airborne radar environments 17 p2461 A83-37821

Numerical stimulation of photochemical air pollution over the Ise Bay District 20 p3013 A83-42202

The simulation of solar radiation 20 p2944 A83-42896

The simulation of temperature-stratified atmospheric boundary layers in a wind tunnel 22 p3256 A83-46492

Laboratory simulation of Venusian lightning 23 p3529 A83-47863

Modelling of long-range transport of sulphur over Europe - A two-year model run and some model experiments 23 p3479 A83-48682

On the treatment of point source emissions in urban air quality modeling 24 p3602 A83-50189

ENVIRONMENT SIMULATORS

NT SOLAR SIMULATORS

NT SPACE SIMULATORS

Fiber optics for electro-magnetic pulse /EMP/ simulators 08 p1047 A83-22495

An experimental investigation of the rhombic EMP simulator under pulse excitation 10 p1411 A83-26492

Design and verification of a cloud field optical simulator 18 p2727 A83-39886

ENVIRONMENTAL CHAMBERS

U TEST CHAMBERS

ENVIRONMENTAL CHEMISTRY

NT AEROTHERMOCHEMISTRY

NT ATMOSPHERIC CHEMISTRY

NT BIOCHEMISTRY

NT BIOGEOCHEMISTRY

NT GEOCHEMISTRY

NT PHYSIOCHEMISTRY

Chemical weathering and the Viking biology experiments on Mars 04 p0567 A83-15577

On the radiocarbon record in banded corals - Exchange parameters and net transport of 14CO2 between atmosphere and surface ocean 09 p1295 A83-24253

Laboratory measurements of dry deposition of acetone over adobe clay soil 09 p1297 A83-25186

ENVIRONMENTAL CONTROL

Environmental control and life support - Partially closed system will save big money 09 p1324 A83-24356

Space station environmental, thermal control and life support /ETCLS/ - Meeting the evolutionary growth challenge 09 p1297 A83-25186

[ASME PAPER 82-WA/AERO-1]

10 p1458 A83-25676

Spacelab ECLS follow-on-development [SAE PAPER 820848] 10 p1458 A83-25757

Control philosophy concepts in complex space heat rejection systems [SAE PAPER 820864] 10 p1384 A83-25764

A hybrid facility for the simulation, development, and validation of ECS microprocessor based controls [SAE PAPER 820867] 10 p1379 A83-25766

Aircraft vehicle equipment improvements via microprocessors [SAE PAPER 820868] 10 p1375 A83-25767

Environmental control of an aircraft pod mounted electronics system [SAE PAPER 820869] 10 p1375 A83-25768

ECS schemes for All Electric Airliners [SAE PAPER 820870] 10 p1375 A83-25769

Evaluating Scroll refrigerant compressors for reducing size and weight of military aircraft ECS [SAE PAPER 820877] 10 p1375 A83-25771

Spacelab ECLS current status --- Environmental Control/Life Support Subsystem [SAE PAPER 820884] 10 p1458 A83-25775

Chemical defense, environmental control systems study [SAE PAPER 820866] 13 p1806 A83-30944

Performance of the Multiple Mirror Telescope (MMT). III Seeing experiments with the MMT 13 p1937 A83-30979

Blueprint of a clean room 13 p1864 A83-31506

New technology for improved clean room operations 13 p1865 A83-31520

Features and testing of clean room apparel 13 p1865 A83-31525

Space Shuttle environmental and life support system (ECLSS) [SAE PAPER 821420] 17 p2562 A83-37977

Ecological monitoring and regulation of the state of the environment 24 p3598 A83-49275

ENVIRONMENTAL ENGINEERING

Psychic effects on the safety and reliability of complex technical systems 02 p0225 A83-13015

Operational considerations on the moon-day project 06 p0720 A83-19148

Terraforming Mars and Venus using machine self-replicating systems /SRS/ 09 p1211 A83-23684

The development of STS payload environmental engineering standards 13 p1811 A83-31197

Environmental stress impact and environmental engineering methods; Proceedings of the Twenty-seventh Annual Technical Meeting on Emerging Environmental Solutions for the Eighties, Los Angeles, CA, May 5-7, 1981, Volume 1 13 p1862 A83-31476

Proposed IES recommended practice on environmental test program management 13 p1862 A83-31478

Enhancement of quality through environmental technology; Proceedings of the Twenty-eighth Annual Technical Meeting, Atlanta, GA, April 21-23, 1982 13 p1864 A83-31507

An in-depth evaluation of mission profile testing: Environmental engineering aspects - Reliability engineering aspects 13 p1864 A83-31510

ENVIRONMENTAL LABORATORIES

Nonlinear phenomena in laboratory and space plasmas 11 p1660 A83-28251

Effective low cost testing - A laboratory perspective 13 p1863 A83-31490

The NASA Space Environment Simulation Laboratory 15 p2125 A83-34194

ENVIRONMENTAL MONITORING

Detection of coastal zone environmental conditions using synthetic aperture radar 01 p0076 A83-10068

The use of near color infrared photography to assess the impact of the oil and natural gas industry on Louisiana's wetlands 01 p0063 A83-10069

Using new methods in monitoring the thermal regime of the Arctic 01 p0075 A83-10828

Advanced operational earth resources satellite systems [AAS 82-128] 02 p0137 A83-11932

Environmental monitoring of the Athabasca Oil Sands using Landsat data 02 p0198 A83-11988

Renewable resources monitoring needs in Manitoba 03 p0346 A83-14228

Toward an operational, satellite-based, wetland monitoring program for the Fraser River Estuary, British Columbia 03 p0345 A83-14234

Environmental monitoring of the Athabasca Oil Sands Region 03 p0346 A83-14238

Remote sensing and waste management 03 p0400 A83-14263

An experimental Landsat Quicklook System for Alaska 03 p0348 A83-14271

Temporary lakes and salt plains in the high plateaus of the Andes /Bolivia/ - A continuing survey of periodic hydrologic phenomena using the geostationary satellite GOES-EST 03 p0360 A83-14574

An optimum statistical technique for ozone profile retrieval from backscattered UV radiances 03 p0360 A83-14632

Automated measurements of atmospheric visibility [AIAA PAPER 83-0436] 05 p0643 A83-16713

Monitoring ecology in inaccessible areas of tropical zones by interpretation of machine processed Landsat-scenes 08 p1127 A83-21937

Application of remote sensing for preparation of nature conservation maps and natural processes dynamics study 08 p1128 A83-21951

Optimal signal discrimination and problems of monitoring --- Russian book 09 p1283 A83-23819

Remote sensing in the global monitoring of environment 09 p1284 A83-24527

Monitoring of seasonal and yearly land-use changes on aerial photography and Landsat imagery - A case study in the Yemen Arab Republic 09 p1285 A83-24538

Monitoring of water quality and environmental changes in the Aswan High Dam reservoir from Landsat imagery 09 p1286 A83-24555

Approaches to desertification monitoring in the Sudan using Landsat data: A test of a geographical data base approach - Preliminary results 09 p1286 A83-24558

Monitoring arid land changes in the Turpan Depression, People's Republic of China 09 p1288 A83-24589

Landsat as an aid in consulting projects in the Middle East and Africa some examples of applications on VBB/SWECO projects 09 p1289 A83-24592

Monitoring land use and land use appropriateness in the central Sudan - A combination of Landsat data and statistical analysis of climatic data 09 p1290 A83-24608

Environmental change detection in the Nile using multidade Landsat imagery 09 p1291 A83-24630

Climate as determined by observations from space 09 p1317 A83-25259

Monitoring of pollutants in the environment --- Russian book 10 p1446 A83-25607

Transport of certain substances through the atmosphere-ocean interface in the region of the Bering Sea 10 p1447 A83-25610

An intercomparison of two radars used in the Montana HIPLEX 11 p1627 A83-27038

Estimation of turbulence severity in precipitation environments by radar 11 p1627 A83-27044

Selected man-made halogenated chemicals in the air and oceanic environment 13 p1873 A83-30883

The cosmic horizons of climatology 13 p1893 A83-31315

On the efficiency and basic design parameters of satellites for continuous observations of elemental natural phenomena 14 p2035 A83-32505

Potential for cross-contamination for payloads in the STS bay [AIAA PAPER 83-1562] 14 p1981 A83-32779

Study of land transformation processes from space and ground observations; Proceedings of the Symposium, Ottawa, Canada, May 16-June 2, 1982 15 p2181 A83-33551

The first decade of regular observation of land transformation from space 15 p2181 A83-33552

A technique for mapping environmental change using digital Landsat data 15 p2181 A83-33561

- Remote sensing techniques for monitoring and managing irrigated lands 15 p2181 A83-33564
- Canadian Landsat studies for monitoring resource development A summary 15 p2182 A83-33567
- A review of current Australian work on the application of Landsat to land transformation processes 15 p2182 A83-33569
- Canadian Landsat studies for monitoring hydrologic conditions and coastal environments - A summary 15 p2183 A83-33579
- Remote-sensing techniques for geographical surveys --- Russian book 15 p2184 A83-34572
- Classification and mapping habitats within the Mississippi River deltaic plain region 15 p2184 A83-34810
- Satellite remote sensing needs and applications in Less Developed Countries 16 p2370 A83-35424
- Effects of past and present surface mining observed through remote sensing techniques 17 p2531 A83-38343
- Utilization of Landsat data to monitor deforestation of Kenya's Mau Forest 17 p2534 A83-38461
- The use of remote sensing in global biosystem studies --- in ecology 19 p2861 A83-42040
- The economic benefits of operational environmental satellites [AAS PAPER 83-188] 20 p3010 A83-43770
- Signature extension versus retraining for multispectral classification of surface mines in arid regions 21 p3165 A83-43894
- Air monitoring - Research needs 21 p3169 A83-45616
- Application of remote sensing techniques to study environmental conditions and natural resources in Antarctic Peninsula 22 p3313 A83-46206
- Predicting eruptions at Mount St. Helens, June 1980 through December 1982 22 p3332 A83-46795
- Seismic precursors to the Mount St. Helens eruptions in 1981 and 1982 22 p3333 A83-46796
- Deformation monitoring at Mount St. Helens in 1981 and 1982 22 p3333 A83-46797
- Gas emissions and the eruptions of Mount St. Helens through 1982 22 p3333 A83-46798
- Monitoring the 1980-1982 eruptions of Mount St. Helens Compositions and abundances of glass 22 p3333 A83-46800
- Ecological monitoring and regulation of the state of the environment 24 p3598 A83-49275
- Information about the environment from spaceborne observations and the national-economic significance and cost effectiveness of this information 24 p3598 A83-49291

ENVIRONMENTAL QUALITY

- NT AIR QUALITY
- NT WATER QUALITY
- Some results from experiments on remote sensing of water quality and oil pollution in the Mediterranean Sea 09 p1286 A83-24557
- Environmental data display 21 p3142 A83-45615
- Application of space imagery for the study of anthropogenic pollution and its impact on the environment [IAF PAPER 83-134] 23 p3478 A83-47286
- ENVIRONMENTAL RESEARCH SATELLITES**
- Performance assessment of future European remote sensing systems 01 p0021 A83-10109
- Configuration design of a closed-loop, pseudogravitational, environmental research facility in low earth orbit [AIAA PAPER 83-0651] 05 p0607 A83-16817
- High-throughput digital SAR processing 21 p3165 A83-43978
- NASA/NOAA implementation of the USAID-sponsored satellite ground station and data processing facility for Bangladesh [IAF PAPER 83-127] 23 p3475 A83-47282

ENVIRONMENTAL SURVEYS

- Cities and the environment: Studies from space --- Russian book 15 p2241 A83-34167
- Survey and analysis of present or potential environmental impact sites in Woburn, Massachusetts 17 p2536 A83-38359

ENVIRONMENTAL TEMPERATURE**U AMBIENT TEMPERATURE****ENVIRONMENTAL TESTS**

- NT COLD WEATHER TESTS
- NT CORROSION TESTS
- NT HIGH TEMPERATURE TESTS
- NT LOW TEMPERATURE TESTS
- NT SALT SPRAY TESTS
- NT UNDERWATER TESTS

- Investigation of the tribochemical influence of air pollution on the rolling friction of various materials being used in a newly developed railroad measuring post --- German thesis 01 p0056 A83-10175

- Testing of complex ECM systems 01 p0057 A83-10746
- A high order language for the analysis of experimental data 01 p0089 A83-11196
- Development of advanced composite materials and geodetic structures for future space systems 01 p0017 A83-11334
- Shuttle contamination and experimentation - DoD implications 03 p0284 A83-13466
- General contamination criteria for optical surfaces --- instrument performance losses in spaceborne conditions 03 p0287 A83-13743
- Space environmental effects on materials 03 p0291 A83-14125
- A study into the degradation of nylon, Kevlar and polyester fabrics when exposed to varying amounts of ultra violet in the laboratory and in natural environment and the effects of varying degrees of heat on the degradation of these fabrics 04 p0463 A83-15439
- The electromagnetic environment for the Space Shuttle orbiter [AIAA PAPER 83-0332] 05 p0604 A83-16661
- The McDonnell Aircraft environmental test laboratory 05 p0599 A83-16931
- Environmentally induced discharges in a solar array 05 p0610 A83-17493
- The effect of environment on fatigue crack growth behavior of 2021 aluminum alloy 05 p0616 A83-17894
- Fatigue spectrum sensitivity of composite joints --- in aircraft structures 06 p0716 A83-17964
- Test tailoring in the 80's --- as applied to Sparrow air-to-air missile environment simulation 07 p0869 A83-21036
- Screening design considerations 07 p0943 A83-21037
- The interaction of high temperature corrosion and mechanical properties of alloys 07 p0893 A83-21470
- The metallography of fatigue in the high strength aluminum alloy 7010 08 p1060 A83-21711
- Influence of environment on fracture 08 p1065 A83-21798
- A spaceborne experiment to determine the radiation sensitivity of microwave bipolar transistors 08 p1080 A83-22371
- Environmental testing of UV-cured acrylate-coated fibers 08 p1073 A83-22488
- Measurements in hostile environments; Proceedings of the International Conference, University of Edinburgh, Edinburgh, Scotland, August 31-September 4, 1981 09 p1264 A83-23358
- Convective heat losses from flat-plate solar collectors in turbulent winds 09 p1293 A83-23883
- The environmental background in gas-filled detectors for X ray astronomy 09 p1268 A83-24107
- Applications of titanium and prospects for the use of AT-series titanium alloys in environments containing chlorides 09 p1235 A83-24404
- The T700-GE-700 engine experience in sand environment 09 p1208 A83-24842
- Thermal storage life of solid-propellant motors 09 p1243 A83-24885
- Low cycle fatigue behaviour of cast nickel-base superalloy IN-738LC in air and in hot corrosive environments 10 p1394 A83-25422
- Amorphous silicon photovoltaic modules 10 p1446 A83-26064
- Qualification testing of large lithium-thionyl chloride batteries for US Air Force Minuteman extended survival power 11 p1539 A83-27191
- Combined environmental reliability testing of guided weapons using acoustic techniques 11 p1590 A83-28401
- Stress screening using multiaxial vibration 11 p1590 A83-28403
- A wind tunnel study of the flow field within and around open-top chambers used for air pollution studies 12 p1750 A83-29134
- Methods to assess the success of test programs 12 p1733 A83-29219
- Polysulfide sealants for aerospace. II - Application and handling 12 p1716 A83-29242
- Designing electronic equipment for random vibration environments; Proceedings of the Meeting, Los Angeles, CA, March 25, 26, 1982 13 p1834 A83-30851
- Design guides for random vibration --- for testing electronic packaging design 13 p1861 A83-30855
- Design for long fatigue life in random vibration environment 13 p1861 A83-30858
- Designing electronic equipment for random vibration environments 13 p1861 A83-30860
- Component lead wire strain relief for random vibration environments 13 p1835 A83-30867

- Anti-icing system design and test optimization --- for shipboard or ground missile launcher components [SAE PAPER 820879] 13 p1809 A83-30948
- Tests and quality of the 3.5 meter primary mirror of the Max-Planck-Institut fuer Astronomie's telescope at Calar Alto 13 p1920 A83-31012
- Influence of external environments on fatigue crack growth in epoxy resin 13 p1825 A83-31047
- Approaches to environmental verification of STS free-flier and pallet payloads 13 p1810 A83-31184
- Environmental stress impact and environmental engineering methods; Proceedings of the Twenty-seventh Annual Technical Meeting on Emerging Environmental Solutions for the Eighties, Los Angeles, CA, May 5-7, 1981 Volume 1 13 p1862 A83-31476
- Proposed IES recommended practice on environmental test program management 13 p1862 A83-31478
- On the certainty of synergistic effects --- in environmental reliability testing 13 p1862 A83-31480
- Benefits of mission profile testing 13 p1862 A83-31481
- Outdoor and laboratory testing of photovoltaic modules 13 p1862 A83-31482
- MIL-STD-810 - An eye to the future --- military standard for environmental testing 13 p1862 A83-31483
- Accelerated weathering of photovoltaic modules employing natural sunlight 13 p1862 A83-31484
- Effective low cost testing - A laboratory perspective 13 p1863 A83-31490
- Burn-in/acceptance test model using TGP growth guideline concepts --- Tracking Growth and Prediction 13 p1863 A83-31492
- Standardization of environmental requirements and related test methods 13 p1863 A83-31501
- MIL-STD-810D - A progress report 13 p1863 A83-31502
- Cost effective utilization of environmental design criteria; MIL-STD-210B updated 13 p1863 A83-31503
- Enhancement of quality through environmental technology; Proceedings of the Twenty-eighth Annual Technical Meeting, Atlanta, GA, April 21-23, 1982 13 p1864 A83-31507
- Tailoring the composite mission profile environments for reliability testing --- for external stores 13 p1864 A83-31508
- An assessment of external stores reliability testing 13 p1864 A83-31509
- The effect of environment on the growth of small fatigue cracks 13 p1824 A83-31539
- The role of the environment on the corrosion cracking of Al-Mg and Al-Li-Mg alloys 14 p1992 A83-32072
- Environmental stress cracking behavior of glass fiber reinforced epoxy resins 14 p1986 A83-32345
- Creep-fatigue-environment interactions --- Book 14 p1993 A83-32650
- Evolution of new materials for space applications [AIAA PAPER 83-0792] 14 p1985 A83-32794
- Composites for extreme environments --- Book 14 p1986 A83-33114
- Environmental effects on graphite fiber reinforced PMR-15 polyimide 14 p1987 A83-33115
- V378A polyimide resin - A new composite matrix for the 1980's 14 p1987 A83-33116
- Space environmental effects on graphite/epoxy composites 14 p1987 A83-33121
- Environmental exposure of carbon/epoxy composite material systems 14 p1987 A83-33123
- Dynamic tests of graphite/epoxy composites in hygrothermal environments 14 p1987 A83-33124
- Service life analysis of rocket motors with internal gas generation 15 p2129 A83-33736
- High temperature time-dependent crack growth 15 p2139 A83-34485
- Effects of environment on intermediate temperature crack growth in superalloys 15 p2139 A83-34488
- Results from a 'small box' realtime molecular contamination monitor on STS-3 [AIAA PAPER 83-0251] 16 p2317 A83-36050
- Fatigue: Environment and temperature effects --- Book 16 p2330 A83-36160
- Overview of temperature and environmental effects on fatigue of structural metals 16 p2330 A83-36161
- Corrosion fatigue crack propagation 16 p2330 A83-36162
- Delta K thresholds in titanium alloys - The role of microstructure, temperature and environment 16 p2331 A83-36164
- The effect of microstructure on the fatigue behavior of Ni base superalloys 16 p2331 A83-36166
- Environment, frequency and temperature effects on fatigue in engineering plastics 16 p2337 A83-36170
- The effect of environment and temperature on the fatigue behavior of titanium alloys 16 p2331 A83-36171
- Effects of frequency on the corrosion fatigue of Udimet 720 in a molten sulfate salt 16 p2332 A83-36191

- A comparison of environmentally-influenced near-threshold fatigue crack growth behavior in high and lower strength steels at conventional frequencies 16 p2332 A83-36195
- Investigation of the fatigue behaviour of some industrial glass reinforced polyesters (GRP) 18 p2655 A83-40205
- The environmental stress corrosion cracking of glass fibre reinforced polyester and epoxy composites 18 p2656 A83-40223
- Effects of corrosive environments on graphite/epoxy composites 18 p2656 A83-40227
- Design and development of advanced-composite shrouds 18 p2662 A83-40297
- Method for a reliability study on photovoltaic modules Application for the qualification of cells and modules 18 p2710 A83-40528
- Qualification and durability tests - Applications for thermal collectors and photovoltaic modules 18 p2710 A83-40531
- Facilities for the study of behaviour in corrosive atmospheres and their application to thermal and photovoltaic converters 18 p2673 A83-40532
- Environmental effects on fibre-reinforced plastics; Proceedings of the Symposium, Imperial College of Science and Technology, London, England, July 12, 13, 1983 20 p2946 A83-42801
- On the accelerated ageing of CFRP 20 p2946 A83-42802
- Analysis of moisture gradients in service and in the laboratory --- in composite materials 20 p2947 A83-42803
- The effect of moisture on the shear properties of carbon fibre composites 20 p2947 A83-42804
- The environmental degradation of notched CFRP in compression 20 p2947 A83-42806
- The effect of composite prebond moisture on adhesive-bonded CFRP-CFRP joints 20 p2947 A83-42807
- The in-service flight testing of some carbon fibre-reinforced plastic components 20 p2933 A83-42808
- Environmental resistance of carbon fibre-reinforced polyether etherketone 20 p2947 A83-42810
- Environmental fatigue of reinforced plastics 20 p2947 A83-42812
- The effects of environmental exposure on the fatigue behaviour of CFRP laminates 20 p2947 A83-42813
- Glass processing in a microgravity environment 20 p2941 A83-43282
- Semiconductor crystal growth and segregation problems on earth and in space 20 p2941 A83-43291
- Viscoelastic behavior of AS/3501-6 Gr/ep composite 21 p3105 A83-44043
- DINS - Lessons learned and successes achieved --- ring laser gyro Dormant Inertial Navigation System for maneuvering reentry vehicles [AAS PAPER 83-084] 21 p3097 A83-44184
- Dust storm simulation for accelerated life testing of solar collector mirrors 21 p3168 A83-45063
- Environmental aging of epoxy composites 22 p3263 A83-46288
- A study of the surface deterioration due to erosion --- of gas turbine blades [ASME PAPER 83-GT-213] 23 p3397 A83-48014
- The kinetics of gas-solid reactions and environmental degradation of nitrogen ceramics 23 p3436 A83-48281

ENVIRONMENTS

- NT AEROSPACE ENVIRONMENTS
- NT CHROMOSPHERE
- NT CISLUNAR SPACE
- NT DEEP SPACE
- NT EARTH ENVIRONMENT
- NT EXTRATERRESTRIAL ENVIRONMENTS
- NT FRICTIONLESS ENVIRONMENTS
- NT GEOMAGNETIC TAIL
- NT HELIUM HYDROGEN ATMOSPHERES
- NT HIGH ALTITUDE ENVIRONMENTS
- NT HIGH GRAVITY ENVIRONMENTS
- NT HIGH TEMPERATURE ENVIRONMENTS
- NT ICE ENVIRONMENTS
- NT INNER RADIATION BELT
- NT INTERPLANETARY SPACE
- NT INTERSTELLAR SPACE
- NT IONOSPHERE
- NT JUPITER ATMOSPHERE
- NT LOW TEMPERATURE ENVIRONMENTS
- NT LOWER IONOSPHERE
- NT MAGNETOPAUSE
- NT MAGNETOSPHERE
- NT MARINE ENVIRONMENTS
- NT MARS ATMOSPHERE
- NT MARS ENVIRONMENT
- NT MESOPAUSE
- NT MESOSPHERE

- NT MIDLATITUDE ATMOSPHERE
- NT NEPTUNE ATMOSPHERE
- NT PLANETARY ATMOSPHERES
- NT PLANETARY ENVIRONMENTS
- NT ROTATING ENVIRONMENTS
- NT SATELLITE ATMOSPHERES
- NT SATURN ATMOSPHERE
- NT SOLAR ATMOSPHERE
- NT SPACECRAFT ENVIRONMENTS
- NT STELLAR ATMOSPHERES
- NT THERMAL ENVIRONMENTS
- NT URANUS ATMOSPHERE
- NT VENUS ATMOSPHERE
- Strain measuring systems and protections for adverse environments 09 p1264 A83-23359
- The effect of genotype and environment on evoked potential parameters during orienting and defensive reactions 16 p2401 A83-36824

ENZYME ACTIVITY

- NT FERMENTATION
- Investigation of the localization of dehydrogenases in aerobic and anaerobic bacteria at the submicroscopic level 01 p0078 A83-10421
- Common mechanism of the intratissue regulation of proliferation on the basis of the principle of the tissue-specific control of the oxidative phosphorylation of mitochondria 01 p0078 A83-10425
- The stereospecificity of the effect of the isomers of flupentixol on the substrate inhibition of brain tyrosine hydroxylase 01 p0079 A83-10536
- The activity of tyrosine hydroxylase in the ganglia of the vegetative nervous system in rabbits during acute experimental emotional stress 01 p0080 A83-10542
- The use of chromatography for determining kallikrein and prekallikrein in canine blood serum 01 p0080 A83-10546
- The possible role of assignment catalysts in the origin of the genetic code 02 p0219 A83-11634
- Oxygen toxicity 02 p0222 A83-12261
- The effect of helium-neon laser irradiation on the membranes of the retina 03 p0374 A83-13610
- The activity of renin in blood plasma, the indicators of central hemodynamics, and the water-electrolyte balance in patients with hypertension 03 p0379 A83-13622
- The role of peptidases in the regulation of vascular tonus 03 p0380 A83-13635
- The cyclase system and lysosome enzyme activity in health and disease 03 p0374 A83-13637
- Regulation of the activity of enzymatic reactions in the brain in the presence of nervous system pathology 03 p0374 A83-13638
- The assay of glycosaminoglycans in the blood serum 03 p0375 A83-14333
- A method for the assessment of enzyme activity in drug metabolism 03 p0381 A83-14335
- The activity of AP-endonuclease in thymocytes of normal and irradiated rats 03 p0376 A83-14877
- The role of catechol-o-methyltransferase in catecholamine transformations in the hypothalamus of rats at long-term intervals after irradiation 03 p0377 A83-14886
- The inhibitory effect of linoleic acid hydroperoxide on the activity of superoxide dismutase --- radioprotective substance 03 p0377 A83-14887
- Peculiarities of the reaction of cortical pyramidal neurons to the cessation of oxygen supply by the effect of cAMP 04 p0520 A83-15890
- The effect of microelemental additions on the activity of certain metallic enzymes, immune stability, and performance of athletes 05 p0672 A83-17155
- Adaptation and resistance to hypoxia in light of the functional activity of the antisytems 05 p0669 A83-17161
- Changes in the affinity of the respiratory enzymes for oxygen as a factor of the physiological regulation of oxygen supply to the tissues 05 p0672 A83-17637
- A circulating inhibitor of $/\text{Na}/+/- + \text{K}/+/-$ ATPase associated with essential hypertension 05 p0672 A83-17794
- The ultracytochemical analysis of nuclear ribonucleoproteins /RNP/ 06 p0795 A83-18981
- The regulation of the biosynthesis of serotonin in the central nervous system 06 p0795 A83-18983
- The effect of short-term hypothermia on the monoamine oxidase enzyme system in the rat brain 06 p0795 A83-18989
- The activity of $\text{Ca}/2 + /$ ATPase and enzymes of cAMP metabolism in the nerve tissue of rats during the early stages of acute radiation damage 06 p0796 A83-19383
- Investigation of cAMP phosphodiesterase activity in brain tissue under general and local irradiation of the head and body of adult animals and embryos 07 p0974 A83-20843

- The effect of the calmodulin inhibitor, trifluoroperazine, on the calcium activation of phosphorilases in the glycosomes of the skeletal muscles in rabbits 07 p0975 A83-20981
- The effect of hypothermia on the glutamate dehydrogenase activity in the brain 07 p0975 A83-20982
- The transport and turnover of aldolase in rat livers during total body irradiation with X-rays 09 p1321 A83-24927
- The reaction of chronically irradiated dogs to radiation as evaluated by changes in the activity of cholinesterase 09 p1321 A83-24932
- Metabolic effect of intermittent exposure to altitude stress on rats and guinea pigs 10 p1453 A83-25670
- Polyamine formation by arginine decarboxylase as a transducer of hormonal, environmental and stress stimuli in higher plants 11 p1639 A83-27830
- Changes in osteoblastic activity due to simulated weightless conditions 11 p1640 A83-27831
- Microbodies in the living cell 12 p1762 A83-29249
- Regulation of glycogenolysis in human muscle in response to epinephrine infusion 13 p1902 A83-30455
- The activity of 5-nucleotidase in leukocytes, erythrocytes, and blood serum of rats with radiation sickness 14 p2062 A83-32061
- The early changes in the activation of nucleoside diphosphatekinase in the brain and liver of rats following total-body gamma-irradiation at an absolutely lethal dose 14 p2062 A83-32062
- The effect of pyridoxine, riboflavin, and glutamic acid on the activity of lysosomal hydrolases in the liver and blood serum of rats during traumatic stress 14 p2066 A83-33330
- State of the kidney and brain Renin-Angiotensin System (RAS) and of the pituitary-adrenal axis in rats with acute neurogenic hypertension 15 p2210 A83-34453
- Renin, kallikrein, and the angiotensin-converting enzyme during a physical load in humans 15 p2213 A83-34959
- UDP-coenzymes in the tissues of the brain glia of humans 16 p2400 A83-36831
- The role of proteolysis in the processing and inactivation of neuropeptides - Its possible connection with certain functions of the brain 16 p2396 A83-36840
- Nonspecific esterases of the extramural ganglia of the autonomous nervous system in rabbits during acute experimental emotional stress 17 p2556 A83-38175
- Electromagnetic and magnetic fields in the treatment of ischemic heart disease 18 p2734 A83-40540
- The processes of proteolysis in the small intestine of rats in the case of the intestinal form of acute radiation sickness 19 p2874 A83-41013
- A low-renin form of hypertension - Characteristics of the functional relationships of the renin-aldosterone pressor system 19 p2881 A83-41439
- An investigation of the proteinase activity in the perilymph of patients with otosclerosis 19 p2883 A83-41830
- Stabilization of the yeast desaturase system by low levels of oxygen 19 p2879 A83-42159
- Effect of prolonged exercise at altitude on the renin-aldosterone system 20 p3034 A83-43482
- Effects of acute moderate-intensity exercise on carnitine metabolism in men and women 20 p3034 A83-43484
- An investigation of methane monooxygenase from *Methylococcus capsulatus* 21 p3186 A83-45378
- Renin-aldosterone and angiotensin-converting enzyme during prolonged altitude exposure 22 p3347 A83-45984
- Circadian clock in *Xenopus* eye controlling retinal serotonin N-acetyltransferase 23 p3495 A83-48086

ENZYMES

- NT ALDOLASE
- NT CHOLINESTERASE
- NT CYSTEAMINE
- NT LYSOZYME
- NT PAPAINE
- Evolutionary roots of catalysis by nicotinamide and flavins in C-H oxidoreductases and in photosynthesis 02 p0219 A83-11633
- The possible mechanism of the solar-biosphere connections --- effect on enzymes 02 p0221 A83-11894
- Quantitation of chlorpromazine-bound calmodulin during chlorpromazine inhibition of gravitropism 11 p1638 A83-27815
- Selective modification of gultathione metabolism 13 p1899 A83-31162
- The evolutionary pattern of aromatic amino acid biosynthesis and the emerging phylogeny of pseudomonad bacteria 20 p3033 A83-42399
- Rapid purification of fluorescent enzymes by ultrafiltration 21 p3105 A83-44858

- Rapid purification of fluorescent enzymes by ultrafiltration 22 p3347 A83-46710
Glutathione reductase in evolution 24 p3617 A83-49620
- EOS**
U LANDSAT SATELLITES
- EOSINOPHILS**
Blood eosinophilia in aviators 08 p1147 A83-22954
- EOSS**
Space station orbit maintenance [AIAA PAPER 83-0347] 05 p0603 A83-17919
- EPE-A**
U EXPLORER 12 SATELLITE
- EPHEMERIDES**
NT PLANET EPHEMERIDES
Four years of photometry of DK Draconis = HR 4665 04 p0548 A83-15975
The second catalog of ephemerides for the relative radial velocities of the components of visual binary stars with known orbits --- Book 05 p0694 A83-17133
Five years of photometry of Lambda Andromedae 12 p1785 A83-28995
Cometary ephemerides for spacecraft flyby missions 15 p2249 A83-35017
The lunar ephemeris ELP 2000 20 p3059 A83-42383
Internal inconsistency of reference system determined by on-board ephemerides of NNSS satellites 23 p3482 A83-48067
- EPHEMERIS TIME**
Eclipse timings in U Geminorum 09 p1353 A83-23737
- EPINEPHRINE**
NT NOREPINEPHRINE
The histochemical and ultrastructural characteristics of the neuron reactions of mammillary nuclei in old animals to injections of adrenaline 09 p1321 A83-25154
Regulation of glycogenolysis in human muscle in response to epinephrine infusion 13 p1902 A83-30455
Effect of hyperoxia on metabolic and catecholamine responses to prolonged exercise 13 p1902 A83-30456
The role of free fatty acids in the accumulation of thrombocytes and the development of myocardial injuries during prolonged adrenalin administration 17 p2555 A83-37237
The adrenoreactivity of the contractile myocardium and coronary arteries in the case of chronic overload and acute ischemic injuries of the heart 18 p2733 A83-40556
- EPITAXY**
NT ELECTROEPITAXY
NT LIQUID PHASE EPITAXY
NT MOLECULAR BEAM EPITAXY
NT VAPOR PHASE EPITAXY
Photosensitive gate structures based on epitaxial layers of Fe-doped GaP 01 p0108 A83-10373
Heteroepitaxial growth of Ge on 111-line Si by vacuum evaporation 03 p0399 A83-14938
Diffusivity and growth rate of silicon in solid-phase epitaxy with an aluminum medium 05 p0691 A83-17768
Epitaxial growth of Hg(1-x)Cd(x)Te by chemical vapor transport 07 p0998 A83-19903
Formation of ultrathin single-crystal silicidic films on Si - Surface and interfacial stabilization of Si-NiSi₂ epitaxial structures 07 p1000 A83-20817
Electrical properties and ion implantation of epitaxial GaN, grown by low pressure metalorganic chemical vapor deposition 08 p1169 A83-22760
Carrier lifetimes in silicon epitaxial layers deposited on oxygen-implanted substrates 08 p1082 A83-22920
Epitaxy 09 p1349 A83-23854
Heteroepitaxial Si films on yttria-stabilized, cubic zirconia substrates 10 p1488 A83-25981
Epitaxial relations in group-IIIa fluoride/Si(111)/heterostructures 10 p1488 A83-25983
Deposition of GaAs epitaxial layers by organometallic CVD - Temperature and orientation dependence 10 p1488 A83-26060
Use of epitaxial ZnSe films, grown from organoelemental compounds, in electron-beam-pumped lasers 10 p1432 A83-26673
Investigation of the features of formation of crystalline structures grown in conditions of microgravity 11 p1661 A83-27447
Enhancement of the superconducting transition temperature T_c in Nb₃Ge by the homoepitaxial technique 12 p1782 A83-29169
Spectroscopy of the isoelectronic nitrogen addition in epitaxial structures based on wide-band solid solutions of the system In-Ga-P-As 13 p1927 A83-30262
Epitaxial crystallization of nylon 6 cast from solution on the surface of poly(p-phenylene terephthalamide) filament 13 p1817 A83-31796
- An approach to solargrade silicon layers epitaxially grown on MG silicon substrates 14 p2090 A83-32318
The growth and characterization of epitaxial solar cells on resolidified metallurgical-grade silicon 16 p2420 A83-35986
Epitaxial growth of Hg(0.7)Cd(0.3)Te by laser-assisted deposition 19 p2903 A83-40741
Photoconverters using epitaxial layers deposited on substrates of metallurgical silicon 19 p2862 A83-42011
Device characterization on monocrystalline silicon grown over SiO₂ by the ELO (epitaxial lateral overgrowth) process 21 p3123 A83-43846
Heteroepitaxial growth of CdTe on GaAs by laser assisted deposition 21 p3219 A83-45492
Recent progress on LADA growth of HgCdTe and CdTe epitaxial layers --- laser assisted deposition 24 p3633 A83-48739
Characterization of epitaxial films of CdTe and CdS grown by hot-wall epitaxy 24 p3636 A83-50182
- EPITHELIUM**
Morphological evidence for natural poxvirus infection in rats 07 p0976 A83-21049
- EPOCHS**
U TIME MEASUREMENT
- EPOXY COMPOUNDS**
NT BORON-EPOXY COMPOUNDS
NT HYOSCINE
- EPOXY MATRIX COMPOSITES**
The modelling of hydrothermal aging in glass fibre reinforced epoxy composites 01 p0022 A83-10700
Role of fibre surface-matrix combination in carbon fibre reinforced epoxy composites 02 p0149 A83-11669
A production engineers view of advanced composite materials 02 p0149 A83-11800
Nonlinear matrix failure criterion for fiber-reinforced composite materials 02 p0150 A83-12062
The relation between the network structure, deformation and failure processes, and mechanical properties of epoxies 02 p0160 A83-12063
The effect of physical aging on the time-dependent properties of carbon-fiber-reinforced epoxy composites 02 p0150 A83-12064
The use of composite materials in aircraft propellers 02 p0136 A83-12966
An experimental study of the strength of a cross-ply glass-reinforced composite in the plane stressed state 03 p0293 A83-14738
Compressive failure and kinking in uniaxially aligned glass-resin composite under superposed hydrostatic pressure 04 p0455 A83-15994
Pulse radiolysis of epoxy-based matrix materials [AIAA PAPER 83-0586] 05 p0617 A83-16805
The fracture of particulate-filled epoxide resins. I 05 p0611 A83-17563
The problem of a crack in an orthotropic strip 06 p0778 A83-19546
Engineering principles of the formation of epoxy resin composites. I Mathematical model of the fluid flow 07 p0875 A83-20439
Elastomermodified epoxy resins for composite applications 07 p0876 A83-20476
Reliability analysis of circumferentially wound FRP flywheels 07 p0950 A83-21625
Hygrothermal aging effects on the micromechanisms of crack extension in glass fibre and carbon fibre composites 08 p1053 A83-21679
A quest for micropolar elastic constants. II 08 p1120 A83-21814
Relation of interfacial adhesion in Kevlar/epoxy systems to surface characterization and composite performance 08 p1055 A83-22716
Effect of fiber-aspect ratio and orientation on the stress-strain behavior of aligned, short-fiber-reinforced, ductile epoxy 08 p1055 A83-22719
Mechanical behavior of thick filament-wound composites tested in transverse compression 09 p1221 A83-23606
Bisimide amine cured epoxy /IME/ resins and composites. II - Ten-degree off-axis tensile and shear properties of Celion 6000/IME composites 09 p1221 A83-23608
Advanced composites structures at Hughes Helicopters, Inc 09 p1202 A83-23645
Post-crazing analysis of glass-epoxy laminates 09 p1223 A83-23941
Transverse moisture sensitivity of aramid/epoxy composites 10 p1388 A83-25626
Compression molded energy storage flywheels 11 p1608 A83-27303
Carbon/epoxy laminates under combined fastener bearing and tension bypass loading [AIAA 83-0967] 12 p1710 A83-29778
An epoxy resin system for composite flywheels 12 p1711 A83-29893
- Life estimation of an S-Glass/epoxy composite under sustained tensile loading 12 p1711 A83-29894
An accumulated-damage fracture criterion for a three-component layered composite 13 p1865 A83-30055
A study of the structure of organic composites reinforced with polyheteroarylene fibers 13 p1815 A83-30058
The effect of the molding pressure on the overall physicochemical properties of carbon composites 13 p1815 A83-30061
Free-volume relaxation during the molding of composite materials 13 p1816 A83-30087
Distributions of fatigue life and fatigue strength in notched specimens of a carbon eight-harness-satin laminate 13 p1816 A83-31621
Environmental stress cracking behavior of glass fiber reinforced epoxy resins 14 p1986 A83-32345
Cryogenic fluid management experiment trunnion fatigue verification 14 p1982 A83-32782
[AIAA PAPER 83-0911] 14 p1982 A83-32782
Filament wound composite thermal isolator structures for cryogenic dewars and instruments --- glass fiber reinforced epoxy laminates for spaceborne equipment 14 p1982 A83-33120
Environmental exposure of carbon/epoxy composite material systems 14 p1987 A83-33123
Curing of epoxy matrix composites 15 p2130 A83-34795
The fracture of composites with allowance for the effects of temperature and humidity 16 p2323 A83-35508
A machine for the mechanical testing of polymers in a three-dimensional stressed state 16 p2364 A83-35513
A tubular braided composite main rotor blade spar 16 p2299 A83-35949
Static fatigue life of Kevlar aramid/epoxy pressure vessels at room and elevated temperatures [AIAA PAPER 83-1328] 16 p2324 A83-36342
Photoelastic determination of stress intensity factors in patched cracked plates 16 p2325 A83-36505
Investigation of the load-carrying capacity and efficiency of thin-walled shells made of epoxy composites 17 p2521 A83-37560
An analysis of models for calculating the strength of aramid fibers in bundles and in a microcomposite 18 p2649 A83-40101
A model of the curing process of epoxy matrix composites 18 p2650 A83-40128
Strength of epoxy resin under multiaxial stress field 18 p2672 A83-40141
Longitudinal shear modulus of unidirectional composites 18 p2652 A83-40161
Vibration characteristics of laminated composite plates 18 p2703 A83-40170
On the knee-point of cross-ply composite 18 p2653 A83-40175
Analysis of mechanical damage growth in notched carbon-epoxy (+, or - 45 deg)ns laminates 18 p2654 A83-40191
On fracture behavior during crack propagation in carbon-fiber composites 18 p2654 A83-40192
Distributions of fatigue life and fatigue strength in notched specimens of a carbon eight-harness-satin laminate 18 p2655 A83-40201
Fatigue behaviour of carbon fiber reinforced epoxy composite materials with edge notch 18 p2655 A83-40202
Fatigue crack growth behavior in the vicinity of interface of dissimilar materials 18 p2705 A83-40204
The modelling of failure processes and the role of the matrix in the failure of carbon fibre reinforced epoxy resin 18 p2655 A83-40208
Performance of carbon fibre reinforced epoxy composites under different environments 18 p2656 A83-40225
Swelling of Kevlar 49/epoxy and S2-glass/epoxy composites 18 p2657 A83-40228
Fractography of carbon/epoxy angle-ply laminates 18 p2660 A83-40273
Synthesis and characterization of bisimide amines and bisimide amine-cured epoxy resins 19 p2823 A83-40924
The effect of moisture on the shear properties of carbon fibre composites 20 p2947 A83-42804
Effect of moisture on the notch sensitivity of carbon fibre composites 20 p2947 A83-42805
Water absorption of glass/epoxy laminates under bending stresses 20 p2947 A83-42809
The effects of environmental exposure on the fatigue behaviour of CFRP laminates 20 p2947 A83-42813
Design, fabrication and test of a composite elevator 21 p3151 A83-44046
Composite helicopter structure tested for crashworthiness 21 p3091 A83-44875
Network structure description and analysis of amine-cured epoxy matrices 22 p3262 A83-46283

Rubber modified matrices --- for epoxy matrix composites 22 p3262 A83-46286

Environmental aging of epoxy composites 22 p3263 A83-46288

Effect of fiber aspect ratio on ultimate properties of short-fiber composites 22 p3264 A83-46297

The effect of moisture on the fatigue resistance of an aramid/epoxy composite 22 p3265 A83-46904

On wave propagation in random particulate composites 23 p3428 A83-48095

Dry wear studies on glass-fibre-reinforced epoxy composites 23 p3428 A83-48154

The effect of temperature on the strength of aramide fibers and microplastics based on them 23 p3428 A83-48440

Statistical analysis of multiple fracture in 0 deg/90 deg/0 deg glass fibre/epoxy resin laminates 24 p3554 A83-50064

EPOXY RESINS

Synthesis and characterization of bisimide amines and bisimide amine-cured epoxy resins 01 p0027 A83-11486

Toughening epoxy resin matrix for glass and carbon fiber composites 02 p0149 A83-11852

Rheological characterization of epoxy prepreg resins 03 p0302 A83-13563

Use of the holophotoelastic method for three-dimensional stress analysis 03 p0344 A83-14942

The effect of moisture and temperature on the properties of an epoxide-polyamide adhesive in relation to its performance in single lap joints 04 p0463 A83-15872

Photoelastic stress analysis of epoxy resin having an inserted metal. I - Residual stress caused by curing 05 p0611 A83-17096

A study on threshold of macro-crack growth in a soft epoxy resin 05 p0618 A83-17101

The fracture of particulate-filled epoxide resins. I 05 p0611 A83-17563

Impact testing of toughened epoxy resin systems 07 p0875 A83-20444

Adiabatic calorimetry for kinetics modeling of epoxy resin systems 07 p0898 A83-20445

Rheological characterization of a toughened epoxy adhesive system as a quality control tool 07 p0942 A83-20446

The dielectric properties of anhydride-cured epoxy potting compounds 07 p0899 A83-20458

High performance, low viscosity resin systems 07 p0899 A83-20465

Elastomermodified epoxy resins for composite applications 07 p0876 A83-20476

Plastic tooling for advanced composites 07 p0876 A83-20481

Aging and performance of structural film adhesives. I - A comparison of two high-temperature curing, epoxy-based systems 07 p0900 A83-21048

Evidence of microscopic crack jumping in an epoxy resin 07 p0901 A83-21085

Impact fatigue strength and reliability for fiber reinforced epoxy resin laminates subjected to repeated impact loads 07 p0877 A83-21624

Bisimide amine cured epoxy /IME/ resins and composites. II - Ten-degree off-axis tensile and shear properties of Celion 6000/IME composites 09 p1221 A83-23608

The characterization of diaminodiphenyl sulfone /DDS/ cured tetraglycidyl 4, 4'diaminodiphenyl methane /TGDDM/ epoxies 09 p1221 A83-23610

A new generation of high performance, rubber free toughened epoxy resin systems 09 p1238 A83-23641

Dynamics and mechanism of cavitation erosion on perspex and epoxy resin tested in a rotating disk device 11 p1551 A83-27422

Characterization of two nitrile-epoxy structural adhesives 12 p1716 A83-29550

Polymer selection and matrix aspects of processing and manufacture of fibre composites 12 p1710 A83-29714

Temperature dependent dynamic shear properties of CFRP 12 p1710 A83-29719

An epoxy resin system for composite flywheels 12 p1711 A83-29893

Influence of external environments on fatigue crack growth in epoxy resin 13 p1825 A83-31047

Thermokinetic modeling of an epoxy resin. I - Chemoviscosity 13 p1825 A83-31048

Dynamic-mechanical response of graphite/epoxy composite laminates and neat resin 13 p1817 A83-31795

Influence of quality control variables on failure of graphite/epoxy under extreme moisture conditions 14 p1987 A83-33125

Generation of thermal strains in GRP. I - Effect of water on the expansion behaviour of unidirectional glass fibre-reinforced laminates. II - The origin of thermal strains in polyester cross-ply laminates 15 p2130 A83-35074

The effect of the transport properties of epoxy based coatings on metallic substrate corrosion 18 p2671 A83-39052

Synthesis and characterization of bisimide amines and bisimide amine-cured epoxy resins 19 p2823 A83-40924

Cavitation erosion characteristics of poly(methyl methacrylate) in a rotating disk device 19 p2824 A83-41851

Removal of histological sections from glass for electron microscopy - Use of Quetol 651 resin and heat 21 p3183 A83-44675

Epon 828 epoxy - A new photoelastic-model material 21 p3117 A83-45165

In situ analysis of the interface --- of composites 22 p3264 A83-46303

Removal of histological sections from glass for electron microscopy - Use of Quetol 651 resin and heat 22 p3346 A83-46709

The curing of a bisphenol A-type epoxy resin with 1,8 diamino-p-menthane 22 p3270 A83-46905

EQUALIZERS (CIRCUITS)

A simplified 'real frequency' technique applied to broad-band multistage microwave amplifiers 07 p0923 A83-21537

Performance of adaptive equalization for staggered QPSK and QPR over frequency-selective LOS microwave channels --- Quadrature Partial Response 19 p2831 A83-41377

A new wideband HF technique for MHz-bandwidth spread-spectrum radio communications 24 p3570 A83-48994

EQUATIONS OF MOTION

NT EULER EQUATIONS OF MOTION

NT HELMHOLTZ VORTICITY EQUATION

NT HYDRODYNAMIC EQUATIONS

NT KINEMATIC EQUATIONS

NT KINETIC EQUATIONS

NT NAVIER-STOKES EQUATION

NT REYNOLDS EQUATION

On spinor equations of motion and their 'possible integrals' 01 p0017 A83-10262

Estimating three-dimensional motion parameters of a rigid planar patch 01 p0097 A83-11419

Perfect fluids in general relativity 02 p0233 A83-12026

Light rays in gravitating, refractive media 02 p0233 A83-12138

Allowance for nonstationary and nonlinear terms in the equations of motion in regard to the solution of problems of ionospheric modeling 02 p0209 A83-12424

A similarity analysis of the droplet trajectory equation 03 p0315 A83-13133

Analysis of some degenerate quadruple collisions 03 p0389 A83-13410

A generalization of Szebehely's equation for three dimensions 03 p0405 A83-13422

Equivalence principle for massive bodies in a generalized theory of gravitation. I, II 03 p0417 A83-13494

On the conditions for the intersection of a satellite orbit with a conical shadow 03 p0407 A83-13669

The dynamical evolution of clusters of nonpoint bodies 03 p0419 A83-13897

Dynamic analysis of multirigid-body system based on the Gauss principle 03 p0391 A83-14509

Ballistic entry motion, including gravity - Constant drag coefficient case 03 p0283 A83-14839

Bounded motion for a modified three-body problem 04 p0545 A83-14985

Investigation of the equations of motion of the heliostats of a tower-type solar electric power plant 04 p0503 A83-15133

The passage of a star by a massive black hole 04 p0554 A83-15638

The reduction of a system of differential equations for the motion of a satellite that is dynamically compressed relative to the center of mass to a special form 04 p0451 A83-15771

A computational method for performing the multiblade coordinate transformation 04 p0446 A83-16029

Robustness of the independent modal-space control method 04 p0528 A83-16116

On resonance in celestial mechanics /A survey/ 04 p0548 A83-16359

SYMBOD - A computer program for the automatic generation of symbolic equations of motion for systems of hinge-connected rigid bodies [AIAA PAPER 83-0013] 05 p0678 A83-16463

On the possibility of balancing rotating flexible shafts 05 p0653 A83-17724

On equations of motion for cross term modified gravitational field equations 05 p0703 A83-17860

On the resonant nonlinear traveling waves in a thin rotating ring 06 p0770 A83-17975

Investigation of regions of the possibility of motion in mechanical systems 06 p0805 A83-17979

Relativistic perturbations of the moon in ELP 2000 06 p0817 A83-18084

Rotor blade flap-lag stability in turbulent flows 06 p0716 A83-18380

Stochasticity in plasmas with electromagnetic waves 06 p0812 A83-18918

Gyro motion boundedness under uncertain angular acceleration about vehicle output axis 06 p0723 A83-19034

The effect of the force structure on the stability of a linear system 06 p0806 A83-19550

A class of soliton solutions of the hydrodynamic equations of motion for ions in a uniform plasma without external fields 07 p0995 A83-20060

On an analogy to the Steklov case for a balanced gyrostat in a Newtonian gravitational force field 07 p0988 A83-20145

Behavior of magnetic dynamic absorber 07 p0945 A83-20282

Optimization of solutions of the equations of motion of shells of revolution to enhance the dynamic-stability parameters 07 p0946 A83-20897

Tether deployment dynamics 07 p0869 A83-21426

Canonical formalism for relativistic dynamics 08 p1160 A83-22010

Real time estimation of ship motions using Kalman filtering techniques 08 p1158 A83-22720

A general method for the solution of self-consistent equations of motion and Maxwell equations 09 p1253 A83-23487

On conditions of the existence of certain classes of solutions of the problem of the motion of a rigid body with a fixed point 09 p1337 A83-23551

Kinematic interpretation of the motion of a gyrostat in one solution of E. I. Kharlamova 09 p1337 A83-23552

Isoconic motions of a rigid body with a fixed point 09 p1337 A83-23553

Construction of a complete solution for one problem of rigid-body dynamics 09 p1337 A83-23554

Motion of a Kovalevskaja gyroscope in the Delaunay case 09 p1337 A83-23555

Methods for the investigation of rigid-body motions and their application to the classification of motions 09 p1337 A83-23556

On an attempt to generalize the Hess solution of the problem concerning the motion of a heavy rigid body with a fixed point 09 p1337 A83-23557

On certain motions of a system of three Lagrange gyroscopes 09 p1337 A83-23558

Stationary motions of two linked bodies 09 p1337 A83-23559

Asymptotic properties of certain motions of an asynchronous gyroscope in a gimbal suspension 09 p1337 A83-23560

Investigation of the sufficient and necessary conditions of the stability of the uniform rotations of a gyrostat about the principal axis 09 p1337 A83-23561

Sufficient conditions of the stability of the regular precessions of a system of n Lagrange gyroscopes 09 p1337 A83-23562

The use of invariant relationships to reduce the order of the system of equations of motion of a vortex-filled heavy rigid body 09 p1337 A83-23564

The representation of a matricant of a linearized system of differential equations of motion in a field of forces possessing potential 09 p1338 A83-23865

Integrable Hamiltonian systems. I - Methods for the integration of Hamiltonian systems. II - Series of integrable systems 09 p1340 A83-25266

Component mode analysis of nonlinear, nonconservative systems [ASME PAPER 83-APM-1] 10 p1472 A83-26447

Equations of motion of the problem of two bodies with variable masses 11 p1669 A83-27453

On the regularization of the Hill problem 11 p1673 A83-28031

Stability criteria in many-body systems. III - Empirical stability regions for corotational, coplanar, hierarchical three-body systems 12 p1786 A83-29108

Stability criteria in many-body systems. IV - Empirical stability parameters for general hierarchical dynamical systems 12 p1786 A83-29109

Solution of equations of problem of motion of a heavy rigid body about a fixed point in the Kowalevskaya's case using theta-function 12 p1775 A83-29115

General equations of motion for an elastic wing and method of solution 12 p1743 A83-29847

Influence of mass representation on the modal analysis of rotating flexible structures [AIAA 83-0915] 12 p1745 A83-29889

Towards a closer cooperation between theoretical and numerical analysis in gas dynamics 12 p1698 A83-29936

Equation of motion for a small rigid sphere in a nonuniform flow 13 p1839 A83-30104

Theory of motion of Saturn's coorbiting satellites 13 p1939 A83-31204

The stability of motion with respect to some of the variables under continuous perturbations 14 p2079 A83-32357

Superintegrability of the Calogero-Moser system 15 p2225 A83-34136

General solution of the Clemmow equation in a three-dimensional cold plasma, with a zero-velocity stream 15 p2235 A83-34273

On physical and material conservation laws 15 p2177 A83-34335

Equations of motion of gyropendulum systems in Rodrigues-Hamilton parameters 15 p2226 A83-34428

The stability of stationary motions of systems of a certain type 15 p2226 A83-34431

A study of the engineering stability of a system of coupled bodies with damping elements 16 p2316 A83-35931

Relativistic rocket motion via Minkowski's formalism 17 p2472 A83-37071

The effect of stochastic modulations on the stability characteristics of hydrodynamic flows --- German thesis 17 p2504 A83-37501

The inertial motion of a gyrost at about a fixed center of mass 17 p2576 A83-38073

Estimation of the value of the small parameter in a linear singularly perturbed system of differential equations 17 p2571 A83-38074

The Hamilton-Jacobi equation and its complementary form 18 p2741 A83-39148

Integrals of motion for the classical two-body problem with drag 18 p2644 A83-39568

Dynamics of momentum biased spacecraft in a near-polar orbit 19 p2809 A83-41143

The effect of coupling between the heat equation and the equations of motion in case of shock-like temperature stresses 20 p3005 A83-42985

Approximate solutions of the equations of motion of a charged particle in the field of a magnetic dipole 20 p3050 A83-43394

Time integration of the equations of motion of a structural system including damping 20 p3007 A83-43448

Discrete mechanics - Some remarks --- numerical method in celestial mechanics 20 p3062 A83-43573

A linear solution of the equations of motion of an earth-orbiting satellite based on a Lie-series 20 p2944 A83-43578

Equations of motion of the restricted problem of three bodies with variable mass 20 p3062 A83-43579

The dynamic analysis of a structure having discrete dampers 21 p3151 A83-44106

Time integration of the motion equations of a damped structure 21 p3152 A83-44359

On the reduction of the order of equations of motion of gyrost at in an axisymmetric field 21 p3199 A83-44461

The use of complex normal coordinates during an investigation of nonlinear systems by the averaging method --- equations of motion for vibration 21 p3199 A83-44638

Structure of the phase space and bifurcations of the equation of motions of a magnetized satellite in a circular-polar-orbit plane 21 p3103 A83-45278

A method of obtaining equations of motion for a dynamically tunable gyroscope 21 p3142 A83-45353

New nonsingular forms of perturbed satellite equations of motion 21 p3095 A83-45469

An analysis of the processes occurring at the cathode of a magnetron oscillator under orbital resonance 22 p3276 A83-45665

Exact solution of some discrete stochastic models with chaos 22 p3354 A83-45936

Stability of rotating liquid drops. I - Uncharged drops 22 p3280 A83-46001

Stability analysis of the motion along re-entry optimal trajectories [IAF PAPER 83-332] 23 p3417 A83-47345

Added fluid mass and the equations of motion of a parachute 23 p3398 A83-48145

A partitioned finite element method for dynamical systems 23 p3471 A83-48166

The dynamics of a rigid body suspended by a string 23 p3504 A83-48451

Equations in Rodrigues-Hamilton parameters for a heavy rigid body rotating about a stationary point 23 p3504 A83-48452

Cases of integrability of equations for the inertial motion of two bodies connected by means of a spherical joint 23 p3504 A83-48453

Stability of the periodic oscillations of a nearly axisymmetrical satellite in the plane of an elliptical orbit 23 p3418 A83-48455

Equations for the small oscillations of an inertial navigation system with allowance for the ellipsoidal of the earth 23 p3421 A83-48456

On some treatment of the equations of motion for cylindrical shells based on an improved theory 23 p3473 A83-48497

The Lie-series method in the problem of the separation of motions in nonlinear mechanics 23 p3505 A83-48527

Practical applications of system identification in flutter testing 24 p3550 A83-49182

Regularization and linearization of the equations of motion in central force-fields 24 p3551 A83-49395

Dynamics of a mobile tank partially filled with liquid

Equations of motion and their linearization 24 p3581 A83-50124

EQUATIONS OF STATE

NT HUGONOT EQUATION OF STATE

Equation of state and phase equilibrium curve for liquid-vapor systems 02 p0243 A83-11657

Eigenvalue sensitivity of digital filters based on the expanded state model 02 p0229 A83-11792

Invariance properties under a reciprocal Backlund transformation in gasdynamics 03 p0320 A83-14566

Approximate equation of state for multicomponent gaseous mixtures 04 p0544 A83-15861

State variable representation of a class of linear shift-variant systems 05 p0680 A83-16911

Linear equations of state for an electrically polarized ceramic 06 p0814 A83-17985

Modeling the shock-wave behavior of multicomponent materials --- for powder metallurgy 06 p0727 A83-18011

'Maximally hard' universe and mass spectrum of primordial black holes 06 p0839 A83-19230

Angles of multivariable root loci [LIDS-P-1147] 06 p0803 A83-19320

Irreducible divisors of lambda-matrices and their applications to multivariable control systems 06 p0803 A83-19386

The decay of a plane shock wave in a two-parameter medium described by an arbitrary equation of state 06 p0760 A83-19438

The pi-meson term in the equation of state of hadron systems 06 p0809 A83-19540

A finite state aerodynamic model for a lifting surface in incompressible flow 07 p0862 A83-19802

The distribution of the state variables in the products of spherical detonation 07 p0880 A83-19963

Global transformations of nonlinear systems 07 p0984 A83-20719

Effect of Stark shift on two photon optical bistability 08 p1164 A83-21888

Perfect fluid spheres in general relativity 08 p1180 A83-22207

Equation of state for reinforced plastic materials subjected to mechanical and thermal loading with the account taken of damage and physical-chemical transformations 09 p1224 A83-23945

Simplified robot arm dynamics for control 09 p1328 A83-24712

Questions concerning the solution of a system of condition equations --- for calculation of planetary orbital elements 11 p1673 A83-28038

On the equation of state of solar wind ions derived from Helios measurements 11 p1691 A83-28302

Parastatistics and the equation of state for the early universe 12 p1791 A83-28994

The state equation of superdense degenerate plasma 12 p1793 A83-29067

Stability of periodic solutions of the random vibration equations 12 p1771 A83-29600

Universal equation of state in the theory of strong turbulence 13 p1933 A83-31332

On the construction of K-consistent difference schemes of gas dynamics 13 p1913 A83-31594

Equation of state of sodium at pressures up to 30 GPa 15 p2237 A83-33783

Response of liquid carbon disulfide to shock compression Equation of state at normal and high densities 20 p3055 A83-42638

Lower bounds on neutron star mass and moment of inertia implied by the millisecond pulsar 21 p3234 A83-44768

A thermodynamic approach to equations of state and melting at mantle and core pressures 22 p3324 A83-45799

The quadrupole oscillations of neutron stars 22 p3377 A83-46260

The radial oscillations of neutron stars 22 p3377 A83-46261

State-space analysis of the dynamic characteristics of a variable thrust liquid propellant rocket engine [IAF PAPER 83-ST-06] 23 p3426 A83-47385

Application of a method of averaging to the study of dithers in non-linear systems 23 p3502 A83-48646

EQUATORIAL ATMOSPHERE

The small-scale turbulence spectrum of the high-latitude and equatorial ionosphere 02 p0203 A83-11679

The role of cross-equatorial tropical cyclone pairs in the southern oscillation 02 p0218 A83-13057

Rocket-borne investigations of the optical emissions of the equatorial ionosphere during periods of moderate and high geomagnetic activity 03 p0356 A83-13220

The tropospheric gas composition of Jupiter's north equatorial belt /NH₃, PH₃, CH₃D, GeH₄, H₂O/ and the Jovian D/H isotopic ratio 04 p0569 A83-15643

Electromagnetic resonances in the equatorial ionosphere 04 p0510 A83-15823

Coordinated airborne and satellite measurements of equatorial plasma depletions [AD-A123689] 05 p0661 A83-17400

Stability dependence of fluxes and bulk transfer coefficients in a tropical boundary layer 06 p0788 A83-18061

Theory of the mesopause semiannual oscillation 06 p0782 A83-18253

Vertical ionization drift velocities and range type spread F in the evening equatorial ionosphere 06 p0785 A83-18308

The low- and equatorial-latitude ionosphere at a height of 500 km in the course of magnetospheric-ionospheric disturbances during September-December 1977 /according to data from the Cosmos-900 satellite/ 06 p0786 A83-18359

A correlation between measured E-region current and geomagnetic daily variation at equatorial latitude 07 p0966 A83-21429

Nighttime VHF and GHz scintillations in the East-Asian sector of the equatorial anomaly 07 p0967 A83-21558

F-region neutral winds and temperatures at equatorial latitudes - Measured and predicted behaviour during geomagnetically quiet conditions 07 p0968 A83-21580

Cloud height differences on Saturn 08 p1189 A83-22934

Stratospheric warming following the El Chichon volcanic eruption 08 p1138 A83-23276

On the equatorial transport of Saturn's ionosphere as driven by a dust-ring current system 09 p1365 A83-24339

VHF amplitude scintillations and associated electron content depletions as observed at Arequipa, Peru [AD-A126952] 09 p1306 A83-24688

Monsoon and teleconnection variability over Australasia during the Southern Hemisphere summers of 1973-77 10 p1450 A83-25386

A morphological study of gigahertz equatorial scintillations in the Asian region 10 p1449 A83-26046

Atmospheric balance of sulphur above an equatorial forest 11 p1615 A83-27671

Theoretical study of multiple equilibria in simple axisymmetric tropical circulations 11 p1633 A83-28087

Influence of the E region dynamo on equatorial spread F 11 p1618 A83-28319

Conjugate studies of an isolated equatorial irregularity region [AD-A127561] 11 p1618 A83-28320

Auroral riometer absorptions and the F-region disturbances observed over a wide range of latitudes 12 p1754 A83-29436

On the quasi-biennial oscillation in equatorial stratospheric temperatures and total ozone 12 p1756 A83-29581

A payload for the study of electric fields and electron density in the equatorial region 13 p1814 A83-30759

The resonance cone technique for exciting electron acoustic waves in equatorial ionosphere 13 p1814 A83-30765

Equatorial depletions in the 630.0 nm airglow at Vanimo --- New Guinea 13 p1881 A83-31538

The effect of the electrodynamic drift caused by magnetospheric processes on the structural features of the polar and equatorial ionosphere 14 p2054 A83-33036

Latitudinal and magnetic flux tube extension of the equatorial spread F irregularities 15 p2195 A83-33938

On the generation and growth of equatorial backscatter plumes. II - Structuring of the west walls of upwellings 15 p2195 A83-33939

Seasonal and solar-related cyclic variations of equatorial F-scattering 15 p2200 A83-34418

Some characteristics of the F2 layer at low and middle latitudes 15 p2200 A83-34419

Study of the deep cloud structure in the equatorial region of Jupiter from Voyager infrared and visible data 15 p2275 A83-34719

Electric field and electron density measurements in the equatorial E-region 16 p2373 A83-35367

In situ studies of electron density during equatorial spread-F 16 p2374 A83-35387

Equatorial F-region ionization differences between March and September, 1979 16 p2375 A83-35388

Mesospheric ionisation over dip equator at sunrise 16 p2375 A83-35392

A nonsymmetric equatorial inertial instability 16 p2385 A83-35476

On symmetric stability and instability of zonal mean flows near the equator 16 p2386 A83-35481

A first order vorticity equation for tropical easterly waves 16 p2386 A83-35486

Interaction of the Monsoon and Pacific Trade Wind System at interannual time scales. I - The equatorial zone 16 p2388 A83-36033

Characterization of the atmospheric aerosol over the eastern equatorial Pacific 16 p2380 A83-36149

Equatorial propagation of axisymmetric magnetogasdynamic shocks with increasing energy. I --- in sun 16 p2440 A83-36542

Discrete chorus emissions recorded at Nainital 16 p2381 A83-36617

Narrow band characteristics of low latitude VLF hiss 16 p2344 A83-36730

Equatorial radio scintillations of ATS-6 beacons-phase. I Huancayo 1974-75 16 p2344 A83-36735

The morphology of a multi-bubble system in the ionosphere 17 p2538 A83-37579

Geometry of depleted plasma regions in the equatorial ionosphere 17 p2539 A83-37606

Near-equatorial magnetospheric particles from approximately 1 eV to approximately 1 MeV 17 p2541 A83-38293

Loss cone fluxes and pitch angle diffusion at the equatorial plane during auroral radio absorption events 17 p2543 A83-38372

Solar cycle effects on radio scintillations at Huancayo 17 p2545 A83-38536

A comparative study of some aspects of low and middle latitude ionospheric absorption 17 p2545 A83-38540

Equatorial radio scintillations of ATS-6 radio beacons. Phase II - Ootacamund 1975-76 17 p2545 A83-38542

The stochastic instability of high-energy protons of the inner radiation belt at low altitudes 18 p2786 A83-39314

Features of the propagation of whistlers in magnetospheric ducts in the equatorial region. I - Ducts with high density 18 p2714 A83-39323

The effect of the conductivity of the E-region on the growth increment of the Rayleigh-Taylor instability in the ionospheric plasma of the equatorial F-region 18 p2714 A83-39331

Ionospheric scintillations 18 p2720 A83-40658

Equatorial disturbance dynamo electric fields 19 p2864 A83-41117

Ionospheric conditions affecting the evolution of equatorial plasma depletions 19 p2864 A83-41118

Variability of the ocean and atmospheric in the equatorial Atlantic (FGGE investigations) 19 p2869 A83-42101

Meteorological investigations during the voyages of the research vessels Akademik Kurchatov and Professor Shtokman in the FGGE program 19 p2868 A83-42114

Variability of meteorological fields in the equatorial Atlantic 19 p2868 A83-42115

Precipitation patterns in the equatorial Atlantic 19 p2868 A83-42117

Radiation studies in the equatorial Atlantic 19 p2867 A83-42119

The structure of the atmosphere in the equatorial zone of the Atlantic in the spring and summer of 1979 19 p2869 A83-42120

Retarding layers in the troposphere over the equatorial Atlantic 19 p2869 A83-42122

Water-vapor content of the near-equatorial atmosphere over the Atlantic Ocean during March-August 1979 19 p2869 A83-42123

Weather conditions in the center of the equatorial Atlantic in the spring of 1979 19 p2869 A83-42124

Polarization fluctuations of VHF transionospheric signal near the crest of the equatorial anomaly 20 p3017 A83-42313

Equatorial ionospheric currents derived from MAGSAT data 20 p3026 A83-43212

A statistical study of the dynamics of the equatorward boundary of the diffuse aurora in the pre-midnight sector 20 p3026 A83-43214

Modeling of the equatorial ionosphere in the hybrid model 21 p3176 A83-45258

Localized plasma depletion in the ionosphere and the equatorial spread F 22 p3334 A83-46888

Modeling the total electron content observations above Ascension Island 22 p3337 A83-47064

EQUATORIAL ELECTROJET

Global dynamo simulation of ionospheric currents and their connection with the equatorial electrojet and counter electrojet - A case study 06 p0783 A83-18296

Regional variations of equatorial electrojet parameters 08 p1134 A83-22308

An investigation of the equatorial electrojet by means of ground-based magnetic measurements in Brazil 08 p1134 A83-22309

Effect of the equatorial counter-electrojet in the Indian region on the geomagnetic solar and lunar daily variations 08 p1134 A83-22310

Studies of the external origin component of Sq by 'canonical' GDS analysis --- Geomagnetic Depth Sounding 08 p1134 A83-22313

The variation of the magnetic field and its interaction with the equatorial electrojet in eastern Senegal 08 p1135 A83-22314

Short wavelength stabilization of the gradient drift instability due to velocity shear --- in equatorial electrojet 12 p1779 A83-28921

Unified theory of type I and type II irregularities in the equatorial electrojet 15 p2195 A83-33937

Spectral characteristics of the geomagnetic field associated with the equatorial electrojet and counter-electrojet in the Indian region 16 p2382 A83-36729

Some features of annual variation in the equatorial geomagnetic field 16 p2382 A83-36733

Depth of the nonconducting layer at the Nigerian dip equator 17 p2537 A83-37578

Lunar modulations of the equatorial electrojet 17 p2544 A83-38373

Dynamo region and the equatorial electrojet in the Jovian atmosphere 17 p2623 A83-38517

The relationship between indices AE and Dst --- reflecting intensities of equatorial ring current and auroral electrojet due to geomagnetic disturbances 21 p3173 A83-44583

Nonlinear theory of type I irregularities in the equatorial electrojet 23 p3482 A83-47869

EQUATORIAL ORBITS

NT STATIONARY ORBITS

Poisson series solution of geosynchronous drift [AIAA PAPER 83-0016] 05 p0601 A83-16465

Optimization of the equatorial transfer orbit with an allowance made for atmospheric drag 09 p1212 A83-24487

On the equatorial orbits of a satellite of a triaxial attracting rigid body 09 p1212 A83-25044

EQUATORIAL REGIONS

On the relationship of the plasmopause to the equatorward boundary of the auroral oval and to the inner edge of the plasma sheet 02 p0207 A83-12380

Raindrop size distribution from microwave scattering measurements in equatorial and tropical climates 04 p0466 A83-15239

Observations of parallel ion energization in the equatorial region 05 p0661 A83-17404

The formation of albedo-electron fluxes in the geomagnetic field 05 p0662 A83-17603

The induced effects of geomagnetic variations in the equatorial region 05 p0665 A83-17866

High resolution topside in situ data of electron densities and VHF/GHz scintillations in the equatorial region [AD-A125353] 06 p0785 A83-18309

Equatorial long waves in geostationary satellite observations and in a multichannel sea surface temperature analysis 08 p1144 A83-22704

Synoptic oscillations of the currents in the FGGE Atlantic equatorial test-region 09 p1320 A83-24941

The electrophotometry of Saturn. I - The distribution of brightness over the equatorial regions in the spectral range of 0.3-0.6 micron 14 p2095 A83-31837

Role of neutral winds in generating irregularities in equatorial F-region 16 p2374 A83-35378

Gigahertz scintillations associated with equatorial patches [AD-A129919] 16 p2341 A83-35417

The effect of islands on low frequency equatorial motions 16 p2393 A83-36976

Saturn's equatorial haze 17 p2620 A83-38113

Equatorial oceanography --- review of research 17 p2554 A83-38322

Spatial-temporal variability of the optical attenuation coefficient of sea water 19 p2870 A83-42106

Observations and modeling of multi-frequency VHF and GHz scintillations in the equatorial region 22 p3327 A83-46046

Numerical simulation of the atmospheric response to equatorial Pacific sea surface temperature anomalies 22 p3340 A83-46844

Interannual variability of the equatorial Pacific - Revisited 22 p3344 A83-46910

Bottomside sinusoidal irregularities in the equatorial F region 22 p3337 A83-47065

EQUATORS

NT MAGNETIC EQUATOR

Distances from auroral zones to the magnetic and geographic equators 02 p0205 A83-11971

New absolute spectroscopic measurement of the solar equatorial rotation rate 15 p2281 A83-34308

EQUILIBRIUM

Collinear relative equilibria of the planar n-body problem 03 p0404 A83-13407

Sufficient indicators of the stability of the equilibrium position and of the existence of limit cycles in nonlinear systems 06 p0807 A83-19604

Synthesis and thermal stability of carborane-containing phosphazenes 23 p3427 A83-47640

EQUILIBRIUM DIAGRAMS

U PHASE DIAGRAMS

EQUILIBRIUM EQUATIONS

A bimodal Maxwellian distribution as the equilibrium solution of the two-particle regime 03 p0399 A83-13117

A comparison of methods for determining turning points of nonlinear equations 04 p0530 A83-15699

Some general methods for constructing different versions of the shell theory --- Russian book 05 p0654 A83-17128

Symmetry and bifurcation in three-dimensional elasticity. I 06 p0776 A83-18928

Impulsive loading of a cylindrical shell with transverse shear and rotatory inertia 11 p1594 A83-28412

Emden-Chandrasekhar axisymmetric, solid-body rotating polytropes. II - Power series solutions to EC associated equations of degree 0 and 2 12 p1793 A83-29070

Non-axisymmetric magnetostatic equilibrium --- in sunspot structures 13 p1963 A83-29879

Certain relationships for operators constructed on the basis of the Green tensor of the equilibrium equation and their use in the theory of composites 15 p2178 A83-34442

Parallel solution of finite element equations 16 p2403 A83-36721

The equilibrium structure of loaded rotating polytropes --- in astronomical bodies study 18 p2764 A83-39000

A singular approximation in the theory of elastoplastic media with microstructures 19 p2858 A83-41218

An equilibrium model finite element analysis for buckling of moderately thick plates 21 p3151 A83-44105

The structure of a equilibrium magnetotail 21 p3172 A83-44505

H-theorem and trend to equilibrium in the kinetic theory of gases 21 p3220 A83-44942

Harmonic acceleration method for dynamic structural analysis 23 p3471 A83-48165

Galerkin method as a tool to investigate the planar and non-planar behavior of curved beams 23 p3471 A83-48171

Elliptic stellar disks - Equilibrium solutions in the presence of a halo and in binary systems 24 p3653 A83-49165

Characterization of equilibrium sets for bilinear systems with feedback control 24 p3621 A83-49923

EQUILIBRIUM FLOW

Stationary shape of bodies ablating in hypersonic flow under the action of radiation heating 04 p0477 A83-15863

A three-dimensional hypersonic gas flow over a slender wing 05 p0589 A83-17412

A note on the logarithmic velocity profile in turbulent boundary layers 08 p1083 A83-21895

Theoretical study of multiple equilibria in simple axisymmetric tropical circulations 11 p1633 A83-28087

The influence of a coastal headland on oceanic boundary currents 15 p2208 A83-34325

A local equilibrium axiom on the flows in relativistic thermodynamics 15 p2239 A83-34410

Stability of relativistic laminar flow equilibria for electrons drifting in crossed fields 17 p2496 A83-37042

Calculation of shock-layer parameters for the hypersonic flow of equilibrium-dissociated air around bodies with bends of the generatrix 19 p2791 A83-41881

EQUILIBRIUM METHODS

Stability of the elastic equilibrium of an infinite plate in the vicinity of a randomly oriented rectilinear crack under plane-stressed state 01 p0059 A83-10684

- The critical equilibrium of a simply supported cylindrical glass-reinforced plastic shell 01 p0059 A83-10689
 A new formulation of hybrid/mixed finite element 02 p0193 A83-12739
 On the theory of stress-assisted diffusion, II 11 p1593 A83-27865
 Numerical problems of nonlinear stability analysis of elastic structures 11 p1599 A83-28719

EQUINOXES

- Dependence of an equinoctial analytical model of ionospheric electron density on solar activity 02 p0209 A83-12423
 Orientation of the JPL Ephemerides, DE 200/LE 200, to the dynamical equinox of J 2000 03 p0410 A83-14763
 Note on the relation between the equinox and Guinot's non-rotating origin 12 p1787 A83-29122
 The semi-diurnal tide at the equinoxes - MF radar observations for 1978-1982 at Saskatoon (52 deg N, 107 deg W) 16 p2386 A83-35487

EQUIPARTITION THEOREM

- Column accretion on to white dwarfs 06 p0827 A83-18168
 Evolution toward equipartition in galaxy clusters and its effect on virial M/L estimates 11 p1681 A83-28271

EQUIPMENT

- The definition of short-period flying qualities characteristics via equivalent systems 14 p1977 A83-32578

EQUIPMENT SPECIFICATIONS

- Commonly misunderstood ATE instrument specifications 01 p0050 A83-10789
 A topological approach to the unification of electromagnetic specifications and standards 01 p0041 A83-11084
 The reliability of the engines of flying vehicles --- Russian book 03 p0289 A83-13813
 Photovoltaic systems measurements - Status and perspectives 04 p0504 A83-15461
 Experience with specifications applicable to certification --- of photovoltaic modules for large-scale application 04 p0504 A83-15463
 ATE accomplishes receiver specification testing with increased speed and throughput 04 p0474 A83-16398
 The agency's approach to normalisation and standards --- for ESA space technology 05 p0621 A83-17435
 Testing explosive ordnance devices for space application 13 p1826 A83-31191
 Effects of fine airborne particles on equipment reliability 13 p1863 A83-31500
 MIL-STD-810D - A progress report 13 p1863 A83-31502
 Cost effective utilization of environmental design criteria; MIL-STD-210B updated 13 p1863 A83-31503
 MIL-STD-810D - A climatic testing update --- environment simulation 13 p1864 A83-31515
 Features and testing of clean room apparel 13 p1865 A83-31525
 Communications performance specifications of the INTELSAT V with maritime communications subsystem 17 p2494 A83-37796
 Guide for qualification testing of aircraft air valves [SAE ARP 986A] 17 p2443 A83-38101
 Component qualification and initial build of the AGT 100 advanced automotive gas turbine [ASME PAPER 83-GT-225] 23 p3465 A83-48023

EQUIVALENCE

- Equivalence principle for massive bodies in a generalized theory of gravitation. I, II 03 p0417 A83-13494
 Equivalence and singularities - An application of computer algebra --- metric calculation in general relativity 12 p1776 A83-29645
 Astrophysical consequences of a violation of the strong equivalence principle 20 p3063 A83-42166
 The method of equivalent systems in the theory of wave propagation --- Russian book 21 p3199 A83-43906
 Test of the principle of equivalence by a null gravitational red-shift experiment 22 p3380 A83-46714

EQUIVALENT CIRCUITS

- Fluxon propagation in Josephson junction transmission lines coupled by resistive networks 01 p0036 A83-10639
 Effects of stray capacitances between transformer windings on the noise characteristics in switching power converters 01 p0040 A83-11012
 Radio-frequency devices based on p-n-p-n transistor equivalents --- Russian book 02 p0167 A83-11973
 Notes on the theory of linear, time-discrete signal processing with a rational sampling rate conversion. I 02 p0165 A83-12989
 Microwave switching with GaAs FETs 03 p0308 A83-13438

- A method of calculating the 'cold' parameters of slow-wave structures of the type comprising networks of coupled resonators 04 p0469 A83-15139

- System analysis of eddy-current measurements 04 p0491 A83-15190
 Equivalent circuit of a coaxial-waveguide junction 04 p0471 A83-15732

- Study of electrical faults in magnetohydrodynamic Faraday generators 04 p0538 A83-16106
 Impedance transformation in fin lines 04 p0474 A83-16209

- Theory of traveling-wave transistors 06 p0752 A83-18753
 CIECA - Application to current programmed switching Dc-Dc converters --- Current Injection Equivalent Circuit Approach 06 p0753 A83-19028

- Input devices for CCDs 06 p0754 A83-19351
 Linear induction motor - Equivalent-circuit model 07 p0916 A83-19630

- Equivalent circuit for an electrostatic probe 07 p0928 A83-20064
 Equivalent circuit of a microwave transition connecting rectangular and circular waveguides 07 p0920 A83-20675

- Improved equivalent network analysis of a dielectric waveguide placed on a ground plane 07 p0922 A83-21173
 Operation and applications of linear pyroelectric arrays 08 p1101 A83-22611

- Variable-structure systems and system zeros 08 p1158 A83-23018
 Measurement of series resistance in IMPATT diodes 09 p1256 A83-24500

- A method of analyzing nonlinear phenomena in radio-receiving apparatus 09 p1257 A83-25159
 The loop antenna with a cylindrical core - Theory and experiment 10 p1405 A83-26826

- Representation of coupled-cavity slow-wave structures by equivalent circuits 12 p1719 A83-29418
 Power MOSFET dynamic large-signal model 12 p1719 A83-29419

- Large-signal, dynamic, negative conductance of gunn devices in sharpless flanges 13 p1831 A83-30229
 Microwave circuit models of semiconductor injection lasers 13 p1849 A83-30232

- Mathematical representation of microwave oscillators by use of the Fliecke diagram 13 p1834 A83-30786
 Stability of override control systems 14 p2074 A83-31928

- Non linear model for shunt current in terrestrial silicon solar cells 14 p2004 A83-32244
 Exact analysis of class E tuned power amplifier with only one inductor and one capacitor in load network 15 p2151 A83-33893

- Electronic circuits for the simulation of physical processes in semiconductor structures by the method of direct analogies 16 p2347 A83-36904
 The Q-value and resistance of the heliospheric resonator model for the 22-year solar cycle 17 p2628 A83-38524

- Phototransistors in digital optical communication systems 19 p2899 A83-40949
 Determination of the parameters of the equivalent circuit of the active region of an FET crystal 20 p2967 A83-42914

- Nonlinear lumped circuit model of GaAs MESFET 20 p2968 A83-43354
 Measurement and modeling of the apparent characteristic impedance of microstrip 21 p3122 A83-43831

- Equivalent-circuit consideration of dual-gate MESFETs at high frequency 21 p3126 A83-44970
 Functional analog integrated microcircuits --- Russian book 21 p3126 A83-45017

- Equivalent ionospheric current systems representing lunar daily variations of the polar geomagnetic field 22 p3327 A83-46052
 An active dummy cell for use in corrosion studies 22 p3267 A83-46701

- Distributed-parameter solar cells - Volt-ampere characteristics under uniform and nonuniform illumination 23 p3477 A83-48397
 Simulators for solving internal inverse heat-conduction problems 24 p3620 A83-50205

- A method for the simulation of the transfer of charge carriers and the distribution of electrostatic potential in semiconductor structures 24 p3575 A83-50208

- ERBE**
 U EARTH RADIATION BUDGET EXPERIMENT

- ERBIUM**
 Reversible nonradiative transfer of excitation energy in a system of strongly interacting particles --- in laser materials 01 p0055 A83-10817

- Erbium glass lasers and their applications 11 p1583 A83-27620

- Channels of energy losses in erbium laser glasses in the stimulated emission process 19 p2853 A83-41186
 Steady-state emission from a Y3Al5O12:Er(3+) laser (lambda = 2.94 microns, T = 300 K) 20 p2998 A83-43806

- ERBIUM ALLOYS**
 Formation and thermal stability of an oxide dispersion in a rapidly solidified Ti-Er alloy 18 p2668 A83-40618

- ERBIUM COMPOUNDS**
 Phase relations and ordering in the system erbia-hafnia 08 p1070 A83-22191

- Operating characteristics of thin thermophotovoltaic cells with minority carrier mirrors and optical mirrors using selective radiators of erbium and ytterbium oxides 14 p2089 A83-32270

- ERECTION**
 U CONSTRUCTION

- ERGATIC PROCESS**
 Ordered and ergodic motions of stars in galaxies 07 p1008 A83-21215

- Choice of parameters for ergatic stabilization systems 20 p3035 A83-43501
 Determination of physically achievable accelerations in the problem of the spatial convergence of a material point --- for ergatic control system synthesis 20 p3035 A83-43502

- Informational evaluation of operator activity in an ergatic system with a learning model 20 p3035 A83-43503
 On the problem of manual control. I 20 p3036 A83-43504

- Application of factor-analysis methods to evaluate the quality of ergatic control systems --- of aircraft landing by human operator 20 p3036 A83-43508
 On the design of ergatic systems for the solution of a two-goal game-theoretical problem of control 20 p3036 A83-43509

- Phase distribution and ergodicity relative to the spatial variable in scattered fields 21 p3201 A83-45506
 Ergodic stream-lines in steady convection 23 p3449 A83-48199

- ERGOMETERS**
 The W170 differentiating test --- arm and leg veloergometer tests 01 p0084 A83-11389

- A nomogram for determining the conditions of the step test --- for physiological loads on bicycle ergometers 05 p0677 A83-17158
 A device controlling the timing and frequency of physical loads 05 p0677 A83-17169

- The diagnostic value of a test with graded physical load for several heart rhythm disorders 14 p2071 A83-33337
 A constant-velocity cycle ergometer for the study of dynamic muscle function 19 p2885 A83-41139

- ERGONOMICS**
 U HUMAN FACTORS ENGINEERING

- EROSION**
 NT RAIN EROSION
 NT SOIL EROSION
 NT WATER EROSION
 NT WIND EROSION

- MPD thruster erosion measurements [AIAA PAPER 82-1884] 02 p0143 A83-12469
 A direct-measurement technique for estimating discharge-chamber lifetime --- for ion thrusters [AIAA PAPER 82-1908] 02 p0144 A83-12483

- Bank erosion and flood plain studies of the Annapolis River - An application of remote sensing data 03 p0348 A83-14262
 New method for monitoring and correlating cavitation noise to erosion capability 04 p0478 A83-16138

- A method of predicting the performance deterioration of a compressor cascade due to sand erosion [AIAA PAPER 83-0178] 05 p0596 A83-16572
 Mapping erosion with airphotos - Panchromatic or black and white infrared 05 p0657 A83-17839

- A model for the accumulation of solar wind radiation damage effects in lunar dust grains, based on recent results concerning implantation and erosion effects 07 p1033 A83-21305
 The Manicouagan impact structure - An analysis of its original dimensions and form 07 p0950 A83-21315

- High temperature erosion and erosion-hot corrosion of superalloys and coatings 07 p0892 A83-21458
 Characterization of particle rebound phenomena in the erosion of turbomachinery 08 p1073 A83-22165

- Processes occurring in an erosion plasma during laser vacuum deposition of films. I - Properties of a laser erosion plasma in the inertial-expansion stage. II - Interaction of laser erosion products with the solid surface 09 p1348 A83-23991

- An example of the application of a procedure for determining the extent of erosional and depositional features and rock and soil units in the Kharga Oasis Region, Egypt, using remote sensing 09 p1290 A83-24603

Ablative radome materials thermal-ablation and erosion modeling 09 p1239 A83-24964

Erosion resistance of Co-Cr-Al coatings containing active element additions 10 p1395 A83-25551

The initial stages of cavitation damage and erosion on copper and brass tested in a rotating disk device 11 p1547 A83-27421

Dynamics and mechanism of cavitation erosion on perspex and epoxy resin tested in a rotating disk device 11 p1551 A83-27422

Boundary layer effects on impingement and erosion 11 p1566 A83-27425

Performance deterioration on turbomachinery with presence of solid particles 11 p1525 A83-27477

Solid particle dynamic behavior through twisted blade rows 11 p1525 A83-27478

Two-phase gas-solid particle flow past bodies with allowance for erosion 11 p1569 A83-28540

Particle collisions in the vicinity of an eroding surface 12 p1718 A83-29156

Morphology of ductile metals eroded by a jet of spherical particles impinging at normal incidence 14 p1993 A83-32624

Hypervelocity erosion of carbon-carbon composites by laser simulation [AIAA PAPER 83-1440] 14 p1986 A83-32711

On the correlation between solid-particle erosion and fracture parameters in SiC 15 p2142 A83-35072

Experimental study on the effects of specimen sizes on erosion 15 p2141 A83-35245

Investigation of gas particle flow in an erosion wind tunnel 15 p2162 A83-35246

High temperature erosion study of INCO 600 metal 15 p2141 A83-35247

Effect of sand erosion on the performance deterioration of a single stage axial flow compressor 16 p2304 A83-35854

Experimental research on cavitation erosion for an oscillating wing profile --- German thesis 17 p2493 A83-37497

Cavitation erosion characteristics of poly(methyl methacrylate) in a rotating disk device 19 p2824 A83-41851

The effect of particle shape and size on erosion of aluminum alloy 1100 at 90 deg impact angles 20 p2955 A83-43408

Use of a chromogenic film for aerial photography of erosion features 21 p3135 A83-43896

A critical study of the erosion of an aluminum alloy by solid spherical particles at normal impingement 21 p3112 A83-44375

The erosion of metals 22 p3268 A83-45897

A simple one-dimensional model for primary turbine blade erosion prediction [ASME PAPER 83-GT-164] 23 p3397 A83-47986

Effect of particle rebound characteristics on erosion of turbomachinery components [ASME PAPER 83-GT-169] 23 p3397 A83-47988

A study of the surface deterioration due to erosion --- of gas turbine blades [ASME PAPER 83-GT-213] 23 p3397 A83-48014

Erosion pattern of twisted blades by particle laden flows [ASME PAPER 83-GT-214] 23 p3397 A83-48015

Surface damage in ceramics - Implications for strength degradation, erosion and wear 23 p3438 A83-48301

Investigation of signs of erosion of agricultural lands on the basis of aerial and space remote sensing data (using the southwestern spurs of the Gissar ridge as an example) 24 p3598 A83-48935

Erosion-corrosion of coatings and superalloys in high velocity hot gases 24 p3562 A83-49481

EROSIVE BURNING

The erosion combustion of a solid fuel under various temperatures of the ventilating flow 07 p0901 A83-19951

Erosive burning of composite solid propellants - Mechanism, correlation, and grain design applications [AIAA PAPER 81-1581] 07 p0902 A83-20418

Burning rate measurements in solid rocket motors [AIAA PAPER 83-0481] 09 p1269 A83-24149

Local admittance measurement in forced longitudinal wave motors --- propellant combustion in solid rocket engines [AIAA PAPER 83-0579] 09 p1220 A83-24150

Effect of erosive burning on pressure and temperature sensitivity --- of composite propellants [IAF PAPER 83-368] 23 p3439 A83-47361

ERROR ANALYSIS

Horizontal correlation of satellite temperature errors 01 p0074 A83-10045

Solution of Burgers' equation with a large Reynolds number 01 p0045 A83-10710

Independent verification & validation /IV & V/ 01 p0103 A83-11112

A dynamic interface error performance simulation - IV&V for the F-4F OGP --- Independent Verification and Validation for Operational Flight Program 01 p0092 A83-11114

Investigating the correlation between reading errors and degraded numerics - Or, do missing dots call the shots 01 p0085 A83-11168

Performance uncertainty analysis 01 p0103 A83-11173

The use of modal control to minimize errors in the analytical reconstruction of flight control sensor signals 01 p0013 A83-11210

Range distance requirements for measuring low and ultralow sidelobe antenna patterns 01 p0033 A83-11366

Error analysis of image representations for sources near to a dissipative earth 01 p0073 A83-11374

Explication of a simple output error based model reference adaptive controller 02 p0229 A83-11791

An experimental determination of the accuracy characteristics of meteorological measurements made by rocket 02 p0213 A83-11979

Fine delay estimation with time integrating correlators 02 p0168 A83-12308

Measurement of the magnetic field components of sea waves 02 p0218 A83-12454

Bit error rate performance of Image Processing Facility high density tape recorders 02 p0179 A83-12681

The hierarchical concept in finite element analysis 02 p0193 A83-12737

Bootstrap stereo error simulations --- autonomous aerial navigation using terrain images 02 p0134 A83-12895

Further developments of Rp and Ap error analysis --- Relative and Absolute precision in floating point arithmetic operations 02 p0231 A83-12926

Assessment of the error in measuring the strength of a constant electric field by the double-Langmuir-probe method 03 p0397 A83-13206

An accurate derivation of the division corrections in a photoelectric meridian circle 03 p0402 A83-13356

On a higher order accurate fully discrete Galerkin approximation to the Navier-Stokes equations 03 p0316 A83-13568

On optimal integration methods for Volterra integral equations of the first kind 03 p0387 A83-13572

Evaluation of Fourier integrals using B-splines 03 p0387 A83-13574

Discrete-analog signal processing --- Russian book 03 p0311 A83-13815

Linear phase-locked loop theory for cyclostationary input disturbances 03 p0311 A83-13854

Performance analysis of digital tanlock loop 03 p0312 A83-13869

Error rates for fading NCFSK signals in an additive mixture of impulsive and Gaussian noise --- noncoherent FSK 03 p0304 A83-13870

Limitations on the calibration of infrared /IR/ transmissometer 03 p0328 A83-13994

Multifocal three-dimensional bootlace lenses 03 p0305 A83-14002

Co-energy methods for elliptic flow and related problems 03 p0384 A83-14080

Optimal interpolation and the Kalman filter --- for analysis of numerical weather predictions 03 p0365 A83-14409

An examination of the characteristics of planetary scale systematic forecast errors 03 p0366 A83-14418

A-posteriori error analysis and adaptive finite element methods for singularly perturbed convection-diffusion equations 03 p0388 A83-14496

Global convergence of output error recursions in colored noise 03 p0386 A83-14592

A tutorial assessment of atmospheric height uncertainties for high-precision satellite altimeter missions to monitor ocean currents 03 p0289 A83-14851

Thermodynamic analysis of causes of differences of values of the thermal conductivity of gases measured by stationary and nonstationary methods 04 p0544 A83-15449

On an evaluation of data impact with respect to Rossby mode in the data assimilation cycle. I - On the impact of satellite wind data with special emphasis on the vertical prediction error correlation 04 p0518 A83-16015

Some accuracy and resolution aspects of computer vision distance measurements 04 p0528 A83-16032

Performance and limits of global models in the Mediterranean 04 p0518 A83-16152

Concerning the processing and the accuracy estimation of results of very long baseline interferometry in a single system of coordinates --- for geodesy 04 p0514 A83-16380

Allowance for the influence of geopotential in the high-precision numerical integration of artificial-earth-satellite orbits 04 p0453 A83-16385

A new technique for the precision DME of microwave landing system 04 p0445 A83-16448

The effect of some systematic errors on the determination of time and latitude, and group corrections 05 p0693 A83-16858

FIR filter structures having low sensitivity and roundoff noise 05 p0623 A83-16913

Direct form expansion of the transfer function for a digital Butterworth low-pass filter 05 p0623 A83-16916

Combined effect of the carrier recovery and symbol timing recovery error on the P/e/ performance of QPR and offset QPR systems --- quadrature partial response 05 p0621 A83-17271

Error rate bounds for differential PSK 05 p0622 A83-17272

A note on errors and uncertainties in NCAR aircraft pyrometer data from MONEX 05 p0644 A83-17275

Error analysis and prevention of cosmic ion-induced soft errors in static CMOS RAMs 05 p0629 A83-17537

The Chebyshev approximation as the solution of the problem of multigoal planning in the case of arbitrarily correlated errors of measurement 06 p0805 A83-18352

Estimation of spectra from speckled images 06 p0763 A83-19040

Adaptive method for the real-time identification of a covariance matrix of measurement errors 06 p0803 A83-19178

Analysis of the effect of dispersion errors of memories on the precision of discrete spectral analysis 06 p0802 A83-19180

Pulse decoding in stretched pulse laser PMM systems 07 p0905 A83-19706

The effect of sampling offset on the Pe performance of partial response systems --- probability of error in signal processing 07 p0909 A83-19750

Error bounds for a spread spectrum multiple access system 07 p0912 A83-19788

Error probability for coherent hybrid slow-frequency-hopped direct-sequence spread-spectrum multiple-access communications 07 p0912 A83-19796

A technique for reducing low-frequency, time-dependent errors present in network-type surveys --- magnetic and gravity drift corrections 07 p0957 A83-19872

Abel inversion with a simple analytic representation for experimental data 07 p0988 A83-19984

Soft error in MOS dynamic RAM 07 p0918 A83-20072

A method for the approximate calculation of the current errors of mismatch in two-coordinate pursuit tracking 07 p0981 A83-20328

Error bounds and error asymptotic behavior for a class of interpolation quadratures --- German thesis 07 p0987 A83-20397

A critical evaluation of the aerodynamical error of a turbulence instrument 07 p0930 A83-20804

High accuracy matrix multiplication with outer product optical processor 07 p0983 A83-20826

On the errors of the Kurucz-Peytreman Fe I oscillator strengths 07 p1024 A83-21226

Orbital error analysis of time synchronization via geostationary broadcast satellite 08 p1048 A83-22039

Resolution improvement in an analog-to-digital converter by the superposed dither signal 08 p1080 A83-22231

Synthesis of sliding discrete Fourier transform and sliding Hadamard transform circuits 08 p1157 A83-22232

Bayes' error probability for noisy and imprecise measurement in pattern recognition 08 p1157 A83-22350

Motion-error immunity in photo coordinate determination - A novel approach to the absolute comparator 08 p1100 A83-22594

Errors in the experimental determination of the parameters of supersonic combustion ramjet engines 08 p1046 A83-22653

Accuracy of univariate, bivariate, and a 'modified double Monte Carlo' technique for finding lower confidence limits of system reliability 08 p1114 A83-22712

On selection effects in pulsar searches 08 p1185 A83-23102

Analysis of the effect of finite register length on the efficiency of digital filters for the detection of signals on a noise background 08 p1082 A83-23159

Error and stability analysis of the finite element solution for the transport equation 08 p1090 A83-23216

Approximate determination of the statistical error in lidar measurements of wind velocity by accounting for the evolution of the aerosol non-uniformities 08 p1143 A83-23245

The sea state correction for Geos 3 and Seasat satellite altimeter data 09 p1318 A83-24293

Nonlinear truncation error analysis of finite difference schemes for the Euler equations [AIAA PAPER 81-0193] 09 p1336 A83-24654

A function space approach to smoothing with applications to model error estimation for flexible spacecraft control 09 p1217 A83-24759

Generalized error coefficients for the multivariable servomechanism problem 09 p1334 A83-24813

On the error behavior of the reduced basis technique for nonlinear finite element approximations 09 p1282 A83-25106

Errors in high-resolution abundance analyses 10 p1501 A83-25577

Principal components analysis of spectral data. II - Error analysis and applications to interstellar reddening, luminosity classification of M supergiants, and the analysis of VV Cephei stars 10 p1493 A83-25658

An algorithm for detecting hardware errors in the data of supermonitors --- of cosmic ray parameters 10 p1420 A83-26104

Sources of methodological errors in calculations of the solar cosmic ray spectrum 10 p1521 A83-26107

Design of model reference adaptive control systems with arbitrarily small error 10 p1468 A83-26557

Error statistics in delta modulation and differential pulse code modulation communication systems 10 p1407 A83-26938

Utilization of the decorrelation properties of discrete spectral transformations for the multialternative recognition of signals on a background of correlated noise 10 p1470 A83-26955

Allowance for antenna errors in the determination of the scattering matrix of a radar target 10 p1407 A83-26959

Selected comment on multiple Doppler analysis --- of radar scanned storm with advection error correction 11 p1628 A83-27051

Precise determination of potential energy curves from spectroscopic data 11 p1653 A83-27525

Computable finite element error bounds for Poisson's equation 11 p1649 A83-27998

Errors due to transverse sensitivity in strain gages 11 p1573 A83-28077

Symbolic error analysis and robot planning 11 p1648 A83-28103

Adjacent-channel and quadrature-channel interference in minimum shift keying 11 p1556 A83-28127

Errors in measuring the temperature-inversion characteristics of the atmospheric boundary layer during radio sounding 11 p1634 A83-28207

Computation of electromagnetic flowmeter characteristics from magnetic field data. II - Errors 12 p1729 A83-29152

STS-1 orbital trajectory reconstruction using unmodelled acceleration estimation 12 p1706 A83-29206

Reverse Velocity Rocket Sled Test Bed for inertial guidance systems 12 p1705 A83-29209

Error estimate for the modified Newton method with applications to the solution of nonlinear, two-point boundary-value problems 12 p1771 A83-29244

Determination of aerosol optical depth from ground measurements 12 p1730 A83-29576

An improved solution to the fourth moment equation for intensity fluctuations --- for waves propagating through random media 12 p1775 A83-29598

On the numerical integration of the Schroedinger equation Numerical tests 12 p1776 A83-29604

Regional Monte Carlo solution of elliptic partial differential equations 12 p1773 A83-29626

A more accurate method for the numerical solution of nonlinear partial differential equations 12 p1773 A83-29671

A method of determining structural flexibility matrix from static experiment data 12 p1747 A83-29944

Calculation of refractive indices using Buchdahl's chromatic coordinate 13 p1918 A83-30208

The effect of errors in the amplitude-phase distribution of a linear antenna on its scattering coefficient 13 p1828 A83-30282

Quality and trends in national weather service forecasts 13 p1886 A83-30545

Error-correcting codes in binary-coded radix-r arithmetic 13 p1910 A83-30796

Approximation of 2-D separable in denominator filters 13 p1910 A83-30873

An objective procedure for detecting and correcting errors in geophysical data. II - Multidimensional applications 13 p1877 A83-30897

Active optics - Don't build a telescope without it 13 p1920 A83-31007

Peculiarities in measuring the velocity vector using a laser anemometer in flow through axisymmetric models 13 p1848 A83-31470

The field error and photometric system of the double long-focus astrophotograph of the Main Astronomical Observatory of the Academy of Sciences of the Ukrainian SSR 14 p2095 A83-31840

The photometric field error of the double wide-angle astrophotograph of the Main Astronomical Observatory of the Academy of Sciences of the Ukrainian Soviet Socialist Republic 14 p2095 A83-31843

Errors in the determination of electron density in the D-region of the ionosphere by the method of partial reflections 14 p2049 A83-31856

The choice and use of normal approximations to transfer-function matrices of multivariable control systems 14 p2074 A83-31932

Statistical characteristics of errors in the measurement of the coordinates of extended targets 14 p2000 A83-32111

Method for calculating the potential accuracy of the estimation of the vector parameter in the presence of random interference parameters 14 p2000 A83-32113

Estimation of the probability of error in the reception of broadband signals 14 p2001 A83-32487

Increasing the accuracy of static deformation measurements 14 p2019 A83-32570

The application of iterated defect correction to variational methods for elliptic boundary value problems 14 p2078 A83-32842

Theory of tracking accuracy of laser systems 14 p2025 A83-33175

Bit error rate evaluation of GSTDN/TRSS communication links 15 p2125 A83-33734

A simple approach to the error analysis of division-free numerical algorithms 15 p2217 A83-33904

Error analysis of certain floating-point on-line algorithms 15 p2217 A83-33905

The design of error checkers for self-checking residue number arithmetic 15 p2217 A83-33909

Techniques to reduce the inherent limitations of fully digit on-line arithmetic 15 p2217 A83-33913

The use of floating-point and interval arithmetic in the computation of error bounds 15 p2218 A83-33914

Concurrent error detection in multiply and divide arrays 15 p2218 A83-33915

Surface temperature measurement errors 15 p2163 A83-33995

The airborne Knollenberg cloud droplet spectrometer probes of DFVLR 15 p2164 A83-34054

A theoretical framework for analysis of lateral position errors in VOR jet-route systems 15 p2121 A83-35273

Computational noise effects on adaptive filter algorithms 16 p2403 A83-35349

Velocity-dependent factors for the Rubakov process for slowly moving magnetic monopoles 16 p2441 A83-35745

Crosstalk and loss of information in holography 16 p2355 A83-35890

A stochastic-dynamic model for the spatial structure of forecast error statistics 16 p2388 A83-36031

Error sources in hybrid computer based flight simulation [AIAA PAPER 83-1090] 16 p2299 A83-36214

Adaptive companded pulse code modulation 16 p2344 A83-36609

The effect of systematic differences between proper stellar motions on the determination of the solar motion parameters 16 p2426 A83-36857

Variances and correlations of errors of rectangular coordinates of selenodetic reference points 16 p2439 A83-36859

Correction to the wing source velocity error in Woodward's USSAERO code 16 p2297 A83-36920

Improvements of the performance of triple hot wire probes 17 p2509 A83-36999

Simple corrections for the temperature sensitivity of hot wires 17 p2509 A83-37000

Adaptive control techniques for reducing settling time 17 p2566 A83-37112

Applying stochastic control theory to robot sensing, teaching, and long term control 17 p2568 A83-37154

Investigation of the systematic errors of the Belgrade NPZT and AGK3 catalogues 17 p2587 A83-37285

Radial velocities of galaxies in neighborhoods of groups of galaxies. I 17 p2602 A83-37883

Piecewise polynomial Galerkin approximation to invariant densities of one-dimensional difference equations 17 p2571 A83-38037

Statistical theory for estimating sampling errors of regional radiation averages based on satellite measurements 17 p2551 A83-38735

Error induced by coordinate systems 17 p2572 A83-38778

Line strength measurements using diode lasers - The nu2 band of H2S 18 p2742 A83-39182

Sensitivity of ozone retrievals in limb-viewing experiments to errors in line-width parameters 18 p2664 A83-39183

Computational errors of difference schemes for calculating discontinuous solutions [AIAA PAPER 83-1938] 18 p2740 A83-39388

How confidently do we know the CO rotation curve of the outer Galaxy? 18 p2769 A83-39648

IRAS follow-up - Problems and prospects 18 p2763 A83-40464

Double galaxies - Redshift measurements, error analysis, and mean mass/luminosity ratio 18 p2778 A83-40485

Signaling performance over a piecewise linear limited channel in the presence of interference and Gaussian noise 19 p2826 A83-40921

On the extraction of tidal information from measurements covering a fraction of a day --- for upper atmosphere meteorology 19 p2865 A83-41128

Sensitivity of some optimal detectors to noise skewness 19 p2839 A83-41364

Autonomous satellite navigation by stellar refraction [AIAA PAPER 83-2211] 19 p2814 A83-41695

Analysis of instrument errors arising in velocity measurement by an LDV based on a Fabry-Perot interferometer 19 p2849 A83-41900

Analysis of the error associated with grid representation of point sources --- for pollutant dispersion 19 p2863 A83-41969

Errors in the referencing of geophysical fields by astronomical methods 19 p2867 A83-42019

The heading of a vehicle moving with roll and trim 19 p2897 A83-42020

Bayesian estimates of vector quantities in the case of microstatistics 19 p2893 A83-42059

Particle size distributions from forward scattered light using the Chahine inversion scheme 20 p3046 A83-42213

Representations of intervals and optimal error bounds 20 p3041 A83-42500

Computational interferometric description of nested flow fields 20 p2988 A83-42527

Improvement in spectral directional emissivity measurement techniques by direct methods 20 p2989 A83-42776

The influence of fabrication defects of tube dispersive waveguides on the shape of the output signal of a matched filter 20 p2967 A83-42911

Strict error estimation of numerical solution of compressible flow in two-dimensional space 20 p2985 A83-43171

Nucleation theory - Is replacement free energy needed? --- error analysis of capillary approximation 20 p3056 A83-43287

Correction of meteor radiant for zenith attraction 20 p3061 A83-43416

Cosmic ray induced soft error rate in VLSI circuits 21 p3123 A83-43844

The dynamical analysis of orbital correction for earth's observatory satellite 21 p3094 A83-44508

Something about to improve the accuracy of testing in low speed wind tunnel 21 p3093 A83-44571

The effect of the emissivity of a surface on the IR measurements of its temperature 21 p3177 A83-45333

Analysis of some low-order finite element schemes for the Navier-Stokes equations 21 p3133 A83-45521

An automatic orthonormalization method for solving stiff boundary-value problems 21 p3198 A83-45524

Optimal symbol-by-symbol detection for duobinary signaling 22 p3272 A83-45739

Assessment of relative error sources in IR DIAL measurement accuracy 22 p3295 A83-46084

Analysis of the errors of location of acoustic-emission sources for one-dimensional objects 22 p3304 A83-46333

Adjustment problems in inertial positioning 22 p3316 A83-46343

Coherence loss and delay observation error in very-long-baseline interferometry 22 p3376 A83-46919

Effect of the coefficient of error propagation on satellite position fixing [IAF PAPER 83-460] 23 p3420 A83-47383

Identification of systematic errors in a numerical weather forecast 23 p3489 A83-47396

Estimation of the analysis error variance of the 500 mb height analyses in the Northern Hemisphere, 1946-79 23 p3490 A83-47409

Improved stress simulation with simple finite element meshes [ASME PAPER 83-GT-89] 23 p3469 A83-47936

The multigrid method for accelerated solution of the discretized Schroedinger equation 24 p3622 A83-48873

An analysis of two-step time discretizations in the solution of the linearized shallow water equations 24 p3575 A83-48875

The influence of the magnitude equation in the proper motions of stars on the determination of stellar astronomical constants 24 p3638 A83-48929

A posteriori errors in the finite element method [ONERA, TP NO. 1983-89] 24 p3622 A83-49408

The accuracy of determining stress concentrations by methods that combine experimental and numerical techniques 24 p3595 A83-49906

Estimation of truncation and aliasing errors involved in DFT computation 24 p3621 A83-49968

Probe correction in near field measurements by pseudo sampling technique 24 p3571 A83-49995

ERROR BAND

U ACCURACY

ERROR CORRECTING CODES

High dynamic range mapping of strong radio sources, with application to 3C84 01 p0115 A83-10208

Statistical correction of projection of radio-sources on the sky and application to the apparent size-redshift and linear size-line width relations 01 p0125 A83-10939

Gravity modeling for airborne applications 01 p0004 A83-11090

Influence of LSI and VLSI technology on the design of error-correction coding systems 02 p0163 A83-11552

Errors in fixed and moving frame of references - Applications for conventional and Doppler radar analysis 02 p0214 A83-12237

An aperture phase compensation technique for off-axis beam synthesis in parabolic reflector antennas 06 p0738 A83-18620

Concatenated error correcting system 07 p0984 A83-19685

Modulation, coding, and interleaving tradeoffs for spread spectrum systems 07 p0904 A83-19695

A low-power, high-throughput maximum-likelihood convolutional decoder chip for NASA's 30/20 GHz program 07 p0917 A83-19754

Viterbi decoder VLSI integrated circuit for bit error correction 07 p0917 A83-19755

A relaxation technique for evaluating stress intensity factors by the finite element method 07 p0949 A83-21439

High-speed decoding technique for slip detection in data transmission systems using modified cyclic block codes 09 p1249 A83-24115

Noise-immune coding of discrete information --- bibliography 1972-1979 09 p1327 A83-24248

Linear cascade codes --- Russian book 09 p1335 A83-25099

Remote sensing - Corrections and data enhancement. II 11 p1601 A83-28189

Error-correcting codes in binary-coded radix-r arithmetic 13 p1910 A83-30796

New syndrome decoder for (n, 1) convolutional codes 13 p1912 A83-31785

Error free computation - A direct method to convert finite-segment p-adic numbers into rational numbers 15 p2217 A83-33903

Asynchronous multiplexing for an optical-fibre local-area network 15 p2144 A83-34523

A modified selective-repeat type-II hybrid ARQ system and its performance analysis --- Automatic Repeat reQuest 16 p2343 A83-36601

Noise immunity of selection algorithms in the whole 18 p2674 A83-39426

Performance of concatenated codes on channels with jamming 19 p2833 A83-41410

Explicit finite difference predictor and convex corrector with applications to hyperbolic partial differential equations 19 p2893 A83-41852

Class of linear cyclic block codes for burst errors occurring in one-, two- and three-dimensional channels 20 p3040 A83-43686

Towards the fundamental limits of optical-fiber communications 21 p3204 A83-44215

Removal of velocity bias in the interpretation of measurements of the azimuthal component of the interplanetary magnetic field 22 p3377 A83-46059

Three-dimensional wind field analysis from dual-Doppler radar data. II - Minimizing the error due to temporal variation 22 p3342 A83-46944

ERROR CORRECTING DEVICES

Approximation techniques of a selective ARQ protocol 01 p0032 A83-11093

High accuracy digital sensor 01 p0053 A83-11118

An examination of reduction techniques for determining the Linke turbidity factor 02 p0212 A83-12960

Design of a microprocessor-based A/D converter with drift and offset correction 03 p0385 A83-13499

Shutterless fixed pattern noise correction for infrared imaging arrays 03 p0325 A83-13731

Digital computational synthesizers of two-level signals with compensation of phase errors 04 p0470 A83-15712

Applying existing safety design techniques to software safety [AIAA PAPER 83-0327] 05 p0678 A83-16656

Parametric correction of control systems --- Russian book 05 p0653 A83-17121

Real-time nonuniformity correction for focal plane arrays using 12-bit digital electronics 08 p1094 A83-22440

A computer-controlled broadband system for measuring scattered fields and for locating scattering centers 09 p1244 A83-23382

NOVA-1 - The 'drag-free' navigation satellite 11 p1534 A83-28780

An experimental verification of laser-velocimeter sampling bias and its correction 12 p1727 A83-28840

Minimization of a class of temperature errors of float-type gyroinstruments 15 p2167 A83-35268

The use of multiple inertial systems to correct for the effects of gravitational anomalies [AIAA PAPER 83-2196] 19 p2796 A83-41681

Autonomous failure detection and correction on Landsat-4 [AIAA PAPER 83-2265] 19 p2817 A83-41735

The determination of the minute volume of the blood by a thermal dilution method 19 p2876 A83-41845

Reducing errors in single-degree-of-freedom gyroscopes 21 p3137 A83-44633

Choice of the optimal correcting moment of a gyrovertical on the basis of an applications program 21 p3141 A83-45309

The layer model and error control for satellite communications 22 p3273 A83-45756

Post-flight compensation for a master navigator error 22 p3253 A83-46966

Comparison of simple position resets and Kalman filter position updates for correcting inertial navigation system errors 22 p3253 A83-46967

ERROR DETECTION CODES

A class of codes with unequal protection of symbols, based on balanced incomplete solvable block-schemes 01 p0094 A83-10567

Inflight parity vector compensation for FDI --- Failure Detection and Isolation 01 p0019 A83-11129

Influence of LSI and VLSI technology on the design of error-correction coding systems 02 p0163 A83-11552

On implementing self-checking microprocessors 02 p0227 A83-11909

Design methods of single-output built-in self-checking circuits for equilibrium codes 10 p1460 A83-25467

Concurrent error detection in multiply and divide arrays 15 p2218 A83-33915

A framework for software fault tolerance in real-time systems 16 p2403 A83-35325

Developments in test software philosophy and techniques 16 p2363 A83-35499

Abstractions for node level passive fault detection in distributed systems 19 p2889 A83-41036

ERROR FUNCTIONS

Procedure for camera calibration with image sequences 02 p0182 A83-12899

Further developments of Rp and Ap error analysis --- Relative and Absolute precision in floating point arithmetic operations 02 p0231 A83-12926

An empirical initial estimate for the solution of Kepler's equation 07 p0868 A83-21427

ERROR SIGNALS

Error-signal response of a phase-locked loop to a coherent chirp signal 03 p0311 A83-13856

Combined effect of the carrier recovery and symbol timing recovery error on the P/e/ performance of QPR and offset QPR systems --- quadrature partial response 05 p0621 A83-17271

Deadbeat error control of discrete multivariable systems 09 p1326 A83-23688

Wide-band nulling performance versus number of pattern constraints for an array antenna 09 p1247 A83-23799

A stable smoothing algorithm --- for digital processing of radar signals 11 p1556 A83-27948

Average error probability for DS-SSMA communications - The Gram-Charlier expansion approach --- Direct Sequence-Spread Spectrum Multiple Access 15 p2147 A83-35117

Estimation of the efficiency of devices for the detection and recognition of signals 16 p2404 A83-35940

Model error estimation for large flexible spacecraft 21 p3103 A83-45134

ERRORS

NT BORESIGHT ERROR

NT INSTRUMENT ERRORS

NT PHASE ERROR

NT PILOT ERROR

NT POSITION ERRORS

NT RANDOM ERRORS

NT RANGE ERRORS

NT ROOT-MEAN-SQUARE ERRORS

NT TRUNCATION ERRORS

NT VELOCITY ERRORS

Spectral radiance errors in remote sensing ground studies due to nearby objects 06 p0779 A83-18576

New error bounds for modulation and coding under mismatch 07 p0909 A83-19745

ERS-1 (ESA SATELLITE)

An imaging microwave radiometer 01 p0020 A83-10006

The microwave payload for the ESA Remote Sensing Satellite /ERS-1/ 03 p0289 A83-14290

The ERS-1 programme of the European Space Agency 14 p1979 A83-33471

ERS-1 - An ice and ocean monitoring mission 20 p2938 A83-42826

An Active Microwave Instrumentation for land imagery and oceanographic observations 22 p3260 A83-46141

Performance simulation of a wind scatterometer 22 p3260 A83-46143

The active microwave instrument (AMI) for ERS-1 [IAF PAPER 83-92] 23 p3424 A83-47261

ERS-1 processing algorithms and disseminated products [IAF PAPER 83-129] 23 p3475 A83-47284

A large deployable antenna structure for the ERS-1 satellite [IAF PAPER 83-361] 23 p3422 A83-47359

ERTS

U LANDSAT SATELLITES

ERTS-B

U LANDSAT 2

ERTS-C

U LANDSAT 3

ERTS-D

U LANDSAT 4

ERYTHROCYTES

The regulation of erythropoiesis /Status of the problem/ 01 p0081 A83-10916

Stability of erythrocyte suspensions layered on stationary and flowing liquids 02 p0169 A83-11840

An approach for determining common cholesterol and its structural-functional fractions in erythrocytes on the basis of the digitonin method 03 p0375 A83-14327

Pulmonary microcirculatory response to localized hypercapnia 05 p0671 A83-17333

The changes in the erythropoiesis-stimulating action of the erythrocytic factors during the blocking of cells of the mononuclear phagocyte system 07 p0972 A83-19921

An investigation of human blood, erythrocytes, and plasma using the method of ESR at 77 K 08 p1150 A83-23022

Beta adrenergic blockade and erythropoietic production in rats after hypoxia and hypovolemia 09 p1321 A83-23875

Enhanced erythrocyte suspension layer stability achieved by surface tension lowering additives 11 p1546 A83-28762

Impaired red cell filterability with elimination of old red blood cells during a 100-km race 13 p1904 A83-30492

A calorimetric approach to investigating the effect of electromagnetic radiation at radio frequencies on the plasmatic membrane of erythrocytes 13 p1900 A83-31334

The activity of 5-nucleotidase in leukocytes, erythrocytes, and blood serum of rats with radiation sickness 14 p2062 A83-32061

The effect of products of erythrocyte degradation on the migration of hemopoietic stem cells in lethally-irradiated mice 14 p2062 A83-32065

The role of erythrocytes in blood coagulation and in blood platelet formation 14 p2065 A83-33319

Erythropoiesis during adaptation to cold 16 p2399 A83-35916

The effect of the kinetics of erythrocyte destruction on the dynamic behavior of the erythropoiesis system 16 p2395 A83-36805

The action of colyones on erythropoiesis (A quantitative evaluation) 16 p2396 A83-36841

The characteristics of the aggregation of erythrocytes in various animals and in humans 19 p2871 A83-40814

The mechanism of the regeneration of erythropoiesis in conditions of local irradiation of bone marrow 19 p2874 A83-41008

The characteristics of the biosynthesis of nucleic acids during the activation of erythroid cell proliferation evoked by prolonged gamma-irradiation 19 p2874 A83-41009

Settling of fixed erythrocyte suspension droplets 21 p3183 A83-44649

ESA

U EUROPEAN SPACE AGENCY

ESA SATELLITES

- NT COS-B SATELLITE
 NT ERS-1 (ESA SATELLITE)
 NT EUROPEAN COMMUNICATIONS SATELLITE
 NT EXOSAT SATELLITE
 NT GEOS SATELLITES (ESA)
 NT HEOS SATELLITES
 NT HIPPARCOS SATELLITE
 NT L-SAT
 NT MAGELLAN MISSION
 NT MARECS MARITIME SATELLITES
 NT MAROTS (ESA)
 NT METEOSAT SATELLITE
 NT OTS (ESA)
 NT TD SATELLITES
 NT TD-1 SATELLITE
- ESA's science programme - The present situation and future perspectives 04 p0451 A83-15667
- Disco - A solar-seismology and heliospheric-structure observatory 05 p0600 A83-17428
- The Infrared Space Observatory /ISO/ - A study for a cooled telescope in space for infrared astronomy 05 p0601 A83-17429
- X-80 - A spectroscopy, transient and timing mission for X-ray astrophysics 05 p0601 A83-17432
- The Prosat Programme --- of ESA satellite communications for maritime and mobile earth terminals 05 p0623 A83-17437
- Access technique for the Italsat SS-TDMA system 07 p0911 A83-19785
- The MAGE family of European solid-propellant apogee boost motors --- for geostationary orbit transfer 11 p1542 A83-27369
- The Navsat aeronavigation system - Possible control-segment concepts 11 p1535 A83-27371
- The ground segment for a European ocean-monitoring satellite ERS-1 20 p2944 A83-42970
- Investigations on an active satellite system for earth kinematics and positioning 22 p3258 A83-46112
- ESA SPACECRAFT**
 NT COS-B SATELLITE
 NT ESA SATELLITES
 NT GIOTTO MISSION
 NT L-SAT
 NT MARECS MARITIME SATELLITES
 NT MAROTS (ESA)
 NT METEOSAT SATELLITE
 NT OTS (ESA)
 NT TD SATELLITES
 NT TD-1 SATELLITE
- Kepler - A mission to the planet Mars 05 p0601 A83-17430
- Sampled control stability of the ESA instrument pointing system 17 p2480 A83-37438
- ESAKI DIODES**
 U TUNNEL DIODES
- ESCAPE CAPSULES**
 MOSES /Manned Orbital Space Escape System/ - A hypothetical application 09 p1214 A83-24887
- ESCAPE SYSTEMS**
 Extension of service life of rigid transfer lines /SMDC/ --- explosive components for aircraft escape systems 03 p0303 A83-14173
- Open seat ejection at high dynamic pressure - A radical approach 04 p0445 A83-15308
- SAFE Association, Annual Symposium, 19th, Las Vegas, NV, December 6-10, 1981, Proceedings 04 p0524 A83-15401
- An analysis of the fatality rate data from 'jettison-canopy' and 'through-the-canopy' ejections from automated airborne escape systems 04 p0443 A83-15403
- Preliminary overview analyses of U.S. Navy Aircrew Automated Escape Systems /AAES/ in-service usage data 04 p0444 A83-15405
- Preliminary generalized thoughts concerning jettisoned vs through-the-canopy ejection escape systems 04 p0444 A83-15406
- Preliminary analyses of flail, windblast and tumble problems and injuries associated with usage of U.S. Navy Aircrew Automated Escape Systems /AAES/ 04 p0444 A83-15407
- U.S. Navy Aircrew Automated Escape Systems /AAES/ In-Service Data Analysis program 04 p0444 A83-15408
- An option for enhanced aircrew survivability 04 p0444 A83-15409
- First stage propulsion for the maximum performance ejection system 04 p0445 A83-15421
- MPES update 1981 --- Navy Maximum Performance Ejection System program 04 p0445 A83-15425
- Easiest ejection seat stability and control analysis capability 04 p0446 A83-15428
- Design and development of Cartridge Actuated Device /CAD/ primer 04 p0464 A83-15433

- Development and testing of a microwave radiometric vertical sensor for application to a vertical seeking aircrew escape system 04 p0447 A83-15437
- Microwave measurements for an attitude reference system design --- thrust vector controlled escape systems 04 p0447 A83-15438
- The United States Navy's injury experience in aircraft mishaps 04 p0445 A83-15441
- Design considerations for a electrical signal transmission subsystem /STS/ for the maximum performance ejection system /MPES/ 04 p0446 A83-15442
- Flight helmets - The British approach 04 p0526 A83-15443
- Aircraft vehicle equipment improvements via microprocessors [SAE PAPER 820868] 10 p1375 A83-25767
- Escape low and hot --- vertical-seeking, steerable ejection seat design for F-14A aircraft 13 p1806 A83-31587
- Performance assessment of a reclined ejection seat 17 p2462 A83-37879
- Finite-element analysis of the T-38 canopy 19 p2797 A83-41044

ESCAPE VELOCITY

- The velocity of escape from the Galaxy in the solar neighbourhood 03 p0413 A83-13317
- The loss of regolith from solar system satellites 09 p1355 A83-24999
- Escape of ejecta from cratered solar system satellites 21 p3224 A83-44740
- Escape velocities of interacting spherical galaxies 21 p3234 A83-44870
- Three-body problem - A test of escape valid even for very small mutual distances [IAF PAPER 83-319] 23 p3515 A83-47340

ESCARPMENTS

- Bouguer gravity profiles across the highland-lowland escarpment on Mars 16 p2439 A83-36784

ESCHERICHIA

- A theoretical analysis of the effect of the photoreactivation of E. Coli cells irradiated by gamma-rays 19 p2874 A83-41004

ESG (GYROSCOPES)

- U ELECTROSTATIC GYROSCOPES

ESKERS

- U GLACIAL DRIFT

ESRO

- U EUROPEAN SPACE AGENCY

ESRO SATELLITES

- U ESA SATELLITES

ESTERS

- NT ACRYLATES
 NT ALKYLATES
 NT CELLULOSE NITRATE
 NT GLUTAMATES
 NT GLYCERIDES
 NT LACTATES
 NT NITRATE ESTERS
 NT NITROGLYCERIN
 NT ORGANIC NITRATES
 NT PETN
 NT POLYCARBONATES
 NT POLYESTERS
 NT POLYETHYLENE TEREPHTHALATE
 NT SODIUM SALICYLATES
 NT STEARATES
- Formation of pyrophosphate on hydroxyapatite with thioesters as condensing agents 05 p0613 A83-17234
- Nonspecific esterases of the extramural ganglia of the autonomic nervous system in rabbits during acute experimental emotional stress 17 p2556 A83-38175
- Cholesterol esters increase the permeability of lecithin bilayer membranes 21 p3184 A83-45223
- The effect of additives on the critical diameter of detonation of nitroesters 24 p3557 A83-49791

ESTIMATES

- NT COST ESTIMATES
 On systems of standards --- set of estimates in astronomy 01 p0101 A83-10139
- Numerical estimates of Hausdorff dimensions --- for problems in turbulence theory 12 p1724 A83-29615
- Theory of transport aircraft weight fractions [SAWE PAPER 1452] 20 p2935 A83-43734
- Contour-based motion estimation 22 p3350 A83-46252

ESTIMATING

- NT ORBITAL POSITION ESTIMATION
 NT PARAMETER IDENTIFICATION
 NT SYSTEM IDENTIFICATION
- A time-invariant state estimator for continuous time systems 02 p0229 A83-11853
- Melnikov's method and averaging 03 p0389 A83-13418

- Estimation of helicopter and target motion for the advanced attack helicopter fire control system 06 p0715 A83-18378
- Estimation of mixed Weibull parameters in life testing 07 p0943 A83-20517
- Improved three subaperture method for elevation angle estimation --- of radar targets 08 p1077 A83-22734
- Estimating the angles of arrival of multiple plane waves 08 p1158 A83-22736
- Separability and estimation of parameters in identification of complex static systems 09 p1326 A83-23977
- Multi-domain adaptive parameter estimation 09 p1249 A83-24702
- Convergence properties of LMS adaptive estimators with unbounded dependent inputs 09 p1330 A83-24743
- A new recursive partitioned estimation algorithm derived from Extended Least Squares technique 09 p1330 A83-24744
- Applied spectral estimation theory --- Russian book 09 p1335 A83-25221
- Spectral estimation for sensor arrays [AD-A129985] 13 p1847 A83-30925
- Methods in optimal estimation theory for problems involving the vibration of dynamic distributed-parameter systems 17 p2570 A83-38925

ESTIMATORS

- Computing the distribution of a random variable via Gaussian quadrature rules 04 p0530 A83-16323
- A practical method for sensor selection in linear estimation --- applied to inertial navigation systems 10 p1465 A83-26531
- Estimators for the 2-parameter Weibull distribution with progressively censored samples 17 p2517 A83-37295

ESTROGENS

- Sexual influence on the control of breathing 13 p1904 A83-30494

ESTUARIES

- Remote sensing of water quality for estuarine environments 01 p0069 A83-10073
- Toward an operational, satellite-based, wetland monitoring program for the Fraser River Estuary, British Columbia 03 p0345 A83-14234
- Delineation of estuarine fronts in the German Bight using airborne laser-induced water Raman backscatter and fluorescence of water column constituents 05 p0646 A83-17715
- Laboratory analysis of techniques for remote sensing of estuarine parameters using laser excitation 06 p0762 A83-18583

ETCHING

- Competing processes of Si molecular beam reactive etching and simultaneous deposition on film and bulk SiO₂ 01 p0108 A83-10623
- Manufacture and measurement of ion-etched X-ray diffraction gratings 02 p0238 A83-12712
- Preparation and analysis of cross-sections of etched and unetched CdSe semiconductor thin films 04 p0504 A83-15477
- Seeding of FPL solution --- in preparation of aluminum surfaces for adhesive bonding 07 p0885 A83-20431
- Compositional depth profiles of chemiplated Cu₂S//Zn,Cd/S heterojunction solar cells 08 p1130 A83-22339
- Evaluation of the P2 and PAA treatments --- sulfuric acid-ferric sulfate etching and phosphoric acid anodizing 09 p1238 A83-23627
- Laser-controlled etching of chromium-doped 100 line-type GaAs 10 p1390 A83-25986
- Compositional depth profile of a native oxide LPCVD MNOS structure using X-ray photoelectron spectroscopy and chemical etching 10 p1391 A83-26062
- The relation between performance and stability of Cd-Chalcogenide/Polysulfide photoelectrochemical cells. I - Model and the effect of photoetching 11 p1546 A83-28297
- CW operation of 1.5 micron GaInAsP/InP buried heterostructure laser with a reactive ion-etched facet 11 p1585 A83-28606
- Structure in carbon/carbon fibre composites as studied by microscopy and etching with chromic acid 12 p1709 A83-29502
- Laser-controlled chemical etching of aluminum 18 p2693 A83-40055
- Selective electrochemical etching of p-CdTe (for photovoltaic cells) 18 p2750 A83-40065
- Effect of photoelectrochemical etching on charge collection efficiency in CdS - An electron beam induced current study 20 p3053 A83-42613
- Laser chemical etching of vias in GaAs 21 p3142 A83-43847
- A new method for the fabrication of submicron thick gallium arsenide membranes 21 p3220 A83-45498

ETHANE

Spectroscopic detection of acetylene and ethane in the terrestrial atmosphere using ground-based solar IR observations 04 p0508 A83-16447

Measurements of stratospheric ethane in the Jovian South Polar Region from infrared heterodyne spectroscopy of the nu9 band near 12 microns 07 p1031 A83-21151

Stratospheric NO2 and upper limits of CH3Cl and C2H6 from measurements at 3.4 microns 15 p2200 A83-34386

ETHERS

Characterization of ether electrolytes for rechargeable lithium cells 02 p0152 A83-12052

ETHYL ALCOHOL

The effect of small doses of ethanol on the minute waves of ultralow activity and the temperature of the brain 07 p0973 A83-20241

Rotational and vibrational spectra of ethynol from quantum-mechanical calculations 07 p0874 A83-21060

Homogeneous nucleation of ethanol and n-propanol in a shock tube 08 p1053 A83-23000

The level of endogenous ethanol and its connection with the voluntary consumption of alcohol by rats 11 p1641 A83-28525

Heat transfer during the boiling of acetone and ethyl alcohol in a thermosiphon with porous capillary structures on the heat-transfer face 11 p1571 A83-28798

The molecular mechanisms of the action of endogenous and exogenous ethanol 12 p1762 A83-29272

Feasibility study on the ethanol-water solar fractionating system 15 p2190 A83-34071

Effects of serotonin on memory impairments produced by ethanol 18 p2736 A83-39934

The Air Canada programme for rehabilitation of the alcoholic employee/pilot 18 p2734 A83-40352

Experimental studies of heat and mass exchange phenomena in the two-component heat pipe 20 p2981 A83-42767

Effect of ethanol and naloxone on control of ventilation and load perception 22 p3348 A83-45996

Improved combustion turbine efficiency with reformed alcohol fuels [ASME PAPER 83-GT-60] 23 p3464 A83-47916

A modified technique for estimation of ethanol in body fluids by gas liquid chromatography 23 p3499 A83-48694

ETHYL COMPOUNDS

Association of triethylammonium perchlorate with bases 01 p0023 A83-11322

Thermal decomposition of tetraethylammonium perchlorate 06 p0726 A83-18458

Optically pumped molecular laser utilizing C2H5Br and C2H5I halogen derivatives of ethane 20 p2996 A83-43779

ETHYLENE

NT VINYLIDENE

Laminated modules with new plastic material based on an ethylene-vinylacetate copolymer --- for solar cells 14 p1986 A83-32226

Determination of ethylene and other reactive hydrocarbons in the atmospheric air at Trombay, Bombay by gas chromatography using a chemiluminescent detector 19 p2849 A83-41984

Numerical modeling of ethylene oxidation in laminar flames 23 p3430 A83-48159

ETHYLENE COMPOUNDS

NT CHLOROETHYLENE

Photothermal degradation of ethylene/vinylacetate copolymer 22 p3270 A83-46717

ETIOLOGY

An evaluation of the carcinogenic effect of radiation at the cellular level 06 p0796 A83-19380

Etiological aspects of indispositions in flight 17 p2561 A83-38945

Etiological factors in space motion sickness 21 p3186 A83-43986

ETTINGSHAUSEN COOLERS

U THERMOELECTRIC COOLING

EUCLIDEAN GEOMETRY

NT ANALYTIC GEOMETRY

NT ANGLE OF ATTACK

NT ANGLES (GEOMETRY)

NT BRAGG ANGLE

NT CARTESIAN COORDINATES

NT CHORDS (GEOMETRY)

NT CONICS

NT DESCRIPTIVE GEOMETRY

NT ELEVATION ANGLE

NT FIXED POINTS (MATHEMATICS)

NT GEODESIC LINES

NT GREAT CIRCLES

NT HEXAGONS

NT LEADING EDGE SWEEP

NT LINES (GEOMETRY)

NT LOCII

NT LOOK ANGLES (TRACKING)

NT OBLATE SPHEROIDS

NT PARABOLAS

NT PARALLELEPIPEDS

NT POINTS (MATHEMATICS)

NT POLYGONS

NT POLYHEDRONS

NT PROJECTIVE GEOMETRY

NT PROLATE SPHEROIDS

NT PYRAMIDS

NT RADII

NT SPHEROIDS

NT SQUARES (MATHEMATICS)

NT SWEEP ANGLE

NT TETRAGONS

NT TORUSES

NT TRAPEZOIDS

NT TRIANGLES

NT TRIGONOMETRY

Oscillation properties of solutions of second order elliptic equations 17 p2572 A83-38466

Optimal spherical designs and numerical integration on the sphere 21 p3198 A83-45522

EUCLIDEAN SPACE

U EUCLIDEAN GEOMETRY

EULER BUCKLING

Flutter of a buckled plate as an example of chaotic motion of a deterministic autonomous system 04 p0501 A83-16339

Optimal finite element discretization - A dynamic programming approach --- for structural analysis of linear elastic systems 06 p0773 A83-18230

EULER EQUATIONS OF MOTION

Certain numerical methods for solving problems of gas dynamics in Euler coordinates 01 p0045 A83-10566

A down-stream boundary procedure for the Euler equations 02 p0174 A83-13021

Comparison of different integration schemes based on the concept of characteristics as applied to the ablated blunt body problem 02 p0132 A83-13022

Geometrical properties of the Euler-Poisson equations of a rigid body about a fixed point 03 p0390 A83-13423

Methods for solving Euler's equations for airfoil and intake flow 03 p0279 A83-14604

Computation of vortex flow around wings using the Euler equations 03 p0279 A83-14605

Numerical experiments with the split-flux-vector form of the Euler equations [AIAA PAPER 83-0122] 05 p0633 A83-16535

New implicit boundary procedures - Theory and applications [AIAA PAPER 83-0123] 05 p0579 A83-16536

A multigrid method for the Euler equations [AIAA PAPER 83-0124] 05 p0580 A83-16537

Finite element formulations for convection dominated flows with particular emphasis on the compressible Euler equations [AIAA PAPER 83-0125] 05 p0633 A83-16538

A class of central bidiagonal schemes with implicit boundary conditions for the solution of Euler's equations [AIAA PAPER 83-0126] 05 p0633 A83-16539

Three-dimensional Euler equation simulation of propeller-wing interaction in transonic flow [AIAA PAPER 83-0236] 05 p0582 A83-16603

An enhanced version of an implicit code for the Euler equations [AIAA PAPER 83-0344] 05 p0584 A83-16669

Flow simulations for general nacelle configurations using Euler equations [AIAA PAPER 83-0539] 05 p0587 A83-16775

Transonic wing-body calculations using Euler equations [AIAA PAPER 83-0501] 05 p0589 A83-16828

Three-dimensional Euler solutions for long-duct nacelles [AIAA PAPER 83-0089] 05 p0590 A83-17905

Finite-volume solutions to the Euler equations in transonic flow [AIAA PAPER 81-1265] 06 p0712 A83-18405

An implicit time marching method for the calculation of transonic flows using Euler equations [ONERA, TP NO. 1982-111] 06 p0712 A83-18437

On a stationary solution for the motion of a rigid body about a fixed point under the influence of a Newtonian force field 07 p0988 A83-20200

A new multifold series general solution of the steady, laminar boundary layers. I - Theory of the multifold series expansion. II - Application theory of the Euler transformation 07 p0925 A83-20278

Hamiltonian description of stratified fluid dynamics 07 p0926 A83-20529

A finite element formulation for steady transonic Euler equations 08 p1042 A83-22129

EULER EQUATIONS OF MOTION

On the symmetric form of systems of conservation laws with entropy 09 p1350 A83-23724

Finite-element method for time-dependent Euler equation --- of inviscid incompressible flow 10 p1413 A83-25462

Euler equations - Implicit schemes and boundary conditions 12 p1695 A83-28959

Compact finite difference schemes for the Euler and Navier-Stokes equations 12 p1722 A83-29096

An overrelaxation method for Euler equations in steady transonic flow 12 p1726 A83-29668

Implicit finite difference simulation of inviscid and viscous compressible flow 12 p1726 A83-29934

Transonic flow calculations using the Euler equations 14 p1971 A83-32981

The rolling of an ellipsoid on a horizontal plane 15 p2226 A83-34432

Coupled Euler/Integral Boundary Layer analysis in transonic flow [AIAA PAPER 83-1806] 17 p2508 A83-38640

An algebraic grid generation method coupled with an Euler solver for simulating three-dimensional flows [AIAA PAPER 83-1807] 17 p2454 A83-38641

Calculation of axisymmetric inlet flowfield using the Euler equations [AIAA PAPER 83-1853] 17 p2457 A83-38681

Efficient solution of the Euler and Navier-Stokes equations with a vectorized multiple-grid algorithm [AIAA PAPER 83-1893] 18 p2634 A83-39359

Implicit methods of second-order accuracy for the Euler equations [AIAA PAPER 83-1925] 18 p2682 A83-39379

Solution of the Euler equations for complex configurations [AIAA PAPER 83-1929] 18 p2635 A83-39381

Implicit upwind methods for the Euler equations [AIAA PAPER 83-1930] 18 p2682 A83-39382

A fast Euler solver for steady flows [AIAA PAPER 83-1940] 18 p2682 A83-39389

High resolution applications of the Osher upwind scheme for the Euler equations [AIAA PAPER 83-1943] 18 p2636 A83-39390

A flexible grid embedding technique with application to the Euler equations [AIAA PAPER 83-1944] 18 p2636 A83-39391

Multiple-gridding of the Euler equations with an implicit scheme [AIAA PAPER 83-1945] 18 p2636 A83-39392

A new stream function formulation for the Euler equations [AIAA PAPER 83-1947] 18 p2636 A83-39393

Analysis by computer of the convergence to steady state of discrete approximations to the Euler equations [AIAA PAPER 83-1951] 18 p2636 A83-39395

Flux vector splitting and approximate Newton methods --- for solution of steady Euler equations [AIAA PAPER 83-1899] 18 p2683 A83-39404

A general perturbation approach for the equations of fluid dynamics [AIAA PAPER 83-1903] 18 p2637 A83-39411

Entropy and vorticity corrections for transonic flows [AIAA PAPER 83-1926] 18 p2637 A83-39413

Implicit conservative characteristic modeling schemes for the Euler equations - A new approach [AIAA PAPER 83-1939] 18 p2683 A83-39416

A nonstationary relaxation method for the Cauchy-Riemann and 1-D Euler equations [AIAA PAPER 83-1901] 18 p2683 A83-39418

Spectral methods for the Euler equations [AIAA PAPER 83-1942] 18 p2683 A83-39420

Two-point implicit scheme for the Euler equations --- for computational fluid dynamics 18 p2686 A83-39917

Upwind schemes and boundary conditions with applications to Euler equations in general geometries 19 p2789 A83-40752

Numerical experiments with the Osher upwind scheme for the Euler equations 20 p2930 A83-43439

Microscopic derivation of plasma electro-hydrodynamics 20 p3050 A83-43568

Nonparametric solution of the Euler equations for steady flow 21 p3127 A83-43827

Statistical solutions to Navier-Stokes system and Euler's systems 21 p3131 A83-44658

Free motions of a nearly spherical deformable solid 21 p3200 A83-45357

An implicit lambda scheme --- for transonic inviscid flow simulation 21 p3089 A83-45581

A low Mach number Euler formulation and application to time-iterative LBI schemes --- Linearized Block Implicit 21 p3134 A83-45592

On a variational approach to conservative hyperbolic systems 22 p3352 A83-45978

Investigation of the three-dimensional transonic flow around an air intake by a finite-volume method for the Euler equations 22 p3249 A83-46463

- Experience with the development of an Euler code for rotor rows
[ASME PAPER 83-GT-36] 23 p3394 A83-47897
The well-posedness of two-dimensional ideal flow
23 p3449 A83-48047

EULER-LAGRANGE EQUATION

- Conservation laws for a dynamical system in group variables 01 p0104 A83-10122
An averaged Lagrangian-finite element technique for the solution of nonlinear vibration problems
02 p0194 A83-12747
Quasi-periodic solutions of the plane three-body problem near Euler's orbits 03 p0404 A83-13416
Approximation of extremal surface elements / hyperbolic type/ by means of characteristic three-dimensional quadrilateral elements 03 p0388 A83-14493
The generalized Lagrangian-mean equations and hydrodynamic stability 06 p0757 A83-19014
A Lagrangian approach to the analysis of nonlinear electromagnetic circuits 07 p0922 A83-20969
Lagrange-type formulation for finite element analysis of non-linear beam vibrations 08 p1120 A83-21805
Multiply-upstream, semi-Lagrangian advective schemes - Analysis and application to a multi-level primitive equation model 08 p1139 A83-22288
Quasi-Lagrangian rezoning of fluid codes maintaining an orthogonal mesh 09 p1259 A83-23721
Lagrange variational equations from Hori's method for canonical systems 12 p1771 A83-29123
A mechanistic model of Eulerian, Lagrangian mean, and Lagrangian ozone transport by steady planetary waves
16 p2379 A83-36136
An Eulerian-Lagrangian method for turbulent combustion
[ONERA, TP NO. 1983-16] 16 p2327 A83-36426
Absolute synchronization - Faster-than-light particles and causality violation 16 p2407 A83-36551
An explicit Lagrangian scheme for solving plane and axisymmetric aerodynamic problems, and the mesh rezoning 21 p3130 A83-44558
Equations of motion for a dynamically tunable gyroscope with n rings 21 p3138 A83-44645
A method of obtaining equations of motion for a dynamically tunable gyroscope 21 p3142 A83-45353
Lagrangian models for turbulent combustion
[ONERA, TP NO. 1983-106] 24 p3554 A83-49417

EURECA (ESA)

- The microgravity payload for the first Eureka mission
17 p2473 A83-37869

EUROPA

- Radar properties of Europa, Ganymede, and Callisto
04 p0570 A83-16233
The geology of Europa 04 p0571 A83-16239
Liquid water and active resurfacing on Europa
08 p1190 A83-23263
Patterns of fracture and tidal stresses on Europa
13 p1961 A83-31203
Voyager photometry of Europa
19 p2922 A83-40782

EUROPE

- Fine mesh models in the U.K. Meteorological Office
04 p0519 A83-16157
Air traffic flow management over Europe
05 p0593 A83-17735
Spectral distribution of solar radiation in the Nordic countries 18 p2713 A83-39115
Experimental data on the typification of synoptic situations and cloud fields over Europe
23 p3486 A83-47128
Modelling of long-range transport of sulphur over Europe - A two-year model run and some model experiments
23 p3479 A83-48682

EUROPEAN AIRBUS

- NT A-300 AIRCRAFT
The A310 - Even better than expected
04 p0445 A83-14952
Flight flutter testing with emphasis on the tip vane method
[ONERA, TP NO. 1982-109] 06 p0717 A83-18435
Trim Tank system for optimizing drag at the center of gravity
[DGLR PAPER 82-030] 09 p1209 A83-24156
Selected topics in licensing Airbus A310
[DGLR PAPER 82-042] 09 p1199 A83-24166
Design and implementation of an active load alleviation system, taking into account the example of a modern transport aircraft
[DGLR PAPER 82-045] 09 p1209 A83-24170
New displays for the next generation of civil aircraft - Airbus A 310 and A 300/600 color cathode tubes
09 p1204 A83-24374
Maintenance of large engines CF6s for the Airbus A310
13 p1807 A83-30073
Astroplane - The Airbus proposal
18 p2762 A83-40456

- ASTROPLANE - A working group of the European Science Foundation
18 p2762 A83-40457
Advanced material application on the European wide body transport aircraft Airbus
[SAWE PAPER 1484] 20 p2935 A83-43751
Ten years of promoting the development of air transport research
23 p3391 A83-47185
Modern digital air-data computer
23 p3405 A83-47186
Experience from flight flutter testing with tip vanes on Airbus
24 p3547 A83-49183
Active gust load alleviation and ride comfort improvement
24 p3549 A83-49193

EUROPEAN COMMUNICATIONS SATELLITE

- A portable program package for geostationary orbit control
05 p0679 A83-17433
New drive system for large antennas
06 p0750 A83-18000
Multicarrier SPINE tests on the orbital test satellite module A
08 p1049 A83-21998
International Conference on Results of Tests and Experiments with the European OTS Satellite, London, England, April 8-10, 1981, Proceedings
13 p1811 A83-30139
High-efficiency satellite antenna
13 p1812 A83-31772
The Italsat preoperational communication satellite program
16 p2342 A83-36500

EUROPEAN INCOHERENT SCATTER RADAR**U EISCAT RADAR SYSTEM (EUROPE)****EUROPEAN LARGE TELECOMM SATELLITE****U L-SAT****EUROPEAN RETRIEVABLE CARRIER****U EURECA (ESA)****EUROPEAN SPACE AGENCY**

- NASA-ESA Spacelab systems and programs; Proceedings of the Seminar, Washington, DC, April 23, 24, 1981
03 p0284 A83-13703
Spacelab - Status and capabilities
03 p0285 A83-13705
International Scientific Conference on Space, 22nd, Rome, Italy, March 25, 26, 1982, Proceedings
04 p0450 A83-15655
The European space agency's programmes today and tomorrow
04 p0450 A83-15657
Advantages and problems of Italian participation in ESA
04 p0451 A83-15662
Earthnet prepares for Landsat-D
05 p0603 A83-17426
The agency's approach to normalisation and standards --- for ESA space technology
05 p0621 A83-17435
ESA procedures to account for inflation
11 p1666 A83-27372
The Earthnet LEDA-2 image catalogue system
11 p1666 A83-27375
The HIPPARCOS space astrometry mission
11 p1670 A83-27732
Fiber optics at ESO. I - Coupling of the CES with the 3.6 m telescope using a 40 m fiber link
13 p1922 A83-31576
Europe in space
16 p2313 A83-35776
Control systems for European satellites
17 p2475 A83-37854
The Sophia antipolis workshop on the relationship between ESA and industry
17 p2471 A83-37870
ESA's new high-performance tone-ranging system
17 p2475 A83-37874
Law and security in outer space: International regional role Focus on the European Space Agency
22 p3370 A83-46311
MACS - The ESA standard for guidance/control and robotics --- Modular Attitude Control Systems
[IAF PAPER 83-346] 23 p3422 A83-47352

EUROPEAN SPACE PROGRAMS

- European sensors on the Space Shuttle
01 p0020 A83-10082
Performance assessment of future European remote sensing systems
01 p0021 A83-10109
The Spacelab program - The future
01 p0017 A83-10431
Italy in millimeter waves activities for space communication
01 p0032 A83-11278
Current topics of SPS realization from a European viewpoint
01 p0069 A83-11283
Objectives of the German Spacelab Mission D1 and its role in the German space program
03 p0286 A83-13718
D1 mission project implementation
03 p0286 A83-13719
International Scientific Conference on Space, 22nd, Rome, Italy, March 25, 26, 1982, Proceedings
04 p0450 A83-15655
The European space agency's programmes today and tomorrow
04 p0450 A83-15657

- The Swedish space programme - Particularly the Viking and Tele-X projects
04 p0450 A83-15658
The Italian national space plan - The origin, rationale and objectives of the Italian space activities plan
04 p0450 A83-15659

- Goals of the new space programme of the Federal Republic of Germany
04 p0450 A83-15660
The San Marco project - Prospects and programs
04 p0452 A83-15666

- ESA's science programme - The present situation and future perspectives
04 p0451 A83-15667
Italian scientific space programs
04 p0451 A83-15668

- Microgravity programmes
04 p0451 A83-15669
The IRIS system - An Italian STS-upper stage
04 p0452 A83-15670

- A Retrievable Carrier for European science and applications
04 p0452 A83-15671
Biotechnology in space laboratories
05 p0669 A83-17111

- The SPINE programme and the associated demonstrations at UNISPACE 82 --- satellite data transmission via Space Information Network Experiment
05 p0622 A83-17427
Spacelab's role in future platform concepts
06 p0721 A83-19244
EURECA - A European free-floating platform
06 p0722 A83-19245

- A unifying concept for future fixed satellite service payloads for Europe
08 p1076 A83-22369
Deutsche Forschungs- und Versuchsanstalt fuer Luft- und Raumfahrt, Annual Report 1981 --- Book
09 p1195 A83-23850

- Status of the Spacelab program
[DGLR PAPER 82-059] 09 p1211 A83-24174
The status of work in the area of Spacelab development
[DGLR PAPER 82-061] 09 p1213 A83-24175
Eureca, a new element of Europe's space transportation systems
[DGLR PAPER 82-062] 09 p1213 A83-24176

- The concept of a retrievable microgravity platform
[DGLR PAPER 82-063] 09 p1213 A83-24177
Utilisation of a modular European orbital propulsion module
[DGLR PAPER 82-078] 09 p1213 A83-24192

- Rendezvous and docking possibilities in future European outer space projects
[DGLR PAPER 82-079] 09 p1211 A83-24193
Broadcast satellites in Europe
10 p1402 A83-25800

- GIRL - The German infrared laboratory for spacelab
11 p1670 A83-27741
The Magellan project --- European spaceborne ultraviolet observatory
11 p1670 A83-27744

- X-80, A European X-ray astrophysics mission
11 p1672 A83-27767
New opportunities for man
12 p1705 A83-29672

- International Conference on Results of Tests and Experiments with the European OTS Satellite, London, England, April 8-10, 1981, Proceedings
13 p1811 A83-30139
Structure and organizational mechanism of the Intercosmos Program
13 p1808 A83-30274

- Europe in space
16 p2313 A83-35776
The evolution of space technology and its economic impact Reflection on the transposition of the European model in the countries of the Third World
18 p2752 A83-39828

- The status of space science and technology in developed countries - The European experience
18 p2643 A83-39830
Review of the European microgravity activities
20 p2939 A83-43253

- The politics of space - The pride of France: A national commitment
21 p3094 A83-45608
Investigations on an active satellite system for earth kinematics and positioning
22 p3258 A83-46112

- IRIS - A new Italian upper stage system
[IAF PAPER 83-25] 23 p3419 A83-47237
Athos, an experimental telecommunication program to promote new platform and payload technologies
[IAF PAPER 83-59] 23 p3419 A83-47246

- The implications of the orbital characteristics of the European Kepler project
23 p3417 A83-48052
Simplified linearly polarised contoured beam reflector antenna for a European coverage requirement
23 p3444 A83-48713

- EUROPEAN SPACE RESEARCH ORGANIZATION**
U EUROPEAN SPACE AGENCY

- EUROPEAN SPACE RESEARCH ORGANIZATION SAT**
U ESA SATELLITES

- EUROPIUM**
Optical transitions of RbMgF₃:Eu²⁺/ and RbMgF₃:Mn²⁺/, Eu²⁺/ 11 p1581 A83-27590

EUTECTIC ALLOYS

A model for the formation of subboundaries in the matrix of eutectic alloys of the system M-MeC --- Ni or Co alloyed with Ta, Nb or Hf carbides 01 p0025 A83-10397

The significance of the dimensionless constant in the rate equation for superplastic flow 02 p0157 A83-12416

Thermal expansion of the directionally solidified Ni3Al-Ni3Nb eutectic alloy and its constituent phases 04 p0461 A83-16006

The modification of Si phase in Al-Si eutectic alloys - Effect of element addition on microstructures of Al-Si and Al-Si-Ge eutectic alloys 07 p0885 A83-20275

A study of the adhesive interaction between plasma-sprayed coatings of eutectic alloys on refractory steels 07 p0888 A83-20695

A study of the structure of liquid aluminum-silicon alloys. I - Hypoeutectic and eutectic melts 07 p0890 A83-20916

Microstructural changes and deformation mechanisms during creep of an unidirectionally solidified gamma/delta and gamma/gamma'-alpha eutectic alloy at elevated temperature 07 p0897 A83-21610

Modeling the creep and fracture of the directionally solidified gamma/gamma'-prime-MeC eutectic 08 p1068 A83-22786

Structure formation in binary refractory carbide eutectics based on niobium and molybdenum 09 p1229 A83-23522

The high-temperature friction of alloys of the system TiN/x/-TiB2 09 p1236 A83-25068

Isothermal oxidation of the COTAC 74 in-situ composite between 800 and 1300 C 10 p1389 A83-26891

Incipient fracture in shock-loaded lamellar metal alloy composites with and without microstructural defects 11 p1547 A83-27436

Investigation of the features of formation of crystalline structures grown in conditions of microgravity 11 p1661 A83-27447

Growth of thin ribbons of aluminum-base regular eutectic compositions and a study of their microstructures 11 p1548 A83-28367

Tensile properties of directionally solidified Ni-Al-Ti-(Ta) gamma/gamma prime eutectic alloys 12 p1714 A83-29415

Effects of cooling rate and modifier concentration on modification of Al-Si eutectic alloys 13 p1820 A83-30324

The properties of the eutectic composite gamma/gamma prime-delta 14 p1986 A83-31946

Subsurface damage during dry sliding wear of Al-Al3Ni eutectic alloy 14 p1993 A83-32623

The effect of heat treatment on the structure and long-term strength of the nickel eutectic gamma/gamma'-prime-MeC - The length memory effect 15 p2137 A83-34017

A study of the structure of liquid aluminum-silicon alloys. II - Hypereutectic melts 15 p2141 A83-35308

The temperature dependence of the ultimate stress for eutectic tungsten alloys with titanium, zirconium, and hafnium carbides 15 p2141 A83-35311

Creep-fatigue-effects in composites 16 p2324 A83-36172

Stress field related to dislocation arrangements observed in the phase boundary of a lamellar in-situ composite 18 p2667 A83-40257

New method of preparation of dispersion-hardening materials Improvement of mechanical properties of as-cast eutectics followed by heavy deformation 18 p2667 A83-40280

Thermal stability in microstructure and rupture strength of directionally solidified Ni-Al-Ti eutectic alloys 19 p2819 A83-40775

Response of MnBi-Bi eutectic to freezing rate changes 20 p2942 A83-43303

Gravitationally induced convection during directional solidification of off-eutectic Mn-Bi alloys 20 p2942 A83-43308

A study of a cellular phase transformation in the ternary Ni-Al-Mo alloy system 20 p2954 A83-43341

Mechanical properties of superplastic Al-Zn eutectoid-base alloys having ultrafine-grained structures 20 p2957 A83-43637

Ni-base MC-carbide reinforced eutectic alloys for jet engine application 21 p3111 A83-44061

Effect of swaging on the 1000 C compressive slow plastic flow characteristics of the directionally solidified eutectic alloy gamma/gamma prime-alpha 21 p3111 A83-44340

Shape of growing crystals of primary phases in eutectic alloys of the systems Fe-Fe2B and Ni-Ni3B 21 p3112 A83-44476

Unidirectional solidification behaviors at high cooling rates in Al-Fe-Mn ternary eutectic alloys 23 p3431 A83-47651

Precipitation in Ni-Mo-Al in-situ composite 23 p3431 A83-47848

EUTECTIC COMPOSITES

Microstructural and dimensional stabilities of a potential gamma/gamma prime-alpha/Mo/ directionally solidified eutectic superalloy under cyclic thermal exposure to 1000 C 04 p0460 A83-15987

Creep of directionally solidified superalloys and eutectic composites 09 p1232 A83-24062

High-temperature composites - Status and future directions 18 p2650 A83-40129

Tensile and compressive deformation and fracture behavior of the Al-Al3Ni eutectic composites at elevated temperatures 18 p2667 A83-40255

Influence of gravity driven convection on the directional solidification of Bi/MnBi eutectic composites 20 p2942 A83-43302

EUTECTIC DIAGRAMS

U PHASE DIAGRAMS

EUTECTICS

NT EUTECTIC ALLOYS

The effect of iron, aluminium, calcium on the vitrification of grain-boundary phases in nitrogen ceramics 05 p0619 A83-17570

Reactions of FeS2, CoS2, and NiS2 electrodes in molten LiCl-KCl electrolytes 07 p0881 A83-20578

EMF measurements on the Li-Al/Ni3S2 couple in molten salt electrolytes 14 p1990 A83-32636

Influence of freezing rate changes of MnBi-Bi eutectic microstructure --- effects of space processing 18 p2643 A83-39899

EVACUATING (TRANSPORTATION)

An FAA analysis of aircraft emergency evacuation demonstrations [SAE PAPER 821486] 17 p2459 A83-38005

EVALUATION

NT TRAINING EVALUATION

Defining the subjective experience of workload 10 p1457 A83-26330

Quantitative indicators for evaluation of basic research programs/projects 19 p2906 A83-41298

The evaluation cycle - In Res evaluation approaches for the eighties 19 p2906 A83-41300

Clinical possibilities in the evaluation of extreme effects --- on humans 23 p3496 A83-47102

EVANESCENCE

Diffraction efficiencies of evanescent-wave holograms - An improved model 08 p1092 A83-22080

Evanescent waves and complex rays for modal propagation in curved open waveguides 20 p3043 A83-43122

EVAPORATION

NT EVAPOTRANSPIRATION

NT PROPELLANT EVAPORATION

NT TRANSPIRATION

Kinetic analysis of evaporation and condensation in a vapor-gas mixture 03 p0315 A83-13118

Chromospheric evaporation in soft X-ray flares 03 p0436 A83-13157

Collision between an evaporating drop and a hot wall 04 p0478 A83-16166

The use of electron-beam evaporation for producing refractory coatings 07 p0888 A83-20691

Sensible heat flux estimated from routine meteorological data by the resistance method 07 p0969 A83-20805

Kinetic theory of evaporation and condensation for a cylindrical condensed phase 10 p1490 A83-25784

Vapor flow through a porous membrane - A throttling process with condensation and evaporation 11 p1567 A83-27859

A theory of nondilute spray evaporation based upon multiple drop interactions 13 p1843 A83-31223

Evaporation from a two-dimensional meniscus [AIAA PAPER 83-1526] 14 p2011 A83-32757

Evaporation and condensation on two parallel plates at finite Reynolds numbers 14 p2094 A83-33379

An outline of approach linking black-hole-evaporation with quantum-field effects in flat spacetime 15 p2262 A83-34531

Using midday surface temperature to estimate daily evaporation from satellite thermal IR data 15 p2188 A83-35288

On the evaporation of shock-compressed metals during expansion 16 p2328 A83-35539

A model for the Priestley-Taylor parameter alpha --- of atmospheric boundary layer 18 p2724 A83-39680

Theory of the Leidenfrost phenomenon 18 p2685 A83-39866

Quantized evaporation from liquid helium 20 p3044 A83-42167

Evaporation from a partially wet forest canopy 21 p3165 A83-44234

Evaporation derived from optical and radio-wave scintillation --- for water balance and mesoscale meteorological studies 22 p3339 A83-46069

EVOKED RESPONSE (PSYCHOPHYSIOLOGY)

Evaporation-limited tropical temperatures as a constraint on climate sensitivity 22 p3340 A83-46847

The interdependence of spray characteristics and evaporation history of fuel sprays in stagnant air [ASME PAPER 83-GT-7] 23 p3440 A83-47880

EVAPORATION RATE

The role of the heat-up period in fuel drop evaporation [AIAA PAPER 83-0068] 05 p0632 A83-16500

Evaporation and ignition of a fuel droplet on a hot surface. IV - Model of evaporation and ignition 13 p1818 A83-31224

Is gasification rate controlling step in polymer ignition? 15 p2142 A83-33724

Further studies on the prediction of spray evaporation rates --- for aircraft fuels 16 p2338 A83-35811

The effect of the real properties of a carrier vapor on the evaporation time of a drop 17 p2506 A83-37814

Steady-state evaporation characteristics of hydrocarbon fuel drops 21 p3117 A83-45587

EVAPORATIVE COOLING

NT FILM COOLING

NT SWEAT COOLING

Dynamic equation of state of a gas with evaporating drops 04 p0544 A83-15445

Inertial effects of the gas motion upon the linear and nonlinear waves in Kelvin-Helmholtz flow 08 p1083 A83-21813

Shuttle Water Spray Boiler flight performance --- lubricant cooling for Orbiter Hydraulic System and APU [SAE PAPER 820885] 10 p1383 A83-25751

Mass, heat, and momentum transfer in laminar and turbulent pipe flow with vaporization of a liquid film 15 p2161 A83-34266

Heat transfer in thin liquid films flowing over horizontal tubes 20 p2981 A83-42771

Gas turbine compressor interstage cooling using methanol [ASME PAPER 83-GT-230] 23 p3466 A83-48026

EVAPORATORS

An experimental study of an annular film-evaporation combustion chamber in a low-power gas turbine engine 09 p1205 A83-23443

Shuttle orbiter flash evaporator operational flight test performance [SAE PAPER 820883] 13 p1812 A83-30926

Monogroove heat pipe development for the space constructible radiator system [AIAA PAPER 83-1431] 14 p2010 A83-32706

Heat transfer in the evaporation and condensation zones of heat pipes intensely heated at the end 15 p2161 A83-34471

The geyser effect in a two-phase thermosyphon 16 p2354 A83-36597

EVAPOROGRAPHY

Remote determination of surface evaporation using thermal IR measurements 01 p0065 A83-10101

EVAPOTRANSPIRATION

Processing of remotely sensed data for mapping thermal inertia, soil moisture and evapotranspiration in semi-arid areas 09 p1288 A83-24585

Estimates of regional evapotranspiration in South-Eastern France using thermal and albedo data from the heat capacity mapping mission satellite 09 p1291 A83-24631

Satellite-derived surface energy balance estimates in the Alaskan sub-Arctic 18 p2721 A83-39112

EVASIVE ACTIONS

Deterministic and stochastic differential games [AIAA PAPER 83-0573] 05 p0682 A83-16799

The capture region of a coasting pursuer 07 p0987 A83-21010

One pursuer and two evaders on the line - A stochastic pursuit-evasion differential game 12 p1773 A83-29245

The effects of non-linear kinematics in optimal evasion 19 p2889 A83-40674

Pursuit-evasion between two realistic aircraft [AIAA PAPER 83-2119] 19 p2894 A83-41944

The optimal evasive maneuver of a fighter against proportional navigation missiles [AIAA PAPER 83-2139] 19 p2807 A83-41961

EVECTION

U LUNAR ORBITS

U ORBIT PERTURBATION

U SOLAR GRAVITATION

EVOKED RESPONSE (PSYCHOPHYSIOLOGY)

The functional asymmetry of the brain and the direct subjective evaluation of loudness 01 p0085 A83-10503

Contrast sensitivity - Psychophysical and evoked potential methods compared 05 p0676 A83-17750

The slow latent auditory evoked potential of humans 07 p0976 A83-19932

The visual function of the nonprojected sections of the cortex and its reflection in the evoked potentials 07 p0973 A83-20353

- Evoked potentials /EP/ and the processing of sensory information in the visual system of humans 07 p0976 A83-20354
- Electrophysiological investigations of color vision in humans 07 p0977 A83-20358
- The effects of various gases on cortical and spinal somatosensory evoked potentials at pressures up to 10 bar 07 p0974 A83-20777
- Evoked potentials of the posterior associative regions of the cerebrum during the discrimination and identification of human facial images 12 p1764 A83-29302
- Vertical fusional response to asymmetric disparities --- of retinal image stimulus 14 p2068 A83-32800
- The age characteristics of cortical auditory evoked potentials 14 p2071 A83-33341
- The effect of spatial-structural stimulus parameters on the evoked potentials in the visual and posterior associative areas of the cortex in humans 14 p2071 A83-33342
- Modifying oculomotor activity in awake subjects increases the amplitude of eye movements during REM sleep 15 p2211 A83-33777
- Brainstem auditory evoked potentials 16 p2398 A83-35902
- The effect of genotype and environment on evoked potential parameters during orienting and defensive reactions 16 p2401 A83-36824
- Comparison of the spatial response properties of the human retina and cortex as measured by simultaneously recorded pattern ERGs and VEPs 19 p2880 A83-40750
- The characteristics of the evoked electrical reactions of the nucleus lateralis posterior of the thalamus of rabbits and their dependence on the functional condition of the cortex and the reticular formation 19 p2879 A83-42092
- The first cortical implant of a multiplexed multi-electrode semiconductor brain electrode 20 p3035 A83-42553
- A cholinergic-sensitive channel in the cat visual system tuned to low spatial frequencies 21 p3183 A83-44364

EVOLUTION (DEVELOPMENT)

- NT ABIOTIC GENESIS
- NT BIOLOGICAL EVOLUTION
- NT CHEMICAL EVOLUTION
- NT GALACTIC EVOLUTION
- NT LUNAR EVOLUTION
- NT PLANETARY EVOLUTION
- NT STELLAR EVOLUTION
- NT STELLAR MASS ACCRETION
- Structure and origin of cometary nuclei 03 p0415 A83-13382
- On the distribution and evolution of clouds and rain over the Vosges and Black Forest mountains - A three-dimensional mesoscale simulation with parameterized microphysics 03 p0368 A83-14437
- The origin of the cosmic X-ray background 04 p0575 A83-16047
- The outer satellites of Jupiter 04 p0570 A83-16230
- The evolution of large-scale structures in the universe. I 04 p0558 A83-16376
- Absolute age of formation of chondrites studied by the /Rb-87/-/Sr-87/ method 05 p0703 A83-16846
- Chaos in the mixmaster universe 05 p0703 A83-17937
- Supernovae and the origin of the solar system 08 p1179 A83-21857
- Evolution of cometary perihelion distances in Oort cloud - Another statistical approach 10 p1492 A83-25511
- Updraft evolution and storm types 11 p1623 A83-26998
- The evolution of quasars 13 p1949 A83-31319
- Internal motions in ten planetary nebulae 17 p2587 A83-37279
- Madley - Growth of a large earth station 23 p3442 A83-47653
- The cosmological evolution of general Bianchi models in the adiabatic regime 24 p3660 A83-49429
- The formation of comets by radiation pressure in the outer protosun. II - Dependence on the radiation-grain coupling. III - Dependence on the anisotropy of the radiation field 24 p3664 A83-49889

EVOLUTION (LIBERATION)

NT GAS EVOLUTION

EXACTNESS

U PRECISION

EXAMINATION

NT EYE EXAMINATIONS

EXCHANGING

NT CHARGE EXCHANGE

NT GAS EXCHANGE

NT ION EXCHANGING

NT RESONANCE CHARGE EXCHANGE

The reaction $H_2 + D_2 \rightarrow 2HD$ - A long history of erroneous interpretation of shock tube results 23 p3429 A83-47633

EXCIMER LASERS

- Pulsed excimer laser annealing of ion implanted silicon - Characterization and solar cell fabrication 02 p0243 A83-12284
- Lasers in the 200-400 nm region - Characteristics and applications 03 p0332 A83-13956
- Picosecond, tunable ArF/asterisk/ excimer laser source 03 p0333 A83-14933
- Survey of lasers for spectroscopic use - Optical and ultraviolet 04 p0485 A83-15802
- An UV-preionized KrF excimer laser with an output energy of 0.42 J 06 p0766 A83-19143
- Determination of the minimum X-ray flux for effective preionization of an XeCl laser 06 p0767 A83-19255
- Compact repetitively pulsed excimer laser 07 p0938 A83-21383
- Analysis, design and construction of rare-gas halide discharge lasers 09 p1271 A83-23695
- Thermal homogeneity in a closed excimer laser cavity 09 p1272 A83-24661
- Generation of 35.5-nm coherent radiation 10 p1429 A83-26115
- Supersonic flow e-beam stabilized discharge excimer lasers 10 p1430 A83-26171
- Characteristics of the laser emission spectrum of a thallium photodissociation laser 10 p1431 A83-26654
- A discharge-pumped repetitively pulsed excimer laser 10 p1435 A83-26948
- Tuning characteristics of broadband excimer lasers 11 p1576 A83-27503
- Kinetics of the triatomic Xe2Cl/asterisk/-laser 11 p1576 A83-27504
- XeF laser beam quality impact of pump-induced medium inhomogeneities 11 p1576 A83-27505
- Arc suppression in excimer laser discharges 11 p1576 A83-27506
- Analysis of the lifetime of a small volume UV preionized discharge XeCl excimer laser 11 p1576 A83-27507
- High spectral brightness extreme ultraviolet generation with excimer lasers 11 p1576 A83-27508
- Injection locking of excimer lasers 11 p1577 A83-27518
- Formation of highly excited Ar and Kr atoms in the case of asymmetric charge transfer of Ar(+) and Kr(+) ions with rare-gas atoms 13 p1915 A83-30019
- High-power-density electron-beam-sustained laser 13 p1849 A83-30256
- Laser induced deposition of zinc oxide 13 p1928 A83-30335
- A high-power, narrow linewidth XeCl(asterisk) oscillator 13 p1852 A83-31058
- Characteristics of a pulsed chemical laser utilizing an H2-F2 mixture and initiated by radiation from an XeCl excimer laser 14 p2022 A83-31903
- Laser action benzimidazoles in various aggregate states 14 p2024 A83-32827
- Metal plasma induced by the bombardment of 308 nm excimer and 585 nm dye laser pulses at low pressure 15 p2235 A83-34368
- Long pulse excimer laser excited by sequenced discharges 16 p2359 A83-35956
- Optimization of electrically excited XeF(C yields A) laser performance 16 p2361 A83-36770
- Differential-absorption-lidar measurement of tropospheric ozone with excimer-Raman hybrid laser 17 p2540 A83-37942
- Deep-ultraviolet spatial-period division using an excimer laser [AD-A122130] 19 p2850 A83-40672
- XeCl excimer laser excited by longitudinal discharge 20 p2995 A83-43597
- Laser induced damage in the ultraviolet 21 p3145 A83-44831
- New technological developments for the remote detection of atmospheric hydroxyl radicals 22 p3288 A83-46072
- Gain on the green (504 nm) excimer band of I2 22 p3299 A83-46726
- Development of compact excimer lasers for remote sensing 23 p3461 A83-47796
- Progress in dye and excimer laser sources for remote sensing 23 p3462 A83-47800
- Multiphoton excitation and frequency tripling in xenon 23 p3463 A83-48579

EXCIMERS

Photolysis of KI/Xe mixtures at 193 nm - Observation of KXe/asterisk/ emission 07 p0933 A83-19977

EXCITATION

- NT ACOUSTIC EXCITATION
- NT ATOMIC EXCITATIONS
- NT HARMONIC EXCITATION
- NT MOLECULAR EXCITATION
- NT SELF EXCITATION
- NT WAVE EXCITATION

- On the excitation of oscillations of the sun /numerical models/ 11 p1689 A83-27651
- An analytical excitation model for an ionizing plasma 19 p2901 A83-40889
- The 'whistler-nozzle' phenomenon 24 p3578 A83-49472

EXCITED STATES

U EXCITATION

EXCITONS

- Donor discrimination and bound exciton spectra in InP 07 p1000 A83-20746
- Raman scattering of light in crystals with the participation of the Bose-Einstein condensate of excitons 11 p1663 A83-28561
- Electroabsorption by Stark effect on room-temperature excitons in GaAs/GaAlAs multiple quantum well structures 14 p2093 A83-33442
- Luminescence of strong exciton transitions 21 p3219 A83-45336

EXCRETION

- The effect of several diuretics on the renal excretion of glycine in dogs 07 p0975 A83-20988
- The role of the kidneys in the pharmacokinetics of novocainamide 07 p0975 A83-20989

EXECUTIVE AIRCRAFT

U GENERAL AVIATION AIRCRAFT

U PASSENGER AIRCRAFT

EXERCISE

U PHYSICAL EXERCISE

EXERCISE PHYSIOLOGY

- Reduction in plasma calcium during exercise in man 01 p0082 A83-10212
- The ensemble of circadian rhythms and the effectiveness of training activities conducted at various times of the day 01 p0083 A83-10518
- Sport gastroenterology - Some results and prospects of development 01 p0083 A83-10519
- The active and passive flexibility of athletes of various specialties 01 p0083 A83-10523
- The changes in the hemodynamics of dogs during exercise of different intensities in the acute adaptation to high altitude 01 p0079 A83-10529
- Assessment of central hemodynamics during arm-crank exercise 01 p0083 A83-11138
- A comparison of the cardiovascular responses to isometric exercise of three different sized muscle groups 01 p0083 A83-11139
- Recovery curves in partially fatigued muscle 01 p0084 A83-11259
- The dependence of immunological changes in athletes in polar regions on the intensity of the physical load 01 p0084 A83-11387
- The effect of physical exercise on changes of lysozyme in the blood of athletes 01 p0084 A83-11388
- The methodological principles for the determination of physical work capacity in young athletes 03 p0382 A83-14352
- The effects of rest and exercise in the cold on substrate mobilization and utilization 04 p0521 A83-15534
- Pericardial massages and their effect on the rehabilitation therapy by means of graded physical loads of patients who have had a myocardial infarction 05 p0673 A83-17172
- Effect of change in P50 on exercise tolerance at high altitude - A theoretical study 05 p0671 A83-17329
- Surfactant homeostasis in the rat lung during swimming exercise 05 p0671 A83-17330
- Autonomic contribution to heart rate recovery from exercise in humans 05 p0675 A83-17335
- Comparison of hemodynamic responses to static and dynamic exercise 05 p0675 A83-17337
- Fate of exogenous glucose during exercise of different intensities in humans 05 p0675 A83-17338
- Criteria for the evaluation of the physical aptitude - Their utilization for the classification of subjects 06 p0799 A83-18339
- Means for increasing athletic fitness - Technical and applied military aspects of athletics --- Russian book 07 p0977 A83-20383
- Response of age forty and over military personnel to an unsupervised, self-administered aerobic training program 07 p0977 A83-20783
- The diagnostic accuracy of exercise electrocardiography - A review 07 p0978 A83-20785
- Effects of ageing on cardiorespiratory changes to moderate physical exercise 09 p1323 A83-24005
- Variations in heart rate (pulse 'drift') in the course of work of constant aerobic intensity in athletes and nonathletes 12 p1765 A83-29316
- Effect of hyperoxia on metabolic and catecholamine responses to prolonged exercise 13 p1902 A83-30456
- Determination of maximal aerobic power during upper-body exercise 13 p1902 A83-30458

Blood osmolality in vitro - Dependence on P(CO₂), lactic acid concentration, and O₂ saturation
13 p1902 A83-30459

Metabolic and cardiorespiratory responses to He-O₂ breathing during exercise
13 p1903 A83-30470

Drinking and water balance during exercise and heat acclimation
13 p1903 A83-30471

Effect of glycogen depletion on the ventilatory response to exercise
13 p1903 A83-30474

Plasma volume shifts during progressive arm and leg exercise
13 p1903 A83-30475

Plasma volume, renin, and vasopressin responses to graded exercise after training
13 p1903 A83-30476

Unusual core temperature decrease in exercising heart-failure patients
13 p1903 A83-30478

Muscle fiber composition and blood ammonia levels after intense exercise in humans
13 p1903 A83-30480

Coupling of ventilation to pulmonary gas exchange during nonsteady-state work in men
13 p1903 A83-30481

Ventilatory and circulatory transients during exercise - New arguments for a neurohumoral theory
13 p1897 A83-30483

Repeated development and regression of exercise-induced cardiac hypertrophy in rats
13 p1898 A83-30489

Skeletal muscle mitochondria and myoglobin, endurance, and intensity of training
13 p1898 A83-30490

Impaired red cell filterability with elimination of old red blood cells during a 100-km race
13 p1904 A83-30492

Effects of beta-adrenergic blockade on O₂ uptake during submaximal and maximal exercise
13 p1904 A83-30497

Anaerobic threshold, blood lactate, and muscle metabolites in progressive exercise
13 p1905 A83-30503

Changes in diastolic coronary resistance during submaximal exercise in conditioned dogs
13 p1898 A83-30504

Cardiovascular responses to exercise as functions of absolute and relative work load
14 p2069 A83-32817

The adaptation of the body to physical load after a loss of blood
14 p2069 A83-33301

The interrelation of the parameters of the cardiorespiratory system in athletes during various conditions
14 p2069 A83-33303

An evaluation of muscle forces according to the electrical activity of muscles during athletic exercises in 'loadless' conditions
14 p2070 A83-33304

The characteristics of the changes of several biochemical parameters of the blood during the testing of the general endurance of middle distance runners
14 p2070 A83-33305

Physiological and biochemical methods for evaluating the functional condition of athletes in cyclical forms of sports
14 p2070 A83-33306

Renin, kallikrein, and the angiotensin-converting enzyme during a physical load in humans
15 p2213 A83-34959

An evaluation of the condition and potential of athletes using indicators of humoral-hormonal reactions
16 p2398 A83-35904

The effect of maximum physical work on the cardiodynamics and microcirculatory bed of young athletes and of individuals not pursuing athletic activities
16 p2398 A83-35907

Reserves of the respiratory system under various conditions of aerobic productivity
16 p2398 A83-35908

Adrenocortical activity in athletes after repeated physical loads during the course of the day
16 p2398 A83-35909

Expiratory and arterial partial pressure relations under different ventilation-perfusion conditions
17 p2558 A83-36996

The physiological advisability of voluntary control of respiration in athletes
17 p2558 A83-38169

The optimal speed of cyclic locomotion in individuals of different ages
17 p2559 A83-38172

The cardiovascular system and the fitness for work of athletes --- Russian book
19 p2880 A83-40983

Alteration of ischemic cardiac function in normal heart by daily exercise
19 p2875 A83-41134

Changes in total body calcium balance with exercise in the rat
19 p2875 A83-41138

A constant-velocity cycle ergometer for the study of dynamic muscle function
19 p2885 A83-41139

Power output and fatigue of human muscle in maximal cycling exercise
19 p2880 A83-41140

The characteristics of heart rhythm disorders in athletes with various types of vegetative regulation
19 p2882 A83-41447

Gravitational effects on human cardiovascular responses to isometric muscle contractions
19 p2884 A83-42049

Lactate in human skeletal muscle after 10 and 30 s of supramaximal exercise
20 p3034 A83-43479

Fluid and electrolyte homeostasis during prolonged exercise at altitude
20 p3034 A83-43481

Breathing patterns during submaximal and maximal exercise in elite oarsmen
20 p3034 A83-43483

Effects of acute moderate-intensity exercise on carnitine metabolism in men and women
20 p3034 A83-43484

Effects of exercise and lack of exercise on glucose tolerance and insulin sensitivity
20 p3035 A83-43485

A comparison of methods for quantitation of metabolites in skeletal muscle
20 p3033 A83-43488

Maximal exercise at extreme altitudes on Mount Everest
22 p3347 A83-45983

Instantaneous cardiac acceleration in the cat elicited by peripheral nerve stimulation
22 p3345 A83-45985

Influence of body CO₂ stores on ventilatory dynamics during exercise
22 p3347 A83-45988

Chronic low-sodium diet in rats - Hormonal and physiological effects during exercise in the heat
22 p3346 A83-45994

Neck muscle loading and fatigue - Systematic variation of headgear weight and center-of-gravity
24 p3618 A83-48878

Effect of confinement in small space flight size cages on insulin sensitivity of exercise-trained rats
24 p3617 A83-48881

EXERTION

U PHYSICAL WORK

EXHAUST DIFFUSERS

Design and development of a nozzle extendible exit cone
[AIAA PAPER 83-1410] 16 p2323 A83-36399

Experimental study of jet-flap diffusers
17 p2448 A83-37534

EXHAUST EMISSION

Impacts of broadened-specification fuels on aircraft turbine engine combustors
01 p0028 A83-10655

Contamination measurements during the firing of the solid propellant apogee insertion motor on the P78-2 /SCATHA/ spacecraft
03 p0284 A83-13751

NOx formation experiments in an MHD simulation facility
04 p0507 A83-16103

Design of a low emission combustor for an automotive gas turbine
[AIAA PAPER 83-0338] 05 p0652 A83-16664

The application of forest classification from Landsat data as a basis for natural hydrocarbon emission estimation and photochemical oxidant model simulations in southeastern Virginia
07 p0957 A83-19848

Gas turbine combustor modelling for calculating pollutant emission
08 p1046 A83-23142

Radiation and smoke from the gas turbine combustor using heavy fuels
09 p1242 A83-23877

Possibilities of improving exhaust emissions and energy consumption in mixed hydrogen-gasoline operation
11 p1589 A83-27334

The effect of fuel injection on NOx emissions and undesirable combustion for hydrogen-fuelled piston engines
11 p1589 A83-27335

Fuel character effects on the TF41 engine combustion system
13 p1807 A83-30190

Postfire sampling of SRMs for contamination sources in high altitude test cells
[AIAA PAPER 83-1448] 14 p1984 A83-32716

The effects of fuel properties upon pollutants present in gas turbine aero-engines
16 p2338 A83-35813

Experimental exhaust plume analysis with MB8 10 N thruster --- Bipropellant for US/German Galileo spacecraft propulsion
[AIAA PAPER 83-1259] 16 p2320 A83-36313

A JT8D low emissions combustor by radial zoning
[AIAA PAPER 83-1324] 16 p2309 A83-36339

Development and operating characteristics of an advanced two-stage combustor
17 p2469 A83-38022

Procedure for the calculation of basic emission parameters for aircraft turbine engines
[SAE AIR 1533] 17 p2469 A83-38104

Investigation of fixed-rake sampling system for the assessment of emission characteristics of gas turbine engines
[ASME PAPER 83-GT-72] 23 p3407 A83-47925

Emissions variability and traversing on production RB211 engines
[ASME PAPER 83-GT-141] 23 p3409 A83-47966

Emissions from enclosed swirl stabilised premixed flames
[ASME PAPER 83-GT-192] 23 p3410 A83-47998

EXHAUST FLOW SIMULATION

NT ATMOSPHERIC ENTRY SIMULATION

Scale model performance test investigation of mixed flow exhaust systems for an energy efficient engine /E3/ propulsion system
[AIAA PAPER 83-0541] 05 p0597 A83-16776

Experimental and theoretical studies on the relationship between engine exhaust and the surrounding flow field --- German thesis
06 p0714 A83-19618

Prediction of the flowfield in laser propulsion devices
[AIAA PAPER 83-1445] 15 p2129 A83-34907

Rocket exhaust plume induced flowfield interaction experiences with the Space Shuttle
[AIAA PAPER 83-1549] 15 p2128 A83-34923

Numerical investigation of three-dimensional transonic flow through air intakes disturbed by a missile plume
[AIAA PAPER 83-1854] 17 p2457 A83-38682

Plume/flowfield jet interaction effects on the Space Shuttle Orbiter during entry
18 p2646 A83-40009

Bell-shaped jet flow into a vacuum and interference effects with affected surfaces
22 p3261 A83-46486

EXHAUST GASES

NT FLUE GASES

The influence of equivalence ratio variation on pollutant formation in a gas turbine type combustor
02 p0136 A83-13095

Gaseous emissions of gas turbine combustors
[AIAA PAPER 83-0242] 05 p0596 A83-16608

Studies of a diffusion flame matrix burner in a combustion chamber with heat exchanger
09 p1225 A83-23334

Concentration of selected vapor and particulate-phase substances in the Lincoln and Holland Tunnels
11 p1613 A83-28699

Thrust reverser exhaust plume reingestion tests for a STOL fighter model
[AIAA PAPER 83-1229] 16 p2307 A83-36293

An application of model testing for the study of rocket exhaust cloud properties
17 p2483 A83-38706

Microphysical properties of the Shuttle exhaust cloud
17 p2536 A83-38707

Lidar remote measurements of Space Shuttle ground cloud emissions
17 p2537 A83-38708

A study of the formation of nitrogen oxides during the combustion of a lean homogeneous mixture in the hybrid combustion chamber of an automotive gas-turbine engine
19 p2821 A83-42134

Experimental investigation of a model of the internal exhaust gas mixer configuration of a turbofan engine in the reverse-thrust mode
19 p2801 A83-42146

EXHAUST JETS

U EXHAUST GASES

EXHAUST NOZZLES

NT CONVERGENT-DIVERGENT NOZZLES

NT TURBINE EXHAUST NOZZLES

Prediction of jet exhaust noise on airframe surfaces during low-speed flight
03 p0282 A83-13160

Pressure transfer function of a JT15D nozzle due to acoustic and convected entropy fluctuations
04 p0533 A83-16319

Effect of swirl on the potential core in two-dimensional ejector nozzles
06 p0712 A83-18416

Analysis of secondary flows for tube-launched rocket configurations
07 p0863 A83-20417

Internal performance prediction for advanced exhaust systems --- for tactical aircraft
08 p1046 A83-22156

A high speed wind tunnel test evaluation of STOL dedicated advanced exhaust nozzle concepts
[AIAA PAPER 83-1225] 16 p2294 A83-36292

Results of tests of a rectangular vectoring/reversing nozzle on an F101 engine
[AIAA PAPER 83-1285] 16 p2308 A83-36322

A static investigation of yaw vectoring concepts on two-dimensional convergent-divergent nozzles
[AIAA PAPER 83-1288] 16 p2294 A83-36324

Three-dimensional compressible viscous analysis of mixer nozzles
[AIAA PAPER 83-1401] 16 p2295 A83-36391

Definition of vectored nonaxisymmetric nozzle plumes --- for aircraft thrust vector control
[AIAA PAPER 83-1290] 16 p2297 A83-36924

Advanced technology exhaust nozzle development
[AIAA PAPER 83-1286] 17 p2451 A83-38080

Exhaust nozzle concepts for STOL tactical aircraft
[AIAA PAPER 83-1226] 18 p2639 A83-39102

Vectoring exhaust systems for STOL tactical aircraft
[ASME PAPER 83-GT-212] 23 p3410 A83-48013

Performance of a forward swept wing fighter utilizing thrust vectoring
[AIAA PAPER 83-2482] 23 p3404 A83-48344

EXHAUST SYSTEMS

Scale model performance test investigation of mixed flow exhaust systems for an energy efficient engine /E3/ propulsion system
[AIAA PAPER 83-0541] 05 p0597 A83-16776

Experimental and theoretical studies on the relationship between engine exhaust and the surrounding flow field --- German thesis
06 p0714 A83-19618

EXISTENCE THEOREMS

- Design and development of a mixer compound exhaust system --- in aircraft turbofan engines 09 p1206 A83-24029
- Measurement of acoustic modes and wall impedance in a turbofan exhaust duct [AIAA PAPER 83-0733] 11 p1651 A83-28015
- Sound propagation in segmented exhaust ducts - Theoretical predictions and comparison with measurements [AIAA PAPER 83-0734] 11 p1651 A83-28016
- The integration of internal combustion engines of the General Aviation - Problems raised by ventilation and exhaust [AAAF PAPER NT 82-16] 14 p1976 A83-33167
- Model test and full-scale checkout of dry-cooled jet runup sound suppressors 23 p3413 A83-48217

EXISTENCE THEOREMS

- Formal convergence characteristics of elliptically constrained incremental Newton-Raphson algorithms 01 p0101 A83-10273
- Partial regularity of suitable weak solutions of the Navier-Stokes equations 02 p0170 A83-12100
- On the restricted three-body problem when the mass parameter is small 03 p0404 A83-13413
- On the existence of periodic solutions of Poincaré's third sort in the general problem of three bodies in three dimensions 03 p0404 A83-13414
- The existence and uniqueness of a solution for a boundary-value problem for an equation of mixed type in a rectangular domain 03 p0388 A83-14495
- Global existence results for discrete velocity models of the Boltzmann equation in several dimensions 03 p0400 A83-14569
- On the nonexistence and existence of global solutions of boundary value problems for quasi-linear parabolic equations --- in propagation of thermal disturbances 05 p0640 A83-17642
- Existence and uniqueness of shock-free transonic flow past symmetrical thin wings at zero incidence 05 p0590 A83-17847
- Existence of a generalized solution in thermoelasticity with two relaxation times. I 06 p0775 A83-18807
- On the swirling flow between rotating coaxial disks - Existence and nonuniqueness 06 p0757 A83-18824
- Absolute stability and absolute instability of control systems with two nonlinear nonstationary elements. II 07 p0984 A83-19997
- Global transformations of nonlinear systems 07 p0984 A83-20719
- Analysis of oscillations in systems with polynomial-type nonlinearities using describing functions 07 p0984 A83-20720
- Design of linear systems with saturating linear control and bounded states 07 p0985 A83-20725
- Cascade of period doublings of tori 08 p1162 A83-22948
- On conditions of the existence of certain classes of solutions of the problem of the motion of a rigid body with a fixed point 09 p1337 A83-23551
- Isoconic motions of a rigid body with a fixed point 09 p1337 A83-23553
- On local controllability 09 p1329 A83-24731
- Stochastic control of randomly varying systems 09 p1331 A83-24770
- Simultaneous design of control systems 09 p1332 A83-24781
- Necessary and sufficient conditions for regulation of linear systems 09 p1333 A83-24794
- Instability and the ill-posed Cauchy problem in elasticity 10 p1437 A83-25310
- An existence theorem for a non linear shell model in large displacements analysis 10 p1438 A83-25463
- Model reference invariant control for a class of unknown multivariable plants 10 p1468 A83-26558
- Volterra-like expansions for solutions of nonlinear integral equations and nonlinear differential equations 13 p1912 A83-30872
- Oblique derivative boundary value problems for nonlinear elliptic systems of second order 14 p2078 A83-33155
- Linear dynamic output feedback - Invariants and stability [AD-A129968] 14 p2077 A83-33447
- Existence of solutions in finite elasticity 15 p2176 A83-34327
- Local theorems of existence and uniqueness in finite elastostatics 15 p2177 A83-34345
- Some results on stability and stabilization of systems with retardation 15 p2222 A83-35127
- Monotonicity methods for nonlinear singular integral and integro-differential equations 18 p2740 A83-39987
- A Liapunov theory for the existence and uniqueness of solutions to boundary value problems 20 p3042 A83-42939
- Multipoint boundary value problem (MPBVP) and spline interpolation 20 p3042 A83-43170

EXITS (DOORS)

U DOORS

EXO BIOLOGY

- The space flight of the Soviet-French crew 01 p0015 A83-10382
- Evolution from space /The Omni Lecture/ and others papers on the origin of life --- Book 01 p0087 A83-10880
- Probing the presently tenuous link between comets and the origin of life 02 p0226 A83-11629
- Cosmic radiobiology --- Russian book 03 p0380 A83-13818
- Chemical weathering and the Viking biology experiments on Mars 04 p0567 A83-15577
- Orbiting Quarantine Facility - The Antaeus report 05 p0601 A83-17575
- The content of phosphoglycerides in *Rhodotorula rubra* in three of its phenotypes as influenced by the lunar environment during the flight of Apollo 16 06 p0794 A83-18369
- The Voyager mission and the origin of life - Selected references 06 p0801 A83-19409
- The NASA Space Biology Program 11 p1636 A83-27790
- Status of joint US/USSR experiments planned for the Cosmos '83 biosatellite mission 11 p1636 A83-27791
- Some karyological observations on plants grown in space 11 p1639 A83-27824
- The morphological and anatomical structure of *Arabidopsis thaliana* /Brassicaceae/ in ontogenesis --- plants for exobiology 11 p1641 A83-28766
- Space vacuum hinders radiopanspermia 12 p1767 A83-29451
- Microbiological problems of closed ecological systems --- Russian book 13 p1906 A83-30425
- SOYCHMBR.I - A model designed for the study of plant growth in a closed chamber [SAE PAPER 820853] 13 p1899 A83-30941
- Cosmochemistry and the origin of life; Proceedings of the Advanced Study Institute, Maratea, Italy, June 1-12, 1981 13 p1899 A83-31151
- Cosmochemistry and the origin of life 13 p1908 A83-31152
- An extensive galactic search for conformer II glycine 14 p2073 A83-33191
- On the optical properties of bacterial grains - I. 15 p2216 A83-34549
- 2.8-3.6-micron spectra of micro-organisms with varying H₂O ice-content 17 p2563 A83-38590
- Life sciences and Space Research XX(1); Proceedings of the Workshops and Topical Meeting, Ottawa, Canada, May 16-June 2, 1982 19 p2871 A83-40826
- Effect of HZE particles and space hadrons on bacteriophages 19 p2871 A83-40834
- Inactivation, mutation induction and repair in *Bacillus subtilis* spores irradiated with heavy ions 19 p2872 A83-40837
- Inactivation probability of heavy ion-irradiated *Bacillus subtilis* spores as a function of the radial distance to the particle's trajectory 19 p2872 A83-40838
- Heavy ion action on yeast cells - Inhibition of ribosomal-RNA synthesis, loss of colony forming ability and induction of mutants 19 p2872 A83-40840
- Experiments with air-dried seeds of *Arabidopsis thaliana* (L.) Heynh. and *Crepis capillaris* (L.) Wallr., aboard Salyut 6 19 p2872 A83-40841
- The development of the vestibular apparatus in conditions of weightlessness 19 p2875 A83-41460
- Possible forms of life in environments very different from the earth 19 p2886 A83-41511
- Life sciences and space research XX(2); Proceedings of the Workshop and Topical Meeting, Ottawa, Canada, May 16-June 2, 1982 19 p2877 A83-42029
- Peculiarities of genital organ formation in *Arabidopsis thaliana* (L.) heynh. under spaceflight conditions 19 p2878 A83-42055
- Biological effects of weightlessness and clinostatic conditions registered in cells of root meristem and cap of higher plants 19 p2878 A83-42056
- Single cell algae and higher plant cell cultures used in space biology [IAF PAPER 83-185] 23 p3494 A83-47302
- Results of space experiment program 'Interferon' [IAF PAPER 83-187] 23 p3498 A83-47303
- Cytological aspects of higher plant ontogenesis under microgravity [IAF PAPER 83-190] 23 p3494 A83-47306
- Preliminary results of Cytos 2 experiment --- for bacteria antibiotic sensitivity during orbital flight [IAF PAPER 83-192] 23 p3494 A83-47307
- Prebiotic evolution on a universal scale. I 23 p3500 A83-48054
- Complete cycle of the individual development of *Arabidopsis thaliana* (L.) Heynh. plants aboard Salyut-7 23 p3496 A83-48515

- Lectures on the planets - The terrestrial planets and life 24 p3673 A83-49460
- The functional system of antigravitation --- Russian book on physiological responses to decreased gravitation 24 p3617 A83-50075

EXOSAT SATELLITE

- Exosat for ground-based observers 13 p1811 A83-30395
- IRAS and Exosat - Europe maintains its contribution to space science 14 p1978 A83-31942
- Ground support software for the Exosat onboard computer 17 p2472 A83-37489
- Exosat - The new extrasolar X-ray observatory 18 p2645 A83-39971
- Exosat/Delta - Demonstrated short-term backup launcher capability through international cooperation [IAF PAPER 83-01] 23 p3418 A83-47227

EXOSPHERE

- The influence of thermospheric winds on exospheric hydrogen on Venus 02 p0266 A83-12570
- Near-earth ultraviolet environment 03 p0358 A83-13974
- On charge exchange and knock-on processes in the exosphere of Io 03 p0434 A83-14214
- Charge exchange in the Io torus and exosphere 05 p0705 A83-17385
- Altitude profile of H in the atmosphere of Venus from Lyman alpha observations of Venera 11 and Venera 12 and origin of the hot exospheric component 07 p1029 A83-20612
- Modern exospheric theories and their observational relevance --- kinetic theory 07 p1031 A83-20839
- Properties of the mesosphere and thermosphere and comparison with CIRA 72 [AD-A129615] 16 p2377 A83-36109
- Neutral temperatures from Thomson scatter measurements Comparisons with the CIRA(1972) [AD-A130290] 16 p2378 A83-36120
- Collisional modification to the exospheric theory of solar wind halo electron pitch angle distributions 22 p3388 A83-46027

EXOTHERMIC REACTIONS

- Estimating the propelling action of explosives 06 p0726 A83-18009
- Critical characteristics of thermal self-ignition in reacting systems with two-stage reactions 07 p0878 A83-19640
- Adiabatic calorimetry for kinetics modeling of epoxy resin systems 07 p0898 A83-20445
- Instability of surface combustion on exposure to laser radiation 10 p1433 A83-26680
- Interaction between SiC fibers and aluminum alloys 13 p1816 A83-31604
- The effect of pressure on the combustion characteristics of melting heterogeneous systems 18 p2663 A83-39162
- Molecular dynamical studies of the dissociation of a diatomic molecular crystal. I - Energy exchange in rapid exothermic reactions 20 p2950 A83-42628

EXPANDABLE STRUCTURES

- NT BALLOONS
- NT BEACON SATELLITES
- NT GAS BAGS
- NT HIGH ALTITUDE BALLOONS
- NT INFLATABLE STRUCTURES
- NT JIMSPHERE BALLOONS
- NT METEOROLOGICAL BALLOONS
- NT MICROBALLOONS
- NT SUPERPRESSURE BALLOONS
- NT TETHERED BALLOONS

EXPANSION

- NT GAS EXPANSION
- NT KARHUNEN-LOEVE EXPANSION
- NT PRANDTL-MEYER EXPANSION
- NT SERIES EXPANSION
- NT THERMAL EXPANSION
- Phase transformations in the mantle and expansion of the earth 16 p2376 A83-35594

EXPANSION WAVES

U ELASTIC WAVES

EXPEDITIONS

- An expedition to East Siberia to observe the total solar eclipse on 31 July 1981 02 p0249 A83-13049

EXPENDABLE STAGES (SPACECRAFT)

- Space Shuttle external tank rocket engine addition 20 p2944 A83-42565

EXPERIENCE

- Positive G tolerance of Indian subjects - Effects of age and flying experience 09 p1323 A83-24004
- An experience-judgement approach to tactical flight training 10 p1458 A83-26337

EXPERIMENT DESIGN

- Experiment control in problems of minimax estimation --- for aircraft longitudinal control 01 p0094 A83-10455

Pattern-recognition analysis of experimental data --- Russian book 03 p0327 A83-13811

Thermal tests concerning spacecraft --- Russian book 03 p0304 A83-13819

Experimental procedure for fast measurement of threshold in fatigue crack propagation 08 p1062 A83-21734

Space Experiments with Particle Accelerators (SEPAC) 15 p2124 A83-34213

The first dedicated life sciences mission - Spacelab 4 19 p2808 A83-42042

Measurement Assurance Program transmittance standards for spectrophotometric linearity testing - Preparation and calibration 20 p2990 A83-42946

The use of graph-analytic methods to solve problems of the operational planning of scientific experiments --- aboard spacecraft 21 p3094 A83-45292

Autonomous Fluid Physics Module (AFPM) - Status and perspectives --- first Spacelab mission payload [IAF PAPER 83-165] 23 p3414 A83-47300

The decay of 'mesotrons' (1939-1943), experimental particle physics in the age of innocence 23 p3540 A83-47765

Study of satellite situations mission 24 p3551 A83-49624

EXPERIMENTAL BREEDER REACTOR 2

Development of high-temperature liquid metal heat pipes for isothermal irradiation assemblies --- for in-pile tests of UO2 space reactor fuel configurations 11 p1538 A83-27129

EXPERIMENTATION

The application of methods of the mathematical theory of experiment in the development of multicomponent radioprotective preparations 23 p3495 A83-48202

EXPERT SYSTEMS

Ad Hoc modeling, expert problem solving, and R&T program evaluation 19 p2907 A83-41304

EXPIRED AIR

Reversal of arterial-to-expired CO2 partial pressure differences during rebreathing in goats 22 p3345 A83-45987

EXPLODING CONDUCTOR CIRCUITS

U CIRCUITS

U EXPLODING WIRES

EXPLODING CONDUCTORS

U EXPLODING WIRES

EXPLODING WIRES

A simple model for plasma temperature in imploded hollow plasma liners 01 p0106 A83-10619

First indication of Ampere tension in solid electric conductors 23 p3445 A83-48592

Simulation of detonation cell kinematics using two-dimensional reactive blast waves 24 p3580 A83-49836

EXPLORATION

NT LUNAR EXPLORATION

NT MINERAL EXPLORATION

NT OIL EXPLORATION

NT SPACE EXPLORATION

EXPLORER SATELLITES

NT COSMIC BACKGROUND EXPLORER SATELLITE

NT DYNAMICS EXPLORER SATELLITES

NT DYNAMICS EXPLORER 1 SATELLITE

NT DYNAMICS EXPLORER 2 SATELLITE

NT EXPLORER 1 SATELLITE

NT EXPLORER 12 SATELLITE

NT EXPLORER 47 SATELLITE

NT EXPLORER 50 SATELLITE

NT EXPLORER 51 SATELLITE

NT EXPLORER 54 SATELLITE

NT EXPLORER 55 SATELLITE

NT INTERNATIONAL SUN EARTH EXPLORER 1

NT INTERNATIONAL SUN EARTH EXPLORER 2

NT INTERNATIONAL SUN EARTH EXPLORER 3

NT INTERNATIONAL SUN EARTH EXPLORERS

NT SOLAR MESOSPHERE EXPLORER

EXPLORER 1 SATELLITE

Prelude to the space age 01 p0130 A83-10463

Explorer 1 - The second age of discovery 23 p3416 A83-48639

EXPLORER 12 SATELLITE

S3-3 satellite instrumentation and data 04 p0511 A83-16286

On ion harmonic structure in auroral zone waves - The effect of ion conic damping of auroral hiss 05 p0661 A83-17398

Comparison of S3-3 polar cap potential drops with the interplanetary magnetic field and models of magnetopause reconnection 17 p2538 A83-37598

EXPLORER 47 SATELLITE

Availability of IMP-7 and IMP-8 data for the IMS period 04 p0511 A83-16278

Dependence of 50-keV upstream ion events at IMP 7 and 8 upon magnetic field bow shock geometry 17 p2599 A83-37588

EXPLORER 50 SATELLITE

Availability of IMP-7 and IMP-8 data for the IMS period 04 p0511 A83-16278

Dependence of 50-keV upstream ion events at IMP 7 and 8 upon magnetic field bow shock geometry 17 p2599 A83-37588

EXPLORER 51 SATELLITE

Optical emissions induced by spacecraft - Atmosphere interactions 07 p0869 A83-21551

The surface glow of the Atmosphere Explorer C and E satellites 22 p3334 A83-46887

EXPLORER 54 SATELLITE

Atmosphere explorer and the IMS 04 p0512 A83-16288

The response of thermospheric atomic nitrogen to magnetic storms 20 p3019 A83-42425

EXPLORER 55 SATELLITE

Atmosphere explorer and the IMS 04 p0512 A83-16288

Conjectures on the origin of the surface glow of space vehicles [AD-A128637] 07 p0870 A83-21555

The surface glow of the Atmosphere Explorer C and E satellites 22 p3334 A83-46887

EXPLOSION SUPPRESSION

The AH-64 nitrogen inerting unit 10 p1375 A83-25895

EXPLOSIONS

NT AERIAL EXPLOSIONS

NT CHEMICAL EXPLOSIONS

NT GAS EXPLOSIONS

NT NUCLEAR EXPLOSIONS

NT THERMONUCLEAR EXPLOSIONS

Shock wave propagation law in the point explosion theory 01 p0047 A83-10912

Spectroscopic studies of the hazards of Li/SOCl2 batteries during anode-limited cell reversal 02 p0202 A83-12056

Transmission effects of explosion-produced dust clouds on downward viewing airborne platforms 08 p1132 A83-22543

Drop explosion under the effect of intense laser radiation 10 p1434 A83-26780

An effort to simulate magnetospheric-ionospheric effects in the presence of seismic phenomena 13 p1880 A83-31328

Calculation of critical branching points in two-parameter bifurcation problems 13 p1913 A83-31371

Lamb pulse observed in nature 18 p2717 A83-39800

Experimental study of the thermal explosion of liquids --- Thesis 22 p3267 A83-46695

A class of self-similar astrophysical explosions 23 p3520 A83-47458

All-Union Symposium on Combustion and Explosion, 7th, Chernogolovka, USSR, October 1983, Proceedings 24 p3555 A83-49758

EXPLOSIVE DEVICES

NT BOMBS (ORDNANCE)

NT EXPLODING WIRES

NT INITIATORS (EXPLOSIVES)

NT PRIMERS (EXPLOSIVES)

NT SHAPED CHARGES

Extension of service life of rigid transfer lines /SMDC/ --- explosive components for aircraft escape systems 03 p0303 A83-14173

Influence of Gaussian fluctuations on a model kinetic system exhibiting explosive behavior 10 p1389 A83-25565

EXPLOSIVE GASES

U FLAMMABLE GASES

EXPLOSIVE WELDING

Acoustic inspection of explosion welded joints in titanium 10 p1436 A83-26220

Titanium-steel interaction under production and operation temperatures 18 p2667 A83-40299

Practical small-scale explosive seam welding 22 p3302 A83-46422

Thermal spraying for cost reduction and efficiency 23 p3467 A83-48637

The detonation-spraying method of coating deposition, its current status and prospects for further development 24 p3590 A83-49083

EXPLOSIVES

NT CELLULOSE NITRATE

NT HYDROGEN AZIDES

NT RDX

NT TRINITROTOLUENE

Transition from combustion to detonation in solid explosives 02 p0151 A83-11659

Detonation properties of 1,3,5-triamino-2,4,6-trinitrobenzene when impacted by hypervelocity projectiles 04 p0464 A83-15473

The cook-off phenomenon of solid propellants 04 p0464 A83-15475

Synthesis of cyclotetramethylene tetranitramine by three stage method 04 p0454 A83-16432

Detonation --- Russian book 06 p0726 A83-18001

The critical pressure of initiation of powdered explosives 06 p0726 A83-18003

A study of detonation initiation in TNT and TH 50/50 by shock waves of short duration 06 p0726 A83-18004

Some aspects of the detonation of explosive mixtures 06 p0726 A83-18005

Detonation characteristics of retarded explosives 06 p0726 A83-18006

The effect of aluminum on the detonation wave profile of greatly diluted Hexogen 06 p0726 A83-18007

Estimating the propelling action of explosives 06 p0726 A83-18009

Thermal decomposition of tetraethylammonium perchlorate 06 p0726 A83-18458

The inhomogeneous development of the decomposition reaction of shock-compressed homogeneous explosives 07 p0880 A83-19960

Structure of a detonation front 07 p0926 A83-20898

Chemical and mechanical technology of propellants and explosives; International Annual Meeting, 12th, Karlsruhe, West Germany, July 1-3, 1981, Reports 09 p1240 A83-23829

Polyvinyl nitrate - A component for propellants and explosives 09 p1240 A83-23831

Problems regarding the manufacture of explosives having a very fine grain 09 p1240 A83-23832

TNT as a component in plastic-bonded explosive 09 p1242 A83-23844

Techniques in the formulation and handling of composite and very-low-density explosives 09 p1242 A83-23845

Manufacture of triaminotrinrobenzene 09 p1242 A83-23846

Penthrite in castable composite explosives 09 p1242 A83-23847

Dependency of the impact sensitivity of beta-HMX on the grain size and effects on the application 09 p1242 A83-23848

Blast waves in free air 09 p1264 A83-25272

Testing explosive ordnance devices for space application 13 p1826 A83-31191

On the loss of stability of detonation waves in long heterogeneous-explosive charges 13 p1843 A83-31372

Shock initiation of high explosives 13 p1826 A83-31722

A study of the steady-state reaction-zone structure of a homogeneous and a heterogeneous explosive 14 p1991 A83-33383

Hexanitrostilbene and its properties 21 p3117 A83-44074

Effect of the number density of heterogeneties on the critical diameter of condensed explosives 22 p3266 A83-46007

Heat resistant explosives produced in Hungary with possible space applications [IAF PAPER 83-357] 23 p3429 A83-47356

Ignition of a thin plate of condensed matter by a heated block 24 p3555 A83-49543

The ignition of a vapor bubble in a liquid 24 p3556 A83-49774

A universal relationship for heat release in the condensed phase and gas microkinetics during the combustion of ballistite powders 24 p3556 A83-49779

Critical diameter of the steady detonation of highly dense explosives - The effect of the shell 24 p3557 A83-49789

The effect of additives on the critical diameter of detonation of nitroesters 24 p3557 A83-49791

Transient processes during the impact initiation of trotyl-hexogen and trotyl-octogen mixtures 24 p3557 A83-49794

The use of Helmholtz coils in the electromagnetic method --- for shock-initiated detonation measurements 24 p3584 A83-49796

Possibility of the steady detonation of condensed explosives in charges without shells in connection with the properties of shock polars 24 p3557 A83-49797

Parameters and regimes of the detonation of condensed explosives 24 p3557 A83-49798

A pulsating detonation front 24 p3557 A83-49799

EXPONENTIAL FUNCTIONS

NT LOGARITHMS

Analysis of maximum-likelihood estimation on a randomly censored sample with a small fraction of failures in the example of exponential distributions 01 p0103 A83-10296

Fast firmware algorithms for square root, sine/cosine, and exponential 01 p0087 A83-11149

- Inclusions and separation of the zeros of exponential trinomials with constant coefficients 03 p0389 A83-14510
- HP-41C programs for Bayesian binomial and exponential interval estimation with a uniform prior on the reliability 07 p0942 A83-20513
- Numerical computation of an important integral function in two-dimensional radiative transfer 07 p1001 A83-21397
- Exponential growth and atmospheric carbon dioxide 09 p1295 A83-24255
- On approximation by the interpolating series of G. Valiron 10 p1470 A83-26475
- GEM --- Generalized exponential Markov process for statistical weather forecasting 17 p2550 A83-38728
- Applications of exponential splines in computational fluid dynamics 19 p2893 A83-40852
- The use of piecewise-exponential functions in transfer theory --- of chemical laser energy characteristics 21 p3146 A83-45222
- General form for representing the Fourier transform 24 p3621 A83-49966

EXPONENTS

- Approximation of an integral exponent by means of quadrature formulas 01 p0102 A83-11263
- Lyapunov exponents for multidimensional orbits 20 p3043 A83-43566

EXPOSURE

- The effect of open-space exposure on the biomechanical properties of a carbon composite 16 p2323 A83-35504

EXPRESSIONS (MATHEMATICS)

U FORMULAS (MATHEMATICS)

EXTARS

- Be components in X-ray binaries 01 p0122 A83-10342
- The problem of X Persei 01 p0123 A83-10350
- Why are essential parts of 'bursters' located in globular clusters 01 p0128 A83-11341
- Einstein Observatory pulse-phase spectroscopy of Hercules X-1 02 p0257 A83-12133
- The theoretically expected X-ray luminosity and the binary nature of Wolf-Rayet runaway stars 03 p0429 A83-14792
- A comparison of the X-ray properties of X Persei and Gamma Cassiopeiae 04 p0554 A83-15629
- A study of X-ray emission from Ap and Am stars 05 p0694 A83-17028
- X Persei - Optical polarization variation on the 580 day binary-like period 06 p0841 A83-19287
- Ultraviolet spectroscopy of V1341 Cygni /equals Cygnus X-2/ 07 p1022 A83-21133
- Optical eclipses and precession effects in the X-ray binary system HD 77581 - 4U 0900-40 07 p1009 A83-21265
- GX 339-4 - X-ray spectra of high and low states 10 p1498 A83-25352
- The instability of the SS 433 precession period 12 p1796 A83-29491
- Stellar rotation as a controller of coronae and chromospheres of giant stars 12 p1797 A83-29952
- Recent optical observations of the X-ray source HO139-68; an AM-Herculis type binary system 13 p1946 A83-30384
- X-ray spectra and light curves of accreting magnetic degenerate dwarfs 14 p2105 A83-33207
- High luminosity X-ray binaries - IUE results 15 p2251 A83-33589
- Einstein observations of high luminosity X-ray binaries 15 p2251 A83-33590
- Solar and late-type dwarfs 15 p2252 A83-33602
- IUE spectrophotometry of X Persei (4U 0352+30) 16 p2425 A83-36656
- Optical photometry of massive X-ray binaries - 4U 1538-52/QV Nor 16 p2425 A83-36666
- The correlated X-ray and optical time variability of TT Arietis 17 p2605 A83-37920
- Irregular X-ray variability in the transient X-ray burst source MXB 1659-29 17 p2605 A83-37921
- Evidence for an about 300 day period in Cygnus X-1 17 p2605 A83-37922
- Gamma-rays and the production of energetic electrons in enshrouding material - A model for the quiescent radio emission from Cygnus X-3 20 p3068 A83-42456
- A search for X-rays from runaway stars 21 p3237 A83-45552
- EXTENDED DURATION SPACE FLIGHT**
- U LONG DURATION SPACE FLIGHT
- EXTENSIONS**
- NT PROLONGATION
- EXTENSOMETERS**
- A facility for precise measurement of mechanical properties at elevated temperatures 09 p1230 A83-23744
- An extensometer for axial strain measurement at high temperature 23 p3459 A83-48604

EXTERNAL STORE SEPARATION

- A new approach to weapon separation aerodynamics 03 p0278 A83-13164
- Advances in methods for predicting store aerodynamic characteristics in proximity to an aircraft [AIAA PAPER 83-0266] 05 p0584 A83-16622
- Application of panel methods to external stores at supersonic speeds 06 p0712 A83-18409
- Store separation from cavities at supersonic flight speeds 09 p1198 A83-24882
- Control techniques to improve Space Shuttle solid rocket booster separation 13 p1811 A83-30164
- Recent improvements in prediction techniques for supersonic weapon separation 19 p2789 A83-41041

EXTERNAL STORES

- NT PODS (EXTERNAL STORES)
- Development of analytical and experimental techniques for determining store airload distributions 02 p0132 A83-13077
- Tailoring the composite mission profile environments for reliability testing --- for external stores 13 p1864 A83-31508
- An assessment of external stores reliability testing 13 p1864 A83-31509
- Improvement of a captive trajectory system by using optical distance sensors --- store separation from aircraft [ONERA, TP NO. 1983-115] 24 p3550 A83-49426

EXTERNAL SURFACE CURRENTS

- Barriers to flashover discharge arcs on Teflon 05 p0618 A83-17496
- Visualization of the electric field around a moving animal by numerical calculation 07 p0976 A83-21172
- Silicon-silicon dioxide interface study by surface inversion currents 08 p1169 A83-21869
- Electrostatic flow field of satellites moving in ionosphere 08 p1050 A83-21881
- Infrared application to the detection of induced surface currents 08 p1103 A83-22845
- The electrostatic-discharge phenomena on Marecs-A 17 p2480 A83-37871
- Laboratory and in flight passive dischargers characterization --- for elimination of electrostatic radiation interference [ONERA, TP NO. 1983-54] 23 p3400 A83-48176

EXTERNAL TANKS

- Multispectral radiation detection of small changes in target emissivity --- ice measurements on space shuttle external tank 03 p0327 A83-13795
- The ET in orbit as a space system material resource [IAF PAPER 82-392] 05 p0603 A83-16924
- Numerical simulation of ice/frost formation on the external tank of the Space Shuttle in varying environments [AIAA PAPER 83-0524] 06 p0722 A83-19592
- Dynamic wind tunnel tests of the simulated Shuttle external cable trays 07 p0869 A83-20412
- Environmental protection system for the Shuttle External Tank Aft Cargo Carrier [SAE PAPER 820880] 10 p1384 A83-25773
- Design and performance of the external tank portion of the Space Shuttle main propulsion system 11 p1535 A83-27471
- Space Shuttle siphon dropout prediction [AIAA PAPER 83-1383] 16 p2321 A83-36374
- Prediction of ice/frost growth on insulated cryogenic tanks 18 p2646 A83-40019
- Space Shuttle external tank rocket engine addition 20 p2944 A83-42565
- Experimental evaluation of a proposed ice suppression system for the Space Shuttle external tank [IAF PAPER 83-ST-08] 23 p3423 A83-47386
- Application of composites and computer graphics in the design of the MH-53E fuel sponson [AIAA PAPER 83-2441] 23 p3403 A83-48329
- EXTERNALLY BLOWN FLAPS**
- Augmentation of fighter aircraft lift and STOL capability by blowing outboard from the wing tips [AIAA PAPER 83-0078] 05 p0578 A83-16507
- Circulation controlled STOL wing optimization [AIAA PAPER 83-0082] 05 p0579 A83-16509
- Some observations on the aerodynamics of an airfoil with a jet exhausting from the lower surface [AIAA PAPER 83-0173] 05 p0580 A83-16569
- Aerodynamic characteristics of a circulation controlled elliptical airfoil with blown jets [AIAA PAPER 83-1794] 17 p2453 A83-38633

EXTINCTION

- NT INTERSTELLAR EXTINCTION
- An examination of instabilities of an electric arc at atmospheric pressure --- French thesis on relation to cathodic material properties 03 p0294 A83-13805
- Mid- and far-infrared extinction coefficients of hydrous silicate minerals 05 p0707 A83-17808
- Environmental effects of an impact-generated dust cloud - Implications for the Cretaceous-Tertiary extinctions 06 p0779 A83-18816

- The interaction of the cretaceous-tertiary extinction bolide with the atmosphere, ocean, and solid earth 13 p1880 A83-31475
- Retrieval of stratospheric aerosol size distribution from atmospheric extinction of solar radiation at two wavelengths 15 p2201 A83-34459
- Thermal neutrons could be a cause of biological extinctions 65 Myr ago 17 p2557 A83-38605
- On the accuracy of IR extinction predictions made by the Navy Aerosol Model 17 p2546 A83-38740
- Optical extinction theorem in the nonlinear theory of optical multistability 21 p3206 A83-44803

EXTINGUISHERS

U FIRE EXTINGUISHERS

EXTINGUISHING

- Flame quenching by turbulence 03 p0295 A83-14848
- The mechanism of lean limit flame extinction 07 p0879 A83-19841
- Numerical study of a confined premixed laminar flame - Oscillatory propagation and wall quenching 07 p0879 A83-19842
- Local quenching due to flame stretch and non-premixed turbulent combustion 09 p1226 A83-24362
- Extinction of premixed flames in a stagnation flow considering general Lewis number 22 p3267 A83-46763

EXTRACTION

NT ION EXTRACTION

EXTRAGALACTIC LIGHT

U EXTRATERRESTRIAL RADIATION

U LIGHT (VISIBLE RADIATION)

EXTRAGALACTIC MEDIA

U INTERGALACTIC MEDIA

EXTRAGALACTIC RADIO SOURCES

NT RADIO GALAXIES

- High dynamic range mapping of strong radio sources, with application to 3C84 01 p0115 A83-10208
- Investigation of the fine structure of radio sources 01 p0124 A83-10841
- Precise optical positions of radio sources in the FK 4-system. II - Results from 28 sources on the northern hemisphere and a preliminary comparison of the optical-radio reference frame 01 p0117 A83-10937
- Statistical correction of projection of radio-sources on the sky and application to the apparent size-redshift and linear size-line width relations 01 p0125 A83-10939
- A rapid outburst of BL Lac at 2.72 GHz 01 p0126 A83-10955
- Optical variability and the redshift of quasars 01 p0126 A83-10970
- Spectra of compact radio sources in galactic nuclei 02 p0250 A83-11578
- MERLIN observations of superluminal radio sources --- Multi Element Radio Linked Interferometer Network 02 p0245 A83-11621
- Evolutionary luminosity functions of extragalactic sources driven by gravitational power 02 p0259 A83-12515
- Complete samples of active extragalactic objects. II - A deep 1.452-GHz VLA survey centered on alpha = 08h 52m 15s, delta = +17deg 16 arcmin 02 p0248 A83-12906
- The distribution of companion galaxies to mirror-symmetric extragalactic radio sources 03 p0420 A83-13940
- Variability of compact radio sources at a wavelength of 1 millimeter 03 p0422 A83-14181
- In situ acceleration in extragalactic radio jets 03 p0423 A83-14185
- The influence of buoyancy on the stability of jets --- in extragalactic radio sources 03 p0427 A83-14755
- Local coupling of surface MHD waves with kinetic Alfvén waves in jets 03 p0428 A83-14776
- An Effelsberg - Green Bank galactic H I absorption line survey. II - Results and interpretation 04 p0549 A83-15027
- The quasar B2 1320 plus 29 04 p0551 A83-15051
- Circular polarization from compact extragalactic radio sources as a result of nonuniform magnetic fields 05 p0697 A83-16986
- Radio continuum emission - A tracer for star formation 06 p0826 A83-18096
- Multiperture infrared photometry of extragalactic radio sources 06 p0828 A83-18180
- The radio structure of 3C303 at 408 MHz 06 p0828 A83-18182
- A search for extended structures near the radio sources 3C 120 and 3C 273 06 p0831 A83-18791
- An interpretation of the decimeter flux variability of extragalactic radio sources 06 p0831 A83-18831
- Infrared properties of serendipitous X-ray quasars 06 p0819 A83-18854

Optical variability and radio structure of extragalactic sources - Evidence of recurrent activity 06 p0838 A83-19224

Low frequency asymptotic spectra of multiple, decelerating adiabatic bursts 06 p0843 A83-19486

Activity in the centers of galaxies 06 p0846 A83-19530

A fast-scan extragalactic source survey at 4.755 GHz. I - Source list and radio spectra 07 p1003 A83-19851

Optical identifications of flat-spectrum radio sources 07 p1003 A83-19853

Flux density measurements of bright extragalactic sources at 36.8 GHz 07 p1006 A83-20564

The rotation measures of radio sources in selected celestial zones - The Perseus arm window 07 p1006 A83-20571

A bisymmetric spiral magnetic field and the spiral arms in our Galaxy 08 p1182 A83-23041

3C 395 - A quasar with asymmetrical radio structure 08 p1176 A83-23078

Further observations of radio sources from the BG survey. II - Mainly extragalactic 08 p1176 A83-23109

The low frequency variability of extragalactic radio sources - Discussion of the properties 09 p1361 A83-24476

Precise optical positions for radio/optical astrometric sources in the southern hemisphere 10 p1493 A83-25654

The reconfinement of jets --- in extragalactic radio sources 10 p1502 A83-25707

Radio and mm-observations of active nuclei 10 p1506 A83-26229

H II regions in M33. I - Radio and H-alpha observations of the H II complex NGC595 11 p1669 A83-27679

Low-frequency flux density variations of QSO 2345-167 11 p1682 A83-28280

Linear polarization observations in selected celestial zones The anticentre region 12 p1784 A83-28867

Rotation measures for compact variable radio sources 12 p1788 A83-29180

Low-frequency variability and predicted superluminal motion in 3C147 13 p1944 A83-30215

Infrared counterparts to 'empty field' steep-spectrum radio sources 13 p1942 A83-31697

Asymmetries in four powerful radio sources 13 p1958 A83-31708

The variability of the optical counterparts of four extragalactic radio sources 14 p2103 A83-33059

Measurement of unambiguous rotation measures of extragalactic sources 14 p2098 A83-33063

X-ray studies of quasars with the Einstein Observatory. III The 3CR sample 14 p2104 A83-33183

Extragalactic 1 millimeter sources - Simultaneous observations at centimeter, millimeter, and visual wavelengths 14 p2098 A83-33184

Neutral hydrogen in the Small Magellanic Cloud 14 p2099 A83-33243

Redshift dependence of the low-frequency turnover of quasars 15 p2255 A83-33828

A radio pulsar in the Large Magellanic Cloud 15 p2246 A83-34219

Pressure collimation of supersonic radio jets 15 p2267 A83-34620

The optical identification content of the Einstein Observatory deep X-ray survey of a region in Pavo 17 p2587 A83-37303

A statistical VLBI study of milli-arcsecond cores in extragalactic radio sources 17 p2588 A83-37304

Results of investigations of extragalactic radio sources in the microwave range 17 p2600 A83-37663

The variability of 3C 273, OJ 287, and PKS 0735+17 in radio and optical emissions 17 p2601 A83-37710

Observations of radio sources by the 22-m radio telescope at the Crimean Astrophysical Observatory and the 14-m radio telescope at the Radio Laboratory of the Helsinki University of Technology at millimeter wavelengths 17 p2590 A83-37712

Further high-resolution observations of faint radio sources and the angular size-flux density relation 17 p2593 A83-38249

Optical identifications of Parkes radio sources using UK Schmidt plates 17 p2593 A83-38253

A sample of 25 extragalactic radio sources having a spectrum peaked around 1 GHz 17 p2594 A83-38420

Are black holes necessary? 17 p2612 A83-38617

Summary results of the Shanghai-Effelsberg VLBI experiment 18 p2754 A83-39006

Relativistic beaming in the central components of double radio quasars 18 p2765 A83-39202

Magnetic fields in galactic jets 18 p2766 A83-39251

Advances in gamma-ray line astronomy 18 p2756 A83-39293

A search for X-ray emission from optically quiet, compact radio sources 19 p2918 A83-41613

High precision astrometry via very-long-baseline radio interferometry - Estimate of the angular separation between the quasars 1038+528A and B 20 p3057 A83-42184

Arcsecond positions for milliarcsecond VLBI nuclei of extragalactic radio sources. II - 207 sources 20 p3057 A83-42185

Large-scale magnetic field in the Perseus spiral arm 20 p3066 A83-42396

Radio observations of steep-spectrum compact sources 20 p3066 A83-42434

Emission mechanism of extragalactic X-ray and radio sources 20 p3070 A83-42784

A search for microwave background diminution towards the cluster 0016 + 16 21 p3223 A83-44429

Search for large-scale extension of the quasars 3C273, 3C345 and 3C380 21 p3223 A83-44453

VLA observations of compact radio sources near the galactic plane 21 p3224 A83-44741

A catalogue of extragalactic radio source identifications 21 p3225 A83-44978

Linear polarization observations in selected celestial zones The Gum nebula area 22 p3372 A83-46264

Precise positions in the FK4 system for ten optical counterparts of extragalactic radio sources 22 p3373 A83-46385

Redshifts of five extragalactic radio sources 22 p3375 A83-46574

Flux density and linear polarization measurements of variable radio sources at 9.00 mm (33.5 GHz) 22 p3380 A83-46575

VLBI maps of 3C 273 and 3C 345 at 2.3 GHz 22 p3376 A83-46972

VLA observations of extragalactic NH3 in IC 342 22 p3381 A83-46981

Extragalactic cosmic rays, active galaxies and quasi-stellar objects 23 p3540 A83-47751

The possibility of using sparse reference-star grids to determine the optical positions of extragalactic radio sources 24 p3644 A83-49827

A VLBI search for compact components in extended high redshift quasars 24 p3668 A83-50079

Black hole electromagnetic fields and negative energy states for charged particles 24 p3668 A83-50092

EXTRAPOLATION

Self-consistent extrapolation of the results of numerical experiments for fluid structures 03 p0389 A83-13537

A re-extrapolation technique in Newton-SOR computer simulation of semiconductor devices --- Successive Over Relaxation 05 p0631 A83-17765

Extrapolation of optimum design based on sensitivity derivatives 12 p1735 A83-28978

Extrapolation techniques for determining stress intensity factors 16 p2368 A83-36507

On extrapolation boundary conditions for the numerical solution of hyperbolic difference schemes 21 p3198 A83-45054

The use of the extrapolation technique in the calibration of radiation-measuring devices in the region of strong band absorption for the rho-sigma-tau water-vapor bands from 0.91 to 0.98 microns 21 p3142 A83-45406

The influence of wind and temperature gradients on outdoor sound propagation - Development and evaluation of a calculation method based on wavefield extrapolation --- Thesis 22 p3354 A83-46694

EXTRASOLAR PLANETS

The stars near at hand 03 p0406 A83-13557

On the detection of other planetary systems by astrometric techniques 05 p0693 A83-17011

New conceptions of unmanned planetary exploration - Extra-solar planetary systems 06 p0816 A83-19149

Formation of planetary systems --- Book 06 p0849 A83-19451

Detection of extra-solar planets 06 p0823 A83-19473

The frequency of planetary systems in the Galaxy 19 p2923 A83-41514

The planetary system of Barnard's star 19 p2911 A83-42163

Emerging solar system in view --- recent observational evidence of extrasolar planet systems 21 p3226 A83-44990

A space-telescope able to see the planets and even the satellites around the nearest stars [IAF PAPER 83-222] 23 p3515 A83-47313

Star-planet systems as progenitors of cataclysmic binaries Tidal effects 23 p3518 A83-47428

EV Lacertae - Is flare activity related to an unseen planet-like companion? 23 p3516 A83-47493

EXTRATERRESTRIAL COMMUNICATION

Attitudes toward interstellar communication - An empirical study 18 p2751 A83-39608

Siblings for SETI --- selection of stars for extraterrestrial communications 22 p3372 A83-47085

EXTRATERRESTRIAL ENVIRONMENTS

NT CHROMOSPHERE

NT CISLUNAR SPACE

NT DEEP SPACE

NT HELIUM HYDROGEN ATMOSPHERES

NT INTERPLANETARY SPACE

NT INTERSTELLAR SPACE

NT JUPITER ATMOSPHERE

NT MARS ATMOSPHERE

NT MARS ENVIRONMENT

NT NEPTUNE ATMOSPHERE

NT PLANETARY ATMOSPHERES

NT PLANETARY ENVIRONMENTS

NT SATELLITE ATMOSPHERES

NT SATURN ATMOSPHERE

NT SOLAR ATMOSPHERE

NT STELLAR ATMOSPHERES

NT URANUS ATMOSPHERE

NT VENUS ATMOSPHERE

Nuclear power - Key to man's extraterrestrial civilization 11 p1540 A83-27220

A proposed new policy for planetary protection 19 p2807 A83-40828

EXTRATERRESTRIAL INTELLIGENCE

We are alone in our Galaxy 03 p0401 A83-14050

A brief survey of the solar system 06 p0849 A83-19463

Pathways of evolution for man and machine 12 p1784 A83-29454

Is mankind unique? 12 p1784 A83-29455

Search for Extraterrestrial Life - A new Commission of the International Astronomical Union 18 p2754 A83-39609

Extraterrestrials - Where are they? --- Book 19 p2907 A83-41501

An explanation for the absence of extraterrestrials on earth 19 p2908 A83-41502

Searches for electromagnetic signals from extraterrestrial beings 19 p2908 A83-41503

Preemption of the Galaxy by the first advanced civilization 19 p2908 A83-41504

Settlements in space, and interstellar travel 19 p2807 A83-41506

Exponential evolution - Implications for intelligent extraterrestrial life 19 p2908 A83-42038

If they are here, where are they? Observational and search considerations --- extraterrestrial artifacts in solar system 21 p3222 A83-44092

On the regularities of development of extraterrestrial civilizations and the search strategy [IAF PAPER 83-271] 23 p3515 A83-47326

Preferred frequencies for SETI observations [IAF PAPER 83-279] 23 p3515 A83-47327

A search strategy for ETI signals with small duty cycle 24 p3637 A83-49604

EXTRATERRESTRIAL LIFE

Evolution from space /The Omni Lecture/ and others papers on the origin of life --- Book 01 p0087 A83-10880

Search for Extraterrestrial Life - A new Commission of the International Astronomical Union 18 p2754 A83-39609

Mars - A contamination potential? 19 p2885 A83-40831

An extraterrestrial habitat on earth - The algal mat of Don Juan Pond 19 p2885 A83-40832

Extraterrestrials - Where are they? --- Book 19 p2907 A83-41501

An explanation for the absence of extraterrestrials on earth 19 p2908 A83-41502

Searches for electromagnetic signals from extraterrestrial beings 19 p2908 A83-41503

Preemption of the Galaxy by the first advanced civilization 19 p2908 A83-41504

Colonies in the asteroid belt, or a missing term in the Drake equation 19 p2908 A83-41509

Possible forms of life in environments very different from the earth 19 p2886 A83-41511

Cosmology and life in the universe 19 p2908 A83-41512

Nucleosynthesis and galactic evolution - Implications for the origin of life 19 p2886 A83-41513

Atmospheric evolution, the Drake equation, and DNA - Sparse life in an infinite universe 19 p2886 A83-41515

Lectures on the planets - The terrestrial planets and life 24 p3673 A83-49460

EXTRATERRESTRIAL MATTER

NT COSMIC GASES

NT COSMIC PLASMA

NT INTERPLANETARY GAS

NT INTERSTELLAR GAS

NT NEUTRAL GASES

- Do oblique impacts produce Martian meteorites
07 p1034 A83-21313
- Accelerator mass spectrometry measurement of cosmogenic Al-26 in terrestrial and extraterrestrial matter
08 p1187 A83-23293
- The role of impact magnetization in the solar system
15 p2276 A83-35006
- Meteorites from Mars?
16 p2437 A83-36571
- Ni isotopic compositions in Allende and other meteorites
16 p2438 A83-36747
- Measurement of Mn-53 in deep-sea iron and stony spherules --- for proof of extraterrestrial origin
16 p2438 A83-36749
- A quarantine protocol for analysis of returned extraterrestrial samples
19 p2885 A83-40830
- Martian gases in an Antarctic meteorite?
19 p2922 A83-40913
- A method for the identification and elimination of contamination during carbon isotopic analyses of extraterrestrial samples
22 p3385 A83-46375
- Chemical and isotopic study of extraterrestrial particles from the ocean floor
24 p3672 A83-49398

EXTRATERRESTRIAL RADIATION

- NT EXTRATERRESTRIAL RADIO WAVES
- NT GALACTIC RADIATION
- NT GALACTIC RADIO WAVES
- NT GAMMA RAY BURSTS
- NT INTERSTELLAR RADIATION
- NT LUNAR RADIATION
- NT PLANETARY RADIATION
- NT PRIMARY COSMIC RAYS
- NT RADIO BURSTS
- NT SOLAR CORPUSCULAR RADIATION
- NT SOLAR COSMIC RAYS
- NT SOLAR ELECTRONS
- NT SOLAR NEUTRINOS
- NT SOLAR PROTONS
- NT SOLAR RADIATION
- NT SOLAR RADIO BURSTS
- NT SOLAR RADIO EMISSION
- NT SOLAR WIND
- NT SOLAR X-RAYS
- NT STELLAR RADIATION
- NT STELLAR WINDS
- NT SUNLIGHT
- NT TYPE 2 BURSTS
- NT TYPE 3 BURSTS
- NT TYPE 4 BURSTS
- NT ZODIACAL LIGHT
- Space radiation effects on structural composites
[AIAA PAPER 83-0591]
05 p0610 A83-16808
- Results from a new search for proton decay
08 p1192 A83-22641
- The origin of cosmic radiation - Status after 70 years of research
09 p1369 A83-23497
- Inactivation, mutation induction and repair in *Bacillus subtilis* spores irradiated with heavy ions
19 p2872 A83-40837
- Radiation safety standards - Space hazards vs. terrestrial hazards
19 p2885 A83-40844
- Genetic risks associated with radiation exposures during space flight
19 p2873 A83-40845
- Radiation exposures during space flight and their measurement
19 p2880 A83-40846
- Cataractogenesis from high-LET radiation and the Casarett model
19 p2873 A83-40848
- Late skin damage in rabbits and monkeys after exposure to particulate radiations
19 p2873 A83-40849
- Apparent superluminal velocities due to the curvature of space
24 p3670 A83-50159

EXTRATERRESTRIAL RADIO WAVES

- NT GALACTIC RADIO WAVES
- NT RADIO BURSTS
- NT SOLAR RADIO BURSTS
- NT SOLAR RADIO EMISSION
- NT TYPE 2 BURSTS
- NT TYPE 3 BURSTS
- NT TYPE 4 BURSTS
- Phenomenology of magnetospheric radio emissions
10 p1519 A83-26618
- Theories of radio emissions and plasma waves --- in Jupiter magnetosphere
10 p1520 A83-26620
- Narrowband electromagnetic emissions from Jupiter's magnetosphere
12 p1799 A83-29707
- The electrical activity of the Venus atmosphere. I
Measurements using descent modules
14 p2111 A83-31968
- On the time spectrum of phase fluctuations of radio waves during the occultation of the near-solar plasma
14 p2114 A83-32101
- The Cherenkov effect and plasma turbulent reactors
17 p2582 A83-37893

EXTRATERRESTRIAL RESOURCES

- Choice of lunar materials as determined by fabrication methods
16 p2313 A83-35613

- Should we make products on the moon?
16 p2313 A83-35774
- An analysis of propulsion options for transport of lunar materials to earth orbit
[AIAA PAPER 83-1344]
16 p2313 A83-36349
- Ideas regarding the utilization of extraterrestrial resources
17 p2471 A83-38620
- Limited aerospace natural resources and their regulation
22 p3368 A83-45817
- Space industrialization. Volumes 1 & 2
22 p3256 A83-45851
- Space manufacturing of nonterrestrial materials
22 p3256 A83-45854
- Materials processing in space
22 p3256 A83-45855
- Asteroidal resources for space manufacturing
22 p3257 A83-45856
- Lunar utilization --- materials resources and cislunar transportation considerations for space industrialization
22 p3257 A83-45857

EXTRATERRESTRIAL ROVING VEHICLES**U ROVING VEHICLES****EXTRAVEHICULAR ACTIVITY**

- HMMU's, AMU's, and MMU's - The development of astronaut maneuvering units
[AAS 82-148]
02 p0140 A83-11936
- Mission 6's EVA to verify capability
05 p0605 A83-17277
- Large space structures, alignment, and extravehicular activities /EVA/ crew support
09 p1213 A83-23585
- A satellite-service approach for long-duration Space Platforms
[SAE PAPER 820851]
10 p1381 A83-25759

EXTRAVEHICULAR MOBILITY UNITS**NT ASTRONAUT MANEUVERING EQUIPMENT**

- STS Manned Maneuvering Unit propulsion system
11 p1644 A83-27469

EXTREMA**U RANGE (EXTREMES)****EXTREME ULTRAVIOLET RADIATION**

- Evaluation of EUV spectra of X-ray binaries Cygnus X-1, Vela X-1, and X Persei --- German thesis
01 p0123 A83-10477
- Observations of grains in the extreme ultraviolet
01 p0104 A83-10859
- Extreme ultraviolet observational data on the solar spectrum
02 p0269 A83-12155
- Optical constants in the extreme ultraviolet and soft X-ray region
02 p0237 A83-12702
- Progress in extreme ultraviolet and soft X-ray multilayer coatings
02 p0238 A83-12704
- X-ray and extreme ultraviolet imaging using layered synthetic microstructures
02 p0240 A83-12724
- Quantum efficiency of opaque CsI photocathodes with channel electron multiplier arrays in the extreme and far ultraviolet
03 p0330 A83-14383
- EUV arcades - Signatures of filament instability
03 p0438 A83-14911
- Magellan - A far- and extreme-ultraviolet spectrographic observatory
05 p0601 A83-17431
- Dichroic beam splitter for extreme-ultraviolet and visible radiation
05 p0651 A83-17878
- The chromospheric evershed flow observed in the EUV spectrum
06 p0852 A83-18122
- The Saturn spectrum in the EUV - Electron excited hydrogen
06 p0848 A83-18316
- High resolution EUV structure of the chromosphere-corona transition region above a sunspot
06 p0855 A83-19130
- Maximizing the quantum efficiency of microchannel plate detectors - The collection of photoelectrons from the interchannel web using an electric field
07 p0872 A83-21377
- EUV branching ratios for ionized nitrogen and oxygen emissions
07 p0991 A83-21396
- EUV indices for low solar activity
09 p1368 A83-23415
- EUV studies of N2 and O2 produced by low energy electron impact
09 p1342 A83-24130
- Study of sulfur-containing molecules in the EUV region. II - Photoabsorption cross section of COS
09 p1343 A83-25131
- Study of sulfur-containing molecules in the EUV region. III Photoexcitation of CS2
09 p1343 A83-25134
- Chromospheric jets - Possible extreme-ultraviolet observations of spicules
10 p1522 A83-26760
- High spectral brightness extreme ultraviolet generation with excimer lasers
11 p1576 A83-27508
- Development of a 1m-normal-incidence-EUV-Telescope
11 p1670 A83-27745
- S II and S III branching ratios in the 600- to 1200-A interval --- applied to modeling of Io plasma torus
11 p1619 A83-28327
- High efficiency spectrographs for the EUV and soft X-rays
13 p1935 A83-30183

- Composite thin-foil bandpass filter for EUV astronomy
Titanium-antimony-titanium
13 p1918 A83-30209
- The role of spicules in heating the solar atmosphere
Implications of EUV observations
13 p1965 A83-31434
- Measured gain for XUV plasma lasers at varying pump intensities
13 p1857 A83-31459
- Anti-Stokes scattering as an XUV radiation source --- for spectroscopy
13 p1818 A83-31810
- The extreme ultraviolet day airglow
15 p2196 A83-33942
- The extreme ultraviolet spectrum of dayside and nightside aurorae - 800-1400 A
15 p2196 A83-33943
- O I (7990 A) emission and radiative entrapment of auroral EUV
15 p2196 A83-33944
- Rocket-borne EUV-visible emission measurements
16 p2373 A83-35369
- Solar EUV and decimetric indices and thermospheric models
16 p2378 A83-36112
- Extreme ultraviolet emission from gas puff plasmas
17 p2582 A83-37611
- Origin of the weakening of EUV emission lines formed in the chromosphere-corona transition zone
18 p2781 A83-39020
- Type I noise storms and the structure of the extreme ultraviolet corona
18 p2782 A83-39035
- Direct measurements of the gradual extreme ultraviolet emission from large solar flares
18 p2782 A83-39038
- Experimental limits of the extreme ultraviolet background
18 p2759 A83-39777
- Generation of extreme ultraviolet radiation at 79 nm by sum frequency mixing
22 p3300 A83-46821
- Linear absorption coefficient of beryllium in the 50-300-A wavelength range --- bandpass filter materials for ultraviolet astronomy instrumentation
23 p3508 A83-47588
- The origin of line-free XUV continuum emission from laser-produced plasmas of the elements Z = 62-74
23 p3511 A83-48586

EXTREMELY HIGH FREQUENCIES

- K-band FET doubling oscillator
02 p0168 A83-13041
- Measurements of K-band antenna patterns
04 p0468 A83-16419
- Industry looks at military exceptionally high frequency bands
05 p0621 A83-18688
- Q-band dielectric-loaded short backfire antenna arrays
06 p0738 A83-18615
- Broad-band characteristics of EHF IMPATT diodes
06 p0753 A83-18768
- Experimental evaluation of a ruby maser at 43 GHz
06 p0753 A83-18773
- Dielectric and optical measurements from 30 to 1000 GHz
07 p0929 A83-20185
- Atmospheric EHF window transparencies near 35, 90, 140, and 220 GHz
09 p1247 A83-23793
- 50-GHz IC components using alumina substrates
10 p1408 A83-25803
- Measurement of relative propagation delay between C- and K-band satellite loops
10 p1403 A83-26076
- Fabrication and investigation of BARITT diodes in the Ka-band --- German thesis
11 p1564 A83-28645
- First results using a K-band maser receiver on the Parkes 64-m radio telescope
13 p1946 A83-30391
- EHF planar module for spatial combining
14 p2007 A83-33074
- Characterisation of the 50-70 GHz band for space communications
14 p2003 A83-33473
- High-performance K-band GaAs power field-effect transistors prepared by molecular beam epitaxy
15 p2150 A83-33846
- Shaped lens antennas
15 p2146 A83-35081
- Cloud particle identification near the melting layer with dual polarization K-band Doppler radar
24 p3614 A83-49721

EXTREMELY LOW FREQUENCIES

- VLF/ELF radiation from the ionospheric dynamo current system modulated by powerful HF signals
09 p1300 A83-23311
- ELF and VLF wave generation by modulated HF heating of the current carrying lower ionosphere
09 p1300 A83-23312
- Plasmaspheric hiss observed in the topside ionosphere at mid and low-latitudes
13 p1882 A83-31631
- A waveguide for low-frequency electromagnetic waves in the upper ionosphere
20 p3017 A83-42331
- Design strategies aid ELF/VLF receivers
22 p3275 A83-46758

EXTREMELY LOW RADIO FREQUENCIES

- Ionospheric ELF radio signal generation due to LF and/or MF radio transmissions. I - Experimental results
02 p0205 A83-12015
- Ionospheric ELF radio signal generation due to LF and/or MF radio transmissions. II - Interpretation
02 p0205 A83-12016

Theory of generation of ULF pulsations by ionospheric modification experiments 09 p1300 A83-23308

Propagation of ULF electromagnetic waves through the ionosphere and geomagnetic pulsations 11 p1617 A83-28118

Quarter-wave ULF pulsations 13 p1881 A83-31535

Plasmaspheric ELF hiss observed by ISIS satellites 14 p2055 A83-33145

Drift boundaries and ULF wave generation near noon at geostationary orbit 20 p3025 A83-43194

Fine structure of the energy spectra of ELF hiss in the upper ionosphere and a possible mechanism of hiss generation (the Intercosmos-14 satellite) 21 p3175 A83-45240

The intensity of low-frequency emissions and the interplanetary magnetic field 21 p3175 A83-45250

EXTREMUM VALUES

NT LIMITS (MATHEMATICS)

NT MAXIMA

NT MINIMA

Upper and lower bounds for the solution to the discrete Lyapunov matrix equation 01 p0102 A83-10964

Nondifferentiable optimization --- Russian book 02 p0231 A83-11975

Statistical extreme-value problems and unique solvability of a three-dimensional Navier-Stokes system under almost any initial conditions 03 p0323 A83-14897

Asymptotic methods in the extreme-value problems of mechanics --- Russian book 04 p0530 A83-15835

The fluctuation of black hole's energy and the upper bound to the temperature of the radiation in the vicinity of black hole 05 p0701 A83-17147

Error rate bounds for differential PSK 05 p0622 A83-17272

Concerning some boundary value problems for a third-order equation and extremal properties of its solutions 06 p0804 A83-17978

Concerning a method of extremal control 06 p0803 A83-19114

New error bounds for modulation and coding under mismatch 07 p0909 A83-19745

Distribution of a life ratio and its application 07 p0943 A83-20516

Legendre transformations and extremum principles 10 p1470 A83-25315

A combinatorial limit to the computing power of VLSI circuits 13 p1908 A83-30793

Equations of the necessary extremum condition for a class of incorrect extreme-value problems --- for optimization of aerodynamic configurations 14 p1972 A83-33011

The use of floating-point and interval arithmetic in the computation of error bounds 15 p2218 A83-33914

Direct observational upper limit to gravitational radiation from millisecond pulsar PSR1937+214 15 p2261 A83-34383

Bounds on the parallel processor speedup 15 p2218 A83-35131

The field of expanded extremals of a controlled process 20 p3039 A83-42922

Extremal statistics in the problem of the detection of pulse processes 21 p3120 A83-44771

Extremum principles for the energy-release problem of elastic-perfectly plastic body subjected to prescribed change of material properties 23 p3470 A83-48093

EXTRUDING

Raman spectroscopic study of ultraoriented solid state extruded polyethylene 01 p0027 A83-10609

Destruction of polyvinyl chloride under extrusion --- toxic hazards in industry 01 p0029 A83-11404

Plane strain extrusion studies by finite element method 02 p0196 A83-12874

Hot extrusion of aluminum composite containing dispersed graphite particles - Study of properties of particle-dispersed aluminum composite II 05 p0611 A83-17103

Properties of cold extruded aluminum-A12O3 powder materials 06 p0731 A83-19088

Fatigue crack propagation response in extruded and cast aluminum alloys 08 p1060 A83-21710

Screw extrusion of double base propellants 09 p1241 A83-23833

Investigations of the extrusion process 09 p1241 A83-23836

The effect of deformation and temperature on the structure and mechanical properties of a high-cobalt alloy 10 p1399 A83-26794

A study of the dynamic conditions of the extrusion of NiTi intermetallic 13 p1820 A83-30683

Temperature fields and deformation resistance during the extrusion of titanium alloys 13 p1820 A83-30685

Stresses in the deformation zone during the extrusion of titanium alloys 13 p1859 A83-30686

The shape of the deformation zone in extrusion 13 p1859 A83-30687

The geometrical factor during the extrusion of complex metal materials 13 p1859 A83-30688

On the cyclic behavior of cast and extruded aluminum alloys. B - Fractography 14 p1992 A83-32343

Load and material flow in hot extrusion of aluminium and copper powder compacts 16 p2329 A83-35607

Extruded composite propellant technology development [AIAA PAPER 83-1272] 16 p2340 A83-36318

The effect of extrusion conditions on the formation of the structure of titanium alloys 17 p2486 A83-37723

Investigation of the fatigue and crack propagation properties of X7091-T7E69 extrusion 17 p2487 A83-37836

A constant amplitude fatigue study of an aluminum powder metallurgy alloy 22 p3269 A83-46024

EYE (ANATOMY)

NT CONJUNCTIVA

NT CORNEA

NT NYSTAGMUS

NT OCULOMOTOR NERVES

NT RETINA

Phantom images of binocular vision in the system of hemispheric relations 01 p0082 A83-10505

Color vision is altered during the suppression phase of binocular rivalry 02 p0222 A83-12067

Changes in the organ of vision under the effect of vibration 03 p0373 A83-13292

A physiological-hygienic evaluation of eye fatigue in women workers of the warping shop at a weaving mill 03 p0379 A83-13612

Growth and aging of the lens 05 p0670 A83-17196

The long-term results of operations for the ultrasonic activation of trabeculae --- antiglaucoma treatment 05 p0674 A83-17213

Optics, the eye, and the brain 15 p2209 A83-33801

The distribution of Na, K, Ca, P, and S in the vestibular apparatus and eye of the larvae of the fish Brachydanio rerio 15 p2210 A83-34937

The objective measurement of anatomical and optical parameters of emmetropic and ametropic eyes 15 p2212 A83-34939

Visual sensations evoked by single electrons and muons 18 p2733 A83-39519

Differences in the description of a visual image at the level of the posterior parietal and inferotemporal cortices of monkeys 18 p2732 A83-39521

EYE DISEASES

NT ASTIGMATISM

NT CATARACTS

NT CONJUNCTIVITIS

NT GLAUCOMA

NT KERATITIS

A case report - Unilateral cycloplegia resulting from careless use of Transderrm-V 02 p0223 A83-12410

An experiment on oxygen permeability through corneal tissue 03 p0373 A83-13291

Color-stress as a method for detecting the focal reaction in endogenous uveitis 03 p0377 A83-13293

Perspectives on the use of stimulating laser therapy in ophthalmology 03 p0374 A83-13601

Concerning the so-called laser stimulation of the macula lutea and the possibility of theoretical interpretation of the mechanism of its action 03 p0378 A83-13602

Stimulation laser therapy for diseases of the cornea with the irradiation of a ruby laser 03 p0378 A83-13604

The effectiveness of stimulating argon laser therapy for some forms of macular dystrophy 03 p0378 A83-13605

The stimulating action of coagulating laser interventions in macular pathologies 03 p0378 A83-13606

A stimulating laser therapy for sclerotic and posttraumatic central dystrophies of the retina 03 p0378 A83-13607

Laser stimulation in the comprehensive therapy of central dystrophies of the retina 03 p0378 A83-13608

Condition of the organum visus in persons performing precision work 03 p0378 A83-13609

Refractive thermo- and laser keratoplasty 05 p0674 A83-17208

The information value of an ultrasonic examination in posttraumatic endophthalmitis 05 p0674 A83-17209

The problem of microcirculation and eye pathology 15 p2210 A83-34940

The diagnosis of changes in the vessels and membranes of eyes using fluorescent angiography 17 p2560 A83-38202

The characteristics of aerospace medical expertise for diseases of the eye 19 p2884 A83-42024

EYE DOMINANCE

The cyclopean eye vs. the sighting-dominant eye as the center of visual direction 02 p0224 A83-12095

EYE EXAMINATIONS

NT ELECTRONYSTAGMOGRAPHY

Condition of the organum visus in persons performing precision work 03 p0378 A83-13609

The information value of an ultrasonic examination in posttraumatic endophthalmitis 05 p0674 A83-17209

Optical devices for investigations of the eye --- Russian book 12 p1767 A83-29331

A comparative evaluation of the simplified tonograph methods of Nesterov and Kal'fa-Vurgaff --- for eye examinations 15 p2212 A83-34938

Procedures for the examination of the visual acuity and of the visual field in civil aeronautics 16 p2396 A83-35578

A device for the biomicroscopic study of the blood vessel bed in the eyeball conjunctiva 16 p2402 A83-36811

The characteristics of aerospace medical expertise for diseases of the eye 19 p2884 A83-42024

EYE MOVEMENTS

NT ELECTRONYSTAGMOGRAPHY

NT NYSTAGMUS

NT SACCADIC EYE MOVEMENTS

A comparison of some effects of three antimition sickness drugs on nystagmic responses to angular accelerations and to optokinetic stimuli 04 p0521 A83-15533

The accuracy of binocular vergence for peripheral stimuli 05 p0675 A83-17747

The dynamics of vertical eye movements in normal human subjects 06 p0797 A83-18192

System-theoretical analysis of the temporal buildup of transient processes in the visual system --- German thesis 06 p0800 A83-18496

Goal-directed movements of cat's eyes in response to electrical stimulation of the lateral geniculate body 07 p0972 A83-19645

The change of parameters of the eyelid motion reaction of an operator during prolonged work 07 p0981 A83-20332

The dependence of the eyelid motion reaction parameters of an operator on the complexity of a visual task 07 p0979 A83-20341

An infrared method for measuring the eyelid motion reaction 07 p0982 A83-20343

Presentation effects and eye-motion behaviors in dynamic visual inspection 07 p0980 A83-20622

Measurement of ocular counterrolling /OCR/ by polarized light 08 p1151 A83-22568

Dynamics of pattern vision 08 p1150 A83-22892

Convergence accommodation --- of eye 09 p1324 A83-24092

The eye movements of cats induced by the electrical stimulation of the lateral geniculate body 10 p1454 A83-26786

Oculomotor response to voluntary head rotations during parabolic flights 11 p1643 A83-27820

Pursuit eye movements - Movement of servomotor type or preprogrammed movements? 13 p1901 A83-30442

Pursuit eye movements and the localization of brief visually perceived events 13 p1901 A83-30443

The characteristics of the interaction of the vestibular-oculomotor and the visual systems in young animals 14 p2063 A83-32565

Design considerations for a real-time ocular counterroll instrument 14 p2073 A83-33108

Modifying oculomotor activity in awake subjects increases the amplitude of eye movements during REM sleep 15 p2211 A83-33777

The conditions contributing to the sensorimotor adaptation of the eye movement system in humans 19 p2883 A83-41835

Zero-latency tracking of predictable targets by time-delay systems 24 p3621 A83-49898

EYE PROTECTION

Optimal conditions for protecting the eyes from solar radiation with vision correction 14 p2073 A83-33314

EYEPIECES

The problem of presbyopia in pilots and its correction with eyeglasses 06 p0798 A83-18338

F**F CENTERS**

U COLOR CENTERS

F DISPLAYS

U F REGION

F LAYER

U F REGION

F REGION

NT F 1 REGION

NT F 2 REGION

Fabry-Perot determinations of midlatitude F-region neutral winds and temperatures from 1975 to 1979 02 p0204 A83-11965

Interaction of neutral and plasma motions in the ionosphere 02 p0206 A83-12154
 Equatorial plasma bubbles - Vertically elongated wedges from the bottomside F layer 02 p0208 A83-12390
 A heating mechanism for the generation of inhomogeneities of the ionospheric F-layer 02 p0208 A83-12420
 A three-dimensional model of the high-latitude F-region with allowance for the noncoincidence of geographical and geomagnetic coordinates 02 p0208 A83-12421
 The use of 1356-A emission intensity to determine parameters of the F-region 03 p0356 A83-13212
 Movements of the mid-latitude ionospheric trough 03 p0362 A83-14751
 The S3-4 ionospheric irregularities satellite experiment - Probe detection of multi-ion component plasmas and associated effects on instability processes 04 p0509 A83-14976
 The anisotropy of high-latitude nighttime F region irregularities 05 p0661 A83-17402
 Observations of the horizontal irregularity of F-layer nightglow in the region of the Brazilian anomaly 05 p0663 A83-17621
 The consequences of high latitude particle precipitation on global thermospheric dynamics 05 p0665 A83-17782
 Two-channel rocket photometer for tracing weak optical emissions at night 06 p0723 A83-18023
 A perpendicular ion beam instability - Solutions to the linear dispersion relation --- for F region ionosphere 06 p0784 A83-18304
 High resolution topside in situ data of electron densities and VHF/GHz scintillations in the equatorial region [AD-A125353] 06 p0785 A83-18309
 Nonlinear evolution of convecting plasma enhancements in the auroral ionosphere. II - Small scale irregularities 06 p0785 A83-18319
 F-region neutral winds and temperatures at equatorial latitudes - Measured and predicted behaviour during geomagnetically quiet conditions 07 p0968 A83-21580
 F-region irregularity drifts deduced from the scintillation measurements by two closely-spaced antennas 08 p1133 A83-22042
 Thermal modulation of the plasma density in ionospheric heating experiments 09 p1300 A83-23306
 The feedback-diffraction theory of ionospheric heating 09 p1300 A83-23307
 HF produced ionospheric electron density irregularities diagnosed by UHF radio star scintillations 09 p1300 A83-23310
 Observations of HF-enhanced plasma line with a 46.8-MHz radar and reinterpretation of previous observations with the 430-MHz radar 09 p1303 A83-23764
 A theoretical study of the high latitude F region's response to magnetospheric storm inputs 09 p1303 A83-23767
 The temporal structure of intensity scintillations near the magnetic equator [AD-A127533] 10 p1449 A83-26048
 Dynamics of the disturbed ionosphere 11 p1614 A83-27401
 Ionospheric observations at Pruhonice during the solar eclipse of April 29, 1976 11 p1616 A83-28111
 Meridional neutral winds in the thermosphere at Arecibo Simultaneous incoherent scatter and airglow observations 11 p1618 A83-28321
 Theoretical modeling of low-latitude Mg 11 p1618 A83-28324
 Monte Carlo calculations of the O⁺/+ velocity distribution in the auroral ionosphere 11 p1619 A83-28328
 The influence of the interplanetary magnetic field on the F region and the upper ionosphere 11 p1620 A83-28743
 Spatial and frequency correlation of a field scattered by small-scale irregularities of the ionospheric F-region 12 p1753 A83-29252
 Horizontal velocity dispersion of medium-scale travelling ionospheric disturbances in the F-region 12 p1754 A83-29433
 Auroral riometer absorptions and the F-region disturbances observed over a wide range of latitudes 12 p1754 A83-29436
 F region ion temperature enhancements resulting from Joule heating 13 p1879 A83-31243
 Generation of ionospheric irregularities by thermal-source - A new mechanism 13 p1881 A83-31533
 Equatorial depletions in the 630.0 nm airglow at Vanimo --- New Guinea 13 p1881 A83-31538
 Dependence of vertical drifts of the ionospheric F-layer at the Leningrad observatory on magnetic activity in the auroral zone 14 p2050 A83-31879

On the formation of daytime troughs in the F-region within the plasmasphere 14 p2053 A83-32697
 Latitudinal and magnetic flux tube extension of the equatorial spread F irregularities 15 p2195 A83-33938
 Plasma waves produced by the xenon ion beam experiment on the Porcupine sounding rocket 15 p2198 A83-34189
 Generation of ultra-violet oxygen emissions with wavelengths of 1304 and 1356 Å by electron collision and some aeronomic consequences 15 p2200 A83-34416
 Extremely high F-region electron temperatures during the maximum of 21st solar cycle 15 p2200 A83-34417
 On the kinetic balance in the ca. maximal part of the daily F-region 15 p2201 A83-34447
 Role of neutral winds in generating irregularities in equatorial F-region 16 p2374 A83-35378
 Equatorial F-region ionization differences between March and September, 1979 16 p2375 A83-35388
 Relationship between electron density and electron temperature as a function of solar activity 16 p2375 A83-35397
 F-region ion composition modeling 16 p2376 A83-35398
 Simple M-factor algorithm for improved estimation of the basic maximum usable frequency of radio waves reflected from the ionospheric F-region 16 p2342 A83-36576
 Millstone Hill incoherent scatter observations of auroral convection over Lambda = 60-75 deg. III - Average patterns versus Kp 17 p2537 A83-37576
 The response of the nighttime F-region to wave disturbances 17 p2539 A83-37650
 The mid-latitude trough in the electron concentration of the ionospheric F-layer - A review of observations and modelling 18 p2712 A83-39069
 F-region dynamo in the evening - Interpretation of equatorial Delta D anomaly found by MAGSAT 18 p2712 A83-39074
 Recombination dynamics in the F-region 18 p2713 A83-39318
 The effect of the conductivity of the E-region on the growth increment of the Rayleigh-Taylor instability in the ionospheric plasma of the equatorial F-region 18 p2714 A83-39331
 Equatorial disturbance dynamo electric fields 19 p2864 A83-41117
 Complexities of the storm-time characteristics of ionospheric total electron content 20 p3016 A83-42305
 Ionospheric plasma bubble encounters or F region bottomside traversals? 20 p3018 A83-42416
 Polarization electric fields in the nighttime F layer at Arecibo 20 p3019 A83-42418
 Observations of large scale F-region irregularities using airglow emissions at 7774 Å and 6300 Å 21 p3170 A83-44245
 Modeling of the meridional distribution of the F-region electron concentration over Ashkhabad during the storm of August 1972 21 p3176 A83-45271
 Investigation of the midlatitude ionospheric trough using ground-based geophysical methods and synchronous measurements from satellites 21 p3177 A83-45287
 Global distribution of the ionospheric F-layer critical frequency f_oF2 21 p3177 A83-45446
 Short-term prediction of HF propagation 21 p3122 A83-45450
 Photochemistry of N2(+) in the daytime F region 22 p3328 A83-46056
 Parametric excitation and suppression of convective plasma instabilities in the high-latitude F region ionosphere 22 p3328 A83-46060
 Ionospheric irregularities and their potential impact on synthetic aperture radars 22 p3275 A83-46535
 Very high latitude F-region irregularities observed by HF-radar backscatter 22 p3334 A83-46889
 The fossil theory of nighttime high latitude F region troughs 22 p3335 A83-47041
 Bottomside sinusoidal irregularities in the equatorial F region 22 p3337 A83-47065
 Telecommunications and the satellite 'Intercosmos-Bulgaria-1300' [IAF PAPER 83-ST-09] 23 p3420 A83-47387
 A scattering theory of VHF transequatorial propagation 24 p3570 A83-49313

F 1 REGION

The possibility of calculating and deterministic method of predicting ionospheric parameters at the heights of the E and F1 regions for particular heliogeophysical conditions 01 p0071 A83-10599
 The correlation of parameters of the F2 and F1 layers of the ionosphere in the case of day-to-day variations 02 p0210 A83-12445

Ion transport in the mid-latitude F1-region 17 p2544 A83-38522

F 2 REGION

The correlation of f_oF2 disturbances with variations in solar radio emission 01 p0129 A83-10592
 The stability of the diurnal variation of the degree of disturbance of f_oF2 during the cycle of solar activity 01 p0071 A83-10593
 The manifestation of solar activity features upon the decay of the 20th cycle in the ionization of the F2 layer 01 p0129 A83-10594
 Diffusion in the high atmosphere 02 p0206 A83-12153
 Mg/+ morphology from visual airglow experiment observations 02 p0208 A83-12396
 The correlation of parameters of the F2 and F1 layers of the ionosphere in the case of day-to-day variations 02 p0210 A83-12445
 Dependence of the parameters of the disturbed midlatitude ionospheric F2-region on local time 02 p0210 A83-12446
 Geographical and seasonal distribution of critical frequencies in the F2-layer during a period of high solar activity 04 p0509 A83-15724
 Improving ionospheric maps using theoretically derived values of f₁/f₂/ 07 p0961 A83-20372
 The variation of the magnetic field and its interaction with the equatorial electrojet in eastern Senegal 08 p1135 A83-22314
 A study of the post-sunset increase in the F2-region electron density at low- and middle latitudes in the Asian zone during sunspot maximum and minimum periods 08 p1135 A83-22315
 Non-linear interaction of decametre radio waves at close frequencies in oblique propagation --- in ionosphere 09 p1300 A83-23313
 The effects of meridional electric fields in the high-latitude ionosphere 11 p1620 A83-28746
 Tropical nightglow observations and predictions from ionospheric models 12 p1754 A83-29432
 The height distribution of electron density in the high-latitude F2-layer 13 p1875 A83-30611
 The effects of neutral air winds on the electron content of the mid-latitude ionosphere and protonosphere in summer 13 p1882 A83-31629
 High latitude neutral atmosphere temperature and concentration measurements from the first Eiscat incoherent scatter observations 13 p1883 A83-31717
 Longitudinal and latitudinal abnormalities in the daily variation of f_oF2 in the South-American region 13 p1883 A83-31719
 Meteorological effects in the F2-layer of the ionosphere 14 p2049 A83-31857
 The reaction of the ionosphere to variations of electric fields during nighttime baylike disturbances 14 p2049 A83-31866
 Some characteristics of the F2 layer at low and middle latitudes 15 p2200 A83-34419
 Implementation of a new characteristic parameter into the IRI sub-peak electron density profile 16 p2374 A83-35386
 Characteristics of low-latitude whistlers and their relation with f_oF2 and magnetic activity 16 p2375 A83-35393
 The statistical model of the F2-layer critical frequency 18 p2713 A83-39316
 Correlations between cyclic increments of F2-layer critical frequencies 18 p2713 A83-39317
 Water vapor in the thermosphere 18 p2719 A83-40086
 Particle precipitation in the ionospheric F2 region at locations in the vicinity of the South-Atlantic Magnetic Anomaly 20 p3017 A83-42312
 A waveguide for low-frequency electromagnetic waves in the upper ionosphere 20 p3017 A83-42331
 f_oF2 response to IMF sector-boundary crossings 20 p3017 A83-42375
 A model for the variations of the critical frequency of F2 layer during the negative phases of ionospheric storms 20 p3024 A83-43173
 The correlations between the typhoon and th(f)_oF(2) of ionosphere 21 p3172 A83-44518
 Possible mechanism for a synphase variation of electron density in the E and F2 regions of the ionosphere 21 p3174 A83-45234
 Estimation of the critical frequency of the F2-layer from the difference of the reflection heights of magnetoionic components 21 p3174 A83-45235
 Reaction of the ionospheric F2 region to a solitary internal gravity wave 21 p3176 A83-45257
 Modeling of the equatorial ionosphere in the hybrid model 21 p3176 A83-45258
 Annual and semiannual periodicities in NmF2 in the African sector 24 p3605 A83-49303

- The accuracy of simple methods for determining the height of the maximum electron concentration of the F2-layer from scaled ionospheric characteristics
24 p3606 A83-49312
- F-4 AIRCRAFT**
F-4F fire control system software support - An integrated approach to ground and flight testing
01 p0015 A83-11228
Application of vector performance optimization to a robust control loop design for a fighter aircraft
07 p0867 A83-21160
Accelerated Mission Testing of the F110 Engine
[AIAA PAPER 83-1235] 16 p2308 A83-36298
F/RF-4 transparency baseline bird impact test program
20 p2932 A83-42533
Scheduled depot maintenance of naval aircraft - How often?
[AIAA PAPER 83-2517] 23 p3392 A83-48361
The F-4 flutter suppression program
24 p3547 A83-49192
- F-5 AIRCRAFT**
The Northrop F-20 avionics mission simulator
[AIAA PAPER 83-0142] 05 p0599 A83-16551
Design and development of the RF-5E aircraft
12 p1700 A83-29015
The F-5 story - Prototype and technology demonstrator
[AIAA PAPER 83-1062] 16 p2301 A83-36473
- F-8 AIRCRAFT**
Implicit adaptive control for a class of MIMO systems --- with application to lateral dynamics of F-8 aircraft
06 p0719 A83-19031
Model reference adaptive control in the presence of measurement noise
17 p2568 A83-37128
Flight-test results using nonlinear control with the F-8C digital fly-by-wire aircraft
[AIAA PAPER 83-2174] 19 p2802 A83-41669
- F-110 AIRCRAFT**
U F-4 AIRCRAFT
- F-14 AIRCRAFT**
PETTS /Programmable Engine Trim Test Set/
01 p0014 A83-10752
Tomorrow's Tomcat
03 p0281 A83-14324
Serviceability evaluation of advanced composite F-14A main-landing-gear-strut doors and overwing fairings
07 p0861 A83-20480
Integrated propulsion-aircraft control evaluation for a current Navy fighter
[AIAA PAPER 83-1236] 16 p2308 A83-36299
F-14 aircraft and propulsion control integration evaluation
[ASME PAPER 83-GT-234] 23 p3411 A83-48029
- F-15 AIRCRAFT**
Integrated flight and fire control development and flight test on an F-15B aircraft
01 p0006 A83-11160
USAF studies fighters for dual-role, all-weather operations
05 p0595 A83-17276
Digital electronic engine control system - F-15 flight test
06 p0718 A83-18406
Flight evaluation of modifications to a digital electronic engine control system in an F-15 airplane
[AIAA PAPER 83-0537] 06 p0718 A83-19593
Integrated systems evaluated on F-15
11 p1528 A83-28700
US fighter options
18 p2641 A83-40665
- F-16 AIRCRAFT**
F-16 voice message system study
01 p0005 A83-11121
Design of direct digital adaptive flight-mode control systems for high-performance aircraft
01 p0013 A83-11179
Advanced fighter technology integrator /AFTI/ F-16 display mechanization
04 p0448 A83-16132
Qualification of the flight-critical AFTI/F-16 digital flight control system --- Advanced Fighter Technology Integration
[AIAA PAPER 83-0060] 05 p0597 A83-16492
Estimating roll coupling instability for highly augmented aircraft
[AIAA PAPER 83-0366] 05 p0598 A83-16673
USAF studies fighters for dual-role, all-weather operations
05 p0595 A83-17276
The General Dynamics F-16 XL fighter aircraft
06 p0717 A83-19411
Technology and modern fighter aircraft - The evolutionary F-16
07 p0865 A83-20598
F-16 pulse Doppler radar /AN/APG-66/ performance
08 p1044 A83-22737
Recent developments in polycarbonate coatings for advanced aircraft
09 p1239 A83-24959
Environmental control of an aircraft pod mounted electronics system
[SAE PAPER 820869] 10 p1375 A83-25768
AFTI/F-16 aeroservoelastic analyses and ground test with a digital flight control system
[AIAA 83-0994] 12 p1704 A83-29888

- The F-16 - A technology demonstrator, a prototype, and a flight demonstrator.
[AIAA PAPER 83-1063] 16 p2301 A83-36467
AFTI/F-16 technology demonstrator
[AIAA PAPER 83-1059] 16 p2301 A83-36474
Super integrated power unit (SIPU) for the F-16 engine start system
[SAE PAPER 821462] 17 p2469 A83-37996
Application of forward sweep wings to an air combat fighter
[AIAA PAPER 83-1833] 17 p2465 A83-38662
F-16XL - GD hatches a new Falcon
18 p2641 A83-40621
US fighter options
18 p2641 A83-40665
MIMO controller design for longitudinal decoupled aircraft motion --- Multi-Input/Multi-Output
[AIAA PAPER 83-2274] 19 p2804 A83-41740
F-16XL shows advances in range, ride
22 p3254 A83-46924
Emergency power for the F-16 aircraft
[ASME PAPER 83-GT-189] 23 p3410 A83-47995
- F-17 AIRCRAFT**
Active control of near frequency coalescence flutter
24 p3549 A83-49191
- F-18 AIRCRAFT**
Four-channel multiplexed resolver-to-digital converter
01 p0009 A83-11100
Software configuration control in a real-time flight test environment
01 p0009 A83-11144
A survey of avionics software support environments
01 p0087 A83-11163
F-18 Hornet high angle of attack /AOA/ program
02 p0137 A83-11809
Wind tunnel correlation study of aerodynamic modeling for F/A-18 wing-store tip-missile flutter
[AIAA 83-1028] 12 p1703 A83-29877
Principal site testing of the F/A-18 at the Naval Air Test Center
14 p1975 A83-32935
Flight fidelity testing of the F/A-18 simulators
[AIAA PAPER 83-1094] 16 p2300 A83-36225
F/A-18A Inflight Engine Condition Monitoring System (IECMS)
[AIAA PAPER 83-1237] 16 p2308 A83-36300
Thrust reverser effects on the tail surface aerodynamics of an F-18 type configuration
[AIAA PAPER 83-1860] 17 p2457 A83-38687
F/A-18 inlet/engine compatibility flight test results
19 p2796 A83-41039
Integrated flight control systems development - The F/A-18A Automatic Carrier Landing System
[AIAA PAPER 83-2162] 19 p2804 A83-41765
F/A-18 high angle of attack departure resistant criteria for control law development
[AIAA PAPER 83-2126] 19 p2806 A83-41950
Investigation of F/A-18A engine throttle usage and parametric sensitivities
[ASME PAPER 83-GT-64] 23 p3407 A83-47919
Subsonic/supersonic aeropropulsive characteristics of nonaxisymmetric nozzles installed on an F-18 model
23 p3411 A83-48215
- F-28 TRANSPORT AIRCRAFT**
The Fokker F28 and a four-engined newcomer
07 p0866 A83-21349
In-flight acoustic measurements in the engine intake of a Fokker F28 aircraft
[AIAA PAPER 83-0677] 10 p1376 A83-25909
- F-104 AIRCRAFT**
F-104 CCV research flight test program
07 p0867 A83-20074
Analysis of the precision of inertial navigation systems --- German thesis
11 p1528 A83-28649
- F-111 AIRCRAFT**
ATE support of RF line replaceable units
01 p0013 A83-10732
Vibration isolation system development for the FB-111 tail pod electronics
05 p0595 A83-16932
From new technology development to operational usefulness B-36, B-58, F-111/FB-111
[AIAA PAPER 83-1046] 16 p2287 A83-36459
AFTI/F-111 mission adaptive wing technology demonstration program
[AIAA PAPER 83-1057] 16 p2301 A83-36468
An integrated maneuver enhancement and gust alleviation mode for the AFTI/F-111 MAW aircraft
[AIAA PAPER 83-2217] 19 p2803 A83-41699
- FAB (PROGRAMMING LANGUAGE)**
U FORTRAN
- FABRICATION**
NT SPACE MANUFACTURING
The electrical characteristics of degenerate InP Schottky diodes with an interfacial layer
01 p0036 A83-10629
Development of a microwave 20 x 20 switch matrix for 30/20 GHz SS-TDMA application
01 p0044 A83-11484
Self-annealed ion implanted solar cells
02 p0202 A83-12290

- Fabrication and use of silicon carbide mirrors for synchrotron radiation
02 p0238 A83-12707
X-ray ultraviolet grating measurements at LURE - Comparison with electromagnetic theory predictions
02 p0238 A83-12710
Development in replicated nickel gratings
02 p0238 A83-12713
Yield considerations in the design and fabrication of GaAs MMICs
03 p0308 A83-13439
Recent developments in infrared acousto-optic tunable filters
03 p0393 A83-13770
Impact of molecular beam epitaxy on millimeter wave and optical systems
03 p0310 A83-13788
Low-loss GeO₂ optical waveguide fabrication using low deposition rate rf sputtering
03 p0395 A83-14392
Self-registered gradually doped source drain extension short channel CMOS/SOS devices
05 p0624 A83-17291
SOI/CMOS circuits fabricated in zone-melting-recrystallized Si films on SiO₂-coated Si substrates
05 p0624 A83-17292
0.15 micron channel-length MOSFET's fabricated using e-beam lithography
05 p0624 A83-17297
Single event error immune CMOS RAM
05 p0629 A83-17538
High power CW single-drift Impatt diodes at W-band
06 p0750 A83-17971
Polarisation preserving single-mode-fibre coupler
06 p0809 A83-18570
Experimental results on junction charge-coupled devices
06 p0752 A83-18760
CdTe/HgCdTe indium-diffused photodiodes
06 p0753 A83-18943
Fabrication and heat treatment of a Ni-base superalloy integrally bladed rotor for small gas turbine engine applications
06 p0732 A83-19102
Evaluation of a process for achieving low between-metal contact resistance in plasma etched polyimide vias --- for integrated circuits
07 p0917 A83-19898
Fabrication technology for aircraft engines --- Russian book
07 p0861 A83-20381
Composite drapability - A too often ignored impacting cost characteristic
07 p0875 A83-20438
Low cost fabrication of sheet structure using a new beta titanium alloy, Ti-15V-3Cr-3Al-3Sn
07 p0886 A83-20469
Knitted fabrics in fiber reinforced structural composites
07 p0876 A83-20470
Composites fabrication cost estimating technique /FACET/ - An automated estimating system
07 p0877 A83-20494
Design considerations for fabrication of sintered alpha-SiC components
08 p1072 A83-22261
Contemporary methods of optical fabrication; Proceedings of the Meeting, San Diego, CA, August 25, 26, 1981
08 p1111 A83-22863
Image transforms with fused fiber optics
08 p1167 A83-22864
Beryllium optical mirrors by vapor deposition
08 p1112 A83-22865
Fabrication of thin glass mirrors on alnico magnets
08 p1112 A83-22866
Fabrication of electroless nickel-plated mirrors on alnico substrates
08 p1112 A83-22867
Diamond machining of infrared refractors utilizing two-axis machine tool technology
08 p1112 A83-22868
Testing diamond turned aspheric optics using computer-generated holographic /CGH/ interferometry
08 p1103 A83-22869
Fabrication of cryogenic mirrors
08 p1112 A83-22870
Polyetheretherketone matrix composites
09 p1221 A83-23605
Fabrication of bonded graphite/polyimide structures for advanced aerospace applications
09 p1210 A83-23636
Problems regarding the manufacture of explosives having a very fine grain
09 p1240 A83-23832
Base-bleed solid propellants with thermoplastic elastomers as binders
09 p1241 A83-23839
Phenomena of static electricity in fabrication and processing of solid propellants
09 p1242 A83-23843
Epitaxy
09 p1349 A83-23854
Yield considerations for ion-implanted GaAs MMIC's
09 p1256 A83-24680
Developments in the design, analysis, and fabrication of advanced technology transmission elements
09 p1274 A83-24832
Development of a new family of improved infrared /IR/ dome ceramics
09 p1239 A83-24952
Nitrogen-stabilized aluminum oxide spinel /ALON/
09 p1345 A83-24954
Fabrication and Josephson behavior of high-Tc superconductor-normal-superconductor microbridges
10 p1410 A83-25988

Stresses during fabrication of cylindrically woven carbon-carbon composites 11 p1543 A83-27462

Railcon anodes fabricated by electron beam lithography for image photon counting detectors 11 p1553 A83-27754

Proton-exchanged optical waveguides in Y-cut lithium niobate 11 p1657 A83-28611

Fabrication and investigation of BARITT diodes in the Ka-band --- German thesis 11 p1564 A83-28645

Optimization of pulling conditions by electronic bombardment of polycrystalline silicon ribbons for solar cells --- French thesis 12 p1750 A83-29946

Carbon fibers produced by pyrolysis of natural gas in stainless steel tubes 13 p1825 A83-30337

Application of the graining process for the fabrication of chopped carbon fiber-aluminium composite 13 p1816 A83-31602

Gas immersion laser diffusion - A new method for making efficient Si solar cells 14 p2041 A83-32234

Zn3P2 thin-film solar cells 14 p2090 A83-32304

Possibilities of ion implantation in silicon solar cell manufacturing 14 p2045 A83-32312

Polycrystalline silicon solar cells utilizing an integral screen printing technique 14 p2045 A83-32314

Recent developments in multi-wire fixed abrasive slicing technique (FAST) --- for low cost silicon wafer production from ingots 14 p2027 A83-32322

Critical technology limits to silicon material and sheet production 14 p2091 A83-32323

Comparison between various ion beam doping procedures and anneal techniques used in manufacturing silicon solar cells 14 p2091 A83-32325

Screen printed SIS-type solar cells 14 p2005 A83-32334

The world's largest 12volt single string photovoltaic module 14 p2046 A83-32337

Design and fabrication of brazed beryllium assemblies [AIAA PAPER 83-0868] 14 p2028 A83-32789

InGaAsP/InP phototransistor-based detectors 15 p2150 A83-33683

All-refractory Josephson logic circuits 15 p2150 A83-33888

Fabrication and investigation of GaInPAs/InP heterolasers 15 p2168 A83-33978

(GaAl)As/GaAs heterojunction bipolar transistors with graded composition in the base 15 p2152 A83-34516

The effect of certain fabrication factors on the errors of a dynamically tuned gyroscope with a displaced center of mass 15 p2167 A83-35264

Introduction to metal matrix composite materials --- Book 16 p2324 A83-35575

Studies of fabrication of carbon fiber reinforced aluminium matrix composite 16 p2324 A83-35606

Very low threshold InGaAsP mesa laser 16 p2359 A83-35955

Fabrication of GaAs bistable optical devices 16 p2412 A83-36069

Metal-metal composites loaded at ultrasonic frequencies 16 p2324 A83-36190

Extruded composite propellant technology development [AIAA PAPER 83-1272] 16 p2340 A83-36318

Sputtering of silicon and its compounds in the electronic stopping region 16 p2421 A83-36713

GaAs microwave devices and circuits with submicron electron-beam defined features 17 p2496 A83-37059

Microstructural effects on properties and new processing techniques of silicon nitride. I - Microstructural effects on mechanical, thermal and thermomechanical properties of silicon nitride 18 p2671 A83-39619

Silicon carbide whiskers from rice hulls - A unique reinforcement 18 p2651 A83-40136

Fabrication of carbon fiber reinforced aluminum composites by roll diffusion bonding method 18 p2659 A83-40262

Fabrication of SiC fiber-aluminum composite materials 18 p2659 A83-40264

Mechanical behavior of silicon carbide whisker reinforced aluminum alloys 18 p2659 A83-40266

Warpage, a nightmare for composite parts producers 18 p2661 A83-40283

Development of structural graphite/epoxy tube for space application 18 p2661 A83-40285

Surface analyses of carbon fibers produced from polyacrylonitrile fibers at low carbonization temperatures 19 p2824 A83-41860

Development of fabrication technology and measurement systems for multimode, single-mode and polarization maintaining optical fibers --- Thesis 19 p2901 A83-42125

Design, fabrication, and qualification of composite carbon/epoxy horizontal stabilizer components 20 p2927 A83-42546

The influence of fabrication defects of tube dispersive waveguides on the shape of the output signal of a matched filter 20 p2967 A83-42911

Design and fabrication of payload for OH emission experiment onboard Spacelab - A case study 21 p3095 A83-43821

The spectral response of BSF silicon solar cells fabricated through masked ion implantation --- Back Surface Field 21 p3166 A83-43843

Laser chemical etching of vias in GaAs 21 p3142 A83-43847

Fabrication of a 360 deg astigmatic rainbow hologram 21 p3136 A83-44153

Fabrication of polarization-maintaining and absorption-reducing fibers 21 p3204 A83-44203

Chirped grating lenses in Ti-indiffused LiNbO3 optical waveguides 21 p3207 A83-44835

Control of composite cure processes 21 p3119 A83-45067

A new method for the fabrication of submicron thick gallium arsenide membranes 21 p3220 A83-45498

Annual review of materials science. Volume 13 22 p3262 A83-45892

Mechanical alloying 22 p3268 A83-45896

Ion mixing 22 p3364 A83-45899

Crystalline silicon as a material for solar cells 22 p3269 A83-45918

Optical waveguides in LiTaO3 formed by proton exchange 22 p3356 A83-45969

Control of composite cure processes 22 p3262 A83-46284

Fabrication of ZrCx/Zr and Cr-CrOx films for practical solar selective absorption systems 22 p3319 A83-46584

Cascade AlGaAs-GaAs solar cell research using molecular beam epitaxy 22 p3319 A83-46606

High efficiency GaAs(1-x)P(x) solar cells fabricated by vacuum metalorganic chemical vapor deposition 22 p3319 A83-46607

Use of column V alkyls in organometallic vapor phase epitaxy (OMVPE) 22 p3266 A83-46608

Materials for infrared low loss fibers 22 p3358 A83-46624

Fabrication and performance of diffraction lenses 22 p3359 A83-46645

Method of construction and fabrication procedures for the A300-rudder unit, using a carbon-fiber type of construction 23 p3391 A83-47211

High-frequency holographic transmission gratings in photoresist 23 p3454 A83-47578

Progress in net shape fabrication of alpha SiC turbine components [ASME PAPER 83-GT-238] 23 p3466 A83-48030

Nitrogen ceramics 1976-1981 23 p3433 A83-48252

Sintering of Si3N4-based materials using the powder bed technique 23 p3435 A83-48268

Fabrication of complex shaped ceramic articles by slip casting and injection molding 23 p3466 A83-48306

High-efficiency Si solar cells by beam processing 24 p3598 A83-48791

Preparation and properties of sputtered a-Si:H:F films 24 p3636 A83-50185

FABRICS

Heat transfer on cylinder covered with close-fitting fabrics. I - Wind penetration through fabrics 02 p0226 A83-13070

Stiffness and strength behaviour of woven fabric composites 03 p0291 A83-13685

An investigation of the shielding effectiveness of FFP-15 fabric relative to bacterial aerosols 05 p0677 A83-17201

Experimental data from a study of the toxic effect on embryos exerted by hexachlorophene - A component of antimicrobial fabrics and synthetic clothes of everyday use 05 p0677 A83-17203

Knitted fabrics in fiber reinforced structural composites 07 p0876 A83-20470

In-plane thermal expansion and thermal bending coefficients of fabric composites 11 p1592 A83-27444

Prepreg, tape and fabric technology for advanced composites 12 p1710 A83-29713

Stiffness and strength properties of woven composites 18 p2703 A83-40177

Thermoelastic analysis of hybrid fabric composites 21 p3106 A83-44120

FABRY-PEROT INTERFEROMETERS

A modular Fabry-Perot interferometer system for imagery and spectrometry 01 p0118 A83-11048

Stable and rugged etalon for the Dynamics Explorer Fabry-Perot interferometer. I - Design and construction 02 p0142 A83-12312

Stable and rugged etalon for the Dynamics Explorer Fabry-Perot interferometer. II - Performance 02 p0142 A83-12313

Linewidth measurements of tunable diode lasers using heterodyne and etalon techniques 02 p0185 A83-12318

Optical coherence effects on a fiber-sensing Fabry-Perot interferometer 03 p0330 A83-14390

The helium 10830 A line in early-type stars - An atlas of Fabry-Perot scans 05 p0698 A83-17003

Optical bistability and self-oscillation of a nonlinear Fabry-Perot interferometer filled with a nematic-liquid-crystal film 05 p0685 A83-17882

A theoretical and experimental analysis of modulated laser fields and power spectra 06 p0766 A83-18908

The optical computer 06 p0810 A83-19240

Cherenkov parametric optical oscillations in a 'double' Fabry-Perot interferometer 07 p0934 A83-20116

Regenerative oscillation in the nonlinear Fabry-Perot interferometer 07 p0994 A83-21596

Multistability at microwave frequencies 08 p1079 A83-22011

TAURUS - The imaging Fabry-Perot at La Silla 09 p1356 A83-25290

A far-infrared Fabry-Perot interferometer and grating spectrometer for balloon-borne astronomy 10 p1419 A83-25458

Influence of a nonlinear active medium on the structure of natural oscillation modes of a Fabry-Perot interferometer 10 p1433 A83-26681

Cerenkov-type optical parametric oscillation in a 'double' Fabry-Perot interferometer 11 p1578 A83-27540

Theory of a Fabry-Perot interferometer with statistically irregular surfaces 11 p1573 A83-27959

A simple fibre Fabry-Perot sensor 12 p1729 A83-29189

A Fabry-Perot etalon with one phase-conjugate mirror 12 p1778 A83-29197

Internal movements in H II regions - The small nebula Sharpless 158 14 p2100 A83-33284

Folded Fabry-Perot quasi-optical ring resonator diplexer Theory and experiment 14 p2027 A83-33457

Fabry-Perot interferograms for amplitude and phase modulated light 15 p2163 A83-33755

High-accuracy wave-number measurements in molecular iodine 15 p2227 A83-33762

Theory and experiment on optical bistability in a Fabry-Perot interferometer with an intracavity nematic liquid-crystal film 16 p2411 A83-35666

Hysteresis and nonlinear thermo-optic waves in a semiconductor Fabry-Perot interferometer 17 p2581 A83-38972

A cryogenic Fabry-Perot for far infrared astronomy 18 p2692 A83-40461

Analysis of instrument errors arising in velocity measurement by an LDV based on a Fabry-Perot interferometer 19 p2849 A83-41900

Fiber-optic spectrum analyzer 21 p3136 A83-44211

Sensitive all-single-mode-fiber resonant ring interferometer 21 p3136 A83-44212

A new method of determining nebular radial velocities from Fabry-Perot interferograms 21 p3222 A83-44415

Resonant modes in a dispersive cavity --- nonlinear optical effects in active interferometer 21 p3206 A83-44802

Optical extinction theorem in the nonlinear theory of optical multistability 21 p3206 A83-44803

Velocity fields in late-type galaxies from H-alpha Fabry-Perot interferometry. IV - Kinematics and dynamics of the SAB(s) spiral NGC 5236 (M83) 22 p3377 A83-46257

OH Pepsips --- polyetanol pressure-scanned interferometric optical spectrometer for atmospheric measurements 22 p3294 A83-46841

Specular reflection cancellation in an interferometer with a phase-conjugate mirror 24 p3628 A83-48905

FABRY-PEROT LASERS

FABRY-PEROT SPECTROMETERS

A modular Fabry-Perot interferometer system for imagery and spectrometry 01 p0118 A83-11048

TAURUS: A wide-field imaging Fabry-Perot spectrometer for astronomy 03 p0401 A83-13324

Dual Fabry-Perot spectrometer measurements of daytime thermospheric temperature and wind velocity - Data analysis procedures 09 p1306 A83-24449

Doppler imaging system: An optical device for measuring vector winds. I - General principles 10 p1423 A83-26643

Cooled grating Fabry-Perot spectrometer for the 10 micron region 14 p2017 A83-32003

Ultra-high precision radial velocity spectrometer 14 p2017 A83-32017

Fabry-Perot spectrometers for the ground-based infrared 18 p2690 A83-40435

PRESTO - A programmable etalon spectrometer for twilight observations 22 p3288 A83-46066

- Taurus observations of the emission-line velocity field of Centaurus A (NGC 5128) 24 p3642 A83-49257
- FACE (ANATOMY)**
 NT NOSE (ANATOMY)
 The effectiveness of various methods of reflex therapy for the postneurtic contraction of mimic muscles 01 p0084 A83-11392
 Metabolic effects of facial cooling in exercise 06 p0796 A83-18190
 Evoked potentials of the posterior associative regions of the cerebrum during the discrimination and identification of human facial images 12 p1764 A83-29302
 Necrotic epitympanitis complicated by paresis of the facial nerve and labyrinthitis 16 p2399 A83-36815
- FACE CENTERED CUBIC LATTICES**
 The growth of gamma-prime precipitates in nickel-base superalloys 04 p0462 A83-16270
 Diffuse electron scattering in the Ti50Ni46Nb4 alloy in the X-phase preprecipitation stage 07 p0889 A83-20860
 Phase composition and phase stability of alloy IN939 07 p0894 A83-21483
 Microstructure and strengthening of superalloys 07 p0896 A83-21603
 Modeling the creep and fracture of the directionally solidified gamma/gamma-prime-McC eutectic 08 p1068 A83-22786
 Recovery and work hardening during high temperature creep of fcc alloys of low stacking fault energy 09 p1231 A83-24055
 On the power-law breakdown during high temperature creep of fcc metals 09 p1231 A83-24059
 Deformation mechanism diagrams - Modifications for engineering applications 09 p1232 A83-24060
 Anelastic relaxation, cyclic creep and stress rupture of gamma prime and oxide dispersion strengthened superalloys 09 p1232 A83-24074
 The tribological properties of highly oriented cobalt and Co-Cr ion platings 10 p1395 A83-25550
 Orientation relationships between bcc Mo and fcc gamma in a Ni-Al-Mo-W superalloy 10 p1398 A83-26284
 On the structure of tilt grain boundaries in cubic metals. I - Symmetrical tilt boundaries. II - Asymmetrical tilt boundaries. III - Generalizations of the structural study and implications for the properties of grain boundaries 11 p1551 A83-28807
 The effect of heat treatment on the structure and long-term strength of the nickel eutectic gamma/gamma-prime-McC - The length memory effect 15 p2137 A83-34017
 Recrystallization of a nickel-base superalloy - Kinetics and microstructural development 15 p2138 A83-34132
 On gamma and gamma-prime phases composition in Ni-base superalloys after high-temperature exposure 15 p2140 A83-34799
 Comments on 'Long term growth of gamma-prime particles' 16 p2330 A83-35984
 Calculations of the binding of hydrogen to fixed interstitial impurities in nickel 18 p2669 A83-40627
 Discontinuous gamma-prime coarsening in a Ni-Al-Mo base superalloy 18 p2669 A83-40628
 Microstructure and mechanical properties of rapidly quenched L1(2) alloys in Ni-Al-X systems 18 p2669 A83-40632
 Effect of swaging on the 1000 C compressive slow plastic flow characteristics of the directionally solidified eutectic alloy gamma/gamma prime-alpha 21 p3111 A83-44340
 Orientation dependence of creep behavior of single crystal gamma-prime (Ni3Al) 22 p3268 A83-45623
 Gamma prime shape changes during creep of a nickel-base superalloy 23 p3432 A83-47855
- FACETS**
 U FLAT SURFACES
- FACSIMILE COMMUNICATION**
 One-way multiaddress satellite data communication system 11 p1557 A83-28133
- FACSIMILE TRANSMISSION**
 U FACSIMILE COMMUNICATION
- FACTOR ANALYSIS**
 Allowance for the mutual influence of factors in the analysis of reliability 04 p0494 A83-15918
 Possible mechanisms for the organization of the structure of the sleep-wakefulness cycle according to the data of factor analysis 06 p0794 A83-18971
 A contribution to the investigation of time-sharing ability --- in human complex task performance 16 p2400 A83-35560
 Application of factor-analysis methods to evaluate the quality of ergatic control systems --- of aircraft landing by human operator 20 p3036 A83-43508
- FACTORIES**
 U INDUSTRIAL PLANTS

FACTORIZATION

- Factors for cubics and quartics 03 p0389 A83-14841
 New implicit boundary procedures - Theory and applications [AIAA PAPER 83-0123] 05 p0579 A83-16536
 Approximate factorization schemes for 3D nonlinear supersonic potential flow [AIAA PAPER 83-0376] 05 p0591 A83-17923
 On the relation between stable matrix fraction factorizations and regulable realizations of linear systems over rings 09 p1333 A83-24795
 Spectral factorization by optimal gain iteration 12 p1770 A83-28998
 Stability analysis of intermediate boundary conditions in approximate factorization schemes [AIAA PAPER 83-1898] 18 p2740 A83-39403
 Factorization method for calculating the three-dimensional flows of a viscous compressible gas 19 p2845 A83-42008
 Approximate-factorization scheme of transonic small-disturbance potential equation 21 p3088 A83-44574

FACULAE

- Active-region evolution and solar rotation variations in solar UV irradiance, total solar irradiance, and soft X rays 05 p0708 A83-17377
 Observations of the wavelength dependence of the average contrast of sunspots 06 p0853 A83-18131
 Brightness of the photosphere and faculae at the limb based on eclipse observations 07 p1027 A83-21269
 Facular influences on the apparent solar shape 08 p1192 A83-23257
 Structure and physics of solar faculae. III - The densities in the chromosphere-corona transition zone 11 p1692 A83-28578
 Magnetohydrostatic model of solar faculae 14 p2116 A83-33220
 The connection of the changes in the radio brightness of the sun with the humps of the magnetic field and the flocculae during a minimum of solar activity 17 p2626 A83-37718
 Solar activity with respect to Ca-plages 17 p2628 A83-38539
 The influence of faculae on solar flux variations 17 p2628 A83-38845
 The dynamical behavior of facular points in the quiet photosphere 18 p2781 A83-39024
 Visibility of facular fields in Mg I b-lines 18 p2781 A83-39025
 Long-term relationships between sunspots, Ca-plages and the ionosphere 18 p2712 A83-39065
 Facular influences on the apparent solar shape 20 p3079 A83-42168
 The Ca II K emission from the sun as a star. II - The plage emission profile 20 p3080 A83-42382
 Photospheric faculae-III-intensity, and magnetic field mapping of a typical element of the photospheric network 23 p3530 A83-47445
 The characteristic size and brightness of facular points in the quiet photosphere 23 p3536 A83-47722
 Variation of the contrast of faculae depending on heliocentric distance 24 p3674 A83-49056

FADING

- NT SELECTIVE FADING
 NT SIGNAL FADING

FAHRENHEIT TEMPERATURE SCALE

- U TEMPERATURE SCALES

FAIL-SAFE SYSTEMS

- Design of an aircraft ice detector using microcomputer electronics to enhance system availability 01 p0009 A83-11097
 The reliability analysis of a dual, physically separated, communicating IMU system 01 p0005 A83-11128
 A microprocessor-based fault-tolerant computer system 02 p0227 A83-11907
 Fail-safe optimal design of complex structures with substructures 03 p0339 A83-13490
 Determining the availability factor for a restorable technical system subject to two types of failure 03 p0337 A83-14099
 Design for safe software [AIAA PAPER 83-0323] 05 p0678 A83-16652
 Applying existing safety design techniques to software safety [AIAA PAPER 83-0327] 05 p0678 A83-16656
 A feedback time constant concept 06 p0803 A83-19038
 A fail-safe node for lightguide digital networks 07 p0992 A83-19712
 Generic faults and architecture design considerations in flight-critical systems 09 p1203 A83-24426
 Performance analysis of some ARQ protocols 15 p2144 A83-33521
 Fail safe logic design 16 p2345 A83-35555

- Reconfiguration of on-board control algorithms 17 p2569 A83-37491
 Fuzzy set theory for improving and evaluating reliability of complex systems 17 p2518 A83-37767
 A selective-repeat ARQ scheme and its throughput analysis 19 p2832 A83-41398
 Restructurable controls for aircraft [AIAA PAPER 83-2255] 19 p2804 A83-41728
 Measures of merit for fault-tolerant systems [AIAA PAPER 83-2259] 19 p2892 A83-41729
 Undetectable critical defects in safety-of-flight structure 20 p2999 A83-42544
 Fail-operational DAFCS for business/commuter aircraft --- Digital Automatic Flight Control System [SAE PAPER 830714] 20 p2937 A83-43324
 Autonomy in military aircraft [AAS PAPER 83-041] 21 p3097 A83-44168
 Autonomy issues for an operational space station [AAS PAPER 83-043] 21 p3095 A83-44170
 Autonomy and fault tolerant design --- for satellite system and components [AAS PAPER 83-044] 21 p3104 A83-44171
 Damage tolerant design using collapse techniques 21 p3164 A83-45591

FAILURE

- NT BURNTHROUGH (FAILURE)
 NT ENGINE FAILURE
 NT STRUCTURAL FAILURE
 NT SYSTEM FAILURES

FAILURE ANALYSIS

- A systematic approach to comprehensive TPS diagnostics for electronic modules --- Test Program Set 01 p0037 A83-10730
 UUT modeling 01 p0091 A83-10743
 A failure model for sealed nickel-cadmium batteries 01 p0068 A83-10795
 Automatic fault diagnosis of a switching regulator 01 p0040 A83-11014
 Inflight parity vector compensation for FDI --- Failure Detection and Isolation 01 p0019 A83-11129
 Investigation of network tree technology as a tool for developing effective fault isolation procedures 01 p0043 A83-11231
 Testability using Logmod --- Logic MOdel method for functional analysis of system design 01 p0029 A83-11232
 Test chips for custom ICs - Six kinds of test structures 02 p0167 A83-11824
 Nonlinear matrix failure criterion for fiber-reinforced composite materials 02 p0150 A83-12062
 An experimental method for determining the maximum stress during spalling 02 p0191 A83-12333
 J series thruster isolator failure analysis [AIAA PAPER 82-1907] 02 p0144 A83-12482
 A unifying strain criterion for fracture of fibrous composite laminates 03 p0291 A83-13340
 Quantitative analysis of delayed fracture observed in stress rate tests on brittle materials 03 p0290 A83-13686
 An optimum inversion method for the remote probing of defective phase shifters in phased arrays 03 p0328 A83-14020
 Determining the availability factor for a restorable technical system subject to two types of failure 03 p0337 A83-14099
 Fractographic studies of graphite/epoxy fatigue specimens 03 p0292 A83-14554
 Present status and future needs for quantitative measurement techniques 04 p0488 A83-15154
 Overview of probabilistic failure prediction and accept-reject decisions 04 p0488 A83-15155
 Characterization of NDE reliability 04 p0492 A83-15211
 Nondestructive evaluation of ceramics 04 p0463 A83-15213
 Probabilistic failure prediction for ceramics 04 p0463 A83-15214
 Allowance for the mutual influence of factors in the analysis of reliability 04 p0494 A83-15918
 Engineering safety analysis via destructive numerical experiments 04 p0500 A83-16198
 On availability of a series-system with imperfect detectors 04 p0494 A83-16429
 Within-panel variability and scaling effects in composite materials --- static strength 05 p0611 A83-16934
 An analysis of impact failure modes for fiber-reinforced composite laminates by using fault tree 05 p0611 A83-17104
 The use of fractography and fracture mechanics in analysing fatigue cracks 05 p0654 A83-17229
 Use of emulation in fault analyses of digital systems 05 p0678 A83-17303
 The characterization of transistor electrical overstress failure probability density functions 05 p0625 A83-17477

- Silicon solar cell damage from electrical overstress
05 p0658 A83-17481
- Rapid annealing in advanced bipolar microcircuits
05 p0627 A83-17516
- Total dose susceptibility of the SBP 9899
05 p0628 A83-17519
- Latchup window tests
05 p0628 A83-17526
- Hardness assurance and overtesting
05 p0653 A83-17529
- A failure mechanism in adaptive arrays
07 p0907 A83-19722
- Use of microanalytical techniques in PC board failure analysis
07 p0920 A83-20474
- Surface characterization and failure analysis of thermally aged, polyimide bonded titanium
07 p0886 A83-20491
- ESCAF - A new and cheap system for complex reliability analysis and computation
07 p0942 A83-20514
- Electromigration-induced failure by edge displacement in fine-line aluminum-0.5% copper thin film conductors
07 p0921 A83-20743
- Limitations and possible extensions to a nonlinear finite element shell-of-revolution model based on Reissner's shell theory
07 p0948 A83-21438
- Determination of the mean time of the absence of defects in objects with a variable period of utilization and diagnostics
08 p1113 A83-22122
- Failure mechanism for alloy KhN67VM under the action of a copper-silver solder
08 p1067 A83-22698
- Characterization of matrix/interface-controlled strength of unidirectional composites
09 p1223 A83-23935
- Post-crazing analysis of glass-epoxy laminates
09 p1223 A83-23941
- Mode-fault diagnosis and a design of testability
09 p1333 A83-24796
- Fault Detection/Location System for intermediate and tail rotor gearboxes
09 p1274 A83-24835
- Design, materials selection and failure analysis
10 p1393 A83-25325
- Statistical analysis of aging-induced degradation /or lifetime/ variations in /Al, Ga/As/GaAs double-heterostructure lasers
10 p1429 A83-26028
- Micromechanical modeling of 3D composites with interface failure
11 p1544 A83-27464
- Compressive fatigue behaviour of a glass fibre-reinforced polyester composite at 300 K and 77 K
12 p1710 A83-29720
- A new design method for m-out-of-n TSC checkers --- Totally Self-Checking for codes
13 p1908 A83-30791
- Statistical correlation between the thermal transition stress of a specimen and its resistance to alternating torsional fatigue
[ASME PAPER 82-WA/DE-15]
13 p1823 A83-31297
- Investigation of thermal effects on weapon system components
13 p1859 A83-31298
- Enhancement of strength in composites reinforced with previously stressed fibers
13 p1868 A83-31618
- Performance testing and module monitoring at the EC Necessary steps to develop cost-effective PV modules
14 p2038 A83-32194
- Reverse bias power dissipation of shadowed or faulty cells in different array configurations
14 p2040 A83-32212
- A statistical model for the time dependent failure of unidirectional composite materials under local elastic load-sharing among fibers
14 p1986 A83-32663
- Influence of quality control variables on failure of graphite/epoxy under extreme moisture conditions
14 p1987 A83-33125
- An approach to accelerated testing
15 p2173 A83-33549
- The failure characteristics of cutting tools machining titanium alloys at high speed
15 p2171 A83-33649
- Analog multifrequency fault diagnosis
15 p2151 A83-33923
- Node-fault diagnosis and a design of testability
15 p2151 A83-33926
- The influence of defects on the operational strength of disks and wheels in engines
15 p2174 A83-33964
- Micro and macro mechanics of crack growth; Proceedings of the Symposium, Louisville, KY, October 13-15, 1981
15 p2179 A83-34476
- Some aspects of crack growth and failure in fibre reinforced composites
15 p2130 A83-35075
- On testing stuck-open faults in CMOS combinational circuits
15 p2153 A83-35141
- Standard failure criteria needed for advanced composites
16 p2324 A83-35771
- An experimental study of the failure of elastoplastic cylindrical shells under combined loading
16 p2365 A83-35929
- Calculation of the forming limit curve at fracture
16 p2366 A83-35980
- Planning and evaluation of fatigue tests in regard to ultrasonic frequency tests
16 p2333 A83-36201
- Prediction of failure probabilities for cleavage fracture from the scatter of crack geometry and of fracture toughness using the weakest link model
16 p2368 A83-36510
- Reliability theory of stochastic fracture processes in sustained loading. I
16 p2369 A83-36623
- A new method for failure detection and location in complex dynamic systems
17 p2565 A83-37094
- A fault tolerant approach to state estimation and failure detection in nonlinear systems
17 p2567 A83-37121
- Microelectronic system reliability prediction
17 p2517 A83-37288
- Comparison of memory chip organizations vs reliability in virtual memories
17 p2517 A83-37290
- Minimizing the average cost of testing coherent systems
17 p2517 A83-37292
- Sequential method for comparing two constant failure-rates
17 p2517 A83-37293
- Optimal number of failures before replacement time
17 p2518 A83-37297
- A pseudo-linear analysis of yielding and crack growth - Strain energy density criterion
17 p2522 A83-38388
- An experimental investigation of fatigue reliability laws
17 p2523 A83-38398
- Fracture strains in biaxially loaded 2024 aluminum tubes
17 p2491 A83-38527
- Safety assessments in fracture-mechanics defect evaluation for biaxial stresses
18 p2696 A83-39256
- Fracture initiation under gross yielding - Strain energy density criterion
18 p2666 A83-39546
- Secondary loading of I-spar caps due to shear deformation of the web
18 p2700 A83-39991
- Analysis of compression failures in fibre composite laminates
18 p2653 A83-40172
- In-plane tensile strength of multidirectional composite laminates
18 p2653 A83-40173
- Probabilistic design on strength of fiber reinforced composite laminates
18 p2654 A83-40182
- The modelling of failure processes and the role of the matrix in the failure of carbon fibre reinforced epoxy resin
18 p2655 A83-40208
- Analysis of Charpy impact failure for unidirectional fiber-reinforced composite laminates by using a computerized fault tree
18 p2655 A83-40212
- Energy absorption of composite materials under crash conditions
18 p2705 A83-40216
- The strength, ductility and failure of thermoplastics reinforced with short-glass fibres
18 p2657 A83-40233
- Fractography of carbon/epoxy angle-ply laminates
18 p2660 A83-40273
- Composite flywheel rotor containment
18 p2709 A83-40294
- Method of investigating the rules of deformation and failure under conditions of low-cycle nonisothermal loading
19 p2855 A83-40763
- Autonomous failure detection and correction on Landsat-4
[AIAA PAPER 83-2265]
19 p2817 A83-41735
- Availability as a function of usage profile
[AIAA PAPER 83-2287]
19 p2855 A83-41747
- Diagnostics of the conditions of gas-turbine engines using models reflecting the dynamics of changes in the controlled parameters
19 p2801 A83-42133
- The environmental degradation of notched CFRP in compression
20 p2947 A83-42806
- On the analysis of creep stability and rupture
20 p3003 A83-42932
- On the automatic solution of nonlinear finite element equations --- for structural analysis
20 p3003 A83-42933
- Energy absorption of composite materials
20 p2948 A83-43148
- The fracture diagram - A new design tool for stiffened panels
20 p3007 A83-43447
- Bilinear failure analysis of fiber composite laminates
21 p3106 A83-44049
- Acoustic emission from graphite/epoxy composite laminates with special reference to delamination
21 p3106 A83-44126
- Compression fatigue behaviour of notched composite laminates
21 p3106 A83-44334
- Main mechanisms for the failures of monolithic integrated circuits
21 p3125 A83-44591
- The ultimate load sensitivity of lipped channel columns to column axis imperfection
21 p3153 A83-44624
- Statistical approach to time-dependent failure of brittle material
21 p3157 A83-44903
- A probabilistic treatment of brittle fracture under nonmonotonically increasing stresses
21 p3159 A83-44923
- Probability distributions for the strength of composite materials. IV - Localized load-sharing with tapering
21 p3159 A83-44926
- Lower-tail approximations for the probability of failure of three-dimensional fibrous composites with hexagonal geometry
21 p3159 A83-44941
- Moireinterferometry for damage analysis of composites
21 p3108 A83-45148
- A stress transfer model for the deformation and failure of polymeric matrices under swelling conditions
22 p3263 A83-46290
- Examination of the development of fatigue damage in metals by the eddy-current method
22 p3303 A83-46325
- Observation of damage growth in compressively loaded laminates
22 p3264 A83-46810
- Plastic composites fight for status --- performance predictability as construction material
23 p3428 A83-47822
- Non-destructive failure prediction in ceramics
23 p3467 A83-48299
- Avionics fault tree analyzer
[AIAA PAPER 83-2452]
23 p3401 A83-48335
- Monte Carlo simulation of the strength of composite fibre bundles
24 p3591 A83-48896
- ### FAILURE MODES
- Defects and disorder in the fast-ion electrode lithium-aluminum
02 p0154 A83-12057
- The relation between the network structure, deformation and failure processes, and mechanical properties of epoxies
02 p0160 A83-12063
- The fracture mechanics of composite materials under axial compression - Brittle fracture
03 p0291 A83-14064
- Effect of stacking sequence on damage propagation and failure modes in composite laminates
03 p0293 A83-14563
- Toroidal shells - Delayed catastrophes under dynamic loading
04 p0499 A83-15881
- An analysis of impact failure modes for fiber-reinforced composite laminates by using fault tree
05 p0611 A83-17104
- CMOS/SOS 4K RAMS hardened to 100 Krads/Si/
05 p0627 A83-17513
- Time dependent low cycle fatigue of PM Astrolay at 1003 K
07 p0893 A83-21475
- Hole nucleation and ductile failure in multiaxial states of stress
08 p1116 A83-21663
- Failure and acoustic-emission response of plasma-sprayed ZrO₂-8 wt% Y₂O₃ coatings
08 p1072 A83-22274
- Characteristics of the spalling fracture of aluminum and aluminum alloys D16 and AMg6 in the temperature range -196 to 600 C
09 p1229 A83-23510
- Failure modes induced in TTL-LS bipolar logics by negative inputs
09 p1253 A83-23696
- On failure modes of unidirectional composites under compressive loading
09 p1223 A83-23937
- Mode-fault diagnosis and a design of testability
09 p1333 A83-24796
- Strength of mechanically fastened composite joints
10 p1439 A83-25880
- Energy absorption in composite tubes
10 p1439 A83-25883
- Characteristics of the spall fracture of copper, nickel, titanium, and iron in the temperature range from -196 to 800 C
11 p1549 A83-28514
- Studies of damage involving aircraft components --- accident-causing metallic component fractures
12 p1699 A83-29371
- A mixed-mode fracture criterion for composite materials
12 p1711 A83-29895
- Vibration-fatigue reliability analysis
13 p1867 A83-30859
- Temperature readjustment factors for application to MIL-HDBK-217C failure rates --- electronic equipment reliability prediction
13 p1837 A83-31516
- Solar cells failure modes and improvement of reverse characteristics
14 p2041 A83-32229
- Development of simulated mission endurance test acceleration factors in determining engine component serviceability and failure mode criticality
[AIAA PAPER 83-1409]
16 p2310 A83-36398
- On mechanical fastening in graphite epoxy composite
18 p2652 A83-40155
- Deformation characteristics and failure modes of center-notched graphite/epoxy laminates
18 p2654 A83-40198
- Long term strength of glass reinforced plastics
18 p2656 A83-40224
- Effects of interfacial reaction on fracture mode and tensile strength of fibres in metal matrix composites
18 p2659 A83-40254
- Thickness and stacking sequence effect on the acoustic emission of CFRP
18 p2660 A83-40271

- On the interaction between local and overall buckling of an asymmetric portal frame 19 p2857 A83-41154
- Restructurable controls for aircraft [AIAA PAPER 83-2255] 19 p2804 A83-41728
- Statistical analysis of lithium iron sulfide status cell cycle life and failure mode 20 p3013 A83-43419
- The effects of cut and edge on the ultimate tensile strength of planar randomly-distributed short fiber composites 21 p3106 A83-44052
- A four-point shear test for graphite/epoxy composites 21 p3107 A83-45068
- Reliability of fiber optic emitters 22 p3360 A83-46654
- Contact stresses at ceramic interfaces 23 p3438 A83-48302
- The idealized structural unit method and its application to deep girder structures 24 p3593 A83-49441
- FAINT OBJECT CAMERA**
- A data analysis facility for the Faint Object Camera 01 p0114 A83-10143
- Faint-object spectrograph optical bench 07 p0872 A83-20462
- Imaging performance of the Faint Object Camera 09 p1266 A83-23584
- High voltage power electronics packaging on NASA's Space Telescope 11 p1539 A83-27155
- Performance of the spectropolarimeter for the Space Telescope faint object spectrograph 14 p2096 A83-32010
- Faint Object Spectrograph (FOS) calibration 14 p2017 A83-32011
- Analysis of synthesized dim galaxy images 14 p2096 A83-32035
- Low light level detectors in astronomy --- Book 21 p3226 A83-45095
- FAIRCHILD MILITARY AIRCRAFT**
- U MILITARY AIRCRAFT
- FAIRINGS**
- Serviceability evaluation of advanced composite F-14A main-landing-gear-strut doors and overwing fairings 07 p0861 A83-20480
- Hybrid composite application to the Boeing 767 wing/body fairing 18 p2640 A83-40244
- FALKNER-SKAN EQUATION**
- Asymptotic solutions of the laminar boundary-layer equations 03 p0323 A83-14675
- Use of limiting solutions of Falkner-Skan-Type equations in the integral method of evaluation of near wakes 05 p0590 A83-17422
- Branching of the Falkner-Skan solutions for gamma less than zero 05 p0642 A83-17942
- Self-similar solutions of the equations of a boundary layer on a moving surface 17 p2506 A83-37635
- Similar velocity profiles of the compressible boundary layer over a rotating cylinder in an axial flow 18 p2681 A83-39349
- A Meksyn series method for the Falkner-Skan equation with mass transfer 21 p3128 A83-44023
- FALLING SPHERES**
- Axis ratios of oscillating raindrops 11 p1628 A83-27046
- Axially symmetric gravitational two-body problem of Cooperstock, Lim, and Hobill 22 p3354 A83-46715
- FALLOUT**
- Ambient airborne solids concentrations including volcanic ash at Hanford, Washington sampling sites subsequent to the Mount St. Helens eruption 07 p0960 A83-20207
- FAN BLADES**
- Mechanical properties of adhesive systems at cryogenic and other temperatures 01 p0027 A83-11490
- Turbofan engine blade pressure and acoustic radiation at simulated forward speed 09 p1205 A83-24026
- Shock waves ahead of a fan with nonuniform blades 09 p1341 A83-24665
- Fluctuating pressure measurements on the fan blades of a turbofan engine during ground and flight tests [AIAA PAPER 83-0679] 10 p1377 A83-25911
- Interaction of fan rotor flow with downstream struts [AIAA PAPER 83-0682] 10 p1377 A83-25912
- Ray-theory and mode-theory predictions of intake-liner performance - A comparison with engine measurements [AIAA PAPER 83-0711] 10 p1475 A83-25927
- Zero-length inlets for subsonic V/STOL aircraft 12 p1696 A83-29012
- Structural tailoring of engine blades (STAEBL) [AIAA 83-0828] 12 p1703 A83-29737
- Dynamic characteristics of the 40- by 80- /80- by 120-foot wind tunnel drive fan blades [AIAA 83-0918] 12 p1704 A83-29846
- Analytical and experimental investigation of bird impact on fan and compressor blading [AIAA 83-0954] 12 p1704 A83-29856
- Method of calculating optimum angular blade pitches in fan with unequally pitched blades 14 p1972 A83-33090
- Containment of turbine engine fan blades 16 p2305 A83-35871
- A study of the control properties of axial fans on the basis of theoretical characteristics of plane cascades 17 p2451 A83-37807
- A technique for the accelerated life testing of fan impellers 18 p2698 A83-39512
- Blade loss transient dynamic analysis of turbomachinery 19 p2800 A83-40864
- Aerodynamic performance of a fan stage utilizing variable inlet guide vanes (VIGV's) for thrust modulation --- subsonic V/STOL aircraft [AIAA PAPER 83-1162] 21 p3088 A83-45508
- The impact of three-dimensional analysis on fan design --- for turbine engines [ASME PAPER 83-GT-136] 23 p3408 A83-47963
- FANLIFT DEVICES**
- U LIFT FANS
- FAR FIELDS**
- The far field of an airfoil 01 p0002 A83-10573
- The response of a fluid-loaded, beam-stiffened plate 01 p0105 A83-11040
- A broad-band constant beamwidth corrugated rectangular horn 01 p0033 A83-11367
- A survey of the near-field far-field inverse scattering inverse source integral equation 01 p0104 A83-11368
- A survey of the physical optics inverse scattering identity 01 p0104 A83-11369
- A note on utilizing far-field phase information 01 p0034 A83-11375
- Theory of the frequency responses of uniform and quasi-taper helical antennas 01 p0034 A83-11378
- Optical damage resistance of lithium niobate waveguides 03 p0393 A83-13759
- The unimoment method for elastic wave scattering problems 04 p0489 A83-15164
- Far field radiated by rectangular patch microstrip antenna 04 p0465 A83-15233
- Method of multiple scales and the problem of aerodynamically generated sound 04 p0533 A83-16100
- Runge's theorem and far field patterns for the impedance boundary value problem in acoustic wave propagation 04 p0533 A83-16365
- Far field conditions in unsteady subsonic flow 05 p0590 A83-17834
- Diffraction-field structure in the Fraunhofer zone 06 p0809 A83-17983
- Study on doubly curved shaped-beam reflector antenna theory 06 p0735 A83-18149
- Distance criteria in near-field and far-field antenna measurements 06 p0740 A83-18640
- Near and far field airborne antenna pattern analysis 06 p0715 A83-18645
- The plane wave synthesis technique for antenna near-field/far-field transformation - Further development 06 p0740 A83-18649
- Quasi-real-time antenna near-field/far-field transformation without phase and amplitude recording 06 p0741 A83-18652
- Complex ray and evanescent wave analysis of parabolic reflector antennas 06 p0743 A83-18685
- A novel technique for the computation of secondary patterns of reflector antennas 06 p0743 A83-18687
- The effect of undersampling and finite truncation of the antenna near-field data on the predicted far-field pattern 06 p0743 A83-18689
- A pole-zero modeling approach to linear array synthesis. I - The unconstrained solution 07 p0913 A83-20368
- Scattering from randomly rough surfaces and the far field approximation 07 p0989 A83-20369
- Phase aberrations and laser output beam quality 08 p1108 A83-22450
- Optical distortion and far field measurements for laser window materials 08 p1108 A83-22458
- Diffraction of an electric polarized wave by a dielectric wedge 08 p1161 A83-22742
- Experiences with two new lightning localization devices 09 p1310 A83-23405
- Analysis of the radiation characteristics of an aperture antenna excited by a periodic pulsed signal 09 p1245 A83-23454
- Combined E- and H-plane phase centers of antenna feeds 09 p1248 A83-23810
- Use of far-field radiation pattern to characterize single-mode symmetric slab waveguides 09 p1254 A83-24118
- Analysis of the effect of heated jet flow on the far field radiation from a noise source [ASME PAPER 82-WA/NCA-4] 10 p1472 A83-25697
- Farfield inflight measurements of high-speed turboprop noise [AIAA PAPER 83-0745] 10 p1377 A83-25947
- Near-field and far-field patterns of phase-locked semiconductor laser arrays 10 p1426 A83-25979
- Comparison of cutoff wavelength measurements for single-mode waveguides 10 p1483 A83-26633
- A GTD study of pyramidal horns for offset reflector antenna applications 10 p1406 A83-26837
- Far-field radiation patterns of elliptical apertures and its annuli 10 p1406 A83-26847
- Far field in transient two-dimensional scattering 10 p1406 A83-26849
- Calculation of the cross-polarization in the far field of waveguide radiators 10 p1412 A83-26888
- On the far-zone distribution of a scattered field - A numerical experiment 11 p1556 A83-27946
- Far field boundary conditions for compressible flows 12 p1725 A83-29649
- Test of large aperture antennas using near-field techniques 13 p1829 A83-31194
- Phased array alignment with planar near-field scanning or determining element excitation from planar near-field data 15 p2146 A83-35082
- Far-field characterization of diode lasers with standard vidicons 17 p2514 A83-37745
- Fraunhofer diffraction by ice crystals suspended in the atmosphere 20 p3028 A83-43465
- Spot size measurements for single-mode fibers - A comparison of four techniques 21 p3204 A83-44202
- Detection of hidden diffractors by coherence measurements 21 p3208 A83-44841
- Far-field distributions of semiconductor phase-locked arrays with multiple contacts 21 p3145 A83-44953
- Phase distribution and ergodicity relative to the spatial variable in scattered fields 21 p3201 A83-45506
- Radiation properties of a vacuum-insulated infinite flat slotted plate antenna in a cold isotropic homogeneous plasma 22 p3274 A83-46526
- Loop antennas for directive transmission into a material half space 22 p3274 A83-46527
- Far field radiated by short-circuited microstrip antenna acting at a quarter-wavelength resonance 23 p3444 A83-48720
- Minimization of farfield acoustic effects in turbulent boundary layer wall pressure fluctuation experiments 24 p3580 A83-49812
- Probe correction in near field measurements by pseudo sampling technique 24 p3571 A83-49995
- FAR INFRARED RADIATION**
- Ac Josephson effect in small-area superconducting tunnel junctions at 604 GHz 01 p0039 A83-10995
- Far-infrared sources in Cygnus X - An extended emission complex at DR 21 and unresolved sources at S106 and ON 2 02 p0251 A83-11589
- The Bubble Nebula - Far-infrared and radio molecular observations of NGC 7635 03 p0412 A83-13304
- Low background spectral response of 30-130-micron detectors from blackbody measurements 03 p0324 A83-13458
- Electron collision strengths for the far-infrared lines of O III --- in Milky Way Galaxy 03 p0419 A83-13933
- Far infrared observations of a star forming region in Serpens 04 p0550 A83-15037
- Interaction of three coherent fields with Doppler broadened serial four-level systems - Application to four-level FIR lasers 06 p0766 A83-18907
- Searches for far-infrared emission from dark clouds - Rho Ophiuchi, Heiles 2, L1529, and L183 07 p1010 A83-19860
- Highly excited /J = 16 to 15/ rotational transitions of CO, at 162.8 microns, in the Orion cloud 07 p1019 A83-20955
- Selective enhancement of the 251-micron line in an optically pumped CH₃OH laser 07 p0937 A83-21360
- Effect of the stratospheric medium temperature on strong lines observed in the far infrared region 07 p0965 A83-21399
- A comparative study of D₂O oscillators emitting at 385 microns 07 p0938 A83-21598
- An optically-pumped multigas far-IR laser 08 p1107 A83-22246
- Bidirectional reflectance distribution function /BRDF/ measurements of sunshield and baffle materials for the Infrared Astronomy Satellite /IRAS/ telescope 08 p1167 A83-22861
- Analysis of the far infrared H₂-He spectrum 09 p1343 A83-25214
- Modulation of far-infrared radiation by electron-hole plasma in indium antimonide 10 p1488 A83-25456
- Interaction of electromagnetic waves with a moving perturbation in a stationary gas 10 p1471 A83-25648
- Backward and forward FIR emission characteristics from D₂O in both Raman and laser regimes 10 p1426 A83-26001

Optical properties of the metals Al, Co, Cu, Au, Fe, Pb, Ni, Pd, Pt, Ag, Ti, and W in the infrared and far infrared
10 p1483 A83-26645

Near-millimeter wave polarizing duplexer/isolator
10 p1483 A83-26646

Application of advanced millimeter/far-infrared sources to collective Thomson scattering plasma diagnostics
10 p1487 A83-26647

Growth of emission in a far infrared laser
11 p1583 A83-27625

The ground state far infrared spectrum of NH₃
12 p1778 A83-29526

The potential for far-infrared astronomy in Australia
13 p1936 A83-30399

Nonlinear far-infrared magnetoabsorption and optically detected magnetoimpurity effect in n-GaAs
13 p1850 A83-30600

FIR NH₃ cascade laser excited by a Q-switch laser
14 p2025 A83-33143

Resonant array bandpass filters for the far infrared
15 p2231 A83-34470

An infrared luminosity function for star-forming molecular clouds
15 p2264 A83-34584

Numerical analysis of an optically pumped D₂O far infrared laser
16 p2358 A83-35430

A high power D₂O laser optimized for microsecond pulse duration
16 p2358 A83-35431

New pulsed far infrared laser lines in D₂O
16 p2359 A83-35959

Infrared observations of OB star formation in NGC 6334
17 p2597 A83-37322

A new stabilization system for optically pumped CW far infrared lasers
17 p2514 A83-37752

Absolute measurement at 1 THz of the optical coupling of a F.I.R. conical antenna with a Josephson detector
17 p2511 A83-37759

The Orion Nebula - Large-scale distribution of far-infrared and submillimeter line emission
18 p2772 A83-39706

Far-infrared CO line emission from Orion-KL
18 p2772 A83-39712

A cryogenic Fabry-Perot for far infrared astronomy
18 p2692 A83-40461

New far infrared observations of the central 30 arcmin of the Galaxy
19 p2912 A83-40681

Large beam observations of the galactic center at 150, 200, and 300 microns
19 p2912 A83-40682

Some considerations on a Michelson spatial interferometer in the far IR
21 p3137 A83-44380

Power broadening and nonlinear FIR magneto-photoconductivity in n-GaAs
21 p3216 A83-44382

Sensitivity of a wide-band far-IR receiver using a Josephson self-oscillator mixer
21 p3125 A83-44387

A two-beam interferometer for dispersive reflection spectroscopy of solids in the far infrared at temperatures between 4 and 300K
21 p3137 A83-44388

Generation of coherent far-infrared radiation using lasers
22 p3296 A83-46497

Observation and assignment of torsional transitions in FIR emission from optically pumped CH₃OH
22 p3299 A83-46743

Low-threshold semiconductor Raman laser
22 p3300 A83-46818

Far infrared absorption in normal H₂ from 77 to 298 K
23 p3507 A83-48649

FAR ULTRAVIOLET RADIATION

NT LYMAN ALPHA RADIATION

Structure of a computer-controlled apparatus for reflection and transmission measurements using thin metallic sheets in the context of astronomical observations in the far ultraviolet region --- German thesis
01 p0117 A83-10478

Wide-band mirrors for vacuum ultraviolet and soft X-ray radiation
02 p0232 A83-11656

Vacuum ultraviolet generation in phase matched carbon monoxide
02 p0185 A83-12403

Transitions in highly ionized silicon --- of extreme ultraviolet solar spectrum
02 p0270 A83-12582

Discussion of the relative efficiency in the vacuum ultraviolet of diffraction gratings with laminar sinusoidal and triangular grooves
02 p0238 A83-12709

Airglow at a height below 40 km in the vacuum ultraviolet
03 p0356 A83-13216

Ultraviolet and vacuum ultraviolet systems; Proceedings of the Meeting, Washington, DC, April 21, 22, 1981
03 p0327 A83-13954

Frequency mixing in the extreme ultraviolet /XUV/ using rare gas halide lasers
03 p0332 A83-13955

Effects of excitation mechanism on linewidth parameters of conventional vacuum ultraviolet /VUV/ discharge line sources
03 p0392 A83-13957

Electron bombardment charge-coupled device /CCD/ detectors for the vacuum ultraviolet
03 p0288 A83-13964

Photon-counting array detectors for space and ground-based studies at ultraviolet and vacuum ultraviolet /VUV/ wavelengths
03 p0327 A83-13965

Near-earth ultraviolet environment
03 p0358 A83-13974

X- and XUV-radiation of the solar corona
04 p0574 A83-15115

Generation of continuously tunable coherent vacuum-ultraviolet radiation /140 to 106 nm/ in zinc vapor
05 p0647 A83-16840

Evolution of chromospheres and coronae in solar mass stars - A far-ultraviolet and soft X-ray comparison of Arcturus /K2 III/ and Alpha Centauri A /G2 V/
05 p0699 A83-17005

The far-UV spectrum of the low-excitation planetary nebula HD 138403
06 p0825 A83-18085

Extremely low-loss hollow core waveguide for VUV light
06 p0810 A83-18951

Tunable VUV radiation generated by two-photon resonant frequency mixing in xenon
07 p0938 A83-21595

Photochemistry of acetylene at 1849 A
08 p1053 A83-22217

Chemical kinetics studied by vacuum-UV spectroscopy in shock tubes
10 p1391 A83-26129

Far-ultraviolet diffuse emission lines from the interstellar medium
10 p1511 A83-26406

Three-dimensional quantum dynamics of H₂O and HOD photodissociation
10 p1480 A83-26459

The diffuse interstellar feature at 4430 A and interstellar extinction in the far-ultraviolet
10 p1516 A83-26756

Vacuum ultraviolet monochromator calibration using measured atomic branching ratios
10 p1484 A83-26857

Recent developments in ultraviolet filters and coatings
11 p1657 A83-27743

A future Japanese program in far-ultraviolet astronomy and solar physics
11 p1671 A83-27747

Photodissociation of NH₃ at 106-200 nm
11 p1655 A83-28527

Status and perspectives of the FEL experiment at Brookhaven
13 p1853 A83-31107

Photon counting photodiode array detector for far ultraviolet (FUV) astronomy
14 p2015 A83-31983

Measurement of absorption line intensities with VUV monochromators
14 p2021 A83-32913

Electron-photon coincidence technique for the absolute calibration of VUV detectors
14 p2021 A83-32914

Solrad 11 observations of the far-ultraviolet background
15 p2245 A83-34116

The electron angular distribution of different rotational branches in the VUV photoelectron spectrum of H₂
16 p2408 A83-35328

Vacuum-ultraviolet refractive index of LiF and MgF₂ in the temperature range 80-300 K
21 p3203 A83-43875

Far ultraviolet observations of the expanding shell in Eridanus
21 p3229 A83-44425

The far UV emission spectrum of H₂
21 p3202 A83-44615

A far-ultraviolet extinction law - What does it mean? --- in interstellar grains
22 p3382 A83-46986

Dependence of auroral FUV emissions on the incidence electron spectrum and neutral atmosphere
22 p3337 A83-47067

Far-ultraviolet and visible observations of flares on dMe stars
23 p3522 A83-47499

Multiphoton excitation and frequency tripling in xenon
23 p3463 A83-48579

Generation of tunable single-frequency continuous-wave coherent vacuum-ultraviolet radiation
24 p3587 A83-48852

Anti-Stokes Raman laser emission at 149 nm in atomic bromine
24 p3587 A83-48853

Far ultraviolet colors of B and Be stars
24 p3669 A83-50100

Far ultraviolet colors of Beta Cephei stars
24 p3669 A83-50101

FARADAY EFFECT

Study of electrical faults in magnetohydrodynamic Faraday generators
04 p0538 A83-16106

Coupled three-dimensional flow and electrical calculations for Faraday MHD generators
04 p0538 A83-16107

Absorption lines, Faraday rotation, and magnetic field estimates for QSO absorption-line clouds
05 p0696 A83-16979

Investigation of the magnetic field of the galaxy
06 p0838 A83-19225

The rotation measures of radio sources in selected celestial zones - The Perseus arm window
07 p1006 A83-20571

A bisymmetric spiral magnetic field and the spiral arms in our Galaxy
08 p1182 A83-23041

Measurement of plasma conductivity using Faraday rotation of submillimeter waves
08 p1169 A83-23139

Is there evidence for universal rotation
08 p1187 A83-23294

An analysis of ultraviolet magneto-optical spectra
09 p1341 A83-23657

Single mode fiber isolator in toroidal configuration
11 p1656 A83-27565

Rotation measures for compact variable radio sources
12 p1788 A83-29180

Measurement of unambiguous rotation measures of extragalactic sources
14 p2098 A83-33063

Some applications of transformation to the space-independent frame in the processes of strong radiation in plasmas
15 p2235 A83-34493

Effects of short-duration loading faults on high-interaction Faraday and diagonal type MHD generators with subsonic or supersonic flow [AIAA PAPER 83-1745]
17 p2581 A83-37221

Stellar and interstellar magnetic fields
18 p2765 A83-39236

The interband Faraday effect and g-factors in Group IV A-VI A semiconductors
19 p2904 A83-40994

Observations of the total electron content of the ionosphere in Havana during the period of low solar activity 1974-1976
20 p3022 A83-43135

A new Faraday rotator using a thick Gd:YIG film grown by liquid-phase epitaxy and its applications to an optical isolator and optical switch
21 p3205 A83-44228

A method for the determination of the integrating constant of total electron content
21 p3170 A83-44284

Combined reciprocal and non-reciprocal birefringence in optical monomode fibres
24 p3627 A83-48744

FARADAY ROTATION

U FARADAY EFFECT

FARM CROPS

NT CORN
NT COTTON
NT RICE
NT SORGHUM
NT SUNFLOWERS
NT WHEAT

A backscatter model for a randomly perturbed periodic surface --- furrowed soils in agricultural fields
01 p0065 A83-10107

Satellite orbital dynamics and observation strategies in support of agricultural applications
01 p0066 A83-10717

Computing and mapping Thiessen weighting factors from digitized district boundaries and climatological station latitudes and longitudes
02 p0217 A83-12964

Land use/land cover mapping from enhanced Landsat imagery of the eastern provinces of the People's Republic of China
03 p0346 A83-14241

A model for microwave emission from vegetation-covered fields
07 p0951 A83-20223

Evaluation of digital SLAR images for an agricultural area
08 p1125 A83-21918

On the economic efficiency of using satellite data to assess the condition of crops
14 p2034 A83-32497

Extension of a uniform canopy reflectance model to include row effects
14 p2035 A83-32612

Estimation of shelter temperatures from operational satellite sounder data --- for farm crop monitoring
18 p2706 A83-39131

Ground truth measurements and results from the interpretation of multispectral data during the Convair project at the Straubing test site (D9)
22 p3310 A83-46137

Wind influence on the backscattering coefficient from crops
22 p3312 A83-46186

A statistical model for radar images of agricultural scenes
22 p3312 A83-46191

Comparison of multifrequency band radars for crop classification
22 p3314 A83-46234

Classification of agricultural crops in radar images
22 p3315 A83-46239

Certain results of a comparison of airborne data with satellite measurements --- spectral brightness and albedo of deserts and agricultural regions
24 p3598 A83-49280

An effort to determine the weed content of agricultural fields in springtime
24 p3598 A83-49283

FARMLANDS

Remote sensing of dielectric media with periodic rough surfaces --- microwave scattering from farmlands
01 p0065 A83-10106

A parametric study of tillage effects on radar backscatter
01 p0065 A83-10108

Landsat for delineation and mapping of saline soils in dryland areas in southern Alberta
03 p0348 A83-14261

Inferring non-point pollution from land cover analysis
15 p2182 A83-33575

- The operating experiences and performance characteristics during the first year of operation of the Crocheted Mt. New Hampshire windfarm
15 p2190 A83-34148
- Monitoring agricultural growth in pronghorn antelope habitat
15 p2184 A83-34813
- Landsat image date selection for an irrigated lands inventory over a large geographical area using general crop phenology and irrigation management data
17 p2532 A83-38357
- A technique for analysis of terrain features in remote sensing - The extraction of linear and circular farmlands
17 p2533 A83-38440
- Remote sensing of tank irrigated areas in Tamil Nadu State, India
20 p3010 A83-42961
- FAST FOURIER TRANSFORMATIONS**
- Evaluation of Fourier integrals using B-splines
03 p0387 A83-13574
- FFT vs. conjugate gradient method for solution of flow equations by pseudo-spectral methods
03 p0322 A83-14614
- Algorithm 49 - Fast Fourier transforms with recursively generated trigonometric functions
04 p0530 A83-15700
- Numerical evaluation of the Rayleigh integral for planar radiators using the FFT
04 p0532 A83-16320
- Sampling approach for fast computation of scattered fields
06 p0736 A83-18569
- A novel technique for the computation of secondary patterns of reflector antennas
06 p0743 A83-18687
- The use of a two-dimensional fast Fourier transformation algorithm for processing information from a linear antenna array
06 p0749 A83-19359
- Modified FFT algorithms with a reduced number of multiplication operations
08 p1154 A83-23169
- Control of cryogenic Fourier transform spectrometer scanning mirrors
09 p1267 A83-23591
- SNR enhancement of narrowband signals in colored noise using adaptive predictors
09 p1327 A83-24703
- Analysis method for Fourier transform spectroscopy
10 p1424 A83-26867
- Progressive phase trends in multi-degree-of-freedom systems
12 p1774 A83-28850
- Application of numerical Fourier transformation on measurements made on board rotating spacecraft
13 p1812 A83-30778
- A parallel-pipeline architecture of the fast polynomial transform for computing a two-dimensional cyclic convolution
13 p1908 A83-30794
- Computation of Faber series with application to numerical polynomial approximation in the complex plane
13 p1912 A83-31364
- A real-data FFT algorithm for image processing applications
14 p2073 A83-32900
- On an algorithm for the simulation of a vector random process
14 p2076 A83-32966
- Fast convolution methods for hexagonally sampled two-dimensional signals
15 p2220 A83-33518
- Fast hardware implementation of the Winograd Fourier transform algorithm
15 p2218 A83-34514
- A spectral-iteration technique for analyzing scattering from arbitrary bodies. I - Cylindrical scatterers with E-wave incidence
15 p2148 A83-35186
- Optimal smoothing of 'noisy' data by fast Fourier transform
15 p2223 A83-35257
- On the application of the fast Fourier transform in simulation problems
16 p2406 A83-36905
- Digital signal processing --- Book
17 p2496 A83-37163
- Fast Fourier transform and convolution algorithms / 2nd revised edition/
17 p2571 A83-37175
- Numerical evaluation of the radiation from un baffled, finite plates using the FFT
18 p2742 A83-39975
- A fast Fourier method for the dynamic analysis of linear structures with frequency dependent properties
20 p3005 A83-42989
- Performance analysis of FFT algorithms on multiprocessor systems
20 p3036 A83-43118
- Application of Winograd's fast Fourier transform (FFT) to the calculation of diffraction optical transfer function (OTF)
21 p3208 A83-44843
- Nonpolynomial finite difference schemes and the use of the fast Fourier transform
21 p3198 A83-45525
- Fast algorithm for the computation of the zero-order Hankel transform
23 p3501 A83-47581
- General form for representing the Fourier transform
24 p3621 A83-49966
- Normalisation of Fourier descriptors of planar shapes
24 p3621 A83-49984
- FAST NEUTRONS**
- Postirradiation fracture toughness of Inconel X-750
18 p2666 A83-39542
- FAST NUCLEAR REACTORS**
- NT EXPERIMENTAL BREEDER REACTOR 2
- FASTENERS**
- NT BOLTS
- NT NUTS (FASTENERS)
- NT PINS
- NT WASHERS (SPACERS)
- Digitized measurements of the shape of corner cracks at fastener holes
03 p0339 A83-13202
- Multisegment eddy current probe
04 p0481 A83-15191
- NDE of fastener hole cracks by the electric current perturbation method
04 p0481 A83-15192
- Strength of mechanically fastened composite joints
10 p1439 A83-25880
- Statistical crack propagation in fastener holes under spectrum loading
[AIAA 83-0808]
12 p1741 A83-29808
- The strength of blade-root fastenings at higher-mode vibrations
13 p1867 A83-31323
- Fatigue crack growth rates for very short cracks developing at fastener holes in 7075 and 7010 aluminum alloys
16 p2330 A83-35982
- On statistical moments of fatigue crack propagation
16 p2368 A83-36501
- Tabulated stress intensity factor solutions for flawed fastener holes
16 p2368 A83-36514
- Design of algorithms to extract data from capacitance sensors to measure fastener hole profiles
19 p2855 A83-41026
- Detection of cracks under installed fasteners in aircraft structures
22 p3304 A83-46769
- FATIGUE (BIOLOGY)**
- NT AUDITORY FATIGUE
- NT FLIGHT FATIGUE
- NT MUSCULAR FATIGUE
- Human factors and the design of display terminals
01 p0085 A83-10253
- A method for the quantitative integral evaluation of fatigue
01 p0085 A83-11400
- Circadian rhythms and fatigue - A discrimination of their effects on performance
02 p0223 A83-12411
- A physiological-hygienic evaluation of eye fatigue in women workers of the warping shop at a weaving mill
03 p0379 A83-13612
- The significance of the level of general physical work capacity in the development of fatigue in workers in conditions of occupational hypokinesia
05 p0673 A83-17194
- Experimental methods and techniques for the investigation of operator activity --- Russian book
07 p0981 A83-20326
- Methods of the measurement of changes in the functional system of a human operator
07 p0981 A83-20334
- The activity of a human operator during vestibular perturbations
07 p0976 A83-20336
- The recognition of the condition of fatigue and emotional stress according to the parameters of a speech signal
07 p0979 A83-20347
- The patterns of several parameters of speech flow of production line operators
07 p0979 A83-20349
- A comprehensive evaluation of the probability of the asthenization of female workers in conditions of nervous stress (using the model of telephone operators on interurban lines)
14 p2071 A83-33323
- An investigation of the recognition ability before and after various visual loads
16 p2399 A83-35915
- Subjective and objective methods in the diagnosis of fatigue
17 p2559 A83-38184
- Integral determination of changes in central nervous system functioning during mental work
17 p2561 A83-38927
- Power output and fatigue of human muscle in maximal cycling exercise
19 p2880 A83-41140
- FATIGUE (MATERIALS)**
- NT ACOUSTIC FATIGUE
- NT BENDING FATIGUE
- NT METAL FATIGUE
- NT STRUCTURAL STRAIN
- NT THERMAL FATIGUE
- NT VOLUMETRIC STRAIN
- On the Markovian models for fatigue accumulation
02 p0190 A83-11863
- Fracture of fatigue-loaded composite laminates
02 p0149 A83-12013
- The extension of the J-integral concept to fatigue cracks
02 p0190 A83-12044
- Toward the nondestructive characterization of fatigue damage in composite materials
03 p0292 A83-14552
- Path dependent nature of fatigue crack growth
04 p0496 A83-15064
- The fatigue behavior of SiSiC
04 p0462 A83-15125
- Effects of closure on the detection probability of fatigue cracks
04 p0490 A83-15186
- Characterization of NDE reliability
04 p0492 A83-15211
- Luminescence fatigue and light-induced electron spin resonance in amorphous silicon-hydrogen alloys
04 p0541 A83-15514
- Decrease in closure and delay of fatigue crack growth in plane strain
04 p0501 A83-16258
- Materials evaluation under fretting conditions; Proceedings of the Symposium, Warminster, PA, June 3, 1981
05 p0652 A83-17251
- Residual stress effects in fatigue; Proceedings of the Symposium, Phoenix, AZ, May 11, 1981
05 p0615 A83-17260
- Stress intensity factors, crack profiles, and fatigue crack growth rates in residual stress fields
05 p0654 A83-17261
- Fatigue initiation in a short glass fibre composite
05 p0612 A83-17569
- Introduction to the fundamentals of fracture mechanics. III - Fatigue crack growth in fracture mechanics representation
05 p0654 A83-17573
- Three-dimensional constitutive relations and ductile fracture --- Book
06 p0774 A83-18477
- Fatigue crack growth theory for ductile material
06 p0774 A83-18480
- Constitutive equations and global criteria for ductile fracture
06 p0774 A83-18491
- Review of the effects of fatigue cracking loads on plane strain fracture toughness
07 p0886 A83-20518
- The fatigue fracture of metals from the standpoint of physics and fracture mechanics
07 p0890 A83-20914
- An improved methodology for predicting random spectrum load interaction effects on fatigue crack growth
08 p1064 A83-21794
- Influence of environment on fracture
08 p1065 A83-21798
- An automated measuring system for analyzing the development of fatigue cracks in the case of nonstationary loading
08 p1113 A83-22404
- Fatigue considerations for FRP composites
09 p1221 A83-23424
- Vibration resistance of conformal coated axial-lead components on printed wiring assemblies
09 p1253 A83-23613
- A stochastic theory of fatigue crack propagation
[AIAA 83-0978]
12 p1740 A83-29785
- Large-amplitude multimode response of clamped rectangular panels to acoustic excitation
[AIAA 83-1033]
12 p1745 A83-29879
- Linear elastic fracture mechanics and fatigue crack growth Residual stress effects
12 p1746 A83-29905
- Influence of external environments on fatigue crack growth in epoxy resin
13 p1825 A83-31047
- Fatigue crack closure after overload
14 p2031 A83-32660
- Theory of fatigue for brittle flaws originating from residual stress concentrations
14 p2032 A83-32974
- Micro and macro mechanics of crack growth; Proceedings of the Symposium, Louisville, KY, October 13-15, 1981
15 p2179 A83-34476
- Fatigue damage and degradation in random short-fiber SMC composite --- sheet molding compound
15 p2130 A83-34794
- An analytic description of the kinetics of fatigue cracks in laminated composites
15 p2180 A83-35041
- Fatigue: Environment and temperature effects --- Book
16 p2330 A83-36160
- High-temperature static fatigue in ceramics
16 p2337 A83-36169
- Environment, frequency and temperature effects on fatigue in engineering plastics
16 p2337 A83-36170
- On statistical moments of fatigue crack propagation
16 p2368 A83-36501
- Analyses of microstructural and chemical effects on fatigue crack growth
17 p2490 A83-38396
- An experimental investigation of fatigue reliability laws
17 p2523 A83-38398
- On the nature of craze development and breakdown during fatigue
18 p2671 A83-39059
- On the probabilistic modeling of fatigue crack growth
18 p2699 A83-39544
- Consideration of short cracks in high stress fatigue design
[ASME PAPER 83-PVP-90]
20 p3009 A83-43730
- The cyclic J-integral as a criterion for fatigue crack growth
21 p3158 A83-44910
- Fatigue crack growth of a corner crack in an attachment lug
21 p3158 A83-44920
- Elastoplastic crack propagation (fatigue and failure)
22 p3305 A83-45977
- Equations of fatigue crack growth
23 p3472 A83-48465
- Development of fatigue cracks in polymethyl methacrylate
23 p3439 A83-48541

FATIGUE DIAGRAMS

U S-N DIAGRAMS

FATIGUE LIFE

Fatigue of graphite/epoxy /0/90/45/-45/s laminates under dual stress levels 02 p0149 A83-12060

Corrosion fatigue of nickel and nickel-base alloys 02 p0156 A83-12223

Life determination under dual-frequency loading, II - Proposed method --- for metals and welded joints 02 p0156 A83-12327

Fatigue life prediction on the basis of the characteristic parameters of the loading process 02 p0156 A83-12328

Cumulative damage and life-estimations in fatigue 02 p0193 A83-12660

The cyclic strength of reinforced magnesium-matrix composites 02 p0151 A83-13038

A theoretical study on fatigue life distribution of metallic materials based on the distribution of surface defects 02 p0197 A83-13065

A pitting model for rolling contact fatigue [ASME PAPER 82-LUB-10] 03 p0335 A83-13506

Low-cycle fatigue and life prediction --- Book 03 p0339 A83-13901

Damage accumulation and fracture life in high-temperature low-cycle fatigue 03 p0339 A83-13905

Prediction capability and improvements of the numerical notch analysis for fatigue loaded aircraft and automotive components 03 p0340 A83-13907

Two decades of progress in the assessment of multiaxial low-cycle fatigue life 03 p0340 A83-13910

Fatigue life evaluation of the A-7E arresting gear hook shank 03 p0277 A83-13912

J-Integral analysis for initiation of notch fatigue crack 03 p0342 A83-14490

Compression fatigue behavior of composites in the presence of delaminations 03 p0293 A83-14562

Effect of stacking sequence on damage propagation and failure modes in composite laminates 03 p0293 A83-14563

Damage mechanism and life prediction of graphite/epoxy composites 03 p0293 A83-14564

What is fatigue damage 03 p0342 A83-14565

Fatigue fracture properties of a Mg-Al-Zn alloy 03 p0300 A83-14600

Application of fatigue-strength analysis to the evaluation of the consequences of local damage and the effects of wing-shell repairs. III - An example of the application of fatigue-strength analysis using a specific fatigue wear 03 p0342 A83-14620

Estimating the life of materials on the basis of the theory of thermal fluctuations 03 p0301 A83-14731

Retirement for cause inspection system design 04 p0488 A83-15159

Fatigue lifetime predictions from ultrasonically detected laminar defects in a graphite-epoxy composite 04 p0454 A83-15180

Cast transage 175 titanium alloy for durability critical structural components 04 p0458 A83-15318

Statistical aspect of fatigue crack propagation from surface defects 05 p0614 A83-17093

A tentative procedure of parameter estimation of Weibull distribution from the Type I censored samples 05 p0653 A83-17094

Effect of transverse direction strain on fracture of notched 0 deg/90 deg GRP laminate under biaxial fatigue 05 p0611 A83-17105

Effect ion implantation on fretting fatigue in Ti-6Al-4V alloy 05 p0614 A83-17257

A study of cumulative fatigue damage in aluminum alloy 2011-T3 05 p0616 A83-17864

Defects and crack shape development in fillet welded joints 05 p0656 A83-17895

Measuring the 'life span' of certain metals under impulse tension 06 p0728 A83-18015

Fatigue sensitivity of composite structure for fighter aircraft 06 p0717 A83-18402

The analysis of operational stresses --- on aircraft during flight 06 p0775 A83-18596

Fatigue life prediction 06 p0769 A83-18599

A review of aero-generator fatigue problems 06 p0781 A83-18939

Effects of defects on fatigue properties of P/M disk alloys 06 p0732 A83-19098

Various criteria for determining the equivalent plastic deformation range in the theory of low-cycle fatigue 06 p0777 A83-19304

Fatigue life estimation - A review of traditional methods. 06 p0770 A83-19612

Fatigue control in prealloyed titanium powder compacts 07 p0883 A83-19832

Fatigue oxidation interaction in a superalloy - Application to life prediction in high temperature low cycle fatigue 07 p0884 A83-20256

Distribution of a life ratio and its application 07 p0943 A83-20516

Fracture mechanics analysis of the effects of residual stress on fatigue life 07 p0946 A83-20521

The effect of absorbed hydrogen on torsional fatigue of 2024-T351 aluminum alloy 07 p0887 A83-20633

The fatigue resistance of aluminum alloy 1201 under programmed and random high-frequency loading 07 p0890 A83-20906

Tensile fatigue of carbon fiber reinforced plastics 07 p0877 A83-20924

Fatigue and creep considerations in the design of turbine components 07 p0949 A83-21461

Low cycle fatigue and life prediction methods 07 p0892 A83-21462

The influence of creep on the high temperature cyclic life of IN738LC 07 p0893 A83-21471

An operational definition of life to crack initiation in high temperature fatigue 07 p0893 A83-21477

Fatigue failure under fretting conditions 07 p0894 A83-21481

High-temperature low-cycle fatigue behaviour of IN738LC alloy in air and in vacuum 07 p0895 A83-21489

Modelling R ratio effects in fatigue crack growth in polymers 08 p1068 A83-21676

Normalization of fatigue crack propagation behavior in polymers 08 p1068 A83-21677

Geometry and size requirements for fatigue life similitude among notched members 08 p1059 A83-21685

Prediction of crack formation life in notched specimens 08 p1117 A83-21686

Deriving a design fatigue resistance curve for analysing crack initiation 08 p1059 A83-21687

Fretting fatigue in a 3-1/2NiCrMoV rotor steel 08 p1059 A83-21690

Fatigue crack propagation response in extruded and cast aluminum alloys 08 p1060 A83-21710

On the interaction of hardening and fatigue damage in the 316 stainless steel 08 p1062 A83-21736

Regularities of similarity and fatigue damage accumulation under irregular loading 08 p1118 A83-21737

The low-cycle fatigue and cyclic behaviour of zirconium 08 p1062 A83-21738

Low-cycle fatigue of base metals and welded joints at elevated temperature - Life prediction, application, transferability 08 p1065 A83-22029

Static fatigue of preoxidized hot-pressed silicon nitride 08 p1071 A83-22201

On Bayes estimation of reliability for the Birnbaum-Saunders fatigue life model [AD-A128477] 08 p1114 A83-22708

Fatigue failure models - Birnbaum-Saunders vs. inverse Gaussian 08 p1114 A83-22709

Fatigue crack propagation in composites with spherical fillers. I 08 p1055 A83-22715

Analysis of closure behavior of small fatigue cracks 09 p1275 A83-23299

Fatigue behavior of solution-treated and quenched Ti-6Al-4V 09 p1228 A83-23344

Fatigue Conference and Exposition, Dearborn, MI, April 14-16, 1982, Proceedings 09 p1276 A83-23416

Cumulative damage analysis 09 p1276 A83-23418

Corrosion and fretting effects on fatigue 09 p1277 A83-23419

Constant amplitude fatigue life assessment models 09 p1277 A83-23420

Variable amplitude fatigue life estimation models 09 p1277 A83-23421

A discussion of methods for estimating fatigue life 09 p1277 A83-23422

Theoretical fatigue life prediction using the cumulative damage approach 09 p1277 A83-23423

Fatigue considerations in use of aluminum alloys 09 p1228 A83-23425

A study of the effect of stresses below the fatigue limit on the life of D16T alloy under programmed loading 09 p1228 A83-23501

Estimation of the cyclic fatigue life of parts subjected to complex loading patterns --- for compressor disks and turbine wheels in aircraft engines 09 p1228 A83-23502

Adhesive stress-strain properties relative to fatigue life of titanium bonded to graphite reinforced plastic 09 p1237 A83-23616

Effects of GTA dressing on the fatigue properties of aluminum alloy welded, butt jointed and fillet welded plates 09 p1274 A83-23650

Analytical description of the aging of polyamide 6 under fatigue fracture 09 p1239 A83-25023

A damage law for predicting the elevated temperature low cycle fatigue life of a martensitic stainless steel 10 p1393 A83-25418

The effect of shear bands on service properties of Ti-6Al-2Sn-4Zr-2Mo-0.1Si forgings 10 p1397 A83-25870

High temperature low cycle fatigue of IN 738 and application of strain range partitioning 10 p1398 A83-26282

Fatigue life estimation using simple fracture mechanics 11 p1594 A83-28402

Turbine blade nonlinear structural and life analysis 12 p1703 A83-29024

A study of the effect of notches and cracks on creep rupture life 12 p1713 A83-29225

An automated finite element procedure for fatigue crack propagation analyses 12 p1737 A83-29748

[AIAA 83-0841] Improved damage-tolerance analysis methodology [AIAA 83-0863] 12 p1738 A83-29751

Effect of stitching on the strength of bonded composite single lap joints [AIAA 83-0969] 12 p1739 A83-29779

Numerical simulation of material fatigue by a thermodynamic approach 12 p1740 A83-29784

Improved fatigue life tracking procedures for Navy aircraft structures [AIAA 83-0805] 12 p1703 A83-29807

Reliability-based fatigue damage predictions under random vibration environments [AIAA 83-0809] 12 p1741 A83-29809

An evaluation of the random bending fatigue life of bonded aluminum joints using various adhesive/primer combinations [AIAA 83-0998] 12 p1744 A83-29873

Acoustic fatigue life analysis - Honeycomb panels subjected to diffuse and progressive random acoustic waves [AIAA 83-1000] 12 p1745 A83-29875

A study on the notch effect on the low cycle fatigue of metals in creep-fatigue interacting conditions at elevated temperature 13 p1820 A83-30240

Experimental verification of properties of S-N fatigue life gages for the purpose of a use of the gages as indicators of the relative severity of operating conditions 13 p1808 A83-30514

Fatigue crack propagation behaviors of AZ31 magnesium alloy at temperatures from room temperature (17 + or - 2 C) to 50 C 13 p1822 A83-30843

Design for long fatigue life in random vibration environment 13 p1861 A83-30858

Statistical correlation between the thermal transition stress of a specimen and its resistance to alternating torsional fatigue [ASME PAPER 82-WA/DE-15] 13 p1823 A83-31297

On life time predictions with the strain range partitioning method 13 p1824 A83-31543

Distributions of fatigue life and fatigue strength in notched specimens of a carbon eight-harness-satin laminate 13 p1816 A83-31621

The residual strength of prefabricated structures made of pressed panels of D16chT alloy and its modifications 14 p2029 A83-32075

The fatigue strength of compressor disks 14 p2030 A83-32387

Filament wound composite thermal isolator structures for cryogenic dewars and instruments --- glass fiber reinforced epoxy laminates for spaceborne equipment 14 p1982 A83-33120

An approach to accelerated testing 15 p2173 A83-33549

Improving the fatigue strength of welded joints --- Book 15 p2171 A83-33626

Effect of processing on fatigue life of Ti-6Al-4Al-4V castings 15 p2135 A83-33641

Residual life prediction for jet engine rotor disks at elevated temperature 15 p2174 A83-33974

Low cycle fatigue behaviour of cast nickel-base superalloy IN738LC at room temperature 15 p2140 A83-34742

Prediction of constant amplitude fatigue lives of precracked specimens from accelerated fatigue data 15 p2140 A83-34743

On improving the fatigue performance of a double-shear lap joint 15 p2180 A83-34744

The fracture mechanism of carbon and boron composites in interlayer shear 16 p2323 A83-35509

Life estimation methods of gas turbine rotating components 16 p2305 A83-35870

Investigation methods on residual stresses in aero engines components 16 p2305 A83-35879

Creep-fatigue-effects in composites 16 p2324 A83-36172

Thermal fatigue analysis --- of turbine components 16 p2366 A83-36173

Life prediction for turbine engine components 16 p2366 A83-36174

- The prediction of fatigue life using ultrasound testing 16 p2367 A83-36184
- Fatigue limits of Cu and Al up to the 10th loading cycles 16 p2332 A83-36189
- Evaluation of fatigue limits and crack growth properties of PM-Mo alloys tested at cyclic frequencies of 200 Hz and 20 kHz 16 p2333 A83-36199
- The fatigue of wind turbine structures 16 p2367 A83-36200
- Static fatigue life of Kevlar aramid/epoxy pressure vessels at room and elevated temperatures [AIAA PAPER 83-1328] 16 p2324 A83-36342
- Estimating the statistical properties of crack growth for small cracks 16 p2333 A83-36504
- Reliability theory of stochastic fracture processes in sustained loading. I 16 p2369 A83-36623
- In-flight computation of helicopter transmission fatigue life expenditure 16 p2301 A83-36921
- Some consequences of the two-parameter model of fatigue-life scatter --- under complex and cyclic loading 17 p2518 A83-37269
- Design of minimum-mass panels with allowance for constraints on fatigue life, and residual and static strength 17 p2520 A83-37536
- A model for determining the reliability of an aircraft wing structure 17 p2521 A83-37638
- Microstructure/strength/fatigue crack growth relations in high temperature P/M aluminum alloys 17 p2488 A83-37844
- Titanium fan disc Structural Life Prediction/Correlation program [SAE PAPER 821437] 17 p2522 A83-37985
- A unified approach to turbine blade life prediction [SAE PAPER 821439] 17 p2468 A83-37987
- A synergistic fracture mechanics approach to fatigue life evaluation 18 p2665 A83-39077
- Disaggregation and a fracture criterion under creep 18 p2698 A83-39484
- Prediction of the fatigue life of Duralumin specimens 18 p2665 A83-39499
- Micromechanisms of fatigue crack growth retardation following overloads 18 p2699 A83-39540
- Fatigue life prediction of notched members based on local strain and elastic-plastic fracture mechanics concepts 18 p2699 A83-39543
- Fatigue life prediction for complex load versus time histories 18 p2700 A83-39995
- A fatigue fracture model for metal-matrix composites 18 p2701 A83-40103
- Fatigue of composite bolted joints under dual load levels 18 p2703 A83-40158
- Strength tests of CFRP joint assembly models for tailplane structure 18 p2703 A83-40159
- A study on the fatigue life estimation of FRP under random loading 18 p2655 A83-40199
- Statistical analysis of composite fatigue life 18 p2655 A83-40200
- Distributions of fatigue life and fatigue strength in notched specimens of a carbon eight-harness-satin laminate 18 p2655 A83-40201
- The prediction of long term viscoelastic properties of fiber reinforced plastics 18 p2655 A83-40210
- Effects of corrosive environments on graphite/epoxy composites 18 p2656 A83-40227
- The comparison of the results of service-spectrum tests with the help of the relative Miner rule --- fatigue life analysis of aircraft structures 18 p2696 A83-40471
- Planning and statistical processing of the results of tests for plotting quantile fatigue curves 19 p2824 A83-40762
- Generic aspects of three-dimensional internal-damage development in fatigue-loaded composite laminates 19 p2819 A83-41035
- Some effects of material property data selection on crack propagation analyses 19 p2821 A83-41200
- Thermal fatigue of gas-turbine blades made of a material based on silicon nitride and silicon carbide 19 p2823 A83-41594
- Service life characteristics of the composite material KAS-1A 19 p2820 A83-41601
- Case depth requirements in carburized gears 20 p2999 A83-43409
- Fatigue life of brittle superconducting alloys in normal and superconducting states 20 p2955 A83-43468
- A crack growth fatigue life under spectrum loading 20 p3009 A83-43692
- The behaviour of short cracks in the sub-critical crack growth regime [ASME PAPER 83-PVP-98] 20 p3009 A83-43732
- A theory for the long-term cyclic strength under high-temperature high-cycle loading 21 p3113 A83-44722
- Engineering formulae for fatigue strength reduction due to crack-like notches 21 p3158 A83-44916
- The effect of the parameters of cyclic loading on the kinetics of deformation and fracture of E182 alloy 21 p3114 A83-45317
- Low-cycle fatigue during symmetric disproportionate deformation 21 p3163 A83-45363
- Fatigue fracture of polycarbonate 22 p3270 A83-46902
- Statistical cumulative damage theory for fatigue life prediction 23 p3468 A83-47595
- Self-similarity of fatigue fracture - Cumulative damage 23 p3472 A83-48466
- Thermal fatigue on a thermally unstable alloy [ONERA, TP NO. 1983-86] 24 p3561 A83-49405
- In-plane and interlaminar shear fatigue characterization of unidirectional GFRP and CFRP, including moisture effects [ONERA, TP NO. 1983-109] 24 p3553 A83-49420
- Analytical determination of the crack path and elastic energy release rate under cyclic loading with allowance for welding stresses 24 p3596 A83-49915
- ### FATIGUE TESTING MACHINES
- DSO-series devices for fatigue testing under repeated impact and harmonic loading with various cycle ratios 02 p0191 A83-12342
- Test stand for fatigue life studies involving superposed mechanical and thermal cyclic stresses 02 p0197 A83-12986
- A resonance-type machine for studying the fatigue properties of composite materials 06 p0762 A83-18518
- Bidirectional coupling of a cracking test machine to a calculator 08 p1112 A83-21764
- Simple reverse bending machine for low cycle fatigue at elevated temperatures 08 p1106 A83-23232
- Unit for corrosion-fatigue testing of samples with stationary and cyclic heating 11 p1550 A83-28620
- A study of the low-cycle fatigue of the structural alloys for cryogenic applications 14 p1998 A83-33018
- A study of the fatigue of structural alloys under repeated static loading with superposed vibration 14 p1998 A83-33019
- A study of the high-cycle fatigue of materials under plane cantilever bending 14 p1998 A83-33020
- An improved method for threshold fatigue crack propagation testing on an electromagnetic resonance type machine 15 p2162 A83-33512
- A new transducer to monitor fatigue crack propagation 15 p2162 A83-33513
- Creep fracture in polymers - Technique and data handling for a statistical characterization 20 p2958 A83-43470
- Use of S/N-sensors for measuring the fatigue damage of materials 20 p2992 A83-43563
- ### FATIGUE TESTS
- Fatigue behaviour of two nickel-base alloys. I - Experimental results on low cycle fatigue, fatigue crack propagation and substructures. II - Physical modelling of the fatigue crack propagation process 01 p0023 A83-10215
- The effect of environment on the high temperature low cycle fatigue behaviour of cast nickel-base IN-738 alloy 01 p0023 A83-10216
- Study of plastic zones in fatigue - A photogrid technique 01 p0058 A83-10276
- Effect of stress frequency on fatigue crack propagation in titanium 01 p0026 A83-10647
- Analysis of accumulated damage in accelerated fatigue testing by the increasing load methods 01 p0059 A83-10686
- Fracture toughness test by impact-fatigue method 02 p0154 A83-11851
- Water-displacing organic corrosion inhibitors - Their effect on the fatigue characteristics of aluminium alloy bolted joints 02 p0148 A83-12014
- Long-term strength of composite compacts under programmed uniaxial tension-compression. I - A comparative analysis of some accumulated damage hypotheses. II - Modification of a hereditary long-term strength criterion 02 p0192 A83-12355
- Induced creep and creep/fatigue of a nickel-base superalloy at ambient temperatures 02 p0157 A83-12415
- Operational summary of an electric propulsion long term test facility [AIAA PAPER 82-1903] 02 p0139 A83-12478
- Quantitative evaluation of fatigue strength of metals containing various small defects or cracks 03 p0338 A83-13197
- Modeling of the frequency effect on fatigue crack propagation in PMMA 03 p0301 A83-13198
- Digitized measurements of the shape of corner cracks at fastener holes 03 p0339 A83-13202
- The effect of load ratio on fatigue crack growth in Ti8-A1-1Mo-1V 03 p0298 A83-13342
- A description of fatigue crack growth in terms of plastic work 03 p0339 A83-13343
- Influence of microstructure on elevated-temperature fatigue resistance of a titanium alloy 03 p0298 A83-13902
- Low-cycle fatigue damage accumulation of aluminum alloys 03 p0299 A83-13903
- An evaluation of four creep-fatigue models for a nickel-base superalloy 03 p0299 A83-13904
- Cumulation of high-temperature low-cycle fatigue damage in two-temperature tests 03 p0299 A83-13906
- Fractographic studies of graphite/epoxy fatigue specimens 03 p0292 A83-14554
- An investigation of cumulative damage development in quasi-isotropic graphite/epoxy laminates 03 p0292 A83-14555
- Characterization of delamination onset and growth in a composite laminate 03 p0293 A83-14560
- Characterizing delamination growth in graphite-epoxy 03 p0293 A83-14561
- Fatigue fracture properties of a Mg-Al-Zn alloy 03 p0300 A83-14600
- Application of fatigue-strength analysis to the evaluation of the consequences of local damage and the effects of wing-shell repairs. III - An example of the application of fatigue-strength analysis using a specific fatigue wear 03 p0342 A83-14620
- Influence of the gaseous environment on fatigue crack propagation in an austenitic steel 03 p0300 A83-14701
- The fracture of constituent particles during fatigue 03 p0301 A83-14705
- Evaluation of the effect of fatigue crack closure 04 p0459 A83-15399
- Microstructural influence on fatigue crack growth near threshold in 7075 Al alloy 04 p0461 A83-16251
- The influence of fatigue stress on the creep behaviour of metals 04 p0462 A83-16275
- The effect of glass fibers filled in polyester on fatigue crack arrest 05 p0611 A83-17106
- Fretting fatigue of Ti-6Al-4V alloy 05 p0614 A83-17258
- Effect of surface residual stresses on the fretting fatigue of a 4130 steel 05 p0615 A83-17264
- The effect of environment on fatigue crack growth behavior of 2021 aluminum alloy 05 p0616 A83-17894
- An evaluation of overload models on the retardation behavior in a Ti-6Al-4V alloy 05 p0616 A83-17896
- Surface damage and near-threshold fatigue crack growth in a Ni-base superalloy in vacuum 05 p0616 A83-17897
- Fatigue spectrum sensitivity of composite joints --- in aircraft structures 06 p0716 A83-17964
- The interlayer strength criteria for carbon composites under cyclic loads 06 p0725 A83-18502
- Fatigue tests under variable-amplitude stresses - Laboratory simulation methods for operational stresses 06 p0775 A83-18597
- Effects of defects on fatigue properties of P/M disk alloys 06 p0732 A83-19098
- Effects of ceramic inclusions on fatigue properties of a powder metallurgical nickel-base superalloy 06 p0732 A83-19101
- Fatigue life estimation - A review of traditional methods. I 06 p0770 A83-19612
- The importance of surface layer on fatigue behavior of a Ti-6Al-4V-alloy 07 p0884 A83-20254
- Fatigue and microstructural properties of quenched Ti-6Al-4V 07 p0885 A83-20262
- Matching materials and structures in vertical axis wind turbines 07 p0953 A83-20434
- Fatigue crack front shape and its effect on fracture toughness measurements 07 p0886 A83-20519
- The fatigue resistance of aluminum alloy 1201 under programmed and random high-frequency loading 07 p0890 A83-20906
- Characteristics of the amplitude distribution of acoustic emission in the nucleation and propagation of fatigue cracks 07 p0943 A83-21405
- Effect of fatigue damage in members of a sectional structure on its damping 07 p0948 A83-21416
- Fatigue crack propagation at elevated temperature in MAR-M002 single crystals 07 p0893 A83-21476
- Fatigue of high-temperature materials at ultrasonic frequencies 07 p0894 A83-21479
- Crack initiation and propagation in a forged nickel-base alloy under high mechanical and thermal loading 07 p0894 A83-21480
- Mechanisms of high cycle fatigue of cast nickel base alloys 07 p0894 A83-21482
- Fatigue-crack initiation in IMI 829 caused by high-temperature fretting 07 p0896 A83-21566
- Impact fatigue strength and reliability for fiber reinforced epoxy resin laminates subjected to repeated impact loads 07 p0877 A83-21624

An empirical approach to determining K for surface cracks 08 p1115 A83-21653

Examination of several mechanical parameters to analyse the plastic fatigue crack initiation in geometrical concentration zones and mechanical notches 08 p1116 A83-21670

The relationship of compliance changes during fatigue loading to the fracture of composite materials 08 p1054 A83-21682

Fatigue crack propagation from crack arrays 08 p1059 A83-21688

Fretting fatigue in a 3-1/2NiCrMoV rotor steel 08 p1059 A83-21690

The effect of overloads upon fatigue crack tip opening displacement and crack tip opening/closing loads in aluminum alloys 08 p1060 A83-21709

R ratio influence and overload effects on fatigue crack mechanisms 08 p1060 A83-21714

Low rates of fatigue crack growth in beta heat treated titanium alloy 08 p1061 A83-21715

The low-cycle fatigue and cyclic behaviour of zirconium 08 p1062 A83-21738

Mode II fatigue crack growth in aluminum alloys and mild steel 08 p1063 A83-21759

Fatigue crack growth under controlled K 08 p1118 A83-21765

Static fatigue of preoxidized hot-pressed silicon nitride 08 p1071 A83-22201

Comparison of static, cyclic, and thermal-shock fatigue in ceramic composites 08 p1055 A83-22268

Optical fiber strength/fatigue experiments 08 p1073 A83-22485

Use of vacuum metallography methods for evaluating the effectiveness of materials with protective coatings 08 p1066 A83-22629

The simulation of fatigue loads in aeronautics 08 p1048 A83-23241

Effect of strain-amplitude change on low-cycle fatigue behavior of pure aluminium at 77 K 09 p1228 A83-23300

Fatigue Conference and Exposition, Dearborn, MI, April 14-16, 1982, Proceedings 09 p1276 A83-23416

Variable amplitude fatigue life estimation models 09 p1277 A83-23421

Fatigue considerations in use of aluminum alloys 09 p1228 A83-23425

A study of the effect of stresses below the fatigue limit on the life of D16T alloy under programmed loading 09 p1228 A83-23501

A study of the effect of the cycle ratio on the fatigue of titanium alloys under high-frequency loading 09 p1228 A83-23503

Measurement of fatigue crack propagation at -70 C with the direct-current potential probe method 09 p1281 A83-24944

Static fatigue of silica in hermetic environments 09 p1240 A83-25207

Accuracy and precision of crack length measurements using a compliance technique 10 p1438 A83-25424

Static and fatigue testing of 2024 Al-SiC /F-9/ T-4 [ASME PAPER 82-WA/AERO-2] 10 p1388 A83-25677

S-N curve inversion of a nickel-base superalloy at elevated temperature 10 p1397 A83-25868

Deformation behavior of blended elemental Ti-6Al-4V compacts 10 p1397 A83-25871

Increasing the fatigue strength of welded joints in PT3V alloy treated with mechanical brushes 10 p1397 A83-26224

Effect of local heating on corrosion fatigue strength of a titanium alloy 10 p1398 A83-26225

Procedure for estimating the fatigue strength of gas turbine blades by method of acoustic emission 10 p1436 A83-26286

Notch effect on torsional low-cycle fatigue 10 p1399 A83-26893

The effect of cycle waveshape on the low cycle fatigue behaviour of 20%Cr-25%Ni-Nb stainless steel at 650 C 11 p1547 A83-27852

Propagation of fatigue cracks under polymodal loading 11 p1547 A83-27853

EUROMECH colloquium on short fatigue cracks 11 p1547 A83-27854

Resonance controlled fatigue crack propagation 11 p1595 A83-28440

A diagram for the discrete growth of a fatigue crack under self-similarity conditions 11 p1597 A83-28480

A study of the strength characteristics of the carbon composite KMu-3L 11 p1544 A83-28483

Method for low-cycle fatigue testing of isothermal and nonisothermal loading 11 p1550 A83-28618

Unit for corrosion-fatigue testing of samples with stationary and cyclic heating 11 p1550 A83-28620

Pulse sensor to monitor the loading process during programmed fatigue tests on specimens of materials and structural elements 11 p1575 A83-28621

Theoretical and experimental investigations regarding crack propagation in sheet metal --- German thesis 11 p1599 A83-28658

Observations of cyclic grain boundary migration in aluminium after large numbers of fatigue cycles 12 p1714 A83-29510

Fatigue tests on fillet welded joints to assess the validity of Miner's cumulative damage rule 12 p1736 A83-29596

Compressive fatigue behaviour of a glass fibre-reinforced polyester composite at 300 K and 77 K 12 p1710 A83-29720

Effect of multiple crack propagation on the high temperature low cycle fatigue of a cast nickel-base alloy 12 p1714 A83-29725

On the effect of residual stresses on crack growth from a hole 12 p1737 A83-29747

[AIAA 83-0840] Delamination-based compression residual-strength prediction model for composites 12 p1738 A83-29756

[AIAA 83-0872] Effect of stitching on the strength of bonded composite single lap joints 12 p1739 A83-29779

[AIAA 83-0969] The effect of acoustic-thermal environments on advanced composite fuselage panels 12 p1744 A83-29857

[AIAA 83-0955] Acoustic fatigue test evaluation of adhesively bonded aluminum fuselage panels using FM 73/BR 127 adhesive/primer system 12 p1744 A83-29874

[AIAA 83-0999] Low cycle fatigue behavior of aluminum/stainless steel composites 12 p1711 A83-29886

[AIAA 83-0806] Fatigue crack propagation behaviors of A231 magnesium alloy at temperatures from room temperature (17 + or - 2 C) to 50 C 13 p1822 A83-30843

Vibration-fatigue reliability analysis 13 p1867 A83-30859

Slow fatigue crack growth and threshold behaviour in IMI 685 --- in titanium alloys 13 p1824 A83-31541

Distributions of fatigue life and fatigue strength in notched specimens of a carbon eight-harness-satin laminate 13 p1816 A83-31621

Processing of fatigue test results for corrosion-affected structural materials 14 p1992 A83-32074

On the cyclic behavior of cast and extruded aluminum alloys. I - Fatigue crack propagation 14 p1992 A83-32342

Comparison of properties of joints prepared by ultrasonic welding and other means 14 p2031 A83-32586

Cryogenic fluid management experiment trunnion fatigue verification 14 p1982 A83-32782

[AIAA PAPER 83-0911] Infrared measurement of specimen temperature profiles during fatigue crack propagation tests 14 p2020 A83-32825

Microstructure, deformation, and corrosion-fatigue behavior of a rapidly solidified Al-Li-Cu-Mn alloy 14 p1996 A83-32890

Subsurface crack initiation in high cycle fatigue in Ti6Al4V and in a typical Martensitic stainless steel 14 p1997 A83-32944

High-frequency fatigue testing of structural steels and alloys at 77 K 14 p1998 A83-33021

Evaluation of the effect of voids in composite main rotor blades 15 p1713 A83-33507

Canadian forces tracker aircraft full-scale fatigue test at the National Aeronautical Establishment 15 p1222 A83-33548

On improving the fatigue performance of a double-shear lap joint 15 p2180 A83-34744

Dynamic fatigue of brittle materials containing indentation line flaws 15 p2180 A83-35064

Evaluation of the effect of voids in composite main rotor blades 16 p2299 A83-35950

Fatigue crack growth rates for very short cracks developing at fastener holes in 7075 and 7010 aluminium alloys 16 p2330 A83-35982

Creep-fatigue-effects in composites 16 p2324 A83-36172

The state of ultrasonic fatigue 16 p2367 A83-36177

Monitoring of high power ultrasonic fatigue systems 16 p2367 A83-36178

Problems arising with fatigue-testing at ultrasonic frequencies in single and double transducer systems 16 p2356 A83-36179

Theoretical considerations 16 p2356 A83-36179

Problems arising with fatigue-testing at ultrasonic frequencies in single and double transducer systems 16 p2331 A83-36180

Practical applications 16 p2331 A83-36180

Method of measuring elastic strain distribution in specimens used for high frequency fatigue testing 16 p2332 A83-36182

The use of various ultrasonic systems for fatigue testing 16 p2367 A83-36183

The prediction of fatigue life using ultrasound testing 16 p2367 A83-36184

Stress distributions in notched specimens loaded statically and dynamically 16 p2367 A83-36185

Review of the application of ultrasonic fatigue test methods for the determination of crack growth and threshold behavior of metallic materials 16 p2332 A83-36186

Fatigue limits of Cu and Al up to 10 to the 10th loading cycles 16 p2332 A83-36189

Metal-metal composites loaded at ultrasonic frequencies 16 p2324 A83-36190

Corrosion fatigue behaviour of 13Cr stainless steel and Ti-6Al-4V at ultrasonic frequency 16 p2332 A83-36192

Corrosion fatigue testing of implant materials (Nb, Ta, stainless steel) at transonic frequencies 16 p2332 A83-36193

The influence of frequency on fatigue crack propagation of some heat resisting alloys using ultrasonic fatigue 16 p2332 A83-36196

Planning and evaluation of fatigue tests in regard to ultrasonic frequency tests 16 p2333 A83-36201

Low cycle fatigue of tubular specimens 17 p2519 A83-37299

Initial strain field and fatigue crack initiation mechanics [ASME PAPER 83-APM-20] 17 p2519 A83-37385

The influence of microstructure on the scatter of the fatigue strength of the titanium alloy TiAl6V4 17 p2491 A83-38473

Fatigue crack growth rate under full yielding condition for 15CDV6 steel 18 p2665 A83-39084

Separate processing of the results of low-cycle and high-cycle fatigue tests --- of aluminum alloys 18 p2665 A83-39500

Utilization of the dynamic characteristics of a structure to evaluate its technological state --- dynamic structural analysis of caissons 18 p2698 A83-39510

Evaluation of the efficiency of the diamond burnishing of gas-turbine-engine parts 18 p2695 A83-39511

A technique for the accelerated life testing of fan impellers 18 p2698 A83-39512

Fatigue life prediction for complex load versus time histories 18 p2700 A83-39995

Strength tests of CFRP joint assembly models for tailplane structure 18 p2703 A83-40159

Fatigue behaviour of carbon fiber reinforced epoxy composite materials with edge notch 18 p2655 A83-40202

Compressive fatigue damage accumulation near holes in graphite/epoxy laminates 18 p2655 A83-40203

Fatigue crack growth behavior in the vicinity of interface of dissimilar materials 18 p2705 A83-40204

Investigation of the fatigue behaviour of some industrial glass reinforced polyesters (GRP) 18 p2655 A83-40205

Effect of combination of glass mat and cloth on the fatigue properties of fibrous composite materials 18 p2655 A83-40206

Effect of defect on the behaviour of composites 18 p2656 A83-40215

Method of investigating the rules of deformation and failure under conditions of low-cycle nonisothermal loading 19 p2855 A83-40763

Dynamic fatigue of a machinable glass-ceramic 19 p2823 A83-40908

Fatigue crack initiation and propagation in several nickel-base superalloys at 650 C 19 p2821 A83-41199

Fracture anomalies of a casting magnesium alloy in low-cycle fatigue 19 p2822 A83-41595

Estimation of the thermal fatigue strength of the blades of full-scale gas-turbine engines 19 p2800 A83-41596

Environmental fatigue of reinforced plastics 20 p2947 A83-42812

The effects of environmental exposure on the fatigue behaviour of CFRP laminates 20 p2947 A83-42813

Post-impact fatigue performance of carbon fibre laminates with non-woven and mixed-woven layers 20 p2948 A83-42814

The strength of GTE structural elements under low-cycle loading 20 p2936 A83-42877

Fatigue crack propagation in random short-fiber SMC composite --- Sheet Molding Compound 20 p2948 A83-43147

Appliance for fatigue tests of materials with symmetrical and asymmetrical loading 20 p2992 A83-43624

Compression fatigue behaviour of notched composite laminates 21 p3106 A83-44334

Load-shedding techniques for fatigue-threshold determination 21 p3161 A83-45149

Computer controlled decreasing Delta-K fatigue threshold test 21 p3162 A83-45184

- Consideration on the fatigue damage of specimens used for composite critical components qualification 22 p3305 A83-46307
- Visualization of fatigue defects by an electrodischarge high-frequency method 22 p3269 A83-46330
- The effect of moisture on the fatigue resistance of an aramid/epoxy composite 22 p3265 A83-46904
- The behaviour of fatigue cracks subject to applied biaxial stress - A review of experimental evidence 23 p3470 A83-48146
- The effect of water vapor on fatigue crack tip mechanics in 7075-T651 aluminum alloy 23 p3432 A83-48147
- Estimating initiation times of secondary fatigue cracks in damage tolerance analysis 23 p3470 A83-48148
- On the transition from near-threshold to intermediate growth rates in fatigue 23 p3432 A83-48149
- Cyclic fatigue behavior of ceramics 23 p3437 A83-48291
- ARALL (aramid-fiber-reinforced aluminum laminate) - A new hybrid composite with exceptional fatigue-resistance properties 23 p3428 A83-48500
- Modern methods for studying the initial stage of the fatigue fracture of metals 23 p3433 A83-48539
- Fatigue crack growth in vacuum and a gaseous environment 23 p3433 A83-48540
- FATTY ACIDS**
- NT CARBOXYLIC ACIDS
- NT PALMITIC ACID
- A mathematical model for the regulation of glycolysis by the oxidation of pyruvate and fatty acids in the myocardium 14 p2064 A83-32957
- A study of the fatty acid composition of the major brain 14 p2065 A83-33316
- The effect of products based on higher fatty acids on the performance characteristics of jet fuels 15 p2143 A83-34500
- The role of free fatty acids in the accumulation of thrombocytes and the development of myocardial injuries during prolonged adrenalin administration 17 p2555 A83-37237
- Effects of acute moderate-intensity exercise on carnitine metabolism in men and women 20 p3034 A83-43484
- FAULT MECHANICS**
- U FRACTURE MECHANICS
- FAULT TOLERANCE**
- Approximation techniques of a selective ARQ protocol 01 p0032 A83-11093
- Economic modeling of fault tolerant flight control systems in commercial applications 01 p0013 A83-11156
- Testability using Logmod --- Logic MModel method for functional analysis of system design 01 p0029 A83-11232
- A microprocessor-based fault-tolerant computer system 02 p0227 A83-11907
- CPU coverage evaluation using automatic fault injection 03 p0385 A83-14842
- Design for safe software [AIAA PAPER 83-0323] 05 p0678 A83-16652
- Fault tolerant techniques for a multiple microprocessor-based space borne packet switch 07 p0906 A83-19714
- Fault detection by adaptive nonlinear filtering 07 p0984 A83-20501
- A microwave approach to fault tolerance in satellite networking 07 p0914 A83-20674
- The influence of software errors on the reliability of data processing systems --- French thesis 08 p1154 A83-22084
- The software-implemented fault tolerance /SIFT/ approach to fault tolerant computing 08 p1155 A83-22825
- Multicomputer systems in real-time sensor data processing - A look at the problems of throughput and reliability 08 p1155 A83-22826
- Generic faults and architecture design considerations in flight-critical systems 09 p1203 A83-24426
- Fault isolation methodology for the L-1011 digital avionic flight control system 09 p1209 A83-24427
- The theory and practice of reliable system design --- Book 09 p1325 A83-24947
- Design methods of single-output built-in self-checking circuits for equilibrium codes 10 p1460 A83-25467
- Application of redundant processing to Space Shuttle 10 p1381 A83-26610
- Galileo spacecraft power distribution and autonomous fault recovery 11 p1539 A83-27149
- Use of a multiprocessor for control of a robotic system 11 p1648 A83-28099
- Fault/maneuver tolerance of aided GPS demodulation/navigation processors in the non-precision approach environment 11 p1529 A83-28787
- The laser gyro as a self-contained inertial navigation aid 12 p1729 A83-29208
- A new design method for m-out-of-n TSC checkers --- Totally Self-Checking for codes 13 p1908 A83-30791
- The design of error checkers for self-checking residue number arithmetic 15 p2217 A83-33909
- Concurrent error detection in multiply and divide arrays 15 p2218 A83-33915
- Control of locally testable duplex system for large-scale implementation 15 p2218 A83-34524
- A framework for software fault tolerance in real-time systems 16 p2403 A83-35325
- Fail safe logic design 16 p2345 A83-35555
- Operational fault-tolerant microcomputer for very high reliability 16 p2403 A83-36963
- A fault tolerant approach to state estimation and failure detection in nonlinear systems 17 p2567 A83-37121
- Reconfiguration of on-board control algorithms 17 p2569 A83-37491
- Full Authority Fault Tolerant Electronic Engine Control systems for advanced high performance engines (FAFTEEC) [SAE PAPER 821398] 17 p2468 A83-37972
- Yield enhancement of bit level systolic array chips using fault tolerant techniques 18 p2679 A83-40389
- Restructurable controls for aircraft [AIAA PAPER 83-2255] 19 p2804 A83-41728
- Measures of merit for fault-tolerant systems [AIAA PAPER 83-2259] 19 p2892 A83-41729
- Reliability considerations in the placement of control system components [AIAA PAPER 83-2260] 19 p2816 A83-41730
- A fault tolerant design for autonomous attitude control of the DSCS-III communication satellite [AIAA PAPER 83-2264] 19 p2816 A83-41734
- Autonomous failure detection and correction on Landsat-4 [AIAA PAPER 83-2265] 19 p2817 A83-41735
- A generalized stage-state method for centralized fault-tolerant flight control system [AIAA PAPER 83-2301] 19 p2892 A83-41759
- New results in fault latency modelling [AIAA PAPER 83-2303] 19 p2888 A83-41760
- Interactive reductions in the number of states in Markov reliability analysis [AIAA PAPER 83-2304] 19 p2894 A83-41761
- Undetectable critical defects in safety-of-flight structure 20 p2999 A83-42544
- Autonomy and fault tolerant design --- for satellite system and components [AAS PAPER 83-044] 21 p3104 A83-44171
- Guidance and control concepts for autonomous spacecraft [AIAA PAPER 83-045] 21 p3099 A83-44172
- A method of designing fault tolerant software 22 p3350 A83-45847
- The purpose, the principles and the problems of fault tolerant systems --- for aircraft gas turbine engines [ASME PAPER 83-GT-59] 23 p3407 A83-47915
- A new approach to fault-tolerant helicopter swashplate control [AIAA PAPER 83-2485] 23 p3412 A83-48345
- FAULT TREES**
- Using fault trees to find design errors in real time software [AIAA PAPER 83-0325] 05 p0678 A83-16654
- Applying existing safety design techniques to software safety [AIAA PAPER 83-0327] 05 p0678 A83-16656
- An analysis of impact failure modes for fiber-reinforced composite laminates by using fault tree 05 p0611 A83-17104
- ESCAF - A new and cheap system for complex reliability analysis and computation 07 p0942 A83-20514
- An analytic method for uncertainty analysis of nonlinear output functions, with applications to fault-tree analysis 08 p1160 A83-22710
- Node-fault diagnosis and a design of testability 15 p2151 A83-33926
- A new approach to system diagnosis --- for fault identification in self-testing systems 15 p2218 A83-35140
- A deductive method for the simulation of faults in Programmable Logic Arrays 15 p2218 A83-35142
- Analysis of Charpy impact failure for unidirectional fiber-reinforced composite laminates by using a computerized fault tree 18 p2655 A83-40212
- Interval reliability for initiating and enabling events 23 p3467 A83-47615
- Avionics fault tree analyzer [AIAA PAPER 83-2452] 23 p3401 A83-48335
- A generator of test sequences for probabilistic systems of the fault diagnostics of digital devices 24 p3575 A83-50207
- FAYALITE**
- Olivine flotation and settling experiments on the join Mg2SiO4-Fe2SiO4 16 p2382 A83-36972
- FBFM (MODULATION)**
- U FEEDBACK FREQUENCY MODULATION
- FCC LATTICES**
- U FACE CENTERED CUBIC LATTICES
- FDMA**
- U FREQUENCY DIVISION MULTIPLE ACCESS
- FEASIBILITY ANALYSIS**
- Design considerations for a multiport multitest machine 01 p0029 A83-10769
- Aerodynamic platform comparison for jet-stream electricity generation 04 p0507 A83-16102
- Inflow disk generator for open-cycle MHD power generation 04 p0538 A83-16104
- Feasibility design for a Surface Effect Catamaran Corvette escort [AIAA PAPER 83-0619] 08 p1173 A83-23246
- A concept of heat pipe engine 11 p1605 A83-27208
- Solar residential total energy system using the sodium heat engine - A concept study 11 p1606 A83-27231
- Reversible chemical reactions for energy storage in a large-scale heat utility 11 p1609 A83-27315
- Photovoltaic retrofit feasibility in the United States 14 p2038 A83-32188
- Advanced Civil Military Aircraft - Technical feasibility assessment [AIAA PAPER 83-1592] 14 p1973 A83-33359
- Feasibility of dry lubrication for limited-duty gas turbine engines [AIAA PAPER 83-1130] 16 p2362 A83-36405
- Analysis of the WINDSAT concept for measuring the global wind field 17 p2551 A83-38737
- Feasibility test of an airborne pulse-Doppler meteorological radar 18 p2726 A83-39872
- The scientific case and feasibility of a three metre balloon telescope 18 p2762 A83-40459
- Technical feasibility of satellite-aided land mobile radio 19 p2834 A83-41416
- Rolling KCl fiber - A feasibility study --- for IR optical communication 22 p3359 A83-46636
- Application of fiber optics to speckle metrology - A feasibility study 22 p3293 A83-46807
- FEATURE EXTRACTION**
- U PATTERN RECOGNITION
- FEDERAL BUDGETS**
- Why billions can and should be spent on space 13 p1934 A83-30832
- United States Federal Photovoltaic Program status 14 p2037 A83-32179
- FEDERAL REPUBLIC OF GERMANY**
- U WEST GERMANY
- FEED SYSTEMS**
- Optimal design of the lateral feed of a turbomachine [AAAF PAPER NT 81-04] 02 p0169 A83-11770
- Prediction of a propellant tank pressure history using state space methods 07 p0873 A83-20419
- FEEDBACK**
- NT NEGATIVE FEEDBACK
- NT NONLINEAR FEEDBACK
- NT POSITIVE FEEDBACK
- NT SENSORY FEEDBACK
- Relationship between carrier-induced index change and feedback noise in diode lasers 02 p0184 A83-12169
- The voluntary regulation of alpha and theta EEG rhythms in humans 02 p0224 A83-12215
- Data transmission rate in a memoryless discrete channel with data feedback 05 p0623 A83-17686
- Optimization and comparison of binary and multistep digital transmission systems with and without quantified feedback --- German thesis 06 p0751 A83-18498
- A water vapor-energy balance model designed for sensitivity testing of climatic feedback processes 08 p1142 A83-23004
- Noise of semiconductor lasers with external feedback 09 p1270 A83-23378
- Gaussian Schell-model sources - An example and some perspectives --- generation of directional light beams 09 p1344 A83-24083
- A new method of quantized feedback for the regeneration of digital signals 10 p1412 A83-26899
- The formation of nonlinear binary sequences 14 p2075 A83-32477
- Confocal optical feedback processing system - An improved optical design 14 p2076 A83-32903
- Efficient phase conjugation under parametric-feedback conditions 15 p2167 A83-33778
- FEEDBACK AMPLIFIERS**
- Concerning convective and absolute instabilities in bounded media --- wave amplifier and generator theory 01 p0036 A83-10416
- A design method of super-wideband pulse amplifiers 03 p0314 A83-14129
- A distributed-feedback tunable laser with dye-activated polymer matrices 04 p0486 A83-16325
- A network modeling and design method for a 2-18-GHz feedback amplifier 07 p0923 A83-21536

A monolithic GaAs DC to 2-GHz feedback amplifier 09 p1256 A83-24682
The complex dynamics of delayed-feedback oscillators /Review/ 09 p1257 A83-25077
Computer-aided design of infrared detector preamplifiers having switched feedback resistors 22 p3292 A83-46604

FEEDBACK CIRCUITS

An analysis of the efficiency of a noise self-compensator with correlation feedback with respect to the suppression coefficient 04 p0470 A83-15143
The effect of reflection on the operation of an O-type TWT under two-signal amplification 04 p0470 A83-15144
Instabilities and chaotic behavior in a hybrid bistable system with a short delay 08 p1163 A83-21886
Rejection of CW interference in QPSK systems using decision-feedback filters 14 p2001 A83-32865
On a regime of the development of oscillations in a spin oscillator 14 p2025 A83-33394

FEEDBACK CONTROL

NT CASCADE CONTROL
Analysis and flight data for a drone aircraft with active flutter suppression 01 p0008 A83-10192
Low-sensitivity observer-compensator design for two-dimensional digital systems 01 p0094 A83-10292
A method for adaptive biocontrol in the multifaceted treatment of patients with cerebral arachnoiditis 01 p0083 A83-10525
The design of robust feedback controllers for partly unknown systems by optimal control procedures 01 p0094 A83-10799
Identification of bilinear systems using relay feedback 01 p0095 A83-10800
Stability multipliers and multivariable circle criteria 01 p0095 A83-10957
Phase-locked-loop control systems using pulse frequency modulation 01 p0095 A83-10958
Decentralized stabilization of a class of non-linear interconnected systems 01 p0095 A83-10959
Computation of the zeros and zero directions of linear multivariable systems 01 p0095 A83-10961
A note on the generalized inverse Nyquist stability criterion 01 p0095 A83-10962
A new method to design non-linear feedback controllers for non-linear systems 01 p0095 A83-10963
Investigations of stability and dynamic performances of switching regulators employing current-injected control 01 p0039 A83-11002
Instabilities in current-mode controlled switching voltage regulators 01 p0039 A83-11003
Time-varying feedback gains for power circuits with active waveshaping 01 p0040 A83-11006
Flux-balanced variable frequency inverter 01 p0040 A83-11010
On the maximum regulation range in boost and buck-boost converters 01 p0040 A83-11013
Large-signal transient response of a switching regulator 01 p0041 A83-11027
Large signal design of a buck converter for high power dc/ac conversion 01 p0041 A83-11028
Microprocessor control for automated gateway transit vehicles 01 p0112 A83-11035
Transmission matrix approach to variable-rate sampled-data systems 01 p0095 A83-11132
PPS - A switch in time --- Programmable Pushbutton Switch 01 p0029 A83-11169
A closed loop test facility for validating flight control software 01 p0015 A83-11226
Transistorized PWM inverter-induction motor drive system 01 p0044 A83-11488
Optimal synchronization systems with time lag in the loop 02 p0229 A83-11534
Robotics for assembly - Design of a feedback sensor, and its use in general insertion procedures --- French thesis 02 p0229 A83-11767
Pole placement and order reduction in two-time-scale control systems through Riccati iteration 02 p0229 A83-11838
Application of matrix singular value properties for evaluating gain and phase margins of multiloop systems --- stability margins for wing flutter suppression and drone lateral attitude control 02 p0230 A83-12457
Feedback control of linear multivariable systems with uncertain description in the frequency domain 02 p0230 A83-12550
Inertial reference for robotic manipulators [ASME PAPER 82-DET-63] 02 p0230 A83-12774
Synthesis of control systems using coordinate-parametric and parametric feedback 03 p0386 A83-13591
Shutterless fixed pattern noise correction for infrared imaging arrays 03 p0325 A83-13731
Compensation electronics for staring focal plane arrays 03 p0326 A83-13734

Cycle slips in phase-locked loops - A tutorial survey 03 p0311 A83-13852
Equivocation as a cause of PLL hangup 03 p0311 A83-13853
False-lock performance improvement in Costas loops 03 p0311 A83-13858
All-pole phase-locked tracking filters 03 p0312 A83-13861
Carrier arraying with coupled phase-locked loops for tracking improvement 03 p0312 A83-13862
A note on the statistical dynamics of two mutually phase-locked oscillators 03 p0312 A83-13864
Phase-locked loops used with masers - Atomic frequency standards 03 p0331 A83-13865
Performance analysis of digital tanlock loop 03 p0312 A83-13869
Stable model reference adaptive control in the presence of bounded disturbances 03 p0386 A83-14590
Transfer function matrix description of decentralized fixed modes 03 p0386 A83-14591
On optimal nonlinear feedback regulation of linear plants 03 p0387 A83-14597
Stability relationships between gyrostats with free, constant-speed, and speed-controlled rotors 03 p0287 A83-14838
Fixed-trim re-entry guidance analysis 03 p0287 A83-14840
Multivariable and optimal systems --- Book 04 p0527 A83-15838
Design of stabilizing controller with incomplete state data for linear stochastic system with multiplicative noise 04 p0527 A83-15923
Robustness of the independent modal-space control method 04 p0528 A83-16116
Improved design technique for uncertain multiple-input-multiple-output feedback systems 04 p0528 A83-16148
Uncertain multiple-input-multiple-output systems with internal variable feedback 04 p0528 A83-16149
Quantitative feedback theory 04 p0528 A83-16185
Principal gains and phases - Insensitive robustness measures for assessing the closed-loop stability property 04 p0529 A83-16186
Analysis of feedback systems with structured uncertainties 04 p0529 A83-16187
Stability margins of diagonally perturbed multivariable feedback systems 04 p0529 A83-16188
Frequency-response design of robust optimal controllers 04 p0529 A83-16189
Multivariable stability-margin optimisation with decoupling and output regulation 04 p0529 A83-16191
Robust control strategy for a linear time-invariant multivariable sampled-data servomechanism problem 04 p0529 A83-16192
Robustness properties of model-reference adaptive control systems 04 p0529 A83-16193
Closed-loop eigenvalue selection for reduced autopilot sensitivity to radome errors [AIAA PAPER 83-0062] 05 p0592 A83-16494
Decoupling of high gain multivariable tracking systems [AIAA PAPER 83-0280] 05 p0592 A83-16625
Computation of optimal feedback strategies for interception in a horizontal plane [AIAA PAPER 83-0281] 05 p0577 A83-16626
Fully controllable heat pipe containing a short electro-osmotic pumping section [AIAA PAPER 83-0317] 05 p0634 A83-16647
Higher-order distributed feedback and generation of light 05 p0648 A83-17049
Model following and pole-placement self-tuners 05 p0680 A83-17579
Self-tuning controller with integral action 05 p0681 A83-17581
A continuous-time approach to discrete-time self-tuning control 05 p0681 A83-17583
Discrete adaptive control of a manipulator arm 05 p0681 A83-17585
Stochastic control in structural design 06 p0771 A83-18208
Dynamics of electrooptic bistable devices with delayed feedback 06 p0810 A83-18904
Load insensitive electro-hydraulic servo system 06 p0769 A83-18924
A feedback time constant concept 06 p0803 A83-19038
CTD MTI radar filter with charge-transfer inefficiency compensation 06 p0754 A83-19043
Angles of multivariable root loci [LIDS-P-1147] 06 p0803 A83-19320
Design of error-actuated controllers for multivariable plants with unknown dynamics and unmeasurable outputs --- for automatic control of industrial processes and gas turbine engines 06 p0718 A83-19385

Feedback representation of precompensators 06 p0803 A83-19387
Pole assignment and minimal feedback design 06 p0803 A83-19388
Time suboptimal feedback control of high order linear systems 06 p0803 A83-19389
A geometric approach to stabilization by output feedback 06 p0804 A83-19390
Generic pole assignment using dynamic output feedback 06 p0804 A83-19391
On the minimality of feedback realizations 06 p0804 A83-19392
A 12 GHz phaselocked divider loop 07 p0917 A83-19757
Design of adaptive controllers using the method of Lyapunov functions 07 p0984 A83-19998
Properties of diode lasers with intensity noise control 07 p0935 A83-20161
Extended perfect model following --- control system synthesis technique 07 p0984 A83-20289
Compensation technique for force balance devices 07 p0929 A83-20548
Analysis of oscillations in systems with polynomial-type nonlinearities using describing functions 07 p0984 A83-20720
Equations for the angles of arrival and departure for multivariable root loci using frequency-domain methods 07 p0985 A83-20724
Design of linear systems with saturating linear control and bounded states 07 p0985 A83-20725
Application of vector performance optimization to a robust control loop design for a fighter aircraft 07 p0867 A83-21160
The problem of guaranteeing robust disturbance rejection in linear multivariable feedback systems 07 p0985 A83-21161
Design of an adaptive observer and its application to an adaptive pole placement controller 07 p0985 A83-21163
Synthesis of feedback systems for specified time domain insensitivity to interaction induced plant ignorance 07 p0985 A83-21165
On the problem of observation spillover in self-adjoint distributed-parameter systems 08 p1156 A83-22044
Construction of a robot manipulating objects in contact - Control through force-feedback --- French thesis 08 p1156 A83-22088
Strictly observable linear systems 08 p1157 A83-22241
Dirichlet boundary control problem for parabolic equations with quadratic cost - Analyticity and Riccati's feedback synthesis 08 p1157 A83-22242
Linear-quadratic optimal control of hereditary differential systems - Infinite dimensional Riccati equations and numerical approximations 08 p1157 A83-22244
An anatomy of industrial robots and their controls 08 p1074 A83-22415
Joint torque control by a direct feedback for industrial robots 08 p1074 A83-22416
Advanced architecture for graphics and image processing 08 p1152 A83-22530
Variable-structure systems and system zeros 08 p1158 A83-23018
Dynamic output feedback controller 08 p1158 A83-23019
The stability of non-linear multivariable systems - Review of frequency domain methods 08 p1158 A83-23172
Design of an integrated control system for a supersonic aircraft power plant 08 p1046 A83-23175
Suboptimal control of discrete stochastic amplitude constrained systems 09 p1326 A83-23687
Deadbeat error control of discrete multivariable systems 09 p1326 A83-23688
A linear programming approach for multivariable feedback control with inequality constraints 09 p1326 A83-23689
The stability of linear multivariable systems 09 p1326 A83-23690
Realization of some analog functions with switchable feedback loops 09 p1253 A83-23694
Robust control of flexible spacecraft 09 p1216 A83-24432
Model reference adaptive control of large structural systems 09 p1327 A83-24433
MOFNM - A method for optimum design of feedback systems --- Multiple Object Function Newton Method 09 p1327 A83-24708
Stability and stabilization of delay systems with sampled feedback 09 p1328 A83-24714
A linear programming approach for multivariable feedback control with inequality constraints 09 p1328 A83-24720
Control design for a wind turbine-generator using output feedback 09 p1293 A83-24721
On local controllability 09 p1329 A83-24731

Controllability conditions and effective controls for nonlinear systems 09 p1329 A83-24734

An eigenstructure approach to noninteracting control synthesis 09 p1331 A83-24753

Optimal control of flexible structures 09 p1217 A83-24755

Fast-sampling tracking systems incorporating Lur'e plants with multiple switching nonlinearities 09 p1331 A83-24762

Global parameterization of feedback systems 09 p1332 A83-24780

Simultaneous design of control systems 09 p1332 A83-24781

The Total Synthesis Problem of linear multivariable control. II - Unity feedback and the design morphism 09 p1332 A83-24782

Reduced order modeling of large space structures via least squares estimation 09 p1217 A83-24785

Improved observer design incorporating modal consideration --- for feedback application to flight control problems 09 p1332 A83-24787

Controller design for asymptotic stability of flexible spacecraft 09 p1217 A83-24788

Multivariable adaptive pole placement 09 p1333 A83-24790

Necessary and sufficient conditions for regulation of linear systems 09 p1333 A83-24794

Robust control/estimator design by frequency-shaped cost functionals 09 p1333 A83-24797

Robustness tests utilizing the structure of modelling error 09 p1333 A83-24798

Performance and robustness trades in log regulator design 09 p1333 A83-24799

Disturbance decoupling, decentralized control and the Riccati equation 09 p1334 A83-24801

A new design for decentralized control with output feedbacks 09 p1334 A83-24802

Analytical verification of undesirable properties of direct model reference adaptive control algorithms 09 p1334 A83-24806

On spectrum placement for linear time invariant delay systems 09 p1334 A83-24808

Generalized error coefficients for the multivariable servomechanism problem 09 p1334 A83-24813

Multivariable stability margins for vehicle flight control systems 09 p1210 A83-24815

Near insensitivity of linear feedback systems 09 p1335 A83-24817

Use of parameter groups in the analysis and design of multivariable feedback systems 09 p1335 A83-24818

Closed-loop asymptotic stability and robustness conditions for large space systems with reduced-order controllers 09 p1218 A83-24819

Applied control theory --- Book 09 p1335 A83-24894

Time suboptimal feedback control design through coordinate transformation 10 p1461 A83-25396

Control of the constrained planar simple inverted pendulum 10 p1461 A83-25397

Feedback control of parametric instabilities 10 p1461 A83-25398

Self-tuning regulators - Non-parametric algorithms 10 p1461 A83-25399

The design of optimal output regulators for linear multivariable systems with constant disturbances 10 p1461 A83-25400

A scheme of feedback compensation for CMG gimbal compliance, using multiple rate sensors --- Control Moment Gyroscope [ASME PAPER 82-WA/DSC-10] 10 p1419 A83-25681

Multivariable system compensation [ASME PAPER 82-WA/DSC-19] 10 p1462 A83-25682

Development of an active optical mirror for astronomical applications 10 p1482 A83-25829

Image quality and high resolution in future telescopes 10 p1482 A83-25832

A new class of stabilizing controllers for uncertain dynamical systems 10 p1462 A83-25997

Characterization of the dynamical response of receivers to fading 10 p1404 A83-26471

Control science and technology for the progress of society; Proceedings of the Eighth Triennial World Congress, Kyoto, Japan, August 24-28, 1981. Volume 1 - Control theory 10 p1463 A83-26501

On stabilization of classes of nonlinear systems with state observers 10 p1463 A83-26505

The internal model principle of regulator theory on differentiable manifolds 10 p1464 A83-26517

On receding horizon feedback control 10 p1464 A83-26518

On the compensation in linear feedback control systems - Transfer functions attainable by realizable linear compensation 10 p1464 A83-26519

Suboptimal feedback control with inaccessible state variables via moving model 10 p1464 A83-26521

The manipulation of interaction effects in multivariable feedback systems 10 p1465 A83-26525

D-decomposition in the space of feedback gains for arbitrary pole regions 10 p1465 A83-26526

An asymptotic analysis of interactions of feedback loops with parasitics in actuators and sensors 10 p1465 A83-26527

New results on stationary stochastic feedback processes 10 p1466 A83-26542

Stochastic control and identification enhancement for the flutter suppression problem 10 p1379 A83-26544

Schemes for multivariable parameter-adaptive deadbeat control 10 p1467 A83-26549

Possible evolution of feedback types and their applications in control of nonstationary plants 10 p1467 A83-26555

Design of model reference adaptive control systems with arbitrarily small error 10 p1468 A83-26557

Model reference invariant control for a class of unknown multivariable plants 10 p1468 A83-26558

A design procedure for linear multi-variable feedback systems 10 p1468 A83-26564

Frequency domain structure for disturbance rejection 10 p1468 A83-26565

Multivariable limit cycle prediction - A new approach 10 p1468 A83-26566

Algebraic and topological aspects of the servo problem for lumped linear systems 10 p1469 A83-26567

Scalar output feedback in linear multivariable systems 10 p1469 A83-26568

Perfect and subperfect regulation in linear multivariable control systems 10 p1469 A83-26569

The linear servomechanism with non-unity feedback 10 p1469 A83-26570

Feedback, optimal sensitivity, and plant uncertainty via multiplicative seminorms 10 p1469 A83-26572

Structural optimality of linear optimal control 10 p1469 A83-26573

Robust control of tracking problem with internal stability for linear structured system 10 p1469 A83-26575

A sensitivity analysis of modal controller for flexible space structures 10 p1385 A83-26587

Closed loop magnetic control of spin rate and pointing normal to the orbit for a polar orbiting spin stabilized satellite 10 p1385 A83-26588

Software for automatic control of spacecraft instruments 10 p1382 A83-26598

Multivariable approach to the problem of structural cross coupling of force feedback electrohydraulic actuators --- for structural testing of aircraft and their components 10 p1379 A83-26601

An optimal guidance law via first order inertial loop 10 p1469 A83-26770

Self-learning of sensor-motor control sequences 11 p1647 A83-27490

Mode structure of a DFB gas laser 11 p1578 A83-27547

Problems associated with correlation-loop adaptive antennas employing hard limiting 11 p1554 A83-27910

The vibro-mass gyroscope 12 p1728 A83-28844

The control of linear multivariable systems in the presence of harmonic disturbances 12 p1769 A83-28845

Robust controller design for linear dynamic systems using approximate models 12 p1770 A83-29521

Multivariable system theory and design --- Book 12 p1770 A83-29536

Control design and performance analysis of a 6 MW wind turbine-generator 12 p1750 A83-29897

Construction of algorithms for the automatic control of the force operations of manipulator robots 13 p1910 A83-30089

Control techniques to improve Space Shuttle solid rocket booster separation 13 p1811 A83-30164

Behavior of phase-locked loops in the presence of large interfering signal 13 p1834 A83-30785

Closed-loop YIG filters stay on frequency 13 p1835 A83-30914

Optical mode control in the free-electron laser 13 p1854 A83-31121

Optimal input/output feedback with structure constraints 13 p1911 A83-31356

Low-cost digital random vibration control (DRVC) technology demonstration 13 p1862 A83-31488

Differential-geometric methods in control theory 13 p1911 A83-31723

Controller design for linear multivariable feedback systems with stable plants, using optimization with inequality constraints 14 p2074 A83-31926

Finite-dimensional servomechanism design for parabolic distributed-parameter systems 14 p2074 A83-31927

Stability of override control systems 14 p2074 A83-31928

An algebraic algorithm for determining the desired gain of multivariable feedback systems 14 p2074 A83-31930

The choice and use of normal approximations to transfer-function matrices of multivariable control systems 14 p2074 A83-31932

Uniform ultimate boundedness of the solutions of uncertain dynamic delay systems with state-dependent and memoryless feedback control 14 p2074 A83-31933

Regulated converter circuit for direct photovoltaic energy feedback into the power grid 14 p2004 A83-32217

Power conditioning in solar photovoltaic array applications 14 p2040 A83-32218

Globally stable nonlinear flight control system 14 p1977 A83-32425

Nondegenerative conditions and physical realizability of multivariable linear feedback systems 14 p2077 A83-33157

Linear dynamic output feedback - Invariants and stability [AD-A129968] 14 p2077 A83-33447

Design of unity feedback systems to achieve arbitrary denominator matrix 14 p2077 A83-33449

Dynamic switching of Type-I/Type-II structures in tracking servosystems 14 p2077 A83-33450

Optimal-control of nonlinear systems 15 p2220 A83-33525

Quasi-dynamical systems and the stabilization of elastic vibrations with controls whose range is restricted to a finite number of values 15 p2220 A83-33875

Using adaptive control to synthesize invariant and partially autonomous automatic stabilization systems 15 p1213 A83-33900

Structural control research and experiments at NASA/LaRC 15 p2220 A83-33968

Information theory and causal information transmission with feedback 15 p2221 A83-35104

On the decoupling of linear systems into single input-multiple output subsystems 15 p2221 A83-35110

Generic pole assignment using dynamic output feedback 15 p2221 A83-35112

Conflict resolution protocols for random multiple-access channels with binary feedback 15 p2147 A83-35122

The Riccati equation, imprimitive actions and symplectic forms --- with application to decentralized optimal control problem 15 p2222 A83-35124

Optimal quantized control 15 p2222 A83-35125

A servo compensator design approach for variable structure systems 15 p2222 A83-35126

Some results on stability and stabilization of systems with retardation 15 p2222 A83-35127

A fast and efficient digital simulation technique for control systems 16 p2404 A83-35348

Aircraft active controls - New era in design 16 p2311 A83-35773

A new approach for the design of multivariable feedback systems 16 p2405 A83-36453

Algorithm for solving a class of phase-lock-loop equations 16 p2347 A83-36476

An automatically controlled predistorter for multilevel quadrature amplitude modulation 16 p2347 A83-36608

Some critical questions about deterministic and stochastic adaptive control algorithms 16 p2406 A83-36978

Parameter estimation and control of distributed systems with application to large deployable antennae 17 p2475 A83-37077

A Z-domain controller design method for sampled-data systems having feedback dynamics 17 p2565 A83-37083

Displacement control of elastic structures - Integral control with a robustness property 17 p2565 A83-37090

Nonlinear multivariable design by total synthesis --- of gas turbine engine control systems 17 p2467 A83-37092

Some necessary conditions for steepest descent controllability 17 p2566 A83-37099

Gain optimization with nonlinear controls 17 p2566 A83-37109

Controller design for uncertain nonlinear systems 17 p2566 A83-37110

Parameter-adaptive state space controller for nonlinear processes 17 p2566 A83-37111

Maximum entropy stochastic approach to control design for uncertain structural systems 17 p2567 A83-37114

Multivariable sensitivity reduction and decentralized control 17 p2567 A83-37118

I-O stability analysis of multiple nonlinear-multivariable systems 17 p2567 A83-37119

Model reference adaptive control with inexact model matching. I 17 p2568 A83-37126

Fundamental issues in guidance and control of uncertain systems 17 p2568 A83-37132

Quadratic weight adjustment for the enhancement of feedback properties 17 p2568 A83-37138

Optimal control for interception and rendezvous problems with delay - A state-feedback realization 17 p2568 A83-37140

Frequency-shaped penalty functions for robust control design 17 p2568 A83-37143

Structural information in robustness analysis 17 p2568 A83-37144

A variable structure approach to robust control of VTOL aircraft 17 p2470 A83-37145

Asymptotic expansions of singularly perturbed Chandrasekhar type of equations 17 p2571 A83-37146

Validation techniques for spot attitude control system development 17 p2477 A83-37439

Design of reaction jet attitude control systems for flexible spacecraft 17 p2479 A83-37471

Testing and investigations of reaction wheels 17 p2479 A83-37478

Software for the closed loop control of experiments on the GEOS spacecraft 17 p2472 A83-37483

Impact of spacecraft design on remote control of satellite operations 17 p2479 A83-37490

Asymptotic unbounded root loci - Formulas and computation 17 p2571 A83-37548

Feedback, minimax sensitivity, and optimal robustness 17 p2569 A83-37549

Singularly perturbed systems with low sensitivity to model reduction 17 p2570 A83-38030

Frequency responses to minimize output disturbances caused by parameter variations and noise 17 p2570 A83-38817

An optimal design approach for the robust controller problem 17 p2570 A83-38818

Robust stability - Parameter-dependent perturbations 17 p2570 A83-38819

On model-following using measured output feedback 17 p2570 A83-38820

A synthesis theory for a class of saturating systems --- in feedback control 17 p2570 A83-38821

The immersion under feedback of a multidimensional discrete-time non-linear system into a linear system 17 p2570 A83-38823

Threshold-wavelength and threshold-temperature dependences of GaInAsP/InP lasers with frequency selective feedback operating in the 1.3- and 1.5-micron regions 18 p2693 A83-40057

Conventional controller design for industrial robots - A tutorial 19 p2824 A83-41295

Control and its applications; Proceedings of the International Conference, Warwick, England, March 23-25, 1981 19 p2890 A83-41476

A new approach to exact model-matching with applications to aircraft systems 19 p2890 A83-41477

Discrete control scheme design for multi input multi output systems 19 p2890 A83-41478

Dominance optimisation in multivariable design 19 p2890 A83-41479

Sensitivity synthesis of systems subject to large parameter variations 19 p2890 A83-41480

An adaptive mechanism for a non-linear control system 19 p2890 A83-41483

The use of structural properties in multivariable model reduction and control system design 19 p2890 A83-41487

A numerical method for the analysis of harmonic balance conditions in multiloop non-linear feedback systems 19 p2891 A83-41489

Design of feedback controllers for nonlinear systems 19 p2891 A83-41491

Regulator design for the F100 turbofan engine 19 p2800 A83-41492

Robustness analysis of a multiloop flight control system [AIAA PAPER 83-2189] 19 p2802 A83-41675

The use of singular value gradients and optimization techniques to design robust controllers for multiloop systems [AIAA PAPER 83-2191] 19 p2891 A83-41677

Control of forward swept wing aeroelastic instabilities using active feedback systems [AIAA PAPER 83-2220] 19 p2803 A83-41701

Pilot modeling and closed-loop analysis of flexible aircraft in the pitch tracking task [AIAA PAPER 83-2231] 19 p2803 A83-41709

Design of reduced order optimal state estimators with applications to stochastic linear optimal regulators [AIAA PAPER 83-2277] 19 p2892 A83-41743

Reduction of large flexible spacecraft models using internal balancing theory [AIAA PAPER 83-2292] 19 p2817 A83-41751

Optimization and closed loop guidance of drag modulated aeroassisted orbital transfer [AIAA PAPER 83-2093] 19 p2810 A83-41923

Acquisition performance of 2nd-order phase-locked loops in the presence of time delay for switched and swept signal conditions 20 p2964 A83-43168

Choice of parameters for ergatic stabilization systems 20 p3035 A83-43501

Deadbeat control in multivariable non-linear time-varying systems with constraints of control inputs 20 p3040 A83-43620

Tracking control of non-linear systems using sliding surfaces, with application to robot manipulators 20 p3040 A83-43621

Airborne radar tracking system based on optimal filtering theory 20 p2932 A83-43696

On stabilizing uncertain systems 21 p3192 A83-44008

Finite-dimensional discrete-time control of linear distributed parameter systems 21 p3192 A83-44009

Solution methods for the enhanced modal control Riccati equation 21 p3193 A83-44018

On modern modal controller for flexible space structures - A sensitivity analysis 21 p3099 A83-44032

General conditions on reduced-order control for ensuring full-order closed-loop asymptotic stability --- of large space structures 21 p3099 A83-44033

Optimal independent modal space control of a flexible system including integral feedback 21 p3193 A83-44034

First order solution of the optimal control problem for distributed parameter elastic system 21 p3193 A83-44040

Nonlinear feedback control of spacecraft slew maneuvers [AAS PAPER 83-002] 21 p3193 A83-44162

Digital control system design for a precision pointing system [AAS PAPER 83-003] 21 p3103 A83-44163

Simulation of hot spot tracking loops [AAS PAPER 83-007] 21 p3104 A83-44166

The stability of a controlled gyrohorizon-compass during the maneuvering of an object 21 p3138 A83-44636

A curvilinear snake arm robot with gripper-axis fibre-optic image processor feedback 21 p3119 A83-44695

Adaptive optical system for astronomical applications 21 p3206 A83-44808

Output feedback pole assignment under system variation --- with CH-46 example 21 p3195 A83-44948

Multivariable feedback: A quasi-classical approach --- Book 21 p3195 A83-45100

Spillover and model error bounding techniques for large scale systems 21 p3195 A83-45104

Numerical implementation of suboptimal output feedback control for large space structures 21 p3195 A83-45105

An alternative view of the optimal output feedback compensator problem 21 p3195 A83-45106

Minimum information approach to regulator design - Numerical methods and illustrative results 21 p3195 A83-45108

Control of a large class of flexible systems 21 p3102 A83-45129

On the uniqueness of the independent modal-space control method 21 p3102 A83-45130

An integrated approach to optimal reduced order control theory 21 p3196 A83-45131

Exact pole assignment using direct or dynamic output feedback 21 p3196 A83-45135

Feedback strategies for partially observable stochastic systems --- Book 21 p3197 A83-45142

Dislocated actuator/sensor positioning and feedback design for flexible structures 21 p3103 A83-45465

Closed-loop control performance sensitivity to parameter variations --- applied to orbiting large space structures 21 p3103 A83-45471

Automation of the thermal spray process [SAE PAPER 820610] 22 p3301 A83-45868

Stabilization and structural assignment of Dirichlet boundary feedback parabolic equations 22 p3351 A83-46093

Linear feedback decoupling - Transfer function analysis 22 p3351 A83-46365

State-feedback decomposition of multivariable systems via block-pole placement 22 p3351 A83-46367

On asymptotically stabilizing feedback control of bilinear systems 22 p3352 A83-46370

Phase-Nulling Fiber Optic Gyro development review 22 p3292 A83-46658

Spectrophon stabilization and offset tuning of a carbon dioxide waveguide laser 22 p3300 A83-46816

The involuntary regulation of the GSR --- Galvanic Skin Response 23 p3497 A83-47108

Control of reflector vibrations in large spaceborne antennas by means of movable dampers 23 p3423 A83-47598

The impact of computers on the test cell of tomorrow --- for gas turbine engine tests [ASME PAPER 83-GT-187] 23 p3409 A83-47993

Application of a method of averaging to the study of dithers in non-linear systems 23 p3502 A83-48646

Asymptotic behavior of the closed loop poles of linear optimal multivariable systems 23 p3502 A83-48676

Reduced-order observers for linear multivariable systems with disturbance and tracking signal accommodation 24 p3620 A83-49896

Design of digital two- and three-term controllers for discrete-time multivariable systems 24 p3620 A83-49897

Characterization of equilibrium sets for bilinear systems with feedback control 24 p3621 A83-49923

Self-error feedback in recursive digital filters 24 p3621 A83-50197

Servo-system design technique utilising sensitivity as a design parameter 24 p3621 A83-50198

Offset problem and k-incremental predictors in self-tuning control 24 p3622 A83-50199

A conditional algorithm for setting a discrete device with memory to a definite state 24 p3622 A83-50206

FEEDBACK FREQUENCY MODULATION

Experimental study of the frequency characteristics of gas ring lasers with additional feedback 01 p0056 A83-11344

Precision phase comparison via communication satellites using loop-back tones 10 p1403 A83-26042

Effectiveness of the frequency-adaptive parallel transmission of discrete signals 10 p1407 A83-26936

Theory on distributed feedback /DFB/ lasers including strong modulations 11 p1578 A83-27548

FEEDFORWARD CONTROL

Stability multipliers and multivariable circle criteria 01 p0095 A83-10957

A novel input filter compensation scheme for switching regulators 01 p0044 A83-11494

Fixed-trim re-entry guidance analysis 03 p0287 A83-14840

Robustness properties of model-reference adaptive control systems 04 p0529 A83-16193

Introduction of feedforward control for an improved optimal regulator system and its application 06 p0804 A83-19393

Extended perfect model following --- control system synthesis technique 07 p0984 A83-20289

Minimal-order realizations for continuous-time 2-power input-output maps 09 p1329 A83-24730

Generalized error coefficients for the multivariable servomechanism problem 09 p1334 A83-24813

Frequency domain structure for disturbance rejection 10 p1468 A83-26565

A novel feedforward compensation canceling input filter-regulator interaction 14 p2007 A83-33133

Frequency responses to minimize output disturbances caused by parameter variations and noise 17 p2570 A83-38817

FEELINGS

U SENSORY FEEDBACK

FEET (ANATOMY)

Restoration of thermoregulatory response to body cooling by cooling hands and feet 03 p0378 A83-13578

An investigation of the Achilles reflex in standing humans 12 p1765 A83-29317

The regulation by the human foot of the balance of the mechanical system of the 'inverted pendulum' type. I - The significance of the speed of motion. II - The role of the position of the center of gravity and temporal programs 23 p3497 A83-47117

FELDSPARS

Thermal annealing of experimentally shocked feldspar crystals 04 p0564 A83-15375

Rock 67015 - A feldspathic fragmental breccia with KREEP-rich melt clasts 07 p1033 A83-21299

Geochemical studies of feldspathic fragmental breccias and the nature of North Ray Crater ejecta 07 p1033 A83-21300

An analytical and experimental study of zoning in plagioclase 22 p3332 A83-46711

FUN with PANURGE - High mass resolution ion microprobe measurements of Mg in Allende inclusions --- meteoritic composition isotope analysis 24 p3672 A83-49350

FELLOWSHIP AIRCRAFT

U F-28 TRANSPORT AIRCRAFT

FEMALES

- Selection and prediction of the athletic results of young female long-jumpers 03 p0382 A83-14353
- Manual parachute ripcord pull-force capability of female naval personnel 04 p0525 A83-15410
- Increased hematuria following hypergravic exposure in middle-aged women 11 p1643 A83-27844
- Some methodological approaches to the evaluation of the morbidity with temporary loss of work capacity of women working in the metro 15 p2212 A83-34934
- The phospholipid content of subfractions of high-density lipoproteins in women with angiographically documented atherosclerosis of the coronary arteries 18 p2735 A83-40543
- The condition of the physiological functions of female workers occupied with visually stressful types of work at a low level of motor activity 19 p2882 A83-41454
- The functional condition of the body and several specific functions of women construction workers engaged in finishing work in hot climatic conditions 19 p2882 A83-41455
- The content of gonadotropin hormones and hydrocortisone in women during adaptation to conditions of high latitudes 23 p3497 A83-47104
- Psychiatric assessment of female fliers at the U.S. Air Force School of Aerospace Medicine (USAFSAM) 24 p3618 A83-48883

FERMENTATION

- Applications of mutant yeast strains with low glycogen storage capability 02 p0220 A83-11827

FERMI LIQUIDS

- Observation of high-field superconductivity of a strongly interacting Fermi liquid in U6Fe 19 p2904 A83-40958
- Ordered pairing in liquid metallic hydrogen 19 p2899 A83-41867

FERMI SURFACES

- Correlation of Fermi-level energy and chemistry at InP /100/ interfaces 08 p1170 A83-22766
- The effect of light soaking on the low temperature photoconductivity of hydrogenated amorphous silicon 18 p2749 A83-39470
- Classical magnetoresistance of a two-dimensional electron gas in a one-dimensional superlattice 20 p3051 A83-42283
- Fermi levels in electrolytes and the absolute scale of redox potentials 20 p2951 A83-43608

FERMI-DIRAC STATISTICS

- Statistical mechanics of light elements at high pressure. V Three-dimensional Thomas-Fermi-Dirac theory --- relevant to Jovian planetary interiors 21 p3242 A83-45563

FERMIONS

- NT ANTINEUTRINOS
- NT BARYONS
- NT CONDUCTION ELECTRONS
- NT FAST NEUTRONS
- NT LEPTONS
- NT MUONS
- NT NEUTRINOS
- NT NEUTRONS
- NT PROTONS
- NT SOLAR NEUTRINOS
- NT SOLAR PROTONS
- NT THERMAL NEUTRONS
- Generalized theory of gravitation and its physical consequences 01 p0127 A83-11292
- Possible new long-range interaction and methods for detecting it 07 p0989 A83-20609
- Upper bound on gauge-fermion masses 07 p0992 A83-20814
- Astrophysical consequences of barytinos 12 p1794 A83-29085
- Fermion-induced monopole-antimonopole annihilation 13 p1954 A83-31606
- On the statistical distribution off massive fermions and bosons in a Friedmann universe 23 p3518 A83-47442

FERRATES

- Hexagonal ferrites for millimeter wave applications 03 p0399 A83-13786

FERRIMAGNETS

- Electromagnetic waves in a doubly periodic array of circular longitudinally magnetized ferrite rods 17 p2494 A83-38477

FERRITES

- Realization of selective microwave networks on the basis of ferrite resonators 04 p0470 A83-15717
- Hexaferrite gate-flanges in the 3-4 millimeter range 04 p0470 A83-15719
- Magnetostatic volume wave propagation in multiple ferrite layers 04 p0473 A83-16076
- Nonreciprocal devices in open-boundary structures for millimeter-wave integrated circuits 05 p0624 A83-17278

Practical millimeter-wave ferrite phase shifters

- 05 p0625 A83-17342
- Cryogenic X-band ferrite phase shifter/attenuator 08 p1079 A83-21977
- Modes of propagation in slot line with layered substrate containing magnetised ferrite 08 p1081 A83-22918
- The low-frequency limit of the application of ferrite circulators 10 p1412 A83-26940
- Natural modes of a periodic array of rectangular longitudinally magnetized ferrite rods 11 p1561 A83-27966
- Nonreciprocal element on the basis of hexaferrites in millimeter-wave masers 11 p1562 A83-27967
- Magnetostatic waves with complex wavenumbers in a lossless ferrite film 15 p2153 A83-35163
- Nonreciprocal phaseshift in ferrite loaded rectangular waveguides 19 p2841 A83-42165
- Analysis of coupled asymmetric microstrip lines on a ferrite substrate 24 p3574 A83-49970

FERRITIC STAINLESS STEELS

- Chemically driven cavity growth 07 p0887 A83-20632
- Oxide scale induced cleavage fracture in an ODS Fe-Cr-Al alloy 18 p2670 A83-40639

FERROALLOYS**U IRON ALLOYS****FERROELECTRICITY**

- Ferroelectricity and coherent phonon generation in piezoelectric composition-modulated structures 01 p0108 A83-10622
- Asymmetry of conductivity along the polarization axis in ferroelectric crystals 04 p0542 A83-15885
- Photovoltaic properties of ferroelectric BaTiO3 thin films RF sputter deposited on silicon 04 p0473 A83-16078
- Piezoelectric and pyroelectric coefficients for ferroelectric crystals with polarizable molecules 05 p0690 A83-17227
- Polarization catastrophe model of static electrification and spokes in the B-ring of Saturn 07 p1028 A83-20083
- Parametric regeneration in ferroelectric resonators 07 p0921 A83-20873
- Ferroelectric crystals for the control of laser radiation --- Russian book 09 p1271 A83-23815
- The features of the atomic structure of pure inorganic ferroelastics 13 p1928 A83-30311
- Applications of ferroelastics 13 p1832 A83-30312
- The dielectric permittivity tensor and its spontaneous rotation in the submillimeter range for the ferroelastics KH3(SeO3)2 and KD3(SeO3)2 13 p1928 A83-30313
- The influence of defects on the switching of the pure ferroelastic KH3(SeO3)2 13 p1928 A83-30314
- The Barkhausen effect and viscous phenomena in gadolinium molybdate single crystals 13 p1928 A83-30315
- Structural studies of new series of crystals 13 p1928 A83-30316
- All-Union Conference on Ferroelectricity, 10th, Minsk, Belorussian SSR, September 19-23, 1982, Proceedings 13 p1930 A83-31301
- Experimental study of the photovoltaic effect in piezoelectric and ferroelectric crystals 13 p1930 A83-31302
- Correlation of the electron spectra and temperatures of phase transformations in solid solutions based on barium titanate 13 p1930 A83-31305
- Viscosity phenomena in ferroelectrics and ferroelastics 13 p1930 A83-31309
- A model for photovoltaic centers in ferroelectrics 14 p2088 A83-32169
- Raman scattering of light during phase transitions in crystals 14 p2092 A83-33038
- The theory of phase transitions in certain systems with electromagnetic interaction and its application to ferroelectrics 14 p2092 A83-33041
- A continuum mechanical approach to the ultrasonic relaxation of ferroelectric materials 15 p2238 A83-34348
- Ferroelectric transducers and sensors 19 p2848 A83-41527
- Channeled acoustic waves - Elastic waves of a new type of polydomain ferroelectrics 24 p3634 A83-48866

FERROFLUIDS

- Theory of lubrication with ferrofluids - Application to short bearings [ASME PAPER 81-LUB-39] 02 p0186 A83-11940
- Overall characteristics of bearings lubricated with ferrofluids [ASME PAPER 82-LUB-14] 03 p0335 A83-13508
- Structured films of magnetizable surfactants 06 p0813 A83-19552
- Flow of a thin fluid layer covered by a magnetizable surfactant 12 p1781 A83-29263

FERROMAGNETIC FILMS

- Propagation of magnetostatic waves in a structure with a tangentially magnetized anisotropic ferrite layer 15 p2152 A83-34711

FERROMAGNETIC MATERIALS**NT FERROFLUIDS****NT FERROMAGNETIC FILMS****NT MAGNETITE**

- Ferromagnetics --- Russian book 09 p1349 A83-23817
- Magnetic semiconductors --- Russian book 14 p2091 A83-32574
- Temperature dependence of the relaxation decay time and the integrated intensity of the photoluminescence from the magnetic semiconductor CdCr2Se4 14 p2085 A83-33429
- Undulator radiation of relativistic electrons in a polydomain ferromagnetic 15 p2150 A83-33782
- New class of materials - Half-metallic ferromagnets 16 p2421 A83-36564
- Direct optical observation of ferromagnetic domains 17 p2585 A83-38611
- Nondestructive inspection by the method of magnetic leakage fields - Theoretical and experimental foundations of the detection of surface cracks of finite and infinite depth 20 p3000 A83-43178
- On the optimum applied field for magnetic particle inspection using direct current 21 p3149 A83-44472

FERROMAGNETIC RESONANCE

- Ferromagnetic resonance g-factor measurement on LUNA 20 soil 03 p0432 A83-13297
- Ferromagnetic resonance intensity - A rapid method for determining lunar glass bead origin 04 p0561 A83-15344
- The Apennine Front core 15007/8 - Irradiational and depositional history 04 p0561 A83-15347
- Nonreciprocal element on the basis of hexaferrites in millimeter-wave masers 11 p1562 A83-27967
- Ferromagnetic resonance and magnetic properties of ALHA 81005 22 p3386 A83-46869

FERROMAGNETISM

- Comparison of magnetic fields computed by finite element and classical series methods 08 p1082 A83-22945
- Ferromagnetics --- Russian book 09 p1349 A83-23817
- Undulator radiation of charged particles moving above a domain structure 10 p1472 A83-26243
- The use of the intrinsic fields of magnetically soft bodies to determine the components of a magnetizing field 14 p2078 A83-31873
- Influence of polarized optical pumping on the ferromagnetism of CdCr2Se4 15 p2237 A83-33798
- Is magnetic flux quantized in a toroidal ferromagnet? 19 p2895 A83-40962

FERROUS METALS

- Modern developments in powder metallurgy. Volume 13 - Ferrous and nonferrous materials --- Book 06 p0730 A83-19082
- Atomic absorption analysis in ferrous metallurgy --- Russian book 21 p3114 A83-45008

FERTILIZERS

- Factors influencing the loss of fertilizer nitrogen into the atmosphere as N2O 20 p3014 A83-42851

FET (TRANSISTORS)**U FIELD EFFECT TRANSISTORS****FETUSES**

- The autoallergic effect of microwaves and their influence on fetus and offspring 05 p0670 A83-17190

FFT**U FAST FOURIER TRANSFORMATIONS****FIBER COMPOSITES**

- NT CARBON FIBER REINFORCED PLASTICS
- NT GLASS FIBER REINFORCED PLASTICS
- Orthogonal fibre composites as micromorphic materials 01 p0044 A83-10274
- Present state of methods for static testing of composites /Review/ 01 p0022 A83-10297
- Shear force effect on the static deformations of straight bars 01 p0059 A83-10587
- Theory of thermal conductivity, heat conduction and convective heat transfer in fiber filled polymer composites 02 p0149 A83-11804
- Determining the composition and homogeneity of polymer-polymer fiber composites 02 p0150 A83-12367
- Rheology of fiber- or flake-filled plastics 02 p0150 A83-12825
- Designing composites for maximum toughness 02 p0151 A83-12970
- Analysis of bonded repairs to damaged fibre composite structures 03 p0291 A83-13200
- A unifying strain criterion for fracture of fibrous composite laminates 03 p0291 A83-13340
- Stiffness-reduction mechanisms in composite laminates 03 p0292 A83-14558

Effect of thermal cycle on the phase boundary of SiC/Ni monofilament composite 04 p0454 A83-14964
 Double torsion fracture toughness test for evaluating transverse cracking in composites 04 p0455 A83-15996
 Short fiber technology 04 p0455 A83-16177
 The fracture of a unidirectional fiber composite with an elastoplastic matrix under compression 06 p0725 A83-18503
 Stress redistribution in the ruptured fiber of a viscoelastic composite 06 p0725 A83-18504
 Length distribution of ruptured fibers in unidirectional composites 06 p0725 A83-18516
 Applications for Nextel in the aerospace industry 07 p0899 A83-20466
 The effect of matrix strain limitations on composite design allowables 07 p0877 A83-20495
 Microstructure of fiber and particulate SiC in 6061 Al composites 07 p0877 A83-20634
 Fracture behaviour of a single-fibre graphite/epoxy model composite containing a broken fibre or cracked matrix 07 p0877 A83-21565
 Fibre length-strength relationships and the fracture of composites 08 p1053 A83-21678
 Monte Carlo simulation of the strength of hybrid composites 08 p1120 A83-21819
 Development of an improved, lightweight insulation material for the Space Shuttle Orbiter's thermal-protection system 08 p1049 A83-22260
 Refractory-ceramic-fiber composites - Progress, needs, and opportunities 08 p1055 A83-22267
 Note on the postbuckling analysis of cross-ply laminated plates with elastically restrained edges and initial curvatures 08 p1123 A83-22414
 An evaluation of certain properties of fiber-reinforced composites through bending tests 08 p1055 A83-22993
 An analysis of delamination in drilling composite materials 09 p1273 A83-23640
 Stochastic models of fracture of unidirectional fiber composites 09 p1222 A83-23927
 The effect of interface structure on the strength of fibrous composite materials 09 p1224 A83-23943
 An estimation of the compressive strength of a fibrous composite 09 p1224 A83-23944
 Manufacture and testing of fibre composite rotor components /Fibre composite flywheel development program for road vehicle applications/ 11 p1667 A83-27308
 Measurement of local stress distributions in damaged composites using an electric analogue 11 p1592 A83-27438
 Redistribution of stresses in a fractured fiber during its delamination from the viscoelastic matrix of a composite material 11 p1597 A83-28471
 Stress distribution in a strongly anisotropic elastic plane with a parabolic cutout 11 p1598 A83-28486
 The calculation of energy storage flywheels of fiber composites with electric energy converter --- German thesis 11 p1590 A83-28666
 Reproducible processing and reliable repeatability in carbon fiber composite 12 p1710 A83-29715
 Fracture toughness/Young's modulus correlation for low-density fibrous silica bodies 12 p1717 A83-29976
 The elastic characteristics of unidirectionally reinforced hybrid composites 13 p1815 A83-30052
 A study of the structure of organic composites reinforced with polyheteroarylene fibers 13 p1815 A83-30058
 Advanced fibers and composites for elevated temperatures --- Book 14 p1986 A83-32173
 A statistical model for the time dependent failure of unidirectional composite materials under local elastic load-sharing among fibers 14 p1986 A83-32663
 A comparison of probabilistic techniques for the strength of fibrous materials under local load-sharing among fibers 15 p2130 A83-34142
 Boundary integral equations for inextensible materials 15 p2130 A83-34341
 Fatigue damage and degradation in random short-fiber SMC composite --- sheet molding compound 15 p2130 A83-34794
 Composite fiber/metal pressure vessels for propulsion systems [AIAA PAPER 83-1329] 16 p2324 A83-36343
 Fibre composites of aluminium with graphite 16 p2325 A83-36525
 The application of polyvinylidene fluoride as an acoustic emission transducer for fibrous composite materials 18 p2695 A83-39622
 Adhesive bonding and composites 18 p2650 A83-40131
 How the interface controls the properties of fibre composites 18 p2651 A83-40143
 On fibre composites with intermittent interlaminar bonding 18 p2651 A83-40151

Stress concentrations in cylindrically orthotropic plates with radial variation of the compliances 18 p2703 A83-40165
 Analysis of compression failures in fibre composite laminates 18 p2653 A83-40172
 Stiffness and strength properties of woven composites 18 p2703 A83-40177
 Buckling of continuous filament composite isogrid panels Theory and experiment 18 p2704 A83-40183
 Damage analysis of fibrous composites 18 p2654 A83-40189
 Effect of combination of glass mat and cloth on the fatigue properties of fibrous composite materials 18 p2655 A83-40206
 A statistical approach to the strength of hybrid composites 18 p2658 A83-40242
 New composite materials with a carbon-titanium carbide hybrid matrix for high temperature application 18 p2658 A83-40245
 Interface interaction in aluminum-carbon system 18 p2658 A83-40247
 Formation of intermetallic compound in composite materials 18 p2658 A83-40248
 Tensile property evaluation of polycrystalline alumina filaments and their composites 19 p2819 A83-41032
 The random variation of stress concentration factors in fibrous composites 20 p3007 A83-43398
 Polar-scan - A nondestructive test method for the inspection of layer orientation and stacking order in advanced fiber composites 21 p3148 A83-43828
 Bilinear failure analysis of fiber composite laminates 21 p3106 A83-44049
 The structural dependence of the anisotropy of the elastic properties of fiber composites 21 p3107 A83-44850
 Probability distributions for the strength of composite materials. IV - Localized load-sharing with tapering 21 p3159 A83-44926
 The role of the matrix in fibrous composite structures 22 p3262 A83-46280
 A study of the thermo-oxidative process and stability of graphite and glass-PMR polyimide composites 22 p3262 A83-46285
 Constitutive relationships for sheet molding materials 22 p3263 A83-46291
 Effect of fiber aspect ratio on ultimate properties of short-fiber composites 22 p3264 A83-46297
 An optical technique for measuring fiber orientation in short fiber composites 22 p3290 A83-46298
 Design of continuous fiber composite structures 22 p3264 A83-46306
 Shear waves in fiber composites 23 p3427 A83-47171
 Hingeless and bearingless main rotor in a fiber composite type of construction for dynamic systems of future helicopters 23 p3402 A83-47195
 Composite interphase characterization 23 p3427 A83-47424
 Stiffness changes in unidirectional composites caused by crack systems. 23 p3428 A83-48602
 The effective moduli of short-fiber composites 23 p3474 A83-48697

FIBER OPTICS

Light transmission optics /2nd edition/ --- Book 01 p0106 A83-10879
 Low loss poly/methyl methacrylate-d5/ core optical fibers 01 p0106 A83-10895
 Fiber optic aircraft multiplex systems - Planning for the 1990s 01 p0006 A83-11180
 Fiber optics wavelength division multiplexing for aircraft applications 01 p0006 A83-11181
 Video distribution requirements for future tactical aircraft 01 p0006 A83-11182
 Description and planned use of a data distribution evaluation system for fiber optic data buses 01 p0006 A83-11183
 Distributed processing and fiber optic communications in air data measurement 01 p0011 A83-11258
 Demonstration of image transmission through fibers by optical phase conjugation 02 p0235 A83-11568
 Sensitive, high-speed thermometry using optical fibers 02 p0175 A83-11569
 Source statistics and the Kerr effect in fiber-optic gyroscopes 02 p0176 A83-11570
 Broadband infrared generation in liquid-bromine-core optical fibers 02 p0183 A83-11571
 Polarization properties of single-polarization fibers 02 p0235 A83-11572
 Fibre-optic laser Doppler anemometer with Bragg frequency shift utilising polarisation-preserving single-mode fibre 02 p0177 A83-12010
 Suppressed turn-on laser regenerative optoelectronic amplifier 02 p0185 A83-12301
 Optical sensor for measurement of position and deformations of models in wind tunnel 02 p0178 A83-12347

OTDR in single-mode fibre at 1.55 micron using a semiconductor laser and PINFET receiver 02 p0185 A83-13042
 Experiments with optical solitons 03 p0390 A83-13428
 Transport of solar energy with optical fibres 03 p0354 A83-13698
 Integrated optical logic devices 03 p0392 A83-13756
 Single-mode fiber-to-channel waveguide coupling 03 p0393 A83-13758
 Development of the multiwavelength monolithic integrated fiber optics terminal 03 p0393 A83-13760
 Components for angular division multiplexing --- for increasing optical fiber information capacity 03 p0394 A83-13775
 Fiber optic pulse compression concept for processing wide bandwidth radar signals 03 p0304 A83-13790
 Ultraviolet measurements, methods and production 03 p0394 A83-13968
 Fiber optics for the future - Wavelength division multiplexing 03 p0395 A83-14122
 Multimode optical fibers as sensing devices 03 p0329 A83-14377
 Electric field detection with a piezoelectric polymer-jacketed single-mode optical fiber 03 p0330 A83-14384
 Transmission of pulse sequences through monomode fibers 03 p0395 A83-14385
 Birefringence variation with temperature in elliptically clad single-mode fibers 03 p0395 A83-14386
 Measurement of stresses in optical fiber and preform 03 p0395 A83-14387
 Paraxial imaging and transforming in a medium with gradient-index Transmittance function 03 p0395 A83-14388
 Loss analysis of laser-fiber coupling and fiber combiner, and its application to wavelength division multiplexing 03 p0395 A83-14389
 Optical coherence effects on a fiber-sensing Fabry-Perot interferometer 03 p0330 A83-14390
 Splicing of single-polarisation fibres by an optical short-pulse method 04 p0534 A83-15235
 Fibre-optic variable delay lines 04 p0534 A83-15236
 Temperature sensing in twisted single-mode fibres 04 p0481 A83-15242
 Low-loss quadruple-clad single-mode lightguides with dispersion below 2 ps/km nm over the 1.28-1.65 micron wavelength range 04 p0534 A83-15243
 Nonreciprocal circuit for laser-diode-to-single-mode-fibre coupling employing a YIG sphere 04 p0534 A83-15245
 BSO/fibre-optic voltmeter with excellent temperature stability 04 p0481 A83-15250
 The resolving power of a reflectometer with compensation of background reflections 04 p0482 A83-15714
 Smoothing of output-signal fading for a fiber ring interferometer, determined by instabilities of the parameters of a one-mode fiber-optic waveguide 04 p0482 A83-15747
 The controlled non-linear evolution of TE and TH ps-pulses in Selfoc fibre 04 p0535 A83-15791
 Spatial coherence of laser light propagating in an optical fibre 04 p0535 A83-15793
 Simple spectral control technique for external cavity laser transmitters 04 p0485 A83-16023
 Fiberoptics technology and its application to propulsion control systems 05 p0595 A83-16772
 [AIAA PAPER 83-0534] Intensity-dependent nonreciprocal phase shift in fiber-optic gyroscopes for light sources with low coherence 05 p0643 A83-16842
 Birefringence correction for single-mode fiber couplers 05 p0684 A83-16843
 Stress-induced single-polarization single-mode fiber 05 p0684 A83-16844
 Fiber-optic technology takes to the air 05 p0592 A83-16867
 Generation of wide-band optical continuum in fiber waveguides 05 p0685 A83-17070
 Metal coated fibers for use in the radiation environment 05 p0685 A83-17480
 Transmission of two-dimensional images through a single optical fiber by wavelength-time encoding 05 p0685 A83-17885
 Single-mode-fiber 1 x N directional coupler 05 p0685 A83-17886
 Review - Progress of coherent optical fibre communication systems 05 p0685 A83-17887
 Observation of bifurcation to chaos in an all-optical bistable system 05 p0686 A83-17935
 Development of fibre optic sensing systems - A review 05 p0647 A83-17938

The application of fibre optics to remote speckle metrology using incoherent light

05 p0647 A83-17939

Predicting 'lifetime' of fibre optics exposed to radiation

05 p0686 A83-17941

Coherent optical-fibre sensors with modulated laser sources

06 p0762 A83-18568

Polarisation preserving single-mode-fibre coupler

06 p0809 A83-18570

Medusa spectroscopy of A400, A576, A1767, and A2124

06 p0820 A83-18856

Extremely low-loss hollow core waveguide for VUV light

06 p0810 A83-18951

Microwave fiber-optic communications systems

07 p0905 A83-19709

USAF ground fiber optic development program

07 p0906 A83-19711

Optical data-transmission equipment for computer systems - Optical data mux

07 p0983 A83-19780

Differential modal delay measurements in graded-index multimode optical waveguides

07 p0992 A83-19781

Stimulated Mandel'shtam-Brillouin scattering in a multimode glass fiber lightguide

07 p0933 A83-20046

Multichannel duplex fiber-optic communication line operating at the wavelength in the region of 1.3 micron

07 p0993 A83-20122

Application of optical fibers to wide-band differential interferometry

07 p0993 A83-20175

Monochromatic photographs of the Cygnus Loop with a fiber-optics image intensifier

07 p1006 A83-20656

A line-scanning system with fiber-optic elements

07 p0929 A83-20776

Optical Kerr effect in fiber gyroscopes - Effects of nonmonochromatic sources

07 p0930 A83-20800

Polarization backscatter analysis of field distributions using fiber optics

07 p0930 A83-20828

Dual GRIN lens wavelength multiplexer --- Graded Refractive Index

07 p0993 A83-20831

Determination of the index profile of optical fibers from transverse interferograms using Fourier theory

07 p0993 A83-20832

Cross-talk fiber-optic temperature sensor

07 p0930 A83-20833

Dynamic thermal response of single-mode optical fiber for interferometric sensors

07 p0930 A83-20834

Wavelength multiplexing in single-mode fiber couplers

07 p0993 A83-20835

Methods for analyzing optical guided wave structures

08 p1164 A83-22470

Fiber optics in adverse environments; Proceedings of the Seminar, San Diego, CA, August 25-27, 1981

08 p1164 A83-22475

Recent progress in the investigation of radiation resistant optical fibers

08 p1164 A83-22476

Radiation damage in optical fibers

08 p1164 A83-22477

X-ray induced transient attenuation at low temperatures in polymer clad silica /PCS/ fibers

08 p1165 A83-22478

Optical fiber composition and radiation hardness

08 p1165 A83-22479

Response of irradiated optical waveguides at low temperatures

08 p1165 A83-22480

Effect of ionizing radiation on fiber-optic waveguides

08 p1165 A83-22481

Vulnerability of fiber optic cables to thermal pulses

08 p1165 A83-22482

Fiber optic cables for severe environment

08 p1165 A83-22483

Cold-induced losses in loose-sheath fiber-optic cables

08 p1165 A83-22484

Optical fiber strength/fatigue experiments

08 p1073 A83-22485

Air-deployed, over-ocean, small, ruggedized optical fiber

08 p1074 A83-22486

Direct bandgap, ionizing-radiation insensitive, photodiode structures

08 p1165 A83-22487

Environmental testing of UV-cured acrylate-coated fibers

08 p1073 A83-22488

Survivability of army fiber optics systems

08 p1165 A83-22489

Space application of fiber optics systems

08 p1165 A83-22490

Fiber optic experiment for the Shuttle long-duration exposure facility

08 p1166 A83-22491

Fiber optic wavelength multiplexing for civil aviation applications

08 p1045 A83-22492

New fiber optic data bus topology

08 p1152 A83-22493

Fiber optics for aircraft engine/inlet control

08 p1046 A83-22494

Fiber optics for electro-magnetic pulse /EMP/ simulators

08 p1047 A83-22495

Wideband analog fiber optic signal link for use in the space/radiation simulator environment

08 p1049 A83-22496

Fiber optic transmitters and receivers for use in high dose-rate ionizing environments

08 p1166 A83-22497

Fiber optics as light-detector probes in the accurate measurement of detonation velocities in two-phase fuel-air explosions

08 p1095 A83-22498

Influence of semiconductor-laser phase noise on coherent optical communication systems

08 p1077 A83-22638

Propagation constants for linearly polarized modes of arbitrarily shaped optical fibers or dielectric waveguides

08 p1166 A83-22639

Image transforms with fused fiber optics

08 p1167 A83-22864

Enhanced bandgap resonant nonlinear susceptibility in quantum-well heterostructures

08 p1167 A83-22917

Enhancement of birefringence in polarisation-maintaining fibres by thermal annealing

08 p1167 A83-22921

A fiber-optic gyrometer in a gravitational field

08 p1105 A83-23165

Towards displacement measurement in remote locations by holographic fiber optics probes

09 p1264 A83-23362

An application of the Ambartsumian invariance principle to the investigation of extended lightguides with random inhomogeneities

09 p1344 A83-23484

Optical communications and laser beam acquisition performances

09 p1245 A83-23528

Use of far-field radiation pattern to characterise single-mode symmetric slab waveguides

09 p1254 A83-24118

Data systems - Optical bus will connect distributed system

09 p1215 A83-24352

Enhancement of fringe visibility in a fibre interferometer

10 p1481 A83-25405

Application of nonlinear oscillator theory to multimode fibers

10 p1481 A83-25406

A shearing, modulating interferometer --- for astronomical observation

10 p1420 A83-25838

Coherence and interferometry through optical fibers --- of stellar interferometers

10 p1482 A83-25847

External cavity controlled operation of a semiconductor diode gain element in series with an optical fiber

10 p1428 A83-26025

Inverse-square wavelength dependence of attenuation in infrared polycrystalline fibers

10 p1482 A83-26116

Laser phase noise effects in fiber-optic signal processors with recirculating loops

10 p1429 A83-26118

Real-time Fourier transformation in dispersive optical fibers

10 p1482 A83-26119

1-Gbit/s code generator and matched filter using an optical fiber tapped delay line

10 p1483 A83-26204

A dual focus fiber optic anemometer for measurements in wet steam

10 p1422 A83-26422

Fibre-optic gyro for sensitive measurement of rotation

10 p1422 A83-26474

Wedge coupling of lasers into multimode fibers

10 p1431 A83-26631

Singular value decomposition using iterative optical processors

10 p1483 A83-26632

Comparison of cutoff wavelength measurements for single-mode waveguides

10 p1483 A83-26633

Bandwidth estimation for multimode optical fibers using the frequency correlation function of speckle patterns

10 p1423 A83-26634

Achieving stability in remote holography using flexible multimode image bundles

10 p1423 A83-26635

Optical-fiber copolymer-film electric-field sensor

10 p1423 A83-26636

Generation of light in optical fibers made of glasses formed from rare-earth ultraphosphate crystals

10 p1432 A83-26670

Determination of the amplitude-frequency characteristics of W-type fiber waveguides

10 p1484 A83-26692

Sound excitation and appearance of additional losses in a single-mode fiber-optic waveguide in the case of the transmission of amplitude-modulated optical waves

10 p1484 A83-26942

Coupling semiconductor lasers to multimode optical fibres

11 p1655 A83-27515

Single mode fiber isolator in toroidal configuration

11 p1656 A83-27565

Transmission code for high-speed fibre-optic data networks

11 p1558 A83-28604

Local velocity measurement of opaque fluid flow using laser Doppler velocimeter with optical dual fiber pickup

12 p1727 A83-28839

A simple fibre Fabry-Perot sensor

12 p1729 A83-29189

New measurement method for polarisation dispersion in single-mode fibres employing frequency-modulated optical signal

12 p1779 A83-29460

Single-polarisation operation of highly birefringent bow-tie optical fibres

12 p1779 A83-29462

Mode analysis of optical fibres using computer-generated matched filters

12 p1779 A83-29463

Stabilisation of single and multimode fibre-optical microbend sensors

12 p1730 A83-29468

Optical fibres with an Al₂O₃-doped silicate core composition

12 p1779 A83-29471

The development of fibre optic microbend sensors

12 p1730 A83-29519

A highly sensitive fiber-optic rotation sensor

13 p1844 A83-30015

Fibre optic development at the AAO

13 p1936 A83-30400

Advances in auroral imaging from space

13 p1814 A83-30768

Phase modulation of coherent light in long multimode fiber light guides

13 p1919 A83-30815

Phase modulation efficiency of coherent light in fiber light guides

13 p1919 A83-30816

On the localization of the resonance state wave function in the complex coordinate method

13 p1919 A83-30961

Broadband guided-wave optical frequency translator using an electro-optical Bragg array

13 p1922 A83-31053

Hybrid modes in circular cylindrical optical fibers

13 p1922 A83-31146

Fiber optics at ESO. I - Coupling of the CES with the 3.6 m telescope using a 40 m fiber link

13 p1922 A83-31576

Sub-10 ps high-gain direct coupled Josephson logic gate

13 p1837 A83-31764

Analysis of decoding in optical-fibre communication systems

13 p1830 A83-31770

Matching of single-mode optical waveguides to semiconductor lasers

14 p2083 A83-31904

Multiple object fiber optic spectroscopy

14 p2017 A83-32012

Multiple object fiber optics spectrograph feed for the Hale telescope

14 p2017 A83-32013

Photon counting Reticon system - Description and performance

14 p2018 A83-32023

Starlab detector system - A wide field, high resolution, photon counting array

14 p2018 A83-32038

The combination of hollow focusing concentrators with fiber-optic waveguides --- for solar energy transmission

14 p2036 A83-32048

A thermo-optical method for the formation of lightguide channels

14 p2084 A83-32122

Mode energy transformation between two connected multimode general square-law-index optical waveguides

14 p2084 A83-32444

Dispersion of tubular modes propagating in multimode optical fibres

14 p2084 A83-32446

Fiber-optic absorption/fluorescence probes for combustion measurements

14 p2020 A83-32902

Hamiltonian analysis of beams in an optical slab guide

15 p2229 A83-33539

InGaAsP photodiodes

15 p2150 A83-33680

Magnetostrictive fiber-optic sensor system for detecting dc magnetic fields

15 p2163 A83-33765

Measurement of fiber birefringence by wavelength scanning Effect of dispersion

15 p2230 A83-33766

Lasing characteristics of a Nd(3+):YAG laser with a long optical-fiber resonator

15 p2168 A83-33812

State-of-the-art survey of multimode fiber optic wavelength division multiplexing

15 p2230 A83-33970

Optoacoustic characteristics of single-mode fiber waveguides

15 p2230 A83-33985

Modal characteristics of step-index concentric-core fiberguides of circular cross section

15 p2231 A83-34468

[AD-A130935] Radiation damage in single-mode optical-fiber waveguides

15 p2231 A83-34469

Heterodyne OTDR at 0.82 micron --- Optical Time-Domain Reflectometry

15 p2231 A83-34513

Asynchronous multiplexing for an optical-fibre local-area network

Determination of the form of the amplitude-frequency response of variable-length optical waveguides
15 p2232 A83-34885

The transmission of two-dimensional and color images through a single fiber by the spectral scanning technique
15 p2232 A83-34889

High-power KrF laser transmission through optical fibers and its application to the triggering of gas switches
16 p2357 A83-35427

Amplification by stimulated Raman scattering in low-loss optical fibers
16 p2358 A83-35514

Optical fiber repeatered transmission systems utilizing SAW filters
16 p2345 A83-35648

Variational approach to nonlinear pulse propagation in optical fibers
16 p2411 A83-35660

Investigation of the state of polarization of light in a single-mode fiber waveguide
16 p2412 A83-35897

Optical nonreciprocity in a ring Raman fiber laser
16 p2359 A83-35898

The stress-optic effect in optical fibers
16 p2412 A83-35964

Coupled multiple waveguide systems
16 p2412 A83-35965

Theory of backward Rayleigh scattering in polarization-maintaining single-mode fibers and its application to polarization optical time domain reflectometry
16 p2412 A83-35967

Novel polarisation phenomena on anisotropic multimoded fibres
16 p2412 A83-36001

Rayleigh scattering in fluoride glass optical fibers
16 p2412 A83-36480

New single-mode single-polarisation optical fiber
16 p2412 A83-36487

Depolarised broadband source --- for optical communication
16 p2412 A83-36488

Receiver design for digital fiber optic transmission systems using Manchester (biphase) coding
16 p2343 A83-36602

Holographic coupler to monomode fiber
16 p2413 A83-36755

Coherence properties and cutoff wavelength determination in dielectric waveguides
16 p2413 A83-36766

Analysis of a directional coupler based on fused single-mode optical fibers
16 p2413 A83-36767

High-temperature optical fiber thermometer
17 p2510 A83-37608

Phenomenon of interference between two light beams propagating in optical fibers having a large path difference
17 p2580 A83-37744

Electrooptical imaging system using wavelength coding
17 p2510 A83-37748

Fiber-optic image transmission system with high resolution
17 p2580 A83-37749

On a method for determining the amplitude-frequency response curve of regular multimode optical waveguides
17 p2580 A83-38502

All-fibre 'Michelson' thermometer
17 p2513 A83-38879

Joint characteristics between polarisation-maintaining single-mode fibres
17 p2580 A83-38884

Design of a fiber-optic data-acquisition network
18 p2743 A83-39435

An interference technique of distance measurement using a fiber-optic waveguide
18 p2688 A83-39436

Optical fiber V-groove transversal filter
18 p2744 A83-40056

Analog fiber-optic measurement line
18 p2690 A83-40097

Determination of the nonreciprocity matrix of a nonstationary single-mode fiber-optic waveguide, with application to a fiber-optic ring interferometer
18 p2690 A83-40098

Polarization noise in single mode fibres and its reduction by depolarizers
18 p2744 A83-40349

Nonlinear conversion of laser radiation in optical fibres and its applications for spectral investigation
18 p2744 A83-40351

Investigation of Brillouin light scattering in crystals and glasses with application to problems of quantum electronics and fiber optics
18 p2694 A83-40609

Theory of multiplicative noise caused by coupling loss and amplitude vector rotation in optical communication channels
19 p2826 A83-40895

Electrical diagnostics of the amplifier operation and a feasibility of signal registration on the basis of the voltage saturation effect in junction laser diodes
19 p2852 A83-40941

Modal birefringence and polarization mode dispersion in single-mode fibers with stress-induced anisotropy
19 p2899 A83-40945

How to detect the gravitationally induced phase shift of electromagnetic waves by optical-fiber interferometry
19 p2846 A83-40967

Middle IR As-S and As-Se glass fibres with optical losses lower than 1 dB/m
19 p2900 A83-41280

Development of fabrication technology and measurement systems for multimode, single-mode and polarization maintaining optical fibers --- Thesis
19 p2901 A83-42125

Synchronous phase detection for optical fiber interferometric sensors
20 p2988 A83-42219

Launching light from semiconductor lasers into plane-ended multimode optical fibers
20 p3046 A83-42220

Polarization-maintaining optical fibers with low dispersion over a wide spectral range
20 p3046 A83-42221

Thermal properties of highly birefringent optical fibers and preforms
20 p3047 A83-42222

Selective nonlinear spectroscopy of inhomogeneously broadened phonon resonances in a disordered medium
20 p2993 A83-42285

Photometer for quasielastic and classical light scattering
20 p2988 A83-42295

Phase conjugation by degenerate four-wave mixing and temporal coherence
20 p3047 A83-42343

Polarisation-holding directional coupler made from elliptically cored fibre having a D section
20 p3047 A83-42477

Acousto-optic phase modulator for single-mode fibres
20 p3047 A83-42479

Efficient backward and forward pumping CW Raman amplification for InGaAsP laser light in silica fibres
20 p2993 A83-42486

Radiation-hardened pure silica-core fibre optics
20 p3047 A83-42487

Performance degradation due to stimulated Raman scattering in wavelength-division-multiplexed optical-fiber systems
20 p3047 A83-42492

Integrated optics, fiber optics and holography; International School on Coherent Optics and Holography, 2nd, Varna, Bulgaria, September 28-October 3, 1981, Proceedings
20 p3048 A83-43774

Wavelength-division multiplexing of channels in fiber-optic communication lines (review)
20 p3048 A83-43776

Mode locking in a fiber laser
20 p2997 A83-43798

Fibre-optic gyroscope
21 p3135 A83-44075

Measurement of axially nonsymmetrical refractive-index distribution of a single-mode fiber by a multidirectional scattering-pattern method
21 p3204 A83-44201

Spot size measurements for single-mode fibers - A comparison of four techniques
21 p3204 A83-44202

Fabrication of polarization-maintaining and absorption-reducing fibers
21 p3204 A83-44203

Depolarization in a single-mode optical fiber
21 p3204 A83-44204

Splicing of single polarization-maintaining fibers
21 p3204 A83-44205

A fluoride glass optical fiber operating in the mid-infrared wavelength range
21 p3204 A83-44206

Performance of Lyot depolarizers with birefringent single-mode fibers
21 p3204 A83-44207

Multimode-optical-fiber Michelson interferometer
21 p3129 A83-44208

An external cavity diode laser sensor
21 p3136 A83-44209

Fiber-optic gyroscopes with broad-band sources
21 p3136 A83-44210

Fiber-optic spectrum analyzer
21 p3136 A83-44211

Sensitive all-single-mode-fiber resonant ring interferometer
21 p3136 A83-44212

Dielectric multilayer thin-film filters for WDM transmission systems --- Wavelength Division Multiplexing in optical fiber communication
21 p3204 A83-44213

An effective nonreciprocal circuit for semiconductor laser-to-optical-fiber coupling using a YIG sphere
21 p3204 A83-44214

Towards the fundamental limits of optical-fiber communications
21 p3204 A83-44215

A single-mode-fiber coupler with a variable coupling ratio
21 p3205 A83-44218

Plastic optical passive devices and their application to a local computer network
21 p3205 A83-44219

A curvilinear snake arm robot with gripper-axis fibre-optic image processor feedback
21 p3119 A83-44695

Review of fiber optic gyroscopes
21 p3140 A83-44820

ALPD (Axial Lateral Plasma Deposition) - A new process for the production of high quality optical fibers
21 p3207 A83-44821

Backscattering observation of radiation damage in optical fibers
21 p3207 A83-44822

Solitons in single mode optical fibres
21 p3207 A83-44823

Optical fibre sensors - Principles and applications
21 p3140 A83-44824

Single mode laser spectral spread repercussions in single-mode optical fiber coherent detection systems
21 p3145 A83-44832

Emission frequency stability in single-mode-fibre optical feedback controlled semiconductor lasers
21 p3145 A83-44954

Bend behaviour of polarising optical fibres
21 p3208 A83-44959

Practical single-polarisation anisotropic fibres
21 p3208 A83-44963

Polarisation-mode dispersion as a bandwidth-limiting factor in a long-haul single-mode optical-transmission system
21 p3208 A83-44964

Comparing the chromatic dispersions of two single-mode silica fibres with pure F and pure GeO₂ doping, respectively
21 p3208 A83-44966

Polarimetric strain gauges using high birefringence fibre
21 p3208 A83-44968

The monomode fiber - A new tool for holographic interferometry
21 p3141 A83-45159

Multimode optical fiber sensors
21 p3142 A83-45415

Rayleigh backscattering in a fiber gyroscope with limited coherence sources
22 p3287 A83-45730

Broad-band ultrasonic sensor based on induced optical phase shifts in single-mode fibers
22 p3287 A83-45731

An all fiber-optic sensor for surface acoustic wave measurements
22 p3287 A83-45735

Continuous laser amplification in a monomode fiber longitudinally pumped by evanescent field coupling
22 p3295 A83-45971

Optimization of an optical fiber for missile guidance applications
22 p3357 A83-46609

16 x 16 optical star coupler using a mixing block with two perfect mirrors
22 p3292 A83-46610

Laser and laser systems reliability; Proceedings of the Conference, Los Angeles, CA, January 28, 29, 1982
22 p3296 A83-46611

Tradeoff between laser diodes and light-emitting diodes (LEDs) for the common weapon control system
22 p3278 A83-46616

Advances in infrared fibers II; Proceedings of the Second Meeting, Los Angeles, CA, January 26-28, 1982
22 p3357 A83-46621

Polycrystalline KRS-5 infrared fibers for power transmission
22 p3357 A83-46622

Infrared glass optical fibers for 2 to 11 micrometer band
22 p3358 A83-46623

Materials for infrared low loss fibers
22 p3358 A83-46624

Fluoride glasses with large optical window for infrared fibers
22 p3358 A83-46625

Progress in heavy metal fluoride glasses for infrared fibers
22 p3358 A83-46626

Preparation of high purity ZnCl₂ for 10.6-micron optical fibers
22 p3358 A83-46627

Material dispersion considerations for infrared fibers
22 p3358 A83-46628

Growth and characterization of single crystal refractory oxide fibers
22 p3358 A83-46629

Broadband infrared generation by stimulated Raman scattering in liquid filled fibers
22 p3297 A83-46631

Electrical transmission lines as models for soliton propagation in infrared fibers
22 p3358 A83-46632

Mode coupling analysis of bending losses in hollow infrared waveguides
22 p3358 A83-46634

GeO₂-Sb₂O₃ glass optical fibers for 2 to 3 microns fabricated by vapor-phase axial deposition (VAD) method
22 p3358 A83-46635

Rolling KCl fiber - A feasibility study --- for IR optical communication
22 p3359 A83-46636

Characterization of fibers for 10.6 micron transmittance
22 p3359 A83-46637

Coherent, single-mode fiber optic for multifunction 10.6 micron helicopter avionics system
22 p3359 A83-46639

Infrared fiber early warning receiver
22 p3255 A83-46640

Infrared heterodyning using silver halide fibers
22 p3359 A83-46641

Radiometric applications of infrared optical fibers
22 p3292 A83-46642

Progress on electro-optic integrated optical devices
22 p3360 A83-46650

Reliability of fiber optic emitters
22 p3360 A83-46654

Narrow diffused stripe GaAs/GaAlAs lasers for high speed integrated optical transmitters
22 p3297 A83-46655

Single-mode fiber systems for deep space communication network
22 p3360 A83-46657

Phase-Nulling Fiber Optic Gyro development review
22 p3292 A83-46658

Wideband frequency conversion in the UV by nine orders of stimulated Raman scattering in a XeCl laser pumped multimode silica fiber
22 p3299 A83-46719

Application of fiber optics to speckle metrology - A feasibility study
22 p3293 A83-46807

- Birefringence and polarization mode dispersion caused by thermal stress in single-mode fibers with various core ellipticities 22 p3360 A83-46813
- State of the art and development potential of fiberoptic rotation sensors --- for inertial navigation 23 p3405 A83-47187
- Single-mode, single-polarization fibers made of birefringent material 23 p3508 A83-47583
- Rayleigh backscattering theory for single-mode optical fibers 23 p3508 A83-47584
- Optical remote sensing of environmental pollution and danger by molecular species using low-loss optical fiber network system 23 p3508 A83-47802
- Soliton analysis with the propagating beam method 23 p3508 A83-48313
- Dynamic sensing for robots - An analysis and implementation 23 p3501 A83-48635
- Combined reciprocal and non-reciprocal birefringence in optical monomode fibres 24 p3627 A83-48744
- A method of calculating the efficiency for coupling light power from a LED into an optical fibre by use of a sphere lens 24 p3627 A83-48745
- Laser bias effect on the receiver sensitivity of passive fibre optic star bus networks 24 p3627 A83-48746
- Fiber-optic gyroscope with polarization-holding fiber 24 p3581 A83-48856
- Monomode-polarization-maintaining fiber directional couplers 24 p3628 A83-48857
- Measurement of polarization mode coupling along a polarization-maintaining optical fiber using a backscattering technique 24 p3628 A83-48858
- Transversely anisotropic optical fibers - Variational analysis of a nonstandard eigenproblem 24 p3628 A83-48968
- Attenuation at 10.6 microns in loaded and unloaded polycrystalline KRS-5 fibers 24 p3629 A83-49017
- Practical two-wavelength multi-demultiplexer - Design and performance 24 p3629 A83-49018
- Ultralow loss single-mode fiber design for 2.5-6-micron band operation 24 p3629 A83-49019
- Ultraviolet four-photon mixing in a multimode silica fiber Raman amplifier 24 p3589 A83-49616
- High-gain optical amplification of laser diode signal by Raman scattering in single-mode fibres 24 p3589 A83-49960
- High-speed pulse-train generation using single-mode-fibre recirculating delay lines 24 p3589 A83-49962
- Fabrication of polarisation-maintaining (3 x 3) single-mode-fibre couplers 24 p3630 A83-49971
- 8 km-long polarisation-maintaining fibre with highly stable polarisation state 24 p3630 A83-49974
- Acousto-optic frequency shifter for single-mode fibres 24 p3630 A83-49978
- Evanescent amplification in a single-mode optical fiber 24 p3630 A83-49980
- Polarisation-preserving coupler with self aligning birefringent fibres 24 p3630 A83-49982
- Gamma-ray irradiation effect on transmission loss for ZrF4-based optical fibres 24 p3630 A83-49985
- Chirped picosecond injection laser pulse transmission in single-mode fibres in the minimum chromatic dispersion region 24 p3630 A83-49988
- Polarisation holding in coiled high-birefringence fibres 24 p3630 A83-49992
- FIBER ORIENTATION**
- Swept composite wing aeroelastic divergence experiments 01 p0009 A83-10193
- A simple approach to determination of stiffness characteristics of unidirectional composites 03 p0291 A83-14491
- Oxidative stabilization of oriented acrylic fibres - Morphological rearrangements 05 p0619 A83-17561
- Use of the flash method to determine the thermal properties of the constituents of a directionally reinforced composite [ONERA, TP NO. 1982-104] 06 p0724 A83-18431
- Thermal behavior of directional reinforced composites subjected to thermal flux pulses [ONERA, TP NO. 1982-105] 06 p0724 A83-18432
- Calculating the elastic characteristics of a unidirectional fiber composite by the method of sections 06 p0725 A83-18501
- The fracture of a unidirectional fiber composite with an elastoplastic matrix under compression 06 p0725 A83-18503
- A study of the effect of low-cycle loading on the mechanical characteristics and structure of a unidirectional organic-fiber-reinforced composite 06 p0725 A83-18505
- Predicting the creep behavior of a unidirectionally reinforced composite with thermorheologically simple structural components 06 p0725 A83-18511
- Probability distributions for the strength of composite materials. III - The effect of fiber arrangement 06 p0776 A83-18912
- Variation of in-plane elastic constants in material design of composite laminates 07 p0949 A83-21623
- Role of local fiber distribution at notch tip in the fracture toughness of FRP 08 p1054 A83-21681
- Fracture analyses of angle-ply laminates 08 p1054 A83-21729
- Effects of processing on the mechanical properties of carbon short-fiber reinforced polycarbonate 08 p1055 A83-22718
- Effect of fiber-aspect ratio and orientation on the stress-strain behavior of aligned, short-fiber-reinforced, ductile epoxy 08 p1055 A83-22719
- Stochastic models of fracture of unidirectional fiber composites 09 p1222 A83-23927
- Characterization of matrix/interface-controlled strength of unidirectional composites 09 p1223 A83-23935
- Determination of fracture toughness of unidirectionally fiber-reinforced composites 09 p1223 A83-23936
- On failure modes of unidirectional composites under compressive loading 09 p1223 A83-23937
- On three-dimensional fibrous flaws in unidirectional fiber reinforced elastic composites 09 p1281 A83-24821
- Wear characteristics of composites - Effect of fiber orientation 12 p1709 A83-29399
- On the multi filament failure problem in unidirectional fiber reinforced composites [AIAA 83-0800] 12 p1737 A83-29733
- The elastic characteristics of unidirectionally reinforced hybrid composites 13 p1815 A83-30052
- Modeling the fracture of thin-walled structural elements of multidirectional layered composites 13 p1865 A83-30054
- An investigation of stress-dependent, temperature-dependent, and time-dependent strains in randomly oriented fiber reinforced composites 14 p1988 A83-33295
- Viscoelastic characterization of a random fiber composite material employing micromechanics 14 p1988 A83-33297
- Longitudinal shear modulus of unidirectional composites 18 p2652 A83-40161
- Analysis of the elastoplastic behavior of (0 deg/90 deg) and + Theta/-Theta) bidirectionally fiber-reinforced ductile matrix composites in uniaxial loading 18 p2653 A83-40174
- Mechanical testing and micrographic examination of prepreg GFRP composites with different pressure-temperature cycles 18 p2653 A83-40176
- Best angles against buckling for rectangular laminates 18 p2704 A83-40186
- A study on fracture mechanism of unidirectional fibrous composites 18 p2654 A83-40190
- Prediction of fracture toughness of unidirectional metal matrix composites 18 p2654 A83-40196
- The environmental stress corrosion cracking of glass fibre reinforced polyester and epoxy composites 18 p2656 A83-40223
- Long term strength of glass reinforced plastics 18 p2656 A83-40224
- Origins of thermal strains in polyester laminates 18 p2657 A83-40230
- The strength of aligned short-fiber carbon, glass, and hybrid carbon/glass composites 18 p2657 A83-40234
- Prediction of the stress-strain curve of unidirectional metal matrix composite 18 p2657 A83-40236
- Fabrication cycle influence on the acoustic emission response of GFRP composites 18 p2660 A83-40270
- Non-destructive testing method of fiber orientation and fiber content in FRP using microwaves 18 p2660 A83-40275
- Microstructure and fracture behaviour of unidirectionally reinforced carbon fiber/carbon composites 18 p2661 A83-40282
- Material design of composite laminates with required in-plane elastic properties 18 p2662 A83-40292
- Photoelastic analysis of the behaviour of curved fibers in composite 18 p2662 A83-40300
- On the off-axis tension test for unidirectional composites 19 p2819 A83-41033
- Fatigue crack propagation in random short-fiber SMC composite --- Sheet Molding Compound 20 p2948 A83-43147
- Effect of fiber aspect ratio on ultimate properties of short-fiber composites 22 p3264 A83-46297
- An optical technique for measuring fiber orientation in short fiber composites 22 p3290 A83-46298
- On the relation between Young's modulus and orientation in carbon fibres 24 p3553 A83-48898
- FIBER REINFORCED COMPOSITES**
- Short fibre reinforced thermoplastics --- Book 01 p0022 A83-10882
- Development of advanced composite materials and geodetic structures for future space systems 01 p0017 A83-11334
- The thermal conductivity of Kevlar fibre-reinforced composites 02 p0149 A83-11667
- Role of fibre surface-matrix combination in carbon fibre reinforced epoxy composites 02 p0149 A83-11669
- Designing parts in fiber composites --- Russian book 02 p0149 A83-12025
- Nonlinear matrix failure criterion for fiber-reinforced composite materials 02 p0150 A83-12062
- Survey of recent research in the analysis of composite plates 02 p0191 A83-12065
- Elastoplastic behavior of a fiber laminate 02 p0150 A83-12340
- Fracture modes of inelastic materials as a function of loading rate and temperature, and associated fracture criteria 02 p0192 A83-12354
- Fatigue behavior of SiC reinforced Ti/6Al-4V/ at 650 C 02 p0150 A83-12414
- Dynamic instability of suddenly heated angle-ply laminated composite cylindrical shells 02 p0194 A83-12742
- A comprehensive theory for planar bending of composite laminates 02 p0195 A83-12760
- An experimental and analytical study of the dynamic response of a linkage fabricated from a unidirectional fiber-reinforced composite laminate [ASME PAPER 82-DET-67] 02 p0187 A83-12775
- Fiber-matrix interactions 02 p0150 A83-12824
- Bending waves in strongly anisotropic elastic plates 02 p0196 A83-12855
- The use of composite patches for repair of aircraft structural parts 02 p0131 A83-12968
- The cyclic strength of reinforced magnesium-matrix composites 02 p0151 A83-13038
- Normalized thermoplastic properties of fiber composites 03 p0291 A83-14065
- Experimental mechanics of fiber reinforced composite materials --- Book 03 p0341 A83-14117
- The effect of shear modulus on the elastic behavior of strongly anisotropic plates 03 p0343 A83-14736
- Deformation characteristics of metal composites with brittle fibers during bending 03 p0293 A83-14817
- Microstructure and fracture of fiber reinforced thermoplastic polyethylene terephthalate /P.E.T./ 03 p0293 A83-14825
- Extension of oblique-incidence method to photo-orthotropic elasticity 03 p0344 A83-14941
- Plasticity analysis of laminated composite plates [ASME PAPER 82-WA/APM-11] 04 p0498 A83-15680
- Stability and vibrations of compressed, aeolotropic, composite cylindrical shells 04 p0499 A83-15689
- Complex moduli of aligned discontinuous fibre-reinforced polymer composites 04 p0455 A83-15988
- A compliant, high failure strain, fibre-reinforced glass-matrix composite 04 p0455 A83-15989
- Carbon fibre-reinforced silicon nitride composite 04 p0455 A83-15990
- On a thermodynamic theory of fiber-reinforced thermoelastic materials with thermo-kinematic constraints 04 p0455 A83-16098
- CAP/polyester reinforcement 04 p0455 A83-16178
- Wave propagation in a unidirectional composite in comparison with that in a layered elastic body 04 p0455 A83-16397
- The fracture mechanics of composite materials under axial compression - Plastic fracture 04 p0456 A83-16402
- Simulated space environmental effects on fiber reinforced polymeric composites [AIAA PAPER 83-0589] 05 p0610 A83-16806
- An analysis of impact failure modes for fiber-reinforced composite laminates by using fault tree 05 p0611 A83-17104
- On the preparation of glass-fibre reinforced aluminum by powder hot extrusion 05 p0611 A83-17110
- Optimization procedure for material composition of composite material structures 06 p0724 A83-18231
- Use of the flash method to determine the thermal properties of the constituents of a directionally reinforced composite [ONERA, TP NO. 1982-104] 06 p0724 A83-18431
- Thermal behavior of directional reinforced composites subjected to thermal flux pulses [ONERA, TP NO. 1982-105] 06 p0724 A83-18432
- A study of the effect of low-cycle loading on the mechanical characteristics and structure of a unidirectional organic-fiber-reinforced composite 06 p0725 A83-18505
- A statistical theory for fibrous media. I - Longitudinal shear 06 p0725 A83-18508
- Predicting the creep behavior of a unidirectionally reinforced composite with thermorheologically simple structural components 06 p0725 A83-18511

Development of a structural, bird impact resistant, de-iced wing leading edge for the de Havilland Dash 8 aircraft using fibre-reinforced composites

06 p0717 A83-18823

Probability distributions for the strength of composite materials. III - The effect of fiber arrangement

06 p0776 A83-18912

A continuum theory for the fracture of metal-matrix composites under compression

06 p0726 A83-19542

Computer simulation of the fracture of composite materials with various degrees of physicochemical interaction between the components

07 p0874 A83-19971

Engineering principles of the formation of epoxy resin composites. I Mathematical model of the fluid flow

07 p0875 A83-20439

Knitted fabrics in fiber reinforced structural composites

07 p0876 A83-20470

Plastic tooling for advanced composites

07 p0876 A83-20481

Elevated temperature repairs of advanced composite structures

07 p0877 A83-20499

An anisotropic strip weakened by an array of cracks

07 p0946 A83-20637

Variation of in-plane elastic constants in material design of composite laminates

07 p0949 A83-21623

Impact fatigue strength and reliability for fiber reinforced epoxy resin laminates subjected to repeated impact loads

07 p0877 A83-21624

Analysis of thermal cracking of unidirectionally reinforced composite structures in the micromechanical range

08 p1054 A83-21680

Role of local fiber distribution at notch tip in the fracture toughness of FRP

08 p1054 A83-21681

Computer simulation of micro and macromechanisms of fibre reinforced composite fracture

08 p1054 A83-21801

Nonlinear micropolar continuum model of a composite reinforced by elements of finite rigidity. I - Equations of motion and constitutive relations

08 p1120 A83-21816

Resin flow during the cure of fiber reinforced composites

08 p1054 A83-21822

Saint-Venant end effects in composites

08 p1054 A83-21823

Optimum elastic design of a reinforced beam

08 p1121 A83-21825

Composite flywheels with rim and hub

08 p1073 A83-21992

Relation of interfacial adhesion in Kevlar/epoxy systems to surface characterization and composite performance

08 p1055 A83-22716

Fatigue considerations for FRP composites

09 p1221 A83-23424

Status and recent developments in Celion carbon fibers

09 p1221 A83-23614

Fracture tough composites - The effect of toughened matrices on the mechanical performance of carbon fiber reinforced laminates

09 p1222 A83-23642

Transient hygrothermal and mechanical stress intensities around cracks

09 p1223 A83-23930

Characterization of matrix/interface-controlled strength of unidirectional composites

09 p1223 A83-23935

On failure modes of unidirectional composites under compressive loading

09 p1223 A83-23937

Non-linear phenomenological models of fibre-reinforced composites

09 p1224 A83-23942

Comparative evaluation of shear test methods for composites

09 p1224 A83-23948

On three-dimensional fibrous flaws in unidirectional fibre reinforced elastic composites

09 p1281 A83-24821

Properties of stresses in composites with ribbon-like fibers

09 p1282 A83-25022

Structural deformation model of spatially reinforced composites

09 p1282 A83-25107

Elasticity theory of composites

10 p1438 A83-25316

On a micromechanical fracture model for cracked reinforced composites

10 p1438 A83-25470

Strength of mechanically fastened composite joints

10 p1439 A83-25880

Heat of reaction, degree of cure, and viscosity of Hercules 3501-6 resin

10 p1400 A83-25882

Instabilities of a finitely deformed fiber-reinforced elastic material

10 p1441 A83-26440

Experimental determination of stresses in damaged composites using an electric analogue

10 p1441 A83-26446

Isothermal oxidation of the COTAC 74 in-situ composite between 800 and 1300 C

10 p1389 A83-26891

Program overview and diesel/flywheel hybrid power train design - Fibre composite flywheel development program for road vehicle applications

11 p1667 A83-27306

Fibre composite rotor selection and design /Fibre composite flywheel development program for road vehicle applications/

11 p1667 A83-27307

1982 advances in aerospace structures and materials; Proceedings of the Winter Annual Meeting, Phoenix, AZ, November 14-19, 1982

11 p1591 A83-27426

On the analysis of adhesive joints in fiber reinforced composite plates and shells

11 p1591 A83-27430

A theory for transverse cracks in composite laminates

11 p1591 A83-27435

Influence of flaw bridging on the stress concentration in composites

11 p1592 A83-27445

Thermomechanical behavior of high-temperature composites; Proceedings of the Symposium, Phoenix, AZ, November 14-19, 1982

11 p1543 A83-27457

Thermal expansion behavior of a thermally degrading organic matrix composite

11 p1543 A83-27460

Effects of matrix viscoelasticity and cracking on fiber composite response during thermal cycling

11 p1592 A83-27461

An experimental and theoretical study of crack propagation in crossply fiber composites

11 p1544 A83-28437

Further comparison of the numerical and experimental buckling behaviors of composite panels

11 p1599 A83-28722

Tensile stress-strain behavior of hybrid composite laminates

12 p1709 A83-28900

The effects of pressure on the carbonization of pitch and pitch/carbon fibre composites

12 p1709 A83-29503

Numerical solutions of the traction problem for a fibre-reinforced material by an integral-equation method

12 p1736 A83-29611

Prepreg, tape and fabric technology for advanced composites

12 p1710 A83-29713

Polymer selection and matrix aspects of processing and manufacture of fibre composites

12 p1710 A83-29714

Processing and property relationships for fibre composites

12 p1710 A83-29716

The quality control and non-destructive evaluation of composite aerospace components

12 p1710 A83-29717

Composites in the construction of the Lear Fan 2100 aircraft

12 p1710 A83-29718

On the multi filament failure problem in unidirectional fiber reinforced composites

[AIAA 83-0800] 12 p1737 A83-29733

Stress intensity factor calculation for designing with fiber reinforced composite materials

[AIAA 83-0835] 12 p1737 A83-29744

Drop weight impact testing of laminates reinforced with Kevlar aramid fibers, E-glass, and graphite

12 p1711 A83-29891

A finite element analysis of composite tension specimens

12 p1711 A83-29892

The relationship between the anisotropy of high-modulus reinforcing fibers and the mechanical and thermophysical properties of fiber composites

13 p1815 A83-30063

Modern propellers for commuter airlines

[SAE PAPER 820719] 13 p1807 A83-30874

Effect of the structure on the strength of the fibrous composite aluminum-carbon strip

13 p1816 A83-31217

Application of the graining process for the fabrication of chopped carbon fiber-aluminum composite

13 p1816 A83-31602

Interaction between SiC fibers and aluminum alloys

13 p1816 A83-31604

Fracture toughness of unidirectional glass/carbon hybrid composites

13 p1816 A83-31616

Enhancement of strength in composites reinforced with previously stressed fibers

13 p1868 A83-31618

Singularity of contact-edge stress in laminated composites under uniform extension

13 p1868 A83-31620

On dynamical description of fiber reinforced composites

13 p1868 A83-31622

Epitaxial crystallization of nylon 6 cast from solution on the surface of poly(p-phenylene terephthalamide) filament

13 p1817 A83-31796

Composite materials applications in the manufacture of helicopters - Design and problems of helicopters

14 p1974 A83-31822

Aluminum-matrix composites reinforced with carbon fibers

14 p1986 A83-32146

Advanced fibers and composites for elevated temperatures --- Book

14 p1986 A83-32173

Mathematical modeling of damage in unidirectional composites

14 p1986 A83-32344

The design of flywheels made of fibrous materials

14 p2046 A83-32378

Nonstationary thermal behavior of directional reinforced composites - Limit of application of thermal property homogenization

[AIAA PAPER 83-1471] 14 p1986 A83-32725

Two coplanar Griffith cracks in an orthotropic semi-infinite medium

14 p2032 A83-32921

Composites for extreme environments --- Book

14 p1986 A83-33114

Environmental effects on graphite fiber reinforced PMR-15 polyimide

14 p1987 A83-33115

Short fiber reinforced composite materials

14 p1988 A83-33294

Evaluation of the effect of voids in composite main rotor blades

15 p2173 A83-33507

On thermal bending of layered composite plates and shells of biomodulus materials

15 p2175 A83-34242

Stress concentration layers in finite deformation of fibre-reinforced elastic materials

15 p2130 A83-34344

Some aspects of crack growth and failure in fibre reinforced composites

15 p2130 A83-35075

Deformation of an elastoviscoplastic composite under complex loading

16 p2364 A83-35503

Studies of fabrication of carbon fiber reinforced aluminium matrix composite

16 p2324 A83-35606

Thermoelasticity of ideal fibre-reinforced materials

16 p2324 A83-35775

Evaluation of the effect of voids in composite main rotor blades

16 p2299 A83-35950

Light aircraft and sailplane structures in reinforced plastics

16 p2299 A83-36065

Stress analysis procedures for the design of fibre-reinforced metallic rocket motor cases

[AIAA PAPER 83-1330] 16 p2367 A83-36344

The load-bearing behavior of shear-stressed square plates of fiber-reinforced composite materials under large deformations --- German thesis

17 p2520 A83-37499

Shrinkage stresses in products of high-modulus composites

17 p2524 A83-38512

Economic evaluation of a standard product of fiber-reinforced composite material in comparison with steel

17 p2483 A83-38875

Fracture behaviour of collimated thermoplastic poly(ethylene terephthalate) reinforced with short E-glass fibre

18 p2649 A83-39055

Matrix/fiber interface effects on Kevlar 49 pressure vessel performance --- for rocket engine cases

18 p2701 A83-40018

An analysis of models for calculating the strength of aramide fibers in bundles and in a microcomposite

18 p2649 A83-40101

Approximate methods for solving the problems of stress concentration near holes in orthotropic plates of composite materials. IV - Stress concentration in plates of directionally reinforced fiber composites

18 p2701 A83-40105

Composites in Japan

18 p2650 A83-40127

High-temperature composites - Status and future directions

18 p2650 A83-40129

A study of relationship between composite strength and mono-filament strength

18 p2651 A83-40135

A new rubber modified resin

18 p2672 A83-40138

Novel fibre/resin interface for improved mechanical properties of composites reinforced with high modulus polyethylene filaments

18 p2651 A83-40144

Longitudinal shear modulus of unidirectional composites

18 p2652 A83-40161

Influence of the polymer matrix on the mechanical response of a unidirectional composite

18 p2653 A83-40179

Probabilistic design on strength of fiber reinforced composite laminates

18 p2654 A83-40182

Study on elasto-plastic fracture toughness of composite materials

18 p2654 A83-40197

A study on the fatigue life estimation of FRP under random loading

18 p2655 A83-40199

The prediction of long term viscoelastic properties of fiber reinforced plastics

18 p2655 A83-40210

Analysis of Charpy impact failure for unidirectional fiber-reinforced composite laminates by using a computerized fault tree

18 p2655 A83-40212

Mechanical behaviours in high velocity tension of composites

18 p2656 A83-40213

Impact damage tolerance of composites reinforced with Kevlar aramid fibers

18 p2656 A83-40214

Energy absorption of composite materials under crash conditions

18 p2705 A83-40216

On the stress wave velocity of fiber reinforced rectangular bar by means of finite prism method

18 p2705 A83-40218

Dynamic stress concentrations in some composite strips with a circular hole under high-velocity tension

18 p2705 A83-40221

Hygrothermal ageing of fibrous composites

18 p2657 A83-40229

Prediction of the stress-strain curve of unidirectional metal matrix composite 18 p2657 A83-40236

Strain analysis in discontinuous fiber-reinforced metals using the Moiregrid method 18 p2657 A83-40237

Theoretical predictions of the strength behavior of short-fiber reinforced metals 18 p2658 A83-40238

Method for estimating effective elastic moduli of dispersely reinforced composite 18 p2658 A83-40239

On the hybrid effect and fracture mode of interlaminated hybrid composites 18 p2658 A83-40241

Weft insertion warp knit for hybrid composites 18 p2658 A83-40243

Effects of compounds as diffusion-barrier coatings between the fiber and the matrix in tungsten fiber reinforced nickel matrix composites 18 p2658 A83-40249

Interfacial interactions in aluminium matrix stainless steel fibre composites 18 p2667 A83-40250

Prospects of metal nitride intermediate layer for FRM 18 p2659 A83-40251

Strengthening effect and interfacial adhesion of boron and silicon carbide fibre reinforced aluminum 18 p2659 A83-40252

Influence of the interface on transverse strength, creep behaviour, and impact behaviour of boron and silicon carbide fibre reinforced aluminum 18 p2659 A83-40253

Mechanical properties of SiC fiber reinforced Al composites 18 p2659 A83-40259

Fabrication of carbon fiber reinforced aluminum composites by roll diffusion bonding method 18 p2659 A83-40262

Squeeze casting of silicon carbide fiber reinforced aluminum 18 p2659 A83-40263

Fabrication of SiC fiber-aluminum composite materials 18 p2659 A83-40264

Fracture behavior and toughness of helical fiber reinforced composite metals 18 p2667 A83-40265

Analysis and evaluation of interfacial delamination energy of notched laminated composites 18 p2660 A83-40272

Non-destructive testing method of fiber orientation and fiber content in FRP using microwave 18 p2660 A83-40275

Warpage, a nightmare for composite parts producers 18 p2661 A83-40283

Kevlar aramid as a fiber reinforcement with emphasis on aircraft 18 p2661 A83-40286

New insights in structural design of composite rotor blades for helicopters 18 p2640 A83-40287

From outer space to the great ocean's depths - An adventure in high performance composite materials 18 p2661 A83-40288

Material design of composite laminates with required in-plane elastic properties 18 p2662 A83-40292

Design and development of advanced-composite shrouds 18 p2662 A83-40297

Photoelastic analysis of the behaviour of curved fibers in composite 18 p2662 A83-40300

An inelastic finite element model of 4D carbon-carbon composite 19 p2819 A83-40866

Environmental effects on fibre-reinforced plastics; Proceedings of the Symposium, Imperial College of Science and Technology, London, England, July 12, 13, 1983 20 p2946 A83-42801

Thermal stresses in an orthotropic elastic half-plane weakened by a Griffith crack 20 p3004 A83-42937

Infinite row of parallel cracks in an orthotropic strip 20 p3004 A83-42938

Effective constitutive equations for fiber-reinforced viscoplastic composites exhibiting anisotropic hardening 20 p3004 A83-42974

Elastic-plastic interaction of Dugdale type cracks and plastified matrix material in self-stressed fibre-reinforced composites 20 p3006 A83-42996

Experiments on highly-nonlinear elastic composites 21 p3106 A83-44048

Designing with fiber reinforced plastics - Planar random composites 21 p3106 A83-44051

The effects of cut and edge on the ultimate tensile strength of planar randomly-distributed short fiber composites 21 p3106 A83-44052

Thermoelastic analysis of hybrid fabric composites 21 p3106 A83-44120

Organic composites based on aromatic-polyamide fibers 21 p3106 A83-44697

Concentrated body force loading of an elastically bridged penny shaped flaw in a unidirectional fibre reinforced composite 21 p3156 A83-44893

An analysis of the energy release rate for non-coplanar crack growth in fiber reinforced composite materials 21 p3107 A83-44913

Lower-tail approximations for the probability of failure of three-dimensional fibrous composites with hexagonal geometry 21 p3159 A83-44941

Fiber-reinforced plastics in aviation and space flight 21 p3107 A83-45088

A semi-automated in-plane loader for materials testing --- of fiber reinforced composites 21 p3108 A83-45162

Quasistatic thermal crack growth in unidirectionally fiber reinforced composite materials 21 p3108 A83-45185

The role of the polymeric matrix in the processing and structural properties of composite materials; Proceedings of the Joint U.S.-Italy Symposium on Composite Materials, Capri, Italy, June 15-19, 1981 22 p3262 A83-46279

Environmental aging of epoxy composites 22 p3263 A83-46288

Effects of matrix characteristics in the processing of short fiber composites 22 p3263 A83-46292

Creep and fracture initiation in fibre reinforced plastics 22 p3264 A83-46296

Low cost energy storage flywheels from structural sheet molding compound 22 p3318 A83-46299

Definition of interphase in composites 22 p3264 A83-46302

Internal stresses in fibre reinforced plastics 22 p3264 A83-46304

Plastic composites fight for status --- performance predictability as construction material 23 p3428 A83-47822

Variational estimates for dispersion and attenuation of waves in random composites. III - Fibre-reinforced materials 23 p3428 A83-48096

ARALL (aramid-fiber-reinforced aluminum laminate) - A new hybrid composite with exceptional fatigue-resistance properties 23 p3428 A83-48500

Elastic and viscoelastic properties of fibre-reinforced composite materials 24 p3553 A83-48895

Monte Carlo simulation of the strength of composite fibre bundles 24 p3591 A83-48896

Oxidation and corrosion of a gamma/gamma-prime-NbC unidirectionally solidified pseudo-eutectic alloy 24 p3563 A83-49492

Note on shear interaction between two fibres 24 p3595 A83-49871

Statistical properties of hybrid composites. I - Recursion analysis 24 p3554 A83-49876

Creep of Kevlar 49 fibre and a Kevlar 49-cement composite 24 p3554 A83-50066

Compressive strength of fiber-reinforced materials 24 p3597 A83-50147

FIBER STRENGTH

A study of residual stresses in boron filaments 02 p0150 A83-12351

Micromechanics 02 p0193 A83-12733

Designing composites for maximum toughness 02 p0151 A83-12970

Measurement of stresses in optical fiber and preform 03 p0395 A83-14387

A study into the degradation of nylon, Kevlar and polyester fabrics when exposed to varying amounts of ultra violet in the laboratory and in natural environment and the effects of varying degrees of heat on the degradation of these fabrics 04 p0463 A83-15439

Stress redistribution in the ruptured fiber of a viscoelastic composite 06 p0725 A83-18504

Fibre length-strength relationships and the fracture of composites 08 p1053 A83-21678

Optical fiber strength/fatigue experiments 08 p1073 A83-22485

Environmental testing of UV-cured acrylate-coated fibers 08 p1073 A83-22488

Status and recent developments in Celion carbon fibers 09 p1221 A83-23614

Damageability evaluation of organic and carbon fiber plastics by nondestructive technique 09 p1224 A83-23947

Room-temperature tensile strength of fibres in boron-aluminum, boron-titanium and graphite-aluminum composites as a function of annealing temperature and time 09 p1225 A83-25148

On the multi filament failure problem in unidirectional fiber reinforced composites [AIAA 83-0800] 12 p1737 A83-29733

Analysis of progressive damage in thin circular laminates due to static-equivalent impact loads [AIAA 83-0997] 12 p1711 A83-29872

Enhancement of strength in composites reinforced with previously stressed fibers 13 p1868 A83-31618

Thermomechanical characterization of graphite/polyimide composites 14 p1987 A83-33117

An analysis of models for calculating the strength of aramid fibers in bundles and in a microcomposite 18 p2649 A83-40101

Inelastic deformation of certain high-modulus reinforcing fibers 18 p2649 A83-40102

Microstructure (microtexture), Structure and surface studies of some carbon fibers 18 p2650 A83-40133

Residual stress in high modulus carbon fibers 18 p2650 A83-40134

A study of relationship between composite strength and mono-filament strength 18 p2651 A83-40135

Effects of carbon fiber strain and resin characteristics on optimum composite performance 18 p2653 A83-40181

Statistical aspects of fibre and bundle strength in hybrid composites 18 p2658 A83-40240

Effects of interfacial reaction on fracture mode and tensile strength of fibres in metal matrix composites 18 p2659 A83-40254

Tensile property evaluation of polycrystalline alumina filaments and their composites 19 p2819 A83-41032

Silicon carbide yarn stimulates development of new composites 19 p2819 A83-41034

An experimental study of the effect of prestressed loose carbon strands on composite strength 20 p2948 A83-43142

The structure of boron in boron fibres 21 p3116 A83-44342

Probability distributions for the strength of composite materials. IV - Localized load-sharing with tapering 21 p3159 A83-44926

Lower-tail approximations for the probability of failure of three-dimensional fibrous composites with hexagonal geometry 21 p3159 A83-44941

Strain modulation measurements of stiffening effects in carbon fibers 23 p3454 A83-47649

The effect of temperature on the strength of aramide fibers and microplastics based on them 23 p3428 A83-48440

On the relation between Young's modulus and orientation in carbon fibres 24 p3553 A83-48898

Statistical properties of hybrid composites. I - Recursion analysis 24 p3554 A83-49876

FIBERGLASS

U GLASS FIBERS

FIBERS

NT BORON FIBERS

NT CARBON FIBERS

NT GLASS FIBERS

NT HAIR

NT METAL FIBERS

NT NYLON (TRADEMARK)

NT REINFORCING FIBERS

NT SYNTHETIC FIBERS

NT VYCOR

Variability of fiber type distributions within human muscles 05 p0674 A83-17328

Chemical deposition of coatings with additions of fibrous fillers 07 p0877 A83-20686

Finite element analysis of radiative transport in fibrous insulation [AIAA PAPER 83-1502] 14 p2010 A83-32741

FIBRILLATION

Fibrillation of the heart at low temperatures 01 p0081 A83-10919

The use of cordarone during acute myocardial infarctions 05 p0674 A83-17221

The transmembrane potentials of the heart cells of rats during fibrillation induced by a decrease in extracellular sodium 10 p1454 A83-26791

Sudden cardiac death - A problem in topology 12 p1762 A83-29250

FIBROBLASTS

NT COLLAGENS

FIBROUS MATERIALS

U FIBERS

FIDELITY

U ACCURACY

FIELD EFFECT TRANSISTORS

NT JFET

GaAs FET circuits handle high power. V - Designers: Prepare for the GaAs FET age 01 p0035 A83-10270

A model for field-sensitive interface states 01 p0109 A83-10631

Anomalous inversion channel formation in enhancement-mode InP metal-insulator-semiconductor field effect transistors 01 p0037 A83-10640

High-power field effect transistors in low-frequency and high-frequency power amplifiers 01 p0038 A83-10802

Microwave field-effect transistors - Theory, design and applications --- Book 01 p0038 A83-10876

An enhancement mode Schottky barrier gate charge-coupled device on a high electron mobility transistor structure 01 p0039 A83-10994

An automatic protection of spacecraft high power lines - The electronic solid state switch /ELSS/ 01 p0021 A83-11005

A compact and comprehensive micro-electronic control system for an unorthodox inverter-converter 01 p0040 A83-11008

Effects of dV/dt in MOSFET and bipolar junction transistor switches 01 p0041 A83-11020

The current status and the principal problems of developing microwave transistors /Review/ 01 p0043 A83-11304

A 1 watt GaAs power amplifier for the NASA 30/20 GHz communication system 01 p0044 A83-11489

Solid state components adapt to sensor environmental demands 02 p0168 A83-12973

K-band FET doubling oscillator 02 p0168 A83-13041

OTDR in single-mode fibre at 1.55 micron using a semiconductor laser and PINFET receiver 02 p0185 A83-13042

Microwave switching with GaAs FETs 03 p0308 A83-13438

Monolithic GaAs FET low-noise amplifiers for X-band applications 03 p0308 A83-13441

Direct-coupled GaAs ring oscillators with self-aligned gates 03 p0308 A83-13558

High performance ion-implanted low noise GaAs MESFET's 03 p0309 A83-13559

A high temperature GaP MESFET 03 p0309 A83-13561

Source-coupling for hybrid focal planes 03 p0326 A83-13733

TiW silicide gate self-alignment technology for ultra-high-speed GaAs MESFET LSI/VLSI's 03 p0314 A83-14514

Gate-drain avalanche breakdown in GaAs power MESFET's 03 p0314 A83-14515

Switching behaviour of Al₂O₃-n GaAs MISFETs 04 p0470 A83-15248

Enhancement of electron velocity in modulation-doped /Al, Ga/As/GaAs FETs at cryogenic temperatures 04 p0470 A83-15251

Bulk and interface gap states in a-Si:H - A comparative study of field effect and capacitance measurements on codeposited samples 04 p0539 A83-15487

Hot-electron induced excess carriers in MOSFET's 05 p0624 A83-17287

The Bloch-FET - A lateral surface superlattice device 05 p0690 A83-17289

Quarter micron low noise GaAs FET's 05 p0624 A83-17293

0.15 micron channel-length MOSFET's fabricated using e-beam lithography 05 p0624 A83-17297

A GaP MESFET for high temperature applications 05 p0625 A83-17348

Reduction of long-term transient radiation response in ion implanted GaAs FETs 05 p0625 A83-17482

Radiation effects on distortion characteristics of power GaAs MESFET amplifiers 05 p0625 A83-17483

The effect of operating conditions on the radiation resistance of VDMOS power FETs --- Vertical Double-diffused MOS 05 p0626 A83-17486

Radiation effects on MOS power transistors 05 p0626 A83-17487

Modeling of ionizing radiation effects in short-channel MOSFETs 05 p0626 A83-17508

Enhanced radiation effects on submicron narrow-channel NMOS 05 p0627 A83-17509

Total dose radiation-bias effects in laser-recrystallized SOI MOSFET's 05 p0627 A83-17510

Gamma-ray irradiation effects on VLSI geometry MOSFETs fabricated on laser recrystallized SOI wafers 05 p0627 A83-17511

Self-aligned phosphorus doped polysilicon gate MOS device radiation hardening 05 p0627 A83-17512

Miniaturization degree of dynamic MOS RAM cells with readout signal gain 05 p0630 A83-17751

An analytical breakdown model for short-channel MOSFET's 05 p0630 A83-17753

Correlation between substrate and gate currents in MOSFET's 05 p0630 A83-17754

A simple model for short-channel effects of a buried-channel MOSFET on the buried insulator 05 p0630 A83-17755

GaAs LSI-directed MESFET's with self-aligned implantation for n/+/-layer technology /SAINT/ 05 p0631 A83-17759

A novel buried-drain DMOSFET structure 05 p0631 A83-17761

FET photodetectors - A combined study using optical and electron-beam stimulation 05 p0631 A83-17762

The effect of parasitic capacitances on the circuit speed of GaAs MESFET ring oscillators 05 p0631 A83-17763

The effect of Al-GaAs interaction on the technology of self-aligned gallium arsenide MESFETs 05 p0631 A83-17771

Power MOSFET characteristics with modified SPICE modeling 05 p0631 A83-17772

Travelling wave power FET with coplanar slow-wave electrode system, modeling and experimental results 06 p0749 A83-17969

Monte Carlo particle simulation of a GaAs short-channel MESFET 06 p0751 A83-18572

Theory of traveling-wave transistors 06 p0752 A83-18753

A monolithic lead sulfide-silicon MOS integrated-circuit structure 06 p0752 A83-18756

Investigation of transient electronic transport in GaAs following high energy injection 06 p0814 A83-18757

Direct comparison of the electron-temperature model with the particle-mesh /Monte-Carlo/ model for the GaAs MESFET 06 p0752 A83-18761

On design and performance of lossy match GaAs MESFET amplifiers 06 p0752 A83-18765

Undoped, semi-insulating GaAs layers grown by molecular beam epitaxy 06 p0815 A83-19262

Microwave fiber-optic communications systems 07 p0905 A83-19709

Characteristics of modulation-doped Al_x/Ga_{1-x}/As/GaAs field-effect transistors - Effect of donor-electron separation 07 p0918 A83-19987

4-GHz high-efficiency broadband FET power amplifiers 07 p0920 A83-20556

Initial results of a high throughput MBE system for device fabrication 07 p0999 A83-20593

The effect of interfacial traps on the stability of insulated gate devices on InP 07 p0921 A83-20742

Monolithic integration of a photodiode and a field-effect transistor on a GaAs substrate by molecular beam epitaxy 07 p0922 A83-21375

A monolithic single-chip X-band four-bit phase shifter 07 p0923 A83-21534

X-band burnout characteristics of GaAs MESFET's 07 p0923 A83-21535

A simplified 'real frequency' technique applied to broad-band multistage microwave amplifiers 07 p0923 A83-21537

RDA requirements for optimum hybrid focal plane performance --- Resistance-Area product for IR detector arrays 08 p1100 A83-22599

Integrating 128-element linear imager for the 1 to 5 microns region 08 p1100 A83-22601

Empirical model for gallium arsenide MESFETs 09 p1251 A83-23348

AC model for MOS transistors from transient-current computations 09 p1252 A83-23349

Comparison between two-dimensional short-channel MOSFET models 09 p1252 A83-23350

New receivers in radio astronomy 09 p1352 A83-23395

0.5 micron GaAs FET for low-noise circuits for Orbital Test Satellite reception 09 p1252 A83-23396

Two-channel receiver for 21 cm wavelength with cooled FET amplifiers 09 p1252 A83-23397

Physics of semiconductor power devices 09 p1254 A83-23853

An MOS dosimeter for use in space 09 p1219 A83-24110

Practical design of 2-4 GHz low intermodulation distortion GaAs FET amplifiers with flat gain response and low noise figure 09 p1255 A83-24348

Theory of triangular-barrier bulk unipolar diodes including minority-carrier effects 09 p1255 A83-24493

Design, fabrication, and evaluation of 2- and 3-bit GaAs MESFET analog-to-digital converter IC's 09 p1256 A83-24678

A monolithic GaAs DC to 2-GHz feedback amplifier 09 p1256 A83-24682

A negative drain conductance property in a super-thin film buried-channel MOSFET on a buried insulator 09 p1256 A83-24685

Numerical comparison of DMOS, VMOS, and UMOS power transistors 09 p1256 A83-24686

Electronically cold microwave artificial resistors 10 p1410 A83-26339

Improving the power-added efficiency of FET amplifiers operating with varying-envelope signals 10 p1410 A83-26340

Fast low-power driver and Schmitt trigger using GaAs MESFET and tunnel diode 10 p1411 A83-26886

Four MOSFETs deliver 600 W of RF power 11 p1562 A83-28155

Finite element iterative techniques for determining the interface boundary between Laplace and Poisson domains - Characteristic analysis of a field effect transistor 11 p1563 A83-28417

A low-noise GaAs FET preamplifier for 21 GHz satellite earth terminals 11 p1563 A83-28591

Development of a measurement technique for qualitative analysis of MOS transistors using Kuhn's method for MOS varactors --- German thesis 11 p1564 A83-28644

Power MOSFET dynamic large-signal model 12 p1719 A83-29419

The COMFET - A new high conductance MOS-gated device 12 p1720 A83-29520

Temperature stabilization of GaAs MESFET oscillators using dielectric resonators 13 p1831 A83-30238

Picosecond Al(x)Ga(1-x) As modulation-doped optical field-effect transistor sampling gate 13 p1832 A83-30341

Glow discharge polycrystalline silicon thin-film transistors 13 p1832 A83-30345

Two-dimensional analysis of hot-electron emission current in MOS FET 13 p1834 A83-30783

Large signal design of GaAs FET oscillators using input dielectric resonators 13 p1836 A83-31149

Theory of heterostructure inversion-mode metal-insulator-semiconductor field effect transistors 13 p1837 A83-31391

Inverted transistor gate with FET load 13 p1837 A83-31769

Near-infrared linear array spectrometer for space applications 14 p2016 A83-31999

Low pressure nitrided-oxide as a thin gate dielectric for MOSFET's 14 p2006 A83-32640

A small geometry MOSFET model for CAD applications 14 p2006 A83-32672

Numerical modeling of power MOSFETs 14 p2007 A83-32673

Delay times in Si MOSFETs in the 4.2-400 K temperature range 14 p2007 A83-32674

The effect of gamma-irradiation on amorphous silicon field effect transistors 14 p2007 A83-33142

Switching characteristics of logic gates addressed by picosecond light pulses 14 p2008 A83-33422

Performance of a microwave amplitude limiter using GaAs MESFET 15 p2149 A83-33522

High-performance K-band GaAs power field-effect transistors prepared by molecular beam epitaxy 15 p2150 A83-33846

Compact dc model of GaAs FET's for large-signal computer calculation 15 p2151 A83-33892

Comments on 'Silicon MESFET digital circuit techniques' 15 p2151 A83-33895

I-V characteristics of MOS FET devices with a variable channel width 15 p2152 A83-34450

Electrical properties of polyacetylene/polysiloxane interface 16 p2344 A83-35444

Schottky barrier height variation with metallurgical reactions in aluminum-titanium-gallium arsenide contacts 16 p2419 A83-35671

Double-injection currents and the field effect in p(+)-nn(+)-silicon-on-sapphire diodes 16 p2346 A83-35946

Modes of operation in dual-gate MESFET mixers 16 p2346 A83-36005

High-power InP MISFETs 16 p2346 A83-36006

Mim gate FET - New GaAs enhancement-mode transistor 16 p2346 A83-36007

High-performance modulation-doped GaAs integrated circuits with planar structures 16 p2347 A83-36477

GaAs integrated digital-to-analogue converter for control of power dual-gate FETs 16 p2347 A83-36479

Integrated surface acoustic wave/field-effect transistor high-speed analog memory 16 p2347 A83-36772

GaAs microwave devices and circuits with submicron electron-beam defined features 17 p2496 A83-37059

On theory and performance of solid-state microwave distributed amplifiers 17 p2497 A83-37799

High-frequency doubler operation of GaAs field-effect transistors 17 p2497 A83-37800

Novel design of travelling-wave FET 17 p2500 A83-38876

Analytical model and characterization of small geometry MOSFET's 18 p2677 A83-40368

A simplified model of short-channel MOSFET characteristics in the breakdown mode 18 p2677 A83-40370

Characterization of electron traps in ion-implanted GaAs MESFET's on undoped and Cr-doped LEC semi-insulating substrates 18 p2750 A83-40372

Ideal FET doping profile 18 p2678 A83-40376

Two-dimensional numerical analysis of the narrow gate effect in MOSFET 18 p2678 A83-40378

Optically controllable S-type negative resistance presented by a combinational connection of photocoupled FET's 18 p2678 A83-40379

An As-P/n(+)-n(-)/ double diffused drain MOSFET for VLSI's 18 p2678 A83-40380

Constant voltage scaling of FETs for high frequency and high power applications 19 p2836 A83-40668

GaAs digital dynamic IC's for applications up to 10 GHz 19 p2837 A83-40793

High-speed logic at 300 K with self-aligned submicrometer-gate GaAs MESFET's 19 p2837 A83-41019

Microwave characteristics of an optically controlled GaAs MESFET 19 p2838 A83-41092

The effect of temperature on hot electron trapping in MOSFET's 19 p2905 A83-41287

High efficiency broadband FET power amplifier for C-band TWTA replacement 19 p2839 A83-41335

- 20 GHz GaAs FET transmitter 19 p2839 A83-41368
- Anodic oxide gate a-Si:H MOSFET 20 p2966 A83-42480
- Comparison of the electrophysical and fundamental approaches to the modeling of GaAs Schottky transistors 20 p3053 A83-42912
- Determination of the parameters of the equivalent circuit of the active region of an FET crystal 20 p2967 A83-42914
- A theory of noise in GaAs FET microwave oscillators and its experimental verification 20 p2968 A83-43349
- X-band self-aligned gate enhancement-mode InP MISFET's 20 p2968 A83-43353
- Nonlinear lumped circuit model of GaAs MESFET 20 p2968 A83-43354
- Ion implanted Si MESFET's with high cutoff frequency 20 p2968 A83-43355
- Measurement and simulation of GaAs FET's under electron-beam irradiation 20 p2968 A83-43357
- Monolithic integration of a double heterostructure light-emitting diode and a field-effect transistor amplifier using molecular beam grown AlGaAs/GaAs 20 p2968 A83-43596
- An analytic approach to optimum oscillator design using S-parameters 21 p3122 A83-43832
- Submicron GaAs microwave FET's with low parasitic gate and source resistances 21 p3123 A83-43848
- A new high-power voltage-controlled differential negative resistance device - The Lambda bipolar power transistor 21 p3123 A83-43850
- Indium phosphide accumulation-mode field-effect transistors 21 p3124 A83-43856
- An empirical model for device degradation due to hot-carrier injection 21 p3124 A83-43857
- Short-channel effects in 0.5-micron source-drain spaced vertical GaAs FET's - A first experimental investigation 21 p3124 A83-43860
- Negative differential resistance in GaAs MESFETs 21 p3125 A83-44951
- Simulation of GaAs submicron FET with hot-electron injection structure 21 p3126 A83-44967
- Equivalent-circuit consideration of dual-gate MESFETs at high frequency 21 p3126 A83-44970
- Noise measurements in ion implanted MOSFETs 21 p3127 A83-45174
- High-frequency admittance of high-electron-mobility transistors (HEMTs) 21 p3127 A83-45175
- Analytical solutions for threshold voltage calculations in ion-implanted IGFETs 21 p3127 A83-45177
- Effect of the velocity-field peak on I-V characteristics of GaAs FET's 21 p3127 A83-45181
- Electron-beam-induced current measurements in silicon-on-insulator films prepared by zone-melting recrystallization 21 p3219 A83-45496
- The effect of impurities on the current-amplification cut-off frequency of field-effect transistors 22 p3277 A83-45675
- Drain-voltage effects on the threshold voltage of a small-geometry MOSFET 23 p3446 A83-48606
- A time-dependent and two-dimensional numerical model for MOSFET device operation 23 p3446 A83-48610
- Highly stable FET DROs using new linear dielectric resonator material --- Dielectric Resonator Oscillators 23 p3446 A83-48723
- A new approach for mm-wave generation 24 p3571 A83-48774
- A 20 GHz band 0.5 W GaAs FET amplifier for satellite communications 24 p3574 A83-49858
- Instabilities in modulation doped field-effect transistors (MODFETs) at 77 K 24 p3574 A83-49972
- New Ga(0.47)In(0.53)As sheet-charge field-effect transistor for long-wavelength optoelectronic integration 24 p3574 A83-49973
- Optical injection locking of X-band FET oscillator using coherent mixing of GaAlAs lasers 24 p3630 A83-49991
- FIELD EMISSION**
- Field-ion microscopy - A review of basic principles and selected applications 05 p0644 A83-16918
- Analysis of airfoil leading edge separation bubbles [AIAA PAPER 83-0300] 05 p0591 A83-17918
- An experimental study of the dynamics of interaction between rarefied gas flows and a solid surface using the method of field-emission microscopy 13 p1932 A83-30664
- Influence of light exposure on the transport properties of a-Si:H films 14 p2088 A83-32238
- Excitation of violent discharge of charged bodies --- planetary rings or interplanetary medium 17 p2609 A83-38414
- 125 kV field emission electron microscope and its application to lattice imaging 20 p2992 A83-43617
- Five milli Newtons field emission thruster testing [IAF PAPER 83-394] 23 p3426 A83-47371

FIELD INTENSITY METERS

- Electric field detection with a piezoelectric polymer-jacketed single-mode optical fiber 03 p0330 A83-14384

FIELD MODE THEORY

- Mode selection with a three-layer dielectric rib waveguide 03 p0393 A83-13762
- TE/11/-to-HE/11/ mode converters for small angle corrugated horns 03 p0305 A83-14003
- A curved-aperture corrugated horn having very low cross-polar performance 03 p0305 A83-14005
- High-frequency propagation in an elevated tropospheric duct 03 p0305 A83-14011
- Characteristics of annular-ring microstrip antenna 04 p0466 A83-15249
- A high power gyrotron operating in the TE/041/ mode 06 p0752 A83-18758
- Asymptotic relations and period doubling bifurcations in a mean-field model of optical bistability 08 p1164 A83-21887
- Electromagnetic fields in twisted coordinate system 08 p1080 A83-22234
- The theory of irregular waveguides and open resonators 08 p1080 A83-22249
- Local momentum representation of a propagator in external gravitational and electromagnetic fields 09 p1338 A83-24212
- Giant Raman optical activity of the 128/cm mode in alpha-quartz 10 p1481 A83-25432
- Mode control in a submillimetre open resonator with a variable iris 10 p1425 A83-25459
- Influence of a nonlinear active medium on the structure of natural oscillation modes of a Fabry-Perot interferometer 10 p1433 A83-26681
- Optical resonators with polarization mixing elements 11 p1656 A83-27568
- Modes of resonance of the Jerusalem cross in frequency-selective surfaces 12 p1718 A83-29438
- Shielded dielectric resonators 12 p1720 A83-29461
- Modes of phase-conjugate resonators with bounded mirrors 15 p2229 A83-33531
- Power and stability of phase-conjugate lasers 15 p2167 A83-33535
- Orthogonality and noarmalization of radiation modes in dielectric waveguides - An alternative derivation 15 p2229 A83-33538
- Quantum theory of optical bistability. III - Atomic fluorescence in a low-Q cavity 16 p2411 A83-35659
- Problems in steady-state theory of a multimode laser with a selective saturable absorber 16 p2359 A83-35896
- Mode coupling phenomena of Tonks-Dattner resonances in an asymmetrically inhomogeneous plasma column 18 p2747 A83-40072
- Classical derivation of the laser rate equation 22 p3300 A83-46814
- FIELD OF VIEW**
- Sensor snap and narrow field-of-view inset for terrain avoidance flight 01 p0010 A83-11188
- Gyrotropic isosex filter 02 p0178 A83-12597
- Off-axis effects in a mosaic Michelson interferometer [AD-A123678] 02 p0179 A83-12609
- AOI displays in simulation --- Area Of Interest 04 p0448 A83-16337
- Cognitive load and the functional field of view 07 p0980 A83-20625
- Image processing for extended depth of field 14 p2020 A83-32905
- The design and study of the aspherical plate corrector of the view field for Cassegrain system 17 p2580 A83-38774
- Wide field of view head-up displays 21 p3091 A83-44690
- Continuous-wave self-pumped phase conjugator with wide field of view 22 p3356 A83-45964
- Forward multiple scattering corrections as a function of detector field of view --- laser beam propagation through atmospheric aerosols 24 p3588 A83-49005
- FIELD STRENGTH**
- NT ELECTRIC FIELD STRENGTH
- NT MAGNETIC FLUX
- The changes in the nerve and cardiac activity in animals of various ages during the application of electromagnetic fields of low frequency and low voltage 02 p0220 A83-11884
- The biological effectiveness of a weak electromagnetic field of infralow frequency 02 p0221 A83-11887
- The reaction of a biological system to adequate or weak low-frequency electromagnetic fields 02 p0221 A83-11889
- The structure of sunspots. IV - Magnetic field strengths in small sunspots and pores 02 p0270 A83-12575
- Stimulated emission from ultrarelativistic electrons in strong electric and magnetic fields 11 p1584 A83-28058

- The low-frequency electromagnetic field in the Venus atmosphere - Evidence from Venera 13 and Venera 14 12 p1798 A83-29483
- Relative field strength of VHF/UHF horizontally polarized waves in 5 to 100-meter range of propagation 14 p2002 A83-33147
- Techniques for measuring the field intensity of radio waves --- Russian book 21 p3121 A83-45042
- Approximate solution of the strongly magnetized hydrogenic problem with the use of an asymptotic property --- application to stellar magnetic fields 24 p3650 A83-48828

FIELD THEORY (ALGEBRA)

- NT CUBIC EQUATIONS
- NT QUADRATIC EQUATIONS
- Variational approach to problems of the interpolation of physical fields --- Russian book on oceanography 24 p3622 A83-49041

FIELD THEORY (PHYSICS)

- NT INSTANTONS
- NT QUANTUM CHROMODYNAMICS
- NT STRONG INTERACTIONS (FIELD THEORY)
- NT UNIFIED FIELD THEORY
- NT WEAK INTERACTIONS (FIELD THEORY)
- The external field of a rotating and charged body in the vector graviton metric theory 01 p0119 A83-10232
- Application of Ampere's force law to railgun accelerators 01 p0036 A83-10613
- Some experimental consequences of the fundamental-length hypothesis --- inquantum electrodynamics 02 p0235 A83-11738
- Radiation from a black hole - A Vaidya-metric-based computation 02 p0254 A83-12027
- Static conformally flat solutions in a general scalar-tensor theory of gravitation 02 p0233 A83-12090
- Field theory analysis and numerical synthesis of symmetrical multiple-branch waveguide couplers 02 p0168 A83-12988
- The energy problem in Einstein's theory of gravitation /Dedicated to the memory of V. A. Fock/ 03 p0416 A83-13426
- The energy-momentum pseudotensor of the gravitational field and the gravitational radiation emitted by an axisymmetric system 03 p0417 A83-13474
- Fundamentals handbook of electrical and computer engineering. Volume 1 Circuits fields and electronics 03 p0314 A83-14047
- Hidden supersymmetry in stochastic dissipative dynamics 04 p0532 A83-15911
- Astrophysical consequences of neutron-antineutron oscillations 04 p0556 A83-15965
- Infinity subtraction in a quantum field theory of charges and monopoles 06 p0805 A83-18330
- Static spherically-symmetric scalar-field theory in general relativity 06 p0835 A83-18894
- Measurability analysis of the linearized gravitational field 06 p0806 A83-19448
- Some remarks on the antidynamo theorem 07 p0996 A83-20140
- Self-similar collision of plane neutrino waves in general relativity 07 p1013 A83-20143
- Concerning problems of optimization in nonlinear optics --- field characteristics and incident radiation 07 p0936 A83-20312
- Algorithmization of computations in a discretely observed gravitational field 07 p0962 A83-20602
- On one type of system with equivalent external gravity effects 07 p0962 A83-20603
- Propagation of vertically and horizontally polarized waves excited by distributions of electric and magnetic sources in irregular stratified spheroidal structures of finite conductivity - Generalized field transforms 08 p1161 A83-22281
- Static plane symmetric disordered radiation in Brans-Dicke theory 08 p1181 A83-22745
- Generalized network representations for small-aperture coupling between dissimilar regions 09 p1254 A83-23804
- The representation of a matricant of a linearized system of differential equations of motion in a field of forces possessing potential 09 p1338 A83-23865
- Application of the Braunbek method to the Maggi-Rubinowicz field representation --- asymptotic evaluation of surface integral representations of optical diffraction by apertures 09 p1338 A83-24090
- Interaction of a plane gravitational wave with a scalar field 09 p1359 A83-24207
- Vacuum static gravitational fields with axial symmetry 09 p1338 A83-24213
- New solutions of Einstein equations from analytic mappings 10 p1471 A83-25408
- Some remarks on zeta function regularization in curved space-times 10 p1472 A83-26094

Gravitational radiation in Robertson-Walker backgrounds 10 p1506 A83-26096
Field theory of planar helix traveling-wave tube 10 p1410 A83-26343
Theoretical aspects of interrelationships between remote-sensing measurements and the state parameters of natural formations 10 p1444 A83-26810
The absorber theory for the Einstein equations in the first approximation 11 p1677 A83-27455
Space-time ordered electromagnetic radiation outside a massive plane 12 p1774 A83-28874
General vacuum-Universe solutions in Brans-Dicke cosmology 12 p1790 A83-28982
Robertson-Walker cosmologies with a trace anomaly effect in their dynamical description 12 p1791 A83-28985
A mathematical solution of general relativistic binary systems 12 p1791 A83-28989
Gauge transformations in soliton theory 12 p1774 A83-29004
Hermitian gravity and supergravity 12 p1774 A83-29029
Organization of parallel computations for the solution of nonlinear problems of field theory using networks 12 p1768 A83-29347
Numerical methods for solving time-dependent quantum-mechanical problems with applications 12 p1776 A83-29606
Unified quantum theory of free-electron devices 13 p1856 A83-31139
Magnetic-charge conjugation and the topological nature of magnetic monopole 13 p1918 A83-31605
Three-dimensional higher-order mode analysis of transition from waveguide to shielded dielectric image line 13 p1837 A83-31771
Dynamic properties of gravitational fields 14 p2079 A83-32351
Microcanonical quantum gravity 14 p2103 A83-33050
Painleve property of anharmonic systems with an external periodic field 15 p2225 A83-34135
On physical and material conservation laws 15 p2177 A83-34335
Transport effects associated with turbulence with particular attention to the influence of helicity 15 p2161 A83-34400
An outline of approach linking black-hole-evaporation with quantum-field effects in flat spacetime 15 p2262 A83-34531
Polarization effects in the diffraction of electromagnetic waves - The role of disclinations 16 p2407 A83-35639
Solutions of Einstein-Maxwell field equations for a static charged perfect fluid sphere 16 p2407 A83-36538
Absolute synchronization - Faster-than-light particles and causality violation 16 p2407 A83-36551
Large numbers hypothesis. II - Electromagnetic radiation 16 p2408 A83-36986
Large numbers hypothesis. IV - The cosmological constant and quantum physics 16 p2408 A83-36987
Alternative variational formulations for first order partial differential systems 17 p2571 A83-37769
Cosmological models with S3 topology 17 p2614 A83-38951
Black holes in neutrino fields 18 p2767 A83-39529
General relativity and matter: A spinor field theory from Fermis to light-years --- Book 19 p2896 A83-41521
Vacuum field, modified cosmical term and non-singular cosmology 20 p3070 A83-42940
Theory of spinors and its application in physics and mechanics --- Russian book 21 p3200 A83-45031
Conducting shells in a pulsed electromagnetic field --- Russian book 21 p3126 A83-45047
Fields of radiation sources in moving media 21 p3200 A83-45049
Nonlinear scattering from a plasma column. I - Theory. II Special cases 22 p3363 A83-46536
A note on electromagnetic 'tidal' force 23 p3503 A83-47418
The complete integration of the Einstein vacuum and the Maxwell-Einstein equations, of type D 23 p3503 A83-48051
Bianchi type-I universes of the Brans-Dicke vacuum theory 23 p3526 A83-48060
Hydrodynamics, fields, and constants in gravitation theory --- Russian book 23 p3527 A83-48450
The stability of the stationary motions of a plane body in the field of a central force 23 p3504 A83-48458
Lichnerowicz-York equation and conformal deformations on maximal slicings in asymptotically flat space-times 24 p3651 A83-49098
The equivalence of perfect fluid space-times and viscous magnetohydrodynamic space-times in general relativity 24 p3651 A83-49099

Scalar-tensor theories of gravitation - Foundations and prospects 24 p3651 A83-49100
Electric-magnetic duality of conformal gravitation 24 p3624 A83-49745

FIGHTER AIRCRAFT

NT ALPHA JET AIRCRAFT
NT F-4 AIRCRAFT
NT F-5 AIRCRAFT
NT F-8 AIRCRAFT
NT F-14 AIRCRAFT
NT F-15 AIRCRAFT
NT F-16 AIRCRAFT
NT F-17 AIRCRAFT
NT F-18 AIRCRAFT
NT F-104 AIRCRAFT
NT F-111 AIRCRAFT
NT HARRIER AIRCRAFT
NT JAGUAR AIRCRAFT
NT YF-12 AIRCRAFT
Departure susceptibility and uncoordinated roll-reversal boundaries for fighter configurations 01 p0012 A83-10176
Minimum-time 180 deg turns of aircraft 01 p0012 A83-10250
The solution of 'real-world' aircraft EMC problems using the AAPG computer program 01 p0041 A83-11085
Integrated CNI avionics maximizes reliability --- communications, navigation, and cooperative identification 01 p0042 A83-11089
The development of JTIDS distributed TDMA /DTDMA/ advanced development model /ADM/ terminals --- Joint Tactical Information Distribution System 01 p0004 A83-11094
Rationalizing Tacair force development in the next decade 01 p0002 A83-11116
Advanced speech technology in fighter cockpits - A new perspective on issues and applications 01 p0005 A83-11125
Strapdown inertial performance needed for the 1990s 01 p0005 A83-11127
Color, pictorial display formats for future fighters 01 p0010 A83-11134
Integrated airframe/propulsion controls technology 01 p0013 A83-11175
Fiber optic aircraft multiplex systems - Planning for the 1990s 01 p0006 A83-11180
F-4F fire control system software support - An integrated approach to ground and flight testing 01 p0015 A83-11228
Applications of autopath technology to terrain/obstacle avoidance 01 p0008 A83-11255
The effects of firing a weapon on the air intake in a subsonic flow [AAAF PAPER NT 81-11] 02 p0132 A83-11772
ACA-ECA or pipedream; Industry needs it - but who will pay 02 p0135 A83-13017
Airframe effects on a top-mounted fighter inlet system 03 p0278 A83-13166
The application of diffraction optics to the LANTIRN head-up display 04 p0447 A83-16131
Simulation of a terrain following system 04 p0445 A83-16333
Augmentation of fighter aircraft lift and STOL capability by blowing outboard from the wing tips [AIAA PAPER 83-0078] 05 p0578 A83-16507
Thrust reversing effects on horizontal tail effectiveness of twin-engine fighter aircraft [AIAA PAPER 83-0086] 05 p0594 A83-16512
The application of energy saving concepts to future fighter/attack aircraft design [AIAA PAPER 83-0092] 05 p0594 A83-16516
A glimpse into the future of air combat --- via computerized cockpit simulators [AIAA PAPER 83-0143] 05 p0599 A83-16552
Trimming high lift for STOL fighters [AIAA PAPER 83-0168] 05 p0598 A83-16566
Decoupling of high gain multivariable tracking systems [AIAA PAPER 83-0280] 05 p0592 A83-16625
Low-speed investigation of the maneuver capability of supersonic fighter wings [AIAA PAPER 83-0426] 05 p0585 A83-16708
Slender wings with leading-edge vortex separation - A challenge for panel-methods and Euler-solvers [AIAA PAPER 83-0562] 05 p0588 A83-16790
The JA37 /VIGGEN/ pilot training concepts ATD preliminary use and 'signs' of effectiveness --- Aircraft Training Device System 05 p0676 A83-17310
Fatigue sensitivity of composite structure for fighter aircraft 06 p0717 A83-18402
Effects of spanwise blowing and reverse thrust on fighter low-speed aerodynamics 06 p0712 A83-18410
Military propulsion technology. I - Fighter power - The need for tomorrow 06 p0718 A83-18948
Military propulsion technology. II - Supersonic V/STOL technology shapes up 06 p0718 A83-18949

Military propulsion technology. III - Materials are the key --- for fighter aircraft engines 06 p0730 A83-18950
US Navy STOVL - Waiting in the wings 06 p0717 A83-19450
The development of advanced composite front fuselage technology 07 p0865 A83-20464
The future for fighter aircraft 07 p0862 A83-20597
Thirty years of fighter armament 07 p0866 A83-20600
Solution of three dimensional interception by inclined plane using the forced singular perturbations technique 07 p0862 A83-21013
Suboptimal filters for INS alignment on a moving base 07 p0865 A83-21019
Dynamics of air combat 07 p0862 A83-21026
Stability of steady sideslip equilibria for high alpha --- supersonic fighter aircraft 09 p1209 A83-24031
Configuration development for a highly maneuverable experimental aircraft with negative sweep rudder units [DGLR PAPER 82-035] 09 p1203 A83-24160
Ground tests for obtaining the airworthiness certificate for an automatic terrain-following system [DGLR PAPER 82-040] 09 p1200 A83-24164
Maneuver load control for reducing the design loads of modern combat aircraft [DGLR PAPER 82-046] 09 p1209 A83-24169
Some aspects of the engine design of future fighter planes [DGLR PAPER 82-071] 09 p1206 A83-24185
Development trends regarding jet engines for future combat aircraft [DGLR PAPER 82-072] 09 p1206 A83-24186
On the design philosophy of fighter aircraft engines [DGLR PAPER 82-073] 09 p1206 A83-24187
Delta canard configuration at high angle of attack 09 p1210 A83-24650
Technical qualities for combat helicopter powerplants 09 p1208 A83-24839
A multifunction integrated approach to providing aircraft inertial data 09 p1200 A83-24853
Now is the time for new fighters 09 p1204 A83-25137
Operational utilization study on new human centrifuge of JASDF. II - Capability and usability of the new systems 10 p1458 A83-26088
Potential uses of two types of stereographic display systems in the airborne fire control environment 10 p1376 A83-26314
Self-tuning fly-by-wire control system 10 p1379 A83-26603
A multifunction integrated approach to providing aircraft inertial data 11 p1528 A83-28595
A core software concept for integrated control 13 p1909 A83-30170
X-29 - Advanced technology demonstrator 13 p1806 A83-31051
Escape low and hot --- vertical-seeking, steerable ejection seat design for F-14A aircraft 13 p1806 A83-31587
AM-X - The export challenger with a foot in two continents 14 p1974 A83-31940
Flight tests verify predictions for F-20 14 p1974 A83-32475
AMRAAM - Tomorrow's Sparrow 14 p1969 A83-32844
Aircraft design philosophy. I - Lee Begin of Northrop 16 p2298 A83-35624
An investigation of motion base cueing and G-seat cueing on pilot performance in a simulator [AIAA PAPER 83-1084] 16 p2401 A83-36209
Real time simulation of mission environments for avionics systems integration [AIAA PAPER 83-1097] 16 p2312 A83-36217
Criteria for optimizing starting cycles for high performance fighter engines [AIAA PAPER 83-1127] 16 p2306 A83-36236
Thrust reverser exhaust plume reingestion tests for a STOL fighter model [AIAA PAPER 83-1229] 16 p2307 A83-36293
A static investigation of yaw vectoring concepts on two-dimensional convergent-divergent nozzles [AIAA PAPER 83-1288] 16 p2294 A83-36324
Fighter engine cycle selection [AIAA PAPER 83-1300] 16 p2310 A83-36412
The application of low-cost demonstrators for advanced fighter technology evaluation [AIAA PAPER 83-1052] 16 p2300 A83-36462
X-29 integrated technology demonstrator and ATF [AIAA PAPER 83-1058] 16 p2301 A83-36469
GE's APG-67 - Fighter radar with a future 16 p2298 A83-36625
Dynamics of air combat 16 p2287 A83-36914
The future of the manned aircraft 16 p2287 A83-36960

Piloted simulation of hover and transition of a vertical attitude takeoff and landing aircraft 17 p2462 A83-37064

Configuration studies for future fighters 17 p2462 A83-37859

Supersonic STOVL research aircraft [SAE PAPER 821375] 17 p2463 A83-37965

Electromechanical primary flight control activation systems for fighter/attack aircraft [SAE PAPER 821435] 17 p2463 A83-37983

Flight at supersonic attitudes [SAE PAPER 821469] 17 p2470 A83-38000

Application of forward sweep wings to an air combat fighter [AIAA PAPER 83-1833] 17 p2465 A83-38662

High angle-of-attack flight dynamics of a forward-swept wing fighter configuration [AIAA PAPER 83-1837] 17 p2470 A83-38666

Status review of a supersonically-biased fighter wing-design study [AIAA PAPER 83-1857] 17 p2465 A83-38684

Aerodynamics critical to the operations of tactical fighters from bomb damaged runways [AIAA PAPER 83-1861] 17 p2465 A83-38688

Survey of inlet development for supersonic aircraft [AIAA PAPER 83-1164] 18 p2638 A83-40473

Air-to-air combat in a plastic dome 18 p2642 A83-40620

Integrated airframe/p propulsion control system architectures (IAPSA) study [AIAA PAPER 83-2158] 19 p2797 A83-41660

Control law design for ejection seats [AIAA PAPER 83-2204] 19 p2797 A83-41688

Impact of aircraft structural dynamics on integrated control design [AIAA PAPER 83-2216] 19 p2798 A83-41698

Computational aerodynamic design of fighter aircraft Progress and pitfalls [AIAA PAPER 83-2063] 19 p2798 A83-41903

Determination of aerodynamic parameters of a fighter airplane from flight data at high angles of attack [AIAA PAPER 83-2066] 19 p2804 A83-41904

Comparison of fixed-base and in-flight simulation results for lateral high order systems [AIAA PAPER 83-2105] 19 p2806 A83-41934

Flight test experience with pilot-induced-oscillation suppressor filters [AIAA PAPER 83-2107] 19 p2806 A83-41936

Poststall flight in close combat [AIAA PAPER 83-2120] 19 p2806 A83-41945

Interception in three dimensions - An energy formulation [AIAA PAPER 83-2121] 19 p2798 A83-41946

An eccentric two-target differential game model for qualitative air-to-air combat analysis [AIAA PAPER 83-2122] 19 p2789 A83-41947

Flight path/nose pointing - A required criterion in future fighter aircraft design [AIAA PAPER 83-2123] 19 p2798 A83-41948

Innovative concepts for tactical STOL [AIAA PAPER 83-2129] 19 p2798 A83-41952

Subsonic roll oscillation experiments on the Standard Dynamics Model [AIAA PAPER 83-2134] 19 p2806 A83-41956

The optimal evasive maneuver of a fighter against proportional navigation missiles [AIAA PAPER 83-2139] 19 p2807 A83-41961

World aeronautical research - III 20 p2927 A83-43033

Grumman's forward swept wing feasibility studies and X-29A technology demonstrator [SAWE PAPER 1454] 20 p2935 A83-43736

Life cycle cost applications to conceptual designs [SAWE PAPER 1479] 20 p3056 A83-43748

Aerodynamic aspects of aircraft dynamics at high angles of attack 21 p3085 A83-43964

Nonlinear control law for piloting aircraft in the air-to-ground attack phase [ONERA, TP NO. 1983-37] 21 p3093 A83-44315

Design impact of composites on fighter aircraft. I - They force a fresh look at the design process 22 p3254 A83-46347

EAGLE/DTA - A life cycle cost model for damage tolerance assessment --- Engine/Aircraft Generalized Life cycle cost Evaluator [ASME PAPER 83-GT-76] 23 p3407 A83-47929

Integrated flight and propulsion operating modes for advanced fighter engines [ASME PAPER 83-GT-194] 23 p3410 A83-47999

A design study of a reaction control system for a V/STOL fighter/attack aircraft [ASME PAPER 83-GT-199] 23 p3410 A83-48002

STOL fighter technology program [ASME PAPER 83-GT-243] 23 p3403 A83-48033

Correlation of flight test and analytic M-on-N air combat exchange ratios --- Many-on-Many 23 p3392 A83-48219

Preliminary design engine thermodynamic cycle selection for advanced fighters [AIAA PAPER 83-2480] 23 p3411 A83-48343

Performance of a forward swept wing fighter utilizing thrust vectoring [AIAA PAPER 83-2482] 23 p3404 A83-48344

Effect of aircraft configuration and control integration on surface actuation [AIAA PAPER 83-2487] 23 p3404 A83-48347

Large-scale wind-tunnel investigation of a close-coupled canard-delta-wing fighter model through high angles of attack [AIAA PAPER 83-2554] 23 p3399 A83-48373

Voice-actuated avionics 24 p3546 A83-48891

Identification and control of flutter on military combat aircraft 24 p3547 A83-49187

Aeroelastic considerations for automatic structural design procedures 24 p3547 A83-49189

Strength-flutter structural optimization of a supersonic cruise combat aircraft 24 p3547 A83-49190

Active gust load alleviation and ride comfort improvement 24 p3549 A83-49193

Subsonic diffuser development of advanced tactical aircraft [AIAA PAPER 83-1168] 24 p3544 A83-49300

Application of optimal control synthesis to integrated vertical flight path and airspeed control for an advanced fighter [AIAA PAPER 83-2560] 24 p3549 A83-49594

FIGURE OF MERIT

Demonstration of a figure of merit for inherent testability 01 p0050 A83-10790

Figures of merit for dispersive birefringent filter materials 02 p0236 A83-12303

A figure of merit for competing communications satellite designs 21 p3221 A83-44533

Statistical performance of the circular harmonic filter for rotation-invariant pattern recognition 22 p3352 A83-46832

FILAMENT WINDING

Effect of resin flexibility on the properties of filament wound tubes 01 p0022 A83-10241

A generalized model for the winding mechanics of polymer composite shells 02 p0187 A83-12363

Simple calculations for the stability of soft, thin-walled mandrels during filament winding [ASME PAPER 82-PVP-1] 02 p0195 A83-12767

Mechanical behavior of thick filament-wound composites tested in transverse compression 09 p1221 A83-23606

Advanced composites structures at Hughes Helicopters, Inc 09 p1202 A83-23645

The design of flywheels made of fibrous materials 14 p2046 A83-32378

Filament wound composite thermal isolator structures for cryogenic dewars and instruments --- glass fiber reinforced epoxy laminates for spaceborne equipment 14 p1982 A83-33120

Static fatigue life of Kevlar aramid/epoxy pressure vessels at room and elevated temperatures [AIAA PAPER 83-1328] 16 p2324 A83-36342

FILAMENT WOUND CONSTRUCTION

U FILAMENT WINDING

FILAMENTS

A study of residual stresses in boron filaments 02 p0150 A83-12351

The geometrical factor during the extrusion of complex metal materials 13 p1859 A83-30688

An X-ray investigation of the dependence on pH of the structure of thick filaments in demembranized fiber bundles of skeletal muscles in vertebrates 16 p2394 A83-36803

Ultrafine filamentary composites 22 p3262 A83-45898

FILAMENTS (SOLAR PHYSICS)

U SOLAR PROMINENCES

FILE MAINTENANCE (COMPUTERS)

Management of astronomical data at Kanazawa Data Center 01 p0113 A83-10129

File structures and data bases for CAD; Proceedings of the Working Conference, Seeheim, West Germany, September 14-16, 1981 09 p1325 A83-25095

Data base organization in computer-aided design systems 11 p1646 A83-28622

FILLERS

A method for calculating the threshold filler concentration for polytetrafluorethylene-matrix composites 02 p0160 A83-12369

Rheology of fiber- or flake-filled plastics 02 p0150 A83-12825

The fracture of particulate-filled epoxide resins. I 05 p0611 A83-17563

Performance properties of conductive PVC composites for EMI shielding applications 07 p0876 A83-20488

Fatigue crack propagation in composites with spherical fillers. I 08 p1055 A83-22715

An analysis of the stress-strain state of a shell structure with a viscoelastic filler of arbitrary shape --- of rocket engines 09 p1219 A83-23426

Stability of three-layer cylindrical shells with a discrete filler under axial compression 11 p1596 A83-28455

Thermophysical properties of filled polymers 16 p2324 A83-35591

The effect of adhesion on the elastic properties of a composite with a disperse filler 18 p2649 A83-39478

Mathematical modeling of the elastic-plastic deformation of composite materials with disperse fillers 18 p2649 A83-39479

Dimensional stability of reinforced matrices 22 p3264 A83-46301

The electroconductivity of composites with binary fillers containing high-conductivity components 24 p3553 A83-49054

FILLING

NT REFILLING

A study of the processes involved in the filling of pipelines with liquid 09 p1258 A83-23444

The influence of undissolved gas on the magnitude of hydraulic shock during the filling of a pipeline 24 p3579 A83-49654

FILM BOILING

Heat transfer during the film boiling of liquids under conditions of free convection 11 p1570 A83-28555

Instability in the film boiling of a moving liquid 11 p1570 A83-28556

Flow film boiling from submerged bodies [AIAA PAPER 83-1529] 14 p2011 A83-32760

Liquid-solid contact and its relationship to improved film boiling heat transfer rates 20 p2980 A83-42761

Superfluid helium (He - II) film boiling on vertical heat transfer surfaces 20 p2981 A83-42763

Subcooled film boiling and the behavior of vapor film on a horizontal wire and a sphere 20 p2981 A83-42764

Forced convection film boiling on a sphere immersed in (a) subcooled or (b) superheated liquid 20 p2981 A83-42770

Study of the accelerated cooling of a very hot wall with a forced flow of subcooled liquid in film boiling regime 20 p2981 A83-42772

The calculation of the film vaporization of hydrocarbons in a hot-air flow 23 p3430 A83-48494

FILM CONDENSATION

An integral method in laminar film condensation of plane and axisymmetric bodies 08 p1083 A83-21893

An analysis of heat transfer during film condensation of stationary vapor on a vertical surface 19 p2843 A83-41566

Film condensation in a tube with counter current vapor flow 20 p2969 A83-42535

Heat transfer characteristics of the two-phase closed thermosyphon (wickless heat pipe) 20 p2981 A83-42765

FILM COOLING

Mass transfer in the neighborhood of jets entering a crossflow [ASME PAPER 82-HT-62] 02 p0173 A83-12802

Experimental and theoretical investigation on three-dimensional film cooling of a flat plate 03 p0315 A83-13345

Experimental investigation on film cooling of a gas turbine blade 03 p0282 A83-13346

Efficiency of combined jet cooling of a plate in conditions of complex heat transfer 10 p1417 A83-26254

Experimental study of a gas film in a tube 11 p1568 A83-28371

Near-wall gaseous films 11 p1569 A83-28375

Three-dimensional film cooling on a flat plate with tangential multi-jets 15 p2156 A83-33774

A theoretical and experimental investigation of flow and heat transfer in film cooling 15 p2161 A83-34268

Profile losses during the release of air onto the surface of nozzle vanes 16 p2288 A83-35590

The introduction of tangential or perpendicular nonisothermal plane jets into a turbulent crossflow for the purpose of film cooling 16 p2350 A83-35799

Interaction of a jet at a lateral angle to a mainstream at low injection rates - An experimental study 16 p2290 A83-35818

A numerical study of the characteristics of a radiant heat flux in a turbine cascade 19 p2844 A83-41570

The effect of cold air jet injection upon the film cooling effectiveness of combustion chamber walls for different injection geometries 20 p2978 A83-42738

Application of the swollen polymer technique to the study of heat transfer on film cooled surfaces 20 p2982 A83-42775

- Film cooling effectiveness of discrete holes measured by mass transfer and laser interferometer 20 p2983 A83-43017
- Film cooling with steam injection through three staggered rows of inclined holes over a straight airfoil [ASME PAPER 83-GT-30] 23 p3446 A83-47892
- Aerodynamic loss penalty produced by film cooling transonic turbine blades [ASME PAPER 83-GT-77] 23 p3395 A83-47930
- Cooling airflow studies at the leading edge of a film-cooled airfoil [ASME PAPER 83-GT-82] 23 p3447 A83-47935
- Effectiveness measurements for a cooling film disrupted by a single jet [ASME PAPER 83-GT-250] 23 p3397 A83-48037

FILM THICKNESS

- Fundamental relations for radiowave ellipsometry of 'thin metal film on dielectric substrate' system 01 p0049 A83-10362
- Two-parameter gap independence in eddy-current thickness gauging on conducting plates, strips, films, and coatings 01 p0057 A83-10368
- A study on thermal behavior of large seal-ring [ASME PAPER 81-LUB-27] 02 p0186 A83-11937
- Characteristics of an oil squeeze film 02 p0186 A83-11939
- Automatic determination of the optical constants of inhomogeneous thin films 02 p0236 A83-12595
- Elastohydrodynamic lubrication of finite line contacts [ASME PAPER 82-LUB-4] 03 p0335 A83-13503
- The effect of specimen thickness and morphology on fracture toughness of thermoplastic polymers 08 p1069 A83-21698
- Effect of the fluid film profile on the performance of magnetohydrodynamic bearings 09 p1273 A83-23345
- Film flow of a liquid on a convergent-nozzle surface 11 p1568 A83-28372
- Optical second-harmonic generation in a thin-film waveguide without control of film thickness 12 p1731 A83-29190
- Effect of inlet shear heating due to sliding on elastohydrodynamic film thickness 13 p1858 A83-30244
- Oil leakage and friction forces of reciprocating O-ring seals considering cavitation 13 p1859 A83-30249
- Design of stable metal-insulator-semiconductor (MIS) solar cells by oxide thickness compensation 14 p2041 A83-32250
- An investigation of the formation of texture in ZnO films during growth --- Russian book 14 p2093 A83-33298
- Thickness dependence of kink temperature and band bending in amorphous silicon 17 p2585 A83-38954
- Thin-film thickness measurements with thermal waves 18 p2689 A83-40060
- The effect of the thickness of the intermediate oxide layers in the metal-semiconductor contact on the properties of solar cells having a Schottky barrier 19 p2862 A83-42013
- Thin oxide film formation on metals 20 p2948 A83-42229
- Optimization of substrate thickness for interdigitated back contact silicon solar cells 20 p3052 A83-42360
- Heat transfer in thin liquid films flowing over horizontal tubes 20 p2981 A83-42771
- Automatic devices for the electromagnetic inspection of the thickness of the coating on small components 20 p2991 A83-43180
- Prediction of interfacial filler thickness for minimum thermal contact resistance 20 p2987 A83-43450
- A nonintrusive laser interferometer method for measurement of skin friction 21 p3138 A83-44677
- Microprocessor controlled microwave radiometer system for measuring the thickness of an oil slick 22 p3343 A83-46108
- Electrical, optical, and structural properties of semitransparent metallic layers 24 p3633 A83-48736
- The effect of the thickness of a protective molybdenum disilicide coating on the maximum operating temperature of heaters 24 p3568 A83-49078

FILTRING

U FILTRATION

FILTRATION

NT SPATIAL FILTRING

- A general diagram for estimating pore size of ultrafiltration and reverse osmosis membranes 02 p0151 A83-11841
- The filtration combustion of fine powders of Group IV B transition metals 07 p0880 A83-19955
- Full-flow debris monitoring and fine filtration for helicopter propulsion systems 09 p1208 A83-24838
- Filtration coefficient and hydraulic permeability of Nafion 125 membranes in metal alkali solutions 10 p1390 A83-26056

- Aviation filters for fuels, oils, hydraulic fluids, and air --- Russian book 12 p1700 A83-28813
- Filtration combustion of gases 14 p1988 A83-32083
- Numerical modelling of the ionospheric filtration of an ULF micropulsation signal 19 p2866 A83-41318
- The effect of an acoustic wave on the aerosol capture efficiency of a granular bed 20 p3014 A83-42977
- Rapid purification of fluorescent enzymes by ultrafiltration 22 p3347 A83-46710

FINANCIAL MANAGEMENT

- Airline planning: Corporate, financial, and marketing --- Book 03 p0400 A83-14046
- ESA procedures to account for inflation 11 p1666 A83-27372
- Land remote sensing in the 1980's 15 p2241 A83-34802
- The entropy of affordability 20 p3042 A83-42569
- Life cycle cost management - An engineer's view [AIAA PAPER 83-2451] 23 p3513 A83-48334

FINE STRUCTURE

- The effect of the characteristics of interstitial solid solution decomposition on the fine structure and properties of cast alloys of molybdenum 01 p0025 A83-10393
- Observations of the infrared fine-structure lines of S III at 18.71 and 33.47 microns in four H II regions 02 p0255 A83-12119
- Electron densities from the semforbidden O IV lambda 1401 multiplet 03 p0430 A83-14809
- EXAFS investigation of dilute Cu impurities in amorphous As2Se3 04 p0540 A83-15502
- Strained spiral vortex model for turbulent fine structure 05 p0639 A83-17357
- NO2A2B2 state properties from Zeeman quantum beats 05 p0684 A83-17652
- The fine structure of sunspot penumbras [AD-A111864] 06 p0852 A83-18123
- A study of the fine structure of titanium sponge 06 p0729 A83-18745
- The fine structure of 3C 84 and 3C 345 at 18-cm wavelength 06 p0819 A83-18780
- The fiber fine structure during solar type IV radio bursts - Observations and theory of radiation in presence of localized whistler turbulence 06 p0857 A83-19514
- Analytical electron microscope study of eight ataxites 07 p1035 A83-21330
- The structure of grain boundaries and their effect on mechanical properties 07 p0896 A83-21606
- Multiconfiguration Hartree-Fock Breit-Pauli results for 2P1/2-2P3/2 transitions in the boron sequence 08 p1162 A83-21985
- Versatile curved crystal spectrometer for laboratory extended X-ray absorption fine structure measurements 08 p1105 A83-23227
- Spectral fine analysis of the extreme helium star BD + 10.2179 deg 09 p1359 A83-24458
- Large anisotropic vibrational correlations in A15 Nb3Ge 13 p1929 A83-30922
- The apparent superluminal motion of the fine-structure components of 3C 120 13 p1948 A83-31256
- Fine structure in high velocity clouds 14 p2109 A83-33274
- High-accuracy wave-number measurements in molecular iodine 15 p2227 A83-33762
- Fine-structure transitions occurring in collisional redistribution of light 15 p2227 A83-33795
- O I (7990 A) emission and radiative entrapment of auroral EUV 15 p2196 A83-33944
- IR maps of M17 in the forbidden O III 88 micron and 52 micron lines and forbidden N III 57 micron line measurements 15 p2245 A83-34098
- The fine-structure constant, magnetic monopoles and dirac charge quantization condition 15 p2225 A83-34275
- Zebra pattern flux density observation during the type IV burst on October 12, 1981 15 p2280 A83-34304
- Evidence of anomalous multiplet line shapes in optically thick, laser-produced plasmas 15 p2236 A83-34997
- Analysis of ultra-fast fine structures of microwave bursts 15 p2284 A83-35220
- On the fine structure of meteoritical taenite/tetrataenite and its interpretation 15 p2277 A83-35300
- Proton excitation of fine-structure transitions in Fe XIV 16 p2410 A83-35652
- The fine structure of the stratospheric flow revealed by differential sounding 16 p2389 A83-36137
- On the statistical stability of solar cyclicity 17 p2628 A83-38561
- Type I noise storms and the structure of the extreme ultraviolet corona 18 p2782 A83-39035
- Fine-structure spectrum of O2-rare gas van der Waals molecules 19 p2897 A83-40770
- High resolution telescope and spectrograph observations of solar fine structure in the 1600 A region 19 p2925 A83-41656

- Observations of fine time structure in solar flare hard X-ray bursts 23 p3534 A83-47695
- Infrared emission lines in planetary nebulae 24 p3639 A83-49133
- The measurement of the cross sections of excitation of several quartet states of the cobalt atom by electron impact 24 p3626 A83-49737

FINES

- Chemical composition of Martian fines 04 p0567 A83-15576
- Shock-induced color changes in nontronite - Implications for the Martian fines 04 p0567 A83-15579

FINGERS

- Studies on a versatile handling system having multijointed fingers 08 p1151 A83-22064

FINISHES

NT ENAMELS

NT GLAZES

- An improved high temperature carbon fiber finish for polyimide composites 07 p0875 A83-20428

FINITE DIFFERENCE THEORY

- A note on using finite differences on the ICL distributed array processor 01 p0090 A83-10712
- The solution of triboengineering problems by numerical methods --- Russian book 02 p0186 A83-11946
- Numerical solutions to natural convection in a channel with porous walls under a transverse magnetic field 02 p0171 A83-12666
- Thermal storage performance calculations by closed form and finite difference solutions [ASME PAPER 82-HT-52] 02 p0172 A83-12799
- The simulation of secondary flow effects in turbulent non-circular passage flows 02 p0173 A83-12902
- Two-stage, two-level finite difference schemes for non-linear parabolic equations 02 p0231 A83-12927
- Time-dependent convection under reduced gravity 02 p0174 A83-12993
- Prediction of single-point temperature statistics in a half-heated grid flow 02 p0175 A83-13096
- A study of transverse turbulent jets in a cross flow --- for gas turbine combustion process modelling 02 p0136 A83-13100
- Numerical experiments on the leading-edge flowfield 03 p0277 A83-13131
- Transient performance of evacuated tubular solar collectors 03 p0352 A83-13478
- Simple phenomenological modeling of transition-region capacitance of forward-biased p-n junction diodes and transistor diodes 03 p0313 A83-13925
- Application of a parallel processor to the solution of finite difference problems 03 p0385 A83-14086
- Adapting iterative algorithms developed for symmetric systems to nonsymmetric systems 03 p0388 A83-14088
- Mesh generation by conformal and quasiconformal mappings 03 p0388 A83-14089
- An empirical investigation of methods for nonsymmetric linear systems 03 p0385 A83-14091
- Finite-difference techniques for vectorized fluid dynamics calculations --- Book 03 p0317 A83-14225
- A novel method to analyze electromagnetic scattering of complex objects 03 p0308 A83-14548
- Finite-difference analysis of EM fields inside complex cavities driven by large apertures 03 p0308 A83-14549
- Stiffness-reduction mechanisms in composite laminates 03 p0292 A83-14558
- Comparison of time integration /finite difference and spectral/ for the non-linear Burgers equation 03 p0389 A83-14603
- A posteriori numerical techniques for enforcing simultaneous conservation of integral invariants upon finite-difference shallow-water equation models 03 p0322 A83-14607
- On a multi-time step procedure to accelerate time-asymptotic flow calculations 03 p0322 A83-14613
- Solution of the Navier-Stokes equations using the finite-difference method of Hermitian type 03 p0322 A83-14615
- Numerical treatment of boundaries in compressible flow problems 03 p0322 A83-14616
- Advances in numerical studies of elastic wave propagation and scattering 04 p0489 A83-15165
- Linear/nonlinear behavior in unsteady transonic aerodynamics 04 p0442 A83-15280
- A fast algorithm for the calculation of transonic flow over wing/body combinations 04 p0442 A83-15283
- Nonlinear aerodynamic modeling of flap oscillations in transonic flow - A numerical validation [AIAA PAPER 81-0073] 04 p0442 A83-15290
- Numerical study of terrain-induced mesoscale motions in a mixed layer 04 p0516 A83-15932
- Fine mesh models in the U.K. Meteorological Office 04 p0519 A83-16157

Duct acoustics - A time dependent difference approach for steady state solutions 04 p0533 A83-16345

A characteristic flux difference splitting for the hyperbolic conservation laws of inviscid gasdynamics [AIAA PAPER 83-0040] 05 p0632 A83-16480

A finite difference method for inverse solutions of 3-D turbulent boundary-layer flow [AIAA PAPER 83-0301] 05 p0634 A83-16639

A new hybrid approach to supersonic aircraft analysis --- and flow field prediction [AIAA PAPER 83-0340] 05 p0584 A83-16666

An enhanced version of an implicit code for the Euler equations [AIAA PAPER 83-0344] 05 p0584 A83-16669

Monotone implicit algorithms for the small-disturbance and full potential equations applied to transonic flows [AIAA PAPER 83-0371] 05 p0585 A83-16677

A new consistent spatial differencing scheme for the transonic full-potential equation [AIAA PAPER 83-0373] 05 p0585 A83-16678

A new approach to truly adaptive grid generation [AIAA PAPER 83-0450] 05 p0681 A83-16722

Adaptive grids generated by elliptic systems --- for computational fluid dynamics [AIAA PAPER 83-0451] 05 p0636 A83-16723

An exploratory study of finite difference grids for transonic unsteady aerodynamics [AIAA PAPER 83-0503] 05 p0587 A83-16752

On a finite-difference method for solving transient viscous flow problems [AIAA PAPER 83-0560] 05 p0637 A83-16788

Calculation of the pressure distribution and streamline pattern around a ring wing using finite difference methods [AIAA PAPER 83-0645] 05 p0588 A83-16812

An implicit finite-difference method for chemical nonequilibrium flow through an axisymmetric supersonic nozzle 05 p0589 A83-16928

Treatment of late time instabilities in finite-difference EMP scattering codes 05 p0628 A83-17532

Construction and investigation of schemes for the calculation of radiative transfer 05 p0640 A83-17645

The use of substantially nonuniform grids in the numerical solution of the Navier-Stokes equations 05 p0640 A83-17646

A high-order difference method for the computation of viscous-gas flows 05 p0590 A83-17648

The calculation of some laminar flows using various discretisation schemes 05 p0642 A83-17900

Approximate factorization schemes for 3D nonlinear supersonic potential flow [AIAA PAPER 83-0376] 05 p0591 A83-17923

A comparison of two explicit time integration schemes applied to the transient heat equation 06 p0757 A83-18467

Acoustics in variable area duct - Finite element and finite difference comparisons to experiment 07 p0990 A83-19809

A three-dimensional modified strongly implicit procedure for heat conduction 07 p0924 A83-19823

Transonic airfoil calculations using solution-adaptive grids 07 p0863 A83-19824

Numerical calculations of ultrasonic fields. I - Transducer near fields 07 p0942 A83-20269

Application of the small-parameter method to the numerical solution of differential equations 07 p0986 A83-20309

Impact of an asteroid or comet in the ocean and extinction of terrestrial life 07 p0950 A83-21314

A finite boundary method for fluid flow field computations 07 p0927 A83-21436

Numerical studies of laminar flame propagation in spherical bombs 08 p1056 A83-22139

MHD channel electrical boundary-layer theory and applications 08 p1168 A83-23131

Numerical prediction of turbulent boundary layer development on a two-dimensional curved wall 08 p1089 A83-23198

Numerical solution of the momentum equations in unsteady incompressible flow 08 p1090 A83-23207

Transient characteristics of flat-plate solar collector 09 p1292 A83-23333

A difference scheme of second-order accuracy with a minimal pattern for hyperbolic equations 09 p1335 A83-23567

Quasi-Lagrangian rezoning of fluid codes maintaining an orthogonal mesh 09 p1259 A83-23721

Spurious solutions in driven cavity calculations 09 p1259 A83-23725

Analysis of circulation-controlled airfoils in transonic flow 09 p1196 A83-24032

Finite difference modeling of rotor flows including wake effects [ONERA, TP NO. 1982-114] 09 p1197 A83-24326

Nonlinear truncation error analysis of finite difference schemes for the Euler equations [AIAA PAPER 81-0193] 09 p1336 A83-24654

Vertical differencing of the primitive equations in sigma coordinates 10 p1450 A83-25382

A time efficient finite differences algorithm for the solution of the meridional flow in turbo compressor impellers [ASME PAPER 82-WA/FE-3] 10 p1413 A83-25683

Transient difference solutions of the inhomogeneous wave equation - Simulation of the Green's function [AIAA PAPER 83-0667] 10 p1473 A83-25904

Finite difference solutions to shocked acoustic waves [AIAA PAPER 83-0671] 10 p1473 A83-25907

A basic code for the prediction of transient three-dimensional turbulent flowfields 11 p1565 A83-27412

Euler equations - Implicit schemes and boundary conditions 12 p1695 A83-28959

MHD free-convection flow in the Stokes problem for a porous vertical plate by finite difference method 12 p1779 A83-28984

High resolution schemes for hyperbolic conservation laws 12 p1771 A83-29085

Compact finite difference schemes for the Euler and Navier-Stokes equations 12 p1722 A83-29096

Steady viscous flows by compact differences in boundary-fitted coordinates 12 p1722 A83-29099

On the numerical integration of the Schroedinger equation in the finite-difference schemes 12 p1776 A83-29603

On the numerical integration of the Schroedinger equation Numerical tests 12 p1776 A83-29604

Adaptive zoning for singular problems in two dimensions 12 p1771 A83-29613

Relationship between the truncation errors of centered finite-difference approximations on uniform and nonuniform meshes 12 p1771 A83-29619

ADI on staggered mesh - A method for the calculation of compressible convection 12 p1724 A83-29621

An explicit finite-difference scheme with exact conservation properties 12 p1772 A83-29624

A segmentation approach to grid generation using biharmonics 12 p1772 A83-29635

Stability of the explicit finite differenced transport equation 12 p1725 A83-29638

A numerical study of the two-dimensional Navier-Stokes equations in vorticity-velocity variables 12 p1725 A83-29639

Solution of burner-stabilized premixed laminar flames by boundary value methods 12 p1712 A83-29642

On local relaxation methods and their application to convection-diffusion equations 12 p1725 A83-29644

Implicit boundary conditions for the solution of the parabolized Navier-Stokes equations for supersonic flows 12 p1697 A83-29648

Stability analysis of numerical boundary conditions and implicit difference approximations for hyperbolic equations 12 p1772 A83-29650

Influence of boundary approximations and conditions on finite-difference solutions 12 p1772 A83-29652

Application of multigrid methods for integral equations to two problems from fluid dynamics 12 p1725 A83-29661

Group velocity interpretation of the stability theory of Gustafsson, Kreiss, and Sundstrom 12 p1776 A83-29665

Numerical calculations of discontinuities by shape preserving splines 12 p1773 A83-29670

A more accurate method for the numerical solution of nonlinear partial differential equations 12 p1773 A83-29671

Fast iterative solution of Poisson equation with Neumann boundary conditions in nonorthogonal curvilinear coordinate systems by a multiple grid method 12 p1726 A83-29898

Some remarks on the numerical solution of tricom-type equations 12 p1726 A83-29932

Implicit finite difference simulation of inviscid and viscous compressible flow 12 p1726 A83-29934

Tracking of interfaces for fluid flow: Accurate methods for piecewise smooth problems. 12 p1726 A83-29937

Shock calculations and the numerical solution of singular perturbation problems 12 p1726 A83-29938

Convergence of approximate solutions to conservation laws --- in parabolic systems and finite difference schemes 12 p1727 A83-29939

The constraints of energy-conserving vertical finite difference on the hydrostatic equations in a NWP model --- Numerical Weather Prediction 13 p1891 A83-30805

On two upwind finite-difference schemes for hyperbolic equations in non-conservative form 13 p1913 A83-31593

A numerical solution to the equations for the dynamics of a viscous incompressible fluid containing dispersed particles 14 p2008 A83-31897

Applying the method of flows to a problem concerning the dynamics of a viscous, stratified fluid 14 p2008 A83-31898

Modification of approximate methods for separating normal stresses on the basis of experimental determinations of their difference or sum 14 p2029 A83-32156

An implicit solution procedure for finite difference modeling of the Stefan problem [AIAA PAPER 83-1527] 14 p2011 A83-32758

An implicit, bidiagonal numerical method for solving the Navier-Stokes equations 14 p2012 A83-32979

Transonic flow calculations using the Euler equations 14 p1971 A83-32981

A more accurate transonic computational method for wing-body configurations 14 p1971 A83-32982

A split-coefficient/locally monotonic scheme for multishocked supersonic flow 14 p1971 A83-32985

An arbitrary-mesh computer program with applications to astrophysics 15 p2254 A83-33817

On one-dimensional stretching functions for finite-difference calculations --- computational fluid dynamics 15 p2224 A83-33821

Influence of transport models and boundary conditions on flame structure 15 p2132 A83-34034

On the comparison of finite difference and finite element time integration schemes for the heat conduction equation 15 p2158 A83-34231

ADI methods for solution of the transient heat conduction problems in spherical geometry 15 p2159 A83-34234

Heat transfer accompanied with melting and freezing for solar heat storage 15 p2190 A83-34235

Computation of the three-dimensional unsteady thermal field in a cooled mirror by a finite difference explicit method 15 p2159 A83-34247

Survey of numerical methods for three-dimensional, unsteady thermal problems 15 p2159 A83-34248

Laminar, natural convection heat transfer in a horizontal gap, bounded by an elliptic and A circular cylinder 15 p2160 A83-34260

Laminar flow heat transfer with axial conduction in a circular tube - A finite difference solution 15 p2160 A83-34262

Isoparametric finite difference energy method for plate bending problems 15 p2176 A83-34322

Axisymmetric vortex flow in a turbine stage under variable operating conditions 15 p2120 A83-34899

Laminar natural convection from a horizontal plate and the influence of plate-edge extensions 16 p2348 A83-35337

Generating exact solutions of the two-dimensional Burgers' equations 16 p2349 A83-35524

Numerical methods for partial differential equations based on power series 16 p2406 A83-35646

Some economical, explicit finite-difference schemes for the primitive equations 16 p2388 A83-36027

A variation on McCormack's method for axisymmetric viscous compressible flows 16 p2352 A83-36093

Analytical characterization of flow fields in side-inlet dump combustors [AIAA PAPER 83-1399] 16 p2322 A83-36389

A 3-D finite difference solution for orthotropic laminated composites using curvilinear coordinates 16 p2369 A83-36559

Navier-Stokes calculations for the vortex wake of a rotor in hover [AIAA PAPER 83-1676] 17 p2444 A83-37184

Finite-difference simulation of transonic separated flow using a full potential boundary layer interaction approach [AIAA PAPER 83-1689] 17 p2502 A83-37189

A hybrid field panel/finite difference method for 3-D potential unsteady transonic flow calculations [AIAA PAPER 83-1690] 17 p2444 A83-37190

Isolation of singular surfaces when using finite-difference methods --- for computing supersonic flow past wing-fuselage combinations 17 p2447 A83-37259

Numerical solution technique for the transient equation of transfer 17 p2506 A83-37866

Some comments on the analysis of electromagnetic fields in inhomogeneous media 17 p2576 A83-38034

Some recent applications of XTRAN3S --- time marching finite difference code for solution of three-dimensional transonic small perturbation flow [AIAA PAPER 83-1811] 17 p2454 A83-38644

Transfinite mappings and their application to grid generation 17 p2573 A83-38783

On application of body conforming curvilinear grids for finite difference solution of external flow 17 p2458 A83-38788

Adaptive gridding for finite difference solutions to heat and mass transfer problems 17 p2508 A83-38790

Test problems, coordinate transformations, and technique for nonsteady compressible flow analysis 17 p2508 A83-38797

Semidirect/marching solutions and elliptic grid generation 17 p2574 A83-38807

Three dimensional grid generation using biharmonics 17 p2574 A83-38809

Assessing the quality of curvilinear coordinate meshes by decomposing the Jacobian matrix 17 p2574 A83-38811

An implicit scheme for water wave problems 17 p2508 A83-38812

Idealized dynamic grid computation of physical systems 17 p2574 A83-38813

Equidistant mesh for gas dynamic calculations 17 p2508 A83-38814

Interacting flow theory and trailing edge separation - No stall 18 p2633 A83-39214

Improving the convergence rate of parabolic ADI methods [AIAA PAPER 83-1897] 18 p2739 A83-39361

Implicit total variation diminishing (TVD) schemes for steady-state calculations [AIAA PAPER 83-1902] 18 p2739 A83-39362

Comparison between the integro-differential technique and the finite - difference method in solving unsteady compressible viscous flow over airfoils [AIAA PAPER 83-1912] 18 p2635 A83-39370

Finite-difference calculations of unsteady premixed flame-flow interactions [AIAA PAPER 83-1917] 18 p2664 A83-39373

Conjugate gradients methods for solution of finite element and finite difference flow problems [AIAA PAPER 83-1923] 18 p2682 A83-39377

Implicit methods of second-order accuracy for the Euler equations [AIAA PAPER 83-1925] 18 p2682 A83-39379

Implicit upwind methods for the Euler equations [AIAA PAPER 83-1930] 18 p2682 A83-39382

Adaptive mesh schemes based on grid speeds [AIAA PAPER 83-1931] 18 p2739 A83-39383

High resolution applications of the Osher upwind scheme for the Euler equations [AIAA PAPER 83-1943] 18 p2636 A83-39390

Application of the implicit McCormack scheme to the PNS equations [AIAA PAPER 83-1956] 18 p2636 A83-39399

A time-split finite-volume algorithm for three-dimensional flow-field simulation [AIAA PAPER 83-1957] 18 p2636 A83-39400

Implicit upwind methods for the compressible Navier-Stokes equations [AIAA PAPER 83-1958] 18 p2682 A83-39401

A general perturbation approach for the equations of fluid dynamics [AIAA PAPER 83-1903] 18 p2637 A83-39411

Multi-dimensional formulation of CSCM - An upwind flux difference eigenvector split method for the compressible Navier-Stokes equations --- Conservative Supra-Characteristics Method [AIAA PAPER 83-1895] 18 p2683 A83-39414

Implicit conservative characteristic modeling schemes for the Euler equations - A new approach [AIAA PAPER 83-1939] 18 p2683 A83-39416

Spectral methods for the Euler equations [AIAA PAPER 83-1942] 18 p2683 A83-39420

An analysis of finite-difference schemes for the numerical solution of the advection equation 18 p2723 A83-39438

Thermal stress concentrations in the transient two-dimensional temperature field. II - Plate with a semi-elliptic notch 18 p2697 A83-39454

On the difference-approximation approach to the solution of systems of nonlinear equations 18 p2740 A83-39476

Two-point implicit scheme for the Euler equations --- for computational fluid dynamics 18 p2686 A83-39917

Upwind schemes and boundary conditions with applications to Euler equations in general geometries 19 p2789 A83-40752

Explicit finite difference predictor and convex corrector with applications to hyperbolic partial differential equations 19 p2893 A83-41852

Boundary conditions for a fourth order hyperbolic difference scheme 20 p3041 A83-42494

An effective numerical method in phase change problems with temperature dependent thermal properties 20 p2971 A83-42670

A finite difference study of natural convection in complex enclosures 20 p2972 A83-42678

Numerical analysis of heat and mass transfer processes during directional solidification in weightlessness 20 p2939 A83-42893

Numerical experiments with the Osher upwind scheme for the Euler equations 20 p2930 A83-43439

Numerical analysis of moving boundary problem in matrix with a thin alternate matrix 21 p3197 A83-44012

ISOMS - A implicit difference scheme for solving complete compressible Navier-Stokes equations---Implicit Second-Order Monotone Scheme 21 p3130 A83-44553

Calculation of three-dimensional turbulent boundary layer on an infinite swept wing 21 p3086 A83-44555

On the numerical solution of head-on vehicle shock-planar incident shock interaction flow 21 p3086 A83-44556

3-D shock-boundary layer solution from Navier-Stokes equations 21 p3087 A83-44563

Numerical calculation of inviscid supersonic flow field around bent nose cones 21 p3087 A83-44564

The discussion on stability and convergence of linear relaxation of transonic steady small perturbation plane potential flows 21 p3087 A83-44565

A comparison of finite element and finite difference solutions of the one- and two-dimensional Burgers' equations 21 p3132 A83-44989

The finite-difference method in wave problems of acoustics --- Russian book 21 p3201 A83-45026

On extrapolation boundary conditions for the numerical solution of hyperbolic difference schemes 21 p3198 A83-45054

Monotonic second-order difference scheme for hyperbolic systems with two independent variables --- in unsteady gas dynamics 21 p3133 A83-45213

Relaxation method for solving a difference biharmonic equation 21 p3198 A83-45214

On a scheme for solving the equations of a viscous heat-conducting gas 21 p3133 A83-45216

Application of the method of parallel chords to solve implicit difference equations of magnetohydrodynamics 21 p3215 A83-45219

Numerical determination of the parameters in high-entropy layers on slightly blunt bodies in supersonic flow 21 p3088 A83-45220

Nonpolynomial finite difference schemes and the use of the fast Fourier transform 21 p3198 A83-45525

On the turbulence-modeling requirements of three-dimensional boundary-layer flows 22 p3248 A83-46456

Finite-difference solutions for laminar boundary layer flows with separation 22 p3249 A83-46459

Calculation of a laminar-turbulent two-dimensional turbine blade boundary layer including surface curvature effects 22 p3249 A83-46464

Emission of electrons from the collector of a thermionic converter 23 p3477 A83-47567

An experimental investigation of a gas turbine disk cooling system [ASME PAPER 83-GT-78] 23 p3447 A83-47931

Subharmonic and chaotic bifurcation structure in optical bistability 23 p3509 A83-48320

A numerical method for potential flows with a free surface 24 p3575 A83-48871

Single cell high order difference methods for the Helmholtz equation 24 p3622 A83-48874

Alternating-triangular difference scheme for solving the Navier-Stokes equations 24 p3576 A83-48946

Finite difference analysis of MHD free-convection flow past an accelerated vertical porous plate 24 p3633 A83-50165

Investigation of a two-dimensional model of an MOS structure 24 p3575 A83-50203

FINITE ELEMENT METHOD

Load distribution on deformed wings in supersonic flow 01 p0002 A83-10180

Finite element analysis of ideal flow over axisymmetric solid body /sphere/ 01 p0045 A83-10277

On the optimization of magnetic field sources in electromechanical energy conversion 01 p0037 A83-10641

Solution of Burgers' equation with a large Reynolds number 01 p0045 A83-10710

Predicting the thermal ratcheting and creep behaviour of a component with a stress concentration 01 p0060 A83-11032

The superconvergence of finite element method solutions in mesh norms 01 p0102 A83-11266

A numerical simulation of three-dimensional transonic flows of compressible perfect fluids around aircraft by use of the finite element and least squares methods [AAAF PAPER NT 81-23] 02 p0169 A83-11779

The solution of triboengineering problems by numerical methods --- Russian book 02 p0186 A83-11946

A finite-element model of the atmospheric boundary layer suitable for use with numerical weather prediction models 02 p0214 A83-12236

The construction of a computational model that uses the finite-element method to solve spatial problems in the theory of elasticity 02 p0191 A83-12341

On a semiglobal finite element method 02 p0231 A83-12661

The hierarchical concept in finite element analysis 02 p0193 A83-12737

Recent advances in reduction methods for instability analysis of structures 02 p0193 A83-12738

A new formulation of hybrid/mixed finite element 02 p0193 A83-12739

Our discrete-Kirchhoff and isoparametric shell elements for nonlinear analysis - An assessment 02 p0193 A83-12740

An averaged Lagrangian-finite element technique for the solution of nonlinear vibration problems 02 p0194 A83-12747

A Newton-Lanczos method for solution of nonlinear finite element equations 02 p0194 A83-12748

Lanczos eigenvalue algorithm for large structures on a minicomputer 02 p0194 A83-12749

A sparse matrix finite element technique for iterative structural optimization 02 p0194 A83-12750

Data management in FEM-based optimization software 02 p0228 A83-12751

An efficient triangular plate bending finite element for crash simulation 02 p0194 A83-12755

Improved method of static and free vibration analysis of thin rectangular plates 02 p0195 A83-12759

Dynamic finite element model for laminated structures 02 p0195 A83-12761

Finite element analysis of moisture effects in graphite-epoxy composites 02 p0150 A83-12762

Nonlinear structural and life analyses of a combustor liner 02 p0195 A83-12764

The application of nonlinear analysis techniques to practical structural design problems 02 p0195 A83-12765

Further developments in the controlled growth approach for optimal structural synthesis [ASME PAPER 82-DET-62] 02 p0232 A83-12773

Vibrational characteristics of packeted bladed disc [ASME PAPER 82-DET-137] 02 p0196 A83-12782

Numerical solutions of radiative heat transfer with convection [ASME PAPER 82-HT-45] 02 p0172 A83-12798

Finite-element simulation of natural convection in three-dimensional enclosures [ASME PAPER 82-HT-71] 02 p0173 A83-12803

A family of hybrid plate elements 02 p0196 A83-12837

A linear finite element approach to the solution of the variational inequalities arising in contact problems of structural dynamics 02 p0196 A83-12838

Block-indexed solution of very large linear equation systems with symmetric DBBF coefficient matrix --- Double Bounded Band Form 02 p0228 A83-12839

Stresses in rotating disc with eccentric hole 02 p0196 A83-12873

Plane strain extrusion studies by finite element method 02 p0196 A83-12874

Numerical solution of subsonic and transonic cascade flows 02 p0132 A83-12901

General hyperbolic difference formulas for linear and quasilinear hyperbolic equations 02 p0231 A83-12905

An iterative method for predicting turbfan inlet acoustics 03 p0391 A83-13135

An algorithm for finite element analysis of partly wrinkled membranes 03 p0338 A83-13147

An analytical and experimental study of the plate tearing mode of fracture 03 p0339 A83-13201

On prediction of wear coefficients in sliding wear [ASLE PREPRINT 82-LC-1B-2] 03 p0333 A83-13231

Radiation view factors by finite elements 03 p0316 A83-13489

A finite element method for solving Helmholtz type equations in waveguides and other unbounded domains 03 p0390 A83-13567

On a higher order accurate fully discrete Galerkin approximation to the Navier-Stokes equations 03 p0316 A83-13568

Analysis of a multilevel iterative method for nonlinear finite element equations 03 p0387 A83-13571

Solution of a unilateral problem using integral equations and finite elements --- French thesis 03 p0390 A83-13809

Computing scattering amplitudes for arbitrary cylinders under incident plane waves 03 p0390 A83-14001

A multi-level iterative method for nonlinear elliptic equations 03 p0388 A83-14077

Multigrid solvers on parallel computers 03 p0385 A83-14079

On the choice of discretization for solving P.D.E.'s on a multi-processor 03 p0385 A83-14090

Synthetic discrete method in structural analysis 03 p0341 A83-14487

A-posteriori error analysis and adaptive finite element methods for singularly perturbed convection-diffusion equations 03 p0388 A83-14496

- Characterizing delamination growth in graphite-epoxy
03 p0293 A83-14561
- Derivative calculation from finite element solutions
03 p0389 A83-14696
- An iteration procedure for reducing the expenses of static, elastoplastic and eigenvalue problems in finite element analysis
03 p0389 A83-14697
- Penalty-finite-element analysis of 3-D Navier-Stokes equations
03 p0323 A83-14699
- A simple yet accurate finite element procedure for computing stress intensity factors
03 p0342 A83-14707
- Evaluation of a new quadrilateral thin plate bending element
03 p0342 A83-14709
- Alternative ways for formulation of hybrid stress elements
03 p0342 A83-14710
- Use of finite element method for determining stress intensity factors with a conic-section simulation model of crack surface
03 p0343 A83-14818
- On the numerical solution of constrained variational problems by boundary and finite elements
04 p0529 A83-14958
- Fenomech '81; Proceedings of the Second International Conference on Finite Elements in Nonlinear Mechanics, Stuttgart, West Germany, August 25-28, 1981. Parts 1, 2 & 3
04 p0465 A83-15001
- Streamline upwind/Petrov-Galerkin formulations for convection dominated flows with particular emphasis on the incompressible Navier-Stokes equations
04 p0475 A83-15005
- On current aspects of finite element computational fluid mechanics for turbulent flows
04 p0475 A83-15006
- Studies on plastic structures - Stability, anisotropic hardening, cyclic loads
04 p0495 A83-15012
- One-dimensional finite element analysis of thermal ablation with pyrolysis
04 p0475 A83-15014
- Nonlinear analysis of elasto-plastic shells by hybrid stress finite elements
04 p0495 A83-15017
- Finite element analysis of plates with nonlinear properties
04 p0495 A83-15018
- Computer graphics displays of nonlinear calculations
04 p0526 A83-15019
- A simple finite element for elastic-plastic deformations of shells
04 p0495 A83-15020
- The plastic node method - A new method of plastic analysis
04 p0495 A83-15021
- Growth and stability of interacting surface flaws of arbitrary shape
04 p0495 A83-15060
- Elastic-plastic finite element analysis of dynamic fracture
04 p0495 A83-15062
- Analytical solution for embedded elliptical cracks, and finite element alternating method for elliptical surface cracks, subjected to arbitrary loadings
04 p0496 A83-15063
- Stress intensity factors for two cracks emanating from two holes and approaching each other
04 p0496 A83-15065
- The unimoment method for elastic wave scattering problems
04 p0489 A83-15164
- The use of an error index to improve numerical solutions for unsteady lifting airfoils
04 p0442 A83-15281
- A new method of finite element structure discretization
04 p0498 A83-15549
- A global local finite element analysis of axisymmetric scattering of elastic waves
[ASME PAPER 82-WA/APM-3]
04 p0498 A83-15686
- A theory of substructure modal synthesis
[ASME PAPER 82-WA/APM-29]
04 p0499 A83-15693
- Stress measurement at the threads of nut-bolt assemblies using the finite element method --- German thesis
04 p0487 A83-15846
- The dynamics of plane supporting structures - A computer-aided experimental analysis of structure dynamic problems with interactive method of test --- German thesis
04 p0499 A83-15847
- A penalty duality method for the Budiansky-Sanders shell model
04 p0501 A83-16310
- Finite element thermal analysis of an icing protective system
[AIAA PAPER 83-0113]
05 p0632 A83-16528
- Finite element formulations for convection dominated flows with particular emphasis on the compressible Euler equations
[AIAA PAPER 83-0125]
05 p0633 A83-16538
- A fast finite element method for transonic potential flow calculations
[AIAA PAPER 83-0507]
05 p0587 A83-16755
- Simplified Laplace transform inversion for unsteady surface element method
[AIAA PAPER 83-0527]
05 p0638 A83-16830
- Three-dimensional analysis of /0/90/s and /90/0/s laminates with a central circular hole
05 p0653 A83-16933
- Evaluation of finite-element software packages for stress analysis of laminated composites
05 p0678 A83-16936
- SIF of surface cracks and fatigue crack propagation behaviour in a cylindrical bar
05 p0614 A83-17092
- Effects of hole curvature on transient hygrothermal stresses in plates with a hole /moisture and temperature coupling effects/
05 p0611 A83-17107
- Curved elements with polynomials of varying degree
05 p0682 A83-17555
- Elastic-plastic finite element analyses of short cracks
05 p0655 A83-17675
- An elastic-plastic finite element analysis of a compact tension specimen
05 p0655 A83-17721
- Parametric instability of tapered beams by finite element method
05 p0655 A83-17723
- Optimality criterion approach using tapered finite elements with nodal averaging technique for two-dimensional problems
05 p0655 A83-17736
- A finite element formulation for multilayered and thick plates
05 p0655 A83-17737
- A new strategy for stress analysis using the finite element method
05 p0655 A83-17738
- Approximation to bending trial functions for shell triangular finite elements in quadratic parametric representation
05 p0655 A83-17739
- An improved rectangular element for plate bending analysis
05 p0656 A83-17740
- Finite-element solution of the incompressible Navier-Stokes equations
05 p0641 A83-17743
- Prediction of secondary vortex flowfields induced by multiple free-jets issuing in close proximity
[AIAA PAPER 83-0289]
05 p0642 A83-17916
- Shape determination of structures based on the inverse variational principle/the finite element approach
06 p0772 A83-18212
- Parameterization in finite element analysis --- in optimal structural design
06 p0772 A83-18216
- Large scale structural optimization by finite elements
06 p0772 A83-18226
- Interactive optimum design system --- for two dimensional elastic structures
06 p0773 A83-18228
- Optimal finite element discretization - A dynamic programming approach --- for structural analysis of linear elastic systems
06 p0773 A83-18230
- Crack separation energy rates for inclined cracks in an elastic-plastic material
06 p0774 A83-18479
- Finite deformation constitutive relations including ductile fracture damage
06 p0774 A83-18490
- A finite element analysis of planar circulators using arbitrarily shaped resonators
06 p0753 A83-18772
- Solution of bifurcation problems and limit load problems in certain nonlinear boundary-value problems of continuum mechanics
06 p0777 A83-19322
- Evaluation of fracture toughness /J sub Ic/ using single specimen fracture test augmented by finite element analysis
07 p0883 A83-19670
- Acoustics in variable area duct - Finite element and finite difference comparisons to experiment
07 p0990 A83-19809
- Application of the finite-element method to one-dimensional flame propagation problems
07 p0878 A83-19818
- A superelement analysis of stiffened shells --- Russian book on aircraft fuselage structures
07 p0865 A83-20392
- Computer-aided design of complex composite material systems and structures
07 p0877 A83-20498
- Preconditioning and two-level multigrid methods of arbitrary degree of approximation
07 p0986 A83-20508
- Transonic flow calculations by a finite element method
07 p0864 A83-21023
- Finite-element analysis of layered waveguides for piezoelectric surface waves using analytical solutions for semi-infinite media
07 p0922 A83-21174
- Limitations and possible extensions to a nonlinear finite element shell-of-revolution model based on Reissner's shell theory
07 p0948 A83-21438
- A relaxation technique for evaluating stress intensity factors by the finite element method
07 p0949 A83-21439
- A finite element model for thin-walled members
07 p0949 A83-21443
- The application of the theorems of structural variation to finite element problems
07 p0949 A83-21446
- Constraint equations from rigid elements including initial strains
07 p0949 A83-21447
- Finite element strength analysis of rotating shell-plate structures
07 p0949 A83-21448
- Nonlinear analysis of the statics of thin axisymmetric shells by the finite element method
08 p1114 A83-21629
- Analysis and repair of flaws in thick structures
08 p1115 A83-21654
- Two stress intensity factor calculation methods and solutions for various three-dimensional crack problems
08 p1116 A83-21660
- Near-crack tip finite strain analysis
08 p1116 A83-21662
- Hole nucleation and ductile failure in multiaxial states of stress
08 p1116 A83-21663
- A finite element analysis of creep deformation in a specimen containing a macroscopic crack
08 p1117 A83-21694
- The influence of specimen geometry on fracture of unwelded and welded steel specimens - Comparison of experimental results with FEM-calculation
08 p1060 A83-21707
- An analysis of fatigue crack growth under yielding conditions
08 p1060 A83-21708
- Fracture mechanisms in the peeling failure of adhesive joints
08 p1069 A83-21730
- Dynamic steady antiplane shear crack growth in an elastic-plastic material
08 p1119 A83-21779
- Some effects of inelastic constitutive models on crack tip fields in steady quasistatic growth
08 p1119 A83-21793
- Lagrange-type formulation for finite element analysis of non-linear beam vibrations
08 p1120 A83-21805
- On the numerical stability of the finite element method
08 p1159 A83-21879
- Nodal averaging technique in the optimality criterion approach using tapered finite elements
08 p1121 A83-21889
- Consideration of the local shape of the terrain in height interpolation with the aid of finite elements
08 p1129 A83-22031
- On the accuracy of J-integral value evaluated by finite element method for mixed mode
08 p1122 A83-22068
- On the convergence of the finite element approximation of eigenfrequencies and eigenvectors to Maxwell's boundary value problem
08 p1159 A83-22077
- The stability of thin shells of revolution under gravitational or thermal loading - Modeling by means of curved finite elements --- French thesis
08 p1122 A83-22087
- A finite element formulation for steady transonic Euler equations
08 p1042 A83-22129
- Space basis for weakly solenoidal functions --- incompressible fluid dynamics
08 p1084 A83-22277
- Development of a two-dimensional finite-element PBL model and two preliminary model applications
08 p1140 A83-22299
- Quantitative geometric characterization of two-dimensional flaws via liquid crystals tomography
08 p1113 A83-22409
- Design with several eigenvalue constraints by finite elements and linear programming
08 p1122 A83-22411
- Study on the elastic-plastic buckling strength of plate structures
08 p1123 A83-22422
- A transonic quasi-3D analysis for gas turbine engines including split-flow capability for turbofans
08 p1042 A83-22647
- Investigation of solution of Navier-Stokes equations using a variational formulation
08 p1085 A83-22648
- Analysis of progressive plastic buckling in cylindrical shell as contact problem
08 p1123 A83-22772
- Computations in limit analysis for plastic plates
08 p1123 A83-22942
- Comparison of magnetic fields computed by finite element and classical series methods
08 p1082 A83-22945
- On the inclusion principle for the hierarchical finite element method
08 p1159 A83-22946
- Different finite element formulations for the Navier-Stokes equations
08 p1088 A83-23185
- On the finite element simulation of incompressible turbulent flow in general two-dimensional geometries
08 p1088 A83-23187
- Prediction of developing turbulent flow by the finite element method
08 p1088 A83-23189
- A finite element method for the shallow water equations
08 p1089 A83-23201
- A finite element solution of compressible flow through cascades of turbomachines
08 p1089 A83-23203
- Error and stability analysis of the finite element solution for the transport equation
08 p1090 A83-23216
- Finite element analysis of mixed convection applied to the storage of solar energy
08 p1091 A83-23219
- J-integral analysis for cracks emanated from elliptical holes
09 p1275 A83-23298
- The thermal stressed state of nozzle vanes under shutdown conditions
09 p1277 A83-23513
- A finite-element study of the stress-strain state of the turbofan rotor of an aircraft gas-turbine engine
09 p1205 A83-23515
- Finite-element methods for steady solidification problems
09 p1338 A83-23723

Spurious solutions in driven cavity calculations
09 p1259 A83-23725

An algorithm for kinetoelastodynamic analysis of plane mechanisms with rectilinear elements
09 p1280 A83-24505

Numerical interpretations of creep buckling behavior of columns
09 p1282 A83-25105

On the error behavior of the reduced basis technique for nonlinear finite element approximations
09 p1282 A83-25106

Finite-element method for time-dependent Euler equation --- of inviscid incompressible flow
10 p1413 A83-25462

The study of dynamic fracture propagation using a special finite element technique
[ASME PAPER 82-WA/DE-13]
10 p1439 A83-25680

A finite element procedure for studying the acoustic radiation of a vibrating plate
[ASME PAPER 82-WA/NCA-3]
10 p1472 A83-25698

A finite element thermal modelling of modular space radiators
[SAE PAPER 820865]
10 p1384 A83-25765

Micromechanical predictions of crack initiation, propagation and crack growth resistance in boron/aluminum composites
10 p1389 A83-25879

On the unsymmetric eigenproblem for the buckling of shells under pressure loading
10 p1440 A83-26434

Three-dimensional elastoplastic finite element analysis
10 p1442 A83-26767

Deformation work density fracture criterion for composite materials
10 p1442 A83-26771

Numerical calculation of local convective heat transfer coefficients over air-cooled vane surfaces
10 p1418 A83-26772

Linear analysis by the finite element method of the dynamics of axisymmetric structures subjected to arbitrary loads
10 p1442 A83-26819

Optimization of acoustic liners by the hybrid finite element-integral approach
[AIAA PAPER 83-0670]
10 p1478 A83-26917

Finite element analysis of dynamic energy transfer in a Stirling engine regenerator
11 p1665 A83-27271

A finite element method for construction of dynamical theories of layered plates
11 p1591 A83-27429

Geometrically nonlinear analysis of layered composite shells
11 p1591 A83-27431

Micromechanical modeling of 3D composites with interface failure
11 p1544 A83-27464

Finite-element solution of three-dimensional electromagnetic problems
11 p1560 A83-27893

Computable finite element error bounds for Poisson's equation
11 p1649 A83-27998

The evolution of the moon - A finite element approach
11 p1686 A83-28385

Nonlinear bending of bimodular-material plates
11 p1544 A83-28410

Finite element iterative techniques for determining the interface boundary between Laplace and Poisson domains - Characteristic analysis of a field effect transistor
11 p1563 A83-28417

A novel boundary infinite element
11 p1649 A83-28418

Influence of crack closure on the stress intensity factor for plates subjected to bending - A 3-D finite element analysis
11 p1595 A83-28436

Research on the thermomechanical stress in turbine disks under thermal manipulations --- German thesis
11 p1531 A83-28667

Numerical problems of nonlinear stability analysis of elastic structures
11 p1599 A83-28719

Thermoelastic stress analysis of anisotropic composite sandwich plates by finite element method
11 p1599 A83-28721

Estimating singularity powers with finite elements
11 p1599 A83-28723

Geometrically non-linear formulation for two dimensional curved beam elements
11 p1600 A83-28725

Calculation of the natural frequencies and steady state response of thin plates in bending by an improved rectangular element
11 p1600 A83-28726

Penalty-finite element methods in mechanics; Proceedings of the Winter Annual Meeting, Phoenix, AZ, November 14-19, 1982
12 p1717 A83-28851

The penalty function method in mechanics - A review of recent advances
12 p1717 A83-28852

Reduced first order differential equation with optimal control finite element penalty functions --- applied to convection-radiation heat transfer and boundary layer problems
12 p1721 A83-28853

Numerical solution of large deformation problems involving surface contact and impact
12 p1734 A83-28854

A penalty finite element algorithm for parabolic flow problems
12 p1721 A83-28855

Standard and asymptotic finite element methods for incompressible viscous flows
12 p1721 A83-28856

Fractional calculus - A different approach to the analysis of viscoelastically damped structures
12 p1734 A83-28965

An alternating method for analysis of surface-flawed aircraft structural components
12 p1734 A83-28966

Buckled plate vibrations and large amplitude vibrations using high-order triangular elements
12 p1734 A83-28967

Finite element modeling techniques for constrained layer damping
12 p1735 A83-28976

Orthogonal polynomials as variable-order finite element shape functions
12 p1770 A83-28977

A finite element method for high Reynolds number viscous fluid flow using two step explicit scheme
12 p1724 A83-29442

Stability analysis of numerical boundary conditions and implicit difference approximations for hyperbolic equations
12 p1772 A83-29650

Influence of boundary approximations and conditions on finite-difference solutions
12 p1772 A83-29652

A multigrid method for the transonic full potential equation discretized with finite elements on an arbitrary body fitted mesh
12 p1697 A83-29657

Finite element interpolation error bounds with applications to eigenvalue problems
12 p1773 A83-29705

Auxiliary convergence criteria for Mindlin plate elements and their application to the four-node quadrilateral
[AIAA 83-0834]
12 p1737 A83-29743

Stress intensity factor calculation for designing with fiber reinforced composite materials
[AIAA 83-0835]
12 p1737 A83-29744

An automated finite element procedure for fatigue crack propagation analyses
[AIAA 83-0841]
12 p1737 A83-29748

Finite deformation analysis of shells - A hybrid finite element method based on assumed stress-function vector and rotation tensor
[AIAA 83-0861]
12 p1738 A83-29749

Elastic-plastic behavior of coldworked holes
[AIAA 83-0865]
12 p1738 A83-29753

An equivalent continuum representation of structures composed of repeated elements
[AIAA 83-1007]
12 p1740 A83-29794

An adaptive finite element technique for plate structures
[AIAA 83-1009]
12 p1740 A83-29795

Application of multiple objective optimization techniques to finite element model tuning --- for flutter analysis of T-38 aircraft horizontal stabilizer
[AIAA 83-1010]
12 p1740 A83-29796

Creation and checking of load transformation matrices for modally coupled systems using the acceleration method with recursive equations
[AIAA 83-0816]
12 p1742 A83-29815

Vibration characteristics of hexagonal radial rib and hoop platforms
[AIAA 83-0822]
12 p1742 A83-29819

Nonlinear structural dynamics analysis using a modified modal method
[AIAA 83-0824]
12 p1742 A83-29820

Fractional calculus in the transient analysis of viscoelastically damped structures
[AIAA 83-0901]
12 p1743 A83-29841

Thermorheological analysis of high voltage electronic module potting
[AIAA 83-0903]
12 p1720 A83-29842

A refined finite element for vibration analysis of twisted blades based on beam theory
[AIAA 83-0917]
12 p1743 A83-29845

Application of the nonlinear finite element method to crashworthiness analysis of aircraft seats
[AIAA 83-0929]
12 p1699 A83-29855

Large-amplitude vibration of laminated composite plates of arbitrary shape
[AIAA 83-1035]
12 p1745 A83-29880

Influence of mass representation on the modal analysis of rotating flexible structures
[AIAA 83-0915]
12 p1745 A83-29889

An automated technique for improving modal matrices by means of experimentally obtained dynamic data
[AIAA 83-0881]
12 p1746 A83-29890

A finite element analysis of composite tension specimens
12 p1711 A83-29892

Use of the finite-element method for natural convection in a horizontally confined infinite layer of fluid
12 p1726 A83-29899

Calculation of quenching stresses with and without transformation effects
12 p1746 A83-29912

Variational methods in elasticity and in elastoplasticity for multilayered structures --- French thesis
12 p1747 A83-29947

The finite-element method in solutions of boundary value problems for anisotropic plates of composite materials. I
Refined theories for anisotropic plates and finite-element approximations
13 p1866 A83-30059

Experimental demonstration of static shape control --- for large space structure development
13 p1812 A83-30165

An analysis of the natural vibrations of the rotors of centrifugal compressor machines
13 p1859 A83-30310

Finite element analysis of the buckling of variable thickness discs
13 p1867 A83-30845

Structural analysis of the mirror of the University of Texas 7.6 m Telescope
13 p1938 A83-31002

Finite element analysis of lossy waveguides - Application to microstrip lines on semiconductor substrate
13 p1836 A83-31143

An algorithm for constructing shape functions for a rectangular finite element
13 p1867 A83-31322

A computational study of finite element methods for second order linear two-point boundary value problems
13 p1912 A83-31362

Application of the 2-D discrete-ordinates method to multiple scattering of laser radiation
13 p1857 A83-31460

Robust active vibration damping of finite element structures in space flight
13 p1868 A83-31624

A non-conforming piecewise quadratic finite element on triangles --- for flow computation
13 p1844 A83-31638

Elasto-plastic analysis of anisotropic plates and shells by the Semiloof element
13 p1868 A83-31639

Anisotropic elasto-plastic finite element analysis of thick and thin plates and shells
13 p1868 A83-31640

Finite element, boundary element and coupled analysis of unbounded problems in elastostatics
13 p1868 A83-31641

Geometrically nonlinear formulation for the curved shell elements
13 p1868 A83-31642

A note on universal matrices for triangular finite elements for the quasi-harmonic equation
13 p1913 A83-31643

A mixed-mode crack analysis of rotating disk using finite element method
14 p2031 A83-32658

Finite element analysis of radiative transport in fibrous insulation
[AIAA PAPER 83-1502]
14 p2010 A83-32741

Two-dimensional deforming finite element methods for surface ablation
[AIAA PAPER 83-1555]
14 p2012 A83-32773

The application of iterated defect correction to variational methods for elliptic boundary value problems
14 p2078 A83-32842

Surface roughness effects on the stress analysis of adhesive joints
14 p2032 A83-32843

A finite element algorithm for computational fluid dynamics
14 p2078 A83-32978

Design for minimum stress concentration by finite elements and linear programming
14 p2033 A83-33111

Local buckling of thin tensioned plate with a crack
14 p2033 A83-33374

Finite elements and characteristics applied to advection-diffusion equations
15 p2157 A83-33864

Three-dimensional non-linear variational analysis of a non homogeneous heat conduction problem - Finite element results
15 p2158 A83-34230

On the comparison of finite difference and finite element time integration schemes for the heat conduction equation
15 p2158 A83-34231

Appropriate finite element techniques for heat transfer problems with high gradients and ablation
15 p2159 A83-34236

Charring ablation by finite element
15 p2159 A83-34237

The determination of hygrothermal stress development in anisotropic composites
15 p2175 A83-34239

On thermal bending of layered composite plates and shells of bimodulus materials
15 p2175 A83-34242

Unified finite element approach for coupled thermal stress waves
15 p2175 A83-34244

Survey of numerical methods for three-dimensional, unsteady thermal problems
15 p2159 A83-34248

The consistent method for computing derived boundary quantities when the Galerkin FEM is used to solve thermal and/or fluids problems
15 p2159 A83-34252

Accuracy aspects of the finite element method in free convection heat transfer problems
15 p2160 A83-34256

Exact finite elements for conduction and convection
15 p2160 A83-34263

Numerical evaluating of the instantaneous temperature field in turbulent flow and heat flux on the wall with variable boundary conditions and heat source in turbulent flow
15 p2161 A83-34270

- A study of shear factors in reduced-selective integration Mindlin beam elements 15 p2175 A83-34313
- Unconditionally stable implicit-explicit algorithms for coupled thermal stress waves 15 p2176 A83-34317
- A nonlinear, semi-analytical finite element analysis for nearly axisymmetric solids 15 p2176 A83-34318
- A simple selectively integrated torsion-flexure coupled tapered beam element with transverse shear deformation 15 p2176 A83-34319
- Estimation of the fundamental frequencies of shallow shells by a finite element-isodeformation contour method 15 p2176 A83-34320
- A variable power singular element for analysis of fracture mechanics problems 15 p2176 A83-34321
- Nonlinear statics and dynamics of thin axisymmetric shells by high precision finite elements 15 p2177 A83-34347
- Field redistribution in finite elements - A mathematical alternative to reduced integration 15 p2179 A83-34561
- Reflections on the computational approximation of elastic incompressibility 15 p2179 A83-34562
- Quarter-point elements for curved crack fronts 15 p2179 A83-34565
- A reinvestigation of post-buckling behaviour of elastic circular plates using a simple finite element formulation 15 p2179 A83-34566
- Geometrically nonlinear formulation for the axis-symmetric transition finite elements 15 p2179 A83-34567
- Modification of the finite element method for solving two-dimensional elastic and plastic contact problems 15 p2180 A83-35036
- The calculation of electromagnetic fields by numerical methods 16 p2406 A83-35517
- Optimum design for potential flows 16 p2288 A83-35525
- Fortran computer program for inextensional bending of a doubly curved shell triangular element 16 p2365 A83-35643
- An accurate scalar potential finite element method for linear, two-dimensional magnetostatics problems 16 p2406 A83-35645
- Investigation of flow field in a turbocompressor by the finite element method 16 p2290 A83-35834
- Numerical solution of the problem of flame propagation by the use of the random element method [AIAA PAPER 83-0600] 16 p2326 A83-36062
- Stability of short Beck and Leipholz columns on elastic foundation 16 p2366 A83-36098
- Finite element methods for internal flow calculations [AIAA PAPER 83-1404] 16 p2296 A83-36415
- Methods of static and dynamic calculations of structures with cyclic symmetries [ONERA, TP NO. 1983-14] 16 p2367 A83-36424
- The mean transverse shear in stratified anisotropic plates [ONERA, TP NO. 1983-15] 16 p2368 A83-36425
- A multigrid finite element method for the calculation of transonic potential flows [ONERA, TP NO. 1983-18] 16 p2296 A83-36427
- A minicomputer finite elements program for microgravity hydroelastic analysis --- of spacecraft flexible propellant tanks 16 p2317 A83-36499
- Extrapolation techniques for determining stress intensity factors 16 p2368 A83-36507
- On the electrical potential analysis of a cracked fracture mechanics test specimen using the finite element method 16 p2368 A83-36509
- Fracture mechanics deliberation of lugs 16 p2368 A83-36515
- A viscoelastic-viscoplastic constitutive equation and its finite element implementation 16 p2369 A83-36557
- A simple efficient hidden line algorithm 16 p2404 A83-36558
- Effect of heat transfer of melt/solid interface shape and solute segregation in Edge-Defined Film-Fed growth - Finite element analysis 16 p2354 A83-36715
- Finite element computation with parallel VLSI 16 p2403 A83-36720
- Parallel solution of finite element equations 16 p2403 A83-36721
- Evaluation of J-integral value by using finite element method 16 p2369 A83-36968
- A general method of determination of finite element interpolation polynomials 17 p2570 A83-37022
- Identification of distributed parameter systems using finite element approximation 17 p2565 A83-37095
- Finite-element mathematical model of a gas turbine engine in unsteady flow 17 p2467 A83-37252
- The use of the finite-element method to calculate unsteady temperatures in the cross section of a thin-wall structure 17 p2503 A83-37255
- Generalization of the results of calculations of the stressed state of structures with cutouts --- such as wing and fuselage combinations 17 p2518 A83-37268
- On the formulation of the finite-element method in heat-conduction problems for aircraft structures 17 p2520 A83-37515
- Analytical control of the shape of the polygons used in the finite-element method 17 p2521 A83-37644
- Piecewise polynomial Galerkin approximation to invariant densities of one-dimensional difference equations 17 p2571 A83-38037
- On conforming mixed finite element methods for incompressible viscous flow problems 17 p2507 A83-38057
- Algorithms for determining invertible two- and three-dimensional quadratic isoparametric finite element transformations 17 p2572 A83-38569
- Dynamic elasto-plastic response of shells in an acoustic medium - EPSA code 17 p2524 A83-38570
- A two-step approach to finite element ordering 17 p2572 A83-38574
- An infinite element and a formula for numerical quadrature over an infinite interval 17 p2572 A83-38575
- Finite element triangular meshing optimization for pure torsion 17 p2525 A83-38576
- General boundary conditions for the wave equation around non-homogeneous scatterers 17 p2576 A83-38618
- Transfinite mappings and their application to grid generation 17 p2573 A83-38783
- An error estimate for a finite-element approximation of an elliptic variational inequality formulation of a Hele-Shaw moving-boundary problem 18 p2739 A83-39254
- Finite element analysis in computational fluid dynamics [AIAA PAPER 83-1918] 18 p2682 A83-39374
- Progress in finite element techniques for transonic flows [AIAA PAPER 83-1919] 18 p2635 A83-39375
- Transonic flow calculations using triangular finite elements [AIAA PAPER 83-1922] 18 p2635 A83-39376
- Conjugate gradients methods for solution of finite element and finite difference flow problems [AIAA PAPER 83-1923] 18 p2682 A83-39377
- Transonic Euler simulations by means of finite element explicit schemes [AIAA PAPER 83-1924] 18 p2635 A83-39378
- New discretization and solution techniques for incompressible viscous flow problems [AIAA PAPER 83-1921] 18 p2683 A83-39415
- Spectral methods for the Euler equations [AIAA PAPER 83-1942] 18 p2683 A83-39420
- A method for obtaining stress intensity factor by F.E.M. and its application to dynamic problem. II - A treatment for mixed mode cracks 18 p2697 A83-39451
- Growth of ring-shaped edge cracks under reversed torsional fatigue 18 p2697 A83-39452
- Numerical analysis of 3-D potential flow in axial flow turbomachines 18 p2684 A83-39458
- An algorithm for solving the nonisothermal thermoplasticity problem on the basis of the finite element method 18 p2698 A83-39502
- A singular element for a new experimental method of fracture toughness determination 18 p2699 A83-39539
- Stress intensity factor for semi-elliptical surface cracks loaded by stress gradients 18 p2699 A83-39545
- Fracture initiation under gross yielding - Strain energy density criterion 18 p2666 A83-39546
- Design for temperature and thermal buckling constraints employing a noneigenvalue formulation 18 p2646 A83-40011
- Stress analysis and strength of adhesive bonded joints under bending loads 18 p2703 A83-40156
- Application of the finite element method to determine the moisture content of composites under transient conditions 18 p2656 A83-40226
- Finite element methods for transonic flow analysis 19 p2789 A83-40854
- An inelastic finite element model of 4D carbon-carbon composite 19 p2819 A83-40866
- Analysis of a thin-walled pressurized torus in contact with a plane --- aircraft tires study [AIAA PAPER 82-0702] 19 p2856 A83-40869
- Stress concentration around circular cutouts in laminated composite cylindrical shells - Experimental investigation and finite element analysis 19 p2857 A83-40883
- An overview of the general programme - Finite element analysis of structures (FEAST) 19 p2857 A83-40887
- Finite-element analysis of the T-38 canopy 19 p2797 A83-41044
- Assessment of rotor-fuselage coupling on vibration predictions using a simple finite element model 19 p2857 A83-41075
- A displacement formulation for the finite element elastic-plastic problem 19 p2857 A83-41153
- Topology-finite-element method for solving electromagnetic field problems 19 p2896 A83-41277
- Reduced order control design benefits and costs of frequency-shaped LQG methodology --- [AIAA PAPER 83-2229] 19 p2891 A83-41708
- Finite element computational fluid mechanics --- Book 19 p2844 A83-41874
- Application of the hybrid method of finite elements to strength analysis of axially symmetric shell-plate structures 20 p3001 A83-42935
- On the simplified hybrid-combined method --- for solving boundary value problems of elliptic equations 20 p3041 A83-42495
- Residual strength predictions for ballistically damaged aircraft 20 p3001 A83-42540
- Finite element model tuning via multiple objective optimization techniques 20 p3002 A83-42542
- An approximate transformation for nonlinear transient heat conduction problems 20 p2971 A83-42667
- Heat flux display and heat transmission coefficient calculation with the finite element method 20 p2971 A83-42669
- On the numerical solution of nonlinear problems of transient heat conduction 20 p3003 A83-42895
- Nonlinear finite element analysis and ADINA: Proceedings of the Fourth Conference, MIT, Cambridge, MA, June 15-17, 1983 20 p3003 A83-42926
- Determination and simulation of stable crack growth in ADINA 20 p3003 A83-42927
- The use of NONSAP to compare the Von Mises and a modified Von Mises yield criteria 20 p3003 A83-42928
- On elastic-plastic analysis of l-beams in bending and torsion 20 p3003 A83-42929
- Fracture mechanics J-integral calculations in thermo-elasto-plasticity 20 p3003 A83-42931
- On the analysis of creep stability and rupture 20 p3003 A83-42932
- On the automatic solution of nonlinear finite element equations --- for structural analysis 20 p3003 A83-42933
- Analysis of surface cracks in plates and shells using the line-spring model and ADINA 20 p3003 A83-42934
- Variational geometry - A new method for modifying part geometry for finite element analysis 20 p3041 A83-42935
- A fast Fourier method for the dynamic analysis of linear structures with frequency dependent properties 20 p3005 A83-42989
- A finite element analysis of heat transfer in solid with radiation and ablation 20 p2983 A83-43015
- Praxis-oriented results processing in the calculation of electromagnetic fields by discretization methods 20 p2967 A83-43027
- Finite element analysis of the effect of a non-planar solid-liquid interface on the lateral solute segregation during unidirectional solidification 20 p2943 A83-43312
- Dual analysis of plane stress problems by commonly based finite elements 20 p3008 A83-43646
- Algorithmic mass-factoring of finite element model analyses [SAWE PAPER 1451] 20 p3009 A83-43733
- Trends in interactive finite element modeling [SAWE PAPER 1489] 20 p3037 A83-43756
- Application of finite element analysis techniques to the derivation of advanced composite structure weight [SAWE PAPER 1490] 20 p3009 A83-43757
- Finite element approximations in transient analysis --- of flexible structures 21 p3150 A83-44024
- Buckling finite element analysis of flat plates with a rectangular hole 21 p3150 A83-44025
- Dynamic analysis of viscoelastic structures using incremental finite element method 21 p3150 A83-44026
- Reanalysis and design in structural dynamics 21 p3151 A83-44031
- Peculiarities in stress solutions in laminated composites 21 p3105 A83-44047
- An equilibrium model finite element analysis for buckling of moderately thick plates 21 p3151 A83-44105
- Finite element model to determine K(I) 21 p3153 A83-44548
- Finite element methods in aerodynamics 21 p3086 A83-44551
- Families of variation principle for the semi-inverse problem and the A-type hybrid problem on the S2-stream sheet in radial turbomachines and the extensions and applications of semi-inverse problem to the mixed-type turbomachines 21 p3130 A83-44552
- The influence of the 3-dimensional transition-section onto the aerodynamical uniformity in test section 21 p3087 A83-44567

Comparison of finite element solutions with analytical and experimental data for elastic-plastic cracked problems 21 p3156 A83-44894

A FEM analysis of crack arrest experiments 21 p3157 A83-44905

Analysis of cracks with multiple branches 21 p3159 A83-44927

Large increments technique in the elastic-plastic analysis 21 p3159 A83-44932

Constrained finite elements for singular boundary value problems --- applied to fracture mechanics 21 p3160 A83-44987

A comparison of finite element and finite difference solutions of the one- and two-dimensional Burgers' equations 21 p3132 A83-44989

A new approach to the dynamic analysis of structures using fixed frequency dynamic stiffness matrices 21 p3160 A83-45051

Finite element analysis of 3-ply laminated conical shell for flutter 21 p3160 A83-45052

Finite element models and system identification of large space structures 21 p3196 A83-45115

Three-dimensional elastic-plastic finite element analysis of small surface cracks 21 p3162 A83-45182

On an efficient algorithm for the Dirichlet variational-difference problem 21 p3198 A83-45215

Combined experimental and numerical method for determining stress concentrations 21 p3163 A83-45316

Analysis of some low-order finite element schemes for the Navier-Stokes equations 21 p3133 A83-45521

Nonlinear panel flutter using high-order triangular finite elements 21 p3164 A83-45590

Integrated thermal-structural approach for shells of revolution 21 p3164 A83-45596

The finite element method: A basic introduction (2nd edition) 22 p3304 A83-45745

Finite elements in fracture mechanics 22 p3304 A83-45768

Introduction to the method of finite elements 22 p3305 A83-45770

Finite element procedures in fracture mechanics 22 p3305 A83-45771

Numerical studies involving fracture mechanics samples 22 p3305 A83-45774

Finite-element model of two-dimensional problems involving moving objects of inspection 22 p3304 A83-46331

Stability of vertical discretization schemes for semi-implicit primitive equation models - Theory and application 23 p3489 A83-47394

Improved stress simulation with simple finite element meshes [ASME PAPER 83-GT-89] 23 p3469 A83-47936

Boundary conditions for the potential equation in transonic internal flow calculation [ASME PAPER 83-GT-135] 23 p3396 A83-47962

Stiffness derivative finite element technique to determine nodal weight functions with singularity elements [ASME PAPER 83-GT-224] 23 p3470 A83-48022

A singular hybrid finite element analysis of boundary-layer stresses in composite laminates 23 p3470 A83-48098

Economical stiffness formulations for nonlinear finite elements 23 p3470 A83-48162

Dynamic finite element analysis of nonaxisymmetric structures 23 p3471 A83-48163

Solutions of plates on a heterogeneous elastic foundation 23 p3471 A83-48164

A partitioned finite element method for dynamical systems 23 p3471 A83-48166

Alternate stress and conjugate strain measures, and mixed variational formulations involving rigid rotations, for computational analyses of finitely deformed solids, with application to plates and shells. I - Theory 23 p3471 A83-48167

Finite strip method with X-spline functions 23 p3502 A83-48168

Nonlinear viscoelastic stress analysis - A finite element approach 23 p3471 A83-48169

A brief note on the 'local least squares' stress smoothing technique 23 p3471 A83-48172

A least squares finite element scheme for transonic flow around harmonically oscillating airfoils 24 p3543 A83-48872

An analysis of two-step time discretizations in the solution of the linearized shallow water equations 24 p3575 A83-48875

Optimisation of cylindrically orthotropic annular plates with simply supported edges subjected to a constraint on fundamental frequency 24 p3591 A83-48899

The use of finite elements in the shape of a plane parallelogram for the analysis of plates and shells 24 p3592 A83-49033

A finite element solution to the equations of a mathematical model for turbomachine blades 24 p3593 A83-49057

Numerical generation of boundary-fitted coordinate systems with optimal control of orthogonality [ONERA, TP NO. 1983-82] 24 p3622 A83-49401

Mixed and hybrid non-linear variational analysis of a three dimensional heat conduction problem - Finite element results [ONERA, TP NO. 1983-83] 24 p3577 A83-49402

A posteriori errors in the finite element method [ONERA, TP NO. 1983-89] 24 p3622 A83-49408

Finite element analysis of steadily moving contact fields 24 p3593 A83-49437

A three-dimensional nonlinear analysis of cross-ply rectangular composite plates 24 p3593 A83-49439

A curvilinear triangular finite element for plate bending by a hybrid method of assumed displacements supplemented with assumed stresses 24 p3593 A83-49442

Analysis of the elastic vibrations of manipulators by the finite element method 24 p3594 A83-49447

A numerical study of the plastic adaptation of plates and shells of revolution by equilibrium finite elements 24 p3594 A83-49645

Real-time parameter identification in a class of distributed systems using Lyapunov design method. I - Theory 24 p3620 A83-49895

Formulation of the resolving relationships of the finite element method for elasticity problems. II 24 p3595 A83-49902

A finite element study of the nonstationary temperature fields of bodies of revolution 24 p3596 A83-49909

FINITE IMPULSE RESPONSE FILTERS

U FIR FILTERS

FINITE VOLUME METHOD

Explicit and implicit corrected viscosity schemes for the computation of steady transonic flows 03 p0279 A83-14606

Finite-volume solutions to the Euler equations in transonic flow [AIAA PAPER 81-1265] 06 p0712 A83-18405

Calculation of transonic potential flow past three-dimensional configurations 12 p1698 A83-29930

Modular method for centrifugal compressor performance prediction 13 p1804 A83-31169

Efficient computation of volume in flow predictions 14 p2012 A83-32994

An experience in mesh generation for three-dimensional calculation of potential flow around a rotating propeller 17 p2458 A83-38798

A time-split finite-volume algorithm for three-dimensional flow-field simulation [AIAA PAPER 83-1957] 18 p2636 A83-39400

3-D calculation of transonic viscous flows by an implicit method [AIAA PAPER 83-1953] 18 p2637 A83-39412

A finite-volume, adaptive grid algorithm applied to planetary entry flowfields 20 p2930 A83-43440

Finite volume calculation of three-dimensional potential flow around a propeller 21 p3089 A83-45577

Investigation of the three-dimensional transonic flow around an air intake by a finite-volume method for the Euler equations 22 p3249 A83-46463

FINNED BODIES

Upstream influence in sharp fin-induced shock wave turbulent boundary-layer interaction 04 p0442 A83-15296

Impedance transformation in fin lines 04 p0474 A83-16209

Missile Datcom status report - Body and fin alone methodology [AIAA PAPER 83-0181] 05 p0581 A83-16574

Techniques for roll tailoring for missiles with wrap-around fins [AIAA PAPER 83-0463] 05 p0598 A83-16731

Aerodynamic estimation techniques for aerostats and airships 06 p0712 A83-18404

Aerodynamic characteristics for a slender missile with wrap-around fins 09 p1198 A83-24881

Certain features of transverse flow past a cylinder with longitudinal fins 11 p1569 A83-28551

Heat transfer in a latent heat storage device with finned annular tube heat exchanger --- German thesis 11 p1570 A83-28665

Empirical expressions for fin-line design 13 p1836 A83-31147

Calculation method of the optimum configurations of the extended surfaces with simultaneous conductive, convective and radiative heat transfer in heat exchanger 18 p2686 A83-39932

Equivalent angle-of-attack method for estimating nonlinear aerodynamics of missile fins 18 p2638 A83-40010

FINS

NT COOLING FINS

NT NOSE FINS

Fin geometry for minimum entropy generation in forced convection 03 p0315 A83-13483

On-board instrumentation for test vehicles with varying roll rates [AIAA PAPER 83-0570] 05 p0595 A83-16797

Aerodynamics of wrap-around fins 07 p0863 A83-21011

Static and damage tolerance tests of an advanced composite vertical fin for L-1011 aircraft [AIAA 83-0970] 12 p1701 A83-29780

Thermal cycling in compact plate-fin heat exchangers --- in aircraft gas turbines 15 p2123 A83-34253

Calculation of viscous supersonic flows over finned bodies [AIAA PAPER 83-1667] 17 p2443 A83-37178

Flowfield scaling in sharp fin-induced shock wave turbulent boundary layer interaction [AIAA PAPER 83-1754] 17 p2446 A83-37227

Conical similarity of shock/boundary layer interactions generated by swept fins [AIAA PAPER 83-1756] 17 p2446 A83-37229

The evaluation of the rolling moments induced by wraparound fins [AIAA PAPER 83-1840] 17 p2470 A83-38669

Aerodynamics of wraparound fins 18 p2638 A83-40007

Aerodynamic characteristics of missile control fins in nonlinear flow fields [AIAA PAPER 83-2083] 19 p2792 A83-41917

Enhancement of heat transfer 20 p2970 A83-42659

The one-dimensional analysis of fin assembly heat transfer 20 p2986 A83-43365

FIR FILTERS

System identification techniques for adaptive signal processing 02 p0229 A83-11821

Design of FIR digital filters using tapped cascaded FIR subfilters 02 p0167 A83-11822

FIR filter structures having low sensitivity and roundoff noise 05 p0623 A83-16913

Fast algorithms for linear prediction and system identification filters with linear phase 05 p0680 A83-16914

A new realization of a digital filter using a number theory transform 08 p1157 A83-22233

Restoration of bilinearly distorted images. I - Finite impulse response linear digital filtering 08 p1101 A83-22672

A simplified approach to the design of apodised SAW filters 10 p1408 A83-25503

The use of derivative techniques in astronomical spectroscopy 12 p1786 A83-29080

Performance of a fast algorithm for FIR system identification using least-squares analysis 13 p1911 A83-31725

Efficient positive coefficient algorithm for image processing 13 p1911 A83-31776

Memory requirements for the hardware implementation of decimators 15 p2218 A83-33924

A new approach to FIR digital filters with fewer multipliers and reduced sensitivity 15 p2151 A83-33927

Systolic and SIMD algorithms for digital filtering 15 p2219 A83-35148

The detection of unresolved targets using the Hough transform 21 p3120 A83-44276

General form for representing the Fourier transform 24 p3621 A83-49966

FIRE CONTROL

Integrated flight and fire control development and flight test on an F-15B aircraft 01 p0006 A83-11160

Development and evaluation of advanced air-to-air missile fire control algorithms and displays 01 p0006 A83-11191

Maximizing survivability and effectiveness of air-to-ground gunnery using a moveable gun 01 p0006 A83-11192

Use of the onboard simulation concept for the integrated flight and fire control program 01 p0007 A83-11201

Dynamic characteristics of an integrated flight and fire control system 01 p0013 A83-11208

F-4F fire control system software support - An integrated approach to ground and flight testing 01 p0015 A83-11228

The Aquila - A versatile, cost-effective military tool shows its potential 04 p0447 A83-16399

Phoenix missile system - Still the one to beat 04 p0441 A83-16452

Estimation of helicopter and target motion for the advanced attack helicopter fire control system 06 p0715 A83-18378

Estimation and prediction for maneuvering target trajectories 10 p1373 A83-26261

- Potential uses of two types of stereographic display systems in the airborne fire control environment
10 p1376 A83-26314
- Integrated systems evaluated on F-15
11 p1528 A83-28700
- The significant elements of the reliability and maintainability programs for the modernized Cobra helicopter weapons/weapons control systems
13 p1863 A83-31499
- Microprocessor-based optimal controllers for a helicopter turret control system
15 p2122 A83-35138
- Concepts for improved gun fire control systems
15 p2223 A83-35139
- GE's APG-67 - Fighter radar with a future
16 p2298 A83-36625
- Design and analysis of a digitally controlled integrated flight/fire control system
17 p2460 A83-37063
- Nonlinear control law for piloting aircraft in the air-to-ground attack phase
[ONERA, TP NO. 1983-37] 21 p3093 A83-44315
- Judgments of relative motion in tactical displays
[AD-A129722] 22 p3349 A83-46699
- FIRE DAMAGE**
The use of space imagery to evaluate forest fire damage
14 p2034 A83-32496
- FIRE EXTINGUISHERS**
Evaluation of advanced airplane fire extinguishants
[AIAA PAPER 83-1141] 17 p2459 A83-38076
- Powder pack protection for aircraft dry bays
20 p2931 A83-42558
- FIRE FIGHTING**
Potential applications of remote sensing to fire service planning
15 p2241 A83-34812
- Use of Landsat data to develop a fuels database for a wildland fire simulation model
15 p2187 A83-34847
- FIRE PREVENTION**
Flammability handbook for electrical insulation
09 p1221 A83-24895
- Fire mosaics in southern California and northern Baja California
09 p1292 A83-25287
- Integrating non-first order automated meteorological observations into national weather forecasting and analysis programs
13 p1891 A83-30593
- Effectiveness of seat cushion blocking layer materials against cabin fires
[SAE PAPER 821484] 17 p2459 A83-38003
- The survivable aircraft fire
20 p2931 A83-43407
- FIRE RETARDANTS**
U FLAME RETARDANTS
- FIREBALLS**
ASCORECORD 3 DP two-coordinate measuring instrument in the service of the European Fireball Programme
02 p0183 A83-13046
- The energy spectrum of cosmic fireballs
16 p2431 A83-36672
- FIREPROOFING**
Optimization of fire blocking layers for aircraft seating
[SAWE PAPER 1468] 20 p2931 A83-43742
- FIRES**
NT FOREST FIRES
Combustion toxicology: Principles and test methods ---
Book 09 p1227 A83-24903
- A model of freely burning pool fires
16 p2325 A83-35789
- Infrasonic and internal gravity waves in the atmosphere during large fires
23 p3485 A83-48503
- FIREWORKS**
U PYROTECHNICS
- FIRING (IGNITING)**
NT ROCKET FIRING
NT STATIC FIRING
NT TEST FIRING
A dynamic model of turbojet in starting at high altitude
16 p2304 A83-35846
- FIRING TIME**
U BURNING TIME
- FIRMWARE**
Cost-effective approaches for extending the useful life of ATE and test program sets
01 p0088 A83-10762
- Fast firmware algorithms for square root, sine/cosine, and exponential
01 p0087 A83-11149
- FIRST AID**
Emergency care for burns --- Russian book
23 p3498 A83-48150
- FISHERIES**
Application of remote sensing techniques in oceanographic studies of the British Columbia Salmon Fishery
03 p0347 A83-14258
- FISHTAILING**
U YAW
- FISSION**
Fission track studies of xenolithic chondrites - Implications regarding brecciation and metamorphism
02 p0267 A83-12840

FISSION PRODUCTS

- Heavy element fission products on earth --- Russian book
02 p0204 A83-11923
- Terrestrial fission xenon - Choice of primordial isotopic composition
22 p3329 A83-46376

FISSURES (GEOLOGY)

- Episodic rifting and volcanism at Krafla in North Iceland - Growth of large ground fissures along the plate boundary
07 p0957 A83-19870

FITNESS

NT FLIGHT FITNESS

NT PHYSICAL FITNESS

- The psychological fitness of the ground personnel in charge of airspace security depending on the civil aviation authority Evaluation at recruiting, disorders observed during the period of employment
08 p1151 A83-22970

- The fitness for work of humans and the problems of its increase
19 p2882 A83-41458

FITZGERALD-LORENTZ CONTRACTION

U LORENTZ CONTRACTION

FIX

U FIXING

FIXED POINT ARITHMETIC

- Finite precision rational arithmetic - An arithmetic unit
15 p2217 A83-33908

FIXED POINTS (MATHEMATICS)

- Geometrical properties of the Euler-Poisson equations of a rigid body about a fixed point
03 p0390 A83-13423

- On conditions of the existence of certain classes of solutions of the problem of the motion of a rigid body with a fixed point
09 p1337 A83-23551
- Kinematic interpretation of the motion of a gyrost at in one solution of E. I. Khariamova
09 p1337 A83-23552

- Isoconic motions of a rigid body with a fixed point
09 p1337 A83-23553

- Construction of a complete solution for one problem of rigid-body dynamics
09 p1337 A83-23554
- Motion of a Kovalevskaya gyroscope in the Delaunay case
09 p1337 A83-23555

- On an attempt to generalize the Hess solution of the problem concerning the motion of a heavy rigid body with a fixed point
09 p1337 A83-23557

- Asymptotic properties of certain motions of an asynchronous gyroscope in a gimbal suspension
09 p1337 A83-23560

- Fractal basin boundaries, long-lived chaotic transients, and unstable-unstable pair bifurcation
10 p1471 A83-25794

- Solution of equations of problem of motion of a heavy rigid body about a fixed point in the Kowalevskaya's case using theta-function
12 p1775 A83-29115

FIXED WINGS

- Effects of amplitude of oscillation on the wear of dry bearings containing PTFE
[ASME PAPER 81-LUB-6] 02 p0186 A83-11942
- Fixed wing and rotary wing flight testing of Navstar GPS as a civilian navigation system
07 p0865 A83-19777

FIXED-WING AIRCRAFT

U AIRCRAFT CONFIGURATIONS

U FIXED WINGS

FIXING

- Nitrogen fixation by lightning activity in a thunderstorm
15 p2197 A83-34039

FLAME FRONTS

U FLAME PROPAGATION

FLAME HOLDERS

- Influence of confinement on flame acceleration due to repeated obstacles
07 p0878 A83-19836
- Features of the dynamics of gas combustion in closed vessels under various laws for the change in the flame surface
07 p0880 A83-19952
- Further study on the prediction of liquid fuel spray capture by v-gutter downstream of a plain orifice injector under uniform cross air flow
16 p2351 A83-35810
- A study of lean extinction limit for pilot flame holder
16 p2325 A83-35821
- Heat liberation and heat transfer in flame tubes
20 p2974 A83-42696

FLAME INTERACTION

U CHEMICAL REACTIONS

U FLAME PROPAGATION

FLAME IONIZATION

- Structure of a premixed concentric jet flame at main flame blow-off
08 p1056 A83-22065
- Temperature and optimum ionization in the micro diffusion flame
08 p1056 A83-22343
- The effect of the fuel quality on the degree of combustion product ionization in gas-turbine engines
14 p1988 A83-32078
- On the computation of ionization levels in rocket exhaust flames
22 p3261 A83-45716
- On large eddy structure and turbulent mixing in flames
24 p3557 A83-49809

FLAME PROBES

- High repetition rate, high resolution back-lit, shadow, and schlieren photography of gaseous and liquid mass-transport phenomena and flames
01 p0052 A83-11061

- The accuracy of mass-spectrometer soundings in investigations of the flame structure of condensed systems
07 p0928 A83-19956

- Probe-shift error in remote diagnostics of volume-radiation sources
[AIAA PAPER 83-1541] 14 p2011 A83-32765

- Rotational Raman interferometric measurement of flame temperatures
22 p3294 A83-46840

FLAME PROPAGATION

- Performance predictions for confined swirling flows
01 p0045 A83-10663

- A theory of the limits of flame propagation on the surface of a combustible material
02 p0151 A83-11958

- Boundary integral equation method calculations of surface regression effects in flame spreading
03 p0294 A83-13488

- The conditions of flame propagation in metal particle suspensions in air
03 p0295 A83-14059

- The autonomy of shock waves in a sonic downstream state - The case of detonation
03 p0320 A83-14570

- Turbulent flow structure effect on diffusion and premixed flame propagation
03 p0295 A83-14602

- Flame quenching by turbulence
03 p0295 A83-14848

- Flames as gasdynamic discontinuities
04 p0457 A83-16262

- Flame propagation with a sequential reaction mechanism
04 p0457 A83-16362

- Nonadiabatic nonisobaric propagation of a planar premixed flame - Constant-volume enclosure
[AIAA PAPER 83-0239] 05 p0612 A83-16605

- On the modeling of turbulent premixed flames
[AIAA PAPER 83-0241] 05 p0612 A83-16607

- Measurement of the pressure-velocity correlation in turbulent reactive flows
[AIAA PAPER 83-0400] 05 p0612 A83-16693

- Grid adaption for problems with separation, cell Reynolds number, shock-boundary layer interaction, and accuracy
[AIAA PAPER 83-0449] 05 p0636 A83-16721

- Aerodynamic features of turbulent flames
[AIAA PAPER 83-0470] 05 p0636 A83-16737

- Dynamic behavior of turbulent flow in a widely-spaced co-axial jet diffusion flame combustor
[AIAA PAPER 83-0575] 05 p0637 A83-16800

- Mixing in jet flames by laser Rayleigh scattering
[AIAA PAPER 83-0403] 05 p0612 A83-16827

- A new kind of spin combustion
07 p0878 A83-19641

- Application of the finite-element method to one-dimensional flame propagation problems
07 p0878 A83-19818

- Ignition, propagation, and structure of deflagrations and detonations - Stable species concentration of a turbulent premixed methane-air flame
07 p0878 A83-19835

- Influence of confinement on flame acceleration due to repeated obstacles
07 p0878 A83-19836

- Laminar burning velocities of hydrogen-air and hydrogen-air-steam flames
07 p0878 A83-19837

- The mechanism of lean limit flame extinction
07 p0879 A83-19841

- Numerical study of a confined premixed laminar flame - Oscillatory propagation and wall quenching
07 p0879 A83-19842

- Features of the dynamics of gas combustion in closed vessels under various laws for the change in the flame surface
07 p0880 A83-19952

- The combustion of substances with a liquid reaction layer
07 p0880 A83-19953

- The filtration combustion of fine powders of Group IV B transition metals
07 p0880 A83-19955

- An experimental study of the stationary propagation of a flame in a tube under conditions of weightlessness
07 p0868 A83-19957

- The asymptotic structure of a counterflow premixed flame for large activation energies
07 p0882 A83-21166

- Flame propagation through dust clouds of carbon, coal, aluminium and magnesium in an environment of zero gravity
07 p0882 A83-21352

- Flames with impinging jets
07 p0882 A83-21423

- Structure of a premixed concentric jet flame at main flame blow-off
08 p1056 A83-22065

- Numerical studies of laminar flame propagation in spherical bombs
08 p1056 A83-22139

- Lift-off characteristics of turbulent jet diffusion flames
08 p1056 A83-22140

- Experimental study on inhibited diffusion and premixed flames in a counterflow system
08 p1057 A83-22347

Steady state diffusion flame structure with Lewis number variations 08 p1057 A83-22392

A comparison of techniques for reconstructing axisymmetric reacting flow fields from absorption measurements 08 p1057 A83-22393

NO₂ formation in laminar flames 08 p1057 A83-22397

Transient processes during the formation of a combustion surface in hydraulically controlled solid-propellant rocket engines 09 p1220 A83-23435

On the changes in the structure of steady plane flames as their speed increases 09 p1225 A83-23747

Local quenching due to flame stretch and non-premixed turbulent combustion 09 p1226 A83-24362

A diffusion combustor and methane-air flame propagation in concentration gradient fields 09 p1226 A83-24366

Estimation of pressure fields in combustion of vapour clouds 09 p1262 A83-24419

Stratification instability of switching front in an active trigger diffusive medium --- oscillations and wave processes during combustion 10 p1471 A83-25893

Flame spread in an opposed flow with a linear velocity gradient 10 p1390 A83-25897

Sensitivity analysis for premixed, laminar, steady state flames 10 p1390 A83-25898

Acoustic imaging for diagnostics of chemically reacting systems [AIAA PAPER 83-0761] 10 p1476 A83-25955

A study on the hydrogen-oxygen diffusion flame in high speed flow 10 p1391 A83-26199

An asymptotic theory of condensed two-phase flame propagation 12 p1712 A83-29000

One-dimensional stability of a combustion process in a magnetic field 12 p1781 A83-29268

The effect of a standing acoustic wave transverse to the flow on a turbulent flame 14 p1989 A83-32087

The propagation of a curved flame front in a specified gas-flow field 14 p1989 A83-32088

The influence of the temperature dependence of diffusivities on the dynamics of flame fronts 14 p1989 A83-32125

Investigations on a reaction model for turbulent diffusion flames 15 p2155 A83-33662

On effects due to thermal expansion and Lewis number in spherical flame propagation 15 p2131 A83-33722

On flame stretch 15 p2131 A83-33723

Numerical methods in laminar flame propagation; Proceedings of the Workshop, Aachen, West Germany, October 12-14, 1981 15 p2131 A83-34026

Discussion of test problem A --- numerical solutions of laminar flame propagation 15 p2131 A83-34027

Activation-energy asymptotics of the plane premixed flame 15 p2131 A83-34028

Theoretical implications of nonequal diffusivities of heat and matter on the stability of a plane premixed flame 15 p2132 A83-34029

The effect of Lewis number greater than unity on an unsteady propagation flame with one-step chemistry 15 p2132 A83-34030

Discussion of test problem B --- numerical methods in flame propagation 15 p2132 A83-34031

On the use of adaptive grids in numerically calculating adiabatic flame speeds 15 p2132 A83-34032

Results of a study of several transport algorithms for premixed, laminar steady-state flames 15 p2132 A83-34033

Influence of transport models and boundary conditions on flame structure 15 p2132 A83-34034

Toward the formulation of a global local equilibrium kinetics model for laminar hydrocarbon flames 15 p2132 A83-34035

Time-dependent simulation of flames in hydrogen-oxygen-nitrogen mixtures 15 p2132 A83-34036

Mechanism of flame propagation in hydrogen-air and methane-air systems 15 p2132 A83-34037

Critical conditions for the combustion of macroheterogeneous systems of the type fuel-inert material 15 p2134 A83-35318

Regular reflection of detonation waves 16 p2350 A83-35723

Turbulent flame propagation in swirl stabilized flames 16 p2326 A83-35824

Numerical solution of the problem of flame propagation by the use of the random element method [AIAA PAPER 83-0600] 16 p2326 A83-36062

Influence of laminar flame speed on the blowoff velocity of bluff-body stabilized flames [AIAA PAPER 83-1327] 16 p2326 A83-36341

Laser applications to combustion research [AIAA PAPER 83-1360] 16 p2360 A83-36358

Analysis of turbulent diffusion flames using unique relationships from laminar flame calculations [AIAA PAPER 83-1364] 16 p2326 A83-36360

An Eulerian-Lagrangian method for turbulent combustion [ONERA, TP NO. 1983-16] 16 p2327 A83-36426

Controlling mechanisms of flame spread 17 p2484 A83-37043

The detailed processes involved in flame spread over solid fuels 17 p2484 A83-37044

Correlating downward flame spread rates for thick fuel beds 17 p2484 A83-37045

Modelling the fuel temperature effect on flame spread limits in opposed flow 17 p2484 A83-37046

Prediction of metal fire spread in high pressure oxygen 17 p2484 A83-37047

Towards wind-aided flame spread along a horizontal charring slab - The steady-flow problem 17 p2484 A83-37048

Fire spread mechanisms along steel cylinders in high pressure oxygen 17 p2485 A83-38026

A two-dimensional flow model of laser supported combustion waves [AIAA PAPER 83-1718] 17 p2507 A83-38088

On the propagation laws of combustion waves in solids (pyrotechnic reactions) 17 p2486 A83-38995

The detection property of a curved flame front 18 p2663 A83-39167

Ignition and flame propagation studies with adaptive numerical grids 18 p2664 A83-40310

Acoustic signature from flames as a combustion diagnostic tool 19 p2820 A83-40860

Flame velocity for the onset of detonation 19 p2820 A83-40861

Fast deflagration waves 21 p3130 A83-44462

Diagnostic possibilities on the basis of premixed flame noise levels 22 p3265 A83-45718

Velocity statistics in premixed turbulent flames 22 p3265 A83-45719

A calculation of wrinkled flames 22 p3267 A83-46761

Comments on rates of creeping spread of flames over thermally thin fuels 22 p3267 A83-46764

Flashback in prevaporizing/premixing combustion systems [ASME PAPER 83-GT-94] 23 p3429 A83-47940

Turbulent flame propagation and combustion in spark ignition engines 23 p3429 A83-48156

An experimental study of the effects of gravity on flame spread in high oxygen concentration environments 23 p3430 A83-48158

Numerical modeling of ethylene oxidation in laminar flames 23 p3430 A83-48159

Turbulent premixed combustion - Further discussions on the scales of fluctuations [ONERA, TP NO. 1983-67] 23 p3430 A83-48188

Hydrodynamical coupling between the motion of a flame front and the upstream gas flow 24 p3577 A83-49297

Unsteady regimes of the convective combustion of a porous powder fuel 24 p3555 A83-49539

The effect of the acceleration of the external force on the evolution of a combustion site in a closed vessel 24 p3555 A83-49759

The mechanism of acoustic emission from a turbulent gas flame 24 p3555 A83-49762

Visualization of two-dimensional nonstationary flows of combustible media 24 p3555 A83-49766

Optimum conditions for the acceleration of the flame of gas mixtures at discontinuous obstacles in large volume 24 p3555 A83-49768

Characteristics of the supersonic combustion of nonmixed gases in ducts 24 p3556 A83-49778

Combustion regimes with laser-induced plasma 24 p3556 A83-49782

Combustion-wave propagation along a thin layer of a material during a gas-phase reaction between fuel and oxidizer 24 p3556 A83-49786

On large eddy structure and turbulent mixing in flames 24 p3557 A83-49809

FLAME QUENCHING

U EXTINGUISHING

U QUENCHING (COOLING)

FLAME RETARDANTS

Flame-retardant polymeric materials. Volume 3 --- Book 02 p0160 A83-11944

Synthesis and characteristics of poly(bis(dichloromaleimides)/ 05 p0610 A83-17475

Thermal performance of aircraft polyurethane seat cushions 09 p1238 A83-23849

Effectiveness of seat cushion blocking layer materials against cabin fires [SAE PAPER 82-1484] 17 p2459 A83-38003

A new brominated polymeric additive for flame retardant glass-filled polybutylene terephthalate 19 p2824 A83-41854

The development of flame retarded thermoplastic polyurethane elastomers 21 p3116 A83-44665

Effect of ammonium halides on the combustion of polystyrene 21 p3116 A83-44666

FLAME SPECTROSCOPY

Flame diagnosis with electron beam method. Research on elementary reactions in flames during suppression by electron beam fluorescence --- German thesis 01 p0022 A83-10173

Spatially precise laser diagnostics for combustion 01 p0055 A83-11060

Temperature profile of a stoichiometric CH₄/N₂O flame from laser excited fluorescence measurements on OH 02 p0152 A83-12080

Concentration profiles of NH and OH in a stoichiometric CH₄/N₂O flame by laser excited fluorescence and absorption 02 p0152 A83-12081

Spatially resolved IR absorption spectroscopy by optical Stark modulation 03 p0295 A83-14376

Instantaneous CARS thermometry in turbulent flames 03 p0295 A83-14847

Spectral characteristics of the aerodynamic field of a turbulent diffusion flame at a low Froude number 04 p0480 A83-16443

Flow visualization in combustion gases using planar laser-induced fluorescence [AIAA PAPER 83-0405] 05 p0643 A83-16694

The total emissivities of high-temperature flames 07 p0879 A83-19840

The application of coherent anti-Stokes Raman scattering to turbulent combustion thermometry 07 p0879 A83-19844

The accuracy of mass-spectrometer soundings in investigations of the flame structure of condensed systems 07 p0928 A83-19956

Doppler-free polarization spectroscopy of diatomic molecules in flame reactions 08 p1056 A83-21884

Fiber optics as light-detector probes in the accurate measurement of detonation velocities in two-phase fuel-air explosions 08 p1095 A83-22498

Laser-saturated fluorescence measurements of OH concentration in flames 09 p1225 A83-23749

Laser fluorescence measurements of the OH concentration in a combustion boundary layer 09 p1226 A83-24367

Raman oxygen detection for combustion control and regulation 10 p1425 A83-26876

Minority species concentration measurements in flames using the photoacoustic and photothermal deflection technique 11 p1572 A83-27617

Spatially resolved temperature measurements in a flame using laser-excited two-line atomic fluorescence and diode-array detection 13 p1817 A83-30746

Instantaneous Ramanography of a turbulent diffusion flame 13 p1817 A83-30747

Laser induced fluorescence and absorption measurements of NO in NH₃/O₂ and CH₄/air flames 13 p1818 A83-30969

10-Hz coherent anti-Stokes Raman spectroscopy apparatus for turbulent combustion studies 14 p2020 A83-32823

Simultaneous CARS and luminosity measurements in a bluff-body combustor [AIAA PAPER 83-1481] 15 p2134 A83-34915

Kr(+) and Ar(+) laser-excited fluorescence of CN in a flame 17 p2485 A83-37746

Nitric oxide formation in an ammonia-doped methane-oxygen low pressure flame 17 p2485 A83-38028

Fluorescence measurements of OH in a turbulent flame --- A feasibility study 19 p2820 A83-40859

Picosecond laser-spectroscopy measurement of hydroxyl fluorescence lifetime in flames 20 p2949 A83-42347

Spectroscopic analysis of the chemiluminescence from lead oxide flames 20 p2950 A83-42579

Dynamic measurements in gas flowfields using rotational Raman spectroscopy 20 p2950 A83-42580

Statistical processing of multiplexed data from turbulent flames 20 p2950 A83-42581

Recent high-resolution resonant refractivity studies of a sodium-seeded flame 21 p3110 A83-44680

Fire flame radiation 22 p3265 A83-45717

The collision half-width for the R(0) line of the nu₃ band of methane 22 p3355 A83-46268

Rotational Raman interferometric measurement of flame temperatures 22 p3294 A83-46840

Trace species analysis of flames by resonance CARS [ONERA, TP NO. 1983-66] 23 p3430 A83-48187

Hydrodynamical coupling between the motion of a flame front and the upstream gas flow 24 p3577 A83-49297

A thermal-fluctuation spectroscopy study of the combustion of ballistite powders 24 p3556 A83-49776

The use of the techniques of holographic interferometry in qualitative studies of gas-dynamic flows with chemical reactions 24 p3584 A83-49780

FLAME SPRAYING

- Structure-property relationships in flame sprayed nickel base powder coatings 06 p0733 A83-19110
- Techniques for the production of flame and plasma spray powders 06 p0769 A83-19112
- Studies on luminous and non-luminous flames with spray combustor. II - Case of swirl combustor 21 p3109 A83-44067
- Modern techniques for depositing thermally sprayed ceramic coatings with specified performance characteristics 24 p3568 A83-49084

FLAME STABILITY

- Methods for calculating the stabilization limits of a flame of inhomogeneous mixtures using a bluff body 02 p0136 A83-11512
- Influence of hydrodynamics and diffusion upon the stability limits of laminar premixed flames 04 p0457 A83-16261
- Flames as gasdynamic discontinuities 04 p0457 A83-16262
- An experimental study of the stationary propagation of a flame in a tube under conditions of weightlessness 07 p0868 A83-19957
- The effect of viscosity on hydrodynamic stability of a plane flame front 08 p1057 A83-22395
- Solution of burner-stabilized premixed laminar flames by boundary value methods 12 p1712 A83-29642
- Instabilities, pattern formation, and turbulence in flames 13 p1818 A83-31080
- Flow measurement in a model combustion chamber [AIAA PAPER 83-1550] 14 p1990 A83-32771
- Theoretical implications of nonequal diffusivities of heat and matter on the stability of a plane premixed flame 15 p2132 A83-34029
- Semi implicit calculation method of the flow field in a duct with the flame stabilized by a step --- for aircraft engine combustion chamber design 16 p2303 A83-35820
- Experimental research of the mechanism of flame stabilization in two phase mixture 16 p2325 A83-35822
- The influence of flame stabiliser pressure loss on mixing, combustion performance and flame stability 16 p2325 A83-35823
- Turbulent flame propagation in swirl stabilised flames 16 p2326 A83-35824
- Laser light scattering technique in the diagnostics of sprays in isothermal and burning conditions 16 p2351 A83-35825
- Influence of laminar flame speed on the blowoff velocity of bluff-body stabilized flames [AIAA PAPER 83-1327] 16 p2326 A83-36341
- Temperature characteristics of turbulent, premixed flames stabilised on a step 21 p3110 A83-44974
- Dynamic behavior of a bluff-body diffusion flame 21 p3110 A83-45584
- Instability and coherent structures in jet flames 22 p3266 A83-46458
- A calculation of wrinkled flames 22 p3267 A83-46761
- Hydrodynamical coupling between the motion of a flame front and the upstream gas flow 24 p3577 A83-49297
- FLAME TEMPERATURE**
- Centrifugal mixing - A comparison of temperature profiles in nonrecirculating swirling and nonswirling flames 02 p0152 A83-12076
- Measured and predicted soot profiles in a gas turbine combustor 02 p0136 A83-12077
- Two-line atomic fluorescence temperature measurement in flames - An experimental study 02 p0179 A83-12608
- Instantaneous CARS thermometry in turbulent flames 03 p0295 A83-14847
- The effect of turbulence on the formation of large superequilibrium concentrations of atoms and free radicals in diffusion flames 06 p0727 A83-19426
- Temperature measurements in a radially symmetric flame using holographic interferometry 07 p0879 A83-19845
- Temperature and optimum ionization in the micro diffusion flame 08 p1056 A83-22343
- Flame annealing of arsenic and boron implanted silicon 08 p1170 A83-22768
- Premixed, turbulent combustion of a sudden-expansion flow 09 p1225 A83-23748
- Radiation and smoke from the gas turbine combustor using heavy fuels 09 p1242 A83-23877
- Spatially resolved temperature measurements in a flame using laser-excited two-line atomic fluorescence and diode-array detection 13 p1817 A83-30746
- Calculation of the characteristics of submerged combustion 14 p1988 A83-32084
- The influence of the temperature dependence of diffusivities on the dynamics of flame fronts 14 p1989 A83-32125

- Cross-correlation of velocity and temperature in a premixed turbulent flame 14 p1990 A83-32941
- On flame stretch 15 p2131 A83-33723
- Rayleigh thermometry with low power laser sources [AIAA PAPER 83-1554] 15 p2165 A83-34925
- Model for double-base propellants combustion, without and with additives [AIAA PAPER 83-1197] 16 p2339 A83-36273
- Rotational Raman interferometric measurement of flame temperatures 22 p3294 A83-46840

FLAMEOUT

- Lewis number effects on the structure and extinction of diffusion flames due to strain 01 p0023 A83-10897
- Extinction of premixed flames in a stagnation flow considering general Lewis number 22 p3267 A83-46763

FLAMES

- NT DIFFUSION FLAMES
- NT PREMIXED FLAMES
- Theory of laminar flames --- Book 09 p1227 A83-24946
- Use of planar laser-induced fluorescence for the study of combustion flowfields [AIAA PAPER 83-1361] 18 p2688 A83-39263
- Studies on luminous and non-luminous flames with spray combustor. II - Case of swirl combustor 21 p3109 A83-44067

FLAMMABILITY

- Flame-retardant polymeric materials. Volume 3 --- Book 02 p0160 A83-11944
- The development and application of a full-scale wide-body test article to study the behavior of interior materials during a post crash fire 06 p0719 A83-18373
- The mechanism of lean limit flame extinction 07 p0879 A83-19841
- Flammability handbook for electrical insulation 09 p1221 A83-24895
- Polymer ignition - A review 14 p1999 A83-33400
- Flames near rich flammability limits, with particular reference to the hydrogen - Air and similar systems 15 p2132 A83-34038
- A relationship between the flash point, boiling point and the lean limit of flammability of liquid fuels 16 p2325 A83-35791
- Flammability testing --- at European Space Agency 17 p2483 A83-37872
- The survivable aircraft fire 20 p2931 A83-43407
- Rheological behavior of FM-9 solutions and correlation with flammability test results and interpretations --- fuel thickening additive 21 p3117 A83-44856
- FLAMMABLE GASES**
- NT GASEOUS FUELS
- Decomposition of hydrogen azide in shock waves 10 p1391 A83-26185

FLANGES

- The lubrication of roller bearing ribs - Hydrodynamic approach 01 p0056 A83-10225
- Performance of an angular flange aeroelastic wind energy converter 13 p1870 A83-30200

FLAP CONTROL

- U AIRCRAFT CONTROL
- U FLAPS (CONTROL SURFACES)

FLAPPING

- Nonlinear flapping vibrations of rotating blades 02 p0197 A83-13004
- A simplified model of the influence of elastic pitch variations on the rotor flapping dynamics 07 p0866 A83-21025
- A closed-form analysis of rotor blade flap-lag stability in hover and low-speed forward flight in turbulent flow [AIAA 83-0986] 12 p1702 A83-29864
- Coupled flap-torsional response of a rotor blade in forward flight due to atmospheric turbulence excitations 19 p2801 A83-41073
- On approximating higher-order rotor dynamics in helicopter stability-derivative models [AIAA PAPER 83-2088] 19 p2805 A83-41920

FLAPS (CONTROL SURFACES)

- NT EXTERNALLY BLOWN FLAPS
- NT JET FLAPS
- NT LEADING EDGE FLAPS
- NT LEADING EDGE SLATS
- NT TRAILING-EDGE FLAPS
- NT VORTEX FLAPS
- NT WING FLAPS

- Nonlinear aerodynamic modeling of flap oscillations in transonic flow - A numerical validation [AIAA PAPER 81-0073] 04 p0442 A83-15290
- Analysis, design, and test of a graphite/polyimide Shuttle orbiter body flap segment 09 p1216 A83-23637
- Flow over a biconic configuration with an afterbody compression flap - A comparative numerical study [AIAA PAPER 83-1668] 17 p2444 A83-37179

- Transonic wind tunnel test on an oscillating flap [AIAA PAPER 83-2132] 19 p2793 A83-41954
- Application of unsteady laminar triple-deck theory to viscous-inviscid interactions from an oscillating flap in supersonic and subsonic flow 21 p3086 A83-44457

FLARE STARS

- Astrophysical observations on Mt. Maidanak 01 p0124 A83-10846
- HEAO 1 observations of quiescent X-ray emission from flare stars 02 p0256 A83-12129
- A correlation between the age of a stellar aggregate and the color parameters of its member flare stars 03 p0408 A83-13881
- A0535 +26 - A hard X-ray observation of the 1977 December flare-up with the Prognos 6 Signe II experiment 04 p0554 A83-15633
- An unusual microwave flare with 56 second oscillations on the M dwarf L726-8 A 05 p0700 A83-17032
- A superflare in EV Lacertae 06 p0830 A83-18783
- High-energy observations of stellar flares - Comparison with the sun 07 p1012 A83-20031
- Coordinated Einstein and IUE observations of a disaripions brusques type flare event and quiescent emission from Proxima Centauri 10 p1514 A83-26729
- Statistical description of a simulacrum for eruptive variables 11 p1678 A83-27700
- On the possibility of discovering flare stars in their quiet state 13 p1943 A83-30004
- Detection of flare like events and their relationship to presumed spot regions on V471 Tau - A solar-stellar connection 13 p1951 A83-31420
- First observations of stellar coronal structure - The coronae of AR Lacertae 13 p1951 A83-31421
- The flare activity of V 780 Tau 13 p1941 A83-31555
- VLBI observations of a radio flare of Circinus X-1 14 p2099 A83-33228
- A catalog and identification charts of the Pleiades flare stars 15 p2244 A83-33751
- Discovery of a flare star near Sirius 15 p2247 A83-34560
- The origin of anomalous Balmer decrements in the spectra of eruptive stars 17 p2600 A83-37657
- Brightness variations of the star HD 29697 17 p2590 A83-37705
- Photometric investigations of the short-period brightness variability in Nova Cygni 1975 (V1500 Cyg) in a continuum 17 p2590 A83-37707
- Observations of the nonflare variability of EV Lacertae 18 p2763 A83-40481
- Starspots and stellar flares on EV Lac and YZ CMi 19 p2914 A83-40708
- Bright, rapid, highly polarized radio spikes from the M dwarf AD Leonis 22 p3376 A83-45629
- A model for A 0538-066 - The fast flaring pulsar 22 p3379 A83-46563
- Global and photospheric physical parameters of active dwarf stars 23 p3520 A83-47478
- Optical photometry of flares and flare statistics 23 p3516 A83-47488
- EV Lacertae - Is flare activity related to an unseen planet-like companion? 23 p3516 A83-47493
- An unusual flare on EV Lac 23 p3521 A83-47494
- Optical and ultraviolet stellar flare spectroscopy 23 p3521 A83-47495
- Observations of H-beta and He II lambda 4686 lines in the spectra of flares of UV Cet-type stars 23 p3521 A83-47497
- IUE spectra of the BY Dra/flarestar AU Mic 23 p3522 A83-47500
- Quiescent and flaring radio emission from dMe stars 23 p3522 A83-47503
- On activities of UV Cet-type flare stars and of T Tau-type stars 23 p3524 A83-47533
- Flares on red dwarf stars as a result of the dynamical response of the chromosphere to the heating 23 p3525 A83-47546
- Outburst period-energy relations in cataclysmic novae 23 p3527 A83-48072
- Phenomenological models of antflare stars 24 p3663 A83-49636
- FLARED BODIES**
- Hyperballistic vehicle dynamics 02 p0132 A83-13078
- FLARES**
- A flare in the millimetre to IR spectrum of 3C273 24 p3669 A83-50105
- FLASH LAMPS**
- Blocking the negative delta waves in the rabbit visual cortex by light flashes 06 p0795 A83-18972
- Performance of parallel-driven flashlamps suitable for photoinitiated lasers 11 p1579 A83-25751
- Passive mode locking of flashlamp-pumped dye lasers in the 508-583 nm range 14 p2026 A83-33411

- Dye laser spectrum narrowing by 'double pulse' flashlamp pumping 15 p2169 A83-34369
- Lasing and fluorescent characteristics of nine, new, flashlamp-pumpable, coumarin dyes in ethanol and ethanol:water 21 p3143 A83-44193

FLASH POINT

- A relationship between the flash point, boiling point and the lean limit of flammability of liquid fuels 16 p2325 A83-35791

FLASH TUBES

- U FLASH LAMPS

FLASH WELDING

- Effects of HAZ size and hardness variation on the performance of DC flash welds --- heat affected zone 21 p3151 A83-44056

FLASHBACK

- Flashback in prevaporizing/premixing combustion systems [ASME PAPER 83-GT-94] 23 p3429 A83-47940

FLASHING (VAPORIZING)

- Critical flashing flows in nozzles with subcooled inlet conditions 15 p2157 A83-33996

FLAT COAXIAL TRANSMISSION LINES

- U MICROSTRIP TRANSMISSION LINES

FLAT LAYERS

- Absorption and lateral shift of beams incident upon lossy multilayered media 08 p1161 A83-22670
- Critical conditions of the combustion of plane layers of polymethyl methacrylate on substrates of various thickness and thermal conductivity 24 p3555 A83-49760

FLAT PLATES

- Free convection fluctuating boundary layer on a horizontal plate 01 p0044 A83-10124
- Mixed convection over a horizontal heated flat plate [ASME PAPER 82-HT-75] 02 p0173 A83-12804
- Experimental and theoretical investigation on three-dimensional film cooling of a flat plate 03 p0315 A83-13345
- Transient performance of evacuated tubular solar collectors 03 p0352 A83-13478
- Laminar and turbulent boundary layers on moving, nonisothermal continuous flat surfaces 03 p0316 A83-13486
- 50 per cent more output power from an albedo-collecting flat panel using bifacial solar cells 03 p0354 A83-13700

- Boundary-layer diffusion on a plate with inhomogeneous chemical properties 03 p0323 A83-14900
- Effect of suction and blowing on boundary-layer transition [AIAA PAPER 83-0043] 05 p0578 A83-16483
- Turbulent properties of a flat plate boundary layer with mass addition and diffusion flame [AIAA PAPER 83-0471] 05 p0636 A83-16738
- Temperature distribution in a plate produced by a moving heat source --- with application to recrystallization of amorphous silicon thin films [AIAA PAPER 83-0530] 05 p0690 A83-16769

- An asymptotic analysis of free convection boundary layer on a horizontal flat plate due to small fluctuations in surface temperature 05 p0638 A83-17321

- Construction of pointwise bounds for solutions of the problem of flow on a uniformly heated moving continuous flat surface 05 p0640 A83-17552

- The analysis of a flat plate twist reflector Cassegrain aerial using GTD 06 p0715 A83-18646

- GTD analysis of reflector antennas with general rim shapes 06 p0743 A83-18690

- An experimental investigation of heat transfer near the leading edge of inclined flat plate in hypersonic flow 08 p1041 A83-22071

- An experimental study of unsteady heat transfer from a flat plate to an oscillating air flow 08 p1084 A83-22239

- Nonlinear hydrodynamic pressure on an accelerating plate 08 p1084 A83-22377

- Quantitative geometric characterization of two-dimensional flaws via liquid crystals thermography 08 p1113 A83-22409

- On the OLP prediction of the unstable modes of the flat plate turbulent boundary layer 08 p1089 A83-23197

- Transient characteristics of flat-plate solar collector 09 p1292 A83-23333

- Low Reynolds number flow between interrupted flat plates 09 p1259 A83-23878

- Heat transfer from interrupted plates 09 p1259 A83-23879

- Classification and stability criteria of separated flows 09 p1259 A83-24010

- One-dimensional problem of the identification of temperature distribution in an infinite plate 09 p1263 A83-25101

- A numerical and experimental investigation of turbulent heat transport of an axisymmetric jet impinging on a flat plate [ASME PAPER 82-WA/HT-55] 10 p1413 A83-25695

- Shock induced unsteady flat plate boundary layers and transitions 10 p1414 A83-26147

- Slip flow of a viscous fluid past an inclined flat plate 12 p1721 A83-28846

- Distortion in turbulence upstream of a flat plate and induced pressure fluctuations 12 p1723 A83-29383

- Thermal stresses in partially absorbing flat plate due to sudden interruption of steady-state asymmetric radiation. I Convective cooling at rear surface. II - Convective cooling at front surface 12 p1747 A83-29922

- Reliability and performance experience with flat-plate photovoltaic modules 14 p2038 A83-32195

- Operational experience with intermediate flat-plate photovoltaic systems 14 p2038 A83-32196

- Thermal structure of a flat plate turbulent boundary layer diffusion flame 14 p2013 A83-33092

- The cancellation of a sound-excited Tollmien-Schlichting wave with plate vibration 14 p2013 A83-33377

- Three-dimensional film cooling on a flat plate with tangential multi-jets 15 p2156 A83-33774

- Thermal cycling in compact plate-fin heat exchangers --- in aircraft gas turbines 15 p2123 A83-34253

- A dynamic simulation of a flat-plate collector system 15 p2191 A83-34409

- Description of finite deformations of thin shells by means of the coordinates of reference and actual configurations 15 p2178 A83-34438

- On the current distribution for open surfaces 15 p2154 A83-35190

- Calculation of flow past a small projection directed toward the flow 16 p2288 A83-35531

- Nonlinear bending analyses of heated sandwich plates and shells by the boundary element method 16 p2369 A83-36728

- Calculation of the amplification rates of a three-dimensional Tollmien-Schlichting wave in the boundary layer of an incompressible fluid 17 p2503 A83-37262

- An electrogasdynamic boundary layer on a dielectric plate 17 p2505 A83-37523

- Wake interference of a row of normal flat plates arranged side by side in a uniform flow 17 p2505 A83-37571

- The effect of a sudden change in the motion of a plate surface on flow in a laminar boundary layer in supersonic flow 17 p2450 A83-37634

- Allowing for the effect of a weak inhomogeneity in a boundary-layer flow on its stability characteristics 17 p2506 A83-37812

- Operational experience with flat-plate photovoltaic systems 17 p2536 A83-38019

- Free convection flow on a nonisothermal flat plate under nonuniform gravity 18 p2681 A83-39347

- Correlations concerning turbulent natural convection Influence of pressure and nature of the gas 18 p2685 A83-39851

- Recent developments in zeta-sandwich/plate structures 18 p2703 A83-40168

- Solar thermal collectors 18 p2709 A83-40522

- The integral scale of turbulence in an analysis of a boundary-layer flow on a permeable plate 19 p2846 A83-42136

- Flow and heat transfer past a semi-infinite vertical plate with oscillating plate temperature 20 p2977 A83-42720

- Experimental mixed convection from a large, vertical plate in a horizontal flow 20 p2980 A83-42754

- Numerical study of heat transfer system with staggered array of vertical flat plates used at low Reynolds number 20 p2980 A83-42755

- Three-space hidden surface removal using boundary traversal logic 20 p3036 A83-42798

- Vapor flow reversal in the condensation zone of a simulated flat-plate heat pipe 20 p2984 A83-43023

- Synthetic method in thermal boundary layer transition 20 p2987 A83-43650

- Buckling finite element analysis of flat plates with a rectangular hole 21 p3150 A83-44025

- Calculation of the heating of layered bodies 21 p3163 A83-45351

- Status of flat-plate photovoltaic systems for applications in developing countries 22 p3318 A83-46096

- Structure of turbulent boundary layer on an oscillating flat plate 22 p3282 A83-46430

- Response of a turbulent boundary layer to a pulsation of the external flow with and without adverse pressure gradient 22 p3248 A83-46434

- First-order equivalent current and corner diffraction scattering from flat plate structures 23 p3442 A83-47829

- Convective heat transfer on flat plate at very high temperature and pressure gradient [ASME PAPER 83-GT-113] 23 p3448 A83-47946

- On the calculation of separation bubbles 23 p3449 A83-48119

- The use of the method of dividing grids for studying plastic deformations in the stress concentration region 24 p3596 A83-49917

FLAT SURFACES

- Acoustic-wave diffraction by a plate moving near a flat surface 01 p0105 A83-11319

- Diffusion slipping of a binary gas mixture of moderate density along a flat surface 09 p1259 A83-23983

- The pressure on a flat surface of arbitrary orientation past which a strongly underexpanded jet of rarefied gas flows 09 p1197 A83-24484

- Multisection planar focusing lenses as concentrators of solar radiation 14 p2036 A83-32047

- The motion of an ellipsoid along a rough plane with slip 14 p2079 A83-32359

- Ray-trace analysis and data reduction methods for the Ritchey-Common test --- for optically flat surfaces 16 p2413 A83-36763

- Scattering of thermal emission from a flat surface in a medium with fluctuating permittivity 19 p2861 A83-41804

- Measurement of stresses on the surface of a plane barrier in a strongly underexpanded rarefied-gas jet 19 p2849 A83-41896

- A computer model for transient heat transfer to liquid helium 20 p2985 A83-43222

- High-frequency scattering from the edges of impedance discontinuities on a flat plane 23 p3442 A83-47830

FLATS (LANDFORMS)

- NT TIDAL FLATS

FLATTENING

- The interpretation of the major non-hydrostatic anomalies of the earth 07 p0963 A83-20974

FLAW DETECTION

- U NONDESTRUCTIVE TESTS

FLAWS

- U DEFECTS

FLEET SATELLITE COMMUNICATION SYSTEM

- FLTSATCOM solar array degradation 11 p1541 A83-27253

- FLTSATCOM - Current and future 19 p2833 A83-41401

FLEETSATCOM

- U FLEET SATELLITE COMMUNICATION SYSTEM

FLEXIBILITY

- Effect of resin flexibility on the properties of filament wound tubes 01 p0022 A83-10241

- The aerodynamics of flexible membranes 08 p1042 A83-22990

- Structural dynamics studies of rotating bladed-disk assemblies coupled with flexible shaft motions [AIAA PAPER 83-0919] 14 p1976 A83-32787

- A flexible waveguide for millimeter waves 17 p2497 A83-37756

FLEXIBLE BODIES

- NT FLEXIBLE SPACECRAFT

- On the damping effect of sloshing fluid on flexible rotor systems [ASME PAPER 82-DET-140] 02 p0196 A83-12783

- A minimum strain energy approach for obtaining optimal unbalance distribution in flexible rotors 03 p0335 A83-13491

- A study of the dynamic behavior of flexible rotors --- French thesis 03 p0337 A83-14103

- Transient dynamics during the Space Shuttle based manufacture of structural components - General formulation of the problem [AIAA PAPER 83-0432] 05 p0600 A83-16711

- On the possibility of balancing rotating flexible shafts 05 p0653 A83-17724

- Stability of two-bladed aeroelastic rotors on flexible supports 06 p0717 A83-18387

- Optimal control of flexible structures 09 p1217 A83-24755

- An application of robust servomechanisms to control of flexible structures. I - Modelling and synthesis 10 p1385 A83-26586

- A computational technique for optimizing correction weights and axial location of balance planes of rotating shafts 11 p1589 A83-28121

- Generation of shock waves in one-dimensional systems by a moving source 11 p1599 A83-28544

- Flow-acoustic interaction near a flexible wall 12 p1777 A83-29230

- Influence of mass representation on the modal analysis of rotating flexible structures [AIAA 83-0915] 12 p1745 A83-29889

- System identification of large flexible structures by using simple continuum models 13 p1812 A83-29995

A minicomputer finite elements program for microgravity hydroelastic analysis --- of spacecraft flexible propellant tanks 16 p2317 A83-36499

On the shape and orientation control of orbiting shallow spherical shell structure 17 p2479 A83-37472

The theory for a flexible slat 17 p2451 A83-37810

Aircraft flexible tanks general design and installation recommendations [SAE ARP 1664] 17 p2464 A83-38102

Dynamic contact problem of flexible orthotropic plates and shells with allowance for transverse shear 18 p2702 A83-40123

Stability of the Shuttle on-orbit flight control system for a class of flexible payloads [AIAA PAPER 83-2178] 19 p2815 A83-41672

Pilot modeling and closed-loop analysis of flexible aircraft in the pitch tracking task [AIAA PAPER 83-2231] 19 p2803 A83-41709

A modal analysis of flexible aircraft dynamics with handling qualities implications [AIAA PAPER 83-2074] 19 p2805 A83-41911

A computer program for system dynamic synthesis of flexible structures from component data 20 p3002 A83-42543

Experimental transonic studies of a three-dimensional adaptive-wall wind tunnel 20 p2928 A83-42548

Principles of sensor and actuator location in distributed systems 21 p3192 A83-44002

Optimal independent modal space control of a flexible system including integral feedback 21 p3193 A83-44034

Response in passing through critical speed of arbitrarily distributed flexible rotor system. I - Case without gyroscopic effect. II - Case with gyroscopic effect 21 p3148 A83-45475

An optimal active control system with Fourier transformed states for a flexible structure in space [IAF PAPER 83-68] 23 p3421 A83-47250

In situ balancing of flexible rotors using influence coefficient balancing and the unified balancing approach [ASME PAPER 83-GT-178] 23 p3465 A83-47989

FLEXIBLE SPACECRAFT

Development of dynamics and control simulation of large flexible space systems 02 p0141 A83-12456

Computation of a degree of controllability via system discretization --- with application to flexible spacecraft control 03 p0287 A83-14844

The stability of rotation of a rigid body with flexible elements 04 p0453 A83-15378

The stability of motion of a flexible cable with loads in a Newtonian force field 04 p0453 A83-15380

Design of space structure control systems using on-off thrusters [AIAA PAPER 81-1847] 04 p0453 A83-16121

The optimal projection approach to fixed-order compensation - Numerical methods and illustrative results --- for large flexible spacecraft design [AIAA PAPER 83-0303] 05 p0680 A83-16641

Effect of solar radiation disturbance on a flexible beam in orbit [AIAA PAPER 83-0431] 05 p0607 A83-16710

Aeroelastic behavior of hypersonic re-entry vehicles [AIAA PAPER 83-0033] 06 p0723 A83-19577

Optimization of the Eulerian turn of a nonlinear flexible object --- for spacecraft with appendages 07 p0872 A83-19936

Ten-channel vibration sensor --- for future large flexible space structures 09 p1219 A83-23595

Dynamics of a spacecraft during extension of flexible appendages 09 p1216 A83-24431

Robust control of flexible spacecraft 09 p1216 A83-24432

Singular value analysis of deformable systems --- of flexible large space structures 09 p1216 A83-24747

Digital stochastic control of distributed-parameter systems --- large flexible space structures 09 p1216 A83-24754

Singular value analysis of the model error sensitivity suppression technique --- for flexible spacecraft control 09 p1217 A83-24757

Experimental results for active structural control --- of large space structures 09 p1217 A83-24758

A function space approach to smoothing with applications to model error estimation for flexible spacecraft control 09 p1217 A83-24759

The decentralized control of large flexible space structures 09 p1217 A83-24786

Controller design for asymptotic stability of flexible spacecraft 09 p1217 A83-24788

Problems in the application of multivariable adaptive control to flexible spacecraft 09 p1217 A83-24792

Closed-loop asymptotic stability and robustness conditions for large space systems with reduced-order controllers 09 p1218 A83-24819

A sensitivity analysis of modal controller for flexible space structures 10 p1385 A83-26587

An investigation of quasi-inertial attitude control for a solar power satellite 12 p1707 A83-29050

Experimental demonstration of static shape control --- for large space structure development 13 p1812 A83-30165

A comparison of control techniques for large flexible systems 17 p2475 A83-37070

Parameter estimation and control of distributed systems with application to large deployable antennae 17 p2475 A83-37077

Modeling rotational dynamics of a flexible space platform for application of multilevel attitude control 17 p2476 A83-37108

Spillover prevention via proper synthesis/placement of actuators and sensors --- on large space structures 17 p2476 A83-37157

Lumped parameter dynamic models for large space structures with flexible and rigid parts 17 p2477 A83-37444

Recent advances in the control of large flexible spacecraft 17 p2478 A83-37468

Damping-augmentation mechanism for flexible spacecraft 17 p2478 A83-37469

The effect of flexible satellite elasticity on orientation accuracy 17 p2479 A83-37470

Design of reaction jet attitude control systems for flexible spacecraft 17 p2479 A83-37471

Progress in modelling and control of flexible spacecraft 18 p2646 A83-39094

Attitude stability of flexible asymmetric dual spin spacecraft [AIAA PAPER 83-2177] 19 p2815 A83-41671

The earth's horizon - A reference for sub arc minute attitude sensing on flexible space structures [AIAA PAPER 83-2179] 19 p2815 A83-41673

Robustness of flexible spacecraft control to actuator and sensor model errors [AIAA PAPER 83-2190] 19 p2815 A83-41676

Attitude stabilization of flexible spacecraft during stationkeeping maneuvers [AIAA PAPER 83-2226] 19 p2815 A83-41706

Adaptive parameter estimation for a flexible structure Effects of spillover [AIAA PAPER 83-2244] 19 p2891 A83-41720

Design of reduced order optimal state estimators with applications to stochastic linear optimal regulators [AIAA PAPER 83-2277] 19 p2892 A83-41743

Robust active vibration damping of flexible spacecraft [AIAA PAPER 83-2289] 19 p2816 A83-41749

Reduction of large flexible spacecraft models using internal balancing theory [AIAA PAPER 83-2292] 19 p2817 A83-41751

Robust control system design techniques for large flexible space structures having non-co-located sensors and actuators [AIAA PAPER 83-2294] 19 p2817 A83-41753

Mathematical modelling of a flexible beam under gravity 21 p3150 A83-43982

Engineering science and mechanics; Proceedings of the International Symposium, Tainan, Republic of China, December 29-31, 1981. Parts 1 & 2 21 p3117 A83-44001

Modal cost analysis as an aid in control system design for large space structures 21 p3098 A83-44005

Effect of deploying acceleration on a flexible antenna of a spin-satellite 21 p3099 A83-44015

Dynamics of Tisserand's frame for an elastic spacecraft with stored angular momentum 21 p3099 A83-44016

Solution methods for the enhanced modal control Riccati equation 21 p3193 A83-44018

On modern modal controller for flexible space structures - A sensitivity analysis 21 p3099 A83-44032

The determination of the degree of controllability for dynamic systems with repeated eigenvalues 21 p3193 A83-44039

Application of identification techniques to remote manipulator system flight data [AAS PAPER 83-083] 21 p3100 A83-44183

Dynamics and control of large flexible spacecraft; Proceedings of the Third Symposium, Blacksburg, VA, June 15-17, 1981 21 p3101 A83-45101

A definition of the degree of controllability for fuel-optimal systems 21 p3195 A83-45102

Control of a flexible satellite via elimination of observation spillover 21 p3101 A83-45103

Approximation techniques for optimal modal control of flexible systems 21 p3101 A83-45107

The control of a flexible square plate in space 21 p3101 A83-45110

Modeling and control of flexible space structures 21 p3101 A83-45111

On the rigid body motion and shape distortion evaluation for large flexible spacecraft 21 p3101 A83-45112

Damped response of spacecraft with flexible deploying appendages 21 p3101 A83-45113

On adaptive regulation of flexible spacecraft 21 p3101 A83-45114

An approximation technique for the control and identification of hybrid systems 21 p3196 A83-45116

Stability and robustness of control systems for large space structures 21 p3102 A83-45119

Stability augmentation for large space structures by modal dashpots and modal springs 21 p3102 A83-45121

Dynamics of flexible hybrid satellites - Evaluation and computation of a symbolic formalism 21 p3102 A83-45122

Optimal distributed control of a flexible spacecraft during a large-angle rotational maneuver 21 p3102 A83-45126

Generalized frequency-shaped KTC and Riccati approaches for space structure control 21 p3196 A83-45128

Control of a large class of flexible systems 21 p3102 A83-45129

Active control of large flexible spacecraft - A new design approach based on minimum information modelling of parameter uncertainties 21 p3196 A83-45133

Model error estimation for large flexible spacecraft 21 p3103 A83-45134

Dislocated actuator/sensor positioning and feedback design for flexible structures 21 p3103 A83-45465

Adaptive control of a flexible beam using least square lattice filters 22 p3351 A83-46099

Experimental implementation of parameter adaptive control on a free-free beam 22 p3351 A83-46100

Dynamic modeling of flexible spacecraft - A general program for simulation and control [IAF PAPER 83-339] 23 p3421 A83-47348

On the controllability and control law design for an orbiting large flexible antenna system [IAF PAPER 83-340] 23 p3422 A83-47349

A new approach to the dynamics and control analysis of a class of large flexible spacecraft [IAF PAPER 83-408] 23 p3422 A83-47376

The features of the space structures dynamic design [IAF PAPER 83-409] 23 p3423 A83-47377

Active vibration control of a cantilevered beam - A study of control actuators --- for large space structures [IAF PAPER 83-ST-11] 23 p3423 A83-47388

Mathematical model of a moving system with low-stiffness elastic elements 24 p3624 A83-49670

FLEXIBLE WINGS

Investigation of dynamic characteristics of an elastic wing due to correction of mass and stiffness matrices [AIAA PAPER 83-0653] 05 p0595 A83-16818

FLEXING

Fracture statistics of surface brittle materials under flexure 02 p0189 A83-11673

Higher order flexural transients in a beam 05 p0654 A83-17322

Vibrations of initially imperfect circular plates including the shear and rotatory inertial effects 06 p0773 A83-18394

The method of initial parameters as applied to the flexural vibrations of beams with hinges and oscillators 06 p0777 A83-19317

Further considerations on the problem of torsion and flexure of prismatical beams 18 p2700 A83-39555

Flexure of beams with certain curvilinear cross sections 21 p3152 A83-44463

Nonlinear flexural vibrations of initially deflected cross-ply laminated plates with elastically restrained edges 24 p3591 A83-48894

FLEXURE**U FLEXING****FLICKER**

Uniform noise in Gunn oscillators 04 p0471 A83-15745

Inhibitory influence of unstimulated rods in the human retina - Evidence provided by examining cone flicker 17 p2558 A83-37771

The mechanisms of flicker noise in Josephson junctions 22 p3276 A83-45673

FLICKER FUSION FREQUENCY
U CRITICAL FLICKER FUSION**FLIGHT ALTITUDE**

New results regarding aerotriangulation with statoscope data 08 p1092 A83-22033

Medical problems peculiar to airline pilots 14 p2067 A83-32461

On the use of height rules in off-route airspace 15 p2121 A83-35274

Wind-tunnel simulation of the actual conditions of high-altitude flight 17 p2447 A83-37507

Height measurement by quadrilateration 18 p2674 A83-39252

FLIGHT CHARACTERISTICS

Departure susceptibility and uncoordinated roll-reversal boundaries for fighter configurations

01 p0012 A83-10176
Analytical consequences of increasing the mass of a glider 03 p0281 A83-14617
F-104 CCV research flight test program 07 p0867 A83-20074

Prediction of the aerodynamic loads on helicopter blades in hovering and axial flight using lifting line theory 07 p0864 A83-21016
A unifying framework for longitudinal flying qualities criteria 09 p1209 A83-24429
Aerodynamics of asymmetric sabot discard 09 p1198 A83-24892

Development and validation of the V/STOL aerodynamics and stability and control manual 12 p1696 A83-29020
Determination of horizontal tail load and hinge moment characteristics from flight data --- on Learjet Model 55 Longhorn 13 p1805 A83-30162
The definition of short-period flying qualities characteristics via equivalent systems 14 p1977 A83-32578

Unique flight characteristics of the AD-1 oblique-wing research airplane 14 p1975 A83-32588
CF34 upgrades Challenger capabilities 15 p2122 A83-35315
In-flight simulation at the U.S. Air Force and Naval Test Pilot Schools [AIAA PAPER 83-1078] 16 p2299 A83-36206
Space Shuttle stability and control derivatives estimated from the first entry 17 p2470 A83-37065
Determination of the equivalent noise level contour for a passenger jet aircraft over a place in the case of quasi-steady flight regimes 17 p2577 A83-37535
Flight at supersonic attitudes [SAE PAPER 821469] 17 p2470 A83-38000
Status and concerns for preferred orientation control of high performance anti-air tactical missiles [AIAA PAPER 83-2198] 19 p2802 A83-41683
Suggested changes in large aircraft flying qualities criteria [AIAA PAPER 83-2071] 19 p2805 A83-41908
Comparison of the Bode envelope criterion with other criteria [AIAA PAPER 83-2073] 19 p2805 A83-41910
A modal analysis of flexible aircraft dynamics with handling qualities implications [AIAA PAPER 83-2074] 19 p2805 A83-41911
Estimation of nonlinear aerodynamics from transport airplane certification maneuvers - A system identification approach [AIAA PAPER 83-2065] 20 p2938 A83-43811
First flight performance of the control system of the inertial upper stage [AAS PAPER 83-086] 21 p3096 A83-44186
Ground simulation investigation of helicopter decelerating instrument approaches 21 p3090 A83-45461

FLIGHT CLOTHING

Improved headgear for rotary wing Navy/Marine Corps aircrewmembers 04 p0525 A83-15422
Helicopter personnel fire-resistant flotation jacket 04 p0525 A83-15427
Flight helmets - The British approach 04 p0526 A83-15443

Study of +Gz protection given by an anti 'G' suit worn on top of a liquid cooled suit 09 p1324 A83-24003
The influence of waterproofing failure on the thermal insulation of sealed flightsuits used in military aviation 14 p2072 A83-32467

FLIGHT COMPUTERS

U AIRBORNE/SPACEBORNE COMPUTERS

FLIGHT CONDITIONS

Detection of clear air turbulence using a diagnostic Richardson number tendency formulation 01 p0074 A83-10177

Building a small format, in-house aerial photography system 03 p0329 A83-14274
Fog visibility and ceilings [AIAA PAPER 83-0207] 05 p0666 A83-16584

Aerodynamic penalties of heavy rain on landing airplanes 06 p0714 A83-18403
Research on contaminated wings, current issues --- concerning icing conditions and aerodynamic effects [AIAA PAPER 83-0277] 06 p0715 A83-19584

Dynamics of air combat 07 p0862 A83-21026
Possible improvements in meteorology for aircraft navigation 09 p1199 A83-23373
Automated profiling of the troposphere 09 p1313 A83-24036

Optimum siting of NEXRAD to detect hazardous weather at airports 09 p1313 A83-24037

Optimal design of a baro/radio supported inertial altitude system [DGLR PAPER 82-041] 09 p1204 A83-24165
Flight effects for jet-airframe interaction noise [AIAA PAPER 83-0784] 10 p1376 A83-25965
The CWSU - A renewed effort to aid IFR pilots --- Center Weather Service Units 13 p1886 A83-30548
Dynamics of air combat 16 p2287 A83-36914
Generalized maximum specific range performance 16 p2301 A83-36918
Verification of numerically produced flight weather products 17 p2548 A83-38705
Operational aspects of Delta air lines meteorological department 17 p2551 A83-38746
Development of low cost RPVs under Indian conditions 20 p2934 A83-43701
Meteorology for the pilot (4th revised and enlarged edition) --- Russian book 21 p3178 A83-43907
Four-dimensional flight management using colour CRT displays 21 p3081 A83-44689
Aviation climatology 23 p3486 A83-47126

FLIGHT CONTROL

NT AUTOMATIC FLIGHT CONTROL
NT AUTOMATIC LANDING CONTROL
NT FLY BY WIRE CONTROL
NT POINTING CONTROL SYSTEMS
NT THRUST VECTOR CONTROL
The MCP-100 - A turnkey system for implementing multivariable flight control laws 01 p0009 A83-11101
On the certification of digital computer programs for flight safety 01 p0002 A83-11115
Color, pictorial display formats for future fighters 01 p0010 A83-11134
An experiment in assessment of flight control software development techniques 01 p0092 A83-11177
Design of direct digital adaptive flight-mode control systems for high-performance aircraft 01 p0013 A83-11179
Use of the onboard simulation concept for the integrated flight and fire control program 01 p0007 A83-11201
Dynamic characteristics of an integrated flight and fire control system 01 p0013 A83-11208
Application of model reference adaptive control to a relaxed static stability transport aircraft 01 p0013 A83-11209
The use of modal control to minimize errors in the analytical reconstruction of flight control sensor signals 01 p0013 A83-11210
A closed loop test facility for validating flight control software 01 p0015 A83-11226
High speed data link concepts for military aircraft 01 p0010 A83-11233
Advanced automatic terrain following/terrain avoidance control concepts study 01 p0013 A83-11254
Distributed processing and fiber optic communications in air data measurement 01 p0011 A83-11258
Air-to-air missiles - Flight test in the 80's 02 p0134 A83-11805
A fast microprocessor communication network design for interprocessor communications for an integrated flight control system 02 p0133 A83-11902
Implementation of a laboratory model Yaw Damper digital filter 02 p0230 A83-11908
The Talos guidance system 02 p0141 A83-12858
Individual blade control independent of a swashplate 04 p0446 A83-16027
Spacecraft computer resource margin management --- of Project Galileo Orbiter in-flight reprogramming task 04 p0527 A83-16118
Effects of control saturation on the command response of statically unstable aircraft [AIAA PAPER 83-0065] 05 p0598 A83-16497
Thrust reversing effects on horizontal tail effectiveness of twin-engine fighter aircraft [AIAA PAPER 83-0086] 05 p0594 A83-16512
The Northrop F-20 avionics mission simulator [AIAA PAPER 83-0142] 05 p0599 A83-16551
Piloting techniques on the backside --- of drag curve 05 p0598 A83-16927
Computer models cut USAF test costs 06 p0719 A83-18274
Spin prediction techniques 06 p0719 A83-18401
Investigation of the longitudinal motion of a flight vehicle by the method of the separation of motions 07 p0867 A83-20144
Constrained eigenvalue/eigenvector assignment - Application to flight control systems 07 p0867 A83-21006
Generic faults and architecture design considerations in flight-critical systems 09 p1203 A83-24426
Fault isolation methodology for the L-1011 digital avionics flight control system 09 p1209 A83-24427
Integration of navigation resources in modern avionics systems 09 p1200 A83-24852
A multifunction integrated approach to providing aircraft inertial data 09 p1200 A83-24853

The Integrated Inertial Navigation System - AN/ASN-132 09 p1201 A83-24855
Now is the time for new fighters 09 p1204 A83-25137
Radio-electronic guidance systems --- Russian book 10 p1402 A83-25622
The Special Research Area of Flight Control, Colloquium, Brunswick, West Germany, September 9, 10, 1981, Reports 10 p1374 A83-26476
Integrated flight path control system 10 p1378 A83-26477
Structure and mode of operation of an interactive onboard four-dimensional flight path control system 10 p1378 A83-26478
The research aircraft of the Special Research Area 'Flight Control' as scientific test stand 10 p1376 A83-26484
Improved simulation of ground reflections --- of radio navigation signals for flight control 10 p1374 A83-26486
Stochastic control and identification enhancement for the flutter suppression problem 10 p1379 A83-26544
A radio guidance algorithm for M Series rockets that are used to launch Japanese scientific satellites 10 p1382 A83-26593
Integrated systems evaluated on F-15 11 p1528 A83-28700
Integration and flight demonstrations of the Integrated Inertial Sensor Assembly /IISA/ 11 p1529 A83-28785
Heavy-lift airship dynamics 12 p1704 A83-29016
Flight testing the Low Cost Inertial Guidance System 12 p1700 A83-29210
Automation of preplanning as a means for improving quality in connection with flight operational control. I 12 p1699 A83-29372
AFTI/F-16 aeroservoelastic analyses and ground test with a digital flight control system 12 p1704 A83-29888
[AIAA 83-0994] 12 p1704 A83-29888
Development and test of an integrated sensory system for advanced aircraft 13 p1807 A83-30159
In-flight simulation of a digitally implemented direct force mode --- for flight control 14 p1977 A83-32933
Aircraft active controls - New era in design 16 p2311 A83-35773
Propulsion control sensor sharing opportunities [AIAA PAPER 83-0536] 16 p2318 A83-36059
Indoctrination of Navy test pilots to vectored thrust flight in the X-22A in-flight simulator 16 p2299 A83-36205
A missile flight control system using boundary layer thrust vector control [AIAA PAPER 83-1149] 16 p2293 A83-36246
Flight/propulsion control system integration [AIAA PAPER 83-1238] 16 p2308 A83-36301
AFTI/F-111 mission adaptive wing technology demonstration program [AIAA PAPER 83-1057] 16 p2301 A83-36468
Design and analysis of a digitally controlled integrated flight/fire control system 17 p2460 A83-37063
Recursive relationships for body axis rotation rates 17 p2575 A83-37074
Modal synthesis of missile autopilot control law 17 p2476 A83-37152
One new method of dynamic flight control 17 p2569 A83-37447
Reconfiguration of on-board control algorithms 17 p2569 A83-37491
Robotic testing for digital systems --- for software in avionics and flight control systems [SAE PAPER 821422] 17 p2563 A83-37979
The all electric airplane-benefits and challenges [SAE PAPER 821434] 17 p2463 A83-37982
Electromechanical primary flight control activation systems for fighter/attack aircraft [SAE PAPER 821435] 17 p2463 A83-37983
Flight test of the HX-I radio-controlled hybrid airship [AIAA PAPER 83-1992] 17 p2466 A83-38917
Automation of preplanning as a means for enhancing quality in operational flight control. II 18 p2638 A83-39222
A global HF telecommand system for long duration balloon flights 18 p2639 A83-39813
Training pilots for testing airplanes with modern flight control systems 18 p2736 A83-40340
Control configured vehicle as a new generation aircraft 19 p2801 A83-40884
A summary of NASA/FAA experiments concerning helicopter IFR airworthiness criteria 19 p2794 A83-41079
An electromechanical primary flight control actuation system for military transport aircraft [AIAA PAPER 83-2195] 19 p2802 A83-41680

The Air Force ejection seat as a vehicle for digital flight control
[AIAA PAPER 83-2205] 19 p2798 A83-41689

Integrated task-tailored control augmentation synthesis --- for multi-axis air-to-air tracking
[AIAA PAPER 83-2215] 19 p2803 A83-41697

An integrated maneuver enhancement and gust alleviation mode for the AFTI/F-111 MAW aircraft
[AIAA PAPER 83-2217] 19 p2803 A83-41699

Aeroelastic interactions with flight control (A survey paper)
[AIAA PAPER 83-2219] 19 p2803 A83-41700

Hovering limit cycles - A man-in-the-loop approach
[AIAA PAPER 83-2232] 19 p2803 A83-41710

Handling qualities criteria for STOL flight path control for approach and landing
[AIAA PAPER 83-2106] 19 p2806 A83-41935

Divergence suppression system for a forward swept wing configuration with wing-mounted stores
[AIAA PAPER 83-2125] 19 p2806 A83-41949

Phoenix GCS - Some considerations which influence the design of computer assisted ground control stations for RPV
20 p2932 A83-43714

Space Shuttle entry flight control overview
[AAS PAPER 83-082] 21 p3096 A83-44182

First flight performance of the control system of the inertial upper stage
[AAS PAPER 83-086] 21 p3096 A83-44186

Nonlinear control law for piloting aircraft in the air-to-ground attack phase
[ONERA, TP NO. 1983-37] 21 p3093 A83-44315

Experience with flight test trajectory guidance
21 p3091 A83-45470

Flight simulation for an inertial navigation system
23 p3420 A83-47178

Integrated flight and propulsion operating modes for advanced fighter engines
[ASME PAPER 83-GT-194] 23 p3410 A83-47999

F-14 aircraft and propulsion control integration evaluation
[ASME PAPER 83-GT-234] 23 p3411 A83-48029

The calculation of optimal paths with singular control segments --- for flight vehicle trajectories
23 p3501 A83-48246

Bucking the current --- electric actuators for V/STOL aircraft
24 p3547 A83-48887

Integrated flight/propulsion control system architectures for a high speed aircraft
[AIAA PAPER 83-2563] 24 p3549 A83-49595

Integrated control system concept for high-speed aircraft
[AIAA PAPER 83-2564] 24 p3549 A83-50074

FLIGHT CREWS
NT SPACECREWS

Psychological and electroencephalographic changes with aging in relation to aircrew performance
02 p0225 A83-12253

Stress coping and the U.S. Navy aircrew factor mishap
02 p0225 A83-12408

Preliminary overview analyses of U.S. Navy Aircrew Automated Escape Systems /AAES/ in-service usage data
04 p0444 A83-15405

Preliminary analyses of flail, windblast and tumble problems and injuries associated with usage of U.S. Navy Aircrew Automated Escape Systems /AAES/
04 p0444 A83-15407

U.S. Navy Aircrew Automated Escape Systems /AAES/ In-Service Data Analysis program
04 p0444 A83-15408

An option for enhanced aircrew survivability
04 p0444 A83-15409

Manual parachute ripcord pull-force capability of female naval personnel
04 p0525 A83-15410

USAF Aerospace Biotechnology Research and Development Program
04 p0525 A83-15420

Improved headgear for rotary wing Navy/Marine Corps aircrewmnen
04 p0525 A83-15422

Mission specific survival equipment for helicopter aircrew
04 p0525 A83-15426

Design and development of Cartridge Actuated Device /CAD/ primer
04 p0464 A83-15433

Development and testing of a microwave radiometric vertical sensor for application to a vertical seeking aircrew escape system
04 p0447 A83-15437

Hypertension and orthostatic hypotension in applicants for flying training and aircrew
06 p0797 A83-18197

Designing patrol aircraft for the crew
06 p0800 A83-18811

Sudden incapacitation - USAF experience, 1970-80
07 p0978 A83-20787

Flight, flight duty, and rest times - A comparison between the regulations of different countries
10 p1454 A83-25667

Application of advanced speech technology /AST/ in manned penetration bombers
10 p1459 A83-26302

Development of a simulator certification /SIMCERT/ methodology for SAC --- Air Force aircrew training regulation
10 p1459 A83-26306

VOR/DME automated station selection algorithm
11 p1528 A83-28597

Hypoxia - USAF experience 1970-1980
12 p1764 A83-28936

Stresses affecting the cockpit personnel and automation
12 p1767 A83-29373

An investigation of the microcirculatory bed in flightcrew members with conjunctivitis during the initial appearance of cerebral atherosclerosis
13 p1905 A83-30949

Degradation of psychomotor performance under 16-18 Hz sinusoidal vibration
14 p2067 A83-32460

Aviation medicine training for aircrew in the 1980's
14 p2067 A83-32463

Airline safety and labor relations law - Balancing rights and responsibility
15 p2240 A83-34475

Head and/or torso cooling during simulated cockpit heat stress
15 p2216 A83-34979

Minimal coronary artery disease and continuation of flying status
15 p2214 A83-34988

Toward an understanding of the work capacity of the flight crew
16 p2400 A83-35597

Canadian forces air combat helmet - The selection
17 p2562 A83-37878

Human factors approach in certification flight test
[SAE PAPER 821340] 17 p2562 A83-37951

Etiological aspects of indispositions in flight
17 p2561 A83-38945

Pointers to diagnosis of psychiatric illness in aircrew
18 p2737 A83-40354

The information content of functional tests in the elucidation of the causes of repolarization disorders of the myocardium in flight personnel
21 p3188 A83-45299

FLIGHT FATIGUE
Pilot fatigue - A deadly cover-up --- Book
09 p1199 A83-24901

Flight, flight duty, and rest times - A comparison between the regulations of different countries
10 p1454 A83-25667

A physiological and hygienic evaluation of vibration in the cabin of the Mi-4 helicopter
14 p2073 A83-33325

A model for prediction of resynchronization after time-zone flights
15 p2214 A83-34983

Naval aviation mishaps and fatigue
15 p2215 A83-34985

The prevention of flight fatigue by a method of physical training
23 p3499 A83-48570

FLIGHT FITNESS
Hypertension and orthostatic hypotension in applicants for flying training and aircrew
06 p0797 A83-18197

Disease risk factors and the flight surgeon - A strategy to keep pilots flying
08 p1147 A83-22963

Some considerations on lumbar pains and diseases of the intervertebral disk to civilian aircrewmnen
08 p1148 A83-22974

The significance of several physiological parameters during the assessment of the flight fitness of student pilots
14 p2068 A83-32466

Problems of fitness posed by vertebral pathology in flight personnel
16 p2397 A83-35584

Practical aspects of the medical check-up of nonprofessional pilots
16 p2397 A83-35585

Return to flying after head injuries - A review
18 p2734 A83-40355

FLIGHT HAZARDS
NT METEOROID HAZARDS

In-flight lightning data measurement system for fleet application - Flight test results
01 p0009 A83-11087

Approach to payload contamination integration
03 p0286 A83-13748

The role of endogenous circadian rhythmicity in Air-Force flight accidents due to pilot error
04 p0521 A83-15402

First stage propulsion for the maximum performance ejection system
04 p0445 A83-15421

Thunderstorms and aviation - Operational forecasting programs at the National Severe Storms Forecast Center
[AIAA PAPER 83-0442] 05 p0666 A83-16716

Sudden incapacitation - USAF experience, 1970-80
07 p0978 A83-20787

Remote sensing of problem birds in aviation
08 p1043 A83-21876

Management of bird problem in Indian airlines
08 p1043 A83-21877

Bird strikes to aircraft and associated hazards and problems regarding the safety of aircraft operations
08 p1043 A83-21878

Space flight and meteoroids
08 p1048 A83-21883

Laser and millimeter-wave backscatter of transmission cables
08 p1043 A83-22523

Optimum siting of NEXRAD to detect hazardous weather at airports
09 p1313 A83-24037

'Scaling' analysis of the ice accretion process on aircraft surfaces
[ASME PAPER 82-WA/HT-39] 10 p1373 A83-25693

Conflict recognition and collision probability in connection with horizontal evasion maneuvers
10 p1373 A83-26481

The design of wind shear filters
10 p1378 A83-26483

Radar detection of low level wind shear affecting aircraft terminal navigation
11 p1529 A83-28784

Application of VAS multispectral imagery to aviation forecasting --- VISSR Atmospheric Sounder for GOES satellites
13 p1887 A83-30561

Short-range prediction of mesoscale windfields
13 p1888 A83-30567

Man-made debris in low earth orbit - A threat to future space operations
15 p2125 A83-33740

Grid-scale turbulence coefficients and their connection with clear air turbulence
16 p2391 A83-36845

Measured cloud data obtained in Northwest and Great Lakes United States and northern Canada during icing certification tests
17 p2549 A83-38719

Numerical simulation of the atmosphere during a CAT encounter
17 p2553 A83-38764

CAT detection and forecasting using operational NMC analysis data
17 p2553 A83-38765

The survivable aircraft fire
20 p2931 A83-43407

Airports as a threat to public safety --- Book
22 p3251 A83-46420

Repeatability and continuous duration of meteorological conditions that are complex for aviation in the northern European territory of the USSR
23 p3486 A83-47130

Wind shear - A danger for flight
23 p3492 A83-48225

Cryogenic liquids and aviation --- biological effects and safety hazards
23 p3499 A83-48695

Droplet spectra and liquid water content measurements in aircraft icing environments
[AD-A122516] 24 p3614 A83-49718

Characteristics of icing conditions in wintertime stratiform clouds
24 p3614 A83-49719

Microphysical influences on aircraft icing
24 p3546 A83-49722

FLIGHT INSTRUMENTS
NT APPROACH INDICATORS
NT ATTITUDE INDICATORS
NT AUTOMATIC PILOTS
NT HORIZON SCANNERS
NT RADIO ALTIMETERS

Holographic HUDs de-mystified
01 p0010 A83-11171

A cost effective approach to design evaluation of advanced system display switchology
01 p0093 A83-11200

Secondary air data measurement technology --- pressure transducers for RPVs, drones, cruise missiles and fighter backup systems
01 p0011 A83-11261

The complete book of cockpits
02 p0135 A83-11575

Mass-produced laser gyros
02 p0176 A83-11628

Advanced P-3 flight station studies
04 p0447 A83-15429

Simulator studies to develop and improve flight attitude information
04 p0448 A83-16334

Assessment of future solid rocket motor flight instrumentation/data needs
09 p1219 A83-24888

Avionics analyzed. III - The hidden sensors
17 p2461 A83-38471

A history of electronic flight instruments - through tomorrow
19 p2799 A83-41532

Method of thermodynamic function control and of damage analysis regarding aircraft engines with the aid of flight data recording systems --- German thesis
19 p2800 A83-41850

Military systems acceptance criteria --- for digital avionic systems
22 p3247 A83-45844

General aviation goes digital - Many advantages, but some problems
23 p3406 A83-48640

FLIGHT MECHANICS
The fundamental geometrical and aerodynamic characteristics of aircraft and rockets --- Russian book
01 p0003 A83-10669

The attainability domain of a coasting vehicle
10 p1380 A83-26073

Fundamentals of flight --- Book
13 p1803 A83-30152

On an algorithm for the simplified integration of dynamic systems --- for flight trajectory analysis
13 p1914 A83-30724

Recursive relationships for body axis rotation rates
17 p2575 A83-37074

- Balloon materials and designs 18 p2640 A83-39806
- Analytic solution for a cruising plane change maneuver [AIAA PAPER 83-2095] 19 p2810 A83-41924
- Interception in three dimensions - An energy formulation [AIAA PAPER 83-2121] 19 p2798 A83-41946
- Separation of time scales in aircraft trajectory optimization [AIAA PAPER 83-2136] 19 p2799 A83-41958
- Energy state revisited --- for minimum-time aircraft climbs [AIAA PAPER 83-2138] 19 p2799 A83-41960
- Universities - Have they a role in aeronautical research? Flight mechanics, avionics and space 20 p2927 A83-42619
- Dynamics of Tisserand's frame for an elastic spacecraft with stored angular momentum 21 p3099 A83-44016

FLIGHT OPERATIONS

- NT CREW PROCEDURES (INFLIGHT)**
- The Space Shuttle operator's manual --- Book 01 p0019 A83-11501
- Sky Hook to help ships launch Harrier 03 p0282 A83-13575
- Shuttle and Spacelab flight operations 03 p0285 A83-13708
- Loran-C RNAV - The best near-term solution to air operations in northeastern North America 06 p0716 A83-18822
- Fuel savings in air transport 06 p0714 A83-19150
- Noise-reducing takeoff and landing procedures and the potential for their operational use in the Airbus A300 [DGLR PAPER 82-032] 09 p1199 A83-24158
- The IRAS project organisation and mission operations 11 p1534 A83-28210
- C-141 operations in Operation Bright Star 82 12 p1699 A83-29203
- Flight operations: A study of flight deck management --- Book 15 p2120 A83-33767

FLIGHT OPTIMIZATION

- Optimization of variable-altitude flyback maneuvers --- for rocket-propelled lifting vehicles [AIAA PAPER 83-0282] 05 p0594 A83-16627
- Maximum endurance and maximum penetration trajectories for horizontal gliding flight [AIAA PAPER 83-0283] 05 p0594 A83-16628
- Possible improvements in meteorology for aircraft navigation 09 p1199 A83-23373
- Drive and flight optimization of a winged space transport vehicle with rocket and ramjet propulsion [DGLR PAPER 82-076] 09 p1216 A83-24190
- New on board equipments /PMS, FMS/ and the ATC system - Evolution or revolution 09 p1204 A83-24859
- Energy conservation in air transportation - The Canadian Air Traffic Control Effort 12 p1699 A83-29393
- Advanced navigation systems and fuel conservation 15 p2120 A83-33545
- Optimal turning climb-out and descent of commercial jet aircraft [SAE PAPER 821468] 17 p2464 A83-37999
- The effects of non-linear kinematics in optimal evasion 19 p2889 A83-40674
- Flight management systems - What are they and why are they being developed? [AIAA PAPER 83-2235] 19 p2803 A83-41712
- Optimal symmetric flight with an intermediate vehicle model [AIAA PAPER 83-2238] 19 p2798 A83-41715
- Flight software for optimal trajectories in transport aircraft [AIAA PAPER 83-2241] 19 p2796 A83-41718
- 4 D fuel-optimal guidance in the presence of winds [AIAA PAPER 83-2242] 19 p2796 A83-41719
- Optimization and closed loop guidance of drag modulated aeroassisted orbital transfer [AIAA PAPER 83-2093] 19 p2810 A83-41923
- The optimal evasive maneuver of a fighter against proportional navigation missiles [AIAA PAPER 83-2139] 19 p2807 A83-41961
- Optimal short range trajectories for helicopters [AIAA PAPER 83-2140] 19 p2799 A83-41962
- Subsonic airplane configurations for maximum range for endurance [AIAA PAPER 83-2536] 23 p3405 A83-48370
- Wing extensions for improving climb performance [AIAA PAPER 83-2556] 23 p3405 A83-48375
- Generalized flight optimization equations for commercial aircraft 24 p3548 A83-50135

FLIGHT PATHS

- NT GLIDE PATHS**
- Estimation of aircraft fuel consumption 01 p0008 A83-10186

- A nonlinear smoothing procedure for the reconstruction of flight trajectories on the basis of radar data 03 p0280 A83-14494
- Novel airborne technique for aircraft noise measurements above the flight path 04 p0533 A83-15316
- The maneuvering flight path display - An update 04 p0447 A83-16130
- Flight path design issues for the TOPEX mission --- Ocean Topography Experiment [AIAA PAPER 83-0197] 05 p0599 A83-16581
- Piloting techniques on the backside --- of drag curve 05 p0598 A83-16927
- Automation of on-board flightpath management 07 p0867 A83-21002
- Analysis of target coverage for an unstabilized 35 mm panoramic strike camera 08 p1100 A83-22596
- An integrated multisensor aircraft track recovery system for remote sensing 10 p1374 A83-26266
- Integrated flight path control system 10 p1378 A83-26477
- Structure and mode of operation of an interactive onboard four-dimensional flight path control system 10 p1378 A83-26478
- Analysis of in-trail following dynamics of CDTI-equipped aircraft --- Cockpit Displays of Traffic Information 13 p1807 A83-30161
- Computer model of a collision-avoidance system for air traffic control 15 p2121 A83-35275
- All weather heliports and airway system - The future need 16 p2312 A83-36073
- The COMPAS system for more efficient approach traffic --- for aircraft 18 p2639 A83-39345
- Optimal symmetric flight with an intermediate vehicle model [AIAA PAPER 83-2238] 19 p2798 A83-41715
- Vertical flight path and speed control autopilot design using total energy principles [AIAA PAPER 83-2239] 19 p2804 A83-41716
- Handling qualities criteria for STOL flight path control for approach and landing [AIAA PAPER 83-2106] 19 p2806 A83-41935
- Flight path/nose pointing - A required criterion in future fighter aircraft design [AIAA PAPER 83-2123] 19 p2798 A83-41948
- Aircraft trajectories for reduced noise impact 21 p3089 A83-43971
- Flight trajectories with maximum tangential thrust in a central Newtonian field 21 p3095 A83-45291
- Flight frequency determination 22 p3251 A83-46776
- Application of optimal control synthesis to integrated vertical flight path and airspeed control for an advanced fighter [AIAA PAPER 83-2560] 24 p3549 A83-49594

FLIGHT PERFORMANCE**U FLIGHT CHARACTERISTICS****FLIGHT PLANS**

- A simple Lagrangian forecast system with aviation forecast potential 17 p2550 A83-38727
- Operational aspects of Delta air lines meteorological department 17 p2551 A83-38746
- Meteorological data requirements for fuel efficient flight 17 p2552 A83-38760
- The Air Force Global Weather Central computer flight planning system 17 p2552 A83-38761

FLIGHT RECORDERS

- Flight data recorders - An investigator's tool 21 p3092 A83-44877
- Analysis of general aviation accidents using ATC radar records 23 p3400 A83-48218

FLIGHT RULES**NT INSTRUMENT FLIGHT RULES****NT VISUAL FLIGHT RULES****FLIGHT SAFETY**

- On the certification of digital computer programs for flight safety 01 p0002 A83-11115
- An experiment in assessment of flight control software development techniques 01 p0092 A83-11177
- The crowded sky 02 p0137 A83-12643
- Existing time limit for overwater operations - Its validity 03 p0281 A83-13170
- SAFE Association, Annual Symposium, 19th, Las Vegas, NV, December 6-10, 1981, Proceedings 04 p0524 A83-15401
- USAF Aerospace Biotechnology Research and Development Program 04 p0525 A83-15420
- Human factors dilemmas in the quest for aviation safety 04 p0444 A83-15423
- Mission specific survival equipment for helicopter aircrew 04 p0525 A83-15426
- Negative transfer - A threat to flying safety 04 p0523 A83-15541
- Safety attitudes of a general aviation pilot population 04 p0523 A83-15542

- Clinical aviation medicine --- Book 05 p0674 A83-17300
- The peculiarities of medical support for helicopter flights 05 p0675 A83-17698
- A proposed simple and safe aircraft take-off or landing procedure with wing roughness or protuberances [AIAA PAPER 83-0604] 06 p0718 A83-19594
- Remarks on the systematic tonal audiometry of the ground personnel in charge of airspace security 08 p1148 A83-22972
- Microlights -The state of the art 09 p1195 A83-23685
- The organization of medical facilities for flight safety 09 p1322 A83-23975
- Increasing flight safety under shear wind conditions by modifying thrust regulation systems and existing cockpit instrumentation [DGLR PAPER 82-033] 09 p1209 A83-24159
- Aircraft separation assurance - Systems design 09 p1201 A83-24863
- Viewpoints on selection of collision avoidance systems 09 p1202 A83-24874
- Pilot fatigue - A deadly cover-up --- Book 09 p1199 A83-24901
- Airline safety and labor relations law - Balancing rights and responsibility 15 p2240 A83-34475
- Locus of control, self-serving biases, and attitudes towards safety in general aviation pilots 15 p2215 A83-34980
- On the use of height rules in off-route airspace 15 p2121 A83-35274
- Space-station crew-safety requirements 16 p2315 A83-36408
- Flight tests of tow wire forces while flying a racetrack pattern 16 p2301 A83-36919
- Operational aspects of Delta air lines meteorological department 17 p2551 A83-38746
- Wakes from arrays of buildings --- flight safety 17 p2508 A83-38766
- Safety in the skies 19 p2794 A83-41467
- Undetectable critical defects in safety-of-flight structure 20 p2999 A83-42544
- Autonomy issues for an operational space station [AAS PAPER 83-043] 21 p3095 A83-44170
- Hazards of loose harness during flying 23 p3499 A83-48693

FLIGHT SIMULATION

- Improved g-cueing system --- for motion simulation in combat pilot training simulators 01 p0013 A83-10178
- Investigation of constant turn-rate dynamics models in filters for airborne vehicle tracking 01 p0096 A83-11190
- Computer animated representations to optically observe numerical evaluations 01 p0092 A83-11199
- A new use for NWC's wind machine - Parachute testing 04 p0449 A83-15309
- A new concept for aircraft dynamic stability testing 04 p0449 A83-15310
- Cross-coupling between longitudinal and lateral aircraft dynamics in a spiral dive 04 p0449 A83-15312
- Flight simulation - Avionic systems and aero medical aspects; Proceedings of the International Conference, London, England, April 6, 7, 1982 04 p0441 A83-16326
- Pilot judgements of distance, height and glide slope angle from computer generated landing scenes 04 p0524 A83-16327
- Putting texture in perspective --- flight simulation by application of computer generated imagery techniques 04 p0524 A83-16330
- Simulation of a terrain following system 04 p0445 A83-16333
- Simple CIG - An approach to visual simulation for procedure training --- Computer Image Generation 04 p0450 A83-16335
- Improving the data base generation process for flight simulator data bases [AIAA PAPER 83-0138] 05 p0598 A83-16547
- Assessment of advanced fighter powered approach simulations [AIAA PAPER 83-0141] 05 p0598 A83-16550
- Measurement of the frequency response of a digital autopilot [AIAA PAPER 83-0326] 05 p0605 A83-16655
- Radio Technical Commission for Aeronautics, Technical Symposium and Annual Assembly Meeting, Washington, DC, November 18-20, 1981, Proceedings 05 p0577 A83-17301
- Boeing gains real-time flight data 06 p0719 A83-18270
- Computer models cut USAF test costs 06 p0719 A83-18274
- The analysis of operational stresses --- on aircraft during flight 06 p0775 A83-18596

Experimental comparison of simulation methods of aeronautic type loading
[ONERA, TP NO. 1982-130] 06 p0775 A83-18598

Effective aerodynamic parameter evaluation from free flight tests 07 p0866 A83-21005

Dynamics of air combat 07 p0862 A83-21026

Evaluation of the sensitivity and intrusion of workload estimation techniques in piloting tasks emphasizing mediational activity 07 p0980 A83-21075

Dynamic stability of a buoyant quad-rotor aircraft 08 p1047 A83-22160

Researchers study methods to combat effects of wind shear 08 p1043 A83-22175

Method of designing a program module for the simulation of complex dynamic systems on a hybrid computer --- for flight simulation 08 p1154 A83-22184

Visual simulation and image realism II; Proceedings of the Conference, San Diego, CA, August 27, 28, 1981 08 p1102 A83-22830

Pilot task profiles, human factors, and image realism 08 p1047 A83-22836

A simulation model for the analysis of the dynamic behavior of a helicopter rotor under nonstationary limit flight conditions 08 p1044 A83-23220

The simulation of fatigue loads in aeronautics 08 p1048 A83-23241

Simulation of the acoustic environment by a launch vehicle at lift-off and its vibratory effects on its structures [ONERA, TP NO. 1982-117] 09 p1212 A83-24328

Computer generated cockpit engine displays 10 p1376 A83-26309

A visual channel theory approach to pilot performance and simulator imagery 10 p1456 A83-26311

Procedure for an evaluation of control systems on the basis of human factor considerations 10 p1460 A83-26479

A compact inflow control device for simulating flight fan noise [AIAA PAPER 83-0680] 11 p1651 A83-28005

Cardiac function monitored by impedance cardiography during changing seatback angles and anti-G suit inflation 12 p1766 A83-28930

Helicopter flight testing, simulation and real-time analysis 12 p1701 A83-29391

Minuteman inertial guidance assessment - The next best thing to flight tests 13 p1811 A83-30160

In-flight simulation of a digitally implemented direct force mode --- for flight control 14 p1977 A83-32933

The United States Air Force and the use of in-flight simulation 14 p1975 A83-32937

A method of grouping pilots before carrying out experiments in flight simulators 14 p2071 A83-32955

An algorithm of flight simulation on a dynamic stand of support type 15 p2123 A83-34429

Propulsion system simulation technique for scaled wind tunnel model testing 16 p2311 A83-35850

Flight Simulation Technologies Conference, Niagara Falls, NY, June 13-15, 1983, Collection of Technical Papers 16 p2287 A83-36203

Indoctrination of Navy test pilots to vectored thrust flight in the X-22A in-flight simulator [AIAA PAPER 83-1076] 16 p2299 A83-36205

In-flight simulation at the U.S. Air Force and Naval Test Pilot Schools [AIAA PAPER 83-1078] 16 p2299 A83-36206

Sinusoidal integration for simulation of second-order systems [AIAA PAPER 83-1086] 16 p2406 A83-36210

Spectral decontamination of a real-time helicopter simulation [AIAA PAPER 83-1087] 16 p2299 A83-36211

Analysis of a real-time application [AIAA PAPER 83-1088] 16 p2406 A83-36212

Benchmarks for a computer system for NASA's Shuttle procedures simulator [AIAA PAPER 83-1089] 16 p2314 A83-36213

Error sources in hybrid computer based flight simulation [AIAA PAPER 83-1090] 16 p2299 A83-36214

Use of flight test results to improve the flying qualities simulation of the B-52H weapon system trainer [AIAA PAPER 83-1091] 16 p2300 A83-36215

Real time simulation of mission environments for avionics systems integration [AIAA PAPER 83-1097] 16 p2312 A83-36217

The man-vehicle systems research facility - A new NASA aeronautical R & D facility [AIAA PAPER 83-1098] 16 p2312 A83-36218

Data base considerations for a tactical environment simulation [AIAA PAPER 83-1099] 16 p2312 A83-36219

Ejector nozzle test results at simulated flight conditions for an advanced supersonic transport propulsion system [AIAA PAPER 83-1287] 16 p2309 A83-36323

Dynamics of air combat 16 p2287 A83-36914

Piloted simulation of hover and transition of a vertical attitude takeoff and landing aircraft 17 p2462 A83-37064

An assessment of flow-field simulation and measurement [AIAA PAPER 83-1721] 17 p2509 A83-37210

Validation of the in-orbit checkout of the IRAS gyroscopes using computer simulations 17 p2481 A83-37475

Wind-tunnel simulation of the actual conditions of high-altitude flight 17 p2447 A83-37507

A six-degree of freedom heavy lift airship flight simulation [AIAA PAPER 83-1988] 17 p2466 A83-38914

An atmospheric sounding balloon with ballast - An automatic numerical model for its manufacture and simulation of its evolution 18 p2640 A83-39804

JT9D performance deterioration results from a simulated aerodynamic load test 19 p2800 A83-41040

The effects of engine and height-control characteristics on helicopter handling qualities 19 p2802 A83-41078

A summary of NASA/FAA experiments concerning helicopter IFR airworthiness criteria 19 p2794 A83-41079

Adaptive control of variable flow ducted rockets [AIAA PAPER 83-2202] 19 p2797 A83-41686

Pilot modeling and closed-loop analysis of flexible aircraft in the pitch tracking task [AIAA PAPER 83-2231] 19 p2803 A83-41709

Status of the development of handling criteria for VSTOL transition [AIAA PAPER 83-2103] 19 p2806 A83-41932

New flying qualities criteria for relaxed static longitudinal stability [AIAA PAPER 83-2104] 19 p2806 A83-41933

Comparison of fixed-base and in-flight simulation results for lateral high order systems [AIAA PAPER 83-2105] 19 p2806 A83-41934

Ascent performance and abort analysis for a Future Space Transportation System [AIAA PAPER 83-2112] 19 p2817 A83-41939

Poststall flight in close combat [AIAA PAPER 83-2120] 19 p2806 A83-41945

Aeroservoelasticity in the time domain --- for YF-16 aircraft 21 p3093 A83-43965

Development of terrain-following displays for the tornado aircraft 21 p3091 A83-44687

Multiwavelength operation of an acousto-optic deflector --- for laser flight simulation displays 21 p3140 A83-44839

Ground simulation investigation of helicopter decelerating instrument approaches 21 p3090 A83-45461

Space Shuttle response to ascent wind profiles 21 p3097 A83-45464

Flight simulation for an inertial navigation system 23 p3420 A83-47178

Studies concerning model technology in the European Transonic Wind Tunnel (ETW) 23 p3412 A83-47197

The mathematical model for space flight visual simulation by computer generated image [IAF PAPER 83-350] 23 p3418 A83-47355

Added fluid mass and the equations of motion of a parachute 23 p3398 A83-48145

FLIGHT SIMULATORS

NT COCKPIT SIMULATORS

Optical information for descent in flight simulation 01 p0085 A83-11137

Sensor snap and narrow field-of-view inset for terrain avoidance flight 01 p0010 A83-11188

A closed loop test facility for validating flight control software 01 p0015 A83-11226

Flight simulator display capability significantly advanced 02 p0135 A83-12935

Meteorological inputs to flight simulators 04 p0515 A83-15323

Assessing pilot performance and mental workload in training simulators 04 p0524 A83-16329

Characteristics of flight simulator visual systems 04 p0450 A83-16331

Simulator studies to develop and improve flight attitude information 04 p0448 A83-16334

Colour flight deck displays 04 p0448 A83-16336

AOI displays in simulation --- Area Of Interest 04 p0448 A83-16337

'A total G-force environment dynamic flight simulator' - A new dimension in flight simulation [AIAA PAPER 83-0139] 05 p0599 A83-16548

The Northrop F-20 avionics mission simulator [AIAA PAPER 83-0142] 05 p0599 A83-16551

DC-9 Super 80 digital flight guidance system simulation techniques for certification 05 p0592 A83-17305

The JA37 /VIGGEN/ pilot training concepts ATD preliminary use and 'signs' of effectiveness --- Aircraft Training Device System 05 p0676 A83-17310

Rockwell B-1B design to be studied in new cab 06 p0719 A83-18271

Real-time scenarios aid McDonnell weapons work 06 p0719 A83-18272

Ames expands rotorcraft capability 06 p0719 A83-18273

An optimal control approach to the design of moving flight simulators 07 p0868 A83-19949

Realistic 'feel' in flight simulators is based on precise control loading 08 p1048 A83-23240

Evaluation of 20 workload measures using a psychomotor task in a moving-base aircraft simulator 10 p1455 A83-25998

A comparison of color versus black and white visual display as indicated by bombing performance in the 2B35 TA-4J flight simulator 10 p1376 A83-26313

Integrated control/display unit vs. dedicated control heads for radio tuning in a KC-135 flight simulator 10 p1459 A83-26318

Training effectiveness evaluation of device 2F117 - OFT for CH-46 helicopter 10 p1456 A83-26326

Simulator fidelity and flight test data - Improving the flight performance of the B-52H WST production unit flight station simulator [AIAA PAPER 83-1075] 16 p2299 A83-36204

Advanced display techniques for training the multi-member tactical air crew [AIAA PAPER 83-1079] 16 p2302 A83-36207

A visual cueing model for terrain-following applications [AIAA PAPER 83-1081] 16 p2401 A83-36208

Simulator performance definition by cue synchronization analysis [AIAA PAPER 83-1092] 16 p2312 A83-36216

Application of experimentally derived pilot perceptual angular response transfer functions [AIAA PAPER 83-1100] 16 p2402 A83-36220

Design of a real-time CGSI system [AIAA PAPER 83-1101] 16 p2341 A83-36221

Compensation for time delay in flight simulator visual-display systems [AIAA PAPER 83-1080] 16 p2312 A83-36222

Old problem/new solutions - Motion cuing algorithms revisited [AIAA PAPER 83-1082] 16 p2404 A83-36223

Visually-coupled systems as simulation devices [AIAA PAPER 83-1083] 16 p2312 A83-36224

Flight fidelity testing of the F/A-18 simulators [AIAA PAPER 83-1094] 16 p2300 A83-36225

Simulator applications and technology [AIAA PAPER 83-2172] 19 p2807 A83-41667

Conditions of the generalized similarity of simulators to aircraft 20 p3036 A83-43505

Heart rate variability, cardiac mechanics, and subjectively evaluated stress during simulator flight 21 p3186 A83-43988

Comparison of color and black-and-white visual displays as indicated by bombing performance in the 2B35 TA-4J flight simulator 21 p3092 A83-44692

FLIGHT STABILITY TESTS

A-10 stall/post-stall testing - A status update 02 p0137 A83-11808

F-18 Hornet high angle of attack /AOA/ program 02 p0137 A83-11809

Flight data on liquid-filled shell for spin-up instabilities [AIAA PAPER 83-2143] 19 p2811 A83-41965

Aeromechanical stability of a hingeless rotor in hover and forward flight - Analysis and wind tunnel tests 24 p3548 A83-50141

FLIGHT STRESS (BIOLOGY)

NT SPACE FLIGHT STRESS

Recovery curves in partially fatigued muscle 01 p0084 A83-11259

The influence of differential physical conditioning regimens on simulated aerial combat maneuvering tolerance [AD-A126486] 02 p0223 A83-12406

Psychological problems of the activities of operators - Three conferences in Zvenigorod 03 p0382 A83-13280

Numerical and psychopathological data bearing upon 700 certifications of civil aviation flight personnel 06 p0799 A83-18333

Ergonomic analysis and evaluation procedures for cockpit operating positions 09 p1324 A83-23496

Pilot fatigue - A deadly cover-up --- Book 09 p1199 A83-24901

Etiological aspects of indispositions in flight 17 p2561 A83-38945

Heart rate variability, cardiac mechanics, and subjectively evaluated stress during simulator flight 21 p3186 A83-43988

Comparative cardiovascular responses to 70 head up tilt in pilots and non-pilots 23 p3499 A83-48691

Changes in the urinary levels of electrolytes, uric acid and 17 OHCS with graded heat stress 23 p3499 A83-48692

FLIGHT TECHNICAL ERROR

U PILOT ERROR

FLIGHT TEST VEHICLES

The application of low-cost demonstrators for advanced fighter technology evaluation
[AIAA PAPER 83-1052] 16 p2300 A83-36462

Aerospace technology demonstrators/research and operational options
[AIAA PAPER 83-1054] 16 p2300 A83-36465

The Northrop Flying Wing prototypes
[AIAA PAPER 83-1047] 16 p2287 A83-36471

Active flutter suppression using eigenspace and linear quadratic design techniques
[AIAA PAPER 82-2222] 19 p2803 A83-41702

Advanced propan testbed - 'A progress report'
[SAWE PAPER 1453] 20 p2937 A83-43735

FLIGHT TESTS

NT FLIGHT STABILITY TESTS

NT SPACE TRANSPORTATION SYSTEM FLIGHTS

NT SPACE TRANSPORTATION SYSTEM 1 FLIGHT

NT SPACE TRANSPORTATION SYSTEM 2 FLIGHT

NT SPACE TRANSPORTATION SYSTEM 3 FLIGHT

NT SPACE TRANSPORTATION SYSTEM 4 FLIGHT

NT SPACE TRANSPORTATION SYSTEM 6 FLIGHT

NT SPACE TRANSPORTATION SYSTEM 7 FLIGHT

NT SPACE TRANSPORTATION SYSTEM 8 FLIGHT

Application of pulse code modulation technology to aircraft dynamics data acquisition
01 p0008 A83-10182

Advanced facility for processing aircraft dynamic test data
01 p0013 A83-10189

In-flight structural dynamic characteristics of the XV-15 tilt-rotor research aircraft
01 p0008 A83-10191

Analysis and flight data for a drone aircraft with active flutter suppression
01 p0008 A83-10192

Attempt to determine the power demand of a helicopter control system on the basis of flight tests
01 p0012 A83-10439

The evolution of Navy Flight Line EW testers from AN/ALM-66 to AN/USM-406C
01 p0014 A83-10739

In-flight lightning data measurement system for fleet application - Flight test results
01 p0009 A83-11087

A dynamic interface error performance simulation - IV&V for the F-4F OFP --- Independent Verification and Validation for Operational Flight Program
01 p0092 A83-11114

Unaided tactical guidance flight test results
01 p0005 A83-11140

Software configuration control in a real-time flight test environment
01 p0009 A83-11144

Integrated flight and fire control development and flight test on an F-15B aircraft
01 p0006 A83-11160

F-4F fire control system software support - An integrated approach to ground and flight testing
01 p0015 A83-11228

Air-to-air missiles - Flight test in the 80's
02 p0134 A83-11805

Wake vortex attenuation flight tests - A status report
02 p0134 A83-11806

Data acquisition/reduction system for flight testing general aviation aircraft
02 p0135 A83-11903

Space flight test of MDT-2A --- pulsed plasma microthruster
[AIAA PAPER 82-1874] 02 p0143 A83-12462

Software and system level tests of a test flight mercury ion thruster subsystem
[AIAA PAPER 82-1912] 02 p0145 A83-12485

Reliability and maintainability aspects of a 'fleet' of prototype helicopters
02 p0131 A83-12654

U.S. Army considers Aquila RPV ready to field
02 p0135 A83-13025

Lift-off ignition overpressure - A correlation --- full-scale measurements on Titan vehicle launch conditions
02 p0140 A83-13086

Flight test of the 747-JT9D for airframe noise
03 p0281 A83-13163

In-flight deflection measurement of the HiMAT aeroelastically tailored wing
03 p0281 A83-13167

Sky Hook to help ships launch Harrier
03 p0282 A83-13575

Operation of a helicopter on sloping ground. II
03 p0280 A83-14624

The A310 - Even better than expected
04 p0445 A83-14952

The Air Force Flight Test Center Palletized Airborne Water Spray System
[AIAA PAPER 83-0030] 05 p0594 A83-16472

Evaluation of a rocket burnout velocity from ground and free flight tests
[AIAA PAPER 83-0036] 05 p0602 A83-16476

Development of a flight test maneuver autopilot for a highly maneuverable aircraft
[AIAA PAPER 83-0061] 05 p0597 A83-16493

Plasma diagnostics package assessment of the STS-3 orbiter environment and systems for science
[AIAA PAPER 83-0253] 05 p0604 A83-16612

Thermal environment for payload/cargo integration
[AIAA PAPER 83-0330] 05 p0607 A83-16659

On-board instrumentation for test vehicles with varying roll rates
[AIAA PAPER 83-0570] 05 p0595 A83-16797

Flight testing of the Space Shuttle
05 p0605 A83-16972

USAF studies fighters for dual-role, all-weather operations
05 p0595 A83-17276

Long-range Falcon - Flight-test Dassault Falcon 50
06 p0716 A83-18074

XH-59A ABC aircraft flight tests at Ft. Rucker, Alabama
06 p0716 A83-18148

Digital electronic engine control system - F-15 flight test
06 p0718 A83-18406

Icing analysis of an unprotected aircraft radome
06 p0791 A83-18413

Loran-C RNAV - The best near-term solution to air operations in northeastern North America
06 p0716 A83-18822

Flight evaluation of modifications to a digital electronic engine control system in an F-15 airplane
[AIAA PAPER 83-0537] 06 p0718 A83-19593

The MCA method, a flight test technique to determine the thrust of jet aircraft in flight --- Mass Consumption Acceleration
07 p0865 A83-19661

Fixed wing and rotary wing flight testing of Navstar GPS as a civilian navigation system
07 p0865 A83-19777

F-104 CCV research flight test program
07 p0867 A83-20074

Flight test results of an active flutter suppression system
08 p1047 A83-22164

Design, construction, and testing of an experimental propeller in the 750 PS performance class
[DGLR PAPER 82-066] 09 p1206 A83-24180

Flight testing with hot JP-4 fuel --- in helicopter suction fuel systems
09 p1208 A83-24831

Flight tests of integrated navigation by least squares adjustment
09 p1202 A83-24871

Assessment of future solid rocket motor flight instrumentation/data needs
09 p1219 A83-24888

Qualification of the Space Shuttle Orbiter Radiator system
[SAE PAPER 820886] 10 p1384 A83-25776

Flight effects on fan noise with static and wind tunnel comparisons
[AIAA PAPER 83-0678] 10 p1377 A83-25910

Fluctuating pressure measurements on the fan blades of a turbofan engine during ground and flight tests
[AIAA PAPER 83-0679] 10 p1377 A83-25911

The design and flight test of an engine inlet bulk acoustic liner
[AIAA PAPER 83-0781] 10 p1378 A83-25963

The research aircraft of the Special Research Area 'Flight Control' as scientific test stand
10 p1376 A83-26484

Estimation regarding the feasibility of using larger distances in measurements with L2F systems in flight tests --- Laser-two-Focus
10 p1431 A83-26487

The reusable Space Shuttle Main Engine prepares for long life
11 p1542 A83-27470

Helicopter flight noise tests about the influence of rotor-rotational and forward speed changes on the characteristics of the imitted sound
[AIAA PAPER 83-0672] 11 p1650 A83-28002

The extended Kalman filter and its use in estimating aerodynamic derivatives
11 p1531 A83-28183

Development and testing of Skyship 500
11 p1530 A83-28191

Integrated systems evaluated on F-15
11 p1528 A83-28700

FAA helicopter NAVSTAR GPS flight testing
11 p1529 A83-28788

NASA aerial applications wake interaction research --- particle trajectories in aircraft induced wakes
12 p1699 A83-28899

Analysis of engine usage data for tactical systems
[AIAA PAPER 81-1370] 12 p1703 A83-29011

VOR area navigation - Techniques and results
12 p1700 A83-29205

Flight testing the Low Cost Inertial Guidance System
12 p1700 A83-29210

Helicopter flight testing, simulation and real-time analysis
12 p1701 A83-29391

The application of a sub-scale flight demonstrator as a cost effective approach to aircraft development
12 p1701 A83-29395

Dash 8 - Canada's new commuter
12 p1701 A83-29675

Determination of horizontal tail load and hinge moment characteristics from flight data --- on Learjet Model 55 Longhorn
13 p1805 A83-30162

Excessive roll damping can cause roll ratchet
13 p1808 A83-30171

Apache on the war path - The Hughes AH-64 in production at last
14 p1974 A83-31939

The B-1 gets airborne again 14 p1974 A83-31941

Ground and in-flight testing of new portable oxygen generators 14 p2072 A83-32465

Flight tests verify predictions for F-20 14 p1974 A83-32475

Sun-powered aircraft designs 14 p1974 A83-32577

Unique flight characteristics of the AD-1 oblique-wing research airplane 14 p1975 A83-32588

Space Shuttle base heating
[AIAA PAPER 83-1544] 14 p1981 A83-32767

Dynamic taxi response (have bounce) testing of the C-5A aircraft
[AIAA PAPER 83-1024] 14 p1975 A83-32783

Society of Flight Test Engineers, Annual Symposium, 12th, Dayton, OH, September 16-18, 1981, Proceedings. 14 p1969 A83-32926

A cost effective quick-response test station 14 p1977 A83-32927

Flight development and certification - How efficient can it be? 14 p1975 A83-32929

Flight testing the Hustler 500 14 p1975 A83-32930

Airspeed calibrations on a stretch YC-141B aircraft 14 p1975 A83-32931

Flight test and predicted pressure data comparison on aircraft modifications 14 p1975 A83-32932

Sidestick controller design requirements 14 p1977 A83-32934

Principal site testing of the F/A-18 at the Naval Air Test Center 14 p1975 A83-32935

Use of simulated ice shapes in known icing certification 14 p1973 A83-32936

The United States Air Force and the use of in-flight simulation 14 p1975 A83-32937

Performance flight testing --- Book 15 p2122 A83-33621

Aerial testing of an N2 laser fluorosensor system 15 p2169 A83-34467

Application of system identification flight analysis techniques to the pitch-heave dynamics of an air cushion vehicle 15 p2241 A83-34852

Simulator fidelity and flight test data - Improving the flight performance of the B-52H WST production unit flight station simulator
[AIAA PAPER 83-1075] 16 p2299 A83-36204

Use of flight test results to improve the flying qualities simulation of the B-52H weapon system trainer
[AIAA PAPER 83-1091] 16 p2300 A83-36215

Natural laminar flow data from full-scale flight and wind-tunnel experiments 16 p2296 A83-36409

Variable sweep wing design
[AIAA PAPER 83-1051] 16 p2300 A83-36461

YAV-8B flight demonstration program
[AIAA PAPER 83-1055] 16 p2300 A83-36466

Large jet aircraft validation and demonstrations - An overview of Boeing experience
[AIAA PAPER 83-1049] 16 p2301 A83-36472

AFTI/F-16 technology demonstrator
[AIAA PAPER 83-1059] 16 p2301 A83-36474

A technique to determine lift and drag polars in flight 16 p2296 A83-36913

Flight tests of tow wire forces while flying a racetrack pattern 16 p2301 A83-36919

HiMAT onboard flight computer system architecture and qualification 17 p2467 A83-37061

Piloted simulation of hover and transition of a vertical attitude takeoff and landing aircraft 17 p2462 A83-37064

Investigation of flow past an aircraft wing section in flight and in a wind tunnel 17 p2447 A83-37506

Dornier Do 24 TT (technology testbed) experimental amphibian 17 p2462 A83-37857

NGT sub-scale flight demonstrator - A cost-effective approach to aircraft development --- Next Generation Trainer
[SAE PAPER 821341] 17 p2462 A83-37952

Space Shuttle environmental and life support system (ECLSS)
[SAE PAPER 821420] 17 p2562 A83-37977

U.S. Army helicopter icing developments
[SAE PAPER 821504] 17 p2459 A83-38011

Flight test of the HX-1 radio-controlled hybrid airship
[AIAA PAPER 83-1992] 17 p2466 A83-38917

Flight testing and operational demonstrations of a modern non-rigid airship
[AIAA PAPER 83-1999] 17 p2466 A83-38920

An imaging telescope for soft gamma-ray astronomy - The preliminary in-flight tests 18 p2756 A83-39287

Balloon film strain measurement 18 p2641 A83-39807

Training pilots for testing airplanes with modern flight control systems 18 p2736 A83-40340

US fighter options 18 p2641 A83-40665

F/A-18 inlet/engine compatibility flight test results 19 p2796 A83-41039

- Algorithms for real-time flutter identification
[AIAA PAPER 83-2223] 19 p2859 A83-41703
- Integrated flight control systems development - The F/A-18A Automatic Carrier Landing System
[AIAA PAPER 83-2162] 19 p2804 A83-41765
- Determination of aerodynamic parameters of a fighter airplane from flight data at high angles of attack
[AIAA PAPER 83-2066] 19 p2804 A83-41904
- Applications of state estimation in aircraft flight-data analysis
[AIAA PAPER 83-2087] 19 p2798 A83-41919
- Filtering flight data prior to aerodynamic system identification
[AIAA PAPER 83-2098] 19 p2798 A83-41928
- Identification of aerodynamic coefficients using flight testing data
[AIAA PAPER 83-2099] 19 p2798 A83-41929
- Flight test experience with pilot-induced-oscillation suppressor filters
[AIAA PAPER 83-2107] 19 p2806 A83-41936
- The application and results of a new flight test technique
[AIAA PAPER 83-2137] 19 p2799 A83-41959
- The in-service flight testing of some carbon fibre-reinforced plastic components
20 p2933 A83-42808
- Autogas flight test in a Cessna 150 airplane
[SAE PAPER 830706] 20 p2933 A83-43317
- Flight investigation of natural laminar flow on the Bellanca Skyrocket II
20 p2933 A83-43326
- Aeracoustic flight test of four single engine propellers
[SAE PAPER 830731] 20 p2936 A83-43328
- Estimation of nonlinear aerodynamics from transport airplane certification maneuvers - A system identification approach
[AIAA PAPER 83-2065] 20 p2938 A83-43811
- The tasks and organization of the flight testing of airplanes and helicopters --- Russian book
21 p3091 A83-43901
- DSCS III A-1 ACS flight experience --- evaluation and testing of Attitude Control System
[AAS PAPER 83-085] 21 p3100 A83-44185
- An experimental investigation of turbulent base heat transfer in hypersonic flow
21 p3087 A83-44569
- Extracting the comprehensive characteristics in terms of similar parameters from flight test
21 p3091 A83-44570
- Experience with flight test trajectory guidance
21 p3091 A83-45470
- Designed to be stalled --- T-46A training aircraft
22 p3254 A83-46349
- Problems in determining aircraft polar curves from test-flight data
22 p3254 A83-46489
- F-16XL shows advances in range, ride
22 p3254 A83-46924
- Pneumatic rotor blade deicing
22 p3254 A83-46926
- The Integrated Technology and Flight Research Rotor Technology demonstrators for the 1985-1995 timeframe
22 p3255 A83-46928
- Flight test evaluation of Loran-C in Alaska
22 p3252 A83-46955
- An improved propeller for general-aviation aircraft
23 p3406 A83-47194
- Correlation of flight test and analytic M-on-N air combat exchange ratios --- Many-on-Many
23 p3392 A83-48219
- Simulations used in the development and flight test of the HiMAT vehicle
[AIAA PAPER 83-2505] 23 p3404 A83-48355
- A flight test of laminar flow control leading-edge systems
[AIAA PAPER 83-2508] 23 p3404 A83-48356
- NOTAR - The viable alternative to a tail rotor
[AIAA PAPER 83-2527] 23 p3404 A83-48365
- Survey of aeroelastic wind tunnel and flight testing methods at MBB
24 p3550 A83-49181
- Experience from flight flutter testing with tip vanes on Airbus
24 p3547 A83-49183
- FLIGHT TIME**
- Designing a mini-RPV for a world endurance record
01 p0001 A83-11000
- Advanced propulsion for future planetary spacecraft
02 p0148 A83-13083
- Rocket rendezvous at preassigned destinations with optimum exit trajectories
04 p0452 A83-16433
- Cruise flight of a tail mounted ramjet
16 p2303 A83-35805
- New systems for extending the useful float duration of standard zero-pressure balloon flights
18 p2640 A83-39805
- FLIGHT TRAINING**
- NT SPACE FLIGHT TRAINING
- Toward 'combat realistic' tests, evaluations, exercises - and training
01 p0015 A83-11237
- Psychological factors responsible for wastage among trainees during ab initio flying training
02 p0225 A83-12257
- A study of self-initiated elimination from the flight training.
04 p0523 A83-16008
- Total simulation for airline applications /Line Oriented Flight Training/
05 p0676 A83-17306
- The role of simulation in general aviation
05 p0671 A83-17307
- Improving simulation training through research
05 p0676 A83-17309
- Hypertension and orthostatic hypotension in applicants for flying training and aircrew
06 p0797 A83-18197
- The determination of the functional reliability of pilots during training on a flight-training simulator
07 p0980 A83-20884
- Training effectiveness evaluation of device 2F117 - OFT for CH-46 helicopter
10 p1456 A83-26326
- Sex differences in the transfer of training of basic flight skills
10 p1457 A83-26336
- An experience-judgement approach to tactical flight training
10 p1458 A83-26337
- Current Air Force navigator training
12 p1766 A83-29202
- B-52 operations in the Bright Star 82 exercise
12 p1699 A83-29204
- A study of self-initiated eliminating from the flight training.
VI - Personality traits of flying students related to self-initiated elimination.
15 p2214 A83-33543
- In-flight simulation at the U.S. Air Force and Naval Test Pilot Schools
[AIAA PAPER 83-1078] 16 p2299 A83-36206
- Advanced display techniques for training the multi-member tactical air crew
[AIAA PAPER 83-1079] 16 p2302 A83-36207
- A visual cueing model for terrain-following applications
[AIAA PAPER 83-1081] 16 p2401 A83-36208
- Simulation which simulates less
18 p2642 A83-40619
- Hypertension and orthostatic hypotension in applicants for spaceflight training and spacecrews - A review of medical standards
19 p2884 A83-42048
- General aviation safety - How safe? Its implication for flying and theory training
21 p3089 A83-44878
- FLIGHT VEHICLES**
- Intelligent control of tactical target cueing --- by subsonic flight vehicles
02 p0133 A83-12879
- Free rotation of a flight vehicle as a rigid body
04 p0531 A83-15382
- Theory and design of flight-vehicle engines --- Russian book
08 p1046 A83-22651
- Electronic devices in automatic systems --- Russian book on flight vehicle control
10 p1408 A83-25624
- Current studies at Calspan utilizing short-duration flow techniques
10 p1379 A83-26128
- An approximate analytical method for calculating the trajectories of a flight vehicle in the atmosphere
14 p1979 A83-32364
- Perturbation methods in mechanics
14 p1972 A83-33001
- Dynamic stability of a flight vehicle near a perturbed surface
14 p1977 A83-33008
- A study of the statistical dynamics of flight vehicles
14 p1977 A83-33009
- Method of calculating radiative heat transfer for computer-aided analysis systems --- in flight vehicle structures
17 p2505 A83-37524
- FLIP-FLOPS**
- Single event upset sensitivity of low power Schottky devices
05 p0629 A83-17542
- Optically controllable S-type negative resistance presented by a combinational connection of photocoupled FET's
18 p2678 A83-40379
- GaAs digital dynamic IC's for applications up to 10 GHz
19 p2837 A83-40793
- A superconducting flip-flop using two interacting weak links
20 p2966 A83-42604
- FLIR DETECTORS**
- Four-channel multiplexed resolver-to-digital converter
01 p0009 A83-11100
- Multiscenario imaging sensor autoprocessor --- for target recognition
01 p0007 A83-11224
- TF/TA by means of integrated FLIR and radar sensors --- terrain following-terrain avoidance displays using forward looking infrared imagery
01 p0010 A83-11240
- The A6E /TRAM/ all-weather weapon system --- Target Recognition and Attack Multisensor
01 p0008 A83-11260
- Calibration of a transfer radiometer in support of the Navy forward looking infrared systems /FLIR/ program
08 p1104 A83-22876
- Calibration support of the AN/AAM-60 common forward-looking infrared /FLIR/ test bench
08 p1104 A83-22886
- Effects of tilt of a four-bar pattern on the minimum resolvable temperature difference /MRTD/ --- of FLIR detectors
08 p1105 A83-22899
- Techniques for pseudo-dc restoration and dynamic range enhancement of scanned infrared imagery
08 p1105 A83-22900
- Bo 105 rotor blade influence on the Calipso FLIR in the mast-mounted observation platform Ophelia
08 p1044 A83-23249
- Comparison of imaging infrared detection algorithms
09 p1265 A83-23529
- Comparative study of edge-thinning algorithms for target identification
09 p1265 A83-23530
- Target acquisition and extraction from cluttered backgrounds
09 p1204 A83-23531
- Target classification algorithms for video and forward looking infrared /FLIR/ imagery
09 p1266 A83-23541
- Gallium arsenide infrared windows for high-speed airborne applications
09 p1345 A83-24958
- Infrared visibility prediction by statistical methods
11 p1619 A83-28340
- Application of aerial thermography to determine physical states in wildlife
15 p2187 A83-34848
- FLOATING**
- Floated gyro dynamical behavior during slew testing
[AIAA PAPER 83-2182] 19 p2848 A83-41674
- FLOATING POINT ARITHMETIC**
- Use of multifunctional computers with decentralized control for digital signal processing with floating point decimal representation --- German thesis
01 p0031 A83-10476
- Implementation of the DAST ARW II control laws using an 8086 microprocessor and an 8087 floating-point coprocessor --- drones for aeroelasticity research
02 p0227 A83-11910
- Further developments of Rp and Ap error analysis --- Relative and Absolute precision in floating point arithmetic operations
02 p0231 A83-12926
- Solving nonlinear systems with least significant bit accuracy
04 p0530 A83-15698
- Error free computation - A direct method to convert finite-segment p-adic numbers into rational numbers
15 p2217 A83-33903
- A simple approach to the error analysis of division-free numerical algorithms
15 p2217 A83-33904
- Error analysis of certain floating-point on-line algorithms
15 p2217 A83-33905
- CADAC - A controlled-precision decimal arithmetic unit
15 p2217 A83-33907
- Finite precision rational arithmetic - An arithmetic unit
15 p2217 A83-33908
- Fully digit on-line networks
15 p2217 A83-33912
- Techniques to reduce the inherent limitations of fully digit on-line arithmetic
15 p2217 A83-33913
- The use of floating-point and interval arithmetic in the computation of error bounds
15 p2218 A83-33914
- FLOOD CONTROL**
- Application of Landsat imagery to flood control and management of agricultural land - A case study of northern India
03 p0345 A83-14233
- FLOOD PLAINS**
- Bank erosion and flood plain studies of the Annapolis River - An application of remote sensing data
03 p0348 A83-14262
- Analysis of effects after typhoon 8115 in coastal area and fields in Hokkaido, Northern Japan, using Landsat MSS data
17 p2534 A83-38453
- FLOODS**
- Causes of flood streamlines observed on Landsat images and their use as indicators of floodways
15 p2183 A83-34151
- FLOORS**
- Advanced lightweight, fire retardant floor paneling for aircraft
[AIAA PAPER 83-2442] 23 p3403 A83-48330
- FLOQUET THEOREM**
- Aeroelasticity of helicopter rotors in forward flight
05 p0654 A83-17316
- Modal control of an unstable periodic orbit
13 p1808 A83-29994
- Some analysis methods for rotating systems with periodic coefficients
14 p2032 A83-32987
- Wave scattering and guidance by dielectric waveguides with periodic surfaces
15 p2229 A83-33537
- Magnetic roll/way attitude control of a momentum biased near polar orbit satellite
17 p2478 A83-37459
- FLORA**
- U PLANTS (BOTANY)
- FLOW CHAMBERS**
- Numerical computation of three-dimensional convective flows in horizontal and tilted containers
22 p3284 A83-46488

FLOW CHARACTERISTICS

NT BOUNDARY LAYER STABILITY
 NT FLAME STABILITY
 NT FLOW DISTRIBUTION
 NT FLOW STABILITY
 NT FLOW VELOCITY
 NT MAGNETOHYDRODYNAMIC STABILITY
 NT WEIBEL INSTABILITY
 Flow characteristics around a circular cylinder with a slit. II Effect of boundary layer suction
 02 p0175 A83-13069
 Nonequilibrium flow over delta wings with detached shock waves
 03 p0277 A83-13126
 Flow behavior and heat transfer around a circular cylinder at high blockage ratios
 03 p0315 A83-13344
 Structure of turbulence in heat and mass transfer --- Book
 03 p0317 A83-14453
 Characteristics of coherent structures in complex turbulent shear flows
 03 p0318 A83-14465
 Some characteristics of turbulent flows at elevated temperatures
 03 p0318 A83-14468
 Visualizations of turbulent structures of wakes and boundary layers
 03 p0319 A83-14481
 Visualization study of the axisymmetric mixing layer of a high Reynolds number jet
 03 p0320 A83-14482
 Conditionally averaged patterns of coherent events in a wall-bounded turbulent flow
 03 p0320 A83-14483
 The role of orderly structures in the vorticity balance of the turbulent velocity fields of unrestricted shear flows
 04 p0443 A83-15921
 Predictions of the structure of turbulent, particle-laden, round jets
 [AIAA PAPER 83-0066]
 05 p0632 A83-16498
 Attachment of ventilated jets to rough boundaries
 06 p0713 A83-18964
 Certain effects and paradoxes in aerodynamics and hydraulics --- Russian book
 07 p0925 A83-20379
 Embedded flow characteristics of sharp-edged rectangular wings
 08 p1042 A83-22152
 Fluid flow and heat transfer in the separated region of a circular cylinder with wake control
 08 p1084 A83-22238
 Flow characteristics and methods of flow calculation of high-speed compressible flow through pipe orifices
 09 p1257 A83-23332
 The aerodynamic properties of the DISA nozzle unit for calibrating and testing hot-wire probes, in particular multiple sensor probes at moderate velocities
 09 p1267 A83-23700
 Observation of streamwise rotation in the near-wall region of a turbulent boundary layer
 10 p1414 A83-25782
 Experimental method for determining the dynamic properties of gas flows
 10 p1417 A83-26293
 Certain features of transverse flow past a cylinder with longitudinal fins
 11 p1569 A83-28551
 Autorotation --- in fluid dynamics
 13 p1804 A83-31079
 The role of coherent structures in the development of a uniformly strained turbulent wake
 15 p2155 A83-33661
 Parametric excitation of oscillations in a liquid flowing out of a container
 16 p2350 A83-35717
 New trends in combustion research for gas turbine engines
 16 p2303 A83-35806
 An experimental investigation of three-dimensional unsteady flow in an axial flow turbine
 [AIAA PAPER 83-1170]
 16 p2294 A83-36257
 PANAIR Pilot Code application to subsonic nacelle type interior flows
 [AIAA PAPER 83-1369]
 16 p2295 A83-36365
 Nozzles producing a free-vortex flow at the exit section and flow characteristics in these nozzles
 17 p2447 A83-37264
 Gas turbine engines
 17 p2467 A83-37274
 Experimental study of jet-flap diffusers
 17 p2448 A83-37534
 Mathematical modeling of unsteady coherent structures in the near-wall region of a turbulent boundary layer
 17 p2506 A83-37632
 Application of curvilinear coordinate generation techniques to the computation of internal flows
 17 p2458 A83-38791
 Laminar boundary layers behind detonation waves
 18 p2684 A83-39450
 Calculation of various diffuser flows with inlet swirl and inlet distortion effects
 19 p2789 A83-40863
 The motion of compressible fluids and inhomogeneous media
 19 p2845 A83-41877
 A method for calculating and analyzing the properties of a vertical nonisothermal jet with allowance for the buoyancy force
 19 p2794 A83-42131
 Heat transfer and flow characteristics of jets impinging on a concave hemispherical plate
 20 p2979 A83-42743

Analysis of spiral-groove face seals for liquid oxygen [ASLE PREPRINT 83-AM-4B-2]
 20 p2999 A83-43339
 On the structure of wall-bounded turbulent flows
 21 p3128 A83-43930
 Flow characteristics in the curved rectangular channels
 Visualization of secondary flow
 21 p3129 A83-44064
 The effect of injection and suction on the characteristics of the viscous sublayer in a turbulent flow
 21 p3133 A83-45346
 Vortex flow in nature and technology --- Book
 22 p3279 A83-45775
 Some characteristics of pulsating or flapping jets
 22 p3283 A83-46449
 Heat transfer characteristics for jet array impingement with initial crossflow
 [ASME PAPER 83-GT-28]
 23 p3393 A83-47891
 Distinction between different types of impeller and diffuser rotating stall in a centrifugal compressor with vaneless diffuser
 [ASME PAPER 83-GT-61]
 23 p3395 A83-47917
 An investigation of the flow characteristics and of losses in radial nozzle cascades
 [ASME PAPER 83-GT-126]
 23 p3396 A83-47955
 Strong pressure waves in air-breathing engines
 23 p3398 A83-48216
 Approximate unsteady fluid jet properties from one-dimensional theory
 [ASME PAPER 83-FE-25]
 23 p3450 A83-48236
 Flow visualization by light sheet
 [ONERA, TP NO. 1983-105]
 24 p3583 A83-49416
 On the organized motion of a turbulent plane jet
 24 p3577 A83-49464

FLOW COEFFICIENTS

NT DISCHARGE COEFFICIENT
 Heat transfer and dynamics of supersonic air flow past cavities
 02 p0170 A83-11872
 The calculation of the coefficient-optimal total pressure of a system of plane shock waves
 09 p1258 A83-23447

FLOW DEFLECTION

Shock fitting in the numerical analysis of supersonic conical flows
 01 p0003 A83-11269
 Asymptotic expansions for the problem of boundary layer formation
 01 p0047 A83-11273
 Analysis of flows of an equilibrium dissociated, ionized, and radiating gas by the method of large particles
 01 p0003 A83-11275
 Solution of the transonic integral equation using a polar coordinate formulation
 03 p0279 A83-14572
 Space Shuttle third flight /STS-3/ entry RCS analysis --- Reaction Control System
 [AIAA PAPER 83-0116]
 05 p0604 A83-16530
 Regular or catastrophic evolution of steady flows depending on parameters --- in aerodynamics
 05 p0638 A83-17318
 A numerical transformation solution procedure for closely coupled canard-wing transonic flows
 [AIAA PAPER 83-0502]
 06 p0714 A83-19591
 The boundary element method applied to the creeping motion of a sphere
 08 p1087 A83-23182
 The prediction of the drag on structural beams
 08 p1088 A83-23194
 Formation of streamwise vortices in the flow past a corner
 10 p1371 A83-25569
 Motion of a spherical particle in a viscous nonisothermal fluid
 11 p1566 A83-27705
 Body with minimum wave drag in a twisted hypersonic flow
 11 p1526 A83-27712
 Supersonic flow past a thin cone with an asymmetric tip
 11 p1526 A83-27716
 The effect of the mechanisms of heterogeneous catalytic reactions on the heat flux in hypersonic flow past a blunted body
 13 p1804 A83-30675
 Initial observations of the subsurface structure and short-term variability of the seaward deflection of the Gulf Stream off Charleston, South Carolina
 14 p2060 A83-33085
 Solution of the problem of flow past a permeable plate with separation of jets
 15 p2162 A83-35316
 Three-dimensional turbulent boundary layers on bielliptic bodies in flows of a compressible gas at angle of attack
 16 p2289 A83-35704
 Flow past a nonconducting wedge in magnetohydrodynamics
 16 p2415 A83-35710
 A study of supersonic nonstationary flow past conical bodies
 16 p2289 A83-35722
 Numerical simulation of hypersonic viscous flow over cones at very high incidence
 [AIAA PAPER 83-1669]
 17 p2444 A83-37180
 Isolation of singular surfaces when using finite-difference methods --- for computing supersonic flow past wing-fuselage combinations
 17 p2447 A83-37259
 Investigation of flow past an aircraft wing section in flight and in a wind tunnel
 17 p2447 A83-37506

Three-dimensional hypersonic flow past a body of finite thickness
 17 p2448 A83-37528
 On initial and boundary conditions for the Navier-Stokes equations in the Helmholtz form
 17 p2505 A83-37529
 Calculation of transonic noncircular flow past a highly oblate ellipsoid
 17 p2449 A83-37538
 Comparison of computational and experimental data concerning flow past axisymmetric air intakes in regimes with an expelled shock wave
 17 p2449 A83-37541
 Wake interference of a row of normal flat plates arranged side by side in a uniform flow
 17 p2505 A83-37571
 Boundary layer separation over a rotating cylinder in a flow of an incompressible fluid
 17 p2506 A83-37804
 A numerical study of slow nonisothermal flows past axisymmetrical bodies
 17 p2506 A83-37805
 The theory for a flexible slat
 17 p2451 A83-37810
 The effect of an increase in the temperature factor of a cone on the parameters of the base region
 17 p2451 A83-37811
 Plane flow past an air-supported soft cylindrical shell
 17 p2522 A83-38099
 A study of heat and mass transfer in flows past bodies of various shapes with allowance for injection
 19 p2844 A83-41577
 The principles governing the formation of circulation zones in the wake of mechanical and jet screens in confined flows
 19 p2794 A83-42147
 Heat transfer in a turbulent boundary layer behind a two-dimensional bluff body at different Pr numbers
 20 p2977 A83-42722
 Flow past and radiant heating of blunt bodies moving at angles of attack alpha greater than or equal to 0 deg
 20 p2929 A83-42878
 Similarity law for hypersonic flow past asymmetrically blunt bodies
 20 p2929 A83-42879
 Heat transfer during ionized-gas flow past bodies
 20 p2929 A83-42880
 Synthetic method in thermal boundary layer transition
 20 p2987 A83-43650
 Some characteristics of the unsteady wake flow past a circular cylinder
 22 p3282 A83-46442
 Calculation of deflected-walled backward-facing step flows Effects of angle of deflection on the performance of four models of turbulence
 [ASME PAPER 83-FE-16]
 23 p3450 A83-48233
 Analysis of turbulent flow past a class of semi-infinite bodies
 [ASME PAPER 83-FE-32]
 23 p3450 A83-48237
 The effect of injection in the boundary layer on supersonic flow past an oscillating cone
 23 p3400 A83-48654
 Calculation of stellar-wind flow past an x-ray source
 23 p3528 A83-48662

FLOW DIRECTION INDICATORS

NT WIND VANES
 Directional gas-flow measurement with pyroelectric anemometers (PA)
 17 p2512 A83-38532
 Modified calibration technique of a five-hole probe for high flow angles
 21 p3141 A83-44975

FLOW DISTORTION

Coherent structures and studies of perturbed and unperturbed jets
 01 p0046 A83-10894
 Measurement of bursting period and test of surface renewal model in a turbulent boundary layer disturbed by a cylinder
 03 p0318 A83-14462
 The dominant coherent structure of the circular jet organized by controlled perturbation
 03 p0318 A83-14463
 Concerning the center of pressure of bodies --- supersonic flow interactions with variable surface configurations
 04 p0441 A83-15089
 Distortion of turbulence in flows with parallel streamlines
 04 p0479 A83-16263
 Axial-compressor flow distortion with water ingestion [AIAA PAPER 83-0004]
 05 p0596 A83-16456
 On the nonexistence and existence of global solutions of boundary value problems for quasi-linear parabolic equations --- in propagation of thermal disturbances
 05 p0640 A83-17642
 On the deformation of the rectangular turbulent jet cross-section
 05 p0640 A83-17703
 Three-dimensional stability of vortex arrays
 06 p0758 A83-19022
 A numerical study of the lateral interaction between an axisymmetric jet issuing into vacuum and an obstacle
 06 p0760 A83-19431
 An approximate solution to the non-self-similar problem concerning the motion of a piston following an instantaneous impact
 06 p0760 A83-19441
 Rapid distortion of small-scale turbulence by an axisymmetric contraction
 08 p1084 A83-22381
 Numerical calculation of the separation and connection of two-dimensional supersonic flows in channels with discontinuous boundaries
 08 p1046 A83-22658

- Flow disturbance induced by the DISA triaxial hot-wire probe 55P91 09 p1267 A83-23699
- Investigation of the distortion of shock-fronts in real gases 10 p1414 A83-26140
- The response of a multistage compressor to an azimuthal distortion 10 p1378 A83-26923
- Development of finite-amplitude disturbances in a Poiseuille flow 11 p1566 A83-27706
- Free convection boundary layers over humps and indentations 11 p1569 A83-28405
- Shock reflection transition in three-dimensional steady flow about interfering bodies 12 p1696 A83-28960
- Distortion in turbulence upstream of a flat plate and induced pressure fluctuations 12 p1723 A83-29383
- Equation of motion for a small rigid sphere in a nonuniform flow 13 p1839 A83-30104
- On the investigation of axisymmetric discontinuous flows using interferometry 16 p2349 A83-35538
- Experiments and mathematical simulation of plate distortion simulators 16 p2351 A83-35817
- The prediction of performance of turbojet engine with distorted inlet flow and its experimental studies 16 p2303 A83-35832
- Variation of rotor blade vibration due to interaction of inlet and outlet distortion 16 p2305 A83-35882
- Aircraft engine inlet pressure distortion testing in a ground test facility [AIAA PAPER 83-1233] 16 p2307 A83-36296
- Numerical investigation of three-dimensional transonic flow through air intakes disturbed by a missile plume [AIAA PAPER 83-1854] 17 p2457 A83-38682
- A disturbance of the upper atmosphere caused by flow around an isolated mountain 18 p2730 A83-40077
- Calculation of various diffuser flows with inlet swirl and inlet distortion effects 19 p2789 A83-40863
- Longitudinal vortices in wind tunnel wall boundary layers 20 p2928 A83-42622
- The effect of small temperature gradients on flow in a continuous flow electrophoresis chamber 20 p2951 A83-43276
- The influence of free-stream disturbances on low Reynolds number airfoil experiments 21 p3088 A83-44676
- A theory of rotating stall of multistage axial compressors. I - Small disturbances [ASME PAPER 83-GT-44] 23 p3394 A83-47904
- A theory of rotating stall of multistage axial compressors. II - Finite disturbances [ASME PAPER 83-GT-45] 23 p3394 A83-47905
- Flow past a sphere at low Mach and Knudsen numbers 24 p3544 A83-48931
- Propagation of finite amplitude disturbances in the weakly non-parallel boundary layer 24 p3580 A83-49832
- ### FLOW DISTRIBUTION
- Coherent structures in turbulent flow 01 p0046 A83-10885
- A model for periodic structures in turbulent boundary layers 01 p0046 A83-10889
- Experimental methods in turbulent structure research 01 p0046 A83-10891
- Coherent structures in turbulent combustion 01 p0023 A83-10899
- Flowfield surveying techniques used in the NSWCHypervelocity wind tunnel no. 9 01 p0052 A83-11064
- Flow visualization in natural convection 01 p0052 A83-11070
- Probing of the unsteady reacting muzzle exhaust flow of 20 MM gun [ASME PAPER 82-HT-34] 02 p0172 A83-12792
- Large-scale vortex-lattice model for the locally separated flow over wings 03 p0277 A83-13127
- Numerical study of flowfields about asymmetric external conical corners 03 p0277 A83-13130
- Numerical experiments on the leading-edge flowfield 03 p0277 A83-13131
- Blunt fin-induced shock wave/turbulent boundary-layer interaction 03 p0277 A83-13132
- Numerical simulation of steady supersonic flow over spinning bodies of revolution 03 p0277 A83-13140
- Oblique impingement of a round jet on a plane surface 03 p0278 A83-13145
- Assessment of inflow control structure effectiveness and design system development 03 p0281 A83-13161
- Self-consistent extrapolation of the results of numerical experiments for fluid structures 03 p0389 A83-13537
- Spectral modeling of linear mechanisms in nonhomogeneous turbulent flows --- French thesis 03 p0317 A83-14104
- A single-level, numerical model suitable for complex terrain 03 p0369 A83-14452
- Numerical solution for fully developed flow in heated curved tubes 03 p0322 A83-14587
- Turbulent flow structure effect on diffusion and premixed flame propagation 03 p0295 A83-14602
- Flow past a profile at angle of attack to a transonic flow 04 p0441 A83-15083
- Shock-fitting bicharacteristic algorithm for three-dimensional scarfed nozzle flowfields 04 p0442 A83-15278
- A fast algorithm for the calculation of transonic flow over wing/body combinations 04 p0442 A83-15283
- Shock tube diagnostics utilizing laser Raman scattering 04 p0481 A83-15287
- The flow field in a suddenly enlarged combustion chamber 04 p0476 A83-15288
- Upstream influence in sharp fin-induced shock wave turbulent boundary-layer interaction 04 p0442 A83-15296
- A comparative study of time-marching and space-marching numerical methods --- for flowfield codes 04 p0476 A83-15297
- An approximation method for the stability analysis of plates in the flow of an incompressible fluid 04 p0497 A83-15392
- The influence of a flow field on the stability of the force-free magnetic field 04 p0536 A83-15595
- On the flow field around a Savonius rotor 04 p0505 A83-15798
- Heat transfer for flows past non-isothermal bodies --- Russian book 04 p0476 A83-15830
- Analytical profiling of turbine blades 04 p0449 A83-16010
- Mathematical model for the analysis of wind-turbine wakes 04 p0507 A83-16108
- An experimental study of the unsteady response of the rotor blades of an axial flow compressor operating in the rotating stall regime [AIAA PAPER 83-0001] 05 p0577 A83-16454
- Computation of supersonic viscous flows around pointed bodies at large incidence [AIAA PAPER 83-0034] 05 p0578 A83-16474
- A shock-fitting solution of the supersonic flowfield in a rounded internal corner [AIAA PAPER 83-0038] 05 p0578 A83-16478
- Computation of shock wave/target interaction [AIAA PAPER 83-0039] 05 p0632 A83-16479
- Computations of two-phase supersonic nozzle flows by a space-marching method [AIAA PAPER 83-0041] 05 p0578 A83-16481
- Orthogonal decomposition techniques to identify convected flow structures [AIAA PAPER 83-0048] 05 p0632 A83-16484
- Autototation of an elliptic airfoil [AIAA PAPER 83-0130] 05 p0580 A83-16543
- Passive shock wave/boundary layer control for transonic airfoil drag reduction [AIAA PAPER 83-0137] 05 p0580 A83-16546
- Measurements and predictions for nonevaporating sprays in a quiescent environment [AIAA PAPER 83-0151] 05 p0633 A83-16558
- Numerical simulation of near-critical and unsteady subcritical inlet flow fields [AIAA PAPER 83-0175] 05 p0580 A83-16570
- Experimental study of flows in a two-dimensional inlet model [AIAA PAPER 83-0176] 05 p0581 A83-16571
- Laminar viscous flow-field prediction of Shuttle-like vehicle aerodynamics [AIAA PAPER 83-0211] 05 p0581 A83-16586
- An efficient method for supersonic viscous flow field calculations [AIAA PAPER 83-0222] 05 p0582 A83-16592
- Navier-Stokes computations of the projectile base flow with and without base injection [AIAA PAPER 83-0224] 05 p0582 A83-16594
- Calculations of a plane turbulent jet [AIAA PAPER 83-0286] 05 p0634 A83-16631
- Confined swirling flow predictions [AIAA PAPER 83-0316] 05 p0634 A83-16646
- A new hybrid approach to supersonic aircraft analysis --- and flow field prediction [AIAA PAPER 83-0340] 05 p0584 A83-16666
- Flow measurements of an airfoil with deflected spoiler [AIAA PAPER 83-0365] 05 p0584 A83-16672
- Numerical study of a ramjet dump combustor flow field [AIAA PAPER 83-0421] 05 p0585 A83-16704
- Aerodynamic features of turbulent flames [AIAA PAPER 83-0470] 05 p0636 A83-16737
- Space Shuttle heating analysis with variation in angle of attack and surface condition [AIAA PAPER 83-0486] 05 p0586 A83-16747
- Flow simulations for general nacelle configurations using Euler equations [AIAA PAPER 83-0539] 05 p0587 A83-16775
- Flow fields and aerodynamic characteristics for hypersonic missiles with mid-fuselage inlets [AIAA PAPER 83-0542] 05 p0587 A83-16777
- Investigations on the effects of discrete wingtip jets [AIAA PAPER 83-0546] 05 p0587 A83-16781
- Flow visualization studies of bodies with square cross sections [AIAA PAPER 83-0563] 05 p0637 A83-16791
- Unsteady natural convection about a sphere at small Grashof number 05 p0639 A83-17358
- Prediction of secondary vortex flowfields induced by multiple free-jets issuing in close proximity [AIAA PAPER 83-0289] 05 p0642 A83-17916
- Real gas flow fields about three dimensional configurations [AIAA PAPER 83-0581] 05 p0591 A83-17931
- The Oseen model for internal separated flows 05 p0642 A83-17943
- Two- and three-dimensional rotational structures in a cavitating wake 06 p0756 A83-18145
- The far nonlinear field in transonic flows past nonlifting profiles 06 p0713 A83-19442
- The configuration of subsonic zones generated during supersonic flow past a spherically blunted cylinder at large angles of attack 06 p0713 A83-19443
- Experimental and theoretical studies on the relationship between engine exhaust and the surrounding flow field --- German thesis 06 p0714 A83-19618
- A note on the specification of freestream velocity in the calculation of the boundary layer flow around bodies of revolution at incidence 07 p0862 A83-19665
- Flowfield experiments on a DF chemical laser 07 p0932 A83-19815
- Measurements of reactive recirculating jet mixing in a combustor 07 p0924 A83-19819
- Analysis of secondary flows for tube-launched rocket configurations 07 p0863 A83-20417
- Effects of plume impingement on a momentum bias communications satellite 07 p0872 A83-20420
- An analytical and experimental comparison of the flow field of an advanced swept turboprop [AIAA PAPER 83-0189] 07 p0864 A83-21080
- Flow widening through a Darrieus wind turbine - Theory and experiment 07 p0955 A83-21082
- Homogeneity of lava flows - Chemical data for historic Mauna Loa eruptions 07 p0965 A83-21321
- Marangoni-effect velocity distribution due to time-oscillatory temperature gradients in zero-gravity environment 07 p0927 A83-21345
- A finite boundary method for fluid flow field computations 07 p0927 A83-21436
- Unsteady transonic flow over wings including inviscid/viscous interaction 08 p1042 A83-22132
- A comparison of techniques for reconstructing axisymmetric reacting flow fields from absorption measurements 08 p1057 A83-22393
- Effects of flow fields in optical systems 08 p1108 A83-22454
- An observation on the origin of secondary flow in straight noncircular ducts 08 p1086 A83-23122
- The boundary element method applied to the creeping motion of a sphere 08 p1087 A83-23182
- Natural convection in a rotating annulus 08 p1090 A83-23209
- Effect of the fluid film profile on the performance of magnetohydrodynamic bearings 09 p1273 A83-23345
- Flow patterns in semiclosed cavities of spindle-operated valves and the valve flow rates 09 p1258 A83-23428
- Calculation of three-dimensional transonic flow past elongated bodies 09 p1196 A83-23570
- Investigation of the flow in a jet produced by two nozzles 09 p1197 A83-24045
- An experimental study of the operation of a vortex tube 09 p1260 A83-24230
- On the application of the integral invariants and decay laws of vorticity distributions [AD-A128456] 09 p1262 A83-24421
- Unsteady concentration distribution and the flow of a binary mixture in a cone and plate viscometer 09 p1262 A83-24502
- Effect of the Prandtl number and mass transfer on the unsteady incompressible boundary layers near the three-dimensional asymmetric stagnation point 09 p1262 A83-24507
- Effect of the volute casing on the flow in radial-flow blowers 09 p1263 A83-24649
- Oil flow separation patterns on an ogive forebody 09 p1198 A83-24662
- Mean flowfields in axisymmetric combustor geometries with swirl 09 p1263 A83-24668
- Influence of finite slot size on boundary layer with suction or injection 09 p1263 A83-24676
- Aeroacoustic computation of cylinder wake flow [AIAA PAPER 83-0736] 10 p1476 A83-25940
- An experimental investigation of wake edge tones [AIAA PAPER 83-0741] 10 p1476 A83-25944

Conditional sampling with a laser velocimeter --- for tone-excited jet and rotating propeller blade
[AIAA PAPER 83-0756] 10 p1420 A83-25953

Shock diffraction computations over complex structures 10 p1417 A83-26196

Sound propagation through fluctuating flows - Its significance in aeroacoustics
[AIAA PAPER 83-0697] 10 p1477 A83-26448

Flow around a normal plate of finite width immersed in a turbulent boundary layer 10 p1418 A83-26630

Automatic recognition of mesocyclones from single Doppler radar data 11 p1630 A83-27088

A basic code for the prediction of transient three-dimensional turbulent flowfields 11 p1565 A83-27412

Turbofan mixer nozzle flowfield - A benchmark experimental study 11 p1525 A83-27419

Concentration of vorticity and spiral vortices 11 p1566 A83-27703

On the deformation of the cross section of a rectangular turbulent jet 11 p1567 A83-27708

Theoretical and experimental study of the flow of a viscous fluid near the line of intersection of cylindrical and plane surfaces 11 p1525 A83-27709

On the simulation of the hypervelocity regime of flow past bodies in wind tunnels 11 p1526 A83-27714

Three-dimensional supersonic ideal-gas flow past a body with a tail assembly 11 p1526 A83-27721

Effect of initial conditions on constant pressure mixing between two turbulent streams 11 p1567 A83-27875

Incidence angle effects on convected gust airfoil noise [AIAA PAPER 83-0765] 11 p1652 A83-28022

A study of flow in a short cavity with one-way fluid inlet and outlet 11 p1570 A83-28794

Investigation of the tip clearance flow inside and at the exit of a compressor rotor passage. II - Turbulence properties 12 p1695 A83-28843

A wind tunnel study of the flow field within and around open-top chambers used for air pollution studies 12 p1750 A83-29134

Prediction of high speed propeller flow fields using a three-dimensional Euler analysis [AIAA PAPER 83-0188] 12 p1697 A83-29535

Three-dimensional boundary conditions in supersonic flow 12 p1697 A83-29654

Computation of steady laminar flow over a circular cylinder with third-order boundary conditions 12 p1725 A83-29664

Experimental data needs for computational fluid dynamics - A position paper 13 p1840 A83-30627

The force effect on a sphere of an underexpanded jet issuing from a transonic nozzle 13 p1842 A83-30678

Viscous shock-layer flowfield analysis by an explicit-implicit method [AIAA PAPER 83-1423] 14 p1970 A83-32702

Heating analysis of bent-nose bionics at high angles of attack using the parabolized Navier-Stokes equations [AIAA PAPER 83-1507] 14 p1970 A83-32744

Viscous real gas flowfields about three dimensional configurations [AIAA PAPER 83-1511] 14 p1970 A83-32748

Computation of two-dimensional jet interaction flow field [AIAA PAPER 83-1546] 14 p1971 A83-32769

Flow field description for the reaction control system of the Space Shuttle Orbiter [AIAA PAPER 83-1548] 14 p1981 A83-32770

A more accurate transonic computational method for wing-body configurations 14 p1971 A83-32982

Numerical solution of transonic wing flowfields 14 p1971 A83-32984

Bow wave patterns 14 p2012 A83-32990

Vorticity at the shock foot in inviscid flow 14 p1971 A83-32993

Turbulent boundary layer associated with periodic rotating wakes --- from axial flow turbomachine rotors 14 p1972 A83-33373

On flame stretch 15 p1231 A83-33723

An empirical method for computing leeside centerline heating on the Space Shuttle Orbiter 15 p2120 A83-33731

The structure of a turbulent wake behind a cruciform circular cylinder. II - The streamwise development of turbulent flow field 15 p2158 A83-34007

Impact of Monex-79 data on the objective analysis of the wind field over the Indian region 15 p2206 A83-34746

Prediction of the flowfield in laser propulsion devices [AIAA PAPER 83-1445] 15 p2129 A83-34907

Improvements in rocket engine nozzle and high altitude plume computations [AIAA PAPER 83-1547] 15 p2130 A83-34922

Rocket exhaust plume induced flowfield interaction experiences with the Space Shuttle [AIAA PAPER 83-1549] 15 p2128 A83-34923

Investigation of gas particle flow in an erosion wind tunnel 15 p2162 A83-35246

Numerical processing of flow-visualization pictures Measurement of two-dimensional vortex flow 16 p2348 A83-35341

Calculation of flow past a small projection directed toward the flow 16 p2288 A83-35531

Calculation of subsonic flow past rectangular wings and their combinations on the basis of a discrete vortex scheme 16 p2288 A83-35541

The effect of acoustic perturbations on the flow structure in a boundary layer with an unfavorable pressure gradient 16 p2289 A83-35705

Flow past a nonconducting wedge in magnetohydrodynamics 16 p2415 A83-35710

A finite hybrid numerical analysis of the internal and external transonic flow fields of inlets 16 p2289 A83-35814

Experiments and mathematical simulation of plate distortion simulators 16 p2351 A83-35817

Semi implicit calculation method of the flow field in a duct with the flame stabilized by a step --- for aircraft engine combustion chamber design [ONERA, TP NO. 1983-52] 16 p2303 A83-35820

A study of lean extinction limit for pilot flame holder 16 p2325 A83-35821

Applications of computational techniques in the design of ramjet engines 16 p2290 A83-35828

Investigation of flow field in a turbocompressor by the finite element method 16 p2290 A83-35834

Application of streamline iteration and relative flow field methods to the calculation of the subsonic flow field of S1 stream surface of turbomachinery 16 p2290 A83-35836

Tip clearance flow in a compressor rotor passage at design and off-design conditions 16 p2291 A83-35855

A model of axial impeller stall 16 p2292 A83-35878

Comparison of techniques for predicting 3-D viscous flows over ablated shapes [AIAA PAPER 83-0345] 16 p2292 A83-36051

Three-dimensional flow studies on a slotted transonic wind tunnel wall 16 p2293 A83-36086

Similarity considerations of isothermal turbulent recirculating flowfields in axisymmetric bluff-body near wakes [AIAA PAPER 83-1203] 16 p2294 A83-36279

Unsteady aerodynamics in open cavities applications to rocket propulsion [AIAA PAPER 83-1314] 16 p2295 A83-36335

Analytical characterization of flow fields in side-inlet dump combustors [AIAA PAPER 83-1399] 16 p2322 A83-36389

New flows in a circular Couette system with co-rotating cylinders 17 p2501 A83-37028

An approximate calculation of laminar boundary layer flow of an incompressible fluid 17 p2501 A83-37049

Unsteady flow field, lift and drag measurements of impulsively started elliptic cylinder and circular-arc airfoil [AIAA PAPER 83-1711] 17 p2502 A83-37205

An assessment of flow-field simulation and measurement [AIAA PAPER 83-1721] 17 p2509 A83-37210

Effect of suction on the wake structure of a three-dimensional turret [AIAA PAPER 83-1738] 17 p2445 A83-37217

Flowfield scaling in sharp fin-induced shock wave turbulent boundary layer interaction [AIAA PAPER 83-1754] 17 p2446 A83-37227

Supersonic flow field analysis for a twin-engine aircraft model 17 p2448 A83-37521

Structure of the flow of an inviscid gas near an isolated stagnation point 17 p2505 A83-37526

Transonic flow at the break point of a profile with a free streamline 17 p2448 A83-37527

Aerodynamic simulation - A key technology not only for aviation 17 p2451 A83-37860

The effect of pressure-velocity correlation in a premixed, planar, turbulent flame 17 p2485 A83-38029

Modeling of turbulent flow fields through cascade of airfoils at stall conditions [AIAA PAPER 83-1743] 17 p2452 A83-38091

A flow analysis procedure based on velocity potentials [AIAA PAPER 83-1818] 17 p2508 A83-38650

A multiple separation model for multielement airfoils [AIAA PAPER 83-1844] 17 p2456 A83-38672

Surface pressures induced on a flat plate with in-line and side-by-side dual jet configurations [AIAA PAPER 83-1849] 17 p2456 A83-38677

Ideal incompressible hydrodynamics in terms of the vortex momentum density 17 p2509 A83-38961

An update on non-stationary oblique shock-wave reflections Actual isopycnics and numerical experiments 18 p2681 A83-39212

Flow development in the vicinity of the sharp trailing edge on bodies impulsively set into motion. II 18 p2632 A83-39213

Supersonic-nitrogen flow-field measurements with the resonant Doppler velocimeter 18 p2689 A83-40054

Flow state of composite materials in the forging die during the molding process 18 p2661 A83-40281

Unsteady aspects of a low mach number jet 18 p2638 A83-40500

Measuring laser flow fields with a 64-channel heterodyne interferometer 19 p2847 A83-41102

Hypersonic flow behind a lifting body 19 p2790 A83-41206

The effect of viscosity on flow in the circulation region in front of a plane obstacle perpendicular to the axis of an underexpanded supersonic jet 19 p2790 A83-41254

Flow distribution in parallel connected manifolds for evacuated tubular solar collectors 19 p2862 A83-41538

Interference during flow around a wing and an axisymmetric nacelle 19 p2791 A83-41879

Allowance for finite Mach numbers in hypersonic asymptotics for blunt axisymmetric bodies 19 p2791 A83-41880

Variant of the Tamm and Mott-Smith solution for describing the structure of a gasdynamic shock in a monatomic gas 19 p2845 A83-41882

Mathematical description of the flow of a gas and suspended particles around a body with allowance for the effect of reflected particles 19 p2845 A83-41897

Calculation of dusty-gas flow around a sphere with allowance for the effect of reflected particles 19 p2845 A83-41898

Computational interferometric description of nested flow fields 20 p2988 A83-42527

Numerical calculations of a confined two-dimensional turbulent isothermal mixing layer 20 p2969 A83-42528

Dynamic measurements in gas flowfields using rotational Raman spectroscopy 20 p2950 A83-42580

Local heat transfer rates from two adjacent spheres in turbulent axisymmetric flow 20 p2976 A83-42719

Flow structure in continuous flow electrophoresis chambers 20 p2950 A83-43275

Maldistributed inlet flow effects on turbulent heat transfer and pressure drop in a flat rectangular duct 20 p2986 A83-43363

A finite-volume, adaptive grid algorithm applied to planetary entry flowfields 20 p2930 A83-43440

A grid overlapping scheme for flowfield computations about multicomponent configurations 20 p2930 A83-43443

Spin-up from rest in a differentially rotating cylinder 20 p2986 A83-43444

Computation of reacting flowfield with radiation interaction in chemical lasers 20 p2995 A83-43445

The two-dimensional laminar wake with initial asymmetry 20 p2930 A83-43454

A study of the unsteady flow field of an airfoil with deflected spoiler [AIAA PAPER 83-2131] 20 p2931 A83-43810

Vortex flow over delta and double-delta wings 21 p3085 A83-43975

Families of variation principle for the semi-inverse problem and the A-type hybrid problem on the S2-stream sheet in radial turbomachines and the extensions and applications of semi-inverse problem to the mixed-type turbomachines 21 p3130 A83-44552

Numerical calculation of inviscid supersonic flow field around bent nose cones 21 p3087 A83-44564

An investigation of the effect of the nonuniform field feature around a delta-wing on the separated vortex breakdown 21 p3087 A83-44566

A simplified calculation method for the nonequilibrium wake of the blunt-cone body 21 p3087 A83-44568

Calculations of the one-dimensional nonequilibrium nozzle flow 21 p3130 A83-44573

White-light speckle method for obtaining an equi-velocity map of a whole flow field 21 p3138 A83-44683

Numerical determination of the parameters in high-entropy layers on slightly blunt bodies in supersonic flow 21 p3088 A83-45220

Analytical and experimental study of flow through an axial turbine stage with a nonuniform inlet radial temperature profile [AIAA PAPER 83-1175] 21 p3088 A83-45510

Topological analysis of computed three-dimensional viscous flow fields 22 p3248 A83-46457

Considerations of the vorticity fields on wings 22 p3249 A83-46465

The structure of flows with unsteady boundary conditions 22 p3284 A83-46477

- A method of flow field determination for moderately skewed, three-dimensional flows 22 p3285 A83-47015
- An investigation of surface flow pattern and pressure distribution for viscous, sonic flow over hemisphere-cylinder at incidence 22 p3286 A83-47029
- Combustion experiments with a new burner air distribution concept [ASME PAPER 83-GT-31] 23 p3406 A83-47893
- Inlet-fan flow field computation [ASME PAPER 83-GT-41] 23 p3394 A83-47901
- Isothermal predictions of recirculating turbulent flowfields of confined dual coaxial jets behind an axisymmetric bluff body [ASME PAPER 83-FE-14] 23 p3450 A83-48232
- Lagrangian models for turbulent combustion [ONERA, TP NO. 1983-106] 24 p3554 A83-49417
- ### FLOW EQUATIONS
- NT HELMHOLTZ VORTICITY EQUATION
- NT VON KARMAN EQUATION
- NT VORTICITY EQUATIONS
- An iteration method and solvability conditions for Navier-Stokes-type equations 01 p0045 A83-10822
- Fundamentals of compressible flow --- Book 01 p0045 A83-10883
- Similarity solutions and experiment for turbulent wakes 03 p0315 A83-13116
- Steady symmetrical problem of a stratified fluid 03 p0316 A83-13693
- Co-energy methods for elliptic flow and related problems 03 p0384 A83-14080
- Finite-difference techniques for vectorized fluid dynamics calculations --- Book 03 p0317 A83-14225
- Inhomogeneous flow calculations by spectral methods - Mono-domain and multi-domain techniques [ONERA, TP NO. 1982-67] 03 p0320 A83-14527
- Invariance properties under a reciprocal Backlund transformation in gasdynamics 03 p0320 A83-14566
- FFT vs. conjugate gradient method for solution of flow equations by pseudo-spectral methods 03 p0322 A83-14614
- On current aspects of finite element computational fluid mechanics for turbulent flows 04 p0475 A83-15006
- Properties of parallel-surfaces coordinate systems --- for balance equations in computational fluid dynamics 04 p0530 A83-15817
- A class of central bidiagonal schemes with implicit boundary conditions for the solution of Euler's equations [AIAA PAPER 83-0126] 05 p0633 A83-16539
- Compressible flow analysis about three-dimensional wing surfaces using a combination technique [AIAA PAPER 83-0183] 05 p0581 A83-16575
- A study with sensitivity analysis of the k-epsilon turbulence model applied to jet flows [AIAA PAPER 83-0285] 05 p0633 A83-16630
- A finite difference method for inverse solutions of 3-D turbulent boundary-layer flow [AIAA PAPER 83-0301] 05 p0634 A83-16639
- Monotone implicit algorithms for the small-disturbance and full potential equations applied to transonic flows [AIAA PAPER 83-0371] 05 p0585 A83-16677
- Transonic wing-body calculations using Euler equations [AIAA PAPER 83-0501] 05 p0589 A83-16828
- A finite element formulation for steady transonic Euler equations 08 p1042 A83-22129
- A refined PUMPIN /Pressure Update by Multiple Path Integration/ method for updating pressures in the numerical solution of the incompressible fluid equations 08 p1088 A83-23188
- A finite element method for the shallow water equations 08 p1089 A83-23201
- Prediction of rough-wall skin friction and heat transfer 09 p1263 A83-24657
- Equations for the general two-dimensional supersonic flow 09 p1198 A83-25112
- Qualitative analysis of equations describing quasi-one-dimensional nonequilibrium flow in channels 11 p1569 A83-28535
- Solitary waves on a viscous fluid film down a vertical wall 12 p1721 A83-29002
- The flow between two finite rotating disks enclosed by a cylinder 12 p1723 A83-29229
- Stability of the explicit finite differenced transport equation 12 p1725 A83-29638
- Numerical solution of the equations of compressible viscous flow 12 p1698 A83-29933
- A two-equation turbulence model for two-phase flows 13 p1839 A83-30109
- Integral techniques --- for turbulence modeling 13 p1841 A83-30632
- Velocity and length scales in turbulent flows - A review of approaches 13 p1841 A83-30633
- Solutions to the boundary value problem with velocity correlations in stratified flow through circular pipe. I 14 p2012 A83-32968
- An implicit, bidiagonal numerical method for solving the Navier-Stokes equations 14 p2012 A83-32979
- Numerical integration of the unsteady-flow equations for a two-dimensional supersonic free jet 15 p2162 A83-34977
- The basic equations of hodograph method in three dimensional flow 16 p2291 A83-35840
- Near-wake computations with Reynolds stress models [AIAA PAPER 83-1696] 17 p2445 A83-37194
- k-epsilon equation for compressible reciprocating engine flows 17 p2507 A83-38021
- Vortex evolution 18 p2679 A83-39009
- Calculation of turbulent diffusion flame using the coherent flame sheet model [AIAA PAPER 83-1322] 18 p2663 A83-39108
- Numerical solution of the Reynolds stress equations in a developing duct flow [AIAA PAPER 83-1883] 18 p2634 A83-39353
- A comparative study of the nonuniqueness problem of the potential equation --- for transonic flow past airfoils [AIAA PAPER 83-1888] 18 p2634 A83-39357
- Efficient solution of the Euler and Navier-Stokes equations with a vectorized multiple-grid algorithm [AIAA PAPER 83-1893] 18 p2634 A83-39359
- Improving the convergence rate of parabolic ADI methods [AIAA PAPER 83-1897] 18 p2739 A83-39361
- A new stream function formulation for the Euler equations [AIAA PAPER 83-1947] 18 p2636 A83-39393
- Application of the implicit MacCormack scheme to the PNS equations [AIAA PAPER 83-1956] 18 p2636 A83-39399
- A method for solving the transonic full-potential equation for general configurations [AIAA PAPER 83-1889] 18 p2637 A83-39402
- Hodographic study of transverse magnetohydrodynamic flows 18 p2746 A83-39855
- Finite element methods for transonic flow analysis 19 p2789 A83-40854
- Coherence in chaos turbulence 19 p2901 A83-40963
- The evolution of large-horizontal-scale disturbances in marginally stable, inviscid, shear flows. I - Derivation of the amplitude evolution equations 19 p2842 A83-41022
- Flow distribution in parallel connected manifolds for evacuated tubular solar collectors 19 p2862 A83-41538
- Variant of the Tamm and Mott-Smith solution for describing the structure of a gasdynamic shock in a monatomic gas 19 p2845 A83-41882
- Evolution equations for the vorticity distribution function in the two-dimensional case 20 p2987 A83-43513
- A Meksyn series method for the Falkner-Skan equation with mass transfer 21 p3128 A83-44023
- Similarity solutions of the boundary-layer equations for a stretching wall 21 p3129 A83-44459
- Evolution scheme to compute periodic solutions of first-order nonlinear equations containing translation operators 21 p3197 A83-44468
- Considerations on the transport-theorem for extensive flow properties 22 p3284 A83-46476
- Effect of crossflow on the vortex-layer-type three-dimensional flow separation 22 p3250 A83-47018
- Integration of equations of atmospheric dynamics using a semiimplicit dissipative scheme 23 p3488 A83-47158
- On the geometry of vortex lines in magnetofluid flows 23 p3510 A83-47604
- Performance evaluation of centrifugal compressor impellers using three-dimensional viscous flow calculations [ASME PAPER 83-GT-62] 23 p3395 A83-47918
- Boundary conditions for the potential equation in transonic internal flow calculation [ASME PAPER 83-GT-135] 23 p3396 A83-47962
- The well-posedness of two-dimensional ideal flow 23 p3449 A83-48047
- ### FLOW FIELDS
- ### U FLOW DISTRIBUTION
- ### FLOW GEOMETRY
- Transient response of the solar wind to changes in flow geometry 02 p0271 A83-12588
- The touching pair of equal and opposite uniform vortices 03 p0314 A83-13111
- Large-scale structure of the core of a spiral discontinuity in a fluid 04 p0475 A83-15082
- Characteristics of a turbulent boundary layer on the concave surface of a 90-degree bend 04 p0475 A83-15094
- Flames as gasdynamic discontinuities 04 p0457 A83-16262
- Laminar viscous flow-field prediction of Shuttle-like vehicle aerodynamics [AIAA PAPER 83-0211] 05 p0581 A83-16586
- Interaction of a pair of curved wall jets after a circular cylinder [AIAA PAPER 83-0290] 05 p0584 A83-16632
- Regular or catastrophic evolution of steady flows depending on parameters --- in aerodynamics 05 p0638 A83-17318
- Effect of inserts on the shaping of fine-particle conveying flows in cylindrical nozzles 05 p0639 A83-17409
- Nonlinear analysis of cavity flows around arbitrarily shaped bluff bodies in a constrained flow 06 p0758 A83-19020
- Three-dimensional stability of vortex arrays 06 p0758 A83-19022
- The far nonlinear field in transonic flows past nonlifting profiles 06 p0713 A83-19442
- The configuration of subsonic zones generated during supersonic flow past a spherically blunted cylinder at large angles of attack 06 p0713 A83-19443
- Spectral methods for flows in complex geometries [AIAA PAPER 83-0229] 06 p0761 A83-19583
- The shape of low Reynolds number jets 07 p0926 A83-20527
- Asymmetric supercritical flow past a double wedge with embedded shocks 08 p1041 A83-21811
- Thermoconvective heat transfer in a rectangular cavity with constant wall cooling rate 08 p1090 A83-23211
- Symmetric marching technique /SMT/ for the efficient solution of discretized Poisson equation on non-rectangular regions 08 p1091 A83-23218
- Mean flowfields in axisymmetric combustor geometries with swirl 09 p1263 A83-24668
- Near field pressure fluctuations of an elliptic jet [AIAA PAPER 83-0663] 10 p1472 A83-25901
- Amplification of non-linear standing waves in a cylindrical cavity with varying cross section 10 p1414 A83-26143
- Experimental method for determining the dynamic properties of gas flows 10 p1417 A83-26293
- Regular structures in a plane triple jet 10 p1418 A83-26627
- On the deformation of the cross section of a rectangular turbulent jet 11 p1567 A83-27708
- Theoretical and experimental study of the flow of a viscous fluid near the line of intersection of cylindrical and plane surfaces 11 p1525 A83-27709
- Experimental investigation of geometry and flow effects on acoustic radiation from duct inlets [AIAA PAPER 83-0713] 11 p1651 A83-28012
- Experimental study of the motion of rising vortex rings 11 p1569 A83-28533
- Calculation of fully developed turbulent flows in ducts of arbitrary cross-section 12 p1723 A83-29231
- On the motion of a spherical fluid film 13 p1839 A83-30092
- Flow in curved pipes 13 p1843 A83-31086
- The propagation of a curved flame front in a specified gas-flow field 14 p1989 A83-32088
- Thin axisymmetric cavities in flow past a body in a longitudinal gravitational field 14 p2008 A83-32158
- Vorticity at the shock foot in inviscid flow 14 p1971 A83-32993
- A novel property of the displacement thickness in three-dimensional boundary-layer theory 14 p2013 A83-33381
- ADI methods for solution of the transient heat conduction problems in spherical geometry 15 p2159 A83-34234
- Swirl characteristics of an S-shaped air intake with both horizontal and vertical offsets 16 p2289 A83-35621
- The shape-factor relationship for turbulent boundary layers 16 p2289 A83-35622
- The effect of acoustic perturbations on the flow structure in a boundary layer with an unfavorable pressure gradient 16 p2289 A83-35705
- Topology of vortices in conical flow [AIAA PAPER 83-1664] 17 p2443 A83-37176
- A numerical investigation for curved pipe flow at high Reynolds number [ASME PAPER 83-APM-18] 17 p2504 A83-37376
- The effect of the geometrical parameters of an air intake with a central body on drag relative to the fluid streamline in the case when there is an incompressible-gas flow around it 17 p2448 A83-37531
- Calculation of steady two-dimensional turbulent flow in a curved channel 18 p2684 A83-39481
- Real gas flows over complex geometries at moderate angles of attack 18 p2638 A83-40004
- Finite element methods for transonic flow analysis 19 p2789 A83-40854
- On the propagation of an intense shock wave in a pipe of variable cross section 19 p2845 A83-41887
- Flow in the base region of a channel in non-self-similar regimes 19 p2792 A83-41894

- Study of asymptotic incompressible flow in curved ducts using a multi-grid technique 20 p2969 A83-42532
- Heat transfer in the turbulent swirling flow in a channel of complex shape 20 p2976 A83-42714
- Cross flow influence upon impinging convective heat transfer in circular arrays of jets - A general correlation 20 p2978 A83-42741
- A study of turbulence models for predicting round and plane heated jets 20 p2979 A83-42745
- Prediction of curved channel flow with an extended k-epsilon model of turbulence 21 p3134 A83-45578
- A study of turbulent flow downstream of an abrupt pipe expansion 21 p3134 A83-45582
- Structure of turbulent boundary layer on an oscillating flat plate 22 p3282 A83-46430
- The preferred-mode coherent structure in the near field of an axisymmetric jet with and without excitation 22 p3283 A83-46451
- The effect of forcing on the mixing-layer region of a round jet 22 p3283 A83-46452
- Cross-hatching - An interaction between shock and turbulent boundary layer 22 p3286 A83-47030
- On the geometry of vortex lines in magnetofluid flows 23 p3510 A83-47604
- On the influence of the diffuser inlet shape on the performance of a centrifugal compressor stage [ASME PAPER 83-GT-9] 23 p3406 A83-47881
- A streamline curvature method for calculating S1 stream surface flow [ASME PAPER 83-GT-16] 23 p3393 A83-47885
- A configuration to improve the aerodynamics and scope of can-annular combustors [ASME PAPER 83-GT-37] 23 p3406 A83-47898
- Entropy production rates from viscous flow calculations. II Flow in a rectangular elbow [ASME PAPER 83-GT-71] 23 p3512 A83-47924
- Annular jets of different diameter ratios 23 p3449 A83-48142
- Prediction of sudden expansion flows using the boundary-layer equations [ASME PAPER 83-FE-11] 23 p3450 A83-48230
- Multiple jet mixing in a rectangular duct - Centre-plane behaviour [ASME PAPER 83-FE-35] 23 p3399 A83-48238
- Efficient computational grid generation for three-dimensional aircraft configurations [AIAA PAPER 83-2557] 23 p3405 A83-48376
- On the asymptotic structure of interaction in a laminar axisymmetric wake 23 p3451 A83-48653
- Dynamics of an elliptical vortex 23 p3452 A83-48656

FLOW MEASUREMENT

- Experimental investigation of the influence of Reynolds number and of shaft and gradient effects on flow measurements using spherical five-hole sondes --- German thesis 01 p0045 A83-10473
- Measurements in shear layers in transonic flows with a laser transit anemometer 01 p0003 A83-10697
- A comparison of characteristic features of coherent turbulent structures found using the Variable Interval Time Average /VITA/ technique and using the pattern recognition technique 01 p0046 A83-10895
- Research programme and measurement techniques in the water towing tank of DFVLR in Goettingen 01 p0052 A83-11058
- Flow visualization study in low specific speed pump impeller passages 01 p0053 A83-11073
- Application of a laser interferometer skin-friction meter in complex flows 01 p0053 A83-11075
- Optical methods of flow diagnostics in turbomachinery 01 p0053 A83-11076
- Performance of LDI in predicting density profiles of compressible boundary layers --- laser differential interferometry 01 p0053 A83-11078
- Measurements and visualizations of unsteady flow /low speed/ [AAAF PAPER NT 81-14] 02 p0176 A83-11774
- X-wire sounding in an air inlet at high angle of attack [AAAF PAPER NT 81-15] 02 p0132 A83-11775
- Three-dimensional or unsteady boundary layers [AAAF PAPER NT 81-16] 02 p0169 A83-11776
- The use of forced Rayleigh scattering to study laminar and turbulent flows 02 p0169 A83-11855
- Assessment of candidate combustor configurations as test beds for modeling complex flows [ASME PAPER 82-HT-36] 02 p0172 A83-12793
- Laser velocimeter for large wind tunnels 03 p0324 A83-13171
- Modified gauge for time-resolved skin-friction measurements 03 p0329 A83-14172
- Measurement of the structure of the streamwise vorticity field in a turbulent boundary-layer 03 p0317 A83-14455
- The influence of Reynolds number on characteristics of turbulent boundary layers 03 p0318 A83-14461

- Measurement of bursting period and test of surface renewal model in a turbulent boundary layer disturbed by a cylinder 03 p0318 A83-14462
- Characteristics of coherent structures in complex turbulent shear flows 03 p0318 A83-14465
- Measurement of turbulence correlations in a two-dimensional supersonic wake 03 p0278 A83-14470
- Applications of flow visualization techniques in aerodynamics [ONERA, TP NO. 1982-68] 03 p0330 A83-14528
- Experimental and theoretical investigations on the turbulence in transonic shock boundary layer interactions [ONERA, TP NO. 1982-77] 03 p0279 A83-14531
- Laser velocimetric analysis of the flow downstream of missile aft-bodies [ONERA, TP NO. 1982-94] 03 p0279 A83-14543
- The effects of surface roughness on the flow past circular cylinders at high Reynolds numbers 03 p0321 A83-14584
- Strouhal numbers of rectangular cylinders 03 p0321 A83-14585
- Simultaneous measurement of stagnation temperature and specific flow rate in a hypersonic gas flow 04 p0481 A83-15447
- On the flow field around a Savonius rotor 04 p0505 A83-15798
- Fluid dynamics of inducers - A review 04 p0478 A83-16137
- Investigation of wall induced modifications to vortex shedding from a circular cylinder 04 p0478 A83-16143
- The use of multiple wall probes to identify coherent flow patterns in the viscous wall region 04 p0479 A83-16265
- The effect of the thermal prong-wire interaction on the response of a cold wire in gaseous flows /air, argon and helium/ 04 p0479 A83-16266
- A method for measuring the stagnation temperature of short-duration gas flows using a radiation-calorimetric transducer 04 p0483 A83-16393
- Effect of suction and blowing on boundary-layer transition [AIAA PAPER 83-0043] 05 p0578 A83-16483
- Constant-temperature hot-wire anemometer practice in supersonic flows. I - The normal wire [AIAA PAPER 83-0050] 05 p0642 A83-16485
- Reduction of flow-measurement uncertainties in laser velocimeters with nonorthogonal channels [AIAA PAPER 83-0051] 05 p0642 A83-16486
- Two-component LDA measurement in a two-phase turbulent jet [AIAA PAPER 83-0052] 05 p0642 A83-16487
- Measurements of the near wake of an airfoil in unsteady flow [AIAA PAPER 83-0127] 05 p0580 A83-16540
- Measurements and predictions for nonevaporating sprays in a quiescent environment [AIAA PAPER 83-0151] 05 p0633 A83-16558
- Flow measurements of an airfoil with deflected spoiler [AIAA PAPER 83-0365] 05 p0584 A83-16672
- Preliminary measurements of velocity, density and total temperature fluctuations in compressible subsonic flow [AIAA PAPER 83-0384] 05 p0635 A83-16684
- Measurements on a projectile with an asymmetric afterbody at transonic speeds [AIAA PAPER 83-0545] 05 p0587 A83-16780
- Experimental investigation of the confluent boundary layer of a multielement low speed airfoil [AIAA PAPER 83-0566] 05 p0588 A83-16793
- An experimental study of the vortex tube - Where the vortex chamber includes a divergent tube 05 p0639 A83-17375
- Quantitative measurement of density and velocity in compressible flows using laser-induced iodine fluorescence [AIAA PAPER 83-0049] 05 p0646 A83-17903
- Turbulence measurements in a compressible reattaching shear layer [AIAA PAPER 83-0299] 05 p0591 A83-17917
- The turbulence transport properties of a supersonic boundary layer on a sharp cone at angle-of-attack [AIAA PAPER 83-0456] 05 p0591 A83-17927
- Boundary-layer development on circular cylinders 06 p0756 A83-18235
- Separated measurement of gas flows through different compartments of a partially pressurized suit 06 p0800 A83-18345
- Characteristics of the evolution of a dynamic turbulent boundary layer in the gas veil region after a porous section 06 p0756 A83-18444
- High Reynolds number shear stress measurements --- flight test results [AIAA PAPER 83-0053] 06 p0713 A83-19578

- Velocity field characteristics of a swirling flow combustor [AIAA PAPER 83-0314] 06 p0761 A83-19586
- Experimental determination of blade forces through stationary and nonstationary pressure measurements on interfering double cascades --- German thesis 06 p0714 A83-19616
- Short duration heat transfer studies at high free-stream temperatures [ASME PAPER 82-GT-129] 07 p0924 A83-19673
- Effect of pulsed slot suction on a turbulent boundary layer 07 p0863 A83-19825
- Measurement of three dimensional flow field behind an impeller by means of periodic multi-sampling with a slanted hot wire 07 p0929 A83-20276
- An experimental study of turbulent free convection boundary layer in air along a vertical plate using LDV 07 p0925 A83-20279
- An experimental investigation of turbulent wake behind 'S'-shaped profiles 07 p0926 A83-20502
- A system for phase and intermittency measurements in periodically turbulent flows 08 p1091 A83-21980
- Turbulence quantities of a turbulent boundary layer over a d-type rough surface 08 p1084 A83-22067
- Measurements and imaging method of blood flow profile in human heart 08 p1151 A83-22237
- A comparison of techniques for reconstructing axisymmetric reacting flow fields from absorption measurements 08 p1057 A83-22393
- Instantaneous velocity field measurements in unsteady gas flow by speckle velocimetry 08 p1101 A83-22616
- Isothermal models of gas-turbine combustors 08 p1057 A83-23097
- Improved light-scattering cavitation nuclei classifier 08 p1106 A83-23229
- Apparatus for simultaneous temperature and heat-flow measurements under transient conditions 08 p1106 A83-23235
- A yawmeter for steady and low-frequency unsteady flows 08 p1106 A83-23296
- Flow characteristics and methods of flow calculation of high-speed compressible flow through pipe orifices 09 p1257 A83-23332
- The structure of the turbulent atmospheric boundary layer 09 p1309 A83-23354
- Calculation of pressure losses in the diffusers of mixing afterburners 09 p1205 A83-23445
- The relationship between the aerodynamics of a combustion chamber and the dynamics of heat release 09 p1205 A83-23446
- The new hydrodynamic visualization laboratory of the aerodynamics division 09 p1210 A83-23676
- Some aspects of measuring the structure of non-isothermic turbulence by simultaneous application of DISA's LDA and hot-wire anemometer 09 p1259 A83-23697
- Classification and stability criteria of separated flows 09 p1259 A83-24010
- Joint measurements of radial velocity and scalars in a turbulent diffusion flame 09 p1226 A83-24365
- The structure of a separating turbulent boundary layer. IV - Effects of periodic free-stream unsteadiness 09 p1261 A83-24414
- Computed and measured turbulence in axisymmetric reciprocating engines 09 p1207 A83-24669
- Turbine meters for liquid measurement 09 p1270 A83-25143
- A study of thermal convection and heat transfer --- Russian book 09 p1264 A83-25246
- Some new results on edge-tone oscillations in high-speed subsonic jets [AIAA PAPER 83-0665] 10 p1473 A83-25902
- Porous-plug flowfield mechanisms for reducing supersonic jet noise [AIAA PAPER 83-0774] 10 p1378 A83-25959
- The measurement of the steady flow resistance of porous materials --- for noise suppression in aircraft turbofan engine ducts [AIAA PAPER 83-0779] 10 p1477 A83-25961
- Measurements of a supersonic velocity in a nitrogen flow using inverse Raman spectroscopy 10 p1420 A83-26114
- Measurement and calculation of shock attenuation in a channel with perforated walls 10 p1414 A83-26141
- Optical studies of shock generated transient supersonic base flows 10 p1371 A83-26142
- Measurement of instantaneous flow rate through estimation of velocity profiles 10 p1417 A83-26268
- Measuring techniques in transonic and supersonic flows in cascades and turbomachines; Proceedings of the Symposium, Ecole Centrale de Lyon, Ecully, Rhone, France, October 15, 16, 1981 10 p1421 A83-26409

- Investigation of the Reynolds-number effects on probe measurements in supersonic flow 10 p1372 A83-26410
- The influence of Reynolds number and a gradient correction method for five-hole pressure probes 10 p1421 A83-26411
- Characteristics of aerodynamic five-hole-probes in transonic and supersonic flow regimes 10 p1421 A83-26412
- Effects of flow unsteadiness on the time-mean response of a Kiel-type total pressure probe - Preliminary investigation 10 p1421 A83-26414
- Measurements and data reduction problems behind the rotor of a transonic axial flow compressor in the hub region 10 p1372 A83-26417
- A dual focus fiber optic anemometer for measurements in wet steam 10 p1422 A83-26422
- Regular structures in a plane triple jet 10 p1418 A83-26627
- Complementary use of a tri-axial hot film probe and a five hole pitot tube to determine vehicle wake characteristics 11 p1571 A83-27416
- Boundary layer behavior on rough surfaces in the presence of a turbulent wake 11 p1565 A83-27417
- Coherent structures in rectangular jets 11 p1565 A83-27418
- Theoretical and experimental study of the flow of a viscous fluid near the line of intersection of cylindrical and plane surfaces 11 p1525 A83-27709
- Investigation of the length and wave structure of the gasdynamic part in straight and spreading gas jets 11 p1567 A83-27718
- Turbulence measurements in wall jets along strongly concave surfaces 11 p1567 A83-27861
- Experimental study of a gas film in a tube 11 p1568 A83-28371
- Measurement of the velocity vector of gas flow 11 p1574 A83-28554
- Improved calibration of hot-wire anemometers 11 p1574 A83-28574
- Engineering applications of laser velocimetry; Proceedings of the Symposium, Phoenix, AZ, November 14-19, 1982 12 p1727 A83-28830
- Laser velocimetry - Problems and opportunities 12 p1727 A83-28831
- Some solutions to the problems and pitfalls of laser velocimetry in a large transonic wind tunnel 12 p1704 A83-28832
- Flow measurements using a laser two-focus anemometer in a high-speed centrifugal and a multistage axial compressor 12 p1695 A83-28835
- Flow measurements using a laser-2-focus velocimeter in a high-pressure ratio centrifugal impeller 12 p1695 A83-28836
- A laser-Doppler velocimeter technique for in situ local measurement of dilute two-phase suspension flows 12 p1720 A83-28837
- Local velocity measurement of opaque fluid flow using laser Doppler velocimeter with optical dual fiber pickup 12 p1727 A83-28839
- Laser velocimeter measurements in highly turbulent recirculating flows 12 p1721 A83-28841
- Application of a three-sensor hot-wire probe for incompressible flow 12 p1728 A83-28963
- A technique for exact determination of the parietal pressure in a flow 12 p1724 A83-29389
- An examination of natural convection between two horizontal walls --- French thesis 12 p1727 A83-29945
- Investigation of the gain in a CO₂ GDL behind wedge-shaped and contoured nozzles. I - The experimental setup, the repetitively pulsed system for gain measurement 13 p1849 A83-30042
- Separation of time-averaged turbulence components by laser-induced fluorescence 13 p1839 A83-30102
- Study of a circular jet at low Reynolds numbers and with impact on a wall --- French thesis 13 p1840 A83-30127
- Conference on Complex Turbulent Flows: Comparison of Computation and Experiment, Stanford University, Stanford, CA, September 3-6, 1980, Proceedings. Volume 1 - Objectives, evaluation of data, specifications of test cases, discussion and position papers 13 p1840 A83-30626
- Contributions to the theory of uncertainty analysis for single-sample experiments 13 p1913 A83-30628
- Conference on Complex Turbulent Flows: Comparison of Computation and Experiment, Stanford University, Stanford, CA, September 14-18, 1981, Proceedings. Volume 3 - Comparison of computation with experiment, and computers' summary reports 13 p1842 A83-30644
- Annual review of fluid mechanics, Volume 15 --- Book 13 p1842 A83-31076
- The turbulent wall jet - Measurements and modeling 13 p1843 A83-31085
- Peculiarities in measuring the velocity vector using a laser anemometer in flow through axisymmetric models 13 p1848 A83-31470
- A sensor for flow measurements near the surface of a compressor blade 14 p2019 A83-32400
- Nonintrusive pressure measurement with laser-induced iodine fluorescence 14 p2019 A83-32724
- [AIAA PAPER 83-1468] 14 p2019 A83-32724
- Flow measurement in a model combustion chamber [AIAA PAPER 83-1550] 14 p1990 A83-32771
- Separated trailing-edge flow at a transonic Mach number 14 p1971 A83-32976
- An experimental study of entraining, stress-driven, stratified flow in an annulus 14 p2013 A83-33382
- Hot-wire anemometry --- Book 15 p2162 A83-33618
- Flow measurement engineering handbook 15 p2163 A83-33620
- Measurements of the periodic velocity oscillations near the wall in unsteady turbulent channel flow 15 p2154 A83-33652
- Experimental investigations in transonic highly separated, turbulent flow 15 p2119 A83-33665
- Turbulent flow induced by a jet in a cavity-measurements and 3D numerical simulation 15 p2155 A83-33666
- The assessment of numerical diffusion in upwind difference calculations of turbulent recirculating flows 15 p2155 A83-33667
- Turbulent and mean flow measurements in an incompressible axisymmetric boundary layer with incipient separation 15 p2156 A83-33668
- The structure of a turbulent wake behind a cruciform circular cylinder. II - The streamwise development of turbulent flow field 15 p2158 A83-34007
- Laser tomography for simultaneous concentration and temperature measurement in reacting flows 15 p2165 A83-34924
- [AIAA PAPER 83-1553] 15 p2165 A83-34924
- Studies on the turbulent flow field of an enclosed fast plasma jet 15 p2236 A83-35239
- A high-performance low-cost constant-temperature hot-wire anemometer 15 p2166 A83-35258
- Triple hot-wire technique for simultaneous measurements of instantaneous velocity components in turbulent flows 15 p2166 A83-35259
- Numerical processing of flow-visualization pictures Measurement of two-dimensional vortex flow 16 p2348 A83-35341
- The effect of acoustic perturbations on the flow structure in a boundary layer with an unfavorable pressure gradient 16 p2289 A83-35705
- Separated flows on a concave conical wing 16 p2289 A83-35707
- The relationship between the aerodynamic and acoustic characteristics of coaxial jets 16 p2408 A83-35712
- A study of a supersonic three-dimensional jet flow in a duct 16 p2289 A83-35718
- Boundary layer development in a supersonic intake 16 p2290 A83-35826
- Experience in the development of computer-controlled high response probe diagnostics for turbomachines 16 p2355 A83-35851
- Optical flow measurements in a transonic turbine stage 16 p2291 A83-35867
- Flow measurements within rotating stall cells in single and multistage axial-flow compressors 16 p2292 A83-35873
- Flow in rotating stall cells of a low speed axial flow compressor 16 p2292 A83-35874
- High angle-of-attack cascade measurements and analysis 16 p2292 A83-35875
- The effects of large heat release on a two dimensional mixing layer 16 p2351 A83-36055
- [AIAA PAPER 83-0472] 16 p2351 A83-36055
- Investigation of two plane parallel jets 16 p2352 A83-36084
- Seven-hole cone probes for high angle flow measurement Theory and calibration 16 p2356 A83-36085
- Application of fluidics to instrumentation in hostile environments 16 p2352 A83-36247
- [AIAA PAPER 83-1150] 16 p2352 A83-36278
- Single-wire swirl flow turbulence measurements [AIAA PAPER 83-1202] 16 p2352 A83-36278
- NASA low-speed centrifugal compressor for fundamental research 16 p2312 A83-36353
- [AIAA PAPER 83-1351] 16 p2295 A83-36355
- Aerodynamic measurements about a rotating propeller with a laser velocimeter [AIAA PAPER 83-1354] 16 p2295 A83-36355
- The measurements of dynamical parameters of low temperature plasma flows by means of ultrasound 16 p2417 A83-36881
- On 'saddle-backed' velocity distributions in a three-dimensional turbulent free jet [AIAA PAPER 83-1677] 17 p2444 A83-37185
- Interaction of multiple supersonic jets with a transonic flow field [AIAA PAPER 83-1680] 17 p2444 A83-37186
- An assessment of flow-field simulation and measurement [AIAA PAPER 83-1721] 17 p2509 A83-37210
- Measurements of compressible secondary flow in a circular S-duct [AIAA PAPER 83-1739] 17 p2446 A83-37218
- Theoretical and experimental study of a dual-flow circuit breaker nozzle flow [AIAA PAPER 83-1748] 17 p2503 A83-37223
- Flowfield scaling in sharp fin-induced shock wave turbulent boundary layer interaction [AIAA PAPER 83-1754] 17 p2446 A83-37227
- Characteristics of supersonic gas flow and heat transfer in the shadow region of a sharp cone 17 p2447 A83-37261
- Variation of heat transfer coefficients in the transition region of a flow at supersonic velocities 17 p2447 A83-37263
- Experimental study of the flow of a viscous compressible gas through a cylindrical channel and through a porous insert 17 p2447 A83-37265
- Investigation of the parameters of a boundary layer before the inlet of a supersonic air intake mounted under the surface of a triangular plate 17 p2448 A83-37533
- The effect of an increase in the temperature factor of a cone on the parameters of the base region 17 p2451 A83-37811
- Sound scattering by a vortex wake behind a cylinder 17 p2578 A83-38049
- A miniature, directional surface-fence gage for three-dimensional turbulent boundary layer measurements [AIAA PAPER 83-1722] 17 p2511 A83-38089
- Bow shock structure from laboratory and satellite experimental results 17 p2544 A83-38516
- Directional gas-flow measurement with pyroelectric anemometers (PA) 17 p2512 A83-38532
- A thermistor probe for use in laser Doppler anemometry 17 p2512 A83-38861
- Laminar boundary layer stability experiments on a cone at Mach 8.1 - Sharp cone [AIAA PAPER 83-1761] 18 p2633 A83-39264
- Measurements of the three-dimensional boundary layers on conical bodies at Mach 3 and Mach 5 [AIAA PAPER 83-1675] 18 p2633 A83-39266
- Holographic measurement of transition and turbulent bursting in supersonic axisymmetric boundary layers [AIAA PAPER 83-1724] 18 p2633 A83-39269
- A study on the fluctuation concentration field in a turbulent jet 18 p2687 A83-40336
- Methods of laser Doppler anemometry --- Russian book 18 p2692 A83-40605
- Freestream turbulence effects on compressor cascade wake 19 p2789 A83-41051
- Measuring laser flow fields with a 64-channel heterodyne interferometer 19 p2847 A83-41102
- Laser anemometry velocity measurements in a heated turbulent flow 19 p2843 A83-41322
- The calculation of planar inlet flows --- German thesis 19 p2844 A83-41809
- An electrical balance for aerodynamic investigations 19 p2849 A83-41883
- The measurement of pressure pulsations by means of piezoelectric transducers 19 p2849 A83-41891
- Pressure measurements of coaxial jet of high mean-velocity ratio 20 p2969 A83-42348
- An experimental investigation of a low heat flux, wickless heat pipe 20 p2969 A83-42350
- Mobilities of various mass-identified positive ions in helium, neon, and argon 20 p2950 A83-42637
- Study of O₂ (1-Delta) production in a glow discharge at large molar flow rates --- considering possibility of initiating iodine laser with discharged oxygen 20 p2994 A83-42643
- Measurements of the turbulent energy and temperature balances in an axisymmetric buoyant plume in a stably stratified environment 20 p2973 A83-42686
- Wake interference for a heated oscillating cylinder 20 p2980 A83-42753
- Two parametric flow measurement in gas-liquid two-phase flow 20 p2981 A83-42773
- Triple hot-wire technique for measurements of turbulence in heated flows 20 p2989 A83-42774
- Frequency response of cold wires and thermocouples used for temperature measurements in gaseous flows 20 p2982 A83-42778
- Photothermal measurements of thermal diffusivities 20 p2989 A83-42779
- Problems of mechanics and heat transfer in space technology 20 p2939 A83-42876

Raman anemometry, a method for component-selective velocity measurements of particles in a flow
20 p2990 A83-42950

Scaling of the bursting frequency in turbulent boundary layers
20 p2985 A83-43097

An experimental study of heat induced surface-tension driven flow
20 p2940 A83-43269

Measurement of surface rheological effects on a rotating flow
20 p2986 A83-43271

Surface tension driven flow in glass melts and model fluids
20 p2941 A83-43284

An interferometric investigation of separated forced convection in laminar flow past cavities
20 p2986 A83-43360

Heat transfer to a fluid in radial, outward flow between two coaxial stationary or corotating disks
20 p2986 A83-43362

Experiments on a crossflow heat exchanger with tubes of lenticular shape
20 p2986 A83-43364

Measurements of turbulent Prandtl number in a plane jet
20 p2986 A83-43366

A method for experimental analysis of the shock-boundary layer interaction in cascades
[ONERA, TP NO. 1983-48] 21 p3086 A83-44322

Turbulence measurements in a developing mixing layer with mild destabilising curvature
21 p3131 A83-44678

LDA signal discrimination in two-phase flows
21 p3140 A83-44971

Measurements of some features of turbulence in wall-proximity
21 p3132 A83-44973

Modified calibration technique of a five-hole probe for high flow angles
21 p3141 A83-44975

Experimental and numerical investigation of a turbulent boundary layer subjected to a sudden transverse strain
22 p3247 A83-46004

Has a small-scale structure in turbulence been experimentally verified?
22 p3281 A83-46005

Effect of driven-wall motion on a turbulent boundary layer
22 p3247 A83-46429

Experimental study of two- and three-dimensional boundary layer separation
22 p3248 A83-46432

Response of a turbulent boundary layer to a pulsation of the external flow with and without adverse pressure gradient
22 p3248 A83-46434

Natural and forced vortex shedding
22 p3282 A83-46440

Vortex shedding from a circular cylinder in oscillatory flow
22 p3282 A83-46441

Experimental analysis of the wake behind an isolated cambered airfoil
22 p3248 A83-46443

Influence of wall vibrations on a flow with boundary-layer separation at a convex edge
22 p3282 A83-46444

Turbulence structures in the wake of an oscillating airfoil
22 p3248 A83-46446

Diffusion of heat as a passive contaminant in a slightly pulsating jet
22 p3283 A83-46450

Measured velocity fluctuations inside the mixing layer of a supersonic jet
22 p3249 A83-46468

Experimental method for pressure-velocity correlation measurements in three-dimensional turbulent boundary layers
22 p3291 A83-46469

Cryogenic-wind-tunnel technology - A way to measurement at higher Reynolds numbers
22 p3256 A83-46484

Laser optical measurements of density and temperature in flowing gases
22 p3291 A83-46487

A contribution to the numerical description of rotating two-phase flow --- Thesis
22 p3285 A83-46693

Experimental techniques in three-dimensional turbulent boundary layers
22 p3285 A83-47013

Measurements in a pressure-driven and a shear-driven three-dimensional turbulent boundary layer
22 p3285 A83-47014

A method of flow field determination for moderately skewed, three-dimensional flows
22 p3285 A83-47015

Experimental study of the boundary layer on a turbomachinery rotor blade
22 p3250 A83-47022

Some measurements in the intermittent region of a turbulent boundary layer along a corner
22 p3286 A83-47025

An evaluation of the final discussion of the IUTAM Symposium on three-dimensional boundary layers
22 p3286 A83-47036

Boundary layer and loss measurements on the rotor of an axial-flow turbine
[ASME PAPER 83-GT-4] 23 p3392 A83-47878

An experimental and computational study of transonic three-dimensional flow in a turbine cascade
[ASME PAPER 83-GT-12] 23 p3393 A83-47884

Measurements of secondary flows within a cascade of curved blades and in the wake of the cascade
[ASME PAPER 83-GT-24] 23 p3393 A83-47889

Statistical characteristics of velocity, concentration, mass transport, and momentum transport for coaxial jet mixing in a confined duct
[ASME PAPER 83-GT-39] 23 p3447 A83-47899

Flow in a turbine cascade. II - Measurement of flow trajectories by ethylene detection
[ASME PAPER 83-GT-69] 23 p3395 A83-47922

The structure of turbulence in homogeneous and stratified rotating fluids
23 p3448 A83-48039

A digital technique for the simultaneous measurement of streamwise and lateral velocities in turbulent flows
23 p3458 A83-48117

An experimental study of low Reynolds number turbulent circular jet flow
[ASME PAPER 83-FE-36] 23 p3451 A83-48239

Computational-experimental study of the gas dynamics of two-dimensional symmetric nozzles having a region of constant height and two contour bend points in the critical section
23 p3400 A83-48661

The effect of free-stream turbulence on turbulent boundary layers
23 p3453 A83-48677

Studies of flows through N-sequential orifices
[ASME PAPER 83-FE-22] 23 p3453 A83-48678

Proposal for the measuring molecular velocity vector with single-pulse coherent Raman spectroscopy
23 p3459 A83-48709

Dimension measurements for geostrophic turbulence
24 p3609 A83-49294

Precautions that have to be taken in applying LDV to combustion chambers
[ONERA, TP NO. 1983-112] 24 p3583 A83-49423

Two focus laser velocimeter applied to measurements in an experimental centrifugal compressor
[ONERA, TP NO. 1983-113] 24 p3583 A83-49424

On the structure and resolution of wall-pressure fluctuations associated with turbulent boundary-layer flow
24 p3578 A83-49471

The use of the techniques of holographic interferometry in qualitative studies of gas-dynamic flows with chemical reactions
24 p3584 A83-49780

Symposium on Turbulence, 7th, University of Missouri-Rolla, Rolla, MO, September 21-23, 1983, Proceedings
24 p3584 A83-49801

On the development of turbulent boundary layer in open channel flows
24 p3579 A83-49804

Turbulent wall jet issued from a Coanda nozzle
24 p3580 A83-49808

A microprocessor controlled data acquisition and processing system for hot-wire anemometry
24 p3584 A83-49810

Measurement of velocity-temperature correlations of different orders in hot turbulent flows
24 p3584 A83-49814

The frequency response of cold wires
24 p3584 A83-49815

Advanced techniques for transverse vorticity measurements
24 p3584 A83-49816

Using numerical techniques to improve the performance of triple hot-wire probes
24 p3585 A83-49817

Digital thermal anemometry
24 p3585 A83-49818

Pattern recognition study of coherent motion in a transpired turbulent boundary layer
24 p3580 A83-49819

Vortex pairing in a Karman vortex street
24 p3580 A83-49821

Simultaneous stereoscopic visual and anemometer measurements in a convected frame of reference
24 p3585 A83-49823

Three-component laser-Doppler anemometry measurements in a circular mixing tube
24 p3585 A83-49824

A 3-D laser Doppler velocimeter for use in high-speed flows
24 p3585 A83-49825

A three component velocity measurement in an open channel by a combination of LDA and hot film anemometry
24 p3585 A83-49826

Space-correlation measurement of attaching jets by the new scanning laser Doppler velocimeter using a diffraction grating
24 p3585 A83-49827

Recent applications of a laser velocimeter in the Langley 4by 7-meter Wind Tunnel
24 p3586 A83-50145

FLOW PATTERNS
U FLOW DISTRIBUTION
FLOW RATE
U FLOW VELOCITY
FLOW REGULATORS
NT FUEL FLOW REGULATORS
Flow patterns in semiclosed cavities of spindle-operated valves and the valve flow rates
09 p1258 A83-23428

Investigation of the combined regulation of the intermediate stage of a centrifugal compressor by an axial regulating apparatus and a two-row diffuser
14 p2028 A83-33149

Controlling the Mach number of a transonic wind tunnel by means of a supersonic diffuser
17 p2451 A83-37641

A flight test of laminar flow control leading-edge systems
[AIAA PAPER 83-2508] 23 p3404 A83-48356

FLOW RESISTANCE
NT AERODYNAMIC DRAG
NT FRICTION DRAG
NT SUPERSONIC DRAG
NT VISCOUS DRAG
Sensible heat flux estimated from routine meteorological data by the resistance method
07 p0969 A83-20805

Determination of the cavitation boundary in liquid flows through constricting devices
09 p1258 A83-23432

The measurement of the steady flow resistance of porous materials --- for noise suppression in aircraft turbofan engine ducts
[AIAA PAPER 83-0779] 10 p1477 A83-25961

Hydrodynamic fluctuation due to the discontinuity of flow impedance
12 p1721 A83-29001

Airflow resistivity instrument for in situ measurement on the earth's ground surface
14 p2020 A83-32824

Solution of the equations of an unsteady boundary layer
16 p2349 A83-35533

Profile losses during the release of air onto the surface of nozzle vanes
16 p2288 A83-35590

Heat transfer and drag in a turbulent boundary layer with a pressure gradient
19 p2844 A83-41576

Experimental study of the effect of pulsations on the development of flow-core velocity oscillations and wall friction in a convergent channel
24 p3576 A83-48950

Heat transfer and flow resistance in the turbulent pipe flow of a fluid with near-critical state parameters
24 p3576 A83-49120

FLOW SEPARATION
U BOUNDARY LAYER SEPARATION
U SEPARATED FLOW
FLOW STABILITY
NT BOUNDARY LAYER STABILITY
NT FLAME STABILITY
NT MAGNETOHYDRODYNAMIC STABILITY
NT WEIBEL INSTABILITY
Performance predictions for confined swirling flows
01 p0045 A83-10663

A model for periodic structures in turbulent boundary layers
01 p0046 A83-10889

Coherent structures and studies of perturbed and unperturbed jets
01 p0046 A83-10894

Jet noise and the effects of jet forcing
01 p0105 A83-10898

Stability of differential rotation in stars
01 p0126 A83-10943

A review and assessment of methods for prediction of the dynamic stability of air cushions
01 p0112 A83-11038

Instability of an extended tangential discontinuity - The first term of the wave-vector expansion
02 p0169 A83-11641

Instability of the three-dimensional distorted stratospheric polar vortex at the onset of the sudden warming
02 p0214 A83-12239

Wave instability in the polar region of Venus
02 p0264 A83-12241

On the stability of almost parallel boundary layer flows
02 p0174 A83-13019

The stability of swirling flows at large Reynolds number when subjected to disturbances with large azimuthal wavenumber
03 p0314 A83-13114

Noise and flow structure of a tone-excited jet
03 p0391 A83-13136

Eigenvalue problems on infinite intervals
03 p0387 A83-13569

Flow instability and turbulence
03 p0317 A83-14454

Coherent structures in free jets
03 p0318 A83-14464

The autonomy of shock waves in a sonic downstream state - The case of detonation
03 p0320 A83-14570

Stability of nonparallel developing flow in an annulus
03 p0323 A83-14698

The influence of buoyancy on the stability of jets --- in extragalactic radio sources
03 p0427 A83-14755

The two-dimensional oscillations of straight vortex filaments with a power-law distribution of vorticity
04 p0474 A83-14948

Nonlinear hydrodynamic stability of some simple rotational flows
04 p0475 A83-14962

Radiative stability of interstellar masers - A variational technique
04 p0549 A83-14990

Stability of flows with discontinuity surfaces
04 p0475 A83-15077

The resonant effect of time-dependent boundary distortion on the stability and secondary regimes of a viscous fluid flow
04 p0477 A83-15879

- Stability problems for inelastic solids with defects and imperfections 04 p0500 A83-16099
- Taylor-Goertler vortices in fully developed or boundary-layer flows Linear theory 04 p0479 A83-16267
- The organized shear layer due to oscillations of a turbulent jet through an axisymmetric cavity 04 p0480 A83-16343
- Unsteady flows about a Joukowski airfoil in the presence of moving vortices [AIAA PAPER 83-0129] 05 p0580 A83-16542
- Modes of shock wave oscillations on spike-tipped bodies [AIAA PAPER 83-0544] 05 p0587 A83-16779
- Motion in the interiors and atmospheres of Jupiter and Saturn - Scale analysis, anelastic equations, barotropic stability criterion 05 p0703 A83-16960
- A unified instability criterion for heterogeneous shear flows 05 p0640 A83-17551
- A non-geostrophic study in a barotropic system 05 p0668 A83-17554
- Instability of a convergent spherical shock wave 05 p0640 A83-17647
- On the thermal and hydrodynamic stability of a fluid in a vertical slot 05 p0641 A83-17722
- Dynamic stabilisation of Rayleigh-Taylor instability 05 p0641 A83-17821
- Parameters controlling the spacing of streamwise vortices on concave walls [AIAA PAPER 83-0380] 05 p0591 A83-17924
- Stability of mean monsoon zonal flow 06 p0792 A83-18991
- The generalized Lagrangian-mean equations and hydrodynamic stability 06 p0757 A83-19014
- Wave-induced longitudinal-vortex instability in shear flows 06 p0757 A83-19015
- Three-dimensional stability of vortex arrays 06 p0758 A83-19022
- Finite-amplitude convection in mixtures with concentration-dependent heat sources 06 p0760 A83-19427
- The stability of flows near an infinite wedge or cone situated in supersonic gas flow 07 p0863 A83-20315
- Formation of turbulence around flow singularities 07 p0927 A83-21341
- On spatial and temporal stability in three dimensional fluid flows 07 p0927 A83-21343
- On certain aspects of three-dimensional instability of parallel flows 07 p0927 A83-21353
- The aerodynamics of flexible membranes 08 p1042 A83-22990
- Finite-amplitude stability of a zonal shear flow 08 p1141 A83-23001
- On the nonlinear stability of slowly varying time-dependent viscous flows 08 p1086 A83-23096
- On the interaction of a sound pulse with the shear layer of an axisymmetric jet. II - Heated jets 09 p1340 A83-23704
- A weakly non-linear theory of barotropic instability 09 p1311 A83-23887
- Classification and stability criteria of separated flows 09 p1259 A83-24010
- The theory of stability of spatially periodic parallel flows 09 p1261 A83-24409
- Non-axisymmetric instability of a rotating layer of fluid 09 p1261 A83-24411
- The stability and disturbance-amplification characteristics of vertical mixed convection flow 09 p1261 A83-24413
- Boundary-layer transition on a rotating cone in still fluid 09 p1262 A83-24417
- Viscous stability of compressible axisymmetric jets 09 p1341 A83-24651
- Fluid mechanics instabilities 09 p1264 A83-25150
- Dynamic instabilities in radiation-heated boiler tubes for solar central receivers [ASME PAPER 82-WA/HT-8] 10 p1445 A83-25692
- Nearfield observations of tones generated from supersonic jet flows [AIAA PAPER 83-0706] 10 p1478 A83-26449
- Local estimates and stability of viscous flows in an exterior domain 10 p1418 A83-26774
- The response of a multistage compressor to an azimuthal distortion 10 p1378 A83-26923
- Prediction of the surge line of axial multistage compressor 10 p1373 A83-26924
- Sound generation by instability waves in a low Mach number jet [AIAA PAPER 83-0661] 11 p1650 A83-28001
- The stability of liquid menisci 11 p1662 A83-28356
- A short look at nonlinear hydrodynamic stability theory 11 p1569 A83-28404
- The stability of certain Riemann ellipsoids --- rotating liquids 11 p1569 A83-28461
- On the self-excited circumferential nonuniformity of a potential fluid flow near a circular cascade of profiles 11 p1569 A83-28534
- Calculation of drag and heat transfer for viscous quasi-stabilized flow of supercritical helium in a pipe 11 p1570 A83-28552
- Single-mode theory of diffusive layers in thermohaline convection 11 p1570 A83-28755
- Axial wavenumber measurements in axisymmetric jets 12 p1696 A83-28974
- Thermal convection instability of liquid metals of magneto-hydrodynamics 12 p1780 A83-29053
- Secondary instability of wall-bounded shear flows 12 p1723 A83-29234
- Stability of two-dimensional hyperbolic initial boundary value problems for explicit and implicit schemes 12 p1772 A83-29647
- Asymptotics of solutions of the Orr-Sommerfeld equation describing unstable oscillations at large Reynolds numbers 13 p1839 A83-30091
- Secondary instability of plane channel flow to subharmonic three-dimensional disturbances 13 p1839 A83-30101
- Effect of rotation on the stability of a bounded cylindrical layer of fluid heated from below 13 p1839 A83-30105
- A theoretical prediction of the fluid buckling frequency 13 p1839 A83-30108
- Compressible Rayleigh-Taylor instability 13 p1840 A83-30111
- Thresholds for the onset of fluid and magnetofluid turbulence 13 p1840 A83-30413
- Experiments on wave number selection in rotating Couette-Taylor flow 13 p1842 A83-30918
- On the loss of stability of detonation waves in long heterogeneous-explosive charges 13 p1843 A83-31372
- Nonstationary phenomena in flows of a viscous reactive fluid 14 p1989 A83-32091
- Contribution of baroclinic mechanism in the formation of the depression during MONEX-79 14 p2056 A83-32404
- Negative viscosity effect in large-scale turbulence Long-wave instability of a periodic system of eddies 14 p2009 A83-32422
- Stability properties of cylindrically curved mean flows --- in atmosphere 14 p2058 A83-32469
- Stability criteria for convection at small Prandtl numbers 14 p2009 A83-32516
- Compressibility effects in turbulent shear layers 14 p2012 A83-32998
- Performance benefits of the direct generation of steam in line-focus solar collectors 15 p2189 A83-33989
- The stability of a rotating fluid cylinder as a figure of equilibrium --- as model for various celestial bodies 15 p2271 A83-34755
- Effect of the Coriolis force and slowly varying flow on the Kelvin-Helmholtz instability 15 p2161 A83-34783
- Instabilities in a stratified fluid having one critical level. I - Results. II - Explanation of gravity wave instabilities using the concept of overreflection. III - Kelvin-Helmholtz instabilities as overreflected waves 16 p2384 A83-35458
- A nonsymmetric equatorial inertial instability 16 p2385 A83-35476
- Barotropic instability of the polar night jet stream 16 p2385 A83-35477
- On symmetric stability and instability of zonal mean flows near the equator 16 p2386 A83-35481
- Theory of waves in the shear flows of an inhomogeneous compressible fluid 16 p2349 A83-35530
- The aerodynamics of hypersonic velocities (On flows with low Mach numbers) 16 p2288 A83-35535
- Kelvin-Helmholtz instability in relativistic mechanics 16 p2427 A83-35715
- A numerical study of the instability of a tangential velocity discontinuity in compressible gases 16 p2350 A83-35716
- Effect of heat transfer augmentation on two-phase flow instabilities in a vertical boiling channel 16 p2350 A83-35800
- On the localized stability of vortices 16 p2290 A83-35819
- Study of instabilities in axial flow compressors 16 p2292 A83-35877
- Unsteady, exponentially-varying standing waves in boundary layers [AIAA PAPER 83-0045] 16 p2351 A83-36041
- The transfer of angular momentum by vortex disturbances during the loss of stability in a plane, axially symmetric shear flow 16 p2392 A83-36872
- Stability of relativistic laminar flow equilibria for electrons drifting in crossed fields 17 p2496 A83-37042
- Subharmonic three-dimensional disturbances [AIAA PAPER 83-1759] 17 p2503 A83-37231
- Stability experiments in rotating-disk flow [AIAA PAPER 83-1760] 17 p2503 A83-37232
- The effect of stochastic modulations on the stability characteristics of hydrodynamic flows --- German thesis 17 p2504 A83-37501
- Forced oscillations of a viscous incompressible fluid in a seminfinite channel 17 p2505 A83-37628
- Turbulence structure in stably stratified open-channel flow 18 p2680 A83-39204
- The linear development of Goertler vortices in growing boundary layers 18 p2680 A83-39205
- On unstable oscillations in a viscous-fluid flow through an infinite channel 18 p2684 A83-39480
- Steady and time-dependent Rayleigh-Benard convection under influence of shear flows 18 p2685 A83-39891
- Two-component Benard convection - Interfacial deformation, oscillatory instabilities and the onset of turbulence 18 p2685 A83-39892
- Morphological and convective instabilities during solidification 18 p2686 A83-39902
- Non-linear systems of a fluid mechanical type and an algebraic model of stability of a stationary flow. I - Theory. II Application 18 p2687 A83-40002
- Bounds on the growth of perturbations to non-parallel steady flow on the barotropic beta plane 18 p2729 A83-40036
- The stability of the elliptically deformed rotation of an ideal incompressible fluid in a Coriolis force field 18 p2687 A83-40079
- Interfacial progressive gravity waves in a two-layer shear flow 18 p2687 A83-40499
- Unsteady aspects of a low mach number jet 18 p2638 A83-40500
- The evolution of large-horizontal-scale disturbances in marginally stable, inviscid, shear flows. I - Derivation of the amplitude evolution equations 19 p2842 A83-41022
- Regimes of mixed convection in a vertical layer whose boundaries undergo unsteady deformation 19 p2842 A83-41205
- Stability of the stationary plane-parallel convective motion of a chemically active medium 19 p2842 A83-41261
- Hydrodynamic instability of axisymmetric flows of an ideal fluid with an interface 19 p2844 A83-41579
- Growth of fluctuations near the Benard-Marangoni convective instability 19 p2845 A83-41997
- Stability of separated flow at a surface with a bend point 19 p2793 A83-42009
- Effect of curvature on the thermal stability of a fluid between two long vertical coaxial cylinders 20 p2973 A83-42682
- Linear stability analysis of heated parallel channels 20 p2981 A83-42768
- Instabilities in the slit-jet flow field 20 p2984 A83-43096
- Instabilities of dynamic thermocapillary liquid layers. I Convective instabilities 20 p2985 A83-43098
- Steady thermocapillary flows and their stability 20 p2986 A83-43270
- A discrete vortex simulation of Kelvin-Helmholtz instability 20 p2987 A83-43453
- Experimental and theoretical investigation of the stability of a linear vortex with a deformed core 20 p2987 A83-43517
- Parametric excitation of electrohydrodynamic surface waves 20 p3051 A83-43671
- Experimentation with turbulent flows experiencing the effects of an adverse pressure gradient [ONERA, TP NO. 1983-36] 21 p3085 A83-44314
- Small-disturbance stability of a non-isothermal tube flow of power law fluids. I - Derivation of the Orr-Sommerfeld equation extended. II - Numerical solution of the problem 21 p3129 A83-44349
- On the instability of internal Alfvén-gravity waves in stratified shear flows 21 p3171 A83-44469
- A universal Strouhal law 21 p3130 A83-44538
- A critical layer dominated by non-parallel effects in a rotating barotropic flow 21 p3132 A83-44940
- Spatial amplification and Squire's theorem 21 p3132 A83-44946
- Wave propagation, instability, and breakdown of vortices 22 p3280 A83-45904
- Structure and stability of streets of finite vortices 22 p3280 A83-45909
- Zigzag instability and axisymmetric rolls in Rayleigh-Benard convection - The effects of curvature 22 p3280 A83-45939
- Turbulence modulated by a coherent shear wave in a wall boundary layer 22 p3282 A83-46431
- Vortices, stability, and turbulence 22 p3285 A83-46718
- Oscillatory bifurcations in singular perturbation theory. I Slow oscillations. II - Fast oscillations 22 p3353 A83-46921

- Supersonic stabilization of a tangential shear in a thin atmosphere 22 p3285 A83-46938
- Stabilization of tangential shear instability in shallow water with 'supersonic' fluid flow 22 p3285 A83-46939
- Recent developments in surface-tension driven instabilities [IAF PAPER 83-144] 23 p3446 A83-47289
- Finite amplitude evolution of mixing layers in the presence of solid boundaries 23 p3449 A83-48043
- The evolution of a nonlinear wave train on the background of a stratified shear flow that is losing stability 23 p3451 A83-48557
- Characteristic lengths in the wavy vortex state of Taylor-Couette flow 24 p3576 A83-48920
- Experimental evidence of intermittencies associated with a subharmonic bifurcation --- in Rayleigh-Benard hydrodynamic instability 24 p3577 A83-49296
- Spinning modes on axisymmetric jets. I 24 p3578 A83-49469
- The stability of the flows of a homogeneous atmosphere of finite thickness 24 p3673 A83-49529
- Instabilities of a cylindrical liquid sheet in the presence of two gaseous flows 24 p3578 A83-49647
- An approach to estimating spectral energy transfer due to nonlinear interactions --- during transition to turbulence of two-dimensional wake 24 p3580 A83-49829
- Three dimensional disturbances propagated from a tunnel side wall to a mixing layer 24 p3580 A83-49831
- Propagation of finite amplitude disturbances in the weakly non-parallel boundary layer 24 p3580 A83-49832
- Variational formulation for the equilibrium condition of a conducting fluid in an electric field 24 p3624 A83-50195
- FLOW THEORY**
- NT MIXING LENGTH FLOW THEORY**
- Load distribution on deformed wings in supersonic flow 01 p0002 A83-10180
- A theoretical model for coherent structures in wall turbulence 03 p0319 A83-14478
- The theory of rotating and oscillating blade rows in a subsonic flow through an annular channel 03 p0279 A83-14492
- Momentum theory, dynamic inflow, and the vortex-ring state 04 p0443 A83-16026
- A diffusion equation illustrating spectral theory for boundary layer stability [AD-A123209] 04 p0479 A83-16182
- Taylor-Görtler vortices in fully developed or boundary-layer flows Linear theory 04 p0479 A83-16267
- On the disputes about open separation --- in three dimensional flow [AIAA PAPER 83-0296] 05 p0634 A83-16636
- Some applications of a generalized aerodynamic forces and moments theory [AIAA PAPER 83-0543] 05 p0587 A83-16778
- Investigation of unsteady flow problems 05 p0638 A83-16897
- A unified instability criterion for heterogeneous shear flows 05 p0640 A83-17551
- Heat transfer - A review of 1981 literature 05 p0682 A83-17701
- Existence and uniqueness of shock-free transonic flow past symmetrical thin wings at zero incidence 05 p0590 A83-17847
- A new theory of the energy spectrum --- in viscous boundary layer shear flow 06 p0756 A83-18056
- On the theory of compressible fluids 06 p0756 A83-18071
- On the swirling flow between rotating coaxial disks - Existence and nonuniqueness 06 p0757 A83-18824
- Nonlinear analysis of cavity flows around arbitrarily shaped bluff bodies in a constrained flow 06 p0758 A83-19020
- A two-scale semiempirical theory for turbulent boundary layers and jets 06 p0760 A83-19428
- On numerical methods of subsonic lifting surface theory 07 p0864 A83-21012
- A note on the logarithmic velocity profile in turbulent boundary layers 08 p1083 A83-21895
- An asymptotic study of the macroscopic behavior of a mixture of two viscous fluids 08 p1085 A83-22770
- A semi analytic method for viscous flows in the vicinity of singular corners 08 p1090 A83-23213
- On a deferred-correction procedure for determination of central-difference solutions to the Navier-Stokes equations 08 p1090 A83-23214
- The theory of stability of spatially periodic parallel flows 09 p1261 A83-24409
- The evolution of Tollmien-Schlichting waves near a leading edge 09 p1261 A83-24410
- Non-axisymmetric instability of a rotating layer of fluid 09 p1261 A83-24411

- Steady three-dimensional convection at high Prandtl numbers 09 p1261 A83-24412
- The rotational motions of compressible fluids. II 09 p1262 A83-24501
- Adiabatic shearing of incompressible fluids with temperature-dependent viscosity 10 p1414 A83-25873
- Flame spread in an opposed flow with a linear velocity gradient 10 p1390 A83-25897
- Some fundamental aspects of shock wave-turbulent boundary interactions in transonic flow 10 p1371 A83-26145
- Stability limits and transition times of wave-induced wall boundary layers 10 p1415 A83-26151
- Boundary layer influenced shock structure 10 p1415 A83-26154
- Microscopic structure of the Mach-type reflection of weak shock waves 10 p1415 A83-26156
- Admissibility criteria for propagating phase boundaries in a van der Waals fluid 10 p1490 A83-26773
- Local estimates and stability of viscous flows in an exterior domain 10 p1418 A83-26774
- A study of irregular-shaped particle deposition in turbulent flows and application to gas turbines 11 p1525 A83-27480
- On the application of linearized theory to multi-element aerofoils. I - Tandem flat plate aerofoils 11 p1526 A83-27874
- Evaluation of a stochastic model of particle dispersion in a turbulent round jet 11 p1568 A83-28104
- On one characteristic internal scale of turbulent diffusion 11 p1665 A83-28113
- Spatial Fourier modes controlling Navier-Stokes flow 11 p1568 A83-28236
- A short look at nonlinear hydrodynamic stability theory 11 p1569 A83-28404
- An application of the modified zero-fourth-cumulant approximation to homogeneous axisymmetric Boussinesq turbulence 12 p1722 A83-29006
- Compressible Rayleigh-Taylor instability 13 p1840 A83-30111
- Contribution to the spectral study of slightly inhomogeneous and anisotropic turbulent flows --- French thesis 13 p1840 A83-30130
- Fundamentals of flight --- Book 13 p1803 A83-30152
- Thresholds for the onset of fluid and magnetofluid turbulence 13 p1840 A83-30413
- Multiscale model equations for turbulent convection and convective overshoot --- relevant to study of solar or stellar evolution 13 p1952 A83-31432
- Unsteady transonic small disturbance approximation with strong shock waves 14 p1972 A83-32995
- Second approximation of quadrupole wing theory in lifting surface theory 14 p1972 A83-33004
- Remarks on the evolution of methods of calculation for propellers and rotors [AAAF PAPER NT 82-03] 14 p1972 A83-33161
- A theoretical model of the coherent structure of the turbulent boundary layer in zero pressure gradient 15 p2155 A83-33656
- Application of the triple-deck theory of viscous-inviscid interaction to bodies of revolution 16 p2288 A83-35345
- Unsteady, exponentially-varying standing waves in boundary layers [AIAA PAPER 83-0045] 16 p2351 A83-36041
- Constraints on the invariant functions of axisymmetric turbulence 16 p2351 A83-36083
- The correct use of dimensional analysis [ONERA, TP NO. 1983-2] 16 p2402 A83-36417
- Interactions of isolated vortices. II - Modon generation by monopole collision 16 p2353 A83-36546
- Irrational flow within boundary layer and wake 16 p2354 A83-36979
- Boundary layers on characteristic surfaces for time-dependent rotating flows 17 p2504 A83-37377
- Some remarks on transonic potential flow theory 17 p2504 A83-37380
- Amplitude-dependent stability of boundary-layer flow with a strongly non-linear critical layer 17 p2509 A83-38924
- The linear development of Goertler vortices in growing boundary layers 18 p2680 A83-39205
- The breaking of axisymmetric slender liquid bridges 18 p2680 A83-39206
- A streamline coordinate system for distorted two-dimensional shear flows 18 p2680 A83-39208
- Steady reflection, absorption and transmission of small disturbances by a screen of dusty gas 18 p2680 A83-39209
- Interacting flow theory and trailing edge separation - No stall 18 p2633 A83-39214
- Application of Padeapproximation to turbulence problem 18 p2686 A83-39919

- Helical structures, fractal dimensions and renormalization-group approach in homogeneous turbulence 19 p2842 A83-41167
- Incompressible fluid mechanics --- French book 20 p2969 A83-42172
- A second-order turbulence model for two-phase flows 20 p2983 A83-43011
- A theory for flow separation 20 p2985 A83-43099
- Low-Reynolds-number flow past a cylindrical body 20 p2985 A83-43103
- A view of the triple deck --- low speed boundary layer theory 20 p2930 A83-43120
- Generation of a countable set of homoclinic flows through bifurcation 20 p3043 A83-43564
- A self-similar flow behind an exponential shock with radiative heat flux. II 20 p3076 A83-43659
- Fingers in a Hele-Shaw cell with surface tension 21 p3127 A83-43926
- Some recent progress in the analysis of transonic internal flows 21 p3085 A83-44019
- Local similarity solution of the Tricomi equation in the elliptic coordinates 21 p3197 A83-44021
- Application of unsteady laminar triple-deck theory to viscous-inviscid interactions from an oscillating flap in supersonic and subsonic flow 21 p3086 A83-44457
- Unified unsteady supersonic/hypersonic theory of flow past double wedge airfoils 21 p3086 A83-44465
- Weakly contracting systems and attractors of the Galerkin approximations of the Navier-Stokes equations on the two-dimensional toroid 21 p3130 A83-44657
- Effects of variable fluid properties and boundary conditions on thermal convection 21 p3131 A83-44854
- Eigenvalues of the Orr-Sommerfeld equation in an unbounded domain 21 p3132 A83-44938
- A method of obtaining three-dimensional spectra in a homogeneous turbulence --- French thesis 21 p3133 A83-45084
- The flapping motion of a turbulent plane jet - A workable relationship to wave-guide theory 22 p3283 A83-46453
- Considerations on the transport-theorem for extensive flow properties 22 p3284 A83-46476
- What can be achieved by similarity laws? --- for fluid dynamics 22 p3284 A83-46481
- A theory of weak shocks 22 p3287 A83-47095
- A theory of rotating stall of multistage axial compressors. III - Limit cycles [ASME PAPER 83-GT-46] 23 p3394 A83-47906
- Introduction to two-dimensional turbulence 23 p3448 A83-48038
- The well-posedness of two-dimensional ideal flow 23 p3449 A83-48047
- The influence of two-dimensional turbulence on diffusion 23 p3449 A83-48049
- Progress in calculation of the interaction between a perfect fluid and a viscous fluid [ONERA, TP NO. 1983-61] 23 p3398 A83-48182
- Steady wall flows in the light of the generalized Karman theory 23 p3451 A83-48538
- Theory for saturation stress difference in torsion versus other types of deformation at low temperatures 23 p3473 A83-48601
- The basic aerodynamics of floatation 23 p3453 A83-48679
- Comments on the theory of local interaction in a rarefied gas 24 p3543 A83-48926
- Overnormalized theory of hydrodynamic turbulence 24 p3624 A83-49536
- The multiple scales concept for modelling turbulent flows. II - Reynolds stresses and turbulent fluxes of a passive scalar contaminant, algebraic modelling, and a simplified model using the Boussinesq hypothesis 24 p3578 A83-49646
- Instabilities of a cylindrical liquid sheet in the presence of two gaseous flows 24 p3578 A83-49647
- Transition prediction based on a differential field theory of turbulence 24 p3580 A83-49830
- Fractional analysis of Reynolds stress distribution in complex shear flows 24 p3581 A83-50127
- Flow of a dipolar fluid due to suddenly accelerated flat plate 24 p3581 A83-50149
- FLOW VELOCITY**
- NT SOLAR WIND VELOCITY**
- Velocity distribution due to thermal Marangoni effect in a liquid column 01 p0044 A83-10123
- Application of the Carafoli method to the supersonic flow around a cruciform wing 01 p0003 A83-10581
- Measurements in shear layers in transonic flows with a laser transit anemometer 01 p0003 A83-10697
- A comparison of characteristic features of coherent turbulent structures found using the Variable Interval Time Average (VITA) technique and using the pattern recognition technique 01 p0046 A83-10895

A half-wing near a wall at high angles of attack in a pulsed flow
[AAAF PAPER NT 81-12] 02 p0132 A83-11773

Stability of erythrocyte suspensions layered on stationary and flowing liquids 02 p0169 A83-11840

Correlations between temperature and velocity fluctuations in the wall region of turbulent flow 02 p0170 A83-11869

An exact solution to the problem of diffusion in a periodic velocity field and turbulent diffusion 02 p0170 A83-11954

Determination of return-flow velocity in the case of the orientation of the geomagnetic dipole along the nondisturbed velocity of the solar wind 02 p0208 A83-12419

Thermal Marangoni convection in a floating zone. Microgravity experiment during the TEXUS 11lb rocket flight 02 p0138 A83-12995

The velocity field induced by a helical vortex filament 03 p0277 A83-13113

Direct measurement of laser velocimeter bias errors in a turbulent flow 03 p0323 A83-13139

Use of breakdown coefficients in turbulent jets to determine the universal exponent μ 03 p0363 A83-13273

The influence of Reynolds number on characteristics of turbulent boundary layers 03 p0318 A83-14461

On the spreading of a turbulent spot in the absence of a pressure gradient 03 p0321 A83-14578

Comparison of conditional sampling and averaging techniques in a turbulent boundary layer 03 p0321 A83-14583

Stability of nonparallel developing flow in an annulus 03 p0323 A83-14698

Experimental study of the large-scale structure of inhomogeneous turbulence 04 p0475 A83-15079

A model for the backflow mean velocity profile 04 p0476 A83-15295

Simultaneous measurement of stagnation temperature and specific flow rate in a hypersonic gas flow 04 p0481 A83-15447

The role of orderly structures in the vorticity balance of the turbulent velocity fields of unrestricted shear flows 04 p0443 A83-15921

A study of the efficiency of a gas screen on a rough surface 04 p0478 A83-16162

Distortion of turbulence in flows with parallel streamlines 04 p0479 A83-16263

Using single-point velocity probability distributions for characterizing turbulent flows 04 p0480 A83-16391

The use of the method of generalized self-similarity for computing turbulent boundary layers 04 p0480 A83-16392

Measurements of the near wake of an airfoil in unsteady flow
[AIAA PAPER 83-0127] 05 p0580 A83-16540

Five-hole pitot probe time-mean velocity measurements in confined swirling flows
[AIAA PAPER 83-0315] 05 p0634 A83-16645

Confined swirling flow predictions
[AIAA PAPER 83-0316] 05 p0634 A83-16646

Fully controllable heat pipe containing a short electro-osmotic pumping section
[AIAA PAPER 83-0317] 05 p0634 A83-16647

Effect of inserts on the shaping of fine-particle conveying flows in cylindrical nozzles 05 p0639 A83-17409

On velocity correlations in homogeneous isotropic turbulence 06 p0756 A83-18073

Boundary-layer development on circular cylinders 06 p0756 A83-18235

Time-dependent solutions of multimode convection equations 06 p0757 A83-19018

Instantaneous two-component laser anemometry and temperature measurements in a complex flow model combustor
[AIAA PAPER 83-0334] 06 p0765 A83-19587

A note on the specification of freestream velocity in the calculation of the boundary layer flow around bodies of revolution at incidence 07 p0862 A83-19665

A new multifold series general solution of the steady, laminar boundary layers. I - Theory of the multifold series expansion. II - Application theory of the Euler transformation 07 p0925 A83-20278

Response of parallel-flow and counterflow heat exchangers to sinusoidal flow rate changes of large amplitude 07 p0925 A83-20290

A class of exact solutions of the Navier-Stokes equations - Plane unsteady flow 07 p0927 A83-21171

Formation of turbulence around flow singularities 07 p0927 A83-21341

A note on the logarithmic velocity profile in turbulent boundary layers 08 p1083 A83-21895

Experimental determination of one-dimensional spectra in high-speed boundary layers 08 p1084 A83-22379

Structures and flow reversal in turbulent plane jets 08 p1085 A83-22383

Potential flow around a thin oblate body of revolution 08 p1085 A83-22743

Prediction of turbulent fields, including fluctuating velocities correlations and approximate spectra, by means of a simplified second-order closure scheme - The round free jet and developed pipe flow 08 p1088 A83-23186

Prediction of developing turbulent flow by the finite element method 08 p1088 A83-23189

A yawmeter for steady and low-frequency unsteady flows 08 p1106 A83-23296

Flow patterns in semiclosed cavities of spindle-operated valves and the valve flow rates 09 p1258 A83-23428

The aerodynamic properties of the DISA nozzle unit for calibrating and testing hot-wire probes, in particular multiple sensor probes at moderate velocities 09 p1267 A83-23700

On the changes in the structure of steady plane flames as their speed increases 09 p1225 A83-23747

An experimental study of the mixing of countertwisted turbulent jets in the initial section of an annular duct 09 p1260 A83-24228

Experimental and theoretical investigation of backward-facing step flow 09 p1262 A83-24420

The supersonic combustion around a truncated cone 09 p1198 A83-24504

On the calculation of the velocity induced by a vortex-source cone 09 p1198 A83-25024

Flame spread in an opposed flow with a linear velocity gradient 10 p1390 A83-25897

Turbulent static pressure fluctuations away from flow boundaries
[AIAA PAPER 83-0754] 10 p1420 A83-25952

An application of the molecular beam time-of-flight technique to measurements of thermal boundary layer effects on mass sampling from a shock tube 10 p1371 A83-26134

Measurement and calculation of shock attenuation in a channel with perforated walls 10 p1414 A83-26141

Heating-rate measurements over 30 deg and 40 deg /half-angle/ blunt cones in air and helium in the Langley expansion tube facility 10 p1371 A83-26146

Measurement of instantaneous flow rate through estimation of velocity profiles 10 p1417 A83-26268

Estimation and correction of advection effects with single and multiple, conventional and Doppler radars 11 p1630 A83-27071

Complementary use of a tri-axial hot film probe and a five hole pitot tube to determine vehicle wake characteristics 11 p1571 A83-27416

Film flow of a liquid on a convergent-nozzle surface 11 p1568 A83-28372

On the self-excited circumferential nonuniformity of a potential fluid flow near a circular cascade of profiles 11 p1569 A83-28534

Fast motions of a gas in a porous medium 11 p1569 A83-28539

Laser velocimetry - Problems and opportunities 12 p1727 A83-28831

Laser anemometer using a Fabry-Perot interferometer for measuring mean velocity and turbulence intensity along the optical axis in turbomachinery 12 p1727 A83-28834

Nonlinear resonant interactions in internal cavity flows 12 p1721 A83-28972

Hydrodynamic fluctuation due to the discontinuity of flow impedance 12 p1721 A83-29001

The velocity perturbations above the orifice of an acoustically excited cavity in grazing flow 12 p1777 A83-29235

The method of successive approximations in the problem of a boundary layer with longitudinal and transverse pressure differentials 12 p1723 A83-29284

The use of turning disk electrode 12 p1723 A83-29380

Spatial periodicity of the longitudinal gradient of the average static pressure in a pulsed turbulent flow 12 p1723 A83-29381

A numerical study of the two-dimensional Navier-Stokes equations in vorticity-velocity variables 12 p1725 A83-29639

Velocity measurements in an axisymmetric laminar flow using an optical technique of visualization in coherent light 12 p1726 A83-29704

Hydrodynamics and heat transfer in turbulent zero-momentum wakes 13 p1838 A83-30046

Velocity and length scales in turbulent flows - A review of approaches 13 p1841 A83-30633

Excitation of circular flow of a fluid by a rotating velocity field 13 p1842 A83-30909

Peculiarities in measuring the velocity vector using a laser anemometer in flow through axisymmetric models 13 p1848 A83-31470

A determination of microturbulent velocity on the basis of Fe I Fraunhofer lines -- for solar photospheric motions 14 p2113 A83-31833

Investigation of the simultaneous variable solution for velocity and pressure in incompressible fluid flow problems
[AIAA PAPER 83-1519] 14 p2010 A83-32752

Flow film boiling from submerged bodies
[AIAA PAPER 83-1529] 14 p2011 A83-32760

Solutions to the boundary value problem with velocity correlations in stratified flow through circular pipe. I 14 p2012 A83-32968

The structure of a turbulent wake behind a cruciform circular cylinder. I - The mean velocity field 14 p2013 A83-33091

A novel property of the displacement thickness in three-dimensional boundary-layer theory 14 p2013 A83-33381

A dynamical and visual study on the oscillatory turbulent boundary layer 15 p2154 A83-33653

Dynamics of an unsteady turbulent boundary layer 15 p2154 A83-33654

Critical flashing flows in nozzles with subcooled inlet conditions 15 p2157 A83-33996

On the use of adaptive grids in numerically calculating adiabatic flame speeds 15 p2132 A83-34032

Toward the formulation of a global local equilibrium kinetics model for laminar hydrocarbon flames 15 p2132 A83-34035

Assessment of two computational procedures for spray combustors 15 p2160 A83-34255

Effect of the Coriolis force and slowly varying flow on the Kelvin-Helmholtz instability 15 p2161 A83-34783

Solution of the equations of an unsteady boundary layer 16 p2349 A83-35533

The aerodynamics of hypersonic velocities (On flows with low Mach numbers) 16 p2288 A83-35535

A numerical study of the instability of a tangential velocity discontinuity in compressible gases 16 p2350 A83-35716

A model of axial impeller stall 16 p2292 A83-35878

Influence of laminar flame speed on the blowoff velocity of bluff-body stabilized flames
[AIAA PAPER 83-1327] 16 p2326 A83-36341

Mesoturbulence --- in solar photosphere 16 p2440 A83-36852

Glow discharge in a fast longitudinal gas flow 16 p2418 A83-36939

Investigations of particle-grid turbulence 16 p2354 A83-36957

The detailed processes involved in flame spread over solid fuels 17 p2484 A83-37044

Correlating downward flame spread rates for thick fuel beds 17 p2484 A83-37045

On 'saddle-backed' velocity distributions in a three-dimensional turbulent free jet
[AIAA PAPER 83-1677] 17 p2444 A83-37185

Microscales and correlation tensors in the viscous turbulent sublayer 17 p2504 A83-37391

A version of a single-beam laser time-of-flight method for measuring flight velocity 17 p2510 A83-37642

A supersonic velocity field in the region of interference between a wing and a body having a common apex 17 p2451 A83-37802

A numerical study of slow nonisothermal flows past axisymmetrical bodies 17 p2506 A83-37805

Some remarks on the selection of sensors for correlation velocity measurement systems 17 p2512 A83-38534

A flow analysis procedure based on velocity potentials
[AIAA PAPER 83-1818] 17 p2508 A83-38650

The structure of a separating turbulent boundary layer. V Frequency effects on periodic unsteady free-stream flows 18 p2681 A83-39217

Similar velocity profiles of the compressible boundary layer over a rotating cylinder in an axial flow 18 p2681 A83-39349

A study on the fluctuation concentration field in a turbulent jet 18 p2687 A83-40336

The hydrodynamic structure of accelerating turbulent boundary layers 19 p2842 A83-41252

On an approximate solution to the problem of unsteady flow around two-dimensional and axisymmetric bodies moving at high variable velocity 19 p2792 A83-41886

A class of exact solutions of the laminar-boundary-layer equations 19 p2845 A83-41892

Measurement of the velocity of a three-dimensional flow by hot-wire anemometers 19 p2850 A83-42017

Calculation of the flow rate characteristic of a jet-throttling hydraulic distributor with allowance for the ejection properties of a tube-plate system 19 p2799 A83-42128

Velocity measurements in a turbulent natural convection boundary layer 20 p2973 A83-42684

- Tests of subgrid models in the near-wall region using represented velocity fields 20 p2985 A83-43101
- Experiments on flow through one to four inlets of the orifice and Borda type 20 p2986 A83-43235
- Velocities of ejection of comets by Jupiter and Saturn 20 p3061 A83-43414
- Statistical characteristics of turbulent bursts 20 p2987 A83-43514
- Kinematics of velocity and vorticity correlations in turbulent flow 21 p3128 A83-43929
- Spectral relationships between velocity and temperature fluctuations in turbulent shear flows 21 p3128 A83-43932
- Real-time measurements of spatial velocity distribution with a laser Doppler imaging system 21 p3136 A83-44151
- A method of streamline curvature for calculating transonic velocities in turbomachinery 21 p3087 A83-44557
- Computation of turbulent flow through constrictions 21 p3130 A83-44588
- Velocity measurements in a confined swirl driven recirculating flow 21 p3131 A83-44682
- White-light speckle method for obtaining an equi-velocity map of a whole flow field 21 p3138 A83-44683
- Velocity-pressure gradient correlation in reactive turbulent flows 21 p3132 A83-44999
- Molecular velocity distribution functions in an argon normal shock wave at Mach number 7 22 p3366 A83-46008
- Response of variations of free stream velocity on inviscid and incompressible flow past a wavy plate 22 p3281 A83-46393
- Unsteady Kutta condition of a plunging airfoil 22 p3248 A83-46438
- Measured velocity fluctuations inside the mixing layer of a supersonic jet 22 p3249 A83-46468
- Extinction of premixed flames in a stagnation flow considering general Lewis number 22 p3267 A83-46763
- Experimental study of the boundary layer on a turbomachinery rotor blade 22 p3250 A83-47022
- Asymmetries in Stokes profiles of magnetic lines - A linear analysis in terms of velocity gradients --- in solar atmosphere active regions 23 p3536 A83-47720
- Three-dimensional flow measurements in a turbine scroll [ASME PAPER 83-GT-128] 23 p3396 A83-47957
- Local heat transfer rates from two adjacent spheres in turbulent flow 23 p3451 A83-48624
- Correlation of pulsational velocities of the dispersed phase in jet flows 23 p3452 A83-48657
- Proposal for the measuring molecular velocity vector with single-pulse coherent Raman spectroscopy 23 p3459 A83-48709
- Effect of wall scattering on SNR in off-axis differential-type laser Doppler velocimetry 24 p3581 A83-48747
- Two focus laser velocimeter applied to measurements in an experimental centrifugal compressor [ONERA, TP NO. 1983-113] 24 p3583 A83-49424
- New applications of laser velocimetry in ONERA wind-tunnels [ONERA, TP NO. 1983-114] 24 p3550 A83-49425
- Investigation of the jet parameters of a source of accelerated gas flow for an aerodynamic test facility 24 p3545 A83-49659
- On the development of turbulent boundary layer in open channel flows 24 p3579 A83-49804
- Strong adverse pressure gradient effects on supersonic turbulent boundary layer 24 p3545 A83-49806
- Turbulence-induced statistical bias in laser anemometry 24 p3584 A83-49811
- Measurement of velocity-temperature correlations of different orders in hot turbulent flows 24 p3584 A83-49814
- Advanced techniques for transverse vorticity measurements 24 p3584 A83-49816
- FLOW VISUALIZATION**
- NT NUMERICAL FLOW VISUALIZATION**
- Flow visualization reveals causes of Shuttle nonlinear aerodynamics 01 p0002 A83-10181
- Structure of air flow separation over wind wave crests 01 p0075 A83-10725
- The role of coherent structures in modelling turbulence and mixing; Proceedings of the International Conference, Madrid, Spain, June 25-27, 1980 01 p0045 A83-10884
- Experimental methods in turbulent structure research 01 p0046 A83-10891
- Investigations of eddy coherence in jet flows 01 p0003 A83-10892
- Initiation, evolution and global consequences of coherent structures in turbulent shear flows 01 p0046 A83-10893
- Flow visualization in natural convection 01 p0052 A83-11070
- Quantitative interpretation of flow visualizations coupling video technics and microcomputer 01 p0052 A83-11071
- Flow visualization and data analysis of self-sustained shock oscillations on a spiked body at Mach 3 01 p0003 A83-11072
- Flow visualization study in low specific speed pump impeller passages 01 p0053 A83-11073
- The water tunnel - A helpful simulation facility for the aircraft industry 01 p0014 A83-11080
- Measurements and visualizations of unsteady flow /low speed/ [AAAF PAPER NT 81-14] 02 p0176 A83-11774
- The use of forced Rayleigh scattering to study laminar and turbulent flows 02 p0169 A83-11855
- A synthesis and model of turbulence structure in the wall region 03 p0317 A83-14456
- Visualizations of turbulent structures of wakes and boundary layers 03 p0319 A83-14481
- Visualization study of the axisymmetric mixing layer of a high Reynolds number jet 03 p0320 A83-14482
- Applications of flow visualization techniques in aerodynamics [ONERA, TP NO. 1982-68] 03 p0330 A83-14528
- Comparison of conditional sampling and averaging techniques in a turbulent boundary layer 03 p0321 A83-14583
- On the flow field around a Savonius rotor 04 p0505 A83-15798
- Modification of vortex shedding in the synchronization range [ASME PAPER 81-WA/FE-25] 04 p0478 A83-16142
- Mechanisms of inlet-vortex formation 04 p0479 A83-16260
- Oscillations of an unstable mixing layer impinging upon an edge 04 p0479 A83-16264
- Experimental evaluation of shockless supercritical airfoils in cascade [AIAA PAPER 83-0003] 05 p0577 A83-16455
- Experimental study of a four-jet impingement flow using visualization techniques --- with applications to high performance VTOL aircraft [AIAA PAPER 83-0171] 05 p0633 A83-16568
- Flow visualization in combustion gases using planar laser-induced fluorescence [AIAA PAPER 83-0405] 05 p0643 A83-16694
- Chemically reacting turbulent shear layers [AIAA PAPER 83-0475] 05 p0636 A83-16739
- Flow visualization studies of bodies with square cross sections [AIAA PAPER 83-0563] 05 p0637 A83-16791
- Visualization studies of turbulent transition flows in a porous medium [AIAA PAPER 83-0654] 05 p0638 A83-16819
- Water tunnel construction for continuous mode flow visualization [AIAA PAPER 83-0657] 05 p0599 A83-16821
- Holographic interferometry by a non-silver film process 05 p0645 A83-17320
- Visualization of heat transfer from arrays of impinging jets 05 p0640 A83-17702
- Examination of the two-flux model for radiative transfer in particular systems 05 p0641 A83-17705
- Quantitative measurement of density and velocity in compressible flows using laser-induced iodine fluorescence [AIAA PAPER 83-0049] 05 p0646 A83-17903
- Smoke visualization in wind tunnels 06 p0763 A83-18813
- A new surface-streamline flow-visualization technique 06 p0763 A83-19016
- Turbulence and waves in a rotating tank [AD-A128174] 06 p0758 A83-19024
- A laser anemometer seeding technique for combustion flows with multiple stream injection 07 p0928 A83-19843
- An experimental investigation of turbulent wake behind 'S'-shaped profiles 07 p0926 A83-20502
- An improved schlieren system and some new results on acoustically excited jets 08 p1162 A83-21806
- Flow visualization methods for separated three-dimensional shock wave/turbulent boundary-layer interactions 08 p1042 A83-22136
- Structures and flow reversal in turbulent plane jets 08 p1085 A83-22383
- Instantaneous pressure fields at a corner associated with vortex impingement 08 p1086 A83-23092
- Flow-excited resonances in covered cavities 09 p1340 A83-23339
- The new hydrodynamic visualization laboratory of the aerodynamics division 09 p1210 A83-23676
- Flow disturbance induced by the DISA triaxial hot-wire probe 55P91 09 p1267 A83-23699
- An experimental investigation of the factors governing the dynamic structure and intensity of atmospheric vortices 09 p1313 A83-23969
- Hydrodynamic visualization of the flow in a model of an axial flow turbomachine 09 p1261 A83-24336
- Moire deflectometry with deferred analysis 09 p1269 A83-24442
- Visualization of multijet impingement flow 09 p1198 A83-24652
- Formation of streamwise vortices in the flow past a corner 10 p1371 A83-25569
- Observation of streamwise rotation in the near-wall region of a turbulent boundary layer 10 p1414 A83-25782
- Acoustic imaging for diagnostics of chemically reacting systems [AIAA PAPER 83-0761] 10 p1476 A83-25955
- The boundary layer behind a shock wave incident on a leading edge 10 p1372 A83-26148
- Determination of shock tube boundary layer parameter utilizing flow marking 10 p1415 A83-26150
- 1 MHz bandwidth, real-time Schlieren techniques in a linear transonic cascade 10 p1422 A83-26419
- Three dimensional holographic flow visualization 10 p1422 A83-26420
- Optical methods for performance evaluation of two-dimensional transonic turbine profiles in steam 10 p1422 A83-26421
- Visualization studies of a shear driven three-dimensional recirculating flow 11 p1565 A83-27411
- The development of detached shock waves in gas-solid suspension flow 11 p1566 A83-27483
- LIF and chemiluminescence methods for the flow diagnostics of supersonic mixing chemical lasers --- laser induced fluorescence 11 p1580 A83-27581
- Development of finite-amplitude disturbances in a Poiseuille flow 11 p1566 A83-27706
- Experimental study of the motion of rising vortex rings 11 p1569 A83-28533
- Optically recording interferometer for velocity measurements with subnanosecond resolution 11 p1575 A83-28706
- A study of flow in a short cavity with one-way fluid inlet and outlet 11 p1570 A83-28794
- Velocity measurements in an axisymmetric laminar flow using an optical technique of visualization in coherent light 12 p1726 A83-29704
- Periodic and irregular convective self-oscillations in an ellipsoid 13 p1843 A83-31343
- Digital image processing of flow visualization photographs 14 p2020 A83-32906
- Turbulent spots, wave packets, and growth 14 p2013 A83-33378
- A dynamical and visual study on the oscillatory turbulent boundary layer 15 p2154 A83-33653
- Aerosol formation in a mixing layer --- for flow visualization 15 p2163 A83-33660
- Laser generated smoke for fluid flow visualization 15 p2164 A83-33997
- The characteristics of low-speed streaks in the near-wall region of a turbulent boundary layer 16 p2348 A83-35336
- Experimental study of the interaction of thermals 16 p2349 A83-35529
- On the investigation of axisymmetric discontinuous flows using interferometry 16 p2349 A83-35538
- Thrust reverser exhaust plume reingestion tests for a STOL fighter model [AIAA PAPER 83-1229] 16 p2307 A83-36293
- New flows in a circular Couette system with co-rotating cylinders 17 p2501 A83-37028
- A visualization study of wakes at large distances from the wing 17 p2511 A83-37809
- A study of the concentration field of a round jet by a quantitative visualization method 17 p2507 A83-38065
- Particle sizing in two-phase flows from scattered laser power spectra and laser attenuation 17 p2511 A83-38205
- Coordinate system control - Adaptive meshes 17 p2573 A83-38787
- High-speed laser visualization of detonation-sprayed particles 18 p2688 A83-39172
- An update on non-stationary oblique shock-wave reflections Actual isopycnics and numerical experiments 18 p2681 A83-39212
- A sounding rocket experiment on the Marangoni convection 18 p2644 A83-39912
- New method for visualizing temperature distributions using thermochromism 18 p2689 A83-39918
- Supersonic-nitrogen flow-field measurements with the resonant Doppler velocimeter 18 p2689 A83-40054
- An experimental study of the transformation of a free spherical volume of a light gas to a vortex ring 19 p2843 A83-41273

Laser anemometry velocity measurements in a heated turbulent flow 19 p2843 A83-41322
Computational interferometric description of nested flow fields 20 p2988 A83-42527
Flow visualization investigation of choking cascade turns 20 p2989 A83-42564
Visualization of heat transfer 20 p2970 A83-42654
Speckle velocimetry study of vortex pairing in a low-Re unexcited jet 21 p3128 A83-43928
Flow characteristics in the curved rectangular channels Visualization of secondary flow 21 p3129 A83-44064
Real-time measurements of spatial velocity distribution with a laser Doppler imaging system 21 p3136 A83-44151
Processing of infrared thermal images for aerodynamic research [ONERA, TP NO. 1983-32] 21 p3137 A83-44310
Visualization of three-dimensional vortex flows [ONERA, TP NO. 1983-34] 21 p3085 A83-44312
A technique for evaluation of three-dimensional behavior in turbulent boundary layers using computer augmented hydrogen bubble-wire flow visualization 21 p3131 A83-44679
White-light speckle method for obtaining an equi-velocity map of a whole flow field 21 p3138 A83-44683
Hybrid processing for phase measurement in metrology and flow diagnostics 22 p3294 A83-46837
The mixing layer - An example of quasi two-dimensional turbulence 23 p3448 A83-48042
Hydrodynamic visualization of the flow phenomena characterizing air intakes [ONERA, TP NO. 1983-103] 24 p3583 A83-49414
Flow visualization by light sheet [ONERA, TP NO. 1983-105] 24 p3583 A83-49416
The use of coloured smoke to visualize secondary flows in a turbine-blade cascade 24 p3545 A83-49466
Visualization of two-dimensional nonstationary flows of combustible media 24 p3555 A83-49766
Investigation of flow visualization techniques for detecting turbulent bursts 24 p3585 A83-49820
Smoke wire visualization of the external region of a two dimensional jet 24 p3585 A83-49822
Simultaneous stereoscopic visual and anemometer measurements in a convected frame of reference 24 p3585 A83-49823

FLOWMETERS

NT HOT-WIRE FLOWMETERS
Performance and temperature stability of an air mass flowmeter based on a self-heated thermistor 04 p0481 A83-15100
Constant-temperature hot-wire anemometer practice in supersonic flows. II - The inclined wire [AIAA PAPER 83-0508] 05 p0643 A83-16756
Apparatus for simultaneous temperature and heat-flow measurements under transient conditions 08 p1106 A83-23235
Turbine meters for liquid measurement 09 p1270 A83-25143
Computation of electromagnetic flowmeter characteristics from magnetic field data. II - Errors 12 p1729 A83-29152
Airflow resistivity instrument for in situ measurement on the earth's ground surface 14 p2020 A83-32824
Flow measurement engineering handbook 15 p2163 A83-33620
Dynamic behaviour and stability of thermistor air flowmeters 17 p2512 A83-38531
Modified calibration technique of a five-hole probe for high flow angles 21 p3141 A83-44975
Long-wave acoustic flowmeter 24 p3586 A83-49925

FLTSATCOM

U FLEET SATELLITE COMMUNICATION SYSTEM

FLUCTUATION

U VARIATIONS

FLUCTUATION THEORY

Adiabatic vs. isothermal - Two pictures of galaxy origin 01 p0127 A83-11291
Ray methods in random media 03 p0390 A83-13979
Estimating the life of materials on the basis of the theory of thermal fluctuations 03 p0301 A83-14731
Investigation of fluctuations in a varactor frequency-tripier 04 p0471 A83-15738
Approximate formulas for the fluctuation spectra of waves propagating in a turbulent medium 04 p0531 A83-15761
Analysis of time fluctuations in synchronous information networks --- German thesis 04 p0467 A83-15839
A measure of the incompleteness of a statistical description and irreversibility Fluctuation-dissipation relation /FDR/ for multiparticle distribution functions 07 p1001 A83-20607

The spectrum of strong intensity fluctuations of light beams in randomly irregular media 07 p0937 A83-20875
Fluctuations of radio-wave emergence angles in the case of scattering in the spherically stratified ionosphere 09 p1245 A83-23469
A kinetic equation for the correlation functions of a quantum system interacting with a Gaussian thermostat 09 p1350 A83-25080
Influence of Gaussian fluctuations on a model kinetic system exhibiting explosive behavior 10 p1389 A83-25565
A random-motion model of fluctuations in a nearly transparent medium 10 p1471 A83-26033
An investigation of cosmic ray fluctuations during Forbush decreases 10 p1523 A83-26101
Fluctuation-dissipation relations in the scattering problem and the method of fluctuations in the kinetic theory of gases 10 p1490 A83-26246
Optimization of the position of the dynamic range of a radar receiver relative to the mean power of reflected-signal fluctuations 10 p1407 A83-26932
Optical bistability and fluctuations 11 p1656 A83-27532
Fluctuations of optical radiation on an inclined path 11 p1556 A83-27944
Nonlinear wave interaction and fluctuations in plasmas 11 p1659 A83-28233
Langmuir probe characteristic modulated with random fluctuations 11 p1661 A83-28708
Hydrodynamic fluctuation due to the discontinuity of flow impedance 12 p1721 A83-29001
Note on the evolution of massive stars 12 p1794 A83-29083
Fluctuations of the parameters of the longitudinal waves of an electric field in a turbulent-plasma flow 12 p1780 A83-29259
Measurement of the phase difference between fluctuating signals received by orthogonally polarized antennas 13 p1828 A83-30283
Measurement of the noise of a magnetron oscillator 13 p1833 A83-30708
Phase fluctuations of a wave caused by ionospheric irregularities 14 p2049 A83-31860
A measuring complex for investigating the fluctuations of short-wave radio signals --- Russian book 14 p2002 A83-33300
Receiver-aperture averaging effects for the intensity fluctuation of a beam wave in the turbulent atmosphere 15 p2168 A83-33811
Unified approach to weak turbulence 15 p2239 A83-34543
Elimination of the standard big bang singularity and particle horizon through quantum conformal fluctuations 17 p2614 A83-38962
The role of current fluctuations in the control circuit of the active element in a Thompson oscillator 19 p2840 A83-41777
Low-frequency fluctuations of oscillations in a gyrotron caused by thermal noise 19 p2840 A83-41779
Phase noise in semiconductor lasers - A theoretical approach 20 p2994 A83-42792
Estimation of the parameters of the phase distribution function of a radio signal 20 p2964 A83-42904
Fluctuations in bounded plasma-molecular systems 21 p3215 A83-45389
The electromagnetic field in a randomly inhomogeneous medium Phase-space representation 21 p3201 A83-45391
Intensity fluctuations due to a deeply modulated phase screen. I - Theory. II - Results --- spectrum analysis for wave propagation through irregular environments 24 p3606 A83-49309

FLUE GASES

The atmospheric oxidation of flue gases from a coal-fired power plant - A comparison between smog chamber and airborne plume sampling 15 p2193 A83-33503
Recuperator alloys for high-temperature waste heat recovery 21 p3111 A83-43950
Calculated droplet size distributions and opacities of condensed sulfuric acid aerosols 22 p3321 A83-46898

FLUID AMPLIFICATION

U FLUID AMPLIFIERS

FLUID AMPLIFIERS

Effect of outlet diffusers on vortex amplifier characteristics 11 p1568 A83-28174
Upgrading vortex amplifier performance by matched ejectors 11 p1568 A83-28175
A fluidic/pneumatic interface amplifier 17 p2501 A83-37117
Analysis of the frequency response of a fluid amplifier using unsteady flow characteristics 17 p2504 A83-37399

FLUID BOUNDARIES

NT GAS-SOLID INTERFACES
NT JET BOUNDARIES
NT LIQUID-LIQUID INTERFACES
NT LIQUID-SOLID INTERFACES
NT LIQUID-VAPOR INTERFACES
The response of a fluid-loaded, beam-stiffened plate 01 p0105 A83-11040
Nonlinear modal analysis of penetrative convection --- in stratified fluids under astrophysical and geophysical conditions 03 p0320 A83-14523
Finite-amplitude convective motions in a solute layer with solid boundaries 04 p0477 A83-15878
The resonant effect of time-dependent boundary distortion on the stability and secondary regimes of a viscous fluid flow 04 p0477 A83-15879
Radial and frictional forces in misaligned radial face seals with a non-Newtonian fluid 06 p0768 A83-18050
Rayleigh-Taylor instability at the interface of conducting and nonconducting fluids in a variable magnetic field 11 p1658 A83-27704
A numerical implementation of the variational method for solving certain problems in hydrodynamics --- free-surface oscillations of ideal incompressible fluid in axisymmetric cavity 11 p1569 A83-28460
Instability in the film boiling of a moving liquid 11 p1570 A83-28556
Regimes of mixed convection in a vertical layer whose boundaries undergo unsteady deformation 19 p2842 A83-41205
The problem of the interaction of a supersonic wedge with an interface between two gases 19 p2790 A83-41258
The modeling of inverse problems of heat conduction with movable phase transition boundaries 19 p2844 A83-41571
Growth of fluctuations near the Benard-Marangoni convective instability 19 p2845 A83-41997
Convection in a horizontal fluid layer having a shear-free upper surface and uniform volumetric energy sources 20 p2972 A83-42672
Direct numerical simulation of the turbulent momentum and heat transfer in an internally heated fluid layer 20 p2972 A83-42673
Effects of variable fluid properties and boundary conditions on thermal convection 21 p3131 A83-44854
The parametric excitation of internal waves and convective instabilities in a fluid layer heated from above 22 p3322 A83-45639
On a class of non-static perfect fluid spheres in general relativity 23 p3527 A83-48572

FLUID DYNAMICS

NT AERODYNAMICS
NT AEROTHERMODYNAMICS
NT COMPUTATIONAL FLUID DYNAMICS
NT CYLINDRICAL PLASMAS
NT ELASTOHYDRODYNAMICS
NT ELECTROHYDRODYNAMICS
NT GAS DYNAMICS
NT HYDRODYNAMICS
NT HYPERSONICS
NT MAGNETOHYDRODYNAMICS
NT RAREFIED GAS DYNAMICS
NT ROTOR AERODYNAMICS
NT SUPERSONICS
NT VORTEX SHEDDING

Flow visualization study in low specific speed pump impeller passages 01 p0053 A83-11073
Some characteristics of turbulent flows at elevated temperatures 03 p0318 A83-14468
A comparison of spectral and cospectral characteristics of dynamic and thermal turbulent fields in weakly stratified boundary layers 03 p0319 A83-14475
A time-dependent ice sheet model - Preliminary results 03 p0359 A83-14505
Fluid dynamics of inducers - A review 04 p0478 A83-16137
Investigation of unsteady flow problems 05 p0638 A83-16897
Geophysical fluid dynamics --- Book 05 p0640 A83-17650
Spouts in a bed of silica powder associated with fluidization by outgassing of adsorbed water 06 p0756 A83-18400
Experiments on natural convection heat transfer in low aspect ratio enclosures 07 p0924 A83-19822
Certain effects and paradoxes in aerodynamics and hydraulics --- Russian book 07 p0925 A83-20379
Hamiltonian description of stratified fluid dynamics 07 p0926 A83-20529
Shock dynamics in non-uniform media 09 p1262 A83-24422
Pressure measurements of a rotating liquid for impulsive coning motion 09 p1263 A83-24877

- Fluid-dynamical aspects of laser-metal interaction
 10 p1416 A83-26172
- Fluid mechanics in crystal growth - The 1982 Freeman
 scholar lecture 10 p1401 A83-26626
- The dynamics of a viscous incompressible fluid in Hilbert
 space with allowance for the boundary conditions
 10 p1418 A83-26944
- Stability analysis of numerical boundary conditions and
 implicit difference approximations for hyperbolic
 equations 12 p1772 A83-29650
- Influence of boundary approximations and conditions
 on finite-difference solutions 12 p1772 A83-29652
- Velocity and length scales in turbulent flows - A review
 of approaches 13 p1841 A83-30633
- Autrotation --- in fluid dynamics 13 p1804 A83-31079
- Progress in boundary element methods. Volume 2
 15 p2224 A83-33852
- Fluid structure interaction 15 p2157 A83-33858
- Low-resolution numerical simulation of decaying
 two-dimensional turbulence 16 p2385 A83-35470
- The dynamics of localized vortex perturbations (vortex
 charges) in a baroclinic fluid 16 p2392 A83-36865
- On a general fluid dynamical theory of discrete unstable
 spiral modes in disk-shaped galaxies 18 p2764 A83-39008
- Laser diagnostic methods - A summary
 [AIAA PAPER 83-1683] 18 p2688 A83-39100
- Implicit total variation diminishing (TVD) schemes for
 steady-state calculations 18 p2739 A83-39362
- [AIAA PAPER 83-1902] 18 p2739 A83-39362
- The BDPU - A microgravity fluid sciences facility ---
 Bubble Drops and Particles in liquid matrices Unit
 [IAF PAPER 83-163] 23 p3414 A83-47298
- Annular jets of different diameter ratios
 23 p3449 A83-48142
- Direct method for investigating the dynamics of
 liquid-filled bodies 24 p3624 A83-49672
- On turbulent spots 24 p3580 A83-49828
- Dynamics of a mobile tank partially filled with liquid
 Equations of motion and their linearization 24 p3581 A83-50124

FLUID FILLED SHELLS

- NT LIQUID FILLED SHELLS
- The dynamic stability of a liquid-gas oscillatory system
 under the effect of vibration 03 p0341 A83-14075
- Vibration effects in bodies containing a gas-liquid
 medium 06 p0760 A83-19547
- The use of invariant relationships to reduce the order
 of the system of equations of motion of a vortex-filled
 heavy rigid body 09 p1337 A83-23564
- Normal oscillations of an ideal compressible fluid in
 rotating elastic vessels 13 p1838 A83-30012
- Fluid structure interaction 15 p2157 A83-33858
- Calculation of transfer functions in internal problems of
 the unsteady hydroelasticity of cylindrical and spherical
 shells 18 p2702 A83-40117
- Natural convection with volumetric energy sources in
 a fluid bounded by a spherical segment 20 p2972 A83-42676
- Natural convection in a spherical annulus filled with heat
 generating fluid 20 p2972 A83-42677
- Effect of curvature on the thermal stability of a fluid
 between two long vertical coaxial cylinders
 20 p2973 A83-42682
- An investigation into the effect of coolant flow on the
 vibration characteristics of hollow blades conveying fluid
 [ASME PAPER 83-GT-217] 23 p3470 A83-48017
- The effect of viscosity on the forced vibrations of a
 fluid-filled elastic shell [ASME PAPER 83-APM-34] 23 p3471 A83-48242
- Calculation of the oscillation-damping decrement of a
 low-viscosity fluid rotating in a cylindrical vessel --- in
 weightlessness conditions 23 p3452 A83-48659
- Unsteady thermal convection in a cylindrical vessel in
 the case of lateral heat injection 23 p3452 A83-48668
- Thermocapillary convection in a two-layer system
 23 p3452 A83-48669

FLUID FILMS

- NT SQUEEZE FILMS
- The Marangoni wave in ripples on an air-water interface
 covered by a spreading film 01 p0069 A83-11047
- Dynamics of rotor bearing systems supported by floating
 ring bearings [ASME PAPER 81-LUB-37] 02 p0186 A83-11938
- An experimental investigation of the vaporous/gaseous
 cavity characteristics of an eccentric journal bearing
 [ASLE PREPRINT 82-LC-3A-1] 03 p0333 A83-13230
- Estimating the severity of shaft vibrations within fluid
 film journal bearings [ASME PAPER 82-LUB-1] 03 p0335 A83-13502
- Transient lubricating films with inertia
 [ASME PAPER 82-LUB-12] 03 p0335 A83-13507

- Overall characteristics of bearings lubricated with
 ferrofluids [ASME PAPER 82-LUB-14] 03 p0335 A83-13508
- Fluid film dynamic coefficients in mechanical face
 seals [ASME PAPER 82-LUB-34] 03 p0336 A83-13515
- Investigation of the effects of initial fluid film profile on
 pumping ring operation [ASME PAPER 82-LUB-35] 03 p0336 A83-13516
- Surface roughness effects in hydrodynamic lubrication
 - The flow factor method [ASME PAPER 82-LUB-45] 03 p0337 A83-13523
- The non-linear response of hydrodynamic seals
 04 p0487 A83-16346
- IR optical properties of thin CO, NO, CH₄, HCl, N₂O,
 O₂, N₂ and Ar cryofilms [AIAA PAPER 83-0244] 05 p0684 A83-16610
- The liquid-gas interface in grooved face seals
 06 p0768 A83-18048
- Structured films of magnetizable surfactants
 06 p0813 A83-19552
- Free energy loss during the breakdown of liquid films
 08 p1087 A83-23141
- Effect of the fluid film profile on the performance of
 magnetohydrodynamic bearings 09 p1273 A83-23345
- Heat transfer between two-phase flow and a nozzle wall
 under conditions of entrainment of droplets from the
 surface of a condensed film 09 p1258 A83-23431
- An experimental study of an annular film-evaporation
 combustion chamber in a low-power gas turbine engine
 09 p1205 A83-23443
- Film flow of a liquid on a convergent-nozzle surface
 11 p1568 A83-28372
- Solitary waves on a viscous fluid film down a vertical
 wall 12 p1721 A83-29002
- Flow of a thin fluid layer covered by a magnetizable
 surfactant 12 p1781 A83-29263
- Parametric method for solving problems of heat transfer
 for the film flow of a fluid 13 p1838 A83-30045
- On the motion of a spherical fluid film
 13 p1839 A83-30092
- Infrared optical properties of solid mixtures of molecular
 species at 20K [AIAA PAPER 83-1452] 14 p2084 A83-32717
- Surface tension effects in a space radiator condenser
 with capillary liquid drainage [AIAA PAPER 83-1525] 14 p2011 A83-32756
- Mass, heat, and momentum transfer in laminar and
 turbulent pipe flow with vaporization of a liquid film
 15 p2161 A83-34266
- A three-dimensional analysis of thermohydrodynamic
 performance of sector-shaped, tilting-pad thrust bearings
 [ASME PAPER 82-LUB-3] 18 p2695 A83-39943
- Melting and wetting behavior in oxygen films
 19 p2905 A83-41158
- Heat transfer in thin liquid films flowing over horizontal
 tubes 20 p2981 A83-42771
- Analysis of spiral-groove face seals for liquid oxygen
 [ASLE PREPRINT 83-AM-4B-2] 20 p2999 A83-43339
- The spreading of a viscous fluid on a horizontal
 surface 20 p2987 A83-43515
- A model for the film flow of a fluid along the surface
 of a convergent nozzle 20 p2987 A83-43516
- Inertia effects of the dynamics of a disk levitated by
 incompressible laminar fluid flow [ASME PAPER 83-GT-149] 23 p3464 A83-47968
- Wave flows of a thin liquid film in reduced gravity
 24 p3576 A83-48942

FLUID FILTERS

- NT AIR FILTERS
- A study of the structural strength and ductility of nickel
 screens --- for aircraft hydraulic system filters
 07 p0940 A83-20910
- Aviation filters for fuels, oils, hydraulic fluids, and air ---
 Russian book 12 p1700 A83-28813

FLUID FLOW

- NT ADIABATIC FLOW
- NT AIR CURRENTS
- NT AIR FLOW
- NT AIR JETS
- NT ANNULAR FLOW
- NT AXIAL FLOW
- NT AXISYMMETRIC FLOW
- NT BAROTROPIC FLOW
- NT BASE FLOW
- NT BELTRAMI FLOW
- NT BENARD CELLS
- NT BLOOD FLOW
- NT BOUNDARY LAYER FLOW
- NT BOUNDARY LAYER SEPARATION
- NT CAPILLARY FLOW
- NT CASCADE FLOW
- NT CAVITATION FLOW
- NT CHANNEL FLOW

- NT COAXIAL FLOW
- NT COMBUSTIBLE FLOW
- NT COMPRESSIBLE FLOW
- NT CONICAL FLOW
- NT CONTINUUM FLOW
- NT CONVECTIVE FLOW
- NT CORE FLOW
- NT CORNER FLOW
- NT COUETTE FLOW
- NT COUNTERFLOW
- NT CRITICAL FLOW
- NT CROSS FLOW
- NT DUCTED FLOW
- NT EQUILIBRIUM FLOW
- NT FREE FLOW
- NT FREE MOLECULAR FLOW
- NT FUEL FLOW
- NT GAS FLOW
- NT HARTMANN FLOW
- NT HEAD (FLUID MECHANICS)
- NT HEAD FLOW
- NT HELICAL FLOW
- NT HYPERSONIC FLOW
- NT HYPERVELOCITY FLOW
- NT INCOMPRESSIBLE FLOW
- NT INLET FLOW
- NT INVISCID FLOW
- NT ISOTHERMAL FLOW
- NT JET FLOW
- NT JET MIXING FLOW
- NT JET STREAMS (METEOROLOGY)
- NT KNUDSEN FLOW
- NT LAMINAR FLOW
- NT LIQUID FLOW
- NT MAGNETOHYDRODYNAMIC FLOW
- NT MASS FLOW
- NT MERIDIONAL FLOW
- NT MOLECULAR FLOW
- NT MULTIPHASE FLOW
- NT NONEQUILIBRIUM FLOW
- NT NONUNIFORM FLOW
- NT NOZZLE FLOW
- NT ONE DIMENSIONAL FLOW
- NT OPEN CHANNEL FLOW
- NT ORIFICE FLOW
- NT OSCILLATING FLOW
- NT OUTLET FLOW
- NT PARALLEL FLOW
- NT PERIPHERAL JET FLOW
- NT PIPE FLOW
- NT PLASTIC FLOW
- NT POTENTIAL FLOW
- NT PRESSURE HEADS
- NT PROPELLANT TRANSFER
- NT RADIAL FLOW
- NT RAYLEIGH-BENARD CONVECTION
- NT REATTACHED FLOW
- NT RECIRCULATIVE FLUID FLOW
- NT REVERSED FLOW
- NT SECONDARY FLOW
- NT SEPARATED FLOW
- NT SHEAR FLOW
- NT SINGLE-PHASE FLOW
- NT SLIP FLOW
- NT SMALL PERTURBATION FLOW
- NT SOLIDS FLOW
- NT STAGNATION FLOW
- NT STEADY FLOW
- NT STEAM FLOW
- NT STOKES FLOW
- NT STRATIFIED FLOW
- NT SUBCRITICAL FLOW
- NT SUBSONIC FLOW
- NT SUPERCAVITATING FLOW
- NT SUPERCRITICAL FLOW
- NT SUPERSONIC FLOW
- NT SUPERSONIC JET FLOW
- NT THREE DIMENSIONAL FLOW
- NT TRANSITION FLOW
- NT TRANSONIC FLOW
- NT TURBULENT FLOW
- NT TWO DIMENSIONAL FLOW
- NT TWO PHASE FLOW
- NT UNIFORM FLOW
- NT UNSTEADY FLOW
- NT VERTICAL AIR CURRENTS
- NT VISCOUS FLOW
- NT WALL FLOW
- NT WATER FLOW
- NT WEDGE FLOW

Flow of a non-Newtonian second-order fluid under an
 enclosed rotating disc with uniform suction and injection
 02 p0171 A83-12663

Laminar and turbulent boundary layers on moving,
 nonisothermal continuous flat surfaces
 03 p0316 A83-13486

Flames as gasdynamic discontinuities
04 p0457 A83-16262

Engineering principles of the formation of epoxy resin composites. I Mathematical model of the fluid flow
07 p0875 A83-20439

Fluid motions in the solar chromosphere-corona transition region. I - Line widths and Doppler shifts for C IV
07 p1038 A83-21147

Acoustic fluidization --- of dry rock landslides
10 p1519 A83-25900

Fluid mechanics in crystal growth - The 1982 Freeman scholar lecture
10 p1401 A83-26626

Fluid shifts in vascular and extravascular compartments of humans during and after simulated weightlessness
11 p1642 A83-27793

On the solution of the time-dependent inertial-frame equation of radiative transfer in moving media to $O(v/c)$ --- largest velocity dependent term
12 p1796 A83-29610

Use of the finite-element method for natural convection in a horizontally confined infinite layer of fluid
12 p1726 A83-29899

Compressible Rayleigh-Taylor instability
13 p1840 A83-30111

Fluid flow in the contact line region of a mixture of alkanes - 98 percent hexane and 2 percent octane
[AIAA PAPER 83-1528] 14 p2011 A83-32759

Flow measurement engineering handbook
15 p2163 A83-33620

Boundary element methods; Proceedings of the Third International Seminar, Irvine, CA, July 7-9, 1981
19 p2896 A83-41516

The role of fluid flow phenomena in the Czochralski growth of oxides
20 p3053 A83-43292

The diffusion of a fluid through a highly elastic spherical membrane
22 p3281 A83-46390

FLUID INJECTION
NT GAS INJECTION
NT LIQUID INJECTION
NT WATER INJECTION

Flow of a non-Newtonian second-order fluid under an enclosed rotating disc with uniform suction and injection
02 p0171 A83-12663

Fluid injection to a laminar boundary layer with variable wall mass and heat flux
[ASME PAPER 82-HT-61] 02 p0173 A83-12801

Experimental and theoretical investigation on three-dimensional film cooling of a flat plate
03 p0315 A83-13345

Compressible boundary-layer flow at a three-dimensional stagnation point with massive blowing
03 p0322 A83-14672

A study of the efficiency of a gas screen on a rough surface
04 p0478 A83-16162

Injection into a turbulent boundary layer through porous surfaces with different surface geometries
[AIAA PAPER 83-0295] 05 p0634 A83-16635

Influence of finite slot size on boundary layer with suction or injection
09 p1263 A83-24676

Supersonic diffusers with reverse flow injection
[ASME PAPER 82-WA/FE-7] 10 p1413 A83-25684

A theoretical and experimental investigation of flow and heat transfer in film cooling
15 p2161 A83-34268

The distribution of the disperse fraction of a polydisperse jet injected into a gas flow
15 p2161 A83-34472

The introduction of tangential or perpendicular nonisothermal plane jets into a turbulent crossflow for the purpose of film cooling
16 p2350 A83-35799

Experiments in dilution jet mixing
[AIAA PAPER 83-1201] 16 p2352 A83-36277

Injection slot location for boundary-layer control in shock-induced separation
19 p2789 A83-41050

The effect of injection and suction on the characteristics of the viscous sublayer in a turbulent flow
21 p3133 A83-45346

Axial flow past a cylinder with uniform injection
23 p3451 A83-48499

The effect of injection in the boundary layer on supersonic flow past an oscillating cone
23 p3400 A83-48654

FLUID JET AMPLIFIERS
U FLUID AMPLIFIERS

FLUID JETS
NT AIR JETS
NT FREE JETS
NT GAS JETS
NT HYDRAULIC JETS

Radio structures of Seyfert galaxies. IV - Jets in NGC 1068 and NGC 4151
05 p0697 A83-16985

A numerical study of the lateral interaction between an axisymmetric jet issuing into vacuum and an obstacle
06 p0760 A83-19431

Atomization of impinging liquid jets in a supersonic crossflow
[AD-A130714] 07 p0924 A83-19806

Penetration and breakup of slurry jets in a supersonic stream
16 p2352 A83-36094

Computational and experimental study of the effect of mass transfer on liquid jet break-up
[AIAA PAPER 83-1400] 16 p2353 A83-36390

An experimental study of the interaction between two hypersonic wakes
20 p2931 A83-43521

Approximate unsteady fluid jet properties from one-dimensional theory
[ASME PAPER 83-FE-25] 23 p3450 A83-48236

FLUID MANAGEMENT
Long term storage of cryogenics in space
01 p0029 A83-11487

Cryogenic fluid management experiment trunnion fatigue verification
[AIAA PAPER 83-0911] 14 p1982 A83-32782

Prospective of tethered system in space station operations
[IAF PAPER 83-41] 23 p3416 A83-47242

FLUID MECHANICS
NT AERODYNAMICS
NT AEROTHERMODYNAMICS
NT COMPUTATIONAL FLUID DYNAMICS
NT CYLINDRICAL PLASMAS
NT ELASTOHYDRODYNAMICS
NT ELECTROHYDRODYNAMICS
NT FLUID DYNAMICS
NT GAS DYNAMICS
NT HYDRODYNAMICS
NT HYDROMECHANICS
NT HYDROSTATICS
NT HYPERSONICS
NT MAGNETOHYDRODYNAMICS
NT MAGNETOHYDROSTATICS
NT RAREFIED GAS DYNAMICS
NT ROTOR AERODYNAMICS
NT SUPERSONICS
NT VORTEX SHEDDING

Quantitative interpretation of flow visualizations coupling video technics and microcomputer
01 p0052 A83-11071

Multiple grid methods for equations of the second kind with applications in fluid mechanics --- Thesis
02 p0170 A83-11899

A study and variational approach to biharmonic equations applied in unbounded domains - Applications in mechanics
03 p0388 A83-14571

Conference on Numerical Methods in Fluid Mechanics, 4th, Ecole Nationale Supérieure de Techniques Avancées, Paris, France, October 7-9, 1981, Proceedings
03 p0322 A83-14601

Investigation of unsteady flow problems
05 p0638 A83-16897

Fluid mechanics of mechanical seals; Proceedings of the Winter Annual Meeting, Phoenix, AZ, November 14-19, 1982
06 p0768 A83-18046

A new theory of the energy spectrum --- in viscous boundary layer shear flow
06 p0756 A83-18056

Heat Transfer and Fluid Mechanics Institute, Meeting, 28th, California State University, Sacramento, CA, June 28, 29, 1982, Proceedings
06 p0757 A83-18451

Computer simulation of fluid-physics-module operations on the first Spacelab flight
08 p1049 A83-22373

A statistical solution to the Navier-Stokes system in the case of infinite average energy
09 p1260 A83-24235

Fluid mechanics instabilities
09 p1264 A83-25150

The development of mechanics - The role of fluid mechanics
11 p1568 A83-28125

Kernel estimates as a basis for general particle methods in hydrodynamics
12 p1724 A83-29617

Finite-sized fluid particle in a nonuniform moving grid
12 p1725 A83-29627

The choice of numerical boundary conditions for hyperbolic systems
12 p1772 A83-29653

Annual review of fluid mechanics, Volume 15 --- Book
13 p1842 A83-31076

Universal equation of state in the theory of strong turbulence
13 p1933 A83-31332

The fluid mechanics of slender wing rock --- vortex shedding of delta configurations
[AIAA PAPER 83-1810] 17 p2454 A83-38643

Vortex flows
[AIAA PAPER 83-1812] 17 p2454 A83-38645

Incompressible fluid mechanics --- French book
20 p2969 A83-42172

Engineering science and mechanics; Proceedings of the International Symposium, Tainan, Republic of China, December 29-31, 1981. Parts 1 & 2
21 p3117 A83-44001

Vortex motion; Proceedings of the Colloquium, Goettingen, West Germany, November 1982
22 p3279 A83-45901

Recent contributions to fluid mechanics
22 p3283 A83-46454

Publication on the occasion of the 65th birthday of Prof. Dr.-Ing. Erich Truckenbrodt; Scientific Colloquium, Technische Universität München, Munich, West Germany, February 1, 1982, Reports
22 p3284 A83-46482

Recent work at the Franco-German research institute Saint-Louis in the field of fluid mechanics
22 p3284 A83-46494

Autonomous Fluid Physics Module (AFPM) - Status and perspectives --- first Spacelab mission payload
[IAF PAPER 83-165] 23 p3414 A83-47300

FLUID PRESSURE
Characteristics of an oil squeeze film
02 p0186 A83-11939

Multi-grid solution of Neumann pressure problem for viscous flows using primitive variables
[AIAA PAPER 83-0557] 05 p0637 A83-16786

Nonlinear hydrodynamic pressure on an accelerating plate
08 p1084 A83-22377

The calculation of the coefficient-optimal total pressure of a system of plane shock waves
09 p1258 A83-23447

The Green function of an infinite, fluid loaded membrane
09 p1278 A83-23705

Upgrading vortex amplifier performance by matched ejectors
11 p1568 A83-28175

Collapse by ponding of shells --- stability analysis
11 p1594 A83-28411

Unsteady boundary layer with self-induced pressure near a rapidly heated section of the surface of a flat plate in supersonic flow
11 p1527 A83-28536

Role of the pressure anisotropy in the relativistic pulsar wind
12 p1793 A83-29060

Nonintrusive pressure measurement with laser-induced iodine fluorescence
[AIAA PAPER 83-1468] 14 p2019 A83-32724

A fluidic/pneumatic interface amplifier
17 p2501 A83-37117

Experiments on flow through one to four inlets of the orifice and Borda type
20 p2986 A83-43235

FLUID ROTOR GYROSCOPES
Vibrations in fluid-filled rotor and the gyroscopic effect --- German thesis
06 p0735 A83-18493

A study of the hydrodynamic moment acting on a solid body in a float suspension
21 p3138 A83-44642

FLUID SWITCHING ELEMENTS
Development of gas gap cryogenic thermal switch
20 p2962 A83-43249

FLUID TRANSPARATION
U TRANSPARATION

FLUID-SOLID INTERACTIONS
Free vibrations of plates in fluid using finite and infinite elements
01 p0058 A83-10279

An approximation method for the stability analysis of plates in the flow of an incompressible fluid
04 p0497 A83-15392

A study of internal waves generated by the rapid horizontal motion of cylinders and spheres
06 p0760 A83-19433

An unsteady interactive separation process --- from downstream moving wall
08 p1042 A83-22131

Statistical flow-oscillator modeling of vortex-shedding
09 p1196 A83-23337

Shock wave diffraction at a sharp edge and the effect of baffles in a shock tube
10 p1416 A83-26164

Fluid structure interaction
12 p2157 A83-33858

Recent studies at NASA-Langley of vortical flows interacting with neighboring surfaces
15 p2120 A83-33972

Cutting fluid performance in fine grinding
15 p2172 A83-35248

Unstable flow in the region of the interaction of an underexpanded jet with a barrier
17 p2450 A83-37567

Flow control in a shock layer on a body of revolution
19 p2845 A83-41878

The effect of viscosity on the interaction of an underexpanded jet with an infinite plane barrier perpendicular to its axis
19 p2792 A83-41895

Aerodynamic drag of a cone in two-phase flow
19 p2792 A83-41899

Effect of particle presence on the incompressible inviscid flow through a two dimensional compressor cascade
20 p2928 A83-42562

On vortex formation and interaction with solid boundaries
22 p3280 A83-45902

Analogies between oscillation and rotation of bodies induced or influenced by vortex shedding
22 p3280 A83-45905

Surface interaction of lubricant greases
23 p3439 A83-48546

FLUIDIC CIRCUITS
NT FLIP-FLOPS

Fluidic elements, areas of their application and reliability assurance
02 p0170 A83-12199

An aggregate complex of fluidic integrated modules
02 p0171 A83-12200
Back-to-back test for determining the pumping losses
in a Stirling cycle machine 11 p1588 A83-27290
Dual mode reaction-jet, thrust-vector controls for small
missiles
[AIAA PAPER 83-1148] 16 p2318 A83-36245

FLUIDICS

Propulsion and fluid management - Station keeping will
eat energy on a new scale 09 p1220 A83-24360
Effect of outlet diffusers on vortex amplifier
characteristics 11 p1568 A83-28174
Upgrading vortex amplifier performance by matched
ejectors 11 p1568 A83-28175
Application of fluidics to instrumentation in hostile
environments
[AIAA PAPER 83-1150] 16 p2352 A83-36247
Fluidic control systems for projectiles
[AIAA PAPER 83-1151] 16 p2352 A83-36248
Space-correlation measurement of attaching jets by the
new scanning laser Doppler velocimeter using a diffraction
grating 24 p3585 A83-49827

FLUIDIZED BED PROCESSORS

Combustion of condensed two-component systems with
spatially separated components
03 p0294 A83-14052
Spouts in a bed of silica powder associated with
fluidization by outgassing of adsorbed water
06 p0756 A83-18400
A new concept in high density power - The rotating bed
reactor revisited --- space tug propulsion systems
[AIAA PAPER 83-1332] 16 p2320 A83-36345
The silicide coating of refractory metals and their alloys
in a fluidized bed at relatively low temperatures
20 p2957 A83-42259
Observations on the characteristics of a fluidized bed
for the thermal shock testing of brittle ceramics
21 p3116 A83-44333

FLUIDS

Electric pulse-time densimeters --- Russian book
10 p1419 A83-25617
Giant resonances as oscillations of two elastically
coupled fluids 15 p2228 A83-33794

FLUORESCENCE

NT PHOSPHORESCENCE
NT RESONANCE FLUORESCENCE
NT X RAY FLUORESCENCE
Flame diagnosis with electron beam method. Research
on elementary reactions in flames during suppression by
electron beam fluorescence --- German thesis
01 p0022 A83-10173
Two-line atomic fluorescence temperature
measurement in flames - An experimental study
02 p0179 A83-12608
Scanning delay generator for measurement of kinetic
decays using laser-induced fluorescence techniques
02 p0181 A83-12823
Ultraviolet /UV/ sensitive phosphors for silicon imaging
detectors 03 p0288 A83-13967
Fluorescence yields from photodissociation of SO₂ at
1060-1330 A 03 p0392 A83-14661
Fluorescent dye penetrant inspection of silicon nitride
bearing surfaces 04 p0462 A83-15176
Flow visualization in combustion gases using planar
laser-induced fluorescence
[AIAA PAPER 83-0405] 05 p0643 A83-16694
Simultaneous multiple-point velocity measurements
using laser-induced iodine fluorescence
05 p0646 A83-17884
Quantitative measurement of density and velocity in
compressible flows using laser-induced iodine
fluorescence
[AIAA PAPER 83-0049] 05 p0646 A83-17903
Photodissociation yields of CS₂ at 1060-1520 A
06 p0807 A83-18042
Experimental feasibility of the airborne measurement of
absolute oil fluorescence spectral conversion efficiency
06 p0793 A83-18581
Performance evaluation of UV sources for lidar
fluoresensing of oil films 06 p0765 A83-18582
A semiclassical study of laser-induced atomic
fluorescence from Na₂, K₂ and NaK
[AD-A127849] 07 p0991 A83-21051
Fluorescence yields from photodissociation of OCS at
1060-1240 A 07 p0882 A83-21056
Fluorescence yield from photodissociation of CH₄ at
1060-1420 A 07 p0991 A83-21192
Ultraviolet fluorescence by optical pumping with extreme
ultraviolet line radiation 08 p1110 A83-22646
Earth limb emission analysis of Spectral Infrared Rocket
Experiment /SPIRE/ data at 2.7 micrometers
08 p1051 A83-22851
EA study of solar concentrator panels with fluorescent
compounds 06 p1131 A83-22911
Radiative lifetimes in Fe II using selective laser
excitation 09 p1341 A83-23651

Laser-saturated fluorescence measurements of OH
concentration in flames 09 p1225 A83-23749
Rethinking automation in NDT applications
09 p1275 A83-23920
Overremoval propensities of the prewash hydrophilic
emulsifier fluorescent penetrant process
09 p1275 A83-23921
A further development of the fluorescent gated gas
scintillation proportional counter
09 p1268 A83-24105
Superfluorescent transients of an inhomogeneously
broadened Q-switched nuclear-magnetic-resonance
system 10 p1426 A83-25795
The uranyl ion, fluorescent and fluorine-like - A review
10 p1390 A83-26061
Enhanced optical spectroscopies at surfaces -
Fluorescence and Raman scattering
11 p1655 A83-27509
Determination of accurate dissociation limits and
interatomic interactions at large internuclear distances
11 p1653 A83-27526
Cooperative effects and transverse coherence in
superfluorescence 11 p1577 A83-27536
Transverse and phase effects in light control by light -
Pump dynamics in superfluorescence
11 p1577 A83-27538
LIF and chemiluminescence methods for the flow
diagnostics of supersonic mixing chemical lasers --- laser
induced fluorescence 11 p1580 A83-27581
Evaluation of microencapsulated penetrant inspection
12 p1734 A83-29594
Separation of time-averaged turbulence components by
laser-induced fluorescence 13 p1839 A83-30102
Spatially resolved temperature measurements in a flame
using laser-excited two-line atomic fluorescence and
diode-array detection 13 p1817 A83-30746
Laser studies of electronic energy transfer in atomic
copper 13 p1851 A83-30957
Laser induced fluorescence and absorption
measurements of NO in NH₃/O₂ and CH₄/air flames
13 p1818 A83-30969
Fluorescence branching ratios from the A²Sigma +
(v-prime = 0) state of NO 14 p2081 A83-31936
Fluorescent plastic coatings for improving ultraviolet
and blue response of cooled silicon charge-injection devices
(CIDs) 14 p2015 A83-31984
Nonintrusive pressure measurement with laser-induced
iodine fluorescence
[AIAA PAPER 83-1468] 14 p2019 A83-32724
The dependence of the fluorescence and absorption
spectra of anthracene vapor on concentration
14 p2082 A83-32828
Fiber-optic absorption/fluorescence probes for
combustion measurements 14 p2020 A83-32902
Ultraviolet continuum and H₂ fluorescent emission in
Herbig-Haro objects 43 and 47
14 p2107 A83-33231
Picosecond streak camera fluorimetry - A review
14 p2022 A83-33415
Multiple fluorescent scattering of N₂ ultraviolet
emissions in the atmospheres of the earth and Titan
15 p2274 A83-33932
A model for superradiance and superfluorescence in
free-electron lasers 15 p2169 A83-34274
Aerial testing of an N₂ laser fluorosensor system
15 p2169 A83-34467
Fluorescent excitation of photospheric Fe K-alpha
emission during solar flares 15 p2284 A83-35218
Time-resolved fluorescence spectra of rotationally
cooled NO₂ 16 p2408 A83-35331
Quantum theory of optical bistability. III - Atomic
fluorescence in a low-Q cavity 16 p2411 A83-35659
Redistribution - Why half a collision is better than a whole
one --- spectra of scattered light from perturbed atomic
system 17 p2484 A83-37075
Kr(+) and Ar(+) laser-excited fluorescence of CN in a
flame 17 p2485 A83-37746
Single-pulse gas thermometry at low temperatures using
two-photon laser-induced fluorescence in NO-N₂
mixtures 17 p2511 A83-37944
Infrared and microwave fluorescence of carbon
monoxide in comets 17 p2608 A83-38412
Use of planar laser-induced fluorescence for the study
of combustion flowfields
[AIAA PAPER 83-1361] 18 p2688 A83-39263
Fluorescence measurements of OH in a turbulent
flame --- A feasibility study 19 p2820 A83-40859
Initiation of superfluorescence in a three-level
'swept-gain' amplifier 19 p2853 A83-41178
Superfluorescence pulse shape
20 p2993 A83-42289
Picosecond laser-spectroscopy measurement of
hydroxyl fluorescence lifetime in flames
20 p2949 A83-42347
Atomic fluorescence study of high temperature
aerodynamic levitation 20 p2939 A83-43256

Lasing and fluorescent characteristics of nine, new,
flashlamp-pumpable, coumarin dyes in ethanol and
ethanol:water 21 p3143 A83-44193
Superfluorescence in a cavity
21 p3143 A83-44197
Propagation, transverse, diffraction effects, and
coherent pump dynamics in three-level superfluorescence
and light control by light 21 p3144 A83-44801
Fluorescence from polystyrene - Photochemical
processes in polymeric systems, 7
21 p3110 A83-44857
Rapid purification of fluorescent enzymes by
ultrafiltration 21 p3105 A83-44858
The lasing capacity of pyrenes in the gas phase
21 p3146 A83-45386
Lidar remote-sensing - Fluorescence and differential
reflectance experiments 21 p3166 A83-45420
Laser-induced fluorescence technique for velocity field
measurements in subsonic gas flows
22 p3287 A83-45962
Picosecond fluorescence in spinach chloroplasts
22 p3346 A83-46672
Laser-induced fluorescence spectroscopy for
combustion diagnostics 23 p3455 A83-47656
Remote sensing of OH in the atmosphere using the
technique of laser-induced fluorescence
23 p3457 A83-47792
The effect of fluorescence decay time on echo-signal
kinetics in the case of remote laser sounding of water
bodies 23 p3493 A83-48505
Plasma electron density measurements by the laser-
and collision-induced fluorescence method
24 p3631 A83-48819
Feasibility of airborne detection of laser-induced
fluorescence emissions from green terrestrial plants
24 p3598 A83-49008
Fluorescent window as wavelength shifter for a
polysulfide containing photoelectrochemical cell
24 p3601 A83-50183

FLUORESCENT EMISSION**U FLUORESCENCE****FLUORIDES**

NT BARIUM FLUORIDES
NT BORON FLUORIDES
NT CALCIUM FLUORIDES
NT COPPER FLUORIDES
NT DEUTERIUM FLUORIDES
NT HYDROFLUORIC ACID
NT LITHIUM FLUORIDES
NT MAGNESIUM FLUORIDES
NT METAL FLUORIDES
NT NICKEL FLUORIDES
NT POLYVINYL FLUORIDE
NT SULFUR FLUORIDES
NT URANIUM FLUORIDES
Rayleigh scattering in ZrF₄-based glasses
04 p0534 A83-15247
Iodine monofluoride B 3Pi/0+/- to X 1Sigma+ lasing
from collisionally pumped states
05 p0651 A83-17653
Rydberg states of SiF in the vacuum ultraviolet
06 p0808 A83-19007
Characteristics of the electron beam pumped iodine
monofluoride laser 07 p0938 A83-21590
The effect of fluoride contamination on the durability
of PAA surfaces --- preparation of aluminum alloy surfaces
for adhesive bonding by phosphoric acid anodize
solution 09 p1230 A83-23625
Infrared optics hot pressed from fluoride glass
09 p1239 A83-24973
Epitaxial relations in group-IIa fluoride/Si/111/
heterostructures 10 p1488 A83-25983
A single mode /F₂+/-asterisk color-center laser for
application in optical pumping of helium
11 p1578 A83-27543
Mode structure of a DFB gas laser
11 p1578 A83-27547
Performance of a cylindrical phase-change thermal
energy storage unit 12 p1749 A83-28969
Kinetics of crystallization of ZrF₄-BaF₂-LaF₃ glass by
differential scanning calorimetry
12 p1717 A83-29972
Light induced drift of CH₃F 19 p2853 A83-41181
Fluoride glasses with large optical window for infrared
fibers 22 p3358 A83-46625
Gamma-ray irradiation effect on transmission loss for
ZrF₄-based optical fibres 24 p3630 A83-49985

FLUORINATION

Experimental study of electrochemical fluorination of
trichloroethylene 04 p0456 A83-15870

FLUORINE**NT FLUORINE ISOTOPES**

The determination of parameters of recombining
laser-produced plasmas by means of X-ray spectroscopy
09 p1347 A83-23654

Fluorocarbon combustion studies. VI - Competitive combustion reactions of fluorocarbons burning with fluorine 14 p1991 A83-32942

Half-widths of neutral fluorine spectral lines 19 p2897 A83-40714

Formation of free fluorine atoms by laser-collisional initiation of the CH3F + F2 reaction 20 p2997 A83-43789

Energy lost in formation of fluorine atoms in the course of electron-beam dissociation of fluorine and fluoride molecules 20 p2997 A83-43797

Comparing the chromatic dispersions of two single-mode silica fibres with pure F and pure GeO2 doping, respectively 21 p3208 A83-44966

Measurement of relative oscillator strengths for Ti I, III Weak transitions from levels a3F(3, 4) (0.02 eV, 0.05 eV), a5F(1-5) (0.81 eV-0.85 eV), a1D(2) (0.90 eV), a3P(0-3) (1.05 eV-1.07 eV) with solar analysis --- for spectrum analysis of cool stars 22 p3388 A83-46538

FLUORINE COMPOUNDS

NT BARIUM FLUORIDES

NT BORON FLUORIDES

NT CALCIUM FLUORIDES

NT COPPER FLUORIDES

NT DEUTERIUM FLUORIDES

NT DIFLUORO COMPOUNDS

NT FLUORIDES

NT FLUORINE ORGANIC COMPOUNDS

NT FLUOROCARBONS

NT FLUOROHYDROCARBONS

NT HYDROFLUORIC ACID

NT LITHIUM FLUORIDES

NT MAGNESIUM FLUORIDES

NT METAL FLUORIDES

NT NICKEL FLUORIDES

NT POLYTETRAFLUOROETHYLENE

NT POLYVINYL FLUORIDE

NT SULFUR FLUORIDES

NT URANIUM FLUORIDES

Ultraviolet absorption spectra of FNO3 and HOF --- in stratosphere 15 p2194 A83-34041

FLUORINE ISOTOPES

Warm CNO nucleosynthesis as a possible enrichment mechanism for oxygen and fluorine isotopes --- stellar burning 05 p0699 A83-17014

FLUORINE ORGANIC COMPOUNDS

NT FLUOROCARBONS

NT FLUOROHYDROCARBONS

NT POLYVINYL FLUORIDE

Electron-tunneling measurements on TSeF-TCNQ 11 p1662 A83-28073

Magnetic anisotropy of the organic conductors /TMTTF/2X 11 p1662 A83-28075

Fluoroelastomers --- materials for hostile fluid environments 16 p2336 A83-36066

Millimeter wave spectroscopic studies of collision-induced energy transfer processes in the (C-13)H3F laser 22 p3301 A83-46823

FLUORINE COMPOUNDS

NT DIFLUORO COMPOUNDS

NT FLUORINE ORGANIC COMPOUNDS

NT FLUOROCARBONS

NT FLUOROHYDROCARBONS

NT POLYTETRAFLUOROETHYLENE

FLUOROCARBONS

Calculation of SF6-/SF6 and Cl-/CFC13 electron attachment cross sections in the energy range 0-100 meV 05 p0613 A83-17231

A statistical analysis of Umkehr measurements of 32-46 km ozone 07 p0957 A83-20803

Stratospheric N2O, CF2Cl2, and CFC13 composition studies utilizing in situ cryogenic, whole air sampling methods 13 p1873 A83-30891

[AD-A128389] 13 p1873 A83-30891

Global distribution and southern hemispheric trends of atmospheric CCl3F 14 p2056 A83-31920

Fluorocarbon combustion studies. VI - Competitive combustion reactions of fluorocarbons burning with fluorine 14 p1991 A83-32942

Is there any chlorine monoxide in the stratosphere? 17 p2546 A83-38625

Simultaneous detection of FC-11, FC-12 and FC-22, through 8 to 13 micrometers IR solar observations from the ground 19 p2862 A83-41113

Yield of excited iodine atoms during many-photon dissociation of CF3I and (CF3)3CI 20 p2993 A83-42287

Crosslinking of fluorocarbon elastomers - Characterization of crosslinking system to obtain transparent, tough materials 22 p3270 A83-46906

The atmospheric lifetime experiment. III - Lifetime methodology and application to three years of CFCL3 data 24 p3606 A83-49330

FLUOROHYDROCARBONS

Experimental study of electrochemical fluorination of trichloroethylene 04 p0456 A83-15870

Formation of free fluorine atoms by laser-collisional initiation of the CH3F + F2 reaction 20 p2997 A83-43789

FLUOROMICA

U MICA

FLUOROPOLYMERS

NT POLYTETRAFLUOROETHYLENE

NT POLYVINYL FLUORIDE

NT TEFLON (TRADEMARK)

FLUOROSCOPY

Field investigation of techniques for remote laser sensing of oceanographic parameters 10 p1419 A83-25643

A small, battery-operated fluoroscopic system - Lixiscope with X-ray generator 16 p2355 A83-35761

FLUTING

U GROOVING

FLUTTER

NT PANEL FLUTTER

NT SUBSONIC FLUTTER

NT SUPERSONIC FLUTTER

NT TRANSONIC FLUTTER

Unsteady Newton-Busemann flow theory. III - Frequency dependence and indicial response 04 p0476 A83-15149

The effect of backlash and trailing-edge strips on the flutter speed of a two-dimensional model of a tailplane with tab 06 p0716 A83-18068

Friction damping of flutter in gas turbine engine airfoils 09 p1206 A83-24038

Stochastic control and identification enhancement for the flutter suppression problem 10 p1379 A83-26544

On the critical speed of empennage flutter with allowance for the rudder 12 p1704 A83-29286

Application of multiple objective optimization techniques to finite element model tuning --- for flutter analysis of T-38 aircraft horizontal stabilizer [AIAA 83-1010] 12 p1740 A83-29796

Design of the flutter suppression system for DAST ARW-1R - A status report 12 p1702 A83-29868

Active suppression of aeroelastic instabilities on a forward swept wing [AIAA 83-0991] 12 p1704 A83-29869

Anti-flutter control concept using a reduced non-linear dynamic model of elastic structure aircraft [AIAA 83-0993] 12 p1704 A83-29870

On measuring transonic dips in the flutter boundaries of a supercritical wing in the wind tunnel [AIAA 83-1031] 12 p1703 A83-29878

Performance of an angular flange aeroelastic wind energy converter 13 p1870 A83-30200

Stability study of a tilt-rotor aircraft model 13 p1806 A83-31172

Effects of friction dampers on aerodynamically unstable rotor stages [AIAA PAPER 83-0848] 14 p1976 A83-32791

Active flutter suppression using eigenspace and linear quadratic design techniques [AIAA PAPER 82-2222] 19 p2803 A83-41702

Algorithms for real-time flutter identification [AIAA PAPER 83-2223] 19 p2859 A83-41703

Divergence suppression system for a forward swept wing configuration with wing-mounted stores [AIAA PAPER 83-2125] 19 p2806 A83-41949

FLUTTER ANALYSIS

Prediction of transonic flutter for a supercritical wing by modified strip analysis 01 p0058 A83-10190

Analysis and flight data for a drone aircraft with active flutter suppression 01 p0008 A83-10192

Application of matrix singular value properties for evaluating gain and phase margins of multiloop systems --- stability margins for wing flutter suppression and drone lateral attitude control 02 p0230 A83-12457

Aerodynamic characteristics of a slotted vs smooth-skin supercritical wing model 04 p0443 A83-15324

A program system for dynamic analysis of aeronautical structures /HAJIF-II/ 04 p0497 A83-15545

System identification and aircraft flutter 04 p0497 A83-15546

Numerical prediction of choking flutter of axial compressor blades [AIAA PAPER 83-0006] 05 p0596 A83-16458

A root locus based flutter synthesis procedure [AIAA PAPER 83-0063] 05 p0653 A83-16495

Dynamic analysis of constant-lift and free-tip rotors 06 p0773 A83-18386

Flight flutter testing with emphasis on the tip vane method [ONERA, TP NO. 1982-109] 06 p0717 A83-18435

On the stability of boundary-layer flow over a spring-mounted piston 06 p0757 A83-19017

The effect of aerodynamic coupling between the blades of a cascade on the aerodynamic damping of blade vibrations and the onset of blading flutter 06 p0777 A83-19312

FLUTTER ANALYSIS

Flutter of orthotropic panels in supersonic flow using affine transformations 07 p0944 A83-19821

The effect of the geometric parameters of a compressor cascade on the threshold of the self-excited flexural vibration of the blades due to cascade flutter 07 p0946 A83-20911

Flight test results of an active flutter suppression system 08 p1047 A83-22164

State-space aeroelastic modeling and its application in flutter calculation 10 p1442 A83-26761

Application of laser holographic interferometry to vibration analysis of aircraft beam structure model 10 p1442 A83-26765

The excitation of a fluid-loaded plate stiffened by a semi-infinite array of beams 11 p1594 A83-27995

Optimum cone angles in aeroelastic flutter 11 p1599 A83-28720

Unified panel flutter theory with viscous damping effects 12 p1734 A83-28968

Near-real-time flutter boundary prediction from turbulence excited response [AIAA 83-0814] 12 p1741 A83-29814

Flutter and forced response of mistuned rotors using standing wave analysis [AIAA 83-0845] 12 p1742 A83-29823

Flutter analysis of advanced turbopropellers [AIAA 83-0846] 12 p1742 A83-29824

Calculation of unsteady aerodynamic coefficients using transonic time domain methods [AIAA 83-0885] 12 p1697 A83-29833

Effects of viscosity on transonic-aerodynamic and aeroelastic characteristics of oscillating airfoils [AIAA 83-0888] 12 p1697 A83-29835

Flutter analysis of a transport wing using XTRAN3S [AIAA 83-0922] 12 p1743 A83-29848

Aeroelastic considerations for continuous patrol/high altitude surveillance platforms [AIAA 83-0924] 12 p1702 A83-29850

Describing function flutter analysis for transonic flow Extension and comparison with time marching analysis [AIAA 83-0958] 12 p1744 A83-29859

Airfoil shape and thickness effects on transonic airloads and flutter [AIAA 83-0959] 12 p1702 A83-29860

Vibration and flutter of advanced composite lifting surfaces [AIAA 83-0961] 12 p1744 A83-29861

The design, testing and analysis of aeroelastically tailored transonic flutter model wings [AIAA 83-1027] 12 p1702 A83-29876

Wind tunnel correlation study of aerodynamic modeling for F/A-18 wing-store tip-missile flutter [AIAA 83-1028] 12 p1703 A83-29877

Transonic interference effects in testing of oscillating airfoils [AIAA 83-1032] 12 p1698 A83-29883

Bending effects on structural dynamic instabilities of transonic wings [AIAA 83-0920] 12 p1745 A83-29887

Supersonic flow past a body with prescribed oscillations of its surface 13 p1803 A83-30002

Test demonstration of digital control of wing/store flutter 13 p1805 A83-30163

A three degree-of-freedom, typical section flutter analysis using harmonic transonic air forces [AIAA PAPER 83-0960] 14 p2032 A83-32797

Compressible helicoidal surface theory for propeller aerodynamics and noise 14 p1971 A83-32986

Rigid-body structural mode coupling on a forward swept wing aircraft 19 p2797 A83-41046

Transonic flutter model study of a supercritical wing and winglet 19 p2857 A83-41048

Transonic wind tunnel test on an oscillating flap [AIAA PAPER 83-2132] 19 p2793 A83-41954

Flutter investigation of a repaired T-38 horizontal stabilizer using NASTRAN 20 p3002 A83-42541

Finite element model tuning via multiple objective optimization techniques 20 p3002 A83-42542

Unsteady aerodynamic forces and flutter analysis for a wing-aileon-tab configuration 20 p3008 A83-43688

Optical design and aeroelastic investigation of segmented windmill rotor blades 21 p3166 A83-44028

Finite element analysis of 3-ply laminated conical shell for flutter 21 p3160 A83-45052

Design of a candidate flutter suppression control law for DAST ARW-2--- Drones for Aerodynamic and Structural Testing Aeroelastic Research Wing [AIAA PAPER 83-2221] 23 p3402 A83-47125

Cascade flutter analysis of cantilevered blades [ASME PAPER 83-GT-129] 23 p3408 A83-47958

Flutter of mistuned turbomachinery rotors [ASME PAPER 83-GT-153] 23 p3465 A83-47979

On the energy characteristics of the aerodynamic matrix and the relationship to possible flutter 23 p3398 A83-48144

- Evaluation of four subcritical response methods for on-line prediction of flutter onset in wind tunnel tests 23 p3413 A83-48212
- Effects of angle of attack on transonic flutter of a supercritical wing 23 p3403 A83-48213
- International Symposium on Aeroelasticity, Nuremberg, West Germany, October 5-7, 1981, Collected Papers [DGLR BERICHT 82-01] 24 p3543 A83-49176
- Unsteady airloads on supercritical wings 24 p3544 A83-49179
- Survey of aeroelastic wind tunnel and flight testing methods at MBB 24 p3550 A83-49181
- Practical applications of system identification in flutter testing 24 p3550 A83-49182
- Experience from flight flutter testing with tip vanes on Airbus 24 p3547 A83-49183
- Identification and control of flutter on military combat aircraft 24 p3547 A83-49187
- Strength-flutter structural optimization of a supersonic cruise combat aircraft 24 p3547 A83-49190
- Active control of near frequency coalescence flutter 24 p3549 A83-49191
- The F-4 flutter suppression program 24 p3547 A83-49192

FLUX (RATE PER UNIT AREA)

U FLUX DENSITY

FLUX (RATE)

- NT HEAT FLUX
- NT MAGNETIC FLUX
- NT SOLAR FLUX

- Energetic electron fluxes and ionospheric absorption during the August event 1972 09 p1301 A83-23672
- The evaluation of predictive schemes for the growth or decay of rain areas 11 p1624 A83-27000

FLUX DENSITY

- NT CURRENT DENSITY
- NT ELECTRON FLUX DENSITY
- NT ILLUMINANCE
- NT IRRADIANCE
- NT LUMINANCE
- NT LUMINOUS INTENSITY
- NT NEUTRON FLUX DENSITY
- NT PARTICLE FLUX DENSITY
- NT PHOTON DENSITY
- NT PROTON FLUX DENSITY
- NT RADIANCE
- NT RADIANT FLUX DENSITY
- NT SOLAR CONSTANT
- NT SOLAR FLUX DENSITY
- NT SOUND INTENSITY
- ULF geomagnetic power near L = 4. VII - A Conjugate area study of power controlled by solar wind quantities 05 p0660 A83-17391
- Reaction of metal-target vaporization to energy-flux modulation 06 p0765 A83-18445
- Methods for the recovery of the spectral density of the energy brightness of natural objects on the basis of integral measurements 07 p0951 A83-19916
- Rapid variability in 3C273 at 1 mm 07 p1008 A83-21202
- Dynamic properties of gravitational fields 14 p2079 A83-32351
- Zebra pattern flux density observation during the type IV burst on October 12, 1981 15 p2280 A83-34304
- An upper limit to the microwave continuum radiation from Comet Austin (1982g) 15 p2248 A83-34650
- Observations of galaxies of high surface brightness at 102 MHz 17 p2594 A83-38550
- A simple scheme for daytime estimates of the surface fluxes from routine weather data 18 p2724 A83-39675
- A neutrino-dominated universe? 18 p2777 A83-39782
- A quantitative description of the spatial distribution and dynamics of the energy flux in the continuous aurora 22 p3327 A83-46053

FLUX MAPPING

U FLUX DENSITY

U MAPPING

FLUX QUANTIZATION

- Variations in short-wave solar radiation 01 p0129 A83-10598
- Fluxon propagation in Josephson junction transmission lines coupled by resistive networks 01 p0036 A83-10639
- Reynolds stresses and differential rotation. II - Mean-field models 02 p0174 A83-12976
- Comparison of absolute photoelectron fluxes measured on AE-C and AE-E with theoretical fluxes and predicted and measured N2 2PG 3371A volume emission rates 08 p1137 A83-23118
- Trapped flux readout for an electrostatically supported superconducting gyroscope 11 p1576 A83-28786
- Modeling of the interaction of a confined electron beam with an electromagnetic wave in distributed-emission magnetron-type systems 13 p1833 A83-30703

- Remote sensing of a flux transfer event with energetic particles 13 p1966 A83-31230
- The use of METEOSAT for solar radiation mapping 14 p2049 A83-31845
- Quantitative intensity measurements using a soft X-ray streak camera 14 p2022 A83-33417
- Observations and modeling of downward radiative fluxes /Solar and Infrared/ in urban/rural areas 18 p2712 A83-39114
- Meteosat measurements of vertical fluxes in thunderstorms 20 p3031 A83-42966
- A practical approach to flux measurements of long duration in the marine atmospheric surface layer 22 p3338 A83-45710
- A measurement of the IR flux from a radio lobe 23 p3526 A83-47871

FLUXMETERS

- U MAGNETIC MEASUREMENT
- U MEASURING INSTRUMENTS

FLY ASH

- Ambient airborne solids concentrations including volcanic ash at Hanford, Washington sampling sites subsequent to the Mount St. Helens eruption 07 p0960 A83-20207
- Fatigue crack propagation in composites with spherical fillers. I 08 p1055 A83-22715

FLY BY WIRE CONTROL

- Air data systems for airplanes of the 1990's 01 p0004 A83-11099
- F-104 CCV research flight test program 07 p0867 A83-20074
- Nonlinear filter for pilot's remnant attenuation 09 p1209 A83-24436
- A discrete tracking control law for nonlinear plants --- applied to F-8 aircraft stall recovery 10 p1378 A83-26503
- Self-tuning fly-by-wire control system 10 p1379 A83-26603
- In-flight simulation of a digitally implemented direct force mode --- for flight control 14 p1977 A83-32933
- Redundancy Management of Shuttle flight control rate gyroscopes and accelerometers 17 p2474 A83-37123
- Validation of the KC-10 refueling boom digital control system [SAE PAPER 821421] 17 p2463 A83-37978
- Flight-test results using nonlinear control with the F-8C digital fly-by-wire aircraft [AIAA PAPER 83-2174] 19 p2802 A83-41669
- Flight clearance of the Jaguar fly by wire aircraft. I 22 p3254 A83-45845
- Flight clearance of the Jaguar-fly-by-wire aircraft. II 22 p3255 A83-45846
- Effect of aircraft configuration and control integration on surface actuation [AIAA PAPER 83-2487] 23 p3404 A83-48347

FLYBY MISSIONS

- NT ASTEROID MISSIONS
- NT GIOTTO MISSION
- NT GRAND TOURS
- NT VOYAGER 1977 MISSION
- A theoretical study of Comet Halley's spectrum in the infrared range 03 p0407 A83-13841
- Outer-planet probe/flyby missions [AIAA PAPER 83-0522] 05 p0600 A83-16767
- By Jupiter: Odysseys to a giant --- Book 05 p0704 A83-17118
- Micron-sized particles detected near Saturn by the Voyager plasma wave instrument 11 p1684 A83-27357
- The Comet Halley flyby I.R. sounder 'I.K.S.' --- infrared spectrometer 11 p1670 A83-27740
- Cometary probe of the Venera-Halley mission 15 p2124 A83-35011
- Planet-A mission to Halley 15 p2124 A83-35012
- Cometary ephemerides for spacecraft flyby missions 15 p2249 A83-35017
- Dust modelling of fast flyby missions - Implications of in situ measurements 15 p2128 A83-35022
- Giotta - The European spacecraft to flyby Halley's comet 17 p2473 A83-37862
- The Voyager mission to Uranus and beyond 18 p2644 A83-39967
- Return to Jupiter - Project Galileo 18 p2644 A83-40344
- To Uranus and beyond 21 p3240 A83-44326

FLYING BEDSTEAD AIRCRAFT

U FLYING PLATFORMS

FLYING EJECTION SEATS

- Preliminary analyses of flail, windblast and tumble problems and injuries associated with usage of U.S. Navy Aircrew Automated Escape Systems /AAES/ 04 p0444 A83-15407
- Escape low and hot --- vertical-seeking, steerable ejection seat design for F-14A aircraft 13 p1806 A83-31587

- Vertical seeking ejection seat boosts pilots odds 18 p2641 A83-40305
- Hazards of loose harness during flying 23 p3499 A83-48693

FLYING PERSONNEL

- NT AIRCRAFT PILOTS
- NT ASTRONAUTS
- NT COSMONAUTS
- NT FLIGHT CREWS
- NT PILOTS (PERSONNEL)
- NT SPACECREWS
- NT TEST PILOTS
- Numerical and psychopathological data bearing upon 700 certifications of civil aviation flight personnel 06 p0799 A83-18333
- A presentation of a new protocol for the evaluation of color sense in aeronautics 08 p1147 A83-22956
- The pressure problems of the middle ear in flight personnel - The importance of impedancemetric examinations 08 p1147 A83-22958
- Extrasystoles and the fitness of flight personnel - The contribution of the stress EKG tests 08 p1147 A83-22961
- The importance of determining the systole timing of the left ventricle in the selection of flight personnel 08 p1147 A83-22962
- The detection of drug addiction among flight personnel 08 p1148 A83-22965
- Some considerations on lumbar pains and diseases of the intervertebral disk to civilian aircrewmembers 08 p1148 A83-22974
- Echocardiography in assessment of cardiovascular problems of Air Force personnel 09 p1323 A83-24006
- The chemoprophylaxis of malaria in flight personnel 14 p2067 A83-32452
- Current barotraumatic otitis of the commercial flight personnel in civil aviation 14 p2067 A83-32454
- Problems of fitness posed by vertebral pathology in flight personnel 16 p2397 A83-35584
- Psychiatric assessment of female fliers at the U.S. Air Force School of Aerospace Medicine (USAFSAM) 24 p3618 A83-48883

FLYING PLATFORM STABILITY

U AERODYNAMIC STABILITY

U FLYING PLATFORMS

- Lidar meteorology 01 p0073 A83-10016
- On the rotary wing concept for jet stream electricity generation 04 p0507 A83-16111
- Transmission effects of explosion-produced dust clouds on downward viewing airborne platforms 08 p1132 A83-22543
- Bo 105 rotor blade influence on the Calipso FLIR in the mast-mounted observation platform Ophelia 08 p1044 A83-23249
- Putting the microlight to work 09 p1195 A83-23686
- Aeroelastic considerations for continuous patrol/high altitude surveillance platforms [AIAA 83-0924] 12 p1702 A83-29850
- The UTIC hard X-ray balloon-borne platform 13 p1936 A83-30396
- Airborne reconnaissance in the civilian sector - Agricultural monitoring from high-altitude powered platforms 18 p2706 A83-39939
- ASTROPLANE - A European airborne observatory for infrared astronomy 18 p2762 A83-40455
- Pointing requirements for space station science [AAS PAPER 83-061] 21 p3095 A83-44174

FLYING QUALITIES

U FLIGHT CHARACTERISTICS

FLYING SPOT SCANNERS

- Multiwavelength operation of an acousto-optic deflector --- for laser flight simulation displays 21 p3140 A83-44839

FLYING WING AIRCRAFT

U TAILLESS AIRCRAFT

FLYWHEELS

- Reliability analysis of circumferentially wound FRP flywheels 07 p0950 A83-21625
- Composite flywheels with rim and hub 08 p1073 A83-21992
- Study on composite flywheels for energy storage 08 p1131 A83-22701
- Construction of an optimal filter in the problem of the flywheel control of an artificial earth satellite 09 p1218 A83-25041
- Energy utilization of electric and hybrid vehicles 11 p1667 A83-27164
- Recent advances in composite flywheel containment design technology 11 p1589 A83-27302
- Compression molded energy storage flywheels 11 p1608 A83-27303
- Twin disk composite flywheel 11 p1609 A83-27304

- Program overview and diesel/flywheel hybrid power train design - Fibre composite flywheel development program for road vehicle applications 11 p1667 A83-27306
- Fibre composite rotor selection and design /Fibre composite flywheel development program for road vehicle applications/ 11 p1667 A83-27307
- Manufacture and testing of fibre composite rotor components /Fibre composite flywheel development program for road vehicle applications/ 11 p1667 A83-27308
- Analysis of fixed-base flywheel systems for electric utility applications 11 p1609 A83-27310
- The calculation of energy storage flywheels of fiber composites with electric energy converter --- German thesis 11 p1590 A83-28666
- An epoxy resin system for composite flywheels 12 p1711 A83-29893
- The design of flywheels made of fibrous materials 14 p2046 A83-32378
- Material behavior in connection with flywheel friction welding of superalloys 15 p2137 A83-33965
- Composite flywheel rotor containment 18 p2709 A83-40294
- Fabrication and spin tests of composite flywheels 18 p2709 A83-40295
- Low cost energy storage flywheels from structural steel molding compound 22 p3318 A83-46299
- Controllabilization and observabilization of the attitude control system with flywheel [IAF PAPER 83-341] 23 p3422 A83-47350
- Choice of parameters for a flywheel energy storage system --- for spacecraft 24 p3552 A83-49674
- FM/PM (MODULATION)**
- The superposition principle in acoustics 04 p0533 A83-15450
- Numerical calculation of spectra for digital FM signals 07 p0909 A83-19747
- FOAMING**
- The effect of oceanic whitecaps and foams on pulse-limited radar altimeters 10 p1452 A83-25973
- FOAMS**
- NT METAL FOAMS**
- Detection of strength limiting defects in cellular glasses by dielectric measurements 03 p0302 A83-13248
- Some properties of foamed material-aluminium composites 05 p0611 A83-17108
- Removable foam encapsulants 09 p1237 A83-23617
- Debris from spallation of foam insulation of cryogenic fuel tanks in space launch systems [AIAA PAPER 83-1457] 14 p1980 A83-32718
- Microstructure of semi-crystalline thermoplastics structural foams 16 p2336 A83-35569
- On the application of an integral equation method for the solution of heat transfer problems in heterogeneous and cellular media 20 p2971 A83-42664
- Reinforced polyester structural foam 22 p3264 A83-46300
- FOCI**
- NT PLASMA FOCUS**
- The properties of focused fields --- for optical beams 15 p2147 A83-35152
- FOCUSING**
- NT DEFOCUSING**
- NT SELF FOCUSING**
- Toroidal mirror with adjustable bending radius for X-ray imaging 02 p0237 A83-12699
- Focussing of submillimeter radiation guided by a dielectric sheet 04 p0535 A83-15810
- Problem of accurate intensity measurements in focused laser beams 10 p1433 A83-26683
- Evaluation of the thermal focal length produced in a repetitively pulsed solid-state laser 13 p1857 A83-31379
- Investigation of the spherical and chromatic aberrations of the 400/2000 double wide-angle astrophotograph 14 p2095 A83-31839
- Multisection planar focusing lenses as concentrators of solar radiation 14 p2036 A83-32047
- The combination of hollow focusing concentrators with fiber-optic waveguides --- for solar energy transmission 14 p2036 A83-32048
- Primary-focus operation of shaped dual-reflector antennas 15 p2149 A83-35199
- Electrostrictive limit and focusing effects in pulsed photoacoustic detection 18 p2692 A83-39261
- Microwave radio meteorology - Fading by beam focusing 19 p2833 A83-41405
- Theoretical studies in isoelectric focusing --- mathematical modeling and computer simulation for biologicals purification process 20 p2951 A83-43280
- Effect of focusing and detection lenses on the Raman frequency spectrum in a laser plasma 21 p3210 A83-44132
- Computer simulation of model isoelectric focusing experiments 22 p3266 A83-45760
- Focusing antennas usage in locating acoustic sources [ONERA, TP NO. 1983-75] 23 p3505 A83-48190
- Theory of phase conjugation by degenerate four-wave mixing using spatially varying pump beams 24 p3623 A83-48978
- Axial irradiance and optimum focusing of laser beams 24 p3588 A83-49015
- FOETUSES**
- U FETUSES**
- FOG**
- Combustion-related pollutants of polydisperse single-composition aerosols and advection fog formation 01 p0070 A83-10226
- A statistical method of forecasting radiation-fog at the Rhein-Main-Airport 02 p0214 A83-12300
- Drop-size distribution of fog droplets determined from transmission measurements in the 0.53-10.1-microns wavelength range 03 p0365 A83-14378
- Fog visibility and ceilings [AIAA PAPER 83-0207] 05 p0666 A83-16584
- Fogwater composition in southern California [AIAA PAPER 83-0362] 05 p0659 A83-16671
- Numerical simulation of fog formation and liquid water content on polydisperse multi-composition aerosols due to combustion-related pollutants 07 p0963 A83-21038
- Effect of the aerosol on fog microstructure 08 p1140 A83-22355
- Measurements of the properties of wintertime fog and haze in West Germany - A preliminary report on project 'Meppen 80' 08 p1141 A83-22549
- Optical properties of model aerosols growing into fogs 08 p1135 A83-22551
- A comparison between the calculated and measured characteristics of an advection fog and a stratus over ice 09 p1316 A83-25229
- A method of calculating fluxes and the influx of long-wave and solar radiation in a model of low clouds and fogs 09 p1317 A83-25235
- The use of geostationary satellite imagery for observing and forecasting movement of New England sea fog 13 p1886 A83-30552
- Radiation-fog intensities associated with surface synoptic patterns at Albany, New York 13 p1890 A83-30592
- Explanation for the inverse partial polarization of fog glories compared with rainbows and fogbows 14 p2057 A83-32413
- Simultaneous determination of complex refractive index and size distribution of airborne and water-suspended particles from light scattering measurements 14 p2052 A83-32440
- The influence of atmospheric aerosol on the life cycle radiation fog 15 p2205 A83-34066
- The prediction of the dissipation of radiation fogs over Sofia airport 15 p2206 A83-34415
- An approximate procedure to isolate single scattering contribution to lidar returns from fogs 15 p2207 A83-35290
- Fogwater chemistry in an urban atmosphere 16 p2372 A83-36128
- An investigation of the spectral transmission of a crystalline cloud medium 16 p2392 A83-36869
- The Fog Project - 1982 17 p2549 A83-38721
- Forecasting upslope stratus and fog in the central plains 17 p2550 A83-38725
- DFVLR-remote slant visual range (SVR) and wind vector measuring systems 17 p2552 A83-38750
- Organic films on atmospheric aerosol particles, fog droplets, cloud droplets, raindrops, and snowflakes 18 p2719 A83-40329
- Accelerated precipitation of water fogs due to acoustic action of a CO2 laser pulse 20 p3028 A83-42278
- A dynamic model for the production of H(+), NO3(-), and SO4(2-) in urban fog 20 p3013 A83-42844
- Effect of a CO2 laser pulse on transmission through fog at visible and IR wavelengths 24 p3588 A83-49003
- Mechanisms of radiation fog formation on four consecutive nights 24 p3611 A83-49678
- FOG DISPERSAL**
- Diffusion mechanism of the interaction of aerosol drops and the possibility of controlling this mechanism by means of electromagnetic radiation 13 p1874 A83-30043
- A two-dimensional model of the electrocoagulation-hygroscopic dissipation of warm fogs 18 p2724 A83-39442
- FOIL BEARINGS**
- Advanced development of air-lubricated foil thrust bearings [ASLE PREPRINT 82-LC-6B-1] 03 p0335 A83-13246
- Analysis of gas lubricated compliant thrust bearings [ASME PAPER 82-LUB-39] 03 p0336 A83-13518
- Analysis of gas-lubricated foil journal bearings [ASME PAPER 82-LUB-40] 03 p0336 A83-13519
- Test experience with turbine-end foil bearing equipped gas turbine engines [ASME PAPER 83-GT-73] 23 p3407 A83-47926
- FOILS (MATERIALS)**
- NT METAL FOILS**
- H atom detection and energy analysis by use of thin foils and TOF technique --- Time Of Flight apparatus 05 p0644 A83-16923
- Extended capabilities of a vibrating-reed internal friction apparatus 07 p0932 A83-21385
- FOKKER AIRCRAFT**
- NT F-28 TRANSPORT AIRCRAFT**
- FOKKER BOND TESTERS**
- U ADHESION TESTS**
- FOKKER F 28 AIRCRAFT**
- U F-28 TRANSPORT AIRCRAFT**
- FOKKER-PLANCK EQUATION**
- An exact solution to a certain non-linear random vibration problem 02 p0233 A83-12868
- Numerical modeling of the energy spectrum of the cosmic ray Forbush decrease 07 p1040 A83-21504
- Stochastic diffusion in inverse square fields - General formulation for interplanetary gas 07 p1028 A83-21576
- A model description of fluxes of high-energy protons trapped by the geomagnetic field 10 p1523 A83-26103
- Suprathermal electron energy deposition in plasmas with the Fokker-Planck method 21 p3215 A83-45520
- Quantum statistics of parametric oscillation 22 p3356 A83-45930
- FOLDING STRUCTURES**
- Designing an umbrella-type folding antenna 22 p3272 A83-45688
- FOLDS (GEOLOGY)**
- The use of space images to study tectonics and to predict antimony-mercury mineralization in the Southern Tien Shan 07 p0950 A83-19905
- Reconstruction of the strike-slip faults of the Adycha-Taryn region 23 p3483 A83-48110
- FOLIAGE**
- Application of computer axial tomography /CAT/ to measuring crop canopy geometry --- corn and soybeans 01 p0065 A83-10096
- FOOD**
- An evaluation of microorganisms for unconventional food regeneration schemes in CELSS - Research recommendations [SAE PAPER 820852] 13 p1899 A83-30940
- FOOD CHAIN**
- Use of Landsat data to predict the trophic state of Minnesota lakes 07 p0952 A83-21432
- FOOD INTAKE**
- The antihypoxic effectiveness of alimentary fasting 02 p0219 A83-11521
- Effects of time and duration of exposure to 12% O2 and prior food deprivation on hypoxic hypophagia of rats 04 p0519 A83-15536
- The opioid peptide dynorphin, circadian rhythms, and starvation 05 p0669 A83-16940
- The tolerance to physical loads among patients with ischemic heart disease as a function of diet and the time when food is taken 05 p0673 A83-17173
- The nutritional and microbiological aspects of the onboard meal for pilots of international airlines 08 p1148 A83-22967
- FOOD PROCESSING**
- NT CANNING**
- FORBIDDEN BANDS**
- Proposed Mg V, Fe XIV and forbidden Fe XVII line identifications in the EUV solar spectrum 03 p0438 A83-14907
- Ansaes and the precession of central stars in planetary nebulae - The cases of NGC 5189 and NGC 6826 07 p1008 A83-21208
- High spectral resolution observations of forbidden Si II lines in the planetary nebula IC 418 at the CES spectrograph 09 p1356 A83-25294
- On the observability of forbidden lines 14 p2086 A83-31938
- Bright emission lines in new Seyfert galaxies 15 p2269 A83-34676
- The expansion velocity field within the planetary nebula NGC 7008 17 p2587 A83-37290
- Isophotes of a field in the Cygnus Loop photographed in the forbidden O III and forbidden N II + H-alpha lines 17 p2613 A83-38632
- FORBIDDEN TRANSITIONS**
- Discovery of a large, high-excitation planetary nebula at l = 136 deg, b = -5 deg 03 p0411 A83-14781
- Forbidden line emission from highly ionized atoms in tokamak plasmas 04 p0538 A83-16060
- Spatial-kinematical models for planetary nebulae - NGC 2371-2 05 p0701 A83-17671
- Electron impact excitation of forbidden transitions in Si IX 06 p0835 A83-19012

- Observations of the red auroral oxygen lines in nine comets 06 p0822 A83-19074
- A determination of the collision relaxation constants for a forbidden transition by means of nonlinear polarization spectroscopy for a three-level gas in a magnetic field 06 p0809 A83-19541
- Observations of the 145.5 micron O I forbidden emission line in the Orion Nebula 07 p1023 A83-21155
- Multiconfiguration Hartree-Fock Breit-Pauli results for 2P1/2-2P3/2 transitions in the boron sequence 08 p1162 A83-21985
- Observations of M42 in the O III 52 and 88-micron forbidden lines, the O I 63-micron forbidden line, and the N III 57-micron forbidden line 09 p1362 A83-24977
- Transition probabilities for forbidden lines in the 3p4 configuration. III --- in astrophysics 09 p1362 A83-24986
- Neon forbidden lines in Nova Aql 1982 11 p1682 A83-28291
- N I /3466 A/ and N I /5200 A/ emissions from various nighttime and daytime auroras 11 p1618 A83-28317
- Line ratios for O VII --- solar spectra 13 p1965 A83-31712
- Distribution of forbidden neutral carbon emission in the ring nebula (NGC 6720) 15 p2257 A83-34093
- Electron density in solar atmosphere from forbidden lines 16 p2440 A83-36545
- An H-alpha forbidden N II survey of the nuclei of a complete sample of spiral galaxies 17 p2602 A83-37827
- Electron impact excitation of forbidden transitions in Ca XV 17 p2579 A83-38367
- Expected intensities of solar forbidden lines emitted from 2p(k) (k = 2, 3, 4) configurations 18 p2780 A83-39018
- Stark interference effects in a weak magnetic field on the 6S-7S forbidden transition of cesium 19 p2898 A83-41180
- Determinations of S III, O IV, and Ne V abundances in planetary nebulae from infrared lines 19 p2919 A83-41630
- Rapid variations in forbidden emission line profiles in a Seyfert 2 galaxy 20 p3065 A83-42329
- Probabilities for transition processes crucial to Li lasers 22 p3295 A83-45945
- Identification of forbidden transitions in the nu-4 band of (N-14)H3 by intracavity laser-Stark spectroscopy 22 p3355 A83-45966

FORBUSH DECREASES

- The modulation characteristics of the Forbush effect 02 p0273 A83-11727
- Quasi-periodic variations of cosmic-ray anisotropy 02 p0274 A83-11729
- Unusual characteristics of the cosmic ray intensity increase of September 17-18, 1979 02 p0276 A83-12393
- Numerical modeling of the energy spectrum of the cosmic ray Forbush decrease 07 p1040 A83-21504
- An investigation of cosmic ray fluctuations during Forbush decreases 10 p1523 A83-26101

FORBUSH EFFECT**U FORBUSH DECREASES****FORCE**

- A resistance strain gauge for measuring force 11 p1574 A83-28518
- Force and moment in incompressible flows 14 p2012 A83-32991

FORCE DISTRIBUTION

- Application of Ampere's force law to railgun accelerators 01 p0036 A83-10613
- Force distribution in a shell loaded tangentially along a circle 04 p0500 A83-16049
- Calculation of the lift distribution and aerodynamic derivatives of quasi-static elastic aircraft 06 p0712 A83-18151
- Compensation technique for force balance devices 07 p0929 A83-20548
- Mechanisms of cavity growth in creep 07 p0887 A83-20629
- Stabilization of the stationary motions of mechanical systems 14 p2079 A83-32358
- Force balance in the magnetospheres of Jupiter and Saturn 17 p2620 A83-38114
- On the force fluctuations acting on a circular cylinder in crossflow from subcritical up to transcritical Reynolds numbers 23 p3398 A83-48118
- Determination of autonomous three-dimensional force fields from a two-parameter family of orbits 24 p3644 A83-49393

FORCE FIELDS**U FIELD THEORY (PHYSICS)****FORCE-FREE MAGNETIC FIELDS**

- The influence of a flow field on the stability of the force-free magnetic field 04 p0536 A83-15595

- The determination of the alpha factor of force-free magnetic field and the forecast for the solar proton flares 05 p0707 A83-16852
- Invariant structures of magnetic flux tubes 06 p0838 A83-19229
- Theory of quadrupolar sunspots and the active region of August, 1972 15 p2279 A83-34291
- The final state of a solar flare 20 p3080 A83-42376
- Magnetohydrodynamic stability of line-tied coronal arcades. I - Force-free magnetic fields without embedded prominences 20 p3081 A83-43073
- The storage processes of magnetic energy in solar flares 21 p3242 A83-44301
- The mechanism of acceleration of ring current during a substorm of magnetosphere 21 p3171 A83-44302

FORCED CONVECTION

- Heat transfer by laminar forced flow against a rotating disk 01 p0044 A83-10227
- A groundwater convection model for Rio Grande rift geothermal resources 02 p0203 A83-11831
- Fin geometry for minimum entropy generation in forced convection 03 p0315 A83-13483
- Integral method to thermally developing laminar flow in a duct subjected to external radiation and convection [AIAA PAPER 83-0529] 05 p0637 A83-16768
- Heat conduction in an undulating heating wire 06 p0756 A83-18063
- Numerical calculation of pressure loss and forced convective heat transfer in rotating channels of arbitrary rectangular cross section 08 p1083 A83-21634
- An experimental study of unsteady heat transfer from a flat plate to an oscillating air flow 08 p1084 A83-22239
- The effect of forced and free convection in the discharge of a pressurized gas 08 p1090 A83-23210
- Heat transfer from interrupted plates 09 p1259 A83-23879
- Fluid mechanics in crystal growth - The 1982 Freeman scholar lecture 10 p1401 A83-26626
- Oscillatory convection in sunspots 14 p2115 A83-32541
- Combined free and forced laminar convection in a vertical channel 15 p2160 A83-34257
- Combined convection in an annulus applied to a thermal storage problem 15 p2191 A83-34259
- Unsteady forced convective heat transfer from a hot film in non-reversing and reversing shear flow 18 p2681 A83-39348

Heat transfer in turbulent flows

- 20 p2970 A83-42652
- Buoyancy effect on heat transfer in forced channel flows 20 p2971 A83-42661
- Heat transfer 1982; Proceedings of the Seventh International Conference, Technische Universitaet Muenchen, Munich, West Germany, September 6-10, 1982. Volume 3 - General papers: Forced convection, mixed convection 20 p2975 A83-42700
- Combined natural and forced convection in vertical ducts 20 p2979 A83-42749
- Natural, mixed and forced convection in a vertical channel with asymmetric uniform heating 20 p2979 A83-42750
- Forced convection film boiling on a sphere immersed in (a) subcooled or (b) superheated liquid 20 p2981 A83-42770
- Advances in cryogenic engineering. Volume 27 - Proceedings of the Cryogenic Engineering Conference, San Diego, CA, August 11-14, 1981 20 p2960 A83-43220
- An interferometric investigation of separated forced convection in laminar flow past cavities 20 p2986 A83-43360
- Low Reynolds number flow heat exchangers; Proceedings of the Fourth Advanced Study Institute, Ankara, Turkey, July 13-24, 1981 21 p3133 A83-45099

FORCED VIBRATION**U FORCED VIBRATION****FORCED VIBRATION**

- Introduction to the vibration of mechanical systems with internal impacts --- Czech book 01 p0060 A83-10877
- Nonlinear forced oscillations of a rotating shaft carrying an unsymmetrical rotor at the major critical speed 07 p0939 A83-20288
- Numerical calculation of the translational forced oscillations of a sloshing liquid in axially symmetric tanks 07 p0926 A83-21003
- The use of natural modes to describe the forced vibrations of asymmetric shafts on flexible supports 07 p0947 A83-21091
- Covariance analysis of oscillatory systems under combined periodic and random forced vibrations 08 p1160 A83-21862

- Statistical flow-oscillator modeling of vortex-shedding 09 p1196 A83-23337
- Automatic optimization of oscillations in a vibratory system 10 p1462 A83-26066
- Numerical analysis of flexural vibrations of rotors resting on elastic supports 11 p1589 A83-27724
- Vibrations of a shallow shell with an attached mass distributed on part of its surface 12 p1735 A83-29276
- A revised version of the transfer matrix method to analyze one-dimensional structures [AIAA 83-0825] 12 p1742 A83-29821
- Flutter and forced response of mistuned rotors using standing wave analysis 12 p1742 A83-29823
- Collisional forcing of raindrop oscillations 13 p1893 A83-31042
- On small forced oscillations of a nonlinear acoustic resonator 13 p1915 A83-31331
- Vibrational characteristics of a nonlinear system associated with asymmetry in the elastic response 14 p2029 A83-32157
- Forced oscillations of system with nonlinear restoring force 14 p2080 A83-32519
- Some analysis methods for rotating systems with periodic coefficients 14 p2032 A83-32987
- Forced vibrations and their damping 14 p2033 A83-33484
- Analysis of forced vibration by reduced impedance method. III - Damped vibration 15 p2174 A83-34008
- Analysis of forced vibration by reduced impedance method. IV Proposition and application of multiple reduced impedance method 15 p2174 A83-34009
- Excitation and vibration of flexible bladed disks under operating and simulated operation conditions 16 p2305 A83-35881
- Variation of rotor blade vibration due to interaction of inlet and outlet distortion 16 p2305 A83-35882
- Design of dry-friction dampers for turbine blades 16 p2306 A83-35883
- Forced and self-excited vibrations of gas-turbine assemblies with perfect and perturbed symmetry 16 p2311 A83-36791
- Solution of problems in the dynamics of noncircular cylindrical shells in a liquid 17 p2521 A83-37573
- Natural and forced oscillations of open resonance systems based on dielectric disk resonators 17 p2500 A83-38986
- Normal vibrations of a finite-length cylinder with a restrained lateral surface 18 p2701 A83-40114
- Topology of the invariant manifolds of period-doubling attractors for some forced nonlinear oscillators 19 p2895 A83-41166
- Periodically forced linear oscillator with impacts - Chaos and long-period motions 20 p3042 A83-42649
- Determination of the resonance frequency spectrum of the forced vibration of current leads 21 p3138 A83-44634
- Analysis of an axial compressor blade vibration based on wave reflection theory 23 p3409 A83-47970
- [ASME PAPER 83-GT-151] The effect of viscosity on the forced vibrations of a fluid-filled elastic shell 23 p3471 A83-48242
- [ASME PAPER 83-APM-34] Vibration and radiation of a shell of revolution under circumferential loading 23 p3472 A83-48468

FORCED VIBRATORY MOTION EQUATIONS**U FORCED VIBRATION****FOREARM**

- The formation of the vascular-receptor relations in the forearm muscles of humans 07 p0978 A83-20993
- An investigation of the rigidity of a human muscle depending on its length 12 p1766 A83-29318
- Effect of blood volume on forearm venous and cardiac stroke volume during exercise 22 p3347 A83-45995

FOREBODIES**NT ABLATIVE NOSE CONES****NT NOSE CONES****NT ROCKET NOSE CONES**

- Reductions in parachute drag due to forebody wake effects 04 p0443 A83-15315
- Analysis of viscous transonic flow over aircraft forebodies and afterbodies 16 p2295 A83-36362
- [AIAA PAPER 83-1366] Aerodynamics of pointed forebodies at high angles of attack 19 p2793 A83-41942
- [AIAA PAPER 83-2117] Dynamics of forebody flow separation and associated vortices 19 p2793 A83-41943
- [AIAA PAPER 83-2118]

FORECASTING**NT LONG RANGE WEATHER FORECASTING****NT NOWCASTING****NT NUMERICAL WEATHER FORECASTING****NT PERFORMANCE PREDICTION****NT PREDICTION ANALYSIS TECHNIQUES**

- NT STATISTICAL WEATHER FORECASTING
 NT TECHNOLOGICAL FORECASTING
 NT WEATHER FORECASTING
- Utility operating strategy and requirements for wind power forecast 13 p1869 A83-30192
- Worldwide aviation outlook --- for passenger and freight traffic 1982-1992 16 p2297 A83-36952
- [AIAA PAPER 83-1597] 16 p2297 A83-36952
- Predicting eruptions at Mount St. Helens, June 1980 through December 1982 22 p3332 A83-46795
- Seismic precursors to the Mount St. Helens eruptions in 1981 and 1982 22 p3333 A83-46796
- Deformation monitoring at Mount St. Helens in 1981 and 1982 22 p3333 A83-46797
- Solar-flare prognostication by the empirical-statistical approach 24 p3674 A83-48992
- FORECASTS**
 U FORECASTING
- FOREIGN POLICY**
 NT INTERNATIONAL COOPERATION
 NT INTERNATIONAL RELATIONS
 NT OUTER SPACE TREATY
- FORENSIC SCIENCES**
 U LAW (JURISPRUDENCE)
- FOREST FIRE DETECTION**
- Determination of forest fire spread rates from infrared photographs 03 p0350 A83-14307
- Processing infrared images for fire management applications 08 p1094 A83-22434
- Fire mosaics in southern California and northern Baja California 09 p1292 A83-25287
- The use of space imagery to evaluate forest fire damage 14 p2034 A83-32496
- On the determination of the physical characteristics of forest fires by methods of microwave radiometry 14 p2035 A83-32501
- The effect of tree crowns on the microwave emission of forest fires 17 p2535 A83-38977
- FOREST FIRES**
- Integrating non-first order automated meteorological observations into national weather forecasting and analysis programs 13 p1891 A83-30593
- Preparation of a 1:25000 Landsat map for assessment of burnt area on Etajima Island 15 p2183 A83-34152
- Some environmental effects of forest fires in interior Alaska 20 p3015 A83-43430
- FOREST MANAGEMENT**
- The application of remote sensing in southern Alberta's mountain pine beetle management 03 p0347 A83-14257
- A Spot-Landsat comparison simulation in a forested region - Ermenonville 1980 08 p1126 A83-21929
- The visual interpretation of Landsat imagery - The possibilities of the utilization of Landsat imagery improved for forestry studies in tropical regions 08 p1127 A83-21935
- Prospects for multitemporal studies focusing on a forested region - Proof of clear-cutting 08 p1127 A83-21939
- Monitoring recent changes in extent of natural forests in Kenya using remote sensing techniques 08 p1127 A83-21940
- On a method of forest mapping 10 p1444 A83-26825
- Use of Landsat satellite data for multitemporal analysis of Landes forest lumbering. (Nezer forest test site) 15 p2181 A83-33559
- Forest management applications of Landsat data in a geographic information system 15 p2185 A83-34823
- Cartographic modeling - Procedures for extending the utility of remotely sensed data 15 p2186 A83-34830
- Remote-sensing technology applied to forest assessment in California 17 p2528 A83-38152
- Sensor data for forest policy information 17 p2530 A83-38166
- The classification of forest species types using gradient analysis and spectral data 17 p2531 A83-38340
- Utilization of Landsat data to monitor deforestation of Kenya's Mau Forest 17 p2534 A83-38461
- A technique for phenological observations in measurements of the spectral brightness coefficients of vegetation 23 p3476 A83-48111
- The use of the Monte Carlo method in investigating the influence of the dimensions of a conifer on the angular dependence of its coefficient of spectral brightness 23 p3476 A83-48114
- FORESTS**
 NT RAIN FORESTS
- Seasat L-band radar response to forest vegetation in eastern Virginia 01 p0063 A83-10061
- The use of R.B.V., colour additive viewer and M.S.S. products in the British Columbia Forest Inventory Depletion Monitoring Program --- Return Beam Vidicon and Multispectral Scanning 03 p0346 A83-14246
- Landsat-based forest mapping in Ontario north of latitude 52 deg north 03 p0347 A83-14253
- Multitemporal analysis of Landsat data for forest cutover mapping - A trial of two procedures 03 p0347 A83-14254
- Predicting forest land attributes from aerial photo interpretation variables 03 p0347 A83-14259
- The application of forest classification from Landsat data as a basis for natural hydrocarbon emission estimation and photochemical oxidant model simulations in southeastern Virginia 07 p0957 A83-19848
- Some air-photo scale effects on Douglas-fir damage type interpretation 10 p1443 A83-25967
- Remote sensing as a means for units of landscape in forest regions - Applications to the Ambazac Mountains (Limousin, France) 14 p2034 A83-32170
- Spectral signatures obtained from Landsat digital data for forest vegetation and land-use mapping in India 14 p2036 A83-33350
- Seasonal variation of monoterpenes in the atmosphere of a pine forest 15 p2194 A83-34040
- VHF propagation over hilly, forested terrain 15 p2148 A83-35184
- Air pollutants and forest decline 16 p2372 A83-35764
- Aerial photograph interpretation to update and refine LUNR forest land classifications --- New York State Land Use and Natural Resource Inventory 17 p2530 A83-38338
- The use of small scales for a stereoscopic dual chamber with a 'VHF-homing' system for the inventory and monitoring of natural renewable resources 17 p2533 A83-38447
- Evaporation from a partially wet forest canopy 21 p3165 A83-44234
- Mapping of deciduous forest cover using simulated Landsat-D TM data 22 p3311 A83-46166
- Detecting forest canopy change due to insect activity using Landsat MSS 22 p3318 A83-46765
- FORGING**
- Internal shear forging for missiles 01 p0056 A83-10975
- Necklace structure obtained by forging astroloy supersolidus-sintered preforms 02 p0154 A83-11666
- New high-strength aluminum alloy V950ch 03 p0296 A83-13251
- The production of dispersion strengthened aluminium parts by powder forging 06 p0731 A83-19087
- P/M Astroloy obtained by forcing or hiping supersolidus sintered preforms 06 p0732 A83-19100
- Fabrication and heat treatment of a Ni-base superalloy integrally bladed rotor for small gas turbine engine applications 06 p0732 A83-19102
- The occurrence of shear bands in nonisothermal, hot forging of Ti-6Al-2Sn-4Zr-2Mo-0.1Si 07 p0884 A83-20253
- Crack initiation and propagation in a forged nickel-base alloy under high mechanical and thermal loading 07 p0894 A83-21480
- The evolution of the forging processes on discs 07 p0941 A83-21492
- Forging Astroloy supersolidus-sintered preforms - Necklace structure achievement 07 p0896 A83-21502
- Properties and structures of hot isostatic pressed and hot isostatic pressed plus forged superalloys 09 p1236 A83-25286
- Effect of grain flow on creep properties of heat-resistant aluminium-alloy forgings 10 p1394 A83-25473
- The effect of shear bands on service properties of Ti-6Al-2Sn-4Zr-2Mo-0.1Si forgings 10 p1397 A83-25870
- A model for the behavior of the titanium alloy Ti-6 percent Al-4 percent V in the hot forging regime 11 p1551 A83-28808
- Effect of multiple heating at the partial forging of workpieces made of TiAl6V4 12 p1713 A83-29369
- Recent advancements in titanium near-net-shape technology 15 p2171 A83-33633
- Development of process models to produce a dual-property titanium alloy compressor disk 15 p2134 A83-33634
- Flow state of composite materials in the forging die during the molding process 18 p2661 A83-40281
- A constant amplitude fatigue study of an aluminum powder metallurgy alloy 22 p3269 A83-46024
- FORM**
 U SHAPES
- FORM PERCEPTION**
 U SPACE PERCEPTION
- FORMALDEHYDE**
- Formaldehyde absorption towards OH sources 02 p0260 A83-12531
- Formaldehyde formation in a H₂O/CO₂ ice mixture under irradiation by fast ions 03 p0424 A83-14196
- Mode specificity in the unimolecular dissociation of formaldehyde /H₂CO yields H₂ + CO/, a two-mode model 05 p0613 A83-17654
- 3.508 micron-HeXe-laser line absorption by formaldehyde monomer and dimer and by nitrogen dioxide monomer and dimer without and in the presence of argon 05 p0684 A83-17871
- VLA observations of the 6-cm H₂CO absorption towards Sgr A West 06 p0828 A83-18184
- High density molecular gas in the Rho Ophiuchi cloud 07 p1024 A83-21221
- Photodissociation of HCHO in air - CO and H₂ quantum yields at 220 and 300 K 08 p1163 A83-22216
- Six-centimeter H₂CO observations - Envelopes of dark clouds 10 p1499 A83-25373
- Formaldehyde toward Cas A - Cloud sizes and H₂ densities 10 p1501 A83-25496
- Rates and mechanisms of formaldehyde pyrolysis and oxidation 10 p1388 A83-26201
- Time-resolved infrared-ultraviolet double resonance spectroscopy of formaldehyde 11 p1653 A83-27528
- VLA observations of H₂ in DR 21 12 p1785 A83-28884
- The Corona Australis dark cloud 13 p1946 A83-30389
- Detection of HCO(+) and HCN absorption towards three galactic H II-regions 13 p1954 A83-31570
- A survey of formaldehyde in the Cepheus OB3 molecular cloud 13 p1958 A83-31709
- Formaldehyde and OH in the Orion molecular clouds 15 p2265 A83-34597
- The relative locations of the Sgr A molecular clouds and continuum sources 19 p2912 A83-40679
- The distribution of 6 centimeter H₂CO in Orion Molecular Cloud 1 20 p3074 A83-43090
- H₂ densities and masses of the molecular clouds close to the galactic center 21 p3231 A83-44452
- 'CARS' study of vibrationally excited H₂ formed in formaldehyde photolysis 23 p3430 A83-48181
- [ONERA, TP NO. 1983-60] 4.8-GHz H₂CO maser emission in Sgr B2 24 p3660 A83-49388
- Formaldehyde, cold neutral hydrogen and dust distribution in a globular filament in Taurus 24 p3669 A83-50096
- FORMALISM**
- The polarization characteristics of coherent transient phenomena in two-photon resonance 09 p1346 A83-25091
- Dynamics of flexible hybrid satellites - Evaluation and computation of a symbolic formalism 21 p3102 A83-45122
- FORMAT**
- Standardization of computer compatible tape formats for remote sensing data 01 p0064 A83-10075
- FORMATES**
- Nearly noncritically phase-matched UV generation at 3547 A in NaCHO₂ 19 p2851 A83-40929
- FORMIC ACID**
- Quantum chemical studies of a model for peptide bond formation Formation of formamide and water from ammonia and formic acid 07 p0976 A83-21052
- Aqueous-phase source of formic acid in clouds 20 p3028 A83-43555
- FORMING TECHNIQUES**
 NT BLANKING (CUTTING)
 NT CASTING
 NT COLD ROLLING
 NT COLD WORKING
 NT ELECTROFORMING
 NT EXTRUDING
 NT FORGING
 NT HOT WORKING
 NT INJECTION MOLDING
 NT INVESTMENT CASTING
 NT METAL DRAWING
 NT METAL SPINNING
 NT PRESSING (FORMING)
 NT PROPELLANT CASTING
 NT ROLL FORMING
 NT SLIP CASTING
 NT STAMPING
- Computer-aided control of sheet metal forming processes 02 p0161 A83-12086
- The forming limit diagram of sheet metals and effects of strain path changes on formability - A dislocation treatment 03 p0301 A83-14704
- Contribution to the determination of forming limit curves for titanium and aluminum - Proposal of an intrinsic criterion --- French thesis 04 p0459 A83-15840
- Modern developments in powder metallurgy. Volume 14 - Special materials --- Book 06 p0731 A83-19096
- Experimental examination of several material hypotheses on the basis of mutual predetermination of stress-strain and creep curves --- German thesis 07 p0873 A83-20393

- Superplastic forming/weld-brazing of titanium skin-stiffened compression panels 07 p0886 A83-20467
- Superplastic forming characterization of titanium alloys 07 p0889 A83-20850
- Anisotropy of bulk-formability in 2024-T351 aluminum plates and bars 08 p1058 A83-21664
- Screw extrusion of double base propellants 09 p1241 A83-23833
- Investigations of the extrusion process 09 p1241 A83-23836
- Prediction of strain recovery during solid-phase forming of thermoplastics 10 p1400 A83-26350
- Superplastic forming and diffusion bonding 11 p1589 A83-28176
- The generation of residual stresses in metal-forming processes 12 p1715 A83-29908
- The geometrical factor during the extrusion of complex metal materials 13 p1859 A83-30688
- Sheet forming of titanium alloys 15 p2135 A83-33637
- Forming SPF/DB structure --- Superplastic Forming/Diffusion Bonding of metal sheets 15 p2171 A83-33638
- Aspects of metallography and manufacturing technology regarding the superplastic forming of TiAl6V4 15 p2136 A83-33961
- Discontinuity sources in manufacturing processes --- for metals 17 p2523 A83-38400
- A new construction method of carbon fibre hybrid GRP moulds in vacuum forming process 18 p2662 A83-40290
- Development of forming limits for superplastic formed fine grain 7475 Al 20 p2954 A83-43343

FORMULAS (MATHEMATICS)

- On the approximate calculation of double integrals 07 p0987 A83-20510
- Proton-nucleus total inelastic cross sections - An empirical formula for E greater than 10 MeV 08 p1192 A83-22747

FORSTERITE

- Olivine flotation and settling experiments on the join Mg2SiO4-Fe2SiO4 16 p2382 A83-36972
- Cumberland Falls chondritic inclusions. II - Trace element contents of forsterite chondrites and meteorites of similar redox state 24 p3672 A83-49349

FORTAN

- A note on using finite differences on the ICL distributed array processor 01 p0090 A83-10712
- A general precompiler for algebraic manipulation 12 p1768 A83-29110
- Fortran computer program for inextensional bending of a doubly curved shell triangular element 16 p2365 A83-35643

FORWARD LOOKING INFRARED DETECTORS

U FLIR DETECTORS

FORWARD SCATTERING

- The method of forward scattering amplitude in a theory of hydrogen line broadening in a plasma 01 p0106 A83-10375
- Interaction and competition between forward and backscattering in stimulated Raman scattering 05 p0649 A83-17058
- Stimulated Raman scattering by particles captured in a trap 10 p1431 A83-26651
- Frequency dependence of degenerate four-wave mixing at the band edge of InAs 11 p1581 A83-27597
- Investigation of domains of validity of approximation methods in forward light scattering from long absorbing cylinders 11 p1657 A83-27845
- Radiative heat transfer in absorbing, emitting and anisotropically scattering boundary layer flows [AIAA PAPER 83-1504] 14 p2010 A83-32742
- Electromagnetic scattering by magnetic spheres 15 p2224 A83-33805
- Comparison of radiative transfer approximations for a highly forward scattering planar medium 18 p2680 A83-39181
- Particle size distributions from forward scattered light using the Chanine inversion scheme 20 p3046 A83-42213
- Forward multiple scattering corrections as a function of detector field of view --- laser beam propagation through atmospheric aerosols 24 p3588 A83-49005
- Laboratory evaluations of six PMS forward scattering spectrometer probes --- for precipitation particle measurement 24 p3583 A83-49708

FOSSIL FUELS

NT CRUDE OIL

NT NATURAL GAS

NT PEAT

- Development and application of advanced diagnostics methods in fossil fuel combustion studies 07 p0902 A83-20436
- Distribution of and changes in industrial carbon dioxide production 09 p1295 A83-24256

FOSSIL METEORITE CRATERS

U FOSSILS

U METEORITE CRATERS

FOSSILS

- Amino acids from the Late Precambrian Thule Group, Greenland 02 p0219 A83-11636
- The Cretaceous-Tertiary transition 10 p1448 A83-25650
- Organic molecules as chemical fossils - The molecular fossil record 13 p1899 A83-31160

FOULING

- Correlation and prediction of thermophoretic and inertial effects on particle deposition from non-isothermal turbulent boundary layers 11 p1566 A83-27481
- Combustion system processes leading to corrosive deposits 20 p2949 A83-42246

FOUNDATIONS

- A method for the mathematical description and solution of boundary value problems in the deformation mechanics of shells on continuous or discrete elastic supports 13 p1867 A83-31321
- Stability of short Beck and Leipholz columns on elastic foundation 16 p2366 A83-36098
- Ground couplings and measurement frequency ranges of vibration transducers 17 p2510 A83-37733
- Solutions of plates on a heterogeneous elastic foundation 23 p3471 A83-48164
- The control of a four-axis gimbal suspension 23 p3459 A83-48457

FOUNDRIES

- New developments in foundry engineering --- Russian book 10 p1395 A83-25628

FOUR BODY PROBLEM

- Central configurations of four bodies with one inferior mass 03 p0404 A83-13406
- Collinear relative equilibria of the planar n-body problem 03 p0404 A83-13407
- Analysis of some degenerate quadruple collisions 03 p0389 A83-13410
- Stability criteria in many-body systems. V - On the totality of possible hierarchical general four-body systems 12 p1787 A83-29117

FOURIER ANALYSIS

NT FOURIER SERIES

- The light curves of RR Lyrae field stars 02 p0251 A83-11593
- A time Fourier analysis of zonal averaged ozone heating rates 03 p0361 A83-14651
- Fourier spectroscopy of the C-12C-13 and /C-13/2 Ballik-Ramsay system --- in cool carbon star atmospheres 05 p0700 A83-17023
- Principles governing the structure of coherent video preprocessors 05 p0645 A83-17660
- Determination of the index profile of optical fibers from transverse interferograms using Fourier theory 07 p0993 A83-20832
- Chaos in the semiclassical N-atom Jaynes-Cummings model - Failure of the rotating-wave approximation 10 p1481 A83-25797
- Coherence and interferometry through optical fibers --- of stellar interferometers 10 p1482 A83-25847
- Optical reconstruction of wideband Fourier and Fresnel acoustic holograms 10 p1421 A83-26295
- The distribution of quasars from a small area survey 10 p1512 A83-26702
- Spatial Fourier modes controlling Navier-Stokes flow 11 p1568 A83-28236
- Spectral analysis algorithms for the laser velocimeter - A comparative study 12 p1728 A83-28961
- Application of numerical Fourier transformation on measurements made on board rotating spacecraft 13 p1812 A83-30778
- A nonorthogonal spectral analysis of time series --- in geophysics 15 p2200 A83-34421
- Theoretical and numerical methods for the nonlinear Fourier analysis of shallow-water wave data 17 p2577 A83-38940
- Conjugate duality and the exponential Fourier spectrum --- Book 20 p3040 A83-42204
- Fourier analysis of the wave number of unstable waves in a spiral beam-plasma system 20 p3050 A83-43397
- Fourier processing with phase-reflection gratings 22 p3287 A83-45959
- Frequency analysis of Beta Cephei variables in NGC 6231 24 p3659 A83-49373

FOURIER SERIES

- Fourier series of functions having a fractional-logarithmic derivative 02 p0231 A83-11638
- Spectral method solutions for some laminar channel flows with separation 03 p0315 A83-13138
- The Fourier-Chebyshev approximation for time series with a great many terms --- for describing motions of celestial bodies 06 p0817 A83-17991

- Nonlinear analysis of cavity flows around arbitrarily shaped bluff bodies in a constrained flow 06 p0758 A83-19020

- Number of terms required in the Fourier expansion of the reflection function for optically thick atmospheres 18 p2743 A83-39179

- The Fourier method in problems of the mechanics of layered media with nontraditional contact conditions 24 p3593 A83-49040

FOURIER TRANSFORMATION

NT FAST FOURIER TRANSFORMATIONS

- Generalized formulas for the computation of the discrete Fourier transformation 01 p0102 A83-10285
- Fourier transform perturbation solution of elliptic equations with small nonlinearities 01 p0102 A83-10495
- A survey of the physical optics inverse scattering identity 01 p0104 A83-11369
- Computer tracking of moving objects using a Fourier-domain filter based on a model of the human visual system 01 p0097 A83-11420
- Discrete Fourier transforms of nonuniformly spaced data 02 p0231 A83-12925
- Evaluation of Fourier integrals using B-splines 03 p0387 A83-13574
- Multiplex holographic filtering through contact screens 03 p0326 A83-13772
- A stochastic Fourier transform approach to scattering from perfectly conducting randomly rough surfaces 03 p0306 A83-14014
- Fourier transform spectrometry in relation to other passive spectrometers 04 p0482 A83-15804
- Full-wave analysis of microstrip resonator and open-circuit end effect 04 p0473 A83-16208
- Binary multiplexing and the phase-retrieval problem 05 p0643 A83-16836
- Speckle reduction by a rotating aperture at the Fourier transform plane 05 p0647 A83-17940
- The parametric discrete Fourier transformation 06 p0802 A83-18028
- Algorithm of the two-dimensional Fourier transformation with a mixed base 06 p0802 A83-18031
- The use of the intraperiod symmetry of harmonic basis functions to compute the discrete Fourier transformation 06 p0802 A83-18039
- Seeing-independent definitions of the solar limb position 06 p0818 A83-18537
- Computationally efficient discrete cosine transform algorithm 06 p0803 A83-18574
- The plane wave synthesis technique for antenna near-field/far-field transformation - Further development 06 p0740 A83-18649
- Fourier transform-iteration for antenna pattern synthesis 06 p0743 A83-18686
- Calculation of complex Fourier coefficients using natural splines 06 p0804 A83-18898
- Product device analysis for radar applications 06 p0749 A83-19050
- TRAPATT oscillators with active harmonic tuning --- German thesis 07 p0919 A83-20396
- Numerical computation of an important integral function in two-dimensional radiative transfer 07 p1001 A83-21397
- Synthesis of sliding discrete Fourier transform and sliding Hadamard transform circuits 08 p1157 A83-22232
- Partially coherent optical processing of images 08 p1093 A83-22427
- Fourier transform image tracker and stabilizer 08 p1099 A83-22584
- Fourier transform of a polygonal shape function and its application in electromagnetics 09 p1247 A83-23789
- Remote determination of the structure constant profile from amplitude scintillation data using Tikhonov's regularized inverse method --- Fourier transform for solving convolution equations 09 p1311 A83-23795
- Self-imaging effect in physical radiometry 09 p1268 A83-24100
- High frequency behavior of the tilt spectrum of atmospheric turbulence 09 p1249 A83-24439
- Fourier spectroscopy of the /C-12/ /C-13/ and /C-13/2 Phillips system 09 p1361 A83-24519
- The processing of periodically sampled multidimensional signals 10 p1402 A83-25641
- Numerical conformal mapping and analytic continuation 10 p1470 A83-25875
- Real-time Fourier transformation in dispersive optical fibers 10 p1482 A83-26119
- Far field in transient two-dimensional scattering 10 p1406 A83-26849
- Digital image reconstruction of microwave holograms 10 p1424 A83-26855
- Simple method for image deblurring 10 p1484 A83-26860
- Reducing the effects of ghostlines in a step-record Fourier spectrometer 10 p1424 A83-26870

- Line positions and strengths in the /001/, /110/, and /030/ bands of HDO 10 p1481 A83-26877
- Accuracy of an optical open area radiometer 12 p1729 A83-29147
- The effect of aberrations on the quality of the optical Fourier transformation 13 p1918 A83-30444
- Modified signals. I - Basic properties of modified signals. II - Results of computerized simulation 13 p1829 A83-30728
- Isolation and molecular identification of ultramicro contaminants by Fourier transform infrared spectroscopy 13 p1848 A83-31522
- Fresnel detour-phase circular computer generated holograms 14 p2083 A83-31948
- Unifying approach to spectral estimation 14 p2075 A83-32432
- High-speed optical Fourier transformer 14 p2085 A83-33425
- Lensless Fourier holography applied to nondestructive testing - Experimental results 15 p2163 A83-33754
- Small interferometer for Fourier spectrometry 15 p2163 A83-33789
- Signal restoration from phase by projections onto convex sets 15 p2220 A83-33809
- A numerical method based on the Fourier-Fourier transform approach for modeling 1-D electron plasma evolution --- in earth bow shock region 15 p2233 A83-33823
- Global fringe search techniques for VLIBI 15 p2245 A83-33839
- Switched-capacitor realization of a discrete Fourier transformer 15 p2151 A83-33925
- Photoexcitations in trans-(CH)₃ - A Fourier-transform infrared study 16 p2420 A83-35748
- A two-scanning mirror Fourier transform interferometer for plasma diagnostics 17 p2511 A83-37755
- Systolic processor for computing the Wigner distribution 17 p2564 A83-38882
- On the Stokes wave in shallow water - Perspective in the context of spectral-transform theory 17 p2577 A83-38938
- Nonlinear Fourier analysis of localized wave fields described by the Korteweg-deVries equation 17 p2577 A83-38939
- A survey of methods for iterative signal restoration 19 p2830 A83-41376
- Discrete Fourier transformation and its applications to power spectra estimation --- Book 19 p2893 A83-41849
- Air broadened NO linewidths in a temperature range of atmospheric interest 20 p3044 A83-42626
- Algorithm for the fast computation of the two-dimensional discrete Fourier transformation 20 p3041 A83-42903
- Discrete Fourier transform processor based on the prime-factor algorithm 20 p3037 A83-43169
- Modified method of estimating space-time spectra from polar-orbiting satellite data. I - The frequency transform method. II - The wavenumber transform method 20 p3032 A83-43463
- A Fourier transform technique that measures phase delays between ultrasonic impulses with sufficient accuracy to determine residual stresses in metals 20 p3000 A83-43560
- Hardware-based Fourier transforms - Algorithms and architectures 20 p3037 A83-43681
- Application of the one-dimensional Fourier transform for tracking moving objects in noisy environments 21 p3194 A83-44278
- The stress intensity factor for the double cantilever beam 21 p3158 A83-44914
- The stochastic properties of the parametric discrete Fourier transform 22 p3353 A83-45661
- Electric microfield distributions in strongly coupled plasmas 22 p3361 A83-45935
- Estimation of truncation and aliasing errors involved in DFT computation 24 p3621 A83-49968
- FOURIER-BESSEL TRANSFORMATIONS**
- Point source radiation of a solid-fluid interface - Numerical solution using a Fourier-Bessel transformation [ONERA, TP NO. 1982-110] 06 p0807 A83-18436
- A 'periodic' solution for an axisymmetric deformable elastic paraboloid of revolution 09 p1282 A83-25019
- FRACTIONATION**
- NT CHEMICAL FRACTIONATION
- Numerical simulation of crystal fractionation in shergottite meteorites 04 p0563 A83-15363
- Fractionation of mineral species by electrophoresis 07 p1029 A83-20235
- Feasibility study on the ethanol-water solar fractionating system 15 p2190 A83-34071
- FRACTOGRAPHY**
- Determination of the stressed state of bodies with defects using the method of holographic photoelasticity 02 p0191 A83-12337
- TEM observations of dislocation emission at crack tips in aluminium 03 p0298 A83-13679
- Fractographic studies of graphite/epoxy fatigue specimens 03 p0292 A83-14554
- Analytical methods in eddy current NDE 04 p0490 A83-15188
- Inversion algorithms for crack-like flaws 04 p0492 A83-15204
- A study on threshold of macro-crack growth in a soft epoxy resin 05 p0618 A83-17101
- The use of fractography and fracture mechanics in analysing fatigue cracks 05 p0654 A83-17229
- A study of the deformation and fracture of structural elements of composite materials by speckle-holographic interferometry 06 p0675 A83-18513
- Reversible reaction between MC and M/273/C/6/ in a NiCrWTi cast superalloy 07 p0885 A83-20274
- The effect of the structure factor on the formation of the fracture surface in molybdenum alloys 07 p0889 A83-20900
- Stereoscopic depth analysis by thermal wave transmission for nondestructive evaluation 07 p0931 A83-21373
- Microstructural analysis of the cold working effect on the fracture toughness of weld metal in HSLA steel welds 08 p1061 A83-21726
- Fractographic identification of subcritical to critical crack growth transition mechanisms in ceramics 08 p1069 A83-21743
- Quantitative fractography and dislocation interpretations of the cyclic cleavage crack growth process 08 p1123 A83-23224
- New method of determining the onset of ring cracking 08 p1106 A83-23233
- Fracture properties of aluminum alloys 10 p1393 A83-25322
- The shielding of excess phases during fracture under plane strain conditions and its effect on the fracture toughness 11 p1549 A83-28481
- On the cyclic behavior of cast and extruded aluminum alloys. B - Fractography 14 p1992 A83-32343
- The evaluation of tempered martensite embrittlement in 4130 steel by instrumented Charpy V-notch testing 16 p2329 A83-35689
- Effect of structure on the type of fracture of titanium alloy VT3-1 16 p2330 A83-36025
- A fractographic study of corrosion-fatigue crack propagation in a duplex stainless steel 17 p2490 A83-38397
- Fractography of carbon/epoxy angle-ply laminates 18 p2660 A83-40273
- Recent developments in quantitative fractography 21 p3114 A83-44950
- Gel electrode imaging of fatigue cracks in titanium 22 p3268 A83-45624
- FRACTURE MECHANICS**
- On crack kinking and curving 01 p0058 A83-10282
- Thermal activation analysis of the structural stability of refractory alloys and computer simulation of the fracture process 01 p0024 A83-10391
- Energy criteria of the brittle fracture of materials with initial stresses 01 p0059 A83-10676
- The relationship between the solutions to mixed dynamic problems for a continuous elastic medium and a lattice 02 p0189 A83-11655
- The effect of grain structure on the fracture behavior and tensile properties of an Al-Li-Cu alloy 02 p0154 A83-11865
- Application of finite-part integrals to the singular integral equations of crack problems in plane and three-dimensional elasticity 02 p0190 A83-12001
- On the J-integral blunting line for soft materials 02 p0190 A83-12045
- The effect of hydrogen on the microfracture mechanism of titanium alloys 02 p0156 A83-12208
- Fracture of thermoelastic reinforced shells from a probabilistic viewpoint 02 p0191 A83-12335
- Fracture modes of inelastic materials as a function of loading rate and temperature, and associated fracture criteria 02 p0192 A83-12354
- The load-carrying capacity of hollow composite rods in torsion 02 p0192 A83-12364
- Micromechanics 02 p0193 A83-12733
- Evaluation of the tentative JI-R curve testing procedure by round robin tests of HY130 steel 02 p0158 A83-12832
- Creep fracture by coupled power-law creep and diffusion under multiaxial stress 02 p0197 A83-12930
- Dynamic fracture of a beam or plate under tensile loading 03 p0339 A83-13338
- A study of the effect of internal microstresses on the development of delayed fracture in maraging steels 03 p0298 A83-13595
- Dynamic spalling in rarefaction waves 03 p0339 A83-13596
- Time-of-flight measurements of the mass-to-charge ratio of positive ion emission accompanying fracture --- related to crack propagation in materials 03 p0302 A83-13681
- Solution of the axisymmetric problem for an elastic body with a cylindrical crack 03 p0339 A83-13692
- Fatigue life evaluation of the A-7E arresting gear hook shank 03 p0277 A83-13912
- The fracture mechanics of composite materials under axial compression - Brittle fracture 03 p0291 A83-14064
- Mechanisms of fatigue damage in boron/aluminum composites 03 p0292 A83-14557
- A simple yet accurate finite element procedure for computing stress intensity factors 03 p0342 A83-14707
- The fracture mechanics of microsphere-filled composites 03 p0293 A83-14739
- Elastic-plastic finite element analysis of dynamic fracture 04 p0495 A83-15062
- Analytical solution for embedded elliptical cracks, and finite element alternating method for elliptical surface cracks, subjected to arbitrary loadings 04 p0496 A83-15063
- Review of progress in quantitative nondestructive evaluation. Volume 1 - Proceedings of the Eighth USAF/Defense Advanced Research Projects Agency Symposium on Quantitative Nondestructive Evaluation, University of Colorado, Boulder, CO, August 2-7, 1981 04 p0487 A83-15151
- Probabilistic fracture mechanics 04 p0496 A83-15153
- Mechanisms which influence the applicability of fracture mechanics for short cracks 04 p0496 A83-15184
- A theory of eddy current NDE for cracks in nonmagnetic materials 04 p0490 A83-15187
- An antiplane problem concerning crack propagation in a lattice 04 p0497 A83-15388
- Fracture mechanics in the presence of electric fields --- for piezoelectrics 04 p0539 A83-15393
- Impact machines /The fundamentals of complex design/ --- Russian book 04 p0487 A83-15834
- Mechanism of interfacial bond failure 04 p0463 A83-15873
- Estimates and asymptotics of the stress-strain state of a three-dimensional body with a crack in the theory of elasticity and the theory of creep 04 p0500 A83-15884
- The fracture mechanics of composite materials under axial compression - Plastic fracture 04 p0456 A83-16402
- Damage mechanics approach to the orientations of slip bands and related cracking in polycrystalline metals 05 p0614 A83-17090
- Influence of tensile pre-strain on fatigue crack closure in aluminum alloy 2017-T3 05 p0614 A83-17095
- Fracture behavior of polymers by Charpy impact tests 05 p0618 A83-17100
- The use of fractography and fracture mechanics in analysing fatigue cracks 05 p0654 A83-17229
- An improved dislocation approach in solving three-dimensional boundary value problems 05 p0681 A83-17324
- Introduction to the fundamentals of fracture mechanics. III - Fatigue crack growth in fracture mechanics representation 05 p0654 A83-17573
- Damage to structures by high-cycle fatigue 05 p0655 A83-17672
- The short crack problem 05 p0655 A83-17673
- The growth of small fatigue cracks in 7075-T6 aluminum 05 p0616 A83-17674
- Three-dimensional constitutive relations and ductile fracture --- Book 06 p0774 A83-18477
- Experimental and numerical study of the different stages in ductile rupture - Application to crack initiation and stable crack growth 06 p0774 A83-18484
- Stability of tearing fracture in structural steels 06 p0728 A83-18486
- A thermodynamic description of the running crack problem 06 p0774 A83-18489
- Finite deformation constitutive relations including ductile fracture damage 06 p0774 A83-18490
- Constitutive equations and global criteria for ductile fracture 06 p0774 A83-18491
- Elastic-plastic fields in steady crack growth 06 p0774 A83-18492
- The fracture of a unidirectional fiber composite with an elastoplastic matrix under compression 06 p0725 A83-18503
- The deformation and fracture mechanisms of coarse-grained textured alpha-titanium alloys 06 p0729 A83-18748
- Mixed mode plane stress ductile fracture 06 p0775 A83-18909
- Fracture behavior of blended elemental P/M titanium alloys 06 p0731 A83-19094

A study of the principles underlying the deformation and fracture of a polycrystalline molybdenum alloy under high-temperature cyclic creep. I - The long-term strength and creep 06 p0733 A83-19307

A continuum theory for the fracture of metal-matrix composites under compression 06 p0726 A83-19542

Why ductile fracture mechanics 07 p0944 A83-19669

Stationary subsonic motion of a crack in an elastic strip 07 p0944 A83-19944

Computer simulation of the fracture of composite materials with various degrees of physicochemical interaction between the components 07 p0874 A83-19971

Double-cantilever-beam testing of a transversely isotropic fibrous silica material [ACS PAPER 61-B-81F] 07 p0898 A83-20170

Effect of fracture surface roughness on growth of short fatigue cracks 07 p0884 A83-20257

The evaluation of the fracture energy of materials in the presence of frictional contact force according to structural changes 07 p0939 A83-20324

Materials characterization and fracture mechanics of a space grade dielectric silicone insulation 07 p0899 A83-20456

A summary of fracture mechanics concepts 07 p0945 A83-20520

Fracture mechanics analysis of the effects of residual stress on fatigue life 07 p0946 A83-20521

Continuous cavity nucleation and creep fracture 07 p0887 A83-20631

An anisotropic strip weakened by an array of cracks 07 p0946 A83-20637

Peripheral edge crack around a spherical cavity under uniaxial tension field 07 p0946 A83-20642

The fatigue fracture of metals from the standpoint of physics and fracture mechanics 07 p0890 A83-20914

Boundary element method in fracture mechanics 07 p0947 A83-20925

Analytical and experimental fracture mechanics --- Book 07 p0948 A83-21098

The exact form of caustics in mixed-mode fracture - A comparison with approximate solutions 07 p0948 A83-21342

The effect of hot corrosion on creep and fracture behaviour of cast nickel-based superalloy IN738LC 07 p0895 A83-21490

Advances in fracture research; Proceedings of the Fifth International Conference on Fracture, Cannes, France, March 29-April 3, 1981. Volumes 1, 2, 3, 4, 5, & 6 08 p1115 A83-21651

Observations on prediction of non-self-similar subcritical crack growth and stress intensity distributions 08 p1115 A83-21652

Evaluation of process zone by using Jext integral under large scale yielding - Structure of J integral 08 p1116 A83-21658

On the maximum-energy-release-rate criterion for fracture under combined loads 08 p1116 A83-21659

An integral equations method for resolution, in opening mode, of the problem of plane cracks at free surface 08 p1116 A83-21661

Mechanical model and mathematical analysis for ductile fracture 08 p1116 A83-21665

Analysis of thermal cracking of unidirectionally reinforced composite structures in the micromechanical range 08 p1054 A83-21680

Propagation of damage in elastic and plastic solids 08 p1116 A83-21684

Fracture and fatigue crack propagation in bearing steels 08 p1059 A83-21689

The relation between microstructural fracture processes and macroscopic crack tip characterizing parameters during the stable growth of cracks 08 p1117 A83-21699

The implications of recent developments in elastic plastic fracture mechanics on the growth of stress corrosion cracks 08 p1061 A83-21719

On the critical problems in physico-mechano-structural foundations of fracture 08 p1117 A83-21724

A J based engineering usage of fracture mechanics 08 p1117 A83-21725

Fracture analyses of angle-ply laminates 08 p1054 A83-21729

High strain fracture analysis 08 p1062 A83-21739

The mechanism and mechanics of subcritical crack propagation in hot-pressed SiC above 1000 C 08 p1069 A83-21740

Metallographic aspects of creep fracture in a cast Ni-Cr-base alloy 08 p1062 A83-21745

The fracture characteristics of Al and Al-5% Mg at elevated temperatures 08 p1062 A83-21747

On the relation between the creep mechanism and creep fracture 08 p1118 A83-21748

Plane stress fracture under biaxial loading 08 p1062 A83-21749

A technique for measuring crack length and load in compact fracture mechanics specimens using strain gauges 08 p1118 A83-21763

Acoustic emission in rock fracture analysis 08 p1113 A83-21769

Damage tolerance assessment of the A-7D aircraft structure 08 p1044 A83-21771

Application of systems analysis methods to fracture control 08 p1118 A83-21772

The crack tip stress intensification associated with crack propagation and arrest 08 p1118 A83-21778

In-situ study of deformation and initiation of ductile fracture at a notch-root 08 p1119 A83-21789

A comparative study on different methods to measure the crack opening displacement 08 p1064 A83-21790

Inelastic analysis of surface flaws using the line-spring model 08 p1119 A83-21792

Advancements in macroscopic fracture mechanics 08 p1064 A83-21795

Progress in the practical applications of fracture mechanics 08 p1119 A83-21796

Crack-tip singularity fields in nonlinear fracture mechanics - A survey of current status 08 p1064 A83-21797

Practical application of fracture mechanics 08 p1119 A83-21799

Computer simulation of micro and macromechanisms of fibre reinforced composite fracture 08 p1054 A83-21801

Nonlinear micropolar continuum model of a composite reinforced by elements of finite rigidity. I - Equations of motion and constitutive relations 08 p1120 A83-21816

Interlaminar fracture of composite materials 08 p1054 A83-21820

The experimental evaluation on the brittle fracture characterization under the mixed mode 08 p1122 A83-22069

Effects of morphology and hardness of inclusions on ductile fracture 08 p1066 A83-22078

Evaluation of creep crack growth criteria for IN-100 at elevated temperature 08 p1066 A83-22142

Physics of fracture /The Sosman Lecture/ --- crack propagation and crack-tip phenomena in structural ceramics 08 p1070 A83-22188

Controlled flaws in ceramics - A comparison of Knoop and Vickers indentation 08 p1070 A83-22193

Moving Griffith crack in an orthotropic material 08 p1123 A83-22722

Minimum silicon wafer thickness for ID wafering 08 p1132 A83-22924

J-integral analysis for cracks emanated from elliptical holes 09 p1275 A83-23298

Analysis of closure behavior of small fatigue cracks 09 p1275 A83-23299

Constant amplitude fatigue life assessment models 09 p1277 A83-23420

Shearing in inhomogeneous media --- Russian book on fracture mechanics 09 p1278 A83-23823

The relation between surface energy and effective fracture energy for grain boundary fracture 09 p1279 A83-23869

Fracture of composite materials; Proceedings of the Second USA-USSR Symposium, Lehigh University, Bethlehem, PA, March 9-12, 1981 09 p1222 A83-23926

Stochastic models of fracture of unidirectional fiber composites 09 p1222 A83-23927

Two approaches in fracture mechanics of composites 09 p1222 A83-23929

Some peculiarities of fracture in heterogeneous materials 09 p1223 A83-23932

Influence of stress interaction on the behavior of off-axis unidirectional composites 09 p1223 A83-23934

Determination of fracture toughness of unidirectionally fiber-reinforced composites 09 p1223 A83-23936

The relationship of stiffness changes in composite laminates to fracture-related damage mechanisms 09 p1223 A83-23940

Creep and fracture of engineering materials and structures; Proceedings of the International Conference, University College of Swansea, Swansea, Wales, March 24-27, 1981 09 p1279 A83-24051

A unifying view of the kinetics of creep cavity growth 09 p1279 A83-24066

Grain boundary sliding and fracture of metal bicrystals at high temperatures 09 p1232 A83-24068

Mechanisms of creep deformation and fracture in single and two-phase Si-Al-O-N ceramics 09 p1238 A83-24072

Change in geometry of surface cracks during alternating tension and bending 09 p1280 A83-24137

The lateral buckling-fracture stability of thin-sheet structural components with deep cracks 09 p1280 A83-24648

The boundary integral method for the solution of planar multicrack problems of linear elastostatics --- German thesis 09 p1281 A83-24846

The topography of the core-region around cracks under modes I, II and III of fracture 09 p1282 A83-25050

New physical trends in experimental mechanics --- Book 09 p1243 A83-25096

Application of fracture mechanics for selection of metallic structural materials --- Book 10 p1392 A83-25317

Concepts of fracture mechanics 10 p1392 A83-25318

Fracture properties of wrought stainless steels 10 p1392 A83-25321

Design, materials selection and failure analysis 10 p1393 A83-25325

On a micromechanical fracture model for cracked reinforced composites 10 p1438 A83-25470

On path-independent integrals and fracture criteria in non-linear fracture dynamics 10 p1438 A83-25471

Mechanics aspects of NDE by sound and ultrasound 10 p1436 A83-25571

Segregation to interphase boundaries in liquid-phase sintered Tungsten alloys 10 p1396 A83-25866

Energy absorption in composite tubes 10 p1439 A83-25883

Microstructure and tensile ductility in a beta heat treated titanium alloy 10 p1398 A83-26280

Changes in properties and fracture behavior of tungsten-heavy metals during liquid-phase sintering 10 p1399 A83-26892

A theoretical study on the running crack path by energy balance method 10 p1442 A83-26968

Fracture control and its application within the agency's programmes 11 p1536 A83-27374

1982 advances in aerospace structures and materials; Proceedings of the Winter Annual Meeting, Phoenix, AZ, November 14-19, 1982 11 p1591 A83-27426

A theory for transverse cracks in composite laminates 11 p1591 A83-27435

Incipient fracture in shock-loaded lamellar metal alloy composites with and without microstructural defects 11 p1547 A83-27436

Curved crack growth in brittle solids under farfield compression 11 p1592 A83-27439

Thermomechanical behavior of high-temperature composites; Proceedings of the Symposium, Phoenix, AZ, November 14-19, 1982 11 p1543 A83-27457

The formulation of a crack growth equation for short cracks 11 p1547 A83-27855

The behaviour of short cracks 11 p1593 A83-27857

Fatigue life estimation using simple fracture mechanics 11 p1594 A83-28402

Fracture estimation - Norton-Hoff regularization and an augmented Lagrangian 11 p1595 A83-28433

Some remarks on elastic fracture mechanics 11 p1595 A83-28434

An investigation of the stress intensity factor for a finite internally cracked plate by using variational method 11 p1595 A83-28441

On the fundamental basis of fracture mechanics 11 p1596 A83-28444

Redistribution of stresses in a fractured fiber during its delamination from the viscoelastic matrix of a composite material 11 p1597 A83-28471

Estimates and approximation formulas in the problem of elasticity theory concerning a plane normal crack 11 p1597 A83-28472

Interaction of a surface wave with a crack situated on a curved surface 11 p1597 A83-28475

The method of boundary interpolation in fracture mechanics problems 11 p1597 A83-28476

An analysis of the durability characteristics of aircraft structures on the basis of fracture mechanics 11 p1597 A83-28477

The use of linear fracture mechanics for processing the results of residual strength tests 11 p1597 A83-28479

A diagram for the discrete growth of a fatigue crack under self-similarity conditions 11 p1597 A83-28480

Determination of the stress intensity factors for short cracks initiated by stress raisers 11 p1598 A83-28485

On the question of damage and fracture criteria in creep 11 p1549 A83-28501

Correlation between the energy characteristics of fracture - Crack propagation and spalling 11 p1598 A83-28503

Changes in the fracture characteristics of graphite under low-temperature neutron irradiation 11 p1551 A83-28506

- A morphological study of the fracture mechanisms of unidirectionally reinforced thermoplastics 11 p1544 A83-28512
- Characteristics of the spall fracture of copper, nickel, titanium, and iron in the temperature range from -196 to 800 C 11 p1549 A83-28514
- Theoretical and experimental investigations regarding crack propagation in sheet metal --- German thesis 11 p1599 A83-28658
- Indentation fracture transitions in polymethylmethacrylate 12 p1716 A83-29160
- Problem of a crack in a transversely isotropic sandwich plate 12 p1735 A83-29410
- Structures, Structural Dynamics and Materials Conference, 24th, Lake Tahoe, NV, May 2-4, 1983, Collection of Technical Papers. Part 1 - Structures and materials. Part 2 - Structural dynamics 12 p1736 A83-29729
- Dynamic crack propagation analysis using a new path-independent integral and moving isoparametric elements [AIAA 83-0838] 12 p1737 A83-29746
- A stochastic theory of fatigue crack propagation [AIAA 83-0978] 12 p1740 A83-29785
- Statistical crack propagation in fastener holes under spectrum loading [AIAA 83-0808] 12 p1741 A83-29808
- Residual stress and stress relaxation; Proceedings of the Twenty-eighth Sagamore Army Materials Research Conference, Lake Placid, NY, July 13-17, 1981 12 p1746 A83-29901
- Linear elastic fracture mechanics and fatigue crack growth Residual stress effects 12 p1746 A83-29905
- Finite element analysis of slow crack growth 12 p1747 A83-29942
- Modeling the fracture of thin-walled structural elements of multidirectional layered composites 13 p1865 A83-30054
- An accumulated-damage fracture criterion for a three-component layered composite 13 p1865 A83-30055
- Allowing for temperature in descriptions of the delayed fracture of inelastic materials 13 p1865 A83-30056
- Allowing for the coalescence of microcracks in a statistical kinetic model for the fracture of materials under uniaxial tension 13 p1866 A83-30057
- The fracture of 15Kh1M1F steel in creep as a function of the type of structure 13 p1819 A83-30067
- Experimental study of the fatigue fracture of the aluminum alloy AU4G1-T3 and the austenitic stainless steel Type 316 --- French thesis 13 p1819 A83-30144
- Semiempirical, quantum mechanical calculation of hydrogen embrittlement in metals 13 p1820 A83-30598
- Observation of voids and cracks on ductile fracture process in tensile test of 5083 aluminum alloy plate 13 p1822 A83-30842
- On the relation between stable crack growth and fatigue 13 p1867 A83-31540
- Low temperature fatigue fracture of metals and alloys 13 p1824 A83-31585
- A calculation of the asymptotic behavior of 'intensity coefficients' in approaching corner and conical points 14 p2077 A83-31895
- The development of the foundations of fracture mechanics for materials with initial stresses 14 p2029 A83-32151
- Modelling of fracture process zones and singularity dominated zones 14 p2029 A83-32341
- Structural parameters in a continuum model of ductile fracture 14 p1992 A83-32382
- Path-independent integrals, energy release rates, and general solutions of near-tip fields in mixed-mode dynamic fracture mechanics 14 p2031 A83-32652
- Effect of bending moment on the dynamic fracture of a beam or plate under tensile loading 14 p2031 A83-32653
- Effect of shear and rotary inertia on dynamic fracture of a beam or plate in tensile loading 14 p2031 A83-32654
- A Mohr-circle graphical method for stress intensity factors in cracked plates under different loadings 14 p2031 A83-32656
- Arrest of fast Mode-I fracture in an elastic-viscoplastic transition zone 14 p2031 A83-32657
- Mechanics and mechanisms of fracture 14 p2032 A83-32808
- Progress in boundary element methods. Volume 2 15 p2224 A83-33852
- Fracture mechanics stress analysis 15 p2173 A83-33855
- The ductile fracture of metals - A microstructural viewpoint 15 p2138 A83-34131
- A variable power singular element for analysis of fracture mechanics problems 15 p2176 A83-34321
- Mechanics of fracture of rubber-like materials 15 p2142 A83-34329
- Interaction of cracks in elastic media 15 p2177 A83-34349
- Micro and macro mechanics of crack growth; Proceedings of the Symposium, Louisville, KY, October 13-15, 1981 15 p2179 A83-34476
- Micro and macro mechanics aspects of time-dependent crack growth 15 p2138 A83-34477
- Hydrogen-assisted crack-growth in titanium alloys 15 p2139 A83-34481
- High temperature time-dependent crack growth 15 p2139 A83-34485
- Temperature dependence of creep crack growth in aluminum alloy RR58 15 p2139 A83-34487
- Quarter-point elements for curved crack fronts 15 p2179 A83-34565
- Fracture morphology of graphite/epoxy composites 15 p2130 A83-34793
- The fracture of composites with allowance for the effects of temperature and humidity 16 p2323 A83-35508
- The fracture mechanism of carbon and boron composites in interlayer shear 16 p2323 A83-35509
- Determination of stresses in an infinite plate with a kinked or branched crack 16 p2365 A83-35550
- A fracture mechanics analysis of indentation-induced Palmqvist crack in ceramics 16 p2336 A83-35572
- Strain rate sensitivity effects in cyclic deformation and fatigue fracture 16 p2332 A83-36188
- On the electrical potential analysis of a cracked fracture mechanics test specimen using the finite element method 16 p2368 A83-36509
- Fracture mechanics deliberation of lugs 16 p2368 A83-36515
- Mixed mode fracture analysis of rectilinear anisotropic plates using singular boundary elements 16 p2369 A83-36555
- A nonlinear energy analysis for mixed mode fracture 17 p2518 A83-37271
- Isoparametric finite element analysis of large elasto-plastic strain problems and its applications in fracture mechanics 17 p2518 A83-37272
- Defects, fracture and fatigue; Proceedings of the Second International Symposium, Mont Gabriel, Quebec, Canada, May 30-June 5, 1982 17 p2489 A83-38376
- The effect of homo- and heterogeneous mechanisms coupling on microcrack nucleation in metals 17 p2490 A83-38385
- Motion of the crack under constant loading and at high constant temperature 17 p2523 A83-38389
- Sudden twisting of partially bonded cylindrical rods 17 p2523 A83-38392
- Experimental stress intensity distributions by optical methods 17 p2523 A83-38395
- On cracking instability in plates containing circular holes 17 p2523 A83-38399
- Energy criteria for the brittle fracture of composite materials with initial stresses 17 p2523 A83-38503
- Dynamic fields near a crack tip growing in an elastic-perfectly-plastic solid 17 p2524 A83-38528
- A map of fracture mechanisms for tungsten 17 p2492 A83-38874
- Fracture of notched polycarbonate under hydrostatic pressure 18 p2670 A83-39049
- Non-singular stresses effects on two interacting equal collinear cracks 18 p2696 A83-39076
- A synergistic fracture mechanics approach to fatigue life evaluation 18 p2665 A83-39077
- A simple model of stress intensity range threshold and crack closure stress 18 p2665 A83-39081
- Safety assessments in fracture-mechanics defect evaluation for biaxial stresses 18 p2696 A83-39256
- Fracture of an aluminum alloy at the prespalling stage 18 p2666 A83-39504
- A technique for the accelerated life testing of fan impellers 18 p2698 A83-39512
- Stress intensity factors in two bonded elastic layers containing cracks perpendicular to and on the interface. I Analysis. II - Solution and results 18 p2698 A83-39535
- Fatigue life prediction of notched members based on local strain and elastic-plastic fracture mechanics concepts 18 p2699 A83-39543
- Fracture mechanics in design - Particular reference to the thickness effect on the risk of unstable fracture 18 p2699 A83-39547
- Discussion - 'The Mises elastic-plastic boundary as the core region in fracture criteria' by P. S. Theocaris and N. P. Andrianopoulos 18 p2699 A83-39550
- Further remarks on an exact solution for crack problems 18 p2699 A83-39551
- A fatigue fracture model for metal-matrix composites 18 p2701 A83-40103
- Factors affecting the interlaminar fracture energy of graphite/epoxy laminates 18 p2651 A83-40152
- Fracture mechanics for delamination problems in composite materials 18 p2652 A83-40153
- Damage analysis of fibrous composites 18 p2654 A83-40189
- A study on fracture mechanism of unidirectional fibrous composites 18 p2654 A83-40190
- On fracture behavior during crack propagation in carbon-fiber composites 18 p2654 A83-40192
- Damage and fracture of tridirectional composites 18 p2704 A83-40194
- Fracture analysis of composite materials 18 p2704 A83-40195
- Fracture mechanism of short glass fiber reinforced polyamide thermoplastics 18 p2657 A83-40232
- Deformation and fracture of strongly textured Ti alloy sheets in uniaxial tension 18 p2669 A83-40630
- Stretch forming and fracture of strongly textured Ti alloy sheets 18 p2669 A83-40631
- Flow localization accompanying the intergranular fracture of Ni3Al 18 p2670 A83-40641
- Microfracture model for hydrogen embrittlement of austenitic steels 18 p2670 A83-40643
- Some effects of material property data selection on crack propagation analyses 19 p2821 A83-41200
- Contour invariants of the fracture theory for thermoelastic bodies 19 p2858 A83-41215
- A criterion for predicting creep fracture mechanisms 19 p2858 A83-41290
- Technical fracture mechanics --- German book 19 p2858 A83-41522
- Fracture anomalies of a casting magnesium alloy in low-cycle fatigue 19 p2822 A83-41595
- A theoretical analysis of the effect of short cracks on the endurance limit of materials 19 p2859 A83-41597
- Diffraction of SH waves by a moving crack 19 p2860 A83-41999
- Creep of structures - A continuous damage mechanics approach 20 p3001 A83-42520
- Fracture mechanics J-integral calculations in thermo-elasto-plasticity 20 p3003 A83-42931
- A comparison of exact and model solutions for the initiation of debond fracture 20 p3004 A83-42973
- Fracture mechanics for delamination problems in composite materials 20 p3007 A83-43143
- A study of the time dependence of the breaking stresses during spalling in copper, nickel, and titanium 20 p2956 A83-43523
- The opening of a crack in the elastic region under the effect of a moving load 20 p3008 A83-43524
- Reliability theory of stochastic fracture processes in sustained loading. II - Stochastic loading 20 p3008 A83-43582
- Structural stability considerations in elastic-plastic fracture mechanics [ASME PAPER 83-PVP-40] 20 p3009 A83-43728
- Consideration of short cracks in high stress fatigue design [ASME PAPER 83-PVP-90] 20 p3009 A83-43730
- The role of grain boundaries in high-temperature deformation and fracture 20 p2957 A83-43775
- Brittle fracture near holes --- Russian book 21 p3150 A83-43911
- Some geometrical observations on crack front profiles in PMMA double torsion specimens 21 p3152 A83-44330
- Effect of thickness on plastic zone size in BCS theory of fracture --- Bilby, Cottrell and Swinden 21 p3155 A83-44882
- Application of electrical analog technique in fracture mechanics 21 p3155 A83-44883
- A comparison of the J (asterisk) integral with other methods of post yield fracture mechanics 21 p3155 A83-44886
- Some consequences of a fracture criterion for oriented polymers based on electron spin resonance spectroscopy 21 p3156 A83-44889
- A new singular integral equation for the classical crack problem in plane and antiplane elasticity 21 p3156 A83-44890
- On the modelling of the process region at crack growth 21 p3156 A83-44891
- Numerical analysis of fast mode-I fracture of a strip of viscoplastic work-hardening material 21 p3156 A83-44892
- 3-D elastic-plastic investigation of fracture parameters in side-grooved compact specimen 21 p3157 A83-44906
- The use of the method of lines in 3-D fracture mechanics analyses with application to compact tension specimens 21 p3158 A83-44911
- On the small crack fracture mechanics 21 p3159 A83-44924
- Concentration of elastic stresses near dies, cracks, thin inclusions, and reinforcements --- Russian book 21 p3160 A83-45025

Improved moiré interferometry and applications in fracture mechanics, residual stress and damaged composites 21 p3160 A83-45144

A hybrid technique for improved K determination from photoelastic data 21 p3161 A83-45156

Fracture properties of metals under rapid heating and loading 21 p3114 A83-45158

Fracture mechanics approach to fatigue crack initiation from deep notches 21 p3162 A83-45187

A theory for the Bilby-Cottrell mechanism of crack nucleation in metals 21 p3115 A83-45364

Dynamics of a rupture-shear crack at the interface of two elastic materials 21 p3164 A83-45394

Finite elements in fracture mechanics 22 p3304 A83-45768

Introduction to engineering fracture mechanics 22 p3304 A83-45769

Finite element procedures in fracture mechanics 22 p3305 A83-45771

Structures with cracks in the case of superimposed normal and shear stresses 22 p3305 A83-45772

Fracture mechanics of plates and shells 22 p3305 A83-45773

Numerical studies involving fracture mechanics samples 22 p3305 A83-45774

An axisymmetric problem for an elastic medium with a spherical inclusion weakened by an interface crack 23 p3468 A83-47172

Flow localization and fracture in materials exhibiting structural superplasticity 23 p3469 A83-47853

Extremum principles for the energy-release problem of elastic-perfectly plastic body subjected to prescribed change of material properties 23 p3470 A83-48093

The behaviour of fatigue cracks subject to applied biaxial stress - A review of experimental evidence 23 p3470 A83-48146

The crack problem for a nonhomogeneous plane [ASME PAPER 83-APM-35] 23 p3471 A83-48243

Self-similarity of fatigue fracture - Cumulative damage 23 p3472 A83-48466

Delamination of composites under compression 23 p3472 A83-48467

Stability and fracture of a plate with two slits under tension 23 p3473 A83-48474

Modern methods for studying the initial stage of the fatigue fracture of metals 23 p3433 A83-48539

Stiffness changes in unidirectional composites caused by crack systems. 23 p3428 A83-48602

The stress-strain state at the point of accumulation of collinear cracks 24 p3591 A83-48927

Mechanical parameters applied to the propagation of creep cracks 24 p3591 A83-48995

Calculation of energy changes in the Griffith problem 24 p3592 A83-49027

Strain energy density fracture criterion in elastodynamic mixed mode crack propagation 24 p3594 A83-49863

Statistical analysis of multiple fracture in 0 deg/90 deg/0 deg glass fibre/epoxy resin laminates 24 p3554 A83-50064

FRACTURE RESISTANCE

U FRACTURE STRENGTH

FRACTURE STRENGTH

Determination of fracture toughness from stretch zone width measurement in predeformed AISI type 4340 steel 01 p0024 A83-10217

Correlation between fracture toughness K_{IC} for a plane stress system and mechanical properties 01 p0024 A83-10298

Precipitation hardening and the resistance to brittle fracture of low alloy steels containing vanadium 01 p0025 A83-10396

Calculating the limiting state of refractory alloys under high-cycle loading 01 p0026 A83-10687

Recommendations for the measurement of R-curves using centre-cracked panels 01 p0026 A83-11029

Determination of fracture toughness of ductile materials using a reinforced double cantilever beam specimen 01 p0026 A83-11030

X-ray analysis of the transformed zone in partially stabilized zirconia /PSZ/ 02 p0159 A83-11675

Effect of water on the crazing of a crosslinked poly/methylmethacrylate/ 02 p0159 A83-11676

Fracture toughness test by impact-fatigue method 02 p0154 A83-11851

Toughening epoxy resin matrix for glass and carbon fiber composites 02 p0149 A83-11852

Fracture of fatigue-loaded composite laminates 02 p0149 A83-12013

Fracture diagrams for the case of monotonic loading at elevated temperatures --- in aluminum alloys 02 p0156 A83-12326

The effect of the shape and size of a fatigue crack on the cyclic fracture toughness of titanium alloy VT9 02 p0156 A83-12330

Evaluation of the fracture toughness of tungsten at high temperatures 02 p0157 A83-12339

Fracture modes of inelastic materials as a function of loading rate and temperature, and associated fracture criteria 02 p0192 A83-12354

The role of the generalized fracture toughness in fracture mechanics [ASME PAPER 82-PVP-21] 02 p0157 A83-12768

Structure and fracture character of V95 alloy sheets in relation to impurity content and aging conditions 03 p0297 A83-13254

Effect of composition and structure on the properties of wrought aluminum alloys of the D16 type 03 p0297 A83-13255

Effect of particles of the insoluble phase Al₉FeNi on the kinetics of fatigue crack propagation in alloy AK4-1 03 p0297 A83-13256

A comparison of the geometry dependence of several nonlinear fracture toughness parameters 03 p0298 A83-13339

A unifying strain criterion for fracture of fibrous composite laminates 03 p0291 A83-13340

Variations of various fracture parameters during the process of subcritical crack growth 03 p0298 A83-13341

Indentation microfracture in the Palmqvist crack regime - Implications for fracture toughness evaluation by the indentation method 03 p0290 A83-13725

Damage accumulation and fracture life in high-temperature low-cycle fatigue 03 p0339 A83-13905

Tensile fracture behaviors of helical fiber reinforced composites 03 p0291 A83-13975

A combination of statistics and subcritical crack extension 03 p0342 A83-14703

Fracture toughness of high-strength laminate sheets containing plastic layers of high elastic modulus 03 p0293 A83-14728

Estimating the life of materials on the basis of the theory of thermal fluctuations 03 p0301 A83-14731

A thermoelectric method of stress analysis for plates weakened by holes 03 p0343 A83-14733

The effect of alloying on the strength of vanadium 03 p0301 A83-14737

An experimental study of the strength of a cross-ply glass-reinforced composite in the plane stressed state 03 p0293 A83-14738

Deformation characteristics of metal composites with brittle fibers during bending 03 p0293 A83-14817

A compendium of sources of fracture toughness and fatigue crack growth data for metallic alloys. II 03 p0301 A83-14822

Microstructure and fracture of fiber reinforced thermoplastic polyethylene terephthalate /P.E.T./ 03 p0293 A83-14825

Fracture toughness of polycrystalline beta-alumina 03 p0303 A83-14921

A mechanical model to predict elastic-plastic fracture toughness in high strength materials 04 p0458 A83-15061

Nondestructive evaluation of ceramics 04 p0463 A83-15213

Methods for determining the crack growth rate during the testing of materials for cyclic fracture toughness 04 p0497 A83-15395

Carbon fibre-reinforced silicon nitride composite 04 p0455 A83-15990

Double torsion fracture toughness test for evaluating transverse cracking in composites 04 p0455 A83-15996

Fracture toughness - A rationalization of the role of microstructure in an alpha-beta titanium alloy 04 p0460 A83-16003

A study on threshold of macro-crack growth in a soft epoxy resin 05 p0618 A83-17101

Characterization of fracture surface, pores and inclusions in sintered Ti-6Al-4V 05 p0615 A83-17548

Transformation toughening of beta double prime-alumina by incorporation of zirconia 05 p0619 A83-17558

The fracture of particulate-filled epoxide resins. I 05 p0611 A83-17563

Critical microstructures for microcracking in Al₂O₃-ZrO₂ composites 06 p0733 A83-17954

The effect of temperature on the spalling fracture of polymer materials 06 p0734 A83-18012

The relationship between the spall resistance and the spall plate thickness 06 p0770 A83-18013

The strength of VT6 titanium under shock-wave loading 06 p0727 A83-18014

Dependence of fracture toughness of alumina on grain size and test technique 06 p0734 A83-18051

Slow growth of microcracks - Evidence for one type of ZrO₂ toughening 06 p0734 A83-18054

The plastic work spent in ductile fracture 06 p0774 A83-18485

Stability of tearing fracture in structural steels 06 p0728 A83-18486

A quantitative description of fracture toughness under plane stress conditions by the R-curve method 06 p0774 A83-18487

Stress redistribution in the ruptured fiber of a viscoelastic composite 06 p0725 A83-18504

Biomechanical aspects of the fracture resistance of the vertebral column of humans under impact overloads in the head-pelvis direction 06 p0798 A83-18509

Length distribution of ruptured fibers in unidirectional composites 06 p0725 A83-18516

Influence of load biaxiality on the fracture load of center cracked sheets 06 p0776 A83-18911

The effect of the deformation history and loading cycle ratio on the cyclic fracture toughness characteristics of VT9 alloy 06 p0733 A83-19303

The relationship between the time to failure and the minimum creep rate during long-term loading under plane stressed state 06 p0733 A83-19309

The effect of rapid heating on the short-term strength characteristics of 28Kh3SNMVFA and 30KhGSA steels 06 p0733 A83-19311

Effects of specimen size on strength of sintered silicon nitride 06 p0735 A83-19319

Evaluation of fracture toughness /J sub I/ using single specimen fracture test augmented by finite element analysis 07 p0883 A83-19670

The fracture characteristics of porous sintered molybdenum 07 p0883 A83-19968

The effect of loading rates, temperature and moisture on the fracture toughness of polycarbonate 07 p0899 A83-20497

Review of the effects of fatigue cracking loads on plane strain fracture toughness 07 p0886 A83-20518

Fatigue crack front shape and its effect on fracture toughness measurements 07 p0886 A83-20519

A summary of fracture mechanics concepts 07 p0945 A83-20520

Evidence of microscopic crack jumping in an epoxy resin 07 p0901 A83-21085

Low cycle fatigue and life prediction methods 07 p0892 A83-21462

Fracture mechanics and crack growth in fatigue 07 p0892 A83-21464

High temperature fatigue of a superalloy for cast turbine wheel 07 p0893 A83-21478

Fracture behaviour of a single-fibre graphite/epoxy model composite containing a broken fibre or cracked matrix 07 p0877 A83-21565

High-temperature fracture of hot-pressed AlN ceramics 07 p0901 A83-21567

Characterization of AlN ceramics containing long-period polytypes 07 p0901 A83-21569

Advances in fracture research; Proceedings of the Fifth International Conference on Fracture, Cannes, France, March 29-April 3, 1981. Volumes 1, 2, 3, 4, 5, & 6 08 p1115 A83-21651

The fracture toughness of high strength engineering alloys containing short cracks 08 p1058 A83-21655

Comparison of impact testing on Charpy V-notch specimens and WOL-1X-specimens 08 p1058 A83-21672

Experimental determination of high loading rate effects on fracture toughness of aluminum alloys 08 p1058 A83-21673

Fibre length-strength relationships and the fracture of composites 08 p1053 A83-21678

Role of local fiber distribution at notch tip in the fracture toughness of FRP 08 p1054 A83-21681

The relationship of compliance changes during fatigue loading to the fracture of composite materials 08 p1054 A83-21682

Fracture mechanical studies of the strength resulting from polymer interdiffusion 08 p1068 A83-21696

Shear bands and fracture in crystalline polymers 08 p1069 A83-21697

The effect of specimen thickness and morphology on fracture toughness of thermoplastic polymers 08 p1069 A83-21698

Constitutive relations including ductile fracture damage - Application to cracked bodies 08 p1117 A83-21700

Study of fracture criteria for ductile rupture of A508 steel 08 p1059 A83-21701

On the effects of pre-loading on the fracture toughness of A533B-1 steel 08 p1059 A83-21702

Numerical modelling of warm prestress effect using a damage function for cleavage fracture 08 p1060 A83-21703

The influence of specimen geometry on stable crack growth for a high strength steel 08 p1060 A83-21704

- Experimental studies of stable crack growth
08 p1060 A83-21705
- Effect of specimen size of J1c for a Ni-Cr-Mo rotor steel in the upper shelf region
08 p1060 A83-21706
- The influence of specimen geometry on fracture of unwelded and welded steel specimens - Comparison of experimental results with FEM-calculation
08 p1060 A83-21707
- The influence of prior austenite grain size and stress ratio on near threshold fatigue crack growth behavior in high strength steel
08 p1061 A83-21716
- Contiguity and the fracture process of WC-Co alloys
08 p1061 A83-21721
- On the critical problems in physico-mechano-structural foundations of fracture
08 p1117 A83-21724
- Microstructural analysis of the cold working effect on the fracture toughness of weld metal in HSLA steel welds
08 p1061 A83-21726
- Significance of pop-in fracture in high nickel cryogenic steel weldments
08 p1061 A83-21727
- Fracture toughness of simulated H.A.Z. --- heat affected zone
08 p1061 A83-21728
- Threshold Delta-K values and non-closure of fatigue cracks
08 p1061 A83-21733
- Fracture strength and toughness of engineering nitrogen ceramics
08 p1069 A83-21741
- The significance of microstructure to the fracture toughness of partially-stabilized zirconia
08 p1069 A83-21742
- Conditions for toughening of particulate brittle composites
08 p1054 A83-21744
- Plane stress fracture under biaxial loading
08 p1062 A83-21749
- Simplified determination of J-integral and its availability as a strain intensity parameter at notch tip
08 p1118 A83-21750
- Instability problems in ductile fracture
08 p1063 A83-21752
- Development of the nonlinear energy method for fracture toughness determination
08 p1063 A83-21753
- The fracture toughness-microstructure relationship of alumina-based ceramics
08 p1069 A83-21768
- The influence of microstructure and geometric factors on the stress state and the fracture toughness of ceramics
08 p1070 A83-21780
- Residual stress effects on fracture toughness measurements
08 p1064 A83-21791
- The effect of dispersoids on the ductile fracture toughness of Al-Mg-Si alloys
08 p1065 A83-22015
- Fracture of nickel-base superalloy single crystals
08 p1065 A83-22018
- On the accuracy of J-integral value evaluated by finite element method for mixed mode
08 p1122 A83-22068
- A relationship between the fracture strength and the fracture surface markings of brittle plastic plates
08 p1070 A83-22070
- Application of the J concept to alumina at high temperatures
08 p1070 A83-22192
- Dynamic fracture toughnesses of reaction-bonded silicon nitride
08 p1071 A83-22197
- High-temperature environmental strength degradation of a hot-pressed silicon nitride - An experimental test [ACS PAPER 117-B-81F]
08 p1071 A83-22198
- Failure mechanism for alloy KhN67VM under the action of a copper-silver solder
08 p1067 A83-22698
- Reasons for the reduction in the fracture toughness of alloy KhN77TYuR-VD at room temperature
08 p1067 A83-22699
- Effects of processing on the mechanical properties of carbon short-fiber reinforced polycarbonate
08 p1055 A83-22718
- Modeling the creep and fracture of the directionally solidified gamma/gamma-prime-McC eutectic
08 p1068 A83-22786
- Strength conditions for molybdenum and molybdenum-base low alloys in complex stressed state at high temperatures
09 p1229 A83-23509
- Characteristics of the spalling fracture of aluminum and aluminum alloys D16 and AMg6 in the temperature range -196 to 600 C
09 p1229 A83-23510
- Fracture tough composites - The effect of toughened matrices on the mechanical performance of carbon fiber reinforced laminates
09 p1222 A83-23642
- The influence of metallurgical factors on the fracture toughness of 7010 and 7050 aluminium alloys
09 p1230 A83-23677
- Stable crack growth during fracture toughness testing in Ti-6Al-4V alloy
09 p1230 A83-23916
- Interrelation of material microstructure, ultrasonic factors, and fracture toughness of a two-phase titanium alloy
09 p1231 A83-23922
- Determination of fracture toughness of unidirectionally fiber-reinforced composites
09 p1223 A83-23936
- Comparative evaluation of shear test methods for composites
09 p1224 A83-23948
- A comparison of the performances of titanium alloys under conditions of a limiting-state similarity
09 p1234 A83-24380
- The effect of hydrogen on the fracture toughness of titanium alloys
09 p1235 A83-24398
- Hydrogen in the welded joints of titanium alloys
09 p1235 A83-24399
- The effect of a gas-saturated layer on the corrosion stability and mechanical strength of titanium alloys
09 p1235 A83-24403
- Determination of the fracture toughness of polycarbonate using an energy approach
09 p1239 A83-25049
- Flaws responsible for slow cracking in the delayed fracture of alumina
09 p1240 A83-25205
- Elastic properties of hafnium and zirconium oxides stabilized with praseodymium or terbium oxide
09 p1240 A83-25209
- Transformation strengthening of beta double prime-Al₂O₃ with tetragonal ZrO₂
09 p1240 A83-25210
- Fracture test methods
10 p1392 A83-25319
- Fracture properties of carbon and alloy steels
10 p1392 A83-25320
- Fracture properties of wrought stainless steels
10 p1392 A83-25321
- Fracture properties of aluminum alloys
10 p1393 A83-25322
- Fracture properties of titanium alloys
10 p1393 A83-25323
- Fracture properties of superalloys
10 p1393 A83-25324
- Experimental determination of stresses in damaged composites using an electric analogue
10 p1441 A83-26446
- Deformation work density fracture criterion for composite materials
10 p1442 A83-26771
- Crack deflection processes. I - Theory
11 p1595 A83-28424
- Compliance calibration of a family of short rod and short bar fracture toughness specimens
11 p1548 A83-28435
- A new method of determining J1c of steel by means of single specimen
11 p1548 A83-28442
- The shielding of excess phases during fracture under plane strain conditions and its effect on the fracture toughness
11 p1549 A83-28481
- The effect of temperature and heat treatment on the fracture toughness of powder-metallurgy tungsten
11 p1549 A83-28482
- The effect of the annealing conditions on the cyclic fracture toughness of the magnesium alloy VMD-10
11 p1549 A83-28488
- The effect of block cyclic loading on the deformability and strength of structural materials under conditions of plane stressed state. II - The limiting states /yield and strength/
11 p1549 A83-28504
- A method for testing metals for fracture toughness under vibration loading at high temperatures
11 p1549 A83-28505
- The theoretical strength of metals
11 p1549 A83-28513
- Strength and fracture toughness of reaction-bonded Si₃N₄
12 p1716 A83-29398
- Fracture behavior of hybrid composite laminates [AIAA 83-0804]
12 p1710 A83-29736
- Carbon/epoxy laminates under combined fastener bearing and tension bypass loading [AIAA 83-0967]
12 p1710 A83-29778
- A strain-limit strength theory for metals [AIAA 83-1013]
12 p1740 A83-29797
- Effect of indenter geometry on controlled-surface-flaw fracture toughness
12 p1717 A83-29975
- Fracture toughness/Young's modulus correlation for low-density fibrous silica bodies
12 p1717 A83-29976
- Mechanical properties of sintered and nitrided laser-synthesized silicon powder
12 p1717 A83-29977
- Method of high-speed loading in determining fracture
13 p1823 A83-31218
- Application of the acoustic emission method in repeated determinations of fracture toughness characteristics
13 p1823 A83-31219
- The strength of blade-root fastenings at higher-mode vibrations
13 p1867 A83-31323
- On the dependence of fracture toughness on metallurgical factors
13 p1824 A83-31586
- Fracture toughness of unidirectional glass/carbon hybrid composites
13 p1816 A83-31616
- The residual strength of prefabricated structures made of pressed panels of D16chT alloy and its modifications
14 p2029 A83-32075
- The critical angles of shock-wave collision in porous media in the low-pressure region
14 p1992 A83-32095
- The effect of recrystallization on the fracture toughness of tungsten
14 p1992 A83-32147
- Engineering property comparisons of 7050-T73651, 7010-T7651 and 7010-T73651 aluminium alloy plate
14 p1992 A83-32340
- The fracture toughness of interlayers in joints with layers of different moduli under static tension
14 p2030 A83-32384
- A comment on the multispecimen R curve approach to crack initiation toughness testing
14 p2031 A83-32664
- Mechanical properties of BCC metals; Proceedings of the U.S.-Japan Seminar, Honolulu, HI, March 23-27, 1981
14 p1995 A83-32874
- Toughness and ductility of aluminum-lithium alloys prepared by powder metallurgy and ingot metallurgy
14 p1996 A83-32886
- The use of the acoustic emission method for studying the strength and ductility of materials at low temperatures
14 p1997 A83-33014
- The resistance of structural materials to fracture during impact bending
14 p2033 A83-33015
- A study of the temperature dependence of the mechanical characteristics of structural alloys under impact tension
14 p1997 A83-33016
- Elastic properties and fracture behavior of graphite/polyimide composites at extreme temperatures
14 p1987 A83-33119
- Fracture characterization of a random fiber composite material
14 p1988 A83-33296
- Numerical analysis of ductile fracture experiments using single-edge notched tension specimens
15 p2134 A83-33511
- An improved method for threshold fatigue crack propagation testing on an electromagnetic resonance type machine
15 p2162 A83-33512
- J(Ic) measurement point determination for HY130, CMS-9, and Inconel Alloy 718
15 p2134 A83-33514
- Laser welding of a titanium alloy
15 p2135 A83-33643
- The effect of heat treatment on the structure and long-term strength of the nickel eutectic gamma/gamma-prime-McC - The length memory effect
15 p2137 A83-34017
- Dislocation shielding of a crack in a quasi continuum approximation
15 p2179 A83-34479
- Effects of environment and internal hydrogen on the sustained load cracking of Ti-6211
15 p2139 A83-34482
- High-temperature embrittlement of tungsten
15 p2140 A83-35042
- The effect of thermal shock on the substructure and strength of single-crystal cubic boron nitride
15 p2142 A83-35043
- On the correlation between solid-particle erosion and fracture parameters in SiC
15 p2142 A83-35072
- The temperature dependence of the ultimate stress for eutectic tungsten alloys with titanium, zirconium, and hafnium carbides
15 p2141 A83-35311
- A machine for the mechanical testing of polymers in a three-dimensional stressed state
16 p2364 A83-35513
- Prediction of failure probabilities for cleavage fracture from the scatter of crack geometry and of fracture toughness using the weakest link model
16 p2368 A83-36510
- The relationship between the structure and cyclic fracture toughness of alpha titanium alloys
16 p2335 A83-36890
- The principles governing changes in the hot brittleness of aluminum alloys of the system Al-Cu-Mg
16 p2335 A83-36895
- Intergranular crack-deflection toughening in silicon carbide
16 p2337 A83-36948
- Tensile loading of a plate with a crack near a reinforced hole filled with an elastic disk
17 p2521 A83-37643
- Fatigue of high-strength powder metallurgy aluminum alloys
17 p2487 A83-37835
- Titanium fan disc Structural Life Prediction/Correlation program [SAE PAPER 821437]
17 p2522 A83-37985
- On the crack energy density and energy release rate for an elasto-plastic crack
18 p2697 A83-39456
- The fracture toughness of structural alloys under cyclic loading. I, II
18 p2665 A83-39498
- A singular element for a new experimental method of fracture toughness determination
18 p2699 A83-39539
- Postirradiation fracture toughness of Inconel X-750
18 p2666 A83-39542
- Damage tolerance evaluation of adhesively laminated titanium
18 p2666 A83-39994
- Analysis of flexure strength data of ceramics
18 p2672 A83-39996

An experimental study of the thermal cycling of composite materials with disperse reinforcement 18 p2649 A83-40104

Strength of epoxy resin under multiaxial stress field 18 p2672 A83-40141

Stress and strength analysis of composite laminates at delamination 18 p2651 A83-40149

On fibre composites with intermittent interlaminar bonding 18 p2651 A83-40151

Prediction of fracture toughness of unidirectional metal matrix composites 18 p2654 A83-40196

Study on elasto-plastic fracture toughness of composite materials 18 p2654 A83-40197

Mechanical behaviours in high velocity tension of composites 18 p2656 A83-40213

Properties of composite box beams under combined impact loading 18 p2705 A83-40222

Long term strength of glass reinforced plastics 18 p2656 A83-40224

The strength, ductility and failure of thermoplastics reinforced with short-glass fibres 18 p2657 A83-40233

The strength of aligned short-fiber carbon, glass, and hybrid carbon/glass composites 18 p2657 A83-40234

Fracture behavior and toughness of helical fiber reinforced composite metals 18 p2667 A83-40265

Microstructure and fracture behaviour of unidirectionally reinforced carbon fiber/carbon composites 18 p2661 A83-40282

Oxide scale induced cleavage fracture in an ODS Fe-Cr-Al alloy 18 p2670 A83-40639

The effect of hydrogen on the fracture toughness and subcritical crack growth behavior of alpha + beta titanium alloys 19 p2821 A83-40801

The cyclic fracture toughness, K_{IC}, of aluminum alloys 19 p2821 A83-40802

The effect of crack closure and estimation of the cyclic fracture toughness of structural alloys 19 p2856 A83-40803

The bending of a laterally cracked beam clamped at its ends 19 p2856 A83-40807

The wedging of a square specimen with a lateral crack 19 p2856 A83-40808

Slow crack growth behavior in transformation-toughened Al₂O₃-ZrO₂(Y₂O₃) ceramics 19 p2823 A83-40907

Mechanical, thermal, and microstructural properties of neutron-irradiated SiC [ACS PAPER 66-N-82] 19 p2823 A83-40909

Determination of stable crack growth resistance of ductile material using an RDCB specimen --- Reinforced Double Cantilever Beam 20 p2954 A83-42830

The fracture diagram - A new design tool for stiffened panels 20 p3007 A83-43447

Investigation of the mechanism of failure under low-cycle nonisothermal load --- for structural steels 20 p2956 A83-43562

An energy approach to evaluating the crack resistance of materials 20 p3008 A83-43622

Evaluation of fracture toughness of thermomechanical-processed 7079 alloy using double torsion bend test 20 p2957 A83-43635

Tear test on 7075 and 7475 alloys by use of kahn type specimens 20 p2957 A83-43636

Fracture toughness measurement of cast magnesium alloy by cylindrical specimen with ring-shaped crack 21 p3111 A83-44107

Fracture toughness of composite adherend adhesive joints under mixed mode I and III loading 21 p3115 A83-44121

Crack-front shape effects in the double torsion test 21 p3152 A83-44329

A theory for the long-term cyclic strength under high-temperature high-cycle loading 21 p3113 A83-44722

The effect of molybdenum on the ductility of a niobium alloy precipitation-hardened by zirconium nitrides 21 p3113 A83-44846

Fracture toughness tests on an aluminum alloy using a chevron notch bend specimen 21 p3113 A83-44899

A loading device for the creation of mixed mode in fracture mechanics 21 p3158 A83-44919

Estimation of transverse-shear fracture toughness for an HSLA steel 21 p3114 A83-44921

A probabilistic treatment of brittle fracture under nonmonotonically increasing stresses 21 p3159 A83-44923

Simultaneous measurements of stress intensity and toughness for fast-running cracks in steel 21 p3114 A83-45154

Plane-stress fracture testing of finite sheets under biaxial loads 21 p3161 A83-45161

An engineering interpretation of pop-in arrest and tearing arrest in terms of static crack arrest, K_{IC}(a) 21 p3162 A83-45186

Recovery behavior of hydrogen charged 7075-T6 aluminum 22 p3268 A83-45625

A constant amplitude fatigue study of an aluminum powder metallurgy alloy 22 p3269 A83-46024

A new method for the determination of the critical value of crack tip opening displacement at the initiation of crack growth using a single three-point bend specimen 22 p3305 A83-46025

Creep and fracture initiation in fibre reinforced plastics 22 p3264 A83-46296

An edge-cracked Mode II fracture specimen 22 p3306 A83-46804

Fatigue fracture of polycarbonate 22 p3270 A83-46902

Effect of grinding variables on strength of hot pressed silicon nitride [ASME PAPER 83-GT-203] 23 p3465 A83-48004

Contribution of the strength-porosity relationship of reaction bonded silicon nitride 23 p3436 A83-48280

High temperature fatigue failure in pressureless sintered silicon nitride 23 p3437 A83-48289

Effect of deformation on the fracture of Si₃N₄ and sialon 23 p3437 A83-48290

The fracture behaviour of hot-pressed silicon nitride between room temperature and 1400 C 23 p3437 A83-48292

Surface damage in ceramics - Implications for strength degradation, erosion and wear 23 p3438 A83-48301

Stiffness changes in unidirectional composites caused by crack systems. 23 p3428 A83-48602

Effect of zirconium content on properties of type D16 alloy plates 24 p3559 A83-48804

Fracture behavior of the Space Shuttle thermal protection system 24 p3568 A83-48961

Fracture toughness and limiting strength of cermets 24 p3560 A83-49327

Effect of texture and grain size on the fracture behaviour of hot rolled Mg, Mg-12.5 percent Li and Mg-5 percent Ti alloys 24 p3566 A83-49648

Characteristics of brittle fracture under general combined modes including those under bi-axial tensile loads 24 p3594 A83-49866

The stability of plates near a sharp defect in the case of the initial biaxial plane stressed state 24 p3596 A83-49908

The strength of the hard-alloy components of high-pressure apparatus for the synthesis of superhard materials 24 p3567 A83-49911

Determination of anisotropy during the analysis of the long-term strength under conditions of plane stressed state 24 p3596 A83-49912

The effect of heating on the strength and elasticity of precipitation-hardened molybdenum alloys 24 p3567 A83-49914

The disentanglement time of the craze fibrils in polymethylmethacrylate 24 p3569 A83-50068

Macroscopic fracture surface energy of unidirectional metal matrix composites - Experiment and theory 24 p3554 A83-50069

FRACTURE TOUGHNESS

U FRACTURE STRENGTH

FRACTURES (MATERIALS)

The deformation and fracture of Beta HMX 02 p0161 A83-12030

Reflective and refractive scattering of ultraviolet radiation caused by state of the art optical grinding and polishing techniques 02 p0237 A83-12701

Quantitative analysis of delayed fracture observed in stress rate tests on brittle materials 03 p0290 A83-13686

The fracture of constituent particles during fatigue 03 p0301 A83-14705

Metal fracture kinetics in the submicrosecond life range 04 p0460 A83-15887

An investigation and classification of the fractures of refractory nickel-base PM alloys 06 p0729 A83-18747

Fracture of composite materials; Proceedings of the Second USA-USSR Symposium, Lehigh University, Bethlehem, PA, March 9-12, 1981 09 p1222 A83-23926

Flaws and defects of structural carbon fibers 09 p1238 A83-23950

Calculation of the forming limit curve at fracture 16 p2366 A83-35980

Effect of structure on the type of fracture of titanium alloy VT-3-1 16 p2330 A83-36025

Processing-related fracture origins. I - Observations in sintered and isostatically hot-pressed Al₂O₃/ZrO₂ composites 16 p2337 A83-36945

Processing-related fracture origins. II - Agglomerate motion and cracklike internal surfaces caused by differential sintering 16 p2337 A83-36946

Processing-related fracture origins. III - Differential sintering of ZrO₂ agglomerates in Al₂O₃/ZrO₂ composite 16 p2337 A83-36947

Boundary element methods in creep and fracture --- Book 17 p2518 A83-37159

Defects, fracture and fatigue; Proceedings of the Second International Symposium, Mont Gabriel, Quebec, Canada, May 30-June 5, 1982 17 p2489 A83-38376

Prediction of damage sites ahead of a moving heat source 17 p2522 A83-38387

A pseudo-linear analysis of yielding and crack growth - Strain energy density criterion 17 p2522 A83-38388

Creep cavitation and fracture due to a stress concentration in 2-1/4 Cr-1 Mo 17 p2490 A83-38390

Gasdynamic approach to solving the problem of the fracture of a brittle rod by an intense shock wave 19 p2845 A83-41888

High temperature deformation and fracture phenomena of polypphase Si₃N₄ materials 23 p3437 A83-48287

Fiber fracture in reinforced thermoplastic processing 24 p3553 A83-48998

FRACTURING

NT CRUSTAL FRACTURES

Fracto-emission from pentaerythritol tetranitrate and cyclotetramethylene tetranitramine single crystals 02 p0152 A83-12281

Microstructural study of the deformation and fracture behavior of a sintered tungsten-base composite 06 p0732 A83-19104

Hydrogen-induced fracture phenomena in a BCC titanium alloy 08 p1061 A83-21717

Fracture assessment in ductile tearing situations 08 p1063 A83-21751

Development of a microfracture model for high rate tensile damage 09 p1279 A83-24071

A fracture criterion for edge-bonded bimaterial bodies 10 p1439 A83-25878

Microscopic aspects of the effect of friction reducers at the lubrication limit --- French thesis 11 p1590 A83-28663

Mechanical properties and fracture behaviour of ZrO₂-Y₂O₃ ceramics 18 p2670 A83-39050

Fracture behaviour of collimated thermoplastic poly(ethylene terephthalate) reinforced with short E-glass fibre 18 p2649 A83-39055

Observations on the fracture and deformation behaviour during annealing of residually stressed polycrystalline aluminium oxides 18 p2671 A83-39058

On the hybrid effect and fracture mode of interlaminated hybrid composites 18 p2658 A83-40241

FRAGMENTATION

Physical parameters of meteoroids undergoing quasicontinuous crushing in the atmosphere. I - Methods of parameter determination 03 p0432 A83-13373

Accumulation and fragmentation in protoplanetary and protosatellite systems 04 p0557 A83-16034

Complete fragmentation of the parent bodies of Themis, Eos, and Koronis families 08 p1175 A83-22928

On the initial mass function and the fragmentation of molecular clouds 09 p1363 A83-24994

Monte Carlo simulations of the initial stellar mass function 11 p1682 A83-28279

Power-law asymptotic mass distributions for systems of accreting or fragmenting bodies 15 p2264 A83-34587

Containment of turbine engine fan blades 16 p2305 A83-35871

Fragmentation of the universe 24 p3671 A83-50166

FRAME PHOTOGRAPHY

Motion detection using Hough techniques 01 p0097 A83-11418

Motion and image differencing --- computer analysis of dynamic scenes 01 p0097 A83-11425

Nonlinear image operators for nulling 3-space translations 01 p0100 A83-11465

Multiframe image point matching and 3-D surface reconstruction 12 p1728 A83-28949

FRAMES

NT AIRFRAMES

NT CHASSIS

NT UNDERCARRIAGES

Bracketing of the eigenfrequencies of spatial skeletons. I, II 06 p0777 A83-19198

Damped second-order Rayleigh-Timoshenko beam vibration in space - An exact complex dynamic member stiffness matrix 11 p1595 A83-28421

Interactive graphical preprocessing of three-dimensional framed structures 11 p1646 A83-28718

A simple mixed formulation for elastica problems 11 p1600 A83-28724

Effective constitutive relations for the microstructure of periodic frames [AIAA 83-1006] 12 p1740 A83-29793

Radiation exchange in large space structures and frames [AIAA PAPER 83-1462] 14 p2032 A83-32721

- On the interaction between local and overall buckling of an asymmetric portal frame 19 p2857 A83-41154
- Design concepts for low cost composite engine frames [AIAA PAPER 83-2445] 23 p3411 A83-48331
- FRANCE**
- The use of the SPOT satellite for remote sensing of land use in the Mediterranean region - A first assessment of simulated images of Corsica 17 p2534 A83-38459
- FRANCK-CONDON PRINCIPLE**
- r-centroids and Franck-Condon factors for the b(prim)-X and b(prim)-b band systems of the NO(+) molecule 15 p2228 A83-35000
- Franck-Condon analysis of thermal and vibrational excitation effects on the ozone Hartley continuum 18 p2713 A83-39180
- FRANZHOEFER LINE DISCRIMINATORS**
- Use of the Franzhofer line discriminator (FLD) for remote sensing of materials stimulated to luminescence by the sun 23 p3458 A83-47793
- FRANZHOEFER LINES**
- Observations of global-scale photospheric Fraunhofer line shifts 06 p0857 A83-19515
- An investigation of the nickel abundance in the solar atmosphere 14 p2113 A83-31829
- A determination of the total photospheric velocity field on the basis of the Fraunhofer lines of various elements 14 p2113 A83-31830
- A determination of microturbulent velocity on the basis of Fe I Fraunhofer lines --- for solar photospheric motions 14 p2113 A83-31833
- On the depth dependence of the solar rotation velocity determined from Fraunhofer lines 15 p2281 A83-34307
- Investigation of the damping constant for profiles of neutral iron lines in the undisturbed solar photosphere 16 p2440 A83-36851
- Telluric spectra from 4690 to 5525 A in a humid atmosphere 21 p3169 A83-43873
- Applications of the Fraunhofer-diffraction method for plasma-wave measurements 24 p3633 A83-49900
- FRANZHOEFER REGION**
- U. FAR FIELDS
- FREDHOLM EQUATIONS**
- Determination of thermal stresses in disks with the Boundary Element Method 01 p0058 A83-10574
- Multiple grid methods for equations of the second kind with applications in fluid mechanics --- Thesis 02 p0170 A83-11899
- Galerkin methods for second kind integral equations with singularities 03 p0387 A83-13573
- The use of integral equations of the second kind to study diffraction by thin screens 07 p0914 A83-20862
- On the problem of two coplanar cracks inside an infinite isotropic elastic solid 07 p0949 A83-21440
- A numerical method for the solution of static and dynamic three-dimensional elasticity problems 08 p1122 A83-21892
- Numerical experiments involving Galerkin and collocation methods for linear integral equations of the first kind 12 p1771 A83-29098
- Numerical solutions of the traction problem for a fibre-reinforced material by an integral-equation method 12 p1736 A83-29611
- A natural interpolation formula for Cauchy-type singular integral equations with generalized kernels 12 p1772 A83-29643
- Application of multigrid methods for integral equations to two problems from fluid dynamics 12 p1725 A83-29661
- The solution of a class of paired integral equations in problems of diffraction theory 13 p1915 A83-31374
- On complex poles in scattering theory 16 p2407 A83-35698
- FREDHOLM OPERATORS**
- U. FREDHOLM EQUATIONS
- U. OPERATORS (MATHEMATICS)
- FREE ATMOSPHERE**
- Blast waves in free air 09 p1264 A83-25272
- An improved model for the calculation of profiles of C/n-squared and epsilon in the free atmosphere from background profiles of wind, temperature and humidity 11 p1623 A83-26994
- The potential of high atmospheric layers 11 p1620 A83-28730
- Radiation-aerosols interaction - Applications to remote sensing and for calculation of the radiative balance --- French thesis 12 p1756 A83-29949
- Retrieval of clear sky moisture profiles using the 183 GHz water vapor line 22 p3342 A83-46950
- FREE BOUNDARIES**
- Solution of a free-boundary problem for elliptic equations 01 p0102 A83-11264
- Optimization problems with free boundaries 02 p0231 A83-11652

- Surface tension driven flows in micro-gravity conditions 02 p0174 A83-12904
- The role of orderly structures in the vorticity balance of the turbulent velocity fields of unrestricted shear flows 04 p0443 A83-15921
- Finite-element methods for steady solidification problems 09 p1338 A83-23723
- Theoretical justification of the method of successive approximations for stationary problems of the mechanics of viscous fluids with free boundaries 09 p1261 A83-24323
- Conditional analysis of intermittency in the near wake of a circular cylinder 10 p1414 A83-25783
- Axially symmetric jet flows 11 p1564 A83-26975
- Solitary waves on a viscous fluid film down a vertical wall 12 p1721 A83-29002
- Nonlinear interfacial progressive waves near a boundary in a Boussinesq fluid 13 p1839 A83-30106
- Variational principles and free-boundary problems --- Book 15 p2223 A83-33749
- Connectivity methods for free boundary problems - 2 phase heat flow 15 p2159 A83-34238
- Exact solutions of a free-boundary problem for the Stokes system 19 p2846 A83-42061
- A numerical method for potential flows with a free surface 24 p3575 A83-48871
- FREE CONVECTION**
- NT. BENARD CELLS
- NT. RAYLEIGH-BENARD CONVECTION
- Velocity distribution due to thermal Marangoni effect in a liquid column 01 p0044 A83-10123
- Free convection fluctuating boundary layer on a horizontal plate 01 p0044 A83-10124
- The Marangoni wave in ripples on an air-water interface covered by a spreading film 01 p0069 A83-11047
- Flow visualization in natural convection 01 p0052 A83-11070
- Numerical solutions to natural convection in a channel with porous walls under a transverse magnetic field 02 p0171 A83-12666
- Natural convection heat transfer between eccentric horizontal cylinders [ASME PAPER 82-HT-43] 02 p0172 A83-12796
- Effect of aspect ratio on heat transfer in shallow enclosures [ASME PAPER 82-HT-44] 02 p0172 A83-12797
- Finite-element simulation of natural convection in three-dimensional enclosures [ASME PAPER 82-HT-71] 02 p0173 A83-12803
- Finite element, stream function-vorticity solution of steady laminar natural convection 02 p0173 A83-12903
- Time-dependent convection under reduced gravity 02 p0174 A83-12993
- Heat transfer in a parallelogram shaped enclosure. II Free convection in infinitely stacked parallelogram shaped enclosure. III - Combined free convection and radiation heat transfer 02 p0175 A83-13071
- Numerical simulation of natural convection in concentric and eccentric horizontal cylindrical annuli 03 p0315 A83-13484
- Laminar and turbulent natural convection in the annulus between horizontal concentric cylinders 03 p0315 A83-13485
- Numerical modeling of the development of a combustion nucleus in a closed vessel under the conditions of natural convection 03 p0295 A83-14054
- Large Prandtl number finite-amplitude thermal convection with Maxwell viscoelasticity --- earth mantle rheological model 03 p0304 A83-14521
- Nonlinear modal analysis of penetrative convection --- in stratified fluids under astrophysical and geophysical conditions 03 p0320 A83-14523
- Applicability of the Boussinesq approximation to solve problems of nonstationary concentrational natural convection 04 p0475 A83-15093
- MHD free-convection flow in the Stokes problem for a porous vertical plate 04 p0538 A83-15985
- Laminar free convection on a vertical nonisothermal plate under strong injection 04 p0478 A83-16164
- The unsteady collision of free-convective boundary layers 04 p0480 A83-16363
- An asymptotic analysis of free convection boundary layer on a horizontal flat plate due to small fluctuations in surface temperature 05 p0638 A83-17321
- Unsteady natural convection about a sphere at small Grashof number 05 p0639 A83-17358
- Influence of small-amplitude undulations on turbulent convection in an axisymmetric pipe flow - Experiments and numerical prediction 05 p0641 A83-17704
- On the thermal and hydrodynamic stability of a fluid in a vertical slot 05 p0641 A83-17722
- Numerical calculation of two-dimensional natural convection in isothermal open cavities 05 p0641 A83-17742

- Natural convection from a horizontal cylinder at small Grashof numbers 05 p0641 A83-17744
- Buoyancy-induced two-dimensional vertical flows in a thermally stratified environment 06 p0756 A83-18375
- Finite-amplitude convection in mixtures with concentration-dependent heat sources 06 p0760 A83-19427
- Experiments on natural convection heat transfer in low aspect ratio enclosures 07 p0924 A83-19822
- An experimental study of the stationary propagation of a flame in a tube under conditions of weightlessness 07 p0868 A83-19957
- An experimental study of turbulent free convection boundary layer in air along a vertical plate using LDV 07 p0925 A83-20279
- Effect of vibration on natural convection heat transfer from vertical fin arrays 08 p1083 A83-21894
- An asymptotic theory of natural convection --- French thesis 08 p1084 A83-22091
- An experimental and theoretical investigation of the onset of convection in rotating spherical shells 08 p1086 A83-23094
- Laminar natural convection along vertical corners and rectangular channels 08 p1090 A83-23208
- The effect of forced and free convection in the discharge of a pressurized gas 08 p1090 A83-23210
- Thermoconvective heat transfer in a rectangular cavity with constant wall cooling rate 08 p1090 A83-23211
- Numerical calculation of the heat transfer by natural convection in a cubical enclosure 08 p1090 A83-23212
- The use of the theory of thermal regularity in investigating the effect of radiation on free convection 09 p1258 A83-23448
- Free convection flow of water at 4 C past an infinite porous plate with constant suction and free stream velocity 09 p1258 A83-23600
- A study of thermal convection and heat transfer --- Russian book 09 p1264 A83-25246
- Convection induced by insulated boundaries in a square 10 p1413 A83-25781
- Fluid mechanics in crystal growth - The 1982 Freeman scholar lecture 10 p1401 A83-26626
- Free convection boundary layers over humps and indentations 11 p1569 A83-28405
- Heat transfer during the film boiling of liquids under conditions of free convection 11 p1570 A83-28555
- Single-mode theory of diffusive layers in thermohaline convection 11 p1570 A83-28755
- MHD free-convection flow in the Stokes problem for a porous vertical plate by finite difference method 12 p1779 A83-28984
- A 2D model of turbulent solar induced flows in passive air collectors 12 p1749 A83-29039
- Use of the finite-element method for natural convection in a horizontally confined infinite layer of fluid 12 p1726 A83-29899
- On partial spectral expansions with natural convection in spherical annulus enclosures as an example 12 p1726 A83-29900
- An examination of natural convection between two horizontal walls --- French thesis 12 p1727 A83-29945
- Effect of rotation on the stability of a bounded cylindrical layer of fluid heated from below 13 p1839 A83-30105
- The effect of natural convection on the concentration limits of ignition for combustible mixtures in a closed container 14 p1988 A83-32081
- Airborne measurements of the free convective internal boundary layer during the sea breeze 14 p2057 A83-32442
- Stability criteria for convection at small Prandtl numbers 14 p2009 A83-32516
- Measurement of thermoacoustic convection heat transfer phenomenon [AIAA PAPER 83-1422] 14 p2009 A83-32701
- Pressure effects on triple correlations in turbulent convective flows 15 p2156 A83-33669
- Accuracy aspects of the finite element method in free convection heat transfer problems 15 p2160 A83-34256
- Combined free and forced laminar convection in a vertical channel 15 p2160 A83-34257
- Combined convection in an annulus applied to a thermal storage problem 15 p2191 A83-34259
- Laminar, natural convection heat transfer in a horizontal gap, bounded by an elliptic and A circular cylinder 15 p2160 A83-34260
- Nonlinear convection in a rotating layer - Amplitude expansions and normal forms 15 p2161 A83-34324
- Laminar natural convection from a horizontal plate and the influence of plate-edge extensions 16 p2348 A83-35337

A model to determine open or closed cellular convection 16 p2384 A83-35463

The effect of thermal boundary conditions on the heat transport in vertical channels heated from below 16 p2349 A83-35557

Free convection about a sphere at small Grashof number 16 p2349 A83-35558

Structure of the free convective internal boundary layer above the coastal area 16 p2390 A83-36494

Effects of mass transfer on the hydromagnetic flow past a vertical limiting surface 16 p2416 A83-36534

Analysis of transient natural convection flow at high Prandtl number using a matched asymptotic expansion technique 16 p2354 A83-36596

Existence of a steady state of a natural convective flow in a confined medium 17 p2507 A83-38066

Period doubling and chaos in partial differential equations for thermosolutal convection 17 p2576 A83-38606

Free convection flow on a nonisothermal flat plate under nonuniform gravity 18 p2681 A83-39347

Hall effects on an oscillatory MHD flow in the Stokes problem past an infinite vertical porous plate. I 18 p2746 A83-39752

Correlations concerning turbulent natural convection 18 p2685 A83-39851

Influence of pressure and nature of the gas 18 p2685 A83-39851

Melt temperature fluctuations - Causes and response of the solidification front --- in low gravity environments 18 p2643 A83-39895

Convection in melts and crystal growth 18 p2685 A83-39896

Solar thermal collectors 18 p2709 A83-40522

The effects of parallel viscosity on stationary convection in plasmas 19 p2901 A83-41172

A numerical study of the effect of free convection on the development of a vertical semifinite turbulent gas jet 19 p2844 A83-41568

Thermal processes in resonance tubes 19 p2845 A83-41890

Natural convection heat transfer in cavities and cells 20 p2971 A83-42662

Convection in a horizontal fluid layer having a shear-free upper surface and uniform volumetric energy sources 20 p2972 A83-42672

Direct numerical simulation of the turbulent momentum and heat transfer in an internally heated fluid layer 20 p2972 A83-42673

Numerical study of the interaction of natural convection with radiation in nongray gases in a narrow vertical cavity 20 p2972 A83-42674

Natural convection with volumetric energy sources in a fluid bounded by a spherical segment 20 p2972 A83-42676

Natural convection in a spherical annulus filled with heat generating fluid 20 p2972 A83-42677

A finite difference study of natural convection in complex enclosures 20 p2972 A83-42678

Numerical simulation of laminar natural convection in shallow inclined enclosures 20 p2973 A83-42680

Natural convection in an open cavity 20 p2973 A83-42681

Effect of curvature on the thermal stability of a fluid between two long vertical coaxial cylinders 20 p2973 A83-42682

Overshooting and damped oscillations of transient natural convection flows in cavities 20 p2973 A83-42683

Velocity measurements in a turbulent natural convection boundary layer 20 p2973 A83-42684

Combined natural and forced convection in vertical ducts 20 p2979 A83-42749

Natural, mixed and forced convection in a vertical channel with asymmetric uniform heating 20 p2979 A83-42750

Holographic interferometry studies of temperature profiles in thermal boundary layer in free convection and bubble boiling 20 p2980 A83-42760

Free convection in hydromagnetic flows in a vertical wavy channel 20 p2982 A83-42971

Nonlinear convection 20 p2982 A83-43005

Ground based studies for the space processing of lead-tin-telluride 20 p2943 A83-43310

Numerical solution of natural convection in eccentric annuli 20 p2987 A83-43451

Mass transfer and free convection through a porous medium by the presence of a rotating fluid 21 p3131 A83-44853

Effects of variable fluid properties and boundary conditions on thermal convection 21 p3131 A83-44854

A numerical method to solve the steady-state Navier-Stokes equations for natural convection in enclosures 22 p3284 A83-46472

Mechanism for transition to turbulence in buoyant plume flow 23 p3451 A83-48623

Unsteady thermal convection in a cylindrical vessel in the case of lateral heat injection 23 p3452 A83-48668

Thermocapillary convection in a two-layer system 23 p3452 A83-48669

Stability of convection rolls in the presence of a horizontal magnetic field 24 p3632 A83-49643

Magnetohydrodynamic free convective effect for an incompressible viscous fluid past an infinite limiting surface 24 p3633 A83-50158

Finite difference analysis of MHD free-convection flow past an accelerated vertical porous plate 24 p3633 A83-50165

FREE ELECTRON LASERS

Floating wire measurement of transverse magnetic field errors in a planar free-electron laser wiggler 01 p0054 A83-10611

Self-focusing effects in free electron lasers 02 p0184 A83-12084

On the gain of the free electron laser /FEL/ amplifier for a nonmonoenergetic beam 02 p0184 A83-12271

Improved orotron performance in the 50- to 75-GHz frequency region 03 p0314 A83-14516

Saturation characteristics of a free-electron laser with a large undulator length 04 p0485 A83-15904

Steady-state pulses in a laser amplifier with a delayed swept gain 05 p0647 A83-16837

The stochastic behavior of electrons in free electron lasers with variable parameter wigglers 05 p0650 A83-17145

Coherent emission from electron clusters in free-electron lasers 06 p0765 A83-17981

Nonlinear saturation of free electron lasers around gyroresonance 07 p0936 A83-20526

A new millimeter free electron laser using a relativistic beam with spiraling electrons 07 p0936 A83-20544

The critical number of photons in free-electron devices - A quantum effect 07 p0936 A83-20756

Analysis of a class of free electron laser using a periodic static magnetic field 07 p0937 A83-20825

Concerning one feature of energy conversion in diffraction-radiation generator/free-electron laser systems 09 p1272 A83-24219

Efficiency of free-electron lasers with a scattered electron beam 10 p1426 A83-25791

Intense free electron laser harmonic generation in a longitudinal magnetic wiggler 10 p1426 A83-25792

Quantum/classical mode evolution in free electron laser oscillators 10 p1426 A83-26004

FEL's with Bragg reflection resonators - Cyclotron autoresonance masers versus ubitrons 10 p1427 A83-26005

Three-dimensional propagation in free-electron laser amplifiers 10 p1427 A83-26006

e-guns and depressed collectors for two-stage free electron lasers 10 p1427 A83-26008

Free electron laser small signal gain measurement at 10.6 microns 10 p1427 A83-26009

Three-dimensional theory of free electron lasers with an axial guide field 10 p1427 A83-26010

Theory of a nonwiggler collective free electron laser in uniform magnetic field 10 p1427 A83-26011

A free electron laser oscillator based on a cyclotron-undulator interaction 10 p1427 A83-26012

Finite-temperature effects in free-electron lasers 10 p1427 A83-26013

Design and operation of a collective millimeter-wave free-electron laser 10 p1427 A83-26014

The prospects of an X-ray free electron laser using stimulated resonance transition radiation 10 p1427 A83-26015

Laser induced bunch lengthening on the ACO storage ring FEL 10 p1428 A83-26016

An optimized multicomponent wiggler design for a free electron laser oscillator 10 p1428 A83-26017

Electron spectrum measurements for a tapered-wiggler free-electron laser 10 p1428 A83-26018

Laser light backscattering off an electron beam-plasma system 10 p1428 A83-26019

Results of the Los Alamos Free-Electron Laser Experiment 10 p1428 A83-26021

Undulator radiation of charged particles moving above a domain structure 10 p1472 A83-26243

Multimode theory of free-electron laser oscillators 10 p1431 A83-26275

Effects of electron energy spread on self-excitation of free-electron lasers 10 p1431 A83-26466

Optics and resonator design issues for high-power free electron lasers 11 p1579 A83-27570

Stimulated emission from ultrarelativistic electrons in strong electric and magnetic fields 11 p1584 A83-28058

Kinetic description of a dynamically coupled free-electron-and molecular gas laser 11 p1584 A83-28239

The role of plasma turbulence for wave excitation in a free-electron-laser combined with a molecular and plasma medium. 13 p1925 A83-30418

Free-electron generators of coherent radiation - /Volumes 8 & 9/ 13 p1852 A83-31101

Relationship of FEL physics to accelerator physics --- Free Electron Laser 13 p1852 A83-31102

Additional experimental results from the Stanford 3 micron FEL 13 p1852 A83-31103

The Stanford Superconducting Linear Accelerator --- for powering free electron laser 13 p1917 A83-31104

Results of the first phase of the ACO storage ring laser experiment 13 p1852 A83-31105

Optical klystron spontaneous emission and gain --- as undulator for free electron laser 13 p1852 A83-31106

Status and perspectives of the FEL experiment at Brookhaven 13 p1853 A83-31107

FEL program at the Adone storage ring 13 p1853 A83-31108

A free-electron laser for the storage ring BESSY 13 p1853 A83-31109

U.K. free-electron laser proposal 13 p1853 A83-31110

Theory of a free-electron laser with gain expansion 13 p1853 A83-31111

A note on the Madey gain-spread theorem --- concerning energy change experienced by electrons in free electron laser 13 p1853 A83-31112

Kinetic theory of a free-electron laser amplifier with guide magnetic field 13 p1853 A83-31113

An experiment on FEL efficiency enhancement with a variable wiggler 13 p1853 A83-31114

Spontaneous spectrum and small-signal gain for a tapered wiggler free-electron laser 13 p1853 A83-31115

Pulse propagation in the tapered wiggler 13 p1854 A83-31116

Optical pulse evolution in the Stanford free-electron laser and in a tapered wiggler 13 p1854 A83-31117

Axial expansion of the electron pulse in a free-electron laser 13 p1854 A83-31118

The effect of space charge fields due to finite length electron beams in the free-electron laser 13 p1854 A83-31119

Hamiltonian picture of the free-electron laser - Multimode, super mode and all that 13 p1854 A83-31120

Optical mode control in the free-electron laser 13 p1854 A83-31121

Resonator mode structure --- in free electron lasers 13 p1854 A83-31122

Millimeter-wave generation by a single-pass, Compton-regime, variable-parameter free-electron laser 13 p1854 A83-31123

Microtron free-electron laser experiment 13 p1854 A83-31124

The FEL-microtron activity at the C.N.E.N. Frascati Center Progress and perspectives 13 p1854 A83-31125

Experimental results from the HDL orotron - A tunable source of coherent millimeter wave radiation 13 p1855 A83-31126

Spectral studies of millimeter wave emission from intense, relativistic electron beams in combined guiding and wiggler magnetic fields 13 p1855 A83-31127

High current, high voltage accelerators as free-electron lasers drivers 13 p1917 A83-31128

Experimental study of axial magnetic field effects on the operation of a millimeter-wave free-electron laser 13 p1855 A83-31129

The effect of an axial guide field on free-electron lasers 13 p1855 A83-31130

Design considerations of a Compton scattering free-electron laser with an axial electrical field 13 p1855 A83-31131

Nonlinear saturation mechanisms and improvement in free-electron lasers 13 p1855 A83-31132

Gain-enhanced free-electron laser with an electromagnet pump field 13 p1855 A83-31133

Saturation of side-band instabilities in a free-electron laser 13 p1855 A83-31134

A diagnostic device for bunched electron beams --- for free electron lasers 13 p1855 A83-31135

TOK-transverse optical klystron and converter physics and figures 13 p1856 A83-31136

Free-electron coherent relativistic scatterer for UV generation 13 p1856 A83-31137

Measurements of the stimulated Cerenkov interaction at optical wavelengths 13 p1856 A83-31138

Unified quantum theory of free-electron devices 13 p1856 A83-31139

A quantum approach to realizable wigglers of free-electron lasers 13 p1856 A83-31140

- The application of free-electron lasers to the transmission of energy in space 13 p1856 A83-31141
- A two-dimensional numerical model of the tapered wiggler free-electron laser 13 p1856 A83-31142
- Nonlinear self-consistent theory of the orotron 13 p1857 A83-31380
- Effects of space charge on the performance of an orotron 13 p1857 A83-31392
- Relativistic quasi-optical Cerenkov oscillator with Wood anomalies 14 p2023 A83-32116
- Free-electron lasers and prospects of their utilization 14 p2024 A83-32592
- Mirrors that are electron transparent for use in free-electron-laser oscillators 15 p2167 A83-33760
- Initiation of a pulsed-beam free-electron-laser oscillator 15 p2168 A83-33796
- Drift velocity measurements in relativistic electron beams --- for free electron laser experiments 15 p2168 A83-33843
- A model for superradiance and superfluorescence in free-electron lasers 15 p2169 A83-34274
- Parametric interaction and backward wave oscillation in stimulated Compton scattering 15 p2169 A83-34372
- Free-electron lasers and their applications 15 p2169 A83-34398
- Free-electron lasers 16 p2358 A83-35725
- Mode structure of a tapered-wiggler free-electron laser stable oscillator 16 p2360 A83-35960
- Free electron lasers [AIAA PAPER 83-1727] 17 p2513 A83-37213
- A general theory of the Raman-type free-electron laser 17 p2514 A83-38039
- Effects of rectangular boundaries in a linearly polarized wiggler free electron laser [AIAA PAPER 83-1729] 17 p2514 A83-38090
- A general theory of the Raman-type free-electron laser 17 p2514 A83-38206
- Synchrotron instability for long pulses in free electron laser oscillators 17 p2515 A83-38970
- Spontaneous radiation from relativistic electrons in a tapered undulator 18 p2743 A83-40410
- Photon antibunching effect and statistical properties of single-mode emission in free-electron lasers 18 p2694 A83-40411
- Operating conditions for free-electron lasers 19 p2851 A83-40918
- Demonstration of a two-stage backward-wave-oscillator free-electron laser 19 p2852 A83-41157
- Stimulated emission from a relativistic electron beam in a variable-parameter longitudinal magnetic wiggler 19 p2853 A83-41192
- Small-signal gain in lethargic and conventional laser amplifiers 19 p2853 A83-41198
- Wiggler-free free electron waveguide laser in a uniform axial magnetic field - Single particle treatment 20 p2994 A83-42587
- Cylindrical Gaussian-Hermite modes in rectangular waveguide resonators --- for free electron lasers 20 p2968 A83-43375
- Electron-diffractive mode selection in free electron lasers 20 p2995 A83-43632
- A visible free electron laser in France 21 p3143 A83-43984
- An increase in laser gain to free electrons by means of laser radiation from an external source 21 p3145 A83-45202
- Absorption and stimulated radiation of quanta of an external inhomogeneous electromagnetic field of free electrons 21 p3145 A83-45204
- Second-harmonic photons from the interaction of free electrons with intense laser radiation 22 p3294 A83-45929
- Unstable electrostatic beam modes in free-electron-laser systems 22 p3295 A83-45942
- Photon statistics of the free-electron-laser startup 22 p3295 A83-45943
- Study of gain, bandwidth, and tunability of a millimeter-wave free-electron laser operating in the collective regime 22 p3295 A83-46016
- Synchrotron radiation of wiggled electron beam in rectangular waveguide 22 p3296 A83-46269
- Generation of high power, very coherent radiation by interaction of a free electron laser with a molecular (or ionic) medium 23 p3463 A83-48573
- Evolution of spontaneous and coherent radiation in the free-electron-laser oscillator 24 p3586 A83-48838
- FREE ELECTRONS**
- Theory of nonlinear optical absorption associated with free carriers in semiconductors 02 p0233 A83-12267
- Forces acting on free carriers in semiconductors of inhomogeneous composition I, II 11 p1663 A83-28449
- Internal photoemission from quantum well heterojunction superlattices by phononless free-carrier absorption 20 p3054 A83-43593
- Bistable cyclotron resonance in semiconductors 24 p3635 A83-49743
- FREE ENERGY**
- NT GIBBS FREE ENERGY
- Theoretical calculation of conformational energies of polytetrafluoroethylene 01 p0027 A83-10606
- Free energy loss during the breakdown of liquid films 08 p1087 A83-23141
- Role of ions in heteromolecular nucleation - Free energy change of hydrated ion clusters 09 p1308 A83-25180
- Standard free energy of formation of iron iodide 11 p1546 A83-28299
- Nucleation theory - Is replacement free energy needed? --- error analysis of capillary approximation 20 p3056 A83-43287
- FREE FALL**
- Physiological factors affecting military high altitude high opening /HALO/ operations 04 p0521 A83-15435
- Perceived orientation in free-fall dependson visual, postural, and architectural factors 06 p0799 A83-18194
- Relativistic tidal forces 06 p0845 A83-19507
- Gyrational motion of disks during free-fall 13 p1839 A83-30107
- Experimental measurements of material damping in free fall with tuneable excitation [AIAA PAPER 83-0858] 14 p1985 A83-32796
- Attitude control for experiments in microgravity [AIAA PAPER 83-2261] 19 p2816 A83-41731
- Thermocapillary motion of bubbles inside drops --- in free fall environment with axisymmetric surface temperature field 20 p2940 A83-43279
- FREE FLIGHT**
- Evaluation of a rocket burnout velocity from ground and free flight tests [AIAA PAPER 83-0036] 05 p0602 A83-16476
- Effective aerodynamic parameter evaluation from free flight tests 07 p0866 A83-21005
- Roll resonance probability for ballistic missiles with random configurational asymmetry 13 p1809 A83-30173
- Comparisons of STS-1 experimental and predicted heating rates 15 p2125 A83-33729
- FREE FLIGHT TEST APPARATUS**
- Methodology for a multiparametric study of the combustion of metal particles in a free-falling chamber 24 p3555 A83-49767
- FREE FLOW**
- The deterministic description of the coherent structure of free shear layers 01 p0046 A83-10886
- Experimental study of the development of free turbulent flows in stratified flows 02 p0170 A83-11871
- Development of analytical and experimental techniques for determining store airload distributions 02 p0132 A83-13077
- Transport processes in turbulent boundary layer under high-level free stream turbulence 03 p0318 A83-14467
- On the spreading of a turbulent spot in the absence of a pressure gradient 03 p0321 A83-14578
- The role of orderly structures in the vorticity balance of the turbulent velocity fields of unrestricted shear flows 04 p0443 A83-15921
- Free stream noise and transition measurements in a Mach 3.5 pilot quiet tunnel [AIAA PAPER 83-0042] 05 p0598 A83-16482
- Aircraft icing roughness features and its effect on the icing process [AIAA PAPER 83-0111] 05 p0666 A83-16527
- A new consistent spatial differencing scheme for the transonic full-potential equation [AIAA PAPER 83-0373] 05 p0585 A83-16678
- New results, a review and synthesis of the mechanism of turbulence production in boundary layers and its modification [AIAA PAPER 83-0377] 05 p0635 A83-16681
- Water tunnel construction for continuous mode flow visualization [AIAA PAPER 83-0657] 05 p0599 A83-16821
- Effect of turbulent viscosity of the external flow on heat transfer in a turbulent boundary layer 06 p0759 A83-19152
- Heat and mass transfer at high free-stream turbulence as a function of injection rate 06 p0759 A83-19157
- Parameters for the simulation of high temperature blown shock layers 07 p0924 A83-19829
- Freestream turbulence and transonic flow over a 'bump' model 08 p1042 A83-22147
- Influence of free-stream turbulence on turbulent boundary layer heat transfer and mean profile development. I - Experimental data. II - Analysis of results 09 p1259 A83-23876
- The structure of a separating turbulent boundary layer. IV - Effects of periodic free-stream unsteadiness 09 p1261 A83-24414
- Freestream turbulence effects on attached subsonic turbulent boundary layers 09 p1198 A83-24656
- Atmospheric definition for Shuttle aerothermodynamic investigations 09 p1212 A83-24883
- Near wall region behavior of unsteady layers with favorable and adverse pressure gradients 11 p1565 A83-27413
- Second order closure for variable density free shear layer 15 p2156 A83-33672
- Contouring tunnel walls to achieve free-air flow over a transonic swept wing [AIAA PAPER 83-1725] 17 p2445 A83-37211
- The relative effects of Reynolds number and turbulence in transonic flow [AIAA PAPER 83-1726] 17 p2445 A83-37212
- Characteristics of supersonic gas flow and heat transfer in the shadow region of a sharp cone 17 p2447 A83-37261
- Nozzles producing a free-vortex flow at the exit section and flow characteristics in these nozzles 17 p2447 A83-37264
- Transonic flow at the break point of a profile with a free streamline 17 p2448 A83-37527
- Similarity solutions of free shear flows with mean Reynolds stress turbulence models 17 p2506 A83-37868
- The structure of a separating turbulent boundary layer. V Frequency effects on periodic unsteady free-stream flows 18 p2681 A83-39217
- An experimental study of the transformation of a free spherical volume of a light gas to a vortex ring 19 p2843 A83-41273
- Effects of free stream turbulence intensity and integral length scale on heat transfer from a circular cylinder in crossflow 20 p2976 A83-42711
- A universal Strouhal law 21 p3130 A83-44538
- ISOMS - A implicit difference scheme for solving complete compressible Navier-Stokes equations --- Implicit Second-Order Monotone Scheme 21 p3130 A83-44553
- The influence of free-stream disturbances on low Reynolds number airfoil experiments 21 p3088 A83-44676
- Response of variations of free stream velocity on inviscid and incompressible flow past a wavy plate 22 p3281 A83-46393
- The effect of free-stream turbulence on turbulent boundary layers 23 p3453 A83-48677
- Free-stream turbulence effects on the heat transfer through the turbulent boundary layer behind a fence 24 p3578 A83-49573
- FREE JETS**
- Permissible model sizes for measurements in free-jet supersonic wind tunnels 02 p0132 A83-13000
- Flow instability and turbulence 03 p0317 A83-14454
- Coherent structures in free jets 03 p0318 A83-14464
- Some problems of second order modelling of mass transfer in a turbulent gas mixture 03 p0319 A83-14480
- A vortex-street model of the flow in the similarity region of a two-dimensional free turbulent jet 03 p0322 A83-14588
- Prediction of secondary vortex flowfields induced by multiple free-jets issuing in close proximity [AIAA PAPER 83-0289] 05 p0642 A83-17916
- Hot-film anemometer measurements in a starting turbulent jet 07 p0924 A83-19826
- The shape of low Reynolds number jets 07 p0926 A83-20527
- Prediction of turbulent flames, including fluctuating velocities correlations and approximate spectra, by means of a simplified second-order closure scheme - The round free jet and developed pipe flow 08 p1088 A83-23186
- Eddy viscosity in axisymmetric swirling jets 09 p1263 A83-25025
- Acoustic evaluation of DNW free jet shear layer correction using a model jet [AIAA PAPER 83-0757] 10 p1476 A83-25954
- Comparison of measured and predicted flight effects on high-bypass coaxial jet exhaust noise [AIAA PAPER 83-0749] 10 p1478 A83-26450
- Coherent structures in rectangular jets 11 p1565 A83-27418
- Numerical integration of the unsteady-flow equations for a two-dimensional supersonic free jet 15 p2162 A83-34977
- On 'saddle-backed' velocity distributions in a three-dimensional turbulent free jet [AIAA PAPER 83-1677] 17 p2444 A83-37185

- Optimal mode of operation of a pulsed aerodynamic test facility with a free-flowing jet 17 p2448 A83-37522
- A study on the fluctuation concentration field in a turbulent jet 18 p2687 A83-40336
- Diffusive separation of binary mixtures of CO₂-H₂ in a sonic-orifice expansion 21 p3128 A83-43934

FREE MOLECULAR FLOW

- Equivalent circuit for an electrostatic probe 07 p0928 A83-20064
- Interaction of high-velocity rarefied flow with the surface of a solid body 20 p2950 A83-42883
- Gas flow through a cylindrical tube under free molecular conditions 20 p2985 A83-43105
- Forces and moments acting on axisymmetric bodies rotating arbitrarily in free molecular flow 24 p3545 A83-49657

FREE OSCILLATIONS

U FREE VIBRATION

FREE RADICALS

- NT HYDROXYL RADICALS
- Is cell aging caused by respiration-dependent injury to the mitochondrial genome 02 p0220 A83-11834
- Free radical propulsion concept 03 p0289 A83-13141
- Free radicals induced by UV light in aqueous solutions of DNA with various amounts of protein at 77 K 06 p0796 A83-19377
- The effect of turbulence on the formation of large superequilibrium concentrations of atoms and free radicals in diffusion flames 06 p0727 A83-19426
- Laboratory and astronomical measurement of the millimeter wave spectrum of the ethynyl radical CCH 06 p0845 A83-19520
- An investigation of human blood, erythrocytes, and plasma using the method of ESR at 77 K 08 p1150 A83-23022
- Simultaneous measurements of vertical distributions of stratospheric NO₃ and O₃ at different periods of the night 09 p1296 A83-24273
- Kinetics of reactions between free radicals and surfaces /aerosols/ applicable to atmospheric chemistry 09 p1297 A83-25187
- Difference frequency laser spectroscopy of the nu₃ band of the CH₃ radical 10 p1480 A83-26451
- The rotational spectrum and hyperfine structure of the methylene radical CH₂ studied by far-infrared laser magnetic resonance spectroscopy 10 p1480 A83-26452
- The laser magnetic resonance spectrum of the nu₂ band of the methylene radical CH₂ 10 p1480 A83-26453
- The equilibrium geometry, potential function, and rotation-vibration energies of CH₂ in the X3B1 ground state 10 p1480 A83-26454
- Difference frequency laser spectroscopy of the nu₁ band of the HO₂ radical 11 p1655 A83-28526
- Impact sensitivity of gamma-irradiated HMX 13 p1826 A83-31674
- Pulsed laser photolysis study of the reaction between O(3P) and HO₂ 14 p1991 A83-33104
- The microwave and far-infrared spectra of the CH radical 14 p2083 A83-33234
- Resonant and nonresonant processes in the formation of CH(+) by radiative association 17 p2578 A83-37342

FREE STREAM EFFECTS

U FREE FLOW

FREE STREAMS

U FREE FLOW

FREE VIBRATION

- Free torsional vibration of thick isotropic incompressible circular cylindrical shell subjected to uniform external pressure 01 p0058 A83-10272
- Free vibrations of plates in fluid using finite and infinite elements 01 p0058 A83-10279
- Qualitative analysis of free oscillations in a quasi-harmonic resonance circuit 01 p0036 A83-10417
- Survey of recent research in the analysis of composite plates 02 p0191 A83-12065
- Small transverse vibrations of circular laminate plates 02 p0191 A83-12334
- Non-linear vibrations of orthotropic rectangular plates under in-plane forces 02 p0193 A83-12667
- Improved method of static and free vibration analysis of thin rectangular plates 02 p0195 A83-12759
- Improved numerical computation of uniform beam characteristic values and characteristic functions 02 p0197 A83-13001
- Vibrations of split beams 02 p0197 A83-13002
- Vibrations of conical shells with variable thickness 02 p0197 A83-13073
- Load-frequency relations for a clamped shallow circular arch 03 p0338 A83-13148

- Free vibrations and the stability of annular plates under nonuniform tension and compression 04 p0497 A83-15390
- Free out-of-plane vibration of a ring elastically supported at several points 04 p0499 A83-15690
- Free vibrations of a composite shell system 04 p0500 A83-16050
- Rayleigh-Ritz vibration analysis of rectangular Mindlin plates subjected to membrane stresses 04 p0500 A83-16181
- Transverse vibration of clamped trapezoidal plates having rectangular orthotropy 04 p0501 A83-16338
- Axisymmetric vibrations of an isotropic elastic non-homogeneous circular plate of linearly varying thickness 04 p0501 A83-16342
- Vibrations of initially imperfect circular plates including the shear and rotatory inertial effects 06 p0773 A83-18394
- Numerical solution of the problem of the bending and free vibrations of a plate 06 p0776 A83-19120
- Axisymmetric vibrations of conical shells with variable thickness 07 p0945 A83-20281
- On the buckling and vibration of antisymmetric angle-ply laminated circular cylindrical shells 07 p0946 A83-20639
- Dynamic analysis of thin elastic noncircular conical shells 07 p0948 A83-21346
- Free vibration of cantilever quadrilateral plates 10 p1439 A83-25825
- Free-surface oscillations of a liquid in a cylindrical container under longitudinal vibrations 11 p1569 A83-28458
- A numerical implementation of the variational method for solving certain problems in hydrodynamics --- free-surface oscillations of ideal incompressible fluid in axisymmetric cavity 11 p1569 A83-28460
- Vibrations of a shallow shell with an attached mass distributed on part of its surface 12 p1735 A83-29276
- Nonlinear structural dynamics analysis using a modified modal method [AIAA 83-0824] 12 p1742 A83-29820
- A revised version of the transfer matrix method to analyze one-dimensional structures [AIAA 83-0825] 12 p1742 A83-29821
- Large-amplitude vibration of laminated composite plates of arbitrary shape [AIAA 83-1035] 12 p1745 A83-29880
- Nonlinear analysis of composite circular plates [AIAA 83-1036] 12 p1745 A83-29881
- The effect of specimen size on J(R) resistance curve in limited amounts of crack growth 12 p1715 A83-29943
- Free vibration analysis of rectangular plates --- Book 13 p1866 A83-30134
- Free vibrations of an isotropic nonhomogeneous infinite plate of linearly varying thickness 14 p2029 A83-32150
- Vibrations of Mindlin's circular plates with variable thickness 14 p2033 A83-33094
- Free vibrations of antisymmetric angle-ply laminated circular cylindrical panels 16 p2365 A83-35641
- Free vibrations of simply supported cylindrical shells of oval cross section 16 p2366 A83-36090
- Transverse vibrations of nonuniform rectangular orthotropic plates 16 p2366 A83-36097
- Vibrations of cantilevered circular cylindrical shells Shallow versus deep shell theory 16 p2369 A83-36958
- On the three-dimensional vibrations of the cantilevered rectangular parallelepiped 17 p2521 A83-37729
- Free vibration of circular-segment-shaped membranes and plates of rectangular orthotropy 17 p2522 A83-37730
- A new approach to free vibration analysis using boundary elements 17 p2522 A83-37734
- Natural and forced oscillations of open resonance systems based on dielectric disk resonators 17 p2500 A83-38986
- Vibrations of noncircular cylindrical shells 18 p2697 A83-39460
- Vibrations of cantilevered doubly-curved shallow shells 18 p2700 A83-39557
- 'Non-linear normal modes' and the generalized Ritz method in the problems of vibrations of non-linear elastic continuous systems 18 p2700 A83-39570
- On a method for the investigation of nonlinear periodic vibrations of circular plates 18 p2702 A83-40121
- Vibration characteristics of laminated composite plates 18 p2703 A83-40170
- Acoustic pulses excited by impacts on objects - Their analytical representation and spectra 20 p3000 A83-43645
- Method for improving incomplete modal coupling 21 p3152 A83-44545

- Free motions of a nearly spherical deformable solid 21 p3200 A83-45357
- Free vibration of a circular cylindrical shell elastically restrained by axially spaced springs 23 p3468 A83-47594
- Flexural vibrations of clamped polygonal and circular plates having rectangular orthotropy 23 p3469 A83-47600
- Vibrations of blades with variable thickness and curvature by shell theory [ASME PAPER 83-GT-152] 23 p3469 A83-47978
- An investigation into the effect of coolant flow on the vibration characteristics of hollow blades conveying fluid [ASME PAPER 83-GT-217] 23 p3470 A83-48017
- Nonlinear flexural vibrations of initially deflected cross-ply laminated plates with elastically restrained edges 24 p3591 A83-48894
- FREEFIGHTER AIRCRAFT**
- U F-5 AIRCRAFT
- FREEZING**
- NT ZONE MELTING
- Use of the holophotoelastic method for three-dimensional stress analysis 03 p0344 A83-14942
- Two severe freezes in Brazil - Precursors and synoptic evolution 10 p1450 A83-25390
- Heat transfer accompanied with melting and freezing for solar heat storage 15 p2190 A83-34235
- Operational effects of increased freeze point fuels in military airplanes [AIAA PAPER 83-1139] 17 p2492 A83-38077
- Influence of freezing rate changes of MnBi-Bi eutectic microstructure --- effects of space processing 18 p2643 A83-39899
- Effect of freezing on sulfur dioxide dissolved in supercooled droplets 19 p2863 A83-41973
- Response of MnBi-Bi eutectic to freezing rate changes 20 p2942 A83-43303
- Transient Workman-Reynolds freezing potentials --- at ice-water interfaces causing thunderstorm electrification and aircraft static 24 p3610 A83-49337
- FREEZING POINTS**
- U MELTING POINTS
- FREIGHT**
- U CARGO
- FREIGHTERS**
- A new class ACV - Tanker-freighter 15 p2243 A83-35053
- FRENCH SATELLITES**
- Space activities in France - Present and future 04 p0451 A83-15661
- TDMA demand assignment operation in Telecom 1 business services network 07 p0911 A83-19783
- The AUREOL-3 satellite 18 p2645 A83-39572
- The infra-red horizon sensor on board the Aureol-3 satellite 18 p2647 A83-39583
- On board and ground equipment for TV broadcast applications State of the art and evolution [IAF PAPER 83-75] 23 p3441 A83-47254
- FRENCH SPACE PROGRAMS**
- The space flight of the Soviet-French crew 01 p0015 A83-10382
- Space activities in France - Present and future 04 p0451 A83-15661
- Spot and remote sensing applications for arid and semi-arid lands 09 p1284 A83-24532
- State of the art in materials science in microgravity 17 p2471 A83-38330
- The Arcad-3 project --- aboard Franco-Soviet AUREOL-3 satellite 18 p2715 A83-39571
- French-Soviet data processing system for Arcad-3 experiments 18 p2648 A83-39587
- The politics of space - The pride of France: A national commitment 21 p3094 A83-45608
- FRENKEL DEFECTS**
- Sintering of mixtures of tungsten and rhenium powders 03 p0300 A83-14223
- FREEON**
- A study on two-phase, two-component Stirling engine 11 p1665 A83-27328
- Alternate thermal control coolant fluid investigation for the NASA Space Transportation System [AIAA PAPER 83-1493] 14 p1980 A83-32738
- FREQUENCIES**
- NT BEAT FREQUENCIES
- NT BROADBAND
- NT BRUNT-VAISALA FREQUENCY
- NT C BAND
- NT CARRIER FREQUENCIES
- NT CRITICAL FREQUENCIES
- NT CYCLOTRON FREQUENCY
- NT EXTREMELY HIGH FREQUENCIES
- NT EXTREMELY LOW FREQUENCIES
- NT EXTREMELY LOW RADIO FREQUENCIES
- NT HIGH FREQUENCIES
- NT INFRASONIC FREQUENCIES

NT INTERMEDIATE FREQUENCIES
 NT LOW FREQUENCIES
 NT MAXIMUM USABLE FREQUENCY
 NT MICROWAVE FREQUENCIES
 NT NYQUIST FREQUENCIES
 NT PLASMA FREQUENCIES
 NT RADIO FREQUENCIES
 NT RESONANT FREQUENCIES
 NT SUPERHIGH FREQUENCIES
 NT SWEEP FREQUENCY
 NT ULTRAHIGH FREQUENCIES
 NT VERY HIGH FREQUENCIES
 NT VERY LOW FREQUENCIES

An investigation of the frequency dependence of the biological effectiveness of a magnetic field in the range of the micropulsations of the geomagnetic field /0.01-100 Hz/ 02 p0221 A83-11886

A comparative analysis of the amplitude-frequency characteristics of the microphone potentials of humans as determined by experiments and with a mathematical model 12 p1764 A83-29304
 Effects of frequency on the corrosion fatigue of Udimet 720 in a molten sulfate salt 16 p2332 A83-36191
 The influence of frequency on fatigue crack propagation of some heat resisting alloys using ultrasonic fatigue 16 p2332 A83-36196

FREQUENCY ASSIGNMENT

Determination of minimum cost interference between services sharing the same frequency bands 04 p0465 A83-15074

Frequency scaling at millimetre wave frequencies 06 p0745 A83-18716

Future satellite systems - Market demand assessment 07 p0910 A83-19762

Algorithms for the optimization of an isolated frequency band for a group of radio-electronic devices of one type according to EMC-assurance conditions 10 p1407 A83-26935

The broadcasting-satellite service - Freedom or control 15 p2144 A83-34652
 Domestic broadcasting-satellite systems - The need for a common standard and the case for block allotment planning 19 p2829 A83-41349

Optimum frequency assignment for satellite SCPC systems 19 p2829 A83-41358
 Demand-assignment schemes for SCPC FDMA satellite systems with contiguous spot beams 19 p2835 A83-41553

Economics of spectrum allocation 22 p3273 A83-45755

The international politics of the orbit-spectrum issue --- concerning communication satellites 22 p3367 A83-45809

The genesis of the 1985/87 ITU world administrative radio conference on the use of the geostationary-satellite orbit and the planning (1) of space services utilizing it 22 p3367 A83-45811

FREQUENCY BANDS

U FREQUENCIES

FREQUENCY CONTROL

NT AUTOMATIC FREQUENCY CONTROL

Flux-balanced variable frequency inverter 01 p0040 A83-11010

Locking bandwidth asymmetry in injection-locked GaAlAs lasers 04 p0483 A83-15231

FM sideband injection locking of diode lasers 04 p0483 A83-15240

Frequency control of high-frequency quartz resonators 05 p0630 A83-17685

Extremely linear electrically tunable active receiving antenna 06 p0751 A83-18616
 Calculation of the frequency spectrum of an electron beam in a klystron with premodulation 07 p0921 A83-20855

Continuously tunable coherent spectroscopy for the 0.1-1.0-THz region 07 p0931 A83-21357
 Theory of line narrowing and frequency selection in an injection locked laser 07 p0938 A83-21600

Infra-red homodyne receiver with acousto-optically controlled local oscillator 11 p1657 A83-28616
 A monolithically integrated wide-tunable sine oscillator --- Thesis 11 p1564 A83-28642

Frequency-tunable lasers --- Russian book 13 p1851 A83-30846

Electronic control of the difference frequency between two semiconductor lasers 14 p2024 A83-32420
 Principle of piezoelectric frequency-tunable transducer 19 p2846 A83-40920

Most reliable messenger - MM-waves get through 22 p3275 A83-46757

FREQUENCY CONVERSION

U FREQUENCY CONVERTERS

FREQUENCY CONVERTERS

NT DOWN-CONVERTERS

NT FREQUENCY DIVIDERS

NT FREQUENCY MULTIPLIERS

NT FREQUENCY SYNTHESIZERS

NT PARAMETRIC FREQUENCY CONVERTERS

NT UP-CONVERTERS

On the design and test of an advanced containment structure for PM machines --- in aircraft electrical power systems 01 p0012 A83-11206

Frequency mixing in the extreme ultraviolet /XUV/ using rare gas halide lasers 03 p0332 A83-13955
 Conversion of 3-micron infrared radiation in cesium vapor 05 p0649 A83-17055

Stimulated Raman scattering in a multipass cell filled with CO₂ 07 p0935 A83-20125
 Two-phase frequency-conversion type spectrum analyzer for low-frequency noise measurement 07 p0929 A83-20547

An ultra-low-drift dc amplifier for use with photomultipliers 09 p1267 A83-23743
 Broadband guided-wave optical frequency translator using an electro-optical Bragg array 13 p1922 A83-31053

Phase-matched frequency conversion in coupled waveguides 15 p2231 A83-33986
 Radio reception by the phase-quantization method with prior frequency conversion 19 p2825 A83-40825

12 GHz band satellite broadcasting receiver with direct converting system 19 p2829 A83-41353
 Wideband frequency conversion in the UV by nine orders of stimulated Raman scattering in a XeCl laser pumped multimode silica fiber 22 p3299 A83-46719

FREQUENCY DISCRIMINATORS

Improved acquisition in phase-locked loops with sawtooth phase detectors 03 p0312 A83-13866
 Performance of narrow-band Manchester coded FSK with discriminator detection 16 p2343 A83-36604

Double-square frequency-selective surfaces and their equivalent circuit 21 p3121 A83-44958
 Frequency-selective combine directional couplers designed as novel filters and multiplexers 21 p3126 A83-44965

FREQUENCY DISTRIBUTION

An attempt to expose the statistical effects of usual radio emissions on variations of polar-substorm elements 02 p0210 A83-12437

Spatial-frequency characteristics of receptive fields of the cat visual cortex in cases of homogeneous and inhomogeneous backgrounds 03 p0376 A83-14362
 Solar altitude frequency tables 08 p1136 A83-22617

The mean number of scatterings during radiative transfer with frequency redistribution 13 p1943 A83-30094
 The relationship between the strength of the IMF and the frequency of magnetic pulsations on the ground and in the solar wind 15 p2199 A83-34362

Frequency and geographical distribution of ancient meteorite falling in China 16 p2438 A83-36724
 Scaling of the bursting frequency in turbulent boundary layers 20 p2985 A83-43097

Frequency gap formation in electromagnetic cyclotron wave distributions --- in magnetosphere 20 p3025 A83-43193
 The estimate of probability distribution of the dominant frequencies for the lightning during an eclipse of the sun 21 p3179 A83-44587

Global distribution of the ionospheric F-layer critical frequency f0F₂ 21 p3177 A83-45446
 Frequency analysis of the rapidly oscillating Ap star HR 1217 (HD 24712) 24 p3643 A83-49352

FREQUENCY DIVIDERS

A 12 GHz phaselocked divider loop 07 p0917 A83-19757
 Analysis of the properties of systems of frequency-time signals 08 p1078 A83-23158

A versatile CMOS rate multiplier/variable divider 19 p2837 A83-40791

FREQUENCY DIVISION MULTIPLE ACCESS

Diversity ALOHA - A random access scheme for satellite communications 13 p1827 A83-30225
 Adaptive control of satellite EIRP to reduce outage caused by fading --- Effective Isotropically Radiated Power 16 p2344 A83-36611

Non-linear distortion analysis in frequency division multi-access satellite communication systems 18 p2674 A83-39093
 Implication of a color multibeam communications satellite in the 30/20 GHz bands 19 p2827 A83-41328

Comparative study of FDMA, TDMA and hybrid 30/20 GHz satellite communications systems for small users 19 p2832 A83-41390
 Combined FDMA-TDMA - A cost effective technique for digital satellite communication networks 19 p2834 A83-41414

Demand-assignment schemes for SCPC FDMA satellite systems with contiguous spot beams 19 p2835 A83-41553

FREQUENCY DIVISION MULTIPLEXING

Digital satellites with time and frequency divided channels 07 p0904 A83-19691
 Millimeter-wave hybrid coupled reflection amplifiers and multiplexers 07 p0922 A83-21527

A method of increasing satellite link capacity 08 p1078 A83-22994
 Development of a 60-channel FDM-TDM transmultiplexer 17 p2497 A83-37789

Third-order distortion of television and sound multiplexed signals in satellite FM systems 17 p2493 A83-37793
 Performance of adaptive equalization for staggered QPSK and QPR over frequency-selective LOS microwave channels --- Quadrature Partial Response 19 p2831 A83-41377

Frequency-selective combine directional couplers designed as novel filters and multiplexers 21 p3126 A83-44965
 Optical systolic array processor using residue arithmetic 22 p3350 A83-46834

Increasing the shipborne telemetric systems capacity with the channel frequency division [IAF PAPER 83-89] 23 p3441 A83-47260
 30 GHz band low noise receiver for 30/20 GHz single-conversion transponder 24 p3570 A83-49857

FREQUENCY HOPPING

On initial acquisition of FH/TH Spread Spectrum signal --- Frequency-Hopping/Time-Hopping 07 p0904 A83-19678
 Modulation, coding, and interleaving tradeoffs for spread spectrum systems 07 p0904 A83-19695

Coding tradeoffs for improved performance of FH/MFSK systems in partial band noise 07 p0909 A83-19751
 Computer simulation of a frequency hop system and a direct sequence-frequency hop hybrid system in a collocated environment 07 p0909 A83-19752

Effects of time-selective fading on slow-frequency-hopped DPSK spread-spectrum communications 07 p0912 A83-19793
 Error probability for coherent hybrid slow-frequency-hopped direct-sequence spread-spectrum multiple-access communications 07 p0912 A83-19796

A comparison of schemes for coarse acquisition of frequency-hopped spread-spectrum signals 11 p1553 A83-26972
 Performance of concatenated codes on channels with jamming 19 p2833 A83-41410

FREQUENCY MEASUREMENT

Application to variable-frequency transducers of ONERA studies on the stability of crystal oscillators 02 p0178 A83-12344
 Accurate frequency and intensity measurements of the infrared spectra of atmospheric molecules 03 p0294 A83-13981

Instantaneous simultaneous signal detecting 05 p0625 A83-17344
 2.5-THz frequency difference measurements in the visible using metal-insulator-metal diodes 06 p0764 A83-19253

Latitudinal variation of chorus frequency observed in the topside ionosphere 08 p1133 A83-22035
 Determination of laser frequencies by mixing experiments between two submillimeter lasers 08 p1107 A83-22245

Direct frequency measurements of transitions at 520 THz /576 nm/ in iodine and 260 THz /1.15 micron/ in neon 08 p1110 A83-22633
 Direct frequency measurement of the I₂-stabilized He-Ne 473-THz /633-nm/ laser 08 p1110 A83-22634

Comparison of cutoff wavelength measurements for single-mode waveguides 10 p1483 A83-26633
 Optimization of an electrodynamic basis for determination of the resonant frequencies of microwave cavities partially filled with a dielectric 13 p1831 A83-30234

Trends in microwave counter technology 13 p1836 A83-30975
 Results of international comparisons using methane-stabilized He-Ne lasers at 3.39 microns and iodine-stabilized He-Ne lasers at 633 nm 13 p1856 A83-31279

Optically pumped FIR lasers phase-locked by Stark effect applied to precise optical frequency measurements 13 p1847 A83-31287
 Simultaneous multimode pressure-induced frequency-shift measurements in shock-compressed organic liquid mixtures by use of reflected broadband coherent anti-Stokes Raman scattering 15 p2131 A83-33800

Relative performances of central and dipole frequency soundings over a layered earth 15 p2202 A83-34748
 Measurement of the spectral-frequency and correlation parameters and characteristics of laser radiation --- Russian book 16 p2360 A83-36439

Estimation of the frequency of a PSK signal with an unknown law of formation 21 p3120 A83-44774
 Estimation of f0F2 from interferences appearing on AGC data of ISS-b topside sounder 21 p3178 A83-45447
 Vernier fringe-counting device for laser wavelength measurements 23 p3454 A83-47645

FREQUENCY MODULATION

NT FEEDBACK FREQUENCY MODULATION
 NT FM/PM (MODULATION)
 NT FREQUENCY SHIFT KEYING
 NT PULSE FREQUENCY MODULATION
 NT PULSE FREQUENCY MODULATION TELEMETRY
 Determination of the parameters of the attraction regime of a nonautonomous phase-locked loop system
 01 p0035 A83-10286
 A strip-type generator of heterodyne frequencies
 01 p0044 A83-11312
 Group time and bandwidth of signals modulated simultaneously in amplitude and frequency
 01 p0032 A83-11335
 FM sideband injection locking of diode lasers
 04 p0483 A83-15240
 Nonequidistant discrete frequency modulated signals of complex form 04 p0467 A83-15749
 High-rate amplitude and frequency modulation of semiconductor lasers 04 p0486 A83-16218
 Quasi-static calculation of noise parameters of a magnetron-type backward wave tube
 06 p0750 A83-18026
 Coherent optical-fibre sensors with modulated laser sources 06 p0762 A83-18568
 Measurement of time dependent optical gain using frequency modulation spectroscopy
 06 p0763 A83-18955
 Linear frequency modulation derived polyphase pulse compression codes 06 p0748 A83-19035
 Line-rate energy dispersal waveforms for FM TV
 07 p0910 A83-19763
 FM spectroscopy detection of stimulated Raman gain
 07 p0937 A83-20798
 Parasitic frequency modulation of a millimeter-wave BWT and its elimination 07 p0921 A83-20882
 The impact of mismatch on the performance of coded narrow-band FM with limiter/discriminator detection
 07 p0916 A83-21198
 Theory of FM noise of single-mode injection lasers
 08 p1110 A83-22919
 The application of phase shift keying in an incoherent optical correlometer of linear-FM signals
 09 p1245 A83-23460
 Oscillations in an acoustooptic bistable device
 09 p1345 A83-24638
 Random modulation - A review
 10 p1402 A83-25639
 FM-SCPC system and equipments for satellite communication --- Single Channel Per Carrier
 10 p1404 A83-26084
 Frequency modulation spectroscopy and frequency domain optical memories 11 p1656 A83-27594
 High-speed direct single-frequency modulation with large tuning rate and frequency excursion in cleaved-coupled-cavity semiconductor lasers
 13 p1850 A83-30332
 Autocorrelation compression filter for radio pulses with linear frequency modulation 13 p1829 A83-30729
 The effect of the limitation of the spectrum of a linear-FM signal with intrapulse phase shift keying on the characteristics of optimal reception
 13 p1829 A83-30734
 Improvements to a pulse compression radar matched filter 13 p1836 A83-31175
 Generation and reception of spread-spectrum signals
 14 p2002 A83-33075
 Tone-burst modulated color-center-laser spectroscopy
 15 p2167 A83-33758
 Complete experimental evaluation of the carrier dependence of the refractive index from the frequency modulation spectra of single mode injection lasers
 15 p2168 A83-33841
 Frequency modulation of Gunn oscillator by low magnetic flux 15 p2151 A83-33894
 The calculation of polarization characteristics of systems by the symbolic method 17 p2510 A83-37693
 Third-order distortion of television and sound multiplexed signals in satellite FM systems 17 p2493 A83-37793
 Analysis of the effect of intense structural noise on a radio system with pseudonoise signals
 17 p2494 A83-38484
 Multigigahertz-bandwidth linear-frequency-modulated filters using a superconductive stripline
 19 p2836 A83-40747
 Continuous wave (CW) Doppler free two-photon frequency modulated (FM) spectroscopy
 21 p3139 A83-44816

Enhanced frequency modulation in cleaved-coupled-cavity semiconductor lasers with reduced spurious intensity modulation 22 p3299 A83-46722

FREQUENCY MODULATION PHOTOMULTIPLIERS

An ultra-low-drift dc amplifier for use with photomultipliers 09 p1267 A83-23743

FREQUENCY MULTIPLIERS

The load characteristics of frequency multipliers
 01 p0043 A83-11309
 Investigation of fluctuations in a varactor frequency-tripler 04 p0471 A83-15738
 Efficient frequency doubling of radiation emitted by a multistage neodymium laser 05 p0648 A83-17040
 Frequency doubling in a LiNbO3 thin film deposited on sapphire 07 p0993 A83-20730
 Interaction in frequency doubling of ultrashort laser pulses 10 p1434 A83-26693
 High-efficiency Q-to-W-band MIC frequency doubler
 11 p1563 A83-28609
 Determination of the law of variation of magnetic induction in sectioned M-type multipliers
 13 p1833 A83-30702
 High-frequency doubler operation of GaAs field-effect transistors 17 p2497 A83-37800
 A versatile CMOS rate multiplier/variable divider
 19 p2837 A83-40791
 Analysis of the operation of a Gunn diode under conditions of frequency multiplication
 19 p2840 A83-41786
 Fast beam deflectors based on phase matching
 21 p3206 A83-44815
 Frequency multiplication with a Schottky diode in the short-wave region of the millimeter band
 22 p3276 A83-45672
 Frequency-doubled CO2 lidar measurement and diode laser spectroscopy of atmospheric CO2
 22 p3288 A83-46073

FREQUENCY RANGES**NT RADIO RANGE**

A line-scanning system with fiber-optic elements
 07 p0929 A83-20776
 A new procedure for improving the solution stability and extending the frequency range of the EBCM --- Extended Boundary Condition Method for EM absorption and scattering in biological dielectric objects
 10 p1460 A83-26839
 Transformation of the matrix of generalized impedances in the case of frequency variation --- for antenna radiation pattern calculations 11 p1556 A83-27945

FREQUENCY REGULATION**U FREQUENCY CONTROL****FREQUENCY RESPONSE**

Frequency fluctuations of radio waves propagating in a turbulent atmosphere 01 p0030 A83-10402
 Two methods for the analysis of multifrequency regimes of microwave amplifiers 01 p0036 A83-10414
 Asymptotic formulas for the dielectric response function of a relativistic plasma 01 p0107 A83-10905
 Theory of the frequency responses of uniform and quasi-taper helical antennas 01 p0034 A83-11378
 Feedback control of linear multivariable systems with uncertain description in the frequency domain
 02 p0230 A83-12550
 All-pole phase-locked tracking filters
 03 p0312 A83-13861
 Unsteady Newton-Busemann flow theory. III - Frequency dependence and indicial response
 04 p0476 A83-15149
 Helicopter vibration reduction by local structural modification 04 p0500 A83-16028
 Frequency-response design of robust optimal controllers 04 p0529 A83-16189
 Measurement of the frequency response of a digital autopilot
 05 p0605 A83-16655
 [AIAA PAPER 83-0326] GaAs/GaAlAs heterojunction bipolar transistors with cutoff frequencies above 10 GHz
 05 p0624 A83-17285
 A stable solution to the Wiener-Hopf equation in the frequency domain on the basis of the complexity principle 05 p0681 A83-17659
 Automatic determination of frequency response parameters and distortion in resonant microwave cavities 06 p0750 A83-17970
 Limits of VSWR for optimal broadband capacitively loaded cylindrical antennas versus their length
 06 p0741 A83-18661
 Frequency and phase fluctuations of radio waves during propagation in the Venus atmosphere
 06 p0848 A83-19353
 Temperature dependence of SAW dispersive delay lines 07 p0918 A83-20073
 Response of parallel-flow and counterflow heat exchangers to sinusoidal flow rate changes of large amplitude 07 p0925 A83-20290

Equations for the angles of arrival and departure for multivariable root loci using frequency-domain methods
 07 p0985 A83-20724

Complex-frequency poles and creeping-wave transients in electromagnet-wave scattering
 07 p0916 A83-21545

Spatial frequency response and resolution in holography 08 p1092 A83-22081
 Solc filter engineering 08 p1166 A83-22572
 Cryogenic frequency domain optical mass memory
 08 p1166 A83-22808

The stability of non-linear multivariable systems - Review of frequency domain methods 08 p1158 A83-23172
 Determination of amplitude-frequency response of thermoacoustic oscillations in a liquid at supercritical pressures 09 p1260 A83-24050
 High frequency behavior of the tilt spectrum of atmospheric turbulence 09 p1249 A83-24439
 An unbiased adaptive method for retrieval of sinusoidal signals in colored noise 09 p1331 A83-24773
 Robust control/estimator design by frequency-shaped cost functionals 09 p1333 A83-24797
 Use of parameter groups in the analysis and design of multivariable feedback systems
 09 p1335 A83-24818

GG-pseudo-band method for the design of multivariable control systems 10 p1464 A83-26520
 Frequency domain structure for disturbance rejection
 10 p1468 A83-26565

Frequency limitations and optimal step size for the two-point central difference derivative algorithm with applications to human eye movement data
 10 p1460 A83-26650

The broad-band scattering response of periodic arrays
 10 p1405 A83-26832

The low-frequency limit of the application of ferrite circulators 10 p1412 A83-26940
 Modeling of optical impedance spectroscopy
 11 p1572 A83-27530

Frequency modulation spectroscopy and frequency domain optical memories 11 p1656 A83-27594
 Frequency dependence of degenerate four-wave mixing at the band edge of InAs 11 p1581 A83-27597
 A designer's guide to digital filters
 11 p1648 A83-28151

Tubes in space - Very much alive
 11 p1562 A83-28160

An investigation of the resonance characteristics of the cardiovascular system 12 p1765 A83-29309
 Physical frequency limitations of 2-terminal devices
 12 p1719 A83-29420

Modes of resonance of the Jerusalem cross in frequency-selective surfaces 12 p1718 A83-29438
 Frequency-domain identification of transmission-zero locations of linear multivariable plants
 12 p1769 A83-29469

The spatial frequency and the temporal characteristics of masking 13 p1900 A83-30432
 Spatial frequency and the temporal characteristics of the perception of the form of complex gratings --- visual perception test 13 p1901 A83-30434
 Speaking in a random fashion --- random vibration testing of electronic equipment 13 p1914 A83-30852
 Forced vibrations and their damping
 14 p2033 A83-33484

Temperature control of line-focus solar collectors
 15 p2189 A83-33993

Pupillary escape intensified by large pupillary size
 15 p2211 A83-34873

Determination of the form of the amplitude-frequency response of variable-length optical waveguides
 15 p2232 A83-34885

A matrix of the frequency characteristics of a combustion zone 15 p2133 A83-34898

An ellipsoidal frequency selective surface
 15 p2146 A83-35080

Statistical analysis and wavenumber-frequency spectra of the 500 mb geopotential along 50 deg S
 16 p2387 A83-35493

Response of a supersonic inlet to downstream perturbations
 [AIAA PAPER 83-2017] 16 p2296 A83-36403

New phase-shifting technique for group-type unidirectional transducers used in surface-acoustic-wave filters 16 p2347 A83-36482

Coherence properties and cutoff wavelength determination in dielectric waveguides
 16 p2413 A83-36766

Analysis of the frequency response of a fluid amplifier using unsteady flow characteristics
 17 p2504 A83-37399

Ground couplings and measurement frequency ranges of vibration transducers 17 p2510 A83-37733

On a method for determining the amplitude-frequency response curve of regular multimode optical waveguides
 17 p2580 A83-38502

- The dependence between spatial and spatial-frequency characteristics of the receptive fields of the visual cortex in cats 19 p2871 A83-40812
- High-precision test of the universality of the Josephson voltage-frequency relation 19 p2837 A83-40959
- The calibration and performance of a microstrip six-port reflectometer 19 p2837 A83-41082
- Maximum energy spectral window with frequency domain constraints 19 p2839 A83-41344
- Estimated performance of a QPR digital microwave radio in the presence of frequency selective fading --- Quadrature Partial Response 19 p2833 A83-41406
- Discrete control scheme design for multi input multi output systems 19 p2890 A83-41478
- 4-layer inductive grid FSS at 45 deg incidence --- Frequency Selective Surfaces 20 p2963 A83-42478
- Frequency response of cold wires and thermocouples used for temperature measurements in gaseous flows 20 p2982 A83-42778
- Hybrid frequency-domain coding of speech signals 20 p2965 A83-43685
- A cholinergic-sensitive channel in the cat visual system tuned to low spatial frequencies 21 p3183 A83-44364
- Improved feed network for group-type unidirectional transducers 21 p3126 A83-44960
- Generalized frequency-shaped KTC and Riccati approaches for space structure control 21 p3196 A83-45128
- The response of normal shocks in diffusers [AIAA PAPER 81-1431] 21 p3089 A83-45580
- The effect of impurities on the current-amplification cut-off frequency of field-effect transistors 22 p3277 A83-45675
- Modelling of a multivariable system on the basis of frequency data 22 p3351 A83-45979
- Acoustic surface wave band filters with weighted fan transducers 23 p3445 A83-47569
- Performance of two tripole arrays as frequency-selective surfaces 23 p3444 A83-48710
- Passbands and stopbands for an electromagnetic waveguide with a periodically varying cross section 24 p3573 A83-48969
- The frequency response of cold wires 24 p3584 A83-49815
- FREQUENCY REUSE**
- Satellite clusters and frequency reuse 07 p0904 A83-19690
- Conservation of the geostationary spectrum 07 p0910 A83-19760
- Geostationary communications satellite orbit utilization strategies for the 1980s 07 p0910 A83-19761
- A statistical study of abnormal depolarization 14 p2000 A83-32419
- Theoretical model for calculating rain-induced crosspolarisation 17 p2495 A83-38878
- Implication of a color multibeam communications satellite in the 30/20 GHz bands 19 p2827 A83-41328
- FREQUENCY SCANNING**
- Single frequency scanning laser as a plasma diagnostic 08 p1111 A83-23230
- Measurement of fiber birefringence by wavelength scanning Effect of dispersion 15 p2230 A83-33766
- Performance degradation in fast frequency-scanned circular arrays 15 p2148 A83-35188
- Analysis and design of frequency scanned transmission gratings 18 p2676 A83-40651
- FREQUENCY SHIFT**
- The possibility of laboratory detection of long-period gravitational waves 01 p0125 A83-10904
- Electro-optic-waveguide frequency translator in LiNbO₃ fabricated by proton exchange 02 p0235 A83-11566
- Investigation of pressure shifts of frequencies in a system of successive transitions of the ^N-14/H₃ molecule in the nu₂-excited vibrational state 02 p0234 A83-11692
- Fibre-optic laser Doppler anemometer with Bragg frequency shift utilising polarisation-preserving single-mode fibre 02 p0177 A83-12010
- Influence of an axial magnetic field on the frequency shifts in a two-mode He-Ne/CH₄ laser 03 p0331 A83-13589
- The superposition principle in acoustics 04 p0533 A83-15450
- A two-grating method for combined beam splitting and frequency shifting in a two-component laser-Doppler velocimeter 05 p0645 A83-17352
- Observations of global-scale photospheric Fraunhofer line shifts 06 p0857 A83-19515
- Parametric decay of electromagnetic waves in a magnetized vacuum 07 p0988 A83-20043
- Frequency-shift of self-trapped light --- due to decrease in resonant frequency of plasma cavity 08 p1168 A83-22391
- Backward stimulated Raman scattering in shock-compressed benzene 08 p1057 A83-22643

- Doppler frequency effects due to source, medium, and receiver motions of constant velocity [AIAA PAPER 83-0702] 10 p1474 A83-25922
- Interaction in frequency doubling of ultrashort laser pulses 10 p1434 A83-26693
- On the accuracy of frequency determination by an autoregressive spectral estimator --- of astronomical spectra 11 p1669 A83-27636
- Evaluation of the light shift in a frequency standard based on Raman induced Ramsey resonance 12 p1729 A83-29192
- Optimization of an electrodynamic basis for determination of the resonant frequencies of microwave cavities partially filled with a dielectric 13 p1831 A83-30234
- Plasma shifts of the Lyman lines to shorter wavelengths in C VI 13 p1926 A83-30919
- Simultaneous multimode pressure-induced frequency-shift measurements in shock-compressed organic liquid mixtures by use of reflected broadband coherent anti-Stokes Raman scattering 15 p2131 A83-33800
- Acousto-optic frequency shifter for single-mode fibres 24 p3630 A83-49978
- FREQUENCY SHIFT KEYING**
- Error rates for fading NCFSK signals in an additive mixture of impulsive and Gaussian noise --- noncoherent FSK 03 p0304 A83-13870
- A general analysis of anti-jam communication systems 07 p0904 A83-19694
- Capacity and coding in the presence of fading and jamming 07 p0905 A83-19697
- Error rates for narrowband Manchester coded digital FM 07 p0909 A83-19748
- Coding tradeoffs for improved performance of FH/MFSK systems in partial band noise 07 p0909 A83-19751
- Advances in Serial MSK modems 07 p0917 A83-19789
- S/N and error rate evaluation for an optical FSK-heterodyne detection system using semiconductor lasers 07 p0994 A83-21594
- Correlation function and spectral density of continuous-phase discrete FSK radio signals 08 p1078 A83-23157
- Analysis of the properties of systems of frequency-time signals 08 p1078 A83-23158
- A comparative analysis of the noise immunity of methods for processing FSK signals with split values of frequencies on a noise background 09 p1251 A83-25081
- NCFSK performance improvements by selection diversity in Gaussian and impulsive noise environments 10 p1401 A83-25501
- Random modulation - A review 10 p1402 A83-25639
- Adjacent-channel and quadrature-channel interference in minimum shift keying 11 p1556 A83-28127
- Demonstration of multilevel multichannel optical frequency shift keying (FSK) with cleaved-coupled-cavity (C3) semiconductor lasers 13 p1922 A83-31784
- Performance of narrow-band Manchester coded FSK with discriminative detection 16 p2343 A83-36604
- Regenerative/non-regenerative satellite systems using differentially-detected MSK 19 p2829 A83-41360
- Performance of concatenated codes on channels with jamming 19 p2833 A83-41410
- Wideband frequency-shift keying with a spectrally bistable cleaved-coupled-cavity semiconductor laser 24 p3630 A83-49976

FREQUENCY SHIFT KEYING

- FREQUENCY STABILITY**
- A strip-type generator of heterodyne frequencies 01 p0044 A83-11312
- Performance measures for phase-locked loops - A tutorial 03 p0311 A83-13851
- False-lock performance improvement in Costas loops 03 p0311 A83-13858
- Phase-locked loops used with masers - Atomic frequency standards 03 p0331 A83-13865
- Passive frequency stability of pulsed CO₂ lasers 05 p0647 A83-16919
- Phase noise in signal sources /Theory and applications/ --- Book 05 p0622 A83-17350
- The dispersion characteristics of generators of diffraction radiation in the millimeter-wavelength range 06 p0750 A83-18141
- Properties of diode lasers with intensity noise control 07 p0935 A83-20161
- Frequency stabilization of GaAlAs laser using a Doppler-free spectrum of the Cs-D₂ line 07 p0938 A83-21593
- Multistability at microwave frequencies 08 p1079 A83-22011
- Frequency-stabilized transversely excited atmospheric /TEA/ CO₂ lasers for coherent infrared radar systems 08 p1109 A83-22515
- Programmable transmitters for coherent laser radars 08 p1109 A83-22517

- Frequency stabilization of internal-mirror He-Ne lasers 09 p1272 A83-24443
- Mode effects in second harmonic generation and their uses for laser stabilization 10 p1425 A83-25404
- Frequency reproducibility of ring He-Ne/CH₄ lasers 10 p1433 A83-26686
- Nonlinear optical indication in frequency-stabilization systems --- for metal vapor lasers 11 p1583 A83-27955
- Gas-lens effect and cavity design of some frequency-stabilized He-Ne lasers 13 p1849 A83-30213
- Temperature stabilization of GaAs MESFET oscillators using dielectric resonators 13 p1831 A83-30238
- Behavior of phase-locked loops in the presence of large interfering signal 13 p1834 A83-30785
- Subharmonic sampling for the measurement of short-term stability of microwave oscillators 13 p1837 A83-31290
- A compact hydrogen maser with exceptional long-term stability 13 p1856 A83-31292
- Electronic control of the difference frequency between two semiconductor lasers 14 p2024 A83-32420
- Natural fluctuations of the emission frequency of an He-Ne/CH₄ 3.39 micron laser 16 p2359 A83-35895
- Scaling laws for the intrapulse frequency stability of an injection mode selected TEA CO₂ laser 16 p2360 A83-35961
- Frequency-domain criteria of instability for phase-locked loops 17 p2570 A83-38485
- Spectral dispersion of modulated signals due to oscillator phase instability - White and random walk phase model 19 p2837 A83-40922
- A structure function representation theorem with applications to frequency stability estimation 19 p2894 A83-41027
- A proposal of a new dielectric resonator construction for MIC's 19 p2838 A83-41085
- Modeling of frequency random walk instability and effects on spectral spreading 19 p2832 A83-41394
- Analysis of the temperature stability of the frequency of a SAW oscillator 19 p2840 A83-41784
- Stabilization of a microwave oscillator using a resonance Raman transition in a sodium beam 20 p2965 A83-42346
- New approach towards frequency stabilisation of linewidth-narrowed semiconductor lasers 20 p2994 A83-42493
- Ultra-stable laser clock - Second generation 20 p2989 A83-42576
- Estimation of parameters in models for Cesium beam atomic clocks 20 p2990 A83-42944
- Influence of transit effects on frequency resonances in gas lasers 20 p2997 A83-43799
- Emission frequency stability in single-mode-fibre optical feedback controlled semiconductor lasers 21 p3145 A83-44954
- Spectrophone stabilization and offset tuning of a carbon dioxide waveguide laser 22 p3300 A83-46816
- Stability of a detuned single mode homogeneously broadened ring laser 23 p3462 A83-48319
- Highly stable FET DROs using new linear dielectric resonator material --- Dielectric Resonator Oscillators 23 p3446 A83-48723
- An analysis of the international comparison results of helium-neon lasers stabilized by saturated absorption in I-127 (review) 24 p3589 A83-49736
- FREQUENCY STANDARDS**
- Phase-locked loops used with masers - Atomic frequency standards 03 p0331 A83-13865
- A demonstration of relative positioning using conventional GPS Doppler receivers 07 p0865 A83-19779
- Evaluation of the light shift in a frequency standard based on Raman induced Ramsey resonance 12 p1729 A83-29192
- Performance of the four NRC long-beam primary cesium clocks Cs V, Cs VIA, Cs VIB, and Cs VIC 13 p1847 A83-31293
- Modeling of frequency random walk instability and effects on spectral spreading 19 p2832 A83-41394
- Longitudinal Ramsey-fringe spectroscopy in a calcium beam --- for optical frequency standard 23 p3509 A83-48707
- FREQUENCY SYNCHRONIZATION**
- Modification of vortex shedding in the synchronization range [ASME PAPER 81-WA/FE-25] 04 p0478 A83-16142
- Synchronization of lasers with intracavity second harmonic generation 05 p0648 A83-17039
- Estimating the number of cycle slippings in synchronization systems with discontinuous nonlinearity --- multivariable phase control 09 p1249 A83-24490
- Synchronization effects in a submillimeter Josephson self-oscillator 10 p1409 A83-25812

- Precision phase comparison via communication satellites using loop-back tones 10 p1403 A83-26042
- Noise analysis of a PSK carrier recovery DPLL 11 p1559 A83-26973

FREQUENCY SYNTHESIZERS

- Digital computational synthesizers of two-level signals with compensation of phase errors 04 p0470 A83-15712
- Digital PLL frequency synthesizers: Theory and design 19 p2839 A83-41529

FREQUENCY TRANSLATION**U FREQUENCY CONVERTERS****FRESH WATER**

- Current and density structure in shelf waters due to fresh water discharge - A numerical study 08 p1089 A83-23202
- Fresh water springs detection and discharge evaluation using thermal I.R. surveys along sea shores in areas affected by poor precipitations 09 p1288 A83-24578
- The brightness temperature of sea ice and fresh-water ice in the frequency range 500 MHz to 37 GHz 22 p3313 A83-46205

FRESNEL DIFFRACTION

- Fresnel ripple mapping of water-cooled laser mirrors 08 p1108 A83-22457
- The converging prolate spheroidal functions and their use in Fresnel optics 11 p1657 A83-27846
- Barrier insertion loss versus Fresnel number and secondary parameters 11 p1652 A83-28187
- Observation of Fresnel-type fading at Delhi, a low midlatitude station, over half a solar cycle 13 p1881 A83-31545
- Fresnel detour-phase circular computer generated holograms 14 p2083 A83-31948
- Modes of phase-conjugate resonators with bounded mirrors 15 p2229 A83-33531
- Asymptotic solution for the diffraction of an electromagnetic plane wave by a cylinder-tipped half-plane 15 p2144 A83-33806
- Diffraction optics 21 p3207 A83-44837
- Image formation by multifacet holograms 22 p3294 A83-46835

FRESNEL INTEGRALS

- The superradiance of a polyatomic system with allowance for the Coulomb interaction 09 p1273 A83-25090

FRESNEL LENSES

- The image-forming properties of multiple-zone Fresnel lenses in the millimeter-wavelength range 02 p0175 A83-11539
- Properties of a Fresnel sandwich as an optical resonator 04 p0535 A83-15886
- Minimax optimization of two-dimensional Cartesian and Fresnel lens phased arrays 08 p1161 A83-22474
- Study of a photovoltaic concentrating system like 'Sophocle' in fluctuating mode 14 p2039 A83-32200
- Performance of 1 kw peak concentrating photovoltaic array 14 p2039 A83-32201
- Photovoltaic concentrator module characterization 14 p2039 A83-32202
- Lambertian analysis of mirrors and Fresnel lenses for solar concentration 14 p2043 A83-32271
- Stationary nonimaging concentrator as a second stage element in tracking systems 15 p2190 A83-34074

FRESNEL REFLECTORS

- Generalized model for wire grid polarizers 08 p1098 A83-22564
- Photovoltaic concentrator technology in the USA 14 p2042 A83-32261

FRESNEL REGION

- Optical reconstruction of wideband Fourier and Fresnel acoustic holograms 10 p1421 A83-26295
- Focusing antennas usage in locating acoustic sources [ONERA, TP NO. 1983-75] 23 p3505 A83-48190

FRESNEL-KIRCHHOFF INTEGRALS**U FRESNEL INTEGRALS****FRETING**

- Materials evaluation under fretting conditions; Proceedings of the Symposium, Warminster, PA, June 3, 1981 05 p0652 A83-17251
- Occurrence of fretting in practice and its simulation in the laboratory 05 p0652 A83-17252
- A new machine for studying surface damage due to wear and fretting 05 p0652 A83-17253
- An evaluation of fretting at small slip amplitudes 05 p0614 A83-17254
- Effect ion implantation on fretting fatigue in Ti-6Al-4V alloy 05 p0614 A83-17257
- Review of factors that influence fretting wear 05 p0652 A83-17259
- Effect of surface residual stresses on the fretting fatigue of a 4130 steel 05 p0615 A83-17264
- Fatigue failure under fretting conditions 07 p0894 A83-21481

- Fatigue-crack initiation in IMI 829 caused by high-temperature fretting 07 p0896 A83-21566
- The fretting fatigue behaviour of the titanium alloy IMI 829 at temperatures up to 600 C 11 p1547 A83-27851

FRETING CORROSION

- Friction oxidation characteristics [ASLE PREPRINT 82-LC-3B-2] 03 p0334 A83-13236
- A vibration analysis of a bearing/cartridge interface for a fretting corrosion study [ASME PAPER 82-LUB-19] 03 p0335 A83-13510
- Evaluation of fretting corrosion by means of a new device for the control of oscillation amplitude 05 p0652 A83-17255
- An electrochemical method for investigating corrosion in rubbing surfaces 05 p0652 A83-17256
- Fretting fatigue of Ti-6Al-4V alloy 05 p0614 A83-17258
- Fretting fatigue in a 3-1/2NiCrMoV rotor steel 08 p1059 A83-21690
- Application of the equivalent initial damage method to fretting fatigue 08 p1059 A83-21691
- Corrosion and fretting effects on fatigue 09 p1277 A83-23419
- Factors leading to the formation of surface oxide layer on metal during cyclic loading under conditions of fretting corrosion 14 p1992 A83-32071

FRICTION**NT AERODYNAMIC DRAG****NT DRY FRICTION****NT FLOW RESISTANCE****NT FRICTION DRAG****NT INTERNAL FRICTION****NT KINETIC FRICTION****NT SKIN FRICTION****NT SLIDING FRICTION****NT STATIC FRICTION****NT SUPERSONIC DRAG****NT VISCOUS DRAG**

- On the behaviour of a cracked elastic body with /or without/ friction 02 p0189 A83-11856
- Correlation of tensile and shear strengths of metals with their friction properties [ASLE PREPRINT 82-LC-UB-1] 03 p0296 A83-13226

- Theoretical and applied problems of the friction, wear and lubrication of machines --- Russian book 07 p0939 A83-20320

- A sliding-beam X-ray technique for the investigation of thin surface layers of a metal deformed under friction 07 p0929 A83-20322

- New systems with the application of gaseous lubrication for the investigation of the friction and wear of machine and instrument parts 07 p0939 A83-20323

- The evaluation of the fracture energy of materials in the presence of frictional contact force according to structural changes 07 p0939 A83-20324

- Friction damping of flutter in gas turbine engine airfoils 09 p1206 A83-24038

- The friction mechanism for accelerating particles in interplanetary space 17 p2614 A83-38847

- Friction and wear of iron and nickel in sodium hydroxide solutions 24 p3559 A83-48922

- The formulation of plane contact problems of elasticity theory for the wear of interacting bodies 24 p3594 A83-49533

FRICTION COEFFICIENT**U COEFFICIENT OF FRICTION****FRICTION DRAG****NT AERODYNAMIC DRAG****NT SUPERSONIC DRAG****NT VISCOUS DRAG**

- Hot wire gauges for skin friction measurement /design, calibration, applications/ 02 p0178 A83-12349
- Friction drag and other design parameters for acoustic face sheets --- for aircraft noise reduction [AIAA PAPER 83-0780] 10 p1477 A83-25962

- A semi-empirical approach for the prediction of aft-body drag of supersonic projectiles with base bleeding 15 p2119 A83-33489

- Friction drag measurements of acoustic surfaces [AIAA PAPER 83-1356] 16 p2296 A83-36414

- Viscous effects on the performance of cone-derived waveriders [AIAA PAPER 83-2084] 19 p2792 A83-41918

FRICTION FACTOR

- Nonlinear systems that are gyrostat superpositions 02 p0232 A83-11953
- Effects of friction in tensile and compressive stress problems for a rigid circular disk in an infinite plate 02 p0197 A83-13066

- The effect of hysteretic friction on the errors of gyroinstruments 06 p0764 A83-19181

- Radiation friction in the problem of emission from an oscillator in a coherent state 14 p2081 A83-33399

- Friction damping studies in multiple turbine blade systems by lumped mass method 20 p3002 A83-42571

- Blade platform friction damping tests on a model blade (methods and results) 20 p3002 A83-42572

- Generalization of results of experimental and numerical studies of heat transfer in flows with increased external turbulence on the bases of two-parameter models of turbulence 20 p2977 A83-42724

- A friction factor correlation for the offset strip-fin matrix 20 p2984 A83-43022

- Heat transfer and friction loss characteristics of pin fin cooling configuration [ASME PAPER 83-GT-123] 23 p3448 A83-47952

- Calculation of friction and heat transfer on the profile of a turbomachine cascade 23 p3399 A83-48449

FRICTION LOSS COEFFICIENT**U FRICTION FACTOR****FRICTION MEASUREMENT**

- Investigation of the tribochemical influence of air pollution on the rolling friction of various materials being used in a newly developed railroad measuring post --- German thesis 01 p0056 A83-10175

- Hot wire gauges for skin friction measurement /design, calibration, applications/ 02 p0178 A83-12349

- Modified gauge for time-resolved skin-friction measurements 03 p0329 A83-14172

- A laser interferometer for measuring skin friction in three-dimensional flows [AIAA PAPER 83-0385] 05 p0643 A83-16685

- Extended capabilities of a vibrating-reed internal friction apparatus 07 p0932 A83-21385

- The high-temperature friction of alloys of the system TiN/x/-TiB2 09 p1236 A83-25068

- The wear resistance of chromium-base alloys during high-temperature friction 10 p1396 A83-25633

- Measurement of stresses on the surface of a plane barrier in a strongly underexpanded rarefied-gas jet 19 p2849 A83-41896

FRICTION PRESSURE DROP**U SKIN FRICTION****FRICTION REDUCTION**

- The use of powdered metals as antifriction additions to plastic lubricants 01 p0027 A83-10459

- The solution of triboengineering problems by numerical methods --- Russian book 02 p0186 A83-11946

- Chemicothermal treatment of alloy VT6 to improve antifriction properties 05 p0614 A83-17134

- The effect of thin lubricant films and the methods of their application on the friction of several materials of bearings with a gaseous lubricant 07 p0939 A83-20321

- On tuned bladed disk dynamics - Some aspects of friction related mistuning 08 p1120 A83-21807

- Microscopic aspects of the effect of friction reducers at the lubrication limit --- French thesis 11 p1590 A83-28663

- Oil leakage and friction forces of reciprocating O-ring seals considering cavitation 13 p1859 A83-30249

- Research on non-planar wall geometries for turbulence control and skin-friction reduction 14 p1969 A83-31975

- Effects of friction dampers on aerodynamically unstable rotor stages [AIAA PAPER 83-0848] 14 p1976 A83-32791

- Effects of MoS2 concentration on friction 15 p2143 A83-35244

- Self-lubricating antifriction materials (Review) 17 p2483 A83-38870

FRICTION WELDING

- Material behavior in connection with flywheel friction welding of superalloys 15 p2137 A83-33965

FRICTIONLESS ENVIRONMENTS

- The frictionless contact of cracked elastic bodies 09 p1283 A83-25108

FRINGE PATTERNS**U DIFFRACTION PATTERNS****FRONTAL AREAS (METEOROLOGY)****U FRONTS (METEOROLOGY)****FRONTS (METEOROLOGY)****NT COLD FRONTS****NT WARM FRONTS**

- Mesoscale structures of vortices in polar air streams 02 p0218 A83-13058

- A numerical study of the influence of the planetary boundary layer and moisture on frontal structure 03 p0367 A83-14432

- The subtropical front - Satellite observations during FRONTS 80 03 p0369 A83-14503

- Surface signatures of a dry nocturnal gust front 10 p1451 A83-25391

- Characteristics of frontal zones determined from spaced antenna VHF radar observations 11 p1622 A83-26980

- Exponential size distributions of raindrops and vertical air motions deduced from zenith-pointing Doppler radar in a frontal precipitation 11 p1622 A83-26989
- Comparison of tropopause height and frontal boundary locations based on radar and radiosonde data [AD-A128467] 12 p1757 A83-28915
- Numerical modeling of an atmospheric front with a cloud system and precipitation 14 p2056 A83-32367
- Case studies of aerosol size distribution and chemistry during passages of a cold and a warm front 20 p3014 A83-43427
- Dynamical processes in the atmosphere and the use of models 21 p3179 A83-44389
- FROST**
- A search for frosts in Comet Bowell /1980b/ 06 p0833 A83-18874
- Numerical simulation of ice/frost formation on the external tank of the Space Shuttle in varying environments [AIAA PAPER 83-0524] 06 p0722 A83-19592
- Two severe freezes in Brazil - Precursors and synoptic evolution 10 p1450 A83-25390
- Reflectance spectra of SO₂ frosts contaminated by sodium and their implication on Io 17 p2615 A83-37363
- Prediction of ice/frost growth on insulated cryogenic tanks 18 p2646 A83-40019
- FROSTBITE**
- Rheological properties of the arterial and venous blood of rats following intravital icing of the extremities 21 p3185 A83-45325
- Cryogenic liquids and aviation --- biological effects and safety hazards 23 p3499 A83-48695
- FROZEN SOILS**
- U PERMAFROST
- FRUSTRUMS**
- Nosetip bluntness effects on cone frustum boundary layer transition in hypersonic flow [AIAA PAPER 83-1763] 18 p2633 A83-39265
- FUEL CELL CATALYSTS**
- U ELECTROCATALYSTS
- FUEL CELL POWER PLANTS**
- Fuel cell power plants for automotive applications 13 p1871 A83-31092
- Coal gas as a feed fuel for phosphoric acid fuel cell power plants 20 p3012 A83-42952
- Fuel cell power plants for electric utilities and hydrogen 20 p3013 A83-43640
- Advanced electrolysis development for hydrogen-cycle peak shaving for electric utilities 22 p3320 A83-46779
- FUEL CELLS**
- NT HYDROGEN OXYGEN FUEL CELLS
- NT PHOSPHORIC ACID FUEL CELLS
- NT REGENERATIVE FUEL CELLS
- Catalytic autothermal reforming increases fuel cell flexibility 02 p0201 A83-11794
- Batteries and fuel cells: Design, employment, chemistry --- German book 03 p0355 A83-14041
- The effect of thickness on the performance of molten carbonate fuel cell cathodes 04 p0506 A83-15869
- Research on oxidation by air and tempering of Raney nickel electrocatalysts for the H₂ anodes of alkali combustion materials cells --- German thesis 06 p0726 A83-18494
- The structure of the double layer at the mercury-phosphoric acid interface from studies of adsorption of thiourea and its implications on oxygen reduction kinetics --- in fuel cells 07 p0879 A83-19876
- Molten carbonate fuel cell performance model 07 p0953 A83-19884
- Simple porous electrode models for molten carbonate fuel cells 07 p0953 A83-19891
- The equilibrium constant for the reversible reaction $\text{H}_2\text{S} + 3\text{H}_2\text{O} + \text{Li}_0.66\text{K}_0.34/2 \text{ CO}_3$ yields $4\text{H}_2 + \text{CO}_2 + \text{Li}_0.66\text{K}_0.34/2 \text{ SO}_4$ at elevated temperature --- in molten carbonate fuel cells 07 p0954 A83-20590
- Porous perovskite electrode as molten carbonate cathode --- in fuel cells 07 p0955 A83-20596
- Coating applications for the molten carbonate fuel cell 10 p1445 A83-25538
- A zinc paste primary battery --- for electric vehicles 10 p1445 A83-26052
- Assessment of phosphoric acid and trifluoromethane sulfonic acid fuel cells for vehicular powerplants 11 p1602 A83-27162
- Abuse resistant high rate lithium/thionyl chloride cells 11 p1604 A83-27180
- Acid fuel cell technologies for vehicular power plants 11 p1604 A83-27185
- Status of solid polymer electrolyte fuel cell technology and potential for transportation applications 11 p1604 A83-27186
- Pore size engineering applied to starved electrochemical cells and batteries 11 p1305 A83-27201
- Evaluation of tetrafluorethane-1,2-disulfonic acid as a fuel cell electrolyte 11 p1546 A83-28300
- Advanced Vehicle system concepts --- nonpetroleum passenger transportation 13 p1935 A83-31094
- Energy Storage in a fuel cell with bipolar membranes burning acid and hydroxide 13 p1872 A83-31599
- Hydrogen as a fuel 15 p2193 A83-35302
- High-temperature solid oxide fuel cell - Technical status 24 p3601 A83-49954
- FUEL COMBUSTION**
- Tests of blending and correlation of distillate fuel properties 01 p0028 A83-11050
- Multifuel evaluation of rich/quench/lean combustor 01 p0023 A83-11492
- NOx results from two combustors tested on medium BTU coal gas 01 p0070 A83-11493
- A theory of the limits of flame propagation on the surface of a combustible material 02 p0151 A83-11958
- Mathematical modeling of homogeneous-heterogeneous reactions in monolithic catalysts 02 p0152 A83-13093
- Hydrogen oxidation kinetics in gaseous detonations 02 p0153 A83-13097
- A study of transverse turbulent jets in a cross flow --- for gas turbine combustion process modelling 02 p0136 A83-13100
- Boundary integral equation method calculations of surface regression effects in flame spreading 03 p0294 A83-13488
- An experimental study of transient combustion in low-gas heterogeneous systems 03 p0294 A83-14053
- Numerical modeling of the development of a combustion nucleus in a closed vessel under the conditions of natural convection 03 p0295 A83-14054
- An experimental study of fuel combustion in a high-temperature air counterflow 03 p0295 A83-14056
- Combustion of a layer of fuel in a flow of oxidizer over its surface 03 p0295 A83-14058
- The conditions of flame propagation in metal particle suspensions in air 03 p0295 A83-14059
- An experimental study and modeling of heat transfer in boilers of small and medium power --- French thesis 04 p0456 A83-15841
- NOx formation experiments in an MHD simulation facility 04 p0507 A83-16103
- A double reaction zone model and perturbation analysis for finite rate kinetics in hydrocarbon fuel combustors [AIAA PAPER 83-0599] 05 p0612 A83-16810
- Diagnostics of single particle boron combustion [AIAA PAPER 83-0070] 05 p0613 A83-17904
- A study of inter-phase exchange laws in spray combustion modeling [AIAA PAPER 83-0152] 05 p0613 A83-17910
- A laser anemometer seeding technique for combustion flows with multiple stream injection 07 p0928 A83-19843
- The application of coherent anti-Stokes Raman scattering to turbulent combustion thermometry 07 p0879 A83-19844
- Effects of envelope flames on drop gasification rates in turbulent diffusion flames 07 p0879 A83-19846
- Features of the dynamics of gas combustion in closed vessels under various laws for the change in the flame surface 07 p0880 A83-19952
- Development and application of advanced diagnostics methods in fossil fuel combustion studies 07 p0902 A83-20436
- CO₂-laser-induced deflagration of fuel/oxygen mixtures 07 p0882 A83-20732
- Investigation of slurry fuel performance for use in a ramjet propulsor 07 p0902 A83-21014
- Flame propagation through dust clouds of carbon, coal, aluminium and magnesium in an environment of zero gravity 07 p0882 A83-21352
- Steady state diffusion flame structure with Lewis number variations 08 p1057 A83-22392
- Fiber optics as light-detector probes in the accurate measurement of detonation velocities in two-phase fuel-air explosions 08 p1095 A83-22498
- On the changes in the structure of steady plane flames as their speed increases 09 p1225 A83-23747
- Future fuels for turbojet engines and their impacts on combustion chambers and fuel systems [DGLR PAPER 82-089] 09 p1242 A83-24201
- Local quenching due to flame stretch and non-premixed turbulent combustion 09 p1226 A83-24362
- A diffusion combustor and methane-air flame propagation in concentration gradient fields 09 p1226 A83-24366
- Gas-phase ignition of premixed fuel by catalytic bodies in stagnation flow 09 p1226 A83-24368
- Droplet size effects on NO_x/x/ formation in a one-dimensional monodisperse spray combustion system [ASME PAPER 82-JPGC-GT-10] 09 p1227 A83-25268
- Catalytic combustion with steam injection [ASME PAPER 82-JPGC-GT-23] 09 p1294 A83-25271
- Spray combustion processes - A review [ASME PAPER 82-WA/HT-86] 10 p1390 A83-25691
- A study on the ignition of a fuel droplet in high temperature stagnant gas 10 p1391 A83-26197
- Propagation at 10 microns through smoke produced by atmospheric combustion of diesel fuel 10 p1447 A83-26641
- Fuel character effects on the TF41 engine combustion system 13 p1807 A83-30190
- Evaporation and ignition of a fuel droplet on a hot surface. IV - Model of evaporation and ignition 13 p1818 A83-31224
- A new approach to soot control in Diesel engines by fuel-drop charging 13 p1859 A83-31225
- Numerical optimization studies of axisymmetric unsteady sprays 13 p1843 A83-31368
- The combustion stability of a wedge 14 p1989 A83-32086
- The effect of a standing acoustic wave transverse to the flow on a turbulent flame 14 p1989 A83-32087
- The formation of nitrogen oxides in a nonequilibrium turbulent diffusion flame 14 p1989 A83-32090
- The rules governing changes in combustion characteristics for competing reactions 14 p1989 A83-32092
- Group combustion models and laser diagnostic methods in sprays - A review 14 p1990 A83-32938
- Fluorocarbon combustion studies. VI - Competitive combustion reactions of fluorocarbons burning with fluorine 14 p1991 A83-32942
- Determination of mass transfer number of polymers from heats of gasification 15 p2142 A83-33725
- A matrix of the frequency characteristics of a combustion zone 15 p2133 A83-34898
- CARS diagnostics of high pressure and temperature gases --- Coherent Anti-Stokes Raman Spectroscopy [AIAA PAPER 83-1478] 15 p2133 A83-34913
- Critical conditions for the combustion of macroheterogeneous systems of the type fuel-inert material 15 p2134 A83-35318
- A relationship between the flash point, boiling point and the lean limit of flammability of liquid fuels 16 p2325 A83-35791
- Combustion instability in liquid fuel ramjets 16 p2303 A83-35804
- New trends in combustion research for gas turbine engines 16 p2303 A83-35806
- Group combustion of liquid fuel sprays [AIAA PAPER 83-0150] 16 p2326 A83-36044
- Methanol combustion in a CF6I-80A engine combustor [AIAA PAPER 83-1138] 16 p2339 A83-36241
- Effect of fuel composition on Navy aircraft engine hot section components [AIAA PAPER 83-1147] 16 p2306 A83-36244
- Small turbine engine experience with high density fuels [AIAA PAPER 83-1177] 16 p2339 A83-36262
- Application of 3D aerodynamic/combustion model to combustor primary zone study [AIAA PAPER 83-1265] 16 p2308 A83-36316
- Laser applications to combustion research [AIAA PAPER 83-1360] 16 p2360 A83-36358
- Calculation of a pressure rise during the burning of a plane supersonic hydrogen jet in a supersonic slipstream 17 p2485 A83-37806
- The ignition of a fuel on contact with an oxidizer 18 p2663 A83-39159
- Theory of the combustion of condensed substances with blowing past them 18 p2663 A83-39163
- The cold locking of the duct of a gas-liquid mixer by burning fuel jets 18 p2663 A83-39168
- The laser ignition of compact mixed compositions 18 p2663 A83-39171
- Effect of using emulsions of high nitrogen containing fuels and water in a gas turbine combustor on NO_x and other emissions [ASME PAPER 82-GT-224] 18 p2673 A83-39992
- Modeling solid-fuel ramjet combustion, including radiation to the fuel surface 18 p2649 A83-40021
- Structure and extinction of convective diffusion flames with general Lewis numbers 18 p2664 A83-40312
- Fuel-air explosions; Proceedings of the International Conference, McGill University, Montreal, Canada, November 4-6, 1981 19 p2820 A83-41523
- Optical recording of nonstationary processes of mixture formation and combustion --- atomized jet droplets characteristics 19 p2850 A83-42141

- Increasing the combustion efficiency of fuel in an air-heating chamber operating on a pre vaporized fuel
19 p2801 A83-42151
- Heat liberation and heat transfer in flame tubes
20 p2974 A83-42696
- Rheological behavior of FM-9 solutions and correlation with flammability test results and interpretations --- fuel thickening additive
21 p3117 A83-44856
- Dynamic behavior of a bluff-body diffusion flame
21 p3110 A83-45584
- Comments on rates of creeping spread of flames over thermally thin fuels
22 p3267 A83-46764
- Mixing and fuel atomisation effects on premixed combustion performance
[ASME PAPER 83-GT-55] 23 p3407 A83-47911
- All-Union Symposium on Combustion and Explosion, 7th, Chernogolovka, USSR, October 1983, Proceedings
24 p3555 A83-49758
- A theoretical study of the nonstationary combustion of a gasifiable solid fuel during a pressure drop
24 p3569 A83-49763
- The effect of the pressure and molecular properties of gases on turbulent combustion
24 p3555 A83-49764
- The formation of carbon monoxide during turbulent diffusion combustion --- for aircraft gas turbine combustion chambers
24 p3569 A83-49769
- Fluctuations during the combustion of fuels
24 p3556 A83-49785
- Combustion-wave propagation along a thin layer of a material during a gas-phase reaction between fuel and oxidizer
24 p3556 A83-49786
- ### FUEL CONSUMPTION
- Estimation of aircraft fuel consumption
01 p0008 A83-10186
- Improved solution of optimal impulsive fixed-time rendezvous
02 p0139 A83-13081
- The cleaning of the exterior of the aircraft
03 p0277 A83-14325
- Powerplants. I --- turbofan engine design for aircraft
04 p0449 A83-14951
- Rolls-Royce RB 211-535 power plant
04 p0449 A83-15311
- Fuel-optimal aircraft trajectories with fixed arrival times
04 p0446 A83-16115
- Efficiency improved turboprop
[AIAA PAPER 83-0059] 05 p0596 A83-16491
- The application of energy saving concepts to future fighter/attack aircraft design
[AIAA PAPER 83-0092] 05 p0594 A83-16516
- Optimization of variable-altitude flyback maneuvers --- for rocket-propelled lifting vehicles
[AIAA PAPER 83-0282] 05 p0594 A83-16627
- Loran-C RNAV - The best near-term solution to air operations in northeastern North America
06 p0716 A83-18822
- Fuel savings in air transport
06 p0714 A83-19150
- Optimal processing of the correction data of an aircraft fuel-measurement system
06 p0718 A83-19177
- The automated cockpit
07 p0866 A83-20849
- The Fokker F28 and a four-engined newcomer
07 p0866 A83-21349
- PW 4000 - A radically new jet engine being developed in the USA
08 p1046 A83-23239
- Structures and mechanisms - Streamlining for fuel economy
09 p1216 A83-24361
- Minimum-fuel, impulsive transfers between adjacent orbits --- German thesis
09 p1212 A83-24845
- Energy conservation in air transportation - The Canadian Air Traffic Control Effort
12 p1699 A83-29393
- All-electric vs conventional aircraft - The production/operational aspects
14 p1974 A83-32576
- Advanced turboprop cargo aircraft systems study
14 p1974 A83-32582
- Advanced navigation systems and fuel conservation
15 p2120 A83-33545
- New concept in hovercraft design diesel versus gas turbines
15 p2242 A83-34860
- Some aspects of development of power plant optimum control to increase aircraft fuel efficiency
16 p2303 A83-35841
- Flight management concepts development for fuel conservation
16 p2304 A83-35843
- Effect of fuel composition on Navy aircraft engine hot section components
[AIAA PAPER 83-1147] 16 p2306 A83-36244
- Concepts for increased power and enhanced fuel conservation with newly patented multiple power-cycle gas turbine engines
[AIAA PAPER 83-1209] 16 p2307 A83-36282
- Measured effect of wind generation on the fuel consumption of an isolated diesel power system
16 p2371 A83-36410
- The recipe for re-engining jet transports
[SAE PAPER 821441] 17 p2463 A83-37989
- Parametric study of factors affecting the fuel efficiency of advanced turboprop airplanes
[AIAA PAPER 83-1823] 17 p2464 A83-38655
- Meteorological data requirements for fuel efficient flight
17 p2552 A83-38760
- 4 D fuel-optimal guidance in the presence of winds
[AIAA PAPER 83-2242] 19 p2796 A83-41719
- Weight reduction for fuel economy
[SAWE PAPER 1469] 20 p2935 A83-43743
- Minimum-fuel aeroassisted coplanar orbit transfer using lift-modulation
[AIAA PAPER 83-2094] 20 p2944 A83-43812
- On the minimum fuel consumption switching surfaces
21 p3193 A83-44013
- Wing tip devices for energy conservation and other purposes Experimental and analytical work in progress at the Lockheed-Georgia Company
21 p3086 A83-44358
- A definition of the degree of controllability for fuel-optimal systems
21 p3195 A83-45102
- Saving fuel with the wide-chord fan
23 p3411 A83-48174
- Design integration of laminar flow control for transport aircraft
[AIAA PAPER 83-2440] 24 p3547 A83-49577
- ### FUEL CONTAMINATION
- J series thruster isolator failure analysis
[AIAA PAPER 82-1907] 02 p0144 A83-12482
- Deposition and blade fouling of gas turbines by fuel impurities and additives
07 p0941 A83-21456
- The removal of metals from a jet fuel using a manganese catalyst
11 p1552 A83-28775
- The effect of the fuel quality on the degree of combustion product ionization in gas-turbine engines
14 p1988 A83-32078
- Monitoring the contamination of jet fuels by corrosion inhibitors
23 p3440 A83-48544
- ### FUEL CONTROL
- Closed-loop engine fuel system simulation
[SAE PAPER 821374] 17 p2468 A83-37964
- A definition of the degree of controllability for fuel-optimal systems
21 p3195 A83-45102
- Parallel induction - A simple fuel control method for hydrogen engines
21 p3148 A83-45426
- ### FUEL CORROSION
- Mechanisms of the microbial corrosion of aluminum alloys
06 p0726 A83-18550
- High temperature erosion and erosion-hot corrosion of superalloys and coatings
07 p0892 A83-21458
- Test program to demonstrate the stability of hydrazine in propellant tanks
[AIAA PAPER 83-1382] 16 p2340 A83-36373
- ### FUEL FLOW
- #### NT PROPELLANT TRANSFER
- Three-dimensional model of spray combustion in gas turbine combustors
01 p0011 A83-10652
- Lewis number effects on the structure and extinction of diffusion flames due to strain
01 p0023 A83-10897
- Methods for calculating the stabilization limits of a flame of inhomogeneous mixtures using a bluff body
02 p0136 A83-11512
- J series thruster isolator failure analysis
[AIAA PAPER 82-1907] 02 p0144 A83-12482
- The generation of electric currents by the turbulent flow of dielectric liquids. I - Long pipes
12 p1722 A83-29089
- Vapor flow into a capillary propellant-acquisition device
[AIAA PAPER 83-1380] 16 p2321 A83-36371
- Modelling the fuel temperature effect on flame spread limits in opposed flow
17 p2484 A83-37046
- ### FUEL FLOW REGULATORS
- Electrohydraulic fuel-flow regulator for gas-turbine-engine control systems
16 p2311 A83-36793
- ### FUEL INJECTION
- Transient thermal boundary layer in heating of droplet with internal circulation - Evaluation of assumptions
02 p0175 A83-13098
- Break-up and droplet formation of slurry jets
[AIAA PAPER 83-0067] 05 p0632 A83-16499
- Trajectory with diffusion method for predicting the fuel distribution in a transverse stream
[AIAA PAPER 83-0336] 05 p0596 A83-16662
- Transverse jet break-up and atomization with rapid vaporization along the trajectory
[AIAA PAPER 83-0419] 05 p0597 A83-16702
- Investigation of a dual inlet side dump combustor using liquid fuel injection
[AIAA PAPER 83-0420] 05 p0609 A83-16703
- A study of inter-phase exchange laws in spray combustion modeling
[AIAA PAPER 83-0152] 05 p0613 A83-17910
- Atomization of impinging liquid jets in a supersonic crossflow
[AD-A130714] 07 p0924 A83-19806
- Hot-film anemometer measurements in a starting turbulent jet
07 p0924 A83-19826
- A laser anemometer seeding technique for combustion flows with multiple stream injection
07 p0928 A83-19843
- Premixed combustion in a turbulent boundary layer with injection
09 p1225 A83-23750
- Catalytic combustion with steam injection
[ASME PAPER 82-JPGC-GT-23] 09 p1294 A83-25271
- The effect of fuel injection on NOx emissions and undesirable combustion for hydrogen-fuelled piston engines
11 p1589 A83-27335
- Numerical optimization studies of axisymmetric unsteady sprays
13 p1843 A83-31368
- Effect of air, liquid and injector geometry variables upon the performance of a plain-jet airblast atomizer
16 p2351 A83-35809
- A JT8D low emissions combustor by radial zoning
[AIAA PAPER 83-1324] 16 p2309 A83-36339
- LOX/hydrocarbon injector performance
[AIAA PAPER 83-1390] 16 p2322 A83-36380
- Influence of atomizer design features on mean drop size
19 p2800 A83-40865
- The effect of the wave injection of a fluid jet into a gas cross-stream
19 p2794 A83-42155
- Hydrogen aspiration in a direct injection type diesel engine its effects on smoke and other engine performance parameters
20 p2998 A83-42956
- A reverse flow chamber for small turbomachines
[ONERA, TP NO. 1983-30] 21 p3092 A83-44309
- Aerodynamic-wave break-up of liquid sheets in swirling airflows and combustor modules
[AIAA PAPER 83-1204] 21 p3133 A83-45511
- The Rolls-Royce annular vaporizer combustor
[ASME PAPER 83-GT-49] 23 p3407 A83-47908
- Three-dimensional modeling of horseshoe vortex flows
[ASME PAPER 83-GT-191] 23 p3397 A83-47997
- Experimental investigation of fuel distribution in a transverse stream
[ASME PAPER 83-GT-207] 23 p3410 A83-48008
- ### FUEL OILS
- Use of pyrolysis-derived fuel in a gas turbine engine
[ASME PAPER 83-GT-96] 23 p3440 A83-47942
- ### FUEL PRODUCTION
- Developing technologies for synthetic fuels
01 p0068 A83-10658
- New sources for fuel and materials --- from plants
05 p0658 A83-16937
- The properties of fuel fractions obtained by the hydrogenation of Kansk-Achinsk coal
10 p1401 A83-26920
- A viable process for producing hydrogen synfuel using nuclear fusion heat
11 p1605 A83-27210
- Hydrogen energy creeps forward --- hydrogen fuel production and storage
13 p1869 A83-30000
- Future U.S. jet fuels - A refiner's viewpoint
13 p1826 A83-30187
- Gaseous fuel generation by magma-thermal conversion of biomass
13 p1870 A83-30196
- The lunar factory --- for production of construction materials and spacecraft fuels
17 p2471 A83-38622
- Fuels from solar energy - How soon?
24 p3599 A83-48808
- ### FUEL PUMPS
- Flow visualization study in low specific speed pump impeller passages
01 p0053 A83-11073
- Model studies of the dynamic characteristics of the pumps and turbines of liquid propellant rocket engines in transition regimes
08 p1052 A83-22660
- Component life reduction due to use of AVGAS in gas turbine engines
16 p2305 A83-35869
- The analysis and testing of blade platform friction dampers used in the high pressure fuel turbopump (HPFTP) of the Space Shuttle Main Engine (SSME)
20 p2946 A83-42570
- ### FUEL SPRAYS
- Three-dimensional model of spray combustion in gas turbine combustors
01 p0011 A83-10652
- Characteristic time ignition model extended to an annular gas turbine combustor
01 p0011 A83-10666
- Liquid fuel spray ignition predictions for JP-10
04 p0464 A83-16113
- Break-up and droplet formation of slurry jets
[AIAA PAPER 83-0067] 05 p0632 A83-16499
- The role of the heat-up period in fuel drop evaporation
[AIAA PAPER 83-0068] 05 p0632 A83-16500
- Effect of liquid phase decomposition on fuel droplet distribution function
[AIAA PAPER 83-0069] 05 p0632 A83-16501
- Measurements and predictions for nonevaporating sprays in a quiescent environment
[AIAA PAPER 83-0151] 05 p0633 A83-16558

- Prediction of liquid fuel spray capture by v-gutter downstream of plain orifice injector under uniform cross air-flow
[AIAA PAPER 83-0153] 05 p0596 A83-16559
- A study of inter-phase exchange laws in spray combustion modeling
[AIAA PAPER 83-0152] 05 p0613 A83-17910
- Effects of envelope flames on drop gasification rates in turbulent diffusion flames 07 p0879 A83-19846
- The ignition of a drop of fuel behind the front of a shock wave 07 p0901 A83-19961
- Degradation and characterization of antimiting kerosene 09 p1242 A83-24035
- Droplet size effects on NO_x/ formation in a one-dimensional monodisperse spray combustion system
[ASME PAPER 82-JPGC-GT-10] 09 p1227 A83-25268
- Application of digital image analysis techniques to antimiting fuel spray characterization
[ASME PAPER 82-WA/HT-23] 10 p1401 A83-25690
- Spray combustion processes - A review
[ASME PAPER 82-WA/HT-86] 10 p1390 A83-25691
- A theory of nondilute spray evaporation based upon multiple drop interactions 13 p1843 A83-31223
- Evaporation and ignition of a fuel droplet on a hot surface. IV - Model of evaporation and ignition 13 p1818 A83-31224
- A new approach to soot control in Diesel engines by fuel-drop charging 13 p1859 A83-31225
- Numerical optimization studies of axisymmetric unsteady sprays 13 p1843 A83-31368
- Group combustion models and laser diagnostic methods in sprays - A review 14 p1990 A83-32938
- Assessment of two computational procedures for spray combustors 15 p2160 A83-34255
- Effect of air, liquid and injector geometry variables upon the performance of a plain-jet airblast atomizer 16 p2351 A83-35809
- Further study on the prediction of liquid fuel spray capture by v-gutter downstream of a plain orifice injector under uniform cross air flow 16 p2351 A83-35810
- Further studies on the prediction of spray evaporation rates --- for aircraft fuels 16 p2338 A83-35811
- The effect of fuel atomization on soot-free combustion in a prevaporizing combustor 16 p2303 A83-35812
- Laser light scattering technique in the diagnostics of sprays in isothermal and burning conditions 16 p2351 A83-35825
- Group combustion of liquid fuel sprays
[AIAA PAPER 83-0150] 16 p2326 A83-36044
- Hydrodynamics and heat transfer in sphere assemblages Cylindrical cell models 21 p3131 A83-44928
- Steady-state evaporation characteristics of hydrocarbon fuel drops 21 p3117 A83-45587
- The interdependence of spray characteristics and evaporation history of fuel sprays in stagnant air
[ASME PAPER 83-GT-7] 23 p3440 A83-47880
- Mixing and fuel atomisation effects on premixed combustion performance
[ASME PAPER 83-GT-55] 23 p3407 A83-47911
- The effect of hydrocarbon structure upon fuel sooting tendency in a turbulent spray diffusion flame
[ASME PAPER 83-GT-90] 23 p3440 A83-47937
- Spray characteristics of plain-jet airblast atomizers
[ASME PAPER 83-GT-138] 23 p3448 A83-47965
- Modelling of soot formation in spray combustors
[ASME PAPER 83-GT-190] 23 p3429 A83-47996
- Experimental investigation of fuel distribution in a transverse stream
[ASME PAPER 83-GT-207] 23 p3410 A83-48008
- Drop size measurements in evaporating realistic sprays of emulsified and neat fuels
[ASME PAPER 83-GT-231] 23 p3440 A83-48027
- On-line calibration technique for laser diffraction droplet sizing instruments
[ASME PAPER 83-GT-232] 23 p3458 A83-48028
- FUEL SYSTEMS**
NT AIRCRAFT FUEL SYSTEMS
Closed-loop engine fuel system simulation
[SAE PAPER 821374] 17 p2468 A83-37964
- FUEL TANK PRESSURIZATION**
Prediction of a propellant tank pressure history using state space methods 07 p0873 A83-20419
- FUEL TANKS**
NT WING TANKS
Trim Tank system for optimizing drag at the center of gravity
[DGLR PAPER 82-030] 09 p1209 A83-24156
- Interface and transport phenomena under reduced gravity. II - Surfaces and wetting 09 p1263 A83-24645
- The AH-64 nitrogen inerting unit 10 p1375 A83-25895
- Debris from spallation of foam insulation of cryogenic fuel tanks in space launch systems
[AIAA PAPER 83-1457] 14 p1980 A83-32718
- Parametric excitation of oscillations in a liquid flowing out of a container 16 p2350 A83-35717
- Performance tests of two inert gas generator concepts for airplane fuel tank inerting
[AIAA PAPER 83-1140] 17 p2464 A83-38078
- Aircraft flexible tanks general design and installation recommendations
[SAE ARP 1664] 17 p2464 A83-38102
- FUEL TESTS**
Tests of blending and correlation of distillate fuel properties 01 p0028 A83-11050
- A carbon-13 and proton nuclear magnetic resonance study of some experimental referee broadened-specification /ERBS/ turbine fuels 01 p0028 A83-11482
- The effect of the jet fuel temperature on wear rates during the friction of sliding and rolling 04 p0464 A83-16145
- A rapid method for determining the initial boiling point and the saturated-vapor pressure of petroleum products --- jet fuel tests in railroad tank cars 07 p0931 A83-20962
- Flight testing with hot JP-4 fuel --- in helicopter suction fuel systems 09 p1208 A83-24831
- Development of high-temperature liquid metal heat pipes for isothermal irradiation assemblies --- for in-pile tests of UO₂ space reactor fuel configurations 11 p1538 A83-27129
- Some fuel effects on carbon formation in gas turbine combustors 12 p1717 A83-29392
- Jet fuels based on West Siberian oils 14 p1999 A83-32077
- The effect of products based on higher fatty acids on the performance characteristics of jet fuels 15 p2143 A83-34500
- Feasibility of a full-scale degrader for antimiting kerosene
[AIAA PAPER 83-1137] 16 p2339 A83-36240
- Thermal stability of alternative aircraft fuels
[AIAA PAPER 83-1143] 16 p2339 A83-36243
- Small turbine engine experience with high density fuels
[AIAA PAPER 83-1177] 16 p2339 A83-36262
- Testing of antimiting kerosene in the DC-10/KC-10 fuel system simulator
[SAE PAPER 821485] 17 p2492 A83-38004
- Operational effects of increased freeze point fuels in military airplanes
[AIAA PAPER 83-1139] 17 p2492 A83-38077
- Operation of an aircraft engine using liquefied methane fuel 20 p2927 A83-43239
- Autogas flight test in a Cessna 150 airplane
[SAE PAPER 830706] 20 p2933 A83-43317
- Comparison-effects of broadened property jet fuels on older and modern J79 combustors
[ASME PAPER 83-GT-81] 23 p3407 A83-47934
- Monitoring the contamination of jet fuels by corrosion inhibitors 23 p3440 A83-48544
- FUEL VALVES**
Fast acting valve for a quasi-steady MPD arcjet
[AIAA PAPER 82-1886] 02 p0144 A83-12470
- Fast acting hydrocarbon valve 08 p1112 A83-23295
- FUEL-AIR RATIO**
Methods for calculating the stabilization limits of a flame of inhomogeneous mixtures using a bluff body 02 p0136 A83-11512
- The conditions of flame propagation in metal particle suspensions in air 03 p0295 A83-14059
- Design of a low emission combustor for an automotive gas turbine
[AIAA PAPER 83-0338] 05 p0652 A83-16664
- Laminar burning velocities of hydrogen-air and hydrogen-air-stem flames 07 p0878 A83-19837
- Countercurrent jet combustion of a hydrocarbon fuel in air 07 p0882 A83-21422
- Sooting tendency of fuels containing polycyclic aromatics in a research combustor 08 p1073 A83-23138
- Prediction of turbulent mixing in confined co-axial reacting jets 08 p1088 A83-23191
- An experimental study of an annular film-evaporation combustion chamber in a low-power gas turbine engine 09 p1205 A83-23443
- Using a global hydrogen-air combustion model in turbulent reacting flow calculations 09 p1227 A83-24667
- Mechanism of flame propagation in hydrogen-air and methane-air systems 15 p2132 A83-34037
- FUELING**
U REFUELING
- FUELS**
NT AIRCRAFT FUELS
NT AUTOMOBILE FUELS
NT CRYOGENIC ROCKET PROPELLANTS
NT DIESEL FUELS
NT DOUBLE BASE ROCKET PROPELLANTS
NT FOSSIL FUELS
NT FUEL OILS
NT GASEOUS FUELS
NT GASOLINE
NT HIGH ENERGY FUELS
NT HYDROCARBON FUELS
NT HYDROGEN FUELS
NT HYPERGOLIC ROCKET PROPELLANTS
NT JET ENGINE FUELS
NT JP-4 JET FUEL
NT KEROSENE
NT LIQUID FUELS
NT LIQUID ROCKET PROPELLANTS
NT METAL FUELS
NT METAL PROPELLANTS
NT MONOPROPELLANTS
NT NUCLEAR FUELS
NT PEAT
NT SLURRY PROPELLANTS
NT SOLID ROCKET PROPELLANTS
NT SYNTHETIC FUELS
- FULL SCALE TESTS**
A study on thermal behavior of large seal-ring
[ASME PAPER 81-LUB-27] 02 p0186 A83-11937
- The development and application of a full-scale wide-body test article to study the behavior of interior materials during a post crash fuel fire 06 p0719 A83-18373
- Full scale test of the C22 target in the ONERA S1MA wind tunnel
[ONERA, TP NO. 1982-95] 06 p0717 A83-18430
- The JEFF Craft Air Cushion vehicle - A unique naval platform
[AIAA PAPER 83-0637] 08 p1173 A83-22425
- Model and full-scale studies of the exhaust noise from a bypass engine in flight
[AIAA PAPER 83-0751] 11 p1531 A83-28019
- The behaviour of large solar power stations in the Swiss Alps 14 p2037 A83-32182
- Principal site testing of the F/A-18 at the Naval Air Test Center 14 p1975 A83-32935
- Canadian forces tracker aircraft full-scale fatigue test at the National Aeronautical Establishment 15 p2122 A83-33548
- Full-scale measurements of blade-vortex interaction noise 16 p2298 A83-35947
- Natural laminar flow data from full-scale flight and wind-tunnel experiments 16 p2296 A83-36409
- Testing of a five-channel spectrophotometer on the AZT-8 telescope 17 p2590 A83-37695
- Advanced technology wing structure
[SAWE PAPER 1487] 20 p3009 A83-43754
- Testing of a full-scale staged combustor operating with a synthetic liquid fuel
[ASME PAPER 83-GT-27] 23 p3464 A83-47890
- Model test and full-scale checkout of dry-cooled jet runup sound suppressors 23 p3413 A83-48217
- FUMES**
Smoke/fumes in the cockpit 21 p3187 A83-43997
- FUNCTION GENERATORS**
An n-th power function generator and an n-th rooter in current mode 07 p0922 A83-21175
- Special-purpose trigonometric function generators 08 p1152 A83-22187
- FUNCTION SPACE**
NT BANACH SPACE
NT HILBERT SPACE
- Evolution of singularities of potential flows in collisionless media and transformations of caustics in three-dimensional space 05 p0683 A83-17135
- Existence of a generalized solution in thermoelasticity with two relaxation times. I 06 p0775 A83-18807
- Space basis for weakly solenoidal functions --- incompressible fluid dynamics 08 p1084 A83-22277
- FUNCTIONAL ANALYSIS**
NT BANACH SPACE
NT CONVOLUTION INTEGRALS
NT FOURIER TRANSFORMATION
NT FREDHOLM EQUATIONS
NT HARMONIC ANALYSIS
NT HILBERT SPACE
NT HILBERT TRANSFORMATION
NT INTEGRAL EQUATIONS
NT INTEGRAL TRANSFORMATIONS
NT J INTEGRAL
NT LAPLACE TRANSFORMATION
NT SINGULAR INTEGRAL EQUATIONS
NT VOLTERRA EQUATIONS
NT WIENER HOPF EQUATIONS
NT ZONAL HARMONICS

Linear functional differential equations as semigroups on product spaces 08 p1156 A83-22025
 Projected Newton methods for optimization problems with wimple constraints 09 p1331 A83-24767
 Optimum sensitivity derivatives of objective functions in nonlinear programming 14 p2076 A83-32992
 The use of the asymptotic method of short-time space for solving systems of differential and algebraic equations 14 p2078 A83-33010
 Optimal-control of nonlinear systems 15 p2220 A83-33525
 The analysis and design of nonlinear systems with the aid of functional power series 19 p2889 A83-40982
 Finite-element model of two-dimensional problems involving moving objects of inspection 22 p3304 A83-46331

Navier-Stokes equations and nonlinear functional analysis --- Book 22 p3284 A83-46692

FUNCTIONAL DESIGN SPECIFICATIONS

LAMMR: A new generation satellite microwave radiometer - Its concepts and capabilities --- Large Antenna Multichannel Microwave Radiometer 01 p0021 A83-10116
 The agency's approach to normalisation and standards --- for ESA space technology 05 p0621 A83-17435
 The impact of missions on the preliminary design of an ABC rotor [SAWE PAPER 1501] 20 p2935 A83-43760

FUNCTIONAL INTEGRATION

An introduction to nonlinear filtering and functional integration 09 p1329 A83-24737
 Applications of functional integrals to wave propagation problems [AD-A112841] 09 p1339 A83-24739
 Product integration over infinite intervals. I - Rules based on the zeros of Hermite polynomials 13 p1912 A83-31363
 Stabilization of linear dynamic systems 14 p2076 A83-33007

FUNCTIONALS

Determination of higher order accelerations by a functional method 17 p2575 A83-37023

FUNCTIONS (MATHEMATICS)

NT ABEL FUNCTION
 NT ANALYTIC FUNCTIONS
 NT ASYMPTOTES
 NT BOOLEAN FUNCTIONS
 NT COMPOSITE FUNCTIONS
 NT CONFORMAL MAPPING
 NT COORDINATE TRANSFORMATIONS
 NT COSINE SERIES
 NT DISCRETE FUNCTIONS
 NT DISCRIMINANT ANALYSIS (STATISTICS)
 NT DISTRIBUTION FUNCTIONS
 NT DISTURBING FUNCTIONS
 NT ELLIPTIC FUNCTIONS
 NT ENTIRE FUNCTIONS
 NT ERROR FUNCTIONS
 NT EXPONENTIAL FUNCTIONS
 NT FOURIER TRANSFORMATION
 NT FOURIER-BESSEL TRANSFORMATIONS
 NT FRESNEL INTEGRALS
 NT GAMMA FUNCTION
 NT GREEN FUNCTION
 NT HAMILTONIAN FUNCTIONS
 NT HANKEL FUNCTIONS
 NT HARMONIC FUNCTIONS
 NT HYPERBOLIC FUNCTIONS
 NT HYPERGEOMETRIC FUNCTIONS
 NT KERNEL FUNCTIONS
 NT LAGUERRE FUNCTIONS
 NT LAPLACE TRANSFORMATION
 NT LEGENDRE FUNCTIONS
 NT LIAPUNOV FUNCTIONS
 NT LINEAR TRANSFORMATIONS
 NT LOGARITHMS
 NT LORENTZ TRANSFORMATIONS
 NT MATHIEU FUNCTION
 NT MAXWELL-BOLTZMANN DENSITY FUNCTION
 NT MELLIN TRANSFORMS
 NT MEROMORPHIC FUNCTIONS
 NT MODULATION TRANSFER FUNCTION
 NT MONOTONE FUNCTIONS
 NT NORMAL DENSITY FUNCTIONS
 NT OPTICAL TRANSFER FUNCTION
 NT ORTHOGONAL FUNCTIONS
 NT ORTHONORMAL FUNCTIONS
 NT PENALTY FUNCTION
 NT PERIODIC FUNCTIONS
 NT POINT SPREAD FUNCTIONS
 NT POISSON DENSITY FUNCTIONS
 NT PROBABILITY DENSITY FUNCTIONS
 NT PROBABILITY DISTRIBUTION FUNCTIONS
 NT RAMP FUNCTIONS
 NT RATIONAL FUNCTIONS

NT RAYLEIGH DISTRIBUTION
 NT RECURSIVE FUNCTIONS
 NT SCHWARZ-CHRISTOFFEL TRANSFORMATION
 NT SINE SERIES
 NT SPACE-TIME FUNCTIONS
 NT SPHERICAL HARMONICS
 NT SPLINE FUNCTIONS
 NT STEP FUNCTIONS
 NT STRESS FUNCTIONS
 NT TIME FUNCTIONS
 NT TRANSCENDENTAL FUNCTIONS
 NT TRANSFER FUNCTIONS
 NT TRIGONOMETRIC FUNCTIONS
 NT WALSH FUNCTION
 NT WEIBULL DENSITY FUNCTIONS
 NT WEIGHTING FUNCTIONS

Fourier series of functions having a fractional-logarithmic derivative 02 p0231 A83-11638
 Nondifferentiable optimization --- Russian book 02 p0231 A83-11975
 Applications of transfinite /'blending-function'/ interpolation to the approximate solution of elliptic problems 03 p0388 A83-14085
 Convolution equations in multidimensional spaces --- Russian book 05 p0681 A83-17120
 On two-layer models and the similarity functions for the PBL 06 p0789 A83-18246
 The numerical evaluation of one-dimensional Cauchy principal value integrals 06 p0804 A83-18899
 A model function for ocean microwave brightness temperatures 09 p1320 A83-24311
 Boundary value problems of mathematical physics and related questions in the theory of functions. 14 --- Russian book 09 p1339 A83-24316
 Shear center in aerofoil sections with special reference to circular arc aerofoil blades [ASME PAPER 82-WA/DE-19] 10 p1439 A83-25699

Mass function for massive stars 11 p1677 A83-27676
 On the integration of functions of elliptical motion 11 p1673 A83-28043
 The use of the method of multisegment argument-transformation for the high-precision hardware implementation of elementary functions 12 p1768 A83-29348
 The use of elements of the theory of R-functions to analyze receivers of composite signals with redundancy 13 p1828 A83-30288
 Functional formulation of magnetohydrodynamic turbulence in a rotating frame of reference 14 p2087 A83-32919
 On one-dimensional stretching functions for finite-difference calculations --- computational fluid dynamics 15 p2224 A83-33821
 Notes on the associated alpha-functions and related integrals --- for variable eclipsing binary star studies 15 p2249 A83-34791
 The earth-moon tidal force function 16 p2426 A83-36783
 Further applications of the singularity function method to plate problems 18 p2701 A83-40048
 Fast special-purpose processors for the computation of elementary functions 19 p2888 A83-41423

FUNGI

NT ACTINOMYCETES
 NT MICROSPORES
 NT SPORES
 NT YEAST
 Influence of zero gravity simulation on time course of mitosis in microplasmidia of Physarum polycephalum 19 p2878 A83-42057

FUNGICIDES

NT CAFFEINE
 NT GUANINES
 NT URIC ACID

FUNNELS

Characteristics of the regular reflection of a shock wave from the walls of a conical funnel 17 p2507 A83-38072

FURAN RESINS

NT KEVLAR (TRADEMARK)
 NT POLYAMIDE RESINS

FURANS

NT TETRAHYDROFURAN

FURLABLE ANTENNAS

Designing an umbrella-type folding antenna 22 p3272 A83-45688

FURNACES

NT IMAGE FURNACES
 NT SOLAR FURNACES
 NT VACUUM FURNACES
 Heating unit for high-temperature mechanical tests 19 p2824 A83-40764
 Non luminous gas radiation - Approximate emissivity models 20 p2974 A83-42692

Air jet levitation furnace system for observing glass microspheres during heating and melting 20 p2963 A83-43265

FUSELAGE MOUNTING

U AIRCRAFT PRODUCTION

FUSELAGES

The application of nonlinear analysis techniques to practical structural design problems 02 p0195 A83-12765

Numerical simulation of wing-fuselage interference 03 p0277 A83-13129

A study of the corrosion activity of the fuselage condensate of passenger aircraft 04 p0445 A83-15398

An evaluation of Space Shuttle Orbiter forward fuselage surface pressures - Comparison with wind tunnel and theoretical predictions [AIAA PAPER 83-0119] 05 p0606 A83-16532

Numerical simulation of wing-fuselage aerodynamic interaction [AIAA PAPER 83-0225] 05 p0582 A83-16595

Computation of three-dimensional boundary layers at fuselages [AIAA PAPER 83-0455] 05 p0586 A83-16725

Numerical computation of transonic flow about wing-fuselage configurations on a vector computer [AIAA PAPER 83-0499] 05 p0587 A83-16751

Flow fields and aerodynamic characteristics for hypersonic missiles with mid-fuselage inlets [AIAA PAPER 83-0542] 05 p0587 A83-16777

Theoretical and experimental evaluation of transmission loss of cylinders --- as idealized aircraft fuselages 07 p0990 A83-19808

A superelement analysis of stiffened shells --- Russian book on aircraft fuselage structures 07 p0865 A83-20392

The development of advanced composite front fuselage technology 07 p0865 A83-20464

Fuselage-lifting surfaces interaction in unsteady subsonic flow --- French thesis 08 p1041 A83-22093

Application of the matrix method of forces for the calculation of aircraft structures 08 p1123 A83-23221

Calculation of three-dimensional transonic flow past elongated bodies 09 p1196 A83-23570

Simulation of propfan noise impact on a fuselage --- by newly developed siren [AIAA PAPER 83-0715] 10 p1475 A83-25930

Direct measurement of transmission loss of aircraft structures using the acoustic intensity approach 11 p1530 A83-28185

On an algorithm for solving the incomplete eigenvalue problem in the vibration analysis of complex structures of fuselage type 12 p1735 A83-29278

The effect of acoustic-thermal environments on advanced composite fuselage panels [AIAA 83-0955] 12 p1744 A83-29857

Acoustic fatigue test evaluation of adhesively bonded aluminum fuselage panels using FM 73/BR 127 adhesive/primer system [AIAA 83-0999] 12 p1744 A83-29874

Isolation of singular surfaces when using finite-difference methods --- for computing supersonic flow past wing-fuselage combinations 17 p2447 A83-37259

Generalization of the results of calculations of the stressed state of structures with cutouts --- such as wing and fuselage combinations 17 p2518 A83-37268

Aerodynamic loads on the rear part of a fuselage behind a swept wing in supersonic flow 17 p2450 A83-37562

Convoir 990 transonic flow-field simulation about the forward fuselage [AIAA PAPER 83-1785] 17 p2452 A83-38626

The combination of a geometry generator with transonic design and analysis algorithms [AIAA PAPER 83-1862] 17 p2457 A83-38689

Apparent-mass coefficients for isosceles triangles and cross sections formed by two circles --- in slender body fuselage aerodynamics 21 p3091 A83-43973

Three-dimensional boundary-layer calculations in design aerodynamics 22 p3251 A83-47034

Automatized bonding process for load-bearing aircraft cellular structural components in light contour systems 23 p3391 A83-47198

FUSIFORM SHAPES

U CONES

FUSION (MELTING)

Reactions between Ni-Cr-B-Si matrices and carbide additives in coatings during fusion treatment 10 p1400 A83-25533

FUSION REACTORS

Ion gun tritium permeation testing [AIAA PAPER 82-1940] 02 p0157 A83-12502
 A viable process for producing hydrogen synfuel using nuclear fusion heat 11 p1605 A83-27210

Thermochemical hydrogen production based on
magnetic fusion 20 p3049 A83-42954

FUSION WELDING

NT ARC WELDING
NT BRAZING
NT ELECTRON BEAM WELDING
NT GAS TUNGSTEN ARC WELDING
NT GAS WELDING
NT PLASMA ARC WELDING

Technological advances in welding and other joining
processes --- Book 05 p0652 A83-17117
Some aspects of welding on the structure and properties
of titanium alloys 15 p2135 A83-33645

FUZZY SETS

Dynamic programming, fuzzy sets, and the modeling of
R&D management control Systems 08 p1159 A83-22348

Test of a fuzzy set based decision model as an aid in
solving human factors design problems 10 p1470 A83-26324

A fuzzy algorithm to compute transonic profile flow
12 p1696 A83-28973

Principles for the adaptation of logical integrating
computing structures for the implementation of fuzzy
algorithm 16 p2403 A83-36902

Fuzzy set theory for improving and evaluating reliability
of complex systems 17 p2518 A83-37767

Robot planning with fuzzy sets 21 p3194 A83-44696

FUZZY SYSTEMS

Fuzzy differential equations and their possible use in
meteorology 09 p1316 A83-25145

A design method for nonlinear control systems based
upon partial knowledge about controlled objects 10 p1465 A83-26528

Fuzzy-probabilistic algorithms in identification of fuzzy
systems 10 p1466 A83-26541

F4H AIRCRAFT

U F-4 AIRCRAFT

F8U AIRCRAFT

U F-8 AIRCRAFT

G**G FORCE**

U ACCELERATION (PHYSICS)

GADOLINIUM

Synthesis and investigation of GdScO₃ single crystals,
activated by Nd(3+) ions 13 p1849 A83-30263

The Barkhausen effect and viscous phenomena in
gadolinium molybdate single crystals 13 p1928 A83-30315

GAGES

U MEASURING INSTRUMENTS

GAIN (AMPLIFICATION)

U AMPLIFICATION

GALACTIC CLUSTERS

NT VIRGO GALACTIC CLUSTER

Mapping the Local Supercluster

Galactic clusters 01 p0115 A83-10206
01 p0124 A83-10569

Intergalactic gas in galactic clusters, the microwave
background radiation and cosmology 01 p0124 A83-10839

Clusters of galaxies --- optical observation data
01 p0127 A83-11290

Three-dimensional structure of the universe and regions
devoid of galaxies 01 p0128 A83-11342

The cross-correlation of the Zwicky and Shane-Wirtanen
catalogs of galaxies 02 p0245 A83-11610

Evolution of the cluster X-ray luminosity function slope
02 p0254 A83-12101

The halos of rich clusters of galaxies. I - An infall model
for the Coma Cluster 02 p0254 A83-12102

The evolution of radio galaxies - A VLA survey of
high-redshift clusters of galaxies 02 p0246 A83-12103

X-ray-imaging observations of clusters of galaxies
02 p0259 A83-12194

Evolution of rich clusters of galaxies 02 p0260 A83-12522

21 cm line observations of cD galaxies 02 p0261 A83-12546

The age spread and initial mass function of NGC 3293
- Implications for the formation of clusters 02 p0248 A83-12911

The gravitational evolution of structure in a scale-free
universe 03 p0412 A83-13301

Electronographic photometry in the galactic cluster M
37 03 p0402 A83-13364

The estimation of galaxy angular correlation functions
03 p0408 A83-13930

Star formation in a cooling flow 03 p0419 A83-13934

The distribution of companion galaxies to
mirror-symmetric extragalactic radio sources 03 p0420 A83-13940

Flocculent and grand design spiral structure in field,
binary and group galaxies 03 p0420 A83-13941

Flocculent and grand design spiral arm structure in
cluster galaxies 03 p0420 A83-13942

The structure of groups of galaxies in the Ursa
Major/Canes Venatici region. I - A discussion of the results
of an H I survey 03 p0409 A83-13944

The relationships between morphological type and
quantitative measures in the cluster environment 03 p0421 A83-14140

On the large-scale variations of M/L --- mass to light
ratio in universe 03 p0422 A83-14176

An approximately 300 Mpc void of rich clusters of
galaxies 03 p0422 A83-14177

The four-point function in the BBGKY hierarchy --- galaxy
correlation in clustering pattern 03 p0422 A83-14178

The neutral hydrogen deficiency of the cluster A262
03 p0422 A83-14180

On the origin of the voids in the galaxy distribution
03 p0425 A83-14216

The distribution of relative distances of double
galaxies 03 p0426 A83-14693

Perturbation of the magnitude-redshift relation in an
inhomogeneous relativistic model. II - Correction to the
Hubble law behind clusters 03 p0427 A83-14758

How well is gas mixed in clusters of galaxies
03 p0428 A83-14767

Galactic neutrino models 03 p0429 A83-14778

Monte-Carlo simulations of galaxy systems. IV - Static
properties for galaxies in supercluster cells. V - Computer
models of galaxy fields 04 p0545 A83-14987

The estimation of the mean density in the universe
04 p0549 A83-14992

V Zw 311 - The once and future cD 04 p0551 A83-15602

Coma quasars 04 p0551 A83-15603

Polarization in NGC 7789 and the membership of blue
stragglers 04 p0553 A83-15621

Post-Newtonian approximations in scale covariant
gravitation 04 p0556 A83-15960

The evolution of large-scale structures in the universe.
I 04 p0558 A83-16376

Giant voids in the universe 05 p0695 A83-16845

Spectroscopy of galaxies in distant clusters. I - First
results for 3C 295 and 0024 + 1654 05 p0696 A83-16980

The curvature of radio jets and tails in the intracluster
media of Abell 1446 and 2220 05 p0696 A83-16981

The galactic content of groups of galaxies
05 p0696 A83-16982

Filamentary structure in the Shane-Wirtanen galaxy
distribution 05 p0700 A83-17025

Common properties of clusters of galaxies containing
radio halos and implications for models of radio halo
formation 06 p0825 A83-18092

On the gravitational radius - Velocity dispersion
correlation for clusters of galaxies 06 p0827 A83-18172

Tidal compression of the Local Supercluster
06 p0828 A83-18183

Is there a ring around Milky Way 06 p0828 A83-18419

Spectroscopic identification of white dwarfs in galactic
clusters. II - NGC 2516 06 p0830 A83-18548

Cluster galaxies with Seyfert properties 06 p0830 A83-18778

U, B, V photometry of nests of interacting galaxies
06 p0819 A83-18826

The fluctuations in the instantaneous virial mass of
stationary gravitating systems 06 p0831 A83-18828

Medusa spectroscopy of A400, A576, A1767, and
A2124 06 p0820 A83-18856

Some properties of the centers of cD galaxies
06 p0821 A83-19052

On the possibility of cluster membership for the cepheid
V Centauri 06 p0822 A83-19073

Isolated triplets of galaxies: Virial mass - Luminosity
ratios 06 p0836 A83-19201

Morphology of compact galaxies. II 06 p0836 A83-19202

Galaxies with very elongated shapes 06 p0837 A83-19205

Observations of the Coma Cluster of galaxies /A 1656/
at frequency 102.5 MHz 06 p0838 A83-19218

Physical conditions in interacting galaxies, in
components of isolated pairs, and in isolated galaxies
06 p0838 A83-19220

Effect of variable obscuration on the clustering of
galaxies 06 p0839 A83-19265

Relaxation and tidal stripping in rich clusters of galaxies.
I - Evolution of the mass distribution 06 p0839 A83-19267

Carbon stars in Local Group galaxies

06 p0839 A83-19274

CCD photometry of Abell clusters. I - Magnitudes and
redshifts for 84 brightest cluster galaxies 06 p0842 A83-19476

Galaxy clusters with multiple components. II - Abell
115 06 p0842 A83-19477

Numerical simulations of the decay of satellite galaxy
orbits 06 p0824 A83-19478

Superclusters as nondissipative pancakes - Flattening
06 p0843 A83-19479

The peculiar velocity field in flattened superclusters
06 p0845 A83-19521

Problems in stellar statistics 06 p0846 A83-19537

Intergalactic gas in galaxy clusters - Scattering and
polarization of the radio emission of a central source
07 p1014 A83-20663

Stellar dynamical processes in the evolution of galaxies
and galaxy clusters 07 p1016 A83-20767

Tidal distension in protostructures - The shapes of
galaxies and systems of galaxies 07 p1017 A83-20937

The NGC 1961 group of galaxies 07 p1018 A83-20954

A distance scale from the infrared magnitude/H I
velocity-width relation. IV - The morphological type
dependence and scatter in the relation; the distances to
nearby groups 07 p1019 A83-21101

The X-ray morphology of Abell 1367 07 p1019 A83-21103

Dynamical friction on extended objects --- during
gravitational interaction with non-colliding particles
07 p1023 A83-21205

Bias in observed nearby clusters of galaxies
07 p1008 A83-21206

Holes in cosmology 07 p1026 A83-21253

Hierarchical merging and the structure of elliptical
galaxies 08 p1181 A83-23027

The nature of the cluster surrounding 3C 295
08 p1181 A83-23028

A QSO in a rich, distant cluster of galaxies
08 p1186 A83-23260

The orientation in space of spiral galaxies in the local
supercluster 09 p1359 A83-24457

Perturbation of the magnitude-redshift relation in an
inhomogeneous relativistic model. III - Redshift effect
intrinsic to clusters of galaxies 09 p1354 A83-24462

WSRT radio observations at 1.4 GHz of 32 Abell clusters
of distance class 3 and 4 09 p1354 A83-24513

408 MHz observations of clusters of galaxies. II - The
Coma and Perseus superclusters 09 p1355 A83-24522

CCD camera observations of nearby rich clusters. I -
R photometry of brightest galaxies 09 p1355 A83-24998

An absorption feature and filamentary structures in the
central galaxy of the Centaurus cluster, NGC 4696
09 p1365 A83-25296

On semi-degenerate equilibrium configurations of a
collisionless self-gravitating Fermi gas 10 p1500 A83-25482

Inner ring structures in galaxies as distance indicators.
IV - Distances to several groups, clusters, the Hercules
supercluster, and the value of the Hubble constant
10 p1502 A83-25701

A survey by HEAO 1 of clusters of galaxies. III - The
complete Abell catalog 10 p1496 A83-26351

Markarian galaxies and voids in the galaxy distribution
10 p1507 A83-26352

Paired quasars near NGC 2639 - Evidence for quasars
in superclusters 10 p1507 A83-26353

Normal modes of relaxation in stellar systems -
Dynamical friction and thermalization 10 p1510 A83-26392

Flocculent and grand design spiral galaxies in groups -
Time scales for the persistence of grand design spiral
structures 10 p1512 A83-26705

Cluster collapse and radio source morphology
11 p1679 A83-27993

Multifrequency radio observations of 3C 28, 76.1, 186
and 319 11 p1674 A83-28264

Evolution toward equipartition in galaxy clusters and
its effect on virial M/L estimates 11 p1681 A83-28271

X-ray observations of the southern cluster CA 0340-538
and the Horologium supercluster 11 p1681 A83-28274

A test for transverse motions of clusters of galaxies
11 p1675 A83-28396

On the variability of the two brightest stars in the galactic
cluster IC 2391 12 p1789 A83-28861

Analysis of optical imagery for Seyfert's Sextet and VV
172 12 p1784 A83-28880

Global value of Hubble constant 13 p1946 A83-30382

- Spectra of radio galaxies in clusters
13 p1946 A83-30386
- A survey of galaxy redshifts. V - The two-point position and velocity correlations
13 p1949 A83-31401
- A new evaluation of the four-point galaxy correlation function amplitudes
13 p1949 A83-31402
- Neutral hydrogen in X-ray cluster galaxies - A1367
13 p1949 A83-31404
- Core radii determination for eleven southern clusters of galaxies
13 p1955 A83-31665
- The Horologium-Reticulum supercluster of galaxies
13 p1956 A83-31682
- An observational study of the dynamics of binary galaxies
13 p1942 A83-31696
- The geometry of two superclusters Coma-A1367 and Perseus-Pisces
13 p1958 A83-31732
- Observations of the interacting galaxy pair NGC 4490/85
13 p1959 A83-31754
- A catalog of hierarchical subclustering in the Turner-Gott groups
14 p2098 A83-33153
- Can graininess in the early universe make galaxies?
14 p2103 A83-33178
- Cosmological self-similar shock waves and galaxy formation
14 p2103 A83-33179
- The evolution of clusters of galaxies. I - Very rich clusters
14 p2104 A83-33180
- The Cancer Cluster - An unbound collection of groups
14 p2098 A83-33181
- Redshift quantization in compact groups of galaxies
14 p2104 A83-33182
- Search for neutral hydrogen in the early universe
14 p2107 A83-33236
- Towards a study of southern distant clusters of galaxies
14 p2099 A83-33240
- A proper motion survey in the area of the galactic cluster in Coma Berenices
14 p2100 A83-33255
- Are dominant central galaxies the proto-nuclei of rich clusters?
14 p2101 A83-33468
- Einstein X-ray observations of clusters of galaxies
15 p2252 A83-33601
- Statistical genesis of a lognormal distribution as a source of properties observed in the clumping of galaxies
15 p2253 A83-33703
- The galaxy as fundamental calibrator of the extragalactic distance scale. I - The basic scale factors of the galaxy and two kinematic tests of the long and short distance scales
15 p2255 A83-34076
- CCD photometry of Abell clusters. II - Surface photometry of 249 cluster galaxies
15 p2255 A83-34077
- Effects of galaxy collisions on the structure and evolution of galaxy clusters. I - Mass and luminosity functions and background light
15 p2255 A83-34078
- Spherical simulations of holes and honeycombs in Friedman universes
15 p2256 A83-34080
- Redshift modifications to HEAO A-1 cluster X-ray luminosities
15 p2256 A83-34081
- Accretion-driven star formation in central dominant galaxies in X-ray clusters
15 p2256 A83-34082
- A note on the formation of clusters of galaxies
15 p2256 A83-34083
- Enhanced radio emission in merging galaxies
15 p2256 A83-34088
- Some properties of radio galaxies in clusters
15 p2261 A83-34495
- A new ring galaxy in the Abell 1631 cluster of galaxies
15 p2247 A83-34504
- Effects of spherically-symmetric gravitational lenses produced by galaxies and clusters
15 p2262 A83-34538
- A search for Beta Cephei stars in NGC 6231
15 p2265 A83-34591
- A narrow-line radio galaxy behind the Fornax cluster
15 p2266 A83-34610
- 21 centimeter observations of supercluster galaxies - The bridge between Coma and A1367
15 p2266 A83-34613
- On the association of galaxies and QSOs
15 p2266 A83-34614
- Groups of galaxies. III - The CfA survey
16 p2423 A83-35971
- Multifrequency WSRT observations of the radio galaxy 3C 31 --- Westerbork Synthesis Radio Telescope
16 p2426 A83-36699
- X-ray observations of radio-jet galaxies
16 p2433 A83-36704
- WSRT radio observations at 1.4 GHz of 22 Abell clusters of distance class 5
17 p2587 A83-37282
- Dynamical evolution of a compact group of galaxies
17 p2599 A83-37356
- Multicolor photometry of the galaxy Markarian 141, a component of a binary system
17 p2590 A83-37711
- The dynamics of rich clusters of galaxies. II - The Perseus cluster
17 p2591 A83-37776
- Are wide-angle radio-tail QSOs members of clusters of galaxies? I - VLA maps at 20 cm of 117 radio quasars
17 p2602 A83-37777
- Surface brightness and effective radius for elliptical galaxies
17 p2602 A83-37780
- The evolution of galaxies in clusters. III - Photometry of 17 intermediate redshift clusters
17 p2591 A83-37826
- Radial velocities of galaxies in neighborhoods of groups of galaxies. I
17 p2602 A83-37883
- Radial velocities of galaxies in neighborhoods of groups of galaxies. II
17 p2602 A83-37884
- On the connection between Seyfert galaxies and neighboring objects
17 p2603 A83-37886
- Spectroscopy of galaxies in distant clusters. II - The population of the 3C 295 cluster
17 p2603 A83-37901
- The spatial correlation function of rich clusters of galaxies
17 p2603 A83-37902
- Discovery of a quasar with a wide angle radio tail in a distant cluster of galaxies
17 p2603 A83-37903
- An assessment of the completeness and correctness of the Abell catalogue
17 p2606 A83-38235
- Distance and model dependence of observational galaxy cluster concepts
17 p2610 A83-38427
- The association of QSOs with field and cluster galaxies
17 p2612 A83-38591
- Diffuse radio emission from the Coma cluster of galaxies at decimetre wavelengths
18 p2764 A83-39191
- The galactic extinction of extragalactic objects. I - The csc b law and the extinction coefficient
18 p2767 A83-39592
- Masses and mystery in the local group --- of galaxies
18 p2771 A83-39670
- Radio data on clusters of galaxies from the Culgoora circular array
18 p2760 A83-40326
- The spatial covariance function for rich clusters of galaxies
18 p2778 A83-40486
- Numerical experiments on the clustering of galaxies
19 p2917 A83-41608
- Radio and X-ray observations of the radio halo source in A1367
19 p2917 A83-41609
- On the density of galaxy quartets and the statistical likelihood of discordant redshift groups
19 p2917 A83-41610
- On the mass and extent of the Coma Cluster of galaxies
19 p2917 A83-41611
- Correlation functions in a filamentary clustering prescription
19 p2920 A83-41644
- The collapse and violent relaxation of N-body systems - Mass segregation and the secondary maximum
20 p3066 A83-42430
- The X-ray luminosity function of very rich clusters and the luminosity-richness relation
20 p3070 A83-43037
- X-ray survey of clusters of galaxies with the Einstein Observatory
20 p3071 A83-43038
- The IC 698 group of galaxies
20 p3071 A83-43039
- CCD photometry of the BL Lacertae object 1400+162 and the associated group of galaxies
20 p3059 A83-43040
- Further observations and analysis of quasars near companion galaxies
20 p3060 A83-43041
- Empirical indicators of the evolution of clusters of galaxies
20 p3074 A83-43131
- Magnitude-redshift relation in clusters, groups and pairs of galaxies
20 p3075 A83-43393
- The cluster of galaxies SC0316-44 - Does it rotate?
21 p3228 A83-44402
- A search for microwave background diminution towards the cluster 0016 + 16
21 p3223 A83-44429
- Are galaxy properties specific for their parent clusters?
21 p3231 A83-44446
- The cluster around 3 C 130
21 p3223 A83-44456
- Positions of stars in regions of 14 southern galactic clusters
21 p3225 A83-44976
- Pair correlations in an expanding universe for a multicomponent system
21 p3235 A83-45526
- Two-dimensional spectrophotometry of the cores of X-ray luminous clusters
21 p3235 A83-45529
- The Ursa Major supercluster. II - A statistical analysis of the radio survey
22 p3379 A83-46570
- X-ray, optical, and radio observations of the blue galaxy Butcher-Oemler 6 in the 3C 295 cluster
22 p3380 A83-46976
- The X-ray emitting gas in poor clusters with central dominant galaxies
22 p3381 A83-46977
- Radiative accretion of intracluster gas onto dominant galaxies in poor clusters
22 p3381 A83-46978
- Globular cluster systems in the Hydra I elliptical galaxies. II
22 p3381 A83-46979
- Expected number of multiple QSOs from galaxy and QSO surface density data
22 p3383 A83-47006
- The Hydra I cluster of galaxies. II - First results from H I observations
23 p3518 A83-47433
- The trivariate (radio, optical, X-ray) luminosity function of cD galaxies. I - New Westerbork observations of 22 cD galaxies and Einstein observations of A 1918 and A 2317. II - The fuelling of radio sources
23 p3518 A83-47437
- ESO 438-G 9 - A Seyfert galaxy with unusual properties
23 p3519 A83-47444
- Galaxy groups - Correlations between luminosities, velocity dispersions, and virial radii
23 p3519 A83-47456
- A class of self-similar astrophysical explosions
23 p3520 A83-47458
- The large-scale structure of the universe
23 p3526 A83-47825
- The effect of a magnitude cut-off on the spectral shift anomaly of galaxies in the Perseus supercluster
23 p3526 A83-47847
- Accretion of intracluster gas by a galaxy
24 p3653 A83-49167
- Simulations of galaxy mergers
24 p3642 A83-49259
- Galaxy formation - Some comparisons between theory and observation
24 p3657 A83-49267
- Proto-galactic perturbations
24 p3658 A83-49365
- Frequency analysis of Beta Cephei variables in NGC 6231
24 p3659 A83-49373
- High-resolution optical observations of NGC 3379. II
24 p3663 A83-49846
- On the derivation of the East-West profile
24 p3663 A83-49846
- Galaxies in clusters - Alignments, formation from pancakes, and tidal forces
24 p3664 A83-49998
- Large scale structure in the direction of the Indus supercluster
24 p3649 A83-50024
- Objective prism radial velocities for clusters of galaxies near the South Galactic Pole
24 p3649 A83-50025
- Clustering and alignment of quasars
24 p3649 A83-50026
- Clustering of QSO's and galaxies
24 p3649 A83-50027
- Poor evidence of merging in loose galaxy groups
24 p3668 A83-50088
- ### GALACTIC COSMIC RAYS
- Relationship between various solar-activity indices and long-term variations of cosmic-ray intensity
18 p2784 A83-39308
- Galactic cosmic rays and N2 dissociation on Titan
19 p2921 A83-40780
- Investigation of the characteristics of proton fluxes via the Venera 13 and 14 probes
19 p2925 A83-41245
- Blast waves with cosmic-ray pressure
22 p3390 A83-47004
- Composition and origin of cosmic rays; Proceedings of the Advanced Study Institute, Erice, Italy, June 20-30, 1982
23 p3538 A83-47735
- Introduction to the galactic cosmic radiation
23 p3538 A83-47736
- On the origin of low energy anomalous component of galactic cosmic rays
23 p3539 A83-47744
- Cosmic-ray acceleration by diffusive shocks - Cut-off energy
23 p3539 A83-47747
- Cosmic ray sources
23 p3539 A83-47749
- Extragalactic cosmic rays, active galaxies and quasi-stellar objects
23 p3540 A83-47751
- Effectiveness of HZE-particles onto different biological systems in the Biostack Experiments on Apollo 16, and 17 and on ASTP
23 p3494 A83-47764
- Experimental tests of the 'invisible' axion --- elementary particles in cosmology
24 p3658 A83-49292
- Galactic gamma radiation - The contribution from discrete sources
24 p3675 A83-50080
- ### GALACTIC EVOLUTION
- Mapping the Local Supercluster
01 p0115 A83-10206
- Origin and evolution of galaxies; Proceedings of the International School of Cosmology and Gravitation, Course, 7th, Erice, Italy, May 11-23, 1981
01 p0127 A83-11287
- Reflections on the formation of galaxies in the frame of Lemaitre's cosmology
01 p0127 A83-11289
- Adiabatic vs. isothermal - Two pictures of galaxy origin
01 p0127 A83-11291
- Formation of galaxies in G-variable cosmologies
01 p0127 A83-11294
- Primary nucleosynthesis in the galactic disk
02 p0252 A83-11599
- Evolution of the cluster X-ray luminosity function slope
02 p0254 A83-12101
- The evolution of radio galaxies - A VLA survey of high-redshift clusters of galaxies
02 p0246 A83-12103
- X-ray illumination of globular cluster puzzles --- globular cluster X ray sources as clues to Milky Way Galaxy age and evolution
02 p0255 A83-12117
- Extranuclear clues to the origin and evolution of activity in galaxies
02 p0258 A83-12190

- X-ray-imaging observations of clusters of galaxies
02 p0259 A83-12194
- Evolutionary luminosity functions of extragalactic sources driven by gravitational power
02 p0259 A83-12515
- Evolution of rich clusters of galaxies
02 p0260 A83-12522
- On the nature of the stellar population in the nucleus of the Sd galaxy NGC 7793
03 p0414 A83-13336
- The dynamical evolution of clusters of nonpoint bodies
03 p0419 A83-13897
- Dissipationless galaxy formation and the r to the 1/4-power law
03 p0420 A83-13935
- On the large-scale variations of M/L --- mass to light ratio in universe
03 p0422 A83-14176
- An approximately 300 Mpc void of rich clusters of galaxies
03 p0422 A83-14177
- Abundance of lithium in unevolved halo stars and old disk stars - Interpretation and consequences
04 p0550 A83-15043
- V Zw 311 - The once and future cD
04 p0551 A83-15602
- Large-scale background temperature and mass fluctuations due to scale-invariant primeval perturbations
04 p0554 A83-15646
- Giant voids in the universe
05 p0695 A83-16845
- The galactic content of groups of galaxies
05 p0696 A83-16982
- The warping of disk galaxies. I - Theory
05 p0697 A83-16992
- The evolution of galaxies - Expectations and observations
05 p0702 A83-17825
- Common properties of clusters of galaxies containing radio halos and implications for models of radio halo formation
06 p0825 A83-18092
- High frequency radio continuum observations of bright spiral galaxies
06 p0817 A83-18095
- On the gravitational radius - Velocity dispersion correlation for clusters of galaxies
06 p0827 A83-18172
- H I observations of high-luminosity elliptical galaxies
06 p0819 A83-18853
- On the existence of cosmological evolutionary effects.
I - A morphological selection effect in the counts of quasars
06 p0834 A83-18880
- Some properties of the centers of cD galaxies
06 p0821 A83-19052
- The distant open cluster Tombaugh 2
06 p0836 A83-19056
- The galactic abundance of deuterium - A test for cosmological models
06 p0837 A83-19215
- Activity of nuclei of galaxies in double systems
06 p0838 A83-19222
- Optical variability and radio structure of extragalactic sources - Evidence of recurrent activity
06 p0838 A83-19224
- Relaxation and tidal stripping in rich clusters of galaxies.
I - Evolution of the mass distribution
06 p0839 A83-19267
- Superclusters as nondissipative pancakes - Flattening
06 p0843 A83-19479
- A simple theory of how spiral galaxies acquire their principal global properties
06 p0843 A83-19483
- The motions of the stars and their significance in galactic astronomy /Karl Schwarzschild Lecture 1982/
06 p0824 A83-19532
- G and K stars as indicators of the galactic evolution
06 p0846 A83-19535
- Problems in stellar statistics
06 p0846 A83-19537
- The origin and evolution of galaxies; Proceedings of the International School of Cosmology and Gravitation, Course, 7th, Erice, Italy, May 11-23, 1981
07 p1015 A83-20757
- Theory and evidence about the origin of cosmological structure
07 p1015 A83-20760
- Structure in the universe and fluctuations in the cosmic microwave background
07 p1015 A83-20761
- Large-scale fluctuations in the mass distribution and the microwave background - Nature and evolution
07 p1016 A83-20762
- Primordial stars - The precursors to galaxy formation
07 p1016 A83-20764
- The chemical evolution of galaxies
07 p1016 A83-20766
- Stellar dynamical processes in the evolution of galaxies and galaxy clusters
07 p1016 A83-20767
- Evolution of faint galaxies
07 p1016 A83-20769
- Epilogue - Do we understand how galaxies formed
07 p1017 A83-20771
- Analysis of the large-scale structure of the universe
07 p1017 A83-20935
- Tidal distension in protostructures - The shapes of galaxies and systems of galaxies
07 p1017 A83-20937
- Two-dimensional simulation of the gravitational superclustering of collisionless particles
07 p1018 A83-20940
- Time evolution of disk galaxies undergoing stochastic self-propagating star formation
07 p1020 A83-21112
- The effects of induced star formation on the evolution of the galaxy. II - The galactic ecosystem
07 p1020 A83-21117
- Holes in cosmology
07 p1026 A83-21253
- Pregalactic very massive objects and their cosmological consequences
08 p1178 A83-21843
- Supernovae and the formation of galaxies
08 p1179 A83-21858
- The L varies as σ to the n power relation for the bulge components of disk galaxies
08 p1181 A83-23032
- From dwarfs to giants - Signposts of galaxy formation
08 p1187 A83-23284
- How galaxies acquire their neutrino haloes
08 p1187 A83-23285
- Cosmological density fluctuations produced by sources of radiation at z greater than 100
09 p1363 A83-24997
- On semi-degenerate equilibrium configurations of a collisionless self-gravitating Fermi gas
10 p1500 A83-25482
- The kinematic properties of faint elliptical galaxies
10 p1493 A83-25704
- Is there nonluminous matter in dwarf spheroidal galaxies
10 p1504 A83-25740
- Some implications of nonluminous matter in dwarf spheroidal galaxies
10 p1504 A83-25741
- The cosmological evolution and luminosity function of X-ray selected active galactic nuclei
10 p1510 A83-26399
- Quasar evolution - Not a deficit at 'low' redshifts
10 p1511 A83-26701
- Flocculent and grand design spiral galaxies in groups - Time scales for the persistence of grand design spiral structures
10 p1512 A83-26705
- Neutral hydrogen in isolated galaxies. II - The large angular diameter galaxies
11 p1668 A83-27106
- Evolution toward equipartition in galaxy clusters and its effect on virial M/L estimates
11 p1681 A83-28271
- On the energy distribution function for a one-dimensional gravitational system
11 p1682 A83-28293
- On the evolution of the spiral galaxies in the Virgo cluster
12 p1794 A83-29177
- Self-regulating star formation - The rate limit set by ionizing photons
12 p1796 A83-29544
- The r - and s -process nuclei in the early history of the galaxy - HD 122563
13 p1952 A83-31430
- The formation of disc galaxies
13 p1953 A83-31552
- Stochastic effects in the chemical evolution of galaxies
13 p1956 A83-31687
- Infrared colors of a complete sample of faint galaxies
13 p1957 A83-31694
- The weight, shape, and speed of the universe
14 p2103 A83-33049
- Can graininess in the early universe make galaxies?
14 p2103 A83-33178
- Cosmological self-similar shock waves and galaxy formation
14 p2103 A83-33179
- The evolution of clusters of galaxies. I - Very rich clusters
14 p2104 A83-33180
- The ages of the disks of S0 galaxies
14 p2098 A83-33186
- Search for neutral hydrogen in the early universe
14 p2107 A83-33236
- The spectrum of the extragalactic background light
14 p2107 A83-33237
- Convective mixing length and the galactic carbon to oxygen ratio
14 p2107 A83-33241
- How can we approach the study of cosmology?
15 p2254 A83-33753
- Collisionless matter and galaxy formation
15 p2255 A83-33818
- Very red, yet H I rich galaxies
15 p2255 A83-33826
- Effects of galaxy collisions on the structure and evolution of galaxy clusters. I - Mass and luminosity functions and background light
15 p2255 A83-34078
- A note on the formation of clusters of galaxies
15 p2256 A83-34083
- Monte Carlo simulations of the evolution of galactic nuclei containing massive, central black holes
15 p2256 A83-34084
- Detection of 10 to the 10th solar masses of hot gas in the normal elliptical galaxy NGC 5846 with the Einstein satellite
15 p2259 A83-34119
- Dwarf elliptical galaxies
15 p2259 A83-34120
- DDO integrated photometry of globular clusters and initial chemical evolution of the galaxy
15 p2262 A83-34536
- Two-colour photometry of a sample of faint galaxies
15 p2248 A83-34606
- 21 centimeter observations of supercluster galaxies - The bridge between Coma and A1367
15 p2266 A83-34613
- NGC 1275 - A burgeoning elliptical galaxy
15 p2267 A83-34622
- Temperature fluctuations in the background radiation in the entropy theory of galaxy formation
15 p2269 A83-34680
- Metallicity gradient in the galaxy and its origin
15 p2270 A83-34681
- Synthesized colors and spectra for galaxies of normal chemical composition
15 p2270 A83-34753
- Chemical evolution of the galactic halo. I - Effects of possible mass segregation mechanisms
15 p2272 A83-34779
- Can secondary infall produce flat rotation curves?
17 p2596 A83-37314
- Simulation models for the evolution of cloud systems.
I Introduction and preliminary simulations
17 p2596 A83-37315
- Dynamical evolution of a compact group of galaxies
17 p2599 A83-37356
- Cyclic phase changes of interstellar medium
17 p2599 A83-37357
- The energy and momentum of slow drift spiral density waves
17 p2600 A83-37645
- Stochastic self-propagating star formation in three-dimensional disk galaxy simulations
17 p2604 A83-37907
- Bright radio sources at 178 MHz - Flux densities, optical identifications and the cosmological evolution of powerful radio galaxies
17 p2606 A83-38241
- Simulations of galaxy mergers. II
17 p2593 A83-38244
- Direct dissipationless formation of filaments in the large-scale matter distribution
17 p2607 A83-38259
- Nitrogen and oxygen as indicators of primordial enrichment
17 p2608 A83-38402
- The distribution of violently relaxed matter in galaxies
17 p2609 A83-38418
- Stochastic star formation and chemical evolution of dwarf irregular galaxies
17 p2609 A83-38423
- The canonical anticorrelation between Y and Z in galactic globular clusters and the case of the pulsars in M15
17 p2609 A83-38425
- New actinide chronometer production ratios and the age of the Galaxy
17 p2610 A83-38429
- An evolutionary scheme for active-nucleus objects --- in galaxies
17 p2610 A83-38548
- The expansion of the universe as a driving mechanism for the evolution of correlations
17 p2614 A83-38967
- Colliding and merging galaxies. II - S0 galaxies with polar rings
18 p2767 A83-39589
- On the local standard of rest --- comoving with young objects in gravitational field of spiral galaxies
18 p2768 A83-39633
- Elliptical galaxies - Can rotation be effective in determining their shapes?
18 p2775 A83-39748
- Galaxy formation
18 p2776 A83-39774
- Nucleosynthesis and galactic evolution - Implications for the origin of life
19 p2886 A83-41513
- The ultimate fate of the universe --- Book
20 p3063 A83-42173
- Simulations of galaxy mergers - Cannibalism and dynamical friction
20 p3066 A83-42431
- Cross section for the reaction C-12(e,p)B-11; and its relevance to the formation of B-11 in active galaxies
20 p3068 A83-42464
- Primordial quantum fluctuations and the origin of galaxies
20 p3070 A83-42787
- Nonlinear evolution of large-scale structure in the universe
20 p3070 A83-43035
- The Riemann disks. I - Equilibrium and secular evolution
20 p3071 A83-43051
- Empirical indicators of the evolution of clusters of galaxies
20 p3074 A83-43131
- Cluster analysis of the nonlinear evolution of large-scale structure in an axion/gravitino/photino-dominated universe
21 p3227 A83-44200
- Abundance gradients in galaxies in the Sculptor and Centaurus groups
21 p3233 A83-44750
- Kinematical and chemical evolution of the galactic disc
21 p3233 A83-44754
- Pair correlations in an expanding universe for a multicomponent system
21 p3235 A83-45526
- The rate of star formation in normal disk galaxies
21 p3235 A83-45531
- Velocity fields in late-type galaxies from H-alpha Fabry-Perot interferometry. IV - Kinematics and dynamics of the SAB(s) spiral NGC 5236 (M83)
22 p3377 A83-46257
- Globular clusters and the early chemical history of galactic halos
22 p3378 A83-46409

Three-dimensional numerical model of the formation of large-scale structure in the Universe 22 p3378 A83-46539

Very large spiral galaxies 22 p3374 A83-46540

Luminosity function of high-redshift quasars 22 p3376 A83-46975

Planetary nebulae and the chemical evolution of galaxies 24 p3653 A83-49158

Accretion of intracluster gas by a galaxy 24 p3653 A83-49167

Internal kinematics and dynamics of galaxies; Proceedings of the Symposium, Universite de Franche-Comte, Besancon, France, August 9-13, 1982 24 p3654 A83-49201

The origin of dwarf spheroidal galaxies 24 p3654 A83-49216

Distribution and motions of atomic hydrogen in lenticular galaxies 24 p3655 A83-49219

Neutral hydrogen mapping of three SO galaxies 24 p3641 A83-49220

On the evolution of perturbed gas disks 24 p3655 A83-49224

Magnetic fields and spiral structure 24 p3656 A83-49230

Disk stability --- and barred galaxies 24 p3641 A83-49234

Formation of rings and lenses --- in disk galaxies 24 p3657 A83-49245

Observational evidence for mergers --- of galaxies 24 p3657 A83-49256

Kinematics and evolution of NGC 5128 24 p3642 A83-49258

Simulations of galaxy mergers 24 p3642 A83-49259

On the formation and dynamics of shells around elliptical galaxies 24 p3657 A83-49260

Collisions and merging of disk galaxies 24 p3642 A83-49261

S0 and smooth-arm Sa's within the Hubble sequence 24 p3657 A83-49263

The formation of galaxies 24 p3657 A83-49266

Galaxy formation - Some comparisons between theory and observation 24 p3657 A83-49267

Four-colour uvby and H-beta photometry of A5 to G0 stars brighter than 8.3 m 24 p3642 A83-49317

Proto-galactic perturbations 24 p3658 A83-49365

Gravitational instability for a multifluid medium in an expanding universe 24 p3660 A83-49430

Far ultraviolet observations of Population II 24 p3662 A83-49562

Star formation and abundance gradients in the galaxy 24 p3664 A83-49997

Galaxies in clusters - Alignments, formation from pancakes, and tidal forces 24 p3664 A83-49998

The stellar processing of helium 24 p3665 A83-50039

The helium abundances of G-K main sequence halo and disk stars, the helium galactic abundance evolution and the astrometric satellite Hipparcos 24 p3666 A83-50046

On the pregalactic He/H abundance ratio derived from planetary nebulae 24 p3667 A83-50054

Primordial helium abundance determinations using galactic H II regions 24 p3667 A83-50056

Pregalactic helium abundance determination from extragalactic H II regions 24 p3667 A83-50057

Chemical evolution of the galactic halo. II - Enrichment in primary elements 24 p3670 A83-50154

GALACTIC MAGNETIC FIELDS

U INTERSTELLAR MAGNETIC FIELDS

GALACTIC NUCLEI

Photometric observations of active nuclei 01 p0124 A83-10840

The galactic center - Structure and kinematics from 21-cm line measurements 01 p0125 A83-10941

Tracks of heavy and superheavy cosmic nuclei in olivines of extraterrestrial origin 01 p0130 A83-11339

Thick supercritical accretion disks and active galactic nuclei 01 p0128 A83-11340

Spectra of compact radio sources in galactic nuclei 02 p0250 A83-11578

VLA observations of the Seyfert galaxy NGC 1068 02 p0252 A83-11609

Radio jets in NGC 4151 02 p0254 A83-12108

A nuclear spectroscopic survey of disk galaxies. II - Galaxies with emission lines not excited by stellar photoionization 02 p0254 A83-12109

Time variations of the neutral hydrogen absorption spectrum of NGC 1275 /3C 84/ 02 p0254 A83-12110

Theory of electron-positron showers in double radio sources 02 p0255 A83-12111

Precessing jets in Sagittarius A - Gas dynamics in the central parsec of the galaxy 02 p0255 A83-12113

The nature of the central parsec of the Galaxy 02 p0255 A83-12114

Extranuclear clues to the origin and evolution of activity in galaxies 02 p0258 A83-12190

Physical processes in jets from active galaxies 03 p0412 A83-13151

Luminosity limits for funnels in thick accretion discs 03 p0414 A83-13325

On the nature of the stellar population in the nucleus of the Sd galaxy NGC 7793 03 p0414 A83-13336

A nuclear spectroscopic survey of field disk galaxies 03 p0406 A83-13553

Kinematics of gas clouds in Seyfert nuclei and quasars 03 p0418 A83-13876

On gaseous disks in Seyfert 1 nuclei 03 p0423 A83-14187

The nucleus of M81 - Simultaneous 2.3 and 8.3 GHz Mark III VLBI observations 03 p0423 A83-14188

Two-color CCD observations of the galactic center region 03 p0409 A83-14190

The influence of buoyancy on the stability of jets --- in extragalactic radio sources 03 p0427 A83-14755

VLBI observations of the core sources of a sample of spiral galaxies 03 p0411 A83-14777

The detection of extranuclear emission lines in the Seyfert galaxies Mk10 and Mk79 03 p0430 A83-14811

Ly-alpha absorption at a high velocity in NGC1275 03 p0411 A83-14923

Observations of bipolar planetary nebula 19W32 04 p0551 A83-15050

A spectroscopic method for determining the luminosities of spiral galaxies and estimating their stellar population 04 p0551 A83-15601

V Zw 311 - The once and future cD 04 p0551 A83-15602

A spectroscopic investigation of the nebulosity around low-luminosity quasars 04 p0551 A83-15604

The heating of dust in the broad-line regions of active galaxies and quasars 04 p0551 A83-15605

VLA observations of H I absorption in the nuclei of Seyfert and active galaxies 04 p0552 A83-15609

Low surface brightness spiral galaxies. I - Neutral hydrogen content and location in the infrared Fisher-Tully diagram 04 p0552 A83-15610

Structure of the M33 nucleus 04 p0552 A83-15611

X-rays from quasars and active galaxies 04 p0555 A83-15822

The X-ray jets of Centaurus A and M87 04 p0558 A83-16369

Are there black holes in quasars 05 p0696 A83-16862

Detection of a compact radio source near the center of a gravitational lens - Quasar image or galactic core 05 p0696 A83-16939

Radio structures of Seyfert galaxies. IV - Jets in NGC 1068 and NGC 4151 05 p0697 A83-16985

Dynamo action in a supermassive rotator and the active galactic nuclei 05 p0697 A83-16988

VLBI observations of the nucleus and jet of M87 05 p0697 A83-16989

The infrared emission from the elliptical galaxy NGC 1052 05 p0697 A83-16990

Polarization of compact sources in the galactic center 05 p0698 A83-16994

M supergiants and star formation at the galactic center 05 p0698 A83-17001

On the inner ring of HII regions in NGC 3351 05 p0701 A83-17669

NGC 6503 - Rotation, mass and physical conditions in galaxy nucleus 06 p0824 A83-18017

MERLIN observations of compact sources with very steep radio spectra 06 p0825 A83-18082

MR 2251-178 - A nearby QSO embedded in a giant H II envelope 06 p0827 A83-18163

VLA observations of the 6-cm H2CO absorption towards Sgr A West 06 p0828 A83-18184

Spectrophotometry of the nucleus of the galaxy Arakelyan 144 06 p0831 A83-18792

Q351 + 026 - A QSO spawned by interacting galaxies 06 p0832 A83-18851

New bright Seyfert Galaxies 06 p0819 A83-18852

Infrared properties of serendipitous X-ray quasars 06 p0819 A83-18854

The radio continuum morphology of NGC 4631 at 2.7 and 8.1 GHz 06 p0833 A83-18858

Some properties of the centers of cD galaxies 06 p0821 A83-19052

Reddening of the narrow-line regions of active galaxies and the intrinsic Balmer decrement 06 p0835 A83-19053

Further comments on the radio emission of the nuclei of spiral galaxies 06 p0836 A83-19203

Activity of nuclei of galaxies in double systems 06 p0838 A83-19222

On the possibility of gas being swept out of a galaxy under the influence of the radiation pressure of an active nucleus 06 p0838 A83-19223

The absence of rapid X-ray variability in active galaxies 06 p0839 A83-19272

Are there any shock-heated galaxies 06 p0839 A83-19273

The reddening of active galactic nuclei 06 p0841 A83-19298

The nuclear radio source of the X-ray Galaxy NGC 2110 06 p0823 A83-19299

Bubbles, jets, and clouds in active galactic nuclei 06 p0843 A83-19484

Feeding quasars with stellar winds 06 p0843 A83-19485

Thick accretion disks around black holes /Karl Schwarzschild Lecture 1981/ 06 p0846 A83-19529

Activity in the centers of galaxies 06 p0846 A83-19530

Spectroscopic observations of two very red objects toward the galactic center 07 p1004 A83-19861

Inner ring structures in galaxies as distance indicators. III - Distances to 453 spiral and lenticular galaxies 07 p1013 A83-20080

Photographic surface photometry of the Milky Way. III - Photometry of the central area of the Galaxy in the ultraviolet 07 p1006 A83-20560

A possible mechanism for the recurrent activity in galaxy nuclei 07 p1014 A83-20652

Observations of the galaxies Markaryan 673 and 686 07 p1014 A83-20653

Ionized gas clouds and the origin of the apparent variability of the compact galactic-center radio source 07 p1014 A83-20654

High-resolution radio observations of the Seyfert galaxy NGC 1068 07 p1018 A83-20944

Optical and radio structure of the quasar PKS 0812 + 02 07 p1019 A83-21105

Radio structure and optical kinematics of the cD galaxy Hydra A /3C 218/ 07 p1019 A83-21108

Asymmetric structure in the nuclei of NGC 1275 and 3C 345 07 p1020 A83-21110

Cosmic rays from active galactic nuclei and in metagalactic space 07 p1040 A83-21152

Spectroscopy of the fuzz associated with four quasars 07 p1023 A83-21154

New H2O masers in the galactic center region 07 p1025 A83-21247

Full-implicit continuous eulerian scheme in the spherical coordinates and its applications to solar phenomena --- from radio galaxies 08 p1191 A83-22034

On the origin of relativistic particles and gamma-rays in quasars 08 p1181 A83-23030

A clamshell for Blandford-Rees jets --- from radio galaxies 08 p1181 A83-23034

The supernovae near the nuclei of M31 and the Galaxy 08 p1182 A83-23040

Extinction to ionized gas at the galactic center 08 p1182 A83-23044

Confirmation of the luminous connection between NGC 4319 and Markarian 205 08 p1184 A83-23079

Do galactic bulge X-ray sources evolve into millisecond pulsars 08 p1186 A83-23261

The centre of the Galaxy 08 p1187 A83-23289

Comparison of infrared and optical positions for sources in the direction of the galactic center 09 p1351 A83-23318

Can all quasars be gravitationally lensed Seyfert's nuclei 09 p1359 A83-24451

NGC 6240 - A unique interacting galaxy 09 p1361 A83-24475

RGU photometry of a southern starfield near the galactic centre /SA 158/ 09 p1354 A83-24515

Velocity field and physical conditions in the active lenticular galaxy NGC 3998 09 p1363 A83-24989

IUE observations of variable Seyfert 1 galaxies 09 p1356 A83-25297

The composite UV emission spectrum of Seyfert 1 galaxies 10 p1500 A83-25486

Nuclear activity in the barred spiral galaxy NGC 3660 from radio, optical, and X-ray observations 10 p1500 A83-25488

The reconfinement of jets --- in extragalactic radio sources 10 p1502 A83-25707

Kinematics of the late M stars in the galactic nuclear bulge 10 p1503 A83-25721

Highly compact structures in galactic nuclei and quasars 10 p1496 A83-25858

Active nuclei of galaxies; Goutelas Spring School, 5th, Goutelas, France, April 6-10, 1981, Proceedings 10 p1506 A83-26226

Seyfert and active galaxies 10 p1506 A83-26227

Active nuclei - Observations, classifications, and observational constraints 10 p1506 A83-26228

Radio and mm-observations of active nuclei 10 p1506 A83-26229

- Physical conditions in the emission regions of active galactic nuclei 10 p1506 A83-26230
- Models of massive black holes in the active galactic nuclei 10 p1507 A83-26231
- Toward explaining Seyfert galaxies 10 p1507 A83-26357
- Nearby galaxies with Seyfert-like nuclei 10 p1496 A83-26358
- The dynamics and fueling of active nuclei 10 p1508 A83-26359
- Optical spectrophotometry of the nuclear region of M51. II - Further evidence for nuclear activity 10 p1496 A83-26361
- CCD photometry of the center of M31 10 p1508 A83-26364
- The cosmological evolution and luminosity function of X-ray selected active galactic nuclei 10 p1510 A83-26399
- A wind and shock model for active galactic nuclei 10 p1511 A83-26401
- The nature of the ionizing source of the nuclear gas in NGC 1052 10 p1511 A83-26402
- VLBI observations of the nucleus of Centaurus A 10 p1497 A83-26403
- Spherical accretion onto quasars 10 p1512 A83-26704
- Star formation in the semistellar nucleus of M33 10 p1512 A83-26709
- Comptonization effects in spherical accretion onto black holes 10 p1515 A83-26739
- Anomalous radio continuum features in edge-on spiral galaxies 10 p1516 A83-26748
- Millimeter-wavelength outbursts in the elliptical galaxy NGC 1052 10 p1516 A83-26749
- The distance to M33 based on a new study of its Cepheids 10 p1516 A83-26752
- Detection of sulfur in the galactic center 10 p1516 A83-26754
- X-ray and optical studies of emission-line Markarian galaxies 11 p1668 A83-27103
- Active galaxies and the diffuse gamma-ray background 11 p1694 A83-28389
- The gas distribution in the central region of the Galaxy. IV A survey of neutral hydrogen in the region $1 = 349$ to 13 deg, $b = 10$ to 10 deg, and absolute value of v less than 350 km/s 12 p1789 A83-28864
- The supersonic nozzles of the galaxies 12 p1795 A83-29364
- H76-alpha recombination line emission near Sgr A 13 p1947 A83-30392
- The ultraviolet spectrum of the Seyfert galaxies NGC 3516 and NGC 5548 13 p1949 A83-31405
- Star bursts and the extraordinary galaxy NGC 3690 13 p1950 A83-31409
- Variability at 5 GHz in low luminosity radio nuclei of galaxies and quasars 13 p1941 A83-31568
- The galaxy NGC 1365 13 p1941 A83-31577
- Remarkable kinematics of the ionized gas in the nucleus of NGC 1365 13 p1957 A83-31700
- A dust lane in NGC 6251 13 p1958 A83-31714
- The kinematics and structure of the Galaxy at high galactic latitudes 14 p2101 A83-31834
- Dark matter in spiral galaxies 14 p2103 A83-33100
- Spatially extended narrow emission-line gas in the Seyfert galaxy NGC 4151 14 p2104 A83-33187
- Extended soft X-ray emission from NGC 4151 14 p2104 A83-33188
- Are dominant central galaxies the proto-nuclei of rich clusters? 14 p2101 A83-33468
- Observations of ultraviolet spectra of H II regions and galaxies with IUE 15 p2251 A83-33598
- Einstein Observatory results on active galactic nuclei 15 p2252 A83-33600
- The velocity field in the central region of the galaxy Markarian 538 15 p2252 A83-33701
- A method for estimating the mass of the central bodies in active galaxy nuclei and quasars 15 p2253 A83-33704
- Central condensations in Seyfert galaxies. I 15 p2253 A83-33712
- Observations of neutral hydrogen in radio-loud and interacting galaxies 15 p2255 A83-33827
- Monte Carlo simulations of the evolution of galactic nuclei containing massive, central black holes 15 p2256 A83-34084
- Star-burst galactic nuclei 15 p2256 A83-34087
- The distribution of ionized gas in the nuclei of spiral galaxies 15 p2256 A83-34089
- VLA observations of massive star formation in spiral nuclei 15 p2259 A83-34121
- The gas density and distribution within 2 parsecs of the galactic center 15 p2259 A83-34122
- A new ring galaxy in the Abell 1631 cluster of galaxies 15 p2247 A83-34504
- A study of the long-term variability in radio emission of active galaxies 15 p2262 A83-34529
- The virial mass of the nucleus of M32 15 p2263 A83-34559
- Quasar evolution and gravitational collapse 15 p2267 A83-34618
- Gravitational radiation from particles falling along the symmetry axis into a Kerr black hole - The momentum radiated 15 p2269 A83-34640
- An interpretation of the low energy gamma ray emission from Seyfert nuclei in terms of annihilation radiation from a hot plasma 16 p2431 A83-36667
- A galaxy with a 3.2×2.2 sq kpc H II region surrounding its nucleus 16 p2431 A83-36671
- The radio structure of Sgr A 16 p2431 A83-36676
- The elliptical galaxy NGC 4696 - CCD observations of an absorbing lane 16 p2433 A83-36698
- Morphology of optical forms of N galaxies 17 p2588 A83-37308
- The transitory nature of the filaments in NGC 5128 (Centaurus A) 17 p2596 A83-37309
- Spectroscopic evidence for activity in the nuclei of normal spiral galaxies 17 p2596 A83-37311
- Low-ionization active galactic nuclei - X-ray or shock heated? 17 p2598 A83-37345
- Infrared polarization in the direction to the galactic center 17 p2588 A83-37360
- An H-alpha forbidden N II survey of the nuclei of a complete sample of spiral galaxies 17 p2602 A83-37627
- Spectroscopy of galaxies in distant clusters. II - The population of the 3C 295 cluster 17 p2603 A83-37901
- Continuum reddening of Seyfert 1 nuclei 17 p2607 A83-38260
- The forbidden O III electron temperature and density structure in the nucleus of NGC 1068 17 p2609 A83-38419
- A sample of 25 extragalactic radio sources having a spectrum peaked around 1 GHz 17 p2594 A83-38420
- An evolutionary scheme for active-nucleus objects --- in galaxies 17 p2610 A83-38548
- Dynamics of the radiating gas in the quasar PHL 5200 and in kindred objects 17 p2610 A83-38549
- The distinction between Seyfert 1 and Seyfert 2 galaxies 17 p2610 A83-38552
- Gravitational waves and the activity in galactic nuclei and quasars 17 p2612 A83-38827
- The compact radio source 41.9+58 in M82 as a young plerion 17 p2613 A83-38837
- Relativistic beaming in the central components of double radio quasars 18 p2765 A83-39202
- Active galactic nuclei as clusters of accreting black holes 18 p2766 A83-39248
- The central powerhouse of active galactic nuclei 18 p2766 A83-39249
- Positron annihilation radiation from the nuclei of Seyfert Galaxies 18 p2786 A83-39296
- On the determination of $R(O)---$ distance to center of Milky Way Galaxy 18 p2758 A83-39636
- Globular clusters and the distance to the galactic centre 18 p2771 A83-39668
- A model for the emission spectrum of active galactic nuclei 18 p2774 A83-39740
- On the hypothesis of ejection of supermassive black holes from centers of galaxies and its application to quasar-galaxy associations 18 p2775 A83-39758
- Positron annihilation radiation from Seyfert nuclei and the cosmic diffuse gamma-ray background 18 p2775 A83-39762
- The galactic center; Proceedings of the Workshop, California Institute of Technology, Pasadena, CA, January 7, 8, 1982 19 p2911 A83-40676
- Observations of the galactic center in the radio band 19 p2911 A83-40677
- Molecular gas near the galactic center - Recent contributions from radioastronomy 19 p2912 A83-40678
- The relative locations of the Sgr A molecular clouds and continuum sources 19 p2912 A83-40679
- Depression of molecular emission in the line of sight of Sgr A West 19 p2912 A83-40680
- New far infrared observations of the central 30 arcmin of the Galaxy 19 p2912 A83-40681
- Large beam observations of the galactic center at 150, 200, and 300 microns 19 p2912 A83-40682
- Balloon observation of the central bulge of our Galaxy in near infrared radiation 19 p2912 A83-40683
- Infrared observations of the ionized gas in the galactic center 19 p2912 A83-40684
- B-alpha and Ne II line spectroscopy in the vicinity of the galactic center source IRS 16 19 p2908 A83-40685
- Spatial and spectral studies of the galactic center near 10 microns 19 p2908 A83-40686
- OI and OIII in Sgr A - Neutral and ionized gas at the galactic center 19 p2912 A83-40687
- Two micron observations of C-120 and C-130 in the red giant sources IRS 7, IRS 12, and IRS 19 19 p2912 A83-40688
- Mapping and imaging of the galactic center in the near infrared 19 p2909 A83-40689
- The position of the infrared source IRS 16 in the galactic center region relative to a visual field star 19 p2909 A83-40690
- Observations of continuum X-ray and gamma-ray emission from the galactic center 19 p2913 A83-40691
- Observations of gamma-ray line emission from the galactic center region 19 p2913 A83-40692
- Observations of the galactic center with the GSFC low-energy gamma-ray spectrometer - Preliminary results 19 p2909 A83-40693
- Emission in the 0.3 to 1.0 MeV range from the galactic center region 19 p2913 A83-40694
- On the origin of the positron annihilation radiation from the direction of the galactic center 19 p2913 A83-40695
- The intensity and spectrum of galactic center beta (+) annihilation protons after Compton scattering 19 p2913 A83-40696
- The compact source at the galactic center 19 p2913 A83-40697
- Positron production near a 1,000,000 solar mass black hole 19 p2913 A83-40698
- Gas motions in the central region and their interpretation 19 p2913 A83-40699
- Triaxiality and the galactic center 19 p2913 A83-40700
- Comparison of galactic center with other galaxies 19 p2913 A83-40701
- Radio observations of the galactic center - Future directions 19 p2914 A83-40702
- Future directions in X-ray/gamma-ray observations 19 p2909 A83-40703
- A search for X-ray emission from optically quiet, compact radio sources 19 p2918 A83-41613
- The distribution of molecular clouds in the nuclear region of NGC 1068 19 p2918 A83-41614
- Neutral hydrogen absorption in early spiral galaxies 19 p2920 A83-41645
- Optical spectroscopy of the radio-loud nuclei of spiral galaxies - Starbursts or monsters? 20 p3057 A83-42179
- The temperature of molecular gas in the galactic center region 20 p3064 A83-42195
- A faint star astrometric grid for the galactic center 20 p3058 A83-42199
- The spectral appearance of active galactic nuclei undergoing bursts of star formation 20 p3065 A83-42388
- The emission-line gas in quasars and active nuclei 20 p3069 A83-42468
- Implications for the nature of core-dominant radio sources 20 p3069 A83-42468
- Evidence for a highly polarized continuum in the nucleus of NGC 1068 20 p3069 A83-42469
- Tracing the gas in galaxies 20 p3069 A83-42625
- A 10 micron survey of star formation in galactic nuclei 20 p3071 A83-43043
- Virgo spiral galaxies 20 p3071 A83-43043
- cD galaxy dynamics and an aged ridge (jet) in 3C 338 20 p3071 A83-43050
- Position angle variation of the major axis of some galaxies 20 p3061 A83-43378
- Super-Eddington luminosity characteristics of active galactic nuclei 21 p3230 A83-44439
- H2 densities and masses of the molecular clouds close to the galactic center 21 p3231 A83-44452
- VLBI observations of NGC 4151, Mk 231 and other galaxies with broad emission line nuclei 21 p3224 A83-44753
- Is the polarization of NGC1068 evidence for a non-thermal source? 21 p3235 A83-45058
- Two-dimensional spectrophotometry of the cores of X-ray luminous clusters 21 p3235 A83-45529
- The dynamics of dissipatively heated spherical accretion --- onto black holes 21 p3238 A83-45561
- High-resolution images of the Galactic Centre 22 p3375 A83-46560
- The galactic nucleus 22 p3375 A83-46561
- The high-ionization optical spectrum of the Seyfert galaxy Tololo 0109-383 22 p3379 A83-46568
- An infrared and optical investigation of galactic nuclei with compact radio sources 22 p3380 A83-46974
- Rotation curves and masses of galaxies 23 p3520 A83-47463
- Sources of extragalactic cosmic rays - Photons and neutrinos as probes 23 p3540 A83-47750
- Relativistic particles and gamma-rays in quasars and active galactic nuclei 23 p3540 A83-47761

Physical conditions in nucleus of Seyfert Galaxy NGC 7469. II - Spectrophotometric investigation 23 p3527 A83-48443

Rotation, mass and physical conditions in nucleus of spiral galaxy NGC 7537 23 p3527 A83-48444

Survey of OH masers at 1665 MHz. II - Galactic longitude 340 deg to the galactic centre 24 p3650 A83-48984

H₂O masers in the galactic plane. I - Longitude 340 deg to the galactic centre 24 p3650 A83-48985

A radio search for galactic center planetary nebulae 24 p3639 A83-49155

Planetary nebulae and Seyfert galaxies - Similarities and differences 24 p3640 A83-49159

Narrow-band photometry of normal and Seyfert galaxies 24 p3653 A83-49160

Gas in the nucleus of the Seyfert galaxy NGC 4151 24 p3653 A83-49161

Relative intensities of hydrogen lines in the spectra of quasars and the nuclei of Seyfert galaxies 24 p3653 A83-49164

High velocity HI in the inner 5 kpc of M31 24 p3640 A83-49205

3 micron spectroscopy of IRS7 towards the Galactic Centre 24 p3658 A83-49363

Active galactic nuclei - IUE results on continuum, emission and absorption lines 24 p3661 A83-49559

GALACTIC RADIATION

NT GALACTIC RADIO WAVES

Are classical Be stars sources of hard X-rays 01 p0116 A83-10343

Photometric observations of active nuclei 01 p0124 A83-10840

The far-infrared disk of M51 02 p0250 A83-11581

The 11-year variation of the isotropic and anisotropic flux of galactic cosmic rays 02 p0273 A83-11726

Modulation of the monoenergetic spectrum of galactic cosmic rays 02 p0276 A83-12417

Absorption of fluxes of galactic cosmic rays in the atmosphere during 1961-1980 02 p0208 A83-12418

A 1415 MHz survey of Seyfert and related galaxies. III 03 p0402 A83-13361

Neutral hydrogen in the vicinity of galactic radio sources - The supernova remnant W28 03 p0417 A83-13654

Diffuse galactic gamma-ray line emission from nucleosynthetic Fe-60, Al-26, and Na-22 - Preliminary limits from HEAO 3 03 p0439 A83-14210

Samples of the Milky Way --- isotopic abundances in Galactic cosmic rays 03 p0426 A83-14599

Galactic neutrino models 03 p0429 A83-14778

Cosmic ray origin above 10 to the 18th eV - Galactic or extragalactic 04 p0575 A83-14983

X-rays from quasars and active galaxies 04 p0555 A83-15822

The X-ray jets of Centaurus A and M87 04 p0558 A83-16369

The infrared emission from the elliptical galaxy NGC 1052 05 p0697 A83-16990

Gamma-ray emission from the galactic anticenter at MeV energies 05 p0698 A83-16995

Cosmic ray north-south anisotropy - The role of the interplanetary magnetic field 05 p0709 A83-17378

A list of ultraviolet excess galaxies 05 p0695 A83-17819

Transport and propagation of cosmic rays in galaxies. II - The effect of a galactic wind on the mean lifetime and age distribution of non-decaying cosmic rays 06 p0857 A83-18077

High frequency radio continuum observations of bright spiral galaxies 06 p0817 A83-18095

Ultraviolet spectrum of the sky background at different galactic latitudes 06 p0830 A83-18545

A study of the two-dimensional luminosity distribution of NGC 3379 06 p0833 A83-18855

Spectral and morphological investigation of galaxies with ultraviolet excess. IV 06 p0838 A83-19219

Optical variability and radio structure of extragalactic sources - Evidence of recurrent activity 06 p0838 A83-19224

Radio frequency observations of galactic X-ray sources 06 p0845 A83-19524

Spectrophotometry of four galaxies of high surface brightness 07 p1007 A83-20665

Ultrahigh-energy cosmic rays 07 p1039 A83-20851

Variable extragalactic objects - Identification and analysis of a complete sample to B = 21 07 p1007 A83-20938

Theoretical quasar emission-line profiles. I - Curve-of-growth effects on observed profiles 07 p1019 A83-21104

Optical and radio structure of the quasar PKS 0812 -- 02 07 p1019 A83-21105

A non-spherically symmetric model for absorption regions near quasars 07 p1019 A83-21107

IUE observations of Markarian 3 and 6 - Reddening and the nonstellar continuum 07 p1019 A83-21109

Cosmic rays from active galactic nuclei and in metagalactic space 07 p1040 A83-21152

Einstein observations of supernova remnants 08 p1174 A83-21855

A radio galaxy at high redshift undergoing strong stellar evolution 08 p1191 A83-23280

The Hubble sequence of masses 09 p1359 A83-24454

A simple model for the distribution of light in spherical galaxies 09 p1363 A83-24988

The gamma-ray colour of the Milky Way and the cosmic-ray electron density 09 p1363 A83-24992

On semi-degenerate equilibrium configurations of a collisionless self-gravitating Fermi gas 10 p1500 A83-25482

The diffuse gamma radiation from the local spiral arm 10 p1523 A83-25483

Imaging X-ray observations of Markarian 279 10 p1492 A83-25582

X-ray observations of the Antennae /NGC 4038/39/ 10 p1494 A83-25738

Large-scale variations in the 11-year cycle of cosmic rays 10 p1523 A83-26108

High-resolution radio and X-ray observations of the supernova remnant W28 10 p1497 A83-26375

Related galaxies with different redshifts 10 p1511 A83-26699

Discovery of X-ray bursts from GX 3+1 /4U 1744-26/ 10 p1515 A83-26732

CO emission in the outer Galaxy between longitudes 50 deg and 72 deg 10 p1516 A83-26753

Solar cycle variations of cosmic ray intensity and large-scale structure of the heliosphere 11 p1693 A83-27386

LMC and galactic extinction 11 p1682 A83-28278

Spectroscopic changes in the Seyfert galaxy NGC 3783 11 p1682 A83-28290

Active galaxies and the diffuse gamma-ray background 11 p1694 A83-28389

VLF ionosonde and long-distance propagation anomalies produced by galactic Cen X-4 X-ray burst in May 1979 12 p1753 A83-29430

A new installation for studying the sidereal anisotropy of cosmic rays 13 p1846 A83-30394

Stellar contributions to the hard X-ray galactic ridge 13 p1951 A83-31423

Time-resolved spectrophotometry of the emission lines in the galactic X-ray source H2252-035 13 p1940 A83-31427

The strength of Paschen-alpha in the Seyfert 1.9 galaxy V Zwicky 317 13 p1952 A83-31441

Analysis of synthesized dim galaxy images 14 p2096 A83-32035

A method for determining the age of cosmic rays in the Galaxy 14 p2116 A83-32598

Spatially extended narrow emission-line gas in the Seyfert galaxy NGC 4151 14 p2104 A83-33187

Extended soft X-ray emission from NGC 4151 14 p2104 A83-33188

The galactic gamma-ray source population 14 p2104 A83-33189

The X-ray properties of normal galaxies 15 p2252 A83-33599

Interstellar H-alpha emission along the galactic equator 15 p2257 A83-34095

The galaxy's 157 micron (C II) emission - Observations by means of a spectroscopic lunar occultation technique 15 p2246 A83-34125

Cosmic ray density gradients perpendicular to the solar equatorial plane 16 p2441 A83-36732

X-ray observations of 20 3CR radio galaxies and their environs 17 p2596 A83-37305

Mrk 744 and Mrk 1066 - Two Seyfert galaxies with strong absorption-line spectra 17 p2596 A83-37306

2-165 keV observations of active galaxies and the diffuse background 17 p2596 A83-37307

A multifrequency study of star formation in the blue compact dwarf galaxy I Zw 36 17 p2596 A83-37310

Rapid X-ray variability from the Seyfert 1 galaxy NGC 4051 17 p2598 A83-37344

Multicolor photometry of the galaxy Markarian 141, a component of a binary system 17 p2590 A83-37711

New galaxies with ultraviolet excess. IV 17 p2591 A83-37882

On Markarian 6 and the problem of the intermediate Sy 1.5 type 17 p2602 A83-37885

Measurements of galactic plane gamma-ray emission in the energy range 10-80 MeV 17 p2629 A83-37931

The elemental and isotopic composition of galactic cosmic ray nuclei 17 p2630 A83-38283

Observations of galaxies of high surface brightness at 102 MHz 17 p2594 A83-38550

Status and future of high energy diffuse gamma-ray astronomy 18 p2785 A83-39276

The observation of the galactic anticenter region by the balloon borne gamma-ray telescope Natalya-1 18 p2785 A83-39282

Low and medium energy gamma-ray astronomy - Present status and future aspects 18 p2756 A83-39283

Advances in gamma-ray line astronomy 18 p2756 A83-39293

Changes in interstellar atomic abundances from the galactic plane to the halo 18 p2768 A83-39630

The large scale dust distribution in the inner galaxy 18 p2770 A83-39654

Cosmic rays and magnetic fields in the galaxy 18 p2786 A83-39655

COS-B gamma-ray measurements and the large-scale distribution of interstellar matter 18 p2786 A83-39658

Positron annihilation radiation from Seyfert nuclei and the cosmic diffuse gamma-ray background 18 p2775 A83-39762

Hydrostatic-equilibrium distribution of cosmic rays and the magnetic field in the galactic halo 18 p2778 A83-40489

Is the 6-ms binary pulsar the remnant of a bright galactic X-ray source? 20 p3076 A83-43552

A method for determining the age of cosmic rays in the galaxy 21 p3245 A83-44506

A deep survey of galaxies 22 p3372 A83-46377

Central distribution of the near-infrared colours in two early-type spirals 22 p3375 A83-46572

X-ray, optical, and radio observations of the blue galaxy Butcher-Oemler 6 in the 3C 295 cluster 22 p3380 A83-46976

Implications of HEAO 3 data for the acceleration and propagation of galactic cosmic rays 22 p3390 A83-47003

A measurement of the IR flux from a radio lobe 23 p3526 A83-47871

The galactic extinction towards Maffei 1 24 p3643 A83-49360

CCD surface photometry of two southern active galaxies, NGC 1316 and 1052 24 p3659 A83-49378

Automated two-dimensional galaxy photometry 24 p3648 A83-50018

Galaxy number-magnitude counts 24 p3648 A83-50020

Broad emission lines of QSOs are consistent with rotating supermassive stars 24 p3670 A83-50112

GALACTIC RADIO WAVES

A search for short time variability in the radio emission from active galaxies 01 p0118 A83-10968

The jet in M87 02 p0250 A83-11580

Radio structures of Seyfert galaxies. IV - Jets in NGC 1068 and NGC 4151 05 p0697 A83-16985

The radio continuum morphology of NGC 4631 at 2.7 and 8.1 GHz 06 p0833 A83-18858

Further comments on the radio emission of the nuclei of spiral galaxies 06 p0836 A83-19203

Observations of the Coma Cluster of galaxies /A 1656/ at frequency 102.5 MHz 06 p0838 A83-19218

Observational constraints on galaxy-IGM interactions in the Virgo cluster 06 p0839 A83-19266

High-resolution radio observations of the Seyfert galaxy NGC 1068 07 p1018 A83-20944

Asymmetric structure in the nuclei of NGC 1275 and 3C 345 07 p1020 A83-21110

A survey of the distribution of wavelength 2.8 cm radio continuum in nearby galaxies. III - A small sample of irregular and blue compact galaxies 07 p1025 A83-21246

Infrared observations of the jet in M87 10 p1493 A83-25706

Observations of the interacting galaxy pair NGC 4490/85 13 p1959 A83-31754

Preliminary results of a galactic background survey at 45 MHz 14 p2099 A83-33246

Enhanced radio emission in merging galaxies 15 p2256 A83-34088

A study of the long-term variability in radio emission of active galaxies 15 p2262 A83-34529

Radio observations of interacting galaxies NGC 7714 (Markarian 538) - NGC 7715 (ARP 284, VV 51), and Radio quasar UB1 15 p2269 A83-34678

Galactic emission of OH at 1720 MHz as a tracer of spiral arms 18 p2769 A83-39652

Cosmic rays and magnetic fields in the galaxy 18 p2786 A83-39655

GALACTIC ROTATION

The galactic center - Structure and kinematics from 21-cm line measurements 01 p0125 A83-10941

Implications of gravitational interactions for the angular momenta of galaxies 01 p0126 A83-10965

Rotational properties of 23 Sb galaxies 02 p0250 A83-11579

Cosmic turbulence and the angular momenta of astronomical systems 02 p0252 A83-11598

- Dynamics of elliptical galaxies and other spheroidal components 02 p0246 A83-12189
- Optical study of the morphology and velocity field of the galaxy NGC 6946 02 p0259 A83-12518
- Orbital eccentricity in a logarithmic potential 02 p0249 A83-12924
- The dynamical evolution of clusters of nonpoint bodies 03 p0419 A83-13897
- Steady wave model of spiral galaxies and its application in cosmogony 04 p0549 A83-14995
- Triaxial equilibrium models for elliptical galaxies with slow figure rotation 05 p0697 A83-16987
- NGC 6503 - Rotation, mass and physical conditions in galaxy nucleus 06 p0824 A83-18017
- Statistics of structure and rotation parameters of disk galaxies 06 p0836 A83-19172
- The rotation of elliptical galaxies - An application of the theory of tidal torques 06 p0843 A83-19481
- A simple theory of how spiral galaxies acquire their principal global properties 06 p0843 A83-19483
- Radio structure and optical kinematics of the cD galaxy Hydra A /3C 218/ 07 p1019 A83-21108
- The effects of induced star formation on the evolution of the galaxy. II - The galactic ecosystem 07 p1020 A83-21117
- On the methods for determining galaxy velocity dispersions 07 p1009 A83-21236
- Galactic spiral structure and the gas motion near and beyond the corotation resonance 07 p1026 A83-21261
- Rotational velocities and central velocity dispersions for a sample of S0 galaxies 08 p1182 A83-23035
- Rotation, mass and excitation of the spiral galaxy NGC 3893 10 p1502 A83-25655
- The kinematic properties of faint elliptical galaxies 10 p1493 A83-25704
- Dynamics of yet more ellipticals and bulges 10 p1508 A83-26360
- The ratio of the unseen halo mass to the luminous disk mass in NGC 891 10 p1512 A83-26707
- Modeling of steady, rotational, transonic winds from rotating stars and galaxies 10 p1512 A83-26708
- Orbital configurations for gas in elliptical galaxies 10 p1497 A83-26751
- Dynamic effects of the angular asymmetry of stellar motions in galaxies 10 p1516 A83-26901
- Clarification of the angular momentum/mass relation $J = pM$ -squared/ for astronomical objects 11 p1669 A83-27699
- Intergalactic and galactic magnetic fields - An updated test 11 p1679 A83-27990
- Are there correlations between radio and optical axes of radio galaxies 12 p1785 A83-28996
- Global shearing modes of galactic disks 12 p1794 A83-29079
- Investigation of the outer regions of the galactic halo 13 p1946 A83-30383
- Stellar orbits in a triaxial galaxy. I - Orbits in the plane of rotation 13 p1950 A83-31411
- Roche's limit in a galaxy. II - The effects of rotation 13 p1953 A83-31558
- Rotation curve of the edge-on spiral galaxy NGC 5907: disc and halo masses 13 p1957 A83-31698
- The kinematics and structure of the Galaxy at high galactic latitudes 14 p2101 A83-31834
- Measurement of unambiguous rotation measures of extragalactic sources 14 p2098 A83-33063
- Dark matter in spiral galaxies 14 p2103 A83-33100
- The masses of spiral galaxies 14 p2107 A83-33242
- Neutral hydrogen in the Small Magellanic Cloud 14 p2099 A83-33243
- The rotation curve of our Galaxy - How well do we know it? 14 p2107 A83-33245
- Estimating the tumble rates of galaxy halos 15 p2257 A83-34090
- Mass model of spiral galaxies disk 15 p2262 A83-34535
- The virial mass of the nucleus of M32 15 p2263 A83-34559
- Unusual rotation curve of the Galaxy NGC 2814 15 p2269 A83-34677
- A survey of galaxy redshifts. IV - The data 16 p2423 A83-35972
- The rotation of spiral galaxies 16 p2428 A83-36014
- Can secondary infall produce flat rotation curves? 17 p2596 A83-37314
- Drift-rotational gravitational instability in galaxies 17 p2600 A83-37646
- Numerical investigation of the generation of global spiral structure in interacting galaxies 17 p2603 A83-37889
- Stochastic self-propagating star formation in three-dimensional disk galaxy simulations 17 p2604 A83-37907
- Spiral structure and gas motion in M81 17 p2610 A83-38547
- The stability of a differentially rotating disk of stars 17 p2610 A83-38551
- Kinematics, dynamics and structure of the Milky Way; Proceedings of the Workshop on the Milky Way, Vancouver, British Columbia, Canada, May 17-19, 1982 18 p2767 A83-39626
- On the local standard of rest --- comoving with young objects in gravitational field of spiral galaxies 18 p2768 A83-39633
- Determination of AR ($R =$ distance to galactic center) --- product of Oort's rotational constant and distance to Galactic center 18 p2758 A83-39639
- The rotation curve of the Galaxy 18 p2770 A83-39659
- A model for the galaxy with rising rotational velocity 18 p2770 A83-39660
- Globular clusters and the potential well of the Galaxy 18 p2771 A83-39669
- NGC 3200 - Is this what our Galaxy is like? 18 p2771 A83-39672
- Elliptical galaxies - Can rotation be effective in determining their shapes? 18 p2775 A83-39748
- Dynamics of the stellar component of the bulge of M31 19 p2918 A83-41617
- The noninteracting spiral pair, NGC 450/UGC 807 20 p3060 A83-43048
- The cluster of galaxies SC0316-44 - Does it rotate? 21 p3228 A83-44402
- Periodic orbits in elliptical galaxies 21 p3223 A83-44445
- Neutral hydrogen observations of double spiral galaxies. II NGC 3958/3963, NGC 5289/5290, NGC 5673/IC 1 029, NGC 5107/5112 21 p3226 A83-44982
- Rotation curves and masses of galaxies 23 p3520 A83-47463
- Rotation, mass and physical conditions in nucleus of spiral galaxy NGC 7537 23 p3527 A83-48444
- Gas in the nucleus of the Seyfert galaxy NGC 4151 24 p3653 A83-49161
- Transfer of angular momentum in a galactic disk by the interaction of clouds of interstellar gas 24 p3653 A83-49166
- Internal kinematics and dynamics of galaxies; Proceedings of the Symposium, Universitede Franche-Comte, Besancon, France, August 9-13, 1982 24 p3654 A83-49201
- Systematics of H II rotation curves 24 p3654 A83-49202
- H I velocity fields and rotation curves 24 p3654 A83-49203
- Comparison of global 21 cm velocity profiles with H-alpha rotation curves 24 p3640 A83-49206
- H I observations of the irregular galaxy IC 10 24 p3640 A83-49207
- The CO rotation curve of the Milky Way - Accuracy and implications 24 p3654 A83-49209
- Rotation curve and mass model for the edge-on galaxy NGC 5907 24 p3641 A83-49211
- Mass distribution and dark halos 24 p3654 A83-49215
- Relation between star formation and angular momentum in spiral galaxies 24 p3655 A83-49225
- Spiral structure - Density waves or material arms? 24 p3656 A83-49231
- Attacking the problem of a selfconsistent bar --- stellar orbits in barred galaxies 24 p3641 A83-49239
- Dynamics of early-type galaxies 24 p3657 A83-49246
- New phenomena in triaxial stellar systems 24 p3641 A83-49250
- The manifold of elliptical galaxies 24 p3657 A83-49265
- Galaxies rotation curves - A catalogue 24 p3645 A83-49845
- A preliminary investigation of proper motions of faint stars in the Hazard 8hr region 24 p3647 A83-50009
- GALACTIC STRUCTURE**
- On the widths of dust layers in galaxies 01 p0119 A83-10266
- Investigation of the fine structure of radio sources 01 p0124 A83-10841
- The theoretical expected galactic distribution of WR runaway stars 01 p0125 A83-10935
- Multiperture photometry of galaxies. II - Near-infrared observations of six isolated objects 01 p0117 A83-10940
- The galactic center - Structure and kinematics from 21-cm line measurements 01 p0125 A83-10941
- Bulge X-ray sources and Novae in M31 01 p0118 A83-10951
- Accurate optical positions of M 82 knots 01 p0118 A83-10954
- Clusters of galaxies --- optical observation data 01 p0127 A83-11290
- Rotational properties of 23 Sb galaxies 02 p0250 A83-11579
- The jet in M87 02 p0250 A83-11580
- Primary nucleosynthesis in the galactic disk 02 p0252 A83-11599
- VLA observations of the Seyfert galaxy NGC 1068 02 p0252 A83-11609
- The halos of rich clusters of galaxies. I - An infall model for the Coma Cluster 02 p0254 A83-12102
- Einstein Observatory solid state spectrometer observations of M87 and the Virgo cluster 02 p0254 A83-12104
- X-ray spectroscopy of the galaxy M87 - Radiative accretion of the hot plasma halo 02 p0254 A83-12105
- The nature of the central parsec of the Galaxy 02 p0255 A83-12114
- Abundances in five nearby galactic H II regions from infrared forbidden lines 02 p0255 A83-12118
- Stellar populations in the Galaxy 02 p0258 A83-12179
- Gas in the galactic halo 02 p0258 A83-12184
- Extranuclear clues to the origin and evolution of activity in galaxies 02 p0258 A83-12190
- The galaxy NGC 1566 - Distribution and kinematics of the ionized gas 02 p0260 A83-12519
- Neutral hydrogen in binary and multiple galaxies 02 p0248 A83-12908
- UBV-/H-beta/ photometry of luminous stars between l equals 335 deg and l equals 6 deg 03 p0402 A83-13365
- The problem of deriving galactic spiral structure from the stellar velocity field - Statistical modeling 03 p0418 A83-13657
- The galactic distribution, birthrate, and luminosity evolution of pulsars 03 p0418 A83-13658
- On the history of the wave theory of spiral structure 03 p0418 A83-13675
- Flocculent and grand design spiral structure in field, binary and group galaxies 03 p0420 A83-13941
- Flocculent and grand design spiral arm structure in cluster galaxies 03 p0420 A83-13942
- A mass estimate for the companion to the 'Cartwheel' galaxy 03 p0421 A83-13953
- A comparison of galaxy images on new and old POSS prints 03 p0409 A83-14137
- The relationships between morphological type and quantitative measures in the cluster environment 03 p0421 A83-14140
- An optical and radio investigation of the radio galaxy 3C 305 03 p0423 A83-14186
- On gaseous disks in Seyfert 1 nuclei 03 p0423 A83-14187
- Photographic surface photometry of the Milky Way. IV - The Northern Milky Way in the ultraviolet spectral region 03 p0430 A83-14798
- Monte-Carlo simulations of galaxy systems. IV - Static properties for galaxies in supercluster cells. V - Computer models of galaxy fields 04 p0545 A83-14987
- New high resolution radio observations of NGC 4258. III - VLA and WSRT observations of the anomalous arms 04 p0545 A83-15032
- NGC 1961 - Stripping of a supermassive spiral galaxy 04 p0550 A83-15036
- The Galactic abundance gradient from supernova remnant observations 04 p0550 A83-15038
- Photographic photometry of galaxies using the INMP. I - The lenticulars NGC404 and NGC524 --- Interactive Numerical Mapping Package 04 p0546 A83-15046
- The quasar B2 1320 plus 29 04 p0551 A83-15051
- V Zw 311 - The once and future cD 04 p0551 A83-15602
- A spectroscopic investigation of the nebulosity around low-luminosity quasars 04 p0551 A83-15604
- Further examples of companion galaxies with discordant redshifts and their spectral peculiarities 04 p0552 A83-15606
- Structure of the M33 nucleus 04 p0552 A83-15611
- Supergiants and the galactic metallicity gradient. I - 27 late-type supergiants in the inner-arm regions 04 p0553 A83-15623
- The distribution of infrared obscuration in NGC 7331 - Evidence for a massive molecular ring 04 p0555 A83-15649
- A method of investigating the structure of the observed field of the Galaxy and the metagalaxy 04 p0547 A83-15773
- The X-ray jets of Centaurus A and M87 04 p0558 A83-16369
- Giant voids in the universe 05 p0695 A83-16845

The galactic content of groups of galaxies
05 p0696 A83-16982

Radio structures of Seyfert galaxies. IV - Jets in NGC 1068 and NGC 4151
05 p0697 A83-16985

VLBI observations of the nucleus and jet of M87
05 p0697 A83-16989

The warping of disk galaxies. I - Theory
05 p0697 A83-16992

The equilibrium of a galactic bar. II - Stellar-dynamical counterparts of the s-type Riemann ellipsoids
05 p0697 A83-16993

Stable polar gas disks in triaxial S0 galaxies
05 p0700 A83-17026

NGC 6503 - Rotation, mass and physical conditions in galaxy nucleus
06 p0824 A83-18017

Kinematics of elliptical-like galaxies with dust lanes
06 p0826 A83-18157

The Seyfert 1 galaxy NGC 4593. I - Variability of the UV spectrum and physical conditions in the broad line emitting region
06 p0826 A83-18161

A 2.2-micron map of NGC 5128
06 p0827 A83-18171

Is there a ring around Milky Way
06 p0828 A83-18419

Neutral hydrogen in two extremely isolated galaxies
06 p0829 A83-18534

The galaxy Markaryan 348
06 p0830 A83-18779

The fine structure of 3C 84 and 3C 345 at 18-cm wavelength
06 p0819 A83-18780

A search for extended structures near the radio sources 3C 120 and 3C 273
06 p0831 A83-18791

The nature of the galactic H I superhells
06 p0831 A83-18793

0351+026 - A QSO spawned by interacting galaxies
06 p0832 A83-18851

Statistics of structure and rotation parameters of disk galaxies
06 p0836 A83-19172

Morphology of compact galaxies. II
06 p0836 A83-19202

Spectral observations of M 82
06 p0822 A83-19204

Galaxies with very elongated shapes
06 p0837 A83-19205

Spectral and morphological investigation of galaxies with ultraviolet excess. IV
06 p0838 A83-19219

Optical variability and radio structure of extragalactic sources - Evidence of recurrent activity
06 p0838 A83-19224

Relaxation and tidal stripping in rich clusters of galaxies. I - Evolution of the mass distribution
06 p0839 A83-19267

Massive neutrinos in large-scale gravitational clustering
06 p0839 A83-19270

Preferred orbit planes in the gravitational field of a tumbling spheroidal galaxy
06 p0843 A83-19480

The rotation of elliptical galaxies - An application of the theory of tidal torques
06 p0843 A83-19481

Gravitationally induced spurs in spiral galaxies - An example in M31
06 p0843 A83-19488

The H I absorption in NGC 5128 /Centaurus A/
06 p0845 A83-19522

Radio studies of galactic structure
06 p0846 A83-19536

The peculiar radio galaxy 3C 433
07 p1010 A83-19855

Inner ring structures in galaxies as distance indicators. III - Distances to 453 spiral and lenticular galaxies
07 p1013 A83-20080

Internal motions in planetary nebulae - NGC 7354, I 289 and Hu 1-2
07 p1014 A83-20570

New observations of positive high velocity clouds
07 p1014 A83-20572

The structure of spiral arm S6 in the Andromeda Nebula
07 p1007 A83-20666

Disc stability and halo mass
07 p1016 A83-20768

Tidal distension in protostructures - The shapes of galaxies and systems of galaxies
07 p1017 A83-20937

A distance scale from the infrared magnitude/H I velocity-width relation. IV - The morphological type dependence and scatter in the relation; the distances to nearby groups
07 p1019 A83-21101

Theoretical quasar emission-line profiles. I - Curve-of-growth effects on observed profiles
07 p1019 A83-21104

A non-spherically symmetric model for absorption regions near quasars
07 p1019 A83-21107

Radio structure and optical kinematics of the cD galaxy Hydra A /3C 218/
07 p1019 A83-21108

Asymmetric structure in the nuclei of NGC 1275 and 3C 345
07 p1020 A83-21110

The spatial distribution of H II regions in NGC 4321
07 p1020 A83-21111

Time evolution of disk galaxies undergoing stochastic self-propagating star formation
07 p1020 A83-21112

The molecular gas distribution in M51
07 p1020 A83-21113

Absorption by halo gas in the direction of M13
07 p1020 A83-21118

Abnormal extinction and dust properties in M 16, M 17, NGC 6357 and the Ophiuchus dark cloud
07 p1025 A83-21241

Full-implicit continuous eulerian scheme in the spherical coordinates and its applications to solar phenomena --- from radio galaxies
08 p1191 A83-22034

Hierarchical merging and the structure of elliptical galaxies
08 p1181 A83-23027

The L varies as sigma to the n power relation for the bulge components of disk galaxies
08 p1181 A83-23032

Infrared mapping and UBVRI photometry of the spiral galaxy NGC 1566
08 p1175 A83-23033

A clamshell for Blandford-Rees jets --- from radio galaxies
08 p1181 A83-23034

Rotational velocities and central velocity dispersions for a sample of S0 galaxies
08 p1182 A83-23035

Optical emission in the radio lobes of radio galaxies. II - New observations of 21 radio lobes
08 p1175 A83-23036

A bisymmetric spiral magnetic field and the spiral arms in our Galaxy
08 p1182 A83-23041

The galactic spheroid
08 p1182 A83-23042

Infrared photometry of the halo of M87
08 p1176 A83-23080

Color gradients in galactic spheroids. II - Gradient as a function of luminosity and morphology
09 p1356 A83-23317

Systems of galaxies --- properties, structure and evolution
09 p1358 A83-23914

RGU photometry of a southern starfield near the galactic centre /SA 158/
09 p1354 A83-24515

Velocity field and physical conditions in the active lenticular galaxy NGC 3998
09 p1363 A83-24989

New light on faint stars. III - Galactic structure towards the South Pole and the Galactic thick disc
09 p1363 A83-24991

A quasi-stable stellar system with prolate inner and oblate outer parts
09 p1363 A83-25001

Models for elliptical galaxies. I - Oblate spheroids with anisotropy. II - Oblate spheroids with realistic rotation curves
09 p1364 A83-25004

An absorption feature and filamentary structures in the central galaxy of the Centaurus cluster, NGC 4696
09 p1365 A83-25296

RGU photometry in a field of the galactic bulge
10 p1493 A83-25662

Inner ring structures in galaxies as distance indicators. IV - Distances to several groups, clusters, the Hercules supercluster, and the value of the Hubble constant
10 p1502 A83-25701

Anisotropic velocity dispersions in spherical galaxies
10 p1502 A83-25705

Infrared observations of the jet in M87
10 p1493 A83-25706

Is there nonluminous matter in dwarf spheroidal galaxies
10 p1504 A83-25740

Some implications of nonluminous matter in dwarf spheroidal galaxies
10 p1504 A83-25741

Resolution in normal galaxies
10 p1496 A83-25856

Highly compact structures in galactic nuclei and quasars
10 p1496 A83-25858

Can galactic halos be made of axions
10 p1507 A83-26270

Axions and the evolution of structure in the universe
10 p1507 A83-26271

The dynamics and fueling of active nuclei
10 p1508 A83-26359

Dynamics of yet more ellipticals and bulges
10 p1508 A83-26360

The role of the gas in propagating star formation
10 p1508 A83-26363

VLBI observations of the nucleus of Centaurus A
10 p1497 A83-26403

CO emission and the optical disk in the giant Sc galaxy M101
10 p1511 A83-26405

Flocculent and grand design spiral galaxies in groups - Time scales for the persistence of grand design spiral structures
10 p1512 A83-26705

Effects of environment on neutral hydrogen distribution for disk galaxies in the Virgo Cluster area
10 p1512 A83-26706

The ratio of the unseen halo mass to the luminous disk mass in NGC 891
10 p1512 A83-26707

One-dimensional periodic flows with a shock transition - Application to the density wave theory of spiral structure
10 p1512 A83-26711

Orbital configurations for gas in elliptical galaxies
10 p1497 A83-26751

Sensitive mapping of E and S0 galaxies in search of H I content differences between supernovae and non-supernovae producing galaxies
11 p1668 A83-27104

Globular cluster orbits and the galactic mass distribution
11 p1676 A83-27109

H II regions in M33. I - Radio and H-alpha observations of the H II complex NGC595
11 p1669 A83-27679

Further radio observations of the supernova remnant in NGC 4449 and a candidate remnant in NGC 4656
11 p1678 A83-27697

Cluster collapse and radio source morphology
11 p1679 A83-27993

Regular strings of H II regions and superclouds in spiral galaxies - Clues to the origin of cloudy structure
11 p1680 A83-28256

Hydromagnetic wave heating of the galactic corona
11 p1681 A83-28262

On the energy distribution function for a one-dimensional gravitational system
11 p1682 A83-28293

The gas distribution in the central region of the Galaxy. IV A survey of neutral hydrogen in the region l = 349 to 13 deg, b = 10 to 10 deg, and absolute value of v less than 350 km/s
12 p1789 A83-28864

On the origin of the solar system and the exceptional position of the sun in the galaxy
12 p1792 A83-29055

Large-scale flow of interstellar gas in galactic spiral waves - Effects of thermal balance and self-gravitation
12 p1793 A83-29065

The supersonic nozzles of the galaxies
12 p1795 A83-29364

Dissipative structures in galaxies
12 p1795 A83-29378

Further evidence for M87's massive, dark halo
13 p1950 A83-31407

Thermal conduction and heating by nonthermal electrons in the X-ray halo of M87
13 p1950 A83-31408

The radial distribution of H II regions in spiral galaxies
13 p1950 A83-31410

Stellar orbits in a triaxial galaxy. I - Orbits in the plane of rotation
13 p1950 A83-31411

An exact solution for an isothermal gas cloud with fast differential rotation
13 p1953 A83-31561

The galaxy NGC 1365
13 p1941 A83-31577

The Horologium-Reticulum supercluster of galaxies
13 p1956 A83-31682

An arcsec radio jet in NGC 1275 (Perseus A)
13 p1957 A83-31692

Rotation curve of the edge-on spiral galaxy NGC 5907: disc and halo masses
13 p1957 A83-31698

A dust lane in NGC 6251
13 p1958 A83-31714

Pairs of spiral galaxies with magnitude differences greater than one
13 p1943 A83-31736

Structure of the local interstellar medium and the line of sight to Alpha Oph
13 p1960 A83-31790

The kinematics and structure of the Galaxy at high galactic latitudes
14 p2101 A83-31834

An investigation of the star cluster NGC 6913 (M 29)
14 p2095 A83-31835

Density gradients for disc- and halo-stars in the direction of the globular cluster NGC 7006
14 p2103 A83-33056

Spatially extended narrow emission-line gas in the Seyfert galaxy NGC 4151
14 p2104 A83-33187

The masses of spiral galaxies
14 p2107 A83-33242

Neutral hydrogen related to Gould's belt
14 p2109 A83-33275

A method for estimating the mass of the central bodies in active galaxy nuclei and quasars
15 p2253 A83-33704

Nonlinear effects in a gravitating plasma disk subject to a poloidal magnetic field
15 p2254 A83-33721

The galaxy as fundamental calibrator of the extragalactic distance scale. I - The basic scale factors of the galaxy and two kinematic tests of the long and short distance scales
15 p2255 A83-34076

CCD photometry of Abell clusters. II - Surface photometry of 249 cluster galaxies
15 p2255 A83-34077

Effects of galaxy collisions on the structure and evolution of galaxy clusters. I - Mass and luminosity functions and background light
15 p2255 A83-34078

Enhanced radio emission in merging galaxies
15 p2256 A83-34088

Estimating the tumble rates of galaxy halos
15 p2257 A83-34090

On the equilibrium configurations of prolate, axisymmetric stellar systems
15 p2257 A83-34091

Inversion symmetry of radio lobes in extragalactic sources
15 p2261 A83-34384

Comparison between 'normal' double and single galaxies
15 p2246 A83-34445

- A new ring galaxy in the Abell 1631 cluster of galaxies 15 p2247 A83-34504
- Pressure collimation of supersonic radio jets 15 p2267 A83-34620
- Unusual rotation curve of the Galaxy NGC 2814 15 p2269 A83-34677
- Theory of the stability of flat subsystems of galaxies 15 p2269 A83-34679
- Dissipative effects in the gaseous subsystems of flat galaxies 15 p2271 A83-34754
- Surface photometry of edge-on galaxies. III - Luminosity distributions in eight galaxies 16 p2422 A83-35676
- The new Milky Way 16 p2423 A83-35762
- The radio structure of Sgr A 16 p2431 A83-36676
- Effective H I diameters of galaxies 16 p2432 A83-36695
- Morphology of optical forms of N galaxies 17 p2588 A83-37308
- The transitory nature of the filaments in NGC 5128 (Centaurus A) 17 p2596 A83-37309
- Analysis of box orbits in a triaxial galaxy 17 p2588 A83-37312
- The stability of a magnetically confined radio jet 17 p2596 A83-37313
- Radio continuum observations of the bar of NGC 1097 17 p2588 A83-37347
- Multicolor photometry of bright patches in the galaxy NGC 4303 17 p2589 A83-37655
- The dynamics of rich clusters of galaxies. II - The Perseus cluster 17 p2591 A83-37776
- Structure and stellar content of dwarf elliptical galaxies 17 p2602 A83-37781
- Numerical investigation of the generation of global spiral structure in interacting galaxies 17 p2603 A83-37889
- Stellar and gaseous dynamics of triaxial galaxies 17 p2592 A83-37905
- Stochastic self-propagating star formation in three-dimensional disk galaxy simulations 17 p2604 A83-37907
- Simulations of galaxy mergers. II 17 p2593 A83-38244
- The distribution of violently relaxed matter in galaxies 17 p2609 A83-38418
- Discovery of a Wolf-Rayet star in NGC 6822 17 p2594 A83-38428
- Observable properties of non-axisymmetric galaxies. I 17 p2595 A83-38581
- Geometrical parameters 17 p2611 A83-38588
- A new model for barred spiral galaxies 17 p2612 A83-38599
- Why is M87 jet one sided in appearance? 17 p2612 A83-38828
- Shocks in spiral galaxies 17 p2612 A83-38828
- On a general fluid dynamical theory of discrete unstable spiral modes in disk-shaped galaxies 18 p2764 A83-39008
- Colliding and merging galaxies. II - S0 galaxies with polar rings 18 p2767 A83-39589
- Kinematics, dynamics and structure of the Milky Way; Proceedings of the Workshop on the Milky Way, Vancouver, British Columbia, Canada, May 17-19, 1982 18 p2767 A83-39626
- New trends in Milky Way research 18 p2767 A83-39627
- Local galactic structure and velocity field 18 p2768 A83-39635
- The large-scale structure of atomic hydrogen --- in Galaxy 18 p2768 A83-39641
- Large-scale structure of H I in the outer Galaxy 18 p2768 A83-39642
- More H I shells and supershells or a new explanation of 'noncircular motions' in the Galaxy 18 p2768 A83-39643
- Low latitude absorption spectra 18 p2768 A83-39644
- The distribution of molecular clouds in the Galaxy 18 p2769 A83-39645
- Kinematics of molecular clouds - Evidence for agglomeration in spiral arms 18 p2769 A83-39646
- The distribution of HII regions in the outer Galaxy 18 p2769 A83-39649
- Galactic emission of OH at 1720 MHz as a tracer of spiral arms 18 p2769 A83-39652
- Galactic HII regions, anomalous 1720 MHz OH clouds and spiral structure in the Galaxy 18 p2769 A83-39653
- The large scale dust distribution in the inner galaxy 18 p2770 A83-39654
- The distribution of stars in the Galaxy 18 p2770 A83-39656
- Optical spiral structure between $l = 30$ deg and 70 deg --- of Milky Way Galaxy 18 p2770 A83-39657
- A model for the galaxy with rising rotational velocity 18 p2770 A83-39660
- Cloud-particle galactic gas dynamics and star formation 18 p2770 A83-39662
- Spiral modes and the Milky Way 18 p2770 A83-39663
- A modal approach to spiral structure - Two examples --- of galaxy models 18 p2770 A83-39664
- Molecular clouds in spiral galaxies 18 p2771 A83-39671
- Elliptical galaxies - Can rotation be effective in determining their shapes? 18 p2775 A83-39748
- Hydrodynamic and turbulent motions in the galactic disk 18 p2775 A83-39755
- What is a spiral galaxy? 18 p2775 A83-39756
- Jet activity in the Seyfert galaxy MKN 335 18 p2777 A83-39779
- Double galaxies - Redshift measurements, error analysis, and mean mass/luminosity ratio 18 p2778 A83-40485
- A modification of the Newtonian dynamics as a possible alternative to the hidden mass hypothesis 19 p2917 A83-41606
- A modification of the Newtonian dynamics - Implications for galaxies 19 p2917 A83-41607
- Scalloped disk galaxies - A Kelvin-Helmholtz instability? 19 p2918 A83-41618
- The structure of the Carina dwarf elliptical galaxy 20 p3064 A83-42319
- Simulations of galaxy mergers - Cannibalism and dynamical friction 20 p3066 A83-42431
- Photometry of resolved galaxies. III - GR 8 20 p3059 A83-42436
- The magellanic irregular galaxy DDO 155 20 p3067 A83-42440
- Alignment of faint galaxy images - Cosmological distortion and rotation 20 p3070 A83-43036
- Does the association of quasars with galaxies depend on the morphological type of galaxy? 20 p3071 A83-43042
- cD galaxy dynamics and an aged ridge (jet) in 3C 338 20 p3071 A83-43050
- The Riemann disks. II - Stability 20 p3071 A83-43052
- Spiral gravitational potentials and the mass growth of molecular clouds 20 p3071 A83-43053
- Stellar-statistical investigations in the vicinity of the sun 20 p3075 A83-43381
- Self-modulation and envelope solitons of spiral density waves --- in approximation of galactic structure 20 p3075 A83-43386
- Luminosity distribution in galaxies. II - A study of accidental and systematic errors with application to NGC 3379 21 p3222 A83-44118
- The nature of the nebula around BL Lacertae 21 p3222 A83-44401
- The quick convolution of galaxy profiles, with application to power-law intensity distributions 21 p3234 A83-44764
- Focusing of high-Mach number jets by an ambient medium --- in radio galaxies 21 p3235 A83-45530
- Shell structure in NGC 5128 22 p3372 A83-45627
- Size distributions of H II regions in galaxies. I - Irregular galaxies 22 p3372 A83-46380
- Three-dimensional numerical model of the formation of large-scale structure in the Universe 22 p3378 A83-46539
- Some constraints on the color-magnitude diagram of giants in the galactic spheroid 22 p3382 A83-46991
- The tensor virial theorem for subsystems --- with application to elliptical galaxies 23 p3519 A83-47452
- The large-scale structure of the universe 23 p3526 A83-47825
- A radio search for galactic center planetary nebulae 24 p3639 A83-49155
- Internal kinematics and dynamics of galaxies; Proceedings of the Symposium, Universit  de Franche-Comte, Besancon, France, August 9-13, 1982 24 p3654 A83-49201
- Systematics of H II rotation curves 24 p3654 A83-49202
- Vertical motion and the thickness of HII disks - Implications for galactic mass models 24 p3654 A83-49213
- Do spiral galaxies have a variable disk thickness? 24 p3654 A83-49214
- Mass distribution and dark halos 24 p3654 A83-49215
- Distribution and motions of atomic hydrogen in lenticular galaxies 24 p3655 A83-49219
- Theory of spiral structure --- of Milky Way Galaxy 24 p3655 A83-49221
- Quasi-stationary spiral structure in galaxies 24 p3655 A83-49222
- Model calculations on the large scale distribution of bubbles in galaxies 24 p3655 A83-49226
- Velocity structures in the vertical extensions of spiral arms 24 p3655 A83-49227
- Possible evidence for Lin's three-wave interaction mechanism at corotation in the galaxy NGC 1566 24 p3655 A83-49229
- Conflicts and directions in spiral structure --- in disk galaxies 24 p3656 A83-49232
- Disk stability --- and barred galaxies 24 p3641 A83-49234
- Numerical experiments on the response mechanism of barred spirals 24 p3656 A83-49237
- Onset of stochasticity in barred spirals 24 p3641 A83-49238
- The barred galaxy NGC 7741 24 p3656 A83-49243
- Hydrodynamical models of offcentered barred spirals 24 p3657 A83-49244
- Formation of rings and lenses --- in disk galaxies 24 p3657 A83-49245
- Dynamics of early-type galaxies 24 p3657 A83-49246
- Models of ellipticals and bulges 24 p3641 A83-49247
- Dust and gas in triaxial galaxies 24 p3657 A83-49255
- Observational evidence for mergers --- of galaxies 24 p3657 A83-49256
- Centaurus A - The nearest active galaxy 24 p3660 A83-49444
- Ap stars and galactic structure 24 p3663 A83-49607
- A program for investigating the kinematics of stars in the main meridional section of the Galaxy 24 p3645 A83-49637
- Standard photometric diameters of galaxies 24 p3645 A83-49842
- Narrow-band photometry of G and K stars near the North Galactic Pole 24 p3645 A83-49851
- Radial velocities for early type stars in six galactic regions 24 p3664 A83-49854
- Application of star count data to studies of galactic structure 24 p3664 A83-49885
- The detection of variable stars in the south galactic cap 24 p3647 A83-50006
- Intensity estimation from pixel data --- for stellar and galactic magnitude determination 24 p3648 A83-50013
- Fast shape analysis of galaxies 24 p3648 A83-50019
- Galactic helium and stellar population colors 24 p3666 A83-50051
- Poor evidence of merging in loose galaxy groups 24 p3668 A83-50088

GALAXIES

NT ANDROMEDA GALAXIES

NT BARRED GALAXIES

NT DISK GALAXIES

NT DWARF GALAXIES

NT ELLIPTICAL GALAXIES

NT GALACTIC CLUSTERS

NT MAGELLANIC CLOUDS

NT MILKY WAY GALAXY

NT RADIO GALAXIES

NT SEYFERT GALAXIES

NT SPIRAL GALAXIES

NT VIRGO GALACTIC CLUSTER

Data retrieval in the metacatalogue of galaxies

01 p0115 A83-10157

The compiled catalogue of galaxies in machine-readable form and its statistical investigation

01 p0115 A83-10158

On the widths of dust layers in galaxies

01 p0119 A83-10266

Markarian 914 is a galactic object, lick H-alpha 233

01 p0118 A83-10969

Double galaxy investigations. I - Observations

02 p0245 A83-11993

Double galaxy investigations. II - The redshift periodicity in optically observed pairs

02 p0246 A83-12106

Molecular clouds in galaxies

02 p0259 A83-12193

Null influence of possible local extragalactic perturbations on tests of redshift-distance laws

04 p0550 A83-15047

Quasars near companion galaxies - A comment on Arp's statistics

04 p0555 A83-15647

Density of quasars around companion galaxies

04 p0555 A83-15648

Intermediate band filter spectrophotometry of bright galaxies. II - Data reductions

05 p0694 A83-17663

A list of ultraviolet excess galaxies

05 p0695 A83-17819

Cosmic density wave and its observable vestiges - Maximum scale of inhomogeneities in the distribution of galaxies and features in the distribution of absorption-line redshifts of quasars

05 p0702 A83-17850

Distances of galaxies from the apparent size distribution of Dark Clouds. II - NGC 224, NGC 2841 and NGC 7331

05 p0695 A83-17861

The 'black' regions of the Universe
06 p0830 A83-18776

Physical conditions in interacting galaxies, in components of isolated pairs, and in isolated galaxies
06 p0838 A83-19220

Observations of galaxies with ultraviolet continuum at 102 MHz
06 p0823 A83-19221

Observations of the galaxies Markaryan 673 and 686
07 p1014 A83-20653

Long-period variables in the galactic bulge - Evidence for a young super-metal-rich population
08 p1182 A83-23043

H I line studies of galaxies. II - The 21-cm-width as an extragalactic distance indicator
09 p1359 A83-24453

Calibrated B, V surface photometry of X-ray cD galaxies
09 p1360 A83-24469

Estimation of reddening at low galactic latitudes from the Lick galaxy counts
09 p1363 A83-24990

On estimates of the galaxy correlation function
09 p1355 A83-25007

On the deconvolution of brightness profiles of galaxies from seeing - Application to NGC 3379
10 p1494 A83-25834

Markarian galaxies and voids in the galaxy distribution
10 p1507 A83-26352

H I absorption in the peculiar galaxy UGC 6081
10 p1516 A83-26750

Observations of low redshift H I in Stephan's Quintet
11 p1668 A83-27105

An atlas of H II regions in 125 galaxies
11 p1668 A83-27107

Spectroscopic survey of southern compact and bright-nucleus galaxies. V
11 p1680 A83-28257

Analysis of optical imagery for Seyfert's Sextet and VV 172
12 p1784 A83-28880

Redshifts for 115 galaxies near the equator
12 p1787 A83-29176

21-cm observations of galaxies in groups and multiplets
12 p1787 A83-29178

A search for large-scale lineations in the apparent distribution of galaxies
12 p1788 A83-29490

A survey of galaxy redshifts. V - The two-point position and velocity correlations
13 p1949 A83-31401

The statistics of gravitational lenses - Apparent changes in the luminosity function of distant sources due to passage of light through a single galaxy
13 p1949 A83-31403

A variable radio source in the clumpy irregular galaxy Markarian 297
13 p1952 A83-31442

Extended H I emission associated with the low-surface-brightness companions of the S0 galaxy NGC 4026
13 p1956 A83-31681

Infrared colors of a complete sample of faint galaxies
13 p1957 A83-31694

Surface photometry of NGC 4656/4657
15 p2245 A83-33829

Effects of spherically-symmetric gravitational lenses produced by galaxies and clusters
15 p2262 A83-34538

Two-colour photometry of a sample of faint galaxies
15 p2248 A83-34606

CO observations of the galaxies in the Leo triplet - NGC 3623, NGC 3627, and NGC 3628
15 p2267 A83-34624

Stability of star clusters as galactic satellites. I - Motion in the cluster orbital plane
16 p2424 A83-36631

Stability of star clusters as galactic satellites. II - Motion perpendicular to the cluster orbital plane
16 p2425 A83-36632

Further statistics on the M/L ratios in early-type galaxies
16 p2430 A83-36650

The irregular distribution of galaxies and the anisotropies in the microwave background photons
17 p2598 A83-37343

Predicted source counts for normal and active galaxies at 10-100 microns
17 p2607 A83-38258

Statistical investigation of the space distribution of quasars and of their association with galaxies
18 p2764 A83-38996

The galactic extinction of extragalactic objects. I - The csc b law and the extinction coefficient
18 p2767 A83-39592

Comparison of galactic center with other galaxies
19 p2913 A83-40701

Search for Wolf-Rayet features in the spectra of giant HII regions. I - Observations in NGC 300, NGC 604, NGC 5457 and He2-10
19 p2910 A83-41066

Probable association of UX Piscium with a galaxy
20 p3058 A83-42323

The statistics of quasar-galaxy separations
20 p3070 A83-42788

Photometric classification of normal galaxies and their redshift determination
20 p3062 A83-43653

Galaxies, quasars, and beyond - The Space Telescope
[AAS PAPER 83-168] 20 p3063 A83-43768

On the apparent association of quasars and Arp's companion galaxies
21 p3233 A83-44744

Escape velocities of interacting spherical galaxies
21 p3234 A83-44870

A deep survey of galaxies
22 p3372 A83-46377

Estimated energy and momentum input to the interstellar medium for several external galaxies
23 p3519 A83-47448

Spectrophotometric investigation of the irregular galaxy NGC 2814
24 p3653 A83-49163

Geometrical analysis of catalogs of galaxies
24 p3640 A83-49168

Optical features associated with the extended H I envelope of M83
24 p3641 A83-49212

H I observations of the interacting galaxies - VV 371 and VV 329
24 p3655 A83-49218

The stability of axisymmetric galaxy models with anisotropic dispersions
24 p3641 A83-49248

Observational evidence for mergers --- of galaxies
24 p3657 A83-49256

The anomalous spectral shift of mixed pairs of galaxies
24 p3661 A83-49452

A methodology for determination of extragalactic distances
24 p3661 A83-49453

Photometric studies of faint galaxies on deep UKST plates with COSMOS
24 p3648 A83-50021

Galaxy redshifts from objective prism spectra
24 p3648 A83-50023

GALAXY AIRCRAFT

U C-5 AIRCRAFT

GALERKIN METHOD

Boundary value problems for a class of equations containing a derivative with respect to time
01 p0102 A83-11315

Buckling of polar orthotropic annular plates under inplane radial pressures
02 p0190 A83-12002

A two-dimensional isoparametric Galerkin finite element for acoustic-flow problems
02 p0234 A83-12778

[ASME PAPER 82-DET-97] 02 p0234 A83-12778

Analysis of global expansion methods: Weakly asymptotically diagonal systems --- Book
03 p0387 A83-13500

On a higher order accurate fully discrete Galerkin approximation to the Navier-Stokes equations
03 p0316 A83-13568

Galerkin methods for second kind integral equations with singularities
03 p0387 A83-13573

A multi-level iterative method for nonlinear elliptic equations
03 p0388 A83-14077

Derivative calculation from finite element solutions
03 p0389 A83-14696

Full-wave analysis of microstrip resonator and open-circuit end effect
04 p0473 A83-16208

Hybrid-mode analysis of a microstrip-slot resonator
04 p0474 A83-16210

The convergence speed of projection methods in eigenvalue problems
05 p0682 A83-17640

A numerical technique for the determination of propagation characteristics of inhomogeneous planar optical waveguides
05 p0686 A83-17892

Application of the finite-element method to one-dimensional flame propagation problems
07 p0878 A83-19818

Computation of periodic solutions for polynomial nonlinear equations
07 p0986 A83-20067

Projection methods in non-self-adjoint problems of mathematical physics
07 p0986 A83-20310

Finite-element methods for steady solidification problems
09 p1338 A83-23723

Character and stability of axisymmetric thermal convection in spheres and spherical shells --- model for heat transfer in planetary interiors
09 p1365 A83-24126

Spatial Fourier modes controlling Navier-Stokes flow
11 p1568 A83-28236

Numerical experiments involving Galerkin and collocation methods for linear integral equations of the first kind
12 p1771 A83-29098

Convergence of Galerkin approximations for the Korteweg-de Vries equation
13 p1912 A83-31360

A computational study of finite element methods for second order linear two-point boundary value problems
13 p1912 A83-31362

Appropriate finite element techniques for heat transfer problems with high gradients and ablation
15 p2159 A83-34236

The consistent method for computing derived boundary quantities when the Galerkin FEM is used to solve thermal and/or fluids problems
15 p2159 A83-34252

Numerical calculations of low-frequency TE fields in arbitrarily shaped inhomogeneous lossy dielectric cylinders
16 p2407 A83-35407

The effect of thermal boundary conditions on the heat transport in vertical channels heated from below
16 p2349 A83-35557

Investigation of flow field in a turbocompressor by the finite element method
16 p2290 A83-35834

Piecewise polynomial Galerkin approximation to invariant densities of one-dimensional difference equations
17 p2571 A83-38037

Finite element methods for transonic flow analysis
19 p2789 A83-40854

On the simplified hybrid-combined method --- for solving boundary value problems of elliptic equations
20 p3041 A83-42495

Further convergence results for the weighted Galerkin method of numerical solution of Cauchy-type singular integral equations
20 p3041 A83-42497

Aspects of Galerkin approximations for hydrodynamic simulations
20 p2972 A83-42675

Nonlinear convection
20 p2982 A83-43005

Nonlinear vibrations of a clamped rectangular plate with initial deflection and initial edge displacement. I - Theory
21 p3153 A83-44622

Weakly contracting systems and attractors of the Galerkin approximations of the Navier-Stokes equations on the two-dimensional toroid
21 p3130 A83-44657

Galerkin method as a tool to investigate the planar and non-planar behavior of curved beams
23 p3471 A83-48171

GALILEAN SATELLITES

NT CALLISTO
NT EUROPA
NT GANYMEDE
NT IO

Satellites of Jupiter --- Book 04 p0569 A83-16226

Orbital evolution of the Galilean satellites
04 p0570 A83-16228

Structure and thermal evolution of the Galilean satellites
04 p0570 A83-16229

Composition of the surfaces of the Galilean satellites
04 p0570 A83-16232

Interpreting the cratering record - Mercury to Ganymede and Callisto
04 p0570 A83-16234

Cratering time scales for the Galilean satellites
04 p0548 A83-16235

Cartography and nomenclature for the Galilean satellites
04 p0572 A83-16250

Satellite tour design for the Galileo mission
[AIAA PAPER 83-0101] 05 p0602 A83-16822

Formation of the Galilean satellites in a gaseous nebula
05 p0703 A83-16957

Jupiter --- Book 09 p1366 A83-24900

Orbital evolution of the Galilean satellites - Capture into resonance
10 p1492 A83-25510

The influence of short-period perturbations on the motion of the Galilean satellites of Jupiter
11 p1673 A83-28039

On the nature of the interaction of the Jovian magnetosphere with the icy Galilean satellites
15 p2273 A83-33930

Global multispectral mosaics of the icy Galilean satellites
18 p2779 A83-40321

Plasma ion-induced molecular ejection on the Galilean satellites - Energies of ejected molecules
22 p3387 A83-46886

GALILEO MISSION

U GALILEO PROJECT

GALILEO PROBE

Assessment of contamination in the Shuttle bay
03 p0286 A83-13746

Galileo Atmospheric Entry Probe System - Design, development, and test
[AIAA PAPER 83-0098] 05 p0605 A83-16520

Galileo atmospheric entry probe mission description
[AIAA PAPER 83-0100] 06 p0722 A83-19580

Parameters for the simulation of high temperature blown shock layers
07 p0924 A83-19829

Effect of low Reynolds number turbulence amplification on the Galileo probe flowfield
18 p2645 A83-40023

GALILEO PROJECT

Galileo - Mission to Jupiter 02 p0263 A83-11793

Galileo mission overview
[AIAA PAPER 83-0096] 05 p0603 A83-17906

Interplanetary trajectory design for the Galileo mission
[AIAA PAPER 83-0099] 05 p0602 A83-17908

Navigation of the Galileo mission
[AIAA PAPER 83-0102] 05 p0605 A83-17909

Galileo 1986 on Centaur
07 p0868 A83-20644

Galileo Institute for Astronomy (IFA) charge-coupled device (CCD) system
14 p2015 A83-31989

Return to Jupiter - Project Galileo
18 p2644 A83-40344

GALILEO SPACECRAFT

Spacecraft computer resource margin management --- of Project Galileo Orbiter in-flight reprogramming task
04 p0527 A83-16118

- A radiation-hardened star scanner for spacecraft guidance and control 04 p0454 A83-16119
- Satellite tour design for the Galileo mission [AIAA PAPER 83-0101] 05 p0602 A83-16822
- Radiation effects on spacecraft materials for Jupiter and near-earth Orbits 05 p0608 A83-17498
- The Galileo spacecraft system design [AIAA PAPER 83-0097] 05 p0608 A83-17907
- Progress in 800 x 800 charge-coupled device /CCD/ imager development and applications 08 p1051 A83-22603
- Galileo spacecraft power distribution and autonomous fault recovery 11 p1539 A83-27149
- Near-infrared mapping spectrometer for investigation of Jupiter and its satellites 14 p1983 A83-32000
- Charge-coupled device (CCD) television camera for NASA's Galileo mission to Jupiter 14 p1983 A83-32024
- Experimental investigation of bipropellant exhaust plume flowfield, heating, and contamination, and comparison with the CONTAM computer model predictions [AIAA PAPER 83-1447] 14 p1984 A83-32715
- Experimental exhaust plume analysis with MBB 10 N thruster --- Bipropellant for US/German Galileo spacecraft propulsion [AIAA PAPER 83-1259] 16 p2320 A83-36313
- Galileo spacecraft high gain antenna offset calibration 17 p2474 A83-37147
- Return to Jupiter - Project Galileo 18 p2644 A83-40344
- Development of the functional simulator for the Galileo attitude and articulation control system [AIAA PAPER 83-2299] 19 p2817 A83-41757
- GALL**
- Gall bladder disease in a 30 year follow up study - Its association with ischemic disease 08 p1147 A83-22959
- GALLIUM**
- NT GALLIUM ISOTOPES
- Long wavelength Pb/1-x/Sn/x/Te homostructure diode lasers having a gallium-doped cladding layer 07 p0937 A83-21369
- Defects in electron-irradiated, gallium-doped silicon --- in solar cells 10 p1489 A83-26213
- Performance of Si:Ga infrared detectors under reduced background fluxes 11 p1669 A83-27695
- Determination of natural radiative lifetimes of the 5p2 P state in Ga I and 6p2 P state in In I using a pulsed dye laser 16 p2410 A83-36653
- Growth rate dependence of the interface distribution coefficient in the system Ge-Ga 16 p2421 A83-36714
- GALLIUM ANTIMONIDES**
- Defects in amorphous III-V compounds 04 p0542 A83-15531
- Nonlinear optical studies of picosecond relaxation times of electrons in n-GaAs and n-GaSb 06 p0814 A83-19260
- Incorporation of Sb in GaAs(1-x)Sb(x) (x less than 0.15) by molecular beam epitaxy 16 p2420 A83-36013
- Crystal growth of GaSb under microgravity conditions [IAF PAPER 83-153] 23 p3413 A83-47292
- GALLIUM ARSENIDE LASERS**
- Direct observation of picosecond light pulses from a pulse-current pumped semiconductor laser 01 p0054 A83-10615
- Source statistics and the Kerr effect in fiber-optic gyroscopes 02 p0176 A83-11570
- Luminescence spectra of stripe-geometry laser heterostructures in GaAs-Al/x/Ga/1-x/As 02 p0183 A83-11695
- Optical phase modulation in an injection locked AlGaAs semiconductor laser 02 p0184 A83-12168
- Narrow strip AlGaAs lasers using double current confinement 02 p0185 A83-12276
- Very narrow graded-barrier single quantum well lasers grown by metalorganic chemical vapor deposition 02 p0185 A83-12279
- High-power single-mode AlGaAs laser diodes 03 p0331 A83-13875
- Calculated threshold current of GaAs quantum well lasers 03 p0331 A83-13918
- Theoretical analysis of single-mode AlGaAs-GaAs double heterostructure lasers with channel-guide structure 03 p0332 A83-13920
- Influence of hot carriers on the temperature dependence of threshold in 1.3-micron InGaAsP lasers 03 p0332 A83-14930
- High quantum efficiency InGaAsP/InP lasers 03 p0333 A83-14931
- Continuous wave high-power, high-temperature semiconductor laser phase-locked arrays 03 p0333 A83-14932
- Optoelectronic digital/analogue converter-emitter 04 p0534 A83-15241
- Pulsed-power performance and stability of 880 nm GaAlAs/GaAs oxide-stripe lasers 04 p0486 A83-16215
- Catastrophic degradation level of visible and infrared GaAlAs lasers 05 p0647 A83-16941
- Influence of lateral waveguiding properties on the longitudinal mode spectrum for semiconductor lasers 05 p0648 A83-16944
- Determination of the parameters of injection laser amplifiers based on GaAlAs heterostructures from superluminescence characteristics 05 p0649 A83-17060
- High-performance single-mode AlGaAs Gaussian channel substrate planar laser diodes 06 p0765 A83-18566
- Measurement of very-high-speed photodetectors with picosecond InGaAsP film lasers 06 p0809 A83-18573
- High power single mode InGaAsP lasers fabricated by single step liquid phase epitaxy 06 p0767 A83-19254
- Dispersion of the group velocity refractive index in GaAs double heterostructure lasers 07 p0938 A83-21592
- Transient and stationary properties in bistable operation of a GaAs laser coupled to an external resonator 08 p1106 A83-21885
- Enhanced indium phosphide substrate protection for liquid phase epitaxy growth --- of indium-gallium-arsenide-phosphide double heterostructure lasers 08 p1107 A83-22331
- Prediction of transverse-mode selection in double heterojunction lasers by an ambipolar excess carrier diffusion solution 08 p1107 A83-22332
- InGaAsP/InP undercut mesa laser with planar polyimide passivation 08 p1110 A83-22752
- High optical power CW operation in visible spectral range by window V-channeled substrate inner stripe lasers 08 p1110 A83-22753
- GaAs laser beacon for satellite communications 09 p1214 A83-23582
- Short-cavity single-frequency InGaAsP buried-heterostructure lasers 09 p1272 A83-24112
- Effects of 140 Mbit/s operation on degradation of GaAlAs DH lasers 09 p1272 A83-24113
- Detection at Gbit/s rates with a TJS GaAlAs laser 10 p1425 A83-25426
- Statistical analysis of aging-induced degradation /or lifetime/ variations in /Al, Ga/As/GaAs double-heterostructure lasers 10 p1429 A83-26028
- High-frequency impedance of proton-bombarded injection lasers 10 p1429 A83-26071
- The study and manufacture of Ga-Al-As double heterojunction laser diodes emitting in the visible spectrum --- French thesis 11 p1585 A83-28627
- Phase-locked (GaAl)As laser emitting 1.5 W CW per mirror 13 p1850 A83-30330
- Nonlinear far-infrared magnetoabsorption and optically detected magnetoimpurity effect in n-GaAs 13 p1850 A83-30600
- GaAs/GaAlAs active-passive-interference laser 13 p1858 A83-31768
- Investigation of CW operation of a GaAs laser pumped by an electron beam 14 p2022 A83-31906
- Electronic control of the difference frequency between two semiconductor lasers 14 p2024 A83-32420
- Short cavity InGaAsP/InP lasers with dielectric mirrors 14 p2027 A83-33436
- New large optical cavity laser with distributed active layers 14 p2027 A83-33437
- Degenerate four-wave mixing in room-temperature GaAs/GaAlAs multiple quantum well structures 15 p2230 A83-33840
- GaAs/(GaAl)As deep Zn-diffused channelled-substrate laser 16 p2358 A83-35454
- Direct amplitude modulation of short-cavity GaAs lasers up to X-band frequencies 17 p2514 A83-38042
- Phase-locked InGaAsP laser array with diffraction coupling 18 p2693 A83-40051
- Reliability of constricted double-heterojunction AlGaAs diode lasers 18 p2693 A83-40052
- Room-temperature optically triggered bistability in twin-stripe lasers 18 p2693 A83-40400
- Carrier leakage and temperature dependence of InGaAsP lasers 19 p2850 A83-40732
- Streak camera study of short pulse generation in an optically pumped GaAs/(GaAl)As laser 19 p2850 A83-40735
- Anomalous longitudinal mode behavior of a deep Zn-diffused GaAs/GaAlAs laser 19 p2850 A83-40736
- Long-lived GaAlAs laser diodes with multiple quantum well active layers grown by organometallic vapor phase epitaxy 19 p2850 A83-40744
- Analysis of diode laser properties. II 19 p2851 A83-40934
- Superluminescent damping of relaxation resonance in the modulation response of GaAs lasers 20 p2995 A83-43592
- Investigation of the refractive index profiles of multilayer Ga(1-x)Al(x)As laser heterostructures 20 p2997 A83-43796
- GaAs optoelectronic integrated light sources 21 p3125 A83-44226
- A 1.59 micron wavelength GaInAsP/InP distributed feedback laser with first-order grating on anti-meltback layer 21 p3144 A83-44500
- Wavelength tuning of GaInAsP/InP integrated laser with butt-jointed built-in distributed Bragg reflector 21 p3145 A83-44952
- Emission frequency stability in single-mode-fibre optical feedback controlled semiconductor lasers 21 p3145 A83-44954
- Generation of single-longitudinal-mode gigabit-rate optical pulses from semiconductor lasers through harmonic-frequency sinusoidal modulation 21 p3145 A83-44956
- Nonlinear optics with a diode-laser light source 22 p3356 A83-45963
- Proton damage in laser diodes and light-emitting diodes (LEDs) 22 p3296 A83-46618
- Narrow diffused stripe GaAs/GaAlAs lasers for high speed integrated optical transmitters 22 p3297 A83-46655
- Two-photon pumped synchronously mode-locked bulk GaAs laser 22 p3298 A83-46668
- Reliability of InGaAsP/InP buried heterostructure 1.3 micron lasers 22 p3301 A83-46824
- A study of optical amplification in a double heterostructure GaAs device using the density matrix approach 22 p3301 A83-46825
- Longitudinal mode spectrum of GaAs injection lasers under high-frequency microwave modulation 24 p3586 A83-48780
- Bandwidth-limited picosecond pulse generation in a synchronously pumped GaAs laser containing a variable absorber diode 24 p3586 A83-48783
- Ultrashort optical pulse generation from microwave modulated AlGaAs diode laser with Selfoc rod resonator 24 p3588 A83-49611
- GALLIUM ARSENIDES**
- NT ALUMINUM GALLIUM ARSENIDES
- GaAs FET circuits handle high power. V - Designers: Prepare for the GaAs FET age 01 p0035 A83-10270
- Switched optoelectronic microwave load 01 p0035 A83-10295
- Semiconducting and other major properties of gallium arsenide 01 p0108 A83-10605
- Hot electrons in a GaAs heterolayer at low temperature 01 p0109 A83-10626
- Microwave field-effect transistors - Theory, design and applications --- Book 01 p0038 A83-10876
- Metalorganic chemical vapor deposition of very thin /approximately 2 micron/, oriented GaAs layers on tungsten substrates 01 p0110 A83-10989
- Tunable electroluminescence from GaAs doping superlattices 01 p0110 A83-10991
- Deep photoluminescence band related to oxygen in gallium arsenide 01 p0110 A83-10993
- An enhancement mode Schottky barrier gate charge-coupled device on a high electron mobility transistor structure 01 p0039 A83-10994
- Photoelectrochemical cells based on GaAs/0.6/P/0.4/epilayers - Stabilization and luminescent properties 01 p0069 A83-10997
- A 1 watt GaAs power amplifier for the NASA 30/20 GHz communication system 01 p0044 A83-11489
- Some features of the continuous operation of Gunn diodes 02 p0166 A83-11545
- A study of silicon and GaAs solar cells, and their optical coupling by means of a dichroic mirror --- French thesis 02 p0200 A83-11764
- Simulation of non steady-state transport in GaAs and InP millimeter IMPATT diodes 02 p0167 A83-11799
- Ellipsometric study of silicon nitride on gallium arsenide 02 p0242 A83-11812
- Depth distributions and range parameters for He implanted in Si and GaAs 02 p0242 A83-12283
- Raman scattering characterization of Ga/1-x/Al/x/As/GaAs heterojunctions - Epilayer and interface 02 p0243 A83-12289
- Epitaxial growth of Fe on GaAs by metalorganic chemical vapor deposition in ultrahigh vacuum 02 p0243 A83-12291
- Ga/0.80/In/0.20/As 1.20-eV high quantum efficiency junction for multijunction solar cells 02 p0243 A83-12292
- Current oscillations in semi-insulating GaAs associated with field-enhanced capture of electrons by the major deep donor EL2 02 p0243 A83-12294
- Microwave switching with GaAs FETs 03 p0308 A83-13438

Yield considerations in the design and fabrication of GaAs MMICs 03 p0308 A83-13439

Broadband monolithic integrated power amplifiers in gallium arsenide 03 p0308 A83-13440

Monolithic GaAs FET low-noise amplifiers for X-band applications 03 p0308 A83-13441

Flip-chip BeO technology applied to GaAs active aperture radars 03 p0308 A83-13442

Direct-coupled GaAs ring oscillators with self-aligned gates 03 p0308 A83-13558

High performance ion-implanted low noise GaAs MESFET's 03 p0309 A83-13559

Liquid encapsulated Czochralski growth of low dislocation GaAs 03 p0399 A83-13784

Planar doped barriers by molecular beam epitaxy for millimeter wave devices 03 p0310 A83-13785

Real space transfer electron device oscillator - A new candidate for the near millimeter range 03 p0310 A83-13797

TiW silicide gate self-alignment technology for ultra-high-speed GaAs MESFET LSI/VLSI's 03 p0314 A83-14514

Gate-drain avalanche breakdown in GaAs power MESFET's 03 p0314 A83-14515

Switching behaviour of Al₂O₃-n GaAs MISFETs 04 p0470 A83-15248

Enhancement of electron velocity in modulation-doped /Al, Ga/As/GaAs FETs at cryogenic temperatures 04 p0470 A83-15251

Defects in amorphous III-V compounds 04 p0542 A83-15531

Antireflection layers for GaAs solar cells 04 p0507 A83-16068

Selenium doping of molecular beam epitaxial GaAs using SnSe₂ 04 p0544 A83-16094

Gallium arsenide ICs in space and nuclear radiation environments [AIAA PAPER 83-0165] 05 p0623 A83-16565

GaAs/GaAlAs heterojunction bipolar transistors with cutoff frequencies above 10 GHz 05 p0624 A83-17285

Ion-implanted s lateral PNP transistors 05 p0624 A83-17288

Quarter micron low noise GaAs FET's 05 p0624 A83-17293

Numerical simulation of GaAs/GaAlAs heterojunction bipolar transistors 05 p0624 A83-17294

Semiconductor structures for repeated velocity overshoot 05 p0690 A83-17295

Electron transport in GaAs n/+/-p/-n/+/- submicron diodes 05 p0624 A83-17296

Reduction of long-term transient radiation response in ion implanted GaAs FETs 05 p0625 A83-17482

Radiation effects on distortion characteristics of power GaAs MESFET amplifiers 05 p0625 A83-17483

Ionizing radiation response of GaAs JFETs and DCFL circuits 05 p0626 A83-17503

Dependence of normally-off GaAs JFET performance on device structure 05 p0631 A83-17756

The effect of parasitic capacitances on the circuit speed of GaAs MESFET ring oscillators 05 p0631 A83-17763

The effect of Al-GaAs interaction on the technology of self-aligned gallium arsenide MESFETs 05 p0631 A83-17771

Design of a 13% efficient n-GaAs/1-x/P/x/ semiconductor-liquid junction solar cell 05 p0658 A83-17801

Monte Carlo particle simulation of a GaAs short-channel MESFET 06 p0751 A83-18572

Noise in short n/+/-n/-n/+/- GaAs diodes 06 p0751 A83-18751

Investigation of transient electronic transport in GaAs following high energy injection 06 p0814 A83-18757

Direct comparison of the electron-temperature model with the particle-mesh /Monte-Carlo/ model for the GaAs MESFET 06 p0752 A83-18761

On design and performance of lossy match GaAs MESFET amplifiers 06 p0752 A83-18765

Broad-band characteristics of EHF IMPATT diodes 06 p0753 A83-18768

Broad-band GaAs monolithic amplifier using negative feedback 06 p0753 A83-18774

Nonlinear optical studies of picosecond relaxation times of electrons in n-GaAs and n-GaSb 06 p0814 A83-19260

Undoped, semi-insulating GaAs layers grown by molecular beam epitaxy 06 p0815 A83-19262

Radiation effects on modulation-doped GaAs-Al_x/Ga/1-x/As heterostructures 06 p0815 A83-19263

20-GHz bandwidth GaAs photodiode 06 p0754 A83-19264

Regenerative photoelectrochemical cells using polymer-coated n-GaAs photoanodes in contact with aqueous electrolytes 07 p0952 A83-19882

Surface acoustic wave memory correlator on semi-insulating GaAs 07 p0918 A83-19982

Residual double acceptors in bulk GaAs 07 p0998 A83-19989

X-ray photoelectron spectroscopic study of the oxide removal mechanism of GaAs /100/ molecular beam epitaxial substrates in situ heating 07 p0881 A83-19994

Quantum corrections to the galvanomagnetic coefficients of quasi-two-dimensional electrons of InSb/GaAs heteroepitaxial structures 07 p0999 A83-20049

The development of millimetre wave mixer diodes 07 p0919 A83-20181

Manufacture and study of Diffused Gallium Arsenide IMPATT Diodes in the Ku-band --- German thesis 07 p0919 A83-20399

Physiochemical effects of heating gold thin films on gallium arsenide 07 p0882 A83-20591

Surface and redox reactions at GaAs in various electrolytes --- of photoelectrochemical cells 07 p0955 A83-20595

Study of the thermal conversion of semi-insulating GaAs:Cr with cathodoluminescence, photoluminescence, and secondary ion mass spectrometry 07 p1000 A83-20747

Addressing and control of high-speed logic circuits with picosecond light pulses 07 p0921 A83-20793

Absence of the Gunn effect in p-In_{0.53}/Ga_{0.47}/As 07 p1000 A83-21374

Monolithic integration of a photodiode and a field-effect transistor on a GaAs substrate by molecular beam epitaxy 07 p0922 A83-21375

Monolithic voltage controlled oscillator for X- and Ku-bands 07 p0922 A83-21529

A monolithic single-chip X-band four-bit phase shifter 07 p0923 A83-21534

X-band burnout characteristics of GaAs MESFET's 07 p0923 A83-21535

Interface states and internal photoemission in p-type GaAs metal-oxide-semiconductor surfaces 08 p1066 A83-22338

AlGaAs/GaAs heterojunction charge-coupled devices /CCDs/ for visible/near infrared imaging applications 08 p1080 A83-22604

EL2 distributions in doped and undoped liquid encapsulated Czochralski GaAs --- deep donor concentration 08 p1169 A83-22756

New experimental evidence of surface ripples on gallium arsenide in laser annealing 08 p1169 A83-22758

Spectral tuning of shallow-junction surface-emitting light-emitting diodes /LEDs/ through gamma-ray irradiation 08 p1170 A83-22846

A model for the collection of minority carriers generated in the depletion region of a Schottky barrier solar cell 08 p1170 A83-22910

Molecular beam epitaxial double heterojunction bipolar transistors with high current gains 08 p1081 A83-22916

High-speed GaAlAs-GaAs heterojunction bipolar transistors with near-ballistic operation 08 p1082 A83-22922

Empirical model for gallium arsenide MESFETs 09 p1251 A83-23348

0.5 micron GaAs FET for low-noise circuits for Orbital Test Satellite reception 09 p1252 A83-23396

Future applications and limitations for digital GaAs IC technology 09 p1255 A83-24347

Practical design of 2-4 GHz low intermodulation distortion GaAs FET amplifiers with flat gain response and low noise figure 09 p1255 A83-24348

Measurement of series resistance in IMPATT diodes 09 p1256 A83-24500

Design, fabrication, and evaluation of 2- and 3-bit GaAs MESFET analog-to-digital converter IC's 09 p1256 A83-24678

Ka-band monolithic GaAs balanced mixers 09 p1256 A83-24679

Yield considerations for ion-implanted GaAs MMIC's 09 p1256 A83-24680

A monolithic GaAs DC to 2-GHz feedback amplifier 09 p1256 A83-24682

Monolithic GaAs interdigitated couplers 09 p1256 A83-24683

High-voltage two-dimensional simulations of permeable base transistors 09 p1256 A83-24684

Gallium arsenide infrared windows for high-speed airborne applications 09 p1345 A83-24958

Electron traps in GaAs/1-x/P/x/ alloys 10 p1488 A83-25985

Laser-controlled etching of chromium-doped 100 line-type GaAs 10 p1390 A83-25986

Amplification of total-reflection-mode acoustic surface waves in n-type GaAs films 10 p1410 A83-25987

Deposition of GaAs epitaxial layers by organometallic CVD - Temperature and orientation dependence 10 p1488 A83-26060

Use of a superlattice to enhance the interface properties between two bulk heterolayers 10 p1489 A83-26214

Design of interdigitated capacitors and their application to gallium arsenide monolithic filters 10 p1410 A83-26341

Space applications of gallium arsenide solar cells 11 p1541 A83-27258

Status of GaAs solar cells for space power applications 11 p1542 A83-27259

Nondivergent monochromatic X-ray beams from Ge and GaAs monocrystals 11 p1577 A83-27523

Transient phenomena in optical bistability 11 p1656 A83-27531

New GaAs Impatt theory explains mm-wave operation 11 p1562 A83-28158

A method for producing heat pipes for cooling semiconductor photovoltaic cells and the heat pipe characteristics 11 p1553 A83-28366

A low-noise GaAs FET preamplifier for 21 GHz satellite earth terminals 11 p1563 A83-28591

Transferred-electron effect in In_{0.53}/Ga_{0.47}/As 11 p1663 A83-28601

Miniaturization of monolithic amplifiers on GaAs at 10 GHz 12 p1719 A83-29409

The technology of metal semiconductor contacts - Application to the manufacture of microwave modulators and limiters on GaAs --- French thesis 12 p1720 A83-29948

Nonlinear properties of GaAs Gunn diodes in the short-wave part of the millimeter-wave range 13 p1830 A83-30017

Temperature stabilization of GaAs MESFET oscillators using dielectric resonators 13 p1831 A83-30238

Spectroscopy of the isoelectronic nitrogen addition in epitaxial structures based on wide-band solid solutions of the system In-Ga-P-As 13 p1927 A83-30262

Harmonic Gunn oscillators allow frequency growth 13 p1835 A83-30912

Effects of very low growth rates on GaAs grown by molecular beam epitaxy at low substrate temperatures 13 p1929 A83-31064

Electrical measurements on n(+)-GaAs-undoped Ga(0.6)Al(0.4)As-n-GaAs 13 p1836 A83-31065

Defect nature of the 0.4-eV center in O-doped GaAs [AD-A129932] 13 p1930 A83-31068

Large signal design of GaAs FET oscillators using input dielectric resonators 13 p1836 A83-31149

The electrical behavior of GaAs-insulator interfaces - A discrete energy interface state model 13 p1931 A83-31386

High-speed GaAs heterojunction bipolar phototransistor grown by molecular beam epitaxy 13 p1837 A83-31759

Integral packaging for millimetre-wave GaAs IMPATT diodes prepared by molecular beam epitaxy 13 p1838 A83-31777

Stable tantalum silicide Schottky barrier on n-type gallium arsenide evaluated at elevated temperatures 13 p1838 A83-31779

High efficiency GaAs solar cells for concentrator and flat plate arrays 14 p2042 A83-32260

Role of photoluminescence in the efficiency of a Ga(1-x)Al(x)As-GaAs solar cell 14 p2043 A83-32269

750 suns concentrator modules using GaAs solar cells 14 p2043 A83-32272

Growth and characterization of Ga(0.47)In(0.53)As films on InP substrates using triethylgallium, triethylindium, and arsine 14 p2092 A83-32643

The characteristics of Au-Ge-based ohmic contacts to n-GaAs including the effects of aging 14 p2006 A83-32671

Switching characteristics of logic gates addressed by picosecond light pulses 14 p2008 A83-33422

Specific site location of S and Si in ion-implanted GaAs 14 p2093 A83-33445

Low-noise, low power dissipation GaAs monolithic broad-band amplifiers 14 p2008 A83-33459

Performance of a microwave amplitude limiter using GaAs MESFET 15 p2149 A83-33522

Recent advances in the performance and reliability of InGaAsP: LED's for lightwave communication systems 15 p2229 A83-33677

Wavelength tuning of GaAs LED's through surface effects 15 p2149 A83-33679

InGaAsP photodiodes 15 p2150 A83-33680

Magnetoresistance anisotropy due to the 2D-electron subsystem at a GaAs/AlGaAs interface 15 p2237 A83-33784

Determination of diffusion length of electron beam induced minority carriers in polycrystalline GaAs 15 p2238 A83-33844

- High-performance K-band GaAs power field-effect transistors prepared by molecular beam epitaxy 15 p2150 A83-33846
- Fabrication of GaAs-Mo-Si structures by metalorganic chemical vapor deposition and laser annealing 15 p2238 A83-33848
- Compact dc model of GaAs FET's for large-signal computer calculation 15 p2151 A83-33892
- Double heterojunction Al(x)Ga(1-x)As/GaAs bipolar transistors (DHBJT's) by MBE with a current gain of 1650 15 p2151 A83-33916
- Laser cathode ray tube with a semiconductor double-heterostructure screen 15 p2163 A83-33921
- (GaAl)As/GaAs heterojunction bipolar transistors with graded composition in the base 15 p2152 A83-34516
- Liquid phase epitaxial growth of ZnSnP2 on GaAs 15 p2238 A83-34697
- Low temperature annealing of Be-implanted GaAs 16 p2418 A83-35438
- A study of the 0.1-eV conversion acceptor in GaAs 16 p2419 A83-35443
- Transmission electron microscopy of GaAs permeable base transistor structures grown by vapor phase epitaxy 16 p2419 A83-35450
- Numerical and experimental study of a GaAs transferred electron device without transit-time limitation 16 p2345 A83-35523
- Schottky barrier height variation with metallurgical reactions in aluminum-titanium-gallium arsenide contacts 16 p2419 A83-35671
- A correlation of atomic and electrical measurements of Cr and residual donors in thermally processed semi-insulating GaAs 16 p2419 A83-35672
- The quantized Hall effect 16 p2420 A83-35763
- Dispersion of the refractive index of GaAs and Al(x)Ga(1-x)As 16 p2420 A83-35970
- Mim gate FET - New GaAs enhancement-mode transistor 16 p2346 A83-36007
- Incorporation of Sb in GaAs(1-x)Sb(x) (x less than 0.15) by molecular beam epitaxy 16 p2420 A83-36013
- Fabrication of GaAs bistable optical devices 16 p2412 A83-36069
- High-performance modulation-doped GaAs integrated circuits with planar structures 16 p2347 A83-36477
- GaAs integrated digital-to-analogue converter for control of power dual-gate FETs 16 p2347 A83-36479
- Polarisation-dependent gain-current relationship in GaAs-AlGaAs MQW laser diodes --- Multi-Quantum-Well 16 p2360 A83-36481
- Dynamic behaviour of a GaAs-AlGaAs MQW laser diodes --- Multi-Quantum-Well 16 p2360 A83-36485
- Bulk unipolar diodes in MBE GaAs 16 p2347 A83-36486
- Electrochemical measurements on the photoelectrochemical reduction of aqueous carbon dioxide on p-gallium phosphide and p-gallium arsenide semiconductor electrodes 16 p2328 A83-36741
- GaAs microwave devices and circuits with submicron electron-beam defined features 17 p2496 A83-37059
- Gallium arsenide and related compounds 1982; International Symposium, 10th, Albuquerque, NM, September 19-22, 1982, Contributed Papers --- Book 17 p2584 A83-37160
- Influence of radiative recombination on the minority-carrier transport in direct band-gap semiconductors 17 p2496 A83-37617
- An enhanced sensitivity null ellipsometry technique for studying films on substrates - Application to silicon nitride on gallium arsenide 17 p2584 A83-37618
- High-frequency doubler operation of GaAs field-effect transistors 17 p2497 A83-37800
- An experimental study of unsteady transport phenomena in GaAs --- French thesis 17 p2585 A83-38430
- TDEG in In(0.53)Ga(0.47)As-InP heterojunction grown by chloride VPE --- two-dimensional electron gas 17 p2585 A83-38880
- Ultrafast GaAs microwave PIN diode 17 p2500 A83-38883
- A two-stage monolithic buffer amplifier for 20 GHz satellite communication 18 p2676 A83-39272
- On the optical evaluation of the EL2 deep level concentration in semi-insulating GaAs 18 p2750 A83-40062
- Characterization of electron traps in ion-implanted GaAs MESFET's on undoped and Cr-doped LEC semi-insulating substrates 18 p2750 A83-40372
- 100 GHz bandwidth planar GaAs Schottky photodiode 18 p2679 A83-40397
- High-speed GaAlAs/GaAs p-i-n photodiode on a semi-insulating GaAs substrate 19 p2836 A83-40742
- Low compensation vapor phase epitaxial gallium arsenide 19 p2903 A83-40745
- Accumulation mode Ga(0.47)In(0.53)As insulated gate field-effect transistors 19 p2836 A83-40746
- GaAs digital dynamic IC's for applications up to 10 GHz 19 p2837 A83-40793
- Avalanche InP/InGaAs heterojunction phototransistor 19 p2899 A83-40948
- High-speed logic at 300 K with self-aligned submicrometer-gate GaAs MESFET's 19 p2837 A83-41019
- Microwave characteristics of an optically controlled GaAs MESFET 19 p2838 A83-41092
- The dependence of the polarization and intensity of recombination radiation on the spin orientation of current carriers in GaAs semiconductors 19 p2905 A83-41221
- The design and manufacture of a GaAs solar cell by liquid phase epitaxy --- French thesis 19 p2862 A83-41813
- Low cost process for ohmic contacts on GaAs/Ga(1-x)Al(x)As concentrator solar cells based on palladium and gold deposition 20 p2965 A83-42353
- Field ionised impurity scattering in an AlGaAs/GaAs two-dimensional electron gas 20 p3052 A83-42485
- Hole transport in pure and doped GaAs 20 p3052 A83-42599
- Optical and crystallographic properties and impurity incorporation of Ga(x)In(1-x)As (with x between 0.44 and 0.49) grown by liquid phase epitaxy, vapor phase epitaxy, and metal organic chemical vapor deposition 20 p3053 A83-42606
- Comparison of the electrophysical and fundamental approaches to the modeling of GaAs Schottky transistors 20 p3053 A83-42912
- A theory of noise in GaAs FET microwave oscillators and its experimental verification 20 p2968 A83-43349
- Nonlinear lumped circuit model of GaAs MESFET 20 p2968 A83-43354
- Measurement and simulation of GaAs FET's under electron-beam irradiation 20 p2968 A83-43357
- A quantitative comparison between calculated and measured conversion losses of a novel beam-lead GaAs Schottky-barrier mixer diode with minimized parasitics 20 p2968 A83-43359
- An analytic approach to optimum oscillator design using S-parameters 21 p3122 A83-43832
- Proton implantation isolation for microwave monolithic circuits 21 p3123 A83-43845
- Laser chemical etching of vias in GaAs 21 p3142 A83-43847
- Submicron GaAs microwave FET's with low parasitic gate and source resistances 21 p3123 A83-43848
- Application of thermal pulse annealing to ion-implanted GaAlAs/GaAs heterojunction bipolar transistors 21 p3123 A83-43851
- A three-terminal double junction GaAs/GaAlAs cascade solar cell 21 p3166 A83-43853
- Self-aligned submicron gate digital GaAs integrated circuits 21 p3124 A83-43854
- Further investigations on the operating modes of millimeter-wave Gunn oscillators 21 p3124 A83-43859
- Short-channel effects in 0.5-micron source-drain spaced vertical GaAs FET's - A first experimental investigation 21 p3124 A83-43860
- Small-radii curved rib waveguides in GaAs/GaAlAs using electron-beam lithography 21 p3205 A83-44222
- Power broadening and nonlinear FIR magneto-photoconductivity in n-GaAs 21 p3216 A83-44382
- Characteristics of the photoluminescence of GaAs films obtained by molecular-beam epitaxy 21 p3217 A83-44542
- The effect of external factors (heat treatment, deformation, and irradiation) on the luminescence of GaAs (review) 21 p3217 A83-44593
- Negative differential resistance in GaAs MESFETs 21 p3125 A83-44951
- Simulation of GaAs submicron FET with hot-electron injection structure 21 p3126 A83-44967
- Planar, ion-implanted bipolar devices in GaAs 21 p3127 A83-45172
- Effect of the velocity-field peak on I-V characteristics of GaAs FET's 21 p3127 A83-45181
- Twisted double-heterostructure GaAs-(AlGa)As laser 21 p3146 A83-45484
- Heteroepitaxial growth of CdTe on GaAs by laser assisted deposition 21 p3219 A83-45492
- High-efficiency (21.4 pct) Ga0.75 In0.25 As/GaAs (Eg = 1.15 eV) concentrator solar cells and the influence of lattice mismatch on performance 21 p3169 A83-45493
- A new method for the fabrication of submicron thick gallium arsenide membranes 21 p3220 A83-45498
- Rapid thermal annealing of Be, Si, and Zn implanted GaAs using an ultrahigh power argon arc lamp 21 p3220 A83-45500
- Three-guide optical couplers in GaAs 22 p3356 A83-45734
- Co-60 gamma-ray and electron irradiation damage of GaAs single crystals and solar cells 22 p3364 A83-46274
- High efficiency GaAs(1-x)P(x) solar cells fabricated by vacuum metalorganic chemical vapor deposition 22 p3319 A83-46607
- Neutron damage effects in laser diodes 22 p3297 A83-46619
- Transient response of nonlinear ring resonators using GaAs with photon energy below band gap 22 p3360 A83-46652
- Switching of a GaAs bistable etalon - External switching on and off, regenerative pulsations, transverse effects, and lasing 22 p3360 A83-46653
- Modification of optical properties of GaAs-Ga(1-x)Al(x)As superlattices due to band mixing 22 p3365 A83-46725
- Characteristics of Schottky diodes with microcluster interface 22 p3278 A83-46729
- Optical studies of In(x)Ga(1-x)As-GaAs strained multiquantum well structures 22 p3365 A83-46730
- Sputtered Schottky barrier solar cells on p-type GaAs 22 p3319 A83-46733
- Resonant tunneling through quantum wells at frequencies up to 2.5 THz 22 p3365 A83-46737
- Characterization of WSi(x)/GaAs Schottky contacts 22 p3278 A83-46739
- pAl(x)Ga(1-x)AspGaAs-nGaAs heterostructure concentrator photocells synthesized by liquid-gas-phase epitaxy 22 p3366 A83-46787
- Studies of electroluminescence in pAlGaAs-pGaAs-nGaAs heterophotocells with distributed parameters 23 p3477 A83-47565
- Waveguide light modulators using the Keldysh-Franz effect in gallium arsenide 23 p3507 A83-47570
- Study of deep-level defects and annealing effects in undoped and Sn-doped GaAs solar cells irradiated by one-MeV electrons 23 p3427 A83-48605
- Low-frequency noise in GaAs current limiters 23 p3446 A83-48607
- AlGaAs/GaAs cascade solar cell computer modeling under high solar concentration 23 p3478 A83-48616
- Mismatch and electron mobility in MBE Ga(x)In(1-x)As epitaxial layers on InP substrates 23 p3512 A83-48701
- Current oscillations in semiconductor diodes under streaming instability conditions 23 p3512 A83-48719
- A new approach for mm-wave generation 24 p3571 A83-48774
- Electrical characteristics of Be-implanted GaAs diodes annealed with an ultrahigh power argon arc lamp 24 p3572 A83-48788
- Dissipation and dynamic nonlinear behavior in the quantum Hall regime 24 p3635 A83-48921
- Optical bistability in GaSe 24 p3629 A83-49530
- Study of defect annealing by supercurrent proton beam irradiation and of radiation defect profiles in GaAs by the positron annihilation method 24 p3636 A83-49748
- A 20 GHz band 0.5 W GaAs FET amplifier for satellite communications 24 p3574 A83-49858
- High-performance millimetre-wave mixer diodes fabricated using a deep mesa etch approach 24 p3574 A83-49959
- High-speed Schottky photodiode on semi-insulating GaAs 24 p3574 A83-49961
- Instabilities in modulation doped field-effect transistors (MODFETs) at 77 K 24 p3574 A83-49972
- Hot-electron noise generation in gallium-arsenide Schottky-barrier diodes 24 p3574 A83-49993
- GALLIUM COMPOUNDS**
- NT ALUMINUM GALLIUM ARSENIDES
- NT GALLIUM ANTIMONIDES
- NT GALLIUM ARSENIDES
- NT GALLIUM NITRIDES
- NT GALLIUM PHOSPHIDES
- Magnetic and crystallographic characteristics of R2Ni2Ga and R2Ni2Al compounds --- rare earth compounds 03 p0299 A83-14153
- Improvements on the electrical and luminescent properties of reactive molecular beam epitaxially grown GaN films by using AlN-coated sapphire substrates 08 p1169 A83-22759
- Electrical properties and ion implantation of epitaxial GaN, grown by low pressure metalorganic chemical vapor deposition 08 p1169 A83-22760
- A study of the interaction between titanium and gallium 14 p1992 A83-32148
- The anomalous kinetics of cathode luminescence in GaN:Zn 19 p2903 A83-40822

GALLIUM ISOTOPES

Observation of Gamow-Teller strength distribution in the reaction Ga-71(p,n)Ge-71 for application to solar-neutrino detection 24 p3674 A83-48919

GALLIUM NITRIDES

Properties of Al_x/Ga_{1-x}/N films prepared by reactive molecular beam epitaxy 01 p0109 A83-10624
The capacitance-voltage characteristics of m-i-n GaN light emitting diodes --- metal-insulator-n-type semiconductor 17 p2496 A83-7649
Properties and ion implantation of Al(x)Ga(1-x)N epitaxial single crystal films prepared by low pressure metalorganic chemical vapor deposition 21 p3220 A83-45499

GALLIUM PHOSPHIDES

Photosensitive gate structures based on epitaxial layers of Fe-doped GaP 01 p0108 A83-10373
A high temperature GaP MESFET 03 p0309 A83-13561
Visible and infrared waveguiding in proton implanted n-type GaP 03 p0393 A83-13768
Defects in amorphous III-V compounds 04 p0542 A83-15531
A GaP MESFET for high temperature applications 05 p0625 A83-17348
Design of a 13% efficient n-GaAs/1-x/P/x/ semiconductor-liquid junction solar cell 05 p0658 A83-17801

Optical techniques for implant process diagnosis in GaP 07 p0998 A83-19897
Infrared to visible up-conversion using GaP light-emitting diodes 07 p0992 A83-19990
Strong photoinduced infrared absorption in GaP 07 p0999 A83-20745

Electron traps in GaAs/1-x/P/x/ alloys 10 p1488 A83-25985
Chemically induced interface states in photoelectrochemical cells 10 p1446 A83-26207
The electrical properties of GaP MOS structures 13 p1831 A83-30268

Electrochemical measurements on the photoelectrochemical reduction of aqueous carbon dioxide on p-gallium phosphide and p-gallium arsenide semiconductor electrodes 16 p2328 A83-36741
Comparative study of surface acoustic wave and photocurrent spectroscopies in GaP 20 p3053 A83-42601

Resistivity and mobility of GaP at 300 K 20 p3054 A83-43358
Silicon-gallium-phosphide heterostructures with a (Si₂)x(GaP)_{1-x} 22 p3366 A83-46783
GaP/Al(x)Ga(1-x)P heterojunction transistors for high-temperature electronic applications 24 p3572 A83-48917

GALVANIC CELLS

U. ELECTROLYTIC CELLS

GALVANIC SKIN RESPONSE

The conditions of the development and the regularities of the patterns of the skin-galvanic response 04 p0522 A83-15778
Electrogustometric investigations during manned space flight 06 p0796 A83-18186
Biofeedback as an important mechanism in the success of teaching humans to control the skin-galvanic reaction 07 p0979 A83-20330
The involuntary regulation of the GSR --- Galvanic Skin Response 23 p3497 A83-47108

GALVANOMAGNETIC EFFECTS

Quantum corrections to the galvanomagnetic coefficients of quasi-two-dimensional electrons of InSb/GaAs heteroepitaxial structures 07 p0999 A83-20049
Galvanomagnetic and thermoelectric properties of p-Pb(1-x)Ge(x)Te in a 80-300 K temperature range 21 p3216 A83-44488
Kinetic phenomena in nondegenerate narrow-gap semiconductors --- Russian book 23 p3511 A83-47121

Supermetallic conductivity of graphite intercalated with iodine monochloride 24 p3634 A83-48864

GALVANOMAGNETISM

U. GALVANOMAGNETIC EFFECTS

GALVANOMETERS

Galvanometric devices --- Russian book 02 p0176 A83-11947

GAME THEORY

Game-theoretical approach to the detection of radar signals on a background of unknown noise 01 p0030 A83-10408
Conflict of interest wind modeling in aircraft response study 03 p0281 A83-13158
Two person zero sum differential games and singular surfaces [AIAA PAPER 83-0572] 05 p0682 A83-16798
Deterministic and stochastic differential games [AIAA PAPER 83-0573] 05 p0682 A83-16799

The application of game theory to the synthesis of an optimal system of symbol data transmission 05 p0623 A83-17689
Concerning a method of extremal control 06 p0803 A83-19114
Game-theoretical evaluation of capacity in the case of channel parameters that are unknown to the operator 07 p0985 A83-20772

The capture region of a coasting pursuer 07 p0987 A83-21010
Optimal sample-at-a-time processing of signals on a background of noise with an arbitrary distribution 09 p1251 A83-25162

An optimal guidance law via first order inertial loop 10 p1469 A83-26770
One pursuer and two evaders on the line - A stochastic pursuit-evasion differential game 12 p1773 A83-29245

Game systems of adaptive control 14 p2076 A83-32962
Potential estimates of the time lag of a signal in conditions of strict conflict 18 p2674 A83-39429

Pursuit-evasion between two realistic aircraft [AIAA PAPER 83-2119] 19 p2894 A83-41944
An eccentric two-target differential game model for qualitative air-to-air combat analysis [AIAA PAPER 83-2122] 19 p2789 A83-41947

On the design of ergatic systems for the solution of a two-goal game-theoretical problem of control 20 p3036 A83-43509
First application of the mathematical theory of cooperative games of two persons in problems of communications theory 23 p3444 A83-48521

GAMMA FUNCTION

Modified gamma aerosol model for the marine environment 08 p1136 A83-22553
A new formula for raindrop terminal velocity 11 p1627 A83-27033

GAMMA GLOBULIN

Morphofunctional changes of the lymphoid tissue of the respiratory organs following the administration of gamma-globulin 18 p2733 A83-40582

GAMMA RADIATION

U. GAMMA RAYS

GAMMA RAY ASTRONOMY

Investigation of cosmic gamma-ray bursts 01 p0130 A83-10844
Radio measurements in the fields of gamma-ray sources. I - CG 195 + 04 01 p0117 A83-10949
Results of multiyear observations of fluxes of superhigh-energy gamma-ray quanta from Cyg X-3 02 p0272 A83-11706
Investigation of fluxes of electrons and gamma quanta with energies exceeding 30 MeV at heights of 300-350 km 02 p0272 A83-11709
High-energy astrophysics 02 p0245 A83-13103
A neutral hydrogen survey of the southern galactic plane for /b/ less than 10 deg 03 p0413 A83-13310
Very high-energy gamma-ray astronomy --- workshop review 05 p0693 A83-16860
Gamma-ray emission from the galactic anticenter at MeV energies 05 p0698 A83-16995
Comments on the gamma-ray burst catalog of Mazets et al. /1981a/ 05 p0710 A83-17820
Discrete sources of cosmic gamma rays 06 p0857 A83-18087

The propagation of energetic ions in magnetic loops and gamma-ray emission from solar flares 06 p0857 A83-19511

Gamma ray transients and related astrophysical phenomena; Proceedings of the Workshop, La Jolla, CA, August 5-8, 1981 07 p1010 A83-20001
10 June 1974 transient 07 p1039 A83-20014
Search for time variations in 511 keV flux by ISEE-3 gamma-ray spectrometer 07 p1039 A83-20016
Inverse Compton gamma-ray from pulsars. I - The Vela pulsar 07 p1017 A83-20932
A low energy gamma ray observation of the region containing CG 195 + 4 07 p1008 A83-21209
Asymptotic solution of the transfer equation for linearly polarized X-ray and gamma radiation 07 p1026 A83-21264

The centre of the Galaxy 08 p1187 A83-23289
Gamma ray detection with long NaI/Tl/ scintillator bars 09 p1268 A83-24104

The gamma-ray colour of the Milky Way and the cosmic-ray electron density 09 p1363 A83-24992
The distribution of gamma-burst sources in the sky and the burst of June 13, 1979 09 p1369 A83-25047
The diffuse gamma radiation from the local spiral arm 10 p1523 A83-25483

Gamma-ray astronomy and the local interstellar medium 10 p1504 A83-25724
High-resolution radio and X-ray observations of the supernova remnant W28 10 p1497 A83-26375

Gamma astronomy of the sun and study of solar cosmic rays 11 p1693 A83-28675
Gamma-ray imaging with a rotating modulator 12 p1708 A83-28895
Spectral observations of atmospheric gamma-ray background 13 p1967 A83-31473
The galactic gamma-ray source population 14 p2104 A83-33189
Detection of 2 x 10 to the 15th to 2 x 10 to the 16th eV gamma-rays from Cygnus X-3 14 p2117 A83-33227

A method for estimating the mass of the central bodies in active galaxy nuclei and quasars 15 p2253 A83-33704
Relativistic thermal plasmas - Effects of magnetic fields 15 p2266 A83-34617

Einstein observations of the Rho Ophiuchi dark cloud - An X-ray Christmas tree 15 p2267 A83-34628
Spatial variation for flares observed with the gamma ray spectrometer aboard the SMM satellite 15 p2284 A83-35223

An interpretation of the low energy gamma ray emission from Seyfert nuclei in terms of annihilation radiation from a hot plasma 16 p2431 A83-36667
The energy spectrum of cosmic fireballs 16 p2431 A83-36672

On the possible nature of the gamma source SG 195 + 4 17 p2601 A83-37686
Observations of gamma radiation at 10 to the 12th eV from the X-ray source Cyg X-3 at the Tien-Shan installation in 1977 and 1978 17 p2589 A83-37687
On the variation of the 4.8-hour period of Cyg X-3 17 p2601 A83-37688

Extragalactic gamma-ray astronomy 17 p2590 A83-37775
Measurements of galactic plane gamma-ray emission in the energy range 10-80 MeV 17 p2629 A83-37931

New activity in the Dorado gamma-ray burst source 17 p2630 A83-38829
Slowing down, quantum effects and magnetic fields in pulsars 18 p2766 A83-39242
Radio pulsars behaviour above 50 MeV 18 p2755 A83-39243
Search for pulsars inside the gamma-ray sources error boxes 18 p2755 A83-39244

Gamma-ray astronomy in perspective of future space experiments; Proceedings of the Symposium, Ottawa, Canada, May 16-June 2, 1982 18 p2755 A83-39275
Status and future of high energy diffuse gamma-ray astronomy 18 p2785 A83-39276
Current wisdom and future possibilities for gamma-ray sources within high-energy astronomy 18 p2755 A83-39277

Gamma rays from giant-molecular clouds 18 p2785 A83-39278
Prospects in instrumentation for future space experiments 18 p2755 A83-39279

An imaging telescope for high energy gamma-ray astronomy 18 p2755 A83-39281
The observation of the galactic anticenter region by the balloon borne gamma-ray telescope Natalya-1 18 p2785 A83-39282

Low and medium energy gamma-ray astronomy - Present status and future aspects 18 p2756 A83-39283
Imaging systems using modulation and coded aperture masks --- for gamma ray telescopes 18 p2756 A83-39284

An imaging telescope for soft gamma-ray astronomy - The preliminary in-flight tests 18 p2756 A83-39287
Sigma - A new gamma-ray space observatory with high angular resolution for 1985 and beyond --- Satellite d'Imagerie Gamma Monte sur Ariane 18 p2756 A83-39288

A directional gamma-ray telescope using coded aperture techniques 18 p2756 A83-39289
The Oriented Scintillation Spectrometer Experiment for the Gamma-Ray Observatory 18 p2756 A83-39290
Figaro - An experiment for pulsar and variable source studies in the MeV range 18 p2688 A83-39291

May 1980 low energy gamma-ray observations with the 'MISO' telescope 18 p2756 A83-39292
Advances in gamma-ray line astronomy 18 p2756 A83-39293

Gamma-ray spectroscopy - Status and prospects 18 p2647 A83-39294
Positron annihilation radiation from the nuclei of Seyfert galaxies 18 p2786 A83-39296

Catalogue of gamma-bursts detected by the Soviet-French experiment 'Signe 2M' (Venera-11, 12 and Prognoz-7) 18 p2786 A83-39303
Gamma radiation as a tracer of the local interstellar gas 18 p2768 A83-39631

Radiation spectrum of optically thin relativistic electron-positron plasma 18 p2774 A83-39734

- The galactic center; Proceedings of the Workshop, California Institute of Technology, Pasadena, CA, January 7, 8, 1982 19 p2911 A83-40676
- Observations of continuum X-ray and gamma-ray emission from the galactic center 19 p2913 A83-40691
- Observations of gamma-ray line emission from the galactic center region 19 p2913 A83-40692
- Emission in the 0.3 to 1.0 MeV range from the galactic center region 19 p2913 A83-40694
- On the origin of the positron annihilation radiation from the direction of the galactic center 19 p2913 A83-40695
- The intensity and spectrum of galactic center beta (+) annihilation protons after Compton scattering 19 p2913 A83-40696
- Future directions in X-ray/gamma-ray observations 19 p2909 A83-40703
- Candidates for a gamma-ray burster optical counterpart 19 p2911 A83-41648
- Gamma ray astronomy 19 p2911 A83-42162
- Gamma-rays and the production of energetic electrons in enshrouding material - A model for the quiescent radio emission from Cygnus X-3 20 p3068 A83-42456
- The high-energy spectrum of hot accretion disks 20 p3073 A83-43072
- Discovery of a redshift $z = 1.2$ quasar with a flat radio spectrum in the field of the gamma-ray source CG 195+04 20 p3073 A83-43081
- A method to improve the visibility of time-variable gamma-ray sources in structured background 21 p3245 A83-44451
- Analysis methods for results in gamma-ray astronomy 21 p3226 A83-45565
- Pulsar electrodynamics - Cylindrical model and radio and gamma-ray radiation 22 p3379 A83-46559
- Blast waves with cosmic-ray pressure 22 p3390 A83-47004
- Gamma-ray observations from Hinotori 23 p3535 A83-47696
- Gamma-ray line emission from SS433 23 p3527 A83-48073
- The Sneg-3 gamma-ray astronomy experiment 23 p3517 A83-48405
- A system of active data-storage for experiments on gamma-ray transients 23 p3500 A83-48416
- Investigation of gamma-ray transients on Venera 11 and 12 and Prognoz 7 23 p3517 A83-48419
- Gamma-ray line features from the Crab Nebula in the energy range 50-2000 keV 24 p3659 A83-49370
- Ultra high energy gamma rays from Cygnus X3 24 p3667 A83-50076
- Galactic gamma radiation - The contribution from discrete sources 24 p3675 A83-50080
- GAMMA RAY BURSTS**
- Investigation of cosmic gamma-ray bursts 01 p0130 A83-10844
- Gamma-ray bursts and the collapse of a white dwarf 02 p0252 A83-11611
- Radiation for a strongly-magnetized plasma - The case of predominant scattering --- in models for X-ray pulsars and gamma-ray bursters 04 p0548 A83-14977
- Persistent X-ray emission from a gamma-ray burst source 05 p0701 A83-17799
- Comments on the gamma-ray burst catalog of Mazets et al. (1981a) 05 p0710 A83-17820
- Comments on the gamma-ray burst log N / greater than S / log S point of Beurle et al 06 p0858 A83-18888
- Gamma-ray burst systematics 07 p1038 A83-20002
- A review of the 1979 March 5 transient 07 p1011 A83-20003
- Frequency of gamma-ray bursts greater than 3×10 to the -6th erg/sq cm 07 p1039 A83-20004
- Observation of gamma-ray bursts from 10 keV to 9 MeV 07 p1039 A83-20005
- Gamma-ray burst observations by the HEAO-3 high-resolution gamma-ray spectrometer 07 p1039 A83-20006
- Observations of a gamma-ray burst and other sources with a large-area, balloon-borne detector 07 p1039 A83-20007
- Search for associations of radio pulses and gamma ray bursts 07 p1004 A83-20008
- Gamma ray burst positions 07 p1004 A83-20009
- Statistical study of gamma-ray burst source locations 07 p1004 A83-20010
- The observational consequences of an intrinsic burst luminosity distribution 07 p1011 A83-20011
- Derivation of the luminosity of a gamma ray burst 07 p1011 A83-20012
- Gamma-ray burst spectra 07 p1039 A83-20013
- Time variations of an absorption feature in the spectrum of the gamma-ray burst on 1980 April 19 07 p1011 A83-20015
- The low energy spectra of gamma-ray bursts 07 p1039 A83-20018
- On the interpretation of gamma-ray burst continua and possible cyclotron absorption lines 07 p1011 A83-20019
- Emission mechanisms of the March 5th 1979 gamma ray transient 07 p1039 A83-20021
- Surface and magnetospheric physics of neutron stars and gamma-ray bursts 07 p1011 A83-20022
- Gamma-ray bursts from young neutron stars 07 p1011 A83-20023
- Precursors to gamma-ray bursts in the asteroid impact scenario 07 p1012 A83-20024
- Proton deceleration in a neutron star atmosphere 07 p1012 A83-20025
- Solar energetic photon transients - 50 keV-100 MeV 07 p1036 A83-20030
- Evidence for delayed second phase acceleration in solar flares 07 p1037 A83-20033
- Solar flare energetics 07 p1037 A83-20035
- The Burst and Transient Source Experiment for the Gamma-Ray Observatory 07 p1005 A83-20037
- Modulated Multiple Slit Camera for improved localization of gamma ray bursts 07 p1005 A83-20038
- Proposed hard X-ray imaging and gamma ray burst studies for XTE --- X-ray Timing Explorer 07 p1005 A83-20040
- Ion chamber gamma burst detector 07 p1005 A83-20041
- Can gamma-ray bursts originate from low-mass binaries 08 p1186 A83-23281
- Supplementary information for some gamma-ray bursts by SAS-2 anticoincidence dome data 09 p1360 A83-24467
- Size of a gamma-ray burster optical emitting region 09 p1361 A83-24697
- The distribution of gamma-burst sources in the sky and the burst of June 13, 1979 09 p1369 A83-25047
- Thermoluminescence in sediments and historical supernovae explosions 11 p1619 A83-28430
- Nuclear fission in the neutron stars and gamma-ray bursts 12 p1794 A83-29088
- Observations of fast, transient gamma-ray phenomena --- Thesis 15 p2277 A83-33698
- On the nature of two gamma bursts with spectral evolutions observed by the KONUS experiment 15 p2286 A83-34123
- A search for very high energy gamma-ray transients from Cygnus X-3 and PSR 0531 16 p2441 A83-36639
- Gravitational settling in layers accreted on neutron stars and its relations to gamma ray bursts 16 p2430 A83-36643
- H0547-14 - X-ray flux from a weak gamma-ray burst? 17 p2598 A83-37340
- On the possible nature of the gamma source SG 195-4 17 p2601 A83-37686
- Observations of gamma radiation at 10 to the 12th eV from the X-ray source Cyg X-3 at the Tien-Shan installation in 1977 and 1978 17 p2589 A83-37687
- On the variation of the 4.8-hour period of Cyg X-3 17 p2601 A83-37688
- Possible observation of a burst of cosmic-ray events in the form of extensive air showers 17 p2629 A83-37738
- Quantized synchrotron radiation as a cause of gamma-ray bursts 17 p2629 A83-38050
- New activity in the Dorado gamma-ray burst source 17 p2630 A83-38829
- The role of proton cyclotron emission near accreting magnetic neutron stars 18 p2765 A83-39199
- Gamma-ray bursts and neutron stars 18 p2766 A83-39246
- Advances in gamma-ray line astronomy 18 p2756 A83-39293
- Gamma-ray spectroscopy - Status and prospects 18 p2647 A83-39294
- Gamma-ray bursts - The current status 18 p2756 A83-39297
- Developments in high-precision gamma-ray burst source studies 18 p2786 A83-39298
- Nature of gamma-ray burst sources 18 p2766 A83-39299
- Techniques for fine gamma-ray burst spectroscopy 18 p2757 A83-39300
- Gamma-ray burst localization with the international solar polar mission 18 p2647 A83-39301
- Problems in the analysis of gamma-ray burst spectra 18 p2786 A83-39302
- Catalogue of gamma-bursts detected by the Soviet-French experiment 'Signe 2M' (Venera-11, 12 and Prognoz-7) 18 p2786 A83-39303
- X-ray emission associated with gamma-ray bursts 18 p2775 A83-39759
- Constraints on gamma-ray bursters from soft X-ray transients 18 p2787 A83-39959
- Non-absorption dips in the spectra of gamma-ray bursts 18 p2777 A83-39962
- Observations of cosmic gamma-ray bursts in the Konus experiment on Venera 13 and 14 19 p2925 A83-41249
- Optical candidates for the 1978 November 19 gamma-ray burst source 19 p2911 A83-41647
- Candidates for a gamma-ray burster optical counterpart 19 p2911 A83-41648
- Analysis of the Konus catalog of gamma-ray bursts with the thermal synchrotron model 20 p3073 A83-43069
- Prospects for the study of gamma-ray-burst sources 21 p3226 A83-45297
- Investigation of gamma-ray transients by means of unmanned spacecraft 23 p3424 A83-48401
- Instruments and detectors for the registration of gamma-ray transients 23 p3425 A83-48402
- Physical calibration of instruments for the detection of transients --- of gamma-ray bursts by satellite detectors 23 p3425 A83-48403
- Ground tests of instruments for the detection of transients --- of gamma-ray bursts 23 p3425 A83-48404
- Estimation of the false detection of X-ray and gamma-ray transients --- in spaceborne experiments 23 p3425 A83-48407
- Ballistic support of optimal conditions for the performance of stereo gamma-ray transient experiments on Venera 11 and 12 23 p3418 A83-48408
- Determination of the coordinates of transient gamma-ray sources on the basis of delays in the passage of transients at various points of space 23 p3517 A83-48409
- Identification of the coordinates of a transient gamma-ray source with star-catalog coordinates 23 p3517 A83-48410
- Determination of the attitude of the Prognoz station in the problem of the localization of X-ray and gamma-ray sources 23 p3425 A83-48411
- Processing of data from the Sneg-2MP experiment --- onboard gamma-ray bursts detector 23 p3425 A83-48412
- The data processing and transfer system for the Sneg-2MZ experiment --- onboard gamma-ray bursts detector 23 p3425 A83-48413
- System for the rapid processing of data in experiments involving the search for gamma-ray transients 23 p3501 A83-48414
- Rapid processing of scientific data of the stereo gamma-ray transient experiment on Venera 11 and 12 23 p3500 A83-48415
- The application of a graphic display for the analysis of scientific telemetry data in experiments involving the search for gamma-ray transients on Prognoz 6 and 7 23 p3500 A83-48417
- Preliminary results on gamma-ray transients in the Konus experiment on Venera 11 and 12 23 p3517 A83-48418
- On a possible evolutionary link between certain gamma-ray flare sources and nearby pulsars 23 p3527 A83-48421
- GAMMA RAY LASERS**
- Upconversion of laser radiation to gamma-ray energies 11 p1577 A83-27533
- The gain of a solid-state gamma-ray laser 14 p2023 A83-32162
- Setting up the Sagnac experiment in a gamma-ray ring interferometer --- Russian book 23 p3453 A83-47122
- GAMMA RAY OBSERVATORY**
- The Burst and Transient Source Experiment for the Gamma-Ray Observatory 07 p1005 A83-20037
- The Oriented Scintillation Spectrometer Experiment for the Gamma-Ray Observatory 18 p2756 A83-39290
- Scientific satellite data communications 19 p2813 A83-41341
- GAMMA RAY SPECTRA**
- Diffuse galactic gamma-ray line emission from nucleosynthetic Fe-60, Al-26, and Na-22 - Preliminary limits from HEAO 3 03 p0439 A83-14210
- Gamma-ray burst spectra 07 p1039 A83-20013
- Gamma ray lines from solar flares and cosmic transients 07 p1011 A83-20020
- A third-generation small spectroscopy experiment for hard transient events 07 p1005 A83-20039
- On the origin of relativistic particles and gamma-rays in quasars 08 p1181 A83-23030
- A new method for measuring radon exhalation 09 p1296 A83-24278
- Spectral observations of atmospheric gamma-ray background 13 p1967 A83-31473
- The energy spectrum of cosmic fireballs 16 p2431 A83-36672
- May 1980 low energy gamma-ray observations with the 'MISO' telescope 18 p2756 A83-39292
- Gamma-ray spectroscopy - Status and prospects 18 p2647 A83-39294

GAMMA RAY SPECTROMETERS

- Problems in the analysis of gamma-ray burst spectra
18 p2786 A83-39302
- Positron annihilation radiation from Seyfert nuclei and the cosmic diffuse gamma-ray background
18 p2775 A83-39762
- Non-absorption dips in the spectra of gamma-ray bursts
18 p2777 A83-39962
- The high-energy spectrum of hot accretion disks
20 p3073 A83-43072
- Gamma-ray observational constraints on the origin of the optical continuum emission from the white-light flare of 1980 July 1
22 p3389 A83-47010
- Relativistic particles and gamma-rays in quasars and active galactic nuclei
23 p3540 A83-47761
- Expected high-frequency radiation from the 1.5-ms pulsar
24 p3670 A83-50113

GAMMA RAY SPECTROMETERS

- A direct observation of solar neutrons following the 0118 UT flare on 1980 June 21
05 p0708 A83-17035
- Gamma-ray burst observations by the HEAO-3 high-resolution gamma-ray spectrometer
07 p1039 A83-20006
- Search for time variations in 511 keV flux by ISEE-3 gamma-ray spectrometer
07 p1039 A83-20016
- Two years orbital performance summary of Stirling cycle mechanical refrigerators
08 p1053 A83-22847
- The position sensitive low energy detector on board the ZEBRA telescope --- for gamma and X-ray astronomy
18 p2647 A83-39286
- The Oriented Scintillation Spectrometer Experiment for the Gamma-Ray Observatory
18 p2756 A83-39290
- Gamma-ray spectroscopy - Status and prospects
18 p2647 A83-39294
- Computer simulation study of multiple germanium gamma-ray sensor arrays
18 p2756 A83-39295
- Observations of the galactic center with the GSFC low-energy gamma-ray spectrometer - Preliminary results
19 p2909 A83-40693
- Modeling and deconvolution for reconstruction of airborne gamma ray radiometer data
22 p3288 A83-46125

GAMMA RAY TELESCOPES

- Gamma ray detection with long NaI/Tl scintillator bars
09 p1268 A83-24104
- The choice of an astatic system for the regulation of the rotational velocity of a dc electric motor for azimuthal mountings of a gamma-telescope
17 p2496 A83-37720
- Prospects in instrumentation for future space experiments
18 p2755 A83-39279
- An imaging telescope for high energy gamma-ray astronomy
18 p2755 A83-39281
- The observation of the galactic anticenter region by the balloon borne gamma-ray telescope Natalya-1
18 p2785 A83-39282
- Imaging systems using modulation and coded aperture masks --- for gamma ray telescopes
18 p2756 A83-39284
- The position sensitive low energy detector on board the ZEBRA telescope --- for gamma and X-ray astronomy
18 p2647 A83-39286
- An imaging telescope for soft gamma-ray astronomy - The preliminary in-flight tests
18 p2756 A83-39287
- A directional gamma-ray telescope using coded aperture techniques
18 p2756 A83-39289
- Figaro - An experiment for pulsar and variable source studies in the MeV range
18 p2688 A83-39291
- May 1980 low energy gamma-ray observations with the 'MISO' telescope
18 p2756 A83-39292

GAMMA RAYS

- NT GAMMA RAY BURSTS
- Airborne measurement of surficial soil moisture using natural terrestrial gamma radiation
01 p0066 A83-10120
- The longitudinal radioisotopic gamma-tomograph GPR-1
01 p0050 A83-10558
- Study of diffuse cosmic and atmospheric gamma radiation using a spark chamber in the energy range 4 MeV-100 MeV
02 p0271 A83-11606
- Partial inelasticity coefficients K-gamma in pi-A and pA interactions
02 p0234 A83-11734
- Investigation of azimuth effects in gamma families with total energies of 30-1000 TeV
02 p0274 A83-11740
- What is it possible to say about the breakdown of scaling according to data of the Pamir experiment
02 p0274 A83-11741
- The structure of gamma families and its relation to the formation of jets. II
02 p0274 A83-11742
- Correlation between the number and energy flux of hadrons and gamma quanta. III
02 p0274 A83-11743
- Experimental studies of superfamily halos. IV --- in cosmic ray showery
02 p0274 A83-11744
- Characteristics of inelastic interactions with high transverse momenta of secondary particles
02 p0274 A83-11747

- The interrelation of cosmic gamma-rays and interstellar gas in the range 165-180 deg
03 p0414 A83-13329
- High-energy gamma-ray light curve of PSR0531+21
03 p0409 A83-14175
- Secondary electron spectra in interstellar clouds, and the bremsstrahlung gamma-ray luminosity
03 p0439 A83-14211
- High energy gamma-rays from black holes
03 p0439 A83-14721
- The local interstellar medium as traced by gamma rays
04 p0550 A83-15048
- Radiation effects in IRAS extrinsic infrared detectors
05 p0645 A83-17484
- Ionizing radiation effects on power MOSFETs during high speed switching
05 p0625 A83-17485
- The effect of operating conditions on the radiation resistance of VDMOS power FETs --- Vertical Double-diffused MOS
05 p0626 A83-17486
- EPROM erasure in transient and total dose gamma environments --- Electrically Programmable Read Only Memory
05 p0626 A83-17507
- The damage equivalence of electrons, protons, and gamma rays in MOS devices
05 p0628 A83-17533
- A comparison of radiation damage in transistors from cobalt-60 gamma rays and 2.2 MeV electrons
05 p0629 A83-17534
- Generation of a radio signal by a low-power gamma-ray source in the atmosphere
06 p0787 A83-19338
- Spectral tuning of shallow-junction surface-emitting light-emitting diodes /LEDs/ through gamma-ray irradiation
08 p1170 A83-22846
- The pattern of the conductivity and the permeability of cells at short periods following gamma-irradiation
09 p1321 A83-24930
- The comparative radioprotective effect of adenylates during short-term and long-term gamma-irradiation
09 p1321 A83-24931
- Active galaxies and the diffuse gamma-ray background
11 p1694 A83-28389
- Low energy gamma ray enhancement observed during a stratospheric balloon flight
13 p1967 A83-31474
- Impact sensitivity of gamma-irradiated HMX
13 p1826 A83-31674
- The early changes in the activation of nucleoside diphosphatekinase in the brain and liver of rats following total-body gamma-irradiation at an absolutely lethal dose
14 p2062 A83-32062
- The response of the lymph and blood coagulation systems to gamma-radiation at high altitudes
14 p2062 A83-32064
- The effect of gamma-irradiation on amorphous silicon field effect transistors
14 p2007 A83-33142
- Kosmos 856 and Kosmos 914 measurements of high-energy diffuse gamma rays
15 p2286 A83-33706
- The pulse profile of the Crab pulsar in the energy range 45 keV-1.2 MeV
15 p2268 A83-34638
- Strongly acidic polypeptides as inhibitors of the repair of single-strand DNA breaks caused by gamma-irradiation
16 p2393 A83-35919
- The halo effect in a nuclear-electromagnetic cascade
17 p2629 A83-37647
- An exact-time registration system for observations of very-high-energy gamma-quanta
17 p2510 A83-37719
- Nature of gamma-ray burst sources
18 p2766 A83-39299
- The biosynthesis of cholesterol in the tissues of irradiated rats
18 p2731 A83-39520
- COS-B gamma-ray measurements and the large-scale distribution of interstellar matter
18 p2786 A83-39658
- A theoretical analysis of the effect of the photoreactivation of E. Coli cells irradiated by gamma-rays
19 p2874 A83-41004
- The relative biological effectiveness of neutrons in conditions of mixed gamma and neutron irradiation
19 p2874 A83-41007
- The characteristics of the biosynthesis of nucleic acids during the activation of erythroid cell proliferation evoked by prolonged gamma-irradiation
19 p2874 A83-41009
- Elastic and inelastic scattering of gamma rays from V3Si
19 p2905 A83-41537
- Annealing behaviour of gamma-ray-induced electron traps in LEC n-InP
20 p3052 A83-42482
- Electric conduction of low density polyethylene induced by high dose rate gamma rays
20 p3052 A83-42598
- Registration of transition X-radiation at gamma = 1000-10,000 by the photon-counting method
20 p2991 A83-43535
- The effect of irradiation temperature on radiation processes in MOS structures
21 p3217 A83-44544

An identification for 'Geminga' (2CG 195+04) 1E 0630+178 - A unique object in the error box of the high-energy gamma-ray source

- 22 p3372 A83-45628
- Co-60 gamma-ray and electron irradiation damage of GaAs single crystals and solar cells
22 p3364 A83-46274
- Gamma-ray lines and neutrons from solar flares
23 p3535 A83-47698
- Characteristics of gamma-ray line flares as observed in hard X-ray emissions and other phenomena
23 p3535 A83-47699
- Damages of the superhelical structures of nuclear DNA by gamma-rays and heavy ions
23 p3495 A83-48201
- The radiosensitivity of colony forming units in diffuse chambers contained in the bone marrow and the spleen of mice during gamma-irradiation at various conditions of oxygenation
23 p3495 A83-48205
- The effect of a constant magnetic field and gamma-radiation on the hereditary structure of somatic cells - The effect of the combination of a constant magnetic field and ionizing radiation on the blood lymphocytes of humans in vitro
23 p3498 A83-48210
- Positrons in cosmic rays and the galactic gamma radiation associated with them
24 p3675 A83-49173
- Gamma-ray irradiation effect on transmission loss for ZrF4-based optical fibres
24 p3630 A83-49985

GANGLIA

- NT NERVES
- NT NEURONS
- The activity of tyrosine hydroxylase in the ganglia of the vegetative nervous system in rabbits during acute experimental emotional stress
01 p0080 A83-10542
- The basal ganglia-circa 1982 - A review and commentary
02 p0222 A83-11826
- A histochemical study of the rat spinal cord, spinal ganglia, and adrenal glands under local vibration
05 p0670 A83-17192

GANYMED

- Pedestal craters on Ganymede
03 p0133 A83-13832
- Constraints on the expansion of Ganymede and the thickness of the lithosphere
04 p0560 A83-15334
- Radar properties of Europa, Ganymede, and Callisto
04 p0570 A83-16233
- Craters and basins on Ganymede and Callisto - Morphological indicators of crustal evolution
04 p0570 A83-16237
- The geology of Ganymede
04 p0571 A83-16238
- Color photometry of surface features on Ganymede and Callisto
05 p0704 A83-16963
- Interpretation of integrated-disk photometry of Callisto and Ganymede
07 p1032 A83-21290
- Ganymede and Callisto
08 p1188 A83-22774
- The evolution of tectonic features on Ganymede
08 p1189 A83-22938
- Voyager 2 observations of energetic particle variations in the Ganymede wake region - A possible acceleration mechanism
17 p2618 A83-37581

GAPS

- NT ENERGY GAPS (SOLID STATE)
- NT SPARK GAPS
- J. E. Keeler's discovery of a gap in the outer part of the A ring
11 p1683 A83-27351
- Aerothermal environment in control surface gaps in hypersonic flow - An overview
14 p1970 A83-32732
- [AIAA PAPER 83-1483]
- Eccentric ringlet in the Maxwell gap at 1.45 Saturn radii
23 p3528 A83-47818

GARMENTS

- The effects of variations in garment protection on clean room cleanliness levels
05 p0677 A83-16930
- Evaluation of a Reverse Gradient Garment for prevention of bed-rest deconditioning
10 p1458 A83-25664
- A tumble test for determining the level of detachable particles associated with clean room garments and clean room wipers
13 p1865 A83-31524

GARNETS

- NT YTTRIUM-ALUMINUM GARNET
- NT YTTRIUM-IRON GARNET
- Experimental determination of the spinel-garnet boundary in a Martian mantle composition
04 p0559 A83-15330
- Effects of pressure and temperature on the physical behavior of mantle-relevant olivine, orthopyroxene and garnet. I Compressibility, thermal properties and macroscopic Gruenisen parameters
16 p2383 A83-36975
- Solidus and liquidus temperatures and mineralogies for anhydrous garnet-lherzolite to 15 GPa
17 p2546 A83-38698

Effects of pressure and temperature on the physical behavior of mantle-relevant olivine, orthopyroxene and garnet. II Infrared absorption and microscopic Grueisen parameters 22 p3332 A83-46716

GARP
U GLOBAL ATMOSPHERIC RESEARCH PROGRAM

GARP ATLANTIC TROPICAL EXPERIMENT
The inclusion of moist downdraft effects in the Arakawa-Schubert cumulus parameterization 03 p0368 A83-14445

Results from studies of the intertropical convergence zone in GATE 05 p0668 A83-17700

The use of GATE data for the analysis of polar wind 07 p0970 A83-20894

ANMRC data assimilation for the Southern Hemisphere 08 p1138 A83-22283

Numerical weather prediction studies from the FGGE Southern Hemisphere data base 08 p1138 A83-22285

Vertical mass transport in cumulonimbus clouds on day 261 of GATE 08 p1140 A83-22297

Rainfall rates derived from Nimbus 5 observations analysed against GATE radar rainfall 09 p1314 A83-24121

Synoptic oscillations of the currents in the FGGE Atlantic equatorial test-region 09 p1320 A83-24941

Life cycles of convective cells in organized mesoscale systems in gate 11 p1626 A83-27026

A radiation model using hourly meteorological data with results from GATE 11 p1632 A83-27972

A composite analysis of the boundary layer accompanying a tropical squall line 13 p1891 A83-30803

Basic state energy budget analysis for phases 1, 2 and 3 of GATE 13 p1891 A83-30806

A first order vorticity equation for tropical easterly waves 16 p2386 A83-35486

A comparison of calculated and radar-located precipitation in GATE 19 p2868 A83-41586

GAS ANALYSIS
NT OZONOMETRY
Design considerations for aerodynamically quenching gas sample probes [ASME PAPER 82-HT-39] 02 p0172 A83-12794

Gas analysis techniques for high temperature corrosion testing 02 p0149 A83-12834

Analysis points to meteorite coming from Mars 02 p0268 A83-13024

Laser resonant optoacoustic gas-analyzer for the monitoring of trace contaminants of the atmosphere 06 p0764 A83-19183

Oxygen isotopes in eucrites, shergottites, nakhlites, and chassignites 08 p1187 A83-21639

Detection of trace quantities of dimethylacetamide during the curing process of a polyimide film 09 p1237 A83-23623

Semiautomatic nondispersive infrared analyzer apparatus for CO2 air sample analyses 09 p1295 A83-24258

Carbon monoxide mixing ratio inference from gas filter radiometer data 09 p1306 A83-24450

High-sensitivity atmospheric gas analysis based on intracavity laser detection of scattered radiation 10 p1392 A83-26685

Analysis method for Fourier transform spectroscopy 10 p1424 A83-26867

A laser-based technique for the measurement of hydrogen at local areas in metals 11 p1547 A83-27331

The optimal design for spectral gas analyzers of atmospheric pollution 11 p1573 A83-28201

Separate determination of the nitrogen oxides NO, NO2, and NOx/ in city air by an automatic gas analyzer and a chemical method 11 p1613 A83-28202

Isotopic analysis of nanomole gas samples by means of dynamic flow mass spectrometry 13 p1845 A83-30255

Laser methods for the control of atmospheric gases and gases which pollute the atmosphere 14 p2052 A83-32560

Quantitative intracavity spectroscopy 14 p2052 A83-32561

Fiber-optic absorption/fluorescence probes for combustion measurements 14 p2020 A83-32902

Coherent anti-Stokes Raman spectroscopic modeling for combustion diagnostics 14 p2021 A83-33173

The laser-induced Schlieren effect in sodium-nitrogen mixtures [AIAA PAPER 83-1467] 15 p2165 A83-34911

Design and performance of the Stratospheric Aerosol and Gas Experiment II (SAGE II) instrument 17 p2511 A83-38056

Gas emissions and the eruptions of Mount S. Helens through 1982 22 p3333 A83-46798

GAS ATOMIZATION

Comparison of the quench rates attained in gas-atomized powders and melt-spun ribbons of Co- and Ni-base superalloys - Influence on resulting microstructures [ONERA, TP NO. 1982-132] 04 p0460 A83-15993

GAS BAGS
A new static-launch method for plastic balloons 18 p2642 A83-39816

GAS BEARINGS

Advanced development of air-lubricated foil thrust bearings [ASLE PREPRINT 82-LC-6B-1] 03 p0335 A83-13246

An experimental investigation of the stability of externally pressurized gas-lubricated porous thrust bearings [ASME PAPER 82-LUB-38] 03 p0336 A83-13517

Analysis of gas lubricated compliant thrust bearings [ASME PAPER 82-LUB-39] 03 p0336 A83-13518

Analysis of gas-lubricated foil journal bearings [ASME PAPER 82-LUB-40] 03 p0336 A83-13519

The effect of two sided surface roughness on ultra-thin gas films 06 p0769 A83-18390

Influence of gas inertia forces generated within the stabilizing restrictor on dynamic characteristics of externally pressurized thrust gas bearings. I - Case of laminar flow at the capillary restriction 07 p0939 A83-20292

A study on characteristics of surface-restriction compensated gas bearing with T-shaped grooves 07 p0939 A83-20293

Influence of gas inertia forces generated within the stabilizing restrictor on dynamic characteristics of externally pressurized thrust gas bearings. II - Case of turbulent flow at the capillary restriction 09 p1273 A83-23336

Dynamic behavior of fluid bearings - Linear and nonlinear study --- French thesis 11 p1589 A83-28631

Ceramic-beryllium composites for gas bearings 14 p1986 A83-31916

Analysis of externally pressurized gas-lubricated conical bearings 16 p2363 A83-36941

Moving-wave gas seal [ASLE PREPRINT 83-AM-5A-2] 20 p2999 A83-43333

Gas bearings. I - Dynamic analysis and solution method 21 p3147 A83-44374

Hypersonic dynamic testing of ablating models with three-degree-of-freedom gas bearings 23 p3412 A83-48135

Gas bearings. II - Design data for centrally loaded partial arc journal bearings 23 p3466 A83-48155

Steady-state characteristics of aerostatic porous rectangular thrust bearings incorporating the effects of velocity slip, anisotropy and tilt 24 p3590 A83-48825

GAS CHROMATOGRAPHY

Data enhancement and analysis through mathematical deconvolution of signals from scientific measuring instruments 01 p0051 A83-11055

High-voltage spark atomic emission detector for gas chromatography 02 p0153 A83-13108

The composition of the products of the combustion of pyropowder at atmospheric pressure 07 p0880 A83-19954

Chromatographic and mass-spectrometric determinations of traces of organic substances in the atmosphere --- Russian book 09 p1299 A83-25250

Venera 13 and Venera 14 gas-chromatography analysis of the Venus atmosphere composition 12 p1798 A83-29478

Gas-chromatographic analysis of the chemical composition of the Venusian atmosphere on the descent modules of the Venera-13 and Venera-14 probes 14 p2111 A83-31962

Fluorocarbon combustion studies. VI - Competitive combustion reactions of fluorocarbons burning with fluorine 14 p1991 A83-32942

Determination of ethylene and other reactive hydrocarbons in the atmospheric air at Trombay, Bombay by gas chromatography using a chemiluminescent detector 19 p2849 A83-41984

Synthesis and thermal stability of carborane-containing phosphazenes 23 p3427 A83-47640

Determination of the thermal stability of oils by pyrolytic gas chromatography 23 p3439 A83-48547

A modified technique for estimation of ethanol in body fluids by gas liquid chromatography 23 p3499 A83-48694

GAS COMPOSITION

NT CARBON DIOXIDE CONCENTRATION
Gas analysis techniques for high temperature corrosion testing 02 p0149 A83-12834

Rapid monitoring of the acid-base and gas composition of the blood 03 p0375 A83-14334

GAS DENSITY

The tropospheric gas composition of Jupiter's north equatorial belt /NH3, PH3, CH3D, GeH4, H2O/ and the Jovian D/H isotopic ratio 04 p0569 A83-15643

On the siting of noble gases in E-chondrites 04 p0572 A83-16356

Structure of a reflected planar shock wave 05 p0640 A83-17416

An investigation of the genotypic conditionality of the gas composition and acid-base state indicators of the blood during various effects on the body 09 p1323 A83-25152

Attachment of low-energy electrons to O2 molecules in some gases and liquids - An instrument for measuring concentrations of electronegative impurities in gases 10 p1422 A83-26468

Calculation of the parameter for the quality of the least-squares fit in investigating atmospheric pollution by resonance absorption 11 p1613 A83-28204

Effects of low concentrations of chlorine on pulmonary function in humans 13 p1905 A83-30509

Temperature and concentration measurements in an internal combustion engine using laser Raman spectroscopy [AIAA PAPER 83-1551] 14 p1990 A83-32772

Laboratory simulation of tunable diode laser remote measurement of atmospheric gases using topographic targets 17 p2510 A83-37741

The problem of the excess of noble gases in the atmosphere of Venus 17 p2619 A83-37816

Direct statistical simulation of collisional relaxation in gas mixtures with large differences in concentration 18 p2751 A83-39151

Correlations concerning turbulent natural convection Influence of pressure and nature of the gas 18 p2685 A83-39851

Martian gases in an Antarctic meteorite? 19 p2922 A83-40913

Gaseous contaminants in the atmosphere and changes of the global climate 21 p3169 A83-45334

Trapped noble gases indicate lunar origin for Antarctic meteorite 22 p3386 A83-46867

Relationship between thermal-radiation characteristics and concentrations of trace gases in different layers of the atmosphere 23 p3488 A83-47160

2.7 measurements of HONO, NO3, and NO2 by long-path differential optical absorption spectroscopy in the Los Angeles Basin 23 p3478 A83-47779

Numerical simulation of the effects of changes of the gas composition of the atmosphere on climate 24 p3609 A83-49278

GAS COOLED REACTORS
NT HIGH TEMPERATURE GAS COOLED REACTORS
Advances in NASA research on nuclear-pumped lasers 11 p1579 A83-27558

Design considerations for nuclear reactor gas turbine space power systems [ASME PAPER 83-GT-20] 23 p3426 A83-47886

GAS COOLING
Star formation in a cooling flow 03 p0419 A83-13934

Inversion of the vibrational level populations during the kinetic cooling of a moving gas 04 p0483 A83-15091

Numerical study of the dependence of the efficiency of the gas-screen cooling of perforated gas-turbine blades on cascade parameters 05 p0589 A83-16955

Tests of vacuum vs helium in a solar telescope 06 p0818 A83-18577

Analytic and experimental study of the efficiency of a cooling-gas blanket downstream of a single row of identical rectangular orifices in a wall 06 p0759 A83-19158

Efficiency of combined jet cooling of a plate in conditions of complex heat transfer 10 p1417 A83-26254

Stability characteristics of a boundary gas layer recombining on a cooled wall 19 p2843 A83-41272

Model test and full-scale checkout of dry-cooled jet runup sound suppressors 23 p3413 A83-48217

Cooling of the primordial gas by molecular hydrogen 24 p3663 A83-49635

Calculation of a boundary layer with phase transformations --- oxygen condensation at cooled surface 24 p3579 A83-49661

GAS DENSITY
The peculiarities of the external respiration and gas exchange during the respiration of helium-oxygen mixtures having various concentrations of oxygen 01 p0082 A83-10488

The thermal conductivity of oxygen 02 p0244 A83-12094

The interrelation of cosmic gamma-rays and interstellar gas in the range 1.65-180 deg 03 p0414 A83-13329

Reconstructing the vertical profile of the ozone density in the atmosphere on the basis of measurements of the absorption of solar infrared radiation 03 p0362 A83-14830

- The relation between magnetic field and gas density in interstellar clouds 06 p0840 A83-19276
- New observations of a region of the Magellanic Stream 07 p1010 A83-19857
- Time evolution of disk galaxies undergoing stochastic self-propagating star formation 07 p1020 A83-21112
- Noble gas components in clasts and separates of the Abee meteorite 08 p1188 A83-21642
- Formaldehyde toward Cas A - Cloud sizes and H2 densities 10 p1501 A83-25496
- Molecular beam technique for recording chemical species behind incident shock waves 10 p1391 A83-26184
- Dependence of interstellar depletion on hydrogen column density - Possibilities and implications 10 p1513 A83-26716
- Structure of dense molecular gas in TMC 1 from observations of three transitions of HC3N 10 p1513 A83-26717
- The distribution of atomic and molecular hydrogen in the Galactic plane 11 p1681 A83-28260
- Investigation of supersonic plane underexpanded jets by the laser schlieren method 11 p1584 A83-28538
- Ozone density distribution in the mesosphere /50-90 km/ measured by the SME limb scanning near infrared spectrometer 12 p1750 A83-28903
- Measurements of NO2 in the earth's stratosphere using a limb scanning visible light spectrometer 12 p1751 A83-28908
- A mesospheric ozone profile at sunset 12 p1756 A83-29582
- Human respiration at rest in rapid compression and at high pressures and gas densities 13 p1902 A83-30467
- On the kinetic theory of dense gases 13 p1932 A83-30656
- Calculation of the kinetic coefficients for a moderately dense gas 13 p1932 A83-30657
- Approximate method of solving the kinetic equation for moderately dense gases near a boundary temperature jump in a binary mixture 13 p1933 A83-31467
- Second order closure for variable density free shear layer 15 p2156 A83-33672
- The gas density and distribution within 2 parsecs of the galactic center 15 p2259 A83-34122
- Termolecular ionic recombination at high ambient gas density 16 p2414 A83-35326
- Density and temperature variations in pulsed discharge lasers 16 p2358 A83-35453
- On the investigation of axisymmetric discontinuous flows using interferometry 16 p2349 A83-35538
- An approximate method for solving a kinetic equation for moderately dense gases near a boundary - The slip of a binary mixture 16 p2350 A83-35711
- On the distribution of nitrogen dioxide in the high-latitude stratosphere 16 p2379 A83-36138
- On the possibly low H2 formation rate in dense clouds 17 p2598 A83-37349
- Time-resolved two-dimensional concentration measurements in an acoustically driven flow 19 p2841 A83-40856
- Cyanoacetylene as a density probe of molecular clouds 20 p3067 A83-42443
- Optical properties of a laser plasma near a solid surface in a dense gas 21 p3211 A83-44146
- A distribution function for a gas under conditions of escape flow 21 p3176 A83-45263
- The effect of inhomogeneity on the nonlinear stabilization of the acoustic oscillations of a heat-releasing medium in a limited volume 23 p3513 A83-48651
- NGC 3992 - A galaxy without a massive halo 24 p3654 A83-49217
- Theory of spiral structure --- of Milky Way Galaxy 24 p3655 A83-49221
- GAS DETECTORS**
- Modification of a commercial NOx detector for high sensitivity 03 p0328 A83-14168
- Detection of trace concentrations of H2 in air by coherent active Raman spectroscopy 10 p1423 A83-26657
- Pd-SiO2-GaAs MIS diode for hydrogen detection 12 p1728 A83-29038
- Palladium-silicondioxide-silicon structures as hydrogen sensors in electrolytes 12 p1712 A83-29464
- Ozone precursor monitor for investigating air pollution 15 p2162 A83-33488
- Pd/a-Si:H metal-insulator-semiconductor Schottky barrier diode for hydrogen detection 15 p2150 A83-33845
- Some recent steps in the evolution of gaseous detectors 16 p2355 A83-35627
- Characteristics of semiconductor gas sensors. I - Steady state gas response 17 p2512 A83-38535
- The detection of photons with gaseous detectors 18 p2688 A83-39280

- Determination of ethylene and other reactive hydrocarbons in the atmospheric air at Trombay, Bombay by gas chromatography using a chemiluminescent detector 19 p2849 A83-41984
- Hydrogen embrittlement measurement using new palladium probe [SAE PAPER 820604] 22 p3287 A83-45865
- Semiconductor detector for the selective detection of atomic hydrogen 23 p3454 A83-47643
- GAS DISCHARGE COUNTERS**
- U GAS DISCHARGE TUBES**
- GAS DISCHARGE TUBES**
- NT THYRATRONS**
- Gas discharge lasers --- Russian book 01 p0054 A83-10673
- Measurement of the excited-atom density in a discharge in neon by laser resonance fluorescence 03 p0396 A83-13185
- Lightweight ozonizer for field and airborne use 03 p0329 A83-14169
- He-Ne laser generation of 1.15-1.20 microns in a hollow copper cathode 04 p0485 A83-15950
- Transversely excited Sr/ + / recombination laser 06 p0767 A83-19251
- A high-density effusive target of atomic hydrogen 08 p1162 A83-21981
- Mode-medium interactions --- high power CO2 laser output instability 08 p1109 A83-22461
- Service life of a copper bromide vapor laser 10 p1432 A83-26674
- The physics of electric-discharge CO2-lasers --- Russian book 12 p1731 A83-28815
- Injection gas electronics --- Russian book 13 p1832 A83-30523
- Simple and efficient preionization system for gaseous lasers 13 p1857 A83-31472
- Investigation of strata in small-scale He-Ne lasers 17 p2515 A83-38488
- A selfsustained discharge multiatmospheric CO2 laser with electron-beam preionization 20 p2995 A83-43633
- Compact uniform field electrode profiles --- for use in TEA laser 21 p3143 A83-44191
- Analysis of temporal-length limitations in XeCl lasers 23 p3460 A83-47605
- GAS DISCHARGES**
- Wide aperture self-sustained discharge KrF and XeCl lasers 01 p0055 A83-10984
- The structure of electron avalanches at high E/P --- electric field - pressure relations 02 p0241 A83-11956
- A direct-measurement technique for estimating discharge-chamber lifetime --- for ion thrusters [AIAA PAPER 82-1908] 02 p0144 A83-12483
- Uniformity of an externally sustained steady-state volume discharge 03 p0392 A83-13196
- Kinetic processes in the HgBr/B-X//HgBr2 dissociation laser 03 p0331 A83-13917
- Atmospheric- and supraatmospheric-pressure CO2 lasers with a self-maintained discharge 04 p0483 A83-15256
- Physicomechanical properties of polytetrafluorethylene treated by a high-frequency gas-discharge plasma 04 p0463 A83-15397
- Metastable atom density in helium, neon, and argon glow discharges 04 p0538 A83-16059
- Photoionization of nitrogen and oxygen mixtures by radiation from a gas discharge 06 p0811 A83-18439
- Initiation of a high-power nonself-sustained volume discharge in molecular gases by ultraviolet radiation from a plasma cathode 07 p0996 A83-20127
- An RF-primed all-halogen gas plasma microwave high-power receiver protector 07 p0922 A83-21530
- The effect of forced and free convection in the discharge of a pressurized gas 08 p1090 A83-23210
- Plasma layers near the electrodes of a cesium diode - Cathode layer 09 p1348 A83-23989
- Interaction of electromagnetic waves with a moving perturbation in a stationary gas 10 p1471 A83-25648
- Experimental study of an axial discharge in a turbulent gas flow 10 p1430 A83-26252
- Thermal physics of transverse-discharge copper vapor lasers 10 p1433 A83-26682
- The construction of systems of equations describing gas discharges containing several species of atoms and ions, including stepwise processes, negative ions, and the spatial variation of the temperatures 15 p2237 A83-35271
- Plasma formation in a gas-liner pinch 16 p2414 A83-35617
- Long pulse excimer laser excited by sequenced discharges 16 p2359 A83-35956
- Unipolar currents and electrostatic probe characteristics in a gas discharge plasma 17 p2582 A83-37613

- A kinetic model of the sustained discharge HgBr laser 17 p2514 A83-38207
- Effect of water vapor on an externally maintained gas discharge 18 p2746 A83-39860
- High-efficiency infrared xenon laser excited by a UV preionized discharge 19 p2852 A83-40947
- Measurement of high-voltage pulses employing a quartz Pockels cell 20 p2990 A83-42790
- A kinetic study of the high-frequency instability of a discharge in gases 20 p3050 A83-43510
- XeCl excimer laser excited by longitudinal discharge 20 p2995 A83-43597
- Externally sustained RF discharges in electronegative gases 21 p3211 A83-44143
- Lasing on the B-X band of cadmium moniodide (CdI) and (Cd-114I) in a UV-preionized, transverse discharge 21 p3146 A83-45481
- The secondary light emissions of a gaseous medium in the strong field of a standing electromagnetic wave 23 p3508 A83-48091
- GAS DISSOCIATION**
- Analysis of flows of an equilibrium dissociated, ionized, and radiating gas by the method of large particles 01 p0003 A83-11275
- Dissociative recombination of electrons and molecular ions 02 p0234 A83-12175
- Free radical propulsion concept 03 p0289 A83-13141
- Ion aging effects on the dissociative-attachment instability in CO2 lasers 04 p0484 A83-15792
- Heat transfer in the turbulent flow of dissociating and vibrationally relaxing gas in a channel with rough walls 04 p0477 A83-15862
- Mode specificity in the unimolecular dissociation of formaldehyde /H2CO yields H2 + CO/, a two-mode model 05 p0613 A83-17654
- Long contact effect between active nitrogen and carbon monoxide - N2 dissociation to N/S-/ 05 p0613 A83-17872
- Dissociative excitation of SO2 by controlled electron impact --- Jupiter emission 08 p1190 A83-23116
- Investigation of the electrokinetic properties and of the dissociation of O2 molecules in an oxygen discharge 09 p1348 A83-23987
- Production of negative ions by dissociative electron attachment to SO2 10 p1478 A83-25552
- Comparison of photon stimulated dissociation of gas phase and chemisorbed CO 10 p1389 A83-25556
- Interactions between neutral dissociation and ionization continua in N2O 10 p1479 A83-25560
- A shock tube study of DF dissociation 10 p1389 A83-25561
- Theory of dissociative recombination 10 p1479 A83-25991
- The acceleration of molecular hydrogen clouds through radiative dissociation 10 p1508 A83-26369
- Experimental investigation of the glow of certain fragments observed in cometary spectra 11 p1679 A83-27887
- Dissociation of CO2 in a nonequilibrium plasma 13 p1925 A83-30647
- The Delta band dissociation of nitric oxide - A potential mechanism for coupling thermospheric variations to the mesosphere and stratosphere 13 p1877 A83-30894
- The dissociative recombination of O2(+) - The quantum yield of O(1S) and O(1D) 13 p1916 A83-31248
- Vibrational relaxation and dissociation of strongly excited ozone molecules 14 p2081 A83-31905
- Dissociation of CO2(2+) ions into CO(+) and O(+) fragments 17 p2486 A83-38469
- Galactic cosmic rays and N2 dissociation on Titan 19 p2921 A83-40780
- Dissociative recombination in low-energy e-H2(+) collisions 19 p2898 A83-41194
- The kinetic theory of H2 dissociation --- in interstellar molecular clouds 19 p2918 A83-41624
- Production of O(-) from CO2 by dissociative electron attachment 19 p2898 A83-41863
- The photodissociation of nitromethane at 193 nm 20 p2950 A83-42629
- Photofragmentation of nitromethane in a molecular beam at 193 nm 20 p2950 A83-42630
- Photofragment spectroscopy and dynamics of the visible photodissociation of ozone 20 p3044 A83-42632
- Measurement of the branching ratio for the dissociative recombination of H3(+) + e 21 p3202 A83-44199
- A spectroscopic study of the translation of predissociations of the molecular ions HeH(+) and N2(+) and of dissociations of N2(+) and NO(+) ions by collision with an atomic target --- French thesis 21 p3202 A83-45085
- Nonequilibrium plasmachemical process of CO2 decomposition in a supersonic microwave discharge 21 p3215 A83-45397

- Evolution of weak discontinuities in the unsteady flow of thermally conducting dissociating gases 21 p3134 A83-45598
- Bohr effect data for blood gas calculations 22 p3348 A83-45999
- 'CARS' study of vibrationally excited H₂ formed in formaldehyde photolysis [ONERA, TP NO. 1983-60] 23 p3430 A83-48181
- Angular intensity distribution of Balmer-alpha emission excited by electron impact on H₂ 24 p3626 A83-49431

GAS DYNAMICS

- NT AERODYNAMICS
- NT AEROTHERMODYNAMICS
- NT HYPERSONICS
- NT RAREFIED GAS DYNAMICS
- NT ROTOR AERODYNAMICS
- NT SUPERSONICS
- Some exact solutions describing unsteady plane gas flows with shocks 01 p0045 A83-10493
- Certain numerical methods for solving problems of gas dynamics in Euler coordinates 01 p0045 A83-10566
- Nonstationary flow in gas lines 01 p0045 A83-10582
- The influence of magnetospheric processes on the dynamics of neutral gas at ionospheric heights 01 p0071 A83-10603
- Fundamentals of compressible flow --- Book 01 p0045 A83-10883
- Structure and dynamics of supersonic jets 01 p0126 A83-10946
- Numerical analysis of the dispersion of detonation products 01 p0047 A83-11274
- A theoretical investigation of the distribution of electron concentration in the positive column of a glow discharge with a longitudinal flow of gas 02 p0240 A83-11514
- Computational model of a diffuse discharge on electrodes in a weakly ionized plasma 02 p0241 A83-11952
- Precessing jets in Sagittarius A - Gas dynamics in the central parsec of the galaxy 02 p0255 A83-12113
- A bimodal Maxwellian distribution as the equilibrium solution of the two-particle regime 03 p0399 A83-13117
- Kinetic analysis of evaporation and condensation in a vapor-gas mixture 03 p0315 A83-13118
- Dusty gas-dynamics in real comets 03 p0416 A83-13389
- A relativistic gas in a gravitational field 03 p0417 A83-13527
- Three-dimensional unsteady hypersonic flow of a relaxing gas past a thin wing 03 p0278 A83-13592
- Kinematics of gas clouds in Seyfert nuclei and quasars 03 p0418 A83-13876
- The dynamical destruction of shocked gas clouds 03 p0419 A83-13928
- An analytical study of the flow of a two-phase mixture in a nozzle with allowance for gas-dynamic division 03 p0316 A83-14060
- Invariance properties under a reciprocal Backlund transformation in gasdynamics 03 p0320 A83-14566
- Global existence results for discrete velocity models of the Boltzmann equation in several dimensions 03 p0400 A83-14569
- The nonuniqueness and instability of steady-state combustion modes in a boundary layer with intense injection 03 p0296 A83-14898
- Boundary conditions for equations of the two-temperature gas dynamics of a binary mixture with significantly different component masses 04 p0544 A83-15085
- Probabilistic analysis of plane random waves of gas dynamics 04 p0544 A83-15086
- Three-component gasdynamic model for the interaction of the solar wind with the interstellar medium 04 p0551 A83-15088
- The interference of oblique shocks of a particular family in a hypersonic flow 04 p0441 A83-15090
- Inversion of the vibrational level populations during the kinetic cooling of a moving gas 04 p0483 A83-15091
- Simultaneous measurement of stagnation temperature and specific flow rate in a hypersonic gas flow 04 p0481 A83-15447
- The velocity gradient of B361 04 p0553 A83-15618
- Equations for the dynamics of a vibrationally nonequilibrium gas under conditions of anharmonicity in the molecular vibrations 04 p0544 A83-15775
- On a modified differential approximation method in radiative gas dynamics 04 p0544 A83-15819
- The diagnostics of disturbances in components of turbojet engines with gasdynamics parameter monitoring 04 p0449 A83-15850
- Laminar flow of vapor flux in the condensation region of heat tubes 04 p0477 A83-15864

- Nonlinear problem of heat and mass transfer to a particle in a gas flow at low Reynolds numbers 04 p0477 A83-15876
- Flames as gasdynamic discontinuities 04 p0457 A83-16262
- The transitory phase of the establishment of supercritical shock when a strong shock emerges from a dense medium in a gas 04 p0480 A83-16442
- A characteristic flux difference splitting for the hyperbolic conservation laws of inviscid gasdynamics [AIAA PAPER 83-0040] 05 p0632 A83-16480
- Predictions of the structure of turbulent, particle-laden, round jets [AIAA PAPER 83-0066] 05 p0632 A83-16498
- The entropy of a gas of hard spheres with respect to the group of space-time translations 05 p0691 A83-17138
- Nonlinear theory of a positive column in a magnetic field 05 p0688 A83-17361
- Comparison of gas dynamic model with steady solar wind flow around Venus 05 p0704 A83-17383
- Calculation of the flow of a dust-laden gas over a disk and the flat end of a cylinder 05 p0639 A83-17406
- Structure of a reflected planar shock wave 05 p0640 A83-17416
- Construction and investigation of schemes for the calculation of radiative transfer 05 p0640 A83-17645
- A high-order difference method for the computation of viscous-gas flows 05 p0590 A83-17648
- Structure of normal shock waves in a gas-particle mixture 05 p0642 A83-17837
- Complementary variational principles for radiation heat transfer in an absorbing medium 05 p0642 A83-17838
- Solar wind flow about the terrestrial planets. II - Comparison with gas dynamic theory and implications for solar-planetary interactions 06 p0847 A83-18278
- Alternation of derivatives is no criterion for choosing an entropy function --- during free thermal relaxation of gas 06 p0815 A83-18325
- A self-similar flow in generalized Roche model with increasing energy 06 p0833 A83-18878
- A new surface-streamline flow-visualization technique 06 p0763 A83-19016
- The behavior of two-dimensional nonplane-parallel vortex flows of inviscid gas 06 p0758 A83-19118
- Gas-dynamic processes in a gas layer heated by high-intensity radiation during target acceleration 06 p0813 A83-19436
- Computing three-dimensional transonic gas flow through an axial-turbine stage 06 p0713 A83-19437
- The spectrum of gas-dynamic perturbations and stability of supersonic plasma flow under Joule heating 06 p0813 A83-19439
- The motion and sedimentation of a cloud of heated particles 07 p0924 A83-19639
- Equivalent circuit for an electrostatic probe 07 p0928 A83-20064
- The stability of flows near an infinite wedge or cone situated in supersonic gas flow 07 p0863 A83-20315
- Solution of two-dimensional problems of radiating-gas dynamics 07 p0925 A83-20319
- Analysis of similarity in thermophysics --- Russian book 07 p0925 A83-20382
- Lectures on nonlinear waves and shocks --- Book 07 p0925 A83-20391
- On the passage of a shock wave through a dusty-gas layer 07 p0927 A83-21354
- Centred compression-wave in polytropic gas, and its disintegration 07 p0917 A83-21449
- Application of modified BGK-equations to the calculation of the shock wave structure in Xe-He mixtures 08 p1083 A83-21817
- Marangoni convection-induced bubble motion 08 p1086 A83-23124
- The use of Bessel function and Jacobi polynomial in radial vibrations of a gas in an infinite cylindrical tube 08 p1091 A83-23217
- Numerical method for solving radiative-transfer equations in one-dimensional problems of radiative gas-dynamics 09 p1258 A83-23568
- The statistical particle-in-cell method for multicomponent gases 09 p1350 A83-23571
- The influence of mathematical viscosity on the difference solution in problems of two-temperature gas dynamics 09 p1347 A83-23573
- On the theory of hydrodynamic fluctuations in nonequilibrium systems 09 p1350 A83-23599
- On the symmetric form of systems of conservation laws with entropy 09 p1350 A83-23724
- Numerical modeling of nonstationary processes during sputtering and interaction of an erosion laser flare 09 p1274 A83-23992

- Nonlinear truncation error analysis of finite difference schemes for the Euler equations [AIAA PAPER 81-0193] 09 p1336 A83-24654
- The kinematics of the Ori A SO emission zone 09 p1363 A83-24996
- Shock capturing using flux-corrected transport algorithms with adaptive gridding 10 p1415 A83-26161
- Experimental method for determining the dynamic properties of gas flows 10 p1417 A83-26293
- Radiative energy receiver for high performance energy conversion cycles 11 p1602 A83-27138
- Billiard ball echo model --- atomic recoil model of photo, Raman and grating echoes in gases 11 p1654 A83-27615
- Investigation of the length and wave structure of the gasdynamic part in straight and spreading gas jets 11 p1567 A83-27718
- Optically thick radiatively driven shocks near QSOs 11 p1681 A83-28273
- Fast motions of a gas in a porous medium 11 p1569 A83-28539
- Two-phase gas-solid particle flow past bodies with allowance for erosion 11 p1569 A83-28540
- Speed of propagation of infinitesimal disturbances in a relativistic gas 11 p1650 A83-28695
- A radial temperature gradient in swirling gas flow 11 p1570 A83-28797
- Three-dimensional, two-phase supersonic nozzle flows 12 p1695 A83-28955
- Wave interaction in radiative gas dynamics 12 p1775 A83-29032
- Numerical boundary condition procedures and multigrid methods; Proceedings of the Symposium, NASA Ames Research Center, Moffett Field, CA, October 19-22, 1981 12 p1772 A83-29646
- Towards a closer cooperation between theoretical and numerical analysis in gas dynamics 12 p1698 A83-29936
- On the maximal invariance group and the general solution of the one-dimensional equations of gas dynamics 13 p1839 A83-30083
- Molecular gas dynamics 13 p1931 A83-30651
- A method for the integral transformation of the Boltzmann equation - Analytical studies 13 p1932 A83-30658
- The interaction of supersonic multiphase flows 13 p1842 A83-30677
- Theory of thermophoresis of moderately large aerosol particles 13 p1933 A83-30820
- Heat waves near meteor bodies moving in the atmosphere at hypersonic velocities 13 p1880 A83-31329
- On small forced oscillations of a nonlinear acoustic resonator 13 p1915 A83-31331
- Classification of difference schemes of gas dynamics by the method of differential approximation. I - One-dimensional case 13 p1844 A83-31592
- On the construction of K-consistent difference schemes of gas dynamics 13 p1913 A83-31594
- A calculation of the gas flow in a zone of energy release during a cylindrical explosion 14 p2008 A83-31896
- The propagation of a curved flame front in a specified gas-flow field 14 p1989 A83-32088
- The homogeneous property and flux splitting in gas dynamics 14 p2094 A83-32124
- The large-particle method in gas dynamics - A computational experiment --- Russian book 14 p2009 A83-32600
- High velocity clouds - Review of observational properties 14 p2109 A83-33273
- Shock waves in dusty gas with radiation effects 15 p2157 A83-33873
- Estimating the tumble rates of galaxy halos 15 p2257 A83-34090
- Dissipative effects in the gaseous subsystems of flat galaxies 15 p2271 A83-34754
- A gas-dynamic analogy of the motion and equilibrium of magnetizable and polarizable media 16 p2415 A83-35713
- Symposium on High Temperature Gas Dynamics, Liblice, Czechoslovakia, September 15-19, 1981, Proceedings 16 p2354 A83-36876
- Gas-dynamic stability of two-component plasma streams 16 p2417 A83-36928
- Gas dynamic effects in stimulated Raman scattering [AIAA PAPER 83-1685] 17 p2575 A83-37187
- An electrogasdynamic boundary layer on a dielectric plate 17 p2505 A83-37523
- Limits to the averaging of the total pressure of nonuniform gas flows 17 p2450 A83-37565
- Collisions of massive gas clouds with primordial chemical composition 17 p2603 A83-37892
- Equidistant mesh for gas dynamic calculations 17 p2508 A83-38814
- Shocks in spiral galaxies 17 p2612 A83-38828

Features of the numerical solution of gasdynamic problems with many interacting discontinuities 18 p2680 A83-39152

The computation of inviscid rotational gasdynamic flows using an alternate velocity decomposition [AIAA PAPER 83-1900] 18 p2637 A83-39405

Cloud-particle galactic gas dynamics and star formation 18 p2770 A83-39662

On corotating high-z HI --- in inner Galaxy 18 p2770 A83-39665

Gas dynamics in the circumstellar Nebula on the Becklin-Neugebauer source 18 p2772 A83-39711

Three gas clumps near the edge of the visible Orion Nebula 18 p2773 A83-39722

Shock damping in an ultrarelativistic gas 18 p2778 A83-40503

Two-dimensional outflow of an inhomogeneous streaming gas into a vacuum 19 p2842 A83-41208

A simple example of a classical gauge transformation 19 p2899 A83-41876

Variant of the Tamm and Mott-Smith solution for describing the structure of a gasdynamic shock in a monatomic gas 19 p2845 A83-41882

Gasdynamic approach to solving the problem of the fracture of a brittle rod by an intense shock wave 19 p2845 A83-41888

Factorization method for calculating the three-dimensional flows of a viscous compressible gas 19 p2845 A83-42008

Determination of full pressure losses in stepped annular diffusers with rectilinear outer walls and a uniform velocity field at the inlet 19 p2800 A83-42130

Calculation of heat transfer from polydisperse flows of gas suspensions in straight ducts and pipes 19 p2846 A83-42135

Heat transfer at hyperbolic flight velocities - Physical model and theoretical and experimental studies 20 p2929 A83-42882

The gasdynamic momentum of flow in axisymmetric channels 20 p2982 A83-42886

Heat and mass exchange of a droplet in a polyatomic gas 21 p3220 A83-43933

An analogy of the motion of a two-phase medium consisting of an incompressible phase and a gas phase with the motion of a gas 21 p3131 A83-44848

The force effect of a supersonic flow of a dust-filled gas on a blunt body 21 p3088 A83-45347

Invariant transformations of kinetic equations 23 p3512 A83-47176

Characteristic method applied to blast waves in a dusty gas 24 p3576 A83-48989

Fast winds in planetary nebulae 24 p3652 A83-49149

Theoretical studies of gas flow in barred spirals galaxies 24 p3656 A83-49240

Hydrodynamical models of offcentered barred spirals 24 p3657 A83-49244

Interstellar matter in elliptical galaxies 24 p3657 A83-49252

Two hidden symmetries of the equations of ideal gasdynamics, and the general solution in a case of non-uniform entropy distribution 24 p3577 A83-49467

Nonlinear tridimensional propagation of acoustic waves in radiative gas dynamics 24 p3625 A83-49522

The use of the techniques of holographic interferometry in qualitative studies of gas-dynamic flows with chemical reactions 24 p3584 A83-49780

GAS EVOLUTION

Shock-induced devolatilization of calcite 04 p0559 A83-15306

Dependence of hydrogen evolution from a Si-H on boron doping and substrate potential 04 p0541 A83-15518

The hydrogen evolution process on a Ni-28 percent Mo alloy 06 p0728 A83-18146

A new method for measuring radon exhalation 09 p1296 A83-24278

Coal gasification using solar energy 13 p1872 A83-31612

Bulk modulus technique for determining void content changes due to solid propellant gas evolution [AIAA PAPER 83-1119] 16 p2338 A83-36230

The effect of gas bubble evolution on the energy efficiency in water electrolysis --- Thesis 22 p3266 A83-46688

GAS EXCHANGE

The exchange of CO₂ between the ocean and atmosphere 02 p0205 A83-11980

Seasonal carbon dioxide exchange between the regolith and atmosphere of Mars - Experimental and theoretical studies 04 p0568 A83-15588

Models for a comparative functional analysis of gas exchange organs in vertebrates 05 p0671 A83-17326

Effect of change in P₅₀ on exercise tolerance at high altitude - A theoretical study 05 p0671 A83-17329

Influence of abdominal restriction on gas exchange during +Gz stress in dogs 11 p1637 A83-27809

Oxygen uptake and elimination of nonmetabolic CO₂ excess in an initial period of heavy muscular exercise 12 p1765 A83-29315

Coupling of ventilation to pulmonary gas exchange during nonsteady-state work in men 13 p1903 A83-30481

Liquid ventilation in dogs - An apparatus for normobaric and hyperbaric studies 13 p1898 A83-30510

Some comments on the exchange of CO₂ across the air-sea interface 13 p1869 A83-30879

Closed microbial ecosystems as gas exchange units in CELSS --- Controlled Environment Life Support System [SAE PAPER 820857] 13 p1907 A83-30943

The radon cycle and its daughters - An application to the study of troposphere-stratosphere exchanges 13 p1883 A83-31720

Effects of beta-adrenergic blockade on ventilation and gas exchange during exercise in humans 14 p2068 A83-32816

Does Venus breathe? 15 p2275 A83-34725

Expiratory and arterial partial pressure relations under different ventilation-perfusion conditions 17 p2558 A83-36996

Several mechanisms of the transport of oxygen and its utilization in the skeletal muscles during acute hemic hypoxia 17 p2555 A83-37240

Pulmonary gas exchange in cats under a heat load 17 p2555 A83-37247

Air-sea fluxes of transient atmospheric species 20 p3021 A83-42850

Oxygen and carbon dioxide exchange between the Arctic Ocean and the atmosphere 21 p3182 A83-45398

Pulmonary gas exchange on the summit of Mount Everest 22 p3347 A83-45982

The relationship between blood flow, partial pressure, and oxygen demand in the human cortex (A theory of tissue gas exchange) 23 p3497 A83-47113

GAS EXPANSION

On the total axial-symmetric expansion of a supersonic stream 01 p0003 A83-11329

Stochastic modeling of uniformly expanding rarefied gases 02 p0243 A83-11654

The evolution of supernova remnants and the structure of the interstellar medium 08 p1178 A83-21849

Gas flow in an overexpanded axisymmetric nozzle 09 p1197 A83-24046

Investigation of supersonic plane underexpanded jets by the laser schlieren method 11 p1584 A83-28538

The effect of nonequilibrium on the expansion of CO₂ issuing into a rarefied medium 13 p1842 A83-30679

An energetic, bisymmetrically expanding H₂ remnant 14 p2104 A83-33190

The similarity of condensation processes in expanding CO₂ jets 16 p2349 A83-35527

Acceleration of impurity ions during plasma expansion into vacuum 16 p2417 A83-36935

The expansion velocity field within the planetary nebula NGC 7008 17 p2587 A83-37280

The hybrid model and its application for studying free expansion --- of hot gas cylinders into vacuum 18 p2681 A83-39218

Free expansion of three-dimensional jets of an ideal gas 19 p2790 A83-41207

The expansion of a plasma into a vacuum - Basic phenomena and processes and applications to space plasma physics 20 p3048 A83-42177

Nonequilibrium expansion of halogens in short nozzles --- Russian book 23 p3392 A83-47123

The influence of boundaries and electrical currents on plasma jet expansion into vacuum --- in laser thrusters [IAF PAPER 83-398] 23 p3426 A83-47373

GAS EXPLOSIONS

Temperature measurements at an implosion focus 04 p0474 A83-14950

Numerical modeling of a high-explosive-driven plasma generator with allowance for radiative transfer and wall evaporation 04 p0538 A83-16171

The effect of thermal relaxation on the damping of a high-intensity shock wave in a two-phase medium 06 p0815 A83-19548

The propagation of powerful blast waves in a gas-particle mixture 07 p0878 A83-19633

Point explosion in an exponential atmosphere with a nonzero asymptote --- for stellar and planetary atmospheric models 09 p1359 A83-24221

Generation of the patterns in gaseous detonations 10 p1415 A83-26158

Decomposition of hydrogen azide in shock waves 10 p1391 A83-26185

A calculation of the gas flow in a zone of energy release during a cylindrical explosion 14 p2008 A83-31896

Process of the transition from none-dimensional explosion-induced flows to one-dimensional ones 23 p3452 A83-48660

The mechanism of acoustic emission from a turbulent gas flame 24 p3555 A83-49762

GAS FLOW

NT AIR CURRENTS

NT AIR FLOW

NT CONTINUUM FLOW

NT EQUILIBRIUM FLOW

NT FREE MOLECULAR FLOW

NT JET STREAMS (METEOROLOGY)

NT KNUDSEN FLOW

NT MERIDIONAL FLOW

NT MOLECULAR FLOW

NT NONEQUILIBRIUM FLOW

NT PIPE FLOW

NT SLIP FLOW

NT TRANSITION FLOW

NT VERTICAL AIR CURRENTS

The thermoacoustic effect in a resonance tube having one open end 02 p0233 A83-11516

Energetic activity in a star-forming molecular cloud core - A disk constrained bipolar outflow in NGC 2071 02 p0251 A83-11590

Measurements and visualizations of unsteady flow /flow speed/ [AAAF PAPER NT 81-14] 02 p0176 A83-11774

A neutral vortex induced by an auroral arc 02 p0209 A83-12429

The absorption of electromagnetic radiation in an advanced propulsion system 02 p0147 A83-12507

Measurements of energy distribution and thrust for microwave plasma coupling of electrical energy to hydrogen for propulsion [AIAA PAPER 82-1951] 02 p0147 A83-12508

Transient response of the solar wind to changes in flow geometry 02 p0271 A83-12588

High-speed motion picture camera experiments of cavitation in dynamically loaded journal bearings [ASME PAPER 82-LUB-18] 03 p0335 A83-13509

Star formation in a cooling flow 03 p0419 A83-13934

Transonic disk accretion of barytropic gas onto black holes 03 p0427 A83-14714

A self-similar flow of self-gravitating gas behind a shock wave with increasing energy. I 04 p0557 A83-15978

Unidirectional unsteady flow of an instantaneously heated gas out of a cylinder with various locations of the heating zones 04 p0479 A83-16172

Acoustic streaming in swirling flow and the Ranque-Hilsch /vortex-tube/ effect 04 p0479 A83-16259

The effect of the thermal prong-wire interaction on the response of a cold wire in gaseous flows /air, argon and helium/ 04 p0479 A83-16266

A method for measuring the stagnation temperature of short-duration gas flows using a radiation-calorimetric transducer 04 p0483 A83-16393

Transient flow analysis of the AEDC/HPDE MHD generator [AIAA PAPER 83-0395] 05 p0686 A83-16691

Vacuum technology /2nd revised and enlarged edition/ --- Book 05 p0621 A83-17112

Aerodynamic drag in two-phase flows 05 p0589 A83-17408

An experimental unit for investigating two-phase flows 05 p0639 A83-17410

Linear approximation of the reflection of a shock wave from a concave wall 05 p0639 A83-17414

Diagnostics of a discontinuity in a self-similar gas flow 05 p0639 A83-17415

Separated measurement of gas flows through different compartments of a partially pressurized suit 06 p0800 A83-18345

Characteristics of the evolution of a dynamic turbulent boundary layer in the gas veil region after a porous section 06 p0756 A83-18444

On the possibility of gas being swept out of a galaxy under the influence of the radiation pressure of an active nucleus 06 p0838 A83-19223

The peculiar velocity field in flattened superclusters 06 p0845 A83-19521

The heating effect in resonance tubes --- German thesis 06 p0761 A83-19623

Influence of gas inertia forces generated within the stabilizing restrictor on dynamic characteristics of externally pressurized thrust gas bearings. I - Case of laminar flow at the capillary restriction 07 p0939 A83-20292

Time evolution of discontinuities at the wave head in a non-equilibrium two-phase flow of a mixture of a gas and dusty particles 07 p0927 A83-21338

Characterization of particle rebound phenomena in the erosion of turbomachinery 08 p1073 A83-22165

Effects of flow fields in optical systems 08 p1108 A83-22454

Instantaneous velocity field measurements in unsteady gas flow by speckle velocimetry 08 p1101 A83-22616

A new type of boundary layer in a rapidly rotating gas 08 p1086 A83-23098

On the Balmer progression in the expanding shell of Pleione 08 p1185 A83-23106

Transient behavior of nonlinear thermal effects in an intense light beam in a uniform gas flow 09 p1271 A83-23988

Gas flow in an overexpanded axisymmetric nozzle 09 p1197 A83-24046

Heat transfer during nonlinear gas oscillations in a pipe open at one end 09 p1260 A83-24227

An accurate determination of the thermal conductivity of argon at high temperatures 10 p1415 A83-26152

Microscopic structure of the Mach-type reflection of weak shock waves 10 p1415 A83-26156

Molecular beam technique for recording chemical species behind incident shock waves 10 p1391 A83-26184

Shock wave structure in gas-particle mixtures at low Mach numbers 10 p1416 A83-26186

A comparison of measured and computed energy exchanger performance 10 p1417 A83-26195

Calculation of heat transfer in smooth pipes with turbulent flow of gaseous heat-carriers with constant and variable physical properties 10 p1417 A83-26255

Spherical accretion onto quasars 10 p1512 A83-26704

Investigation of thermal self-defocusing of intense beams in homogeneous gas flows 10 p1435 A83-26784

Steady flow examination of a cryocooler 11 p1564 A83-27289

The development of detached shock waves in gas-solid suspension flow 11 p1566 A83-27483

On analytical models of gas flow and chemical lasers 11 p1580 A83-27583

Kinetic model of a structural suspension of particles in a gas 11 p1665 A83-27715

Supersonic flow past a thin cone with an asymmetric tip 11 p1526 A83-27716

Vapor flow through a porous membrane - A throttling process with condensation and evaporation 11 p1567 A83-27859

Experimental study of the motion of rising vortex rings 11 p1569 A83-28533

Measurement of the velocity vector of gas flow 11 p1574 A83-28554

A self-similar flow of self-gravitating gas behind a shock wave with radiation heat flux. I 12 p1791 A83-28992

Large-scale flow of interstellar gas in galactic spiral waves - Effects of thermal balance and self-gravitation 12 p1793 A83-29065

Wave processes in solids-laden gas flows 12 p1724 A83-29443

Shock calculations and the numerical solution of singular perturbation problems 12 p1726 A83-29938

A simple model of a coronal hole 13 p1964 A83-30369

Filtration combustion of gases 14 p1988 A83-32083

Heat-transfer distributions on bionics at incidence in hypersonic-hypervelocity He, N₂, air, and CO₂ flows [AIAA PAPER 83-1508] 14 p1970 A83-32745

Viscous real gas flowfields about three dimensional configurations [AIAA PAPER 83-1511] 14 p1970 A83-32748

An inviscid three-dimensional analysis of the Space Shuttle main engine hot-gas manifold [AIAA PAPER 83-1523] 14 p1984 A83-32754

A split-coefficient/locally monotonic scheme for multishocked supersonic flow 14 p1971 A83-32985

Analysis of self-similar problems of imploding shock waves by the method of characteristics 14 p2013 A83-33386

On flame stretch 15 p2131 A83-33723

The distribution of the disperse fraction of a polydisperse jet injected into a gas flow 15 p2161 A83-34472

Investigation of gas particle flow in an erosion wind tunnel 15 p2162 A83-35246

Unsteady gas flow into vacuum through a perforated barrier 16 p2349 A83-35536

Calculation of a laminar flow of a compressible gas in plane curvilinear ducts with heat transfer 16 p2349 A83-35701

Computation of tridimensional gas flow with recirculation and combustion [ONERA, TP NO. 1983-49] 16 p2350 A83-35807

Nozzle contour optimization for nonuniform rocket flow [AIAA PAPER 83-1253] 16 p2319 A83-36309

Unsteady aerodynamics in open cavities applications to rocket propulsion [AIAA PAPER 83-1314] 16 p2295 A83-36335

Vapor flow into a capillary propellant-acquisition device [AIAA PAPER 83-1380] 16 p2321 A83-36371

Glow discharge in a fast longitudinal gas flow 16 p2418 A83-36939

Stationary flow of gas at very high temperatures and relativistic speeds 17 p2595 A83-37032

Controlling mechanisms of flame spread 17 p2484 A83-37043

Modeling study of a CW HF optical resonance transfer laser model [AIAA PAPER 83-1700] 17 p2513 A83-37197

Characteristics of supersonic gas flow and heat transfer in the shadow region of a sharp cone 17 p2447 A83-37261

Experimental study of the flow of a viscous compressible gas through a cylindrical channel and through a porous insert 17 p2447 A83-37265

Gas turbine engines 17 p2467 A83-37274

Radio continuum observations of the bar of NGC 1097 17 p2588 A83-37347

Boundary layer separation from the moving surface of a body in a supersonic gas flow 17 p2448 A83-37509

Structure of the flow of an inviscid gas near an isolated stagnation point 17 p2505 A83-37526

On a method for the closure of the energy equation formulated relative to the total enthalpy in the case of turbulent flow in a boundary layer 17 p2505 A83-37530

Calculation of three-dimensional supersonic flows with allowance for the real properties of the gas 17 p2449 A83-37539

A numerical study of slow nonisothermal flows past axisymmetrical bodies 17 p2506 A83-37805

Directional gas-flow measurement with pyroelectric anemometers (PA) 17 p2512 A83-38532

High-speed motion picture camera experiments of cavitation in dynamically loaded journal bearings [ASME PAPER 82-LUB-18] 18 p2695 A83-39944

Real gas flows over complex geometries at moderate angles of attack 18 p2638 A83-40004

An experimental study of the transformation of a free spherical volume of a light gas to a vortex ring 19 p2843 A83-41273

Gas flow through rotameters 19 p2849 A83-41870

Dynamic measurements in gas flowfields using rotational Raman spectroscopy 20 p2950 A83-42580

Heat transfer at the tip of an unshrouded turbine blade 20 p2975 A83-42706

Heat transfer to pulsating, turbulent gas flow 20 p2975 A83-42707

Two parametric flow measurement in gas-liquid two-phase flow 20 p2981 A83-42773

Frequency response of cold wires and thermocouples used for temperature measurements in gaseous flows 20 p2982 A83-42778

Gas flow through a cylindrical tube under free molecular conditions 20 p2985 A83-43105

Hydraulic analogy for isentropic flow through a nozzle 21 p3129 A83-44071

Velocity and turbulence measurements in combustion systems 21 p3131 A83-44684

Laser-induced fluorescence technique for velocity field measurements in subsonic gas flows 22 p3287 A83-45962

Laser optical measurements of density and temperature in flowing gases 22 p3291 A83-46487

The influence of stretch on a premixed flame with two-step kinetics 22 p3267 A83-46760

Optical plasmatron [IAF PAPER 83-399] 23 p3509 A83-47374

The collapse of a gas bubble attached to a solid wall by a shock wave and the induced impact pressure [ASME PAPER 83-FE-3] 23 p3450 A83-48228

Rarefied gas flow in a cylindrical annulus 24 p3575 A83-48738

Theory of thermophoresis of nonvolatile liquid aerosol particles 24 p3575 A83-48861

Theoretical studies of gas flow in barred spirals galaxies 24 p3656 A83-49240

Hydrodynamical coupling between the motion of a flame front and the upstream gas flow 24 p3577 A83-49297

GAS GENERATOR ENGINES

U ENGINES

U GAS GENERATORS

GAS GENERATORS

Lightweight ozonizer for field and airborne use 03 p0329 A83-14169

Performance testing of a three-bed molecular sieve oxygen generator 04 p0524 A83-15307

Base-bleed solid propellants with thermoplastic elastomers as binders 09 p1241 A83-23839

MX Launcher gas generator development 15 p2125 A83-33737

Hydrazine gas generator performance on Space Shuttle [AIAA PAPER 83-1381] 16 p2321 A83-36372

Aspects of the T56 power section usage/operating costs [AIAA PAPER 83-1408] 16 p2310 A83-36397

Application of a hot gas high pressure rotary vane motor to aircraft APU starting [SAE PAPER 821464] 17 p2469 A83-37997

Evaluation of advanced airplane fire extinguishants [AIAA PAPER 83-1141] 17 p2459 A83-38076

Performance tests of two inert gas generator concepts for airplane fuel tank inerting [AIAA PAPER 83-1140] 17 p2464 A83-38078

Cryogenic gas engines --- Russian book 21 p3117 A83-43925

A new-technology gas generator for medium-power shaft-turbine engines 23 p3406 A83-47217

GAS GIANT PLANETS

NT JUPITER (PLANET)

NT NEPTUNE (PLANET)

NT SATURN (PLANET)

NT URANUS (PLANET)

NT URANUS RINGS

On resonance in celestial mechanics /A survey/ 04 p0548 A83-16359

Mysteries of the ringed planets --- colloquium review 05 p0703 A83-16861

Infrared views of the giant planets 07 p1005 A83-20150

The extraordinary voyages through the region of the giant planets 08 p1048 A83-22049

Theory for the motion of the four giant planets - The TOP 82 solution 13 p1941 A83-31556

The atmospheres of the outer planets 14 p2113 A83-33482

Methane photochemistry in the outer planets 15 p2273 A83-33550

Planetary magnetic fields 15 p2274 A83-34399

A new view on the origin of comets and other minor bodies 15 p2248 A83-34688

The interiors of the giant planets - 1983 16 p2439 A83-36789

The giant planets and their satellites; Proceedings of the Symposium, Ottawa, Canada, May 16-June 2, 1982 17 p2620 A83-38106

The giant planets and their satellites - Report on the Cospar Symposium, Ottawa, Canada, May 18-21, 1982 17 p2620 A83-38107

Outer planets satellites 17 p2622 A83-38268

Desaturation of H₂ quadrupole lines in the atmospheres of the outer planets 20 p3078 A83-43077

On the origin of comets 21 p3228 A83-44297

Planetary spin and satellite formation 21 p3224 A83-44761

Cosmogonical implications of elemental and isotopic abundances in atmospheres of the giant planets 21 p3241 A83-44991

Statistical mechanics of light elements at high pressure. V Three-dimensional Thomas-Fermi-Dirac theory --- relevant to Jovian planetary interiors 21 p3242 A83-45563

Solar system ice - Amorphous or crystalline? 24 p3671 A83-48809

Inertia coefficient considerations and the structure of Jovian planets 24 p3672 A83-49396

Lectures on the planets - The exploration of the giant planets 24 p3673 A83-49461

Helium and deuterium in the outer solar system 24 p3665 A83-50042

GAS GUNS

The methods and results of the diagnosis of the detonation spraying of coatings 07 p0940 A83-20692

GAS HEATING

The effect of environments on the thermal stability of titanium hydride 04 p0459 A83-15471

The effect of changes in the turbulent flow structure of the unsteady heat transfer during the heating of gases and liquids in pipes 04 p0478 A83-16163

Unidirectional unsteady flow of an instantaneously heated gas out of a cylinder with various locations of the heating zones 04 p0479 A83-16172

Gain and efficiency of a traveling wave heat engine 04 p0480 A83-16312

On photochemical heating of cometary comae - The cases of H₂O and CO-rich comets 06 p0845 A83-19518

Why are broad emission lines seen in Seyfert galaxies and not in BL Lacertae objects 10 p1507 A83-26355

Thermal physics of transverse-discharge copper vapor lasers 10 p1433 A83-26682

- Determination of vibrational exchange constants in N₂ from heating of gas 13 p1917 A83-31466
Microwave-energy coupling in a nitrogen-breakdown plasma 17 p2582 A83-37612
Thermal processes in resonance tubes 19 p2845 A83-41890
Neutral and ion gas heating by auroral electron precipitation 20 p3019 A83-42421
Several generation parameters of a CO₂ gasdynamic laser with a high-temperature regenerative-heat-transfer heater of the working gas 24 p3588 A83-48936
Regenerative electric heater of gas for a gasdynamic laser 24 p3588 A83-48937

GAS INJECTION

- The nonuniqueness and instability of steady-state combustion modes in a boundary layer with intense injection 03 p0296 A83-14898
Flow of a rarefied gas past a sphere under the conditions of surface injection 04 p0442 A83-15099
Laminar free convection on a vertical nonisothermal plate under strong injection 04 p0478 A83-16164
Structure of a reflected planar shock wave 05 p0640 A83-17416
Calculation of parameters of a near wake produced by injection of an annular jet into the base region 05 p0590 A83-17424
A solution to the problem of multiparameter optimization in calculating flow around bodies with injection 06 p0712 A83-18143
Turbulent boundary layer on a permeable wall with vectored injection of similar or dissimilar gases at different angles to the surface 06 p0759 A83-19153
Heat and mass transfer at high free-stream turbulence as a function of injection rate 06 p0759 A83-19157
Analytic and experimental study of the efficiency of a cooling-gas blanket downstream of a single row of identical rectangular orifices in a wall 06 p0759 A83-19158
Fast acting hydrogen valve 08 p1112 A83-23295
Application of the method of unconditional optimization to solve an inverse boundary value problem with a free boundary 10 p1371 A83-25614
Penetration into a supersonic flow of a jet injected through a convex cylindrical surface 11 p1526 A83-27722
Near-wall gaseous films 11 p1569 A83-28375
Calculation of a gas-vapor-liquid heat screen on an adiabatic wall by means of h-d diagrams 11 p1570 A83-28795
Mixed laminar convection on a vertical surface under conditions of strong injection 11 p1571 A83-28799
Experimental investigation of multiple jets in a cross-flow [AIAA PAPER 83-1545] 14 p1971 A83-32768
Three-dimensional film cooling on a flat plate with tangential multi-jets 15 p2156 A83-33774
The theoretical advantages and practical considerations of gas replenishment techniques in long-duration scientific ballooning [AD-A129841] 18 p2640 A83-39802
The base pressure of bodies of revolution with gas injection through the body surface into a supersonic flow 19 p2790 A83-41265
Thermodynamic efficiency of air injection into the radial clearance of the turbine of a turbojet engine 19 p2801 A83-42139
Refinement of the limiting relative friction law for a permeable plate with gas injection 21 p3133 A83-45345
Film cooling with steam injection through three staggered rows of inclined holes over a straight airfoil [ASME PAPER 83-GT-30] 23 p3446 A83-47892
- GAS IONIZATION**
NT ATMOSPHERIC IONIZATION
NT AURORAL IONIZATION
NT FLAME IONIZATION
The hygienic characteristic of the air environment in buildings during artificial ionization 01 p0086 A83-11396
X-ray nebular models 02 p0253 A83-11992
High repetition rate mini TEA CO₂ laser using a semiconductor preionizer 02 p0185 A83-12816
Miniature, sealed TEA-CO₂ lasers with integral semiconductive preionization 03 p0332 A83-14166
The effects of the coronal gas on the champagne phase 03 p0430 A83-14810
Gas breakdown on the surface of metallic mirrors due to radiation from a pulsed /periodic pulsed/ CO₂ laser 04 p0484 A83-15263
Investigation of the ionization relaxation of shock-wave heated krypton with an HCN laser interferometer --- German thesis 04 p0536 A83-15842
A fast wave of gas-ionization in a laser beam 05 p0686 A83-16892
Investigation of preionization CO and CO₂ lasers operating in the active zone of a stationary nuclear reactor 05 p0650 A83-17085

- A scaling model for plasma columns produced by CO₂ laser-induced breakdown in a solenoidal field 05 p0688 A83-17368
Approximate correction for the effect of injectants on the ionization level in the boundary layer of a blunt body and in its near wake 05 p0590 A83-17423
Discharge in an electromagnetic shock tube with preionization of xenon 06 p0811 A83-18440
Transition from steady-state to pulsed gas breakdown near the surface of a target subjected to laser radiation 07 p0935 A83-20124
Numerical modeling of optical-breakdown waves in gases 07 p0996 A83-20303
High-power microwave energy coupling to nitrogen during breakdown 07 p0997 A83-20731
On plasma transport in the vicinity of the rings of Saturn - A siphon flow mechanism 07 p1036 A83-21508
Powerful electroionization laser on Xe infrared atomic transitions 07 p0938 A83-21589
The doubly excited autoionizing states of H₂ 08 p1163 A83-22220
Unimolecular reaction paths of electronically excited species. IV - The C(II)de 2Sigma plus g state of CO₂/plus/ 08 p1163 A83-22999
A new class of atomic states - The 'Wannier-ridge' resonances 09 p1342 A83-24143
Experimental study on the ionization of argon gas in a non-equilibrium state behind reflected shock waves 10 p1490 A83-26174
New experimental results upon ionizational relaxation of a shock heated xenon plasma 10 p1487 A83-26175
Number density of the 5s states during the ionisation relaxation of shock heated krypton 10 p1479 A83-26176
Collisional excitation and ionisation of NO behind shock waves 10 p1479 A83-26177
The investigation of ionization phenomena in a 800 mm shock-tube 10 p1487 A83-26178
The nature of the ionizing source of the nuclear gas in NGC 1052 10 p1511 A83-26402
A theoretical study of ionization phenomena and radiative behaviors behind a strong shock in argon gas 10 p1487 A83-26967
Dynamics of the two-photon photodissociation of NO₂ - A molecular beam multiphoton ionization study of NO photofragment internal energy distributions 11 p1653 A83-27492
Experimental verification of the breakdown of the electric dipole rotational selection rule in electron impact ionization-excitation of N₂ 11 p1653 A83-27493
Analysis of the lifetime of a small volume UV preionized discharge XeCl excimer laser 11 p1576 A83-27507
Photoionisation of krypton atoms in 'strong' electric fields 11 p1653 A83-27512
Multiphoton ionization and third-harmonic generation in atoms and molecules 11 p1579 A83-27556
Above threshold ionisation - Multiphoton ionization involving continuum-continuum transitions 11 p1654 A83-27557
High-power electro-ionization CO₂ - Lasers for laser technology 11 p1580 A83-27574
High efficiency infrared xenon laser excited by a U.V. preionized discharge 11 p1580 A83-27579
Corona preionization technique for CO₂ TEA lasers 11 p1580 A83-27580
Ionisation and appearance potentials of CH₄ by electron impact 12 p1778 A83-29925
A photoelectron spectroscopic study of (3 + 1) resonant multiphoton ionization of NO and NH₃ 13 p1916 A83-30964
Doubly differential cross sections of secondary electron ejected from gases by electron impact - 50-400 eV on N₂ 13 p1916 A83-31353
Simple and efficient preionization system for gaseous lasers 13 p1857 A83-31472
The spectral properties of filamentary, physically inhomogeneous prominences. II - Hydrogen (second level excitation, ionization) 14 p2113 A83-31832
Electron kinetics in the atmosphere in conditions of repeated air breakdown 14 p2049 A83-31864
Spectroscopic investigation of laser-initiated low-pressure plasmas in atmospheric gases [AD-A130571] 14 p1990 A83-32916
Preionization kinetics of an X-ray preionized XeCl gas discharge laser 14 p2025 A83-33144
Quasi-continuous excitation regime of electric-discharge exciplex lasers 15 p2168 A83-33980
Multiphoton ionization of nitrogen dioxide - Four photon spectroscopy of the np sigma(u) Rydberg series 15 p2227 A83-34013
Microwave-energy coupling in a nitrogen-breakdown plasma 17 p2582 A83-37612
Dissociation of CO₂(2+) ions into CO(+) and O(+) fragments 17 p2486 A83-38469

- Penning ionization in the field of a light wave 17 p2583 A83-38964
Charge transfer and ionisation processes involving multiply charged ions in collision with atomic hydrogen 18 p2742 A83-39447
Two-photon-ionization mass spectroscopy of ammonia clusters in a pulsed supersonic nozzle beam 20 p3044 A83-42631
Ionizational instability due to a surface wave and its effect on the structure of a steady microwave discharge 21 p3210 A83-44139
The Knudsen ion layer problem in the theory of the collisionless sheath 21 p3212 A83-44356
The high-ionization optical spectrum of the Seyfert galaxy Tololo 0109-383 22 p3379 A83-46568
Study of the autoionising states of the hydrogen atom in intense magnetic fields by the complex coordinate coupled-channel formalism 23 p3506 A83-48576
Core level excitation of simple gases 24 p3625 A83-48737
Propagation velocity of an ionization front maintained by a relativistic electron beam 24 p3632 A83-48860
Secondary ionisation processes in laser-induced cascade ionisation 24 p3627 A83-49837
Hydrogen and helium ionization structure of gaseous nebulae 24 p3671 A83-50170
- GAS JETS**
Coherent structures in free jets 03 p0318 A83-14464
Are thick accretion disks the 'central engine' for astrophysical jets 03 p0431 A83-14875
Two types of jets and origin of macrospicules --- in solar atmosphere 03 p0437 A83-14902
An exact solution for a high-temperature jet stream 04 p0480 A83-16390
Calculation of the dispersal of a layer of granular material by a supersonic gas jet 05 p0639 A83-17407
An experimental investigation of the dispersion of a gas jet in a coflowing stream of air 08 p1042 A83-23215
Principles governing the mixing of transverse jets 09 p1196 A83-23439
Investigation of the flow in a jet produced by two nozzles 09 p1197 A83-24045
Calculation of thermal radiation from jets by the Monte-Carlo method 09 p1260 A83-24047
Regular structures in a plane triple jet 10 p1418 A83-26627
Investigation of the length and wave structure of the gasdynamic part in straight and spreading gas jets 11 p1567 A83-27718
Investigation of supersonic plane underexpanded jets by the laser schlieren method 11 p1584 A83-28538
The freezing of the translational degrees of freedom of molecules in multiphase flows 13 p1933 A83-30672
Calculation of the characteristics of submerged combustion 14 p1988 A83-32084
Computational method for Chaplygin function 14 p2012 A83-32969
The similarity of condensation processes in expanding CO₂ jets 16 p2349 A83-35527
Free expansion of three-dimensional jets of an ideal gas 19 p2790 A83-41207
A numerical study of the effect of free convection on the development of a vertical semifinite turbulent gas jet 19 p2844 A83-41568
A numerical analysis of the development of a system of jets in the mixing region of countertwisted annular flows 19 p2844 A83-41569
The measurement of pressure pulsations by means of piezoelectric transducers 19 p2849 A83-41891
The effect of viscosity on the interaction of an underexpanded jet with an infinite plane barrier perpendicular to its axis 19 p2792 A83-41895
Measurement of stresses on the surface of a plane barrier in a strongly underexpanded rarefied-gas jet 19 p2849 A83-41896
A method for calculating and analyzing the properties of a vertical nonisothermal jet with allowance for the buoyancy force 19 p2794 A83-42131
The effect of the wave injection of a fluid jet into a gas cross-stream 19 p2794 A83-42155
Viscous interaction of an underexpanded jet with a supersonic wake 20 p2982 A83-42885
Analytical description of a hypersonic gas jet flowing into a medium at rest or into a supersonic wake 23 p3400 A83-48673
Calculation of the attached mass for a supersonic gas jet 24 p3576 A83-48938
Numerical study of the interaction of supersonic viscous gas jets in the presence of nonequilibrium physicochemical processes 24 p3588 A83-49122
Investigation of the jet parameters of a source of accelerated gas flow for an aerodynamic test facility 24 p3545 A83-49659

GAS LASERS

NT CARBON DIOXIDE LASERS
 NT CARBON MONOXIDE LASERS
 NT DF LASERS
 NT EXCIMER LASERS
 NT HCL ARGON LASERS
 NT HCN LASERS
 NT HELIUM-NEON LASERS
 NT HF LASERS
 NT KRYPTON FLUORIDE LASERS
 NT NITROGEN LASERS
 NT TEA LASERS
 NT ULTRAVIOLET LASERS
 NT XENON CHLORIDE LASERS
 NT XENON FLUORIDE LASERS
 Gas discharge lasers --- Russian book
 01 p0054 A83-10673
 Raman gain in 12-micron NH₃ lasers
 02 p0183 A83-11560
 The effect of a weak axial magnetic field on a He-Cd laser
 02 p0184 A83-12085
 Dispersion-induced instability in CW laser oscillators
 02 p0184 A83-12270
 Gas laser mode-locking using an external acoustooptic modulator with a potential application to passive ring gyroscopes
 02 p0185 A83-12589
 Nonlinear interaction between elliptically polarized waves in a ring gas laser in a magnetic field
 03 p0316 A83-13586
 Investigation of the mode competition in an He-Ne/CH₄ laser with independent variation of the mode spacing and spatial shift
 05 p0648 A83-17046
 Influence of electron heating during recombination of copper atoms in copper halide vapor lasers on their output parameters
 05 p0650 A83-17068
 Iodine monofluoride B 3Pi/0 + / to X 1Sigma+ lasing from collisionally pumped states
 05 p0651 A83-17653
 Regular and chaotic behaviour of multimode gas lasers
 05 p0651 A83-17893
 Formation of a non-Gaussian intensity profile in a laser with inhomogeneous mirrors
 07 p0934 A83-20110
 Nuclear-reactor pumped lasers excited by ion-ion neutralization
 07 p0936 A83-20728
 Optical bistabilities, phase transitions, and Q-switch characteristics of an N₂O laser with a saturable NH₃ absorber
 07 p0937 A83-20791
 Selective enhancement of the 251-micron line in an optically pumped CH₃OH laser
 07 p0937 A83-21360
 Powerful electroionization laser on Xe infrared atomic transitions
 07 p0938 A83-21589
 Tunable VUV radiation generated by two-photon resonant frequency mixing in xenon
 07 p0938 A83-21595
 New technique for measurement of upper laser level decay rates in gas laser plasmas
 07 p0938 A83-21597
 A comparative study of D₂O oscillators emitting at 385 microns
 07 p0938 A83-21598
 An optically-pumped multigas far-IR laser
 08 p1107 A83-22246
 The possibility of stimulated three-photon emission in molecular media
 09 p1270 A83-23492
 Electron beam energy branching in a gas mixture
 09 p1343 A83-23678
 High power operation of a CW 28-micron water vapor laser
 10 p1425 A83-25428
 A mechanism for producing inversion in gas lasers
 10 p1426 A83-25894
 Spectroscopy and efficiency of the /Hg-200/Br-81 and /Zn-64/I photodissociation lasers
 10 p1426 A83-26003
 Pumping of gas lasers by runaway-electron beams
 10 p1430 A83-26241
 Pumping of pulsed gas lasers by bulk and sliding spark discharges
 10 p1431 A83-26464
 Quantum and quasiclassical lasing regimes
 10 p1432 A83-26663
 Frequency reproducibility of ring He-Ne/CH₄ lasers
 10 p1433 A83-26686
 Resonances of the polarization of gas laser radiation under mode self-locking conditions
 10 p1433 A83-26688
 High-pressure NH₃-N₂ laser
 10 p1434 A83-26689
 High-resolution line-shape analyses of the pulsed cuprous chloride-laser oscillator and amplifier
 10 p1435 A83-26878
 On the interpretation of interferograms of cavity turbulence --- in laser cavity medium
 11 p1577 A83-27516
 New types of mode locking in stimulated radiation in optical resonators
 11 p1578 A83-27539
 Mode structure of a DFB gas laser
 11 p1578 A83-27547

Advances in NASA research on nuclear-pumped lasers
 11 p1579 A83-27558
 Stepwise excitation - A limiting process in pulsed gas lasers
 11 p1582 A83-27601
 Comparison of He-Kr+ / laser oscillations in transverse and longitudinal hollow - Cathode discharges
 11 p1582 A83-27603
 Kinetic description of a dynamically coupled free-electron-and molecular gas laser
 11 p1584 A83-28239
 Injection gas electronics --- Russian book
 13 p1832 A83-30523
 Heavy ion beam pumped He-Ar laser
 13 p1852 A83-31060
 Enhanced HgBr(B2Sigma+ - X2Sigma+) emission at low pressures --- blue-green laser
 13 p1852 A83-31062
 Simple and efficient preionization system for gaseous lasers
 13 p1857 A83-31472
 Gas laser with a phase anisotropy in an axial magnetic field for arbitrary relative excitation of the active medium
 14 p2022 A83-31902
 Preionization kinetics of an X-ray preionized XeCl gas discharge laser
 14 p2025 A83-33144
 Quasi-continuous excitation regime of electric-discharge exciplex lasers
 15 p2168 A83-33980
 New pulsed far infrared laser lines in D₂O
 16 p2359 A83-35959
 Molecular gas lasers: Physics and application
 18 p2693 A83-39983
 High-efficiency infrared xenon laser excited by a UV preionized discharge
 19 p2852 A83-40947
 Xenon laser action in discharge and electron-beam excited Ar-Xe mixture
 19 p2853 A83-41183
 Longitudinal voltage distribution in transverse RF discharge waveguide lasers
 20 p2994 A83-42592
 Routes to chaotic output from a single-mode, dc-excited laser
 20 p2994 A83-42650
 Low temperature operation of an S₂ laser using radio frequency simmer discharges
 20 p2994 A83-42794
 Mechanism of pulse emission from high-pressure electric-discharge He-Ar, He-Kr, and He-Xe infrared lasers
 20 p2996 A83-43783
 Influence of the inhomogeneity of the process of energy deposition on the gain coefficient of high-power gas lasers
 20 p2997 A83-43795
 Influence of transit effects on frequency resonances in gas lasers
 20 p2997 A83-43799
 Laser action in xenon pumped by pulsed beams of runaway electrons
 20 p2997 A83-43800
 Laser spark with a continuous channel in air
 20 p2998 A83-43803
 Transport of a relativistic electron beam in a dense gas
 21 p3143 A83-44134
 Noise of He-Cd laser and its suppression
 21 p3143 A83-44156
 A 28 micron water-vapor laser interferometer for plasma diagnostics
 21 p3144 A83-44381
 The lasing capacity of pyrenes in the gas phase
 21 p3146 A83-45386
 Lasing on the B-X band of cadmium moniodide (CdI) and (Cd-114I) in a UV-preionized, transverse discharge
 21 p3146 A83-45481
 Laser and laser systems reliability; Proceedings of the Conference, Los Angeles, CA, January 28, 29, 1982
 22 p3296 A83-46611
 A 1.5 W CW optically pumped 12.08 microns NH₃ laser
 23 p3462 A83-48317
 Problems encountered in the development of 1-10-kw industrial lasers
 23 p3462 A83-48431
 Relative efficiency of Hg-200Br-79, HgBr-79, and HgBr electric discharge lasers
 24 p3586 A83-48781
 Inhomogeneity effects in a gas laser
 24 p3587 A83-48842

GAS LIQUEFACTION

U CONDENSING

GAS LUBRICANTS

The effect of two sided surface roughness on ultra-thin gas films
 06 p0769 A83-18390
 The effect of thin lubricant films and the methods of their application on the friction of several materials of bearings with a gaseous lubricant
 07 p0939 A83-20321
 New systems with the application of gaseous lubrication for the investigation of the friction and wear of machine and instrument parts
 07 p0939 A83-20323

GAS LUBRICATED BEARINGS

U GAS BEARINGS

GAS MASERS

NT HYDROGEN MASERS

Stimulated bremsstrahlung masers
 16 p2361 A83-36771
 An electron cyclotron maser instability for astrophysical plasmas
 21 p3227 A83-43944

GAS MIXTURES

NT AIR
 NT ALVEOLAR AIR
 NT COMPRESSED AIR
 NT DETONABLE GAS MIXTURES
 NT EXPIRED AIR
 Morphology of corrosion products formed on cobalt and nickel in argon-oxygen-chlorine mixtures at 1000 K
 01 p0024 A83-10247
 Sources of photoionization in transversely excited atmospheric CO₂ lasers
 01 p0055 A83-10978
 Exergie /4th revised and enlarged edition/ --- German book
 02 p0244 A83-12325
 Kinetic analysis of evaporation and condensation in a vapor-gas mixture
 03 p0315 A83-13118
 Absorption at 10 micron in CO₂-He and CO₂-N₂ mixtures at elevated temperatures
 03 p0392 A83-13497
 Influence of an axial magnetic field on the frequency shifts in a two-mode He-Ne/CH₄ laser
 03 p0331 A83-13589
 Some problems of second order modelling of mass transfer in a turbulent gas mixture
 03 p0319 A83-14480
 How well is gas mixed in clusters of galaxies
 03 p0428 A83-14767
 Boundary conditions for equations of the two-temperature gas dynamics of a binary mixture with significantly different component masses
 04 p0544 A83-15085
 Applicability of the Boussinesq approximation to solve problems of nonstationary concentrational natural convection
 04 p0475 A83-15093
 Approximate equation of state for multicomponent gaseous mixtures
 04 p0544 A83-15861
 On the existence of a second detonation front for two-phase mixtures of hydrogen-oxygen-nitrogen and aluminum particles
 04 p0457 A83-16444
 Ignition of confined gaseous mixtures by hot surfaces and hot wires
 05 p0612 A83-16606
 [AIAA PAPER 83-0240] Quasi-CW lasing of a Ne-Xe-HCl mixture excited by an electric discharge
 05 p0650 A83-17083
 Exchange of energy and momentum between gases at different temperatures
 05 p0691 A83-17359
 Structure of normal shock waves in a gas-particle mixture
 05 p0642 A83-17837
 Slowing down of rubidium-induced nuclear spin relaxation of Xe-129 gas in a magnetic field
 05 p0684 A83-17934
 Photoionization of nitrogen and oxygen mixtures by radiation from a gas discharge
 06 p0811 A83-18439
 Measurement of temperature conductivity of pure fluids and binary mixtures with the aid of dynamic light scattering in the general region of the critical point --- German thesis
 06 p0757 A83-18521
 Corrosion of 310 stainless steel in H₂-H₂O-H₂S gas mixtures Studies at constant temperature and fixed oxygen potential
 07 p0885 A83-20265
 The effects of various gases on cortical and spinal somatosensory evoked potentials at pressures up to 10 bar
 07 p0974 A83-20777
 Problems with the computation of the shock structure in binary gas mixtures using the direct simulation Monte Carlo method
 07 p0927 A83-21340
 Application of modified BGK-equations to the calculation of the shock wave structure in Xe-He mixtures
 08 p1083 A83-21817
 Transport coefficients of ternary gas mixtures
 08 p1170 A83-21988
 Mechanism of thermal electron attachment to O₂ as studied by observing isotope effects of attachment rates for /O-18/2 systems
 08 p1163 A83-22218
 An optically-pumped multigas far-IR laser
 08 p1107 A83-22246
 The statistical particle-in-cell method for multicomponent gases
 09 p1350 A83-23571
 Diffusion slipping of a binary gas mixture of moderate density along a flat surface
 09 p1259 A83-23983
 A further development of the fluorescent gated gas scintillation proportional counter
 09 p1268 A83-24105
 A boundary layer with selective suction
 09 p1260 A83-24226
 An approximate method for calculating the transfer coefficients of multicomponent mixtures --- transport properties of gases
 09 p1350 A83-24232
 Excitation of the O₂/a 1Delta g/ state by low energy electrons in O₂-N₂ mixtures
 10 p1478 A83-25554
 Resonance absorption measurements of atom concentrations in reacting gas mixtures. IX - Measurements of O atoms in oxidation of H₂ and D₂
 10 p1480 A83-26182
 Frequency reproducibility of ring He-Ne/CH₄ lasers
 10 p1433 A83-26686
 Rotational relaxations in a high pressure N₂ laser
 10 p1435 A83-26858

- B/C mixing and vibrational relaxation in XeF
11 p1654 A83-27586
- A proportional counter/image intensifier system for the detection of low energy X-rays
11 p1657 A83-27756
- Experimental study of the motion of rising vortex rings
11 p1569 A83-28533
- The third virial coefficient for nonpolar gases and their mixtures
11 p1665 A83-28559
- Electron drift velocities in gas mixtures of He, N₂, and CO₂
11 p1655 A83-28707
- Thermal diffusion in gases --- Russian book
12 p1723 A83-29341
- Hydrodynamic equations for partially ionized multicomponent gas mixtures with higher approximations to the transport coefficients
13 p1925 A83-30653
- On the kinetic theory of dense gases
13 p1932 A83-30656
- The kinetic theory of gas mixtures
13 p1932 A83-30666
- Certain aspects of the kinetic theory of reacting gases and its applications to relaxation aerodynamics
13 p1932 A83-30667
- Flow of a gas mixture near a catalytic surface
13 p1932 A83-30669
- A statistical model of nonstationary nonequilibrium processes in rarefied multicomponent chemically reacting gases
13 p1933 A83-30673
- The effect of boundary conditions on the flow of a polyatomic gas mixture in a supersonic nozzle --- in gasdynamic lasers
13 p1850 A83-30676
- Thermal conductivity of yttrium oxide in the temperature range 400-2100 C in different gaseous media
13 p1826 A83-31468
- The effect of natural convection on the concentration limits of ignition for combustible mixtures in a closed container
14 p1988 A83-32081
- A model equation for the probability distribution of the velocity and concentration during turbulent mixing and diffusive combustion of gases
14 p1988 A83-32085
- Infrared optical properties of solid mixtures of molecular species at 20K
[AIAA PAPER 83-1452]
14 p2084 A83-32717
- Intermolecular potentials from NMR data - H₂-N₂O and H₂-CO₂
15 p2227 A83-33631
- Diffusion and thermal diffusion in multicomponent mixtures of nonequilibrium ionized gases in a magnetic field
15 p2233 A83-34022
- Properties of a gasdynamic NO₂ laser
15 p2169 A83-34023
- Time-dependent simulation of flames in hydrogen-oxygen-nitrogen mixtures
15 p2132 A83-34036
- Flames near rich flammability limits, with particular reference to the hydrogen - Air and similar systems
15 p2132 A83-34038
- Miniature 250 Hz, TEA CO₂ laser using H₂ buffered gas mixture
15 p2170 A83-35251
- Experimental study of the interaction of thermals
16 p2349 A83-35529
- A Trimix saturation dive to 660 m studies of cognitive performance, mood and sleep quality
16 p2400 A83-35565
- Electron thermalization in gas mixtures
16 p2410 A83-35667
- A study of lean extinction limit for pilot flame holder
16 p2325 A83-35821
- Interaction of oblique shock and detonation waves
16 p2352 A83-36088
- Analysis of turbulent diffusion flames using unique relationships from laminar flame calculations
[AIAA PAPER 83-1364]
16 p2326 A83-36360
- The effects of chemical kinetics on the ignition of confined propane-air mixtures by hot particles and hot wires
[AIAA PAPER 83-1365]
16 p2326 A83-36361
- The determination of transport coefficients in multicomponent gas mixtures
16 p2354 A83-36882
- The effect of insulin on the reaction of the coronary and systemic blood circulation during the inspiration of hypoxic mixtures
17 p2555 A83-37239
- The viscosity and thermal conductivity of gas mixtures at high densities
17 p2505 A83-37568
- Direct statistical simulation of collisional relaxation in gas mixtures with large differences in concentration
18 p2751 A83-39151
- Degenerate regimes of heterogeneous combustion and extinction of a particle in a gaseous oxidizer
18 p2663 A83-39157
- Absorptivity of nitric oxide in the fundamental vibrational band
18 p2742 A83-39185
- Electron drift velocity in molecular gas rare gas mixtures
20 p3049 A83-42577
- Heavy gas mixtures for wind tunnel use
20 p2938 A83-42623
- Measurements of the conduction of heat in water vapor, nitrogen and mixtures of these gases in an extended temperature range
20 p2972 A83-42671
- Diffusive separation of binary mixtures of CO₂-H₂ in a sonic-orifice expansion
21 p3128 A83-43934
- Problems with a direct simulation Monte Carlo method applied to the shock structure in a binary gas mixture
21 p3132 A83-44945
- Atmospheric-pressure electroionization CO₂ laser using CO₂-N₂-H₂O mixtures
22 p3300 A83-46785
- The condition of the pulmonary blood flow and central hemodynamics in healthy humans during the breathing of a helium-oxygen mixture
23 p3497 A83-47115
- Core level excitation of simple gases
24 p3625 A83-48737
- Flow of a gas mixture in a cylindrical channel at intermediate Knudsen numbers
24 p3576 A83-48940
- Reaction mechanism of Ni-20Cr in mixtures of SO₂+O₂
24 p3565 A83-49513
- Experimental study of the parameters of a binary-mixture plasma jet
24 p3632 A83-49660
- An investigation of the pulsed-discharge radiation in mixtures of ZnI₂, CdI₂, and HgI₂ with helium and neon --- in metal vapor lasers
24 p3589 A83-49742
- Optimum conditions for the acceleration of the flame of gas mixtures at discontinuous obstacles in large volume
24 p3555 A83-49768

GAS PHASES

U VAPOR PHASES

GAS PIPES

Nonstationary flow in gas lines

01 p0045 A83-10582

Nonlinear oscillations of a gas in a pipe open at one end

10 p1417 A83-26288

Acoustic waves in a Rijke tube with radiation impedance

12 p1777 A83-29382

GAS POCKETS

Experimental study of the interaction of thermals

16 p2349 A83-35529

GAS PRESSURE

Dependence of the sign of the pressure shift of molecular lines upon the type of disturbing gas

02 p0234 A83-11680

Sources of pressure in lithium thionyl chloride batteries

02 p0202 A83-12054

The thermal conductivity of oxygen

02 p0244 A83-12094

Hot isostatic pressing technology. III - Diffusional bonding

02 p0156 A83-12296

High-pressure tunable CW waveguide CO₂ lasers

04 p0483 A83-15255

An approximate solution to the non-self-similar problem concerning the motion of a piston following an instantaneous impact

06 p0760 A83-19441

The effect of a high-pressure gaseous environment on the content of sodium, potassium, and water in the blood and tissues of white rats

07 p0973 A83-20246

The effects of various gases on cortical and spinal somatosensory evoked potentials at pressures up to 10 bar

07 p0974 A83-20777

Measurement of dynamic pressure in shock tube by streak photography

10 p1421 A83-26135

An experimental investigation of the internal methane pressure in hydrogen attack

14 p1994 A83-32682

Optimal mode of operation of a pulsed aerodynamic test facility with a free-flowing jet

17 p2448 A83-37522

Limits to the averaging of the total pressure of nonuniform gas flows

17 p2450 A83-37565

A gas pressure sintering process for producing dense Si₃N₄

23 p3435 A83-48274

The ignition of a vapor bubble in a liquid

24 p3556 A83-49774

Ignition of crystalline hexogen with adiabatic compression of the adjacent gas pocket

24 p3557 A83-49792

GAS REACTORS

Magnetogasdynamic effects on the growth of transverse acoustic waves in a reacting gas

18 p2744 A83-39149

GAS SPECTROSCOPY

NT FLAME SPECTROSCOPY

Measurements of intensities and self- and foreign-gas-broadened half-widths of spectral lines in the CO fundamental band

02 p0234 A83-11574

Spectroscopy of molecular rotation in gases and liquids --- Russian book

03 p0392 A83-13816

Coherent polarization methods of nonlinear gas spectroscopy in a longitudinal magnetic field

04 p0456 A83-15759

Measurement of time dependent optical gain using frequency modulation spectroscopy

06 p0763 A83-18955

A determination of the collision relaxation constants for a forbidden transition by means of nonlinear polarization spectroscopy for a three-level gas in a magnetic field

06 p0809 A83-19541

Continuously tunable coherent spectroscopy for the 0.1-1.0-THz region

07 p0931 A83-21357

Self-broadening in the millimeter-wave spectrum of ozone

07 p0991 A83-21395

Discrepancies between balloon-borne IR atmospheric spectra and corresponding synthetic spectra calculated line by line around 825 per cm

09 p1306 A83-24440

Spectral effects of intermolecular interactions in gases --- Russian book

10 p1478 A83-25520

Periphery of absorption bands as a specific form of the manifestation of intermolecular interaction in gases

10 p1478 A83-25521

Collision-induced absorption spectra of simple molecular systems

10 p1448 A83-25523

Investigation of absorption line profiles of molecular gases by methods of laser spectroscopy

10 p1419 A83-25525

Modeling of optical impedance spectroscopy

11 p1572 A83-27530

Short and middle range remote sensing of atmospheric gases using Raman lidar --- French thesis

11 p1585 A83-28640

Scattering of light by an intense saturating pulse in a resonance medium

14 p2078 A83-31901

Spectroscopy of atmospheric gases --- Russian book

14 p2052 A83-32555

Infrared heterodyne spectroscopy of seven gases in the vicinity of chlorine monoxide lines

14 p1990 A83-32915

CARS diagnostics of high pressure and temperature gases --- Coherent Anti-Stokes Raman Spectroscopy [AIAA PAPER 83-1478]

15 p2133 A83-34913

A relation between Holstein's photon escape transmission factor and the equivalent width --- for resonance radiation in gases

15 p2228 A83-34999

Mass spectrometry in the stratosphere

16 p2354 A83-35402

State-selective electron capture by C(2+), C(3+), N(2+), and Ar(2+) ions in rare gases

17 p2579 A83-38365

Metastable excitation measurements in CO and N₂ by high-resolution electron impact, using a low work function detector

17 p2579 A83-38368

An approximation of the mean velocity in the theory of spectral line broadening in gases

19 p2897 A83-40823

Optical splitter for dynamic range enhancement of optical multichannel detectors

19 p2847 A83-41098

Absorption of H₂S at DF laser wavelengths

19 p2852 A83-41108

Remote sensing of stratospheric and mesospheric winds by gas correlation electrooptic phase-modulation spectroscopy

22 p3328 A83-46063

140 GHz microwave spectrometer for the detection of gaseous chemical species

22 p3293 A83-46744

Optical and laser remote sensing

23 p3455 A83-47766

Interferometric measurements of atmospheric species

23 p3456 A83-47775

Detection of trace gases using high-resolution IR spectroscopy

23 p3456 A83-47776

Gaseous correlation spectrometric measurements --- remote sensing of gases in atmosphere

23 p3456 A83-47777

Measurements of atmospheric trace gases by long path differential UV/visible absorption spectroscopy

23 p3456 A83-47778

Remote detection of gases by gas correlation spectroradiometry

23 p3456 A83-47780

CARS - The only tool for the diagnostics of reactive media?

23 p3430 A83-48192

Core level excitation of simple gases

24 p3625 A83-48737

Radiation characteristics of vibrationally nonequilibrium CO₂ gas in the spectral region 12-19 microns

24 p3626 A83-49117

Applications of mass spectrometry techniques to autoclave curing of materials

24 p3559 A83-50143

Nonlinear plasma spectroscopy of the hydrogen Balmer-alpha line

24 p3627 A83-50196

GAS STREAMS

The effect of the neutral solar-wind component upon the interaction of the solar system with the interstellar gas stream

03 p0419 A83-13883

Instability and atomization of a liquid layer adjacent to a gas stream

05 p0635 A83-16665

[AIAA PAPER 83-0339]

05 p0635 A83-16665

Energy balance in a contracted glow discharge in a longitudinal gas flow

06 p0811 A83-18441

- Analysis of additional absorption components of MgII lines in Algol in terms of a model of gas stream
13 p1955 A83-31668
- Measurement of high gas-stream temperature using dynamic thermocouples
16 p2355 A83-35556
- Effects of properties and location in the plume on droplet diameter for injection in a supersonic stream
16 p2351 A83-36080
- Computational and experimental study of the effect of mass transfer on liquid jet break-up
[AIAA PAPER 83-1400]
16 p2353 A83-36390
- GAS TEMPERATURE**
- Application of light polarization technique to the generalized line-reversal method for gaseous temperature measurements
02 p0181 A83-12814
- Boundary conditions for equations of the two-temperature gas dynamics of a binary mixture with significantly different component masses
04 p0544 A83-15085
- Exchange of energy and momentum between gases at different temperatures
05 p0691 A83-17359
- An implicit scheme for determining temperature in the presence of radiative-conductive heat transfer
05 p0691 A83-17644
- Physical conditions in H II/OH maser regions
06 p0825 A83-18088
- Thermal behavior and insulation of a cryogenic wind tunnel
[ONERA, TP NO. 1982-89]
06 p0720 A83-18427
- Classical thermodynamics of homogeneous systems based upon Carnot's general axiom
06 p0815 A83-18929
- Investigation of the vibrational temperature kinetics in a TEA CO₂ laser
07 p0934 A83-20113
- Experimental study on inhibited diffusion and premixed flames in a counterflow system
08 p1057 A83-22347
- An evaluation of the thermal two-phase-state parameter given the nonstationary turbulence of a two-phase flow in a tube
09 p1258 A83-23441
- Measurement of temperatures in a shock tube by coherent anti-Stokes Raman spectroscopy /CARS/
10 p1421 A83-26136
- Temperature measurement of detonation using UV-absorption of O₂
10 p1421 A83-26137
- Investigation of the optical inhomogeneities of the active medium of a fast-flow CO₂ laser with mixing
10 p1433 A83-26677
- Experimental investigation of the optimum specific input energy on a subsonic CO EDL --- Electric Discharge Laser
11 p1580 A83-27577
- Doubly ionized aluminium - A diagnostic of cooling gas in the galactic corona
15 p2266 A83-34600
- Density and temperature variations in pulsed discharge lasers
16 p2358 A83-35453
- Experimental study of the interaction of thermals
16 p2349 A83-35529
- Measurement of high gas-stream temperature using dynamic thermocouples
16 p2355 A83-35556
- Determination of gas temperature from spectral lines with complex structure
16 p2356 A83-35938
- A new concept in high density power - The rotating bed reactor revisited --- space tug propulsion systems
[AIAA PAPER 83-1332]
16 p2320 A83-36345
- Ammonia as a molecular cloud thermometer
16 p2431 A83-36678
- The chemical composition and thermal history of the ice of a cometary nucleus
16 p2425 A83-36679
- Thermal effects on a high altitude airship
[AIAA PAPER 83-1984]
17 p2460 A83-38912
- Unsteady method of measuring the thermal conductivity of gases at high temperatures
18 p2751 A83-39867
- The temperature of molecular gas in the galactic center region
20 p3064 A83-42195
- Prediction of gas emissivity for a wide range of process conditions
20 p2974 A83-42691
- Correlation between the gas heating and the contraction of an RF discharge in hydrogen
21 p3210 A83-44140
- The effect of gas on dust temperature in comets
24 p3650 A83-48955
- GAS TRANSPORT**
- The regulation of erythropoiesis /Status of the problem/
01 p0081 A83-10916
- On the two-dimensional transport of stratospheric trace gases in isentropic coordinates
02 p0214 A83-12240
- Transport of aurorally produced N₂D⁺ by winds in the high latitude thermosphere
04 p0508 A83-14967
- The dynamics of oxygen transport from the capillaries to the nerve cells of the brain
08 p1145 A83-22104
- Numerical modeling of a zonally averaged stratospheric ozone field
09 p1305 A83-24215
- CO₂ and radon 222 as tracers for atmospheric transport
09 p1295 A83-24257
- The mathematical kinetics of reacting gases --- Russian book
09 p1227 A83-25220
- Fluctuation-dissipation relations in the scattering problem and the method of fluctuations in the kinetic theory of gases
10 p1490 A83-26246
- Kinetic enrichment of hydrogen at interfaces and voids by dislocation sweep-in of hydrogen
10 p1398 A83-26279
- Gas-kinetic magnetic resonance in N₂ and CO gases
11 p1654 A83-28062
- A device for the formation and investigation of spherical artificial phospholipid membranes
13 p1895 A83-30305
- Regional gas distributions and single-breath washout curves in head-down position
13 p1903 A83-30469
- Analytical methods for solving the Boltzmann equation
13 p1932 A83-30652
- On the kinetic theory of dense gases
13 p1932 A83-30656
- The global distribution of atmospheric carbon dioxide.
I Aspects of observations and modeling. II - A review of provisional background observations, 1978-1980
13 p1876 A83-30876
- Observations of neutral hydrogen in radio-loud and interacting galaxies
15 p2255 A83-33827
- A mechanistic model of Eulerian, Lagrangian mean, and Lagrangian ozone transport by steady planetary waves
16 p2379 A83-36136
- On the distribution of nitrogen dioxide in the high-latitude stratosphere
16 p2379 A83-36138
- Stratospheric NO₂. III - The effects of large-scale horizontal transport
16 p2379 A83-36139
- O₂ transport during two forms of stagnant hypoxia following acid and base infusions
17 p2554 A83-36992
- Several mechanisms of the transport of oxygen and its utilization in the skeletal muscles during acute hemic hypoxia
17 p2555 A83-37240
- Measurement of helium gas transmission through aerostat material
[AIAA PAPER 83-1986]
17 p2483 A83-38913
- Surface light-induced drift of a rarefied gas
17 p2515 A83-38959
- Steady reflection, absorption and transmission of small disturbances by a screen of dusty gas
18 p2680 A83-39209
- Deuterium transport and trapping in aluminum alloys
18 p2669 A83-40629
- A study of transport processes in a high-temperature boundary layer on an ablating graphite surface
19 p2842 A83-41259
- Cumulus cloud transport of transient tracers
20 p3021 A83-42842
- Deep earthquakes beneath Mount St. Helens - Evidence for magmatic gas transport
22 p3333 A83-46801
- Seasonal variations in the vertically integrated water vapor transport fields over the Southern Hemisphere
23 p3489 A83-47399
- GAS TUNGSTEN ARC WELDING**
- Effects of GTA dressing on the fatigue properties of aluminum alloy welded, butt jointed and fillet welded plates
09 p1274 A83-23650
- Welding iridium heat source capsules for space missions
20 p2998 A83-42300
- GAS TURBINE ENGINES**
- NT BRISTOL-SIDDELEY BS 53 ENGINE
NT HYDROGEN ENGINES
NT J-79 ENGINE
NT JET ENGINES
NT PULSEJET ENGINES
NT RAMJET ENGINES
NT SUPERSONIC COMBUSTION RAMJET ENGINES
NT T-56 ENGINE
NT T-64 ENGINE
NT TF-41 ENGINE
NT TURBOFAN ENGINES
NT TURBOJET ENGINES
NT TURBOPROP ENGINES
- Automatic plotting of the results of bench tests of turbine engines
01 p0011 A83-10444
- Three-dimensional model of spray combustion in gas turbine combustors
01 p0011 A83-10652
- Fuel property effects on Air Force gas turbine engines - Program genesis
01 p0028 A83-10653
- Effect of oxygen addition on ignition of aero-gas turbine at simulated altitude facility
01 p0011 A83-10660
- Characteristic time ignition model extended to an annular gas turbine combustor
01 p0011 A83-10666
- The theory of aircraft engines --- Russian book
01 p0011 A83-10675
- Identification and model reduction of multivariable continuous systems via a block-pulse functions scheme
01 p0094 A83-10708
- The first implementation of ATLAS for testing gas turbine engines
01 p0001 A83-10750
- Digital engine control for V/STOL and V/TOL aircraft
01 p0012 A83-10871
- Optical methods of flow diagnostics in turbomachinery
01 p0053 A83-11076
- Multifuel evaluation of rich/quench/lean combustor
01 p0023 A83-11492
- Low temperature /650 to 700 C/ burner rig testing
02 p0158 A83-12835
- Composite fan exit guide vanes for high bypass ratio gas turbine engines
03 p0282 A83-13159
- Experimental investigation on film cooling of a gas turbine blade
03 p0282 A83-13346
- The icing of aircraft gas turbine engines
03 p0280 A83-14619
- Automated ultrasonic dimensional and defect inspection of complex geometry gas turbine airfoil shapes
04 p0488 A83-15158
- An enhancement for the ultrasonic test bed to inspect engine disk bolt holes
04 p0488 A83-15160
- The application of the state-of-the-art NDE techniques to defect detection in silicon carbide structural ceramics
04 p0463 A83-15177
- Mechanisms of inlet-vortex formation
04 p0479 A83-16260
- Gaseous emissions of gas turbine combustors
[AIAA PAPER 83-0242]
05 p0596 A83-16608
- Swirling flow in a research combustor
[AIAA PAPER 83-0313]
05 p0612 A83-16644
- Small gas turbine combustor study - Combustor liner evaluation
[AIAA PAPER 83-0337]
05 p0596 A83-16663
- Design of a low emission combustor for an automotive gas turbine
[AIAA PAPER 83-0338]
05 p0652 A83-16664
- Effectiveness of turbine engine diagnostic systems
[AIAA PAPER 83-0535]
05 p0597 A83-16773
- The entropy efficiency of blade machines
05 p0597 A83-16953
- Numerical study of the dependence of the efficiency of the gas-screen cooling of perforated gas-turbine blades on cascade parameters
05 p0589 A83-16955
- Application of optimization to aircraft engine disk synthesis
06 p0718 A83-18213
- Fabrication and heat treatment of a Ni-base superalloy integrally bladed rotor for small gas turbine engine applications
06 p0732 A83-19102
- Preventing the strength failure of machines by vibrodiagnostic methods. II - The use of vibrodiagnostics for preventing the failure of certain parts and assemblies of gas-turbine engines
06 p0770 A83-19314
- Unbalance response analysis of a complete turbomachine
07 p0938 A83-19674
- P/M dual-property wheels for small engines
07 p0938 A83-19834
- Effect of broad properties fuel on injector performance in a reverse flow combustor
[AIAA PAPER 83-0154]
07 p0867 A83-21079
- Precision casting for gas turbine engines
07 p0941 A83-21347
- Cleaning gas turbine compressors - Some service experience with a wet-wash system
07 p0867 A83-21350
- High temperature alloys for gas turbines 1982; Proceedings of the Conference, Liege, Belgium, October 4-6, 1982
07 p0891 A83-21451
- The corrosion resistance of protective coatings
07 p0891 A83-21454
- Mechanisms of hot corrosion
07 p0891 A83-21455
- Deposition and blade fouling of gas turbines by fuel impurities and additives
07 p0941 A83-21456
- High temperature erosion and erosion-hot corrosion of superalloys and coatings
07 p0892 A83-21458
- High temperature stability of pack aluminide coatings on IN38LC
07 p0941 A83-21459
- Fatigue and creep considerations in the design of turbine components
07 p0949 A83-21461
- The interaction of high temperature corrosion and mechanical properties of alloys
07 p0893 A83-21470
- Fatigue failure under fretting conditions
07 p0894 A83-21481
- Cyclic rig and engine testing of ceramic turbine components
08 p1072 A83-22262
- Evaluation of air-cooled Si₃N₄ vanes
08 p1072 A83-22263
- Influence coefficients of variable geometry free gas turbine engines
08 p1111 A83-22321
- A transonic quasi-3D analysis for gas turbine engines including split-flow capability for turbofans
08 p1042 A83-22647
- Current problems in the testing of aircraft engines
08 p1046 A83-22652
- Features of the selection of the basic parameters of cooled GTE turbines
08 p1046 A83-22655

Gas turbine combustor modelling for calculating pollutant emission 08 p1046 A83-23142

Rotating strain gage instrumentation for gas turbine engines 09 p1264 A83-23360

Evaluation of the technical state of aircraft gas-turbine engines from thermogasdynamic parameters with allowance for the natural scatter of state parameters 09 p1205 A83-23430

A mathematical model for a turboshaft gas-turbine engine with an optimum control program for high-level computer-aided design 09 p1205 A83-23436

Determination of the region of efficient use for microturbines with working medium recirculation 09 p1205 A83-23440

An experimental study of an annular film-evaporation combustion chamber in a low-power gas turbine engine 09 p1205 A83-23443

The thermal stressed state of nozzle vanes under shutdown conditions 09 p1277 A83-23513

Radiation and smoke from the gas turbine combustor using heavy fuels 09 p1242 A83-23877

Friction damping of flutter in gas turbine engine airfoils 09 p1206 A83-24038

Prospects for the use of heat exchangers in aircraft gas turbines [DGLR PAPER 82-088] 09 p1207 A83-24200

New instrumentation for advanced turbine research 09 p1270 A83-25142

NASA clean catalytic combustor program [ASME PAPER 82-JPGC-GT-11] 09 p1227 A83-25269

Catalyst durability evaluation for advanced gas turbine engines [ASME PAPER 82-JPGC-GT-21] 09 p1274 A83-25270

Coatings in industrial gas turbines - Experience and further requirements 10 p1388 A83-25539

Thermal barrier coatings for thermal insulation and corrosion resistance in industrial gas turbine engines 10 p1400 A83-25542

The high temperature impact-sliding wear and oxidation resistance of several cobalt-based oxide-containing detonation gun coatings 10 p1394 A83-25544

Procedure for estimating the fatigue strength of gas turbine blades by method of acoustic emission 10 p1436 A83-26286

The effect of mass ratio of Ti to Al on the hot corrosion of quaternary 75Ni-13.5Cr-11.5/Ti + Al/ alloys 10 p1400 A83-26898

Large parabolic dish collectors with small gas-turbine, Stirling engine or photovoltaic power conversion systems 11 p1610 A83-27329

Separation characteristics of the T700 engine inlet particle separator 11 p1530 A83-27479

A software package for computing the three-dimensional stressed state of the blades of gas-turbine engines 11 p1598 A83-28507

The interaction between a separated blade and the armor ring 11 p1531 A83-28510

The influence of electrode potential on the corrosion of gas turbine alloys in sulfate melts 11 p1550 A83-28672

Three-dimensional viscous analysis of ducts and flow splitters 12 p1696 A83-29010

Some fuel effects on carbon formation in gas turbine combustors 12 p1717 A83-29392

Structural tailoring of engine blades (STAEBL) [AIAA 83-0828] 12 p1703 A83-29737

Minimum contact magnetic sensing of turbine blade speed 13 p1807 A83-30175

A general-purpose oil for ground-based gas-turbine engines 14 p1998 A83-32076

The effect of the fuel quality on the degree of combustion product ionization in gas-turbine engines 14 p1988 A83-32078

The fatigue strength of compressor disks 14 p2030 A83-32387

Development of counter-rotating innershaft support bearing technology --- for aircraft gas turbine engines 14 p1976 A83-32587

On the question of calculating the pressurization start-up regimes of a gas-turbine plant 14 p2027 A83-32651

Effects of friction dampers on aerodynamically unstable rotor stages [AIAA PAPER 83-0848] 14 p1976 A83-32791

Thermal cycling in compact plate-fin heat exchangers --- in aircraft gas turbines 15 p2123 A83-34253

Vibrational diagnostics of gas-turbine blades 15 p2180 A83-35040

Temperature and composition measurements in a research gas turbine combustion chamber 16 p2302 A83-35790

New trends in combustion research for gas turbine engines 16 p2303 A83-35806

Combustor modelling by assembly of well-stirred reactors 16 p2325 A83-35808

Effect of air, liquid and injector geometry variables upon the performance of a plain-jet airblast atomizer 16 p2351 A83-35809

The effects of fuel properties upon pollutants present in gas turbine aero-engines 16 p2338 A83-35813

Experimental investigation on the role of flexbars and metallic end seals in squeeze film dampers --- of gas turbine engines 16 p2361 A83-35862

Component life reduction due to use of AVGAS in gas turbine engines 16 p2305 A83-35869

Life estimation methods of gas turbine rotating components 16 p2305 A83-35870

A contribution to airworthiness certification of gas turbine disks 16 p2305 A83-35872

Stress analysis of critical areas of low-pressure compressor-disc assembly of a developmental aero-engine 16 p2305 A83-35880

Criteria for optimizing starting cycles for high performance fighter engines [AIAA PAPER 83-1127] 16 p2306 A83-36236

Eccentric end wear in cylindrical roller bearings can be predicted and prevented [AIAA PAPER 83-1132] 16 p2361 A83-36237

Simulation of advanced engine lubrication and rotor dynamics systems - Rig design and fabrication [AIAA PAPER 83-1133] 16 p2306 A83-36238

Advanced propfan engine characteristics and technology needs [AIAA PAPER 83-1155] 16 p2306 A83-36250

The performance of single-shaft gas turbine load compressor auxiliary power units [AIAA PAPER 83-1159] 16 p2306 A83-36251

Numerical calculations of time dependent three-dimensional viscous flows in a blade passage with tip clearance [AIAA PAPER 83-1171] 16 p2294 A83-36258

A survey of trends in modern turbine technology [AIAA PAPER 83-1174] 16 p2306 A83-36260

Small turbine engine experience with high density fuels [AIAA PAPER 83-1177] 16 p2339 A83-36262

Effects of interstage diffuser flow distortion on the performance of a 15.41-centimeter tip diameter axial power turbine [AIAA PAPER 83-1179] 16 p2307 A83-36263

Experiments in dilution jet mixing [AIAA PAPER 83-1201] 16 p2352 A83-36277

Concepts for increased power and enhanced fuel conservation with newly patented multiple power-cycle gas turbine engines [AIAA PAPER 83-1209] 16 p2307 A83-36282

Nondestructive evaluation methods for implementation of damage-tolerant designed gas turbine engine components [AIAA PAPER 83-1232] 16 p2307 A83-36295

United Kingdom military engine usage, condition and maintenance systems experience [AIAA PAPER 83-1239] 16 p2308 A83-36302

Importance of inlet boundary conditions for numerical simulation of combustor flows [AIAA PAPER 83-1263] 16 p2308 A83-36314

Advanced techniques for gas and metal temperature measurements in gas turbine engines [AIAA PAPER 83-1291] 16 p2302 A83-36325

Application of thin film strain gages and thermocouples for measurement on aircraft engine parts [AIAA PAPER 83-1292] 16 p2302 A83-36326

Instrumental problems in small gas turbine engines [AIAA PAPER 83-1293] 16 p2302 A83-36327

Development trends in engine durability --- for USAF aircraft gas turbines [AIAA PAPER 83-1297] 16 p2309 A83-36329

A JT8D low emissions combustor by radial zoning [AIAA PAPER 83-1324] 16 p2309 A83-36339

The performance of an annular vane swirler --- to aid in modeling gas turbine combustor flowfields and swirling confined flow turbulence [AIAA PAPER 83-1326] 16 p2309 A83-36340

A comprehensive method for preliminary design optimization of axial gas turbine stages. II - Code verification [AIAA PAPER 83-1403] 16 p2309 A83-36393

The impact of engine usage on life cycle cost [AIAA PAPER 83-1406] 16 p2310 A83-36395

LCC evaluation of advanced engine damage tolerance goals for a hot-section disk --- in aircraft engines [AIAA PAPER 83-1407] 16 p2310 A83-36396

Development of simulated mission endurance test acceleration factors in determining engine component serviceability and failure mode criticality [AIAA PAPER 83-1409] 16 p2310 A83-36398

Configuration selection and technology transition in 5000 SHP class engines [AIAA PAPER 83-1411] 16 p2310 A83-36400

Feasibility of dry lubrication for limited-duty gas turbine engines [AIAA PAPER 83-1130] 16 p2362 A83-36405

Propulsion prototypes at General Electric [AIAA PAPER 83-1053] 16 p2310 A83-36463

Technology and engine demonstrator programs [AIAA PAPER 83-1064] 16 p2310 A83-36464

Forced and self-excited vibrations of gas-turbine assemblies with perfect and perturbed symmetry 16 p2311 A83-36791

Electrohydraulic fuel-flow regulator for gas-turbine-engine control systems 16 p2311 A83-36793

Nonlinear multivariable design by total synthesis --- of gas turbine engine control systems 17 p2467 A83-37092

Finite-element mathematical model of a gas turbine engine in unsteady flow 17 p2467 A83-37252

Gas turbine engines 17 p2467 A83-37274

Full Authority Fault Tolerant Electronic Engine Control systems for advanced high performance engines (FAFTEEC) [SAE PAPER 821398] 17 p2468 A83-37972

Microcomputer brings digital power to the small aircraft gas turbine [SAE PAPER 821402] 17 p2468 A83-37975

Utilization of computer aided design for the development of advanced turbomachinery components [SAE PAPER 821423] 17 p2468 A83-37980

A unified approach to turbine blade life prediction [SAE PAPER 821439] 17 p2468 A83-37987

727, B-52 retrofit with PW2037 meeting today's requirements [SAE PAPER 821443] 17 p2463 A83-37991

Repairing gas turbine hot section airfoils today [SAE PAPER 821487] 17 p2469 A83-38006

Experiences in repair of hot section gas turbine components [SAE PAPER 821490] 17 p2469 A83-38008

The Coanda/refraction concept for gas turbine engine test cell noise suppression [SAE AIR 1813] 17 p2471 A83-38105

Solution of viscous internal flows on curvilinear grids generated by the Schwarz-Christoffel transformation 17 p2508 A83-38796

Advanced techniques for measurement of strain and temperature in a turbine engine [AIAA PAPER 83-1296] 18 p2688 A83-39106

Longitudinal modes of gas oscillations in the main combustion chamber of gas-turbine engines 18 p2641 A83-39169

Evaluation of the efficiency of the diamond burnishing of gas-turbine-engine parts 18 p2695 A83-39511

Composite engine duct fabrication 18 p2631 A83-39941

The feasibility of water injection into the turbine coolant to permit gas turbine contingency power for helicopter application [ASME PAPER 83-GT-66] 18 p2642 A83-39993

Blade loss transient dynamic analysis of turbomachinery 19 p2800 A83-40864

Use of mixed performance criteria in gas turbine engine controller design 19 p2800 A83-41482

Large scale aeroengine compressor test facility 19 p2807 A83-41534

Thermal fatigue of gas-turbine blades made of a material based on silicon nitride and silicon carbide 19 p2823 A83-41594

Estimation of the thermal fatigue strength of the blades of full-scale gas-turbine engines 19 p2800 A83-41596

A criteria approach to estimating the accumulation of the working medium mass and energy in the gas-air circuit of gas-turbine engines when analyzing transient regimes 19 p2800 A83-42126

A study of the characteristics of short hydrodynamic dampers of aircraft engine motors with allowance for turbulization of the working fluid in the damper clearance 19 p2800 A83-42129

Diagnostics of the conditions of gas-turbine engines using models reflecting the dynamics of changes in the controlled parameters 19 p2801 A83-42133

A study of the formation of nitrogen oxides during the combustion of a lean homogeneous mixture in the hybrid combustion chamber of an automotive gas-turbine engine 19 p2821 A83-42134

The effect of supercritical pressure gradients on heat transfer in turbine nozzle cascades 19 p2801 A83-42140

An experimental study of ball bearings in the combined supports of the rotors of gas-turbine engines 19 p2855 A83-42144

A study of the effect of the combustion process on mass transfer in the primary zone of the combustion chamber of a gas-turbine engine 19 p2801 A83-42150

- A study of the gas-dynamic efficiency of the labyrinth seals of gas-turbine engines with a profiled stator wall
19 p2801 A83-42153
- Mathematical modeling of gas-turbine engines with heat regeneration
19 p2801 A83-42154
- Recent developments in high temperature coatings for gas turbine airfoils
20 p2953 A83-42254
- Tapered roller bearings for turbine engines
20 p2998 A83-42559
- Gas turbine engine cascade wind tunnel with automatic data acquisition and control
20 p2938 A83-42563
- A family of small low cost gas turbines for unmanned vehicle systems
20 p2936 A83-42616
- Pressure loss and heat transfer through multiple rows of short pin fins
20 p2975 A83-42709
- Experimental investigation of heat transfer by a single- and a triple-row round jets impinging on semi-cylindrical concave surfaces
20 p2929 A83-42740
- The strength of GTE structural elements under low-cycle loading
20 p2936 A83-42877
- Study of convective heat transfer in gas turbine combustion chambers
20 p2984 A83-43024
- Small gas turbines and their applications in the field of high-speed surface craft
21 p3147 A83-44371
- Hovercraft auxiliary power units (APUs)
21 p3147 A83-44372
- Demands on the air system of modern aircraft engines
22 p3255 A83-46491
- Increased energy exploitation in cooled high-temperature turbines
23 p3406 A83-47202
- A new-technology gas generator for medium-power shaft-turbine engines
23 p3406 A83-47217
- Design considerations for nuclear reactor gas turbine space power systems
[ASME PAPER 83-GT-20] 23 p3426 A83-47886
- Testing of a full-scale staged combustor operating with a synthetic liquid fuel
[ASME PAPER 83-GT-27] 23 p3464 A83-47890
- Combustion experiments with a new burner air distribution concept
[ASME PAPER 83-GT-31] 23 p3406 A83-47893
- The Rolls-Royce annular vaporizer combustor
[ASME PAPER 83-GT-49] 23 p3407 A83-47908
- Measurements of heat transfer distribution over the surfaces of highly loaded turbine nozzle guide vanes
[ASME PAPER 83-GT-53] 23 p3394 A83-47910
- A small engine high temperature core research programme
[ASME PAPER 83-GT-56] 23 p3407 A83-47912
- Techniques for obtaining detailed heat transfer coefficient measurements within gas turbine blade and vane cooling passages
[ASME PAPER 83-GT-58] 23 p3447 A83-47914
- The purpose, the principles and the problems of fault tolerant systems --- for aircraft gas turbine engines
[ASME PAPER 83-GT-59] 23 p3407 A83-47915
- Performance evaluation of centrifugal compressor impellers using three-dimensional viscous flow calculations
[ASME PAPER 83-GT-62] 23 p3395 A83-47918
- A CAD method for centrifugal compressor impellers
[ASME PAPER 83-GT-65] 23 p3395 A83-47920
- Investigation of fixed-rake sampling system for the assessment of emission characteristics of gas turbine engines
[ASME PAPER 83-GT-72] 23 p3407 A83-47925
- Test experience with turbine-end foil bearing equipped gas turbine engines
[ASME PAPER 83-GT-73] 23 p3407 A83-47926
- EAGLE/DTA - A life cycle cost model for damage tolerance assessment --- Engine/Aircraft Generalized Life cycle cost Evaluator
[ASME PAPER 83-GT-76] 23 p3407 A83-47929
- Use of pyrolysis-derived fuel in a gas turbine engine
[ASME PAPER 83-GT-96] 23 p3440 A83-47942
- Automated diagnostic system for engine maintenance --- vibration data extraction from gas turbine engines
[ASME PAPER 83-GT-103] 23 p3408 A83-47943
- Automotive gas turbine ceramic component testing
[ASME PAPER 83-GT-112] 23 p3464 A83-47945
- Experimental study of the three-dimensional flow field in an annular turbine nozzle guidevane
[ASME PAPER 83-GT-120] 23 p3396 A83-47949
- Measurement and analyses of heat flux data in a turbine stage. I - Description of experimental apparatus and data analysis
[ASME PAPER 83-GT-121] 23 p3408 A83-47950
- Measurement and analyses of heat flux data in a turbine stage. II - Discussion of results and comparison with predictions
[ASME PAPER 83-GT-122] 23 p3408 A83-47951
- Three-dimensional flow measurements in a turbine scroll
[ASME PAPER 83-GT-128] 23 p3396 A83-47957
- Emissions variability and traversing on production RB211 engines
[ASME PAPER 83-GT-141] 23 p3409 A83-47966
- An investigation into the effect of side-plate clearance in an uncentralized squeeze-film damper
[ASME PAPER 83-GT-176] 23 p3464 A83-47975
- Developments in air cooling of gas turbine vanes and blades
[ASME PAPER 83-GT-160] 23 p3409 A83-47984
- Ceramic Applications in Turbine Engines (CATE) development testing
[ASME PAPER 83-GT-179] 23 p3465 A83-47990
- A comparative study of the influence of different means of turbine cooling on gas turbine performance
[ASME PAPER 83-GT-180] 23 p3465 A83-47991
- Built-In Test Equipment (BITE) on the Garrett model GTCP331 APU digital electronic control unit --- for gas turbine aircraft auxiliary power system
[ASME PAPER 83-GT-186] 23 p3409 A83-47992
- The impact of computers on the test cell of tomorrow --- for gas turbine engine tests
[ASME PAPER 83-GT-187] 23 p3409 A83-47993
- Three-dimensional modeling of horseshoe vortex flows
[ASME PAPER 83-GT-191] 23 p3397 A83-47997
- Emissions from enclosed swirl stabilised premixed flames
[ASME PAPER 83-GT-192] 23 p3410 A83-47998
- A comparison of Navy and contractor gas turbine acquisition cost
[ASME PAPER 83-GT-198] 23 p3410 A83-48001
- Ceramic components for high-temperature vehicular gas turbines - State of the art of the German ceramic program
[ASME PAPER 83-GT-205] 23 p3465 A83-48006
- Erosion pattern of twisted blades by particle laden flows
[ASME PAPER 83-GT-214] 23 p3397 A83-48015
- An investigation into the effect of coolant flow on the vibration characteristics of hollow blades conveying fluid
[ASME PAPER 83-GT-217] 23 p3470 A83-48017
- Gas turbine performance improvement by retrofit of advanced technology
[ASME PAPER 83-GT-222] 23 p3465 A83-48020
- Strain isolated ceramic coatings
[ASME PAPER 83-GT-223] 23 p3465 A83-48021
- Component qualification and initial build of the AGT 100 advanced automotive gas turbine
[ASME PAPER 83-GT-225] 23 p3465 A83-48023
- Progress in net shape fabrication of alpha SiC turbine components
[ASME PAPER 83-GT-238] 23 p3466 A83-48030
- Economic aspects of advanced coal-fired gas turbine locomotives
[ASME PAPER 83-GT-241] 23 p3514 A83-48031
- The coal-fired gas turbine locomotive - A new look
[ASME PAPER 83-GT-242] 23 p3466 A83-48032
- Development of the single crystal alloys CM SX-2 and CM SX-3 for advanced technology turbine engines
[ASME PAPER 83-GT-244] 23 p3432 A83-48034
- Squeeze-film damper technology. I - Prediction of finite length damper performance
[ASME PAPER 83-GT-247] 23 p3466 A83-48035
- Aluminide coatings on superalloys
[ONERA, TP NO. 1983-68] 23 p3432 A83-48189
- US national programs in ceramics for energy conversion
23 p3438 A83-48308
- Status report 1981 on the German BMFT-sponsored programme 'Ceramic components for vehicular gas turbines'
23 p3438 A83-48309
- The use of ceramics for engines
23 p3439 A83-48636
- Evaluation of three fluid-film models for use in uncentralized squeeze-film damper bearing analysis
24 p3590 A83-48923
- Supersonic V/STOL - Tandem fan concepts
[AIAA PAPER 83-2567] 24 p3549 A83-49597
- The formation of carbon monoxide during turbulent diffusion combustion --- for aircraft gas turbine combustion chambers
24 p3569 A83-49769
- A finite element study of the nonstationary temperature fields of bodies of revolution
24 p3596 A83-49909
- ### GAS TURBINES
- Gas corrosion characteristics of nickel-base alloys
01 p0025 A83-10392
- Diffusion welding for water-cooled gas turbine applications
02 p0187 A83-12071
- Measured and predicted soot profiles in a gas turbine combustor
02 p0136 A83-12077
- Oxidation-resistant materials for hot gas turbines and jet power plants. II
02 p0148 A83-12298
- The influence of equivalence ratio variation on pollutant formation in a gas turbine type combustor
02 p0136 A83-13095
- High temperature corrosion on high temperature materials Metallographic, scanning electron microscopic and microanalytical tests
04 p0458 A83-15124
- Short duration heat transfer studies at high free-stream temperatures
[ASME PAPER 82-GT-129] 07 p0924 A83-19673
- IN939 - Metallurgy, properties and performance
07 p0892 A83-21465
- Blade repair and recovery --- in gas turbines
07 p0941 A83-21496
- Diffusion bonding of superalloys for gas turbines
07 p0941 A83-21503
- Use of fiber-like materials to augment cycle life of thick, thermoprotective-seal coatings --- for gas turbine engine components
08 p1072 A83-22271
- Isothermal models of gas-turbine combustors
08 p1057 A83-23097
- The mechanism of the stabilization of turbine oil by antioxidants
09 p1238 A83-23868
- A computer model for gas turbine blade cooling analysis
[ASME PAPER 82-JPGC-GT-6] 09 p1208 A83-25267
- Sputter-ion plating of coatings for protection of gas-turbine blades against high-temperature oxidation and corrosion
10 p1394 A83-25472
- A study of irregular-shaped particle deposition in turbulent flows and application to gas turbines
11 p1525 A83-27480
- Correlation and prediction of thermophoretic and inertial effects on particle deposition from non-isothermal turbulent boundary layers
11 p1566 A83-27481
- The design and construction of a low power gas turbine for solar energy conversion - An analytical model of operation of the installation in a variable mode --- French thesis
11 p1612 A83-28647
- A study of a solar central power plant with a gas turbine - Project Sirocco modelling and control --- French thesis
11 p1612 A83-28652
- 18:1 pressure ratio axial/centrifugal compressor demonstration program
12 p1732 A83-29013
- Convective heat transfer in rotating cylindrical cavity
[ASME PAPER 82-GT-151] 13 p1840 A83-30239
- A theoretical and experimental investigation of flow and heat transfer in film cooling
15 p2161 A83-34268
- Flow-loss, efficiency, and change-of-state calculations for fluid-flow engines and heat exchangers
15 p2162 A83-34976
- Temperature dependent deformation mechanisms of Alloy 718 in low cycle fatigue
16 p2331 A83-36168
- Liquid fuel cyclone combustors for gas turbine applications
[AIAA PAPER 83-1205] 16 p2361 A83-36280
- Effect of using emulsions of high nitrogen containing fuels and water in a gas turbine combustor on NOx and other emissions
[ASME PAPER 82-GT-224] 18 p2673 A83-39992
- Tests of a solar receiver for a solar gas turbine module with Re = 1500-4000
19 p2862 A83-42015
- The components of gas turbines: Materials and strength (2nd revised and enlarged edition) --- Russian book
21 p3147 A83-43912
- A reverse flow chamber for small turbomachines
[ONERA, TP NO. 1983-30] 21 p3092 A83-44309
- Velocity measurements in a confined swirl driven recirculating flow
21 p3131 A83-44682
- Velocity and turbulence measurements in combustion systems
21 p3131 A83-44684
- Use of flight engine technology in stationary industrial gas turbines and diesel motors
23 p3464 A83-47203
- Film cooling with steam injection through three staggered rows of inclined holes over a straight airfoil
[ASME PAPER 83-GT-30] 23 p3446 A83-47892
- Pressure recovery of collectors with annular curved diffusers
[ASME PAPER 83-GT-35] 23 p3394 A83-47896
- Statistical characteristics of velocity, concentration, mass transport, and momentum transport for coaxial jet mixing in a confined duct
[ASME PAPER 83-GT-39] 23 p3447 A83-47899
- Heat transfer experiments in high aspect ratio rectangular channel with epoxied short pin fins
[ASME PAPER 83-GT-57] 23 p3447 A83-47913
- Improved combustion turbine efficiency with reformed alcohol fuels
[ASME PAPER 83-GT-60] 23 p3464 A83-47916
- An experimental investigation of a gas turbine disk cooling system
[ASME PAPER 83-GT-78] 23 p3447 A83-47931
- Full coverage discrete hole wall cooling - Discharge coefficients
[ASME PAPER 83-GT-79] 23 p3447 A83-47932
- Cascade flutter analysis of cantilevered blades
[ASME PAPER 83-GT-129] 23 p3408 A83-47958
- Brazing of silicon nitride
23 p3437 A83-48286
- Non-destructive evaluation of ceramic gas turbine components by X-rays and other methods
23 p3468 A83-48300

- Certain aspects of the application of high-temperature coatings to gas-turbine blades 24 p3590 A83-49089
- GAS VALVES**
A pulsed molecular beam for laser spectroscopy 16 p2410 A83-36554
- GAS VISCOSITY**
The influence of mathematical viscosity on the difference solution in problems of two-temperature gas dynamics 09 p1347 A83-23573
On the viscosity of monatomic and diatomic gases at intermediate temperatures 13 p1931 A83-30098
The viscosity and thermal conductivity of gas mixtures at high densities 17 p2505 A83-37568
- GAS WELDING**
NT BRAZING
Welding technology / 2nd edition/ --- Book 13 p1858 A83-30142
Exploiting MIG-welding developments --- Book 15 p2171 A83-33630
- GAS-GAS INTERACTIONS**
NT ASSOCIATION REACTIONS
Exchange of energy and momentum between gases at different temperatures 05 p0691 A83-17359
Attachment of low-energy electrons to O₂ molecules in some gases and liquids - An instrument for measuring concentrations of electronegative impurities in gases 10 p1422 A83-26468
Experimental study of the interaction of thermals 16 p2349 A83-35529
- GAS-ION INTERACTIONS**
Electron loss from fast one-electron ions colliding with He, N₂, and Ar 01 p0105 A83-10194
Ionisation of H₂ by fast protons and multiply charged ions of He, Li, C, N and O 01 p0105 A83-10857
The mobilities of NO₃⁻, NO₂⁻, NO⁺, and Cl⁻ in N₂ - A measure of inelastic energy loss 05 p0684 A83-17656
Ion kinetics, minor neutral and excited constituents in the D region with a high level of ionization. I - Formulation of the problem and a general scheme for the processes 06 p0786 A83-18360
The role of ion-molecule reactions in the conversion of N₂O₅ to HNO₃ in the stratosphere 08 p1137 A83-23114
Temperature dependence of three-body association reactions from 45 to 400 K - The reactions N₂⁺ + N₂ yields Na⁺ + N₂ and O₂⁺ + 2O₂ yields O₄⁺ + O₂ 10 p1391 A83-26458
Charge transfer of doubly charged and trebly charged ions with atomic hydrogen at thermal energies 13 p1916 A83-31352
Charge transfer of O(3+) ions in collisions with atomic hydrogen 13 p1916 A83-31354
Transport properties for the nitrogen system - N₂, N, N(+) and E [AIAA PAPER 83-1474] 14 p2094 A83-32728
Excited states created in charge transfer collisions between atoms and highly charged ions 16 p2409 A83-35636
Ion-neutral collision frequency variations in the lower thermosphere from incoherent scatter measurements 17 p2545 A83-38538
Single collision ion-molecule reactions at thermal energy Rotational and vibrational distributions from N(+) + CO yields N + CO(+) 19 p2897 A83-40771
Investigation of the dynamics and threshold behavior of negative ion-neutral reactions 20 p2949 A83-42578
Ion-molecule syntheses of interstellar molecular hydrocarbons through C₄H - Toward molecular complexity 22 p3377 A83-46258
- GAS-LIQUID INTERACTIONS**
NT AIR SEA ICE INTERACTIONS
NT AIR WATER INTERACTIONS
Dynamic equation of state of a gas with evaporating drops 04 p0544 A83-15445
Sound velocity and critical mass throughput in one- and two-component gas-liquid flows --- German thesis 06 p0761 A83-19621
Sulfur dioxide absorption, oxidation, and oxidation inhibition in falling drops - An experimental/modeling approach 09 p1298 A83-25194
Attachment of low-energy electrons to O₂ molecules in some gases and liquids - An instrument for measuring concentrations of electronegative impurities in gases 10 p1422 A83-26468
Direct-contact air/molten salt heat exchange for solar thermal systems 11 p1607 A83-27234
The relation between the molecular emissivity and the molecular absorptivity of the surfaces of bodies 13 p1817 A83-30665
Calculation of the characteristics of submerged combustion 14 p1988 A83-32084
Preliminary results of Texas 8 experiments on effects of surface tension minimum [IAF PAPER 83-151] 23 p3446 A83-47291

- Theory of thermophoresis of nonvolatile liquid aerosol particles 24 p3575 A83-48861
Instabilities of a cylindrical liquid sheet in the presence of two gaseous flows 24 p3578 A83-49647
- GAS-METAL INTERACTIONS**
Investigation of the tribochemical influence of air pollution on the rolling friction of various materials being used in a newly developed railroad measuring post --- German thesis 01 p0056 A83-10175
Sulfidation properties of Fe-Cr alloys at 1073 K in H₂S-H₂ atmospheres of sulfur pressures 0.01 and 0.00001 Pa 01 p0024 A83-10244
Morphology of corrosion products formed on cobalt and nickel in argon-oxygen-chlorine mixtures at 1000 K 01 p0024 A83-10247
Gas saturation of the surface layers of welded joints of alloy OT4 after full and partial annealing in vacuum 01 p0025 A83-10448
Influence of the gaseous environment on fatigue crack propagation in an austenitic steel 03 p0300 A83-14701
The effect of oxidation and gas saturation processes on the mechanical properties of titanium alloys VT1-0 and VT14 04 p0458 A83-15396
Influence of corrosion deposits on near-threshold fatigue crack growth behavior in 2XXX and 7XXX series aluminum alloys 04 p0460 A83-16005
An experimental study of the thermal accommodation coefficients of inert gases on a tungsten surface 04 p0457 A83-16169
The effect of sulfur containing environment on the high temperature low cycle fatigue of a cast Ni-base alloy 04 p0461 A83-16252
On the existence of a second detonation front for two-phase mixtures of hydrogen-oxygen-nitrogen and aluminum particles 04 p0457 A83-16444
The effect of environment on fatigue crack growth behavior of 2021 aluminum alloy 05 p0616 A83-17894
Hydrogen in titanium, niobium, and tantalum 06 p0727 A83-17960
The hydrogen evolution process on a Ni-28 percent Mo alloy 06 p0728 A83-18146
Steel in equilibrium with hydrogen at room temperature --- German thesis 06 p0729 A83-18499
Hydrogen permeation and diffusion in niobium 07 p0884 A83-20259
The effect of absorbed hydrogen on torsional fatigue of 2024-T351 aluminum alloy 07 p0887 A83-20633
Hydrogen-induced fracture phenomena in a BCC titanium alloy 08 p1061 A83-21717
A criterion for hydrogen-induced fracture 08 p1063 A83-21760
A study of the kinetic characteristics of hydrogen interaction with alpha titanium and a titanium-niobium alloy 09 p1235 A83-24394
The effect of hydrogen on the fracture toughness of titanium alloys 09 p1235 A83-24398
A study of the oxidation and gas saturation of beta titanium alloys 09 p1235 A83-24400
The effect of a gas-saturated layer on the corrosion stability and mechanical strength of titanium alloys 09 p1235 A83-24403
Effects of hydrogen on near-threshold crack propagation in niobium 10 p1396 A83-25867
The interaction of hydrogen with traps and its solubility in a maraging steel 10 p1399 A83-26793
Hydrogen absorption and embrittlement of tantalum at cathodic deposition 10 p1399 A83-26897
Direct contact droplet heat exchangers for thermal management in space 11 p1564 A83-27137
Experimental investigation of metal hydride reaction beds 11 p1545 A83-27214
The phase-change behavior of hydrogen in niobium and in niobium-vanadium alloys 11 p1545 A83-27496
The oxidation of carbon on nickel - Effects of surface morphology 11 p1545 A83-28170
Application of nuclear reaction analysis to stress-induced hydrogen migration in titanium 13 p1820 A83-30182
Stress corrosion and hydrogen induced cracking behaviour in an Al alloy 13 p1820 A83-30325
Semiempirical, quantum mechanical calculation of hydrogen embrittlement in metals 13 p1820 A83-30598
Evidence for pseudo bridge bonding of c(2 x 2)-O on Ni(100) 13 p1817 A83-30920
Cluster studies of CO adsorption. III - CO on small Cu clusters 13 p1817 A83-30965
Distribution of internal energy in NO vibrationally excited by a hot platinum surface 13 p1818 A83-30970
Hydrogen solubility in rhenium at pressure up to 90 kb 13 p1824 A83-31333
Hydrogen in pure aluminum solidified unidirectionally 13 p1824 A83-31601

- The effect of nitrogen- and hydrogen-containing media on the refractory properties of nickel-base alloys 14 p1993 A83-32388
Stress corrosion cracking and hydrogen embrittlement 14 p1995 A83-32809
Hydrogen effects in metals 14 p1995 A83-32875
Hydrogen permeability and diffusivity in nickel and Ni-base alloys 14 p1997 A83-32950
Exploiting MIG-welding developments --- Book 15 p2171 A83-33630
Influence of hydrogen additions on high-temperature superplasticity of titanium alloys 15 p2135 A83-33639
A study of the diffusion of oxygen in alpha-titanium oxidized in the temperature range 460-700 C 15 p2133 A83-34699
Measurement of hydrogen permeation through nickel by oscillation method 16 p2328 A83-35602
Photoelectrocatalysis on silicon in solar light 16 p2328 A83-36775
Phenomenological study of metal-plasma systems in the presence of coupled electrical, chemical, and thermal effects 16 p2328 A83-36877
Drastic reduction of adsorption of CO and H₂ on (111)-type Pd layers 16 p2328 A83-36990
Trapping of hydrogen by oxygen and nitrogen impurities in niobium, vanadium and tantalum 17 p2491 A83-38856
The effect of nitrogen on the combustion of aluminum 18 p2663 A83-39161
Penetration of sulfur through preformed protective oxide scales 18 p2666 A83-39854
A comparison of microvoid sizes in nickel base alloys tested in air and in the presence of hydrogen 18 p2668 A83-40614
Calculations of the binding of hydrogen to fixed interstitial impurities in nickel 18 p2669 A83-40627
Deuterium transport and trapping in aluminum alloys 18 p2669 A83-40629
Results of apparent atomic oxygen reactions on Ag, C, and Os exposed during the Shuttle STS-4 orbits 19 p2820 A83-41125
Interaction between hydrogen and intermetallic compounds 19 p2820 A83-42010
High temperature corrosion; Proceedings of the International Conference, San Diego, CA, March 2-6, 1981 20 p2951 A83-42226
First stages of gas-metal interactions 20 p2948 A83-42227
Initial oxidation of metals and alloys 20 p2948 A83-42228
Thin oxide film formation on metals 20 p2948 A83-42229
High temperature oxidation of chromium 20 p2951 A83-42231
High temperature oxidation of hafnium and its alloys 20 p2952 A83-42233
Cyclic oxidation of superalloys 20 p2952 A83-42234
Diffusion processes in Al₂O₃ scales - Void growth, grain growth, and scale growth 20 p2952 A83-42238
Corrosion of nickel in SO₂ atmospheres at elevated temperatures 20 p2952 A83-42240
The oxidation behavior of a model molybdenum/tungsten-containing alloy in air alone and in air with trace levels of NaCl(g) 20 p2952 A83-42241
Thermodynamic analyses of the high temperature corrosion of alloys in gases containing more than one reactant 20 p2949 A83-42242
Some effects of environment on high temperature mechanical behavior of alloys 20 p2953 A83-42245
New perspectives on hot corrosion mechanisms 20 p2949 A83-42248
Microstructural features of low temperature hot corrosion in nickel and cobalt base MCrAlY coating alloys 20 p2953 A83-42249
Hydrogen diffusion and hydride formation at the metal-hydride interface 21 p3109 A83-43963
Hydrogen embrittlement of 7075 series aluminum alloys 21 p3112 A83-44368
Quantum motion of chemisorbed hydrogen on Ni surfaces 21 p3218 A83-45198
Kinetics of hydrogen absorption by alpha-zirconium 23 p3429 A83-47635
The effect of hydrogen induced surface asperities of fatigue crack closure in ultrahigh strength steel 23 p3431 A83-47850
On the influence of internal hydrogen on fatigue thresholds of HSLA steel 23 p3432 A83-47851
Fatigue crack growth in vacuum and a gaseous environment 23 p3433 A83-48540
Oxidation theory of alloys 24 p3561 A83-49478
The influence of secondary processes on the mechanism of scales growth on metals and alloys 24 p3561 A83-49480

- Erosion-corrosion of coatings and superalloys in high velocity hot gases 24 p3562 A83-49481
- The effects of metal pretreatment and oxide grain size on the oxidation of cobalt 24 p3562 A83-49485
- Internal and external sulphidation of Ni77Cr16Fe7 alloys 24 p3565 A83-49510
- The kinetics and mechanism of the attack of MCr-type alloys in oxygen-sulphur environments at 700 C 24 p3565 A83-49511
- The sulfidation properties of iron-nickel alloys at low sulfur pressures 24 p3565 A83-49512
- Reaction mechanism of Ni-20Cr in mixtures of SO₂+O₂ 24 p3565 A83-49513
- The sulfidation behavior of nickel chromium and nickel-aluminum binary alloys with and without yttrium 24 p3565 A83-49514
- A study of the mechanism of magnesium oxidation 24 p3556 A83-49784
- A new statistical model of the hydrogen embrittlement of steel 24 p3567 A83-50070

GAS-SOLID INTERACTIONS**NT GAS-METAL INTERACTIONS**

- Oxygen atom reaction with Shuttle materials at orbital altitudes - Data and experiment status [AIAA PAPER 83-0073] 05 p0617 A83-16503
- Reducing the gas permeability of porous ceramics by means of magnesium oxide coatings 07 p0900 A83-20712
- The gas-grain interaction in the interstellar medium - Thermal accommodation and trapping 07 p1021 A83-21120
- Heterogeneous atmospheric chemistry --- Book 09 p1297 A83-25176
- Effect of the mechanism of gas-to-particle conversion on the evolution of aerosol size distributions 09 p1308 A83-25178
- Neutral and charged clusters in the atmosphere - Their importance and potential role in heterogeneous catalysis 09 p1297 A83-25179
- Chemical reactions with aerosols 09 p1297 A83-25182
- The effects of hydrogen in stabilizing the electrical properties of n-Pb/0.8/Sn/0.2/Te thin films 10 p1488 A83-25455
- Shock wave structure in gas-particle mixtures at low Mach numbers 10 p1416 A83-26186
- On reactions between silicon and nitrogen. I - Mechanisms 12 p1712 A83-29501
- The problem of boundary conditions in the kinetic theory of gases 13 p1932 A83-30661
- Boundary conditions on a solid surface in a flow of a rarefied gas 13 p1932 A83-30662
- The relation between the molecular emissivity and the molecular absorptivity of the surfaces of bodies 13 p1817 A83-30665
- Studies of the orientational ordering transition in nitrogen adsorbed on graphite 18 p2750 A83-39925
- The problem of the interaction of a supersonic wedge with an interface between two gases 19 p2790 A83-41258
- Interaction of high-velocity rarefied flow with the surface of a solid body 20 p2950 A83-42883
- Ground state energy and structure of physisorbed monolayers of linear molecules 23 p3429 A83-47636
- The kinetics of gas-solid reactions and environmental degradation of nitrogen ceramics 23 p3436 A83-48281
- Oxidation behaviour of beta-prime silalons in oxygen and carbon dioxide 23 p3436 A83-48284

GAS-SOLID INTERFACES

- A determination of the potential of the interatomic interaction on the basis of the function for the single scattering of a gas by a surface 09 p1339 A83-24491
- Ion injection from the surface of bodies moving in a gas 12 p1781 A83-29295
- The statistical mechanics of transport processes at a phase boundary and the problem of boundary conditions 13 p1932 A83-30663
- An experimental study of the dynamics of interaction between rarefied gas flows and a solid surface using the method of field-emission microscopy 13 p1932 A83-30664
- Flow of a gas mixture near a catalytic surface 13 p1932 A83-30669
- Quasi-liquefaction in the surface layers of cometary nuclei. I - The static layer at the threshold of quasi-liquefaction 14 p2102 A83-31836
- A nonequilibrium system consisting of a gas, a surface, and a solid body in problems of relaxational gas dynamics 16 p2349 A83-35526
- Kinetics of interfacial reactions of gases on metals and oxides 20 p2949 A83-42239

- The turbulent electrode effect as influenced by interfacial ion transfer --- between atmosphere and aerodynamically rough earth surface 24 p3607 A83-49334

GASDYNAMIC LASERS

- Gasdynamic laser --- Book 03 p0332 A83-14100
- Simple arrangement for spatially scanning gain measurements in CW lasers 03 p0332 A83-14165
- The angular divergence of radiation from flowing gas lasers 04 p0483 A83-15258
- A handbook of gasdynamic lasers --- in Russian 04 p0485 A83-15831
- The dependence of the resonator efficiency of a CO₂ gasdynamic laser on the laser mixture parameters 04 p0486 A83-16387
- Numerical investigation of the nozzle flow of a vibrationally nonequilibrium medium of a CO₂ gasdynamic laser 05 p0649 A83-17050
- Approximate method for calculations of unstable telescopic resonators --- carbon dioxide gasdynamic laser design 05 p0649 A83-17061
- Thermal gasdynamic laser utilizing rotational transitions in hydrogen halides with energy transfer from H₂ molecules 05 p0649 A83-17065
- High-temperature selective gasdynamic continuous CO₂ laser 06 p0765 A83-18450
- Small signal gain measurements for the 00/0/1-02/0/0 and 00/0/1-10/0/0 bands in a flowing-gas CW CO₂ laser 06 p0766 A83-18945
- The effect of the nozzle profile on the characteristics of a gas-dynamic laser 06 p0767 A83-19440
- Experimental verification of a computational model for a combustion-product CO₂-GDL for high stagnation temperatures 06 p0767 A83-19556
- Shock-tube investigation of jet flows from slotted and wedge-shaped nozzles --- for gasdynamic lasers 06 p0767 A83-19565
- Model for pure source flow chemical lasers 07 p0932 A83-19817
- Optically pumped sodium-dimer supersonic-beam laser 07 p0933 A83-19981
- Investigation of the active medium in a fast-flow closed-cycle industrial CO₂ laser 07 p0933 A83-20105
- Production of electronically excited bismuth in a supersonic flow 07 p0936 A83-20726
- A supersonic multikilohertz pulsed HF chemical laser 07 p0936 A83-20729
- Compact repetitively pulsed excimer laser 07 p0938 A83-21383
- Pulsed visible laser flow and acoustics 08 p1108 A83-22459
- Optical distortion due to gas-dynamic motion in a photolytically pumped cylindrical laser cavity 10 p1428 A83-26022
- High gain CO chemical laser produced in a shock tunnel 10 p1429 A83-26168
- Use of unstable resonators in CW chemical lasers with radial flow of a gas mixture 10 p1431 A83-26652
- Investigation of the optical inhomogeneities of the active medium of a fast-flow CO₂ laser with mixing 10 p1433 A83-26677
- Experimental investigation of the optimum specific input energy on a subsonic CO EDL --- Electric Discharge Laser 11 p1580 A83-27577
- Gradually mixing model used to calculate mixing nonequilibrium flow --- in chemical and mixing gasdynamic lasers 11 p1582 A83-27616
- Investigation of supersonic plane underexpanded jets by the laser schlieren method 11 p1584 A83-28538
- Gain dynamics of a degenerate three-level system excited by a rectangular pumping-signal pulse 11 p1584 A83-28563
- Investigation of the gain in a CO₂ GDL behind wedge-shaped and contoured nozzles. I - The experimental setup, the repetitively pulsed system for gain measurement 13 p1849 A83-30042
- High-repetition-rate CO₂-lasers 13 p1850 A83-30645
- Interpretation of vibrational relaxation channels on the basis of gas-dynamic measurements 13 p1850 A83-30668
- The use of the small-parameter method for analyzing flows of vibrationally nonequilibrium gases with allowance for the anharmonicity of vibrations 13 p1933 A83-30671
- The effect of boundary conditions on the flow of a polyatomic gas mixture in a supersonic nozzle --- in gasdynamic lasers 13 p1850 A83-30676
- Influence of a counterpressure on the operation of a CO₂ gasdynamic laser emitting of 18.4 microns 14 p2023 A83-31914
- Properties of a gasdynamic NO₂ laser 15 p2169 A83-34023

- A study of the CO₂-GDL gain behind wedge-shaped and contoured nozzles. II - Measurement results. Comparison of experimental data with calculations 15 p2169 A83-34474

- Glow discharge in a fast longitudinal gas flow 16 p2418 A83-36939
- An experimental study of downstream mixing CO₂ laser [AIAA PAPER 83-1703] 17 p2513 A83-37200
- Performance characteristics of a transverse-flow, oxygen-iodine chemical laser in a low gas-flow velocity 17 p2513 A83-37609
- Calculation of optimal lasing regimes for CW supersonic electroionization CO lasers 18 p2692 A83-39516
- The effect of diffusion on the energy characteristics of molecular lasers 18 p2693 A83-39525
- Temperature requirements and corrosion rates in combustion driven hydrogen fluoride supersonic diffusion lasers 19 p2850 A83-40857
- Simple model for base pressure effects in source flow chemical lasers 19 p2850 A83-40858
- Computation of reacting flowfield with radiation interaction in chemical lasers 20 p2995 A83-43445
- Calculation of the maximum output power of a continuous-flow CO₂ laser 20 p2997 A83-43794
- determination of the rate constants used in design calculations relating to low-temperature CO₂-D₂ gasdynamic lasers 20 p2998 A83-43801
- Nonequilibrium expansion of halogens in short nozzles --- Russian book 23 p3392 A83-47123
- Several generation parameters of a CO₂ gasdynamic laser with a high-temperature regenerative-heat-transfer heater of the working gas 24 p3588 A83-48936
- Regenerative electric heater of gas for a gasdynamic laser 24 p3588 A83-48937
- Numerical study of the interaction of supersonic viscous gas jets in the presence of nonequilibrium physicochemical processes 24 p3588 A83-49122

GASEOUS CAVITATION**U CAVITATION FLOW****U GAS FLOW****GASEOUS DIFFUSION**

- Assessment of contamination in the Shuttle bay 03 p0286 A83-13746
- Influence of hydrodynamics and diffusion upon the stability limits of laminar premixed flames 04 p0457 A83-16261
- Evolutionary effects of helium diffusion in population II stars 06 p0840 A83-19286
- Thermochemical treatment of porous materials 07 p0892 A83-21460
- Stochastic diffusion in inverse square fields - General formulation for interplanetary gas 07 p1028 A83-21576
- Diffusion slipping of a binary gas mixture of moderate density along a flat surface 09 p1259 A83-23983
- The diffusion constants of hydrogen, nitrogen, and carbon in solid solutions and binary phases with titanium 09 p1235 A83-24395
- Stratification instability of switching front in an active trigger diffusive medium --- oscillations and wave processes during combustion 10 p1471 A83-25893
- Uptake of excess CO₂ by an outcrop-diffusion model of the ocean 13 p1869 A83-30877
- A model equation for the probability distribution of the velocity and concentration during turbulent mixing and diffusive combustion of gases 14 p1988 A83-32085
- A study of the diffusion of oxygen in alpha-titanium oxidized in the temperature range 460-700 C 15 p2133 A83-34699
- Measurement of hydrogen permeation through nickel by oscillation method 16 p2328 A83-35602
- Numerical calculations and wind tunnel experiments on gas diffusion in thermally stratified flow over a ridge 16 p2390 A83-36495
- The diffusion capability of the hematoparenchymatous barrier for oxygen during the breathing of helium-oxygen gas mixtures 17 p2555 A83-37245
- Numerical stimulation of photochemical air pollution over the Isle Bay District 20 p3013 A83-42202
- Diffusion processes in Al₂O₃ scales - Void growth, grain growth, and scale growth 20 p2952 A83-42238
- A thermal mechanism for the escape of neutral hydrogen from the earth's atmosphere 20 p3027 A83-43415
- Diffusive separation of binary mixtures of CO₂-H₂ in a sonic-orifice expansion 21 p3128 A83-43934
- Low-temperature oxygen diffusion in alpha titanium characterized by Auger sputter profiling 21 p3113 A83-44608
- Kinetics of hydrogen absorption by alpha-zirconium 23 p3429 A83-47635
- Oxidation theory of alloys 24 p3561 A83-49478
- Examination of the growth of NiO on Ni using magnetic resonance techniques 24 p3562 A83-49486

GASEOUS FUELS

Combustion characteristics of hydrogen-carbon monoxide based gaseous fuels

01 p0023 A83-11491

Numerical modeling of the development of a combustion nucleus in a closed vessel under the conditions of natural convection

03 p0295 A83-14054

Features of the dynamics of gas combustion in closed vessels under various laws for the change in the flame surface

07 p0880 A83-19952

A study on the hydrogen-oxygen diffusion flame in high speed flow

10 p1391 A83-26199

Gaseous fuel generation by magma-thermal conversion of biomass

13 p1870 A83-30196

The formation of nitrogen oxides in a nonequilibrium turbulent diffusion flame

14 p1989 A83-32090

Liquid fuel cyclone combustors for gas turbine applications

16 p2361 A83-36280

GASEOUS ROCKET PROPELLANTS

Performance data comparison of the inert gas RIT 10 --- as ion thruster propellant

02 p0146 A83-12498

Determination of absorption coefficients in shock heated propellant mixtures for laser-heated rocket thrusters

10 p1387 A83-26170

GASES

NT AIR
NT ALVEOLAR AIR
NT ARGON
NT ARGON ISOTOPES
NT ARGON PLASMA
NT BOUNDARY LAYER PLASMAS
NT CARBON DIOXIDE
NT CARBON MONOXIDE
NT CESIUM PLASMA
NT CHARGED PARTICLES
NT COLD GAS
NT COLD PLASMAS
NT COLLISIONAL PLASMAS
NT COLLISIONLESS PLASMAS
NT COMPRESSED AIR
NT COMPRESSED GAS
NT CONDUCTION ELECTRONS
NT COSMIC GASES
NT DENSE PLASMAS
NT DETONABLE GAS MIXTURES
NT DEUTERIUM
NT DEUTERIUM PLASMA
NT DIATOMIC GASES
NT DISSOLVED GASES
NT ELECTRON PLASMA
NT ELLIPTICAL PLASMAS
NT EXHAUST GASES
NT EXPIRED AIR
NT FLAMMABLE GASES
NT FLUE GASES
NT GAS MIXTURES
NT GAS STREAMS
NT GRAY GAS
NT HEAVY NUCLEI
NT HELIUM
NT HELIUM ATOMS
NT HELIUM ISOTOPES
NT HELIUM PLASMA
NT HIGH PRESSURE OXYGEN
NT HIGH TEMPERATURE AIR
NT HIGH TEMPERATURE GASES
NT HIGH TEMPERATURE PLASMAS
NT HYDROGEN
NT HYDROGEN ATOMS
NT HYDROGEN IONS
NT HYDROGEN ISOTOPES
NT HYDROGEN PLASMA
NT IDEAL GAS
NT INTERPLANETARY GAS
NT INTERSTELLAR GAS
NT IONIZED GASES
NT KRYPTON
NT LASER PLASMAS
NT LIQUEFIED GASES
NT LIQUID HELIUM
NT LIQUID HELIUM 2
NT LIQUID HYDROGEN
NT LIQUID NITROGEN
NT LIQUID OXYGEN
NT LORENTZ GAS
NT METALLIC PLASMAS
NT MICROPLASMAS
NT MOLECULAR GASES
NT MONATOMIC GASES
NT NATURAL GAS
NT NEON
NT NEON ISOTOPES
NT NEUTRAL GASES
NT NITROGEN

NT NITROGEN IONS
NT NITROGEN PLASMA
NT NONGRAY GAS
NT NONPOLAR GASES
NT NUCLEI (NUCLEAR PHYSICS)
NT OXYGEN
NT OXYGEN ATOMS
NT OXYGEN IONS
NT OXYGEN ISOTOPES
NT OXYGEN PLASMA
NT OXYGEN 18
NT OZONE
NT OZONIDES
NT POLAR GASES
NT POLYATOMIC GASES
NT RADON
NT RADON ISOTOPES
NT RARE GASES
NT RAREFIED GASES
NT RAREFIED PLASMAS
NT REAL GASES
NT RELATIVISTIC PLASMAS
NT RESIDUAL GAS
NT ROTATING PLASMAS
NT SOLAR WIND
NT SOLIDIFIED GASES
NT STELLAR WINDS
NT STRONGLY COUPLED PLASMAS
NT THERMAL PLASMAS
NT TRITIUM
NT XENON
NT XENON ISOTOPES
NT XENON 129
NT XENON 133

Sound emission from moving sources in an inhomogeneous gaseous medium

12 p1777 A83-29257

Nonlinear theory for acoustic beams --- Russian book

21 p3201 A83-45028

GASIFICATION

NT COAL GASIFICATION
Thermochemical conversion of biomass - Gasification by flash pyrolysis study
06 p0780 A83-18556
Effects of envelope flames on drop gasification rates in turbulent diffusion flames
07 p0879 A83-19846
Is gasification rate controlling step in polymer ignition?
15 p2142 A83-33724
Determination of mass transfer number of polymers from heats of gasification
15 p2142 A83-33725
Solar gasification of carbonaceous materials
15 p2190 A83-34069

GASKETS

Shielding techniques tackle EMI excesses. V - EMI shielding
01 p0035 A83-10271
Pressure concentrations due to plastic deformation of thin films or gaskets between anvils
01 p0028 A83-10610

GASOLINE

The properties of fuel fractions obtained by the hydrogenation of Kansk-Achinsk coal
10 p1401 A83-26920
Possibilities of improving exhaust emissions and energy consumption in mixed hydrogen-gasoline operation
11 p1589 A83-27334
The effect of a standing acoustic wave transverse to the flow on a turbulent flame
14 p1989 A83-32087
Aviation gasoline - Issues and answers
[SAE PAPER 830705] 20 p2959 A83-43316
Autogas flight test in a Cessna 150 airplane
[SAE PAPER 830706] 20 p2933 A83-43317

GASP

U GLOBAL AIR SAMPLING PROGRAM

GASTROINTESTINAL SYSTEM

NT INTESTINES
NT STOMACH
Sport gastroenterology - Some results and prospects of development
01 p0083 A83-10519
Ultrasonic study of the gall bladder
03 p0381 A83-14342

GATE (EXPERIMENT)

U GARP ATLANTIC TROPICAL EXPERIMENT

GATES (CIRCUITS)

NT THRESHOLD GATES
Photosensitive gate structures based on epitaxial layers of Fe-doped GaP
01 p0108 A83-10373
Logic delays of 5-micron resistor coupled Josephson logic
01 p0039 A83-10996
Fast LSI based on current switches --- Russian book
02 p0168 A83-12374
Direct-coupled GaAs ring oscillators with self-aligned gates
03 p0308 A83-13558
TiW silicide gate self-alignment technology for ultra-high-speed GaAs MESFET LSI/VLSI's
03 p0314 A83-14514
Gate-drain avalanche breakdown in GaAs power MESFET's
03 p0314 A83-14515

Hexaferrite gate-flanges in the 3-4 millimeter range
04 p0470 A83-15719

Current-waveform dependence of punchthrough probability in a Josephson tunnel junction

04 p0473 A83-16072

Blister formation in Pd gate MIS hydrogen sensors

05 p0645 A83-17290

Correlation between substrate and gate currents in MOSFET's

05 p0630 A83-17754

The effect of interfacial traps on the stability of insulated gate devices on InP

07 p0921 A83-20742

Circuit analysis, logic simulation, and design verification for VLSI

07 p0923 A83-21539

Direct-coupled Josephson exclusively or gate with a high gain and a wide margin

11 p1563 A83-28615

The COMFET - A new high conductance MOS-gated device

12 p1720 A83-29520

Picosecond Al(x)Ga(1-x) As modulation-doped optical field-effect transistor sampling gate

13 p1832 A83-30341

Sub-10 ps high-gain direct coupled Josephson logic gate

13 p1837 A83-31764

Inverted transistor gate with FET load

13 p1837 A83-31769

Switching characteristics of logic gates addressed by picosecond light pulses

14 p2008 A83-33422

Optical logic array processor using shadowgrams

15 p2230 A83-33808

A PISO JCCD filter with high-speed linear charge injection --- serial-in, parallel-out junction charge coupled devices

15 p2151 A83-33890

A deductive method for the simulation of faults in Programmable Logic Arrays

15 p2218 A83-35142

The dV/dt capability of field-controlled thyristors

18 p2678 A83-40374

Two-dimensional numerical analysis of the narrow gate effect in MOSFET

18 p2678 A83-40378

Accumulation mode Ga(0.47)In(0.53)As insulated gate field-effect transistors

19 p2836 A83-40746

High-speed logic at 300 K with self-aligned submicrometer-gate GaAs MESFET's

19 p2837 A83-41019

Anodic oxide gate a-Si:H MOSFET

20 p2966 A83-42480

X-band self-aligned gate enhancement-mode InP MISFET's

20 p2968 A83-43353

Submicron GaAs microwave FET's with low parasitic gate and source resistances

21 p3123 A83-43848

Self-aligned submicron gate digital GaAs integrated circuits

21 p3124 A83-43854

Equivalent-circuit consideration of dual-gate MESFETs at high frequency

21 p3126 A83-44970

GAUGE INVARIANCE

Some remarks on zeta function regularization in curved space-times

10 p1472 A83-26094

On often used gauge transformations in gravitational radiation-reaction calculations.

12 p1791 A83-29027

Hamiltonian formulation of the gauge theory of gravitation Pure-gravity case.

12 p1792 A83-29046

A simple example of a classical gauge transformation

19 p2899 A83-41876

Reference systems in gravitation theory --- Russian book

21 p3234 A83-45043

General consideration of electronic transitions in many-electron atoms and ions

23 p3506 A83-48577

GAUGE THEORY

Cosmology and unified gauge theory

04 p0558 A83-16441

Upper bound on gauge-fermion masses

07 p0992 A83-20814

Gauge transformations in soliton theory

12 p1774 A83-29004

Hamiltonian structure of the theory of gravity with $R + T(2)$ type of Lagrangian

12 p1775 A83-29043

Hamiltonian formulation for a translation gauge theory of gravitation

12 p1792 A83-29045

The KS-transformation in hypercomplex form

12 p1786 A83-29103

Magnetic-charge conjugation and the topological nature of magnetic monopole

13 p1918 A83-31605

Primordial nucleosynthesis and scale-covariant cosmology

18 p2774 A83-39736

GAUSS EQUATION

Dynamic analysis of multirigid-body system based on the Gauss principle

03 p0391 A83-14509

GAUSS FUNCTION

U GAUSS EQUATION

GAUSSIAN DISTRIBUTIONS

U NORMAL DENSITY FUNCTIONS

GAUSSIAN NOISE

U RANDOM NOISE

GAUSSMETERS

U MAGNETOMETERS

GAW-2 AIRFOIL

Modifying a general aviation airfoil for supercritical flight

09 p1196 A83-24039

GC-130 AIRCRAFT

U C-130 AIRCRAFT

GCR (REACTORS)

U GAS COOLED REACTORS

GDOF

U GEOMETRIC DILUTION OF PRECISION

GEAR TEETH

Tooth profile analysis of circular-cut, spiral-bevel gears
[ASME PAPER 82-DET-79] 02 p0187 A83-12776
Report on advanced transmission system integration tests --- of Blackhawk helicopters 09

Design of an advanced 500-HP helicopter transmission 09 p1208 A83-24834
Combined effects of rim thickness and pitch diameter on spur gear tooth stresses 19 p2854 A83-41074

GEARS

Magnetic inspection of the quality of surface hardening of teeth of large gears 01 p0057 A83-10367
Tooth profile analysis of circular-cut, spiral-bevel gears [ASME PAPER 82-DET-79] 02 p0187 A83-12776
Reliability model for planetary gear trains [ASME PAPER 82-DET-81] 02 p0187 A83-12777
Fault Detection/Location System for intermediate and tail rotor gearboxes 09 p1274 A83-24835
Gears and their vibration: A basic approach to understanding gear noise --- Book 15 p2171 A83-33616
Case depth requirements in carburized gears 20 p2999 A83-43409

GEL PERMEATION CHROMATOGRAPHY

U LIQUID CHROMATOGRAPHY

GELATINS

Some characteristics of and measurements on dichromated gelatin reflection holograms 21 p3140 A83-44838

GELS

NT DOUBLE BASE ROCKET PROPELLANTS

NT SILICA GEL

The GEL electrode - A new method of detecting fatigue cracks 18 p2668 A83-40612
Gels and gel-derived glasses in the Na₂O-B₂O₃-SiO₂ system --- containerless melting in space 20 p2941 A83-43288
Glass shell manufacturing in space 20 p2941 A83-43290

GEMINI PROJECT

The human presence in space 22 p3347 A83-45861

GEMINID METEOROIDS

Geminid meteor shower as observed on the long base 05 p0695 A83-17830

GENERAL AVIATION AIRCRAFT

NT AGRICULTURAL AIRCRAFT

NT DO-28 AIRCRAFT

NT YAK 40 AIRCRAFT

Thunder power for executive and ag-aircraft 01 p0011 A83-10866
Data acquisition/reduction system for flight testing general aviation aircraft 02 p0135 A83-11903
A microcomputer-based system for noise characteristics analysis 02 p0227 A83-11915
Cross-coupling between longitudinal and lateral aircraft dynamics in a spiral dive 04 p0449 A83-15312
Safety attitudes of a general aviation pilot population 04 p0523 A83-15542
GASAP - A general aviation airplane analysis and synthesis program 05 p0594 A83-16488
[AIAA PAPER 83-0054]
Aerodynamic investigation of closely coupled lifting surfaces with positive and negative stagger for general aviation applications 05 p0578 A83-16489
[AIAA PAPER 83-0057]
Aerodynamic optimization, comparison, and trim design of canard and conventional high performance general aviation configurations 05 p0594 A83-16490
[AIAA PAPER 83-0058]
A dynamic model for aircraft poststall departure 05 p0595 A83-16674
[AIAA PAPER 83-0367]
The role of simulation in general aviation 05 p0671 A83-17307
Computer-based pre-simulator training 05 p0676 A83-17308
Long-range Falcon - Flight-test Dassault Falcon 50 06 p0716 A83-18074
Design and development of a mixer compound exhaust system --- in aircraft turbofan engines 09 p1206 A83-24029
Development trend in general aviation 09 p1195 A83-24153
[DGLR PAPER 82-026]
The consideration of operational aspects for utility-/commuter aircraft, taking into account the example of the Dornier 228 09 p1199 A83-24171
[DGLR PAPER 82-047]
New technology in general aviation 09 p1203 A83-24172
[DGLR PAPER 82-048]

Performance improvements of single-engine business airplanes by the integration of advanced technologies [DGLR PAPER 82-064] 09 p1203 A83-24178

A steady state performance model for general aviation spark-ignition piston engines 11 p1530 A83-27163
Determination of horizontal tail load and hinge moment characteristics from flight data --- on Learjet Model 55 Longhorn 13 p1805 A83-30162

The integration of internal combustion engines of the General Aviation - Problems raised by ventilation and exhaust [AAAF PAPER NT 82-16] 14 p1976 A83-33167

The future of the U.S. aviation system [AIAA PAPER 83-1594] 14 p1973 A83-33360
CF34 upgrades Challenger capabilities 15 p2122 A83-35315

Development and application of a liquid-cooled V-8 piston engine for general aviation aircraft [AIAA PAPER 83-1342] 16 p2309 A83-36347
New technologies for general aviation 17 p2443 A83-37856

The application of a liquid-cooled V-8 piston engine to general aviation aircraft [SAE PAPER 821446] 17 p2468 A83-37994

Advanced airfoil design for general aviation propellers [AIAA PAPER 83-1791] 17 p2453 A83-38631
Air traffic control problems in the field of general aviation 17 p2460 A83-38931

A simulation study of the low-speed characteristics of a light twin with an engine-out [AIAA PAPER 83-2128] 19 p2806 A83-41951
Influence of airplane components on rotational aerodynamic data for a typical single-engine airplane [AIAA PAPER 83-2135] 19 p2793 A83-41957

An improved method for predicting lateral-directional dynamic stability characteristics [SAE PAPER 830711] 20 p2937 A83-43321
Optimum configuration for a 10-passenger business turbofan jet airplane 21 p3091 A83-43967
General aviation safety - How safe? Its implication for flying and theory training 21 p3089 A83-44878
Airports as a threat to public safety --- Book 22 p3251 A83-46420

An improved propeller for general-aviation aircraft 23 p3406 A83-47194

OLGA - A gust-alleviation system for general-aviation aircraft --- Open Loop Gust Alleviation 23 p3412 A83-47212

Propulsion system integration as applied to business jet aircraft [ASME PAPER 83-GT-227] 23 p3403 A83-48024

Analysis of general aviation accidents using ATC radar records 23 p3400 A83-48218
General aviation goes digital - Many advantages, but some problems 23 p3406 A83-48640

Ultralight aircraft safety and regulation 24 p3546 A83-48885

GENERAL AVIATION WHITCOMB AIRFOIL

U GAW-2 AIRFOIL

GENERAL DYNAMICS AIRCRAFT

NT B-58 AIRCRAFT

NT CANADAIR AIRCRAFT

NT CV-990 AIRCRAFT

NT F-111 AIRCRAFT

GENERAL DYNAMICS MILITARY AIRCRAFT

U MILITARY AIRCRAFT

GENETIC CODE

Expected frequencies of codon use as a function of mutation rates and codon fitnesses 01 p0081 A83-11033

Immunoglobulin genes 01 p0082 A83-11408
The possible role of assignment catalysts in the origin of the genetic code 02 p0219 A83-11634

The effect of activators of cAMP accumulation on separate stages of the cell genome expression during acute radiation damage of the animal. V Investigations of the sedimentation characteristics of RNP-particles released from the cell nuclei of irradiated animals and of animals protected with serotonin 03 p0376 A83-14878

Oxidative peptide /and amide/ formation from Schiff base complexes 06 p0800 A83-18247
Globular proteins, GU wobbling, and the evolution of the genetic code 06 p0794 A83-18248

Stages of emerging life - Five principles of early organization 06 p0801 A83-18250

The chemical structure of DNA sequence signals for RNA transcription 06 p0796 A83-19408
The systemic determination of the activity of neurons in behavior 08 p1145 A83-22118

A model for the development of genetic translation 17 p2557 A83-38899
Changes in the amino acid code 19 p2877 A83-42039

Experimental studies related to the origin of the genetic code and the process of protein synthesis - A review 19 p2879 A83-42156

Evolution of the amino acid code - Inferences from mitochondrial codes 20 p3033 A83-42397

GENETIC ENGINEERING

New sources for fuel and materials --- from plants 05 p0658 A83-16937

An investigation of the strength of action and the interaction of genes determining the differences in the stem length of *Arabidopsis thaliana* (L.) Heynh. (three hybrid cross) 18 p2733 A83-40573

Methylotrophic bacteria - Biochemical diversity and genetics 22 p3345 A83-45724

GENETICS

NT GENETIC CODE

NT MUTATIONS

Hybridization of the DNA of purple phototrophic bacteria 01 p0078 A83-10423
The prognostic significance of several traits in studying the functioning of the oxygen homeostasis system of humans in the genetic aspect 01 p0082 A83-10491

The gas composition and the acid-base state of the blood in twins when breathing a hypoxic gas mixture 01 p0082 A83-10492

The genetic danger of microwaves of nonthermal intensity and its hygienic aspects 05 p0670 A83-17202

The structure of DNA and the transformation of cells 06 p0795 A83-18980

The genetics of immunoglobulins - Successes and problems 06 p0795 A83-18982
Evidence of genetic differences in acute hypoxia survival 07 p0974 A83-20781

An investigation of the genotypic conditionality of the gas composition and acid-base state indicators of the blood during various effects on the body 09 p1323 A83-25152

Transitions and transversions in evolutionary descent - An approach to understanding 12 p1762 A83-29421

The effect of the radiation dose rate on the formation of double-strand DNA breaks 14 p2062 A83-32063
Immunoglobulin genes 14 p2065 A83-33326

Syzers: the modeling of fundamental characteristics of molecular-biological organization - The correspondence between general properties of genetic processes and the structural peculiarities of macromolecular assemblies 16 p2395 A83-36810

Genetic predispositions in human learning of motor actions 17 p2559 A83-38173

Negatively supercoiled simian virus 40 DNA contains Z-DNA segments within transcriptional enhancer sequences 17 p2557 A83-38607

Genetic risks associated with radiation exposures during space flight 19 p2873 A83-40845
DNA fusion product of phage P2 with plasmid pBR322 - A new phasmid 21 p3183 A83-44860

Methylotrophic bacteria - Biochemical diversity and genetics 22 p3345 A83-45724

GENITOURINARY SYSTEM

NT TESTES

NT UTERUS

GEOASTROPHYSICS

U ASTROPHYSICS

U GEOPHYSICS

GEOBOTANY

Refinement of schemes of soil-geobotanic classification by means of space imagery 14 p2034 A83-32494

Geobotanical techniques for discriminating serpentine rock types in Western United States 17 p2533 A83-38448

Applications of remote sensing to geobotanical prospecting for non-renewable resources 17 p2534 A83-38449

GEOCENTRIC COORDINATES

Data on time and polar motion - Immediate accessibility 01 p0111 A83-10131

A three-dimensional model of the high-latitude F-region with allowance for the noncoincidence of geographical and geomagnetic coordinates 02 p0208 A83-12421

Corrected geomagnetic pole coordinates 07 p0965 A83-21189

The use of the geopotential model in the orbital method of the coordinate determination of stations 11 p1616 A83-28050

Linear perturbations of the coordinates of satellites in ellipsoidal orbits due to the effect of atmospheric drag in the standard gravitational field of the earth 11 p1532 A83-28053

JPL pulsar timing observations. II - Geocentric arrival times 22 p3372 A83-46266

Combined least squares solution using terrestrial and Doppler observations 22 p3317 A83-46361
Results of the first observations with the Doppler astrometric receiver DOP-2 --- satellite tracking for geocentric coordinate determination 23 p3421 A83-48065

- Position of the station Borowiec in the Doppler observation campaign WEDOC 80
23 p3482 A83-48066
- Internal inconsistency of reference system determined by on-board ephemerides of NNSS satellites
23 p3482 A83-48067
- The geocentric zones of the bright planets
24 p3644 A83-49608

GEOCHEMISTRY

NT BIOGEOCHEMISTRY

- Impact events at the Cretaceous-Paleogene boundary
01 p0129 A83-11325
- The geochemistry of rare earth elements in the metamorphic rocks of the Kola series
01 p0073 A83-11500
- Beryllium-10 in Australasian tektites - Evidence for a sedimentary precursor
02 p0264 A83-12066
- The geochemical coherence of Pu and Nd and the Pu-244/U-238 ratio of the early solar system
02 p0267 A83-12843
- An electrochemical study of Ni²⁺ / Co²⁺ / and Zn²⁺ / ions in melts of composition CaMgSi₂O₆
02 p0152 A83-12845
- Effects of fractional crystallization and cumulus processes on mineral composition trends of some lunar and terrestrial rock series
04 p0559 A83-15332
- Comparative geochemistry of Apollo 16 surface soils and samples from cores 64002 and 60002 through 60007
04 p0561 A83-15351
- Remote determination of humus content in soils
04 p0502 A83-15889
- Geochemistry and petrogenesis of Archean metavolcanic amphibolites from Fiskensæset, S. W. Greenland
04 p0514 A83-16353
- Nonequilibrium condensation and ultrapotassium impactites
05 p0706 A83-17472
- Variations of delta S-34/SO₄²⁻, delta O-18/H₂O¹⁸, and Cl/SO₄ ratio in rainwater over northern Israel, from the Mediterranean coast to Jordan Rift Valley and Golan Heights
05 p0665 A83-17843
- Arid soils as a source of atmospheric carbon monoxide
07 p0959 A83-20198
- Clay mineralogy of the Cretaceous-Tertiary boundary clay --- in search for asteroid ejecta
07 p1029 A83-20301
- Phase transitions and mantle discontinuities
07 p0962 A83-20838
- The ophiolitic Bath-Dunrobin formation, Jamaica - Significance for Cretaceous plate margin evolution in the north-western Caribbean
07 p0963 A83-21042
- Sulfide saturation of basalt and andesite melts at high pressures and temperatures
07 p0963 A83-21045
- A model for the formation of the earth's core
07 p0965 A83-21284
- Siderophile trace elements in the earth's oceanic crust and upper mantle
07 p0965 A83-21285
- The lunar nearside highlands - Evidence of resurfacing
07 p1032 A83-21288
- Do oblique impacts produce Martian meteorites
07 p1034 A83-21313
- Strangways Crater, Northern Territory, Australia - Siderophile element enrichment and lithophile element fractionation
07 p0950 A83-21316
- Homogeneity of lava flows - Chemical data for historic Mauna Loa eruptions
07 p0965 A83-21321
- Chemical weathering and diagenesis of a cold desert soil from Wright Valley, Antarctica - An analog of Martian weathering processes
07 p0951 A83-21325
- Experimental investigation of the partitioning of phosphorus between metal and silicate phases - Implications for the earth, moon and eucrite parent body
08 p1190 A83-22997
- Rare earth elements in the sedimentary cycle - A pilot study of the first leg
11 p1616 A83-28078
- Rare earth elements in these sedimentary cycle - A pilot study of the first leg
12 p1748 A83-29554
- Problems in the geochemistry of radiogenic isotopes
13 p1960 A83-30725
- Noble gas constraints on the layered structure of the mantle
14 p2051 A83-31922
- Annual review of earth and planetary sciences. Volume 11 --- Book
14 p2034 A83-33477
- Radioactive nuclear waste stabilization - Aspects of solid-state molecular engineering and applied geochemistry
14 p2083 A83-33478
- Terrestrial inert gases - Isotope tracer studies and clues to primordial components in the mantle
14 p2055 A83-33481
- Phase transformations in the mantle and expansion of the earth
16 p2376 A83-35594
- Pre-Keweenaw anorthosite inclusions in the Keweenaw Beaver Bay and Duluth Complexes, northeastern Minnesota
16 p2382 A83-36971
- The isotopic composition of primary xenon and the fission of Pu-244 --- on earth
17 p2619 A83-37818

- Approaches to detection of geochemical stress in vegetation
17 p2528 A83-38149
- Prospecting in glaciated terrain - Integrating airborne and Landsat MSS
17 p2528 A83-38151
- Geochemical evolution of the crust and mantle
17 p2543 A83-38325
- Carbon isotopic variation in spectral type II diamonds
17 p2545 A83-38603
- Carbon isotopic variation within individual diamonds
17 p2545 A83-38604
- Solidus and liquidus temperatures and mineralogies for anhydrous garnet-ilmenite to 15 GPa
17 p2546 A83-38698
- Evolution of the oceans and continents
18 p2715 A83-39495
- Pb, Sr, Nd and Hf isotopic evidence of multiple sources for Oahu, Hawaii basalts
18 p2718 A83-39957
- The start of sulfur oxidation in continental environments
19 p2864 A83-40903
- About 2.2 billion years ago
19 p2922 A83-40913
- Martian gases in an Antarctic meteorite?
19 p2864 A83-41109
- Dynamic compression of diopside and salite to 200 GPa --- in earth's mantle
19 p2864 A83-41109
- The oxidation-reduction conditions on the Venus surface according to data from the Konrads geochemical indicator on the Venera 13 and 14 probes
19 p2922 A83-41232
- Geochemistry and tectonic affinities of a Proterozoic bimodal igneous suite, west Texas
19 p2867 A83-41866
- Isotope and geochemical glaciology --- Russian book
21 p3169 A83-43902
- Handbook of isotope geochemistry --- in Russian
21 p3239 A83-43909
- Radiogenic isotopes and crustal evolution
22 p3323 A83-45781
- The carbon-oxygen system at present and in the Precambrian
22 p3323 A83-45782
- Geosphere interactions and earth chemistry
22 p3323 A83-45784
- The role of oxidation-reduction reactions in the earth's early history
22 p3324 A83-45793
- A two-layer convective mantle with an internal boundary layer
22 p3324 A83-45794
- Lead isotope systematics of some igneous rocks from the Egyptian Shield
22 p3332 A83-46704
- Origin of Archean anorthosites - Evidence from the Bad Vermilion Lake anorthosite complex, Ontario
22 p3332 A83-46705
- Petrologic monitoring of 1981 and 1982 eruptive products from Mount St. Helens
22 p3333 A83-46799
- Monitoring the 1980-1982 eruptions of Mount St. Helens
22 p3333 A83-46800
- Compositions and abundances of glass
22 p3386 A83-46871
- Possible lunar source areas of meteorite ALHA 81005
22 p3386 A83-46871
- Geochemical remote sensing information
22 p3386 A83-46871
- Rare gases from the undepleted mantle?
23 p3483 A83-48080
- Geography of trace elements: Global dispersion --- Russian book
23 p3483 A83-48250
- The efficiency of coupled processes in connection with geochemical and biogeological evolution
23 p3485 A83-48508
- Phase relations in the MgO-SiO₂ system under the P-T parameters of the mantle's transition region
24 p3604 A83-48951
- Geochemistry of the impactites of the Ianis'iarvi, Kara, and El'gygytyn craters
24 p3671 A83-48952
- Cometary matter in the environment
24 p3598 A83-49105
- Rb-Sr, Sm-Nd, K-Ca, O, and H isotopic study of Cretaceous-Tertiary boundary sediments, Caravaca, Spain
24 p3672 A83-49399
- Evidence for an oceanic impact site
24 p3673 A83-49555
- The first finding of suessite on the earth
24 p3673 A83-49555

GEOCHRONOLOGY

- Comment on 'Thermoluminescence of meteorites and their terrestrial ages'
02 p0267 A83-12850
- Geology and terrestrial age of the Derrick Peak meteorite occurrence, Antarctica
03 p0434 A83-14318
- Mars - Stratigraphy and gravimetry of Olympus Mons and its aureole
04 p0566 A83-15565
- Chronology and petrogenesis of young achondrites, Shergotty, Zagami, and ALHA77005 - Late magmatism on a geologically active planet
04 p0572 A83-16355
- The abiogenic synthesis of amino acids under conditions imitating an ash-gas cloud during volcanic eruptions
06 p0800 A83-17987
- Do oblique impacts produce Martian meteorites
07 p1034 A83-21313
- Precise age determinations and petrogenetic studies using the K-Ca method
07 p1035 A83-21335

- Importance of the Lu-Hf isotopic system in studies of planetary chronology and chemical evolution
08 p1190 A83-22996
- Quaternary geochronology of the Western Desert
09 p1286 A83-24549
- The Cretaceous-Tertiary transition
10 p1448 A83-25650
- The dating of the earliest sediments on earth --- containing biogenic markers
13 p1899 A83-31157
- Large-scale impact cratering on the terrestrial planets
15 p2277 A83-35033
- Eruption age of a Pleistocene basalt from Ar-40-Ar-39 analysis of partially degassed xenoliths
16 p2381 A83-36599
- A megastructural end to Geologic Time
18 p2754 A83-39607
- The geologic record of climatic change
18 p2730 A83-40327
- Origin of Espanola Island and the age of terrestrial life on the Galapagos Islands
19 p2864 A83-40902
- The continental crust
20 p3020 A83-42819
- Simple energy balance model resolving the seasons and the continents - Application to the astronomical theory of the ice ages
20 p3021 A83-42841
- Age dependence of oceanic intraplate seismicity and implications for lithospheric evolution
21 p3169 A83-43824
- Ion microprobe identification of 4,100-4,200 Myr-old terrestrial zircons
21 p3174 A83-45059
- Lead isotope systematics of some igneous rocks from the Egyptian Shield
22 p3332 A83-46704
- Uppermantle anisotropy and the oceanic lithosphere
22 p3333 A83-46878
- Analytic comparison of apparent polar wander paths
24 p3608 A83-50175

GEOCORONAL EMISSIONS

- Near-earth ultraviolet environment
03 p0358 A83-13974

GEODESIC LINES

- Allowance for near and far zones in the calculation of geoid heights and plumbline deviations
01 p0072 A83-10853
- Null geodesics in the static Ernst space-time
06 p0828 A83-18328
- Relative lateration across the Los Angeles basin using a satellite laser ranging system
07 p0952 A83-21524
- Closed geodesics
09 p1340 A83-25263
- Prestressed geodesic 3-nets
12 p1740 A83-29781
- [AIAA 83-0972] A model that realizes the soliton and the chaos simultaneously
14 p2080 A83-32518
- A geodesic lens antenna for 360 deg azimuthal coverage
15 p2146 A83-35085

GEODESY

NT CELESTIAL GEODESY

- Defense Mapping Agency /DMA/ overview of mapping, charting, and geodesy /MC&G/ applications of digital image pattern recognition
02 p0200 A83-12877
- Derivation of the harmonic coefficients C₂₁ and S₂₁ using parameters of the secular motion of the earth's poles
04 p0514 A83-16381
- Very-long-baseline radio interferometry - The Mark III system for geodesy, astrometry, and aperture synthesis
05 p0693 A83-16938
- Information search and retrieval in the areas of astronomy and geodesy --- Russian book
07 p1001 A83-20375
- Handbook on higher geodesy /computational aspects/ --- Russian book
07 p0962 A83-20376
- Applications of deformation analysis in geodesy and geodynamics
07 p0962 A83-20837
- The interpretation of the major non-hydrostatic anomalies of the earth
07 p0963 A83-20974
- The effects of atmospheric turbulence on telescopic observations
07 p1010 A83-21525
- The topology of geodesically complete space-times
08 p1180 A83-22204
- Current investigations at TsNIIGAIK in the area of physical geodesy
08 p1136 A83-22788
- Solution of systems of linear equations with a sparse matrix --- for geodesy, photogrammetry and navigation
08 p1159 A83-22789
- Optimal signal discrimination and problems of monitoring --- Russian book
09 p1283 A83-23819
- On the wave number spectrum of oceanic mesoscale variability observed by the SEASAT altimeter
15 p2207 A83-33490
- Global mesoscale variability from collinear tracks of SEASAT altimeter data
15 p2207 A83-33491
- Earth's flattening effect on the tidal forcing field
16 p2381 A83-36618
- Planetary geodesy --- surveys of planets other than earth
17 p2622 A83-38301
- Status of the geopotential --- earth gravity measurement
17 p2542 A83-38303

- Radio interferometry --- VLBI for geodesy
 - 17 p2542 A83-38304
- Polar motion and earth rotation
 - 17 p2525 A83-38305
- Satellite altimetry --- geodetic applications
 - 17 p2482 A83-38306
- Satellite positioning --- for geodesy
 - 17 p2475 A83-38307
- New techniques --- in geodesy
 - 17 p2542 A83-38308
- Utilization of the Trident radar system for air navigation, photogrammetry, and geodesy at the National Geographic Institute: First results - Ongoing tests
 - 18 p2639 A83-40623
- The oblateness effect on the extraterrestrial solar radiation
 - 19 p2864 A83-40769
- The contributions of the Zentralinstitut fuer Physik der Erde to the MERIT project --- Monitor Earth-Rotation and Intercompare the Techniques of observation and analysis
 - 20 p3022 A83-41312
- Laser ranging to artificial earth satellites and to the moon
 - 22 p3288 A83-46110
- Present capabilities and trends
 - 22 p3288 A83-46110
- International Symposium on Geodetic Networks and Computations, Munich, West Germany, August 31-September 5, 1981, Proceedings. Volume 4 - Modern observation techniques for terrestrial networks
 - 22 p3315 A83-46336
- Inertial technology applications to geodetic networks
 - 22 p3291 A83-46342
- Which information can you get out of an inertial system and what can you do with it?
 - 22 p3291 A83-46344
- Orientation of geodetic networks by gyro azimuths
 - 22 p3316 A83-46345
- Orientation information of levelling and gravity measurements in threedimensional regional networks
 - 22 p3317 A83-46355
- On the interpolation of gravity anomalies and deflections of the vertical in mountainous terrain
 - 22 p3317 A83-46356
- International Symposium on Geodetic Networks and Computations, Munich, West Germany, August 31-September 5, 1981, Proceedings. Volume 5 - Network analysis models
 - 22 p3317 A83-46359
- Deformation of the Australian plate - Preliminary findings from laser ranging to the LAGEOS satellite
 - 22 p3317 A83-46363
- Quaternion algebra applied to polygon theory in three dimensional space --- Thesis
 - 22 p3353 A83-46697
- Equations for the small oscillations of an inertial navigation system with allowance for the ellipsoidality of the earth
 - 23 p3421 A83-48456
- GEODETTIC ACCURACY**
 - Geodesy by radio interferometry - A critical review
 - 01 p0070 A83-10021
 - Concerning the calculation of geodetic heights
 - 01 p0072 A83-10852
 - Allowance for near and far zones in the calculation of geoid heights and plumbline deviations
 - 01 p0072 A83-10853
 - Precision of the determination of the mutual location of points on the basis of satellite observations
 - 03 p0356 A83-13296
 - A review of geodetic and geodynamic satellite Doppler positioning
 - 07 p0871 A83-20836
 - Adjustment problems in inertial positioning
 - 22 p3316 A83-46343
 - Which information can you get out of an inertial system and what can you do with it?
 - 22 p3291 A83-46344
 - Combination of leveling and gravity data for detecting real crustal movements
 - 22 p3316 A83-46353
 - Accuracy analysis of the Finnish Laser Geodimeter Traverse
 - 22 p3317 A83-46360
- GEODETTIC COORDINATES**
 - Data on time and polar motion - Immediate accessibility
 - 01 p0111 A83-10131
 - A three-dimensional model of the high-latitude F-region with allowance for the noncoincidence of geographical and geomagnetic coordinates
 - 02 p0208 A83-12421
 - Concerning the processing and the accuracy estimation of results of very long baseline interferometry in a single system of coordinates --- for geodesy
 - 04 p0514 A83-16380
 - A dynamic method for determining the axis of rotation and coordinates of the center of mass of a planet from orbital data
 - 05 p0707 A83-17676
 - Concerning a method for the determination of initial geodetic data
 - 05 p0664 A83-17679
 - A check for the pole coordinates of asteroid 22 Kalliope
 - 07 p1008 A83-21203
 - The existence of teleconnections in the geopotential field of the Northern Hemisphere
 - 09 p1315 A83-24942
 - Coordinate systems --- of Jupiter
 - 10 p1497 A83-26624

- Selenodetic network of reference points for the far side of the moon
 - 13 p1961 A83-31099
- Orientation of geodetic networks by gyro azimuths
 - 22 p3316 A83-46345
- A contribution to 3D-operational geodesy. I - Principle and observational equations of terrestrial type. II - Concepts of solution
 - 22 p3317 A83-46354
- Test computations of threedimensional geodetic networks with observables in geometry and gravity space
 - 22 p3317 A83-46357
- Three-dimensional adjustment of geodetic networks using gravity field data
 - 22 p3317 A83-46358
- International Symposium on Geodetic Networks and Computations, Munich, West Germany, August 31-September 5, 1981, Proceedings. Volume 5 - Network analysis models
 - 22 p3317 A83-46359
- Combined least squares solution using terrestrial and Doppler observations
 - 22 p3317 A83-46361
- GEODETTIC SATELLITES**
 - NT GEOS 1 SATELLITE
 - NT GEOS 2 SATELLITE
 - NT GEOS 3 SATELLITE
 - The antenna phase center in satellite radio-Doppler geodetic systems
 - 03 p0287 A83-14860
 - On the question of correlation in satellite geodesy networks
 - 04 p0514 A83-16382
 - Allowance for the influence of geopotential in the high-precision numerical integration of artificial-earth-satellite orbits
 - 04 p0453 A83-16385
 - Numerical prediction of the motion of high-altitude geodetic satellites
 - 17 p2472 A83-37724
 - New method for the reduction of satellite data applicable to geodesy
 - 22 p3316 A83-46339
 - On the use of orbital methods for development of satellite geodetic networks
 - 22 p3316 A83-46341
 - An investigation on the optimization of the space objects Observations for the East-European satellite triangulation
 - 22 p3259 A83-46364
 - Satellite technology developments in gravity research [IAF PAPER 83-223]
 - 23 p3414 A83-47314
- GEODETTIC SURVEYS**
 - Miniature interferometer terminals for earth surveying /MITES/ - Geodetic results and multipath effects
 - 01 p0070 A83-10022
 - Relative lateration across the Los Angeles basin using a satellite laser ranging system
 - 07 p0952 A83-21524
 - The application of near-nadir Delta-k radar techniques to geodetic altimetry and oceanographic remote sensing
 - 08 p1144 A83-22677
 - International Symposium on Geodetic Networks and Computations, Munich, West Germany, August 31-September 5, 1981, Proceedings. Volume 4 - Modern observation techniques for terrestrial networks
 - 22 p3315 A83-46336
 - Modern observation techniques for terrestrial networks
 - 22 p3316 A83-46337
 - Inertial technology applications to geodetic networks
 - 22 p3291 A83-46342
 - Adjustment problems in inertial positioning
 - 22 p3316 A83-46343
 - Which information can you get out of an inertial system and what can you do with it?
 - 22 p3291 A83-46344
 - International Symposium on Geodetic Networks and Computations, Munich, West Germany, August 31-September 5, 1981, Proceedings. Volume 7 - Combination of horizontal, vertical and gravity networks
 - 22 p3316 A83-46351
 - Combination of horizontal, vertical and gravity networks - A review
 - 22 p3316 A83-46352
 - International Symposium on Geodetic Networks and Computations, Munich, West Germany, August 31-September 5, 1981, Proceedings. Volume 5 - Network analysis models
 - 22 p3317 A83-46359
 - Results of the first observations with the Doppler astrolabe receiver DOG-2 --- satellite tracking for geocentric coordinate determination
 - 23 p3421 A83-48065
- GEODETTIC METERS**
 - Accuracy analysis of the Finnish Laser Geodimeter Traverse
 - 22 p3317 A83-46360
- GEODYNAMICS**
 - The application of space technology to geodynamics - An overview
 - 01 p0070 A83-10020
 - A kinematic thermal history of the earth's mantle
 - 02 p0212 A83-13101
 - Concerning the problem of the relationship between geoid undulations and tectonic structures
 - 04 p0514 A83-16379
 - Deep asymmetry and geodynamical evolution
 - 06 p0787 A83-18926
 - Numerical modeling of intraplate deformation - Simple mechanical models of continental collision
 - 07 p0961 A83-20230
 - Applications of deformation analysis in geodesy and geodynamics
 - 07 p0962 A83-20837

- Geodynamics of the Baikal-Stanovoy seismic belt
 - 07 p0963 A83-20975
- The tides of the planet earth /2nd edition/ --- Book
 - 09 p1307 A83-24948
- The possibility of using space photographs to study the dynamics of tectonic processes /Using the example of the Turan plate/
 - 10 p1443 A83-26801
- The use of a system of four radio telescopes in solving a number of problems of astrometry and geodynamics by means of VLBI
 - 11 p1673 A83-28028
- Models of crustal deformation
 - 17 p2543 A83-38328
- A dynamical basis for crustal deformation and seismotectonic block movements in central Europe
 - 17 p2546 A83-38697
- The dynamic earth
 - 20 p3020 A83-42815
- Dynamics of the earth's core and the geodynamo
 - 22 p3323 A83-45780
- Magnetometer arrays and geodynamics
 - 22 p3323 A83-45785
- NASA geodynamics program
 - 22 p3329 A83-46109
- Laser ranging to artificial earth satellites and to the moon
 - 22 p3288 A83-46110
- Present capabilities and trends
 - 22 p3288 A83-46110
- Investigations on an active satellite system for earth kinematics and positioning
 - 22 p3258 A83-46112
- Information from space and the prediction of exogenous processes --- in tectonics
 - 23 p3483 A83-48106
- GEOELECTRICITY**
 - NT TELLURIC CURRENTS
 - Some possibilities of identifying the effect of geoelectric inhomogeneities on the polarization of geomagnetic pulsations at midlatitudes
 - 02 p0210 A83-12440
 - The nature of the vertical component of the geoelectric field during magnetic disturbances
 - 05 p0664 A83-17626
 - The spatial distribution of disturbances of the vertical component of the geoelectric field, accompanying an intensification of magnetic activity
 - 05 p0664 A83-17627
 - On the resolving power of the VLF method
 - 11 p1558 A83-28346
 - Impacts of solar and auroral storms on power line systems
 - 14 p2053 A83-32899
 - Electromagnetic induction studies --- of earth lithosphere and asthenosphere
 - 17 p2543 A83-38311
- GEOFACTURES**
 - U GEOLOGICAL FAULTS
- GEOGRAPHIC APPLICATIONS PROGRAM**
 - Conversion of raster coded images to polygonal data structures
 - 15 p2165 A83-34838
- GEOGRAPHIC INFORMATION SYSTEMS**
 - Analytical plotter for data input into geo-based information systems
 - 02 p0180 A83-12683
 - Computer-assisted photo interpretation system
 - 02 p0180 A83-12684
 - A position-based resource mapping study of the Kananaskis Valley using Landsat
 - 03 p0345 A83-14232
 - Office automation in resource-management - The future is now --- agricultural land use map dissemination
 - 03 p0348 A83-14269
 - An experimental Landsat Quicklook System for Alaska
 - 03 p0348 A83-14271
 - Remote sensing: An input to geographic information systems in the 1980's; Proceedings of the Seventh Pecora Symposium, Sioux Falls, SD, October 18-21, 1981
 - 15 p2184 A83-34801
 - Sub-regional information system formation using multi-resolution remote sensing products
 - 15 p2239 A83-34807
 - Remote sensing data integration into a geographic information system for the creation of a biogenic hydrocarbon inventory of the San Francisco Bay area
 - 15 p2185 A83-34819
 - Hierarchical modeling for image classification
 - 15 p2185 A83-34820
 - Integration and manipulation of remotely sensed and other data in geographic information systems
 - 15 p2185 A83-34821
 - An overview of remote sensing input to geographic information systems
 - 15 p2185 A83-34822
 - Forest management applications of Landsat data in a geographic information system
 - 15 p2185 A83-34823
 - Compressing interpreted satellite imagery for geographic information systems applications over extensive regions
 - 15 p2185 A83-34824
 - From ecological test site to geographic information system Lessons for the 1980's
 - 15 p2185 A83-34825
 - GIS information layers derived from Landsat classification --- Geographic Information Systems
 - 15 p2185 A83-34826

- The wetlands inventory of the Northern Great Plains -
An example of operational remote sensing and data management 15 p2185 A83-34827
- The development and application of a county-level geographic data base 15 p2186 A83-34828
- A 'user friendly' geographic information system in a color interactive digital image processing system environment 15 p2186 A83-34829
- Cartographic modeling - Procedures for extending the utility of remotely sensed data 15 p2186 A83-34830
- Combining land use data acquired from Landsat with soil map data using an information system 15 p2186 A83-34833
- Some technical considerations on the evolution of the IBIS system --- Image Based Information System 15 p2186 A83-34834
- Use of remote sensing inputs in geographic information systems for watershed management 15 p2186 A83-34836
- Generalized balanced ternary - An approach to handling spatial data 15 p2165 A83-34841
- A geographic information system for New Mexico 15 p2187 A83-34843
- Oregon's Statewide Landuse Inventory - Remote sensing input to geographic information systems 15 p2187 A83-34844
- A geographic data base for Texas pecan 16 p2370 A83-35740
- Remote-sensing technology applied to forest assessment in California 17 p2528 A83-38152
- The system of physical spatial units ('Naturraumliche Gliederung') as an aid in the evaluation of satellite data 22 p3311 A83-46165
- A hybrid structure for the storage and manipulation of very large spatial data sets 24 p3619 A83-49195
- GEOGRAPHY**
NT HYPISOGRAPHY
NT OROGRAPHY
- Remote-sensing techniques for geographical surveys --- Russian book 15 p2184 A83-34572
- GEOTIDS**
Concerning the calculation of geodetic heights 01 p0072 A83-10852
- Allowance for near and far zones in the calculation of geoid heights and plumbline deviations 01 p0072 A83-10853
- Concerning the problem of the relationship between geoid undulations and tectonic structures 04 p0514 A83-16379
- Direct integration of Stokes' undulation and Vening Meinesz's deflection equations for geographically defined gravity anomaly blocks 07 p0958 A83-19873
- Phase transformations in the transition zone of the mantle and possible changes in the earth's radius 07 p0961 A83-20273
- Thermal parameters of the oceanic lithosphere estimated from geoid height data 08 p1144 A83-22363
- Current investigations at TsNIGAIK in the area of physical geodesy 08 p1136 A83-22788
- Roughness of the marine geoid from Seasat altimetry 09 p1317 A83-24280
- The determination of geoid undulations and gravity anomalies from Seasat altimeter data 09 p1318 A83-24282
- The modern geoid and ancient plate boundaries 12 p1752 A83-29172
- Global isostatic geoid anomalies for plate and boundary layer models of the lithosphere 13 p1882 A83-31590
- The Indian Ocean gravity low - Evidence for an isostatically uncompensated depression in the upper mantle 15 p2202 A83-34726
- Palaeocontinental configurations and geoid anomalies 16 p2376 A83-35997
- GEOLOGICAL FAULTS**
NT AFRICAN RIFT SYSTEM
NT SAN ANDREAS FAULT
- Lithospheric flexure at fracture zones 02 p0212 A83-12870
- Convective thinning of the lithosphere - A mechanism for the initiation of continental rifting 02 p0212 A83-12871
- Tectonic history of the Tharsis region, Mars 04 p0565 A83-15556
- Episodic rifting and volcanism at Krafla in North Iceland - Growth of large ground fissures along the plate boundary 07 p0957 A83-19870
- Vertical movements following a dip-slip earthquake 07 p0958 A83-20094
- Continental rifting and the implications for plate tectonic reconstructions 07 p0961 A83-20228
- Geodynamics of the Baikal-Stanovoy seismic belt 07 p0963 A83-20975
- Focal depths and fault plane solutions of earthquakes under the Tibetan plateau 08 p1135 A83-22366

- The evolution of tectonic features on Ganymede 08 p1189 A83-22938
- NNE-SSW fault system in part of the Gulf of Suez and its bearing on oil exploration 09 p1286 A83-24551
- Analysis of the fault and block structure of the Bashkir anticlinorium on the basis of space photographs 10 p1443 A83-26803
- Grabens, basin tectonics, and the maximum total expansion of the moon 12 p1799 A83-29965
- On the size distribution of solid jointings --- in rocks formed by geological fracture processes 13 p1873 A83-30005
- Features of the spread of faults around meteorite craters (the El'gygytyn crater taken as an example) 13 p1962 A83-31347
- Geology, structure, and tectonics of the Pajarito fault zone in the Espanola basin of the Rio Grande rift, New Mexico 16 p2370 A83-36970
- Crustal processes at spreading centers 17 p2543 A83-38327
- On a new type of rotation-tectonic lines in the earth's lithosphere 18 p2715 A83-39533
- Introduction - Processes of continental rifting 19 p2866 A83-41856
- Constraints on rift thermal processes from heat flow and uplift 19 p2867 A83-41857
- Back arc thrusting in the eastern Sunda arc, Indonesia - A consequence of arc-continent collision 22 p3322 A83-45742
- Precise leveling across active faults in California 22 p3329 A83-46362
- Deformation monitoring at Mount St. Helens in 1981 and 1982 22 p3333 A83-46797
- Information from space and the prediction of exogenous processes --- in tectonics 23 p3483 A83-48106
- Transregional faults in the northeastern part of the USSR appearing in space photographs 23 p3483 A83-48107
- Analysis of the pattern of geological joints from an interpretation of aerospace photographs (using the Pechenga ore region as an example) 23 p3476 A83-48109
- Reconstruction of the strike-slip faults of the Adycha-Taryn region 23 p3483 A83-48110
- GEOLOGICAL SURVEYS**
Basic principles underlying the application of space images to small-scale geological mapping 07 p0950 A83-19907
- Geologic interpretation of texture in Seasat and SIR-A radar images 08 p1126 A83-21921
- Geologic observations of the northern boundary of the Caribbean plate across central America as seen by Seasat and SIR-A 08 p1128 A83-21947
- Geology and image processing 08 p1129 A83-22525
- Remote sensing - A significant exploration tool for the geoscientist 09 p1286 A83-24550
- Tectonics of west central New Mexico and adjacent Arizona - A remote sensing and field study in arid and semi-arid areas 09 p1287 A83-24573
- Use of Landsat multispectral scanner data in geologic mapping of the Meatiq Dome, central Eastern Desert, Egypt 09 p1289 A83-24591
- Application of visual interpretation and digital processing of Landsat data for the preparation of a geological interpretation map of southwestern Egypt at a scale of 1:500,000 09 p1289 A83-24598
- A practical attempt at correlation of rock units from CCT print out --- Computer Compatible Tapes 09 p1291 A83-24627
- Information from spectral and textural features for geological interpretation of Landsat imagery of the eastern Sahara 09 p1291 A83-24634
- The investigation and mapping of terrain with the utilization of remote sensing information --- Russian book 09 p1292 A83-25223
- Hydrogeologic studies abroad --- Russian book 09 p1292 A83-25247
- The Cretaceous-Tertiary transition 10 p1448 A83-25650
- Results of the investigation of the oil and gas deposits of Tadzhikistan on the basis of space photographs 10 p1444 A83-26805
- The use of space imagery for geocryological mapping 14 p2034 A83-32492
- Using Landsat imagery interpretation for underground water prospectation around Qena Province, Egypt 15 p2187 A83-35276
- The application of aerial techniques in geocryological explorations --- Russian book 16 p2370 A83-36446
- Geological mapping of the moon 17 p2615 A83-37012
- Application of remote sensing techniques in mineral resources survey - A case study pertaining to Singbhum Shear Zone, Bihar, India 17 p2527 A83-38133

- Geological exploration and landuse using Landsat data, Sierra Leone, West Africa 17 p2527 A83-38137
- The application of remote sensing techniques to regional geological survey in China 17 p2527 A83-38138
- Mapping of hydrothermally altered rocks using airborne multispectral scanner data, Marysville, Utah, mining district 17 p2528 A83-38140
- Operational use of a block adjustment technique in the realization of an accurate radar mosaic --- for mineral assessment and geological survey of Gabon 17 p2533 A83-38442
- Global satellite remote sensing for energy, minerals and other resources 17 p2534 A83-38450
- Correlation between the SIR-A radar survey, the Landsat data, and the IR surveys in the Corinth canal zone 17 p2534 A83-38451
- Aerial photography and scanning aerial methods in engineering geological investigations --- Russian book 21 p3166 A83-45013
- Geologic thermal-inertia mapping using HCMM satellite data 22 p3309 A83-46130
- The use of the Space Shuttle for land remote sensing 22 p3259 A83-46146
- Geological mapping from spaceborne imaging radars Kentucky-Virginia, USA 22 p3313 A83-46222
- Mapping and analysis of aerial conductivity measurements from INPUT system over geothermal areas 22 p3314 A83-46233
- Mineralogical information from a new airborne thermal infrared multispectral scanner 23 p3475 A83-47816
- GEOLOGY**
NT CONES (VOLCANOES)
NT GEOCHRONOLOGY
NT GEOMORPHOLOGY
NT GLACIOLOGY
NT HYDROGEOLOGY
NT LITHOLOGY
NT LUNAR GEOLOGY
NT MARS VOLCANOES
NT OROGRAPHY
NT PETROGRAPHY
NT PETROLOGY
NT PHOTOGEOLOGY
NT RADAR GEOLOGY
NT STRUCTURAL PROPERTIES (GEOLOGY)
NT TECTONICS
NT VOLCANOES
NT VOLCANOLOGY
- International Geoscience and Remote Sensing Symposium, Washington, DC, June 8-10, 1981, Digest, Volumes 1 & 2 01 p0061 A83-10001
- Astronomic geology - Its subject and general problems 04 p0502 A83-15400
- Geology and image processing 08 p1129 A83-22525
- Archean diamond-bearing mantle in the expanding-earth model 13 p1873 A83-30020
- Annual review of earth and planetary sciences. Volume 11 --- Book 14 p2034 A83-33477
- The investigation of social-psychological factors of occupational injuries in geological-survey work 16 p2401 A83-36819
- The application of space imagery to geology and mineral exploration in the USSR - A case history 17 p2527 A83-38128
- The continental crust 20 p3020 A83-42819
- Data from remote sensing in the geographical information system - The construction of territorial data banks 20 p3011 A83-43137
- Geological development of the earth during the Precambrian --- Russian book 21 p3174 A83-45035
- Inter-layered clay stacks in Jurassic shales 21 p3174 A83-45060
- The use of thermal infrared images in geologic mapping 22 p3309 A83-46131
- The efficiency of coupled processes in connection with geochemical and biogeological evolution 23 p3485 A83-48508
- The origin of the iridium anomaly at the Cretaceous-Tertiary boundary 24 p3671 A83-48954
- GEOMAGNETIC ANOMALIES**
U MAGNETIC ANOMALIES
- GEOMAGNETIC CROTCHETS**
U SUDDEN IONOSPHERIC DISTURBANCES
- GEOMAGNETIC EFFECTS**
U MAGNETIC EFFECTS
- GEOMAGNETIC EQUATOR**
U MAGNETIC EQUATOR
- GEOMAGNETIC FIELD**
U GEOMAGNETISM
- GEOMAGNETIC LATITUDE**
Ion whistlers in mid-latitude trough of light ions 02 p0205 A83-11999
- Geographical and seasonal distribution of critical frequencies in the F2-layer during a period of high solar activity 04 p0509 A83-15724

Latitude dependence of geomagnetic storm after-effects in ionospheric absorption 18 p2712 A83-39064

GEOMAGNETIC MICROPULSATIONS

An investigation of the frequency dependence of the biological effectiveness of a magnetic field in the range of the micropulsations of the geomagnetic field /0.01-100 Hz/ 02 p0221 A83-11886

A cross spectral analysis of high-latitude Pc 5 pulsations in the morning sector 02 p0207 A83-12386

Stare and GEOS 2 observations of a storm time Pc 5 ULF pulsation 02 p0208 A83-12387

The nature of the source of packets of fading long-period geomagnetic pulsations 02 p0210 A83-12439

Heavy O⁺/ ions in the earth's radiation belt as a possible source of Pc1-2 geomagnetic pulsations 02 p0211 A83-12453

Average diurnal variations of the intensity of geomagnetic pulsations in the period ranges of pc 2-pc 5 observed at Fuerstenfeldbruck during the years 1960-1971 03 p0357 A83-13300

Pulsing hiss, pulsating aurora and micropulsations 03 p0361 A83-14744

Antarctic observations available for IMS correlative analyses 04 p0513 A83-16300

The hydromagnetic oscillation of individual shells of the geomagnetic field 05 p0660 A83-17392

PC 4 - PC 1 magnetic pulsations at synchronous orbit and their relation to pulsations on the ground 05 p0660 A83-17393

Characteristics of geomagnetic micropulsations in the earth's equatorial zone 05 p0664 A83-17628

Multisatellite observations of resonant hydromagnetic waves 05 p0664 A83-17777

Pc 1-2 observations of heavy ion effects by synchronous satellite ATS-6 05 p0664 A83-17779

Pi 2 pulsations - High latitude results 05 p0664 A83-17780

Analysis of pulsations --- of geomagnetic fields 05 p0664 A83-17781

A theory of forced magnetohydrodynamic waves 05 p0689 A83-17867

Pi2 magnetic pulsations, auroral break-ups, and the substorm current wedge - A case study 05 p0665 A83-17868

Ground magnetometer detection of a large-M Pc 5 pulsation observed with the STARE radar 06 p0783 A83-18292

Comparison of phase and amplitude structures of Pc 5 pulsations in the morning and afternoon sectors 07 p0966 A83-21514

Correlations between ground observations of Pi 2 geomagnetic pulsations and satellite plasma density observations 08 p1137 A83-23111

Pc 1 pulsation activity at Ottawa 09 p1303 A83-23763

Ionospheric electric field pulsations - A comparison between VLF results from an ionospheric heating experiment and STARE 09 p1304 A83-23770

160 m pulsations in the magnetosphere of the earth possibly caused by oscillations of the sun 11 p1615 A83-27665

Statistical properties of geomagnetic pulsations at the Fuerstenfeldbruck Observatory determined by means of pulsation indices. I - Method and cross-correlation 11 p1617 A83-28117

PC1 wave generation by sudden impulses 13 p1881 A83-31531

Polarization characteristics of Pi 2 pulsations and implications for their source mechanisms - Influence of the westward travelling surge 13 p1882 A83-31633

Local time asymmetry in the characteristics of Pc5 magnetic pulsations 13 p1883 A83-31634

Propagation properties of hydromagnetic waves in a hot plasma and right-hand polarized Pc1 and Pc5 13 p1883 A83-31635

Correlated irregular magnetic pulsations and optical emissions observed at Siple Station, Antarctica 15 p2195 A83-33936

The relationship between the strength of the IMF and the frequency of magnetic pulsations on the ground and in the solar wind 15 p2199 A83-34362

Associated geomagnetic and ionospheric variations 15 p2199 A83-34363

First results of micropulsation activity observed by SABRE --- Sweden and Britain auroral Radar Experiment 15 p2199 A83-34364

Conjugate observations of Pc 5 electric fields with a geostationary satellite and a ground radar facility 17 p2538 A83-37596

Maps of the polarizations of high latitude Pi 2's 17 p2538 A83-37599

A double-resonance Pc 5 pulsation 17 p2539 A83-37602

Oscillations in the earth's magnetosphere with a period of 160 minutes caused by the pulsations of the sun 17 p2539 A83-37716

A facility for measuring geomagnetic micropulsations at L'Aquila, Italy 19 p2847 A83-41163

Numerical modelling of the ionospheric filtration of an ULF micropulsation signal 19 p2866 A83-41318

The evolution of pearls in the earth's magnetosphere 20 p3023 A83-43156

Propagation characteristics of hydromagnetic waves in a cold plasma mixed with a hot plasma and right-hand polarized Pc1 and Pc5 20 p3024 A83-43163

PD 1 pearl-electron interactions on the L = 4.2 magnetic shell 20 p3024 A83-43191

The rate of occurrence of dayside Pc 3,4 pulsations - The L-value dependence of the IMF cone angle effect 20 p3025 A83-43200

Remote determination of the outer radial limit of stormtime Pc5 wave occurrence using geosynchronous satellites 20 p3025 A83-43202

Reflection of MHD-waves in the PC4-5 period range at ionospheres with non-uniform conductivity distributions 20 p3026 A83-43204

Satellite observations of Pi 2 activity at synchronous orbit 22 p3326 A83-46040

The localization of Pi 2 pulsations - Ground-satellite observations 22 p3326 A83-46041

Comparative study of magnetic Pc 1 pulsations observed at low and high latitudes - Source region and generation mechanism of periodic hydromagnetic emissions 22 p3329 A83-46502

Compressional Pc 4 pulsations observed at synchronous orbit 22 p3329 A83-46503

Polarization patterns of Pi 2 magnetic pulsations and the substorm current wedge 22 p3336 A83-47057

Simultaneous geomagnetic and radio auroral observations 24 p3605 A83-49302

GEOMAGNETIC PULSATIONS**NT GEOMAGNETIC MICROPULSATIONS**

Evidence for interactions between Pc 1 hydromagnetic waves and energetic positive ions near the plasmapause 02 p0208 A83-12392

Midlatitude oscillations of the geomagnetic field and their connection with the dynamics of processes in the ionosphere 02 p0209 A83-12434

The fading of ultralow-frequency waves in the transition region --- solar wind geomagnetic-pulsations in magnetosphere 02 p0210 A83-12438

Some possibilities of identifying the effect of geoelectric inhomogeneities on the polarization of geomagnetic pulsations at midlatitudes 02 p0210 A83-12440

The possibility of exciting geomagnetic pulsations in the case of the radial direction of the interplanetary magnetic field 02 p0211 A83-12451

Pulsed reconnection as a possible source of icpl pulsations --- of geomagnetic field 02 p0211 A83-12452

Ground-Satellite correlative study of a giant pulsation event 03 p0357 A83-13299

Pulsing hiss, pulsating aurora and micropulsations 03 p0361 A83-14744

Arrays of magnetometers operated in NW Europe 04 p0512 A83-16294

Detailed correlations of magnetic field and riometer observations at L = 4.2 with pulsating aurora 05 p0660 A83-17394

Structure of the spatial distribution of the amplitude and polarization characteristics of Pi2 geomagnetic pulsations in the region of the activation of auroras 05 p0663 A83-17615

Penetration of geomagnetic pulsations from one polar cap to the other 05 p0663 A83-17616

The role of ground arrays of magnetometers in the study of pulsation resonance regions 05 p0664 A83-17776

Pulsations in magnetic field and ion flux observed at L = 4.5 on August 5, 1972 06 p0783 A83-18290

Charged particle behavior in low-frequency geomagnetic pulsations. III - Spin phase dependence 06 p0783 A83-18291

Schumann resonances at high latitudes 07 p0957 A83-19635

The importance of B-gradient drift in high beta magnetospheric plasma instabilities 07 p0958 A83-20087

Morphology of spatial patterns in Pi 1-2 magnetic field pulsation activity - A review 07 p0965 A83-21428

Reflection of Alfvén waves by nonuniform ionospheres 07 p0968 A83-21585

High-beta theory of low-frequency magnetic pulsations 09 p1303 A83-23762

Propagation of ULF electromagnetic waves through the ionosphere and geomagnetic pulsations 11 p1617 A83-28118

Observations of quasistatic electric fields on the GEOS and ISEE satellites 11 p1621 A83-28770

The employment of the pulsation data of Nagycenk observatory for the study of the effect of the interplanetary magnetic field on the geomagnetic pulsations 12 p1753 A83-29236

Features of the relationship between the spatial-temporal behavior of pulsations of decreasing period with magnetic activity 13 p1876 A83-30614

Quarter-wave ULF pulsations 13 p1881 A83-31535

On the possibility that certain types of geomagnetic pulsations have an ionospheric origin 14 p2050 A83-31869

Large-amplitude ion bounce wave in the magnetosphere near L = 3 15 p2202 A83-34737

STARE radar observations of a Pg pulsation --- giant pulsations 17 p2538 A83-37592

Drift wave model for geomagnetic pulsations in a high beta plasma 17 p2538 A83-37593

Relationship between the intensification of the 6300-Å emission at midlatitudes and geomagnetic pulsations 18 p2714 A83-39336

Diagnostics of the daytime cusp in the case of the northern direction of the interplanetary field according to data from the chain of automatic magnetic-variation stations in the Antarctic 18 p2714 A83-39341

Type IPDP magnetic pulsations and the development of their sources --- Intervals of Pulsations of Diminishing Periods 20 p3018 A83-42412

Plasma drift measurements with the electron beam experiment on GEOS-2 during long period pulsations on April 7, 1979 20 p3025 A83-43201

Geos 2 plasma drift velocity measurements associated with a storm time Pc5 pulsation 20 p3027 A83-43216

A theory of long period magnetic pulsations. III - Local field line oscillations 20 p3027 A83-43218

The dynamic parameters of an autooscillatory model of geomagnetic pulsations 21 p3175 A83-45248

Method for identifying the structure of the anomalous field of geomagnetic pulsations at midlatitudes 21 p3176 A83-45267

Modes of pulsating auroras and related geomagnetic pulsations 22 p3330 A83-46508

Long-duration Pc5 pulsations observed by geostationary satellites 22 p3334 A83-46890

PiC magnetic pulsations and variations of the ionospheric electric field and conductivity 24 p3606 A83-49307

The employment of the pulsation data of Nagycenk observatory for the study of the effect of the interplanetary magnetic field on the geomagnetic pulsations 12 p1753 A83-29236

Features of the relationship between the spatial-temporal behavior of pulsations of decreasing period with magnetic activity 13 p1876 A83-30614

Quarter-wave ULF pulsations 13 p1881 A83-31535

On the possibility that certain types of geomagnetic pulsations have an ionospheric origin 14 p2050 A83-31869

Large-amplitude ion bounce wave in the magnetosphere near L = 3 15 p2202 A83-34737

STARE radar observations of a Pg pulsation --- giant pulsations 17 p2538 A83-37592

Drift wave model for geomagnetic pulsations in a high beta plasma 17 p2538 A83-37593

Relationship between the intensification of the 6300-Å emission at midlatitudes and geomagnetic pulsations 18 p2714 A83-39336

Diagnostics of the daytime cusp in the case of the northern direction of the interplanetary field according to data from the chain of automatic magnetic-variation stations in the Antarctic 18 p2714 A83-39341

Type IPDP magnetic pulsations and the development of their sources --- Intervals of Pulsations of Diminishing Periods 20 p3018 A83-42412

Plasma drift measurements with the electron beam experiment on GEOS-2 during long period pulsations on April 7, 1979 20 p3025 A83-43201

Geos 2 plasma drift velocity measurements associated with a storm time Pc5 pulsation 20 p3027 A83-43216

A theory of long period magnetic pulsations. III - Local field line oscillations 20 p3027 A83-43218

The dynamic parameters of an autooscillatory model of geomagnetic pulsations 21 p3175 A83-45248

Method for identifying the structure of the anomalous field of geomagnetic pulsations at midlatitudes 21 p3176 A83-45267

Modes of pulsating auroras and related geomagnetic pulsations 22 p3330 A83-46508

Long-duration Pc5 pulsations observed by geostationary satellites 22 p3334 A83-46890

PiC magnetic pulsations and variations of the ionospheric electric field and conductivity 24 p3606 A83-49307

GEOMAGNETIC STORMS

U MAGNETIC STORMS**GEOMAGNETIC TAIL**

On the convective mechanism for formation of the plasma sheet in the magnetospheric tail 02 p0204 A83-11963

The properties of ionospheric O⁺/ ions as observed in the magnetotail boundary layer and northern plasma lobe 02 p0207 A83-12383

A two-dimensional simulation of the interaction of the plasma sheet with the lobes of the earth's magnetotail 06 p0782 A83-18287

Energetic ion beam in the earth's magnetotail lobe 07 p0958 A83-20086

On reconnection and plasmoids in the geomagnetic tail 07 p0966 A83-21512

Current sheet acceleration of ions in the geomagnetic tail and the properties of ion bursts observed at the lunar distance 08 p1137 A83-23119

Exit of boundary layer plasma from the distant magnetotail 09 p1305 A83-24342

Neutral sheet current interruption and field-aligned current generation by three-dimensional driven reconnection 09 p1306 A83-24343

Active plasmas near planets and stars 11 p1679 A83-28240

Dielectric currents in the low-latitude boundary layer and geomagnetic tail 15 p2202 A83-34734

Model field flux conservation and the Beard magnetotail model - Two corrections 17 p2539 A83-37607

The viscous-like magnetospheric convection and the length of the earth's magnetotail 20 p3023 A83-43160

New observations of plasma vortices and insights into their interpretation --- in magnetotail plasma sheet 20 p3026 A83-43203

A nonlinear kinetic energy principle for two-dimensional collision-free plasmas 21 p3209 A83-43940

The structure of an equilibrium magnetotail 21 p3172 A83-44505

Scattering and precipitation of particles of the magnetotail under the action of the dawn-dusk electric field 21 p3172 A83-44522

Self-consistent theory of three-dimensional convection in the geomagnetic tail 22 p3326 A83-46036

Development of substorm activity in multiple-onset substorms at synchronous orbit 22 p3326 A83-46038

- Plasma regimes in the deep geomagnetic tail - ISEE 3
22 p3334 A83-46891
- Energetic particles in the vicinity of a possible neutral
line in the plasma sheet 22 p3334 A83-47038
- Observations of ion streaming during substorms
22 p3335 A83-47039
- A statistical study of large electric field events in the
earth's magnetotail 22 p3335 A83-47040
- Average configuration of the distant (less than
220-earth-radii) magnetotail - Initial ISEE-3 magnetic field
results 23 p3482 A83-47866
- The convective mechanism of the formation of the
plasma sheet in the magnetospheric tail 23 p3484 A83-48380
- Magnetospheric tail dynamics 23 p3485 A83-48554

GEOMAGNETICALLY TRAPPED PARTICLES

U RADIATION BELTS

GEOMAGNETISM

- Rocket observations of high-amplitude Alfvén waves
theoretically explained through their interaction with polar
light electrons --- German thesis 01 p0070 A83-10169
- The network of automatic magnetographs in the
Antarctic Geographic Polygon project for the investigation
of near-earth space 01 p0072 A83-10837
- The beginnings of magnetospheric physics
01 p0072 A83-11284
- The Biot-Savart formula for an equilibrium plasma ---
in magnetosphere 02 p0240 A83-11646
- Experimental studies of geomagnetic effects in cosmic
rays and the spectrum of the increase effect before
magnetic storms 02 p0273 A83-11713
- Investigation of high-energy electrons by the
Interkosmos-17 satellite 02 p0273 A83-11714
- The effect of geomagnetic disturbances on human
biorhythms 02 p0222 A83-11878
- The effect of the solar-geomagnetic situation on
monolayers of cells and the distant intercellular interactions
at high latitudes 02 p0220 A83-11881
- The state of the adrenal cortex function in healthy
individuals during changes in geomagnetic activity
02 p0222 A83-11882
- Low-strength ULF magnetic fields and the condition of
the adaptive reserve in experimental animals 02 p0220 A83-11883
- Determination of the magnetospheric current system
parameters and development of experimental
geomagnetic field models based on data from IMP and
HEOS satellites 02 p0204 A83-11961
- Energetic particle losses and trapping boundaries as
deduced from calculations with a realistic magnetic field
model 02 p0204 A83-11962
- A quantitative model of geomagnetic activity
02 p0207 A83-12379
- Field-aligned current and the auroral electrojets in the
post-noon quadrant 02 p0207 A83-12381
- Correlations of magnetospheric ion composition with
geomagnetic and solar activity 02 p0207 A83-12382
- A broadband VLF burst associated with ring current
electrons 02 p0207 A83-12385
- Thermospheric response observed over Fritz Peak,
Colorado, during two large geomagnetic storms near solar
cycle maximum 02 p0208 A83-12391
- Determination of return-flow velocity in the case of the
orientation of the geomagnetic dipole along the
nondisturbed velocity of the solar wind 02 p0208 A83-12419
- Investigation of processes in the thermosphere during
magnetic disturbances 02 p0209 A83-12430
- Dependence of magnetic activity on the orientation of
the geomagnetic dipole relative to the interplanetary
magnetic field 02 p0209 A83-12433
- Concerning the nature of geomagnetic-field oscillations
produced by solar flares 02 p0210 A83-12435
- Spatial-temporal analysis of 60-year field variations
according to data from the global network of
observatories 02 p0210 A83-12441
- The geoeffectiveness of the meridional component of
the large-scale magnetic field of the sun 02 p0210 A83-12442
- Experimental verification of theoretical calculations of
geomagnetic cutoff rigidity 02 p0210 A83-12443
- Measurement of the magnetic field components of sea
waves 02 p0218 A83-12454
- The 11-year variation of the western drift of the magnetic
center of the earth 02 p0211 A83-12455
- June-July 1974 proton-flare region. III - The geomagnetic
activity during the declining phase of the complex
process 02 p0271 A83-12863
- Electrons with energies of hundreds of MeV in near-earth
space 03 p0438 A83-13208
- Particle acceleration during the development of
tearing-mode discontinuity --- in cosmic plasma 03 p0356 A83-13209

- Comparison between the hot spot and geomagnetic field
reference frames 04 p0508 A83-14957
- Solar interaction regions, geomagnetic indices and the
troposphere 04 p0508 A83-14965
- Neutral line motion due to reconnection in two-ribbon
solar flares and magnetospheric substorms 04 p0509 A83-14974
- The effect of a geomagnetic field and
neuro-psychological stress on the electrical resistance in
biologically active points of the skin 04 p0523 A83-15787
- The relationship between the statistical characteristics
of the anomalous magnetic field and the upper,
magnetically active mantle of the earth 04 p0510 A83-16036
- The IMS source book: Guide to the International
Magnetospheric Study data analysis 04 p0511 A83-16276
- S3-3 satellite instrumentation and data 04 p0511 A83-16286
- Magsat data availability 04 p0512 A83-16289
- Antarctic observations available for IMS correlative
analyses 04 p0513 A83-16300
- The July 29, 1977 magnetic storm - Observations and
modeling of energetic particles at synchronous orbit 04 p0513 A83-16306
- ISEE work on collisionless shocks - CDAW-3, the
meeting and the results July 23-26, 1979 --- Coordinated
Data Analysis Workshop 04 p0513 A83-16307
- ISEE-magnetopause observations - Workshop results
04 p0513 A83-16308
- Magnetic field compression at the dayside
magnetopause 05 p0660 A83-17388
- ULF geomagnetic power near $L = 4$. VII - A Conjugate
area study of power controlled by solar wind quantities
05 p0660 A83-17391
- Ionospheric and geomagnetic variations at
mid-latitudes 05 p0662 A83-17596
- The formation of albedo-electron fluxes in the
geomagnetic field 05 p0662 A83-17603
- Investigation of the filling and emptying of plasma tubes
with allowance for ion inertia --- in ionosphere 05 p0663 A83-17610
- Application of method of pattern recognition for the
classification of geomagnetic disturbances at the epoch
of the solar-activity maximum 05 p0663 A83-17614
- Field-aligned currents in the magnetosphere 05 p0663 A83-17617
- The use of the method of natural orthogonal components
to identify and analyze 60-year variations of the
geomagnetic field 05 p0663 A83-17619
- The effect of random irregularities on the field strength
of radio waves in the region of caustics 05 p0663 A83-17624
- Parametric resonance of the bounce oscillations of
particles with a magnetoacoustic wave propagating
transverse to the geomagnetic field 05 p0664 A83-17625
- The spatial distribution of disturbances of the vertical
component of the geoelectric field, accompanying an
intensification of magnetic activity 05 p0664 A83-17627
- Mechanism of the stationary biaxial dynamo 05 p0664 A83-17629
- Certain characteristics of the geomagnetic field
variations over the past 700,000 years 05 p0664 A83-17630
- The consequences of high latitude particle precipitation
on global thermospheric dynamics 05 p0665 A83-17782
- The induced effects of geomagnetic variations in the
equatorial region 05 p0665 A83-17866
- A new theory about the origin of the earth's magnetic
field 06 p0782 A83-18020
- Ground magnetometer detection of a large-M Pc 5
pulsation observed with the STARE radar 06 p0783 A83-18292
- Dynamics of magnetosphere-ionosphere coupling
including turbulent transport 06 p0784 A83-18305
- Boundaries of the trapping and loss of
outer-radiation-belt particles, conditioned by the
magnetospheric magnetic field 06 p0857 A83-18358
- Low-frequency noise during an intense magnetic
storm 06 p0786 A83-18367
- Convective dynamos with intermediate and strong
fields 06 p0813 A83-18932
- Analysis of geodynamo equations by means of
perturbation theory 06 p0787 A83-18933
- The amplitude modulation of the short-period oscillations
of the earth's electromagnetic field 06 p0787 A83-19421
- Late precambrian Keweenawian asymmetric polarities
as analyzed by axial offset dipole geomagnetic models 07 p0957 A83-19871
- Improving ionospheric maps using theoretically derived
values of $f(0)F/2f$ 07 p0961 A83-20372

- Effect of geomagnetic activity on the changes of
atmospheric circulation in the northern hemisphere 07 p0950 A83-20601
- Optimal processing of satellite-derived magnetic
anomaly data 07 p0963 A83-20972
- Magnetospheric convection effects at mid-latitudes. II
- A coordinated Chatanika/Saint-Santin study of the April
10-14, 1978, magnetic storm 07 p0964 A83-21061
- Characteristics of gaps in discrete dayside auroras
07 p0965 A83-21186
- Corrected geomagnetic pole coordinates 07 p0965 A83-21189
- A correlation between measured E-region current and
geomagnetic daily variation at equatorial latitude 07 p0966 A83-21429
- The magnetic poles of the earth 07 p0966 A83-21430
- Observation of an IMF sector effect in the Y magnetic
field component at geostationary orbit 07 p0968 A83-21582
- Satellite systems for the acquisition and processing of
geomagnetic data 08 p1133 A83-22082
- Solar and lunar seasonal variations in the American
sector 08 p1133 A83-22302
- Interpretation of seasonal variations of S and L --- solar
and lunar geomagnetic variations 08 p1133 A83-22303
- A study of quiet day magnetic field variations in East
Asia at sunspot minimum 08 p1134 A83-22304
- Dynamics of the global Sq-field --- current distribution
and geomagnetic variations 08 p1134 A83-22305
- On the position of the Sq /H/ focus in years of sunspot
minimum --- solar quiet day geomagnetic variations 08 p1134 A83-22306
- Sq and L currents in the ionosphere --- solar quiet and
lunar tidal effects on ionospheric and geomagnetic
variations 08 p1134 A83-22307
- An investigation of the equatorial electrojet by means
of ground-based magnetic measurements in Brazil 08 p1134 A83-22309
- Effect of the equatorial counter-electrojet in the Indian
region on the geomagnetic solar and lunar daily
variations 08 p1134 A83-22310
- Bi-diurnal geomagnetic variations 08 p1134 A83-22311
- Normal and anomalous geomagnetic fields separated
by solving the eigenvalue problem 08 p1134 A83-22312
- Studies of the external origin component of Sq by
'canonical' GDS analysis --- Geomagnetic Depth
Sounding 08 p1134 A83-22313
- The variation of the magnetic field and its interaction
with the equatorial electrojet in eastern Senegal 08 p1135 A83-22314
- Geomagnetic westward drift using the correlation
coefficient 08 p1138 A83-22358
- Hydromagnetic waves in inhomogeneous plasmas 09 p1347 A83-23394
- The effect of the geomagnetic field on the diffusion of
meteor trails 09 p1301 A83-23477
- The decrease in the earth's magnetic dipole moment 09 p1302 A83-23675
- International Geomagnetic Reference Field - The third
generation 09 p1302 A83-23711
- Some new methods in geomagnetic field modeling
applied to the 1960-1980 epoch 09 p1302 A83-23712
- The IGS proposal for the new International Geomagnetic
Reference Field 09 p1302 A83-23713
- A proposed International Geomagnetic Reference Field
for 1965-1985 09 p1302 A83-23714
- Comparison of candidate IGRF models --- International
Geomagnetic Reference Field 09 p1302 A83-23715
- Evaluation of IGRF 1980 candidate models ---
International Geomagnetic Reference Field 09 p1302 A83-23716
- Assessment of models proposed for the 1981 revision
of the IGRF --- International Geomagnetic Reference
Field 09 p1302 A83-23717
- Comparison of IGRF models with North American
magnetic data 09 p1302 A83-23718
- A comparison of the proposed IGRF models - Internal
and relative consistencies 09 p1302 A83-23719
- A preliminary assessment of International Geomagnetic
Reference Field models for Australia 09 p1302 A83-23720
- Plasma rest frame frequencies and polarizations of the
low-frequency upstream waves - ISEE 1 and 2
observations 09 p1302 A83-23757
- Solar wind control of the low-latitude asymmetric
magnetic disturbance field 09 p1303 A83-23768
- A dynamic model for the auroral field line plasma in the
presence of field-aligned current 09 p1304 A83-23769

The periodic variations in the atmospheric electric, electrotelluric, and geomagnetic fields according to data from the observatory at Dusheti

09 p1304 A83-23981
Crustal geomagnetic field - Two-dimensional intermediate-wavelength spatial power spectra

09 p1305 A83-24139
Exit of boundary layer plasma from the distant magnetotail

09 p1305 A83-24342
Neutral sheet current interruption and field-aligned current generation by three-dimensional driven reconnection

09 p1306 A83-24343
Short-period geomagnetic, atmospheric and earth-rotation variations

09 p1306 A83-24455
Direct inversion of one-dimensional magnetotelluric data

09 p1308 A83-25069
Inductive coupling between idealized conductors and its significance for the geomagnetic coast effect

10 p1447 A83-25435

An analogue model of the geomagnetic induction in the South Indian Ocean

10 p1448 A83-25440

Magnetosphere-ionosphere relationships

10 p1448 A83-25604

Secular variations in the geomagnetic field caused by processes in the magnetosphere

10 p1448 A83-25606

The relative importance of geomagnetic effects in the observed secular, eleven-year, and solar-diurnal variations of cosmic rays

10 p1523 A83-26102

A model description of fluxes of high-energy protons trapped by the geomagnetic field

10 p1523 A83-26103

Coronal disturbances and their terrestrial effects

/Tutorial Lecture/ 11 p1686 A83-27377

IMF control of the earth's magnetosphere

11 p1614 A83-27390

Magnetic structure of the boundary layer --- explaining magnetospheric convection

11 p1614 A83-27391

The earth's ring current: Causes, generation, and decay

- /Tutorial Lecture/ 11 p1614 A83-27393

Geomagnetic induction effects in ground-based systems

11 p1615 A83-27403

Relation of the B sub z component of the interplanetary magnetic field to the generation of the semi-annual wave in Kp-indices

11 p1616 A83-28106

Solar causes of geomagnetic storms during the world retrospective interval 20.3-5.5. 1976

11 p1616 A83-28107

Relation of absorption of radio waves to solar X-rays and to Lyman-alpha radiation at the time of low solar and geomagnetic activity

11 p1616 A83-28110

The shape of the solar corona on 23 October, 1976 and geomagnetic activity

11 p1691 A83-28115

The significance of the long-term pattern of geomagnetic activity for forecasting

11 p1616 A83-28116

The self-focusing of whistler waves

11 p1660 A83-28250

Stability of electron distributions within the earth's bow shock

11 p1617 A83-28307

Three-dimensional current flow and particle precipitation in a westward travelling surge /observed during the barium-GEOS rocket experiment/

11 p1618 A83-28316

Conjugate studies of an isolated equatorial irregularity region

[AD-A127561] 11 p1618 A83-28320

Interpolation and transformations of maps --- French thesis

11 p1601 A83-28632

Determining the polarity of sectors of the interplanetary magnetic field on the basis of variations in the geomagnetic field at high latitudes

11 p1620 A83-28739

Interplanetary magnetic field polarity, the geomagnetic ring current, and the precipitation of particles at middle latitudes

11 p1620 A83-28740

The interplanetary magnetic field and the absorption of radio waves in the auroral zone

11 p1620 A83-28741

The effects of the interplanetary magnetic field in the lower ionosphere at middle latitudes

11 p1620 A83-28742

The physics of slow MHD waves in the ionospheric plasma --- Russian book

12 p1750 A83-28828

Geomagnetic reversal frequency since the Late Cretaceous

12 p1752 A83-29171

Hydromagnetic waves in a differentially rotating sphere --- applied to geomagnetic secular variations

12 p1752 A83-29226

The stabilizing role of differential rotation on hydromagnetic waves --- applied geomagnetic secular variations

12 p1752 A83-29227

Energy estimates for latent-heat driven convection in the earth's core

12 p1753 A83-29238

Direct relations between solar activity and atmospheric circulation, its effect on changes of weather and climate

12 p1758 A83-29405

Auroral oval dynamics in relation to solar wind-magnetosphere interaction

12 p1756 A83-29703

Geomagnetic excursions and climate change

12 p1756 A83-29712

Features of radio-aurora observations at the high-latitude station Mirnyi

13 p1875 A83-30605

N-S radio-aurora forms

13 p1875 A83-30606

Dynamics of sporadic E layers during magnetic disturbances

13 p1875 A83-30610

Dynamics of a charged-particle beam --- injected into ionosphere along geomagnetic field lines

13 p1875 A83-30612

An instrument for DC electric field and AC electric and magnetic field measurements aboard

'INTERCOSMOS-BULGARIA-1300' satellite

13 p1813 A83-30757

Field and wave measurements aboard the Aureol-3 spacecraft

13 p1813 A83-30758

Response of nightside auroral-oval boundaries to the interplanetary magnetic field

13 p1947 A83-31233

Finite parallel wavelengths and ionospheric structuring

13 p1879 A83-31239

On changes in atmospheric circulation after the entry of the earth into a solar corpuscular system

13 p1879 A83-31267

An analysis of several ionospheric parameters associated with the South Atlantic Geomagnetic Anomaly by means of VLF waves

13 p1880 A83-31471

Generation of Alfvén waves in an anomalous resistivity region

13 p1881 A83-31528

Correlation and spectral properties of random potential vector fields --- for analysis of magnetic and gravity anomalies

14 p2050 A83-31874

The drift of barium ion clouds and the electric field over Volgograd

14 p2051 A83-31886

Possible effects of distant field sources in Sq variations

14 p2051 A83-31889

Geomagnetic effects of solar flares in the polar cap

14 p2051 A83-31892

The interaction of magnetic fields at the boundary of the earth's magnetosphere

14 p2052 A83-32534

The generation of small-scale magnetic fields --- by solar wind in earth magnetosphere

14 p2115 A83-32554

Induction in power transmission lines during geomagnetic disturbances

14 p2053 A83-32898

Impacts of solar and auroral storms on power line systems

14 p2053 A83-32899

Results from the Magsat mission

15 p2195 A83-33773

Comment on 'An evaluation of three predictors of geomagnetic activity' by R. E. Holzer and J. A. Slavin

15 p2197 A83-33950

The Indian Ocean gravity low - Evidence for an isostatically uncompensated depression in the upper mantle

15 p2202 A83-34726

Hall current effect on tearing mode instability --- possible cause of magnetic field reconnection in space

15 p2202 A83-34736

Coordinated rocket campaign on Heiss Island --- for upper atmosphere sounding during auroral disturbances

16 p2372 A83-35362

Characteristics of low-latitude whistlers and their relation with f0F2 and magnetic activity

16 p2375 A83-35393

Use of a superconductive magnetic gradiometer near magnetic objects

16 p2354 A83-35449

How continents break up

16 p2377 A83-36020

Investigations of the internal geomagnetic field by means of a global model of the earth's crust

16 p2381 A83-36616

Spectral characteristics of the geomagnetic field associated with the equatorial electrojet and counter-electrojet in the Indian region

16 p2382 A83-36729

Some features of annual variation in the equatorial geomagnetic field

16 p2382 A83-36733

The sector structure of the interplanetary magnetic field and the midlatitude sporadic-E-layer

17 p2537 A83-37054

The Janet/Busch oscillator - A multivibratory dissipative structure relevant to dynamic theories of geomagnetic flux reversals

17 p2537 A83-37082

Depth of the nonconducting layer at the Nigerian dip equator

17 p2537 A83-37578

Electron current disruption and parallel electric fields associated with electrostatic ion cyclotron waves

17 p2538 A83-37582

On the structure of the magnetic slow switch-off shock

17 p2538 A83-37594

Systematics of the equatorward diffuse auroral boundary

17 p2538 A83-37595

A note on the accuracy of the auroral electrojet indices

17 p2539 A83-37604

An estimate of the distances to the outer sources of geomagnetic variations

17 p2539 A83-37700

Wavy patterns of ionospheric electron density profiles triggered by TID - Observation results of the electron density by TAIYO satellite

17 p2540 A83-37825

Induced geomagnetic variation and crustal evolution of the southern peninsula of India

17 p2528 A83-38144

Mapping the earth's magnetic and gravity fields from space Current status and future prospects

17 p2540 A83-38146

Geomagnetic models and the solar cycle effect

17 p2540 A83-38230

Modeling planetary magnetospheres

17 p2542 A83-38299

Geomagnetism of earth's core

17 p2542 A83-38309

Magnetic anomalies --- Magsat studies

17 p2543 A83-38310

Electromagnetic induction studies --- of earth lithosphere and asthenosphere

17 p2543 A83-38311

Lunar modulations of the equatorial electrojet

17 p2544 A83-38373

Dependence of ionospheric drift speed on geomagnetic activity

17 p2495 A83-38544

Physical constraints for the analysis of the geomagnetic secular variation

17 p2546 A83-38695

Sensitivity study of orbital atmospheric density models

17 p2546 A83-38755

Correlation of cosmic-ray intensity with geomagnetic Kp index and solar-magnetic-field reversal

17 p2630 A83-38868

Determination of the cross-section configuration of interplanetary flare MHD-disturbances on a sphere with a radius of 1 AU

18 p2713 A83-39311

The structure of polar cusps according to measurements of the magnetic field in the dayside part of the magnetosphere

18 p2714 A83-39325

Boundaries of the penetration of proton fluxes with energies of 5-90 MeV into the polar caps during geomagnetic disturbances

18 p2714 A83-39330

Magnetic field of a model of a three-dimensional magnetospheric-ionospheric current system on the surface of a nonconducting earth

18 p2714 A83-39338

Variations of the geomagnetic field in the northern polar cap, independent of the interplanetary magnetic field

18 p2714 A83-39339

On the possibility of recovering zone III currents from ground data

18 p2714 A83-39340

DC magnetic field observations on board the AUREOL-3 satellite - The TRAC experiment

18 p2647 A83-39579

Measurements of the VLF electric and magnetic components of waves and DC electric field on board the AUREOL-3 spacecraft The TBF-ONCH experiment

18 p2715 A83-39580

Recent ISEE observations of the magnetopause and low latitude boundary layer - A review

18 p2718 A83-39950

The use of Magsat data to determine secular variation

18 p2719 A83-40323

The relationship of total Birkeland currents to the merging electric field

19 p2865 A83-41126

The existence and planetary character of a jerk in the secular variation of the geomagnetic field in 1912-1913

19 p2866 A83-41324

VLF emissions at low latitudes and geomagnetic activity

19 p2866 A83-41564

15-Myr periodicity in the frequency of geomagnetic reversals since 100 Myr

20 p3015 A83-42169

Two different R-N geomagnetic reversals with identical VGP paths recorded at the same site --- reverse-normal virtual geomagnetic pole

20 p3015 A83-42170

Variations of the geomagnetic field at at Mbour (Senegal) and Bangui (Central Africa) between 1955 and 1981

20 p3017 A83-42314

f0F2 response to IMF sector-boundary crossings

20 p3017 A83-42375

Longitudinal structure of substorm injections at synchronous orbit

20 p3018 A83-42413

The Joule heat production rate and the particle energy injection rate as a function of the geomagnetic indices AE and AL

20 p3019 A83-42420

The response of thermospheric atomic nitrogen to magnetic storms

20 p3019 A83-42425

An empirical relationship between electron temperature and electron density in the subauroral electron-density trough

20 p3022 A83-43133

Geomagnetic and ionospheric disturbances of internal meteorological type - A synergistic approach to disturbances

20 p3022 A83-43134

Solar-cycle variation in the secular magnetic changes at observatories and secular-measurement stations

20 p3022 A83-43136

Non-recurrent geomagnetic disturbances from high-speed streams

20 p3023 A83-43157

Electron precipitation equatorward of the auroral oval and the mantle aurora in the midday sector
20 p3023 A83-43161

On the ring current energy injection rate --- effect of geomagnetic storms
20 p3023 A83-43162

Computer simulation studies of VLF triggered emissions deformation of distribution function by trapping and detrapping --- of resonant electrons in inhomogeneous geomagnetic field
20 p3024 A83-43186

Transfer of pulsation-related wave activity across the magnetopause - Observations of corresponding spectra by ISEE-1 and ISEE-2
20 p3025 A83-43199

Matching long term periodicities of geomagnetic reversals and galactic motions of the solar system
20 p3057 A83-43206

Geomagnetic implications of a simple IMF model
21 p3170 A83-44246

Identification of the discontinuities at the magnetopause
21 p3173 A83-44580

Methods of computation of geomagnetic field at greater altitude in a local region
21 p3173 A83-44585

Computer synthesis of geomagnetic palaeosecular variations
21 p3173 A83-44992

Short-period variations of the rate of change of solar activity as a possible geoefficient parameter
21 p3174 A83-45227

Nonrecurring M-disturbances of the geomagnetic field
21 p3175 A83-45246

A moving source of the secular variations in the geomagnetic field at the boundary between the core and the mantle
21 p3175 A83-45251

The main publications of the annual mean values of the elements of the geomagnetic field of the world network of magnetic observatories
21 p3176 A83-45253

The drift of the Brazilian anomaly
21 p3176 A83-45255

Comparison of an empirical magnetic-field model based on HEOS-1,2 data with an analytical two-dipole model of the magnetosphere
21 p3176 A83-45268

Observations on the magnetically conjugate upper ionosphere of signals from a Soviet midlatitude VLF transmitter
21 p3177 A83-45284

Spatial, spectral, and angular structures of electron fluxes with energies of 30-210 keV at low altitudes during a magnetically quiet period
21 p3245 A83-45288

Dynamics of the earth's core and the geodynamo
22 p3323 A83-45780

The effect of local perturbations of the geomagnetic field on cosmic ray cutoff rigidities at Jungfraujoch and Kiel
22 p3390 A83-46035

Magnetospheric processes preceding the onset of an isolated substorm - A case study of the March 31, 1978, substorm
22 p3326 A83-46039

Equivalent ionospheric current systems representing lunar daily variations of the polar geomagnetic field
22 p3327 A83-46052

Development of the barium shaped charge technique in Japan --- for studying magnetic field configurations in upper atmosphere
22 p3270 A83-46525

Localized plasma depletion in the ionosphere and the equatorial spread F
22 p3334 A83-46888

Earth's magnetic field as a radiator to detect cosmic ray electrons of energy greater than 10 to the 12th eV
22 p3390 A83-47043

The shift of the auroral electron precipitation boundaries in the dawn-dusk sector in association with geomagnetic activity and interplanetary magnetic field
22 p3336 A83-47058

Whistler induced charged particle precipitation and distortion of geomagnetic field
22 p3337 A83-47074

Inferring electric fields and currents from ground magnetometer data - A test with theoretically derived inputs
22 p3337 A83-47077

Comment on 'geomagnetic and solar wind cycles, 1900-1975' by Joan Feynman
22 p3338 A83-47078

The effect of sudden changes of the geomagnetic field on several physiological indicators of healthy humans
23 p3498 A83-47119

The relationships between disappearing solar filaments, coronal mass ejections, and geomagnetic activity
23 p3481 A83-47734

Earth magnetic field fluctuations produced by filamentation instabilities of electromagnetic heater waves
23 p3482 A83-47868

The dependence of the indices of auroral electrojets on the IMF Bz component and on the solar wind velocity
23 p3484 A83-48385

Cyclic variation of solar wind parameters on geomagnetically quiet days
23 p3484 A83-48386

Characteristics of the rhythm of solar, geomagnetic, and atmospheric phenomena and their relation to the earth rotation
23 p3484 A83-48387

Structure of South Atlantic anomaly in maximum of 21st solar cycle by satellite IC-Bulgaria-1300 data
23 p3485 A83-48447

Occurrence probability of solar-geomagnetic-weather relations
24 p3605 A83-49305

Determination of the latitude of Sq focus and its relation to the electrojet variations
24 p3606 A83-49306

GEOMETRIC DILUTION OF PRECISION
Height measurement by quadrilateration
18 p2674 A83-39252

GPS user errors resulting from one 'bad' satellite in the navigation solution
22 p3254 A83-46971

GEOMETRIC RECTIFICATION (IMAGERY)
Using radar image simulation to assess relative geometric distortions inherent in radar imagery
01 p0030 A83-10054

Interpretation of geometric structure from image boundaries
02 p0182 A83-12891

Geometric constraints for interpreting images of common structural elements - Orthogonal trihedral vertices
02 p0182 A83-12898

Some effects on the GCP success rate --- Ground Control Points for satellite image rectification
03 p0349 A83-14285

The need for cross-fertilization between the fields of profile inversion and computed tomography --- in test pattern reconstruction
03 p0329 A83-14291

Coordinate transformation during the geometric correction of the space scanner imagery of the earth
03 p0350 A83-14313

The digital image processing system MOBI-DIVAH
03 p0352 A83-14944

Rectification of Seasat radar on Landsat MSS with the aid of digital image correlation
03 p0352 A83-14946

A geometrical approach to polygonal dissimilarity and shape matching
04 p0528 A83-16033

Geometric rectification of radar imagery using digital elevation models
07 p0952 A83-21431

The geometric correction of Landsat-type imagery using perturbation techniques
15 p2183 A83-33689

The classification of forest species types using gradient analysis and spectral data
17 p2531 A83-38340

Geometric constraints in multispectral scanner data
17 p2532 A83-38361

Preprocessing of side-looking airborne radar data
20 p2990 A83-42968

Production and analysis of output data products for Landsat-4 in the engineering check-out phase
[AAS PAPER 83-158] 20 p3011 A83-43762

Comparative study of data acquired by various types of remote sensors
22 p3308 A83-46120

Geometric registration and rectification of spaceborne SAR imagery
22 p3290 A83-46213

Image restoration by convex projections in the presence of noise
22 p3294 A83-46828

The computer-aided matching and geometric alignment of images
24 p3582 A83-49045

Saturn's pole - geometric correction based on voyager UVS and radio occultations
24 p3673 A83-49890

GEOMETRICAL ACUSTICS
Weak and short waves in inhomogeneous isotropic elastic materials. I
08 p1160 A83-22227

Ray-theory and mode-theory predictions of intake-liner performance - A comparison with engine measurements [AIAA PAPER 83-0711]
10 p1475 A83-25927

Propagation of shock waves through nonuniform and random media
10 p1416 A83-26163

Modeling of long-range acoustic transmissions through cyclonic and anticyclonic eddies
[AD-A129125] 14 p2081 A83-33023

Intensity of focused sonic booms in straight flight at constant altitude
18 p2742 A83-39424

Relation between the actual and nominal boundaries of an extended defect in ultrasonic examination of a thick sheet
22 p3303 A83-46326

Weakly nonlinear high frequency waves
22 p3354 A83-47091

GEOMETRICAL HYDROMAGNETICS
U MAGNETOHYDRODYNAMICS

GEOMETRICAL OPTICS
Waveguide-type solutions for light beams with nonlocal self-defocusing in the geometric-optics approximation
01 p0054 A83-10816

Light transmission optics /2nd edition/ --- Book
01 p0106 A83-10879

Holographic HUDs de-mystified
01 p0010 A83-11171

Image quality and lens aberrations of an aerial camera
02 p0177 A83-11989

Optical analysis of solar energy tubular absorbers
02 p0202 A83-12596

Optical components and systems for synchrotron radiation - An introduction
02 p0237 A83-12692

Phase-space performances of optimized and conventional synchrotron radiation grazing incidence mirrors
02 p0237 A83-12696

Traditions of optical fabrication
02 p0237 A83-12697

Analysis of the throughput of a grazing incidence monochromator using transmission gratings
02 p0239 A83-12714

Transport of solar energy with optical fibres
03 p0354 A83-13698

A hybrid MM-geometrical optics technique for the treatment of wire antennas mounted on a curved surface
03 p0307 A83-14037

A simple model for relative air mass
03 p0370 A83-14644

Plane-wave scattering by bodies of revolution with absorbing coatings
04 p0466 A83-15728

The controlled non-linear evolution of TE and TH ps-pulses in Selfoc fibre
04 p0535 A83-15791

Dual offset reflectors shaped for zero crosspolarisation with asymmetric feed pattern
04 p0468 A83-16204

Geometrical optical characteristics of the Schwarzschild scanning antenna - Comparison with the Cassegrain antenna
04 p0468 A83-16205

A vector approach to numerical computation of view factors and application to space heating --- for spacecraft
[AIAA PAPER 83-0157] 05 p0606 A83-16561

Approximate method for calculations of unstable telescopic resonators --- carbon dioxide gasdynamic laser design
05 p0649 A83-17061

A ray theory of three-dimensional photoelasticity
05 p0683 A83-17848

Offset dual reflector synthesis as a boundary-value problem
06 p0743 A83-18684

Breakdown wave in the self-consistent field of an electromagnetic wave beam
07 p0995 A83-20061

A general diffraction theory - A new approach
08 p1164 A83-22469

Radiation characteristics of tapered slab waveguides
08 p1166 A83-22674

The development of numerical methods for solving the radiative transfer equation
09 p1340 A83-25258

Integral representation for geometric optics solutions --- of field autocorrelation functions and diffusion tensors for nonuniform plasmas
10 p1485 A83-25786

Interferometry with the multiple mirror telescope and conventional telescopes
10 p1495 A83-25845

Steady-state point-source excitation of a laminated composite
10 p1441 A83-26442

Improved simulation of ground reflections --- of radio navigation signals for flight control
10 p1374 A83-26486

Design of antireflection coatings for textured silicon solar cells
11 p1612 A83-27983

Refraction and absorption in plasma atmospheres
13 p1927 A83-31573

Performance of the spectropolarimeter for the Space Telescope faint object spectrograph
14 p2096 A83-32010

On the nonlinear aberrations with self-deflection of a light beam in a moving medium
14 p2025 A83-33397

Anisotropic propagation of magnetogasdynamic sonic waves in conducting and radiating atmosphere
15 p2235 A83-34546

The properties of focused fields --- for optical beams
15 p2147 A83-35152

Collection efficiency of a spectrograph for distributed sources
16 p2357 A83-36762

Possible optical scheme of a telescope with a main spherical mirror with a diameter of 20-25 m
17 p2590 A83-37690

Invariant curves of point mappings and natural oscillations of open resonators
17 p2499 A83-38479

Diffraction on a segmented telescope mirror
17 p2580 A83-38567

The method of complex rays --- extended to antenna electromagnetic fields
19 p2894 A83-40797

A spectral approach to the physical theory of diffraction
19 p2894 A83-40798

New technique for the evaluation of the scattering cross-sections of radar corner reflectors
20 p2963 A83-42364

Approximating point-set images by line segments using a variation of the Hough transform
21 p3190 A83-44271

Wave refraction in an isotropic medium with anisotropic inhomogeneities
21 p3200 A83-45260

Complex geometrical optics for the study of reflector antennas
21 p3121 A83-45409

Fields of wide-aperture resonators formed by plane mirrors
22 p3294 A83-45653

Effects of a rough boundary surface on polarization of the scattered field from an inhomogeneous medium
22 p3314 A83-46231

Short waves on long waves --- spatial changes of gravity waves
22 p3344 A83-46912

Directionality of the radiation of a misaligned cavity with a lens-like medium
23 p3460 A83-47166

A model of the random phase screen in the problem of the thermal self-defocusing of light 23 p3462 A83-48090

Factorization of the transfer matrix for symmetrical optical systems 24 p3628 A83-48980

Matrix decompositions for nonsymmetrical optical systems 24 p3629 A83-48981

Light scattering by randomly oriented cubes and parallelepipeds --- for interpretation of observed data from planetary atmospheres 24 p3671 A83-49009

Radiation from a rough surface and its polarization properties. I - Method of calculation 24 p3623 A83-49118

Applied optics (2nd revised edition) --- Russian book 24 p3629 A83-49411

GEOMETRICAL THEORY OF DIFFRACTION

Stability of an economical difference scheme for the solution of a boundary value problem of diffraction 01 p0104 A83-11271

A hybrid diffraction technique - General theory and applications 01 p0104 A83-11357

Geometrical theory of dispersion distortions of signals with limited spectrum 02 p0163 A83-11685

A note on some common diffraction link loss models 02 p0165 A83-12628

An attenuation function for multiple knife-edge diffraction --- of electromagnetic waves in communication systems 02 p0165 A83-12629

An evaluation of Longley-Rice and GTD propagation models 03 p0305 A83-14009

Inversion of scattering data of the shadow region of discontinuities 04 p0492 A83-15205

Criteria of applicability for the geometrical theory of diffraction 04 p0531 A83-15763

High frequency scattering by a thin dielectric slab 06 p0737 A83-18611

The analysis of a flat plate twist reflector Cassegrain aerial using GTD 06 p0715 A83-18646

An asymptotic high frequency analysis of the radiation from sources on perfectly-conducting structures with an impedance surface patch 06 p0715 A83-18647

Diffraction from cylindrically truncated planar surfaces with application to an aperture matched horn design 06 p0742 A83-18666

Radiation patterns of a quarter-wave monopole on a finite ground plane --- for aircraft antennas 06 p0715 A83-18682

GTD analysis of reflector antennas with general rim shapes 06 p0743 A83-18690

Pattern prediction for a focused reflector antenna using GTD and near-field to far-field transformations 06 p0744 A83-18691

Phase aberrations and laser output beam quality 08 p1108 A83-22450

A general diffraction theory - A new approach 08 p1164 A83-22469

The radiation of a horn antenna 08 p1078 A83-23152

A geometrical theory for the resonant frequencies and Q-factors of some triangular microstrip patch antennas 09 p1246 A83-23778

High frequency scattering by a thin lossless dielectric slab 09 p1247 A83-23790

On the collimation phase error computation of a space-fed planar phased array 09 p1247 A83-23797

Application of the Braunkel method to the Maggi-Rubinowicz field representation --- asymptotic evaluation of surface integral representations of optical diffraction by apertures 09 p1338 A83-24090

A GTD study of pyramidal horns for offset reflector antenna applications 10 p1406 A83-26837

Barrier insertion loss versus Fresnel number and secondary parameters 11 p1652 A83-28187

On a method of the asymptotic theory of diffraction 14 p2079 A83-32104

Diffraction by the secondary reflector of a Cassegrain antenna of revolution 19 p2825 A83-40795

The method of complex rays --- extended to antenna electromagnetic fields 19 p2894 A83-40797

A spectral approach to the physical theory of diffraction 19 p2894 A83-40798

Coupling between two conical horns placed side by side 20 p2963 A83-42368

Fraunhofer diffraction by ice crystals suspended in the atmosphere 20 p3028 A83-43465

Ray methods for waves in elastic solids with applications to scattering by cracks --- Book 21 p3160 A83-45139

High-frequency scattering from the edges of impedance discontinuities on a flat plane 23 p3442 A83-47830

The finite ground plane effect on the microstrip antenna radiation patterns 23 p3443 A83-47839

Possible generalization of the Kirchhoff approximation in problems of wave diffraction by transparent inhomogeneous objects 23 p3504 A83-48484

Simple formula for the RCS of a finite hollow circular cylinder 24 p3571 A83-49994

GEOMETRODYNAMICS

U RELATIVITY

GEOMETRY

NT ANALYTIC GEOMETRY

NT ANGLE OF ATTACK

NT ANGLES (GEOMETRY)

NT BRAGG ANGLE

NT CARTESIAN COORDINATES

NT CHORDS (GEOMETRY)

NT COLLINEARITY

NT CONICS

NT CRACK GEOMETRY

NT CURVATURE

NT CURVES (GEOMETRY)

NT CUSPS (MATHEMATICS)

NT DESCRIPTIVE GEOMETRY

NT DIFFERENTIAL GEOMETRY

NT DUCT GEOMETRY

NT ELEVATION ANGLE

NT EUCLIDEAN GEOMETRY

NT FIXED POINTS (MATHEMATICS)

NT FLOW GEOMETRY

NT GEODESIC LINES

NT GREAT CIRCLES

NT HEXAGONS

NT HOMOTOPY THEORY

NT IMBEDDINGS (MATHEMATICS)

NT INVARIANT IMBEDDINGS

NT LEADING EDGE SWEEP

NT LIE GROUPS

NT LINES (GEOMETRY)

NT LOCI

NT LOOK ANGLES (TRACKING)

NT METRIC SPACE

NT NOZZLE GEOMETRY

NT OBLATE SPHEROIDS

NT PARABOLAS

NT PARALLELEPIPEDS

NT POINTS (MATHEMATICS)

NT POLYGONS

NT POLYHEDRONS

NT PROJECTIVE GEOMETRY

NT PROLATE SPHEROIDS

NT PYRAMIDS

NT RADII

NT RIEMANN MANIFOLD

NT SPECIMEN GEOMETRY

NT SPHEROIDS

NT SPINOR GROUPS

NT SQUARES (MATHEMATICS)

NT SWEEP ANGLE

NT TANK GEOMETRY

NT TENSOR ANALYSIS

NT TETRAGONS

NT TOPOLOGY

NT TORUSES

NT TRAPEZOIDS

NT TRIANGLES

NT TRIGONOMETRY

NT VECTOR ANALYSIS

NT VORTICITY

A geometric approach to stabilization by output feedback 06 p0804 A83-19390

The value distribution of holomorphic maps --- Russian book 12 p1774 A83-29336

A parallel algorithm for determining convex hulls of sets of points in two dimensions 15 p2218 A83-35115

Computational topology - A study of topological manipulations and interrogations in computer graphics and geometric modeling 18 p2740 A83-40339

GEOMORPHOLOGY

Drumlin fields and glaciated mountains - A contrast in geomorphic perception from Seasat radar images 01 p0064 A83-10078

Imaging radar observations of volcanic features in Medicine Lake Highland, California 01 p0064 A83-10079

Morphometric consistency with the Hausdorff-Besicovich dimension 02 p0203 A83-11844

Application of Landsat imagery to flood control and management of agricultural land - A case study of northern India 03 p0345 A83-14233

Tharsis volcanoes - Separation distances, relative ages, sizes, morphologies, and depths of burial 04 p0565 A83-15560

Craters and basins on Ganymede and Callisto - Morphological indicators of crustal evolution 04 p0570 A83-16237

The geology of Europa 04 p0571 A83-16239

The geology of Io 04 p0571 A83-16240

Hot spots of Io 04 p0571 A83-16244

The bilateral symmetry of circular impact structures - of astrophysics 05 p0706 A83-17473

Super high altitude photography for coastal geomorphology --- from approximately 20 km altitude 05 p0657 A83-17840

Geomorphological mapping using Landsat imagery - A case study in Argentina 05 p0657 A83-17841

Some comparative aspects of SLAR and airphoto images for geomorphologic and geologic interpretation 05 p0657 A83-17842

New morphostructural data obtained from the interpretation of space images of the BAM region 07 p0950 A83-19906

The utilization of SLAR and the Landsat satellites in geomorpho-pedological surveys performed in the Venezuelan Amazon - Methodology and initial results 08 p1126 A83-21924

Comparison of Landsat and SPOT spectral signatures for the case of sandstone outcrops of the Bandiagara Plateau of Mali 08 p1127 A83-21944

Structural geomorphology of Rajasthan basin, India-interpreted through Landsat imagery and aerial photos 09 p1291 A83-24626

Comment on 'A schematic model of crater modification by gravity' by H. J. Melosh 09 p1367 A83-25075

Classification of arid geomorphic surfaces using Landsat spectral and textural features 10 p1443 A83-25968

The possibility of using space photographs to study the dynamics of tectonic processes /Using the example of the Turan plate/ 10 p1443 A83-26801

Structural-geomorphological interpretation of lineaments revealed from space photographs in the north of the European part of the USSR 10 p1443 A83-26802

Analysis of the panoramas of the Venera 13 and Venera 14 landing sites 12 p1798 A83-29484

The internal structure of the earth and its concentric faults 13 p1880 A83-31348

Transition zones between the continents and the oceans --- Russian book 15 p2200 A83-34375

Glacial geologic interpretation of southeastern Wisconsin through diazo enhancement of Landsat multispectral imagery 15 p2186 A83-34839

Examples of sequential radar images from Washington, Arizona and Alaska 15 p2187 A83-34842

Bouguer gravity profiles across the highland-lowland escarpment on Mars 16 p2439 A83-36784

The morphometric index - The profile characteristic of a crater in the process of denudation 17 p2615 A83-37016

The NOAA satellites - A largely neglected tool in the land sciences 17 p2529 A83-38154

A megastructural end to Geologic Time 18 p2754 A83-39607

The use of space imagery to subdivide the structure of swamp masses 18 p2706 A83-40589

Venus - Identification of banded terrain in the mountains of Ishtar Terra 19 p2922 A83-40912

Geological-morphological analysis of Venera 13 and 14 panoramas 19 p2922 A83-41231

Morphological volcanology --- Russian book 21 p3165 A83-45001

Interpretation of Landsat imagery - A case study of lineations in a part of north-western Himalaya, India 22 p3309 A83-46134

Desertification in Kaokoland (northern South West Africa/Namibia) - Field evidence, recognition in satellite imagery, mapping of spatial distribution by satellite image interpretation (Landsat 1) 22 p3309 A83-46135

A complex selective key to identify genetic relief forms on satellite images /for education and training in geomorphological interpretation/ 22 p3313 A83-46216

GEON (TRADEMARK)

U POLYVINYL CHLORIDE

GEOPHYSICAL FLUIDS

Geophysical fluid dynamics --- Book 05 p0640 A83-17650

Development of a turbulence closure model for geophysical fluid problems 17 p2507 A83-38227

Heat transfer mechanism in a thermally stratified turbulent flow 20 p2973 A83-42688

The earth's core 20 p3020 A83-42816

GEOPHYSICAL OBSERVATORIES

NT OSO-8

NT POGO

Remote ground-based observations of terrestrial airglow emissions and thermospheric dynamics at Calgary, Alberta, Canada 08 p1135 A83-22360

The main publications of the annual mean values of the elements of the geomagnetic field of the world network of magnetic observatories 21 p3176 A83-45253

GEOPHYSICAL SATELLITES

NT EXPLORER 12 SATELLITE

NT INTERCOSMOS SATELLITES

NT OSO-8

NT POGO

- Optical tracking of synchronous earth's satellites for geophysical purposes 07 p0958 A83-19874
Field and wave measurements aboard the Aureol-3 spacecraft 13 p1813 A83-30758
Choosing artificial satellites for studies of the earth's rotation on the basis of optical detection and ranging data 14 p2048 A83-31838

GEOPHYSICS

- International Geoscience and Remote Sensing Symposium, Washington, DC, June 8-10, 1981, Digest. Volumes 1 & 2 01 p0061 A83-10001
Passive microwave remote sensing for meteorology 01 p0073 A83-10015
Geophysical inversion and remote probing are inverse scattering problems 01 p0048 A83-10110
Handbook of physics. Volume 49 - Geophysics III. Part 6 --- Book 02 p0206 A83-12151
The thermal physics of glaciers --- Russian book 05 p0657 A83-17132
The fundamental precision limit of optical gyros 06 p0763 A83-19142
Continental rifting and the implications for plate tectonic reconstructions 07 p0961 A83-20228
Paleomagnetism --- Russian book 07 p0962 A83-20387
The interpretation of the major non-hydrostatic anomalies of the earth 07 p0963 A83-20974
Polar auroras. Number 30 - Complex investigations of the dynamics of polar auroras --- Russian book 07 p0964 A83-21176
The relationship between surface topography, gravity anomalies, and temperature structure of convection 08 p1135 A83-22365
Continental lithospheric thickness and deglaciation induced true polar wander 09 p1305 A83-24337
Mathematical models in geophysics 09 p1309 A83-25242
The physical geography of the world's oceans --- Russian book 10 p1452 A83-25598
Progress in solar-terrestrial physics; Proceedings of the Fifth International Symposium, Ottawa, Canada, May 17-22, 1982. Parts 1-7 11 p1686 A83-27376
On the theory of electromagnetic induction in the earth by ocean currents 12 p1757 A83-29963
An objective procedure for detecting and correcting errors in geophysical data. II - Multidimensional applications 13 p1877 A83-30897
A two step linear statistical technique using leaps and bounds procedure for retrieval of geophysical parameters from microwave radiometric data 15 p2194 A83-33692
A nonorthogonal spectral analysis of time series --- in geophysics 15 p2200 A83-34421
Electromagnetic scattering from subterranean obstacles in a stratified ground 16 p2341 A83-35409
Synthesis of geophysical data with space-acquired imagery - A review 17 p2540 A83-38147
Random fluctuations, persistence, and quasi-persistence in geophysical and cosmical periodicities - A sequel 17 p2525 A83-38231
Dynamic compression of diopside and salite to 200 GPa --- in earth's mantle 19 p2864 A83-41109
Errors in the referencing of geophysical fields by astronomical methods 19 p2867 A83-42019
The spectral matrix, eigenvalues, and principal components in the analysis of multichannel geophysical data 21 p3119 A83-44230
Evolution of the earth 22 p3322 A83-45776
Electrical conduction in mantle materials 22 p3324 A83-45798
Reviews of space science - Legacy of the IGY 24 p3597 A83-48893
Determination of the geocentric gravitational constant from satellite observations 24 p3604 A83-48933
- GEOPOTENTIAL**
NT **GEOPOTENTIAL HEIGHT**
Evaluation of 15th-order harmonics in the geopotential from analysis of resonant orbits 04 p0509 A83-15451
Derivation of the harmonic coefficients C21 and S21 using parameters of the secular motion of the earth's poles 04 p0514 A83-16381
Expansion of planetary gravitational potential in a system of fundamental solutions of the Laplace equation 04 p0514 A83-16383
Allowance for the influence of geopotential in the high-precision numerical integration of artificial-earth-satellite orbits 04 p0453 A83-16385
The climatology of the geopotential of the 500 mb surface of the northern hemisphere as obtained by natural orthogonal functions in the wave number region 06 p0793 A83-19249
Optical tracking of synchronous earth's satellites for geophysical purposes 07 p0958 A83-19874
Deformation, gravity, and potential changes due to volcanic loading of the crust 07 p0961 A83-20231

- Algorithmization of computations in a discretely observed gravitational field 07 p0962 A83-20602
On one type of system with equivalent external gravity effects 07 p0962 A83-20603
The mean annual variation of the geopotential of the 500 mb surface for the Northern Hemisphere in wavenumber space 09 p1313 A83-24120
Motion of an earth satellite. II - Nonlinear perturbations 11 p1532 A83-28034
The effect of resonance perturbations from a planet's gravitational field on the motion of a satellite 11 p1532 A83-28041
The use of the geopotential model in the orbital method of the coordinate determination of stations 11 p1616 A83-28050
A method for studying temperature fields during stratospheric warmings 11 p1633 A83-28206
Accuracy of the earth's gravity field models 12 p1752 A83-29221
The global stress field in the lithosphere obtained from the satellite gravitational harmonics 12 p1752 A83-29222
Interpolation with respect to the vertical of the relative geopotential and temperature 13 p1884 A83-30293
Statistical analysis and wavenumber-frequency spectra of the 500 mb geopotential along 50 deg S 16 p2387 A83-35493
The influence of errors in determining the geopotential on the determination of a satellite orbit 16 p2313 A83-35501
The earth-moon tidal force function 16 p2426 A83-36783
Status of the geopotential --- earth gravity measurement 17 p2542 A83-38303
Satellite orbit perturbations due to the deforming potential of centrifugal forces 18 p2645 A83-39977
Directions of axes of the earth's ellipsoid of inertia derived from satellite orbit dynamics 19 p2860 A83-41317
A planetary density model and the normal gravitational field of the earth 19 p2866 A83-41475
Collocations and thirtieth order resonant harmonics --- for determining earth's gravitational field 20 p3023 A83-43153
Distribution of deviations of geopotential from standard-atmosphere values above the Northern Hemisphere 23 p3486 A83-47134
Orbital rates of earth satellites at resonances to test the accuracy of earth gravity field models 24 p3550 A83-48768
- GEOPOTENTIAL HEIGHT**
Concerning the calculation of geodetic heights 01 p0072 A83-10852
Allowance for near and far zones in the calculation of geoid heights and plumbline deviations 01 p0072 A83-10853
Algorithm for computing the first- and second-order partial derivatives of geopotential on the basis of artificial-earth-satellite coordinates 05 p0664 A83-17680
The existence of teleconnections in the geopotential field of the Northern Hemisphere 09 p1315 A83-24942
On the nonlinear versus linearized lower boundary conditions for topographically forced stationary long waves 10 p1450 A83-25384
Autocorrelation of Northern Hemisphere geopotential heights 10 p1450 A83-25388
Satellite-in situ measurement intercomparisons at Wallops Island, Virginia --- comparative atmospheric sounding 12 p1760 A83-29688
A numerical study of the divergence of spherical harmonic series of the gravity and height anomalies at the earth's surface 14 p2051 A83-31899
Three-dimensional teleconnections in the zonally asymmetric height field during the Northern Hemisphere winter 16 p2390 A83-36490
An analysis of geopotential height at 300 mbar in the frequency wavenumber domain along 50 deg N in observed and modelled January climate 16 p2391 A83-36584
On single station forecasting - The geopotential height, its vertical and times structure and 500 mbar ARMA prediction 16 p2391 A83-36586
The accuracy of the low-degree geopotential - Implications for ocean dynamics 16 p2393 A83-36600
Satellite altimetry determination of differences between mean sea-level heights and testing geopotential models 17 p2525 A83-38145
Space-time spectral analyses of Northern Hemisphere geopotential heights 18 p2728 A83-40028
Some singularities and irregularities in the seasonal progression of the 700 mb height field 22 p3338 A83-45702

- Interannual variability and predictability of 500 mb geopotential heights over the Northern Hemisphere 23 p3489 A83-47400
The influence of the tropics on the prediction of ultralong waves. I - Tropical wind field 23 p3490 A83-47405
Supra-annual variations of geopotential heights in the subtropical stratosphere 24 p3609 A83-48814

GEORGIA

- Distribution of Georgia tektites 03 p0435 A83-14322

GEOS SATELLITES (ESA)

- The use of satellite information in weather forecasting at the Pacific Weather Centre 03 p0364 A83-14277
Diurnal radiation budget - Four months assembled into an annual mean 03 p0370 A83-14646
Remote control of satellites and applied automation 10 p1382 A83-26597
Software for automatic control of spacecraft instruments 10 p1382 A83-26598
Parametric study of intersatellite CO2 laser data links 11 p1535 A83-27605
Observations of quasistatic electric fields on the GEOS and ISEE satellites 11 p1621 A83-28770
Software for the closed loop control of experiments on the GEOS spacecraft 17 p2472 A83-37483

GEOS SATELLITES (ESRO)**U GEOS SATELLITES (ESA)****GEOS 1 SATELLITE**

- The availability of GEOS data for IMS research 04 p0511 A83-16282
Observations on the GEOS 1 satellite of whistler mode signals transmitted by the Omega navigation system transmitter in northern Norway 13 p1878 A83-31234

GEOS 2 SATELLITE

- Stare and GEOS 2 observations of a storm time Pc 5 ULF pulsation 02 p0208 A83-12387
The availability of GEOS data for IMS research 04 p0511 A83-16282
Conjugate observations of Pc 5 electric fields with a geostationary satellite and a ground radar facility 17 p2538 A83-37596

GEOS 3 SATELLITE

- Global mean sea surface computation using GEOS 3 altimeter data 07 p0971 A83-20238
Southern Hemisphere western boundary current variability revealed by GEOS 3 altimeter 07 p0971 A83-20545
The sea state correction for Geos 3 and Seasat satellite altimeter data 09 p1318 A83-24293

GEOS-B SATELLITE**U GEOS 2 SATELLITE****GEOS-C SATELLITE****U GEOS 3 SATELLITE****GEOSTATIONARY OPERATIONAL ENVIRON SATS****U GOES SATELLITES****GEOSTATIONARY PLATFORMS****U SYNCHRONOUS PLATFORMS****GEOSTATIONARY SATELLITES****U SYNCHRONOUS SATELLITES****GEOSTROPHIC WIND**

- Some features of the spatial structure of the Arctic Ocean ice cover in connection with turbulent friction and geostrophic capture of tide waves 01 p0077 A83-10833
Predictability of quasi-geostrophic planetary waves in global and hemispheric domains 03 p0366 A83-14417
Baroclinic nonlinear exchanges of energy and potential enstrophy in the quasi-geostrophic two-layer model 03 p0369 A83-14520
Analysis of the diurnal oscillation of surface geostrophic wind over Western Europe 04 p0516 A83-15855
Wave-interactions in quasi-geostrophic uniform potential vorticity flow 04 p0516 A83-15927
A study of the adequacy of quasi-geostrophic dynamics for modeling the effect of cyclone waves on the larger scale flow 04 p0516 A83-15929
Forced, stationary waves in a linear, stratified, quasi-geostrophic atmosphere 04 p0516 A83-15930
A modulated point-vortex model for geostrophic, beta-plane dynamics [AD-A126704] 05 p0639 A83-17355
Airborne radar altimeter measurements of geostrophic and ageostrophic winds over irregular topography 05 p0668 A83-17447
Momentum balance of gravity flows 06 p0789 A83-18255
Synoptic-scale vertical motion computed by the quasi-geostrophic omega-equation 06 p0793 A83-19250
The use of GATE data for the analysis of polar wind 07 p0970 A83-20894
Numerical simulation of nonlinear jet streak adjustment 08 p1140 A83-22300

On the predictability of quasi-geostrophic flow - The effects of beta and baroclinicity 08 p1142 A83-23002

A conservation law for small-amplitude quasi-geostrophic disturbances on a zonally asymmetric basic flow 08 p1142 A83-23007

The structure of an atmospheric warm front and its interaction with the boundary layer 09 p1310 A83-23355

Objective wind forecast on the basis of geostrophic wind 09 p1314 A83-24122

A hemispheric barotropic quasi-geostrophic model of the atmosphere with conservation of the degrees of potential vorticity 09 p1315 A83-24934

Linear non-divergent mass-wind laws on the sphere 11 p1633 A83-28080

The dynamic response of the high-latitude thermosphere and geostrophic adjustment 11 p1618 A83-28318

Satellite-in situ measurement intercomparisons at Wallops Island, Virginia --- comparative atmospheric sounding 12 p1760 A83-29688

The dynamics of singular geostrophic vortices in a two-level model of the atmosphere (ocean) 13 p1873 A83-30026

Forecasting foehn winds at Anchorage, Alaska 13 p1888 A83-30566

Prospects for prediction of zonal wind oscillations 13 p1889 A83-30575

Ageostrophic winds and vertical motion fields accompanying upper level jet streak propagation during the Red River Valley tornado outbreak 13 p1890 A83-30587

Distribution of Antarctic Intermediate Water over the Blake Plateau 14 p2061 A83-33087

A conception of normal mode expansion procedure applied to a limited-area model. II - Linear aspects. III - Derivation and theoretical discussion of a nonlinear approach --- of geostrophic balance 15 p2207 A83-35096

Effects of baroclinicity on resistance laws for the atmospheric boundary layer over a slightly inclined terrain 16 p2385 A83-35469

Statistical analysis and wavenumber-frequency spectra of the 500 mb geopotential along 50 deg S 16 p2387 A83-35493

Energy equation of non-equilibrium states in the earth's atmosphere 19 p2867 A83-41319

The establishment of hydrostatic and quasi-geostrophic balance in synoptic-scale disturbances in a polytropic turbulent atmosphere 19 p2867 A83-41581

A rotary-spectrum analysis of the horizontal flow over central Europe 21 p3181 A83-45404

On the relevance of two-dimensional turbulence to geophysical fluid motions 23 p3448 A83-48041

Dimension measurements for geostrophic turbulence 24 p3609 A83-49294

GEOSYNCHRONOUS ORBITS

Orbital ring systems and Jacob's ladders. I 01 p0016 A83-10702

Earth based synchronization for navigation satellite constellations 01 p0019 A83-11091

The crowded sky 02 p0137 A83-12643

The Los Alamos synchronous orbit data set 04 p0511 A83-16285

Poisson series solution of geosynchronous drift [AIAA PAPER 83-0016] 05 p0601 A83-16465

A split delta-V technique for drift control of geosynchronous spacecraft 05 p0601 A83-16466

Observations of field-aligned energetic electron and ion distributions near the magnetopause at geosynchronous orbit 05 p0660 A83-17389

A portable program package for geostationary orbit control 05 p0679 A83-17433

The Quad aperture /hoop/column/ antenna for advanced communications missions in the 1990's 06 p0738 A83-18621

Orbit utilization - Current regulations 07 p0910 A83-19759

Conservation of the geostationary spectrum 07 p0910 A83-19760

Geostationary communications satellite orbit utilization strategies for the 1980s 07 p0910 A83-19761

Optical tracking of synchronous earth's satellites for geophysical purposes 07 p0958 A83-19874

Is occupation an appropriation - The status of a commercial facility in geosynchronous orbit 07 p1003 A83-21620

Military manoeuvres in synchronous orbit 07 p0868 A83-21622

Cost-efficient transport of loads in geostationary orbit and in near-earth circular orbits [DGLR PAPER 82-077] 09 p1211 A83-24191

Deployment of a long-tethered connection between two bodies in orbit 09 p1212 A83-25042

Geostationary satellite orbital geometry and coverage area variations due to the attitude control errors 10 p1380 A83-25504

Synchronous orbit performance of Hughes Aircraft Company solar arrays - Update 11 p1541 A83-27252

The MAGE family of European solid-propellant apogee boost motors --- for geostationary orbit transfer 11 p1542 A83-27369

On the propagation and control of geosynchronous orbits 13 p1809 A83-29996

Time-optimized north-south stationkeeping 13 p1809 A83-30172

Monitoring of the location of the magnetospheric ring current by means of synchronous magnetic-field measurements in geostationary orbit and on the earth's surface 14 p2051 A83-31890

Alpha-s/epsilon-H measurements of thermal control coatings over four years at geosynchronous altitude --- ratio of solar absorptance to infrared hemispherical emittance 15 p2127 A83-34909

[AIAA PAPER 83-1450] 15 p2127 A83-34909

Avoiding the Van Allen belt in low-thrust transfer to geosynchronous orbit 16 p2314 A83-36047

[AIAA PAPER 83-0195] 16 p2314 A83-36047

Propulsion system tradeoff studies for geosynchronous satellites 16 p2319 A83-36288

[AIAA PAPER 83-1218] 16 p2319 A83-36288

A comparison between advanced chemical and MPD propulsion for geocentric missions [AIAA PAPER 83-1391] 16 p2322 A83-36381

Digital control loops for TELECOM 1 AOCs --- Altitude and Orbit Control System 17 p2477 A83-37440

Geosynchronous satellite list - 1983 18 p2644 A83-39973

A high-precision phase-comparison experiment using a geostationary satellite 19 p2826 A83-41028

Orbit utilization in the US Broadcast Satellite Service 19 p2829 A83-41350

India's domestic satellite communication system - INSAT 19 p2831 A83-41379

Drift boundaries and ULF wave generation near noon at geostationary orbit 20 p3025 A83-43194

Lateral drift compensation for satellites in non-equatorial synchronous orbits through attitude control 21 p3099 A83-44017

Operational aspects of the injection of spacecraft into geostationary orbit 21 p3095 A83-44042

Tracking geosynchronous satellites by very-long-baseline interferometry 21 p3098 A83-45468

Geostationary junk - Problem for the future 22 p3256 A83-45723

The international politics of the orbit-spectrum issue --- concerning communication satellites 22 p3367 A83-45809

The legal status of the geostationary orbit 22 p3368 A83-45814

Communication satellites in the geostationary orbit --- Book 22 p3274 A83-45911

Development of substorm activity in multiple-onset substorms at synchronous orbit 22 p3326 A83-46038

Satellite observations of Pi 2 activity at synchronous orbit 22 p3326 A83-46040

Synthetic aperture radar imaging from an inclined geosynchronous orbit 22 p3315 A83-46238

Orbital debris management - International cooperation for the control of a growing safety hazard 23 p3415 A83-47324

[IAF PAPER 83-254] 23 p3415 A83-47324

Summary of environmentally induced electrical discharges on the P78-2 (SCATHA) satellite 23 p3423 A83-48127

Improved estimate of the channel capacity of the geostationary orbit 23 p3444 A83-48516

GEOSYNCLINES

Tectonic zonality in early Precambrian formations in southern Siberia 13 p1880 A83-31340

GEOTECHNICAL ENGINEERING

Terrain analysis for geotechnical engineering studies related to a part of Chandrapur district, Maharashtra - India 09 p1290 A83-24604

GEOTEMPERATURE

Modes of mantle convection and the removal of heat from the earth's interior 02 p0212 A83-12872

A kinematic thermal history of the earth's mantle 02 p0212 A83-13101

Comparison between the hot spot and geomagnetic field reference frames 04 p0508 A83-14957

The ilmenite/titano-magnetite assemblage - Kinetics of re-equilibration 04 p0509 A83-15305

On the thermal state of the earth's mantle 20 p3017 A83-42373

Destabilization of a 650 km chemical boundary layer and its bearing on the evolution of the continental crust 21 p3171 A83-44363

Regional geothermal exploration in Egypt 21 p3165 A83-44599

Temperature profiles in the earth 22 p3323 A83-45777

Terrestrial heat flow history and temperature profiles 22 p3324 A83-45795

Initial state of the earth and its early evolution 22 p3324 A83-45797

Cooling of the earth - A constraint on paleotectonic hypotheses 22 p3325 A83-45800

The minimum mantle viscosity of an accreting earth 23 p3529 A83-47856

GEOTHERMAL ENERGY CONVERSION

Gaseous fuel generation by magma-thermal conversion of biomass 13 p1870 A83-30196

GEOTHERMAL ENERGY UTILIZATION

The economical utilization of geothermal energy --- German thesis 17 p2535 A83-37505

GEOTHERMAL RESOURCES

NT VOLCANCES

A groundwater convection model for Rio Grande rift geothermal resources 02 p0203 A83-11831

Radar and infrared remote sensing of geothermal features at Pilgrim Springs, Alaska 02 p0198 A83-12036

Main advances and needs on the study of geothermal resources in Chile by using remote sensing techniques 08 p1127 A83-21946

Use of remote sensing techniques to study geothermal resources in arid and semi-arid zones in Chile 09 p1288 A83-24577

Regional geothermal exploration in Egypt 21 p3165 A83-44599

Use of remote sensing techniques to study water resources in Los Andes Ranges, Chile 22 p3313 A83-46203

Mapping and analysis of aerial conductivity measurements from INPUT system over geothermal areas 22 p3314 A83-46233

GEOTHERMAL TECHNOLOGY

NT GEOTHERMAL ENERGY CONVERSION

NT GEOTHERMAL ENERGY UTILIZATION

The economical utilization of geothermal energy --- German thesis 17 p2535 A83-37505

GEOTHERMOMETRY

U GEOTEMPERATURE

GEOTROPISM

Plants, gravity, and mechanical stresses 02 p0220 A83-11835

How stems bend up 02 p0220 A83-11836

The effect of phototropism and chemotropism in the absence of geotropism on the orientation of higher plants 07 p0974 A83-20967

The mode of gravity sensing in plant cells 11 p1638 A83-27811

Linkage between gravity perception and response in the grass leaf-sheath pulvinus 11 p1638 A83-27812

Protein synthesis in geostimulated root caps 11 p1638 A83-27814

Quantitation of chlorpromazine-bound calmodulin during chlorpromazine inhibition of gravitropism 11 p1638 A83-27815

A reevaluation of the role of abscisic acid in root gravitropism 11 p1638 A83-27816

The mechanics of gravitropic bending in leafy dicot stems 11 p1638 A83-27817

Gravitropic basis of leaf blade nastic curvatures 11 p1639 A83-27828

GEP TELESCOPES

U PARTICLE TELESCOPES

GERDIEN ARC HEATERS

U ARC HEATING

U HEATING EQUIPMENT

GERMAN DEMOCRATIC REPUBLIC

U EAST GERMANY

GERMANATES

Infrared transmitting germanate glasses 09 p1346 A83-24962

Enhancement of the superconducting transition temperature Tc in Nb3Ge by the homoepitaxial technique 12 p1782 A83-29169

Photovoltaic effect in thin Bi12GeO20 films 20 p3051 A83-42263

GERMANIDES

Preparation, tunneling, resistivity, and critical current measurements on homogeneous high T sub c A15 Nb3Ge thin films [AD-A125657] 04 p0543 A83-16074

GERMANIUM

NT GERMANIUM ISOTOPES

Heteroepitaxial growth of Ge on 111-line Si by vacuum evaporation 03 p0399 A83-14938

Chemical bonding in amorphous semiconductors 04 p0541 A83-15516

Electronic properties of doped glow-discharge amorphous germanium 04 p0542 A83-15530

- Determination of the aluminum content in high-purity germanium by laser multistage photoionization of atoms
10 p1432 A83-26667
- Nondivergent monochromatic X-ray beams from Ge and GaAs monocrystals
11 p1577 A83-27523
- Microscopic processes in low-power laser annealing of ion-implanted Ge
11 p1661 A83-28068
- The optical properties and applications of germanium semiconductor single crystals
11 p1657 A83-28368
- Spectroscopic search for fractional charge in ultrapure semiconductors
13 p1929 A83-30595
- Ge-seeded crystallisation on SiO₂ by using a slider system with RF heated strip heater
13 p1931 A83-31758
- Pulsed electron beam annealing of ion implanted germanium for photovoltaic devices
14 p2088 A83-32239
- Picosecond transient orientational and concentration gratings in germanium
14 p2093 A83-33427
- Direct free-hole absorption induced in germanium by 1.06 micron picosecond pulses
14 p2093 A83-33428
- High pressure studies of Ge using synchrotron radiation
16 p2419 A83-35455
- Growth rate dependence of the interface distribution coefficient in the system Ge-Ga
16 p2421 A83-36714
- Efficient and durable AR coatings for Ge in the 8-11.5 micron band using synthesized refractive indices by evaporation of homogeneous mixtures
16 p2413 A83-36756
- Positron and electron channeling radiation from germanium
17 p2585 A83-38955
- Computer simulation study of multiple germanium gamma-ray sensor arrays
18 p2756 A83-39295
- Photoconductor developments at the Battelle-Institut e.v., Frankfurt am Main
18 p2691 A83-40442
- High sensitivity with a germanium detector in integrating mode
18 p2691 A83-40447
- Electrical conductivity of a low-temperature two-dimensional medium
20 p3051 A83-42273
- Wideband heterodyne detection in the far infrared with extrinsic Ge photocoductors
20 p3048 A83-42583
- Thermophysical properties of germanium for thermal analysis of growth from the melt
20 p2943 A83-43315
- Nonlinear oscillations and chaos in electrical breakdown in Ge
21 p3124 A83-43889
- Three holes bound to a double acceptor - Be(+) in germanium
21 p3218 A83-45199
- An active dummy cell for use in corrosion studies
22 p3267 A83-46701

GERMANIUM ALLOYS

- Hydrogenated a-Si_x/Ge_{1-x}/ - A potential solar cell material
04 p0542 A83-15871
- High temperature creep properties of alpha Ti-Ti5Ge3
18 p2667 A83-40256
- Solidification studies of Nb-Ge alloys at large degrees of supercooling
20 p2940 A83-43261

GERMANIUM COMPOUNDS

- NT GERMANATES
NT GERMANIDES
NT GERMANIUM OXIDES
- Thin germanium nitride films grown by thermal reaction process
04 p0543 A83-16077
- Large anisotropic vibrational correlations in A15 Nb3Ge
13 p1929 A83-30922
- Crystallization of germanium-silicon solid solution from the vapour phase in microgravity conditions
18 p2644 A83-39914
- Galvanomagnetic and thermoelectric properties of p-Pb(1-x)Ge(x)Te in a 80-300 K temperature range
21 p3216 A83-44488

GERMANIUM ISOTOPES

- Observation of Gamow-Teller strength distribution in the reaction Ga-71(p,n)Ge-71 for application to solar-neutrino detection
24 p3674 A83-48919

GERMANIUM OXIDES

- Low-loss GeO₂ optical waveguide fabrication using low deposition rate rf sputtering
03 p0395 A83-14392
- Photoelectrochemical processes in bismuth germanium oxide, Bi₂GeO₂₀ single crystals
07 p0954 A83-20581
- New configurations for high-efficiency prism couplers with application to GeO₂ optical waveguides
10 p1483 A83-26638

GERMICIDES**U BACTERICIDES****GERONTOLOGY**

- The effect of hypoxia on the functional condition of the external respiratory system in mature and old age
12 p1765 A83-29310
- The leading problems of contemporary age physiology, biochemistry, and biophysics and the investigations of the school of A. V. Nagornyi
14 p2065 A83-33322

Heredity, aging, and longevity of humans

- 18 p2735 A83-40572

GHOSTS

- Reducing the effects of ghostlines in a step-record Fourier spectrometer
10 p1424 A83-26870

GIACOBINI-ZINNER COMET

- The relationship between nongravitational effects in the motion of the Giacobini-Zinner and Brooks 2 comets and solar activity
11 p1672 A83-27883

GIANT STARS

- NT CARBON STARS
NT RED GIANT STARS
- A possible CH subdwarf
01 p0118 A83-11498
- Metal abundances of RR Lyrae stars in globular clusters
02 p0251 A83-11592
- Strong CN stars in the globular cluster NGC 1851
02 p0248 A83-12910
- Photoelectric radial velocities. X - The orbits of four spectroscopic binaries in the Clube selected areas
03 p0401 A83-13309
- The X-ray transient 3A 1431-409 - A highly active RS CVn system
03 p0414 A83-13332
- Studies on the spectra of K-giants. I - Physical parameters and Fe and Ti abundances for 26 K-giants
03 p0419 A83-13927
- The temperature dependence of rotation and turbulence in giant stars
03 p0424 A83-14202
- Carbon, nitrogen, and oxygen abundances in G8-K3 giant stars
03 p0430 A83-14802
- Abundances in metal-poor stars. I - The globular clusters NGC 2808, NGC 3201, NGC 6397, and M 22
03 p0430 A83-14805
- Further observational evidence for a coronal boundary line in the cool star region of the H-R diagram
04 p0553 A83-15626
- A comparison of observed and theoretical luminosity functions of carbon stars and late M giants
04 p0553 A83-15627
- On the formation of carbon star characteristics and the production of neutron-rich isotopes in asymptotic giant branch stars of small core mass
04 p0555 A83-15651
- The space density distribution of late-type giants in the solar neighbourhood
04 p0547 A83-15969
- Studies on the spectra of K-giants. II - Abundance determinations for K-giants from very strong iron lines
06 p0827 A83-18170
- A kinematic and abundance survey at the galactic poles
06 p0833 A83-18859
- Carbon, nitrogen, and iron-peak abundances for giants in the remote globular clusters NGC 7006 and Pal 13
06 p0835 A83-19051
- Observations of RR Lyrae with the ANS satellite
06 p0821 A83-19057
- H-alpha emission and mass loss from metal-poor giants
06 p0840 A83-19285
- Radial velocities of a random sample of K giant stars and implications concerning multiplicity among giant stars in clusters
08 p1185 A83-23084
- Evidence of non-LTE in photospheric lines of G and K giants
08 p1185 A83-23087
- Four-colour photometry of some globular cluster giants in the Galaxy and the Magellanic Clouds
10 p1492 A83-25487
- The abundance of M71 and 47 Tucanae
10 p1501 A83-25576
- Errors in high-resolution abundance analyses
10 p1501 A83-25577
- Carbon and nitrogen abundances in giant stars of the metal-poor globular cluster M15
10 p1503 A83-25712
- Closed and open magnetic fields in stellar winds
10 p1510 A83-26391
- Identification and properties of the M giant/X-ray system HD 154791 = 2A 1704+241
10 p1514 A83-26730
- A color-magnitude diagram for Leo II
11 p1668 A83-27108
- Stellar 5 min oscillations
11 p1677 A83-27667
- HR 6522 - A previously unknown multiperiodic Delta Scuti star
12 p1784 A83-28859
- Stellar rotation as a controller of coronae and chromospheres of giant stars
12 p1797 A83-29952
- Investigation of the outer regions of the galactic halo
13 p1946 A83-30383
- Numerical simulation of radiative transfer in circumstellar dust shells. II - Ellipsoidal shells
13 p1959 A83-31741
- A photometric atlas of the spectrum of Gamma Tauri 5186-8700A
14 p2097 A83-33054
- Density gradients for disc- and halo-stars in the direction of the globular cluster NGC 7006
14 p2103 A83-33056
- Stellar diameter measurements by two-aperture interferometry in the infrared
14 p2099 A83-33208
- Blue compact dwarf galaxies. II - Near-infrared studies and stellar populations
15 p2257 A83-34092

Revised list of pulsating stars with ultra-short periods

- 15 p2247 A83-34530

The chemical composition of Algol systems. II - The carbon and nitrogen abundances of the secondaries of U Cep and U Sge
15 p2265 A83-34593

A possible explanation of the Blazhko effect in RR Lyrae
15 p2265 A83-34599

Photometric and spectroscopic observations of the peculiar M giant HD 139216 (Tau4 Serpentis)
16 p2423 A83-35683

Direct evidence for a massive galactic halo
16 p2424 A83-35989

Molecular hydrogen lines in the infrared spectra of M-giant stars
16 p2433 A83-36700

Do all barium stars have a white dwarf companion?
17 p2604 A83-37917

The symbiotic star H1-36
17 p2606 A83-38238

Concentrations in the local association. III - Late-type bright giants, ages and abundances
17 p2607 A83-38256

Multiband optical and infrared photometry of CH Cygni
17 p2613 A83-38841

A lambda 10830 vs X-ray correlation among late-type stars
18 p2767 A83-39600

Orbital and chemical properties of globular clusters and halo stars
18 p2770 A83-39667

Optical and infrared photometry of TX Canum Venaticorum
18 p2763 A83-40480

Abundances in metal-poor stars. III - Eleven field giants
19 p2914 A83-40721

On the evolutionary status of bright, low-mass X-ray sources
19 p2919 A83-41634

The evolution of a stripped giant-neutron star binary
19 p2920 A83-41635

The reddening, metal abundance, and luminosity of high-luminosity G-type stars
20 p3063 A83-42191

Narrow- and intermediate-band H-alpha and O I 7774
20 p3058 A83-42322

A photometry and reiticon spectroscopy of SX Cassiopeiae
20 p3058 A83-42322

Chromospheric and coronal emissions from the giants in the Hyades
20 p3072 A83-43060

Stationary flows in the circumstellar envelopes of M giants
20 p3072 A83-43063

Outer atmospheres of cool stars. XIII - Capella at critical phases
21 p3237 A83-45553

Spectra of the blue CN and CH bands for a CN-enhanced giant in the open cluster IC 4651
22 p3377 A83-46382

Some constraints on the color-magnitude diagram of giants in the galactic spheroid
22 p3382 A83-46991

The possible long-period eclipsing binary BM Eri
23 p3520 A83-47462

Effects of stellar mass loss on the formation of planetary nebulae
24 p3652 A83-49148

Visible and UV observations of the giant early-type members of the Large Magellanic Cloud
24 p3658 A83-49366

The distribution of carbon and M-type giants in the Magellanic Clouds
24 p3664 A83-49881

A perspective review of supermetallicity studies. I --- of giant stars and star clusters
24 p3664 A83-50000

GIBBS FREE ENERGY

A local equilibrium axiom on the flows in relativistic thermodynamics
15 p2239 A83-34410

GIBBS PHENOMENON

A pseudospectral scheme for the numerical calculation of shocks
12 p1725 A83-29622

Grain boundary segregation in Ni and binary Ni alloys doped with sulfur
14 p1993 A83-32677

GIMBALLESS INERTIAL NAVIGATION

Mass-produced laser gyros
02 p0176 A83-11628

GIMBALS

Asymptotic properties of certain motions of an asynchronous gyroscope in a gimbal suspension
09 p1337 A83-23560

A scheme of feedback compensation for CMG gimbal compliance, using multiple rate sensors --- Control Moment Gyroscope
[ASME PAPER 82-WA/DSC-10]

Pointing requirements for space station science
[AAS PAPER 83-061]
21 p3095 A83-44174

Equations of motion for a dynamically tunable gyroscope with n rings
21 p3138 A83-44645

Precise setting of devices in gimbal suspensions with misalignment of the axes
21 p3141 A83-45308

The control of a four-axis gimbal suspension
23 p3459 A83-48457

GIOTTO MISSION

Radio metric orbit determination for the Giotto mission to Comet Halley
[AIAA PAPER 83-0196]
05 p0605 A83-16580

The Giotto dust protection system --- for encounters with comet Halley
05 p0607 A83-17434

SUBJECT INDEX

The experiment PIA of the ESA mission Giotto, a device for the analysis of the mass of the smallest particles which are released from Halley's comet
09 p1218 A83-23383

Analog signal processing in the dust particle experiment of the Giotto mission
09 p1218 A83-23384

Attitude perturbations of the Giotto spacecraft in the dust cloud of Comet Halley
14 p1979 A83-33472

The Giotto mission to Halley's Comet
15 p2124 A83-35013

Impact induced plasma during a cometary fly-by
15 p2128 A83-35021

Hypervelocity impact on the Giotto Halley mission dust shield - Momentum exchange and measurement
15 p2128 A83-35023

A capacitor impact sensor (CIS) on board Giotto for detection of cometary dust particles
15 p2129 A83-35024

The detection of energetic cometary and solar particles by the EPONA instrument on the Giotto mission --- Energetic Particle Onset Admonitor
15 p2129 A83-35025

Automatic controls on board planetary probes
17 p2480 A83-37493

Giotto - The European spacecraft to flyby Halley's comet
17 p2473 A83-37862

Mass spectrometer experiments for the European space probe Giotto
17 p2482 A83-37863

The electronic system of the Halley Multicolour Camera (HMC)
17 p2482 A83-37864

Determination of the mass flow and electron content of the coma of Halley's comet using Doppler measurements of signals from the Giotto probe
18 p2777 A83-39784

Requirements on the reaction control subsystem for the Giotto spacecraft generated from consideration of spacecraft dynamics
21 p3099 A83-44014

GIRDERS
The idealized structural unit method and its application to deep girder structures
24 p3593 A83-49441

GLACIAL DRIFT
Drumlin fields and glaciated mountains - A contrast in geomorphic perception from Seasat radar images
01 p0064 A83-10078

Geology and terrestrial age of the Derrick Peak meteorite occurrence, Antarctica
03 p0434 A83-14318

Ice sculpture in the Martian outflow channels
04 p0566 A83-15568

GLACIERS
Interpretation of mono-pulse ice radar soundings on two Peruvian glaciers
01 p0064 A83-10089

The thermal physics of glaciers --- Russian book
05 p0657 A83-17132

A quantitative determination of the microorganisms in microbiological investigations of Antarctic glaciers
06 p0794 A83-18350

Analysis and retracking of continental ice sheet radar altimeter waveforms
09 p1305 A83-24288

Continental lithospheric thickness and deglaciation induced true polar wander
09 p1305 A83-24337

Regime of the Filchner-Ronne ice shelves, Antarctica
12 p1754 A83-29448

Mathematical model of the glaciers-ocean-atmosphere system
24 p3610 A83-49556

GLACIOFLUVIAL DEPOSITS
U GLACIAL DRIFT

GLACIOLOGY
Drumlin fields and glaciated mountains - A contrast in geomorphic perception from Seasat radar images
01 p0064 A83-10078

Use of Seasat synthetic aperture radar and Landsat multispectral scanner subsystem data for Alaskan glaciology studies
09 p1305 A83-24287

The glaciation of Mars
13 p1962 A83-31318

A theory of stochastic resonance in climatic change
16 p2387 A83-35696

Orbital forcing, climatic interactions, and glaciation cycles
16 p2379 A83-36133

Dynamic effects from mantle phase transitions on true polar wander during ice ages
17 p2546 A83-38613

Orbital forcing of the inception of the Laurentide ice sheet?
18 p2718 A83-39960

Some aspects of the application of space photographs in the compilation of glaciological maps
18 p2706 A83-40125

Isotope and geochemical glaciology --- Russian book
21 p3169 A83-43902

Cryolithogenesis --- Russian book
21 p3169 A83-43919

GLANDS
The arterial vascular bed of the human mesenteric lymph nodes
03 p0380 A83-13644

GLANDS (ANATOMY)
NT ADRENAL GLAND
NT ENDOCRINE GLANDS
NT PANCREAS

NT PINEAL GLAND
NT PITUITARY GLAND
NT SALIVARY GLANDS
NT TESTES
NT THYMUS GLAND
NT THYROID GLAND

GLASS
NT BOROSILICATE GLASS
NT GLASS FIBERS
NT METALLIC GLASSES
NT PYROCERAM (TRADEMARK)
NT S GLASS
NT SILICA GLASS
NT VYCOR

Detection of strength limiting defects in cellular glasses by dielectric measurements
03 p0302 A83-13248

The El'gygytyn meteorite - Probable composition
03 p0434 A83-13896

The fracture mechanics of microsphere-filled composites
03 p0293 A83-14739

Rayleigh scattering in ZrF₄-based glasses
04 p0534 A83-15247

KREEP glass and the exotic provenance and formation of polymict breccia 66055
04 p0560 A83-15341

The Apollo 15 yellow impact glasses - Chemistry, petrology, and exotic origin
04 p0560 A83-15342

Ferromagnetic resonance intensity - A rapid method for determining lunar glass bead origin
04 p0561 A83-15344

Thermophysical properties of quartz glass
04 p0464 A83-16167

Impact glasses from some astrombles on the territory of the USSR
05 p0706 A83-17470

Characterization and crystallization of Y-Si-Al-O-N glass
06 p0734 A83-18053

Dissolution of a stationary bubble in a glassmelt with reversible chemical reaction - Rapid forward reaction rate constant
06 p0735 A83-19318

The effect of materials and processes on package reliability
07 p0920 A83-20473

Diaplectic labradorite glass from the Manicouagan impact crater. I - Physical properties, crystallization, structural and genetic implications
07 p0950 A83-21046

Cooling rates for glass containing lunar compositions
07 p1035 A83-21324

Glass formation - A contemporary view
08 p1070 A83-22190

Fabrication of thin glass mirrors on alnico magnets
08 p1112 A83-22866

Infrared optics hot pressed from fluoride glass
09 p1239 A83-24973

Generation of light in optical fibers made of glasses formed from rare-earth ultraphosphate crystals
10 p1432 A83-26670

Calculation of refractive indices using Buchdahl's chromatic coordinate
13 p1918 A83-30208

Increasing the numerical aperture of a glass-polymer light guide
13 p1919 A83-30814

The polarization control of tone-transmission brightness in a holographic image of light-scattering surfaces and layers
14 p2019 A83-32132

Chalcogenide glasses - Promising materials for quantum electronics. I - The interaction and structure of As-S glasses
14 p2088 A83-32167

Sulphur content and sulphur isotope composition of orange and black glasses in Apollo 17 drive tube 74002/1
15 p2274 A83-34497

Dynamic fatigue of brittle materials containing indentation line flaws
15 p2180 A83-35064

Physical properties of disordered structures (Molecular-kinetic and thermodynamic processes in inorganic glasses and polymers) --- Russian book
16 p2337 A83-36438

Formation and characterization of oxynitride glasses in the Si-Ca-Al-O-N and Si-Ca-Al,B-O-N systems
18 p2671 A83-39056

Optical properties of oxide glasses containing nickel microgranules
18 p2649 A83-39060

Effects of titanate coupling agents on the mechanical properties of poly (vinyl chloride)-glass flake composites
18 p2651 A83-40147

Dynamic fatigue of a machinable glass-ceramic
19 p2823 A83-40908

Air jet levitation furnace system for observing glass microspheres during heating and melting
20 p2963 A83-43265

Glass processing in a microgravity environment
20 p2941 A83-43282

Experimental observation of the thermocapillary driven motion of bubbles in a molten glass under low gravity conditions
20 p2941 A83-43283

Surface tension driven flow in glass melts and model fluids
20 p2941 A83-43284

GLASS FIBER REINFORCED PLASTICS

Preliminary study of the effects of a reversible chemical reaction on gas bubble dissolution --- for space glass refining
20 p2941 A83-43285

Gels and gel-derived glasses in the Na₂O-B₂O₃-SiO₂ system --- containerless melting in space
20 p2941 A83-43288

Glass shell manufacturing in space
20 p2941 A83-43290

On the nature of the accumulation effect in laser-induced damage to optical materials
21 p3203 A83-43862

Siloxanes, silanes, and silazanes in the preparation of ceramics and glasses
[ACS PAPER 17-B-81]
21 p3115 A83-44095

Plating on glass for hermetic seal
[SAE PAPER 820613]
22 p3302 A83-45871

Monitoring the 1980-1982 eruptions of Mount St. Helens
Compositions and abundances of glass
22 p3333 A83-46800

Design of glass-faced helicopter windshields for survival in a particle impact environment
[AIAA PAPER 83-2439]
23 p3403 A83-48328

The effect of nonequilibrium physical-chemical processes in the boundary layer on the ablation of quartz glass
23 p3452 A83-48665

GLASS COATINGS
Component interaction in a glass-ceramic layer
07 p0900 A83-20710

Fluctuation and scattering properties of RF sputtered glass thin film optical waveguides
13 p1919 A83-30781

Porous metallic membrane produced by the fiber metallurgy
18 p2667 A83-40137

Thermal stability of compositions consisting of molybdenum disilicide, quartz, and glass
24 p3568 A83-49080

A study of the interaction between coatings and alloys based on refractory metals
24 p3560 A83-49081

Heat resistance of coatings based on aluminoborosilicate glass and disilicides of refractory metals
24 p3569 A83-49092

Protective coatings for niobium based on refractory glasses and molybdenum disilicide
24 p3569 A83-49095

GLASS FIBER REINFORCED PLASTICS
Effect of resin flexibility on the properties of filament wound tubes
01 p0022 A83-10241

The critical equilibrium of a simply supported cylindrical glass-reinforced plastic shell
01 p0059 A83-10689

The modelling of hydrothermal aging in glass fibre reinforced epoxy composites
01 p0022 A83-10700

Toughening epoxy resin matrix for glass and carbon fiber composites
02 p0149 A83-11852

Optical flaw detector
02 p0188 A83-12161

The use of composite materials in aircraft propellers
02 p0136 A83-12966

The strength of the fibre-polymer interface in short glass fibre-reinforced polypropylene
03 p0291 A83-13682

The effects of humidity on fatigue due to shear stress in unidirectional composites - Attempts at interpretation and a summing up
[ONERA, TP NO. 1982-98]
03 p0292 A83-14546

An experimental study of the strength of a cross-ply glass-reinforced composite in the plane stressed state
03 p0293 A83-14738

Compressive failure and kinking in uniaxially aligned glass-resin composite under superposed hydrostatic pressure
04 p0455 A83-15994

The effect of glass fibers filled in polyester on fatigue crack arrest
05 p0611 A83-17106

Fatigue initiation in a short glass fibre composite
05 p0612 A83-17569

A spectroscopic study of the features seen in the thermal curing of the binder P-2M --- phenol formaldehyde matrix material for glass fiber reinforced plastics
05 p0619 A83-17693

Effect of water on the interlaminar fracture behaviour of glass fibre-reinforced polyester composite
06 p0724 A83-17966

Calculating the elastic characteristics of a unidirectional fiber composite by the method of sections
06 p0725 A83-18501

A statistical theory for fibrous media. I - Longitudinal shear
06 p0725 A83-18508

A comparative study of the light transmission, acoustic emission, and thermal effects of a glass-reinforced plastic under mechanical loads
06 p0725 A83-18519

The problem of a crack in an orthotropic strip
06 p0778 A83-19546

A study of the thermo-oxidation process and stability of graphite and glass/PMR polyimide composites
07 p0877 A83-20490

Reliability analysis of circumferentially wound FRP flywheels
07 p0950 A83-21625

Hydrothermal aging effects on the micromechanisms of crack extension in glass fibre and carbon fibre composites
08 p1053 A83-21679

Effect of fiber-aspect ratio and orientation on the stress-strain behavior of aligned, short-fiber-reinforced, ductile epoxy 08 p1055 A83-22719

Determination of fracture toughness of unidirectionally fiber-reinforced composites 09 p1223 A83-23936

Post-crazing analysis of glass-epoxy laminates 09 p1223 A83-23941

A corrugated core theory of sandwich plates 09 p1280 A83-24512

Energy absorption in composite tubes 10 p1439 A83-25883

A Monte Carlo simulation of the strength of laminated hybrid composites 10 p1389 A83-26965

Compression molded energy storage flywheels 11 p1608 A83-27303

An experimental and theoretical study of crack propagation in crossply fiber composites 11 p1544 A83-28437

Thermal stresses in a partially restrained orthotropic plate with a source and sink of heat 11 p1596 A83-28464

On the determination of the load-carrying capacity of the glass-plastic propeller blade of an aircraft 12 p1703 A83-29294

Compressive fatigue behaviour of a glass fibre-reinforced polyester composite at 300 K and 77 K 12 p1710 A83-29720

Fracture behavior of hybrid composite laminates [AIAA 83-0804] 12 p1710 A83-29736

Life estimation of an S-Glass/epoxy composite under sustained tensile loading 12 p1711 A83-29894

Modeling the fracture of thin-walled structural elements of multidirectional layered composites 13 p1865 A83-30054

An accumulated-damage fracture criterion for a three-component layered composite 13 p1865 A83-30055

Fracture toughness of unidirectional glass/carbon hybrid composites 13 p1816 A83-31616

Environmental stress cracking behavior of glass fiber reinforced epoxy resins 14 p1986 A83-32345

Filament wound composite thermal isolator structures for cryogenic dewars and instruments --- glass fiber reinforced epoxy laminates for spaceborne equipment 14 p1982 A83-33120

An investigation of stress-dependent, temperature-dependent, and time-dependent strains in randomly oriented fiber reinforced composites 14 p1988 A83-33295

Fracture characterization of a random fiber composite material 14 p1988 A83-33296

Viscoelastic characterization of a random fiber composite material employing micromechanics 14 p1988 A83-33297

Generation of thermal strains in GRP. I - Effect of water on the expansion behaviour of unidirectional glass fibre-reinforced laminates. II - The origin of thermal strains in polyester cross-ply laminates 15 p2130 A83-35074

The fracture mechanism of carbon and boron composites in interlayer shear 16 p2323 A83-35509

Investigation of anisotropic problems in the mechanics of deformable bodies by the holographic moiré method 16 p2355 A83-35512

SEM observations of the initiation and propagation of cracks in a short fibre-reinforced thermoplastic composite under stress 16 p2323 A83-35568

A tensile testing technique for fibre-reinforced composites at impact rates of strain 16 p2324 A83-35981

Fracture behaviour of collimated thermoplastic poly(ethylene terephthalate) reinforced with short E-glass fibre 18 p2649 A83-39055

Composite materials in aircraft structures 18 p2650 A83-40130

How the interface controls the properties of fibre composites 18 p2651 A83-40143

Mechanical testing and micrographic examination of prepreg GFRP composites with different pressure-temperature cycles 18 p2653 A83-40176

Photoelastic analysis of the effect of residual stress on the deformation of unidirectional glass fiber reinforced plastic at the wedge indentation 18 p2654 A83-40193

Investigation of the fatigue behaviour of some industrial glass reinforced polyesters (GRP) 18 p2655 A83-40205

Effect of combination of glass mat and cloth on the fatigue properties of fibrous composite materials 18 p2655 A83-40206

Effect of time on the mechanical behavior of laminated composites 18 p2655 A83-40211

A study of spallation in phenolic-resin based woven roving glass fibre reinforced composite material 18 p2656 A83-40219

Properties of composite box beams under combined impact loading 18 p2705 A83-40222

The environmental stress corrosion cracking of glass fibre reinforced polyester and epoxy composites 18 p2656 A83-40223

Long term strength of glass reinforced plastics 18 p2656 A83-40224

Swelling of Kevlar 49/epoxy and S2-glass/epoxy composites 18 p2657 A83-40228

Origins of thermal strains in polyester laminates 18 p2657 A83-40230

Fracture mechanism of short glass fiber reinforced polyamide thermoplastics 18 p2657 A83-40232

The strength, ductility and failure of thermoplastics reinforced with short-glass fibres 18 p2657 A83-40233

The strength of aligned short-fiber carbon, glass, and hybrid carbon/glass composites 18 p2657 A83-40234

Statistical aspects of fibre and bundle strength in hybrid composites 18 p2658 A83-40240

Fabrication cycle influence on the acoustic emission response of GFRP composites 18 p2660 A83-40270

A contribution to non-destructive inspection of fibrous plastics composites with an emphasis on application of AE techniques 18 p2660 A83-40274

A new construction method of carbon fibre hybrid GRP moulds in vacuum forming process 18 p2662 A83-40290

Deformation and stress of antenna made of glass fiber reinforced plastics under wind force 18 p2662 A83-40296

Stress concentration around circular cutouts in laminated composite cylindrical shells - Experimental investigation and finite element analysis 19 p2857 A83-40883

Thermoplastic aromatic polyimide composites 19 p2819 A83-40925

A new brominated polymeric additive for flame retardant glass-filled polybutylene terephthalate 19 p2824 A83-41854

Water absorption of glass/epoxy laminates under bending stresses 20 p2947 A83-42809

The hydrolytic stability of glass fiber reinforced poly(butylene terephthalate), poly(ethylene terephthalate) and polycarbonate 20 p2948 A83-42834

Fatigue crack propagation in random short-fiber SMC composite --- Sheet Molding Compound 20 p2948 A83-43147

Design, fabrication and test of a composite elevator 21 p3151 A83-44046

On stress analysis of anisotropic composites through transmission optical patterns - Isochromatics and isopachics 21 p3108 A83-45166

A preliminary study of composite reaction injection molding 22 p3263 A83-46287

Time dependent properties of injection moulded composites 22 p3263 A83-46293

Rheology of reinforced thermoplastics and its application to injection-molding. IV - Transient injection capillary flow and injection-molding 22 p3265 A83-46901

Dry wear studies on glass-fibre-reinforced epoxy composites 23 p3428 A83-48154

Fiber fracture in reinforced thermoplastic processing 24 p3553 A83-48998

In-plane and interlaminar shear fatigue characterization of unidirectional GFRP and CFRP, including moisture effects [ONERA, TP NO. 1983-109] 24 p3553 A83-49420

Statistical analysis of multiple fracture in 0 deg/90 deg/0 deg glass fibre/epoxy resin laminates 24 p3554 A83-50064

GLASS FIBERS

Osmosis in composite materials 01 p0022 A83-10240

Electroconducting glass fibres produced by ion-exchange and reduction treatments 02 p0159 A83-11674

Effects of amplitude of oscillation on the wear of dry bearings containing PTFE [ASME PAPER 81-LUB-6] 02 p0186 A83-11942

On the preparation of glass-fibre reinforced aluminum by powder hot extrusion 05 p0611 A83-17110

Stimulated Mandel'shtam-Brillouin scattering in a multimode glass fiber lightguide 07 p0933 A83-20046

Automated inspection of metallized glass fiber 07 p0944 A83-21415

X-ray induced transient attenuation at low temperatures in polymer clad silica /PCS/ fibers 08 p1165 A83-22478

Drop weight impact testing of laminates reinforced with Kevlar aramid fibers, E-glass, and graphite 12 p1711 A83-29891

Fracture toughness/Young's modulus correlation for low-density fibrous silica bodies 12 p1717 A83-29976

The effect of multiple-scattering in measuring the radiation properties of absorbing and scattering media [AIAA PAPER 83-1454] 15 p2161 A83-34910

Rayleigh scattering in fluoride glass optical fibres 16 p2412 A83-36480

Integrated optical waveguiding structures made by silver ion-exchange in glass. I - The propagation characteristics of stripe ion-exchanged waveguides: A theoretical and experimental investigation 16 p2413 A83-36768

Integrated optical waveguiding structures made by silver ion-exchange in glass. II - Directional coupler and bends 16 p2414 A83-36769

X-ray diffraction analysis at high temperature on two ceramic systems 21 p3116 A83-44127

A fluoride glass optical fiber operating in the mid-infrared wavelength range 21 p3204 A83-44206

A study of the thermo-oxidative process and stability of graphite and glass-PMR polyimide composites 22 p3262 A83-46285

In situ analysis of the interface --- of composites 22 p3264 A83-46303

Advances in infrared fibers II; Proceedings of the Second Meeting, Los Angeles, CA, January 26-28, 1982 22 p3357 A83-46621

Polycrystalline KRS-5 infrared fibers for power transmission 22 p3357 A83-46622

Infrared glass optical fibers for 2 to 11 micrometer band 22 p3358 A83-46623

Materials for infrared low loss fibers 22 p3358 A83-46624

Fluoride glasses with large optical window for infrared fibers 22 p3358 A83-46625

Progress in heavy metal fluoride glasses for infrared fibers 22 p3358 A83-46626

Preparation of high purity ZnCl₂ for 10.6-micron optical fibers 22 p3358 A83-46627

Material dispersion considerations for infrared fibers 22 p3358 A83-46628

Pulse compression by stimulated Brillouin scattering 22 p3297 A83-46630

GeO₂-Sb₂O₃ glass optical fibers for 2 to 3 microns fabricated by vapor-phase axial deposition (VAD) method 22 p3358 A83-46635

Ultralow loss single-mode fiber design for 2.5-6-micron band operation 24 p3629 A83-49019

GLASS LASERS

Energy transfer and lasing in phosphate glasses activated with chromium, ytterbium, and erbium 03 p0331 A83-13594

An ultra-short-pulsed laser with adjustable parameters 04 p0484 A83-15264

A two-channel picosecond parametric spectrometer with high temporal resolution 04 p0481 A83-15267

Spectral characteristics of the extraction of excitation energy from neodymium glass amplifiers 05 p0649 A83-17051

Polarized fluorescence line narrowing measurements of Nd laser glasses - Evidence of stimulated emission cross section anisotropy 06 p0767 A83-19258

Passively Q-switched laser utilizing concentrated Li-Nd-La phosphate glass 07 p0933 A83-20102

Observation of the population inversion of O VIII levels in a laser plasma 07 p0996 A83-20126

Generation of 3-psec pulses in a laser with concentrated neodymium phosphate glass 10 p1432 A83-26661

Spectral composition of the radiation emitted from a concentrated LiNdLa phosphate glass laser with a Q switch made of an LiF crystal with F₂/- centers 10 p1432 A83-26662

New data on nonradiative relaxation of impurity center excitations in laser materials 11 p1581 A83-27591

A long pulse width neodymium-doped glass rod laser amplifier with a moving input laser beam 11 p1581 A83-27592

Erbium glass lasers and their applications 11 p1583 A83-27620

A ruby laser in an electron-beam field 14 p2023 A83-32133

Spectral development of picosecond pulses of mode-locked Nd-glass lasers 14 p2026 A83-33412

Future development of high-power solid-state laser systems 16 p2358 A83-35884

Channels of energy losses in erbium laser glasses in the stimulated emission process 19 p2853 A83-41186

Effect of resonant absorption of laser-induced plasma on temporal resolved spectrum and temporal integrated spectrum 20 p3050 A83-43177

Intelligent attenuator for laser pulse energy and power stabilization 21 p3145 A83-44833

Second-harmonic emission from laser-plasma interactions 22 p3363 A83-46273
Picosecond photofragmentation experiments with a repetitively pulsed mode-locked Nd:phosphate glass laser system 22 p3266 A83-46684
Coherent pulse propagation in the infrared on the picosecond time scale 23 p3462 A83-48314
The effect of the mode structure of laser radiation on the stability of lead azide 24 p3557 A83-49795

GLASSY CARBON
Electrodeposition of zinc on glassy carbon from ZnCl₂ and ZnBr₂ electrolytes 20 p2951 A83-43420
Thermochemical ablation of the glass-graphite surface of a blunt cone at the spreading line in a three-dimensional boundary layer 24 p3579 A83-49662

GLAUCOMA
Laser treatment of open-angle glaucoma: Randomized comparative studies - Cyclotrabeculospasms and trabeculoplasty 05 p0674 A83-17212
The long-term results of operations for the ultrasonic activation of trabeculae --- antiglaucoma treatment 05 p0674 A83-17213
Timolol maleate - Side effects on healthy nonglaucomatous volunteers 12 p1764 A83-28937
A comparative evaluation of the simplified tonograph methods of Nesterov and Kal'fa-Vurgaft --- for eye examinations 15 p2212 A83-34938

GLAUERT COEFFICIENT
U AERODYNAMIC FORCES
U MACH NUMBER

GLAZES
Performance of laser-glazed zirconia thermal barrier coatings in cyclic oxidation and corrosion burner rig tests 01 p0027 A83-10300

GLIDE ANGLES
U GLIDE PATHS

GLIDE PATHS
Pilot judgements of distance, height and glide slope angle from computer generated landing scenes 04 p0524 A83-16327
Maximum endurance and maximum penetration trajectories for horizontal gliding flight [AIAA PAPER 83-0283] 05 p0594 A83-16628
Simulated fan-beam radar imagery --- use in assessing aircraft approach-to-landing paths 18 p2675 A83-40302
Carrier landing simulation results of precision flight path controllers in manual and automatic approach [AIAA PAPER 83-2072] 19 p2796 A83-41909
Approximation to the optimization of a coast-glide trajectory 23 p3403 A83-48223

GLIDE SLOPES
U GLIDE PATHS

GLIDERS
NT ASSET GLIDERS
NT BOOSTGLIDE VEHICLES
NT HANG GLIDERS
NT HYPERSONIC GLIDERS
Analytical consequences of increasing the mass of a glider 03 p0281 A83-14617
The ULS experimental ultralight glider made of polymer composites. I - Genesis of the program and construction of the glider 03 p0281 A83-14621
First results of boundary layer research flights with three powered gliders during the field experiment PUKK 06 p0793 A83-18996
Ultralight sounder - An airborne system for studying the planetary boundary layer 13 p1803 A83-30787
Light aircraft and sailplane structures in reinforced plastics 16 p2299 A83-36065

GLIDING
Entry vehicle performance in low-heat-load trajectories 02 p0139 A83-13079
Asset and prime - Gliding re-entry test vehicles 18 p2645 A83-39972

GLOBAL AIR POLLUTION
Global distribution of stratospheric aerosols by satellite measurements 09 p1306 A83-24675
July 1981 NASA workshop on passive remote sensing of the troposphere 09 p1283 A83-24889
Climatic effects of atmospheric carbon dioxide 13 p1893 A83-31200
Global distribution and southern hemispheric trends of atmospheric CCl₃F 14 p2056 A83-31920
Measurement of weak organic acidity in precipitation from remote areas of the world 16 p2372 A83-36129
Active measures for reducing the global climatic impacts of escalating CO₂ concentrations [IAF PAPER 83-106] 23 p3488 A83-47269
Background concentration of ozone, dust, and nitrogen and sulfur compounds in the atmosphere (according to worldwide data) 24 p3602 A83-49102
On the concentration of mercury in the atmosphere in background regions 24 p3604 A83-49108

GLOBAL AIR SAMPLING PROGRAM
Cloud encounter statistics in the 28.5-43.5 KFT altitude region from four years of GASP observations 17 p2550 A83-38733

GLOBAL ATMOSPHERIC RESEARCH PROGRAM
NT GARP ATLANTIC TROPICAL EXPERIMENT
On some characteristics of the atmospheric boundary layer in the Indian Ocean during the GARP cruise 02 p0212 A83-11846
Available potential energy in the northern hemisphere during the FGGE year 04 p0515 A83-15853
On an evaluation of data impact with respect to Rossby mode in the data assimilation cycle. I - On the impact of satellite wind data with special emphasis on the vertical prediction error correlation 04 p0518 A83-16015
Results of the First GARP Global Experiment 06 p0787 A83-17992
Global-scale weekly and monthly energetics during January and February 1979 06 p0790 A83-18259
A ubiquitous wavenumber-5 anomaly in the Southern Hemisphere during FGGE --- First Garp Global Experiment 06 p0792 A83-18472
Large-scale two-dimensional turbulence in the atmosphere 08 p1143 A83-23013
The First GARP Global Experiment. Volume 2 - Polar aerosols, extensive cloudiness, and radiation --- Russian book 09 p1316 A83-25226
The results of aircraft investigations of cloudiness and radiation carried out over the eastern Arctic during the Second Observational Period of the Global Weather Experiment 09 p1316 A83-25228
Objective analysis and assimilation of observational data from FGGE --- First GARP Global experiment 13 p1891 A83-30804
The global atmospheric research program - 1979-1982 17 p2525 A83-38320
Large-scale energy transformations in the high latitudes of the Northern Hemisphere 18 p2728 A83-40026
Variability of the ocean and atmospheric in the equatorial Atlantic (FGGE investigations) 19 p2869 A83-42101
Meteorological investigations during the voyages of the research vessels Akademik Kurchatov and Professor Shtokman in the FGGE program 19 p2868 A83-42114
The SE trade during the FGGE 19 p2868 A83-42116
Meteorological conditions in the Atlantic FGGE study area 19 p2869 A83-42121
Seasonal distributions of diabatic heating during the first GARP global experiment 21 p3172 A83-44470
The influence of the tropics on the prediction of ultralong waves. I - Tropical wind field 23 p3490 A83-47405

GLOBAL POSITIONING SYSTEM
NAVSTAR GPS - State of development and future of this global navigation system 02 p0134 A83-13009
Trend analysis concerning the displays and the keyboard of GPS navigation receivers for different applications 02 p0135 A83-13010
Accuracy and availability of various modern navigation procedures 02 p0134 A83-13013
A wide-band omnidirectional vertical shaped-beam collinear array 03 p0307 A83-14038
Total dose response of STL and I2L logic devices --- Schottky Transistor Logic 05 p0627 A83-17517
GPS control segment capabilities 07 p0871 A83-19764
The integrated transfer subsystem /ITS/ - A GPS-to-GPS data link 07 p0871 A83-19765
The Navstar Global Positioning System six-plane 18-satellite constellation 07 p0871 A83-19766
Advances in tactical weapon guidance through GPS 07 p0871 A83-19767
GPS L-band communication concept 07 p0871 A83-19768
Fixed wing and rotary wing flight testing of Navstar GPS as a civilian navigation system 07 p0865 A83-19777
Ionospheric scintillation measurements using the Global Positioning System 07 p0911 A83-19778
A demonstration of relative positioning using conventional GPS Doppler receivers 07 p0865 A83-19779
Navstar equipments accuracy compared with experimental results 09 p1201 A83-24861
Multiconfiguration Kalman filter design for high-performance GPS navigation 10 p1373 A83-26262
Fault/maneuver tolerance of aided GPS demodulation/navigation processors in the non-precision approach environment 11 p1529 A83-28787
FAA helicopter NAVSTAR GPS flight testing 11 p1529 A83-28788
Synergistic integration of JTIDS/GPS technology --- Joint Tactical Information Distribution System 11 p1529 A83-28789
Computer simulation of a differential GPS for civil applications 11 p1529 A83-28790

Reliability of NAVSTAR GPS for civil aviation 11 p1529 A83-28791
NAVSTAR-GPS at sea 12 p1700 A83-29207
Integrated GPS, DLMS, and radar altimeter measurements for improved terrain determination 12 p1700 A83-29212
An advanced single-channel NAVSTAR GPS multiplex receiver with up to eight pseudochannels 12 p1700 A83-29213
Benefits of integrating GPS and Inertial Navigation Systems 12 p1700 A83-29214
Analysis and test of ceramic substrates for packaging of leadless chip carriers 13 p1834 A83-30861
GPS test experience under MIL-STD-1540 guidelines 13 p1810 A83-31181
Satrack - Review and update 21 p0397 A83-44693
Marine gravity measurement from fixed wing aircraft 22 p3288 A83-46111
International Symposium on Geodetic Networks and Computations, Munich, West Germany, August 31-September 5, 1981, Proceedings. Volume 4 - Modern observation techniques for terrestrial networks 22 p3315 A83-46336
Geodesy and the global positioning system 22 p3252 A83-46338
Consequences of Gravsat and GPS - New concept of geodetic networks 22 p3316 A83-46340
A strategy for buildup to the operational Navstar GPS constellation 22 p3253 A83-46961
Navigating low altitude satellites using the current four Navstar/GPS satellites 22 p3259 A83-46962
Experimental results of using the GPS for Landsat 4 onboard navigation 22 p3253 A83-46963
Applications of time transfer using Navstar GPS 22 p3253 A83-46964
The Navstar GPS 22 p3253 A83-46965
Differential operation of NAVSTAR GPS 22 p3253 A83-46968
Collins avionics NAVSTAR GPS advanced digital receiver 22 p3253 A83-46969
GPS navigation using three satellites and a precise clock 22 p3253 A83-46970
GPS user errors resulting from one 'bad' satellite in the navigation solution 22 p3254 A83-46971
Principles and present status --- of Navstar GPS for sea and air navigation 23 p3401 A83-48733
GPS for Marine navigation 23 p3401 A83-48734

GLOBULAR CLUSTERS
NT HORIZONTAL BRANCH STARS
Why are essential parts of 'burstors' located in globular clusters 01 p0128 A83-11341
Metal abundances of RR Lyrae stars in globular clusters 02 p0251 A83-11592
TiO band strengths in metal-rich globular clusters. V - 47 Tucanae 02 p0255 A83-12116
X-ray illumination of globular cluster puzzles --- globular cluster X ray sources as clues to Milky Way Galaxy age and evolution 02 p0255 A83-12117
Do black holes exist at the centres of globular clusters 02 p0260 A83-12525
On the origin of the globular cluster system of M87 02 p0261 A83-12909
Strong CN stars in the globular cluster NGC 1851 02 p0248 A83-12910
Variable stars in the globular cluster NGC 6293 02 p0248 A83-12912
Absolute ultraviolet fluxes of elliptical galaxies as observed with the Astronomical Netherlands Satellite /ANS/ 03 p0415 A83-13363
Color-magnitude studies of globular clusters. I - The bright stars in NGC 362 03 p0406 A83-13556
Is NGC 1851-UV5 a binary star in a globular cluster 03 p0421 A83-14139
The mass of the anomalous cepheid in the globular cluster NGC 5466 03 p0424 A83-14203
Dynamical evolution of globular clusters. I 03 p0427 A83-14718
Abundances in metal-poor stars. I - The globular clusters NGC 2808, NGC 3201, NGC 6397, and M 22 03 p0430 A83-14805
Abundances in metal-poor stars. II - The anomalous globular cluster Omega Centauri 04 p0550 A83-15041
A statistical method for determining ages of globular clusters by fitting isochrones 04 p0547 A83-15619
Abundances of the elements in six stars in the globular cluster M22 04 p0553 A83-15620
What has happened in the cores of globular clusters 04 p0555 A83-15650
The extended giant branches of intermediate age globular clusters in the Magellanic Clouds. III 05 p0697 A83-16991
Carbon, nitrogen, and iron-peak abundances for giants in the remote globular clusters NGC 7006 and Pal 13 06 p0835 A83-19051

A search for globular clusters around the edge-on spiral galaxy NGC 55 06 p0839 A83-19269

The ages and compositions of old clusters 06 p0840 A83-19283

Evolutionary effects of helium diffusion in population II stars 06 p0840 A83-19286

Age calibrations of Magellanic Cloud clusters 06 p0843 A83-19489

Stability limits for 'isothermal' cores in globular cluster models - Two-component systems 06 p0844 A83-19490

Radio frequency observations of galactic X-ray sources 06 p0845 A83-19524

Star clusters and stellar evolution. I - Improved synthetic color-magnitude diagrams for the oldest clusters 07 p1012 A83-20077

Positions, magnitudes, and colors for stars in the globular cluster M15 07 p1006 A83-20566

The color-magnitude diagram for stars in the central part of the globular cluster NGC 7089 / M 2/ 07 p1006 A83-20573

A search for globular clusters around the edge-on late-type spiral galaxy NGC 253 07 p1020 A83-21114

Absorption by halo gas in the direction of M13 07 p1020 A83-21118

Photometry of bright stars in nucleus of globular cluster M 3 08 p1174 A83-22276

White dwarfs and neutron stars in globular cluster X-ray sources 08 p1187 A83-23287

A comment on the colors of globular clusters in elliptical galaxies 09 p1357 A83-23728

Age and metal abundance of a globular cluster, as derived from Stromgren photometry 09 p1364 A83-25289

On the stellar content of the galactic globular cluster M5 10 p1499 A83-25372

Four-colour photometry of some globular cluster giants in the Galaxy and the Magellanic Clouds 10 p1492 A83-25487

The abundance of M71 and 47 Tucanae 10 p1501 A83-25576

Errors in high-resolution abundance analyses 10 p1501 A83-25577

Faint star studies in the Magellanic Clouds. I - RICHFLD photographic photometry in NGC 2257 10 p1493 A83-25708

Double-mode RR Lyrae variables in M15 10 p1502 A83-25709

Photometric studies of composite stellar systems. V - Infrared photometry of star clusters in the Magellanic clouds 10 p1494 A83-25710

The chemical inhomogeneity of M22 10 p1502 A83-25711

Carbon and nitrogen abundances in giant stars of the metal-poor globular cluster M15 10 p1503 A83-25712

On searches for pulsed emission with application to four globular cluster X-ray sources - NGC 1851, 6441, 6624, and 6712 10 p1503 A83-25713

Chemical separation in horizontal-branch stars 10 p1514 A83-26727

Globular cluster orbits and the galactic mass distribution 11 p1676 A83-27109

Search for new variable stars in NGC 5927, 5946, and 6144 11 p1668 A83-27113

The cyanogen inhomogeneity of NGC 362 11 p1669 A83-27114

The globular cluster NGC 6544 12 p1784 A83-28865

Observed radii and structural parameters of clusters in the SMC. II 12 p1784 A83-28870

Photoelectric photometry of star clusters in M31. VIII 12 p1788 A83-29488

X-ray evidence for white dwarf binaries in globular clusters 13 p1952 A83-31444

Discovery of a nitrogen-rich UV-bright star in the globular cluster M5 13 p1952 A83-31445

Density gradients for disc- and halo-stars in the direction of the globular cluster NGC 7006 14 p2103 A83-33056

Survey of H-alpha emission in globular cluster red giants 14 p2105 A83-33196

The chemical composition of NGC 288 14 p2110 A83-33460

Radial velocities of stars in M12 (NGC 6216) and M56 (NGC 6779) and UV-bright stars in globular clusters 14 p2110 A83-33464

Are dominant central galaxies the proto-nuclei of rich clusters? 14 p2101 A83-33468

IUE observations of globular clusters and blue horizontal branch stars 15 p2244 A83-33594

X-ray diagnostics of globular clusters 15 p2251 A83-33595

Color-magnitude photometry of 47 Tucanae to M(V) = +9 15 p2260 A83-34127

DDO photometry and metallic abundances of E and SO galaxies and globular clusters of the LMC and SMC 15 p2262 A83-34534

DDO integrated photometry of globular clusters and initial chemical evolution of the galaxy 15 p2262 A83-34536

Chemical evolution of the galactic halo. I - Effects of possible mass segregation mechanisms 15 p2272 A83-34779

Photoelectric catalogue of globular clusters in the Andromeda Nebula M31 and its companions NGC 147, NGC 185, and NGC 205 15 p2249 A83-34785

Photographic photometry in globular clusters - Comparison of techniques 15 p2249 A83-34788

Stability of star clusters as galactic satellites. I - Motion in the cluster orbital plane 16 p2424 A83-36631

Stability of star clusters as galactic satellites. II - Motion perpendicular to the cluster orbital plane 16 p2425 A83-36632

IUE observations of the nucleus of the galactic globular cluster NGC 2808 16 p2429 A83-36634

An ultraviolet approach to M 15 16 p2429 A83-36638

Predicted and observed UV spectrum of M5 16 p2430 A83-36652

Positions, magnitudes and colours for stars in the core of M 3 17 p2587 A83-37278

Spectroscopic analysis of dwarf and subgiant stars in 47 Tucanae 17 p2597 A83-37318

The chemical composition of stars in globular clusters 17 p2602 A83-37828

A comparison between observed and theoretical H-R diagrams for the young LMC star cluster NGC 1866 17 p2604 A83-37915

The abundance scale of the galactic globular clusters 17 p2607 A83-38247

Post-collapse evolution of globular clusters 17 p2607 A83-38261

The galactic globular cluster system - Helium content versus metallicity 17 p2609 A83-38424

The canonical anticorrelation between Y and Z in galactic globular clusters and the case of the pulsators in M15 17 p2609 A83-38425

The metal abundances of RR Lyrae stars in the globular clusters NGC 3201, NGC 4590, and NGC 6171 18 p2767 A83-39595

Orbital and chemical properties of globular clusters and halo stars 18 p2770 A83-39667

Globular clusters and the distance to the galactic centre 18 p2771 A83-39668

Globular clusters and the potential well of the Galaxy 18 p2771 A83-39669

Positions, magnitudes, and colors for stars in the globular cluster M92 19 p2910 A83-41053

NGC 6256, a galactic globular cluster 19 p2915 A83-41059

Abundances in globular cluster red giants. V - The metal-rich globular clusters 19 p2919 A83-41631

Core collapse with strong encounters --- for celestial systems 19 p2920 A83-41636

The velocity dispersion of the globular clusters in the Fornax dwarf galaxy 19 p2920 A83-41646

On the age of M92 and M15 20 p3063 A83-42187

The globular cluster NGC 6638 20 p3058 A83-42188

Magnitudes and colours of stars of central part of globular cluster M15 21 p3223 A83-44487

The evolutionary state and pulsation characteristics of red variables in globular clusters 21 p3236 A83-45544

The ellipticities of globular clusters and the second parameter problem 21 p3237 A83-45556

The main sequence of the globular cluster M22 22 p3377 A83-46381

Spectra of the blue CN and CH bands for a CN-enhanced giant in the open cluster IC 4651 22 p3377 A83-46382

Integrated magnitudes and colors of clusters in the magellanic clouds and Fornax system 22 p3373 A83-46401

Globular clusters and the early chemical history of galactic halos 22 p3378 A83-46409

Detectability of globular cluster systems in distant galaxies 22 p3378 A83-46410

Abundance sensitive parameters for red giants in globular clusters 22 p3378 A83-46545

Observations of red variable stars in globular clusters 22 p3378 A83-46546

M and S stars in the Magellanic Clouds 22 p3374 A83-46548

Globular cluster systems in the Hydra I elliptical galaxies. II 22 p3381 A83-46979

The kinematics of globular clusters in the Large Magellanic Cloud 22 p3381 A83-46982

The Al I-cyanogen correlation in the spectra of globular cluster red giants and the origin of intracluster heavy element variations 22 p3382 A83-46992

A search for neutral hydrogen near nine globular clusters 23 p3519 A83-47443

Ellipticity variations within some globular clusters of the Galaxy and the Magellanic Clouds 23 p3516 A83-47455

Colour magnitude diagram for central stars of globular cluster M 15 23 p3517 A83-48441

Dynamics of globular cluster systems 24 p3642 A83-49262

Far ultraviolet observations of Population II 24 p3662 A83-49562

The variable stars in the field of the globular cluster NGC 6681 24 p3646 A83-49883

Primordial helium in galactic globular clusters 24 p3666 A83-50047

Globular cluster colour-magnitude diagrams - Possible evidence for helium abundance variations 24 p3666 A83-50048

Helium content in globular clusters - The R-method 24 p3666 A83-50049

Helium abundances in globular star clusters 24 p3666 A83-50050

Variable stars in NGC 6397 24 p3649 A83-50153

GLOBULES

On the origin and structure of isolated dark globules 03 p0423 A83-14191

GLOBULINS

NT GAMMA GLOBULIN

The role of Fc-receptors of lymphocytes, macrophages, and other mammalian cells during the immune processes 01 p0082 A83-11406

Immunoglobulin genes 01 p0082 A83-11408

The genetics of immunoglobulins - Successes and problems 06 p0795 A83-18982

Immunoglobulin genes 14 p2065 A83-33326

The complement-fixing capability of aggregated immunoglobulins with various molecular weights 15 p2211 A83-34965

The content of immunoglobulins in the blood serum of patients with various forms of chronic inflammation of the middle ear 19 p2883 A83-41826

GLOMERULUS

Alterations in glomerular and tubular dynamics during simulated weightlessness 11 p1636 A83-27795

GLOSSARIES

U DICTIONARIES

GLOVES

Ergonomic aspects of aircraft keyboard design - The effects of gloves and sensory feedback on keying performance 04 p0526 A83-15900

GLOW

U LUMINESCENCE

GLOW DISCHARGES

Plasma science and technology --- Book on plasma chemistry, polymerization, deposition and surface treatment 01 p0022 A83-10875

Multikilowatt electron beams for pumping CW ion lasers 01 p0039 A83-10987

Stratification of a glow discharge in a gas flow at high energy inputs 01 p0108 A83-11321

A theoretical investigation of the distribution of electron concentration in the positive column of a glow discharge with a longitudinal flow of gas 02 p0240 A83-11514

Miniature, sealed TEA-CO₂ lasers with integral semiconductive preionization 03 p0332 A83-14166

Effect of discharge conditions on characteristics of hydrogenated amorphous silicon deposited by DC glow discharge decomposition 04 p0539 A83-15498

Optical properties of a-Si:H and a-SiC_{1-x}:H films prepared by glow-discharge deposition 04 p0541 A83-15522

Metastable atom density in helium, neon, and argon glow discharges 04 p0538 A83-16059

Ion extraction from a plasma through a conical orifice 05 p0687 A83-16920

A mechanism for the formation and breakdown of O₁ levels in the positive column of a glow discharge in O₂ 05 p0689 A83-17691

Energy balance in a contracted glow discharge in a longitudinal gas flow 06 p0811 A83-18441

The glow of an I₂/Ar mixture issuing from a quenching device at atmospheric pressure 07 p0932 A83-19958

Optogalvanic effects in the obstructed glow discharge 07 p0994 A83-19983

Spatial and temporal evolution of the thermal-ionizational instability 07 p0994 A83-20054

Studies of a glow discharge electron beam 07 p0997 A83-20733

The role of acceleration processes in the formation of nanosecond volume discharges in dense gases 07 p0998 A83-20867

- Investigation of the electrokinetic properties and of the dissociation of O₂ molecules in an oxygen discharge
09 p1348 A83-32987
- Several features of the free glow discharge
10 p1487 A83-26238
- A critical generalization of the results of experimental studies of the thermal and electrical characteristics of a glow discharge
11 p1660 A83-28557
- Glow discharge polycrystalline silicon thin-film transistors
13 p1832 A83-30345
- Mechanisms of glow-discharge compression
13 p1925 A83-30646
- A model for analysis of optical measurements carried on a-Si:H films for photovoltaic applications
14 p2041 A83-32253
- The effect of glow discharge excitation frequency on the performance of microcrystalline Si:H thin films and devices
14 p2043 A83-32279
- Large area and high efficiency A-Si:H solar cell
14 p2044 A83-32284
- Novel plasma chemical methods for doping a-Si:H
14 p2044 A83-32290
- Electronic properties of doped amorphous SiO(x)
14 p2089 A83-32291
- Effects of artificial excitation upon a low Reynolds number Mach 2.5 jet
14 p2081 A83-32996
- Pd/a-Si:H metal-insulator-semiconductor Schottky barrier diode for hydrogen detection
15 p2150 A83-33845
- Visible signatures of the multi-step transition to a beam-plasma-dicharge
15 p2234 A83-34195
- Glow discharge in a fast longitudinal gas flow
16 p2418 A83-36939
- Mechanism for the loss of fast electrons from a Penning glow discharge
16 p2418 A83-36940
- The energy of thermal electrons in electron beam created helium discharges
17 p2583 A83-38965
- Anode-plasma parameters of a high-voltage glow discharge of about 150 kV
18 p2746 A83-39863
- Model of Burgers turbulence for turbulent ionization waves
18 p2747 A83-39916
- Molecular gas lasers: Physics and application
18 p2693 A83-39983
- Study of O₂ (1-Delta) production in a glow discharge at large molar flow rates --- considering possibility of initiating iodine laser with discharged oxygen
20 p2994 A83-42643
- On the anomaly of the electrical field strength in the magnetized positive column of glow discharges at small currents
21 p3212 A83-44351
- Coronal and collisional - Radiative model of the plasma for the case of hydrogen glow discharge
21 p3212 A83-44353
- The hollow cathode glow discharge analysed by optogalvanic and other studies --- Thesis
22 p3267 A83-46689
- Comment on 'Stimulated bremsstrahlung masers'
22 p3299 A83-46741
- The secondary light emissions of a gaseous medium in the strong field of a standing electromagnetic wave
23 p3508 A83-48091
- Current-channel formation dynamics in a non-self-maintained discharge plasma
24 p3632 A83-49116
- GLUCOSE**
- The assay of glycosaminoglycans in the blood serum
03 p0375 A83-14333
- Several metabolic effects of a glucose-insulin-potassium mixture on patients with acute myocardial infarctions
05 p0674 A83-17218
- Fate of exogenous glucose during exercise of different intensities in humans
05 p0675 A83-17338
- Increased gluconeogenesis in hyper-G stressed rats
11 p1637 A83-27805
- Effect of denervation and reinnervation on oxidation of 6-(C-14) glucose by rat skeletal muscle homogenates
12 p1763 A83-29551
- The role of the middle hypothalamus structures in the regulation of the glucose content in the blood and the glycogen content in the liver
13 p1895 A83-30304
- The effect of glucose concentration and pH on hydrogen production by Rhodopseudomonas sphaeroides VM 81
15 p2193 A83-35303
- Effects of exercise and lack of exercise on glucose tolerance and insulin sensitivity
20 p3035 A83-43485
- Androgens enhance in vivo 2-deoxyglucose uptake by rat striated muscle
22 p3346 A83-46706
- GLUCOSIDES**
- An approach for determining common cholesterol and its structural-functional fractions in erythrocytes on the basis of the digitonin method
03 p0375 A83-14327
- The effect of strophanthine and celanide on the blood circulation and metabolism in the brain
07 p0975 A83-20983
- The pharmacology of cardioactive compounds in early ontogenesis --- Russian book
21 p3184 A83-45027
- GLUONS**
- Glueballs --- atoms of color formed by gluons
01 p0105 A83-10239
- The structure of gamma families and its relation to the formation of jets. II
02 p0274 A83-11742
- GLUTAMATES**
- The effect of hypothermia on the glutamate dehydrogenase activity in the brain
07 p0975 A83-20982
- The mechanism of kainic acid neurotoxicity
23 p3495 A83-48087
- GLUTAMIC ACID**
- The effect of pyridoxine, riboflavin, and glutamic acid on the activity of lysosomal hydrolases in the liver and blood serum of rats during traumatic stress
14 p2066 A83-33330
- GLUTATHIONE**
- Selective modification of glutathione metabolism
13 p1899 A83-31162
- Glutathione reductase in evolution
24 p3617 A83-49620
- GLYCERIDES**
- The lipid balance of technical flight personnel between 50 and 55 years old in commercial and civil aviation
06 p0798 A83-18340
- The content of phosphoglycerides in Rhodotorula rubra in three of its phenotypes as influenced by the lunar environment during the flight of Apollo 16
06 p0794 A83-18369
- GLYCERINS**
- U GLYCEROLS**
- GLYCEROLS**
- Effect of hydrogen bonding on the vibrational dephasing time in glycerol
07 p0874 A83-21054
- GLYCINE**
- The effect of several diuretics on the renal excretion of glycine in dogs
07 p0975 A83-20988
- Piezooptical properties of crystals of triglycine sulfate doped with L-alpha-alanine
13 p1930 A83-31304
- The effect of growth conditions on the polarization of triglycine sulfate doped with L-alpha-alanine
13 p1930 A83-31306
- Epsilon nonlinearity of doped triglycine sulfate crystals depending on conditions of growth
13 p1930 A83-31307
- The effect of various types of defects on the physical properties of crystals of the triglycine sulfate group
13 p1930 A83-31308
- Relaxation of the pyroelectric response of single crystals of triglycine sulfate doped with metal ions
13 p1931 A83-31310
- The nature of temperature anomalies of the piezooptical coefficient in crystals of the triglycine sulfate group
14 p2087 A83-32127
- An extensive galactic search for conformer II glycine
14 p2073 A83-33191
- A continuum mechanical approach to the ultrasonic relaxation of ferroelectric materials
15 p2238 A83-34348
- Growth of triglycine sulfate (TGS) crystals by solution technique
20 p2941 A83-43294
- GLYCOGENS**
- The content of glycogen in muscles and the effect of the carbohydrate saturation method on the physical aerobic work capacity of athletes and nonathletes
01 p0083 A83-10520
- The content and distribution of glycogen in the brain following an experimental craniocerebral injury
01 p0079 A83-10527
- Applications of mutant yeast strains with low glycogen storage capability
02 p0220 A83-11827
- The significance of glucocorticoids in the regulation of the resynthesis of glycogen in the postexercise period and the mechanism of their action
04 p0520 A83-15898
- The effect of the calmodulin inhibitor, trifluoroperazine, on the calcium activation of phosphorylases in the lysosomes of the skeletal muscles in rabbits
07 p0975 A83-20981
- The role of the middle hypothalamus structures in the regulation of the glucose content in the blood and the glycogen content in the liver
13 p1895 A83-30304
- Regulation of glycogenolysis in human muscle in response to epinephrine infusion
13 p1902 A83-30455
- Effect of glycogen depletion on the ventilatory response to exercise
13 p1903 A83-30474
- GLYCOLYSIS**
- The effect of glycolysis blockage in the vascular wall on the phasic activity of the smooth muscles
01 p0080 A83-10544
- The energy metabolism in the brains of rats exposed to mechanical asphyxia
07 p0972 A83-19923
- The problem of tissue adaptation to hypoxia
09 p1322 A83-25168
- A mathematical model for the regulation of glycolysis by the oxidation of pyruvate and fatty acids in the myocardium
14 p2064 A83-32957
- The condition of glycolysis in the heart during necrosis produced after the preliminary action of stress
14 p2066 A83-33339
- GLYCOSIDES**
- U GLUCOSIDES**
- GOAL THEORY**
- The Chebyshev approximation as the solution of the problem of multigoal planning in the case of arbitrarily correlated errors of measurement
06 p0805 A83-18352
- On the design of ergatic systems for the solution of a two-goal game-theoretical problem of control
20 p3036 A83-43509
- Planning in time - Windows and durations for activities and goals
21 p3198 A83-43951
- GOALS**
- The interaction of the dominant and the conditioned reflex as the functional unity of the organization of behavior
21 p3189 A83-45371
- GOBI DESERT**
- Origin of desert loess from some experimental observations
05 p0656 A83-16849
- GODDARD EXPERIMENT PACKAGE TELESCOPE**
- U PARTICLE TELESCOPES**
- GOES SATELLITES**
- NOAA/NESS satellite snowmapping techniques
01 p0061 A83-10012
- Delineation of cold-prone areas using nighttime SMS/GOES thermal data Effects of soils and water
02 p0216 A83-12961
- Solar radiation estimation using GOES satellite data
03 p0364 A83-14267
- Geostationary satellites ATS-6 and SMS/GOES - Description, position and data availability during IMS
04 p0511 A83-16283
- Reliability of enhanced infrared /EIR/ geostationary satellite data at high latitudes
08 p1137 A83-22925
- The use of stereoscopic satellite observation in the determination of the emissivity of cirrus
12 p1761 A83-29700
- Real-time stereoscopic applications using the GOES operational satellites --- stereo images and graphics for meteorological interpretation
12 p1761 A83-29702
- The use of VAS satellite data in weather analysis, prediction and diagnosis
13 p1887 A83-30560
- Application of VAS multispectral imagery to aviation forecasting --- VISSR Atmospheric Sounder for GOES satellites
13 p1887 A83-30561
- Preliminary efforts in developing a technique that uses satellite data for analyzing precipitation from extratropical cyclones
13 p1887 A83-30562
- Determination of thunderstorm heights and intensities from GOES infrared data
13 p1888 A83-30564
- A mesoscale, climatologically-based forecast technique for Colorado
13 p1888 A83-30568
- The GOES operational support system (GOSS)
17 p2548 A83-38710
- Analysis of rapid interval GOES data for the 9 July 1982 New Orleans airliner crash
17 p2553 A83-38767
- An interactive system for compositing digital radar and satellite data
18 p2726 A83-39869
- The life cycle of a tornadic cloud as seen from a geosynchronous satellite
20 p3031 A83-43436
- Estimating the solar zenith dependence of the clear-sky planetary albedo for land surfaces from the GOES satellite
20 p3010 A83-43474
- GOLD**
- NT GOLD ISOTOPES**
- Dependence of barrier height on energy gap in Au n-type GaAs/1-x/P/x/ Schottky diodes
02 p0242 A83-11784
- Tribological properties and X-ray photoelectron spectroscopy studies of ion-plated gold on nickel and iron
02 p0157 A83-12650
- Optical properties of gold-magnesia selective cermets --- for solar collectors
04 p0504 A83-15482
- Suppression of bulk modes in SAW transversal filters by gold transducers
09 p1255 A83-24119
- Studies of the reduction of oxygen on gold in molten Li₂CO₃-K₂CO₃ at 650 C
10 p1390 A83-26054
- Evidence for effective-mass states of a gold-related doubly charged donor in silicon
11 p1661 A83-28071
- Evidence that the gold donor and acceptor in silicon are two levels of the same defect
13 p1928 A83-30340
- Self-interstitial and vacancy contributions to silicon self-diffusion determined from the diffusion of gold in silicon
13 p1929 A83-30342
- Stopping of 200-GeV gold nuclei in nuclear emulsions
18 p2743 A83-40416
- Gold as a reliable internal pressure calibrant at high temperatures
20 p2959 A83-42596

Photovoltaic effect in gold-indium selenide Schottky barriers 24 p3634 A83-48912

GOLD ALLOYS

A two-dimensional phase separation on the spherical surface of the metallic glass Au₅₅Pb_{22.5}Sb_{22.5} 03 p0399 A83-14937

GOLD COATINGS

Physicochemical effects of heating gold thin films on gallium arsenide 07 p0882 A83-20591
Photovoltaic properties of Au-merocyanine-TiO₂ sandwich cells. I - Dark electrical properties and transient effects. II - Properties of illuminated cells and effects of doping with electron acceptors 11 p1661 A83-27494

The characteristics of Au-Ge-based ohmic contacts to n-GaAs including the effects of aging 14 p2006 A83-32671

GOLD ISOTOPES

Relativistic calculation of atomic M-shell ionization by protons [AD-A130664] 13 p1918 A83-31351

GOLD PLATE

U GOLD COATINGS

GONIOMETERS

NT RADIOGONIOMETERS

Potential accuracy of the goniometer section of a complex short-range navigation system 10 p1375 A83-26929

GOODNESS OF FIT

Two-dimensional goodness-of-fit testing in astronomy 07 p1007 A83-20942
A modified Kolmogorov-Smirnov test for Weibull distributions with unknown location and scale parameters 23 p3467 A83-47619

GOSS (SUPPORT SYSTEM)

U GROUND OPERATIONAL SUPPORT SYSTEM

GOVERNMENT PROCUREMENT

Tarps test program set / parallel development of avionics and its support capability/ 01 p0014 A83-10755
Aeronautical research - Some current influences and trends /The Second Sir Frederick Page Lecture/ 02 p0131 A83-12851
Strict liability in military aviation cases - Should it apply? 18 p2753 A83-39045
Prime contractor/subcontractor product liability exposure under government contracts 18 p2753 A83-39693

Durability and damage tolerance control plans for U.S. Air Force aircraft 19 p2797 A83-41045

GOVERNMENT/INDUSTRY RELATIONS

Future land remote sensing data and services - A commercial perspective 02 p0244 A83-11933
Aeronautical research - Some current influences and trends /The Second Sir Frederick Page Lecture/ 02 p0131 A83-12851
The role of the research establishments in the developing world of aerospace 06 p0711 A83-18963

Face to face for industry on NASA high technology 07 p1003 A83-20649

Technology transfer - A case history of success 07 p1003 A83-20650

Intellectual property rights in space ventures 07 p1001 A83-21386

Industrial innovation policy - Lessons from American history 07 p1001 A83-21421

The U.S. Coast Guard SES - Buying an off-the-shelf vessel [AIAA PAPER 83-0620] 08 p1172 A83-22169

Issues surrounding the commercialization of civil land remote sensing from space 12 p1783 A83-29915

United States space law: National and international regulation. I --- Book 13 p1934 A83-30137

United States Federal Photovoltaic Program status 14 p2037 A83-32179

The Space Transportation Company Inc. [SAE PAPER 821368] 17 p2586 A83-37961

Legislative developments affecting the aviation industry 1981-1982 18 p2752 A83-39043

Strict liability in military aviation cases - Should it apply? 18 p2753 A83-39045

New technologies from aerospace development 18 p2631 A83-39343

Prime contractor/subcontractor product liability exposure under government contracts 18 p2753 A83-39693

Space Station architectural issues as viewed by the user community - Commercial user mission concerns [AIAA PAPER 83-7100] 19 p2808 A83-42085

Universities - Have they a role in aeronautical research? Contribution to RAeS discussion evening --- university department planning for aeronautical research 20 p3056 A83-42620

The significance of a strong value-added industry to the successful commercialization of Landsat [AAS PAPER 83-185] 20 p3011 A83-43769

Comfort criteria and/or national requirements in the issuance of a license for air service in Canada 22 p3367 A83-45807

Airline subsidies --- a historical review 22 p3369 A83-45833

Deregulation of aviation in the United States 22 p3369 A83-45834

The 'legislative hearing' on IATA traffic conferences Creative procedure in a high stakes setting 22 p3370 A83-45838

The Freedom of Information Act - Its impact on civil aviation 22 p3370 A83-45839

Law and security in outer space - Implications for private enterprise 22 p3371 A83-46320

Law and security in outer space - Private sector interests 22 p3371 A83-46321

Law and security in outer space from the viewpoint of private industry 22 p3372 A83-46322

Research and development of helicopters in Europe 22 p3255 A83-46929

The need for additional Space Shuttle Orbiters [IAF PAPER 83-02] 23 p3413 A83-47228

The commercial Centaur family [IAF PAPER 83-233] 23 p3514 A83-47316

Competition in space - Government vs. industry 23 p3514 A83-47322

The law applicable to the use of space for commercial activities [IAF PAPER 83-253] 23 p3514 A83-47323

Push to commercialize space runs into budget cutbacks, boondoggle charges, and fear of high risks 23 p3514 A83-47820

Comparative cost of military aircraft - Fiction versus fact [AIAA PAPER 83-2565] 23 p3392 A83-48378

GOVERNMENTS

The management of federal research programs. I - Variations in techniques. II - Patterns of management 19 p2907 A83-41303

GRABENS

U GEOLOGICAL FAULTS

GRADIENT INDEX OPTICS

Raising damage thresholds of gradient-index antireflecting surfaces by pulsed laser irradiation 01 p0055 A83-10977

Demonstration of image transmission through fibers by optical phase conjugation 02 p0235 A83-11568

Multimode optical fibers as sensing devices 03 p0329 A83-14377

Paraxial imaging and transforming in a medium with gradient-index Transmittance function 03 p0395 A83-14388

Differential modal delay measurements in graded-index multimode optical waveguides 07 p0992 A83-19781

Beam aberration in phase conjugation by degenerate four-wave mixing in optical waveguides 07 p0993 A83-20152

Dual GRIN lens wavelength multiplexer --- Graded Refractive Index 07 p0993 A83-20831

Cold-induced losses in loose-sheath fiber-optic cables 08 p1165 A83-22484

Use of far-field radiation pattern to characterize single-mode symmetric slab waveguides 09 p1254 A83-24118

Application of nonlinear oscillator theory to multimode fibers 10 p1481 A83-25406

CW electro-optical characteristics of graded-index waveguide separate-confinement heterostructure lasers with proton-delineated stripe 10 p1430 A83-26202

Wedge coupling of lasers into multimode fibers 10 p1431 A83-26631

Sharp bends with low losses in dielectric optical waveguides 10 p1483 A83-26637

Determination of the amplitude-frequency characteristics of W-type fiber waveguides 10 p1484 A83-26692

Single-polarisation operation of highly birefringent bow-tie optical fibres 12 p1779 A83-29462

Mode analysis of optical fibres using computer-generated matched filters 12 p1779 A83-29463

Stabilisation of single and multimode fibre-optical microbend sensors 12 p1730 A83-29468

The development of fibre optic microbend sensors 12 p1730 A83-29519

Uniform and graded multilayers as X-ray optical elements 13 p1845 A83-30212

Mode energy transformation between two connected multimode general square-law-index optical waveguides 14 p2084 A83-32444

Dispersion of tubular modes propagating in multimode optical fibres 14 p2084 A83-32446

Hamiltonian analysis of beams in an optical slab guide 15 p2229 A83-33539

Modal characteristics of step-index concentric-core fiberguides of circular cross section [AD-A130935] 15 p2231 A83-34468

Reliability of graded-index lightguides 15 p2232 A83-34886

Attenuation in planar optical waveguides - Comparison of theory and experiment 16 p2412 A83-35966

Long delay time for lasing in very narrow graded barrier single-quantum-well lasers 16 p2360 A83-36008

Integrated optical waveguiding structures made by silver ion-exchange in glass. I - The propagation characteristics of stripe ion-exchanged waveguides: A theoretical and experimental investigation 16 p2413 A83-36768

Phenomenon of interference between two light beams propagating in optical fibers having a large path difference 17 p2580 A83-37744

Polarization-maintaining optical fibers with low dispersion over a wide spectral range 20 p3046 A83-42221

Coherent image amplification and optical phase conjugation with photorefractive materials 21 p3206 A83-44799

Multimode optical fiber sensors 21 p3142 A83-45415

Twisted double-heterostructure GaAs-(AlGa)As laser 21 p3146 A83-45484

The propagation of surface waves in graded-index slab waveguides with an irregular section 22 p3355 A83-45648

Optical wave propagation in form-birefringent media and waveguides 22 p3356 A83-45732

Numerical field solution for an arbitrary asymmetrical graded-index planar waveguide 22 p3356 A83-45733

A method of calculating the efficiency for coupling light power from a LED into an optical fibre by use of a sphere lens 24 p3627 A83-48745

Transversely anisotropic optical fibers - Variational analysis of a nonstandard eigenproblem 24 p3628 A83-48968

GRADIENTS

NT ELECTRON DENSITY PROFILES

NT POTENTIAL GRADIENTS

NT PRESSURE GRADIENTS

NT TEMPERATURE GRADIENTS

NT THERMOCLINES

Conjugate gradient method for the solution of linear equations - Application to molecular electronic structure calculations 12 p1778 A83-29640

Metallicity gradient in the galaxy and its origin 15 p2270 A83-34681

Preparative density gradient electrophoresis of cells and cell organelles - A new separation chamber 22 p3266 A83-45764

GRADIOMETERS

U MAGNETOMETERS

GRADUATION

U CALIBRATING

GRAIN BOUNDARIES

NT TRANSGRANULAR CORROSION

A model for the formation of subboundaries in the matrix of eutectic alloys of the system M-MeC --- Ni or Co alloyed with Ta, Nb or Hf carbides 01 p0025 A83-10397

A nucleus-free mechanism of irregular grain growth in metals 01 p0026 A83-10450

Investigation of the hydrogen-influenced tendency toward cold cracking in high-strength low-alloy fine-grained structural steel, with regard to the implant experiment --- German thesis 01 p0026 A83-10469

The scale effect in the elastic properties of polycrystalline materials 01 p0026 A83-10677

The effect of grain structure on the fracture behavior and tensile properties of an Al-Li-Cu alloy 02 p0154 A83-11865

The size of grains formed during dynamic recrystallization in ultrasonically loaded aluminum 02 p0155 A83-12205

Critical grain size corresponding to the superplastic transition 02 p0156 A83-12207

Crystal size and orientation in ice grown by droplet accretion in wet and spongy regimes 02 p0214 A83-12238

Ultrafine grain structures in alloys with recrystallization annealing 03 p0297 A83-13263

The asymmetric contrast and structure of antiphase boundaries in Ni₄Mo alloy 03 p0299 A83-14155

A search for diffuse band profile variations in the rho Ophiuchi cloud 03 p0423 A83-14194

Intergranular corrosion mechanism in Al-Mn alloys 04 p0457 A83-14963

Grain boundary diffusion mechanisms in metals 04 p0460 A83-16001

The influence of grain structure on the ductility of the Al-Cu-Li-Mn-Cd alloy 2020 04 p0460 A83-16004

- Laser annealing study of the grain size effect in polycrystalline silicon Schottky diodes
04 p0542 A83-16067
- Thorium segregation to grain boundaries in Ir + 0.3% W alloys containing 5-1000 ppm thorium
04 p0462 A83-16273
- Grain size and prestrain dependences of deformation behaviour of pure nickel at 4.2 K
05 p0614 A83-17088
- The effect of iron, aluminium, calcium on the vitrification of grain-boundary phases in nitrogen ceramics
05 p0619 A83-17570
- Anti-phase domain boundary tubes in NiAl --- crystal defect structures
05 p0616 A83-17792
- Texture and grain boundary strengthening in hot rolled magnesium - 12.5 at.% lithium alloy
05 p0616 A83-17951
- Decomposition processes in an Al-5 percent Zn-1 percent Mg alloy. III - Reversion of GP-zones
05 p0617 A83-17953
- Critical microstructures for microcracking in Al₂O₃-ZrO₂ composites
06 p0733 A83-17954
- Dependence of fracture toughness of alumina on grain size and test technique
06 p0734 A83-18051
- Slow growth of microcracks - Evidence for one type of ZrO₂ toughening
06 p0734 A83-18054
- Mechanics and mechanisms of intergranular cavitation in creeping alloys
06 p0728 A83-18478
- Problems in environmentally-affected creep crack growth
06 p0728 A83-18481
- Creep cavitation of grain interfaces
06 p0728 A83-18483
- Characteristics of the formation of the structure and properties of refractory niobium-base high alloys
06 p0729 A83-18746
- The importance of the excitation volume in determination of surface recombination velocity
06 p0814 A83-18755
- Grain boundary migration during sintering
06 p0730 A83-19078
- Determination of grain boundary barrier height and interface states by a focused laser beam
07 p0999 A83-19992
- Microstructure and grain-boundary composition of hot-pressed silicon nitride with yttria and alumina
07 p0898 A83-20166
- Precipitation of T₁ phase in α phase + T₁ type Al-4.2%Cu-1.3%Li alloy
07 p0885 A83-20294
- Rapidly solidified structure and grain refinement of aluminum containing titanium
07 p0885 A83-20295
- Intergranular cavitation in creeping alloys
07 p0887 A83-20627
- Models of creep cavitation and their interrelationships
07 p0887 A83-20628
- Mechanisms of cavity growth in creep
07 p0887 A83-20629
- Mechanisms of intergranular cavity nucleation and growth during creep
07 p0887 A83-20630
- Continuous cavity nucleation and creep fracture
07 p0887 A83-20631
- Determination of surface recombination velocity at a grain boundary using electron-beam-induced current
07 p0999 A83-20736
- The effect of the structure factor on the formation of the fracture surface in molybdenum alloys
07 p0889 A83-20900
- Structural characteristics of boundary regions and their effect on the development of microplastic strain in molybdenum with grain-boundary nickel segregations
07 p0891 A83-20922
- Characteristics of the oxide phase formation during the low-temperature oxygenation of niobium alloys
07 p0891 A83-20923
- Grain boundary pore chains in cast nickel base superalloys
07 p0894 A83-21486
- Investigation of the surface grain refinement for superalloys castings
07 p0895 A83-21499
- The nature and origin of previous particle boundary precipitates in P/M superalloys
07 p0895 A83-21501
- The structure of grain boundaries and their effect on mechanical properties
07 p0896 A83-21606
- Microstructures in cold-rolled polycrystalline aluminium
07 p0897 A83-21608
- Advances in understanding of boundary strengthening
07 p0897 A83-21609
- Dynamics of microstructural changes in a superplastic aluminium alloy
07 p0897 A83-21611
- Creep deformation induced substructure in polycrystalline molybdenum
07 p0897 A83-21612
- Superplastic deformation of an oxide-dispersion strengthened superalloy
07 p0897 A83-21613
- Creep fracture behavior of austenitic stainless steels from 550 to 800 C
08 p1062 A83-21746
- Effect of rate of heating for hardening on the structure of alloys VT23 and VT6
08 p1067 A83-22691
- The effect of structural components on the energy of intergranular fracture --- in Mo and W alloys
08 p1068 A83-22784
- The relation between surface energy and effective fracture energy for grain boundary fracture
09 p1279 A83-23869
- The effect of strain and concurrent grain growth on the superplastic behaviour of the Ti-6Al-4V alloy
09 p1230 A83-23871
- Dislocation creep in subgrain-forming pure metals and alloys
09 p1231 A83-24052
- A unifying view of the kinetics of creep cavity growth
09 p1279 A83-24066
- Cavitation in nickel during oxidation and creep
09 p1232 A83-24067
- Grain boundary sliding and fracture of metal bicrystals at high temperatures
09 p1232 A83-24068
- Creep crack extension by grain-boundary cavitation
09 p1279 A83-24070
- Mechanisms of creep deformation and fracture in single and two-phase Si-Al-O-N ceramics
09 p1238 A83-24072
- Microstructural aspects of the creep of alloys based on Nimonic 80A
09 p1232 A83-24075
- A new simple casting technique - The Flying Wheel Casting
09 p1274 A83-24123
- A conduction model for semiconductor-grain-boundary-semiconductor barriers in polycrystalline-silicon films
09 p1350 A83-24497
- Interstellar grain composition and the infrared spectrum of OH26.5+0.6
09 p1362 A83-24985
- Superplasticity --- and relation to grain size
10 p1392 A83-25308
- Effect of grain flow on creep properties of heat-resistant aluminium-alloy forgings
10 p1394 A83-25473
- Role of grain boundary segregation in diffusional creep
10 p1396 A83-25859
- Grain boundary sliding and stress concentration during creep
10 p1396 A83-25860
- Segregation to interphase boundaries in liquid-phase sintered Tungsten alloys
10 p1396 A83-25866
- A study of the structure of grain boundaries with special misorientations in tungsten
10 p1399 A83-26795
- Junction geometry in Cu₂S/CdS or Cu₂S/Cd/1-x/ZnS solar cells prepared by the solution reaction method
11 p1611 A83-27978
- Grain boundary effects in polycrystalline silicon solar cells. I - Solution of the three-dimensional diffusion equation by the Green's function method. II - Numerical calculation of the limiting parameters and maximum efficiency
11 p1611 A83-27981
- Relative influence of grain boundaries and intragrain defects on the photocurrents obtained with Bridgman polysilicon
11 p1661 A83-27985
- An electron microscopy study of the interaction between dislocations and grain boundaries during deformation
11 p1550 A83-28547
- Development of preferential intergranular oxides in nickel-aluminum alloys at high temperatures
11 p1550 A83-28668
- On the structure of tilt grain boundaries in cubic metals. I - Symmetrical tilt boundaries. II - Asymmetrical tilt boundaries. III - Generalizations of the structural study and implications for the properties of grain boundaries
11 p1551 A83-28807
- Grain-boundary diffusion in metals
12 p1713 A83-29240
- Observations of cyclic grain boundary migration in aluminium after large numbers of fatigue cycles
12 p1714 A83-29510
- A brittle to ductile transition in NiAl of a critical grain size
12 p1714 A83-29726
- Identification and resolution of a material defect in high strength beryllium
12 p1715 A83-29755
- [AIAA 83-0871]
Metallographic features of the subendritic structure of aluminum alloy ingots
13 p1819 A83-30065
- Distribution of impurity elements in titanium alloys
13 p1819 A83-30086
- A study of changes in the grain-boundary structure during the recrystallization of a magnesium alloy following small deformations
13 p1821 A83-30740
- Crystallographic features of subgranular structure and their relationship to the deformation texture
13 p1822 A83-30741
- The multiplicity of factors causing intergranular fracture
13 p1822 A83-30742
- The effect of environment on the growth of small fatigue cracks
13 p1824 A83-31539
- On the dependence of fracture toughness on metallurgical factors
13 p1824 A83-31586
- Grain boundary diffusion in columnar structure polycrystalline materials
13 p1931 A83-31765
- Grain boundaries and intragrain defects dependence of local and global electronic and photovoltaic properties of CGE polysilicon
14 p2088 A83-32233
- Study of the grain boundary effects in n-p junction polycrystalline Si solar cells
14 p2088 A83-32236
- The influence of grain-boundary recombination and grain size on the I(V)-characteristics of polycrystalline silicon solar cells
14 p2004 A83-32247
- Segregation of impurities at grain boundaries and other compositional inhomogeneities in chill-casted silicon ingots
14 p2090 A83-32309
- Grain boundary photocurrent enhancement in solar cells made by laser diffusion
14 p2046 A83-32332
- Grain boundary segregation in Ni and binary Ni alloys doped with sulfur
14 p1993 A83-32677
- Crack nucleation in tungsten on crystallographic planes and on grain boundaries of twist misorientation
14 p1997 A83-32946
- Diffusive relaxation of stress concentrations at grain boundary cavities in elevated temperature creep
14 p2033 A83-33452
- Efficiency of the a-Si:H solar cell and grain size of SnO₂ transparent conductive film
15 p2189 A83-33922
- Cyclic stress relaxation of polycrystalline metals at elevated temperature
15 p2138 A83-34145
- Cavity nucleation during fatigue crack growth caused by linkage of grain boundary cavities
15 p2139 A83-34489
- Temperature effects on fatigue thresholds and structure sensitive crack growth in a nickel-base superalloy
15 p2139 A83-34740
- A structural-kinetic criterion of superplasticity
15 p2141 A83-35306
- Nickel diffusion in the M/Mc phase boundaries
15 p2141 A83-35310
- Carrier recombination at grain boundaries and the effective recombination velocity
16 p2419 A83-35674
- Strengthening mechanisms in hot-rolled magnesium and magnesium alloys
16 p2330 A83-36070
- Intergranular crack-deflection toughening in silicon carbide
16 p2337 A83-36948
- Superplasticity - A review of data
16 p2335 A83-36959
- Effects of triaxial stressing on creep cavitation of grain boundaries
16 p2335 A83-36961
- A study relating slip steps and substructure produced during creep of an Al-Zn alloy
17 p2486 A83-37298
- Theory of beam induced current characterization of grain boundaries in polycrystalline solar cells
17 p2535 A83-37614
- The effect of extrusion conditions on the formation of the structure of titanium alloys
17 p2486 A83-37723
- Grain boundary phenomena in n-type CdTe films grown by hot wall vacuum evaporation
17 p2584 A83-38215
- Boundary conditions at grain boundaries
17 p2584 A83-38220
- Effect of rigid grains separation on the diffusive growth of crack-like cavities on grain boundaries
17 p2491 A83-38526
- Studies of nucleation mechanisms and the role of residual stresses in the grain boundary cavitation of a superalloy
17 p2491 A83-38857
- On the mechanism of serrated grain boundary formation in Ni-based superalloys
17 p2492 A83-38859
- Constitutive behavior and crack tip fields for materials undergoing creep-constrained grain boundary cavitation
17 p2492 A83-38860
- Density of gap states of silicon grain boundaries determined by optical absorption
18 p2750 A83-40063
- The role of non-equilibrium grain boundary structure in strain induced grain boundary migration (recrystallization after small strains)
18 p2668 A83-40613
- Diffusion induced grain boundary migration in Ni-C alloys
18 p2668 A83-40615
- Discontinuous gamma-prime coarsening in a Ni-Al-Mo base superalloy
18 p2669 A83-40628
- Observations of grain boundary sliding during superplastic deformation
18 p2669 A83-40635
- Characterization of grain boundaries in polycrystalline solar cells using a computerized electron beam induced current system
20 p2988 A83-42299
- Influence of carbon and hydrogen segregation on the electrical properties of grain boundaries in polycrystalline silicon sheets
20 p3051 A83-42351
- The effect of grain size on fatigue growth of short cracks
20 p2954 A83-43346
- Thermomechanical treatment for producing an ultrafine-grained structure in superplastic alloys
20 p2956 A83-43496
- The role of grain boundaries in high-temperature deformation and fracture
20 p2957 A83-43775
- On subcritical crack growth in ceramics as influenced by grain size and energy-dissipative mechanisms
21 p3116 A83-44122

- Relationship between grain boundary segregation and heat-treatment parameters in an aluminum alloy 21 p3111 A83-44338
- Optical properties and grain boundary effects in CuInSe_2 21 p3167 A83-44606
- Electron-beam-induced current measurements in silicon-on-insulator films prepared by zone-melting recrystallization 21 p3219 A83-45496
- Grain-boundary segregation in titanium-vanadium low alloys 23 p3431 A83-47181
- Microstructure development in silicon nitride 23 p3436 A83-48279
- Effect of grain size on the resistivity of polycrystalline material 23 p3512 A83-48611
- Structure and properties of vanadium maraging steels 24 p3559 A83-48805
- The effects of metal pretreatment and oxide grain size on the oxidation of cobalt 24 p3562 A83-49485
- Examination of the growth of NiO on Ni using magnetic resonance techniques 24 p3562 A83-49486
- Effect of texture and grain size on the fracture behaviour of hot rolled Mg, Mg-12.5 percent Li and Mg-5 percent Ti alloys 24 p3566 A83-49648
- Stress corrosion cracking and intergranular corrosion of 2017 aluminum alloy 24 p3566 A83-49861
- Microanalytical investigation of sintered SiC. II - Study of the grain boundaries of sintered SiC by high resolution Auger electron spectroscopy 24 p3569 A83-50071
- GRAINS**
- Grain alignment in the intergalactic magnetic field 15 p2263 A83-34552
- GRAINS (FOOD)**
- NT CORN
- NT RICE
- NT SORGHUM
- NT WHEAT
- GRAMMARS**
- An attribute grammar for the semantic analysis of Ada --- Book 21 p3191 A83-45140
- GRAND TOURS**
- NT VOYAGER 1977 MISSION
- Nuclear electric propulsion mission to Neptune [AIAA PAPER 82-1870] 02 p0137 A83-12459
- Satellite tour design for the Galileo mission [AIAA PAPER 83-0101] 05 p0602 A83-16822
- Virtual center arraying 07 p0916 A83-21199
- The extraordinary voyages through the region of the giant planets 08 p1048 A83-22049
- To Uranus and beyond 21 p3240 A83-44326
- GRANITE**
- Path dependence of acoustic velocity and attenuation in experimentally deformed Westerly granite 07 p0959 A83-20096
- Surface deformation of Westerly granite during creep 07 p0959 A83-20097
- Petrology and chemistry of two 'large' granite clasts from the moon 24 p3673 A83-50172
- GRANULAR MATERIALS**
- Model calculations of the molecular composition of interstellar grain mantles 03 p0427 A83-14757
- Calculation of the dispersal of a layer of granular material by a supersonic gas jet 05 p0639 A83-17407
- Presolar grains in micro-inclusions of iron meteorites 15 p2276 A83-35003
- The structure and properties of powder metallurgy aluminum alloys with transition metals 16 p2334 A83-36885
- The effect of the stress pattern on the ductility of aluminum-alloy powder compacts 16 p2334 A83-36886
- The effective lifetime in semicrystalline silicon --- for solar cells 23 p3512 A83-48618
- GRAPH THEORY**
- Sampling considerations for multilevel crossing analysis --- in pattern recognition 01 p0098 A83-11430
- Parallel implementations of a structural analysis algorithm --- for pattern recognition 01 p0100 A83-11457
- Image recognition by matching relational structures 01 p0100 A83-11468
- Air traffic flow control systems - Modelling and evaluation 10 p1374 A83-26602
- A graph-theoretic algorithm for hierarchical decomposition of dynamic systems with applications to estimation and control 13 p1911 A83-31071
- A parallel computation of connected components 15 p2218 A83-35114
- On graph theoretic approach to n- and (2n-1) stage interconnection networks 15 p2219 A83-35134
- Some methods of parallel organization of mass computations 16 p2403 A83-36903
- A two-step approach to finite element ordering 17 p2572 A83-38574
- A distance measure between attributed relational graphs for pattern recognition 19 p2889 A83-41297

GRAPHIC ARTS

- Graphical representation of prism coupling into thin films 20 p3047 A83-42223

GRAPHITE

- Electrical resistance of hot-pressed TiC-SiC-C composites 03 p0302 A83-14815
- A compliant, high failure strain, fibre-reinforced glass-matrix composite 04 p0455 A83-15989
- Plasma-spraying of a refractory coating on graphite 07 p0900 A83-20700
- A study of the formation conditions and refractory properties of silicon carbide and boron carbide coatings on GMZ-grade graphite 07 p0900 A83-20706
- Cadmium telluride films on foreign substrates 07 p1000 A83-20750
- Bragg-reflection profiles of graphite and alkali-graphite intercalation compounds - Comparison of double-axis and triple-axis spectrometer results 07 p0932 A83-21380
- Development of solvent insensitive graphite reinforced thermoplastic composites 09 p1221 A83-23609
- Room-temperature tensile strength of fibres in boron-aluminium, boron-titanium and graphite-aluminium composites as a function of annealing temperature and time 09 p1225 A83-25148
- Melting transition of near-monolayer xenon films on graphite - A computer simulation study 10 p1390 A83-25798
- Changes in the fracture characteristics of graphite under low-temperature neutron irradiation 11 p1551 A83-28506
- Drop weight impact testing of laminates reinforced with Kevlar aramid fibers, E-glass, and graphite 12 p1711 A83-29891
- Carbon fibers produced by pyrolysis of natural gas in stainless steel tubes 13 p1825 A83-30337
- An investigation of the possibilities for lowering the detection limits of elements in a graphite laser torch using the intracavity method for the registration of atomic absorption 14 p2020 A83-32826
- Environmental effects on graphite fiber reinforced PMR-15 polyimide 14 p1987 A83-33115
- Thermophysical properties data on graphite/polyimide composite materials 14 p1987 A83-33118
- A quasi-three dimensional analysis of thermal ablation from a hypersonic missile 15 p2159 A83-34254
- Recession behavior of graphitic nozzles in simulated rocket motors [AIAA PAPER 83-1317] 16 p2320 A83-36338
- The conspicuous absence of normal graphite grains in the small Magellanic Cloud 17 p2608 A83-38263
- Studies of the orientational ordering transition in nitrogen adsorbed on graphite 18 p2750 A83-39925
- Three-dimensional energy band in graphite and lithium-intercalated graphite 19 p2904 A83-40971
- A study of transport processes in a high-temperature boundary layer on an ablating graphite surface 19 p2842 A83-41259
- Ground state energy and structure of physisorbed monolayers of linear molecules 23 p3429 A83-47636
- Supermetallic conductivity of graphite intercalated with iodine monochloride 24 p3634 A83-48864
- Physicochemical means of reducing the synthesis temperature of refractory coatings for nonmetallic materials 24 p3568 A83-49079
- Experimental investigation of the reflection coefficients of graphites heated in different gaseous media 24 p3569 A83-49119
- High temperature corrosion of pure nickel and nickel-20 percent chromium alloy in the presence of calcium sulfate and graphite 24 p3563 A83-49497
- Intercalation of alkali metals in graphite under high pressure 24 p3569 A83-49554
- Moessbauer study of the lattice location of Co-57 implanted in graphite 24 p3636 A83-49756
- A reversible graphite-lithium negative electrode for electrochemical generators 24 p3558 A83-49946
- GRAPHITE-EPOXY COMPOSITES**
- Fatigue of graphite/epoxy 10/90/45/-45/s laminates under dual stress levels 02 p0149 A83-12060
- Finite element analysis of moisture effects in graphite-epoxy composites 02 p0150 A83-12762
- Analysis of bonded repairs to damaged fibre composite structures 03 p0291 A83-13200
- Rheological characterization of epoxy prepreg resins 03 p0302 A83-13563
- Damage documentation in composites by stereo radiography 03 p0292 A83-14553
- Fractographic studies of graphite/epoxy fatigue specimens 03 p0292 A83-14554
- An investigation of cumulative damage development in quasi-isotropic graphite/epoxy laminates 03 p0292 A83-14555
- The dependence of transverse cracking and delamination on ply thickness in graphite/epoxy laminates 03 p0292 A83-14559

- Characterization of delamination onset and growth in a composite laminate 03 p0293 A83-14560
- Characterizing delamination growth in graphite-epoxy 03 p0293 A83-14561
- Compression fatigue behavior of composites in the presence of delaminations 03 p0293 A83-14562
- Effect of stacking sequence on damage propagation and failure modes in composite laminates 03 p0293 A83-14563
- Damage mechanism and life prediction of graphite/epoxy composites 03 p0293 A83-14564
- Application of the ultrasonic testbed to graphite/organic composites 04 p0454 A83-15179
- Fatigue lifetime predictions from ultrasonically detected laminar defects in a graphite-epoxy composite 04 p0454 A83-15180
- Characterization of stability mechanisms in advanced composites 04 p0454 A83-15181
- Mechanisms of degradation of graphite composites in a simulated space environment [AIAA PAPER 83-0590] 05 p0610 A83-16807
- Space radiation effects on structural composites [AIAA PAPER 83-0591] 05 p0610 A83-16808
- Acceptance testing of graphite/epoxy composite parts using an acoustic emission monitoring technique 05 p0653 A83-16874
- Within-panel variability and scaling effects in composite materials --- static strength 05 p0611 A83-16934
- An equation for bolt clampup relaxation in transient environments 05 p0611 A83-16935
- Fatigue spectrum sensitivity of composite joints --- in aircraft structures 06 p0716 A83-17964
- Design and manufacture of composite tubes for compression applications 07 p0874 A83-20427
- Delamination in graphite/epoxy laminates 07 p0875 A83-20437
- HPLC evaluation of MY 720 II --- High Performance Liquid Chromatography-tetraglycidylated methylenedianiline used in epoxy graphite composites 07 p0875 A83-20441
- Material characterization and specification development for 350 F curing epoxy-graphite materials 07 p0875 A83-20443
- Impact testing of toughened epoxy resin systems 07 p0875 A83-20444
- Acousto-ultrasonic evaluation of impact-damaged graphite epoxy composites 07 p0875 A83-20454
- The effect of defects on the strength of composite sandwich assemblies 07 p0876 A83-20461
- The development of a precision composite spacecraft antenna reflector 07 p0920 A83-20463
- Serviceability evaluation of advanced composite F-14A main-landing-gear-strut doors and overwing fairings 07 p0861 A83-20480
- Demonstration of repairability and repair quality on graphite/epoxy structural subelements 07 p0861 A83-20485
- Fracture behaviour of a single-fibre graphite/epoxy model composite containing a broken fibre or cracked matrix 07 p0877 A83-21565
- Reliability analysis of circumferentially wound FRP flywheels 07 p0950 A83-21625
- Interlaminar fracture of composite materials 08 p1054 A83-21820
- Sonic fatigue of advanced composite panels in thermal environments 08 p1055 A83-22166
- Graphite/epoxy material characteristics and design techniques for airborne instrument application 08 p1055 A83-22595
- Study on composite flywheels for energy storage 08 p1131 A83-22701
- The influence of environmental effects on the mechanical properties of graphite/epoxy laminates 09 p1221 A83-23369
- Polyetheretherketone matrix composites 09 p1221 A83-23605
- Sealants - Uses in composite structures 09 p1236 A83-23615
- Damage and repair of the APS graphite/epoxy composite skins due to Columbia first flight April 12-14, 1981 --- Aft Propulsion System 09 p1210 A83-23633
- Graphite epoxy satellite structure development program 09 p1216 A83-23644
- Advanced methods for damage analysis in graphite-epoxy composites 09 p1222 A83-23648
- Delamination of T300/5208 graphite/epoxy laminates 09 p1223 A83-23938
- Stress singularities in laminated composites 09 p1223 A83-23939
- The interface crack between dissimilar anisotropic composite materials [ASME PAPER 83-APM-6] 10 p1441 A83-26443
- Deformation work density fracture criterion for composite materials 10 p1442 A83-26771
- Twin disk composite flywheel 11 p1609 A83-27304

Thermal expansion of graphite epoxy 11 p1543 A83-27443

Edge effects in composites by moire interferometry 11 p1594 A83-28076

Advanced design structural considerations when introducing new materials and construction methods 12 p1701 A83-29394

Wear characteristics of composites - Effect of fiber orientation 12 p1709 A83-29399

Space radiation environment effects on selected properties of advanced composite materials [AIAA 83-0803] 12 p1710 A83-29735

Fracture behavior of hybrid composite laminates [AIAA 83-0804] 12 p1710 A83-29736

A new look at commonly used failure theories in composite laminates [AIAA 83-0837] 12 p1710 A83-29745

Collapse analysis of cylindrical composite panels with cutouts [AIAA 83-0875] 12 p1738 A83-29759

Static and damage tolerance tests of an advanced composite vertical fin for L-1011 aircraft [AIAA 83-0970] 12 p1701 A83-29780

Stability analysis of Centaur-in-Shuttle composite corrugated adapters [AIAA 83-1003] 12 p1707 A83-29791

Analysis of progressive damage in thin circular laminates due to static-equivalent impact loads [AIAA 83-0997] 12 p1711 A83-29872

A finite element analysis of composite tension specimens 12 p1711 A83-29892

A mixed-mode fracture criterion for composite materials 12 p1711 A83-29895

First design details of the all-composite Lear Fan 13 p1806 A83-30829

X-29 - Advanced technology demonstrator 13 p1806 A83-31051

Interlaminar shear properties of graphite fiber, high-performance resin composites 13 p1816 A83-31794

Dynamic-mechanical response of graphite/epoxy composite laminates and neat resin 13 p1817 A83-31795

Space environmental effects on graphite/epoxy composites 14 p1987 A83-33121

Effects of extreme aircraft storage and flight environments on graphite/epoxy 14 p1987 A83-33122

Dynamic tests of graphite/epoxy composites in hygrothermal environments 14 p1987 A83-33124

Fracture morphology of graphite/epoxy composites 15 p2130 A83-34793

Optimal design of high speed rotating graphite/epoxy shafts 15 p2172 A83-34796

Low-kilovoltage radiography of composites 16 p2363 A83-35759

Process-induced residual thermal stresses in advanced fiber-reinforced composite laminates 17 p2483 A83-37366

Design of an aerobatic aircraft wing using advanced composite materials [SAE PAPER 821346] 17 p2463 A83-37955

Manufacturing methods for composite graphite hole generation [SAE PAPER 821418] 17 p2516 A83-37976

Composite materials in aircraft structures 18 p2650 A83-40130

Factors affecting the interlaminar fracture energy of graphite/epoxy laminates 18 p2651 A83-40152

Fracture mechanics for delamination problems in composite materials 18 p2652 A83-40153

On mechanical fastening in graphite epoxy composite 18 p2652 A83-40155

Fatigue of composite bolted joints under dual load levels 18 p2703 A83-40158

Predicted elastic constants of transversely isotropic composites containing anisotropic fibers 18 p2652 A83-40160

In-plane tensile strength of multidirectional composite laminates 18 p2653 A83-40173

Compressive buckling of graphite-epoxy composite circular cylindrical shells 18 p2704 A83-40184

Damage analysis of fibrous composites 18 p2654 A83-40189

Analysis of mechanical damage growth in notched carbon-epoxy (+ or - 45 deg)ns laminates 18 p2654 A83-40191

Deformation characteristics and failure modes of center-notched graphite/epoxy laminates 18 p2654 A83-40198

Statistical analysis of composite fatigue life 18 p2655 A83-40200

Compressive fatigue damage accumulation near holes in graphite/epoxy laminates 18 p2655 A83-40203

Creep behaviour of carbon-epoxy (+ or - 45 deg)2s laminates 18 p2655 A83-40209

Effects of corrosive environments on graphite/epoxy composites 18 p2656 A83-40227

Effect of stacking sequence in cross-ply graphite/epoxy laminates on acoustic emission results 18 p2661 A83-40276

Development of advanced composite fabrication for aerospace structures 18 p2661 A83-40278

Development of structural graphite/epoxy tube for space application 18 p2661 A83-40285

Design, manufacture and test of graphite composite wing box test structure 18 p2641 A83-40291

Temperature dependence of mechanical and thermal expansion properties of T300/5208 graphite/epoxy 20 p2947 A83-42811

A finite element analysis of heat transfer in solid with radiation and ablation 20 p2983 A83-43015

Fracture mechanics for delamination problems in composite materials 20 p3007 A83-43143

Interlaminar stresses at a hole in a composite member subjected to in-plane loading 20 p3007 A83-43146

An analysis and comparison of the tribological behavior of two polymers sliding against a polymeric composite [ASLE PREPRINT 83-AM-8A-1] 20 p2958 A83-43334

Weight control program for a graphite/epoxy aircraft [SAWE PAPER 1485] 20 p2948 A83-43752

Viscoelastic behavior of AS/3501-6 Gr/ep composite 21 p3105 A83-44043

Residual stresses and their effects in composite laminates 21 p3105 A83-44045

Bi-linear failure analysis of fiber composite laminates 21 p3106 A83-44049

Wave propagation in a graphite/epoxy laminate 21 p3151 A83-44050

Fracture toughness of composite adherend adhesive joints under mixed mode I and III loading 21 p3115 A83-44121

Acoustic emission from graphite/epoxy composite laminates with special reference to delamination 21 p3106 A83-44126

Compression fatigue behaviour of notched composite laminates 21 p3106 A83-44334

Composite materials: Quality assurance and processing; Proceedings of the Symposium, St. Louis, MO, October 20, 1981 21 p3107 A83-45065

Quality assurance of graphite/epoxy by high-performance liquid chromatography 21 p3149 A83-45066

A four-point shear test for graphite/epoxy composites 21 p3107 A83-45068

Void formation and transport during composite laminate processing - An initial model framework 21 p3107 A83-45070

Calculation of cure process variables during cure of graphite/epoxy composites 21 p3107 A83-45071

Characterization of quick-cure and vacuum-bag cure composites 21 p3119 A83-45073

Out-of-plane deformation of balanced and symmetric composites as measured by holographic interferometry 21 p3108 A83-45153

Characterization of the matrix glass transition in carbon-epoxy laminates using the CSD test geometry --- centro-symmetric deformation 22 p3262 A83-46282

Observation of damage growth in compressively loaded laminates 22 p3264 A83-46810

Effects of 0.5-MeV electrons on the interlaminar shear and flexural strength properties of graphite fiber composites 24 p3553 A83-48901

GRAPHITE-POLYIMIDE COMPOSITES

A study of the thermo-oxidation process and stability of graphite and glass/PMR polyimide composites 07 p0877 A83-20490

Graphite/polyimide technology overview and Space Shuttle Orbiter applications 09 p1221 A83-23634

Celion/Larc-160 graphite/polyimide composite processing techniques and properties 09 p1222 A83-23635

Fabrication of bonded graphite/polyimide structures for advanced aerospace applications 09 p1210 A83-23636

Analysis, design, and test of a graphite/polyimide Shuttle orbiter body flap segment 09 p1216 A83-23637

Design, fabrication and test of graphite/polyimide composite joints and attachments [AIAA 83-0907] 12 p1739 A83-29763

Dynamic mechanical characterization of cure of a polyimide-graphite fiber composite (PMR 15/Celion 6000) 13 p1816 A83-31793

Interlaminar shear properties of graphite fiber, high-performance resin composites 13 p1816 A83-31794

Composites for extreme environments --- Book 14 p1986 A83-33114

V378A polyimide resin - A new composite matrix for the 1980's 14 p1987 A83-33116

Thermomechanical characterization of graphite/polyimide composites 14 p1987 A83-33117

Elastic properties and fracture behavior of graphite/polyimide composites at extreme temperatures 14 p1987 A83-33119

Composite engine duct fabrication 18 p2631 A83-39941

Lower-curing-temperature PMR polyimides 19 p2823 A83-40923

On the off-axis tension test for unidirectional composites 19 p2819 A83-41033

A study of the thermo-oxidative process and stability of graphite and glass-PMR polyimide composites 22 p3262 A83-46285

Effects of 0.5-MeV electrons on the interlaminar shear and flexural strength properties of graphite fiber composites 24 p3553 A83-48901

GRAPHS (CHARTS)

NT BOND GRAPHS

Graphical analysis method for a retarding potential analyzer and its application to the real-time measurements of ion temperature in space plasmas 02 p0142 A83-12818

Enhancement of a graph drawing package 04 p0527 A83-15147

A logarithmic reflection chart for presentation of antenna impedance 10 p1411 A83-26844

A reevaluation of the meaning of capacitance plots for Schottky-barrier-type diodes 11 p1564 A83-28712

The use of graph-analytic methods to solve problems of the operational planning of scientific experiments --- aboard spacecraft 21 p3094 A83-45292

GRASHOF NUMBER

Natural convection from a horizontal cylinder at small Grashof numbers 05 p0641 A83-17744

Free convection about a sphere at small Grashof number 16 p2349 A83-35558

GRASSES

NT SORGHUM

Growth response and spectral characteristics of a short Spartina alterniflora salt marsh irrigated with freshwater and sewage effluent 10 p1443 A83-25645

Radiometric estimation of biomass and nitrogen content of Alicia grass 14 p2035 A83-32616

GRASSHOPPERS

Aerial survey of crop losses due to grasshoppers /Orthoptera - Acrididae/ in Saskatchewan 03 p0347 A83-14255

GRASSLANDS

Landsat for delineation and mapping of saline soils in dryland areas in southern Alberta 03 p0348 A83-14261

The influence of time of year and the colors of prairie flora bloom on their spectral behavior and that of the prairie where they are found 08 p1126 A83-21928

Inventory and evaluation of rangeland in the Cimarron National Grassland, Kansas 15 p2184 A83-34806

GRASSMANN ALGEBRA

U VECTOR SPACES

GRATINGS

The excitation of a metal-bar grating by a current passing across one of the gaps 05 p0630 A83-17594

GRATINGS (SPECTRA)

Visible ultraviolet optical design of toroidal mirror-toroidal grating combinations 02 p0237 A83-12695

Discussion of the relative efficiency in the vacuum ultraviolet of diffraction gratings with laminar sinusoidal and triangular grooves 02 p0238 A83-12709

X-ray ultraviolet grating measurements at LURE - Comparison with electromagnetic theory predictions 02 p0238 A83-12710

Grazing incidence gratings and mirrors - Case studies 02 p0238 A83-12711

Manufacture and measurement of ion-etched X-ray diffraction gratings 02 p0238 A83-12712

Development in replicated nickel gratings 02 p0238 A83-12713

Analysis of the throughput of a grazing incidence monochromator using transmission gratings 02 p0239 A83-12714

Fabrication of transmission gratings for use in X-ray astronomy 02 p0240 A83-12725

Determination of the vibrating phase by a time-averaged shadow moire method 03 p0395 A83-14396

Higher-order distributed feedback and generation of light 05 p0648 A83-17049

Diffraction efficiency of out-of-phase amplitude-phase volume holograms 05 p0644 A83-17080

Propagation and conversion of light waves in corrugated waveguide structures 05 p0685 A83-17081

A two-grating method for combined beam splitting and frequency shifting in a two-component laser-Doppler velocimeter 05 p0645 A83-17352

Three-wave mixing and light diffraction by transient light induced gratings for the study of fast relaxation processes 05 p0651 A83-17888

A new method for simultaneous complex addition and subtraction --- of two input optical signals with holographic grating 05 p0646 A83-17890

Diffraction-field structure in the Fraunhofer zone 06 p0809 A83-17983

Monochromatic imaging from UV to IR using a subtractive double monochromator 06 p0762 A83-18579

Time-resolved X-ray transmission grating spectrometer for studying laser-produced plasmas 07 p0928 A83-20163

A three-dimensional pattern recognition technique for inspection of missing parts in assemblies 07 p0942 A83-20452

Influence of transient absorber gratings on the pulse parameters of passively mode-locked CW dye ring lasers 07 p0937 A83-21362

Wavefront distortion introduced by sampling with a hole grating --- high power laser beam diagnostics 08 p1108 A83-22455

Phase grating effects in pulsed CO₂ electric discharge lasers 08 p1109 A83-22462

Rigorous coupled-wave analysis of pure reflection gratings 09 p1338 A83-24099

Moire deflectometry with deferred analysis 09 p1269 A83-24442

Design of dielectric grating antennas for millimeter-wave applications 10 p1402 A83-25816

Submicrometer periodicity gratings as artificial anisotropic dielectrics 10 p1482 A83-25978

High power TEA CO₂ laser tuned by a holographic grating 12 p1731 A83-29196

Stigmatism conditions of concave holographic gratings utilized at normal incidence 12 p1730 A83-29384

Cooled grating array spectrometer for 0.6-5 microns 14 p2016 A83-31998

Cooled grating Fabry-Perot spectrometer for the 10 micron region 14 p2017 A83-32003

European Southern Observatory (ESO) coudeechelle spectrometer 14 p2084 A83-32005

Grens for a Ritchey-Chretien (R-C) telescope --- grating-on-lens corrector optics 14 p2096 A83-32008

Stellar spectrograph using aberration corrected concave holographic grating 14 p2017 A83-32009

Dynamic free-carrier holograms in semiconductors 14 p2084 A83-32164

Wave scattering and guidance by dielectric waveguides with periodic surfaces 15 p2229 A83-33537

Spatiotemporal variation of chromatic and achromatic contrast thresholds 15 p2215 A83-33802

Underlying psychometric function for detecting gratings and identifying spatial frequency 15 p2214 A83-33803

Iterative solutions for electromagnetic scattering by gratings 15 p2224 A83-33804

Diffraction of light by a perfectly conducting biaxial periodic surface 15 p2231 A83-34367

0.81 micron band AlGaAs/GaAs double-channel planar buried-heterostructure laser with large optical cavity 15 p2169 A83-34517

Experimental and theoretical investigations of the influence of a saturation grating in an absorber on pulse generation in a passively mode-locked dye laser 16 p2359 A83-35887

A cooled grating spectrometer for Tingo 18 p2690 A83-40430

Irspec --- cooled grating array IR spectrometer for use with New Technology Telescope 18 p2690 A83-40433

Cooled grating spectrometer 18 p2690 A83-40433

Analysis and design of frequency scanned transmission gratings 18 p2676 A83-40651

Efficient spectral narrowing of a XeCl TEA laser 18 p2694 A83-40662

Deep-ultraviolet spatial-period division using an excimer laser [AD-A122130] 19 p2850 A83-40672

Two-dimensional modeling of the MIS grating solar cell 20 p3054 A83-43356

Restoration of out-of-focused color photographic images 20 p2992 A83-43631

Chirped grating lenses in Ti:indiffused LiNbO₃ optical waveguides 21 p3207 A83-44835

New grating spectrometer with increased throughput 21 p3140 A83-44840

Detection of hidden diffractors by coherence measurements 21 p3208 A83-44841

Moireinterferometry for damage analysis of composites 21 p3108 A83-45148

Double ion exchanged chirp grating lens in lithium niobate waveguides 21 p3208 A83-45483

The element pattern in the theory of diffraction gratings and Rayleigh's hypothesis 22 p3271 A83-45652

Fourier processing with phase-reflection gratings 22 p3287 A83-45959

Wavelength-selective absorption enhancement in thin-film solar cells 22 p3319 A83-46735

Three-dimensional vector coupled-wave analysis of planar-grating diffraction 23 p3507 A83-47577

High-frequency holographic transmission gratings in photoresist 23 p3454 A83-47578

Diffraction characteristics of planar absorption gratings 23 p3509 A83-48706

Fringe addition in moireanalysis 24 p3582 A83-49010

Chirped grating lenses on Nb₂O₅ transition waveguides 24 p3629 A83-49020

Space-correlation measurement of attaching jets by the new scanning laser Doppler velocimeter using a diffraction grating 24 p3585 A83-49827

GRAVIMETERS

The possibility of laboratory detection of long-period gravitational waves 01 p0125 A83-10904

Possible systematic errors in OVM pendulum apparatus 02 p0177 A83-11955

The precise measurement of gravitational acceleration using a laser interferometric technique 04 p0481 A83-15275

Applications of an orbiting gravity gradiometer 14 p1983 A83-31900

GRAVIMETRY

A spaceborne superconducting gravity gradiometer for mapping the earth's gravity field 01 p0020 A83-10025

Inversion of gravity gradients for density information 01 p0070 A83-10067

Covariational analysis of the correlation between lunar relief and the acceleration due to gravity 03 p0432 A83-13369

A technique for reducing low-frequency, time-dependent errors present in network-type surveys --- magnetic and gravity drift corrections 07 p0957 A83-19872

Direct integration of Stokes' undulation and Vening Meinesz's deflection equations for geographically defined gravity anomaly blocks 07 p0958 A83-19873

NNE-SSW fault system in part of the Gulf of Suez and its bearing on oil exploration 09 p1286 A83-24551

Interpolation and transformations of maps --- French thesis 11 p1601 A83-28632

Wave of gravitational experiments in space 11 p1683 A83-28694

Prospects for the detection of gravity wave bursts 13 p1846 A83-30359

Quantum nondemolition measurements on coupled harmonic oscillators --- for gravitational radiation detection 16 p2355 A83-35651

Gravimetry --- recent advances (1979-82) 17 p2542 A83-38302

Status of the geopotential --- earth gravity measurement 17 p2542 A83-38303

Excitation of the earth's eigenvibrations by gravitational radiation from astrophysical sources 19 p2915 A83-41164

Results from an absolute gravity survey in the United States 22 p3322 A83-45743

Marine gravity measurement from fixed wing aircraft 22 p3288 A83-46111

International Symposium on Geodetic Networks and Computations, Munich, West Germany, August 31-September 5, 1981, Proceedings. Volume 7 - Combination of horizontal, vertical and gravity networks 22 p3316 A83-46351

Combination of horizontal, vertical and gravity networks - A review 22 p3316 A83-46352

Combination of leveling and gravity data for detecting real crustal movements 22 p3316 A83-46353

A contribution to 3D-operational geodesy. I - Principle and observational equations of terrestrial type. II - Concepts of solution 22 p3317 A83-46354

Orientation information of levelling and gravity measurements in three-dimensional regional networks 22 p3317 A83-46355

Test computations of three-dimensional geodetic networks with observables in geometry and gravity space 22 p3317 A83-46357

Three-dimensional adjustment of geodetic networks using gravity field data 22 p3317 A83-46358

GRAVIRECEPTORS

NT OTOLITH ORGANS

Characteristics of statoliths from rootcaps and coleoptiles 11 p1637 A83-27810

Striated organelles in hair cells of rat inner ear maculas - Description and implication for transduction 11 p1638 A83-27818

Gravity receptors in a microcrustacean water flea - Sensitivity of antennal-socket setae in Daphnia magna 11 p1639 A83-27823

Reversible loss of gravitropic sensitivity in maize roots after tip application of calcium chelators 16 p2394 A83-36017

Gravity and the cells of gravity receptors in mammals 19 p2877 A83-42046

The state of gravity sensors and peculiarities of plant growth during different gravitational loads 19 p2878 A83-42050

GRAVITATION

NT GRAVITY ANOMALIES

NT LUNAR GRAVITATION

NT LUNAR GRAVITATIONAL EFFECTS

NT PLANETARY GRAVITATION

NT REDUCED GRAVITY

NT SOLAR GRAVITATION

Deformation, gravity, and potential changes due to volcanic loading of the crust 07 p0961 A83-20231

Thermodynamic fluctuations and gravitational instabilities 07 p1018 A83-20950

The unit gravitational charge /hc/4/ 1/2 /the uniton/, the structure of the electron and muon, and their anomalous magnetic moments 11 p1655 A83-27498

Quantum gravity and the 'flatness problem' of the standard big bang universe 17 p2614 A83-38963

Results from an absolute gravity survey in the United States 22 p3322 A83-45743

GRAVITATION THEORY

The external field of a rotating and charged body in the vector graviton metric theory 01 p0119 A83-10232

Origin and evolution of galaxies; Proceedings of the International School of Cosmology and Gravitation, Course, 7th, Erice, Italy, May 11-23, 1981 01 p0127 A83-11287

Generalized theory of gravitation and its physical consequences 01 p0127 A83-11292

Perfect fluids in general relativity 02 p0233 A83-12026

Static conformally flat solutions in a general scalar-tensor theory of gravitation 02 p0233 A83-12090

The gravitational evolution of structure in a scale-free universe 03 p0412 A83-13301

The energy problem in Einstein's theory of gravitation /Dedicated to the memory of V. A. Fock/ 03 p0416 A83-13426

Equivalence principle for massive bodies in a generalized theory of gravitation. I, II 03 p0417 A83-13494

Space-time layers in gravitation theory 03 p0390 A83-13528

Quantum formalism in gravitation quantitative application to the Titius-Bode law 03 p0411 A83-14867

Gravitation without black holes 03 p0431 A83-14876

Post-Newtonian approximations in scale covariant gravitation 04 p0556 A83-15960

Static plane-symmetric solution of a scalar-tensor theory of gravitation 04 p0557 A83-16368

Manifestations of a cosmological density of compact objects in quasar light 05 p0696 A83-16978

Does gravitation reveal its secret 06 p0816 A83-19246

Clocks and gravity 06 p0806 A83-19446

The unified field theory, combining Kaluza's five-dimensional and Weyl's conformal theories 06 p0806 A83-19449

Relativistic tidal forces 06 p0845 A83-19507

Theory of gravitation 07 p1013 A83-20403

Analysis of the large-scale structure of the universe 07 p1017 A83-20935

The nonuniqueness of the limit transition from Brans-Dicke theory to Einstein theory 07 p0990 A83-20970

Perfect fluids in the Einstein-Cartan theory 07 p0990 A83-21065

Solution of the gravitational polytropic equations by using the quasi-invariance group --- stellar evolution model 08 p1180 A83-22060

Black holes and the stability of gravitation 08 p1180 A83-22202

Interaction of massless scalar field and charged dust in nonrigid rotation 08 p1181 A83-22744

Consequences of a new experimental determination of the quadrupole moment of the sun for gravitation theory 08 p1186 A83-23238

The fourth test of General Relativity 09 p1357 A83-23855

On semi-degenerate equilibrium configurations of a collisionless self-gravitating Fermi gas 10 p1500 A83-25482

A new approach to scale-invariant gravity /or: A variable-mass embedding for general relativity/ 10 p1501 A83-25497

Pregeometric origin of the big bang 10 p1506 A83-26092

Algebraic programming of Hamiltonian formalism in general relativity - Application to inhomogeneous space-times 10 p1506 A83-26093

Some remarks on zeta function regularization in curved space-times 10 p1472 A83-26094

On the energy distribution function for a one-dimensional gravitational system 11 p1682 A83-28293

Wave of gravitational experiments in space 11 p1683 A83-28694

Classical and quantum models of strong cosmic censorship 12 p1774 A83-28873

Geometrical mass of charged particle in Brans-Dicke theory 12 p1774 A83-28875

Herrmitian gravity and supergravity 12 p1774 A83-29029

Cosmological consequences of the existence of the unit gravitational charge (Planck's constant \times speed of light/4) exp 1/2 12 p1792 A83-29042

Hamiltonian structure of the theory of gravity with $R + T(2)$ type of Lagrangian 12 p1775 A83-29043

Hamiltonian formulation for a translation gauge theory of gravitation 12 p1792 A83-29045

Hamiltonian formulation of the gauge theory of gravitation Pure-gravity case. 12 p1792 A83-29046

Gravitational Debye-Hueckel theory for a Newtonian cosmology 12 p1793 A83-29061

Magnetogravitational instability of a finitely-conducting medium with variable streaming motion 12 p1793 A83-29072

Scale covariance and post-Newtonian approximations in the framework of General Relativity 12 p1796 A83-29549

Chronometrically invariant variations in the Einstein gravitation theory 13 p1944 A83-30099

Limiting density of matter as a universal law of nature 13 p1947 A83-30798

Supersymmetry and supergravity 13 p1914 A83-31163

On the stability of gravitating liquid bodies containing small solid cores 13 p1962 A83-31272

Supergravity '81; Proceedings of the First School, Trieste, Italy, April 22-May 6, 1981 13 p1915 A83-31400

A scalar field with self-interaction leads to the absence of a singularity in cosmology 14 p2102 A83-32424

Quantum cosmology and stationary states 14 p2102 A83-33046

Exact solutions for the early universe in general scalar-tensor theories 14 p2102 A83-33047

Microcanonical quantum gravity 14 p2103 A83-33050

Zero-energy theorem for scale-invariant gravity 15 p2224 A83-33791

Magnetic monopoles and evaporating black holes 15 p2254 A83-33793

Perturbation of an exact strong-gravity solution 15 p2225 A83-34414

Computation of Jupiter interior models from gravitational inversion theory 15 p2275 A83-34720

Evolution of a homogeneous universe with a posthydrodynamic stress-energy tensor for the ultrarelativistic medium 15 p2270 A83-34751

Tensorial rank of gravitational theories in flat space-time 16 p2407 A83-36553

Large numbers hypothesis. IV - The cosmological constant and quantum physics 16 p2408 A83-36987

Spinning fluids in the Einstein-Cartan theory 16 p2408 A83-36989

On a nonlinear and Lorentz-invariant version of Newtonian gravitation 18 p2741 A83-39197

Representation of a gravitational field by means of a hypercomplex potential 18 p2767 A83-39528

Primordial nucleosynthesis and scale-covariant cosmology 18 p2774 A83-39736

Charged particle motion on and off the equatorial plane of a magnetic star in Rosen's bimetric gravity 18 p2775 A83-39754

Quantum gravity - A unified model of existence? 18 p2776 A83-39773

Variable gravity theories 18 p2741 A83-39776

Relativistic thermodynamics of irreversible processes in a static gravitational field; a theory of phenomenological heat conduction 18 p2777 A83-39780

Recent developments in scalar-tensor theories of gravity 18 p2741 A83-39781

Rastall's and related theories are conservative gravitational theories although physically inequivalent to general relativity 18 p2741 A83-40417

General solutions for the field of a charged particle in Brans-Dicke theory of gravitation 18 p2741 A83-40418

Kepler and two-body problems in bimetric Machian gravitation 18 p2763 A83-40625

$N = 1$ supergravity with nonminimal coupling - A class of models 19 p2895 A83-40961

A scalar-tensor theory of gravity incorporating Mach's principle 19 p2895 A83-41170

Spatially homogeneous and anisotropic cosmological solution in Brans-Dicke theory 19 p2916 A83-41282

A bimetric Machian approach to gravitation 19 p2916 A83-41285

On a gravitational hypothesis 19 p2896 A83-41563

Cylindrically symmetric Einstein-Maxwell-massless scalar field equations 21 p3199 A83-44367

Reference systems in gravitation theory --- Russian book 21 p3234 A83-45043

The first steps in quantum gravitation and Planck's quantities 21 p3200 A83-45050

A possible approach to the description of topological transitions in quantum gravitation theory 21 p3201 A83-45382

Non-Einsteinian gravitational Lagrangians assuring cosmological solutions without collapse 22 p3380 A83-46753

The influence of quantum effects on the structure of space-time near singularities in general relativity 23 p3504 A83-48445

Hydrodynamics, fields, and constants in gravitation theory --- Russian book 23 p3527 A83-48450

Soliton collision in general relativity 24 p3650 A83-48918

Nonlinear gravitational-field equations in the special theory of relativity 24 p3623 A83-49063

Cosmological term in a nonsingular cosmological model of the Einstein-Cartan gravitation theory 24 p3651 A83-49067

Scalar-tensor theories of gravitation - Foundations and prospects 24 p3651 A83-49100

Gravitational instability for a multilfluid medium in an expanding universe 24 p3660 A83-49430

The anthropic principle and the actual size of the universe 24 p3661 A83-49523

Non-equilibrium relativistic cosmology 24 p3663 A83-49650

Electric-magnetic duality of conformal gravitation 24 p3624 A83-49745

GRAVITATIONAL COLLAPSE

NT BLACK HOLES (ASTRONOMY)

NT WHITE HOLES (ASTRONOMY)

A comparison of the entropies of collapsing stars and black holes 01 p0119 A83-10234

On the collapse dynamics of cold stars with a phase transition in the interior 01 p0119 A83-10264

Explaining supernova explosions 01 p0117 A83-10570

The lower end of the main sequence 01 p0124 A83-10571

Shock induced star formation - The effects of magnetic fields and turbulence 01 p0126 A83-10945

Homologous collapse and deleptonization of an evolved stellar core 02 p0252 A83-11601

Gamma-ray bursts and the collapse of a white dwarf 02 p0252 A83-11611

Transport of neutrinos, radiation and energetic particles in accretion flows 02 p0276 A83-12031

Evolutionary luminosity functions of extragalactic sources driven by gravitational power 02 p0259 A83-12515

Gravitational radiation from collapsing rotating stellar cores 02 p0260 A83-12523

3D models for self-gravitating, rotating magnetic interstellar clouds 02 p0260 A83-12537

A statistical method for determining ages of globular clusters by fitting isochrones 04 p0547 A83-15619

Collapse of iron stellar cores 04 p0554 A83-15637

A numerical study of the effects of ambipolar diffusion on the collapse of magnetic gas clouds 05 p0698 A83-16997

Neutrino escape, nuclear dissociation, and core collapse and/or explosion 05 p0700 A83-17027

Nuclear forces and the properties of matter at high temperature and density 06 p0826 A83-18098

Neutrino emission spectra of collapsing degenerate stellar cores - Calculations by the Monte Carlo method 06 p0832 A83-18843

Massive neutrinos in large-scale gravitational clustering 06 p0839 A83-19270

Superclusters as nondissipative pancakes - Flattening 06 p0843 A83-19479

Black hole explosions 07 p1013 A83-20404

Production of the Be-9 isotope induced by neutrinos generated through gravitational stellar collapse 07 p1015 A83-20668

Two-dimensional simulation of the gravitational superclustering of collisionless particles 07 p1018 A83-20940

Supernovae: A survey of current research; Proceedings of the Advanced Study Institute, Cambridge University, Cambridge, England, June 29-July 10, 1981 08 p1176 A83-21826

The fate of massive stars - Collapse, bounce and shock formation 08 p1177 A83-21829

Supernovae for pedestrians --- collapse phase described by self-similar solutions 08 p1177 A83-21831

Shock stagnation and neutrino losses in stellar collapse 08 p1177 A83-21832

Computer simulations of stellar collapse and supernovae explosions - Non-rotating and rotating models 08 p1177 A83-21833

The boundary between explosion and collapse in very massive objects 08 p1178 A83-21842

Supernovae and the formation of galaxies 08 p1179 A83-21858

Hydrodynamic collapse --- of stars 08 p1179 A83-22030

Novikov-type coordinates for HJ separable metrics --- in relation to gravitational collapse 08 p1180 A83-22203

Perfect fluid spheres in general relativity 08 p1180 A83-22207

Self-similar stellar collapse 08 p1184 A83-23069

Signatures of stellar collapse in electron-type neutrinos 08 p1186 A83-23267

Gravitational collapse and fragmentation of isothermal, non-rotating, cylindrical clouds 10 p1500 A83-25492

Models of the formation of the solar nebula 10 p1521 A83-25508

Cluster collapse and radio source morphology 11 p1679 A83-27993

Gravitational collapse of pressureless inhomogeneous spheroids 11 p1681 A83-28275

Lepton loss and entropy generation in stellar collapse 12 p1791 A83-28987

Asymptotic freedom and entropy in a perpetually oscillating universe 12 p1794 A83-29166

Gravitational instability - The second approximation in the linear long-wave theory 13 p1948 A83-31253

Stellar collapses in the galaxy 13 p1952 A83-31443

The collapse of a fast rotating interstellar gas cloud 13 p1956 A83-31679

A numerical method for the study of the gravothermal instability in star clusters 13 p1958 A83-31707

The effect of the existence of a single coordinate system of curvature on the properties of the boundary between the R and T regions and the energy-momentum tensor --- in stellar gravitational collapse 14 p2102 A83-32131

Thin charged shells and the violation of the third law of black hole mechanics 14 p2102 A83-33044

The equilibria of rotating, isothermal clouds. I - Method of solution. II - Structure and dynamical stability 14 p2104 A83-33195

Does stellar collapse produce supernovae or black holes? 15 p2254 A83-33814

Magnetorotational collapse of an iron stellar core 15 p2254 A83-33815

An outline of approach linking black-hole-evaporation with quantum-field effects in flat spacetime 15 p2262 A83-34531

A limit for gravitational collapse 15 p2263 A83-34545

Encounters of binaries. I - Equal energies 15 p2265 A83-34596

Quasar evolution and gravitational collapse 15 p2267 A83-34618

Interstellar magnetic fields 15 p2273 A83-35010

Bulk viscosity of degenerate neutrinos 17 p2629 A83-37932

Direct dissipationless formation of filaments in the large-scale matter distribution 17 p2607 A83-38259

Post-collapse evolution of globular clusters 17 p2607 A83-38261

On the collapse of neutron stars and stellar cores to pion-condensed stars 18 p2776 A83-39766

Electron capture during gravitational collapse in type II supernovae 19 p2916 A83-41169

Cosmic censorship and curvature growth 19 p2916 A83-41283

Core collapse with strong encounters --- for celestial systems 19 p2920 A83-41636

The effect of trapped lepton number and entropy on the outcome of stellar collapse 19 p2920 A83-41638

Oxygen neutronization in accreting white dwarfs 20 p3065 A83-42381

The collapse and violent relaxation of N-body systems - Mass segregation and the secondary maximum 20 p3066 A83-42430

Cosmological estimate of the age of stars exploding as Type I supernovae 20 p3075 A83-43537

3-D simulations of the collapse of nonspherical interstellar clouds 21 p3230 A83-44438

Transport properties of neutrinos in stellar collapse. I Bulk viscosity of collapsing stellar cores 21 p3230 A83-44444

- A search for X-rays from runaway stars 21 p3237 A83-45552
- Phase transitions in dense stars 23 p3519 A83-47446
- Material and electromagnetic sources of the Kerr-Newman geometry --- of collapsed rotating star 23 p3525 A83-47602
- Vibrating-dust spheres in the Reissner-Nordstrom metric 23 p3525 A83-47603
- Softening effects in the equation of state and influence of general relativity on the outcome of stellar collapse 23 p3527 A83-48061
- The breakdown of the connectedness of physical space --- in cosmology and during gravitational collapse 24 p3651 A83-49060
- Some exact models for nonspherical collapse. I 24 p3651 A83-49096
- Some exact models for nonspherical collapse. II 24 p3651 A83-49097
- Galaxy formation - Some comparisons between theory and observation 24 p3657 A83-49267
- Proto-galactic perturbations 24 p3658 A83-49365
- GRAVITATIONAL CONSTANT**
- Zero age main sequence models with variable G 02 p0261 A83-12865
- The determination of the gravitational constant and the detection of gravitational radiation in a cosmic laboratory 05 p0702 A83-17851
- Stability of a 1 solar mass star with decreasing gravitational constant 11 p1678 A83-27688
- Determination of the geocentric gravitational constant from satellite observations 24 p3604 A83-48933
- GRAVITATIONAL EFFECTS**
- NT GRAVITATIONAL LENSES.
- NT LAGRANGIAN EQUILIBRIUM POINTS
- NT LUNAR GRAVITATIONAL EFFECTS
- NT STELLAR GRAVITATION
- Implications of gravitational interactions for the angular momenta of galaxies 01 p0126 A83-10965
- Gravity modeling for airborne applications 01 p0004 A83-11090
- Formation of galaxies in G-variable cosmologies 01 p0127 A83-11294
- Plants, gravity, and mechanical stresses 02 p0220 A83-11835
- Gravitation, phase transitions, and the big bang 02 p0259 A83-12220
- Oscillations of a satellite with compensating devices in an elliptical orbit 03 p0287 A83-13204
- The distribution of companion galaxies to mirror-symmetric extragalactic radio sources 03 p0420 A83-13940
- Ballistic entry motion, including gravity - Constant drag coefficient case 03 p0283 A83-14839
- Self-gravitation in Saturn's rings 03 p0435 A83-14863
- The precise measurement of gravitational acceleration using a laser interferometric technique 04 p0481 A83-15275
- Further evidence for a mass movement origin of the Olympus Mons Aureole 04 p0566 A83-15566
- Problem of detecting quantum-gravity effects 04 p0555 A83-15709
- Structure and thermal evolution of the Galilean satellites 04 p0570 A83-16229
- 'A total G-force environment dynamic flight simulator' - A new dimension in flight simulation [AIAA PAPER 83-0139] 05 p0599 A83-16548
- Dynamical models and our Virgo-centric deviation from Hubble flow 05 p0696 A83-16976
- Tidal compression of the Local Supercluster 06 p0828 A83-18183
- Momentum balance of gravity flows 06 p0789 A83-18255
- Gravitationally induced spurs in spiral galaxies - An example in M31 06 p0843 A83-19488
- The motion of short-wavelength photons in gravitating, refractive media 06 p0845 A83-19508
- On one type of system with equivalent external gravity effects 07 p0962 A83-20603
- Dynamical friction on extended objects --- during gravitational interaction with non-colliding particles 07 p1023 A83-21205
- Charged dust in Saturn's magnetosphere 07 p1035 A83-21326
- Effect of compressibility on the Rayleigh-Taylor instability 08 p1085 A83-22386
- Nature of the Kirkwood gaps in the asteroid belt 08 p1176 A83-23259
- Stationary motions of two linked bodies 09 p1337 A83-23559
- Thermal and gravitational instability of a model hydrogen plasma in the presence of a radiation field 09 p1347 A83-23598
- Gravitational three-body problem in 120 deg axial coordinates 09 p1339 A83-24437
- Comment on 'A schematic model of crater modification by gravity' by H. J. Melosh 09 p1367 A83-25075
- Determination of the masses of Saturn and Uranus from an analysis of the motion of the minor planets /944/ Hidalgo and /2060/ Chiron 10 p1492 A83-25490
- Velocity fluctuations in the interstellar medium due to the gravitational interaction with the system of stars 10 p1500 A83-25491
- Evolution of cometary perihelion distances in Oort cloud - Another statistical approach 10 p1492 A83-25511
- Gravitational lenses 10 p1505 A83-25899
- Stellar disruption by tidal forces 10 p1507 A83-26232
- Bending waves in Saturn's rings 11 p1683 A83-27353
- The role of dissipation in shepherding of ring particles 11 p1683 A83-27354
- The absorber theory for the Einstein equations in the first approximation 11 p1677 A83-27455
- International Union of Physiological Sciences, Annual Meeting, 4th, San Diego, CA, October 10-15, 1982, Proceedings 11 p1635 A83-27776
- The effect of gravity on plant cells 11 p1635 A83-27777
- The first plants to fly on Shuttle 11 p1635 A83-27778
- Human tolerance to rotation at different G's 11 p1642 A83-27784
- Cardiovascular and endocrine effects of gravitational stresses /LBNP/ - The influence of angiotensin-converting enzyme inhibition with captopril 11 p1642 A83-27798
- Estimation of skeletal muscle mass from body creatine content 11 p1637 A83-27803
- Restraint hypothermia in cold-exposed rats at 3 G and 1 G 11 p1637 A83-27806
- Altered auditory function in rats exposed to hypergravic fields 11 p1637 A83-27808
- The mode of gravity sensing in plant cells 11 p1638 A83-27811
- Linkage between gravity perception and response in the grass leaf-sheath pulvinus 11 p1638 A83-27812
- Role of auxin and protons in plant shoot gravitropism 11 p1638 A83-27813
- Quantitation of chlorpromazine-bound calmodulin during chlorpromazine inhibition of gravitropism 11 p1638 A83-27815
- A reevaluation of the role of abscisic acid in root gravitropism 11 p1638 A83-27816
- The mechanics of gravitropic bending in leafy dicot stems 11 p1638 A83-27817
- Oculomotoric response to voluntary head rotations during parabolic flights 11 p1643 A83-27820
- Reversal of early pattern formation in inverted amphibian eggs 11 p1638 A83-27821
- Gravito-inertial sensitivity of the spider - Araneus sericatus 11 p1639 A83-27822
- Gravitropic basis of leaf blade nastic curvatures 11 p1639 A83-27828
- Velocity-change distribution in the problem of long-period comets 11 p1672 A83-27885
- The effect of resonance perturbations from a planet's gravitational field on the motion of a satellite 11 p1532 A83-28041
- On the motion of geostationary satellites in the earth's gravitational field 11 p1532 A83-28055
- The effect of gravity on freely growing crystals 11 p1662 A83-28171
- Why weakly non-linear effects are small in a zero-pressure cosmology 11 p1682 A83-28283
- About the non-existence of additional analytical integral in the problem of satellite's motion under the gravitational attraction of a triaxial rigid body 12 p1787 A83-29120
- A theoretical prediction of the fluid buckling frequency 13 p1839 A83-30108
- Global value of Hubble constant 13 p1946 A83-30382
- Regional gas distributions and single-breath washout curves in head-down position 13 p1903 A83-30469
- Gravity dependence of phases III, IV, and V in single-breath washout curves 13 p1904 A83-30495
- Gravity deflections of lightweighted mirrors 13 p1922 A83-31028
- Metrology mount development and verification for a large spaceborne mirror 13 p1939 A83-31030
- The renormalized coupling constant in an open static Einstein universe 13 p1954 A83-31607
- Tidal compression of a star by a large black hole. I Mechanical evolution and nuclear energy release by proton capture 13 p1959 A83-31747
- Thin axisymmetric cavities in flow past a body in a longitudinal gravitational field 14 p2008 A83-32158
- Measurement of thermoacoustic convection heat transfer phenomenon [AIAA PAPER 83-1422] 14 p2009 A83-32701
- Binary-single star scattering. I - Numerical experiments for equal masses 14 p2105 A83-33209
- New opportunities in space - Research in microgravity 15 p2123 A83-33544
- Stationary axially symmetric perturbations of the Reissner-Nordstrom black hole. I - Equations for the perturbations 15 p2254 A83-33771
- Does Venus breathe? 15 p2275 A83-34725
- Some results of studies of the effect of weightlessness on the growth of an epiphytic orchid 15 p2211 A83-34967
- Reversible loss of gravitropic sensitivity in maize roots after tip application of calcium chelators 16 p2394 A83-36017
- Nonstationary shaping filters for simulation of gravity uncertainty effects on missile trajectories 17 p2472 A83-37072
- Can secondary infall produce flat rotation curves? 17 p2596 A83-37314
- Plasma effects in the formation, evolution and present configuration of the Saturnian ring system 17 p2621 A83-38120
- Nonuniformity of the earth's rotation within a day 17 p2545 A83-38562
- The motion of a stationary satellite in the neighbourhood of the equilibrium points of a central potential perturbed by the J(22) term 17 p2472 A83-38941
- Long-period tidal forcing of Indian monsoon rainfall - An hypothesis 18 p2722 A83-39124
- Weak dynamical effects in the Uranian ring system 18 p2779 A83-39604
- Fragmentation, protostellar winds, and star formation 18 p2774 A83-39728
- Melt temperature fluctuations - Causes and response of the solidification front --- in low gravity environments 18 p2643 A83-39895
- Oscillatory thermocapillary convection in floating zones under normal- and micro-gravity 18 p2643 A83-39901
- Gravitational influence on binary alloy melt equilibria 18 p2644 A83-39905
- Sensitivity on nonequilibrium chemical systems to gravitational field 18 p2751 A83-39910
- Marangoni effects under electric fields 18 p2686 A83-39911
- How to detect the gravitationally induced phase shift of electromagnetic waves by optical-fiber interferometry 19 p2846 A83-40967
- A determination of gravitational perturbations in the intermediate motion of artificial earth satellites 19 p2809 A83-41546
- Power series for perturbations in the intermediate motion of artificial earth satellites caused by atmospheric attraction 19 p2809 A83-41548
- Gravitational model effects on ICBM accuracy [AIAA PAPER 83-2296] 19 p2810 A83-41755
- Life sciences and space research XX(2); Proceedings of the Workshop and Topical Meeting, Ottawa, Canada, May 16-June 2, 1982 19 p2877 A83-42029
- Experimental and theoretical analysis of the influence of gravity at the cellular level - A review 19 p2877 A83-42043
- Gravity and positional homeostasis of the cell 19 p2877 A83-42044
- Research on the adaptation of skeletal muscle to hypogravity Past and future directions 19 p2877 A83-42047
- Gravitational effects on human cardiovascular responses to isometric muscle contractions 19 p2884 A83-42049
- The state of gravity sensors and peculiarities of plant growth during different gravitational loads 19 p2878 A83-42050
- Calcium movements and the cellular basis of gravitropism 19 p2878 A83-42051
- Gravitational effects on plant growth hormone concentration 19 p2878 A83-42052
- The lunar ephemeris ELP 2000 20 p3059 A83-42383
- Gravity-driven convection studies in compound semiconductor crystal growth by physical vapor transport 20 p3054 A83-43297
- The shape of the small satellites of Saturn - Gravitational equilibrium vs solid-state strength 20 p3079 A83-43586
- Mathematical modelling of a flexible beam under gravity 21 p3150 A83-43982
- Stability of a self-gravitating partially ionized plasma 21 p3212 A83-44357
- Effects of simulated increased gravity on the rate of aging of rats - Implications for the rate of living theory of aging 21 p3183 A83-44575
- Gravitational radiation reaction in the binary pulsar and the quadrupole-formula controversy 21 p3235 A83-45197

Nonlinear electromagnetics in vacuo - Gravitational effects 21 p3201 A83-45413
Gravity-induced emf in superionic conductor RbAg415 22 p3364 A83-45621
On the mechanism of the gravitational differentiation in the inner earth 22 p3324 A83-45792
Materials processing in the reduced-gravity environment of space 22 p3257 A83-45895
Hypergravic fields and parallel controllers for thermoregulation 22 p3346 A83-45998
Computer simulations of gravitational encounters between pairs of binary star systems 22 p3377 A83-46389
A large millimeter wave antenna 22 p3375 A83-46748
Cytological aspects of higher plant ontogenesis under microgravity [IAF PAPER 83-190] 23 p3494 A83-47306
Magnetic equilibrium in coronal arcades 23 p3537 A83-47727
Gravitational anisotropies of gyromagnetic ratios and tests of general relativity 23 p3503 A83-47876
An experimental study of the effects of gravity on flame spread in high oxygen concentration environments 23 p3430 A83-48158
Stability of the periodic oscillations of a nearly axisymmetrical satellite in the plane of an elliptical orbit 23 p3418 A83-48455
Nonaxisymmetric equilibrium shapes of a drop on a plane 23 p3452 A83-48670
A noncanonical analytic solution to the J2 perturbed two-body problem 24 p3550 A83-48763
Stabilizing a cold disk with a 1/r force law 24 p3656 A83-49236
The effects experienced by a point electric dipole in a gravity field 24 p3623 A83-49455
Galaxies in clusters - Alignments, formation from pancakes, and tidal forces 24 p3664 A83-49998

GRAVITATIONAL FIELDS
NT STELLAR GRAVITATION
Topology of cosmological models near critical points 01 p0125 A83-10907
Light rays in gravitating, refractive media 02 p0233 A83-12138
Deflections of the vertical on the farside of the moon 02 p0268 A83-12866
The energy-momentum pseudotensor of the gravitational field and the gravitational radiation emitted by an axisymmetric system 03 p0417 A83-13474
Conformal-plane gravitational fields of a viscous fluid 03 p0390 A83-13526
A relativistic gas in a gravitational field 03 p0417 A83-13527
Space-time layers in gravitation theory 03 p0390 A83-13528
A refined gravity model from Lageos /GEM-L2/ 03 p0358 A83-13549
On the motion of a body whose dynamical structure is variable 03 p0419 A83-13885
The study of toroidal magnetic configurations in a spherically symmetric gravitational field with applications to coronal loops and transients 04 p0573 A83-14988
Gravity field model of Mars in spherical harmonics up to degree and order eighteen 04 p0564 A83-15553
Toroidal solutions of the Gegenbauer equation --- for space gravitational and plasma problems 04 p0532 A83-15961
The law governing the variation of the anomalous gravitational field with the survey altitude 04 p0510 A83-16037
On the possibility for a fourth test of general relativity in earth's gravitational field 05 p0683 A83-17148
Concerning a method for the determination of initial geodetic data 05 p0664 A83-17679
On equations of motion for cross term modified gravitational field equations 05 p0703 A83-17860
Translation effect of reference system on harmonic coefficients of gravitational potential 06 p0817 A83-18018
The fluctuations in the instantaneous virial mass of stationary gravitating systems 06 p0831 A83-18828
Measurability analysis of the linearized gravitational field 06 p0806 A83-19448
On an analogy to the Steklov case for a balanced gyrostat in a Newtonian gravitational force field 07 p0988 A83-20145
On a stationary solution for the motion of a rigid body about a fixed point under the influence of a Newtonian force field 07 p0988 A83-20200
Algorithmization of computations in a discretely observed gravitational field 07 p0962 A83-20602
On one type of system with equivalent external gravity effects 07 p0962 A83-20603

Variation of e/m in the five-dimensional theory of gravitation, electromagnetism, and scalar field 07 p0989 A83-20852
Rayleigh-Taylor instability with spatially varying acceleration - An illustration 08 p1168 A83-22378
A fiber-optic gyrometer in a gravitational field 08 p1105 A83-23165
Consequences of a new experimental determination of the quadrupole moment of the sun for gravitation theory 08 p1186 A83-23238
Inflation and time asymmetry in the universe 08 p1186 A83-23272
Local momentum representation of a propagator in external gravitational and electromagnetic fields 09 p1338 A83-24212
Vacuum static gravitational fields with axial symmetry 09 p1338 A83-24213
Results of a study of the gravitational field, figure, and internal structure of Mars 09 p1367 A83-25280
The absorber theory for the Einstein equations in the first approximation 11 p1677 A83-27455
Resonance transition scattering in vacuum in the presence of an external gravitational field 11 p1649 A83-27456
The rotation number of bounded orbits in a central field 12 p1787 A83-29116
Accuracy of the earth's gravity field models 12 p1752 A83-29221
Soliton configurations of interacting zero-mass fields 13 p1913 A83-30095
On the possibility of using a Laplace series for the gravitational potential at the surface of a planet. II 13 p1949 A83-31268
Periodic motions of a satellite in the gravitational field of a rotating rigid body 13 p1809 A83-31397
Applications of an orbiting gravity gradiometer 14 p1983 A83-31900
Dynamic properties of gravitational fields 14 p2079 A83-32351
Nonlinear effects in a gravitating plasma disk subject to a poloidal magnetic field 15 p2254 A83-33721
New general relativistic effect by means of charged-particle interferometry 15 p2224 A83-33792
Collisionless matter and galaxy formation 15 p2255 A83-33818
The universal solution of Einstein's equations of general relativity. I - Gravitation 15 p2226 A83-34550
The accuracy of the low-degree geopotential - Implications for ocean dynamics 16 p2393 A83-36600
Earth's flattening effect on the tidal forcing field 16 p2381 A83-36618
The planar inverse problem with four monoparametric families of curves --- for coplanar cofocal elliptical orbits in autonomous gravitational field 16 p2426 A83-36691
Drift-rotational gravitational instability in galaxies 17 p2600 A83-37646
The gravitational field and density distribution inside Mars 17 p2619 A83-37696
Mapping the earth's magnetic and gravity fields from space Current status and future prospects 17 p2540 A83-38146
Turbulence in a self-gravitating gaseous disk. II - Turbulence spectra 17 p2610 A83-38553
On the nonlinear theory for the stability of a rotating gravitating disk 17 p2614 A83-38848
Gravitational radiation of plasmas - Bremsstrahlung 18 p2744 A83-39522
Representation of a gravitational field by means of a hypercomplex potential 18 p2767 A83-39528
On the local standard of rest --- comoving with young objects in gravitational field of spiral galaxies 18 p2768 A83-39633
Velocity distribution of stars and relaxation in the galactic disk 18 p2768 A83-39640
Compressible, conductive, steady MHD flow in a gravitational field --- applied to mass flow in sunspots 18 p2784 A83-39733
Sensitivity on nonequilibrium chemical systems to gravitational field 18 p2751 A83-39910
Renormalizability of quantum gravity with cosmological constant 18 p2777 A83-39923
Gravitational scintillation, anisotropies of background radiation and density inhomogeneities of cosmic matter 18 p2777 A83-40364
State space of the gravitational field in the Hamiltonian approach to general relativity 19 p2895 A83-40821
A planetary density model and the normal gravitational field of the earth 19 p2866 A83-41475
The classical inverse scattering problem for a spherically symmetric gravitational field 19 p2917 A83-41493
A simple example of a classical gauge transformation 19 p2899 A83-41876
The gravitational field and brain function 19 p2877 A83-42045

A gravitationally stable Bok globule 20 p3067 A83-42442
Spiral gravitational potentials and the mass growth of molecular clouds 20 p3071 A83-43053
Collocations and thirtieth order resonant harmonics --- for determining earth's gravitational field 20 p3023 A83-43153
The gravitational potential due to uniform disks and rings 20 p3061 A83-43571
Bifurcations and phase transitions of self-gravitating and uniformly rotating fluid 21 p3232 A83-44737
Investigation of the lunar gravitational field according to measurements of the trajectories of Soviet artificial lunar satellites 21 p3241 A83-45276
Test of the principle of equivalence by a null gravitational red-shift experiment 22 p3380 A83-46714
Satellite technology developments in gravity research [IAF PAPER 83-223] 23 p3414 A83-47314
Inference of variations in the gravity field from satellite-to-satellite range rate 23 p3482 A83-47814
Orbital rates of earth satellites at resonances to test the accuracy of earth gravity field models 24 p3550 A83-48768
Relativistic kinetic equation for inelastically interacting particles in a gravitational field 24 p3636 A83-49062
Occupation of quasi-bound states by electrons in a Schwarzschild field 24 p3651 A83-49066
Lichnerowicz-York equation and conformal deformations on maximal slicings in asymptotically flat space-times 24 p3651 A83-49098
Determination of autonomous three-dimensional force fields from a two-parameter family of orbits 24 p3644 A83-49393
Regularization and linearization of the equations of motion in central force-fields 24 p3551 A83-49395

GRAVITATIONAL LENSES
Detection of a compact radio source near the center of a gravitational lens - Quasar image or galactic core 05 p0696 A83-16939
Gravitational lenses 05 p0701 A83-17773
Cepstrum analysis of interfering delayed signals as a tool for detecting gravitational lenses 06 p0830 A83-18777
Optical variability of QSOs and gravitational lenses in galactic haloes 08 p1186 A83-23273
Can all quasars be gravitationally lensed Seyfert's nuclei 09 p1359 A83-24451
Highly compact structures in galactic nuclei and quasars 10 p1496 A83-25858
Gravitational lenses 10 p1505 A83-25899
A test for transverse motions of clusters of galaxies 11 p1675 A83-28396
Gravitational lens effects of neutrino astronomical objects 12 p1789 A83-28878
The statistics of gravitational lenses - Apparent changes in the luminosity function of distant sources due to passage of light through a single galaxy 13 p1949 A83-31403
Effects of spherically-symmetric gravitational lenses produced by galaxies and clusters 15 p2262 A83-34538
Image distortion by gravitational lensing 17 p2605 A83-37924
Corrections for the gravitational deflection of light in the case of observations with an astrolabe 17 p2594 A83-38406
The caustics of gravitational 'lenses' 20 p3071 A83-43047
On the behaviour of test matter in the neighbourhood of caustics of homogeneous cosmological models 20 p3074 A83-43377
Gravitational lenses with angular momentum 21 p3228 A83-44407
Expected number of multiple QSOs from galaxy and QSO surface density data 22 p3383 A83-47006

GRAVITATIONAL POTENTIAL
U GRAVITATIONAL FIELDS
GRAVITATIONAL RADIATION
U GRAVITATIONAL WAVES
GRAVITATIONAL WAVE ANTENNAS
Research on tunable antenna to detect continuous gravitational wave at low frequency 05 p0700 A83-17144
Efficiency of a gravitational detector with interference of quantum states 07 p1012 A83-20042
Coupling of a high-Q gravitational-wave antenna with the resonator of a capacitive sensor of oscillations 11 p1572 A83-27454
Development and test at T equals 4.2 K of a capacitive resonant transducer for cryogenic gravitational-wave antennas 11 p1574 A83-28426
Prospects for the detection of gravity wave bursts 13 p1846 A83-30359
High-energy gravitational antennas - A theoretical approach 15 p2261 A83-34405

- Thermal and superconducting properties of an aluminium alloy for gravitational wave antennae below 1 K 17 p2492 A83-38864
- Compressed quantum states of a harmonic oscillator in the problem of detecting gravitational waves 19 p2896 A83-41495
- Remote quantum mechanical detection of gravitational radiation 22 p380 A83-46752
- A proposed back action evading read-out for a gravitational wave detector 23 p3459 A83-48593
- GRAVITATIONAL WAVES**
- Parametric interaction between gravitational and electromagnetic radiations 01 p0124 A83-10901
- The possibility of laboratory detection of long-period gravitational waves 01 p0125 A83-10904
- Some aspects of gravitational waves in an isotropic background universe 01 p0127 A83-11295
- Timing observations of the binary pulsar PSR 1913 + 16 02 p0253 A83-11616
- Fermi normal co-ordinate system and electromagnetic detectors of gravitational waves. I - Calculation of the metric 02 p0254 A83-12028
- Gravitational radiation from collapsing rotating stellar cores 02 p0260 A83-12523
- High-energy astrophysics 02 p0245 A83-13103
- The energy-momentum pseudotensor of the gravitational field and the gravitational radiation emitted by an axisymmetric system 03 p0417 A83-13474
- The effect of a strong gravitational wave on an anisotropic plasma 03 p0397 A83-13534
- Collisional relaxation of a plasma in the field of a plane gravitational wave 04 p0536 A83-15711
- The determination of the gravitational constant and the detection of gravitational radiation in a cosmic laboratory 05 p0702 A83-17851
- On crossing the Cauchy horizon of a Reissner-Nordstroem black-hole 06 p0824 A83-17972
- Gowdy three-handle and S/3/ inhomogeneous cosmological models 06 p0828 A83-18324
- Gravitational radiation of the binary pulsar PSR 1913 + 16 06 p0837 A83-19210
- Self-similar collision of plane neutrino waves in general relativity 07 p1013 A83-20143
- The importance of the binary pulsar for general relativity 07 p1015 A83-20406
- Gravitational waves and red shifts - A space experiment for testing relativistic gravity using multiple time-correlated radio signals 08 p1180 A83-22212
- An upper limit on the stochastic background of ultralow-frequency gravitational waves 08 p1184 A83-23076
- Upper limits on the isotropic gravitational radiation background from pulsar timing analysis 08 p1184 A83-23077
- Ultra-low phase noise superconducting-cavity stabilised microwave oscillator with application to gravitational radiation detection 09 p1253 A83-23663
- Interaction of a plane gravitational wave with a scalar field 09 p1359 A83-24207
- New solutions of Einstein equations from analytic mappings 10 p1471 A83-25408
- Gravitational radiation in Robertson-Walker backgrounds 10 p1506 A83-26096
- Energy, momentum and angular momentum of gravitational radiation from a particle plunging into a non-rotating black hole 11 p1679 A83-28070
- Gravitational radiation from a plasma in a magnetic field 11 p1683 A83-28566
- The evolution of shear and gravitational wave perturbations of Friedmann models and the isotropy of the universe 12 p1790 A83-28889
- On often used gauge transformations in gravitational radiation-reaction calculations. 12 p1791 A83-29027
- Loss of angular momentum in a binary system due to collisionless particles as monopoles or gravitinos - Does it exceed the gravitational radiation emission in the binary system PSR 1913 + 16? 12 p1792 A83-29037
- Is cooling of a neutron star due to gravitational radiation 12 p1793 A83-29058
- Prospects for the detection of gravity wave bursts 13 p1846 A83-30359
- Colliding plane gravitational and electromagnetic waves 13 p1947 A83-30519
- Torsional oscillations of neutron stars 13 p1956 A83-31678
- Microcanonical quantum gravity 14 p2103 A83-33050
- Modeling sources of gravitational radiation 15 p2254 A83-33816
- The minimum period and the gap in periods of cataclysmic binaries 15 p2258 A83-34108
- Direct observational upper limit to gravitational radiation from millisecond pulsar PSR1937 + 214 15 p2261 A83-34383

- Limits from the timing of pulsars on the cosmic gravitational wave background 15 p2264 A83-34583
- The influence of gravitational wave momentum losses on the centre of mass motion of a Newtonian binary system 15 p2265 A83-34592
- Gravitational radiation from particles falling along the symmetry axis into a Kerr black hole - The momentum radiated 15 p2269 A83-34640
- Non-conservative evolution of low-mass, close binaries with gravitational radiation and systemic mass losses 15 p2272 A83-34777
- Recovery of long-wavelength mean gravity anomalies for the dedicated gravitational satellite (GRAVSAT) mission 15 p2203 A83-34850
- Quantum nondemolition measurements on coupled harmonic oscillators --- for gravitational radiation detection 16 p2355 A83-35651
- Gravitational waves and the activity in galactic nuclei and quasars 17 p2612 A83-38827
- The effect of a gravitational wave at the contact of conductors 17 p2585 A83-38952
- Representation of a gravitational field by means of a hypercomplex potential 18 p2767 A83-39528
- Excitation of the earth's eigenvibrations by gravitational radiation from astrophysical sources 19 p2915 A83-41164
- Gravitational radiation from a particle with zero orbital angular momentum plunging into a Kerr black hole 19 p2916 A83-41171
- Contractive states and the standard quantum limit for monitoring free-mass positions --- by gravitational wave interferometers 21 p3199 A83-43861
- Detection of gravitational wave by spacecraft 21 p3228 A83-44295
- An interaction between gravitational and electromagnetic waves 21 p3232 A83-44730
- Gravitational radiation reaction in the binary pulsar and the quadrupole-formula controversy 21 p3235 A83-45197
- Axially symmetric gravitational two-body problem of Cooperstock, Lim, and Hobill 22 p3354 A83-46715
- On calculation of magnetic-type gravitation and experiments 22 p3354 A83-46751
- Infrasonic and internal gravity waves in the atmosphere during large fires 23 p3485 A83-48503
- Soliton collision in general relativity 24 p3650 A83-48918
- Quantum dissipative processes and gravitational entropy of the universe 24 p3663 A83-49749
- GRAVITONS**
- The external field of a rotating and charged body in the vector graviton metric theory 01 p0119 A83-10232
- Cosmological constant and absence of particle creation 10 p1505 A83-25799
- Quantum dissipative processes and gravitational entropy of the universe 24 p3663 A83-49749
- GRAVITY**
- U GRAVITATION**
- GRAVITY ANOMALIES**
- Venus gravity - Analysis of Beta Regio 02 p0266 A83-12571
- Covariational analysis of the correlation between lunar relief and the acceleration due to gravity 03 p0432 A83-13369
- Interpretation of gravity and magnetic anomalies on the basis of space imagery 03 p0359 A83-14309
- Mars - Stratigraphy and gravimetry of Olympus Mons and its aureole 04 p0566 A83-15565
- The law governing the variation of the anomalous gravitational field with the survey altitude 04 p0510 A83-16037
- Concerning the problem of the relationship between geoid undulations and tectonic structures 04 p0514 A83-16379
- Direct integration of Stokes' undulation and Vening Meinesz's deflection equations for geographically defined gravity anomaly blocks 07 p0958 A83-19873
- The interpretation of the major non-hydrostatic anomalies of the earth 07 p0963 A83-20974
- Venus gravity anomalies and their correlations with topography 08 p1188 A83-22364
- The relationship between surface topography, gravity anomalies, and temperature structure of convection 08 p1135 A83-22365
- The determination of geoid undulations and gravity anomalies from Seasat altimeter data 09 p1318 A83-24282
- The modern geoid and ancient plate boundaries 12 p1752 A83-29172
- Correlation and spectral properties of random potential vector fields --- for analysis of magnetic and gravity anomalies 14 p2050 A83-31874
- A numerical study of the divergence of spherical harmonic series of the gravity and height anomalies at the earth's surface 14 p2051 A83-31899

- The Indian Ocean gravity low - Evidence for an isostatically uncompensated depression in the upper mantle 15 p2202 A83-34726
- Recovery of long-wavelength mean gravity anomalies for the dedicated gravitational satellite (GRAVSAT) mission 15 p2203 A83-34850
- The interior of Venus and Tectonic implications 17 p2616 A83-37411
- Investigation of the isostatic state of the Elysium dome on Mars by gravity models 17 p2623 A83-38696
- The use of multiple inertial systems to correct for the effects of gravitational anomalies [AIAA PAPER 83-2196] 19 p2796 A83-41681
- Direct conversion of LOS acceleration data to vertical gravity anomalies - A new approach --- Line Of Sight 20 p3062 A83-43587
- On the interpolation of gravity anomalies and deflections of the vertical in mountainous terrain 22 p3317 A83-46356
- Constraints on the structure of the Himalaya from an analysis of gravity anomalies and a flexural model of the lithosphere 23 p3482 A83-47811
- GRAVITY GRADIENT SATELLITES**
- NT ATS 1
- NT ATS 6
- The effect of atmospheric drag on the single-axis gravity gradient stabilization of an artificial satellite 03 p0287 A83-13203
- The effect of displacing the center of a protective sphere on the oscillations of a body acted upon by Lorentz forces under conditions of resonance --- stability of rotating electrostatically protected satellite under resonant vibration 04 p0452 A83-15772
- Nonlinear resonances in the problem of the motion of a body near the center of mass when acted upon by Lorentz forces 09 p1212 A83-24486
- Parametric excitation of a high altitude gravity gradient satellite 12 p1705 A83-29106
- GRAVITY GRADIOMETERS**
- A spaceborne superconducting gravity gradiometer for mapping the earth's gravity field 01 p0020 A83-10025
- Inversion of gravity gradients for density information 01 p0070 A83-10067
- Maximum precision of the measurement of gravity gradients 07 p0989 A83-20854
- Inertial technology applications to geodetic networks 22 p3291 A83-46342
- Satellite technology developments in gravity research [IAF PAPER 83-223] 23 p3414 A83-47314
- GRAVITY WAVES**
- NT BAROCLINIC WAVES**
- Variational normal mode balancing in the Navy operational data assimilation system --- for numerical weather prediction 03 p0366 A83-14410
- Towards the optimum control of gravity waves and ageostrophic circulations for data assimilation 03 p0366 A83-14411
- Formulation of a modal-split-explicit time integration method for use in the UCLA atmospheric general circulation model 03 p0366 A83-14416
- HF Doppler observations of gravity waves during the 16 February 1980 solar eclipse 03 p0362 A83-14748
- Radiation damping of acoustic-gravity waves in a nonisothermal atmosphere 03 p0362 A83-14828
- The energetics of the lower thermosphere in the presence of internal gravity waves 03 p0362 A83-14834
- A measurement of the tidal variations of atmospheric pressure and their relationship with geomagnetic disturbances 03 p0362 A83-14835
- Internal gravity waves in the solar atmosphere. II - Effects of radiative damping 04 p0575 A83-15639
- Excitation of acoustic-gravity waves by sources moving in the atmosphere at an angle to the horizon 04 p0510 A83-15758
- An analysis of wave-turbulence interaction 04 p0516 A83-15931
- Fine altitude resolution radar observations of upper-tropospheric and lower-stratospheric winds and waves 04 p0517 A83-15937
- Instability and confined chaos in a nonlinear dispersive wave system --- application to gravity waves in deep water 05 p0638 A83-17354
- Observation of atmospheric waves generated by cyclone centres 06 p0791 A83-18422
- Convection and gravity waves in two layer models. I - Overstable modes driven in conducting boundary layers --- of solar and stellar models 06 p0835 A83-18934
- The theory of the interaction of gravity waves with hydrodynamic turbulence 06 p0793 A83-19563
- Incremental linear normal mode initialization in four-dimensional data assimilation --- for numerical weather forecasting 08 p1138 A83-22284

Application of WKB theory to turbulence layers in the vicinity of critical levels --- in winter hemisphere for internal gravity wave propagation 09 p1311 A83-23888

The instability of the gravity-inertia wave and its relation to low-level jet and heavy rainfall 09 p1311 A83-23889

A small-component model of the nonlinear interactions between internal gravity waves 09 p1308 A83-25052

Synthetic aperture radar imaging of ocean waves during the Marineland experiment 10 p1453 A83-26497

Estimates of ocean wavelength and direction from X- and L-band synthetic aperture radar data collected during the Marineland Experiment 10 p1453 A83-26498

Joint observations of gravity wave activity in vertical winds in the troposphere and lower stratosphere over a 63 km baseline obtained with clear-air VHF radars at Platteville and Sunset, Colorado 11 p1623 A83-26991

A mechanism of gravity wave excitation observable with atmospheric radars 11 p1623 A83-26992

On waves in non-isothermal, compressible, ionized and viscous atmospheres 11 p1677 A83-27654

Atmospheric internal gravity waves as a source of quasiperiodic variations of the cosmic ray secondary component and their likely solar origin 11 p1615 A83-27664

Intensity variations of the IGW source and the ionospheric response during the substorm of September 18, 1974 --- Internal Gravity Wave 11 p1615 A83-27952

Generation of the internal gravity waves of auroral electrojets 11 p1620 A83-28747

Nonlinearity effects in the spectrum of surface gravity waves 13 p1894 A83-30038

Utilization of satellite and surface observations in a gravity wave study 13 p1887 A83-30554

Gravitational character of cold surges during winter MONEX 13 p1891 A83-30802

Magneto-atmospheric waves 13 p1878 A83-31083

Visible continuum emission and gravity waves 13 p1881 A83-31536

Slow waves near the mesopause 14 p2059 A83-32860

Seasat synthetic aperture radar observations of wave-current and wave-topographic interactions 15 p2207 A83-33493

Nonlinear features of internal waves off Baja California as observed from the Seasat imaging radar 15 p2208 A83-33496

An upper boundary condition permitting internal gravity wave radiation in numerical mesoscale models 15 p2203 A83-33878

The spectrum of temperature oscillations in the neighborhood of the inertial frequency according to POLYMODE data --- Atlantic Ocean temperature measurement analysis 15 p2209 A83-34356

Experiments on solitary internal Kelvin waves 16 p2348 A83-35343

Analysis of gravity-wave induced instabilities and turbulence viscosity parameters from optical emissions 16 p2374 A83-35377

Stratified turbulence and the mesoscale variability of the atmosphere 16 p2385 A83-35471

Internal gravity waves in Titan's atmosphere observed by Voyager radio occultation 16 p2436 A83-35738

A numerical model of gravity wave breaking and stress in the mesosphere 16 p2380 A83-36140

Linear conversion of magnetogravity waves in an exponential atmosphere 16 p2434 A83-36931

Experiments on the generation of internal waves in a stratified fluid 17 p2502 A83-37201

[AIAA PAPER 83-1704] 17 p2502 A83-37201

Wavy patterns of ionospheric electron density profiles triggered by TID - Observation results of the electron density by TAIYO satellite 17 p2540 A83-37825

Numerical simulation of the atmosphere during a CAT encounter 17 p2553 A83-38764

The instability of hydromagnetic planetary-gravity waves in a zonal flow and transverse magnetic field 18 p2711 A83-39021

Sea pressure waves 18 p2731 A83-39444

HF Doppler measurements of mesospheric gravity wave momentum fluxes 18 p2718 A83-40044

Interfacial progressive gravity waves in a two-layer shear flow 18 p2687 A83-40499

Study of internal gravity waves in the lower troposphere from observations of the nocturnal sky airglow (01) 5577 A in Ashkhabad 20 p3016 A83-42309

Analysis of airglow image data 20 p3016 A83-42310

Turbulence originating from convectively stable internal waves 20 p3020 A83-42838

Nonlinear interaction of magnetogravity waves with Alfvén and sound waves 21 p3211 A83-44344

On the instability of internal Alfvén-gravity waves in stratified shear flows 21 p3171 A83-44469

The modeling of nonlinear wave processes --- Russian book 21 p3213 A83-45016

Reaction of the ionospheric F2 region to a solitary internal gravity wave 21 p3176 A83-45257

Analysis of MARSEN synthetic aperture radar wave imagery --- in Maritime Satellite North Sea experiment 22 p3343 A83-46156

Cross modulation of VLF and LF waves by gravity waves --- in nocturnal D region 22 p3332 A83-46533

Localized plasma depletion in the ionosphere and the equatorial spread F 22 p3334 A83-46888

Short waves on long waves --- spatial changes of gravity waves 22 p3344 A83-46912

Supersonic stabilization of a tangential shear in a thin atmosphere 22 p3285 A83-46938

Some experiments in variational normal mode initialization in data assimilation --- for gravity waves 23 p3489 A83-47395

Short-period atmospheric gravity waves - A study of their statistical properties and source mechanisms 23 p3489 A83-47402

Diagnostic study of the momentum balance in the Northern Hemisphere winter stratosphere 23 p3491 A83-47411

Features characterizing the backscattering of radio signals by ocean waves 23 p3493 A83-48102

The spatial and temporal structure of internal inertial-gravity and topographic waves in the sea at frequencies close to the inertial frequency 23 p3493 A83-48563

GRAVSAT SATELLITE

Recovery of long-wavelength mean gravity anomalies for the dedicated gravitational satellite (GRAVSAT) mission 15 p2203 A83-34850

Consequences of Gravsat and GPS - New concept of geodetic networks 22 p3316 A83-46340

Satellite technology developments in gravity research [IAF PAPER 83-223] 23 p3414 A83-47314

GRAY GAS

Two-dimensional radiation in absorbing-emitting-scattering media using the P-N approximation 02 p0171 A83-12786

[ASME PAPER 82-HT-19] 02 p0171 A83-12786

Radiative transfer in spectrally dissimilar absorbing-emitting-scattering adjacent mediums 04 p0476 A83-15294

Non luminous gas radiation - Approximate emissivity models 20 p2974 A83-42692

Two-dimensional energy transfer in radiatively participating media with conduction by the P-N approximation 20 p2974 A83-42697

GRAZING INCIDENCE

Aberrations grazing incidence systems and their reduction or toleration --- in astronomical X ray imagery 02 p0237 A83-12693

Properties and performance of grazing incidence reflectors --- optical system errors due to synchrotron radiation 02 p0237 A83-12694

Phase-space performances of optimized and conventional synchrotron radiation grazing incidence mirrors 02 p0237 A83-12696

Traditions of optical fabrication 02 p0237 A83-12697

New design of mirror bending block --- grazing incidence X-ray optics 02 p0237 A83-12698

Toroidal mirror with adjustable bending radius for X-ray imaging 02 p0237 A83-12699

Bent approximations to synchrotron radiation optics 02 p0237 A83-12700

Optical constants in the extreme ultraviolet and soft X-ray region 02 p0237 A83-12702

Grazing incidence gratings and mirrors - Case studies 02 p0238 A83-12711

Analysis of the throughput of a grazing incidence monochromator using transmission gratings 02 p0239 A83-12714

Surface and figure characterization of grazing incidence optics 02 p0239 A83-12718

Metrological evaluation of grazing incidence mirrors 02 p0239 A83-12722

Grazing incidence relay optics 02 p0240 A83-12723

High resolution X-ray scattering measurements 02 p0240 A83-12729

Grazing impacts on Mars - A record of lost satellites 04 p0560 A83-15335

Dual-frequency microwave backscatter from the ocean at low grazing angles Comparison with theory 05 p0645 A83-17708

Optical design of a grazing-incidence X-ray imaging telescope 06 p0810 A83-19145

Grazing incidence optics - New techniques for high sensitivity spectroscopy in the space ultraviolet 14 p2084 A83-32018

X-ray spectrograph design 14 p2021 A83-32910

Grazing incidence toroidal mirror pairs in imaging and spectroscopic applications 21 p3204 A83-44150

GRAZING LANDS

U GRASSLANDS

GREASES

The effect of the soap cation on the antiscuff and antiwear properties of lubricant greases 14 p1998 A83-32079

Surface interaction of lubricant greases 23 p3439 A83-48546

GREAT BRITAIN

U UNITED KINGDOM

GREAT CIRCLES

An axial meridian circle 24 p3645 A83-49640

GREAT LAKES (NORTH AMERICA)

NT LAKE MICHIGAN

NT LAKE ONTARIO

A framework for analysis of temporal and spatial patterns of land use changes in Michigan's coastal zone 15 p2186 A83-34835

GREAT PLAINS CORRIDOR (NORTH AMERICA)

Drought-induced wind erosion in southwestern Kansas, U.S.A. - Integration of Landsat, Seasat, and airborne multispectral data 09 p1290 A83-24606

Composite study of comma clouds and their association with severe weather over the Great Plains 13 p1890 A83-30584

Estimating irrigation water use and withdrawal of ground water on the high plains, U.S.A. 15 p2181 A83-33563

Landsat image date selection for an irrigated lands inventory over a large geographical area using general crop phenology and irrigation management data 17 p2532 A83-38357

Forecasting upslope stratus and fog in the central plains 17 p2550 A83-38725

Mesoscale analysis of surface variables during the severe storm outbreak of 10-11 April 1979 20 p3030 A83-42515

The impacts of different satellite data on rain estimation schemes 22 p3342 A83-46949

GREAT SALT LAKE (UT)

Computer mapping of shoreline fluctuations by satellite Great Salt Lake, Utah, U.S.A. 09 p1287 A83-24571

GREENEE

Correlation between the SIR-A radar survey, the Landsat data, and the IR surveys in the Corinth canal zone 17 p2534 A83-38451

GREEN FUNCTION

Mean dyadic Green's function for remote sensing of a two layer random medium 01 p0063 A83-10066

A computational alternative for variational expressions that involve dyadic Green functions --- for electromagnetic scattering 01 p0103 A83-11373

Radiation from a dipole in the presence of a grounded gyromagnetic slab 03 p0312 A83-13914

Numerical evaluation of principal value integral by Gauss-Laguerre quadrature 04 p0530 A83-15299

A diagram technique in the theory of relaxation processes 04 p0544 A83-15912

Integral representation of electromagnetic fields in inhomogeneous anisotropic media 04 p0532 A83-16451

The Green's function along the microstrip substrate from a horizontal magnetic dipole 07 p0920 A83-20727

The Green function of an infinite, fluid loaded membrane 09 p1278 A83-23705

Comments on 'Singularity in Green's function and its numerical evaluation' 09 p1248 A83-23803

Transient difference solutions of the inhomogeneous wave equation - Simulation of the Green's function [AIAA PAPER 83-0667] 10 p1473 A83-25904

On the spectral expansion of the electric and magnetic dyadic Green's functions in cylindrical harmonics 10 p1472 A83-26037

Comparison of the methods used to describe the process of scattering of a guided mode by an inhomogeneous part of a dielectric waveguide 10 p1484 A83-26672

Analysis of microstrip wraparound antennas using dyadic Green's function 10 p1374 A83-26830

Dyadic Green's functions for a coaxial line 10 p1411 A83-26845

Analytical and numerical techniques in the Green's function treatment of microstrip antennas and scatterers 11 p1553 A83-27896

Grain boundary effects in polycrystalline silicon solar cells. I - Solution of the three-dimensional diffusion equation by the Green's function method. II - Numerical calculation of the limiting parameters and maximum efficiency 11 p1611 A83-27981

Certain relationships for operators constructed on the basis of the Green tensor of the equilibrium equation and their use in the theory of composites

- 15 p2178 A83-34442
- Dephasing in steady-state and time-varying spectroscopy 20 p3044 A83-42264
- Multipoint boundary value problem (MPBVP) and spline interpolation 20 p3042 A83-43170
- Using the Green's function in studies of stiffened plates 21 p3162 A83-45305
- Integral-equation solution for half planes bonded together or in contact and containing internal cracks or holes 23 p3473 A83-48495
- Green's function solution and applications for cracks emanating from a circular hole in an infinite sheet 24 p3594 A83-49599

GREEN THEOREM**U GREEN FUNCTION****GREENHOUSE EFFECT**

- Optimal weighting of data to detect climatic change - Application to the carbon dioxide problem 07 p0969 A83-20216
- Feedback mechanisms in the climate system affecting future levels of carbon dioxide 09 p1294 A83-24252
- On the relationship between the greenhouse effect, atmospheric photochemistry, and species distribution 09 p1296 A83-24268
- Climatic effects of atmospheric carbon dioxide 13 p1893 A83-31200
- The cosmic horizons of climatology 13 p1893 A83-31315
- Optical properties of the Martian atmosphere and radiative heat exchange 16 p2435 A83-35359
- General circulation model experiments on the climatic effects due to a doubling and quadrupling of carbon dioxide concentration 20 p3031 A83-42843
- The response of the ocean to changes in the greenhouse effect 23 p3493 A83-48564

GREENLAND

- Surface elevation contours of Greenland and Antarctic ice sheets 09 p1305 A83-24286

GRIDS

- Simple formulas for transmission through periodic metal grids or plates 01 p0033 A83-11359
- Multigrid solvers on parallel computers 03 p0385 A83-14079
- Interaction of electromagnetic waves in a classical supergrating 04 p0471 A83-15766
- A multi-grid method for the computation of viscous/inviscid interactions on airfoils [AIAA PAPER 83-0234] 05 p0582 A83-16602
- A survey of grid generation techniques in computational fluid dynamics [AIAA PAPER 83-0447] 05 p0636 A83-16719
- Three-dimensional grid generation using elliptic equations with direct grid distribution control [AIAA PAPER 83-0448] 05 p0636 A83-16720
- Adaptive grids generated by elliptic systems --- for computational fluid dynamics [AIAA PAPER 83-0451] 05 p0636 A83-16723
- An exploratory study of finite difference grids for transonic unsteady aerodynamics [AIAA PAPER 83-0503] 05 p0587 A83-16752
- Phenomenal coherence of moving visual patterns 05 p0676 A83-16865
- The use of substantially nonuniform grids in the numerical solution of the Navier-Stokes equations 05 p0640 A83-17646
- Transonic airfoil calculations using solution-adaptive grids 07 p0863 A83-19824
- 2-D coordinate grid generation by a vortex singularity method 07 p0864 A83-21018
- Shock capturing using flux-corrected transport algorithms with adaptive gridding 10 p1415 A83-26161
- Hidden line elimination in projected grid surfaces 11 p1646 A83-27122
- Spatial frequency and the temporal characteristics of the perception of the form of complex gratings --- visual perception test 13 p1901 A83-30434
- The characteristics of the discrimination of gratings depending on their spectra --- visual perception 13 p1901 A83-30435
- The evaluation of spatial frequency --- human perception of grids 13 p1901 A83-30436
- The electrostatic potential of a two-layer three-element symmetric array 13 p1833 A83-30718
- Aberrations of holographic toroidal grating systems 14 p2021 A83-32909
- Theoretical and experimental study of metal grid angular filters for sidelobe suppression 15 p2154 A83-35179

GRIDS (MATHEMATICS)**U COMPUTATIONAL GRIDS****GRIFFITH CRACK**

- Crack propagation in bending thin plates 03 p0342 A83-14567

- Influence of load biaxiality on the fracture load of center cracked sheets 06 p0776 A83-18911
- An anisotropic strip weakened by an array of cracks 07 p0946 A83-20637
- Moving Griffith crack in an orthotropic material 08 p1123 A83-22722
- Double slip plane crack model 11 p1595 A83-28423
- Two coplanar Griffith cracks in an orthotropic semi-infinite medium 14 p2032 A83-32921
- Diffraction of plane harmonic waves by cracks 15 p2174 A83-34006
- Experimental determination of critical defects in polymers under conditions of impact fracture 19 p2824 A83-42066
- Thermal stresses in an orthotropic elastic half-plane weakened by a Griffith crack 20 p3004 A83-42937
- An energy approach to evaluating the crack resistance of materials 20 p3008 A83-43622
- Interaction of shear waves with a Griffith crack situated in an infinitely long elastic strip 21 p3155 A83-44885
- On crack branching and curving in a finite body 21 p3156 A83-44887
- A Griffith crack shielded by a dislocation pile-up 21 p3157 A83-44908
- Critical loading conditions and stress intensity factors for partial or entire closure of a Griffith crack under thermo-mechanical loading 21 p3157 A83-44909
- Equations of fatigue crack growth 23 p3472 A83-48465
- Calculation of energy changes in the Griffith problem 24 p3592 A83-49027

GRINDING (COMMINUTION)

- Fine ammonium perchlorate manufacture by the use of the vibro-energy mill wet grinding process 09 p1240 A83-23830

GRINDING (MATERIAL REMOVAL)**NT METAL GRINDING**

- Reflective and refractive scattering of ultraviolet radiation caused by state of the art optical grinding and polishing techniques 02 p0237 A83-12701
- Determination of residual surface stresses caused by grinding in polycrystalline Al₂O₃ 08 p1071 A83-22199
- Image transforms with fused fiber optics 08 p1167 A83-22864
- Generation of off-axis aspherics --- optical surfaces for telescopes 13 p1921 A83-31015
- Cutting fluid performance in fine grinding 15 p2172 A83-35248
- Effect of grinding variables on strength of hot pressed silicon nitride [ASME PAPER 83-GT-203] 23 p3465 A83-48004
- GRINDING MACHINES**
- Computer-controlled polishing of telescope mirror segments 12 p1778 A83-29145
- Computer-controlled polishing of telescope mirror segments -13 p1921 A83-31017
- GRINDING MILLS**
- Fine ammonium perchlorate manufacture by the use of the vibro-energy mill wet grinding process 09 p1240 A83-23830

GROOVES**NT V GROOVES**

- Discussion of the relative efficiency in the vacuum ultraviolet of diffraction gratings with laminar sinusoidal and triangular grooves 02 p0238 A83-12709
- The liquid-gas interface in grooved face seals 06 p0768 A83-18048
- Dielectric image line groove antennas for millimeterwaves 06 p0738 A83-18613
- A study on characteristics of surface-restriction compensated gas bearing with T-shaped grooves 07 p0939 A83-20293
- Design analysis of a self-acting spiral-groove ring seal for counter-rotating shafts --- o ring seals [AIAA PAPER 83-1134] 16 p2361 A83-36239
- The influence of surface dents and grooves on traction in sliding EHD point contacts 17 p2516 A83-37823
- Axisymmetric bluff-body drag reduction using circumferential grooves [AIAA PAPER 83-1788] 17 p2453 A83-38628
- 3-D elastic-plastic investigation of fracture parameters in side-grooved compact specimen 21 p3157 A83-44906

GROOVING

- Manufacture and measurement of ion-etched X-ray diffraction gratings 02 p0238 A83-12712

GROUND BASED CONTROL**NT AIR TRAFFIC CONTROL****NT RADAR APPROACH CONTROL**

- A portable program package for geostationary orbit control 05 p0679 A83-17433
- GPS control segment capabilities 07 p0871 A83-19764

GPS L-band communication concept

- 07 p0871 A83-19768
- Satellite television broadcasting systems in the USSR 10 p1402 A83-25877
- Experimental system for computer network via satellite /CS/. III - Network control processor 10 p1403 A83-26079
- Software for automatic control of spacecraft instruments 10 p1382 A83-26598
- The Navsat aeronavigation system - Possible control-segment concepts 11 p1535 A83-27371
- The IRAS ground station and operations control centre at Chilton 11 p1533 A83-28211
- Ground operations software at the IRAS Operations Control Centre --- IR Astronomical Satellite 11 p1533 A83-28215
- A ground loop attitude control system for Anik B 17 p2479 A83-37484
- Flight-test results using nonlinear control with the F-8C digital fly-by-wire aircraft [AIAA PAPER 83-2174] 19 p2802 A83-41669
- A ground control system for UMA --- unmanned aircraft 20 p2932 A83-43713
- Phoenix GCS - Some considerations which influence the design of computer assisted ground control stations for RPV 20 p2932 A83-43714
- Extended uses of the Aquila RPV system 20 p2934 A83-43716
- Digital simulation and control of the Machan UMA 20 p2932 A83-43718
- A flight control and navigation system for small RPVs 20 p2932 A83-43723
- On the structure and functions of the ISS-b satellite control systems 21 p3098 A83-45439
- Operations of ISS-b at Kashima station and their result --- with description of satellite tracking, telemetry and command 21 p3098 A83-45441
- Orbit and attitude of ISS-b 21 p3098 A83-45442
- GROUND CREWS**
- The psychological fitness of the ground personnel in charge of airspace security depending on the civil aviation authority Evaluation at recruiting, disorders observed during the period of employment 08 p1151 A83-22970
- Remarks on the systematic tonal audiometry of the ground personnel in charge of airspace security 08 p1148 A83-22972
- Effect of length of service on ground crew hearing threshold 15 p2211 A83-33541
- GROUND EFFECT**
- A note on the calculation of sound propagation over impedance jumps and screens 02 p0234 A83-13006
- Numerical studies of atmospheric flows over and around large-scale mountains 03 p0367 A83-14422
- GROUND EFFECT (AERODYNAMICS)**
- Oblique impingement of a round jet on a plane surface 03 p0278 A83-13145
- A method for estimating the propulsion induced aerodynamic characteristics of STOL aircraft in ground effect [AIAA PAPER 83-0169] 05 p0594 A83-16567
- Ground effects on aircraft noise for a wide-body commercial airplane 09 p1340 A83-24034
- Subsonic dynamic stall in pitching and plunging oscillations including large ground interference effects [AIAA 83-0889] 12 p1697 A83-29836
- A study of the motion of thin-section wings of complex configurations near a solid surface 14 p1972 A83-33005
- The effect of windstream on the aerodynamic characteristics of an airfoil moving near a perturbed surface 14 p1972 A83-33006
- Dynamic stability of a flight vehicle near a perturbed surface 14 p1977 A83-33008
- A viscous vortex pair in ground effect 16 p2348 A83-35344
- Motion of aircraft trailing vortices near the ground [AIAA PAPER 83-2130] 19 p2793 A83-41953
- Problem of the motion of a thin airfoil near a wavy boundary 24 p3576 A83-48945
- The effect of damage in structural elements on the ground resonance of a helicopter 24 p3547 A83-49446
- Characteristics of the ground vortex developed by various V/STOL jets at forward speeds [AIAA PAPER 83-2494] 24 p3545 A83-49585
- GROUND EFFECT (COMMUNICATIONS)**
- A topological approach to the unification of electromagnetic specifications and standards 01 p0041 A83-11084
- An evaluation of Longley-Rice and GTD propagation models 03 p0305 A83-14009
- Scattering by wires near a material half-space 03 p0306 A83-14017

- A long range propagation experiment to investigate the incidence of anomalous propagation in the N.W. Atlantic
06 p0746 A83-18726
- MTI processing and Weibull-distributed ground clutter
06 p0748 A83-19047
- The efficiency of a directional triorthogonal antenna system used for the polarization processing of signals under conditions of earth reflection
09 p1250 A83-24910
- Real axis integration of Sommerfeld integrals - Source and observation points in air
10 p1403 A83-26038
- Improved simulation of ground reflections --- of radio navigation signals for flight control
10 p1374 A83-26486
- Considerations for the design of ground clutter cancelers for weather radars
11 p1626 A83-27023
- Horizontal dipole antenna above an imperfectly conducting ground fed by a two-wire line
13 p1828 A83-30648
- Antenna gain measurements by an extended version of the NBS extrapolation method
13 p1829 A83-31281
- Method for determining the electrical properties of the underlying surface on inhomogeneous paths from measurements of the fields of VLF radio stations
14 p2050 A83-31882
- VHF propagation over hilly, forested terrain
15 p2148 A83-35184
- Maximum power penetration through an electrically small aperture
15 p2149 A83-35191
- The finite ground plane effect on the microstrip antenna radiation patterns
23 p3443 A83-47839
- GROUND EFFECT MACHINES**
- NT CUSHIONCRAFT GROUND EFFECT MACHINE
- NT HOVERCRAFT GROUND EFFECT MACHINES
- Material effects on the dynamic stability of a flexible skirted air cushion
[AIAA PAPER 83-0369] 05 p0692 A83-16675
- U.S. Navy high performance ship concept formulation
[AIAA PAPER 83-0626] 08 p1173 A83-22172
- LCAC - from test craft to production design --- air cushion vehicles for amphibious assault landing operations
[AIAA PAPER 83-0622] 08 p1173 A83-22423
- The JEFF Craft Air Cushion vehicle - A unique naval platform
[AIAA PAPER 83-0637] 08 p1173 A83-22425
- Computer studies of ACV heave performance as a function of vent valve proportional control parameters
15 p2241 A83-33547
- Canadian Symposium on Air Cushion Technology, 16th, Charlottetown, Prince Edward Island, Canada, October 19-21, 1982, Preprints
15 p2241 A83-34851
- Application of system identification flight analysis techniques to the pitch-heave dynamics of an air cushion vehicle
15 p2241 A83-34852
- An over-view of UTIAS research on the dynamic stability of air cushion vehicles
15 p2242 A83-34853
- Computer studies of ACV heave performance as a function of vent valve control parameters
15 p2123 A83-34854
- How to improve air cushion vehicle performance with VUMP equipped wave-forming keels --- Vent-pump
15 p2242 A83-34855
- An innovative type of icebreaker for the arctic environment
15 p2242 A83-34856
- Performance of the advanced twin gimbal fan aeromobile
16 on varied terrain in 1982 15 p2242 A83-34857
- Technical aspects of the AEROBAC AB-7
15 p2242 A83-34858
- 'Larus' and 'VP-1' tested in winter 1982
15 p2242 A83-34859
- New concept in hovercraft design diesel versus gas turbines
15 p2242 A83-34860
- ACV lift air systems - More puff for less power
15 p2242 A83-34861
- AP.1-88 craft 001 prototype clearance trials
15 p2242 A83-34862
- Operational deployment of the air cushion vehicle
15 p2242 A83-34864
- Combat damage - A unique element
15 p2243 A83-34865
- Canadian Symposium on Air Cushion Technology, 15th, Toronto, Canada, September 29, 30, 1981, Proceedings
15 p2243 A83-35051
- From Voyageur on - The exploitation of an opportunity to develop a Canadian air cushion vehicle industry --- developing Canadian Air Cushion Vehicle Industry
15 p2243 A83-35052
- A new class ACV - Tanker-freighter
15 p2243 A83-35053
- Dynamic modeling of an air cushion vehicle
15 p2243 A83-35054
- Computer studies of ACV heave dynamics stabilization
15 p2243 A83-35055
- Developments in air cushion vehicle spray suppression
15 p2243 A83-35056
- A design synthesis model for ACV/SES lift systems
15 p2243 A83-35057
- Skirts - Time for a new look?
15 p2243 A83-35058
- The Transportation Development Centre contribution to air cushion technology
15 p2244 A83-35059
- LACV-30 supportability
15 p2244 A83-35062
- Design and experimentation within the Mobility Development Laboratory (MDL) utilizing the Static and Dynamic Test Machines
20 p2938 A83-42549
- The basic aerodynamics of floatation
23 p3453 A83-48679
- GROUND HANDLING**
- Spacelab ground processing
03 p0284 A83-13707
- The United Nations Convention on International Multimodal Transport of Goods /1980/ - Discussion of the operations of pick-up and delivery with particular attention to the air mode
06 p0816 A83-18100
- DOD/Shuttle payload ground handling operations at Kennedy Space Center
13 p1811 A83-31196
- Impact of stretching wide-bodied aircraft on existing airport facilities
14 p1978 A83-33351
- [AIAA PAPER 83-1578] 14 p1978 A83-33351
- Identifying aircraft and airport compatibility - A straightforward approach to complexity
14 p1978 A83-33354
- [AIAA PAPER 83-1582] 14 p1978 A83-33354
- Interaction of the small commuter operation within the hub terminal
[AIAA PAPER 83-1584] 14 p1973 A83-33355
- GROUND OPERATIONAL SUPPORT SYSTEM**
- Ground operations software at the IRAS Operations Control Centre --- IR Astronomical Satellite
11 p1533 A83-28215
- The GOES operational support system (GOSS)
17 p2548 A83-38710
- GROUND STATE**
- The ground state of superdense quark-lepton matter
01 p0124 A83-10813
- Amorphous solid and bipolaronic ground-state
04 p0540 A83-15507
- Theoretical study of NH₂ - Potential curves, transition moments, and photodissociation cross sections
05 p0684 A83-17655
- Vibration-rotation transition probabilities for the ground electronic chi/1/-sigma/+/- state of HD
05 p0701 A83-17670
- Long contact effect between active nitrogen and carbon monoxide - N₂ dissociation to N/S-4/
05 p0613 A83-17872
- The asymptotic theory of resonance charge exchange between diatomics
06 p0807 A83-18044
- Excitation rate coefficients from the ground state of atomic hydrogen to the n = 2 and n = 3 levels
06 p0811 A83-18185
- Coronal line intensities for ions with fine-structured ground states - Si X
06 p0854 A83-18532
- The spectrum of neutral sulfur /S I/ in the vacuum ultra-violet
06 p0808 A83-18817
- Calculated line positions and intensities for the nu1 plus nu3 and nu1 plus nu2 plus nu3 minus nu2 bands of N/14/O-16/2
06 p0808 A83-18944
- Rates for some reactions in the mass range 39 is less than or equal to A which is less than or equal to 45 --- stellar nuclear reactions
06 p0841 A83-19291
- Light-induced drift in cascade excitation of levels --- laser effects on atomic energy levels
07 p0934 A83-20117
- Theoretical determination of the X 1Sigma g + potential of Cs2 using relativistic effective core potentials
07 p0991 A83-21055
- The doubly excited autoionizing states of H2
08 p1163 A83-22220
- Ab initio spin-orbit coupling constants for potential exotic interstellar molecules
08 p1183 A83-23049
- Effective collision strengths for electron excitation of the ground state of O VII to the 2/3/S and 2/3/P states
09 p1347 A83-23652
- A new class of optical multistabilities and instabilities induced by atomic coherence
10 p1481 A83-25434
- The laser magnetic resonance spectrum of the nu2 band of the methylene radical CH2
10 p1480 A83-26453
- The equilibrium geometry, potential function, and rotation-vibration energies of CH2 in the X3B1 ground state
10 p1480 A83-26454
- Determination of accurate dissociation limits and interatomic interactions at large internuclear distances
11 p1653 A83-27526
- The ground state of an atom moving in a medium
11 p1654 A83-28067
- The ground state far infrared spectrum of NH3
12 p1778 A83-29526
- Laboratory measurement of the 4(04)-3(13) 70 GHz transition of ground-state methylene (CH2)
13 p1916 A83-31453
- Ab initio calculation of the X 1 Sigma + state of CsH
14 p2083 A83-33106
- Radiative recombination of the ground state of lithium-like ions
17 p2578 A83-37934
- Measured electron-impact ionization of Be-like ions: B(+), C(2+), N(3+), and O(4+)
18 p2743 A83-40406
- Single collision ion-molecule reactions at thermal energy
Rotational and vibrational distributions from N(+) + CO yields N + CO(+) 19 p2897 A83-40771
- Transport properties of ground state nitrogen atoms
19 p2906 A83-40773
- First detection of the ground-state J(K) = 1(0)-0(0) submillimeter transition of interstellar ammonia
20 p3069 A83-42473
- Ground state energy and structure of physisorbed monolayers of linear molecules
23 p3429 A83-47636
- New calculation of the properties of the positronium ion
24 p3626 A83-48845
- GROUND STATIONS**
- NT DEEP SPACE INSTRUMENTATION FACILITY
- NT EARTH TERMINALS
- NT POLYSTATION DOPPLER TRACKING SYSTEM
- Earth stations for satellite telecommunications - State of the art and perspectives
01 p0031 A83-10430
- Mobile earth station for synchronous satellite tracking
01 p0019 A83-10915
- Ground-Satellite correlative study of a giant pulsation event
03 p0357 A83-13299
- Inventory of major operational and planned ground-based astronomical telescopes of the countries represented in the European Science Foundation /second edition, 1982/ 03 p0402 A83-13357
- Narrow multibeam satellite ground station antenna employing a linear array with a geosynchronous arc coverage of 60 deg. l - Theory
03 p0305 A83-14004
- The San Marco project - Prospects and programs
04 p0452 A83-15666
- Novel technique for antenna gain measurement in satellite earth stations
04 p0468 A83-16022
- The attitude control performance of the BSE and its influence on the received television signal strengths on the ground
04 p0453 A83-16420
- Switching control system for access to a broadcast satellite from multiple earth stations
04 p0468 A83-16422
- The Sirio-1 timing experiment
04 p0469 A83-16450
- Earthnet prepares for Landsat-D
05 p0603 A83-17426
- The role of ground arrays of magnetometers in the study of pulsation resonance regions
05 p0664 A83-17776
- Radomes for satellite communication earth-stations
06 p0742 A83-18677
- Satellite communication in presence of multipath fading
07 p0903 A83-19659
- Broadcasting satellites and the system of the United States Satellite Broadcasting Company
07 p0904 A83-19680
- Pre-operational tests of high-speed /56 kbps/ transmission over MARISAT
07 p0870 A83-19702
- GPS control segment capabilities
07 p0871 A83-19764
- GPS L-band communication concept
07 p0871 A83-19768
- Light route TDMA for business communications
07 p0911 A83-19784
- Access technique for the Italsat SS-TDMA system
07 p0911 A83-19785
- Mitelnet - A private network using TDMA
07 p0911 A83-19787
- 30-20 GHz domestic satellite communication system experiments
08 p1075 A83-21997
- The 'Orbita-RV' satellite sound broadcasting and newspaper column transmission system
10 p1402 A83-25876
- Satellite television broadcasting systems in the USSR
10 p1402 A83-25877
- The use of the geopotential model in the orbital method of the coordinate determination of stations
11 p1616 A83-28050
- A new baseband linearizer for more efficient utilization of earth station amplifiers used for QPSK transmission
11 p1556 A83-28130
- Symbiosis between a terrestrial-based integrated services digital network and a digital satellite network
11 p1557 A83-28132
- One-way multiaddress satellite data communication system
11 p1557 A83-28133
- VOR/DME automated station selection algorithm
11 p1528 A83-28597
- A cost effective quick-response test station
14 p1977 A83-32927
- 6/4 GHz band small capacity omni-use terminal satellite system
15 p2143 A83-33508

- Correlations of solar insolation and wind data for SOLMET stations 15 p2197 A83-33991
Aperture averaging of scintillation for space-to-ground optical communication applications 15 p2144 A83-34454
Uplink depolarisation control in TV feeder link earth stations 15 p2144 A83-34520
Hook whistlers observed at low latitude ground station Varanasi 16 p2382 A83-36780
Control systems for European satellites 17 p2475 A83-37854
Ground receiving station for meteorological satellite data 17 p2475 A83-37855
Particulate extinction models for sun photometer measurements taken at high mountain stations 19 p2865 A83-41162
A 12 GHz Downconverter for direct broadcast satellite ground station 19 p2829 A83-41354
India's domestic satellite communication system - INSAT 19 p2831 A83-41379
Interference to satellite earth stations due to scatter of terrestrial transmissions by aircraft 19 p2835 A83-41554
Aussat - A milestone in Australia's communication history 21 p3120 A83-44535
Methodological requirements in information gathered by an extensive network of ground-based meteorological and specialized stations 21 p3181 A83-45023
Operations of ISS-b at Kashima station and their result --- with description of satellite tracking, telemetry and command 21 p3098 A83-45441
NASA/NOAA implementation of the USAID-sponsored satellite ground station and data processing facility for Bangladesh [IAF PAPER 83-127] 23 p3475 A83-47282
A transportable satellite earth station for television outside broadcast contributions 23 p3442 A83-47652
Madley - Growth of a large earth station 23 p3442 A83-47653
Position of the station Borowiec in the Doppler observation campaign WEDOC 80 23 p3482 A83-48066
Internal inconsistency of reference system determined by on-board ephemerides of NNSS satellites 23 p3482 A83-48067
Optimal conditions for determinations of polar coordinates from lunar laser ranging 23 p3483 A83-48069

GROUND SUPPORT EQUIPMENT

- NT GROUND OPERATIONAL SUPPORT SYSTEM
Bubble technology for automatic test equipment/ground support equipment /ATE/GSE/ applications 01 p0037 A83-10748
Visible and infrared spin scanning radiometer /VISSR/ atmospheric sounder /VAS/ ground data system 02 p0142 A83-12679
Insights into contamination control for the Shuttle Payload Integration Facility /SPIF/ at the Eastern Launch Site /ELS/ 03 p0284 A83-13749
An experimental support center for operational use of remotely sensed data 08 p1124 A83-21908
KSC ground support operations and equipment for the space transportation system 11 p1533 A83-27474
STS cargo processing at the Kennedy Space Center 11 p1533 A83-27475
The IRAS ground station and operations control centre at Chilton 11 p1533 A83-28211
DOD/Shuttle payload ground handling operations at Kennedy Space Center 13 p1811 A83-31196
Direct-current power supply units GVG 800/350 24 p3549 A83-50115

GROUND SUPPORT SYSTEMS

- The ground support program to prepare for microgravity experiments of the Spacelab D1 mission 02 p0139 A83-12999
Some advances in ground systems for air traffic control 05 p0593 A83-17734
USAF ground fiber optic development program 07 p0906 A83-19711
Design of a hydrodynamic support system for the Saturn V launch vehicle - A case problem [ASME PAPER 82-WA/DE-29] 10 p1381 A83-25679
AISA - Program for automated treatment of aeronautical data --- for civil aviation applications 16 p2311 A83-35598
Weather support to the Space Transportation System 17 p2553 A83-38770

GROUND TESTS

- NT COLD FLOW TESTS
NT PRELAUNCH TESTS
NT STATIC FIRING
Evaluation of a rocket burnout velocity from ground and free flight tests [AIAA PAPER 83-0036] 05 p0602 A83-16476

- The role of CFD in aeropropulsion ground testing --- Computational Fluid Dynamics [AIAA PAPER 83-0149] 05 p0599 A83-16557
Compact installation for testing vectored-thrust engines 08 p1047 A83-22158
Ground tests for obtaining the airworthiness certificate for an automatic terrain-following system [DGLR PAPER 82-040] 09 p1200 A83-24164
Experiments of Omega for aviation 09 p1201 A83-24862
Hyperthermal environment simulation for development of thermal protection systems [SAE PAPER 820881] 10 p1381 A83-25774
Qualification of the Space Shuttle Orbiter Radiator system [SAE PAPER 820886] 10 p1384 A83-25776
AFTI/F-16 aeroservoelastic analyses and ground test with a digital flight control system [AIAA 83-0994] 12 p1704 A83-29888
Aerospace Testing Seminar, 6th, Los Angeles, CA, March 11-13, 1981, Proceedings 13 p1809 A83-31176
Systems environmental testing and redundancy vs Shuttle on-orbit repair/satellite retrieval 13 p1810 A83-31180
PAM-D test program --- Payload Assist Module-Delta 13 p1810 A83-31182
The use of onboard computers for satellite testing 13 p1815 A83-31187
Satellite assembly, integration, and test and analysis 13 p1810 A83-31189
Ground and in-flight testing of new portable oxygen generators 14 p2072 A83-32465
A system for spacecraft attitude determination using laser techniques 14 p1981 A83-33148
Ground simulation of engine operation at altitude 16 p2312 A83-35863
Improvement of a large analytical model using test data 19 p2856 A83-40870
Orbital performance of a one-year lifetime superfluid helium dewar based on ground testing and computer modelling 20 p2962 A83-43247
Bubble motion in a rotating liquid body --- ground based tests for space shuttle experiments 20 p2940 A83-43272
Ground tests of instruments for the detection of transients --- of gamma-ray bursts 23 p3425 A83-48404
Large space structures raise testing challenges 24 p3551 A83-48888

GROUND TRACKS

- NT SATELLITE GROUND TRACKS
The total solar eclipse on June 11, 1983 15 p2281 A83-34571

GROUND TRUTH

- Multifrequency microwave radiometer measurements of soil moisture 03 p0351 A83-14855
Results from a comparison of ground and satellite observations of cloud shapes 09 p1317 A83-25236
Vertical structure and dynamics of Mesoscale Wave Disturbance (MWD) inferred from GOES satellite imagery and ground truth data 13 p1887 A83-30553
Metropolitan expansion and population density patterns in third world supercities as indicated by integration of space and ground data 15 p2182 A83-33573
The application of Landsat, geochemical, and phytogeographical methods to mineral exploration in vegetated regions 15 p2184 A83-34809
Some ground truth considerations in inland water quality surveys 20 p3010 A83-42960
A multi-frequency measurement of thermal microwave emission from soils - The effect of soil texture and surface roughness 22 p3308 A83-46103
Ground truth measurements and results from the interpretation of multispectral data during the Convoir project at the Straubing test site (D9) 22 p3310 A83-46137
Ground truth collection for a visual interpretation of SAR-580 imagery on the B1-site in Belgium 22 p3310 A83-46139

GROUND WATER

- A groundwater convection model for Rio Grande rift geothermal resources 02 p0203 A83-11831
Evaluating depth to shallow groundwater using heat capacity mapping mission /HCMM/ data 03 p0351 A83-14668
Application of Landsat imagery in groundwater investigations in a semi-arid hard-rock region of the State of Gujarat /India/ 09 p1288 A83-24584
Hydrogeologic studies abroad --- Russian book 09 p1292 A83-25247
Estimating irrigation water use and withdrawal of ground water on the high plains, U.S.A. 15 p2181 A83-33563

- Using Landsat imagery interpretation for underground water prospection around Qena Province, Egypt 15 p2187 A83-35276
Discrimination of growth and water stress in wheat by various vegetation indices through clear and turbid atmospheres 17 p2526 A83-37620
Multispectral remote sensing of saline seeps 22 p3314 A83-46228

GROUND WAVE PROPAGATION

- Radiation patterns of a quarter-wave monopole on a finite ground plane --- for aircraft antennas 06 p0715 A83-18682
Acoustic ground impedance meter 17 p2510 A83-37732

GROUND WIND

- Observations of oceanic surface-wind fields from the Nimbus-7 microwave radiometer 03 p0372 A83-14861
Wind streaks in Tharsis and Elysium - Implications for sediment transport by slope winds 04 p0567 A83-15573
Intercomparisons of upper air and surface winds in an urban region 06 p0781 A83-18238
Convective heat losses from flat-plate solar collectors in turbulent winds 09 p1293 A83-23883
Dynamical and microphysical observations in 2 Oklahoma squall lines. I - Radar measurements. II - In-situ measurements 11 p1622 A83-26984
Combined radar and aircraft analysis of a Doppler radar 'black hole' region in an Oklahoma squall line 11 p1622 A83-26985
Acoustic measurements of the wind velocity at the Venera 13 and Venera 14 landing sites 12 p1798 A83-29482
The upslope effect 13 p1888 A83-30565
Wind velocity at the Venus surface according to acoustic measurements 14 p1983 A83-31961
Measurements of katabatic winds between Dome C and Dumont d'Urville 15 p2207 A83-34747
Observations and models of simple nocturnal slope flows 16 p2384 A83-35467
Procedure for generating ground wind environments for Shuttle liftoff studies 18 p2687 A83-40024
Analysis of nighttime drainage winds in Boulder, Colorado during 1980 20 p3030 A83-42510
The relationship between the surface wind field and convective precipitation over the St. Louis area 22 p3338 A83-45703
A boundary-layer-scale model of mountain upslope flow [AD-A130312] 22 p3340 A83-46226
The structure of the Asian monsoon surface wind field over the ocean 22 p3342 A83-46946

GROUND-AIR-GROUND COMMUNICATION

- A long range propagation experiment to investigate the incidence of anomalous propagation in the N.W. Atlantic 06 p0746 A83-18726
The future of civil avionics 17 p2461 A83-37819

GROUND-TO-AIR MISSILES

- U SURFACE TO AIR MISSILES

GROUP BEHAVIOR

- U GROUP DYNAMICS

GROUP DYNAMICS

- On the maximal invariance group and the general solution of the one-dimensional equations of gas dynamics 13 p1839 A83-30083
The psychology of intergroup relations --- Russian book 23 p3499 A83-47096

GROUP THEORY

- A model that realizes the soliton and the chaos simultaneously 14 p2080 A83-32518
Group-theory properties of crystal vibrations with allowance for spatial symmetry 14 p2092 A83-33040
Methods of static and dynamic calculations of structures with cyclic symmetries [ONERA, TP NO. 1983-14] 16 p2367 A83-36424
Homogenization and linear thermoelasticity 17 p2523 A83-38465
Optimal spherical designs and numerical integration on the sphere 21 p3198 A83-45522
Invariant transformations of kinetic equations 23 p3512 A83-47176
Fluid turbulence and the renormalization group - A preliminary calculation of the eddy viscosity 24 p3575 A83-48848

GROUP VELOCITY

- Continuous separable regulation of group delay and phase of the carrier frequency of a signal in an acoustic delay line 01 p0038 A83-10807
Threshold and dispersion effects in the anti-Stokes Raman laser 02 p0183 A83-11559
Dispersion of the group velocity refractive index in GaAs double heterostructure lasers 07 p0938 A83-21592

SUBJECT INDEX

- Group velocity interpretation of the stability theory of Gustafsson, Kreiss, and Sundstrom
 - 12 p1776 A83-29665
- Theory of radiation in an anisotropic plasma
 - 18 p2746 A83-39741
- Effect of group velocity mismatch on the measurement of ultrashort optical pulses via second harmonic generation
 - 22 p3293 A83-46822
- An analysis of two-step time discretizations in the solution of the linearized shallow water equations
 - 24 p3575 A83-48875

GROUP 1A COMPOUNDS

- U ALKALI METAL COMPOUNDS

GROUP 7A COMPOUNDS

- U HALOGEN COMPOUNDS

GROUP 2B COMPOUNDS

- Phonons in Group II B-Group VI A semiconductors /Review/
 - 06 p0815 A83-19573

GROUP 3A COMPOUNDS

- Calculation of the electronic spectrum of Group III A-Group V A compounds and solid solutions based on these compounds using the model-pseudopotential method
 - 14 p2091 A83-32594

GROUP 5A COMPOUNDS

- Calculation of the electronic spectrum of Group III A-Group V A compounds and solid solutions based on these compounds using the model-pseudopotential method
 - 14 p2091 A83-32594

GROUP 5B COMPOUNDS

- The principles underlying the precipitation hardening of Group V-VI refractory metals
 - 06 p0729 A83-18749

GROUP 6A COMPOUNDS

- Preparation of high purity II-VI compounds by laser annealing
 - 14 p2090 A83-32303

GROUP 6B COMPOUNDS

- The principles underlying the precipitation hardening of Group V-VI refractory metals
 - 06 p0729 A83-18749

GROWTH

- NT CROP GROWTH
- NT CRYSTAL GROWTH
- NT CZOCHRALSKI METHOD
- NT DIRECTIONAL SOLIDIFICATION (CRYSTALS)
- NT ELECTROEPITAXY
- NT EPITAXY
- NT HYDROTHERMAL CRYSTAL GROWTH
- NT LIQUID PHASE EPITAXY
- NT MOLECULAR BEAM EPITAXY
- NT VAPOR PHASE EPITAXY
- NT VEGETATION GROWTH
 - Growth and aging of the lens
 - 05 p0670 A83-17196
 - Repeated development and regression of exercise-induced cardiac hypertrophy in rats
 - 13 p1898 A83-30489
 - The turnover of mitochondrial proteins in the livers of rats of various ages
 - 15 p2211 A83-34964
 - The hypertrophy of cells and hyperplasia of ultrastructures in spleen parenchyma of mice as a consequence of acute stress
 - 16 p2395 A83-36833
 - Asymmetrical hypertrophy of the myocardium in patients with hypertension (According to echocardiographic data)
 - 17 p2559 A83-38180
 - The decrease in the functional ability of the hypertrophic heart due to disorders of cellular adaptation to oxygen
 - 18 p2731 A83-39496
 - Water droplet growth at precritical radii
 - 24 p3611 A83-49686

GRUMMAN AIRCRAFT

- NT A-6 AIRCRAFT
- NT F-14 AIRCRAFT
- NT F-111 AIRCRAFT

GRUNEISEN CONSTANT

- Thermal Gruneisen parameters of CdAl₂O₄, beta-Si₂N₄, and other phenacite-type compounds
 - 01 p0027 A83-10621
- A thermodynamic approach to equations of state and melting at mantle and core pressures
 - 22 p3324 A83-45799

GUANINES

- Globular proteins, GU wobbling, and the evolution of the genetic code
 - 06 p0794 A83-18248

GUANOSINES

- Opposing actions of dibutyryl cyclic AMP and GMP on temperature in conscious guinea-pigs
 - 12 p1762 A83-29530

GUAYULE

- Contrast enhancement applied to Guayule distribution in Mexico for commercial rubber production
 - 09 p1290 A83-24617

GUIDANCE (MOTION)

- NT AIRCRAFT GUIDANCE
- NT BEAM RIDER GUIDANCE
- NT COMMAND GUIDANCE
- NT INERTIAL GUIDANCE
- NT MAP MATCHING GUIDANCE
- NT MIDCOURSE GUIDANCE

- NT REENTRY GUIDANCE
- NT RENDEZVOUS GUIDANCE
- NT SATELLITE GUIDANCE
- NT SPACECRAFT GUIDANCE
- NT STRAPDOWN INERTIAL GUIDANCE
- NT TERMINAL GUIDANCE

- Advances in tactical weapon guidance through GPS
 - 07 p0871 A83-19767
- An experimental system for automatic guidance of ground vehicle following the commanded guidance route on map
 - 10 p1469 A83-26606
- Facility problems due to test tailoring --- at Pacific Missile Test Center
 - 13 p1811 A83-31479
- Fundamental issues in guidance and control of uncertain systems
 - 17 p2568 A83-37132
- Robot programming
 - 21 p3191 A83-44069
- Navigation, guidance and control curriculum at the Air Force Academy
 - 21 p3220 A83-44167
- [AAS PAPER 83-021]
 - 21 p3091 A83-45470
- Experience with flight test trajectory guidance
 - 21 p3091 A83-45470

GUIDANCE SENSORS

- Sensor snap and narrow field-of-view inset for terrain avoidance flight
 - 01 p0010 A83-11188
- The A6E /TRAM/ all-weather weapon system --- Target Recognition and Attack Multisensor
 - 01 p0008 A83-11260
- Determination of the orientation of a sensor trihedron using angular information
 - 07 p0988 A83-19938
- Radio-electronic guidance systems --- Russian book
 - 10 p1402 A83-25622
- A practical method for sensor selection in linear estimation --- applied to inertial navigation systems
 - 10 p1465 A83-26531
- Spacecraft attitude sensing based on the earth's radiation
 - 11 p1536 A83-27373
- Terrain profile matching for missile guidance
 - 11 p1527 A83-28164
- Understanding Kalman filters - How to extract the maximum information from imperfect measurement
 - 11 p1648 A83-28167
- Algorithm development for infra-red air-to-air guidance systems - How to separate the wheat from the chaff: A simple approach to target detection
 - 11 p1528 A83-28178
- A highly sensitive fiber-optic rotation sensor
 - 13 p1844 A83-30015
- Development and test of an integrated sensory system for advanced aircraft
 - 13 p1807 A83-30159
- Development of methods for calibration and testing gyroscopic instruments for GW applications
 - 16 p2354 A83-35498
- Reliability testing for GW systems
 - 16 p2363 A83-35500
- An advanced star tracker design using the charge injection device
 - 17 p2481 A83-37465
- Failure detection and correction in low orbit satellite attitude control system --- for SPOT earth observation satellite
 - 17 p2479 A83-37492
- Peacekeeper - Guidance system flight readiness review
 - 19 p2814 A83-41736
- [AIAA PAPER 83-2269]
 - 19 p2814 A83-41736
- Laser gyro for instrumentation of advanced missile guidance system testing
 - 19 p2848 A83-41737
- [AIAA PAPER 83-2271]
 - 19 p2848 A83-41737
- A sun acquisition sensor for spacecraft guidance and control
 - 19 p2817 A83-41744
- [AIAA PAPER 83-2284]
 - 19 p2817 A83-41744
- Optimization of an optical fiber for missile guidance applications
 - 22 p3357 A83-46609
- Dynamic sensing for robots - An analysis and implementation
 - 23 p3501 A83-48635
- Missile guidance electromagnetic sensors
 - 24 p3546 A83-48769
- Broadband sensors for lethal defense suppression
 - 24 p3570 A83-48770
- Electro-optic and infrared sensors
 - 24 p3581 A83-48772
- mm-wave sensors for missile guidance
 - 24 p3546 A83-48773

GUIDE VANES

- NT JET VANES
 - Optimal design of the lateral feed of a turbomachine
 - 02 p0169 A83-11770
 - Composite fan exit guide vanes for high bypass ratio gas turbine engines
 - 03 p0282 A83-13159
 - Effect of variable guide vanes on the performance of a high-bypass turbofan engine
 - 09 p1205 A83-24028
 - The performance of an annular vane swirler --- to aid in modeling gas turbine combustor flowfields and swirling confined flow turbulence
 - 16 p2309 A83-36340
 - [AIAA PAPER 83-1326]
 - 16 p2309 A83-36340
 - A study of the control properties of axial fans on the basis of theoretical characteristics of plane cascades
 - 17 p2451 A83-37807

GUN LAUNCHERS

- Aerodynamic performance of a fan stage utilizing variable inlet guide vanes (VIGV's) for thrust modulation --- subsonic V/STOL aircraft
 - [AIAA-PAPER 83-1162]
 - 21 p3088 A83-45508
- Measurements of heat transfer distribution over the surfaces of highly loaded turbine nozzle guide vanes
 - [ASME PAPER 83-GT-53]
 - 23 p3394 A83-47910
- Experimental study of the three-dimensional flow field in an annular turbine nozzle guidevane
 - [ASME PAPER 83-GT-120]
 - 23 p3396 A83-47949
- Wall boundary layer development near the tip region of an IGV of an axial flow compressor
 - [ASME PAPER 83-GT-171]
 - 23 p3396 A83-47972

GULF OF ALASKA

- The impact of TIROS N soundings on the analysis of a cyclone in the Gulf of Alaska, Oct. 21-22, 1979
 - 03 p0365 A83-14406

GULF OF MEXICO

- On the circulation of the western Gulf of Mexico - A satellite view
 - 01 p0076 A83-10113
- Helicopter IFR - The economics of schedule regularity [SAE PAPER 821501]
 - 17 p2459 A83-38009

GULF STREAM

- Survey of a Gulf Stream frontal filament
 - 09 p1320 A83-24338
- The thermohaline driving mechanism of oceanic jet streams
 - 12 p1761 A83-29553
- Low-frequency current and temperature variability from Gulf Stream frontal eddies and atmospheric forcing along the southeast U.S. outer continental shelf
 - 14 p2059 A83-33076
- Gulf Stream frontal statistics from Florida Straits to Cape Hatteras derived from satellite and historical data
 - 14 p2060 A83-33077
- Comparison of the TIROS-N satellite and aircraft measurements of Gulf Stream surface temperatures
 - 14 p2060 A83-33080
- On Gulf Stream variability and meanders over the Blake Plateau at 30 deg N
 - 14 p2060 A83-33081
- Gulf Stream meanders off North Carolina during winter and summer 1979
 - 14 p2060 A83-33082
- Subsurface energetics of the Gulf Stream cyclonic frontal zone off Onslow Bay, North Carolina
 - 14 p2060 A83-33083
- Temperature and current variability of a Gulf Stream meander observed off Onslow Bay, August 1977
 - 14 p2060 A83-33084
- Initial observations of the subsurface structure and short-term variability of the seaward deflection of the Gulf Stream off Charleston, South Carolina
 - 14 p2060 A83-33085
- Cape Romain and the Charleston Bump - Historical and recent hydrographic observations
 - 14 p2060 A83-33086
- Distribution of Antarctic Intermediate Water over the Blake Plateau
 - 14 p2061 A83-33087
- Seasat synthetic aperture radar observations of wave-current and wave-topographic interactions
 - 15 p2207 A83-33493
- An observation of the surface circulation in a Gulf Stream frontal perturbation
 - 19 p2869 A83-41131
- Airborne dual laser excitation and mapping of phytoplankton photopigments in a Gulf Stream Warm Core Ring
 - 20 p3032 A83-42210

GULFS

- NT GULF OF ALASKA
- NT GULF OF MEXICO

GUM NEBULA

- Star formation in Bok globules and low-mass clouds. I - The cometary globules in the Gum Nebula
 - 07 p1024 A83-21228
- The Gum Nebula - New photometric and spectrophotometric results
 - 13 p1958 A83-31735
- Magnetic field structure in the Gum Nebula area
 - 21 p3236 A83-45539
- Linear polarization observations in selected celestial zones The Gum nebula area
 - 22 p3372 A83-46264

GUM VULCANIZATES

- U VULCANIZED ELASTOMERS

GUMBEL THEORY

- U RANGE (EXTREMES)

GUMS (SUBSTANCES)

- Features of a transparent antistatic resin
 - 07 p0899 A83-20489

GUN LAUNCHERS

- Electric rail gun projectile acceleration to high velocity [AIAA PAPER 82-1939]
 - 02 p0146 A83-12501
- Fatigue crack propagation from crack arrays
 - 08 p1059 A83-21688
- Innovative energy storage for ground-based launch systems
 - [AIAA PAPER 83-1348]
 - 16 p2314 A83-36352
 - Acceleration measurements in a high G environment
 - 17 p2509 A83-37131
- Fast electromagnetic launchers
 - 21 p3125 A83-44103

GUN PROPELLANTS

GUN PROPELLANTS

The composition of the products of the combustion of
pyropowder at atmospheric pressure

07 p0880 A83-19954

A combustion theory for very high regression-rate solid
propellant

[AIAA PAPER 83-1196] 16 p2339 A83-36272

The stability of the steady-state combustion of
gunpowder under conditions of constant light flux

18 p2663 A83-39165

Nonstationary combustion regimes of porous
gunpowders

18 p2663 A83-39166

GUN TURRETS

Microprocessor-based optimal controllers for a
helicopter turret control system

15 p2122 A83-35138

Microprocessor controlled optimal helicopter turret
control system

17 p2462 A83-37148

GUNFIRE

The effects of firing a weapon on the air intake in a
subsonic flow

[AAAF PAPER NT 81-11] 02 p0132 A83-11772

Probing of the unsteady reacting muzzle exhaust flow
of 20 MM gun

[ASME PAPER 82-HT-34] 02 p0172 A83-12792

Analysis of missile response to gunfire --- vibration and
shock on captive-carry configuration aboard aircraft

13 p1806 A83-31511

Concepts for improved gun fire control systems

15 p2223 A83-35139

GUNN DIODES

NT TRANSFERRED ELECTRON DEVICES

Conditions of domain suppression in Gunn diodes under
relaxation

01 p0043 A83-11307

The effect of IR radiation on generation in Gunn
diodes

01 p0044 A83-11311

A strip-type generator of heterodyne frequencies

01 p0044 A83-11312

Some features of the continuous operation of Gunn
diodes

02 p0166 A83-11545

Solid state components adapt to sensor environmental
demands

02 p0168 A83-12973

Uniform noise in Gunn oscillators

04 p0471 A83-15745

A multiple-device cavity oscillator using both magnetic
and electric coupling mechanisms

06 p0753 A83-18769

Millimeter-wave hybrid coupled reflection amplifiers and
multiplexers

07 p0922 A83-21527

Certain peculiarities of the noise characteristics of Gunn
diodes

08 p1082 A83-23170

Millimeter-wave /W-band/ quartz image guide Gunn
oscillator

10 p1409 A83-25815

Image line Gunn diode combiner oscillators

11 p1563 A83-28593

Nonlinear properties of GaAs Gunn diodes in the
short-wave part of the millimeter-wave range

13 p1830 A83-30017

Large-signal, dynamic, negative conductance of Gunn
devices in sharpless flanges

13 p1831 A83-30229

Harmonic Gunn oscillators allow frequency growth

13 p1835 A83-30912

8 GHz tunable Gunn oscillator in WR-137 waveguide

15 p2150 A83-33870

Frequency modulation of Gunn oscillator by low
magnetic flux

15 p2151 A83-33894

Optimization of the autodyne mode of operation of
Gunn-diodes

15 p2153 A83-34892

Investigation of the effect of the increase of the maximum
generation frequency of Gunn diodes

15 p2154 A83-35174

Dielectric resonator stabilization of a Gunn diode
oscillator

17 p2495 A83-37021

A millimeter-wave oscillator, stabilized by a disk-shaped
dielectric resonator

18 p2677 A83-40095

Domain modes of operation of a Gunn diode in an
external variable field

19 p2840 A83-41785

Analysis of the operation of a Gunn diode under
conditions of frequency multiplication

19 p2840 A83-41786

Further investigations on the operating modes of
millimeter-wave Gunn oscillators

21 p3124 A83-43859

GUNN EFFECT

Absence of the Gunn effect in $p\text{-In}/0.53/\text{Ga}/0.47/\text{As}$

07 p1000 A83-21374

Computer simulation of negative-differential-conductivity
effects, including trapping --- Gunn effect

09 p1255 A83-24499

Monte Carlo simulation of a millimeter-wave Gunn-effect
relaxation oscillator

18 p2677 A83-40369

Nonlinear lumped circuit model of GaAs MESFET

20 p2968 A83-43354

GUNPOWDER

U GUN PROPELLANTS

GUNS (ORDNANCE)

NT PRECISION GUIDED PROJECTILES

Maximizing survivability and effectiveness of
air-to-ground gunnery using a moveable gun

01 p0006 A83-11192

Thirty years of fighter armament

07 p0866 A83-20600

Investigation of thermal effects on weapon system
components

13 p1859 A83-31298

Analysis of missile response to gunfire environment ---
vibration and shock effects on captive-carry configuration
aboard aircraft

13 p1806 A83-31495

GUST ALLEVIATORS

Design and implementation of an active load alleviation
system, taking into account the example of a modern
transport aircraft

[DGLR PAPER 82-045] 09 p1209 A83-24170

Application of optimal control theory to aircraft gust load
alleviation

19 p2802 A83-41484

An integrated maneuver enhancement and gust
alleviation mode for the AFTI/F-111 MAW aircraft

[AIAA PAPER 83-2217] 19 p2803 A83-41699

Aeroelastic interactions with flight control (A survey
paper)

[AIAA PAPER 83-2219] 19 p2803 A83-41700

OLGA - A gust-alleviation system for general-aviation
aircraft --- Open Loop Gust Alleviation

23 p3412 A83-47212

Active gust load alleviation and ride comfort
improvement

24 p3549 A83-49193

GUST LOADS

A program system for dynamic analysis of aeronautical
structures /HAJIF-II/

04 p0497 A83-15545

Vibration of airfoils in sinusoidal oblique gust

[AIAA PAPER 83-0005] 05 p0577 A83-16457

Study of rotor gust response by means of the local
momentum theory

06 p0719 A83-18379

The acoustic response of a propeller subjected to gusts
incident from various inflow angles

[AIAA PAPER 83-0692] 11 p1651 A83-28010

Incidence angle effects on convected gust airfoil noise

[AIAA PAPER 83-0765] 11 p1652 A83-28022

Noise generation by a finite span swept airfoil

[AIAA PAPER 83-0768] 11 p1652 A83-28023

Aerodynamic theory for wing with side edge passing
subsonically through a gust

14 p1971 A83-32977

The dynamic bending load on a satellite launcher due
to inclined lift-off

17 p2480 A83-37572

Application of optimal control theory to aircraft gust load
alleviation

19 p2802 A83-41484

Theoretical gust response prediction of a Joukowski
airfoil

20 p2928 A83-42536

GUSTATORY PERCEPTION

U TASTE

GUSTS

Dynamic simulation in wind tunnels

01 p0014 A83-11079

Surface signatures of a dry nocturnal gust front

10 p1451 A83-25391

Short-range prediction of mesoscale windfields

13 p1888 A83-30567

Wind turbines in simulated gusts

[AAAF PAPER NT 82-13] 14 p2048 A83-33164

Information retrieval from wide-band meteorological data

- An example 17 p2552 A83-38758

An analysis of spanwise gust gradient data

17 p2553 A83-38762

Interactions of airfoils with gusts and concentrated
vortices in unsteady transonic flow

[AIAA PAPER 83-1691] 18 p2633 A83-39267

GUY WIRES

Refined design of self-expanding stayed column for use
in space

02 p0142 A83-12753

Toward the nondestructive characterization of fatigue
damage in composite materials

03 p0292 A83-14552

GYMNASTICS

U PHYSICAL EXERCISE

GYRATION

NT AUTOROTATION

NT COUNTER ROTATION

NT EARTH ROTATION

NT MOLECULAR ROTATION

NT PLANETARY ROTATION

NT PRECESSION

NT QUENCHING (ATOMIC PHYSICS)

NT ROTATION

NT SATELLITE ROTATION

NT SOLAR ROTATION

NT STELLAR ROTATION

Gyrational motion of disks during free-fall

13 p1839 A83-30107

Dynamics of gyro-elastic continua

[AIAA PAPER 83-0826] 14 p2032 A83-32795

GYRATORS

NT MICROWAVE FILTERS

GYROCOMPASSES

Development of inertial navigation and its employment
in measurement technology

05 p0592 A83-16900

Instability of a gyroscopic compass under resonance
due to variable moments on the rotor

06 p0764 A83-19549

A two-degree-of-freedom gyrocompass

16 p2356 A83-35936

A theory for gyroscopic compasses in the light of
analogies with elastic systems

21 p3137 A83-44626

The stability of a controlled gyrohorizon-compass during
the maneuvering of an object

21 p3138 A83-44636

A vector-kinematic approach to problems related to the
use of a gyrocompass in orbit

21 p3101 A83-44644

GYROFREQUENCY

Source regions deduced from attenuation bands in VLF
saucers

02 p0208 A83-12388

Active region magnetic fields inferred from simultaneous
VLA microwave maps, X-ray spectroheliograms, and
magnetograms

02 p0270 A83-12574

The role of gyro-resonance radiation in the slowly varying
component of the solar radio emission

06 p0856 A83-19168

Whistler-mode propagation at frequencies near the
electron gyrofrequency

13 p1927 A83-31645

Hydromagnetic waves in the magnetosphere

17 p2542 A83-38300

Energetic electron precipitation due to gyroresonant
interactions in the magnetosphere involving coherent VLF
waves with slowly varying frequency

22 p3326 A83-46042

Simulations of beam excited minor species
gyroharmonics in the Porcupine experiment

22 p3337 A83-47075

GYROINTERACTION

U MAGNETIC RIGIDITY

GYROMAGNETISM

NT GYROFREQUENCY

Radiation from a dipole in the presence of a grounded
gyromagnetic slab

03 p0312 A83-13914

Influence of gyroradius and dissipation on the Alfvén
wave continuum

07 p0997 A83-20538

Natural modes of a periodic array of rectangular
longitudinally magnetized ferrite rods

11 p1561 A83-27966

Coherent gyromagnetic emission --- in astrophysical
objects

13 p1944 A83-30362

Level crossing and polarization rotation in doubly
resonant third-harmonic generation in I2

16 p2358 A83-35658

Electromagnetic waves in a doubly periodic array of
circular longitudinally magnetized ferrite rods

17 p2494 A83-38477

Gyromagnetic perturbation of a slow-wave structure
partially loaded by a dielectric

19 p2841 A83-41824

Gravitational anisotropies of gyromagnetic ratios and
tests of general relativity

23 p3503 A83-47876

GYROPLANES

U HELICOPTERS

GYROS

U GYROSCOPES

GYROSCOPES

NT ATTITUDE GYROS

NT CONTROL MOMENT GYROSCOPES

NT CRYOGENIC GYROSCOPES

NT ELECTROSTATIC GYROSCOPES

NT FLUID ROTOR GYROSCOPES

NT GYROCOMPASSES

NT GYROSCOPIC PENDULUMS

NT GYROSTABILIZERS

NT LASER GYROSCOPES

NT OPTICAL GYROSCOPES

NT ROTARY GYROSCOPES

NT TUNING FORK GYROSCOPES

Gas laser mode-locking using an external acoustooptic
modulator with a potential application to passive ring
gyroscopes

02 p0185 A83-12589

Kinematic interpretation of the motion of a gyrost at
one solution of E. I. Kharlamova

09 p1337 A83-23552

Motion of a Kovalevskia gyroscopic in the Delaunay
case

09 p1337 A83-23555

On an attempt to generalize the Hess solution of the
problem concerning the motion of a heavy rigid body with
a fixed point

09 p1337 A83-23557

On certain motions of a system of three Lagrange
gyroscopes

09 p1337 A83-23558

Stationary motions of two linked bodies

- Redundancy Management of Shuttle flight control rate gyroscopes and accelerometers 17 p2474 A83-37123
- Validation of the in-orbit checkout of the IRAS gyroscopes using computer simulations 17 p2481 A83-37475
- Estimation of the value of the small parameter in a linear singularly perturbed system of differential equations 17 p2571 A83-38074
- Kalman filter formulations for transfer alignment of strapdown inertial units 18 p2739 A83-40303
- Dynamics of Tisserand's frame for an elastic spacecraft with stored angular momentum 21 p3099 A83-44016
- Certain properties of gyroscopic systems in relation to the Hertzian concept in mechanics 21 p3199 A83-44627
- The effect of manufacturing imperfections on the accuracy of inertial navigation systems 21 p3097 A83-44631
- Reducing errors in single-degree-of-freedom gyroscopes 21 p3137 A83-44633
- Determination of the resonance frequency spectrum of the forced vibration of current leads 21 p3138 A83-44634
- Orientation of geodetic networks by gyro azimuths 22 p3136 A83-46345
- Gyromotors --- Russian book 23 p3441 A83-48475
- GYROSCOPIC COUPLING**
- 3 x 2 channel waveguide gyroscope couplers - Theory 02 p0177 A83-12171
- GYROSCOPIC DRIFT**
- U GYROSCOPES
- U GYROSCOPIC STABILITY
- GYROSCOPIC PENDULUMS**
- From the pendulum to the laser gyroscope 05 p0644 A83-16899
- Equations of motion of gyropendulum systems in Rodrigues-Hamilton parameters 15 p2226 A83-34428
- Conservation laws for some separable gyroscopic dynamical systems 24 p3624 A83-50125
- Computer analysis of the operation of a pendulum accelerometer 24 p3586 A83-50211
- GYROSCOPIC STABILITY**
- The effect of imbalance in a dynamically adjustable gyroscope on its dynamics and accuracy 01 p0050 A83-10688
- The effect of resonance properties of a dynamically adjustable gyroscope on the stability of a gyro-stabilized platform 01 p0050 A83-10692
- Stability relationships between gyrostats with free, constant-speed, and speed-controlled rotors 03 p0287 A83-14838
- An investigation of the properties of systems of two-degrees-of-freedom force gyroscopes 04 p0453 A83-15377
- Equilibrium positions of a satellite gyrostat in a circular orbit 06 p0723 A83-18355
- NAPC gyroscopic moment test facility 06 p0720 A83-18407
- Vibrations in fluid-filled rotor and the gyroscopic effect --- German thesis 06 p0735 A83-18493
- Gyro motion boundedness under uncertain angular acceleration about vehicle output axis 06 p0723 A83-19034
- The effect of hysteretic friction on the errors of gyroinstruments 06 p0764 A83-19181
- Active damping of the nutation of the rotor of a noncontact gyroscope 06 p0764 A83-19182
- Instability of a gyroscopic compass under resonance due to variable moments on the rotor 06 p0764 A83-19549
- Certain classes of exact solutions to the problem of motion of a system of Lagrangian gyroscopes 06 p0807 A83-19606
- Stationary motions of a gyrostat with deformable plates and their stability in a Newtonian central force field 07 p0872 A83-19937
- On an analogy to the Steklov case for a balanced gyrostat in a Newtonian gravitational force field 07 p0988 A83-20145
- Asymptotic properties of certain motions of an asynchronous gyroscope in a gimbal suspension 09 p1337 A83-23560
- Investigation of the sufficient and necessary conditions of the stability of the uniform rotations of a gyrostat about the principal axis 09 p1337 A83-23561
- Sufficient conditions of the stability of the regular precessions of a system of n Lagrange gyroscopes 09 p1337 A83-23562
- On the stabilization of an unbalanced Lagrange gyroscope at rest 09 p1337 A83-23563
- Analysis of the force characteristics of the suspension of a cryogenic gyroscope 11 p1574 A83-28466

- Parametric oscillations of a gyropendulum under random excitations 11 p1574 A83-28496
- Features of the digital-computer simulation of a dynamically tunable gyroscope 11 p1574 A83-28497
- Gyroscopic attitude and stabilization systems --- Russian book 12 p1727 A83-28819
- The laser gyro as a self-contained inertial navigation aid 12 p1729 A83-29208
- The vibrating cylinder gyro 12 p1730 A83-29516
- Determination of the transfer functions of a dynamically tunable gyroscope 14 p2019 A83-32159
- Stability of gyro with harmonic nonlinearity in spinning vehicle. 14 p1984 A83-33129
- The effect of certain fabrication factors on the errors of a dynamically tuned gyroscope with a displaced center of mass 15 p2167 A83-35264
- Minimization of a class of temperature errors of float-type gyroinstruments 15 p2167 A83-35268
- On the choice of parameters for a single-rotor corrected gyrocompass 16 p2356 A83-35937
- Angular motion of a spinning projectile with a viscous liquid payload 17 p2470 A83-37067
- A new strapdown attitude algorithm 17 p2460 A83-37068
- The inertial motion of a gyrostat about a fixed center of mass 17 p2576 A83-38073
- Floated gyro dynamical behavior during slow testing [AIAA PAPER 83-2182] 19 p2848 A83-41674
- Stability analysis of gyroscopic systems by matrix methods 19 p2848 A83-41746
- [AIAA PAPER 83-2286] 19 p2848 A83-41746
- Vibrations of a conservative, gyroscopic system 20 p2959 A83-42984
- On the reduction of the order of equations of motion of gyrostat in an axisymmetric field 21 p3199 A83-44461
- A theory for gyroscopic compasses in the light of analogies with elastic systems 21 p3137 A83-44626
- The dynamics of a two-gimbal elastically suspended gyroscope 21 p3137 A83-44632
- The stability of a controlled gyrohorizon-compass during the maneuvering of an object 21 p3138 A83-44636
- A study of the moment of elastic unbalance in a gyroscopic instrument in the case of the main resonance 21 p3138 A83-44640
- A method for determining the inertial-dissipative parameters of an astatic gyroscope 21 p3138 A83-44641
- A study of the hydrodynamic moment acting on a solid body in a float suspension 21 p3138 A83-44642
- The efficiency of compact damping systems for gyroscopes under conditions of angular vibration of the base 21 p3138 A83-44643
- Choice of the optimal correcting moment of a gyrovertical on the basis of an applications program 21 p3141 A83-45309
- Determination of the probability characteristics of perturbation moments in gyroscopes with an electrostatic suspension 21 p3142 A83-45352
- Cases of integrability of equations for the inertial motion of two bodies connected by means of a spherical joint 23 p3504 A83-48453
- The control of a four-axis gimbal suspension 23 p3459 A83-48457
- GYROSTABILIZERS**
- The effect of resonance properties of a dynamically adjustable gyroscope on the stability of a gyro-stabilized platform 01 p0050 A83-10692
- Errors of a biaxial gyro-stabilizer under random vibrations of the base 12 p1729 A83-29321
- Magnetogyrogravitational system of three-axis orbital orientation and stabilization of the AUREOL-3 satellite 18 p2645 A83-39582
- Optimal magnetic bearing control for high speed momentum wheels 19 p2855 A83-41733
- [AIAA PAPER 83-2263] 19 p2855 A83-41733
- The application of gyroscopes in remotely piloted vehicles 20 p2936 A83-43708
- On the reduction of the order of equations of motion of gyrostat in an axisymmetric field 21 p3199 A83-44461
- GYROSTATS**
- U GYROSCOPES
- GYROTURNS**
- U CYCLOTRON RESONANCE DEVICES
- GYROTROPISM**
- Gyrotropic waveguides --- Book 05 p0625 A83-17373
- The singular edge in problems of diffraction by inhomogeneities with a gyrotropic medium 06 p0754 A83-19356
- Resonance nonreciprocal effects during wave propagation in layered gyrotropic media and periodic structures with gyrotropic filling 14 p2003 A83-32114

- Self-diffraction of light waves in gyrotropic crystals 19 p2899 A83-40997
- Emission from a moving charge during the instantaneous appearance of gyration in the medium 20 p3043 A83-42874

H

H ALPHA LINE

- Intrinsic reddening of Be stars and its relation with H-alpha emission intensities 01 p0120 A83-10311
- Observation of the H-alpha line of Be stars 01 p0120 A83-10319
- Intensifier-dissector-scanner observations of the bright northern Be stars 01 p0116 A83-10321
- Oe star spectra in the red and near infrared 01 p0121 A83-10331
- Portrait of an unusual group of sunspots 01 p0129 A83-10572
- Markarian 914 is a galactic object, lick H-alpha 233 01 p0118 A83-10969
- Spectra of SN 1980k in NGC 6946 02 p0247 A83-12549
- Evidence for starspots on single solar-like stars 02 p0262 A83-12918
- Irregularities of the limb of the solar disk in white light 03 p0436 A83-13676
- Aperture synthesis observations of recombination lines from compact H II regions V - NGC 7538 03 p0430 A83-14803
- Mass loss in Alpha Cygni - Synthetic H-alpha profiles 04 p0553 A83-15624
- Spectroscopic observations of Delta Orionis 04 p0556 A83-15971
- Properties and nature of Be and shell stars 7A. 88 Her - Observational data, their reduction and basic evaluation 05 p0694 A83-17668
- The H-alpha emission line in the star HDE 245770 = A0535 + 26 06 p0830 A83-18786
- Observations of the Orion nebula in H-alpha, forbidden N II and H-beta lines 06 p0834 A83-18892
- New H-alpha emission stars in galactic dark clouds 06 p0823 A83-19207
- H-alpha emission and mass loss from metal-poor giants 06 p0840 A83-19285
- Vertical distribution of glow in H-alpha and in the 1PGN2 band at polar-cusp latitudes 07 p0964 A83-21178
- Supernova remnants in M31 08 p1179 A83-21851
- Observations of H-alpha and microwave brightening caused by a distant solar flare 08 p1192 A83-23073
- High dispersion investigation of CP stars around the H-alpha line 09 p1356 A83-25300
- Brightness oscillations of the sun's chromosphere in K and H-alpha 10 p1521 A83-25494
- The dependence of H-alpha on chromospheric activity in G and K main-sequence stars 10 p1516 A83-26759
- An atlas of H II regions in 125 galaxies 11 p1668 A83-27107
- A search for weak H-alpha emission line pre-main-sequence stars 11 p1669 A83-27117
- H II regions in M33. I - Radio and H-alpha observations of the H II complex NGC595 11 p1669 A83-27679
- Dynamics of solar filaments. II - Mass motions in an active region filament from H-alpha center to limb observations 11 p1690 A83-27681
- Flare asymmetry as seen in offband H-alpha filtergrams 11 p1692 A83-28577
- A white-light /Fe X/H-alpha coronal transient observation to 10 solar radii 11 p1693 A83-28587
- Spectral line profiles from spherical shells 12 p1789 A83-28877
- High-resolution H-alpha observations of Gamma Cas and Pi Aqr 12 p1788 A83-29181
- Emission-line profiles for selected planetary nebulae and symbiotic stars, V1016 Cygni, and HM Sagittae 12 p1797 A83-29959
- Optical counterpart of the radio event accompanying the 3B flare of 13 May 1981 13 p1963 A83-29984
- H76-alpha recombination line emission near Sgr A 13 p1947 A83-30392
- Investigation of the radial velocities of chromospheric spicules 13 p1965 A83-31393
- An H-alpha survey of southern hemisphere active chromosphere stars 13 p1951 A83-31419
- The Gum Nebula - New photometric and spectrophotometric results 13 p1958 A83-31735
- The Cygnus X region. XIII - The dark cloud between IC 1318b and c 13 p1959 A83-31743
- OSO-8 observations of a quiescent prominence - A comparison of Lyman-alpha with theoretical intensities 13 p1966 A83-31756
- Survey of H-alpha emission in globular cluster red giants 14 p2105 A83-33196

- H-alpha emission in F-K high luminosity stars 14 p2108 A83-33271
- The H 166 alpha recombination line in the Carina Nebula 14 p2109 A83-33276
- Catalog of H-alpha emission stars in the region of the Orion Nebula 15 p2244 A83-33752
- Interstellar H-alpha emission along the galactic equator 15 p2257 A83-34095
- Calculation of the H-alpha profile at bright points in flares 15 p2282 A83-34767
- A surge observed in H alpha and C IV 15 p2285 A83-35228
- The expansion velocity field within the planetary nebula NGC 7008 17 p2587 A83-37280
- Spectroscopic evidence for activity in the nuclei of normal spiral galaxies 17 p2596 A83-37311
- H-alpha line profiles in B stars - Comparison of theory and observations 17 p2597 A83-37324
- The relationship between variations in the brightness of hydrogen flocculi in active regions on the sun 17 p2625 A83-37666
- An H-alpha forbidden N II survey of the nuclei of a complete sample of spiral galaxies 17 p2602 A83-37827
- Isophotes of a field in the Cygnus Loop photographed in the forbidden O III and forbidden N II + H-alpha lines 17 p2613 A83-38832
- Dependence of radio emission in large H alpha flares 1967-1970 upon the orientation of the local solar magnetic field 18 p2782 A83-39040
- Morphology of H-alpha filaments and filament channel systems --- of solar magnetic field 18 p2783 A83-39195
- Novel mirror telescope for prominences 18 p2755 A83-39225
- Balmer-alpha and Balmer-beta emission cross sections for low-energy H collisions with He and H2 18 p2743 A83-40408
- A survey of H-alpha emission in normal galaxies 20 p3063 A83-42181
- Narrow- and intermediate-band H-alpha and O I 7774 A photometry and reticon spectroscopy of SX Cassiopeiae 20 p3058 A83-42322
- The X-ray emission of subflares 21 p3244 A83-45254
- H-alpha observations of four novae in M31 21 p3226 A83-45534
- Velocity fields in late-type galaxies from H-alpha Fabry-Perot interferometry. IV - Kinematics and dynamics of the SAB(s) spiral NGC 5236 (M83) 22 p3377 A83-46257
- The behavior of H-alpha in the 16-day cepheid X Cygni 22 p3378 A83-46413
- A comparison of high resolution optical and radio observations of W3 23 p3519 A83-47450
- The H-alpha cyclonic spectra of a flare loop system on 1981 April 27 23 p3536 A83-47714
- Prediction of shock wave and flux velocities for a powerful solar flare from measurements of the H-alpha line broadening 23 p3538 A83-48390
- Comparison of global 21 cm velocity profiles with H-alpha rotation curves 24 p3640 A83-49206
- A nebula around Nova BT Monocerotis 24 p3643 A83-49389
- Transfer of H I Lyman-alpha radiation in optically thick media 24 p3674 A83-49632
- A second catalog of the profile of the H-alpha line in 55 Be stars 24 p3645 A83-49839
- The Rosette nebula. I - An absolutely calibrated photoelectric H-alpha surface photometry 24 p3645 A83-49848
- Nonlinear plasma spectroscopy of the hydrogen Balmer-alpha line 24 p3627 A83-50196
- H BETA LINE**
- The absolute H-beta flux from NGC 7027 02 p0251 A83-11585
- Observations of the Orion nebula in H-alpha, forbidden N II and H-beta lines 06 p0834 A83-18892
- Intermediate-band photometry of stars in three clusters containing classical Cepheids 07 p1004 A83-19863
- Rocket measurements of the vertical profile of H-beta emission and the background at 4600 A at high latitudes 07 p0964 A83-21179
- Six clusters in Puppis-Vela 09 p1352 A83-23321
- Remarkable kinematics of the ionized gas in the nucleus of NGC 1365 13 p1957 A83-31700
- Burst of star formation in detached extragalactic H II regions - A qualitative analysis 15 p2272 A83-34786
- The effects of seeing on spectral line measurements in Seyfert 1 galaxies 17 p2604 A83-37906
- The variability of the spectrum of Arakelian 120 18 p2757 A83-39590
- Balmer-alpha and Balmer-beta emission cross sections for low-energy H collisions with He and H2 18 p2743 A83-40408

H LINES

- NT H ALPHA LINE
- NT H BETA LINE
- The method of forward scattering amplitude in a theory of hydrogen line broadening in a plasma 01 p0106 A83-10375
- The galactic center - Structure and kinematics from 21-cm line measurements 01 p0125 A83-10941
- A distinct shell structure in H I-line-emission at intermediate galactic latitudes 01 p0118 A83-10953
- Time variations of the neutral hydrogen absorption spectrum of NGC 1275 /3C 84/ 02 p0254 A83-12110
- Interstellar molecular hydrogen 02 p0258 A83-12182
- 2-4 micrometer spectroscopy of the compact H II region G 45.13 + 0.14 A 02 p0260 A83-12520
- 21 cm line observations of cD galaxies 02 p0261 A83-12546
- A search for meter-wavelength hydrogen recombination lines, and constraints on the parameters of the ionized interstellar gas 03 p0418 A83-13656
- An Effelsberg - Green Bank galactic H I absorption line survey. II - Results and interpretation 04 p0549 A83-15027
- New bright Seyfert Galaxies 06 p0819 A83-18852
- A search for resonance polarization in stars with enhanced Ca II H and K emission 06 p0821 A83-19062
- Do the W44 and W28 molecular clouds show evidence of a shock 06 p0840 A83-19278
- Internal motions in planetary nebulae - NGC 7354, I 289 and Hu 1-2 07 p1014 A83-20570
- H I line studies of galaxies. II - The 21-cm-width as an extragalactic distance indicator 09 p1359 A83-24453
- A measurement of the 'missing' Q/6/ line of H2 in Orion 09 p1364 A83-25008
- Helium atoms in the interstellar and interplanetary medium. I - Prognoz-5 and Prognoz-6 satellite observations of scattered ultraviolet radiation in the H I 1216 A and He I 584 A lines 09 p1364 A83-25036
- A search for neutral hydrogen in radio galaxies 10 p1492 A83-25477
- NGC 315 - High-velocity H I in an active elliptical galaxy 10 p1511 A83-26404
- The Corona Australis dark cloud 13 p1946 A83-30389
- Detection of H2 emission in Herbig-Haro object No. 101 13 p1957 A83-31703
- The Mg II h and k lines in Vega 13 p1959 A83-31742
- The spectral properties of filamentary, physically inhomogeneous prominences. II - Hydrogen (second level excitation, ionization) 14 p2113 A83-31832
- Ultraviolet continuum and H2 fluorescent emission in Herbig-Haro objects 43 and 47 14 p2107 A83-33231
- Reddening indicators for quasars and Seyfert 1 galaxies 15 p2256 A83-34086
- Stellar chromospheric temperatures 15 p2262 A83-34539
- Bright emission lines in new Seyfert galaxies 15 p2269 A83-34676
- Hydrogen line ratios of low redshift QSO's 16 p2430 A83-36658
- Molecular hydrogen lines in the infrared spectra of M-giant stars 16 p2433 A83-36700
- Multicolor photometry of bright patches in the galaxy NGC 4303 17 p2589 A83-37655
- The origin of anomalous Balmer decrements in the spectra of eruptive stars 17 p2600 A83-37657
- The Balmer decrement in moving stellar envelopes 17 p2600 A83-37658
- The relative intensities of hydrogen lines in moving media --- stellar spectra 17 p2600 A83-37659
- The formation of hydrogen lines in quiescent prominences 17 p2625 A83-37669
- The behavior of emissions in the spectrum of Gamma Cassiopeia from September to November 1977 and in September and October 1979 17 p2601 A83-37708
- Integrated magnitudes and mean colors of DDO dwarf galaxies in the UVB system. II - Distances, luminosities, and H I properties 17 p2602 A83-37779
- On Markaryan 6 and the problem of the intermediate Sy 1.5 type 17 p2602 A83-37885
- The infrared luminosity-H I profile width-surface brightness relation, and the cosmological expansion 17 p2612 A83-38826
- Hydrogen line broadening in the presence of a magnetic field with the unified classical path theory 21 p3230 A83-44434
- Are galaxy properties specific for their parent clusters? 21 p3231 A83-44446
- High spatial and temporal resolution observations of the solar Ca II H line 21 p3244 A83-45569

- Observations of red variable stars in globular clusters 22 p3378 A83-46546
- H I Lyman-alpha in the sun - The effects of partial redistribution in the line wings 22 p3389 A83-47001
- Stellar activity and calcium emission variability 23 p3521 A83-47492
- The timescales of variations in continuum and hydrogen lines during stellar flares 23 p3521 A83-47498
- RS CVn stars - Chromospheric phenomena 23 p3522 A83-47512
- The optical flare --- observations in solar visible spectra 23 p3532 A83-47675
- Relative intensities of hydrogen lines in the spectra of quasars and the nuclei of Seyfert galaxies 24 p3653 A83-49164

H WAVES

- A solution to the problem of H-polarized electromagnetic wave diffraction by piecewise linear cylindrical surfaces 05 p0623 A83-17593
- Semicircular-waveguide radiator with circular polarization 09 p1257 A83-24925
- Electrodynamic analysis of a model of a two-reflector antenna with strict allowance for the interaction between reflectors 13 p1828 A83-30280
- Experimental study of the electrodynamic properties of an open cylinder in a rectangular waveguide 17 p2498 A83-38478
- On a class of integro-summator equations of diffraction theory 18 p2741 A83-39490
- Scattering of an H-polarized wave by a screen with narrow slots 23 p3445 A83-48487

H-53 HELICOPTER

- The super stallion --- CH-53E helicopter design features 16 p2299 A83-36075

H-60 HELICOPTER

- The UH-60A Black Hawk - A world-wide force multiplier 02 p0135 A83-12934
- The T700-GE-700 engine experience in sand environment 09 p1208 A83-24842

HABITABILITY

- Human capabilities: Long residence - An uncharted field 09 p1325 A83-24359

HABITATS

- Waterfowl habitat inventory of Alberta, Saskatchewan and Manitoba by remote sensing 03 p0346 A83-14244
- Digital colour enhancement of Landsat data for mapping vegetation of barrenground caribou winter range in northern Manitoba 03 p0347 A83-14249
- Integration of Landsat imagery into a program for aerial surveying of deer populations in Alberta 03 p0347 A83-14252
- Landsat-derived land-cover classifications for locating potential Kestrel nesting habitat 07 p0952 A83-21435
- Identification and monitoring of Australian plague locust habitats from Landsat 14 p2035 A83-32610
- Classification and mapping habitats within the Mississippi River deltaic plain region 15 p2184 A83-34810
- Monitoring agricultural growth in pronghorn antelope habitat 15 p2184 A83-34813
- Utilization of remote sensing in wetland management 15 p2184 A83-34814

HABITS

- A device for increasing the feedback and speeding the process of forming occupational habits 07 p0981 A83-20338

HABITUATION (LEARNING)

- Vestibular habituation with gimbal mounted tumbling device 09 p1322 A83-24002

HADRONS

- NT BARYONS
- NT MESONS
- NT MUONS
- NT VECTOR MESONS
- Interpretations of changes in the character of the interaction of hadrons at an energy greater than 10 to the 14th eV 02 p0235 A83-11736
- Correlation between the number and energy flux of hadrons and gamma quanta. III 02 p0274 A83-11743
- Neutral pions from the fragmentation region of an impinging hadron at E sub 0 approximately equal to 10 to the 13th eV 02 p0274 A83-11748
- The interaction of hadrons and the nuclear composition of primary cosmic rays with energies of 200-2000 TeV according to the energy spectrum of hadrons in showers 02 p0275 A83-11755
- The relative number of hadrons in an extensive air shower with the number of particles N -- 10 to the 4th to 10 to the 6th 02 p0276 A83-11760
- Energy spectra of hadrons and leptons in the atmosphere 06 p0858 A83-19346
- On the acoustic registration of cascades and single strongly ionized particles 06 p0764 A83-19350

The pi-meson term in the equation of state of hadron systems 06 p0809 A83-19540

The quark-hadron phase transition and the temperature of the MW background radiation 12 p1792 A83-29030

Heavy particle with long life in cosmic rays above 10 to the 17th eV 12 p1801 A83-29036

High-energy hadrons produced by cosmic-ray muons in the earth as a source of background in proton-decay experiments 15 p2228 A83-33780

Effect of HZE particles and space hadrons on bacteriophages 19 p2871 A83-40834

Possible explanation for scaling violation in hadron interactions above 1000 TeV 20 p3082 A83-42291

Particle identification using the angular distribution of transition X-radiation quanta 20 p3046 A83-43532

HAFNIUM

NT HAFNIUM ISOTOPES

HAFNIUM ALLOYS

Short-range stratification in Ti-Zr, Ti-Hf, and Zr-Hf alloys and lattice instability 08 p1068 A83-22783

The effect of hafnium on the phase composition and the mechanical and corrosion properties of cobalt alloys 10 p1395 A83-25632

High temperature oxidation of hafnium and its alloys 20 p2952 A83-42233

Structural instability of the Laves phases Hf(x)Zr(1-x)V2 23 p3431 A83-47180

The effect of Hf additions on oxidation behaviour of Ni3Al 24 p3565 A83-49515

HAFNIUM CARBIDES

A reevaluation of the mechanical properties of molybdenum- and tungsten-based alloys containing hafnium and carbon 07 p0885 A83-20264

HAFNIUM COMPOUNDS

NT HAFNIUM CARBIDES

NT HAFNIUM OXIDES

Some properties of r.f.-sputtered hafnium nitride coatings 02 p0160 A83-12653

Optical properties of CVD-coated TiN, ZrN and HfN 12 p1779 A83-29511

Thermal stability of hafnium and titanium nitride diffusion barriers in multilayer contacts to silicon 14 p2006 A83-32644

HAFNIUM ISOTOPES

Importance of the Lu-Hf isotopic system in studies of planetary chronology and chemical evolution 08 p1190 A83-22996

Pb, Sr, Nd and Hf isotopic evidence of multiple sources for Oahu, Hawaii basalts 18 p2718 A83-39957

Hf chronometer for the early solar system 20 p3076 A83-43539

HAFNIUM OXIDES

Phase relations and ordering in the system erbia-hafnia 08 p1070 A83-22191

Hydrothermal oxidation of Hf metal chips in the preparation of monoclinic HfO2 powders 08 p1071 A83-22196

Initial characterization of partially stabilized HfO2 single crystals 08 p1072 A83-22257

Elastic properties of hafnium and zirconium oxides stabilized with praseodymium or terbium oxide 09 p1240 A83-25209

HAIL

Criteria for the formation and water content of cumulus clouds 03 p0364 A83-14097

An approach to the radar investigation of the cell structure of hail processes 04 p0515 A83-15722

Mathematical description of the shape of conical hydrometeors 04 p0517 A83-15941

Radar backscattering of microwaves by spongy ice spheres 04 p0517 A83-15942

A comparative study of the rates of development of potential graupel and hail embryos in high plains storms 06 p0790 A83-18265

Antenna beam patterns and dual-wavelength processing --- for radar hail detection 07 p0969 A83-20806

The development of the cumulonimbus clouds which move along a valley 09 p1313 A83-23964

On the measurement of hail cells by radar and hailpads 11 p1624 A83-27002

First-echo characteristics of the NHRE area --- National Hail Research Experiment 11 p1625 A83-27011

The effects of mismatched antenna beam patterns on dual-wavelength processing --- for hail detection 11 p1630 A83-27083

Hail growth in an Okalahoma multicell storm 22 p3341 A83-46854

Multidimensional analysis of hailpatterns in the Grossversuch IV experiment 22 p3342 A83-46941

HAILSTONES

U HAIL

HAILSTORMS

Investigation of the radio characteristics of hailstorm clouds 02 p0212 A83-11691

Case study of a hailstorm in Colorado. I - Radar echo structure and evolution 06 p0790 A83-18263

Case study of a hailstorm in Colorado. II - Particle growth processes at mid-levels deduced from in-situ measurements 06 p0790 A83-18264

The variable nature of thunderstorm updrafts and precipitation 09 p1313 A83-23962

Comparison of radar observations of a devastating hailstorm and a cloudburst at Jan Smuts airport 09 p1313 A83-23965

Complex radar methods of hail cloud structure, evolution dynamics and microstructure 09 p1313 A83-23967

Vertical air mass flux properties in the northeast Colorado hailstorm of 22 July 1976 11 p1623 A83-26996

An attenuation-correction technique for dual-wavelength analyses --- of meteorological radar signals 11 p1571 A83-27081

Case study of a hailstorm in Colorado. III - Airflow from triple-Doppler measurements 16 p2384 A83-35466

Hail growth in an Okalahoma multicell storm 22 p3341 A83-46854

A technique for investigating graupel and hail development 22 p3342 A83-46940

HAIR

Interrelated striated elements in vestibular hair cells of the rat 13 p1895 A83-30022

HALF PLANES

Radiation from two plane waveguides formed by three half-planes 05 p0623 A83-17592

A novel approach to the solution of a problem concerning contact interaction between a semiinfinite stringer and a half-plane 06 p0778 A83-19601

The Sommerfeld half-plane problem revisited. II - The factoring of a matrix of analytic functions 10 p1471 A83-25461

The problem of the intersection of two half-planes with reinforced edges 11 p1597 A83-28470

A temperature problem for a half-plane with a crack 11 p1598 A83-28489

Theory of optical-radiation diffraction by a nontransparent half-plane in a turbulent atmospheric layer 12 p1779 A83-29256

The scattering of waves described by the Klein-Gordon equation by an inclined half-plane 13 p1913 A83-30082

A model that realizes the soliton and the chaos simultaneously 14 p2080 A83-32518

Asymptotic solution for the diffraction of an electromagnetic plane wave by a cylinder-tipped half-plane 15 p2144 A83-33806

A concentrated couple acting on an elastic half-plane 17 p2522 A83-38100

Optimum recursive filtering of noisy two-dimensional data with sequential parameter identification 21 p3192 A83-43955

Reduction of the probiem of diffraction by parallel half-planes to the Riemann boundary value problem 21 p3121 A83-44779

Integral-equation solution for half planes bonded together or in contact and containing internal cracks or holes 23 p3473 A83-48495

A thermoelasticity problem for a half-plane with a partially contacting crack 23 p3473 A83-48543

HALF SPACES

Radiation patterns of interfacial dipole antennas 02 p0165 A83-12631

Scattering by wires near a material half-space 03 p0306 A83-14017

Plane-strain surface waves in a laminated composite [ASME PAPER 82-WA/APM-21] 04 p0498 A83-15681

New formulas for the electromagnetic field of a vertical electric dipole in a dielectric or conducting half-space near its horizontal interface [AD-A125370] 04 p0468 A83-16054

Generalised hybrid-network parameters for electromagnetic coupling between dissimilar regions through a small aperture 04 p0473 A83-16206

The thermal-stress state of a two-temperature half-space with a periodically varying surface-temperature 04 p0502 A83-16403

An improved dislocation approach in solving three-dimensional boundary value problems 05 p0681 A83-17324

Coupled magnetoelastoc problem in elastic half-space 07 p0948 A83-21170

Surface impedance and wave tilt interpretation over horizontally stratified media 08 p1160 A83-22028

Ignition of a combustible half space 08 p1057 A83-22738

A boundary value problem in the propagation of sound in a rarefied gas 09 p1341 A83-24485

Axisymmetric problem of a flat interface annular crack between an elastic layer and a half-space 10 p1440 A83-26424

A longitudinal impact of a slender viscoelastic bar 13 p1866 A83-30449

The diffraction of longitudinal shear waves by a rigid tunnel inclusion in an elastic half-space 14 p2030 A83-32379

Subsonic steady motion of a uniform load over the surface of a thermoelastic half space 15 p2175 A83-34243

Electromagnetic scattering from subterranean obstacles in a stratified ground 16 p2341 A83-35409

On the excitation of elastic waves in a half-space containing a horizontal elastic cylindrical inclusion 16 p2365 A83-35549

On waves of general type propagating at the interface between an elastic half-space and a liquid 16 p2369 A83-36549

The solution of elasticity problems for the half-space by the method of Green and Collins 17 p2525 A83-38619

Annular punch on a transversely isotropic layer bonded to a half-space 19 p2859 A83-41540

Axisymmetric torsion of an elastic half-space with an elastic washer 21 p3154 A83-44720

Loop antennas for directive transmission into a material half space 22 p3274 A83-46527

Radiation of the half-space and layer of a nonequilibrium plasma with active molecules 23 p3510 A83-48392

Scattering of electromagnetic waves by the edge of a semiinfinite dielectric slab imbedded in an ideally conducting half-space 23 p3445 A83-48486

HALIDES

NT ALKALI HALIDES

NT AMMONIUM BROMIDES

NT AMMONIUM CHLORIDES

NT BARIUM FLUORIDES

NT BORON FLUORIDES

NT BROMIDES

NT CALCIUM FLUORIDES

NT CARBON TETRACHLORIDE

NT CESIUM IODIDES

NT CHLORIDES

NT COPPER CHLORIDES

NT COPPER FLUORIDES

NT DICHLORIDES

NT FLUORIDES

NT HYDROBROMIC ACID

NT HYDROCHLORIC ACID

NT HYDROFLUORIC ACID

NT HYDROGEN CHLORIDES

NT LITHIUM CHLORIDES

NT LITHIUM FLUORIDES

NT MAGNESIUM CHLORIDES

NT MAGNESIUM FLUORIDES

NT METAL HALIDES

NT NICKEL FLUORIDES

NT NITROSYL CHLORIDES

NT NITROXYCHLORIDES

NT POTASSIUM BROMIDES

NT POTASSIUM CHLORIDES

NT POTASSIUM IODIDES

NT SILICON TETRACHLORIDE

NT SILVER HALIDES

NT SILVER IODIDES

NT SODIUM CHLORIDES

NT SODIUM IODIDES

NT SULFUR CHLORIDES

NT SULFUR FLUORIDES

NT TETRACHLORIDES

NT URANIUM FLUORIDES

NT ZINC CHLORIDES

Structural features of conducting quasi-one-dimensional organic halides and pseudohalides 02 p0148 A83-11815

Thermal gasdynamic laser utilizing rotational transitions in hydrogen halides with energy transfer from H2 molecules 05 p0649 A83-17065

HALL ACCELERATORS

Theory of ion acceleration with closed electron drift [AIAA PAPER 82-1919] 02 p0241 A83-12490

Experimental investigation of a Hall-current accelerator [AIAA PAPER 82-1920] 02 p0241 A83-12491

HALL COEFFICIENT

U HALL EFFECT

HALL CURRENTS

U ELECTRIC CURRENT

U HALL EFFECT

HALL EFFECT

Temperature dependence of the Hall factor and the conductivity mobility in p-type silicon 01 p0109 A83-10628

Hall-effect devices as strain and pressure sensors 02 p0180 A83-12812

The effects of heat treatments on the transport properties of Cu/x/S thin films 04 p0543 A83-16083

Hall effects on MHD flow through a porous straight channel 04 p0539 A83-16434

Residual double acceptors in bulk GaAs 07 p0998 A83-19989

Electrophysical properties of single crystals of n-Cd/x/Hg/1-x/Te /x ranging from 0.24 to 0.40/ 09 p1350 A83-24250

The Hall effect in a unipolar inductor - A possible mechanism for a dynamo and an antidynamo --- pulsar model 09 p1364 A83-25088

Approximation of atmospheric radio noise in the Arctic by the Hall model 09 p1251 A83-25166

Drift-resistive interchange and tearing modes in cylindrical geometry 13 p1923 A83-30114

Anomalous quantum Hall effect - An incompressible quantum fluid with fractionally charged excitations 13 p1914 A83-30923

Defect nature of the 0.4-eV center in O-doped GaAs [AD-A129932] 13 p1930 A83-31068

Fractional quantum numbers in solids 13 p1930 A83-31164

Hall effects on non-linear Hartmann-Ekman layers 14 p2087 A83-33455

Ionospheric and Birkeland current distributions inferred from the MAGSAT magnetometer data 15 p2196 A83-33940

Heat and mass transfer of an oscillatory flow with Hall current 15 p2236 A83-34557

Hall current effect on tearing mode instability --- possible cause of magnetic field reconnection in space 15 p2202 A83-34736

A correlation of atomic and electrical measurements of Cr and residual donors in thermally processed semi-insulating GaAs 16 p2419 A83-35672

Fractional quantization of the Hall effect 16 p2420 A83-35750

The quantized Hall effect 16 p2420 A83-35763

Temperature dependence of electrical transport properties of n-type solar grade polycrystalline silicon 17 p2584 A83-38210

Hall effects on an oscillatory MHD flow in the Stokes problem past an infinite vertical porous plate. I 18 p2746 A83-39752

Hall effects on MHD free-convection flow in the Stokes problem for a vertical porous plate 18 p2746 A83-39765

On the optical evaluation of the EL2 deep level concentration in semi-insulating GaAs 18 p2750 A83-40062

Fractional quantization of the Hall effect - A hierarchy of incompressible quantum fluid states 19 p2895 A83-41160

The nonlinear generation of a steady magnetic field in a conducting sphere placed in an oscillatory magnetic field 20 p3049 A83-42585

Dissipation and dynamic nonlinear behavior in the quantum Hall regime 24 p3635 A83-48921

Hall effect in a boundary layer flow --- over MHD generator walls 24 p3633 A83-50150

Heat and mass transfer of an oscillatory flow with Hall current. II 24 p3633 A83-50164

The gravitational instability of a rotating plasma in the presence of finite Larmor radius, Hall currents and suspended particles 24 p3633 A83-50168

HALL GENERATORS

Loading schemes for a 50 MWth diagonally connected MHD generator 01 p0106 A83-10659

HALLEY'S COMET

Towards the encounter with Halley's comet 01 p0123 A83-10376

Halley's comet during its 1835 return 01 p0118 A83-11338

Halley's comet is expected 02 p0249 A83-13050

A theoretical study of Comet Halley's spectrum in the infrared range 03 p0407 A83-13841

The estimates of the magnetic field in Halley's comet 03 p0431 A83-14872

Radio metric orbit determination for the Giotto mission to Comet Halley [AIAA PAPER 83-0196] 05 p0605 A83-16580

The Giotto dust protection system --- for encounters with comet Halley 05 p0607 A83-17434

The experiment PIA of the ESA mission Giotto, a device for the analysis of the mass of the smallest particles which are released from Halley's comet 09 p1218 A83-23383

Analog signal processing in the dust particle experiment of the Giotto mission 09 p1218 A83-23384

The swarm of meteoroid bodies produced by the Halley's comet 09 p1364 A83-25274

The rediscovery of Halley's comet 10 p1496 A83-26123

Evolution of the orbits of Halley's comet, the Orionids, and the eta-Aquarids over 15,000 years 10 p1498 A83-26903

The Comet Halley flyby I.R. sounder 'I.K.S.' --- infrared spectrometer 11 p1670 A83-27740

Scientific instrumentation of PLANET-A VUV imaging of the hydrogen coma of Halley 11 p1537 A83-27746

Astrometry and photometry of comet P/Halley in October and November 1982 13 p1943 A83-31727

P/Halley - First signs of activity? --- nucleus ice vaporization 13 p1943 A83-31729

Electrodynamics of submicron dust in the cometary coma 13 p1958 A83-31733

Attitude perturbations of the Giotto spacecraft in the dust cloud of Comet Halley 14 p1979 A83-33472

Magnetic field distribution in the tail of Halley's Comet found from the kinematics of a plasma formation 15 p2271 A83-34772

Recent researches into solid bodies and magnetic fields in the solar system; Proceedings of the Topical Meeting and Symposium, Ottawa, Canada, May 16-June 2, 1982 15 p2124 A83-35001

Cometary probe of the Venera-Halley mission 15 p2124 A83-35011

Planet-A mission to Halley 15 p2124 A83-35012

The Giotto mission to Halley's Comet 15 p2124 A83-35013

Modelling the neutral gas environment of comets with special application to P/Halley 15 p2273 A83-35014

The Halley dust model 15 p2273 A83-35015

Dust hazard near Halley Comet in case of the Vega project 15 p2128 A83-35016

Cometary ephemerides for spacecraft flyby missions 15 p2249 A83-35017

The derivation of Halley parameters from observations 15 p2273 A83-35018

The infrared synthetic spectrum of comet Halley 15 p2273 A83-35019

Impact induced plasma during a cometary fly-by 15 p2128 A83-35021

Dust modelling of fast flyby missions - Implications of in situ measurements 15 p2128 A83-35022

Hypervelocity impact on the Giotto Halley mission dust shield - Momentum exchange and measurement 15 p2128 A83-35023

The detection of energetic cometary and solar particles by the EPONA instrument on the Giotto mission --- Energetic Particle Onset Admonitor 15 p2129 A83-35025

Analysis of the nucleus and circumnuclear area of Comet Halley with the 'I.K.S.' infrared sounder from the 'Vega' flyby probes --- Venera satellite-borne IR imaging spectrometer 15 p2249 A83-35026

Wide field ultraviolet observations of Comet Halley with the FAUST Spacelab I instrument 15 p2250 A83-35027

Preparing for Halley's comet 15 p2250 A83-35319

Japan's Halley's Comet probes 16 p2314 A83-35777

The attitude and orbit control system for GIOTTO, ESA's Halley encounter mission 17 p2476 A83-37435

Giotto - The European spacecraft to flyby Halley's comet 17 p2473 A83-37862

Mass spectrometer experiments for the European space probe Giotto 17 p2482 A83-37863

Determination of the mass flow and electron content of the coma of Halley's comet using Doppler measurements of signals from the Giotto probe 18 p2777 A83-39784

Halley's Comet - Orbital elements evolution 20 p3061 A83-43390

Temporal variations of the absolute magnitude of Halley's comet 22 p3375 A83-46576

Lectures on the planets: The comets - Halley's Comet 24 p3661 A83-49459

HALOCARBONS

NT CHLOROCARBONS

NT FLUOROCARBONS

Absolute band strengths of halocarbons F-11 and F-12 in the 8- to 16-micron region 09 p1296 A83-24269

Halocarbon measurements in the Southern Hemisphere since 1977 15 p2194 A83-34046

Physical properties of dihalocarbene modified rubbers 18 p2672 A83-40139

Henry's Law constants and the air-sea exchange of various low molecular weight halocarbon gases 18 p2705 A83-40645

The atmospheric lifetime experiment. I - Introduction, instrumentation, and overview 24 p3606 A83-49328

HALOGEN COMPOUNDS

NT ALKALI HALIDES

NT AMMONIUM BROMIDES

NT AMMONIUM CHLORIDES

NT AMMONIUM PERCHLORATES

NT BARIUM FLUORIDES

NT BORON FLUORIDES

NT BROMIDES

NT BROMINE COMPOUNDS

NT CALCIUM FLUORIDES

NT CARBON TETRACHLORIDE

NT CESIUM IODIDES

NT CHLORATES

NT CHLORIDES

NT CHLORINE COMPOUNDS

NT CHLORINE OXIDES

NT COPPER CHLORIDES

NT COPPER FLUORIDES

NT DICHLORIDES

NT DIFLUORO COMPOUNDS

NT FLUORIDES

NT FLUORINE COMPOUNDS

NT FLUORINE ORGANIC COMPOUNDS

NT FLUOROCARBONS

NT FLUOROHYDROCARBONS

NT HALIDES

NT HALOCARBONS

NT HYDROBROMIC ACID

NT HYDROCHLORIC ACID

NT HYDROFLUORIC ACID

NT HYDROGEN CHLORIDES

NT IODIDES

NT IODINE COMPOUNDS

NT LITHIUM CHLORIDES

NT LITHIUM FLUORIDES

NT LITHIUM IODATES

NT LITHIUM PERCHLORATES

NT MAGNESIUM CHLORIDES

NT MAGNESIUM FLUORIDES

NT METAL FLUORIDES

NT METAL HALIDES

NT NICKEL FLUORIDES

NT NITROSYL CHLORIDES

NT NITROXYCHLORIDES

NT POLYTETRAFLUOROETHYLENE

NT POTASSIUM BROMIDES

NT POTASSIUM CHLORIDES

NT POTASSIUM IODIDES

NT SILICON TETRACHLORIDE

NT SILVER HALIDES

NT SILVER IODIDES

NT SODIUM CHLORIDES

NT SODIUM IODIDES

NT SULFUR CHLORIDES

NT SULFUR FLUORIDES

NT TETRACHLORIDES

NT URANIUM FLUORIDES

NT ZINC CHLORIDES

Selected man-made halogenated chemicals in the air and oceanic environment 13 p1873 A83-30883

Optically pumped molecular laser utilizing C2H5Br and C2H5I halogen derivatives of ethane 20 p2996 A83-43779

HALOGENATION

NT BROMINATION

NT FLUORINATION

HALOGENS

NT BROMINE

NT CHLORINE

NT FLUORINE

NT FLUORINE ISOTOPES

NT IODINE

NT IODINE ISOTOPES

The thermodynamic principles of calorizing 07 p0887 A83-20679

An RF-primed all-halogen gas plasma microwave high-power receiver protector 07 p0922 A83-21530

Nonequilibrium expansion of halogens in short nozzles --- Russian book 23 p3392 A83-47123

HALOS

The halos of rich clusters of galaxies. I - An infall model for the Coma Cluster 02 p0254 A83-12102

X-ray spectroscopy of the galaxy M87 - Radiative accretion of the hot plasma halo 02 p0254 A83-12105

Gas in the galactic halo 02 p0258 A83-12184

Massive neutrino halos in an expanding universe 03 p0427 A83-14754

Common properties of clusters of galaxies containing radio halos and implications for models of radio halo formation 06 p0825 A83-18092

Absorption by halo gas in the direction of M13 07 p1020 A83-21118

Optical variability of QSOs and gravitational lenses in galactic haloes 08 p1186 A83-23273

RGU photometry in a field of the galactic bulge 10 p1493 A83-25662

Can galactic halos be made of axions 10 p1507 A83-26270

Investigation of the outer regions of the galactic halo 13 p1946 A83-30383

Further evidence for M87's massive, dark halo 13 p1950 A83-31407

Thermal conduction and heating by nonthermal electrons in the X-ray halo of M87 13 p1950 A83-31408

- Rotation curve of the edge-on spiral galaxy NGC 5907: disc and halo masses 13 p1957 A83-31698
- Chemical enrichment in halo planetary nebulae 14 p2110 A83-33282
- Theory of the stability of flat subsystems of galaxies 15 p2269 A83-34679
- Bulge-halo effects in barred galaxies 16 p2426 A83-36688
- Considerations arising from the faint absolute magnitude of halo RR Lyrae variables and an error in the Cepheid PLC relation --- Period-Luminosity-Color 16 p2432 A83-36692
- Hydrostatic-equilibrium distribution of cosmic rays and the magnetic field in the galactic halo 18 p2778 A83-40489
- Collisional modification to the exospheric theory of solar wind halo electron pitch angle distributions 22 p3388 A83-46027
- Globular clusters and the early chemical history of galactic halos 22 p3378 A83-46409
- Neutral interstellar gas in the lower galactic halo 22 p3381 A83-46983
- Transient X-ray rings around dwarf novae 23 p3526 A83-47874
- Elliptic stellar disks - Equilibrium solutions in the presence of a halo and in binary systems 24 p3653 A83-49165
- Mass distribution and dark halos 24 p3654 A83-49215
- NGC 3992 - A galaxy without a massive halo 24 p3654 A83-49217
- HAMILTON-JACOBI EQUATION**
- A method for constructing explicit solutions to a simplified version of the spatial circular restricted three-body problem 03 p0408 A83-13898
- Solution of equations of problem of motion of a heavy rigid body about a fixed point in the Kowalevskaya's case using theta-function 12 p1775 A83-29115
- Lagrange variational equations from Hori's method for canonical systems 12 p1771 A83-29123
- The Hamilton-Jacobi equation and its complementary form 18 p2741 A83-39148
- HAMILTONIAN FUNCTIONS**
- The molecular vibration-rotation Hamiltonian in the Bargmann-Hilbert space 02 p0234 A83-11573
- Analysis of H₂O vibration-rotation spectra in the visible region 03 p0392 A83-13354
- The determination of the derivatives in Brown's lunar theory 03 p0405 A83-13421
- On the motion of a body whose dynamical structure is variable 03 p0419 A83-13885
- Comments on Aksnes' intermediary --- in theory of artificial satellite orbits 04 p0452 A83-16358
- Gowdy three-handle and S/3- inhomogeneous cosmological models 06 p0828 A83-18324
- Intermittent behaviour in non-linear-Hamiltonian systems far from equilibrium 06 p0805 A83-18329
- Hamiltonian description of stratified fluid dynamics 07 p0926 A83-20529
- Analytical theory of the libration of the moon 08 p1190 A83-23125
- The use of invariant relationships to reduce the order of the system of equations of motion of a vortex-filled heavy rigid body 09 p1337 A83-23564
- Simple relationship between the geometric and Hamiltonian representations of integrable nonlinear equations 09 p1339 A83-24325
- Uniform semiclassical quantization of regular and chaotic classical dynamics on the Henon-Heiles surface 09 p1344 A83-25215
- Approximate constants of motion for classically chaotic vibrational dynamics - Vague tori, semiclassical quantization, and classical intramolecular energy flow 09 p1344 A83-25216
- Integrable Hamiltonian systems. I - Methods for the integration of Hamiltonian systems. II - Series of integrable systems 09 p1340 A83-25266
- The variations in eccentricity and apse precession rate of a narrow ring perturbed by a close satellite 10 p1492 A83-25512
- Algebraic programming of Hamiltonian formalism in general relativity - Application to inhomogeneous space-times 10 p1506 A83-26093
- A simple approach to Hamiltonian structures of soliton equations. I. 12 p1775 A83-29040
- Hamiltonian structure of the theory of gravity with R + T(2) type of Lagrangian 12 p1775 A83-29043
- Hamiltonian formulation for a translation gauge theory of gravitation 12 p1792 A83-29045
- Hamiltonian formulation of the gauge theory of gravitation Pure-gravity case. 12 p1792 A83-29046
- On the double averaged three-body problem 12 p1787 A83-29118
- Natural Poisson structures of Nonlinear plasma dynamics 13 p1924 A83-30415
- Hamiltonian picture of the free-electron laser - Multimode, super mode and all that 13 p1854 A83-31120
- Energy characteristics of an electromagnetic field and an extraneous particle in a dispersive medium 14 p2079 A83-32168
- Hamiltonian analysis of beams in an optical slab guide 15 p2229 A83-33539
- Hamiltonian formulation of the second-order drift equations of motion --- for charged particles in fixed electromagnetic fields in high temperature plasmas 15 p2232 A83-33781
- Superintegrability of the Calogero-Moser system 15 p2225 A83-34136
- A resonance problem of two degrees of freedom --- for artificial earth satellite orbits 15 p2124 A83-34390
- The Hamiltonian formalism of one-dimensional systems of hydrodynamic type and the Bogoliubov-Whitham averaging method 18 p2741 A83-39477
- Problem of three rigid bodies - Conversion of the Hamiltonian to Delaunay and Andoyer variables 18 p2759 A83-39976
- State space of the gravitational field in the Hamiltonian approach to general relativity 19 p2895 A83-40821
- The stability of the permanent rotations of an asymmetric heavy rigid body 19 p2895 A83-41202
- Nearly Hamiltonian two-dimensional nonconservative periodic systems 19 p2896 A83-41204
- Equations in Rodrigues-Hamilton parameters for a heavy rigid body rotating about a stationary point 23 p3504 A83-48452
- Fundamental equation of two body problem in relativistic analytical mechanics 24 p3624 A83-50126
- HAND (ANATOMY)**
- NT FINGERS**
- Restoration of thermoregulatory response to body cooling by cooling hands and feet 03 p0378 A83-13578
- HANDBOOKS**
- NT USER MANUALS (COMPUTER PROGRAMS)**
- The Space Shuttle operator's manual --- Book 01 p0019 A83-11501
- Fundamentals handbook of electrical and computer engineering. Volume 1 Circuits fields and electronics 03 p0314 A83-14047
- A handbook of gasdynamic lasers --- in Russian 04 p0485 A83-15831
- Thermophysical properties of materials at low temperatures: A handbook /2nd revised and enlarged edition/ 05 p0610 A83-17129
- Flammability handbook for electrical insulation 09 p1221 A83-24895
- Flow measurement engineering handbook 15 p2163 A83-33620
- Polymer materials - Properties and applications (A handbook) --- in Russian 15 p2142 A83-34574
- The handbook of antenna design. Volumes 1 & 2 17 p2493 A83-37158
- Handbook of isotope geochemistry --- in Russian 21 p3239 A83-43909
- Polymer materials - Toxic properties /Handbook/ --- in Russian 21 p3117 A83-45006
- Metals handbook. Volume 6 - Welding, brazing, and soldering /9th edition/ 24 p3590 A83-50121
- HANDLES**
- How to get a grip on TADS/PNVS --- Target Acquisition Detection System/Pilot's Night Vision System 10 p1459 A83-26316
- HANDLING EQUIPMENT**
- Studies on a versatile handling system having multijointed fingers 08 p1151 A83-22064
- HANDLING QUALITIES**
- U CONTROLLABILITY**
- HANG GLIDERS**
- Microlights -The state of the art 09 p1195 A83-23685
- HANKEL FUNCTIONS**
- Axisymmetric problem of a flat interface annular crack between an elastic layer and a half-space 10 p1440 A83-26424
- Fast algorithm for the computation of the zero-order Hankel transform 23 p3501 A83-47581
- HARDENERS**
- Synthesis and characterization of bisimide amines and bisimide amine-cured epoxy resins 01 p0027 A83-11486
- HARDENING (MATERIALS)**
- NT CARBURIZING**
- NT HOT PRESSING**
- NT NITRIDING**
- NT PRECIPITATION HARDENING**
- NT PULSE HEATING**
- NT SHOT PEENING**
- NT STRAIN HARDENING**
- NT WORK HARDENING**
- Prediction of the hardening of magnesium alloy VMD10 from high-temperature test data 01 p0025 A83-10395
- The strengthening of hard alloys by ultrasonic oscillations. I - The effect of ultrasound on the physicomachanical properties of hard alloys 02 p0159 A83-13040
- System identification for yield limits and hardening moduli in discrete elastic-plastic structures by nonlinear programming 04 p0494 A83-14959
- Studies on plastic structures - Stability, anisotropic hardening, cyclic loads 04 p0495 A83-15012
- Finite endochronic theory for ratcheting and cyclic plasticity 04 p0500 A83-16096
- On the interaction of hardening and fatigue damage in the 316 stainless steel 08 p1062 A83-21736
- The microstructure and resistance properties of titanium alloys following hardening from the liquid state 09 p1234 A83-24383
- The properties, structure, and transformations of hardened titanium-niobium alloys with /alpha-prime + omega + beta/, /omega + beta/, and beta structures 09 p1235 A83-24391
- Transformation strengthening of beta double prime-Al₂O₃ with tetragonal ZrO₂ 09 p1240 A83-25210
- Methods of producing dispersion-strengthened cast alloys based on aluminum 10 p1395 A83-25629
- The crystalline structure of gas-saturated beta titanium alloys 11 p1550 A83-28546
- Thermal and transformation stresses 12 p1746 A83-29902
- Structural features of solid solutions in magnesium-yttrium alloys 16 p2334 A83-36888
- On the question of hardening during plastic deformation 17 p2521 A83-37544
- A remark on the definition of hardening, softening and perfectly plastic behavior 19 p2860 A83-42000
- Magnetic, electrical, and mechanical properties of 12KhN3A and 12Kh2N4A steels and of case-hardened layers on them 21 p3111 A83-43879
- Distortional hardening rules for metal plasticity 21 p3113 A83-44547
- The use of the internal friction method for studying laser-irradiated materials 21 p3115 A83-45502
- HARDENING (SYSTEMS)**
- A low-risk hardened computer for today's spacecraft programs 21 p3190 A83-43999
- HARDNESS**
- NT KNOOP HARDNESS**
- NT MICROHARDNESS**
- Effects of morphology and hardness of inclusions on ductile fracture 08 p1066 A83-22078
- Controlled flaws in ceramics - A comparison of Knoop and Vickers indentation 08 p1070 A83-22193
- An analysis of shot peening 12 p1733 A83-29446
- Thermomechanical treatment of the Elinvor alloy 44NkHMT using plain shear 13 p1823 A83-31216
- The variation of hardness in Lucas Syalon ceramics 18 p2671 A83-39061
- Studies on the metastable phase retention and hardness in zirconia ceramics 20 p2958 A83-42782
- HARDNESS TESTS**
- Equivalence of indentation and compressive creep tests on a WC/Co hardmetal 04 p0460 A83-15997
- The relation between hardness-indentation processes and the stress-strain curve of metallic materials 12 p1713 A83-29363
- Lamination and microlamination in parts made of Tsm2A alloy sheet --- molybdenum alloy 13 p1823 A83-31215
- HARDWARE**
- A data analysis facility for the Faint Object Camera 01 p0114 A83-10143
- Human factors and intelligent products 01 p0085 A83-10254
- Cost-effective approaches for extending the useful life of ATE and test program sets 01 p0088 A83-10762
- Emulation, a cost effective alternative for replacing obsolete ATE 01 p0088 A83-10763
- The U.S. Air Force and U.S. Navy Standard Central Air Data Computer 01 p0009 A83-11120
- An integrated support software system for the VHSC era 01 p0089 A83-11165
- Incorporating ISPS into a commercial CAD system 01 p0092 A83-11195
- Integrated and transferable hardware/software checkout --- of digitally controlled flight systems 01 p0093 A83-11249
- Life Cycle Cost analysis of standard avionics hardware and software 01 p0112 A83-11256
- Spacelab software for science applications 03 p0285 A83-13710
- Hardware and software configuration control - History and current status 05 p0621 A83-17313

- Hardware simulation facility for 120-Mbit/s QPSK/TDMA system 07 p0914 A83-20554
- Automatic hardware synthesis 07 p0923 A83-21540
- The use of the method of multisetting argument-transformation for the high-precision hardware implementation of elementary functions 12 p1768 A83-29348
- Reducing the cost for airborne instrumentation hardware testing 14 p1978 A83-32928
- Deterioration trending enhances jet engine hardware durability assessment and part management [AIAA PAPER 83-1234] 16 p2308 A83-36297
- The use of production hardware for the development of control laws --- LSI for engine control [ASME PAPER 83-GT-6] 23 p3406 A83-47879
- Soviet manned space flight hardware 23 p3423 A83-48630

HARMONIC ANALYSIS**NT ZONAL HARMONICS**

- Improvement of the theories of Jupiter and Saturn by harmonic analysis 02 p0247 A83-12533
- Rotation-invariant digital pattern recognition using circular harmonic expansion 02 p0230 A83-12593
- Optical pattern recognition using circular harmonic expansion 02 p0178 A83-12594
- Evaluation of 15th-order harmonics in the geopotential from analysis of resonant orbits 04 p0509 A83-15451
- On the analysis of Hopf bifurcations 07 p0989 A83-20641
- M2 ocean tide at Cobb seamount from Seasat altimeter data 09 p1318 A83-24291
- Double Schottky-barrier diode power sensor 11 p1560 A83-27894
- On a method for the representation of images in the process of their arrival 13 p1910 A83-30617
- The singular integral problem in surfaces 15 p2148 A83-35187
- A numerical method for the analysis of harmonic balance conditions in multiloop non-linear feedback systems 19 p2891 A83-41489
- Power series for perturbations in the intermediate motion of artificial earth satellites caused by atmospheric attraction 19 p2809 A83-41548
- Methods of computation of geomagnetic field at greater altitude in a local region 21 p3173 A83-44585
- Analysis of the periodic variations of atmospheric pressure over Greece 21 p3181 A83-45408
- Harmonic response of a tunable Solc filter 22 p3357 A83-46088
- Harmonic acceleration method for dynamic structural analysis 23 p3471 A83-48165

HARMONIC EXCITATION

- The induced radiation of linear oscillators in a spatially inhomogeneous variable field 06 p0750 A83-18142
- Strange attractor in the nonautonomous Van der Pol equation 06 p0806 A83-19368
- A method for the analysis of the stationary regime of a nonlinear electric circuit under polyharmonic external excitation 12 p1719 A83-29345
- Intracavity second harmonic excitation under the action of an external signal on a Q-switched solid-state ring laser 14 p2023 A83-31907
- A three degree-of-freedom, typical section flutter analysis using harmonic transonic air forces [AIAA PAPER 83-0960] 14 p2032 A83-32797
- Observations of odd-half cyclotron harmonic emissions in a shell-Maxwellian laboratory plasma 22 p3362 A83-46047

HARMONIC FUNCTIONS

- Inclusions and separation of the zeros of exponential trinomials with constant coefficients 03 p0389 A83-14510
- The use of the intraperiod symmetry of harmonic basis functions to compute the discrete Fourier transformation 06 p0802 A83-18039
- On the spectral expansion of the electric and magnetic dyadic Green's functions in cylindrical harmonics 10 p1472 A83-26037

HARMONIC GENERATIONS

- Approximation of the distribution functions of the phase and phase cosine of the sum of a harmonic signal and noise 01 p0031 A83-10411
- Transient pulse evolution of active mode locking in an intracavity frequency-doubled laser 01 p0054 A83-10642
- On the distribution of second harmonic emission from a laser-produced plasma 02 p0241 A83-12082
- Continuous-wave garnet ring laser emitting single-mode linearly polarized radiation and intracavity second harmonic generation in LiIO₃ 03 p0330 A83-13584
- Synchronization of lasers with intracavity second harmonic generation 05 p0648 A83-17039
- Efficient frequency doubling of radiation emitted by a multistage neodymium laser 05 p0648 A83-17040

- Third-harmonic generation in a pulsed supersonic jet of xenon 05 p0651 A83-17879
- Harmonic generation with noncollinear laser beams - Application to pulse stacking 06 p0766 A83-18958
- Third-harmonic generation in a semiconductor with negative differential resistance 06 p0754 A83-19337
- Dynamics of harmonic generation in a laser plasma 07 p0995 A83-20059
- Propagation of interacting first and second optical harmonics in a nonlinear active medium 07 p0934 A83-20118
- The polarization characteristics of coherent transient phenomena in two-photon resonance 09 p1346 A83-25091
- Mode effects in second harmonic generation and their uses for laser stabilization 10 p1425 A83-25404
- Intense free electron laser harmonic generation in a longitudinal magnetic wiggler 10 p1426 A83-25792
- Generalized description of harmonic generation in a transverse optical klystron 10 p1427 A83-26007
- Generation of 35.5-nm coherent radiation 10 p1429 A83-26115
- Interaction in frequency doubling of ultrashort laser pulses 10 p1434 A83-26693
- Squeezed states in harmonic generation of a laser beam 10 p1435 A83-26971
- High spectral brightness extreme ultraviolet generation with excimer lasers 11 p1576 A83-27508
- Multiphoton ionization and third-harmonic generation in atoms and molecules 11 p1579 A83-27556
- Band-reject filters suppress second harmonics 11 p1562 A83-28161
- Optical second-harmonic generation in a thin-film waveguide without control of film thickness 12 p1731 A83-29190
- Subharmonic generation in Josephson junction fluxon oscillators biased on Fiske steps 13 p1832 A83-30355
- Radio emission by parallel acceleration mechanism --- applied to solar bursts 15 p2279 A83-34289
- Investigation of the effect of the increase of the maximum generation frequency of Gunn diodes 15 p2154 A83-35174
- Level crossing and polarization rotation in doubly resonant third-harmonic generation in I₂ 16 p2358 A83-35658
- Spectral decontamination of a real-time helicopter simulation [AIAA PAPER 83-1087] 16 p2299 A83-36211
- Harmonic generation of radiation in a steep density profile 18 p2748 A83-40512
- Nearly noncritically phase-matched UV generation at 3547 Å in NaCHO₂ 19 p2851 A83-40929
- Second harmonic generation by optically travelling long range surface polaritons 19 p2853 A83-41191
- Second-harmonic generation on reflection from a monomolecular Langmuir layer 20 p3047 A83-42282
- Ultra-wideband millimetre-wave self-oscillating mixer 20 p2966 A83-42366
- Rectification and harmonic generation with metal-insulator-metal diodes in the mid-infrared 20 p3048 A83-43600
- Further investigations on the operating modes of millimeter-wave Gunn oscillators 21 p3124 A83-43859
- Nonlinear scattering from a plasma column. I - Theory. II Special cases 22 p3363 A83-46536
- Enhancement of high-harmonic gyrotron gain by a dielectric rod 22 p3279 A83-46750
- Effect of group velocity mismatch on the measurement of ultrashort optical pulses via second harmonic generation 22 p3293 A83-46822
- Generation of higher harmonics of an intense laser beam in a plasma 22 p3363 A83-46935
- Theory of prism coupling with a nonlinear optical waveguide Second harmonic generation 23 p3507 A83-47559
- A new approach for mm-wave generation 24 p3571 A83-48774

HARMONIC GENERATORS

- Applied nonlinear-optics: Second-harmonic generators and parametric light-generators --- Russian book 05 p0650 A83-17126
- Prediction and control of harmonic phase sequence in power convertors 07 p0916 A83-19631
- Modified numerical method for solving the nonlinear mixer pumping problem 08 p1079 A83-21975
- Hyperabrupt junction varactor diodes for millimeter-wavelength harmonic generators 10 p1409 A83-25820
- Optical second-harmonic generation with long-range surface plasmons 16 p2360 A83-36562
- Bernstein mode quasi-optical gyroklystron [AD-A130124] 17 p2497 A83-37760

HARMONIC MOTION**NT SIMPLE HARMONIC MOTION****HARMONIC OSCILLATION**

- Vibration-induced change of flow in the annular space between two concentric pipes 03 p0320 A83-14506
- Peculiarities of the appearance of subharmonic and subultraharmonic resonances in systems which are described by Duffing's equation 04 p0531 A83-15379
- Forced oscillations of system with nonlinear restoring force 14 p2080 A83-32519
- Higher harmonic control for the jet smooth ride 14 p1977 A83-33096
- Energetics and optimum motion of oscillating lifting surfaces --- energy losses of rigid wings [AIAA PAPER 83-1710] 17 p2445 A83-37204
- High space harmonic perturbations in travelling wave tubes 17 p2497 A83-37757
- Spacecraft model verification using swept sine data analysis 22 p3303 A83-45748
- Subharmonic vibration of a rotor rotating in rolling-contact bearings 23 p3467 A83-48459
- A least squares finite element scheme for transonic flow around harmonically oscillating airfoils 24 p3543 A83-48872
- Calculation of modal characteristics from measured quasi-normal mode information 24 p3591 A83-49185

HARMONIC OSCILLATORS

- Flux-balanced variable frequency inverter 01 p0040 A83-11010
- Analog computer simulation of a Duffing oscillator and comparison with statistical linearization 02 p0233 A83-12869
- Broad-band bias-current-tuned IMPATT oscillator for 100-200 GHz 06 p0753 A83-18767
- On a model for multiphoton excitation of molecules in a strong laser field 06 p0766 A83-19003
- Excitation of an infinite periodic structure by a local harmonic source with an imprecisely specified frequency 06 p0749 A83-19333
- The stability of two-terminal oscillators with high harmonic content --- German thesis 07 p0919 A83-20394
- TRAPATT oscillators with active harmonic tuning --- German thesis 07 p0919 A83-20396
- A kinetic equation for the correlation functions of a quantum system interacting with a Gaussian thermostat 09 p1350 A83-25080
- A monolithically integrated wide-tunable sine oscillator --- Thesis 11 p1564 A83-28642
- The use of the small-parameter method for analyzing flows of vibrationally nonequilibrium gases with allowance for the anharmonicity of vibrations 13 p1933 A83-30671
- Harmonic Gunn oscillators allow frequency growth 13 p1835 A83-30912
- A simple model for radiation damping 14 p2102 A83-33045
- On the registration of the classical force acting on a quantum oscillator 14 p2080 A83-33395
- Transformations of the perturbed two-body problem to unperturbed harmonic oscillators 15 p2246 A83-34392
- Quantum nondemolition measurements on coupled harmonic oscillators --- for gravitational radiation detection 16 p2355 A83-35651
- Small-signal theory of a large-orbit electron-cyclotron harmonic maser 18 p2694 A83-40516
- Spectral dispersion of modulated signals due to oscillator phase instability - White and random walk phase model 19 p2837 A83-40922
- A structure function representation theorem with applications to frequency stability estimation 19 p2894 A83-41027
- Compressed quantum states of a harmonic oscillator in the problem of detecting gravitational waves 19 p2896 A83-41495
- Operation of a millimeter-wave harmonic gyrotron 21 p3125 A83-43386
- Radiation from an oscillator in media with periodic inhomogeneity 21 p3215 A83-45392
- Quantum nondemolition measurements via quadratic coupling --- for gravitational radiation detection 24 p3623 A83-48827

HARMONIC RADIATION

- Radiated electromagnetic waves in an inhomogeneous magnetoplasma near the upper hybrid frequency 10 p1487 A83-26697
- The rate of convergence of the parameters of adaptive filters with quasi-harmonic input signals 11 p1561 A83-27934
- Detection of the Z-dependence of laser-plasma corona temperature in a study of half-integer harmonic radiation 11 p1658 A83-28063
- On the resolving power of the VLF method 11 p1558 A83-28346

- Ground observations of power line radiation coupled to the ionosphere and magnetosphere
 - 14 p2053 A83-32895
- Power-line harmonic radiation and the electron slot
 - 14 p2053 A83-32896
- Satellite observations of power line harmonic radiation
 - 14 p2053 A83-32897

HARMONICS

- NT HARMONIC EXCITATION
- NT HARMONIC GENERATIONS
- NT HARMONIC OSCILLATION
- NT SIMPLE HARMONIC MOTION
- NT SPHERICAL HARMONICS
- NT SUPERHARMONICS
- NT ZONAL HARMONICS
- Second-harmonic diffraction field in nonlinear propagation of transversely limited surface acoustic wave beams
 - 04 p0473 A83-16058
- Mechanism for chaos in the Duffing equation
 - 10 p1472 A83-26969
- Approximate method for calculating the characteristics of a magnetron at frequencies above the higher temporal harmonics
 - 13 p1833 A83-37074
- Collocations and thirtieth order resonant harmonics --- for determining earth's gravitational field
 - 20 p3023 A83-43153

HARNESSES

- Hazards of loose harness during flying
 - 23 p3499 A83-48693

HARRIER AIRCRAFT

- Sky Hook to help ships launch Harrier
 - 03 p0282 A83-13575
- Operational test and evaluation of the molecular sieve On-Board Oxygen Generation System /OBOGS/ in the AV-8A 'Harrier'
 - 04 p0525 A83-15417
- Supersonic Harrier - One step closer
 - 04 p0449 A83-16371
- Fiber-optic technology takes to the air
 - 05 p0592 A83-16867
- Investigation of thermal effects on weapon system components
 - 13 p1859 A83-31298
- YAV-8B flight demonstration program
 - 16 p2300 A83-36466
- [AIAA PAPER 83-1055]
 - 16 p2300 A83-36466
- A variable structure approach to robust control of VTOL aircraft
 - 17 p2470 A83-37145
- Development of thrust augmentation technology for the Pegasus vectored thrust engine
 - 17 p2468 A83-37966
- [SAE PAPER 821390]
 - 17 p2468 A83-37966
- Simulation evaluation of flight controls and display concepts for VTOL shipboard operations
 - 19 p2789 A83-41668
- [AIAA PAPER 83-2173]
 - 19 p2789 A83-41668

HARTMANN FLOW

- Cyclic wave action in the stable operation of a Hartmann-Sprenger tube
 - 10 p1414 A83-26144
- Hall effects on non-linear Hartmann-Ekman layers
 - 14 p2087 A83-33455
- The measurement of pressure pulsations by means of piezoelectric transducers
 - 19 p2849 A83-41891

HARTREE APPROXIMATION

- Multiconfiguration Hartree-Fock Breit-Pauli results for 2P1/2-2P3/2 transitions in the boron sequence
 - 08 p1162 A83-21985
- A semiempirical self-consistent field Hartree-Fock crystal orbital approach to the infinite tetraza porphrin nickel/II system
 - 11 p1661 A83-28072
- State-to-state differential and integral cross sections for vibrational-rotational excitation and elastic scattering of electrons by N2 at 5-50 eV - Calculations using extended-basis-set Hartree-Fock wave functions
 - 20 p3045 A83-42634

HARTREE-APPLETON APPROXIMATION

- U HARTREE APPROXIMATION

HARTREE-FOCK APPROXIMATION

- U HARTREE APPROXIMATION

HARTREE-FOCK-SLATER METHOD

- The Hartree-Fock method in the theory of the nucleus --- Russian book
 - 21 p3202 A83-45030

HASTELLOY (TRADEMARK)

- An evaluation of fretting at small slip amplitudes
 - 05 p0614 A83-17254
- The anodic dissolution of a Ni-base superalloy
 - 12 p1713 A83-29401
- Porous metallic membrane produced by the fiber metallurgy
 - 18 p2667 A83-40137
- Oxidation of carburized Hastelloy X
 - 18 p2670 A83-40640
- Long-term ageing characteristics of Hastelloy alloy X
 - 24 p3567 A83-50067

HAWKER SIDDELEY AIRCRAFT

- NT HARRIER AIRCRAFT

HAWKEYE SATELLITES

- A correlation between auroral kilometric radiation and field-aligned currents
 - 05 p0661 A83-17396

HAYNES STELLITE

- U STELLITE (TRADEMARK)

HAZARDS

- NT AIRCRAFT HAZARDS
- NT FLIGHT HAZARDS
- NT METEOROID HAZARDS
- NT OPERATIONAL HAZARDS
- NT RADIATION HAZARDS
- NT TOXIC HAZARDS
- The effect of dangerous motions on kinesthesia
 - 05 p0672 A83-17152
- Hazards in the manufacture of RDX and HMX
 - 15 p2143 A83-33874
- Geostationary junk - Problem for the future
 - 22 p3256 A83-45723

HAZE

- Detection of regional air pollution episodes utilizing satellite data in the visual range
 - 01 p0069 A83-10044
- More about the influence of the aerosol correction on the results of total ozone amount
 - 01 p0070 A83-10289
- Polarization studies of the Venus UV contrasts - Cloud height and haze variability
 - 02 p0266 A83-12567
- The effects of haze on resolution on small scale aerial photography
 - 03 p0329 A83-14283
- Arctic haze and perturbations in the solar radiation fluxes at Barrow, Alaska
 - 03 p0370 A83-14642
- Arctic haze and the Arctic gas and aerosol sampling program /AGASP/ [AIAA PAPER 83-0439]
 - 05 p0659 A83-16714
- Measurements of the properties of wintertime fog and haze in West Germany - A preliminary report on project 'Meppen 80'
 - 08 p1141 A83-22549
- Atmospheric aerosols in the polar regions
 - 09 p1316 A83-25231
- Venus -Mesospheric hazes of ice, dust, and acid aerosols
 - 10 p1518 A83-25507
- Simultaneous determination of complex refractive index and size distribution of airborne and water-suspended particles from light scattering measurements
 - 14 p2052 A83-32440
- High altitude Venus haze from Pioneer Venus limb scans
 - 14 p2112 A83-32606
- Infrared optical properties of a coal-fired power plant plume
 - 16 p2372 A83-36760
- The clouds are hazes of Venus
 - 17 p2617 A83-37417
- Saturn's equatorial haze
 - 17 p2620 A83-38113
- On the aerosol particle size distribution spectrum in Alaskan air mass systems - Arctic haze and non-haze episodes
 - 18 p2729 A83-40043
- Vertical distribution of scattering hazes in Titan's upper atmosphere
 - 19 p2921 A83-40778
- The coefficient of haze as a measure of particulate elemental carbon
 - 22 p3321 A83-46775

HAZE DETECTION

- Evidence for a central Eurasian source area of arctic haze in Alaska
 - 02 p0203 A83-11626

HC-1 HELICOPTER

- U CH-47 HELICOPTER

HCL ARGON LASERS

- Short-cavity hydrogen-halide laser
 - 22 p3296 A83-46086

HCL LASERS

- NT HCL ARGON LASERS

HCMM

- U HEAT CAPACITY MAPPING MISSION

HCN LASERS

- Investigation of the ionization relaxation of shock-wave heated krypton with an HCN laser interferometer --- German thesis
 - 04 p0536 A83-15842
- Absorption of HCN-laser rays with inverse bremsstrahlung in a krypton atom field --- German thesis
 - 06 p0811 A83-18520
- Experimental study of submillimeter radiation patterns produced by HCN waveguide laser and HCN laser-excited oversized hollow dielectric waveguide
 - 17 p2514 A83-37763
- A compact CW HCN gas laser with RF-excited discharge
 - 19 p2852 A83-40946

HD-1 GROUND EFFECT MACHINES

- U HOVERCRAFT GROUND EFFECT MACHINES

HEAD (ANATOMY)

- NT CRANIUM
- NT INTRACRANIAL CAVITY
- NT SKULL
- Investigation of cAMP phosphodiesterase activity in brain tissue under general and local irradiation of the head and body of adult animals and embryos
 - 07 p0974 A83-20843
- Head and/or torso cooling during simulated cockpit heat stress
 - 15 p2216 A83-34979
- Basilar skull fracture in U.S. Army aircraft accidents --- helmet design for pilot protection
 - 18 p2737 A83-40359

HEAD (FLUID MECHANICS)

- NT HEAD FLOW
- NT PRESSURE HEADS
- Dependence of the head of a centrifugal inclined Archimedeian screw pump on the volume of cavitation cavities in the flow area of the pump
 - 24 p3579 A83-49653

HEAD (PRESSURE)

- U PRESSURE HEADS

HEAD FLOW

- On the numerical solution of head-on vehicle shock-planar incident shock interaction flow
 - 21 p3086 A83-44556

HEAD MOVEMENT

- Analysis of the perception of motion concomitant with a lateral motion of the head
 - 02 p0224 A83-12096
- Comparison of respirator protection factors measured by two quantitative fit test methods
 - 02 p0226 A83-12409
- Oculomotoric response to voluntary head rotations during parabolic flights
 - 11 p1643 A83-27820
- Neck muscle loading and fatigue - Systematic variation of headgear weight and center-of-gravity
 - 24 p3618 A83-48878

HEAD-UP DISPLAYS

- Holographic HUDs de-mystified
 - 01 p0010 A83-11171
- TF/TA by means of integrated FLIR and radar sensors --- terrain following-terrain avoidance displays using forward looking infrared imagery
 - 01 p0010 A83-11240
- The application of diffraction optics to the LANTIRN head-up display
 - 04 p0447 A83-16131
- Head up display operational problems
 - 04 p0448 A83-16135
- Colour flight deck displays
 - 04 p0448 A83-16336
- Applications of head-up displays in commercial transport aircraft
 - 09 p1204 A83-24428
- Some perceptual effects of differential luminance induced by the use of a monocular head-up display
 - 10 p1456 A83-26305
- Automatic return in multifunction control logic --- for fighter cockpits
 - 10 p1459 A83-26317
- A history of electronic flight instruments - through tomorrow
 - 19 p2799 A83-41532
- Wide field of view head-up displays
 - 21 p3091 A83-44690

HEADACHE

- The psychiatric point of view on pilot headaches
 - 06 p0797 A83-18335
- Computer tomography of the brain during migraine (Review)
 - 19 p2883 A83-41463

HEALING

- NT WOUND HEALING

HEALTH

- NT HEALTH PHYSICS
- NT MENTAL HEALTH
- NT PUBLIC HEALTH
- Disease risk factors and the flight surgeon - A strategy to keep pilots flying
 - 08 p1147 A83-22963
- Development of an occupational health data base system
 - 15 p2239 A83-34990
- The problems of health protection in polar expeditions and their importance for space flights
 - 15 p2214 A83-35049

HEALTH PHYSICS

- NT PUBLIC HEALTH
- Incidence of a disease with a temporary loss of work capacity in miners in the northeastern USSR
 - 01 p0083 A83-10557
- Occupational skin hazards from ultraviolet /UV/ exposures
 - 03 p0380 A83-13973
- Physical exercise as a method in support of therapy
 - 05 p0673 A83-17175
- Radio-frequency hazards in the VLF to MF band
 - 05 p0677 A83-17250
- The organization of medical facilities for flight safety
 - 09 p1322 A83-23975
- Thermodynamic properties of tissue impacted by CO2 laser
 - 11 p1635 A83-27520
- Physical stress during work and the incidence of disease in workers
 - 17 p2559 A83-38185
- A prognostic investigation of the functional condition of administration and management workers
 - 21 p3187 A83-44663

HEAO

- NT HEAO 1
- NT HEAO 2
- NT HEAO 3
- The HEAO experience - design through operations
 - 17 p2473 A83-37482
- Scientific satellite data communications
 - 19 p2813 A83-41341

HEAO A

- U HEAO 1

HEAO B

U HEAO 2

HEAO C

U HEAO 3

HEAO 1

A new X-ray pulsar with a 67-millisecond period in the constellation Equuleus 05 p0693 A83-17008

HEAO A-2 soft X-ray source catalog 07 p1005 A83-20076

A survey by HEAO 1 of clusters of galaxies. III - The complete Abell catalog 10 p1496 A83-26351

HEAO project - Revisited --- attitude control system design for spaceborne astronomy 10 p1385 A83-26585

Redshift modifications to HEAO A-1 cluster X-ray luminosities 15 p2256 A83-34081

HEAO 1 high-energy X-ray observations of Centaurus X-3 22 p3383 A83-46996

HEAO 2

An X-ray image of Tycho's supernova remnant 02 p0250 A83-11583

Einstein Observatory solid state spectrometer observations of M87 and the Virgo cluster 02 p0254 A83-12104

Einstein Observatory pulse-phase spectroscopy of Hercules X-1 02 p0257 A83-12133

A giant X-ray flare in the Hyades 06 p0845 A83-19525

The X-ray morphology of Abell 1367 07 p1019 A83-21103

X-ray spectroscopy and imagery of supernova remnants with the Einstein Observatory 08 p1179 A83-21854

Einstein observations of supernova remnants 08 p1174 A83-21855

An X-ray survey of supernova remnants in the Large Magellanic Cloud 08 p1179 A83-21856

A new AM Her-like X-ray source 08 p1176 A83-23268

Imaging X-ray observations of Markarian 279 10 p1492 A83-25582

Einstein observations of three classical Cepheids 10 p1494 A83-25714

X-ray observations of 4U 1626-67 by the monitor counter on the Einstein /HEAO 2/ observatory 10 p1510 A83-26385

Coordinated Einstein and IUE observations of a disaritions brusques type flare event and quiescent emission from Proxima Centauri 10 p1514 A83-26729

Einstein observations of cool stars 15 p2250 A83-33586

Einstein observations of hot stars 15 p2251 A83-33588

Einstein X-ray observations of cataclysmic variables 15 p2251 A83-33593

Einstein observations of supernova remnants 15 p2251 A83-33597

Einstein Observatory results on active galactic nuclei 15 p2252 A83-33600

Einstein X-ray observations of clusters of galaxies 15 p2252 A83-33601

The optical identification content of the Einstein Observatory deep X-ray survey of a region in Pavo 17 p2587 A83-37303

Constraints on gamma-ray bursters from soft X-ray transients 18 p2787 A83-39959

Einstein Observations of X-ray emission from A stars 20 p3068 A83-42452

X-ray survey of clusters of galaxies with the Einstein Observatory 20 p3071 A83-43038

The detection of X rays from Jupiter 22 p3387 A83-47037

X-ray observations of stellar flares 23 p3522 A83-47502

HEAO 3

The abundance of the actinides in the cosmic radiation as measured on HEAO 3 02 p0272 A83-11619

Gamma-ray burst observations by the HEAO-3 high-resolution gamma-ray spectrometer 07 p1039 A83-20006

Evidence for delayed second phase acceleration in solar flares 07 p1037 A83-20033

Implications of HEAO 3 data for the acceleration and propagation of galactic cosmic rays 22 p3390 A83-47003

Significance of ultraheavy cosmic rays 23 p3539 A83-47738

HEARING

NT BINAURAL HEARING

Current aspects of prophylaxis and treatment of hearing disorders in patients with Meniere's disease 05 p0672 A83-16950

Sensory systems: Hearing --- Russian book 07 p0972 A83-19926

The evolution of the structural-functional organization of the organ of hearing of vertebrates 07 p0972 A83-19933

The role of the sections of the hearing system in the localization of the source of sound 07 p0972 A83-19934

A cytochemical investigation of the hearing system during acoustic stimulation 07 p0972 A83-19935

Incorporation of a test of selective attention in a pilot selection battery 10 p1457 A83-26335

The asymmetry of the sensitivity of the auditory system of humans determined by a method of constant stimuli 12 p1764 A83-29301

HEARING LOSS

U AUDITORY DEFECTS

HEART

NT CARDIAC AURICLES

NT CARDIAC VENTRICLES

NT MYOCARDIUM

Heart and liver energetics in mountain voles of the genus *Microtus juldaschi-caruthersi* /mammalia/ 02 p0219 A83-11661

Repeated development and regression of exercise-induced cardiac hypertrophy in rats 13 p1898 A83-30489

On the possibility to determine integral characteristics of the cardiac electric generator from extracardiac electric and magnetic measurements 14 p2072 A83-32799

HEART DISEASES

NT CORONARY ARTERY DISEASE

The changes in the structural components of the walls of the small vessels and the composition of the peripheral blood during immune and hypoxic effects on the heart 01 p0078 A83-10487

Fibrillation of the heart at low temperatures 01 p0081 A83-10919

A correlation analysis of macrometric parameters of the pulmonary heart during chronic nonspecific diseases of the lungs 01 p0084 A83-11391

The adaptive properties of the major arterial vessels 03 p0379 A83-13620

The integral EKG, the ventricular gradient, the differential EKG, and their diagnostic possibilities 03 p0379 A83-13621

The diagnostic significance of the integral assessment of myocardial ischemia in patients with ischemic heart disease for the computerized monitoring of the EKG during the treadmill test 03 p0379 A83-13624

The diagnostic possibilities of ultrasonic sector scanning of the heart 03 p0380 A83-13625

Mechanism for the appearance of spiral waves in active media, associated with the phenomenon of critical curvature --- in damaged myocardium tissues 03 p0376 A83-14364

The tolerance to physical loads among patients with ischemic heart disease as a function of diet and the time when food is taken 05 p0673 A83-17173

The effect of xenogenous cerebrospinal fluid on the course of experimental hypercholesterolemia 05 p0670 A83-17187

Clinical and EKG criteria for disorders of the cardiac rhythm in the weak sinus node syndrome 05 p0674 A83-17216

Emotional stresses and their role in cerebrovisceral disturbances 05 p0672 A83-17598

Acceleration-induced ventricular tachycardia in asymptomatic men - Relation to mitral valve prolapse 06 p0797 A83-18196

The lipid balance of technical flight personnel between 50 and 55 years old in commercial and civil aviation 06 p0798 A83-18340

The diagnostic accuracy of exercise electrocardiography - A review 07 p0978 A83-20785

The effect of physical exercise on the ultrastructure of the damaged myocardium 07 p0974 A83-20845

The content of ubiquinone and vitamin E in rat tissues during experimental focal myocarditis and hypoxic hypoxia 07 p0974 A83-20980

An attempt to prevent weather-aggravated cardiovascular diseases 07 p0978 A83-20995

Preventive screening as a method for the early detection of cardiovascular disease in railroad workers 07 p0978 A83-20996

The prognosis of acute cardiovascular diseases using the biorhythm curves of the patients 07 p0978 A83-20997

Gall bladder disease in a 30 year follow up study - Its association with ischemic disease 08 p1147 A83-22959

Cardiac localizations of sarcoidosis - The importance of the continuous electrocardiogram 08 p1148 A83-22964

The condition of the hypothalamic-hypophysial-adrenal system during sudden cardiac death 09 p1322 A83-23982

The value of echocardiography in diagnosing diseases of the cardiovascular system 11 p1643 A83-28801

The condition of the contractile function of the myocardium and the hemodynamics in patients with heart diseases according to echocardiography 11 p1644 A83-28802

Sudden cardiac death - A problem in topology 12 p1762 A83-29250

Blood lactate threshold in some well-trained ischemic heart disease patients 13 p1902 A83-30452

Unusual core temperature decrease in exercising heart-failure patients 13 p1903 A83-30478

The diagnostic value of a test with graded physical load for several heart rhythm disorders 14 p2071 A83-33337

The condition of glycolysis in the heart during necrosis produced after the preliminary action of stress 14 p2066 A83-33339

Basal insulinemia in healthy males and in males with ischemic heart disease of 20-59 years of age (population study) 16 p2400 A83-36836

The application of noninvasive methods for the study of patients with ischemic heart disease 16 p2400 A83-36838

The relation between the degree of cardiodynamic disorders and the volume of myocardial injuries during cytotoxic actions on the heart 17 p2555 A83-37236

The optimal speed of cyclic locomotion in individuals of different ages 17 p2559 A83-38172

Characteristics of the left ventricular blood expulsion phase during arterial hypertension and aortal stenosis 17 p2559 A83-38176

Mechanisms of the regulation of high cardiac output in patients with hypertension (angiocardiographic investigation) 17 p2559 A83-38177

Electromagnetic and magnetic fields in the treatment of ischemic heart disease 18 p2734 A83-40540

The differential diagnosis of functional murmurs and defects of the heart using ultrasonic pulse Doppler detection 18 p2734 A83-40541

The condition of peripheral hemodynamics and the effect on it of several drugs in patients with chronic ischemic heart disease and left ventricular insufficiency 18 p2735 A83-40546

The effect of disorders of lipid metabolism on the rheological properties of blood in patients with ischemic heart disease 18 p2735 A83-40548

The effect of calcium on the diastolic phases in healthy individuals and in patients with heart failure 18 p2735 A83-40549

The development of hypertrophy of the heart in the case of hypertension 19 p2881 A83-41430

Pulmonary blood circulation in patients with various types of hypertensive hearts 19 p2881 A83-41433

The pharmacology of cardioactive compounds in early ontogenesis --- Russian book 21 p3184 A83-45027

The information content of functional tests in the elucidation of the causes of repolarization disorders of the myocardium in flight personnel 21 p3188 A83-45299

Physiological aspects of cardiohemodynamics during hypertension 21 p3188 A83-45304

HEART FUNCTION

NT HEART MINUTE VOLUME

The pulmonary circulation and the right ventricular function in experimental models of high-altitude acute edema of the lungs 01 p0080 A83-10543

Assessment of central hemodynamics during arm-crank exercise 01 p0083 A83-11138

The general patterns and types of the hemodynamic changes during myocardial infarction 03 p0379 A83-13619

The effects of nonachlazine on the energy supply of the heart contractile activity during experimental myocardial infarction 03 p0374 A83-13628

The effect of cordamine and mesatone on the EKG under conditions of acute microwave irradiation 03 p0374 A83-13629

Indices of hemodynamics in patients with hypertension according to echocardiography data 03 p0381 A83-14345

The relationship between length and force in the cardiac muscle - Electromechanical coupling during deformation of the myocardium 03 p0376 A83-14363

The adaptation of the heart to chronic high-altitude hypoxia 04 p0522 A83-15780

Static and dynamic components of the heterometric regulation of myocardial contractions of the auricle and ventricle 04 p0520 A83-15893

The changes in cardiac activity during physical exercises in an athletic arena and swimming pool following prolonged antihypertensive hypokinesia /based on biotelemetry data/ 05 p0673 A83-17171

The results of focused and projector ultrasonic Doppler cardiovascularulography /a study of patients with pulmonary normotension and hypertension/ 05 p0674 A83-17215

Morphological and functional peculiarities of the myocardium during extreme coronary insufficiency 05 p0671 A83-17219

A method for the quantitative evaluation of the contractile function of the myocardium 05 p0675 A83-17695

Use of phase spectral information in assessment of frequency contents of ECG waveforms 07 p0980 A83-19627

Signal processing for recovery of cardiac conducting system activity 07 p0980 A83-19628

The prevention of disorders of the contractile function of the heart during stress by means of preliminary adaptation of the animals to hypoxia 07 p0972 A83-19920

The changes in the activity of the intracardiac ganglionic-synaptic apparatus during the interaction of sympathetic and parasympathetic regulatory effects on the rhythm of the pacemaker 07 p0973 A83-20243

The effect of a magnetic field on the patterns of the frequency changes and the content of serotonin in the isolated heart of frogs 07 p0974 A83-20968

An autoradiographic investigation of protein synthesis by the muscles and interstitial elements of the myocardium during the formation of compensatory hyperfunction of the heart 07 p0974 A83-20976

Morphofunctional features of the cardiac neural structures in adapting to physical loads in experiments 07 p0975 A83-20994

The relationship between isometric and isotonic contractile responses of the myocardium of mammals 08 p1145 A83-22111

Measurements and imaging method of blood flow profile in human heart 08 p1151 A83-22237

Echocardiography in assessment of cardiovascular problems of Air Force personnel 09 p1323 A83-24006

The contractile function of the heart and the ultrastructure of the cardiomyocytes during prolonged hypokinesia in growing animals 09 p1322 A83-25169

The content of creatine phosphate and the activity of creatine phosphokinase in the mitochondria of cardiomyocytes in myocardial infarctions in rats subjected to emotional and painful stress 09 p1322 A83-25170

Alterations in mitochondria and sarcoplasmic reticulum from heart and skeletal muscle of horizontally casted primates 11 p1640 A83-27835

Cardiac function monitored by impedance cardiography during changing seatback angles and anti-G suit inflation 12 p1766 A83-28930

Variations in heart rate (pulse 'drift') in the course of work of constant aerobic intensity in athletes and nonathletes 12 p1765 A83-29316

Afferent activity in the cardiac branches of vagus nerves after intracoronary and intravenous administration of anticardiac cytotoxic serum 13 p1895 A83-30301

Physiological assessment of right-side and left-side cardiohemodynamics in patients with hypertension 13 p1906 A83-31395

Problems in aerospace medicine posed by mitral valve prolapse 14 p2067 A83-32451

Polymeric prostaglandin PGb_x and other prostaglandin polymers prolong survival of the heart of the hypoxic mouse 14 p2064 A83-32688

A method for the calculation of the spatial position of the dipole generators of multipole model of the equivalent generator of the heart 14 p2073 A83-32958

The effect of exogenous amino acids on the cardiac contractile function and the metabolism of nitrogen compounds during anoxia 14 p2066 A83-33336

Heart function and certain mechanisms for its regulation when simulating the adaptation to hypoxia by administering 2,4-dinitrophenol 15 p2210 A83-34958

A cholinergic mechanism for the regulation of the cardiac function during acute transitory coronary insufficiency 15 p2210 A83-34961

The effect of stress on the extensibility and the contractile function of the myocardium 15 p2211 A83-34962

Emotional excitation and parameters of cardiac activity during muscular work 17 p2558 A83-37238

Characteristics of the left ventricular blood expulsion phase during arterial hypertension and aortal stenosis 17 p2559 A83-38176

Indicators of the cardiovascular system function during the work activity of scientific workers 17 p2560 A83-38200

The decrease in the functional ability of the hypertrophic heart due to disorders of cellular adaptation to oxygen 18 p2731 A83-39496

The evaluation of the functional condition of the heart in patients with ischemic heart disease at early stages of graded physical loading 18 p2734 A83-40542

Stress-induced injuries of the nonischemic regions of the heart in experimental infarction and their prevention 18 p2732 A83-40551

The mechanism of the heart diastole 19 p2871 A83-40815

Alteration of ischemic cardiac function in normal heart by daily exercise 19 p2875 A83-41134

Effects of hyperbaric oxygen exposure at 31.3 ATA on spontaneously beating cat hearts 19 p2875 A83-41136

The determination of the cardiac output during physical loading of increasing strength by a modified rebreathing method 23 p3498 A83-47120

ATP-regulated K(+) channels in cardiac muscle 23 p3495 A83-48088

Pathophysiologic effects of acceleration stress in the miniature swine 24 p3617 A83-48876

Correlations between ejection times measured from the carotid pulse contour and the impedance cardiogram 24 p3617 A83-48877

The change in cardiac activity under increased pressure according to data from vector analysis 24 p3618 A83-49070

The dependence of the functional activity of the heart on mental activity 24 p3618 A83-49547

HEART MINUTE VOLUME

The stroke and minute volumes of the heart, the demand for oxygen, and their changes under the influence of physical loads 08 p1146 A83-22776

The metrological possibilities of the tetrapolar transthoracic impedance rheoplethysmography method in clinical conditions 13 p1906 A83-30306

Rheographic investigations of the stroke volume of the heart in antiorthostatic hypokinesia 15 p2214 A83-35047

Effect of blood volume on forearm venous and cardiac stroke volume during exercise 22 p3347 A83-45995

HEART RATE

NT ARRRHYTHMIA

NT BRADYCARDIA

NT SYSTOLE

NT TACHYCARDIA

A comparison of the cardiovascular responses to isometric exercise of three different sized muscle groups 01 p0083 A83-11139

The changes in the nerve and cardiac activity in animals of various ages during the application of electromagnetic fields of low frequency and low voltage 02 p0220 A83-11884

Dynamics of heart rate and blood pressure in the evaluation of the functional condition of swimmers 03 p0382 A83-14350

The dependence of the character of the recovery of pulse on the rhythm of the heart and the lability of the sinusoid nodes in athletes after step loads 03 p0382 A83-14355

The correlation of the parameters of the cardiac rhythm with the physical work capacity of humans during the adaptation to high-altitude hypoxia 04 p0522 A83-15781

The peculiarities of the functioning of the cardiovascular system and its regulator mechanisms in swimmers depending on the initial condition of the vegetative nervous system 04 p0522 A83-15782

A theoretical analysis of the regularities of the Bainbridge reflex --- heart rate acceleration by blood pressure increase 04 p0520 A83-15894

Clinical and EKG criteria for disorders of the cardiac rhythm in the weak sinus node syndrome 05 p0674 A83-17216

Autonomic contribution to heart rate recovery from exercise in humans 05 p0675 A83-17335

Comparison of hemodynamic responses to static and dynamic exercise 05 p0675 A83-17337

The stroke and minute volumes of the heart, the demand for oxygen, and their changes under the influence of physical loads 08 p1146 A83-22776

Circadian variations in tolerance to +Gz acceleration 11 p1642 A83-27783

Hormonal changes in antiorthostatic rats 11 p1637 A83-27800

Gravito-inertial sensitivity of the spider - Araneus sericatus 11 p1639 A83-27822

The circadian rhythm of the body temperature, arterial pressure, and heart rate 12 p1765 A83-29311

Variations in heart rate (pulse 'drift') in the course of work of constant aerobic intensity in athletes and nonathletes 12 p1765 A83-29316

Metabolic and cardiorespiratory responses to He-O₂ breathing during exercise 13 p1903 A83-30470

Changes in the vegetative balance of an organism during experimental hypokinesia 14 p2061 A83-31972

Problems in aerospace medicine posed by mitral valve prolapse 14 p2067 A83-32451

Automatic activity and workload during learning of a simulated aircraft carrier landing task 14 p2071 A83-32690

Cardiorespiratory responses to exercise distributed between the upper and lower body [AD-A130505] 14 p2069 A83-32821

An ionic mechanism of the Woodwors staircase --- electromechanical coupling in myocardium cells 16 p2395 A83-36806

An investigation of the rhythmoinotropic dependence in the heart during accidentally varying heartbeat rhythm 17 p2555 A83-37235

The effect of inverted gymnastic exercises on the hemodynamic and respiratory indicators of students 17 p2559 A83-38171

The application of a method of the variability of the heart rate for the evaluation of an operator's activity 19 p2884 A83-42023

Heart rate variability, cardiac mechanics, and subjectively evaluated stress during simulator flight 21 p3186 A83-43988

The observation of influence on the characteristics of cardiovascular response during bed rest 21 p3187 A83-44517

Instantaneous cardiac acceleration in the cat elicited by peripheral nerve stimulation 22 p3345 A83-45985

The changes in the cardiac rhythm of air traffic controllers using automated systems 23 p3497 A83-47112

HEART VALVES

Acceleration-induced ventricular tachycardia in asymptomatic men - Relation to mitral valve prolapse 06 p0797 A83-18196

The pathological and physiological characteristics of the deficiencies of the mitral valve in animals as a consequence of high-altitude hypoxia 11 p1641 A83-28764

HEAT

NT DRY HEAT

NT HEAT OF DISSOCIATION

NT PROCESS HEAT

HEAT ACCLIMATIZATION

The effect of succinic acid on work capacity and recovery during muscle activity in conditions of various ambient temperatures 03 p0382 A83-14351

Heat loss and tissue metabolism in white mice during the recovery after acute hypothermia 04 p0520 A83-15896

The activity of the sympathetic-adrenal system as an indicator of athletes' adaptation to physical loads at high temperatures 05 p0672 A83-17154

Sweat composition in exercise and in heat 05 p0675 A83-17332

Does heat acclimation lower the rate of metabolism elicited by muscular exercise 06 p0796 A83-18191

The functional condition of the mitochondria of the mucous membrane of the small intestine under thermal stresses 08 p1145 A83-22113

The effect of multiple exposures to radiative heat on the resistance of the body to convective heating and total cooling 09 p1321 A83-25157

The characteristics of the thermoregulation in rats adapted to heat during the effect of cold 09 p1321 A83-25158

The specific characteristics of heat stress during the microwave irradiation of mammals (Theoretical analysis) 12 p1762 A83-29274

Nitrogen metabolism during heat stress 12 p1765 A83-29314

Human frontal sweat rate and lactate concentration during heat exposure and exercise 13 p1903 A83-30468

Drinking and water balance during exercise and heat acclimation 13 p1903 A83-30471

Blood volume and protein responses to skin heating and cooling in resting subjects 13 p1903 A83-30477

Sweating efficiency in acclimated men and women exercising in humid and dry heat 13 p1904 A83-30499

The shifts in the blood circulation system during the effect of high external temperature on an organism 14 p2063 A83-32096

Scheduling work and rest for the hot ambient conditions with radiant heat source 16 p2396 A83-35561

Physiological and hygienic aspects of artificial heat adaptation (Review of the literature) 16 p2397 A83-35596

The pattern of physical and mental work capacity depending on the level of hyperthermia in athletes 17 p2559 A83-38170

Canine blood volume and cardiovascular function during hyperthermia 20 p3033 A83-43476

Cognitive performance during a heat acclimatization regimen 21 p3187 A83-43992

HEAT BALANCE

The efficiency of several techniques and preparations for accelerating the adaptation and increasing the work capacity of sailors in the tropics

- 21 p3188 A83-45300
The physiological stability of humans to ergothermal effects 21 p3188 A83-45343
The functional system of human thermal adaptability 23 p3497 A83-47105

HEAT BALANCE

The application of energy and entropy balances for treatment of flow and temperature data at a real wall in an unsteady state

- 06 p0759 A83-19237
Transfer processes at the air-sea interface 09 p1317 A83-23352
Optimization of heat transfer in an incompressible-fluid boundary layer with allowance for the heat-balance equation 12 p1723 A83-29279
The thermal structure and energy balance of the Uranian upper atmosphere 13 p1961 A83-31202
Heat balance for the high-temperature component of a solar flare 15 p2279 A83-34294
A dynamic simulation of a flat-plate collector system 15 p2191 A83-34409

The thermal balance of the lower atmosphere of Venus

- 17 p2617 A83-37419
Numerical experiments with a stochastic zonal climate model 22 p3340 A83-46846
Evaporation-limited tropical temperatures as a constraint on climate sensitivity 22 p3340 A83-46847

HEAT BUDGET

NT ATMOSPHERIC HEAT BUDGET

- Budget of the temperature variance in a turbulent plane jet 05 p0641 A83-17707
The influence of poloidal motions and latent heat release on the equilibrium ice extent in a simple climate model 21 p3180 A83-44703

HEAT CAPACITY

U SPECIFIC HEAT

HEAT CAPACITY MAPPING MISSION

Some examples of the utility of HCMM data in geologic remote sensing --- Heat Capacity Mapping Mission

- 01 p0065 A83-10099
Snow hydrology studies using data from the Heat Capacity Mapping Mission 01 p0065 A83-10102
Construction and interpretation of a thermal inertia image using airborne data 03 p0348 A83-14260
Evaluating depth to shallow groundwater using heat capacity mapping mission /HCMM/ data 03 p0351 A83-14668

A contribution to the study of the sea surface temperature by remote sensing by means of the HCMM space experiment --- French thesis

- 08 p1143 A83-22086
Estimates of regional evapotranspiration in South-Eastern France using thermal and albedo data from the heat capacity mapping mission satellite 09 p1291 A83-24631

A simulation model supporting HCMM investigation on geological objectives --- heat capacity mapping mission

- 15 p2188 A83-35287
Enhanced Landsat and HCMM imagery for mineral exploration in contrasting areas of subtropical humid and semi-arid terrain 17 p2528 A83-38150

Enhanced thermal mapping with Landsat and HCMM digital data

- 17 p2531 A83-38351
Satellite-derived surface energy balance estimates in the Alaskan sub-Arctic 18 p2721 A83-39112

An analysis of the ground temperature and reflectivity pattern about St. Louis, Missouri, using HCMM satellite data

- 18 p2724 A83-39679
Geologic thermal-inertia mapping using HCMM satellite data 22 p3309 A83-46130

HEAT CONDUCTION

U CONDUCTIVE HEAT TRANSFER

HEAT CONTENT

U ENTHALPY

HEAT DISSIPATION

U COOLING

HEAT DISSIPATION CHILLING

U COOLING

HEAT EFFECTS

U TEMPERATURE EFFECTS

HEAT EQUATIONS

U THERMODYNAMICS

HEAT EXCHANGERS

NT TUBE HEAT EXCHANGERS

Heat and mass transfer apparatuses in cryogenics --- Russian book

- 01 p0028 A83-10672
The simulation of secondary flow effects in turbulent non-circular passage flows 02 p0173 A83-12902

High-temperature ceramic heat exchanger element for a solar thermal receiver

- 03 p0352 A83-13476
A study of different techniques for cooling solar cells in centralized concentrator photovoltaic power plants --- French thesis 03 p0355 A83-14109

Improved formulations for the analysis of convecting and radiating finned surfaces

- 04 p0476 A83-15292
An experimental study and modeling of heat transfer in boilers of small and medium power --- French thesis 04 p0456 A83-15841

Comparisons of paraffin wax storage subsystem models using liquid heat transfer media

- 06 p0780 A83-18553
Radiation heat exchange in a solar cavity-type receiver at various times 07 p0953 A83-20138

Response of parallel-flow and counterflow heat exchangers to sinusoidal flow rate changes of large amplitude

- 07 p0925 A83-20290
Shuttle engine problems spark broad review 08 p1052 A83-22176

Transient analysis of a natural circulation solar water heater with a heat exchanger

- 08 p1132 A83-23129
Studies of a diffusion flame matrix burner in a combustion chamber with heat exchanger 09 p1225 A83-23334

Low Reynolds number flow between interrupted flat plates

- 09 p1259 A83-23878
Heat transfer from interrupted plates 09 p1259 A83-23879

Regenerative shaft engines for helicopters, multipurpose and feeder service aircraft

- [DGLR PAPER 82-087] 09 p1207 A83-24199
Prospects for the use of heat exchangers in aircraft gas turbines [DGLR PAPER 82-088] 09 p1207 A83-24200

Thermal control - Heat buses will operate like a public utility

- 09 p1216 A83-24358
Direct contact droplet heat exchangers for thermal management in space 11 p1564 A83-27137

Direct-contact air/molten salt heat exchange for solar thermal systems

- 11 p1607 A83-27234
The ideal adiabatic cycle - A rational basis for Stirling engine analysis 11 p1664 A83-27264

General method for optimization of Stirling engines

- 11 p1586 A83-27268
Steady flow examination of a cryocooler 11 p1564 A83-27289

Back-to-back test for determining the pumping losses in a Stirling cycle machine

- 11 p1588 A83-27290
Heat transfer in a latent heat storage device with finned annular tube heat exchanger --- German thesis 11 p1570 A83-28665

Emulsification of thermal energy storage materials in an immiscible fluid

- 14 p2046 A83-32347
An automated on-orbit thermal acquisition device --- reusable heat rejectors for space platforms [AIAA PAPER 83-1465] 14 p1982 A83-32723

Heat exchangers: Theory and practice --- Book

- 15 p2154 A83-33619
Thermal cycling in compact plate-fin heat exchangers --- in aircraft gas turbines 15 p2123 A83-34253

Flow-loss, efficiency, and change-of-state calculations for fluid-flow engines and heat exchangers

- 15 p2162 A83-34976
Effect of heat transfer augmentation on two-phase flow instabilities in a vertical boiling channel 16 p2350 A83-35800

A method for modeling heat exchangers

- 16 p2353 A83-36595
Optimal control of a bilinear solar collector/heat exchange system 17 p2535 A83-37150

Calculation method of the optimum configurations of the extended surfaces with simultaneous conductive, convective and radiative heat transfer in heat exchanger

- 18 p2686 A83-39932
Mathematical modeling of gas-turbine engines with heat regeneration 19 p2801 A83-42154

Application of logic-algebraic and numerical methods to multidimensional heat exchange problems in regions of complex geometry filled with uniform or composite media

- 20 p2971 A83-42668
Study of a thermosyphon with a counter-flow heat exchanger 20 p2972 A83-42679

Flow reversal in turbulent mixed convection

- 20 p2980 A83-42756
Heat transfer 1982; Proceedings of the Seventh International Conference, Technische Universitaet Muenchen, Munich, West Germany, September 6-10, 1982. Volume 6 - General papers: Combined heat and mass transfer, particle heat transfer, heat exchangers, industrial heat transfer, heat transfer in energy utilization 20 p2983 A83-43013

Design of shell-and-tube heat exchangers to avoid flow-induced vibration

- 20 p2984 A83-43021
A friction factor correlation for the offset strip-fin matrix 20 p2984 A83-43022

Cryogenic gas engines --- Russian book

- 21 p3117 A83-43925
Low Reynolds number flow heat exchangers; Proceedings of the Fourth Advanced Study Institute, Ankara, Turkey, July 13-24, 1981 21 p3133 A83-45099

Optimal thermodynamics of thermal exchanges

- [ONERA, TP NO. 1983-78] 23 p3512 A83-48193

HEAT FLOW

U HEAT TRANSMISSION

HEAT FLUX

A switched continuous-wave sonic anemometer for measuring surface heat fluxes

- 01 p0050 A83-10722
A transient one-dimensional inverse heat conduction problem with overspecified data at one boundary 02 p0174 A83-12932

Heat transfer with bubble formation - Results of the TEXUS IIIB experiment

- 02 p0138 A83-12998
On the definition of the flux of sensible heat --- in atmosphere 03 p0364 A83-13276

Momentum and temperature fluxes in a shock wave - Turbulence interaction

- 03 p0318 A83-14469
Heat transfer with ablation in a finite slab subjected to time variant heat fluxes [AIAA PAPER 83-0582] 05 p0637 A83-16802

A simple parameterization of the surface fluxes of sensible and latent heat during daytime compared with the Penman-Monteith concept

- 05 p0667 A83-17440
Budget of the temperature variance in a turbulent plane jet 05 p0641 A83-17707

Heat-transfer rate measurements obtained in a highly erosive two-phase flow field --- of solid rocket motor exhaust environments

- [AIAA PAPER 83-0584] 05 p0610 A83-17932
Thermal behavior of directional reinforced composites subjected to thermal flux pulses [ONERA, TP NO. 1982-105] 06 p0724 A83-18432

Startup conditions of alkali-metal vaporization from rectangular channels --- in heat pipes

- 06 p0756 A83-18446
Propagation of spherical shock waves in an exponential medium with radiation heat flux 06 p0834 A83-18879

Sensible heat flux estimated from routine meteorological data by the resistance method

- 07 p0969 A83-20805
Some comments on Beck's solution of the inverse problem of heat conduction through the use of Duhamel's theorem 08 p1087 A83-23144

Apparatus for simultaneous temperature and heat-flow measurements under transient conditions

- 08 p1106 A83-23235
Method to increase the bandwidth of heat fluxmeters 08 p1106 A83-23236

Calculation of thermal radiation from jets by the Monte-Carlo method

- 09 p1260 A83-24047
Current studies at Calspan utilizing short-duration flow techniques 10 p1379 A83-26128

Exact solution of the thermal boundary-layer equations for an arbitrary heat-flux distribution on a surface in a flow

- 10 p1417 A83-26253
Heat load limits in laser mirrors with a cooled porous backing 10 p1430 A83-26256

Albedo, internal heat flux, and energy balance of Saturn

- 11 p1684 A83-27359
Conductive flux in flaring solar chromospheres deduced from the linear polarization observations 11 p1691 A83-27685

Results of an experimental determination of limiting heat fluxes in two-phase thermosiphons

- 11 p1570 A83-28792
The effect of a passive cross-stream temperature gradient on the evolution of temperature variance and heat flux in grid turbulence 12 p1723 A83-29233

The effect of the mechanisms of heterogeneous catalytic reactions on the heat flux in hypersonic flow past a blunted body

- 13 p1804 A83-30675
Parameterization of the surface fluxes of heat and momentum for the convective atmospheric boundary layer 14 p2056 A83-32402

A heat-flux history length scale for the nocturnal boundary layer

- 14 p2058 A83-32473
The seasonal variation of the thermal structure of the atmosphere of Uranus 14 p2112 A83-32608

Calorimetry with heat flux transducers - Comparison with a suit calorimeter

- 14 p2072 A83-32819
Measurements in the heated turbulent boundary layer on a mildly curved convex surface 15 p2155 A83-33657

Numerical evaluating of the instantaneous temperature field in turbulent flow and heat flux on the wall with variable boundary conditions and heat source in turbulent flow

- 15 p2161 A83-34270
Typical influences of moisture on profile measurements in the marine atmospheric surface layer 16 p2388 A83-35796

Determining latent heat flux at sea - A comparison between wind-wave interaction and profile methods

- 16 p2388 A83-35797
Estimation of the average exchanges in momentum and latent heat between the atmosphere and the oceans with Seasat observations 16 p2393 A83-36982

Features of the simulation of the catalytic properties of surfaces in subsonic and hypersonic flows 17 p2447 A83-37508

A discretized-intensity method proposed for two-dimensional systems enclosing radiative and conductive media 17 p2506 A83-37865

A simple scheme for daytime estimates of the surface fluxes from routine weather data 18 p2724 A83-39675

Critical heat flux in a closed two-phase thermosyphon 18 p2684 A83-39849

Characteristics of a film-type heat-flux transducer 18 p2689 A83-39868

A comparison between radiation fluxes and heat influxes calculated with various transmission functions in a clear sky 18 p2719 A83-40083

Measurement of heat flux through the ocean surface 19 p2870 A83-42112

An experimental investigation of a low heat flux, wickless heat pipe 20 p2969 A83-42350

Critical heat flux in flow boiling of helium 20 p2981 A83-42769

A technique for measuring energy absorption from high energy laser radiation 20 p2989 A83-42781

Radiative-convective heat transfer and heat shielding for spacecraft descending to the earth's surface and to the surfaces of other solar-system planets 20 p2945 A83-42881

Reduction of electron thermal conductivity by ion acoustic turbulence 21 p3210 A83-44131

Evaporation derived from optical and radio-wave scintillation --- for water balance and mesoscale meteorological studies 22 p3339 A83-46069

Comments on rates of creeping spread of flames over thermally thin fuels 22 p3267 A83-46764

Measurement and analyses of heat flux data in a turbine stage. II - Discussion of results and comparison with predictions [ASME PAPER 83-GT-122] 23 p3408 A83-47951

HEAT GAIN

U HEATING

HEAT GENERATION

The relationship between the aerodynamics of a combustion chamber and the dynamics of heat release 09 p1205 A83-23446

Cogeneration using a thermionic combustor 11 p1608 A83-27300

A study of the steady-state reaction-zone structure of a homogeneous and a heterogeneous explosive 14 p1991 A83-33383

A review of the literature concerning resuscitation from hypothermia. II - Selected rewarming protocols 15 p2214 A83-34978

Heat evolution investigated by a liquid crystal film technique during fracture in metals 16 p2330 A83-35978

Natural convection in a spherical annulus filled with heat generating fluid 20 p2972 A83-42677

HEAT ISLANDS

Urban albedo as a function of the urban structure - A model experiment 01 p0069 A83-10720

Enhancement and initiation of a cumulus by a heat island 20 p3032 A83-43462

HEAT MEASUREMENT

A switched continuous-wave sonic anemometer for measuring surface heat fluxes 01 p0050 A83-10722

Method for measuring specific heats in intense magnetic fields at low temperatures using capacitance thermometry 02 p0180 A83-12813

Calorimetric measurements of thermal control surfaces of operational satellites 05 p0605 A83-16505

[AIAA PAPER 83-0075] Decomposition processes in an Al-5 percent Zn-1 percent Mg alloy. III - Reversion of GP-zones 05 p0617 A83-17953

An experimental heat-transfer investigation of an advanced winged entry vehicle at Mach 10 [AIAA PAPER 83-0409] 06 p0714 A83-19589

Adiabatic calorimetry for kinetics modeling of epoxy resin systems 07 p0898 A83-20445

Heat capacity measurements - Progress in experimental techniques 07 p0926 A83-20503

Method to increase the bandwidth of heat fluxmeters 08 p1106 A83-23236

Multiwavelength laser rate calorimetry on various infrared window materials 09 p1346 A83-24967

Dynamic instabilities in radiation-heated boiler tubes for solar central receivers [ASME PAPER 82-WA/HT-8] 10 p1445 A83-25692

Kinetics of crystallization of ZrF₄-BaF₂-LaF₃ glass by differential scanning calorimetry 12 p1717 A83-29972

A calorimetric approach to investigating the effect of electromagnetic radiation at radio frequencies on the plasmatic membrane of erythrocytes 13 p1900 A83-31334

Total radiant power measurement of laser diode by a calorimetric method 13 p1858 A83-31774

Calorimetry with heat flux transducers - Comparison with a suit calorimeter 14 p2072 A83-32819

A calorimetric method for the measurement of the Stefan-Boltzmann constant 15 p2164 A83-34412

Characteristics of a film-type heat-flux transducer 18 p2689 A83-39868

Mathematical analysis for radiometric calorimetry of a radiating sphere 20 p3055 A83-42943

Heat capacities of liquid metals above 1500 K 20 p2954 A83-43255

Convective heat transfer on flat plate at very high temperature and pressure gradient [ASME PAPER 83-GT-113] 23 p3448 A83-47946

Measurement and analyses of heat flux data in a turbine stage. I - Description of experimental apparatus and data analysis [ASME PAPER 83-GT-121] 23 p3408 A83-47950

Measurement and analyses of heat flux data in a turbine stage. II - Discussion of results and comparison with predictions [ASME PAPER 83-GT-122] 23 p3408 A83-47951

HEAT OF COMBUSTION

Determination of mass transfer number of polymers from heats of gasification 15 p2142 A83-33725

HEAT OF DISSOCIATION

Studies on thermal decomposition of double-base propellants 09 p1243 A83-24884

HEAT OF FUSION

Low temperature latent heat thermal energy storage - Heat storage materials 12 p1749 A83-28943

HEAT OF VAPORIZATION

Low temperature volatilization on the moon 04 p0562 A83-15352

Determination of mass transfer number of polymers from heats of gasification 15 p2142 A83-33725

A magnetogasdynamic model for a capillary discharge with wall vaporization 21 p3215 A83-45350

HEAT PIPES

Performance investigation of a long, slender heat pipe for thermal energy storage applications --- for solar residential heating 01 p0068 A83-10651

The effect of the parameters of metal-fiber capillary structures on the maximum heat-transfer capability of thermal pipes 02 p0169 A83-11515

Capillary priming characteristics of a high capacity dual passage heat pipe [ASME PAPER 82-HT-14] 02 p0171 A83-12784

Testing of the energy module of a parabolocylindrical solar installation 04 p0503 A83-15130

Laminar flow of vapor flux in the condensation region of heat tubes 04 p0477 A83-15864

Investigation of the characteristics of heat transfer in the heating zone of heat pipes with metal fiber capillary structures 04 p0477 A83-15865

Use of thermocapillary migration in a controllable heat valve 04 p0477 A83-16093

A study of the characteristics of a thermal diode heat pipe in the direct and reverse modes of operation 04 p0478 A83-16165

Thermal Canister Experiment on OSS-1 [AIAA PAPER 83-0254] 05 p0609 A83-16613

Fully controllable heat pipe containing a short electro-osmotic pumping section [AIAA PAPER 83-0317] 05 p0634 A83-16647

Performance characteristics of the double-wall artery high capacity heat pipe [AIAA PAPER 83-0318] 05 p0634 A83-16648

Radiant heating tests of several liquid metal heat-pipe sandwich panels [AIAA PAPER 83-0319] 05 p0635 A83-16649

Startup conditions of alkali-metal vaporization from rectangular channels --- in heat pipes 06 p0756 A83-18446

Priming considerations of heat pipes in zero-G 06 p0757 A83-18454

Transient shutdown of an axial-groove liquid trap heat pipe thermal diode 06 p0759 A83-19161

The effect of soldering on the characteristics of heat pipes with a liquid-metal heat-transfer agent 09 p1258 A83-23449

The results of an experimental investigation of the effect of vibration loading parameters on the working characteristics of heat pipes 09 p1259 A83-23924

The effect of porous-surface defects on the thermophysical characteristics of the wicks of heat pipes 09 p1260 A83-24229

Thermal control - Heat buses will operate like a public utility 09 p1216 A83-24358

A heat pipe simulation technique for spacecraft thermal testing under variable orientation [SAE PAPER 820860] 10 p1383 A83-25760

Long titanium heat pipes for high-temperature space radiators 11 p1537 A83-27127

Artery heat pipes for space power systems 11 p1537 A83-27128

Development of high-temperature liquid metal heat pipes for isothermal irradiation assemblies --- for in-pile tests of UO₂ space reactor fuel configurations 11 p1538 A83-27129

A concept of heat pipe engine 11 p1605 A83-27208

U.K. Consortium Stirling engine programme 11 p1588 A83-27285

Direct-energy-conversion implications of space nuclear reactors 11 p1542 A83-27297

Thermionic technology infrastructure for space power 11 p1542 A83-27298

A method for producing heat pipes for cooling semiconductor photovoltaic cells and the heat pipe characteristics 11 p1553 A83-28366

Development and production of advanced cooling techniques for hybrid microcircuits 13 p1837 A83-31518

Aluminum/ammonia heat pipe gas generation and long term system impact for the Space Telescope's Wide Field Planetary Camera [AIAA PAPER 83-1428] 14 p2009 A83-32704

High-capacity honeycomb panel heat pipes for space radiators [AIAA PAPER 83-1430] 14 p2010 A83-32705

Monogroove heat pipe development for the space constructible radiator system [AIAA PAPER 83-1431] 14 p2010 A83-32706

Performance limits for smooth-wall, gravity-assisted heat pipes [AIAA PAPER 83-1433] 14 p2010 A83-32707

Development and test of a space reactor core heat pipe [AIAA PAPER 83-1530] 14 p2011 A83-32761

Thermal behavior of axially grooved heat pipes aboard a rocket 15 p2158 A83-33999

Heat transfer in the evaporation and condensation zones of heat pipes intensely heated at the end 15 p2161 A83-34471

Axial-grooved variable-conductance heat pipes - The Marangoni effect [AIAA PAPER 83-1429] 15 p2161 A83-34904

Critical heat flux in a closed two-phase thermosyphon 18 p2684 A83-39849

Heat transfer performance of an inclined two-phase closed thermosyphon 18 p2684 A83-39850

Investigation of the unsteady modes of operation of gas-regulated heat pipes with gas dissolving in the heat carrier 19 p2845 A83-41991

An experimental investigation of a low heat flux, wickless heat pipe 20 p2969 A83-42350

Film condensation in a tube with counter current vapor flow 20 p2969 A83-42535

Heat transfer characteristics of the two-phase closed thermosyphon (wickless heat pipe) 20 p2981 A83-42765

Heat pipes - Thermal diodes 20 p2981 A83-42766

Experimental studies of heat and mass exchange phenomena in the two-component heat pipe 20 p2981 A83-42767

Vapor flow reversal in the condensation zone of a simulated flat-plate heat pipe 20 p2984 A83-43023

The effect of the diode property of heat pipes on the thermal regime of solar collectors 21 p3168 A83-45272

HEAT PUMPS

Analysis of two-phase flow solar collectors with application to heat pumps 03 p0353 A83-13481

Metal hydride heat pump 11 p1605 A83-27211

Two phase thermal control systems for spacecraft instrumentation [AIAA PAPER 83-1491] 14 p1982 A83-32736

Solar operated water-ammonia absorption heat pump for air-conditioning - Modelling and simulation 15 p2192 A83-34674

Performance of a hybrid solar heating system of the solar laboratory at the JRC-ISPRRA 18 p2710 A83-40533

A strategy for optimization of wind energy systems 20 p3012 A83-43371

HEAT RADIATORS

NT SPACECRAFT RADIATORS

Capillary priming characteristics of a high capacity dual passage heat pipe [ASME PAPER 82-HT-14] 02 p0171 A83-12784

Enhancement of radiation cooling by means of reflectors 13 p1872 A83-31614

An automated on-orbit thermal acquisition device --- reusable heat rejectors for space platforms [AIAA PAPER 83-1465] 14 p1982 A83-32723

Axial-grooved variable-conductance heat pipes - The Marangoni effect [AIAA PAPER 83-1429] 15 p2161 A83-34904

- Thermal performance of radiative cooling panels
16 p2353 A83-36594
- HEAT REGULATION**
U TEMPERATURE CONTROL
- HEAT REJECTION DEVICES**
U HEAT RADIATORS
- HEAT RESISTANCE**
U THERMAL RESISTANCE
- HEAT RESISTANT ALLOYS**
NT MOLYBDENUM ALLOYS
NT NIMONIC ALLOYS
NT NIOBIUM ALLOYS
NT REFRACTORY METAL ALLOYS
NT RHENIUM ALLOYS
NT TANTALUM ALLOYS
NT TUNGSTEN ALLOYS
NT UDIMET ALLOYS
NT WASPALOY
- A new diffusion-inhibited oxidation-resistant coating for superalloys 01 p0024 A83-10299
High temperature aerospace materials prepared by powder metallurgy 02 p0153 A83-11508
X-ray powder diffraction evidence for the incorporation of W and Mo into M23C6 extracted from high-temperature alloys 02 p0154 A83-11670
A new approach to the weldability of nickel-base as-cast and powder metallurgy superalloys 02 p0155 A83-12069
High-temperature electron beam welding of the nickel-base superalloy IN-738 LC 02 p0155 A83-12072
Improving the weldability of Ni-base superalloy 713C 02 p0155 A83-12073
The structure of rapidly solidified Al-Fe-Cr alloys 02 p0157 A83-12412
Microstructural changes during superplastic deformation of powder-consolidated nickel-base superalloy IN-100 02 p0158 A83-12931
A nuclear gamma resonance study of TiAl containing Fe-57 impurity 02 p0159 A83-13039
Effect of silicon on the structure and properties of heat resistant aluminum alloy D21 03 p0297 A83-13258
Heat resistant and corrosion resistant aluminum alloys hardened with oxide phase 03 p0297 A83-13262
An evaluation of four creep-fatigue models for a nickel-base superalloy 03 p0299 A83-13904
Cumulation of high-temperature low-cycle fatigue damage in two-temperature tests 03 p0299 A83-13906
The influence of different deposition parameters on the aluminum content in alloy coatings obtained by cathodic sputtering [ONERA, TP NO. 1982-86] 03 p0300 A83-14538
High temperature corrosion on high temperature materials: Metallographic, scanning electron microscopic and microanalytical tests 04 p0458 A83-15124
Test bed for quantitative NDE - Inversion results 04 p0490 A83-15175
Microstructural and dimensional stabilities of a potential gamma/gamma prime-alpha/Mo/ directionally solidified eutectic superalloy under cyclic thermal exposure to 1000 C 04 p0460 A83-15987
Comparison of the quench rates attained in gas-atomized powders and melt-spun ribbons of Co- and Ni-base superalloys - Influence on resulting microstructures [ONERA, TP NO. 1982-132] 04 p0460 A83-15993
Micromechanism-dependent model of the high-temperature strength and lifetime of particle-hardened alloys 04 p0461 A83-16174
Investigation of the electron-beam weldability of a heat-resistant iron-based superalloy /A286/ 04 p0461 A83-16175
Particle-coarsening, sigma-0 and tertiary creep 04 p0462 A83-16268
The growth of gamma-prime precipitates in nickel-base superalloys 04 p0462 A83-16270
Surface damage and near-threshold fatigue crack growth in a Ni-base superalloy in vacuum 05 p0616 A83-17897
An investigation of heat-affected zone hot cracking in alloy 800 06 p0728 A83-18399
Recent approaches to the development of corrosion resistant coatings --- for Nickel and Cobalt based superalloys used for gas turbines [ONERA, TP NO. 1982-106] 06 p0769 A83-18433
Parameters influencing particle boundary precipitation in superalloy powders 06 p0732 A83-19097
Effects of ceramic inclusions on fatigue properties of a powder metallurgical nickel-base superalloy 06 p0732 A83-19101
Fabrication and heat treatment of a Ni-base superalloy integrally bladed rotor for small gas turbine engine applications 06 p0732 A83-19102
- Fatigue oxidation interaction in a superalloy - Application to life prediction in high temperature low cycle fatigue 07 p0884 A83-20256
Anelastic relaxation controlled cyclic creep and cyclic stress rupture behavior of an oxide dispersion strengthened alloy 07 p0885 A83-20263
Reversible reaction between MC and M₂₃C₆/ in a NiCrWTi cast superalloy 07 p0885 A83-20274
Models of creep cavitation and their interrelationships 07 p0887 A83-20628
The effect of heating on the structure of ZhS6F alloy in the directionally solidified blades of gas-turbine engines 07 p0889 A83-20905
Requirements of constitutive models for two nickel-base superalloys 07 p0891 A83-21071
High temperature alloys for gas turbines 1982; Proceedings of the Conference, Liege, Belgium, October 4-6, 1982 07 p0891 A83-21451
Superalloy technology - Today and tomorrow 07 p0891 A83-21452
Recent approaches to the development of corrosion resistant coatings 07 p0891 A83-21453
Mechanisms of hot corrosion 07 p0891 A83-21455
Comparison of hot-salt corrosion test procedures 07 p0892 A83-21457
High temperature erosion and erosion-hot corrosion of superalloys and coatings 07 p0892 A83-21458
High temperature stability of pack aluminide coatings on IN38LC 07 p0941 A83-21459
Thermochemical treatment of porous materials 07 p0892 A83-21460
Fatigue and creep considerations in the design of turbine components 07 p0949 A83-21461
Low cycle fatigue and life prediction methods 07 p0892 A83-21462
High cycle fatigue properties of cast nickel base superalloys IN 738LC and IN 939 07 p0892 A83-21463
Fracture mechanics and crack growth in fatigue 07 p0892 A83-21464
Creep strengthening mechanisms 07 p0892 A83-21466
Creep damage and fracture --- in wrought and cast precipitation-hardened superalloys 07 p0892 A83-21468
Effect of coatings on the mechanical properties of superalloys 07 p0893 A83-21469
The interaction of high temperature corrosion and mechanical properties of alloys 07 p0893 A83-21470
The influence of creep on the high temperature cyclic life of IN738LC 07 p0893 A83-21471
Some interactions of creep and fatigue in IN 738 LC at 850 C 07 p0893 A83-21472
Factors influencing the creep behaviour of a cast Ni-Cr-base alloy 07 p0893 A83-21474
Time dependent low cycle fatigue of PM Astroloy at 1003 K 07 p0893 A83-21475
An operational definition of life to crack initiation in high temperature fatigue 07 p0893 A83-21477
High temperature fatigue of a superalloy for cast turbine wheel 07 p0893 A83-21478
Fatigue of high-temperature materials at ultrasonic frequencies 07 p0894 A83-21479
Mechanisms of high cycle fatigue of cast nickel base alloys 07 p0894 A83-21482
Phase composition and phase stability of alloy IN939 07 p0894 A83-21483
Alloy design for nickel-base superalloys 07 p0894 A83-21484
Grain boundary pore chains in cast nickel base superalloys 07 p0894 A83-21486
The effects of section size, coating and environment on creep rupture behaviour of superalloys 07 p0894 A83-21487
The influence of applied coatings on the creep fracture of IN 738 LC 07 p0894 A83-21488
High-temperature low-cycle fatigue behaviour of IN738LC alloy in air and in vacuum 07 p0895 A83-21489
The effect of hot corrosion on creep and fracture behaviour of cast nickel-based superalloy IN738LC 07 p0895 A83-21490
Vader - A new melting and casting technology 07 p0895 A83-21491
The relationship between structure, properties and processing in powder metallurgy superalloys 07 p0895 A83-21493
Precision casting of turbine blades and vanes 07 p0941 A83-21494
Welding of PM-superalloys 07 p0895 A83-21495
Blade repair and recovery --- in gas turbines 07 p0941 A83-21496
- Microporosity formation in investment castings of nickel-base superalloys: Metallurgical effects, thermal modelling and foundry assessment 07 p0895 A83-21497
Investigation of the surface grain refinement for superalloys castings 07 p0895 A83-21499
The nature and origin of previous particle boundary precipitates in P/M superalloys 07 p0895 A83-21501
Diffusion bonding of superalloys for gas turbines 07 p0941 A83-21503
The solid-state reaction of silicon nitride with an Ni-base alloy 07 p0874 A83-21568
Microstructure and strengthening of superalloys 07 p0896 A83-21603
Superplastic deformation of an oxide-dispersion strengthened superalloy 07 p0897 A83-21613
Fatigue of cast nickelbase superalloys at 850 C 08 p1064 A83-21783
Growth of small fatigue cracks at high temperature - Applicability of conventional fracture mechanics 08 p1064 A83-21785
Fracture of nickel-base superalloy single crystals 08 p1065 A83-22018
Metallurgical instabilities during the high temperature low cycle fatigue of nickel-base superalloys 08 p1065 A83-22019
Heating unit for mechanical testing of heat-resistant alloys at high temperatures 08 p1066 A83-22631
Physicochemical fundamentals of the development of heat-resistant niobium alloys 08 p1067 A83-22694
Thermal softening of Inconel MA 6000 alloy 09 p1228 A83-23343
Estimation of the cyclic fatigue life of parts subjected to complex loading patterns --- for compressor disks and turbine wheels in aircraft engines 09 p1228 A83-23502
A comparative analysis of certain characteristics of the long-term softening of heat-resistant and refractory metals 09 p1228 A83-23504
The effectiveness of plastic surface treatments for strengthening parts operating under elevated temperatures 09 p1278 A83-23517
On the power-law breakdown during high temperature creep of fcc metals 09 p1231 A83-24059
Creep of directionally solidified superalloys and eutectic composites 09 p1232 A83-24062
A theoretical consideration of the microstructural origins of friction stress in a cast gamma prime-strengthened superalloy 09 p1232 A83-24063
Factors controlling the creep behavior of a nickel-base superalloy 09 p1232 A83-24065
Anelastic relaxation, cyclic creep and stress rupture of gamma prime and oxide dispersion strengthened superalloys 09 p1232 A83-24074
A study of the oxidation and gas saturation of beta titanium alloys 09 p1235 A83-24400
Properties and structures of hot isostatic pressed and hot isostatic pressed plus forged superalloys 09 p1236 A83-25286
Fracture properties of superalloys 10 p1393 A83-25324
Post-weld heat-treatment cracking in superalloys 10 p1393 A83-25407
High temperature low cycle fatigue of MAR-M 509 superalloy. I - The influence of temperature on the low cycle fatigue behaviour from 20 to 1100 C. II - The influence of oxidation at high temperature 10 p1393 A83-25417
Low cycle fatigue behaviour of cast nickel-base superalloy IN-738LC in air and in hot corrosive environments 10 p1394 A83-25422
Effect of grain flow on creep properties of heat-resistant aluminium-alloy forgings 10 p1394 A83-25473
Low-pressure-plasma-deposited coatings formed from mechanically alloyed powders 10 p1394 A83-25532
Influence of coatings and hot corrosion on the fatigue behaviour of nickel-based superalloys 10 p1394 A83-25540
The structure and interdiffusional degradation of aluminide coatings on oxide-dispersion-strengthened alloys 10 p1394 A83-25541
Erosion resistance of Co-Cr-Al coatings containing active element additions 10 p1395 A83-25551
The effect of cerium on high temperature tensile and creep behavior of a superalloy 10 p1396 A83-25864
S-N curve inversion of a nickel-base superalloy at elevated temperature 10 p1397 A83-25868
Nickel-base superalloys - Physical metallurgy of recycling 10 p1398 A83-26277
The effect of mass ratio of Ti to Al on the hot corrosion of quaternary 75Ni-13.5Cr-11.5Ti + Al/ alloys 10 p1400 A83-26898
The identification of the sulfide NaCrS₂ in nickel-base superalloys during corrosion in sulfate melts 11 p1550 A83-28671

- The anodic dissolution of a Ni-base superalloy 12 p1713 A83-29401
- Soviet superalloy ZHS6-K, effect of B/C modification --- increased boron and decreased carbon concept for castability improvement 12 p1714 A83-29508
- Decomposition of sigma phase in a Ni-Cr-W system 12 p1714 A83-29723
- Effect of boride stress rupture properties of an FeNiCr-base alloy 13 p1820 A83-30323
- Solution of gamma-prime phase in nickel heat-resistant aging alloys 13 p1823 A83-31214
- Creep-fatigue-environment interactions --- Book 14 p1993 A83-32650
- Creep and high temperature deformation of simple metals and superalloys 14 p1995 A83-32807
- Oxide dispersion hardened mechanically alloyed materials for high temperatures 15 p2137 A83-33963
- Material behavior in connection with flywheel friction welding of superalloys 15 p2137 A83-33965
- Microstructure and hot corrosion resistance of aluminide coating on a nickel-base superalloy in 738LC 15 p2137 A83-33973
- The effect of microstructure on the mechanical properties of an iron-based superalloy after prolonged exposure to 750 C heat 15 p2137 A83-34001
- Effect of cyclic stress on creep rupture strength of a cast superalloy with high Al and Ti contents 15 p2137 A83-34002
- Recrystallization of a nickel-base superalloy - Kinetics and microstructural development 15 p2138 A83-34132
- Cold deformation of a nickel-base superalloy 15 p2138 A83-34134
- High temperature time-dependent crack growth 15 p2139 A83-34485
- Micromechanisms of creep crack growth in nickel based superalloys 15 p2139 A83-34486
- Effects of environment on intermediate temperature crack growth in superalloys 15 p2139 A83-34488
- Cavity nucleation during fatigue crack growth caused by linkage of grain boundary cavities 15 p2139 A83-34489
- Temperature effects on fatigue thresholds and structure sensitive crack growth in a nickel-base superalloy 15 p2139 A83-34740
- On gamma and gamma-prime phases composition in Ni-base superalloys after high-temperature exposure 15 p2140 A83-34799
- High temperature erosion study of INCO 600 metal 15 p2141 A83-35247
- Emission spectrochemical analysis of main components in superalloys using electrolytic iron dilution-high frequency induction melting and centrifugal cast samples 16 p2329 A83-35603
- Comments on 'Long term growth of gamma-prime particles' 16 p2330 A83-35984
- The effect of microstructure on the fatigue behavior of Ni-base superalloys 16 p2331 A83-36166
- Temperature dependent deformation mechanisms of Alloy 718 in low cycle fatigue 16 p2331 A83-36168
- The influence of frequency on fatigue crack propagation of some heat resisting alloys using ultrasonic fatigue 16 p2332 A83-36196
- Hot corrosion of aluminide coatings on nickel-base superalloys in oxidizing and reducing conditions [ONERA, TP NO. 1983-12] 16 p2333 A83-36422
- Statistical modeling of fatigue-crack growth in a nickel-base superalloy 16 p2333 A83-36502
- Dimensional stability of Superinvar 16 p2334 A83-36751
- Elevated temperature aluminum alloys for aerospace 17 p2488 A83-37843
- Microstructure/strength/fatigue crack growth relations in high temperature P/M aluminum alloys 17 p2488 A83-37844
- Studies of nucleation mechanisms and the role of residual stresses in the grain boundary cavitation of a superalloy 17 p2491 A83-38857
- On the mechanism of serrated grain boundary formation in Ni-based superalloys 17 p2492 A83-38859
- High-temperature composites - Status and future directions 18 p2650 A83-40129
- The high temperature creep of dispersion strengthened Ni-Al₂O₃ alloy 18 p2667 A83-40258
- Discontinuous gamma-prime coarsening in a Ni-Al-Mo base superalloy 18 p2669 A83-40628
- Cyclic creep and stress rupture of a mechanically alloyed oxide dispersion and precipitation strengthened nickel-base superalloy 18 p2669 A83-40633
- Creep crack growth behavior of several structural alloys --- superalloys 18 p2669 A83-40636
- The effect of structural dispersity on the high-temperature strength of prestrained steels and alloys 19 p2821 A83-40804
- Fatigue crack initiation and propagation in several nickel-base superalloys at 650 C 19 p2821 A83-41199
- Microstructural contributions to friction stress and recovery kinetics during creep of the nickel-base superalloy IN738LC 19 p2822 A83-42026
- Cyclic oxidation of superalloys 20 p2952 A83-42234
- Low temperature hot corrosion 20 p2953 A83-42252
- Electrochemical assessment of MCrAlY coating alloys at 750 and 900 C in air and CO/CO₂ mixtures 20 p2953 A83-42253
- Recent developments in high temperature coatings for gas turbine airfoils 20 p2953 A83-42254
- Coatings for balanced environmental/mechanical behavior 20 p2998 A83-42255
- Coatings containing chromium, aluminum, and silicon for high temperature alloys 20 p2953 A83-42260
- Improved performance thermal barrier coatings 20 p2957 A83-42261
- Modeling of diffusion processes during carburization of alloys --- surface precipitation reactions 20 p2954 A83-42523
- Recuperator alloys for high-temperature waste heat recovery 21 p3111 A83-43950
- Ni-base MC-carbide reinforced eutectic alloys for jet engine application 21 p3111 A83-44061
- Microstructure of a plasma-sprayed superalloy coating/substrate 21 p3116 A83-44336
- Effect of modification on the ductility of alloy ZrNi6K 21 p3113 A83-44484
- The aging response of a welded iron-based superalloy 22 p3268 A83-45727
- Phase composition and phase stability of a high-chromium nickel-based superalloy, IN939 22 p3269 A83-46395
- Process and structural aspects of melt-spun nickel-base superalloy ribbons 22 p3269 A83-46396
- The construction and testing of pilot installations for making diffusion connections and for depositing layers on high-alloy engine components 23 p3440 A83-47206
- Precipitation in Ni-Mo-Al in-situ composite 23 p3431 A83-47848
- Gamma prime shape changes during creep of a nickel-base superalloy 23 p3432 A83-47855
- Development of the single crystal alloys CM SX-2 and CM SX-3 for advanced technology turbine engines [ASME PAPER 83-GT-244] 23 p3432 A83-48034
- Aluminide coatings on superalloys [ONERA, TP NO. 1983-68] 23 p3432 A83-48189
- Hot isostatic pressing of oxide dispersion strengthened superalloy parts 23 p3439 A83-48725
- Notch sensitivity of high-alloy nickel alloys 24 p3559 A83-48803
- Analysis of nickel- and iron-base heat resisting alloys by spark source mass spectrometry 24 p3554 A83-49326
- Effect of heat treatments on the creep behaviour of a Ni-base single crystal superalloy [ONERA, TP NO. 1983-102] 24 p3561 A83-49413
- High temperature corrosion of metals and alloys; Proceedings of the Third International Symposium, Mount Fuji, Japan, November 17-20, 1982 24 p3561 A83-49476
- Protective coatings against hot corrosion 24 p3590 A83-49479
- Erosion-corrosion of coatings and superalloys in high velocity hot gases 24 p3562 A83-49481
- Alloy design for hot corrosion resistance 24 p3562 A83-49482
- High temperature oxidation of Fe-20Cr-4Al alloys with small additions of Sc, Y or Er 24 p3563 A83-49493
- Oxidation of high alloyed steels 24 p3563 A83-49494
- Hot corrosion of iron- and nickel-base superalloys caused by deposit of calcium sulfate 24 p3563 A83-49498
- Effect of hot corrosion on strength and fracture of a nickel-base superalloy subjected to creep-fatigue interaction 24 p3563 A83-49499
- A fundamental basis for using the platinum group elements as alloying additions in nickel-base alloys to improve high temperature corrosion 24 p3564 A83-49501
- Hot corrosion resistance of nickel-base superalloys and aluminide coatings to molten Na₂SO₄-NiSO₄-NaCl salt 24 p3564 A83-49503
- Hot corrosion behaviour of a cobalt-free, nickel-base superalloy 24 p3564 A83-49504
- The study of the effect of cobalt on the hot corrosion resistance of nickel-based high temperature alloys 24 p3564 A83-49507
- High temperature oxidation of Ni-25Cr-15W alloy 24 p3565 A83-49517
- Corrosion resistance of some composite coatings on Ni-base superalloy 24 p3566 A83-49521
- A high performance wrought nickel-base superalloy El-929 24 p3567 A83-50065
- Long-term ageing characteristics of Hastelloy alloy X 24 p3567 A83-50067
- ## HEAT SHIELDING
- ### NT REENTRY SHIELDING
- ### NT REUSABLE HEAT SHIELDING
- Tests of a thermal acoustic shield with a supersonic jet 01 p0105 A83-10183
- Electromagnetic transducer with temperature-compensating shield 01 p0049 A83-10363
- Parameters for the simulation of high temperature blown shock layers 07 p0924 A83-19829
- A near omnidirectional sunshade for cryogenic instruments [SAE PAPER 820842] 10 p1383 A83-25754
- Calculation of a gas-vapor-liquid heat screen on an adiabatic wall by means of h-d diagrams 11 p1570 A83-28795
- Mixed laminar convection on a vertical surface under conditions of strong injection 11 p1571 A83-28799
- TPS is more than tiles [AIAA PAPER 83-1486] 14 p1980 A83-32733
- Thermal-protection requirements for near-earth aero-assisted orbital-transfer vehicle missions [AIAA PAPER 83-1513] 14 p1982 A83-32750
- Ablation of carbonaceous materials in a hydrogen-helium arc-jet flow [AIAA PAPER 83-1561] 14 p1998 A83-32778
- Structural analysis of Shuttle orbiter penetration tiles [AIAA PAPER 83-0914] 14 p2032 A83-32788
- Aerospace technology demonstrators/research and operational options [AIAA PAPER 83-1054] 16 p2300 A83-36465
- ## HEAT SOURCES
- ### NT GEOTHERMAL RESOURCES
- A multiple step random walk Monte Carlo method for heat conduction involving distributed heat sources [ASME PAPER 82-HT-25] 02 p0171 A83-12788
- On invariant solutions of the equation of nonlinear heat conduction with a source 05 p0640 A83-17643
- Finite-amplitude convection in mixtures with concentration-dependent heat sources 06 p0760 A83-19427
- A universal heat source for active thermal inspection 13 p1860 A83-30837
- Recent developments in the analysis and design of extended surface 15 p2157 A83-33994
- Prediction of damage sites ahead of a moving heat source 17 p2522 A83-38387
- A perturbation method for nonlinear, one-dimensional conduction with heat generation 20 p2971 A83-42665
- Convection in a horizontal fluid layer having a shear-free upper surface and uniform volumetric energy sources 20 p2972 A83-42672
- Direct numerical simulation of the turbulent momentum and heat transfer in an internally heated fluid layer 20 p2972 A83-42673
- Perturbation of the zonal flow by a local heat source 21 p3181 A83-45329
- The effect of a heat source on the large-scale pressure and wind fields (a quasi-barotropic model) 21 p3181 A83-45330
- Binaries as a heat source in stellar dynamics - Release of binding energy 22 p3376 A83-45632
- ## HEAT STORAGE
- Performance investigation of a long, slender heat pipe for thermal energy storage applications --- for solar residential heating 01 p0068 A83-10651
- Fusible pellet transport and storage of heat [ASME PAPER 82-HT-32] 02 p0171 A83-12790
- Thermal storage performance calculations by closed form and finite difference solutions [ASME PAPER 82-HT-52] 02 p0172 A83-12799
- An experimental study of single medium thermocline thermal energy storage [ASME PAPER 82-HT-53] 02 p0173 A83-12800
- Thermal energy storage units for solar electric power plants 04 p0503 A83-15132
- Liquid phase thermochemical energy conversion systems - An application of Diels-Alder chemistry 05 p0658 A83-17149
- Two applications of a numerical approach of heat transfer process within rock beds 06 p0780 A83-18551
- Comparisons of paraffin wax storage subsystem models using liquid heat transfer media 06 p0780 A83-18553
- Solar energy storage by the reversible reaction - N₂O₄ yields 2NO₂ - Theoretical and experimental results 06 p0780 A83-18554

- A further study on the theory of 'falling ponds' --- for solar pond heat storage 06 p0780 A83-18555
- The effect of crystal size on the thermal energy storage capacity of thickened Glauber's salt 06 p0780 A83-18562
- Finite element analysis of mixed convection applied to the storage of solar energy 08 p1091 A83-23219
- Optimal control of solar heating and off-peak energy storage installations 09 p1293 A83-23882
- Design and construction of the 'Solar One' thermal storage subsystem 11 p1606 A83-27230
- Comparison of advanced thermal and electrical storage for parabolic dish solar thermal power systems 11 p1606 A83-27232
- Evaluation and application of solid thermal energy carriers in a high temperature solar central receiver system 11 p1607 A83-27235
- Thermal energy storage - Air Force user considerations in various modes of operation 11 p1609 A83-27305
- Thermal energy storage media for advanced compressed air energy storage systems 11 p1609 A83-27312
- AQUASTOR - A computer model for cost analysis of aquifer thermal energy storage coupled with district heating or cooling systems 11 p1609 A83-27314
- Cost and performance of thermal storage concepts in solar thermal systems, Phase 2-liquid metal receivers 11 p1609 A83-27316
- High-temperature molten salt solar thermal systems 11 p1609 A83-27317
- Analysis and test results for a molten salt thermal energy storage system 11 p1610 A83-27318
- Composite salt/ceramic media for thermal energy storage applications 11 p1610 A83-27319
- Computer simulation of transient energy storage in a packed-bed of iron spheres with liquid-metal through-flow by numerical inversion of Laplace transforms 11 p1610 A83-27320
- Storing solar energy in thermally stratified tanks 11 p1610 A83-27321
- Heat transfer in a latent heat storage device with finned annular tube heat exchanger --- German thesis 11 p1570 A83-28665
- Low temperature latent heat thermal energy storage - Heat storage materials 12 p1749 A83-28943
- Use of some simple statistical models in solar meteorology 12 p1757 A83-28944
- Performance of a cylindrical phase-change thermal energy storage unit 12 p1749 A83-28969
- Emulsification of thermal energy storage materials in an immiscible fluid 14 p2046 A83-32347
- An implicit solution procedure for finite difference modeling of the Stefan problem [AIAA PAPER 83-1527] 14 p2011 A83-32758
- Thermal energy storage development for solar electrical power and process heat applications 15 p2189 A83-33987
- Heat transfer accompanied with melting and freezing for solar heat storage 15 p2190 A83-34235
- Combined convection in an annulus applied to a thermal storage problem 15 p2191 A83-34259
- Alternative energy sources IV; Proceedings of the Fourth Miami International Conference, Miami Beach, FL, December 14-16, 1981. Volume 1 - Solar Collectors Storage 15 p2191 A83-34374
- Optimal control of a bilinear solar collector/heat exchange system 17 p2535 A83-37150
- Recuperator alloys for high-temperature waste heat recovery 21 p3111 A83-43950
- Net energy analysis of district solar heating with seasonal heat storage 24 p3599 A83-49649
- Investigations of sodium acetate trihydrate for solar latent heat storage, controlling the melting point 24 p3601 A83-50179

HEAT STROKE

- Nitrogen metabolism during heat stress 12 p1765 A83-29314
- Work-heat tolerance in endurance-trained rats 13 p1897 A83-30466
- Chronic low-sodium diet in rats - Hormonal and physiological effects during exercise in the heat 22 p3346 A83-45994

HEAT TESTS

U HIGH TEMPERATURE TESTS

HEAT TOLERANCE

- Physiological criteria of upper limits of body heating 02 p0223 A83-12256
- Study of + Gz protection given by an anti 'G' suit worn on top of a liquid cooled suit 09 p1324 A83-24003
- The limitation of human performance in extreme heat conditions 10 p1459 A83-26307
- Role of bacterial endotoxins of intestinal origin in rat heat stress mortality 13 p1896 A83-30454
- Work-heat tolerance in endurance-trained rats 13 p1897 A83-30466

- Role of surface area-to-mass ratio and work efficiency in heat intolerance 13 p1904 A83-30493
- Results of an experimental evaluation of the thermal stress of operators 14 p2073 A83-33324
- Inherent variability in heat-stress decision rules 16 p2402 A83-36475
- Changes in the urinary levels of electrolytes, uric acid and 17 OHCS with graded heat stress 23 p3499 A83-48692

HEAT TRANSFER

- NT AERODYNAMIC HEAT TRANSFER
- NT CONDUCTIVE HEAT TRANSFER
- NT CONVECTIVE HEAT TRANSFER
- NT HYPERSONIC HEAT TRANSFER
- NT LAMINAR HEAT TRANSFER
- NT RADIATIVE HEAT TRANSFER
- NT SUPERSONIC HEAT TRANSFER
- NT TURBULENT HEAT TRANSFER
- Free convection fluctuating boundary layer on a horizontal plate 01 p0044 A83-10124
- Heat transfer by laminar forced flow against a rotating disk 01 p0044 A83-10227
- Heat and mass transfer apparatuses in cryogenics --- Russian book 01 p0028 A83-10672
- On the application of variable shear double exposure interferometer for the study of heat transfer to or from solid surfaces 01 p0051 A83-11056
- The effect of the parameters of metal-fiber capillary structures on the maximum heat-transfer capability of thermal pipes 02 p0169 A83-11515
- The thermoacoustic effect in a resonance tube having one open end 02 p0233 A83-11516
- A solution to the inverse coefficient problem of thermal conductivity --- in heat transfer 02 p0161 A83-11517
- Some features of the continuous operation of Gunn diodes 02 p0166 A83-11545
- Analysis and computation of heat transfer around a cylinder in argon plasma cross flow [ASME PAPER 82-HT-30] 02 p0171 A83-12789
- Fusible pellet transport and storage of heat [ASME PAPER 82-HT-32] 02 p0171 A83-12790
- Design considerations for aerodynamically quenching gas sample probes [ASME PAPER 82-HT-39] 02 p0172 A83-12794
- Heat transfer with bubble formation - Results of the TEXUS IIIB experiment 02 p0138 A83-12998
- Analytical experimental heat transfer in dry sliding of polymeric composites [ASLE PREPRINT 82-LC-2B-1] 03 p0333 A83-13233
- Flow behavior and heat transfer around a circular cylinder at high blockage ratios 03 p0315 A83-13344
- Collection of solar energy at specified output temperature 03 p0353 A83-13582
- Analysis and evaluation of extended surface thermal systems --- Book 03 p0317 A83-14114
- Numerical solution for fully developed flow in heated curved tubes 03 p0322 A83-14587
- The comparative performance of selected solar global models 03 p0370 A83-14634
- Flow of a conducting rotating fluid above a disc under uniform suction 03 p0323 A83-14724
- One-dimensional finite element analysis of thermal ablation with pyrolysis 04 p0475 A83-15014
- Heat transport in porous cometary nuclei 04 p0551 A83-15369
- Heat transfer for flows past non-isothermal bodies --- Russian book 04 p0476 A83-15830
- An experimental study and modeling of heat transfer in boilers of small and medium power --- French thesis 04 p0456 A83-15841
- A seasonal global climate model with an equivalent meridional atmospheric circulation 04 p0515 A83-15852
- Investigation of the characteristics of heat transfer in the heating zone of heat pipes with metal fiber capillary structures 04 p0477 A83-15865
- Nonlinear problem of heat and mass transfer to a particle in a gas flow at low Reynolds numbers 04 p0477 A83-15876
- Numerical study of wall heat transfer in the recirculating flow region of a confined jet 04 p0477 A83-16124
- The effect of changes in the turbulent flow structure of the unsteady heat transfer during the heating of gases and liquids in pipes 04 p0478 A83-16163
- Performance characteristics of the double-wall artery high capacity heat pipe [AIAA PAPER 83-0318] 05 p0634 A83-16648
- A numerical study of phase change energy transport in two-dimensional rectangular enclosures [AIAA PAPER 83-0321] 05 p0635 A83-16650
- An experimental facility for the investigation of the two-dimensional Stefan problem [AIAA PAPER 83-0322] 05 p0635 A83-16651

- Grid adaption for problems with separation, cell Reynolds number, shock-boundary layer interaction, and accuracy [AIAA PAPER 83-0449] 05 p0636 A83-16721
- Heat transfer with ablation in a finite slab subjected to time variant heat fluxes [AIAA PAPER 83-0582] 05 p0637 A83-16802
- An analytical approach to thermal modeling of Bridgman-type crystal growth. I - One-dimensional analysis 05 p0638 A83-17235
- On the nonexistence and existence of global solutions of boundary value problems for quasi-linear parabolic equations --- in propagation of thermal disturbances 05 p0640 A83-17642
- Heat transfer - A review of 1981 literature 05 p0682 A83-17701
- A steady state linear ablation problem 05 p0641 A83-17706
- A literature survey on numerical heat transfer 05 p0641 A83-17741
- Momentum and heat transfers in the surface layer over a frozen sea 06 p0788 A83-18059
- The thermal behavior of oscillating squeeze films [ASME PAPER 81-LUB-26] 06 p0768 A83-18388
- Thermal behavior and insulation of a cryogenic wind tunnel [ONERA, TP NO, 1982-89] 06 p0720 A83-18427
- Heat Transfer and Fluid Mechanics Institute, Meeting, 28th, California State University, Sacramento, CA, June 28, 29, 1982, Proceedings 06 p0757 A83-18451
- An analytical investigation of mass flow, pressure and temperature in a flat-plate solar collector 06 p0779 A83-18452
- Unsteady heating of a complex solid body by a hot gaseous jet --- erosion effects of missile exhaust on its launcher 06 p0721 A83-18455
- Models for stellar coronae - The effects of coronal heating with long dissipation scale lengths 06 p0829 A83-18542
- Two applications of a numerical approach of heat transfer process within rock beds 06 p0780 A83-18551
- Comparisons of paraffin wax storage subsystem models using liquid heat transfer media 06 p0780 A83-18553
- Comparison of computational and flight data concerning heat transfer for axisymmetric bodies moving along a trajectory at freestream Mach of not greater than 5 06 p0713 A83-19570
- The heating effect in resonance tubes --- German thesis 06 p0761 A83-19623
- Short duration heat transfer studies at high free-stream temperatures [ASME PAPER 82-GT-129] 07 p0924 A83-19673
- An experimental study of turbulent free convection boundary layer in air along a vertical plate using LDV 07 p0925 A83-20279
- Optimal design of thermophysical measuring systems --- for heat transfer measurement in turbine blades 07 p0930 A83-20957
- Development of mixed time partition procedures for thermal analysis of structures 07 p0949 A83-21445
- An experimental investigation of heat transfer near the leading edge of inclined flat plate in hypersonic flow 08 p1041 A83-22071
- Fluid flow and heat transfer in the separated region of a circular cylinder with wake control 08 p1084 A83-22238
- Quantitative geometric characterization of two-dimensional flaws via liquid crystals thermography 08 p1113 A83-22409
- Ignition of a combustible half space 08 p1057 A83-22738
- The role of latent heat release in baroclinic waves - Without beta-effect 08 p1142 A83-23005
- Numerical study on flow behaviour and heat transfer in the vicinity of starting point of transpiration 08 p1090 A83-23206
- The effect of forced and free convection in the discharge of a pressurized gas 08 p1090 A83-23210
- Numerical calculation of the heat transfer by natural convection in a cubical enclosure 08 p1090 A83-23212
- The effect of soldering on the characteristics of heat pipes with a liquid-metal heat-transfer agent 09 p1258 A83-23449
- Heat transfer during nonlinear gas oscillations in a pipe open at one end 09 p1260 A83-24227
- Thermal homogeneity in a closed excimer laser cavity 09 p1272 A83-24661
- A study of thermal convection and heat transfer --- Russian book 09 p1264 A83-25246
- An analysis of the thermal entrainment effect on jet impinging heat transfer [ASME PAPER 82-WA/HT-54] 10 p1413 A83-25694

- Efficiency of combined jet cooling of a plate in conditions of complex heat transfer 10 p1417 A83-26254
- Calculation of heat transfer in smooth pipes with turbulent flow of gaseous heat-carriers with constant and variable physical properties 10 p1417 A83-26255
- Evaluation and application of solid thermal energy carriers in a high temperature solar central receiver system 11 p1607 A83-27235
- Improved Stirling engine performance using jet impingement 11 p1588 A83-27288
- The effect of the nonuniformity of supersonic flow with shocks on friction and heat transfer in plane channels 11 p1526 A83-27710
- Thermal stresses in a partially restrained orthotropic plate with a source and sink of heat 11 p1596 A83-28464
- Calculation of drag and heat transfer for viscous quasi-stabilized flow of supercritical helium in a pipe 11 p1570 A83-28552
- Heat transfer in a latent heat storage device with finned annular tube heat exchanger --- German thesis 11 p1570 A83-28665
- Results of an experimental determination of limiting heat fluxes in two-phase thermosiphons 11 p1570 A83-28792
- An analysis of the thermal state of plane channels with allowance for the mutual influence of the processes in the wall and in the fluid 11 p1570 A83-28796
- Heat transfer during the boiling of acetone and ethyl alcohol in a thermosiphon with porous capillary structures on the heat-transfer face 11 p1571 A83-28798
- Comparison of laser anemometer measurements and theory in an annular turbine cascade with experimental accuracy determined by parameter estimation 12 p1695 A83-28833
- A 2D model of turbulent solar induced flows in passive air collectors 12 p1749 A83-29039
- Implicit boundary conditions for the solution of the parabolized Navier-Stokes equations for supersonic flows 12 p1697 A83-29648
- Hydrodynamics and heat transfer in turbulent zero-momentum wakes 13 p1838 A83-30046
- The basic types of conjugate problems of heat and mass transfer 13 p1838 A83-30048
- Heat transfer performance of metal fiber sintered surfaces 13 p1840 A83-30521
- Metal-hydride energy-technological processing of hydrogen 13 p1871 A83-31375
- Nonstationary phenomena in flows of a viscous reactive fluid 14 p1989 A83-32091
- Intrinsic thermocouple analysis using multinode unsteady surface element method [AIAA PAPER 83-1437] 14 p2019 A83-32709
- Prediction of thermal conductivity and viscosity for some fluids in the near-critical region [AIAA PAPER 83-1475] 14 p2094 A83-32729
- Alternate thermal control coolant fluid investigation for the NASA Space Transportation System [AIAA PAPER 83-1493] 14 p1980 A83-32738
- Heating analysis of bent-nose biconics at high angles of attack using the parabolized Navier-Stokes equations [AIAA PAPER 83-1507] 14 p1970 A83-32744
- Heat-transfer distributions on biconics at incidence in hypersonic-hypervelocity He, N₂, air, and CO₂ flows [AIAA PAPER 83-1508] 14 p1970 A83-32745
- Fluid flow in the contact line region of a mixture of alkanes - 98 percent hexane and 2 percent octane [AIAA PAPER 83-1528] 14 p2011 A83-32759
- Flow film boiling from submerged bodies [AIAA PAPER 83-1529] 14 p2011 A83-32760
- Development and test of a space reactor core heat pipe [AIAA PAPER 83-1530] 14 p2011 A83-32761
- Overview of D.C. casting --- Direct-Chill solid-liquid interface shape prediction using heat transfer models 14 p1995 A83-32878
- Thermal properties of some asphaltic concrete mixes [AIAA PAPER 83-1598] 14 p1978 A83-33361
- Benchmark determination of Shuttle Orbiter entry aerodynamic heat-transfer data 15 p2119 A83-33730
- Thermal analysis and control of electronic equipment --- Book 15 p2143 A83-33747
- Thermal behavior of axially grooved heat pipes aboard a rocket 15 p2158 A83-33999
- Numerical methods in thermal problems. Volume 2 - Proceedings of the Second International Conference, Venice, Italy, July 7-10, 1981 15 p2158 A83-34226
- Appropriate finite element techniques for heat transfer problems with high gradients and ablation 15 p2159 A83-34236
- Connectivity methods for free boundary problems - 2 phase heat flow 15 p2159 A83-34238
- The determination of hygrothermal stress development in anisotropic composites 15 p2175 A83-34239
- Survey of numerical methods for three-dimensional, unsteady thermal problems 15 p2159 A83-34248
- Unsteady heat transfer from circular cylinder immersed in impulsively started flow 15 p2159 A83-34249
- New results in transient heat transfer analysis by the boundary integral equation method 15 p2159 A83-34250
- The consistent method for computing derived boundary quantities when the Galerkin FEM is used to solve thermal and/or fluids problems 15 p2159 A83-34252
- A quasi-three dimensional analysis of thermal ablation from a hypersonic missile 15 p2159 A83-34254
- A dynamic simulation of a flat-plate collector system 15 p2191 A83-34409
- The thermal mechanism of barrier destruction by a transonic jet of rocket propellant combustion products 15 p2172 A83-34473
- Heat and mass transfer of an oscillatory flow with Hall current 15 p2236 A83-34557
- Heat loss optimisation of a concentric cylindrical solar collector employing a cobalt oxide selective absorber 15 p2192 A83-34675
- A theoretical and experimental study of non-adiabatic wall effects on transonic shock/boundary layer interaction [AIAA PAPER 83-1421] 15 p2120 A83-34901
- Critical conditions for the combustion of macroheterogeneous systems of the type fuel-inert material 15 p2134 A83-35318
- Nonstationary temperature fields during the heat treatment of titanium disks of complex configurations 16 p2361 A83-35589
- Calculation of a laminar flow of a compressible gas in plane curvilinear ducts with heat transfer 16 p2349 A83-35701
- Effect of heat transfer augmentation on two-phase flow instabilities in a vertical boiling channel 16 p2350 A83-35800
- The effects of large heat release on a two dimensional mixing layer [AIAA PAPER 83-0472] 16 p2351 A83-36055
- Thermal stability of alternative aircraft fuels [AIAA PAPER 83-1143] 16 p2339 A83-36243
- Prediction of stagnation flow heat transfer on turbomachinery airfoils [AIAA PAPER 83-1173] 16 p2294 A83-36259
- Computational and experimental study of the effect of mass transfer on liquid jet break-up [AIAA PAPER 83-1400] 16 p2353 A83-36390
- Heat and mass transfer and hydrodynamics of swirling flows in axisymmetric channels --- Russian book 16 p2353 A83-36437
- Heat transfer performance of ceramic regenerator matrices with sine-duct shaped passages 16 p2353 A83-36592
- A method for modeling heat exchangers 16 p2353 A83-36595
- Effect of heat transfer of melt/solid interface shape and solute segregation in Edge-Defined Film-Fed growth - Finite element analysis 16 p2354 A83-36715
- Theoretical and experimental study of momentum and heat transfer between alumina particles and a d.c. plasma jet 16 p2362 A83-36878
- Unsteady nonsimilar laminar boundary-layer flows with heat and mass transfer 17 p2501 A83-37024
- Computer in analysis and design --- for heat transfer analysis 17 p2504 A83-37275
- Artificially thickened turbulent boundary layers for studying heat transfer and skin friction on rough surfaces 17 p2504 A83-37396
- On a method for the closure of the energy equation formulated relative to the total enthalpy in the case of turbulent flow in a boundary layer 17 p2505 A83-37530
- Numerical solution technique for the transient equation of transfer 17 p2506 A83-37866
- Numerical model for dynamic and thermal developments of a pulsed laminar ducted flow 17 p2506 A83-37867
- Adaptive gridding for finite difference solutions to heat and mass transfer problems 17 p2508 A83-38790
- The effect of strong heat addition on the convergence of implicit schemes [AIAA PAPER 83-1914] 18 p2635 A83-39371
- Calculation method of the optimum configurations of the extended surfaces with simultaneous conductive, convective and radiative heat transfer in heat exchanger 18 p2686 A83-39932
- The effect of the interference of traveling and stationary waves on time variations of the large-scale circulation 18 p2728 A83-40030
- Buoyancy effects and the manifolding of single ended absorber tubes 19 p2861 A83-40765
- Flow and heat transfer on a disk rotating beneath a forced vortex 19 p2841 A83-40853
- Stagnation point heat transfer for jet impingement to a plane surface 19 p2842 A83-40879
- Stability of the stationary plane-parallel convective motion of a chemically active medium 19 p2842 A83-41261
- Stability characteristics of a boundary gas layer recombining on a cooled wall 19 p2843 A83-41272
- Heat transfer in energy problems --- Book 19 p2843 A83-41524
- An analysis of heat transfer during film condensation of stationary vapor on a vertical surface 19 p2843 A83-41566
- Heat transfer and drag in a turbulent boundary layer with a pressure gradient 19 p2844 A83-41576
- A study of heat and mass transfer in flows past bodies of various shapes with allowance for injection 19 p2844 A83-41577
- Constraints on rift thermal processes from heat flow and uplift 19 p2867 A83-41857
- Calculation of heat transfer from polydisperse flows of gas suspensions in straight ducts and pipes 19 p2846 A83-42135
- The effect of supercritical pressure gradients on heat transfer in turbine nozzle cascades 19 p2801 A83-42140
- The effect of rotation on heat transfer in the radial slot passage of a turbine blade 19 p2794 A83-42149
- Heat transfer 1982; Proceedings of the Seventh International Conference, Technische Universitaet Muenchen, Munich, West Germany, September 6-10, 1982. Volume 1 - Review and keynote papers 20 p2970 A83-42651
- Prediction of transport properties related to heat transfer 20 p2970 A83-42656
- Advanced boundary-layer theory in heat transfer 20 p2970 A83-42657
- Heat transfer 1982; Proceedings of the Seventh International Conference, Technische Universitaet Muenchen, Munich, West Germany, September 6-10, 1982. Volume 2 - General papers: Conduction, natural convection, environmental heat transfer, radiation 20 p2971 A83-42663
- Finite analytic numerical solution of heat transfer and flow past a square channel cavity 20 p2975 A83-42703
- Heat transfer at the tip of an unshrouded turbine blade 20 p2975 A83-42706
- Heat transfer to pulsating, turbulent gas flow 20 p2975 A83-42707
- Effects of free stream turbulence intensity and integral length scale on heat transfer from a circular cylinder in crossflow 20 p2976 A83-42711
- Heat transfer in the turbulent swirling flow in a channel of complex shape 20 p2976 A83-42714
- Influence of temperature and concentration boundary layers at separation on heat and mass transfer in separated flows 20 p2976 A83-42715
- Effects of molecular vibrational relaxation of stagnation heat transfer 20 p2976 A83-42716
- Flow and heat transfer past a semi-infinite vertical plate with oscillating plate temperature 20 p2977 A83-42720
- Heat transfer in a turbulent boundary layer behind a two-dimensional bluff body at different Pr numbers 20 p2977 A83-42722
- Modification of the turbulent temperature field in strongly heated air flows 20 p2977 A83-42726
- Convex curvature effects on the heated turbulent boundary layer 20 p2978 A83-42733
- Profile analysis of heat/mass transfer across the plane wall-jet 20 p2978 A83-42742
- Heat transfer augmentation in an axisymmetric impinging jet 20 p2979 A83-42744
- Effect of semi-confinement on impingement heat transfer 20 p2979 A83-42746
- Heat transfer 1982; Proceedings of the Seventh International Conference, Technische Universitaet Muenchen, Munich, West Germany, September 6-10, 1982. Volume 4 - General papers: Pool boiling, flow boiling, measuring techniques 20 p2980 A83-42757
- Steam chugging analysis in single-vent vapor injection 20 p2980 A83-42758
- Liquid-solid contact and its relationship to improved film boiling heat transfer rates 20 p2980 A83-42761
- The dryout region in frictionally heated sliding contacts 20 p2980 A83-42762
- Superfluid helium (He - II) film boiling on vertical heat transfer surfaces 20 p2981 A83-42763
- Heat transfer characteristics of the two-phase closed thermosyphon (wickless heat pipe) 20 p2981 A83-42765
- Heat pipes - Thermal diodes 20 p2981 A83-42766
- Experimental studies of heat and mass exchange phenomena in the two-component heat pipe 20 p2981 A83-42767

Critical heat flux in flow boiling of helium
20 p2981 A83-42769

Heat transfer in thin liquid films flowing over horizontal tubes
20 p2981 A83-42771

Study of the accelerated cooling of a very hot wall with a forced flow of subcooled liquid in film boiling regime
20 p2981 A83-42772

Two applications of thermal network correction techniques
20 p2982 A83-42780

Numerical analysis of heat and mass transfer processes during directional solidification in weightlessness
20 p2939 A83-42893

Free convection in hydromagnetic flows in a vertical wavy channel
20 p2982 A83-42971

Heat transfer 1982; Proceedings of the Seventh International Conference, Technische Universitaet Muenchen, Munich, West Germany, September 6-10, 1982. Volume 6 - General papers: Combined heat and mass transfer, particle heat transfer, heat exchangers, industrial heat transfer, heat transfer in energy utilization
20 p2983 A83-43013

Heat and mass transfer in transpiration cooled turbine blades
20 p2983 A83-43014

A finite element analysis of heat transfer in solid with radiation and ablation
20 p2983 A83-43015

Modelling of the irreversibility of the heat and mass transfer - Similarity of irreversibility
20 p2983 A83-43016

Heat and mass transfer in a low speed turbulent boundary layer with condensation
20 p2984 A83-43018

A friction factor correlation for the offset strip-fin matrix
20 p2984 A83-43022

A computer model for transient heat transfer to liquid helium
20 p2985 A83-43222

Transient heat transfer in superfluid helium
20 p2986 A83-43223

Analysis of coolant entrance boundary shape of porous region to control cooling along exit boundary
20 p2986 A83-43361

Heat transfer to a fluid in radial, outward flow between two coaxial stationary or corotating disks
20 p2986 A83-43362

The one-dimensional analysis of fin assembly heat transfer
20 p2986 A83-43365

Heat and mass exchange of a droplet in a polyatomic gas
21 p3220 A83-43933

Numerical analysis of moving boundary problem in matrix with a thin alternate matrix
21 p3197 A83-44012

Heat transfer in unsteady flow past a heated impulsively started circular cylinder
21 p3128 A83-44022

Heat transfer for elastico-viscous flow between two rotating porous discs
21 p3129 A83-44072

Peripheral temperature variation in the walls of noncircular ducts
21 p3129 A83-44247

An experimental investigation into the effect of changes in the geometry of a slot nozzle on the heat transfer characteristics of an impinging air jet
21 p3131 A83-44851

Unsteady Couette flow and heat transfer in a dusty gas
21 p3131 A83-44855

Heat and mass transfer toward bluff bodies
21 p3133 A83-45348

Calculation of the circulation, heat budget, and moisture cycle of the atmosphere for July on the basis of a model of the general circulation of the atmosphere
23 p3488 A83-47152

Hot spot heat transfer - Its application to Venus and implications to Venus and earth
23 p3528 A83-47812

An experimental investigation of endwall heat transfer and aerodynamics in a linear vane cascade
[ASME PAPER 83-GT-52] 23 p3394 A83-47909

Heat transfer experiments in high aspect ratio rectangular channel with epoxied short pin fins
[ASME PAPER 83-GT-57] 23 p3447 A83-47913

Optimisation of homogeneous thermal insulation layers
23 p3449 A83-48097

Optimal thermodynamics of thermal exchanges
[ONERA, TP NO. 1983-78] 23 p3512 A83-48193

The effect of heat release and injection on the structure of a laminar hypersonic flow behind a body
23 p3399 A83-48534

The effect of nonequilibrium physical-chemical processes in the boundary layer on the ablation of quartz glass
23 p3452 A83-48665

Heat transfer and flow resistance in the turbulent pipe flow of a fluid with near-critical state parameters
24 p3576 A83-49120

Experimental investigation of heat transfer with interaction of a density discontinuity with a turbulent boundary layer on the permeable surface of a rectangular channel
24 p3577 A83-49121

Free-stream turbulence effects on the heat transfer through the turbulent boundary layer behind a fence
24 p3578 A83-49573

Heat and mass transfer of an oscillatory flow with Hall current. II
24 p3633 A83-50164

HEAT TRANSFER COEFFICIENTS

Turbulent momentum and heat transfer in thermally-stratified flows
02 p0170 A83-11870

Heat transfer and dynamics of supersonic air flow past cavities
02 p0170 A83-11872

Friction and heat transfer from plates to normally-incident axisymmetric turbulent jets
02 p0170 A83-11874

Fluid injection to a laminar boundary layer with variable wall mass and heat flux
[ASME PAPER 82-HT-61] 02 p0173 A83-12801

Laminar and turbulent boundary layers on moving, nonisothermal continuous flat surfaces
03 p0316 A83-13486

Generalized laminar heat transfer from the surface of a rotating disk
03 p0323 A83-14673

Thermodynamic analysis of causes of differences of values of the thermal conductivity of gases measured by stationary and nonstationary methods
04 p0544 A83-15449

Visualization of heat transfer from arrays of impinging jets
05 p0640 A83-17702

Influence of small-amplitude undulations on turbulent convection in an axisymmetric pipe flow - Experiments and numerical prediction
05 p0641 A83-17704

The development of thermal boundary layers in airfoil-cascade flows with off-design angles of attack
06 p0713 A83-19155

An experimental heat-transfer investigation of an advanced winged entry vehicle at Mach 10
[AIAA PAPER 83-0409] 06 p0714 A83-19589

Effect of Delta T- and spatially varying heat transfer coefficient on thermal stress resistance of brittle ceramics measured by the quenching method
07 p0898 A83-20171

An experimental study of unsteady heat transfer from a flat plate to an oscillating air flow
08 p1084 A83-22239

Some comments on Beck's solution of the inverse problem of heat conduction through the use of Duhamel's theorem
08 p1087 A83-23144

A nonstationary approach to the investigation of heat transfer in the cooling ducts of turbine blades
09 p1258 A83-23429

Heat transfer between two-phase flow and a nozzle wall under conditions of entrainment of droplets from the surface of a condensed film
09 p1258 A83-23431

The effect of the nonisothermality of an airfoil surface on the local values of the heat transfer coefficient
09 p1196 A83-23438

Heat transfer from interrupted plates
09 p1259 A83-23879

Convective heat losses from flat-plate solar collectors in turbulent winds
09 p1293 A83-23883

Hydraulics of a channel with a linear jet array --- heat transfer coefficient enhancement by transpiration cooling
09 p1260 A83-24049

A boundary layer with selective suction
09 p1260 A83-24226

The effect of porous-surface defects on the thermophysical characteristics of the wicks of heat pipes
09 p1260 A83-24229

An approximate method for calculating the transfer coefficients of multicomponent mixtures --- transport properties of gases
09 p1350 A83-24232

Determination of the temperature dependence of the heat conductivity coefficient of a composite material from the data of a nonstationary experiment
09 p1224 A83-24233

Numerical calculation of local convective heat transfer coefficients over air-cooled vane surfaces
10 p1418 A83-26772

Temperature fields in conditions of intense porous cooling
11 p1568 A83-28374

Heat transfer during the film boiling of liquids under conditions of free convection
11 p1570 A83-28555

Heat loss coefficients and effective tau-alpha products for flat-plate collectors with diathermanous covers
12 p1749 A83-28939

Wave processes in solids-laden gas flows
12 p1724 A83-29443

The temperature field of plates and infinite prismatic bodies of complex cross section in the case of a heat transfer coefficient that varies in time
13 p1838 A83-30047

The influence of heat-transfer factors on results of the thermal optimization of solar power plants
14 p2036 A83-32050

Emulsification of thermal energy storage materials in an immiscible fluid
14 p2046 A83-32347

Monogroove heat pipe development for the space constructible radiator system
[AIAA PAPER 83-1431] 14 p2010 A83-32706

Surface tension effects in a space radiator condenser with capillary liquid drainage
[AIAA PAPER 83-1525] 14 p2011 A83-32756

Evaporation from a two-dimensional meniscus
[AIAA PAPER 83-1526] 14 p2011 A83-32757

Comparisons of STS-1 experimental and predicted heating rates
15 p1225 A83-33729

Recent developments in the analysis and design of extended surface
15 p2157 A83-33994

A theoretical and experimental investigation of flow and heat transfer in film cooling
15 p2161 A83-34268

Heat transfer in the evaporation and condensation zones of heat pipes intensely heated at the end
15 p2161 A83-34471

Hypersonic shock tunnel heat transfer tests of the Space Shuttle SILTS pod configuration
[AIAA PAPER 83-1535] 15 p2127 A83-34921

The geyser effect in a two-phase thermosyphon
16 p2354 A83-36597

Variation of heat transfer coefficients in the transition region of a flow at supersonic velocities
17 p2447 A83-37263

Gas turbine engines
17 p2467 A83-37274

Heat transfer performance of an inclined two-phase closed thermosyphon
18 p2684 A83-39850

Solar thermal collectors
18 p2709 A83-40522

The mean coefficients of heat transfer from gas to turbine nozzle blade at high Reynolds numbers
19 p2846 A83-42075

Enhancement of heat transfer
20 p2970 A83-42659

Cryogenic heat transfer - He-4 Kapitza conductances including phase change effects
20 p2971 A83-42660

Heat flux display and heat transmission coefficient calculation with the finite element method
20 p2971 A83-42669

Heat liberation and heat transfer in flame tubes
20 p2974 A83-42696

Heat transfer to turbulent pipe flows with swirl and following a sudden enlargement
20 p2975 A83-42704

Heat transfer characteristics and boundary layer development about heating and cooling rotating blunt bodies at supersonic speeds
20 p2929 A83-42710

Local heat transfer rates from two adjacent spheres in turbulent axisymmetric flow
20 p2976 A83-42719

Viscous dissipation effects on heat transfer from turbulent flow with high Prandtl number fluids
20 p2977 A83-42723

A new approach for calculating heat transfer characteristics of turbulent wall flows
20 p2977 A83-42725

Coefficients for the combined heat- and momentum-transfer in laminar and turbulent boundary layers
20 p2977 A83-42728

Heat transfer enhancement using vortex generators
20 p2978 A83-42731

Predictions of heat transfer in turbine blades with a 2-equation model of turbulence
20 p2929 A83-42732

Cooling of a rotating disk by means of an impinging jet
20 p2978 A83-42739

Experimental investigation of heat transfer by a single- and a triple-row round jets impinging on semi-cylindrical concave surfaces
20 p2929 A83-42740

Heat transfer and flow characteristics of jets impinging on a concave hemispherical plate
20 p2979 A83-42743

A study of turbulence models for predicting round and plane heated jets
20 p2979 A83-42745

Heat transfer from a turbulent, swirling, impinging jet
20 p2979 A83-42747

Acoustic enhancement of heat transfer in plane channels
20 p2929 A83-42751

Wake interference for a heated oscillating cylinder
20 p2980 A83-42753

Experimental mixed convection from a large, vertical plate in a horizontal flow
20 p2980 A83-42754

Numerical study of heat transfer system with staggered array of vertical flat plates used at low Reynolds number
20 p2980 A83-42755

Application of the swollen polymer technique to the study of heat transfer on film cooled surfaces
20 p2982 A83-42775

Problems of mechanics and heat transfer in space technology
20 p2939 A83-42876

Heat transfer during ionized-gas flow past bodies
20 p2929 A83-42880

Experiments on a crossflow heat exchanger with tubes of lenticular shape
20 p2986 A83-43364

Observations on the characteristics of a fluidized bed for the thermal shock testing of brittle ceramics
21 p3116 A83-44333

- Hydrodynamics and heat transfer in sphere assemblages Cylindrical cell models 21 p3131 A83-44928
- Calculation of the heating of layered bodies 21 p3163 A83-45351
- Transient thermal stresses in a rectangular plate due to variation of heat-transfer coefficients on upper and lower surfaces 22 p3306 A83-46391
- Heat transfer characteristics for jet array impingement with initial crossflow [ASME PAPER 83-GT-28] 23 p3393 A83-47891
- Techniques for obtaining detailed heat transfer coefficient measurements within gas turbine blade and vane cooling passages [ASME PAPER 83-GT-58] 23 p3447 A83-47914
- Heat transfer and friction loss characteristics of pin fin cooling configuration [ASME PAPER 83-GT-123] 23 p3448 A83-47952
- Local heat transfer rates from two adjacent spheres in turbulent flow 23 p3451 A83-48624

HEAT TRANSMISSION

- NT AERODYNAMIC HEAT TRANSFER
- NT CONDUCTIVE HEAT TRANSFER
- NT CONVECTIVE HEAT TRANSFER
- NT HEAT TRANSFER
- NT HYPERSONIC HEAT TRANSFER
- NT LAMINAR HEAT TRANSFER
- NT RADIATIVE HEAT TRANSFER
- NT SUPERSONIC HEAT TRANSFER
- NT TURBULENT HEAT TRANSFER
- The propagation of thermal radiation in the case of the random refraction of beams in a medium with fluctuating permittivity 04 p0531 A83-15733
- Transport theory of semiconductor energy conversion 04 p0544 A83-16087
- Hot spots of lo 04 p0571 A83-16244
- Apparatus for simultaneous temperature and heat-flow measurements under transient conditions 08 p1106 A83-23235
- The penny-shaped interface crack with heat flow. I - Perfect contact [ASME PAPER 83-APM-10] 10 p1440 A83-26428
- Monopole heat --- generated by elementary particle interactions 13 p1960 A83-31789
- Critical-cone channeling of thermal phonons at a sapphire-metal interface 19 p2903 A83-40954
- Numerical computation of the matrix Riccati equation for heat propagation during Space Shuttle reentry 20 p3041 A83-42550
- Frequency domain analysis of entropy generation through heat flow 24 p3575 A83-48908
- Propagation of heat waves in parametric media 24 p3576 A83-48948
- Heat loss measurements on an enclosure for high temperature batteries 24 p3599 A83-49926

HEAT TREATMENT

- NT ANNEALING
- NT LASER ANNEALING
- NT NITRIDING
- NT PULSE HEATING
- NT STRESS RELIEVING
- NT TEMPERING
- Determining the temperature to which sheets of alloy D16T have been heated from the structure and properties 01 p0025 A83-10445
- Microstructural study of a high-strength stress-corrosion resistant 7075 aluminum alloy 02 p0153 A83-11663
- Comments on 'The influence of Mg contents on the formation and reversion of Guinier-Preston zones in Al-4.5 at percent Zn-xMg alloys' 02 p0154 A83-11671
- A study of the structure and properties of aluminum-magnesium alloys with high magnesium contents after various deformation and heat treatment schedules 02 p0155 A83-12203
- A study of the processes of second phase precipitation in titanium alloy VT30 02 p0155 A83-12204
- Recovery treatment of Al27-1 alloy 03 p0297 A83-13264
- A study of the ordering kinetics of an equiatomic cobalt-platinum alloy using the method of nuclear gamma resonance 03 p0299 A83-14156
- The effect of heat treatment conditions on the fine structure and mechanical properties of titanium alloy VT3-1 03 p0300 A83-14158
- Magnetic changes accompanying the thermal decomposition of nontronite /in air/ and its relevance to Martian mineralogy 04 p0567 A83-15580
- Transport mechanisms for Mg/Zn3P2 junctions 04 p0543 A83-16071
- The effects of heat treatments on the transport properties of Cu/x/S thin films 04 p0543 A83-16083
- Heat-treatment studies on thin-film CdS/Cu/x/S solar cells 04 p0507 A83-16084
- The thermophysical characteristics of two-phase titanium alloys and the optimum heat treatment schedules 05 p0614 A83-16952

- Thermodynamic assessment of heat treatments for a Co-Cr-Mo alloy 05 p0615 A83-17565
- Critical microstructures for microcracking in Al2O3-ZrO2 composites 06 p0733 A83-17954
- The effect of temperature on the spalling fracture of polymer materials 06 p0734 A83-18012
- Characterization and crystallization of Y-Si-Al-O-N glass 06 p0734 A83-18053
- Characteristics of the formation of the structure and properties of refractory niobium-base high alloys 06 p0729 A83-18746
- The aging response of a high-strength P/M aluminum alloy 06 p0731 A83-19091
- Processing effects on microstructure and elevated temperature properties of an ODS Fe-Al-Mo P/M alloy 06 p0732 A83-19099
- The effect of rapid heating on the short-term strength characteristics of 28Kh3SNMVFA and 30KhGSA steels 06 p0733 A83-19311
- The effects of heat treatment and composition on the stress corrosion cracking resistance of Inconel alloy X-750 07 p0884 A83-20255
- Influence of hot isostatic processing and heat treatment variables on the tensile properties of cast Transage 175 alloy, Ti-2.5Al-13V-7Sn-2Zr 07 p0886 A83-20471
- Physicochemical effects of heating gold thin films on gallium arsenide 07 p0882 A83-20591
- IN939 - Metallurgy, properties and performance 07 p0892 A83-21465
- The effect of soaking times on the mechanical properties of rapidly solidified aluminium alloys 07 p0896 A83-21571
- Low rates of fatigue crack growth in beta heat treated titanium alloy 08 p1061 A83-21715
- Fracture toughness of simulated H.A.Z. --- heat affected zone 08 p1061 A83-21728
- The polymorphic alpha-beta transformation in commercial titanium under rapid heating 08 p1066 A83-22055
- A comparison of reducing and oxidizing heat treatments of hot-pressed silicon nitride 08 p1070 A83-22189
- Effect of rate of heating for hardening on the structure of alloys VT23 and VT6 08 p1067 A83-22691
- Recrystallization of nickel alloy KhN62BMKTYu during hot deformation and quenching 08 p1067 A83-22700
- Principles governing texture formation in alloys undergoing phase transitions during various treatments 08 p1068 A83-22782
- Fabrication of cryogenic mirrors 08 p1112 A83-22870
- Al-Si peaked Schottky barriers 08 p1170 A83-22903
- Fine metal fibers as engineering materials 09 p1230 A83-23611
- The influence of metallurgical factors on the fracture toughness of 7010 and 7050 aluminium alloys 09 p1230 A83-23677
- Temperature fields in metals treated with electron beams 09 p1231 A83-23994
- Effect of annealing in buffer gas at 800-1000 C on the mechanical properties of x 10 NiCrAlTi 32 20 type alloys 09 p1233 A83-24138
- The effect of welding and heat treatment on the structure and properties of high-strength titanium alloys 09 p1235 A83-24392
- The effect of heat treatment on hydrogen diffusion and solubility in titanium alloys at room temperature 09 p1235 A83-24393
- Post-weld heat-treatment cracking in superalloys 10 p1393 A83-25407
- Microstructure and tensile ductility in a beta heat treated titanium alloy 10 p1398 A83-26280
- The effect of heat treatment on some properties of electrodeposited nickel and chromium coatings 10 p1399 A83-26896
- The effect of the melt heat treatment time on the properties of lithium lubricants with additives 10 p1401 A83-26921
- The effect of temperature and heat treatment on the fracture toughness of powder-metallurgy tungsten 11 p1549 A83-28482
- Effect of multiple heating at the partial forging of workpieces made of TiAl6V4 12 p1713 A83-29369
- Spall studies of differently treated 2024 Al specimens 13 p1824 A83-31376
- Effect of heat treatment on the bulk diffusion length of EFG ribbon silicon --- Edge-defined Film-fed Growth 14 p2092 A83-32670
- Effect of heat-treatment on the fatigue behavior 15 p2135 A83-33636
- Laser heat treatment - The state of the art 15 p2172 A83-33770
- Investigation and application of high density W-Ni-Fe alloys 15 p2137 A83-33975

- The effect of heat treatment on the structure and long-term strength of the nickel eutectic gamma/gamma-prime-MeC - The length memory effect 15 p2137 A83-34017
- The influence of creep and transformation plasticity in the analysis of stresses due to heat-treatment 15 p2175 A83-34240
- Effect of vacuum-treatment on mechanical properties of W-Ni-Fe heavy alloy 15 p2140 A83-35067
- Nonstationary temperature fields during the heat treatment of titanium disks of complex configurations 16 p2361 A83-35589
- Schottky barrier height variation with metallurgical reactions in aluminum-titanium-gallium arsenide contacts 16 p2419 A83-35671
- Effect of structure on the type of fracture of titanium alloy VT3-1 16 p2330 A83-36025
- Origin of acoustic emission in Al-Zn-Mg alloys. II Copper-containing quaternary alloys 16 p2334 A83-36567
- The effect of heat treatment on the mechanical properties of a mechanically alloyed 2000 series aluminum alloy 17 p2488 A83-37849
- Heat treatment, microstructure and mechanical property correlations in Al-Li-Cu and Al-Li-Mg PM alloys 17 p2489 A83-37850
- Heat treatment, structure and properties of nonferrous alloys --- Book 19 p2822 A83-41465
- Tear test on 7075 and 7475 alloys by use of kahn type specimens 20 p2957 A83-43636
- Relationship between grain boundary segregation and heat-treatment parameters in an aluminium alloy 21 p3111 A83-44338
- Grain-boundary segregation in titanium-vanadium low alloys 23 p3431 A83-47181
- Surface modification of materials by laser irradiation 23 p3467 A83-48427
- Alloying of surface layers during laser treatment 23 p3433 A83-48430
- Experimental investigation of the reflection coefficients of graphites heated in different gaseous media 24 p3569 A83-49119
- Effect of heat treatments on the creep behaviour of a Ni-base single crystal superalloy [ONERA, TP NO. 1983-102] 24 p3561 A83-49413
- The effect of heating on the strength and elasticity of precipitation-hardened molybdenum alloys 24 p3567 A83-49914

HEATING

- NT AERODYNAMIC HEATING
- NT ARC HEATING
- NT ATMOSPHERIC HEATING
- NT BAKING
- NT BASE HEATING
- NT ELECTRON CYCLOTRON HEATING
- NT GAS HEATING
- NT IONOSPHERIC HEATING
- NT KINETIC HEATING
- NT LASER HEATING
- NT PLASMA HEATING
- NT PULSE HEATING
- NT RADIANT HEATING
- NT RADIO FREQUENCY HEATING
- NT RESISTANCE HEATING
- NT SHOCK HEATING
- NT SOLAR HEATING
- NT SPACE HEATING (BUILDINGS)
- NT SUPERHEATING
- NT TRANSIENT HEATING
- NT WATER HEATING
- Adiabatic heating at a dislocation pile-up avalanche 03 p0291 A83-14497
- A universal heat source for active thermal inspection 13 p1860 A83-30837
- On the preferential acceleration and heating of solar wind heavy ions 13 p1964 A83-31226
- Population inversion due to separate shift and heating of light and heavy holes in semiconductors 19 p2905 A83-41174

HEATING EQUIPMENT

- NT BOILERS
- NT EVAPORATORS
- NT FURNACES
- NT IMAGE FURNACES
- NT SOLAR FURNACES
- NT VACUUM FURNACES
- NT VAPORIZERS
- Elevated temperature repairs of advanced composite structures 07 p0877 A83-20499
- A set for the dynamic measurement of the thermophysical properties of materials at high temperatures 07 p0930 A83-20960
- Heating unit for mechanical testing of heat-resistant alloys at high temperatures 08 p1066 A83-22631

f-Chart - Predictions and measurements --- of solar heating systems 09 p1293 A83-23880
Thermodynamics based on the Hahn-Banach theorem - The Clausius inequality 16 p2422 A83-36100
Review of helicopter icing protection systems [AIAA PAPER 83-2529] 23 p3401 A83-48367
Regenerative electric heater of gas for a gasdynamic laser 24 p3588 A83-48937
The effect of the thickness of a protective molybdenum disilicide coating on the maximum operating temperature of heaters 24 p3568 A83-49078

HEAVING

Computer studies of ACV heave performance as a function of vent valve proportional control parameters 15 p2241 A83-33547
Application of system identification flight analysis techniques to the pitch-heave dynamics of an air cushion vehicle 15 p2241 A83-34852
Computer studies of ACV heave performance as a function of vent valve control parameters 15 p2123 A83-34854
Computer studies of ACV heave dynamics stabilization 15 p2243 A83-35055

HEAVY COSMIC RAY PRIMARIES

U HEAVY NUCLEI
U PRIMARY COSMIC RAYS

HEAVY ELEMENTS

NT CALIFORNIUM ISOTOPES
NT PLUTONIUM 238
NT PLUTONIUM 244
Primary nucleosynthesis in the galactic disk 02 p0252 A83-11599
Heavy element fission products on earth --- Russian book 02 p0204 A83-11923
The ages and compositions of old clusters 06 p0840 A83-19283
Absorption-line spectroscopy of close pairs of QSOs 13 p1954 A83-31582
The hypothesis of the preferential acceleration of heavy elements in the cosmic plasma 14 p2116 A83-32544
Magnetorotational collapse of an iron stellar core 15 p2254 A83-33815
Design consideration for tungsten heavy metal [SAWE PAPER 1486] 20 p2957 A83-43753

HEAVY IONS

Heavy O⁺/+ ions in the earth's radiation belt as a possible source of Pc1-2 geomagnetic pulsations 02 p0211 A83-12453
The effect of heavy ions on mammalian cells. I - The cytogenic effects during the irradiation of Chinese hamster cells induced by accelerated ions of helium, carbon, and neon 03 p0377 A83-14884
Radiobiological research in space 04 p0519 A83-15675
Pc 1-2 observations of heavy ion effects by synchronous satellite ATS-6 05 p0664 A83-17779
The effect of heavy ions on mammalian cells. II - The evaluation of the relative biological effectiveness of accelerated ions of helium, carbon, and neon according to cytogenetic parameters 06 p0796 A83-19381
Heavy ions in the outer Kronian magnetosphere --- Saturn 07 p1036 A83-21509
Recent developments in ion mass spectrometers in the energy range below 100 KeV 13 p1813 A83-30752
Heavy ion beam pumped He-Ar laser 13 p1852 A83-31060
On the preferential acceleration and heating of solar wind heavy ions 13 p1964 A83-31226
Preferential perpendicular acceleration of heavy ionospheric ions by interactions with electrostatic hydrogen cyclotron waves 13 p1966 A83-31237
Temporal variations of nucleonic abundances in solar flare energetic particle events. I - Well-connected events 13 p1965 A83-31436
Sputtering of UF₄ by high energy heavy ions 16 p2421 A83-36712
Heavy ion plasmas in the outer magnetosphere 18 p2718 A83-39948
Inactivation, mutation induction and repair in *Bacillus subtilis* spores irradiated with heavy ions 19 p2872 A83-40837
Inactivation probability of heavy ion-irradiated *Bacillus subtilis* spores as a function of the radial distance to the particle's trajectory 19 p2872 A83-40838
Effect of heavy ions on bacterial spores 19 p2872 A83-40839
Heavy ion action on yeast cells - Inhibition of ribosomal-RNA synthesis, loss of colony forming ability and induction of mutants 19 p2872 A83-40840
Results on artemia cysts, lettuce and tobacco seeds in the Biobloc 4 experiment flown aboard the Soviet biosatellite Cosmos 1129 19 p2872 A83-40842
Cataractogenesis from high-LET radiation and the Casarett model 19 p2873 A83-40848

Late skin damage in rabbits and monkeys after exposure to particulate radiations 19 p2873 A83-40849
Heating of heavy ions on auroral field lines 19 p2865 A83-41121
Elastic scattering of heavy ions and the compressibility of nuclear matter 19 p2899 A83-41535
Selective nonresonant acceleration of He-3(2+) and heavy ions by H(+) cyclotron waves --- in solar flares 19 p2925 A83-41657
Generation of Alfvén-ion cyclotron waves on auroral field lines in the presence of heavy ions 20 p3025 A83-43195
Enhanced adhesion from high energy ion irradiation 22 p3365 A83-46703
Effectiveness of HZE-particles onto different biological systems in the Biostack Experiments on Apollo 16, and 17 and on ASTP 23 p3494 A83-47764
Damages of the superhelical structures of nuclear DNA by gamma-rays and heavy ions 23 p3495 A83-48201

HEAVY LIFT AIRSHIPS

Preliminary report on the engineering development of the Magnus Aerospace Corp LTA 20-1 heavy-lift aircraft 22 p3365 A83-28193
Investigation of possible LTA craft application to solve national economy problems 11 p1527 A83-28194
Heavy-lift airship dynamics 12 p1704 A83-29016
Dynamic analysis of the Magnus Aerospace Corporation LTA 20-1 heavy-lift aircraft [AIAA PAPER 83-1977] 17 p2466 A83-38908
A six-degree of freedom heavy lift airship flight simulation [AIAA PAPER 83-1988] 17 p2466 A83-38914
Development of the Magnus Aerospace Corporation's rotating-sphere airship [AIAA PAPER 83-2003] 17 p2466 A83-38922

HEAVY LIFT HELICOPTERS

Warm cycle propulsion for the 1990's heavy lift helicopters 09 p1208 A83-24840

HEAVY LIFT LAUNCH VEHICLES

Prediction of corridor effect from the launching of the satellite power system --- air pollutant concentration into narrow band of latitude 03 p0360 A83-14519

HEAVY NUCLEI

Tracks of heavy and superheavy cosmic nuclei in olivines of extraterrestrial origin 01 p0130 A83-11339
Interaction of the aluminum nucleus with an energy of approximately 1 TeV per nucleon in a photoemulsion 02 p0274 A83-11737
Multiple-nucleon interactions of relativistic heavy nuclei of cosmic rays with Ag and Br nuclei, and characteristics of interactions with a high multiplicity of shower particles in the energy range of 4-400 GeV/nucleon 02 p0274 A83-11739
Samples of the Milky Way --- isotopic abundances in Galactic cosmic rays 03 p0426 A83-14599
Cosmic-ray record in solar system matter 06 p0857 A83-18814
The propagation of ultraheavy cosmic ray nuclei 06 p0858 A83-19297
Heavy particle with long life in cosmic rays above 10 to the 17th eV 12 p1801 A83-29036
Cosmic-ray abundances of Sn, Te, Xe, and Ba nuclei measured on HEAO 3 13 p1953 A83-31446
Search for short-term increases of the flux of heavy cosmic-ray nuclei according to Prognostic-satellite data 14 p2117 A83-33392
On nucleosynthesis in supernovae beyond the iron peak 15 p2254 A83-33716
Steady flow approximations to the helium r-process 15 p2263 A83-34541
The waiting point approximation in R-process calculations --- of astrophysical nucleosynthesis 15 p2263 A83-34542
Extremely high multiplicities in high-energy nucleus-nucleus collisions 17 p2629 A83-37737
Stopping of 200-GeV gold nuclei in nuclear emulsions 18 p2743 A83-40416
Electron capture during gravitational collapse in type II supernovae 19 p2916 A83-41169
Significance of ultraheavy cosmic rays 23 p3539 A83-47738
Detectors of ultraheavy cosmic rays 23 p3455 A83-47754
Measurement of the relative composition of the cosmic-ray iron group with lexan polycarbonate 24 p3676 A83-50163

HEAVY WATER

Absorption spectra of deuterated water at DF laser wavelengths 02 p0211 A83-12601
An analysis of the absorption spectrum of heavy water vapor in the region of 1.06 microns 05 p0684 A83-17694
A comparative study of D₂O oscillators emitting at 385 microns 07 p0938 A83-21598

Backward and forward FIR emission characteristics from D₂O in both Raman and laser regimes 10 p1426 A83-26001
A high energy D₂O submillimeter laser for plasma diagnostics 10 p1431 A83-26648
Numerical analysis of an optically pumped D₂O far infrared laser 16 p2358 A83-35430
A high power D₂O laser optimized for microsecond pulse duration 16 p2358 A83-35431
New pulsed far infrared laser lines in D₂O 16 p2359 A83-35959

HEF (HIGH ENERGY FUELS)**U HIGH ENERGY FUELS****HEIGHT**

SEASAT wave height measurement - A comparison with sea-truth data and a wave forecasting model - Application to the geographic distribution of strong sea states in storms 09 p1319 A83-24302
The maximum possibilities of using information about constant height in an inertial navigation system 15 p2126 A83-34427
Improved cloud motion wind vector and altitude assignment using VAS --- Visible Infrared Spin-Scan Radiometer Atmospheric Sounder 18 p2722 A83-39132
Height measurement by quadrilateration 18 p2674 A83-39252

HEISENBERG THEORY

Method for generating discrete soliton equations. I. II 14 p2080 A83-32517
Quantum theory of laser-radiation scattering by electrons in magnetic fields 24 p3587 A83-48841

HELICAL ANTENNAS

A band-switched resonant quadrifilar helix 01 p0034 A83-11376
Theory of the frequency responses of uniform and quasi-taper helical antennas 01 p0034 A83-11378
Characteristics of modified spiral and helical antennas 02 p0164 A83-12003
Balanced helical antenna with tapered open ends 03 p0307 A83-14130
A ship-borne helical array antenna for maritime satellite communication 06 p0741 A83-18655

HELICAL FLOW

The jet in M87 02 p0250 A83-11580
Helical wave and K-H instability in Type I comet tails. I - Waves of infinitesimal amplitude in incompressible plasma 06 p0832 A83-18850
Helicity and alpha-effect of simple convection cells --- in solar envelope 10 p1520 A83-25378
Helical-flow CO₂ laser 11 p1585 A83-28705
Compressible helicoidal surface theory for propeller aerodynamics and noise 14 p1971 A83-32986
Helical structures, fractal dimensions and renormalization-group approach in homogeneous turbulence 19 p2842 A83-41167

HELICAL INDUCERS

Fluid dynamics of inducers - A review 04 p0478 A83-16137
On the allowance for intrinsic magnetic field in the theory of the shaping of helical relativistic electron beams 09 p1257 A83-25087
Suction performance of high speed cryogenic inducers [AIAA PAPER 83-1387] 16 p2321 A83-36377

HELICAL WINDINGS

Tensile fracture behaviors of helical fiber reinforced composites 03 p0291 A83-13975
A study of the stressed state of a helically reinforced composite in shear 03 p0343 A83-14740
Fracture behavior and toughness of helical fiber reinforced composite metals 18 p2667 A83-40265
Electromagnetic-wave propagation in a conducting waveguide loaded with a tape helix 24 p3572 A83-48963

HELICOPTER ATTITUDE INDICATORS

U ATTITUDE INDICATORS
U HELICOPTERS

HELICOPTER CONTROL

Attempt to determine the power demand of a helicopter control system on the basis of flight tests 01 p0012 A83-10439
A concept for reducing helicopter IFR landing weather minimums - Offshore 02 p0133 A83-12099
Individual blade control independent of a swashplate 04 p0446 A83-16027
Wind tunnel results showing rotor vibratory loads reduction using higher harmonic blade pitch 06 p0719 A83-18385
Identification of certain dynamic characteristics of a helicopter-autopilot system by means of simulation 08 p1047 A83-23222
Multivariable stability margins for vehicle flight control systems 09 p1210 A83-24815
Microprocessor-based optimal controllers for a helicopter turret control system 15 p2122 A83-35138

- Helicopter IFR approaches into major terminals using RNAV, MLS, and CDTI 19 p2794 A83-41042
- Effects of rotor inertia and rpm control on helicopter handling qualities [AIAA PAPER 83-2070] 19 p2805 A83-41907
- On approximating higher-order rotor dynamics in helicopter stability-derivative models [AIAA PAPER 83-2088] 19 p2805 A83-41920
- Output feedback pole assignment under system variation --- with CH-46 example 21 p3195 A83-44948
- Ground simulation investigation of helicopter decelerating instrument approaches 21 p3090 A83-45461
- Helicopter avionic systems certification 22 p3255 A83-45849
- Coherent, single-mode fiber optic for multifunction 10.6 micron helicopter avionics system 22 p3359 A83-46639
- A new approach to fault-tolerant helicopter swashplate control [AIAA PAPER 83-2485] 23 p3412 A83-48345
- Evaluation of control and display configurations for helicopter shipboard operations [AIAA PAPER 83-2486] 23 p3405 A83-48346
- NOTAR - The viable alternative to a tail rotor [AIAA PAPER 83-2527] 23 p3404 A83-48365
- ### HELICOPTER DESIGN
- Helicopter blade tips [AAAF PAPER NT 81-19] 02 p0132 A83-11778
- Military potential of the ABC 02 p0134 A83-12097
- The UH-60A Black Hawk - A world-wide force multiplier 02 p0135 A83-12934
- Helicopter rotor performance evaluation using oscillatory airfoil data 03 p0278 A83-13172
- Fail-safe optimal design of complex structures with substructures 03 p0339 A83-13490
- Principles of helicopter design and construction --- Serbo-Croatian book 03 p0281 A83-14042
- Helicopter vibration reduction by local structural modification 04 p0500 A83-16028
- Helicopter technology for the 1990s 04 p0446 A83-16372
- Ames expands rotorcraft capability 06 p0719 A83-18273
- Evolution of the application of composite materials to helicopters 06 p0716 A83-18376
- Composite technology in the UK helicopter industry 06 p0716 A83-18377
- Helicopter evolution 06 p0711 A83-18384
- An investigation of the aerodynamics of an RAE swept tip using a model rotor [ONERA, TP NO. 1982-76] 06 p0712 A83-18426
- Lowering of the first blade number harmonic cell vibrations of a helicopter by reduction of rotor blade retention forces via appropriate bending-torsion coupling of the rotor blade --- German thesis 06 p0714 A83-19619
- The Hummercraft 07 p0866 A83-21033
- Will technology make the helicopter competitive 07 p0866 A83-21574
- Studies on an acceleration platform and at the time of a simulated crash of helicopter antirash seats 08 p1043 A83-22976
- Development of the basic methods needed to predict helicopters' aeroelastic behaviour [ONERA, TP NO. 1982-75] 08 p1124 A83-23248
- Developmental trends in helicopter design [DGLR PAPER 82-065] 09 p1203 A83-24179
- An approach to helicopter power selection 09 p1207 A83-24828
- Developments in the design, analysis, and fabrication of advanced technology transmission elements 09 p1274 A83-24832
- Design of an advanced 500-HP helicopter transmission 09 p1208 A83-24834
- Development of a variable-load energy absorber --- for helicopter seats 10 p1373 A83-25896
- Theoretical study on the design of low noise rotor blade section 10 p1478 A83-26966
- Helicopter flight noise tests about the influence of rotor-rotational and forward speed changes on the characteristics of the imitted sound [AIAA PAPER 83-0672] 11 p1650 A83-28002
- Design, analysis and test of composite curved frames for helicopter fuselage structure [AIAA 83-1005] 12 p1741 A83-29805
- Aeroelastic tailoring of rotor blades for vibration reduction in forward flight [AIAA 83-0916] 12 p1701 A83-29844
- Identification of helicopter rotor dynamic models [AIAA 83-0988] 12 p1702 A83-29866
- A discretized asymptotic method for unsteady helicopter rotor airloads [AIAA 83-0989] 12 p1697 A83-29867
- Rotorshaft torqueometer --- to increase helicopter performance 13 p1807 A83-30174
- Development of two airfoil sections for helicopter rotor blades 13 p1805 A83-31623
- The helicopter preliminary design process 13 p1806 A83-31812
- Composite materials applications in the manufacture of helicopters - Design and problems of helicopters 14 p1974 A83-31822
- Apache on the war path - The Hughes AH-64 in production at last 14 p1974 A83-31939
- Boeing Vertol - The leading edge of technology 14 p1969 A83-33095
- Higher harmonic control for the jet smooth ride 14 p1977 A83-33096
- Smooth and simple - The Bell Model 680 bearingless main rotor 14 p1975 A83-33098
- The fenestron on a helicopter [AAAF PAPER NT 82-18] 14 p1976 A83-33169
- A tubular braided composite main rotor blade spar 16 p2299 A83-35949
- Evaluation of the effect of voids in composite main rotor blades 16 p2299 A83-35950
- The super stallion --- CH-53E helicopter design features 16 p2299 A83-36075
- The Ka-26 helicopter --- Russian book 16 p2300 A83-36448
- Super choppers --- helicopters with counter rotating rotors 17 p2465 A83-38700
- DFVLR research on helicopter noise 18 p2631 A83-39346
- The dynamics of a helicopter rotor structure 18 p2639 A83-39485
- New insights in structural design of composite rotor blades for helicopters 18 p2640 A83-40287
- Blade design for reduced helicopter vibration 19 p2797 A83-41076
- Investigations of hingeless rotor stability 20 p2933 A83-43674
- The impact of missions on the preliminary design of an ABC rotor [SAWE PAPER 1501] 20 p2935 A83-43760
- Composite helicopter structure tested for crashworthiness 21 p3091 A83-44875
- Consideration on the fatigue damage of specimens used for composite critical components qualification 22 p3305 A83-46307
- Kaman's new directions --- helicopter development 22 p3247 A83-46925
- Research and development of helicopters in Europe 22 p3255 A83-46929
- Hingeless and bearingless main rotor in a fiber composite type of construction for dynamic systems of future helicopters 23 p3402 A83-47195
- The system ARIS and its employment in the development of future helicopters 23 p3402 A83-47196
- Studies and designs for a new helicopter cockpit 23 p3402 A83-47210
- Design of glass-faced helicopter windshields for survival in a particle impact environment [AIAA PAPER 83-2439] 23 p3403 A83-48328
- Application of composites and computer graphics in the design of the MH-53E fuel sponson [AIAA PAPER 83-2441] 23 p3403 A83-48329
- A conceptual design program for educational purposes [AIAA PAPER 83-2473] 23 p3403 A83-48339
- Formulation of a helicopter preliminary design course [AIAA PAPER 83-2521] 23 p3404 A83-48363
- NOTAR - The viable alternative to a tail rotor [AIAA PAPER 83-2527] 23 p3404 A83-48365
- Design and technology influences - 'Maturity' at introduction of the 214ST [AIAA PAPER 83-2528] 23 p3404 A83-48366
- Review of helicopter icing protection systems [AIAA PAPER 83-2529] 23 p3401 A83-48367
- Optimal controller design for a helicopter using its lower order dynamic model [AIAA PAPER 83-2550] 23 p3412 A83-48371
- LHX - The US Army wants 5,000 - Industry needs the business 23 p3405 A83-48642
- Transonic effects on helicopter rotor blades 24 p3544 A83-49178
- The effect of damage in structural elements on the ground resonance of a helicopter 24 p3547 A83-49446
- Developments in UK rotor blade technology [AIAA PAPER 83-2525] 24 p3548 A83-49589
- Commonality potential of future public service helicopters and Army light utility helicopters [AIAA PAPER 83-2553] 24 p3546 A83-49593
- Force-transmitting structures in blades for helicopter rotors, wind-tunnel blowers, and wind turbines [DGLR PAPER 82-013] 24 p3597 A83-50138
- Parametric tip effects for conformable rotor applications 24 p3548 A83-50140
- ### HELICOPTER ENGINES
- Engine technology for the next decade 02 p0136 A83-12098
- A mathematical model for a turboshaft gas-turbine engine with an optimum control program for high-level computer-aided design 09 p1205 A83-23436
- Regenerative shaft engines for helicopters, multipurpose and feeder service aircraft [DGLR PAPER 82-087] 09 p1207 A83-24199
- Recent developments in digital control for helicopter powerplants 09 p1207 A83-24829
- FAA approved S-76A in-flight power assurance and trending procedure 09 p1207 A83-24830
- Helicopter engine development - New standards for the '80s 09 p1208 A83-24837
- Full-flow debris monitoring and fine filtration for helicopter propulsion systems 09 p1208 A83-24838
- Technical qualities for combat helicopter powerplants 09 p1208 A83-24839
- Composite engine inlet particle separator swirl frame --- CAD for T700 helicopter engine centrifugal filter 09 p1208 A83-24841
- The T700-GE-700 engine experience in sand environment 09 p1208 A83-24842
- The super stallion --- CH-53E helicopter design features 16 p2299 A83-36075
- Accelerated simulated mission endurance test of a turboshaft engine for military attack helicopter application [AIAA PAPER 83-1359] 16 p2309 A83-36357
- The feasibility of water injection into the turbine coolant to permit gas turbine contingency power for helicopter application [ASME PAPER 83-GT-66] 18 p2642 A83-39993
- Status report - DARPA/NASA convertible turbofan/turboshaft engine program [ASME PAPER 83-GT-196] 23 p3410 A83-48000
- ### HELICOPTER PERFORMANCE
- Multifunction CO2 NOE sensor - A status report --- Nap-Of-the-Earth 01 p0010 A83-11147
- Helicopter blade tips [AAAF PAPER NT 81-19] 02 p0132 A83-11778
- Military potential of the ABC 02 p0134 A83-12097
- Reliability and maintainability aspects of a 'fleet' of prototype helicopters 02 p0131 A83-12654
- The UH-60A Black Hawk - A world-wide force multiplier 02 p0135 A83-12934
- A note on the general scaling of helicopter blade-vortex interaction noise [ONERA, TP NO. 1982-32] 03 p0391 A83-13375
- Operation of a helicopter on sloping ground. I 03 p0280 A83-14618
- Operation of a helicopter on sloping ground. II 03 p0280 A83-14624
- Mission specific survival equipment for helicopter aircrew 04 p0525 A83-15426
- Studies of aerofoils and blade tips for helicopters 05 p0589 A83-17317
- XH-59A ABC aircraft flight tests at Ft. Rucker, Alabama 06 p0716 A83-18148
- A simulation model for the analysis of the dynamic behavior of a helicopter rotor under nonstationary limit flight conditions 08 p1044 A83-23220
- Acoustic measurements of a full-scale coaxial helicopter [AIAA PAPER 83-0722] 10 p1375 A83-25933
- Performance of a Strapdown Ring Laser Gyro Tetrad Inertial Navigation System in a helicopter flight environment 11 p1528 A83-28781
- FAA helicopter NAVSTAR GPS flight testing 11 p1529 A83-28788
- Helicopter flight testing, simulation and real-time analysis 12 p1701 A83-29391
- Rotor-vortex interaction noise [AIAA PAPER 83-0720] 12 p1777 A83-29950
- Boeing Vertol - The leading edge of technology 14 p1969 A83-33095
- The Ka-26 helicopter --- Russian book 16 p2300 A83-36448
- Analytical and experimental investigation of a bearingless hub-absorber 19 p2797 A83-41077
- The effects of engine and height-control characteristics on helicopter handling qualities 19 p2802 A83-41078
- LHX system design for improved performance and affordability --- Light Helicopter 19 p2797 A83-41080
- Optimal short range trajectories for helicopters [AIAA PAPER 83-2140] 19 p2799 A83-41962
- The impact of missions on the preliminary design of an ABC rotor [SAWE PAPER 1501] 20 p2935 A83-43760

HELICOPTER PROPELLER DRIVE

- The tasks and organization of the flight testing of airplanes and helicopters --- Russian book 21 p3091 A83-43901
- Helicopter noise [ONERA, TP NO. 1983-80] 23 p3506 A83-48195
- HELICOPTER PROPELLER DRIVE**
- Developments in the design, analysis, and fabrication of advanced technology transmission elements 09 p1274 A83-24832
- Report on advanced transmission system integration tests --- of Blackhawk helicopters 09 p1274 A83-24833
- In-flight computation of helicopter transmission fatigue life expenditure 16 p2301 A83-36921
- HELICOPTER ROTORS**
- U ROTARY WINGS**
- HELICOPTER TAIL ROTORS**
- Wind tunnel results showing rotor vibratory loads reduction using higher harmonic blade pitch 06 p0719 A83-18385
- Fault Detection/Location System for intermediate and tail rotor gearboxes 09 p1274 A83-24835
- A study of helicopter rotor noise, with special reference to tail rotors, using an acoustic wind tunnel 12 p1777 A83-29403
- Keeled rotors for diffusion by a captive vortex [AAAF PAPER NT 82-17] 14 p1972 A83-33168
- The fenestron on a helicopter [AAAF PAPER NT 82-18] 14 p1976 A83-33169
- A jointless and bearingless tail rotor of fiber-reinforced-composite construction 23 p3402 A83-47215
- HELICOPTER WAKES**
- Vortex theory for hovering rotors 03 p0278 A83-13144
- Momentum theory, dynamic inflow, and the vortex-ring state 04 p0443 A83-16026
- Rotor hovering performance using the method of fast free wake analysis 08 p1042 A83-22162
- Obscuration by helicopter-produced snow clouds 08 p1043 A83-22357
- The structure of trailing vortices generated by model rotor blades 12 p1696 A83-29404
- Navier-Stokes calculations for the vortex wake of a rotor in hover [AIAA PAPER 83-1676] 17 p2444 A83-37184
- The use of actuator-disc dynamic inflow for helicopter flap-lag stability 19 p2797 A83-41081
- HELICOPTERS**
- NT AH-1G HELICOPTER
- NT AH-64 HELICOPTER
- NT BO-105 HELICOPTER
- NT CH-46 HELICOPTER
- NT CH-47 HELICOPTER
- NT H-53 HELICOPTER
- NT H-60 HELICOPTER
- NT HEAVY LIFT HELICOPTERS
- NT MILITARY HELICOPTERS
- NT OH-58 HELICOPTER
- NT UH-1 HELICOPTER
- Reliability model for planetary gear trains [ASME PAPER 82-DET-81] 02 p0187 A83-12777
- Helmet mounted display symbology for helicopter landing on small ships 04 p0448 A83-16134
- The peculiarities of medical support for helicopter flights 05 p0675 A83-17698
- Helicopter icing - Testing and certification 06 p0716 A83-18381
- A concept for reducing helicopter IFR landing weather minimums - Onshore 07 p0865 A83-21034
- Equivalent G/E of helicopter rotor blades --- shear modulus to Young's modulus ratio 08 p1122 A83-22151
- Finite difference modeling of rotor flows including wake effects [ONERA, TP NO. 1982-114] 09 p1197 A83-24326
- Wind tunnel study of icing and de-icing on oscillating rotor blades [ONERA, TP NO. 1982-116] 09 p1199 A83-24327
- Flight testing with hot JP-4 fuel --- in helicopter suction fuel systems 09 p1208 A83-24831
- How to get a grip on TADS/PNVS --- Target Acquisition Detection System/Pilot's Night Vision System 10 p1459 A83-26316
- A physiological and hygienic evaluation of vibration in the cabin of the Mi-4 helicopter 14 p2073 A83-33325
- The spine and the helicopter 16 p2397 A83-35582
- Spectral decontamination of a real-time helicopter simulation [AIAA PAPER 83-1087] 16 p2299 A83-36211
- Microprocessor controlled optimal helicopter turret control system 17 p2462 A83-37148
- Offshore helicopter operations - Gulf of Mexico [SAE PAPER 821366] 17 p2459 A83-37960

- Helicopter IFR - The economics of schedule regularity [SAE PAPER 821501] 17 p2459 A83-38009
- The integration of multiple avionic sensors and technologies for future military helicopters 18 p2639 A83-40301
- Assessment of rotor-fuselage coupling on vibration predictions using a simple finite element model 19 p2857 A83-41075
- FAA rotorcraft icing regulations and directions 22 p3251 A83-46927
- The emerging need for improved helicopter navigation 22 p3252 A83-46930
- Technology transfer from the aircraft sector to other sectors as exemplified by helicopter technology 23 p3391 A83-47190

HELIOCENTRIC ORBITS

U SOLAR ORBITS

HELIOGRAPHS

U SPECTROHELIOGRAPHS

HELIOGRAPHY

U SPECTROHELIOGRAPHS

HELIOGRAPHY

U SPECTROHELIOGRAPHS

HELIOGRAPHY

U SPECTROHELIOGRAPHS

HELIOGRAPHY

U SPECTROHELIOGRAPHS

HELIOGRAPHY

U SPECTROHELIOGRAPHS

HELIOGRAPHY

U SPECTROHELIOGRAPHS

HELIOGRAPHY

U SPECTROHELIOGRAPHS

HELIOGRAPHY

U SPECTROHELIOGRAPHS

HELIOGRAPHY

U SPECTROHELIOGRAPHS

HELIOGRAPHY

U SPECTROHELIOGRAPHS

HELIOGRAPHY

U SPECTROHELIOGRAPHS

HELIOGRAPHY

U SPECTROHELIOGRAPHS

HELIOGRAPHY

U SPECTROHELIOGRAPHS

HELIOGRAPHY

U SPECTROHELIOGRAPHS

HELIOGRAPHY

U SPECTROHELIOGRAPHS

HELIOGRAPHY

U SPECTROHELIOGRAPHS

HELIOGRAPHY

U SPECTROHELIOGRAPHS

HELIOGRAPHY

U SPECTROHELIOGRAPHS

HELIOGRAPHY

U SPECTROHELIOGRAPHS

HELIOGRAPHY

U SPECTROHELIOGRAPHS

HELIOGRAPHY

U SPECTROHELIOGRAPHS

HELIOGRAPHY

U SPECTROHELIOGRAPHS

HELIOGRAPHY

U SPECTROHELIOGRAPHS

HELIOGRAPHY

U SPECTROHELIOGRAPHS

HELIOGRAPHY

U SPECTROHELIOGRAPHS

HELIOGRAPHY

U SPECTROHELIOGRAPHS

HELIOGRAPHY

U SPECTROHELIOGRAPHS

HELIOGRAPHY

U SPECTROHELIOGRAPHS

HELIOGRAPHY

U SPECTROHELIOGRAPHS

HELIOGRAPHY

U SPECTROHELIOGRAPHS

HELIOGRAPHY

U SPECTROHELIOGRAPHS

HELIOGRAPHY

U SPECTROHELIOGRAPHS

HELIOGRAPHY

U SPECTROHELIOGRAPHS

HELIOGRAPHY

U SPECTROHELIOGRAPHS

HELIOGRAPHY

U SPECTROHELIOGRAPHS

HELIOGRAPHY

U SPECTROHELIOGRAPHS

HELIOGRAPHY

U SPECTROHELIOGRAPHS

HELIOGRAPHY

U SPECTROHELIOGRAPHS

HELIOGRAPHY

U SPECTROHELIOGRAPHS

HELIOGRAPHY

U SPECTROHELIOGRAPHS

HELIOGRAPHY

U SPECTROHELIOGRAPHS

HELIOGRAPHY

U SPECTROHELIOGRAPHS

HELIOGRAPHY

HELIOSTATS

- A methodology of evaluation and design of fields of focusing heliostats --- French thesis 02 p0201 A83-11768
- Determination of the interference between the elements of a central-receiver solar system 02 p0201 A83-11848
- Automatic methods for the adjustment of faceted solar-energy concentrators and heliostats 04 p0503 A83-15131
- Investigation of the equations of motion of the heliostats of a tower-type solar electric power plant 04 p0503 A83-15133
- Prospects for the construction of solar furnaces for industry 06 p0781 A83-19236
- Radiation heat exchange in a solar cavity-type receiver at various times 07 p0953 A83-20138
- Area utilization efficiency of a sloping heliostat system for solar concentration 08 p1130 A83-22618
- Design, fabrication, and initial testing of solar one receiver 11 p1606 A83-27229
- Solar thermionic energy converter experiment 11 p1608 A83-27301

HELIPORTS

- All weather heliports and airway system - The future need 16 p2312 A83-36073

HELIUM

- NT HELIUM ATOMS
- NT HELIUM IONS
- NT HELIUM ISOTOPES
- NT LIQUID HELIUM
- NT LIQUID HELIUM 2
- The Crab Nebula's progenitor 02 p0253 A83-11623
- Absorption at 10 micron in CO₂-He and CO₂-N₂ mixtures at elevated temperatures 03 p0392 A83-13497
- The era of superheavy-particle dominance and big bang nucleosynthesis 03 p0439 A83-13653
- He I lines in B stars - Comparison of non-local thermodynamic equilibrium models with observations 03 p0424 A83-14200
- Operating efficiencies in pulsed carbon dioxide lasers 03 p0333 A83-14934
- Metastable atom density in helium, neon, and argon glow discharges 04 p0538 A83-16059
- The helium 10830 A line in early-type stars - An atlas of Fabry-Perot scans 05 p0698 A83-17003
- Tests of vacuum vs helium in a solar telescope 06 p0818 A83-18577
- Propagation effects in the hydrogen-to-helium ratio in the solar cosmic rays 06 p0856 A83-19170
- Evolutionary effects of helium diffusion in population II stars 06 p0840 A83-19286
- Explosive helium burning in supernovae - A source of r-process elements 07 p1022 A83-21140
- New technique for measurement of upper laser level decay rates in gas laser plasmas 07 p0938 A83-21597
- Scattering of thermal He beams by crossed atomic and molecular beams. V - Anisotropic intermolecular potentials for He + CO₂, N₂O, C₂N₂ 08 p1163 A83-22215
- Helium purge flow prevention of atmospheric contamination of cryogenically cooled optics on orbiting infrared telescopes 08 p1074 A83-22723
- M dependence in the analysis of NH₃-He microwave double resonance experiments 09 p1343 A83-25133
- Chemical separation in horizontal-branch stars 10 p1514 A83-26727
- A single mode /F₂+/-asterisk color-center laser for application in optical pumping of helium 11 p1578 A83-27543
- A new method for determining the helium abundance in the solar atmosphere /Invited Review/ 11 p1689 A83-27642
- Cosmological implications of helium and deuterium abundances on Jupiter and Saturn 11 p1686 A83-28388
- Calculation of drag and heat transfer for viscous quasi-stabilized flow of supercritical helium in a pipe 11 p1570 A83-28552
- The third virial coefficient for nonpolar gases and their mixtures 11 p1665 A83-28559
- Helium abundance variations in the solar wind [AD-A129760] 13 p1964 A83-29991
- Pressure broadening of CO infrared lines perturbed by H₂ and He 13 p1916 A83-30968
- Thermal conductivity of yttrium oxide in the temperature range 400-2100 C in different gaseous media 13 p1826 A83-31468
- Helium cyclotron emission from accreting magnetized neutron stars 13 p1958 A83-31726
- Non-LTE analysis of subliminous O-star. V - The binary system HD 128220 13 p1959- A83-31745
- Explosive helium burning at constant pressures 17 p2598 A83-37352

- The galactic globular cluster system - Helium content versus metallicity 17 p2609 A83-38424
- Measurement of helium gas transmission through aerostat material [AIAA PAPER 83-1986] 17 p2483 A83-38913
- Primordial nucleosynthesis and scale-covariant cosmology 18 p2774 A83-39736
- Balmer-alpha and Balmer-beta emission cross sections for low-energy H collisions with He and H₂ 18 p2743 A83-40408
- Search for Wolf-Rayet features in the spectra of giant HII regions. I - Observations in NGC 300, NGC 604, NGC 5457 and He2-10 19 p2910 A83-41066
- He D3 as a diagnostic for the hard and soft X-rays from solar flares 20 p3081 A83-43074
- Can population III stars generate primordial helium? 20 p3075 A83-43538
- Noise of He-Cd laser and its suppression 21 p3143 A83-44156
- The helium abundance and the isotropy of the universe 21 p3234 A83-44766
- A He-Sr laser with a mean power of 3 W 21 p3147 A83-45504
- Photon and helium energy spectra above 1 TeV for primary cosmic rays 21 p3246 A83-45575
- The solar O III spectrum. II - Longer wavelengths, line widths, and the He II Lyman alpha radiation field 22 p3388 A83-46263
- Secondary ionisation processes in laser-induced cascade ionisation 24 p3627 A83-49837
- ESO Workshop on Primordial Helium, Garching, West Germany, February 2, 3, 1983, Proceedings 24 p3664 A83-50030
- The primordial helium abundance and the age of the universe 24 p3665 A83-50034
- The stellar processing of helium 24 p3665 A83-50039
- Helium production by low and intermediate mass stars 24 p3665 A83-50040
- The protosolar helium abundance 24 p3675 A83-50041
- Helium and deuterium in the outer solar system 24 p3665 A83-50042
- Helium abundances from young stars and open clusters 24 p3666 A83-50043
- The helium abundance of halo dwarfs 24 p3666 A83-50044
- Observational evidence for helium production in stars - The helium abundance of hot subdwarfs, central stars of planetary nebulae, very massive O-stars and OBN-stars 24 p3666 A83-50045
- The helium abundances of G-K main sequence halo and disk stars, the helium galactic abundance evolution and the astrometric satellite Hipparcos 24 p3666 A83-50046
- Primordial helium in galactic globular clusters 24 p3666 A83-50047
- Globular cluster colour-magnitude diagrams - Possible evidence for helium abundance variations 24 p3666 A83-50048
- Helium content in globular clusters - The R-method 24 p3666 A83-50049
- Helium abundances in globular star clusters 24 p3666 A83-50050
- Galactic helium and stellar population colors 24 p3666 A83-50051
- Helium in supernova remnants 24 p3666 A83-50052
- Determining helium abundances in H II regions 24 p3666 A83-50053
- On the pregalactic He/H abundance ratio derived from planetary nebulae 24 p3667 A83-50054
- Calculation of stellar structure. III - Solar models that satisfy the necessary conditions for a unique solution to the stellar structure equations 24 p3675 A83-50091
- HELIUM AFTERGLOW**
- Helium radiation diffusion in prominences 06 p0855 A83-19135
- The energy of thermal electrons in electron beam created helium discharges 17 p2583 A83-38965
- HELIUM ATOMS**
- Energy loss of slowly moving magnetic monopoles in matter 08 p1192 A83-22640
- Helium atoms in the interstellar and interplanetary medium. I - Prognoz-5 and Prognoz-6 satellite observations of scattered ultraviolet radiation in the H I 1216 Å and He I 584 Å lines 09 p1364 A83-25036
- Observation and quasistatic analysis of structure in microwave ionization of highly excited helium atoms 13 p1915 A83-30597
- Rotational and vibrational-rotational relaxation in collisions of CO₂(01¹/0) with He atoms 13 p1916 A83-30953
- Quantized evaporation from liquid helium 20 p3044 A83-42167

HELIUM COMPOUNDS

A spectroscopic study of the translation of predissociations of the molecular ions HeH⁺(+) and N₂⁺(+) and of dissociations of N₂⁺(+) and NO⁺(+) ions by collision with an atomic target --- French thesis 21 p3202 A83-45085

HELIUM HYDROGEN ATMOSPHERES

Radiative heat transfer near the stagnation point of a blunt body with an intensely vaporizing surface in the three-dimensional hypersonic flow of a hydrogen-helium mixture 06 p0712 A83-18357

The hydrogen to helium ratio in Jupiter and Saturn 06 p0849 A83-19465

Experimental study of the pure rotational S1 line of the H₂-He spectrum induced by an absorption defect collision due to collisional interference effects 12 p1778 A83-29390

Ablation of carbonaceous materials in a hydrogen-helium arc-jet flow [AIAA PAPER 83-1561] 14 p1998 A83-32778

The spectra of Wolf-Rayet stars. I - Optical line strengths and the hydrogen-to-helium ratios in WN type stars 14 p2105 A83-33201

Effect of variations of opacity and helium-hydrogen ratio on pulsational instability 15 p2263 A83-34548

The interiors of the giant planets - 1983 16 p2439 A83-36789

Statistical mechanics of light elements at high pressure. V Three-dimensional Thomas-Fermi-Dirac theory --- relevant to Jovian planetary interiors 21 p3242 A83-45563

Hydrogen and helium ionization structure of gaseous nebulae 24 p3671 A83-50170

HELIUM IONS

Depth distributions and range parameters for He implanted in Si and GaAs 02 p0242 A83-12283

Helium resonance and dispersion effects on geostationary Alfvén/ion cyclotron waves 02 p0207 A83-12384

Dielectronic satellite spectra for highly-charged helium-like ions. VII - Calcium spectra: Theory and comparison with SMM observations 03 p0420 A83-13948

On the systematics of line ratios along the helium isoelectronic sequence 04 p0554 A83-15645

Excitation of atoms by collisions with ions - Photon-ion angle correlation measurements for determining the scattering amplitudes in magnetic substates for He⁺/+ + He and He⁺/+ + Ne systems --- German thesis 06 p0808 A83-18524

2P⁰/ resonances in He⁻/ 06 p0808 A83-19004

Binary encounter calculations for electron capture from noble gases by He²⁺/ 08 p1167 A83-21987

Measurement of the 1s2p2p-prime 4Pe resonance in He⁻/ photodetachment 08 p1163 A83-22644

Theory of cosmic ray spectra 13 p1966 A83-30423

Observation and quasistatic analysis of structure in microwave ionization of highly excited helium atoms 13 p1915 A83-30597

Channeling contrast microscopy - Application to semiconductor structures 13 p1929 A83-31067

The volumes of He⁺(+) and H⁺(+) in H II regions - The Orion Nebula 15 p2263 A83-34551

Energy and charge distribution of energetic helium ions in the outer radiation belt of the earth 18 p2787 A83-39954

The helium-iodine laser 18 p2694 A83-40664

Selective nonresonant acceleration of He-3(2+) and heavy ions by H⁺(+) cyclotron waves --- in solar flares 19 p2925 A83-41657

Mobilities of various mass-identified positive ions in helium, neon, and argon 20 p2950 A83-42637

Frequency gap formation in electromagnetic cyclotron wave distributions --- in magnetosphere 20 p3025 A83-43193

Observation of the ion composition by Ionosphere Sounding Satellite 21 p3178 A83-45457

Large-scale counterstreaming of H⁺(+) and He⁺(+) along plasmaspheric flux tubes 22 p3335 A83-47051

Characteristics of thermal and suprathermal ions associated with the dayside plasma trough as measured by the dynamics explorer retarding ion mass spectrometer 22 p3335 A83-47053

Primordial helium abundance determinations using galactic H II regions 24 p3667 A83-50056

Pregalactic helium abundance determination from extragalactic H II regions 24 p3667 A83-50057

HELIUM ISOTOPES

Fluxes of electromagnetic radiation, energetic particles, and solar wind from the region of a helium-3-rich flare 02 p0269 A83-11718

Statistical mechanics of dilute liquid mixtures of He³ in He⁴ 05 p0691 A83-17228

The effect of heavy ions on mammalian cells. II - The evaluation of the relative biological effectiveness of accelerated ions of helium, carbon, and neon according to cytogenetic parameters 06 p0796 A83-19381

Primitive helium in diamonds 08 p1136 A83-22687

Selective acceleration of He-3 in solar flare particles by radiation pressure 10 p1521 A83-25731

Helium on Venus - Implications for uranium and thorium 12 p1797 A83-28924

Cooling liquid He-3 to around 100 micro-K 14 p1999 A83-31921

Noble gas constraints on the layered structure of the mantle 14 p2051 A83-31922

A helium-3 cooled bolometer system for one millimeter continuum observations 17 p2510 A83-37751

Constraints on evolution of earth's mantle from rare gas systematics 17 p2545 A83-38598

Dynamics of the textures of the order parameter in superfluid He-3 19 p2904 A83-40996

The breakdown of nuclear quasi-equilibrium in highly compact binaries and the origin of the 2-3 hour gap in the orbital period distribution of cataclysmic variables 19 p2921 A83-41653

The rate of the He-3(p,e+ nu) - He-4 reaction --- source of high energy solar neutrinos 21 p3244 A83-45564

Neutrinos, the He-4 abundance, and stellar evolution 24 p3665 A83-50033

He-4 determinations from radio recombination lines --- of interstellar matter 24 p3667 A83-50055

Detection of the 3.46 cm line of interstellar He-3(+) (He-3(+) / H(+)) ratios 24 p3667 A83-50062

HELIUM PLASMA

A laser-based measurement of electron collision rates for excited states of ionised helium in a plasma 03 p0398 A83-14662

A high-current magnetically stabilized plasma column for fast current-reversal and penetration studies 04 p0538 A83-16062

High-power microwave energy coupling to nitrogen during breakdown 07 p0997 A83-20731

Steady flow approximations to the helium r-process 15 p2263 A83-34541

Stark-shifts of the He II spectral lines 20 p3049 A83-42340

Plasma electron density measurements by the laser- and collision-induced fluorescence method 24 p3631 A83-48819

Energy distribution functions of electrons in low-temperature helium-neon plasma at low pressures 24 p3632 A83-49113

HELIUM STARS

U B STARS

HELIUM 2

U HELIUM ISOTOPES

U LIQUID HELIUM

HELIUM 3

U HELIUM ISOTOPES

HELIUM 4

U HELIUM ISOTOPES

HELIUM-NEON LASERS

Experimental study of the frequency characteristics of gas ring lasers with additional feedback 01 p0056 A83-11344

Laser schlieren microphone for optoacoustic spectroscopy 02 p0178 A83-12600

Influence of an axial magnetic field on the frequency shifts in a two-mode He-Ne/CH₄ laser 03 p0331 A83-13589

The stimulating effect of a helium-neon laser in acute inflammatory processes of the eye 03 p0378 A83-13603

The effect of helium-neon laser irradiation on the membranes of the retina 03 p0374 A83-13610

Treatment of degenerative-dystrophic diseases of the vertebral column by a helium-neon laser 03 p0381 A83-14341

Spectrum control of laser radiation by means of linear phase anisotropy, induced in an amplifying or absorbing medium by an external magnetic field 04 p0484 A83-15268

He-Ne laser generation of 1.15-1.20 microns in a hollow copper cathode 04 p0485 A83-15950

Opto-optical modulation in N-/p-methoxybenzylidene/p-butylaniline 05 p0647 A83-16833

An investigation of the dislocation density of a wave front in light fields having a speckle structure 05 p0647 A83-16889

Investigation of the mode competition in an He-Ne/CH₄ laser with independent variation of the mode spacing and spatial shift 05 p0648 A83-17046

Two-frequency helium-neon laser in a transverse magnetic field 05 p0650 A83-17078

Measurement of time dependent optical gain using frequency modulation spectroscopy 06 p0763 A83-18955

Determination of grain boundary barrier height and interface states by a focused laser beam
07 p0999 A83-19992

Development of a two-directional seam tracking system with laser sensor
07 p0940 A83-20524

Direct frequency measurements of transitions at 520 THz /576 nm/ in iodine and 260 THz /1.15 micron/ in neon
08 p1110 A83-22633

Direct frequency measurement of the 12-stabilized He-Ne 473-THz /633-nm/ laser
08 p1110 A83-22634

Frequency stabilization of internal-mirror He-Ne lasers
09 p1272 A83-24443

Mode effects in second harmonic generation and their uses for laser stabilization
10 p1425 A83-25404

Frequency reproducibility of ring He-Ne/CH4 lasers
10 p1433 A83-26686

He-Ne laser in the near infrared of the type LG-1-LR
10 p1435 A83-26881

The mechanism of the effect of strations on the output power of a helium-neon laser
11 p1584 A83-28522

Gas-lens effect and cavity design of some frequency-stabilized He-Ne lasers
13 p1849 A83-30213

International intercomparison of laser power measurements in the visible region
13 p1856 A83-31278

Results of international comparisons using methane-stabilized He-Ne lasers at 3.39 microns and iodine-stabilized He-Ne lasers at 633 nm
13 p1856 A83-31279

Single-mode operation of Doppler-broadened lasers by injection locking
15 p2167 A83-33761

Radiation characteristics of a multimode linear Zeeman laser
15 p2170 A83-34703

Natural fluctuations of the emission frequency of an He-Ne/CH4 3.39 micron laser
16 p2359 A83-35895

Investigation of strata in small-scale He-Ne lasers
17 p2515 A83-38488

He-Ne laser frequencies near 2.4 microns and their application to hydrogen fluoride detection
19 p2851 A83-40928

Optimal physical parameters for a high-power He-Ne laser
20 p2995 A83-42949

Continuous laser amplification in a monomode fiber longitudinally pumped by evanescent field coupling
22 p3295 A83-45971

Reliability factors in gas lasers
22 p3296 A83-46612

Estimated lifetime of an He-Ne microwave-pumped laser using a spectroscopic method
23 p3460 A83-47558

An analysis of the international comparison results of helium-neon lasers stabilized by saturated absorption in I-127 (review)
24 p3589 A83-49736

An investigation of the pulsed-discharge radiation in mixtures of ZnI2, CdI2, and HgI2 with helium and neon --- in metal vapor lasers
24 p3589 A83-49742

Evanescent amplification in a single-mode optical fibre
24 p3630 A83-49980

HELIUM-OXYGEN ATMOSPHERES

The peculiarities of the external respiration and gas exchange during the respiration of helium-oxygen mixtures having various concentrations of oxygen
01 p0082 A83-10488

The effect of a normoxic helium-oxygen gas mixture on the consumption of oxygen by the tissues of the liver and lungs in white rats
01 p0078 A83-10489

The effect of the replacement of nitrogen of the air by helium on external respiration
01 p0078 A83-10490

Metabolic and cardiorespiratory responses to He-O2 breathing during exercise
13 p1903 A83-30470

Breathing He-O2 shifts the lung pressure-volume curve of the dog
13 p1897 A83-30479

The diffusion capability of the hematoaparenchymatous barrier for oxygen during the breathing of helium-oxygen gas mixtures
17 p2555 A83-37245

The condition of the pulmonary blood flow and central hemodynamics in healthy humans during the breathing of a helium-oxygen mixture
23 p3497 A83-47115

HELIX TUBES

U TRAVELING WAVE TUBES

HELIXES

U CURVES (GEOMETRY)

HELLMANN-FEYNMAN THEOREM

Expectation values for Morse oscillators
23 p3506 A83-47629

HELMET MOUNTED DISPLAYS

Helmet mounted display symbology for helicopter landing on small ships
04 p0448 A83-16134

The importance of cabin guide marks in visual flying Application of this idea to the design of night vision aides, of the visual helmet type
14 p2071 A83-32458

Visually-coupled systems as simulation devices [AIAA PAPER 83-1083]
16 p2312 A83-36224

HELMETS

Improved headgear for rotary wing Navy/Marine Corps aircrewmenn
04 p0525 A83-15422

Flight helmets - The British approach
04 p0526 A83-15443

Quantitative electromyography - Response of the neck muscles to conventional helmet loading
14 p2072 A83-32693

Canadian forces air combat helmet - The selection
17 p2562 A83-37878

Basilar skull fracture in U.S. Army aircraft accidents --- helmet design for pilot protection
18 p2737 A83-40359

Neck muscle loading and fatigue - Systematic variation of headgear weight and center-of-gravity
24 p3618 A83-48878

HELMHOLTZ EQUATIONS

Development of a sound radiation model for a finite-length duct of arbitrary shape
03 p0391 A83-13134

A finite element method for solving Helmholtz type equations in waveguides and other unbounded domains
03 p0390 A83-13567

Separation of the boundary conditions of a shallow spherical shell
04 p0500 A83-16048

The method of the variation of constants for the Helmholtz equation, illustrated by the problem of diffraction by an inhomogeneous sphere
06 p0806 A83-19354

The ac field around a plane crack in a metal surface when the skin depth is large
07 p0929 A83-20268

Analytic continuation applied to microwave apertures
08 p1095 A83-22471

A theoretical investigation of the sound radiation fields associated with a Bellmouth inlet [AIAA PAPER 83-0710]
10 p1474 A83-25926

An iterative method for the Helmholtz equation
12 p1771 A83-29097

Volume integrals of ellipsoids associated with the inhomogeneous Helmholtz equation
12 p1775 A83-29528

Polyspheroidal periodic functions
21 p3198 A83-45211

The beam propagation method - An analysis of its applicability --- to integrated optics
24 p3627 A83-48748

Single cell high order difference methods for the Helmholtz equation
24 p3622 A83-48874

HELMHOLTZ RESONATORS

Laser schlieren microphone for optoacoustic spectroscopy
02 p0178 A83-12600

The velocity perturbations above the orifice of an acoustically excited cavity in grazing flow
12 p1777 A83-29235

HELMHOLTZ VORTICITY EQUATION

The use of invariant relationships to reduce the order of the system of equations of motion of a vortex-filled heavy rigid body
09 p1337 A83-23564

The analytic continuation of solutions of the generalized axially symmetric Helmholtz equation
10 p1470 A83-26775

On initial and boundary conditions for the Navier-Stokes equations in the Helmholtz form
17 p2505 A83-37529

HELOS (SATELLITE)

U EXOSAT SATELLITE

HEMATOLOGY

The changes in the structural components of the walls of the small vessels and the composition of the peripheral blood during immune and hypoxic effects on the heart
01 p0078 A83-10487

The simultaneous measurement of four functional parameters of blood platelets
01 p0080 A83-10553

A quantitative determination of the hemodepressive effect of some alkylating agents
03 p0374 A83-13633

Rapid monitoring of the acid-base and gas composition of the blood
03 p0375 A83-14334

The rheology of the blood --- Russian book
04 p0520 A83-15828

The role of the lung in the formation of the rheological properties of the blood
05 p0670 A83-17183

The phospholipid composition of blood platelets in healthy individuals and in individuals with diabetes mellitus
05 p0674 A83-17205

The comparative radioprotective effect of adenylylates during short-term and long-term gamma-irradiation
09 p1321 A83-24931

The hematological changes during the adaptation to polar conditions
11 p1644 A83-28803

Ultraviolet-irradiated blood - Photochemistry, immunological action
16 p2393 A83-35920

The action of colyones on erythropoiesis (A quantitative evaluation)
16 p2396 A83-36841

Circulating macromolecular complexes in rats following radiation, thermal, and combined trauma
19 p2874 A83-41011

HEMATOPOIESIS

The significance of cellular contacts for the differentiation of precursor cells of hemopoietic stroma in long-term bone marrow cultures
01 p0080 A83-10548

The radioprotective effect of a gaseous hypoxic mixture on hemopoiesis in mice
03 p0377 A83-14889

The cytokinetics and morphology of hemopoiesis during chronic irradiation --- Russian book
05 p0669 A83-17122

Stromal bone-marrow cells and the hemopoietic environment
05 p0671 A83-17207

The effect of products of erythrocyte degradation on the migration of hemopoietic stem cells in lethally-irradiated mice
14 p2062 A83-32065

Erythropoiesis during adaptation to cold
16 p2399 A83-35916

The action of colyones on erythropoiesis (A quantitative evaluation)
16 p2396 A83-36841

The kinetics of hemopoiesis and its clinical significance
19 p2882 A83-41451

The effect of an antioxidant on the recovery of hemopoiesis and the aggregation of thrombocytes
21 p3186 A83-45380

Age-related characteristics of the postirradiation regeneration of the blood system
23 p3495 A83-48206

HEMATOPOIETIC SYSTEM

The changes in the hemopoietic system and the small intestine mucosa during the breathing of pure oxygen under atmospheric pressure
03 p0374 A83-13632

The effect of adeturon on the survival and the blood system of mice under the effect of various types of ionizing radiation
03 p0376 A83-14880

HEMATURIA

Increased hematuria following hypergravic exposure in middle-aged women
11 p1643 A83-27844

HEMISPHERE CYLINDER BODIES

Hyperballistic vehicle dynamics
02 p0132 A83-13078

Turbulent shear flow behind hemisphere-cylinder placed on ground plane
15 p2119 A83-33664

Pseudospectral approximation in a three-dimensional Navier-Stokes code
19 p2841 A83-40876

An investigation of surface flow pattern and pressure distribution for viscous, sonic flow over hemisphere-cylinder at incidence
22 p3286 A83-47029

HEMISPHERES

Induction and deduction as the function of different hemispheres --- of brain
19 p2870 A83-40810

HEMODYNAMIC RESPONSES

The blood flow in bronchial vessels during hypoxia
01 p0078 A83-10481

The effect of a mountain climate on the condition of the respiratory-hemodynamic function in miners suffering from the initial stages of pneumoconiosis
01 p0082 A83-10482

The changes in the hemodynamics of dogs during exercise of different intensities in the acute adaptation to high altitude
01 p0079 A83-10529

The hemodynamic responses of normotensive and hypertensive rats to injections of prostaglandins and indomethacin
01 p0079 A83-10538

Assessment of central hemodynamics during arm-crank exercise
01 p0083 A83-11138

A comparison of the cardiovascular responses to isometric exercise of three different sized muscle groups
01 p0083 A83-11139

The changes of several cerebral hemodynamic indicators during the action of physical factors
01 p0084 A83-11395

Two types of adaptation reactions of the blood circulation apparatus
03 p0379 A83-13616

The general patterns and types of the hemodynamic changes during myocardial infarction
03 p0379 A83-13619

A theoretical analysis of the regularities of the Bainbridge reflex --- heart rate acceleration by blood pressure increase
04 p0520 A83-15894

The peptide DSIP as a factor for raising the resistance of animals to emotional stress
04 p0521 A83-16414

The state of hepatic circulation under the combined effect of lead and electromagnetic fields
05 p0673 A83-17159

Cerebral circulation and the hemodynamics of lesser circulation in patients with bronchial asthma in combination with systemic arterial hypertension
05 p0673 A83-17162

The effect of clonidine on the central and renal hemodynamics of individuals with hypertension during the administration of orthostatic probes --- side effects of antihypertensive treatments
05 p0674 A83-17198

The effect of dopamine on coronary circulation
05 p0671 A83-17220

Pulmonary microcirculatory response to localized hypercapnia 05 p0671 A83-17333

Regional circulatory responses to head-out water immersion in anesthetized dog 05 p0672 A83-17339

An experimental study of the effects of hypobaric hypoxia on the cerebral blood flow and the metabolism of the brain 06 p0794 A83-18342

The coefficient of capillary filtration in the skeletal muscles during changes in their hemodynamics 07 p0973 A83-20360

The effect of a magnetic field on the patterns of the frequency changes and the content of serotonin in the isolated heart of frogs 07 p0974 A83-20968

An investigation of the participation of the venous return in the pressor changes of systemic hemodynamics by means of the automatic control of its size 08 p1145 A83-22107

The interrelationship of the intracranial pressure, the blood volume of the skull cavity, and the total blood flow of the brain 08 p1145 A83-22108

An experimental study of the encephalic hemodynamic variations connected with flight and position with respect to the flight axes on Alouette III in a healthy subject 08 p1148 A83-22966

The effect of low frequency vibrations on the human cardio-circulatory system - A measurement technique and results for an 18 Hz sinusoidal vibration 08 p1149 A83-22978

Central hemodynamics during stepwise increasing water immersion 08 p1149 A83-22984

The hemodynamic reactions of animals to episodic stimulations of the ventromedial hypothalamus during acute emotional stress 09 p1321 A83-25151

Noninvasive echo-Doppler duplex measurements of common femoral artery blood flow variables during supine exercise and post-occlusive reactive hyperemia 10 p1455 A83-26120

Short term /1 and 3 day/ cardiovascular adjustments to suspension antihorsthosis in rats 11 p1640 A83-27842

The reaction of the central blood circulation of healthy individuals to the decompression of various areas of the body 12 p1764 A83-29306

The phase character of the compensatory reactions of the cardiovascular system during active orthostatic tests 12 p1765 A83-29307

The thermal condition and systemic blood circulation of the human body in the case of moderate (physiological) levels of cooling 12 p1765 A83-29313

Variations in heart rate (pulse 'drift') in the course of work of constant aerobic intensity in athletes and nonathletes 12 p1765 A83-29316

The problem of sudden coronary death in the light of mathematical catastrophe theory 13 p1900 A83-30093

Effects of hypercapnia, hypoxia, and rebreathing on circulatory response to apnea 13 p1902 A83-30463

Dynamic response of local pulmonary blood flow to alveolar gas tensions - Analysis 13 p1789 A83-30473

Ventilatory and circulatory transients during exercise - New arguments for a neurohumoral theory 13 p1897 A83-30483

Hypoxic pulmonary hypertension in the mast cell-deficient mouse 13 p1897 A83-30485

Cardiovascular responses to treadmill exercise in rats 13 p1898 A83-30488

Effects of training 13 p1898 A83-30488

Changes in diastolic coronary resistance during submaximal exercise in conditioned dogs 13 p1898 A83-30504

Physiological assessment of right-side and left-side cardiohemodynamics in patients with hypertension 13 p1906 A83-31395

The microcirculatory condition during burn shock in rats after a prolonged limitation of motor activity 14 p2061 A83-31973

The shifts in the blood circulation system during the effect of high external temperature on an organism 14 p2063 A83-32096

Vasopressin and the cardiovascular system 14 p2063 A83-32097

Hemodynamic effects of Dextran 40 on hemorrhagic shock during hyperbaria and hyperbaric hyperoxia 14 p2064 A83-32687

Renin, kallikrein, and the angiotensin-converting enzyme during a physical load in humans 15 p2213 A83-34959

The effect of maximum physical work on the cardiodynamics and microcirculatory bed of young athletes and of individuals not pursuing athletic activities 16 p2398 A83-35907

Hemodynamic shifts in response to isometric loads in humans in the case of various initial indicators of systemic blood circulation 16 p2398 A83-35910

The characteristics of thermoregulation and blood circulation during prolonged exposure to low temperature 16 p2398 A83-35912

Hemodynamic responses during prolonged sitting 17 p2558 A83-36995

The effect of inverted gymnastic exercises on the hemodynamic and respiratory indicators of students 17 p2559 A83-38171

Hemodynamic indicators, the phasic pattern of the systole of the left and right ventricles of the heart, and the condition of pulmonary blood circulation and microcirculation in patients with hypertension during treatment with adelfane esidrex 17 p2559 A83-38178

The condition of peripheral hemodynamics and the effect on it of several drugs in patients with chronic ischemic heart disease and left ventricular insufficiency 18 p2735 A83-40546

The effect of seduxen on hemodynamic reactions in patients with hypertension during emotional stress 18 p2735 A83-40550

The effect of long-acting nitrates on hemodynamic indicators in patients with acute myocardial infarcts 18 p2736 A83-40580

The change in the reaction of systemic and regional blood circulation to immobilization stress in rats in the case of pharmacological desympathization 19 p2871 A83-40816

Gender differences in hypoxic vascular response of isolated sheep lungs 19 p2875 A83-41135

The therapeutic effect of the cardioselective beta-blocker tenormin and its effect on parameters of the central, intracardiac, and regional hemodynamics in patients with hypertension 19 p2881 A83-41428

Differences in the response of systemic blood circulation to loading tests depending on the sex and age of the subject 19 p2881 A83-41431

The relationship of hormonal and hemodynamic parameters during emotional stress in healthy individuals and patients with hypertension 19 p2881 A83-41435

Canine blood volume and cardiovascular function during hyperthermia 20 p3033 A83-43476

Heart rate variability, cardiac mechanics, and subjectively evaluated stress during simulator flight 21 p3186 A83-43988

Hemodynamic effects of lactated ringer's solution on hemorrhagic shock during exposure to hyperbaric air and hyperbaric hyperoxia 21 p3182 A83-43991

The observation of influence on the characteristics of cardiovascular response during bed rest 21 p3187 A83-44517

The position of the body and the regulation of blood circulation --- Russian book 21 p3184 A83-45002

Physiological aspects of cardiohemodynamics during hypertension 21 p3188 A83-45304

The effect of controlled hyperthermia on several hemodynamic parameters in experimental conditions 21 p3185 A83-45324

The condition of the pulmonary blood flow and central hemodynamics in healthy humans during the breathing of a helium-oxygen mixture 23 p3497 A83-47115

The interaction of cardiac ventricles in intact dogs during 3-5 days of high altitude adaptation 23 p3496 A83-48566

Changes in the microcirculation in mesentery rats during hyperoxia 23 p3496 A83-48568

Comparative cardiovascular responses to 70 head up tilt in pilots and non-pilots 23 p3499 A83-48691

The dependence of the functional activity of the heart on mental activity 24 p3618 A83-49547

HEMODYNAMICS

NT LOWER BODY NEGATIVE PRESSURE

A case of recording changes in the rhythm of systoles on an ophthalmotonogram 03 p0377 A83-13294

The 'volume-dependent' form of essential hypertension 03 p0379 A83-13617

The hemodynamic parallels between the types of central and cerebral blood circulation in individuals with normal arterial pressure 03 p0379 A83-13618

The adaptive properties of the major arterial vessels 03 p0379 A83-13620

The activity of renin in blood plasma, the indicators of central hemodynamics, and the water-electrolyte balance in patients with hypertension 03 p0379 A83-13622

Indices of hemodynamics in patients with hypertension according to echocardiography data 03 p0381 A83-14345

The effects of rest and exercise in the cold on substrate mobilization and utilization 04 p0521 A83-15534

The rheology of the blood --- Russian book 04 p0520 A83-15828

Comparison of hemodynamic responses to static and dynamic exercise 05 p0675 A83-17337

The effect of strophanthine and celanide on the blood circulation and metabolism in the brain 07 p0975 A83-20983

The changes in the venous endothelium after acute hemodynamic disorders 07 p0975 A83-20992

The physiology and pathology of the venous blood circulation of the lower extremities --- Russian book 09 p1322 A83-23822

The condition of the contractile function of the myocardium and the hemodynamics in patients with heart diseases according to echocardiography 11 p1644 A83-28802

An investigation of the hemodynamics of a human in an antihorsthatic position using a method of mathematical modeling 14 p2069 A83-32959

The problem of microcirculation and eye pathology 15 p2210 A83-34940

Electroencephalogram indicators and hypoxic shifts in patients with hypertension with different hemodynamic variations 15 p2213 A83-34951

The application of euphylline electrophoresis with sinusoidal modulated currents in the treatment of patients with transitory disorders of the brain blood circulation 15 p2213 A83-34972

The effect of insulin on the reaction of the coronary and systemic blood circulation during the inspiration of hypoxic mixtures 17 p2555 A83-37239

Hemodynamic interrelations of the systemic and pulmonary blood circulation in the case of hypertension 19 p2880 A83-41426

Systemic and renal hemodynamics in hypertension 19 p2881 A83-41429

The condition of hemodynamics in pulmonary blood circulation in patients with hypertension combined with chronic heart disease 19 p2881 A83-41432

HEMOGLOBIN

NT OXYHEMOGLOBIN

Cooperative deoxygenation of haemoglobin - Asymmetry of binding and subunit differences 05 p0676 A83-17795

Structural and functional changes in the hemoglobin of irradiated dogs 06 p0796 A83-19379

The resonance interaction between low-intensity microwave radiation in the millimeter range and hemoglobin 09 p1321 A83-24929

Skeletal muscle mitochondria and myoglobin, endurance, and intensity of training 13 p1898 A83-30490

Hemophilic bacteria in the nasopharynx of healthy individuals 14 p2066 A83-33334

The physiological mechanisms for supplying the energy requirements of an organism during a decrease in the concentration of hemoglobin in the blood 23 p3496 A83-48567

HEMOPERFUSION

The automatic stabilization of pressure in the main arteries during changes in the blood flow 01 p0080 A83-10545

HEMORRHAGES

Hemorrhagic tolerance of rats at sea level after acute exposure to high altitude 12 p1762 A83-28934

Hemodynamic effects of Dextran 40 on hemorrhagic shock during hyperbaria and hyperbaric hyperoxia 14 p2064 A83-32687

HEMOSTASIS

U HEMOSTATICS

HEMOSTATICS

The system of the regulation of the aggregation condition of the blood in patients with ischemic heart disease 19 p2882 A83-41453

HENRY LAW

Henry's Law constants and the air-sea exchange of various low molecular weight halocarbon gases 18 p2705 A83-40645

HEOS SATELLITES

Comparison of an empirical magnetic-field model based on HEOS-1,2 data with an analytical two-dipole model of the magnetosphere 21 p3176 A83-45268

HEPARINS

The hormonal dependence of the initial stages of heparin clearance during immobilization stress in rats 07 p0973 A83-20242

HEPTANES

Shock initiated ignition in heptane-oxygen-argon mixtures 10 p1391 A83-26198

HERBIG-HARO OBJECTS

The ultraviolet continuous and emission-line spectra of the Herbig-Haro objects HH 2 and HH 1 02 p0256 A83-12125

The ultraviolet spectrum of Herbig-Haro object 2H 03 p0425 A83-14219

The visible and ultraviolet continuum from a Herbig-Haro object in the core of M 16 /NGC 6611/ 03 p0428 A83-14773

Herbig-Haro Objects 46 and 47 - Evidence for bipolar ejection from a young star 05 p0700 A83-17031

New candidate Herbig-Haro objects 06 p0819 A83-18797

- The near-infrared spectrum of the Herbig Ae-Be stars
06 p0844 A83-19497
- Water-vapor masers located near Herbig-Haro objects
07 p1021 A83-21126
- Observations of H₂ emission from molecular clouds and Herbig-Haro objects
08 p1183 A83-23055
- The exciting stars of Herbig-Haro objects
08 p1183 A83-23056
- Jets from pre-main-sequence stars - As 353A and its associated Herbig-Haro objects
08 p1185 A83-23083
- A two-micron survey of southern Herbig-Haro objects
10 p1492 A83-25479
- Detection of H₂ emission in Herbig-Haro object No. 101
13 p1957 A83-31703
- Ultraviolet continuum and H₂ fluorescent emission in Herbig-Haro objects 43 and 47
14 p2107 A83-33231
- HH 1 and HH 2 - The results of an eruptive event in the Cohen-Schwartz star?
15 p2258 A83-34102
- The 1D-3P transition in atomic oxygen induced by collisions with atomic hydrogen
17 p2578 A83-37341
- Proper motions of Herbig-Haro objects. III - HH-7 through -11, HH-12, and HH-32
18 p2757 A83-39603
- Infrared observations of low-mass star formation in Orion - HH objects
18 p2758 A83-39720
- A survey of high-velocity molecular gas in the vicinity of Herbig-Haro objects. I
19 p2919 A83-41627
- On the contributions of the Orion reflection nebulosity to the continuous UV spectrum of the Herbig-Haro objects HH 1 and HH 2 and of the C-S Star
19 p2921 A83-41650
- Optical study of a possible bipolar flow associated with Herbig-Haro 12
20 p3069 A83-42472
- Spectrophotometry of low excitation Herbig-Haro objects
21 p3230 A83-44435
- Herbig-Haro objects in the dust globule ESO 210-6A
22 p3382 A83-46990
- Hydrodynamic models of Herbig-Haro objects
24 p3658 A83-49358
- Ammonia observations of the Herbig-Haro objects HH24-27
24 p3658 A83-49359
- HERCULES AIRCRAFT**
U C-130 AIRCRAFT
- HEREDITY**
The effect of genotype and environment on evoked potential parameters during orienting and defensive reactions
16 p2401 A83-36824
- Genetic predispositions in human learning of motor actions
17 p2559 A83-38173
- Heredity, aging, and longevity of humans
18 p2735 A83-40572

HERCULES AIRCRAFT

U C-130 AIRCRAFT

HEREDITY

- The effect of genotype and environment on evoked potential parameters during orienting and defensive reactions
16 p2401 A83-36824
- Genetic predispositions in human learning of motor actions
17 p2559 A83-38173
- Heredity, aging, and longevity of humans
18 p2735 A83-40572

HERMES SATELLITE

U COMMUNICATIONS TECHNOLOGY SATELLITE

HERMETIC SEALS

- Plating on glass for hermetic seal
[SAE PAPER 820613]
22 p3302 A83-45871

HERMITIAN POLYNOMIAL

- Solution of the Navier-Stokes equations using the finite-difference method of Hermitian type
03 p0322 A83-14615
- Recursive algorithms for two-dimensional smoothing using bicubic hermite polynomial
09 p1336 A83-24717

Hermitian gravity and supergravity

- Product integration over infinite intervals. I - Rules based on the zeros of Hermite polynomials
12 p1774 A83-29029

Application of Wiener-Hermite expansion to strong plasma turbulence

Application of Wiener-Hermite expansion to nonstationary random vibration of a Duffing oscillator

17 p2575 A83-37389

HERTZSPRUNG-RUSSELL DIAGRAM

- Mass loss in Alpha Cygni - Synthetic H-Alpha profiles
04 p0553 A83-15624

Further observational evidence for a coronal boundary line in the cool star region of the H-R diagram

04 p0553 A83-15626

Color-magnitude diagrams and ages of two young Magellanic cloud clusters

06 p0835 A83-19054

Sunlike stars

06 p0841 A83-19424

G and K stars as indicators of the galactic evolution

06 p0846 A83-19535

Studies of luminous stars in nearby galaxies. VIII - The Small Magellanic Cloud

07 p1020 A83-21115

On the photometric differences between luminous OBA type stars in the LMC with and without P Cygni characteristics

07 p1023 A83-21212

MK spectral classification in the Praesepe lower main sequence

09 p1354 A83-24022

Status of evolution of F, G, and K field stars contained in the Fe/H abundance ratio catalogue

10 p1492 A83-25478

Double-mode RR Lyrae variables in M15

10 p1502 A83-25709

A color-magnitude diagram for Leo II

11 p1668 A83-27108

The globular cluster NGC 6544

12 p1784 A83-28865

Note on the evolution of massive stars

12 p1794 A83-29083

Blue edges of the Delta-Scuti instability strip - Theory in comparison with observations

12 p1794 A83-29087

The upper end of the main series --- stars with greatest absolute brightness

12 p1795 A83-29365

Radial velocities of stars in M12 (NGC 6218) and M56 (NGC 6779) and UV-bright stars in globular clusters

14 p2110 A83-33464

A comparison between observed and theoretical H-R diagrams for the young LMC star cluster NGC 1866

17 p2604 A83-37915

The brightest supergiants --- stellar evolution in extragalactic systems

18 p2754 A83-39224

Very massive stars - Evolution with mass loss. I - The hydrogen and helium burning phase

18 p2775 A83-39744

NGC 6256, a galactic globular cluster

19 p2915 A83-41059

Period determination of the Delta Scuti star HR 5005

19 p2910 A83-41063

Some constraints on the color-magnitude diagram of giants in the galactic spheroid

22 p3382 A83-46991

Distances of the central stars and their position in the HR diagram

24 p3639 A83-49154

Study of the variability of the Delta Scuti stars. VI

Pulsational behaviour of HR 1392 (69 Tau). VII - The problem of stability and monopole periodicity in 20 CVn

24 p3663 A83-49847

HERZBERG BANDSThe altitude dependence of the O₂/A₃Sigma u + / vibrational distribution in the terrestrial nightglow

04 p0508 A83-14971

Implication for stratospheric composition of a reduced absorption cross section in the Herzberg continuum of a molecular oxygen

07 p0958 A83-20088

HETEROCYCLIC COMPOUNDS

NT ADENOSINE DIPHOSPHATE

NT ADENOSINE TRIPHOSPHATE

NT ADENOSINES

NT ALKALOIDS

NT ASCORBIC ACID

NT ATROPINE

NT AZOLES

NT CAFFEINE

NT CARBAZOLES

NT CARNITINE

NT CYCLIC AMP

NT GUANINES

NT HYOSCINE

NT MORPHINE

NT NICOTINAMIDE

NT PHTHALOCYANIN

NT PYRIDOXINE

NT PYRROLES

NT RDX

NT RIBOFLAVIN

NT TETRAHYDROFURAN

NT THIAMINE

NT TOCOPHEROL

NT TRYPTOPHAN

NT URACIL

NT URIC ACID

Synthesis and characteristics of poly[bis(dichloromaleimides)/

05 p0610 A83-17475

HETERODYNING

NT OPTICAL HETERODYNING

Heterodyne detection of microwave signals by thin-film superconducting elements

04 p0471 A83-15743

An SIS receiver for the 3 mm wavelength range --- Superconductor Insulator Superconductor

04 p0472 A83-15811

Experimental comparison of heterodyne and direct detection for pulsed differential absorption CO₂ lidar

09 p1272 A83-24444

Submillimetric heterodyne techniques for space

11 p1537 A83-27735

Trends in microwave counter technology

13 p1836 A83-30975

Heterodyne detection of lower hybrid waves in a plasma by microwave scattering

21 p3211 A83-44343

HETEROGENEITY

Compositional heterogeneity of tephros from the 1980 eruptions of Mount St. Helens

07 p0961 A83-20237

Heterogeneous atmospheric chemistry --- Book

09 p1297 A83-25176

Effect of the number density of heterogeneities on the critical diameter of condensed explosives

22 p3266 A83-46007

HETEROJUNCTION DEVICES

Low threshold InGaAsP/InP lasers with microcleaved mirrors suitable for monolithic integration

01 p0055 A83-10981

Room-temperature CW operation in the visible spectral range of 680-700 nm by AlGaAs double heterojunction lasers

01 p0055 A83-10983

Electrolyte electroreflectance study of laser annealing effects of the CdTe/Hg/0.8/Cd/0.2/Te/111/ system

01 p0110 A83-10992

An enhancement mode Schottky barrier gate charge-coupled device on a high electron mobility transistor structure

01 p0039 A83-10994

Luminescence spectra of stripe-geometry laser heterostructures in GaAs-Al_xGa_{1-x}As

02 p0183 A83-11695

Narrow strip AlGaAs lasers using double current confinement

02 p0185 A83-12276

Very narrow graded-barrier single quantum well lasers grown by metalorganic chemical vapor deposition

02 p0185 A83-12279

Raman scattering characterization of Ga_{1-x}Al_x/Al_xAs/GaAs heterojunctions - Epilayer and interface

02 p0243 A83-12289

Valency control of glow discharge produced a-SiC:H and its application to heterojunction solar cells

03 p0354 A83-13649

Real space transfer electron device oscillator - A new candidate for the near millimeter range

03 p0310 A83-13797

Theoretical analysis of single-mode AlGaAs-GaAs double heterostructure lasers with channel-guide structure

03 p0332 A83-13920

A p-n heterojunction model for the thin-film CuInSe₂/CdS solar cell

03 p0355 A83-14513

High quantum efficiency InGaAsP/InP lasers

03 p0333 A83-14931

High-power individually addressable monolithic array of constricted double heterojunction large-optical-cavity lasers

03 p0333 A83-14935

Photoelectric properties of nSiC-pSi heterojunctions

04 p0539 A83-15128

Optoelectronic digital/analogous convertor-emitter

04 p0534 A83-15241

Enhancement of electron velocity in modulation-doped /Al, Ga/As/GaAs FETs at cryogenic temperatures

04 p0470 A83-15251

Material parameters of In_{1-x}Ga_xAs_y/P_{1-y}/ and related binaries

04 p0542 A83-16064

Transport mechanisms for Mg/Zn₃P₂ junctions

04 p0543 A83-16071

Single-mode lasers for optical communications

04 p0486 A83-16213

'Nonwaveguide'-mode semiconductor injection lasers

04 p0486 A83-16214

High-rate amplitude and frequency modulation of semiconductor lasers

04 p0486 A83-16218

Catastrophic degradation level of visible and infrared GaAlAs lasers

05 p0647 A83-16941

Spatial mode discrimination and control in high-power single-mode constricted double-heterojunction large-optical-cavity diode lasers

05 p0648 A83-16942

Determination of the parameters of injection laser amplifiers based on GaAlAs heterostructures from superluminescence characteristics

05 p0649 A83-17060

GaAs/GaAlAs heterojunction bipolar transistors with cutoff frequencies above 10 GHz

05 p0624 A83-17285

Ion-implanted

s lateral PNP transistors

05 p0624 A83-17288

Numerical simulation of GaAs/GaAlAs heterojunction bipolar transistors

05 p0624 A83-17294

A monolithic lead sulfide-silicon MOS integrated-circuit structure

06 p0752 A83-18756

Direct modulation of semiconductor injection lasers

06 p0765 A83-18762

Mode partition noise characteristics in high-speed modulated laser diodes

06 p0766 A83-18902

Role of the conductivity of the confining layers in DH-laser spatial hole burning effects

06 p0766 A83-18903

Theory for nonequilibrium behavior of anisotropy graded heterojunctions

06 p0814 A83-18961

Common anion heterojunctions - CdTe-CdHgTe

06 p0814 A83-18962

Stability of the horizontal transverse modes of the planar stripe lasers with deep Zn-diffusion

06 p0766 A83-19141

High power single mode InGaAsP lasers fabricated by single step liquid phase epitaxy

06 p0767 A83-19254

Photovoltaic properties of cadmium sulfide/trivalent-metal phthalocyanine heterojunction devices

06 p0754 A83-19259

- Radiation effects on modulation-doped GaAs-Al_x/Ga_{1-x}/As heterostructures 06 p0815 A83-19263
- Optically pumped 1.55-micron double heterostructure Ga_x/Al_y/In_{1-x-y}/As/Al_u/In_{1-u}/As lasers grown by molecular beam epitaxy 07 p0933 A83-19986
- Characteristics of modulation-doped Al_x/Ga_{1-x}/As/GaAs field-effect transistors - Effect of donor-electron separation 07 p0918 A83-19987
- Quantum corrections to the galvanomagnetic coefficients of quasi-two-dimensional electrons of InSb/GaAs heteroepitaxial structures 07 p0999 A83-20049
- Third-order optical nonlinearity induced by effective mass gradient in heterostructures [AD-A130018] 07 p0994 A83-21364
- Dispersion of the group velocity refractive index in GaAs double heterostructure lasers 07 p0938 A83-21592
- Frequency stabilization of GaAlAs laser using a Doppler-free spectrum of the Cs-D2 line 07 p0938 A83-21593
- Modal solutions of active dielectric waveguides by approximate methods 07 p0924 A83-21626
- Enhanced indium phosphide substrate protection for liquid phase epitaxy growth of indium-gallium-arsenide-phosphide double heterostructure lasers 08 p1107 A83-22331
- Prediction of transverse-mode selection in double heterojunction lasers by an ambipolar excess carrier diffusion solution 08 p1107 A83-22332
- Compositional depth profiles of chemiplated Cu₂S/Zn,Cd/S heterojunction solar cells 08 p1130 A83-22339
- Multilongitudinal mode operation in angled stripe buried heterostructure lasers 08 p1107 A83-22342
- Direct bandgap, ionizing-radiation insensitive, photodiode structures 08 p1165 A83-22487
- AlGaAs/GaAs heterojunction charge-coupled devices /CCDs/ for visible/near infrared imaging applications 08 p1080 A83-22604
- Analysis of distributed-feedback diode lasers with gain-induced waveguiding 08 p1110 A83-22671
- Diode laser threshold current density and lasing wavelength as functions of active region thickness 08 p1110 A83-22751
- High optical power CW operation in visible spectral range by window V-channelled substrate inner stripe lasers 08 p1110 A83-22753
- Effect of grain boundaries on the minority carrier diffusion length in InP solar cells 08 p1170 A83-22908
- Molecular beam epitaxial double heterojunction bipolar transistors with high current gains 08 p1081 A83-22916
- Enhanced bandgap resonant nonlinear susceptibility in quantum-well heterostructures 08 p1167 A83-22917
- High-speed GaAlAs-GaAs heterojunction bipolar transistors with near-ballistic operation 08 p1082 A83-22922
- Short-cavity single-frequency InGaAsP buried-heterostructure lasers 09 p1272 A83-24112
- Effects of 140 Mbit/s operation on degradation of GaAlAs DH lasers 09 p1272 A83-24113
- Future applications and limitations for digital GaAs IC technology 09 p1255 A83-24347
- Continuous 300-K laser operation of strained superlattices 10 p1426 A83-25977
- Heteroepitaxial Si films on yttria-stabilized, cubic zirconia substrates 10 p1488 A83-25981
- CW electro-optical characteristics of graded-index waveguide separate-confinement heterostructure lasers with proton-delineated stripe 10 p1430 A83-26202
- Use of a superlattice to enhance the interface properties between two bulk heterolayers 10 p1489 A83-26214
- New materials for solar cells - Tandem cells 10 p1446 A83-26882
- Semiconductor lasers 11 p1576 A83-27502
- Optimal design of Pb_{1-x}/Sn_x/Te double heterostructure injection lasers 11 p1583 A83-27622
- Gain spectra of quantum-well lasers 11 p1584 A83-28605
- CW operation of 1.5 micron GaInAsP/InP buried heterostructure laser with a reactive ion-etched facet 11 p1585 A83-28606
- Ga_{0.47}/In_{0.53}/As/Al_{0.48}/In_{0.52}/As m-well LEDs emitting at 1.6 microns 11 p1664 A83-28613
- The study and manufacture of Ga-Al-As double heterojunction laser diodes emitting in the visible spectrum --- French thesis 11 p1585 A83-28627
- Static model of DH laser 12 p1732 A83-29417
- Study of electronically active defects in GaAlAs:Sn devices and their role in degradation --- French thesis 13 p1830 A83-30129
- Picosecond Al(x)Ga(1-x) As modulation-doped optical field-effect transistor sampling gate 13 p1832 A83-30341
- Electro-optical light modulation in InGaAsP/InP double heterostructure diodes 13 p1918 A83-30343
- Modal analysis of separate-confinement heterojunction lasers with inhomogeneous cladding layers 13 p1851 A83-30750
- Bistable operation and nonuniform output in an injection heterostructure laser 13 p1851 A83-30907
- Passive mode locking of buried heterostructure lasers with nonuniform current injection 13 p1852 A83-31057
- Low-current-threshold (GaAl)As visible lasers with emission wavelengths below 750 nm 13 p1857 A83-31378
- Interfacial stability of SnO₂/n-Si and In₂O₃/Sn/n-Si heterojunction solar cells 13 p1931 A83-31384
- Barrier at the interface between amorphous silicon and transparent conducting oxides and its influence on solar cell performance 13 p1871 A83-31389
- Theory of heterostructure inversion-mode metal-insulator-semiconductor field effect transistors 13 p1837 A83-31391
- High-speed GaAs heterojunction bipolar phototransistor grown by molecular beam epitaxy 13 p1837 A83-31759
- GaAs/GaAlAs active-passive-interference laser 13 p1858 A83-31768
- New mechanism for bistable operation of closely coupled twin stripe lasers 13 p1858 A83-31783
- High-blocked heterojunction and Schottky barrier solar cells 14 p2004 A83-32242
- Role of photoluminescence in the efficiency of a Ga(1-x)Al(x)As-GaAs solar cell 14 p2043 A83-32269
- 8 percent efficiency a-SiC:H/a-Si:H heterojunction solar cells 14 p2043 A83-32276
- Electrodeposited CdS/CdTe heterojunction solar cells 14 p2044 A83-32280
- Thin film heterojunction CdS/Cu ternary alloys solar cells with minority carrier mirrors 14 p2044 A83-32281
- Large area CdS/Cu(x)S thin film solar cells produced by electrophoretic deposition 14 p2044 A83-32282
- Photovoltaic performance of CdS heterojunctions on polycrystalline silicon 14 p2044 A83-32293
- Thin film Cu₂S/CdS junctions produced by evaporation and sputtering - Effect of thermal treatments in vacuum 14 p2089 A83-32297
- Cadmium sulfide polyacetylene photovoltaic heterojunction 14 p2090 A83-32305
- An XPS study of Cu(x)S formed on Zn(0.15)Cd(0.85)S --- for solar cells 14 p2092 A83-32639
- New large optical cavity laser with distributed active layers 14 p2027 A83-33437
- A high-power, single-mode laser with twin-ridge-substrate structure 14 p2027 A83-33438
- Bistability and slow oscillation in an external cavity semiconductor laser 14 p2027 A83-33440
- InGaAsP/InP phototransistor-based detectors 15 p2150 A83-33683
- Optical comparator - A new application for avalanche phototransistors 15 p2229 A83-33684
- Magnetoresistance anisotropy due to the 2D-electron subsystem at a GaAs/AlGaAs interface 15 p2237 A83-33784
- Double heterojunction Al(x)Ga(1-x)As/GaAs bipolar transistors (DHBJT's) by MBE with a current gain of 1650 15 p2151 A83-33916
- Laser cathode ray tube with a semiconductor double-heterostructure screen 15 p2163 A83-33921
- Fabrication and investigation of GaInPAs/InP heterolayers 15 p2168 A83-33978
- (GaAl)As/GaAs heterojunction bipolar transistors with graded composition in the base 15 p2152 A83-34516
- Temporal and spectral characteristics of rapidly gain-switched GaAs/GaAlAs buried-heterostructure lasers 15 p2170 A83-34522
- Cuprous oxide-indium-tin oxide thin film photovoltaic cells 16 p2371 A83-35451
- The growth of Cu₂S on polished or etched single crystal CdS substrates 16 p2419 A83-35573
- Microscopic investigations of semiconductor interfaces 16 p2419 A83-35670
- The quantized Hall effect 16 p2420 A83-35763
- Generation of coherent picosecond pulses using mode-locked semiconductor lasers 16 p2358 A83-35886
- Very low threshold InGaAsP mesa laser 16 p2359 A83-35955
- Synthetic nonlinear semiconductors 16 p2420 A83-35957
- Current injection in multiquantum well lasers 16 p2359 A83-35958
- Ohmic contacts for laser diodes 16 p2346 A83-35988
- Incorporation of Sb in GaAs(1-x)Sb(x) (x less than 0.15) by molecular beam epitaxy 16 p2420 A83-36013
- High-performance modulation-doped GaAs integrated circuits with planar structures 16 p2347 A83-36477
- Polarisation-dependent gain-current relationship in GaAs-AlGaAs MOW laser diodes --- Multi-Quantum-Well 16 p2360 A83-36481
- Dynamic behaviour of a GaAs-AlGaAs MQW laser diodes --- Multi-Quantum-Well 16 p2360 A83-36485
- Preparation and properties of Si/SnO₂ heterojunctions 16 p2347 A83-36737
- Photovoltaic and structural properties of CuInSe₂/CdS solar cells 16 p2371 A83-36744
- Beam-propagation analysis of stripe-geometry semiconductor lasers - Threshold behavior 17 p2514 A83-38043
- Allowance for the skin effect in a superconductor-semiconductor-superconductor structure 17 p2499 A83-38487
- TDEG in In(0.53)Ga(0.47)As-InP heterojunction grown by chloride VPE --- two-dimensional electron gas 17 p2585 A83-38880
- Analysis of photon-induced changes in the performance of amorphous silicon solar cells 18 p2708 A83-39467
- Reliability of constricted double-heterojunction AlGaAs diode lasers 18 p2693 A83-40052
- Threshold-wavelength and threshold-temperature dependences of GaInAsP/InP lasers with frequency selective feedback operating in the 1.3- and 1.5-micron regions 18 p2693 A83-40057
- Implications of velocity overshoot in heterojunction transit-time diodes 18 p2679 A83-40387
- Planar structure AlGaAs/GaAs PIN photodiode grown by MOCVD 18 p2679 A83-40388
- Carrier leakage and temperature dependence of InGaAsP lasers 19 p2850 A83-40732
- Effect of an active layer thickness on lateral and longitudinal modes of a gain guiding laser with a tapered stripe structure 19 p2850 A83-40737
- A nondestructive method for predicting laser emission wavelength from photocurrent spectra of GaAlAs double heterostructure wafers 19 p2851 A83-40930
- High-efficiency and high-power AlGaAs/GaAs laser 19 p2851 A83-40935
- The stresses and photoelastic effects in stripe geometry GaAs-GaAlAs DH lasers with masked and selective thermal oxidation (MSTO) structure 19 p2851 A83-40936
- Graded barrier single quantum well lasers - Theory and experiment 19 p2851 A83-40937
- Avalanche InP/InGaAs heterojunction phototransistor 19 p2899 A83-40948
- Phototransistors in digital optical communication systems 19 p2899 A83-40949
- The CdS-CuInSe₂ solar cell interface - Thermodynamic considerations 20 p2949 A83-42352
- Field ionised impurity scattering in an AlGaAs/GaAs two-dimensional electron gas 20 p3052 A83-42485
- High efficiency GaInAs/Inp heterojunction IMPATT diodes 20 p2968 A83-43350
- Internal photoemission from quantum well heterojunction superlattices by phononless free-carrier absorption 20 p3054 A83-43593
- Monolithic integration of a double heterostructure light-emitting diode and a field-effect transistor amplifier using molecular beam grown AlGaAs/GaAs 20 p2968 A83-43596
- Radiative characteristics of injection lasers with short resonators 20 p2996 A83-43788
- Application of thermal pulse annealing to ion-implanted GaAlAs/GaAs heterojunction bipolar transistors 21 p3123 A83-43851
- A three-terminal double junction GaAs/GaAlAs cascade solar cell 21 p3166 A83-43853
- Modulation characteristics of constricted double-heterojunction AlGaAs laser diodes 21 p3144 A83-44216
- Electrical and optical properties of n-CdS/P-Si and n(Zn(x)-Cd(1-x))S/P-Si heterojunction solar cells 21 p3167 A83-44607
- Simulation of GaAs submicron FET with hot-electron injection structure 21 p3126 A83-44967
- Photovoltaic properties of sputtered n-CdO films on p-Cu₂O 21 p3218 A83-45178
- Twisted double-heterostructure GaAs-(Al)GaAs laser 21 p3146 A83-45484
- Optical stability of narrow stripe, proton-isolated AlGaAs double heterostructure lasers with gain guiding 21 p3147 A83-45485
- Neutron damage effects in laser diodes 22 p3297 A83-46619
- Switching of a GaAs bistable etalon - External switching on and off, regenerative pulsations, transverse effects, and lasing 22 p3360 A83-46653

- Narrow diffused stripe GaAs/GaAlAs lasers for high speed integrated optical transmitters 22 p3297 A83-46655
- Electronic wavelength tuning with semiconductor integrated etalon interference lasers 22 p3299 A83-46723
- Optical studies of In(x)Ga(1-x)As-GaAs strained multiquantum well structures 22 p3365 A83-46730
- Epitaxial InP/fluoride/InP(001) double heterostructures grown by molecular beam epitaxy 22 p3365 A83-46732
- Silicon-gallium-phosphide heterostructures with a (Si₂)x(GaP)_{1-x} 22 p3366 A83-46783
- Two-dimensional quantum-mechanical confinement of electrons in DH lasers by strong magnetic fields 22 p3300 A83-46819
- Reliability of InGaAsP/InP buried heterostructure 1.3 micron lasers 22 p3301 A83-46824
- A study of optical amplification in a double heterostructure GaAs device using the density matrix approach 22 p3301 A83-46825
- In₂O₃ heterojunction photocells using compounds of type A(II)B(IV)C₂(V) 23 p3445 A83-47564
- Studies of electroluminescence in pAlGaAs-pGaAs-nGaAs heterophotocells with distributed parameters 23 p3477 A83-47565
- New types of high efficiency solar cells based on a-Si 24 p3598 A83-48787
- Heterojunction formation in (CdZn)S/CuInSe₂ ternary solar cells 24 p3634 A83-48790
- Polarization photosensitivity of n-Ge-p-CdGeP₂ heterostructures 24 p3628 A83-48863
- GaP/Al(x)Ga(1-x)P heterojunction transistors for high-temperature electronic applications 24 p3572 A83-48917
- Dissipation and dynamic nonlinear behavior in the quantum Hall regime 24 p3635 A83-48921
- GaAlAs buried-heterostructure lasers grown by a two-step MOCVD process 24 p3590 A83-49963
- Instabilities in modulation doped field-effect transistors (MODFETs) at 77 K 24 p3574 A83-49972
- New Ga(0.47)In(0.53)As sheet-charge field-effect transistor for long-wavelength optoelectronic integration 24 p3574 A83-49973
- New negative-resistance device by a CHIRP superlattice --- coherent heterointerfaces for reflection and penetration 24 p3636 A83-49981
- ### HETEROJUNCTIONS
- Hot electrons in a GaAs heterolayer at low temperature 01 p0109 A83-10626
- Epitaxial relations in group-IIIa fluoride/Si₃N₄/heterostructures 10 p1488 A83-25983
- Photosensitivity spectra of InAs-PbS heterojunctions 11 p1663 A83-28520
- Theory of silicon superlattices - Electronic structure and enhanced mobility 11 p1664 A83-28710
- The peculiarities of current transmission in degenerate semiconductor-semiconductor heterojunctions 14 p2087 A83-32128
- Reduced threshold current temperature dependence in double heterostructure lasers due to separate p-n and heterojunctions 19 p2852 A83-40938
- Space-charge waves in multilayered heterostructures --- acoustic plasma modes 20 p3053 A83-42600
- Transient capacitance spectroscopy on large quantum well heterostructures 20 p3053 A83-42614
- Energy levels and alloy scattering in InP-In(Ga)As heterojunctions 22 p3365 A83-46738
- HgCdTe heterojunctions 24 p3571 A83-48742
- ### HEURISTIC METHODS
- Occlusion analysis in time-varying imagery 01 p0100 A83-11463
- Criteria of applicability for the geometrical theory of diffraction 04 p0531 A83-15763
- Optimization of manipulator workspace 11 p1552 A83-27486
- On a method of frozen coefficients in the synthesis of linear controllers 13 p1910 A83-30079
- Field redistribution in finite elements - A mathematical alternative to reduced integration 15 p2179 A83-34561
- Distribution design of logical database schemas 20 p3038 A83-43117
- ### HEXAGONAL CELLS
- Hexagonal ferrites for millimeter wave applications 03 p0399 A83-13786
- Stacking fault energy and texture changes during the polygonization of alpha titanium alloys 03 p0300 A83-14162
- Oscillatory internal friction associated with hydride precipitation in alpha-titanium 04 p0462 A83-16257
- The deformation and fracture mechanisms of coarse-grained textured alpha-titanium alloys 06 p0729 A83-18748
- Precipitation of T1 phase in α + T1/ type Al-4.2%Cu-1.3%Li alloy 07 p0885 A83-20294
- Characterization of AlN ceramics containing long-period polytypes 07 p0901 A83-21569
- A modulus method of determining the type of rolling texture in sheets of hexagonal metals 08 p1066 A83-22627
- Deformation of polycrystalline alpha-SiC 09 p1239 A83-24073
- Effect of alpha phase morphology on mechanical properties of commercial purity titanium 10 p1393 A83-25401
- Alpha-beta interface sliding in Ti-Mn alloys 10 p1398 A83-26285
- Strengthening mechanisms in hot-rolled magnesium and magnesium alloys 16 p2330 A83-36070
- Distribution of aluminum, molybdenum, and zirconium among phases in Ti-Al-Mo-Zr alloys 16 p2335 A83-36898
- Kinetics of hydrogen absorption by alpha-zirconium 23 p3429 A83-47635
- ### HEXAGONS
- Fast convolution methods for hexagonally sampled two-dimensional signals 15 p2220 A83-33518
- ### HEXANITROSTILBENE
- A parametric study of the synthesis of 2,2',4,4',6,6'-hexanitrostilbene from trinitrotoluene and sodium hypochlorite 13 p1818 A83-31672
- ### HEXOGENES (TRADEMARK)
- A study of detonation initiation in TNT and TH 50/50 by shock waves of short duration 06 p0726 A83-18004
- Detonation characteristics of retarded explosives 06 p0726 A83-18006
- The effect of aluminum on the detonation wave profile of greatly diluted Hexogen 06 p0726 A83-18007
- A study of the microstructure of cast compositions --- of TNT-Hexogene explosives 06 p0726 A83-18008
- A case of quasi-isentropic compression of a medium 14 p2027 A83-32094
- Ignition of crystalline hexogen with adiabatic compression of the adjacent gas pocket 24 p3557 A83-49792
- ### HF LASERS
- Numerical modeling of processes occurring in the cavity of a CW chemical HF laser on the basis of Navier-Stokes equations 03 p0332 A83-14061
- Refractive index of HF from 2.5 microns to 2.9 microns 03 p0332 A83-14393
- Continuous-wave reaction-product chemical lasers /review/ 05 p0648 A83-17038
- Pulsed high-pressure chemical HF laser with electric-discharge initiation 05 p0650 A83-17084
- Experiments with active phase matching of parallel-amplified multiline HF laser beams by a phase-locked Mach-Zehnder interferometer 06 p0765 A83-18591
- Influence of translational and rotational relaxation on the specific energy characteristics of a CW chemical HF laser 07 p0933 A83-20103
- A supersonic megahertz pulsed HF chemical laser 07 p0936 A83-20729
- Medium induced phase aberrations in continuous wave /CW/ hydrogen fluoride chemical lasers 08 p1109 A83-22460
- Continuous-wave HF R-branch laser demonstration 08 p1110 A83-22637
- Rotational nonequilibrium influences in CW HF/DF chemical lasers 10 p1429 A83-26167
- Shock/Ludwig-tube driven HF laser 10 p1429 A83-26169
- LIF and chemiluminescence methods for the flow diagnostics of supersonic mixing chemical lasers --- laser induced fluorescence 11 p1580 A83-27581
- Laser action during the induction period of photoinitiated F₂/H₂ chain reactions 11 p1580 A83-27582
- Theoretical simulation of a pulsed HF optical resonance transfer laser 11 p1585 A83-28703
- Ab initio studies of the CO₂-HF and N₂O-HF complexes 13 p1818 A83-30966
- Characteristics of a pulsed chemical laser utilizing an H₂-F₂ mixture and initiated by radiation from an XeCl excimer laser 14 p2022 A83-31903
- Rotational energy transfer in HF 15 p2227 A83-34014
- HF chemical laser amplification properties in homologous turbulent shear flow 15 p2170 A83-35250
- The status of rotational nonequilibrium in HF chemical lasers [AIAA PAPER 83-1699] 17 p2513 A83-37196
- Modeling study of a CW HF optical resonance transfer laser model [AIAA PAPER 83-1700] 17 p2513 A83-37197
- Temperature requirements and corrosion rates in combustion driven hydrogen fluoride supersonic diffusion lasers 19 p2850 A83-40857
- Energy lost in formation of fluorine atoms in the course of electron-beam dissociation of fluorine and fluoride molecules 20 p2997 A83-43797
- Pulsed chemical HF laser utilizing a mixture of technical-grade C₃H₈ and SF₆ and initiated by an electric discharge 20 p2998 A83-43802
- Continuous-wave HF optical resonance transfer laser model 22 p3296 A83-46087
- Numerical study of the interaction of supersonic viscous gas jets in the presence of nonequilibrium physicochemical processes 24 p3588 A83-49122
- ### HXX HELICOPTER
- ### U H-53 HELICOPTER
- ### HIBERNATION
- Effects of exposure to low O₂ or high CO₂ environments on respiration in hibernating hamsters and ground squirrels 04 p0520 A83-16009
- A pronounced decrease in the metabolism of warm-blooded animals caused by endogenous substances from the tissues of hibernants in the state of hibernation 07 p0971 A83-19643
- The character of protein synthesis in the brains of hibernating mammals 13 p1900 A83-31342
- ### HICAT (RADAR TECHNIQUE)
- ### U HIGH RESOLUTION COVERAGE ANTENNAS
- ### HICAT PROJECT
- ### U HIGH RESOLUTION COVERAGE ANTENNAS
- ### HIERARCHIES
- ### NT BBKY HIERARCHY
- Recursive generation of hierarchical data structures for multidimensional digital images 01 p0097 A83-11414
- A VLSI pyramid machine for hierarchical parallel image processing 01 p0090 A83-11447
- The hierarchical concept in finite element analysis 02 p0193 A83-12737
- Optimization and filtering of linear systems of finite dimension by hierarchical calculation --- French thesis 08 p1156 A83-22089
- Hierarchical merging and the structure of elliptical galaxies 08 p1181 A83-23027
- The modelling of hierarchical systems of spatial-temporal synchronous connections of the human brain 10 p1462 A83-25625
- Stability criteria in many-body systems. V - On the totality of possible hierarchical general four-body systems 12 p1787 A83-29117
- A graph-theoretic algorithm for hierarchical decomposition of dynamic systems with applications to estimation and control 13 p1911 A83-31071
- Method for generating discrete soliton equations. I. II 14 p2080 A83-32517
- A participative approach to program evaluation 19 p2906 A83-41299
- Priority setting in complex problems 19 p2907 A83-41302
- Hierarchical strategy for machinery maintenance [AIAA PAPER 83-2497] 23 p3441 A83-48352
- ### HIGH ACCELERATION
- A standardized instrumentation methodology for assessing ejection seat performance 04 p0525 A83-15412
- Acceleration measurements in a high G environment 17 p2509 A83-37131
- The hydrodynamic forces acting on a cylinder set in motion in an impulsive manner 19 p2843 A83-41264
- Effect of Rayleigh accelerations applied to an initially moving fluid --- in circular cylinders under low gravity associated with space flight 20 p2940 A83-43274
- ### HIGH ALTITUDE
- Physiological factors affecting military high altitude high opening /HALO/ operations 04 p0521 A83-15435
- Super high altitude photography for coastal geomorphology --- from approximately 20 km altitude 05 p0657 A83-17840
- Deployment of a spin parachute in the altitude region of 260,000 ft 07 p0869 A83-20413
- Chemoreceptor sensitivity in adaptation to high altitude 07 p0977 A83-20780
- Hemorrhagic tolerance of rats at sea level after acute exposure to high altitude 12 p1762 A83-28934
- Missile guidance design tradeoffs for high-altitude air defense 13 p1812 A83-30168
- The use of high altitude aerial photography (1:120,000) for range condition/trend determination 15 p2187 A83-34845
- Wind-tunnel simulation of the actual conditions of high-altitude flight 17 p2447 A83-37507
- Numerical prediction of the motion of high-altitude geodetic satellites 17 p2472 A83-37724
- ### HIGH ALTITUDE BALLOONS
- ### NT JIMSPHERE BALLOONS
- ### NT SUPERPRESSURE BALLOONS
- Some characteristics of clear-air turbulence in the middle stratosphere 04 p0517 A83-15938

Transformation of wind energy by a high-altitude power plant 04 p0507 A83-16112
New thermal and trajectory model for high-altitude balloons 14 p1974 A83-32579
The use of stratospheric balloons in astronomy - Sun-pointing nacelles for the study of the solar UV spectrum 16 p2427 A83-36955
The radiation controlled balloon (RACoon) 18 p2640 A83-39803
Instantaneous, predictable balloon system descent from high altitude 18 p2640 A83-39808
Detection of solar neutrons on a long duration balloon flight 18 p2784 A83-39820

HIGH ALTITUDE BREATHING

The physiological mechanisms of the rehabilitary action of a mountain climate 01 p0078 A83-10480
The effect of a mountain climate on the condition of the respiratory-hemodynamic function in miners suffering from the initial stages of pneumoconiosis 01 p0082 A83-10482
The pulmonary circulation and the right ventricular function in experimental models of high-altitude acute edema of the lungs 01 p0080 A83-10543
OBOGS and OBIGGS - The application of molecular sieves to aircrew breathing and aircraft survivability --- On-Board Oxygen Generator System and On-Board Inert Gas Generator System 04 p0525 A83-15430
Arterial oxygen saturation at altitude using a nasal cannula 04 p0521 A83-15537
Acclimatization to high altitude in goats with ablated carotid bodies 19 p2875 A83-41132
Pulmonary gas exchange on the summit of Mount Everest 22 p3347 A83-45982
Methods of increasing the tolerance of humans to acute hypoxia 23 p3496 A83-47101

HIGH ALTITUDE ENVIRONMENTS

The changes in the hemodynamics of dogs during exercise of different intensities in the acute adaptation to high altitude 01 p0079 A83-10529
Effects of time and duration of exposure to 12% O2 and prior food deprivation on hypoxic hypophagia of rats 04 p0519 A83-15536
The correlation of the parameters of the cardiac rhythm with the physical work capacity of humans during the adaptation to high-altitude hypoxia 04 p0522 A83-15781
Earth limb altitude determination for the Solar Mesosphere Explorer [AIAA PAPER 83-0429] 05 p0603 A83-17926
Moisture sounding at millimeter wavelengths /94/183 GHz/ at high altitudes 08 p1098 A83-22557
Review of some nonlocal-thermodynamic-equilibrium high-altitude 4.3 micron background effects 08 p1136 A83-22854
The effect of the pharmacological blocking of the alpha and beta adrenoreceptors on the development of experimental high-altitude acute pulmonary edema 09 p1322 A83-25171
Neuropsychological functioning after prolonged high altitude exposure in mountaineering 10 p1455 A83-25665
A dynamic model of turbojet in starting at high altitude 16 p2304 A83-35846
Cold stress at high altitudes 21 p3183 A83-44073
Methods of computation of geomagnetic field at greater altitude in a local region 21 p3173 A83-44585
High altitude physiology and medicine --- Book 21 p3188 A83-45090

HIGH ALTITUDE FLIGHT

U HIGH ALTITUDE

HIGH ALTITUDE PRESSURE

Effect of oxygen addition on ignition of aero-gas turbine at simulated altitude facility 01 p0011 A83-10660

HIGH ALTITUDE TESTS

The adrenoreactivity of the vessels of the small intestine in cats during the process of high altitude adaptation 07 p0973 A83-20245
Postfire sampling of SRMs for contamination sources in high altitude test cells [AIAA PAPER 83-1448] 14 p1984 A83-32716
Ground simulation of engine operation at altitude 16 p2312 A83-35863

HIGH ASPECT RATIO

An asymptotic expression of lift slope of elliptic wing with high aspect ratio 01 p0002 A83-10125
Near field pressure fluctuations of an elliptic jet [AIAA PAPER 83-0663] 10 p1472 A83-25901
The structure of trailing vortices generated by model rotor blades 12 p1696 A83-29404
Calculation of a turbulent boundary layer of an incompressible fluid over swept wings of large aspect ratios 17 p2451 A83-37803
An iterative extended boundary condition method for solving the absorption characteristics of lossy dielectric objects of large aspect ratios --- under exposure to incident plane wave radiation 21 p3189 A83-43833

Heat transfer experiments in high aspect ratio rectangular channel with epoxied short pin fins [ASME PAPER 83-GT-57] 23 p3447 A83-47913

HIGH ASPECT RATIO WINGS

U SLENDER WINGS

HIGH CURRENT

The physics of power rectifiers at very high current levels - Electric and thermal aspects --- French thesis 02 p0166 A83-11699
The MAJIC-FET - A high speed power switch with low on-resistance --- Modulated Admittance Junction Injection Controlled 02 p0167 A83-11798
A high-current magnetically stabilized plasma column for fast current-reversal and penetration studies 04 p0538 A83-16062
High current, high voltage accelerators as free-electron lasers drivers 13 p1917 A83-31128
Propagation of intense relativistic electron beams through drift tubes with perturbed walls 16 p2345 A83-35747
Antennas for nonsinusoidal waves. II - Sensors 16 p2342 A83-35781
Plasma pump sources for lasers 16 p2416 A83-35892
Measurement of laser photoelectron image degradation at high current densities 16 p2356 A83-35969
First indication of Ampere tension in solid electric conductors 23 p3445 A83-48592

HIGH DISPERSION SPECTROGRAPHS

Ultraviolet spectra of planetary nebulae. IX - High-dispersion observations of NGC 7662 03 p0402 A83-13334
The width of echelle orders in IUE images as derived with the astronomical image display and analysis /AIDA/ system in Tuebingen 03 p0411 A83-14799
High dispersion investigation of CP stars around the H-alpha line 09 p1356 A83-25300
On the need for a new spectroscopic standard for MK spectral type B0 III 15 p2250 A83-35321
Spectroscopic study of three supergiants of type F8 17 p2601 A83-37680
The narrow ultraviolet emission lines of the red dwarf Au Microscopii (dM1.6e) 17 p2605 A83-37939

HIGH ECCENTRIC LUNAR OCCULTATION SATELLITE U EXOSAT SATELLITE

HIGH ENERGY ASTRONOMY OBSERVATORIES

U HEO

HIGH ENERGY ASTRONOMY OBSERVATORY A

U HEO 1

HIGH ENERGY ASTRONOMY OBSERVATORY B

U HEO 2

HIGH ENERGY ASTRONOMY OBSERVATORY C

U HEO 3

HIGH ENERGY ASTRONOMY OBSERVATORY 1

U HEO 1

HIGH ENERGY ASTRONOMY OBSERVATORY 2

U HEO 2

HIGH ENERGY ASTRONOMY OBSERVATORY 3

U HEO 3

HIGH ENERGY ELECTRONS

NT RELATIVISTIC ELECTRON BEAMS

Concerning a new component of the radiation belts 02 p0272 A83-11708
Investigation of fluxes of electrons and gamma quanta with energies exceeding 30 MeV at heights of 300-350 km 02 p0272 A83-11709
Investigation of high-energy electrons by the Intercosmos-17 satellite 02 p0273 A83-11714
The possibility of detecting electrons with an energy greater than 20 MeV in the region of the Brazilian magnetic anomaly 02 p0210 A83-12444
Fast-particle production in a parametrically unstable electron plasma 03 p0397 A83-13191
Electrons with energies of hundreds of MeV in near-earth space 03 p0438 A83-13208
The dynamics of energetic electrons according to Intercosmos-19 satellite observations in April 1979 03 p0439 A83-13217
The Los Alamos synchronous orbit data set 04 p0511 A83-16285
Investigation of transient electronic transport in GaAs following high energy injection 06 p0814 A83-18757
Electromagnetic cyclotron-loss-cone instability associated with weakly relativistic electrons 06 p0812 A83-18919
Distribution functions of the number of cascade electrons at various stages of the development of a shower in lead at high energies 06 p0858 A83-19347
High-energy solid-state electronics --- Russian book 07 p0919 A83-20388
Quantitative study of substorm-associated VLF phase anomalies and precipitating energetic electrons on November 13, 1979 07 p0966 A83-21513
Observation of suprathermal electrons produced by stimulated Raman scattering processes 08 p1168 A83-22376

Energetic electron fluxes and ionospheric absorption during the August event 1972 09 p1301 A83-23672
The differential energy spectra of electrons having energies of 0.3-3 MeV on the basis of data from the satellite Prognoz 4 10 p1523 A83-26109
Study on the onsets of solar energetic electron events 11 p1692 A83-28579

Quantitative study of substorm-associated VLF phase anomalies and precipitating energetic electrons 14 p2055 A83-33146

On the use of artificially injected energetic electrons as indicators of magnetospheric electric fields parallel to the magnetic lines of force 15 p2197 A83-34180
Evidence for beam-stimulated precipitation of high energy electrons --- in magnetosphere 15 p2198 A83-34186

Elastic and inelastic scattering of high-energy electrons and X-rays by NH3, CH4 and H2O molecules 16 p2409 A83-35333

Mechanism for the loss of fast electrons from a Penning glow discharge 16 p2418 A83-36940
Loss cone fluxes and pitch angle diffusion at the equatorial plane during auroral radio absorption events 17 p2783 A83-38372

Mechanism of the formation near the earth of a halo of electrons with energies in the hundreds of MeV 18 p2713 A83-39313

High energy electrons at altitudes 500 km near the equator 18 p2787 A83-39955
Creation of high-energy electron tails by means of the modified two-stream instability 18 p2747 A83-40496

Ground-based observations of subauroral energetic-electron arcs 19 p2865 A83-41122
Magnetic drifts at lo - Depletion of 10-MeV electrons at Voyager 1 encounter due to a forbidden zone 20 p3077 A83-42406

Electron energy deposition in the middle atmosphere 20 p3019 A83-42419

Neutral and ion gas heating by auroral electron precipitation 20 p3019 A83-42421
The propagation of extra-relativistic cosmic ray electron in the interstellar medium 21 p3245 A83-44577
Measurements of high-energy electrons in the radiation belt by the Bulgaria-1300 satellite 21 p3245 A83-45296

Suprathermal electron energy deposition in plasmas with the Fokker-Planck method 21 p3215 A83-45520
Earth's magnetic field as a radiator to detect cosmic ray electrons of energy greater than 10 to the 12th eV 22 p3390 A83-47043

Evidence for the E x B drift of pulsating auroras 22 p3336 A83-47059

Satellite observations of energetic electron precipitation during the 1979 solar eclipse and companions with rocket measurements 23 p3480 A83-47468
Energetic electrons as an energy transport mechanism in solar flares 23 p3532 A83-47672
Properties of the corona generated by the incidence of intense CO2 laser pulses on spherical targets 24 p3631 A83-48820

Dielectric surface discharges - Effects of combined low-energy and high-energy incident electrons 24 p3572 A83-48900

HIGH ENERGY FUELS

Penetration and breakup of slurry jets in a supersonic stream 16 p2352 A83-36094
Small turbine engine experience with high density fuels [AIAA PAPER 83-1177] 16 p2339 A83-36262

HIGH ENERGY INTERACTIONS

NT LIGHT-CONE EXPANSION

NT STRONG INTERACTIONS (FIELD THEORY)

Large detectors and photomultipliers in experiments at CERN 01 p0051 A83-10872
Stratification of a glow discharge in a gas flow at high energy inputs 01 p0108 A83-11321
Interpretations of changes in the character of the interaction of hadrons at an energy greater than 10 to the 14th eV 02 p0235 A83-11736
The PAMIR-ANI experiments and quantum chromodynamics 02 p0274 A83-11745
Derivation of vertical muon spectra at superhigh energies from our predicted primary cosmic-ray spectrum using machine interaction parameters and Feynman scaling hypothesis 06 p0857 A83-18136
Two-body relaxation in relativistic thermal plasmas 07 p1017 A83-20930
Proton-nucleus total inelastic cross sections - An empirical formula for E greater than 10 MeV 08 p1192 A83-22747

Energy spectrum of cosmic ray primaries at super high energies estimated from the recent balloon-borne calorimeter measurements 09 p1369 A83-24700
Heavy particle with long life in cosmic rays above 10 to the 17th eV 12 p1801 A83-29036

- Conference on the Application of Accelerators in Research and Industry, 7th, North Texas State University, Denton, TX, November 8-10, 1982, Proceedings
13 p1917 A83-30176
- Space radiation interaction mechanisms in materials [AIAA PAPER 80-0588] 13 p1918 A83-31299
- Inelastic p-air cross section at energies between 10,000-1,000,000 TeV estimated from air-shower experiments 17 p2629 A83-37736
- Extremely high multiplicities in high-energy nucleus-nucleus collisions 17 p2629 A83-37737
- Cosmic rays and high-energy interactions - Is there a necessity for a new phenomenon? 17 p2630 A83-38942
- Status and future of high energy diffuse gamma-ray astronomy 18 p2785 A83-39276
- Radiation spectrum of optically thin relativistic electron-positron plasma 18 p2774 A83-39734
- A high-energy, laser accelerator for electrons using the inverse Cherenkov effect 20 p2994 A83-42586
- The high-energy spectrum of hot accretion disks 20 p3073 A83-43072
- Ionization effects and transition radiation of relativistic charged particles 20 p3045 A83-43526
- Eikonal phase shift analyses of carbon-carbon scattering 20 p3046 A83-43580
- Channeling, radiation, and reactions in crystals at high energies --- Russian book 21 p3218 A83-45048
- Ultra high energy cosmic rays 23 p3539 A83-47743
- Positrons in cosmic rays and the galactic gamma radiation associated with them 24 p3675 A83-49173
- HIGH FIELD MAGNETS**
- Performance results of a 300 MWth generator at high magnetic field [AIAA PAPER 83-0394] 05 p0686 A83-16690
- Observation of high-field superconductivity of a strongly interacting Fermi liquid in U6Fe 19 p2904 A83-40958
- HIGH FREQUENCIES**
- The influence of characteristics of an HF discharge on the oscillation level of a hydrogen maser 01 p0055 A83-10925
- Industry looks at military exceptionally high frequency bands 05 p0621 A83-16868
- High frequency scattering by a thin dielectric slab 06 p0737 A83-18611
- The performance of adaptive antennas in HF communications 06 p0739 A83-18625
- Adaptive antenna studies for HF communications 06 p0739 A83-18635
- High-frequency scattering from offset reflectors 06 p0740 A83-18648
- HF propagation - What we know and what we need to know 06 p0747 A83-18733
- Ionospheric modification by high power radio waves 09 p1299 A83-23302
- Observations of fluxes of suprathermal electrons accelerated by HF excited instabilities 09 p1300 A83-23309
- HF produced ionospheric electron density irregularities diagnosed by UHF radio star scintillations 09 p1300 A83-23310
- The ionosphere as a limiting factor in HF radio communication 09 p1244 A83-23386
- Analytical model of a magnetron 09 p1252 A83-23461
- Sonic diagnostics of HF discharges 09 p1347 A83-23660
- Observations of HF-enhanced plasma line with a 46.8-MHz radar and reinterpretation of previous observations with the 430-MHz radar 09 p1303 A83-23764
- High frequency scattering by a thin lossless dielectric slab 09 p1247 A83-23790
- On the relationship between the intensity of the sporadic radio emission of the earth's magnetosphere in the 0.7-2.3 MHz frequency range and fluxes of soft electrons /0.2-10 keV/ 09 p1307 A83-25035
- Experimental investigation of modal power distribution in a duct at high frequency [AIAA PAPER 83-0731] 10 p1475 A83-25938
- A study of a high-frequency polarized-wave field penetrating a plasma in a transition region with a diffused boundary 10 p1487 A83-26800
- Coefficient perturbation adaptive HF array 11 p1555 A83-27914
- A comparison of different devices for phase shift measurement at high frequency 19 p2840 A83-41556
- Production of auroral zone E region irregularities by powerful HF heating 20 p3020 A83-42427
- Analysis of HF interference with application to digital communications 20 p2965 A83-43684
- Short-term prediction of HF propagation 21 p3122 A83-45450
- Cosmic noise observations at high radio frequencies 21 p3226 A83-45452
- The effects of the ionosphere on the extent of the radio horizon at high frequency band 21 p3178 A83-45453
- High frequency radio noise 22 p3273 A83-45882
- Visualization of fatigue defects by an electrodischarge high-frequency method 22 p3269 A83-46330
- Observation of HF noise in an intense aurora by the sounding rocket S-310JA-7 22 p3331 A83-46516
- HF Doppler measurement in the auroral ionosphere 22 p3332 A83-46524
- High-frequency scattering from the edges of impedance discontinuities on a flat plane 23 p3442 A83-47830
- A new wideband HF technique for MHz-bandwidth spread-spectrum radio communications 24 p3570 A83-48994
- HIGH GAIN**
- Decentralized stabilization of a class of non-linear interconnected systems 01 p0095 A83-10959
- Design of E-plane cosecant square beam horn antennas based on ray theory and their radiation characteristics 03 p0308 A83-14135
- Decoupling of high gain multivariable tracking systems [AIAA PAPER 83-0280] 05 p0592 A83-16625
- Q-switched semiconductor diode lasers 07 p0938 A83-21591
- Molecular beam epitaxial double heterojunction bipolar transistors with high current gains 08 p1081 A83-22916
- Direct-coupled Josephson exclusively or gate with a high gain and a wide margin 11 p1563 A83-28615
- InP:Fe photoconductors as photodetectors 15 p2150 A83-33685
- A geodesic lens antenna for 360 deg azimuthal coverage 15 p2146 A83-35085
- HIGH GRAVITY (ACCELERATION)**
- U HIGH GRAVITY ENVIRONMENTS
- HIGH GRAVITY ENVIRONMENTS**
- Parametric study of acceleration effects on burning rates of metallized solid propellants 02 p0161 A83-13084
- Acceleration measurements in a high G environment 17 p2509 A83-37131
- HIGH INTENSITY LASERS**
- U HIGH POWER LASERS
- HIGH LATITUDES**
- U POLAR REGIONS
- HIGH LEVEL LANGUAGES**
- NT ADA (PROGRAMMING LANGUAGE)
- An Atlas implementation for the '80s 01 p0091 A83-10740
- ADATLAS - The test language of the future 01 p0091 A83-10741
- Voice ATLAS 01 p0091 A83-10742
- HOML compiler - High Order Microcode Language 01 p0092 A83-11194
- A high order language for the analysis of experimental data 01 p0089 A83-11196
- Jovial language control procedures with a view toward Ada 01 p0092 A83-11198
- ADA, an introduction: ADA reference manual, /July 1980/ --- Book 01 p0093 A83-11503
- Cellular array processing simulation 02 p0228 A83-12881
- ESACAP - A minicomputer-oriented network-analysis program 03 p0385 A83-13847
- Electronic Circuit Analysis Language /ECAL/ 04 p0470 A83-15550
- DARTS - A software manufacturing technology [AIAA PAPER 83-0324] 05 p0678 A83-16653
- AML - A manufacturing language 11 p1646 A83-28100
- A general precompiler for algebraic manipulation 12 p1768 A83-29110
- A basis for the quantitative comparison of computer number systems 15 p2217 A83-33906
- CADAC - A controlled-precision decimal arithmetic unit 15 p2217 A83-33907
- Integrated verification and testing system (IVTS) for HAL/S programs 15 p2219 A83-33971
- Experiments in automatic microcode generation 19 p2888 A83-41037
- Using English as a high-level robot command language 21 p3191 A83-44080
- HIGH MELTING COMPOUNDS**
- U REFRACTORY MATERIALS
- HIGH POWER LASERS**
- B-X transitions in HgCl and HgI --- for high power UV-visible lasers 01 p0055 A83-10980
- Recent development in high speed cinematographic and interferometric studies of high power laser target interaction 01 p0052 A83-11067
- A high-power polarised coherent TE N2 laser 02 p0183 A83-12011
- High power single-frequency laser at 1.32 microns using Nd:YAG 02 p0183 A83-12083
- Studies of organic molecules as saturable absorbers at 193 nm 02 p0184 A83-12268
- High-power multiple-stripe injection lasers with channel guides 02 p0184 A83-12269
- Picosecond amplification and kinetic studies of XeCl 02 p0184 A83-12272
- Development in replicated nickel gratings 02 p0238 A83-12713
- Dynamic saturation of optical transitions in high-power molecular lasers 03 p0331 A83-13588
- Optical damage resistance of lithium niobate waveguides 03 p0393 A83-13759
- High-power single-mode AlGaAs laser diodes 03 p0331 A83-13875
- Continuous wave high-power, high-temperature semiconductor laser phase-locked arrays 03 p0333 A83-14932
- High-power individually addressable monolithic array of constricted double heterojunction large-optical-cavity lasers 03 p0333 A83-14935
- Polymeric passive laser shutters 04 p0484 A83-15265
- Single-mode lasers for optical communications 04 p0486 A83-16213
- Pulsed-power performance and stability of 880 nm GaAlAs/GaAs oxide-stripe lasers 04 p0486 A83-16215
- The effect of giant laser pulses on a quasi-stationary plasma torch 05 p0687 A83-16893
- Spatial mode discrimination and control in high-power single-mode constricted double-heterojunction large-optical-cavity diode lasers 05 p0648 A83-16942
- Efficient frequency doubling of radiation emitted by a multistage neodymium laser 05 p0648 A83-17040
- Analysis of the energetics of a chemical oxygen-iodine laser 05 p0648 A83-17047
- Stability of compensation regimes for nonlinear distortions of beams with any polarization 05 p0650 A83-17077
- Dye lasers --- in tunable high-power modes 05 p0650 A83-17224
- Femtosecond white-light continuum pulses 05 p0651 A83-17876
- Dichroic beam splitter for extreme-ultraviolet and visible radiation 05 p0651 A83-17878
- An UV-preionized KrF excimer laser with an output energy of 0.42 J 06 p0766 A83-19143
- High power single mode InGaAsP lasers fabricated by single step liquid phase epitaxy 06 p0767 A83-19254
- Single longitudinal mode operation of high power multiple-stripe injection lasers 06 p0767 A83-19256
- Rapid-flow combined-action industrial CO2 laser 07 p0933 A83-20104
- Investigation of the active medium in a fast-flow closed-cycle industrial CO2 laser 07 p0933 A83-20105
- Investigation of the vibrational temperature kinetics in a TEA CO2 laser 07 p0934 A83-20113
- Advances in laser and MIAB welding techniques 07 p0940 A83-20523
- Laser beam welding of aluminum alloy 5456 07 p0940 A83-20525
- Metal drilling investigation by means of different high power laser radiation 07 p0940 A83-21031
- Powerful electroionization laser on Xe infrared atomic transitions 07 p0938 A83-21589
- Theoretical analysis of electron-beam-excited KrF laser performance - New F2 concentration optimization 07 p0938 A83-21599
- Theory of line narrowing and frequency selection in an injection locked laser 07 p0938 A83-21600
- New CH3OH laser lines pumped with a fine-tuned high-power CO2-TEA laser 08 p1107 A83-22247
- Wavefront distortions in power optics; Proceedings of the Meeting, San Diego, CA, August 27, 28, 1981 08 p1107 A83-22449
- Phase aberrations and laser output beam quality 08 p1108 A83-22450
- Limitations on the use of root-mean-square /rms/ phase to describe beam quality characteristics --- of high power lasers 08 p1108 A83-22451
- Aberrations in high power laser systems 08 p1108 A83-22452
- Overview of aero-optical phenomena --- in pulsed and continuous wave laser-target interactions 08 p1108 A83-22453
- Effects of flow fields in optical systems 08 p1108 A83-22454
- Wavefront distortion introduced by sampling with a hole grating --- high power laser beam diagnostics 08 p1108 A83-22455
- Fresnel ripple mapping of water-cooled laser mirrors 08 p1108 A83-22457

Mode-medium interactions --- high power CO₂ laser
 output instability 08 p1109 A83-22461
 Intracresonator phase conjugation --- for high power
 lasers 08 p1109 A83-22463
 Pseudo-conjugation/compensation of high-power
 optical trains 08 p1164 A83-22464
 Adaptive optics - Problems and prospects
 08 p1109 A83-22465
 Wavefront sensing and control aspects in a high energy
 laser optical train 08 p1109 A83-22467
 Liquid crystals as large aperture waveplates and circular
 polarizers 08 p1166 A83-22571
 High power operation of a CW 28-micron water vapor
 laser 10 p1425 A83-25428
 High power pulsed FIR laser lines from CD₃OH
 10 p1425 A83-25429
 Backward and forward FIR emission characteristics from
 D₂O in both Raman and laser regimes
 10 p1426 A83-26001
 Results of the Los Alamos Free-Electron Laser
 Experiment 10 p1428 A83-26021
 A high energy D₂O submillimeter laser for plasma
 diagnostics 10 p1431 A83-26648
 Analysis of multistage dissociation of polyatomic
 molecules 10 p1480 A83-26679
 Problem of accurate intensity measurements in focused
 laser beams 10 p1433 A83-26683
 Electric-discharge CW industrial CO₂ laser
 10 p1433 A83-26687
 High-pressure NH₃-N₂ laser 10 p1434 A83-26689
 Injection locking of excimer lasers
 11 p1577 A83-27518
 Suprathermal electron pumping of X-ray lasers
 11 p1577 A83-27521
 Optics and resonator design issues for high-power free
 electron lasers 11 p1579 A83-27570
 Diatomic molecules as storage media for high energy
 lasers 11 p1580 A83-27573
 High-power electro-ionization CO₂ - Lasers for laser
 technology 11 p1580 A83-27574
 Experimental investigation of the optimum specific input
 energy on a subsonic CO EDL --- Electric Discharge
 Laser 11 p1580 A83-27577
 The physics of electric-discharge CO₂-lasers --- Russian
 book 12 p1731 A83-28815
 High power TEA CO₂ laser tuned by a holographic
 grating 12 p1731 A83-29196
 The high-power iodine laser --- Book
 13 p1849 A83-30135
 High-power-density electron-beam-sustained laser
 13 p1849 A83-30256
 Runaway self-absorption in multikilowatt CO₂ lasers
 13 p1850 A83-30328
 Phase-locked (GaAl)As laser emitting 1.5 W CW per
 mirror 13 p1850 A83-30330
 A high-power, narrow linewidth XeCl(asterisk)
 oscillator 13 p1852 A83-31058
 Resonator mode structure --- in free electron lasers
 13 p1854 A83-31122
 Millimeter-wave generation by a single-pass,
 Compton-regime, variable-parameter free-electron laser
 13 p1854 A83-31123
 Microtron free-electron laser experiment
 13 p1854 A83-31124
 Design considerations of a Compton scattering
 free-electron laser with an axial electrical field
 13 p1855 A83-31131
 International intercomparison of laser power
 measurements in the visible region
 13 p1856 A83-31278
 High-power continuously tunable atmospheric-pressure
 CO₂ laser operating in the superregenerative amplification
 regime 14 p2023 A83-31915
 Influences of thermal effects on high power CW outputs
 of b-axis Nd:YAP lasers 14 p2024 A83-32596
 Pulsed gain and thermal lensing of Nd:LiYF₄
 14 p2025 A83-33401
 Femtosecond optical pulses 14 p2025 A83-33402
 A high-power, single-mode laser with
 twin-ridge-substrate structure 14 p2027 A83-33438
 An experimental study of the absorption mechanisms
 in laser-matter interaction at high energies - The effect
 of wavelength --- French thesis
 15 p2232 A83-33699
 High-power KrF laser transmission through optical fibers
 and its application to the triggering of gas switches
 16 p2357 A83-35427
 A high power D₂O laser optimized for microsecond pulse
 duration 16 p2358 A83-35431
 Future development of high-power solid-state laser
 systems 16 p2358 A83-35884
 Plasma pump sources for lasers
 16 p2416 A83-35892
 Long pulse excimer laser excited by sequenced
 discharges 16 p2359 A83-35956

High-power, long-pulse CO₂ laser transversely excited
 by a damped oscillating discharge through dielectric
 electrodes 17 p2513 A83-36998
 Modeling of overlap thermal blooming in smoke
 [AIAA PAPER 83-1719] 17 p2503 A83-37208
 Electrically triggered multimodule KrF laser system with
 narrow-linewidth output 18 p2692 A83-39092
 Proposal for high-power radiative-collisional lasers
 [AD-A122225] 19 p2850 A83-40671
 High-efficiency and high-power AlGaAs/GaAs laser
 19 p2851 A83-40935
 High-efficiency infrared xenon laser excited by a UV
 preionized discharge 19 p2852 A83-40947
 Demonstration of a two-stage backward-wave-oscillator
 free-electron laser 19 p2852 A83-41157
 Intracavity pumped NH₃ laser using a very small
 cavity 19 p2853 A83-41184
 A technique for measuring energy absorption from high
 energy laser radiation 20 p2989 A83-42781
 Long pulse DCM dye laser 20 p2994 A83-42793
 Optimal physical parameters for a high-power He-Ne
 laser 20 p2995 A83-42949
 A self-sustained discharge multiatmospheric CO₂ laser
 with electron-beam preionization 20 p2995 A83-43633
 Polarization of picosecond light pulses in nonlinear
 isotropic media 20 p2995 A83-43634
 High-power rhodamine 6G laser with an extended
 service life 20 p2996 A83-43778
 Formation of the spatial structure of radiation in
 solid-state laser systems by apodizing and hard
 apertures 20 p2996 A83-43786
 Influence of the inhomogeneity of the process of energy
 deposition on the gain coefficient of high-power gas
 lasers 20 p2997 A83-43795
 Plastics for high-power laser applications - A review
 21 p3115 A83-43861
 Compact uniform field electrode profiles --- for use in
 TEA laser 21 p3143 A83-44191
 Improved welding penetration of a 10-kW industrial
 laser 21 p3146 A83-45480
 Study of gain, bandwidth, and tunability of a
 millimeter-wave free-electron laser operating in the
 collective regime 22 p3295 A83-46016
 Carbon dioxide waveguide laser design for maximum
 output power at specified frequency offset 22 p3299 A83-46747
 Atmospheric-pressure electroionization CO₂ laser using
 CO₂-N₂-H₂O mixtures 22 p3300 A83-46785
 Chaotic and periodic emission of high power solid state
 lasers 23 p3462 A83-48318
 Problems encountered in the development of 1-10-kw
 industrial lasers 23 p3462 A83-48431
 Generation of high power, very coherent radiation by
 interaction of a free electron laser with a molecular (or
 ionic) medium 23 p3463 A83-48573
 Laser welding of PM materials 23 p3467 A83-48724
 High-power, subpicosecond 10-micron pulse
 generation 24 p3587 A83-48851
 Optimization of corona-discharge photoionization
 sources for CO₂ lasers 24 p3587 A83-48909
 A theoretical model for multiple-pulse laser-induced
 damage to metal mirrors 24 p3587 A83-48911
 Thermophysical characteristics of coaxial high-power
 laser chambers 24 p3588 A83-49123

HIGH PRESSURE
 Direct conversion from amorphous to beta-Si₃N₄ under
 high pressure 02 p0160 A83-11677
 Relaxation kinetics of a high-pressure inert-gas
 plasma 03 p0397 A83-13194
 Equipment for development of better end-face seals -
 A progress review
 [ASLE PREPRINT 82-LC-5C-1] 03 p0334 A83-13244
 High-pressure tunable CW waveguide CO₂ lasers
 04 p0483 A83-15255
 Open seat ejection at high dynamic pressure - A radical
 approach 04 p0445 A83-15308
 Optical investigations in the megabar range using a
 chamber consisting of a rounded cone and a flat
 foundation 07 p0902 A83-20044
 The effect of a high-pressure gaseous environment on
 the content of sodium, potassium, and water in the blood
 and tissues of white rats 07 p0973 A83-20246
 High-pressure NH₃-N₂ laser 10 p1434 A83-26689
 Human respiration at rest in rapid compression and at
 high pressures and gas densities 13 p1902 A83-30467
 Density-functional theory for solid nitrogen and carbon
 dioxide at high pressure 13 p1929 A83-30958
 Equation of state of sodium at pressures up to 30
 GPa 15 p2237 A83-33783
 CARS diagnostics of high pressure and temperature
 gases --- Coherent Anti-Stokes Raman Spectroscopy
 [AIAA PAPER 83-1478] 15 p2133 A83-34913

High pressure studies of Ge using synchrotron
 radiation 16 p2419 A83-35455
 High-pressure growth of polycrystalline molybdenum
 disulphide 16 p2337 A83-36071
 Structural phase transitions in crystals at high
 pressure 19 p2904 A83-40980
 High-temperature, high-pressure optical cells
 20 p2959 A83-42297
 High pressure measurements on photopumped low
 threshold Al(x)Ga(1-x)As quantum well lasers
 20 p2994 A83-42595
 Response of liquid carbon disulfide to shock
 compression Equation of state at normal and high
 densities 20 p3055 A83-42638
 Detonation propulsion experiments and theory --- for
 spacecraft in high pressure planetary atmospheres
 21 p3105 A83-45585
 Thermal conductivity of minerals at high pressure - The
 effect of phase transitions 22 p3322 A83-45741

HIGH PRESSURE OXYGEN
 Prediction of metal fire spread in high pressure oxygen
 17 p2484 A83-37047
 Fire spread mechanisms along steel cylinders in high
 pressure oxygen 17 p2485 A83-38026

HIGH Q
U Q FACTORS
HIGH RESOLUTION
 A Michelson interferometer for high resolution of shot
 start movement using a CO₂ laser
 01 p0052 A83-11068
 High resolution imaging from the ground
 02 p0246 A83-12188
 High resolution soft X-ray optics: Proceedings of the
 Meeting, Brookhaven, NY, November 18-20, 1981
 02 p0239 A83-12721
 Solar corona at high resolution
 02 p0271 A83-12727
 Progress report on the high resolution spectrograph for
 the Space Telescope 03 p0288 A83-13971
 Recent results in the analysis of high-resolution infrared
 atmospheric transmission spectra 03 p0358 A83-13983
 High-resolution atmospheric spectroscopy using a diode
 laser heterodyne spectrometer 03 p0327 A83-13984
 High resolution planetary albedos - Values and
 variability 05 p0660 A83-16906
 Observations of the solar wind with high temporal
 resolution 06 p0853 A83-18362
 Broadband high-resolution receivers for the
 sub-millimeter region 07 p0913 A83-20184
 Fundamental properties of high-resolution
 sideways-looking radar 08 p1075 A83-21994
 Resolution improvement in an analog-to-digital converter
 by the superposed dither signal 08 p1080 A83-22231
 A complete sample of intermediate-strength radio
 sources selected from the GB/GB2 1400-MHz surveys.
 III - High-resolution observations and optical identifications
 of sources with normal or flat spectra 09 p1351 A83-23315
 Ring laser gyroscopes - Charge-coupled device /CCD/
 readout and signal processing for high resolution
 applications 09 p1267 A83-23590
 Optical observations of active galaxies and quasars at
 high angular resolution 10 p1496 A83-25857
 High-resolution line-shape analyses of the pulsed
 cuprous chloride-laser oscillator and amplifier
 10 p1435 A83-26878
 High resolution schemes for hyperbolic conservation
 laws 12 p1771 A83-29095
 Analysis of the high-resolution Mg XI X-ray spectra. IV
 Derivation of the plasma densities to the 'low-density'
 limit 13 p1943 A83-29983
 High-resolution observations of solar radio bursts at 2,
 6, and 20 cm wavelength 13 p1963 A83-29986
 High efficiency spectrographs for the EUV and soft
 X-rays 13 p1935 A83-30183
 Performance of the Multiple Mirror Telescope (MMT).
 IX - Doing science with the MMT 13 p1937 A83-30985
 Speckle interferometry and related techniques with
 advanced technology optical telescope 13 p1920 A83-31011
 High spectral resolution lidar system with atomic blocking
 filters for measuring atmospheric parameters
 [AD-A129929] 13 p1857 A83-31463
 European Southern Observatory (ESO) coudeechelle
 spectrometer 14 p2084 A83-32005
 Grazing incidence optics - New techniques for high
 sensitivity spectroscopy in the space ultraviolet
 14 p2084 A83-32018
 Spatial lattice filter for high-resolution spectral analysis
 of array data 14 p2075 A83-32434
 Picosecond spectrochronography 14 p2022 A83-33418

- Microwave and hard X-ray observations of a solar flare with a time resolution better than 100 ms
15 p2280 A83-34302
- Superresolution of multiple noise sources in antenna beam
15 p2148 A83-35180
- Simultaneous scanning optical and acoustic microscopy
16 p2356 A83-36478
- The use of high horizontal resolution satellite temperature and moisture profiles to initialize a mesoscale numerical weather prediction model - A severe weather event case study
18 p2725 A83-39687
- IFU - A multi-detector IR spectrometer
18 p2690 A83-40432
- Recording of interferograms on normal high resolution plates using a CO₂ laser at 10.6 microns
19 p2847 A83-41103
- Principles of high resolution NMR in solids (2nd revised and enlarged edition) --- Book
19 p2820 A83-41466
- High resolution lattice images of G.P. zones in an Al-3.97 wt pct Cu alloy --- Guinier-Preston
20 p2956 A83-43613
- High resolution spectroscopy using picosecond pulse trains
21 p3140 A83-44818
- New results of airborne measurements with a sensitive high resolution 90 GHz radiometer
22 p3309 A83-46124
- The European SAR-580 project --- high resolution Synthetic Aperture Radar data evaluation
22 p3310 A83-46136
- The High Spectral Resolution Lidar
23 p3458 A83-47803
- High-sensitivity material with reversible photo-induced anisotropy
23 p3459 A83-48315
- FUN with PANURGE - High mass resolution ion microprobe measurements of Mg in Allende inclusions --- meteoritic composition isotope analysis
24 p3672 A83-49350
- High-resolution imaging of inhomogeneities in superconducting tunnel junctions by scanning with a modulated electron beam
24 p3636 A83-49757
- High-resolution optical observations of NGC 3379. II - On the derivation of the East-West profile
24 p3663 A83-49846
- HIGH RESOLUTION COVERAGE ANTENNAS**
- The use of multiple transmitting antennas to provide beamwidth reduction for H.F. pulse radars with sector coverage
06 p0738 A83-18623
- HIGH REYNOLDS NUMBER**
- Solution of Burgers' equation with a large Reynolds number
01 p0045 A83-10710
- Visualization study of the axisymmetric mixing layer of a high Reynolds number jet
03 p0320 A83-14482
- The effects of surface roughness on the flow past circular cylinders at high Reynolds numbers
03 p0321 A83-14584
- A simple model of mixing and chemical reaction in a turbulent shear layer
[AD-A128220]
06 p0758 A83-19021
- Local isotropy and anisotropy in a high-Reynolds-number turbulent boundary layer
06 p0758 A83-19023
- Fully developed turbulent flow in a pipe - An intermediate layer
06 p0759 A83-19321
- High Reynolds number shear stress measurements --- flight test results
[AIAA PAPER 83-0053]
06 p0713 A83-19578
- On the finite element simulation of incompressible turbulent flow in general two-dimensional geometries
08 p1088 A83-23187
- A finite element method for high Reynolds number viscous fluid flow using two step explicit scheme
12 p1724 A83-29442
- Elliptic-vortex method for incompressible flow at high Reynolds number
12 p1724 A83-29609
- High-Re solutions for incompressible flow using the Navier-Stokes equations and a multigrid method
12 p1725 A83-29659
- Asymptotics of solutions of the Orr-Sommerfeld equation describing unstable oscillations at large Reynolds numbers
13 p1839 A83-30091
- Cryogenic wind tunnels for high Reynolds number testing
14 p1977 A83-32175
- A statistical mechanical model for two dimensional turbulence
14 p2009 A83-32510
- A numerical study of the Burgers turbulence at extremely large Reynolds numbers
14 p2009 A83-32520
- A new facility and technique for two-dimensional aerodynamic testing
14 p1977 A83-32585
- A numerical investigation for curved pipe flow at high Reynolds number
[ASME PAPER 83-APM-18]
17 p2504 A83-37376
- The application of splines to the numerical solution of the Navier-Stokes equations at high Reynolds numbers
17 p2505 A83-37629
- Amplitude-dependent stability of boundary-layer flow with a strongly non-linear critical layer
17 p2509 A83-38924
- Investigation of transonic Ludwig tubes. I - Starting process in the case of an upstream valve
18 p2684 A83-39459
- A vortex sheet method for calculating separated two-dimensional flows
19 p2789 A83-40855
- Interaction between two spherical particles in a stationary flow of a viscous fluid at larger Reynolds numbers
19 p2843 A83-41263
- The mean coefficients of heat transfer from gas to turbine nozzle blade at high Reynolds numbers
19 p2846 A83-42075
- A theory for flow separation
20 p2985 A83-43099
- Cryogenic-wind-tunnel technology - A way to measurement at higher Reynolds numbers
22 p3256 A83-46484
- The dynamics of two-dimensional ideal MHD
23 p3510 A83-48046
- Alternating-triangular difference scheme for solving the Navier-Stokes equations
24 p3576 A83-48946
- HIGH SPEED**
- Flow characteristics and methods of flow calculation of high-speed compressible flow through pipe orifices
09 p1257 A83-23332
- Farfield inflight measurements of high-speed turboprop noise
[AIAA PAPER 83-0745]
10 p1377 A83-25947
- Acoustic measurements on aerofoils moving in a circle at high speed
[AIAA PAPER 83-0674]
11 p1650 A83-28003
- Measurements and predictions of turboprop noise at high cruise speed
[AIAA PAPER 83-0689]
11 p1651 A83-28008
- A coronal transient associated with a high-speed type II burst
14 p2116 A83-33219
- Review of prior work in high-speed machining --- of metals and alloys
15 p2171 A83-33646
- Titanium - A model material for analysis of the high speed machining process
15 p2171 A83-33647
- Tapered roller bearings for turbine engines
20 p2998 A83-42559
- High velocity HI in the inner 5 kpc of M31
24 p3640 A83-49205
- HIGH SPEED CAMERAS**
- High repetition rate, high resolution back-lit, shadow, and schlieren photography of gaseous and liquid mass-transport phenomena and flames
01 p0052 A83-11061
- Recent development in high speed cinematographic and interferometric studies of high power laser target interaction
01 p0052 A83-11067
- Light-in-flight recording - High-speed holographic motion pictures of ultrafast phenomena
07 p0928 A83-20153
- High-speed television camera and video tape recording system for motion analysis
08 p1097 A83-22531
- International Symposium of Biomechanics Cinematography and High Speed Photography, 2nd, San Diego, CA, August 24-26, 1981, Proceedings
08 p1102 A83-22790
- Adaptive control algorithm design for high-speed cameras
09 p1269 A83-24778
- Vacuum chamber trajectory measurement by high speed cinematography
22 p3287 A83-45975
- High-speed photography
24 p3586 A83-50116
- HIGH SPEED FLIGHT**
- U HIGH SPEED
- HIGH SPEED TRANSPORTATION**
- U RAPID TRANSIT SYSTEMS
- HIGH STRENGTH**
- High performance, low viscosity resin systems
07 p0899 A83-20465
- HIGH STRENGTH ALLOYS**
- NT ASTROLOY (TRADEMARK)
- NT HIGH STRENGTH STEELS
- NT MARAGING STEELS
- Ultrasonic tomography for nondestructive evaluation
02 p0188 A83-11505
- New high-strength aluminum alloy V95och
03 p0296 A83-13251
- Softening schedules for aging pressed semifinished products made from high-strength aluminum alloy V95pch
03 p0296 A83-13252
- Effect of zirconium additives on the properties of plates of type V95pch alloy
03 p0296 A83-13253
- Structure and fracture character of V95 alloy sheets in relation to impurity content and aging conditions
03 p0297 A83-13254
- Increasing the corrosion resistance of alloy AK8
03 p0297 A83-13257
- Recovery treatment of Al27-1 alloy
03 p0297 A83-13264
- Structural transformations in nonmagnetic alloy 03KhN40MTYuBr in the hardening process
03 p0297 A83-13266
- The effect of load ratio on fatigue crack growth in Ti8-Al-1Mo-1V
03 p0298 A83-13342
- The effect of the initial structure on the characteristics of beta solid solution decomposition in high-strength titanium alloy VT22
03 p0300 A83-14157
- The effect of superplastic deformation on subsequent service properties of fine grained 7475 Al
07 p0883 A83-19672
- The occurrence of shear bands in nonisothermal, hot forging of Ti-6Al-2Sn-4Zr-2Mo-0.1Si
07 p0884 A83-20253
- Comparison of several accelerated laboratory tests for the determination of localized corrosion resistance of high-performance alloys
08 p1066 A83-22650
- Mechanical properties of a high-strength aluminum alloy under impact loading
09 p1229 A83-23511
- Phase equilibria in Ti-Al-Zr-W and Ti-Al-Zr-Mo-W alloy systems
09 p1234 A83-24386
- The mechanical properties and phase composition of Ti-Al-Zr-W-Fe alloys
09 p1234 A83-24388
- The effect of welding and heat treatment on the structure and properties of high-strength titanium alloys
09 p1235 A83-24392
- The effect of ITMT's and P/N processing on the microstructure and mechanical properties of the X7091 alloy --- Intermediate Thermal Mechanical Treatments
10 p1398 A83-26281
- Stress corrosion and hydrogen induced cracking behaviour in an Al alloy
13 p1820 A83-30325
- The effect of loading mode on the stress-corrosion cracking of aluminum alloy 5083
14 p1994 A83-32680
- Metallography of fatigue crack initiation in an overaged high-strength aluminum alloy
14 p1994 A83-32681
- High-frequency fatigue testing of structural steels and alloys at 77 K
14 p1998 A83-33021
- High-strength powder metallurgy aluminum alloys; Proceedings of the Symposium, Dallas, TX, February 17, 18, 1982
17 p2487 A83-37832
- Fatigue of high-strength powder metallurgy aluminum alloys
17 p2487 A83-37835
- Effects of microstructure and aging treatment on the fatigue crack growth behavior of high strength P/M aluminum alloy X7091
17 p2487 A83-37837
- Stress-corrosion cracking and hydrogen embrittlement in P/M X7091 and I/M 7075
17 p2488 A83-37841
- A high strength Al Li-Mn alloy with high modulus
17 p2489 A83-37852
- Grain-boundary segregataion in titanium-vanadium low alloys
23 p3431 A83-47181
- The construction and testing of pilot installations for making diffusion connections and for depositing layers on high-alloy engine components
23 p3440 A83-47206
- Notch sensitivity of high-alloy nickel alloys
24 p3559 A83-48803
- Effect of thermomechanical treatment on mechanical properties of 2024 aluminum alloy
24 p3566 A83-49862
- The strength of the hard-alloy components of high-pressure apparatus for the synthesis of superhard materials
24 p3567 A83-49911
- The microstructure of an aluminum alloy at early stages of spall damage
24 p3567 A83-49913
- HIGH STRENGTH STEELS**
- NT MARAGING STEELS
- Precipitation hardening and the resistance to brittle fracture of low alloy steels containing vanadium
01 p0025 A83-10396
- Investigation of the hydrogen-influenced tendency toward cold cracking in high-strength low-alloy fine-grained structural steel, with regard to the implant experiment --- German thesis
01 p0026 A83-10469
- The use of fractography and fracture mechanics in analysing fatigue cracks
05 p0654 A83-17229
- The effect of rapid heating on the short-term strength characteristics of 28Kh3SNMVFA and 30KhGSA steels
06 p0733 A83-19311
- The influence of specimen geometry on stable crack growth for a high strength steel
08 p1060 A83-21704
- The use of the plastic crack tip opening displacement to correlate fatigue crack growth data for a structural steel
08 p1060 A83-21713
- The influence of prior austenite grain size and stress ratio on near threshold fatigue crack growth behavior in high strength steel
08 p1061 A83-21716
- Mechanism of SCC and hydrogen-induced delayed cracking
08 p1061 A83-21718
- A study of stress corrosion cracking in high strength steels using acoustic emission techniques
08 p1064 A83-21770
- A new method of determining J_{IC} of steel by means of single specimen
11 p1548 A83-28442
- Mechanism of corrosion fatigue crack propagation in high strength steels
11 p1548 A83-28446
- On the relation between stable crack growth and fatigue
13 p1867 A83-31540

Hydrogen-induced cracking in 4340-type steel - Effects of composition, yield strength, and H2 pressure 14 p1994 A83-32678

Ductility and the abrasive wear of an ultrahigh strength steel 15 p2141 A83-35242

Near-threshold fatigue crack propagation of several high strength steels 16 p2334 A83-36512

The structure and mechanical properties of the high-strength powder metallurgy steel 60Kh2 following thermomechanical treatment 17 p2492 A83-38872

Strengthening mechanism of nitrided layers of alloy steels 21 p3112 A83-44478

A FEM analysis of crack arrest experiments 21 p3157 A83-44905

Simultaneous measurements of stress intensity and toughness for fast-running cracks in steel 21 p3114 A83-45154

The metal chemistry of complex alloying --- Russian book 23 p3431 A83-47098

The effect of hydrogen induced surface asperities of fatigue crack closure in ultrahigh strength steel 23 p3431 A83-47850

On the influence of internal hydrogen on fatigue thresholds of HSLA steel 23 p3432 A83-47851

Effect of heat treatment on the mechanical properties of maraging steel 24 p3559 A83-48806

HIGH TEMPERATURE

Performance of laser-glazed zirconia thermal barrier coatings in cyclic oxidation and corrosion burner rig tests 01 p0027 A83-10300

High-temperature ceramic heat exchanger element for a solar thermal receiver 03 p0352 A83-13476

A simplified method of generating layer sequences for SiC polytypes 03 p0399 A83-13683

A GaP MESFET for high temperature applications 05 p0625 A83-17348

Anisotropy of kinetic properties of rhenium at high temperatures 06 p0728 A83-18443

A new explanation of the high effective temperatures in pulsar radioemissions 06 p0831 A83-18819

An improved high temperature carbon fiber finish for polyimide composites 07 p0875 A83-20428

The Magnuswirl turbine wheel - The unique solution for the high temperature cruise missile 09 p1274 A83-23647

The thermodynamic properties of diatomic molecules at elevated temperatures - Role of continuum and metastable states 11 p1665 A83-27495

The production of titanium-nickel intermetallics by self-propagating high-temperature synthesis 11 p1547 A83-27921

The high-temperature shape-memory effect in titanium-nickel intermetallics 15 p2138 A83-34019

High-temperature optical fiber thermometer 17 p2510 A83-37608

High-temperature, high-pressure optical cells 20 p2959 A83-42297

Collisional quenching of A 2Sigma(+) OH at elevated temperatures 20 p2950 A83-42633

Heat loss measurements on an enclosure for high temperature batteries 24 p3599 A83-49926

High temperature batteries with a solid sulphate electrolyte 24 p3601 A83-49955

HIGH TEMPERATURE AIR

High-temperature adsorption of air oxygen by silicon nitride powders 02 p0161 A83-13034

An experimental study of fuel combustion in a high-temperature air counterflow 03 p0295 A83-14056

K-distributed phase differences in turbulent random phase screens 09 p1267 A83-24085

An investigation of energy separation in a vortex tube 11 p1569 A83-28376

Analytical method for determining the nonequilibrium parameters of an air plasma in a Laval nozzle 13 p1922 A83-30044

The interdependence of spray characteristics and evaporation history of fuel sprays in stagnant air [ASME PAPER 83-GT-7] 23 p3440 A83-47880

High temperature oxidation of Ni-25Cr-15W alloy 24 p3565 A83-49517

HIGH TEMPERATURE ALLOYS

U HEAT RESISTANT ALLOYS

HIGH TEMPERATURE ENVIRONMENTS

Morphology of corrosion products formed on cobalt and nickel in argon-oxygen-chlorine mixtures at 1000 K 01 p0024 A83-10247

High-temperature superconductivity --- Book 01 p0110 A83-10878

Crystal structure and electrical resistance of MoS2-NbS2 alloys obtained by the method of self-propagating high-temperature synthesis 02 p0161 A83-13036

A high temperature GaP MESFET 03 p0309 A83-13561

The combined effect of noise, vibration, and high temperatures on the condition of the sympathetic-adrenal system in sailors 03 p0379 A83-13615

The effect of succinic acid on work capacity and recovery during muscle activity in conditions of various ambient temperatures 03 p0382 A83-14351

Continuous wave high-power, high-temperature semiconductor laser phase-locked arrays 03 p0333 A83-14932

Spectral selectivity of high-temperature solar absorbers. II Effects of interference 04 p0505 A83-15488

A finite temperature lambda-phi-4 model and a de Sitter-Friedmann transition in the early universe 04 p0551 A83-15597

The activity of the sympathetic-adrenal system as an indicator of athletes' adaptation to physical loads at high temperatures 05 p0672 A83-17154

The use of the tracking reaction during the normalization of several work-related factors 05 p0677 A83-17697

Military propulsion technology. III - Materials are the key --- for fighter aircraft engines 06 p0730 A83-18950

The self-propagating high-temperature synthesis of aluminides. I - A thermodynamic analysis 07 p0883 A83-19964

Evacuated, load-bearing powder insulation for high temperature applications 08 p1087 A83-23136

Measurements in hostile environments; Proceedings of the International Conference, University of Edinburgh, Edinburgh, Scotland, August 31-September 4, 1981 09 p1264 A83-23358

In-plane interferometric strain/displacement measurement at high temperatures 09 p1264 A83-23363

High temperature thermal strain measurement using laser speckles 09 p1264 A83-23364

High-temperature moire interferometry 09 p1264 A83-23365

The application of the J-integral to small specimens of ductile material to be exposed to high temperatures and high levels of irradiation 09 p1233 A83-24079

Report on advanced transmission system integration tests --- of Blackhawk helicopters 09 p1274 A83-24833

The use of coatings in high temperature battery systems 10 p1445 A83-25536

100% oxygen breathing during acute heat stress - Effect on sweat composition 10 p1454 A83-25669

Hyperthermal environment simulation for development of thermal protection systems [SAE PAPER 820881] 10 p1381 A83-25774

Long titanium heat pipes for high-temperature space radiators 11 p1537 A83-27127

An epoxy resin system for composite flywheels 12 p1711 A83-29893

Determination of threshold stress intensity for crack growth at high temperature in silicon carbide ceramics 14 p1999 A83-32975

Results of an experimental evaluation of the thermal stress of operators 14 p2073 A83-33324

Oxide dispersion hardened mechanically alloyed materials for high temperatures 15 p2137 A83-33963

On gamma and gamma-prime phases composition in Ni-base superalloys after high-temperature exposure 15 p2140 A83-34799

High temperature erosion study of INCO 600 metal 15 p2141 A83-35247

A kinetic model of high temperature fatigue crack growth 16 p2331 A83-36175

A review of the role of frequency on fatigue crack initiation and growth at elevated temperatures 16 p2332 A83-36194

Application of fluidics to instrumentation in hostile environments [AIAA PAPER 83-1150] 16 p2352 A83-36247

Inherent variability in heat-stress decision rules 16 p2402 A83-36475

Experiences in repair of hot section gas turbine components [SAE PAPER 821490] 17 p2469 A83-38008

A method for ensuring the proper operation of an optical instrument for measuring the temperature of the blades of a high-temperature turbine 19 p2799 A83-42152

High temperature corrosion; Proceedings of the International Conference, San Diego, CA, March 2-6, 1981 20 p2951 A83-42226

Disorders of the peripheral nervous system in conditions of a hot, humid climate 24 p3618 A83-49072

Li/SOCI2 cells for high temperature applications 24 p3600 A83-49940

HIGH TEMPERATURE FLUIDS

NT HIGH TEMPERATURE AIR

NT HIGH TEMPERATURE GASES

HIGH TEMPERATURE GASES

Hydrothermal oxidation of Hf metal chips in the preparation of monoclinic HfO2 powders 08 p1071 A83-22196

On the interaction of a sound pulse with the shear layer of an axisymmetric jet. II - Heated jets 09 p1340 A83-23704

HIGH TEMPERATURE GAS COOLED REACTORS
Oxidation of carburized Hastelloy X 18 p2670 A83-40640

HIGH TEMPERATURE GASES
NT HIGH TEMPERATURE AIR
Gas corrosion characteristics of nickel-base alloys 01 p0025 A83-10392

Hot galactic gas and narrow line quasar absorption systems 02 p0253 A83-11620

Analysis of accumulated damage in gas-turbine blade material during thermal cycling and vibration in a gas stream 03 p0301 A83-14732

Relativistic shocks in a Sygne gas 03 p0431 A83-14873

The thermal conductivity of rare gases in a wide range of temperatures 04 p0544 A83-15448

Thermodynamic analysis of causes of differences of values of the thermal conductivity of gases measured by stationary and nonstationary methods 04 p0544 A83-15449

An exact solution for a high-temperature jet stream 04 p0480 A83-16390

A method for measuring the stagnation temperature of short-duration gas flows using a radiation-calorimetric transducer 04 p0483 A83-16393

Approximate correction for the effect of injectants on the ionization level in the boundary layer of a blunt body and in its near wake 05 p0590 A83-17423

High-temperature selective gasdynamic continuous CO2 laser 06 p0765 A83-18450

Combined /radiative-convective/ heat transfer from laminar and turbulent radiating flows in cooled ducts 06 p0759 A83-19160

On the possibility of detecting very hot gas through absorption-line studies 06 p0839 A83-19268

The total emissivities of high-temperature flames 07 p0879 A83-19840

Solution of two-dimensional problems of radiating-gas dynamics 07 p0925 A83-20319

Analysis of similarity in thermophysics --- Russian book 07 p0925 A83-20382

The influence of mathematical viscosity on the difference solution in problems of two-temperature gas dynamics 09 p1347 A83-23573

An accurate determination of the thermal conductivity of argon at high temperatures 10 p1415 A83-26152

Thermal conductivity measurement in high temperature argon by the shock perturbation and Mach reflection methods 10 p1415 A83-26153

Shock tube measurements of IR radiation in hot gas/particle mixtures 10 p1416 A83-26189

A study on the ignition of a fuel droplet in high temperature stagnant gas 10 p1391 A83-26197

Investigation of the length and wave structure of the gasdynamic part in straight and spreading gas jets 11 p1567 A83-27718

Radiative-convective heat transfer during turbulent flow of carbon dioxide in a plane channel 11 p1570 A83-28793

Calculation of a gas-vapor-liquid heat screen on an adiabatic wall by means of h-d diagrams 11 p1570 A83-28795

Acoustic waves in a Rijke tube with radiation impedance 12 p1777 A83-29382

Detection of 10 to the 10th solar masses of hot gas in the normal elliptical galaxy NGC 5846 with the Einstein satellite 15 p2259 A83-34119

CARS diagnostics of high pressure and temperature gases --- Coherent Anti-Stokes Raman Spectroscopy [AIAA PAPER 83-1478] 15 p2123 A83-34913

Creep/corrosion of two nickel alloys in combustion gas 16 p2329 A83-35692

Symposium on High Temperature Gas Dynamics, Liblice, Czechoslovakia, September 15-19, 1981, Proceedings 16 p2354 A83-36876

The determination of transport coefficients in multicomponent gas mixtures 16 p2354 A83-36882

Stationary flow of gas at very high temperatures and relativistic speeds 17 p2595 A83-37032

Gas turbine engines 17 p2467 A83-37274

The hybrid model and its application for studying free expansion --- of hot gas cylinders into vacuum 18 p2681 A83-39218

Unsteady method of measuring the thermal conductivity of gases at high temperatures 18 p2751 A83-39867

A numerical study of the characteristics of a radiant heat flux in a turbine cascade 19 p2844 A83-41570

Thermodynamic efficiency of air injection into the radial clearance of the turbine of a turbojet engine 19 p2801 A83-42139

The effect of soot particles on the thermodynamic condition of heated gases at various temperatures 19 p2821 A83-42145

High temperature corrosion resistance of ceramic thermal barrier coatings 20 p2957 A83-42262

Prediction of gas emissivity for a wide range of process conditions 20 p2974 A83-42691

Heat transfer at hyperbolic flight velocities - Physical model and theoretical and experimental studies 20 p2929 A83-42882

Titanium alpha-nitrogen solid solution formed by high temperature nitriding - Diffusion of nitrogen, hardness, and crystallographic parameters 20 p2954 A83-43340

Recuperator alloys for high-temperature waste heat recovery 21 p3111 A83-43950

Nonequilibrium expansion of halogens in short nozzles --- Russian book 23 p3392 A83-47123

Erosion-corrosion of coatings and superalloys in high velocity hot gases 24 p3562 A83-49481

Unsteady regimes of the convective combustion of a porous powder fuel 24 p3555 A83-49539

Combustion-wave propagation along a thin layer of a material during a gas-phase reaction between fuel and oxidizer 24 p3556 A83-49786

HIGH TEMPERATURE LUBRICANTS

Wear and friction of high-temperature self-lubricating composites [ASLE PREPRINT 82-LC-28-2] 03 p0334 A83-13234

A general-purpose oil for ground-based gas-turbine engines 14 p1998 A83-32076

HIGH TEMPERATURE MATERIALS

U REFRACTORY MATERIALS

HIGH TEMPERATURE NUCLEAR REACTORS

NT HIGH TEMPERATURE GAS COOLED REACTORS

HIGH TEMPERATURE PLASMAS

Wave motions and wave heating in the upper solar atmosphere 03 p0435 A83-13154

The permittivity of an ultrarelativistic plasma 03 p0397 A83-13536

Effects of nuclear forces on ion thermalization in high-temperature plasmas 05 p0687 A83-17013

On uniform limits in the propagation of electromagnetic waves in a hot plasma 06 p0812 A83-18820

Theory of the double layer --- in hot and cold plasma acceleration 07 p0995 A83-20062

On the nature of the high-temperature component of the interstellar plasma 08 p1179 A83-22053

Charge exchange of C/6+ and O/8+ ions with hydrogen atoms - Strong coupling calculation 10 p1486 A83-25885

International Conference on Plasma Physics, Goteborg, Sweden, June 9-15, 1982, Proceedings. Part 1 11 p1658 A83-28226

Nonlinear dynamical models of plasma turbulence 11 p1659 A83-28230

Recent topics in physics of hot plasmas in space environment 11 p1680 A83-28247

The effect of longitudinal waves on the input conductance of a ring aperture antenna 12 p1780 A83-29261

Propagation properties of hydromagnetic waves in a hot plasma and right-hand polarized Pc1 and Pc5 13 p1883 A83-31635

Whistler-mode propagation at frequencies near the electron gyrofrequency 13 p1927 A83-31645

Neutral current sheets in the formation of reversed magnetic configurations 14 p2086 A83-32531

Nonhydrodynamic problems of a plasma focus 14 p2086 A83-32549

Hamiltonian formulation of the second-order drift equations of motion --- for charged particles in fixed electromagnetic fields in high temperature plasmas 15 p2232 A83-33781

Mathematical modeling of plasmas --- Russian book 15 p2233 A83-34164

Calculation of free-free Gaunt factors in hot dense plasmas 16 p2415 A83-35664

Line radiation from a hot, optically thin plasma - Collision strengths and emissivities --- in stellar atmospheres 16 p2416 A83-35974

Instability problems in plasma diagnostics --- Russian book 16 p2416 A83-36434

Emission, absorption, and tunneling of whistler waves in an inhomogeneous magnetic field 17 p2581 A83-37034

Measurement of ionisation rate coefficients of nitrogen ions 18 p2742 A83-39448

Further observations on resonance cones in non-Maxwellian plasmas 18 p2749 A83-40660

The high-energy spectrum of hot accretion disks 20 p3073 A83-43072

Bremsstrahlung produced by electrons in a hot plasma 21 p3213 A83-44653

Dielectronic recombination 21 p3213 A83-44654

Numerical fits to important rates in high temperature astrophysical plasmas 22 p3380 A83-46573

Relativistic corrections for the conventional, classical Nyquist theorem 23 p3510 A83-47607

Thermal evolution of flare plasma 23 p3532 A83-47669

HIGH TEMPERATURE RESEARCH

Self-propagating high temperature synthesis - A Soviet method for producing ceramic materials 08 p1071 A83-22254

A ceramic nozzle for the NASA-Langley 2.4-m /8.0-ft/ high temperature structures tunnel 08 p1072 A83-22264

A small engine high temperature core research programme [ASME PAPER 83-GT-56] 23 p3407 A83-47912

HIGH TEMPERATURE TESTS

The effect of environment on the high temperature low cycle fatigue behaviour of cast nickel-base IN-738 alloy 01 p0023 A83-10216

Electromagnetic transducer with temperature-compensating shield 01 p0049 A83-10363

Prediction of the hardening of magnesium alloy VMD10 from high-temperature test data 01 p0025 A83-10395

Reflections on solar collectors at elevated temperatures /260-1000 C/ --- French thesis 02 p0201 A83-11766

Some observations on creep crack growth 02 p0190 A83-12043

Fracture diagrams for the case of monotonic loading at elevated temperatures --- in aluminum alloys 02 p0156 A83-12326

The effect of the stacking fault energy on the characteristics of the high-temperature creep of nickel-cobalt alloys 02 p0157 A83-12331

Evaluation of the fracture toughness of tungsten at high temperatures 02 p0157 A83-12339

The early stage of Ni3Al layer growth in NiAl/Ni diffusion couples 02 p0157 A83-12413

J series thruster thermal test results [AIAA PAPER 82-1906] 02 p0144 A83-12481

Cumulation of high-temperature low-cycle fatigue damage in two-temperature tests 03 p0299 A83-13906

Role of the strain history on the flow law for high temperature creep 04 p0457 A83-14998

High temperature corrosion on high temperature materials Metallographic, scanning electron microscopic and microanalytical tests 04 p0458 A83-15124

Micromechanism-dependent model of the high-temperature strength and lifetime of particle-hardened alloys 04 p0461 A83-16174

The effect of sulfur containing environment on the high temperature low cycle fatigue of a cast Ni-base alloy 04 p0461 A83-16252

On dislocation-incoherent particle interactions at high temperatures 04 p0461 A83-16254

Thorium segregation to grain boundaries in Ir + 0.3% W alloys containing 5-1000 ppm thorium 04 p0462 A83-16273

Alexandrite-laser performance at high temperature 05 p0647 A83-16838

Effect of heating time at high temperatures on the structure and properties of brazed joints 05 p0652 A83-16884

The thermal diffusion and heat conduction of solid and liquid titanium 06 p0727 A83-17982

Recording shock waves by means of Manganin transducers and the pressures of the graphite-diamond transition at elevated temperatures 06 p0761 A83-18010

Characterization and crystallization of Y-Si-Al-O-N glass 06 p0734 A83-18053

A study of the principles underlying the deformation and fracture of a polycrystalline molybdenum alloy under high-temperature cyclic creep. I - The long-term strength and creep 06 p0733 A83-19307

A study of the principles underlying the deformation and fracture of a polycrystalline molybdenum alloy under high-temperature cyclic creep. II - Structural changes during creep 06 p0733 A83-19308

The effect of rapid heating on the short-term strength characteristics of 28Kh3SNMVFA and 30KhGSA steels 06 p0733 A83-19311

Short duration heat transfer studies at high free-stream temperatures [ASME PAPER 82-GT-129] 07 p0924 A83-19673

The stressed state of cylindrical specimens during thermal-stability testing 07 p0897 A83-19969

Fatigue oxidation interaction in a superalloy - Application to life prediction in high temperature low cycle fatigue 07 p0884 A83-20256

High temperature adhesives 07 p0898 A83-20449

High-temperature protection of materials --- Russian book 07 p0873 A83-20676

Diffusion processes at the metal-coating interface 07 p0873 A83-20677

A study of the high-temperature creep and long-term strength of a niobium alloy with a complex coating in an oxidizing medium 07 p0887 A83-20683

Protection of niobium and molybdenum against high-temperature oxidation 07 p0888 A83-20688

High-temperature creep of unalloyed niobium in vacuum 07 p0889 A83-20903

A set for the dynamic measurement of the thermophysical properties of materials at high temperatures 07 p0930 A83-20960

A two-pyroxene thermometer 07 p0931 A83-21323

Fatigue crack propagation at elevated temperature in MAR-M002 single crystals 07 p0893 A83-21476

Fatigue-crack initiation in IMI 829 caused by high-temperature fretting 07 p0896 A83-21566

High-temperature fracture of hot-pressed AlN ceramics 07 p0901 A83-21567

An incremental crack growth model for high temperature rupture in metals 08 p1059 A83-21695

Crack growth mechanism maps 08 p1117 A83-21731

Creep crack growth characterization of austenitic stainless steel 08 p1061 A83-21732

Fracture strength and toughness of engineering nitrogen ceramics 08 p1069 A83-21741

Creep fracture behavior of austenitic stainless steels from 550 to 800 C 08 p1062 A83-21746

The fracture characteristics of Al and Al-5% Mg at elevated temperatures 08 p1062 A83-21747

Measurements and mechanisms of crack growth at elevated temperatures up to 1273 K 08 p1063 A83-21762

Effect of hold times on the elevated temperature fatigue crack growth behavior of Inconel 718 alloy 08 p1064 A83-21782

On fatigue crack initiation and propagation at elevated temperature 08 p1064 A83-21784

Growth of small fatigue cracks at high temperature - Applicability of conventional fracture mechanics 08 p1064 A83-21785

Influence of thermomechanical processing on elevated temperature slow plastic flow properties of B2 aluminide Fe-39.8at.% Al 08 p1065 A83-22017

Metallurgical instabilities during the high temperature low cycle fatigue of nickel-base superalloys 08 p1065 A83-22019

Low-cycle fatigue of base metals and welded joints at elevated temperature - Life prediction, application, transferability 08 p1065 A83-22029

Application of the J concept to alumina at high temperatures 08 p1070 A83-22192

High-temperature environmental strength degradation of a hot-pressed silicon nitride - An experimental test [ACS PAPER 117-B-81F] 08 p1071 A83-22198

Solar receiver cavity insulation evaluation 08 p1130 A83-22275

Heating unit for mechanical testing of heat-resistant alloys at high temperatures 08 p1066 A83-22631

Simple reverse bending machine for low cycle fatigue at elevated temperatures 08 p1106 A83-23232

High-sensitivity resistivity technique for studies of defect behavior 08 p1106 A83-23234

Strain measurement of acoustically excited aircraft structures at elevated temperatures 09 p1265 A83-23366

The effectiveness of plastic surface treatments for strengthening parts operating under elevated temperatures 09 p1278 A83-23517

The effect of oxygen on the mechanical properties of niobium alloys 09 p1229 A83-23523

Celion/Larc-160 graphite/polyimide composite processing techniques and properties 09 p1222 A83-23635

A facility for precise measurement of mechanical properties at elevated temperatures 09 p1230 A83-23744

Deformation and dislocation behaviour in metals and single-phase alloys at elevated temperatures 09 p1231 A83-24054

Recovery and work hardening during high temperature creep of fcc alloys of low stacking fault energy 09 p1231 A83-24055

Work hardening and recovery rates of internal stress in pure metals and alloys 09 p1231 A83-24056

On the power-law breakdown during high temperature creep of fcc metals 09 p1231 A83-24059

The role of aging in the modeling of elevated temperature deformation 09 p1232 A83-24064

Grain boundary sliding and fracture of metal bicrystals at high temperatures 09 p1232 A83-24068

Mechanisms of creep deformation and fracture in single and two-phase Si-Al-O-N ceramics 09 p1238 A83-24072

Deformation of polycrystalline alpha-SiC 09 p1239 A83-24073

A comprehensive study of the thermophysical properties of titanium alloys in the temperature range 750-1700 K 09 p1234 A83-24379

Stress relaxation in titanium alloys at high temperatures 09 p1234 A83-24382

Absorption of 9.6-micron CO₂ laser radiation by CO₂ at elevated temperatures 09 p1272 A83-24447

Thermal shock testing of optical ceramics 09 p1221 A83-24965

The high-temperature friction of alloys of the system TiN/x/-TiB₂ 09 p1236 A83-25068

Effect of high-temperature exposure in air on strength of hot-pressed silicon nitride 09 p1240 A83-25211

Study of the constitutive creep laws using biaxial relaxation tests 10 p1393 A83-25416

High temperature low cycle fatigue of MAR-M 509 superalloy. I - The influence of temperature on the low cycle fatigue behaviour from 20 to 1100 C. II - The influence of oxidation at high temperature 10 p1393 A83-25417

Thermal degradation of solar collector surfaces 10 p1445 A83-25535

The wear resistance of chromium-base alloys during high-temperature friction 10 p1396 A83-25633

High temperature embrittlement of Ni and Ni-Cr alloys by trace elements 10 p1396 A83-25863

Thermionic converters for terrestrial applications 11 p1608 A83-27299

Analysis of transient thermal responses in a carbon-carbon composite 11 p1543 A83-27459

The high-temperature enthalpy and specific heat of borides in the system niobium-boron 11 p1548 A83-27925

Thermal degradation of aramids. I - Pyrolysis/gas chromatography/mass spectrometry of poly(1,3-phenylene isophthalamide/ and poly(1,4-phenylene terephthalamide/ 11 p1543 A83-28199

Thermal degradation of aramids. II - Pyrolysis/gas chromatography/mass spectrometry of some model compounds of poly(1,3-phenylene isophthalamide/ and poly(1,4-phenylene terephthalamide/ 11 p1551 A83-28200

A method for testing metals for fracture toughness under vibration loading at high temperatures 11 p1549 A83-28505

Development of preferential intergranular oxides in nickel-aluminum alloys at high temperatures 11 p1550 A83-28668

The morphological and structural development of internal oxides in nickel-aluminum alloys at high temperatures 11 p1550 A83-28669

A model for the behavior of the titanium alloy Ti-6 percent Al-4 percent V in the hot forging regime 11 p1551 A83-28808

A unified analysis of high-temperature creep rates from a point of view of recovery 12 p1712 A83-29224

High temperature deformation mechanism of aluminum 12 p1713 A83-29413

A study on the notch effect on the low cycle fatigue of metals in creep-fatigue interacting conditions at elevated temperature 13 p1820 A83-30240

Creep-fatigue-environment interactions --- Book 14 p1993 A83-32650

A new method for measuring optical properties of semitransparent materials at high temperatures [AIAA PAPER 83-1500] 14 p2085 A83-32739

Ceramic tube development for solar receiver applications [AIAA PAPER 83-1501] 14 p2047 A83-32740

Creep and high temperature deformation of simple metals and superalloys 14 p1995 A83-32807

High temperature oxidation studies of Al-3wt pctLi, Al-4.2wt pctMg and Al-3wt pctLi-2wt pctMg alloys 14 p1996 A83-32891

Elastic properties and fracture behavior of graphite/polyimide composites at extreme temperatures 14 p1987 A83-33119

Effects of extreme aircraft storage and flight environments on graphite/epoxy 14 p1987 A83-33122

A new transducer to monitor fatigue crack propagation 15 p2162 A83-33513

The effect of microstructure on the mechanical properties of an iron-based superalloy after prolonged exposure to 750 C heat 15 p2137 A83-34001

Low cycle fatigue of aluminum at elevated temperatures 15 p2138 A83-34133

High temperature time-dependent crack growth 15 p2139 A83-34485

High-temperature embrittlement of tungsten 15 p2140 A83-35042

High temperature internal oxidation behaviour of dilute Ni-Al alloys 15 p2140 A83-35068

Strengthening of polyphase Si₃N₄ materials through oxidation 15 p2143 A83-35073

A high temperature straining stage (300-1000 K) for a 200 kV microscope 15 p2166 A83-35253

On the serration in Al-Mg alloys at elevated temperatures 16 p2329 A83-35604

Experimental evaluation of ablative elastomeric insulators --- for thermal protection of liquid fueled propulsion system combustors 16 p2336 A83-35861

High-temperature static fatigue in ceramics 16 p2337 A83-36169

Creep-fatigue-effects in composites 16 p2324 A83-36172

Creep behavior of aluminum-nickel alloys 17 p2491 A83-38475

High-temperature bending tests on powder metallurgy materials during exploratory studies 17 p2484 A83-38873

High temperature uniaxial tensile stress rupture strength of sintered alpha SiC 18 p2671 A83-39051

High temperature creep properties of alpha Ti-Ti₅Ge₃ 18 p2667 A83-40256

The high temperature creep of dispersion strengthened Ni-Al₂O₃ alloy 18 p2667 A83-40258

Heating unit for high-temperature mechanical tests 19 p2824 A83-40764

The effect of structural dispersity on the high-temperature strength of prestrained steels and alloys 19 p2821 A83-40804

Precision bending apparatus for high temperature measurement 19 p2819 A83-41289

A method for investigating the damping capacity of the blades of turbomachines under the effect of high temperatures and centrifugal forces 19 p2859 A83-41598

High temperature oxidation of hafnium and its alloys 20 p2952 A83-42233

The influence of oxides in high-temperature wear 20 p2953 A83-42244

Some effects of environment on high temperature mechanical behavior of alloys 20 p2953 A83-42245

Heat capacities of liquid metals above 1500 K 20 p2954 A83-43255

A dynamic technique for measurements of thermophysical properties at high temperatures 20 p2991 A83-43257

A simplified approach for evaluating secondary stresses in elevated temperature design [ASME PAPER 83-PVP-51] 20 p3009 A83-43727

Micro-crack initiation, propagation and threshold in elevated temperature inelastic fatigue [ASME PAPER 83-PVP-97] 20 p3009 A83-43731

Development of a new weight saving tile material for the Shuttle orbiter [SAWE PAPER 1457] 20 p2959 A83-43738

The role of grain boundaries in high-temperature deformation and fracture 20 p2957 A83-43775

X-ray diffraction analysis at high temperature on two ceramic systems 21 p3116 A83-44127

Observations on the characteristics of a fluidized bed for the thermal shock testing of brittle ceramics 21 p3116 A83-44333

Mechanical properties of A8 and A85 aluminum at elevated temperatures 21 p3112 A83-44482

Interfacial layers in high-temperature-oxidized NiCrAl 21 p3113 A83-44619

A theory for the long-term cyclic strength under high-temperature high-cycle loading 21 p3113 A83-44722

High temperature deformation and fracture phenomena of polyphase Si₃N₄ materials 23 p3437 A83-48287

Time-temperature effects in nitride and carbide ceramics 23 p3437 A83-48288

High temperature fatigue failure in pressureless sintered silicon nitride 23 p3437 A83-48289

Effect of deformation on the fracture of Si₃N₄ and sialon 23 p3437 A83-48290

High temperature/pressure testing of heat resistant runway materials 23 p3413 A83-48349

[AIAA PAPER 83-2492] 23 p3413 A83-48349

An extensometer for axial strain measurement at high temperature 23 p3459 A83-48604

GaP/Al(x)Ga(1-x)P heterojunction transistors for high-temperature electronic applications 24 p3572 A83-48917

Properties of isostatically hot-pressed silicon nitride [ACS PAPER 168-B-83] 24 p3568 A83-48962

Certain aspects of the application of high-temperature coatings to gas-turbine blades 24 p3590 A83-49089

High temperature in situ experimentation in HVEM instrumentation and application to materials science [ONERA, TP NO. 1983-88] 24 p3583 A83-49407

High temperature oxidation and surface segregation of sulfur 24 p3563 A83-49491

Mechanism of peg growth and influence on scale adhesion 24 p3563 A83-49495

High temperature corrosion of pure nickel and nickel-20 percent chromium alloy in the presence of calcium sulfate and graphite 24 p3563 A83-49497

Studies on the corrosion resistance of MCrAlY alloys at high temperatures 24 p3564 A83-49506

Environmental effects on high temperature creep properties of Ni - 20 Cr - W alloys in air, vacuum and helium 24 p3565 A83-49516

Influence of nitrogen and carbon in the base steel on the transformation temperature of the alloy layer of an aluminized steel sheet for high temperature use 24 p3566 A83-49519

A study of the deformation properties of an isotropic carbon material at elevated temperatures 24 p3554 A83-49666

A photoelectric scanning system, OSS-50-1300, for measuring thermal deformations in specimens of degradable composites 24 p3585 A83-49918

High-temperature solid oxide fuel cell - Technical status 24 p3601 A83-49954

HIGH THRUST

Ion accelerator systems for high power 30-cm thruster operation [AIAA PAPER 82-1893] 02 p0144 A83-12474

Tiny engine combines muscle and fast response 16 p2318 A83-35766

An analysis of the parameters determining the maximum thrust of ramjet engines 19 p2800 A83-42127

Tapered roller bearings for turbine engines 20 p2998 A83-42559

High and low thrust acceleration 24 p3551 A83-49625

HIGH VACUUM

Adsorption and excess fission Xe - Adsorption of Xe on vacuum crushed minerals 04 p0564 A83-15376

HIGH VOLTAGES

Application of transistor emitter-open turn-off scheme to high voltage power inverters 01 p0041 A83-11019

A high voltage, high power pulsed TWT power supply for space application 01 p0021 A83-11022

A gated resonant inverter power processor for pulsed loads 01 p0041 A83-11023

High voltage equipment parts evaluation tests --- for airborne power supplies 01 p0042 A83-11204

Planar multijunction high voltage solar cell chip 03 p0355 A83-13923

Space Shuttle Orbiter charging 07 p0872 A83-20415

High-voltage power supply materials evaluation 07 p0920 A83-20487

High-voltage two-dimensional simulations of permeable base transistors 09 p1256 A83-24684

High-voltage source of constant voltage 10 p1408 A83-25349

High voltage power electronics packaging on NASA's Space Telescope 11 p1539 A83-27155

High voltage distribution and grounding in high power spacecraft 11 p1539 A83-27156

Reliability modeling of high voltage batteries 11 p1540 A83-27200

High current, high voltage accelerators as free-electron lasers drivers 13 p1917 A83-31128

A high temperature straining stage (300-1000 K) for a 200 kV microscope 15 p2166 A83-35253

Establishment of the steady state during the switching on of a high-power high-voltage transistor 17 p2499 A83-38496

Anode-plasma parameters of a high-voltage glow discharge of about 150 kV 18 p2746 A83-39863

High voltage optoelectronic switching in diamond 18 p2677 A83-40066

Radial isolated Blumlein electron beam generator 20 p3045 A83-42293

Measurement of high-voltage pulses employing a quartz Pockels cell 20 p2990 A83-42790

A new technique for high voltage power transistor 21 p3124 A83-44055

HIGHLANDS

Temporary lakes and salt plains in the high plateaus of the Andes /Bolivia/ - A continuing survey of periodic hydrologic phenomena using the geostationary satellite GOES-EST 03 p0360 A83-14574

The role of lithospheric stress in the support of the Tharsis rise 04 p0565 A83-15557

The lunar nearside highlands - Evidence of resurfacing 07 p1032 A83-21288

Pollutant transfer in upland regions by occult precipitation 11 p1613 A83-28393

Palisa catena - Small volcano chains in the western part of the central highlands 16 p2438 A83-36779

HIGHLY ECCENTRIC ORBIT SATELLITES

HIGHLY ECCENTRIC ORBIT SATELLITES

U HEOS SATELLITES

HIGHLY MANEUVERABLE AIRCRAFT

- HiMAT onboard flight computer system architecture and qualification 17 p2467 A83-37061
The application and results of a new flight test technique
[AIAA PAPER 83-2137] 19 p2799 A83-41959
Simulations used in the development and flight test of the HiMAT vehicle
[AIAA PAPER 83-2505] 23 p3404 A83-48355

HIGHWAYS

- Satellite imagery - Application to a highway project in an arid region - Prospects offered by SPOT simulation 08 p1172 A83-21970

HIJACKING

U AIR PIRACY

HILBERT SPACE

NT BANACH SPACE

- The molecular vibration-rotation Hamiltonian in the Bargmann-Hilbert space 02 p0234 A83-11573
Weak global controllability of nonlinear systems 08 p1156 A83-22043
Iterative procedures for constrained and unilateral optimization problems 09 p1331 A83-24765
The dynamics of a viscous incompressible fluid in Hilbert space with allowance for the boundary conditions 10 p1418 A83-26944
Force and moment in incompressible flows 14 p2012 A83-32991
Explicit Hilbert-space representations of atomic and molecular photoabsorption spectra - Computational studies of Stieltjes-Tchebycheff functions 24 p3625 A83-48826

HILBERT TRANSFORMATION

- Quadrature sampling with high dynamic range 06 p0749 A83-19049
A method for the representation of a discrete signal in a complex form on the basis of its Hilbert transformation 08 p1078 A83-23160
An integral equation connected with the Jacobi polynomials 09 p1336 A83-24371

HILL CURVES

U HILL METHOD

HILL DETERMINANT

- The stability of bi-parametric damped oscillations 24 p3597 A83-50131

HILL LUNAR THEORY

- Origin of the moon - Capture by gas drag of the earth's primordial atmosphere 20 p3079 A83-43590

HILL METHOD

- Method for constructing families of three-dimensional periodic orbits in the Hill problem 06 p0721 A83-18351
Families of three-dimensional periodic orbits of the Hill problem and their stability 09 p1212 A83-25026
Theory on distributed feedback /DFB/ lasers including strong modulations 11 p1578 A83-27548
On the regularization of the Hill problem 11 p1673 A83-28031
On the stability of close binaries in hierarchical three-body systems 12 p1787 A83-29113
A qualitative investigation of the motion of asteroids of the Hecuba type 17 p2594 A83-38563
Hill's stability in the elliptic restricted three-body model including body shape 18 p2754 A83-39007

HILLER MILITARY AIRCRAFT

U MILITARY AIRCRAFT

HILSCH TUBES

- Acoustic streaming in swirling flow and the Ranque-Hilsch /vortex-tube/ effect 04 p0479 A83-16259
An experimental study of the vortex tube - Where the vortex chamber includes a divergent tube 05 p0639 A83-17375
Computer modelling of turbulent recirculating flows in engineering applications 08 p1088 A83-23192
An experimental study of the operation of a vortex tube 09 p1260 A83-24230
An investigation of energy separation in a vortex tube 11 p1569 A83-28376

HIMALAYAS

- Neuropsychological functioning after prolonged high altitude exposure in mountaineering 10 p1455 A83-25665
High altitude atmospheric water vapour measurements in the Himalayan region 19 p2867 A83-40891
Constraints on the structure of the Himalaya from an analysis of gravity anomalies and a flexural model of the lithosphere 23 p3482 A83-47811

HIMAT

U HIGHLY MANEUVERABLE AIRCRAFT

HINDRANCE

U CONSTRAINTS

HINGE MOMENTS

U TORQUE

HINGED ROTOR BLADES

U HINGES

U ROTARY WINGS

HINGELESS ROTORS

U RIGID ROTORS

HINGES

- SYMBOL - A computer program for the automatic generation of symbolic equations of motion for systems of hinge-connected rigid bodies
[AIAA PAPER 83-0013] 05 p0678 A83-16463
The method of initial parameters as applied to the flexural vibrations of beams with hinges and oscillators 06 p0777 A83-19317

HIPPARCOS SATELLITE

- The HIPPARCOS space astrometry mission 11 p1670 A83-27732
The coordination of space and ground-based parallax programs for improvement of the stellar luminosity function 18 p2767 A83-39629

HIPPOCAMPUS

- Long-term posttetanic potentiation in the hippocampus 01 p0081 A83-10917

HISS

- Pulsing hiss, pulsating aurora and micropulsations 03 p0361 A83-14744
Auroral hiss, Z mode radiation, and auroral kilometeric radiation in the polar magnetosphere - DE 1 observations
[AD-A125914] 06 p0784 A83-18302
Plasmaspheric hiss observed in the topside ionosphere at midand low-latitudes 13 p1882 A83-31631
Plasmaspheric ELF hiss observed by ISIS satellites 14 p2055 A83-33145
Parametric excitation of 'cold' ion-Bernstein waves by whistler waves 15 p2235 A83-34492
Narrow band characteristics of low latitude VLF hiss 16 p2344 A83-36730
Electron pitch-angle scattering by low frequency waves at the geomagnetic equator 17 p2545 A83-38602
Pulsing hiss and associated phenomena - A morphological study 18 p2712 A83-39066
Fine structure of the energy spectra of ELF hiss in the upper ionosphere and a possible mechanism of hiss generation (the Intercoms-14 satellite) 21 p3175 A83-45240
Standing wave patterns in VLF hiss 22 p3326 A83-46044
Comparison between the arrival direction of auroral hiss and the location of aurora observed at Syowa Station 22 p3329 A83-46504
Wave normal direction of auroral hiss observed by the S-31QJA-5 rocket 22 p3331 A83-46515
A theoretical study of plasmaspheric hiss generation 22 p3336 A83-47055
On the origin of plasmaspheric hiss - Ray path integrated amplification 22 p3336 A83-47056

HISTOCHEMICAL ANALYSIS

- Histochemical changes in muscles and liver during physical loads and overheating /experimental investigation/ 05 p0669 A83-17174
A histochemical study of the rat spinal cord, spinal ganglia, and adrenal glands under local vibration 05 p0670 A83-17192
Variability of fiber type distributions within human muscles 05 p0674 A83-17328
The ultracytochemical analysis of nuclear ribonucleoproteins /RNP/ 06 p0795 A83-18981
The morphological characteristics of the myons of the masticatory muscle of mammals and humans 07 p0975 A83-20990
The changes in the liver and muscles due to the effect of physical exercise during overheating in different water regimes 14 p2061 A83-31974
Topical and systemic effects of the oil AER-M-O 261g batch no. 4 in mice - Anatomopathological and histological findings 17 p2557 A83-38946

HISTOGRAMS

- Histometric indicators of the structure of the femoral and crural muscles of children, adolescents, and young men 07 p0978 A83-20991
Histogram-based algorithms for scene matching 09 p1266 A83-23538
Histogram concavity analysis as an aid in threshold selection --- in image processing 13 p1911 A83-31073
Acquisition and manipulation of image statistics 21 p3139 A83-44787
Histogram deconvolution - An aid to automated classifiers 22 p3350 A83-46253
Picture information measures for similarity retrieval 22 p3290 A83-46255

HISTOLOGY

- Histological and histochemical investigations of the locomotor system during general hypoxia 03 p0375 A83-13640

- The effects on rat bones of a prolonged centrifugation - Results of a morphometrical analysis 06 p0794 A83-18341

- A histopathological study on hearts in ischaemic heart disease fatalities 09 p1323 A83-24009
The blood supply of the trachea and bronchi of rats 18 p2733 A83-40584

- The distribution of streptomycin in the structures of the inner ear following its parenteral administration (a histoautoradiographic investigation) 19 p2875 A83-41443

- Removal of histological sections from glass for electron microscopy - Use of Quetol 651 resin and heat 21 p3183 A83-44675

- The effect of a constant magnetic field on the identified neurons and the glia-neuronal interrelations in isolated nerve system of the Helix lucorum 21 p3185 A83-45376

- Removal of histological sections from glass for electron microscopy - Use of Quetol 651 resin and heat 22 p3346 A83-46709

- Type II collagen-induced autoimmune endolymphatic hydrops in guinea pig 23 p3495 A83-47819
Circulating antibodies to aortic elastin and their significance in atherosclerosis in humans 23 p3499 A83-48674

HISTORIES

NT CASE HISTORIES

- The beginnings of magnetospheric physics 01 p0072 A83-11284
Recent progress in V/STOL technology 02 p0131 A83-12852
The shy eccentric who fathered the rocket 03 p0439 A83-14049
Supernovae: A survey of current research - Introduction --- review of supernova research 08 p1173 A83-21827
The historical supernovae 08 p1174 A83-21846
JPL and the American space program - A history of the Jet Propulsion Laboratory --- Book 09 p1369 A83-25098
Historical review and current plans --- for space stations 11 p1533 A83-27500
Radio astronomy at Dover Heights 13 p1935 A83-30360
The history of V/STOL aircraft. II 14 p1969 A83-33097
Rangers 3-5 - America's first lunar landing attempts 16 p2313 A83-35611
The history of V/STOL aircraft 16 p2299 A83-36074
The development of studies of Venus 17 p2615 A83-37402
Some lessons from NACA/NASA aerodynamic studies following World War II

- [AIAA PAPER 83-1856] 17 p2443 A83-38683
A history of prevailing ideas about the general circulation of the atmosphere 18 p2730 A83-40318
A history of numerical weather prediction in the United States 18 p2730 A83-40319
Satellite communications 21 p3119 A83-43819
The reaction motors division - Thiokol Chemical Corporation --- management history of aerospace rocket engine products 23 p3415 A83-47330
A study of early Korean rockets (1377-1600) 23 p3540 A83-47331
[IAF PAPER 83-291] 23 p3540 A83-47331
Project Rover - The United States nuclear rocket program 23 p3425 A83-47334
[IAF PAPER 83-301] 23 p3419 A83-47335
Communications satellites - The experimental years 23 p3416 A83-48626
[IAF PAPER 83-302] 23 p3416 A83-48631
The evolution of the Soyuz programme 23 p3416 A83-48632
The Soviet cosmonaut team, 1960-1971 23 p3416 A83-48632
The Soviet cosmonaut team, 1971-1983 23 p3416 A83-48632
Explorer 1 - The second age of discovery 23 p3416 A83-48639

HLLV

U HEAVY LIFT LAUNCH VEHICLES

HMX

- The deformation and fracture of Beta HMX 02 p0161 A83-12030
Fracto-emission from pentaerythritol tetranitrate and cyclotetramethylene tetranitramine single crystals 02 p0152 A83-12281
Synthesis of cyclotetramethylene tetranitramine by three stage method 04 p0454 A83-16432
Application of solid-phase transition kinetics to the properties of HMX 07 p0901 A83-19827
Dependency of the impact sensitivity of beta-HMX on the grain size and effects on the application 09 p1242 A83-23848

- Impact sensitivity of gamma-irradiated HMX
13 p1826 A83-31674
- Hazards in the manufacture of RDX and HMX
15 p2143 A83-33874
- Model and chemistry of HMX combustion
[AIAA PAPER 83-1195] 16 p2339 A83-36271
- HNST**
U HEXANITROSTILBENE
- HODOGRAPHS**
Kinematic interpretation of the motion of a gyrostat in one solution of E. I. Khariamova
09 p1337 A83-23552
- Isoconic motions of a rigid body with a fixed point
09 p1337 A83-23553
- Construction of a complete solution for one problem of rigid-body dynamics
09 p1337 A83-23554
- Motion of a Kovalevskaja gyroscope in the Delaunay case
09 p1337 A83-23555
- Investigation of types of root loci of Fourth-order linear and linearized systems --- automatic pilot control system
11 p1647 A83-27448
- Anti-clockwise rotation of the wind hodograph. I - Theoretical study
13 p1893 A83-31045
- The basic equations of hodograph method in three dimensional flow
16 p2291 A83-35840
- Hodographic study of transverse magnetohydrodynamic flows
18 p2746 A83-39855
- Note on the axisymmetric sonic jet
20 p2930 A83-43123
- HOGBACKS**
U RIDGES
- HOHMANN TRAJECTORIES**
U ELLIPTICAL ORBITS
U TRANSFER ORBITS
- HOHMANN TRANSFER ORBITS**
U ELLIPTICAL ORBITS
U TRANSFER ORBITS
- HOLDERS**
NT FLAME HOLDERS
High temperature in situ experimentation in HVEM instrumentation and application to materials science [ONERA, TP NO. 1983-88] 24 p3583 A83-49407
- HOLE BURNING**
The thermal mechanism of barrier destruction by a transonic jet of rocket propellant combustion products
15 p2172 A83-34473
- Photoacoustic time-domain holography of weak picosecond pulses
24 p3629 A83-49610
- HOLE DISTRIBUTION (ELECTRONICS)**
The inverse population of the light-hole band on pumping at cyclotron resonance
05 p0690 A83-16895
- HOLE DISTRIBUTION (MECHANICS)**
Effects of friction in tensile and compressive stress problems for a rigid circular disk in an infinite plate
02 p0197 A83-13066
- NDE of fastener hole cracks by the electric current perturbation method
04 p0491 A83-15192
- The quantitative use of Rayleigh waves to locate and size subsurface holes
04 p0491 A83-15202
- Constrained optimization of monopulse circular aperture distribution in the presence of blockage
10 p1375 A83-26835
- Elastic-plastic behavior of coldworked holes
12 p1738 A83-29753
- [AIAA 83-0865] 12 p1738 A83-29753
- Fatigue crack growth rates for very short cracks developing at fastener holes in 7075 and 7010 aluminum alloys
16 p2330 A83-35982
- Seven-hole cone probes for high angle flow measurement Theory and calibration
16 p2356 A83-36085
- Periodic problem of the plane theory of elasticity for an infinite plane with cracks and holes
18 p2698 A83-39505
- The use of the method of dividing grids for studying plastic deformations in the stress concentration region
24 p3596 A83-49917
- HOLE GEOMETRY (MECHANICS)**
The plane nonlinear problem of stress distribution around holes
01 p0059 A83-10691
- Modification of stress concentration due to circular holes in tensile strips by taper and elliptical cut outs - A comparative study
02 p0193 A83-12668
- A thermoelectric method of stress analysis for plates weakened by holes
03 p0343 A83-14733
- An enhancement for the ultrasonic test bed to inspect engine disk bolt holes
04 p0488 A83-15160
- The quantitative use of Rayleigh waves to locate and size subsurface holes
04 p0491 A83-15202
- Optimization of reinforcement for a class of openings in plate structures
04 p0499 A83-15695
- Effects of hole curvature on transient hygrothermal stresses in plates with a hole /moisture and temperature coupling effects/
05 p0611 A83-17107
- Quantitative use of Rayleigh waves to locate and size subsurface holes
07 p0942 A83-20272
- Peripheral edge crack around a spherical cavity under uniaxial tension field
07 p0946 A83-20642
- Modification of stress concentration due to circular holes in tension strips by taper and elliptical cut-outs - A comparative study
08 p1121 A83-21882
- Narrow optical hole burning and related effects in ruby
12 p1782 A83-29198
- Reduction of stress concentration around a hole in a uniaxially loaded plate
12 p1736 A83-29447
- On the effect of residual stresses on crack growth from a hole
12 p1737 A83-29747
- [AIAA 83-0840] 12 p1737 A83-29747
- Mathematical modeling of damage in unidirectional composites
14 p1986 A83-32344
- Low Reynolds number shear flow along an elliptic hole in a wall
14 p2009 A83-32522
- Tabulated stress intensity factor solutions for flawed fastener holes
16 p2368 A83-36514
- Creep cavitation and fracture due to a stress concentration in 2-1/4 Cr-1 Mo
17 p2490 A83-38390
- On cracking instability in plates containing circular holes
17 p2523 A83-38399
- A partially contacting crack in a plate with an elliptic hole
17 p2524 A83-38509
- Stress concentration in a circular cylindrical shell weakened by a large hole
18 p2697 A83-39482
- On mechanical fastening in graphite epoxy composite
18 p2652 A83-40155
- Stress distribution around hole of angle-ply laminates under uni-axial tension
18 p2652 A83-40166
- Dynamic stress concentrations in some composite strips with a circular hole under high-velocity tension
18 p2705 A83-40221
- Design of algorithms to extract data from capacitance sensors to measure fastener hole profiles
19 p2855 A83-41026
- An integral equation approach for simultaneous solution of rectangular hole and rectangular block problems
20 p3004 A83-42972
- Interlaminar stresses at a hole in a composite member subjected to in-plane loading
20 p3007 A83-43146
- Brittle fracture near holes --- Russian book
21 p3150 A83-43911
- Optimization of openings in plates under plane stress
21 p3164 A83-45588
- Detection of cracks under installed fasteners in aircraft structures
22 p3304 A83-46769
- Nonlinear antiplane strain of a body weakened by a lune-shaped recess
24 p3594 A83-49527
- Stress concentration near two circular holes connected by a narrow slit
24 p3595 A83-49904
- The stability of plates near a sharp defect in the case of the initial biaxial plane stressed state
24 p3596 A83-49908
- HOLE MOBILITY**
Evidence for low diffusivity and mobility of minority carriers in highly doped Si and interpretation
06 p0814 A83-19261
- Optical properties of fast-diffusing solid-state plasmas
19 p2904 A83-40976
- Hole transport in pure and doped GaAs
20 p3052 A83-42599
- Acoustic and optical-phonon-limited mobilities in p-type silicon within the deformation-potential theory
21 p3219 A83-45497
- HOLES**
Three-dimensional analysis of /0/90/s and /90/0/s laminates with a central circular hole
05 p0653 A83-16933
- Green's function solution and applications for cracks emanating from a circular hole in an infinite sheet
24 p3594 A83-49599
- HOLES (ELECTRON DEFICIENCIES)**
Investigation of plasma waves in silicon with the help of MOS structures --- German thesis
01 p0108 A83-10171
- Theory of nonlinear optical absorption associated with free carriers in semiconductors
02 p0233 A83-12267
- Polarized fluorescence line narrowing measurements of Nd laser glasses - Evidence of stimulated emission cross section anisotropy
06 p0767 A83-19258
- Electrochemical studies of photocorrosion of n-CdSe
07 p0952 A83-19881
- Generation of holes during the disintegration of dislocations and mechanoluminescence of metals
08 p1170 A83-22781
- A model for the collection of minority carriers generated in the depletion region of a Schottky barrier solar cell
08 p1170 A83-22910
- On the possibility of microwave generation in the case of avalanche processes in dipole domains
09 p1252 A83-23468
- Physical limitations of present thin film solar cells
14 p2043 A83-32275
- Charge collection in a-Si:H solar cells
14 p2043 A83-32278
- Direct free-hole absorption induced in germanium by 1.06 micron picosecond pulses
14 p2093 A83-33428
- Theory of electron-hole kinetics in amorphous semiconductors under illumination - Application to solar cells
17 p2584 A83-38213
- Carrier leakage and temperature dependence of InGaAsP lasers
19 p2850 A83-40732
- Optical properties of fast-diffusing solid-state plasmas
19 p2904 A83-40976
- Population inversion due to separate shift and heating of light and heavy holes in semiconductors
19 p2905 A83-41174
- Three holes bound to a double acceptor - Be(+) in germanium
21 p3218 A83-45199
- Ultrasonic modulation of persistent spectral holes in crystals
21 p3219 A83-45486
- Growth of phase-space density holes --- in plasma
22 p3361 A83-46010
- The significance of interference effects in thin film Cu2S/CdS solar cells
23 p3478 A83-48619
- HOLLOW CATHODES**
Experimental investigation of an argon hollow cathode [AIAA PAPER 82-1890] 02 p0241 A83-12472
- Thermal runaway phenomenon of a neutralizer hollow cathode
02 p0241 A83-12473
- Effect of cathode keeper potential on the discharge characteristics and stability in a 5 cm diameter ion thruster
02 p0145 A83-12486
- [AIAA PAPER 82-1914] 02 p0145 A83-12486
- A model for mercury orificed hollow cathodes - Theory and experiment
02 p0147 A83-12513
- Baffle aperture design model for electron bombardment thrusters
02 p0148 A83-13091
- Phenomenological model describing orificed, hollow cathode operation
04 p0454 A83-15276
- He-Ne laser generation of 1.15-1.20 microns in a hollow copper cathode
04 p0485 A83-15950
- IR and UV laser activity in a slit-shaped copper hollow cathode --- German thesis
06 p0768 A83-19617
- Cull laser with a helical hollow cathode discharge
08 p1106 A83-21978
- Comparison of He-Kr/ + / laser oscillations in transverse and longitudinal hollow - Cathode discharges
11 p1582 A83-27603
- Mechanism for the loss of fast electrons from a Penning glow discharge
16 p2418 A83-36940
- The helium-iodine laser
18 p2694 A83-40664
- Spectral quality of He-Zn II and He-cd II hollow cathode metal vapor lasers in the magnetic fields
22 p3300 A83-46820
- HOLMIUM**
NT HOLMIUM ISOTOPES
Three wavelength laser emission in Ho:YLF via sequential cascade
11 p1578 A83-27544
- HOLMIUM ISOTOPES**
Relativistic calculation of atomic M-shell ionization by protons
13 p1918 A83-31351
- [AD-A130664]
- HOLOGRAPHY**
Simultaneous diffraction of two waves at a reflection volume hologram
04 p0535 A83-15795
- Contributions of amplitude and phase modulation to diffraction efficiency in three-dimensional reflective holograms
10 p1422 A83-26470
- Digital image reconstruction of microwave holograms
10 p1424 A83-26855
- Experimental observation of amplification of beams by dynamic surface holograms
20 p2998 A83-43807
- HOLOGRAPHIC INTERFEROMETRY**
Optical methods of flow diagnostics in turbomachinery
01 p0053 A83-11076
- Quantitative deformation measurement with virtual-image holographic interferometry --- Dutch thesis
02 p0176 A83-11897
- Determination of the stressed state of bodies with defects using the method of holographic photoelasticity
02 p0191 A83-12337
- A study of the stress-strain state of composites with disperse reinforcement using speckle holographic interferometry
02 p0178 A83-12370
- On-line acquisition and analysis for holographic nondestructive evaluation
03 p0337 A83-13873
- Dual field interferometry by speckle photography - A study of applications and limits of utilization --- French thesis
03 p0328 A83-14101
- Large deformation whole-field measurements of isotropic plates by sandwich hologram interferometry
03 p0341 A83-14399
- Applications of flow visualization techniques in aerodynamics [ONERA, TP NO. 1982-68] 03 p0330 A83-14528

Laser holographic interferometry for an unsteady airfoil in dynamic stall
[AIAA PAPER 83-0388] 05 p0643 A83-16688

Multiple-aperture three-dimensional image construction utilizing fringe-modulated speckle patterns
05 p0643 A83-16835

Holographic interferometry by a non-silver film process
05 p0645 A83-17320

A study of the deformation and fracture of structural elements of composite materials by speckle-holographic interferometry
06 p0775 A83-18513

A method for calculating the surface displacement field of a solid body from double-exposure holographic interferometry data
06 p0764 A83-19315

Temperature measurements in a radially symmetric flame using holographic interferometry
07 p0879 A83-19845

Light-in-flight recording - High-speed holographic motion pictures of ultrafast phenomena
07 p0928 A83-20153

Moiré method to determine separate frequency contributions in vibration patterns
07 p0928 A83-20154

Computer-aided speckle pattern interferometry
07 p0928 A83-20155

A study of process-related residual stresses by holographic and speckle-interferometric techniques
07 p0946 A83-20912

Orthogonal in-plane and out-of-plane fringe maps in holographic interferometry
08 p1101 A83-22635

Testing diamond turned aspheric optics using computer-generated holographic /CGH/ interferometry
08 p1103 A83-22869

Optical second differentiation by shearing moiré deflectometry
09 p1269 A83-24441

The determination of electron density profiles from refraction measurements obtained using holographic interferometry
10 p1418 A83-25427

Speckle interferometry, speckle holography, speckle spectroscopy, and reconstruction of high-resolution images from space telescope data
10 p1419 A83-25833

Rotation interferometry - A new technique for achieving high angular resolution
10 p1419 A83-25837

Real-time holographic interferometry of moving objects in oppositely directed beams
10 p1420 A83-25891

Three dimensional holographic flow visualization
10 p1422 A83-26420

Study of deformed samples using an interferometer attached to the sample
10 p1422 A83-26469

Application of laser holographic interferometry to vibration analysis of aircraft beam structure model
10 p1442 A83-26765

Real-time holographic interferometry - A microcomputer system for the measurement of vector displacements
10 p1424 A83-26873

Automated processing of holographic interferograms in determining the deformations of diffusely reflecting objects
11 p1574 A83-28499

Limitation to the accuracy of interferometrically measured electron density profiles of laser-produced plasmas
11 p1661 A83-28709

High power TEA CO₂ laser tuned by a holographic grating
12 p1731 A83-29196

A review of holographic nondestructive evaluation at Lawrence Livermore National Laboratory
12 p1734 A83-29589

Holographic information processing using nonstationary fields --- Russian book
13 p1846 A83-30621

A holographic surface measurement of the Texas 4.9-m antenna at 86 GHz
13 p1847 A83-31283

Determination of stress intensity factors by holographic interferometry
14 p2019 A83-32073

Interferometric analysis for small rotation
15 p2164 A83-34397

Method of improving image quality in holographic interferometers
15 p2164 A83-34424

The opening of a natural macrocrack
16 p2365 A83-35551

Investigation of the temperature field in the active rod of a laser
16 p2359 A83-35939

The properties of holographic gratings in silicon crystals recorded by means of ultrashort light pulses
16 p2412 A83-35944

Holographic measurement of transition and turbulent bursting in supersonic axisymmetric boundary layers
[AIAA PAPER 83-1724] 18 p2633 A83-39269

Holographic laser scanners for multidirectional scanning
19 p2847 A83-41100

Holographic technique for simultaneous measurement of displacement and tilt
19 p2847 A83-41101

Recording of interferograms on normal high resolution plates using a CO₂ laser at 10.6 microns
19 p2847 A83-41103

Automatic fringe analysis with a computer image-processing system
19 p2847 A83-41106

Computational interferometric description of nested flow fields
20 p2988 A83-42527

Holographic interferometry studies of temperature profiles in thermal boundary layer in free convection and bubble boiling
20 p2980 A83-42760

Application of the swollen polymer technique to the study of heat transfer on film cooled surfaces
20 p2982 A83-42775

Multiplexed speckle and holographic interferometry with color encoding by white-light processing
21 p3134 A83-43872

Temporal and interference fringe analysis of excimer TEM01 zone laser modes
21 p3142 A83-43874

Pulsed holographic nondestructive testing on aircraft
21 p3149 A83-44828

Measurement of curvature and bending stiffness of thin carbon composite plates using holographic interferometry
21 p3155 A83-44829

Diffracting optics
21 p3207 A83-44837

Out-of-plane deformation of balanced and symmetric composites as measured by holographic interferometry
21 p3108 A83-45153

The monomode fiber - A new tool for holographic interferometry
21 p3141 A83-45159

Stress analysis by combination of holographic interferometry and boundary-integral method
21 p3161 A83-45160

On stress analysis of anisotropic composites through transmission optical patterns - Isochromatics and isopachics
21 p3108 A83-45166

Holographic plasma interferometry in the infrared spectrum. II - Using nonlinear effects to increase the sensitivity
23 p3454 A83-47554

Design of an experiment to determine deformations using holographic interferometry
23 p3454 A83-47560

Blade vibration measurements on centrifugal compressors by means of telemetry and holographic interferometry
[ASME PAPER 83-GT-131] 23 p3408 A83-47959

Converging shock on laser plasma - Density profiles by holographic interferometry
23 p3510 A83-48316

Holographic device for rectilinear surface discharge visualization
[ONERA, TP NO. 1983-104] 24 p3583 A83-49415

Interference holographic diagnostics of a detached shock wave using a model
24 p3632 A83-49664

The use of the techniques of holographic interferometry in qualitative studies of gas-dynamic flows with chemical reactions
24 p3584 A83-49780

Stroboscopic holography in studying the vibration of parts of complex shapes
24 p3586 A83-49919

HOLOGRAPHIC SPECTROSCOPY

Dynamic free-carrier holograms in semiconductors
14 p2084 A83-32164

HOLOGRAPHIC SUBTRACTION

Real-time optical interferometric image subtraction by wave polarization
02 p0177 A83-12309

A new method for simultaneous complex addition and subtraction --- of two input optical signals with holographic grating
05 p0646 A83-17890

HOLOGRAPHY

NT ACOUSTICAL HOLOGRAPHY
NT MICROWAVE HOLOGRAPHY
NT WHITE LIGHT HOLOGRAPHY
Holographic HUDs de-mystified
01 p0010 A83-11171

Quantitative deformation measurement with virtual-image holographic interferometry --- Dutch thesis
02 p0176 A83-11897

Optical pattern recognition using circular harmonic expansion
02 p0178 A83-12594

Holographic display of 3D digital data
03 p0324 A83-13437

Multiplex holographic filtering through contact screens
03 p0326 A83-13772

Dual field interferometry by speckle photography - A study of applications and limits of utilization --- French thesis
03 p0328 A83-14101

An automated production holography test facility
04 p0488 A83-15157

Nondestructive evaluation of materials by optical correlation
04 p0492 A83-15219

The application of diffraction optics to the LANTIRN head-up display
04 p0447 A83-16131

Holographic aberration compensation with partially coherent light
05 p0643 A83-16834

Diffraction efficiency of out-of-phase amplitude-phase volume holograms
05 p0644 A83-17080

Holography and the deformation of metals --- Russian book
05 p0644 A83-17119

Unstrained single deblurring filter made from blurred PSF and doubly blurred PSF --- Point Spread Function
06 p0762 A83-18589

Internal reflections in bleached reflection holograms
06 p0762 A83-18593

Rainbow holographic aberrations and the bandwidth requirements
06 p0762 A83-18594

Diffraction efficiencies of evanescent-wave holograms - An improved model
08 p1092 A83-22080

Parameter extraction by holographic filtering
08 p1157 A83-22428

Holographic beam shaping for optical heterodyne arrays in laser radars
08 p1097 A83-22519

A method of automatic image reconstruction from holograms by a homomorphic system of logarithmic transform type
08 p1101 A83-22625

Towards displacement measurement in remote locations by holographic fiber optics probes
09 p1264 A83-23362

Measurement of oscillator strengths in the ultraviolet by magneto-optical rotation
09 p1341 A83-23656

Holographic intensity correlator with a laser electron beam tube for inputting images for processing
10 p1422 A83-26467

Contributions of amplitude and phase modulation to diffraction efficiency in three-dimensional reflective holograms
10 p1422 A83-26470

Achieving stability in remote holography using flexible multimode image bundles
10 p1423 A83-26635

Projection moiré with moving gratings for automated 3-D topography
10 p1484 A83-26868

Holographic local-oscillator beam multiplexing for array heterodyne detection
10 p1425 A83-26875

Holography at X-ray wavelengths
11 p1572 A83-27534

The detection of shape discrepancies between a material surface and a reference model using a moirébeginning from a specific grid
12 p1729 A83-29377

Stigmatism conditions of concave holographic gratings utilized at normal incidence
12 p1730 A83-29384

Single-polarisation operation of highly birefringent bow-tie optical fibres
12 p1779 A83-29462

Holographic nondestructive evaluation - Status and future
12 p1734 A83-29593

Holographic recording of optical signals that vary in time in nonstationary-reference-wave devices
13 p1846 A83-30623

Holographic memory for data with a periodic structure, with imaging of the scatterer into the hologram plane during recording
13 p1846 A83-30624

Holographic recording on board the Salyut-6 space station
13 p1815 A83-30813

Fresnel detour-phase circular computer generated holograms
14 p2083 A83-31948

Stellar spectrograph using aberration corrected concave holographic grating
14 p2017 A83-32009

An investigation of the effect of polarizing radiation, scattered by an optically inhomogeneous layer, on the quality of its holographic image
14 p2019 A83-32126

The polarization control of tone-transmission brightness in a holographic image of light-scattering surfaces and layers
14 p2019 A83-32132

Real-time edge enhancement in four-wave mixing with photorefractive BGO crystals
14 p2084 A83-32450

Binary holographic LO beam multiplexer for IR imaging detector arrays
14 p2021 A83-32908

Aberrations of holographic toroidal grating systems
14 p2021 A83-32909

Real-time holography and wave-front conjugation by stimulated scattering
15 p2229 A83-33529

Lessons Fourier holography applied to nondestructive testing - Experimental results
15 p2163 A83-33754

Criteria of light sensitivity of media and optimization of hologram recording
15 p2163 A83-33981

Synthesis of holographic components for optical data storage and transmission systems allowing for characteristics of semiconductor laser radiation
15 p2163 A83-33983

Investigation of anisotropic problems in the mechanics of deformable bodies by the holographic moirémethod
16 p2355 A83-35512

Crosstalk and loss of information in holography
16 p2355 A83-35890

Holographic coupler to monomode fiber
16 p2413 A83-36755

Image reconstruction of long-wavelength holograms by maximum entropy method
17 p2511 A83-38036

Practical application of the optimal Wiener-Kolmogoroff filtering algorithm in quasi-holographic systems
18 p2739 A83-40099

Statistical analysis of a holographic system intended for the Space Shuttle
19 p2817 A83-41099

Phase-conjugate wavefront generation in four-wave mixing with photorefractive Bi₁₂GeO₂₀ (BGO) crystals
19 p2900 A83-41555

Holographic installation for SAW visualization
20 p2990 A83-42910

Dual-beam encoding for color holographic construction
20 p2992 A83-43630

Integrated optics, fiber optics and holography; International School on Coherent Optics and Holography, 2nd, Varna, Bulgaria, September 28-October 3, 1981, Proceedings 20 p3048 A83-43774

Coordinate transformations via multifacet holographic optical elements 21 p3134 A83-43871

Fabrication of a 360 deg astigmatic rainbow hologram 21 p3136 A83-44153

Dynamic holograms in semiconductors 21 p3138 A83-44698

Some characteristics of and measurements on dichromated gelatin reflection holograms 21 p3140 A83-44838

Multiwavelength operation of an acousto-optic deflector --- for laser flight simulation displays 21 p3140 A83-44839

Low-noise multicolor archival storage with broad source interferometric imaging 22 p3294 A83-46829

Image formation by multifacet holograms 22 p3294 A83-46835

Gaussian beam effects in far-field in-line holography 22 p3294 A83-46836

Volume vector holograms with opposed reference beams 23 p3453 A83-47168

High-frequency holographic transmission gratings in photoresist 23 p3454 A83-47578

Processing signals the optical way 23 p3508 A83-47821

High-sensitivity material with reversible photo-induced anisotropy 23 p3459 A83-48315

Real-time image deblurring using four-wave mixing 24 p3628 A83-48750

Photochemical time-domain holography of weak picosecond pulses 24 p3629 A83-49610

HOLMORPHISM

U ANALYTIC FUNCTIONS

HOMEOSTASIS

The prognostic significance of several traits in studying the functioning of the oxygen homeostasis system of humans in the genetic aspect 01 p0082 A83-10491

Concerning the interrelationship between protein, fat, and carbohydrate metabolisms 01 p0081 A83-10560

The recovery of temperature homeostasis of mammals under microwave irradiation 16 p2394 A83-35922

Fluid and electrolyte homeostasis during prolonged exercise at altitude 20 p3034 A83-43481

HOMING

A comparison between the pseudomeasurement and extended Kalman observers 09 p1328 A83-24715

HOMING DEVICES

Solid state, 95 GHz tracking radar system 02 p0133 A83-11918

Understanding Kalman filters - How to extract the maximum information from imperfect measurement 11 p1648 A83-28167

Algorithm development for infra-red air-to-air guidance systems - How to separate the wheat from the chaff: A simple approach to target detection 11 p1528 A83-28178

Estimation enhancement by trajectory modulation for homing missiles 17 p2461 A83-37135

A sensible approach to realizing mmW seeker systems 17 p2498 A83-37896

New target models for homing missile guidance [AIAA PAPER 83-2166] 19 p2795 A83-41662

Design of an integrated strapdown guidance and control system for a tactical missile [AIAA PAPER 83-2169] 19 p2796 A83-41665

Missile guidance electromagnetic sensors 24 p3546 A83-48769

Semi-active radar guidance 24 p3546 A83-48771

Electro-optic and infrared sensors 24 p3581 A83-48772

HOMODYNE RECEPTION

Measurement of scattering parameters at 35 GHz using amplitude-modulated homodyne detection 04 p0474 A83-16212

Instantaneous simultaneous signal detecting 05 p0625 A83-17344

Infra-red homodyne receiver with acousto-optically controlled local oscillator 11 p1657 A83-28616

Local-oscillator excess-noise suppression for homodyne and heterodyne detection --- in laser communication system 20 p3047 A83-42342

HOMOGENEITY

Stationarity of magnetohydrodynamic fluctuations in the solar wind 05 p0709 A83-17381

Nonparametric methods of homogeneity testing of precipitation fields 09 p1311 A83-23673

Thermal homogeneity in a closed excimer laser cavity 09 p1272 A83-24661

Waves in stratified homogeneous elastic media - The method of boundary integrals in nonstationary problems of dynamics --- Russian book 12 p1774 A83-28826

Homogeneity conditions for elastic membranes 17 p2525 A83-38849

HOMOGENEOUS TURBULENCE

Using single-point velocity probability distributions for characterizing turbulent flows 04 p0480 A83-16391

Atmospheric diffusion of a passive contaminant in a spatially homogeneous flow with transverse velocity [AIAA PAPER 83-0272] 05 p0633 A83-16623

Simple subgrid scale stresses models for homogeneous isotropic turbulence 05 p0638 A83-17315

On velocity correlations in homogeneous isotropic turbulence 06 p0756 A83-18073

Homogeneous and isotropic turbulence on the sphere --- in atmosphere 08 p1142 A83-23012

Conclusions on the basis of similarity characteristics of Reynolds stresses of nearly homogeneous turbulent shear flows 09 p1263 A83-25110

An application of the modified zero-fourth-cumulant approximation to homogeneous axisymmetric Boussinesq turbulence 12 p1722 A83-29006

Direct simulation of homogeneous turbulence at low Reynolds numbers 13 p1841 A83-30640

Homogeneous turbulence 13 p1843 A83-31081

Negative viscosity effect in large-scale turbulence Long-wave instability of a periodic system of eddies 14 p2009 A83-32422

A statistical mechanical model for two dimensional turbulence 14 p2009 A83-32510

A model of three-dimensional transfer in non-isotropic homogeneous turbulence 15 p2156 A83-33670

A theoretical study of radiative cooling in homogeneous and isotropic turbulence 15 p2156 A83-33671

Direct simulation of homogeneous turbulent shear flows on the Illiac IV computer - Applications to compressible and incompressible modeling 15 p2156 A83-33674

Technical improvements for direct numerical simulation of homogeneous three-dimensional turbulence 15 p2156 A83-33820

Unified approach to weak turbulence 15 p2239 A83-34543

Passive scalar fluctuations in intermittent turbulence with applications to wave propagation 18 p2687 A83-40415

Helical structures, fractal dimensions and renormalization-group approach in homogeneous turbulence 19 p2842 A83-41167

New representation of Navier-Stokes equations governing self-similar homogeneous turbulence 20 p2970 A83-42648

Multiple scales for modelling turbulent flows. I - A multiple scales model for the kinetic energy of the turbulence and variance of a passive scalar 21 p3129 A83-44460

A method of obtaining three-dimensional spectra in a homogeneous turbulence --- French thesis 21 p3133 A83-45084

On the question of the power law of the decay of grid turbulence 23 p3452 A83-48671

HOMOGENIZATION

U HOMOGENIZING

HOMOGENIZING

Homogenization and linear thermoelasticity 17 p2523 A83-38465

HOMOJUNCTIONS

Long wavelength Pb/1-x/Sn/x/Te homostructure diode lasers having a gallium-doped cladding layer 07 p0937 A83-21369

HOMOSPHERE

NT MIDDLE ATMOSPHERE

NT STRATOSPHERE

HOMOTOPY THEORY

A quasi-Newton versus a homotopy method for nonlinear structural analysis 16 p2369 A83-36560

HONEYCOMB CORES

Shear modulus of core materials with arbitrary polygonal shape 02 p0193 A83-12735

Electrical discharge machining of aluminum honeycomb core 07 p0940 A83-20500

HONEYCOMB STRUCTURES

NT HONEYCOMB CORES

Honeycomb mirrors of borosilicate glass 10 p1436 A83-25831

Acoustic fatigue life analysis - Honeycomb panels subjected to diffuse and progressive random acoustic waves [AIAA 83-1000] 12 p1745 A83-29875

Manufacture of large glass honeycomb mirrors --- for astronomical telescopes 13 p1921 A83-31013

High-capacity honeycomb panel heat pipes for space radiators [AIAA PAPER 83-1430] 14 p2010 A83-32705

Thermal behavior of laboratory models of honeycomb-covered solar ponds 17 p2535 A83-37050

Metal honeycomb to porous wireform substrate diffusion bond evaluation 18 p2695 A83-39620

Bonded aluminum honeycomb - Aircraft flight surface primary structure application 21 p3091 A83-43972

Non destructive testing of honeycomb structures by computerized thermographic systems --- for spacecraft applications [IAF PAPER 83-419] 23 p3415 A83-47378

Interaction of shock waves of air with a porous screen 23 p3452 A83-48658

HONING

The time series modelling of non-Gaussian engineering processes 08 p1073 A83-22006

HORIZON

NT RADIO HORIZONS

The moon illusion revisited --- eye accommodation to visible texture accompanied by apparent shifts in size 06 p0799 A83-18193

HORIZON SCANNERS

Horizon line scanning telephotometry 03 p0325 A83-13496

Earth limb altitude determination for the Solar Mesosphere Explorer [AIAA PAPER 83-0429] 05 p0603 A83-17926

On the choice of parameters for a single-rotor corrected gyrocompass 16 p2356 A83-35937

Attitude measurement and estimation of solar observation satellites 17 p2478 A83-37451

The infra-red horizon sensor on board the Aureol-3 satellite 18 p2647 A83-39583

The earth's horizon - A reference for sub arc minute attitude sensing on flexible space structures [AIAA PAPER 83-2179] 19 p2815 A83-41673

Modeling of the atmosphere for analysis of horizon sensor performance 22 p3261 A83-46599

Horizon sensor errors calculated by computer models compared with errors measured in orbit 22 p3261 A83-46600

HORIZON SENSING

U HORIZON SCANNERS

HORIZONTAL BRANCH STARS

The rotation of horizontal-branch stars. I - Members of the field 08 p1184 A83-23062

Chemical separation in horizontal-branch stars 10 p1514 A83-26727

Properties of G-type stars from uvby photometry 14 p2108 A83-33261

IUE observations of globular clusters and blue horizontal branch stars 15 p2244 A83-33594

IUE observations of the nucleus of the galactic globular cluster NGC 2808 16 p2429 A83-36634

An ultraviolet approach to M 15 16 p2429 A83-36638

The chemical composition of stars in globular clusters 17 p2602 A83-37828

The ellipticities of globular clusters and the second parameter problem 21 p3237 A83-45556

The magnetic fields of the helium-weak B stars 22 p3377 A83-46265

HORIZONTAL FLIGHT

Maximum endurance and maximum penetration trajectories for horizontal gliding flight [AIAA PAPER 83-0283] 05 p0594 A83-16628

The determination of the functional reliability of pilots during training on a flight-training simulator 07 p0980 A83-20884

The attainability domain of a coasting vehicle 10 p1380 A83-26073

HORIZONTAL ORIENTATION

A review of resonance response in large, horizontal-axis wind turbines 03 p0354 A83-13696

Perceived orientation in free-fall dependson visual, postural, and architectural factors 06 p0799 A83-18194

Hormonal and renal responses to plasma volume expansion after horizontal restraint in the rhesus monkey 11 p1636 A83-27799

Use of the finite-element method for natural convection in a horizontally confined infinite layer of fluid 12 p1726 A83-29899

Whirl flutter analysis of a horizontal-axis wind turbine with a two-bladed teetering rotor 19 p2861 A83-40766

Determination of the horizontal and vertical distribution of clouds from infrared satellite sounding data 22 p3340 A83-46140

HORIZONTAL STABILIZERS

U STABILIZERS (FLUID DYNAMICS)

HORIZONTAL TAIL SURFACES

Thrust reversing effects on horizontal tail effectiveness of twin-engine fighter aircraft [AIAA PAPER 83-0086] 05 p0594 A83-16512

The effect of backlash and trailing-edge strips on the flutter speed of a two-dimensional model of a tailplane with tab 06 p0716 A83-18068

Strength tests of CFRP joint assembly models for tailplane structure 18 p2703 A83-40159

- Aerodynamics propulsion and longitudinal control requirements for a tilt-nacelle V/STOL with control vanes submerged in the nacelle slipstream
[AIAA PAPER 83-2513] 23 p3404 A83-48357
- HORMONE METABOLISMS**
- Intracerebroventricular injections of cholecystokinin decreases the activity of the dopaminergic and serotonergic systems in the brain
02 p0219 A83-11519
- The activity of prostaglandin synthetase in brain tissues during radiation sickness in experimental animals
03 p0375 A83-13639
- The significance of glucocorticoids in the regulation of the resynthesis of glycogen in the postexercise period and the mechanism of their action
04 p0520 A83-15898
- Emotional stresses and their role in cerebrovisceral disturbances
05 p0672 A83-17598
- Current ideas about the mechanism of the action of glucocorticoid hormones
05 p0672 A83-17599
- The effect of prostaglandin F₂-alpha on the thermoregulatory peculiarities in rabbits
07 p0973 A83-20362
- The functional morphology of the submaxillary salivary glands of rats during age-related disorders of endocrine regulation
07 p0974 A83-20978
- Several indicators of the EKG and metabolic processes during an experimental coronary spasm in rats exposed to conditions of hypoxia in combination with hypercapnia
07 p0975 A83-20986
- Analgesic intestinal peptides - New agents of bodily defense
07 p0975 A83-21000
- Free-running activity rhythms in the rat - Entrainment by melatonin
08 p1146 A83-22689
- Hydro-electrolytic and hormonal modifications linked to extended decubitus in an antiorthostatic position
08 p1149 A83-22982
- Multiple hormonal changes during water immersion - An analog of weightlessness
08 p1149 A83-22988
- Hydroelectrolytic and hormonal modifications related to prolonged bedrest in antiorthostatic position
11 p1641 A83-27344
- ADH responses to volume shifts in the low pressure system --- AntiDiuretic Hormone
11 p1636 A83-27781
- Computer simulation analysis of the behavior of renal-regulating hormones during hypogravic stress
11 p1642 A83-27794
- Effects of antiorthostatic position at -4 deg on hydromineral balance
11 p1642 A83-27797
- Cardiovascular and endocrine effects of gravitational stresses /LBNP/ - The influence of angiotensin-converting enzyme inhibition with captopril
11 p1642 A83-27798
- Hormonal and renal responses to plasma volume expansion after horizontal restraint in the rhesus monkey
11 p1636 A83-27799
- Hormonal changes in antiorthostatic rats
11 p1637 A83-27800
- Effects of age and sex on hormonal responses to weightlessness simulation
11 p1643 A83-27841
- Plasma volume, renin, and vasopressin responses to graded exercise after training
13 p1903 A83-30476
- Exercise training, sex hormones, and lipoprotein relationships in men
13 p1903 A83-30487
- Vasopressin and the cardiovascular system
14 p2063 A83-32097
- The internalization and intracellular conversions of biologically active polypeptides and their receptors
14 p2065 A83-33320
- An evaluation of the condition and potential of athletes using indicators of humoral-hormonal reactions
16 p2398 A83-35904
- Inhibition of hypoxia-induced ADH release by meclofenamate in the conscious dog --- AntiDiuretic Hormone
17 p2554 A83-36993
- Changes of the hormonal spectrum of the blood under the effect of microwaves in the centimeter range
18 p2733 A83-40571
- The relationship of hormonal and hemodynamic parameters during emotional stress in healthy individuals and patients with hypertension
19 p2881 A83-41435
- Effects of hypoxia on norepinephrine release and metabolism in dog pulmonary artery
22 p3346 A83-45989
- The effect of the neuropeptides vasopressin and fragments of corticotrophin on the cardiovascular and respiratory system of humans at rest and during physical loading
23 p3497 A83-47116
- On the functional state of the pituitary-adrenal-axis in rats under different conditions of motor activity
23 p3496 A83-48448

HORMONES

- NT ADRENOCORTICOTROPIN (ACTH)
NT ALDOSTERONE
NT CORTICOSTEROIDS
NT CORTISONE

- NT ESTROGENS
NT PITUITARY HORMONES
NT PROSTAGLANDINS
NT THYROXINE
- The opioid peptide dynorphin, circadian rhythms, and starvation
05 p0669 A83-16940
- The hormonal dependence of the initial stages of heparin clearance during immobilization stress in rats
07 p0973 A83-20242
- Role of auxin and protons in plant shoot gravitropism
11 p1638 A83-27813
- The search for the 'sleep hormone'
13 p1900 A83-31314
- The metabolism of lipoproteins in conditions of experimental hyperthyrosis
17 p2556 A83-38125
- Gravitational effects on plant growth hormone concentration
19 p2878 A83-42052
- Androgens enhance in vivo 2-deoxyglucose uptake by rat striated muscle
22 p3346 A83-46706
- HORN ANTENNAS**
- A broad-band constant beamwidth corrugated rectangular horn
01 p0033 A83-11367
- Ground station antenna crosspolarisation measurements with an imperfectly polarised ancillary antenna
02 p0164 A83-11986
- TE/11/-to-HE/11/ mode converters for small angle corrugated horns
03 p0305 A83-14003
- A curved-aperture corrugated horn having very low cross-polar performance
03 p0305 A83-14005
- Design of E-plane cosecant square beam horn antennas based on ray theory and their radiation characteristics
03 p0308 A83-14135
- A phased horn with a main lobe of elliptical cross section
05 p0623 A83-17690
- Axially symmetric radiation patterns from flanged E-plane sectoral horn feeds
06 p0736 A83-18421
- Feeds for reflector antennas - A review
06 p0741 A83-18656
- Optimisation methods applied to horn antennas
06 p0741 A83-18657
- Beamshaping of sectoral and pyramidal horns with stepped amplitude distribution
06 p0741 A83-18659
- Effect of the polarization squirt of small horn antennas
06 p0741 A83-18662
- Diffraction from cylindrically truncated planar surfaces with application to an aperture matched horn design
06 p0742 A83-18666
- The use of integral equations of the second kind to study diffraction by thin screens
07 p0914 A83-20862
- The radiation of a horn antenna
08 p1078 A83-23152
- A wide-band low-sidelobe disc-o-cone antenna
09 p1248 A83-23805
- Symmetrical crossed rectangular horn for a circularly polarized multiple-beam reflector antenna
09 p1248 A83-23811
- Hybrid-mode, shielded, offset parabolic antenna
09 p1248 A83-23874
- A GTD study of pyramidal horns for offset reflector antenna applications
10 p1406 A83-26837
- Nonperiodic electromagnetic fields in a sectoral horn
11 p1555 A83-27932
- Antenna gain measurements by an extended version of the NBS extrapolation method
13 p1829 A83-31281
- Effects of choke-load position on radiation properties in double-choked small horn antennas
13 p1830 A83-31778
- Recent developments in millimeter-wave antennas
15 p2145 A83-35078
- A common-aperture X- and S-band four-function feedcone --- hornfeed design for antennas of Deep Space Network
15 p2126 A83-35086
- Time domain sensors for radiated impulsive measurements
15 p2166 A83-35178
- Absolute measurement at 1 THz of the optical coupling of a F.I.R. conical antenna with a Josephson detector
17 p2511 A83-37759
- Radio-astronomy antennas for 3 deg K cosmic radiation measurements
17 p2494 A83-38059
- A pyramidal horn antenna with identical E- and H-plane patterns
17 p2494 A83-38064
- Coupling between two conical horns placed side by side
20 p2963 A83-42368
- HOSPITALS**
- The use of computers at hospitals in the Ukrainian SSR
01 p0086 A83-10562
- HOT AIR**
- U HIGH TEMPERATURE AIR
- HOT ATOMS**
- The possible effects of translationally excited nitrogen atoms on lower thermospheric odd nitrogen
07 p0968 A83-21588

HOT CORROSION

- NT TEMPERATURE DEPENDENCE

- Oxidation-resistant materials for hot gas turbines and jet power plants. II
02 p0148 A83-12298
- Gas analysis techniques for high temperature corrosion testing
02 p0149 A83-12834
- Low temperature /650 to 700 C/ burner rig testing
02 p0158 A83-12835
- High-temperature adsorption of air oxygen by silicon nitride powders
02 p0161 A83-13034
- Sulfidation-oxidation of nickel and cobalt - Reactions between the metals and their sulfates
03 p0296 A83-13122
- The influence of superficially applied oxide powders on the high-temperature oxidation behavior of Cr₂O₃-forming alloys
03 p0296 A83-13124
- High temperature corrosion on high temperature materials Metallographic, scanning electron microscopic and microanalytical tests
04 p0458 A83-15124
- Protection of niobium and molybdenum against high-temperature oxidation
07 p0888 A83-20688
- A high-temperature protective coating for tantalum alloys
07 p0889 A83-20707
- Recent approaches to the development of corrosion resistant coatings
07 p0891 A83-21453
- Mechanisms of hot corrosion
07 p0891 A83-21455
- Comparison of hot-salt corrosion test procedures
07 p0892 A83-21457
- High temperature erosion and erosion-hot corrosion of superalloys and coatings
07 p0892 A83-21458
- High temperature stability of pack aluminide coatings on IN38LC
07 p0941 A83-21459
- Effect of coatings on the mechanical properties of superalloys
07 p0893 A83-21469
- The interaction of high temperature corrosion and mechanical properties of alloys
07 p0893 A83-21470
- Alloy design for nickel-base superalloys
07 p0894 A83-21484
- The effects of section size, coating and environment on creep rupture behaviour of superalloys
07 p0894 A83-21487
- The effect of hot corrosion on creep and fracture behaviour of cast nickel-based superalloy IN738LC
07 p0895 A83-21490
- Fatigue-crack initiation in IMI 829 caused by high-temperature fretting
07 p0896 A83-21566
- The high-temperature corrosion of aluminum-rich coatings in an atmosphere of sulfur vapor containing oxygen
08 p1068 A83-23243
- A study of the stability of protective coatings against sulfide-oxide corrosion
09 p1229 A83-23512
- A study of the oxidation and gas saturation of beta titanium alloys
09 p1235 A83-24400
- High temperature low cycle fatigue of MAR-M 509 superalloy. I - The influence of temperature on the low cycle fatigue behaviour from 20 to 1100 C. II - The influence of oxidation at high temperature
10 p1393 A83-25417
- Low cycle fatigue behaviour of cast nickel-base superalloy IN-738LC in air and in hot corrosive environments
10 p1394 A83-25422
- Sputter-ion plating of coatings for protection of gas-turbine blades against high-temperature oxidation and corrosion
10 p1394 A83-25472
- Low-pressure-plasma-deposited coatings formed from mechanically alloyed powders
10 p1394 A83-25532
- Coatings in industrial gas turbines - Experience and further requirements
10 p1388 A83-25539
- Influence of coatings and hot corrosion on the fatigue behaviour of nickel-based superalloys
10 p1394 A83-25540
- Thermal barrier coatings for thermal insulation and corrosion resistance in industrial gas turbine engines
10 p1400 A83-25542
- New results on the oxidation and hot corrosion of silicide overlay coatings on nickel-based alloys
10 p1388 A83-25545
- Erosion resistance of Co-Cr-Al coatings containing active element additions
10 p1395 A83-25551
- The effect of temperature on the kinetics of high-temperature salt corrosion in ZhS6K alloy
10 p1395 A83-25631
- Effect of local heating on corrosion fatigue strength of a titanium alloy
10 p1398 A83-26225
- Protective coating test and microstructure of coated turbine blades made of nickel-base alloy IN 100
10 p1399 A83-26895
- The effect of mass ratio of Ti to Al on the hot corrosion of quaternary 75Ni-13.5Cr-11.5/Ti + Al/ alloys
10 p1400 A83-26898
- Correlation and prediction of thermophoretic and inertial effects on particle deposition from non-isothermal turbulent boundary layers
11 p1566 A83-27481
- Emission properties of titanium alloys under heating in air
11 p1548 A83-28370

The identification of the sulfide NiCrS₂ in nickel-base superalloys during corrosion in sulfate melts 11 p1550 A83-28671

The influence of electrode potential on the corrosion of gas turbine alloys in sulfate melts 11 p1550 A83-28672

Microanalytical investigations of plasma-sprayed coatings providing protection against corrosion by hot gases 12 p1713 A83-29370

The effect of nitrogen- and hydrogen-containing media on the refractory properties of nickel-base alloys 14 p1993 A83-32388

High temperature corrosion and use of coatings for protection 14 p1995 A83-32810

High temperature oxidation studies of Al-3wt pctLi, Al-4.2wt pctMg and Al-3wt pctLi-2wt pctMg alloys 14 p1996 A83-32891

Microstructure and hot corrosion resistance of aluminide coating on a nickel-base superalloy in 738LC 15 p2137 A83-33973

High temperature internal oxidation behaviour of dilute Ni-Al alloys 15 p2140 A83-35068

Creep/corrosion of two nickel alloys in combustion gas 16 p2329 A83-35692

Hot corrosion of aluminide coatings on nickel-base superalloys in oxidizing and reducing conditions [ONERA, TP NO. 1983-12] 16 p2333 A83-36422

Computer simulation for the intergranular corrosion of Alloy 800 16 p2335 A83-36899

Penetration of sulfur through preformed protective oxide scales 18 p2666 A83-39854

High temperature corrosion; Proceedings of the International Conference, San Diego, CA, March 2-6, 1981 20 p2951 A83-42226

High temperature oxidation of chromium 20 p2951 A83-42231

The analysis of oxidation and hot corrosion data - A statistical approach 20 p2951 A83-42232

High temperature oxidation of hafnium and its alloys 20 p2952 A83-42233

Cyclic oxidation of superalloys 20 p2952 A83-42234

Corrosion of nickel in SO₂ atmospheres at elevated temperatures 20 p2952 A83-42240

The oxidation behavior of a model molybdenum/tungsten-containing alloy in air alone and in air with trace levels of NaCl(g) 20 p2952 A83-42241

Thermodynamic analyses of the high temperature corrosion of alloys in gases containing more than one reactant 20 p2949 A83-42242

Influence of oxide scales on high temperature corrosion erosion behavior of alloys 20 p2952 A83-42243

Hot corrosion of Sialons 20 p2957 A83-42247

New perspectives on hot corrosion mechanisms 20 p2949 A83-42248

Microstructural features of low temperature hot corrosion in nickel and cobalt base MCrAlY coating alloys 20 p2953 A83-42249

Mechanism of low temperature hot corrosion 20 p2953 A83-42250

Cobalt oxide-SO₂/SO₃ reactions in cobalt-sodium mixed sulfate formation and low temperature hot corrosion 20 p2949 A83-42251

Low temperature hot corrosion 20 p2953 A83-42252

Electrochemical assessment of MCrAlY coating alloys at 750 and 900 C in air and CO/CO₂ mixtures 20 p2953 A83-42253

Improved performance thermal barrier coatings 20 p2957 A83-42261

High temperature corrosion resistance of ceramic thermal barrier coatings 20 p2957 A83-42262

Recuperator alloys for high-temperature waste heat recovery 21 p3111 A83-43950

Interfacial layers in high-temperature-oxidized NiCrAl 21 p3113 A83-44619

High temperature corrosion of metals and alloys; Proceedings of the Third International Symposium, Mount Fuji, Japan, November 17-20, 1982 24 p3561 A83-49476

Defects and transport properties in oxides and sulfides 24 p3554 A83-49477

Protective coatings against hot corrosion 24 p3590 A83-49479

Erosion-corrosion of coatings and superalloys in high velocity hot gases 24 p3562 A83-49481

Alloy design for hot corrosion resistance 24 p3562 A83-49482

The microstructure of high-temperature oxide scales on nickel 24 p3562 A83-49483

Strains in the oxide scales and the substrate metals during oxidation 24 p3562 A83-49487

Selective surface oxidation of Fe-30 Ni alloy 24 p3562 A83-49488

Effect of oxygen pressure on the high temperature oxidation of Ni-Cr alloys 24 p3562 A83-49489

Al₂O₃ scales on ODS alloys --- oxide dispersion strengthened 24 p3563 A83-49490

High temperature oxidation of Fe-20Cr-4Al alloys with small additions of Sc, Y or Er 24 p3563 A83-49493

Electrochemical studies of corrosion of iron, nickel and nickel alloys in alkali sulfate melt 24 p3563 A83-49496

High temperature corrosion of pure nickel and nickel-20 percent chromium alloy in the presence of calcium sulfate and graphite 24 p3563 A83-49497

Hot corrosion of iron- and nickel-base superalloys caused by deposit of calcium sulfate 24 p3563 A83-49498

Effect of hot corrosion on strength and fracture of a nickel-base superalloy subjected to creep-fatigue interaction 24 p3563 A83-49499

Effect of sensitization on the hot corrosion behaviour of stainless steels in the temperature range of 600-900 C 24 p3563 A83-49500

A fundamental basis for using the platinum group elements as alloying additions in nickel-base alloys to improve high temperature corrosion 24 p3564 A83-49501

The role of silicon in protection of Ni-base alloys against hot corrosion 24 p3564 A83-49502

Hot corrosion resistance of nickel-base superalloys and aluminide coatings to molten Na₂SO₄-NiSO₄-NaCl salt 24 p3564 A83-49503

Hot corrosion behaviour of a cobalt-free, nickel-base superalloy 24 p3564 A83-49504

Hot corrosion of Ni-20Cr base alloys induced by Na₂SO₄-NaCl mixtures 24 p3564 A83-49505

Studies on the corrosion resistance of MCrAlY alloys at high temperatures 24 p3564 A83-49506

The study of the effect of cobalt on the hot corrosion resistance of nickel-based high temperature alloys 24 p3564 A83-49507

The kinetics and mechanism of the attack of MCr-type alloys in oxygen-sulphur environments at 700 C 24 p3565 A83-49511

The sulfidation properties of iron-nickel alloys at low sulfur pressures 24 p3565 A83-49512

The effect of Hf additions on oxidation behaviour of Ni₃Al 24 p3565 A83-49515

Effect of bond metal on durability of thermal barrier coating 24 p3565 A83-49518

New results on hot corrosion of silicon ceramics 24 p3569 A83-49520

Corrosion resistance of some composite coatings on Ni-base superalloy 24 p3566 A83-49521

HOT CYCLE PROPULSION SYSTEM

U TIP DRIVEN ROTORS

HOT ELECTRONS

Hot electrons in a GaAs heterolayer at low temperature 01 p0109 A83-10626

On the influence of a plasma hot component on whistler propagation beyond the plasmopause 02 p0206 A83-12020

Influence of hot carriers on the temperature dependence of threshold in 1.3-micron InGaAsP lasers 03 p0332 A83-14930

Photovoltaic emf in conditions of the heating of charge carriers by light 04 p0539 A83-15127

Dispersion relations for hot electrons 04 p0542 A83-16066

Hot-electron luminescence in aged electrodeposited CdSe liquid-junction solar cell 05 p0658 A83-16946

Hot-electron induced excess carriers in MOSFET's 05 p0624 A83-17287

Correlation between substrate and gate currents in MOSFET's 05 p0630 A83-17754

Experimental evidence for the acceleration of thermal electrons by ion cyclotron waves in the magnetosphere 07 p0966 A83-21515

Mechanism of thermal electron attachment to O₂ as studied by observing isotope effects of attachment rates for /O-18/2 systems 08 p1163 A83-22218

Observation of suprathermal electrons produced by stimulated Raman scattering processes 08 p1168 A83-22376

Observations of fluxes of suprathermal electrons accelerated by HF excited instabilities 09 p1300 A83-23309

Influence of diffusion of hot carriers on collection efficiency of solar cells - a-Si:H 09 p1292 A83-23665

The use of a microprocessor in the KM-3 instrumentation for measuring electron temperature and electron velocity distribution --- satellite ionospheric sounding 10 p1386 A83-25339

Two-dimensional analysis of hot-electron emission current in MOS FET 13 p1834 A83-30783

Calculation of velocity overshoot, velocity autocorrelation and hot electron noise in semiconductors from the small signal microwave mobility 14 p2006 A83-32668

The possibility of measuring the directional part of the spectra of superthermal electrons by means of the incoherent scattering of radio waves 14 p2054 A83-33030

Energy distribution of thermal electrons at the height of lower-E-region 16 p2373 A83-35366

The instability of two plasmons and suprathermal electrons in the laser-matter interaction --- French thesis 17 p2583 A83-38224

The energy of thermal electrons in electron beam created helium discharges 17 p2583 A83-38965

The effect of temperature on hot electron trapping in MOSFET's 19 p2905 A83-41287

An empirical model for device degradation due to hot-carrier injection 21 p3124 A83-43857

Simulation of GaAs submicron FET with hot-electron injection structure 21 p3126 A83-44967

Expulsion of a magnetic field by a hot electron cloud 21 p3214 A83-45209

Relativistic corrections for the conventional, classical Nyquist theorem 23 p3510 A83-47607

Hot-electron noise generation in gallium-arsenide Schottky-barrier diodes 24 p3574 A83-49993

HOT EXTRUDING

U EXTRUDING

HOT FORMING

U HOT WORKING

HOT GAS SYSTEMS

U HIGH TEMPERATURE GASES

HOT GASES

U HIGH TEMPERATURE GASES

HOT JET EXHAUST

U HIGH TEMPERATURE GASES

U JET EXHAUST

HOT JETS

U JET FLOW

HOT PLASMAS

U HIGH TEMPERATURE PLASMAS

HOT PRESSING

Hot isostatic pressing of niobium carbide 01 p0167 A83-10218

Comments on 'Kinetics of densification during hot-pressing of aluminium nitride' 02 p0159 A83-11672

Hot isostatic pressing technology. III - Diffusional bonding 02 p0156 A83-12296

Recrystallization of silicon nitride powders during hot pressing 02 p0160 A83-13033

The effect of CaF₂ addition on the oxidation of hot-pressed materials based on silicon nitride 02 p0161 A83-13035

Electrical resistance of hot-pressed TiC-SiC-C composites 03 p0302 A83-14815

Investigation of sintering and HIPing conditions of silicon nitride 03 p0303 A83-14919

Fabrication and characterization of Si₃N₄ ceramics without additives by high pressure hot-pressing 03 p0303 A83-14920

Fracture toughness of polycrystalline beta-alumina 03 p0303 A83-14921

HIP treatment on non-oxide ceramics 05 p0617 A83-17097

Failure probability of hot-pressed silicon-nitride 05 p0618 A83-17098

Oxidation of silicon nitride hot pressed with Y₂O₃ + MgO 05 p0619 A83-17564

Hot isostatic pressing technology. IV - Production of powders of titanium alloy Ti6Al4V and steel X5CrNi18 9 using the REP procedure 06 p0727 A83-17959

Production of high quality parts by hot pressing metal particulates 06 p0769 A83-19081

Stainless steel and nickel base powders for the production of parts via extrusion and hot isostatic pressing 06 p0730 A83-19083

The critical role of titanium in hot isostatically pressed maraging steels 06 p0730 A83-19086

The superplastic hot pressing of Ti6Al4V powders 06 p0731 A83-19095

P/M Astroloy obtained by forcing or HIPing superalloys sintered preforms 06 p0732 A83-19100

Effect of temporary alloying by hydrogen /hydrovac/ on the vacuum hot pressing and microstructure of titanium alloy powder compacts 07 p0883 A83-19833

The properties of rolled powder-metallurgy-alloy products 07 p0883 A83-19966

Microstructure and grain-boundary composition of hot-pressed silicon nitride with yttria and alumina 07 p0898 A83-20166

Processing ternary sulfide ceramics - Powder preparation, sintering, and hot-pressing 07 p0898 A83-20167

Practical applications of hot-isostatic pressing diagrams - Four case studies 07 p0884 A83-20260

Influence of hot isostatic processing and heat treatment variables on the tensile properties of cast Transage 175 alloy, Ti-2.5Al-13V-7Sn-2Zr 07 p0886 A83-20471

High cycle fatigue properties of cast nickel base superalloys IN 738LC and IN 939

Hot Isostatic Pressing of alloy IN-718

The nature and origin of previous particle boundary precipitates in P/M superalloys

High-temperature fracture of hot-pressed AlN ceramics

The mechanism and mechanics of subcritical crack propagation in hot-pressed SiC above 1000 C

Hot-pressed MgAl₂O₄ for ultraviolet /UV/, visible, and infrared /IR/ optical requirements

Infrared optics hot pressed from fluoride glass

The deformation resistance of pressed strips of powder-metallurgy alloys

Effect of hot-pressing temperature on the thermal diffusivity/conductivity of SiC/AlN composites

Effect of high-temperature exposure in air on strength of hot-pressed silicon nitride

Properties and structures of hot isostatically pressed and hot isostatically pressed plus forged superalloys

Microstructures and mechanical properties of hot isostatically pressed powder metallurgy alloy APK-1

A study of the possibility of producing multilayer materials based on titanium

Vacuum hot pressing of large near net shape spar fittings

Effect of processing on fatigue life of Ti-6Al-4Al-4V castings

The effects of weld-repair and hot isostatically pressing on the fracture properties of Ti-5Al-2.5Sn ELI castings

Powder metallurgy and hot isostatic pressing (HIP) of the titanium alloy TiAl6V4

Application of electron beam welding to hot isostatically pressed nickel-base materials

Processing-related fracture origins. I - Observations in sintered and isostatically hot-pressed Al₂O₃/ZrO₂ composites

The effect of the crystallization conditions of diamonds under high-temperature shock compression on their optical properties

Hot isostatic pressing of niobium C-103 alloy shapes

Effects of HAZ size and hardness variation on the performance of DC flash welds --- heat affected zone

Microstructures and subcritical crack growth in oxidized hot-pressed Si₃N₄

Creep behaviour of hot isostatically pressed niobium alloy powder compacts

Hot-isostatic-pressing technology (HIP). V - Properties and processing of HIP-Stellite 6

Equipment for the hot isostatic pressing of metal powders

Effect of grinding variables on strength of hot pressed silicon nitride

[ASME PAPER 83-GT-203]

Stress assisted hot formation of ceramics

Hot pressing of aluminium nitride

Microstructure development in silicon nitride

Oxidation kinetics of hot-pressed silicon nitride

The fracture behaviour of hot-pressed silicon nitride between room temperature and 1400 C

Hot isostatic pressing of ceramics

The effect of hot-pressing conditions on the structure and mechanical properties of boron carbide

Hot isostatic pressing of oxide dispersion strengthened superalloy parts

Properties of isostatically hot-pressed silicon nitride [ACS PAPER 168-B-83]

Hot-isostatic-pressing technology (HIP). VI - The development of a powder-metallurgy alloy of the type NiCr15Ag1Cu1

The kinetics of metal powder consolidation during hot pressing in porous shells. III - An experimental study

HOT STARS

NT A STARS

NT B STARS

NT BLUE STARS

NT O STARS

NT WHITE DWARF STARS

NT WOLF-RAYET STARS

Determination of the inclination of rotational axes and rotational velocity from the line profiles of rotating stars

Evidence for accretion activity and obscured hot component stars in W Serpentis type binaries

On C3 molecules in diffuse interstellar clouds

Photometry of symbiotic stars in the UBV_RJHKLMN system. III - AX Per, AG Dra, BF Cyg, V 443 Her, and YY Her

The hot halo subdwarf binary system HZ-22

Extreme ultraviolet spectrophotometry of the hot DA white dwarf HZ 43 - Detection of He II in the stellar atmosphere

Properties and nature of Be and shell stars: 7 B.88 Her - An important clue to understanding the Be phenomenon

Properties and nature of Be and shell stars. II - A notable correlation between the long-term spectral and photometric variations of V 1294 Aql /HD 184 279/

Properties and nature of Be and shell stars 7A. 88 Her - Observational data, their reduction and basic evaluation

Physical conditions in interacting galaxies, in components of isolated pairs, and in isolated galaxies

Four-color photometry of RZ Ophiuchi and its accretion disk

A study of visual double stars with early type primaries. I - Spectroscopic results

A study of visual double stars with early type primaries. II - Photometric results

An X-ray emitting bubble in the Cep OB3 association

Be and shell stars observed with the 13-color photometric system

CH Cygni 1981-82 - Now a shell star

A proposed observational test of the temperature structure in hot stellar atmospheres

An investigation of the region around the emission nebula IC 1848

An investigation of the region around the emission nebula NGC 1499

The discovery of nonradial instability strips for hot, evolved stars

Mass loss from hot stars

Einstein observations of hot stars

Observational aspects of chromospheres and coronae in hot stars

Star-burst galactic nuclei

Nonradial g-mode oscillations of warm neutron stars

Possible evidence for the driving of the winds of hot stars by Alfvén waves

Non-thermal phenomena in the atmosphere of hot subdwarfs X-ray upper limit for BD-3deg2179

The binary central star of the planetary nebula LT-5

Mass loss, levitation, accretion, and the sharp-lined features in hot white dwarfs

The symbiotic star H1-36

Mode constraints on nonradial pulsations from polarization data

Do pulsating PG1159-035 stars put constraints on stellar evolution?

Determination of effective temperatures for hot stars from integrated fluxes

The discovery of a hot stellar wind

Late stages of stellar evolution. II - Mass loss and the transition of asymptotic giant branch stars into hot remnants

Fast winds in planetary nebulae

Four-colour photometry of eclipsing binaries. XVII - Light curves of DM Virginis

Far ultraviolet observations of Population II

Subsurface-structure determination using photothermal laser-beam deflection

Suction effects on the structure of turbulent boundary layer on a heated porous wall

Heat transfer for flows past non-isothermal bodies --- Russian book

Thermal stresses in a semiinfinite orthotropic plate heated by a heating region moving along the end face

Evaporation and ignition of a fuel droplet on a hot surface. IV - Model of evaporation and ignition

Laminar natural convection from a horizontal plate and the influence of plate-edge extensions

Effect of surface roughness on the delayed transition on 9:1 heated ellipsoids

Recent developments in surface-tension driven instabilities

[IAF PAPER 83-144]

Photovoltaic power for walk-in coolers

Suction effects on the structure of turbulent boundary layer on a heated porous wall

Heat transfer for flows past non-isothermal bodies --- Russian book

Thermal stresses in a semiinfinite orthotropic plate heated by a heating region moving along the end face

Evaporation and ignition of a fuel droplet on a hot surface. IV - Model of evaporation and ignition

Laminar natural convection from a horizontal plate and the influence of plate-edge extensions

Effect of surface roughness on the delayed transition on 9:1 heated ellipsoids

Recent developments in surface-tension driven instabilities

[IAF PAPER 83-144]

Photovoltaic power for walk-in coolers

Production of deformable nickel-molybdenum PM alloys. I - A study of alloy sintering and structure and development of heat treatment schedules

Analysis of ductile deformation processes on the basis of a mixed variational principle

Hot extrusion of aluminum composite containing dispersed graphite particles - Study of properties of particle-dispersed aluminum composite II

Texture and grain boundary strengthening in hot rolled magnesium - 12.5 at. % lithium alloy

The occurrence of shear bands in nonisothermal, hot forging of Ti-6Al-2Sn-4Zr-2Mo-0.1Si

Principles governing texture formation in alloys undergoing phase transitions during various treatments

Hydrogen plasticizing of refractory titanium alloys

The effect of hydrogen plasticization in alloys of titanium with aluminum

Hot-rolled silicon carbide-aluminum composites

The effect of shear bands on service properties of Ti-6Al-2Sn-4Zr-2Mo-0.1Si forgings

A model for the behavior of the titanium alloy Ti-6 percent Al-4 percent V in the hot forging regime

An analysis of the stress-strain state in the internal deformation zone during hot forming

The effect of scandium on the high-temperature ductility of the binary alloy Al-6.5 pct Mg

Load and material flow in hot extrusion of aluminum and copper powder compacts

Production of deformable nickel-molybdenum powder metallurgy alloys. II - The structure and mechanical properties of the alloys following hot working and heat treatment

Strain aging of Ti-6242 at hot-working temperatures

Evaluation of fracture toughness of thermomechanical-processed 7079 alloy using double torsion bend test

Stress assisted hot formation of ceramics

Effect of texture and grain size on the fracture behaviour of hot rolled Mg, Mg-12.5 percent Li and Mg-5 percent Ti alloys

Hot-FILM ANEMOMETERS

Hot-film anemometer measurements in a starting turbulent jet

Turbulent static pressure fluctuations away from flow boundaries

[AIAA PAPER 83-0754]

Complementary use of a tri-axial hot film probe and a five hole pitot tube to determine vehicle wake characteristics

The measurement of cloud droplet concentration with a hot film probe

A note on the measurement of transverse velocity fluctuations with heated cylindrical sensors at small mean velocities

Digital thermal anemometry

Simultaneous stereoscopic visual and anemometer measurements in a convected frame of reference

A three component velocity measurement in an open channel by a combination of LDA and hot film anemometry

HOT-WIRE ANEMOMETERS

X-wire sounding in an air inlet at high angle of attack
[AAAF PAPER NT 81-15] 02 p0132 A83-11775

Constant-temperature hot-wire anemometer practice in supersonic flows. I - The normal wire
[AIAA PAPER 83-0050] 05 p0642 A83-16485

Preliminary measurements of velocity, density and total temperature fluctuations in compressible subsonic flow
[AIAA PAPER 83-0384] 05 p0635 A83-16684

Constant-temperature hot-wire anemometer practice in supersonic flows. II - The inclined wire
[AIAA PAPER 83-0508] 05 p0643 A83-16756

Effects of Mach number on the development of a subsonic rectangular jet
07 p0863 A83-19805

Measurement of three dimensional flow field behind an impeller by means of periodic multi-sampling with a slanted hot wire
07 p0929 A83-20276

A system for phase and intermittency measurements in periodically turbulent flows
08 p1091 A83-21980

Some aspects of measuring the structure of non-isothermic turbulence by simultaneous application of DISA's LDA and hot-wire anemometer
09 p1259 A83-23697

Improved calibration of hot-wire anemometers
11 p1574 A83-28574

Application of a three-sensor hot-wire probe for incompressible flow
12 p1728 A83-28963

Hot-wire anemometry --- Book
15 p2162 A83-33618

A high-performance low-cost constant-temperature hot-wire anemometer
15 p2166 A83-35258

Triple hot-wire technique for simultaneous measurements of instantaneous velocity components in turbulent flows
15 p2166 A83-35259

Single-wire swirl flow turbulence measurements
[AIAA PAPER 83-1202] 16 p2352 A83-36278

Improvements of the performance of triple hot wire probes
17 p2509 A83-36999

Simple corrections for the temperature sensitivity of hot wires
17 p2509 A83-37000

Measurement of the velocity of a three-dimensional flow by hot-wire anemometers
19 p2850 A83-42017

Turbulence measurements in a developing mixing layer with mild destabilising curvature
21 p3131 A83-44678

A flying hot-wire system
21 p3138 A83-44681

A digital technique for the simultaneous measurement of streamwise and lateral velocities in turbulent flows
23 p3458 A83-48117

A microprocessor controlled data acquisition and processing system for hot-wire anemometry
24 p3584 A83-49810

Measurement of velocity-temperature correlations of different orders in hot turbulent flows
24 p3584 A83-49814

Using numerical techniques to improve the performance of triple hot-wire probes
24 p3585 A83-49817

Digital thermal anemometry
24 p3585 A83-49818

HOT-WIRE FLOWMETERS

Simultaneous measurement of stagnation temperature and specific flow rate in a hypersonic gas flow
04 p0481 A83-15447

A critical evaluation of the aerodynamical effect of a turbulence instrument
07 p0930 A83-20804

A method of measuring the thermal conductivity of orthogonal anisotropic materials by a transient hot wire method
08 p1092 A83-22240

Effect of combined roll and pitch angles on triple hot-wire measurements of mean and turbulence structure
09 p1267 A83-23698

Flow disturbance induced by the DISA triaxial hot-wire probe 55P91
09 p1267 A83-23699

The aerodynamic properties of the DISA nozzle unit for calibrating and testing hot-wire probes, in particular multiple sensor probes at moderate velocities
09 p1267 A83-23700

Instantaneous turbulence profiles in the wake of an oscillating airfoil
12 p1695 A83-28951

A sensor for flow measurements near the surface of a compressor blade
14 p2019 A83-32400

Numerical study of the effect of an embedded surface-heat source on the separation bubble of supersonic flow
[AIAA PAPER 83-1753] 17 p2446 A83-37226

An examination of hot-wire length corrections
18 p2692 A83-40501

Triple hot-wire technique for measurements of turbulence in heated flows
20 p2989 A83-42774

HOT-WIRE TURBULENCE METERS

U HOT-WIRE FLOWMETERS

U TURBULENCE METERS

HOUSEKEEPING (SPACECRAFT)

On the application of housekeeping data to ISS-b operations
21 p3096 A83-45444

HOUSINGS

NT COWLINGS
NT RADOMES

Recent advances in composite flywheel containment design technology
11 p1589 A83-27302

Composite flywheel rotor containment
18 p2709 A83-40294

HOVERCRAFT

U GROUND EFFECT MACHINES

HOVERCRAFT GROUND EFFECT MACHINES

The British Hovercraft Corporation's Ap.1-88 hovercraft
[AIAA PAPER 83-0634] 08 p1173 A83-22424

Development of the 'Neova' light hovercraft series
15 p2244 A83-35060

HOVERING

Vortex theory for hovering rotors
03 p0278 A83-13144

Dynamic analysis of constant-lift and free-tip rotors
06 p0773 A83-18386

Prediction of the aerodynamic loads on helicopter blades in hovering and axial flight using lifting line theory
07 p0864 A83-21016

The aeroelastic behavior of curved helicopter blades in hovering and axial flight
07 p0866 A83-21017

Rotor hovering performance using the method of fast free wake analysis
08 p1042 A83-22162

A closed-form analysis of rotor blade flap-lag stability in hover and low-speed forward flight in turbulent flow
[AIAA 83-0986] 12 p1702 A83-29864

Navier-Stokes calculations for the vortex wake of a rotor in hover
[AIAA PAPER 83-1676] 17 p2444 A83-37184

Hover and transition flight performance of a twin tilt-nacelle V/STOL configuration
[AIAA PAPER 83-1824] 17 p2465 A83-38656

Assessment of rotor-fuselage coupling on vibration predictions using a simple finite element model
19 p2857 A83-41075

The use of actuator-disc dynamic inflow for helicopter flap-lag stability
19 p2797 A83-41081

Hovering limit cycles - A man-in-the-loop approach
[AIAA PAPER 83-2232] 19 p2803 A83-41710

Status of the development of handling criteria for VSTOL transition
[AIAA PAPER 83-2103] 19 p2806 A83-41932

HOVERING STABILITY

Rotor blade flap-lag stability in turbulent flows
06 p0716 A83-18380

Dynamic stability of a buoyant quad-rotor aircraft
08 p1047 A83-22160

Measured inplane stability characteristics in hover for an advanced bearingless rotor
[AIAA 83-0987] 12 p1702 A83-29865

Aeroelastic stability of an elastic circulation control rotor blade in hover
[AIAA PAPER 83-0985] 14 p1975 A83-32785

Aeromechanical stability of a hingeless rotor in hover and forward flight - Analysis and wind tunnel tests
24 p3548 A83-50141

HR DIAGRAM

U HERTZSPRUNG-RUSSELL DIAGRAM

HRB-1 HELICOPTER

U CH-46 HELICOPTER

HTGR

U HIGH TEMPERATURE GAS COOLED REACTORS

HTPB PROPELLANTS

Parametric study of acceleration effects on burning rates of metallized solid propellants
02 p0161 A83-13084

Bonding agents for AP and nitramine/HTPB composite propellants
[AIAA PAPER 83-1199] 16 p2340 A83-36275

HU-1 HELICOPTER

U UH-1 HELICOPTER

HUBBLE CONSTANT

On the neutrino mass and the Lemaitre model
01 p0119 A83-10235

Towards a new scale of extragalactic distances
01 p0118 A83-11337

Shifts of spectral lines emitted from stars
03 p0431 A83-14947

Dynamical models and our Virgo-centric deviation from Hubble flow
05 p0696 A83-16976

Extragalactic distance scale, Malmquist bias and Hubble constant
06 p0828 A83-18179

Towards a unification of the parameters underlying elementary particles and cosmology
06 p0835 A83-18896

A distance scale from the infrared magnitude/H I velocity-width relation. IV - The morphological type dependency and scatter in the relation; the distances to nearby groups
07 p1019 A83-21101

Holes in cosmology
07 p1026 A83-21253

Age and metal abundance of a globular cluster, as derived from Stromgren photometry
09 p1364 A83-25289

Tracking back to the big bang

11 p1683 A83-28767

Five crucial tests of the cosmic distance scale using the Galaxy as fundamental standard
13 p1935 A83-30356

Global value of Hubble constant
13 p1946 A83-30382

Radioactive models of type 1 supernovae
13 p1952 A83-31431

A special law of variation for Hubble's parameter
15 p2261 A83-34411

The expansion of the universe as a driving mechanism for the evolution of correlations
17 p2614 A83-38967

HUBBLE DIAGRAM

The Hubble diagram of quasars and the deceleration parameter q sub 0
01 p0119 A83-10228

The Hubble diagram for quasars and quasars
03 p0426 A83-14694

Luminosity evolution of QSOs
05 p0695 A83-16856

The Hubble diagram of quasars showing interplanetary scintillation
06 p0836 A83-19167

CCD photometry of Abell clusters. I - Magnitudes and redshifts for 84 brightest cluster galaxies
06 p0842 A83-19476

Optical variability, absolute luminosity, and the Hubble diagram for QSOs
21 p3235 A83-45527

The effect of a magnitude cut-off on the spectral shift anomaly of galaxies in the Perseus supercluster
23 p3526 A83-47847

S0 and smooth-arm Sa's within the Hubble sequence
24 p3657 A83-49263

HUBS

Measurements and data reduction problems behind the rotor of a transonic axial flow compressor in the hub region
10 p1372 A83-26417

Effects of compressor hub treatment on stator stall margin and performance
[AIAA PAPER 83-1352] 16 p2362 A83-36354

Quasi-three-dimensional turbomachinery flow calculations on multiple hub-to-shroud stream surfaces
[AIAA PAPER 83-1820] 17 p2455 A83-38652

Blade design for reduced helicopter vibration
19 p2797 A83-41076

Analytical and experimental investigation of a bearingless hub-absorber
19 p2797 A83-41077

HUGHES AIRCRAFT

NT AH-64 HELICOPTER

HUGHES MILITARY AIRCRAFT

U MILITARY AIRCRAFT

HUGONIOT ADIABAT

U HUGONIOT EQUATION OF STATE

On the evaporation of shock-compressed metals during expansion
16 p2328 A83-35539

HULLS (STRUCTURES)

NT SHIP HULLS

Aerodynamic estimation techniques for aerostats and airships
06 p0712 A83-18404

HUMAN BEHAVIOR

A method for investigating human factor aspects of aircraft accidents and incidents

04 p0523 A83-15899

Pilot performance and stress - Search for a killer
07 p0979 A83-20075

The systemic quantization of behavior --- of animals and humans
08 p1150 A83-22116

A preliminary study using surface electromyography of the behavior of air traffic controllers according to the density of traffic
08 p1148 A83-22971

Mandatory processing of the background in the detection of objects in scenes
10 p1456 A83-26319

Sustained search - Number of background characters, target type, and time on watch
10 p1456 A83-26321

A study of human behavior in adverse stress
16 p2400 A83-35700

Behavioral thermoregulation
16 p2399 A83-35914

The function of dream sleep
18 p2732 A83-39961

The interaction of the dominant and the conditioned reflex as the functional unity of the organization of behavior
21 p3189 A83-45371

HUMAN BEINGS

The ontogeny of the functional asymmetry of the human brain
01 p0082 A83-10507

Morphological criteria for the individual variability of the human brain
03 p0380 A83-13643

The dynamics of vertical eye movements in normal human subjects
06 p0797 A83-18192

The effect of multiple exposures to radiative heat on the resistance of the body to convective heating and total cooling
09 p1321 A83-25157

The invariance of visual identification in the right and left hemispheres of the human brain
13 p1901 A83-30441

- Time course of posthyperventilation breathing in humans depends on alveolar CO₂ tension 13 p1903 A83-30491
- Hemophilic bacteria in the nasopharynx of healthy individuals 14 p2066 A83-33334
- An automatic system for the medical monitoring of the functional condition of a human 15 p2215 A83-34947
- Methodological principles of the investigation of the influence of the interaction of sensory systems on psychic processes 16 p2401 A83-36818
- HUMAN BODY**
- The omega-potential - A quantitative indicator of the condition of the structure of the brain and the organism. II - The possibilities and limitations of the use of the omega-potential for rapid evaluations of the condition of the human body 02 p0222 A83-12212
- Methods for calculating the optimal and allowable irradiation levels during radiant heating 03 p0379 A83-13613
- Age-related patterns of lateral movement preferences 05 p0673 A83-17156
- Variability of fiber type distributions within human muscles 05 p0674 A83-17328
- The effect on the human body of a high concentration of carbon dioxide and hypokinesia 07 p0978 A83-20883
- Cinematography data systems at the Naval Biodynamics Laboratory 08 p1102 A83-22791
- Targets for three-dimensional /3-D/ tracking of human impact test subjects 08 p1102 A83-22792
- Combination of accelerometer and photographically derived kinematic variables defining three-dimensional rigid body motion 08 p1102 A83-22793
- Automatic measurement of body surfaces using rasterstereography. I - Image scan and control point measurement 10 p1420 A83-25971
- Whole-body vibration and International Standard ISO 2631 - A critique 10 p1458 A83-25999
- An investigation of the Achilles reflex in standing humans 12 p1765 A83-29317
- An investigation of the rigidity of a human muscle depending on its length 12 p1766 A83-29318
- Humanscale 7/8/9 --- Book on human factors engineering information 13 p1906 A83-30154
- Determination of maximal aerobic power during upper-body exercise 13 p1902 A83-30458
- Effects of water immersion on plasma catecholamines in normal humans 13 p1902 A83-30465
- Human respiration at rest in rapid compression and at high pressures and gas densities 13 p1902 A83-30467
- Acute mountain sickness, antacids, and ventilation during rapid, active ascent of Mount Rainier 14 p2068 A83-32684
- An investigation of the biodynamic properties of the human body under general low-frequency vibration 17 p2560 A83-38189
- The structural-functional organization of the fibrous framework of the Achilles tendon in humans 17 p2560 A83-38199
- The position of the body and the regulation of blood circulation --- Russian book 21 p3184 A83-45002
- HUMAN CENTRIFUGES**
- 'A total G-force environment dynamic flight simulator' - A new dimension in flight simulation [AIAA PAPER 83-0139] 05 p0599 A83-16548
- Operational utilization study on new human centrifuge of JASDF. II - Capability and usability of the new systems 10 p1458 A83-26088
- Operational utilization study on new human centrifuge of JASDF. III - Measurement of a three-axis acceleration force in human centrifuge 10 p1458 A83-26089
- Operational utilization study on new human centrifuge of JASDF. IV - Test and evaluation of anti-g system 10 p1458 A83-26090
- Circadian variations in tolerance to +Gz acceleration 11 p1642 A83-27783
- Human tolerance to rotation at different G's 11 p1642 A83-27784
- The application of positive pressure breathing for improving +Gz acceleration tolerance 12 p1764 A83-28931
- HUMAN ENGINEERING**
- U. HUMAN FACTORS ENGINEERING
- HUMAN FACTORS ENGINEERING**
- NT. MOTION SIMULATION
- Human factors and the design of display terminals 01 p0085 A83-10253
- Human factors and intelligent products 01 p0085 A83-10254
- The active-operator principle in engineering psychology 01 p0085 A83-10380
- Maximizing ATE throughput 01 p0087 A83-10727
- F-16 voice message system study 01 p0005 A83-11121

- Integrated perceptual information for designers 01 p0029 A83-11136
- HHMU's, AMU's, and MMU's - The development of astronaut maneuvering units [AAS 82-148] 02 p0140 A83-11936
- Ergonomic evaluation of two-hand control location 02 p0225 A83-12088
- Visual scanning behavior and pilot workload 02 p0225 A83-12405
- Human performance can drastically affect critical systems operation 02 p0225 A83-12975
- Psychic effects on the safety and reliability of complex technical systems 02 p0225 A83-13015
- Systemic approach in the psychological analysis of man-computer interaction 03 p0383 A83-13283
- Investigation of the nonlinear control signal amplification in the case of a continuous tracking problem --- German book 03 p0384 A83-14112
- Evaluation procedures to be used during the development of CAD systems 04 p0465 A83-15146
- SAFE Association, Annual Symposium, 19th, Las Vegas, NV, December 6-10, 1981, Proceedings 04 p0524 A83-15401
- The role of endogenous circadian rhythmicity in Air-Force flight accidents due to pilot error 04 p0521 A83-15402
- Preliminary generalized thoughts concerning ejection fail phenomena 04 p0443 A83-15404
- Investigation of the motion of the center of mass of an occupant under ejection accelerations 04 p0525 A83-15411
- The human factor in mishaps - Psychological anomalies of attention 04 p0523 A83-15413
- The 1981 Naval and Marine Corps aviation anthropometry survey and applications 04 p0525 A83-15414
- USAF Aerospace Biotechnology Research and Development Program 04 p0525 A83-15420
- Human factors dilemmas in the quest for aviation safety 04 p0444 A83-15423
- A review of naval aviation on-board oxygen generating systems 04 p0526 A83-15432
- Flight helmets - The British approach 04 p0526 A83-15443
- Negative transfer - A threat to flying safety 04 p0523 A83-15541
- The optimal shift schedule of work in industry 04 p0522 A83-15785
- A method for investigating human factor aspects of aircraft accidents and incidents 04 p0523 A83-15899
- Ergonomic aspects of aircraft keyboard design - The effects of gloves and sensory feedback on keying performance 04 p0526 A83-15900
- Advanced Aircrew Display Symposium, 5th, Patuxent River, MD, September 15, 16, 1981, Proceedings 04 p0447 A83-16126
- Human engineering in aircraft and system design 04 p0446 A83-16127
- Color selection and verification testing for airborne color CRT displays 04 p0524 A83-16128
- Characteristics of flight simulator visual systems 04 p0450 A83-16331
- Human factors of future air traffic control systems 05 p0677 A83-17732
- Designing patrol aircraft for the crew 06 p0800 A83-18811
- Biofeedback as an important mechanism in the success of teaching humans to control the skin-galvanic reaction 07 p0979 A83-20330
- Handbook on engineering psychology --- in Russian 07 p0982 A83-20389
- Pilot task profiles, human factors, and image realism 08 p1047 A83-22836
- Image quality and observer performance 08 p1150 A83-22891
- Human aspects of integrated navigation in the air 09 p1323 A83-23370
- Ergonomic analysis and evaluation procedures for cockpit operating positions 09 p1324 A83-23496
- Human capabilities: Long residence - An uncharted field 09 p1325 A83-24359
- Selection and experimental comparison of computer input devices --- Book 09 p1325 A83-24902
- Integration of a crewman into a high performance spaceplane [SAE PAPER 820850] 10 p1383 A83-25758
- The effects of extended practice on the evaluation of visual display codes 10 p1456 A83-26000
- Human Factors Society, Annual Meeting, 25th, Rochester, NY, October 12-16, 1981, Proceedings 10 p1456 A83-26301
- Application of advanced speech technology /AST/ in manned penetration bombers 10 p1459 A83-26302

- Human factors in equipment development for the Space Shuttle - A study of the general purpose work station 10 p1459 A83-26310
- Human factors in the application of large screen electronic displays to transport flight station design 10 p1376 A83-26312
- Potential uses of two types of stereographic display systems in the airborne fire control environment 10 p1376 A83-26314
- How to get a grip on TADS/PNVS --- Target Acquisition Detection System/Pilot's Night Vision System 10 p1459 A83-26316
- The model human processor - A model for making engineering calculations of human performance 10 p1459 A83-26323
- Test of a fuzzy set based decision model as an aid in solving human factors design problems 10 p1470 A83-26324
- Procedure for an evaluation of control systems on the basis of human factor considerations 10 p1460 A83-26479
- Wheelchair analysis - A CAD/CAM application 10 p1401 A83-26578
- Humanscale 7/8/9 --- Book on human factors engineering information 13 p1906 A83-30154
- Humanscale 4/5/6 --- Book on human factors engineering information 13 p1906 A83-30155
- Microbiological problems of closed ecological systems --- Russian book 13 p1906 A83-30425
- Thermal control system for a Manned Space Station [SAE PAPER 820836] 13 p1906 A83-30933
- Space Station crew operations impact on ECLSS design [SAE PAPER 820839] 13 p1906 A83-30934
- An evaluation of microorganisms for unconventional food regeneration schemes in CELSS - Research recommendations [SAE PAPER 820852] 13 p1899 A83-30940
- Compatibility and resource competition between modalities of input, central processing, and output --- in human task performance in military aircraft 15 p2215 A83-34075
- The subjective equivalence of sinusoidal and random whole-body vibration in the sitting position - An experimental study using the 'floating reference vibration' method 16 p2401 A83-35563
- A calculation and interference test apparatus for the simulation of mental stress 16 p2402 A83-35566
- The spine and the helicopter 16 p2397 A83-35582
- The pilot seat and the vertebral column 16 p2397 A83-35583
- Bring cohesion to handling-qualities engineering 16 p2298 A83-35772
- The man-vehicle systems research facility - A new NASA aeronautical R & D facility [AIAA PAPER 83-1098] 16 p2312 A83-36218
- Human factors approach in certification flight test [SAE PAPER 821340] 17 p2562 A83-37951
- A hygienic and physiological evaluation of the main ergonomic characteristics of metal-cutting machine tools 19 p2885 A83-41456
- The 'human factor' and production organization 19 p2885 A83-41836
- Man, machine and configuration - Human factors versus hardware in avionic display design 21 p3189 A83-44686
- Aircraft keyboard ergonomics - A review 21 p3189 A83-44691
- Human factors in air traffic control 21 p3189 A83-44881
- The reliability and the quality of the functioning of ergatic systems --- Russian book 21 p3189 A83-45034
- Space technology - The art and science of ergonomics 21 p3092 A83-45605
- Experimental evaluation of the visual efficiency of candidate devices for the display of meteorological radar data 23 p3453 A83-47146

HUMAN PATHOLOGY

- Concerning the interrelationship between protein, fat, and carbohydrate metabolisms 01 p0081 A83-10560
- The pathological anatomy of shock lung 01 p0081 A83-11390
- Heterotopic ossifications in regions of the elbow joint and their treatment with ultrasound 01 p0084 A83-11393
- The stimulating action of coagulating laser interventions in macular pathologies 03 p0378 A83-13606
- Two types of adaptation reactions of the blood circulation apparatus 03 p0379 A83-13616
- The state of the vestibular-analyzer function in patients with infectious-allergic bronchial asthma 03 p0381 A83-14337

Pneumomediastinography in the investigation of the thymus gland in patients with myasthenia 03 p0381 A83-14340

Prevalence of selected pathology among currently certified active airmen 04 p0521 A83-15535

Computer tomography applied to the study of inflammatory diseases of the brain /a survey of the literature/ 05 p0673 A83-17179

Diseases of the nervous system in miners of the far north and problems of prevention 05 p0673 A83-17193

The diagnosis of latent vestibular disorders in patients with otosclerosis 07 p0978 A83-20877

The determination of the circulating immune complexes in humans 07 p0978 A83-20999

Gall bladder disease in a 30 year follow up study - Its association with ischemic disease 08 p1147 A83-22959

Some considerations on lumbar pains and diseases of the intervertebral disk to civilian aircrewmembers 08 p1148 A83-22974

An investigation of human blood, erythrocytes, and plasma using the method of ESR at 77 K 08 p1150 A83-23022

The physiology and pathology of the venous blood circulation of the lower extremities --- Russian book 09 p1322 A83-23822

The condition of the hypothalamic-hypophyseal-adrenal system during sudden cardiac death 09 p1322 A83-23982

A histopathological study on ischaemic heart disease fatalities 09 p1323 A83-24009

The problem of sudden coronary death in the light of mathematical catastrophe theory 13 p1900 A83-30093

Problems in aerospace medicine posed by mitral valve prolapse 14 p2067 A83-32451

The pathology of crisis and medical transport of mental patients in acute conditions 14 p2067 A83-32453

Maxillary intrasinus benign expansive processes that inflate and/or destroy the sinus boney walls (five case studies) Interest in their knowledge for aeronautical medicine 14 p2067 A83-32462

The use of a combined pressure and medication treatment for the rehabilitation and recovery of the functions of the locomotor system 14 p2070 A83-33307

Pulmonary complications during acute disorders of the cerebral blood circulation 14 p2070 A83-33311

The pathology of the immune system during injury 14 p2066 A83-33327

The diagnostics, treatment, and prophylactic measures for the initial appearances of brain blood insufficiencies 15 p2212 A83-34927

The dependence of the origin of acute disorders of the brain blood circulation on the changes of meteorological factors 15 p2212 A83-34929

Some methodological approaches to the evaluation of the morbidity with temporary loss of work capacity of women working in the metro 15 p2212 A83-34934

The problem of microcirculation and eye pathology 15 p2210 A83-34940

Environmentally induced cholinergic urticaria and anaphylaxis 15 p2214 A83-34989

Problems of fitness posed by vertebral pathology in flight personnel 16 p2397 A83-35584

Necrotic epitympanitis complicated by paresis of the facial nerve and labyrinthitis 16 p2399 A83-36815

The pattern of the functional condition of the vestibular analyzer in patients with cervical osteochondrosis combined with a vertebral artery syndrome 16 p2399 A83-36826

Mathematical modelling in studies of the pathology of the visual nerve 16 p2400 A83-36835

Methods for determining the extent of myocardial infarction 16 p2400 A83-36837

The application of noninvasive methods for the study of patients with ischemic heart disease 16 p2400 A83-36838

Several indicators of the functional condition of the immune system in normal and pathological situations 16 p2400 A83-36842

Physical stress during work and the incidence of disease in workers 17 p2559 A83-38185

The cerebral blood circulation of patients with vibration disease during treatment at health resorts 17 p2560 A83-38191

The diagnostics of the subclinical stage of vibration sickness 17 p2561 A83-38926

The reaction of the human lymphocyte chromosome to graded doses of neutrons during irradiation in vitro 19 p2874 A83-41006

The diagnostic value of the otolithic reflex in patients with chronic suppurative inflammation of the middle ear 19 p2881 A83-41441

The content of immunoglobulins in the blood serum of patients with various forms of chronic inflammation of the middle ear 19 p2883 A83-41826

The diagnostic informativity of drugs used for revealing intralabyrinthine hydrops according to data of audiological and biochemical investigations 19 p2883 A83-41828

An investigation of the proteinase activity in the perilymph of patients with otosclerosis 19 p2883 A83-41830

The prevalence of pathologies of the vestibular apparatus among patients referred to a consultation clinic 19 p2883 A83-41831

The cervical test in vertebral-basilar insufficiency 19 p2883 A83-41832

An appraisal of the value of vitamin B12 in the prevention of motion sickness 20 p3034 A83-42372

Age-specific morbidity among Navy-pilots 24 p3618 A83-48880

HUMAN PERFORMANCE

NT ASTRONAUT PERFORMANCE

NT OPERATOR PERFORMANCE

NT PILOT PERFORMANCE

Rotational invariance in visual pattern recognition by pigeons and humans 02 p0224 A83-12068

Circadian rhythms and fatigue - A discrimination of their effects on performance 02 p0223 A83-12411

A possible approach to a systems classification of the actions of a human operator 03 p0383 A83-13278

Psychophysical research on memory sensory patterns 03 p0383 A83-13285

Aspects of discussion concerning the psychology and physiology of vision 03 p0373 A83-13288

Methods for determining the morphometric characteristics of muscles during movement in humans 03 p0384 A83-13645

The effect of microelemental additions on the activity of certain metallic enzymes, immune stability, and performance of athletes 05 p0672 A83-17155

Autonomic contribution to heart rate recovery from exercise in humans 05 p0675 A83-17335

Evoked potentials /EP/ and the processing of sensory information in the visual system of humans 07 p0976 A83-20354

Effects of travel across time zones /jet-lag/ on exercise capacity and performance 07 p0977 A83-20782

Response of age forty and over military personnel to an unsupervised, self-administered aerobic training program 07 p0977 A83-20783

Pattern recognition approach to human sleep EEG analysis and determination of sleep stages 08 p1150 A83-22051

Image quality and observer performance 08 p1150 A83-22891

The model human processor - A model for making engineering calculations of human performance 10 p1459 A83-26323

Methodological investigation of vibration effects on performance of three tasks 10 p1460 A83-26325

The asymmetry of the sensitivity of the auditory system of humans determined by a method of constant stimuli 12 p1764 A83-29301

Circadian rhythms of work capacity, the activity of the sympathoadrenal system and myocardial infarction 12 p1765 A83-29308

The identification of clear and defocused images during short periods of the presentation of visual objects 13 p1901 A83-30433

Human sinus arrhythmia as an index of vagal cardiac outflow 13 p1904 A83-30498

Effects of low concentrations of chlorine on pulmonary function in humans 13 p1905 A83-30509

The current technique for radar control room lighting of the French Air Force 14 p2071 A83-32457

The effect of T and B lymphocytes on the phagocytotic activity of polymorphonuclear neutrophils in the peripheral blood of humans 14 p2070 A83-33333

Underlying psychometric function for detecting gratings and identifying spatial frequency 15 p2214 A83-33803

The human element in air traffic control - Aeromedical aspects, problems, and prescriptions 15 p2214 A83-34981

Interactions of alcohol and caffeine on human reaction time 15 p2215 A83-34984

The relationship between aerobic fitness and certain cardiovascular risk factors 15 p2214 A83-34987

A stimulative mechanism of human adaptation to situations of sensory deprivation 15 p2215 A83-35048

Thermal reaction and manual performance during cold exposure while wearing cold-protective clothing 16 p2401 A83-35559

Circadian rhythm amplitude - Is it related to rhythm adjustment and/or worker motivation? 16 p2396 A83-35562

Digitex - A microcomputer-digitizer facility for automated testing of motor performance during discrete positioning movements 16 p2402 A83-35567

A study of human behavior in adverse stress 16 p2400 A83-35700

The optimal speed of cyclic locomotion in individuals of different ages 17 p2559 A83-38172

Genetic predispositions in human learning of motor actions 17 p2559 A83-38173

Age-related changes of interneuronal connections in the cerebral cortex of humans 17 p2560 A83-38193

Effects of serotonin on memory impairments produced by ethanol 18 p2736 A83-39934

Accurate visual measurement of three-dimensional moving patterns 18 p2734 A83-39936

Human nutrition in the north 18 p2735 A83-40566

Shadows of thought - Shifting lateralization of human brain electrical patterns during brief visuomotor task 19 p2884 A83-41225

The fitness for work of humans and the problems of its increase 19 p2882 A83-41458

Task variables determine which biological clock controls circadian rhythms in human performance 20 p3035 A83-43546

The working capacity of humans in mountains --- Russian book 21 p3186 A83-43922

Carbon monoxide and human performance in a single and dual task methodology 21 p3187 A83-43993

Performance of concurrent tasks - A psychophysiological analysis of the reciprocity of information-processing resources 21 p3189 A83-44366

Ozone and high ventilation effects on pulmonary function and endurance performance 22 p3347 A83-45992

Evidence against saturation of contrast adaptation in the human visual system 22 p3349 A83-46755

Performance evaluation tests for environmental research (PETER) - Moran and computer batteries 24 p3618 A83-48882

Multi-oscillatory control of circadian rhythms in human performance 24 p3619 A83-50109

HUMAN REACTIONS

Principles of differentiation of the self-evaluation scales in psychophysiological investigations 01 p0085 A83-10504

An investigation of the connection between solar activity and the severity of the consequences of traffic accidents in Moscow 02 p0222 A83-11880

The effect of cold on the thermoregulatory reactions of humans in Siberia 02 p0223 A83-12218

The structure of qualitative individual peculiarities of emotionality 05 p0676 A83-17181

Design and fabrication of a portable device to measure the response time to a luminous stimulus 06 p0800 A83-18343

Time of day noise adjustments or 'penalties' 08 p1162 A83-22230

Whole-body vibration and International Standard ISO 2631 - A critique 10 p1458 A83-25999

Detection and identification of moving targets 11 p1644 A83-27900

The reaction of the central blood circulation of healthy individuals to the decompression of various areas of the body 12 p1764 A83-29306

Vertical fusional response to asymmetric disparities --- of retinal image stimulus 14 p2068 A83-32800

An investigation of the hemodynamics of a human in an antiorthostatic position using a method of mathematical modeling 14 p2069 A83-32959

Time-of-day corrections in measures of aircraft noise exposure 14 p2081 A83-33024

Studies of the reactions of human operators in regard to the tracking of moving targets 15 p2215 A83-34900

Sociological studies for the evaluation of the response reaction level of the population to noise 15 p2215 A83-34974

Evaluation of an experimental central warning system with a synthesized voice component 15 p2216 A83-34982

Interactions of alcohol and caffeine on human reaction time 15 p2215 A83-34984

The subjective equivalence of sinusoidal and random whole-body vibration in the sitting position - An experimental study using the 'floating reference vibration' method 16 p2401 A83-35563

Operator's activities at CRT terminals - A behavioural approach 16 p2400 A83-35564

A study of human behavior in adverse stress 16 p2400 A83-35700

Application of experimentally derived pilot perceptual angular response transfer functions [AIAA PAPER 83-1100] 16 p2402 A83-36220

The effect of genotype and environment on evoked potential parameters during orienting and defensive reactions 16 p2401 A83-36824

- Emotional components of self-reports and interpersonal judgments 18 p2737 A83-40558
The stability of physiological and psychological functions of humans during the action of extreme factors --- Russian book 19 p2880 A83-40981

HUMAN TOLERANCES

- Investigations of adaptation and solar activity 02 p0220 A83-11877
The influence of differential physical conditioning regimens on simulated aerial combat maneuvering tolerance [AD-A126486] 02 p0223 A83-12406
A comparison of several methods for measuring variable occupational noise for their hygienic evaluation 03 p0379 A83-13614
The establishment of safe levels of local vibration 05 p0677 A83-17195
Biomechanical aspects of the fracture resistance of the vertebral column of humans under impact overloads in the head-pelvis direction 06 p0798 A83-18509
The effect of low frequency vibrations on the human cardio-circulatory system - A measurement technique and results for an 18 Hz sinusoidal vibration 08 p1149 A83-22978
The results of an investigation of the intermittent effects of low temperature on the human body 09 p1322 A83-23973
The changes of the protein metabolism characteristics during the acclimatization of humans in the Arctic 09 p1322 A83-23974
Human capabilities: Long residence - An uncharted field 09 p1325 A83-24359
Medical standards for experimental human use in acceleration stress research 10 p1454 A83-25671
The limitation of human performance in extreme heat conditions 10 p1450 A83-26307
Human tolerance to rotation at different G's 11 p1642 A83-27784
The effect of vision on the endurance by humans of the continuous action of Coriolis acceleration 12 p1764 A83-29273
The asymmetry of the functional condition of the cerebral hemispheres during the adaptation to new climatic and geographical conditions 12 p1764 A83-29303
Human frontal sweat rate and lactate concentration during heat exposure and exercise 13 p1903 A83-30468
Impact protection in air transport passenger seat design [SAE PAPER 821391] 17 p2459 A83-37967
Effects of exercise and lack of exercise on glucose tolerance and insulin sensitivity 20 p3035 A83-43485
Effects of strength training on g tolerance 21 p3186 A83-43989
The acquisition and validation of the surface electromyogram signal for evaluating muscle fatigue 21 p3187 A83-43998
The physiological stability of humans to ergothermal effects 21 p3188 A83-45343
Methods of increasing the tolerance of humans to acute hypoxia 23 p3496 A83-47101
Clinical possibilities in the evaluation of extreme effects --- on humans 23 p3496 A83-47102
The functional system of human thermal adaptability 23 p3497 A83-47105
- HUMAN WASTES**
NT SWEAT
- HUMIDITY**
Measuring $\frac{1}{C}$ sub T -squared, $\frac{1}{C}$ sub Q -squared, and $\frac{1}{C}$ sub TQ in the unstable surface layer, and relations to the vertical fluxes of heat and moisture --- atmospheric temperature and humidity 03 p0363 A83-13274
The ECMWF humidity analysis and its general impact on global forecasts and on the forecast in the Mediterranean area in particular 04 p0519 A83-16161
The effects of humidity on the processing and performance of a structural adhesive 07 p0899 A83-20453
Correlation of surface humidity and integrated atmospheric water vapour determined from infrared measurements --- at mountain sites 10 p1451 A83-25460
Modelling the height, temperature and relative humidity of a well-mixed planetary boundary layer over a water surface 12 p1758 A83-29131
Sweating efficiency in acclimated men and women exercising in humid and dry heat 13 p1904 A83-30499
Relative humidity distribution in the vicinity of the warm conveyor belt 13 p1889 A83-30574
The measurement of the humidity spectrum and of the concentration of the cloud condensation nuclei 15 p2164 A83-34055

- The measurement of the size distribution of atmospheric ice nuclei, taking into consideration humidity 15 p2204 A83-34057
Condensation growth of droplet spectra 15 p2205 A83-34060
Effect of humidity on jet engine axial-flow compressor performance 16 p2304 A83-35856
Temperature and humidity swings in sealed electronic equipment containers 18 p2676 A83-39258
Modeling of multiphase atmospheric aerosols 20 p3015 A83-43429
Disorders of the peripheral nervous system in conditions of a hot, humid climate 24 p3618 A83-49072
Temperature and humidity spectra in cloud- and cloud-free air and associated cloud electrical and microphysical characteristics 24 p3611 A83-49681

HUMIDITY MEASUREMENT

- The possibility of measuring the moisture content of the upper layers of the atmosphere using radiometric techniques 03 p0359 A83-14308
Determination of atmospheric water vapor content in moderate optical paths by radiometric measurements 08 p1136 A83-22853
Venera 13 and Venera 14 measurements of the water vapor content in the Venus atmosphere 12 p1798 A83-29480
MIL-STD-810 - An eye to the future --- military standard for environmental testing 13 p1862 A83-31483
Experience related to the employment of a highly sensitive humidity probe with miniature humidity sensor on a barium fluoride basis - Comparison with a Lyman alpha-hygrometer 18 p2723 A83-39260
The field of the absolute humidity of air in a zone of frontal divisions 18 p2724 A83-39487
An analysis and comparison of five water droplet measuring instruments 18 p2727 A83-39883
The measurement of moisture in the stratosphere by radiosondes 19 p2868 A83-41587
A note on the new type hygrometer using the photochemical reaction $\text{H}_2\text{O} + \text{h}\nu(\text{Ly}\alpha\text{-line}) \rightarrow \text{OH} + \text{H}$ and metastable $\text{OH}\cdot\text{OH} + \text{h}\nu(\text{wavelength} = 309 \text{ nm})$ 22 p3331 A83-46520
Experimental thermal-microwave radiometric determination of the moisture content of a cloudy atmosphere 23 p3487 A83-47139
Information content, accuracy, and optimal conditions of indirect ground-based thermal-microwave radiometric measurements of the integral water-vapor content of the atmosphere, and the water content and effective temperature of clouds 23 p3487 A83-47140
A method for determining water-vapor content in the atmosphere on the basis of joint infrared and microwave radiometric measurements 23 p3487 A83-47141
Ozone and water vapor monitoring using a ground-based lidar system 23 p3481 A83-47794
A two-frequency 1.35-cm radiometer 23 p3459 A83-48490

HURRICANES

- C-band stepped frequency radiometry for hurricane probing 01 p0074 A83-10103
Assimilation of remotely-sensed rainfall rates in a moist primitive-equation model 03 p0368 A83-14436
Intense atmospheric vortices; Proceedings of the Joint Symposium, Reading, Berks., England, July 14-17, 1981 05 p0667 A83-17113
Rainfall patterns observed by digitized radar during the landfall of Hurricane Frederic /1979/ 08 p1139 A83-22293
WSR-57 radar observations during the landfall of Hurricane Frederic 11 p1623 A83-26990
Reflectivity structure of Hurricane David /1979/ from two radars at Miami 11 p1631 A83-27090
Evolution of the structure of precipitating convection in Hurricane Allen 11 p1631 A83-27091
Meso- and convective-scale characteristics common to several mature hurricanes 11 p1631 A83-27092
Radar imagery of an asymmetric double eye in Hurricane Frederic 11 p1631 A83-27093
Stereoscopic observations of hurricanes and tornadic thunderstorms from geosynchronous satellites 12 p1761 A83-29698
Seasat synthetic aperture radar observations of wave-current and wave-topographic interactions 15 p2207 A83-33493
Imaging radar observations of directional properties of ocean waves 15 p2208 A83-33494
The motion of a solid body along the smooth surface of the earth --- with reference to hurricane motion theory 18 p2724 A83-39441
Hurricane Allen and island obstacles 18 p2730 A83-40047
Atlantic hurricane season of 1982 20 p3030 A83-42512
Eastern North Pacific tropical cyclones of 1982 20 p3030 A83-42513

HUSTLER AIRCRAFT

U B-58 AIRCRAFT

HUYGENS PRINCIPLE

- Huygens' principle and radiation tails in a weak Schwarzschild field 10 p1517 A83-26945
Wave propagation in random media - A comparison of two theories 24 p3623 A83-48979

HYBRID CIRCUITS

- All devices to all pins - Modular architecture and flexible switching provides this capability even for future upgrades 01 p0037 A83-10759
Optical-waveguide hybrid coupler 02 p0235 A83-11567
Generalised hybrid-network parameters for electromagnetic coupling between dissimilar regions through a small aperture 04 p0473 A83-16206
Hybrid substrate attach evaluation techniques --- in production of microcircuits 07 p0919 A83-20460
Instabilities and chaotic behavior in a hybrid bistable system with a short delay 08 p1163 A83-21886
RDA requirements for optimum hybrid focal plane performance --- Resistance-Area product for IR detector arrays 08 p1100 A83-22599
E-plane W-band printed-circuit balanced mixer 10 p1409 A83-25818
Hybrid optical-digital signal processing applied to an optimal nonlinear phase estimator 10 p1406 A83-26861
Stress level evaluation of a Printed Wiring Assembly containing large hybrid packages 13 p1837 A83-31486
Development and production of advanced cooling techniques for hybrid microcircuits 13 p1837 A83-31518
An algebraically derived nonlinear control theory 17 p2566 A83-37098
Hybrid time and space integrating processors for spread spectrum applications 19 p2846 A83-41097
Hybrid optical-digital image processing system for pattern recognition 21 p3194 A83-44826
Analytical noise/performance modeling of detector charge-coupled device (CCD) hybrid devices 22 p3292 A83-46603
Residue arithmetic circuit design based on integrated optics 22 p3350 A83-46659

HYBRID COMPUTERS

- Method of designing a program module for the simulation of complex dynamic systems on a hybrid computer --- for flight simulation 08 p1154 A83-22184
Motivation for a combined data flow-control flow processor 08 p1155 A83-22827
Organization of the structure and computational process of a multiprocessor hybrid computing system with a network analog processor 12 p1768 A83-29346
Error sources in hybrid computer based flight simulation 16 p2299 A83-36214
[AIAA PAPER 83-1090] Software for hybrid computing systems. I - Systems of analog and hybrid programming automation 19 p2888 A83-41421
A hybrid structure for the storage and manipulation of very large spatial data sets 24 p3619 A83-49195
Software for hybrid systems. II - Systems software 24 p3620 A83-50202

HYBRID NAVIGATION SYSTEMS

- The Integrated Inertial Navigation System AN/ASN-132 11 p1528 A83-28596
On the shape and orientation control of orbiting shallow spherical shell structure 17 p2479 A83-37472

HYBRID PROPELLANTS

- The production of a hypergolic hybrid propellant 09 p1241 A83-23837

HYBRID PROPULSION

- The design and technology development for A 150 mlb resistojet for H₂ or NH₃ [AIAA PAPER 82-1949] 02 p0146 A83-12506
The relative attractiveness of electric and hybrid passenger cars 11 p1667 A83-27159
A summary of EHV propulsion technology --- Electric and Hybrid Vehicle 13 p1934 A83-31087
Development history of the Hybrid Test Vehicle 13 p1934 A83-31088
EHV systems technology - A look at the principles and current status --- Electric and Hybrid Vehicle 13 p1934 A83-31093

HYBRID STRUCTURES

- The elastic characteristics of unidirectionally reinforced hybrid composites 13 p1815 A83-30052
The effect of friction on the delamination of heterogeneous materials 13 p1865 A83-30053
Fracture toughness of unidirectional glass/carbon hybrid composites 13 p1816 A83-31616
A statistical approach to the strength of hybrid composites 18 p2658 A83-40242

SUBJECT INDEX

- An approximation technique for the control and identification of hybrid systems 21 p3196 A83-45116
- Dynamics of flexible hybrid satellites - Evaluation and computation of a symbolic formalism 21 p3102 A83-45122
- Statistical proeprieties of hybrid composites. I - Recursion analysis 24 p3554 A83-49876
- HYBRIDS (BIOLOGY)**
- U GENETIC ENGINEERING
- HYDRATION**
- Hydration of lithium beta-alumina 09 p1227 A83-25213
- ADH responses to volume shifts in the low pressure system --- AntiDiuretic Hormone 11 p1636 A83-27781
- Radiation damage enhancement of the penetration of water into silica glass 13 p1931 A83-31382
- HYDRAULIC ACTUATORS**
- U ACTUATORS
- U HYDRAULIC EQUIPMENT
- HYDRAULIC ANALOGIES**
- Ship waves and lee waves 13 p1892 A83-31038
- Hydraulic analogy for isentropic flow through a nozzle 21 p3129 A83-44071
- HYDRAULIC CONTROL**
- Electrohydraulic fuel-flow regulator for gas-turbine-engine control systems 16 p2311 A83-36793
- Recovery system for the Lockheed Aquila R.P.V. 20 p2938 A83-43724
- An analytical design of electrohydraulic position servo systems with variable structure 21 p3118 A83-44038
- HYDRAULIC EQUIPMENT**
- NT AIRCRAFT HYDRAULIC SYSTEMS
- Computer-aided design within the framework of the algorithmic selection procedure for the design with catalogs --- German thesis 04 p0487 A83-15844
- Zeta corrosion of mechanical seals 06 p0768 A83-18047
- Load insensitive electro-hydraulic servo system 06 p0769 A83-18924
- Automated testing systems with hydraulic force excitation /review/ 08 p1074 A83-22632
- A study of the processes involved in the filling of pipelines with liquid 09 p1258 A83-23444
- Design of a hydrodynamic support system for the Saturn V launch vehicle - A case problem [ASME PAPER 82-WA/DE-29] 10 p1381 A83-25679
- Shuttle Water Spray Boiler flight performance --- lubricant cooling for Orbiter Hydraulic System and APU [SAE PAPER 820885] 10 p1383 A83-25751
- Multivariable approach to the problem of structural cross coupling of force feedback electrohydraulic actuators --- for structural testing of aircraft and their components 10 p1379 A83-26601
- Design of hydraulic output unit for 15 kW free-piston Stirling engine 11 p1587 A83-27277
- Design of a hydraulic output Stirling engine 11 p1587 A83-27278
- The design and evaluation of a hydraulic actuation system for a legged rough-terrain vehicle 11 p1552 A83-27485
- A machine for the mechanical testing of polymers in a three-dimensional stressed state 16 p2364 A83-35513
- Calculation of the flow rate characteristic of a jet-throttling hydraulic distributor with allowance for the ejection properties of a tube-plate system 19 p2799 A83-42128
- Theoretical and experimental investigation of the gradual stop of a turbomachine 20 p2982 A83-43004
- HYDRAULIC FLUIDS**
- Long eddies in sheared flows 13 p1842 A83-30915
- Topical and systemic effects of the oil AER-M-O 261g batch no. 4 in mice - Anatomopathological and histological findings 17 p2557 A83-38946
- Determination of storage stability of hydraulic fluids for use in missiles [ASLE PREPRINT 83-AM-1A-1] 20 p2958 A83-43331
- HYDRAULIC HEATING SOURCES**
- U HEAT SOURCES
- U HYDRAULIC EQUIPMENT
- HYDRAULIC JETS**
- Hydraulics of a channel with a linear jet array --- heat transfer coefficient enhancement by transpiration cooling 09 p1260 A83-24049
- HYDRAULIC PUMPS**
- U HYDRAULIC EQUIPMENT

HYDRAULIC SHOCK

- The influence of undissolved gas on the magnitude of hydraulic shock during the filling of a pipeline 24 p3579 A83-49654

HYDRAULIC SYSTEMS

U HYDRAULIC EQUIPMENT

HYDRAULIC TEST TUNNELS

- The water tunnel - A helpful simulation facility for the aircraft industry 01 p0014 A83-11080
- Nonlinear analysis of cavity flows around arbitrarily shaped bluff bodies in a constrained flow 06 p0758 A83-19020
- The effect of an elastic wall on the boundary layer 10 p1413 A83-25593
- Natural and forced vortex shedding 22 p3282 A83-46440

HYDRAULIC VALVES

U HYDRAULIC EQUIPMENT

U VALVES

HYDRAULICS

- Certain effects and paradoxes in aerodynamics and hydraulics --- Russian book 07 p0925 A83-20379
- Computational hydraulics --- Book 13 p1840 A83-30132
- Heat transfer and flow resistance in the turbulent pipe flow of a fluid with near-critical state parameters 24 p3576 A83-49120

HYDRAZINE ENGINES

- Augmented electrothermal hydrazine thruster development 09 p1220 A83-24890
- Monomethylhydrazine versus hydrazine fuels - Test results using flight qualified 100 LBF and 5 LBF bipropellant engine configurations [AIAA PAPER 83-1257] 16 p2340 A83-36311
- Hydrazine gas generator performance on Space Shuttle [AIAA PAPER 83-1381] 16 p2321 A83-36372
- Test program to demonstrate the stability of hydrazine in propellant tanks [AIAA PAPER 83-1382] 16 p2340 A83-36373
- Contamination measurements during operation of hydrazine thrusters on the P78-2 (SCATHA) satellite 23 p3426 A83-48130

HYDRAZINES

NT METHYLYDRAZINE

- Reductive destruction of hydrazines as an approach to hazard control 12 p1712 A83-29094
- Test program to demonstrate the stability of hydrazine in propellant tanks [AIAA PAPER 83-1382] 16 p2340 A83-36373
- Infrared optical properties of solid monomethyl hydrazine, N2O4, and N2H4 at cryogenic temperatures 23 p3508 A83-47585
- Remote sensing of hydrazine compounds using a dual mini-TEA CO2 laser DIAL system --- differential-absorption LIDAR 23 p3456 A83-47769

HYDRIDES

NT ALUMINUM HYDRIDES

NT CARBORANE

NT CESIUM HYDRIDES

NT LITHIUM ALUMINUM HYDRIDES

NT METAL HYDRIDES

NT PHOSPHINES

NT SILANES

NT SODIUM HYDRIDES

NT ZIRCONIUM HYDRIDES

- Optical absorption above the optical gap of amorphous silicon hydride 04 p0541 A83-15520
- Crystal chemistry of RT5H/D/x, RT2H/D/x and RT3H/D/x hydrides based on intermetallic compounds of CaCu5, MgCu2, MgZn2 and PuN3 structure types 04 p0457 A83-16043
- Vibrational energy transfer from OH to other gaseous hydrides 10 p1480 A83-26457
- A system of hydrogen-powered vehicles with liquid organic hydrides 11 p1668 A83-27340
- Effects of Ca additions on some Mg-alloy hydrides 21 p3110 A83-45422
- The Mg2Ni0.75M0.25 alloys (M = 3d element) - Their application to hydrogen storage 21 p3168 A83-45423

HYDROACOUSTICS

U UNDERWATER ACOUSTICS

HYDROAEROMECHANICS

U AERODYNAMICS

HYDROBROMIC ACID

- Rate constant for the reaction of O/3P/ with HBr from 221 to 455 K 09 p1227 A83-25136
- Spectral distribution of CO2 vibrational states produced by collisions with fast hydrogen atoms from laser photolysis of HBr 10 p1478 A83-25555
- Spectral ranges for determining the concentration of hydrogen bromide and hydrogen fluoride in the earth's atmosphere 13 p1872 A83-30036

HYDROCARBON FUEL PRODUCTION

HYDROCARBON COMBUSTION

- Temperature profile of a stoichiometric CH4/N2O flame from laser excited fluorescence measurements on OH 02 p0152 A83-12080
- Concentration profiles of NH and OH in a stoichiometric CH4/N2O flame by laser excited fluorescence and absorption 02 p0152 A83-12081
- Observation of vapor generation preceding the ignition of liquid n-decane and l-decene by CO2 laser radiation 02 p0152 A83-13094
- Rate and additive influences on the oxidation of HCN 02 p0153 A83-13099
- An experimental study of fuel combustion in a high-temperature air counterflow 03 p0295 A83-14056
- Effect of liquid phase decomposition on fuel droplet distribution function [AIAA PAPER 83-0069] 05 p0632 A83-16501
- Flow visualization in combustion gases using planar laser-induced fluorescence [AIAA PAPER 83-0405] 05 p0643 A83-16694
- A double reaction zone model and perturbation analysis for finite rate kinetics in hydrocarbon fuel combustors [AIAA PAPER 83-0599] 05 p0612 A83-16810
- Ignition, propagation, and structure of deflagrations and detonations - Stable species concentration of a turbulent premixed methane-air flame 07 p0878 A83-19835
- Influence of confinement on flame acceleration due to repeated obstacles 07 p0878 A83-19836
- The total emissivities of high-temperature flames 07 p0879 A83-19840
- The mechanism of lean limit flame extinction 07 p0879 A83-19841
- Effect of molecular structure on incipient soot formation 07 p0879 A83-19847
- The ignition of a drop of fuel behind the front of a shock wave 07 p0901 A83-19961
- Countercurrent jet combustion of a hydrocarbon fuel in air 07 p0882 A83-21422
- The origin and nature of 'prompt' nitric oxide in flames 08 p1056 A83-22344
- Sooting tendency of fuels containing polycyclic aromatics in a research combustor 08 p1073 A83-23138
- Premixed, turbulent combustion of a sudden-expansion flow 09 p1225 A83-23748
- Premixed combustion in a turbulent boundary layer with injection 09 p1225 A83-23750
- A diffusion combustor and methane-air flame propagation in concentration gradient fields 09 p1226 A83-24366
- Direct measurements of O-atom reactions with HCN and C2H2 behind shock waves 10 p1391 A83-26183
- Experimental investigation of shock initiated methane-combustion near a wall 10 p1391 A83-26200
- Catalytic combustion of propane/air mixtures on platinum 11 p1546 A83-28600
- The effect of the fuel quality on the degree of combustion product ionization in gas-turbine engines 14 p1988 A83-32078
- A simple model for carbon monoxide in laminar and turbulent hydrocarbon diffusion flames 14 p1990 A83-32939
- Toward the formulation of a global local equilibrium kinetics model for laminar hydrocarbon flames 15 p2132 A83-34035
- Interpretation of optical measurements of soot in flames [AIAA PAPER 83-1516] 15 p2134 A83-34926
- The formation of NO(x) from nitrogen-containing additives in premixed methane flames 17 p2485 A83-38027
- Nitric oxide formation in an ammonia-doped methane-oxygen low pressure flame 17 p2485 A83-38028
- The kinetics of oxygenated hydrocarbons in high intensity combustion [AIAA PAPER 83-1144] 17 p2485 A83-38082
- Soot formation in pyrolysis of acetylene, allene and 1,3-butadiene 18 p2664 A83-39274
- Effect of ammonium halides on the combustion of polystyrene 21 p3116 A83-44666
- Fire flame radiation 22 p3265 A83-45717
- The collision half-width for the R(0) line of the nu3 band of methane 22 p3355 A83-46268
- The effect of hydrocarbon structure upon fuel sooting tendency in a turbulent spray diffusion flame [ASME PAPER 83-GT-90] 23 p3440 A83-47937
- Numerical modeling of ethylene oxidation in laminar flames 23 p3430 A83-48159
- Trace species analysis of flames by resonance CARS [ONERA, TP NO. 1983-66] 23 p3430 A83-48187

HYDROCARBON FUEL PRODUCTION

NT ATMOSPHERIC ENERGY SOURCES

- Thermochemical conversion of biomass - Gasification by flash pyrolysis study 06 p0780 A83-18556
Methane synthesis on nickel by a solid-state ionic method 08 p1056 A83-22324
Use of pyrolysis-derived fuel in a gas turbine engine [ASME PAPER 83-GT-96] 23 p3440 A83-47942

HYDROCARBON FUELS

- NT DIESEL FUELS
NT FOSSIL FUELS
NT GASOLINE
NT JET ENGINE FUELS
NT JP-4 JET FUEL

- The effect of additive compositions on the oxidation stability of T-6 fuel 01 p0028 A83-10458
Fuel property effects on Air Force gas turbine engines - Program genesis 01 p0028 A83-10653
Developing technologies for synthetic fuels 01 p0068 A83-10658

- A carbon-13 and proton nuclear magnetic resonance study of some experimental referee broadened-specification /ERBS/ turbine fuels 01 p0028 A83-11482

- Catalytic autothermal reforming increases fuel cell flexibility 02 p0201 A83-11794
New sources for fuel and materials --- from plants 05 p0658 A83-16937

- CO₂-laser-induced deflagration of fuel/oxygen mixtures 07 p0882 A83-20732
Further studies on the ignition and flame quenching of quiescent dust clouds 07 p0882 A83-21351

- Droplet size effects on NO/x/ formation in a one-dimensional monodisperse spray combustion system [ASME PAPER 82-JPGC-GT-10] 09 p1227 A83-25268

- Shock initiated ignition in heptane-oxygen-argon mixtures 10 p1391 A83-26198
The generation of electric currents by the turbulent flow of dielectric liquids. II - Pipes of finite length 12 p1722 A83-29158

- Hydrocarbon rocket engines for earth-to-orbit vehicles 15 p2129 A83-33735
The effect of fuel atomization on soot-free combustion in a prevaporizing combustor 16 p2303 A83-35812

- The effects of chemical kinetics on the ignition of confined propane-air mixtures by hot particles and hot wires [AIAA PAPER 83-1365] 16 p2326 A83-36361

- LOX/hydrocarbon injector performance [AIAA PAPER 83-1390] 16 p2322 A83-36380
Performance study using natural gas, hydrogen-supplemented natural gas and hydrogen in AVL research engine 21 p3168 A83-45425

- Steady-state evaporation characteristics of hydrocarbon fuel drops 21 p3117 A83-45587

- HYDROCARBON POISONING**
Measurements of benzene, toluene and xylenes in urban air 24 p3603 A83-50192

- HYDROCARBONS**
NT ACETYLENE
NT ALKANES
NT ANTHRACENE
NT BENZENE
NT BUTADIENE
NT CAROTENE
NT CYCLIC HYDROCARBONS
NT DIPHENYL COMPOUNDS
NT ETHANE
NT ETHYLENE
NT HEPTANES
NT KEROGEN
NT METHANE
NT METHYLENE
NT NATURAL GAS
NT PARAFFINS
NT PENTANES
NT PROPANE
NT PROPYLENE
NT PYRENES
NT STILBENE
NT VINYLIDENE

- A Lagrangian long-range transport model with atmospheric boundary layer chemistry 05 p0667 A83-17443
Acetylene terminated fluorenone and its use with fluorenone polyesters 05 p0619 A83-17572

- The application of forest classification from Landsat data as a basis for natural hydrocarbon emission estimation and photochemical oxidant model simulations in southeastern Virginia 07 p0957 A83-19848

- Photoassisted heterogeneous catalysis - Definition and hydrocarbon and chlorocarbon oxidations 09 p1297 A83-25188

- An analysis of the reflection spectrum of Jupiter from 1500 A to 1740 A 10 p1518 A83-25736

- Difference frequency laser spectroscopy of the nu3 band of the CH₃ radical 10 p1480 A83-26451

- Experimental investigation of the glow of certain fragments observed in cometary spectra 11 p1679 A83-27887

- Hard carbon coatings with low optical absorption 13 p1825 A83-30326

- The microwave and far-infrared spectra of the CH radical 14 p2083 A83-33234
Ozone precursor monitor for investigating air pollution 15 p2162 A83-33488

- Laboratory measurements of ion-molecule reactions pertaining to interstellar hydrocarbon synthesis 15 p2269 A83-34645

- Remote sensing data integration into a geographic information system for the creation of a biogenic hydrocarbon inventory of the San Francisco Bay area 15 p2185 A83-34819

- The kinetics of surface craze growth in polycarbonate exposed to normal hydrocarbons 15 p2142 A83-35070

- Photoexcitations in trans-(CH)_x - A Fourier-transform infrared study 16 p2420 A83-35748
Resonant and nonresonant processes in the formation of CH(+) by radiative association 17 p2578 A83-37342

- The photochemistry of anthropogenic nonmethane hydrocarbons in the troposphere 20 p3013 A83-42849

- Autothermal reforming of aliphatic and aromatic hydrocarbon liquids 20 p2946 A83-42955
Methods and results of gas chromatographic-mass spectrometric determination of volatile organic substances in an urban atmosphere 20 p3015 A83-43431

- Ion-molecule syntheses of interstellar molecular hydrocarbons through C₄H - Toward molecular complexity 22 p3377 A83-46258

- The calculation of the film vaporization of hydrocarbons in a hot-air flow 23 p3430 A83-48494
The effect of the dispersion medium on the properties of complex Li lubricants 23 p3439 A83-48545

- HYDROCHLORIC ACID**
Growth of aqueous solution droplets of HNO₃ and HCl in the atmosphere 08 p1133 A83-23008
Inverse distribution of populations of vibrational levels in the A²Sigma state of the HCl/ + - / ion excited by electron impact 09 p1271 A83-24000

- HCl in rocket exhaust clouds - Atmospheric dispersion, acid aerosol characteristics, and acid rain deposition 11 p1613 A83-28698

- A study of the kinetics and mechanisms of the degradation of polybutadiene rubber due to thermal oxidation in vaporized hydrochloric acid 18 p2672 A83-39170

- Prospects for using titanium alloys in the manufacture of apparatus for the hydrochloric acid hydrolysis of yeast 19 p2821 A83-40805

- HYDROCYANIC ACID**
Rate and additive influences on the oxidation of HCN 02 p0153 A83-13099

- H₂CN/plus/-nN₂ clustering formation and the atmosphere of Titan 05 p0703 A83-16863
A 3.4-mm HCN and continuum survey of dark clouds 06 p0819 A83-18834

- Heteropolypeptides on Titan 06 p0801 A83-19405
Ground-based infrared spectroscopic measurements of atmospheric hydrogen cyanide 07 p0956 A83-20212

- HCN J = 1-0 observations in L 673 and S 235B - Two different cases of hyperfine anomalies 10 p1499 A83-25368

- Direct measurements of O-atom reactions with HCN and C₂H₂ behind shock waves 10 p1391 A83-26183
Structure of dense molecular gas in TMC 1 from observations of three transitions of HC₃N 10 p1513 A83-26717

- Radiolysis of aqueous solutions of hydrogen cyanide (pH about 6) - Compounds of interest in chemical evolution studies 12 p1767 A83-29424

- Excitation of the rotational levels of interstellar HCN 13 p1948 A83-31258
Detection of HCO(+) and HCN absorption towards three galactic H II-regions 13 p1954 A83-31570

- HCN formation on Jupiter - The coupled photochemistry of ammonia and Acetylene 15 p2275 A83-34718
Discrete variable theory of triatomic photodissociation 16 p2327 A83-36519

- HYDRODYNAMIC COEFFICIENTS**
Motion of a circular cylinder in a rectangular channel 11 p1567 A83-27720

- A numerical implementation of the variational method for solving certain problems in hydrodynamics --- free-surface oscillations of ideal incompressible fluid in axisymmetric cavity 11 p1569 A83-28460

- Hydrodynamic fluctuation due to the discontinuity of flow impedance 12 p1721 A83-29001

- A study of the hydrodynamic moment acting on a solid body in a float suspension 21 p3138 A83-44642

- HYDRODYNAMIC EQUATIONS**
NT HELMHOLTZ VORTICITY EQUATION

- Instability of an extended tangential discontinuity - The first term of the wave-vector expansion 02 p0169 A83-11641

- Convection in pulsating stars. I - Nonlinear hydrodynamics. II - RR Lyrae convection and stability 02 p0257 A83-12137

- Allowance for nonstationary and nonlinear terms in the equations of motion in regard to the solution of problems of ionospheric modeling 02 p0209 A83-12424

- Investigation of processes in the thermosphere during magnetic disturbances 02 p0209 A83-12430
A relativistic gas in a gravitational field 03 p0417 A83-13527

- Equations for deep moist convection that include moisture phase transitions 03 p0371 A83-14827
Relativistic shocks in a Sygne gas 03 p0431 A83-14873

- The relativistic hydrodynamics of a superfluid 05 p0696 A83-16886
An asymptotic method of calculating large-scale atmospheric motions 05 p0667 A83-17223

- A class of soliton solutions of the hydrodynamic equations of motion for ions in a uniform plasma without external fields 07 p0995 A83-20060
Asymptotic solution of the diatomic Boltzmann equation 07 p0926 A83-20531

- Equations of anisotropic hydrodynamics for electron component of the ionospheric plasma 07 p0968 A83-21583
Solution of the gravitational polytrope equations by using the quasi-invariance group --- stellar evolution model 08 p1180 A83-22060

- Nonlinear theory of strata in a low-temperature plasma 08 p1169 A83-23163
On the theory of hydrodynamic fluctuations in nonequilibrium systems 09 p1350 A83-23599

- Quasi-Lagrangian rezoning of fluid codes maintaining an orthogonal mesh 09 p1259 A83-23721
The time-dependence of non-planar accretion discs 09 p1364 A83-25003

- Some cosmochemical consequences of a turbulent protoplanetary cloud 10 p1501 A83-25509
Flare loop radiative hydrodynamics. IV - Dynamic evolution of unstable semiempirical loop models 10 p1522 A83-26743

- On disk accretion --- in binary stars and black holes 12 p1791 A83-28986

- The effect of electromagnetic forces on the hydrodynamics of a melt in the process of high-frequency floating zone melting 12 p1782 A83-29269

- Numerical calculations of discontinuities by shape preserving splines 12 p1773 A83-29670
Hydrodynamics and heat transfer in turbulent zero-momentum wakes 13 p1838 A83-30046

- Hydrodynamic equations for partially ionized multicomponent gas mixtures with higher approximations to the transport coefficients 13 p1925 A83-30653
Loss of water from Venus. I - Hydrodynamic escape of hydrogen 13 p1961 A83-31209

- Interaction delay in weakly relativistic hydrodynamics 13 p1933 A83-31330
Numerical simulation of nonstationary hydrodynamic phenomena in solar flares 14 p2115 A83-32537

- Long-period oscillations in the atmosphere 14 p2058 A83-32851
Certain aspects of the optimum design of hydrodynamic lifting complexes 14 p1972 A83-33002

- Ideal incompressible hydrodynamics in terms of the vortex momentum density 17 p2509 A83-38961
The Hamiltonian formalism of one-dimensional systems of hydrodynamic type and the Bogoliubov-Whitham averaging method 18 p2741 A83-39477

- The problem of the predictability of the atmosphere and certain questions relating to the hydrodynamic theory of long-term weather prediction 19 p2867 A83-41580

- Application of the method of parallel chords to solve implicit difference equations of magnetohydrodynamics 21 p3215 A83-45219

- Some experiments in variational normal mode initialization in data assimilation --- for gravity waves 23 p3489 A83-47395

- Combined penalty multiplier optimization methods to enforce integral invariants conservation --- for shallow water equations 23 p3489 A83-47397

- Analysis and interpretation of wave solutions of atmospheric dynamics for low latitudes 24 p3609 A83-49052

- Hydrodynamic models of Herbig-Haro objects 24 p3658 A83-49358

- Critical phenomena in detonation associated with an impulse loss 24 p3557 A83-49800

HYDRODYNAMIC RAM EFFECT

The hydrodynamic forces acting on a cylinder set in motion in an impulsive manner 19 p2843 A83-41264

HYDRODYNAMIC STABILITY**U FLOW STABILITY****HYDRODYNAMICS****NT CYLINDRICAL PLASMAS****NT ELASTOHYDRODYNAMICS****NT ELECTROHYDRODYNAMICS****NT MAGNETOHYDRODYNAMICS**

Hydrodynamical models of rotating magnetic winds

01 p0123 A83-10354

Linear analysis of an oscillatory instability of radiative shock waves 02 p0251 A83-11588

Surface roughness effects in hydrodynamic lubrication - The flow factor method

[ASME PAPER 82-LUB-45] 03 p0337 A83-13523

Hydrodynamical models of presolar nebula formation

03 p0418 A83-13838

Hydrodynamical calculations of accretion disks in close binary systems. I - Method. II - Models

03 p0428 A83-14765

Numerical evaluation of principal value integral by Gauss-Laguerre quadrature 04 p0530 A83-15299

Influence of hydrodynamics and diffusion upon the stability limits of laminar premixed flames

04 p0457 A83-16261

Influence of radiative losses on the hydrodynamics of a laser plasma corona 05 p0687 A83-17072

Mathematical models of the hydrodynamics of the cochlea of the inner ear 07 p0972 A83-19927

Hydrodynamic collapse --- of stars

08 p1179 A83-22030

Nonlinear hydrodynamic pressure on an accelerating plate 08 p1084 A83-22377

The structure of mathematical models in environmental hydrodynamics problems 09 p1299 A83-25245

Comments on the dynamical effects of radiative viscosity --- in astrophysics 10 p1503 A83-25719

Normal modes of relaxation in stellar systems - Dynamical friction and thermalization

10 p1510 A83-26392

One-dimensional periodic flows with a shock transition - Application to the density wave theory of spiral structure 10 p1512 A83-26711

Meridional circulation in rotating stars. V - Cooling white dwarfs 10 p1515 A83-26735

QUIPS - Time-dependent properties of quasi-invariant self-gravitating polytropes 10 p1515 A83-26737

Necessary conditions for the stability of rotating Newtonian stellar models 10 p1515 A83-26741

A short look at nonlinear hydrodynamic stability theory 11 p1569 A83-28404

Hydrodynamical models of type II supernovae

12 p1792 A83-29057

A treatment of three dimensional incompressible turbulence 12 p1722 A83-29068

Kernel estimates as a basis for general particle methods in hydrodynamics 12 p1724 A83-29617

Ice and suspended matter as hydrothermodynamic tracers on the basis of data from multispectral satellite surveys --- Russian book 14 p2059 A83-32575

An arbitrary-mesh computer program with applications to astrophysics 15 p2254 A83-33817

The infall of a star into a massive black hole

15 p2269 A83-34641

Level surface approach for uniformly rotating, axisymmetric polytropes --- used for astronomical models 15 p2269 A83-34642

On the choice of boundary conditions for the matching of kinetic to hydrodynamic polar wind models

16 p2376 A83-35787

Heat and mass transfer and hydrodynamics of swirling flows in axisymmetric channels --- Russian book

16 p2353 A83-36437

The effect of stochastic modulations on the stability characteristics of hydrodynamic flows --- German thesis

17 p2504 A83-37501

On an experimental possibility of investigating the hydrodynamic interaction of particles at low Reynolds numbers 17 p2505 A83-37556

Singular matrix inversion in fluid dynamics computations 17 p2571 A83-37735

The detection property of a curved flame front

18 p2663 A83-39167

The breaking of axisymmetric slender liquid bridges

18 p2680 A83-39206

Hydrodynamic and turbulent motions in the galactic disk

18 p2775 A83-39755

Elastic scattering of heavy ions and the compressibility of nuclear matter 19 p2899 A83-41535

Self-similar solutions for the interaction regions of colliding winds --- in interstellar space

19 p2918 A83-41622

The motion of compressible fluids and inhomogeneous media 19 p2845 A83-41877

A study of the characteristics of short hydrodynamic dampers of aircraft engine motors with allowance for turbulization of the working fluid in the damper clearance

19 p2800 A83-42129

Meridional circulation in rotating stars. VI - The effects of anisotropic eddy viscosity 20 p3068 A83-42457

Aspects of Galerkin approximations for hydrodynamic simulations 20 p2972 A83-42675

Dynamic methods in plasma physics

22 p3363 A83-46496

Hydrodynamics, fields, and constants in gravitation theory --- Russian book 23 p3527 A83-48450

Overnormalized theory of hydrodynamic turbulence

24 p3624 A83-49536

HYDROELASTICITY

Free vibrations of plates in fluid using finite and infinite elements 01 p0058 A83-10279

Hydroelastic effects of separated flow

08 p1084 A83-22144

The anomalous Doppler effect and the radiation instability of oscillator motion in hydrodynamics

09 p1260 A83-24214

A minicomputer finite elements program for microgravity hydroelastic analysis --- of spacecraft flexible propellant tanks

16 p2317 A83-36499

Calculation of transfer functions in internal problems of the unsteady hydroelasticity of cylindrical and spherical shells

18 p2702 A83-40117

The effect of viscosity on the forced vibrations of a fluid-filled elastic shell

[ASME PAPER 83-APM-34] 23 p3471 A83-48242

Evaluation of three fluid-film models for use in uncanceled squeeze-film damper bearing analysis

24 p3590 A83-48923

Direct method for investigating the dynamics of liquid-filled bodies 24 p3624 A83-49672

HYDROELECTRIC POWER STATIONS

Ice distribution and winter surface circulation patterns, Kachemak Bay, Alaska 02 p0198 A83-12038

Developments in tidal power 11 p1606 A83-27226

Source reliability in a combined wind-solar-hydro system 15 p2190 A83-34147

HYDROFLUORIC ACID

Precision collisional lineshapes by difference-frequency laser spectroscopy 03 p0294 A83-13982

Semiclassical vibrational spectra for diatomic molecules - Application to HF, CO, and NO

09 p1342 A83-24131

Spectral ranges for determining the concentration of hydrogen bromide and hydrogen fluoride in the earth's atmosphere 13 p1872 A83-30036

Rotational energy transfer in HF

15 p2227 A83-34014

He-Ne laser frequencies near 2.4 microns and their application to hydrogen fluoride detection

19 p2851 A83-40928

HYDROFOIL BOATS**U HYDROFOIL CRAFT****HYDROFOIL CRAFT**

Intermediate size hydrofoil investigations

[AIAA PAPER 83-0618] 08 p1172 A83-22168

Distributed microprocessor application for marine systems monitor and control

[AIAA PAPER 83-0630] 08 p1173 A83-22173

Automated navigation and collision avoidance for high-speed surface craft

[AIAA PAPER 83-0631] 08 p1173 A83-22174

HYDROFOIL OSCILLATIONS

Experimental research on cavitation erosion for an oscillating wing profile --- German thesis

17 p2493 A83-37497

HYDROFOILS**NT KEELS****HYDROGEN****NT DEUTERIUM****NT DEUTERIUM PLASMA****NT HYDROGEN ATOMS****NT HYDROGEN IONS****NT HYDROGEN ISOTOPES****NT HYDROGEN PLASMA****NT LIQUID HYDROGEN****NT METALLIC HYDROGEN****NT TRITIUM**

The isotopic composition of cyclonic precipitation

02 p0216 A83-12952

Calculation of the probability of a pycnonuclear reaction in magnetized hydrogen --- at pulsar surfaces

03 p0417 A83-13538

Neutral hydrogen in the vicinity of galactic radio sources - The supernova remnant W28 03 p0417 A83-13654

On the chemistry of H₂O, H₂ and meteoritic ions in the mesosphere and lower thermosphere

04 p0508 A83-14969

Line positions and strengths in the H₂ quadrupole spectrum 05 p0700 A83-17024

Blister formation in Pd gate MIS hydrogen sensors

05 p0645 A83-17290

Neutral hydrogen observations towards the Puppis Window of the Milky Way 05 p0701 A83-17665

Vibration-rotation transition probabilities for the ground electronic chi¹/1-sigma/ + / state of HD

05 p0701 A83-17670

Cosmological molecular hydrogen and the distortion of the relic radiation spectrum 05 p0710 A83-17804

Design of a XeF-pumped second Stokes amplifier for blue-green production in H₂ 05 p0651 A83-17877

Thermodynamics of silicon nitridation - Effect of hydrogen

[ACS PAPER 33-B-80P] 06 p0734 A83-18052

The Saturn spectrum in the EUV - Electron excited hydrogen 06 p0848 A83-18316

The combined effect of mass loss and overshooting. II - The evolution of 10-solar-mass to 30-solar-mass stars during core hydrogen burning 06 p0829 A83-18544

Propagation effects in the hydrogen-to-helium ratio in the solar cosmic rays 06 p0856 A83-19170

The dynamic polarizability of highly excited hydrogen-like states 06 p0809 A83-19185

Evolutionary effects of helium diffusion in population II stars 06 p0840 A83-19286

Effect of temporary alloying by hydrogen /hydrovac/ on the vacuum hot pressing and microstructure of titanium alloy powder compacts 07 p0883 A83-19833

Optical studies of H I-rich southern galaxies. II - The low-visibility spiral NGC 1079 07 p1010 A83-19856

The filtration combustion of fine powders of Group IV B transition metals 07 p0880 A83-19955

Hydrogen permeation and diffusion in niobium

07 p0884 A83-20259

Photodissociation of HCHO in air - CO and H₂ quantum yields at 220 and 300 K 08 p1163 A83-22216

The diffusion constants of hydrogen, nitrogen, and carbon in solid solutions and binary phases with titanium

09 p1235 A83-24395

The effect of hydrogen plasticization in alloys of titanium with aluminum 09 p1235 A83-24397

Potential energy surface for the study of inelastic collisions between nonrigid CO and H₂

09 p1343 A83-25135

H₂ production in comets. 10 p1500 A83-25374

The effects of hydrogen in stabilizing the electrical properties of n-Pb/0.8/Sn/0.2/Te thin films

10 p1488 A83-25455

Temperature measurement of detonation using UV-absorption of O₂ 10 p1421 A83-26137

Rotational relaxation of H₂ in nozzle flow

10 p1416 A83-26180

CO emission and the optical disk in the giant Sc galaxy M101 10 p1511 A83-26405

Detection of trace concentrations of H₂ in air by coherent active Raman spectroscopy 10 p1423 A83-26657

Effects of environment on neutral hydrogen distribution for disk galaxies in the Virgo Cluster area

10 p1512 A83-26706

Neutral hydrogen in isolated galaxies. II - The large angular diameter galaxies 11 p1668 A83-27106

A laser-based technique for the measurement of hydrogen at local areas in metals

11 p1547 A83-27331

Hydriding and dehydriding kinetics of Mg₂Ni above and below the structural phase transition

11 p1545 A83-27332

High orbital angular momentum states in H₂ and D₂

11 p1653 A83-27491

The phase-change behavior of hydrogen in niobium and in niobium-vanadium alloys 11 p1545 A83-27496

Abstraction vs insertion in O(1D) + H₂ - OH + H

11 p1545 A83-27497

Diatomic molecules as storage media for high energy lasers 11 p1580 A83-27573

Gaseous equilibria in the C-H-O ternary system at 500-2000 K, 0.1-10 atm 11 p1666 A83-28670

Pd-SiO₂-GaAs MIS diode for hydrogen detection

12 p1728 A83-29038

Palladium-silicondioxide-silicon structures as hydrogen sensors in electrolytes 12 p1712 A83-29464

Approaches for reducing the insulator-metal transition pressure in hydrogen 13 p1929 A83-30599

Pressure broadening of CO infrared lines perturbed by H₂ and He 13 p1916 A83-30968

Loss of water from Venus. I - Hydrodynamic escape of hydrogen 13 p1961 A83-31209

Hydrogen solubility in rhenium at pressure up to 90 kb

13 p1824 A83-31333

Moessbauer spectroscopy of amorphous silicon-tin-hydrogen alloys 13 p1931 A83-31387

Neutral hydrogen in X-ray cluster galaxies - A1367

13 p1949 A83-31404

Hydrogen in pure aluminum solidified unidirectionally

13 p1824 A83-31601

Theoretical studies of H₂-H₂ collisions. V - Ab initio calculations of relaxation phenomena in parahydrogen gas 14 p2083 A83-33102

Intermolecular potentials from NMR data - H₂-N₂O and H₂-CO₂ 15 p2227 A83-33631

Influence of hydrogen additions on high-temperature superplasticity of titanium alloys 15 p2135 A83-33639

Hydrogen vibration on Si(111) 7 x 7 - Evidence for a unique chemisorption site 15 p2131 A83-33897

Calculation of the electrostatic field strength above the lunar surface covered by a hydrogen monolayer 15 p2276 A83-34770

A critical analysis of the results of treatment of heliometric observations of the moon 15 p2276 A83-34771

The electron angular distribution of different rotational branches in the VUV photoelectron spectrum of H₂ 16 p2408 A83-35328

Hydrogen line ratios of low redshift QSO's 16 p2430 A83-36658

Effective H I diameters of galaxies 16 p2432 A83-36695

Photoelectrocatalysis on silicon in solar light 16 p2328 A83-36775

Drastic reduction of adsorption of CO and H₂ on (111)-type Pd layers 16 p2328 A83-36990

Rotational excitation of OH by H₂ - Calculations in intermediate coupling 17 p2579 A83-38364

Hydrogen in Luna-24 regolith 18 p2779 A83-39534

Storage and transportation of merchant hydrogen 18 p2708 A83-39563

A comparison of microvoid sizes in nickel base alloys tested in air and in the presence of hydrogen 18 p2668 A83-40614

Metal-hydrogen systems; Proceedings of the Miami International Symposium, Miami Beach, FL, April 13-15, 1981 19 p2818 A83-40850

Geocoronal imaging with Dynamics Explorer - A first look 19 p2864 A83-41116

The nonstationary coherent spectroscopy of the Raman scattering of gaseous hydrogen in the region of Dicke narrowing 19 p2898 A83-41496

The detection of H₂ in cool carbon stars 19 p2921 A83-41651

Interaction between hydrogen and intermetallic compounds 19 p2820 A83-42010

Neutral hydrogen absorption in Mrk 6, NGC 3810, 1506+34, and NGC 1068 20 p3063 A83-42180

Desaturation of H₂ quadrupole lines in the atmospheres of the outer planets 20 p3078 A83-43077

Semimetal cascades - Solid state precursors to spacecraft slush hydrogen refrigerators 20 p2961 A83-43233

Limits to intergalactic neutral hydrogen from photoionization absorption in ultraviolet quasar spectra 20 p3075 A83-43385

Characteristics of the hydrogen plasticizing of titanium alloys 20 p2956 A83-43499

D/H ratios in meteorites - Some results and implications 21 p3240 A83-44232

The far UV emission spectrum of H₂ 21 p3202 A83-44615

The Mg₂Ni_{0.75}Mg_{0.25} alloys (M = 3d element) - Their application to hydrogen storage 21 p3168 A83-45423

Nonthermal escape of hydrogen and deuterium from Venus and implications for loss of water 22 p3387 A83-47081

Far infrared absorption in normal H₂ from 77 to 298 K 23 p3507 A83-48649

Nonequilibrium electron velocity distribution and temperature in thermalization of low-energy electrons in molecular hydrogen 24 p3625 A83-48798

High velocity HI in the inner 5 kpc of M31 24 p3640 A83-49205

HI observations of the irregular galaxy IC 10 24 p3640 A83-49207

Gas at large radii --- in spiral galaxies 24 p3654 A83-49210

NGC 3992 - A galaxy without a massive halo 24 p3654 A83-49217

HI in the barred spiral galaxies NGC 1365 and NGC 1097 24 p3656 A83-49241

Sensitive search for HI in E and SO galaxies 24 p3657 A83-49253

Neutral hydrogen observations of the dwarf elliptical galaxies NGC 185 and NGC 205 24 p3642 A83-49254

Neutral hydrogen observations of double spiral galaxies. III NGC 3504/3512, NGC 4085/4088, IC 65/UGC 622, NGC 797/801. IV NGC 4618/4625, NGC 4016/4017, NGC 3725/UGC 6528, UGC 725/728, NGC 2336/IC 467 24 p3658 A83-49314

Angular intensity distribution of Balmer-alpha emission excited by electron impact on H₂ 24 p3626 A83-49431

On the pregalactic He/H abundance ratio derived from planetary nebulae 24 p3667 A83-50054

Influence of hydrogen reduction on photoelectro-chemical behavior of anodic oxidized n-TiO₂ layers 24 p3559 A83-50178

HYDROGEN AIR FUEL CELLS

U HYDROGEN OXYGEN FUEL CELLS

HYDROGEN ATOMS

The method of forward scattering amplitude in a theory of hydrogen line broadening in a plasma 01 p0106 A83-10375

Energy values and sum rules for hydrogenic atoms in magnetic fields of arbitrary strength using numerical wave functions - Comparison with variational results 02 p0257 A83-12145

An atomic hydrogen propulsion system [AIAA PAPER 82-1934] 02 p0146 A83-12500

The influence of thermospheric winds on exospheric hydrogen on Venus 02 p0266 A83-12570

Microwave plasma generation of hydrogen atoms for rocket propulsion 02 p0148 A83-13090

Concerning one of the possible causes of irregular variations of the hydrogen emission of the upper atmosphere 03 p0356 A83-13219

Resonance structure of the photoionization cross section of atomic hydrogen in an electric field 04 p0534 A83-15903

H atom detection and energy analysis by use of thin foils and TOF technique --- Time Of Flight 05 p0644 A83-16923

Three-photon excitation of hydrogen Rydberg states 05 p0684 A83-17880

Excitation rate coefficients form the ground state of atomic hydrogen to the n = 2 and n = 3 levels 06 p0811 A83-18185

Elastic and inelastic scattering of electrons by atomic hydrogen at intermediate energies in a coupled-channel second-order potential model 06 p0808 A83-19008

Charge transfer in H/ + /-H and H/ + /-D collisions within the energy range 0.1-150 eV 06 p0809 A83-19243

21 centimeter H I absorption at z = 0.437 against the extended radio structure of 3C 196 06 p0839 A83-19271

Quantization rules and instabilities of highly excited hydrogen atom in a strong magnetic field 07 p0991 A83-20605

Altitude profile of H in the atmosphere of Venus from Lyman alpha observations of Venera 11 and Venera 12 and origin of the hot exospheric component 07 p1029 A83-20612

A high-density effusive target of atomic hydrogen 08 p1162 A83-21981

Persistence of two-state resonances in a hydrogen atom under the influence of a periodic impulsive field 08 p1162 A83-21984

Energy loss of slowly moving magnetic monopoles in matter 08 p1192 A83-22640

A hydrogen molecular crystal in a multiparticle approximation 09 p1350 A83-25094

X-ray and nuclear-magnetic studies on the system niobium-titanium-hydrogen 09 p1236 A83-25149

Atomic hydrogen associated with the high-velocity flow in NGC 2071 10 p1505 A83-25748

Charge exchange of C/6+/ and O/8+/ ions with hydrogen atoms - Strong coupling calculation 10 p1486 A83-25885

Generation and application of coherent radiation at Lyman-alpha 11 p1583 A83-27619

The theory of the quadratic Zeeman effect for highly excited hydrogen atoms 11 p1654 A83-28056

State-selective electron capture by N/2+/ ions in atomic hydrogen using collision spectroscopy 11 p1654 A83-28220

Charge transfer reaction of O(3+) + H yields O(2+) + H(+) in low energy collision 12 p1777 A83-29005

Hydrogen and lithium atoms in a strong electric field 13 p1915 A83-30266

Excimer laser photolysis studies of translational-to-vibrational energy transfer in collisions of H and D atoms with CO [AD-A129931] 13 p1916 A83-30952

Charge transfer of doubly charged and trebly charged ions with atomic hydrogen at thermal energies 13 p1916 A83-31352

Charge transfer of O(3+) ions in collisions with atomic hydrogen 13 p1916 A83-31354

Atomic and molecular hydrogen in the circumstellar envelopes of late-type stars 13 p1956 A83-31680

Extended H I emission associated with the low-surface-brightness companions of the S0 galaxy NGC 4026 13 p1956 A83-31681

The spectral properties of filamentary, physically inhomogeneous prominences. II - Hydrogen (second level excitation, ionization) 14 p2113 A83-31832

The hydrogen atom in weak electric and magnetic fields 14 p2082 A83-32140

Electron capture into excited states of hydrogen 14 p2082 A83-32525

On the intensity ratio of emission lines of Na I D1 to D2 in prominences 15 p2278 A83-34280

Elastic scattering of electrons by hydrogen atoms in the 2S state 16 p2410 A83-35654

Excitation mechanisms for hydrogen atoms in an inverse-brush-cathode discharge 16 p2415 A83-35668

The 1D-3P transition in atomic oxygen induced by collisions with atomic hydrogen 17 p2578 A83-37341

Charge transfer and ionisation processes involving multiply charged ions in collision with atomic hydrogen 18 p2742 A83-39447

The infrared spectrum of HNO 18 p2742 A83-39857

Balmer-alpha and Balmer-beta emission cross sections for low-energy H collisions with He and H₂ 18 p2743 A83-40408

Modification of the photoionization of hydrogen by a low-frequency laser 18 p2743 A83-40409

Compression of spin-polarized hydrogen to high density 19 p2897 A83-40974

Scaling laws for hydrogen-like atoms in magnetic fields of arbitrary strength 20 p3045 A83-43080

A thermal mechanism for the escape of neutral hydrogen from the earth's atmosphere 20 p3027 A83-43415

H NMR study of hydrogen motion in the beta phase of the Mg₂NiH(x) system 21 p3109 A83-43962

Coronal and collisional - Radiative model of the plasma for the case of hydrogen glow discharge 21 p3212 A83-44353

Quantum motion of chemisorbed hydrogen on Ni surfaces 21 p3218 A83-45198

Total and partial cross sections for electron capture in collisions of hydrogen atoms with fully stripped ions 22 p3361 A83-45927

Remote quantum mechanical detection of gravitational radiation 22 p3380 A83-46752

The reaction H₂ + D₂ - 2HD - A long history of erroneous interpretation of shock tube results 23 p3429 A83-47633

Semiconductor detector for the selective detection of atomic hydrogen 23 p3454 A83-47643

Study of the autoionising states of the hydrogen atom in intense magnetic fields by the complex coordinate coupled-channel formalism 23 p3506 A83-48576

Radiative and thermal widths of Landau-excited hydrogen atoms in very strong magnetic fields 23 p3527 A83-48578

Line emission from charge transfer with atomic hydrogen at thermal energies 24 p3650 A83-48830

Atomic photoionization in a strong magnetic field 24 p3626 A83-48833

Elastic scattering of electrons by the 2s state of atomic hydrogen at intermediate energies 24 p3626 A83-48846

Observations of the neutral hydrogen in the barred spiral galaxies NGC 3992 and NGC 4731 24 p3656 A83-49242

Electron collisional rate coefficients for low-level transitions in hydrogen 24 p3626 A83-49386

Elastic scattering of electrons by hydrogen atoms in a laser field 24 p3626 A83-49432

Observations of interstellar deuterium 24 p3667 A83-50059

HYDROGEN AZIDES

Decomposition of hydrogen azide in shock waves 10 p1391 A83-26185

HYDROGEN BONDS

A structural interpretation of the infrared absorption spectra of a-Si:H:O alloys 04 p0541 A83-15515

Dependence of hydrogen evolution from a-Si:H on boron doping and substrate potential 04 p0541 A83-15518

Electronic phase transition of molecular hydrogen in the method of an approximating electron-density functional --- bond charge formation in spin polarized biradical state 04 p0456 A83-15704

Effect of hydrogen bonding on the vibrational dephasing time in glycerol 07 p0874 A83-21054

A laboratory study of the infrared spectra of interstellar ices 10 p1502 A83-25653

Calculations of the binding of hydrogen to fixed interstitial impurities in nickel 18 p2669 A83-40627

Hydrogen diffusion and hydride formation at the metal-hydride interface 21 p3109 A83-43963

HYDROGEN CHLORIDES

NT HYDROCHLORIC ACID

Destruction of polyvinyl chloride under extrusion --- toxic hazards in industry 01 p0029 A83-11404

The corrosion resistance of titanium-ruthenium alloys in a salt-acid medium 09 p1235 A83-24401
Interaction of hydrogen chloride and water with oxide surfaces, III - Titanium dioxide 22 p3267 A83-46700
Coherent pulse propagation in the infrared on the picosecond time scale 23 p3462 A83-48314

HYDROGEN CLOUDS

NT ORION NEBULA

The new catalogue of optical HII-regions 01 p0115 A83-10163
Spectral energy distribution /119 - 685 nm/ in 16 shell stars and a tentative model for accreting Be stars 01 p0123 A83-10352
Motion of the sun in the interstellar medium 01 p0124 A83-10845
HI in the Small Magellanic Cloud re-examined, II 01 p0124 A83-10869
The origin of the infrared /C I/ emission - H II or H I regions 01 p0125 A83-10926
A modular Fabry-Perot interferometer system for imagery and spectrometry 01 p0118 A83-11048
Observations of C-12O/J=2-1/ emission in the Large and Small Magellanic Clouds 02 p0255 A83-12112
Temperatures and their variation within interstellar H I structures 02 p0255 A83-12115
Abundances in five nearby galactic H II regions from infrared forbidden lines 02 p0255 A83-12118
Observations of the infrared fine-structure lines of S III at 18.71 and 33.47 microns in four H II regions 02 p0255 A83-12119
Interstellar molecular hydrogen 02 p0258 A83-12182
The galaxy NGC 1566 - Distribution and kinematics of the ionized gas 02 p0260 A83-12519
2-4 micrometer spectroscopy of the compact H II region G 45.13 + 0.14 A 02 p0260 A83-12520
Formaldehyde absorption towards OH sources 02 p0260 A83-12531
Neutral hydrogen in binary and multiple galaxies 02 p0248 A83-12908
The Bubble Nebula - Far-infrared and radio molecular observations of NGC 7635 03 p0412 A83-13304
Spectral types in the direction of the Magellanic Stream 03 p0401 A83-13307
A neutral hydrogen survey of the southern galactic plane for /b/ less than 10 deg 03 p0413 A83-13310
The interrelation of cosmic gamma-rays and interstellar gas in the range l:65-180 deg 03 p0414 A83-13329
The nature of the radio emission from the star-gas-dust complex W1 03 p0417 A83-13655
The structure of groups of galaxies in the Ursa Major/Canes Venatici region. I - A discussion of the results of an H I survey 03 p0409 A83-13944
Wolf-Rayet stars and an extraordinary star-forming region in the barred spiral galaxy NGC 5430 deg 03 p0421 A83-14138
The neutral hydrogen deficiency of the cluster A262 03 p0422 A83-14180
The visible and ultraviolet continuum from a Herbig-Haro object in the core of M 16 /NGC 6611/ 03 p0428 A83-14773
Infrared emission and star formation in NGC 5253 03 p0429 A83-14794
Aperture synthesis observations of recombination lines from compact H II regions V - NGC 7538 03 p0430 A83-14803
The effects of the coronal gas on the champagne phase 03 p0430 A83-14810
The detection of extranuclear emission lines in the Seyfert galaxies Mk10 and Mk79 03 p0430 A83-14811
Ly-alpha absorption at a high velocity in NGC1275 03 p0411 A83-14923
The velocity structure of S54 and S142 04 p0548 A83-14980
An Effelsberg - Green Bank galactic H I absorption line survey. II - Results and interpretation 04 p0549 A83-15027
Fine structure in high velocity clouds near the south celestial pole 04 p0549 A83-15029
Far infrared observations of a star forming region in Serpens 04 p0550 A83-15037
The giant spiral galaxy M 101. VIII - Star formation in H I-H II associations 04 p0550 A83-15045
The local interstellar medium as traced by gamma rays 04 p0550 A83-15048
VLA observations of H I absorption in the nuclei of Seyfert and active galaxies 04 p0552 A83-15609
Low surface brightness spiral galaxies. I - Neutral hydrogen content and location in the infrared Fisher-Tully diagram 04 p0552 A83-15610
The distribution of neutral atomic hydrogen in our galaxy beyond the solar circle 04 p0552 A83-15613
The H II regions of Messier 8 04 p0552 A83-15615

VLBI measurements of the relative position of the 1665 MHz and 1667 MHz OH masers toward W49N and NGC 6334N 04 p0552 A83-15616
A radial velocity survey of the H II region S101 04 p0556 A83-15952
Surface photometry of the H II region - S254-S257 04 p0547 A83-15962
Ring nebulae associated with Of stars - Statistics, classification, origin 04 p0557 A83-15976
Physical conditions in H II/OH maser regions 06 p0825 A83-18088
Radio continuum emission - A tracer for star formation 06 p0826 A83-18096
A new near-infrared source in the molecular cloud associated with S106 06 p0826 A83-18097
Optical polarization in the H II region S 156 06 p0826 A83-18155
Detection of molecular hydrogen emission from G 333.6-0.2 06 p0827 A83-18162
MR 2251-178 - A nearby QSO embedded in a giant H II envelope 06 p0827 A83-18163
The radiation field and the molecular hydrogen photodissociation rate within spherically symmetric inhomogeneous clouds 06 p0828 A83-18181
Neutral hydrogen in two extremely isolated galaxies 06 p0829 A83-18534
The nature of the galactic H I supershells 06 p0831 A83-18793
The neutral hydrogen distribution near the Rosette Nebula and the association Monoceros OB 2 06 p0831 A83-18830
Disk accretion by dynamical friction - A model for the dynamical evolution of giant molecular clouds 06 p0832 A83-18836
H I observations of high-luminosity elliptical galaxies 06 p0819 A83-18853
The radio continuum morphology of NGC 4631 at 2.7 and 8.1 GHz 06 p0833 A83-18858
An accurate position for the 6-cm OH masers in W3 06 p0820 A83-18868
Spatial observations of dust emission in NGC 7027 06 p0833 A83-18869
The relation between magnetic field and gas density in interstellar clouds 06 p0840 A83-19276
On scaling the magnetic field strength in interstellar clouds Resolution of the 'B versus n dilemma' 06 p0840 A83-19277
Observations of the extinction and excitation of the molecular hydrogen emission in Orion 06 p0840 A83-19279
Gravitationally induced spurs in spiral galaxies - An example in M31 06 p0843 A83-19488
The 157 micron /C II/ emission from NGC 2024 - Core and halo components 06 p0844 A83-19494
The H I absorption in NGC 5128 /Centaurus A/ 06 p0845 A83-19522
Radio studies of galactic structure 06 p0846 A83-19536
New observations of a region of the Magellanic Stream 07 p1010 A83-19857
New observations of positive high velocity clouds 07 p1014 A83-20572
Observations of the new OH maser source G43.2-0.1 07 p1007 A83-20670
An X-ray emitting bubble in the Cep OB3 association 07 p1018 A83-20948
Highly excited /J = 16 to 15/ rotational transitions of CO, at 162.8 microns, in the Orion cloud 07 p1019 A83-20955
The spatial distribution of H II regions in NGC 4321 07 p1020 A83-21111
The molecular gas distribution in M51 07 p1020 A83-21113
Modeling of G333.6-0.2 as a spherical H II region 07 p1021 A83-21122
Observations of the 145.5 micron O I forbidden emission line in the Orion Nebula 07 p1023 A83-21155
Temporal variation of the Jovian H I Lyman-alpha emission /1979-1982/ 07 p1031 A83-21158
Westerbork H I observations of the H II region W3 07 p1008 A83-21217
NGC 2359 - The H II-region driven by the WR-star HD 56925 07 p1024 A83-21218
The morphology and dynamics of the halo of the 30 Doradus Nebula 07 p1025 A83-21237
Neutral hydrogen in the Cas OB6 association 07 p1025 A83-21242
Supernova remnants in M31 08 p1179 A83-21851
The H I distribution in an extremely faint dwarf irregular galaxy M81 dwA 08 p1182 A83-23038
Ionized gas in active molecular cloud cores 08 p1182 A83-23046
An optical study of IC 1470 08 p1183 A83-23048
Observations of H2 emission from molecular clouds and Herbig-Haro objects 08 p1183 A83-23055

H I observations of active and interacting galaxies 09 p1356 A83-23316
Thermal and gravitational instability of a model hydrogen plasma in the presence of a radiation field 09 p1347 A83-23598
Optical observations of the LMC H II region N 11 09 p1354 A83-24468
Aperture synthesis observations of the 21 cm Zeeman effect 09 p1361 A83-24473
Emission-line spectra of H II regions - Dependence on metal abundances in the atmosphere of the ionizing star and in the nebular gas 09 p1361 A83-24482
Excitation conditions in HII regions 09 p1361 A83-24514
Morphology of the ionized gas in NGC 1313 09 p1355 A83-24525
A rediscussion of sulfur abundances in Magellanic Clouds and galactic H II regions 10 p1498 A83-25358
A search for neutral hydrogen in radio galaxies 10 p1492 A83-25477
Formaldehyde toward Cas A - Cloud sizes and H2 densities 10 p1501 A83-25496
The galactic gradient in electron temperature from observations of low-density H II regions 10 p1503 A83-25722
X-ray and ultraviolet observations of extragalactic H II regions 10 p1508 A83-26365
VLA observations of warm NH3 associated with mass outflows in W51 10 p1508 A83-26368
The acceleration of molecular hydrogen clouds through radiative dissociation 10 p1508 A83-26369
Infrared spectroscopy of the sources in S235 and its implication for the line excess problem 10 p1509 A83-26371
Infrared line and radio continuum emission of circumstellar ionized regions 10 p1509 A83-26372
NGC 315 - High-velocity H I in an active elliptical galaxy 10 p1511 A83-26404
Nebular dust and extinction in ionized nebulae. I - The Balmer decrement 10 p1513 A83-26712
Dependence of interstellar depletion on hydrogen column density - Possibilities and implications 10 p1513 A83-26716
The nature of NML Cygnus 10 p1513 A83-26719
H I absorption in the peculiar galaxy UGC 6081 10 p1516 A83-26750
Sensitive mapping of E and S0 galaxies in search of H I content differences between supernovae and non-supernovae producing galaxies 11 p1668 A83-27104
Observations of low redshift H I in Stephan's Quintet 11 p1668 A83-27105
An atlas of H II regions in 125 galaxies 11 p1668 A83-27107
Intensity and extinction irregularities in the H2 emission from Orion 11 p1676 A83-27120
H II regions in M33. I - Radio and H-alpha observations of the H II complex NGC595 11 p1669 A83-27679
The neutral gas toward HD 93206 11 p1679 A83-27992
Regular strings of H II regions and superclouds in spiral galaxies - Clues to the origin of cloudy structure 11 p1680 A83-28256
The distribution of atomic and molecular hydrogen in the Galactic plane 11 p1681 A83-28260
Astrophysical properties of a luminous Wolf-Rayet type object in the core of the extragalactic H II region IC 132 from an analysis of its lambda-banda-lambda 1200-6000 A spectrum 11 p1681 A83-28265
J = 2-1 CO and H2O observations of the molecular cloud G35.2-0.74 11 p1682 A83-28288
The gas distribution in the central region of the Galaxy. IV A survey of neutral hydrogen in the region 1 = 349 to 13 deg, b = 10 to 10 deg, and absolute value of v less than 350 km/s 12 p1789 A83-28864
The compact H II region S235A - Observations and interpretation 12 p1789 A83-28876
The ratio of deuterium to hydrogen in interstellar space. V The line of sight to Epsilon Persei 12 p1790 A83-28882
A high-latitude H I-cloud with optical emission 12 p1785 A83-28883
VLA observations of H2 in DR 21 12 p1785 A83-28884
Soft X-ray diagnostics of the kinematics of high-velocity clouds 12 p1793 A83-29064
Large-scale flow of interstellar gas in galactic spiral waves - Effects of thermal balance and self-gravitation 12 p1793 A83-29065
The dust distribution in some small H II regions 12 p1794 A83-29084
Infrared images of southern HII regions 13 p1935 A83-30385
Observations of the 1-0 transition of CO towards southern HII regions 13 p1946 A83-30387

- L1642 - A dust cloud in a cometary globule?
13 p1946 A83-30388
- H I observations of the high-velocity system in NGC 1275
13 p1950 A83-31406
- The radial distribution of H II regions in spiral galaxies
13 p1950 A83-31410
- UV radiation field inside dense clouds - Its possible existence and chemical implications
13 p1950 A83-31413
- Formation of OB clusters - W33 complex
13 p1950 A83-31417
- The origin of the nonthermal radio emission in normal disk galaxies
13 p1953 A83-31559
- Detection of HCO(+) and HCN absorption towards three galactic H II regions
13 p1954 A83-31570
- Aperture synthesis observations of Orion B at 2.695 and 8.085 GHz
13 p1941 A83-31572
- The-micron spectrometry in sharpless-106
13 p1956 A83-31676
- Observations of the interacting galaxy pair NGC 4490/85
13 p1959 A83-31754
- An investigation of the region around the emission nebula IC 1848
14 p2101 A83-31826
- An energetic, bisymmetrically expanding H I remnant
14 p2104 A83-33190
- Search for neutral hydrogen in the early universe
14 p2107 A83-33236
- Neutral hydrogen in the Small Magellanic Cloud
14 p2099 A83-33243
- The rotation curve of our Galaxy - How well do we know it?
14 p2107 A83-33245
- High velocity clouds - Review of observational properties
14 p2109 A83-33273
- Fine structure in high velocity clouds
14 p2109 A83-33274
- Neutral hydrogen related to Gould's belt
14 p2109 A83-33275
- Detection of two new water vapor emission sources in the southern hemisphere
14 p2109 A83-33277
- Internal movements in H II regions - The small nebula Sharpless 158
14 p2100 A83-33284
- Observations of ultraviolet spectra of H II regions and galaxies with IUE
15 p2251 A83-33598
- Observations of neutral hydrogen in radio-loud and interacting galaxies
15 p2255 A83-33827
- A fragmentary cold H I cloud near W3 and W4
15 p2255 A83-33834
- Interstellar H-alpha emission along the galactic equator
15 p2257 A83-34095
- IR maps of M17 in the forbidden O III 88 micron and 52 micron lines and forbidden N III 57 micron line measurements
15 p2245 A83-34098
- Warm H I halos around molecular clouds
15 p2257 A83-34099
- VLA observations of massive star formation in spiral nuclei
15 p2259 A83-34121
- The volumes of He(+) and H(+) in H II regions - The Orion Nebula
15 p2263 A83-34551
- CO observations of the galaxies in the Leo triplet - NGC 3623, NGC 3627, and NGC 3628
15 p2267 A83-34624
- The structure of bright-rimmed molecular clouds
15 p2267 A83-34625
- A study of H-alpha velocities in NGC 1499, NGC 7000, and IC 1318B/C
15 p2267 A83-34626
- The M17 SW molecular cloud
15 p2267 A83-34627
- Unusual rotation curve of the Galaxy NGC 2814
15 p2269 A83-34677
- Burst of star formation in detached extragalactic H II regions - A qualitative analysis
15 p2272 A83-34786
- Radiative excitation and the intensities of radio recombination lines
16 p2429 A83-36627
- Emission and absorption at 6 cm from excited OH associated with compact H II regions
16 p2430 A83-36644
- A galaxy with a 3.2 x 2.2 sq kpc H II region surrounding its nucleus
16 p2431 A83-36671
- The spatial power spectrum of galactic neutral hydrogen from observations of the 21-cm emission line
16 p2432 A83-36696
- Neutral hydrogen absorption in the quasar 3C 268.4 - Possible evidence for galactic halo clouds
17 p2598 A83-37346
- On the possibly low H2 formation rate in dense clouds
17 p2598 A83-37349
- Far-infrared and CO observations of NGC 6357 and regions surrounding NGC 6357 and NGC 6334
17 p2591 A83-37784
- An H-alpha forbidden N II survey of the nuclei of a complete sample of spiral galaxies
17 p2602 A83-37827
- Collisions of massive gas clouds with primordial chemical composition
17 p2603 A83-37892
- The galactic abundance gradient --- in H II regions
17 p2606 A83-38237
- Spiral structure and gas motion in M81
17 p2610 A83-38547
- The H2O maser flare in Orion A
17 p2613 A83-38838
- Interstellar electron density
18 p2765 A83-39198
- The H I extent and deficiency of spiral galaxies in the Virgo cluster
18 p2767 A83-39588
- The precision of velocity measurements from H I profiles
18 p2757 A83-39593
- Radio observations of compact H II regions
18 p2757 A83-39594
- VLA observations of MWC 349 at 15 and 23 GHz
18 p2757 A83-39597
- Local galactic structure and velocity field
18 p2768 A83-39635
- The velocity fields of gas and stars within five kpc of the sun
18 p2768 A83-39637
- A comparison of the velocity fields of young stellar objects and of Sharpless H II regions
18 p2758 A83-39638
- The large-scale structure of atomic hydrogen --- in Galaxy
18 p2768 A83-39641
- Large-scale structure of H I in the outer Galaxy
18 p2768 A83-39642
- More H I shells and supershells or a new explanation of 'noncircular motions' in the Galaxy
18 p2768 A83-39643
- Low latitude absorption spectra
18 p2768 A83-39644
- The distribution of molecular clouds in the Galaxy
18 p2769 A83-39645
- The distribution of HII regions in the outer Galaxy
18 p2769 A83-39649
- CO(J = 2-1) observations of galactic HII-regions
18 p2769 A83-39650
- Galactic HII regions, anomalous 1720 MHz OH clouds and spiral structure in the Galaxy
18 p2769 A83-39653
- Radial distribution of atomic and molecular hydrogen from propagating star formation
18 p2770 A83-39661
- On corotating high-z HI --- in inner Galaxy
18 p2770 A83-39665
- Physical conditions of the Orion Nebula derived from optical and ultraviolet data
18 p2771 A83-39703
- CO and shocks related to the evolution of the Orion Nebula
18 p2771 A83-39704
- Recent progress on molecular hydrogen in Orion
18 p2772 A83-39710
- Gas dynamics in the circumstellar Nebula on the Becklin-Neugebauer source
18 p2772 A83-39711
- Far-infrared CO line emission from Orion-KL
18 p2772 A83-39712
- Compact continuum radio sources in the Orion Nebula
18 p2773 A83-39721
- Hydrodynamic and turbulent motions in the galactic disk
18 p2775 A83-39755
- A balloon-borne cooled telescope for far IR astronomy
18 p2762 A83-40460
- BG 1937+21 - An extended radio source towards the millisecond pulsar PSR 1937+21
19 p2909 A83-40729
- Search for Wolf-Rayet features in the spectra of giant HII regions. I - Observations in NGC 300, NGC 604, NGC 5457 and He2-10
19 p2910 A83-41066
- The kinetic theory of H2 dissociation --- in interstellar molecular clouds
19 p2918 A83-41624
- Neutral hydrogen absorption in early spiral galaxies
19 p2920 A83-41645
- Cool neutral hydrogen in the direction of an anonymous OB association
20 p3064 A83-42194
- The molecular cloud-H II region complexes associated with Sh 90 and Sh 235
20 p3065 A83-42378
- Biconical nebulae and early-type stars - A model for S 106
20 p3065 A83-42386
- Evidence of hourly variations in the deuterium Lyman line profiles toward Epsilon Persei
20 p3065 A83-42389
- The spatial distribution of shocked gas in the Orion nebula
20 p3067 A83-42445
- A far-infrared study of the N/O abundance ratio in galactic H II regions
20 p3072 A83-43055
- Primordial star formation - The role of molecular hydrogen
20 p3072 A83-43057
- Star formation within OB subgroups - Implosion by multiple sources
20 p3073 A83-43086
- An investigation of faint stars in a region of the Magellanic Stream
21 p3222 A83-44413
- The bright stellar content of the giant galactic H II region NGC 3603
21 p3229 A83-44420
- Abundance gradients in galaxies in the Sculptor and Centaurus groups
21 p3233 A83-44750
- Radio images of the bipolar H II region S106
21 p3236 A83-45542
- Velocity fields in late-type galaxies from H-alpha Fabry-Perot interferometry. IV - Kinematics and dynamics of the SAB(s) spiral NGC 5236 (M83)
22 p3377 A83-46257
- A study of low surface brightness spiral galaxies. II
22 p3377 A83-46262
- Optical surface photometry, infrared photometry, and H II region spectrophotometry
22 p3377 A83-46262
- Size distributions of H II regions in galaxies. I - Irregular galaxies
22 p3372 A83-46380
- Remote quantum mechanical detection of gravitational radiation
22 p3380 A83-46752
- Interpretation of neutral hydrogen spin temperature measurements --- interstellar matter
22 p3381 A83-46984
- A search for neutral hydrogen near nine globular clusters
23 p3519 A83-47443
- A comparison of high resolution optical and radio observations of W3
23 p3519 A83-47450
- On the origin of H2 in T Tau stars
23 p3524 A83-47537
- Masses of interstellar gas clouds
23 p3526 A83-47621
- Morphology and kinematics of planetary nebulae
24 p3638 A83-49129
- Planetary nebulae in Local Group galaxies
24 p3640 A83-49157
- Spectrophotometric investigation of the irregular galaxy NGC 2814
24 p3653 A83-49163
- Relative intensities of hydrogen lines in the spectra of quasars and the nuclei of Seyfert galaxies
24 p3653 A83-49164
- Systematics of H II rotation curves
24 p3654 A83-49202
- HI velocity fields and rotation curves
24 p3654 A83-49203
- A high resolution HI survey of M31
24 p3640 A83-49204
- Comparison of global 21 cm velocity profiles with H-alpha rotation curves
24 p3640 A83-49206
- The distribution of molecular clouds in spiral galaxies
24 p3654 A83-49208
- Optical features associated with the extended HI envelope of M83
24 p3641 A83-49212
- HI observations of the interacting galaxies - VV 371 and VV 329
24 p3655 A83-49218
- Distribution and motions of atomic hydrogen in lenticular galaxies
24 p3655 A83-49219
- Neutral hydrogen mapping of three SO galaxies
24 p3641 A83-49220
- OH maser emission at 4765 MHz in W3
24 p3659 A83-49371
- H II regions --- review of IUE studies
24 p3662 A83-49568
- Cooling of the primordial gas by molecular hydrogen
24 p3663 A83-49635
- Spectral observations and physical modeling of Sharpless 121
24 p3646 A83-49884
- Determining helium abundances in H II regions
24 p3666 A83-50053
- Primordial helium abundance determinations using galactic H II regions
24 p3667 A83-50056
- Pregalactic helium abundance determination from extragalactic H II regions
24 p3667 A83-50057
- Are three systematic observational effects on abundance determinations in giant extragalactic H II regions?
24 p3667 A83-50058
- Detection of the 3.46 cm line of interstellar He-3(+) (He-3(+)/H(+)) ratios
24 p3667 A83-50062
- Detection of an extended soft X-ray source H 2326-79 in the southern sky
24 p3668 A83-50085
- Formaldehyde, cold neutral hydrogen and dust distribution in a globular filament in Taurus
24 p3669 A83-50096
- Hydrogen and helium ionization structure of gaseous nebulae
24 p3671 A83-50170

HYDROGEN COMPOUNDS

NT ALUMINUM HYDRIDES
NT CARBORANE
NT CESIUM HYDRIDES
NT DEUTERIDES
NT DEUTERIUM COMPOUNDS
NT DEUTERIUM FLUORIDES
NT HEAVY WATER
NT HYDRIDES
NT HYDROCYANIC ACID
NT HYDROGEN PEROXIDE
NT HYDROGEN SULFIDE
NT LITHIUM ALUMINUM HYDRIDES
NT METAL HYDRIDES
NT PHOSPHINES
NT SILANES
NT SODIUM HYDRIDES
NT ZIRCONIUM HYDRIDES

Thermal gasdynamic laser utilizing rotational transitions in hydrogen halides with energy transfer from H2 molecules
05 p0649 A83-17065

HYDROGEN CYANIDES

U HYDROCYANIC ACID

HYDROGEN DEUTERIUM OXIDE

U HEAVY WATER

HYDROGEN EMBRITTLEMENT

Effect of grain size on the brittleness of titanium

01 p0025 A83-10447

Investigation of the hydrogen-influenced tendency toward cold cracking in high-strength low-alloy fine-grained structural steel, with regard to the implant experiment --- German thesis

01 p0026 A83-10469

The effect of hydrogen gas on high-grade iron and steel at high and medium pressure --- German thesis

01 p0026 A83-10471

The effect of hydrogen on the microfracture mechanism of titanium alloys

02 p0156 A83-12208

Research of hydrogen-induced cracking and stress corrosion cracking in an aluminum alloy

02 p0156 A83-12222

Hydrogen in titanium, niobium, and tantalum

06 p0727 A83-17960

The hydrogen evolution process on a Ni-28 percent Mo alloy

06 p0728 A83-18146

Steel in equilibrium with hydrogen at room temperature --- German thesis

06 p0729 A83-18499

Influence of sulfur, phosphorus, and antimony segregation on the intergranular hydrogen embrittlement of nickel

07 p0885 A83-20261

Chemically driven cavity growth

07 p0887 A83-20632

The effect of absorbed hydrogen on torsional fatigue of 2024-T351 aluminum alloy

07 p0887 A83-20633

The metallography of fatigue in the high strength aluminium alloy 7010

08 p1060 A83-21711

Hydrogen-induced fracture phenomena in a BCC titanium alloy

08 p1061 A83-21717

Mechanism of SCC and hydrogen-induced delayed cracking

08 p1061 A83-21718

A criterion for hydrogen-induced fracture

08 p1063 A83-21760

A study of stress corrosion cracking in high strength steels using acoustic emission techniques

08 p1064 A83-21770

Effect of ion-plated aluminum coating on hydrogen gas embrittlement of ultrahigh strength maraging steel

09 p1230 A83-23918

The effect of heat treatment on hydrogen diffusion and solubility in titanium alloys at room temperature

09 p1235 A83-24393

A study of the kinetic characteristics of hydrogen interaction with alpha titanium and a titanium-niobium alloy

09 p1235 A83-24394

The evaluation of the serviceability of AT series titanium alloys in conditions of current hydrolysis production from the point of view of hydrogen embrittlement

09 p1235 A83-24396

The effect of hydrogen on the fracture toughness of titanium alloys

09 p1235 A83-24398

Hydrogen in the welded joints of titanium alloys

09 p1235 A83-24399

Effects of hydrogen on near-threshold crack propagation in niobium

10 p1396 A83-25867

Kinetic enrichment of hydrogen at interfaces and voids by dislocation sweep-in of hydrogen

10 p1398 A83-26279

The interaction of hydrogen with traps and its solubility in a maraging steel

10 p1399 A83-26793

Hydrogen absorption and embrittlement of tantalum at cathodic deposition

10 p1399 A83-26897

Strain localization and hydrogen embrittlement

12 p1714 A83-29722

Application of nuclear reaction analysis to stress-induced hydrogen migration in titanium

13 p1820 A83-30182

Stress corrosion and hydrogen induced cracking behaviour in an Al alloy

13 p1820 A83-30325

Semiempirical, quantum mechanical calculation of hydrogen embrittlement in metals

13 p1820 A83-30598

The effect of hydrogen on the temperature of the thermoelastic martensitic transformation in titanium-nickel intermetallics

13 p1822 A83-30744

Aging embrittlement behavior of Al-Zn-Mg alloy after stress-corrosion treatment

13 p1825 A83-31603

The effect of nitrogen- and hydrogen-containing media on the refractory properties of nickel-base alloys

14 p1993 A83-32388

Hydrogen-induced cracking in 4340-type steel - Effects of composition, yield strength, and H₂ pressure

14 p1994 A83-32678

The effect of loading mode on the stress-corrosion cracking of aluminum alloy 5083

14 p1994 A83-32680

An experimental investigation of the internal methane pressure in hydrogen attack

14 p1994 A83-32682

Stress corrosion cracking and hydrogen embrittlement

14 p1995 A83-32809

Mechanical properties of BCC metals; Proceedings of the U.S.-Japan Seminar, Honolulu, HI, March 23-27, 1981

14 p1995 A83-32874

Hydrogen effects in metals

14 p1995 A83-32875

On the criteria for hydrogen assisted fracture at the threshold stress intensity

14 p1997 A83-32947

Hydrogen permeability and diffusivity in nickel and Ni-base alloys

14 p1997 A83-32950

Hydrogen-assisted crack-growth in titanium alloys

15 p2139 A83-34481

Effects of environment and internal hydrogen on the sustained load cracking of Ti-6211

15 p2139 A83-34482

Measurement of hydrogen permeation through nickel by oscillation method

16 p2328 A83-35602

Hydrogen embrittlement of titanium and its alloys

16 p2334 A83-36884

Stress-corrosion cracking and hydrogen embrittlement in P/M X7091 and I/M 7075

17 p2488 A83-37841

A fractographic study of corrosion-fatigue crack propagation in a duplex stainless steel

17 p2490 A83-38397

Trapping of hydrogen by oxygen and nitrogen impurities in niobium, vanadium and tantalum

17 p2491 A83-38856

Deuterium transport and trapping in aluminum alloys

18 p2669 A83-40629

Microfracture model for hydrogen embrittlement of austenitic steels

18 p2670 A83-40643

The effect of hydrogen on the fracture toughness and subcritical crack growth behavior of alpha+beta titanium alloys

19 p2821 A83-40801

Muon trapping and Knight shift at a dilute structural defect in zinc --- around hydrogenlike interstitial impurity

19 p2904 A83-40977

Superdiffusion of 4 T-hydrogen in vanadium

21 p3111 A83-43887

Hydrogen diffusion and hydride formation at the metal-hydride interface

21 p3109 A83-43963

Hydrogen embrittlement of 7075 series aluminum alloys

21 p3112 A83-44368

Recovery behavior of hydrogen charged 7075-T6 aluminum

22 p3268 A83-45625

Hydrogen embrittlement measurement using new palladium probe

22 p3287 A83-45865

[SAE PAPER 820604]

23 p3429 A83-47635

Kinetics of hydrogen absorption by alpha-zirconium

23 p3429 A83-47635

The effect of hydrogen induced surface asperities of fatigue crack closure in ultrahigh strength steel

23 p3431 A83-47850

On the influence of internal hydrogen on fatigue thresholds of HSLA steel

23 p3432 A83-47851

A new statistical model of the hydrogen embrittlement of steel

24 p3567 A83-50070

HYDROGEN ENGINES

An atomic hydrogen propulsion system

02 p0146 A83-12500

[AIAA PAPER 82-1934]

The ideas of F. A. Tsander and an assessment of the application of jet engines for the acceleration of aerospace vehicles

08 p1052 A83-22657

Fast acting hydrogen valve

08 p1112 A83-23295

A systems analysis comparing conventional and hydrogen powered rail locomotives

11 p1667 A83-27213

The effect of fuel injection on NO_x emissions and undesirable combustion for hydrogen-fuelled piston engines

11 p1589 A83-27335

Performance study using natural gas, hydrogen-supplemented natural gas and hydrogen in AVL research engine

21 p3168 A83-45425

Parallel induction - A simple fuel control method for hydrogen engines

21 p3148 A83-45426

HYDROGEN FLUORIDES

U HYDROFLUORIC ACID

HYDROGEN FUELS

Combustion characteristics of hydrogen-carbon monoxide based gaseous fuels

01 p0023 A83-11491

Metallurgy of rechargeable hydrides

02 p0153 A83-11509

Particle size distribution of Ni microprecipitates in LaNi₅ used for hydrogen storage

02 p0202 A83-12295

Measurements of energy distribution and thrust for microwave plasma coupling of electrical energy to hydrogen for propulsion

[AIAA PAPER 82-1951]

02 p0147 A83-12508

Hydrogen oxidation kinetics in gaseous detonations

02 p0153 A83-13097

Hydrogen release from ZrNiH_{2.88} and ZrCoH_{2.88} hydrides in the presence of ethylene, ethane, and argon

04 p0456 A83-15888

The effect of turbulence on the formation of large superequilibrium concentrations of atoms and free radicals in diffusion flames

06 p0727 A83-19426

Laminar burning velocities of hydrogen-air and hydrogen-air-steam flames

07 p0878 A83-19837

Laser fluorescence measurements of the OH concentration in a combustion boundary layer

09 p1226 A83-24367

Using a global hydrogen-air combustion model in turbulent reacting flow calculations

09 p1227 A83-24667

A viable process for producing hydrogen synfuel using nuclear fusion heat

11 p1605 A83-27210

Is LH₂ the high cost option for aircraft fuel

11 p1552 A83-27215

Modeling and evaluation of designs for solid hydrogen storage beds

11 p1610 A83-27333

Possibilities of improving exhaust emissions and energy consumption in mixed hydrogen-gasoline operation

11 p1589 A83-27334

Hydrogen energy creeps forward --- hydrogen fuel production and storage

13 p1869 A83-30000

Hydrogen fuel - Universal energy

13 p1871 A83-31504

Flames near rich flammability limits, with particular reference to the hydrogen - Air and similar systems

15 p2132 A83-34038

Hydrogen as a fuel

15 p2193 A83-35302

Hydrogen fuel for space conditioning of buildings

15 p2193 A83-35305

Calculation of a pressure rise during the burning of a plane supersonic hydrogen jet in a supersonic slipstream

17 p2485 A83-37806

Status of hydrogen development for aircraft in five countries - A Canadian perspective

18 p2708 A83-39562

Hydrogen aspiration in a direct injection type diesel engine its effects on smoke and other engine performance parameters

20 p2998 A83-42956

Fuel cell power plants for electric utilities and hydrogen

20 p3013 A83-43640

Model of a cryogenic liquid-hydrogen pipeline for an airport ground distribution system

20 p3013 A83-43641

Performance study using natural gas, hydrogen-supplemented natural gas and hydrogen in AVL research engine

21 p3168 A83-45425

Effects of external burning on spike-induced separated flow

23 p3398 A83-48132

An airline view of LH₂ as a fuel for commercial aircraft

23 p3440 A83-48598

HYDROGEN IONS

A search for meter-wavelength hydrogen recombination lines, and constraints on the parameters of the ionized interstellar gas

03 p0418 A83-13656

Aperture synthesis observations of recombination lines from compact H II regions V - NGC 7538

03 p0430 A83-14803

0351+026 - A QSO spawned by interacting galaxies

06 p0832 A83-18851

Physical conditions in interacting galaxies, in components of isolated pairs, and in isolated galaxies

06 p0838 A83-19220

Charge transfer in H/ + /-H and H/ + /-D collisions within the energy range 0.1-150 eV

06 p0809 A83-19243

Optical orientation of a dense sodium charge-exchange target for producing polarized protons and H⁻ ions

07 p0992 A83-20604

Acceleration of hydrogen ions and conic formation along auroral field lines

07 p0966 A83-21516

A membrane collector of solar-wind hydrogen

10 p1387 A83-25351

On the formation of HCO⁺ / + / and HOC⁺ / + / from the reaction between H₃⁺ / + / and CO

10 p1392 A83-26461

On the possibility to measure the high altitude light ion concentrations with Eiscat

13 p1883 A83-31716

Effect of screening due to free mobile charges on the binding energy of an H(-) ion

14 p2083 A83-33223

The volumes of He(+) and H(+) in H II regions - The Orion Nebula

15 p2263 A83-34551

Observation of autoionising states in H₂ and D₂ above 30 eV by electron impact

18 p2743 A83-40317

Dissociative recombination in low-energy e-H₂⁺ (+) collisions

19 p2898 A83-41194

Measurement of the branching ratio for the dissociative recombination of H₃⁺ (+) + e

21 p3202 A83-44199

The effect of magnetospheric convection on the concentration of H(+) ions in the plasmasphere

21 p3175 A83-45243

Large-scale counterstreaming of H(+) and He(+) along plasmaspheric flux tubes

22 p3335 A83-47051

Characteristics of thermal and suprathermal ions associated with the dayside plasma trough as measured by the dynamics explorer

22 p3335 A83-47053

retarding ion mass spectrometer

HYDROGEN ISOTOPES

- Nonlinear interaction of high-current H(+) and H(-) ion beams 23 p3509 A83-47553
 N2(+) first-negative emission cross sections for low-energy H(+) and H impact on N2 24 p3626 A83-48831
 New calculation of the properties of the positronium ion 24 p3626 A83-48845
 Possible evidence for Lin's three-wave interaction mechanism at corotation in the galaxy NGC 1566 24 p3655 A83-49229

HYDROGEN ISOTOPES

- NT DEUTERIUM
 NT METALLIC HYDROGEN
 NT TRITIUM
 Isotopic anomalies of H2 and C in the peat from the Tunguska meteorite impact area 02 p0263 A83-11960
 Isotopy of the hydrosphere --- Russian book 23 p3480 A83-47150

HYDROGEN MASERS

- The influence of characteristics of an HF discharge on the oscillation level of a hydrogen maser 01 p0055 A83-10925
 Pumping of H II/OH masers - IR line overlaps and collisional excitation by H2 03 p0427 A83-14756
 Atomic clocks for astrophysical measurements 11 p1572 A83-27729
 A compact hydrogen maser with exceptional long-term stability 13 p1856 A83-31292

HYDROGEN OXYGEN ENGINES

- Weak and strong ignition. II - Sensitivity of the hydrogen-oxygen system 02 p0152 A83-12079
 LOX/LH2 propulsion system for launch vehicle upper stage. I System study 12 p1708 A83-29416
 Optimized high-energy propulsion for multimission applications [AIAA PAPER 83-1247] 16 p2319 A83-36305
 Advanced LOX/H2 engine technologies for future OTVs [AIAA PAPER 83-1312] 16 p2320 A83-36333
 Performance of a low thrust LO2/LH2 engine with a 300:1 area ratio nozzle [AIAA PAPER 83-1313] 16 p2320 A83-36334
 Dynamic response of the LE-5 rocket engine liquid oxygen pump [AIAA PAPER 83-1385] 16 p2321 A83-36375
 Preliminary turbopump configuration for the HM60 engine [AIAA PAPER 83-1386] 16 p2321 A83-36376
 Small LOX/LH2 turbopump for a 1-ton thrust class rocket engine [AIAA PAPER 83-1388] 16 p2322 A83-36378
 Progression on the design of the high thrust hydrogen/oxygen engine HM60 17 p2483 A83-38335

HYDROGEN OXYGEN FUEL CELLS

- The choice of low-temperature hydrogen fuel cells: Acidic - or alkaline 21 p3168 A83-45424
 Kinetics of the reaction $O + HO_2$ yields $OH + O_2$ from 229 to 372 K 05 p0613 A83-17232
 The state distribution of OH radicals photodissociated from H2O2 at 193 and 248 nm 10 p1389 A83-25562
 Aqueous oxidation of SO2 by hydrogen peroxide 13 p1817 A83-30882
 Hydrogen peroxide and sulfur (IV) in Los Angeles cloud water 15 p2194 A83-34050

HYDROGEN PLASMA

- NT DEUTERIUM PLASMA
 Ionisation of H2 by fast protons and multiply charged ions of He, Li, C, N and O 01 p0105 A83-10857
 Radiation hydrodynamics on a static fluid 02 p0242 A83-12982
 Diagnostics of a plasma jet by grid electrodes 06 p0814 A83-19559
 Temperature minimum in the electrical conductivity and viscosity of a dense degenerate hydrogen plasma 07 p0995 A83-20066
 Titan's gas and plasma torus 07 p1036 A83-21510
 Gain scaling of short-wavelength plasma-recombination lasers 08 p1110 A83-22636
 Thermal and gravitational instability of a model hydrogen plasma in the presence of a radiation field 09 p1347 A83-23598
 Hydrogen passivation of defects in silicon ribbon grown by the edge-defined film-fed growth process 10 p1489 A83-26215
 X-ray photoelectron spectroscopy study of hydrogen plasma interactions with a tin oxide surface 13 p1818 A83-31063
 Numerical study of overpopulation density for laser oscillation in recombining hydrogen plasmas 15 p2170 A83-34998

- Broadening of Lyman lines of hydrogen and hydrogenic ions by low-frequency fields in dense plasmas 16 p2415 A83-35662
 Excitation mechanisms for hydrogen atoms in an inverse-brush-cathode discharge 16 p2415 A83-35668
 Acceleration of impurity ions during plasma expansion into vacuum 16 p2417 A83-36935
 Analysis of laser light scattered by cold, dense hydrogen plasmas produced in a Z pinch 17 p2581 A83-37040

- Effective proton-proton potential in hydrogen plasmas 18 p2747 A83-40413
 The generation of intense fluxes of negative ions 19 p2902 A83-41497
 Correlation between the gas heating and the contraction of an RF discharge in hydrogen 21 p3210 A83-44140
 Nonlinear interaction of high-current H(+) and H(-) ion beams 23 p3509 A83-47553
 Simultaneous measurement of magnetic field direction and ion temperature in a plasma by collective scattering with a CO2 laser 24 p3630 A83-48786

HYDROGEN PRODUCTION

- Catalytic autothermal reforming increases fuel cell flexibility 02 p0201 A83-11794
 Operation of a steady-state pH-differential water electrolysis cell 04 p0506 A83-16041
 Production of hydrogen by direct thermal decomposition of water - Preliminary investigations 04 p0506 A83-16042
 Hydrogen as a vector for central receiver solar utilities 04 p0506 A83-16044
 Applications of porous flow-through electrodes. I - An experimental study on the hydrogen evolution reaction on packed bed electrodes 07 p0954 A83-20587
 The photoreduction of water - A study of a model system --- French thesis 08 p1056 A83-22083
 Present status of R&D for hydrogen production from water in Japan 09 p1292 A83-23701
 Chemically induced interface states in photoelectrochemical cells 10 p1446 A83-26207
 On-site production of electrolytic hydrogen for generator cooling 11 p1605 A83-27209
 A viable process for producing hydrogen synfuel using nuclear fusion heat 11 p1605 A83-27210
 Current research in advanced water electrolysis in the United States and abroad 11 p1552 A83-27216
 Clean-up and processing of coal-derived gas for hydrogen applications 11 p1611 A83-27336
 Hydrogen fuel - Universal energy 13 p1871 A83-31504
 Solar generator performance with load matching to water electrolysis - Longterm averages and range of instantaneous efficiencies 14 p2038 A83-32191
 Theoretical and experimental aspects of a two-step short cycle, based on ZnO and CdO intended for storage of solar energy 14 p2046 A83-32348
 Visible light induced cleavage of water into hydrogen and oxygen in colloidal and microheterogeneous systems 15 p2131 A83-33862
 A solar-hydrogen economy for U.S.A. 15 p2192 A83-34866
 The question of the hydrogen infrastructure for motor vehicles 15 p2243 A83-34869
 The effect of glucose concentration and pH on hydrogen production by Rhodospseudomonas sphaeroides VM 81 15 p2193 A83-35303
 Cost-effective methods for hydrogen production 15 p2193 A83-35304
 Industrial water electrolysis - Present and future 18 p2664 A83-39560
 An assessment of large-scale solar hydrogen production in Canada 18 p2708 A83-39561
 Thermal efficiency of the magnesium-iodine cycle for thermochemical hydrogen production 20 p2950 A83-42953
 Thermochemical hydrogen production based on magnetic fusion 20 p3049 A83-42954
 Autothermal reforming of aliphatic and aromatic hydrocarbon liquids 20 p2946 A83-42955
 The mechanism of the action of small amounts of metals in increasing currents at photo electrodes 21 p3108 A83-43949
 Production of hydrogen by direct thermal decomposition of water 21 p3168 A83-45421
 Advanced electrolysis development for hydrogen-cycle peak shaving for electric utilities 22 p3320 A83-46779
 The testing of electrodes for alkaline solution water electrolysis 23 p3430 A83-48594
 Iron oxide electrodes for photoelectrolysis of water 23 p3430 A83-48595
 Technological aspects of sulfur dioxide depolarized electrolysis for hydrogen production 23 p3430 A83-48596

- Resource and energy management of synfuels production with hydrogen and oxygen requirements from electrolysis 23 p3477 A83-48597
 Synergistic effects for the TiO2/RuO2/Pt photodissociation of water 24 p3601 A83-50184

HYDROGEN RECOMBINATIONS

- Microwave plasma generation of hydrogen atoms for rocket propulsion 02 p0148 A83-13090
 A search for meter-wavelength hydrogen recombination lines, and constraints on the parameters of the ionized interstellar gas 03 p0418 A83-13656
 Angular fluctuations in the temperature of the cosmic background radiation in a universe with massive neutrinos 03 p0439 A83-13886
 Cross sections for photo-ionisation and photo-recombination of hydrogenic atoms in strong magnetic fields --- of pulsars and accreting neutron stars 07 p0991 A83-21223
 The doubly excited autoionizing states of H2 08 p1163 A83-22220
 Development of improved hydrogen recombination in sealed nickel-cadmium aerospace cells 11 p1540 A83-27198
 The H 166 alpha recombination line in the Carina Nebula 14 p2109 A83-33276
 Radiative excitation and the intensities of radio recombination lines 16 p2429 A83-36627
 Radio recombination lines and the distance to quasars 17 p2608 A83-38401
 The spectral features in the microwave background spectrum due to energy release in the early universe 19 p2914 A83-40707
 Dissociative recombination in low-energy e-H2(+) collisions 19 p2898 A83-41194

HYDROGEN SULFIDE

- Sulfidation properties of Fe-Cr alloys at 1073 K in H2S-H2 atmospheres of sulfur pressures 0.01 and 0.00001 Pa 01 p0024 A83-10244
 The equilibrium constant for the reversible reaction $H_2S + 3H_2O + Li_0.66K_0.34/2 CO_3$ yields $4H_2 + CO_2 + Li_0.66K_0.34/2 SO_4$ at elevated temperature --- in molten carbonate fuel cells 07 p0954 A83-20590
 The contribution of volcanoes to the global atmospheric sulfur budget 13 p1877 A83-30886
 Hydrogen sulfide in a circumstellar envelope 13 p1958 A83-31734
 Line strength measurements using diode lasers - The nu2 band of H2S 18 p2742 A83-39182
 Absorption of H2S at DF laser wavelengths 19 p2852 A83-41108
 On the detectability of H2S in Jupiter 21 p3239 A83-40087
 Fe-Ni-S-O layer phase in C2M carbonaceous chondrites - A hydrous sulphide? 23 p3529 A83-48079
 Reduction of molecular sulphur by methanogenic bacteria 23 p3495 A83-48081

HYDROGEN 2

U DEUTERIUM

HYDROGEN 3

U TRITIUM

HYDROGEN-BASED ENERGY

- Metallurgy of rechargeable hydrides 02 p0153 A83-11509
 Storing energy in metal hydrides - A review of the physical metallurgy 07 p0955 A83-21562
 Present status of R&D for hydrogen production from water in Japan 09 p1292 A83-23701
 Theory of the computer code RET 1 for the calculation of space-time dependent temperature and composition properties of metal hydride hydrogen storage beds 11 p1545 A83-27337
 Porous metal hydride compacts - Preparation, properties and use 11 p1545 A83-27338
 Magnesium for hydrogen storage 11 p1545 A83-27339
 A system of hydrogen-powered vehicles with liquid organic hydrides 11 p1668 A83-27340
 Hydrogen energy creeps forward --- hydrogen fuel production and storage 13 p1869 A83-30000
 Metal-hydride energy-technological processing of hydrogen 13 p1871 A83-31375
 Hydrogen fuel - Universal energy 13 p1871 A83-31504
 A solar-hydrogen economy for U.S.A. 15 p2192 A83-34866
 A study of the hydriding kinetics of Mg-(10-20 w/o) LaNi5 15 p2133 A83-34867
 A kinetic model of hydrogen absorption in CeMg12 15 p2193 A83-34868
 Hydrogen energy in Canada - I Proceedings of the First Hydrogen Energy Symposium, University of Western Ontario, London, Canada, May 1, 1981 15 p2193 A83-35301
 Status of hydrogen development for aircraft in five countries - A Canadian perspective 18 p2708 A83-39562

- The case for solar/hydrogen energy
20 p3012 A83-42951
Advanced electrolysis development for hydrogen-cycle
peak shaving for electric utilities
22 p3320 A83-46779

HYDROGENATION

- Effect of discharge conditions on characteristics of
hydrogenated amorphous silicon deposited by DC glow
discharge decomposition 04 p0539 A83-15498
Effects of prolonged illumination on the properties of
hydrogenated amorphous silicon
04 p0540 A83-15512
Light-induced metastable effects in hydrogenated
amorphous silicon 04 p0540 A83-15513
Luminescence fatigue and light-induced electron spin
resonance in amorphous silicon-hydrogen alloys
04 p0541 A83-15514
Studies of thin-film growth of sputtered hydrogenated
amorphous silicon 04 p0541 A83-15517
The role of hydrogen in amorphous silicon films
deposited by the pyrolytic decomposition of silane
04 p0541 A83-15519
Optical properties of a-Si:H and a-SiC_x:H films
prepared by glow-discharge deposition
04 p0541 A83-15522
States in the gap of amorphous hydrogenated silicon
04 p0541 A83-15524
Hydrogenated a-Si/x/Ge/1-x/- A potential solar cell
material 04 p0542 A83-15871
Effect of hydrogen on the deposition rate for planar RF
magnetron sputtering of hydrogenated amorphous
silicon 04 p0543 A83-16082
Anodic oxidation of a-Si:H films
06 p0814 A83-18567
Photoconductivity in amorphous Si:H:Cl films
07 p0999 A83-20741
Hydrogen plasticizing of refractory titanium alloys
09 p1229 A83-23524
Transient photoconductivity studies of the light soaked
state of hydrogenated amorphous silicon
10 p1488 A83-25982
Amorphous silicon photovoltaic modules
10 p1446 A83-26064
The properties of fuel fractions obtained by the
hydrogenation of Kansk-Achinsk coal
10 p1401 A83-26920
Magnesium for hydrogen storage
11 p1545 A83-27339
Study of gap states in a-Si:H by transient current
spectroscopy 14 p2089 A83-32251
Highly conductive boron doped Si-layers prepared by
plasma decomposition of SiH₄ 14 p2089 A83-32252
A model for analysis of optical measurements carried
on a-Si:H films for photovoltaic applications
14 p2041 A83-32253
Large area and high efficiency A-Si:H solar cell
14 p2044 A83-32284
Large area hydrogenated amorphous silicon for
photovoltaic application 14 p2044 A83-32289
Novel plasma chemical methods for doping a-Si:H
14 p2044 A83-32290
Reversible photoinduced modification of
electron-capture cross section at localized states in
Alpha-Si:H 14 p2093 A83-33446
Density of the gap states in undoped and doped glow
discharge a-Si:H 16 p2421 A83-36740
Effect of boron doping and its profile on characteristics
of p-i-n a-Si:H solar cells 16 p2371 A83-36742
High performance hydrogenated amorphous silicon
solar cells made at a high deposition rate by glow discharge
of disilane 16 p2371 A83-36774
Light-induced effects in indium tin oxide/n-i-p
hydrogenated amorphous silicon solar cells
18 p2707 A83-39463
Origin of the photo-induced changes in hydrogenated
amorphous silicon 18 p2750 A83-39473
Stability of Pd/Nb₂O₅/amorphous hydrogenated silicon
solar cells 20 p3011 A83-42356
Energy barrier height variations of Pd-Si Schottky diodes
induced by deuterium 31 p3123 A83-43849
Effects of Ca additions on some Mg-alloy hydrides
21 p3110 A83-45422
Investigation of in-situ sputtered a-Si(H) by AES
24 p3636 A83-50180

HYDROGEOLOGY

- Application of remote sensing data to hydrogeological
purposes in the Fezzan Region-Lybia
09 p1287 A83-24566
Hydrogeologic studies abroad --- Russian book
09 p1292 A83-25247
The efficiency of using space imagery in hydrogeological
studies 14 p2034 A83-32493
Using Landsat imagery interpretation for underground
water prospecting around Qena Province, Egypt
15 p2187 A83-35276

- Geological features of the present-day and ancient
oceans 18 p2715 A83-39532

HYDROGRAPHY

- Survey paper on remote sensing techniques to map
snow cover 01 p0061 A83-10011
The subtropical front - Satellite observations during
FRONTS 80 03 p0369 A83-14503
Fresh water springs detection and discharge evaluation
using thermal I.R. surveys along sea shores in areas
affected by poor precipitations 09 p1288 A83-24578
SEASAT-derived - ocean surface topography -
Comparison with coincident Kuroshio hydrographic data
10 p1452 A83-25975
Cape Romain and the Charleston Bump - Historical and
recent hydrographic observations
14 p2060 A83-33086
Causes of flood streamlines observed on Landsat
images and their use as indicators of floodways
15 p2183 A83-34151
Spatial variability of soil hydraulics and remotely sensed
soil parameters 21 p3165 A83-44674
Hydrograph simulation and analysis from
Landsat-imagery of tropical zones
22 p3312 A83-46202

HYDROKINETICS**U HYDROMECHANICS****HYDROLOGY****NT HYDROGEOLOGY**

- Snow hydrology studies using data from the Heat
Capacity Mapping Mission 01 p0065 A83-10102
Temporary lakes and salt plains in the high plateaus
of the Andes /Bolivia/- A continuing survey of periodic
hydrologic phenomena using the geostationary satellite
GOES-EST 03 p0360 A83-14574
Landsat-data for distributed hydrological models
08 p1127 A83-21934
Remote sensing of water quality in Flaming Gorge
Reservoir Wyoming-Utah, USA 08 p1128 A83-21948
Use of Seasat synthetic aperture radar and Landsat
multispectral scanner subsystem data for Alaskan
glaciology studies 09 p1305 A83-24287
Assessment and management of water resources from
satellite derived data - Indian example
09 p1286 A83-24553
Hydrologic data collection using satellite systems
09 p1286 A83-24554
The feasibility of thermal inertia mapping for detection
of perched water tables in semi-arid irrigated lands
09 p1288 A83-24583
Application of Landsat imagery in groundwater
investigations in a semi-arid hard-rock region of the State
of Gujarat /India/ 09 p1288 A83-24584
Natural water containment site identification in the arid
mountains of Djibouti 09 p1289 A83-24595
Landsat image investigation of major surface structures,
topography, and hydrology in Qatar
09 p1290 A83-24610
The utility of Landsat for monitoring the ephemeral water
and herbage resources of arid lands - An example of
rangeland management in the Channel Country of
Australia 09 p1290 A83-24614
Hydrological analysis of the Machar region based on
Landsat satellite processed data
09 p1291 A83-24623
Automatic classification of Lake Qarun water by digital
processing of Landsat MSS data
09 p1291 A83-24624
A noninteractive procedure for land-use determination
10 p1443 A83-25642
Vegetation classification based on Advanced Very High
Resolution Radiometer /AVHRR/ satellite imagery
10 p1443 A83-25646
Observations from space of hydrophysical phenomena
in the Black Sea 10 p1453 A83-26809
Classification of Landsat data for hydrologic application,
Everglades National Park 12 p1748 A83-29916
Canadian Landsat studies for monitoring hydrologic
conditions and coastal environments - A summary
15 p2183 A83-33579
A streamflow model based on Landsat imagery for the
Wasatch Mountains 17 p2531 A83-38348
Enhanced thermal mapping with Landsat and HCMM
digital data 17 p2531 A83-38351
Multidate Landsat water quality models
17 p2531 A83-38352
The ocean --- chemical composition
20 p3032 A83-42820
Soil moisture remote sensing applications studies of the
USDA-ARS 22 p3312 A83-46201

HYDROLOGY MODELS

- Evaporation from a partially wet forest canopy
21 p3165 A83-44234
The influence of poloidal motions and latent heat release
on the equilibrium ice extent in a simple climate model
21 p3180 A83-44703

- Hydrograph simulation and analysis from
Landsat-imagery of tropical zones
22 p3312 A83-46202
Modeling inland water quality using Landsat data
23 p3475 A83-47223

HYDROLYSIS

- The evaluation of the serviceability of AT series titanium
alloys in conditions of current hydrolysis production from
the point of view of hydrogen embrittlement
09 p1235 A83-24396
Prospects for using titanium alloys in the manufacture
of apparatus for the hydrochloric acid hydrolysis of yeast
19 p2821 A83-40805
The hydrolytic stability of glass fiber reinforced
poly(butylene terephthalate), poly(ethylene terephthalate)
and polycarbonate 20 p2948 A83-42834
In situ analysis of the interface --- of composites
22 p3264 A83-46303
The hydrolytic stability of some commercially available
polycarbonates 22 p3270 A83-46907

HYDROMAGNETIC FLOW**U MAGNETOHYDRODYNAMIC FLOW****HYDROMAGNETIC STABILITY****U MAGNETOHYDRODYNAMIC STABILITY****HYDROMAGNETIC WAVES****U MAGNETOHYDRODYNAMIC WAVES****HYDROMAGNETICS****U MAGNETOHYDRODYNAMICS****HYDROMAGNETISM****U MAGNETOHYDRODYNAMICS****HYDROMECHANICS****NT ELASTOHYDRODYNAMICS****NT ELECTROHYDRODYNAMICS****NT HYDRODYNAMICS****NT HYDROSTATICS****NT MAGNETOHYDRODYNAMICS****NT MAGNETOHYDROSTATICS****Shock wave propagation law in the point explosion****theory 01 p0047 A83-10912****Hydromechanical dynamics of aircraft landing gear****06 p0717 A83-18925****HYDROMETEOROLOGY****NT MARINE METEOROLOGY****The Pacific Ocean --- Russian book****02 p0218 A83-12375****Case study of a hailstorm in Colorado. II - Particle growth****processes at mid-levels deduced from in-situ****measurements 06 p0790 A83-18264****Use of the radar differential reflectivity radar technique****for observing convective systems 09 p1313 A83-23966****Statistics and the analysis of hydrometeorological data****--- Russian book 10 p1451 A83-25623****Snowfall rate obtained from radar reflectivity within a****50km range 11 p1625 A83-27015****The statistical characterization of rain areas in terms****of fractals 11 p1628 A83-27049****Monitoring of radar systems through weather echoes****11 p1629 A83-27058****Hydrometeor characteristics in the May 2, 1979 squall****line in Central Oklahoma as obtained from radar differential****reflectivity measurements during SESAME****11 p1629 A83-27063****Distribution of ocean surface temperature in connection****with features of atmospheric processes and****hydrometeorological fields /According to POLYMODE****data/ 11 p1634 A83-28208****Subjective probabilistic quantitative precipitation****forecasts - Some experimental results. 13 p1886 A83-30546****Some model differences and their implications for****forecasting southern California rains 13 p1886 A83-30551****Modes of variability in annual hemispheric water vapor****and transport fields 16 p2385 A83-35474****Bulk parameterization of the snow field in a cloud****model 22 p3338 A83-45709****The impacts of different satellite data on rain estimation****schemes 22 p3342 A83-46949****Methods of active and passive radar detection in****meteorology 23 p3487 A83-47137****The effect of the inertia of hydrometeors on the statistical****characteristics of a radar signal 23 p3487 A83-47142****Remote sensing of precipitable water by a thermal****infrared multichannel approach 23 p3488 A83-47268****[IAF PAPER 83-105] 23 p3488 A83-47268****5-cm radar echoes and their microphysical significance****in Florida cumuli 24 p3612 A83-49697****Characteristics of the weak echo region in an intense****high plains thunderstorm as determined by a penetrating****aircraft 24 p3616 A83-49733****HYDRONIUM IONS****Merged electron-ion beam experiments. V - Dissociative****recombination of OH(+), H₂O(+), H₃O(+), and D₃O(+)****23 p3511 A83-48583**

HYDROPONICS

HYDROPONICS

Plant growth and mineral recycle trade-offs in different scenarios for a CELSS --- Closed Ecological Life Support System
[SAE PAPER 820855] 13 p1907 A83-30942

HYDROPOWER STATIONS

U HYDROELECTRIC POWER STATIONS

HYDROSPHERE (EARTH)

U EARTH HYDROSPHERE

HYDROSTATIC PRESSURE

Thermoelastic temperature changes in poly/methyl methacrylate/ at high hydrostatic pressure - Experimental 01 p0027 A83-10607
Allowing for the effect of hydrostatic pressure on the viscoelastic shear of polymers 02 p0160 A83-12368
On the compatibility of thermal and hydrostatic equilibrium in thin radiative accretion disks 02 p0260 A83-12527
Thermally isolated coronal loops in hydrostatic equilibrium 02 p0270 A83-12579
Compressive failure and kinking in uniaxially aligned glass-resin composite under superposed hydrostatic pressure 04 p0455 A83-15994
Significance of the measurement of colloidal-oncotic and hydrostatic pressures in lung capillaries for the diagnosis of edema of the lungs 05 p0673 A83-17177
Radial and frictional forces in misaligned radial face seals with a non-Newtonian fluid 06 p0768 A83-18050
The distensibility of the veins of skeletal muscles during shifts in the level of hydrostatic venous pressure 08 p1145 A83-22109
On the unsymmetric eigenproblem for the buckling of shells under pressure loading 10 p1440 A83-26434
Effect of central vascular engorgement and immersion on various lung volumes 13 p1905 A83-30507
The role of cosmic rays in hydrostatic equilibrium of the galactic halo 16 p2441 A83-36528
Will diamond transform under Megabar pressures? 16 p2421 A83-36563
Fracture of notched polycarbonate under hydrostatic pressure 18 p2670 A83-39049
Control of superplastic cavitation by hydrostatic pressure --- in aluminum alloys 20 p2954 A83-43342
Analysis of multirecess conical hydrostatic thrust bearings under rotation 21 p3147 A83-44373
Inelastic buckling of cylindrical shells subjected to axial tension and external pressure 21 p3164 A83-45597
Investigation of the effect of uniform compression on the angle of the optical axes of olivine single crystals 23 p3485 A83-48509

HYDROSTATICS

NT MAGNETOHYDROSTATICS

The constraints of energy-conserving vertical finite difference on the hydrostatic equations in a NWP model --- Numerical Weather Prediction 13 p1891 A83-30805

A non-reflective upper boundary condition for limited-height hydrostatic models 15 p2203 A83-33877

Computation of Jupiter interior models from gravitational inversion theory 15 p2275 A83-34720

The establishment of hydrostatic and quasi-geostrophic balance in synoptic-scale disturbances in a polytropic turbulent atmosphere 19 p2867 A83-41581
Hydrostatic reaction of the sun to local disturbances 20 p3080 A83-42379

HYDROTHERMAL CRYSTAL GROWTH

Hydrothermally altered impact melt rock and breccia - Contributions to the soil of Mars 04 p0567 A83-15578

Instabilities of dynamic thermocapillary liquid layers. I
Convective instabilities 20 p2985 A83-43098

HYDROTHERMAL STRESS ANALYSIS

The effects of humidity on fatigue due to shear stress in unidirectional composites - Attempts at interpretation and a summing up
[ONERA, TP NO. 1982-98] 03 p0292 A83-14546

The effect of moisture and temperature on the properties of an epoxide-polyamide adhesive in relation to its performance in single lap joints 04 p0463 A83-15872

Transient hygrothermal and mechanical stress intensities around cracks 09 p1223 A83-23930

Influence of the polymer matrix on the mechanical response of a unidirectional composite 18 p2653 A83-40179

Performance of carbon fibre reinforced epoxy composites under different environments 18 p2656 A83-40225

HYDROTHERMAL SYSTEMS

The modelling of hydrothermal aging in glass fibre reinforced epoxy composites 01 p0022 A83-10700

HYDROX ENGINES

U HYDROGEN OXYGEN ENGINES

HYDROXIDES

NT LITHIUM HYDROXIDES

NT SODIUM HYDROXIDES

The characterization of carbon dioxide absorbing agents for life support equipment; Proceedings of the Winter Annual Meeting, Phoenix, AZ, November 14-19, 1982 11 p1644 A83-28329

Carbon dioxide scrubbing materials in life support equipment 11 p1644 A83-28330

Chemical and physical factors affecting the absorption capability of calcium hydroxide based carbon dioxide absorbents 11 p1645 A83-28333

Model for the absorption rate of gaseous CO₂ by solid hydroxides 11 p1645 A83-28337

Absorption of carbon dioxide by solid hydroxide sorbent beds in closed-loop atmospheric revitalization system 11 p1645 A83-28338

Energy Storage in a fuel cell with bipolar membranes burning acid and hydroxide 13 p1872 A83-31599

HYDROXYCORTICOSTEROID

NT CORTISONE

HYDROXYL COMPOUNDS

NT ALCOHOLS

NT BISPHENOLS

NT ETHYL ALCOHOL

NT METHYL ALCOHOLS

NT POLYVINYL ALCOHOL

The use of hydroxyacids as geochemical indicators 17 p2547 A83-38852

HYDROXYL EMISSION

Formaldehyde absorption towards OH sources 02 p0260 A83-12531

An interpretation of OH maser observations in W3/OH/ 03 p0413 A83-13313

Observations of cool stars at 20, 25, and 33 microns 03 p0421 A83-14149

Infrared observations of OH/IR stars 03 p0411 A83-14812

VLBL measurements of the relative position of the 1665 MHz and 1667 MHz OH masers toward W49N and NGC 6334N 04 p0552 A83-15616

Stokes polarimetry of main-line OH emission from stellar masers 04 p0553 A83-15617

Physical conditions in H II/OH maser regions 06 p0825 A83-18088

An accurate position for the 6-cm OH masers in W3 06 p0820 A83-18868

Do the W44 and W28 molecular clouds show evidence of a shock 06 p0840 A83-19278

Observations of the new OH maser source G43.2-0.1 07 p1007 A83-20670

A high-resolution 2.2 micron polarization map of OH 0739-14 07 p1007 A83-20934

Formation of OB clusters - OH maser observations 07 p1021 A83-21128

The Corona Australis dark cloud 13 p1946 A83-30389

First results using a K-band maser receiver on the Parkes 64-m radio telescope 13 p1946 A83-30391

VLA observations of the 2pi(3/2)J=3/2 OH masers associated with Orion A 13 p1940 A83-31415

Intensity variations and ratios of (9-4) and (7-3) hydroxyl bands in nightglow at Poona 13 p1882 A83-31632

Measurement of the height of the hydroxyl-emission layer in the Moscow area 14 p2051 A83-31884

Slow waves near the mesopause 14 p2059 A83-32860

Formaldehyde and OH in the Orion molecular clouds 15 p2265 A83-34597

Electronically resonant CARS detection of OH [AIAA PAPER 83-1477] 15 p2133 A83-34912

Emission and absorption at 6 cm from excited OH associated with compact H II regions 16 p2430 A83-36644

Rotational excitation of OH by H₂ - Calculations in intermediate coupling 17 p2579 A83-38364

Galactic emission of OH at 1720 MHz as a tracer of spiral arms 18 p2769 A83-39652

Galactic HII regions, anomalous 1720 MHz OH clouds and spiral structure in the Galaxy 18 p2769 A83-39653

Fluorescence measurements of OH in a turbulent flame --- A feasibility study 19 p2820 A83-40859

Nightglow intensity variations in the O₂(0-1) atmospheric band, the NaD lines, the OH(6-2) band, the yellow-green continuum at 5750 A and the oxygen green line 20 p3016 A83-42308

Picosecond laser-spectroscopy measurement of hydroxyl fluorescence lifetime in flames 20 p2949 A83-42347

The peculiar circumstellar envelope around IRC+ 10420 20 p3065 A83-42377

The nature of OH/IR stars. I - Infrared Mira variables 20 p3066 A83-42393

The H₂O/OH maser 342.01+0.25 - A case of supernova-induced star formation? 20 p3066 A83-42394

Measurement of the OH rotational temperature at Mawson, East Antarctica 20 p3024 A83-43164

Altitude profiles of OH and O₂ near infrared airglows in the evening twilight 20 p3027 A83-43402

Design and fabrication of payload for OH emission experiment onboard Spacelab - A case study 21 p3095 A83-43821

The disappearance of OH from Comet P/Encke 21 p3227 A83-44086

Quasi-thermal excitation of the satellite lines of OH at 5 cm 21 p3233 A83-44747

OH airglow phenomena during the 5-6 July 1982 total lunar eclipse 22 p3328 A83-46082

The surface glow of the Atmosphere Explorer C and E satellites 22 p3334 A83-46887

The magnetic field of the NGC 2024 molecular cloud - Detection of OH line Zeeman splitting 23 p3518 A83-47431

Spectral channel of a digital radio spectrometer with an analysis band of 180 kHz 24 p3581 A83-48959

Survey of OH masers at 1665 MHz. II - Galactic longitude 340 deg to the galactic centre 24 p3650 A83-48984

Atlas of main-line OH masers in the galactic longitude range 3 to 60 deg 24 p3638 A83-48986

New H₂O masers associated with main-line OH masers in the galactic longitude range 3 to 60 deg 24 p3638 A83-48987

OH maser emission at 4765 MHz in W3 24 p3659 A83-49371

Ammonia absorption toward W3(OH) - 0.3 arcsec resolution maps in the (2,2) line 24 p3668 A83-50078

HYDROXYL RADICALS

Pumping of H II/OH masers - IR line overlaps and collisional excitation by H₂ 03 p0427 A83-14756

Determination of the rotational excitation temperature in solar type stars 04 p0556 A83-15598

Kinetics of the reaction of hydroxyl radicals with nitric acid 05 p0613 A83-17230

Kinetics of the reaction O + HO₂ yields OH + O₂ from 229 to 372 K 05 p0613 A83-17232

The photoproduction of circumstellar OH maser shells 06 p0833 A83-18871

Rate constants for the reaction of OH with SO₂ at low pressure 07 p0882 A83-21059

The kinetics of the reaction of OH with ClO 08 p1056 A83-22214

Laser-saturated fluorescence measurements of OH concentration in flames 09 p1225 A83-23749

Laser fluorescence measurements of the OH concentration in a combustion boundary layer 09 p1226 A83-24367

Shock-tube absorption measurements of OH using a remotely located dye laser 09 p1269 A83-24438

Vibrational population distribution in the hydroxyl night airglow 09 p1306 A83-24640

Interstellar grain composition and the infrared spectrum of OH26.5+0.6 09 p1362 A83-24985

The state distribution of OH radicals photodissociated from H₂O₂ at 193 and 248 nm 10 p1389 A83-25562

Vibrational energy transfer from OH to other gaseous hydrides 10 p1480 A83-26457

Abstraction vs insertion in O/1D/ + H₂ - OH + H 11 p1545 A83-27497

The low-lying 2-sigma-minus states of OH 11 p1655 A83-28528

A general circulation model study of atmospheric carbon monoxide 13 p1876 A83-30884

The pure rotation spectrum of the hydroxyl radical and the solar oxygen abundance 13 p1965 A83-31701

Absolute rate constants for the hydroxyl radical reactions with CH₃SH and C₂H₅SH at room temperature 14 p1991 A83-33105

Balloon borne LIDAR measurements of stratospheric hydroxyl radical 16 p2380 A83-36144

Relative rate constants for the reactions of atomic oxygen with HO₂ and OH radicals 16 p2327 A83-36711

Submillimeter detection of stratospheric OH and further line assignments in the stratospheric emission spectrum 17 p2540 A83-37764

Photodissociation processes in the OH molecule 17 p2579 A83-38468

Spectral line parameters for the pure rotation bands of solar OH 18 p2783 A83-39186

Hydroxyl concentration measurements in the NH₃-NO-O₂ reaction in postflame gases 18 p2664 A83-40311

Collisional quenching of A 2Sigma(+) OH at elevated temperatures 20 p2950 A83-42633

- Correlation of the ozone formation rates with hydroxyl radical concentrations in the propylene-nitrogen oxide-dry air system - Effective ozone formation rate constant
21 p3110 A83-45617
- New technological developments for the remote detection of atmospheric hydroxyl radicals
22 p3288 A83-46072
- OH Pepsios --- polyetalon pressure-scanned interferometric optical spectrometer for atmospheric measurements
22 p3294 A83-46841
- Rocket-based investigations of O(3P), O2(a1-delta/g) and excited OH ($v = 1, 2$) during the solar eclipse of 26 February 1979
23 p3481 A83-47471
- OH(X2II) state distribution from HNO3 and H2O2 photodissociation at 193 nm
23 p3429 A83-47639
- Remote sensing of OH in the atmosphere using the technique of laser-induced fluorescence
23 p3457 A83-47792
- Development of compact excimer lasers for remote sensing
23 p3461 A83-47796
- HYGIENE**
- Hygienic evaluation of clothing made of chemical fibers
05 p0677 A83-17191
- A physiological and hygienic evaluation of the work regime of operators who are working in current energy production in Kirghizia
11 p1643 A83-28765
- Radiation hygiene --- Russian book
12 p1762 A83-28825
- Physiological and hygienic aspects of artificial heat adaptation (Review of the literature)
16 p2397 A83-35596
- New norms for electromagnetic radiation in the microwave range
17 p2562 A83-38181
- New principles in the improvement of the normalization of local vibration
17 p2562 A83-38182
- A hygienic evaluation of the chemical composition of air in living accommodations
17 p2562 A83-38201
- HYGAL PROPERTIES**
- Finite element analysis of moisture effects in graphite-epoxy composites
02 p0150 A83-12762
- Hygrothermal aging effects on the micromechanisms of crack extension in glass fibre and carbon fibre composites
08 p1053 A83-21679
- The aging of electroluminophors in the presence of moisture
13 p1831 A83-30264
- Hygrothermal ageing of fibrous composites
18 p2657 A83-40229
- Environmental aging of epoxy composites
22 p3263 A83-46288
- A stress transfer model for the deformation and failure of polymeric matrices under swelling conditions
22 p3263 A83-46290
- HYGROMETERS**
- Infrared device for simultaneous measurement of fluctuations of atmospheric carbon dioxide and water vapor
03 p0324 A83-13275
- On the calibration and temperature behaviour of single-beam infrared hygrometers
12 p1728 A83-29137
- Venera 13 and Venera 14 measurements of the water vapor content in the Venus atmosphere
12 p1798 A83-29480
- Water-vapor content in the Venusian atmosphere according to data from the Venera-13 and Venera-14 probes
14 p2111 A83-31963
- Experience related to the employment of a highly sensitive humidity probe with miniature humidity sensor on a barium fluoride basis - Comparison with a Lyman alpha-hygrometer
18 p2723 A83-39260
- A note on the new type hygrometer using the photochemical reaction $\text{H}_2\text{O} + \text{h}\nu(\text{Ly-alpha line}) \rightarrow \text{metastable OH} + \text{H}$, and $\text{OH-OH} + \text{h}\nu(\text{wavelength} = 309 \text{ nm})$
22 p3331 A83-46520
- HYGROSCOPICITY**
- Effects of moisture, residual thermal curing stresses, and mechanical load on the damage development in quasi-isotropic laminates
03 p0292 A83-14556
- Transverse moisture sensitivity of aramid/epoxy composites
10 p1388 A83-25626
- A two-dimensional model of the electrocoagulation-hygroscopic dissipation of warm fogs
18 p2724 A83-39442
- The effect of moisture on the fatigue resistance of an aramid/epoxy composite
22 p3265 A83-46904
- HYOSCINE**
- A case report - Unilateral cycloplegia resulting from careless use of Transderm-V
02 p0223 A83-12410
- HYPERBARIC CHAMBERS**
- Physiological aspects and scope of hyperbaric oxygen therapy
02 p0223 A83-12259
- Effects of hyperbaric oxygen on anaerobic organisms
02 p0222 A83-12260
- Current trends in hyperbaric oxygen therapy
02 p0223 A83-12262
- Multiparameter monitoring of the awake brain under hyperbaric oxygenation
13 p1897 A83-30486
- Estimation of human susceptibility to the high-pressure nervous syndrome
13 p1905 A83-30505
- Liquid ventilation in dogs - An apparatus for normobaric and hyperbaric studies
13 p1898 A83-30510
- Drug disposition under hyperbaric and hyperbaric hyperoxic conditions - Meperidine in the dog
14 p2064 A83-32686
- Force and duration of muscle twitch contractions in humans at pressures up to 70 bar
14 p2068 A83-32812
- Salicylate pharmacokinetics in the dog at 6 ATA in air and at 2.8 ATA in 100 percent oxygen
21 p3182 A83-43987
- Hemodynamic effects of lactated ringer's solution on hemorrhagic shock during exposure to hyperbaric air and hyperbaric hyperoxia
21 p3182 A83-43991
- HYPERBOLIC COORDINATES**
- Conformal hyperbolicity of Lorentzian warped products
06 p0841 A83-19445
- HYPERBOLIC DIFFERENTIAL EQUATIONS**
- General hyperbolic difference formulas for linear and quasilinear hyperbolic equations
02 p0231 A83-12905
- Plane stress problems of the elastic perfectly-plastic medium
03 p0341 A83-14486
- Approximation of extremal surface elements /hyperbolic type/ by means of characteristic three-dimensional quadrilateral elements
03 p0388 A83-14493
- A family of flux-correction methods to avoid overshoot occurring with solutions of unsteady flow problems
03 p0322 A83-14608
- Boundary stabilization of hyperbolic systems with no dissipative conditions
04 p0530 A83-16196
- A characteristic flux difference splitting for the hyperbolic conservation laws of inviscid gasdynamics [AIAA PAPER 83-0040]
05 p0632 A83-16480
- A difference scheme of second-order accuracy with a minimal pattern for hyperbolic equations
09 p1335 A83-23567
- Adaptive Nystroem-Runge-Kutta methods for systems of second-order ordinary differential equations
10 p1470 A83-25589
- Euler equations - Implicit schemes and boundary conditions
12 p1695 A83-28959
- Stability of two-dimensional hyperbolic initial boundary value problems for explicit and implicit schemes
12 p1772 A83-29647
- Numerical methods based on additive splittings for hyperbolic partial differential equations
13 p1912 A83-31361
- On two upwind finite-difference schemes for hyperbolic equations in non-conservative form
13 p1913 A83-31593
- The homogeneous property and flux splitting in gas dynamics
14 p2094 A83-32124
- Numerical solution of hyperbolic equations by method of bicharacteristics
14 p2078 A83-32922
- Explicit finite difference predictor and convex corrector with applications to hyperbolic partial differential equations
19 p2893 A83-41852
- Boundary conditions for a fourth order hyperbolic difference scheme
20 p3041 A83-42494
- Control of distributed hyperbolic systems - "What does a tokamak and a large spacecraft have in common?"
21 p3192 A83-44011
- Finite-dimensional controllers for hyperbolic systems
21 p3196 A83-45118
- Monotonic second-order difference scheme for hyperbolic systems with two independent variables --- in unsteady gas dynamics
21 p3133 A83-45213
- Weakly nonlinear high frequency waves
22 p3354 A83-47091
- A theory of weak shocks
22 p3287 A83-47095
- Propagation of heat waves in parametric media
24 p3576 A83-48948
- HYPERBOLIC FUNCTIONS**
- The global hyperbolicity of the dependence domain of a closed achronal set in general relativity
09 p1338 A83-23597
- High resolution schemes for hyperbolic conservation laws
12 p1771 A83-29095
- Stability analysis of numerical boundary conditions and implicit difference approximations for hyperbolic equations
12 p1772 A83-29650
- The choice of numerical boundary conditions for hyperbolic systems
12 p1772 A83-29653
- Self-adjusting grid methods for one-dimensional hyperbolic conservation laws
15 p2224 A83-33822
- Implicit methods of second-order accuracy for the Euler equations [AIAA PAPER 83-1925]
18 p2682 A83-39379
- High resolution applications of the Osher upwind scheme for the Euler equations [AIAA PAPER 83-1943]
18 p2636 A83-39390
- On extrapolation boundary conditions for the numerical solution of hyperbolic difference schemes
21 p3198 A83-45054
- HYPERBOLIC NAVIGATION**
- NT LORAN C
NT SHORAN
- HYPERBOLIC REENTRY**
- Heat transfer at hyperbolic flight velocities - Physical model and theoretical and experimental studies
20 p2929 A83-42882
- HYPERBOLIC SPACE**
- U HYPERBOLIC COORDINATES
- HYPERBOLIC SYSTEMS**
- Null test for hyperbolic convex mirrors
06 p0809 A83-18578
- Tracking of interfaces for fluid flow: Accurate methods for piecewise smooth problems.
12 p1726 A83-29937
- Optical system design study for the University of Texas 300-inch telescope
13 p1920 A83-30998
- On a variational approach to conservative hyperbolic systems
22 p3352 A83-45978
- Interactions of fast and slow waves in hyperbolic systems with two time scales
23 p3504 A83-48245
- HYPERBOLIC TRAJECTORIES**
- Criteria of hyperbolic and hyperbolic-elliptical motion in capture theory
11 p1673 A83-28032
- The averaged, hyperbolic, restricted three-body problem
17 p2594 A83-38564
- HYPERCAPNIA**
- Human breathing patterns on mouthpiece or face mask during air, CO2, or low O2
03 p0378 A83-13579
- Effects of exposure to low O2 or high CO2 environments on respiration in hibernating hamsters and ground squirrels
04 p0520 A83-16009
- Pulmonary microcirculatory response to localized hypercapnia
05 p0671 A83-17333
- Several indicators of the EKG and metabolic processes during an experimental coronary spasm in rats exposed to conditions of hypoxia in combination with hypercapnia
07 p0975 A83-20986
- An investigation of the genotypic conditionality of the gas composition and acid-base state indicators of the blood during various effects on the body
09 p1323 A83-25152
- The thermoregulatory activity of the intercostal muscles in conditions of a hypercapnic load
10 p1454 A83-26790
- Blood osmolality during in vivo changes of CO2 pressure
13 p1902 A83-30460
- Effects of hypercapnia, hypoxia, and rebreathing on heart rate response during apnea
13 p1902 A83-30462
- Effects of hypercapnia, hypoxia, and rebreathing on circulatory response to apnea
13 p1902 A83-30463
- The direct reactions of smooth muscles of the major cerebral arteries to acute hypoxia and hypercapnia
14 p2061 A83-31971
- Effect of hypoxia and hypercapnia on catecholamine content in cat carotid body
14 p2064 A83-32822
- The breathing patterns of humans during hypercapnia and hypoxia
17 p2558 A83-37243
- The regulation of the breathing pattern during muscular activity in conditions of normal and altered chemoreceptor stimulation
17 p2558 A83-37244
- The duration of inhalation and exhalation in growing hypercapnia and the effect of additional resistive inspiratory resistance
17 p2558 A83-37246
- The reaction of respiratory neurons of rats to increasing hypercapnia
19 p2879 A83-42095
- HYPERFINE STRUCTURE**
- HCN J = 1-0 observations in L 673 and S 235B - Two different cases of hyperfine anomalies
10 p1499 A83-25368
- The rotational spectrum and hyperfine structure of the methylene radical CH2 studied by far-infrared laser magnetic resonance spectroscopy
10 p1480 A83-26452
- The nuclear hyperfine structure of deuterated ammonia
13 p1958 A83-31730
- The effect of hyperfine structure on stellar abundance analysis
21 p3233 A83-44752
- The detection of vinyl cyanide in TMC-1
21 p3236 A83-45541
- Hyperfine structure measurements for lines of astrophysical interest in Mn I
24 p3658 A83-49364
- HYPERGEOMETRIC FUNCTIONS**
- An integral equation connected with the Jacobi polynomials
09 p1336 A83-24371
- Computational method for Chaplygin function
14 p2012 A83-32969
- Representation of a gravitational field by means of a hypercomplex potential
18 p2767 A83-39528
- HYPERGEOMETRY**
- U HYPERSPACES

HYPERGLYCEMIA

HYPERGLYCEMIA

What is to be thought of induced hyperglycemia in aviation medicine in 1981 08 p1147 A83-22952
Increased gluconeogenesis in hyper-G stressed rats 11 p1637 A83-27805

HYPERGOLIC ROCKET PROPELLANTS

Orbit manoeuvres with finite thrust - A study and presentation of results 03 p0283 A83-13846
The production of a hypergolic hybrid propellant 09 p1241 A83-23837

HYPERION

Crater numbers and geological histories of Iapetus, Enceladus, Tethys and Hyperion 08 p1191 A83-23290
Eight-color photometry of Hyperion, Iapetus, and Phoebe 11 p1684 A83-27366
Hyperion - Collisional disruption of a resonant satellite 16 p2436 A83-35739

HYPERKINESIA

Carbohydrate feeding during prolonged strenuous exercise can delay fatigue 19 p2880 A83-41141
On the functional state of the pituitary-adrenal-axis in rats under different conditions of motor activity 23 p3496 A83-48448

HYPEROXIA

Oxygen toxicity 02 p0222 A83-12261
The mechanisms of the effect of the adaptation to cold on the resistance of an organism to hyperoxia 04 p0520 A83-15897
100% oxygen breathing during acute heat stress - Effect on sweat composition 10 p1454 A83-25669
Endotoxin protects against hyperoxic alterations in lung endothelial cell metabolism 13 p1896 A83-30453
Effect of hyperoxia on metabolic and catecholamine responses to prolonged exercise 13 p1902 A83-30456
Potentiation of oxygen toxicity in rats by dietary protein or amino acid deficiency 13 p1897 A83-30461
Tissue ammonia and amino acids in rats at various oxygen pressures 13 p1897 A83-30472
Multiparameter monitoring of the awake brain under hyperbaric oxygenation 13 p1897 A83-30486
Drug disposition under hyperbaric and hyperbaric hyperoxic conditions - Meperidine in the dog 14 p2064 A83-32686
Hemodynamic effects of Dextran 40 on hemorrhagic shock during hyperbaria and hyperbaric hyperoxia 14 p2064 A83-32687
Hyperpnea of exercise at various PIO₂ in normal and carotid body-denervated ponies 14 p2064 A83-32820
Mechanisms of defense against the toxic action of oxygen and methods for the utilization of the reactive forms of oxygen in living systems 16 p2395 A83-36809
Effects of hyperbaric oxygen exposure at 31.3 ATA on spontaneously beating cat hearts 19 p2875 A83-41136

Oxygen toxicity in cultured aortic endothelium Selenium-induced partial protective effect 20 p3033 A83-43478
Salicylate pharmacokinetics in the dog at 6 ATA in air and at 2.8 ATA in 100 percent oxygen 21 p3182 A83-43987

Hemodynamic effects of lactated ringer's solution on hemorrhagic shock during exposure to hyperbaric air and hyperbaric hyperoxia 21 p3182 A83-43991
Changes in the microcirculation in mesentery rats during hyperoxia 23 p3496 A83-48568

HYPERPLANES

Multispectral image classification by the separating hyperplanes method - A computer program 08 p1124 A83-21906

HYPERPNEA

Effect of glycogen depletion on the ventilatory response to exercise 13 p1903 A83-30474
Time course of posthyperventilation breathing in humans depends on alveolar CO₂ tension 13 p1903 A83-30491
Hyperpnea of exercise at various PIO₂ in normal and carotid body-denervated ponies 14 p2064 A83-32820
Breathing patterns during submaximal and maximal exercise in elite oarsmen 20 p3034 A83-43483

HYPERSONIC AIRCRAFT

NT HYPERSONIC GLIDERS

Parametric study of hypersonic three-dimensional configurations 11 p1527 A83-28537
An analytical comparison of two wing structures for Mach 5 cruise airplanes [AIAA 83-0974] 12 p1701 A83-29806
The future of the manned aircraft 16 p2287 A83-36960

HYPERSONIC BOUNDARY LAYER

Flowfield surveying techniques used in the NSWC hypervelocity wind tunnel no. 9 01 p0052 A83-11064

Calculation of a three-dimensional boundary layer on a triangular plate of finite length in a hypersonic flow 04 p0441 A83-15081

The effect of an entropy layer on the propagation of unsteady perturbations in a boundary layer --- of hypersonic viscous gas 16 p2288 A83-35534

A study of transport processes in a high-temperature boundary layer on an ablating graphite surface 19 p2842 A83-41259

Flow in a hypersonic boundary layer on a delta wing of finite length at angle of attack 20 p2931 A83-43522

HYPERSONIC COMBUSTION

On the choice of the optimal total wedge angle for the air intake of a hypersonic ramjet engine 08 p1046 A83-22656

The ideas of F. A. Tsander and an assessment of the application of jet engines for the acceleration of aerospace vehicles 08 p1052 A83-22657

HYPERSONIC FLIGHT

Synergetic maneuvering of winged spacecraft for orbital plane change 02 p0139 A83-13080
Introductory aerothermodynamics of advanced space transportation systems [AIAA PAPER 83-0406] 05 p0585 A83-16695

A one-dimensional unsteady model of dual mode scramjet operation [AIAA PAPER 83-0422] 05 p0597 A83-16705

Optimum wing sizing of a single-stage-to-orbit vehicle 09 p1218 A83-24880

Review of shock tube and shock tunnel advancements at NAL 10 p1379 A83-26127

HYPERSONIC FLOW

Analysis of flows of an equilibrium dissociated, ionized, and radiating gas by the method of large particles 01 p0003 A83-11275

Turbulent boundary-layer flow over re-entry bodies including roughness effects 03 p0278 A83-13146

Three-dimensional unsteady hypersonic flow of a relaxing gas past a thin wing 03 p0278 A83-13592

Simultaneous measurement of stagnation temperature and specific flow rate in a hypersonic gas flow 04 p0481 A83-15447

Stationary shape of bodies ablating in hypersonic flow under the action of radiation heating 04 p0477 A83-15863

Effects of large oscillation amplitude on axisymmetric vehicle longitudinal static and dynamic stability in hypersonic flow [AIAA PAPER 83-0215] 05 p0581 A83-16587

Calculation of viscous hypersonic flow over a severely indented nosetip [AIAA PAPER 83-0226] 05 p0582 A83-16596

A three-dimensional hypersonic gas flow over a slender wing 05 p0589 A83-17412

Flow over flat and axisymmetric bodies moving at high variable velocities 05 p0589 A83-17413

Radiative heat transfer near the stagnation point of a blunt body with an intensely vaporizing surface in the three-dimensional hypersonic flow of a hydrogen-helium mixture 06 p0712 A83-18357

Measurement of the particle size distribution in a pulsed hypersonic flow facility 07 p0924 A83-19816

An experimental investigation of heat transfer near the leading edge of inclined flat plate in hypersonic flow 08 p1041 A83-22071

Evaluation of total body heat transfer in hypersonic flow 08 p1042 A83-22150

Hypersonic viscous flows in a streamline coordinate system 08 p1090 A83-23205

An asymptotic solution near the separation point of a shock layer in the case of hypersonic flow around pointed bodies 09 p1197 A83-24483

The supersonic combustion around a truncated cone 09 p1198 A83-24504

Computation of hypersonic viscous flow over a body with mass transfer and/or spin 09 p1198 A83-24878

Body with minimum wave drag in a twisted hypersonic flow 11 p1526 A83-27712

The effect of the mechanisms of heterogeneous catalytic reactions on the heat flux in hypersonic flow past a blunted body 13 p1804 A83-30675

Knudsen layer characteristics for a highly cooled blunt body in hypersonic rarefied flow [AIAA PAPER 83-1424] 14 p1970 A83-32703

Aerothermal environment in control surface gaps in hypersonic flow - An overview [AIAA PAPER 83-1483] 14 p1970 A83-32732

Heat-transfer distributions on bionics at incidence in hypersonic-hypervelocity He, N₂, air, and CO₂ flows [AIAA PAPER 83-1508] 14 p1970 A83-32745

Analysis of aerothermal loads on spherical dome protuberances [AIAA PAPER 83-1557] 14 p1971 A83-32775

Comparison of techniques for predicting 3-D viscous flows over ablated shapes [AIAA PAPER 83-0345] 16 p2292 A83-36051

Parabolized Navier-Stokes solutions for hypersonic flow fields [AIAA PAPER 83-0580] 16 p2293 A83-36061

Hypersonic flows over bionics using a variable-effective-gamma, Parabolized-Navier-Stokes code [AIAA PAPER 83-1666] 17 p2443 A83-37177

Numerical simulation of hypersonic viscous flow over cones at very high incidence [AIAA PAPER 83-1669] 17 p2444 A83-37180

Theory of vortex interaction on a blunt cone 17 p2448 A83-37511

Three-dimensional hypersonic flow past a body of finite thickness 17 p2448 A83-37528

Pressure distribution on a wedge and cone in a hypersonic nonequilibrium gas flow 17 p2449 A83-37555

Nonequilibrium hypersonic air flow past blunt bodies 17 p2450 A83-37630

Aerodynamic characteristics of thin wings in a nonequilibrium hypersonic gas flow 17 p2450 A83-37640

Laminar boundary layer stability experiments on a cone at Mach 8.1 - Sharp cone [AIAA PAPER 83-1761] 18 p2633 A83-39264

Nosetip bluntness effects on cone frustum boundary layer transition in hypersonic flow [AIAA PAPER 83-1763] 18 p2633 A83-39265

Real gas flows over complex geometries at moderate angles of attack 18 p2638 A83-40004

Hypersonic flow behind a lifting body 19 p2790 A83-41206

Allowance for finite Mach numbers in hypersonic asymptotics for blunt axisymmetric bodies 19 p2791 A83-41880

Calculation of shock-layer parameters for the hypersonic flow of equilibrium-dissociated air around bodies with bends of the generatrix 19 p2791 A83-41881

Similarity law for hypersonic flow past asymmetrically blunt bodies 20 p2929 A83-42879

Unified unsteady supersonic/hypersonic theory of flow past double wedge airfoils 21 p3086 A83-44465

An experimental investigation of turbulent base heat transfer in hypersonic flow 21 p3087 A83-44569

Chemical equilibrium laminar or turbulent three-dimensional viscous shock-layer flows 23 p3398 A83-48133

A method for calculating the regime of strong viscous interaction on a delta wing 23 p3400 A83-48664

Analytical description of a hypersonic gas jet flowing into a medium at rest or into a supersonic wake 23 p3400 A83-48673

Comments on the theory of local interaction in a rarefied gas 24 p3543 A83-48926

HYPERSONIC GLIDERS

Hermes - A manned European system 17 p2474 A83-38333

HYPERSONIC HEAT TRANSFER

An experimental heat-transfer investigation of an advanced winged entry vehicle at Mach 10 [AIAA PAPER 83-0409] 06 p0714 A83-19589

The effect of the nonuniformity of supersonic flow with shocks on friction and heat transfer in the channel of a hypersonic ramjet engine 08 p1046 A83-22654

Nonequilibrium hypersonic air flow past blunt bodies 17 p2450 A83-37630

Asymptotic theory of three-dimensional hypersonic radiating-gas flow past bodies 23 p3399 A83-48531

HYPERSONIC INLETS

Application of numerical methods to the calculation of the characteristics of supersonic and hypersonic jet-engine air intakes 17 p2448 A83-37532

HYPERSONIC REENTRY

NT UNCONTROLLED REENTRY (SPACECRAFT)
On the flight derived/aerodynamic data base performance comparisons for the NASA Space Shuttle entries during the hypersonic regime [AIAA PAPER 83-0115] 05 p0606 A83-16529

Hypersonic Mach number and real gas effects on Space Shuttle Orbiter aerodynamics [AIAA PAPER 83-0343] 05 p0584 A83-16668

Shuttle Orbiter boundary-layer transition - A comparison of flight and wind tunnel data [AIAA PAPER 83-0485] 05 p0586 A83-16746

Aeroelastic behavior of hypersonic re-entry vehicles [AIAA PAPER 83-0033] 06 p0723 A83-19577

Heat waves near meteor bodies moving in the atmosphere at hypersonic velocities 13 p1880 A83-31329

Viscous real gas flowfields about three dimensional configurations [AIAA PAPER 83-1511] 14 p1970 A83-32748

A strongly implicit simultaneous variable solution procedure for velocity and pressure in fluid flow problems
[AIAA PAPER 83-1569] 14 p2012 A83-32781

Hypersonic viscous flows past general bodies at angle of attack and yaw 15 p2119 A83-33728

Synthesis of terminal control sequence algorithms with the use of moving-point guidance --- in hypersonic spacecraft reentry 17 p2477 A83-37446

The effect of unsteadiness on the aerodynamic and thermal characteristics of bodies braking in a gas 17 p2449 A83-37554

The numerical analysis of the plasma sheath surrounding a slender sphere-cone 21 p3087 A83-44559

HYPERSONIC SHOCK

The interference of oblique shocks of a particular family in a hypersonic flow 04 p0441 A83-15090

The effect of the nonuniformity of supersonic flow with shocks on friction and heat transfer in the channel of a hypersonic ramjet engine 08 p1046 A83-22654

Analytical method of characteristics applied to the azimuthally dependent solar wind 15 p2281 A83-34601

Hypersonic shock tunnel heat transfer tests of the Space Shuttle SILTS pod configuration [AIAA PAPER 83-1535] 15 p2127 A83-34921

On an approximate solution to the problem of unsteady flow around two-dimensional and axisymmetric bodies moving at high variable velocity 19 p2792 A83-41886

Molecular velocity distribution functions in an argon normal shock wave at Mach number 7 22 p3366 A83-46008

Asymptotic theory of three-dimensional hypersonic radiating-gas flow past bodies 23 p3399 A83-48531

HYPERSONIC SPEED

Hyperballistic vehicle dynamics 02 p0132 A83-13078

Flow fields and aerodynamic characteristics for hypersonic missiles with mid-fuselage inlets [AIAA PAPER 83-0542] 05 p0587 A83-16777

A quasi-three dimensional analysis of thermal ablation from a hypersonic missile 15 p2159 A83-34254

Hypersonic dynamic testing of ablating models with three-degree-of-freedom gas bearings 23 p3412 A83-48135

HYPERSONIC VEHICLES

NT HYPERSONIC AIRCRAFT

NT HYPERSONIC GLIDERS

NT LIFTING REENTRY VEHICLES

Pan Air versus S/HABP - An evaluation of two diverse approaches to supersonic missile aerodynamic analysis --- Advanced Panel Pilot Code and Supersonic/Hypersonic Arbitrary Body Program 05 p0578 A83-16460

Hypersonic slender-wedge analysis with gradual change in angle of attack 11 p1526 A83-27864

Features of the simulation of the catalytic properties of surfaces in subsonic and hypersonic flows 17 p2447 A83-37508

The maximum aerodynamic efficiency of conical wing-body combinations at high supersonic speeds 19 p2790 A83-41266

HYPERSONIC WAKES

Features of the effect of admixtures on the characteristics of a region perturbed by a body moving at hypersonic velocity 19 p2792 A83-41893

An experimental study of the interaction between two hypersonic wakes 20 p2931 A83-43521

A simplified calculation method for the nonequilibrium wake of the blunt-cone body 21 p3087 A83-44568

The effect of heat release and injection on the structure of a laminar hypersonic flow behind a body 23 p3399 A83-48534

HYPERSONIC WIND TUNNELS

NT CASCADE WIND TUNNELS

NT SHOCK TUNNELS

The testing in BIA hypersonic gun tunnel 10 p1380 A83-26133

Shock strength modification for reduced heat transfer to lifting re-entry vehicles 10 p1372 A83-26160

A study of hypersonic low-density gas flows in low-pressure blowdown wind tunnels using pressure tanks 13 p1804 A83-30680

Low L/D aerobrake test at Mach 10 14 p1970 A83-32746

[AIAA PAPER 83-1509] 14 p1970 A83-32746

New transformations of S4 Modane hypersonic wind tunnel for ramjet missiles tests [ONERA, TP NO. 1983-24] 16 p2313 A83-36433

Developing mass spectrometric techniques for boundary layer measurement in hypersonic high enthalpy test facilities 18 p2689 A83-39937

HYPERSONICS

Computations of projectile Magnus effect at transonic velocities [AIAA PAPER 83-0237] 05 p0583 A83-16604

HYPERSPACES

Convolution equations in multidimensional spaces --- Russian book 05 p0681 A83-17120

Inter-class discrimination using synthetic discriminant functions /SDFs/ 09 p1266 A83-23539

On the global geometry of the Stephani universe 19 p2916 A83-41284

HYPERTENSION

NT POLYPEPTIDES

HYPERTENSION

Arterial hypertension and the level of professional work capacity of industrial workers 01 p0083 A83-10512

The 'volume-dependent' form of essential hypertension 03 p0379 A83-13617

The activity of renin in blood plasma, the indicators of central hemodynamics, and the water-electrolyte balance in patients with hypertension 03 p0379 A83-13622

The use of prostaglandin E2 during the treatment of essential hypertension which proceeds with high blood pressure 03 p0379 A83-13623

Clinical aspects of the disruption of the water-electrolyte metabolism during essential hypertension 03 p0381 A83-14343

Indices of hemodynamics in patients with hypertension according to echocardiography data 03 p0381 A83-14345

Cerebral circulation and the hemodynamics of lesser circulation in patients with bronchial asthma in combination with systemic arterial hypertension 05 p0673 A83-17162

Arterial hypertonia in miners working in deep mines 05 p0673 A83-17167

The reaction of the hypophyseal-adrenal system to emotional stress in patients with hypertension 05 p0674 A83-17200

A rare case of pulmonary hypertension 05 p0674 A83-17206

The results of focused and projector ultrasonic Doppler cardioaivulography /a study of patients with pulmonary normotension and hypertension/ 05 p0674 A83-17215

A circulating inhibitor of /Na+/ + K+/++ ATPase associated with essential hypertension 05 p0672 A83-17794

Hypertension and orthostatic hypotension in applicants for flying training and aircrew 06 p0797 A83-18197

The local cerebral blood flow and the local vascular reactivity during brain contusions in an experiment under conditions of arterial normal tension and hypertension 06 p0795 A83-18978

The condition of the resistive vessels of the extremities in rats with spontaneous /hereditary/ hypertension 07 p0975 A83-20985

Preventive screening as a method for the early detection of cardiovascular disease in railroad workers 07 p0978 A83-20996

The role of catecholamines in the development of spontaneous arterial hypertension in spontaneously hypertensive rats 08 p1146 A83-22119

Cardiovascular and endocrine effects of gravitational stresses /LBNP/ - The influence of angiotensin-converting enzyme inhibition with captopril 11 p1642 A83-27798

Psychological stress induces sodium and fluid retention in men at high risk for hypertension 12 p1763 A83-28925

Hypoxic pulmonary hypertension in the mast cell-deficient mouse 13 p1897 A83-30485

Physiological assessment of right-side and left-side cardiohemodynamics in patients with hypertension 13 p1906 A83-31395

State of the kidney and brain Renin-Angiotensin System (RAS) and of the pituitary-adrenal axis in rats with acute neurogenic hypertension 15 p2210 A83-34453

Electroencephalogram indicators and hypoxic shifts in patients with hypertension with different hemodynamic variations 15 p2213 A83-34951

The effect of magnetotherapy on the cardiovascular system of patients with hypertension 15 p2213 A83-34971

Hemodynamic shifts in response to isometric loads in humans in the case of various initial indicators of systemic blood circulation 16 p2398 A83-35910

Characteristics of the left ventricular blood expulsion phase during arterial hypertension and aortal stenosis 17 p2559 A83-38176

Mechanisms of the regulation of high cardiac output in patients with hypertension (angiocardiographic investigation) 17 p2559 A83-38177

Asymmetrical hypertrophy of the myocardium in patients with hypertension (According to echocardiographic data) 17 p2559 A83-38180

Drug therapy of hypertension in drivers 17 p2561 A83-38930

The effect of seduxen on hemodynamic reactions in patients with hypertension during emotional stress 18 p2735 A83-40550

The significance of the strength of the central nervous system in the variability of the reaction in sick persons to acetylcholin 18 p2736 A83-40578

Hemodynamic interrelations of the systemic and pulmonary blood circulation in the case of hypertension 19 p2880 A83-41426

The character of water-sodium changes in the bodies of patients with hypertension under the influence of various types of hypotensive therapies 19 p2881 A83-41427

The therapeutic effect of the cardioselective beta-blocker tenormin and its effect on parameters of the central, intracardiac, and regional hemodynamics in patients with hypertension 19 p2881 A83-41428

Systemic and renal hemodynamics in hypertension 19 p2881 A83-41429

The development of hypertrophy of the heart in the case of hypertension 19 p2881 A83-41430

The condition of hemodynamics in pulmonary blood circulation in patients with hypertension combined with chronic heart disease 19 p2881 A83-41432

Pulmonary blood circulation in patients with various types of hypertensive hearts 19 p2881 A83-41433

Parameters of the vegetative regulation of the cardiovascular system during the early development of hypertension 19 p2881 A83-41434

The relationship of hormonal and hemodynamic parameters during emotional stress in healthy individuals and patients with hypertension 19 p2881 A83-41435

The mathematical selection of information criteria for the differential diagnosis of renovascular hypertonia and hypertension 19 p2881 A83-41436

Prostaglandins of the renal vascular bed during arterial hypertension of various etiologies 19 p2881 A83-41437

A low-renin form of hypertension - Characteristics of the functional relationships of the renin-aldosterone pressor system 19 p2881 A83-41439

The EKG and physical work capacity in patients with hypertension 19 p2882 A83-41452

The semantic structure of interpersonal evaluations and self-evaluations in individuals with normal and elevated arterial pressure 19 p2885 A83-41838

Hypertension and orthostatic hypotension in applicants for spaceflight training and spacecrews - A review of medical standards 19 p2884 A83-42048

The functional condition of the brain during early forms of arterial hypertension in young individuals 21 p3187 A83-44661

Neurogenic conception as a basis for the investigation of the cerebral pathogenesis of hypertension 21 p3187 A83-44662

Physiological aspects of cardiohemodynamics during hypertension 21 p3188 A83-45304

HYPERTHERMIA

Physiological criteria of upper limits of body heating 02 p0223 A83-12256

The modification with methylated hematoporphyrin of the combined effect of radiation and hyperthermia in experiments on asynchronous and synchronous cell cultures 03 p0376 A83-14881

The role of central and peripheral serotonergic mechanisms 04 p0520 A83-15895

Histochemical changes in muscles and liver during physical loads and overheating /experimental investigation/ 05 p0669 A83-17174

The effect of prostaglandin F2-alpha on the thermoregulative peculiarities in rabbits 07 p0973 A83-20362

Degradation of the phospholipids of the outer and inner membranes of mitochondria under exposure to low temperature 07 p0974 A83-20844

The limitation of human performance in extreme heat conditions 10 p1459 A83-26307

Prostacyclin-induced hyperthermia - Implication of a protein mediator 11 p1641 A83-28756

Nitrogen metabolism during heat stress 12 p1765 A83-29314

Opposing actions of dibutyl cyclic AMP and GMP on temperature in conscious guinea-pigs 12 p1762 A83-29530

Role of bacterial endotoxins of intestinal origin in rat heat stress mortality 13 p1896 A83-30454

Work-heat tolerance in endurance-trained rats 13 p1897 A83-30466

Unusual core temperature decrease in exercising heart-failure patients 13 p1903 A83-30478

Role of surface area-to-mass ratio and work efficiency in heat intolerance 13 p1904 A83-30493

Effect of triiodothyronine on body temperature at rest and during exercise in dogs 13 p1898 A83-30508

Head and/or torso cooling during simulated cockpit heat stress 15 p2216 A83-34979

- The human element in air traffic control - Aeromedical aspects, problems, and prescriptions 15 p2214 A83-34981
- Hyperthermic responses to central injections of some peptide and non-peptide opioids in the guinea-pig 16 p2394 A83-36719
- Peptide and non-peptide opioid-induced hyperthermia in rabbits 16 p2396 A83-36985
- Pulmonary gas exchange in cats under a heat load 17 p2555 A83-37247
- The pattern of physical and mental work capacity depending on the level of hyperthermia in athletes 17 p2559 A83-38170
- The characteristics of the vasomotor reactions in the skeletal muscles and skin of cats during heat stress 19 p2871 A83-40817
- The functional condition of the body and several specific functions of women construction workers engaged in finishing work in hot climatic conditions 19 p2882 A83-41455
- Canine blood volume and cardiovascular function during hyperthermia 20 p3033 A83-43476
- The effect of controlled hyperthermia on several hemodynamic parameters in experimental conditions 21 p3185 A83-45324
- The physiological stability of humans to ergothermal effects 21 p3188 A83-45343
- Chronic low-sodium diet in rats - Hormonal and physiological effects during exercise in the heat 22 p3346 A83-45994

HYPERTONIA

U OSMOSIS

HYPERTROPHY

U GROWTH

HYPERVELOCITY

- Introductory aerothermodynamics of advanced space transportation systems 05 p0585 A83-16695
[AIAA PAPER 83-0406]

HYPERVELOCITY ACCELERATORS

U HYPERVELOCITY GUNS

HYPERVELOCITY CRATERING

U HYPERVELOCITY PROJECTILES

U PROJECTILE CRATERING

HYPERVELOCITY FLOW

- Heat-transfer distributions on bionics at incidence in hypersonic-hypervelocity He, N₂, air, and CO₂ flows [AIAA PAPER 83-1508] 14 p1970 A83-32745

HYPERVELOCITY GUNS

- Magnetic acceleration of interstellar probes 01 p0016 A83-10703

HYPERVELOCITY IMPACT

- Detonation properties of 1,3,5-triamino-2,4,6-trinitrobenzene when impacted by hypervelocity projectiles 04 p0464 A83-15473
- The Giotto dust protection system --- for encounters with comet Halley 05 p0607 A83-17434
- Cratering experiments in sands and a trial for general scaling law 07 p0950 A83-21318
- Hypervelocity erosion of carbon-carbon composites by laser simulation [AIAA PAPER 83-1440] 14 p1986 A83-32711
- Hypervelocity impact on the Giotto Halley mission dust shield - Momentum exchange and measurement 15 p2128 A83-35023
- Designing space vehicle shields for meteoroid protection - A new analysis 15 p2128 A83-35028
- The critical energy density and the inelasticity coefficient for asteroidal catastrophic collisions 15 p2250 A83-35029
- High-velocity impact experiments needed to improve our understanding of the asteroids 15 p2250 A83-35030
- Some consequences of meteoroid impacts on Saturn's rings 22 p3388 A83-47086

HYPERVELOCITY LAUNCHERS

- Electric rail gun projectile acceleration to high velocity [AIAA PAPER 82-1939] 02 p0146 A83-12501
- Fast electromagnetic launchers 21 p3125 A83-44103

HYPERVELOCITY PROJECTILES

- Electromagnetic projectile acceleration utilizing distributed energy sources 01 p0036 A83-10620
- Electric rail gun projectile acceleration to high velocity [AIAA PAPER 82-1939] 02 p0146 A83-12501
- Computations of projectile Magnus effect at transonic velocities [AIAA PAPER 83-0237] 05 p0583 A83-16604
- A semi-empirical approach for the prediction of aft-body drag of supersonic projectiles with base bleeding 15 p2119 A83-33489
- High-velocity impact experiments needed to improve our understanding of the asteroids 15 p2250 A83-35030
- Hypervelocity acceleration techniques - A review of existing capabilities and prospects for future developments 15 p2125 A83-35032

HYPERVELOCITY WIND TUNNELS

NT CASCADE WIND TUNNELS

NT SHOCK TUNNELS

- Flowfield surveying techniques used in the NSW hypervelocity wind tunnel no. 9 01 p0052 A83-11064

- On the simulation of the hypervelocity regime of flow past bodies in wind tunnels 11 p1526 A83-27714
- Parameter estimation for thermocouples imbedded in Space Shuttle wind tunnel test articles with a nonisothermal wall [AIAA PAPER 83-1533] 15 p2127 A83-34920

HYPERVENTILATION

- A study of the local irregularity of the ventilation of the lungs 01 p0082 A83-10485
- Time course of posthyperventilation breathing in humans depends on alveolar CO₂ tension 13 p1903 A83-30491
- Influence of body CO₂ stores on ventilatory dynamics during exercise 22 p3347 A83-45988

HYPERVEOLEMIA

- The 'volume-dependent' form of essential hypertension 03 p0379 A83-13617

HYPNOSIS

- The practical application of hypnosis in the athletic activity of young athletes 01 p0082 A83-10506
- Psychotherapy during the treatment of seasickness 03 p0381 A83-14344

HYPOCAPNIA

- Blood osmolality during in vivo changes of CO₂ pressure 13 p1902 A83-30460
- Inhibition of hypoxia-induced ADH release by meclofenamate in the conscious dog --- AntiDiuretic Hormone 17 p2554 A83-36993

HYPODYNAMIA

- Metabolism during hypodynamia --- Russian book 02 p0221 A83-11950
- Effect of suspension hypokinesia/hypodynamia on glucocorticoid receptor levels in rat hindlimb muscles 11 p1640 A83-27836

HYPOELASTICITY

- Surface instability and splitting in compressed brittle elastic solids containing crack arrays [ASME PAPER 82-WA/APM-16] 04 p0498 A83-15682

HYPOKINESIA

- Disturbances of conditioned reflex activity during hypokinesia in rats and the normalizing effect of motor loads 01 p0079 A83-10534
- The changes in cardiac activity during physical exercises in an athletic arena and swimming pool following prolonged antithrostatic hypokinesia /based on biotelemetry data/ 05 p0673 A83-17171
- The significance of the level of general physical work capacity in the development of fatigue in workers in conditions of occupational hypokinesia 05 p0673 A83-17194
- The peculiarities of the functional condition of the adrenal cortex in old rats during immobilization stress 05 p0672 A83-17600
- The effect of 24, 25-dihydroxycalciferol on the chemical composition of the bone tissue of rats during hypokinesia 06 p0795 A83-18987
- The behavior of blood serum proteins separated by electrophoresis in animals during hypokinesia 06 p0795 A83-19373
- The hormonal dependence of the initial stages of heparin clearance during immobilization stress in rats 07 p0973 A83-20242
- The effect on the human body of a high concentration of carbon dioxide and hypokinesia 07 p0978 A83-20883

- The effect of azaperone on the dynamics of the stress-reaction and the content of catecholamines in the adrenal glands of rats during immobilization stress 07 p0975 A83-20984

- The contractile function of the heart and the ultrastructure of the cardiomyocytes during prolonged hypokinesia in growing animals 09 p1322 A83-25169

- Calcium-phosphorous metabolism and prevention of its disorders in hypokinetic rats 11 p1636 A83-27788
- Hormonal changes in antithrostatic rats 11 p1637 A83-27800

- Changes in osteoblastic activity due to simulated weightless conditions 11 p1640 A83-27831
- Is suppression of bone formation during simulated weightlessness related to glucocorticoid levels 11 p1640 A83-27833

- Effect of suspension hypokinesia/hypodynamia on glucocorticoid receptor levels in rat hindlimb muscles 11 p1640 A83-27836

- Synthesis of amino acids in weight bearing and non-weight bearing leg muscles of suspended rats 11 p1640 A83-27838

- Weightlessness hypokinesia - Significance of motor unit studies 11 p1640 A83-27839
- Short term /1 and 3 day/ cardiovascular adjustments to suspension antithrostatic rats 11 p1640 A83-27842

- Changes in the vegetative balance of an organism during experimental hypokinesia 14 p2061 A83-31972

- The microcirculatory condition during burn shock in rats after a prolonged limitation of motor activity 14 p2061 A83-31973

- Bone tissue of hypokinetic rats - Effects of 24,25-dihydroxycalciferol and varying phosphorus content in the diet 14 p2064 A83-32692

- Rheographic investigations of the stroke volume of the heart in antithrostatic hypokinesia 15 p2214 A83-35047

- Nonspecific esterases of the extramural ganglia of the autonomous nervous system in rabbits during acute experimental emotional stress 17 p2556 A83-38175

- Morphological changes in the adenohypophysis during the recovery period following single individually-graded physical loads 17 p2556 A83-38196

- The effect of a decreased functional load on a skeletal muscle 17 p2560 A83-38197

- The condition of the physiological functions of female workers occupied with visually stressful types of work at a low level of motor activity 19 p2882 A83-41454

- Tibial changes in experimental disuse osteoporosis in the monkey 19 p2876 A83-41859

- The effect of hypokinesia on lipid metabolism in adipose tissue [IAF PAPER 83-189] 23 p3494 A83-47305

- On the functional state of the pituitary-adrenal-axis in rats under different conditions of motor activity 23 p3496 A83-48448

HYPOTENSION

- The effects of hypotensive drugs on the humoral factors of the regulation of blood circulation 03 p0380 A83-13631

- Hypertension and orthostatic hypotension in applicants for flying training and aircrew 06 p0797 A83-18197

- ADH responses to volume shifts in the low pressure system --- AntiDiuretic Hormone 11 p1636 A83-27781

- The intensity of kininergic reactions of the cardiovascular system for various levels of the activity of the kallikrein-kinin system in blood plasma 14 p2064 A83-32569

- Hypertensive and orthostatic hypotension in applicants for spaceflight training and spacecrews - A review of medical standards 19 p2884 A83-42048

HYPOTHALAMUS

- The role of catechol-o-methyltransferase in catecholamine transformations in the hypothalamus of rats at long-term intervals after irradiation 03 p0377 A83-14886

- The regulation of the defense functions of organisms --- Russian book 04 p0520 A83-15826

- The peripheral and central effects of gamma-aminobutyric acid on the vascular thermoregulatory reaction in rabbits 07 p0973 A83-20361

- The effect of prostaglandin F₂-alpha on the thermoregulative peculiarities in rabbits 07 p0973 A83-20362

- The characteristics of the mechanism of action of cyproheptadine /peritol/ on the activity of the hypothalamo-hypophysial-adrenal system 07 p0974 A83-20979

- The condition of the hypothalamo-hypophysial-adrenal system during sudden cardiac death 09 p1322 A83-23982

- The role of the middle hypothalamus structures in the regulation of the glucose content in the blood and the glycogen content in the liver 13 p1895 A83-30304

- The role of suprachiasmatic nuclei of the anterior hypothalamus in the organization of the circadian rhythms of locomotor activity in rats 14 p2063 A83-32564

- The effect of electrostimulation of the hypothalamus on the methylation of DNA from the livers of rats 19 p2876 A83-41844

- Serotonin in individual hypothalamic nuclei of rats after space flight on biosatellite COSMOS 1129 [IAF PAPER 83-188] 23 p3494 A83-47304

HYPOTHERMIA

- Fibrillation of the heart at low temperatures 01 p0081 A83-10919

- Restoration of thermoregulatory response to body cooling by cooling hands and feet 03 p0378 A83-13578

- Heat loss and tissue metabolism in white mice during the recovery after acute hypothermia 04 p0520 A83-15896

- The effect of short-term hypothermia on the monoamine oxidase enzyme system in the rat brain 06 p0795 A83-18989

- The response of the surfactant system and the air-blood barrier of the lungs to overall acute hypothermia
07 p0974 A83-20977
- The effect of hypothermia on the glutamate dehydrogenase activity in the brain
07 p0975 A83-20982
- Restraint hypothermia in cold-exposed rats at 3 G and 1 G
11 p1637 A83-27806
- Opposing actions of dibutyl cyclic AMP and GMP on temperature in conscious guinea-pigs
12 p1762 A83-29530
- A review of the literature concerning resuscitation from hypothermia. I - The problem and general approaches
14 p2068 A83-32689
- A review of the literature concerning resuscitation from hypothermia. II - Selected rewarming protocols
15 p2214 A83-34978
- Impaired memory registration and speed of reasoning caused by low body temperature
19 p2880 A83-41133
- Cold stress at high altitudes
21 p3183 A83-44073
- Rheological properties of the arterial and venous blood of rats following intravital icing of the extremities
21 p3185 A83-45325
- ## HYPOTHESES
- NT VORTICITY TRANSPORT HYPOTHESIS
Closure hypotheses from the method of smoothing for coherent wave propagation in discrete random media
07 p0989 A83-20792
- Large numbers hypothesis. II - Electromagnetic radiation
16 p2408 A83-36986
- ## HYPOTONIA
- An investigation of the rigidity of a human muscle depending on its length
12 p1766 A83-29318
- ## HYPOVENTILATION
- A study of the local irregularity of the ventilation of the lungs
01 p0082 A83-10485
- The physiological advisability of voluntary control of respiration in athletes
17 p2558 A83-38169
- ## HYPOVOLEMIA
- Morphological and functional peculiarities of the myocardium during extreme coronary insufficiency
05 p0671 A83-17219
- Beta adrenergic blockade and erythropoietic production in rats after hypoxia and hypovolemia
09 p1321 A83-23875
- ## HYPOXIA
- The blood flow in bronchial vessels during hypoxia
01 p0078 A83-10481
- The age-related peculiarities of the development of hypoxia in skeletal muscles during acute hypoxic hypoxia
01 p0078 A83-10483
- The stages of hypoxic loads
01 p0082 A83-10484
- The changes in the structural components of the walls of the small vessels and the composition of the peripheral blood during immune and hypoxic effects on the heart
01 p0078 A83-10487
- The gas composition and the acid-base state of the blood in twins when breathing a hypoxic gas mixture
01 p0082 A83-10492
- The antihypoxic effectiveness of alimentary fasting
02 p0219 A83-11521
- Effect of short term exposure to hypoxia on systolic time intervals
02 p0223 A83-12252
- Augmentation of the resistance of the myocardium to pituitrin damage via adaptation to hypoxia
03 p0373 A83-13598
- Histological and histochemical investigations of the locomotor system during general hypoxia
03 p0375 A83-13640
- The oxygen effect and the adaptive reactions of cells.
IX - The dependence of the radioprotective effectiveness of gaseous hypoxia on its degree and duration in neonatal and adult mice
03 p0376 A83-14879
- The radioprotective effect of a gaseous hypoxic mixture on hemopoiesis in mice
03 p0377 A83-14889
- Effects of time and duration of exposure to 12% O₂ and prior food deprivation on hypoxic hypophagia of rats
04 p0519 A83-15536
- Arterial oxygen saturation at altitude using a nasal cannula
04 p0521 A83-15537
- The adaptation of the heart to chronic high-altitude hypoxia
04 p0522 A83-15780
- The correlation of the parameters of the cardiac rhythm with the physical work capacity of humans during the adaptation to high-altitude hypoxia
04 p0522 A83-15781
- Effects of exposure to low O₂ or high CO₂ environments on respiration in hibernating hamsters and ground squirrels
04 p0520 A83-16009
- Adaptation and resistance to hypoxia in light of the functional activity of the antisystems
05 p0669 A83-17161
- The improvement of the myocardial resistance to pituitrin via adaptation to hypoxia
05 p0670 A83-17186
- Comparative brain oxygenation and mitochondrial redox activity in turtles and rats
05 p0671 A83-17327
- Attenuation of hypoxic pulmonary vasoconstriction by pulsatile flow in dog lungs
05 p0672 A83-17336
- Changes in the affinity of the respiratory enzymes for oxygen as a factor of the physiological regulation of oxygen supply to the tissues
05 p0672 A83-17637
- An experimental study of the effects of hypobaric hypoxia on the cerebral blood flow and the metabolism of the brain
06 p0794 A83-18342
- A rheological investigation of the circulatory system during high-altitude hypoxia and an orthostatic test
06 p0798 A83-19374
- The prevention of disorders of the contractile function of the heart during stress by means of preliminary adaptation of the animals to hypoxia
07 p0972 A83-19920
- The changes in the erythropoiesis-stimulating action of the erythrocytic factors during the blocking of cells of the mononuclear phagocyte system
07 p0972 A83-19921
- The effect of adrenalectomy and hydrocortisone on the carbohydrate metabolism in the lungs and myocardium during chronic hypoxia
07 p0972 A83-19922
- Effects of hypoxia on the luminance threshold for target detection
07 p0977 A83-20778
- Chemoreceptor sensitivity in adaptation to high altitude
07 p0977 A83-20780
- Evidence of genetic differences in acute hypoxia survival
07 p0974 A83-20781
- The content of ubiquinone and vitamin E in rat tissues during experimental focal myocarditis and hypoxic hypoxia
07 p0974 A83-20980
- Several indicators of the EKG and metabolic processes during an experimental coronary spasm in rats exposed to conditions of hypoxia in combination with hypercapnia
07 p0975 A83-20986
- Beta adrenergic blockade and erythropoietic production in rats after hypoxia and hypovolemia
09 p1321 A83-23875
- An investigation of the genotypic conditionality of the gas composition and acid-base state indicators of the blood during various effects on the body
09 p1323 A83-25152
- The sympathicoadrenal system during hypoxic conditions
09 p1321 A83-25153
- The problem of tissue adaptation to hypoxia
09 p1322 A83-25168
- The architectonics of the arterial bed in the brain hemispheres of rats during normal conditions and after a stay at a 'height' of 5600 m
10 p1454 A83-26788
- The pathological and physiological characteristics of the deficiencies of the mitral valve in animals as a consequence of high-altitude hypoxia
11 p1641 A83-28764
- Hypoxia - USAF experience 1970-1980
12 p1764 A83-28936
- The effect of hypoxia on the functional condition of the external respiratory system in mature and old age
12 p1765 A83-29310
- Physiological mechanisms for fatigue from strenuous muscular activity
13 p1900 A83-30302
- Effect of increased blood oxygen affinity on skeletal muscle surface oxygen pressure fields
13 p1897 A83-30457
- Effects of hypercapnia, hypoxia, and rebreathing on heart rate response during apnea
13 p1902 A83-30462
- Effects of hypercapnia, hypoxia, and rebreathing on circulatory response to apnea
13 p1902 A83-30463
- Hypoxic pulmonary hypertension in the mast cell-deficient mouse
13 p1897 A83-30485
- The direct reactions of smooth muscles of the major cerebral arteries to acute hypoxia and hypercapnia
14 p2061 A83-31971
- The effect of products of erythrocyte degradation on the migration of hemopoietic stem cells in lethally-irradiated mice
14 p2062 A83-32065
- An evaluation of the possibility of predicting the individual radiosensitivity of rats by their reaction to hypoxia and the administration of adrenocorticotropin
14 p2062 A83-32069
- The aminergic control of the cerebral arteries
14 p2063 A83-32099
- Polymeric prostaglandin PGBx and other prostaglandin polymers prolong survival of the heart of the hypoxic mouse
14 p2064 A83-32688
- Barometric pressures at extreme altitudes on Mt. Everest
14 p2068 A83-32811
- Site of pulmonary hypoxic vasoconstriction studied with arterial and venous occlusion
14 p2064 A83-32814
- Hyperpnea of exercise at various PIO₂ in normal and carotid body-denervated ponies
14 p2064 A83-32820
- Effect of hypoxia and hypercapnia on catecholamine content in cat carotid body
14 p2064 A83-32822
- The effect of stress on the tensility, Starling's mechanism, and resistance of the myocardium to hypoxia
14 p2066 A83-33335
- Changes of sidman avoidance behaviour of rats induced by hypoxia
15 p2209 A83-33542
- Electroencephalogram indicators and hypoxic shifts in patients with hypertension with different hemodynamic variations
15 p2213 A83-34951
- Heart function and certain mechanisms for its regulation when simulating the adaptation to hypoxia by administering 2,4-dinitrophenol
15 p2210 A83-34958
- Electron-microscope cytochemical study of ribonucleoprotein particles in cerebral cortex neurons in a posthypoxic period
16 p2395 A83-36812
- The role of cellular membranes in the resistance of plants to hypoxia and anoxia
16 p2396 A83-36839
- O₂ transport during two forms of stagnant hypoxia following acid and base infusions
17 p2554 A83-36992
- Inhibition of hypoxia-induced ADH release by meclofenamate in the conscious dog --- AntiDiuretic Hormone
17 p2554 A83-36993
- Hypoxic constriction of alveolar and extra-alveolar vessels in isolated pig lungs
17 p2555 A83-36994
- The effect of insulin on the reaction of the coronary and systemic blood circulation during the inspiration of hypoxic mixtures
17 p2555 A83-37239
- Several mechanisms of the transport of oxygen and its utilization in the skeletal muscles during acute hemic hypoxia
17 p2555 A83-37240
- The breathing patterns of humans during hypercapnia and hypoxia
17 p2558 A83-37243
- The regulation of the breathing pattern during muscular activity in conditions of normal and altered chemoreceptor stimulation
17 p2558 A83-37244
- The diffusion capability of the hematoparenchymatous barrier for oxygen during the breathing of helium-oxygen gas mixtures
17 p2555 A83-37245
- The functional condition of the respiratory center during the coughing reflex in normoxic and hypoxic conditions
17 p2556 A83-37249
- Effects of various levels of hypoxia on plasma catecholamines at rest and during exercise
18 p2734 A83-40361
- Age-related peculiarities of the functional condition of the vascular system in patients with bronchial asthma in the case of mountain-climate therapy
18 p2735 A83-40569
- The change in the impulse activity of bulbar respiratory neurons in conditions of acute hypoxia
19 p2871 A83-40813
- The role of changes in the concentration of oxygen in the case of the reproductive death of cells in vitro. III - The modification of the radiosensitivity by oxygen-reducing compounds
19 p2874 A83-41005
- The modification of the intestinal syndrome with the aid of a gas hypoxic mixture at various conditions of the irradiation of animals
19 p2874 A83-41015
- Predicting radiation damage on the basis of the response of an organism to acute hypoxia
19 p2875 A83-41018
- Gender differences in hypoxic vascular response of isolated sheep lungs
19 p2875 A83-41135
- Oxygen deficit and stores at onset of muscular exercise in humans
19 p2880 A83-41137
- Fluid and electrolyte homeostasis during prolonged exercise at altitude
20 p3034 A83-43481
- Effect of prolonged exercise at altitude on the renin-aldosterone system
20 p3034 A83-43482
- Effect of catecholamine depletion on ventilatory control in unanesthetized normoxic and hypoxic rats
20 p3033 A83-43486
- Effects of chronic hypoxia on pulmonary vascular responses to biogenic amines
20 p3033 A83-43487
- Modification by sulpiride, pimozide, or domperidone of apomorphine's effects on learning in hypoxic rats
21 p3183 A83-43995
- The characteristics of the immunological reactivity of humans in conditions of a mountain climate
21 p3188 A83-45341
- Pulmonary gas exchange on the summit of Mount Everest
22 p3347 A83-45982
- Maximal exercise at extreme altitudes on Mount Everest
22 p3347 A83-45983
- Renin-aldosterone and angiotensin-converting enzyme during prolonged altitude exposure
22 p3347 A83-45984
- Site and sensitivity for stimulation of hypoxic pulmonary vasoconstriction
22 p3345 A83-45986
- Effects of hypoxia on norepinephrine release and metabolism in dog pulmonary artery
22 p3346 A83-45989
- Effect of ethanol and naloxone on control of ventilation and load perception
22 p3348 A83-45996
- Methods of increasing the tolerance of humans to acute hypoxia
23 p3496 A83-47101

The interaction of cardiac ventricles in intact dogs during 3-5 days of high altitude adaptation 23 p3496 A83-48566

The physiological mechanisms for supplying the energy requirements of an organism during a decrease in the concentration of hemoglobin in the blood 23 p3496 A83-48567

HYPSOGRAPHY

The validity of hypsometric maps of the moon and planets 17 p2614 A83-37008
The interior of Venus and Tectonic implications 17 p2616 A83-37411

HYPSOMETERS

A low-power hypsometer-type barometer for remote weather stations 10 p1423 A83-26496

HYSTERESIS

Hysteresis and stochastic phenomena in nonlinear optical systems 04 p0534 A83-15257
Experimental study of hysteresis phenomena in a diffraction-radiation generator 06 p0754 A83-19335
The phenomenon of hysteresis in the reflection of light at a boundary with a nonlinear medium in the presence of a transition layer 07 p0992 A83-19973
Transient and stationary properties in bistable operation of a GaAs laser coupled to an external resonator 08 p1106 A83-21885
A one-dimensional-map model for noise-induced transitions between bistable states 11 p1649 A83-28066
Magnetoplasma lamination due to microwave gyroresonant heating 15 p2237 A83-35269
Hysteresis and nonlinear thermooptic waves in a semiconductor Fabry-Perot interferometer 17 p2581 A83-38972
Aerodynamic aspects of aircraft dynamics at high angles of attack 21 p3085 A83-43964

I BEAMS

Optimal design of thin walled I beams for extreme natural frequency of torsional vibrations 09 p1276 A83-23340
On elastic-plastic analysis of I-beams in bending and torsion 20 p3003 A83-42929

IAPETUS

Crater numbers and geological histories of Iapetus, Enceladus, Tethys and Hyperion 08 p1191 A83-23290
The dark side of Iapetus 10 p1518 A83-25513
Eight-color photometry of Hyperion, Iapetus, and Phoebe 11 p1684 A83-27366
Albedo asymmetry of Iapetus 17 p2623 A83-38601

ICBM (MISSILES)

U INTERCONTINENTAL BALLISTIC MISSILES

ICE

NT BAY ICE
NT GLACIERS
NT ICE FLOES
NT ICEBERGS
NT LAKE ICE
NT LAND ICE
NT SEA ICE
Rheology of ices - A key to the tectonics of the ice moons of Jupiter and Saturn 01 p0129 A83-11497
Scattering by single ice needles and plates at 30 GHz 02 p0141 A83-12624
Structure and origin of cometary nuclei 03 p0415 A83-13382
Thermal- and plasma-induced molecular redistribution on the icy satellites 03 p0133 A83-13831
Formaldehyde formation in a H₂O/CO₂ ice mixture under irradiation by fast ions 03 p0424 A83-14196
Charge deposition on ice particles by positive streamers 04 p0518 A83-16018
Mass-radius relationships in icy satellites after Voyager 05 p0703 A83-16958
Compression of ice VII to 500 kbar --- possible solid modifications of planetary water 05 p0707 A83-17844
Effects on skylight at South Pole Station, Antarctica, by ice crystal precipitation in the atmosphere 06 p0778 A83-18585
The effects of shape on electromagnetic scattering by ice crystals 06 p0746 A83-18717
Polarization catastrophe model of static electrification and spokes in the B-ring of Saturn 07 p1028 A83-20083
Properties of amorphous H₂O ice and origin of the 3.1-micron absorption 07 p1024 A83-21224
The dynamic tensile strength of ice and ice-silicate mixtures 08 p1129 A83-22367

A theoretical determination of capture efficiency of small columnar ice crystals by large cloud drops 08 p1142 A83-23010

Ice in Comet Bowell 08 p1186 A83-23275
The stability of ground ice in the equatorial region of Mars 09 p1366 A83-25072

A laboratory study of the infrared spectra of interstellar ices 10 p1502 A83-25653
Thermal infrared constraints on ammonia ice particles as candidates for clouds in the atmosphere of Saturn 11 p1684 A83-27361

The effect of the charge of the surface of ice grains and the nucleus of a comet on the rate of their sublimation 11 p1679 A83-27876

The durability of dust matrices formed during the sublimation of dusty ice --- in comets 11 p1679 A83-27888

On the size, shape, and orientation of noctilucent cloud particles 11 p1616 A83-28094
Cl-36 and Mn-53 in Antarctic meteorites and (Be-10)-(Cl-36) dating of Antarctic ice 12 p1797 A83-29175

The attenuation and scattering of infrared radiation by polydisperse systems comprising platelets and cylinders of ice 13 p1883 A83-30029
A statistical study of abnormal depolarization 14 p2000 A83-32419

Observation of ice mantles toward HD 29647 14 p2107 A83-33232

Ice particles in circular orbits around the sun 14 p2101 A83-33288

Comment on Mars residual North Polar Cap - Earth-based spectroscopic confirmation of water ice as a major constituent and evidence for hydrated minerals' by Roger N. Clark and Thomas B. McCord 14 p2113 A83-33470

On the effect of radiative exchange in the 8 to 12 micron spectral region on the diffusional growth of ice crystals 15 p2205 A83-34062

Interstellar ice grains in the Taurus molecular clouds 15 p2261 A83-34385

A calorimetric method for the measurement of the Stefan-Boltzmann constant 15 p2164 A83-34412
Studies of proton-irradiated cometary-type ice mixtures 15 p2270 A83-34716

The cohesive and adhesive strength of ice --- adhering to stainless steel, titanium, and anodized aluminum engineering structures 15 p2130 A83-35069

Dry ice II, a new polymorph of CO₂ 16 p2437 A83-35996

Single- and multiple-crater induced nosetip transition 16 p2293 A83-36078

Status of laboratory experiments on ice mixtures and on the 12 micron H₂O ice feature --- suggesting interstellar IR absorption 16 p2431 A83-36670

The chemical composition and thermal history of the ice of a cometary nucleus 16 p2425 A83-36679
Saturn's ionosphere - A corona of ice particles? 16 p2438 A83-36781

The polarization structure of backscattering by water-droplet and ice clouds 18 p2730 A83-40080
Impact experiments on ice --- for understanding cratering on Callisto and Mimas 18 p2779 A83-40322

Charged particle erosion of frozen volatiles in ice grains and comets 19 p2914 A83-40728

The lifetime of cometary ice nuclei and the secular decrease of the brightness of periodic comets 19 p2915 A83-40820

Effect of ice-induced cross-polarization on digital earth-space links 19 p2833 A83-41400
Fraunhofer diffraction by ice crystals suspended in the atmosphere 20 p3028 A83-43465

The heterogeneous condensation of interstellar ice grains 20 p3077 A83-43665
Tidal dissipation in small viscoelastic ice moons - The case of Enceladus 21 p3239 A83-44082

The impact of ice along satellite-to-earth paths on 11-GHz depolarization statistics 22 p3275 A83-46531

An experimental study of the ice column habit transitions --- crystal growth in atmosphere 24 p3611 A83-49690

Evidence for the production of ice particles in clouds due to aircraft penetrations 24 p3612 A83-49691
An airborne comparison of three PMS probes --- for precipitation particle measurement 24 p3613 A83-49707

ICE ENVIRONMENTS

Measurements of ice depolarization at 28.56 GHz using the COMSTAR beacon simultaneously with a 16.5 GHz polarization diversity radar 01 p0032 A83-11354
An innovative type of icebreaker for the arctic environment 15 p2242 A83-34856

ICE FLOES

Some features of the spatial structure of the Arctic Ocean ice cover in connection with turbulent friction and geostrophic capture of tide waves 01 p0077 A83-10833

ICE FORMATION

NT CLOUD GLACIATION

Ice detector evaluation for aircraft hazard warning and undercooled water content measurements 01 p0009 A83-10187

Ice distribution and winter surface circulation patterns, Kachemak Bay, Alaska 02 p0198 A83-12038
Crystal size and orientation in ice grown by droplet accretion in wet and spongy regimes 02 p0214 A83-12238

A similarity analysis of the droplet trajectory equation 03 p0315 A83-13133

Automatic apparatus for nucleation investigations --- crystalline phase detection 03 p0329 A83-14171
Radar backscattering of microwaves by spongy ice spheres 04 p0517 A83-15942

The Air Force Flight Test Center Palletized Airborne Water Spray System [AIAA PAPER 83-0030] 05 p0594 A83-16472

An analytical evaluation of the icing properties of several low and medium speed airfoils [AIAA PAPER 83-0109] 05 p0579 A83-16525

Aircraft icing roughness features and its effect on the icing process [AIAA PAPER 83-0111] 05 p0666 A83-16527

NASA Lewis Research Center's program on icing research [AIAA PAPER 83-0204] 05 p0577 A83-16582

Helicopter icing - Testing and certification 06 p0716 A83-18381

Icing analysis of an unprotected aircraft radome 06 p0791 A83-18413

Correlation of slant path ice depolarization events at 28.56 GHz with radar reflectivity structure and the determination of ice depolarization statistics for Wallops Island, Virginia 06 p0744 A83-18700

Research on contaminated wings, current issues --- concerning icing conditions and aerodynamic effects [AIAA PAPER 83-0277] 06 p0715 A83-19584

Numerical simulation of ice/frost formation on the external tank of the Space Shuttle in varying environments [AIAA PAPER 83-0524] 06 p0722 A83-19592

Microwave Ice Accretion Measurement Instrument /MIAMI/ 08 p1045 A83-22163

Wind tunnel study of icing and de-icing on oscillating rotor blades [ONERA, TP NO. 1982-116] 09 p1199 A83-24327

"Scaling" analysis of the ice accretion process on aircraft surfaces [ASME PAPER 82-WA/HT-39] 10 p1373 A83-25693

Operation of ILS during snow and ice conditions 11 p1527 A83-27969

Use of simulated ice shapes in known icing certification 14 p1973 A83-32936

The dependence of ice formation on the evolution of the liquid phase 15 p2204 A83-34052

Numerical simulation of airfoil ice accretion [AIAA PAPER 83-0112] 16 p2297 A83-36042

U.S. Army helicopter icing developments [SAE PAPER 821504] 17 p2459 A83-38011

Preliminary results of the AFGL icing study [AD-A129843] 17 p2549 A83-38718

Measured cloud data obtained in Northwest and Great Lakes United States and northern Canada during icing certification tests 17 p2549 A83-38719

Determination of supercooled liquid water content by measuring rime rate 18 p2721 A83-39116

Prediction of ice/frost growth on insulated cryogenic tanks 18 p2646 A83-40019

Effects of growth temperatures and surface roughness on crystal orientation of ice accreted in a dry regime 18 p2729 A83-40041

The short-range forecasting of meteorological conditions of the icing of aircraft on the ground and the runway at the Sofia airport 19 p2868 A83-41585

Experimental comparison of icing cloud instruments [AIAA PAPER 83-0026] 19 p2794 A83-42099

The influence of radiative transfer on the mass and heat budgets of ice crystals falling in the atmosphere 22 p3341 A83-46851

Hail growth in an Oklahoma multicell storm 22 p3341 A83-46854
FAA rotorcraft icing regulations and directions 22 p3251 A83-46927

A technique for investigating graupel and hail development 22 p3342 A83-46940

Solar system ice - Amorphous or crystalline? 24 p3671 A83-48809

- Observation of ice aggregation at temperatures near -50
C 24 p3612 A83-49699
- Droplet spectra and liquid water content measurements in aircraft icing environments
[AD-A122516] 24 p3614 A83-49718
- Characteristics of icing conditions in wintertime stratiform clouds 24 p3614 A83-49719
- Microphysical influences on aircraft icing 24 p3546 A83-49722
- Radar and aircraft observations of generating cells --- tropospheric cumulus-like clouds generating ice crystals 24 p3615 A83-49723

ICE MAPPING

- Survey paper on remote sensing techniques to map snow cover 01 p0061 A83-10011
- The application of microwave remote sensing for snow and ice research 01 p0064 A83-10088
- Accuracy of operational snow and ice charts 01 p0074 A83-10090
- Microwave radiance of early fall sea ice at 1.55 cm 01 p0076 A83-10091
- Satellite laser altimeter for measurement of ice sheet topography 01 p0021 A83-10092
- Ice-sheet dynamics by satellite laser altimetry 01 p0064 A83-10093
- Tidal phenomena in Arctic Ocean ice /according to space data/ 01 p0077 A83-10832
- The utilization of infrared /IR/ aerial and space observations of Arctic seas in navigation and during the solution of other national-economic problems 01 p0077 A83-10836
- Multispectral radiation detection of small changes in target emissivity --- ice measurements on space shuttle external tank 03 p0327 A83-13795
- An algorithm to interface Nimbus-7 SMMR data with the AES ice modelling grid for the Beaufort Sea 03 p0372 A83-14284
- The permanently sparse areas of ice cover in the open regions of the Okhotsk Sea 04 p0519 A83-15058
- Analysis and retracking of continental ice sheet radar altimeter waveforms 09 p1305 A83-24288
- Sea ice motion measurements from Seasat SAR images 09 p1320 A83-24313
- Nimbus 7 SMMR observations of the Bering Sea ice cover during March 1979 10 p1452 A83-26345
- On the seasonal sea ice cover of the Sea of Okhotsk 10 p1452 A83-26346
- Norwegian remote sensing experiment in a marginal ice zone 13 p1894 A83-31198
- Ice and suspended matter as hydrothermodynamic tracers on the basis of data from multispectral satellite surveys --- Russian book 14 p2059 A83-32575
- Mapping snow and ice and other land cover categories in south-central Alaska 17 p2532 A83-38355
- Some aspects of the application of space photographs in the compilation of glaciological maps 18 p2706 A83-40125
- Radarsat - The challenge of daily satellite ice reconnaissance 19 p2861 A83-41342
- ERS-1 - An ice and ocean monitoring mission 20 p2938 A83-42826

ICE NUCLEI

- A comparative study of the rates of development of potential graupel and hail embryos in high plains storms 06 p0790 A83-18265
- Observation of ice crystal formation in lower Arctic atmosphere 06 p0790 A83-18266
- Ice nucleus characteristics of Mount St. Helens effluents 07 p0969 A83-20210
- Ice crystal observations at 1.8 cm wavelength using a polarization diversity radar 11 p1629 A83-27066
- The measurement of the size distribution of atmospheric ice nuclei, taking into consideration humidity 15 p2204 A83-34057
- Destruction of ice grains in T Tauri stars 20 p3068 A83-42450
- An application of chemical kinetic theory and methodology to characterize the ice nucleating properties of aerosols used for weather modification 22 p3342 A83-46942
- Contact ice nucleation by submicron atmospheric aerosols 24 p3612 A83-49692
- Measurements of natural ice nuclei with a continuous flow diffusion chamber 24 p3612 A83-49693
- Ice crystal and ice nucleus measurements in cap clouds 24 p3614 A83-49713

ICE OBSERVATION**U ICE REPORTING****ICE PACKS****U SEA ICE****ICE PREVENTION**

- Design of an aircraft ice detector using microcomputer electronics to enhance system availability 01 p0009 A83-11097
- The icing of aircraft gas turbine engines 03 p0280 A83-14619

- NASA Lewis Research Center's program on icing research [AIAA PAPER 83-0204] 05 p0577 A83-16582
- Experimental evaluation of a proposed ice suppression system for the Space Shuttle external tank [IAF PAPER 83-ST-08] 23 p3423 A83-47386
- ICE REPORTING**
- Observation of sea ice properties with the Nimbus-7 SMMR --- Scanning Multispectral Microwave Radiometer 01 p0076 A83-10008
- Provision of ice information to icebreaker-transport vessels in the Arctic 01 p0077 A83-10827
- Microwave remote sensing of sea ice 08 p1143 A83-21958
- Surface elevation contours of Greenland and Antarctic ice sheets 09 p1305 A83-24286
- Ice crystal observations at 1.8 cm wavelength using a polarization diversity radar 11 p1629 A83-27066
- Preliminary results of the AFGL icing study [AD-A129843] 17 p2549 A83-38718
- Synthetic aperture radar studies of sea ice 22 p3344 A83-46204
- Spectral - Spatial analysis of microwave sea ice data 22 p3344 A83-46207

ICE SHELVES**U LAND ICE****ICEBERGS**

- Ice-sheet dynamics by satellite laser altimetry 01 p0064 A83-10093
- Applications of Robert's gradient operator for the digital enhancement of icebergs from SAR imagery 03 p0349 A83-14278

ICING**U ICE FORMATION****ICL COMPUTERS**

- A note on using finite differences on the ICL distributed array processor 01 p0090 A83-10712

IDEAL FLUIDS

- Finite element analysis of ideal flow over axisymmetric solid body /sphere/ 01 p0045 A83-10277
- Free vibrations of plates in fluid using finite and infinite elements 01 p0058 A83-10279
- The transport equation for the strain rate tensor and the description of an ideal incompressible fluid by a set of dynamic equations 02 p0169 A83-11642
- Perfect fluids in general relativity 02 p0233 A83-12026
- Jet flow of an ideal liquid past a flexible shell 06 p0760 A83-19430
- Perfect fluids in the Einstein-Cartan theory 07 p0990 A83-21065
- The equivalence of perfect fluid space-times and magnetohydrodynamic space-times in general relativity 08 p1180 A83-22206
- Perfect fluid spheres in general relativity 08 p1180 A83-22207
- Spherically symmetric similarity solutions of the equations of radiative relativistic fluids 09 p1262 A83-24508
- A scheme for the analysis of a developed cavitation flow past a wedge 11 p1567 A83-27719
- Motion of a circular cylinder in a rectangular channel 11 p1567 A83-27720
- On the kinematic control of the motion of a vessel with an ideal heavy fluid 11 p1649 A83-28468
- Normal oscillations of an ideal compressible fluid in rotating elastic vessels 13 p1838 A83-30012
- Kelvin-Helmholtz instability in relativistic mechanics 16 p2427 A83-35715
- Self-similar problem concerning the separated flow of an ideal fluid from a diffuser 17 p2446 A83-37258
- The theory for a flexible slat 17 p2451 A83-37810
- The stability of the elliptically deformed rotation of an ideal incompressible fluid in a Coriolis force field 18 p2687 A83-40079
- Hydrodynamic instability of axisymmetric flows of an ideal fluid with an interface 19 p2844 A83-41579
- Incompressible fluid mechanics --- French book 20 p2969 A83-42172
- Rayleigh-Taylor instability and the use of conformal maps for ideal fluid flow 21 p3132 A83-44986
- The dynamics of two-dimensional ideal MHD 23 p3510 A83-48046
- The well-posedness of two-dimensional ideal flow 23 p3449 A83-48047
- On a class of non-static perfect fluid spheres in general relativity 23 p3527 A83-48572
- Dynamics of an elliptical vortex 23 p3452 A83-48656
- The equivalence of perfect fluid space-times and viscous magnetohydrodynamic space-times in general relativity 24 p3651 A83-49099

IDEAL GAS

- Kinematics of a multi-dimensional shock of arbitrary strength in an ideal gas 05 p0642 A83-17846

- Estimate of shock thickness based on entropy production 07 p0926 A83-20530
- Three-dimensional supersonic ideal-gas flow past a body with a tail assembly 11 p1526 A83-27721
- Classification of difference schemes of gas dynamics by the method of differential approximation. I - One-dimensional case 13 p1844 A83-31592
- Isothermal shock wave in magnetogasdynamics 15 p2233 A83-33871
- An asymptotic theory of deflagrations and detonations. I - The steady solutions 16 p2325 A83-35694
- Stationary flow of gas at very high temperatures and relativistic speeds 17 p2595 A83-37032
- Unsteady aerodynamic characteristics of a profile in the transonic flow of an ideal gas 17 p2446 A83-37251
- Three-dimensional hypersonic flow past a body of finite thickness 17 p2448 A83-37528
- Analysis of flow in a conical nozzle with an oblique exit section and in the jet issuing from it 17 p2450 A83-37566
- Self-similar propagation of axisymmetric radiative magnetogasdynamic shocks with increasing energy. II 18 p2746 A83-39753
- Free expansion of three-dimensional jets of an ideal gas 19 p2790 A83-41207
- Viscous interaction of an underexpanded jet with a supersonic wake 20 p2982 A83-42885
- A low Mach number Euler formulation and application to time-iterative LBI schemes --- Linearized Block Implicit 21 p3134 A83-45592
- Isentropic magnetogasdynamic flow of a perfect plasma 22 p3363 A83-46462
- Computational-experimental study of the gas dynamics of two-dimensional symmetric nozzles having a region of constant height and two contour bend points in the critical section 23 p3400 A83-48661
- Analytical description of a hypersonic gas jet flowing into a medium at rest or into a supersonic wake 23 p3400 A83-48673
- Two hidden symmetries of the equations of ideal gasdynamics, and the general solution in a case of non-uniform entropy distribution 24 p3577 A83-49467
- Calculation of three-dimensional supersonic ideal-gas flows in asymmetric nozzles --- for spacecraft engines 24 p3552 A83-49655
- Numerical calculation of mixed flows in plate nozzles --- for spacecraft engines 24 p3552 A83-49656

IDENTIFY FRIEND OR FOE**U IFF SYSTEMS (IDENTIFICATION)****IDENTIFYING**

- NT CROP IDENTIFICATION
- NT IFF SYSTEMS (IDENTIFICATION)
- NT PARAMETER IDENTIFICATION
- NT SYSTEM IDENTIFICATION
- NT TIMBER IDENTIFICATION
- Optimal parameter estimation algorithms in identification problems 17 p2571 A83-37765

IFF SYSTEMS (IDENTIFICATION)

- Integrated CNI avionics maximizes reliability --- communications, navigation, and cooperative identification 01 p0042 A83-11089
- Integrated CNI - A new testing challenge --- Communication, Navigation and Identification 01 p0004 A83-11095
- ICNIA - Lessons learned on sensor integration --- Integrated Communication Navigation Identification Avionics 01 p0004 A83-11096
- Integrated CNI avionics logistics considerations 01 p0103 A83-11157
- Programmable filter technology for integrated communication, navigation and identification systems 01 p0042 A83-11214

IFF (RULES)**U INSTRUMENT FLIGHT RULES****IGFET****U FIELD EFFECT TRANSISTORS****IGNEOUS ROCKS**

- NT ANORTHOSITE
- NT BASALT
- NT GRANITE
- NT MOLDAVITE
- NT PERIDOTITE
- The ilmenite/titano-magnetite assemblage - Kinetics of re-equilibration 04 p0509 A83-15305
- Effects of fractional crystallization and cumulus processes on mineral composition trends of some lunar and terrestrial rock series 04 p0559 A83-15332
- Chemistry and phase relations of VLT volcanic glasses from Apollo 14 and Apollo 17 --- Very Low Titanium 04 p0561 A83-15343
- The polymict eucrites Elephant Moraine A79004 and A79011 and the regolith history of a basaltic achondrite parent body 04 p0562 A83-15359
- Primary igneous carbon in ureilites - Petrological implications 04 p0562 A83-15360

- Geochemistry and petrogenesis of Archaean metavolcanic amphibolites from Fiskenaeset, S. W. Greenland 04 p0514 A83-16353
- The magma ocean from the Fra Mauro shoreline - An overview of the Apollo 14 crust 07 p1032 A83-21294
- Subdivision of the Mg-suite noritic rocks into Mg-gabbro-norites and Mg-norites 07 p1032 A83-21295
- The Cerro Galan ignimbrite 08 p1138 A83-23255
- Sm-Nd studies of Archaean metasediments and metavolcanics from West Greenland and their implications for the earth's early history 09 p1304 A83-23886
- Kinetic effects on trace element partitioning 15 p2274 A83-34498
- Geochemistry and tectonic affinities of a Proterozoic bimodal igneous suite, west Texas 19 p2867 A83-41866
- Lead isotope systematics of some igneous rocks from the Egyptian Shield 22 p3332 A83-46704
- IGNIMBRITE**
- U IGNEOUS ROCKS**
- IGNITERS**
- NT INITIATORS (EXPLOSIVES)
- NT PRIMERS (EXPLOSIVES)
- Pulsed plasma thruster ignitor plug ignition characteristics 23 p3426 A83-48131
- IGNITION**
- NT SOLID PROPELLANT IGNITION
- NT SPARK IGNITION
- Weak and strong ignition. I - Numerical simulations of shock tube experiments 02 p0152 A83-12078
- Weak and strong ignition. II - Sensitivity of the hydrogen-oxygen system 02 p0152 A83-12079
- Observation of vapor generation preceding the ignition of liquid n-decane and l-decene by CO₂ laser radiation 02 p0152 A83-13094
- Ignition of confined gaseous mixtures by hot surfaces and hot wires
- [AIAA PAPER 83-0240] 05 p0612 A83-16606
- CO₂-laser-induced deflagration of fuel/oxygen mixtures 07 p0882 A83-20732
- Further studies on the ignition and flame quenching of quiescent dust clouds 07 p0882 A83-21351
- Ignition of a combustible half space 08 p1057 A83-22738
- Shock initiated ignition in heptane-oxygen-argon mixtures 10 p1391 A83-26198
- Evaporation and ignition of a fuel droplet on a hot surface. IV - Model of evaporation and ignition 13 p1818 A83-31224
- Calculation of critical branching points in two-parameter bifurcation problems 13 p1913 A83-31371
- Titan III ignition overpressure attenuation
- [AIAA PAPER 83-1114] 16 p2318 A83-36228
- The effects of chemical kinetics on the ignition of confined propane-air mixtures by hot particles and hot wires
- [AIAA PAPER 83-1365] 16 p2326 A83-36361
- The homogeneous thermal explosion with dissociation and recombination 22 p3267 A83-46762
- IGNITION LIMITS**
- Effect of oxygen addition on ignition of aero-gas turbine at simulated altitude facility 01 p0011 A83-10660
- An experimental study of transient combustion in low-gas heterogeneous systems 03 p0294 A83-14053
- Titanium ignition by the emission of a CO₂ laser 03 p0299 A83-14062
- On the influence of the plate thickness on the boundary layer ignition for large activation energies 07 p0878 A83-19839
- The ignition of a drop of fuel behind the front of a shock wave 07 p0901 A83-19961
- Gas phase ignition of a composite solid propellant subjected to radiant heating 09 p1243 A83-24369
- Ignition dynamics of fully reactive propellant in stagnation flow 09 p1226 A83-24666
- A study on the ignition of a fuel droplet in high temperature stagnant gas 10 p1391 A83-26197
- The effect of natural convection on the concentration limits of ignition for combustible mixtures in a closed container 14 p1988 A83-32081
- The ignition of disperse heterogeneous systems with consecutive reactions 14 p1988 A83-32082
- Discontinuation of periodic vortex formation behind a stabilizer in an acoustically damped chamber following mixture ignition 14 p1989 A83-32089
- Polymer ignition - A review 14 p1999 A83-33400
- Numerical study of transient laminar combustion in boundary layer flow 15 p2161 A83-34267
- Degenerate regimes of heterogeneous combustion and extinction of a particle in a gaseous oxidizer 18 p2663 A83-39157
- A theory for the ignition of metal particles 18 p2663 A83-39158

- The ignition of a fuel on contact with an oxidizer 18 p2663 A83-39159
- The laser ignition of compact mixed compositions 18 p2663 A83-39171
- Ignition and flame propagation studies with adaptive numerical grids 18 p2664 A83-40310
- Projectile impact ignition characteristics of propellants. III - Effect of particle size and porosity 21 p3117 A83-44998
- Ignition of a thin plate of condensed matter by a heated block 24 p3555 A83-49543
- Thermal self-ignition of a system of hot ignition sites 24 p3555 A83-49771
- Spontaneous combustion and ignition of metals in an oxidizing medium 24 p3556 A83-49773
- The ignition of a vapor bubble in a liquid 24 p3556 A83-49774

IGNITION TEMPERATURE

- NT FLASH POINT
- A study of the ignition characteristics of titanium powders 03 p0299 A83-14051
- The role of the heat-up period in fuel drop evaporation [AIAA PAPER 83-0068] 05 p0632 A83-16500
- Critical characteristics of thermal self-ignition in reacting systems with two-stage reactions 07 p0878 A83-19640
- Is gasification rate controlling step in polymer ignition? 15 p2142 A83-33724
- Mechanical activation of the ignition and combustion of titanium powder 18 p2665 A83-39160
- On an integral method for solving problems of the thermal theory of the ignition of condensed substances 19 p2820 A83-42067

IGY (GEOPHYSICAL YEAR)**U INTERNATIONAL GEOPHYSICAL YEAR****IL-62 AIRCRAFT**

- The employment of a miniature calculating device for the determination of the center of gravity 18 p2642 A83-39220

ILLIAC COMPUTERS**NT ILLIAC 4 COMPUTER****ILLIAC 4 COMPUTER**

- Turbulent structures in wall-bonded shear flows observed via three-dimensional numerical simulations --- using the Illiac 4 computer 01 p0046 A83-10890

ILLUMINANCE

- Calculation of illuminance in the shadow of the external occulting screen of a coronagraph. VI - Theory of tolerances 03 p0330 A83-14695
- The surface illuminance and albedo of a planetary atmosphere with nearly conservative scattering 23 p3529 A83-48559

ILLUMINATING

- Operational considerations on the moon-day project 06 p0720 A83-19148
- Measurement of illumination in the cloud layer of Venus by means of small solar arrays 14 p1984 A83-32043
- The current technique for radar control room lighting of the French Air Force 14 p2071 A83-32457

ILLUMINATION

- Effects of prolonged illumination on the properties of hydrogenated amorphous silicon 04 p0540 A83-15512
- Evaluation of the influence of illumination conditions on results of the spaceborne spectrophotometry of the earth 18 p2719 A83-40594
- Generation of Stokes and anti-Stokes waves initiated by two-photon additional illumination 20 p2996 A83-43782

ILLUSIONS**NT MOON ILLUSION****NT OCULOGRAPHIC ILLUSIONS****NT OPTICAL ILLUSION**

- Apparent movement - Phenomenology, main determinants, and mechanisms 18 p2735 A83-40557
- Depth separation and the Ponzo illusion 22 p3348 A83-45949

ILMENITE

- The ilmenite/titano-magnetite assemblage - Kinetics of re-equilibration 04 p0509 A83-15305
- Redox state of earth's upper mantle from kimberlitic ilmenites 15 p2198 A83-34218

ILS (LANDING SYSTEMS)**U INSTRUMENT LANDING SYSTEMS****ILYUSHIN AIRCRAFT****NT IL-62 AIRCRAFT****ILYUSHIN IL-62 AIRCRAFT****U IL-62 AIRCRAFT****IMAGE ANALYSIS**

- Selected comment on multiple Doppler analysis --- of radar scanned storm with advection error correction 11 p1628 A83-27051
- Survey of model-based image analysis systems 11 p1573 A83-28097

- Automated digital processing of interferograms --- Thesis 11 p1575 A83-28650
- Analysis of optical imagery for Seyfert's Sextet and VV 172 12 p1784 A83-28880
- Analysis of coregistered Landsat, Seasat and SIR-A images of varied terrain types 12 p1748 A83-28909
- Volumetric descriptions of objects from multiple views 12 p1769 A83-28948
- Analysis of the shift-and-add method for imaging through turbulent media 12 p1779 A83-29375
- The interpretation of digital recordings of SIR-A, Seasat, and Landsat data of the Algerian salt deposits 12 p1748 A83-29379
- Evolution of the Venera 13 imagery 12 p1798 A83-29485
- Automated laser speckle interferometry displacement contour analyzer 12 p1730 A83-29587
- On a method for the representation of images in the process of their arrival 13 p1910 A83-30617
- Processing of optical data using a two-beam interferometer 13 p1846 A83-30622
- Holographic recording of optical signals that vary in time in nonstationary-reference-wave devices 13 p1846 A83-30623
- Results of an analysis of space photographs of the moon magnified to a scale of 1:500,000 13 p1961 A83-31100
- An interpretation of weather conditions on the basis of conventional analyses, and of diagnoses utilizing satellite imagery and model parameters 14 p2055 A83-31847
- Resolution classifier --- Bayesian approach for astronomical images 14 p2096 A83-32034
- Analysis of synthesized dim galaxy images 14 p2096 A83-32035
- Real-time fringe-pattern analysis 14 p2021 A83-32912
- A technique for mapping environmental change using digital Landsat data 15 p2181 A83-33561
- Effects of spherically-symmetric gravitational lenses produced by galaxies and clusters 15 p2262 A83-34538
- A comparative study of linear and nonlinear edge finding techniques for Landsat multispectral data 15 p2187 A83-34840
- Cross-polarized radar image anomalies as sensitive measures of L-band vegetation penetration capability 15 p2187 A83-34846
- The problem of the visualization of information and digital image processing 15 p2165 A83-34968
- An algorithm of fast Kotelnikov interpolation --- for optical image simulation 15 p2223 A83-35262
- Digital picture processing. Volumes 1 & 2 /2nd edition/ --- Book 17 p2509 A83-37167
- Evaluation of MSS Landsat imagery over Central Spain 17 p2527 A83-38131
- Landsat analysis of the Yangjiatan tungsten district, Hunan Province, People's Republic of China 17 p2528 A83-38141
- Optimum spectral bands for land cover discrimination 17 p2530 A83-38164
- Delineation of selected urban features utilizing single date and multitemporal Landsat data - A comparative analysis 17 p2586 A83-38356
- Optoelectronic methods of image processing 19 p2846 A83-40985
- Statistical analysis of a holographic system intended for the Space Shuttle 19 p2817 A83-41099
- Automatic fringe analysis with a computer image-processing system 19 p2847 A83-41106
- Analysis of airglow image data 20 p3016 A83-42310
- An interpretation for probabilistic relaxation --- processing mechanisms in image analysis 21 p3194 A83-44263
- Recent developments in quantitative fractography 21 p3114 A83-44950
- The influence of the image scale on the precision of morphotopo analysis from aerial photographs performed by a digital shape recognition analysis 22 p3308 A83-46117
- Effect of differences in categories dispersion patterns on digital image classification results 22 p3308 A83-46118
- Interpretation of Landsat imagery - A case study of lineations in a part of north-western Himalaya, India 22 p3309 A83-46134
- Desertification in Kaokoland (northern South West Africa/Namibia) - Field evidence, recognition in satellite imagery, mapping of spatial distribution by satellite image interpretation (Landsat 1) 22 p3309 A83-46135
- Ground truth collection for a visual interpretation of SAR-580 imagery on the B1-site in Belgium 22 p3310 A83-46139

- Analysis of MARSEN synthetic aperture radar wave imagery --- in Maritime Satellite North Sea experiment
22 p3343 A83-46156
- Multispectral observations of agricultural fields in the Kiskoore test-area
22 p3310 A83-46161
- The system of physical spatial units ('Naturraeumliche Gliederung') as an aid in the evaluation of satellite data
22 p3311 A83-46165
- Parametric studies of SAR-images by means of radar backscattering models
22 p3312 A83-46190
- Characterization of SAR images
22 p3289 A83-46192
- Spectral - Spatial analysis of microwave sea ice data
22 p3344 A83-46207
- A complex selective key to identify genetic relief forms on satellite images /for education and training in geomorphological interpretation/
22 p3313 A83-46216
- Preliminary analysis of Shuttle imaging radar
22 p3313 A83-46223
- Half-fringe photoelasticity - A new approach to whole-field stress analysis
22 p3306 A83-46809
- An interpretation of NOAA-7 scans of the Mediterranean at 1220-1225 GMT on October 7, 1981
23 p3491 A83-48057
- Fringe addition in moireanalysis
24 p3582 A83-49010
- Iconics: Theory and methods of image processing
24 p3582 A83-49042
- The software of an interactive image-processing system
24 p3620 A83-49043
- Intensity estimation from pixel data --- for stellar and galactic magnitude determination
24 p3648 A83-50013
- A straightforward method to calibrate photographic data using stellar images
24 p3648 A83-50014
- IMAGE CONTRAST**
- Drumlin fields and glaciated mountains - A contrast in geomorphic perception from Seasat radar images
01 p0064 A83-10078
- Coherent image fringe contrast measurement with sensing arrays
01 p0051 A83-10863
- Interpretation of geometric structure from image boundaries
02 p0182 A83-12891
- The effects of haze on resolution on small scale aerial photography
03 p0329 A83-14283
- Contrast sensitivity - Psychophysical and evoked potential methods compared
05 p0676 A83-17750
- Assessment of operational techniques for estimating visible spectrum contrast transmittance
08 p1098 A83-22548
- Comparative study of edge-thinning algorithms for target identification
09 p1265 A83-23530
- Real-time statistical tracker for infrared /IR/ focal plane array
09 p1266 A83-23546
- Background influence on visual accommodation - Implications for target acquisition
10 p1456 A83-26320
- A model for calculating the brightness-field contrast of homogeneous objects
10 p1423 A83-26811
- Channeling contrast microscopy - Application to semiconductor structures
13 p1929 A83-31067
- An investigation of the effect of polarizing radiation, scattered by an optically inhomogeneous layer, on the quality of its holographic image
14 p2019 A83-32126
- The polarization control of tone-transmission brightness in a holographic image of light-scattering surfaces and layers
14 p2019 A83-32132
- Real-time edge enhancement in four-wave mixing with photorefractive BGO crystals
14 p2084 A83-32450
- Spatially variant contrast enhancement using local range modification
14 p2021 A83-33177
- Spatiotemporal variation of chromatic and achromatic contrast thresholds
15 p2215 A83-33802
- Spatial and radiometric resolution of the Landsat-3 RBV system --- Return Beam Vidicon
15 p2188 A83-35293
- Measurement of laser photoelectron image degradation at high current densities
16 p2356 A83-35969
- Ridges and valleys on digital images
21 p3193 A83-44251
- Evidence against saturation of contrast adaptation in the human visual system
22 p3349 A83-46755
- IMAGE CONVERTERS**
- NT IMAGE TUBES**
- Methods of measuring the efficiency of X-ray image converters
01 p0049 A83-10360
- Optical-to-optical image conversion with the liquid crystal light valve
03 p0394 A83-13776
- Advances in detectors for astronomical spectroscopy
04 p0547 A83-15806
- Transverse photon bunching and two-photon processes in a parametric scattering field --- in image converters
04 p0482 A83-15906
- Development and performance of a position sensitive proportion counter for the Rosat project
11 p1671 A83-27761
- Calculation of the parameters of the optical system of the image converter of an adaptive industrial robot
12 p1767 A83-29325
- Light-controlled transparencies for storing optical images
13 p1919 A83-30817
- Modified Bowen-Walraven image slicer
14 p2018 A83-32029
- An optical residue processor for computing inner products
16 p2411 A83-35516
- IMAGE CORRELATORS**
- On the correlation structure of random field models of images and textures
01 p0100 A83-11473
- Fast adaptive algorithms for low-level scene analysis - Applications of polar exponential grid /PEG/ representation to high-speed, scale-and-rotation invariant target segmentation
02 p0181 A83-12880
- Automatic reconnaissance-based target-coordinate determinations
02 p0181 A83-12883
- Multiplex holographic filtering through contact screens
03 p0326 A83-13772
- Multiple filter storage --- for optical correlation signal processing
03 p0326 A83-13773
- Rectification of Seasat radar on Landsat MSS with the aid of digital image correlation
03 p0352 A83-14946
- Analysis of spatially correlated images with implications for independent sampling and linear correlator image detection
08 p1105 A83-22901
- Holographic intensity correlator with a laser electron beam tube for inputting images for processing
10 p1422 A83-26467
- Correlation of binarized images
14 p2077 A83-33138
- Amplitude calibration of spaceborne synthetic aperture radars --- Synthetic Aperture Radar
21 p3103 A83-43979
- Dynamic optical cross-correlator using a liquid crystal light valve for real time data input
21 p3207 A83-44827
- Portable real-time coherent optical correlator
22 p3361 A83-46831
- Color coding in quasi-interferometry
24 p3582 A83-49011
- IMAGE ENHANCEMENT**
- Selective image enhancement and restoration
01 p0061 A83-10028
- The magnifying glass - A feature space local expansion for visual analysis --- and image enhancement
01 p0048 A83-10076
- Data enhancement and analysis through mathematical deconvolution of signals from scientific measuring instruments
01 p0051 A83-11055
- Anisotropic filtering operations for image enhancement and their relation to the visual system
01 p0099 A83-11451
- Evaluation of photographic enhancements of Landsat imagery
02 p0198 A83-12035
- Contribution of Landsat imagery to the study of volcanic structures
02 p0211 A83-12641
- Image enhancement through film recorder response contouring
02 p0199 A83-12685
- Enhancement of astronomical images using digital filtration methods
03 p0407 A83-13672
- Application of Landsat imagery to natural resources management in Sierra Leone, West Africa
03 p0347 A83-14247
- Digital colour enhancement of Landsat data for mapping vegetation of bareground caribou winter range in northern Manitoba
03 p0347 A83-14249
- Applications of Robert's gradient operator for the digital enhancement of icebergs from SAR imagery
03 p0349 A83-14278
- Parameter study of synthetic-aperture focusing in ultrasonics
04 p0493 A83-15225
- Putting texture in perspective --- flight simulation by application of computer generated imagery techniques
04 p0524 A83-16330
- OSTA-1/Ocean Color Experiment
[AIAA PAPER 83-0415]
05 p0668 A83-16701
- Method for additional correction of algorithm for the restoration of smeared images
07 p0929 A83-20558
- One form of apodization of telescopes
07 p1009 A83-21275
- Digital image enhancement of noisy scanner imagery
08 p1091 A83-21911
- Composite Seasat-Landsat images from the point of view of thematic interpretation
08 p1125 A83-21916
- Computer-aided soil evaluation methods on Landsat images in cultured landscapes
08 p1126 A83-21933
- Simulation of clutter rejection signal processing for mid-infrared surveillance systems
08 p1094 A83-22438
- Spectral discrimination for long range search/track infrared systems
08 p1094 A83-22442
- Large scale multipurpose interactive image processing facility at ETH-Zurich
08 p1098 A83-22539
- Techniques for pseudo-dc restoration and dynamic range enhancement of scanned infrared imagery
08 p1105 A83-22900
- An inexpensive computer-controlled ultrasonic C-scan system
08 p1105 A83-23099
- Comparative study of edge-thinning algorithms for target identification
09 p1265 A83-23530
- Image analysis using polarized Hough transform and edge enhancer
09 p1265 A83-23532
- Ring laser gyroscopes - Charge-coupled device /CCD/ readout and signal processing for high resolution applications
09 p1267 A83-23590
- Application of the IHS color transform to the processing of multisensor data and image enhancement --- Intensity, Hue and Saturation in satellite remote sensing data
09 p1287 A83-24576
- Contrast enhancement applied to Guayule distribution in Mexico for commercial rubber production
09 p1290 A83-24617
- Digital enhancement of SAR imagery as an aid in geologic data extraction
10 p1443 A83-25970
- Nonlinear filtering of noise-distorted images based on a Markov probability model
10 p1424 A83-26815
- A photodevelopment effect in machines for the continuous processing of photographic film
10 p1424 A83-26823
- Simple method for image deblurring
10 p1484 A83-26860
- Hill shading and the reflectance map
11 p1601 A83-28173
- Deformable mirror with combined piezoelectric and electrostatic actuators
13 p1920 A83-31008
- Real-time edge enhancement in four-wave mixing with photorefractive BGO crystals
14 p2084 A83-32450
- Landsat digital enhancements for change detection in urban environments
14 p2035 A83-32614
- Broad spectral band color image deblurring
14 p2020 A83-32904
- Spatially variant contrast enhancement using local range modification
14 p2021 A83-33177
- Objective procedures for lineament enhancement and extraction --- digital convolution enhanced images
14 p2035 A83-33346
- Method of improving image quality in holographic interferometers
15 p2164 A83-34424
- Glacial geologic interpretation of southeastern Wisconsin through diazo enhancement of Landsat multispectral imagery
15 p2186 A83-34839
- A comparative study of linear and nonlinear edge finding techniques for Landsat multispectral data
15 p2187 A83-34840
- Quantitative evaluation of radiographic imaging variables
16 p2363 A83-35758
- Efficient algorithm for image enhancement
16 p2405 A83-36964
- Image recovery from signal-dependent noise
17 p2511 A83-37950
- Enhanced Landsat and HCMM imagery for mineral exploration in contrasting areas of subtropical humid and semi-arid terrain
17 p2528 A83-38150
- Enhanced thermal mapping with Landsat and HCMM digital data
17 p2531 A83-38351
- Landsat image enhancement in support of seismotectonic studies in Utah
17 p2532 A83-38360
- Method of the coherent spatial filtering of one-dimensional distortions of images using a white-light source
17 p2512 A83-38501
- On solving the problem of the radiation correction of space imagery
18 p2692 A83-40600
- Optical splitter for dynamic range enhancement of optical multichannel detectors
19 p2847 A83-41098
- New trend of atom resolution electron microscopy - Direct observations of atoms, vacancies and impurity atoms in crystal and on-line image analysis
20 p2992 A83-43609
- Optimum recursive filtering of noisy two-dimensional data with sequential parameter identification
21 p3192 A83-43955
- Processing of infrared thermal images for aerodynamic research
[ONERA, TP NO. 1983-32]
21 p3137 A83-44310
- Expedient range enhanced 3-D robot colour vision
21 p3118 A83-44694
- Coherent image amplification and optical phase conjugation with photorefractive materials
21 p3206 A83-44799
- Lithologic mapping using solar infrared
22 p3309 A83-46129
- Image enhancement for determination of agricultural fields using Digital-SLAR data
22 p3313 A83-46211
- Histogram deconvolution - An aid to automated classifiers
22 p3350 A83-46253

- Method of determining optical atmospheric parameters based on space imagery earth-surface
[IAF PAPER 83-102] 23 p3480 A83-47265
- Real-time image deblurring using four-wave mixing
24 p3628 A83-48750
- Noise filtering on an image using the distribution median
24 p3582 A83-49044
- Image enhancement in a dithered picture
24 p3583 A83-49198

IMAGE FILTERS

- SAR squint analysis of directional extended targets --- using Doppler filtering of SAR signal film
01 p0064 A83-10084
- Anisotropic filtering operations for image enhancement and their relation to the visual system
01 p0099 A83-11451
- Iterative design of pupil functions for bipolar incoherent spatial filtering
08 p1164 A83-22429
- Target acquisition and extraction from cluttered backgrounds
09 p1204 A83-23531
- Broad spectral band color image deblurring
14 p2020 A83-32904
- Filtering of noisy images using Markov random field models
15 p2223 A83-35145
- An estimation-theoretic approach to terrain image segmentation
21 p3194 A83-44261
- Color coding in quasi-interferometry
24 p3582 A83-49011
- Noise filtering on an image using the distribution median
24 p3582 A83-49044

IMAGE FURNACES

- Thermal response of solar receiver aperture plates during sun walk-off
[ASME PAPER 82-HT-33] 02 p0202 A83-12791

IMAGE INTENSIFIERS

- NT IMAGE ORTHICONS
- Monochromatic photographs of the Cygnus Loop with a fiber-optics image intensifier
07 p1006 A83-20656
- A proportional counter/image intensifier system for the detection of low energy X-rays
11 p1657 A83-27756
- Image intensifier gain measurements
13 p1848 A83-31455
- Highly versatile computer-controlled television detector system
14 p2015 A83-31985
- Development of a dual microchannel plate intensified charge-coupled device (CCD) speckle camera
14 p2015 A83-31991
- Miniature imaging photon detector
14 p2018 A83-32022
- Biocular magnifiers for use with cathode ray tube (CRT) displays
21 p3139 A83-44786

IMAGE MOTION COMPENSATION

- Analysis of three hierarchical motion compensation systems for synthetic aperture radars
01 p0007 A83-11242
- Determination of displacement vector fields for general camera motions
01 p0097 A83-11421
- Residual recursive displacement estimation --- for motion detection
01 p0100 A83-11464
- The effect of two types of induced-motion displays on perceived location of the induced target
03 p0383 A83-14525
- Aerial camera vibration
03 p0330 A83-14663
- The influence of orbital aberration on the position of points on space photographs
05 p0645 A83-17682
- Image compensation in the presence of thermal blooming --- extended target image reconstruction using adaptive optics
07 p0935 A83-20156
- Fourier transform image tracker and stabilizer
08 p1099 A83-22584
- Motion-error immunity in photo coordinate determination - A novel approach to the absolute comparator
08 p1100 A83-22594
- Bo 105 rotor blade influence on the Calipso FLIR in the mast-mounted observation platform Ophelia
08 p1044 A83-23249
- A study of a correlation tracking method to improve imaging quality of ground-based solar telescopes
10 p1492 A83-25489
- Real-time holographic interferometry of moving objects in oppositely directed beams
10 p1420 A83-25891
- The processing of synthetic aperture radar signals
10 p1404 A83-26473
- Dome induced image motion --- in astronomical telescopes
13 p1920 A83-30999
- Spatiotemporal variation of chromatic and achromatic contrast thresholds
15 p2215 A83-33802
- Image motion compensation for the OGS-3/7 telescopes
21 p3104 A83-44165
- [AAS PAPER 83-006]

IMAGE ORTHICONS

- Features characterizing the formation of signal and noise, common to all TV camera tubes of the superorthicon class
24 p3574 A83-49641

IMAGE PROCESSING

- NT GEOMETRIC RECTIFICATION (IMAGERY)

- A model for simulation and processing of radar images
01 p0061 A83-10026
- Contextual classification of multispectral image data
01 p0061 A83-10027
- Selective image enhancement and restoration
01 p0061 A83-10028
- A method for contours detection, segmentation and classification of Landsat images
01 p0061 A83-10029
- The UCL interactive planetary image processing system /IPIPS/ Application to remote sensing studies in planetary meteorology and oceanography
01 p0128 A83-10051
- A digital Seasat SAR correlation-simulation program
01 p0062 A83-10052
- Using radar image simulation to assess relative geometric distortions inherent in radar imagery
01 p0030 A83-10054
- Landsat images multitemporal analysis
01 p0063 A83-10055
- Rock type discrimination techniques using Landsat and Seasat image data
01 p0063 A83-10057
- The magnifying glass - A feature space local expansion for visual analysis --- and image enhancement
01 p0048 A83-10076
- System software approaches to the analysis of multidimensional data structures
01 p0090 A83-10137
- A data analysis facility for the Faint Object Camera
01 p0114 A83-10143
- Algorithms for smoothing data with periodic and parametric splines
01 p0102 A83-10284
- The real-time image processing problem
01 p0053 A83-11218
- Identification of optimally correlated subsets --- algorithm to allow robust tracking methodology
01 p0096 A83-11220
- Multiscenario imaging sensor autoprocessor --- for target recognition
01 p0007 A83-11224
- Conference on Pattern Recognition and Image Processing, Dallas, TX, August 3-5, 1981, Proceedings
01 p0096 A83-11409
- Probabilistic cluster labeling of imagery data
01 p0096 A83-11410
- A group-linking classifier
01 p0096 A83-11412
- Recursive generation of hierarchical data structures for multidimensional digital images
01 p0097 A83-11414
- Representation of a region as a forest of quad trees --- describing pixels in image processing analysis
01 p0097 A83-11415
- Normalized quadrees with respect to translations --- in image processing
01 p0097 A83-11416
- Approaches to recursive image decomposition
01 p0097 A83-11417
- Motion detection using Hough techniques
01 p0097 A83-11418
- Determination of displacement vector fields for general camera motions
01 p0097 A83-11421
- Shape analysis of segmented objects using moments
01 p0097 A83-11422
- Constraints on optical flow computation --- for image planes
01 p0097 A83-11424
- Motion and image differencing --- computer analysis of dynamic scenes
01 p0097 A83-11425
- Image data compression with the Laplacian pyramid
01 p0098 A83-11426
- An adaptive transform image data compression scheme incorporating pattern recognition procedures
01 p0098 A83-11428
- The GLGS image representation and its application to preliminary segmentation and pre-attentive visual search --- Gray Level Geographic Structure
01 p0098 A83-11431
- On the statistical image segmentation techniques
01 p0098 A83-11432
- An iterative algorithm for multiple threshold detection --- in image processing
01 p0098 A83-11434
- A facet model region growing algorithm --- for image processing
[AD-A125 566] 01 p0098 A83-11435
- The digital edge --- in images
01 p0099 A83-11436
- Description of two hardware convolvers as a part of a general image computer
01 p0089 A83-11437
- Systolic cellular logic - Inexpensive parallel image processors
01 p0089 A83-11438
- 'Bilevel' processing of 'multilevel' pictures
01 p0099 A83-11439
- Microstructure representation through neighborhood relations --- for scene analysis
01 p0099 A83-11440
- Contextual classification on PASM --- multimicroprocessor system for image processing and pattern recognition
01 p0090 A83-11441

- A fast technique for segmentation and recognition of binary patterns --- image processing algorithms
01 p0099 A83-11444
- Texture discrimination using region based primitives
01 p0099 A83-11445
- Architectures for neighborhood processing --- of images by computer serial array processors
01 p0090 A83-11446
- A VLSI pyramid machine for hierarchical parallel image processing
01 p0090 A83-11447
- PUMPS architecture for pattern analysis and image database management --- shared resource multiprocessor computer
01 p0090 A83-11448
- Pattern recognition and digital image processing as applied to remote sensing in India
01 p0067 A83-11450
- Elimination of seams from photomosaics
01 p0099 A83-11452
- Augmented relaxation labeling and dynamic relaxation labeling --- iterative pixel label updating in image processing
01 p0099 A83-11455
- Relaxation labeling using staged updating --- in image processing
01 p0099 A83-11456
- Parallel implementations of a structural analysis algorithm --- for pattern recognition
01 p0100 A83-11457
- Real-time infrared image processing --- onboard aircraft
01 p0011 A83-11459
- Symbolic pattern matching for target acquisition
01 p0008 A83-11460
- Automatic multitemporal segmentation for diachronic analysis of remotely sensed images
01 p0067 A83-11461
- Occlusion analysis in time-varying imagery
01 p0100 A83-11463
- Nonlinear image operators for nulling 3-space translations
01 p0100 A83-11465
- Image recognition by matching relational structures
01 p0100 A83-11468
- Efficient local searching in sparse images
01 p0100 A83-11469
- Generalized correlation measures for use in signal and image processing
01 p0100 A83-11470
- An algorithm for scale invariant segment-matching
01 p0100 A83-11472
- Synthetic generation and estimation in random field models of images
01 p0101 A83-11474
- A simplified procedure for statistical feature extraction in texture processing
01 p0101 A83-11476
- Texture synthesis using a bidimensional Markov model
01 p0101 A83-11477
- Markov Random Field texture models
01 p0101 A83-11478
- Texture simulation using a best-fit model
01 p0101 A83-11479
- Multiple-level representations for texture discrimination
01 p0101 A83-11480
- Automatic feature extraction system - Test bed
01 p0090 A83-11481
- Auxiliary data networks for satellite synthetic aperture radar
02 p0175 A83-11523
- Robots and image processing
02 p0161 A83-11795
- Image restoration - A linear stochastic filtering approach --- Thesis
02 p0176 A83-11900
- Evaluation of photographic enhancements of Landsat imagery
02 p0198 A83-12035
- A comparison of unsupervised classification procedures on Landsat MSS data for an area of complex surface conditions in Basilicata, Southern Italy
02 p0198 A83-12037
- Star - A local network system for real-time management of imagery data
02 p0228 A83-12242
- SIMD image resampling
02 p0228 A83-12243
- Image processing on ZMOB
02 p0228 A83-12244
- Content-addressable read/write memories for image analysis
02 p0227 A83-12246
- PUMPS architecture for pattern analysis and image database management
02 p0227 A83-12247
- PICCOLO logic for a picture database computer and its implementation
02 p0228 A83-12248
- PICAP - A system approach to image processing
02 p0229 A83-12249
- Applications of the Priz light modulator
02 p0236 A83-12307
- Real-time optical interferometric image subtraction by wave polarization
02 p0177 A83-12309
- Technology and future ground processing systems
02 p0199 A83-12678
- Synthetic aperture radar /SAR/ coordinate processing system
02 p0179 A83-12680
- Bit error rate performance of Image Processing Facility high density tape recorders
02 p0179 A83-12681
- Techniques and applications of image understanding; Proceedings of the Meeting, Washington, DC, April 21-23, 1981
02 p0181 A83-12875

- Summary of the DARPA Image Understanding Research Program 02 p0181 A83-12876
- Defense Mapping Agency /DMA/ overview of mapping, charting, and geodesy /MC&G/ applications of digital image pattern recognition 02 p0200 A83-12877
- Application of image understanding to automatic tactical target acquisition 02 p0133 A83-12878
- Intelligent control of tactical target cueing --- by subsonic flight vehicles 02 p0133 A83-12879
- Fast adaptive algorithms for low-level scene analysis - Applications of polar exponential grid /PEG/ representation to high-speed, scale-and-rotation invariant target segmentation 02 p0181 A83-12880
- Cellular array processing simulation 02 p0228 A83-12881
- Reconnaissance applications of image understanding 02 p0200 A83-12882
- Automatic reconnaissance-based target-coordinate determinations 02 p0181 A83-12883
- Hough transform for target detection in infrared imagery 02 p0181 A83-12884
- Dimensional automatic target classification 02 p0182 A83-12886
- Applications of moments to image understanding 02 p0230 A83-12887
- Line finding with subpixel precision 02 p0182 A83-12890
- Computational models for texture analysis and synthesis 02 p0230 A83-12893
- Towards a real time implementation of the Marr and Poggio stereo matcher 02 p0182 A83-12894
- Model-based three-dimensional interpretations of two-dimensional images 02 p0182 A83-12896
- Residue-based image processor for very large scale integration /VLSI/ implementation 02 p0182 A83-12900
- Image smoothing and segmentation by multiresolution pixel linking - Further experiments and extensions 02 p0182 A83-12972
- Feature Identification and Location Experiment 03 p0357 A83-13353
- Toward the robot eye - Isomorphic representation for machine vision 03 p0384 A83-13447
- Conceptual design and requirements of a pushbroom focal plane 03 p0325 A83-13729
- Shutterless fixed pattern noise correction for infrared imaging arrays 03 p0325 A83-13731
- Signal processing for large focal plane arrays 03 p0309 A83-13738
- Quality assessment of remote-sensing data - The SAR case 03 p0344 A83-13845
- Integration of Landsat imagery into a program for aerial surveying of deer populations in Alberta 03 p0347 A83-14252
- Construction and interpretation of a thermal inertia image using airborne data 03 p0348 A83-14260
- Remote sensing software for airborne image analysis 03 p0349 A83-14273
- A field portable reflectance spectrometer 03 p0329 A83-14275
- A refined destriping procedure for Landsat MSS data products 03 p0349 A83-14281
- Investigation of attitude determination program for Landsat image processing 03 p0289 A83-14282
- Some effects on the GCP success rate --- Ground Control Points for satellite image rectification 03 p0349 A83-14285
- Reference quicklook images for monitor of Landsat image data acquisition 03 p0349 A83-14286
- The CCRS SAR processing system 03 p0349 A83-14289
- The need for cross-fertilization between the fields of profile inversion and computed tomography --- in test pattern reconstruction 03 p0329 A83-14291
- A system for the complex processing of aerial and space data for agriculture 03 p0350 A83-14301
- Automation of the search for and recognition of reference zones for precise coordinate control of space imagery 03 p0350 A83-14311
- A method for the digital processing of contour imagery 03 p0329 A83-14312
- Paraxial imaging and transforming in a medium with gradient-index Transmittance function 03 p0395 A83-14388
- The width of echelle orders in IUE images as derived with the astronomical image display and analysis /AIDA/ system in Tuebingen 03 p0411 A83-14799
- Resolution versus speckle relative to geologic interpretability of spaceborne radar images - A survey of user preference 03 p0351 A83-14852
- Estimation of context for statistical classification of multispectral image data 03 p0351 A83-14853
- On geological processes on Venus - Analysis of the relationship between altitude and degree of surface roughness 03 p0435 A83-14868
- Investigations of interpretability of images by different sensors and platforms for small scale mapping 03 p0352 A83-14943
- The digital image processing system MOBI-DIVAH 03 p0352 A83-14944
- Parameter study of synthetic-aperture focusing in ultrasonics 04 p0493 A83-15225
- The effects of surface mapping corrections with synthetic-aperture focusing techniques on ultrasonic imaging 04 p0493 A83-15226
- Advances in detectors for astronomical spectroscopy 04 p0547 A83-15806
- Surface photometry of the H II region - S254-S257 04 p0547 A83-15962
- An interactive procedure to solve the background subtraction problems in IUE high resolution spectra - Application to the image SWP 4616 04 p0547 A83-15972
- A mathematical model for computer image tracking 04 p0528 A83-16030
- Organization of relational models for scene analysis 04 p0528 A83-16031
- Some accuracy and resolution aspects of computer vision distance measurements 04 p0528 A83-16032
- A geometrical approach to polygonal dissimilarity and shape matching 04 p0528 A83-16033
- A description of the Bell Laboratories scanned acoustic microscope 04 p0482 A83-16321
- The use of stereopairs with unknown orientation elements for the solution of the direct and inverse problems of photogrammetry and for the identification of objects 04 p0482 A83-16386
- Shear zone ice deformation using supervised analysis of Seasat data [AIAA PAPER 83-0491] 05 p0668 A83-16748
- The development of a computer controlled camera system for archiving image data [AIAA PAPER 83-0656] 05 p0643 A83-16820
- Binary multiplexing and the phase-retrieval problem 05 p0643 A83-16836
- State variable representation of a class of linear shift-variant systems 05 p0680 A83-16911
- Principles governing the structure of coherent video preprocessors 05 p0645 A83-17660
- Optical coupling of two scanners for the processing of aerial and space images 05 p0645 A83-17681
- Computationally efficient discrete cosine transform algorithm 06 p0803 A83-18574
- Phytoplankton pigment concentrations in the Middle Atlantic Bight - Comparison of ship determinations and CZCS estimates --- Coastal Zone Color Scanner 06 p0793 A83-18580
- Modeling and a correlation algorithm for spaceborne SAR signals 06 p0763 A83-19030
- Estimation of spectra from speckled images 06 p0763 A83-19040
- Transform coding strategies at low rates --- for image transmission 07 p0907 A83-19729
- Digital image processing - A systems approach --- Book 07 p0928 A83-19925
- Computer-aided speckle pattern interferometry 07 p0928 A83-20155
- Inverting a dispersive scene's side-scanned image 07 p0913 A83-20370
- Estimation and choice of neighbors in spatial-interaction models of images 07 p0984 A83-20549
- Method for additional correction of algorithm for the restoration of smeared images 07 p0929 A83-20558
- Reception, preparation, and geometric processing of imagery of meteorological satellites --- German thesis 07 p0951 A83-21069
- Landsat multitemporal color composites 07 p0952 A83-21433
- Landsat-derived land-cover classifications for locating potential Kestrel nesting habitat 07 p0952 A83-21435
- Automated supernova search from photographic plates 08 p1174 A83-21845
- Methodology for thematic image processing using thematic and topographic data bases and base-integrated multi-sensor imagery 08 p1124 A83-21903
- Development of video-rate image processing system in India 08 p1091 A83-21909
- Presentation of a function which makes it possible to follow, independently of the dark-light contrasts, the geological structures in mountainous regions 08 p1125 A83-21910
- Creation of new channels by photographic methods 08 p1125 A83-21913
- Multidensity and its application to Landsat imagery 08 p1125 A83-21915
- Classification of SAR imagery from an agricultural region using digital textural analysis 08 p1125 A83-21917
- Analysis of a multisensor image data set of south San Rafael Swell, Utah 08 p1125 A83-21920
- Renewal of land use data base with the aid of remote sensing 08 p1128 A83-21952
- Studies of object recognition using three-dimensional information 08 p1156 A83-22063
- Image bandwidth compression by pre-compensative interpolation 08 p1075 A83-22235
- A simple speckle smoothing algorithm for synthetic aperture radar images 08 p1093 A83-22349
- Simultaneous multispectral absolute radiometer and transmissometer system 08 p1093 A83-22358
- Processing of images and data from optical sensors; Proceedings of the Meeting, San Diego, CA, August 25, 26, 1981 08 p1093 A83-22426
- Partially coherent optical processing of images 08 p1093 A83-22427
- Digital image processing in Europe - Some highlights 08 p1093 A83-22431
- Image processing and analysis of Saturn's rings 08 p1094 A83-22432
- Processing infrared images for fire management applications 08 p1094 A83-22434
- Multisensor image registration - Experimental verification 08 p1094 A83-22436
- Clutter rejection for infrared surveillance sensors 08 p1094 A83-22437
- Real-time nonuniformity correction for focal plane arrays using 12-bit digital electronics 08 p1094 A83-22440
- Autonomous ship classification by moment invariants 08 p1095 A83-22444
- Detection probability of an object ranking system for an imaging missile seeker 08 p1157 A83-22445
- Noise effects for edge operators 08 p1158 A83-22447
- Experimental studies with a coherent CO2 laser radar 08 p1096 A83-22510
- Design of digital image processing systems; Proceedings of the Meeting, San Diego, CA, August 27, 28, 1981 08 p1097 A83-22524
- Geology and image processing 08 p1129 A83-22525
- Interactive algorithm development system for tactical image exploitation 08 p1097 A83-22527
- Real-time image computer configuration 08 p1152 A83-22528
- Use of array processors in image processing 08 p1152 A83-22529
- Advanced architecture for graphics and image processing 08 p1152 A83-22530
- Programmable image processing element 08 p1097 A83-22532
- System architecture of Vicom digital image processor 08 p1097 A83-22533
- Processing display system architectures 08 p1152 A83-22534
- On-line processing of high resolution imagery from meteorological satellites 08 p1140 A83-22535
- PAR image processing system /PARIPS/ - A testbed for automating image interpretation 08 p1154 A83-22536
- Powerful hardware/software architecture for a minicomputer-based interactive image processing system 08 p1097 A83-22537
- Microprocessor-based image processing system for dedicated applications or interactive image processing 08 p1155 A83-22538
- Large scale multipurpose interactive image processing facility at ETH-Zurich 08 p1098 A83-22539
- Digital reconnaissance imagery processing system for real-time and near-real-time imagery exploitation 08 p1099 A83-22579
- High performance image generators for reconnaissance applications 08 p1099 A83-22580
- Multi-imagery exploitation system /MIES/ tactical scenario analysis 08 p1099 A83-22586
- Validation of a digital simulation of an optical matched filter correlator applied to aerial reconnaissance 08 p1100 A83-22589
- Design of Pel Adaptive DPCM coding based upon image partition 08 p1077 A83-22623
- Restoration of bilinearly distorted images. I - Finite impulse response linear digital filtering 08 p1101 A83-22672
- Hardware-constrained hybrid coding of video imagery 08 p1077 A83-22731
- Dynamic spatial filter for optical signal processing using a liquid crystal light valve 08 p1166 A83-22809
- Microprogrammable high-speed bit slice image processor 08 p1153 A83-22814
- Parallel signal processing for optical satellite detection 08 p1049 A83-22816
- Digital pipelined hardware median filter design for real-time image processing 08 p1153 A83-22817
- Computer-generated images in visual simulation and avionic technologies 08 p1047 A83-22835
- Rural scene perspective transformations 08 p1130 A83-22837

Drift compensation in a mosaic sensor
08 p1103 A83-22839

Thermal infrared pushbroom imagery acquisition and processing --- of NASA's Advanced Land Observing System
08 p1045 A83-22841

Statistical modeling of scene variability
08 p1103 A83-22848

Image transforms with fused fiber optics
08 p1167 A83-22864

Image quality; Proceedings of the Seminar, San Diego, CA, August 27, 28, 1981
08 p1105 A83-22890

Quality metrics of digitally derived imagery and their relation to interpreter performance
08 p1150 A83-22893

Effect of sampling, optical transfer function shape, and anisotropy on subjective image quality
08 p1167 A83-22894

Confirmation of the luminous connection between NGC 4319 and Markarian 205
08 p1184 A83-23079

Comparison of imaging infrared detection algorithms
09 p1265 A83-23529

Image analysis using polarized Hough transform and edge enhancer
09 p1265 A83-23532

Multidimensional clustering - An application to three-dimensional /3D/ surface extraction
09 p1265 A83-23533

Eliminating nearest neighbor searches in estimating target orientation
09 p1204 A83-23535

Optimal performance limits for detection and classification algorithms
09 p1266 A83-23537

Histogram-based algorithms for scene matching
09 p1266 A83-23538

Tracking of obscured targets via generalized correlation measures
09 p1266 A83-23542

Computer mapping of shoreline fluctuations by satellite
Great Salt Lake, Utah, U.S.A.
09 p1287 A83-24571

Application of the IHS color transform to the processing of multisensor data and image enhancement --- Intensity, Hue and Saturation in satellite remote sensing data
09 p1287 A83-24576

The imperial college multi-channel electronic image classifier and its applications to the classification of surface types by multi-spectral analysis
09 p1288 A83-24580

Analysis on the spatial distribution of water quality and pollution sources of a shallow lake by digital image processing
09 p1290 A83-24613

Mapping built up areas using Landsat MSS digital imagery
09 p1291 A83-24629

Image processing in signal-dependent noise
09 p1269 A83-24642

Estimation and identification of two dimensional images
09 p1328 A83-24718

Application of digital image analysis techniques to antismising fuel spray characterization
[ASME PAPER 82-WA/HT-23]
10 p1401 A83-25690

Faint star studies in the Magellanic Clouds. I - RICHFLD photographic photometry in NGC 2257
10 p1493 A83-25708

Hue-saturation-intensity split-spectrum processing of Seasat radar imagery
10 p1387 A83-25969

Mandatory processing of the background in the detection of objects in scenes
10 p1456 A83-26319

Effects of blur and noise on digital imagery interpretability
10 p1456 A83-26322

Holographic intensity correlator with a laser electron beam tube for inputting images for processing
10 p1422 A83-26467

The processing of synthetic aperture radar signals
10 p1404 A83-26473

Design of two-dimensional digital filters for blurred image restoration
10 p1464 A83-26515

Basis for spectral curvature algorithms in remote sensing of chlorophyll
10 p1453 A83-26644

Image processing by a spatial light modulator utilizing the Pockels effect
10 p1484 A83-26658

On the reduction of the distorting effect of the atmosphere in the digital processing of space imagery
10 p1444 A83-26822

Map transformations by optical anamorphic processing
10 p1484 A83-26859

Simple method for image deblurring
10 p1484 A83-26860

Nonlinear local image preprocessing using coherent optical techniques
10 p1484 A83-26863

Coherent optical production of the Hough transform
10 p1484 A83-26866

Complex of programs for the astrometric reduction of photographic observations
10 p1498 A83-26915

Use of computer vision techniques in estimating echo motion
11 p1571 A83-27039

A general interactive system for compositing digital radar and satellite data
11 p1647 A83-27089

X-ray imaging techniques - Modulation collimator and coded mask
11 p1657 A83-27752

Survey of model-based image analysis systems
11 p1573 A83-28097

Analysis of multitemporal Landsat 2 imagery of the Annaba zone of Algeria - April 28, 1977 and February 28, 1978 /Earthnet 20 834/
11 p1600 A83-28145

Remote sensing and cartography for soil use in Algeria: Comparative study of the interpretation of analog imagery /aerial photographs/ and of data treatment of digitized versions of the same images and spacial imagery - Application to the mouth of the Isser wadi /coastal Kabylie/ - Algeria
11 p1600 A83-28146

Land use mapping in lower Chaouia
11 p1601 A83-28147

An analysis of natural features of the Colombian plains by remote sensing
11 p1601 A83-28148

Regional land use research with multitemporal classification - On an image of Thailand
11 p1601 A83-28149

Remote sensing - Corrections and data enhancement. I
11 p1601 A83-28188

Remote sensing - Corrections and data enhancement. II
11 p1601 A83-28189

Remote sensing - Methods and uncertainty in interpretation. II
11 p1601 A83-28190

Automated processing of holographic interferograms in determining the deformations of diffusely reflecting objects
11 p1574 A83-28499

A study and construction of a proton nuclear magnetic resonance tomography device --- French thesis
11 p1575 A83-28630

Design and implementation of the Delft Image Processor DIP-1 --- Thesis
11 p1575 A83-28641

Automated digital processing of interferograms --- Thesis
11 p1575 A83-28650

Model-based three-dimensional interpretations of two-dimensional images
12 p1728 A83-28947

Multiframe image point matching and 3-D surface reconstruction
12 p1728 A83-28949

Detection of edges using range information
12 p1769 A83-28950

Laboratory system for demonstrating spacecraft processing of multispectral image data
12 p1748 A83-29146

Behaviour of a generalised covariance model in picture coding
12 p1769 A83-29470

Coordination of stereo image registration and pixel classification
12 p1731 A83-29918

Anisotropic nonstationary image estimation and its applications. I - Restoration of noisy images. II - Predictive image coding
13 p1845 A83-30223

Information processing in the visual system: Higher visual functions
13 p1900 A83-30426

The mechanisms of the classification of visual images according to spatial signs in normal dogs and after the excision of the parietal and the supertemporal cortices
13 p1896 A83-30439

On a method for the representation of images in the process of their arrival
13 p1910 A83-30617

Digital processing of Spacelab imagery
13 p1846 A83-30769

A parallel-pipeline architecture of the fast polynomial transform for computing a two-dimensional cyclic convolution
13 p1908 A83-30794

Method for automatic compensation of geometrical distortions in astronomical television equipment
13 p1919 A83-30869

Histogram concavity analysis as an aid in threshold selection --- in image processing
13 p1911 A83-31073

Elimination of redundant operations for a fast Sobel operator --- in automatic image segmentation by edge detection
13 p1911 A83-31074

MIDAS - ESO's new image processing system
13 p1942 A83-31581

Information theory and visual displays
13 p1911 A83-31584

Efficient positive coefficient algorithm for image processing
13 p1911 A83-31776

The first color panoramic pictures of the Venus surface transmitted by the Venera 13, 14 probes
14 p2014 A83-31956

Processing of panoramic TV pictures of the Venus surface transmitted by the Venera-13 and Venera-14 descent modules
14 p2014 A83-31957

Galileo Institute for Astronomy (IFA) charge-coupled device (CCD) system
14 p2015 A83-31989

Performance of the International Ultraviolet Explorer for spectral imaging
14 p1983 A83-32019

The atmospheric correction of remote-sensing images
14 p2035 A83-32499

The Laplacian pyramid as a compact image code
14 p2075 A83-32868

Soft decision demodulation and transform coding of images
14 p2076 A83-32872

A real-data FFT algorithm for image processing applications
14 p2073 A83-32900

Analytical tools for nonlinear image restoration
14 p2076 A83-32901

Image processing for extended depth of field
14 p2020 A83-32905

Digital image processing of flow visualization photographs
14 p2020 A83-32906

Transforming images into block stationary behavior
14 p2020 A83-32907

Design considerations for a real-time ocular counterroll instrument
14 p2073 A83-33108

Digital image processing with coherent light - A method and some applications
14 p2021 A83-33174

Determination of quadric surfaces from two projective views
14 p2021 A83-33344

The application of pseudo-Bayesian estimators to remote sensing data - Ideas and examples
14 p2036 A83-33347

Epsilon-separating nonlinear digital filter and its applications
15 p2220 A83-33519

A method of two-dimensional filter image with a nonseparable autocovariance function
15 p2220 A83-33520

Probabilistic cluster labeling of imagery data
15 p2224 A83-33686

Edge and line detection in multidimensional noisy imagery data
15 p2183 A83-33688

Stability of decision rules in pattern recognition problems
15 p2220 A83-33901

Preparation of a 1:25000 Landsat map for assessment of burnt area on Etajima Island
15 p2183 A83-34152

Digital image processing systems and remote sensing
15 p2183 A83-34159

Digitization of a video signal and stress analyses using IR thermography
15 p2178 A83-34401

Photographic photometry in globular clusters - Comparison of techniques
15 p2249 A83-34788

Hierarchical modeling for image classification
15 p2185 A83-34820

Integration and manipulation of remotely sensed and other data in geographic information systems
15 p2185 A83-34821

A 'user friendly' geographic information system in a color interactive digital image processing system environment
15 p2186 A83-34829

Some technical considerations on the evolution of the IBIS system --- Image Based Information System
15 p2186 A83-34834

Conversion of raster coded images to polygonal data structures
15 p2165 A83-34838

A geographic information system for New Mexico
15 p2187 A83-34843

The transmission of two-dimensional and color images through a single fiber by the spectral scanning technique
15 p2232 A83-34889

The problem of the visualization of information and digital image processing
15 p2165 A83-34968

A parallel algorithm for determining convex hulls of sets of points in two dimensions
15 p2218 A83-35115

An efficient source coding technique for data compression of multilevel digitized images
15 p2223 A83-35146

Image source coding using median filter roots
15 p2223 A83-35147

Block Truncation Coding on PASM --- reconfigurable multimicroprocessor for image processing
15 p2219 A83-35149

An optical residue processor for computing inner products
16 p2411 A83-35516

Autonomous earth feature classification - Shuttle and aircraft flight test results
[AIAA PAPER 83-0417]
16 p2370 A83-36054

Design of a real-time CGSI system
[AIAA PAPER 83-1101]
16 p2341 A83-36221

Imagery by radar and tomographical synthesis
[ONERA, TP NO. 1983-5]
16 p2342 A83-36418

Tradeoffs among several synthetic aperture radar image quality parameters - Results of a user survey study
16 p2356 A83-36573

Constrained transform coding and surface fitting
16 p2405 A83-36610

A method of stabilizing the clean algorithm --- for deconvolution of Fourier synthesis point spread functions from radio astronomy images
16 p2425 A83-36646

Automated Foucault test for focus sensing
16 p2413 A83-36764

An investigation of differential sensitivity in the visual perception process in normal individuals and in patients with schizophrenia
16 p2399 A83-36822

Distribution of the two-dimensional DCT coefficients for images --- Discrete Cosine Transform
16 p2357 A83-36909

Efficient algorithm for image enhancement
16 p2405 A83-36964

Photogrammetric processing of space photographs of the moon
17 p2614 A83-37007

Digital picture processing. Volumes 1 & 2 /2nd edition/ --- Book 17 p2509 A83-37167

Method of random image synthesis by means of computer 17 p2563 A83-38032

Image reconstruction of long-wavelength holograms by maximum entropy method 17 p2511 A83-38036

The 8 by 8 display 17 p2564 A83-38061

The role of image processing in mineral exploration - Why stop at Landsat? 17 p2528 A83-38148

Automatic DTM generation from digitized image densities 17 p2531 A83-38342

Land resources inventory assessment by Landsat image processing case study - Kano State, Nigeria (Africa) 17 p2532 A83-38354

International Society for Photogrammetry and Remote Sensing, International Symposium, Toulouse, France, September 13-17, 1982, Transactions. Volume 2 17 p2532 A83-38434

The effect of data reduction on image interpretation 17 p2532 A83-38435

Modeling for visual understanding of remotely sensed images A numerical simulation trial for analytical photointerpretation 17 p2532 A83-38436

The expanded PDCS digital image processing system (EPDCS) 17 p2532 A83-38438

The application of local textural transformation to automatic cartography of a tropical vegetation zone (Sumatra) 17 p2533 A83-38439

The application of Seasat data to the study of the evolution of the Pertuis Breton coastline 17 p2533 A83-38441

The application of SPOT simulated data to the remote sensing of an intertidal environment 17 p2534 A83-38457

The GEMPAK Barnes interactive objective map analysis scheme --- General Meteorological Software Package 17 p2548 A83-38709

Advances in systems for interactive processing and display of meteorological data 17 p2549 A83-38714

Application of sine transform in image processing 17 p2570 A83-38886

Spectral analysis at maximum resolution --- for measurement of astronomical magnetic fields 18 p2755 A83-39238

An interactive system for compositing digital radar and satellite data 18 p2726 A83-39869

Practical application of the optimal Wiener-Kolmogoroff filtering algorithm in quasi-holographic systems 18 p2739 A83-40099

A comparison of several image processing techniques applied to photographically recorded astronomical spectra 19 p2909 A83-40715

Optoelectronic methods of image processing 19 p2846 A83-40985

Image processing in automatic systems for scientific investigations --- Russian book 19 p2889 A83-40986

Stereoperspective in photogrammetry 19 p2846 A83-40988

Generalized chord transformation for distortion-invariant optical pattern recognition 19 p2900 A83-41096

Stationary transform processing of digital images for data compression 19 p2847 A83-41105

Automatic fringe analysis with a computer image-processing system 19 p2847 A83-41106

Image transmission through a turbulent medium using a point reflector and four-wave mixing in BSO crystal --- Bismuth Silicon Oxide 19 p2847 A83-41107

Landsat-D - An end-to-end data system 19 p2813 A83-41339

Two-dimensional hybrid block transform/DPCM coding of images 19 p2832 A83-41388

Optoelectronic methods for increasing the information content of ultrasonic ocular scanograms 19 p2882 A83-41459

Depth-first picture expression viewed from digital picture processing 20 p2989 A83-42646

Image design - Generation of a prescribed image at the output of a band-limited system 20 p3039 A83-42647

Preprocessing of side-looking airborne radar data 20 p2990 A83-42968

Digital image processing - Overview and areas of application 20 p2990 A83-43028

Estimation and identification of two-dimensional images 20 p2991 A83-43404

Nonlinear image processing for optimum composite source coding 20 p3040 A83-43683

Digital line-artifact removal --- image processing 21 p3134 A83-43868

Two-dimensional magneto-optic spatial light modulator for signal processing 21 p3134 A83-43869

Digital image processing using the Apple II microcomputer 21 p3190 A83-43892

A hybrid image classification instructional package 21 p3191 A83-43893

Multiple-window parallel adaptive boundary finding in computer vision 21 p3192 A83-43952

Applications of vector fields to image processing 21 p3135 A83-43953

An image transform coding scheme based on spatial domain considerations 21 p3135 A83-43954

An iterative approach to region growing using associative memories 21 p3191 A83-43956

High-throughput digital SAR processing 21 p3165 A83-43978

Geometrical aspects of interpreting images as a three-dimensional scene 21 p3135 A83-44068

Machine vision for robotics 21 p3135 A83-44078

Ridges and valleys on digital images 21 p3193 A83-44251

An implementation of a computational theory of visual surface interpolation 21 p3136 A83-44252

Rotationally symmetric operators for surface interpolation 21 p3193 A83-44253

Rigid body motion from depth and optical flow --- for computer vision 21 p3194 A83-44254

Processing translational motion sequences 21 p3194 A83-44255

Using shadows in finding surface orientations 21 p3136 A83-44256

3-D shape from contour and selective confirmation 21 p3137 A83-44257

On the information in optical flows --- computer vision 21 p3194 A83-44258

Segmentation of digital curves using linguistic techniques 21 p3194 A83-44259

Matching the task to an image processing architecture --- for overcoming Von Neumann bottleneck 21 p3190 A83-44260

An estimation-theoretic approach to terrain image segmentation 21 p3194 A83-44261

Picture processing - 1982 21 p3194 A83-44262

An interpretation for probabilistic relaxation --- processing mechanisms in image analysis 21 p3194 A83-44263

An operating system interface for transportable image processing software 21 p3191 A83-44264

Quantitative evaluation of some edge-preserving noise-smoothing techniques 21 p3191 A83-44265

An experiment in multispectral, multitemporal crop classification using relaxation techniques 21 p3165 A83-44267

Uniform color scale applications to computer graphics 21 p3190 A83-44268

Fast algorithms for estimating local image properties 21 p3137 A83-44270

Determining 3-D motion and structure of a rigid body using the spherical projection 21 p3118 A83-44273

Representation of three-dimensional motion in dynamic scenes 21 p3118 A83-44275

The detection of unresolved targets using the Hough transform 21 p3120 A83-44276

An approach to the segmentation of textured dynamic scenes 21 p3137 A83-44277

On seeing reddish green and yellowish blue 21 p3187 A83-44365

A new method of determining nebular radial velocities from Fabry-Perot interferograms 21 p3222 A83-44415

A curvilinear snake arm robot with gripper-axis fibre-optic image processor feedback 21 p3119 A83-44695

Acquisition and manipulation of image statistics 21 p3139 A83-44787

Applications of interference coatings in optical processing 21 p3206 A83-44791

Interferometer detection system for optical testing 21 p3139 A83-44797

Optical image processing in coherent and incoherent light - A short comparative review 21 p3207 A83-44825

Hybrid optical-digital image processing system for pattern recognition 21 p3194 A83-44826

Environmental data display 21 p3142 A83-45615

The application of processed Landsat imagery in photo-interpretation 22 p3308 A83-46121

The European SAR-580 project --- high resolution Synthetic Aperture Radar data evaluation 22 p3310 A83-46136

Defining system requirements for acquiring and processing land remote sensing data 22 p3310 A83-46150

Doppler parameter estimation techniques for spaceborne SAR with applications to ocean current measurement 22 p3289 A83-46159

On energy conserving methods in multispectral image processing 22 p3289 A83-46173

Real time SAR-Processor 22 p3290 A83-46209

Automated preprocessing of spaceborne SAR data 22 p3290 A83-46210

Edge detection for synthetic aperture radar and other noisy images 22 p3278 A83-46212

Geometric registration and rectification of spaceborne SAR imagery 22 p3290 A83-46213

SIR-A radar images of sand dunes and volcanic fields 22 p3314 A83-46225

Augmenting Landsat MSS data with topographic information for enhanced registration and classification 22 p3314 A83-46229

Design and implementation of SPIDER - A transportable image processing software package 22 p3350 A83-46251

Neighboring gray level dependence matrix for texture classification 22 p3315 A83-46254

Picture information measures for similarity retrieval 22 p3290 A83-46255

Infrared focal plane array system performance modeling 22 p3292 A83-46597

Technology for large digital mosaics of Landsat data 22 p3318 A83-46766

Image formation by multifacet holograms 22 p3294 A83-46835

Hybrid processing for phase measurement in metrology and flow diagnostics 22 p3294 A83-46837

Information extraction from thematic mapper data [IAF PAPER 83-114] 23 p3475 A83-47275

Satellite image processing for a small country - The Hungarian case [IAF PAPER 83-123] 23 p3475 A83-47280

A development of a high speed image processing system - TIAS 3000 [IAF PAPER 83-125] 23 p3454 A83-47281

The Swedish SPOT data acquisition and processing system [IAF PAPER 83-128] 23 p3475 A83-47283

ERS-1 processing algorithms and disseminated products [IAF PAPER 83-129] 23 p3475 A83-47284

Principles of organization of the on-ground data processing for remote sensing purposes using finite rings and fields [IAF PAPER 83-130] 23 p3501 A83-47285

Application of track spectrometric studies in image processing for remote sensing purposes [IAF PAPER 83-138] 23 p3475 A83-47287

Speckle interferometry observations of Pluto's moon Charon 23 p3516 A83-47439

Fast algorithm for the computation of the zero-order Hankel transform 23 p3501 A83-47581

X-ray tomography applied to NDE of ceramics [ASME PAPER 83-GT-206] 23 p3458 A83-48007

Stereotelevision display devices --- Russian book 23 p3459 A83-48249

Experiments on digital image data comparison --- for Landsat satellite photos 24 p3598 A83-48990

Color coding in quasi-interferometry 24 p3582 A83-49011

Iconics: Theory and methods of image processing 24 p3582 A83-49042

The computer-aided matching and geometric alignment of images 24 p3582 A83-49045

Multilevel computational processes for visual surface reconstruction 24 p3619 A83-49196

IUE data reduction 24 p3644 A83-49558

Methods of image sharpening 24 p3583 A83-49609

Normalisation of Fourier descriptors of planar shapes 24 p3621 A83-49984

Digital processing of objective prism-stellar spectrograms 24 p3648 A83-50022

Automated stellar photometry 24 p3649 A83-50029

IMAGE RECONSTRUCTION

A statistical approach to image segmentation 01 p0098 A83-11433

Microstructure representation through neighborhood relations --- for scene analysis 01 p0099 A83-11440

A general scheme for signal restoration with application to picture processing 01 p0099 A83-11453

A simple contour matching algorithm 01 p0100 A83-11471

Synthetic generation and estimation in random field models of images 01 p0101 A83-11474

Demonstration of image transmission through fibers by optical phase conjugation 02 p0235 A83-11568

Image restoration - A linear stochastic filtering approach --- Thesis 02 p0176 A83-11900

Aberrations grazing incidence systems and their reduction or toleration --- in astronomical X ray imagery 02 p0237 A83-12693

Holographic display of 3D digital data 03 p0324 A83-13437

Enhancement of astronomical images using digital filtration methods 03 p0407 A83-13672

The effect of reference's phase on radio-frequency holographic imaging 03 p0328 A83-14026

The need for cross-fertilization between the fields of profile inversion and computed tomography --- in test pattern reconstruction 03 p0329 A83-14291

Quantitative Time-Of-Flight /TOF/ imaging for nondestructive evaluation by computerized ultrasonic tomography 04 p0493 A83-15224

Quantitative evaluation of real-time synthetic aperture acoustic images [AD-A130062] 04 p0493 A83-15228

Multiple-aperture three-dimensional image construction utilizing fringe-modulated speckle patterns 05 p0643 A83-16835

Diffraction efficiency of out-of-phase amplitude-phase volume holograms 05 p0644 A83-17080

Image compensation in the presence of thermal blooming --- extended target image reconstruction using adaptive optics 07 p0935 A83-20156

Estimation and choice of neighbors in spatial-interaction models of images 07 p0984 A83-20549

Method for additional correction of algorithm for the restoration of smeared images 07 p0929 A83-20558

One-dimensional high resolution image reconstruction on Eta Carinae at 4.6-microns with speckle data 07 p1009 A83-21229

Spatial frequency response and resolution in holography 08 p1092 A83-22081

Analytic continuation applied to microwave apertures 08 p1095 A83-22471

A method of automatic image reconstruction from holograms by a homomorphic system of logarithmic transform type 08 p1101 A83-22625

Restoration of bilinearly distorted images. I - Finite impulse response linear digital filtering 08 p1101 A83-22672

Synthesis of radio holograms by raster scanning using a receiver-transmitter device 09 p1265 A83-23465

Radial multi-slit coding for X-ray imaging of laser microplasmas 09 p1267 A83-23709

Composite two-dimensional phase-restoration procedure 09 p1268 A83-24097

Image reconstruction techniques and target detection 09 p1269 A83-24716

Experiences regarding the accuracy of localization and reconstruction in the case of ultrasonic holography 09 p1270 A83-24943

The reconstruction of images scattered in an inhomogeneous medium --- Russian book 09 p1270 A83-25224

Active optics in astronomy 10 p1481 A83-25828

Active wavefront correction in large telescopes 10 p1482 A83-25830

Speckle interferometry, speckle holography, speckle spectroscopy, and reconstruction of high-resolution images from space telescope data 10 p1419 A83-25833

Real-time holographic interferometry of moving objects in oppositely directed beams 10 p1420 A83-25891

Reconstruction of objects from coded images by simulated annealing 10 p1420 A83-26110

Optical reconstruction of wideband Fourier and Fresnel acoustic holograms 10 p1421 A83-26295

Digital image reconstruction of microwave holograms 10 p1424 A83-26855

Map transformations by optical anamorphic processing 10 p1484 A83-26859

Coherent optical image delay device using a BSO phase-conjugate mirror and its applications 10 p1424 A83-26864

Radio imaging in a receiving system with partial channels 11 p1555 A83-27935

Multiframe image point matching and 3-D surface reconstruction 12 p1728 A83-28949

Analysis of the shift-and-add method for imaging through turbulent media 12 p1779 A83-29375

Aperture analysis of laser speckle interferograms 12 p1730 A83-29588

Methods of reconstruction and visualization of three-dimensional images in X-ray computed tomography --- French thesis 13 p1844 A83-30128

Two-dimensional DPCM image transmission over fading channels 13 p1827 A83-30222

Anisotropic nonstationary image estimation and its applications. I - Restoration of noisy images. II - Predictive image coding 13 p1845 A83-30223

Holographic memory for data with a periodic structure, with imaging of the scatterer into the hologram plane during recording 13 p1846 A83-30624

Spectral estimation for sensor arrays [AD-A129985] 13 p1847 A83-30925

Coherent optical system of modular imaging collectors (COSMIC) telescope array - Astronomical goals and preliminary image reconstruction results 13 p1920 A83-30997

Speckle imaging for planetary research 13 p1939 A83-31208

Analytical tools for nonlinear image restoration 14 p2076 A83-32901

Signal restoration from phase by projections onto convex sets 15 p2220 A83-33809

Method of improving image quality in holographic interferometers 15 p2164 A83-34424

Filtering of noisy images using Markov random field models 15 p2223 A83-35145

On the uniqueness of image reconstruction from the amplitude of radiointerferometric response 16 p2424 A83-36527

Constrained transform coding and surface fitting 16 p2405 A83-36610

Image reconstruction by the speckle-masking method 17 p2592 A83-37949

Method of random image synthesis by means of computer 17 p2563 A83-38032

Image reconstruction of long-wavelength holograms by maximum entropy method 17 p2511 A83-38036

Maximum entropy image reconstruction - A practical non-information-theoretic approach --- for astronomical spectrum restoration 18 p2754 A83-39200

Computerized ultrasonic tomography for testing solid propellant rocket motors 18 p2695 A83-39565

Infrared speckle interferometry, results, true image reconstruction and instrumental plans 18 p2761 A83-40437

X-ray imaging of extended objects using nonoverlapping redundant array 19 p2847 A83-41104

Interferometric displacement sensing in the open atmosphere 19 p2848 A83-41177

A survey of methods for iterative signal restoration 19 p2830 A83-41376

Speckle image reconstruction of solar features 20 p3081 A83-42476

Image design - Generation of a prescribed image at the output of a band-limited system 20 p3039 A83-42647

Dual-beam encoding for color holographic construction 20 p2992 A83-43630

Restoration of out-of-focused color photographic images 20 p2992 A83-43631

Multiplexed speckle and holographic interferometry with color encoding by white-light processing 21 p3134 A83-43872

Fabrication of a 360 deg astigmatic rainbow hologram 21 p3136 A83-44153

Quantitative evaluation of some edge-preserving noise-smoothing techniques 21 p3191 A83-44265

Image restoration by a powerful maximum entropy method 21 p3137 A83-44266

Approximating point-set images by line segments using a variation of the Hough transform 21 p3190 A83-44271

A discrete spatial representation for lateral motion stereo 21 p3118 A83-44274

Image reconstruction by parametric cubic convolution 22 p3350 A83-46250

Image restoration for a defocused optical system 22 p3294 A83-46827

Image restoration by convex projections in the presence of noise 22 p3294 A83-46828

Gaussian beam effects in far-field in-line holography 22 p3294 A83-46836

X-ray tomography applied to NDE of ceramics [ASME PAPER 83-GT-206] 23 p3458 A83-48007

Effects of photon noise on speckle image reconstruction with the Knox-Thompson algorithm --- in astronomy 23 p3459 A83-48312

Real-time image deblurring using four-wave mixing 24 p3628 A83-48750

Phase estimation based on the maximum likelihood criterion 24 p3582 A83-49016

Iconics: Theory and methods of image processing 24 p3582 A83-49042

Multilevel computational processes for visual surface reconstruction 24 p3619 A83-49196

Methods of image sharpening 24 p3583 A83-49609

IMAGE RESOLUTION

Resolution requirements for a soil moisture imaging radar 01 p0020 A83-10039

The effects of photographic noise on pointing precision, detection, and recognition 01 p0050 A83-10714

Wiener estimator for inversion of linear operators and superresolution 01 p0099 A83-11454

Morphometric consistency with the Hausdorff-Besicovich dimension 02 p0203 A83-11844

Image quality and lens aberrations of an aerial camera 02 p0177 A83-11989

High resolution imaging from the ground 02 p0246 A83-12188

High resolution soft X-ray optics; Proceedings of the Meeting, Brookhaven, NY, November 18-20, 1981 02 p0239 A83-12721

Extra-solar astronomy with a 2.4 m normal incidence X-ray telescope at 0.1 arcsec resolution 02 p0247 A83-12726

Solar corona at high resolution 02 p0271 A83-12727

Progress report on the high resolution spectrograph for the Space Telescope 03 p0288 A83-13971

A comparison of galaxy images on new and old POSS prints 03 p0409 A83-14137

The effects of haze on resolution on small scale aerial photography 03 p0329 A83-14283

Results of stereoscopic image simulations for the SPOT HRV carried out at the Gun Lake site in British Columbia 03 p0350 A83-14292

Aerial camera vibration 03 p0330 A83-14663

Resolution versus speckle relative to geologic interpretability of spaceborne radar images - A survey of user preference 03 p0351 A83-14852

The effects of surface mapping corrections with synthetic-aperture focusing techniques on ultrasonic imaging 04 p0493 A83-15226

Some accuracy and resolution aspects of computer vision distance measurements 04 p0528 A83-16032

Rainbow holographic aberrations and the bandwidth requirements 06 p0762 A83-18594

One-dimensional high resolution image reconstruction on Eta Carinae at 4.6-microns with speckle data 07 p1009 A83-21229

The effects of atmospheric turbulence on telescopic observations 07 p1010 A83-21525

A Spot-Landsat comparison simulation in a forested region - Ermenonville 1980 08 p1126 A83-21929

Probabilistic diffraction limited imaging through turbulence 08 p1164 A83-22361

Analytic continuation applied to microwave apertures 08 p1095 A83-22471

The change of limiting resolution of electro-optical systems due to atmospheric effects 08 p1098 A83-22561

Film still looks good --- advantages of conventional cameras for aerial reconnaissance 08 p1099 A83-22587

Image quality; Proceedings of the Seminar, San Diego, CA, August 27, 28, 1981 08 p1105 A83-22890

Quality metrics of digitally derived imagery and their relation to interpreter performance 08 p1150 A83-22893

Effect of sampling, optical transfer function shape, and anisotropy on subjective image quality 08 p1167 A83-22894

Modulation transfer function measurement system /MTFMS/ - A new development in image quality measurement 08 p1105 A83-22898

Effects of tilt of a four-bar pattern on the minimum resolvable temperature difference /MRTD/ --- of FLIR detectors 08 p1105 A83-22899

Techniques for pseudo-dc restoration and dynamic range enhancement of scanned infrared imagery 08 p1105 A83-22900

Image quality experiments for TV reconnaissance at reduced transmission bandwidth 08 p1105 A83-22902

Image resolution and accuracy of measurements of soil moisture with microwave sensors in low earth and geosynchronous orbits 09 p1287 A83-24563

Procedure for the diagnosis of axial electron-optical image defects --- German thesis on electron microscope resolution 09 p1269 A83-24844

Scientific importance of high angular resolution at infrared and optical wavelengths; Proceedings of the Conference, Garching, West Germany, March 24-27, 1981 10 p1494 A83-25826

Atmospheric limitations to high angular resolution imaging 10 p1481 A83-25827

Active optics in astronomy 10 p1481 A83-25828

Active wavefront correction in large telescopes 10 p1482 A83-25830

Image quality and high resolution in future telescopes 10 p1482 A83-25832

Speckle interferometry, speckle holography, speckle spectroscopy, and reconstruction of high-resolution images from space telescope data 10 p1419 A83-25833

On the deconvolution of brightness profiles of galaxies from seeing - Application to NGC 3379 10 p1494 A83-25834

Coherent large telescopes 10 p1494 A83-25836

A shearing, modulating interferometer --- for astronomical observation 10 p1420 A83-25838

Probability of diffraction-limited images in infrared through turbulence experimental results 10 p1420 A83-25839

Imaging by dilute apertures in the presence of atmospheric turbulence 10 p1482 A83-25840

Angular momentum and star formation 10 p1495 A83-25852

Design of two-dimensional digital filters for blurred image restoration 10 p1464 A83-26515

Performance of the Multiple Mirror Telescope (MMT). III Seeing experiments with the MMT 13 p1937 A83-30979

Effects of primary mirror segmentation on telescope image quality 13 p1919 A83-30992

Sub-regional information system formation using multi-resolution remote sensing products 15 p2239 A83-34807

A high temperature straining stage (300-1000 K) for a 200 kV microscope 15 p2166 A83-35253

Measurement of laser photoelectron image degradation at high current densities 16 p2356 A83-35969

Simultaneous scanning optical and acoustic microscopy 16 p2356 A83-36478

Digital picture processing. Volumes 1 & 2 /2nd edition/ --- Book 17 p2509 A83-37167

Possible optical scheme of a telescope with a main spherical mirror with a diameter of 20-25 m 17 p2590 A83-37690

Fiber-optic image transmission system with high resolution 17 p2580 A83-37749

Image quality of the new AGFA-Gevaert aerial-photography films 17 p2511 A83-38058

Aperture synthesis in the infrared 18 p2762 A83-40453

Image design - Generation of a prescribed image at the output of a band-limited system 20 p3039 A83-42647

Spatial resolution of remotely sensed imagery - A review paper 20 p3010 A83-42957

Spatial resolution of thermal wave microscopes 21 p3142 A83-45488

Continuous-wave self-pumped phase conjugator with wide field of view 22 p3356 A83-45964

Remote sensing for coastal areas 22 p3343 A83-46144

Influence of the precipitations and clouds on the performance of a synthetic aperture radar 22 p3289 A83-46197

Low-noise multicolor archival storage with broad source interferometric imaging 22 p3294 A83-46829

High resolution maps with the VLA 24 p3639 A83-49132

High-resolution imaging of inhomogeneities in superconducting tunnel junctions by scanning with a modulated electron beam 24 p3636 A83-49757

IMAGE ROTATION

Rotation modulation phoswich: Design for an image-forming system for the hard X-ray region /greater than 20 keV/ --- German thesis 01 p0116 A83-10475

Rotational invariance in visual pattern recognition by pigeons and humans 02 p0224 A83-12068

Procedure for camera calibration with image sequences 02 p0182 A83-12899

A method of rotating areas on a raster scan graphic display 05 p0644 A83-16871

Rotation interferometry - A new technique for achieving high angular resolution 10 p1419 A83-25837

Real-time holographic interferometry of moving objects in oppositely directed beams 10 p1420 A83-25891

Conceptual kinematic design using homogeneous coordinate transformations [AIAA PAPER 83-2460] 23 p3500 A83-48337

IMAGE TRANSDUCERS

Noise reduction techniques for CCD image sensors 02 p0167 A83-12012

Technical issues in focal plane development; Proceedings of the Meeting, Washington, DC, April 21, 22, 1981 03 p0325 A83-13726

Teal Amber visible focal plane technology 03 p0325 A83-13730

Compensation electronics for staring focal plane arrays 03 p0326 A83-13734

Technical issues in focal plane development for terrestrial resource observations 03 p0326 A83-13735

Large time-delay-and-integration /TDI/ arrays and focal plane structures with intrinsic silicon response 03 p0309 A83-13736

Multi-anode microchannel arrays - New detectors for imaging and spectroscopy in space [AIAA PAPER 83-0105] 05 p0608 A83-16523

Analysis of a linear array taking into account satellite-sensor performances and a digital terrain model 08 p1124 A83-21904

Correction of pixel nonuniformities for solid-state imagers 08 p1094 A83-22441

Evaluation of peak location algorithms with subpixel accuracy for mosaic focal planes 08 p1050 A83-22448

Itek model 2KL sensor - The mini-electro-optical imaging system /Mini EOIS/ 08 p1099 A83-22581

Mosaic focal plane methodologies II; Proceedings of the Conference, San Diego, CA, August 27, 28, 1981 08 p1100 A83-22598

Progress in 800 x 800 charge-coupled device /CCD/ imager development and applications 08 p1051 A83-22603

AlGaAs/GaAs heterojunction charge-coupled devices /CCDs/ for visible/near infrared imaging applications 08 p1080 A83-22604

Modulation transfer function measurement system /MTFMS/ - A new development in image quality measurement 08 p1105 A83-22898

Achieving stability in remote holography using flexible multimode image bundles 10 p1423 A83-26635

Information theory analysis of sensor-array imaging systems for computer vision 12 p1728 A83-28898

Optimization of charge-coupled device (CCD) imager performance for astronomy 14 p2015 A83-31987

Galileo Institute for Astronomy (IFA) charge-coupled device (CCD) system 14 p2015 A83-31989

Charge-coupled device (CCD) television camera for NASA's Galileo mission to Jupiter 14 p1983 A83-32024

IMAGE TUBES

An image-tube camera for cometary spectrography 10 p1498 A83-26911

Multiple object fiber optic spectroscopy 14 p2017 A83-32012

Photon counting Reticon system - Description and performance 14 p2018 A83-32023

Infrared instrumentation on Calar Alto --- mountain-based telescopes for photography 18 p2760 A83-40421

Process for producing laser-formed video calibration markers 21 p3136 A83-44155

IMAGE VELOCITY SENSORS

Fourier transform image tracker and stabilizer 08 p1099 A83-22584

C.C.D. imaging - Solid state sensor now out performs vidicon in tracking application: Back cover illustration contrasts the dimensions of these sensors against the magnified silicon structure of a C.C.D. 11 p1573 A83-28179

Contour-based motion estimation 22 p3350 A83-46252

IMAGERY

NT ACOUSTICAL HOLOGRAPHY

NT AERIAL PHOTOGRAPHY

NT ALL SKY PHOTOGRAPHY

NT ANGIOGRAPHY

NT ASTRONOMICAL PHOTOGRAPHY

NT AUTORADIOGRAPHY

NT BLACK AND WHITE PHOTOGRAPHY

NT CHRONOPHOTOGRAPHY

NT CINEMATOGRAPHY

NT CLOUD PHOTOGRAPHY

NT COLOR INFRARED PHOTOGRAPHY

NT COLOR PHOTOGRAPHY

NT ELECTRO-OPTICAL PHOTOGRAPHY

NT HOLOGRAPHY

NT INFRARED IMAGERY

NT INFRARED PHOTOGRAPHY

NT KINOFORM

NT LUNAR PHOTOGRAPHY

NT MICROWAVE HOLOGRAPHY

NT MICROWAVE IMAGERY

NT NEUTRON RADIOGRAPHY

NT PHOTOMICROGRAPHY

NT PHOTORECONNAISSANCE

NT RADAR IMAGERY

NT RADAR PHOTOGRAPHY

NT RADIOGRAPHY

NT SATELLITE-BORNE PHOTOGRAPHY

NT SCHLIEREN PHOTOGRAPHY

NT SHADOWGRAPH PHOTOGRAPHY

NT SPACEBORNE PHOTOGRAPHY

NT SPECTROHELIOGRAPHS

NT STEREOPHOTOGRAPHY

NT STEREOSCOPY

NT TOMOGRAPHY

NT ULTRAVIOLET PHOTOMETRY

NT WHITE LIGHT HOLOGRAPHY

NT X RAY IMAGERY

NT XEROGRAPHY

IMAGES

NT AFTERIMAGES

NT RETINAL IMAGES

Experimental study of mental rotations in visual representations 16 p2401 A83-36816

Representation of spatial spectrum in terms of the density of luminance differences 18 p2739 A83-40401

IMAGING RADAR

U SYNTHETIC APERTURE RADAR

IMAGING TECHNIQUES

NT IMAGE ENHANCEMENT

NT RADAR IMAGERY

Earth-based and earth orbital observations of solar system bodies 01 p0128 A83-10050

Geological terrain models 01 p0064 A83-10080

Potentials for change detection using Seasat synthetic aperture radar data 01 p0066 A83-10121

Formation of microwave and ultrasonic three-dimensional images by means of antennas with beam scanning during a pulse 01 p0049 A83-10403

Rotation modulation phoswich: Design for an image-forming system for the hard X-ray region /greater than 20 keV/ --- German thesis 01 p0116 A83-10475

An automated mapping satellite system /Mapsat/ 01 p0066 A83-10715

Anisotropic filtering operations for image enhancement and their relation to the visual system 01 p0099 A83-11451

Image registration using generalized Hough transforms 01 p0100 A83-11467

The image-forming properties of multiple-zone Fresnel lenses in the millimeter-wavelength range 02 p0175 A83-11539

High resolution imaging from the ground 02 p0246 A83-12188

Subsurface-structure determination using photothermal laser-beam deflection 02 p0177 A83-12282

Spectroscopic imaging of the thermosphere from the Space Shuttle 02 p0211 A83-12605

Techniques and applications of image understanding; Proceedings of the Meeting, Washington, DC, April 21-23, 1981 02 p0181 A83-12875

Determining optical flow --- distribution of apparent movement velocities of image brightness patterns 02 p0182 A83-12897

Real-time NDE of flaws using a digital acoustic imaging system 03 p0337 A83-13434

3-D machine perception; Proceedings of the Conference, Washington, DC, April 23, 24, 1981 03 p0324 A83-13444

Applications of digital image acquisition in anthropometry 03 p0384 A83-13449

Further developments of electrographic image detectors 03 p0288 A83-13963

The effect of reference's phase on radio-frequency holographic imaging 03 p0328 A83-14026

The effects of surface mapping corrections with synthetic-aperture focusing techniques on ultrasonic imaging 04 p0493 A83-15226

Quantitative evaluation of real-time synthetic aperture acoustic images [AD-A130062] 04 p0493 A83-15228

Acoustic imaging with two dimensional arrays 04 p0493 A83-15229

Test bed for quantitative NDE - Imaging results 04 p0493 A83-15230

Field-ion microscopy - A review of basic principles and selected applications 05 p0644 A83-16918

Analysis of airfoil leading edge separation bubbles [AIAA PAPER 83-0300] 05 p0591 A83-17918

Speckle reduction by a rotating aperture at the Fourier transform plane 05 p0647 A83-17940

Coupling and imaging of Gaussian beams in parallel dielectric slab waveguides 06 p0749 A83-17967

Monochromatic imaging from UV to IR using a subtractive double monochromator 06 p0762 A83-18579

Imaging performance of annular apertures. IV - Apodization and point spread functions. V - Total and partial energy integral functions 06 p0810 A83-18590

Gel electrode imaging of fatigue cracks in aluminum alloys 06 p0730 A83-18941

Proposed hard X-ray imaging and gamma ray burst studies for XTE --- X-ray Timing Explorer 07 p1005 A83-20040

Schlieren visualization of acoustically imaged defects 07 p0929 A83-20174

A three-dimensional pattern recognition technique for inspection of missing parts in assemblies 07 p0942 A83-20452

Measurements and imaging method of blood flow profile in human heart 08 p1151 A83-22237

Thermal effects in photothermal spectroscopy and photothermal imaging 08 p1092 A83-22335

Probabilistic diffraction limited imaging through turbulence 08 p1164 A83-22361

Comparison of transform image coding techniques for compression of tactical imagery 08 p1100 A83-22597

Visual simulation and image realism II; Proceedings of the Conference, San Diego, CA, August 27, 28, 1981 08 p1102 A83-22830

Considerations in the selection and use of calibration equipment for simulators used with thermal imaging systems 08 p1104 A83-22884

Information density and efficiency of two-dimensional /2-D/ sampled imagery 08 p1105 A83-22895

Optical criteria for the prediction of optical system Modulation Transfer Function /MTF/ 08 p1167 A83-22896

Imaging performance of the Faint Object Camera 09 p1266 A83-23584

Self-imaging effect in physical radiometry 09 p1268 A83-24100

A sealed high pressure xenon filled imaging proportional counter with a sensitive area 30cm square 09 p1268 A83-24109

Moire deflectometry with deferred analysis 09 p1269 A83-24442

Image reconstruction techniques and target detection 09 p1269 A83-24716

Spray combustion processes - A review [ASME PAPER 82-WA/HT-86] 10 p1390 A83-25691

Atmospheric limitations to high angular resolution imaging 10 p1481 A83-25827

Acoustic imaging for diagnostics of chemically reacting systems [AIAA PAPER 83-0761] 10 p1476 A83-25955

Reconstruction of objects from coded images by simulated annealing 10 p1420 A83-26110

Doppler imaging system: An optical device for measuring vector winds. I - General principles 10 p1423 A83-26643

The identification of the variation of atherosclerosis plaques by invasive and non-invasive methods 11 p1643 A83-28760

Gamma-ray imaging with a rotating modulator 12 p1708 A83-28895

Conceptual design of a coherent optical system of modular imaging collectors (COSMIC) --- telescope array deployed by space shuttle in 1990's 13 p1938 A83-30996

Channeling contrast microscopy - Application to semiconductor structures 13 p1929 A83-31067

Speckle imaging for planetary research 13 p1939 A83-31208

Instrumentation in astronomy IV; Proceedings of the Fourth Conference, Tucson, AZ, March 8-10, 1982 14 p2014 A83-31976

Highly versatile computer-controlled television detector system 14 p2015 A83-31985

Differential imaging using charge-coupled device (CCD) imagers with on-chip charge storage 14 p2015 A83-31986

Software simulations of the detection of rapidly moving asteroids by a charge-coupled device 14 p2095 A83-31990

Drift scan observations with a charge-coupled device (CCD) 14 p2016 A83-31994

Texas Instruments' virtual phase charge-coupled device (CCD) imager operated in the frontside electron-bombarded mode 14 p2016 A83-31995

New two-dimensional photon camera 14 p2018 A83-32021

Miniature imaging photon detector 14 p2018 A83-32022

Microchannel intensified electrography 14 p2018 A83-32028

Certain characteristics of the use of photothermoplastic materials in remote-sensing imaging systems 14 p2019 A83-32503

Exact analytical solution of the generalized Luneburg lens problem 15 p2230 A83-33807

Imaging of spatial structures in superconducting tunnel junctions by electron-beam scanning 15 p2164 A83-34141

Image quality of active and passive scanners 16 p2356 A83-36123

Electrooptical imaging system using wavelength coding 17 p2510 A83-37748

Energy model of image formation by an optical system 17 p2580 A83-38480

An imaging telescope for high energy gamma-ray astronomy 18 p2755 A83-39281

Imaging systems using modulation and coded aperture masks --- for gamma ray telescopes 18 p2756 A83-39284

The position sensitive low energy detector on board the ZEBRA telescope --- for gamma and X-ray astronomy 18 p2647 A83-39286

An imaging telescope for soft gamma-ray astronomy - The preliminary in-flight tests 18 p2756 A83-39287

A directional gamma-ray telescope using coded aperture techniques 18 p2756 A83-39289

The GEL electrode - A new method of detecting fatigue cracks 18 p2668 A83-40612

Critical-cone channeling of thermal phonons at a sapphire-metal interface 19 p2903 A83-40954

Point spread functions in imaging a Lambert surface from zenith through a thin scattering layer 20 p3011 A83-42964

Many-beam imaging studies of crystal structure of ordered alloys 20 p2992 A83-43610

A versatile thermal imager for RPV applications 20 p2936 A83-43720

Grazing incidence toroidal mirror pairs in imaging and spectroscopic applications 21 p3204 A83-44150

Polychromatic MTF of electrostatic point symmetric electron lenses 21 p3125 A83-44152

Experiments in combining intensity and range edge maps 21 p3137 A83-44272

Scanning radiometer for calibrating thermal imager test targets 21 p3138 A83-44782

Trends in solid state image sensors for remote sensing 22 p3260 A83-46152

Imaging spectrometer - An advanced multispectral imaging concept 22 p3261 A83-46154

High-resolution images of the Galactic Centre 22 p3375 A83-46560

Acoustic imaging of 3D carbon/carbon billets 22 p3304 A83-46770

Doppler imaging of starspots 23 p3516 A83-47513

Aberrated point-spread functions for rotationally symmetric aberrations 24 p3629 A83-49014

Objective prism radial velocities for clusters of galaxies near the South Galactic Pole 24 p3649 A83-50025

IMBEDDINGS (MATHEMATICS)

NT INVARIANT IMBEDDINGS

Application of variational embedding technique to nonlinear heat transfer problems 08 p1084 A83-22149

Symmetric marching technique /SMT/ for the efficient solution of discretized Poisson equation on non-rectangular regions 08 p1091 A83-23218

Variational embedding solutions of radiative heat transfer upon a semi-infinite body with variable thermal properties 21 p3128 A83-44020

IMIDES

Thermal action of laser radiation on imidization 10 p1392 A83-26690

Characterization of geometric isomers of Norbornene end-capped imides 16 p3233 A83-36980

IMINES

Oxidative peptide /and amide/ formation from Schiff base complexes 06 p0800 A83-18247

IMMERSSION

U SUBMERGING

IMMISIBILITY

U SOLUBILITY

IMMITTANCE

U ELECTRICAL IMPEDANCE

IMMOBILIZATION

Closed osteosynthesis and conservative therapy of fresh diaphyseal fractures of the crural bones 03 p0381 A83-14339

The peculiarities of the functional condition of the adrenal cortex in old rats during immobilization stress 05 p0672 A83-17600

Effect of hindlimb immobilization on the fatigability of skeletal muscle 14 p2064 A83-32813

The participation of an insulin-dependent cytoplasmic regulator in carbohydrate metabolism during immobilization 19 p2871 A83-40818

Rhythms in the range of 4.5-12 Hz of the background EEG from the visual and sensorimotor cortex in rats under different patterns of locomotor activity 19 p2876 A83-41565

The changes in the content of catecholamines in the dopamine-synthesizing nuclei of the brain of rats in conditions of immobilization stress 19 p2879 A83-42093

IMMUNITY

The effect of T-activin and hydrocortisone on transplantation immunity 01 p0080 A83-10549

The distribution of functionally different cells in immunocompetent organs after an injection of haloperidol 01 p0080 A83-10550

Immunobiological properties of teichoic acids --- for diagnosing staphylococcal infections 01 p0081 A83-10556

The role of Fc-receptors of lymphocytes, macrophages, and other mammalian cells during the immune processes 01 p0082 A83-11406

The complement and its role in the regulation of immunological reactions 01 p0082 A83-11407

The effect of deficiencies of trace elements on immunity /Review of literature/ 03 p0381 A83-14348

The effect of microelemental additions on the activity of certain metallic enzymes, immune stability, and performance of athletes 05 p0672 A83-17155

The determination of the circulating immune complexes in humans 07 p0978 A83-20999

Analgesic intestinal peptides - New agents of bodily defense 07 p0975 A83-21000

The effect of smoking on the nonspecific resistance of sailors during sea voyages 11 p1644 A83-28805

The changes in the T and B immune systems in sailors during prolonged voyages 13 p1906 A83-30950

The dependence of wound healing on the condition of the immune system 14 p2065 A83-33302

The effect of microwave radiation on several parameters of cellular immunity in conditions of chronic exposure 23 p3495 A83-48207

IMMUNOLOGY

The changes in the structural components of the walls of the small vessels and the composition of the peripheral blood during immune and hypoxic effects on the heart 01 p0078 A83-10487

A comparison of the neural and immunological modulator properties of low molecular weight neuropeptides 01 p0080 A83-10551

Antibodies to streptococcal lipoproteinase in the blood of healthy persons 01 p0083 A83-10554

An analysis of the parameters of the immunoreactive curve 01 p0080 A83-10555

An evolutionary model for the insect vitellins 01 p0081 A83-11034

The dependence of immunological changes in athletes in polar regions on the intensity of the physical load 01 p0084 A83-11387

Immunoglobulin genes 01 p0082 A83-11408

Simultaneous luminescent assessment of the phagocytic and bactericidal functions of the macrophages and neutrophils of human skin exudate 03 p0381 A83-14336

The regulation of the defense functions of organisms --- Russian book 04 p0520 A83-15826

Adaptation and resistance to hypoxia in light of the functional activity of the antisytems 05 p0669 A83-17161

The effect of an electric field of industrial frequency on parameters of natural immunity 05 p0669 A83-17164

The functional characteristics of the immune response stimulators circulating in the blood in a toxic affection of the liver 05 p0670 A83-17182

The autoallergic effect of microwaves and their influence on fetus and offspring 05 p0670 A83-17190

An investigation of the shielding effectiveness of FFP-15 fabric relative to bacterial aerosols 05 p0677 A83-17201

The genetics of immunoglobulins - Successes and problems 06 p0795 A83-18982

Immunoglobulin genes 14 p2065 A83-33326

The pathology of the immune system during injury 14 p2066 A83-33327

The suppression of blood platelet aggregation with immune complexes. I - Clinical investigations 14 p2070 A83-33331

The effect of T and B lymphocytes on the phagocytotic activity of polymorphonuclear neutrophils in the peripheral blood of humans 14 p2070 A83-33333

The determination of circulating immune complexes by a spectrophotometric method 15 p2213 A83-34950

The complement-fixing capability of aggregated immunoglobulins with various molecular weights 15 p2211 A83-34965

Ultraviolet-irradiated blood - Photochemistry, immunological action 16 p2393 A83-35920

Several indicators of the functional condition of the immune system in normal and pathological situations 16 p2400 A83-36842

The regulation of the functions of the immune system 18 p2735 A83-40562

The effect of decimeter waves on the physical and chemical condition of membranes, the chromatin of thymocytes, and the immunological reactivity of an organism 18 p2733 A83-40567

Morphofunctional changes of the lymphoid tissue of the respiratory organs following the administration of gamma-globulin 18 p2733 A83-40582

Coping and immunosuppression - Inescapable but not escapable shock suppresses lymphocyte proliferation 19 p2873 A83-40905

The change of immunobiological reactivity following the combined effects of microwaves, infrasound, and gamma-irradiation 19 p2874 A83-41017

The content of immunoglobulins in the blood serum of patients with various forms of chronic inflammation of the middle ear 19 p2883 A83-41826

Changes in the formation of antibodies caused by the administration of immunomodulators in the respiratory organs 19 p2876 A83-41833

The characteristics of the immunological reactivity of humans in conditions of a mountain climate 21 p3188 A83-45341

Experimental injury of the aorta of rabbits of various ages by immune complexes 21 p3185 A83-45342
 Results of space experiment program 'Interferon' [IAF PAPER 83-187] 23 p3498 A83-47303
 Type II collagen-induced autoimmune endolymphatic hydrops in guinea pig 23 p3495 A83-47819
 Radiation damage and the theory of T-cells of mice - The dynamics of suppressor cells after the effect of radiation 23 p3495 A83-48203
 Circulating antibodies to aortic elastin and their significance in atherosclerosis in humans 23 p3499 A83-48674
 The humoral immune response after injuries of various severities 23 p3496 A83-48675

IMP-H
 U EXPLORER 47 SATELLITE

IMP-J
 U EXPLORER 50 SATELLITE

IMP-7
 U EXPLORER 47 SATELLITE

IMP-8
 U EXPLORER 50 SATELLITE

IMPACT
 NT ECONOMIC IMPACT
 NT ELECTRON IMPACT
 NT HYPERVELOCITY IMPACT
 NT ION IMPACT
 NT PROTON IMPACT
 Reentry vehicle impact error from high altitude transient roll resonance [AIAA PAPER 83-0032] 05 p0602 A83-16473
 Precursors to gamma-ray bursts in the asteroid impact scenario 07 p1012 A83-20024

IMPACT ACCELERATION
 Introduction to the vibration of mechanical systems with internal impacts --- Czech book 01 p0060 A83-10877
 The possibility of using electromagnetic accelerators for studying processes occurring during the high-velocity collision of solids 04 p0465 A83-16388
 An experimental and theoretical study of the rebound of short rods from a solid obstacle 04 p0501 A83-16396
 Targets for three-dimensional /3-D/ tracking of human impact test subjects 08 p1102 A83-22792
 Limiting payload deceleration during ground impact 15 p2122 A83-33726

IMPACT DAMAGE
 NT METEORIC DAMAGE
 NT RAIN IMPACT DAMAGE
 The origin of tektites - settled at last 04 p0558 A83-14953
 Experimental simulation of impact cratering on icy satellites 04 p0570 A83-16236
 The bilateral symmetry of circular impact structures --- of astrolembes 05 p0706 A83-17473
 Laboratory simulation of planetesimal collision 07 p1029 A83-20239
 Acousto-ultrasonic evaluation of impact-damaged graphite epoxy composites 07 p0875 A83-20454
 Chemical systematics among the moldavite tektites 07 p1035 A83-21328
 Advanced methods for damage analysis in graphite-epoxy composites 09 p1222 A83-23648
 Impact damage and erosion in infrared materials 09 p1346 A83-24963
 Comment on 'A schematic model of crater modification by gravity' by H. J. Melosh 09 p1367 A83-25075
 Numerical solution of large deformation problems involving surface contact and impact 12 p1734 A83-28854
 Statistical modeling of ballistic damage and residual strength in composite structures [AIAA 83-1002] 12 p1711 A83-29790
 Analytical and experimental investigation of bird impact on fan and compressor blading [AIAA 83-0954] 12 p1704 A83-29856
 Features of the spread of faults around meteorite craters (the El'gygytyn crater taken as an example) 13 p1962 A83-31347
 Asteroid and comet bombardment of the earth 14 p2095 A83-33483
 Recent researches into solid bodies and magnetic fields in the solar system; Proceedings of the Topical Meeting and Symposium, Ottawa, Canada, May 16-June 2, 1982 15 p2124 A83-35001
 Dust hazard near Halley Comet in case of the Vega project 15 p2128 A83-35016
 Impact induced plasma during a cometary fly-by 15 p2128 A83-35021
 Experimental and theoretical study of the elastoplastic buckling of cylindrical shells under axial impact 18 p2702 A83-40118
 Effect of defect on the behaviour of composites 18 p2656 A83-40215

Residual strength predictions for ballistically damaged aircraft 20 p3001 A83-42540
 The effect of particle shape and size on erosion of aluminum alloy 1100 at 90 deg impact angles 20 p2955 A83-43408
 The erosion of metals 22 p3268 A83-45897
 A study of the surface deterioration due to erosion --- of gas turbine blades [ASME PAPER 83-GT-213] 23 p3397 A83-48014

IMPACT DECELERATION
 U DECELERATION
 U IMPACT ACCELERATION

IMPACT LOADS
 Bursting and bulging of carbon fibre composite discs 01 p0022 A83-10243
 DSO-series devices for fatigue testing under repeated impact and harmonic loading with various cycle ratios 02 p0191 A83-12342
 A numerical study of the buckling process and strength analysis of layered cylindrical shells under axial impact 02 p0192 A83-12358
 Dynamic spalling in rarefaction waves 03 p0339 A83-13596
 Impact machines /The fundamentals of complex design/ --- Russian book 04 p0487 A83-15834
 A new strategy for stress analysis using the finite element method 05 p0655 A83-17738
 The relationship between the spall resistance and the spall plate thickness 06 p0770 A83-18013
 Measuring the 'life span' of certain metals under impulse tension 06 p0728 A83-18015
 Impact of a body on a mass attached to an elastically restrained beam 06 p0770 A83-18070
 Role of impact velocity and chest compression in thoracic injury 06 p0794 A83-18189
 Biomechanical aspects of the fracture resistance of the vertebral column of humans under impact overloads in the head-pelvis direction 06 p0798 A83-18509
 An approximate solution to the non-self-similar problem concerning the motion of a piston following an instantaneous impact 06 p0760 A83-19441
 Optimal control of periodic vibrations of a vibroimpact system 07 p0988 A83-19939
 A numerical solution to problems relating to the vibrations of thin plates acted upon by impact loads 09 p1280 A83-24489
 Space Shuttle solid rocket booster initial water impact loads and dynamics - Analysis, tests, and flight experience [AIAA 83-0956] 12 p1706 A83-29858
 A longitudinal impact of a slender viscoelastic bar 13 p1866 A83-30449
 The impact of compressible liquids 13 p1843 A83-31078
 Dynamic stress intensity factors around a rectangular crack in an infinite plate under impact load 14 p2031 A83-32659
 Designing space vehicle shields for meteoroid protection - A new analysis 15 p2128 A83-35028
 A tensile testing technique for fibre-reinforced composites at impact rates of strain 16 p2324 A83-35981
 Sudden twisting of an external circular crack in an infinite medium with a cylindrical inclusion 16 p2368 A83-36513
 Properties of composite box beams under combined impact loading 18 p2705 A83-40222
 The dynamic collapse of a column impacting a rigid surface 19 p2856 A83-40873
 Similarity in the contact problem for elastic bodies 19 p2858 A83-41217
 Periodically forced linear oscillator with impacts - Chaos and long-period motions 20 p3042 A83-42649
 Acoustic pulses excited by impacts on objects - Their analytical representation and spectra 20 p3000 A83-43645
 Wave propagation in a graphite/epoxy laminate 21 p3151 A83-44050
 Evaluation of dynamic crack instability criteria 21 p3159 A83-44925
 Fracture properties of metals under rapid heating and loading 21 p3114 A83-45158
 Torsional impact response of a penny-shaped crack lying on a bimaterial interface 21 p3162 A83-45188
 Low-velocity impact response of laminated plates 21 p3164 A83-45589
 Impact response of a cracked orthotropic medium 23 p3469 A83-47597
 The vibration of an elastic-plastic plate under the effect of normal impact loads 24 p3592 A83-49030

IMPACT MELTS
 Siderophiles in the Brachina meteorite - Impact melting 02 p0263 A83-11624
 Petrology and shock metamorphism of Pampa del Infierno chondrite 02 p0267 A83-12847

The Apollo 15 yellow impact glasses - Chemistry, petrology, and exotic origin 04 p0560 A83-15342
 Hydrothermally altered impact melt rock and breccia - Contributions to the soil of Mars 04 p0567 A83-15578
 Signs of shock metamorphism in the Kaali meteorite 05 p0706 A83-17464
 Nonequilibrium condensation and ultrapotassium impactites 05 p0706 A83-17472
 Diaplectic labradorite glass from the Manicouagan impact crater. I - Physical properties, crystallization, structural and genetic implications 07 p0950 A83-21046
 Solar system ice - Amorphous or crystalline? 24 p3671 A83-48809
 Geochemistry of the impactites of the lanis'arvi, Kara, and El'gygytyn craters 24 p3671 A83-48952

IMPACT PREDICTION
 Impact of an asteroid or comet in the ocean and extinction of terrestrial life 07 p0950 A83-21314
 Effect of particle rebound characteristics on erosion of turbomachinery components [ASME PAPER 83-GT-169] 23 p3397 A83-47988

IMPACT PRESSURES
 U IMPACT LOADS

IMPACT RESISTANCE
 The Giotto dust protection system --- for encounters with comet Halley 05 p0607 A83-17434
 Role of impact velocity and chest compression in thoracic injury 06 p0794 A83-18189
 A new high impact resin system for advanced composites with 300 F /150 C/ properties 07 p0875 A83-20429
 Impact testing of toughened epoxy resin systems 07 p0875 A83-20444
 The influence of inclusions on the J integral value determined by a Charpy test with digital instrumentation 08 p1124 A83-23242
 Dependency of the impact sensitivity of beta-HMX on the grain size and effects on the application 09 p1242 A83-23848
 Impact damage and erosion in infrared materials 09 p1346 A83-24963
 Impact-resistant transparencies for marine service --- windscreens for aircraft [ASME PAPER 82-WA/OCE-4] 10 p1400 A83-25686
 Impact sensitivity of gamma-irradiated HMX 13 p1826 A83-31674
 The resistance of structural materials to fracture during impact bending 14 p2033 A83-33015
 A study of the temperature dependence of the mechanical characteristics of structural alloys under impact tension 14 p1997 A83-33016
 Submersion of a disk into a compressible fluid at an angle to the free surface 16 p2350 A83-35714
 Impact protection in air transport passenger seat design [SAE PAPER 821391] 17 p2459 A83-37967
 Experimental determination of critical defects in polymers under conditions of impact fracture 19 p2824 A83-42066
 F/RF-4 transparency baseline bird impact test program 20 p2932 A83-42533
 Projectile impact ignition characteristics of propellants. III - Effect of particle size and porosity 21 p3117 A83-44998
 Design of glass-faced helicopter windshields for survival in a particle impact environment 23 p3403 A83-48328

IMPACT SENSITIVITY
 U IMPACT RESISTANCE

IMPACT STRENGTH
 Mechanical properties of a high-strength aluminum alloy under impact loading 09 p1229 A83-23511
 Effects of carbon fiber strain and resin characteristics on optimum composite performance 18 p2653 A83-40181
 A study of the time dependence of the breaking stresses during spalling in copper, nickel, and titanium 20 p2956 A83-43523
 An approach to the evaluation of the impact resistance of a carbon composite 23 p3428 A83-48436

IMPACT TESTING MACHINES
 Impact machines /The fundamentals of complex design/ --- Russian book 04 p0487 A83-15834
 A study of the temperature dependence of the mechanical characteristics of structural alloys under impact tension 14 p1997 A83-33016

IMPACT TESTS
 NT CHARPY IMPACT TEST
 Air bag impact attenuation system for the AQM-34V remote piloted vehicle 01 p0008 A83-10188
 Fracture toughness test by impact-fatigue method 02 p0154 A83-11851

- On the design of containment shields
02 p0195 A83-12766
- Impact induced dehydration of serpentine and the evolution of planetary atmospheres
04 p0564 A83-15374
- Detonation properties of
1,3,5-triamino-2,4,6-trinitrobenzene when impacted by hypervelocity projectiles
04 p0464 A83-15473
- Metal fracture kinetics in the submicrosecond life range
04 p0460 A83-15887
- The use of dynamic impact experiments in the determination of the strain rate sensitivity of metals and alloys
04 p0462 A83-16272
- The possibility of using electromagnetic accelerators for studying processes occurring during the high-velocity collision of solids
04 p0465 A83-16388
- On the preparation of glass-fibre reinforced aluminum by powder hot extrusion
05 p0611 A83-17110
- Impact testing of toughened epoxy resin systems
07 p0875 A83-20444
- Impact fatigue strength and reliability for fiber reinforced epoxy resin laminates subjected to repeated impact loads
07 p0877 A83-21624
- Dynamic impact tests of radiated and temperature conditioned elastomers
09 p1238 A83-23628
- Shock temperatures of SiO₂ and their geophysical implications
09 p1292 A83-25070
- Rain erosion damage in brittle materials
11 p1551 A83-28439
- Drop weight impact testing of laminates reinforced with Kevlar aramid fibers, E-glass, and graphite
12 p1711 A83-29891
- Super strong polymers in planar directions
13 p1826 A83-31250
- Morphology of ductile metals eroded by a jet of spherical particles impinging at normal incidence
14 p1993 A83-32624
- High-velocity impact experiments needed to improve our understanding of the asteroids
15 p2250 A83-35030
- Fracture of an aluminum alloy at the pre-spalling stage
18 p2666 A83-39504
- Impact experiments on ice --- for understanding cratering on Callisto and Mimas
18 p2779 A83-40322
- F/R/F-4 transparency baseline bird impact test program
20 p2932 A83-42533
- Post-impact fatigue performance of carbon fibre laminates with non-woven and mixed-woven layers
20 p2948 A83-42814
- Energy absorption of composite materials
20 p2948 A83-43148

IMPACT TOLERANCES

- Impact protection in air transport passenger seat design
[SAE PAPER 821391]
17 p2459 A83-37967
- Impact damage tolerance of composites reinforced with Kevlar aramid fibers
18 p2656 A83-40214
- Transient processes during the impact initiation of trolyl-hexogen and trolyl-octogen mixtures
24 p3557 A83-49794

IMPATT DIODES

U AVALANCHE DIODES

IMPEDANCE

- NT ACOUSTIC IMPEDANCE
- NT CONTACT RESISTANCE
- NT ELECTRICAL IMPEDANCE
- NT ELECTRICAL RESISTANCE
- NT MECHANICAL IMPEDANCE
- NT REACTANCE
- NT RESPIRATORY IMPEDANCE
- NT SKIN RESISTANCE
- Realization and switching behavior of digital phase modulators for millimeter waves --- German thesis
01 p0035 A83-10168

IMPEDANCE MATCHING

- Impedance of a radiating slot in the ground plane of a microstripline
01 p0033 A83-11362
- Mutual coupling compensation for small, circularly symmetric planar antenna arrays
02 p0164 A83-12006
- Broadband microwave power amplifiers using lumped-element matching and distributed combining techniques
03 p0313 A83-13998
- Analysis of the general nonsymmetrical directional coupler with arbitrary terminations
04 p0474 A83-16211
- Limits of VSWR for optimal broadband capacitively loaded cylindrical antennas versus their length
06 p0741 A83-18661
- Diffraction from cylindrically truncated planar surfaces with application to an aperture matched horn design
06 p0742 A83-18666
- Wideband impedance-matched microstrip resonator antennas
06 p0751 A83-18673
- Matching properties of arbitrarily large dielectric covered phased arrays
09 p1246 A83-23782

- External and internal mutual impedance effects on the radiation patterns of circularly disposed arrays using antennafiers or passive monopoles
09 p1246 A83-23786
- Optimization of lines with small inhomogeneities for wide-band matching
09 p1256 A83-24915
- Electronically cold microwave artificial resistors
10 p1410 A83-26339
- On the effect of absorbing materials on electromagnetic waves with large relative bandwidth
10 p1405 A83-26491
- A logarithmic reflection chart for presentation of antenna impedance
10 p1411 A83-26844
- The wide-band matching area for a small antenna
10 p1406 A83-26848
- Applications of dynamic impedance measurements to aerospace battery cells
11 p1605 A83-27197
- Analysis of fin-line tapers and transitions
12 p1720 A83-29440
- An ideal six-port network consisting of a matched reciprocal lossless five-port and a perfect directional coupler
13 p1831 A83-30231
- Single-element rectangular microstrip antenna for dual-frequency operation
13 p1830 A83-31767
- Matching of single-mode optical waveguides to semiconductor lasers
14 p2083 A83-31904
- Dual frequency microstrip antenna
15 p2144 A83-34512
- Absolute measurement at 1 THz of the optical coupling of a F.I.R. conical antenna with a Josephson detector
17 p2511 A83-37759
- Matching networks in linear phased arrays
17 p2497 A83-37791
- Maximum power transfer for full-wave rectifier circuits
19 p2838 A83-41150
- Improved feed network for group-type unidirectional transducers
21 p3126 A83-44960
- IMPEDANCE MEASUREMENT**
- Instrumentation for the measurement of mobility and mechanical impedance
01 p0057 A83-10588
- Measurement of transfer impedance of thermal blankets --- for spacecraft EMP and SGEMP shielding
05 p0608 A83-17492
- Measurement of the wave impedance of low frequency electromagnetic waves in the earth-ionosphere duct
06 p0747 A83-18731
- An analysis of coplanar waveguides with finite conductor thickness-computation and measurement of characteristic impedance
07 p0918 A83-20070
- Surface impedance and wave tilt interpretation over horizontally stratified media
08 p1160 A83-22028
- Electrochemical impedance diagrams of alloy 600 at active-passive transition potentials
09 p1230 A83-23917
- Effect of substrate thickness on the performance of a circular-disk microstrip antenna
10 p1406 A83-26846
- Modeling of optical impedance spectroscopy
11 p1572 A83-27530
- Measurement of acoustic modes and wall impedance in a turbfan exhaust duct
[AIAA PAPER 83-0733]
11 p1651 A83-28015
- Rectangular dielectric resonator antenna
[AD-A129976]
11 p1558 A83-28608
- Surface acoustic admittance of highly porous open-cell, elastic foams
12 p1776 A83-28849
- Wideband millimeter-wave impedance measurements
13 p1836 A83-30974
- Impedance measurements and photoeffects on Ni electrodes
14 p2091 A83-32633
- The resonant cylindrical dielectric cavity antenna
15 p2148 A83-35175
- Experimental study of the characteristics of top-loaded microstrip monopoles
15 p2149 A83-35195
- Experimental study of the characteristics of coupled top-loaded microstrip monopoles
15 p2149 A83-35196
- On the dielectric properties of semiconducting materials as obtained from impedance measurements on Schottky barriers
16 p2419 A83-35618
- Measurement and modeling of the apparent characteristic impedance of microstrip
21 p3122 A83-43831
- A technique for measuring the effective dielectric constant of a microstrip line
21 p3123 A83-43842
- Measurements and calculations of the impedance of a cylindrical antenna in an isotropic plasma
21 p3211 A83-44300
- Embedding impedance of a millimeter wave Schottky mixer Scaled model measurements and computer simulations
21 p3125 A83-44384
- Microwave automatic impedance measuring schemes using three fixed probes
24 p3573 A83-48970
- IMPEDANCE PROBES**
- NT RADIO FREQUENCY IMPEDANCE PROBES

- An estimate of the errors in measurements of the electron concentration in the ionosphere made with a high-frequency impedance probe
11 p1575 A83-28752
- Acoustic ground impedance meter
17 p2510 A83-37732
- Satellite investigation of the spectral characteristics of irregularities --- of ionospheric electron density
20 p3022 A83-42875
- Microwave automatic impedance measuring schemes using three fixed probes
24 p3573 A83-48970
- IMPELLER BLADES**
- U ROTOR BLADES (TURBOMACHINERY)
- IMPELLERS**
- NT PUMP IMPELLERS
- Experimental investigation of the influence of Reynolds number and of shaft and gradient effects on flow measurements using spherical five-hole sondes --- German thesis
01 p0045 A83-10473
- Basic calibration of a partially-parabolic procedure aimed at centrifugal impeller analysis
[AIAA PAPER 83-0260]
05 p0583 A83-16616
- Measurement of three dimensional flow field behind an impeller by means of periodic multi-sampling with a slanted hot wire
07 p0929 A83-20276
- A solution to inverse problem of quasi three-dimensional flow in centrifugal impeller
09 p1257 A83-23331
- The Magnuswirl turbine wheel - The unique solution for the high temperature cruise missile
09 p1274 A83-23647
- A time efficient finite differences algorithm for the solution of the meridional flow in turbo compressor impellers
[ASME PAPER 82-WA/FE-3]
10 p1413 A83-25683
- Comparison between probe and laser measurements at the outlet of a centrifugal impeller
10 p1421 A83-26418
- Flow measurements using a laser-2-focus velocimeter in a high-pressure ratio centrifugal impeller
12 p1695 A83-28836
- Some aerodynamic and noise studies of flow in centrifugal fans
16 p2408 A83-35864
- Contribution to centrifugal compressor impeller design
16 p2305 A83-35865
- A model of axial impeller stall
16 p2292 A83-35878
- Excitation and vibration of flexible bladed disks under operating and simulated operation conditions
16 p2305 A83-35881
- A computer-aided system for interactive geometric modeling, structural/dynamics analysis and N/C manufacturing/inspection of radial flow compressors
[SAE PAPER 821440]
17 p2493 A83-37988
- Theoretical estimate of the effect of the rotation of impellers on their natural frequencies
18 p2695 A83-39508
- A technique for the accelerated life testing of fan impellers
18 p2698 A83-39512
- Performance evaluation of centrifugal compressor impellers using three-dimensional viscous flow calculations
[ASME PAPER 83-GT-62]
23 p3395 A83-47918
- A CAD method for centrifugal compressor impellers
[ASME PAPER 83-GT-65]
23 p3395 A83-47920
- Effect of relative velocity distribution on efficiency and exit flow of centrifugal impellers
[ASME PAPER 83-GT-74]
23 p3447 A83-47927
- Substructuring and wave propagation - An efficient technique for impeller dynamic analysis
[ASME PAPER 83-GT-150]
23 p3409 A83-47969
- Aerodynamic tests on centrifugal process compressors
Influence of diffuser diameter ratio, axial stage pitch and impeller cut-back
[ASME PAPER 83-GT-172]
23 p3396 A83-47973
- Vibration analysis of radial compressor impellers
[ASME PAPER 83-GT-156]
23 p3469 A83-47982
- Three dimensional inviscid computation of an impeller flow
[ASME PAPER 83-GT-210]
23 p3397 A83-48011
- IMPERFECTIONS**
- U DEFECTS
- IMPINGEMENT**
- NT JET IMPINGEMENT
- Ion beamlet vectoring by grid translation
[AIAA PAPER 82-1895]
02 p0241 A83-12552
- Oscillations of an unstable mixing layer impinging upon an edge
04 p0479 A83-16264
- An analytical evaluation of the icing properties of several low and medium speed airfoils
[AIAA PAPER 83-0109]
05 p0579 A83-16525
- Concerning impingement of shock waves on permeable baffles
05 p0589 A83-17418
- Effects of plume impingement on a momentum bias communications satellite
07 p0872 A83-20420
- Boundary layer effects on impingement and erosion
11 p1566 A83-27425

- Oscillations of impinging shear layers
12 p1695 A83-28953
- An experimental and numerical investigation of the impingement of an oblique shock wave on a body of revolution
[AIAA PAPER 83-1757] 17 p2446 A83-37230
- Prediction of damage sites ahead of a moving heat source
17 p2522 A83-38387
- IMPLANTATION**
- NT ION IMPLANTATION**
- The implantation of sarcoplasmic reticulum membranes in a planar lipid membrane
03 p0375 A83-14359
- Carrier lifetimes in silicon epitaxial layers deposited on oxygen-implanted substrates
08 p1082 A83-22920
- Corrosion fatigue testing of implant materials (Nb, Ta, stainless steel) at transonic frequencies
16 p2332 A83-36193
- IMPLOSIONS**
- Temperature measurements at an implosion focus
04 p0474 A83-14950
- Analysis of self-similar problems of imploding shock waves by the method of characteristics
14 p2013 A83-33386
- Two-dimensional numerical simulation of an inductively driven imploding foil plasma
20 p3049 A83-42590
- IMPULSES**
- The different forms of atmospheric impulse and their conditions of propagation
14 p2052 A83-32412
- IMPURITIES**
- Structure and fracture character of V95 alloy sheets in relation to impurity content and aging conditions
03 p0297 A83-13254
- Role of impurities in silicon solar cell performance
04 p0504 A83-15457
- Determination of trace elements in CuInS₂
04 p0456 A83-15485
- Modification of vitreous As₂Se₃ --- by metallic impurities
04 p0540 A83-15500
- The population of localized states and the photoconductivity of disordered systems
04 p0542 A83-15920
- On particle coarsening during sintering of silicon
04 p0464 A83-16271
- Influence of sulfur, phosphorus, and antimony segregation on the intergranular hydrogen embrittlement of nickel
07 p0885 A83-20261
- Quantum transport in a single layered structure for impurity scattering
07 p1000 A83-21372
- Role of impurities in sintered CdS/Cu₂S solar cells
09 p1292 A83-23666
- The effect of cerium on high temperature tensile and creep behavior of a superalloy
10 p1396 A83-25864
- Segregation to interphase boundaries in liquid-phase sintered Tungsten alloys
10 p1396 A83-25866
- Determination of the aluminum content in high-purity germanium by laser multistage photoionization of atoms
10 p1432 A83-26667
- Clean-up and processing of coal-derived gas for hydrogen applications
11 p1611 A83-27336
- New data on nonradiative relaxation of impurity center excitations in laser materials
11 p1581 A83-27591
- The effect of the chemical composition on the high-cycle and low-cycle fatigue behavior of D16 and V95 alloy sheets under pulsating tension
13 p1819 A83-30068
- Distribution of impurity elements in titanium alloys
13 p1819 A83-30086
- Studies on polycrystalline silicon for solar applications, including characterization of trace elements B, C and Al by charged particles activation analysis
13 p1817 A83-30184
- Spectroscopic search for fractional charge in ultrapure semiconductors
13 p1929 A83-30595
- A Mossbauer study of commercial beryllium
13 p1822 A83-30743
- On the dependence of fracture toughness on metallurgical factors
13 p1824 A83-31586
- Segregation of impurities at grain boundaries and other compositional inhomogeneities in chill-casted silicon ingots
14 p2090 A83-32309
- Impurity diffusion in amorphous silicon and its implications for solar cells
14 p2005 A83-32336
- Grain boundary segregation in Ni and binary Ni alloys doped with sulfur
14 p1993 A83-32677
- Acceleration of impurity ions during plasma expansion into vacuum
16 p2417 A83-36935
- Trapping of hydrogen by oxygen and nitrogen impurities in niobium, vanadium and tantalum
17 p2491 A83-38856
- Convection and impurity distribution in crystal growth in low-gravity environments
18 p2643 A83-39898
- Impurity scattering in partially dielectricized superconductors
19 p2904 A83-41000
- Influence of carbon and hydrogen segregation on the electrical properties of grain boundaries in polycrystalline silicon sheets
20 p3051 A83-42351
- Defect and impurity states in silicon nitride
20 p3053 A83-42603
- Optical and crystallographic properties and impurity incorporation of Ga(x)In(1-x)As (with x between 0.44 and 0.49) grown by liquid phase epitaxy, vapor phase epitaxy, and metal organic chemical vapor deposition
20 p3053 A83-42606
- Impurity distribution in polycrystalline self-bound SiC
21 p3117 A83-45314
- The effect of impurities on the current-amplification cut-off frequency of field-effect transistors
22 p3277 A83-45675
- Deep level impurities and current collection in CdS/CdTe thin-film solar cells
22 p3365 A83-46734
- IMS**
- U INTERNATIONAL MAGNETOSPHERIC STUDY**
- IN-FLIGHT MONITORING**
- In-flight structural dynamic characteristics of the XV-15 tilt-rotor research aircraft
01 p0008 A83-10191
- The evolution of Navy Flight Line EW testers from AN/ALM-66 to AN/USM-406C
01 p0014 A83-10739
- In-flight lightning data measurement system for fleet application - Flight test results
01 p0009 A83-11087
- Develop in-flight acoustic emission monitoring of aircraft to detect fatigue crack growth
04 p0447 A83-15197
- Establishing signal processing and pattern recognition techniques for inflight discrimination between crack-growth acoustic emission and other acoustic waveforms
04 p0491 A83-15198
- An instrument for recording the exceeding of specified levels of an operational parameter of an aircraft
05 p0596 A83-16880
- Optimal processing of the correction data of an aircraft fuel-measurement system
06 p0718 A83-19177
- The MCA method, a flight test technique to determine the thrust of jet aircraft in flight --- Mass Consumption Acceleration
07 p0865 A83-19661
- Improvement of the accuracy of temperature measurement by resistance thermometers --- for in-flight aircraft structures monitoring
08 p1092 A83-22186
- Infrared target array development
09 p1204 A83-23527
- FAA approved S-76A in-flight power assurance and trending procedure
09 p1207 A83-24830
- Fault Detection/Location System for intermediate and tail rotor gearboxes
09 p1274 A83-24835
- Full-flow debris monitoring and fine filtration for helicopter propulsion systems
09 p1208 A83-24838
- Study of an on-board trajectory system for in-flight checking of air-navigation and landing radio aids
09 p1201 A83-24860
- In-flight acoustic measurements in the engine intake of a Fokker F28 aircraft
[AIAA PAPER 83-0677] 10 p1376 A83-25909
- Noise source identification in airplane cabins using acoustic intensity technique
[AIAA PAPER 83-0716] 10 p1475 A83-25931
- Farfield inflight measurements of high-speed turboprop noise
[AIAA PAPER 83-0745] 10 p1377 A83-25947
- Flyover noise measurements for turbo-prop aircraft
[AIAA PAPER 83-0746] 10 p1377 A83-25948
- The incorporation of processing equipment into the electrical power subsystem
11 p1559 A83-27136
- Flight measurements of temperature and pressure on rescued nose cones of the M100 and Oblako meteorological rockets
11 p1634 A83-28373
- An assessment of the Space Shuttle Orbiter thermal environment using flight data
[AIAA PAPER 83-1488] 14 p1980 A83-32734
- Results from a 'small box' realtime molecular contamination monitor on STS-3
[AIAA PAPER 83-0251] 16 p2317 A83-36050
- F/A-18A Inflight Engine Condition Monitoring System (IECMS)
[AIAA PAPER 83-1237] 16 p2308 A83-36300
- Modern technology and airborne engine vibration monitoring systems
[AIAA PAPER 83-1240] 16 p2302 A83-36303
- In-flight computation of helicopter transmission fatigue life expenditure
16 p2301 A83-36921
- Computer performance monitoring during the Centaur launch countdown
17 p2472 A83-37060
- Galileo spacecraft high gain antenna offset calibration
17 p2474 A83-37147
- Failure detection and correction in low orbit satellite attitude control system --- for SPOT earth observation satellite
17 p2479 A83-37492
- DC-9 Super 80 Digital Flight Guidance System integrated system testing
[SAE PAPER 821364] 17 p2467 A83-37959
- Development of a compact real-time turbofan engine dynamic simulation
[SAE PAPER 821401] 17 p2468 A83-37974
- Robust fault detection, isolation, and accommodation to support integrated aircraft control
[AIAA PAPER 83-2161] 19 p2802 A83-41661
- Instrumentation, data acquisition and reduction for a large spaceborne helium dewar
20 p2962 A83-43250
- Observations of severe in-flight environments on airplane composite structural components
20 p2933 A83-43330
- On-board weight and center-of-gravity measurement system with tire-pressure monitoring
23 p3402 A83-47216
- A7E/TF41 Engine Monitoring System (EMS)
[ASME PAPER 83-GT-91] 23 p3408 A83-47938
- INCENTIVES**
- Cost control of aircraft manufacture - A modern approach
08 p1171 A83-23148
- INCIDENCE**
- NT GRAZING INCIDENCE**
- Critical angle of incidence for the flow around spheroids
07 p0862 A83-19668
- Vane camber and angle of incidence effects in fan noise generation
[AIAA PAPER 83-0766] 10 p1377 A83-25956
- Negative incidence flow over a turbine rotor blade
[ASME PAPER 83-GT-23] 23 p3393 A83-47888
- INCIDENT RADIATION**
- Reflections from linearly vibrating objects - Plane mirror at oblique incidence
01 p0104 A83-11358
- Practical problems in the time-domain probing of lossy dielectric media
01 p0034 A83-11372
- Further developments of a general method for deducing average hourly insulations from average daily insulations
02 p0203 A83-11845
- Optical analysis of solar energy tubular absorbers
02 p0202 A83-12596
- Off-axis effects in a mosaic Michelson interferometer
[AD-A123678] 02 p0179 A83-12609
- Measurement of angle resolved light scattering from optical surfaces in the 75 to 750 eV range
02 p0239 A83-12716
- Radiative heat transfer in segregated media
[ASME PAPER 82-HT-16] 02 p0171 A83-12785
- Incident angle modifiers for flat-plate solar collectors - Analysis of measurement and calculation procedures
03 p0353 A83-13480
- Investigations of Mach reflection of a shock wave. I - Configurations and domains of shock reflection
03 p0316 A83-13566
- Extension of oblique-incidence method to photo-orthotropic elasticity
03 p0344 A83-14941
- Spectral selectivity of high-temperature solar absorbers. II Effects of interference
04 p0505 A83-15488
- The method of moving coordinates as a technique for comparing various electrodynamic problems in systems having cylindrical conductors
04 p0467 A83-15746
- Cyclical, broadband economical scanning procedure for determining the direction of incidence of electromagnetic waves --- German thesis
06 p0736 A83-18522
- Effect of the polarization squint of small horn antennas
06 p0741 A83-18662
- Three-dimensional problem of backscattering in stratified, randomly inhomogeneous media
06 p0806 A83-19331
- Processes of the generation of high-energy muons in cosmic rays
06 p0858 A83-19341
- Concerning problems of optimization in nonlinear optics --- field characteristics and incident radiation
07 p0936 A83-20312
- The origin of cosmic radiation - Status after 70 years of research
09 p1369 A83-23497
- The occurrence of detonation in the case of the incidence of a shock wave on a wall
09 p1226 A83-24236
- Velocity measurements of incident and reflected shock waves in various gases and in saturated water vapour
10 p1414 A83-26139
- Double-pass oblique-incidence interferometer for the inspection of nonoptical surfaces
13 p1845 A83-30204
- A spectral-iteration technique for analyzing scattering from arbitrary bodies. II - Conducting cylinders with H-wave incidence
15 p2149 A83-35198
- Calculated transmission profile of an interference filter placed in a convergent beam under various incidence angles --- for nightglow observations
16 p2357 A83-36753
- Asymmetry of proton fluxes in high-latitude zones of the earth's magnetosphere
18 p2784 A83-39329
- Oblique incidence of a strong electromagnetic wave on a cold inhomogeneous electron plasma - Relativistic effects
18 p2748 A83-40508
- A worldwide examination of solar beam-slope angle values
19 p2861 A83-40768
- 4-layer inductive grid FSS at 45 deg incidence --- Frequency Selective Surfaces
20 p2963 A83-42478

- Total internal reflectance optoacoustic spectroscopy
20 p2989 A83-42582
- Radiative transfer in an absorbing and anisotropically scattering slab with reflecting boundaries - The non-azimuthally symmetric case
20 p2974 A83-42699
- Detection of a corner reflector with insonification at angles greater than 45 deg
20 p3000 A83-43183
- An iterative extended boundary condition method for solving the absorption characteristics of lossy dielectric objects of large aspect ratios --- under exposure to incident plane wave radiation
21 p3189 A83-43833
- A simple passive technique for generating short pulses
21 p3143 A83-44187
- Synthesis of optical coatings for the oblique incidence of light
21 p3208 A83-45218
- Analytical yield spectrum approach to electron energy degradation in earth's atmosphere
22 p3327 A83-46055
- Deflection from the incidence plane of a light beam refracted in an absorbing (amplifying) isotropic medium
24 p3629 A83-49552
- INCLUSIONS**
- Micromechanics
02 p0193 A83-12733
- Composites with periodic microstructure
02 p0150 A83-12734
- On neutron-induced and other noble gases in Allende inclusions
02 p0267 A83-12842
- The Eikonal approximation in elastic wave scattering theory
04 p0489 A83-15162
- Inverse scattering at long wavelength - $\Delta\mu = 0$
04 p0489 A83-15163
- An ultra-refractory inclusion from the Ormans carbonaceous chondrite
04 p0558 A83-15301
- Crystallization sequences of Ca-Al-rich inclusions from Allende - An experimental study
04 p0572 A83-16352
- The composition of mineral inclusions in the olivines of pallasites
05 p0706 A83-17465
- Shock-metamorphosed carbonaceous material in impactites
05 p0706 A83-17471
- Effects of ceramic inclusions on fatigue properties of a powder metallurgical nickel-base superalloy
06 p0732 A83-19101
- Schlieren visualization of acoustically imaged defects
07 p0929 A83-20174
- Fluid inclusions in stony meteorites
07 p1033 A83-21306
- Composition and origin of clasts and inclusions in the Abee enstatite chondrite breccia
08 p1188 A83-21645
- Discussion on criteria for crack initiation in the immediate vicinity of the sharp edges of dispersed inclusions
08 p1121 A83-21824
- Acoustic emission during the plastic deformation of aluminium alloys 2024 and 2124
08 p1065 A83-22014
- The effect of dispersoids on the ductile fracture toughness of Al-Mg-Si alloys
08 p1065 A83-22015
- Effects of morphology and hardness of inclusions on ductile fracture
08 p1066 A83-22078
- The influence of inclusions on the J integral value determined by a Charpy test with digital instrumentation
08 p1124 A83-23242
- SH-wave scattering by a cylinder with an interfacial crack
09 p1276 A83-23375
- Methods of producing dispersion-strengthened cast alloys based on aluminum
10 p1395 A83-25629
- Stress couple concentrations for cylindrically bent plates with circular holes or rigid inclusions
10 p1440 A83-26432
- [ASME PAPER 83-APM-5]
- Slip bands along the matrix-inclusion interface
11 p1598 A83-28491
- Nonclassical thermoelasticity equations for piecewise homogeneous media
13 p1865 A83-30051
- The effect of friction on the delamination of heterogeneous materials
13 p1865 A83-30053
- The diffraction of longitudinal shear waves by a rigid tunnel inclusion in an elastic half-space
14 p2030 A83-32379
- On the excitation of elastic waves in a half-space containing a horizontal elastic cylindrical inclusion
16 p2365 A83-35549
- Sudden twisting of an external circular crack in an infinite medium with a cylindrical inclusion
16 p2368 A83-36513
- Pre-Keweenawan anorthositic inclusions in the Keweenawan Beaver Bay and Duluth Complexes, northeastern Minnesota
16 p2382 A83-36971
- Stress concentration coefficient around a three dimensional inclusion in an infinite elastic body
17 p2518 A83-37025
- Ca-Al-rich chondrules and inclusions in ordinary chondrites
17 p2623 A83-38593
- Replacement textures in CAI and implications regarding planetary metamorphism
17 p2623 A83-38851
- Refractory inclusions in the Murchison meteorite
17 p2624 A83-38855
- Statistical aspects of heterogeneous materials
18 p2657 A83-40235
- Analysis of ultrasonic wave scattering for characterization of defects in solids. I - Spherical inclusions and reciprocity
21 p3149 A83-44473
- Impurity distribution in polycrystalline self-bound SiC
21 p3117 A83-45314
- Stress and strength analysis in and around composite inclusions in polymer matrices
22 p3264 A83-46305
- An axisymmetric problem for an elastic medium with a spherical inclusion weakened by an interface crack
23 p3468 A83-47172
- Longitudinal shear in a body with an acute-angled inclusion and an interface crack
23 p3473 A83-48542
- Cumberland Falls chondritic inclusions. II - Trace element contents of forsterite chondrites and meteorites of similar redox state
24 p3672 A83-49349
- INCOHERENCE**
- Error rates for fading NCFSK signals in an additive mixture of impulsive and Gaussian noise --- noncoherent FSK
03 p0304 A83-13870
- Coherent versus incoherent detection for interferometry at infrared wavelengths
10 p1495 A83-25846
- INCOHERENT SCATTER RADAR**
- NT EISCAT RADAR SYSTEM (EUROPE)
- Chatanika radar measurements during the International Magnetospheric Study
04 p0513 A83-16301
- Worldwide incoherent scatter radar measurements
04 p0513 A83-16302
- An empirical electric field model derived from Chatanika radar data
07 p0967 A83-21522
- Variability of the Harang discontinuity as observed by the Chatanika radar and the IMS Alaska magnetometer chain
07 p0967 A83-21559
- Measurement of autocorrelation functions in a bi-static incoherent scatter radar
09 p1249 A83-24694
- Meridional neutral winds in the thermosphere at Arecibo
11 p1618 A83-28321
- Simultaneous incoherent scatter and airglow observations
11 p1618 A83-28321
- Incoherent scatter observations of mid-latitude sporadic-E and comments on its data analysis
12 p1753 A83-29426
- Estimation of the correlation function of incoherent-scatter signals in multiposition radar systems
13 p1829 A83-30726
- Measurement of electric fields in the ionosphere by incoherent scatter radar techniques
13 p1876 A83-30772
- High latitude neutral atmosphere temperature and concentration measurements from the first Eiscat incoherent scatter observations
13 p1883 A83-31717
- Recent incoherent scatter radar results not incorporated in current thermospheric models
16 p2378 A83-36119
- Millstone Hill incoherent scatter observations of auroral convection over $\Lambda = 60-75$ deg. III - Average patterns versus Kp
17 p2537 A83-37576
- EISCAT - The European incoherent scatter radar for studying the polar atmosphere
18 p2716 A83-39775
- Polarization electric fields in the nighttime F layer at Arecibo
20 p3019 A83-42418
- An incoherent scatter study of short- and long-term temperature and atomic oxygen variations in the thermosphere
21 p3173 A83-44671
- Lower thermospheric structure from Millstone Hill incoherent scatter radar measurements. I - Daily mean temperature. II Semidiurnal temperature component
22 p3328 A83-46057
- INCOHERENT SCATTERING**
- First results with Eiscat --- for ionospheric plasma diagnostics
09 p1301 A83-23388
- INCOMPRESSIBILITY**
- On a thermodynamic theory of fiber-reinforced thermoelastic materials with thermo-kinematic constraints
04 p0455 A83-16098
- Comments on anisotropic plastic flow and incompressibility
07 p0946 A83-20638
- Statically permissible stress fields in incompressible media
14 p2030 A83-32353
- The regularity of one-dimensional elastic waves in an incompressible isotropic material
14 p2030 A83-32356
- Reflections on the computational approximation of elastic incompressibility
15 p2179 A83-34562
- INCOMPRESSIBLE BOUNDARY LAYER**
- Effect of the Prandtl number and mass transfer on the unsteady incompressible boundary layers near the three-dimensional asymmetric stagnation point
09 p1262 A83-24507
- Optimization of heat transfer in an incompressible-fluid boundary layer with allowance for the heat-balance equation
12 p1723 A83-29279
- Calculation of the amplification rates of a three-dimensional Tollmein-Schlichting wave in the boundary layer of an incompressible fluid
17 p2503 A83-37262
- Calculation of incompressible turbulent boundary layers over moving wavy surfaces
17 p2507 A83-38083
- [AIAA PAPER 83-1670]
- An interacting boundary layer model for cascades
18 p2635 A83-39372
- [AIAA PAPER 83-1915]
- Refinement of the limiting relative friction law for a permeable plate with gas injection
21 p3133 A83-45345
- Finite-difference solutions for laminar boundary layer flows with separation
22 p3249 A83-46459
- INCOMPRESSIBLE FLOW**
- NT STOKES FLOW
- Magnetohydrodynamic stratified flow past a sphere
01 p0106 A83-10275
- Modeling of three-dimensional turbulent structures around missiles
02 p0131 A83-11769
- [AAAF PAPER NT 81-02]
- Partial regularity of suitable weak solutions of the Navier-Stokes equations
02 p0170 A83-12100
- Finite element, stream function-vorticity solution of steady laminar natural convection
02 p0173 A83-12903
- On the stability of almost parallel boundary layer flows
02 p0174 A83-13019
- Prediction of single-point temperature statistics in a half-heated grid flow
02 p0175 A83-13096
- Spectral method solutions for some laminar channel flows with separation
03 p0315 A83-13138
- The response of static pressure tubes in turbulent flows
03 p0321 A83-14573
- Solution of the Navier-Stokes equations using the finite-difference method of Hermitian type
03 p0322 A83-14615
- Oscillating stagnation point flow
04 p0474 A83-14949
- Obtaining axisymmetric flows from plane-parallel ones
04 p0475 A83-15087
- The use of an error index to improve numerical solutions for unsteady lifting airfoils
04 p0442 A83-15281
- Rotational plane flows of a viscous fluid
04 p0480 A83-16364
- Finite-element solution of the incompressible Navier-Stokes equations
05 p0641 A83-17743
- Computer-aided analysis of three dimensional confined vortex flow
06 p0757 A83-18453
- Boundary layer calculations in the inverse mode for incompressible flows over infinite swept wings
06 p0714 A83-19590
- [AIAA PAPER 83-0454]
- Experimental determination of blade forces through stationary and nonstationary pressure measurements on interfering double cascades --- German thesis
06 p0714 A83-19616
- A finite state aerodynamic model for a lifting surface in incompressible flow
07 p0862 A83-19802
- Aerosound from corner flow and flap flow
07 p0990 A83-19813
- [AIAA PAPER 81-2039]
- A numerical analysis of flow using streamline coordinates - The case of two-dimensional steady incompressible flow
07 p0925 A83-20277
- Methods of the numerical modeling of turbulent flows of an incompressible viscous fluid
07 p0925 A83-20314
- Investigation of solution of Navier-Stokes equations using a variational formulation
08 p1085 A83-22648
- Numerical solution of viscous flows using integral equation methods
08 p1085 A83-22649
- The aerodynamics of flexible membranes
08 p1042 A83-22990
- On the numerical solution of some types of unsteady incompressible viscous flow
08 p1087 A83-23178
- The application of boundary value techniques in the solution of the Navier-Stokes equation
08 p1087 A83-23179
- Integral conditions on the vorticity - Numerical algorithms for the steady and unsteady Navier-Stokes equations
08 p1087 A83-23180
- Investigation of solution of Navier-Stokes equations using a variational formulation
08 p1087 A83-23181
- The boundary element method applied to the creeping motion of a sphere
08 p1087 A83-23182
- Numerical simulation of three dimensional flows in duct
08 p1088 A83-23184
- On the finite element simulation of incompressible turbulent flow in general two-dimensional geometries
08 p1088 A83-23187
- Closure models for rotating two-dimensional turbulence
09 p1314 A83-24129
- On the application of the integral invariants and decay laws of vorticity distributions
09 p1262 A83-24421
- [AD-A128456]
- A higher order panel method applied to vortex sheet roll-up
09 p1198 A83-24658

Finite-element method for time-dependent Euler equation --- of inviscid incompressible flow 10 p1413 A83-25462

Adiabatic shearing of incompressible fluids with temperature-dependent viscosity 10 p1414 A83-25873

Number of modes governing two-dimensional viscous, incompressible flows 10 p1417 A83-26272

The dynamics of a viscous incompressibly fluid in Hilbert space with allowance for the boundary conditions 10 p1418 A83-26944

The development of intermittent turbulence on a swept attachment line including the effects of compressibility 11 p1567 A83-27872

Standard and asymptotic finite element methods for incompressible viscous flows 12 p1721 A83-28856

Application of a three-sensor hot-wire probe for incompressible flow 12 p1728 A83-28963

A treatment of three dimensional incompressible turbulence 12 p1722 A83-29068

Approximate calculation of the aerodynamic characteristics of a cylindrical body of small aspect ratio in an incompressible flow 12 p1696 A83-29287

Elliptic-vortex method for incompressible flow at high Reynolds number 12 p1724 A83-29609

Three-dimensional steady stratified flows - A numerical approach 12 p1724 A83-29616

High-Re solutions for incompressible flow using the Navier-Stokes equations and a multigrid method 12 p1725 A83-29659

An open boundary condition for incompressible stratified flows 12 p1725 A83-29667

Driven cavity flows by efficient numerical techniques 12 p1726 A83-29669

The design and numerical analysis of vortex methods 12 p1727 A83-29940

Parametric method for solving problems of heat transfer for the film flow of a fluid 13 p1838 A83-30045

Low-Reynolds-number airfoils 13 p1804 A83-31082

A numerical solution to the equations for the dynamics of a viscous incompressible fluid containing dispersed particles 14 p2008 A83-31897

Applying the method of flows to a problem concerning the dynamics of a viscous, stratified fluid 14 p2008 A83-31898

Force and moment in incompressible flows 14 p2012 A83-32991

Turbulent and mean flow measurements in an incompressible axisymmetric boundary layer with incipient separation 15 p2156 A83-33668

Direct simulation of homogeneous turbulent shear flows on the Illiac IV computer - Applications to compressible and incompressible modeling 15 p2156 A83-33674

Free and induced oscillations in Poiseuille flow 16 p2349 A83-35642

The correct use of dimensional analysis [ONERA, TP NO. 1983-2] 16 p2402 A83-36417

Solution of the Navier-Stokes equations by a spectral method of subdomains [ONERA, TP NO. 1983-19] 16 p2353 A83-36428

Improved numerical method for unsteady lifting surfaces in incompressible flow 16 p2296 A83-36917

Forced oscillations of a viscous incompressible fluid in a semiinfinite channel 17 p2505 A83-37628

The application of splines to the numerical solution of the Navier-Stokes equations at high Reynolds numbers 17 p2505 A83-37629

On conforming mixed finite element methods for incompressible viscous flow problems 17 p2507 A83-38057

The growth of a magnetic field in the three-dimensional steady flow of an incompressible fluid 17 p2582 A83-38070

Evaluation of factors determining the accuracy of linearized subsonic panel methods [AIAA PAPER 83-1826] 17 p2455 A83-38658

Ideal incompressible hydrodynamics in terms of the vortex momentum density 17 p2509 A83-38961

Airfoil generation with a desktop computer using Lighthill's exact inverse method [AIAA PAPER 83-1867] 18 p2632 A83-39096

Flow of an incompressible fluid in a partially filled, rapidly rotating cylinder with a differentially rotating endcap 18 p2680 A83-39207

Viscosity renormalization based on direct-interaction closure 18 p2681 A83-39215

Computation of leading edge vortices [AIAA PAPER 83-1907] 18 p2634 A83-39366

New discretization and solution techniques for incompressible viscous flow problems [AIAA PAPER 83-1921] 18 p2683 A83-39415

Study of incompressible separated flow using an implicit time-dependent technique [AIAA PAPER 83-1894] 18 p2683 A83-39417

Hodographic study of transverse magnetohydrodynamic flows 18 p2746 A83-39855

Calculation of two-dimensional diffusers 18 p2686 A83-39989

Reynolds stresses for unsteady turbulent flows 19 p2842 A83-40877

Nonsimilar laminar incompressible boundary layer flow over a rotating sphere 19 p2843 A83-41542

Incompressible fluid mechanics --- French book 20 p2969 A83-42172

Study of asymptotic incompressible flow in curved ducts using a multi-grid technique 20 p2969 A83-42532

Effect of particle presence on the incompressible inviscid flow through a two dimensional compressor cascade 20 p2928 A83-42562

Heat transfer in turbulent flows 20 p2970 A83-42652

Numerical study of heat transfer system with staggered array of vertical flat plates used at low Reynolds number 20 p2980 A83-42755

LDA measurements of separated flows and a simple calculation method for the drag of a sharp-edged cylinder 20 p2929 A83-43006

Laminar flow in the interior of a rotating hollow sphere as it is set in motion 20 p2983 A83-43010

A second-order turbulence model for two-phase flows 20 p2983 A83-43011

A general solution to the problem of jet flow past a wedge 20 p2931 A83-43520

Synthetic method in thermal boundary layer transition 20 p2987 A83-43650

Simulation of turbulent flows by a method of point vortices [ONERA, TP NO. 1983-35] 21 p3129 A83-44313

Response of variations of free stream velocity on inviscid and incompressible flow past a wavy plate 22 p3281 A83-46393

Experimental analysis of the wake behind an isolated cambered airfoil 22 p3248 A83-46443

The design of optimum diffusers for incompressible flow 22 p3250 A83-46480

The lift on an aerofoil in starting flow 23 p3398 A83-48121

Analysis of turbulent flow past a class of semi-infinite bodies [ASME PAPER 83-FE-32] 23 p3450 A83-48237

The standing vortex behind a disk normal to uniform flow at small Reynolds number 24 p3577 A83-49468

Flow of a dipolar fluid due to suddenly accelerated flat plate 24 p3581 A83-50149

INCOMPRESSIBLE FLUIDS

NT MICROPOLAR FLUIDS

Magnetic hydrodynamics in processes under extreme conditions --- Russian book 01 p0107 A83-10674

Conservative difference schemes for equations of a viscous incompressible fluid in curvilinear orthogonal coordinates 01 p0047 A83-11267

Asymptotic solutions for the motion of a viscous incompressible fluid filling the cavity of a rotating body 01 p0047 A83-11268

Instability of an extended tangential discontinuity - The first term of the wave-vector expansion 02 p0169 A83-11641

The transport equation for the strain rate tensor and the description of an ideal incompressible fluid by a set of dynamic equations 02 p0169 A83-11642

Flow of a non-Newtonian second-order fluid under an enclosed rotating disc with uniform suction and injection 02 p0171 A83-12663

Vibration-induced change of flow in the annular space between two concentric pipes 03 p0320 A83-14506

Nonlinear waves in superposed fluids --- related to astrophysical phenomena 04 p0549 A83-14982

An approximation method for the stability analysis of plates in the flow of an incompressible fluid 04 p0497 A83-15392

The influence of a flow field on the stability of the force-free magnetic field 04 p0536 A83-15595

Axisymmetric vortex breakdown in rotating fluid within a container 04 p0476 A83-15696

The hydromagnetic viscous boundary layer at the free surface of a rotating baroclinic fluid 05 p0641 A83-17835

Helical wave and K-H instability in Type I comet tails. I - Waves of infinitesimal amplitude in incompressible plasma 06 p0832 A83-18850

Space basis for weakly solenoidal functions --- incompressible fluid dynamics 08 p1084 A83-22277

Two models of truncated Navier-Stokes equations on a two-dimensional torus 08 p1085 A83-22384

Effect of compressibility on the Rayleigh-Taylor instability 08 p1085 A83-22386

A refined PUMPIN /Pressure Update by Multiple Path INtegration/ method for updating pressures in the numerical solution of the incompressible fluid equations 08 p1088 A83-23188

Numerical solution of the momentum equations in unsteady incompressible flow 08 p1090 A83-23207

Error and stability analysis of the finite element solution for the transport equation 08 p1090 A83-23216

Unsteady concentration distribution and the flow of a binary mixture in a cone and plate viscometer 09 p1262 A83-24502

Fluctuating flow induced by a rotating disc 11 p1564 A83-27101

Motion of a spherical particle in a viscous nonisothermal fluid 11 p1566 A83-27705

An analysis of the transient processes of the interaction between elastic bodies of revolution and a fluid 11 p1596 A83-28456

Anomalous quantum Hall effect - An incompressible quantum fluid with fractionally charged excitations 13 p1914 A83-30923

A class of exact solutions of two-dimensional viscous flow 14 p2009 A83-32521

Investigation of the simultaneous variable solution for velocity and pressure in incompressible fluid flow problems [AIAA PAPER 83-1519] 14 p2010 A83-32752

Analysis of a turbulent boundary layer subjected to a strong adverse pressure gradient 14 p2014 A83-33451

Theoretical studies of boundary layers --- Russian book 15 p2158 A83-34163

Solution of the problem of flow past a permeable plate with separation of jets 15 p2162 A83-35316

On the localized stability of vortices 16 p2290 A83-35819

An approximate calculation of laminar boundary layer flow of an incompressible fluid 17 p2501 A83-37049

Subharmonic three-dimensional disturbances [AIAA PAPER 83-1759] 17 p2503 A83-37231

On initial and boundary conditions for the Navier-Stokes equations in the Helmholtz form 17 p2505 A83-37529

The effect of the geometrical parameters of an air intake with a central body on drag relative to the fluid streamline in the case when there is an incompressible-gas flow around it 17 p2448 A83-37531

Calculation of a turbulent boundary layer of an incompressible fluid over swept wings of large aspect ratios 17 p2451 A83-37803

Boundary layer separation over a rotating cylinder in a flow of an incompressible fluid 17 p2506 A83-37804

A study of the control properties of axial fans on the basis of theoretical characteristics of plane cascades 17 p2451 A83-37807

The theory for a flexible slat 17 p2451 A83-37810

Annular squeeze films with inertial effects 18 p2695 A83-39942

The stability of the elliptically deformed rotation of an ideal incompressible fluid in a Coriolis force field 18 p2687 A83-40079

Fractional quantization of the Hall effect - A hierarchy of incompressible quantum fluid states 19 p2895 A83-41160

Drag on a sphere oscillating in a dusty gas 19 p2843 A83-41543

Reflection and refraction of harmonic shear waves in incompressible viscoelastic fluids 19 p2843 A83-41545

Circulation-preserving plane flows of incompressible viscous fluids 20 p2985 A83-43113

Energy stability in the Benard problem for a fluid of second grade 21 p3130 A83-44467

An analogy of the motion of a two-phase medium consisting of an incompressible phase and a gas phase with the motion of a gas 21 p3131 A83-44848

A point vortex method applied to interfacial waves 22 p3280 A83-45906

Inertia effects of the dynamics of a disk levitated by incompressible laminar fluid flow [ASME PAPER 83-GT-149] 23 p3464 A83-47968

On the asymptotic structure of interaction in a laminar axisymmetric wake 23 p3451 A83-48653

Asymptotic theory of turbulent separation 23 p3452 A83-48655

Dynamics of an elliptical vortex 23 p3452 A83-48656

Fluid turbulence and the renormalization group - A preliminary calculation of the eddy viscosity 24 p3575 A83-48848

The turbulence problem - A survey 24 p3576 A83-48925

INCONEL (TRADEMARK)

The effect of microstructure and environment on the crack growth behavior of Inconel 718 alloy at 650 C under fatigue, creep and combined loading

- 04 p0458 A83-14999
Relationships between the structure and the mechanical properties of Inconel 718 06 p0729 A83-18600
The effects of heat treatment and composition on the stress corrosion cracking resistance of Inconel alloy X-750 07 p0884 A83-20255
Anelastic relaxation controlled cyclic creep and cyclic stress rupture behavior of an oxide dispersion strengthened alloy 07 p0885 A83-20263
Effect of hold times on the elevated temperature fatigue crack growth behavior of Inconel 718 alloy 08 p1064 A83-21782
Evaluation of creep crack growth criteria for IN-100 at elevated temperature 08 p1066 A83-22142
Thermal softening of Inconel MA 6000 alloy 09 p1228 A83-23343
J(Ic) measurement point determination for HY130, CMS-9, and Inconel Alloy 718 15 p2134 A83-33514
Creep/corrosion of two nickel alloys in combustion gas 16 p2329 A83-35692
Postirradiation fracture toughness of Inconel X-750 18 p2666 A83-39542

INDENTATION

- Equivalence of indentation and compressive creep tests on a WC/Co hardmetal 04 p0460 A83-15997
Indentation fracture transitions in polymethylmethacrylate 12 p1716 A83-29160
The relation between hardness-indentation processes and the stress-strain curve of metallic materials 12 p1713 A83-29363
Dynamic fatigue of brittle materials containing indentation line flaws 15 p2180 A83-35064
A fracture mechanics analysis of indentation-induced Palmqvist crack in ceramics 16 p2336 A83-35572
An approximate solution to a plane contact elasticity problem 21 p3162 A83-45302

INDEPENDENT VARIABLES

- NT LATTICE PARAMETERS
Analysis of boundary value problems on infinite intervals 08 p1159 A83-22024
Parametrically excited vibrations in theory and practice 14 p2032 A83-32961

INDEXES (DOCUMENTATION)

- Prospects for automated solution of the subject characterization problem in the bibliographic services 01 p0111 A83-10146
The Bibliographical Star Index 01 p0114 A83-10148
The physics of strength and plasticity: A systematic index of the major literature in Russian and in foreign languages 1970-1975. Number 2 - Current and special topics in the plastic deformation of materials --- Russian book 09 p1231 A83-23925
Computer assisted information retrieval 11 p1666 A83-28168
Thermal constants of materials. Number 10 - Li, Na, K, Rb, Cs, Fr. Part 3 - Tables of literature references, appendices, bibliography, index --- Russian book 18 p2672 A83-40602

INDEXES (RATIOS)

- NT KP INDEX
Concerning the nonstationarity of the correlation of solar-wind parameters with the AE and a sub p indices of magnetic activity 02 p0211 A83-12448
Statistics of the logarithmic flare index 06 p0856 A83-19171
Statistical properties of geomagnetic pulsations at the Furstenfeldbruck Observatory determined by means of pulsation indices. I - Method and cross-correlation 11 p1617 A83-28117
A note on the accuracy of the auroral electrojet indices 17 p2539 A83-37604
Coronal index of solar activity. IV - Years 1964-1970 18 p2785 A83-39978
Risk/dispersion index method 19 p2894 A83-41296
Notes on the auroral electrojet indices 20 p3015 A83-42178
Solar indices and solar UV-irradiances 24 p3674 A83-48754

INDIA

- Estimation of wave power potential along the Indian coastline 05 p0658 A83-17849
Remote sensing activities in India 09 p1284 A83-24528
Terrain analysis for geotechnical engineering studies related to a part of Chandrapur district, Maharashtra - India 09 p1290 A83-24604
Structural geomorphology of Rajasthan basin, India-interpreted through Landsat imagery and aerial photos 09 p1291 A83-24626

Utility of Landsat data in mineral exploration - A case study from Orissa, India 17 p2528 A83-38139
Induced geomagnetic variation and crustal evolution of the southern peninsula of India 17 p2528 A83-38144

- Variability of the Indian summer monsoon and tropical circulation features 20 p3029 A83-42505
The importance of remote sensing from space to the Indian subcontinent 20 p3010 A83-42959

INDIAN OCEAN

- On some characteristics of the atmospheric boundary layer in the Indian Ocean during the GARP cruise 02 p0212 A83-11846
An analogue model of the geomagnetic induction in the South Indian Ocean 10 p1448 A83-25440
The electrical conductivity of air over the Indian Ocean 11 p1620 A83-28729
Impact of Monex-79 data on the objective analysis of the wind field over the Indian region 15 p2206 A83-34746
Bathymetry estimates in the southern oceans from Seasat altimetry 20 p3033 A83-43548
The wind field in the western Indian Ocean and the related ocean circulation 23 p3493 A83-47412

INDIAN SPACE PROGRAM

- Attitude sensing of apple --- Ariane Passenger Payload Experiment 02 p0142 A83-12967
Development of video-rate image processing system in India 08 p1091 A83-21909
Space sciences in developing countries - The Indian experience 18 p2787 A83-39829
The role of space communication in promoting national development with specific reference to experiments conducted in India 18 p2752 A83-39841
Developments in ISRO space platforms capability 21 p3095 A83-43816
Design of satellite launch vehicles 21 p3098 A83-43817
Design and fabrication of the Indian cosmic ray payload on board Spacelab-3 - A case study 21 p3095 A83-43822
Satellite based remote sensing program - A perspective in the Indian context 23 p3475 A83-47279
[IAF PAPER 83-122]

INDIAN SPACE RESEARCH ORGANIZATION

U ISRO

INDIAN SPACECRAFT

- Apple - Indian experimental geostationary communication satellite --- Ariane Passenger Payload Experiment 02 p0139 A83-11781
Insat-1 - India's dual spacecraft 02 p0140 A83-12645
Apple attitude acquisition with one - solar panel undeployed 17 p2473 A83-37487
Design summary of the Insat lightweight, deployable solar array 17 p2482 A83-37971
[SAE PAPER 821397]
Selection of spectral bands for Indian Remote Sensing Satellite (IRS) 17 p2530 A83-38163
Optimum spectral bands for land cover discrimination 17 p2530 A83-38164
India's domestic satellite communication system - INSAT 19 p2831 A83-41379

INDICATING INSTRUMENTS

- NT ANEMOMETERS
NT APPROACH INDICATORS
NT ASTROLABES
NT ATTITUDE INDICATORS
NT CLOUD HEIGHT INDICATORS
NT FLOW DIRECTION INDICATORS
NT GYROCOMPASSES
NT HOT-FILM ANEMOMETERS
NT HOT-WIRE ANEMOMETERS
NT LASER ANEMOMETERS
NT MICROWAVE SENSORS
NT POSITION INDICATORS
NT RADIO DIRECTION FINDERS
NT SONIC ANEMOMETERS
NT SPACECRAFT POSITION INDICATORS
NT SPEED INDICATORS
NT STRAIN GAGE BALANCES
NT TACHOMETERS
NT WEIGHT INDICATORS
NT WIND VANES

INDIUM

- Optical and electrical characterization of multiply doped silicon - A study of the Si:/In,Al/ system 04 p0542 A83-16065
Usage of ITO to prevent spacecraft charging --- Indium Tin Oxide 05 p0618 A83-17497
Voltage-current characteristics of a regular system of weakly coupled superconducting particles 15 p2237 A83-33779
Determination of natural radiative lifetimes of the 5p2 P state in Ga I and 6p2 P state in In I using a pulsed dye laser 16 p2410 A83-36653

INDIUM ALLOYS

- Absence of the Gunn effect in p-In/0.53/Ga/0.47/As 07 p1000 A83-21374
Monotectic solidification structure of Al-In alloys 09 p1231 A83-23919
Solidification of hypermonotectic Al-In alloys under microgravity conditions 20 p2942 A83-43304

INDIUM ANTIMONIDES

- Direct-gap group IV semiconductors based on tin 01 p0108 A83-10294
InSb heterodyne receivers for submillimeter astronomy 03 p0405 A83-13463
Characteristics of InSb mixers and backward wave oscillators in a submm heterodyne receiver 04 p0472 A83-15813
Quantum corrections to the galvanomagnetic coefficients of quasi-two-dimensional electrons of InSb/GaAs heteroepitaxial structures 07 p0999 A83-20049
Optical bistability in InSb at room temperature with two-photon excitation 07 p0994 A83-21365
The optical constants of indium antimonide at 1.5 K in the near millimeter wavelength region 08 p1164 A83-22250
Integrating 128-element linear imager for the 1 to 5 microns region 08 p1100 A83-22601
Features of the formation of the recombination properties of InSb-base MOS structures 09 p1349 A83-24210
Modulation of far-infrared radiation by electron-hole plasma in indium antimonide 10 p1488 A83-25456
Investigation of thermoelectromotive force in Al(x)In(1-x)Sb solid solutions 13 p1928 A83-30272
InSb charge-injection device array performance 14 p2015 A83-31979
Two-dimensional infrared speckle interferometry with a 32 x 32 InSb charge-injection device (CID) array 14 p2095 A83-31980
Hybrid packaging approach to improved low-noise operation of photovoltaic InSb detectors 14 p2015 A83-31981
Cleaning chemistry of InSb(100) molecular beam epitaxy substrates 17 p2485 A83-37616
A new InSb charge amplifier for application to a spectrometer array 18 p2691 A83-40446
Conductivity of inversion layers in InSb MIS structures below the 'mobility threshold' 20 p3051 A83-42275
Effects of laser irradiation on the electrophysical properties of an indium antimonide MIS-structure interface 21 p3219 A83-45390
An MIS modulator for the microwave band based on InSb films 22 p3277 A83-45674

INDIUM ARSENIDES

- Ga/0.80/In/0.20/As 1.20-eV high quantum efficiency junction for multijunction solar cells 02 p0243 A83-12292
Frequency dependence of degenerate four-wave mixing at the band edge of InAs 11 p1581 A83-27597
Photosensitivity spectra of InAs-PbS heterojunctions 11 p1663 A83-28520
Transferred-electron effect in In/0.53/Ga/0.47/As 11 p1663 A83-28601
The design and manufacture of an experimental device for irradiation at low temperature and a study of the effects of electron irradiation on type n InAs --- French thesis 17 p2585 A83-38433
Accumulation mode Ga(0.47)In(0.53)As insulated gate field-effect transistors 19 p2836 A83-40746
High-efficiency (21.4 pct) Ga0.75In0.25As/GaAs (Eg = 1.15 eV) concentrator solar cells and the influence of lattice mismatch on performance 21 p3169 A83-45493
Energy levels and alloy scattering in InP-(InGa)As heterojunctions 22 p3365 A83-46738

INDIUM COMPOUNDS

- NT INDIUM ANTIMONIDES
NT INDIUM ARSENIDES
NT INDIUM PHOSPHATES
NT INDIUM PHOSPHIDES
NT INDIUM SULFIDES
NT INDIUM TELLURIDES
Mechanism of current transfer in SiS solar cells based on polycrystalline cadmium telluride In2O3/pCdTe and ITO/pCdTe 14 p2087 A83-32044
Recent advances in ITO/InP and CdS/InP solar cells 14 p2041 A83-32240
Some comments on sprayed ITO/semiconductor solar cells 14 p2043 A83-32268
Properties of tin doped indium oxide thin films prepared by magnetron sputtering 16 p2419 A83-35447
Transparent heat-reflecting coatings for solar applications based on highly doped tin oxide and indium oxide 16 p2371 A83-36738
Light-induced effects in indium tin oxide/n-i-p hydrogenated amorphous silicon solar cells 18 p2707 A83-39463

- In₂O₃ heterojunction photocells using compounds of type A(II)B(IV)C₂(V) 23 p3445 A83-47564
- Photovoltaic properties of In/Trans-polyacetylene/Electrodag + 502 Schottky barrier cells 23 p3477 A83-48613
- Photovoltaic effect in gold-indium selenide Schottky barriers 24 p3634 A83-48912
- Surface modification of polycrystalline p-CuInS₂ and p-CuInSe₂ electrodes for improved solar cell performance 24 p3601 A83-50177
- INDIUM PHOSPHATES**
- Estimation of the band gap of InPO₄ 10 p1489 A83-26210
- INDIUM PHOSPHIDES**
- The electrical characteristics of degenerate InP Schottky diodes with an interfacial layer 01 p0036 A83-10629
- Electron diffusion lengths in p-type InP involved in indium tin oxide/p-InP solar cells 01 p0109 A83-10637
- Anomalous inversion channel formation in enhancement-mode InP metal-insulator-semiconductor field effect transistors 01 p0037 A83-10640
- Low threshold InGaAsP/InP lasers with microcleaved mirrors suitable for monolithic integration 01 p0055 A83-10981
- Simulation of non steady-state transport in GaAs and InP millimeter IMPATT diodes 02 p0167 A83-11799
- Model stabilized terrace InGaAsP lasers on semi-insulating InP 03 p0332 A83-13919
- Influence of hot carriers on the temperature dependence of threshold in 1.3-micron InGaAsP lasers 03 p0332 A83-14930
- High quantum efficiency InGaAsP/InP lasers 03 p0333 A83-14931
- Dielectric constant of semi-insulating indium phosphide 04 p0470 A83-15232
- Material parameters of In_{1-x}Ga_xAs_yP_{1-y} and related binaries 04 p0542 A83-16064
- Measurement of very-high-speed photodetectors with picosecond InGaAsP film lasers 06 p0809 A83-18573
- Picosecond correlation measurements of indium phosphide photoconductors 07 p0917 A83-19978
- Indium phosphide transferred electron oscillators for millimetre-wave frequencies 07 p0919 A83-20180
- The effect of interfacial traps on the stability of insulated gate devices on InP 07 p0921 A83-20742
- Donor discrimination and bound exciton spectra in InP 07 p1000 A83-20746
- Millimeter-wave hybrid coupled reflection amplifiers and multiplexers 07 p0922 A83-21527
- Enhanced indium phosphide substrate protection for liquid phase epitaxy growth of indium-gallium-arsenide-phosphide double heterostructure lasers 08 p1107 A83-22331
- InGaAsP/InP undercut mesa laser with planar polyimide passivation 08 p1110 A83-22752
- Correlation of Fermi-level energy and chemistry at InP /100/ interfaces 08 p1170 A83-22766
- Effect of grain boundaries on the minority carrier diffusion length in InP solar cells 08 p1170 A83-22908
- Non-destructive characterisation of n-type InP epitaxial layers by infrared reflectivity measurements 09 p1349 A83-23667
- Short-cavity single-frequency InGaAsP buried-heterostructure lasers 09 p1272 A83-24112
- A study of impurities and traps in liquid phase epitaxial InP in relation to melt prebaking 10 p1488 A83-26063
- CW operation of 1.5 micron GaInAsP/InP buried heterostructure laser with a reactive ion-etched facet 11 p1585 A83-28606
- Metal-insulator-semiconductor structures in indium phosphorus manufactured by plasma-assisted CVD --- French thesis 11 p1563 A83-28637
- Spectroscopy of the isoelectronic nitrogen addition in epitaxial structures based on wide-band solid solutions of the system In-Ga-P-As 13 p1927 A83-30262
- Laser oscillation at 3.53 microns from Fe(2+) in n-InP:Fe 13 p1850 A83-30327
- Recombination enhanced dislocation glide in InP single crystals 13 p1928 A83-30336
- Electro-optical light modulation in InGaAsP/InP double heterostructure diodes 13 p1918 A83-30343
- Electron transport in InP at high electric fields 13 p1929 A83-30353
- Harmonic Gunn oscillators allow frequency growth 13 p1835 A83-30912
- Recent advances in ITO/InP and CdS/InP solar cells 14 p2041 A83-32240
- Studies on CdS/n-InP PEC solar cells 14 p2042 A83-32258
- Growth and characterization of Ga(0.47)In(0.53)As films on InP substrates using triethylgallium, triethylindium, and arsine 14 p2092 A83-32643
- Short cavity InGaAsP/InP lasers with dielectric mirrors 14 p2027 A83-33436
- InGaAsP photodiodes 15 p2150 A83-33680
- InGaAsP/InP phototransistor-based detectors 15 p2150 A83-33683
- Optical comparator - A new application for avalanche phototransistors 15 p2229 A83-33684
- InP:Fe photoconductors as photodetectors 15 p2150 A83-33685
- Optimum design of n(+)-n-n(+) InP devices in the millimeter-range frequency limitation - RF performances 15 p2151 A83-33917
- Fabrication and investigation of GaInPAs/InP heterolayers 15 p2168 A83-33978
- Very low threshold InGaAsP mesa laser 16 p2359 A83-35955
- High-power InP MISFETs 16 p2346 A83-36006
- TDEG in In(0.53)Ga(0.47)As-InP heterojunction grown by chloride VPE --- two-dimensional electron gas 17 p2585 A83-38880
- Phase-locked InGaAsP laser array with diffraction coupling 18 p2693 A83-40051
- InP surface states and reduced surface recombination velocity 18 p2750 A83-40061
- Impact ionization in (100)-, (110)-, and (111)-oriented InP avalanche photodiodes 18 p2750 A83-40064
- Carrier leakage and temperature dependence of InGaAsP lasers 19 p2850 A83-40732
- Avalanche InP/InGaAs heterojunction phototransistor 19 p2899 A83-40948
- Annealing behaviour of gamma-ray-induced electron traps in LEC n-InP 20 p3052 A83-42482
- High efficiency GaInAs/Inp heterojunction IMPATT diodes 20 p2968 A83-43350
- X-band self-aligned gate enhancement-mode InP MISFET's 20 p2968 A83-43353
- A one-volt p-InP/n-CdSe regenerative photoelectrochemical cell 20 p3013 A83-43421
- CW laser-annealing behavior of Se(+)-implanted InP investigated by ellipsometry 20 p3055 A83-43603
- High-resistivity greater than 10 to the 5th ohm/cm InP layers by liquid phase epitaxy 20 p3055 A83-43604
- Rapid thermal annealing of Se and Be implanted InP using an ultrahigh power argon arc lamp 20 p3055 A83-43605
- Indium phosphide accumulation-mode field-effect transistors 21 p3124 A83-43856
- A 1.59 micron wavelength GaInAsP/InP distributed feedback laser with first-order grating on anti-meltback layer 21 p3144 A83-44500
- Diffusion of zinc into ion implanted iron doped indium phosphide 21 p3218 A83-45179
- Epitaxial InP/fluoride/InP(001) double heterostructures grown by molecular beam epitaxy 22 p3365 A83-46732
- Energy levels and alloy scattering in InP(InGa)As heterojunctions 22 p3365 A83-46738
- Reliability of InGaAsP/InP buried heterostructure 1.3 micron lasers 22 p3301 A83-46824
- Mismatch and electron mobility in MBE Ga(x)In(1-x)As epitaxial layers on InP substrates 23 p3512 A83-48701
- High-field transport properties of In_{0.765}Ga_{0.235}As_{0.5}P_{0.5} 23 p3512 A83-48703
- INDIUM SULFIDES**
- Composition determination of CuInS₂ by a chemical analysis method 04 p0456 A83-15484
- Determination of trace elements in CuInS₂ 04 p0456 A83-15485
- Compositional analysis of CuInS₂ chalcopyrite semiconductor 14 p2089 A83-32257
- INDIUM TELLURIDES**
- Schottky barriers on single-crystal indium telluride 21 p3127 A83-45176
- INDOES**
- NT TRYPTOPHAN
- INDONESIA**
- An investigation methodology for territorial studies in unknown areas /East Kalimantan - Timur, Indonesia/ 08 p1129 A83-21968
- Large scale pressure disturbances over the Indonesian Maritime Continent 09 p1311 A83-23893
- Local circumstances in Java during the total solar eclipse of 1983 09 p1354 A83-24020
- Back arc thrusting in the eastern Sunda arc, Indonesia - A consequence of arc-continent collision 22 p3322 A83-45742
- Development of Indonesian sounding rockets [IAF PAPER 83-379] 23 p3420 A83-47366
- INDOOR AIR POLLUTION**
- A hygienic evaluation of the chemical composition of air in living accommodations 17 p2562 A83-38201
- INDUCED FLUID FLOW**
- U FLUID FLOW
- INDUCTANCE**
- Calculation of the force characteristics and inductance of a suspension electromagnet 13 p1934 A83-30517
- INDUCTION**
- Induction and deduction as the function of different hemispheres --- of brain 19 p2870 A83-40810
- INDUCTION HEATING**
- RFI and ECH plasma generator development for ion thrusters [AIAA PAPER 82-1941] 02 p0146 A83-12503
- Deposition of protective coatings on metals using an induction-plasma jet 07 p0940 A83-22701
- The effect of electromagnetic forces on the hydrodynamics of a melt in the process of high-frequency floating zone melting 12 p1782 A83-29269
- INDUCTION MOTORS**
- Transistorized PWM inverter-induction motor drive system 01 p0044 A83-11488
- The design and control of linear bidirectional stepping motors - Application to machine tools --- French thesis 06 p0750 A83-18495
- Introduction of feedforward control for an improved optimal regulator system and its application 06 p0804 A83-19393
- Linear induction motor - Equivalent-circuit model 07 p0916 A83-19630
- The dynamic braking of a linear induction motor at a variable speed 08 p1080 A83-22224
- Asynchronous induction micromotors for automatic systems --- Russian book 10 p1408 A83-25618
- Linear induction machines - Reflexions on the evaluation of efficiency, and on the choice of secondary resistivity 13 p1832 A83-30448
- Twin-armature rotary-linear induction motor 14 p2006 A83-32426
- INDUCTION SYSTEMS**
- U INTAKE SYSTEMS
- INDUCTORS**
- Push-pull current-fed multiple-output regulated wide-input-range dc/dc power converter with only one inductor and with 0 to 100% switch duty ratio - Operation at duty ratio below 50% 01 p0041 A83-11017
- The thermal limitation of the velocity of annular conductors under inductive axial acceleration 06 p0755 A83-19561
- The Hall effect in a unipolar inductor - A possible mechanism for a dynamo and an antidynamo --- pulsar model 09 p1364 A83-25088
- Optimization of the energy-storage inductors for dc-to-dc converters 14 p2007 A83-33130
- Low-loss unidirectional SAW filters using integrated microinductors 24 p3575 A83-43996
- INDUSTRIAL AREAS**
- A study of the descriptive statistics of turbulent pollution concentration fields in atmospheric air and of meteorological elements for cities with developed industry 05 p0659 A83-16954
- The effect of an electric field of industrial frequency on parameters of natural immunity 05 p0669 A83-17164
- Point discharge current studies near a large pollution source 06 p0781 A83-18417
- INDUSTRIAL ENERGY**
- Thermal infrared sensing applied to energy conservation in building envelopes /Thermosense IV/, Proceedings of the Meeting, Ottawa, Ontario, Canada, September 1-4, 1981 02 p0180 A83-12686
- Prospects for the construction of solar furnaces for industry 06 p0781 A83-19236
- Current aspects of wind-energy utilization - Status and prospects in Bulgaria --- wind resources and site selection for industrial applications 08 p1130 A83-22421
- Can industry afford solar energy 09 p1294 A83-25144
- Direct-contact air/molten salt heat exchange for solar thermal systems 11 p1607 A83-27234
- Development of solar total energy system for industrial sectors 11 p1608 A83-27244
- Continuous-wave industrial electron-beam-controlled CO laser of 10 kW output power 15 p2168 A83-33976
- Industrial water electrolysis - Present and future 18 p2664 A83-39560
- INDUSTRIAL MANAGEMENT**
- NT ENGINEERING MANAGEMENT
- NT PERSONNEL MANAGEMENT
- The optimal shift schedule of work in industry 04 p0522 A83-15785
- The next step in getting the composite story right Industrialisation of manufacturing systems 18 p2752 A83-40277
- Systems analysis and economics --- of space industrialization 22 p3257 A83-45860
- INDUSTRIAL PLANTS**
- NT FOUNDRIES
- CAM networks for the factory of the future [AIAA PAPER 83-0217] 05 p0679 A83-16588
- Stabilization of a class of plants with possible loss of outputs or actuator failures 08 p1157 A83-22418

The lunar factory --- for production of construction materials and spacecraft fuels 17 p2471 A83-38622

INDUSTRIAL SAFETY

Remote sensing applications for mine waste stability monitoring using the acoustic emission method

01 p0062 A83-10036

An investigation of the effect of local vibration at fragmented doses for the substantiation of a model of a sparing regime --- for human body

01 p0083 A83-10528

The yearly individual doses of radiation for personnel who work with sources of ionizing radiation

01 p0085 A83-11402

Destruction of polyvinyl chloride under extrusion --- toxic hazards in industry

01 p0029 A83-11404

A comparison of several methods for measuring variable occupational noise for their hygienic evaluation

03 p0379 A83-13614

A hygienic evaluation of the effectiveness of ultraviolet radiation during the action of industrial poisons on the organism

03 p0375 A83-14347

Engineering safety analysis via destructive numerical experiments

04 p0500 A83-16198

The establishment of safe levels of local vibration

05 p0677 A83-17195

Electromagnetic radiation emissions from visual display units - A review

09 p1324 A83-23885

PIXE analysis of aerosol in the workplace

13 p1872 A83-30181

The contribution of nondestructive testing to quality assurance and industrial safety - Can the taking of risks still be justified

15 p2173 A83-34323

The function of the hypophyseal-adrenal system when exposed to a variable magnetic field of industrial frequency

15 p2210 A83-34931

The investigation of social-psychological factors of occupational injuries in geological-survey work

16 p2401 A83-36819

The control levels of ionizing radiation in the workplace

23 p3499 A83-48569

INDUSTRIES

NT AEROSPACE INDUSTRY

NT AIRCRAFT INDUSTRY

NT DEFENSE INDUSTRY

NT WEAPONS INDUSTRY

A user's viewpoint on computational fluid dynamics

13 p1842 A83-30642

The Sophia antipolis workshop on the relationship between ESA and industry

17 p2471 A83-37870

A prognostic investigation of the functional condition of administration and management workers

21 p3187 A83-44663

INELASTIC BODIES

U RIGID STRUCTURES

INELASTIC COLLISIONS

Partial inelasticity coefficients K-gamma in pi-A and pA interactions

02 p0234 A83-11734

Differences in partial inelasticity coefficients Kpi/0/ for piFe, pFe interactions at energies of 0.5-5 TeV

02 p0235 A83-11735

Characteristics of inelastic interactions with high transverse momenta of secondary particles

02 p0274 A83-11747

Electron distribution function in a weakly ionized plasma in an inhomogeneous electric field. II - Strong fields / energy balance determined by inelastic collisions/

03 p0397 A83-13195

Proton-nucleus total inelastic cross sections - An empirical formula for E greater than 10 MeV

08 p1192 A83-22747

Potential energy surface for the study of inelastic collisions between nonrigid CO and H2

09 p1343 A83-25135

The critical energy density and the inelasticity coefficient for asteroidal catastrophic collisions

15 p2250 A83-35029

Collisions between Rossby solitons --- in shallow atmosphere of rotating planet

18 p2780 A83-40484

Effect of potential fluctuations in a plasma on the population of highly excited atomic states

21 p3211 A83-44145

Collisions and merging of disk galaxies

24 p3642 A83-49261

INELASTIC SCATTERING

Neutral pions from the fragmentation region of an impinging hadron at E sub 0 approximately equal to 10 to the 13th eV

02 p0274 A83-11748

The mobilities of NO3/-, NO2/-, NO/+, and Cl/- in N2 - A measure of inelastic energy loss

05 p0684 A83-17656

Elastic and inelastic scattering of electrons by atomic hydrogen at intermediate energies in a coupled-channel second-order potential model

06 p0808 A83-19008

Computational studies of first-Born scattering cross sections. I - Spectral properties of Bethe surfaces. II - Moment-theory approach

09 p1341 A83-23722

Enhanced optical spectroscopies at surfaces - Fluorescence and Raman scattering

11 p1655 A83-27509

Elastic and inelastic scattering of high-energy electrons and X-rays by NH3, CH4 and H2O molecules

16 p2409 A83-35333

On the dynamics in compressed methane gas at 3 kbar by inelastic neutron scattering

16 p2409 A83-35334

Elastic and inelastic scattering of gamma rays from V3Si

19 p2905 A83-41537

Inelastic scattering effects on photoelectron spectra and ionospheric electron temperature

20 p3019 A83-42422

Relativistic kinetic equation for inelastically interacting particles in a gravitational field

24 p3636 A83-49062

INELASTIC STRESS

On constitutive relations in thermoplasticity

06 p0774 A83-18488

Some theoretical considerations and experimental results concerning elastic-plastic stress-strain relations

06 p0778 A83-19323

Some inelastic effects of thermal cycling on ZrO2-Y2O3 materials

08 p1072 A83-22272

Inelastic deformation of certain high-modulus reinforcing fibers

18 p2649 A83-40102

Effects of complicated deformation history on inelastic deformation behaviour of metals

18 p2705 A83-40334

Micro-crack initiation, propagation and threshold in elevated temperature inelastic fatigue

[ASME PAPER 83-PVP-97] 20 p3009 A83-43731

Large strain inelastic behaviour of cylindrical tubes

23 p3474 A83-48698

INEQUALITIES

Additional necessary conditions for optimal control with state-variable inequality constraints

04 p0527 A83-15945

Thermodynamic inequalities in continuum mechanics

11 p1665 A83-27994

INERT GASES

U RARE GASES

INERTIA

NT INERTIA PRINCIPLE

NT MACH INERTIA PRINCIPLE

Inertial forces on an expanding bubble in motion in a fluid

01 p0047 A83-10921

Transient lubricating films with inertia

[ASME PAPER 82-LUB-12] 03 p0335 A83-13507

Influence of rotary inertia on the fundamental frequency of a cantilever beam

04 p0496 A83-15071

Influence of gas inertia forces generated within the stabilizing restrictor on dynamic characteristics of externally pressurized thrust gas bearings. I - Case of laminar flow at the capillary restriction

07 p0939 A83-20292

On the stabilization of an unbalanced Lagrange gyroscope at rest

09 p1337 A83-23563

Gravito-inertial sensitivity of the spider - Araneus sericatus

11 p1639 A83-27822

On the solution of the time-dependent inertial-frame equation of radiative transfer in moving media to O(v/c) --- largest velocity dependent term

12 p1796 A83-29610

Nonlinear supersonic flutter of panels considering shear deformation and rotary inertia

15 p2176 A83-34315

The motion of a solid body along the smooth surface of the earth --- with reference to hurricane motion theory

18 p2724 A83-39441

Effects of fluid inertia and viscoelasticity on the one-dimensional squeeze-film bearing

[ASLE PREPRINT 83-AM-3E-1] 20 p2999 A83-43336

Analysis of multirecess conical hydrostatic thrust bearings under rotation

21 p3147 A83-44373

Inertia effects of the dynamics of a disk levitated by incompressible laminar fluid flow

[ASME PAPER 83-GT-149] 23 p3464 A83-47968

The effect of fluid inertia in squeeze film damper bearings A heuristic and physical description

[ASME PAPER 83-GT-177] 23 p3465 A83-47976

Cases of integrability of equations for the inertial motion of two bodies connected by means of a spherical joint

23 p3504 A83-48453

Inertia coefficient considerations and the structure of Jovian planets

24 p3672 A83-49396

INERTIA MOMENTS

U MOMENTS OF INERTIA

INERTIA PRINCIPLE

NT MACH INERTIA PRINCIPLE

A method for the computation of inertial properties for general areas

20 p3038 A83-42796

The calculation of robot dynamics using articulated-body inertias

20 p2959 A83-43109

INERTIA WHEELS

U REACTION WHEELS

INERTIAL CONFINEMENT FUSION

The interaction of a relativistic electron beam with a thin target --- French thesis

03 p0398 A83-13806

Interferometric measurement of the electron density in laser-matter interaction --- French thesis

03 p0398 A83-13808

Polymer coating of glass microballoons levitated in a focused acoustic field

20 p2962 A83-43258

Application of microgravity and containerless environments to the investigation of fusion target fabrication technology

20 p2962 A83-43262

Investigation of metallic and metallic glass hollow spheres for fusion target application

20 p2963 A83-43263

Air jet levitation furnace system for observing glass microspheres during heating and melting

20 p2963 A83-43265

Glass shell manufacturing in space

20 p2941 A83-43290

A technique for thick polymer coating of inertial-confinement-fusion targets

21 p3118 A83-44616

A class of similarity solutions for the nonlinear thermal conduction problem

24 p3581 A83-50201

INERTIAL FORCES

U INERTIA

INERTIAL FUSION (REACTOR)

Laser wavelength effect on the thermal conductivity and ablation in plasmas created by a laser --- French thesis

15 p2232 A83-33700

The instability of two plasmons and suprathermal electrons in the laser-matter interaction --- French thesis

17 p2583 A83-38224

INERTIAL GUIDANCE

NT STRAPDOWN INERTIAL GUIDANCE

An optimal guidance law via first order inertial loop

10 p1469 A83-26770

An investigation of quasi-inertial attitude control for a solar power satellite

12 p1707 A83-29050

Reverse Velocity Rocket Sled Test Bed for inertial guidance systems

12 p1705 A83-29209

Flight testing the Low Cost Inertial Guidance System

12 p1700 A83-29210

Minuteman inertial guidance assessment - The next best thing to flight tests

13 p1811 A83-30160

Dual mode reaction-jet, thrust-vector controls for small missiles

16 p2318 A83-36245

[AIAA PAPER 83-1148] Peacekeeper - Guidance system flight readiness review

19 p2814 A83-41736

[AIAA PAPER 83-2269] Laser gyro for instrumentation of advanced missile guidance system testing

19 p2848 A83-41737

[AIAA PAPER 83-2271] Stellar-inertial guidance capabilities for advanced ICBM

19 p2814 A83-41756

[AIAA PAPER 83-2297] Optical angle marker --- for calibrating inertial guidance test equipment

22 p3291 A83-46591

A method for the identification of nonlinear inertial systems

24 p3622 A83-50204

INERTIAL MEASURING UNITS

U INERTIAL PLATFORMS

INERTIAL NAVIGATION

NT GIMBALLESS INERTIAL NAVIGATION

Gravity modeling for airborne applications

01 p0004 A83-11090

Analysis of three hierarchical motion compensation systems for synthetic aperture radars

01 p0007 A83-11242

Development of inertial navigation and its employment in measurement technology

05 p0592 A83-16900

Inertial navigation and optimal filtering --- Russian book

05 p0680 A83-17123

Suboptimal filters for INS alignment on a moving base

07 p0865 A83-21019

Integration of navigation resources in modern avionics systems

09 p1200 A83-24852

A multifunction integrated approach to providing aircraft inertial data

09 p1200 A83-24853

Carrier Aircraft Inertial Navigation System /CAINS/ integrated system approach

09 p1201 A83-24854

The Integrated Inertial Navigation System - AN/ASN-132

09 p1201 A83-24855

The laser gyro - Myth or panacea

09 p1270 A83-24858

Nonlinear Kalman filtering techniques for terrain-aided navigation

10 p1373 A83-26263

Fibre-optic gyro for sensitive measurement of rotation

10 p1422 A83-26474

A practical method for sensor selection in linear estimation --- applied to inertial navigation systems

10 p1465 A83-26531

An azimuth rate inertial navigation system

10 p1382 A83-26768

A multifunction integrated approach to providing aircraft inertial data 11 p1528 A83-28595

The Integrated Inertial Navigation System AN/ASN-132 11 p1528 A83-28596

Space vehicle attitude determination and surface vessel position fixing - A common analytical solution 11 p1536 A83-28598

Analysis of the precision of inertial navigation systems --- German thesis 11 p1528 A83-28649

Guidance and flight control demonstration in a helicopter flight environment using a laser-gyro inertial navigation system 11 p1528 A83-28779

Performance of a Strapdown Ring Laser Gyro Tetrad Inertial Navigation System in a helicopter flight environment 11 p1528 A83-28781

Improved accelerometers for high accuracy strapdown inertial navigation systems 11 p1576 A83-28783

Integration and flight demonstrations of the Integrated Inertial Sensor Assembly /IISA/ 11 p1529 A83-28785

Institute of Navigation, Annual Meeting, 38th, U.S. Air Force Academy, Colorado Springs, CO, June 14-17, 1982, Proceedings 12 p1700 A83-29201

The laser gyro as a self-contained inertial navigation aid 12 p1729 A83-29208

A lab test to find the major error sources in a laser strapdown inertial navigator 12 p1706 A83-29211

Benefits of integrating GPS and Inertial Navigation Systems 12 p1700 A83-29214

The problem of correction in inertial navigation --- Russian book 12 p1706 A83-29330

The maximum possibilities of using information about constant height in an inertial navigation system 15 p2126 A83-34427

Alpha Jet - Further version for the international market 17 p2467 A83-37858

Avionics analyzed. III - The hidden sensors 17 p2461 A83-38471

Navigation, guidance and control curriculum at the Air Force Academy [AAS PAPER 83-021] 21 p3220 A83-44167

DINS - Lessons learned and successes achieved --- ring laser gyro Dormant Inertial Navigation System for maneuvering reentry vehicles [AAS PAPER 83-084] 21 p3097 A83-44184

The effect of manufacturing imperfections on the accuracy of inertial navigation systems 21 p3097 A83-44631

The use of hypercomplex numbers in the algorithms for the operation of a strapdown inertial navigation system 21 p3097 A83-44637

Comparison of simple position resets and Kalman filter position updates for correcting inertial navigation system errors 22 p3253 A83-46967

Flight simulation for an inertial navigation system 23 p3420 A83-47178

State of the art and development potential of fiberoptic rotation sensors --- for inertial navigation 23 p3405 A83-47187

Equations for the small oscillations of an inertial navigation system with allowance for the ellipsoidality of the earth 23 p3421 A83-48456

Integrated navigation systems for aircraft 23 p3402 A83-48735

INERTIAL PLATFORMS

The reliability analysis of a dual, physically separated, communicating IMU system 01 p0005 A83-11128

Inflight parity vector compensation for FDI --- Failure Detection and Isolation 01 p0019 A83-11129

Navigation of the Space Shuttle 09 p1215 A83-24372

CONEX gyroscope 11 p1575 A83-28782

Wheel-speed induced errors in the use of dry-tuned gyros 17 p2509 A83-37156

Space borne attitude measurement units 17 p2481 A83-37474

Dynamic isolation via momentum compensation for precision instrument pointing [AIAA PAPER 83-2176] 19 p2817 A83-41670

The use of multiple inertial systems to correct for the effects of gravitational anomalies [AIAA PAPER 83-2196] 19 p2796 A83-41681

Open-loop residuals and alternate trajectories as a means of validating IMU calibration and alignment performance [AIAA PAPER 83-2252] 19 p2811 A83-41727

Calibration of the aerodynamic coefficient identification package measurements from the shuttle entry flights using inertial measurement unit data [AIAA PAPER 83-2100] 19 p2818 A83-41930

International Symposium on Geodetic Networks and Computations, Munich, West Germany, August 31-September 5, 1981, Proceedings. Volume 4 - Modern observation techniques for terrestrial networks 22 p3315 A83-46336

Inertial technology applications to geodetic networks 22 p3291 A83-46342

Adjustment problems in inertial positioning 22 p3316 A83-46343

Which information can you get out of an inertial system and what can you do with it? 22 p3291 A83-46344

INERTIAL REFERENCE SYSTEMS

Inertial reference for robotic manipulators [ASME PAPER 82-DET-63] 02 p0230 A83-12774

Precise optical positions for radio/optical astrometric sources in the southern hemisphere 10 p1493 A83-25654

HEAO project - Revisited --- attitude control system design for spaceborne astronomy 10 p1385 A83-26585

The maximum possibilities of using information about constant height in an inertial navigation system 15 p2126 A83-34427

Maximum likelihood estimation of stochastic model parameters for inertial systems and components [AIAA PAPER 83-2249] 19 p2892 A83-41725

Precise positions in the FK4 system for ten optical counterparts of extragalactic radio sources 22 p3373 A83-46385

INERTIAL UPPER STAGE

Optimization using sensitivity analysis --- of inertial upper stage design 07 p0872 A83-20411

Reflection characteristics of certain classes of Soviet space objects 07 p0871 A83-21621

Inertial upperstage attitude initialization and update on Space Shuttle 11 p1534 A83-28777

Inertial Upper Stage navigation algorithms evaluation 11 p1536 A83-28778

Inertial upper stage - Upgrading a stopgap proves difficult 14 p1980 A83-31943

Postfire sampling of SRMs for contamination sources in high altitude test cells [AIAA PAPER 83-1448] 14 p1984 A83-32716

First flight performance of the control system of the inertial upper stage [AAS PAPER 83-086] 21 p3096 A83-44186

Chemical orbit transfer vehicles - Options for the future [IAF PAPER 83-11] 23 p3418 A83-47231

INFARCTION

NT MYOCARDIAL INFARCTION

INFECTIOUS

U INFECTIOUS DISEASES

INFECTIOUS DISEASES

NT AIRBORNE INFECTION

NT CONJUNCTIVITIS

NT MENINGITIS

An analysis of the parameters of the immunoreactive curve 01 p0080 A83-10555

The solar-terrestrial links in biology and the phenomenon of frequency 'capture' 02 p0221 A83-11890

Effects of hyperbaric oxygen on anaerobic organisms 02 p0222 A83-12260

Morphological evidence for natural poxvirus infection in rats 07 p0976 A83-21049

The chemoprophylaxis of malaria in flight personnel 14 p2067 A83-32452

INFESTATION

Landsat monitoring of Desert Locust breeding grounds in Africa, the Near East and Southwest Asia 01 p0065 A83-10097

Action plan for remote sensing applications for rice production --- Book [IFAORS-207] 03 p0345 A83-14121

Assessment of spruce budworm defoliation using digital airborne MSS data 03 p0347 A83-14248

Aerial survey of crop losses due to grasshoppers /Orthoptera - Acrididae/ in Saskatchewan 03 p0347 A83-14255

The application of remote sensing in southern Alberta's mountain pine beetle management 03 p0347 A83-14257

Identification and monitoring of Australian plague locust habitats from Landsat 14 p2035 A83-32610

Detecting forest canopy change due to insect activity using Landsat MSS 22 p3318 A83-46765

INFINITE SPAN WINGS

Acoustic-wave diffraction by a plate moving near a flat surface 01 p0105 A83-11319

Calculation of three-dimensional turbulent boundary layer on an infinite swept wing 21 p3086 A83-44555

INFINITY

Conformal Minkowski space-time, I - Relative infinity and proper time 08 p1160 A83-22012

Analysis of boundary value problems on infinite intervals 08 p1159 A83-22024

INFLATABLE DEVICES

U INFLATABLE STRUCTURES

INFLATABLE SPACECRAFT

NT BEACON SATELLITES

INFLATABLE STRUCTURES

NT AIR BAG RESTRAINT DEVICES

NT BALLOONS

NT BEACON SATELLITES

NT GAS BAGS

NT HIGH ALTITUDE BALLOONS

NT JIMSPHERE BALLOONS

NT METEOROLOGICAL BALLOONS

NT MICROBALLOONS

NT SUPERPRESSURE BALLOONS

NT TETHERED BALLOONS

Deflections of inflated cylindrical cantilever beams subjected to bending and torsion 02 p0196 A83-12853

The use of stereophotogrammetry for studying the stress-strain state of a soft spherical shell in air flow 17 p2522 A83-37808

Lighter-Than-Air Systems Conference, Anaheim, CA, July 25-27, 1983, Collection of Technical Papers 17 p2443 A83-38901

Patterning techniques for inflatable LTA vehicles --- Lighter Than Air [AIAA PAPER 83-1983] 17 p2466 A83-38911

INFLATING

The theoretical advantages and practical considerations of gas replenishment techniques in long-duration scientific ballooning [AD-A129841] 18 p2640 A83-39802

INFLUENCE COEFFICIENT

NT STRUCTURAL INFLUENCE COEFFICIENTS

Influence coefficients of variable geometry free gas turbine engines 08 p1111 A83-22321

Use of coefficients of influence to solve some inverse problems in plane elasticity [ASME PAPER 83-APM-23] 17 p2519 A83-37382

In situ balancing of flexible rotors using influence coefficient balancing and the unified balancing approach [ASME PAPER 83-GT-178] 23 p3465 A83-47989

INFORMATION

Teleinformatics, the protection of privacy and the law 22 p3368 A83-45820

INFORMATION ADAPTIVE SYSTEM

Laboratory system for demonstrating spacecraft processing of multispectral image data 12 p1748 A83-29146

INFORMATION DISSEMINATION

Management of astronomical data at Kanazawa Data Center 01 p0113 A83-10129

Euronet-DIANE, the first European network for data transmission 01 p0111 A83-10133

Stability of the decentralized estimation in the JTIDS relative navigation 01 p0008 A83-11253

NASA educational briefs 02 p0244 A83-11819

Office automation in resource-management - The future is now --- agricultural land use map dissemination 03 p0348 A83-14269

Synergistic integration of JTIDS/GPS technology --- Joint Tactical Information Distribution System 11 p1529 A83-28789

Characteristics of sources, channels, and contents for scientific and technical information systems in industrial R and D 15 p2239 A83-33523

Survey of usage of technical report components to establish their most effective organization 15 p2239 A83-34800

ERS-1 processing algorithms and disseminated products [IAF PAPER 83-129] 23 p3475 A83-47284

INFORMATION FLOW

U.S. Navy search and rescue Model Manager 04 p0444 A83-15424

Fourier transform spectrometry in relation to other passive spectrometers 04 p0482 A83-15804

On information flow in relay networks 07 p0908 A83-19734

Computer simulation of fluid-physics-module operations on the first Spacelab flight 08 p1049 A83-22373

Costs and benefits of alternative legal regime for remote sensing 15 p2240 A83-34656

INFORMATION MANAGEMENT

Infrared astronomical data base and catalog of infrared observations 01 p0113 A83-10130

Data in astronomy --- and its management 01 p0114 A83-10152

AEDCS - A computer-aided system design tool for integrated avionics 01 p0089 A83-11176

A file management system for a network of dissimilar computers --- French thesis 04 p0545 A83-15849

Productivity goals drive office automation 18 p2752 A83-40308

The stepwise utilization of meteorological information in numerical analysis 21 p3181 A83-45402

INFORMATION RETRIEVAL

Prospects for automated solution of the subject characterization problem in the bibliographic services 01 p0111 A83-10146

- Aids to the retrieval and evaluation of astronomical data 01 p0114 A83-10149
Retrieval of astronomical information from Padova-Asiago Observatory plates archives 01 p0114 A83-10154
Infrared astronomical data base and catalog of infrared observations 03 p0406 A83-13467
Performance models of distributed databases 07 p0982 A83-19797
The Earthnet LEDA-2 image catalogue system 11 p1666 A83-27375
Computer assisted information retrieval 11 p1666 A83-28168
Data base organization in computer-aided design systems 11 p1646 A83-28622
Semantic representative languages in document retrieval systems - Effects of a representation of meaning involving differences in depth on the system characteristics --- German thesis 11 p1666 A83-28660
Meteorological data assimilation using AFOS 13 p1885 A83-30530
Information retrieval from wide-band meteorological data - An example 17 p2552 A83-38758
Environmental data display 21 p3142 A83-45615
Picture information measures for similarity retrieval 22 p3290 A83-46255
A hybrid structure for the storage and manipulation of very large spatial data sets 24 p3619 A83-49195

INFORMATION SYSTEMS

- NT EARTH RESOURCES INFORMATION SYSTEM
NT GEOGRAPHIC INFORMATION SYSTEMS
NT INFORMATION ADAPTIVE SYSTEM
NT MANAGEMENT INFORMATION SYSTEMS
Standardization of computer compatible tape formats for remote sensing data 01 p0064 A83-10075
Euronet-DIANE, the first European network for data transmission 01 p0111 A83-10133
Prospects for automated solution of the subject characterization problem in the bibliographic services 01 p0111 A83-10146
The development of JTIDS distributed TDMA / DTDMA / advanced development model / ADM / terminals --- Joint Tactical Information Distribution System 01 p0004 A83-11094
Signal conversion in solid-state transducers 02 p0180 A83-12808
Material-testing machine concepts for the integration of material testing into central in-service data acquisition 02 p0189 A83-12987
Analysis of time fluctuations in synchronous information networks --- German thesis 04 p0467 A83-15839
The problem of the maximum data compression in an information system with large data flows 05 p0623 A83-17657
Information search and retrieval in the areas of astronomy and geodesy --- Russian book 07 p1001 A83-20375
Controlling the complexity of menu networks 07 p0983 A83-21041
The development of a land image-based resource information system / LIBRIS / and its application to the assessment and monitoring of Australian arid rangelands 09 p1286 A83-24547
Methodological and systems engineering aspects of environmental pollution monitoring --- Russian book 09 p1299 A83-25248
The design of adaptive information-transfer systems for automatic control --- Russian book 12 p1769 A83-29333
The centralized storm information system at the NOAA Kansas City complex 13 p1885 A83-30535
Computational systems and methods in the automation of investigations and control --- Russian book 13 p1910 A83-30616
Characteristics of sources, channels, and contents for scientific and technical information systems in industrial R and D 15 p2239 A83-33523
Matching remote sensing technology to operational requirements for land resource management in Canada 15 p2187 A83-35278
AISA - Program for automated treatment of aeronautical data --- for civil aviation applications 16 p2311 A83-35598
An automated multichannel measuring system 17 p2563 A83-37674
Lessons learned from the CSIS --- Centralized Storm Information System 17 p2549 A83-38717
Developments in scientific information systems 19 p2907 A83-41291
An overview of a new integrated system for communication, navigation, and identification - The Joint Tactical Information Distribution System 19 p2795 A83-41310
Space Station information systems [AIAA PAPER 83-7105] 19 p2814 A83-42089

- A causal model for analyzing distributed concurrency control algorithms 20 p3038 A83-43116
Distribution design of logical database schemas 20 p3038 A83-43117
Data from remote sensing in the geographical information system - The construction of territorial data banks 20 p3011 A83-43137
The significance of a strong value-added industry to the successful commercialization of Landsat [AAS PAPER 83-185] 20 p3011 A83-43769
Information induced multimodel solutions in multiple decisionmaker problems 21 p3198 A83-44100
New approaches to planetary exploration - Spacecraft and information systems design [IAF PAPER 83-348] 23 p3415 A83-47354

INFORMATION THEORY

- Concerning certain analogies in physics and information theory 01 p0111 A83-10564
Concerning the optimality of discrete-data compression in a four-letter coding system 01 p0094 A83-10565
Generalized correlation measures for use in signal and image processing 01 p0100 A83-11470
Spread spectrum techniques 02 p0163 A83-11921
A one-dimensional logarithmic criterion for the evaluation of multiparametric systems 06 p0803 A83-19176
An experimental study of the concatenated Reed-Solomon/Viterbi channel coding system performance and its impact on space communications 07 p0871 A83-19733
Multicriterial estimation in the synthesis of means for information interaction in complex systems --- cockpit display optimization 08 p1156 A83-22125
Information density and efficiency of two-dimensional /2-D/ sampled imagery 08 p1105 A83-22895
Noise-immune coding of discrete information --- bibliography 1972-1979 09 p1327 A83-24248
Information theory analysis of sensor-array imaging systems for computer vision 12 p1728 A83-28898
Information contained in protein shapes 12 p1763 A83-29547
Information theory and visual displays 13 p1911 A83-31584
The problem of the visualization of information and digital image processing 15 p2165 A83-34968
Information theory and causal information transmission with feedback 15 p2221 A83-35104
A definition of the concept of 'information' and the possibilities of its use in biology 16 p2405 A83-36801
Structural information in robustness analysis 17 p2568 A83-37144
The so-called 'information theory of emotions' 19 p2885 A83-41839
Informational evaluation of operator activity in an ergatic system with a learning model 20 p3035 A83-43503
Removing the polymodality of an a posteriori distribution by using information redundancy 22 p3271 A83-45660
An information theory characterization of radar images and a new definition for radiometric resolution 22 p3289 A83-46194

INFORMATION TRANSMISSION**U DATA TRANSMISSION****INFRARED ABSORPTION**

- Absorption spectra of deuterated water at DF laser wavelengths 02 p0211 A83-12601
Absorption at 10 micron in CO₂-He and CO₂-N₂ mixtures at elevated temperatures 03 p0392 A83-13497
Transmission of CO₂ in the atmosphere of Venus for the spectral region near 7 microns 03 p0434 A83-13836
Below room temperature measurements of the 8-12 micron water vapor continuum absorption 03 p0358 A83-13980
High-resolution atmospheric spectroscopy using a diode laser heterodyne spectrometer 03 p0327 A83-13984
Spatially resolved IR absorption spectroscopy by optical Stark modulation 03 p0295 A83-14376
Drop-size distribution of fog droplets determined from transmission measurements in the 0.53-10.1-microns wavelength range 03 p0365 A83-14378
The transfer of 3.7 micrometer radiation through model cirrus clouds 03 p0371 A83-14655
Reconstructing the vertical profile of the ozone density in the atmosphere on the basis of measurements of the absorption of solar infrared radiation 03 p0362 A83-14830
The law of interstellar absorption in the wave-number interval 0.95/micron to 3.03/microns 04 p0550 A83-15042
Preparation and characteristics of a-Si:Cl:H films 04 p0539 A83-15478
A structural interpretation of the infrared absorption spectra of a-Si:H:O alloys 04 p0541 A83-15515

- An analysis of the absorption spectrum of heavy water vapor in the region of 1.06 microns 05 p0684 A83-17694
Mid- and far-infrared extinction coefficients of hydrous silicate minerals 05 p0707 A83-17808
Infrared absorption of thin metal films - Pt on Si 07 p0992 A83-19980
Residual double acceptors in bulk GaAs 07 p0998 A83-19989
Strong photoinduced infrared absorption in GaP 07 p0999 A83-20745
The three micron 'ice' band in grain mantles --- and their influence in interstellar extinction and polarization 07 p1024 A83-21219
Properties of amorphous H₂O ice and origin of the 3.1-micron absorption 07 p1024 A83-21224
Obscuration by helicopter-produced snow clouds 08 p1043 A83-22357
Discrepancies between balloon-borne IR atmospheric spectra and corresponding synthetic spectra calculated line by line around 825 per cm 09 p1306 A83-24440
Water vapor absorption at isotopic CO₂ laser wavelengths 09 p1269 A83-24446
Absorption of 9.6-micron CO₂ laser radiation by CO₂ at elevated temperatures 09 p1272 A83-24447
Photophoretic spectroscopy - A search for the composition of a single aerosol particle 09 p1297 A83-25183
Inverse-square wavelength dependence of attenuation in infrared polycrystalline fibers 10 p1482 A83-26116
Propagation at 10 microns through smoke produced by atmospheric combustion of diesel fuel 10 p1447 A83-26641
Analysis method for Fourier transform spectroscopy 10 p1424 A83-26867
Absorption and reshaping of 10.6 microns light in pure SF₆ using 1.5 ns, low-intensity incident pulses 11 p1582 A83-27610
Interpretation of temperature dependences of the absorption coefficient in the 8-12 micron atmospheric window on the basis of the generalized line profile 11 p1584 A83-28550
Optical absorption below the absorption edge in Hg/1-x/Cd/x/Te 11 p1658 A83-28714
Tunable diode laser measurements of the band strength and collision halfwidths of nitric oxide 12 p1778 A83-29149
The attenuation and scattering of infrared radiation by polydisperse systems comprising platelets and cylinders of ice 13 p1883 A83-30029
Hard carbon coatings with low optical absorption 13 p1825 A83-30326
Nonlinear far-infrared magnetoabsorption and optically detected magnetoimpurity effect in n-GaAs 13 p1850 A83-30600
The spectrophotometric experiment on the Venera-13 and Venera-14 descent modules. II - Preliminary results of spectrum analysis in the region of H₂O absorption bands 14 p2111 A83-31965
The absorption coefficient of light in the wing of the 4.3 micron band of CO₂ 14 p2082 A83-32556
Refining a radiation model of a stratiform cloud 14 p2058 A83-32856
Direct free-hole absorption induced in germanium by 1.06 micron picosecond pulses 14 p2093 A83-33428
Optically enhanced amorphous silicon solar cells 15 p2189 A83-33847
Diode laser heterodyne observations of silicon monoxide in sunspots - A test of three sunspot models 15 p2281 A83-34643
Molecular absorption bands in the infrared spectra of M giants 15 p2270 A83-34683
N₂ broadening parameters of ozone at 9.6 microns 15 p2203 A83-34995
Photoexcitations in trans-(CH)_x - A Fourier-transform infrared study 16 p2420 A83-35748
Scientific programs for the Spacelab ESO13 grille spectrometer 16 p2317 A83-35784
Parameterization of carbon dioxide 15-micron band absorption and emission 16 p2379 A83-36135
Photoinduced infrared activity in polyacetylene 16 p2421 A83-36565
Status of laboratory experiments on ice mixtures and on the 12 micron H₂O ice feature --- suggesting interstellar IR absorption 16 p2431 A83-36670
Infrared optical properties of a coal-fired power plant plume 16 p2372 A83-36760
Radiometric levitation of spherical carbon aerosol particles using a Nd:YAG laser 16 p2413 A83-36761
Intensity, transition moment, and bandshapes for the second overtone of compressed CO 16 p2410 A83-36796
Infrared absorption intensities of nitrous acid (HONO) fundamental bands 16 p2411 A83-36798

- On the accuracy of IR extinction predictions made by the Navy Aerosol Model 17 p2546 A83-38740
- Absorptivity of nitric oxide in the fundamental vibrational band 18 p2742 A83-39185
- Determination of the attenuation of visible, infrared, and millimeter waves in clouds on the basis of meteorological models 18 p2674 A83-39427
- A lambda 10830 vs X-ray correlation among late-type stars 18 p2767 A83-39600
- A method for on-line corrections of the transmission function in solving the problem of the thermal probing of the atmosphere 18 p2719 A83-40082
- Absorption of H₂S at DF laser wavelengths 19 p2852 A83-41108
- AFGL atmospheric absorption line parameters compilation - 1982 edition 20 p3016 A83-42207
- The photodissociation of nitromethane at 193 nm 20 p2950 A83-42629
- Photofragmentation of nitromethane in a molecular beam at 193 nm 20 p2950 A83-42630
- Photofragment spectroscopy and dynamics of the visible photodissociation of ozone 20 p3044 A83-42632
- Remote sensing applications of pulsed photothermal radiometry 20 p2992 A83-43594
- Temperature dependence of the absorptivity of aluminum targets at the 10.6 microns wavelength 20 p2957 A83-43785
- Quantum cyclotron resonance in silicon 21 p3216 A83-44383
- The experimental measurement of total absorbance by the ozone 9.6 micron band 21 p3109 A83-44507
- Infrared absorption by natural organic aerosol 22 p3321 A83-45635
- Assessment of relative error sources in IR DIAL measurement accuracy 22 p3295 A83-46084
- Infrared glass optical fibers for 2 to 11 micrometer band 22 p3358 A83-46623
- Materials for infrared low loss fibers 22 p3358 A83-46624
- Progress in heavy metal fluoride glasses for infrared fibers 22 p3358 A83-46626
- Preparation of high purity ZnCl₂ for 10.6-micron optical fibers 22 p3358 A83-46627
- Material dispersion considerations for infrared fibers 22 p3358 A83-46628
- Electrical transmission lines as models for soliton propagation in infrared fibers 22 p3358 A83-46632
- Research in infrared hollow waveguides 22 p3358 A83-46633
- Characterization of fibers for 10.6 micron transmittance 22 p3359 A83-46637
- A quasi-continuous record of atmospheric opacity at lambda = 1.1 mm over 34 days at Mauna Kea Observatory 22 p3332 A83-46745
- The Jovian spectrum in the 3-micron window 22 p3388 A83-47082
- Nonequilibrium distribution of particles with doublet levels in the infrared radiation field of a laser 23 p3460 A83-47164
- Possible origins for the 12 microns emission lines in the solar spectrum 23 p3530 A83-47508
- Interferometric measurements of atmospheric species 23 p3456 A83-47775
- Far infrared absorption in normal H₂ from 77 to 298 K 23 p3507 A83-48649
- Attenuation at 10.6 microns in loaded and unloaded polycrystalline KRS-5 fibers 24 p3629 A83-49017
- Ultralow loss single-mode fiber design for 2.5-6-micron band operation 24 p3629 A83-49019
- 8-13 micron spectrophotometry of galaxies. III - The silicate absorption in Markarian 231 24 p3660 A83-49387
- The unexpectedly high solubility of water in cryogenic liquids 24 p3570 A83-50114
- Observationally-based infrared efficiencies and Planck means for circumstellar dust grains 24 p3670 A83-50160
- INFRARED ASTRONOMY**
- Infrared astronomical data base and catalog of infrared observations 01 p0113 A83-10130
- Construction of a 1-3 micron infrared photometer and its test observations 01 p0049 A83-10233
- Infrared photometry of Be stars 01 p0116 A83-10332
- Infrared emission from four Be stars optical counterparts of galactic X-ray sources 01 p0121 A83-10333
- R 136 - WN or O spectral characteristics 01 p0117 A83-10927
- Multiperture photometry of galaxies. II - Near-infrared observations of six isolated objects 01 p0117 A83-10940
- The far-infrared disk of M51 02 p0250 A83-11581
- Far-infrared sources in Cygnus X - An extended emission complex at DR 21 and unresolved sources at S106 and ON 2 02 p0251 A83-11589
- Energetic activity in a star-forming molecular cloud core - A disk constrained bipolar outflow in NGC 2071 02 p0251 A83-11590
- Infrared photometry of the X-ray binary 2A 1822-371 - A model for the ultraviolet, optical, and infrared light curve 02 p0256 A83-12128
- The search for infrared protostars 02 p0246 A83-12195
- Infrared photometry of Hyades dwarfs 02 p0249 A83-12916
- Ultraviolet, optical and infrared astronomy 02 p0250 A83-13105
- The Bubble Nebula - Far-infrared and radio molecular observations of NGC 7635 03 p0412 A83-13304
- The infrared properties of Mira-type variables and other cool stars as determined from JHKL photometry 03 p0412 A83-13305
- A colorimetric mapping of the moon's surface in the 0.62-0.95-micron spectral region 03 p0432 A83-13368
- Optical and infrared observations of bright comets in the range 0.5 micrometers to 20 micrometers 03 p0415 A83-13387
- Infrared astronomy - Scientific/military thrusts and instrumentation; Proceedings of the Meeting, Washington, DC, April 21, 22, 1981 03 p0405 A83-13451
- Infrared spectroscopy in astronomy 03 p0405 A83-13453
- Air Force Geophysics Laboratory /AFGL/ infrared sky survey experiments 03 p0405 A83-13454
- Application of JFets to low background focal planes in space 03 p0308 A83-13456
- Infrared camera for 10-micron astronomy 03 p0324 A83-13457
- InSb heterodyne receivers for submillimeter astronomy 03 p0405 A83-13463
- Infrared astronomical data base and catalog of infrared observations 03 p0406 A83-13467
- SIRE - Transition from free-flyer to Shuttle sortie --- space infrared sensor 03 p0287 A83-13469
- Prediction of infrared /IR/ celestial source counts 03 p0406 A83-13472
- Photometry of symbiotic stars in the UBVRJHKLMN system. III - AX Per, AG Dra, BF Cyg, V 443 Her, and YY Her 03 p0407 A83-13663
- Infrared photometry of periodic comets Encke, Chernykh, Kearns-Kwee, Stephan-Oterma, and Tuttle 03 p0407 A83-13826
- Infrared photometry of HM Sagittae 03 p0408 A83-13891
- A study of the Chamaeleon dark cloud complex - Survey, structure and embedded sources 03 p0420 A83-13945
- Observations of cool stars at 20, 25, and 33 microns 03 p0421 A83-14149
- Two-color CCD observations of the galactic center region 03 p0409 A83-14190
- Mass loss from Wolf-Rayet stars - An analysis of radio and infrared observations of MR 111 /AS 422/ 03 p0424 A83-14198
- Infrared observations of OH/IR stars 03 p0411 A83-14812
- Far infrared observations of a star forming region in Serpens 04 p0550 A83-15037
- Abrupt cutoffs in the optical-infrared spectra of nonthermal sources 04 p0552 A83-15607
- Low surface brightness spiral galaxies. I - Neutral hydrogen content and location in the infrared Fisher-Tully diagram 04 p0552 A83-15610
- The distribution of infrared obscuration in NGC 7331 - Evidence for a massive molecular ring 04 p0555 A83-15649
- Maps of the rings of Uranus at a wavelength of 2.2 microns 05 p0704 A83-16964
- The infrared emission from the elliptical galaxy NGC 1052 05 p0697 A83-16990
- The Infrared Space Observatory /ISO/ - A study for a cooled telescope in space for infrared astronomy 05 p0601 A83-17429
- A 2.2-micron map of NGC 5128 06 p0827 A83-18171
- Multiperture infrared photometry of extragalactic radio sources 06 p0828 A83-18180
- Near infrared spectroscopy of W 51 IRS-2 06 p0818 A83-18541
- A model for the Becklin-Neugebauer infrared point source 06 p0831 A83-18798
- Spatial observations of dust emission in NGC 7027 06 p0833 A83-18869
- Visual and infrared observations of the distant Comets P/Stephan-Oterma /1980g/, Panther /1980u/, and Bowell /1980b/ 06 p0833 A83-18873
- A search for frosts in Comet Bowell /1980b/ 06 p0833 A83-18874
- Identification of some diffuse interstellar features 06 p0835 A83-18895
- Carbon stars in Local Group galaxies 06 p0839 A83-19274
- The 157 micron /C II/ emission from NGC 2024 - Core and halo components 06 p0844 A83-19494
- The near-infrared spectrum of the Herbig Ae-Be stars 06 p0844 A83-19497
- Infrared views of the giant planets 07 p1005 A83-20150
- A high-resolution 2.2 micron polarization map of OH 0739-14 07 p1007 A83-20934
- A distance scale from the infrared magnitude/H I velocity-width relation. IV - The morphological type dependence and scatter in the relation; the distances to nearby groups 07 p1019 A83-21101
- Infrared/optical energy distributions of high-redshift quasars 07 p1019 A83-21102
- Identification of the emission feature near 3.5 microns in the pre-main-sequence star HD 97048 07 p1021 A83-21127
- Infrared photometry of O stars 07 p1021 A83-21129
- Electromechanical device for the support of the oscillating secondary mirror of an infrared telescope 08 p1111 A83-22359
- Development and evaluation of integrated infrared arrays for astronomical applications 08 p1052 A83-22858
- Simultaneous visual-infrared polarimetry of QSOs 08 p1181 A83-23031
- Infrared mapping and UBVRi photometry of the spiral galaxy NGC 1566 08 p1175 A83-23033
- Long-period variables in the galactic bulge - Evidence for a young super-metal-rich population 08 p1182 A83-23043
- The centre of the Galaxy 08 p1187 A83-23289
- Comparison of infrared and optical positions for sources in the direction of the galactic center 09 p1351 A83-23318
- Observations of M42 in the O III 52 and 88-micron forbidden lines, the O I 63-micron forbidden line, and the N III 57-micron forbidden line 09 p1362 A83-24977
- The infrared variability and nature of symbiotic stars. II - RR Tel 09 p1362 A83-24983
- Spatial studies of the middle infrared spectral features in NGC 7027 09 p1364 A83-25006
- Near infrared observations of O stars 09 p1356 A83-25292
- The fate of dust grains in a shock wave originated by a SN explosion 09 p1365 A83-25295
- Satellite-borne infrared Fourier spectrometers for planetary studies 10 p1387 A83-25345
- A rediscussion of sulfur abundances in Magellanic Clouds and galactic H II regions 10 p1498 A83-25358
- Near infrared spectroscopy and infrared photometry of a new WC9 star 10 p1499 A83-25367
- A far-infrared Fabry-Perot interferometer and grating spectrometer for balloon-borne astronomy 10 p1419 A83-25458
- A two-micron survey of southern Herbig-Haro objects 10 p1492 A83-25479
- Further observations of 8-micron polar brightenings of Jupiter 10 p1518 A83-25516
- A laboratory study of the infrared spectra of interstellar ices 10 p1502 A83-25653
- Near infrared photometry. I - Homogenization of near-infrared data from southern bright stars 10 p1493 A83-25659
- Infrared observations of the jet in M87 10 p1493 A83-25706
- Photometric studies of composite stellar systems. V - Infrared photometry of star clusters in the Magellanic clouds 10 p1494 A83-25710
- Scientific importance of high angular resolution at infrared and optical wavelengths; Proceedings of the Conference, Garching, West Germany, March 24-27, 1981 10 p1494 A83-25826
- Speckle interferometry in the infrared 10 p1419 A83-25835
- Imaging by dilute apertures in the presence of atmospheric turbulence 10 p1482 A83-25840
- Interferometric connection of the Canada-France-Hawaii 3.6 metre telescope and the United Kingdom 3.8 metre telescope on Mauna Kea 10 p1495 A83-25843
- Coherent versus incoherent detection for interferometry at infrared wavelengths 10 p1495 A83-25846
- Infrared line and radio continuum emission of circumstellar ionized regions 10 p1509 A83-26372
- Infrared and submillimeter astronomy from space 10 p1497 A83-26700
- X-ray, radio, and infrared observations of the 'rapid burster' /MXB 1730-335/ during 1979 and 1980 10 p1514 A83-26731
- Thermal structure of Saturn from Voyager infrared measurements - Implications for atmospheric dynamics 11 p1684 A83-27360

- Performance of Si:Ga infrared detectors under reduced background fluxes 11 p1669 A83-27695
- Photoconductive detectors for space IR astronomy 11 p1572 A83-27733
- Infrared array detectors --- for astronomical observation 11 p1537 A83-27734
- Advances in infrared and sub-millimeter filters 11 p1572 A83-27736
- Planned NASA Space infrared astronomy experiments 11 p1670 A83-27738
- The Comet Halley flyby I.R. sounder 'I.K.S.' --- infrared spectrometer 11 p1670 A83-27740
- Hardware development and tests in the GIRL project 11 p1670 A83-27742
- The infrared variability and nature of symbiotic stars. III - R Aquarii. IV - RX Puppis. V - Seven more systems 11 p1675 A83-28284
- The 8-13 micron spectrum of IC 2165 11 p1682 A83-28292
- The compact H II region S235A - Observations and interpretation 12 p1789 A83-28876
- Infrared photometry of southern Wolf-Rayet stars 12 p1785 A83-28881
- Infrared photometry of the RS CVn binaries. I - TY Pyxidis 12 p1785 A83-28885
- Infrared images of southern HII regions 13 p1935 A83-30385
- The potential for far-infrared astronomy in Australia 13 p1936 A83-30399
- The strength of Paschen-alpha in the Seyfert 1.9 galaxy V Zwicky 317 13 p1952 A83-31441
- Positions of the SiO masers in Orion-KL - Anisotropy on a scale of 70 AU 13 p1953 A83-31450
- Infrared colors of a complete sample of faint galaxies 13 p1957 A83-31694
- Infrared counterparts to 'empty field' steep-spectrum radio sources 13 p1942 A83-31697
- Optical and IR light curves of VV Puppis 13 p1957 A83-31699
- Superconducting bolometers in astronomical IR equipment. II Threshold sensitivity 14 p2014 A83-31842
- Single photon counters for the infrared 14 p2014 A83-31977
- Integrated infrared detector arrays for low-background applications 14 p1983 A83-31978
- InSb charge-injection device array performance 14 p2015 A83-31979
- Two-dimensional infrared speckle interferometry with a 32 x 32 InSb charge-injection device (CID) array 14 p2095 A83-31980
- Tunable diode laser heterodyne spectrometer for remote observations near 8 microns 14 p2016 A83-32001
- Use of a Fourier transform spectrometer on a balloon-borne telescope and at the multiple mirror telescope (MMT) 14 p2016 A83-32002
- Cooled grating Fabry-Perot spectrometer for the 10 micron region 14 p2017 A83-32003
- The variation of dust temperatures in Maffei 2 14 p2106 A83-33225
- A deep near infrared objective prism survey for carbon stars toward the galactic center and anticenter 14 p2099 A83-33247
- Fourier transform spectroscopy of six stars 14 p2100 A83-33257
- Astrometric and infrared speckle analysis of the visually unresolved binary BD+41.328 deg 14 p2101 A83-33467
- Development of a reaction wheel-based attitude control system for balloon-borne infrared astronomical observation 15 p2119 A83-34000
- Star-burst galactic nuclei 15 p2256 A83-34087
- Blue compact dwarf galaxies. II - Near-infrared studies and stellar populations 15 p2257 A83-34092
- An infrared luminosity function for star-forming molecular clouds 15 p2264 A83-34584
- The infrared variability of OH 0739-14 15 p2266 A83-34602
- The M17 SW molecular cloud 15 p2267 A83-34627
- Infrared observations of Beta Cephei and Delta Scuti stars 16 p2424 A83-36539
- Infrared photometry of the RS CVn binaries. II - JHKL light curves of HR 1099 17 p2587 A83-37277
- Infrared photometry and mass loss rates for Of-type stars 17 p2597 A83-37323
- The near-infrared Cepheid distance scale. I - Preliminary galactic calibration 17 p2588 A83-37325
- The irregular distribution of galaxies and the anisotropies in the microwave background photons 17 p2598 A83-37343
- Infrared polarization in the direction to the galactic center 17 p2588 A83-37360
- The C2H, C2, and CN electronic absorption bands in the carbon star HD 19557 17 p2605 A83-37918
- Predicted source counts for normal and active galaxies at 10-100 microns 17 p2607 A83-38258
- Infrared and microwave fluorescence of carbon monoxide in comets 17 p2608 A83-38412
- 2.8-3.6-micron spectra of micro-organisms with varying H2O ice-content 17 p2563 A83-38590
- Near infrared observations of some of the IRC sources 18 p2754 A83-39201
- Infrared (JHK) photometry of asteroids. II 18 p2757 A83-39605
- The large scale dust distribution in the inner galaxy 18 p2770 A83-39654
- Infrared studies of star formation in Orion 18 p2772 A83-39708
- Infrared observations of low-mass star formation in Orion - HH objects 18 p2758 A83-39720
- ESO Infrared Workshop, 2nd, Garching, West Germany, April 20-23, 1982, Proceedings 18 p2760 A83-40419
- Fabry-Perot spectrometers for the ground-based infrared 18 p2690 A83-40435
- Infrared speckle interferometry, results, true image reconstruction and instrumental plans 18 p2761 A83-40437
- Determination of the atmospheric water vapour content above La Silla and the prospects for FIR observations 18 p2761 A83-40440
- Infrared raster scans and a self optimizing micro-processor system for IR-photometry 18 p2691 A83-40450
- Very Large Telescope (VLT) studies at ESO 18 p2762 A83-40451
- Aperture synthesis in the infrared 18 p2762 A83-40453
- Infrared observations from the NASA Airborne Observatories 18 p2762 A83-40454
- ASTROPLANE - A European airborne observatory for infrared astronomy 18 p2762 A83-40455
- Astroplane - The Airbus proposal 18 p2762 A83-40456
- ASTROPLANE - A working group of the European Science Foundation 18 p2762 A83-40457
- Achievements and promise of balloon IR astronomy 18 p2762 A83-40458
- The scientific case and feasibility of a three metre balloon telescope 18 p2762 A83-40459
- A balloon-borne cooled telescope for far IR astronomy 18 p2762 A83-40460
- A cryogenic Fabry-Perot for far infrared astronomy 18 p2692 A83-40461
- IRAS and its mission 18 p2648 A83-40463
- IRAS follow-up - Problems and prospects 18 p2763 A83-40464
- SIRTF - The Shuttle Infrared Telescope Facility 18 p2763 A83-40465
- A large deployable reflector for infrared and submillimeter astronomy from space 18 p2648 A83-40466
- The galactic center; Proceedings of the Workshop, California Institute of Technology, Pasadena, CA, January 7, 8, 1982 19 p2911 A83-40676
- New far infrared observations of the central 30 arcmin of the Galaxy 19 p2912 A83-40681
- Large beam observations of the galactic center at 150, 200, and 300 microns 19 p2912 A83-40682
- Balloon observation of the central bulge of our Galaxy in near infrared radiation 19 p2912 A83-40683
- Infrared observations of the ionized gas in the galactic center 19 p2912 A83-40684
- B-alpha and Ne II line spectroscopy in the vicinity of the galactic center source IRS 16 19 p2908 A83-40685
- Spatial and spectral studies of the galactic center near 10 microns 19 p2908 A83-40686
- OI and OIII in Sgr A - Neutral and ionized gas at the galactic center 19 p2912 A83-40687
- Two micron observations of C-120 and C-130 in the red giant sources IRS 7, IRS 12, and IRS 19 19 p2912 A83-40688
- Mapping and imaging of the galactic centre in the near infrared 19 p2909 A83-40689
- The position of the infrared source IRS 16 in the galactic center region relative to a visual field star 19 p2909 A83-40690
- Three-micron emission features in Herbig Be/Ae stars and related objects 19 p2909 A83-40722
- The R asteroids reconsidered 19 p2922 A83-40787
- Infrared magnitudes (JHKLM) for 105 chemically peculiar A- and B-stars 19 p2910 A83-41065
- HL Tauri and its circumstellar disk 19 p2921 A83-41652
- Far-infrared and CO observations of Cep F - Implications for star formation in Cepheus OB3 20 p3064 A83-42196
- The spectral and spatial distribution of radiation from Eta Carinae. III - A high-resolution 2.2 micron map and morphological considerations of the evolutionary status 20 p3067 A83-42441
- A 10 micron survey of star formation in galactic nuclei 20 p3071 A83-43043
- Virgo spiral galaxies 20 p3071 A83-43043
- A far-infrared study of the N/O abundance ratio in galactic H II regions 20 p3072 A83-43055
- Far-infrared and submillimeter observations of stellar radiative and wind heating in S140 IRS 20 p3072 A83-43056
- Observations of asteroids in the 3- to 4-micron region 21 p3239 A83-44085
- A near-infrared and optical study of X-ray selected Seyfert Galaxies. I - Observations 21 p3227 A83-44110
- Some considerations on a Michelson spatial interferometer in the far IR 21 p3137 A83-44380
- Spectroscopy and infrared photometry of southern T Tauri stars 21 p3226 A83-44984
- Discovery of an IR echo from a supernova dust cloud 21 p3234 A83-44993
- Infrared observations of R136, the central object of the 30 Doradus Nebula 21 p3236 A83-45538
- 8-13-micron spectral observations of eight moderately extended planetary nebulae 22 p3375 A83-46551
- Central distribution of the near-infrared colours in two early-type spirals 22 p3375 A83-46572
- An infrared and optical investigation of galactic nuclei with compact radio sources 22 p3380 A83-46974
- Herbig-Haro objects in the dust globe ESO 210-6A 22 p3382 A83-46990
- Infrared objects near H2O masers in regions of active star formation. III - Evolutionary phases deduced from IR recombination line and other data 23 p3519 A83-47453
- On the T Tauri nature of the variable star BM Cha 23 p3520 A83-47459
- Infrared studies of molecular ions. I - The nu3 band of NH4(+) 23 p3506 A83-47637
- A measurement of the IR flux from a radio lobe 23 p3526 A83-47871
- Recent work on bipolar nebulae 24 p3638 A83-49130
- 8-13 micron spectrophotometry of galaxies. III - The silicate absorption in Markarian 231 24 p3660 A83-49387
- A flare in the millimetre to IR spectrum of 3C273 24 p3669 A83-50105

INFRARED ASTRONOMY SATELLITE

- Radiation effects in IRAS extrinsic infrared detectors 05 p0645 A83-17484
- Bidirectional reflectance distribution function /BRDF/ measurements of sunshield and baffle materials for the Infrared Astronomy Satellite /IRAS/ telescope 08 p1167 A83-22861
- Computer control of the Infra-Red Astronomical Satellite /IRAS/ 10 p1384 A83-26583
- Scientific objectives of IRAS 11 p1674 A83-28209
- The IRAS project organisation and mission operations 11 p1534 A83-28210
- The IRAS ground station and operations control center at Chilton 11 p1533 A83-28211
- The IRAS spacecraft 11 p1534 A83-28212
- The Dutch Scientific Instrument on board IRAS 11 p1537 A83-28213
- The IRAS telescope 11 p1674 A83-28214
- Ground operations software at the IRAS Operations Control Centre --- IR Astronomical Satellite 11 p1533 A83-28215
- IRAS preliminary science analysis at the OCC 11 p1533 A83-28216
- U.S. data processing for the IRAS project --- by Jet Propulsion Laboratory Scientific Data Analysis System 11 p1674 A83-28217
- IRAS and Exosat - Europe maintains its contribution to space science 14 p1978 A83-31942
- IRAS - The infrared astronomical satellite 15 p2124 A83-34216
- Validation of the in-orbit checkout of the IRAS gyroscopes using computer simulations 17 p2481 A83-37475
- IR-camera for GIRL --- German Infrared Laboratory 18 p2691 A83-40449
- IRAS and its mission 18 p2648 A83-40463
- IRAS follow-up - Problems and prospects 18 p2763 A83-40464
- Progress report on the infrared astronomical satellite cryogenic system 20 p2961 A83-43242
- Orbital performance of a one-year lifetime superfluid helium dewar based on ground testing and computer modelling 20 p2962 A83-43247
- Instrumentation, data acquisition and reduction for a large spaceborne helium dewar 20 p2962 A83-43250

- Emerging solar system in view --- recent observational evidence of extrasolar planet systems
21 p3226 A83-44990
- Orbit prediction for IRAS using vector and analytic techniques --- Infra-Red Astronomical Satellite [IAF PAPER 83-315]
23 p3416 A83-47338
- ### INFRARED DETECTORS
- #### NT FLIR DETECTORS
- Energy gap versus alloy composition and temperature in Hg_{1-x}/Cd_x/Te
[AD-A125659]
01 p0109 A83-10644
- HIRS-AMTS satellite sounding system test - Theoretical and empirical vertical resolving power --- High resolution Infrared Radiation Sounder - Advanced Moisture and Temperature Sounder
02 p0217 A83-12963
- Low background spectral response of 30-130-micron detectors from blackbody measurements
03 p0324 A83-13458
- SIRE - Transition from free-flyer to Shuttle sortie --- space infrared sensor
03 p0287 A83-13469
- Development of Teal Ruby Experiment radiometric test requirements
03 p0325 A83-13728
- Signal conditioning for infrared staring arrays
03 p0326 A83-13732
- Source-coupling for hybrid focal planes
03 p0326 A83-13733
- Epitaxial HgCdTe/CdTe photodiodes for the 1 to 3 micron spectral region
03 p0309 A83-13737
- 1.0 to 2.5 micrometer short wavelength infrared /SWIR/ linear array technology for low background applications
03 p0326 A83-13739
- A two-dimensional analysis of transfer in a charge injection infrared sensor --- French thesis
03 p0310 A83-13801
- Design and implementation of a broadband infrared atmospheric transmissometer
03 p0327 A83-13993
- Limitations on the calibration of infrared /IR/ transmissometer
03 p0328 A83-13994
- Investigations of the apparent temperature of snow cover in the submillimeter wavelength region
04 p0502 A83-15816
- Radiation effects in IRAS extrinsic infrared detectors
05 p0645 A83-17484
- A monolithic lead sulfide-silicon MOS integrated-circuit structure
06 p0752 A83-18756
- Characteristics of Schottky diodes at 10.6 microns
07 p0918 A83-19988
- Photon-assisted tunneling at 246 and 604 GHz in small-area superconducting tunnel junctions
07 p0999 A83-19995
- Clutter rejection for infrared surveillance sensors
08 p1094 A83-22437
- Real-time nonuniformity correction for focal plane arrays using 12-bit digital electronics
08 p1094 A83-22440
- Theory and status of high performance heterodyne detectors
08 p1097 A83-22518
- Transmission effects of explosion-produced dust clouds on downward viewing airborne platforms
08 p1132 A83-22543
- Review of cirrus cloud optical properties and effects on infrared sensors
08 p1135 A83-22544
- Mosaic focal plane methodologies II; Proceedings of the Conference, San Diego, CA, August 27, 28, 1981
08 p1100 A83-22598
- RDA requirements for optimum hybrid focal plane performance --- Resistance-Area product for IR detector arrays
08 p1100 A83-22599
- New 6.5 microns photodiodes for Schottky barrier array applications
08 p1080 A83-22600
- Integrating 128-element linear imager for the 1 to 5 microns region
08 p1100 A83-22601
- Signal processing and compensation electronics for junction field-effect transistor /JFET/ focal plane arrays
08 p1081 A83-22606
- The Teal Ruby Experiment - A potpourri of advanced technology
08 p1051 A83-22607
- Infrared Schottky barrier focal plane array technology
08 p1081 A83-22610
- Modern utilization of infrared technology VII; Proceedings of the Seventh Annual Seminar, San Diego, CA, August 27, 28, 1981
08 p1102 A83-22838
- Drift compensation in a mosaic sensor
08 p1103 A83-22839
- Goal programming for preliminary design and critical technology identification - Application to infrared step-stare moving target detection
08 p1051 A83-22842
- Recent measurements of earth background spatial radiance variations
08 p1103 A83-22843
- Infrared application to the detection of induced surface currents
08 p1103 A83-22845
- Statistical modeling of scene variability
08 p1103 A83-22848
- Radiative transfer and 4.3 micron atmospheric clutter observations --- with balloon-borne sensors
08 p1051 A83-22849
- Development and evaluation of integrated infrared arrays for astronomical applications
08 p1052 A83-22858
- Overview of infrared measurement programs
08 p1103 A83-22862
- Contemporary infrared standards and calibration; Proceedings of the Meeting, San Diego, CA, August 25, 26, 1981
08 p1104 A83-22873
- Infrared calibration facilities at Newark Air Force Station
08 p1047 A83-22875
- Coherence effects in laser testing of long wavelength infrared /LWIR/ sensors
08 p1052 A83-22879
- Calibration of spaceborne thermal detectors
08 p1052 A83-22881
- Electro-optical calibration considerations at intermediate maintenance levels
08 p1104 A83-22883
- Infrared focal plane test station calibration
08 p1104 A83-22885
- Infrared technology for target detection and classification; Proceedings of the Meeting, San Diego, CA, August 25, 26, 1981
09 p1265 A83-23526
- Infrared target array development
09 p1204 A83-23527
- An antitank missile seeker employing an infrared Schottky barrier focal plane array
09 p1253 A83-23544
- Thin-film photoelectromagnetic detectors for infrared radiation
10 p1419 A83-25457
- Correlation of surface humidity and integrated atmospheric water vapour determined from infrared measurements --- at mountain sites
10 p1451 A83-25460
- Signal-to-noise ratio of heterodyne detection - Matrix formalism
10 p1425 A83-26874
- Performance of Si:Ga infrared detectors under reduced background fluxes
11 p1669 A83-27695
- Infrared array detectors --- for astronomical observation
11 p1537 A83-27734
- Infrared visibility prediction by statistical methods
11 p1619 A83-28340
- Informational performance criterion for a photon counter
13 p1832 A83-30318
- Effect of anodic growth temperature on native oxides of n-(Hg, Cd)Te
13 p1929 A83-31066
- Effect of electric fields on long-wavelength response of infra-red detectors
13 p1931 A83-31762
- Single photon counters for the infrared
14 p2014 A83-31977
- Integrated infrared detector arrays for low-background applications
14 p1983 A83-31978
- InSb charge-injection device array performance
14 p2015 A83-31979
- Hybrid packaging approach to improved low-noise operation of photovoltaic InSb detectors
14 p2015 A83-31981
- Proposal for advanced infrared spectrophotometers
14 p2016 A83-31997
- New developments in infra-red sensors for three-axis stabilized satellites
17 p2481 A83-37463
- A helium-3 cooled bolometer system for one millimeter continuum observations
17 p2510 A83-37751
- Optimum coupling of a Gaussian beam to a corner reflector with a four-wavelength antenna
17 p2510 A83-37753
- Absolute measurement at 1 THz of the optical coupling of a F.I.R. conical antenna with a Josephson detector
17 p2511 A83-37759
- An improved chopping secondary design --- of infrared telescopes
18 p2691 A83-40439
- Photoconductor developments at the Battelle-Institut e.v., Frankfurt am Main
18 p2691 A83-40442
- Tests of low-background infrared detectors
18 p2691 A83-40443
- Application of infrared arrays to speckle interferometry
18 p2691 A83-40445
- High sensitivity with a germanium detector in integrating mode
18 p2691 A83-40447
- A method for ensuring the proper operation of an optical instrument for measuring the temperature of the blades of a high-temperature turbine
19 p2799 A83-42152
- Internal photoemission from quantum well heterojunction superlattices by phononless free-carrier absorption
20 p3054 A83-43593
- Sensitivity of a wide-band far-IR receiver using a Josephson self-oscillator mixer
21 p3125 A83-44387
- Spectral responsivity standard for infrared detectors
21 p3138 A83-44781
- Detailed computer modeling of an infrared tracker using simulation of passive infrared equipment (SPIRE) techniques
22 p3292 A83-46594
- Computer-aided infrared sensor thermal design
22 p3292 A83-46602
- Analytical noise/performance modeling of detector charge-coupled device (CCD) hybrid devices
22 p3292 A83-46603
- Computer-aided design of infrared detector preamplifiers having switched feedback resistors
22 p3292 A83-46604
- ### Infrared fiber early warning receiver
- Improved fabrication techniques for infrared bolometers
22 p3293 A83-46742
- Simplified calculation of the effects of jitter on clutter leakage --- performance prediction of mosaic infrared sensor
22 p3294 A83-46830
- IR detectors - Heterodyne and direct
23 p3458 A83-47801
- ### Electro-optic and infrared sensors
- Atmospheric sounding using optical systems
24 p3581 A83-48772
- Harmonic response of a tunable Solc filter
24 p3605 A83-49284
- ### INFRARED FILTERS
- Recent developments in infrared acousto-optic tunable filters
03 p0393 A83-13770
- Solc filter engineering
08 p1166 A83-22572
- Spectral characterization methodology of thin-film optical filters
08 p1104 A83-22880
- Resonant array bandpass filters for the far infrared
15 p2231 A83-34470
- Infrared broad-band filters optimised for observations of Wolf-Rayet stars
18 p2761 A83-40426
- Harmonic response of a tunable Solc filter
22 p3357 A83-46088
- ### INFRARED HORIZON SCANNERS
- #### U HORIZON SCANNERS
- #### U INFRARED SCANNERS
- ### INFRARED IMAGERY
- On the circulation of the western Gulf of Mexico - A satellite view
01 p0076 A83-10113
- Analyzing and mapping regional land use trends by combining Landsat and topographic data
01 p0066 A83-10119
- Satellite imagery - Examples of mesoscale analysis using AVHRR images --- Advanced Very High Resolution Radiometer
01 p0075 A83-10224
- Real-time infrared image processing --- onboard aircraft
01 p0011 A83-11459
- Radar and infrared remote sensing of geothermal features at Pilgrim Springs, Alaska
02 p0198 A83-12036
- A concept for reducing helicopter IFR landing weather minimums - Offshore
02 p0133 A83-12099
- Thermal infrared sensing applied to energy conservation in building envelopes /Thermosense IV/; Proceedings of the Meeting, Ottawa, Ontario, Canada, September 1-4, 1981
02 p0180 A83-12686
- Interpretation of aerial thermographic data
02 p0200 A83-12687
- Hough transform for target detection in infrared imagery
02 p0181 A83-12884
- Technical issues in focal plane development; Proceedings of the Meeting, Washington, DC, April 21, 22, 1981
03 p0325 A83-13726
- Shutterless fixed pattern noise correction for infrared imaging arrays
03 p0325 A83-13731
- Interfacing a focal plane infrared mosaic array and an optical processor
03 p0326 A83-13777
- Environmental monitoring of the Athabasca Oil Sands Region
03 p0346 A83-14238
- Predicting permafrost conditions with infrared sensing techniques
03 p0348 A83-14264
- Infrared observations of Phobos and Deimos from Viking
04 p0569 A83-15594
- Rainfall over the Arabian Sea during the onset of the 1979 monsoon
05 p0668 A83-17793
- Monochromatic imaging from UV to IR using a subtractive double monochromator
06 p0762 A83-18579
- Simulation of IR images of natural backgrounds
06 p0762 A83-18595
- One-dimensional high resolution image reconstruction on Eta Carinae at 4.6-microns with speckle data
07 p1009 A83-21229
- Estimation of the atmospheric path radiance from multispectral infrared images
08 p1133 A83-21926
- Processing infrared images for fire management applications
08 p1094 A83-22434
- Signal processing for staring infrared images
08 p1094 A83-22439
- Automatic classification of infrared ship imagery
08 p1095 A83-22443
- Autonomous ship classification by moment invariants
08 p1095 A83-22444
- Cultural feature and syntax analysis for automatic acquisition
08 p1095 A83-22446
- Noise effects for edge operators
08 p1158 A83-22447
- Weather and thermal electric-optical sensor performance
08 p1098 A83-22545
- Stimulus variables affecting dynamic target acquisition
08 p1045 A83-22590

Charge-coupled device /CCD/ visible light sensor for the Teal Ruby Experiment 08 p1051 A83-22602

Advanced on-focal plane signal processing for nonplanar infrared mosaics 08 p1081 A83-22605

Modern utilization of infrared technology VII; Proceedings of the Seventh Annual Seminar, San Diego, CA, August 27, 28, 1981 08 p1102 A83-22838

Thermal infrared pushbroom imagery acquisition and processing --- of NASA's Advanced Land Observing System 08 p1045 A83-22841

Solid-state Shuttle-launched meteorological sensor 08 p1052 A83-22852

Infrared zoom lens system for target detection 08 p1103 A83-22855

Techniques for pseudo-dc restoration and dynamic range enhancement of scanned infrared imagery 08 p1105 A83-22900

Bo 105 rotor blade influence on the Calipso FLIR in the mast-mounted observation platform Ophelia 08 p1044 A83-23249

Infrared technology for target detection and classification; Proceedings of the Meeting, San Diego, CA, August 25, 26, 1981 09 p1265 A83-23526

Infrared target array development 09 p1204 A83-23527

Comparison of imaging infrared detection algorithms 09 p1265 A83-23529

Comparative study of edge-thinning algorithms for target identification 09 p1265 A83-23530

Target acquisition and extraction from cluttered backgrounds 09 p1204 A83-23531

Eliminating nearest neighbor searches in estimating target orientation 09 p1204 A83-23535

Histogram-based algorithms for scene matching 09 p1266 A83-23538

Target classification algorithms for video and forward looking infrared /FLIR/ imagery 09 p1266 A83-23541

Real-time statistical tracker for infrared /IR/ focal plane array 09 p1266 A83-23546

Infrared remote sensing of the vertical and horizontal distribution of clouds 09 p1312 A83-23954

Application of remote sensing data to hydrogeological purposes in the Fezzan Region-Lybia 09 p1287 A83-24566

Fresh water springs detection and discharge evaluation using thermal I.R. surveys along sea shores in areas affected by poor precipitations 09 p1288 A83-24578

Infrared images of southern Hill regions 13 p1935 A83-30385

Determination of thunderstorm heights and intensities from GOES infrared data 13 p1888 A83-30564

Histogram concavity analysis as an aid in threshold selection --- in image processing 13 p1911 A83-31073

Thermal imaging system with a two-phase ternary mixture of liquids 14 p2014 A83-31947

Near-infrared mapping spectrometer for investigation of Jupiter and its satellites 14 p1983 A83-32000

The importance of cabin guide marks in visual flying Application of this idea to the design of night vision aides, of the visual helmet type 14 p2071 A83-32458

Binary holographic LO beam multiplexer for IR imaging detector arrays 14 p2021 A83-32908

Comparison of the TIROS-N satellite and aircraft measurements of Gulf Stream surface temperatures 14 p2060 A83-33080

Infrared optical constants of PtSi 15 p2230 A83-33850

Remote sensing of the sea-state using the 0.8-1.1 micron spectral band 15 p2209 A83-35292

The enhanced-V - A satellite observable severe storm signature 16 p2389 A83-36038

Image quality of active and passive scanners 16 p2356 A83-36123

Case study of the March 24, 1976 Elton, Louisiana tornado using satellite infrared imagery, Doppler sounder, rawinsonde, and radar observations 17 p2547 A83-37758

Determination of the inhomogeneities of semiconductor materials in the infrared 18 p2744 A83-40405

Aperture synthesis in the infrared 18 p2762 A83-40453

The information content of small-scale multispectral space images (with the Fergana depression and mountain taken as an example) 18 p2707 A83-40592

Recording of interferograms on normal high resolution plates using a CO2 laser at 10.6 microns 19 p2847 A83-41103

The life cycle of a tornadic cloud as seen from a geosynchronous satellite 20 p3031 A83-43436

Pyroelectric IR imaging sensors - The potential for compact inexpensive RPV payloads 20 p2936 A83-43712

A versatile thermal imager for RPV applications 20 p2936 A83-43720

Imaging sensors for an RPV payload 20 p2936 A83-43721

Processing of infrared thermal images for aerodynamic research [ONERA, TP NO. 1983-32] 21 p3137 A83-44310

Spatial resolution of thermal wave microscopes 21 p3142 A83-45488

Lithologic mapping using solar infrared 22 p3309 A83-46129

Geologic thermal-inertia mapping using HCMM satellite data 22 p3309 A83-46130

The use of thermal infrared images in geologic mapping 22 p3309 A83-46131

Infrared focal plane array system performance modeling 22 p3292 A83-46597

Aircraft contrast signatures in the infrared spectral region 22 p3292 A83-46598

Upper-level structure of Oklahoma tornadic storms on 2 May 1979. II - Proposed explanation of 'V' pattern and internal warm region in infrared observations 22 p3341 A83-46853

Estimating surface temperatures from satellite thermal infrared data - A simple formulation for the atmospheric effect 23 p3475 A83-47224

INFRARED INSPECTION

Improving T700 nozzle manufacture 01 p0056 A83-10974

An automated flaw inspection system with the computer processing of results 02 p0188 A83-12163

Uses of infrared thermography in the low-cost solar array program 02 p0180 A83-12689

Stereoscopic depth analysis by thermal wave transmission for nondestructive evaluation 07 p0931 A83-21373

Infrared techniques applied to large solar arrays 08 p1053 A83-22857

Nondestructive corrosion detection under organic films using infrared thermography 09 p1275 A83-23630

Interpretation of the results of thermal inspection with changes in the emitting capacity of the surface of objects of inspection 13 p1860 A83-30836

A universal heat source for active thermal inspection 13 p1860 A83-30837

Infrared measurement of specimen temperature profiles during fatigue crack propagation tests 14 p2020 A83-32825

Thermal wave remote and nondestructive inspection of polymers 20 p2959 A83-43599

INFRARED INSTRUMENTS

NT FLIR DETECTORS

NT INFRARED DETECTORS

NT INFRARED INTERFEROMETERS

NT INFRARED SCANNERS

NT INFRARED SPECTROMETERS

NT INFRARED SPECTROPHOTOMETERS

Infrared device for simultaneous measurement of fluctuations of atmospheric carbon dioxide and water vapor 03 p0324 A83-13275

Infrared astronomy - Scientific/military thrusts and instrumentation; Proceedings of the Meeting, Washington, DC, April 21, 22, 1981 03 p0405 A83-13451

Infrared spectroscopy in astronomy 03 p0405 A83-13453

CIRRIS - A cryogenic infrared /IR/ radiance instrument for Shuttle 03 p0324 A83-13455

Infrared camera for 10-micron astronomy 03 p0324 A83-13457

A climate index indicative of cloudiness derived from satellite infrared sounder data 03 p0371 A83-14658

An infrared method for measuring the eyelid motion reaction 07 p0982 A83-20343

Contemporary infrared standards and calibration; Proceedings of the Meeting, San Diego, CA, August 25, 26, 1981 08 p1104 A83-22873

New design for blackbody simulator cavities 08 p1104 A83-22877

Semiautomatic nondispersive infrared analyzer apparatus for CO2 air sample analyses 09 p1295 A83-24258

The Dutch Scientific Instrument on board IRAS 11 p1537 A83-28213

Infra-red homodyne receiver with acousto-optically controlled local oscillator 11 p1657 A83-28616

On the calibration and temperature behaviour of single-beam infrared hygrometers 12 p1728 A83-29137

Applications of an infrared charge-coupled device Schottky diode array in astronomical instrumentation 14 p2016 A83-31996

Fiber-optic waveguides in the medium infrared range 15 p2231 A83-34879

Integrated-optic elements in the medium infrared range 15 p2231 A83-34882

Automatic laser photometer-polarimeter 21 p3141 A83-45310

Facility for brassboard infrared sensor simulations 22 p3292 A83-46596

Coherent, single-mode fiber optic for multifunction 10.6 micron helicopter avionics system 22 p3359 A83-46639

Non-contact sensing of atmospheric temperature, humidity, and supersaturation 24 p3584 A83-49709

INFRARED INTERFEROMETERS

Multiple telescope infrared interferometry 05 p0694 A83-17425

Diamond machining of infrared refractors utilizing two-axis machine tool technology 08 p1112 A83-22868

Speckle interferometry in the infrared 10 p1419 A83-25835

Coherent versus incoherent detection for interferometry at infrared wavelengths 10 p1495 A83-25846

Measurement of the indices of refraction and the absorption coefficients of dielectric materials in the millimeter wave region 11 p1664 A83-28717

Performance of the Multiple Mirror Telescope (MMT). VIII - MMT as an optical-infrared interferometer and phased array 13 p1937 A83-30984

Infrared speckle imaging - Improvement of the method; results on Miras and protostars 13 p1941 A83-31562

Two-dimensional infrared speckle interferometry with a 32 x 32 InSb charge-injection device (CID) array 14 p2095 A83-31980

Stellar diameter measurements by two-aperture interferometry in the infrared 14 p2099 A83-33208

Small interferometer for Fourier spectrometry 15 p2163 A83-33789

Infrared speckle interferometry, results, true image reconstruction and instrumental plans 18 p2761 A83-40437

Application of infrared arrays to speckle interferometry 18 p2691 A83-40445

The ISO Michelson 18 p2648 A83-40467

Speckle interferometry degraded by irregular motion of a scanning telescope mirror 21 p3135 A83-44148

INFRARED LASERS

The effect of IR radiation on generation in Gunn diodes 01 p0044 A83-11311

Raman gain in 12-micron NH3 lasers 02 p0183 A83-11560

High power single-frequency laser at 1.32 microns using Nd:YAG 02 p0183 A83-12083

433 micron laser heterodyne observations of galactic CO from Mauna Kea 03 p0405 A83-13464

Spectral line inversion for sounding of stratospheric minor constituents by infrared heterodyne technique from balloon altitudes 03 p0325 A83-13723

Gasdynamic laser --- Book 03 p0332 A83-14100

Refractive index of HF from 2.5 microns to 2.9 microns 03 p0332 A83-14393

Influence of hot carriers on the temperature dependence of threshold in 1.3-micron InGaAsP lasers 03 p0332 A83-14930

Critique of tunable infrared lasers 04 p0485 A83-15803

He-Ne laser generation of 1.15-1.20 microns in a hollow copper cathode 04 p0485 A83-15950

'Nonwaveguide'-mode semiconductor injection lasers 04 p0486 A83-16214

Pulsed-power performance and stability of 880 nm GaAlAs/GaAs oxide-stripe lasers 04 p0486 A83-16215

Catastrophic degradation level of visible and infrared GaAlAs lasers 05 p0647 A83-16941

Conversion of 3-micron infrared radiation in cesium vapor 05 p0649 A83-17055

Interaction of three coherent fields with Doppler broadened serial four-level systems - Application to four-level FIR lasers 06 p0766 A83-18907

Spectroscopic study of the mechanism of the linear electrooptic effect 06 p0810 A83-19575

IR and UV laser activity in a slit-shaped copper hollow cathode --- German thesis 06 p0768 A83-19617

Optically pumped 1.55-micron double heterostructure Ga/x/Al/y/In/1-x-y/As/Al/u/In/1-u/As lasers grown by molecular beam epitaxy 07 p0933 A83-19986

Frequency doubling in a LiNbO3 thin film deposited on sapphire 07 p0993 A83-20730

Contribution to the construction of a submillimeter laser - Application to the characterization of various mesomorphic substances --- French thesis 07 p0937 A83-21097

Selective enhancement of the 251-micron line in an optically pumped CH3OH laser 07 p0937 A83-21360

CW recombination laser action in a cadmium vapor arc 07 p0938 A83-21370

Powerful electroionization laser on Xe infrared atomic transitions 07 p0938 A83-21589

A comparative study of D₂O oscillators emitting at 385 microns 07 p0398 A83-21598

Determination of laser frequencies by mixing experiments between two submillimeter lasers 08 p1107 A83-22245

An optically-pumped multigas far-IR laser 08 p1107 A83-22246

New CH₃OH laser lines pumped with a fine-tuned high-power CO₂-TEA laser 08 p1107 A83-22247

Physics and technology of coherent infrared radar: Proceedings of the Meeting, San Diego, CA, August 25, 26, 1981 08 p1095 A83-22499

Experimental measurements of turbulence induced beam spread and wander at 1.06, 3.8, and 10.6 microns 08 p1110 A83-22562

Direct frequency measurements of transitions at 520 THz /576 nm/ in iodine and 260 THz /1.15 micron/ in neon 08 p1110 A83-22633

Direct frequency measurement of the I₂-stabilized He-Ne 473-THz /633-nm/ laser 08 p1110 A83-22634

Infrared calibration facilities at Newark Air Force Station 08 p1047 A83-22875

Coherence effects in laser testing of long wavelength infrared /LWIR/ sensors 08 p1052 A83-22879

Laser transmissometer calibration of long-path atmospheric transmission measurements 08 p1104 A83-22889

Infrared laser spectroscopy of molecular beams 09 p1342 A83-24146

Absorption of 9.6-micron CO₂ laser radiation by CO₂ at elevated temperatures 09 p1272 A83-24447

Infrared optics hot pressed from fluoride glass 09 p1239 A83-24973

Laser-induced damage and two-photon absorption measurements in CdTe 09 p1273 A83-24974

High power operation of a CW 28-micron water vapor laser 10 p1425 A83-25428

High power pulsed FIR laser lines from CD₃OH 10 p1425 A83-25429

Operating conditions of a CW water-vapour laser at 28, 47, 78, 79 and 119 microns 10 p1425 A83-25454

Backward and forward FIR emission characteristics from D₂O in both Raman and laser regimes 10 p1426 A83-26001

Free electron laser small signal gain measurement at 10.6 microns 10 p1427 A83-26009

Laser light backscattering off an electron beam-plasma system 10 p1428 A83-26019

Fluid-dynamical aspects of laser-metal interaction 10 p1416 A83-26172

A high energy D₂O submillimeter laser for plasma diagnostics 10 p1431 A83-26648

Tuning characteristics of multistage stimulated Raman scattering by polaritons in a layer of an LiIO₃ crystal 10 p1432 A83-26671

High-pressure NH₃-N₂ laser 10 p1434 A83-26689

He-Ne laser in the near infrared of the type LG-1-I.R 10 p1435 A83-26881

Three wavelength laser emission in Ho:YLF via sequential cascade 11 p1578 A83-27544

Laser action continuously tunable from 1.98 to 3.76 microns using F₂+ and lithium /F₂+ /A centers in KI 11 p1578 A83-27546

Mode structure of a DFB gas laser 11 p1578 A83-27547

Submillimeter-wave laser emission in carbonyl fluoride 11 p1578 A83-27549

Radio frequency pumped infrared lasers 11 p1580 A83-27576

High efficiency infrared xenon laser excited by a U.V. preionized discharge 11 p1580 A83-27579

Growth of emission in a far infrared laser 11 p1583 A83-27625

New CW two-photon pumped and Raman FIR laser lines in /N-14/H₃ and /N-15/H₃ 11 p1583 A83-27848

Optical multistability in silicon observed with a CW laser at 1.06 microns 11 p1657 A83-27849

Calculation of the parameter for the quality of the least-squares fit in investigating atmospheric pollution by resonance absorption 11 p1613 A83-28204

The optical properties and applications of germanium semiconductor single crystals 11 p1657 A83-28368

CW operation of 1.5 micron GaInAsP/InP buried heterostructure laser with a reactive ion-etched facet 11 p1585 A83-28606

The physics of electric-discharge CO₂-lasers --- Russian book 12 p1731 A83-28815

Operating characteristics of a transverse-excited 16 microns CO₂ laser with profile electrodes and UV-preionization 12 p1732 A83-29408

A passive film gate for mode-locked infrared lasers 13 p1850 A83-30267

Stepwise dependence of a portion of hot molecules on the intensity of exciting radiation 13 p1850 A83-30317

Laser oscillation at 3.53 microns from Fe(2+) in n-InP:Fe 13 p1850 A83-30327

Nonlinear far-infrared magnetoabsorption and optically detected magnetoimpurity effect in n-GaAs 13 p1850 A83-30600

Measurement of high electron drift velocity in a submicron, heavily doped graded gap Al(x)Ga(1-x)As layer 13 p1929 A83-31056

Heavy ion beam pumped He-Ar laser 13 p1852 A83-31060

Additional experimental results from the Stanford 3 micron FEL 13 p1852 A83-31103

U.K. free-electron laser proposal 13 p1853 A83-31110

Microtron free-electron laser experiment 13 p1854 A83-31124

Gain-enhanced free-electron laser with an electromagnetic pump field 13 p1855 A83-31133

Results of international comparisons using methane-stabilized He-Ne lasers at 3.39 microns and iodine-stabilized He-Ne lasers at 633 nm 13 p1856 A83-31279

Optically pumped FIR lasers phase-locked by Stark effect applied to precise optical frequency measurements 13 p1847 A83-31287

Passive mode locking in iodine photodissociation laser 14 p2023 A83-31913

Influence of a counterpressure on the operation of a CO₂ gasdynamic laser emitting of 18.4 microns 14 p2023 A83-31914

Passive mode lockers for lasers generating at a wavelength of 1.06 micron 14 p2025 A83-32832

Binary holographic LO beam multiplexer for IR imaging detector arrays 14 p2021 A83-32908

FIR NH₃ cascade laser excited by a Q-switch laser 14 p2025 A83-33143

Tone-burst modulated color-center-laser spectroscopy 15 p2167 A83-33758

Integrated arrays of 1.3-micron buried-crescent lasers 15 p2168 A83-33842

Collisionless dissociation of molecules due to their interaction with infrared radiation 15 p2227 A83-33984

Measuring atmospheric scattering and extinction at 10 microns using a CO₂ lidar 15 p2201 A83-34464

Numerical analysis of an optically pumped D₂O far infrared laser 16 p2358 A83-35430

A high power D₂O laser optimized for microsecond pulse duration 16 p2358 A83-35431

Natural fluctuations of the emission frequency of an He-Ne/CH₄ 3.39 micron laser 16 p2359 A83-35895

Infrared temperature tunability in GaSe, HgS, and Ti₃AsSe₃ nonlinear devices 16 p2359 A83-35954

New pulsed far infrared laser lines in D₂O 16 p2359 A83-35959

A new stabilization system for optically pumped CW far infrared lasers 17 p2514 A83-37752

Threshold-wavelength and threshold-temperature dependences of GaInAsP/InP lasers with frequency selective feedback operating in the 1.3- and 1.5-micron regions 18 p2693 A83-40057

Intense laser self-focusing in plasmas 18 p2693 A83-40366

A study of ablation by laser irradiation of plane targets at wavelengths 1.05, 0.53, and 0.35 micron 18 p2749 A83-40519

Investigation of processes of the bulk damage of semiconductors under the effect of pulsed infrared laser radiation 18 p2694 A83-40611

Oxygen-induced recombination centers in as-grown Czochralski silicon crystals 19 p2903 A83-40739

Costas loop experiments for a 10.6 micron communications receiver 19 p2826 A83-40896

He-Ne laser frequencies near 2.4 microns and their application to hydrogen fluoride detection 19 p2851 A83-40928

High-efficiency infrared xenon laser excited by a UV preionized discharge 19 p2852 A83-40947

Xenon laser action in discharge and electron-beam excited Ar-Xe mixture 19 p2853 A83-41183

Intracavity pumped NH₃ laser using a very small cavity 19 p2853 A83-41184

Wideband heterodyne detection in the far infrared with extrinsic Ge photocoductors 20 p3048 A83-42583

Picosecond air breakdown studies at 0.53 micron 20 p3051 A83-43598

Rectification and harmonic generation with metal-insulator-metal diodes in the mid-infrared 20 p3048 A83-43600

Mechanism of pulse emission from high-pressure electric-discharge He-Ar, He-Kr, and He-Xe infrared lasers 20 p2996 A83-43783

External-cavity diode laser emitting in the middle infrared range 20 p2998 A83-43804

Chemical laser amplifier using a photon-branched reaction in an aerosol medium 20 p2998 A83-43808

Picosecond damage studies at 0.5 and 1 micron --- laser induced breakdown in optical materials 21 p3203 A83-43864

Temperature effects in AgGaS₂ nonlinear devices 21 p3143 A83-44158

Tunable infrared difference-frequency generation in lithium iodate 21 p3143 A83-44194

A 28 micron water-vapor laser interferometer for plasma diagnostics 21 p3144 A83-44381

A 1.59 micron wavelength GaInAsP/InP distributed feedback laser with first-order grating on anti-meltback layer 21 p3144 A83-44500

Review of laser induced damage thresholds 21 p3144 A83-44784

Window and mirror materials for use at 10.6 micron 21 p3144 A83-44788

Wavelength tuning of GaInAsP/InP integrated laser with butt-jointed built-in distributed Bragg reflector 21 p3145 A83-44952

Wavelength multiplexing of 1.31-micron InGaAsP buried crescent laser arrays 21 p3146 A83-45476

Broadly tunable mode-locked HgCdTe lasers 21 p3146 A83-45478

Assessment of relative error sources in IR DIAL measurement accuracy 22 p3295 A83-46084

Short-cavity hydrogen-halide laser 22 p3296 A83-46086

Generation of coherent far-infrared radiation using lasers 22 p3296 A83-46497

Polycrystalline KRS-5 infrared fibers for power transmission 22 p3357 A83-46622

Broadband infrared generation by stimulated Raman scattering in liquid filled fibers 22 p3297 A83-46631

Tunable diode lasers and laser systems for the 3 to 30 microns infrared spectral region 22 p3297 A83-46638

Infrared heterodyning using silver halide fibers 22 p3359 A83-46641

Two-photon pumped synchronously mode-locked bulk GaAs laser 22 p3298 A83-46668

Observation and assignment of torsional transitions in FIR emission from optically pumped CH₃OH 22 p3299 A83-46743

Assignments of optically pumped CD₃OH laser lines 22 p3299 A83-46746

Millimeter wave spectroscopic studies of collision-induced energy transfer processes in the (C-13)H₃F laser 22 p3301 A83-46823

Reliability of InGaAsP/InP buried heterostructure 1.3 micron lasers 22 p3301 A83-46824

Differential-absorption measurements with fixed-frequency IR and UV lasers --- for pollution monitoring and control 23 p3455 A83-47768

Lidar system analysis for measurement of atmospheric species 23 p3457 A83-47787

Optical remote sensing of environmental pollution and danger by molecular species using low-loss optical fiber network system 23 p3508 A83-47802

A 1.5 W CW optically pumped 12.08 microns NH₃ laser 23 p3462 A83-48317

Experimental investigation of the characteristics of magnetic mirrors at a wavelength of 1.15 micron --- for laser gyroscopes 23 p3459 A83-48493

Transient stimulated Raman scattering of femtosecond laser pulses 24 p3586 A83-48782

High efficiency mid-IR generation by Raman down conversion in liquid nitrogen 24 p3587 A83-48907

Picosecond spectra of gain-switched quaternary lasers 24 p3589 A83-49612

INFRARED MASERS

U INFRARED LASERS

INFRARED PHOTOGRAPHY

NT COLOR INFRARED PHOTOGRAPHY

The utilization of infrared /IR/ aerial and space observations of Arctic seas in navigation and during the solution of other national-economic problems 01 p0077 A83-10836

Mount St. Helens quick response damage assessment using high-altitude infrared photography 02 p0199 A83-12672

Field evaluation of aerial infrared surveys for residential applications 02 p0200 A83-12688

Aerial survey of crop losses due to grasshoppers /Orthoptera - Acrididae/ in Saskatchewan 03 p0347 A83-14255

Determination of forest fire spread rates from infrared photographs 03 p0350 A83-14307

Aerial thermal infrared census of Canada geese in South Dakota 03 p0351 A83-14665

Mapping erosion with airphotos - Panchromatic or black and white infrared 05 p0657 A83-17839

Automatic mapping of lakes for small-scale maps using digital Landsat Imagery 08 p1129 A83-21969

Wax films used as infrared photographic recording medium 08 p1103 A83-22859

- Reliability of enhanced infrared /EIR/ geostationary satellite data at high latitudes 08 p1137 A83-22925
 Digitization of a video signal and stress analyses using IR thermography 15 p2178 A83-34401
 IR-camera for GIRL --- German Infrared Laboratory 18 p2691 A83-40449
 Visualization of heat transfer 20 p2970 A83-42654

INFRARED RADAR

- Physics and technology of coherent infrared radar; Proceedings of the Meeting, San Diego, CA, August 25, 26, 1981 08 p1095 A83-22499
 Military applications of coherent infrared radar 08 p1095 A83-22500
 Overview of technology developments in coherent infrared radar 08 p1109 A83-22501
 Feasibility and design considerations of a global wind sensing coherent infrared radar /WINDSAT/ 08 p1051 A83-22503
 CO2 laser radar systems --- for meteorological measurements 08 p1095 A83-22505
 National Oceanic and Atmospheric Administration's /NOAA/ pulsed, coherent, infrared Doppler lidar - Characteristics and data 08 p1096 A83-22506
 Experimental studies with a coherent CO2 laser radar 08 p1096 A83-22510
 Frequency-stabilized transversely excited atmospheric /TEA/ CO2 lasers for coherent infrared radar systems 08 p1109 A83-22515
 Holographic beam shaping for optical heterodyne arrays in laser radars 08 p1097 A83-22519
 Coherent adaptive speckle tracking 08 p1097 A83-22522
 Holographic local-oscillator beam multiplexing for array heterodyne detection 10 p1425 A83-26875
 Review of laser technology at M.I.T. Lincoln Laboratory 11 p1580 A83-27575
 Coherent IR radar technology 23 p3442 A83-47805

INFRARED RADIATION

- NT FAR INFRARED RADIATION
 NT NEAR INFRARED RADIATION
 Math modeling for prediction of infrared signatures 01 p0106 A83-11221
 Dynamic infrared missile evaluator /DIME/ 01 p0015 A83-11236
 The effect of IR radiation on generation in Gunn diodes 01 p0044 A83-11311
 Broadband infrared generation in liquid-bromine-core optical fibers 02 p0183 A83-11571
 NO infrared radiation in the upper atmosphere 02 p0204 A83-11967
 The parameterization of longwave flux in energy balance climate models 02 p0213 A83-12229
 Airborne measurements of infrared atmospheric radiance and sky noise 03 p0324 A83-13461
 High-resolution lower atmospheric transmission predictions over long paths 03 p0359 A83-13991
 1 millimeter continuum observations of quasars 03 p0422 A83-14182
 Non-LTE atmospheric radiance and transmittance 03 p0360 A83-14638
 Infrared emissivity of water clouds 03 p0371 A83-14654
 Some improvements to the infrared emissivity algorithm including a parameterization of the absorption by water vapor polymers 03 p0371 A83-14659
 Parameterization of the radiative flux divergence in the 15 micron CO2 band in the 30-75 km layer 03 p0362 A83-14752
 Infrared emission and star formation in NGC 5253 03 p0429 A83-14794
 Perturbations in the nodal period of artificial satellites caused by the terrestrial infrared radiation pressure 05 p0602 A83-17858
 Parameterization of outgoing infrared radiation derived from detailed radiative calculations 06 p0789 A83-18252
 Infrared to visible up-conversion using GaP light-emitting diodes 07 p0992 A83-19990
 Multichannel duplex fiber-optic communication line operating at the wavelength in the region of 1.3 micron 07 p0993 A83-20122
 Comparison of ground-based and spacecraft observations of the infrared emission from Venus - The nature of thermal contrasts 07 p1030 A83-20616
 Experimental evidence for collision-induced superradiance 07 p0937 A83-20797
 Identification of the emission feature near 3.5 microns in the pre-main-sequence star HD 97048 07 p1021 A83-21127
 The processing of infrared sky noise by chopping, nodding and filtering 07 p1008 A83-21211
 Atmospheric effects on electro-optical, infrared, and millimeter wave systems performance; Proceedings of the Meeting, San Diego, CA, August 27, 28, 1981 08 p1098 A83-22540

- Measurements of infrared and visible extinction in adverse weather 08 p1140 A83-22546
 Utility of infrared measurements programs --- in support of development, design and operation of military surveillance systems 08 p1051 A83-22840
 Review of some nonlocal-thermodynamic-equilibrium high-altitude 4.3 micron background effects 08 p1136 A83-22854
 Broadband lamp standard for ultraviolet /UV/, visible, and infrared calibration to 6.0 microns 08 p1104 A83-22878
 Some improvements and complements to the infrared emissivity algorithm including a parameterization of the absorption in the continuum region --- for atmospheric radiation transfer 08 p1143 A83-23015
 Attempt to directly simulate cloud-radiation interaction in the case of small cumuli 09 p1312 A83-23957
 Impact damage and erosion in infrared materials 09 p1346 A83-24963
 Shock tube measurements of IR radiation in hot gas/particle mixtures 10 p1416 A83-26189
 A radiation model using hourly meteorological data with results from GATE 11 p1632 A83-27972
 Ga/0.47/In/0.53/As/Al/0.48/In/0.52/As m-well LEDs emitting at 1.6 microns 11 p1664 A83-28613
 On the use of spectral radiance models to obtain irradiances on surfaces of arbitrary orientation 12 p1752 A83-28945
 Resonant upconversion of light at wavelength lambda = 1.06 micron in rubidium vapor 13 p1851 A83-30822
 Solid-state laser having a reflector that transmits IR and UV radiation 13 p1851 A83-30870
 Vibrational relaxation and dissociation of strongly excited ozone molecules 14 p2081 A83-31905
 Optical design of the Diffuse Infrared Background Experiment for NASA's Cosmic Background Explorer 14 p2084 A83-32037
 Optical transmission at 3.39 microns during pulsed laser annealing of silicon 15 p2238 A83-33849
 Interannual variability and climatic noise in satellite-observed outgoing longwave radiation 15 p2195 A83-33884
 Collisionless dissociation of molecules due to their interaction with infrared radiation 15 p2227 A83-33984
 Vibrational energy distribution in molecules excited by infrared radiation in the collisionless regime 16 p2410 A83-35894
 Infrared limb-darkening effects for the earth-atmosphere system 16 p2377 A83-36045
 [AIAA PAPER 83-0161] Observations and modeling of downward radiative fluxes /Solar and Infrared/ in urban/rural areas 18 p2712 A83-39114
 Remote sounding of cloud parameters from a combination of infrared and microwave channels 18 p2721 A83-39119
 IR emission and NO concentration in the case of the significant heating of the upper atmosphere 18 p2713 A83-39322
 Variable infrared radiation from X-ray sources 4U 0115 + 634 and A 0535 + 262 18 p2776 A83-39768
 Observation of proton and electron detachment from an anthracene molecule during pronounced IR many-photon superexcitation 20 p3044 A83-42274
 Beam-gas collision system for excitation cross-section measurements 20 p3044 A83-42294
 Non luminous gas radiation - Approximate emissivity models 20 p2974 A83-42692
 Evaluation of upwelling infrared radiance in a nonequilibrium nonhomogeneous atmosphere 20 p3020 A83-42698
 Experimental and theoretical investigation of nonequilibrium radiation from the jet of the correction engine of the Salyut manned orbital station 20 p2946 A83-42884
 A fluoride glass optical fiber operating in the mid-infrared wavelength range 21 p3204 A83-44206
 The climatological minimum in tropical outgoing infrared radiation - Contributions of humidity and clouds 21 p3179 A83-44395
 Determination of the horizontal and vertical distribution of clouds from infrared satellite sounding data 22 p3340 A83-46140
 Advances in infrared fibers II; Proceedings of the Second Meeting, Los Angeles, CA, January 26-28, 1982 22 p3357 A83-46621
 Mode coupling analysis of bending losses in hollow infrared waveguides 22 p3358 A83-46634
 Infrared synchrotron radiation from electron storage rings 22 p3355 A83-46842
 Infrared cooling in cloudy atmospheres - Precision of grid point selection for numerical models 23 p3491 A83-47416

- Effects of atmospheric obscuration on the propagation of optical/IR radiation 23 p3442 A83-47785
 Radiation characteristics of vibrationally nonequilibrium CO2 gas in the spectral region 12-19 microns 24 p3626 A83-49117
 Observations of dust in planetary nebulae 24 p3639 A83-49135
 Estimates of the applicability of the black-body approximation to the emission of the atmosphere at the horizon 24 p3605 A83-49290
 Catalogue of non stellar molecular maser sources and their probable infrared counterparts in the galactic plane 24 p3642 A83-49321

INFRARED RADIOMETERS

- Satellite imagery - Examples of mesoscale analysis using AVHRR images --- Advanced Very High Resolution Radiometer 01 p0075 A83-10224
 Simulation study of multispectral estimation of sea-surface temperature from infrared observations 02 p0177 A83-12034
 Visible and infrared spin scanning radiometer /VISSR/ atmospheric sounder /VAS/ ground data system 02 p0142 A83-12679
 Mineral identification from orbit - Initial results from the Shuttle multispectral infrared radiometer 03 p0344 A83-13350
 Groundbased infrared measurements using the AMOS/MOTIF facility 03 p0283 A83-13471
 Development of Teal Ruby Experiment radiometric test requirements 03 p0325 A83-13728
 Concerning the determination of the temperature of the ocean surface from multichannel satellite measurements of radiation in infrared atmospheric windows 03 p0372 A83-14316
 Sea surface temperature estimation using the NOAA 6 satellite Advanced Very High Resolution Radiometer 03 p0373 A83-14501
 Local-area atmospheric sounding from satellites 03 p0369 A83-14524
 Calibration of the radiometric asteroid scale using occultation diameters 05 p0704 A83-16969
 Airborne operation of an infrared low-level wind shear prediction system 06 p0791 A83-18412
 Net global thermal emission from the Venusian atmosphere 07 p1030 A83-20613
 The global distribution of water vapor in the middle atmosphere of Venus 07 p1030 A83-20614
 Sea ice classification from infrared thermometry over the North Water, winter 1980/81 08 p1143 A83-21957
 Determination of atmospheric water vapor content in moderate optical paths by radiometric measurements 08 p1136 A83-22853
 Silicon photodiode self-calibration as a basis for radiometry in the infrared 08 p1104 A83-22874
 Calibration of a transfer radiometer in support of the Navy forward looking infrared systems /FLIR/ program 08 p1104 A83-22876
 Electro-optical calibration considerations at intermediate maintenance levels 08 p1104 A83-22883
 Calibration support of the AN/AAM-60 common forward-looking infrared /FLIR/ test bench 08 p1104 A83-22886
 Carbon monoxide mixing ratio inference from gas filter radiometer data 09 p1306 A83-24450
 The IRV-75 infrared radiometers --- for Venera 9 and 10 spacecraft 10 p1387 A83-25346
 The outlook for precipitation measurements from space 11 p1628 A83-27050
 Investigation of the atmospheric aerosols by the visible and IR channels of the AVHRR radiometer on NOAA-6 12 p1755 A83-29568
 Validation of Nimbus-7 temperature-humidity infrared radiometer estimates of cloud type and amount 12 p1759 A83-29679
 Calibration of the VIS-channel of Meteosat-2 12 p1708 A83-29692
 The use of an IR radiometer to investigate the temperature field of a waveguide 13 p1846 A83-30717
 Upper level cloud climatology from an orbiting satellite 13 p1893 A83-31040
 Results from the LIMS experiment for the PMP-1 winter 1978/79 --- Limb Infrared Monitor of the Stratosphere 16 p2383 A83-35381
 Radiometric levitation of spherical carbon aerosol particles using a Nd:YAG laser 16 p2413 A83-36761
 Thunderstorm top structure observed by aircraft overflights with an infrared radiometer 18 p2724 A83-39681
 Total ozone measurements derived from T.O.V.S. radiances --- Tiros Operational Vertical Sounder 18 p2717 A83-39795
 Remote sensing applications of pulsed photothermal radiometry 20 p2992 A83-43594

Scanning radiometer for calibrating thermal imager test targets 21 p3138 A83-44782

The effect of the emissivity of a surface on the IR measurements of its temperature 21 p3177 A83-45333

The use of the extrapolation technique in the calibration of radiation-measuring devices in the region of strong band absorption for the rho-sigma-tau water-vapor bands from 0.91 to 0.98 microns 21 p3142 A83-45406

An investigation of the performance of infrared radiometers for the determination of sea surface temperature from space 22 p3343 A83-46106

Shuttle Multispectral Infrared Radiometer - Preliminary results from the second flight of Columbia 22 p3261 A83-46220

Radiometric applications of infrared optical fibers 22 p3292 A83-46642

Boundary-layer structure over tropical oceans from TIROS-N infrared sounder observations 22 p3342 A83-46951

A method for determining water-vapor content in the atmosphere on the basis of joint infrared and microwave radiometric measurements 23 p3487 A83-47141

Comparison of winter-nocturnal geostationary satellite infrared-surface temperature with shelter-height temperature in Florida 23 p3474 A83-47221

Advanced visible and near-infrared radiometer for earth observation 23 p3424 A83-47270

[IAF PAPER 83-107]

Detonic research infrared radiometer with nanosecond response 23 p3454 A83-47648

Review of NDRE remote sensing program and development of high pressure RF excited CO2 waveguide lasers 23 p3462 A83-47799

Cumulus convection as observed from an airborne infrared radiometer 24 p3615 A83-49726

Estimating the temperature and height of overshooting thunderstorm tops from geostationary satellite infrared data 24 p3615 A83-49727

Interpretation of satellite-observed thunderstorm anvil structure 24 p3615 A83-49729

INFRARED REFLECTION

High-precision tunable infrared reflectometer 02 p0181 A83-12817

Twilight IR brightening over India due to El Chichon's eruption in Mexico 05 p0665 A83-17791

Non-destructive characterisation of n-type InP epitaxial layers by infrared reflectivity measurements 09 p1349 A83-23667

Chemically vapor-deposited black molybdenum films of high IR reflectance and significant solar absorbance 10 p1400 A83-25534

Retrieval of aerosol optical characteristics from polarization measurements of reflected solar radiation above the oceans 12 p1755 A83-29566

Heterodyne OTDR at 0.82 micron --- Optical Time-Domain Reflectometry 15 p2231 A83-34513

Comments on 'Skylab near-infrared observations of clouds indicating supercooled liquid water droplets' 16 p2387 A83-35496

Transparent heat-reflecting coatings for solar applications based on highly doped tin oxide and indium oxide 16 p2371 A83-36738

Infrared specular reflectance of pressed crystal powders and mixtures 16 p2413 A83-36759

Single and multiple pulse catastrophic damage in diamond-turned Cu and Ag mirrors at 10.6, 1.06, and 0.532 microns 21 p3203 A83-43863

Reflectometer measurement of the infra-red reflectance of camouflage paints 21 p3137 A83-44598

Target reflectance measurements for calibration of lidar atmospheric backscatter data 22 p3295 A83-46075

Polarization of reflected 10.6-microns radiation from sublimed sulfur targets --- of carbon dioxide lidar 24 p3582 A83-49013

INFRARED SCANNERS

Matched and optimal filters for the creation of a local-vertical reference --- for spaceborne infrared scanning 03 p0287 A83-13205

Simulation of clutter rejection signal processing for mid-infrared surveillance systems 08 p1094 A83-22438

Future trends in the use of infrared line scanners for airborne reconnaissance 08 p1045 A83-22578

Thermal infrared pushbroom imagery acquisition and processing --- of NASA's Advanced Land Observing System 08 p1045 A83-22841

Considerations in the selection and use of calibration equipment for simulators used with thermal imaging systems 08 p1104 A83-22884

Techniques for pseudo-dc restoration and dynamic range enhancement of scanned infrared imagery 08 p1105 A83-22900

Methods for constructing a local-vertical reference and the evaluation of their effectiveness --- in IR satellite scanning of earth 09 p1219 A83-25045

Remote sensing of row crop structure and component temperatures using directional radiometric temperatures and inversion techniques 10 p1443 A83-25644

Infrared scanning thermography for a quantitativ detection of cavities in a plane slab and a rectangular prism 12 p1733 A83-29143

The measurement of water vapour in thermal emission on studies of Nimbus-7 stratosphere flights for correlative studies of Nimbus-7 12 p1760 A83-29687

Cooled grating Fabry-Perot spectrometer for the 10 micron region 14 p2017 A83-32003

Expanded uses of infrared scanning data in aerodynamic heating materials tests [AIAA-PAPER 83-1542] 14 p1979 A83-32766

The infra-red horizon sensor on board the Aureol-3 satellite 18 p2647 A83-39583

Infrared raster scans and a self optimizing micro-processor system for IR-photometry 18 p2691 A83-40450

A compact high-resolution Michelson Interferometer for Passive Atmospheric Sounding (MIPAS) 22 p3290 A83-46241

Mineralogic information from a new airborne thermal infrared multispectral scanner 23 p3475 A83-47816

INFRARED SIGNATURES

An analytical model to calculate the atmospheric correction on infrared thermal signals 08 p1133 A83-21927

Balloon atmospheric mosaic measurements /BAMM/ IIA phenomenology and band selection 08 p1045 A83-22844

Identification of snow cover and cloud cover on the basis of the spectral brightness of near infrared radiation measured from space 14 p2058 A83-32495

Enhanced crop discrimination using the mid-IR (1.55-1.75 microns) 17 p2530 A83-38165

Target reflectance measurements for calibration of lidar atmospheric backscatter data 22 p3295 A83-46075

Tests of an inversion algorithm for spectrally resolved limb emission 22 p3328 A83-46080

Spectral pattern recognition in IR remote sensing 22 p3288 A83-46085

The use of the Monte Carlo method in investigating the influence of the dimensions of a conifer on the angular dependence of its coefficient of spectral brightness 23 p3476 A83-48114

INFRARED SPECTRA

Passive optical and infrared meteorology 01 p0073 A83-10017

The role of geological surfaces in determining visible-near infra red spectral signatures 01 p0063 A83-10058

A radiation scheme for circulation and climate models 01 p0074 A83-10221

Spectroscopic observations of Be stars especially in the infrared 01 p0121 A83-10330

Oe star spectra in the red and near infrared 01 p0121 A83-10331

The origin of the infrared /C I/ emission - H II or H I regions 01 p0125 A83-10926

Spectroscopic studies of the hazards of Li/SOCl2 batteries during anode-limited cell reversal 02 p0202 A83-12056

Abundances in five nearby galactic H II regions from infrared forbidden lines 02 p0255 A83-12118

Observations of the infrared fine-structure lines of S III at 18.71 and 33.47 microns in four H II regions 02 p0255 A83-12119

The abundances of CH4, CH3D, NH3, and PH3 in the troposphere of Jupiter derived from high-resolution 1100-1200/cm spectra 02 p0264 A83-12143

2-4 micrometer spectroscopy of the compact H II region G 45.13 + 0.14 A 02 p0260 A83-12520

Radio and infrared emission from extended stellar envelopes 03 p0412 A83-13152

Infrared emission spectrophotometric study of the changes produced by TiN coating of metal surfaces in an operating EHD contact [ASLE PREPRINT 82-LC-3C 3] 03 p0333 A83-13229

The infrared spectral properties of frozen volatiles --- in cometary nuclei 03 p0415 A83-13381

Infrared lines from shocked galactic gases 03 p0417 A83-13465

Infrared photometry of periodic comets Encke, Chernykh, Kearns-Kwee, Stephan-Oterma, and Tuttle 03 p0407 A83-13826

The spectrum of Titan in the far-infrared and microwave regions 03 p0133 A83-13827

Far-infrared spectrophotometry of Saturn and its rings 03 p0133 A83-13828

A theoretical study of Comet Halley's spectrum in the infrared range 03 p0407 A83-13841

Accurate frequency and intensity measurements of the infrared spectra of atmospheric molecules 03 p0294 A83-13981

Recent results in the analysis of high-resolution infrared atmospheric transmission spectra 03 p0358 A83-13983

Whatever happened to band models --- for calculating atmospheric IR spectral transmittance 03 p0358 A83-13987

Infrared spectrum of a single aerosol particle by photothermal modulation of structure resonances 03 p0356 A83-14379

On the spectrum of Comet Bradfield 1980 t 03 p0428 A83-14774

The infrared spectrum of interstellar dust --- noting spectroscopic similarity to transmittance of diatomaceous organisms 04 p0526 A83-14981

The heating of dust in the broad-line regions of active galaxies and quasars 04 p0551 A83-15605

The tropospheric gas composition of Jupiter's north equatorial belt /NH3, PH3, CH3D, GeH4, H2O/ and the Jovian D/H isotopic ratio 04 p0569 A83-15643

Composition of the surfaces of the Galilean satellites 04 p0570 A83-16232

Mid- and far-infrared extinction coefficients of hydrous silicate minerals 05 p0707 A83-17808

Q branches in the rotational spectrum of HOCl 05 p0684 A83-17873

A new near-infrared source in the molecular cloud associated with S106 06 p0826 A83-18097

Detection of molecular hydrogen emission from G 333.6-0.2 06 p0827 A83-18162

Infrared observations of V 1016 Cygni 06 p0832 A83-18839

Infrared properties of serendipitous X-ray quasars 06 p0819 A83-18854

New members of*the infrared cluster in the Orion Molecular Cloud 06 p0820 A83-18870

Searches for far-infrared emission from dark clouds - Rho Ophiuchi, Heiles 2, L1529, and L183 07 p1010 A83-19860

Spectroscopic observations of two very red objects toward the galactic center 07 p1004 A83-19861

First infrared measurement of atmospheric NO2 from the ground 07 p0958 A83-20092

A study of peculiar A-type stars in the infrared 07 p1007 A83-20947

Highly excited /J = 16 to 15/ rotational transitions of CO, at 162.8 microns, in the Orion cloud 07 p1019 A83-20955

Properties of amorphous H2O ice and origin of the 3.1-micron absorption 07 p1024 A83-21224

One-dimensional high resolution image reconstruction on Eta Carinae at 4.6-microns with speckle data 07 p1009 A83-21229

SiO isotope emission from Orion - A model for IRC2 07 p1025 A83-21244

Real line strength distributions for random band models 07 p0991 A83-21398

Pressure broadening of OCS in the 10 microns region 07 p0992 A83-21400

Spectral tuning of shallow-junction surface-emitting light-emitting diodes /LEDs/ through gamma-ray irradiation 08 p1170 A83-22846

Earth limb emission analysis of Spectral Infrared Rocket Experiment /SPIRE/ data at 2.7 micrometers 08 p1051 A83-22851

The abundance of CH3D in the atmosphere of Titan, derived from 8- to 14-micron thermal emission 08 p1189 A83-22931

The abundance of water on Jupiter from the Voyager IRIS data at 5 microns 08 p1189 A83-22932

Simultaneous IR and optical light curves of 2A0311-227 08 p1176 A83-23262

The infrared absorption spectrum of water 09 p1342 A83-24147

Discrepancies between balloon-borne IR atmospheric spectra and corresponding synthetic spectra calculated line by line around 825 per cm 09 p1306 A83-24440

Vibrational population distribution in the hydroxyl night airglow 09 p1306 A83-24640

Hot-pressed MgAl2O4 for ultraviolet /UV/, visible, and infrared /IR/ optical requirements 09 p1345 A83-24953

Observations of M42 in the O III 52 and 88-micron forbidden lines, the O I 63-micron forbidden line, and the N III 57-micron forbidden line 09 p1362 A83-24977

Interstellar grain composition and the infrared spectrum of OH26.5 + 0.6 09 p1362 A83-24985

Analysis of the far infrared H2-He spectrum 09 p1343 A83-25214

The C-12/C-13 ratio in Jupiter from the Voyager infrared investigation 10 p1518 A83-25515

A laboratory study of the infrared spectra of interstellar ices 10 p1502 A83-25653

High orbital angular momentum states in H2 and D2 11 p1653 A83-27491

Time-dependence of the infrared spectra of nova dust shells 11 p1681 A83-28277

- The infrared spectrum and variability of Eta Carinae
11 p1682 A83-28285
- Spectral least squares quantification of several atmospheric gases from high resolution infrared solar spectra obtained at the South Pole
12 p1752 A83-29148
- The ground state far infrared spectrum of NH₃
12 p1778 A83-29526
- Infrared and Raman orientation correlation functions of the nu sub 3 vibration of N₂O mixed with rare gases
13 p1916 A83-30963
- Pressure broadening of CO infrared lines perturbed by H₂ and He
13 p1916 A83-30968
- The-micron spectrometry in sharpless-106
13 p1956 A83-31676
- Infrared optical properties of solid mixtures of molecular species at 20K
[AIAA PAPER 83-1452]
14 p2084 A83-32717
- Measurements of infrared optical properties of Al₂O₃ rocket particles
[AIAA PAPER 83-1568]
14 p1985 A83-32780
- The absorption spectrum of (C-12)D₂ in the 1.06-micron region
14 p2048 A83-32833
- The microwave and far-infrared spectra of the CH radical
14 p2083 A83-33234
- Ab initio infrared and Raman spectra
15 p2131 A83-34011
- On the effect of radiative exchange in the 8 to 12 micron spectral region on the diffusional growth of ice crystals
15 p2205 A83-34062
- Infrared light curves of Type I supernovae. II - Late stages
15 p2257 A83-34097
- IR maps of M17 in the forbidden O III 88 micron and 52 micron lines and forbidden N III 57 micron line measurements
15 p2245 A83-34098
- The NH₃ spectrum in Saturn's 5 micron window
15 p2274 A83-34114
- Observations of the line profile of Paschen alpha in 3C 273
15 p2261 A83-34503
- Near-infrared spectroscopy and monochromatic isophotometry of NGC 6302
15 p2248 A83-34586
- Detection of interstellar NH₃ in the far-infrared - Warm and dense gas in Orion-KL
15 p2269 A83-34648
- lo's 4-micron band and the role of adsorbed SO₂
15 p2275 A83-34723
- The non-LTE analysis of carbon lines in the spectra of hot stars. I - C III lambda 4650 and lambda 9710 A triplet lines in the spectra of O stars
15 p2271 A83-34763
- The infrared synthetic spectrum of comet Halley
15 p2273 A83-35019
- IR-spectroscopy of ionosphere from stratospheric balloons
16 p2373 A83-35370
- Amplification by stimulated Raman scattering in low-loss optical fibers
16 p2358 A83-35514
- Simultaneous detection of trace constituents in the middle atmosphere with a small He-cooled, high resolution Michelson interferometer (MIPAS)
16 p2356 A83-36588
- Models of the planetary nebulae II 2003, NGC 3242, 6210, and 7009 - Constraints on the ionizing radiation of the central star
16 p2431 A83-36669
- Molecular hydrogen lines in the infrared spectra of M-giant stars
16 p2433 A83-36700
- X-ray sources in molecular clouds
17 p2597 A83-37316
- Solar emission lines near 12 microns
17 p2624 A83-37350
- Methane on Triton and Pluto - New CCD spectra
17 p2619 A83-37935
- Comparisons among a new soil index and other two- and four-dimensional vegetation indices
17 p2531 A83-38341
- Evidence of high chromospheric activity in Hyades dwarfs from spectroscopic observations
17 p2609 A83-38416
- The main contributions of the international colloquium 'Spectral signatures of remotely sensed objects' in the thermal IR spectral domain
17 p2533 A83-38445
- The infrared luminosity-H I profile width-surface brightness relation, and the cosmological expansion
17 p2612 A83-38826
- Infrared variability of the X-ray binary A0535 + 262
17 p2613 A83-38834
- Multiband optical and infrared photometry of CH Cygni
17 p2613 A83-38841
- Temperature distribution in the atmosphere of the Wolf-Rayet component of V444 Cygni, based on infrared data
17 p2614 A83-38842
- The infrared spectrum of HNO
18 p2742 A83-39857
- Optical and infrared photometry of TX Canum Venaticorum
18 p2763 A83-40480
- Collision-induced absorption in the far infrared spectrum of Titan
19 p2921 A83-40779
- Simultaneous detection of FC-11, FC-12 and FC-22, through 8 to 13 micrometers IR solar observations from the ground
19 p2862 A83-41113
- Determinations of S III, O IV, and Ne V abundances in planetary nebulae from infrared lines
19 p2919 A83-41630
- The 0.9-2.5 micron spectrum of Comet West 1976 VI
19 p2920 A83-41643
- A far red spectrum of Nova LMC 1981
20 p3066 A83-42395
- Infrared spectra of WN stars. I - HD 50896
20 p3068 A83-42448
- Detection of radio emission from the Becklin-Neugebauer object
20 p3069 A83-42474
- Altitude profiles of OH and O₂ near infrared airglows in the evening twilight
20 p3027 A83-43402
- The O IV infrared and ultraviolet flux ratios as temperature and density diagnostics --- of planetary nebulae
21 p3229 A83-44421
- Ultrasonic modulation of persistent spectral holes in crystals
21 p3219 A83-45486
- Near-infrared spectrophotometry of planetary nebulae
21 p3236 A83-45540
- Electron impact excitation of lambda 7990-A multiplet
22 p3355 A83-46061
- Symbiotic stars - Spectrophotometry at 3-4 and 8-13 microns
22 p3375 A83-46550
- 8-13-micron spectral observations of eight moderately extended planetary nebulae
22 p3375 A83-46551
- An infrared study of the eclipsing dwarf nova U Geminorum
22 p3375 A83-46557
- Holographic plasma interferometry in the infrared spectrum. II - Using nonlinear effects to increase the sensitivity
23 p3454 A83-47554
- Infrared optical properties of solid monomethyl hydrazine, N₂O₄, and N₂H₄ at cryogenic temperatures
23 p3508 A83-47585
- The spatial and temporal variability of absorption coefficients of the tropospheric aerosol in the spectral region of 0.4-2.2 microns
23 p3492 A83-48561
- Infrared emission lines in planetary nebulae
24 p3639 A83-49133
- Infrared fluorescence of molecules in comets - The general synthetic spectrum
24 p3669 A83-50098
- INFRARED SPECTROMETERS**
- Cryogenic infrared /IR/ spectral measurements on board the Space Shuttle - CIRIS
03 p0288 A83-13752
- Calibration of an infrared spectrometer and a far-infrared photometer for astronomical applications under low background conditions
06 p0821 A83-18946
- Infrared spectral radiance of the sky
08 p1136 A83-22850
- Total ozone retrieval from infrared Fourier spectrometer radiance measurements
09 p1301 A83-23548
- Satellite-borne infrared Fourier spectrometers for planetary studies
10 p1387 A83-25345
- Rocketborne cryogenic /10 K/ high-resolution interferometer spectrometer flight HIRIS - Auroral and atmospheric IR emission spectra
[AD-A128358]
10 p1423 A83-26642
- The Comet Halley flyby I.R. sounder 'I.K.S.' --- infrared spectrometer
11 p1670 A83-27740
- An IR spectrometry experiment for the Spacelab I mission
[ONERA, TP NO. 1983-98]
14 p1983 A83-31825
- Cooled grating array spectrometer for 0.6-5 microns
14 p2016 A83-31998
- Near-infrared linear array spectrometer for space applications
14 p2016 A83-31999
- Near-infrared mapping spectrometer for investigation of Jupiter and its satellites
14 p1983 A83-32000
- Tunable diode laser heterodyne spectrometer for remote observations near 8 microns
14 p2016 A83-32001
- Use of a Fourier transform spectrometer on a balloon-borne telescope and at the multiple mirror telescope (MMT)
14 p2016 A83-32002
- Cooled grating Fabry-Perot spectrometer for the 10 micron region
14 p2017 A83-32003
- Analysis of the nucleus and circumnuclear area of Comet Halley with the 'I.K.S.' infrared sounder from the 'Vega' flyby probes --- Venera satellite-borne IR imaging spectrometer
15 p2249 A83-35026
- A new spectrometric measurement of atmospheric 60 micron emission
16 p2373 A83-35371
- Scientific programs for the Spacelab ESO13 grille spectrometer
16 p2317 A83-35784
- Controlling the IESO13 spectrometer for spacelab and its data retrieval
16 p2317 A83-35786
- Fabry-Perot spectrometers for the ground-based infrared
18 p2690 A83-40435
- A middle-infrared heterodyne spectrometer to be used at the Cassegrain-focus of medium-size and large astronomical telescopes
18 p2761 A83-40436
- CO₂ measurements with an infrared laser spectrometer on flask samples collected at Jungfraujoch high-altitude research station (3500 meters asl) and with light aircraft up to 8000 meters over Switzerland
20 p3022 A83-42867
- A two-beam interferometer for dispersive reflection spectroscopy of solids in the far infrared at temperatures between 4 and 300K
21 p3137 A83-44388
- INFRARED SPECTROPHOTOMETERS**
- Construction of a 1-3 micron infrared photometer and its test observations
01 p0049 A83-10233
- Far-infrared spectrophotometer for astronomical observations
03 p0405 A83-13462
- Calibration of an infrared spectrometer and a far-infrared photometer for astronomical applications under low background conditions
06 p0821 A83-18946
- The near infrared spectrophotometer for the 182 cm Asiago telescope
12 p1785 A83-28993
- Single photon counters for the infrared
14 p2014 A83-31977
- Proposal for advanced infrared spectrophotometers
14 p2016 A83-31997
- Design of a four-channel simultaneous visual infrared photometer
14 p2096 A83-32030
- Comparison of the Mt. Stromlo/AAO and Caltech/Tololo infrared photometric systems
18 p2757 A83-39599
- Infrared (JHK) photometry of asteroids. II
18 p2757 A83-39605
- Infrared astronomy at ESO
18 p2760 A83-40420
- Infrared instrumentation on Calar Alto --- mountain-based telescopes for photography
18 p2760 A83-40421
- The C.F.H. telescope as an infrared telescope
18 p2760 A83-40422
- The Tingo observatory --- infrared astronomy
18 p2760 A83-40423
- The infrared photometer of the 2 m telescope at Pic du Midi Observatory
18 p2761 A83-40425
- Infrared broad-band filters optimised for observations of Wolf-Rayet stars
18 p2761 A83-40426
- The IR spectrophotometer for the Gornegrat telescope
18 p2761 A83-40428
- Reflective field optics for IR spectrophotometers
18 p2744 A83-40429
- A cooled grating spectrometer for Tingo
18 p2690 A83-40430
- Irspec --- cooled grating array IR spectrometer for use with New Technology Telescope
18 p2690 A83-40431
- IFU - A multi-detector IR spectrometer
18 p2690 A83-40432
- Cooled grating spectrometer
18 p2690 A83-40433
- Future UKIRT instrumentation --- infrared telescope
18 p2690 A83-40434
- A balloon-borne cooled telescope for far IR astronomy
18 p2762 A83-40460
- Infrared photometry of the RS CVn binaries. III - JHK light curves of UV Psc
24 p3645 A83-49841
- INFRARED SPECTROSCOPY**
- Analysis of low-pressure chemical vapor deposited silicon nitride by Rutherford backscattering spectrometry
01 p0110 A83-10990
- Association of triethylammonium perchlorate with bases
01 p0023 A83-11322
- Determination of the activation energies of monomolecular dissociation reactions by means of IR spectroscopy-N-nitrodimethylamine
01 p0023 A83-11323
- Single-scan current-modulated tunable diode laser spectrometer of improved calibration and throughput performance
02 p0179 A83-12607
- Infrared spectroscopy in astronomy
03 p0405 A83-13453
- Infrared /IR/ spectroscopy in support of atmospheric measurements
03 p0294 A83-13985
- Royal Society, Discussion on New Techniques in Optical and Infrared Spectroscopy, London, England, April 21, 22, 1982, Proceedings
04 p0482 A83-15801
- Laser heterodyne spectroscopy
04 p0482 A83-15808
- Infrared spectroscopic study of beta-silicols in the system Si₃N₄-SiO₂-AlN
04 p0464 A83-15998
- Spectroscopic detection of acetylene and ethane in the terrestrial atmosphere using ground-based solar IR observations
04 p0508 A83-16447
- Diameters of Triton and Pluto
05 p0693 A83-16848
- Airborne spectroscopy of Jupiter in the 100- to 300/cm region - Global properties of ammonia gas and ice haze
05 p0703 A83-16961
- A spectroscopic study of the features seen in the thermal curing of the binder P-2M --- phenol formaldehyde matrix material for glass fiber reinforced plastics
05 p0619 A83-17693

Microdamage distribution in the volume of a polymer material under long-term creep 06 p0734 A83-18515

High-resolution near-infrared and millimeter-wave spectroscopy of NGC 7027 06 p0845 A83-19504

Spectroscopic detection of silylene in the infrared multiphoton decomposition of silane --- amorphous silicon film deposition chemistry 07 p0881 A83-19979

Ground-based infrared spectroscopic measurements of atmospheric hydrogen cyanide 07 p0956 A83-20212

Measurements of stratospheric ethane in the Jovian South Polar Region from infrared heterodyne spectroscopy of the nu9 band near 12 microns 07 p1031 A83-21151

Low temperature oxidation of SiC 08 p1072 A83-22259

Infrared photometry of the halo of M87 08 p1176 A83-23080

The characterization of diaminodiphenyl sulfone /DDS/ cured tetraglycidyl 4, 4'diaminodiphenyl methane /TGDDM/ epoxies 09 p1221 A83-23610

Absolute band strengths of halocarbons F-11 and F-12 in the 8- to 16-micron region 09 p1296 A83-24269

Infrared laser optogalvanic spectroscopy of molecules 09 p1227 A83-25132

Infrared spectroscopy of the sources in S235 and its implication for the line excess problem 10 p1509 A83-26371

Optical properties of the metals Al, Co, Cu, Au, Fe, Pb, Ni, Pd, Pt, Ag, Ti, and W in the infrared and far infrared 10 p1483 A83-26645

Cavity phase shift method for high reflectance measurements 11 p1572 A83-27513

Infrared absorption spectroscopy with color center lasers 11 p1653 A83-27529

Inverse Lamb dip spectroscopy using microwave modulation sidebands of CO2 laser lines 13 p1850 A83-30333

Spectroscopic measurements of carbon monoxide in the stratosphere 13 p1877 A83-30890

Isolation and molecular identification of ultramicro contaminants by Fourier transform infrared spectroscopy 13 p1848 A83-31522

Infrared heterodyne spectroscopy of seven gases in the vicinity of chlorine monoxide lines 14 p1990 A83-32915

Infrared spectroscopy of symbiotic stars and the nature of their cool components 15 p2255 A83-33835

Validated band model for NO2 molecular transmittance in the infrared 15 p2201 A83-34457

The stability of oils in aviation systems 15 p2142 A83-34499

The infrared emission spectrum of an argon plasma jet between 4 and 25 microns 15 p2236 A83-35240

Infrared absorption spectroscopy applied to stratospheric profiles of minor constituents [ONERA, TP NO. 1983-99] 16 p2380 A83-36150

Latitudinal distribution of ten stratospheric species deduced from simultaneous spectroscopic measurements 16 p2381 A83-36151

Spatially resolved tunable diode-laser absorption measurements of CO using optical stack shifting 17 p2485 A83-37747

Gas dynamics in the circumstellar Nebula on the Becklin-Neugebauer source 18 p2772 A83-39711

Total atmospheric ozone measured by ground based high resolution infrared spectra - Comparison with Dobson measurements 18 p2716 A83-39786

Atmospheric trace species measured above Haute-Provence observatory 18 p2716 A83-39788

Diffuse reflectance Fourier transform infrared spectroscopic study of chemical bonding and hydrothermal stability of an aminosilane on metal oxide surfaces 18 p2672 A83-40146

The remote monitoring of cloud cover over the ocean in the infrared spectral band 18 p2731 A83-40596

Speckle interferometry of IRC +10216 in the fundamental vibration-rotation lines of CO 20 p3060 A83-43088

External-cavity diode laser emitting in the middle infrared range 20 p2998 A83-43804

Stratospheric diffusion of active species in ozone chemistry The correspondence between the results of spectroscopic measurements and those from a numerical model [ONERA, TP NO. 1983-39] 21 p3171 A83-44317

Advances in infrared and Raman spectroscopy. Volume 9 --- Book 21 p3110 A83-45093

Measurements of minor constituents in the middle atmosphere from IR limb emission spectra - A feasibility study 22 p3328 A83-46062

Spectral pattern recognition in IR remote sensing 22 p3288 A83-46085

Effects of pressure and temperature on the physical behavior of mantle-relevant olivine, orthopyroxene and garnet. II Infrared absorption and microscopic Grueneisen parameters 22 p3332 A83-46716

Ammonium ion rotation in ammonium perchlorate as studied by infrared spectroscopy 23 p3506 A83-47631

Synthesis and thermal stability of carborane-containing phosphazenes 23 p3427 A83-47640

Detection of trace gases using high-resolution IR spectroscopy 23 p3456 A83-47776

Coherent pulse propagation in the infrared on the picosecond time scale 23 p3462 A83-48314

INFRARED STARS

Autonomous star cataloging for space surveillance missions 03 p0406 A83-13468

Prediction of infrared /IR/ celestial source counts 03 p0406 A83-13472

Infrared excesses of stars with intrinsic polarization 06 p0838 A83-19227

The polarization of the infrared cluster in Orion - The spatial distribution of the 3.8 micron polarization 07 p1023 A83-21156

The exciting stars of Herbig-Haro objects 08 p1183 A83-23056

The infrared variability and nature of symbiotic stars. II - RR Tel 09 p1362 A83-24983

Detection of large infrared polarization from L 1551 IRS 5 10 p1500 A83-25476

A two-micron survey of southern Herbig-Haro objects 10 p1492 A83-25479

Infrared spectroscopy of the sources in S235 and its implication for the line excess problem 10 p1509 A83-26371

The nature of NML Cygnus 10 p1513 A83-26719

SIS maser emission from IRC + 10 deg 216 10 p1513 A83-26720

A discussion of the infrared and radio region of the calculated spectral energy distribution of O-type stars 12 p1790 A83-28886

Two newly discovered S stars in a list of faint red objects 12 p1797 A83-29953

The dust around the carbon star IRC +10216 13 p1951 A83-31418

Measurement of the absolute monochromatic flux from Vega at 2.20 and 3.80 microns by comparison with a furnace 13 p1942 A83-31705

Stellar diameter measurements by two-aperture interferometry in the infrared 14 p2099 A83-33208

Narrow-band photometry in the 1-4 micron region - Calibration and applications 14 p2757 A83-33258

VLA positions of OH/IR stars 15 p2245 A83-33833

Far-infrared and CO observations of NGC 6357 and regions surrounding NGC 6357 and NGC 6334 17 p2591 A83-37784

Near infrared observations of some of the IRC sources 18 p2754 A83-39201

Proper motions of Herbig-Haro objects. III - HH-7 through -11, HH-12, and HH-32 18 p2757 A83-39603

Energetic molecular flows in star-forming cloud cores 18 p2773 A83-39719

The peculiar circumstellar envelope around IRC+10420 20 p3065 A83-42377

The nature of OH/IR stars. I - Infrared Mira variables 20 p3066 A83-42393

Infrared colors of the chemically peculiar stars of the upper main sequence 21 p3223 A83-44436

Speckle observations of Eta Carinae 21 p3225 A83-44762

The circumstellar dust of Mu Cephei 21 p3236 A83-45545

INFRARED TELESCOPES

Simulation of mid-infrared clutter rejection. I - One-dimensional LMS spatial filter and adaptive threshold algorithms 02 p0177 A83-12305

Test results of Spacelab 2 infrared telescope focal plane --- photoconductive detector fabrication and JFET transimpedance amplifier design 03 p0405 A83-13452

Air Force Geophysics Laboratory /AFGL/ infrared sky survey experiments 03 p0405 A83-13454

433 micron laser heterodyne observations of galactic CO from Mauna Kea 03 p0405 A83-13464

Shuttle contamination and experimentation - DoD implications 03 p0284 A83-13466

Groundbased infrared measurements using the AMOS/MOTIF facility 03 p0283 A83-13471

The Infrared Space Observatory /ISO/ - A study for a cooled telescope in space for infrared astronomy 05 p0601 A83-17429

Electromechanical device for the support of the oscillating secondary mirror of an infrared telescope 08 p1111 A83-22359

The Teal Ruby Experiment - A potpourri of advanced technology 08 p1051 A83-22607

Helium purge flow prevention of atmospheric contamination of cryogenically cooled optics on orbiting infrared telescopes 08 p1074 A83-22723

Simple infrared telescope with stray-light rejection 08 p1175 A83-22856

Bidirectional reflectance distribution function /BRDF/ measurements of sunshield and baffle materials for the Infrared Astronomy Satellite /IRAS/ telescope 08 p1167 A83-22861

Speckle interferometry in the infrared 10 p1419 A83-25835

Probability of diffraction-limited images in infrared through turbulence experimental results 10 p1420 A83-25839

Imaging by dilute apertures in the presence of atmospheric turbulence 10 p1482 A83-25840

Interferometry with the multiple mirror telescope and conventional telescopes 10 p1495 A83-25845

Infrared and submillimeter astronomy from space 10 p1497 A83-26700

An investigation of the narrow-band photometric system. I - Spectral classification 10 p1498 A83-26906

Infrared telescope in space - IRTs 11 p1670 A83-27739

GIRL - The German infrared laboratory for spacelab 11 p1670 A83-27740

Hardware development and tests in the GIRL project 11 p1670 A83-27742

The IRAS telescope 11 p1674 A83-28214

An orientation platform for a balloon-borne telescope 11 p1537 A83-28575

Performance of the Multiple Mirror Telescope (MMT). V Pointing and tracking of the MMT 13 p1937 A83-30981

Performance of the Multiple Mirror Telescope (MMT). VII Image shrinking in sub-arc second seeing at the MMT and 2.3m telescopes 13 p1919 A83-30983

Performance of the Multiple Mirror Telescope (MMT). X - The first submillimeter phased array 13 p1937 A83-30986

University of California ten meter telescope project 13 p1938 A83-30990

Infrared performance of the University of California Ten Meter Telescope 13 p1938 A83-30991

Plans for a large deployable reflector for submillimeter and infrared astronomy from space 13 p1938 A83-30995

Stressed mirror polishing experiment underway at Kitt Peak National Observatory 13 p1921 A83-31018

Cryogenic testing of mirrors for infrared space telescopes 13 p1939 A83-31026

Two-dimensional infrared speckle interferometry with a 32 x 32 InSb charge-injection device (CID) array 14 p2095 A83-31980

Cryogenic testing of stepper motors 14 p1999 A83-31982

Applications of an infrared charge-coupled device Schottky diode array in astronomical instrumentation 14 p2016 A83-31996

Cooled grating array spectrometer for 0.6-5 microns 14 p2016 A83-31998

Cryogenic infrared radiance instrument for Shuttle (CIRRIIS) telescope 14 p1983 A83-32004

A microprocessor-based position control system for a telescope secondary mirror 17 p2476 A83-37433

ESO Infrared Workshop, 2nd, Garching, West Germany, April 20-23, 1982, Proceedings 18 p2760 A83-40419

Infrared astronomy at ESO 18 p2760 A83-40420

Infrared instrumentation on Calar Alto --- mountain-based telescopes for photography 18 p2760 A83-40421

The C.F.H. telescope as an infrared telescope 18 p2760 A83-40422

The Tingo observatory --- infrared astronomy 18 p2760 A83-40423

Astronomical capability of the U.K. infrared telescope 18 p2761 A83-40424

The infrared photometer of the 2 m telescope at Pic du Midi Observatory 18 p2761 A83-40425

An F/20 millimeter photometer for tingo --- Telescopio Infrarosso Gornegrat 18 p2761 A83-40427

Reflective field optics for IR spectrophotometers 18 p2744 A83-40429

A cooled grating spectrometer for Tingo 18 p2690 A83-40430

Irspec --- cooled grating array IR spectrometer for use with New Technology Telescope 18 p2690 A83-40431

IFU - A multi-detector IR spectrometer 18 p2690 A83-40432

Cooled grating spectrometer 18 p2690 A83-40433

Future UKIRT instrumentation --- infrared telescope 18 p2690 A83-40434

An improved chopping secondary design --- of infrared telescopes 18 p2691 A83-40439

- Use of the 3.6 m telescope for millimeter observations 18 p2761 A83-40441
- Application of infrared arrays to speckle interferometry 18 p2691 A83-40445
- High sensitivity with a germanium detector in integrating mode 18 p2691 A83-40447
- Infrared array photometer 18 p2691 A83-40448
- IR-camera for GIRL --- German Infrared Laboratory 18 p2691 A83-40449
- VLT versus space --- Very Large Telescope 18 p2762 A83-40452
- Aperture synthesis in the infrared 18 p2762 A83-40453
- Astrophysics - The Airbus proposal 18 p2762 A83-40456
- Achievements and promise of balloon IR astronomy 18 p2762 A83-40458
- The scientific case and feasibility of a three metre balloon telescope 18 p2762 A83-40459
- A balloon-borne cooled telescope for far IR astronomy 18 p2762 A83-40460
- The German infrared laboratory GIRL 18 p2763 A83-40462
- SIRTF - The Shuttle Infrared Telescope Facility 18 p2763 A83-40465
- A large deployable reflector for infrared and submillimeter astronomy from space 18 p2648 A83-40466
- The ISO Michelson 18 p2648 A83-40467
- 230-271 GHz cryogenic radiometer 19 p2848 A83-41279
- Integrating and testing the thermal model of the German Infrared Laboratory (GIRL) 20 p2961 A83-43244
- Superfluid-supercritical helium tradeoff analysis for the Shuttle Infrared Telescope Facility (SIRTF) 20 p2962 A83-43245
- Instrumentation, data acquisition and reduction for a large spaceborne helium dewar 20 p2962 A83-43250
- Speckle interferometry degraded by irregular motion of a scanning telescope mirror 21 p3135 A83-44148
- Compact infrared continuous zoom telescope 21 p3139 A83-44783
- Compact refractor telescopes for the thermal infrared 22 p3357 A83-46588

INFRARED TRACKING

- Advanced terrain following radar for LANTIRN --- Low Altitude, Navigation, Targeting Infrared at Night 01 p0007 A83-11241
- Cryo-cooler development for space flight applications 03 p0303 A83-13460
- Optics in ballistic missile defense /BMD/ 03 p0392 A83-13754
- Spectral discrimination for long range search/track infrared systems 08 p1094 A83-22442
- Infrared technology for target detection and classification; Proceedings of the Meeting, San Diego, CA, August 25, 26, 1981 09 p1265 A83-23526
- Infrared target array development 09 p1204 A83-23527
- Intensity correlation techniques for passive optical device detection 09 p1266 A83-23534
- Eliminating nearest neighbor searches in estimating target orientation 09 p1204 A83-23535
- Designing for stray radiation rejection --- of heat seeking missile components 09 p1204 A83-23536
- Real-time statistical tracker for infrared /IR/ focal plane array 09 p1266 A83-23546
- Communications and tracking - Light and IR will help carry high traffic 09 p1215 A83-24354
- Algorithm development for infra-red air-to-air guidance systems - How to separate the wheat from the chaff: A simple approach to target detection 11 p1528 A83-28178
- Pulsed laser beam control by hot spot tracking 20 p2993 A83-42212
- Simulation of hot spot tracking loops [AAS PAPER 83-007] 21 p3104 A83-44166
- Detailed computer modeling of an infrared tracker using simulation of passive infrared equipment (SPIRE) techniques 22 p3292 A83-46594
- INFRARED WINDOWS**
- Emerging optical materials; Proceedings of the Conference, San Diego, CA, August 25, 26, 1981 09 p1345 A83-24951
- Development of a new family of improved infrared /IR/ dome ceramics 09 p1239 A83-24952
- Nitrogen-stabilized aluminum oxide spinel /ALON/ 09 p1345 A83-24954
- Progress in the development of ternary sulfides for use from 8 to 14 microns 09 p1345 A83-24955
- CaLa2S4 - Ceramic window material for the 8 to 14 micron region 09 p1345 A83-24957
- Gallium arsenide infrared windows for high-speed airborne applications 09 p1345 A83-24958

- New advances in chemical vapor deposited /CVD/ infrared transmitting materials 09 p1346 A83-24961
- Infrared transmitting germanate glasses 09 p1346 A83-24962
- Thermostructural evaluation of spinel infrared /IR/ domes 09 p1239 A83-24966
- Multiwavelength laser rate calorimetry on various infrared window materials 09 p1346 A83-24967
- Development of design data for rain impact damage in infrared-transmitting materials 09 p1239 A83-24968
- Calculation of absorption by wings of the H2O monomer in the 8-13 micron atmospheric window 09 p1308 A83-25062
- Mode control in a submillimetre open resonator with a variable iris 10 p1425 A83-25459
- Simultaneous measurements of sea surface temperature by GMS-1 and GMS-2 12 p1761 A83-29701
- The NH3 spectrum in Saturn's 5 micron window 15 p2274 A83-34114
- The effect of the crystallization conditions of diamonds under high-temperature shock compression on their optical properties 18 p2750 A83-39531
- High-temperature, high-pressure optical cells 20 p2959 A83-42297
- Window and mirror materials for use at 10.6 micron 21 p3144 A83-44788
- Fluoride glasses with large optical window for infrared fibers 22 p3358 A83-46625
- The Jovian spectrum in the 3-micron window 22 p3388 A83-47082
- Remote sensing of precipitable water by a thermal infrared multichannel approach [IAF PAPER 83-105] 23 p3488 A83-47268

INFRASONIC FREQUENCIES

- Atmospheric infrasound as a possible factor in the transferring of the effect of solar activity to the biosphere 02 p0221 A83-11891
- Infrasound of cosmic origin in the atmosphere 07 p0962 A83-20606
- Anomalous infrasound from Space Shuttle II and Skylab I 08 p1048 A83-22229
- A hygienic evaluation of the combined effect of infrasound and low-frequency noise on the auditory and vestibular analyzer of compressor operators 15 p2212 A83-34932
- Infrasonic and internal gravity waves in the atmosphere during large fires 23 p3485 A83-48503

INGESTION (BIOLOGY)**NT DRINKING****INGESTION (ENGINES)**

- Thrust reverser exhaust plume reingestion tests for a STOL fighter model [AIAA PAPER 83-1229] 16 p2307 A83-36293
- Space Shuttle siphon dropout prediction [AIAA PAPER 83-1383] 16 p2321 A83-36374

INGOTS

- Metallographic features of the subdendritic structure of aluminum alloy ingots 13 p1819 A83-30065
- Current aspects of the C.G.E. semicrystalline silicon ingots elaboration method 14 p2090 A83-32317
- Casting problems specific to aluminum-lithium alloys 14 p2028 A83-32879
- A comparison of microstructure and tensile properties of P/M and I/M Al-Li-X alloys --- Powder Metallurgy and Ingot Metallurgy 14 p1996 A83-32888
- Embrittlement of P/M X7091 and I/M 7175 aluminium alloys by mercury solutions 16 p2330 A83-35983

INHABITANTS**NT MOUNTAIN INHABITANTS****INHALATION****U RESPIRATION****INHIBITION**

- The characteristics, neuronal mechanisms, and functional significance of cortical inhibition 13 p1895 A83-30303

INHIBITORS**NT WEAR INHIBITORS**

- The effect of cholinesterase inhibitors on the electrically excitable membranes of frog muscle fibers 02 p0219 A83-11520
- A circulating inhibitor of /Na/ + / + K/ + / / ATPase associated with essential hypertension 05 p0672 A83-17794
- The effect of the calmodulin inhibitor, trifluoroperazine, on the calcium activation of phosphorylases in the glycosomes of the skeletal muscles in rabbits 07 p0975 A83-20981
- The inhibition characteristics of the 1 and 3 class receptor fields of the retina in frogs 08 p1144 A83-22102
- Experimental study on inhibited diffusion and premixed flames in a counterflow system 08 p1057 A83-22347
- Linkage between gravity perception and response in the grass leaf-sheath pulvinus 11 p1638 A83-27812

- Quantitation of chlorpromazine-bound calmodulin during chlorpromazine inhibition of gravitropism 11 p1638 A83-27815

- A reevaluation of the role of abscisic acid in root gravitropism 11 p1638 A83-27816
- The electrochemical aspect of the corrosion inhibitor action and ways of increasing the effectiveness of inhibitors 14 p1988 A83-32070
- The action of colyones on erythropoiesis (A quantitative evaluation) 16 p2396 A83-36841
- Catalyzed and inhibited decomposition of ammonium perchlorate 20 p2959 A83-43456
- Tetrachlorophthalicanhydride based chloropolyesters for inhibition of double rocket propellants [IAF PAPER 83-370] 23 p3439 A83-47362

INHOMOGENEITY

- Investigation of the anisotropy of ionospheric inhomogeneities by the differential-phase method 02 p0209 A83-12426
- Experimental study of the large-scale structure of inhomogeneous turbulence 04 p0475 A83-15079
- Modeling surface electromagnetic anomalies using horizontally inhomogeneous layers of finite thickness 05 p0663 A83-17618
- Diffusional transport of ionospheric irregularities 05 p0663 A83-17622
- The creep behavior of inhomogeneously aging bodies 05 p0656 A83-17774
- The singular edge in problems of diffraction by inhomogeneities with a gyrotropic medium 06 p0754 A83-19356
- Correction of pixel nonuniformities for solid-state imagers 08 p1094 A83-22441
- The variations in the spectrum of electron-density inhomogeneities in the lower ionosphere under the effect of high-power electromagnetic radiation 09 p1301 A83-23478
- The propagation of a soliton in a randomly inhomogeneous medium 09 p1336 A83-23485
- Optimization of lines with small inhomogeneities for wide-band matching 09 p1256 A83-24915
- Determination of the inhomogeneities of semiconductor materials in the infrared 18 p2744 A83-40405
- The crack problem for a nonhomogeneous plane [ASME PAPER 83-APM-35] 23 p3471 A83-48243
- Inhomogeneity effects in a gas laser 24 p3587 A83-48842

INITIAL VALUE PROBLEMS**U BOUNDARY VALUE PROBLEMS****INITIATION**

- The critical pressure of initiation of powdered explosives 06 p0726 A83-18003
- Characteristics of the initiation of fast chemical reactions in oxidizer-combustible mixtures 24 p3557 A83-49790

INITIATORS (EXPLOSIVES)**NT EXPLODING WIRES****NT PRIMERS (EXPLOSIVES)**

- A study of detonation initiation in TNT and TH 50/50 by shock waves of short duration 06 p0726 A83-18004
- The effect of the mode structure of laser radiation on the stability of lead azide 24 p3557 A83-49795

INJECTION**NT CARRIER INJECTION****NT FLUID INJECTION****NT FUEL INJECTION****NT GAS INJECTION****NT ION INJECTION****NT LIQUID INJECTION****NT SECONDARY INJECTION****NT WATER INJECTION**

- Approximate correction for the effect of injectants on the ionization level in the boundary layer of a blunt body and in its near wake 05 p0590 A83-17423
- A powder-injection shock-tube facility 10 p1380 A83-26132

INJECTION CARBURETORS**U FUEL INJECTION****INJECTION LASERS**

- Luminescence spectra of stripe-geometry laser heterostructures in GaAs-Al/x/Ga/1-x/As 02 p0183 A83-11695
- Measurement of beam parameters of index-guided and gain-guided single-frequency InGaAsP injection lasers 02 p0183 A83-11982
- Optical phase modulation in an injection locked AlGaAs semiconductor laser 02 p0184 A83-12168
- High-power multiple-stripe injection lasers with channel guides 02 p0184 A83-12269
- Narrow strip AlGaAs lasers using double current confinement 02 p0185 A83-12276
- A proposed new method for damping relaxation oscillations in laser diodes 03 p0330 A83-13560
- Development of the multiwavelength monolithic integrated fiber optics terminal 03 p0393 A83-13760

GHz bandwidth /GaAl/As semiconductor lasers and optical detectors for signal processing applications 03 p0331 A83-13766

Design approach for a thermally compensated injection laser stack transmitter/receiver 03 p0331 A83-13769

'Nonwaveguide'-mode semiconductor injection lasers 04 p0486 A83-16214

A survey of optical nonlinearities - Theory and observation in /AlGa/As injection lasers 04 p0486 A83-16216

Determination of the parameters of injection laser amplifiers based on GaAlAs heterostructures from superluminescence characteristics 05 p0649 A83-17060

Direct modulation of semiconductor injection lasers 06 p0765 A83-18762

A theoretical and experimental analysis of modulated laser fields and power spectra 06 p0766 A83-18908

Injection-locked dye laser pumped and injected by a pulsed xenon-ion laser 06 p0767 A83-19144

Single longitudinal mode operation of high power multiple-stripe injection lasers 06 p0767 A83-19256

Injection locking of wide-aperture TEA CO₂ lasers 07 p0935 A83-20151

Electronic beam steering of semiconductor injection lasers - A theoretical analysis 07 p0935 A83-20162

Theory of FM noise of single-mode injection lasers 08 p1110 A83-22919

Short-cavity single-frequency InGaAsP buried-heterostructure lasers 09 p1272 A83-24112

Single-parameter characterization of bistability in double contact injection lasers 09 p1273 A83-25285

High-frequency impedance of proton-bombarded injection lasers 10 p1429 A83-26071

Semiconductor lasers 11 p1576 A83-27502

Injection locking of excimer lasers 11 p1577 A83-27518

Optimal design of Pb/1-x/Sn/x/Te double heterostructure injection lasers 11 p1583 A83-27622

CW operation of an injection ring laser 11 p1585 A83-28673

Bistable operation of a semiconductor laser 11 p1585 A83-28674

Static model of DH laser 12 p1732 A83-29417

Microwave circuit models of semiconductor injection lasers 13 p1849 A83-30232

Physical nature of the degradation of light emitting diodes and semiconductor lasers 13 p1849 A83-30261

Phase-locked (GaAl)As laser emitting 1.5 W CW per mirror 13 p1850 A83-30330

Injection gas electronics --- Russian book 13 p1832 A83-30523

Bistable operation and nonuniform output in an injection heterostructure laser 13 p1851 A83-30907

Passive mode locking of buried heterostructure lasers with nonuniform current injection 13 p1852 A83-31057

New mechanism for bistable operation of closely coupled twin stripe lasers 13 p1858 A83-31783

Actively coupled index-guided lasers 14 p2024 A83-32448

Short cavity InGaAsP/InP lasers with dielectric mirrors 14 p2027 A83-33436

New large optical cavity laser with distributed active layers 14 p2027 A83-33437

Single-mode operation of Doppler-broadened lasers by injection locking 15 p2167 A83-33761

Complete experimental evaluation of the carrier dependence of the refractive index from the frequency modulation spectra of single mode injection lasers 15 p2168 A83-33841

Long pulse excimer laser excited by sequenced discharges 16 p2359 A83-35956

Current injection in multiquantum well lasers 16 p2359 A83-35958

Scaling laws for the intrapulse frequency stability of an injection mode selected TEA CO₂ laser 16 p2360 A83-35961

Mode selection and frequency tuning by injection in pulsed TEA-CO₂ lasers 16 p2360 A83-35963

Microwave signal generation with injection-locked laser diodes 17 p2515 A83-38887

Breathing, spiking and chaos in a laser with injected signal 17 p2515 A83-38975

Phase-locked InGaAsP laser array with diffraction coupling 18 p2693 A83-40051

Effect of temporal nonstationarity on the spectrum of injection lasers 19 p2852 A83-40940

Radiative characteristics of injection lasers with short resonators 20 p2996 A83-43788

Wavelength tuning of GaInAsP/InP integrated laser with butt-jointed built-in distributed Bragg reflector 21 p3145 A83-44952

Generation of single-longitudinal-mode gigabit-rate optical pulses from semiconductor lasers through harmonic-frequency sinusoidal modulation 21 p3145 A83-44956

Gigabit optical pulse generations in integrated lasers 22 p3298 A83-46681

Longitudinal mode spectrum of GaAs injection lasers under high-frequency microwave modulation 24 p3586 A83-48780

Semiconductor optoelectronic devices for free-space optical communications 24 p3573 A83-48993

Picosecond spectra of gain-switched quaternary lasers 24 p3589 A83-49612

Chirped picosecond injection laser pulse transmission in single-mode fibres in the minimum chromatic dispersion region 24 p3630 A83-49988

Optical injection locking of X-band FET oscillator using coherent mixing of GaAlAs lasers 24 p3630 A83-49991

INJECTION MOLDING

Joining of components moulded in carbon fibre-reinforced thermoplastics 06 p0724 A83-17963

Injection molding ceramics 08 p1111 A83-22255

Effects of processing on the mechanical properties of carbon short-fiber reinforced polycarbonate 08 p1055 A83-22718

Injection molding ceramics to high green densities 15 p2170 A83-33515

Microstructure and properties of injection molded conductive plastics 21 p3106 A83-44059

A preliminary study of composite reaction injection molding 22 p3263 A83-46287

Time dependent properties of injection moulded composites 22 p3263 A83-46293

Rheology of reinforced thermoplastics and its application to injection-molding. IV - Transient injection capillary flow and injection-molding 22 p3265 A83-46901

Fabrication of complex shaped ceramic articles by slip casting and injection molding 23 p3466 A83-48306

INJECTORS

NT VORTEX INJECTORS

Effect of broad properties fuel on injector performance in a reverse flow combustor [AIAA PAPER 83-0154] 07 p0867 A83-21079

Further study on the prediction of liquid fuel spray capture by v-gutter downstream of a plain orifice injector under uniform cross air flow 16 p2351 A83-35810

LOX/hydrocarbon injector performance [AIAA PAPER 83-1390] 16 p2322 A83-36380

INJURIES

NT BACK INJURIES

NT BAROTRAUMA

NT BRAIN DAMAGE

NT BURNS (INJURIES)

NT CRASH INJURIES

NT EJECTION INJURIES

NT FROSTBITE

NT LESIONS

NT NOISE INJURIES

NT PARACHUTING INJURY

NT PARALYSIS

NT PULMONARY LESIONS

NT RADIATION INJURIES

A comparative analysis of the movement of traumatized and healthy extremities during running on a treadmill 01 p0083 A83-10521

The treatment of trauma of the locomotor system in athletes /Study of the work of the athletic clinic for trauma in Austria/ 01 p0084 A83-11385

Role of impact velocity and chest compression in thoracic injury 06 p0794 A83-18189

The pathology of the immune system during injury 14 p2066 A83-33327

The role of free fatty acids in the accumulation of thrombocytes and the development of myocardial injuries during prolonged adrenalin administration 17 p2555 A83-37237

The humoral immune response after injuries of various severities 23 p3496 A83-48675

INLAND WATERS

NT GROUND WATER

Assessment of sedimentation in the Aswan reservoir using Landsat imagery 09 p1288 A83-24586

Passive bathymetric measurements of inland waters with an airborne multi-spectral scanner 09 p1290 A83-24607

Hydrological analysis of the Machar region based on Landsat satellite processed data 09 p1291 A83-24623

Some ground truth considerations in inland water quality surveys 20 p3010 A83-42960

Modeling inland water quality using Landsat data 23 p3475 A83-47223

INLET AIRFRAME CONFIGURATIONS

Problems concerning the external aerodynamics of air-breathing missiles [ONERA, TP NO. 1982-93] 03 p0279 A83-14542

Analysis of complex inlet configurations using a higher-order panel method [AIAA PAPER 83-1828] 17 p2455 A83-38659

INLET FLOW

Assessment of inflow control structure effectiveness and design system development 03 p0281 A83-13161

Effects of approaching flow types on the performances of straight conical diffusers 03 p0316 A83-13565

Inflow disk generator for open-cycle MHD power generation 04 p0538 A83-16104

Mechanisms of inlet-vortex formation 04 p0479 A83-16260

Numerical simulation of near-critical and unsteady subcritical inlet flow fields [AIAA PAPER 83-0175] 05 p0580 A83-16570

Experimental study of flows in a two-dimensional inlet model [AIAA PAPER 83-0176] 05 p0581 A83-16571

Confined swirling flow predictions [AIAA PAPER 83-0316] 05 p0634 A83-16646

Performance prediction of high inlet blockage diffusers [AIAA PAPER 83-0466] 05 p0636 A83-16733

Flow fields and aerodynamic characteristics for hypersonic missiles with mid-fuselage inlets [AIAA PAPER 83-0542] 05 p0587 A83-16777

Strut or guide vane secondary flows and their effect on turbomachinery noise 06 p0807 A83-18414

Self-excited wave oscillations in a water table 08 p1084 A83-22133

A method of predicting unsteady turbulent flows and its application to diffusers with unsteady inlet conditions [AIAA PAPER 82-0349] 09 p1198 A83-24660

Sensitivity of chamber turbulence to intake flows in axisymmetric reciprocating engines 09 p1207 A83-24677

Experimental investigation of geometry and flow effects on acoustic radiation from duct inlets [AIAA PAPER 83-0713] 11 p1651 A83-28012

A study of flow in a short cavity with one-way fluid inlet and outlet 11 p1570 A83-28794

Nonsimilar boundary layers on the leeside of cones at incidence 13 p1804 A83-31591

An axisymmetric nacelle and turbo-prop inlet analysis including power simulation 14 p1970 A83-32584

Investigation of the combined regulation of the intermediate stage of a centrifugal compressor by an axial regulating apparatus and a two-row diffuser 14 p2028 A83-33149

Critical flashing flows in nozzles with subcooled inlet conditions 15 p2157 A83-33996

A finite hybrid numerical analysis of the internal and external transonic flow fields of inlets 16 p2289 A83-35814

A study of lean extinction limit for pilot flame holder 16 p2325 A83-35821

Applications of computational techniques in the design of ramjet engines 16 p2290 A83-35828

The prediction of performance of turbojet engine with distorted inlet flow and its experimental studies 16 p2303 A83-35832

Axisymmetric flow in front of a transonic compressor with unique incidence condition [ONERA, TP NO. 1983-51] 16 p2290 A83-35835

Variation of rotor blade vibration due to interaction of inlet and outlet distortion 16 p2305 A83-35882

Calculation of a simulated 3-D high speed inlet using the Navier-Stokes equations 16 p2293 A83-36255

[AIAA PAPER 83-1165] 16 p2293 A83-36255

An inlet system installed performance prediction program using simplified modeling [AIAA PAPER 83-1167] 16 p2293 A83-36256

Effects of interstage diffuser flow distortion on the performance of a 15.41-centimeter tip diameter axial power turbine [AIAA PAPER 83-1179] 16 p2307 A83-36263

Importance of inlet boundary conditions for numerical simulation of combustor flows [AIAA PAPER 83-1263] 16 p2308 A83-36314

Progress toward the analysis of supersonic inlet flows [AIAA PAPER 83-1371] 16 p2295 A83-36366

Three-dimensional transonic nacelle/inlet flowfield computations using an efficient approximate factorization algorithm [AIAA PAPER 83-1417] 16 p2295 A83-36401

Response of a supersonic inlet to downstream perturbations [AIAA PAPER 83-2017] 16 p2296 A83-36403

Experimental evaluation of inlet turbulence, wall boundary layer, surface finish, and fillet radius on small axial turbine state performance [SAE PAPER 821475] 17 p2469 A83-38001

- Analysis of complex inlet configurations using a higher-order panel method
[AIAA PAPER 83-1828] 17 p2455 A83-38659
- Calculation of axisymmetric inlet flowfield using the Euler equations
[AIAA PAPER 83-1853] 17 p2457 A83-38681
- Supercritical inlet design
[AIAA PAPER 83-1866] 17 p2457 A83-38693
- Determining compressor-inlet airflow in the compact multimission aircraft propulsion simulators in wind-tunnel applications
[AIAA PAPER 83-1231] 18 p2642 A83-39104
- Numerical solution of the Navier-Stokes equations for compressible turbulent two/three dimensional flows in the terminal shock region of an inlet/diffuser
[AIAA PAPER 83-1892] 18 p2634 A83-39358
- Axisymmetric nose inlet effects on supersonic airloads
18 p2638 A83-40008
- Calculation of various diffuser flows with inlet swirl and inlet distortion effects
19 p2789 A83-40863
- The calculation of planar inlet flows --- German thesis
19 p2844 A83-41809
- Determination of full pressure losses in stepped annular diffusers with rectilinear outer walls and a uniform velocity field at the inlet
19 p2800 A83-42130
- Flow visualization investigation of choking cascade turns
20 p2989 A83-42564
- Experiments on flow through one to four inlets of the orifice and Borda type
20 p2986 A83-43235
- Maldistributed inlet flow effects on turbulent heat transfer and pressure drop in a flat rectangular duct
20 p2986 A83-43363
- Aerodynamic performance of a fan stage utilizing variable inlet guide vanes (VIGV's) for thrust modulation --- subsonic V/STOL aircraft
[AIAA PAPER 83-1162] 21 p3088 A83-45508
- Dynamic distortion in a short s-shaped subsonic diffuser with flow separation --- Lewis 8 by 6 foot Supersonic Wind Tunnel
[AIAA PAPER 83-1412] 21 p3092 A83-45515
- Low speed performance of a supersonic axisymmetric mixed compression inlet with auxiliary inlets
[AIAA PAPER 83-1414] 21 p3088 A83-45516
- The design of optimum diffusers for incompressible flow
22 p3250 A83-46480
- Numerical computation of laminar steady-state inlet-aperture flow and the evolving flow after an embankment
22 p3284 A83-46493
- A compact diffuser system for annular combustors
[ASME PAPER 83-GT-43] 23 p3407 A83-47903
- Flow in a turbine cascade. I - Losses and leading-edge effects
[ASME PAPER 83-GT-68] 23 p3395 A83-47921
- Solution of particulate viscous flow in a radial inflow turbine
[ASME PAPER 83-GT-75] 23 p3395 A83-47928
- Optimization of the three-dimensional flow path in the scroll-nozzle system of a radial inflow turbine
[ASME PAPER 83-GT-127] 23 p3396 A83-47956
- Three-dimensional flow measurements in a turbine scroll
[ASME PAPER 83-GT-128] 23 p3396 A83-47957
- Laminar flow in the entrance region of elliptical ducts
[ASME PAPER 83-FE-1] 23 p3449 A83-48226
- Hydrodynamic visualization of the flow phenomena characterizing air intakes
[ONERA, TP NO. 1983-103] 24 p3583 A83-49414
- INLET NOZZLES**
Cast titanium inlet duct development
[AIAA 83-0951] 12 p1695 A83-29776
- Three-dimensional flow measurements in a turbine scroll
[ASME PAPER 83-GT-128] 23 p3396 A83-47957
- INLET PRESSURE**
Choice of the optimal system of shock waves in the inlet part of the diffuser of a supersonic centrifugal compressor
08 p1043 A83-32223
- Aircraft engine inlet pressure distortion testing in a ground test facility
[AIAA PAPER 83-1233] 16 p2307 A83-36296
- INLET TEMPERATURE**
Combined free and forced laminar convection in a vertical channel
15 p2160 A83-34257
- A study of the response of a turbojet engine to the inlet temperature transients
16 p2304 A83-35849
- Analytical and experimental study of flow through an axial turbine stage with a nonuniform inlet radial temperature profile
[AIAA PAPER 83-1175] 21 p3088 A83-45510
- The influence of inlet temperature on energy-separation effects in vortex thermal-transformers
24 p3576 A83-48939
- INLETS (DEVICES)**
U INTAKE SYSTEMS

INNER RADIATION BELT

- The stochastic instability of high-energy protons of the inner radiation belt at low altitudes
18 p2786 A83-39314
- Observations of VLF transmitter-induced depletions of inner zone electrons
20 p3024 A83-43189
- The drift of the Brazilian anomaly
21 p3176 A83-45255

INORGANIC CHEMISTRY

- Inorganic chemistry of earliest sediments - Bioinorganic chemical aspects of the origin and evolution of life
13 p1899 A83-31158

INORGANIC COATINGS

- NT ANODIC COATINGS
NT CERAMIC COATINGS
Inorganic thermal control coatings - A review
[AIAA PAPER 83-0074] 05 p0617 A83-16504
- Phase genesis in heterogeneous inorganic coatings obtained by suspension baking
07 p0873 A83-20678

INORGANIC COMPOUNDS

- NT AMMONIA
The features of the atomic structure of pure inorganic ferroelastics
13 p1928 A83-30311
- Characteristics of the anisotropy of the polarizability of molecules --- Russian book
15 p2227 A83-34700

INORGANIC NITRATES

- NT AMMONIUM NITRATES

INORGANIC PEROXIDES

- NT HYDROGEN PEROXIDE
The characterization of carbon dioxide absorbing agents for life support equipment; Proceedings of the Winter Annual Meeting, Phoenix, AZ, November 14-19, 1982
11 p1644 A83-28329
- Carbon dioxide scrubbing materials in life support equipment
11 p1644 A83-28330
- Review of potassium superoxide characteristics and applications
11 p1644 A83-28331
- PAN concentrations in ambient air in New Jersey
22 p3321 A83-46900

INORGANIC SULFIDES

- NT BISMUTH SULFIDES
NT CADMIUM SULFIDES
NT CALCIUM SULFIDES
NT COPPER SULFIDES
NT HYDROGEN SULFIDE
NT INDIUM SULFIDES
NT LEAD SULFIDES
NT MOLYBDENUM DISULFIDES
NT MOLYBDENUM SULFIDES
NT POLYSULFIDES
NT WURTZITE
NT ZINC SULFIDES
NT ZINBLENDE
- Antimony sulphide thin films
14 p2090 A83-32306
- Temperature effects in AgGaS₂ nonlinear devices
21 p3143 A83-44158
- The metal-insulator transition in oxides and sulfides of 3d metals
24 p3635 A83-49075
- Surface modification of polycrystalline p-CuInS₂ and p-CuSe₂ electrodes for improved solar cell performance
24 p3601 A83-50177

INPUT

- A globally stable adaptive controller for multivariable systems
09 p1332 A83-24789
- Influence of signal level quantization at the input of a beam-forming system on the noise immunity of the receiving section
10 p1404 A83-26289
- New results for the joint input-output identification method
10 p1466 A83-26537
- Optimal input/output feedback with structure constraints
13 p1911 A83-31356
- A novel feedforward compensation canceling input filter-regulator interaction
14 p2007 A83-33133
- Detectors for multinomial input --- for signal detection
14 p2002 A83-33135

INPUT/OUTPUT ROUTINES

- Matrix analysis of mildly nonlinear, multiple-input, multiple-output systems with memory
04 p0474 A83-16322

INSAT SATELLITES

- U INDIAN SPACECRAFT

INSECT DAMAGE

- U INFESTATION

INSECTS

- NT BEETLES
NT DROSOPHILA
NT GRASSHOPPERS
NT LOCUSTS
- An evolutionary model for the insect vitellins
01 p0081 A83-11034
- Gravity receptors in a microcrustacean water flea - Sensitivity of antennal-socket setae in Daphnia magna
11 p1639 A83-27823

INSENSITIVITY

- U SENSITIVITY

INSERTION

- Robotics for assembly - Design of a feedback sensor, and its use in general insertion procedures --- French thesis
02 p0229 A83-11767

INSERTION LOSS

- Curved dielectric optical waveguides with reduced transition losses
02 p0235 A83-12005
- Practical millimeter-wave ferrite phase shifters
05 p0625 A83-17342
- Optimized low-insertion-loss millimeter-wave fin-line and metal insert filters
07 p0919 A83-20178
- Dual GRIN lens wavelength multiplexer --- Graded Refractive Index
07 p0993 A83-20831
- Monolithic GaAs interdigitated couplers
09 p1256 A83-24683
- Optimized waveguide E-plane metal insert filters for millimeter-wave applications
10 p1410 A83-26342
- Barrier insertion loss versus Fresnel number and secondary parameters
11 p1652 A83-28187
- New phase-shifting technique for group-type unidirectional transducers used in surface-acoustic-wave filters
16 p2347 A83-36482
- Radiation losses of E-plane groove-guide bends
18 p2679 A83-40390
- Low insertion-loss, temperature-compensated dielectric filters for microwave integrated circuits
18 p2679 A83-40393
- Measured temperature-dependence of attenuation constant and phase velocity of a superconducting PbAu/SiO₂/Pb microstripline at 10 GHz and 30 GHz
19 p2838 A83-41093
- Small-radii curved rib waveguides in GaAs/GaAlAs using electron-beam lithography
21 p3205 A83-44222
- Ka-band y-circulators in integrated waveguide technology
21 p3125 A83-44955
- Improved feed network for group-type unidirectional transducers
21 p3126 A83-44960
- Acoustic surface wave band filters with weighted fan transducers
23 p3445 A83-47569
- Monomode-polarization-maintaining fiber directional couplers
24 p3628 A83-48857
- Chirped grating lenses on Nb₂O₅ transition waveguides
24 p3629 A83-49020

INSERTS

- NT NOZZLE INSERTS
Photoelastic stress analysis of epoxy resin having an inserted metal. I - Residual stress caused by curing
05 p0611 A83-17096
- Joining of components moulded in carbon fibre-reinforced thermoplastics
06 p0724 A83-17963

INSOLATION

- Further developments of a general method for deducing average hourly insulations from average daily insulations
02 p0203 A83-11845
- Effect of off-south orientation on the performance of collector reflector system in India
03 p0355 A83-14671
- A comment on the insolation at Mercury
05 p0704 A83-16971
- A parameterized model for global insolation under partially cloudy skies
06 p0792 A83-18552
- The insolation at Pluto
08 p1189 A83-22939
- On insolation measurements using pyranometers and solar cell devices
11 p1607 A83-27238
- A probability density function for the clearness index, with applications
12 p1749 A83-28938
- Use of some simple statistical models in solar meteorology
12 p1757 A83-28944
- Determination of surface global radiation using Meteosat images and ground based visibility measurements
12 p1760 A83-29681
- Preliminary research in the measurement of the solar radiation by transient technique
13 p1848 A83-31608
- A simple hourly clear-sky solar radiation model based on meteorological parameters
13 p1894 A83-31611
- Diffuse and global solar spectral irradiance under cloudless skies
13 p1882 A83-31613
- AM/PM - The rating system for photovoltaic modules --- standard based on whole day insolation
14 p2040 A83-32223
- Solar-radiation transfer in the atmosphere in the presence of semitransparent clouds --- satellite multispectral photography
14 p2035 A83-32500
- Correlations of solar insolation and wind data for SOLMET stations
15 p2197 A83-33991
- The effect of orbital element variations on the mean seasonal daily insolation on Mars
16 p2426 A83-36788
- Improvements to a simple physical model for estimating insolation from GOES data
18 p2723 A83-39144
- Predicting daily insolation with hourly cloud height and coverage
18 p2724 A83-39677
- Instrumental effects on the sunshine record
18 p2727 A83-39888

- Orbital forcing of the inception of the Laurentide ice sheet? 18 p2718 A83-39960
- Measurement and analysis of solar radiation data 18 p2719 A83-40521
- The oblateness effect on the extraterrestrial solar radiation 19 p2864 A83-40769
- Analysis of solar-radiation characteristics at the EURELIOS power plant of Adrano 19 p2862 A83-41165
- Detection of a corner reflector with isonification at angles greater than 45 deg 20 p3000 A83-43183
- Statistical comparison of models for estimating solar radiation on inclined surfaces 21 p3166 A83-43899
- Limit of concentration under extended nonhomogeneous light sources 22 p3318 A83-46090
- Evaporation-limited tropical temperatures as a constraint on climate sensitivity 22 p3340 A83-46847
- The effect of atmospheric attenuators with structured vertical distributions on air mass determinations and Langley plot analyses 22 p3341 A83-46858
- An estimate of the solar radiation incident at the top of Pluto's atmosphere 23 p3529 A83-48053
- The hot spot effect of a homogeneous vegetative cover 23 p3476 A83-48113
- Solar insolation upon the Yemen Arab Republic 24 p3608 A83-49623

INSPECTION

- NT INFRARED INSPECTION
- NT X RAY INSPECTION
- Magnetic inspection of the quality of surface hardening of teeth of large gears 01 p0057 A83-10367
- Signal classification for automatic industrial inspection 01 p0029 A83-11442
- Effect of surface roughness of object on amplitude fluctuation of recorded signals during inspection by the shadow method with immersion 03 p0338 A83-14296
- Increased reliability - A critical NDE research goal 04 p0488 A83-15152
- New radiographic inspection system 07 p0941 A83-20173
- A three-dimensional pattern recognition technique for inspection of missing parts in assemblies 07 p0942 A83-20452
- Official liability for insufficient airworthiness - Comments in connection with a supreme-court decision 08 p1171 A83-21898
- A unit for combined inspection of large multilayer parts of composite polymer materials 08 p1113 A83-22401
- Ultrasonic examination of weldments 22 p3303 A83-45726
- Estimating the inspection survivability 23 p3467 A83-47616

INSTABILITY

U STABILITY

INSTALLATION

U INSTALLING

INSTALLING

- Photovoltaic energy systems: Design and installation --- Book 20 p3011 A83-42175

INSTANTONS

- Dynamics of the textures of the order parameter in superfluid He-3 19 p2904 A83-40996

INSTRUCTION SETS (COMPUTERS)

- Some aspects of multimicroprocessor systems 06 p0802 A83-18347
- Program implementation in the application software package NOLINEAR 12 p1768 A83-29541

INSTRUCTIONS

U EDUCATION

INSTRUMENT APPROACH

- Helicopter IFR approaches into major terminals using RNAV, MLS, and CDTI 19 p2794 A83-41042
- Instrument-approach technique for poor-visibility landings 19 p2795 A83-41228

INSTRUMENT COMPENSATION

NT TEMPERATURE COMPENSATION

- Gravity modeling for airborne applications 01 p0004 A83-11090
- Compensation electronics for staring focal plane arrays 03 p0326 A83-13734
- Compensation of scanner error 04 p0482 A83-15917
- Holographic aberration compensation with partially coherent light 05 p0643 A83-16834
- Compensation technique for force balance devices 07 p0929 A83-20548
- A cooled pyrreheliometer with automatic compensation 07 p0931 A83-20964
- Drift compensation in a mosaic sensor 08 p1103 A83-22839
- Smear compensation for a pushbroom scan --- in satellite observations of earth 09 p1218 A83-23545

Dynamic analysis of a precision servosystem for the stabilization of astrophysical instrumentation 10 p1383 A83-25329

High accuracy measurement of the instrumental polarization of the solar coudetelescope at the Okayama Astrophysical Observatory 16 p2423 A83-35684

Design and adjustment of polarization compensators for coudeoptics of stellar telescopes 16 p2423 A83-35686

The effect of self-heating on the dynamical response of bolometric detectors 17 p2513 A83-38862

Reducing errors in single-degree-of-freedom gyroscopes 21 p3137 A83-44633

Optimal properties of a system of single interperiod compensation --- target detection in correlated noise 21 p3120 A83-44776

New developments in foil strain-gage transducers 21 p3141 A83-45151

Laboratory evaluation of an airborne ozone instrument that compensates for altitude/sensitivity effects 21 p3092 A83-45618

Comment on 'Laboratory Evaluation of an airborne ozone instrument that compensates for altitude/sensitivity effects' 22 p3287 A83-45925

On the instrumental and atmospheric stray-light for solar observations 23 p3517 A83-47717

An axial meridian circle 24 p3645 A83-49640

Sparse field stellar photometry 24 p3647 A83-50002

Relativistic reductions for radiointerferometric observables 24 p3649 A83-50151

INSTRUMENT DRIFT

U DRIFT (INSTRUMENTATION)

INSTRUMENT ERRORS

- Effects of thermal noise and interference due to scatterers on VOR system accuracy 01 p0004 A83-11092
- High accuracy digital sensor 01 p0053 A83-11118
- Mechanically dithered RLG at the quantum limit --- Ring Laser Gyro 01 p0053 A83-11130
- Possible systematic errors in OVM pendulum apparatus 02 p0177 A83-11955
- Properties and performance of grazing incidence reflectors --- optical system errors due to synchrotron radiation 02 p0237 A83-12694
- Introduction to precision machining of metal optics 02 p0239 A83-12719
- A special silicon diaphragm pressure sensor with high output and high accuracy 02 p0180 A83-12811
- Direct measurement of laser velocimeter bias errors in a turbulent flow 03 p0323 A83-13139
- General contamination criteria for optical surfaces --- instrument performance losses in spaceborne conditions 03 p0287 A83-13743
- Phase-locked loops used with masers - Atomic frequency standards 03 p0331 A83-13865
- Capabilities and limitations of atmospheric transmission field measurement systems 03 p0359 A83-13995
- Performance and temperature stability of an air mass flowmeter based on a self-heated thermistor 04 p0481 A83-15100
- BSO/fibre-optic voltmeter with excellent temperature stability 04 p0481 A83-15250
- Compensation of scanner error 04 p0482 A83-15917
- A new technique for the precision DME of microwave landing system 04 p0445 A83-16448
- The effect of some systematic errors on the determination of time and latitude, and group corrections 05 p0693 A83-16858
- Concerning the measurement of aircraft acceleration 05 p0595 A83-16876
- The effect of hysteretic friction on the errors of gyroinstruments 06 p0764 A83-19181
- A technique for reducing low-frequency, time-dependent errors present in network-type surveys --- magnetic and gravity drift corrections 07 p0957 A83-19872
- Two-phase frequency-conversion type spectrum analyzer for low-frequency noise measurement 07 p0929 A83-20547
- A critical evaluation of the aerodynamic error of a turbulence instrument 07 p0930 A83-20804
- Maximum precision of the measurement of gravity gradients 07 p0989 A83-20854
- Effect of misaligned ultrasonic transducers on parameters of the shadow inspection method 07 p0932 A83-21412
- Errors in scatterometer-radiometer wind measurement due to rain 08 p1101 A83-22721
- High-sensitivity resistivity technique for studies of defect behavior 08 p1106 A83-23234
- Precision distance measurements in and between satellites 09 p1214 A83-23586
- Precision optical encoder 09 p1267 A83-23588

Discrepancies between balloon-borne IR atmospheric spectra and corresponding synthetic spectra calculated line by line around 825 per cm 09 p1306 A83-24440

Navstar equipments accuracy compared with experimental results 09 p1201 A83-24861

Experiments of Omega for aviation 09 p1201 A83-24862

An algorithm for determining the slope of sensors in measurements of the range and velocity of the relative motions of two satellites 09 p1215 A83-25031

Assessment of the accuracy of electron-temperature measurements by a high-frequency probe 10 p1386 A83-25340

An algorithm for detecting hardware errors in the data of supermonitors --- of cosmic ray parameters 10 p1420 A83-26104

Multiconfiguration Kalman filter design for high-performance GPS navigation 10 p1373 A83-26262

An azimuth rate inertial navigation system 10 p1382 A83-26768

Large symmetric pi transformations for Hadamard transforms 10 p1406 A83-26865

Double Schottky-barrier diode power sensor 11 p1560 A83-27894

Errors due to transverse sensitivity in strain gages 11 p1573 A83-28077

An estimate of the errors in measurements of the electron concentration in the ionosphere made with a high-frequency impedance probe 11 p1575 A83-28752

Accuracy of an optical open area radiometer 12 p1729 A83-29147

A lab test to find the major error sources in a laser strapdown inertial navigator 12 p1706 A83-29211

Errors of a biaxial gyrostabilizer under random vibrations of the base 12 p1729 A83-29321

The design of an automated, high-accuracy antenna test facility 13 p1829 A83-31280

Sampling rate and peak detection requirements for digital shock response spectra calculations 13 p1848 A83-31497

The field error and photometric system of the double long-focus astrophotograph of the Main Astronomical Observatory of the Academy of Sciences of the Ukrainian SSR 14 p2095 A83-31840

Applications of an orbiting gravity gradiometer 14 p1983 A83-31900

Probe-shift error in remote diagnostics of volume-radiation sources [AIAA PAPER 83-1541] 14 p2011 A83-32765

High-accuracy wave-number measurements in molecular iodine 15 p2227 A83-33762

Surface temperature measurement errors 15 p2163 A83-33995

The effect of contamination of the probe surface and coating on the accuracy of the measurement of electron temperature using the Langmuir probe --- in satellite and rocket experiments 15 p2128 A83-34420

Monostatic diffraction-limited lidars - The impact of optical refractive turbulence 15 p2164 A83-34465

The effect of certain fabrication factors on the errors of a dynamically tuned gyroscope with a displaced center of mass 15 p2167 A83-35264

Minimization of a class of temperature errors of float-type gyroinstruments 15 p2167 A83-35268

The design of optimum remote-sensing instruments 15 p2167 A83-35294

Effects of detector coil size and configuration on measurements of the magnetoencephalogram 16 p2401 A83-35452

PMC 190 - A new Photoelectric Meridian Circle of Tokyo Astronomical Observatory. I - Determination of instrumental errors. II - Pinhole system for solar and lunar observations. 16 p2422 A83-35677

Simple corrections for the temperature sensitivity of hot wires 17 p2509 A83-37000

Wheel-speed induced errors in the use of dry-tuned gyros 17 p2509 A83-37156

Testing of a five-channel spectrophotometer on the AZT-8 telescope 17 p2590 A83-37695

Corrections for the gravitational deflection of light in the case of observations with an astrolabe 17 p2594 A83-38406

Instrumental effects on the sunshine record 18 p2727 A83-39888

Estimation of the polarization errors of monopulse direction-finders 18 p2675 A83-40089

The ISO Michelson 18 p2648 A83-40467

High-precision test of the universality of the Josephson voltage-frequency relation 19 p2837 A83-40959

Measuring laser flow fields with a 64-channel heterodyne interferometer 19 p2847 A83-41102

Floated gyro dynamical behavior during slow testing [AIAA PAPER 83-2182] 19 p2848 A83-41674

- Analysis of instrument errors arising in velocity measurement by an LDV based on a Fabry-Perot interferometer 19 p2849 A83-41900
- Errors of a three-axis unit of laser gyroscopes with common initial displacement 19 p2850 A83-42018
- Scattering from a V-shaped groove in the resonance domain --- optical measurement for comparison with theoretical prediction 20 p3046 A83-42215
- Techniques for measuring radiance in sea and air 20 p2988 A83-42216
- Wavelength precision of a Cary model 14R spectrophotometer 20 p2988 A83-42218
- Measurements on the accuracy of pyranometers 21 p3135 A83-43897
- Selecting measurements and controls in log problems 21 p3192 A83-44004
- Speckle interferometry degraded by irregular motion of a scanning telescope mirror 21 p3135 A83-44148
- The solar optical telescope control system [AAS PAPER 83-005] 21 p3104 A83-44164
- Image motion compensation for the OSS-3/7 telescopes [AAS PAPER 83-006] 21 p3104 A83-44165
- Propagation effect on interferometer 21 p3222 A83-44292
- Measurements of cosmic-radiation absolute ionization in the atmosphere 21 p3244 A83-44304
- The effect of manufacturing imperfections on the accuracy of inertial navigation systems 21 p3097 A83-44631
- Reducing errors in single-degree-of-freedom gyroscopes 21 p3137 A83-44633
- A study of the moment of elastic unbalance in a gyroscopic instrument in the case of the main resonance 21 p3138 A83-44640
- X-ray interferometer calibration of microdisplacement transducers 21 p3140 A83-44949
- Metrological investigations and problems in the verification of meteorological equipment 21 p3181 A83-45022
- A simple lower bound on the linearized performance of practical symbol synchronizers 22 p3272 A83-45736
- Horizon sensor errors calculated by computer models compared with errors measured in orbit 22 p3261 A83-46600
- Effect of optical aberrations on scanning Michelson interferometers 22 p3292 A83-46601
- Simplified calculation of the effects of jitter on clutter leakage --- performance prediction of mosaic infrared sensor 22 p3294 A83-46830
- The effects of target-induced speckle, atmospheric turbulence, and beam pointing jitter on the errors in remote sensing measurements 23 p3457 A83-47786
- Assessment of dynamic errors in the measurement of the solar constant 24 p3598 A83-49288
- Sparse field stellar photometry 24 p3647 A83-50002

INSTRUMENT FLIGHT RULES

- A concept for reducing helicopter IFR landing weather minimums - Offshore 02 p0133 A83-12099
- The role of simulation in general aviation 05 p0671 A83-17307
- A concept for reducing helicopter IFR landing weather minimums - Onshore 07 p0865 A83-21034
- Helicopter IFR - The economics of schedule regularity [SAE PAPER 821501] 17 p2459 A83-38009
- Radio-navigation prerequisites for IFR operation of regional airports and civil airfields 17 p2461 A83-38932
- Helicopter IFR approaches into major terminals using RNAV, MLS, and CDTI 19 p2794 A83-41042
- Ground simulation investigation of helicopter decelerating instrument approaches 21 p3090 A83-45461
- The emerging need for improved helicopter navigation 22 p3252 A83-46930

INSTRUMENT LANDING SYSTEMS

- NT ALL-WEATHER LANDING SYSTEMS
- NT AUTOMATIC LANDING CONTROL
- General conditions of operational and technical utilization of ILS during Category III operations 02 p0134 A83-13008
- Instrument Landing Systems /ILS/ at GDR airports. II 09 p1200 A83-23495
- Nonlinear filter for pilot's remnant attenuation 09 p1209 A83-24436
- Study of an on-board trajectography system for in-flight checking of air-navigation and landing radio aids 09 p1201 A83-24860
- Advances related to the measurement and representation of real multipath propagation --- for radio navigation and instrument landing applications 10 p1374 A83-26485
- Operation of ILS during snow and ice conditions 11 p1527 A83-27969

- Improvement of the measurement system for the survey of class-II ILS installations 21 p3090 A83-45401
- A new generation of navigation and landing aids for aviation 23 p3401 A83-47188

INSTRUMENT ORIENTATION

- Effect of off-south orientation on the performance of collector reflector system in India 03 p0355 A83-14671
- An orientation platform for a balloon-borne telescope 11 p1537 A83-28575
- Performance capabilities of photographic flight navigation and sensor orientation systems 16 p2298 A83-36122
- UBVRI photometry of stars useful for checking equipment orientation stability 17 p2591 A83-37786
- Dynamic isolation via momentum compensation for precision instrument pointing [AIAA PAPER 83-2176] 19 p2817 A83-41670
- Altitude determination and calibration for a three-dimensional angular velocimeter with the use of angular information 21 p3200 A83-45354
- Dislocated actuator/sensor positioning and feedback design for flexible structures 21 p3103 A83-45465

INSTRUMENT PACKAGES

- NT APOLLO LUNAR SURFACE EXPERIMENTS PACKAGE
- The International Ultraviolet Explorer --- instrument package 03 p0288 A83-13970
- Fiber optic experiment for the Shuttle long-duration exposure facility 08 p1166 A83-22491
- The IRV-75 infrared radiometers --- for Venera 9 and 10 spacecraft 10 p1387 A83-25346
- The application of thin-film integrated circuits in onboard scientific instrumentation 10 p1408 A83-25347
- The Dutch Scientific Instrument on board IRAS 11 p1537 A83-28213
- Future UKIRT instrumentation --- infrared telescope 18 p2690 A83-40434
- Calibration of the aerodynamic coefficient identification package measurements from the shuttle entry flights using inertial measurement unit data [AIAA PAPER 83-2100] 19 p2818 A83-41930
- Experimental results of using the GPS for Landsat 4 onboard navigation 22 p3253 A83-46963

INSTRUMENTAL ANALYSIS**U AUTOMATION****INSTRUMENTATION****U INSTRUMENTS****INSTRUMENTS**

- A system for the automated thermal design of instruments 09 p1260 A83-24234
- Advanced space instrumentation in astronomy; Proceedings of the Fourth Symposium, Ottawa, Canada, May 20-22, 1982 11 p1669 A83-27726

INSULATED STRUCTURES

- Antennas in conducting media /Review/ 04 p0466 A83-15726

INSULATION

- NT ELECTRICAL INSULATION
- NT MULTILAYER INSULATION
- NT THERMAL INSULATION

INSULATORS

- Experimental study of the sound insulation of various shell configurations 10 p1477 A83-26297
- Arc damage of interelectrode insulators in MHD generators 13 p1924 A83-30198
- Approaches for reducing the insulator-metal transition pressure in hydrogen 13 p1929 A83-30599
- Debris from spallation of foam insulation of cryogenic fuel tanks in space launch systems [AIAA PAPER 83-1457] 14 p1980 A83-32718
- Electrical response of relaxing dielectrics compressed by arbitrary stress pulses 16 p2418 A83-35440
- Dielectric relaxation in insulators slightly damaged by stress pulses 16 p2418 A83-35441

INSULIN

- Several metabolic effects of a glucose-insulin-potassium mixture on patients with acute myocardial infarctions 05 p0674 A83-17218
- Basal insulinemia in healthy males and in males with ischemic heart disease of 20-59 years of age (population study) 16 p2400 A83-36836
- The effect of insulin on the reaction of the coronary and systemic blood circulation during the inspiration of hypoxic mixtures 17 p2555 A83-37239
- The participation of an insulin-dependent cytoplasmic regulator in carbohydrate metabolism during immobilization 19 p2871 A83-40818
- Effects of exercise and lack of exercise on glucose tolerance and insulin sensitivity 20 p3035 A83-43485
- Effect of confinement in small space flight size cages on insulin sensitivity of exercise-trained rats 24 p3617 A83-48881

INTAKE SYSTEMS

- NT AIR INTAKES
- NT CONICAL INLETS
- NT ENGINE INLETS
- NT HELICAL INDUCERS
- NT HYPERSONIC INLETS
- NT INLET AIRFRAME CONFIGURATIONS
- NT NOSE INLETS
- NT SUPERSONIC INLETS
- Methods for solving Euler's equations for airfoil and intake flow 03 p0279 A83-14604
- Mathematical method for the design of the intake branch in the case of centrifugal blade machines --- Book 09 p1263 A83-24850
- Ray-theory and mode-theory predictions of intake-liner performance - A comparison with engine measurements [AIAA PAPER 83-0711] 10 p1475 A83-25927
- The design and combustion performance of practical swirlers for integral rocket/ramjets 12 p1703 A83-28964
- Experiments on flow through one to four inlets of the orifice and Borda type 20 p2986 A83-43235
- A survey of inlet/engine distortion compatibility [AIAA PAPER 83-1166] 21 p3088 A83-45509
- Wall boundary layer development near the tip region of an IGV of an axial flow compressor [ASME PAPER 83-GT-171] 23 p3396 A83-47972

INTEGRAL CALCULUS

- Some methods of integration in function space for use in control and filtering 09 p1329 A83-24738

INTEGRAL EQUATIONS

- NT FREDHOLM EQUATIONS
- NT J INTEGRAL
- NT SINGULAR INTEGRAL EQUATIONS
- NT VOLTERRA EQUATIONS
- NT WIENER HOPF EQUATIONS
- Geophysical inversion and remote probing are inverse scattering problems 01 p0048 A83-10110
- Approximation of an integral exponent by means of quadrature formulas 01 p0102 A83-11263
- A hybrid diffraction technique - General theory and applications 01 p0104 A83-11357
- A survey of the near-field far-field inverse scattering inverse source integral equation 01 p0104 A83-11368
- Boundary value problems of composite media 02 p0233 A83-12763
- Melnikov's method and averaging 03 p0389 A83-13418
- Solution of a unilateral problem using integral equations and finite elements --- French theses 03 p0390 A83-13809
- A simple technique for solving E-field integral equations for conducting bodies at internal resonances 03 p0307 A83-14035
- A formulation of the finite-length narrow slot or strip equation 03 p0313 A83-14036
- Solution of the transonic integral equation using a polar coordinate formulation 03 p0279 A83-14572
- A posteriori numerical techniques for enforcing simultaneous conservation of integral invariants upon finite-difference shallow-water equation models 03 p0322 A83-14607
- On the numerical solution of constrained variational problems by boundary and finite elements 04 p0529 A83-14958
- A calculation of the impulse responses of acoustically reflecting targets 04 p0531 A83-15073
- New computation method for characteristic modes --- eigenvalue equation solution for perfectly conducting object 04 p0466 A83-15234
- Numerical evaluation of the Rayleigh integral for planar radiators using the FFT 04 p0532 A83-16320
- On the integral form of the equation of transfer for a homogeneous sphere 04 p0532 A83-16437
- Integral representation of electromagnetic fields in inhomogeneous anisotropic media 04 p0532 A83-16451
- Calculation of steady and unsteady transonic flows using parametric differentiation and an extended integral equation method [AIAA PAPER 83-0232] 05 p0582 A83-16600
- Use of limiting solutions of Falkner-Skan-Type equations in the integral method of evaluation of near wakes 05 p0590 A83-17422
- Derivation and solution of the transonic integral equation for lifting flows 05 p0590 A83-17553
- Asymptotics of the solution of the Cauchy problem for a class of singularly perturbed systems of integro-differential equations 05 p0682 A83-17833
- The development of a two-dimensional wavepacket in a growing boundary layer 06 p0755 A83-17973
- Concerning some boundary value problems for a third-order equation and extremal properties of its solutions 06 p0804 A83-17978

- Convergence of interpolational cubic splines on nonuniform grids 06 p0804 A83-19599
- New doubly orthogonal functions and their application to pattern synthesis --- in antenna design 07 p0913 A83-20071
- An integral equation method for electromagnetic scattering of guided modes by boundary deformations of dielectric slab waveguides 07 p0913 A83-20367
- Balance laws of continuum physics 07 p0989 A83-20643
- Inversion of Abel's integral equation for experimental data 07 p0987 A83-20734
- An integral equations method for resolution, in opening mode, of the problem of plane cracks at free surface 08 p1116 A83-21661
- Numerical values for integrals of products of simply supported plate functions 08 p1120 A83-21809
- Integral equation formulation for nonlinear bending of plates - Formulation by weighted residual method 08 p1121 A83-21860
- An exact, closed-form, analytical solution to the general synthesis problem 08 p1161 A83-22472
- Angular spectrum representation of scattered electromagnetic fields 08 p1161 A83-22668
- On the existence of branch points in the eigenvalues of the electric field integral equation operator in the complex frequency plane 09 p1253 A83-23787
- Integral equation for the scattered field in the presence of a phase-conjugate mirror 09 p1344 A83-24101
- Solutions of a stationary system of Navier-Stokes equations having an infinite Dirichlet integral 09 p1261 A83-24324
- An integral equation connected with the Jacobi polynomials 09 p1336 A83-24371
- An integral method theorem for heat conduction --- computer aided design of reentry vehicles 09 p1216 A83-24673
- Cylindrical eigencurrents --- during electromagnetic scattering by conducting surfaces 10 p1406 A83-26840
- A numerical solution of singular integral equations without using special collocation points --- in stress analysis problems 11 p1594 A83-28420
- Numerical experiments involving Galerkin and collocation methods for linear integral equations of the first kind 12 p1771 A83-29098
- Solution of the fundamental control problem /FCP/ --- for aircraft 12 p1704 A83-29291
- Volume integrals of ellipsoids associated with the inhomogeneous Helmholtz equation 12 p1775 A83-29528
- Calculation of unsteady small disturbance transonic flow at arbitrary reduced frequency using an extended integral equation method. 12 p1697 A83-29832
- [AIAA 83-0884] 12 p1697 A83-29832
- Integral techniques --- for turbulence modeling 13 p1841 A83-30632
- Horizontal dipole antenna above an imperfectly conducting ground fed by a two-wire line 13 p1828 A83-30648
- A method for the integral transformation of the Boltzman equation - Analytical studies 13 p1932 A83-30658
- Volterra-like expansions for solutions of nonlinear integral equations and nonlinear differential equations 13 p1912 A83-30872
- The solution of a class of paired integral equations in problems of diffraction theory 13 p1915 A83-31374
- On the Benjamin-Ono equation-method for exact solution 14 p2077 A83-32513
- The connection between partial differential equations soluble by inverse scattering and ordinary differential equations of Painleve type 14 p2078 A83-32836
- Oblique derivative boundary value problems for nonlinear elliptic systems of second order 14 p2078 A83-33155
- Exact analytical solution of the generalized Luneburg lens problem 15 p2230 A83-33807
- Superintegrability of the Calogero-Moser system 15 p2225 A83-34136
- General solution of the Clemmow equation in a three-dimensional cold plasma, with a zero-velocity stream 15 p2235 A83-34273
- Notes on the associated alpha-functions and related integrals --- for variable eclipsing binary star studies 15 p2249 A83-34791
- Efficient numerical evaluation of electromagnetic fields due to rectangular patches of electric current 15 p2146 A83-35092
- Diffraction of an H-polarized electromagnetic wave by a circular cylinder with an infinite axial slot 15 p2148 A83-35176
- On the current distribution for open surfaces 15 p2154 A83-35190
- Integro-differential equations of the dynamics of elastic systems in nonstationary flows --- flight vehicle dynamics in turbulent nonseparated flow 16 p2366 A83-35933
- Numerical solutions of three-dimensional time-dependent compressible turbulent integral boundary-layer equations in general curvilinear coordinates [AIAA PAPER 83-1674] 17 p2501 A83-37183
- Sanders' energy-release rate integral for a circumferentially cracked cylindrical shell [ASME PAPER 83-APM-32] 17 p2519 A83-37386
- On a multipoint boundary value problem for integrodifferential-extremal equations with deviating argument of ultraneutral type 17 p2575 A83-38866
- A boundary integral equation method for thermal bending of plates 18 p2697 A83-39425
- On a class of integro-summator equations of diffraction theory 18 p2741 A83-39490
- Intensity moments by path integral techniques for wave propagation through random media, with application to sound in the ocean 18 p2741 A83-40497
- Analytical methods in the theory of elliptic equations --- Russian book 19 p2893 A83-40984
- On the application of an integral equation method for the solution of heat transfer problems in heterogeneous and cellular media 20 p2971 A83-42664
- Exact solutions of certain dual integral equations and their asymptotic properties 20 p3042 A83-43374
- Economical solution technique for boundary integral matrices 20 p3042 A83-43648
- Solitary waves induced by boundary motion 21 p3199 A83-43826
- An inverse integral computational method for compressible turbulent boundary layers 22 p3250 A83-46479
- Distribution of cometary binding energies based on the assumption of steady state 22 p3379 A83-46564
- Hybrid solutions for scattering from perfectly conducting bodies of revolution 23 p3442 A83-47828
- A remark on the solution of the integral equation of planar cracks in three-dimensional elasticity 24 p3595 A83-49869
- ### INTEGRAL FUNCTIONS
- #### U ENTIRE FUNCTIONS
- ### INTEGRAL TRANSFORMATIONS
- #### NT CONVOLUTION INTEGRALS
- #### NT FAST FOURIER TRANSFORMATIONS
- #### NT FOURIER TRANSFORMATION
- #### NT HILBERT TRANSFORMATION
- #### NT LAPLACE TRANSFORMATION
- On the integral form of the equation of transfer for a homogeneous sphere 04 p0532 A83-16437
- An integral method applied to the solution of fluid mechanics problems 04 p0480 A83-16445
- The Abel transformation in the thin-tape diffraction problem 05 p0683 A83-17631
- Conditions of optimality for singular trajectories in the problem of the minimization of a curvilinear integral 06 p0805 A83-17977
- Numerical computation of an important integral function in two-dimensional radiative transfer 07 p1001 A83-21397
- Transformation of the matrix of generalized impedances in the case of frequency variation --- for antenna radiation pattern calculations 11 p1556 A83-27945
- Fast algorithm for the computation of the zero-order Hankel transform 23 p3501 A83-47581
- ### INTEGRATED CIRCUITS
- #### NT LARGE SCALE INTEGRATION
- #### NT LINEAR INTEGRATED CIRCUITS
- #### NT TTL INTEGRATED CIRCUITS
- #### NT VERY LARGE SCALE INTEGRATION
- #### NT VHSIC (CIRCUITS)
- VLSI system design --- Book 01 p0038 A83-10881
- Logic delays of 5-micron resistor coupled Josephson logic 01 p0039 A83-10996
- A predictive tracking EW preprocessor using standard computer instruction set architectures 01 p0088 A83-11133
- Physical principles underlying millimeter-wave integral circuits /Review/ 01 p0043 A83-11301
- Millimeter-wave integral circuits /Review/ 01 p0043 A83-11302
- Integration of solid-state microwave control and protection devices /Review/ 01 p0043 A83-11303
- The Waveform Relaxation method for time-domain analysis of large scale integrated circuits 02 p0167 A83-11797
- Test chips for custom ICs - Six kinds of test structures 02 p0167 A83-11824
- An aggregate complex of fluidic integrated modules 02 p0171 A83-12200
- Solid State Transducer Symposium, Boston, MA, November 18, 19, 1981, Proceedings 02 p0180 A83-12807
- Integrated sensors - Interfacing electronics to a non-electronic world 02 p0180 A83-12809
- Hall-effect devices as strain and pressure sensors 02 p0180 A83-12812
- K-band FET doubling oscillator 02 p0168 A83-13041
- Microwave switching with GaAs FETs 03 p0308 A83-13438
- Yield considerations in the design and fabrication of GaAs MMICs 03 p0308 A83-13439
- Broadband monolithic integrated power amplifiers in gallium arsenide 03 p0308 A83-13440
- Monolithic GaAs FET low-noise amplifiers for X-band applications 03 p0308 A83-13441
- Flip-chip BeO technology applied to GaAs active aperture radars 03 p0308 A83-13442
- Signal conditioning for infrared staring arrays 03 p0326 A83-13732
- Large time-delay-and-integration /TDI/ arrays and focal plane structures with intrinsic silicon response 03 p0309 A83-13736
- Integrated optics and millimeter and microwave integrated circuits; Proceedings of the Conference, Huntsville, AL, November 16-19, 1981 03 p0309 A83-13753
- Radiation loss from a dielectric channel waveguide bend 03 p0393 A83-13767
- Interfacing a focal plane infrared mosaic array and an optical processor 03 p0326 A83-13777
- Integrated-optical techniques for near-millimeter-wave technology 03 p0309 A83-13779
- Progress in millimeter wave integrated-circuit imaging antenna arrays 03 p0327 A83-13780
- Recent advances in dielectric millimeter wave integrated circuits 03 p0309 A83-13781
- Millimeter wave integrated circuit devices based on optoelectronic control 03 p0310 A83-13782
- Silicon technology applicable to monolithic millimeter wave sources 03 p0310 A83-13783
- Millimeter wave integrated circuits for communications and radar applications 03 p0310 A83-13794
- Receiver technology for the millimeter and submillimeter wave regions 03 p0310 A83-13798
- The use of radial integrated circuits for the design of voltage-controlled oscillators --- French thesis 03 p0311 A83-13810
- Unified production planning for integrated circuits --- French thesis 03 p0314 A83-14110
- Dielectric constant of semi-insulating indium phosphide 04 p0470 A83-15232
- An investigation of the magnetically sensitive properties of integral circuit elements having injection feed 04 p0471 A83-15744
- Analog multipliers in radio-electronic equipment --- Russian book 04 p0472 A83-15832
- Multi-anode microchannel arrays - New detectors for imaging and spectroscopy in space [AIAA PAPER 83-0105] 05 p0608 A83-16523
- Gallium arsenide ICs in space and nuclear radiation environments [AIAA PAPER 83-0165] 05 p0623 A83-16565
- Nonreciprocal devices in open-boundary structures for millimeter-wave integrated circuits 05 p0624 A83-17278
- Thermal annealing of radiation damage in CMOS ICs in the temperature range -140 C to +375 C 05 p0627 A83-17515
- Rapid annealing in advanced bipolar microcircuits 05 p0627 A83-17516
- A radiation-hardened 1K-bit dielectrically isolated random access memory 05 p0628 A83-17518
- Latchup window tests 05 p0628 A83-17526
- Transient radiation screening of silicon devices using backside laser irradiation --- for military IC hardness against EMP 05 p0628 A83-17527
- Possibilities of three-dimensional microwave integrated structures 05 p0630 A83-17635
- A process simulation model for multilayer structures involving polycrystalline silicon 05 p0630 A83-17752
- A vertically isolated self-aligned transistor - VIST 05 p0631 A83-17757
- Diffraction models of slot and strip elements of microwave integrated circuits with suspended substrates for the purpose of computer-aided design 06 p0750 A83-17986
- Integrated multiband phased array antenna 06 p0737 A83-18603
- Modeling of charge transfer by surface acoustic waves in a monolithic metal/ZnO/SiO2/Si system 06 p0752 A83-18754
- A monolithic lead sulfide-silicon MOS integrated-circuit structure 06 p0752 A83-18756
- A new type of isolator for millimeter-wave integrated circuits using a nonreciprocal traveling-wave resonator 06 p0752 A83-18764
- Broad-band GaAs monolithic amplifier using negative feedback 06 p0753 A83-18774

Evaluation of a process for achieving low between-metal contact resistance in plasma etched polyimide vias --- for integrated circuits 07 p0917 A83-19898
 Dielectric waveguide - A low-cost technology for millimetre wave integrated circuits 07 p0919 A83-20179
 The development of millimetre wave mixer diodes 07 p0919 A83-20181
 Hybrid substrate attach evaluation techniques --- in production of microcircuits 07 p0919 A83-20460
 Electromigration-induced failure by edge displacement in fine-line aluminum-0.5% copper thin film conductors 07 p0921 A83-20743
 Monolithic integration of a photodiode and a field-effect transistor on a GaAs substrate by molecular beam epitaxy 07 p0922 A83-21375
 Monolithic voltage controlled oscillator for X- and Ku-bands 07 p0922 A83-21529
 A compact broad-band multifunction ECM MIC module 07 p0923 A83-21533
 A monolithic single-chip X-band four-bit phase shifter 07 p0923 A83-21534
 Automatic hardware synthesis 07 p0923 A83-21540
 Design for testability - A survey --- of integrated circuit technology 07 p0923 A83-21541
 A new integrated millimeter-wave transmission line - The fin line 08 p1079 A83-21648
 Real-time nonuniformity correction for focal plane arrays using 12-bit digital electronics 08 p1094 A83-22440
 Programmable image processing element 08 p1097 A83-22532
 Mosaic focal plane methodologies II; Proceedings of the Conference, San Diego, CA, August 27, 28, 1981 08 p1100 A83-22598
 Integrating 128-element linear imager for the 1 to 5 microns region 08 p1100 A83-22601
 Signal processing and compensation electronics for junction field-effect transistor /JFET/ focal plane arrays 08 p1081 A83-22606
 Infrared Schottky barrier focal plane array technology 08 p1081 A83-22610
 New magnetic structures for switching converters 08 p1082 A83-23100
 Experimental study of junctions of dielectric strip waveguides in the millimeter-wave range 09 p1253 A83-23471
 Realization of some analog functions with switchable feedback loops 09 p1253 A83-23694
 An ultra-low-drift dc amplifier for use with photomultipliers 09 p1267 A83-23743
 Characteristics of a new class of diode-switched integrated antenna phase shifter 09 p1247 A83-23798
 Monolithic circuits for millimeter-wave systems 09 p1255 A83-24346
 Future applications and limitations for digital GaAs IC technology 09 p1255 A83-24347
 MMIC technology for microwave radar and communication systems 09 p1255 A83-24349
 Design, fabrication, and evaluation of 2- and 3-bit GaAs MESFET analog-to-digital converter IC's 09 p1256 A83-24678
 Ka-band monolithic GaAs balanced mixers 09 p1256 A83-24679
 Yield considerations for ion-implanted GaAs MMIC's 09 p1256 A83-24680
 A two-stage monolithic IF amplifier utilizing a Ta2O5 capacitor 09 p1256 A83-24681
 A monolithic GaAs DC to 2-GHz feedback amplifier 09 p1256 A83-24682
 Monolithic GaAs interdigitated couplers 09 p1256 A83-24683
 The application of thin-film integrated circuits in onboard scientific instrumentation 10 p1408 A83-25347
 The status of printed millimeter-wave E-plane circuits 10 p1408 A83-25802
 50-GHz IC components using alumina substrates 10 p1408 A83-25803
 Design of dielectric ridge waveguides for millimeter-wave integrated circuits 10 p1408 A83-25804
 Integrated fin-line components and subsystems at 60 and 94 GHz 10 p1409 A83-25806
 V-band low-noise integrated circuit receiver --- for space communication systems 10 p1382 A83-25807
 A quasi-optical polarization-duplexed balanced mixer for millimeter-wave applications 10 p1402 A83-25810
 Millimeter-wave /W-band/ quartz image guide Gunn oscillator 10 p1409 A83-25815
 A limiter for high-power millimeter-wave systems 10 p1409 A83-25821
 A family of special purpose microprogrammable digital signal processor IC's in an LPC vocoder system 10 p1410 A83-26124

Design of interdigitated capacitors and their application to gallium arsenide monolithic filters 10 p1410 A83-26341
 Algorithms for the design of integrated circuits 10 p1412 A83-26926
 Laser bonding of dissimilar semiconductors 11 p1560 A83-27564
 High-efficiency Q-to-W-band MIC frequency doubler 11 p1563 A83-28609
 Fully integrated W-band microstrip oscillator 11 p1563 A83-28610
 A monolithically integrated wide-tunable sine oscillator --- Thesis 11 p1564 A83-28642
 The organization of circuit analysis on array architectures --- Thesis 11 p1564 A83-28648
 Numerical results on the simulation of microstrip elements and units of microwave integrated circuits 12 p1719 A83-29343
 Miniaturization of monolithic amplifiers on GaAs at 10 GHz 12 p1719 A83-29409
 Radiation induced soft fails in space electronics 13 p1812 A83-30185
 Design and performance of W-band broad-band integrated circuit mixers 13 p1831 A83-30230
 Laser-formed connections using polyimide --- on integrated circuits 13 p1832 A83-30346
 Empirical expressions for fin-line design 13 p1836 A83-31147
 Design automation for integrated circuits 13 p1836 A83-31161
 Gigabit logic bipolar technology advanced super self-aligned process technology 13 p1837 A83-31761
 Translinear logic - A new technique in bipolar technology 13 p1838 A83-31787
 Integrated infrared detector arrays for low-background applications 14 p1983 A83-31978
 The effects of nuclear radiation on integrated circuits 14 p2005 A83-32416
 Sputter depth profiling of microelectronic structures 14 p2092 A83-32648
 High resolution acoustic microscopy in superfluid helium 14 p2022 A83-33443
 Low-noise, low power dissipation GaAs monolithic broad-band amplifiers 14 p2008 A83-33459
 All-refractory Josephson logic circuits 15 p2150 A83-33888
 Compact dc model of GaAs FET's for large-signal computer calculation 15 p2151 A83-33892
 Microelectronic pulse generators --- Russian book 15 p2152 A83-34171
 Converters of the levels of logical elements --- Russian book 15 p2152 A83-34174
 Millimeter wave integrated circuits and systems 15 p2153 A83-35077
 On testing stuck-open faults in CMOS combinational circuits 15 p2153 A83-35141
 A new MIC slot-line aerial 15 p2149 A83-35194
 High-performance modulation-doped GaAs integrated circuits with planar structures 16 p2347 A83-36477
 GaAs integrated digital-to-analogue converter for control of power dual-gate FETs 16 p2347 A83-36479
 Integrated surface acoustic wave/field-effect transistor high-speed analog memory 16 p2347 A83-36772
 Developing a technology base for advanced devices and circuits 17 p2496 A83-37057
 GaAs microwave devices and circuits with submicron electron-beam defined features 17 p2496 A83-37059
 Monolithic surface acoustic wave resonator oscillator 17 p2496 A83-37610
 Nonradiative dielectric waveguide circuit components 17 p2497 A83-37761
 Millimeter-wave ICs for precision guided weapons 17 p2498 A83-37894
 Waveguide-to-coax-to-microstrip transitions for millimeter-wave monolithic circuits 17 p2498 A83-37897
 Ultrafast GaAs microwave PIN diode 17 p2500 A83-38883
 Laser-controlled chemical etching of aluminum 18 p2693 A83-40055
 High speed logic operations of all refractory Josephson integrated circuits 18 p2677 A83-40068
 High-speed GaAlAs/GaAs p-i-n photodiode on a semi-insulating GaAs substrate 19 p2836 A83-40742
 A proposal of a new dielectric resonator construction for MIC's 19 p2838 A83-41085
 Substrate optimization for integrated circuit antennas 19 p2826 A83-41087
 Analysis of slow-wave coplanar waveguide for monolithic integrated circuits 19 p2838 A83-41089
 Impact of monolithic microwave integrated circuit development on communications satellites 19 p2828 A83-41334

A technique for analyzing planar dielectric waveguides for millimeter wave integrated circuits 19 p2841 A83-42164
 HMOS 2 - The first step toward VLSI 20 p2967 A83-42824
 Bit-level systolic array circuit for matrix vector multiplication 20 p3037 A83-43167
 Proton implantation isolation for microwave monolithic circuits 21 p3123 A83-43845
 A new high-power voltage-controlled differential negative resistance device - The Lambda bipolar power transistor 21 p3123 A83-43850
 Self-aligned submicron gate digital GaAs integrated circuits 21 p3124 A83-43854
 GaAs optoelectronic integrated light sources 21 p3125 A83-44226
 Main mechanisms for the failures of monolithic integrated circuits 21 p3125 A83-44591
 Ka-band y-circulators in integrated waveguide technology 21 p3125 A83-44955
 Microelectronics --- Russian book 21 p3126 A83-45014
 Functional analog integrated microcircuits --- Russian book 21 p3126 A83-45017
 Measurement of the parameters of digital integrated microcircuits --- Russian book 21 p3126 A83-45040
 A theoretical study and an experimental evaluation of the mutual coupling effects in MIC array antennas 21 p3127 A83-45411
 Novel synthesis method of microwave integrated low-pass filters 21 p3127 A83-45414
 A general-purpose program for nonlinear microwave circuit design 24 p3573 A83-48971
 High-speed Schottky photodiode on semi-insulating GaAs 24 p3574 A83-49961

INTEGRATED ENERGY SYSTEMS

Integrated solar energy system optimization 03 p0352 A83-13477

INTEGRATED OPTICS

Low threshold InGaAsP/InP lasers with microcleaved mirrors suitable for monolithic integration 01 p0055 A83-10981
 Effect of nonuniform piezoelectric films on monolithic surface acoustic wave devices 01 p0039 A83-10986
 Physical principles underlying millimeter-wave integral circuits /Review/ 01 p0043 A83-11301
 Optical-waveguide hybrid coupler 02 p0235 A83-11567
 Guided wave approaches to optical bistability 02 p0235 A83-12167
 Measurement and analysis of periodic coupling in silicon-clad planar waveguides 02 p0235 A83-12170
 Electrical and acoustical crosstalk in integrated optical strip waveguide devices 02 p0168 A83-13044
 Bulk and integrated acousto-optic spectrometers for molecular astronomy with heterodyne spectrometers 03 p0405 A83-13459
 Integrated optics and millimeter and microwave integrated circuits; Proceedings of the Conference, Huntsville, AL, November 16-19, 1981 03 p0309 A83-13753
 Integrated optics strapdown inertial system 03 p0326 A83-13755
 Integrated optical logic devices 03 p0392 A83-13756
 Design criteria for integrated optical devices 03 p0393 A83-13757
 Development of the multiwavelength monolithic integrated fiber optics terminal 03 p0393 A83-13760
 Novel optoelectronic devices prepared by molecular beam epitaxy 03 p0331 A83-13761
 Integrated optics elements for an optical gyro 03 p0326 A83-13763
 Applications of the integrated optical light modulator 03 p0393 A83-13764
 Novel semiconductor lasers for integrated optics 03 p0331 A83-13765
 Radiation loss from a dielectric channel waveguide bend 03 p0393 A83-13767
 Design approach for a thermally compensated injection laser stack transmitter/receiver 03 p0331 A83-13769
 Space-invariant composite matched filters for space-variant processors 03 p0394 A83-13774
 Interfacing a focal plane infrared mosaic array and an optical processor 03 p0326 A83-13777
 Silicon liquid crystal light valves for optical-data processing 03 p0394 A83-13778
 Integrated-optical techniques for near-millimeter-wave technology 03 p0309 A83-13779
 Picosecond signal processing with planar nonlinear integrated optics 03 p0394 A83-13791
 Periodic oscillations and chaos in optical bistability - Possible guided-wave all-optical square-wave oscillators 03 p0394 A83-13792

Potential of integrated optics and integrated millimeter and microwave circuits for future MICOM systems
03 p0310 A83-13799

Optoelectronic digital/analog converter-emitter
04 p0534 A83-15241

An integral-optic correlator with temporal integration
04 p0535 A83-15272

Integral-optic photoreceiving devices
04 p0535 A83-15273

Focussing of submillimeter radiation guided by a dielectric sheet
04 p0535 A83-15810

Simple spectral control technique for external cavity laser transmitters
04 p0485 A83-16023

Effects of cavity length on 20 micron stripe laser waveguiding
04 p0486 A83-16221

Prototyping of an integrated-optics four-digit analog-digital converter
05 p0685 A83-17062

Amplification of light in inhomogeneous waveguides with an adjacent active medium
05 p0685 A83-17076

Propagation and conversion of light waves in corrugated waveguide structures
05 p0685 A83-17081

Review - Progress of coherent optical fibre communication systems
05 p0685 A83-17887

A numerical technique for the determination of propagation characteristics of inhomogeneous planar optical waveguides
05 p0686 A83-17892

Power flux distribution of the guided modes of an asymmetric dielectric slab waveguide
06 p0811 A83-19600

Optically integrated coherently coupled Al_x/Ga_{1-x}/As lasers
07 p0937 A83-21367

Development and evaluation of integrated infrared arrays for astronomical applications
08 p1052 A83-22858

Near-field and far-field patterns of phase-locked semiconductor laser arrays
10 p1426 A83-25979

Rectangular Luneburg-type lenses for integrated optics
10 p1482 A83-26117

Integrated optical ring resonators made by silver ion-exchange in glass
10 p1483 A83-26639

Coupling semiconductor lasers to multimode optical fibres
11 p1655 A83-27515

Acousto-optic measurements of effective refractive indices of guided modes in planar waveguides
12 p1779 A83-29459

The development of fibre optic microend sensors
12 p1730 A83-29519

Integrated optics wave front measurement sensor
13 p1845 A83-30331

Fluctuation and scattering properties of RF sputtered glass thin film optical waveguides
13 p1919 A83-30781

Fabrication of optical waveguides in LiNbO₃ and LiTaO₃ crystals by ion irradiation
13 p1919 A83-30824

A thermooptical method for the formation of lightguide channels
14 p2084 A83-32122

Optical logic array processor using shadowgrams
15 p2230 A83-33808

Integrated arrays of 1.3-micron buried-crescent lasers
15 p2168 A83-33842

Integrated optics - Current status and future prospects
15 p2231 A83-34876

Integrated-optic elements in the medium infrared range
15 p2231 A83-34882

Investigation of the characteristics of an integrated-optic analog-to-digital converter
15 p2232 A83-34890

Dispersion of the refractive index of GaAs and Al(x)Ga(1-x)As
16 p2420 A83-35970

Integrated optical waveguiding structures made by silver ion-exchange in glass. I - The propagation characteristics of stripe ion-exchanged waveguides: A theoretical and experimental investigation
16 p2413 A83-36768

Integrated optical waveguiding structures made by silver ion-exchange in glass. II - Directional coupler and bends
16 p2414 A83-36769

Traveling-wave electrooptic modulator
17 p2580 A83-37750

Isolation spectra for laser diode optical switch
19 p2900 A83-41278

Graphical representation of prism coupling into thin films
20 p3047 A83-42223

Passive planar multibranch optical power divider - Some design considerations
20 p3047 A83-42224

Integrated optical polariser on LiNbO₃:Ti channel waveguides using proton exchange
20 p3047 A83-42483

Monolithic integration of a double heterostructure light-emitting diode and a field-effect transistor amplifier using molecular beam grown AlGaAs/GaAs
20 p2968 A83-43596

Integrated optics, fiber optics and holography; International School on Coherent Optics and Holography, 2nd, Varna, Bulgaria, September 28-October 3, 1981, Proceedings
20 p3048 A83-43774

Integrated-optics photodetector utilizing the external photoelectric effect in a Schottky barrier
20 p3048 A83-43805

An effective nonreciprocal circuit for semiconductor laser-to-optical-fiber coupling using a YIG sphere
21 p3204 A83-44214

Design and performance of an integrated optical digital correlator
21 p3205 A83-44225

GaAs optoelectronic integrated light sources
21 p3125 A83-44226

Picosecond signal sampling and multiplication by using integrated tandem light modulators
21 p3205 A83-44229

Integrated optical microwave spectrum analyser (IOSA) using geodesic lenses
21 p3208 A83-44844

Wavelength tuning of GaInAsP/InP integrated laser with butt-jointed built-in distributed Bragg reflector
21 p3145 A83-44952

Far-field distributions of semiconductor phase-locked arrays with multiple contacts
21 p3145 A83-44953

Wavelength multiplexing of 1.31-micron InGaAsP buried crescent laser arrays
21 p3146 A83-45476

Double ion exchanged chirp grating lens in lithium niobate waveguides
21 p3208 A83-45483

Twisted double-heterostructure GaAs-(AlGa)As laser
21 p3146 A83-45484

Numerical field solution for an arbitrary asymmetrical graded-index planar waveguide
22 p3356 A83-45733

Optical waveguides in LiTaO₃ formed by proton exchange
22 p3356 A83-45969

Integrated optics II; Proceedings of the Meeting, Los Angeles, CA, January 28, 29, 1982
22 p3359 A83-46643

Fabrication and performance of diffraction lenses
22 p3359 A83-46645

Heterodyne receiver on silicon - An exercise in integration
22 p3359 A83-46646

Integrated optical circuits fabricated with laser-written masks
22 p3359 A83-46648

Integrated optical logic devices
22 p3359 A83-46649

Progress on electro-optic integrated optic devices
22 p3360 A83-46650

Narrow diffused stripe GaAs/GaAlAs lasers for high speed integrated optical transmitters
22 p3297 A83-46655

Residue arithmetic circuit design based on integrated optics
22 p3350 A83-46659

Performance of the integrated optic spectrum analyzer
22 p3293 A83-46660

Application of wide band Bragg cells for integrated optic (IO) spectrum analyzers
22 p3293 A83-46661

Advanced integrated optic RF spectrum analyzer
22 p3293 A83-46662

Gigabit optical pulse generations in integrated lasers
22 p3298 A83-46681

Low-loss integrated optical waveguides fabricated by nitrogen ion implantation
22 p3360 A83-46720

Phase-locked semiconductor laser array with separate contacts
22 p3299 A83-46721

Electronic wavelength tuning with semiconductor integrated etalon interference lasers
22 p3299 A83-46723

A bistable hybrid optical device using an integrated modulator with an induced dielectric channel
23 p3507 A83-47561

Waveguide light modulators using the Keldysh-Franz effect in gallium arsenide
23 p3507 A83-47570

1.5 GHz operation of an Al(x)Ga(1-x)As/GaAs modulation-doped photoconductive detector
23 p3446 A83-48712

Coupled-wave theory regarding phase-locked-array lasers
23 p3464 A83-48715

The beam propagation method - An analysis of its applicability --- to integrated optics
24 p3627 A83-48748

Total-internal-reflection electrooptic thin-film modulator
24 p3628 A83-48859

Semiconductor optoelectronic devices for free-space optical communications
24 p3573 A83-48993

New Ga(0.47)In(0.53)As sheet-charge field-effect transistor for long-wavelength optoelectronic integration
24 p3574 A83-49973

INTEGRATION (REAL VARIABLES)

U MEASURE AND INTEGRATION

INTEGRATORS

NT DIGITAL INTEGRATORS

New pulsed laser data-acquisition system
06 p0764 A83-19233

Generic pole assignment using dynamic output feedback
15 p2221 A83-35112

Principles for the adaptation of logical integrating computing structures for the implementation of fuzzy algorithm
16 p2403 A83-36902

INTEGRITY

NT COMPUTER PROGRAM INTEGRITY

INTEGRATION DIFFERENTIAL EQUATIONS

U DIFFERENTIAL EQUATIONS

U INTEGRAL EQUATIONS

INTELLIGENCE

NT ARTIFICIAL INTELLIGENCE

NT EXPERT SYSTEMS

NT EXTRATERRESTRIAL INTELLIGENCE

Electronic intelligence: The analysis of radar signals ---
Book 05 p0622 A83-17374

The enchanted loom --- Book on evolution of intelligence
20 p3033 A83-42174

Scout - A real time intelligence and surveillance system
20 p2934 A83-43717

INTELLIGIBILITY

NT SPEECH RECOGNITION

Masking during speech audiometry and its diagnostic value
19 p2881 A83-41445

INTELSAT SATELLITES

Intelsat VI SS-TDMA
01 p0043 A83-11277

Satellite communications research - The problems of propagation
02 p0163 A83-11820

The INTELSAT propagation measurements programme
06 p0745 A83-18707

Operational measurements of a 4/6-GHz adaptive polarization compensation network employing up/down-link correlation algorithms
06 p0746 A83-18727

INTELSAT: The global telecommunications network ---
Book 07 p0902 A83-19650

Commercial satellite communications for developing areas of the Pacific
07 p0903 A83-19654

120 Mbps TDMA terminal equipment
07 p0903 A83-19658

SS/TDMA operation using INTELSAT VI spacecraft
07 p0910 A83-19772

A cost effective TDMA terminal for Intelsat/Eutelsat applications
07 p0911 A83-19782

Simulation study of DQPSK Intelsat V regenerative/non-regenerative satellite systems ---
Differential Quaternary PSK
07 p0912 A83-19800

4-GHz high-efficiency broadband FET power amplifiers
07 p0920 A83-20556

Summary of Intelsat VI communications performance specifications
07 p0869 A83-20557

The development of global satellite telecommunications
07 p0916 A83-21618

The Intelsat V nickel-hydrogen battery
11 p1542 A83-27330

A new baseband linearizer for more efficient utilization of earth station amplifiers used for QPSK transmission
11 p1556 A83-28130

Alternate architectures and technologies for Intelsat type DSI design --- digital speech interpolation
11 p1558 A83-28141

Maritime communications satellite in-orbit measurements
17 p2475 A83-37794

Communications performance specifications of the INTELSAT V with maritime communications subsystem
17 p2494 A83-37796

Communications performance specifications of the INTELSAT V-A
17 p2494 A83-37797

Design summary of the Intelsat V spacecraft
18 p2646 A83-40014

Equipment design considerations for Intelsat TDMA traffic terminals
19 p2829 A83-41357

Regenerative/non-regenerative satellite systems using differentially-detected MSK
19 p2829 A83-41360

Design considerations for Intelsat V TDMA modems
19 p2830 A83-41361

Intelsat architectures for the 1990s
19 p2830 A83-41370

Intelsat - Making the future happen
21 p3120 A83-44532

A figure of merit for competing communications satellite designs
21 p3221 A83-44533

Madley - Growth of a large earth station
23 p3442 A83-47653

Cochannel and intersymbol interferences in QAM system
24 p3571 A83-49965

INTENSIFICATION
U AMPLIFICATION

INTENSIFIER TUBES

U IMAGE INTENSIFIERS

INTENSIFIERS

NT IMAGE INTENSIFIERS

NT IMAGE ORTHONICS

INTERACTIVE CONTROL

International standards for software structures in astronomy
01 p0113 A83-10140

Consolidated TPS implementation today and tomorrow
01 p0090 A83-10731

EASYCADC - A VAX implementation of a universal user interface for a system of computer aided circuit design /CADC/ programs
01 p0093 A83-11247

- Interactive smoothing of digitized point data
02 p0226 A83-11817
- Interactive computer graphic preprocessing for three-dimensional boundary-integral element analysis
02 p0228 A83-12744
- Data management in FEM-based optimization software
02 p0228 A83-12751
- Critical evaluation of eight semiempirical aerodynamic coefficient prediction programs for missiles and stores [AIAA PAPER 83-0185]
05 p0581 A83-16576
- Controlling the complexity of menu networks
07 p0983 A83-21041
- Interactive algorithm development system for tactical image exploitation
08 p1097 A83-22527
- Real-time image computer configuration
08 p1152 A83-22528
- Powerful hardware/software architecture for a minicomputer-based interactive image processing system
08 p1097 A83-22537
- Large scale multipurpose interactive image processing facility at ETH-Zurich
08 p1098 A83-22539
- Illustration of the applicability of computer aided design packages
09 p1243 A83-24719
- The design of digital filters using interactive optimization
09 p1332 A83-24776
- Selection and experimental comparison of computer input devices --- Book
09 p1325 A83-24902
- Selection of remotely labeled switch functions during dual task performance
10 p1459 A83-26315
- The model human processor - A model for making engineering calculations of human performance
10 p1459 A83-26323
- Integrated flight path control system
10 p1378 A83-26477
- Structure and mode of operation of an interactive onboard four-dimensional flight path control system
10 p1378 A83-26478
- Procedure for an evaluation of control systems on the basis of human factor considerations
10 p1460 A83-26479
- The manipulation of interaction effects in multivariable feedback systems
10 p1465 A83-26525
- Interactive Doppler editing software
11 p1646 A83-27084
- A general interactive system for compositing digital radar and satellite data
11 p1647 A83-27089
- Interactive graphical programming and control of robotic systems
11 p1645 A83-27488
- The display of molecular models with the Ames Interactive Modeling System (AIMS)
12 p1768 A83-29548
- DYSCO - An executive control system for dynamic analysis of synthesized structures
12 p1768 A83-29773
- A numerical weather prediction system utilizing a man/minicomputer/supercomputer interaction
13 p1885 A83-30538
- File allocation in a distributed computer communication network
13 p1909 A83-30788
- Computer-aided interactive structural optimization of printed-circuit-board design
13 p1834 A83-30862
- INTFIS - An interactive package for electronic filter synthesis
16 p2403 A83-35323
- Smoothing of cubic parametric splines
16 p2406 A83-35324
- Interactive fine-tuning of linear-quadratic governors by selective and direct action on the poles of the control system
[ONERA, TP NO. 1983-21]
16 p2404 A83-36430
- The GEMPAK Barnes interactive objective map analysis scheme --- General Meteorological Software Package
17 p2548 A83-38709
- Design and development of a radar control program for the NOAA/WPL pulse-Doppler radars --- Wave Propagation Laboratory
18 p2727 A83-39880
- An interactive weight estimating program for maneuverable reentry vehicles
[SAWE PAPER 1458]
20 p2945 A83-43739
- The use of structural properties in linear multivariable control system design --- Thesis
22 p3352 A83-46690
- INTERACTIVE GRAPHICS**
U COMPUTER GRAPHICS
- INTERATOMIC FORCES**
Cooperative transients in inter-atomic correlation in the presence of an externally applied coherent field - Relation to intrinsic mirrorless optical bistability
03 p0394 A83-13789
- An experimental study of the correlation between the root-mean-square thermal displacements of atoms and the resistance to creep --- of nickel and aluminum alloys
06 p0729 A83-18750
- INTERCALATION**
Metallic conductivity and air stability in copper chloride intercalated carbon fibers
04 p0473 A83-16095
- Supermetallic conductivity of graphite intercalated with iodine monochloride
24 p3634 A83-48864
- Intercalation of alkali metals in graphite under high pressure
24 p3569 A83-49554
- Electrochemical method for studying the reversibility of the lithium intercalation in secondary batteries
24 p3600 A83-49942
- A reversible graphite-lithium negative electrode for electrochemical generators
24 p3558 A83-49946
- INTERCEPTION**
Computation of optimal feedback strategies for interception in a horizontal plane
[AIAA PAPER 83-0281]
05 p0577 A83-16626
- Solution of three dimensional interception by inclined plane using the forced singular perturbations technique
07 p0862 A83-21013
- Optimal guidance laws for missiles with second order characteristics
10 p1383 A83-26769
- Investigation of time-to-go algorithms for air-to-air missiles
17 p2461 A83-37137
- Interception in three dimensions - An energy formulation
[AIAA PAPER 83-2121]
19 p2798 A83-41946
- INTERCEPTOR AIRCRAFT**
U FIGHTER AIRCRAFT
- INTERCEPTORS**
Tiny engine combines muscle and fast response
16 p2318 A83-35766
- Classical vs. modern control system design for terminal guidance of bank-to-turn intercept missiles
[AIAA PAPER 83-2203]
19 p2802 A83-41687
- Control of a spinning, impulsively controlled interceptor
[AIAA PAPER 83-2206]
19 p2815 A83-41690
- INTERCONTINENTAL BALLISTIC MISSILES**
NT MINUTEMAN ICBM
NT MX MISSILE
U.S. and Soviet early warning satellites
14 p1980 A83-31823
- A new measure of ICBM effectiveness that accounts for optimal fuzing
[AIAA PAPER 83-2250]
19 p2894 A83-41726
- Effects of polar motion on ICBM accuracy
[AIAA PAPER 83-2295]
19 p2810 A83-41754
- Gravitational model effects on ICBM accuracy
[AIAA PAPER 83-2296]
19 p2810 A83-41755
- Stellar-inertial guidance capabilities for advanced ICBM
[AIAA PAPER 83-2297]
19 p2814 A83-41756
- INTERCOSMOS SATELLITES**
The dynamics of energetic electrons according to Interkosmos-19 satellite observations in April 1979
03 p0439 A83-13217
- Review of the scientific usage of Interkosmos satellite observations at the Astronomical Institute of the Czechoslovak Academy of Sciences
04 p0546 A83-15101
- Soil cover interpretation on multizonal space photos made by the use of camera 'MKF-6' and 'Fragment' system
08 p1127 A83-21943
- Development of onboard radio-electronic equipment
10 p1408 A83-25328
- A cosmic-ray dosimeter with a semiconductor detector
10 p1387 A83-25344
- Satellite observations of signals from a Soviet mid-latitude VLF transmitter in the magnetic-conjugate region
12 p1753 A83-29429
- Structure and organizational mechanism of the Interkosmos Program
13 p1808 A83-30274
- Spherical ion traps for 'Interkosmos-Bulgaria-1300'
13 p1813 A83-30754
- The ion energy and mass analyzer on board the 'INTERCOSMOS-BULGARIA-1300' satellite
13 p1813 A83-30755
- An instrument for DC electric field and AC electric and magnetic field measurements aboard 'INTERCOSMOS-BULGARIA-1300' satellite
13 p1813 A83-30757
- An instrument for total ion drift velocity measurements aboard the 'Interkosmos-Bulgaria-1300' satellite
13 p1814 A83-30762
- Observations of whistler-type echoes on signals of a ground VLF transmitter on board the 'Interkosmos-19' satellite
16 p2375 A83-35394
- High energy electrons at altitudes 500 km near the equator
18 p2787 A83-39955
- Telecommunications and the satellite
'Interkosmos-Bulgaria-1300'
[IAF PAPER 83-ST-09]
23 p3420 A83-47387
- INTERFACE STABILITY**
Instability and atomization of a liquid layer adjacent to a gas stream
[AIAA PAPER 83-0339]
05 p0635 A83-16665
- The effect of interfacial traps on the stability of insulated gate devices on InP
07 p0921 A83-20742
- Inertial effects of the gas motion upon the linear and nonlinear waves in Kelvin-Helmholtz flow
08 p1083 A83-21813
- Free energy loss during the breakdown of liquid films
08 p1087 A83-23141
- Instability in the film boiling of a moving liquid
11 p1570 A83-28556
- Interfacial stability of SnO₂/n-Si and In₂O₃/n-Si heterojunction solar cells
13 p1931 A83-31384
- The dependence of the shape and stability of captive rotating drops on multiple parameters
17 p2507 A83-38615
- Two-component Benard convection - Interfacial deformation, oscillatory instabilities and the onset of turbulence
18 p2685 A83-39892
- Factors affecting the interlaminar fracture energy of graphite/epoxy laminates
18 p2651 A83-40152
- Interfacial progressive gravity waves in a two-layer shear flow
18 p2687 A83-40499
- Hydrodynamic instability of axisymmetric flows of an ideal fluid with an interface
19 p2844 A83-41579
- Convective and interfacial instabilities during solidification of succinonitrile containing ethanol
20 p2946 A83-43299
- Interfacial chemistry of electrical contacts on GaAs and Al_{0.3}Ga_{0.7}As
21 p3109 A83-44614
- A point vortex method applied to interfacial waves
22 p3280 A83-45906
- Nonaxisymmetric equilibrium shapes of a drop on a plane
23 p3452 A83-48670
- Liquid surface oscillations induced by temperature fluctuation
24 p3576 A83-49024
- INTERFACES**
NT FLUID BOUNDARIES
NT GAS-SOLID INTERFACES
NT JET BOUNDARIES
NT LIQUID-LIQUID INTERFACES
NT LIQUID-SOLID INTERFACES
NT LIQUID-VAPOR INTERFACES
NT SOLID-SOLID INTERFACES
- The rationale for a standard unit-under-test-interface
01 p0037 A83-10754
- Innovation in inertial ATE interfaces
01 p0017 A83-10782
- The strength of the fibre-polymer interface in short glass fibre-reinforced polypropylene
03 p0291 A83-13682
- Surface and interface characterization of advanced materials
08 p1053 A83-22252
- On the structural organization of an onboard interface for space scientific instrumentation
10 p1386 A83-25331
- The penny-shaped interface crack with heat flow. I - Perfect contact
[ASME PAPER 83-APM-10]
10 p1440 A83-26428
- The interface crack behavior in dissimilar anisotropic composites under mixed-mode loading
[ASME PAPER 83-APM-7]
10 p1441 A83-26444
- DOD payload interface verification in the Shuttle era
13 p1810 A83-31179
- Interfacial layers in high-temperature-oxidized NiCrAl
21 p3113 A83-44619
- (HgCd)Te-SiO₂ interface structure
24 p3634 A83-48743
- INTERFACIAL ENERGY**
Molecular-orbital model for metal-sapphire interfacial strength
01 p0023 A83-10612
- Characterization of the interface energetics for N-type cadmium selenide/nonaqueous electrolyte junctions
07 p0881 A83-20585
- Analysis and evaluation of interfacial delamination energy of notched laminated composites
18 p2660 A83-40272
- INTERFACIAL STRAIN**
U INTERFACIAL TENSION
- INTERFACIAL TENSION**
Fiber-matrix interactions
02 p0150 A83-12824
- Surface tension driven flows in micro-gravity conditions
02 p0174 A83-12904
- Effects of morphology and hardness of inclusions on ductile fracture
08 p1066 A83-22078
- Relation of interfacial adhesion in Kevlar/epoxy systems to surface characterization and composite performance
08 p1055 A83-22716
- Marangoni convection-induced bubble motion
08 p1086 A83-23124
- Interface and transport phenomena under reduced gravity. II - Surfaces and wetting
09 p1263 A83-24645
- Alpha-beta interface sliding in Ti-Mn alloys
10 p1398 A83-26285
- Nonlinear behavior and failure mechanisms of three-dimensional carbon-carbon composites
11 p1544 A83-27463
- The effect of gravity on freely growing crystals
11 p1662 A83-28171

- Enhanced erythrocyte suspension layer stability achieved by surface tension lowering additives
11 p1546 A83-28762
- Singularity of contact-edge stress in laminated composites under uniform extension
13 p1868 A83-31620
- Transient thermal Marangoni convection in a liquid bridge
13 p1844 A83-31625
- Interlaminar shear properties of graphite fiber, high-performance resin composites
13 p1816 A83-31794
- Epitaxial crystallization of nylon 6 cast from solution on the surface of poly(p-phenylene terephthalamide) filament
13 p1817 A83-31796
- Interfacial interaction between poly(p-phenylene terephthalamide) filament and nylon 6 matrix crystallized from the melt
13 p1817 A83-31797
- The concept of force and moment as a computational quantity in continuum mechanics
13 p1915 A83-31799
- Surface tension effects in a space radiator condenser with capillary liquid drainage
[AIAA PAPER 83-1525] 14 p2011 A83-32756
- Benard-Marangoni instability in a rotating liquid layer subjected to a transverse magnetic field
18 p2685 A83-39893
- The effect of temperature gradient on the motion of a bubble in reduced gravity
18 p2686 A83-39906
- Thermocapillary migration of bubbles and droplets
18 p2686 A83-39907
- Fatigue crack growth behavior in the vicinity of interface of dissimilar materials
18 p2705 A83-40204
- Fracture mechanism of short glass fiber reinforced polyamide thermoplastics
18 p2657 A83-40232
- Effects of interfacial reaction on fracture mode and tensile strength of fibres in metal matrix composites
18 p2659 A83-40254
- Stress field related to dislocation arrangements observed in the phase boundary of a lamellar in-situ composite
18 p2667 A83-40257
- Natural damped frequencies of an infinitely long column of immiscible viscous liquids
19 p2841 A83-40800
- Annular punch on a transversely isotropic layer bonded to a half-space
19 p2859 A83-41540
- An experimental study of heat induced surface-tension driven flow
20 p2940 A83-43269
- Surface tension driven flow in glass melts and model fluids
20 p2941 A83-43284
- Fingers in a Hele-Shaw cell with surface tension
21 p3127 A83-43926
- Peculiarities in stress solutions in laminated composites
21 p3105 A83-44047
- Stability of rotating liquid drops. I - Uncharged drops
22 p3280 A83-46001
- Recent developments in surface-tension driven instabilities
[IAF PAPER 83-144] 23 p3446 A83-47289
- Preliminary results of Texus 8 experiments on effects of surface tension minimum
[IAF PAPER 83-151] 23 p3446 A83-47291
- INTERFERENCE DRAG**
Calculation of the aerodynamic efficiency of winglets
17 p2446 A83-37257
- Interference during flow around a wing and an axisymmetric nacelle
19 p2791 A83-41879
- INTERFERENCE GRATING**
Simultaneous diffraction of two waves at a reflection volume hologram
04 p0535 A83-15795
- Spectral characterization methodology of thin-film optical filters
08 p1104 A83-22880
- Projection moire with moving gratings for automated 3-D topography
10 p1484 A83-26868
- Applications of interference coatings in optical processing
21 p3206 A83-44791
- Opto-optical light deflection
21 p3207 A83-44834
- INTERFERENCE MONOCHROMATIZATION**
U DIFFRACTION
- INTERFEROGRAMS**
U INTERFEROMETRY
- INTERFEROMETERS**
NT FABRY-PEROT INTERFEROMETERS
NT INFRARED INTERFEROMETERS
NT MACH-ZEHNDER INTERFEROMETERS
NT MICHELSON INTERFEROMETERS
NT MICROWAVE INTERFEROMETERS
NT RADIO INTERFEROMETERS
- On the application of variable shear double exposure interferometer for the study of heat transfer to or from solid surfaces
01 p0051 A83-11056
- Smoothing of output-signal fading for a fiber ring interferometer, determined by instabilities of the parameters of a one-mode fiber-optic waveguide
04 p0482 A83-15747
- Effect of trapped magnetic flux on the threshold curves of three-junction superconducting quantum interference devices
04 p0473 A83-16073
- On the possibility for a fourth test of general relativity in earth's gravitational field
05 p0683 A83-17148
- Dynamic thermal response of single-mode optical fiber for interferometric sensors
07 p0930 A83-20834
- Multidetector intensity interferometers
08 p1092 A83-22327
- Precision optical wavefront measurement
08 p1103 A83-22872
- Coherence and interferometry through optical fibers --- of stellar interferometers
10 p1482 A83-25847
- Fibre-optic gyro for sensitive measurement of rotation
10 p1422 A83-26474
- High-sensitivity laser interferometer based on a multimode optical waveguide
10 p1484 A83-26659
- Measurement of the energy characteristics of a sound field in an interferometer
11 p1650 A83-27451
- Self-calibrating surface measuring machine --- for fabrication of aspheric optical elements
13 p1847 A83-31016
- Telescope alignment with the absolute distance interferometer
13 p1921 A83-31023
- Some results of the application of a selective interference spectrometer to the diagnostics of an inductively coupled plasma
14 p2087 A83-32831
- Real-time fringe-pattern analysis
14 p2021 A83-32912
- New general relativistic effect by means of charged-particle interferometry
15 p2224 A83-33792
- Method of improving image quality in holographic interferometers
15 p2164 A83-34424
- Alternative techniques to GPS/NAVSTAR
17 p2462 A83-38937
- Determination of the nonreciprocity matrix of a nonstationary single-mode fiber-optic waveguide, with application to a fiber-optic ring interferometer
18 p2690 A83-40098
- Contractive states and the standard quantum limit for monitoring free-mass positions --- by gravitational wave interferometers
21 p3199 A83-43881
- Cyclic interferometers for optical testing
21 p3136 A83-44154
- Propagation effect on interferometer
21 p3222 A83-44292
- Interferometric determination of slow movements --- thermal dilatation measurement on laser heated semiconductor surface
21 p3139 A83-44795
- Interferometer detection system for optical testing
21 p3139 A83-44797
- X-ray interferometer calibration of microdisplacement transducers
21 p3140 A83-44949
- A surface-spin-wave interferometer
22 p3276 A83-45671
- Nonlinear antiresonant ring interferometer
22 p3356 A83-45961
- Optical amplitude and polarization multistability in a nonlinear interferometer
22 p3360 A83-46790
- INTERFEROMETRY**
NT DIFFERENTIAL INTERFEROMETRY
NT HOLOGRAPHIC INTERFEROMETRY
NT LASER INTERFEROMETRY
NT MOIRE INTERFEROMETRY
NT VERY LONG BASE INTERFEROMETRY
- Coherent image fringe contrast measurement with sensing arrays
01 p0051 A83-10863
- Flow visualization and data analysis of self-sustained shock oscillations on a spiked body at Mach 3
01 p0003 A83-11072
- The Clark Lake Teepee-Tee telescope
02 p0246 A83-11995
- Optical biasing on quasi-interferometry with coded correlation filtering
02 p0177 A83-12306
- Real-time optical interferometric image subtraction by wave polarization
02 p0177 A83-12309
- Surface and figure characterization of grazing incidence optics
02 p0239 A83-12718
- The proper motions of 26 pulsars
03 p0401 A83-13311
- Interferometer observations of double stars. I
03 p0408 A83-13882
- Speckle interferometry of the spectroscopic binary 94 Aquarii A
03 p0421 A83-14148
- Electrical properties of frozen ground at VHF near Point Barrow, Alaska
03 p0352 A83-14858
- Interferometric determination of curvatures of flexed plate
[ASME PAPER 82-WA/APM-27] 04 p0499 A83-15688
- Prototype of an integrated-optics four-digit analog-digital converter
05 p0685 A83-17062
- Interferometer observations of double stars. II
06 p0819 A83-18788
- On the origin of speckle boiling and its effects in stellar speckle interferometry
06 p0822 A83-19190
- Fast determination of the extent of spatial and temporal coherence
06 p0767 A83-19191
- Interferometric observations of solar limb structure at 2.6 millimeters
06 p0857 A83-19512
- Nondestructive testing in production plants by shearography
07 p0942 A83-20451
- Determination of the index profile of optical fibers from transverse interferograms using Fourier theory
07 p0993 A83-20832
- Speckle interferometric measurements of binary stars. VIII
08 p1175 A83-22749
- Digital speckle interferometry of Juno, Amphitrite and Pluto's moon Charon
09 p1367 A83-25301
- Enhancement of fringe visibility in a fibre interferometer
10 p1481 A83-25405
- Multiple telescope interferometry
10 p1494 A83-25841
- Interferometric connection of the Canada-France-Hawaii 3.6 metre telescope and the United Kingdom 3.8 metre telescope on Mauna Kea
10 p1495 A83-25843
- Interferometry with the multiple mirror telescope and conventional telescopes
10 p1495 A83-25845
- Coherent optical image delay device using a BSO phase-conjugate mirror and its applications
10 p1424 A83-26864
- Thermal expansion of graphite epoxy
11 p1543 A83-27443
- On the interpretation of interferograms of cavity turbulence --- in laser cavity medium
11 p1577 A83-27516
- How to achieve diffraction limited resolution with large space telescopes
11 p1656 A83-27727
- FLUTE or TRIC - Different approaches to optical arrays in space
11 p1536 A83-27728
- Automated digital processing of interferograms --- Thesis
11 p1575 A83-28650
- Acoustical speckle interferometry
12 p1730 A83-29586
- Speckle interferometry and related techniques with advanced technology optical telescope
13 p1920 A83-31011
- Interferometric control of a beam expander consisting of multiple telescopes
13 p1921 A83-31022
- One-dimensional telescope aperture for brightness and velocity speckle interferometry measurements
13 p1939 A83-31029
- Limits on Venus' SO₂ abundance profile from interferometric observations at 3.4 mm wavelength
13 p1961 A83-31211
- Stellar interferometry - Diameters and effective temperatures of five giant stars
13 p1941 A83-31564
- The influence of ionospheric refraction on radio astronomy interferometry
13 p1941 A83-31571
- Speckle interferometry observations of the asteroids Juno and Amphitrite
13 p1943 A83-31751
- Speckle spectroscopy; an application for the multi-anode microchannel array detector system
14 p2017 A83-32016
- First VHF auroral radar interferometer observations
14 p2053 A83-32696
- Complex interferometry
14 p2021 A83-32911
- Picosecond pulse response of broad-band guided-wave interferometric light modulators
14 p2085 A83-33424
- Astrometric and infrared speckle analysis of the visually unresolved binary BD +41.328 deg
14 p2101 A83-33467
- On the investigation of axisymmetric discontinuous flows using interferometry
16 p2349 A83-35538
- High angular resolution observations of alpha Orionis with a rotation shearing interferometer
17 p2592 A83-37940
- Image reconstruction by the speckle-masking method
17 p2592 A83-37949
- An interference technique of distance measurement using a fiber-optic waveguide
18 p2688 A83-39436
- Interferometry in a space-time with torsion
19 p2894 A83-40731
- Synchronous phase detection for optical fiber interferometric sensors
20 p2988 A83-42219
- Visualization of heat transfer
20 p2970 A83-42654
- Speckle-shear interferometry with double Dove prisms
21 p3136 A83-44189
- TV based system for interferogram analysis
21 p3139 A83-44796
- Review of fiber optic gyroscopes
21 p3140 A83-44820
- Method for subaperture testing interferogram reduction --- for large optical systems
22 p3356 A83-45960
- Rotational Raman interferometric measurement of flame temperatures
22 p3294 A83-46840
- Speckle interferometry observations of Pluto's moon Charon
23 p3516 A83-47439
- Interferometric measurements of atmospheric species
23 p3456 A83-47775

- Color coding in quasi-interferometry 24 p3582 A83-49011
- Optical-correlation quasi-interferometry - A new viewpoint on spatial frequency filtering 24 p3582 A83-49012
- INTERFERON**
- Results of space experiment program 'Interferon' [IAF PAPER 83-187] 23 p3498 A83-47303
- INTERGALACTIC MEDIA**
- Einstein Observatory solid state spectrometer observations of M87 and the Virgo cluster 02 p0254 A83-12104
- The optical activity of intergalactic space 03 p0417 A83-13495
- How well is gas mixed in clusters of galaxies 03 p0428 A83-14767
- Cosmic ray origin above 10 to the 18th eV - Galactic or extragalactic 04 p0575 A83-14983
- NGC 1961 - Stripping of a supermassive spiral galaxy 04 p0550 A83-15036
- The dynamics of the intergalactic medium 04 p0556 A83-15957
- Absorption lines, Faraday rotation, and magnetic field estimates for QSO absorption-line clouds 05 p0696 A83-16979
- The curvature of radio jets and tails in the intracuster media of Abell 1446 and 2220 05 p0696 A83-16981
- Observational constraints on galaxy-IGM interactions in the Virgo cluster 06 p0839 A83-19266
- On the possibility of detecting very hot gas through absorption-line studies 06 p0839 A83-19268
- New observations of a region of the Magellanic Stream 07 p1010 A83-19857
- Intergalactic gas in galaxy clusters - Scattering and polarization of the radio emission of a central source 07 p1014 A83-20663
- Wind instability in the clouds around radio galaxies 07 p1015 A83-20664
- Supernovae and the formation of galaxies 08 p1179 A83-21858
- The structure and expansion law of a shock wave in an expanding universe 08 p1181 A83-23026
- Active extragalactic objects in the visible and ultraviolet regions 09 p1353 A83-24015
- Continuous intergalactic extinction 09 p1358 A83-24016
- High-resolution spectroscopy of selected absorption lines toward quasi-stellar objects. I - Lyman-alpha toward PHL 957 10 p1512 A83-26703
- Intergalactic and galactic magnetic fields - An updated test 11 p1679 A83-27990
- Astrophysical properties of a luminous Wolf-Rayet type object in the core of the extragalactic H II region IC 132 from an analysis of its lambda-lambda 1200-6000 A spectrum 11 p1681 A83-28265
- Absorption-line spectroscopy of close pairs of QSOs 13 p1954 A83-31582
- Why high-latitude clouds in our Galaxy and the highly redshifted clouds observed in front of QSOs do not belong to the same parent population 14 p2106 A83-33224
- Search for neutral hydrogen in the early universe 14 p2107 A83-33236
- Physical properties of the intergalactic medium and the Lyman-alpha absorbing clouds 15 p2259 A83-34118
- Detection of 10 to the 10th solar masses of hot gas in the normal elliptical galaxy NGC 5846 with the Einstein satellite 15 p2259 A83-34119
- Intergalactic shock waves 15 p2260 A83-34377
- Grain alignment in the intergalactic magnetic field 15 p2263 A83-34552
- Extragalactic gamma-ray astronomy 17 p2590 A83-37775
- The dynamics of rich clusters of galaxies. II - The Perseus cluster 17 p2591 A83-37776
- Are wide-angle radio-tail QSOs members of clusters of galaxies? I - VLA maps at 20 cm of 117 radio quasars 17 p2602 A83-37777
- The Mount Wilson halo mapping project 18 p2758 A83-39666
- A model for the emission spectrum of active galactic nuclei 18 p2774 A83-39740
- Radio and X-ray observations of the radio halo source in A1367 19 p2917 A83-41609
- Release of protons with energy higher than 10 to the 18th eV from intergalactic magnetic field into interstellar magnetic field 20 p3077 A83-43664
- A search for microwave background diminution towards the cluster 0016 + 16 21 p3223 A83-44429
- The distribution of absorption lines in QSO spectra 21 p3232 A83-44731
- Two-dimensional spectrophotometry of the cores of X-ray luminous clusters 21 p3235 A83-45529
- Diffuse ultraviolet radiation in the intergalactic medium 22 p3378 A83-46549
- Accretion of intracluster gas by a galaxy 24 p3653 A83-49167

- HI observations of the interacting galaxies - VV 371 and VV 329 24 p3655 A83-49218
- Stabilizing a cold disk with a 1/r force law 24 p3656 A83-49236
- Pregalactic helium abundance determination from extragalactic H II regions 24 p3667 A83-50057
- Are there three systematic observational effects on abundance determinations in giant extragalactic H II regions? 24 p3667 A83-50058
- INTERGRANULAR CORROSION**
- Application of X-ray energy dispersive analyses /EDAX/ to determine the penetration depth of one oxide phase /NiAl₂O₄/ in a two-phase oxide internal oxidation zone /NiAl₂O₄+Al₂O₃/ of a binary alloy /Ni-Al/ 01 p0024 A83-10248
- Intergranular corrosion mechanism in Al-Mn alloys 04 p0457 A83-14963
- Mechanics and mechanisms of intergranular cavitation in creeping alloys 06 p0728 A83-18478
- Creep cavitation of grain interfaces 06 p0728 A83-18483
- The effect of superplastic deformation on subsequent service properties of fine grained 7475 Al 07 p0883 A83-19672
- Influence of sulfur, phosphorus, and antimony segregation on the intergranular hydrogen embrittlement of nickel 07 p0885 A83-20261
- Intergranular cavitation in creeping alloys 07 p0887 A83-20627
- Mechanisms of intergranular cavity nucleation and growth during creep 07 p0887 A83-20630
- The influence of applied coatings on the creep fracture of IN 738 LC 07 p0894 A83-21488
- High-temperature environmental strength degradation of a hot-pressed silicon nitride - An experimental test [ACS PAPER 117-B-81F] 08 p1071 A83-22198
- The effect of structural components on the energy of intergranular fracture --- in Mo and W alloys 08 p1068 A83-22784
- Models for intergranular creep crack growth by diffusion 09 p1279 A83-24069
- Grain boundary sliding and stress concentration during creep 10 p1396 A83-25860
- The effects of segregation on the kinetics of intergranular cavity growth under creep conditions 10 p1396 A83-25862
- The multiplicity of factors causing intergranular fracture 13 p1822 A83-30742
- Hydrogen-induced cracking in 4340-type steel - Effects of composition, yield strength, and H₂ pressure 14 p1994 A83-32678
- Computer simulation for the intergranular corrosion of Alloy 800 16 p2335 A83-36899
- Flow localization accompanying the intergranular fracture of Ni3Al 18 p2670 A83-40641
- Thermodynamic mechanism for cation diffusion through an intergranular phase - Application to environmental reactions with nitrogen ceramics 23 p3436 A83-48282
- Effect of Cu addition on intergranular corrosion of Al-5.5 percent Zn-2.5 percent Mg alloy 24 p3566 A83-49860
- Stress corrosion cracking and intergranular corrosion of 2017 aluminum alloy 24 p3566 A83-49861
- INTERIM STAGES (SPACECRAFT)**
- NT INERTIAL UPPER STAGE
- INTERIM UPPER STAGE (STS)**
- U INERTIAL UPPER STAGE
- INTERIOR BALLISTICS**
- Computerized design of CAD --- Charge Activated Devices 04 p0465 A83-15415
- An implicit numerical analysis for two-dimensional, two-phase turbulent interior ballistic flows [AIAA PAPER 83-0561] 05 p0637 A83-16789
- INTERLACING DRAINAGE**
- U DRAINAGE PATTERNS
- INTERLAYERS**
- NT MULTILAYER INSULATION
- Stability of three-layer cylindrical shells with a discrete filler under axial compression 11 p1596 A83-28455
- The fracture toughness of interlayers in joints with layers of different moduli under static tension 14 p2030 A83-32384
- Titanium-steel interaction under production and operation temperatures 18 p2667 A83-40299
- Inter-layered clay stacks in Jurassic shales 21 p3174 A83-45060
- INTERMEDIATE FREQUENCIES**
- Waveguide-bandwidth millimetric mixer with IF to 18 GHz 08 p1079 A83-21972
- Doppler signal processing using IF limiting 11 p1626 A83-27025
- Precision broad-band RF-switched radiometer for the Megahertz and lower Gigahertz range with IF attenuator 13 p1847 A83-31294

- Electronic control of the difference frequency between two semiconductor lasers 14 p2024 A83-32420
- INTERMEDIATE FREQUENCY AMPLIFIERS**
- A two-stage monolithic IF amplifier utilizing a Ta₂O₅ capacitor 09 p1256 A83-24681
- INTERMETALLICS**
- Phase equilibria and certain properties of Ti-TiP-TiNi alloys at 400 C 01 p0024 A83-10385
- A nuclear gamma resonance study of Ti3Al containing Fe-57 impurity 02 p0159 A83-13039
- Effect of particles of the insoluble phase Al₉FeNi on the kinetics of fatigue crack propagation in alloy AK4-1 03 p0297 A83-13256
- Effect of aging on the temperature at which martensitic transformation initiates in a TiNi intermetallic compound 04 p0459 A83-15702
- Observation of an unusual martensitic-transformation sequence in TiNi 04 p0459 A83-15703
- Effect of defect structure upon the mechanical behavior of beta-LiAl through dislocation damping and hardness studies 04 p0460 A83-16002
- Thermal expansion of the directionally solidified Ni3Al-Ni3Nb eutectic alloy and its constituent phases 04 p0461 A83-16006
- Crystal chemistry of RT5H/D/x, RT2H/D/x and RT3H/D/x hydrides based on intermetallic compounds of CaCu₅, MgCu₂, MgZn₂ and PuNi₃ structure types 04 p0457 A83-16043
- Removal of surface strain from rare earth intermetallic compounds by ion-beam planing 05 p0615 A83-17567
- Anti-phase domain boundary tubes in Ni3Al --- crystal defect structures 05 p0616 A83-17792
- An experimental study of the correlation between the root-mean-square thermal displacements of atoms and the resistance to creep --- of nickel and aluminum alloys 06 p0729 A83-18750
- The self-propagating high-temperature synthesis of aluminides. I - A thermodynamic analysis 07 p0883 A83-19964
- Reactions and diffusion between an Al film and a Ti substrate 07 p0874 A83-20252
- Precipitation of T1 phase in /alpha + T1/ type Al-4.2%Cu-1.3%Li alloy 07 p0885 A83-20294
- An electron microscopy study of the structure of V-Al alloys 07 p0890 A83-20919
- Nuclear gamma resonance of Fe-57 impurity atoms in Ti3Al 07 p0890 A83-20920
- The effect of low-temperature annealing on the initial temperature of martensitic transformation in a nickel-titanium intermetallic 07 p0890 A83-20921
- Microstructures and strengthening of aluminum alloys 07 p0896 A83-21605
- Microstructural aspects of the cold deformation of Nimonic alloy 115 07 p0897 A83-21607
- Influence of thermomechanical processing on elevated temperature slow plastic flow properties of B2 aluminide Fe-39.8at.% Al 08 p1065 A83-22017
- Reasons for the reduction in the fracture toughness of alloy KHN77TYuR-VD at room temperature 08 p1067 A83-22699
- The orientation and temperature dependence of the 0.2% proof stress of single crystal Ni3Al/Ti 08 p1067 A83-22750
- Hydrides formed from intermetallic compounds of two transition metals - A special class of ternary alloys 09 p1225 A83-23858
- Thermodynamic and structural aspects of studies on shape-memory alloys based on titanium-nickel intermetallics 09 p1234 A83-24377
- Phase equilibria in the Ti-TiNi₃-Mo region of the Ti-Ni-Mo ternary system 09 p1234 A83-24387
- Methods for the production of titanium-base intermetallic compounds and alloys using self-propagating high-temperature synthesis 09 p1236 A83-24408
- Superconducting properties of a liquid-infiltration Nb-Nb3Sn composite formed during a low-temperature reaction 10 p1489 A83-26216
- Special features of the formation of the joint between platinum and titanium during vacuum diffusion bonding 10 p1397 A83-26219
- Nucleation during solidification of aluminum-titanium alloys 10 p1399 A83-26890
- The production of titanium-nickel intermetallics by self-propagating high-temperature synthesis 11 p1547 A83-27921
- A brittle to ductile transition in NiAl of a critical grain size 12 p1714 A83-29726
- Phase equilibria in alloys of the system Ti-TiRu-TiNi 13 p1819 A83-30069
- A study of the dynamic conditions of the extrusion of NiTi intermetallic 13 p1820 A83-30683
- A study of the ductility of NiTi intermetallics 13 p1821 A83-30690

- The effect of hydrogen on the temperature of the thermoelectric martensitic transformation in titanium-nickel intermetallics 13 p1822 A83-30744
- The dispersion effect during the plastic deformation of titanium-nickel intermetallics 13 p1824 A83-31339
- The mechanical properties and stability of alloys 14 p1991 A83-31945
- A study of the interaction between titanium and gallium 14 p1992 A83-32148
- Heat release during the interphase interaction of titanium with an NiMn melt 14 p1993 A83-32595
- The high-temperature shape-memory effect in titanium-nickel intermetallics 15 p2138 A83-34019
- The texture in diffusion-grown layers of trialuminides MeAl₃ (Me = Ti, V, Ta, Nb, Zr, Hf) and VNi₃ 15 p2140 A83-34798
- Deformation of metals under conditions of transformation plasticity 15 p2140 A83-35045
- An isothermal section of the phase diagram for Ti-TiNi₃-Mo at 900 C 16 p2335 A83-36896
- Investigations of the constitution in the beryllium-rich region of the beryllium-cobalt-nickel system 18 p2665 A83-39174
- The factors underlying the shape memory effect in titanium-nickel intermetallics 18 p2666 A83-39517
- Tensile and compressive deformation and fracture behavior of the Al-Al₃Ni eutectic composites at elevated temperatures 18 p2667 A83-40255
- High temperature creep properties of alpha Ti-Ti₅Ge₃ 18 p2667 A83-40256
- Flow localization accompanying the intergranular fracture of Ni₃Al 18 p2670 A83-40641
- Interaction between hydrogen and intermetallic compounds 19 p2820 A83-42010
- Theoretical and experimental studies of multicomponent nickel alloys 20 p2955 A83-43490
- Intermetallic compounds of the micron- and P-phases of Co₇Mo₆ studied by 1 MV electron microscopy 20 p2956 A83-43616
- The effect of complex alloying on the temperature range of the martensitic transformation in titanium-nickel intermetallics 21 p3113 A83-44845
- X-ray analysis of the crystal structure and thermal expansion of the intermetallic compound (Tb_{0.8}Gd_{0.2})₃Co crystallized in space 23 p3414 A83-47295
- [IAF PAPER 83-159] 23 p3414 A83-47295
- Ordered structures in Ti Al alloys in the composition range from AB to A₂B₃ 23 p3432 A83-48186
- [ONERA, TP NO. 1983-65] 23 p3432 A83-48186
- On the Co-Ti system 24 p3561 A83-49435
- Thermal expansion of refractory metal compounds 24 p3566 A83-49551
- INTERMITTENCY**
- The prediction of the intermittency factor for turbulent shear flows 05 p0635 A83-16683
- [AIAA PAPER 83-0382] 05 p0635 A83-16683
- Intermittent behaviour in non-linear-Hamiltonian systems far from equilibrium 06 p0805 A83-18329
- Intermittency in Josephson junctions 07 p0918 A83-19996
- Conditional analysis of intermittency in the near wake of a circular cylinder 10 p1414 A83-25783
- Experimental evidence of intermittencies associated with a subharmonic bifurcation --- in Rayleigh-Benard hydrodynamic instability 24 p3577 A83-49296
- INTERMODULATION**
- Intermodulation spectra for 2-carrier-level SPC system 07 p0916 A83-21575
- Practical design of 2-4 GHz low intermodulation distortion GaAs FET amplifiers with flat gain response and low noise figure 09 p1255 A83-24348
- The effect of the limitation of the spectrum of a linear-FM signal with intrapulse phase shift keying on the characteristics of optimal reception 13 p1829 A83-30734
- Optimum frequency assignment for satellite SPC systems 19 p2829 A83-41358
- Cross modulation of VLF and LF waves by gravity waves --- in nocturnal D region 22 p3332 A83-46533
- Application of the statistical simulation method to determine the electromagnetic-compatibility factors of radio systems 24 p3571 A83-50209
- INTERMOLECULAR FORCES**
- Theoretical calculation of conformational energies of polytetrafluoroethylene 01 p0027 A83-10606
- Self-consistent extrapolation of the results of numerical experiments for fluid structures 03 p0389 A83-13537
- Experimental and theoretical analysis of the temperature dependence of rotational Raman linewidths of oxygen 07 p0991 A83-21191
- Scattering of thermal He beams by crossed atomic and molecular beams. V - Anisotropic intermolecular potentials for He + CO₂, N₂O, C₂N₂ 08 p1163 A83-22215
- Approximate constants of motion for classically chaotic vibrational dynamics - Vague tori, semiclassical quantization, and classical intramolecular energy flow 09 p1344 A83-25216
- Spectral effects of intermolecular interactions in gases --- Russian book 10 p1478 A83-25520
- On the effectiveness of models of the Boltzmann operator of intermolecular collisions 13 p1932 A83-30660
- Analysis of the influence of intramolecular interactions on the probability of vibration-rotation transitions in linear molecules 14 p2082 A83-32557
- Intermolecular potentials from NMR data - H₂-N₂O and H₂-CO₂ 15 p2227 A83-33631
- Redistribution - Why half a collision is better than a whole one --- spectra of scattered light from perturbed atomic system 17 p2484 A83-37075
- Fine-structure spectrum of O₂-rare gas van der Waals molecules 19 p2897 A83-40770
- Effect of molecular rotation upon charge transport between disordered carbazole units 20 p3053 A83-42602
- The generalized Hubbard model in the theory of trimerizable molecular crystals --- such as Cs(2)(TCNQ)(3)-organic charge transfer salt 21 p3220 A83-45505
- The variational solution of the problem of internal rotation for a series of polyatomic molecules 24 p3627 A83-49741
- INTERMONTANE FLOORS**
- U VALLEYS
- INTERNAL COMBUSTION ENGINES**
- NT BRISTOL-SIDDELEY BS 53 ENGINE
- NT DIESEL ENGINES
- NT GAS TURBINE ENGINES
- NT HELICOPTER ENGINES
- NT HYDROGEN ENGINES
- NT J-79 ENGINE
- NT JET ENGINES
- NT PULSEJET ENGINES
- NT RAMJET ENGINES
- NT SUPERSONIC COMBUSTION RAMJET ENGINES
- NT T-56 ENGINE
- NT T-64 ENGINE
- NT TF-41 ENGINE
- NT TURBOFAN ENGINES
- NT TURBOJET ENGINES
- NT TURBOPROP ENGINES
- NT WANKEL ENGINES
- Test stand for fatigue life studies involving superposed mechanical and thermal cyclic stresses 02 p0197 A83-12986
- Nonadiabatic nonisobaric propagation of a planar premixed flame - Constant-volume enclosure [AIAA PAPER 83-0239] 05 p0612 A83-16605
- The analysis of performance of Stirling engines. I - Computer simulation model 07 p0939 A83-20287
- Energy and entropy balances in a combustion chamber - Analytical solution 09 p1226 A83-24363
- Sensitivity of chamber turbulence to intake flows in axisymmetric reciprocating engines 09 p1207 A83-24677
- Rotary engines 09 p1369 A83-25140
- Temperature and concentration measurements in an internal combustion engine using laser Raman spectroscopy [AIAA PAPER 83-1551] 14 p1990 A83-32772
- The integration of internal combustion engines of the General Aviation - Problems raised by ventilation and exhaust [AAAF PAPER NT 82-16] 14 p1976 A83-33167
- Minimization of energy storage requirements for internal combustion engine hybrid vehicles 17 p2516 A83-37547
- k-epsilon equation for compressible reciprocating engine flows 17 p2507 A83-38021
- INTERNAL ENERGY**
- Energy disposal in charge transfer reactions producing NH₃(+.) - Dependence of the NH₃(+.) + H₂O reaction on NH₃(+.) internal energy 16 p2327 A83-36520
- INTERNAL FRICTION**
- Characteristics of the amplitude dependence of internal friction and Young's modulus defect in solids at low deformation amplitudes 02 p0155 A83-12206
- Dissipation properties and the structure of Ti-Ni-Cu system 04 p0459 A83-15468
- A summary of Viking sample-trench analyses for angles of internal friction and cohesions 04 p0567 A83-15574
- Oscillatory internal friction associated with hydride precipitation in alpha-titanium 04 p0462 A83-16257
- Extended capabilities of a vibrating-reed internal friction apparatus 07 p0932 A83-21385
- A theoretical consideration of the microstructural origins of friction stress in a cast gamma prime-strengthened superalloy 09 p1232 A83-24063
- Interior friction for polycrystalline and monocrystalline high purity nickel at high temperature 11 p1548 A83-28222
- Multimode Rayleigh wave attenuation and Q beta in the crust of the Barents Shelf --- shear wave internal friction 12 p1757 A83-29961
- The effect of hydrogen solubility on the internal friction of V-Ti alloys 14 p1997 A83-32949
- The prediction of fatigue life using ultrasound testing 16 p2367 A83-36184
- Use of high amplitude strains in studying wear and ultrasonic fatigue in metals 16 p2333 A83-36202
- A model of a material with internal friction 17 p2521 A83-37542
- Elevated temperature internal friction due to composite structure in sintered silicon nitrides 18 p2672 A83-40246
- The use of the internal friction method for studying laser-irradiated materials 21 p3115 A83-45502
- The mechanism of elastic energy absorption in boron fibers 24 p3553 A83-49474
- INTERNAL PRESSURE**
- Concerning the formulation of the problem of calculating the stress-strain state in shell-reinforced cylinders by the finite element method 03 p0341 A83-14073
- Simplified multilayer insulation pumpdown calculation approach 12 p1722 A83-29217
- An experimental investigation of the internal methane pressure in hydrogen attack 14 p1994 A83-32682
- Reflections on the computational approximation of elastic incompressibility 15 p2179 A83-34562
- Stability loss during the plastic deformation of shells 15 p2180 A83-35034
- Three dimensional stress state in an internally-pressurized hollow cylinder with a reinforcing ring 18 p2697 A83-39453
- Gold as a reliable internal pressure calibrant at high temperatures 20 p2959 A83-42596
- A note on the problem of an annular crack subjected to an arbitrary normal pressure 20 p3004 A83-42975
- Dynamic finite element analysis of nonaxisymmetric structures 23 p3471 A83-48163
- INTERNAL STRESS**
- U RESIDUAL STRESS
- INTERNAL WAVES**
- NT PLANETARY WAVES
- An isolated internal wave in the thermosphere generated by the auroral electrojet 01 p0071 A83-10597
- The energetics of the lower thermosphere in the presence of internal gravity waves 03 p0362 A83-14834
- Internal reflections in bleached reflection holograms 06 p0762 A83-18593
- The Cauchy problem for the equation of internal waves 06 p0758 A83-19117
- A study of internal waves generated by the rapid horizontal motion of cylinders and spheres 06 p0760 A83-19433
- Two-layer vortices in a rotating stratified fluid 07 p0957 A83-19636
- Application of WKB theory to turbulence layers in the vicinity of critical levels --- in winter hemisphere for internal gravity wave propagation 09 p1311 A83-23888
- Detection of Massachusetts Bay internal waves by the synthetic aperture radar /SAR/ on Seasat 09 p1319 A83-24303
- SAR imagery and surface truth comparisons of internal waves in Georgia Strait, British Columbia, Canada 09 p1319 A83-24305
- A small-component model of the nonlinear interactions between internal gravity waves 09 p1308 A83-25052
- Observation of internal waves in the ocean 10 p1453 A83-26812
- Atmospheric internal gravity waves as a source of quasiperiodic variations of the cosmic ray secondary component and their likely solar origin 11 p1615 A83-27664
- Intensity variations of the IGW source and the ionospheric response during the substorm of September 18, 1974 --- Internal Gravity Wave 11 p1615 A83-27952
- Generation of the internal gravity waves of auroral electrojets 11 p1620 A83-28747
- The scattering of waves described by the Klein-Gordon equation by an inclined half-plane 13 p1913 A83-30082
- Ship waves and lee waves 13 p1892 A83-31038
- The generation of Rossby waves during the disintegration of internal gravity waves 13 p1880 A83-31394
- Slow waves near the mesopause 14 p2059 A83-32860

- Nonlinear features of internal waves off Baja California as observed from the Seasat imaging radar
15 p2208 A83-33496
- An upper boundary condition permitting internal gravity wave radiation in numerical mesoscale models
15 p2203 A83-33878
- Acoustic remote sensing of internal waves in shallow water
15 p2208 A83-34153
- Experiments on solitary internal Kelvin waves
16 p2348 A83-35343
- Internal gravity waves in Titan's atmosphere observed by Voyager radio occultation
16 p2436 A83-35738
- Analysis of viscous-inviscid interaction in transonic internal flows
16 p2293 A83-36081
- Internal-gravity-wave-like variations of temperature, humidity and wind observed in the troposphere downstream of heavy rainfall area
16 p2390 A83-36498
- The detection of internal waves in the atmosphere over the sea on the basis of variations in the microwave self-radiation of the atmosphere and sea surface
16 p2393 A83-36873
- Experiments on the generation of internal waves in a stratified fluid
17 p2502 A83-37201
- [AIAA PAPER 83-1704]
17 p2502 A83-37201
- Sea pressure waves
18 p2731 A83-39444
- HF Doppler measurements of mesospheric gravity wave momentum fluxes
18 p2718 A83-40044
- Study of internal gravity waves in the lower thermosphere from observations of the nocturnal sky airglow (01) 5577
20 p3016 A83-42309
- A in Ashkhabad
20 p3016 A83-42309
- Turbulence originating from convectively stable internal waves
20 p3020 A83-42838
- On the instability of internal Alfvén-gravity waves in stratified shear flows
21 p3171 A83-44469
- Reaction of the ionospheric F2 region to a solitary internal gravity wave
21 p3176 A83-45257
- The parametric excitation of internal waves and convective instabilities in a fluid layer heated from above
22 p3322 A83-45639
- Infrasonic and internal gravity waves in the atmosphere during large fires
23 p3485 A83-48503
- Evolution of axisymmetric distributions of vorticity in an ideal incompressible stratified fluid (the linear description)
23 p3451 A83-48530
- The spatial and temporal structure of internal inertial-gravity and topographic waves in the sea at frequencies close to the inertial frequency
23 p3493 A83-48563
- INTERNATIONAL COMPUTERS LIMITED**
U ICL COMPUTERS
- INTERNATIONAL COOPERATION**
NT OUTER SPACE TREATY
- The space flight of the Soviet-French crew
01 p0015 A83-10382
- Legal-political discrimination in cross-border satellite-mediated TV advertising and publicity - Review of problems
01 p0112 A83-10400
- Advanced operational earth resources satellite systems
02 p0137 A83-11932
- [AAS 82-128]
02 p0137 A83-11932
- NASA-ESA Spacelab systems and programs; Proceedings of the Seminar, Washington, DC, April 23, 24, 1981
03 p0284 A83-13703
- International cooperation in manned space flight - Next steps
04 p0451 A83-15674
- Summary of European IMS workshop
04 p0514 A83-16309
- Environmental contamination in light of space law
05 p0692 A83-16973
- The Montreal Agreement of 1966 and the Malta Agreement of 1965
05 p0692 A83-16975
- International civil aviation in the South Pacific: A perspective --- Book
05 p0591 A83-17116
- 'RARC '83' - International planning for broadcasting satellites at 12 GHz
07 p0906 A83-19717
- The 1985/87 Space Planning Conference --- on use of geostationary satellite orbits for satellite services
07 p0906 A83-19718
- The contribution made by international organizations to the formation of space law
07 p1002 A83-21387
- UNISPACE 82 and beyond
07 p1002 A83-21390
- The Second United Nations conference on the exploration and peaceful uses of outer-space /UNISPACE 82/
07 p1002 A83-21391
- NGOs at UNISPACE 82 --- nongovernmental organizations
07 p1002 A83-21392
- NGO's at UNISPACE 82 - Session on legal and political aspects, Vienna, Aug. 19, 1982
07 p1002 A83-21393
- Report of the second United Nations conference on the exploration and peaceful uses of outer space
07 p1002 A83-21394
- Unispace and space law - Results and perspectives of the Second United Nations' Conference on Outer Space
08 p1171 A83-21896
- Space law in the United Nations - The work of the UN Outer Space Committee in 1982
08 p1171 A83-21897
- International scientific cooperation and legal questions of space exploration --- Russian book
08 p1171 A83-22662
- Trends and prospects of the cooperation of states in the area of space exploration in the framework of international organizations
08 p1171 A83-22665
- Problems of international cooperation in the area of the remote sensing of the earth
08 p1172 A83-22667
- Comparison of candidate IGRF models --- International Geomagnetic Reference Field
09 p1302 A83-23715
- Joint U.S.-Mexican activities in arid land management and desertification control
09 p1284 A83-24531
- Article 22 of the Warsaw Convention - In a state of limbo
09 p1351 A83-25118
- The legal regime of the airspace above the exclusive economic zone
09 p1351 A83-25119
- Managing the Enterprise in space
09 p1211 A83-25123
- Sarsat-Kospas - Satellite search-and-rescue trials presage new international system
09 p1211 A83-25138
- Broadcast satellites in Europe
10 p1402 A83-25800
- Interferometric connection of the Canada-France-Hawaii 3.6 metre telescope and the United Kingdom 3.8 metre telescope on Mauna Kea
10 p1495 A83-25843
- Results of a world survey of computer-aided manufacture
10 p1460 A83-26579
- Status of joint US/USSR experiments planned for the Cosmos '83 biosatellite mission
11 p1636 A83-27791
- The IRAS project organisation and mission operations
11 p1534 A83-28210
- Salyut mission report
11 p1532 A83-28413
- The United Nations resolution from December 10, 1982 concerning the principles for direct television broadcasting by satellites
12 p1783 A83-29366
- Applications of stereoscopic height computations from dual geosynchronous satellite data/joint NASA-Japan stereo project
12 p1761 A83-29699
- MIL-STD-810D - A progress report
13 p1863 A83-31502
- Overview of the European community's activities in photovoltaics
14 p2036 A83-32177
- The French-Soviet experiments ARAKS - Main results --- Artificial Radiation and Aurora between Kerguelen and Soviet Union
15 p2197 A83-34181
- Earth-oriented space activities and their legal implications; Proceedings of the Symposium, McGill University, Montreal, Canada, October 15, 16, 1981
15 p2240 A83-34651
- The broadcasting-satellite service - Freedom or control
15 p2144 A83-34652
- Direct broadcasting satellites - International policy issues
15 p2240 A83-34653
- A new service at the starting line - Direct broadcasting from satellites
15 p2144 A83-34654
- Costs and benefits of alternative legal regime for remote sensing
15 p2240 A83-34656
- The Arcad-3 project --- aboard Franco-Soviet AUREOL-3 satellite
18 p2715 A83-39571
- Air industry cooperation
18 p2631 A83-39692
- International law of territorial boundaries of sea, air, and outer space
18 p2753 A83-39697
- The status of space science and technology in developed countries - The European experience
18 p2643 A83-39830
- Impact of space research and technology on small countries (A case study for Austria)
18 p2788 A83-39834
- Basic space sciences in Africa
18 p2788 A83-39835
- Balloon research and cooperative programmes
18 p2631 A83-39838
- Meteorological satellites and cooperative programmes
18 p2725 A83-39840
- Meteorological satellites and cooperative programs
18 p2725 A83-39842
- Earth survey satellites and cooperative programmes
18 p2706 A83-39843
- Earth survey satellites and cooperative programs
18 p2706 A83-39844
- The Memorandum of Understanding between the United States and Certain ECAC Member States on Pricing Regime between U.S. and Europe
20 p3057 A83-43127
- The space document symbols of the United Nations
20 p3057 A83-43128
- The politics of space - U.S. policy: A drama in 'N' acts
21 p3094 A83-45607
- The interpretation of international conventions supporting a uniform law in international relations
22 p3367 A83-45803
- Security of International Civil Aviation - Role of ICAO
22 p3367 A83-45805
- With regards to the Warsaw Convention - A bad process for false problems --- legal liability in airlaw
22 p3367 A83-45806
- The international politics of the orbit-spectrum issue --- concerning communication satellites
22 p3367 A83-45809
- Space law and international organizations
22 p3367 A83-45810
- Global climate space reflector systems - Some legal issues
22 p3368 A83-45815
- An economic assessment of CCIR's five methods for assuring guaranteed access to the orbit-spectrum resource
22 p3368 A83-45819
- Law and security in outer space: International regional role Focus on the European Space Agency
22 p3370 A83-46311
- International cooperation and competition in space - A current perspective
22 p3370 A83-46312
- The Spacelab program and related legal issues
22 p3371 A83-46313
- Solar power satellites and security considerations - The case for multilateral agreements
22 p3371 A83-46318
- Exosat/Delta - Demonstrated short-term backup launcher capability through international cooperation
23 p3418 A83-47227
- [IAF PAPER 83-01]
23 p3418 A83-47227
- Japanese mission model for space station
23 p3413 A83-47245
- [IAF PAPER 83-53]
23 p3413 A83-47245
- Co-operation to achieve a global meteorological satellite system
23 p3488 A83-47276
- [IAF PAPER 83-119]
23 p3488 A83-47276
- Internationally supported data acquisition for solar system exploration in the 1990's
23 p3420 A83-47309
- [IAF PAPER 83-209]
23 p3420 A83-47309
- Orbital debris management - International cooperation for the control of a growing safety hazard
23 p3415 A83-47324
- [IAF PAPER 83-254]
23 p3415 A83-47324
- PAH-2, HAP, HAC - Will they really get under way this time? --- Franco-German military helicopter program
23 p3405 A83-48641
- Investigations in outer space conducted in the USSR during 1982
24 p3550 A83-48886
- Montreal Protocol - The most recent attempt to modify the Warsaw Convention
24 p3637 A83-49026
- INTERNATIONAL GEOPHYSICAL YEAR**
- The energetics of the general circulation of the atmosphere in southern hemisphere during the IGY. I - The distribution of atmospheric energy
04 p0517 A83-16011
- The energetics of the general circulation of the atmosphere in southern hemisphere during the IGY. II - The cycle of the energetics of the atmosphere in southern hemisphere
14 p2056 A83-32401
- Reviews of space science - Legacy of the IGY
24 p3597 A83-48893
- INTERNATIONAL LAW**
NT AIR LAW
NT SEA LAW
NT SPACE LAW
- The implementation of legal principles governing the use of outer space
06 p0816 A83-19375
- Nationality of airlines - A hidden force in the international air regulation equation
07 p1003 A83-21549
- Additional remarks with respect to the American decree of regarding the suspension of foreign certificates of airworthiness
08 p1171 A83-21899
- International aspects of air traffic control liability. I
11 p1666 A83-27968
- The United Nations resolution from December 10, 1982 concerning the principles for direct television broadcasting by satellites
12 p1783 A83-29366
- For delimiting outer space
15 p2240 A83-34661
- International law of territorial boundaries of sea, air, and outer space
18 p2753 A83-39697
- Outer space in international law
19 p2907 A83-41980
- Are the principles of the Warsaw Convention endangered by recent U.S. court decisions?
20 p3057 A83-43126
- The interpretation of international conventions supporting a uniform law in international relations
22 p3367 A83-45803
- Teleinformatics, the protection of privacy and the law
22 p3368 A83-45820
- Essays in air law
22 p3368 A83-45826
- The Warsaw Convention - Past, present and future
22 p3369 A83-45827
- Interchange of aircraft --- international lease regulations
22 p3369 A83-45832
- Liability and insurance for damage caused by foreign aircraft to third parties on the surface - A possible new approach to an old problem
22 p3369 A83-45835
- International multimodal transport - A legal labyrinth
22 p3369 A83-45837

The legal status of the aircraft commander - Ups and downs of a controversial personality in international law 22 p3370 A83-45842

Law and security in outer space; Proceedings of the Workshop, University of Mississippi, University, MS, May 21, 22, 1982 22 p3370 A83-46309

Security aspects of the current United Nations space law agenda 22 p3371 A83-46315

Arms control - Outer space 22 p3371 A83-46317

The legal status of outer space and relevant issues

Delimitation of outer space and definition of peaceful use 22 p3371 A83-46319

INTERNATIONAL MAGNETOSPHERIC STUDY

The IMS source book: Guide to the International Magnetospheric Study data analysis 04 p0511 A83-16276

Data from ISEE-3 for the IMS period 04 p0511 A83-16277

Availability of IMP-7 and IMP-8 data for the IMS period 04 p0511 A83-16278

Data from ISEE-1 for the IMS period 04 p0511 A83-16279

The International Sun Earth Explorer mission - ISEE-2 04 p0511 A83-16280

The availability of GEOS data for IMS research 04 p0511 A83-16282

Geostationary satellites ATS-6 and SMS/GOES - Description, position and data availability during IMS 04 p0511 A83-16283

Description of P78-2 /SCATHA/ satellite and experiments 04 p0511 A83-16284

Atmosphere explorer and the IMS 04 p0512 A83-16288

The satellite situation center 04 p0502 A83-16290

IMS ground observations on optical aurora and ionospheric absorption made in Northern Europe, with examples of data handling 04 p0512 A83-16291

Examples of multi-instrumental studies on auroral phenomena 04 p0512 A83-16292

Magnetometer networks in Northern Europe 04 p0512 A83-16293

Arrays of magnetometers operated in NW Europe 04 p0512 A83-16294

SBARMO-79; a multi-balloon campaign in the auroral zone 04 p0512 A83-16295

High latitude North American networks operative during the IMS 04 p0512 A83-16296

Midlatitude magnetometer chains during the IMS 04 p0512 A83-16297

Research at United States Antarctic stations during the International Magnetosphere Study 04 p0513 A83-16298

IMS results in Antarctica 04 p0513 A83-16299

Antarctic observations available for IMS correlative analyses 04 p0513 A83-16300

Chatanika radar measurements during the International Magnetospheric Study 04 p0513 A83-16301

Worldwide incoherent scatter radar measurements 04 p0513 A83-16302

The origin and evolution of the coordinated data analysis workshop process --- for International Magnetospheric Study 04 p0513 A83-16303

Status of IMS workshops - CDAW 1: December 1977 events --- Coordinated Data Analysis Workshop 04 p0513 A83-16304

The July 29, 1977 magnetic storm - Observations and modeling of energetic particles at synchronous orbit 04 p0513 A83-16306

ISEE-magnetopause observations - Workshop results 04 p0513 A83-16308

Summary of European IMS workshop 04 p0514 A83-16309

Variability of the Harang discontinuity as observed by the Chatanika radar and the IMS Alaska magnetometer chain 07 p0967 A83-21559

Longitudinal structure of substorm injections at synchronous orbit 20 p3018 A83-42413

INTERNATIONAL PRACTICAL TEMPERATURE

U TEMPERATURE SCALES

INTERNATIONAL RELATIONS

NT INTERNATIONAL COOPERATION

NT OUTER SPACE TREATY

International relations in civil aviation --- Russian book 24 p3637 A83-49200

INTERNATIONAL SOLAR POLAR MISSION

Coronal investigations with occulted spacecraft signals 04 p0574 A83-15117

Automatic controls on board planetary probes 17 p2480 A83-37493

Gamma-ray burst localization with the international solar polar mission 18 p2647 A83-39301

The ISPM Mission - Science objectives and mission overview 21 p3093 A83-43976

INTERNATIONAL SUN AND EARTH EXPLORER A

U INTERNATIONAL SUN EARTH EXPLORER 1

INTERNATIONAL SUN AND EARTH EXPLORER B**U INTERNATIONAL SUN EARTH EXPLORER 2****INTERNATIONAL SUN AND EARTH EXPLORER C****U INTERNATIONAL SUN EARTH EXPLORER 3****INTERNATIONAL SUN EARTH EXPLORER 1**

On the relationship of the plasmopause to the equatorward boundary of the auroral oval and to the inner edge of the plasma sheet 02 p0207 A83-12380

Data from ISEE-1 for the IMS period 04 p0511 A83-16279

ISEE work on collisionless shocks - CDAW-3, the meeting and the results July 23-26, 1979 --- Coordinated Data Analysis Workshop 04 p0513 A83-16307

ISEE-magnetopause observations - Workshop results 04 p0513 A83-16308

Observations of quasistatic electric fields on the GEOS and ISEE satellites 11 p1621 A83-28770

Plasma diagnostics by electron guns and electric field probes on ISEE-1 15 p2233 A83-34184

Stimulation of plasma waves by electron guns on the ISEE-1 satellite 15 p2233 A83-34185

Low-energy (less than 100 eV) ion pitch angle distributions in the magnetosphere by ISEE 1 22 p3326 A83-46034

INTERNATIONAL SUN EARTH EXPLORER 2

The International Sun Earth Explorer mission - ISEE-2 04 p0511 A83-16280

ISEE work on collisionless shocks - CDAW-3, the meeting and the results July 23-26, 1979 --- Coordinated Data Analysis Workshop 04 p0513 A83-16307

ISEE-magnetopause observations - Workshop results 04 p0513 A83-16308

Motion of flux transfer events on 10 November 1977 determined by energetic particles on ISEE 2 18 p2718 A83-39951

INTERNATIONAL SUN EARTH EXPLORER 3

An electric noise component with density 1/1 identified on ISEE 3 02 p0207 A83-12376

Data from ISEE-3 for the IMS period 04 p0511 A83-16277

Accelerometer-enhanced orbit control near the sun-earth L1 libration point [AIAA PAPER 83-0018] 05 p0601 A83-16467

The observation of a coronal transient directed at earth 05 p0708 A83-17036

Observations of upstream ions and low-frequency waves on ISEE 3 06 p0782 A83-18284

Search for time variations in 511 keV flux by ISEE-3 gamma-ray spectrometer 07 p1039 A83-20016

Observations of fast, transient gamma-ray phenomena --- Thesis 15 p2277 A83-33698

Problems in the analysis of gamma-ray burst spectra 18 p2786 A83-39302

ISEE-3 - A late entry in the great comet chase 22 p3372 A83-46348

Correlated particle and magnetic field observations of a large-scale magnetic loop structure behind an interplanetary shock 22 p3380 A83-46892

Average configuration of the distant (less than 220-earth-radii) magnetotail - Initial ISEE-3 magnetic field results 23 p3482 A83-47866

INTERNATIONAL SUN EARTH EXPLORERS

NT INTERNATIONAL SUN EARTH EXPLORER 1

NT INTERNATIONAL SUN EARTH EXPLORER 2

NT INTERNATIONAL SUN EARTH EXPLORER 3

Electrostatic bursts generated by electrons in Landau resonance with whistler mode chorus 11 p1617 A83-28311

An ISEE 3 high time resolution study of interplanetary parameter correlations with magnetospheric activity 20 p3018 A83-42415

INTERNATIONAL SYSTEM OF UNITS

Impact of metrication on data processing [SAWE PAPER 1476] 20 p3037 A83-43746

INTERNATIONAL ULTRAVIOLET EXPLORER

U IUE

INTERNUCLEAR PROPERTIES

Determination of accurate dissociation limits and interatomic interactions at large internuclear distances 11 p1653 A83-27526

INTERPLANETARY DUST

NT METEOROID DUST CLOUDS

NT ZODIACAL DUST

Comets --- Book 03 p0415 A83-13376

Optical and infrared observations of bright comets in the range 0.5 micrometers to 20 micrometers 03 p0415 A83-13387

Interpreting the thermal properties of cometary dust 03 p0415 A83-13388

Cometary dust in the solar system 03 p0416 A83-13390

Laboratory studies of interplanetary dust 03 p0416 A83-13391

Formation of dense solid particles in a protoplanetary cloud 03 p0418 A83-13666

INTERPLANETARY MAGNETIC FIELDS

Infrared photometry of periodic comets Encke, Chernykh, Kearns-Kwee, Stephan-Oterma, and Tuttle 03 p0407 A83-13826

Diffusion of Keplerian motions by a stochastic force. II - Lorentz scattering of interplanetary dusts 03 p0429 A83-14784

The photochemistry and dynamics of a dusty cometary atmosphere 03 p0431 A83-14865

The survival of solar flare tracks in interplanetary dust silicates on deceleration in the earth's atmosphere 04 p0563 A83-15367

Classification of the Johnson Space Center stratospheric dust collection 04 p0563 A83-15368

The structure of cometary dust tails. II - Tail brightness profiles and dust characteristics of comet Arend-Roland, 1957 III 05 p0695 A83-16855

The Giotto dust protection system --- for encounters with comet Halley 05 p0607 A83-17434

A scattering model for the zodiacal light particles 06 p0824 A83-18076

Formation of planetesimals from dust - Simple considerations 06 p0842 A83-19460

Pyroxene whiskers and platelets in interplanetary dust - Evidence of vapour phase growth 08 p1191 A83-23279

The experiment PIA of the ESA mission Giotto, a device for the analysis of the mass of the smallest particles which are released from Halley's comet 09 p1218 A83-23383

Analog signal processing in the dust particle experiment of the Giotto mission 09 p1218 A83-23384

How to maintain the spatial distribution of interplanetary dust 10 p1500 A83-25375

On two mechanisms of disintegration of interplanetary dust grains in cometary heads 10 p1517 A83-26914

A model for the formation of spokes in Saturn's rings 11 p1684 A83-27355

On the evolution of Saturn's 'Spokes' - Theory 11 p1684 A83-27356

A multi-fluid model of an H₂O-dominated dusty cometary atmosphere 11 p1683 A83-28382

The integral equation approach to the study of interplanetary dust 13 p1954 A83-31628

Attitude perturbations of the Giotto spacecraft in the dust cloud of Comet Halley 14 p1979 A83-33472

Dust hazard near Halley Comet in case of the Vega project 15 p2128 A83-35016

The derivation of Halley parameters from observations 15 p2273 A83-35018

Dust modelling of fast flyby missions - Implications of in situ measurements 15 p2128 A83-35022

LDEF - Chemical and isotopic measurements of micrometeoroids by SIMS --- Secondary Ion Mass Spectroscopy from Long Duration Exposure Facility 15 p2129 A83-35031

The magnetosphere - A natural laboratory for the investigation of current problems concerning interplanetary dust 17 p2595 A83-37051

Lorentz forces on the dust in Jupiter's ring 17 p2619 A83-37586

Packing effect of fluffy particles --- conglomerate aggregate of submicron-sized interplanetary dust 17 p2610 A83-38519

Laboratory measurements of D/H ratios in interplanetary dust 23 p3529 A83-48084

INTERPLANETARY FLIGHT

NT ASTEROID MISSIONS

NT GRAND TOURS

NT LONG DURATION SPACE FLIGHT

Venera 13, 14 unmanned interplanetary spacecraft attitude control subsystem 17 p2479 A83-37485

INTERPLANETARY GAS

Stochastic diffusion in inverse square fields - General formulation for interplanetary gas 07 p1028 A83-21576

Helium atoms in the interstellar and interplanetary medium. I - Prognoz-5 and Prognoz-6 satellite observations of scattered ultraviolet radiation in the H I 1216 A and He I 584 A lines 09 p1364 A83-25036

INTERPLANETARY MAGNETIC FIELDS

The 11-year variation of the isotropic and anisotropic flux of galactic cosmic rays 02 p0273 A83-11726

The sector structure of the interplanetary magnetic field and disturbances of the central nervous system 02 p0222 A83-11879

Field-aligned currents and magnetic disturbances in the dayside polar region 02 p0204 A83-11966

Dawn-dusk asymmetry of the tail region of the magnetosphere of Saturn and the interplanetary magnetic field 02 p0263 A83-11969

On the flaring of cometary plasma tails 02 p0257 A83-12144

Dependence of magnetic activity on the orientation of the geomagnetic dipole relative to the interplanetary magnetic field 02 p0209 A83-12433

The possibility of exciting geomagnetic pulsations in the case of the radial direction of the interplanetary magnetic field 02 p0211 A83-12451

Pulsed reconnection as a possible source of icpl pulsations --- of geomagnetic field 02 p0211 A83-12452

Penetration of the solar wind magnetic field into cometary ionospheres 03 p0412 A83-13221

Observations and dynamics of plasma tails --- of comets 03 p0416 A83-13397

Solar wind interaction with comets - Lessons from Venus 03 p0416 A83-13398

Cosmic-ray 13 day oscillation and two-sector interplanetary magnetic field 03 p0439 A83-14874

Magnetic clouds - Voyager observations between 2 and 4 AU 03 p0438 A83-14917

Cosmic ray north-south anisotropy - The role of the interplanetary magnetic field 05 p0709 A83-17378

Structure of the heliospheric current sheet in the early portion of sunspot cycle 21 05 p0708 A83-17379

Quadrupole distortions of the heliospheric current sheet in 1976 and 1977 05 p0708 A83-17380

Stationarity of magnetohydrodynamic fluctuations in the solar wind 05 p0709 A83-17381

Dynamics of the frequency spectrum of fluctuations of the interplanetary magnetic field and cosmic rays 05 p0710 A83-17620

Case studies of the storm time variation of the polar cusp 06 p0782 A83-18288

Magnetospheric convection effects at mid-latitudes. I - Saint-Santin observations 06 p0783 A83-18295

Convection electric fields and ionospheric currents derived from model field-aligned currents at high latitudes [AD-A125082] 06 p0783 A83-18297

Spatial structure of solar wind in 1976 06 p0853 A83-18314

Direction of semi-diurnal anisotropy in relation to interplanetary magnetic fields 06 p0828 A83-18424

The radial evolution of the IMF fluctuations - A comparison with theoretical models 06 p0855 A83-19138

The origins of Birkeland currents 07 p0962 A83-20840

The auroral oval and the sector structure of the interplanetary magnetic field 07 p0964 A83-21184

Observation of an IMF sector effect in the Y magnetic field component at geostationary orbit 07 p0968 A83-21582

Influence of interplanetary magnetic field sector boundary passages on Jovian decametric radio bursts 07 p1036 A83-21587

Polar cap arcs and the open regions 08 p1137 A83-23115

On the nature of magnetic fields in the vicinity of Mars 09 p1366 A83-25039

Magnetosphere-ionosphere relationships 10 p1448 A83-25604

Observations of interplanetary shocks - Recent progress 11 p1687 A83-27384

IMF control of the earth's magnetosphere 11 p1614 A83-27390

Plasma processes within the magnetosphere boundaries 11 p1614 A83-27392

Relation of the B sub z component of the interplanetary magnetic field to the generation of the semi-annual wave in Kp-indices 11 p1616 A83-28106

Cosmic ray modulations related to the interplanetary magnetic field intensity 11 p1694 A83-28301

Study on the onsets of solar energetic electron events 11 p1692 A83-28579

Research on Alfvén fluctuations in the solar wind between 0.29 and 1.0 AU --- German thesis 11 p1693 A83-28656

The solar origin of the interplanetary magnetic field 11 p1683 A83-28738

Determining the polarity of sectors of the interplanetary magnetic field on the basis of variations in the geomagnetic field at high latitudes 11 p1620 A83-28739

Interplanetary magnetic field polarity, the geomagnetic ring current, and the precipitation of particles at middle latitudes 11 p1620 A83-28740

The interplanetary magnetic field and the absorption of radio waves in the auroral zone 11 p1620 A83-28741

The effects of the interplanetary magnetic field in the lower ionosphere at middle latitudes 11 p1620 A83-28742

The influence of the interplanetary magnetic field on the F region and the upper ionosphere 11 p1620 A83-28743

The interplanetary magnetic field and the earth's lower atmosphere 11 p1634 A83-28744

The latitudinal dependence of the IMF polarity during 1975-1981 12 p1792 A83-29035

The employment of the pulsation data of Nagycenk observatory for the study of the effect of the interplanetary magnetic field on the geomagnetic pulsations 12 p1753 A83-29236

The frequency spectrum of variations of the Bz component of the interplanetary magnetic field 13 p1947 A83-30615

Response of nightside auroral-oval boundaries to the interplanetary magnetic field 13 p1947 A83-31233

Does IMF B_y induce the cusp field-aligned currents? 13 p1882 A83-31626

The interaction of magnetic fields at the boundary of the earth's magnetosphere 14 p2052 A83-32534

Dynamical evolution of interplanetary magnetic fields and flows between 0.3 AU and 8.5 AU - Entrainment 14 p2102 A83-32699

Multiple spacecraft observations of interplanetary shocks Four spacecraft determination of shock normals 15 p2255 A83-33929

Intensity distribution of dayside polar soft electron precipitation and the IMF 15 p2199 A83-34358

The relationship between the strength of the IMF and the frequency of magnetic pulsations on the ground and in the solar wind 15 p2199 A83-34362

Helios 1 + Helios 2 - A summary of IMF observations performed in the inner solar system during 1975-1981 15 p2261 A83-34404

Magnetic field distribution in the tail of Halley's Comet found from the kinematics of a plasma formation 15 p2271 A83-34772

Early solar system magnetic fields as recorded in meteorites 15 p2276 A83-35007

Physical interpretation of interdisciplinary solar/interplanetary observations relevant to the 27-29 June 1980 SMY/STIP event no. 5 --- Solar Maximum Year/Study of Interplanetary Traveling Phenomena 15 p2285 A83-35231

Propagation of energetic particles in the solar wind 15 p2286 A83-35235

The sector structure of the interplanetary magnetic field and the midlatitude sporadic-E-layer 17 p2537 A83-37054

Comparison of S3-3 polar cap potential drops with the interplanetary magnetic field and models of magnetopause reconnection 17 p2538 A83-37598

The distribution of chromospheric flares in relation to the sectoral boundaries of the interplanetary magnetic field extrapolated onto the sun 17 p2625 A83-37668

An equivalent ionospheric current system at high latitudes in the Northern Hemisphere for a Bz component of the interplanetary magnetic field greater than zero 17 p2539 A83-37698

Heliospheric magnetic fields and plasmas 17 p2627 A83-38290

Cosmic magnetic fields; Proceedings of the Workshop, Florence, Italy, October 21-23, 1982 18 p2765 A83-39226

Magnetic fields in the interplanetary space 18 p2753 A83-39234

On some properties of MHD turbulence --- in solar wind 18 p2783 A83-39235

The effect of the anisotropy of the random component of the interplanetary magnetic field on the density distribution of cosmic rays 18 p2784 A83-39309

The spectrum of whistler turbulence in the interplanetary plasma 18 p2766 A83-39310

Determination of the cross-section configuration of interplanetary flare MHD-disturbances on a sphere with a radius of 1 AU 18 p2713 A83-39311

Variability of the magnetic field in high-velocity streams of the solar wind 18 p2784 A83-39328

Variations of the geomagnetic field in the northern polar cap, independent of the interplanetary magnetic field 18 p2714 A83-39339

Diagnostics of the daytime cusp in the case of the northern direction of the interplanetary field according to data from the chain of automatic magnetic-variation stations in the Antarctic 18 p2714 A83-39341

The relationship of total Birkeland currents to the merging electric field 19 p2865 A83-41126

The dynamics of charged-particle fluxes and structural features of the interplanetary magnetic field from December 27, 1981 to January 1, 1982 19 p2924 A83-41246

Behavior of the interplanetary and magnetospheric electric fields during very intense storms 20 p3016 A83-42301

Dependence of horizontal polarization of geomagnetic substorm field on IMF and local-time 20 p3016 A83-42304

foF2 response to IMF sector-boundary crossings 20 p3017 A83-42375

The rate of occurrence of dayside Pc 3,4 pulsations - The L-value dependence of the IMF cone angle effect 20 p3025 A83-43200

Ring coupling model - Implications for substorm onsets 20 p3027 A83-43217

Geomagnetic implications of a simple IMF model 21 p3170 A83-44246

A discussion on the properties of MHD shocks in terms of the characteristic velocity 21 p3212 A83-44512

The spiral sector transition regions in the interplanetary magnetic fields 21 p3231 A83-44520

The relationship between indices AE and Dst --- reflecting intensities of equatorial ring current and auroral electrojet due to geomagnetic disturbances 21 p3173 A83-44583

Magnetic disturbances caused by the interplanetary magnetic field in the southern polar cap during the summer 21 p3175 A83-45247

Calculation of the electric fields due to the azimuthal component of the interplanetary magnetic field for the conditions of solstice 21 p3175 A83-45249

The intensity of low-frequency emissions and the interplanetary magnetic field 21 p3175 A83-45250

Triggering of expansive phase intensifications of magnetospheric substorms by northward turnings of the interplanetary magnetic field 22 p3326 A83-46037

Magnetospheric processes preceding the onset of an isolated substorm - A case study of the March 31, 1978, substorm 22 p3326 A83-46039

Removal of velocity bias in the interpretation of measurements of the azimuthal component of the interplanetary magnetic field 22 p3377 A83-46059

Correlated particle and magnetic field observations of a large-scale magnetic loop structure behind an interplanetary shock 22 p3380 A83-46892

A comparison of coronal and interplanetary current sheet inclinations 22 p3389 A83-47046

The shift of the auroral electron precipitation boundaries in the dawn-dusk sector in association with geomagnetic activity and interplanetary magnetic field 22 p3336 A83-47058

The dependence of the indices of auroral electrojets on the IMF Bz component and on the solar wind velocity 23 p3484 A83-48385

INTERPLANETARY MEDIUM

NT INTERPLANETARY DUST

NT INTERPLANETARY GAS

NT METEOROID DUST CLOUDS

NT ZODIACAL DUST

Investigation of the flux of Jupiter electrons with energy not less than 40 keV by the Mars-7 interplanetary probe 02 p0263 A83-11715

On the flaring of cometary plasma tails 02 p0257 A83-12144

Compression of the Venusian ionosphere on May 10, 1979, by the interplanetary shock generated by the solar eruption of May 8, 1979 02 p0264 A83-12377

The distant interplanetary wake of Venus - Plasma observations from Pioneer Venus 02 p0264 A83-12378

Unusual characteristics of the cosmic ray intensity increase of September 17-18, 1979 02 p0276 A83-12393

Concerning the nonstationarity of the correlation of solar-wind parameters with the AE and a sub p indices of magnetic activity 02 p0211 A83-12448

Occurrence of minor particles in summer meteor streams of the Northern Hemisphere 02 p0261 A83-12861

Investigation of electron fluxes with energies of 40-500 keV in quiet periods of solar activity by the methods of correlation and spectral analysis 03 p0438 A83-13207

The turbulence spectrum and velocity of the solar wind at elongations of 90-150 degrees 04 p0575 A83-15754

The observation of a coronal transient directed at earth 05 p0708 A83-17036

The Hubble diagram of quasars showing interplanetary scintillation 06 p0836 A83-19167

A magnetic cloud and a coronal mass ejection 07 p1037 A83-20189

Effects of drift on the transport of cosmic rays. VI - A three-dimensional model including diffusion 07 p1040 A83-21153

Acceleration of low-energy protons and alpha particles at interplanetary shock waves 09 p1357 A83-23753

Models of the formation of the solar nebula 10 p1521 A83-25508

The interplanetary medium and the earth's magnetosphere --- Russian book 10 p1448 A83-25601

A classification of flare states on the sun and isolated disturbances in near-sun, interplanetary, and near-earth space 10 p1521 A83-25602

Certain topics in the energetics of solar-terrestrial relationships 10 p1448 A83-25603

The differential energy spectra of electrons having energies of 0.3-3 MeV on the basis of data from the satellite Prognoz 4 10 p1523 A83-26109

- Coronal disturbances and their terrestrial effects
/Tutorial Lecture/ 11 p1686 A83-27377
- Direct correlations between coronal transients and
interplanetary disturbances 11 p1687 A83-27383
- Comets as indicators of the interplanetary medium
13 p1949 A83-31312
- Temporal variations of nucleonic abundances in solar
flare energetic particle events. I - Well-connected events
13 p1965 A83-31436
- Configuration and structure of the interplanetary
magnetoplasma stream from the intense isolated flare of
November 22, 1977 14 p2114 A83-31852
- On the time spectrum of phase fluctuations of radio
waves during the occultation of the near-solar plasma
14 p2114 A83-32101
- Power-law asymptotic mass distributions for systems of
accreting or fragmenting bodies 15 p2264 A83-34587
- Particle acceleration by coronal and interplanetary shock
waves 15 p2285 A83-35232
- Waves observed upstream of interplanetary shocks
17 p2600 A83-37590
- Excitation of violent discharge of charged bodies ---
planetary rings or interplanetary medium 17 p2609 A83-38414
- Acceleration of particles in interplanetary space
(Survey) 18 p2786 A83-39304
- Investigation of scintillations in near-solar regions of the
interplanetary medium --- for solar wind analysis
18 p2783 A83-39305
- On the possibility of measuring the ion-acoustic
turbulence of the interplanetary plasma and the velocity
of the solar wind by the radio-wave backscattering
technique 18 p2784 A83-39312
- The interplanetary plasma in an 11-year cycle of solar
activity (according to radio-astronomical data)
18 p2784 A83-39327
- The velocity and the density spectrum of the solar wind
from simultaneous three-frequency IPS observations
19 p2923 A83-40709
- Analysis of proton-flux increases in the interplanetary
medium on the basis of Venera 13 and 14 data
19 p2924 A83-41247
- Coupled hydromagnetic wave excitation and ion
acceleration at interplanetary traveling shocks
20 p3066 A83-42404
- Acceleration of nonrelativistic electrons in the
interplanetary medium 21 p3245 A83-45226
- Turbulent generation of outward-traveling interplanetary
Alfvénic fluctuations 24 p3674 A83-49298
- INTERPLANETARY NAVIGATION**
- Navigation of the Galileo mission
[AIAA PAPER 83-0102] 05 p0605 A83-17909
- Ballistics and navigation of the automatic interplanetary
probes Venera-13 and Venera-14 14 p1981 A83-31952
- Interplanetary navigation or the cosmic flipper
16 p2314 A83-35600
- Guidance and control at the near-planet leg of the
'Venera' mission 17 p2475 A83-37486
- INTERPLANETARY PROPULSION**
- U INTERPLANETARY SPACECRAFT
- U ROCKET ENGINES
- INTERPLANETARY SPACE**
- The effect of the large-scale structure of the general
magnetic field of the sun on the intensity and anisotropy
distribution of cosmic rays in interplanetary space
02 p0273 A83-11724
- Spatial structure of solar wind in 1976
06 p0853 A83-18314
- Jovian modulation of interplanetary electrons as
observed with Voyagers 1 and 2 09 p1365 A83-23754
- Ion acceleration at shocks in interplanetary space - A
brief review of recent observations 11 p1676 A83-27385
- Theoretical studies of interplanetary propagation and
acceleration 11 p1676 A83-27387
- Upstream waves and particles /Tutorial Lecture/ --- from
shocks in interplanetary space 11 p1676 A83-27388
- Influence of large-scale inhomogeneities of the
interplanetary plasma on the form of temporal scintillation
spectra 13 p1948 A83-31265
- Acceleration of cosmic rays in interplanetary space as
a consequence of solar activity 14 p2116 A83-32545
- Multiple spacecraft observations of interplanetary
shocks Four spacecraft determination of shock normals
15 p2255 A83-33929
- Modification of the local interstellar gas properties in
the heliospheric interface 16 p2432 A83-36681
- Energetic ions upstream of the earth's bow shock during
an energetic storm particle event 17 p2538 A83-37597
- Plasma boundaries and shocks --- in earth
magnetosphere and interplanetary space 17 p2541 A83-38296
- The friction mechanism for accelerating particles in
interplanetary space 17 p2614 A83-38847
- Cosmic-ray anisotropy in interplanetary space
18 p2786 A83-39760
- Upstream electron oscillations and ion overshoot at an
interplanetary shock wave 19 p2864 A83-41115
- Investigation of the characteristics of proton fluxes via
the Venera 13 and 14 probes 19 p2925 A83-41245
- Variations of cosmic-ray energy in interplanetary
space 20 p3083 A83-43655
- Propagation effects of solar cosmic rays. II - Propagation
correction of peak spectrum 21 p3243 A83-44579
- Measurements on a shock wave generated by a solar
flare 21 p3243 A83-44997
- INTERPLANETARY SPACECRAFT**
- NT GALILEO PROBE
- NT GALILEO SPACECRAFT
- NT JUPITER PROBES
- NT MARINER SPACE PROBES
- NT MARS PROBES
- NT MARS 5 SPACECRAFT
- NT PIONEER SPACE PROBES
- NT PIONEER VENUS SPACECRAFT
- NT PIONEER 2 SPACE PROBE
- NT PIONEER 10 SPACE PROBE
- NT VENERA SATELLITES
- NT VENERA 8 SATELLITE
- NT VENERA 9 SATELLITE
- NT VENERA 10 SATELLITE
- NT VENERA 11 SATELLITE
- NT VENERA 12 SATELLITE
- NT VENUS PROBES
- NT VIKING LANDER SPACECRAFT
- NT VIKING ORBITER SPACECRAFT
- NT VIKING SPACECRAFT
- NT VOYAGER 1 SPACECRAFT
- NT VOYAGER 2 SPACECRAFT
- NT ZOND SPACE PROBES
- Space sail liner --- interplanetary solar-powered cargo
vehicle 01 p0018 A83-11332
- Advanced propulsion for future planetary spacecraft
02 p0148 A83-13083
- Contemporary planetary science 02 p0245 A83-13106
- Low cost planetary science missions
[AIAA PAPER 83-0518] 05 p0600 A83-16763
- Investigation of the optical and meteorological
characteristics of solar cells mounted on Venera
interplanetary probes 14 p1984 A83-32042
- Planet-A mission to Halley 15 p2124 A83-35012
- The Giotto mission to Halley's Comet
15 p2124 A83-35013
- LO2/LH2 propulsion for outer planet orbiter
spacecraft 16 p2320 A83-36330
- [AIAA PAPER 83-1305] 16 p2320 A83-36330
- Plasma effects on Doppler measurements of
interplanetary spacecraft. I - Discontinuities and waves
16 p2429 A83-36635
- Automatic controls on board planetary probes
17 p2480 A83-37493
- Developments in high-precision gamma-ray burst source
studies 18 p2786 A83-39298
- Space applications at the crossroads - Twenty five years
of planetary astronomy [AAS PAPER 83-165] 20 p3079 A83-43765
- New approaches to planetary exploration - Spacecraft
and information systems design [IAF PAPER 83-348] 23 p3415 A83-47354
- INTERPLANETARY TRAJECTORIES**
- Satellite tour design for the Galileo mission
[AIAA PAPER 83-0101] 05 p0602 A83-16822
- Interplanetary trajectory design for the Galileo mission
[AIAA PAPER 83-0099] 05 p0602 A83-17908
- Application of the rectilinear impact pseudostate method
to modeling of third-body effects on interplanetary
trajectories [AIAA PAPER 83-0015] 06 p0721 A83-19576
- The extraordinary voyages through the region of the
giant planets 08 p1048 A83-22049
- Trajectory corrections for flight to short-period comets
in the solar system in 1981-1991 17 p2472 A83-37448
- Space transportation. 22 p3258 A83-45859
- Generation of trajectories by multiple planetary
swingbys [IAF PAPER 83-326] 23 p3417 A83-47342
- INTERPLANETARY TRANSFER ORBITS**
- Rocket rendezvous at preassigned destinations with
optimum exit trajectories 04 p0452 A83-16433
- INTERPOLATION**
- Objective analysis of discontinuous satellite-derived data
fields for grid point interpolation [AD-A122568] 02 p0217 A83-12965
- Notes on the theory of linear, time-discrete signal
processing with a rational sampling rate conversion. I
02 p0165 A83-12989
- On the completeness of multi-variate optimum
interpolation for large-scale meteorological analysis
02 p0217 A83-13051
- Applications of transfinite /'blending-function'/
interpolation to the approximate solution of elliptic
problems 03 p0388 A83-14085
- Optimal interpolation and the Kalman filter --- for analysis
of numerical weather predictions 03 p0365 A83-14409
- Multivariable stability-margin optimisation with
decoupling and output regulation 04 p0529 A83-16191
- A method of rotating areas on a raster scan graphic
display 05 p0644 A83-16871
- Curved elements with polynomials of varying degree
05 p0682 A83-17555
- Calculation of complex Fourier coefficients using natural
splines 06 p0804 A83-18898
- Uniform convergence of interpolation by cubic splines
06 p0804 A83-18900
- Multichannel recovery of quadrature components of
bandpass signals 06 p0748 A83-19046
- Convergence of interpolational cubic splines on
nonuniform grids 06 p0804 A83-19599
- Discrimination of speech and high-speed data using an
adaptive predictor for DSI application --- Digital Speech
Interpolation 07 p0910 A83-19756
- Error bounds and error asymptotic behavior for a class
of interpolation quadratures --- German thesis
07 p0987 A83-20397
- A posteriori improvements for interpolating periodic
splines 07 p0987 A83-20509
- Consideration of the local shape of the terrain in height
interpolation with the aid of finite elements
08 p1129 A83-22031
- On approximation by the interpolating series of G.
Valiron 10 p1470 A83-26475
- The method of boundary interpolation in fracture
mechanics problems 11 p1597 A83-28476
- Interpolation and transformations of maps --- French
thesis 11 p1601 A83-28632
- An interpolation method of randomly distributed
atmospheric data in the height-time domain
12 p1758 A83-29133
- A natural interpolation formula for Cauchy-type singular
integral equations with generalized kernels
12 p1772 A83-29643
- Numerical calculations of discontinuities by shape
preserving splines 12 p1773 A83-29670
- Finite element interpolation error bounds with
applications to eigenvalue problems 12 p1773 A83-29705
- Interpolational and extremal properties of L-spline
functions --- Thesis 13 p1912 A83-30148
- Interpolation with respect to the vertical of the relative
geopotential and temperature 13 p1884 A83-30293
- Product integration over infinite intervals. I - Rules based
on the zeros of Hermite polynomials 13 p1912 A83-31363
- The use of parabolic B-splines in solving interpolation
problems 14 p2077 A83-31894
- Surfaces in computer aided geometric design:
Proceedings of the Conference, Oberwolfach, West
Germany, April 25-30, 1982 15 p2216 A83-33613
- An algorithm of fast Kotelnikov interpolation --- for
optical image simulation 15 p2223 A83-35262
- A general method of determination of finite element
interpolation polynomials 17 p2570 A83-37022
- A flow analysis procedure based on velocity potentials
[AIAA PAPER 83-1818] 17 p2508 A83-38650
- Transfinite mappings and their application to grid
generation 17 p2573 A83-38783
- The numerical differentiation of discrete functions using
polynomial interpolation methods 17 p2564 A83-38795
- Marching grid generation using parabolic partial
differential equations 17 p2574 A83-38810
- Applications of exponential splines in computational fluid
dynamics 19 p2893 A83-40852
- Multipoint boundary value problem (MPBVP) and spline
interpolation 20 p3042 A83-43170
- An implementation of a computational theory of visual
surface interpolation 21 p3136 A83-44252
- Rotationally symmetric operators for surface
interpolation 21 p3193 A83-44253
- The method of alternating integration and interpolation
and its application to the determination and prediction of
spacecraft orbits 21 p3097 A83-45293
- The stepwise utilization of meteorological information
in numerical analysis 21 p3181 A83-45402
- On the interpolation of gravity anomalies and deflections
of the vertical in mountainous terrain 22 p3317 A83-46356

Fringe pattern recognition and interpolation using nonlinear regression analysis 22 p3352 A83-46838
Variational approach to problems of the interpolation of physical fields --- Russian book on oceanography 24 p3622 A83-49041

INTERPOLATORS

U REPEATERS

INTERPRETATION

Image bandwidth compression by pre-compensative interpolation 08 p1075 A83-22235

INTERPROCESSOR COMMUNICATION

The ETH-Multiprocessor EMPRESS - A dynamically configurable MIMD system 05 p0679 A83-17237
Minimization of interprocessor communication for parallel computation 05 p0679 A83-17240
Communication structures in multicomputer systems 07 p0983 A83-19715
On graph theoretic approach to n- and (2n-1) stage interconnection networks 15 p2219 A83-35134

INTERSTELLAR CHEMISTRY

Interstellar molecules 01 p0124 A83-10842
NH₄⁺ - A candidate for comets and interstellar space 01 p0125 A83-10934
Detection of interstellar sodium hydroxide in self-absorption toward the galactic center 02 p0257 A83-12146
Interstellar molecular hydrogen 02 p0258 A83-12182
What are comets made of - A model based on interstellar dust 03 p0415 A83-13380
Laboratory studies of photochemical and spectroscopic phenomena related to comets 03 p0416 A83-13395
Formaldehyde formation in a H₂O/CO₂ ice mixture under irradiation by fast ions 03 p0424 A83-14196
Model calculations of the molecular composition of interstellar grain mantles 03 p0427 A83-14757
Loss of CO⁺ ions by reaction with H₂ in OMC-1 03 p0428 A83-14760
Some H/D exchange reactions involved in the deuteration of interstellar molecules 04 p0552 A83-15614
Dense cloud chemistry. III - The detailed chemical network and the effects of parameter variation --- of interstellar gases 04 p0557 A83-15984
On the n-dependence of the reaction rate for C⁺ + C_n/yields C⁺+n + 1/ in interstellar space 05 p0698 A83-16999
The radiation field and the molecular hydrogen photodissociation rate within spherically symmetric inhomogeneous clouds 06 p0828 A83-18181
Methanol in Orion A - Simultaneous observations of corresponding rotational transitions in the ground and torsionally excited states 06 p0844 A83-19495
Dense cloud chemistry. II - The HCS⁺/+/CS ratio 07 p1018 A83-20946
Fluorescence yields from photodissociation of OCS at 1060-1240 Å 07 p0882 A83-21056
Fluorescence yield from photodissociation of CH₄ at 1060-1420 Å 07 p0991 A83-21192
Structure of molecular clouds. VI - The accuracy of the standard analysis 07 p1023 A83-21210
Theoretical study of AlH₃⁺ - Spin splitting, core polarization, and interstellar chemistry 08 p1180 A83-22219
Experimental studies of the vapor phase nucleation of refractory compounds. II - The condensation of an amorphous magnesium silicate 08 p1071 A83-22223
Formation of complex molecules in TMC-1 --- Taurus Molecular Cloud 08 p1186 A83-23274
H₂ production in comets. 10 p1500 A83-25374
On vibrational excitations of interstellar molecules 10 p1509 A83-26370
Effects of a shock on the molecular composition of a diffuse interstellar cloud 10 p1509 A83-26373
On the formation of HCO⁺/+ and HOC⁺/+ from the reaction between H₃⁺/+ and CO 10 p1392 A83-26461
Further analysis of the possible effects of isotope-selective photodissociation on interstellar carbon monoxide 10 p1513 A83-26715
Surface chemistry of deuterated molecules --- of interstellar molecular clouds 11 p1677 A83-27678
Photodissociation of NH₃ at 106-200 nm 11 p1655 A83-28527
The largest molecules in space - Interstellar dust 13 p1947 A83-31154
X-ray ionization and the Orion molecular cloud 13 p1950 A83-31414
Radiative association and the synthesis of long carbon chain molecules in interstellar clouds 13 p1953 A83-31451
Observations of the 3(1,3)-2(0,2) transition of SO₂ --- in interstellar clouds 13 p1957 A83-31691

Laboratory measurements of ion-molecule reactions pertaining to interstellar hydrocarbon synthesis 15 p2269 A83-34645

Resonant and nonresonant processes in the formation of CH(+) by radiative association 17 p2578 A83-37342

Interstellar photoelectric absorption cross sections, 0.03-10 keV 17 p2604 A83-37910
Rotational excitation of OH by H₂ - Calculations in intermediate coupling 17 p2579 A83-38364

Photodissociation processes in the OH molecule 17 p2579 A83-38468
Equilibrium temperatures of interstellar iron grains 18 p2776 A83-39767

Does CO condense on dust in molecular clouds? 19 p2914 A83-40718
Theory of molecular formation by radiative association in interstellar clouds 19 p2918 A83-41623

Chemical evolution in space - A source of prebiotic molecules 19 p2886 A83-42031
Primordial star formation - The role of molecular hydrogen 20 p3072 A83-43057

Observations of interstellar C₂ toward three heavily reddened stars 20 p3074 A83-43092
Interstellar C₂ in the Ophiuchus clouds 21 p3228 A83-44409

Polymerization induced on interstellar grains by low-energy cosmic rays 21 p3234 A83-44765
The detection of vinyl cyanide in TMC-1 21 p3236 A83-45541

Association reactions of Na(+) and some implications for interstellar chemistry 21 p3238 A83-45571
Synthesis of chain molecules in regions with partially ionized carbon 22 p3382 A83-46987

Charge exchange reactions in astrophysical plasmas 24 p3651 A83-49139
Recombination processes --- for nebular conditions 24 p3651 A83-49140

Time-dependent chemistry. I - Modelling of a static cloud --- in interstellar space 24 p3659 A83-49374
Are three systematic observational effects on abundance determinations in giant extragalactic H II regions? 24 p3667 A83-50058

INTERSTELLAR COMMUNICATION

Attitudes toward interstellar communication - An empirical study 18 p2751 A83-39608
Extraterrestrials - Where are they? --- Book 19 p2907 A83-41501

Searches for electromagnetic signals from extraterrestrial beings 19 p2908 A83-41503
Cosmology and life in the universe 19 p2908 A83-41512

A search strategy for ETI signals with small duty cycle 24 p3637 A83-49604

INTERSTELLAR EXTINCTION

Correlations between BCD parameters of the continuous spectrum and the Balmer decrement of Be stars 01 p0120 A83-10310
Intrinsic reddening of Be stars and its relation with H-alpha emission intensities 01 p0120 A83-10311

Spectroscopic observations of Be stars especially in the infrared 01 p0121 A83-10330
Far-ultraviolet colors of B stars with and without emission lines 01 p0123 A83-10349

Sk 143 - An SMC star with a galactic-type ultraviolet interstellar extinction 01 p0125 A83-10929
2-4 micrometer spectroscopy of the compact H II region G 45.13 + 0.14 A 02 p0260 A83-12520

A photometric map of interstellar reddening within 300 parsecs 03 p0406 A83-13552
The relationship between carbon monoxide abundance and visual extinction in interstellar clouds 03 p0423 A83-14192

A model for interstellar extinction 04 p0548 A83-14979
The law of interstellar absorption in the wave-number interval 0.95/micron to 3.03/microns 04 p0550 A83-15042

The distribution of infrared obscuration in NGC 7331 - Evidence for a massive molecular ring 04 p0555 A83-15649
The peculiar extinction of Herschel 36 04 p0555 A83-15654

Ultraviolet extinction towards far OB associations 04 p0557 A83-15986
HD 29647, a heavily reddened mercury-manganese star 06 p0830 A83-18787

Polarization of early-type stars in Norma 06 p0820 A83-18861
A photometric map of interstellar reddening within 100 PC 06 p0820 A83-18863

Carbon, nitrogen, and iron-peak abundances for giants in the remote globular clusters NGC 7006 and Pal 13 06 p0835 A83-19051

Reddening of the narrow-line regions of active galaxies and the intrinsic Balmer decrement 06 p0835 A83-19053

Infrared excesses of stars with intrinsic polarization 06 p0838 A83-19227
Effect of variable obscuration on the clustering of galaxies 06 p0839 A83-19265

Observations of the extinction and excitation of the molecular hydrogen emission in Orion 06 p0840 A83-19279
The reddening of active galactic nuclei 06 p0841 A83-19298

Dense cores in dark clouds. I - CO observations and column densities of high-extinction regions 06 p0844 A83-19493
Problems in stellar statistics 06 p0846 A83-19537

Structures of Population I in the solar vicinity 06 p0846 A83-19538
Spectroscopic observations of two very red objects toward the galactic center 07 p1004 A83-19861

IUE observations of Markarian 3 and 6 - Reddening and the nonstellar continuum 07 p1019 A83-21109
The wavelength dependence of interstellar polarization in the Large Magellanic Cloud 07 p1020 A83-21116

The three micron 'ice' band in grain mantles --- and their influence in interstellar extinction and polarization 07 p1024 A83-21219
Abnormal extinction and dust properties in M 16, M 17, NGC 6357 and the Ophiuchus dark cloud 07 p1025 A83-21241

Extinction to ionized gas at the galactic center 08 p1182 A83-23044
Interstellar absorption toward HD 14633 08 p1183 A83-23051

Does a 2,200 Å hump observed in an artificial carbonaceous composite account for UV interstellar extinction 08 p1187 A83-23282
NGC 2447 and the reddening and luminosity of normal red giants 09 p1351 A83-23319

Continuous intergalactic extinction 09 p1358 A83-24016
Study of the open cluster IC 1805 09 p1354 A83-24024

Estimation of reddening at low galactic latitudes from the Lick galaxy counts 09 p1363 A83-24990
Principal components analysis of spectral data. II - Error analysis and applications to interstellar reddening, luminosity classification of M supergiants, and the analysis of VV Cephei stars 10 p1493 A83-25658

Peculiar ultraviolet interstellar extinction 10 p1509 A83-26374
Ultraviolet interstellar absorption toward HD 5980 in the Small Magellanic Cloud 10 p1512 A83-26710

Nebular dust and extinction in ionized nebulae. I - The Balmer decrement 10 p1513 A83-26712
The diffuse interstellar feature at 4430 Å and interstellar extinction in the far-ultraviolet 10 p1516 A83-26756

A discussion on the reddening of long period Cepheids in the Magellanic Clouds 11 p1677 A83-27680
LMC and galactic extinction 11 p1682 A83-28278
Anomalous diffuse features in dust-embedded stars 11 p1682 A83-28289

An investigation of the heavily reddened young open cluster Tr 27 on the Walraven photometric systems 12 p1784 A83-28862
The ultraviolet reddening of Be stars 13 p1953 A83-31560

A generalized algorithm for efficient photometric reductions 13 p1941 A83-31569
Absorption spectra of interstellar grains. III - On the origin of the '2200' hump 13 p1955 A83-31664

Structure of the local interstellar medium and the line of sight to Alpha Oph 13 p1960 A83-31790
An investigation of the region around the emission nebula IC 1848 14 p2101 A83-31826

An investigation of the region around the emission nebula NGC 1499 14 p2101 A83-31827
Reddening indicators for quasars and Seyfert 1 galaxies 15 p2256 A83-34086

On the optical properties of bacterial grains - I. 15 p2216 A83-34549
CO adsorption and the optical properties of interstellar grains 16 p2428 A83-36529

Status of laboratory experiments on ice mixtures and on the 12 micron H₂O ice feature --- suggesting interstellar IR absorption 16 p2431 A83-36670
Intrinsic UV colour indices of early-type stars 16 p2432 A83-36684

On the interstellar absorption of light in the Galaxy 16 p2433 A83-36855
Infrared polarization in the direction to the galactic center 17 p2588 A83-37360

Absolute spectrophotometry of four supergiants 17 p2589 A83-37651
Spectrophotometric investigation of the T Tauri type star AS 353 17 p2589 A83-37682

- Calibrations of the reddening, luminosity, and abundance of old disk giants from photometry of stars in M67, NGC 3680, NGC 2420, and the Wolf 630 and Arcturus groups
17 p2591 A83-37782
- Regions of low molecular column density near the galactic plane
17 p2602 A83-37829
- Anomalous reddening of supernovae
17 p2603 A83-37888
- Studies of A and F stars in the region of the North Galactic Pole. V - Interstellar reddening and the uvby-beta intrinsic colour calibration
17 p2593 A83-38246
- Spectrophotometry in the galactic supernova remnants RCW 86, 103 and Kepler
17 p2593 A83-38248
- Continuum reddening of Seyfert 1 nuclei
17 p2607 A83-38260
- The conspicuous absence of normal graphite grains in the small Magellanic Cloud
17 p2608 A83-38263
- The extinction of starlight at wavelengths near 2200 Å
17 p2611 A83-38589
- 2.8-3.6-micron spectra of micro-organisms with varying H₂O ice-content
17 p2563 A83-38590
- A point source of light in an absorbing and scattering plane layer --- interstellar extinction of stellar radiation
18 p2766 A83-39486
- The galactic extinction of extragalactic objects. I - The csc b law and the extinction coefficient
18 p2767 A83-39592
- Gamma radiation as a tracer of the local interstellar gas
18 p2768 A83-39631
- Recent progress on molecular hydrogen in Orion
18 p2772 A83-39710
- Intrinsic polarization and extinction features of early-type stars with emission lines due to X-ray irradiation
18 p2774 A83-39738
- The reddening, metal abundance, and luminosity of high-luminosity G-type stars
20 p3063 A83-42191
- Interstellar proteins and the discovery of a new absorption feature at $\lambda = 2800$ Å
20 p3077 A83-43669
- Notes on the heavily reddened and variable A-type supergiant CD-33.12119 deg
21 p3228 A83-44410
- The intrinsic properties of 29 Cepheids in the Magellanic Clouds
21 p3228 A83-44414
- Studies of the Carina Nebula. V - The near infrared excess of O-type stars and the anomalous extinction law in their environment
21 p3230 A83-44442
- A frequency correlation analysis of pulsar scintillation spectra
21 p3233 A83-44738
- Spectroscopy of the QSO pair Q1228 + 076/G1228 + 077
21 p3225 A83-44767
- The circumstellar dust of Mu Cephei
21 p3236 A83-45545
- The reddening of radio elliptical galaxies
22 p3378 A83-46553
- A far-ultraviolet extinction law - What does it mean? --- in interstellar grains
22 p3382 A83-46986
- Diffuse light near Zeta Orionis and the Horsehead nebula, and anomalous extinction of HD 37903, as measured with the ANS
23 p3516 A83-47441
- The variability of the T Tauri star DI Cephei
23 p3524 A83-47534
- The galactic extinction towards Maffei 1
24 p3643 A83-49360
- 8-13 micron spectrophotometry of galaxies. III - The silicate absorption in Markarian 231
24 p3660 A83-49387
- A perspectivist review of supermetallicity studies. I --- of giant stars and star clusters
24 p3664 A83-50000
- INTERSTELLAR GAS**
- NT NEUTRAL GASES**
- Intergalactic gas in galactic clusters, the microwave background radiation and cosmology
01 p0124 A83-10839
- Interstellar molecules
01 p0124 A83-10842
- Motion of the sun in the interstellar medium
01 p0124 A83-10845
- A distinct shell structure in H I line-emission at intermediate galactic latitudes
01 p0118 A83-10953
- Theoretical models of the mass spectrum of interstellar clouds
02 p0251 A83-11587
- Detection of bipolar CO outflow in Orion
02 p0253 A83-11617
- Hot galactic gas and narrow line quasar absorption systems
02 p0253 A83-11620
- Interstellar turbulence and the kinetics of cosmic rays
02 p0272 A83-11704
- X-ray spectroscopy of the galaxy M87 - Radiative accretion of the hot plasma halo
02 p0254 A83-12105
- Precessing jets in Sagittarius A - Gas dynamics in the central parsec of the galaxy
02 p0255 A83-12113
- Acoustic waves in supernova remnants
02 p0257 A83-12135
- 3D models for self-gravitating, rotating magnetic interstellar clouds
02 p0260 A83-12537
- Determination of the parameters of the interstellar wind from observations of the Lyman-alpha background at large distances from the sun
03 p0412 A83-13210
- An interpretation of OH maser observations in W3/OH/
03 p0413 A83-13313
- The interrelation of cosmic gamma-rays and interstellar gas in the range l:65-180 deg
03 p0414 A83-13329
- Infrared lines from shocked galactic gases
03 p0417 A83-13465
- A search for meter-wavelength hydrogen recombination lines, and constraints on the parameters of the ionized interstellar gas
03 p0418 A83-13656
- The effect of the neutral solar-wind component upon the interaction of the solar system with the interstellar gas stream
03 p0419 A83-13883
- The dynamical destruction of shocked gas clouds
03 p0419 A83-13928
- The neutral hydrogen deficiency of the cluster A262
03 p0422 A83-14180
- Broad line region clouds and the absorbing material in NGC 4151
03 p0423 A83-14189
- The influence of buoyancy on the stability of jets --- in extragalactic radio sources
03 p0427 A83-14755
- Aperture synthesis observations of recombination lines from compact H II regions V - NGC 7538
03 p0430 A83-14803
- The effects of the coronal gas on the champagne phase
03 p0430 A83-14810
- The local interstellar medium as traced by gamma rays
04 p0550 A83-15048
- Three-component gasdynamic model for the interaction of the solar wind with the interstellar medium
04 p0551 A83-15088
- Some H/D exchange reactions involved in the deuteration of interstellar molecules
04 p0552 A83-15614
- The velocity gradient of B361
04 p0553 A83-15618
- Dense cloud chemistry. III - The detailed chemical network and the effects of parameter variation --- of interstellar gases
04 p0557 A83-15984
- On the distribution of interstellar gas in the galactic halo
05 p0698 A83-16996
- Discovery of highly ionized species in the ultraviolet spectrum of Feige 24
05 p0700 A83-17029
- Detection of H/C-17/O plus in Sagittarius B2
05 p0700 A83-17034
- Neutral hydrogen observations towards the Puppis Window of the Milky Way
05 p0701 A83-17665
- On the inner ring of HII regions in NGC 3351
05 p0701 A83-17669
- Shock fronts produced by stellar winds in the interstellar gas
06 p0830 A83-18549
- Disk accretion by dynamical friction - A model for the dynamical evolution of giant molecular clouds
06 p0832 A83-18836
- Physical conditions in interacting galaxies, in components of isolated pairs, and in isolated galaxies
06 p0838 A83-19220
- On the possibility of gas being swept out of a galaxy under the influence of the radiation pressure of an active nucleus
06 p0838 A83-19223
- On the possibility of detecting very hot gas through absorption-line studies
06 p0839 A83-19268
- The relation between magnetic field and gas density in interstellar clouds
06 p0840 A83-19276
- On scaling the magnetic field strength in interstellar clouds Resolution of the 'B versus n dilemma'
06 p0840 A83-19277
- The interstellar medium near the sun. III - Detailed analysis of the line of sight to lambda B Scorpii
06 p0840 A83-19281
- The X-ray surface brightness of Kepler's supernova remnant
06 p0840 A83-19282
- Magnetohydrodynamic shock waves in molecular clouds
06 p0844 A83-19491
- Protostellar rotation - Turbulence and heating of molecular clouds
06 p0844 A83-19492
- A numerical simulation of the magnetospheric gate model for the X-ray bursters
07 p1012 A83-20028
- Ionized gas clouds and the origin of the apparent variability of the compact galactic-center radio source
07 p1014 A83-20654
- Further ultraviolet observations of interstellar gas associated with the supernova remnant S 147
07 p1017 A83-20931
- A collision cross-section for interactions between magnetic diffuse clouds
07 p1018 A83-20943
- An X-ray emitting bubble in the Cep OB3 association
07 p1018 A83-20948
- Absorption by halo gas in the direction of M13
07 p1020 A83-21118
- The gas-grain interaction in the interstellar medium - Thermal accommodation and trapping
07 p1021 A83-21120
- New H₂O masers in the galactic center region
07 p1025 A83-21247
- The evolution of supernova remnants and the structure of the interstellar medium
08 p1178 A83-21849
- Strong spherical shock in a self-gravitating gas
08 p1179 A83-22009
- A survey of ultraviolet interstellar absorption lines
08 p1175 A83-22748
- The H I distribution in an extremely faint dwarf irregular galaxy M81 dwA
08 p1182 A83-23038
- Extinction to ionized gas at the galactic center
08 p1182 A83-23044
- Ionized gas in active molecular cloud cores
08 p1182 A83-23046
- Molecular gas in the W33 region
08 p1183 A83-23047
- Electron and local gas densities in diffuse interstellar clouds from measurements of Ca I absorption
08 p1183 A83-23050
- The high-velocity molecular flows near young stellar objects
08 p1183 A83-23052
- The depletion of calcium in the Rho Ophiuchi cloud
08 p1185 A83-23082
- Formation of complex molecules in TMC-1 --- Taurus Molecular Cloud
08 p1186 A83-23274
- Planetary nebulae
09 p1352 A83-23498
- Point explosion in an exponential atmosphere with a nonzero asymptote --- for stellar and planetary atmospheric models
09 p1359 A83-24221
- 21-cm line observations of 59 lenticular and spiral galaxies
09 p1355 A83-24523
- Morphology of the ionized gas in NGC 1313
09 p1355 A83-24525
- Helium atoms in the interstellar and interplanetary medium. I - Prognoz-5 and Prognoz-6 satellite observations of scattered ultraviolet radiation in the H I 1216 Å and He I 584 Å lines
09 p1364 A83-25036
- Velocity fluctuations in the interstellar medium due to the gravitational interaction with the system of stars
10 p1500 A83-25491
- Gamma-ray astronomy and the local interstellar medium
10 p1504 A83-25724
- J = 2-1 CO observations of molecular clouds with high-velocity gas - Evidence for clumpy outflows
10 p1504 A83-25728
- Some implications of nonluminous matter in dwarf spheroidal galaxies
10 p1504 A83-25741
- Infrared spectroscopy of the sources in S235 and its implication for the line excess problem
10 p1509 A83-26371
- Far-ultraviolet diffuse emission lines from the interstellar medium
10 p1511 A83-26406
- Difference frequency laser spectroscopy of the nu3 band of the CH3 radical
10 p1480 A83-26451
- High-resolution spectroscopy of selected absorption lines toward quasi-stellar objects. I - Lyman-alpha toward PHL 957
10 p1512 A83-26703
- Effects of environment on neutral hydrogen distribution for disk galaxies in the Virgo Cluster area
10 p1512 A83-26706
- Ultraviolet interstellar absorption toward HD 5980 in the Small Magellanic Cloud
10 p1512 A83-26710
- Further analysis of the possible effects of isotope-selective photodissociation on interstellar carbon monoxide
10 p1513 A83-26715
- Dependence of interstellar depletion on hydrogen column density - Possibilities and implications
10 p1513 A83-26716
- Orbital configurations for gas in elliptical galaxies
10 p1497 A83-26751
- Sensitive mapping of E and S0 galaxies in search of H I content differences between supernovae and non-supernovae producing galaxies
11 p1668 A83-27104
- Neutral hydrogen in isolated galaxies. II - The large angular diameter galaxies
11 p1668 A83-27106
- The neutral gas toward HD 93206
11 p1679 A83-27992
- Cluster collapse and radio source morphology
11 p1679 A83-27993
- Regular strings of H II regions and superclouds in spiral galaxies - Clues to the origin of cloudy structure
11 p1680 A83-28256
- Hydromagnetic wave heating of the galactic corona
11 p1681 A83-28262
- Optically thick radiatively driven shocks near QSOs
11 p1681 A83-28273
- X-ray observations of the southern cluster CA 0340-538 and the Horologium supercluster
11 p1681 A83-28274
- The ratio of deuterium to hydrogen in interstellar space. V The line of sight to Epsilon Persei
12 p1790 A83-28882
- On the formation of cometary nuclei in dense globules
12 p1793 A83-29062

- Soft X-ray diagnostics of the kinematics of high-velocity clouds 12 p1793 A83-29064
- Large-scale flow of interstellar gas in galactic spiral waves - Effects of thermal balance and self-gravitation 12 p1793 A83-29065
- High-density gas associated with 'molecular jets' - NGC 1333 and NGC 2071 13 p1953 A83-31449
- Asymmetry of the solar wind in a two-shock model of the heliosphere 13 p1965 A83-31661
- The collapse of a fast rotating interstellar gas cloud 13 p1956 A83-31679
- Structure of the local interstellar medium and the line of sight to Alpha Oph 13 p1960 A83-31790
- The interaction of the solar wind with the interstellar medium - The effect of this interaction on physical processes in near-solar space 14 p2102 A83-32553
- Spatially extended narrow emission-line gas in the Seyfert galaxy NGC 4151 14 p2104 A83-33187
- Extended soft X-ray emission from NGC 4151 14 p2104 A83-33188
- An energetic, bisymmetrically expanding H I remnant 14 p2104 A83-33190
- A fragmentary cold H I cloud near W3 and W4 15 p2255 A83-33834
- The distribution of ionized gas in the nuclei of spiral galaxies 15 p2256 A83-34089
- Interstellar H-alpha emission along the galactic equator 15 p2257 A83-34095
- Warm H I halos around molecular clouds 15 p2257 A83-34099
- Detection of 10 to the 10th solar masses of hot gas in the normal elliptical galaxy NGC 5846 with the Einstein satellite 15 p2259 A83-34119
- The gas density and distribution within 2 parsecs of the galactic center 15 p2259 A83-34122
- Doubly ionized aluminium - A diagnostic of cooling gas in the galactic corona 15 p2266 A83-34600
- On the structure of intermediate- and high-velocity clouds 15 p2266 A83-34605
- 21 centimeter observations of supercluster galaxies - The bridge between Coma and A1367 15 p2266 A83-34613
- CO observations of the galaxies in the Leo triplet - NGC 3623, NGC 3627, and NGC 3628 15 p2267 A83-34624
- A study of H-alpha velocities in NGC 1499, NGC 7000, and IC 1318B/C 15 p2267 A83-34626
- Ring nebulae associated with Wolf-Rayet stars in the Large Magellanic Cloud. III - Kinematics of DEM 39, 231, 240, and 315 15 p2267 A83-34629
- Detection of interstellar NH3 in the far-infrared - Warm and dense gas in Orion-KL 15 p2269 A83-34648
- Theory of the stability of flat subsystems of galaxies 15 p2269 A83-34679
- Galactic magnetic fields 15 p2272 A83-35009
- The role of cosmic rays in hydrostatic equilibrium of the galactic halo 16 p2441 A83-36528
- IUE observations of high velocity interstellar gas tentatively associated with Radio Loop II 16 p2431 A83-36663
- Ammonia as a molecular cloud thermometer 16 p2431 A83-36678
- The chemical composition and thermal history of the ice of a cometary nucleus 16 p2425 A83-36679
- Modification of the local interstellar gas properties in the heliospheric interface 16 p2432 A83-36681
- Effective H I diameters of galaxies 16 p2432 A83-36695
- The spatial power spectrum of galactic neutral hydrogen from observations of the 21-cm emission line 16 p2432 A83-36696
- Spectroscopic evidence for activity in the nuclei of normal spiral galaxies 17 p2596 A83-37311
- Simulation models for the evolution of cloud systems. I Introduction and preliminary simulations 17 p2596 A83-37315
- X-ray sources in molecular clouds 17 p2597 A83-37316
- Collisions of massive gas clouds with primordial chemical composition 17 p2603 A83-37892
- Stellar and gaseous dynamics of triaxial galaxies 17 p2592 A83-37905
- Copernicus observations of C I - Pressures and carbon abundances in diffuse interstellar clouds 17 p2604 A83-37908
- Interstellar absorption lines in the directions of extragalactic objects. I 17 p2593 A83-38250
- Turbulence in a self-gravitating gaseous disk. II - Turbulence spectra 17 p2610 A83-38553
- The H I extent and deficiency of spiral galaxies in the Virgo cluster 18 p2767 A83-39588
- Gamma radiation as a tracer of the local interstellar gas 18 p2768 A83-39631
- On the local standard of rest --- comoving with young objects in gravitational field of spiral galaxies 18 p2768 A83-39633
- Large-scale structure of H I in the outer Galaxy 18 p2768 A83-39642
- How confidently do we know the CO rotation curve of the outer Galaxy? 18 p2769 A83-39648
- The distribution of HII regions in the outer Galaxy 18 p2769 A83-39649
- Radial distribution of atomic and molecular hydrogen from propagating star formation 18 p2770 A83-39661
- Cloud-particle galactic gas dynamics and star formation 18 p2770 A83-39662
- Orion's cloak as a model for supershells of gas around OB associations 18 p2771 A83-39702
- Physical conditions of the Orion Nebula derived from optical and ultraviolet data 18 p2771 A83-39703
- Three gas clumps near the edge of the visible Orion Nebula 18 p2773 A83-39722
- Bipolar gas jets in star-forming regions 18 p2777 A83-40343
- Infrared observations of the ionized gas in the galactic center 19 p2912 A83-40684
- Gas motions in the central region and their interpretation 19 p2913 A83-40699
- Radio observations of the galactic center - Future directions 19 p2914 A83-40702
- A comparison of several image processing techniques applied to photographically recorded astronomical spectra 19 p2909 A83-40715
- Medium size radio continuum loops and their association with HII shells 19 p2915 A83-41060
- Cool neutral hydrogen in the direction of an anonymous OB association 20 p3064 A83-42194
- Observations of H1414+089, QSO with extremely high velocity broad-absorption-line gas 20 p3058 A83-42317
- The molecular cloud-H II region complexes associated with Sh 90 and Sh 235 20 p3065 A83-42378
- The Cygnus X region. XIV - The radio continuum of the North America-Pelican nebulae 20 p3065 A83-42392
- The spatial distribution of shocked gas in the Orion nebula 20 p3067 A83-42445
- First detection of the ground-state J(K) = 1(0)-0(0) submillimeter transition of interstellar ammonia 20 p3069 A83-42473
- Tracing the gas in galaxies 20 p3069 A83-42625
- Synthesis maps of ultraviolet observations of neutral interstellar gas 20 p3073 A83-43084
- Stability of the equilibrium distributions of interstellar gas, cosmic rays, and magnetic field in an external gravitational field 20 p3076 A83-43652
- On the dynamical structure of QSOs and the origin of emission clouds 20 p3076 A83-43654
- Stellar deuterium abundance - A new upper limit in Canopus 21 p3228 A83-44406
- A search for microwave background diminution towards the cluster 0016 + 16 21 p3223 A83-44429
- On the fragmentation of differentially rotating clouds --- in stellar formation 21 p3233 A83-44748
- Abundance gradients in galaxies in the Sculptor and Centaurus groups 21 p3233 A83-44750
- Association reactions of Na(+) and some implications for interstellar chemistry 21 p3238 A83-45571
- Ion-molecule syntheses of interstellar molecular hydrocarbons through C4H - Toward molecular complexity 22 p3377 A83-46258
- IUE observations of stars in the M8 nebula 22 p3379 A83-46566
- The X-ray emitting gas in poor clusters with central dominant galaxies 22 p3381 A83-46977
- Radiative accretion of intracuster gas onto dominant galaxies in poor clusters 22 p3381 A83-46978
- VLA observations of extragalactic NH3 in IC 342 22 p3381 A83-46981
- Neutral interstellar gas in the lower galactic halo 22 p3381 A83-46983
- The kinetic temperature and CH3CCH column density profiles in SGR B2, Orion, and Dr 21 22 p3382 A83-46988
- A search for neutral hydrogen near nine globular clusters 23 p3519 A83-47443
- The interaction of fast particles with frozen gases in T Tau nebulae - The physical background 23 p3524 A83-47536
- Masses of interstellar gas clouds 23 p3526 A83-47621
- Physical conditions in nucleus of Seyfert Galaxy NGC 7469. II - Spectrophotometric investigation 23 p3527 A83-48443
- Planetary nebulae and Seyfert galaxies - Similarities and differences 24 p3640 A83-49159
- Gas in the nucleus of the Seyfert galaxy NGC 4151 24 p3653 A83-49161
- Spectrophotometric investigation of the irregular galaxy NGC 2814 24 p3653 A83-49163
- Transfer of angular momentum in a galactic disk by the interaction of clouds of interstellar gas 24 p3653 A83-49166
- Internal kinematics and dynamics of galaxies; Proceedings of the Symposium, Universite de Franche-Comte, Besancon, France, August 9-13, 1982 24 p3654 A83-49201
- Gas at large radii --- in spiral galaxies 24 p3654 A83-49210
- Theory of spiral structure --- of Milky Way Galaxy 24 p3655 A83-49221
- Model calculations on the large scale distribution of bubbles in galaxies 24 p3655 A83-49226
- Recent TAURUS results on H-alpha velocities in M83 24 p3655 A83-49228
- Theoretical studies of gas flow in barred spirals galaxies 24 p3656 A83-49240
- Observations of the neutral hydrogen in the barred spiral galaxies NGC 3992 and NGC 4731 24 p3656 A83-49242
- Interstellar matter in elliptical galaxies 24 p3657 A83-49252
- Ammonia observations of the Herbig-Haro objects HH24-27 24 p3658 A83-49359
- 4.8-GHz H2CO maser emission in Sgr B2 24 p3660 A83-49388
- Cooling of the primordial gas by molecular hydrogen 24 p3663 A83-49635
- Star formation and abundance gradients in the galaxy 24 p3664 A83-49997
- Primordial helium abundance determinations using galactic H II regions 24 p3667 A83-50056
- Detection of the 3.46 cm line of interstellar He-3(+) (He-3(+)/H(+)) ratios 24 p3667 A83-50062
- Ammonia absorption toward W3(OH) - 0.3 arcsec resolution maps in the (2,2) line 24 p3668 A83-50078
- Detection of an extended soft X-ray source H 2326-79 in the southern sky 24 p3668 A83-50085
- Hydrogen and helium ionization structure of gaseous nebulae 24 p3671 A83-50170
- ### INTERSTELLAR MAGNETIC FIELDS
- Shock induced star formation - The effects of magnetic fields and turbulence 01 p0126 A83-10945
- 3D models for self-gravitating, rotating magnetic interstellar clouds 02 p0260 A83-12537
- Hydromagnetic gravitational instability of an infinite cylinder of a compressible fluid --- in relation to the dynamics of spiral arms of galaxies 04 p0549 A83-14984
- VLBI measurements of the relative position of the 1665 MHz and 1667 MHz OH masers toward W49N and NGC 6334N 04 p0552 A83-15616
- The dynamics of the intergalactic medium 04 p0556 A83-15957
- Vorticity and astrophysical magnetism 04 p0557 A83-15982
- Circular polarization from compact extragalactic radio sources as a result of nonuniform magnetic fields 05 p0697 A83-16986
- Investigation of the magnetic field of the galaxy 06 p0838 A83-19225
- The relation between magnetic field and gas density in interstellar clouds 06 p0840 A83-19276
- On scaling the magnetic field strength in interstellar clouds Resolution of the 'B versus n dilemma' 06 p0840 A83-19277
- A bisymmetric spiral magnetic field and the spiral arms in our Galaxy 08 p1182 A83-23041
- Aperture synthesis observations of the 21 cm Zeeman effect 09 p1361 A83-24473
- Intergalactic and galactic magnetic fields - An updated test 11 p1679 A83-27990
- Magnetic alignment of interstellar dust grains for dominating magnetic effects 12 p1790 A83-28896
- Numerical simulations of collapsing, isothermal, magnetic clouds 13 p1945 A83-30365
- Early Brans-Dicke axisymmetric universe with magnetic field 13 p1958 A83-31731
- The interaction of fast particles with long-wave MHD turbulence 14 p2116 A83-32546
- On the evolution of interacting, magnetized, galactic plasmas 15 p2262 A83-34528
- Grain alignment in the intergalactic magnetic field 15 p2263 A83-34552
- An interesting radio jet in the high-redshift quasar 1857 + 566 15 p2266 A83-34611
- Relativistic thermal plasmas - Effects of magnetic fields 15 p2266 A83-34617
- Galactic magnetic fields 15 p2272 A83-35009
- Interstellar magnetic fields 15 p2273 A83-35010
- Circumvention of Parker's bound on galactic magnetic monopoles 16 p2427 A83-35990
- The role of cosmic rays in hydrostatic equilibrium of the galactic halo 16 p2441 A83-36528

- Polarization of stars in R-associations - Observational data 17 p2611 A83-38555
- Magnetic fields in the cosmos 18 p2764 A83-39087
- Cosmic magnetic fields; Proceedings of the Workshop, Florence, Italy, October 21-23, 1982 18 p2765 A83-39226
- Stellar and interstellar magnetic fields 18 p2765 A83-39236
- Cosmic rays and magnetic fields in the galaxy 18 p2786 A83-39655
- Hydrostatic-equilibrium distribution of cosmic rays and the magnetic field in the galactic halo 18 p2778 A83-40489
- Interaction of a rotating charged black-hole with a uniform magnetic field 19 p2915 A83-40730
- Magnetic bubbles and high-velocity outflows in molecular clouds 19 p2918 A83-41620
- The dynamics of intermediate-scale magnetic fields 19 p2903 A83-42001
- Large-scale magnetic field in the Perseus spiral arm 20 p3066 A83-42396
- Neutron oscillation and the primordial magnetic field 20 p3070 A83-42785
- Determination of the properties of magnetic turbulence in radio sources 20 p3073 A83-43082
- Stability of the equilibrium distributions of interstellar gas, cosmic rays, and magnetic field in an external gravitational field 20 p3076 A83-43652
- Release of protons with energy higher than 10 to the 18th eV from intergalactic magnetic field into interstellar magnetic field 20 p3077 A83-43664
- Magnetic field structure in the Gum Nebula area 21 p3236 A83-45539
- The magnetic field of the NGC 2024 molecular cloud - Detection of OH line Zeeman splitting 23 p3518 A83-47431
- Masses of interstellar gas clouds 23 p3526 A83-47621
- Magnetic paths in the Galaxy - A review of the interstellar magnetic field 24 p3650 A83-48991
- Magnetic fields and spiral structure 24 p3656 A83-49230
- Magnetohydrodynamic effects of a first-order cosmological phase transition 24 p3658 A83-49299
- INTERSTELLAR MASERS**
- Polarization properties of the 86 GHz SiO maser emission from R Cassiopeiae 02 p0251 A83-11591
- The Orion SiO maser - A unique object in the Galaxy 02 p0255 A83-12121
- Formaldehyde absorption towards OH sources 02 p0260 A83-12531
- An interpretation of OH maser observations in W3/OH/ 03 p0413 A83-13313
- Observations of cool stars at 20, 25, and 33 microns 03 p0421 A83-14149
- Pumping of H II/OH masers - IR line overlaps and collisional excitation by H2 03 p0427 A83-14756
- Radiative stability of interstellar masers - A variational technique 04 p0549 A83-14990
- VLBI measurements of the relative position of the 1665 MHz and 1667 MHz OH masers toward W49N and NGC 6334N 04 p0552 A83-15616
- Search for maser emission by water vapor in the nu-2 excited vibrational state 05 p0698 A83-16998
- Physical conditions in H II/OH maser regions 06 p0825 A83-18088
- Observations of variable water maser sources associated with star formation regions 06 p0832 A83-18835
- Observations of SiO maser emission from R Leo during its summer 1981 maximum 06 p0833 A83-18867
- An accurate position for the 6-cm OH masers in W3 06 p0820 A83-18868
- The photoproduction of circumstellar OH maser shells 06 p0833 A83-18871
- SiO isotopic maser emission from VY Canis Majoris 06 p0824 A83-19527
- Observations of the new OH maser source G43.2-0.1 07 p1007 A83-20670
- Water-vapor masers located near Herbig-Haro objects 07 p1021 A83-21126
- Formation of OB clusters - OH maser observations 07 p1021 A83-21128
- SiO isotope emission from Orion - A model for IRc2 07 p1025 A83-21244
- New H2O masers in the galactic center region 07 p1025 A83-21247
- The molecular cloud complex associated with ON 1 10 p1508 A83-26367
- SiS maser emission from IRC + 10 deg 216 10 p1513 A83-26720
- J = 2-1 CO and H2O observations of the molecular cloud G35.2-0.74 11 p1682 A83-28288
- The astronomical objectives of the 6m radiotelescope of the University of NSW 13 p1936 A83-30401
- VLA observations of the 2pi(3/2)J=3/2 OH masers associated with Orion A 13 p1940 A83-31415
- Positions of the SiO masers in Orion-KL - Anisotropy on a scale of 70 AU 13 p1953 A83-31450
- Detection of two new water vapor emission sources in the southern hemisphere 14 p2109 A83-33277
- VLA positions of OH/IR stars 15 p2245 A83-33833
- Transfer of polarized radiation in astronomical masers 15 p2259 A83-34111
- The infrared variability of OH 0739-14 15 p2266 A83-34602
- Radiative excitation and the intensities of radio recombination lines 16 p2429 A83-36627
- Emission and absorption at 6 cm from excited OH associated with compact H II regions 16 p2430 A83-36644
- Far-infrared and CO observations of NGC 6357 and regions surrounding NGC 6357 and NGC 6334 17 p2591 A83-37784
- The H2O maser flare in Orion A 17 p2613 A83-38838
- Investigation of scintillations in near-solar regions of the interplanetary medium --- for solar wind analysis 18 p2783 A83-39305
- Is the SiO maser in Orion associated with a late-type star? 18 p2773 A83-39723
- An analysis of the Orion SiO maser 18 p2773 A83-39724
- Monte Carlo simulation of methanol masers 18 p2778 A83-40478
- The H2O/OH maser 342.01 + 0.25 - A case of supernova-induced star formation? 20 p3066 A83-42394
- Ammonia toward DR21 - A weak maser in ortho-NH3? 21 p3229 A83-44428
- Quasi-thermal excitation of the satellite lines of OH at 5 cm 21 p3233 A83-44747
- Survey of OH masers at 1665 MHz. II - Galactic longitude 340 deg to the galactic centre 24 p3650 A83-48984
- Atlas of main-line OH masers in the galactic longitude range 3 to 60 deg 24 p3638 A83-48986
- New H2O masers associated with main-line OH masers in the galactic longitude range 3 to 60 deg 24 p3638 A83-48987
- Catalogue of non stellar molecular maser sources and their probable infrared counterparts in the galactic plane 24 p3642 A83-49321
- Observations of H2O maser emission in the Large Magellanic Cloud 24 p3659 A83-49368
- OH maser emission at 4765 MHz in W3 24 p3659 A83-49371
- 4.8-GHz H2CO maser emission in Sgr B2 24 p3660 A83-49388
- Ammonia absorption toward W3(OH) - 0.3 arcsec resolution maps in the (2,2) line 24 p3668 A83-50078
- INTERSTELLAR MATTER**
- On the widths of dust layers in galaxies 01 p0119 A83-10266
- Sk 143 - An SMC star with a galactic-type ultraviolet interstellar extinction 01 p0125 A83-10929
- Causal relationship between pulsar long-term intensity variations and the interstellar medium 01 p0126 A83-10948
- The far-infrared disk of M51 02 p0250 A83-11581
- The scattering phase function of interstellar grains - The case of the reflection nebula NGC 7023 02 p0250 A83-11584
- Physical conditions and carbon monoxide abundance in the dark cloud B5 02 p0251 A83-11586
- Linear analysis of an oscillatory instability of radiative shock waves 02 p0251 A83-11588
- Far-infrared sources in Cygnus X - An extended emission complex at DR 21 and unresolved sources at S106 and ON 2 02 p0251 A83-11589
- Novae as sources of nitrogen in galaxies 02 p0253 A83-11612
- Observations of C-12/O/J = 2-1/ emission in the Large and Small Magellanic Clouds 02 p0255 A83-12112
- Temperatures and their variation within interstellar H I structures 02 p0255 A83-12115
- Conversion from /C-12/O/ integrated intensity at 2.6 millimeter wavelength to hydrogen column density --- for probing interstellar medium 02 p0256 A83-12122
- The interstellar absorption-line spectrum of Mu Ophiuchi 02 p0256 A83-12124
- Molecular clouds in galaxies 02 p0259 A83-12193
- The search for infrared protostars 02 p0246 A83-12195
- The solar neighbourhood --- interstellar matter effects on astronomical observations 03 p0412 A83-13153
- Spectral types in the direction of the Magellanic Stream 03 p0401 A83-13307
- A model of the Cygnus Loop 03 p0413 A83-13322
- On C3 molecules in diffuse interstellar clouds 03 p0414 A83-13327
- What are comets made of - A model based on interstellar dust 03 p0415 A83-13380
- Dynamical history of the Oort Cloud 03 p0403 A83-13400
- A photometric map of interstellar reddening within 300 parsecs 03 p0406 A83-13552
- IUE high dispersion spectra of luminous stars in symmetric nebulae 03 p0417 A83-13555
- Protostar fragmentation and star formation in the Taurus dark cloud complex 03 p0418 A83-13659
- Formation of dense solid particles in a protoplanetary cloud 03 p0418 A83-13666
- On the transport and propagation of cosmic rays in galaxies. I - Solution of the steady-state transport equation for cosmic ray nucleons, momentum spectra and heating of the interstellar medium 03 p0439 A83-13943
- A study of the Chamaeleon dark cloud complex - Survey, structure and embedded sources 03 p0420 A83-13945
- On the origin and structure of isolated dark globules 03 p0423 A83-14191
- The relationship between carbon monoxide abundance and visual extinction in interstellar clouds 03 p0423 A83-14192
- A search for NaH in dense molecular clouds - evidence against formation on grains 03 p0423 A83-14193
- A search for diffuse band profile variations in the rho Ophiuchi cloud 03 p0423 A83-14194
- Extreme ultraviolet spectrophotometry of the hot DA white dwarf HZ 43 - Detection of He II in the stellar atmosphere 03 p0424 A83-14206
- Secondary electron spectra in interstellar clouds, and the bremsstrahlung gamma-ray luminosity 03 p0439 A83-14211
- Model calculations of the molecular composition of interstellar grain mantles 03 p0427 A83-14757
- Kinematics of ring-shaped nebulae in the LMC. II - The radial velocity field of N 185 03 p0429 A83-14790
- A model for interstellar extinction 04 p0548 A83-14979
- The infrared spectrum of interstellar dust --- noting spectroscopic similarity to transmittance of diatomaceous organisms 04 p0526 A83-14981
- Silicon monoxide - A component of interstellar grains 04 p0549 A83-14993
- On interstellar linear polarization and grain growth 04 p0549 A83-15026
- An Effelsberg - Green Bank galactic H I absorption line survey. II - Results and interpretation 04 p0549 A83-15027
- Fine structure in high velocity clouds near the south celestial pole 04 p0549 A83-15029
- Far infrared observations of a star forming region in Serpens 04 p0550 A83-15037
- The Galactic abundance gradient from supernova remnant observations 04 p0550 A83-15038
- The giant spiral galaxy M 101. VIII - Star formation in H I-H II associations 04 p0550 A83-15045
- The distribution of neutral atomic hydrogen in our galaxy beyond the solar circle 04 p0552 A83-15613
- The distribution of infrared obscuration in NGC 7331 - Evidence for a massive molecular ring 04 p0555 A83-15649
- Search for maser emission by water vapor in the nu-2 excited vibrational state 05 p0698 A83-16998
- On the n-dependence of the reaction rate for C+ + C/n/yields C+/n + 1/ in interstellar space 05 p0698 A83-16999
- The return of mass and energy to the interstellar medium by winds from early-type stars 05 p0698 A83-17000
- Vibration-rotation transition probabilities for the ground electronic chi/1/-sigma/+/+/- state of HD 05 p0701 A83-17670
- Discrete sources of cosmic gamma rays 06 p0857 A83-18087
- Has P Cygni generated a shock front which emits nonthermal radiation 06 p0829 A83-18526
- The neutral hydrogen distribution near the Rosette Nebula and the association Monoceros OB 2 06 p0831 A83-18830
- A 3.4-mm HCN and continuum survey of dark clouds 06 p0819 A83-18834
- Polarization of early-type stars in Norma 06 p0820 A83-18861
- A photometric map of interstellar reddening within 100 PC 06 p0820 A83-18863
- Spatial observations of dust emission in NGC 7027 06 p0833 A83-18869
- Observations of the Orion nebula in H-alpha, forbidden N II and H-beta lines 06 p0834 A83-18892
- A possible explanation of the variation of the scattering index parameter --- in interstellar medium 06 p0834 A83-18893

- Identification of some diffuse interstellar features
06 p0835 A83-18895
- Observations of the extinction and excitation of the molecular hydrogen emission in Orion
06 p0840 A83-19279
06 p0842 A83-19453
- From clouds to stars
06 p0840 A83-19279
- Dense cores in dark clouds. I - CO observations and column densities of high-extinction regions
06 p0844 A83-19493
- Laboratory millimeter and submillimeter spectrum of HOC
06 p0846 A83-19528
- Dense cloud chemistry. II - The HCS/+/CS ratio
07 p1018 A83-20946
- The magnetic and fluid environment of an ellipsoidal circumstellar plasma cavity
07 p1018 A83-20951
- The gas-grain interaction in the interstellar medium - Thermal accommodation and trapping
07 p1021 A83-21120
- The polarization of the infrared cluster in Orion - The spatial distribution of the 3.8 micron polarization
07 p1023 A83-21156
- The three micron 'ice' band in grain mantles --- and their influence in interstellar extinction and polarization
07 p1024 A83-21219
- Properties of amorphous H₂O ice and origin of the 3.1-micron absorption
07 p1024 A83-21224
- Abnormal extinction and dust properties in M 16, M 17, NGC 6357 and the Ophiuchus dark cloud
07 p1025 A83-21241
- The spatial distribution and spectral characteristics of the diffuse soft X-ray background
07 p1009 A83-21245
- An upper limit on the electron density in Heiles' dust cloud 2 from decimeter-wavelength observations
07 p1026 A83-21263
- Laboratory studies of the condensation and properties of amorphous silicate smokes
07 p1027 A83-21319
- The evolution of supernova remnants and the structure of the interstellar medium
08 p1178 A83-21849
- On the nature of the high-temperature component of the interstellar plasma
08 p1179 A83-22053
- CO emission in directions of some millimeter wavelength continuum sources
08 p1182 A83-23045
- Observations of H₂ emission from molecular clouds and Herbig-Haro objects
08 p1183 A83-23055
- Does a 2,200 Å hump observed in an artificial carbonaceous composite account for UV interstellar extinction
08 p1187 A83-23282
- Photodissociation and radiative processes in interstellar C₂
09 p1356 A83-23658
- The interstellar medium and star formation
09 p1358 A83-23913
- Pressure distribution at the inner boundary of an astropause caused by a compressible stellar wind
09 p1360 A83-24459
- Excitation conditions in HII regions
09 p1361 A83-24514
- Evidence for the detection of X-ray scattering from interstellar dust grains
09 p1355 A83-24699
- Interstellar grain composition and the infrared spectrum of OH26.5 + 0.6
09 p1362 A83-24985
- The diffuse interstellar medium and the CES --- Coude Echelle Spectrograph
09 p1365 A83-25299
- Six-centimeter H₂CO observations - Envelopes of dark clouds
10 p1499 A83-25373
- Grains spin-up by inverse Cerenkov effect --- in interstellar gas
10 p1501 A83-25493
- A laboratory study of the infrared spectra of interstellar ices
10 p1502 A83-25653
- The mass of Tycho's supernova remnant as determined from a high-resolution X-ray map
10 p1504 A83-25725
- Dense cores in dark clouds. II - NH₃ observations and star formation
10 p1504 A83-25727
- The kinetic temperature and density of the Sagittarius B2 molecular cloud from observations of methyl cyanide
10 p1504 A83-25729
- Observations of diffuse interstellar lines toward stars with low column densities of H₂
10 p1505 A83-25746
- Interstellar abundances of oxygen and nitrogen
10 p1505 A83-25747
- The role of the gas in propagating star formation
10 p1508 A83-26363
- CCD photometry of the center of M31
10 p1508 A83-26364
- The ionization equilibrium inside the RHO Ophiuchi cloud
10 p1508 A83-26366
- The acceleration of molecular hydrogen clouds through radiative dissociation
10 p1508 A83-26369
- Effects of a shock on the molecular composition of a diffuse interstellar cloud
10 p1509 A83-26373
- Peculiar ultraviolet interstellar extinction
10 p1509 A83-26374
- CO emission and the optical disk in the giant Sc galaxy M101
10 p1511 A83-26405
- Nebular dust and extinction in ionized nebulae. I - The Balmer decrement
10 p1513 A83-26712
- The polarization of millimeter-wave emission lines in dense interstellar clouds
10 p1513 A83-26713
- Polarization of interstellar radio-frequency lines and magnetic field direction
10 p1513 A83-26714
- Dependence of interstellar depletion on hydrogen column density - Possibilities and implications
10 p1513 A83-26716
- Shock formation of HCO/+/+
10 p1513 A83-26718
- CO emission in the outer Galaxy between longitudes 50 deg and 72 deg
10 p1516 A83-26753
- Detection of sulfur in the galactic center
10 p1516 A83-26754
- Source of the high-velocity molecular flow in Orion
10 p1516 A83-26755
- The diffuse interstellar feature at 4430 Å and interstellar extinction in the far-ultraviolet
10 p1516 A83-26756
- Detection of the J = 1 - 0 transition of CH₃CN
10 p1516 A83-26757
- The state of clouds in a violent interstellar medium
11 p1680 A83-28259
- Cometary Globule 1 --- dense interstellar dust cloud
11 p1675 A83-28270
- The gas distribution in the central region of the Galaxy. IV A survey of neutral hydrogen in the region 1 --- 349 to 13 deg, b --- 10 to 10 deg, and absolute value of v less than 350 km/s
12 p1789 A83-28864
- Magnetic alignment of interstellar dust grains for dominating magnetic effects
12 p1790 A83-28896
- Interstellar carbon in meteorites
12 p1797 A83-28923
- The dust distribution in some small H II regions
12 p1794 A83-29084
- HDE 283809 - A type B star toward the Taurus dark cloud
12 p1796 A83-29495
- Numerical simulations of collapsing, isothermal, magnetic clouds
13 p1945 A83-30365
- Artificial viscosity and the simulation of fragmentation --- of rotating self-gravitating clouds
13 p1945 A83-30368
- Excitation of the rotational levels of interstellar HCN
13 p1948 A83-31258
- High-velocity outflow sources in molecular clouds - The case for low-mass stars
13 p1950 A83-31412
- UV radiation field inside dense clouds - Its possible existence and chemical implications
13 p1950 A83-31413
- X-ray ionization and the Orion molecular cloud
13 p1950 A83-31414
- VLA observations of the 2pi(3/2)J = 3/2 OH masers associated with Orion A
13 p1940 A83-31415
- Formation of OB clusters - W33 complex
13 p1950 A83-31417
- The dust around the carbon star IRC + 10216
13 p1951 A83-31418
- Radiative association and the synthesis of long carbon chain molecules in interstellar clouds
13 p1953 A83-31451
- Detection of HCO(+) and HCN absorption towards three galactic H II-regions
13 p1954 A83-31570
- Star formation and interstellar matter in the Large Magellanic Cloud
13 p1954 A83-31579
- Absorption-line spectroscopy of close pairs of QSOs
13 p1954 A83-31582
- Absorption spectra of interstellar grains. III - On the origin of the '2200' hump
13 p1955 A83-31664
- Stochastic effects in the chemical evolution of galaxies
13 p1956 A83-31687
- The nuclear hyperfine structure of deuterated ammonia
13 p1958 A83-31730
- Hydrogen sulfide in a circumstellar envelope
13 p1958 A83-31734
- The Gum Nebula - New photometric and spectrophotometric results
13 p1958 A83-31735
- An investigation of the region around the emission nebula NGC 1499
14 p2101 A83-31827
- An extensive galactic search for conformer II glycine
14 p2073 A83-33191
- An attempt to resolve pulsar magnetospheres using interstellar scintillations
14 p2106 A83-33214
- Extinct radioactivities - A three-phase mixing model -- for early solar system abundances
14 p2106 A83-33215
- Nonlinear propagation of hydromagnetic waves in high-beta plasmas
14 p2106 A83-33217
- Observation of ice mantles toward HD 29647
14 p2107 A83-33232
- The microwave and far-infrared spectra of the CH radical
14 p2083 A83-33234
- Fragmentation of prestellar clouds by molecule formation
14 p2109 A83-33278
- Interstellar absorption in three Bode fields in the Andromeda Nebula
15 p2253 A83-33702
- Interstellar turbulence and shock waves
15 p2253 A83-33715
- Interstellar ice grains in the Taurus molecular clouds
15 p2261 A83-34385
- On the optical properties of bacterial grains - I.
15 p2216 A83-34549
- The volumes of He(+) and H(+) in H II regions - The Orion Nebula
15 p2263 A83-34551
- Interstellar Ca II and Na I line profiles towards halo OB stars
15 p2264 A83-34585
- Zinc as a tracer of metallicity in the interstellar medium
15 p2266 A83-34604
- The structure of bright-rimmed molecular clouds
15 p2267 A83-34625
- The retention of spallation products in interstellar grains
15 p2270 A83-34717
- Optical observations of the interstellar absorption lines towards the M8 nebula
15 p2272 A83-34790
- CO adsorption and the optical properties of interstellar grains
16 p2428 A83-36529
- Status of laboratory experiments on ice mixtures and on the 12 micron H₂O ice feature --- suggesting interstellar IR absorption
16 p2431 A83-36670
- Prediction of interstellar antiproton flux using a nonuniform galactic disk model
17 p2629 A83-37338
- On the possibly low H₂ formation rate in dense clouds
17 p2598 A83-37349
- Cyclic phase changes of interstellar medium
17 p2599 A83-37357
- Nonconservation of magnetic flux in star formation
17 p2599 A83-37358
- The radio continuum loop G56 - 14 possibly associated with an H I shell
17 p2599 A83-37359
- Copernicus observations of C I - Pressures and carbon abundances in diffuse interstellar clouds
17 p2604 A83-37908
- Dense cores in dark clouds. III - Subsonic turbulence
17 p2604 A83-37909
- Interstellar photoelectric absorption cross sections, 0.03-10 keV
17 p2604 A83-37910
- The galactic abundance gradient --- in H II regions
17 p2606 A83-38237
- The extinction of starlight at wavelengths near 2200 Å
17 p2611 A83-38589
- Interstellar matter in meteorites
18 p2779 A83-39088
- Interstellar electron density
18 p2765 A83-39198
- The large scale dust distribution in the inner galaxy
18 p2770 A83-39654
- COS-B gamma-ray measurements and the large-scale distribution of interstellar matter
18 p2786 A83-39658
- Introduction to the Orion symposium
18 p2758 A83-39700
- Atomic carbon in Orion
18 p2772 A83-39705
- The Orion Nebula - Large-scale distribution of far-infrared and submillimeter line emission
18 p2772 A83-39706
- Intrinsic polarization and extinction features of early-type stars with emission lines due to X-ray irradiation
18 p2774 A83-39738
- Hydrodynamic and turbulent motions in the galactic disk
18 p2775 A83-39755
- Equilibrium temperatures of interstellar iron grains
18 p2776 A83-39767
- Turbulence in the neutral interstellar medium
18 p2777 A83-39778
- Fragmentation of a nonisothermal protostellar cloud
19 p2915 A83-40788
- 230-271 GHz cryogenic radiometer
19 p2848 A83-41279
- The distribution of molecular clouds in the nuclear region of NGC 1068
19 p2918 A83-41614
- Theory of molecular formation by radiative association in interstellar clouds
19 p2918 A83-41623
- The kinetic theory of H₂ dissociation --- in interstellar molecular clouds
19 p2918 A83-41624
- The HCO(+) / HOC(+) abundance ratio in molecular clouds
19 p2919 A83-41625
- Laboratory measurement of the J = 2 goes to 3 rotational transition frequency of H(C-17)O(+-)
19 p2898 A83-41658
- Chemical evolution in space - A source of prebiotic molecules
19 p2886 A83-42031
- Far-infrared and CO observations of Cep F - Implications for star formation in Cepheus OB3
20 p3064 A83-42196
- Evidence of hourly variations in the deuterium Lyman line profiles toward Epsilon Persei
20 p3065 A83-42389
- A gravitationally stable Bok globule
20 p3067 A83-42442
- Comparison of C(+) distributions with new interstellar sources of HCO emission
20 p3067 A83-42444

- Cometary globules in the Gum-Vela complex
20 p3069 A83-42783
- Far-infrared and submillimeter observations of stellar radiative and wind heating in S140 IRS
20 p3072 A83-43056
- Detection of HN-15N(+) and HNN-15(+) in interstellar clouds
20 p3074 A83-43089
- The distribution of 6 centimeter H₂CO in Orion Molecular Cloud 1
20 p3074 A83-43090
- Interstellar C₂ molecules in a Taurus dark cloud
20 p3074 A83-43091
- Discovery of s-process Nd in Allende residue
20 p3078 A83-43093
- Limits to intergalactic neutral hydrogen from photoionization absorption in ultraviolet quasar spectra
20 p3075 A83-43385
- The heterogeneous condensation of interstellar ice grains
20 p3077 A83-43665
- Interstellar proteins and the discovery of a new absorption feature at lambda = 2800 A
20 p3077 A83-43669
- The bright stellar content of the giant galactic H II region NGC 3603
21 p3229 A83-44420
- Far ultraviolet observations of the expanding shell in Eridanus
21 p3229 A83-44425
- 3-D simulations of the collapse of nonspherical interstellar clouds
21 p3230 A83-44438
- The propagation of extra-relativistic cosmic ray electron in the interstellar medium
21 p3245 A83-44577
- Quasi-thermal excitation of the satellite lines of OH at 5 cm
21 p3233 A83-44747
- Polymerization induced on interstellar grains by low-energy cosmic rays
21 p3234 A83-44765
- Common Lyman-alpha absorption lines in the triple QSO PG 1115+08
22 p3376 A83-45626
- Polarization of interstellar molecular radiofrequency absorption lines
22 p3376 A83-45633
- Abundances of carbon-bearing diatomic molecules in diffuse interstellar clouds
22 p3377 A83-46259
- Molecules in celestial objects. IV - IUE observation of CO lines towards Be stars with low reddening
22 p3379 A83-46555
- Neutral interstellar gas in the lower galactic halo
22 p3381 A83-46983
- Interpretation of neutral hydrogen spin temperature measurements --- interstellar matter
22 p3381 A83-46984
- Interstellar polarization, grain growth, and alignment
22 p3381 A83-46985
- A note on compressibility and energy cascade in turbulent molecular clouds
22 p3383 A83-47007
- Tentative detection of the CS(+) molecular ion in diffuse interstellar clouds
23 p3518 A83-47426
- Estimated energy and momentum input to the interstellar medium for several external galaxies
23 p3519 A83-47448
- Galactic propagation of cosmic rays
23 p3539 A83-47748
- A detector to investigate the anomalous component of cosmic rays and its rarer constituents including a possible molecular ion component
23 p3540 A83-47756
- Internal kinematics and dynamics of galaxies; Proceedings of the Symposium, Universitede Franche-Comte, Besancon, France, August 9-13, 1982
24 p3654 A83-49201
- Interstellar matter in elliptical galaxies
24 p3657 A83-49252
- Multiple scattering in the reflection nebula NGC 1999 and the nature of interstellar dust
24 p3659 A83-49376
- H II regions --- review of IUE studies
24 p3662 A83-49568
- Helium in supernova remnants
24 p3666 A83-50052
- He-4 determinations from radio recombination lines --- of interstellar matter
24 p3667 A83-50055
- Observations of interstellar deuterium
24 p3667 A83-50059
- The interstellar lithium abundance
24 p3667 A83-50061
- The fraction of the sky screened by local diffuse dust clouds
24 p3668 A83-50089
- Formaldehyde, cold neutral hydrogen and dust distribution in a globular filament in Taurus
24 p3669 A83-50096
- The radiation field and the molecular hydrogen photodissociation rate within spherically symmetric inhomogeneous clouds
06 p0828 A83-18181
- An interpretation of the flare in the Orion H₂O maser source
06 p0830 A83-18784
- The interstellar medium near the sun. III - Detailed analysis of the line of sight to lambda Sct
06 p0840 A83-19281
- Electron and local gas densities in diffuse interstellar clouds from measurements of Ca I absorption
08 p1183 A83-23050
- Observations of diffuse interstellar lines toward stars with low column densities of H₂
10 p1505 A83-25746
- High-density gas associated with 'molecular jets' - NGC 1333 and NGC 2071
13 p1953 A83-31449
- A galaxy with a 3.2 x 2.2 sq kpc H II region surrounding its nucleus
16 p2431 A83-36671
- The energy spectrum of cosmic fireballs
16 p2431 A83-36672
- Interstellar absorption lines in the directions of extragalactic objects. I
17 p2593 A83-38250
- Observations of an emission nebula associated with the carbon star UV Aur
19 p2914 A83-40716
- Observationally determined Fe II oscillator strengths --- interstellar and quasar absorption spectra
20 p3069 A83-42466
- Monte Carlo estimation of polarization in reflection nebulae
24 p3659 A83-49375
- INTERSTELLAR REDDENING**
U INTERSTELLAR EXTINCTION
- INTERSTELLAR SPACE**
Nuclear waste disposal in space
09 p1211 A83-25126
- Space vacuum hinders radiopanspermia
12 p1767 A83-29451
- Distributed acceleration of cosmic rays
23 p3538 A83-47613
- The spectra of cosmic ray nuclei greater than 1 GeV/nuc
23 p3539 A83-47737
- INTERSTELLAR SPACECRAFT**
Magnetic acceleration of interstellar probes
01 p0016 A83-10703
- Celestial views from nonrelativistic and relativistic interstellar spacecraft
09 p1210 A83-23681
- The interstellar solar sail - Optimization and further analyses
12 p1708 A83-29452
- Optimization of relativistic antimatter rockets [IAAA PAPER 83-1343]
16 p2321 A83-36348
- INTERSTELLAR TRAVEL**
The interstellar solar sail - Optimization and further analyses
12 p1708 A83-29452
- Comets and interstellar travel
12 p1784 A83-29453
- Requirements for rapid transport to the further stars
12 p1784 A83-29456
- Antimatter and distant space flight
12 p1705 A83-29673
- Interstellar travel and communication bibliography - 1982 update
18 p2754 A83-39610
- Interstellar propulsion systems
19 p2818 A83-41505
- Settlements in space, and interstellar travel
19 p2807 A83-41506
- Estimates of expansion time scales
19 p2908 A83-41508
- Colonies in the asteroid belt, or a missing term in the Drake equation
19 p2908 A83-41509
- Mass-, time-, and energy - Characteristics of the interstellar flights during the long proper time of astronautics [IAF PAPER 83-284]
23 p3415 A83-47328
- Relativistic astrodynamics - The problem of payload optimization in a two-star exploration flight with an intermediate powered swing-by [IAF PAPER 83-327]
23 p3415 A83-47343
- INTERSTITIALS**
The effect of the characteristics of interstitial solid solution decomposition on the fine structure and properties of cast alloys of molybdenum
01 p0025 A83-10393
- The crystalline structure of gas-saturated beta titanium alloys
11 p1550 A83-28546
- Self-interstitial and vacancy contributions to silicon self-diffusion determined from the diffusion of gold in silicon
13 p1929 A83-30342
- Calculations of the binding of hydrogen to fixed interstitial impurities in nickel
18 p2669 A83-40627
- Effect of radiation-induced lattice defects in silicon single crystals on the characteristic states of an interstitial muonium atom
20 p3051 A83-42266
- Interstitial CCN measurements --- Cloud Condensation Nuclei
24 p3611 A83-49687
- INTERSYMBOLIC INTERFERENCE**
Performance of IJF-OQPSK modulation schemes in the presence of noise, interchannel and cochannel interference
07 p0905 A83-19699
- Digital modulation techniques for new earth stations
07 p0914 A83-20848
- Performance of IJF-OQPSK and Partial Response /PR/ IJF-OQPSK modems in a nonlinearly amplified and adjacent-channel interference satellite environment
11 p1556 A83-28128
- Cochannel and intersymbol interferences in QAM system
24 p3571 A83-49965
- INTERTROPICAL CONVERGENCE ZONES**
On the causes of formation of two intertropical convergence zones in the western part of the Pacific Ocean and in the Indian Ocean
04 p0517 A83-16012
- Results from studies of the intertropical convergence zone in GATE
05 p0668 A83-17700
- Cloud-cluster-scale circulations and the vorticity budget of synoptic-scale waves over the eastern Atlantic intertropical convergence zone
06 p0792 A83-18470
- Horizontal structure of the atmospheric boundary layer in the intertropical convergence zone
19 p2868 A83-42113
- Easterly waves in the Intertropical Convergence Zone
19 p2868 A83-42118
- Weather conditions in the center of the equatorial Atlantic in the spring of 1979
19 p2869 A83-42124
- INTERVALS**
Eigenvalue problems on infinite intervals
03 p0387 A83-13569
- Mean value and Taylor forms in interval analysis
09 p1335 A83-24370
- The detection of a connection between the extent of short-term memory and the accuracy of the evaluations of time intervals
16 p2401 A83-36820
- Representations of intervals and optimal error bounds
20 p3041 A83-42500
- INTERVERTEBRAL DISKS**
Spinal traumas /dorsal spinal fractures and lumbar disk hernias/ occurring after rapid vibratory phenomena /pumping/ in air combat pilots
08 p1148 A83-22973
- Some considerations on lumbar pains and diseases of the intervertebral disk to civilian aircrewmenn
08 p1148 A83-22974
- A new technique of studying the effects of vibrations on the spine
08 p1148 A83-22977
- INTESTINES**
The changes in the hemopoietic system and the small intestine mucosa during the breathing of pure oxygen under atmospheric pressure
03 p0374 A83-13632
- The adrenoactivity of the vessels of the small intestine in cats during the process of high altitude adaptation
07 p0973 A83-20245
- The functional condition of the mitochondria of the mucous membrane of the small intestine under thermal stresses
08 p1145 A83-22113
- Calcium transport from the intestine and into bone in a rat model simulating weightlessness
11 p1640 A83-27832
- The processes of proteolysis in the small intestine of rats in the case of the intestinal form of acute radiation sickness
19 p2874 A83-41013
- The modification of the intestinal syndrome with the aid of a gas hypoxic mixture at various conditions of the irradiation of animals
19 p2874 A83-41015
- The clinical picture of covered perforated gastric and duodenal ulcers in young individuals
19 p2884 A83-42025
- INTOXICATION**
The effect of chronic alcoholic intoxication on the temporal parameters of the process of 'motor command' organization and on the interhemispheric functional relations in humans
01 p0085 A83-10533
- The Air Canada programme for rehabilitation of the alcoholic employee/pilot
18 p2734 A83-40352
- A modified technique for estimation of ethanol in body fluids by gas liquid chromatography
23 p3499 A83-48694
- INTRACRANIAL CAVITY**
The interrelationship of the intracranial pressure, the blood volume of the skull cavity, and the total blood flow of the brain
08 p1145 A83-22108
- INTRAMOLECULAR STRUCTURES**
Lattice dynamics of solid I₂ under high pressure
23 p3511 A83-47634
- INTRAOCULAR PRESSURE**
A case of recording changes in the rhythm of systoles on an ophthalmotonogram
03 p0377 A83-13294
- A comparative evaluation of the simplified tonograph methods of Nesterov and Kal'fa-Vurgaft --- for eye examinations
15 p2212 A83-34938
- INTRUDER AIRCRAFT**
U A-6 AIRCRAFT

INVALIDITY

U ERRORS

INVARIANCE

NT GAUGE INVARIANCE

Rotational invariance in visual pattern recognition by

pigeons and humans 02 p0224 A83-12068

Invariance properties under a reciprocal Backlund

transformation in gasdynamics 03 p0320 A83-14566

On invariant solutions of the equation of nonlinear heat

conduction with a source 05 p0640 A83-17643

Spontaneously broken complete relativity

07 p0988 A83-20045

Solution of the gravitational polytrope equations by using

the quasi-invariance group --- stellar evolution model

08 p1180 A83-22060

An application of the Ambartsumian invariance principle

to the investigation of extended lightguides with random

inhomogeneities 09 p1344 A83-23484

On an attempt to generalize the Hess solution of the

problem concerning the motion of a heavy rigid body with

a fixed point 09 p1337 A83-23557

The finite-dimensionality of bounded invariant sets for

the Navier-Stokes system and other dissipative systems

09 p1261 A83-24321

The 'Invariant Mechanics' - A new approach to the

study of motion of non-quantum high speed objects

09 p1339 A83-25403

A new approach to scale-invariant gravity /or: A

variable-mass embedding for general relativity/

10 p1501 A83-25497

Invariance and identifiability in adaptive

coordinate-parametric control 10 p1465 A83-26533

On the maximal invariance group and the general

solution of the one-dimensional equations of gas

dynamics 13 p1839 A83-30083

Zero-energy theorem for scale-invariant gravity

15 p2224 A83-33791

Waves in scale-invariant systems

17 p2577 A83-38979

Theory of the invariance of binary nonstationary and

nonlinear sequential machines 20 p3039 A83-42923

Coordinate-invariant conservation laws in Schwarzschild

geometry 20 p3075 A83-43389

Electric-magnetic duality of conformal gravitation

24 p3624 A83-49745

INVARIANT IMBEDDINGS

Properties of parallel-surfaces coordinate systems ---

for balance equations in computational fluid dynamics

04 p0530 A83-15817

Conditions of optimality for singular trajectories in the

problem of the minimization of a curvilinear integral

06 p0805 A83-17977

Pole assignment and minimal feedback design

06 p0803 A83-19388

On conditions of the existence of certain classes of

solutions of the problem of the motion of a rigid body

with a fixed point 09 p1337 A83-23551

The use of invariant relationships to reduce the order

of the system of equations of motion of a vortex-filled

heavy rigid body 09 p1337 A83-23564

The invariant imbedding - Stochastic approximation

algorithm with application to communications satellites

10 p1382 A83-26594

Chronometrically invariant variations in the Einstein

gravitation theory 13 p1944 A83-30099

Real-time solution of linear least-squares estimation

problem with semi-degenerate covariance

17 p2566 A83-37105

Topology of the invariant manifolds of period-doubling

attractors for some forced nonlinear oscillators

19 p2895 A83-41166

Boundary conditions of the second-order differential

equation and the Riccati equation

EQUATIONS 20 p3041 A83-42525

NT CROP INVENTORIES

NT TIMBER INVENTORY

Ecological land classification in the Yukon

03 p0347 A83-14250

The role of aerial photography in multisource

inventories Techniques and tests in applications

research 17 p2532 A83-38362

The use of small scales for a stereoscopic dual chamber

with a 'VHF-homing' system for the inventory and

monitoring of natural renewable resources

17 p2533 A83-38447

INVERSE SCATTERING

Geophysical inversion and remote probing are inverse

scattering problems 01 p0048 A83-10110

Inverse scattering inverse source theory

01 p0048 A83-10111

Inverse scattering for an exterior Dirichlet problem ---

due to metallic cylinder 01 p0104 A83-10494

Radar resonance reflection from sets of plane dielectric

layers --- and possible applications

01 p0031 A83-10614

A survey of the near-field far-field inverse scattering

inverse source integral equation

01 p0104 A83-11368

A survey of the physical optics inverse scattering

identity 01 p0104 A83-11369

Nonuniqueness in inverse source and scattering

problems 01 p0104 A83-11384

Physically motivated approximations in some inverse

scattering problems 02 p0233 A83-12632

Inverse scattering at long wavelength - Delta mu = 0

04 p0489 A83-15163

Inversion of ultrasonic scattering data

04 p0489 A83-15168

Rigorous results on inverse source and inverse

scattering theory --- for use in quantitative nondestructive

evaluation 04 p0490 A83-15172

Inversion of scattering data of the shadow region of

discontinuities 04 p0492 A83-15205

Runge's theorem and far field patterns for the impedance

boundary value problem in acoustic wave propagation

04 p0533 A83-16365

The theory of Dicke superradiation - An exact solution

of the quasi-one-dimensional quantum model

05 p0682 A83-16890

Complete integrability of the quasi-one-dimensional

quantum model of Dicke superradiance

07 p0933 A83-20048

Time domain Born approximation --- for ultrasonic

nondestructive tests 07 p0942 A83-20271

Concerning a modification of the seminverse

method --- for electromagnetic wave propagation

07 p0986 A83-20317

An exact, closed-form, analytical solution to the general

synthesis problem 08 p1161 A83-22472

An augmented technique for backscattering amplitude

inversion in the study of cavities and plane defects

09 p1275 A83-23474

A determination of the potential of the interatomic

interaction on the basis of the function for the single

scattering of a gas by a surface

09 p1339 A83-24491

Direct and inverse problems in scattering theory ---

Russian book 09 p1339 A83-25219

Inverse problems in the laser probing of atmospheric

aerosols 09 p1309 A83-25261

On the inverse scattering and direct linearizing

transforms for the Kadomtsev-Petviashvili equation

09 p1340 A83-25283

The emergence of solitons of the Korteweg-de Vries

equation from arbitrary initial conditions

10 p1471 A83-25464

Theory of the coherent interaction of light pulses and

resonant multilevel media 11 p1584 A83-28059

Gauge transformations in soliton theory

12 p1774 A83-29004

Inverse Compton scattering in a strong magnetic field

12 p1795 A83-29358

Soliton configurations of interacting zero-mass fields

13 p1913 A83-30095

The connection between partial differential equations

soluble by inverse scattering and ordinary differential

equations of Painlevé type 14 p2078 A83-32836

The small dispersion limit of the Korteweg-de Vries

equation. I 14 p2078 A83-32850

Scattering analysis and synthesis of wave trains

14 p2080 A83-33139

Inverse problems of lidar sensing of the atmosphere

--- Book 15 p2195 A83-33768

High-energy gravitational antennas - A theoretical

approach 15 p2261 A83-34405

Inversion procedure for inverse scattering within the

distorted-wave Born approximation

19 p2895 A83-40951

A new method for the numerical solution of nonlinear

evolutionary equations 19 p2895 A83-40995

The classical inverse scattering problem for a spherically

symmetric gravitational field 19 p2917 A83-41493

Inverse problems of the linear theory of radiative transfer

in a plane medium 19 p2897 A83-42063

Inverse methods for remote determination of properties

of optically thick atmospheres 22 p3328 A83-46067

INVERSIONS

NT CENTRIFUGING STRESS

NT MAGNETIC FIELD INVERSIONS

NT POPULATION INVERSION

NT TEMPERATURE INVERSIONS

Inverse Monte Carlo solutions for radiative transfer in

inhomogeneous media 05 p0692 A83-17870

Computation of Jupiter interior models from gravitational

inversion theory 15 p2275 A83-34720

Net-skirt addition to a parachute canopy to prevent

inversion 16 p2297 A83-36911

Differential inversion --- for thermal emission spectrum

of atmosphere [AD-A130984] 17 p2572 A83-38743

An air pollution analytic transport model admitting the

surface and inversion layer effect

21 p3169 A83-44489

INVERTEBRATES

NT BEETLES

NT DROSOPHILA

NT GRASSHOPPERS

NT INSECTS

NT LOCUSTS

NT MICROSPORES

NT PROTOZOA

NT PUPA

NT SPORES

INVERTED CONVERTERS (DC TO AC)

Large signal design of a buck converter for high power

dc/ac conversion 01 p0041 A83-11028

Simple transformerless inverter with automatic

grid-tracking and negligible harmonic content for utility

interactive photovoltaic systems 14 p2004 A83-32216

Large-signal dynamic-stability analysis of synchronised

current-controlled modulators - Application to sine-wave

high-power inverters 14 p2008 A83-33475

INVERTERS

NT STATIC INVERTERS

Estimated power quality for line commutated

photovoltaic residential system 24 p3599 A83-49324

INVESTIGATION

NT ACCIDENT INVESTIGATION

NT AIRCRAFT ACCIDENT INVESTIGATION

NT INTERNATIONAL MAGNETOSPHERIC STUDY

INVESTMENT CASTING

Precision casting for gas turbine engines

07 p0941 A83-21347

Superalloy technology - Today and tomorrow

07 p0891 A83-21452

Microporosity formation in investment castings of

nickel-base superalloys Metallurgical effects, thermal

modelling and foundry assessment

07 p0895 A83-21497

Cast titanium inlet duct development

[AIAA 83-0951] 12 p1695 A83-29776

High-strength aluminum high-quality casting alloy in

aeronautics and astronautics 15 p2136 A83-33955

INVESTMENTS

Industrial innovation policy - Lessons from American

history 07 p1001 A83-21421

Why billions can and should be spent on space

13 p1934 A83-30832

Need for, and financial feasibility of, satellite-aided land

mobile communications 19 p2834 A83-41415

Beyond Percheron - Launch vehicle systems from the

private sector

[AAS PAPER 83-081] 21 p3096 A83-44181

INVISID FLOW

NT STAGNATION FLOW

On a geophysical inviscid vortex

01 p0075 A83-10496

Transient extinction of counter flow diffusion flame

01 p0022 A83-10497

Numerical experiments on the leading-edge flowfield

03 p0277 A83-13131

A theoretical model for coherent structures in wall

turbulence 03 p0319 A83-14478

Transonic shear flow in a three-dimensional channel

03 p0321 A83-14586

Nonlinear hydrodynamic stability of some simple

rotational flows 04 p0475 A83-14962

A fast pseudo-time integration scheme for the solution

of the steady transonic flow problem

04 p0441 A83-15015

- Three-dimensional stability of vortex arrays
06 p0758 A83-19022
- The behavior of two-dimensional nonplane-parallel vortex flows of inviscid gas
06 p0758 A83-19118
- Inviscid axisymmetric jet impingement with recirculating stagnation regions
08 p1042 A83-22130
- Calculation of three-dimensional transonic flow past elongated bodies
09 p1196 A83-23570
- An interaction algorithm for three-dimensional turbulent subsonic aerodynamic juncture region flow
09 p1198 A83-24659
- Finite-element method for time-dependent Euler equation --- of inviscid incompressible flow
10 p1413 A83-25462
- Supersonic flow past a thin cone with an asymmetric tip
11 p1526 A83-27716
- Computation of nonlinear supersonic potential flow over three-dimensional surfaces
12 p1696 A83-29022
- Boundary treatments for implicit solutions to Euler and Navier-Stokes equations
12 p1725 A83-29655
- Implicit finite difference simulation of inviscid and viscous compressible flow
12 p1726 A83-29934
- The design and numerical analysis of vortex methods
12 p1727 A83-29940
- An inviscid three-dimensional analysis of the Space Shuttle main engine hot-gas manifold
[AIAA PAPER 83-1523] 14 p1984 A83-32754
- Computation of nonequilibrium, supersonic three-dimensional inviscid flow over blunt-nosed bodies
14 p1971 A83-32980
- Vorticity at the shock foot in inviscid flow
14 p1971 A83-32993
- Viscous-inviscid interactions in cascades
15 p2120 A83-33790
- Application of the triple-deck theory of viscous-inviscid interaction to bodies of revolution
16 p2288 A83-35345
- A time dependent numerical scheme for three-dimensional inviscid compressible flows in curvilinear coordinates
16 p2290 A83-35815
- Applications of computational techniques in the design of ramjet engines
16 p2290 A83-35828
- Evaluation of a surface panel method coupled with several boundary layer analyses
[AIAA PAPER 83-0011] 16 p2351 A83-36039
- Analysis of viscous-inviscid interaction in transonic internal flows
16 p2293 A83-36081
- A generalization of the Hines' dispersion relation --- for real atmosphere
16 p2377 A83-36108
- An integral analysis of transonic normal shock wave/turbulent boundary layer interactions in internal flow
[AIAA PAPER 83-1402] 16 p2295 A83-36392
- Finite element methods for internal flow calculations
[AIAA PAPER 83-1404] 16 p2296 A83-36415
- Supersonic flow field analysis for a twin-engine aircraft model
17 p2448 A83-37521
- Structure of the flow of an inviscid gas near an isolated stagnation point
17 p2505 A83-37526
- The spiral singularity in the supersonic inviscid flow over a cone
[AIAA PAPER 83-1665] 17 p2451 A83-38084
- Viscous/inviscid analysis of curved sub- or supersonic wall jets
[AIAA PAPER 83-1679] 17 p2452 A83-38086
- High angle of attack inviscid flow calculations over a Shuttle-like vehicle with comparisons to flight data
[AIAA PAPER 83-1798] 17 p2453 A83-38636
- Test problems, coordinate transformations, and technique for nonsteady compressible flow analysis
17 p2508 A83-38797
- A semi-direct solver for compressible three-dimensional rotational flow
[AIAA PAPER 83-1909] 18 p2682 A83-39367
- Transonic Euler simulations by means of finite element explicit schemes
[AIAA PAPER 83-1924] 18 p2635 A83-39378
- Inviscid drag calculations for transonic flows
[AIAA PAPER 83-1928] 18 p2635 A83-39380
- A fast Euler solver for steady flows
[AIAA PAPER 83-1940] 18 p2682 A83-39389
- The computation of inviscid rotational gasdynamic flows using an alternate velocity decomposition
[AIAA PAPER 83-1900] 18 p2637 A83-39405
- Entropy and vorticity corrections for transonic flows
[AIAA PAPER 83-1926] 18 p2637 A83-39413
- A zonal approach for the steady transonic simulation of inviscid rotational flow
[AIAA PAPER 83-1927] 18 p2637 A83-39419
- The evolution of large-horizontal-scale disturbances in marginally stable, inviscid, shear flows. I - Derivation of the amplitude evolution equations
19 p2842 A83-41022
- Global pressure relaxation procedure for flows with strong viscous-inviscid interaction
20 p2969 A83-42555
- Effect of particle presence on the incompressible inviscid flow through a two dimensional compressor cascade
20 p2928 A83-42562
- ONERA research on afterbody viscid/inviscid interaction with special emphasis on base flows
[ONERA, TP NO. 1983-26] 21 p3085 A83-44305
- Application of unsteady laminar triple-deck theory to viscous-inviscid interactions from an oscillating flap in supersonic and subsonic flow
21 p3086 A83-44457
- On the numerical solution of head-on vehicle shock-planar incident shock interaction flow
21 p3086 A83-44556
- Numerical calculation of inviscid supersonic flow field around bent nose cones
21 p3087 A83-44564
- An implicit lambda scheme --- for transonic inviscid flow simulation
21 p3089 A83-45581
- A point vortex method applied to interfacial waves
22 p3280 A83-45906
- The representation of planar separated flow by regions of uniform vorticity
22 p3280 A83-45910
- Axial coherence functions of circular turbulent jets based on an inviscid calculation of damped modes
22 p3281 A83-46002
- Response of variations of free stream velocity on inviscid and incompressible flow past a wavy plate
22 p3281 A83-46393
- Mesh influence on vortex shedding in inviscid flow computations
22 p3249 A83-46471
- Viscid-inviscid interaction analysis on airfoils with an inverse boundary layer approach
22 p3249 A83-46474
- Calculation of three-dimensional, inviscid, rotational flow in axial turbine blade rows
[ASME PAPER 83-GT-119] 23 p3395 A83-47948
- Design of shock-free compressor cascades including viscous boundary layer effects
[ASME PAPER 83-GT-134] 23 p3396 A83-47961
- Three dimensional inviscid computation of an impeller flow
[ASME PAPER 83-GT-210] 23 p3397 A83-48011
- The lift on an aerofoil in starting flow
23 p3398 A83-48121
- Progress in calculation of the interaction between a perfect fluid and a viscous fluid
[ONERA, TP NO. 1983-61] 23 p3398 A83-48182
- A coupling method for the inverse mode calculation of transonic internal flows with a shock wave
[ONERA, TP NO. 1983-62] 23 p3398 A83-48183
- Interaction between the outer inviscid flow and the boundary layer on transonic airfoils
24 p3544 A83-49021
- INVISIBILITY**
U VISIBILITY
- INVOLUNTARINESS**
U INVOLUNTARY ACTIONS
- INVOLUNTARY ACTIONS**
The involuntary regulation of the GSR --- Galvanic Skin Response
23 p3497 A83-47108
- IO**
Tidal heating of Io and orbital evolution of the Jovian satellites
03 p0401 A83-13302
- Io - A volcanic flow model for the hot spot emission spectrum and a thermostatic mechanism
03 p0133 A83-13833
- On charge exchange and knock-on processes in the exosphere of Io
03 p0434 A83-14214
- The geology of Io
04 p0571 A83-16240
- Volcanic eruption plumes on Io
04 p0571 A83-16241
- Volcanic eruptions on Io - Implications for surface evolution and mass loss
04 p0571 A83-16242
- Dynamics and thermodynamics of volcanic eruptions - Implications for the plumes on Io
04 p0571 A83-16243
- Hot spots of Io
04 p0571 A83-16244
- Io's surface - Its phase composition and influence on Io's atmosphere and Jupiter's magnetosphere
04 p0571 A83-16245
- The atmospheres of Io and other satellites
04 p0571 A83-16246
- In situ observations of Io torus plasma
04 p0572 A83-16248
- An interpretation of the near-ultraviolet absorption spectrum of SO₂ - Implications for Venus, Io, and laboratory measurements
05 p0704 A83-16966
- Charge exchange in the Io torus and exosphere
05 p0705 A83-17385
- The proton concentration in the vicinity of the Io plasma torus
05 p0705 A83-17386
- Single and multiple ionization of sulfur atoms by electron impact --- in Io plasma torus
05 p0707 A83-17783
- Identification of radio emission from the Io flux tube
06 p0848 A83-18315
- A deficiency of O III in the Io plasma torus
06 p0848 A83-19296
- Io's sodium cloud - Explanation of the east-west asymmetries, II
06 p0850 A83-19517
- Oscillator strengths and collision strengths for O II and O III
06 p0809 A83-19519
- Departure from corotation of the Io plasma torus - Local plasma production
07 p1028 A83-20190
- Supply of SO₂ for the atmosphere of Io
07 p1036 A83-21523
- The problem of cooling the cold Io torus
09 p1365 A83-23755
- Dawn-dusk electric field asymmetry of the Io plasma torus
09 p1366 A83-24340
- The low-energy plasma in the Jovian magnetosphere
10 p1519 A83-26614
- Spectrophotometric studies of the Io Torus
10 p1519 A83-26617
- Alfven wave propagation in the Io plasma torus
11 p1685 A83-28305
- S II and S III branching ratios in the 600- to 1200-A interval --- applied to modeling of Io plasma torus
11 p1619 A83-28327
- An interpretation of the dawn-dusk asymmetry of UV emission from the Io plasma torus
11 p1686 A83-28391
- Energetic ion losses near Io's orbit
13 p1962 A83-31227
- Oscillator strengths and collision strengths for S II --- atomic spectra of Io plasma torus
13 p1962 A83-31440
- Rocket detection of ultraviolet emission from neutral oxygen and sulfur in the IO Torus
13 p1962 A83-31452
- Io - The near-infrared monitoring program, 1979-1981
14 p2112 A83-32609
- Observed departure of the Io plasma torus from rigid corotation with Jupiter
14 p2113 A83-33233
- Io's atmosphere - Pressure control by regolith cold trapping and surface venting
15 p2274 A83-33931
- Io's 4-micron band and the role of adsorbed SO₂
15 p2275 A83-34723
- Reflectance spectra of SO₂ frosts contaminated by sodium and their implication on Io
17 p2615 A83-37363
- The Io-control of Jupiter's decametric radiation - The Alfven wave model
17 p2620 A83-38115
- Origin and energetics of the Io plasma torus
17 p2621 A83-38116
- Ion cyclotron waves in the Io plasma torus - Polarization reversal of whistler mode noise
19 p2922 A83-41130
- Magnetic drifts at Io - Depletion of 10-MeV electrons at Voyager 1 encounter due to a forbidden zone
20 p3077 A83-42406
- Escape and ionization of atomic oxygen from Io
20 p3078 A83-43078
- Two classes of volcanic plumes on Io
21 p3239 A83-44081
- A two-stage mechanism for escape of Na and K from Io
21 p3241 A83-44994
- The non-Maxwellian energy distribution of ions in the warm Io torus
22 p3387 A83-47072
- Longitudinal asymmetry of the Io plasma torus
23 p3529 A83-47865
- IODATES**
NT LITHIUM IODATES
- IODIDES**
NT CESIUM IODIDES
NT POTASSIUM IODIDES
NT SILVER IODIDES
NT SODIUM IODIDES
- Iron diiodide photodissociation laser
02 p0184 A83-12265
- Threshold of a thallium-iodide photodissociation laser operated at low pressure
04 p0485 A83-16052
- Repetitive passive Q-switching and bistability in lasers with saturable absorbers
08 p1107 A83-22079
- Inverse-square wavelength dependence of attenuation in infrared polycrystalline fibers
10 p1482 A83-26116
- Standard free energy of formation of iron iodide
11 p1546 A83-28299
- Room-temperature mercuric iodide spectrometry for low-energy X-rays
16 p2357 A83-36717
- Characteristics of mercurous bromide and iodide visible lasers
20 p2995 A83-43104
- Interfacial conduction in lithium iodide containing inert oxides
24 p3558 A83-49947
- IODINE**
NT IODINE ISOTOPES
- Simultaneous multiple-point velocity measurements using laser-induced iodine fluorescence
05 p0646 A83-17884
- Current methods for the determination of iodine in the atmosphere
10 p1447 A83-25612

- Nonintrusive pressure measurement with laser-induced iodine fluorescence 14 p2019 A83-32724
[AIAA PAPER 83-1468] 14 p2019 A83-32724
High-accuracy wave-number measurements in molecular iodine 15 p2227 A83-33762
Level crossing and polarization rotation in doubly resonant third-harmonic generation in I₂ 16 p2358 A83-35658
Time-resolved study of the laser optogalvanic effect in I₂ 16 p2360 A83-36716
The effect of an insufficiency of iodine on the growth and formation of bone tissue 18 p2733 A83-40565
Yield of excited iodine atoms during many-photon dissociation of CF₃I and (CF₃)₂CI 20 p2993 A83-42287
Multiple photon echoes in molecular iodine 21 p3202 A83-44195
Lattice dynamics of solid I₂ under high pressure 23 p3511 A83-47634

IODINE COMPOUNDS

- NT CESIUM IODIDES
NT IODIDES
NT LITHIUM IODATES
NT POTASSIUM IODIDES
NT SILVER IODIDES
NT SODIUM IODIDES
Characteristics of the electron beam pumped iodine monofluoride laser 07 p0938 A83-21590
Thermal efficiency of the magnesium-iodine cycle for thermochemical hydrogen production 20 p2950 A83-42953
Supermetallic conductivity of graphite intercalated with iodine monochloride 24 p3634 A83-48864
IODINE ISOTOPES
I-Xe ages of individual Bjurbol chondrules 04 p0562 A83-15356
Shock disturbance of the I-Xe system --- in Bjurbol meteorite 04 p0562 A83-15357
Extinct I-129 in C3 chondrites 07 p1035 A83-21334

IODINE LASERS

- Methods for spectral selection in the region of the 2P_{1/2}-2P_{3/2} transition in an iodine atom under conditions of lasing in a Zeeman inhomogeneous gain profile 05 p0648 A83-17041
Analysis of the energetics of a chemical oxygen-iodine laser 05 p0648 A83-17047
Investigation of a high-efficiency photodissociation laser operating in the free-lasing regime 05 p0649 A83-17054
Determination of the width of the gain profile of an iodine laser with the aid of stimulated Brillouin scattering 05 p0649 A83-17059
Iodine monofluoride B 3P_{1/2} to X 1Sigma⁺ lasing from collisionally pumped states 05 p0651 A83-17653
Quantitative measurement of density and velocity in compressible flows using laser-induced iodine fluorescence [AIAA PAPER 83-0049] 05 p0646 A83-17903
Laser optogalvanic photodetachment spectroscopy - A new technique for studying photodetachment thresholds with application to I⁻/I 07 p0882 A83-21190
Direct frequency measurements of transitions at 520 THz /576 nm/ in iodine and 260 THz /1.15 micron/ in neon 08 p1110 A83-22633
Direct frequency measurement of the I₂-stabilized He-Ne 473-THz /633-nm/ laser 08 p1110 A83-22634
Optical distortion due to gas-dynamic motion in a photolytically pumped cylindrical laser cavity 10 p1428 A83-26022
Photodissociation CW laser using condensation and evaporation for a closed cycle 10 p1430 A83-26235
Numerical modeling of a chemical oxygen-iodine laser 10 p1433 A83-26676
Flashlamp-pumped iodine monobromide laser characteristics 11 p1585 A83-28704
The high-power iodine laser --- Book 13 p1849 A83-30135
Photochemical and photophysical dynamics of I₂ isolated in a rare gas cage 13 p1916 A83-30967
Results of international comparisons using methane-stabilized He-Ne lasers at 3.39 microns and iodine-stabilized He-Ne lasers at 633 nm 13 p1856 A83-31279
Passive mode locking in iodine photodissociation laser 14 p2023 A83-31913
Possibility of operation of a chemical oxygen-iodine laser without a cooled trap 16 p2359 A83-35893
Performance characteristics of a transverse-flow, oxygen-iodine chemical laser in a low gas-flow velocity 17 p2513 A83-37609
The helium-iodine laser 18 p2694 A83-40664
Scattering of light and acoustic disturbances in the atomic iodine laser 20 p2995 A83-42795

- Snowing criteria for cold traps --- utilization in chemical oxygen iodine lasers 21 p3147 A83-45593
Gain on the green (504 nm) excimer band of I₂ 22 p3299 A83-46726
Relative quantum yield of I-asterisk(2P_{1/2}) in the tunable laser UV photodissociation of i-C₃F₇I and n-C₃F₇I - Effect of temperature and exciplex emission 23 p3461 A83-47632
Visible iodine and bromine laser, and coaxial discharge excited strong UV iodine laser 24 p3589 A83-49615
An analysis of the international comparison results of helium-neon lasers stabilized by saturated absorption in I-127 (review) 24 p3589 A83-49736
An investigation of the pulsed-discharge radiation in mixtures of ZnI₂, CdI₂, and HgI₂ with helium and neon --- in metal vapor lasers 24 p3589 A83-49742

ION ACCELERATORS

- Ion accelerator systems for high power 30-cm thruster operation [AIAA PAPER 82-1893] 02 p0144 A83-12474
Theory of ion acceleration with closed electron drift [AIAA PAPER 82-1919] 02 p0241 A83-12490
Radial ion acceleration at a virtual cathode formed in a neutral gas by a relativistic electron beam 03 p0392 A83-13178
Ion extraction from a plasma through a conical orifice 05 p0687 A83-16920
Investigation of the operation of a two-stage accelerator with an anode layer with one power source 06 p0755 A83-19562
Ion acceleration mechanism in electron beams 10 p1486 A83-25992
Accelerator simulation of astrophysical processes 13 p1944 A83-30179
Technology of closed-drift thrusters [AIAA PAPER 83-1398] 16 p2322 A83-36388
Acceleration of impurity ions during plasma expansion into vacuum 16 p2417 A83-36935
Excitation of slow cyclotron waves by an ion beam in a polyhelical relativistic electron beam 21 p3215 A83-45388

ION ACOUSTIC WAVES

- Stimulated scattering of whistler waves by ion acoustic waves in the magnetosphere 01 p0070 A83-10199
Analysis of ion solitons in an unmagnetized plasma 03 p0397 A83-13193
Surface ion-acoustic oscillations in an inhomogeneous plasma 04 p0536 A83-15740
Radiation from a bounded plasma in the case of the scattering of unstable plasma waves by ion-acoustic oscillations 04 p0536 A83-15757
Measurement of ion-acoustic wave velocity in a pulsed plasma 05 p0688 A83-17367
Spiky ion acoustic waves in collisionless auroral plasma 06 p0784 A83-18306
Growth rates of bending KdV solitons 06 p0812 A83-18917
The transport anisotropy effect in a turbulent plasma 06 p0813 A83-19188
Stimulated scattering of space-charge waves in a relativistic electron beam by the ion acoustic wave of a plasma waveguide 07 p0994 A83-20052
Interaction of a coherent wave with a nonisothermal plasma 07 p0995 A83-20057
High-energy ion tail formation in the ion-acoustic instability Three-dimensional quasilinear approach 07 p0996 A83-20534
Stimulated Brillouin scattering of nonducted whistlers 08 p1168 A83-22389
Oblique collision of cylindrical outgoing ion-acoustic solitons 10 p1485 A83-25790
Ion-acoustic soliton propagation in a density well 10 p1487 A83-26698
Ion-acoustic waves in finite geometry 13 p1923 A83-30112
Nonlinear electron Landau damping of ion-acoustic solitons 13 p1923 A83-30115
Solitary drift waves in the presence of magnetic shear 13 p1923 A83-30116
Stimulated Raman backscattering in the presence of ion-acoustic fluctuations 13 p1923 A83-30119
Structure of an excited weakly ionized plasma with a discontinuously moving neutral component 13 p1925 A83-30809
Test wave diagnostics in the afterglow of a microwave discharge 13 p1927 A83-31574
Experimental determination of the velocity and width of plane ion-acoustic solitons propagating in a plasma 14 p2086 A83-32423
Quasilinear evolution of current-driven ion-acoustic instability in a magnetic field 15 p2232 A83-33797
Reflection of an ion-acoustic soliton by plasma inhomogeneities 17 p2581 A83-37036
Formation of ion-acoustic double layers 17 p2581 A83-37037

- Ion-acoustic wave radiation from a point source in a streaming magnetoplasma 17 p2583 A83-38949
On the possibility of measuring the ion-acoustic turbulence of the interplanetary plasma and the velocity of the solar wind by the radio-wave backscattering technique 18 p2784 A83-39312
Reflection dissipation of an ion-acoustic soliton 18 p2748 A83-40505
Unified theory of parametric excitations in magnetized plasma produced by the action of nonmonochromatic driver pump. I Modulated driver pump 18 p2748 A83-40507
Experimental study of launched ion-acoustic waves in a plasma using continuous wave CO₂ laser scattering 19 p2902 A83-41309
Theory of the diffraction of electromagnetic waves by a plasma sphere with allowance for spatial dispersion 19 p2902 A83-41767
Ion-acoustic solitary waves in a magnetized plasma with arbitrary electron equation of state 21 p3209 A83-43937
Reduction of electron thermal conductivity by ion acoustic turbulence 21 p3210 A83-44131
Coupling mechanism of boundary sheaths and wave launcher in a collisionless plasma 21 p3214 A83-45189
Scattering of waves by Langmuir solitons 21 p3214 A83-45190
Plasma boundary motion and the ion-acoustic wave 21 p3214 A83-45195
Effects of ion-acoustic instability on light ion beam transport in deuterium channels 22 p3362 A83-46019
Frequency splitting in stria bursts - Possible roles of low-frequency waves --- in solar radio emission 23 p3537 A83-47731
Stimulated scattering of a large amplitude electromagnetic wave by the eigenmodes of a plasma slab 23 p3511 A83-48574
Soliton experiments in plasmas 24 p3631 A83-48817

ION ATOM INTERACTIONS

- Charge transfer at large scattering angles in asymmetric ion-atom collisions 01 p0105 A83-10195
Charge exchange in the Io torus and exosphere 05 p0705 A83-17385
Charge transfer in H⁺ /-H and H⁺ /-D collisions within the energy range 0.1-150 eV 06 p0809 A83-19243
Binary encounter calculations for electron capture from noble gases by He²⁺ /- 08 p1167 A83-21987
Auger spectroscopy of quasi-molecules 09 p1343 A83-25089
Charge transfer reaction of O(3⁺) + H yields O(2⁺) + H(+) in low energy collision 12 p1777 A83-29005
Particle charge interchange during acceleration in flare regions 15 p2284 A83-35224
Charge transfer and ionisation processes involving multiply charged ions in collision with atomic hydrogen 18 p2742 A83-39447
Charge exchange between atoms and multiply-charged ions 21 p3213 A83-44655
Polymerization induced on interstellar grains by low-energy cosmic rays 21 p3234 A83-44765
Estimation of the rate constant for the reaction N₂(⁺) + O from data on the ion and neutral composition of a diffuse arc 21 p3176 A83-45261
Charge exchange reactions in astrophysical plasmas 24 p3651 A83-49139

ION BEAMS

- Ion beamlet vectoring by grid translation [AIAA PAPER 82-1895] 02 p0241 A83-12552
The influence of stray magnetic fields on ion beam neutralization [AIAA PAPER 82-1945] 02 p0242 A83-12554
Effect of background electron plasma waves on ion-beam neutralization 03 p0396 A83-13179
Dispersion properties of an electron-ion two-beam system in a magnetic field 03 p0392 A83-13186
An evaluation of performances of several types of ion sources capable of delivering monokinetic beams of 10 mA to several keV in the space environment --- French thesis 03 p0398 A83-13803
Contact discontinuities in a cold collision-free two-beam plasma 05 p0689 A83-17382
Upgoing ion beams. I - Microscopic analysis --- of auroral plasma 05 p0681 A83-17399
Removal of surface strain from rare earth intermetallic compounds by ion-beam planing 05 p0615 A83-17567
A perpendicular ion beam instability - Solutions to the linear dispersion relation --- for F region ionosphere 06 p0784 A83-18304
Generation of conic ions by auroral electric fields 06 p0785 A83-18317
Energetic ion beam in the earth's magnetotail lobe 07 p0958 A83-20086

- Surface magic - Making metals tougher
08 p1068 A83-22775
- Excitation of surface cyclotron waves in a solid-state plasma by charged-particle beams
09 p1348 A83-23985
- Superimposed electron and ion beams - Model for an evolving collisionless plasma
10 p1486 A83-25993
- Half-collision aspects of ion photofragment spectroscopy
11 p1654 A83-27584
- A source of the backstreaming ion beams in the foreshock region
11 p1617 A83-28308
- Coherent electromagnetic emission from an electron-ion beam
11 p1584 A83-28564
- Ion-beam-driven electrostatic ion cyclotron instabilities
12 p1751 A83-28920
- Magnetic guiding, focusing and compression of an intense charge-neutral ion beam
13 p1924 A83-30124
- Radioactive ion beams for studying astrophysical nuclear reactions
13 p1917 A83-30178
- Heavy ion beam pumped He-Ar laser
13 p1852 A83-31060
- Channeling contrast microscopy - Application to semiconductor structures
13 p1929 A83-31067
- Comparison between various ion beam doping procedures and anneal techniques used in manufacturing silicon solar cells
14 p2091 A83-32325
- Surface treatments using laser, electron and ion beam processing methods
14 p2028 A83-32803
- Plasma waves produced by the xenon ion beam experiment on the Porcupine sounding rocket
15 p2198 A83-34189
- An overview of ion sputtering physics and practical implications
15 p2238 A83-35063
- Beam-plasma discharge in a Kyoto beam-plasma-type ion source
16 p2414 A83-35426
- An EBIS for atomic physics experiments --- Electron Beam Ion Source
16 p2409 A83-35628
- Self-focusing of multiply charged ions of a laser plasma
17 p2582 A83-38124
- Parametric excitation of a drift wave and associated ion heating by a modulated ion beam
18 p2747 A83-39921
- Measured electron-impact ionization of Be-like ions: B(+), C(2+), N(3+), and O(4+)
18 p2743 A83-40406
- Plasma lenses for the shaping of ion beams
19 p2901 A83-40999
- Quasi-equilibrium states of a pinched electron-ion beam
19 p2902 A83-41499
- Sputtering of SO₂ by high energy ions
19 p2819 A83-41871
- Pulsed ion beam generation with cryogenic-anode diode
20 p2959 A83-42584
- Ion beam sputter deposition of optical coatings
21 p3117 A83-43866
- Damping mechanisms for ion plasma waves excited by a fast ion beam
21 p3210 A83-44128
- Internal contacts to photovoltaic structures using ion beam milling
21 p3167 A83-44604
- Excitation of slow cyclotron waves by an ion beam in a polyhelical relativistic electron beam
21 p3215 A83-45388
- Ion heating due to explosive instability in an ion beam-plasma system
22 p3362 A83-46018
- Effects of ion-acoustic instability on light ion beam transport in deuterium channels
22 p3362 A83-46019
- The distribution of auroral electrostatic shocks below 8000-km altitude
22 p3327 A83-46049
- Observations of ion streaming during substorms
22 p3335 A83-47039
- Observational evidence on the origin of ions upstream of the earth's bow shock
22 p3335 A83-47047
- Simulations of beam excited minor species gyroharmonics in the Porcupine experiment
22 p3337 A83-47075
- Nonlinear interaction of high-current H(+) and H(-) ion beams
23 p3509 A83-47553
- Generation of high-intensity precision ion and atom beams
24 p3632 A83-49553
- Particle charge interchange during acceleration in flare regions
15 p2284 A83-35224
- An EBIS for atomic physics experiments --- Electron Beam Ion Source
16 p2409 A83-35628
- Charge exchange collision experiments with highly charged ions - status report
16 p2414 A83-35630
- Experimental investigation of electron capture by highly charged ions of medium velocities
16 p2409 A83-35633
- Reactions of doubly charged ions at near thermal energies
16 p2409 A83-35634
- Charge exchange of highly charged ions at low energy --- in astrophysical plasmas
16 p2427 A83-35637
- The current state of the theory of the spectra of multiply charged ions
21 p3213 A83-44651
- Electron-induced excitation and ionization of multiply-charged ions
21 p3213 A83-44652
- Charge exchange between atoms and multiply-charged ions
21 p3213 A83-44655
- ION CONCENTRATION**
- Passive binding of Ca/2+/- by fragments of the sarcoplasmic reticulum of frog skeletal muscles
06 p0795 A83-18988
- Ion clustering and proton transport in Nafion membranes and its applications as solid polymer electrolyte
10 p1390 A83-26051
- On the possibility to measure the high altitude light ion concentrations with Eiscat
13 p1883 A83-31716
- Neutral and ion composition of the thermosphere
17 p2541 A83-38277
- A dynamic model for the production of H(+), NO₃(-), and SO₄(2-) in urban fog
20 p3013 A83-42844
- D-region positive and negative ion concentration and mobilities during the February 1979 eclipse
23 p3481 A83-47473
- The pH and ionic composition of stratiform cloud water
23 p3479 A83-48684
- Background variability of the aerosol and ion composition of the atmospheric surface layer
24 p3604 A83-49109
- ION CURRENTS**
- NT ION BEAMS**
- The flexible magnetic field thruster [AIAA PAPER 82-1936]
03 p0290 A83-14374
- A device for measuring plasma structural parameters by means of spherical ion traps
04 p0454 A83-15725
- Determination of plasma potential from the ionic part of the volt-ampere characteristics of an electric probe
11 p1658 A83-27450
- Ion sensor signal fluctuations during spacecraft jet engine operation
17 p2481 A83-37467
- Ion-Pedersen drift and parallel electric field effects on plasma jetting
22 p3327 A83-46048
- Electrical conductivity of the Li₂SO₄-Li₂CO₃ system
24 p3558 A83-49930
- Hall effect in a boundary layer flow --- over MHD generator walls
24 p3633 A83-50150
- ION CYCLOTRON RADIATION**
- Self-focusing of ion cyclotron waves in a plasma
01 p0106 A83-10618
- Ion whistlers in mid-latitude trough of light ions
02 p0205 A83-11999
- Helium resonance and dispersion effects on geostationary Alfvén/ion cyclotron waves
02 p0207 A83-12384
- Wave-particle interactions in the ULF range - GEOS-1 and -2 results
05 p0664 A83-17778
- Pc 1-2 observations of heavy ion effects by synchronous satellite ATS-6
05 p0664 A83-17779
- A perpendicular ion beam instability - Solutions to the linear dispersion relation --- for F region ionosphere
06 p0784 A83-18304
- High-energy tail distributions and resonant wave particle interaction
06 p0785 A83-18318
- Particle simulations of electrostatic emissions near the lower hybrid frequency
06 p0785 A83-18320
- Experimental evidence for the acceleration of thermal electrons by ion cyclotron waves in the magnetosphere
07 p0966 A83-21515
- Convective growth rate of ion cyclotron waves in a H/+/-He/+/- and H/+/-He/+/-O/+/- plasma --- in space
09 p1304 A83-23774
- Ion-beam-driven electrostatic ion cyclotron instabilities
12 p1751 A83-28920
- Geometry effects on ion heating at ion cyclotron frequencies
13 p1923 A83-30117
- Plasma waves produced by the xenon ion beam experiment on the Porcupine sounding rocket
15 p2198 A83-34189
- Electron current disruption and parallel electric fields associated with electrostatic ion cyclotron waves
17 p2538 A83-37582
- On the structure of the magnetic slow switch-off shock
17 p2538 A83-37594
- Propagation of hydromagnetic waves in a rotating plasma
17 p2583 A83-38824
- Finite-width currents, magnetic shear, and the current-driven ion-cyclotron instability
18 p2748 A83-40509
- Ion cyclotron waves in the Io plasma torus - Polarization reversal of whistler mode noise
19 p2922 A83-41130
- Type IPDP magnetic pulsations and the development of their sources --- Intervals of Pulsations of Diminishing Periods
20 p3018 A83-42412
- Generation of auroral arc elements in an inverted-V arc due to ion cyclotron turbulence
20 p3019 A83-42426
- Electromagnetic ion-cyclotron instability in the multi-ion Jovian magnetosphere
20 p3079 A83-43192
- Generation of Alfvén-ion cyclotron waves on auroral field lines in the presence of heavy ions
20 p3025 A83-43195
- Apparent electrostatic ion cyclotron waves in the diffuse aurora
20 p3025 A83-43196
- Modulation of the current-driven ion-cyclotron instability by the potential relaxation instability
21 p3209 A83-43943
- Saturn's magnetosphere - Observations of ion cyclotron waves near the Dione L shell
22 p3387 A83-47045
- Selective destabilization of ion cyclotron modes
24 p3631 A83-48822
- ION DENSITY (CONCENTRATION)**
- NT IONOSPHERIC ION DENSITY**
- NT MAGNETOSPHERIC ION DENSITY**
- NT MAGNETOSPHERIC PROTON DENSITY**
- NT PROTON DENSITY (CONCENTRATION)**
- Predicted electrical conductivity between 0 and 80 km in the Venusian atmosphere
02 p0265 A83-12563
- On the chemistry of H₂O, H₂ and meteoritic ions in the mesosphere and lower thermosphere
04 p0508 A83-14969
- Measurements of the properties of solar wind plasma relevant to studies of its coronal sources
04 p0574 A83-15118
- Variations in ion and neutral composition at Venus - Evidence of solar control of the formation of the predawn bulges in H/+/- and HeI
07 p1029 A83-20611
- Estimation of sulfate deposition
07 p0957 A83-20811
- Hollow probe for measuring ion density in a slightly ionized plasma flow
12 p1728 A83-29008
- Comet Bradfield 1979 X event on 1980 February 6 - Correlation with an interplanetary solar wind disturbance
12 p1796 A83-29545
- Accuracy of mass spectrometric low-temperature plasma diagnostics
13 p1925 A83-30812
- Energetic ion losses near Io's orbit
13 p1962 A83-31227
- Quantitative determination of the outgassing water vapor concentrations surrounding space vehicles from ion mass spectrometer measurements
16 p2316 A83-35401
- [AD-A128648]
Ionic composition of the earth's radiation belts
18 p2787 A83-39953
- Measurement of negative ion concentrations in non-self-maintained Townsend and microwave discharge plasmas
24 p3632 A83-49049
- ION DISTRIBUTION**
- Depth distributions and range parameters for He implanted in Si and GaAs
02 p0242 A83-12283
- Observations of field-aligned energetic electron and ion distributions near the magnetopause at geosynchronous orbit
05 p0660 A83-17389
- On ion harmonic structure in auroral zone waves - The effect of ion conic damping of auroral hiss
05 p0661 A83-17398
- Investigation of the filling and emptying of plasma tubes with allowance for ion inertia --- in ionosphere
05 p0663 A83-17610
- Auroral ion velocity distribution function - Generalized polynomial solution of Boltzmann's equation
07 p0968 A83-21586
- Plasmasphere and its interaction with the ring current
11 p1614 A83-27395
- On the equation of state of solar wind ions derived from Helios measurements
11 p1691 A83-28302
- An alternative interpretation of ion ring distributions observed by the S3-3 satellite
14 p2053 A83-32700
- Application of Wiener-Hermite expansion to strong plasma turbulence
16 p2416 A83-36624
- ISEE/IMP observations of simultaneous upstream ion events
17 p2599 A83-37589
- Thermodynamic properties of ion clusters and their effect on the mechanism of homogeneous nucleation in an ion plasma
18 p2746 A83-39858
- Calculation by the Monte Carlo method in an NpT ensemble
18 p2746 A83-39858
- Coupled hydromagnetic wave excitation and ion acceleration at interplanetary traveling shocks
20 p3066 A83-42404

- Evolution of ion distributions across the nearly perpendicular bow shock - Specularly and non-specularly reflected-gyrating ions 20 p3017 A83-42405
- Modeling of stratospheric ions - A first attempt 21 p3170 A83-44238
- Understanding the middle atmosphere via the laboratory - Ion cluster investigations 21 p3173 A83-44670
- Ion mixing 22 p3364 A83-45899

ION EMISSION

- Formation of the ionization state of a plasma during laser vaporization 01 p0107 A83-10818
- Time-of-flight measurements of the mass-to-charge ratio of positive ion emission accompanying fracture --- related to crack propagation in materials 03 p0302 A83-13681
- Emissions from neutrals and ions in the Jovian magnetosphere 04 p0572 A83-16247

ION ENGINES**NT MERCURY ION ENGINES**

- On-orbit propulsion requirements and performance assessment of ion propulsion subsystems for future GEO large satellite missions [AIAA PAPER 82-1872] 02 p0141 A83-12460
- Advances in series resonant inverter technology and its effect on spacecraft employing electric propulsion [AIAA PAPER 82-1881] 02 p0143 A83-12466
- Magnetoplasma dynamic thruster development [AIAA PAPER 82-1882] 02 p0143 A83-12467
- J series thruster thermal test results [AIAA PAPER 82-1906] 02 p0144 A83-12481
- A direct-measurement technique for estimating discharge-chamber lifetime --- for ion thrusters [AIAA PAPER 82-1908] 02 p0144 A83-12483
- A thrust measurement of an ion engine system [AIAA PAPER 82-1915] 02 p0145 A83-12487
- Inert gas test of two 12-cm magnetostatic thrusters [AIAA PAPER 82-1925] 02 p0145 A83-12494
- Plasma characteristics of a 17 cm diameter line-cusp ion thruster [AIAA PAPER 82-1926] 02 p0145 A83-12495
- Development of a large inert gas ion thruster [AIAA PAPER 82-1927] 02 p0146 A83-12496
- Performance data comparison of the inert gas RIT 10 --- as ion thruster propellant [AIAA PAPER 82-1932] 02 p0146 A83-12498
- Extended-performance 8-cm ion thruster operation [AIAA PAPER 82-1955] 02 p0147 A83-12512
- Ion thruster charge-exchange plasma flow 02 p0148 A83-13089
- Baffle aperture design model for electron bombardment thrusters 02 p0148 A83-13091
- The flexible magnetic field thruster [AIAA PAPER 82-1936] 03 p0290 A83-14374
- Ion flow experiments in a multiple discharge chamber [AIAA PAPER 82-1930] 03 p0398 A83-14398
- Electromagnetic noise from an ion engine system 07 p0873 A83-20424
- Simplification of power electronics for ion thruster neutralizers [AIAA PAPER 82-1880] 07 p0873 A83-21099
- Parallel plate radiofrequency ion thruster [AIAA PAPER 82-1937] 08 p1052 A83-21900
- Design of ion thruster system for satellite position control 10 p1388 A83-26592
- Operation of the J-series thruster using inert gas [AIAA PAPER 82-1929] 10 p1388 A83-26625
- Characterization of advanced electric propulsion systems 15 p2129 A83-33744
- Procedures to integrate electric secondary propulsion systems to large deployable space systems [AIAA PAPER 83-1392] 16 p2322 A83-36382
- Simplified power processing for ion-thruster subsystems [AIAA PAPER 83-1394] 16 p2322 A83-36384
- Technology of closed-drift thrusters [AIAA PAPER 83-1398] 16 p2322 A83-36388
- Simplified power processing for ion-thruster subsystems 18 p2648 A83-39271
- Five milli Newtons field emission thruster testing [IAF PAPER 83-394] 23 p3426 A83-47371

ION EXCHANGE MEMBRANE ELECTROLYTES

- The effect of polymethylene and polyoxyethylene-bis-/2-amino-1,3-diazepinium/ iodides on cell and model membranes 01 p0079 A83-10537
- Transport properties of Nafion membranes for use in three-electrode photoelectrochemical storage cells 02 p0202 A83-12055
- Countercurrent electrolysis in a thin porous membrane 16 p2328 A83-36965
- Solid electrolyte interphase (SEI) electrodes. VI Calcium-Ca(AlCl₄)₂-sulfuryl chloride system 24 p3558 A83-49928

ION EXCHANGING

- Electroconducting glass fibres produced by ion-exchange and reduction treatments 02 p0159 A83-11674

- Integrated optical ring resonators made by silver ion-exchange in glass 10 p1483 A83-26639
- Proton-exchanged optical waveguides in Y-cut lithium niobate 11 p1657 A83-28611
- Sprayed CdS-Cu₂S solar cells. I - Formation of cuprous sulphide 14 p2047 A83-32848
- The distribution of Na, K, Ca, P, and S in the vestibular apparatus and eye of the larvae of the fish *Brachydanio rerio* 15 p2210 A83-34937
- Integrated optical waveguiding structures made by silver ion-exchange in glass. I - The propagation characteristics of stripe ion-exchanged waveguides: A theoretical and experimental investigation 16 p2413 A83-36768
- Integrated optical waveguiding structures made by silver ion-exchange in glass. II - Directional coupler and bends 16 p2414 A83-36769
- Double ion exchanged chirp grating lens in lithium niobate waveguides 21 p3208 A83-45483

ION EXTRACTION

- Ion extraction capabilities of closely spaced grids [AIAA PAPER 82-1894] 02 p0147 A83-12551
- Ion extraction from a plasma through a conical orifice 05 p0687 A83-16920

ION GAGES**U IONIZATION GAGES****ION IMPACT**

- Ionisation of H₂ by fast protons and multiply charged ions of He, Li, C, N and O 01 p0105 A83-10857
- Relative intensity changes of L₃MM Auger transitions in maximal-valent V and Cr compounds under ion bombardment 12 p1778 A83-29543
- Sputtering of UF₄ by high energy heavy ions 16 p2421 A83-36712

ION IMPLANTATION

- CW-laser annealed solar cells 01 p0068 A83-10638
- Depth distributions and range parameters for He implanted in Si and GaAs 02 p0242 A83-12283
- Pulsed excimer laser annealing of ion implanted silicon - Characterization and solar cell fabrication 02 p0243 A83-12284
- Bipolar transistor action in ion implanted diamond 02 p0168 A83-12286
- Self-annealed ion implanted solar cells 02 p0202 A83-12290
- Ion gun tritium permeation testing [AIAA PAPER 82-1940] 02 p0157 A83-12502
- Ion implanting bearing surfaces for corrosion resistance [ASME PAPER 82-LUB-23] 03 p0298 A83-13512
- High performance ion-implanted low noise GaAs MESFET's 03 p0309 A83-13559
- Structural difference rule for amorphous alloy formation by ion mixing 05 p0690 A83-16945
- Effect ion implantation on fretting fatigue in Ti-6Al-4V alloy 05 p0614 A83-17257
- Ion-implanted s lateral PNP transistors 05 p0624 A83-17288
- Reduction of long-term transient radiation response in ion implanted GaAs FETs 05 p0625 A83-17482
- Self-aligned phosphorus doped polysilicon gate MOS device radiation hardening 05 p0627 A83-17512
- GaAs LSI-directed MESFET's with self-aligned implantation for n/+/-layer technology / SAINT/ 05 p0631 A83-17759
- Optical techniques for implant process diagnosis in GaP 07 p0998 A83-19897
- A model for the accumulation of solar wind radiation damage effects in lunar dust grains, based on recent results concerning implantation and erosion effects 07 p1033 A83-21305
- New experimental evidence of surface ripples on gallium arsenide in laser annealing 08 p1169 A83-22758
- Electrical properties and ion implantation of epitaxial GaN, grown by low pressure metalorganic chemical vapor deposition 08 p1169 A83-22760
- Flame annealing of arsenic and boron implanted silicon 08 p1170 A83-22768
- Yield considerations for ion-implanted GaAs MMIC's 09 p1256 A83-24680
- Diffusion of nitrogen in alpha-Ti 10 p1397 A83-25980
- Microscopic processes in low-power laser annealing of ion-implanted Ge 11 p1661 A83-28068
- Effect of ion implantation on creep of molybdenum 11 p1551 A83-28806
- Ion implantation effect on fatigue crack initiation in Ti-24V 12 p1714 A83-29724
- Heat of crystallization and melting point of amorphous silicon 13 p1825 A83-30344
- Limiting ion implantation doses for metals 13 p1821 A83-30737
- Channeling contrast microscopy - Application to semiconductor structures 13 p1929 A83-31067
- Radiation damage enhancement of the penetration of water into silica glass 13 p1931 A83-31382

- Dispersion and luminescence measurements of optical waveguides 13 p1922 A83-31388
- Pulsed electron beam annealing of ion implanted germanium for photovoltaic devices 14 p2088 A83-32239
- Possibilities of ion implantation in silicon solar cell manufacturing 14 p2045 A83-32312
- Status of ion-implanted silicon solar cells 14 p2005 A83-32326
- Optimization of pulsed electron beam annealing process for silicon solar cells 14 p2005 A83-32327
- Silicon solar cells by ion implantation - E-beam and self annealing 14 p2005 A83-32328
- The influence of surface texture and thermal treatment on the performance of laser-annealed silicon solar cells 14 p2045 A83-32330
- Implantation of boron and boron fluoride compounds into silicon for production of solar cells 14 p2005 A83-32331
- Effect of argon implantation on the activation of boron implanted in silicon 14 p2093 A83-33444
- Specific site location of S and Si in ion-implanted GaAs 14 p2093 A83-33445
- Cf-252 plasma desorption in ion implanted mica 15 p2133 A83-34381
- An overview of ion sputtering physics and practical implications 15 p2238 A83-35063
- Low temperature annealing of Be-implanted GaAs 16 p2418 A83-35438
- Structure of ion-implanted and annealed Hg(1-x)Cd(x)Te 16 p2418 A83-35439
- A TEM investigation of the structure of nitrogen-implanted Ti-6Al-4V 16 p2330 A83-36068
- Gallium arsenide and related compounds 1982; International Symposium, 10th, Albuquerque, NM, September 19-22, 1982, Contributed Papers --- Book 17 p2584 A83-37160
- Tribological characteristics of nitrogen (N+) implanted iron 17 p2487 A83-37824
- Comparison between electron-beam and furnace rapid isothermal anneals of phosphorus-implanted solar cells 17 p2584 A83-38217
- Characterization of electron traps in ion-implanted GaAs MESFET's on undoped and Cr-doped LEC semi-insulating substrates 18 p2750 A83-40372
- The role of ion implantation in high temperature oxidation studies 20 p2946 A83-42230
- Ion implantation of Si and Be in Al(0.48)In(0.52)As 20 p3052 A83-42593
- Ion implanted Si MESFET's with high cutoff frequency 20 p2968 A83-43355
- Effect of boron compensation on the photovoltaic properties of amorphous silicon solar cells 20 p3055 A83-43601
- CW laser-annealing behavior of Se(+)-implanted InP investigated by ellipsometry 20 p3055 A83-43603
- Rapid thermal annealing of Se and Be implanted InP using an ultrahigh power argon arc lamp 20 p3055 A83-43605
- The spectral response of BSF silicon solar cells fabricated through masked ion implantation --- Back Surface Field 21 p3166 A83-43843
- Proton implantation isolation for microwave monolithic circuits 21 p3123 A83-43845
- Application of thermal pulse annealing to ion-implanted GaAlAs/GaAs heterojunction bipolar transistors 21 p3123 A83-43851
- Optoelectronic devices based on silicon carbide p-n junctions produced by various processes 21 p3125 A83-44597
- Planar, ion-implanted bipolar devices in GaAs 21 p3127 A83-45172
- Noise measurements in ion implanted MOSFETs 21 p3127 A83-45174
- Analytical solutions for threshold voltage calculations in ion-implanted IGFETs 21 p3127 A83-45177
- Diffusion of zinc into ion implanted iron doped indium phosphide 21 p3218 A83-45179
- Optical stability of narrow stripe, proton-isolated AlGaAs double heterostructure lasers with gain guiding 21 p3147 A83-45485
- Absorption of carbon from residual gases during Ti implantation of alloys 21 p3115 A83-45490
- Properties and ion implantation of Al(x)Ga(1-x)N epitaxial single crystal films prepared by low pressure metalorganic chemical vapor deposition 21 p3220 A83-45499
- Rapid thermal annealing of Be, Si, and Zn implanted GaAs using an ultrahigh power argon arc lamp 21 p3220 A83-45500
- Low-loss integrated optical waveguides fabricated by nitrogen ion implantation 22 p3360 A83-46720
- Correlation among secondary ion mass spectrometry, cross-section transmission electron microscopy, and Rutherford backscattering analyses for defect density and depth distribution determination 22 p3365 A83-46728

- A computer-aided simulation model for the I-V characteristic of M-n-p silicon Schottky-barrier diodes produced by use of low-energy arsenic-ion implantation
23 p3446 A83-48608
- Electrical characteristics of Be-implanted GaAs diodes annealed with an ultrahigh power argon arc lamp
24 p3572 A83-48788
- High-efficiency Si solar cells by beam processing
24 p3598 A83-48791
- Reduction in the localized band-gap states in amorphous silicon by annealing and hydrogen implantation
24 p3634 A83-48793
- Moessbauer study of the lattice location of Co-57 implanted in graphite
24 p3636 A83-49756
- ### ION INJECTION
- Characterization of geostationary particle signatures based on the 'injection boundary' model
11 p1617 A83-28309
- Ion injection from the surface of bodies moving in a gas
12 p1781 A83-29295
- Injections of ions and electrons into the ionosphere and the magnetosphere - Application to measurement of the parallel electric field in the auroral zones --- French thesis
13 p1874 A83-30126
- The ionosphere as a source for magnetospheric ions
17 p2540 A83-38229
- Electric conductivities, electric fields and auroral particle energy injection rate in the auroral ionosphere and their empirical relations to the horizontal magnetic disturbances
17 p2544 A83-38518
- On the injection boundary model and dispersing ion signatures at near-geosynchronous altitudes
19 p2865 A83-41120
- ### ION IRRADIATION
- #### NT PROTON IRRADIATION
- Comparative studies of tunnel injection and irradiation on metal oxide semiconductor structures
01 p0109 A83-10633
- Formaldehyde formation in a H₂O/CO₂ ice mixture under irradiation by fast ions
03 p0424 A83-14196
- The effect of heavy ions on mammalian cells. I - The cytogenic effects during the irradiation of Chinese hamster cells induced by accelerated ions of helium, carbon, and neon
03 p0377 A83-14884
- H₂ production in comets.
10 p1500 A83-25374
- Ion mixing to produce amorphous Mo-Ru superconducting films
10 p1489 A83-26217
- Ion-induced amorphous and crystalline phase formation in Al/Ni, Al/Pd, and Al/Pt thin films
13 p1928 A83-30338
- Fabrication of optical waveguides in LiNbO₃ and LiTaO₃ crystals by ion irradiation
13 p1919 A83-30824
- Temperature-dependent ion mixing and diffusion during sputtering of thin films of CrSi₂ on silicon
19 p2903 A83-40740
- Inactivation probability of heavy ion-irradiated *Bacillus subtilis* spores as a function of the radial distance to the particle's trajectory
19 p2872 A83-40838
- Enhanced adhesion from high energy ion irradiation
22 p3365 A83-46703
- Plasma ion-induced molecular ejection on the Galilean satellites - Energies of ejected molecules
22 p3387 A83-46886
- ### ION MICROSCOPES
- Field-ion microscopy - A review of basic principles and selected applications
05 p0644 A83-16918
- Analysis of airfoil leading edge separation bubbles [AIAA PAPER 83-0300]
05 p0591 A83-17918
- ### ION MOTION
- Ion flow experiments in a multipole discharge chamber [AIAA PAPER 82-1930]
03 p0398 A83-14398
- Auroral ion velocity distribution function - The Boltzmann model revisited
04 p0509 A83-14972
- Observations of parallel ion energization in the equatorial region
05 p0661 A83-17404
- Runaway ions in an expanding plasma
07 p0994 A83-20051
- Evidence for specularly reflected ions upstream from the quasi-parallel bow shock
07 p0959 A83-20193
- Current sheet acceleration of ions in the geomagnetic tail and the properties of ion bursts observed at the lunar distance
08 p1137 A83-23119
- Solar wind deceleration and MHD turbulence in the earth's foreshock region - ISEE 1 and 2 and IMP 8 observations
09 p1303 A83-23758
- Ions upstream of the earth's bow shock - A theoretical comparison of alternative source populations
09 p1303 A83-23759
- Mass composition of substorm-related energetic ion dispersion events
09 p1303 A83-23761
- Ion clustering and proton transport in Nafion membranes and its applications as solid polymer electrolyte
10 p1390 A83-26051
- Electric field enhanced diffusion in trans/CH/x --- battery cells
10 p1446 A83-26053
- Monte Carlo calculations of the O⁺/+/- velocity distribution in the auroral ionosphere
11 p1619 A83-28328
- Quasineutral hybrid simulation of macroscopic plasma phenomena
12 p1782 A83-29634
- Spectroscopic determination of the viscosity of a fully ionized plasma by means of the dynamics of acceleration by a traveling wave
13 p1923 A83-30118
- An instrument for total ion drift velocity measurements aboard the 'Intercomos-Bulgaria-1300' satellite
13 p1814 A83-30762
- The retardation of ions in a degenerate electron gas
14 p2086 A83-32141
- Ion trajectories in a space-charge wave on a relativistic electron beam
18 p2748 A83-40513
- The protective effect of extracellular K(+) in the myocardium during disorders of energy generation
18 p2732 A83-40552
- Upstream electron oscillations and ion overshoot at an interplanetary shock wave
19 p2864 A83-41115
- The Active Magnetospheric Particle Tracer Explorers program
21 p3172 A83-44498
- Quantitative models for the migration of electrolyte gradients in an electric field
22 p3266 A83-45761
- Structure of perpendicular shocks in collisionless plasma
22 p3362 A83-46023
- ### ION OSCILLATION
- #### U PLASMA OSCILLATIONS
- ### ION PLATING
- Tribological properties and X-ray photoelectron spectroscopy studies of ion-plated gold on nickel and iron
02 p0157 A83-12650
- Effect of ion-plated aluminum coating on hydrogen gas embrittlement of ultrahigh strength maraging steel
09 p1230 A83-23918
- Sputter-ion plating of coatings for protection of gas-turbine blades against high-temperature oxidation and corrosion
10 p1394 A83-25472
- The tribological properties of highly oriented cobalt and Co-Cr ion platings
10 p1395 A83-25550
- ### ION PROBES
- The influence of charge transfer on ion probe measurements of laser-produced plasmas
01 p0107 A83-10693
- The S3-4 ionospheric irregularities satellite experiment - Probe detection of multi-ion component plasmas and associated effects on instability processes
04 p0509 A83-14976
- A membrane collector of solar-wind hydrogen
10 p1387 A83-25351
- Hollow probe for measuring ion density in a slightly ionized plasma flow
12 p1728 A83-29008
- Calibration system for satellite and rocket-borne ion mass spectrometers in the energy range from 5 eV/charge to 100 keV/charge
13 p1813 A83-30254
- Some recent advances in energetic ion mass spectrometry
13 p1813 A83-30753
- Ion attitude control circuit operational experience
17 p2478 A83-37466
- Ion microprobe identification of 4,100-4,200 Myr-old terrestrial zircons
21 p3174 A83-45059
- Hydrogen embrittlement measurement using new palladium probe [SAE PAPER 820604]
22 p3287 A83-45865
- FUN with PANURGE - High mass resolution ion microprobe measurements of Mg in Allende inclusions --- meteoritic composition isotope analysis
24 p3672 A83-49350
- ### ION PRODUCTION RATES
- A model for mercury orificed hollow cathodes - Theory and experiment [AIAA PAPER 82-1889]
02 p0147 A83-12513
- Loss of CO⁺/+/- ions by reaction with H₂ in OMC-1
03 p0428 A83-14760
- Phenomenological model describing orificed, hollow cathode operation
04 p0454 A83-15276
- Emissions from neutrals and ions in the Jovian magnetosphere
04 p0572 A83-16247
- Theory of nonstationary kinetic ionization, recombination and population of excited states
06 p0811 A83-18438
- Spatial and temporal evolution of the thermal-ionizational instability
07 p0994 A83-20054
- A one-dimensional model of the atmospheric electric field near the Venusian surface
07 p1030 A83-20619
- Production of negative ions by dissociative electron attachment to SO₂
10 p1478 A83-25552
- On the ionization of the mid-latitude lower ionosphere by precipitating hard electrons
11 p1617 A83-28119
- Ionisation and appearance potentials of CH₄ by electron impact
12 p1778 A83-29925
- Observation and quasistatic analysis of structure in microwave ionization of highly excited helium atoms
13 p1915 A83-30597
- The D region under the conditions of nighttime PCA - The rate of transformation of positive ion clusters and negative ions
14 p2054 A83-33034
- Visible signatures of the multi-step transition to a beam-plasma-dicharge
15 p2234 A83-34195
- The beam-plasma under space-like conditions
15 p2235 A83-34207
- On electron impact ionization cross-sections and rates for multiply charged ions
15 p2236 A83-34609
- Production and physics of highly charged ions; Proceedings of the International Symposium, Stockholm, Sweden, June 1-5, 1982
16 p2409 A83-35626
- Results inferred from electron density measurements at Saskatoon, Canada (L = 4.4) by a partial reflection technique. II - Ion production rates and nitric oxide in the D-region during post-storm periods
18 p2712 A83-39067
- Measurement of ionisation rate coefficients of nitrogen ions
18 p2742 A83-39448
- Recent measurements of electrical conductivity and ion pair production rate, and the ion-ion recombination coefficient derived from them in the lower stratosphere
20 p3027 A83-43401
- Measurement of ionization rates of Ti IX, Ne VI, Ne VII, and O VI
24 p3631 A83-48832
- ### ION PROPULSION
- On-orbit propulsion requirements and performance assessment of ion propulsion subsystems for future GEO large satellite missions [AIAA PAPER 82-1872]
02 p0141 A83-12460
- Experimental investigation of an argon hollow cathode [AIAA PAPER 82-1890]
02 p0241 A83-12472
- Ion accelerator systems for high power 30-cm thruster operation [AIAA PAPER 82-1893]
02 p0144 A83-12474
- Advanced-technology 30-cm-diameter mercury ion thruster [AIAA PAPER 82-1910]
02 p0145 A83-12484
- A thrust measurement of an ion engine system [AIAA PAPER 82-1915]
02 p0145 A83-12487
- Performance design of 10-mN ion thruster [AIAA PAPER 82-1916]
02 p0145 A83-12488
- Operations and performances of a 5 cm diameter ion thruster by using inert gases [AIAA PAPER 82-1924]
02 p0145 A83-12493
- Discharge plasma in a multipole ion thruster [AIAA PAPER 82-1931]
02 p0146 A83-12497
- RFI and ECH plasma generator development for ion thrusters [AIAA PAPER 82-1941]
02 p0146 A83-12503
- A comparison of experimental and computer model results on the charge-exchange plasma flow from a 30 cm mercury ion thruster [AIAA PAPER 82-1946]
02 p0146 A83-12505
- Qualification test results of IAPS 8 cm ion thrusters [AIAA PAPER 82-1954]
02 p0147 A83-12511
- Ion beamlet vectoring by grid translation [AIAA PAPER 82-1895]
02 p0241 A83-12552
- The flexible magnetic field thruster [AIAA PAPER 82-1936]
02 p0147 A83-12553
- Improved ion containment using a ring-cusp ion thruster [AIAA PAPER 82-1928]
07 p0873 A83-21100
- Simplified power processing for ion-thruster subsystems [AIAA PAPER 83-1394]
16 p2322 A83-36384
- Five mill Newtons field emission thruster testing [IAF PAPER 83-394]
23 p3426 A83-47371
- ### ION RECOMBINATION
- Dissociative recombination of electrons and molecular ions
02 p0234 A83-12175
- Recombination of small ions in the troposphere and lower stratosphere
05 p0665 A83-17784
- Theory of nonstationary kinetic ionization, recombination and population of excited states
06 p0811 A83-18438
- Nuclear-reactor pumped lasers excited by ion-ion neutralization
07 p0936 A83-20728
- Amplifications of atomic fluorine, nitrogen ion and XeF lasers
11 p1582 A83-27614
- Termolecular ionic recombination at high ambient gas density
16 p2414 A83-35326
- Radiative recombination of the ground state of lithium-like ions
17 p2578 A83-37934
- Recombination dynamics in the F-region
18 p2713 A83-39318
- Recent measurements of electrical conductivity and ion pair production rate, and the ion-ion recombination coefficient derived from them in the lower stratosphere
20 p3027 A83-43401
- Electric-field-dependent charge-carrier trapping in a one-dimensional organic solid
21 p3216 A83-43888
- ### ION SCATTERING
- Formation of nickel and palladium silicides by a short-pulse light-flash and its application in the metallization of solar cells
21 p3218 A83-45180

ION SOURCES

NT PLASMATRONS

- An evaluation of performances of several types of ion sources capable of delivering monokinetic beams of 10 mA to several keV in the space environment --- French thesis 03 p0398 A83-13803
- Performance characteristics of a microwave plasma disk ion source --- time varying electric propulsion concept [AIAA PAPER 82-1935] 11 p1542 A83-27350
- Anode tufting, arc faulting and plasma nonuniformity in ion sources 12 p1780 A83-29034
- Use of a Cf-252 source in cosmic ray simulation studies on CMOS memories 15 p2152 A83-34519
- Beam-plasma discharge in a Kyoto beam-plasma-type ion source 16 p2414 A83-35426
- An EBIS for atomic physics experiments --- Electron Beam Ion Source 16 p2409 A83-35628
- Discharge with electrostatic containment in order to obtain high performance ion sources 19 p2902 A83-41323
- Phobis, a photon beam ion source for production of highly-charged ions 24 p3627 A83-49750

ION SPECTROMETERS

U MASS SPECTROMETERS

ION STRIPPING

- Total and partial cross sections for electron capture in collisions of hydrogen atoms with fully stripped ions 22 p3361 A83-45927

ION TEMPERATURE

- Graphical analysis method for a retarding potential analyzer and its application to the real-time measurements of ion temperature in space plasmas 02 p0142 A83-12818

- Observations of parallel ion energization in the equatorial region 05 p0661 A83-17404
- New operation mode of a microchannel plate for the detection of low-energy positive ions 06 p0764 A83-19231

- Ion heating due to parametrically driven ion wave turbulence 10 p1485 A83-25779
- On the equation of state of solar wind ions derived from Helios measurements 11 p1691 A83-28302
- Comet Bradfield 1979 X event on 1980 February 6 - Correlation with an interplanetary solar wind disturbance 12 p1796 A83-29545

- F region ion temperature enhancements resulting from Joule heating 13 p1879 A83-31243
- Heat balance for the high-temperature component of a solar flare 15 p2279 A83-34294
- Sputtering of UF₄ by high energy heavy ions 16 p2421 A83-36712

- Ion heating and acceleration by strong magnetosonic waves 19 p2901 A83-40953
- Ion acceleration in the suprathermal region - A Monte Carlo model 19 p2865 A83-41129
- Influences of the ion temperature on the nonlinear electrostatic waves in magnetized plasma 21 p3212 A83-44514

- Observational results of the nighttime ion temperatures in the topside ionosphere by ISS-b 21 p3178 A83-45456

- Ion heating due to explosive instability in an ion beam-plasma system 22 p3362 A83-46018
- Meaning of the vertical profile of ion temperature over the Antarctic 22 p3331 A83-46522

- The non-Maxwellian energy distribution of ions in the warm lo torus 22 p3387 A83-47072
- Simultaneous measurement of magnetic field direction and ion temperature in a plasma by collective scattering with a CO₂ laser 24 p3630 A83-48786

ION TRAPS (INSTRUMENTATION)

- A device for measuring plasma structural parameters by means of spherical ion traps 04 p0454 A83-15725

- On shortening the measurement cycle in a probe experiment with SIT --- Spherical Ion Traps for ionospheric ion density measurement 08 p1133 A83-22278
- Measurement of density irregularities of the ionospheric plasma using a probe with external-grid floating potential on the Cosmos-900 satellite 10 p1386 A83-25336

- Adaptive system for varying the range of sawtooth control voltage depending on the potential of the satellite body in a four-electrode probe experiment 10 p1386 A83-25337
- Spherical ion traps for 'Intercomos-Bulgaria-1300' 13 p1813 A83-30754

- Ionospheric plasma parameters measurement instrument for satellite experiment with sit --- Spherical Ion Trap 14 p2048 A83-31816
- Ion neutralization in helical electron beams 23 p3460 A83-47556

ION-GAS INTERACTIONS

U GAS-ION INTERACTIONS

IONIC COLLISIONS

- Electron loss from fast one-electron ions colliding with He, N₂, and Ar 01 p0105 A83-10194

- Charge transfer at large scattering angles in asymmetric ion-atom collisions 01 p0105 A83-10195

- Test of Sigmund scaling for low collision energies 06 p0807 A83-18043

- Excitation of atoms by collisions with ions - Photon-ion angle correlation measurements for determining the scattering amplitudes in magnetic substrates for He⁺/ + He and He⁺/ + Ne systems --- German thesis 06 p0808 A83-18524

- Oscillator strengths and collision strengths for O II and O III 06 p0809 A83-19519

- A high-density effusive target of atomic hydrogen 08 p1162 A83-21981

- Calculation of the rate coefficients for the electron impact excitation of the n = 2 terms of O IV 08 p1179 A83-21989

- Rotational and vibrational transitions in molecular collisions 09 p1342 A83-24145

- Ionospheric disturbances resulting from ion-neutral coupling 11 p1615 A83-27402

- Half-collision aspects of ion photofragment spectroscopy 11 p1654 A83-27584

- Charge transfer of O(3+) ions in collisions with atomic hydrogen 13 p1916 A83-31354

- Electron impact excitation of positive ions of astrophysical interest. I - Theoretical method 14 p2109 A83-33279
- Electron impact ionization of complex ions 15 p2236 A83-34608

- Charge exchange collision experiments with highly charged ions - status report 16 p2414 A83-35630

- Studies of collision interactions and kinetic energy distribution of eV recoil ions inside Penning traps 16 p2409 A83-35631
- Energy gain and loss spectroscopy of charge changing collisions between multiply charged ions and neutrals 16 p2409 A83-35632

- Experimental investigation of electron capture by highly charged ions of medium velocities 16 p2409 A83-35633
- Reactions of doubly charged ions at near thermal energies 16 p2409 A83-35634

- Excited states created in charge transfer collisions between atoms and highly charged ions 16 p2409 A83-35636
- State-selective electron capture by C(2+), C(3+), N(2+), and Ar(2+) ions in rare gases 17 p2579 A83-38365

- Physical and chemical effects induced by energetic ions on comets 17 p2609 A83-38417
- Dissociative recombination of electrons with NO(+) ions 17 p2579 A83-38521
- Ion-neutral collision frequency variations in the lower thermosphere from incoherent scatter measurements 17 p2545 A83-38538

- Collision strengths for the N = 2 excitation of hydrogenic ions 17 p2583 A83-38960
- Single collision ion-molecule reactions at thermal energy 19 p2897 A83-40771

- Rotational and vibrational distributions from N(+) + CO yields N + CO(+) 19 p2897 A83-40771
- Studies of the photoionization cross section of the 2pi level of nitric oxide 19 p2897 A83-40772
- Vibrational relaxation of NO(+) (v) ions in neutral collisions 19 p2897 A83-40774

- Dissociative recombination in low-energy e-H₂(+) collisions 19 p2898 A83-41194
- Electron excitation of Ca XVII 23 p3506 A83-48580

- IONIC CONDUCTIVITY
- U ION CURRENTS

- IONIC CRYSTALS
- The anomalously small dissipation of electromagnetic waves in an ionic crystal 04 p0474 A83-16413

- High-energy solid-state electronics --- Russian book 07 p0919 A83-20388
- Investigation of mechanisms of damage induced in ionic crystals by pulsed nanosecond laser radiation 18 p2694 A83-40610

- Anomalous electric-field-induced damping of ultrasound in superionic crystals 20 p3051 A83-42265

- IONIC DIFFUSION
- The problem of cooling the cold lo torus 09 p1365 A83-23755

- Termolecular ionic recombination at high ambient gas density 16 p2414 A83-35326

- Atomic diffusion coefficients calculated for transition metals in olivine 17 p2623 A83-38596

- Temperature-dependent ion mixing and diffusion during sputtering of thin films of CrSi₂ on silicon 19 p2903 A83-40740

- A simple theory of mobility for ions in gases 20 p3055 A83-43106

- Diffusion of zinc into ion implanted iron doped indium phosphide 21 p3218 A83-45179

- Thermodynamic mechanism for cation diffusion through an intergranular phase - Application to environmental reactions with nitrogen ceramics 23 p3436 A83-48282

- The turbulent electrode effect as influenced by interfacial ion transfer --- between atmosphere and aerodynamically rough earth surface 24 p3607 A83-49334

IONIC MOBILITY

- A neutral vortex induced by an auroral arc 02 p0209 A83-12429

- The mobilities of NO₃⁻/-, NO₂⁻/-, NO⁺/+, and Cl⁻/- in N₂ - A measure of inelastic energy loss 05 p0684 A83-17656

- Ion wind drag reduction 05 p0689 A83-17914
- Conductivity of the mixed organic electrolyte containing propylene carbonate and 1,2-dimethoxyethane --- for lithium cells 07 p0880 A83-19889

- Mobilities of various mass-identified positive ions in helium, neon, and argon 20 p2950 A83-42637
- A simple theory of mobility for ions in gases 20 p3055 A83-43106

- Analysis and numerical simulation of the effect of ion Pedersen mobility on ionospheric barium clouds 22 p3336 A83-47062

- D-region positive and negative ion concentration and mobilities during the February 1979 eclipse 23 p3481 A83-47473
- Eclipse-related measurements of middle-atmosphere electrical parameters 23 p3481 A83-47474

- IONIC PROPELLANTS
- U ION ENGINES

- IONIC REACTIONS
- Ion kinetics, minor neutral and excited constituents in the D region with a high level of ionization. I - Formulation of the problem and a general scheme for the processes 06 p0786 A83-18360

- The role of ion-molecule reactions in the conversion of N₂O₅ to HNO₃ in the stratosphere 08 p1137 A83-23114

- The uranyl ion, fluorescent and fluorine-like - A review 10 p1390 A83-26061
- Energy dependence of the O(-) transfer reactions of O₃(-) and CO₃(-) with NO and SO₂ 14 p1991 A83-33103

- Laboratory measurements of ion-molecule reactions pertaining to interstellar hydrocarbon synthesis 15 p2269 A83-34645

- IONIC WAVES
- A fast wave of gas-ionization in a laser beam 05 p0686 A83-16892

- Pc 1-2 observations of heavy ion effects by synchronous satellite ATS-6 05 p0664 A83-17779
- Breakdown wave in the self-consistent field of an electromagnetic wave beam 07 p0995 A83-20061

- Electron energy transport in ion waves and its relevance to laser-produced plasmas 07 p0997 A83-20543
- Ion heating due to parametrically driven ion wave turbulence 10 p1485 A83-25779

- Large-amplitude ion bounce wave in the magnetosphere near L = 3 15 p2202 A83-34737
- Damping mechanisms for ion plasma waves excited by a fast ion beam 21 p3210 A83-44128

- Characteristics of the nonlinear suppression of ionization waves 21 p3211 A83-44347

- IONIZATION
- NT ATMOSPHERIC IONIZATION
- NT AURORAL IONIZATION
- NT AUTOIONIZATION
- NT FLAME IONIZATION
- NT GAS IONIZATION
- NT ION PRODUCTION RATES
- NT NONEQUILIBRIUM IONIZATION
- NT PHOTOIONIZATION
- NT SURFACE IONIZATION

- Investigation of processes of the interaction of cosmic-ray muons at an underground depth of 150 mwe 06 p0858 A83-19342

- A model for calculating the probabilistic behavior gasdynamic variables of a jet undergoing physical and chemical transformation 09 p1259 A83-24043

- Excitation conditions in HII regions 09 p1361 A83-24514
- Auger spectroscopy of quasi-molecules 09 p1343 A83-25089

- Studies of the vibrational relaxation of diatomic molecules in a shock heated molecular beam and its application to ionization by electron impact 10 p1479 A83-26179

- The ionization equilibrium inside the RHO Ophiuchi cloud 10 p1508 A83-26366
- Theoretical spectral profiles of laser assisted Penning ionization 11 p1658 A83-27550

- Ionization curves and last scattering surfaces in neutrino-dominated universes 17 p2609 A83-38422

- Model of Burgers turbulence for turbulent ionization waves 18 p2747 A83-39916
- The effect of a non-Maxwellian electron distribution on oxygen and iron ionization balances in the solar corona 19 p2924 A83-41642
- Measurement of ionization rates of Ti IX, Ne VI, Ne VII, and O VI 24 p3631 A83-48832

IONIZATION CHAMBERS

- NT PROPORTIONAL COUNTERS
- Ion chamber gamma burst detector 07 p1005 A83-20041
- Rigidity responses of ionization chambers derived from cosmic-ray time variations 11 p1574 A83-28427
- Ionization effects in real detectors of relativistic charged particles 20 p3045 A83-43527
- Registration of transition X-radiation using a drift chamber with a spatial resolution of 20 microns 20 p2991 A83-43531
- Particle identification with the use of transition radiation by counting the clusters on the particle track 20 p3046 A83-43533

IONIZATION COEFFICIENTS

- Electroabsorption produced mixed injection and its effect on the determination of ionization coefficients --- in low noise avalanche photodiodes 05 p0691 A83-17769
- Experimental ionization rate coefficients of aluminum and silicon ions 06 p0811 A83-18818
- Microwave ionization of Na Rydberg levels 10 p1480 A83-26273
- Analytical solutions for avalanche-breakdown voltages of single-diffused Gaussian junctions 14 p2006 A83-32667
- Staircase solid-state photomultiplier and avalanche photodiodes with enhanced ionization rates ratio 15 p2150 A83-33681
- Effect of electrons produced by ionization on calculated electron-energy distributions 16 p2414 A83-35653
- Impact ionization in (100)-, (110)-, and (111)-oriented InP avalanche photodiodes 18 p2750 A83-40064
- Associative ionization in collisions between two Na(3P) atoms 22 p3361 A83-45926

IONIZATION COUNTERS**U IONIZATION CHAMBERS****U RADIATION COUNTERS****IONIZATION CROSS SECTIONS**

- Ionisation of H₂ by fast protons and multiply charged ions of He, Li, C, N and O 01 p0105 A83-10857
- Resonance structure of the photoionization cross section of atomic hydrogen in an electric field 04 p0534 A83-15903
- Single and multiple ionization of sulfur atoms by electron impact --- in lo plasma torus 05 p0707 A83-17783
- Determination of the minimum X-ray flux for effective preionization of an XeCl laser 06 p0767 A83-19255
- Atomic photoionization 07 p0992 A83-21068
- Cross sections for photo-ionisation and photo-recombination of hydrogenic atoms in strong magnetic fields --- of pulsars and accreting neutron stars 07 p0991 A83-21223
- Electron-sulphur dioxide total ionisation and electron attachment cross-sections 10 p1479 A83-25649
- Relativistic calculation of atomic M-shell ionization by protons [AD-A130664] 13 p1918 A83-31351
- Charge transfer of doubly charged and trebly charged ions with atomic hydrogen at thermal energies 13 p1916 A83-31352
- Doubly differential cross sections of secondary electron ejected from gases by electron impact - 50-400 eV on N₂ 13 p1916 A83-31353
- Electron impact ionization of complex ions 15 p2236 A83-34608
- On electron impact ionization cross-sections and rates for multiply charged ions 15 p2236 A83-34609
- Measured electron-impact ionization of Be-like ions: B(+), C(2+), N(3+), and O(4+) 18 p2743 A83-40406
- Modification of the photoionization of hydrogen by a low-frequency laser 18 p2743 A83-40409
- Studies of the photoionization cross section of the 2p_i level of nitric oxide 19 p2897 A83-40772
- Production of O(-) from CO₂ by dissociative electron attachment 19 p2898 A83-41863
- Electron-induced excitation and ionization of multiply-charged ions 21 p3213 A83-44652
- Double electron excitation in heliumlike ions 22 p3354 A83-45940
- Photoionisation spectrum of Te I - Autoionising series and relative cross section 23 p3506 A83-48584
- Explicit Hilbert-space representations of atomic and molecular photoabsorption spectra - Computational studies of Stieltjes-Tchebycheff functions 24 p3625 A83-48826
- N₂(+) first-negative emission cross sections for low-energy H(+) and H impact on N₂ 24 p3626 A83-48831

- Atomic photoionization in a strong magnetic field 24 p3626 A83-48833
- Recent advances in atomic calculations and experiments of interest in the study of planetary nebulae 24 p3651 A83-49137
- 2P photoionization cross section of SbI 24 p3627 A83-49751

IONIZATION GAGES

- Design and fabrication of the Indian cosmic ray payload on board Spacelab-3 - A case study 21 p3095 A83-43822

IONIZATION POTENTIALS

- Pulsed optical-optical double resonance spectroscopy of the gerade excited states of ⁷Li₂ 11 p1653 A83-27524
- Ionisation and appearance potentials of CH₄ by electron impact 12 p1778 A83-29925
- The effect of a readily ionized element on stellar atmospheres 15 p2270 A83-34686
- The current state of the theory of the spectra of multiply charged ions 21 p3213 A83-44651

IONIZED GASES

- NT ARGON PLASMA
- NT BOUNDARY LAYER PLASMAS
- NT CATIONS
- NT CESIUM PLASMA
- NT CHARGED PARTICLES
- NT COLD PLASMAS
- NT COLLISIONAL PLASMAS
- NT COLLISIONLESS PLASMAS
- NT CONDUCTION ELECTRONS
- NT COSMIC PLASMA
- NT DENSE PLASMAS
- NT ELECTRON PLASMA
- NT ELLIPTICAL PLASMAS
- NT HEAVY NUCLEI
- NT HELIUM PLASMA
- NT HIGH TEMPERATURE PLASMAS
- NT LASER PLASMAS
- NT METALLIC PLASMAS
- NT MICROPLASMAS
- NT NITROGEN PLASMA
- NT NUCLEI (NUCLEAR PHYSICS)
- NT PLASMA CLOUDS
- NT PLASMA JETS
- NT PLASMA LAYERS
- NT PLASMA SHEATHS
- NT PLASMA SLABS
- NT PLASMAS (PHYSICS)
- NT RAREFIED PLASMAS
- NT RELATIVISTIC PLASMAS
- NT ROTATING PLASMAS
- NT SOLAR WIND
- NT STELLAR WINDS
- NT STRONGLY COUPLED PLASMAS
- NT THERMAL PLASMAS
- NT TOROIDAL PLASMAS
- Multikilowatt electron beams for pumping CW ion lasers 01 p0039 A83-10987
- The neutral and ion chemistry of the upper atmosphere 02 p0206 A83-12152
- Very extended ionized gas in radio galaxies. I - A radio, optical and ultraviolet study of PKS 2158-380 03 p0420 A83-13938
- Shock tube diagnostics utilizing laser Raman scattering 04 p0481 A83-15287
- Discovery of highly ionized species in the ultraviolet spectrum of Feige 24 05 p0700 A83-17029
- Nonlinear breaking of waves in an electrically conducting and radiating gas 05 p0642 A83-17836
- Radiative lifetimes of excited Ar II states 06 p0809 A83-19011
- Investigation of the operation of dispersive optical components 07 p0995 A83-20115
- Ionized gas clouds and the origin of the apparent variability of the compact galactic-center radio source 07 p1014 A83-20654
- The morphology and dynamics of the halo of the 30 Doradus Nebula 07 p1025 A83-21237
- EUV branching ratios for ionized nitrogen and oxygen emissions 07 p0991 A83-21396
- Ionized gas in active molecular cloud cores 08 p1182 A83-23046
- Morphology of the ionized gas in NGC 1313 09 p1355 A83-24525
- Stability of an ionized layer in a gas /the atmosphere/ 10 p1449 A83-25989
- Nebular dust and extinction in ionized nebulae. I - The Balmer decrement 10 p1513 A83-26712
- Hydrodynamic equations for partially ionized multicomponent gas mixtures with higher approximations to the transport coefficients 13 p1925 A83-30653
- Structure of an excited weakly ionized plasma with a discontinuously moving neutral component 13 p1925 A83-30809

- Remarkable kinematics of the ionized gas in the nucleus of NGC 1365 13 p1957 A83-31700
- Infall and outflow of S(+3) ions in 15 Monocerotis, Tau Canis Majoris and Iota Orionis 14 p2105 A83-33199
- The distribution of ionized gas in the nuclei of spiral galaxies 15 p2256 A83-34089
- Doubly ionized aluminium - A diagnostic of cooling gas in the galactic corona 15 p2266 A83-34600
- The perturbation region of a weakly ionized plasma near a cold electrode 16 p2415 A83-35706
- The behaviour of excited atoms near stagnation streamline of a blunt body in an ionized gas 16 p2296 A83-36880
- Infrared observations of the ionized gas in the galactic center 19 p2912 A83-40684
- Heat transfer during ionized-gas flow past bodies 20 p2929 A83-42880
- Propagation of an ionizing shock wave in a uniform magnetic field 20 p3050 A83-43511
- A numerical study of the electrical characteristics of the electrode boundary layer of weakly ionized plasmas of molecular gases 20 p3050 A83-43512
- Kinetic theory of transport processes in partially ionized gases --- Thesis 22 p3366 A83-46696
- A thermal-fluctuation spectroscopy study of the combustion of ballistite powders 24 p3556 A83-49776

IONIZED PLASMAS**U PLASMAS (PHYSICS)****IONIZING RADIATION**

- NT ALPHA PARTICLES
- NT BETA PARTICLES
- NT COSMIC RAY SHOWERS
- NT COSMIC RAYS
- NT COSMIC X RAYS
- NT EXTREME ULTRAVIOLET RADIATION
- NT FAR ULTRAVIOLET RADIATION
- NT GALACTIC COSMIC RAYS
- NT GAMMA RAY BURSTS
- NT GAMMA RAYS
- NT LYMAN ALPHA RADIATION
- NT NEAR ULTRAVIOLET RADIATION
- NT PRIMARY COSMIC RAYS
- NT SECONDARY COSMIC RAYS
- NT SOLAR COSMIC RAYS
- NT SOLAR X-RAYS
- NT ULTRAVIOLET RADIATION
- NT X RAYS

The yearly individual doses of radiation for personnel who work with sources of ionizing radiation

- 01 p0085 A83-11402
- Photobiological aspects of the damage of cells by radiation 03 p0377 A83-14927
- The ionizing particle environment near earth --- effects on spacecraft microelectronics [AIAA PAPER 83-0163] 05 p0606 A83-16563
- Metal coated fibers for use in the radiation environment 05 p0685 A83-17480
- Ionizing radiation effects on power MOSFETs during high speed switching 05 p0625 A83-17485
- Barriers to flashover discharge arcs on Teflon 05 p0618 A83-17496
- Radiation-induced charge dynamics in dielectrics 05 p0618 A83-17502
- Ionizing radiation response of GaAs JFETs and DCLF circuits 05 p0626 A83-17503
- Modeling of ionizing radiation effects in short-channel MOSFETs 05 p0626 A83-17508
- Radiation response of two Harris semiconductor radiation hardened 1K CMOS RAMS 05 p0627 A83-17514
- Ionization-induced breakdown and conductivity of satellite dielectrics 05 p0618 A83-17520
- Geometrical considerations in the transient ionization testing of digital logic circuits 05 p0628 A83-17528
- The damage equivalence of electrons, protons, and gamma rays in MOS devices 05 p0628 A83-17533
- Limitations in the use of linear system theory for the prediction of hardened-MOS device response in space satellite environments 05 p0630 A83-17546
- Photoionization of nitrogen and oxygen mixtures by radiation from a gas discharge 06 p0811 A83-18439
- On the acoustic registration of cascades and single strongly ionized particles 06 p0764 A83-19350
- Factors which determine the differences in the biological effectiveness of ionizing radiation with various physical characteristics 06 p0796 A83-19376
- A comparative analysis of the effect of alkylating agents, ionizing radiation, and ultraviolet light on the mammalian cell progression in the mitotic cycle. I - The effect of N-methyl-N'-nitro-N-nitrosoguanine on the passing of various phases of the cycle by HeLa cells 06 p0796 A83-19378
- Effect of ionizing radiation on fiber-optic waveguides 08 p1165 A83-22481

- Direct bandgap, ionizing-radiation insensitive, photodiode structures 08 p1165 A83-22487
Fiber optic transmitters and receivers for use in high dose-rate ionizing environments 08 p1166 A83-22497
- Thermal and gravitational instability of a model hydrogen plasma in the presence of a radiation field 09 p1347 A83-23598
- Amplitude modulation of a nonlinear progressive ionization wave 09 p1347 A83-23661
- DNA damage during the action of ionizing radiation with different physical characteristics 09 p1321 A83-24926
- A general-purpose device for the measurement of thermoluminescent materials 10 p1418 A83-25350
- Plasma column formed by a traveling ionizing electromagnetic wave 10 p1486 A83-25990
- Infrared spectroscopy of the sources in S235 and its implication for the line excess problem 10 p1509 A83-26371
- Radiolysis of aqueous solutions of hydrogen cyanide (pH about 6) - Compounds of interest in chemical evolution studies 12 p1767 A83-29424
- Self-regulating star formation - The rate limit set by ionizing photons 12 p1796 A83-29544
- The possible effect of the natural background of ionizing radiation on the development of mammals 14 p2062 A83-32057
- Prediction of the optical properties of ruby and leucosapphire under the effect of the cosmic plasma 14 p2085 A83-33393
- Endogenous opiates mediate radiogenic behavioral change 15 p2209 A83-34005
- Models of the planetary nebulae II 2003, NGC 3242, 6210, and 7009 - Constraints on the ionizing radiation of the central star 16 p2431 A83-36669
- Role of succinic acid in chemical evolution 17 p2563 A83-38900
- 'Pseudonormal' thymocytes - A peculiar reaction of lymphoid elements of the thymus cortex to high doses of ionizing radiation 19 p2874 A83-41016
- Measurement and detection of radiation --- Book 19 p2848 A83-41520
- Ionization effects and transition radiation of relativistic charged particles 20 p3045 A83-43526
- Ionization effects in real detectors of relativistic charged particles 20 p3045 A83-43527
- Measurements of cosmic-radiation absolute ionization in the atmosphere 21 p3244 A83-44304
- The physical work capacity of rats after the effect of ionizing radiation 23 p3495 A83-48209
- The effect of a constant magnetic field and gamma-radiation on the hereditary structure of somatic cells - The effect of the combination of a constant magnetic field and ionizing radiation on the blood lymphocytes of humans in vitro 23 p3498 A83-48210
- The control levels of ionizing radiation in the workplace 23 p3499 A83-48569

IONOGRAMS

- Numerical separation of overlapping ordinary and extraordinary echoes in digital ionograms 16 p2341 A83-35416
- Automatic calculation of electron density profiles from digital ionograms. III - Processing of bottomside ionograms 16 p2376 A83-35421
- First bistatic oblique-incidence ionograms between digital ionosondes 18 p2720 A83-40659
- Model ionograms of oblique sounding on the Nikolaev-Havana path 21 p3174 A83-45237
- Efficient coding and resonance spike identification for topside ionogram processing 22 p3330 A83-46512
- Interpretation of ionograms in the vicinity of the dayside auroral oval by ray tracing 22 p3332 A83-46532

IONOSONDES

- Instruments for space investigations --- current measuring devices for satellite-borne ionospheric and solar probes 10 p1387 A83-25342
- VLF ionosonde and long-distance propagation anomalies produced by galactic Cen X-4 X-ray burst in May 1979 12 p1753 A83-29430
- The main ionospheric trough according to data from meridional ionosonde networks 14 p2054 A83-33026
- Sond-R, an instrument for vertical probing of ionospheric plasma by means of CLP on board of a geophysical rocket --- Cylindrical Langmuir Probe 15 p2164 A83-34452
- First bistatic oblique-incidence ionograms between digital ionosondes 18 p2720 A83-40659

IONOSPHERE

- NT D REGION
NT E REGION
NT E-2 LAYER
NT F REGION
NT F 1 REGION
NT F 2 REGION

- NT LOWER IONOSPHERE
NT SPORADIC E LAYER
NT UPPER IONOSPHERE
- Installation for the investigation of sporadic radio emission of the earth's ionosphere 02 p0176 A83-11731
- The dynamics of the Venus ionosphere. II - The effects of the time scale of the solar wind dynamic pressure variations 02 p0265 A83-12562
- Penetration of the solar wind magnetic field into cometary ionospheres 03 p0412 A83-13221
- Terrestrial UV environment and emission mechanisms [AIAA PAPER 83-0022] 05 p0659 A83-16470
- On the equatorial transport of Saturn's ionosphere as driven by a dust-ring current system 09 p1365 A83-24339
- Ionosphere --- of Jupiter 10 p1519 A83-26613
- Global characteristics of magnetic flux ropes in the Venus ionosphere 11 p1685 A83-28303
- Injectons of ions and electrons into the ionosphere and the magnetosphere - Application to measurement of the parallel electric field in the auroral zones --- French thesis 13 p1874 A83-30126
- Investigation of the high-latitude ionosphere and magnetosphere of the earth --- Russian book 13 p1874 A83-30601
- Radar auroral observations and ionospheric electric fields 13 p1876 A83-30773
- Quarter-wave ULF pulsations 13 p1881 A83-31535
- Magnetic fields in the ionospheric holes of Venus - Evidence for an intrinsic field? 14 p2053 A83-32698
- Ground observations of power line radiation coupled to the ionosphere and magnetosphere 14 p2053 A83-32895
- Determination of the characteristics of monochromatic VLF waves and parameters of the surrounding plasma on the basis of satellite amplitude wave measurements 15 p2201 A83-34701
- Evidence for helical kink instability in the Venus magnetic flux ropes 15 p2275 A83-34732
- The properties of the low altitude magnetic belt in the Venus ionosphere 16 p2434 A83-35354
- Effects of large-scale magnetic fields in the Venus ionosphere 16 p2434 A83-35355
- IR-spectroscopy of ionosphere from stratospheric balloons 16 p2373 A83-35370
- Replacement of the present sub-peak plasma density profile by a unique expression 16 p2374 A83-35385
- Auroral plasmas in the evening sector - Satellite observations and theoretical interpretations 16 p2382 A83-36620
- The ionosphere of Venus - Observations and their interpretation 17 p2617 A83-37424
- Basic theory and model calculations of the Venus ionosphere 17 p2617 A83-37425
- The interaction of the solar wind with Venus 17 p2618 A83-37426
- Physics of the interaction of the solar wind with the ionosphere of Venus - Flow/field models 17 p2618 A83-37427
- A two-dimensional model of the ionosphere of Venus 17 p2618 A83-37585
- STARE radar observations of a Pg pulsation --- giant pulsations 17 p2538 A83-37592
- Geometry of depleted plasma regions in the equatorial ionosphere 17 p2539 A83-37606
- Long-term relationships between sunspots, Ca-plages and the ionosphere 18 p2712 A83-39065
- The longitudinal asymmetry of the main ionospheric trough 18 p2714 A83-39332
- Numerical experiments in the analysis of mathematical models of the ionosphere 21 p3174 A83-45233
- Symposium on Coordinated Observations of the Ionosphere and the Magnetosphere in the Polar Regions, 4th, Tokyo, Japan, February 23-25, 1981, Proceedings 22 p3329 A83-46501
- Determination of the latitude of Sq focus and its relation to the electrojet variations 24 p3606 A83-49306

IONOSPHERIC ABSORPTION

- U ELECTROMAGNETIC ABSORPTION
U IONOSPHERIC PROPAGATION

IONOSPHERIC COMPOSITION

- Allowance for nonstationary and nonlinear terms in the equations of motion in regard to the solution of problems of ionospheric modeling 02 p0209 A83-12424
- Investigation of frequency distortions of the meteoric component of a signal scattered in the ionosphere 02 p0209 A83-12427
- The correlation of parameters of the F2 and F1 layers of the ionosphere in the case of day-to-day variations 02 p0210 A83-12445
- Disappearing ionospheres on the nightside of Venus 02 p0265 A83-12560

- Observed composition of the ionosphere of Venus - Implications for the ionization peak and the maintenance of the nightside ionosphere 02 p0265 A83-12561
- Results inferred from electron density measurements at Saskatoon, Canada /L = 4.4/ by a partial reflection technique. I - Variations of nitric oxide in the D-region during quiet periods 03 p0362 A83-14747
- Combined mass spectrometric composition measurements of positive and negative ions in the lower ionosphere. II - Negative ions 05 p0665 A83-17787
- Highly sensitive temperature-stable DC amplifier for space probe experiment 08 p1080 A83-22279
- On the ionization of the mid-latitude lower ionosphere by precipitating hard electrons 11 p1617 A83-28119
- Theoretical modeling of low-latitude Mg 11 p1618 A83-28324
- Tropical nightglow observations and predictions from ionospheric models 12 p1754 A83-29432
- Spherical ion traps for 'Intercomsos-Bulgaria-1300' 13 p1813 A83-30754
- Ionospheric plasma parameters measurement instrument for satellite experiment with sit --- Spherical Ion Trap 14 p2048 A83-31816
- Coordinated rocket campaign on Heiss Island --- for upper atmosphere sounding during auroral disturbances 16 p2372 A83-35362
- Aeronomy of the inner planets 17 p2622 A83-38278
- Tests of an ion-chemical model of the D- and lower E-region 18 p2712 A83-39072
- Determining the concentration of two dominant types of ions with the aid of a cylindrical Langmuir probe --- in aerospace environments 19 p2817 A83-41593
- Photolysis of methane and the ionosphere of Uranus 20 p3079 A83-43166
- Variation of aeronomic parameters during the period from the equinox to summer 21 p3175 A83-45241
- Observation of the ion composition by ionosphere Sounding Satellite 21 p3178 A83-45457
- Characteristics of seasonal variations of O(+) ion density troughs in the nighttime topside ionosphere 21 p3178 A83-45458
- E-region nitric oxide concentrations inferred from the 26 February 1979 eclipse expedition 23 p3480 A83-47469
- Positive and negative ion composition measurements in the Dand E-regions during the 26 February 1979 solar eclipse 23 p3480 A83-47470

IONOSPHERIC CONDUCTIVITY

- Dynamic model of the principal types of convection, field-aligned currents, and volumetric structure of the polar ionosphere 02 p0209 A83-12422
- Importance of initial ionospheric conductivity on substorm onset 05 p0665 A83-17788
- Variability of the Harang discontinuity as observed by the Chatanika radar and the IMS Alaska magnetometer chain 07 p0967 A83-21559
- Reflection of Alfven waves by nonuniform ionospheres 07 p0968 A83-21585
- Schumann resonance effects of electrical conductivity perturbations in an exponential atmospheric/ionospheric profile 09 p1307 A83-24693
- Spatial variations of ionospheric conductivity and radar auroral amplitude in the eastward electrojet region during pre-substorm conditions 10 p1447 A83-25427
- Influence of the E region dynamo on equatorial spread F 11 p1618 A83-28319
- The potential of high atmospheric layers 11 p1620 A83-28730
- Joule heating at high latitudes 15 p2196 A83-33941
- Ionospheric and field-aligned current systems in the auroral zone - A concise review 16 p2372 A83-35361
- Calculation of ionospheric conductivity profiles by inverting VLF/LF reflection data. I - Isotropic propagation 16 p2341 A83-35419
- Depth of the nonconducting layer at the Nigerian dip equator 17 p2537 A83-37578
- On the rotation of the polar cap potential pattern and associated polar phenomena 17 p2539 A83-37605
- Ionospheric electrodynamics and irregularities - A review of contributions by U.S. scientists from 1979 to 1982 17 p2541 A83-38275
- Electric conductivities, electric fields and auroral particle energy injection rate in the auroral ionosphere and their empirical relations to the horizontal magnetic disturbances 17 p2544 A83-38518
- The effect of the conductivity of the E-region on the growth increment of the Rayleigh-Taylor instability in the ionospheric plasma of the equatorial F-region 18 p2714 A83-39331
- Ionospheric conditions affecting the evolution of equatorial plasma depletions 19 p2864 A83-41118
- Polarization electric fields in the nighttime F layer at Arecibo 20 p3019 A83-42418

Reflection of MHD-waves in the PC4-5 period range at ionospheres with non-uniform conductivity distributions 20 p3026 A83-43204

Relative contribution of ionospheric conductivity and electric field to the auroral electrojets 22 p3336 A83-47060

Inferring electric fields and currents from ground magnetometer data - A test with theoretically derived inputs 22 p3337 A83-47077

PIC magnetic pulsations and variations of the ionospheric electric field and conductivity 24 p3606 A83-49307

IONOSPHERIC CROSS MODULATION

Non-linear phenomena in the ionosphere traversed by high power radio wave 17 p2495 A83-38541

IONOSPHERIC CURRENTS

NT AURORAL ELECTROJETS

NT ELECTROJETS

NT EQUATORIAL ELECTROJET

Field-aligned current and the auroral electrojets in the post-noon quadrant 02 p0207 A83-12381

A heating mechanism for the generation of inhomogeneities of the ionospheric F-layer 02 p0208 A83-12420

Dynamic model of the principal types of convection, field-aligned currents, and volumetric structure of the polar ionosphere 02 p0209 A83-12422

Barium-cloud drift and the determination of some parameters of field-aligned currents from observations made on Hayes Island 02 p0209 A83-12432

Assessment of the error in measuring the strength of a constant electric field by the double-Langmuir-probe method 03 p0397 A83-13206

Thinning of field-aligned currents 03 p0357 A83-13544

Examples of multi-instrumental studies on auroral phenomena 04 p0512 A83-16292

Detailed correlations of magnetic field and riometer observations at L = 4.2 with pulsating aurora 05 p0660 A83-17394

Relationship between field-aligned currents, diffuse auroral precipitation and the westward electrojet in the early morning sector 05 p0661 A83-17397

Modification of stationary ionospheric current systems under strong ionospheric disturbances 05 p0662 A83-17609

On the nature of homogeneous auroral arcs 05 p0663 A83-17613

Penetration of geomagnetic pulsations from one polar cap to the other 05 p0663 A83-17616

Field-aligned currents in the magnetosphere 05 p0663 A83-17617

Magnetic flux ropes in the Venus ionosphere - Observations and models 06 p0847 A83-18282

Global dynamo simulation of ionospheric currents and their connection with the equatorial electrojet and counter electrojet - A case study 06 p0783 A83-18296

Convection electric fields and ionospheric currents derived from model field-aligned currents at high latitudes [AD-A125082] 06 p0783 A83-18297

Dynamics of magnetosphere-ionosphere coupling including turbulent transport 06 p0784 A83-18305

The origins of Birkeland currents 07 p0962 A83-20840

A correlation between measured E-region current and geomagnetic daily variation at equatorial latitude 07 p0966 A83-21429

A study of quiet day magnetic field variations in East Asia at sunspot minimum 08 p1134 A83-22304

On the position of the Sq /H/ focus in years of sunspot minimum --- solar quiet day geomagnetic variations 08 p1134 A83-22306

Sq and L currents in the ionosphere --- solar quiet and lunar tidal effects on ionospheric and geomagnetic variations 08 p1134 A83-22307

An investigation of the equatorial electrojet by means of ground-based magnetic measurements in Brazil 08 p1134 A83-22309

VLF/ELF radiation from the ionospheric dynamo current system modulated by powerful HF signals 09 p1300 A83-23311

Solar wind control of the low-latitude asymmetric magnetic disturbance field 09 p1303 A83-23768

A possibility to distinguish between ionospheric and magnetospheric origin of low latitude magnetic perturbations 10 p1448 A83-25439

An analogue model of the geomagnetic induction in the South Indian Ocean 10 p1448 A83-25440

Magnetosphere-ionosphere relationships 10 p1448 A83-25604

The stratification of magnetospheric convection and its manifestations in the high-latitude ionosphere 10 p1448 A83-25605

Electric fields in the ionosphere and magnetosphere 11 p1614 A83-27399

Electric currents and voltage drops along auroral field lines 11 p1614 A83-27400

Dynamics of the disturbed ionosphere 11 p1614 A83-27401

Ionospheric disturbances resulting from ion-neutral coupling 11 p1615 A83-27402

Three-dimensional current flow and particle precipitation in a westward travelling surge /observed during the barium-GEOS rocket experiment/ 11 p1618 A83-28316

Comparison of measurements of electromagnetic induction in the magnetosphere of Venus with laboratory simulations 11 p1685 A83-28379

The use of the radio aurora to measure electric fields and currents in the auroral ionosphere 13 p1875 A83-30602

The eastward motion of the radio aurora and auroral loops in the morning sector 13 p1875 A83-30603

Field and wave measurements aboard the Aureol-3 spacecraft 13 p1813 A83-30758

Does IMF B(y) induce the cusp field-aligned currents? 13 p1882 A83-31626

Polarization characteristics of Pi 2 pulsations and implications for their source mechanisms - Influence of the westward travelling surge 13 p1882 A83-31633

Modeling of the development of current systems of a polar magnetic substorm 14 p2050 A83-31868

On the possibility that certain types of geomagnetic pulsations have an ionospheric origin 14 p2050 A83-31869

Field-aligned currents and the structure of the magnetosphere 14 p2050 A83-31872

Currents in the polar-cusp region 14 p2051 A83-31893

Measurement of vehicle potential using a mother-daughter tethered rocket 15 p2127 A83-34212

Dielectric currents in the low-latitude boundary layer and geomagnetic tail 15 p2202 A83-34734

Joule heating and particle precipitation --- in auroral upper atmosphere 16 p2372 A83-35360

Ionospheric and field-aligned current systems in the auroral zone - A concise review 16 p2372 A83-35361

Electric field and electron density measurements in the equatorial E-region 16 p2373 A83-35367

Energy deposition in the polar ionosphere as determined by measurements aboard 'Intercoms-Bulgaria-1300' satellite 16 p2373 A83-35368

High resolution measurements of nighttime ion troughs at Venus - Evidence of electrodynamic perturbations 16 p2435 A83-35403

The morphology of a multi-bubble system in the ionosphere 17 p2538 A83-37579

On the rotation of the polar cap potential pattern and associated polar phenomena 17 p2539 A83-37605

An equivalent ionospheric current system at high latitudes in the Northern Hemisphere for a Bz component of the interplanetary magnetic field greater than zero 17 p2539 A83-37698

Ionospheric electrodynamics and irregularities - A review of contributions by U.S. scientists from 1979 to 1982 17 p2541 A83-38275

Lunar modulations of the equatorial electrojet 17 p2544 A83-38373

Electric conductivities, electric fields and auroral particle energy injection rate in the auroral ionosphere and their empirical relations to the horizontal magnetic disturbances 17 p2544 A83-38518

F-region dynamo in the evening - Interpretation of equatorial Delta D anomaly found by MAGSAT 18 p2712 A83-39074

Field-aligned currents in the polar cap 18 p2714 A83-39324

Magnetic field of a model of a three-dimensional magnetospheric-ionospheric current system on the surface of a nonconducting earth 18 p2714 A83-39338

On the possibility of recovering zone III currents from ground data 18 p2714 A83-39340

DC magnetic field observations on board the AUREOL-3 satellite - The TRAC experiment 18 p2647 A83-39579

The relationship of total Birkeland currents to the merging electric field 19 p2865 A83-41126

Equatorial ionospheric currents derived from MAGSAT data 20 p3026 A83-43212

Equivalent ionospheric current systems representing lunar daily variations of the polar geomagnetic field 22 p3327 A83-46052

The possibility of deducing ionospheric and field-aligned currents from ground magnetic perturbations 22 p3331 A83-46514

Comparison of height-integrated current densities derived from ground-based magnetometer and rocket-borne observations during the Porcupine F3 and F4 flights 22 p3337 A83-47068

Inferring electric fields and currents from ground magnetometer data - A test with theoretically derived inputs 22 p3337 A83-47077

IONOSPHERIC DISTURBANCES

NT IONOSPHERIC STORMS

NT SUDDEN IONOSPHERIC DISTURBANCES

NT TRAVELING IONOSPHERIC DISTURBANCES

Meteorological effects in ionospheric processes /Survey/ 01 p0071 A83-10589

Conditions in the magnetosphere and ionosphere during nighttime sudden commencements that develop against a background of disturbances 01 p0071 A83-10591

The correlation of f0F2 disturbances with variations in solar radio emission 01 p0129 A83-10592

The stability of the diurnal variation of the degree of disturbance of f0F2 during the cycle of solar activity 01 p0071 A83-10593

The problem of energetics in the physics of the ionosphere and approaches to its solution 01 p0071 A83-10596

The influence of magnetospheric processes on the dynamics of neutral gas at ionospheric heights 01 p0071 A83-10603

Estimation of the parameters of disturbances on long-range radio-communication paths 01 p0031 A83-10810

The small-scale turbulence spectrum of the high-latitude and equatorial ionosphere 02 p0203 A83-11679

Distances from auroral zones to the magnetic and geographic equators 02 p0205 A83-11971

Ionospheric disturbances over Japan due to the 18 May 1980 eruption of Mount St. Helens 02 p0206 A83-12019

Electron density profiles in the nighttime high-latitude lower ionosphere, artificially disturbed by high-power radio waves 02 p0209 A83-12425

Dependence of the parameters of the disturbed midlatitude ionospheric F2-region on local time 02 p0210 A83-12446

Stationary large-scale irregularities of the ionosphere 03 p0361 A83-14742

An observational study of the D-region winter anomaly and sudden stratospheric warmings 03 p0362 A83-14746

HF Doppler observations of gravity waves during the 16 February 1980 solar eclipse 03 p0362 A83-14748

The S3-4 ionospheric irregularities satellite experiment - Probe detection of multi-ion component plasmas and associated effects on instability processes 04 p0509 A83-14976

The anisotropy of high-latitude nighttime F region irregularities 05 p0661 A83-17402

Waves generated in the upper ionosphere by a stationary moving source 05 p0662 A83-17586

Ionospheric and geomagnetic variations at mid-latitudes 05 p0662 A83-17596

The modeling of a large-scale region of disturbances arising during the vertical heating of the ionosphere by a field of high-power radio waves 05 p0662 A83-17605

Foreshortened scattering by artificial irregularities, with allowance for total internal reflection from the ionosphere 05 p0662 A83-17607

Modification of stationary ionospheric current systems under strong ionospheric disturbances 05 p0662 A83-17609

Observations of the horizontal irregularity of F-layer nightglow in the region of the Brazilian anomaly 05 p0663 A83-17621

Diffusional transport of ionospheric irregularities 05 p0663 A83-17622

The effect of random irregularities on the field strength of radio waves in the region of caustics 05 p0663 A83-17624

The interaction of flowing plasmas with planetary ionospheres - A Titan-Venus comparison 06 p0847 A83-18281

The role of parametric decay instabilities in generating ionospheric irregularities 06 p0785 A83-18310

The low- and equatorial-latitude ionosphere at a height of 500 km in the course of magnetospheric-ionospheric disturbances during September-December 1977 /according to data from the Cosmos-900 satellite/ 06 p0786 A83-18359

Stability of low-frequency oscillations of the ionospheric plasma in the presence of photoelectrons 06 p0787 A83-19339

Magnetospheric convection effects at mid-latitudes. II - A coordinated Chatanika/Saint-Santin study of the April 10-14, 1978, magnetic storm 07 p0964 A83-21061

Polar auroras. Number 30 - Complex investigations of the dynamics of polar auroras --- Russian book 07 p0964 A83-21176

Bay-like disturbances according to integral-photometer data 07 p0965 A83-21188

On the effect of finite, field-aligned plasma length on a loss-cone instability --- in ionosphere

07 p0967 A83-21518

Rocket and ground-based study of an auroral breakup event

08 p1137 A83-23117

Ionospheric effects of rocket exhaust products - HEAO-C, Skylab

09 p1301 A83-23314

Distance errors related to atmospheric effects at signal frequencies greater than 100 MHz in the case of geodetic systems of measurement. I - Influence of the troposphere. II - Influence of the ionosphere

09 p1301 A83-23387

The scattering of escaping electrons by helicon oscillations in a weakly magnetized plasma --- in ionosphere and magnetosphere

09 p1301 A83-23479

Pc 1 pulsation activity at Ottawa

09 p1303 A83-23763

A theoretical study of the high latitude F region's response to magnetospheric storm inputs

09 p1303 A83-23767

Heater-generated intermediate-scale irregularities - Spatial distribution and spectral characteristics --- in ionosphere

10 p1449 A83-26047

Ionospheric disturbances resulting from ion-neutral coupling

11 p1615 A83-27402

Attenuation of high-frequency radio waves in the lower high-latitude ionosphere, artificially disturbed by high-power radio transmissions

11 p1615 A83-27951

Intensity variations of the IGW source and the ionospheric response during the substorm of September 18, 1974 --- Internal Gravity Wave

11 p1615 A83-27952

Conjugate studies of an isolated equatorial irregularity region

11 p1618 A83-28320

[AD-A127561] The influence of the interplanetary magnetic field on the F region and the upper ionosphere

11 p1620 A83-28743

Ambipolarity in the motion of ionospheric plasma

11 p1620 A83-28745

Features of the development of an ionospheric substorm in various local time sectors

11 p1621 A83-28750

The physics of slow MHD waves in the ionospheric plasma --- Russian book

12 p1750 A83-28828

An investigation of the mid-latitude ionospheric D-region under twilight conditions in summer

12 p1753 A83-29237

High-latitude plasma densities and their relation to riometer absorption

12 p1754 A83-29431

Investigation of ionospheric irregularities by radio holography

13 p1875 A83-30609

Dynamics of sporadic E layers during magnetic disturbances

13 p1875 A83-30610

Preferential perpendicular acceleration of heavy ionospheric ions by interactions with electrostatic hydrogen cyclotron waves

13 p1966 A83-31237

Finite parallel wavelengths and ionospheric structuring

13 p1879 A83-31239

A theory of coherent radar spectra in the auroral E region

13 p1879 A83-31240

An effort to simulate magnetospheric-ionospheric effects in the presence of seismic phenomena

13 p1880 A83-31328

Generation of ionospheric irregularities by thermal-source - A new mechanism

13 p1881 A83-31533

Meteorological effects in the F2-layer of the ionosphere

14 p2049 A83-31857

Phase fluctuations of a wave caused by ionospheric irregularities

14 p2049 A83-31860

The formation of weakly anisotropic irregularities in the high-latitude ionosphere

14 p2049 A83-31861

Modeling of ionospheric-plasmaspheric interactions with allowance for temperature anisotropy

14 p2049 A83-31863

The reaction of the ionosphere to variations of electric fields during nighttime baylike disturbances

14 p2049 A83-31866

The main ionospheric trough according to data from meridional ionosonde networks

14 p2054 A83-33026

Associated geomagnetic and ionospheric variations

15 p2199 A83-34363

Synopsis of D- and E-region electron densities during the energy budget campaign

16 p2373 A83-35364

Heliomagnetic cycle of magnetic-ionospheric and interplanetary activity

18 p2713 A83-39315

Distribution of electric-field potential near a satellite injecting electrons in the steady-state regime in the initial stage of active experiments in the ionosphere

18 p2713 A83-39319

Equatorial disturbance dynamo electric fields

19 p2864 A83-41117

The effect of motions of the ionospheric plasma on the formation of artificial periodic inhomogeneities

19 p2866 A83-41803

Geomagnetic and ionospheric disturbances of internal meteorological type - A synergistic approach to disturbances

20 p3022 A83-43134

Observations of large scale F-region irregularities using airglow emissions at 7774 A and 6300 A

21 p3170 A83-44245

The effect of disturbances of lower ionospheric parameters by powerful radio waves on partially reflected signals

21 p3121 A83-45344

Global distribution of topside spread F

21 p3178 A83-45448

Ionospheric irregularities and their potential impact on synthetic aperture radars

22 p3275 A83-46535

Bottomside sinusoidal irregularities in the equatorial F region

22 p3337 A83-47065

The solar eclipse of 26 February 1979 - Introductory comments

23 p3480 A83-47465

The effect of cold plasmaspheric and ionospheric plasmas on the electron-cyclotron instability of the frontal boundary layer

23 p3484 A83-48384

Modeling of the nonstationary processes of the ionosphere-magnetosphere coupling with allowance for their self-consistency

23 p3484 A83-48389

The storm-time variation of atmospheric disturbance from the data of a global network of vertical-incidence ionospheric sounding stations

23 p3484 A83-48391

IONOSPHERIC DRIFT

Continental effects in the wind field in the upper mesopause region at midlatitudes

02 p0209 A83-12431

Gradient-drift instability of nighttime mid-latitude Es-layers

03 p0361 A83-14745

Magnetospheric convection effects at mid-latitudes. I - Saint-Santin observations

06 p0783 A83-18295

Vertical ionization drift velocities and range type spread F in the evening equatorial ionosphere

06 p0785 A83-18308

Nonlinear evolution of convecting plasma enhancements in the auroral ionosphere. II - Small scale irregularities

06 p0785 A83-18319

Interpretation of auroral radar experiments using a kinetic theory of the two-stream instability

07 p0961 A83-20373

Magnetospheric convection effects at mid-latitudes. III - Theoretical derivation of the disturbance convection pattern in the plasmasphere

07 p0964 A83-21062

Compatibility of Doppler measurements of the drift of auroral scattering at different frequencies

07 p0964 A83-21180

F-region irregularity drifts deduced from the scintillation measurements by two closely-spaced antennas

08 p1133 A83-22042

Midlatitude sporadic-E layers and vertical metallic ion drift profiles

08 p1137 A83-23121

Investigation of the plasma mantle in the earth's magnetosphere. III - Ion acceleration

09 p1307 A83-25034

A test of the cosine relationship using three-radar velocity measurements --- of electron drift in ionospheric E layer

10 p1449 A83-26044

Short wavelength stabilization of the gradient drift instability due to velocity shear --- in equatorial electrojet

12 p1779 A83-28921

Nonlinear limiting mechanism of Buneman-Farley instability --- in auroral ionosphere

13 p1875 A83-30607

An instrument for total ion drift velocity measurements aboard the 'Intercosmos-Bulgaria-1300' satellite

13 p1814 A83-30762

Ionospheric E-region drifts at Sibizmir during 1970-75

13 p1882 A83-31547

The effect of a meridional E x B drift on the thermal plasma at L = 1.4

13 p1882 A83-31630

Dependence of vertical drifts of the ionospheric F-layer at the Leningrad observatory on magnetic activity in the auroral zone

14 p2050 A83-31879

The dynamics of the polar ionosphere in the auroral zone

14 p2054 A83-33031

The effect of the electrodynamic drift caused by magnetospheric processes on the structural features of the polar and equatorial ionosphere

14 p2054 A83-33036

On the generation and growth of equatorial backscatter plumes. II - Structuring of the west walls of upwellings

15 p2195 A83-33939

A first comparison of STARE and EISCAT electron drift velocity measurements --- Scandinavian twin auroral radar experiment and European incoherent scatter facility

17 p2539 A83-37600

The effect of radio waves on the properties of an ionospheric plasma

17 p2539 A83-37699

Ionospheric electrodynamics and irregularities - A review of contributions by U.S. scientists from 1979 to 1982

17 p2541 A83-38275

Dependence of ionospheric drift speed on geomagnetic activity

17 p2495 A83-38544

Measurement of movements in the ionosphere using radio reflections

18 p2712 A83-39070

Correlations between cyclic increments of F2-layer critical frequencies

18 p2713 A83-39317

Ionospheric conditions affecting the evolution of equatorial plasma depletions

19 p2864 A83-41118

Production of auroral zone E region irregularities by powerful HF heating

20 p3020 A83-42427

Dynamics of artificial plasma clouds in 'Spolokh' experiments - Movement pattern

20 p3023 A83-43155

Short wavelength gradient-drift waves at high latitudes

21 p3170 A83-44243

Ion-Pedersen drift and parallel electric field effects on plasma jetting

22 p3327 A83-46048

Parametric excitation and suppression of convective plasma instabilities in the high-latitude F region ionosphere

22 p3328 A83-46060

A new VHF Doppler radar experiment at Syowa Station, Antarctica

22 p3332 A83-46523

HF Doppler measurement in the auroral ionosphere

22 p3332 A83-46524

Modeling of spaced-receiver scintillation measurements --- of drift velocity in ionosphere

22 p3275 A83-46534

Very high latitude F-region irregularities observed by HF-radar backscatter

22 p3334 A83-46889

Evidence for the E x B drift of pulsating auroras

22 p3336 A83-47059

The dependence of the relative backscatter cross section of 1-m density fluctuations in the auroral electrojet on the angle between electron drift and radar wave vector

22 p3337 A83-47066

Earth magnetic field fluctuations produced by filamentation instabilities of electromagnetic heater waves

23 p3482 A83-47868

IONOSPHERIC ELECTRON DENSITY

The mechanism governing the formation of certain types of Es layers in the ionosphere at high latitudes

01 p0071 A83-10600

The role of photochemistry and dynamics in the D region of the ionosphere

01 p0071 A83-10601

Measurements of the inhomogeneities in the polar ionosphere made with an auto-oscillating sonde

01 p0050 A83-10602

Vertical displacements of stratification in the E-layer during sunrise

02 p0205 A83-11996

A comparison between HF partial reflection profiles from the D-region and simultaneous Langmuir probe electron density measurements

02 p0205 A83-12017

A three-dimensional model of the high-latitude F-region with allowance for the noncoincidence of geographical and geomagnetic coordinates

02 p0208 A83-12421

Dependence of an equinoctial analytical model of ionospheric electron density on solar activity

02 p0209 A83-12423

Investigation of the anisotropy of ionospheric inhomogeneities by the differential-phase method

02 p0209 A83-12426

Total electron content structure in the Middle East --- ionosphere during solar maximum

02 p0211 A83-12637

The use of 1356-A emission intensity to determine parameters of the F-region

03 p0356 A83-13212

Results inferred from electron density measurements at Saskatoon, Canada /L = 4.4/ by a partial reflection technique. I - Variations of nitric oxide in the D-region during quiet periods

03 p0362 A83-14747

Movements of the mid-latitude ionospheric trough

03 p0362 A83-14751

The S3-4 ionospheric irregularities satellite experiment - Probe detection of multi-ion component plasmas and associated effects on instability processes

04 p0509 A83-14976

Geographical and seasonal distribution of critical frequencies in the F2-layer during a period of high solar activity

04 p0509 A83-15724

Space environment monitoring by low-altitude operational satellites

04 p0512 A83-16287

Using satellite observed UV intensities to deduce electron density profiles

05 p0659 A83-16471

[AIAA PAPER 83-0023] Relationship between field-aligned currents, diffuse auroral precipitation and the westward electrojet in the early morning sector

05 p0661 A83-17397

The use of a single coupling function for the correction of model profiles of electron density in the ionosphere

05 p0662 A83-17604

Diffusional transport of ionospheric irregularities

05 p0663 A83-17622

High resolution topside in situ data of electron densities and VHF/GHz scintillations in the equatorial region [AD-A125353] 06 p0785 A83-18309

Nonlinear evolution of convecting plasma enhancements in the auroral ionosphere. II - Small scale irregularities 06 p0785 A83-18319

Determination of the electron content of the plasmasphere by means of coherent signals of ATS-6, recorded in Neustrelitz 06 p0786 A83-18361

Comparison of calculated and measured values of electron fluxes for the wide-angle detector in the ARAKS experiment --- on ionospheric electron beam injection 06 p0786 A83-18368

Electron density changes during solar eclipse of 16 Feb. 1980 at Gauhati 06 p0786 A83-18418

A method of estimating the electron density profile of the D layer from a knowledge of the VLF reflection coefficients 07 p0962 A83-20374

Equations of anisotropic hydrodynamics for electron component of the ionospheric plasma 07 p0968 A83-21583

The variation of the magnetic field and its interaction with the equatorial electrojet in eastern Senegal 08 p1135 A83-22314

A study of the post-sunset increase in the F2-region electron density at low-and middle latitudes in the Asian zone during sunspot maximum and minimum periods 08 p1135 A83-22315

Midlatitude sporadic-E layers and vertical metallic ion drift profiles 08 p1137 A83-23121

HF produced ionospheric electron density irregularities diagnosed by UHF radio star scintillations 09 p1300 A83-23310

The variations in the spectrum of electron-density inhomogeneities in the lower ionosphere under the effect of high-power electromagnetic radiation 09 p1301 A83-23478

Diffusion of small-scale artificial irregularities of the upper ionosphere 09 p1301 A83-23491

Studies of the self-focusing instability at Arecibo --- in ionosphere 09 p1303 A83-23765

A simple theoretical model for calculating and parameterizing the ionospheric photoelectron flux 09 p1304 A83-23772

VHF amplitude scintillations and associated electron content depletions as observed at Arequipa, Peru [AD-A126952] 09 p1306 A83-24688

A new ionospheric scattering mechanism 09 p1307 A83-24692

The use of a microprocessor in the KM-3 instrumentation for measuring electron temperature and electron velocity distribution --- satellite ionospheric sounding 10 p1386 A83-25339

Assessment of the accuracy of electron-temperature measurements by a high-frequency probe 10 p1386 A83-25340

An instrument for the direct measurement of electron temperature in the ionosphere 10 p1387 A83-25341

On the dependence of radar aurora amplitude on ionospheric electron density 10 p1447 A83-25438

Meteorological control of the D region - /Tutorial Lecture/ 11 p1615 A83-27407

Ionospheric observations at Pruhonice during the solar eclipse of April 29, 1976 11 p1616 A83-28111

The self-focusing of whistler waves 11 p1660 A83-28250

The effects of meridional electric fields in the high-latitude ionosphere 11 p1620 A83-28746

Changes in the ionosphere caused by longitudinal electric fields 11 p1620 A83-28748

The height distribution of parameters of the auroral ionosphere during a magnetic storm 11 p1621 A83-28749

An estimate of the errors in measurements of the electron concentration in the ionosphere made with a high-frequency impedance probe 11 p1575 A83-28752

An investigation of the mid-latitude ionospheric D-region under twilight conditions in summer 12 p1753 A83-29237

High-latitude plasma densities and their relation to riometer absorption 12 p1754 A83-29431

Prediction of total electron content using the International Reference Ionosphere 12 p1754 A83-29435

Spectra of irregularities of the high-latitude lower ionosphere according to phase VLF measurements 13 p1875 A83-30608

The height distribution of electron density in the high-latitude F2-layer 13 p1875 A83-30611

A payload for the study of electric fields and electron density in the equatorial region 13 p1814 A83-30759

Observations of LHR noise with banded structure by the sounding rocket S29 barium-GEOS 13 p1879 A83-31246

The effects of neutral air winds on the electron content of the mid-latitude ionosphere and protonosphere in summer 13 p1882 A83-31629

Longitudinal and latitudinal abnormalities in the daily variation of 10F2 in the South-American region 13 p1883 A83-31719

Errors in the determination of electron density in the D-region of the ionosphere by the method of partial reflections 14 p2049 A83-31856

On the possibility that certain types of geomagnetic pulsations have an ionospheric origin 14 p2050 A83-31869

Variations of electron density in the D-region 14 p2050 A83-31875

The effect of the winter anomaly of the D-region according to measurements on the Kerguelen Islands 14 p2050 A83-31876

Auger electrons in the auroral ionosphere 14 p2051 A83-31883

On the formation of daytime troughs in the F-region within the plasmasphere 14 p2053 A83-32697

An investigation of the state of the high-latitude ionosphere during substorms 14 p2054 A83-33027

The dynamics of the polar ionosphere in the auroral zone 14 p2054 A83-33031

The electron concentration in the auroral and subauroral zones according to rocket measurements 14 p2054 A83-33035

Recent observations of beam plasma interactions in the ionosphere and a comparison with laboratory studies of the beam plasma discharge 15 p2197 A83-34178

Charged particle measurements from a rocket-borne electron accelerator experiment 15 p2197 A83-34179

The French-Soviet experiments ARAKS - Main results --- Artificial Radiation and Aurora between Kerguelen and Soviet Union 15 p2197 A83-34181

Observations of non-linear processes in the ionosphere 15 p2198 A83-34191

Laboratory simulation of injection particle beams in the ionosphere 15 p2198 A83-34193

Electron beam as a source of electrostatic waves 15 p2228 A83-34205

Excitation of whistler waves by reflected auroral electrons 15 p2199 A83-34359

Extremely high F-region electron temperatures during the maximum of 21st solar cycle 15 p2200 A83-34417

On the kinetic balance in the ca. maximal part of the daily F-region 15 p2201 A83-34447

Synopsis of D- and E-region electron densities during the energy budget campaign 16 p2373 A83-35364

Energy distribution of thermal electrons at the height of lower-E-region 16 p2373 A83-35366

Electric field and electron density measurements in the equatorial E-region 16 p2373 A83-35367

Role of neutral winds in generating irregularities in equatorial F-region 16 p2374 A83-35378

Replacement of the present sub-peak plasma density profile by a unique expression 16 p2374 A83-35385

Implementation of a new characteristic parameter into the IRI sub-peak electron density profile 16 p2374 A83-35386

In situ studies of electron density during equatorial spread-F 16 p2374 A83-35387

Equatorial F-region ionization differences between March and September, 1979 16 p2375 A83-35388

D-region IRI profiles in relation to radio observations 16 p2375 A83-35389

Comparison of A1-absorption data with theoretically computed values based on the International Reference Ionosphere (IRI) 16 p2375 A83-35390

Latitudinal influences on the quiet daytime D-region [AD-A128591] 16 p2375 A83-35391

Relationship between electron density and electron temperature as a function of solar activity 16 p2375 A83-35397

A differential-Doppler study of traveling ionospheric disturbances from Millstone Hill 16 p2376 A83-35418

Automatic calculation of electron density profiles from digital ionograms. III - Processing of bottomside ionograms 16 p2376 A83-35421

Saturn's ionosphere - A corona of ice particles? 16 p2438 A83-36781

Some results of ionospheric slab thickness observations at Lunping 17 p2537 A83-37577

The response of the nighttime F-region to wave disturbances 17 p2539 A83-37650

Wavy patterns of ionospheric electron density profiles triggered by TID - Observation results of the electron density by TAIYO satellite 17 p2540 A83-37825

Ion transport in the mid-latitude F1-region 17 p2544 A83-38522

Non-linear phenomena in the ionosphere traversed by high power radio wave 17 p2495 A83-38541

Results inferred from electron density measurements at Saskatoon, Canada (L = 4.4) by a partial reflection technique. II - Ion production rates and nitric oxide in the D-region during post-storm periods 18 p2712 A83-39067

The mid-latitude trough in the electron concentration of the ionospheric F-layer - A review of observations and modelling 18 p2712 A83-39069

Tests of an ion-chemical model of the D- and lower E-region 18 p2712 A83-39072

Ionospheric scintillations 18 p2720 A83-40658

Ionospheric conditions affecting the evolution of equatorial plasma depletions 19 p2864 A83-41118

Ionospheric characteristics of a detached arc in the evening-sector trough 19 p2865 A83-41123

The local concentration of ionospheric plasma on the basis of data obtained through various methods on the satellite Intercosmos 19 p2817 A83-41590

On the structure function of density fluctuations of ionospheric inhomogeneities 19 p2866 A83-41805

Complexities of the storm-time characteristics of ionospheric total electron content 20 p3016 A83-42305

Inelastic scattering effects on photoelectron spectra and ionospheric electron temperature 20 p3019 A83-42422

Satellite investigation of the spectral characteristics of irregularities --- of ionospheric electron density 20 p3022 A83-42875

An empirical relationship between electron temperature and electron density in the subauroral electron-density trough 20 p3022 A83-43133

Observations of the total electron content of the ionosphere in Havana during the period of low solar activity 1974-1976 20 p3022 A83-43135

Auroral beam/plasma interaction observed directly 20 p3023 A83-43159

Photometric evidence of electron precipitation induced by first HOP whistlers 20 p3024 A83-43187

A method for the determination of the integrating constant of total electron content 21 p3170 A83-44284

Cosmic rays in the upper atmosphere --- Russian book 21 p3174 A83-45019

Possible mechanism for a synapse variation of electron density in the E and F2 regions of the ionosphere 21 p3174 A83-45234

Spatial and temporal variations of the integral electron content in the upper ionosphere 21 p3175 A83-45238

Mathematical model of the three-dimensional structure of the winter polar ionosphere and its variability 21 p3175 A83-45239

The auroral arc as an electrical discharge between the ionosphere and magnetosphere 21 p3175 A83-45242

Reaction of the ionospheric F2 region to a solitary internal gravity wave 21 p3176 A83-45257

Modeling of the equatorial ionosphere in the hybrid model 21 p3176 A83-45258

Interaction of ionospheric photoelectrons with electromagnetic waves 21 p3176 A83-45259

Modeling of the meridional distribution of the F-region electron concentration over Ashkhabad during the storm of August 1972 21 p3176 A83-45271

Ionospheric investigations using Sirio VHF beacon 21 p3177 A83-45417

Observations of the thermal plasma in the topside ionosphere by RPT mission of ISS-b - Electron density, temperature and mean ion mass --- Retarding Potential Trap 21 p3178 A83-45455

Measurement of total electron content by simultaneous reception of ISS-b telemetry signals 21 p3178 A83-45459

The refraction of radiowaves and the vertical gradients of electron density in the day-side ionosphere of Venus 22 p3384 A83-45644

VHF radar observation of auroral E-region irregularities associated with moving-arcs 22 p3330 A83-46511

Ionization by keV electron precipitation in the auroral zone 22 p3331 A83-46517

Time-sharing measurements of ionospheric electron temperature and electron density with the electric field using double probes - An experiment on the Antarctic sounding rocket S-310JA-7 22 p3331 A83-46518

Polar cleft structure and SEC associated plasma irregularities observed by Greenland rocket experiment, 1976 --- Slant E Condition 22 p3331 A83-46519

Interpretation of ionograms in the vicinity of the dayside auroral oval by ray tracing 22 p3332 A83-46532

Ionospheric irregularities and their potential impact on synthetic aperture radars 22 p3325 A83-46535

Very high latitude F-region irregularities observed by HF-radar backscatter 22 p3334 A83-46889

Comparison of model high-latitude electron densities with Millstone Hill observations 22 p3335 A83-47042

Analysis and numerical simulation of the effect of ion Pedersen mobility on ionospheric barium clouds 22 p3336 A83-47062

Modeling the total electron content observations above Ascension Island 22 p3337 A83-47064

The dependence of the relative backscatter cross section of 1-m density fluctuations in the auroral electrojet on the angle between electron drift and radar wave vector 22 p3337 A83-47066

Telecommunications and the satellite 'Interkosmos-Bulgaria-1300' [IAF PAPER 83-ST-09] 23 p3420 A83-47387

Electron density and energetic particle precipitation observed during the eclipse of 26 February 1979 23 p3480 A83-47466

A model of the lower ionosphere above Red Lake, Canada, during the 26 February 1979 solar eclipse 23 p3480 A83-47467

Differential Doppler measurements of the ionosphere during a solar eclipse 23 p3481 A83-47475

Nonlinear theory of type I irregularities in the equatorial electrojet 23 p3482 A83-47869

Spectrum of phase fluctuations in the case of ionospheric sounding 23 p3485 A83-48478

Annual and semiannual periodicities in NmF2 in the African sector 24 p3605 A83-49303

The accuracy of simple methods for determining the height of the maximum electron concentration of the F2-layer from scaled ionospheric characteristics 24 p3606 A83-49312

Response of the total electron content of the ionosphere over North America to the total solar eclipse of 26 February 1979 [AFGL-TR-83-0013] 24 p3608 A83-50144

IONOSPHERIC F-SCATTER PROPAGATION

Spatial and frequency correlation of a field scattered by small-scale irregularities of the ionospheric F-region 12 p1753 A83-29252

Seasonal and solar-related cyclic variations of equatorial F-scattering 15 p2200 A83-34418

A scattering theory of VHF transequatorial propagation 24 p3570 A83-49313

IONOSPHERIC HEATING

A heating mechanism for the generation of inhomogeneities of the ionospheric F-layer 02 p0208 A83-12420

Heating of the ionospheric plasma by high-power radio waves 04 p0510 A83-15768

The modeling of a large-scale region of disturbances arising during the vertical heating of the ionosphere by a field of high-power radio waves 05 p0662 A83-17605

Foreshortened scattering by artificial irregularities, with allowance for total internal reflection from the ionosphere 05 p0662 A83-17607

Modification of stationary ionospheric current systems under strong ionospheric disturbances 05 p0662 A83-17609

The role of parametric decay instabilities in generating ionospheric irregularities 06 p0785 A83-18310

Ionospheric modification by high power radio waves 09 p1299 A83-23302

Ionospheric modification experiments in northern Scandinavia 09 p1299 A83-23304

Solitons and ionospheric modification 09 p1300 A83-23305

Thermal modulation of the plasma density in ionospheric heating experiments 09 p1300 A83-23306

The feedback-diffraction theory of ionospheric heating 09 p1300 A83-23307

Observations of fluxes of suprathermal electrons accelerated by HF excited instabilities 09 p1300 A83-23309

ELF and VLF wave generation by modulated HF heating of the current carrying lower ionosphere 09 p1300 A83-23312

Studies of the self-focusing instability at Arecibo --- in ionosphere 09 p1303 A83-23765

Ionospheric electric field pulsations - A comparison between VLF results from an ionospheric heating experiment and STARE 09 p1304 A83-23770

Heater-generated intermediate-scale irregularities - Spatial distribution and spectral characteristics --- in ionosphere 10 p1449 A83-26047

Heating of thermal ionospheric electrons by suprathermal electrons 12 p1751 A83-28911

Artificial glow and additional ionization in the upper ionosphere in the field of a high-power radio wave 14 p2049 A83-31855

Heating of the polar ionosphere by electric currents at various substorm phases 14 p2049 A83-31865

Observations of plasma heating effects in the ionosphere by a rocket borne electron accelerator 15 p2198 A83-34188

Joule heating and particle precipitation --- in auroral upper atmosphere 16 p2372 A83-35360

Energy deposition in the polar ionosphere as determined by measurements aboard 'Interkosmos-Bulgaria-1300' satellite 16 p2373 A83-35368

New tools for magnetospheric research 17 p2541 A83-38295

Non-linear phenomena in the ionosphere traversed by high power radio wave 17 p2495 A83-38541

Parameters of artificial irregularities according to results of the observation of backscattering during oblique sounding 17 p2547 A83-38989

The thermal self-focusing of a wave beam in an underdense plasma. II, III, IV, V 18 p2745 A83-39617

The Joule heat production rate and the particle energy injection rate as a function of the geomagnetic indices AE and AL 20 p3019 A83-42420

Production of auroral zone E region irregularities by powerful HF heating 20 p3020 A83-42427

Trapping and absorption of plasma waves in thermal small-scale inhomogeneities 21 p3174 A83-45232

Earth magnetic field fluctuations produced by filamentation instabilities of electromagnetic heater waves 23 p3482 A83-47868

Theory of radar detection of solitons during ionospheric heating 24 p3608 A83-49754

IONOSPHERIC ION DENSITY

The possibility of calculating and deterministic method of predicting ionospheric parameters at the heights of the E and F1 regions for particular heliogeophysical conditions 01 p0071 A83-10599

Temperature and solar zenith angle control of D-region positive ion chemistry [AD-A126882] 02 p0204 A83-11970

The properties of ionospheric O+/+ ions as observed in the magnetotail boundary layer and northern plasma lobe 02 p0207 A83-12383

Equatorial plasma bubbles - Vertically elongated wedges from the bottomside F layer 02 p0208 A83-12390

Pioneer Venus observations of plasma and field structure in the near wake of Venus 02 p0264 A83-12394

Mg+/+ morphology from visual airglow experiment observations 02 p0208 A83-12396

The chemistry of metastable species in the Venusian ionosphere 02 p0265 A83-12558

Observations of energetic ions near the Venus ionopause 04 p0558 A83-14968

A device for measuring plasma structural parameters by means of spherical ion traps 04 p0454 A83-15725

A three-dimensional wake model for low earth orbit [AIAA PAPER 83-0309] 05 p0607 A83-16642

Coordinated airborne and satellite measurements of equatorial plasma depletions [AD-A123689] 05 p0661 A83-17400

Role of Rayleigh-Taylor instabilities on prompt striation evolution --- in ionosphere 05 p0661 A83-17401

Investigation of the filling and emptying of plasma tubes with allowance for ion inertia --- in ionosphere 05 p0663 A83-17610

Combined mass spectrometric composition measurements of positive and negative ions in the lower ionosphere. I - Positive ions 05 p0665 A83-17786

Combined mass spectrometric composition measurements of positive and negative ions in the lower ionosphere. II - Negative ions 05 p0665 A83-17787

On the criterion of comparison of MSIS and IRI models by means of optical data 06 p0782 A83-18024

Particle and wave observations of low-altitude ionospheric ion acceleration events 06 p0784 A83-18303

A perpendicular ion beam instability - Solutions to the linear dispersion relation --- for F region ionosphere 06 p0784 A83-18304

Linear theory of the E x B instability with an inhomogeneous electric field --- of ionospheric plasmas 06 p0785 A83-18311

Ion kinetics, minor neutral and excited constituents in the D region with a high level of ionization. I - Formulation of the problem and a general scheme for the processes 06 p0786 A83-18360

The possible role of ionospheric oxygen in the initiation and development of plasma sheet instabilities 07 p0959 A83-20194

Location and source of ionospheric high latitude troughs 07 p0968 A83-21584

Auroral ion velocity distribution function - Generalized polynomial solution of Boltzmann's equation 07 p0968 A83-21586

On shortening the measurement cycle in a probe experiment with SIT --- Spherical Ion Traps for ionospheric ion density measurement 08 p1133 A83-22278

A possible mechanism of ion acceleration in the daytime polar cusps 09 p1308 A83-25046

Measurement of density irregularities of the ionospheric plasma using a probe with external-grid floating potential on the Cosmos-900 satellite 10 p1386 A83-25336

Adaptive system for varying the range of sawtooth control voltage depending on the potential of the satellite body in a four-electrode probe experiment 10 p1386 A83-25337

Theoretical modeling of low-latitude Mg 11 p1618 A83-28324

Ionospheric plasma cloud dynamics via regularized contour dynamics. I - Stability and nonlinear evolution of one-contour models 13 p1874 A83-30125

Invariance in the vertical distribution of O(+)/n sub e in the 130-200 km region 14 p2049 A83-31858

Transformation of the spectrum of energetic protons during the motion through the atmosphere 14 p2054 A83-33033

The D region under the conditions of nighttime PCA - The rate of transformation of positive ion clusters and negative ions 14 p2054 A83-33034

On the kinetic balance in the ca. maximal part of the daily F-region 15 p2201 A83-34447

Solar wind governing the response of Venusian atmosphere and ionosphere 16 p2434 A83-35356

Latitudinal influences on the quiet daytime D-region [AD-A128591] 16 p2375 A83-35391

F-region ion composition modeling 16 p2376 A83-35398

High resolution measurements of nightside ion troughs at Venus - Evidence of electrodynamic perturbations 16 p2435 A83-35403

Ion attitude control circuit operational experience 17 p2478 A83-37466

The ionosphere as a source for magnetospheric ions 17 p2540 A83-38229

Tests of an ion-chemical model of the D- and lower E-region 18 p2712 A83-39072

Recombination dynamics in the F-region 18 p2713 A83-39318

The effect of seasonal asymmetry on the filling of plasma tubes 18 p2714 A83-39334

Ionospheric plasma bubble encounters or F region bottomside traversals? 20 p3018 A83-42416

Modelling of the ion composition of the middle atmosphere 21 p3173 A83-44669

Variation of aeronomical parameters during the period from the equinox to summer 21 p3175 A83-45241

The ion composition and sources of the magnetospheric plasma in the ring current during magnetic storms 21 p3175 A83-45245

Investigation of the midlatitude ionospheric trough using ground-based geophysical methods and synchronous measurements from satellites 21 p3177 A83-45287

Observation of the ion composition by Ionosphere Sounding Satellite 21 p3178 A83-45457

Characteristics of seasonal variations of O(+) ion density troughs in the nighttime topside ionosphere 21 p3178 A83-45458

Photochemistry of N2(+) in the daytime F region 22 p3328 A83-46056

E-region nitric oxide concentrations inferred from the 26 February 1979 eclipse expedition 23 p3480 A83-47469

Positive and negative ion composition measurements in the Dand E-regions during the 26 February 1979 solar eclipse 23 p3480 A83-47470

Steady-state model of the D-region during the February 1979 eclipse 23 p3481 A83-47472

D-region positive and negative ion concentration and mobilities during the February 1979 eclipse 23 p3481 A83-47473

Eclipse-related measurements of middle-atmosphere electrical parameters 23 p3481 A83-47474

Identification of deuterium ions in the ionosphere of Venus 23 p3529 A83-47864

IONOSPHERIC NOISE

NT WHISTLERS

Observations of LHR noise with banded structure by the sounding rocket S29 barium-GEOS 13 p1879 A83-31246

Plasmaspheric hiss observed in the topside ionosphere at midand low-latitudes 13 p1882 A83-31631

Radiation from long conducting tethers moving in the near-earth environment 15 p2235 A83-34407

Fine structure of the energy spectra of ELF hiss in the upper ionosphere and a possible mechanism of hiss generation (the Interkosmos-14 satellite) 21 p3175 A83-45240

IONOSPHERIC PROPAGATION

NT IONOSPHERIC F-SCATTER PROPAGATION

The kinetics of charged particles in the polar ionosphere 01 p0071 A83-10595

Ionospheric ELF radio signal generation due to LF and/or MF radio transmissions. I - Experimental results 02 p0205 A83-12015

Ionospheric ELF radio signal generation due to LF and/or MF radio transmissions. II - Interpretation 02 p0205 A83-12016

A comparison between HF partial reflection profiles from the D-region and simultaneous Langmuir probe electron density measurements 02 p0205 A83-12017

A new approach to mode conversion effects observed in a mid-latitude VLF transmission 02 p0206 A83-12018

Recent results in auroral-zone scintillation studies 02 p0206 A83-12021

Midlatitude oscillations of the geomagnetic field and their connection with the dynamics of processes in the ionosphere 02 p0209 A83-12434

The Venus ionosphere at grazing incidence of solar radiation - Transport of plasma to the night ionosphere 02 p0265 A83-12559

CCIR needs in earth-space radio propagation 02 p0140 A83-12613

Propagation effects on radio range and noise in earth-space telecommunications 02 p0140 A83-12615

VHF parabolic cylinder antenna for incoherent scatter radar research 02 p0168 A83-12636

Echoing mixed-path whistlers near the dawn plasmapause, observed by direction-finding receivers at two Antarctic stations 03 p0362 A83-14750

Horizontally propagating solitary waves in the upper atmosphere 04 p0509 A83-15723

The spectral and polarization characteristics of signal fields of combination frequencies --- in ionosphere 04 p0510 A83-15767

Electromagnetic resonances in the equatorial ionosphere 04 p0510 A83-15823

IMS ground observations on optical aurora and ionospheric absorption made in Northern Europe, with examples of data handling 04 p0512 A83-16291

Beyond the far horizon - USAF's ionosphere-bouncing radar finally set to go 04 p0469 A83-16453

Waves generated in the upper ionosphere by a stationary moving source 05 p0662 A83-17586

Calculation of long-range radio paths by the adiabatic method using a parabolic model of the ionosphere 05 p0663 A83-17611

The most probable trajectories of rays in a plane-stratified scattering medium. I - A linear layer --- in ionosphere 05 p0663 A83-17612

Experimental characteristics of traveling wave-like ionospheric disturbances according to data from the Kaliningrad observatory 05 p0663 A83-17623

The effect of random irregularities on the field strength of radio waves in the region of caustics 05 p0663 A83-17624

Sky-wave radar sea-state sensing - Effects of ionospheric movement and propagation geometry 05 p0645 A83-17709

High resolution topside in situ data of electron densities and VHF/GHz scintillations in the equatorial region [AD-A125353] 06 p0785 A83-18309

Particle simulations of electrostatic emissions near the lower hybrid frequency 06 p0785 A83-18320

Method of remote sensing of horizontal stratification due to an ionospherically reflected powerful radio wave 06 p0786 A83-18321

The INTELSAT propagation measurements programme 06 p0745 A83-18707

Models of the ionospheric D region at noon 06 p0786 A83-18730

Measurement of the wave impedance of low frequency electromagnetic waves in the earth-ionosphere duct 06 p0747 A83-18731

HF propagation - What we know and what we need to know 06 p0747 A83-18733

Results obtained on experimental radio circuits over medium distances 06 p0747 A83-18734

Phase instability of ionospheric propagation and its influence on HF Doppler radar remote sensing 06 p0747 A83-18735

The characteristics of HF propagation paths and their implications in digital communication system design 06 p0747 A83-18736

High frequency sky-wave prediction methods and observational data for high-latitude communication circuits 06 p0747 A83-18737

Schumann resonances at high latitudes 07 p0965 A83-19635

Ionospheric scintillation measurements using the Global Positioning System 07 p0911 A83-19778

Improving ionospheric maps using theoretically derived values of $f(0)F/2$ 07 p0961 A83-20372

A possibility of predicting the Delingier effect on the basis of solar radio emission data --- for ionospheric radio propagation 07 p0963 A83-20865

A study of the radiation from an antenna in a Maxwellian magnetoplasma Application to the in situ sounding of the auroral ionosphere --- French thesis 07 p0964 A83-21093

Nighttime VHF and GHz scintillations in the East-Asian sector of the equatorial anomaly 07 p0967 A83-21558

F-region irregularity drifts deduced from the scintillation measurements by two closely-spaced antennas 08 p1133 A83-22042

Propagation of vertically and horizontally polarized waves excited by distributions of electric and magnetic sources in irregular stratified spheroidal structures of finite conductivity - Generalized field transforms 08 p1161 A83-22281

Scattering and depolarization of electromagnetic waves in irregular stratified spheroidal structures of finite conductivity - Full wave analysis 08 p1161 A83-22282

Ionospheric modification by high power radio waves 09 p1299 A83-23302

The feedback-diffraction theory of ionospheric heating 09 p1300 A83-23307

Observations of fluxes of suprathermal electrons accelerated by HF excited instabilities 09 p1300 A83-23309

Non-linear interaction of decametre radio waves at close frequencies in oblique propagation --- in ionosphere 09 p1300 A83-23313

Coherence time for 430-MHz VLEI 09 p1352 A83-23326

The ionosphere as a limiting factor in HF radio communication 09 p1244 A83-23386

Parameterization of VLF natural modes in a curved waveguide 09 p1244 A83-23404

Fluctuations of radio-wave emergence angles in the case of scattering in the spherically stratified ionosphere 09 p1245 A83-23469

The effect of refraction on the capture of radio waves in the ionospheric waveguide 09 p1245 A83-23470

Energetic electron fluxes and ionospheric absorption during the August event 1972 09 p1301 A83-23672

Splitting and divergence of STARE auroral radar velocities 09 p1304 A83-23771

A new ionospheric scattering mechanism 09 p1307 A83-24692

The method of multiply reflected waves in the problem of the propagation of electromagnetic waves in regular waveguides /Review/ 09 p1250 A83-25076

Approximation of atmospheric radio noise in the Arctic by the Hall model 09 p1251 A83-25166

A morphological study of gigahertz equatorial scintillations in the Asian region 10 p1449 A83-26046

The temporal structure of intensity scintillations near the magnetic equator [AD-A127533] 10 p1449 A83-26048

Measurement of relative propagation delay between C- and K-band satellite loops 10 p1403 A83-26076

Coefficient perturbation adaptive HF array 11 p1555 A83-27914

Wave propagation in a medium with large-scale random irregularities 11 p1556 A83-27956

Interpretation for the R-T coefficient method applied to the propagation of electromagnetic waves through the earth's ionosphere 11 p1616 A83-28108

SFA observations at the Panska Ves observatory - Peculiar events --- ionospheric Sudden Field Anomaly 11 p1616 A83-28109

Relation of absorption of radio waves to solar X-rays and to Lyman-alpha radiation at the time of low solar and geomagnetic activity 11 p1616 A83-28110

Propagation of ULF electromagnetic waves through the ionosphere and geomagnetic pulsations 11 p1617 A83-28118

Various features of VLF waves generated by lightning discharge 11 p1619 A83-28429

The interplanetary magnetic field and the absorption of radio waves in the auroral zone 11 p1620 A83-28741

The effects of the interplanetary magnetic field in the lower ionosphere at middle latitudes 11 p1620 A83-28742

On the role of solar Lyman alpha radiation in radio-wave absorption in the D-region 12 p1753 A83-29406

VLF ionosonde and long-distance propagation anomalies produced by galactic Cen X-4 X-ray burst in May 1979 12 p1753 A83-29430

Reflection of electromagnetic waves from random irregularities in the ionosphere 13 p1828 A83-30285

Correcting low-frequency solar radio source positions for ionospheric refraction 13 p1964 A83-30371

Investigation of the high-latitude ionosphere and magnetosphere of the earth --- Russian book 13 p1874 A83-30601

Spectra of irregularities of the high-latitude lower ionosphere according to phase VLF measurements 13 p1875 A83-30608

Radio aurora magnetic and streaming aspect sensitivities on 6 simultaneous links at 50 MHz 13 p1876 A83-30775

Off-perpendicular propagation of irregularities in middle latitude E(s) layers 13 p1879 A83-31238

An analysis of several ionospheric parameters associated with the South Atlantic Geomagnetic Anomaly by means of VLF waves 13 p1880 A83-31471

Observation of Fresnel-type fading at Delhi, a low midlatitude station, over half a solar cycle 13 p1881 A83-31545

Propagation of VLF atmospherics on 27 kHz 13 p1882 A83-31548

Estimation of effective recombination coefficient and its variation with height for D-region 13 p1882 A83-31549

The influence of ionospheric refraction on radio astronomy interferometry 13 p1941 A83-31571

The solar X-rays and the sudden phase anomalies (SPA) 13 p1883 A83-31721

Dynamic parameters of a magnetized flux of low-energy electrons in the ionosphere 14 p2049 A83-31862

Propagation of a packet of Alfvén waves along the plasmapause 14 p2050 A83-31870

Ionospheric demodulation of signals of radio-broadcasting stations and magnetospheric ELF noise 14 p1999 A83-31880

Method for determining the electrical properties of the underlying surface on inhomogeneous paths from measurements of the fields of VLF radio stations 14 p2050 A83-31882

Overview of power-line radiation and its coupling to the ionosphere and magnetosphere 14 p2001 A83-32893

The possibility of measuring the directional part of the spectra of superthermal electrons by means of the incoherent scattering of radio waves 14 p2054 A83-33030

Plasmaspheric ELF hiss observed by ISIS satellites 14 p2055 A83-33145

Quantitative study of substorm-associated VLF phase anomalies and precipitating energetic electrons 14 p2055 A83-33146

A measuring complex for investigating the fluctuations of short-wave radio signals --- Russian book 14 p2002 A83-33300

The apparent spectral broadening of VLF transmitter signals during transionospheric propagation 15 p2195 A83-33935

Fluctuations of a millimeter-wave beam on a path with back reflection 15 p2145 A83-34702

Experimental study of a multiplicative model of multiple ionospheric reflections 15 p2145 A83-34896

Synopsis of D- and E-region electron densities during the energy budget campaign 16 p2373 A83-35364

Comparison of A1-absorption data with theoretically computed values based on the International Reference Ionosphere (IRI) 16 p2375 A83-35390

Characteristics of low-latitude whistlers and their relation with f0F2 and magnetic activity 16 p2375 A83-35393

Calculation of ionospheric conductivity profiles by inverting VLF/LF reflection data. I - Isotropic propagation 16 p2341 A83-35419

Simple M-factor algorithm for improved estimation of the basic maximum usable frequency of radio waves reflected from the ionospheric F-region 16 p2342 A83-36576

Narrow band characteristics of low latitude VLF hiss 16 p2344 A83-36730

Equatorial radio scintillations of ATS-6 beacons-phase. I Huanacayo 1974-75 16 p2344 A83-36735

Hook whistlers observed at low latitude ground station Varanasi 16 p2382 A83-36780

The response of the nighttime F-region to wave disturbances 17 p2539 A83-37650

Autumn and winter anomalies in ionospheric absorption as measured by riometers 17 p2543 A83-38369

Refractive index surfaces --- for describing EM wave propagation in ionosphere and magnetosphere 17 p2543 A83-38371

Traveling ionospheric disturbances detected by UHF angle-of-arrival measurements 17 p2544 A83-38374

Solar cycle effects on radio scintillations at Huanacayo 17 p2545 A83-38536

A comparative study of some aspects of low and middle latitude ionospheric absorption 17 p2545 A83-38540

Non-linear phenomena in the ionosphere traversed by high power radio wave 17 p2495 A83-38541

Equatorial radio scintillations of ATS-6 radio beacons. Phase II - Ootacamund 1975-76 17 p2545 A83-38542

Parameters of artificial irregularities according to results of the observation of backscattering during oblique sounding 17 p2547 A83-38999

Latitude dependence of geomagnetic storm after-effects in ionospheric absorption 18 p2712 A83-39064
Pulsing hiss and associated phenomena - A morphological study 18 p2712 A83-39066
Tests of an ion-chemical model of the D- and lower E-region 18 p2712 A83-39072
The initial stage of the interaction of high-power radio waves with the plasma of the upper ionosphere 18 p2713 A83-39320
Finding a correlation between the mean level of signals of distant short-wave stations and geoheliophysical conditions 18 p2715 A83-39342
Application of the Monte Carlo method to solving statistical problems of radio-wave propagation in the randomly inhomogeneous ionosphere 18 p2674 A83-39434
Statistical generalization of the formula of ideal radio transmission to the case of long-range short-wave communications 18 p2674 A83-39530
Analytic solution for the two-frequency mutual coherence function for spherical wave propagation 18 p2742 A83-40652
Ionospheric scintillations 18 p2720 A83-40658
First bistatic oblique-incidence ionograms between digital ionosondes 18 p2720 A83-40659
Numerical modelling of the ionospheric filtration of an ULF micropulsation signal 19 p2866 A83-41318
An investigation of the winter anomaly in Czechoslovakia (Survey) --- radio wave absorption in lower ionosphere 19 p2866 A83-41589
Bragg resonator in the ionospheric plasma with an artificial quasi-periodic lattice 19 p2866 A83-41792
Investigation of the propagation of pulsed signals in a modeling multimode waveguide 19 p2836 A83-41800
Polarization fluctuations of VHF transionospheric signal near the crest of the equatorial anomaly 20 p3017 A83-42313
A waveguide for low-frequency electromagnetic waves in the upper ionosphere 20 p3017 A83-42331
A model for the variations of the critical frequency of F2 layer during the negative phases of ionospheric storms 20 p3024 A83-43173
An estimate of the duct life time from low latitude ground observations of whistlers at Varanasi 20 p3028 A83-43591
Refractive effects on very high frequency radio waves through a three-dimensional inhomogeneous ionosphere 21 p3170 A83-44283
Propagation effect on interferometer 21 p3222 A83-44292
The correlations between the typhoon and the f(0)F(2) of ionosphere 21 p3172 A83-44518
Reflection of radio waves from an artificial ionized region 21 p3174 A83-45231
The limits of the applicability of the quasi-homogeneous solution of the wave equation for the thin sporadic E layer 21 p3176 A83-45256
Interaction of ionospheric photoelectrons with electromagnetic waves 21 p3176 A83-45259
Ionospheric absorption of radio waves on reflection by the E layer and by the shielding Es layer 21 p3177 A83-45275
Long-distance HF propagation modes deduced from the simultaneous observation by chirp sounder and ISS-b 21 p3122 A83-45449
Short-term prediction of HF propagation 21 p3122 A83-45450
The effects of the ionosphere on the extent of the radio horizon at high frequency band 21 p3178 A83-45453
Theory of low frequency wave propagation 22 p3273 A83-45889
Standing wave patterns in VLF hiss 22 p3326 A83-46044
In situ measurements of transionospheric VLF wave injection 22 p3326 A83-46045
Observations and modeling of multi-frequency VHF and GHz scintillations in the equatorial region 22 p3327 A83-46046
Parametric excitation and suppression of convective plasma instabilities in the high-latitude F region ionosphere 22 p3328 A83-46060
Full wave calculation for a Gaussian VLF wave injection into the ionosphere 22 p3330 A83-46505
Spatial intensity distribution of whistlers 22 p3330 A83-46506
Cross modulation of VLF and LF waves by gravity waves --- in nocturnal D region 22 p3332 A83-46533
Modeling of spaced-receiver scintillation measurements --- of drift velocity in ionosphere 22 p3275 A83-46534
Telecommunications and the satellite 'Intercosmos-Bulgaria-1300' [IAF PAPER 83-ST-09] 23 p3420 A83-47387

Heater enhanced topside plasma line --- ionospheric modification experiment 23 p3482 A83-47867
Nonlinear theory of type I irregularities in the equatorial electrojet 23 p3482 A83-47869
Spectrum of phase fluctuations in the case of ionospheric sounding 23 p3485 A83-48478
A new wideband HF technique for MHz-bandwidth spread-spectrum radio communications 24 p3570 A83-48994
The method of canonical transformations in classical electrodynamics 24 p3623 A83-49065
Experimental results on satellite scintillations due to field-aligned irregularities at mid-latitudes 24 p3605 A83-49304
A possible cause of the winter disturbance of the ionospheric D-region 24 p3608 A83-49540

IONOSPHERIC REFLECTION

U IONOSPHERIC PROPAGATION

IONOSPHERIC SOUNDING

Statistics of the polarization structure of oblique-sounding signals in the aperture of a linear antenna array 02 p0162 A83-11542
Vertical displacements of stratification in the E-layer during sunrise 02 p0205 A83-11996
Sunrise effect on atmospheric and its relation to the direction of the night noise source 02 p0205 A83-11998
Stimulated plasma instability and nonlinear phenomena in the ionosphere 02 p0211 A83-12638
Rocket-borne investigations of the optical emissions of the equatorial ionosphere during periods of moderate and high geomagnetic activity 03 p0356 A83-13220
Radar observations of an intense plasma beam in the ionosphere /the Aelita-1 experiment/ 03 p0361 A83-14685
A device for measuring plasma structural parameters by means of spherical ion traps 04 p0454 A83-15725
Satellite auroral/ionospheric UV imager [AIAA PAPER 83-0104] 05 p0608 A83-16522
Manifestation of the effect of large-scale ionospheric irregularities in the case of back-oblique sounding 05 p0662 A83-17606
The use of spectral analysis in studying the sporadic-E layer 05 p0666 A83-17949
Particle and wave observations of low-altitude ionospheric ion acceleration events 06 p0784 A83-18303
A method of estimating the electron density profile of the D layer from a knowledge of the VLF reflection coefficients 07 p0962 A83-20374
A spatial filter which suppresses single-ray noise --- for ionospheric sounding 07 p0915 A83-20869
A study of the radiation from an antenna in a Maxwellian magnetoplasma Application to the in situ sounding of the auroral ionosphere --- French thesis 07 p0964 A83-21093
A sounding rocket observation of an apparent wake generated parallel electric field 07 p0967 A83-21521
Ionospheric modification; General Assembly of the International Union of Radio Science, 20th, Washington, DC, August 10-19, 1981, Papers 09 p1299 A83-23301
Investigations in the U.S.S.R. of non-linear phenomena in the ionosphere 09 p1299 A83-23303
Theory of generation of ULF pulsations by ionospheric modification experiments 09 p1300 A83-23308
First results with Eiscat --- for ionospheric plasma diagnostics 09 p1301 A83-23388
Observations of HF-enhanced plasma line with a 46.8-MHz radar and reinterpretation of previous observations with the 430-MHz radar 09 p1303 A83-23764
Field-aligned plasma flow in the quiet, mid-latitude ionosphere deduced from topside soundings 09 p1306 A83-24687
Aircraft laboratory for optical observations in experiments involving active effects upon the earth's ionosphere and magnetosphere 10 p1447 A83-25334
Equipment for measuring ionospheric parameters by means of a cylindrical Langmuir probe and a planar retarding-potential analyzer on the Cosmos-900 satellite 10 p1386 A83-25335
Interference methods for the radio sounding of the ionosphere --- Russian book 10 p1419 A83-25574
On the far-zone distribution of a scattered field - A numerical experiment 11 p1556 A83-27946
Propagation of ULF electromagnetic waves through the ionosphere and geomagnetic pulsations 11 p1617 A83-28118
Measurements of the stability of energetic electron beams in the ionosphere 11 p1617 A83-28312

Incoherent scatter observations of mid-latitude sporadic-E and comments on its data analysis 12 p1753 A83-29426
An onboard navigator for the extremely low-altitude satellite utilizing accelerometers 13 p1812 A83-30167
Observation of a radio-aurora storm by a chain of stations 13 p1875 A83-30604
Features of radio-aurora observations at the high-latitude station Mirnyi 13 p1875 A83-30605
N-S radio-aurora forms 13 p1875 A83-30606
Dynamics of a charged-particle beam --- injected into ionosphere along geomagnetic field lines 13 p1875 A83-30612
Estimation of the correlation function of incoherent-scatter signals in multiposition radar systems 13 p1829 A83-30726
The resonance cone technique for exciting electron acoustic waves in equatorial ionosphere 13 p1814 A83-30765
A retarding potential analyzer for rocket experiments 13 p1814 A83-30766
Measurement of electric fields in the ionosphere by incoherent scatter radar techniques 13 p1876 A83-30772
Bars - A dual bistatic auroral radar system for the study of electric fields in the Canadian sector of the auroral zone 13 p1815 A83-30774
Sounder-accelerated particles observed on ISIS 13 p1966 A83-31235
F region ion temperature enhancements resulting from Joule heating 13 p1879 A83-31243
The HILAT program --- modified TRANSIT navigation satellite for ionospheric sounding 13 p1879 A83-31296
The effects of neutral air winds on the electron content of the mid-latitude ionosphere and protonosphere in summer 13 p1882 A83-31629
Eiscat first plasma line experiment 13 p1883 A83-31715
Variations of electron density in the D-region 14 p2050 A83-31875
Variations of the height of the sporadic E layer in a cycle of solar activity 14 p2050 A83-31878
The main ionospheric trough according to data from meridional ionosonde networks 14 p2054 A83-33026
The electron concentration in the auroral and subauroral zones according to rocket measurements 14 p2054 A83-33035
Subsatellite studies of wave, plasma, and chemical injections from Spacelab 15 p2126 A83-33733
Electric field observations of time constants related to charging and charge neutralization processes in the ionosphere 15 p2198 A83-34211
The Norwegian program using particle accelerators in space 15 p2124 A83-34214
Some characteristics of the F2 layer at low and middle latitudes 15 p2200 A83-34419
Single-channel energospectrometer of low-energy electron and proton fluxes 15 p2128 A83-34448
Generator of steplike voltage sweep --- carried by geophysical rocket to study auroral ionosphere 15 p2152 A83-34449
Coordinated rocket campaign on Heiss Island --- for upper atmosphere sounding during auroral disturbances 16 p2372 A83-35362
D-region IRI profiles in relation to radio observations 16 p2375 A83-35389
Advanced techniques for plasma composition and dynamics measurements 16 p2317 A83-35400
A differential-Doppler study of traveling ionospheric disturbances from Millstone Hill 16 p2376 A83-35418
Automatic calculation of electron density profiles from digital ionograms. III - Processing of bottomside ionograms 16 p2376 A83-35421
Conjugate observations of Pc 5 electric fields with a geostationary satellite and a ground radar facility 17 p2538 A83-37596
Parameters of artificial irregularities according to results of the observation of backscattering during oblique sounding 17 p2547 A83-38989
EISCAT - The European incoherent scatter radar for studying the polar atmosphere 18 p2716 A83-39775
A method for the determination of the integrating constant of total electron content 21 p3170 A83-44284
Nighttime emission of the earth's ionosphere according to Salyut-6 observations 21 p3174 A83-45230
Transionospheric sounding at the boundary of the radio transparency of the ionosphere 21 p3174 A83-45236
Model ionograms of oblique sounding on the Nikolaev-Havana path 21 p3174 A83-45237

- Ionospheric investigations using Sirio VHF beacon
21 p3177 A83-45417
- Operation and experimental results of Ionosphere Sounding Satellite-b (ISS-b, UME-2). I - Outline of ISS-b project
21 p3096 A83-45434
- Topside sounder onboard ISS-b --- Ionosphere Sounding Satellite
21 p3104 A83-45435
- Characteristics of the radio noise receiving equipment --- onboard Ionosphere Sounding Satellite
21 p3104 A83-45436
- The ISS-b retarding potential analyzer --- Ionospheric Sounding Satellite
21 p3104 A83-45437
- Ion mass spectrometer on Ionosphere Sounding Satellite (ISS-b)
21 p3104 A83-45438
- Scheduling of ISS-b operations --- ground station computer algorithm and onboard data recording
Ionosphere Sounding Satellite 21 p3098 A83-45440
- Global distribution of the ionospheric F-layer critical frequency f0F2
21 p3177 A83-45446
- Estimation of f0F2 from interferences appearing on AGC data of ISS-b topside sounder
21 p3178 A83-45447
- Global distribution of topside spread F
21 p3178 A83-45448
- The global distribution of thunderstorm activity observed by the Ionosphere Sounding Satellite (ISS-b)
21 p3182 A83-45451
- Observations of the thermal plasma in the topside ionosphere by RPT mission of ISS-b - Electron density, temperature and mean ion mass --- Retarding Potential Trap
21 p3178 A83-45455
- Observational results of the nighttime ion temperatures in the topside ionosphere by ISS-b
21 p3178 A83-45456
- Observation of the ion composition by Ionosphere Sounding Satellite
21 p3178 A83-45457
- Measurement of total electron content by simultaneous reception of ISS-b telemetry signals
21 p3178 A83-45459
- HF Doppler measurement in the auroral ionosphere
22 p3332 A83-46524
- Interpretation of ionograms in the vicinity of the dayside auroral oval by ray tracing
22 p3332 A83-46532
- The fossil theory of nighttime high latitude F region troughs
22 p3335 A83-47041
- Satellite observations of energetic electron precipitation during the 1979 solar eclipse and comparisons with rocket measurements
23 p3480 A83-47468
- The storm-time variation of atmospheric disturbance from the data of a global network of vertical-incidence ionospheric sounding stations
23 p3484 A83-48391
- Spectrum of phase fluctuations in the case of ionospheric sounding
23 p3485 A83-48478
- IONOSPHERIC STORMS**
- NT Sudden Ionospheric Disturbances
Dynamics of the disturbed ionosphere
11 p1614 A83-27401
- An investigation of the state of the high-latitude ionosphere during substorms
14 p2054 A83-33027
- A comparative study of VHF scintillation and spread F events over Natal and Fortaleza in Brazil
20 p3018 A83-42417
- A model for the variations of the critical frequency of F2 layer during the negative phases of ionospheric storms
20 p3024 A83-43173
- The relation between the onset times of the negative phase of ionospheric storms and the main phase of magnetic storms and a theoretical model
21 p3172 A83-44524
- The distorting effect of ionospheric polar electrojets on the Dst variation
21 p3175 A83-45244
- IONOSPHERIC TEMPERATURE**
- F-region neutral winds and temperatures at equatorial latitudes - Measured and predicted behaviour during geomagnetically quiet conditions
07 p0968 A83-21580
- An instrument for the direct measurement of electron temperature in the ionosphere
10 p1387 A83-25341
- NO and temperature control of the D region
11 p1615 A83-27408
- The thermal self-focusing of a wave beam in an underdense plasma. I - The wave spectrum
13 p1927 A83-31649
- New descriptive temperature model --- for electrons and ions in ionosphere
16 p2375 A83-35396
- Meaning of the vertical profile of ion temperature over the Antarctic
22 p3331 A83-46522
- IONOSPHERIC TILTS**
- The main ionospheric trough according to data from meridional ionosonde networks
14 p2054 A83-33026
- IONOSPHERICS**
- NT DAWN CHORUS
NT HISS
Particle simulations of electrostatic emissions near the lower hybrid frequency
06 p0785 A83-18320
- Electrostatic flow field of satellites moving in ionosphere
08 p1050 A83-21881
- Field and wave measurements aboard the Aureol-3 spacecraft
13 p1813 A83-30758
- The apparent spectral broadening of VLF transmitter signals during transionospheric propagation
15 p2195 A83-33935
- Interaction of ionospheric photoelectrons with electromagnetic waves
21 p3176 A83-45259
- Whistlers --- in earth ionosphere and magnetosphere
22 p3325 A83-45886
- Spectral characteristics of radio noise at low and medium frequencies in the Antarctic topside ionosphere
22 p3330 A83-46507
- IONS**
- NT ANTIPROTONS
NT CATIONS
NT DEUTERONS
NT HEAVY IONS
NT HELIUM IONS
NT HYDROGEN IONS
NT HYDRONIUM IONS
NT LIGHT IONS
NT METAL IONS
NT MOLECULAR IONS
NT NEGATIVE IONS
NT NITROGEN IONS
NT OXYGEN IONS
NT POSITIVE IONS
NT PROTONS
NT RECOIL IONS
NT SOLAR PROTONS
- Properties of ions from spectroscopic data
01 p0105 A83-10202
- Transitions in highly ionized silicon --- of extreme ultraviolet solar spectrum
02 p0270 A83-12582
- Observations of upstream ions and low-frequency waves on ISEE 3
06 p0782 A83-18284
- Role of ions in heteromolecular nucleation - Free energy change of hydrated ion clusters
09 p1308 A83-25180
- IP (IMPACT PREDICTION)**
- U COMPUTERIZED SIMULATION
- IRAS**
- U INFRARED ASTRONOMY SATELLITE
- IRAS-ARAKI-ALCOCK COMET**
- Radio observations of Comet 1983 d
23 p3515 A83-47430
- IRASERS**
- U INFRARED LASERS
- IRIDIUM**
- Relationship between an iridium anomaly and the North American microtektite layer in core RC9-58 from the Caribbean Sea
04 p0563 A83-15370
- Thorium segregation to grain boundaries in Ir + 0.3% W alloys containing 5-1000 ppm thorium
04 p0462 A83-16273
- Mechanisms and criteria for cleavage
08 p1058 A83-21666
- The Cretaceous-Tertiary transition
10 p1448 A83-25650
- Welding iridium heat source capsules for space missions
20 p2998 A83-42300
- The origin of the iridium anomaly at the Cretaceous-Tertiary boundary
24 p3671 A83-48954
- IRIS SATELLITES**
- The IRIS system - An Italian STS-upper stage
04 p0452 A83-15670
- IRIS - A new Italian upper stage system
[IAF PAPER 83-25] 23 p3419 A83-47237
- IRISES (MECHANICAL APERTURES)**
- One form of apodization of telescopes
07 p1009 A83-21275
- Mode control in a submillimetre open resonator with a variable iris
10 p1425 A83-25459
- Calculate waveguide aperture susceptibility
11 p1562 A83-28152
- IRON**
- NT IRON ISOTOPES
NT IRON 57
- Epitaxial growth of Fe on GaAs by metalorganic chemical vapor deposition in ultrahigh vacuum
02 p0243 A83-12291
- Iron metal production in silicate melts through the direct reduction of Fe/II/ by Ti/III/, Cr/II/, and Eu/II/ --- in lunar basalts
02 p0267 A83-12846
- Measurement of relative oscillator strengths for Fe I: Transitions from levels /b-3/-F/2-4/ /2.61 eV-2.56 eV/ - Use of a multipass optical system
03 p0413 A83-13318
- GX 1 + 4: pulse period measurement and detection of phase-variable iron line emission
03 p0402 A83-13330
- Mapping of iron and chromium on the surface of the Ap star Epsilon Ursae Majoris
03 p0418 A83-13880
- Studies on the spectra of K-giants. I - Physical parameters and Fe and Ti abundances for 26 K-giants
03 p0419 A83-13927
- Investigation of the abundance of iron in the nondisturbed solar photosphere. I - Method for calculating theoretical profiles of Fe I. II - Determination of the abundance of Fe I
03 p0436 A83-14686
- Proposed Mg V, Fe XIV and forbidden Fe XVII line identifications in the EUV solar spectrum
03 p0438 A83-14907
- Studies on the spectra of K-giants. II - Abundance determinations for K-giants from very strong iron lines
06 p0827 A83-18170
- The analysis of Fe XIV 5303 coronal emission-line polarization measurements
06 p0854 A83-18535
- Gas-phase high-temperature photoelectron spectroscopy - An investigation of the transition metals iron, cobalt and nickel
06 p0808 A83-19005
- The structural-chemical role of iron in the reaction processes of the soldering of titanium with iron-containing alkali-free aluminoborosilicate glasses
07 p0873 A83-20685
- On the errors of the Kurucz-Peytremann Fe I oscillator strengths
07 p1024 A83-21226
- The asymmetry of photospheric absorption lines. II - The asymmetry of medium-strong Fe I lines in quiet and active regions of the sun
07 p1038 A83-21243
- Measurement of the cross sections for excitation of a singly charged iron ion by electron impact --- stellar spectra
07 p1027 A83-21278
- Energy factors of build-up of X irradiation --- behind iron layer
08 p1114 A83-22628
- Detection of 10 to the 14th-eV iron nuclei in cosmic rays
08 p1192 A83-23252
- Radiative lifetimes in Fe II using selective laser excitation
09 p1341 A83-23651
- Condensation kinetics of iron and silicon in the vapor phase
10 p1490 A83-26192
- Arc measurements of FeII transition probabilities
12 p1789 A83-28863
- Atomic calculations for the Fe XX X-ray lines
12 p1799 A83-28872
- Laser oscillation at 3.53 microns from Fe(2+) in n-InP:Fe
13 p1850 A83-30327
- The oscillator strengths of ionized iron lines --- in solar absorption spectra
14 p2113 A83-31831
- Accuracy of abundance determinations by weighting functions method of curves of growth --- of stars
15 p2263 A83-34556
- Proton excitation of fine-structure transitions in Fe XIV
16 p2410 A83-35652
- Solar flare soft X-ray spectra from the Hinotori. I - Iron line spectra and their time variations of seven X-class flares.
16 p2439 A83-35678
- Observations of the iron emission lines in the X-ray spectrum of the supernova remnant Cassiopeia A
16 p2431 A83-36673
- Tribological characteristics of nitrogen (N+) implanted iron
17 p2487 A83-37824
- Equilibrium temperatures of interstellar iron grains
18 p2776 A83-39767
- Observationally determined Fe II oscillator strengths --- interstellar and quasar absorption spectra
20 p3069 A83-42466
- Interaction mean-free-path of cosmic-ray Fe in air
20 p3083 A83-43667
- Correlation and the 3s2 3p5 2P0 to 3s 3p6 2S, 3s2 3p5 2P0 to 3s2 3p4 3d2S transitions in Fe X
21 p3202 A83-44749
- Resonance and intermediate-coupling effects in electron scattering with highly charged ions. I - Collision strengths for Fe(24+), Se(32+), and Mo(40+). II - Autoionization and dielectronic recombination
24 p3631 A83-48829
- Friction and wear of iron and nickel in sodium hydroxide solutions
24 p3559 A83-48922
- IRON ALLOYS**
- NT AUSTENITIC STAINLESS STEELS
NT CARBON STEELS
NT CHROMIUM STEELS
NT FERRITIC STAINLESS STEELS
NT HIGH STRENGTH STEELS
NT LOW CARBON STEELS
NT MARAGING STEELS
NT MARTENSITIC STAINLESS STEELS
NT NICKEL STEELS
NT STAINLESS STEELS
NT STEELS
- Sulfidation properties of Fe-Cr alloys at 1073 K in H2S-H2 atmospheres of sulfur pressures 0.01 and 0.0001 Pa
01 p0024 A83-10244
- Protection of Fe-Cr-Al alloys in sulfidizing environments by means of an alpha-Al2O3 scale
01 p0024 A83-10245
- Radial distribution studies in a diamond anvil pressure cell
01 p0028 A83-10643

- Effect of nickel plating on Fe-BCu-Mo and -W
02 p0155 A83-12074
- Volume changes accompanying the sintering of compacts from mixtures of titanium and iron powders
02 p0158 A83-12945
- Formation mechanisms of keying or pegging yttrium oxide and increased plasticity of alumina scale on FeCrAlY
03 p0296 A83-13121
- Surface structure of boride layers grown on Fe-C-Ni alloys
03 p0298 A83-13678
- Mechanical properties of ductile Fe-Ni-Zr and Fe-Ni-Zr/Nb or Ta/ amorphous alloys containing fine crystalline particles
05 p0615 A83-17559
- An investigation of heat-affected zone hot cracking in alloy 800
06 p0728 A83-18399
- Processing effects on microstructure and elevated temperature properties of an ODS Fe-Al-Mo P/M alloy
06 p0732 A83-19099
- On the controlling parameters for fatigue-crack threshold at low homologous temperatures
07 p0887 A83-20636
- Investigation of preferred orientation and microstructure in oxide-dispersion-strengthened alloys
08 p1065 A83-22016
- Oxidation characteristics of Fe-Cr-Al-Y and Fe-Cr-Al-Y₂O₃ alloys
08 p1066 A83-22099
- Study of the constitutive creep laws using biaxial relaxation tests
10 p1393 A83-25416
- Grain boundary sliding and stress concentration during creep
10 p1396 A83-25860
- The structure of electrodeposited alloys based on the metals of the iron subgroup
13 p1819 A83-30064
- Limiting ion implantation doses for metals
13 p1821 A83-30737
- Effect of tungsten on the properties of austenitic precipitation-hardening Fe-Cr-Ni alloys
13 p1823 A83-31213
- An experimental investigation of the internal methane pressure in hydrogen attack
14 p1994 A83-32682
- The effect of microstructure on the mechanical properties of an iron-based superalloy after prolonged exposure to 750 C heat
15 p2137 A83-34001
- Effect of vacuum-treatment on mechanical properties of W-Ni-Fe heavy alloy
15 p2140 A83-35067
- Supercooling and structure of levitation melted Fe-Ni alloys
16 p2329 A83-35690
- Dimensional stability of Superalloy
16 p2334 A83-36751
- Reactions between metal and oxide powders in dispersion strengthened alloy
18 p2665 A83-39175
- On the nature of the temperature hysteresis of martensitic transformations in alloys
18 p2666 A83-39518
- An investigation of residual stress of oxide scale affected by the addition rare earth elements in Fe-Cr-Al alloys at 1200 C and 1350 C
20 p2952 A83-42237
- Characterization of metals and alloys by electrical resistivity measurements
21 p3111 A83-43830
- Shape of growing crystals of primary phases in eutectic alloys of the systems Fe-Fe₂B and Ni-Ni₃B
21 p3112 A83-44476
- Effect of iron content on the structure and properties of the AK7 alloy
21 p3112 A83-44477
- Absorption of carbon from residual gases during Ti implantation of alloys
21 p3115 A83-45490
- The aging response of a welded iron-based superalloy
22 p3268 A83-45727
- The effect of nickel on sintering processes in the system Ti-Fe. II - Dilatometric and thermographic studies of the sintering process
23 p3433 A83-48524
- Analysis of nickel- and iron-base heat resisting alloys by spark source mass spectrometry
24 p3554 A83-49326
- Selective surface oxidation of Fe-30 Ni alloy
24 p3562 A83-49488
- High temperature oxidation of Fe-20Cr-4Al alloys with small additions of Sc, Y or Er
24 p3563 A83-49493
- Mechanism of peg growth and influence on scale adhesion
24 p3563 A83-49495
- Electrochemical studies of corrosion of iron, nickel and nickel alloys in alkali sulfate melt
24 p3563 A83-49496
- Hot corrosion of iron- and nickel-base superalloys caused by deposit of calcium sulfate
24 p3563 A83-49498

IRON COMPOUNDS

NT CHROMITES
NT FAYALITE
NT FERRATES
NT FERRITES
NT ILMENITE
NT IRON OXIDES
NT MAGNETITE
NT PYRITES
NT TROLITE

- Iron diiodide photodissociation laser
02 p0184 A83-12265
- Discontinuous precipitation reactions in alpha and gamma phases of meteoritic metal
03 p0133 A83-13724
- The composition and structure of plessite in the Tsarev chondrite
05 p0705 A83-17455
- Investigation of the Tsarev and Northern Kolchik chondrites by Moessbauer spectroscopy
05 p0706 A83-17467
- High magnetic coercivity of meteorites containing the ordered FeNi/tetrateenite/ as the major ferromagnetic constituent
07 p1034 A83-21312
- Viscous flow behavior of four iron-containing silicates with alumina, effects of composition and oxidation condition
07 p0965 A83-21322
- Experimental calibration of the sphalerite cosmobarometer
08 p1190 A83-22998
- Standard free energy of formation of iron iodide
11 p1546 A83-28299
- Low frequency dielectric relaxation in boracites
12 p1709 A83-29555
- The first finding of suessite on the earth
24 p3673 A83-49555

IRON ISOTOPES

- NT IRON 57
Measurement of the relative composition of the cosmic-ray iron group with lexan polycarbonate
24 p3676 A83-50163

IRON METEORITES

- Systematic compositional variations in the Cape York iron meteorite
02 p0267 A83-12848
- Geology and terrestrial age of the Derrick Peak meteorite occurrence, Antarctica
03 p0434 A83-14318
- The Derrick Peak, Antarctica, iron meteorites
03 p0434 A83-14319
- Two new iron meteorites from western Australia
03 p0434 A83-14320
- Investigations of cosmic-ray-produced nuclides in iron meteorites. IV Identification of noble gas abundance anomalies
04 p0559 A83-15304
- The Tucson iron and its relationship to enstatite meteorites
04 p0563 A83-15361
- The effects of C, P, and S on trace element partitioning during solidification in Fe-Ni alloys --- iron meteorites
04 p0564 A83-15372
- The composition and structure of plessite phases in the Chinga ataxite
05 p0706 A83-17463
- Signs of shock metamorphism in the Kaali meteorite
05 p0706 A83-17464
- The composition of mineral inclusions in the olivines of pallasites
05 p0706 A83-17465
- Preatmospheric sizes of the Yamysheva pallasite
05 p0706 A83-17466
- The role of S in the evolution of the parental cores of the iron meteorites
07 p1035 A83-21327
- Determination of the cooling rates and nucleation histories of eight group IVA iron meteorites using local bulk Ni and P variation
08 p1189 A83-22929
- The isotopic composition and concentration of Ag in iron meteorites and the origin of exotic silver
08 p1190 A83-22995
- Plessite formation by discontinuous precipitation reaction from gamma-Fe,Ni in Richardton /H5/ ordinary chondrite
08 p1190 A83-23270
- Investigations of cosmic-ray-produced nuclides in iron meteorites. V - More data on the nuclides of potassium and noble gases, on exposure ages and meteoroid sizes
10 p1518 A83-25452
- Extraterrestrials have landed on Antarctica
11 p1686 A83-28386
- Further finds from the Mundrabilla meteorite shower
14 p2112 A83-33070
- Presolar grains in micro-inclusions of iron meteorites
15 p2276 A83-35003
- Meteorite magnetization and paleointensity
15 p2277 A83-35008
- On the fine structure of meteoritic taenite/tetrateenite and its interpretation
15 p2277 A83-35300
- Measurement of Mn-53 in deep-sea iron and stony spherules --- for proof of extraterrestrial origin
16 p2438 A83-36749
- I-Xe and Ar-40-Ar-39 analyses of silicate from the Eagle Station pallasite and the anomalous iron meteorite Enon
18 p2779 A83-39984
- Nitrogen and xenon in acid residues of iron meteorites
18 p2779 A83-39985
- Experimental investigations of trace element fractionation in iron meteorites. II - The influence of sulfur
20 p3078 A83-43150
- Fission track age and cooling rate of the Marjalahti pallasite
24 p3672 A83-49397

IRON OXIDES

NT CHROMITES
NT ILMENITE
NT MAGNETITE

- Spectral characteristics of the iron oxides with application to the Martian bright region mineralogy
04 p0568 A83-15584
- Open-circuit photopotentials at doped α -Fe₂O₃ electrodes in aqueous solution
07 p0881 A83-20589
- Preparation and characterization of iron oxide thin film electrodes
16 p2347 A83-36743
- Compression, nonstoichiometry and bulk viscosity of wuestite
21 p3174 A83-45061
- Iron oxide electrodes for photoelectrolysis of water
23 p3430 A83-48595

IRON 57

- A nuclear gamma resonance study of Ti₃Al containing Fe-57 impurity
02 p0159 A83-13039
- Nuclear gamma resonance of Fe-57 impurity atoms in Ti₃Al
07 p0890 A83-20920
- A Mossbauer study of commercial beryllium
13 p1822 A83-30743

IROQUOIS HELICOPTER

U UH-1 HELICOPTER

IRRADIANCE

- NT ILLUMINANCE
NT SOLAR CONSTANT
Solar variability
01 p0129 A83-11343
- Calibration of solar cells by the reference cell method - The spectral mismatch problem
03 p0353 A83-13580
- Evaluation of methods for estimating solar irradiance in Canada
03 p0370 A83-14633
- Solar irradiance calculations in the UV and visible using the adjoint discrete ordinates method
03 p0360 A83-14637
- Time and space spectra of earth-emitted radiation at large scales
03 p0370 A83-14648
- Active-region evolution and solar rotation variations in solar UV irradiance, total solar irradiance, and soft X rays
05 p0708 A83-17377
- Relationship between the sky radiance reflected at the sea surface and the downwelling irradiance
07 p0971 A83-20829
- Solar irradiance variations. I - Analysis of modeling techniques and intercomparison of ground-based data
09 p1368 A83-23751
- Mesoscale mapping of available hourly solar irradiance by use of data collected by 'Meteosat'
09 p1315 A83-24633
- Sunspot cycle and associated variation of the solar spectra irradiance
10 p1520 A83-25443
- Solar oscillations observed in the total irradiance
11 p1688 A83-27632
- Solar radiometry - Spectral irradiance measurements
11 p1691 A83-27748
- Solar radiometry - Total irradiance measurements
11 p1691 A83-27750
- A probability density function for the clearness index, with applications
12 p1749 A83-28938
- On the use of spectral radiance models to obtain irradiances on surfaces of arbitrary orientation
12 p1752 A83-28945
- A thermal model of sunspot influence on solar luminosity
13 p1965 A83-31437
- Data on total and spectral solar irradiance
13 p1880 A83-31461
- Diffuse and global solar spectral irradiance under cloudless skies
13 p1882 A83-31613
- Solar collector testing in the European community
14 p2047 A83-32846
- Comparison of calculated and measured atmospheric radiation values for remote sensing purposes
15 p2203 A83-35100
- The solar absolute spectral irradiance 1150-3173 A - May 17, 1982
16 p2439 A83-36153
- Some radiation budget and cloud measurements derived from Meteosat 1 data
18 p2731 A83-40646
- Reduction of solar irradiance by the presence of effective sunspots and variability of solar irradiance by the presence of effective photospheric active features
19 p2924 A83-40916
- Solar irradiance modulation by active regions from 1969 through 1981
19 p2924 A83-41110
- Solar variability in the spectral range 2350-2870 A
20 p3081 A83-42860
- Attenuation of solar irradiance in the stratosphere
Spectrometer measurements between 191 and 207 nm
20 p3021 A83-42861
- The solar absolute spectral irradiance at 1216 A and 1800-3173 A - January 12, 1983
20 p3021 A83-42862
- 27-day variations observed in solar U.V. (120-300 nm) irradiance
24 p3674 A83-48756
- Axial irradiance and optimum focusing of laser beams
24 p3588 A83-49015

IRRADIATION

NT AURORAL IRRADIATION
NT ELECTRON IRRADIATION
NT ION IRRADIATION

NT NEUTRON IRRADIATION
NT PROTON IRRADIATION
NT X RAY IRRADIATION

Methods for calculating the optimal and allowable irradiation levels during radiant heating

03 p0379 A83-13613
The comparative performance of selected solar global models
03 p0370 A83-14634
The Apennine Front core 15007/8 - Irradiation and depositional history
04 p0561 A83-15347

Radiation-induced charge dynamics in dielectrics
05 p0618 A83-17502
Response of irradiated optical waveguides at low temperatures
08 p1165 A83-22480

Effect of ionizing radiation on fiber-optic waveguides
08 p1165 A83-22481
Thermodynamic properties of tissue impacted by CO₂ laser
11 p1635 A83-27520

Optical properties of metal surfaces during laser irradiation
11 p1656 A83-27562
Impact sensitivity of gamma-irradiated HMX
13 p1826 A83-31674

A multi-dimensional differential approximation for absorbing/emitting and anisotropically scattering media with collimated irradiation
[ASME PAPER 82-WA/HT-49]

14 p2008 A83-31937
Formation of amino acids from reactor-irradiated ammonium acetate
17 p2563 A83-38892

Asymmetrical radical formation in D- and L-alanines irradiated with tritium-beta-rays
17 p2563 A83-38897
Reflection effect in close binaries. II - Distribution of emergent radiation from the irradiated component along the line of sight
18 p2764 A83-39188

The biosynthesis of cholesterol in the tissues of irradiated rats
18 p2731 A83-39520
The effect of irradiation and reflectance variability on vegetation condition assessment
20 p3011 A83-42965

The effect of irradiation temperature on radiation processes in MOS structures
21 p3217 A83-44544
Recent cosmic ray exposure history of ALHA 81005
22 p3386 A83-46868

IRREGULARITIES

The role of parametric decay instabilities in generating ionospheric irregularities
06 p0785 A83-18310

IRREVERSIBLE PROCESSES

Heat death and oscillation in model universes containing interacting matter and radiation
03 p0422 A83-14179

Application of Gyarmati's variational principle to laminar stagnation flow problem
06 p0760 A83-19400
A measure of the incompleteness of a statistical description and irreversibility Fluctuation-dissipation relation /FDR/ for multiparticle distribution functions
07 p1001 A83-20607

On the problem of evolution criterion for thermodynamical waves
11 p1665 A83-27863
Strain localization and hydrogen embrittlement
12 p1714 A83-29722

A local equilibrium axiom on the flows in relativistic thermodynamics
15 p2239 A83-34410
Tolman's cosmological models
15 p2272 A83-34782

Modelling of the irreversibility of the heat and mass transfer - Similarity of irreversibility
20 p2983 A83-43016
Optimal thermodynamics of thermal exchanges
[ONERA, TP NO. 1983-78]
23 p3512 A83-48193

Stability of a thin local zone of irreversible deformations
24 p3592 A83-49037

IRRIGATION

A Landsat-based inventory procedure for the estimation of irrigated land in arid areas
09 p1287 A83-24567
The feasibility of thermal inertia mapping for detection of perched water tables in semi-arid irrigated lands
09 p1288 A83-24583

Irrigated agricultural mapping and water demand estimation in arid environments from remote sensing
09 p1289 A83-24601
Monitoring the changing areal extent of irrigated lands of the Gafara Plain, Libya
09 p1291 A83-24622

Estimating irrigation water use and withdrawal of ground water on the high plains, U.S.A.
15 p2181 A83-33563
Remote sensing techniques for monitoring and managing irrigated lands
15 p2181 A83-33564

The role of remotely sensed and other spatial data for predictive modeling - The Umatilla, Oregon, example
15 p2186 A83-34832
Landsat image date selection for an irrigated lands inventory over a large geographical area using general crop phenology and irrigation management data
17 p2532 A83-38357

Remote sensing of tank irrigated areas in Tamil Nadu State, India
20 p3010 A83-42961

IRRITATION

NT TOXICITY AND SAFETY HAZARD

IRROTATIONAL FLOW

U POTENTIAL FLOW

IRS (INDIAN SPACECRAFT)

U INDIAN SPACECRAFT

ISCHEMIA

The determination of the normal /desirable/ body weight for males 40-59 years of age according to the findings of an epidemiological study of cardiovascular diseases
01 p0083 A83-10513

The mechanical properties of the brain in the process of the development of postischemic edema
01 p0079 A83-10526

The diagnostic significance of the integral assessment of myocardial ischemia in patients with ischemic heart disease for the computerized monitoring of the EKG during the treadmill test
03 p0379 A83-13624

Test with graded physical load on bicycle-ergometer and treadmill in patients with chronic ischemic heart disease
03 p0381 A83-14346

The tolerance to physical loads among patients with ischemic heart disease as a function of diet and the time when food is taken
05 p0673 A83-17173
Morphological and functional peculiarities of the myocardium during extreme coronary insufficiency
05 p0671 A83-17219

Several indicators of the EKG and metabolic processes during an experimental coronary spasm in rats exposed to conditions of hypoxia in combination with hypercapnia
07 p0975 A83-20986

The prognosis of acute cardiovascular diseases using the biorhythm curves of the patients
07 p0978 A83-20997

The dependence of the development of complications in patients with an infarction of the myocardium and chronic ischemic heart disease on the state of the electromagnetic field of the earth
08 p1146 A83-22777

Gall bladder disease in a 30 year follow up study - Its association with ischemic disease
08 p1147 A83-22959

A histopathological study on hearts in ischaemic heart disease fatalities
09 p1323 A83-24009
Blood lactate threshold in some well-trained ischemic heart disease patients
13 p1902 A83-30452

The results of the bicycle ergometer test in patients with ischemic heart disease during different body positions
15 p2212 A83-34944

New data about the mechanisms of the adaptation to physical loads during ischemic heart disease and ways of using these data during the rehabilitation of patients with myocardial infarction
15 p2213 A83-34957

The role of adrenergic mechanisms in the development of cerebrovascular disorders during acute myocardial ischemia
15 p2210 A83-34960

Basal insulinemia in healthy males and in males with ischemic heart disease of 20-59 years of age (population study)
16 p2400 A83-36836

The application of noninvasive methods for the study of patients with ischemic heart disease
16 p2400 A83-36838

Electromagnetic and magnetic fields in the treatment of ischemic heart disease
18 p2734 A83-40540

The evaluation of the functional condition of the heart in patients with ischemic heart disease at early stages of graded physical loading
18 p2734 A83-40542

The role of collateral coronary blood flow in the compensation of regional disorders of the energy metabolism of heart muscle during experimental myocardial ischemia
18 p2732 A83-40544

The condition of peripheral hemodynamics and the effect on it of several drugs in patients with chronic ischemic heart disease and left ventricular insufficiency
18 p2735 A83-40546

The effect of disorders of lipid metabolism on the rheological properties of blood in patients with ischemic heart disease
18 p2735 A83-40548

The adrenoreactivity of the contractile myocardium and coronary arteries in the case of chronic overload and acute ischemic injuries of the heart
18 p2733 A83-40556

The neural apparatus of the coronary arteries in normal conditions and in patients with ischemic heart disease
18 p2736 A83-40585

Alteration of ischemic cardiac function in normal heart by daily exercise
19 p2875 A83-41134

The condition of hemodynamics in pulmonary blood circulation in patients with hypertension combined with chronic heart disease
19 p2881 A83-41432

The system of the regulation of the aggregation condition of the blood in patients with ischemic heart disease
19 p2882 A83-41453

ISEE

U INTERNATIONAL SUN EARTH EXPLORERS

ISEE A

U INTERNATIONAL SUN EARTH EXPLORER 1

ISEE B

U INTERNATIONAL SUN EARTH EXPLORER 2

ISEE C

U INTERNATIONAL SUN EARTH EXPLORER 3

ISEE 1

U INTERNATIONAL SUN EARTH EXPLORER 1

ISEE 2

U INTERNATIONAL SUN EARTH EXPLORER 2

ISEE 3

U INTERNATIONAL SUN EARTH EXPLORER 3

ISENTROPE

One-dimensional isentropic compression measurements of multiply loaded polymethylmethacrylate
02 p0191 A83-12280

ISENTROPIC PROCESSES

NT NONISENTROPICITY

On the two-dimensional transport of stratospheric trace gases in isentropic coordinates
02 p0214 A83-12240

Two-dimensional subsonic flow of a compressible medium
08 p1083 A83-22047
Homogeneous nucleation of ethanol and n-propanol in a shock tube
08 p1053 A83-23000

A case of quasi-isentropic compression of a medium
14 p2027 A83-32094
Hydraulic analogy for isentropic flow through a nozzle
21 p3129 A83-44071

ISING MODEL

U FERROMAGNETISM

U MATHEMATICAL MODELS

ISLANDS

NT BERMUDA

NT CUBA

NT GREENLAND

NT INDONESIA

NT JAMAICA

NT JAPAN

NT MALAGASY REPUBLIC

NT PACIFIC ISLANDS

Alicudi project --- photovoltaic solar energy system for electric power supplying
14 p2038 A83-32190
The effect of islands on low frequency equatorial motions
16 p2393 A83-36976

ISOBARIS

Diagnostic equations in isobaric coordinates
08 p1139 A83-22286

ISOBARIS (PRESSURE)

On certain periodicities of atmospheric circulation
11 p1631 A83-27452

ISOCHROMATICS

Appearance aspects of isochromatic mode-1 crack tip fringe loops
11 p1593 A83-27862
Use of coefficients of influence to solve some inverse problems in plane elasticity
[ASME PAPER 83-APM-23]
17 p2519 A83-37382

On stress analysis of anisotropic composites through transmission optical patterns - Isochromatics and isopachics
21 p3108 A83-45166

ISOELECTRONIC SEQUENCE

N I isoelectronic sequence - Observations of 2s/m/2p/n/-2s/m-1/2p/n+1/ intersystem transitions and improved measurements for Cl XI, K XIII, Ca XIV, Sc XV, Ti XVI, and V XVII
01 p0105 A83-10196

C I isoelectronic sequence - Observations of 2s/m/2p/n/-2s/m-1/2p/n+1/ intersystem transitions and improved measurements for Cl XII, K XIV, Ca XV, Sc XVI, Ti XVII, and V XVIII
01 p0105 A83-10198

On the systematics of line ratios along the helium isoelectronic sequence
04 p0554 A83-15645
Magnetic quadrupole transitions in the beryllium isoelectronic sequence
04 p0537 A83-15954

Transition probabilities for forbidden lines in the 3p4 configuration. III --- in astrophysics
09 p1362 A83-24986

Spectroscopy of the isoelectronic nitrogen addition in epitaxial structures based on wide-band solid solutions of the system In-Ga-P-As
13 p1927 A83-30262

Magnetic dipole transitions in the beryllium isoelectronic sequence
15 p2236 A83-34554
Spectra of the ironlike ions from Y XIV to Ag XXII
15 p2228 A83-35298

Isoelectric focusing in space
20 p2940 A83-43281
A unified molecular force field via a model theory of isoelectronic diatomic molecules
21 p3202 A83-43961

Computer simulation of model isoelectronic focusing experiments
22 p3266 A83-45760

ISOLATORS

NT VIBRATION ISOLATORS

A new type of isolator for millimeter-wave integrated circuits using a nonreciprocal traveling-wave resonator
06 p0752 A83-18764

Near-millimeter wave polarizing duplexer/isolator
10 p1483 A83-26646
Single mode fiber isolator in toroidal configuration
11 p1656 A83-27565

ISOMERIZATION

ISOMERIZATION

On the formation of $\text{HCO}^+/\text{HOC}^+$ from the reaction between $\text{H}_3^+/\text{HCO}^+$ and CO

10 p1392 A83-26461
12 p1709 A83-28941

Photochemical storage potential of azobenzenes

12 p1709 A83-28941

ISOMERS

On the possibility of solar-radiation storage in organic photoisomers

14 p2036 A83-32046

Photoinduced infrared activity in polyacetylene

16 p2421 A83-36565

Characterization of geometric isomers of Norbornene end-capped imides

16 p2323 A83-36980

Molecular geometry of cis- and trans-polyacetylene by nutation NMR spectroscopy

23 p3433 A83-47611

ISOPARAMETRIC FINITE ELEMENTS

A new formulation of hybrid/mixed finite element

02 p0193 A83-12739

Our discrete-Kirchhoff and isoparametric shell elements for nonlinear analysis - An assessment

02 p0193 A83-12740

Anisotropic beam theory and applications

02 p0195 A83-12756

A two-dimensional isoparametric Galerkin finite element for acoustic-flow problems

[ASME PAPER 82-DET-97]

02 p0234 A83-12778

Concerning the formulation of the problem of calculating the stress-strain state in shell-reinforced cylinders by the finite element method

03 p0341 A83-14073

Stress intensity factors for two cracks emanating from two holes and approaching each other

04 p0496 A83-15065

A new method of finite element structure discretization

04 p0498 A83-15549

Curved elements with polynomials of varying degree

05 p0682 A83-17555

A finite element formulation for multilayered and thick plates

05 p0655 A83-17737

A new strategy for stress analysis using the finite element method

05 p0655 A83-17738

Approximation to bending trial functions for shell triangular finite elements in quadratic parametric representation

05 p0655 A83-17739

Optimal shape design to minimize stress concentration factors in pressure vessel components

06 p0772 A83-18214

Quality of trial functions in quadratic isoparametric representation of an arc

07 p0949 A83-21441

A note on locking in a shear flexible triangular plate bending element

08 p1123 A83-22947

Optimally discretized finite elements for boundary-layer stresses in composite laminates

09 p1281 A83-24671

The study of dynamic fracture propagation using a special finite element technique

[ASME PAPER 82-WA/DE-13]

10 p1439 A83-25680

Three-dimensional elastoplastic finite element analysis

10 p1442 A83-26767

The stability of elastoplastic arches and cylindrical panels

10 p1442 A83-26821

Three-dimensional finite-element analysis of layered composite plates

11 p1591 A83-27432

Auxiliary convergence criteria for Mindlin plate elements and their application to the four-node quadrilateral

12 p1737 A83-29743

Dynamic crack propagation analysis using a new path-independent integral and moving isoparametric elements

12 p1737 A83-29746

Isoparametric finite difference energy method for plate bending problems

15 p2176 A83-34322

Quarter-point elements for curved crack fronts

15 p2179 A83-34565

Isoparametric finite element analysis of large elasto-plastic strain problems and its applications in fracture mechanics

17 p2518 A83-37272

Algorithms for determining invertible two- and three-dimensional quadratic isoparametric finite element transformations

17 p2572 A83-38569

Elastic-plastic-creep behaviour of a compact-tension specimen

20 p3002 A83-42831

ISOPHOTES

Isophotes of a field in the Cygnus Loop photographed in the forbidden O III and forbidden N II + H-alpha lines

17 p2613 A83-38832

ISOPHOTES

U NOMOGRAPHS

ISOPYCNIC PROCESSES

An update on non-stationary oblique shock-wave reflections Actual isopycnics and numerical experiments

18 p2681 A83-39212

ISOSTATIC PRESSURE

Hot isostatic pressing technology. III - Diffusional bonding

02 p0156 A83-12296

Investigation of sintering and HIPing conditions of silicon nitride

03 p0303 A83-14919

HIP treatment on non-oxide ceramics

05 p0617 A83-17097

Hot isostatic pressing technology. IV - Production of powders of titanium alloy Ti6Al4V and steel X5CrNi18 9 using the REP procedure

06 p0727 A83-17959

Stainless steel and nickel base powders for the production of parts via extrusion and hot isostatic pressing

06 p0730 A83-19083

The critical role of titanium in hot isostatically pressed maraging steels

06 p0730 A83-19086

Practical applications of hot-isostatic pressing diagrams - Four case studies

07 p0884 A83-20260

Influence of hot isostatic processing and heat treatment variables on the tensile properties of cast Transage 175 alloy, Ti-2.5Al-13V-7Sn-2Zr

07 p0886 A83-20471

Hot Isostatic Pressing of alloy IN-718

07 p0895 A83-21500

Advanced processing methods for titanium; Proceedings of the Symposium, Louisville, KY, October 13-15, 1981

15 p2134 A83-33632

The effects of weld-repair and hot isostatic pressing on the fracture properties of Ti-5Al-2.5Sn ELI castings

15 p2135 A83-33642

Powder metallurgy and hot isostatic pressing (HIP) of the titanium alloy TiAl6V4

15 p2137 A83-33962

Application of electron beam welding to hot isostatically pressed nickel-base materials

15 p2137 A83-33966

Hot isostatic pressing of niobium C-103 alloy shapes

18 p2668 A83-40338

Creep behaviour of hot isostatically pressed niobium alloy powder compacts

21 p3111 A83-44332

Hot-isostatic-pressing technology (HIP). V - Properties and processing of HIP-Stellite 6

21 p3114 A83-44936

Equipment for the hot isostatic pressing of metal powders

21 p3148 A83-45312

Hot isostatic pressing of ceramics

23 p3438 A83-48307

Hot isostatic pressing of oxide dispersion strengthened superalloy parts

23 p3439 A83-48725

Hot-isostatic-pressing technology (HIP). VI - The development of a powder-metallurgy alloy of the type NiCr15Ag1Cu1

24 p3561 A83-49450

ISOSTERIC PROCESSES

U ISOPYCNIC PROCESSES

ISOTHERMAL FLOW

Self-similar solutions of isothermal flows behind a strong MHD shock

01 p0108 A83-11328

A study of transverse turbulent jets in a cross flow --- for gas turbine combustion process modelling

02 p0136 A83-13100

Conformal-plane gravitational fields of a viscous fluid

03 p0390 A83-13526

Numerical calculation of two-dimensional natural convection in isothermal open cavities

05 p0641 A83-17742

An isothermal shock wave in a perfectly-conducting and non-homogeneous stellar interior

05 p0702 A83-17811

Approximate solutions for isothermal flows behind strong spherical shocks with variable energy

12 p1722 A83-29056

Strong magnetogasdynamic plane shock in an exponential medium

12 p1780 A83-29059

Isenthalpic predictions of recirculating turbulent flowfields of confined dual coaxial jets behind an axisymmetric bluff body

23 p3450 A83-48232

[ASME PAPER 83-FE-14]

ISOTHERMAL LAYERS

Numerical calculations of a confined two-dimensional turbulent isothermal mixing layer

20 p2969 A83-42528

ISOTHERMAL PROCESSES

Adiabatic vs. isothermal - Two pictures of galaxy origin

01 p0127 A83-11291

On isothermal squeeze films [ASME PAPER 82-LUB-24]

03 p0336 A83-13513

Compression of ice VII to 500 kbar --- possible solid modifications of planetary water

05 p0707 A83-17844

Isothermal shock wave in magnetogasdynamics

15 p2233 A83-33871

High-temperature embrittlement of tungsten

15 p2140 A83-35042

Laser light scattering technique in the diagnostics of sprays in isothermal and burning conditions

16 p2351 A83-35825

A viscoelastic-viscoplastic constitutive equation and its finite element implementation

16 p2369 A83-36557

An isothermal section of the phase diagram for Ti-TiN3-Mo at 900 C

16 p2335 A83-36896

Nonlinear periodic solutions for the isothermal magnetostatic atmosphere

22 p3376 A83-46022

ISOTOPE EFFECT

The isotopic composition of primordial xenon

05 p0706 A83-17461

On the nature of isotopic anomalies in meteorites

05 p0706 A83-17462

The mass-independent fractionation of oxygen - A novel isotope effect and its possible cosmochemical implications

08 p1188 A83-22688

Problems in the geochemistry of radiogenic isotopes

13 p1960 A83-30725

ISOTOPE SEPARATION

Variations in the isotopic composition of xenon under the annealing and selective dissolution of material from the Tsarev meteorite

03 p0432 A83-13524

A method for the identification and elimination of contamination during carbon isotopic analyses of extraterrestrial samples

22 p3385 A83-46375

ISOTOPE SHIFT

U ISOTOPE EFFECT

ISOTOPES

NT ALUMINUM 26
NT ARGON ISOTOPES
NT BARIUM ISOTOPES
NT BERYLLIUM 9
NT BERYLLIUM 10
NT BISMUTH ISOTOPES
NT CALCIUM ISOTOPES
NT CALIFORNIUM ISOTOPES
NT CARBON ISOTOPES
NT CARBON 12
NT CARBON 13
NT CARBON 14
NT CESIUM VAPOR
NT COBALT ISOTOPES
NT COBALT 60
NT DEUTERIUM
NT FLUORINE ISOTOPES
NT GALLIUM ISOTOPES
NT GERMANIUM ISOTOPES
NT GOLD ISOTOPES
NT HAFNIUM ISOTOPES
NT HELIUM ISOTOPES
NT HOLMIUM ISOTOPES
NT HYDROGEN ISOTOPES
NT IODINE ISOTOPES
NT IRON ISOTOPES
NT IRON 57
NT LANTHANUM ISOTOPES
NT LEAD ISOTOPES
NT LITHIUM ISOTOPES
NT LUTETIUM ISOTOPES
NT MAGNESIUM ISOTOPES
NT MANGANESE ISOTOPES
NT MERCURY ISOTOPES
NT METALLIC HYDROGEN
NT NEODYMIUM ISOTOPES
NT NEON ISOTOPES
NT NICKEL ISOTOPES
NT NITROGEN ISOTOPES
NT NITROGEN 15
NT OSMIUM ISOTOPES
NT OXYGEN ISOTOPES
NT OXYGEN 18
NT PLUTONIUM 238
NT PLUTONIUM 244
NT POLONIUM 210
NT POTASSIUM ISOTOPES
NT RADIOACTIVE ISOTOPES
NT RADON ISOTOPES
NT RUBIDIUM ISOTOPES
NT SILICON ISOTOPES
NT SILVER ISOTOPES
NT STRONTIUM ISOTOPES
NT STRONTIUM 87
NT SULFUR ISOTOPES
NT TANTALUM ISOTOPES
NT TELLURIUM
NT THALLIUM ISOTOPES
NT THORIUM ISOTOPES
NT TITANIUM ISOTOPES
NT TRITIUM
NT TUNGSTEN ISOTOPES
NT URANIUM ISOTOPES
NT XENON ISOTOPES
NT XENON 129
NT XENON 133

Isotopic analysis of nanomole gas samples by means of dynamic flow mass spectrometry

13 p1845 A83-30255

Biologically mediated isotope fractionations - Biochemistry, geochemical significance and preservation in the earth's oldest sediments

13 p1899 A83-31159

AFGL trace gas compilation - 1982 version [AD-A130554]

15 p2201 A83-34456

- The isotopic and chemical evolution of Mount St. Helens 16 p2382 A83-36750
 CO 1-0 band isotopic lines as intensity standards 18 p2742 A83-39176
 Rare-gas isotopes in the atmospheres of the terrestrial planets and early stages of the evolution of the solar system 19 p2923 A83-41242
 Isotope and geochemical glaciology --- Russian book 21 p3169 A83-43902
 Isotopic composition of the ocean - Atmospheric system in the geologic past 22 p3323 A83-45788
 Cosmic-ray isotopic composition 23 p3539 A83-47739
 Chemical and isotopic study of extraterrestrial particles from the ocean floor 24 p3672 A83-49398
 Rb-Sr, Sm-Nd, K-Ca, O, and H isotopic study of Cretaceous-Tertiary boundary sediments, Caravaca, Spain
 Evidence for an oceanic impact site 24 p3672 A83-49399

ISOTOPIC ENRICHMENT

- Samples of the Milky Way --- isotopic abundances in Galactic cosmic rays 03 p0426 A83-14599
 Deuterium enrichments in type 3 ordinary chondrites 04 p0562 A83-15355
 On the siting of noble gases in E-chondrites 04 p0572 A83-16356
 Noble gas components in clasts and separates of the Abee meteorite 08 p1188 A83-21642
 Chemical evolution of OB associations 18 p2774 A83-39726

ISOTOPIC LABELING

- Fate of exogenous glucose during exercise of different intensities in humans 05 p0675 A83-17338
 Annual review of earth and planetary sciences. Volume 11 --- Book 14 p2034 A83-33477
 Terrestrial inert gases - Isotope tracer studies and clues to primordial components in the mantle 14 p2055 A83-33481

ISOTROPIC MEDIA

- A study of the creep of thin-walled shells under nonstationary loading 01 p0059 A83-10681
 Some aspects of gravitational waves in an isotropic background universe 01 p0127 A83-11295
 Frequency spectra and dynamics of long-period variations of isotropic and anisotropic fluxes --- of cosmic rays 02 p0273 A83-11728
 Penny-shaped crack in a transversely isotropic plate of finite thickness 02 p0190 A83-12039
 Some axially symmetric thermal stress distributions in an elastic solid containing an annular crack 02 p0191 A83-12050
 Numerical improvement of asymptotic solutions for shells of revolution with application to toroidal shell segments 02 p0194 A83-12741
 A multiple step random walk Monte Carlo method for heat conduction involving distributed heat sources [ASME PAPER 82-HT-25] 02 p0171 A83-12788
 On the concentrated loading of an external elliptical crack 02 p0196 A83-12854
 Stability of a spherical shell with a hollow filler 03 p0341 A83-14072
 Large deformation whole-field measurements of isotropic plates by sandwich hologram interferometry 03 p0341 A83-14399
 Extension of oblique-incidence method to photo-orthotropic elasticity 03 p0344 A83-14941
 Extension and torsion of elastic bars with initial twist 04 p0498 A83-15684
 A global local finite element analysis of axisymmetric scattering of elastic waves [ASME PAPER 82-WA/APM-3] 04 p0498 A83-15686
 Kinetics of the isotropic expansion of an optically transparent plasma in the Compton stage 04 p0536 A83-15710
 Stability of plastic tension 04 p0502 A83-16408
 An elastic-plastic constitutive equation for transversely isotropic materials and its application to the bending of perforated circular plates 05 p0656 A83-17947
 Nonlinear interaction of spherical waves in a homogeneous isotropic plasma 06 p0812 A83-18921
 A constitutive theory for transversely isotropic bimodulus materials with a class of steady wave solutions 07 p0948 A83-21344
 On the problem of two coplanar cracks inside an infinite isotropic elastic solid 07 p0949 A83-21440
 Weak and short waves in inhomogeneous isotropic elastic materials. I 08 p1160 A83-22227
 Thermal stress in a transversely isotropic medium containing a penny-shaped crack [ASME PAPER 83-APM-8] 10 p1440 A83-26427
 A study of a high-frequency polarized-wave field penetrating a plasma in a transition region with a diffused boundary 10 p1487 A83-26800

- A study of the propagation modes and velocities of axisymmetrical waves in an orthotropic hollow cylinder 11 p1596 A83-28453
 A strain-limit strength theory for metals [AIAA 83-1013] 12 p1740 A83-29797
 Transient thermal stress problem in a transversely isotropic finite circular cylinder under three-dimensional temperature field 12 p1747 A83-29924
 Nonclassical thermoelasticity equations for piecewise homogeneous media 13 p1865 A83-30051
 Birefringence of Zn(x)Cd(1-x)S near the isotropic point 13 p1918 A83-30207
 Exact solutions to the nonlinear Boltzmann equation and its models 13 p1932 A83-30655
 The regularity of one-dimensional elastic waves in an incompressible isotropic material 14 p2030 A83-32356
 Linear isotropic elasticity with body forces 15 p2173 A83-33856
 Isoparametric finite difference energy method for plate bending problems 15 p2176 A83-34322
 Finite strain J2 deformation theory 15 p2177 A83-34336
 Inverse problem of three-dimensional elasticity 15 p2178 A83-34434
 A viscoelastic-viscoplastic constitutive equation and its finite element implementation 16 p2369 A83-36557
 Simple waves in a nonlinear-elastic medium 17 p2522 A83-38071
 Reducing scattering to nonscattering problems in radiation heat transfer 18 p2684 A83-39846
 Love surface waves in regularly layered isotropic composites 18 p2701 A83-40113
 Predicted elastic constants of transversely isotropic composites containing anisotropic fibers 18 p2652 A83-40160
 Annular punch on a transversely isotropic layer bonded to a half-space 19 p2859 A83-41540
 Thermal conductivities of a cracked solid 20 p3007 A83-43145
 Measurements and calculations of the impedance of a cylindrical antenna in an isotropic plasma 21 p3211 A83-44300
 Wave refraction in an isotropic medium with anisotropic inhomogeneities 21 p3200 A83-45260
 A twelfth order theory of transverse bending of transversely isotropic plates 21 p3164 A83-45399
 Shear-elastic plates with built-in edge support 21 p3164 A83-45400
 Effects of stepwise variation of albedo on reflectivity and transmissivity of an isotropically scattering slab 23 p3513 A83-48622
 Simple bounds for the stress intensity factors by the method of singular integral equations 24 p3595 A83-49868
 A remark on the solution of the integral equation of planar cracks in three-dimensional elasticity 24 p3595 A83-49869

ISOTROPIC TURBULENCE

- The upper atmosphere of Uranus - A critical test of isotropic turbulence models 03 p0133 A83-13829
 Subgrid scale model for isotropic turbulence [ONERA, TP NO. 1982-80] 03 p0320 A83-14532
 Simple subgrid scale stresses models for homogeneous isotropic turbulence 05 p0638 A83-17315
 On velocity correlations in homogeneous isotropic turbulence 06 p0756 A83-18073
 Noise of a model helicopter rotor due to ingestion of isotropic turbulence 06 p0807 A83-18397
 Local isotropy and anisotropy in a high-Reynolds-number turbulent boundary layer 06 p0758 A83-19023
 Homogeneous and isotropic turbulence on the sphere --- in atmosphere 08 p1142 A83-23012
 Homogeneous turbulence 13 p1843 A83-31081
 A statistical mechanical model for two dimensional turbulence 14 p2009 A83-32510
 A model for the turbulent energy spectrum 14 p2013 A83-33385
 A theoretical study of radiative cooling in homogeneous and isotropic turbulence 15 p2156 A83-33671
 Constraints on the invariant functions of axisymmetric turbulence 16 p2351 A83-36083
 Hydrodynamic and turbulent motions in the galactic disk 18 p2775 A83-39755
 Strong turbulence of a magnetized plasma. I - The generalized Zakharov equations 18 p2747 A83-40073
 Kinematics of velocity and vorticity correlations in turbulent flow 21 p3128 A83-43929
 On the question of the power law of the decay of grid turbulence 23 p3452 A83-48671
 Effects of rotation on isotropic turbulence [ONERA, TP NO. 1983-108] 24 p3577 A83-49419

ISOTROPY**NT ISOTROPIC MEDIA**

- The relationship between the anisotropy of high-modulus reinforcing fibers and the mechanical and thermophysical properties of fiber composites 13 p1815 A83-30063
 Isotropization of arbitrary cosmological expansion given an effective cosmological constant 20 p3064 A83-42269
 Stress-energy density tensor of isotropic homogeneous universe 20 p3075 A83-43388

ISRO

- Developments in ISRO space platforms capability 21 p3095 A83-43816

ISTHMUSES

- Correlation between the SIR-A radar survey, the Landsat data, and the IR surveys in the Corinth canal zone 17 p2534 A83-38451

ITALY

- The Italian national space plan - The origin, rationale and objectives of the Italian space activities plan 04 p0450 A83-15659
 Advantages and problems of Italian participation in ESA 04 p0451 A83-15662
 The San Marco project - Prospects and programs 04 p0452 A83-15666
 Italian scientific space programs 04 p0451 A83-15668
 The Italsat programme 21 p3122 A83-45431
 IRIS - A new Italian upper stage system [IAF PAPER 83-25] 23 p3419 A83-47237

ITERATION**NT ITERATIVE SOLUTION**

- Generalised root iterations for the simultaneous determination of multiple complex zeros 06 p0804 A83-18072
 Determination of the natural frequencies and vibration modes of liquids in vessels of arbitrary shapes 09 p1263 A83-25015
 Spectral factorization by optimal gain iteration 12 p1770 A83-28998
 A calculation of the characteristics of polarized radiation by the method of iterations 13 p1913 A83-30035
 The solution of the equations of the applied theory of elasticity by the method of variational iterations 15 p2178 A83-34433
 Application of streamline iteration and relative flow field methods to the calculation of the subsonic flow field of S1 stream surface of turbomachinery 16 p2290 A83-35836
 An interpretation for probabilistic relaxation --- processing mechanisms in image analysis 21 p3194 A83-44263

ITERATIVE SOLUTION

- Asymptotic rates of convergence for the symmetric successive overrelaxation /SSOR/ iterative method by means of an associated eigenvalue problem 01 p0101 A83-10201
 Digital stochastic iterative procedures for the adaptive adjustment of noise compensation systems - Analysis of convergence and convergence rate 01 p0031 A83-10412
 An iteration method and solvability conditions for Navier-Stokes-type equations 01 p0045 A83-10822
 Transmission matrix approach to variable-rate sampled-data systems 01 p0095 A83-11132
 Choice of iterative parameters in the relaxation method on a sequence of meshes 01 p0102 A83-11265
 An iterative algorithm for multiple threshold detection --- in image processing 01 p0098 A83-11434
 A general scheme for signal restoration with application to picture processing 01 p0099 A83-11453
 Augmented relaxation labeling and dynamic relaxation labeling --- iterative pixel label updating in image processing 01 p0099 A83-11455
 Statistical solution of the inverse problems with application to cosmic-ray experiments 02 p0275 A83-11749
 The Waveform Relaxation method for time-domain analysis of large scale integrated circuits 02 p0167 A83-11797
 Pole placement and order reduction in two-time-scale control systems through Riccati iteration 02 p0229 A83-11838
 A sparse matrix finite element technique for iterative structural optimization 02 p0194 A83-12750
 A convergent method for solving the balance equation --- for atmospheric circulation analysis 02 p0217 A83-13053
 Analysis of a multilevel iterative method for nonlinear finite element equations 03 p0387 A83-13571
 A multi-level iterative method for nonlinear elliptic equations 03 p0388 A83-14077
 The Itpack package for large sparse linear systems 03 p0385 A83-14082
 On preconditioned iterative methods for elliptic partial differential equations 03 p0388 A83-14084
 Vector algorithms for elliptic partial differential equations based on the Jacobi method 03 p0388 A83-14087

Adapting iterative algorithms developed for symmetric systems to nonsymmetric systems 03 p0388 A83-14088

Methods for solving Euler's equations for airfoil and intake flow 03 p0279 A83-14604

An iteration procedure for reducing the expenses of static, elastoplastic and eigenvalue problems in finite element analysis 03 p0389 A83-14697

Factors for cubics and quartics 03 p0389 A83-14841

A variational principle and an algorithm for limit analysis of beams and plates 04 p0495 A83-15013

A comparison of methods for determining turning points of nonlinear equations 04 p0530 A83-15699

A least-square iterative technique for solving time-domain scattering problems 04 p0530 A83-16316

An iterative method for solving an eigenvalue problem 05 p0682 A83-17639

A method of limiting intermediate values of volume fraction in iterative two-fluid computations 05 p0641 A83-17725

A re-extrapolation technique in Newton-SOR computer simulation of semiconductor devices --- Successive Over Relaxation 05 p0631 A83-17765

Iterative solution of the global element equations 05 p0682 A83-17899

Techniques for the solution of MHD generator flows [AIAA PAPER 83-0465] 05 p0689 A83-17928

An iterative eigenvector technique for optimization analysis 06 p0804 A83-18206

The recursive-iterative algorithm for solving the characteristic equation for stabilized spacecraft. II 06 p0723 A83-18353

Fourier transform-iteration for antenna pattern synthesis 06 p0743 A83-18686

On the convergent solution in Kopal's iterative method of solving eclipsing binary orbits 06 p0822 A83-19164

Spectral methods for flows in complex geometries [AIAA PAPER 83-0229] 06 p0761 A83-19583

A three-dimensional modified strongly implicit procedure for heat conduction 07 p0924 A83-19823

Extension of the region of convergence of an iterative method for solving the inverse refraction problem 07 p0989 A83-20853

An empirical initial estimate for the solution of Kepler's equation 07 p0868 A83-21427

Block overrelaxation methods for non-rectangular co-ordinates 07 p0949 A83-21442

An iterative method for finite dimensional structural optimization problems with repeated eigenvalues 07 p0949 A83-21444

On a deferred-correction procedure for determination of central-difference solutions to the Navier-Stokes equations 08 p1090 A83-23214

Iterative procedures for constrained and unilateral optimization problems 09 p1331 A83-24765

Solution of large sparse nonlinear systems by monotone convergent iterations and applications 09 p1336 A83-25109

Riccati transformations in the back-and-forth shooting method for solving two-point boundary-value problems 10 p1465 A83-26524

Identification of high dimensional system by the general parameter method 10 p1466 A83-26534

Singular value decomposition using iterative optical processors 10 p1483 A83-26632

A new procedure for improving the solution stability and extending the frequency range of the EBCM --- Extended Boundary Condition Method for EM absorption and scattering in biological dielectric objects 10 p1460 A83-26839

Certain parallel iterative methods for solving nonlinear equations 10 p1470 A83-26943

Rapid interference suppression using a Kalman filter technique 11 p1554 A83-27906

A computational technique for optimizing correction weights and axial location of balance planes of rotating shafts 11 p1589 A83-28121

Finite element iterative techniques for determining the interface boundary between Laplace and Poisson domains - Characteristic analysis of a field effect transistor 11 p1563 A83-28417

Series solutions of the dispersion relation for linear water waves 11 p1635 A83-28428

An iterative method for the Helmholtz equation 12 p1771 A83-29097

Matrix formulation of the Picard method for parallel computation 12 p1771 A83-29107

Nongradient minimization methods for parallel processing computers. I, II 12 p1767 A83-29243

Error estimate for the modified Newton method with applications to the solution of nonlinear, two-point boundary-value problems 12 p1771 A83-29244

On local relaxation methods and their application to convection-diffusion equations 12 p1725 A83-29644

A multigrid algorithm for steady transonic potential flows around aerofoils using Newton iteration 12 p1697 A83-29656

Application of multigrid methods for integral equations to two problems from fluid dynamics 12 p1725 A83-29661

An automated technique for improving model matrices by means of experimentally obtained dynamic data [AIAA 83-0881] 12 p1746 A83-29890

Fast iterative solution of Poisson equation with Neumann boundary conditions in nonorthogonal curvilinear coordinate systems by a multiple grid method 12 p1726 A83-29898

On an iterative method with fictitious unknowns 13 p1912 A83-30076

Simulation of nonlinear processes in an O-type TWT by an iterative method 13 p1832 A83-30287

Boundary integral equation solution of the Berger equation 13 p1866 A83-30447

An iteration method for solving stochastic boundary value elasticity problems 14 p2029 A83-32155

The application of iterated defect correction to variational methods for elliptic boundary value problems 14 p2078 A83-32842

Three-dimensional phase-conjugate-resonator performance 15 p2229 A83-33532

Iterative solutions for electromagnetic scattering by gratings 15 p2224 A83-33804

Signal restoration from phase by projections onto convex sets 15 p2220 A83-33809

A numerical algorithm for solving inverse problems of two-dimensional wave equations 15 p2223 A83-33819

Progress in computational physics 15 p2216 A83-33868

Fast iterative division of p-adic numbers 15 p2217 A83-33910

A spectral-iteration technique for analyzing scattering from arbitrary bodies. I - Cylindrical scatterers with E-wave incidence 15 p2148 A83-35186

A spectral-iteration technique for analyzing scattering from arbitrary bodies. II - Conducting cylinders with H-wave incidence 15 p2149 A83-35198

The synthetic method in radiative transfer theory 16 p2427 A83-35614

Parallel solution of finite element equations 16 p2403 A83-36721

Triangular system solutions on an optical systolic processor 16 p2403 A83-36752

Numerical solution of the symmetric Riccati equation through Riccati iteration 17 p2571 A83-37139

An iterative algorithm for solving inverse problems in structural dynamics 17 p2525 A83-38571

Conformal mappings onto multiply connected regions with specified boundary shapes 17 p2573 A83-38801

Semidirect/marching solutions and elliptic grid generation 17 p2574 A83-38807

Comparison of fast iterative methods for symmetric systems 18 p2739 A83-39255

Calculations of transonic potential flows by a parameter free procedure [AIAA PAPER 83-1886] 18 p2634 A83-39355

Implicit upwind methods for the Euler equations [AIAA PAPER 83-1930] 18 p2682 A83-39382

Alternating direction adaptive grid generation [AIAA PAPER 83-1937] 18 p2740 A83-39387

Iterative PNS method for attached flows with upstream influence --- Parabolic Navier-Stokes [AIAA PAPER 83-1955] 18 p2636 A83-39398

Flux vector splitting and approximate Newton methods --- for solution of steady Euler equations [AIAA PAPER 83-1899] 18 p2683 A83-39404

A spectral method for the solution of transonic potential flow about an arbitrary two-dimensional airfoil [AIAA PAPER 83-1949] 18 p2637 A83-39406

Algorithm improvements for optical eigenfunction computers 19 p2893 A83-41095

A survey of methods for iterative signal restoration 19 p2830 A83-41376

An iterative scheme for performance modeling of slotted ALOHA packet radio networks 19 p2832 A83-41397

Necessary and sufficient conditions of the convergence asynchronous iterative computational processes when solving systems of linear algebraic equations 19 p2888 A83-41420

A convergence analysis of a numerical method for solving the balance equation --- of atmospheric circulation 20 p3029 A83-42507

Economical solution technique for boundary integral matrices 20 p3042 A83-43648

An iterative approach to region growing using associative memories 21 p3191 A83-43956

Subspace iteration for the eigenvalue problems of self-adjoint differential equations and its applications in the vibration analysis of structures 21 p3151 A83-44109

A low Mach number Euler formulation and application to time-iterative LBI schemes --- Linearized Block Implicit 21 p3134 A83-45592

On the fractal dimension of the Henon attractor 23 p3505 A83-48588

IUE

Archiving and retrieval of data from the International Ultraviolet Explorer /IUE/ mission 01 p0113 A83-10141

Ultraviolet observations of interacting binary Be stars 01 p0122 A83-10347

The problem of X Persei 01 p0123 A83-10350

Evaluation of EUV spectra of X-ray binaries Cygnus X-1, Vela X-1, and X Persei --- German thesis 01 p0123 A83-10477

IUE high dispersion spectra of luminous stars in symmetric nebulae 03 p0417 A83-13555

The International Ultraviolet Explorer --- instrument package 03 p0288 A83-13970

The IUE spectrum of BD + 39 deg 4926 03 p0421 A83-14142

The ultraviolet spectrum of Herbig-Haro object 2H 03 p0425 A83-14219

Luminosities and masses for three central stars of planetary nebulae in the Magellanic Clouds from ultraviolet spectroscopy with the IUE 03 p0425 A83-14220

International Ultraviolet Explorer observations of the R Aquarii jet 03 p0425 A83-14221

The width of echelle orders in IUE images as derived with the astronomical image display and analysis /AIDA/ system in Tuebingen 03 p0411 A83-14799

A study of ultraviolet spectra of Zeta Aur/VV Cep systems. I - Resonance line formation 03 p0430 A83-14800

Ly-alpha absorption at a high velocity in NGC1275 03 p0411 A83-14923

Chromospheric Mg II emission in A5 to K5 main sequence stars from high resolution IUE spectra 04 p0550 A83-15035

An interactive procedure to solve the background subtraction problems in IUE high resolution spectra - Application to the image SWP 4616 04 p0547 A83-15972

Ultraviolet shell formation at V1016 Cygni 05 p0700 A83-17030

Detection of auroral hydrogen Lyman-alpha emission from Uranus 05 p0704 A83-17037

IUE observations of certain short period RS CVn-like stars 06 p0834 A83-18890

The ultraviolet variability of NGC 3783 07 p1017 A83-20929

IUE observations of Markarian 3 and 6 - Reddening and the nonstellar continuum 07 p1019 A83-21109

The planetary nebula IC 3568 - A model based on IUE observations 07 p1021 A83-21124

Temporal variation of the Jovian H I Lyman-alpha emission /1979-1982/ 07 p1031 A83-21158

IUE and other new observations of the slow nova RR Tel 09 p1362 A83-24976

IUE observations of variable Seyfert 1 galaxies 09 p1356 A83-25297

IUE observations of E1405-451 - A new AM Herculis type cataclysmic variable 10 p1505 A83-25744

International Ultraviolet Explorer observations of the peculiar variable spectrum of the eclipsing binary R Arae 10 p1497 A83-26383

Coordinated Einstein and IUE observations of a disarptions brusques type flare event and quiescent emission from Proxima Centauri 10 p1514 A83-26729

IUE observations of X-ray selected Seyfert galaxies 11 p1675 A83-28269

The spectra of late type dwarfs and sub-dwarfs in the near ultraviolet. II - Limits to variability in MglI emission from IUE spectrophotometry 12 p1789 A83-28869

IUE looks at the Algol paradox 13 p1935 A83-30025

The IUE observation of the active binary II Pegasi = HD 224085 13 p1955 A83-31663

Performance of the International Ultraviolet Explorer for spectral imaging 14 p1983 A83-32019

High luminosity X-ray binaries - IUE results 15 p2251 A83-33589

IUE observations of supernova remnants 15 p2251 A83-33596

Observations of ultraviolet spectra of H II regions and galaxies with IUE 15 p2251 A83-33598

IUE observations of five DB white dwarfs 15 p2264 A83-34578

A determination of the composition of the Saturnian stratosphere using the IUE 16 p2436 A83-35736

- IUE observations of the nucleus of the galactic globular cluster NGC 2808 16 p2429 A83-36634
- IUE observations of stars in the M8 nebula 22 p3379 A83-46566
- Einstein and IUE observations of nearby red dwarfs 23 p3521 A83-47485
- The IUE mission 24 p3550 A83-49557
- IUE data reduction 24 p3644 A83-49558
- Active galactic nuclei - IUE results on continuum, emission and absorption lines 24 p3661 A83-49559
- Far ultraviolet observations of BL Lac objects 24 p3661 A83-49560
- The UV spectrum of elliptical galaxies 24 p3662 A83-49561
- Supernovae --- review of IUE observations 24 p3662 A83-49563
- Ultraviolet observations of binary X-ray sources 24 p3662 A83-49564
- IUE observations of cataclysmic variables 24 p3662 A83-49565
- New results on symbiotic stars 24 p3662 A83-49566
- Planetary nebulae - IUE results 24 p3662 A83-49567
- H II regions --- review of IUE studies 24 p3662 A83-49568
- Some aspects of the velocity fields in early-type stars 24 p3662 A83-49569
- Late type stars 24 p3662 A83-49570
- Solar-like activity phenomena in stars 24 p3663 A83-49571
- Chemically peculiar stars 24 p3663 A83-49572
- IUS**
- U INERTIAL UPPER STAGE
- IZSAK ELLIPSOID**
- U ELLIPSOIDS
- U GEODESY

J

J INTEGRAL

- Determination of fracture toughness from stretch zone width measurement in predeformed AISI type 4340 steel 01 p0024 A83-10217
- Key curve analysis of crack-growth-resistance curves 02 p0190 A83-12041
- The extension of the J-integral concept to fatigue cracks 02 p0190 A83-12044
- On the J-integral blunting line for soft materials 02 p0190 A83-12045
- Environmental fatigue crack growth analysis based on elastic-plastic fracture mechanics [ASME PAPER 82-PVP-23] 02 p0196 A83-12769
- Tentative test procedure for determining the plane strain JI-R curve 02 p0158 A83-12831
- Evaluation of the tentative JI-R curve testing procedure by round robin tests of HY130 steel 02 p0158 A83-12832
- J-integral analysis for initiation of notch fatigue crack 03 p0342 A83-14490
- A simple yet accurate finite element procedure for computing stress intensity factors 03 p0342 A83-14707
- The J contour integral in the plastic region 03 p0343 A83-14729
- Mixed mode plane stress ductile fracture 06 p0775 A83-18909
- Evaluation of fracture toughness /J sub lc/ using single specimen fracture test augmented by finite element analysis 07 p0883 A83-19670
- Defect forces, defect couples and path integrals --- J integral study of crack propagation stability 08 p1115 A83-21656
- Evaluation of process zone by using Jext integral under large scale yielding - Structure of J integral 08 p1116 A83-21658
- The relation between microstructural fracture processes and macroscopic crack tip characterizing parameters during the stable growth of cracks 08 p1117 A83-21699
- The influence of specimen geometry on stable crack growth for a high strength steel 08 p1060 A83-21704
- Experimental studies of stable crack growth 08 p1060 A83-21705
- Effect of specimen size of JIc for a Ni-Cr-Mo rotor steel in the upper shelf region 08 p1060 A83-21706
- A J based engineering usage of fracture mechanics 08 p1117 A83-21725
- Fracture toughness of simulated H.A.Z. --- heat affected zone 08 p1061 A83-21728
- Simplified determination of J-integral and its availability as a strain intensity parameter at notch tip 08 p1118 A83-21750

- On the accuracy of J-integral value evaluated by finite element method for mixed mode 08 p1122 A83-22068
- Application of the J concept to alumina at high temperatures 08 p1070 A83-22192
- The influence of inclusions on the J integral value determined by a Charpy test with digital instrumentation 08 p1124 A83-23242
- J-integral analysis for cracks emanated from elliptical holes 09 p1275 A83-23298
- The application of the J-integral to small specimens of ductile material to be exposed to high temperatures and high levels of irradiation 09 p1233 A83-24079
- On path-independent integrals and fracture criteria in non-linear fracture dynamics 10 p1438 A83-25471
- Deformation work density fracture criterion for composite materials 10 p1442 A83-26771
- A comparison of the strain intensity and cyclic J approaches to crack growth 11 p1593 A83-27856
- A new method of determining JIc of steel by means of single specimen 11 p1548 A83-28442
- On the fundamental basis of fracture mechanics 11 p1596 A83-28444
- Dynamic crack propagation analysis using a new path-independent integral and moving isoparametric elements [AIAA 83-0838] 12 p1737 A83-29746
- The effect of specimen size on J(R) resistance curve in limited amounts of crack growth 12 p1715 A83-29943
- Path-independent integrals, energy release rates, and general solutions of near-tip fields in mixed-mode dynamic fracture mechanics 14 p2031 A83-32652
- Plastic rotational factor and J-COD relationship of three point bend specimen 14 p1993 A83-32655
- Limitations of the crack tip blunting line used in the J-sub-IC test procedure 14 p2031 A83-32665
- Numerical analysis of ductile fracture experiments using single-edge notched tension specimens 15 p2134 A83-33511
- J(Ic) measurement point determination for HY130, CMS-9, and Inconel Alloy 718 15 p2134 A83-33514
- Finite strain J2 deformation theory 15 p2177 A83-34336
- Evaluation of J-integral value by using finite element method 16 p2369 A83-36968
- Acoustoelastic determination of forces on a crack in mixed-mode loading 17 p2518 A83-37387
- An axisymmetric-elastodynamic analysis of a crack in orthotropic media using a path-independent integral 17 p2523 A83-38393
- Fracture analysis of composite materials 18 p2704 A83-40195
- Determination and simulation of stable crack growth in ADINA 20 p3003 A83-42927
- Three-dimensional J-integral calculations of part-through surface crack problems 20 p3003 A83-42930
- Fracture mechanics J-integral calculations in thermo-elasto-plasticity 20 p3003 A83-42931
- Analysis of surface cracks in plates and shells using the line-spring model and ADINA 20 p3003 A83-42934
- Estimation of stress and strain at the notch root in the elastic-plastic range using the J-integral 21 p3151 A83-44062
- A comparison of the J(asterisk) integral with other methods of post yield fracture mechanics 21 p3155 A83-44886
- The cyclic J-integral as a criterion for fatigue crack growth 21 p3158 A83-44910
- Some comments on the geometry dependence of the J versus c relation for plane strain crack growth 21 p3158 A83-44912
- J-79 ENGINE**
- Comparison-effects of broadened property jet fuels on older and modern J79 combustors [ASME PAPER 83-GT-81] 23 p3407 A83-47934
- JACKS (ELECTRICAL)**
- U ELECTRIC CONNECTORS
- JACOBI INTEGRAL**
- The use of Bessel function and Jacobi polynomial in radial vibrations of a gas in an infinite cylindrical tube 08 p1091 A83-23217
- Some applications of the Jacobi integral in fixed axes --- for three body problem 11 p1674 A83-28195
- About the non-existence of additional analytical integral in the problem of satellite's motion under the gravitational attraction of a triaxial rigid body 12 p1787 A83-29120
- Orthogonal coordinate meshes with manageable Jacobian 17 p2574 A83-38815
- The general solutions of the doubly periodic cracks 18 p2696 A83-39083

JACOBI MATRIX METHOD

- Vector algorithms for elliptic partial differential equations based on the Jacobi method 03 p0388 A83-14087
- A note on a Runge-Kutta-Chebyshev method 03 p0388 A83-14511
- Computation of periodic solutions for polynomial nonlinear equations 07 p0986 A83-20067
- Error estimate for the modified Newton method with applications to the solution of nonlinear, two-point boundary-value problems 12 p1771 A83-29244
- On an algorithm for solving the incomplete eigenvalue problem in the vibration analysis of complex structures of fuselage type 12 p1735 A83-29278
- An implicit, bidiagonal numerical method for solving the Navier-Stokes equations 14 p2012 A83-32979
- Assessing the quality of curvilinear coordinate meshes by decomposing the Jacobian matrix 17 p2574 A83-38811

JACOBI POLYNOMIALS

U HYPERGEOMETRIC FUNCTIONS

JAGUAR AIRCRAFT

- Flight clearance of the Jaguar fly by wire aircraft. I 22 p3254 A83-45845
- Flight clearance of the Jaguar-fly-by-wire aircraft. II 22 p3255 A83-45846

JAHN-TELLER EFFECT

- Occurrence of the dynamic Jahn-Teller effect in CdTe:Co crystals 19 p2904 A83-40998

JAMAICA

- Analysis of Jamaican lineaments visible in Seasat-SAR imagery 01 p0064 A83-10081
- A Miocene submarine volcano at Low Laiton, Jamaica 02 p0203 A83-11830

JAMMING

- New threat simulator /NETS/ a multi-sensor R & D tool for EW development 01 p0015 A83-11238
- ASPJ update counters the changing threat --- Airborne Self-Protection Jammer System 05 p0592 A83-16866
- A general analysis of anti-jam communication systems 07 p0904 A83-19694
- Capacity and coding in the presence of fading and jamming 07 p0905 A83-19697
- Coding tradeoffs for improved performance of FH/MFSK systems in partial band noise 07 p0909 A83-19751
- AJ/LPI at millimeter wavelengths --- Anti-Jamming/Low Probability of Intercept 07 p0909 A83-19753
- Video compression using sampled data analog devices 08 p1078 A83-22813
- Very high speed integrated circuit /VHSIC/ anti-jam communications chipset and brassboard demonstration 08 p1081 A83-22820
- Transversal filter techniques for adaptive array applications 11 p1554 A83-27905
- Experimental linear phased array with partial adaptivity 11 p1555 A83-27918
- Performance of a direct sequence spread-spectrum system with long period and short period code sequences 13 p1827 A83-30224
- EHF planar module for spatial combining 14 p2007 A83-33074
- Millimeter-wave phased array transmitters for ECM 17 p2498 A83-37896
- Performance of concatenated codes on channels with jamming 19 p2833 A83-41410
- Cochannel and intersymbol interferences in QAM system 24 p3571 A83-49965

JAPAN

- Concentration of atmospheric carbon dioxide over Japan 09 p1295 A83-24261
- Research and development on ocean thermal energy conversion in Japan 11 p1606 A83-27228
- Urbanization of the Tokyo metropolitan area and its thermal condition using Landsat MSS and NOAA-6/AVHRR data 15 p2182 A83-33571
- A study of land transformation processes after the atomic bombing damage in Hiroshima 15 p2182 A83-33572

JAPANESE SPACE PROGRAM

- SEPAK system test in NASDA space chamber --- space experiment with particle accelerator 03 p0284 A83-14850
- Japan's BSE program --- Broadcasting Satellite for Experimental purpose 04 p0468 A83-16415
- Operational broadcasting satellite in Japan 04 p0469 A83-16425
- Japanese satellite programs in X-ray astronomy 11 p1671 A83-27765
- The space race - Here comes Japan --- scientific and communication satellite technology 13 p1808 A83-29999
- Japan's Halley's Comet probes 16 p2314 A83-35777
- Japan's new rocket engine 16 p2323 A83-36572
- Japan's expendable launch vehicles 19 p2812 A83-41373

- Space communications in Japan 22 p3273 A83-45752
- Japanese mission model for space station [IAF PAPER 83-53] 23 p3413 A83-47245
- Research and development of synthetic aperture radar [IAF PAPER 83-94] 23 p3424 A83-47263
- Results of Japanese space processing experiments using the TT-500A rocket [IAF PAPER 83-157] 23 p3414 A83-47294
- Data management scheme for Japanese experiments of FMPT --- First Material Processing Test [IAF PAPER 83-164] 23 p3424 A83-47299
- Centimeter wave propagation experiments using the beacon signals of CS and BSE satellites 23 p3420 A83-47832
- JAPANESE SPACECRAFT**
- Aspects of the satellite broadcasting experiments using the BSE and its in-orbit performance 04 p0468 A83-16416
- Transmission characteristics of transponders --- onboard Japanese experimental broadcasting satellite 04 p0468 A83-16418
- The attitude control performance of the BSE and its influence on the received television signal strengths on the ground 04 p0453 A83-16420
- Up-link power control experiment --- of Japanese Medium-scale Broadcasting Satellite 04 p0468 A83-16421
- Switching control system for access to a broadcast satellite from multiple earth stations 04 p0468 A83-16422
- High definition television broadcasting by satellite 04 p0469 A83-16423
- Transmission system for the television broadcasting satellite 04 p0469 A83-16424
- Operational broadcasting satellite in Japan 04 p0469 A83-16425
- Some topics on the X-ray pulsars and the X-ray bursts observed by the satellite Hakucho 07 p1012 A83-20026
- Measurement of relative propagation delay between C- and K-band satellite loops 10 p1403 A83-26076
- A radio guidance algorithm for M Series rockets that are used to launch Japanese scientific satellites 10 p1382 A83-26593
- On the development of attitude stabilization and control system of a Japanese scientific satellite 10 p1385 A83-26608
- MOS-1 attitude and orbit control system 10 p1385 A83-26609
- Life test report for ETS-III battery 11 p1539 A83-27195
- The space race - Here comes Japan --- scientific and communication satellite technology 13 p1808 A83-29999
- Wave excitation in electron beam experiment on Japanese satellite 'JIKIKEN (EXOS-B)' 15 p2197 A83-34182
- Planet-A mission to Halley 15 p2124 A83-35012
- HINOTORI - A Japanese satellite for solar flare studies 15 p2250 A83-35225
- Japan's Halley's Comet probes 16 p2314 A83-35777
- Spin free analytic platform type guidance and control system --- for attitude control of rocket launcher 17 p2473 A83-37488
- Selection of sensors and spectral bands of Marine Observation Satellite (MOS) - 1 17 p2529 A83-38159
- Snow properties and two channel microwave measurements 17 p2534 A83-38458
- Operation and experimental results of Ionosphere Sounding Satellite-b (ISS-b, UME-2). I - Outline of ISS-b project 21 p3096 A83-45434
- Topside sounder onboard ISS-b --- Ionosphere Sounding Satellite 21 p3104 A83-45435
- Characteristics of the radio noise receiving equipment --- onboard Ionosphere Sounding Satellite 21 p3104 A83-45436
- The ISS-b retarding potential analyzer --- Ionospheric Sounding Satellite 21 p3104 A83-45437
- Ion mass spectrometer on Ionosphere Sounding Satellite (ISS-b) 21 p3104 A83-45438
- On the structure and functions of the ISS-b satellite control systems 21 p3098 A83-45439
- Scheduling of ISS-b operations --- ground station computer algorithm and onboard data recording Ionosphere Sounding Satellite 21 p3098 A83-45440
- Operations of ISS-b at Kashima station and their result --- with description of satellite tracking, telemetry and command 21 p3098 A83-45441
- Orbit and attitude of ISS-b 21 p3098 A83-45442
- Operation of primary processing and data analysis system for ISS --- Ionosphere Sounding Satellite 21 p3098 A83-45443

- On the application of housekeeping data to ISS-b operations 21 p3096 A83-45444
- Automation of satellite control system and its effectiveness in actual operation --- with Ionosphere Sounding Satellite 21 p3098 A83-45445
- Global distribution of the ionospheric F-layer critical frequency f0F2 21 p3177 A83-45446
- Estimation of f0F2 from interferences appearing on AGC data of ISS-b topside sounder 21 p3178 A83-45447
- Global distribution of topside spread F 21 p3178 A83-45448
- Long-distance HF propagation modes deduced from the simultaneous observation by chirp sounder and ISS-b 21 p3122 A83-45449
- The global distribution of thunderstorm activity observed by the Ionosphere Sounding Satellite (ISS-b) 21 p3182 A83-45451
- Cosmic noise observations at high radio frequencies 21 p3226 A83-45452
- Observations of the thermal plasma in the topside ionosphere by RPT mission of ISS-b - Electron density, temperature and mean ion mass --- Retarding Potential Trap 21 p3178 A83-45455
- Observational results of the nighttime ion temperatures in the topside ionosphere by ISS-b 21 p3178 A83-45456
- Observation of the ion composition by Ionosphere Sounding Satellite 21 p3178 A83-45457
- Measurement of total electron content by simultaneous reception of ISS-b telemetry signals 21 p3178 A83-45459
- Control system of TT-500A sounding rocket for materials processing in space 21 p3103 A83-45599
- Development of active microwave sensors in Japan --- for remote sensing satellites 22 p3260 A83-46115
- Japanese free-flying satellites --- as Space Station interface units [IAF PAPER 83-31] 23 p3419 A83-47238
- Studies on Japan's earth resource satellite-1 [IAF PAPER 83-120] 23 p3421 A83-47277
- Introduction to Hinotori --- satellite solar flare mission 23 p3531 A83-47659
- Polarization measurements using the Bragg crystal spectrometers on Hinotori --- soft X-ray emission from solar flares 23 p3532 A83-47668
- JARRING**
- U MECHANICAL SHOCK
- JC-130 AIRCRAFT**
- U C-130 AIRCRAFT
- JEANS THEORY**
- The stability of relativistic gas spheres 06 p0827 A83-18166
- Electric charge in the Kruskal space-time and the Jeans conjecture 06 p0841 A83-19447
- Thermodynamic fluctuations and gravitational instabilities 07 p1018 A83-20950
- Gravitational collapse and fragmentation of isothermal, non-rotating, cylindrical clouds 10 p1500 A83-25492
- Magnetogravitational instability of a finitely-conducting medium with variable streaming motion 12 p1793 A83-29072
- Gravitational instability - The second approximation in the linear long-wave theory 13 p1948 A83-31253
- Turbulence in a self-gravitating gaseous disk. II - Turbulence spectra 17 p2610 A83-38553
- The gravitational instability of a rotating plasma in the presence of finite Larmor radius, Hall currents and suspended particles 24 p3633 A83-50168

JEES

U AUTOMOBILES

JET AIRCRAFT

- NT A-6 AIRCRAFT
- NT A-7 AIRCRAFT
- NT A-300 AIRCRAFT
- NT ALPHA JET AIRCRAFT
- NT B-52 AIRCRAFT
- NT B-58 AIRCRAFT
- NT BOEING 727 AIRCRAFT
- NT BOEING 737 AIRCRAFT
- NT BOEING 747 AIRCRAFT
- NT BOEING 757 AIRCRAFT
- NT BOEING 767 AIRCRAFT
- NT C-5 AIRCRAFT
- NT C-135 AIRCRAFT
- NT C-140 AIRCRAFT
- NT C-141 AIRCRAFT
- NT CV-990 AIRCRAFT
- NT DC 8 AIRCRAFT
- NT DC 9 AIRCRAFT
- NT DC 10 AIRCRAFT
- NT EUROPEAN AIRBUS
- NT F-4 AIRCRAFT
- NT F-5 AIRCRAFT
- NT F-8 AIRCRAFT
- NT F-14 AIRCRAFT
- NT F-15 AIRCRAFT

- NT F-16 AIRCRAFT
- NT F-17 AIRCRAFT
- NT F-18 AIRCRAFT
- NT F-28 TRANSPORT AIRCRAFT
- NT F-104 AIRCRAFT
- NT F-111 AIRCRAFT
- NT IL-62 AIRCRAFT
- NT L-1011 AIRCRAFT
- NT LEAR JET AIRCRAFT
- NT P-3 AIRCRAFT
- NT T-38 AIRCRAFT
- NT TURBOFAN AIRCRAFT
- NT TURBOPROP AIRCRAFT
- NT U-2 AIRCRAFT
- NT YAK 40 AIRCRAFT
- Model-based three-dimensional interpretations of two-dimensional images 02 p0182 A83-12896
- Existing time limit for overwater operations - Its validity 03 p0281 A83-13170
- Long-range Falcon - Flight-test Dassault Falcon 50 06 p0716 A83-18074
- The MCA method, a flight test technique to determine the thrust of jet aircraft in flight --- Mass Consumption Acceleration 07 p0865 A83-19661
- Computer-enhanced analysis of a jet in a cross stream 07 p0924 A83-19804
- The application of a sub-scale flight demonstrator as a cost effective approach to aircraft development 12 p1701 A83-29395
- Large jet aircraft validation and demonstrations - An overview of Boeing experience [AIAA PAPER 83-1049] 16 p2301 A83-36472
- Optimal turning climb-out and descent of commercial jet aircraft [SAE PAPER 821468] 17 p2464 A83-37999
- Propulsion system integration as applied to business jet aircraft [ASME PAPER 83-GT-227] 23 p3403 A83-48024
- JET AIRCRAFT NOISE**
- Jet noise and the effects of jet forcing 01 p0105 A83-10898
- Prediction of jet exhaust noise on airframe surfaces during low-speed flight 03 p0282 A83-13160
- Flight test of the 747-JT9D for airframe noise 03 p0281 A83-13163
- Selected results from the quiet short-haul research aircraft flight research program 03 p0281 A83-13165
- Aeroacoustical characteristics of a mechanical noise suppressor in a nozzle configuration with a central tailcone 03 p0391 A83-13590
- Length and time scales relevant to sound generation in excited jets 04 p0533 A83-15298
- On the radially non-compact source model for subsonic jet noise 05 p0683 A83-16929
- Effect of excitation on coaxial jet noise 07 p0990 A83-19811
- Screech suppression in supersonic jets 07 p0990 A83-19814
- Radiation from a double layer jet --- aerodynamic noise 07 p0990 A83-20364
- Ground effects on aircraft noise for a wide-body commercial airplane 09 p1340 A83-24034
- Viscous stability of compressible axisymmetric jets 09 p1341 A83-24651
- An improved jet noise scaling law which incorporates phase differences due to flight effects [AIAA PAPER 83-0747] 10 p1476 A83-25949
- Flight effects on jet noise sources investigated by model experiments in the DNW [AIAA PAPER 83-0752] 10 p1476 A83-25951
- Tone generation by rotor-downstream strut interaction [AIAA PAPER 83-0767] 10 p1378 A83-25957
- Prediction of high bypass ratio engine static and flyover jet noise [AIAA PAPER 83-0773] 10 p1378 A83-25958
- Porous-plug flowfield mechanisms for reducing supersonic jet noise [AIAA PAPER 83-0774] 10 p1378 A83-25959
- Modified jet noise source model for twin-jet shielding analysis [AIAA PAPER 83-0776] 10 p1477 A83-25960
- Friction drag and other design parameters for acoustic face sheets --- for aircraft noise reduction [AIAA PAPER 83-0780] 10 p1477 A83-25962
- Analysis of jet-airframe interaction noise [AIAA PAPER 83-0783] 10 p1376 A83-25964
- Flight effects for jet-airframe interaction noise [AIAA PAPER 83-0784] 10 p1376 A83-25965
- Nearfield observations of tones generated from supersonic jet flows [AIAA PAPER 83-0706] 10 p1478 A83-26449
- Shock noise features using the SCIPVIS code [AIAA PAPER 83-0705] 10 p1478 A83-26918

- On discrete tones generated by an impinging underexpanded rectangular jet
[AIAA PAPER 83-0729] 10 p1478 A83-26919
- A compact inflow control device for simulating flight fan noise
[AIAA PAPER 83-0680] 11 p1651 A83-28005
- Coaxial supersonic jet-flows, shock structure and related problems with noise-suppression assessment and prediction
[AIAA PAPER 83-0707] 11 p1651 A83-28011
- Model and full-scale studies of the exhaust noise from a bypass engine in flight
[AIAA PAPER 83-0751] 11 p1531 A83-28019
- Turbulence measurements relevant to sound generation of moving jets
[AIAA PAPER 83-0664] 12 p1777 A83-29525
- Aircraft noise and the airport community
[AIAA PAPER 83-1580] 14 p2048 A83-33352
- Effect of length of service on ground crew hearing threshold
15 p2211 A83-33541
- Method for calculating jet noise in the presence of a shielding surface
17 p2577 A83-37253
- Determination of the equivalent noise level contour for a passenger jet aircraft over a place in the case of quasi-steady flight regimes
17 p2577 A83-37535
- A study of the distribution of the noise source strengths in coaxial double jet
17 p2578 A83-37570
- Experimental methods in compressor noise studies
[ONERA, TP NO. 1983-79] 23 p3505 A83-48194
- Model test and full-scale checkout of dry-cooled jet runup sound suppressors
23 p3413 A83-48217
- Noise generation by a low-Mach-number jet
24 p3625 A83-49462
- JET AIRSTREAMS**
U JET STREAMS (METEOROLOGY)
- JET AUGMENTED WING FLAPS**
U JET FLAPS
U WING FLAPS
- JET BOUNDARIES**
Mechanism of pseudo-shock wave in supersonic jet
10 p1373 A83-26425
- JET CONTROL**
Aerodynamic characteristics of a jet controlled projectile
[AIAA PAPER 83-0392] 05 p0585 A83-16689
- A solution to the problem of multiparameter optimization in calculating flow around bodies with injection
06 p0712 A83-18143
- Dual mode reaction-jet, thrust-vector controls for small missiles
[AIAA PAPER 83-1148] 16 p2318 A83-36245
- Fluidic control systems for projectiles
[AIAA PAPER 83-1151] 16 p2352 A83-36248
- A study of the momentum loss of a slot jet propagating along a curved surface
17 p2450 A83-37639
- Stability of the Shuttle on-orbit flight control system for a class of flexible payloads
[AIAA PAPER 83-2178] 19 p2815 A83-41672
- JET DAMPING**
U DAMPING
U SPIN REDUCTION
- JET DRIVE**
U JET PROPULSION
- JET ENGINE FUELS**
NT JP-4 JET FUEL
- The effect of additive compositions on the oxidation stability of T-6 fuel
01 p0028 A83-10458
- Fuel property effects on Air Force gas turbine engines - Program genesis
01 p0028 A83-10653
- Impacts of broadened-specification fuels on aircraft turbine engine combustors
01 p0028 A83-10655
- A carbon-13 and proton nuclear magnetic resonance study of some experimental referee broadened-specification /ERBS/ turbine fuels
01 p0028 A83-11482
- Liquid fuel spray ignition predictions for JP-10
04 p0464 A83-16113
- The effect of the jet fuel temperature on wear rates during the friction of sliding and rolling
04 p0464 A83-16145
- Effects of envelope flames on drop gasification rates in turbulent diffusion flames
07 p0879 A83-19846
- Fuel for future transport aircraft
07 p0901 A83-20082
- A rapid method for determining the initial boiling point and the saturated-vapor pressure of petroleum products --- jet fuel tests in railroad tank cars
07 p0931 A83-20962
- Sooting tendency of fuels containing polycyclic aromatics in a research combustor
08 p1073 A83-23138
- Future fuels for turbojet engines and their impacts on combustion chambers and fuel systems
[DGLR PAPER 82-089] 09 p1242 A83-24201
- The removal of metals from a jet fuel using a manganese catalyst
11 p1552 A83-28775
- A continuous-flow microcalorimeter
11 p1576 A83-28800
- Future U.S. jet fuels - A refiner's viewpoint
13 p1826 A83-30187
- Jet fuels based on West Siberian oils
14 p1999 A83-32077
- The effect of the fuel quality on the degree of combustion product ionization in gas-turbine engines
14 p1988 A83-32078
- The effect of products based on higher fatty acids on the performance characteristics of jet fuels
15 p2143 A83-34500
- Operational effects of increased freeze point fuels in military airplanes
[AIAA PAPER 83-1139] 17 p2492 A83-38077
- Rheological behavior of FM-9 solutions and correlation with flammability test results and interpretations --- fuel thickening additive
21 p3117 A83-44856
- Comparison-effects of broadened property jet fuels on older and modern J79 combustors
[ASME PAPER 83-GT-81] 23 p3407 A83-47934
- Use of pyrolysis-derived fuel in a gas turbine engine
[ASME PAPER 83-GT-96] 23 p3440 A83-47942
- Monitoring the contamination of jet fuels by corrosion inhibitors
23 p3440 A83-48544
- JET ENGINES**
NT BRISTOL-SIDDELEY BS 53 ENGINE
NT J-79 ENGINE
NT PULSEJET ENGINES
NT RAMJET ENGINES
NT SUPERSONIC COMBUSTION RAMJET ENGINES
NT T-56 ENGINE
NT T-64 ENGINE
NT TF-41 ENGINE
NT TURBOFAN ENGINES
NT TURBOJET ENGINES
NT TURBOPROP ENGINES
- ASTF test instrumentation system detail design --- Aeropropulsion System Test Facility
01 p0014 A83-11059
- Effects of cobalt in nickel-base superalloys
07 p0892 A83-21467
- Jet engines for airliners of the next generation
[DGLR PAPER 82-069] 09 p1206 A83-24183
- Development trends regarding jet engines for future combat aircraft
[DGLR PAPER 82-072] 09 p1206 A83-24186
- PW4000 uses JT9D, new technology
10 p1378 A83-26072
- Separation of lower carbonyl compounds as their 2,4-dinitrophenylhydrazones by high-performance liquid chromatography and analytical application from jet engine exhaust
10 p1388 A83-26087
- Residual life prediction for jet engine rotor disks at elevated temperature
15 p2174 A83-33974
- Interaction of a jet at a lateral angle to a mainstream at low injection rates - An experimental study
16 p2290 A83-35818
- Effect of humidity on jet engine axial-flow compressor performance
16 p2304 A83-35856
- Deterioration trending enhances jet engine hardware durability assessment and part management
[AIAA PAPER 83-1234] 16 p2308 A83-36297
- CARS temperature and species measurements in augmented jet engine exhausts --- Coherent Anti-Stokes Raman Spectroscopy
[AIAA PAPER 83-1294] 16 p2309 A83-36328
- Superpotential solution for jet-engine external potential and internal rotational flow interaction
17 p2447 A83-37378
- Ion sensor signal fluctuations during spacecraft jet engine operation
17 p2481 A83-37467
- Application of numerical methods to the calculation of the characteristics of supersonic and hypersonic jet-engine air intakes
17 p2448 A83-37532
- The use of discontinuity surfaces of active and passive disk type for the mathematical modeling of unsteady flows in the circuit of a powerplant with a jet engine
17 p2450 A83-37636
- Experimental and theoretical investigation of nonequilibrium radiation from the jet of the correction engine of the Salyut manned orbital station
20 p2946 A83-42884
- Nonsynchronous whirls of the turbine rotor in aerojet engines
20 p2937 A83-43694
- GATOR-GARD applied coatings extend service lives of critical aerospace components
[SAE PAPER 820611] 22 p3301 A83-45869
- JET EXHAUST**
Some observations on the aerodynamics of an airfoil with a jet exhausting from the lower surface
[AIAA PAPER 83-0173] 05 p0580 A83-16569
- Unsteady heating of a complex solid body by a hot gaseous jet --- erosion effects of missile exhaust on its launcher
06 p0721 A83-18455
- Theory of resistance interference of airfoil wings and engine exhaust
07 p0862 A83-19667
- Conventional profile coaxial jet noise prediction
08 p1162 A83-22128
- Separation of lower carbonyl compounds as their 2,4-dinitrophenylhydrazones by high-performance liquid chromatography and analytical application from jet engine exhaust
10 p1388 A83-26087
- CARS temperature and species measurements in augmented jet engine exhausts --- Coherent Anti-Stokes Raman Spectroscopy
[AIAA PAPER 83-1294] 16 p2309 A83-36328
- Definition of vectored nonaxisymmetric nozzle plumes --- for aircraft thrust vector control
[AIAA PAPER 83-1290] 16 p2297 A83-36924
- The Coanda/refraction concept for gas turbine engine test cell noise suppression
[SAE AIR 1813] 17 p2471 A83-38105
- Scattered visible and ultraviolet solar radiation from condensed altitude control jet plumes
18 p2648 A83-40015
- JET FLAMES**
U FLAMES
U JET FLOW
- JET FLAPS**
Flight test of the 747-JT9D for airframe noise
03 p0281 A83-13163
- Jet wing vortex lattice theory with nonlinear wake and tip flows
[AIAA PAPER 83-0263] 05 p0583 A83-16619
- Progress towards a theory of jet flap thrust recovery
[AIAA PAPER 83-0079] 06 p0717 A83-19579
- Experimental study of jet-flap diffusers
17 p2448 A83-37534
- Aerodynamic characteristics of a circulation controlled elliptical airfoil with blown jets
[AIAA PAPER 83-1794] 17 p2453 A83-38633
- A three-dimensional solution of flows over arbitrary jet-flapped configurations using a higher-order panel method
[AIAA PAPER 83-1846] 17 p2456 A83-38674
- Some characteristics of pulsating or flapping jets
22 p3283 A83-46449
- The flapping motion of a turbulent plane jet - A workable relationship to wave-guide theory
22 p3283 A83-46453
- JET FLIGHT**
U JET AIRCRAFT
- JET FLOW**
NT AIR JETS
NT PERIPHERAL JET FLOW
NT SUPERSONIC JET FLOW
- Investigations of eddy coherence in jet flows
01 p0003 A83-10892
- The effect of a phase velocity difference on the turbulent structure of a jet carrying heavy admixtures
02 p0169 A83-11511
- Higher order boundary layer approximations for some flows of a power law fluid - Related solutions
02 p0169 A83-11858
- The development of jets in stratified fluids
02 p0169 A83-11860
- Mass transfer in the neighborhood of jets entering a crossflow
[ASME PAPER 82-HT-62] 02 p0173 A83-12802
- Noise and flow structure of a tone-excited jet
03 p0391 A83-13136
- Formation of the low-level jet under an inversion
03 p0369 A83-14449
- Numerical study of wall heat transfer in the recirculating flow region of a confined jet
04 p0477 A83-16124
- Analysis of multiple jets in a cross-flow
[ASME PAPER 82-WA/FE-4] 04 p0478 A83-16140
- An exact solution for a high-temperature jet stream
04 p0480 A83-16390
- Break-up and droplet formation of slurry jets
[AIAA PAPER 83-0067] 05 p0632 A83-16499
- A study with sensitivity analysis of the k-epsilon turbulence model applied to jet flows
[AIAA PAPER 83-0285] 05 p0633 A83-16630
- Transverse jet break-up and atomization with rapid vaporization along the trajectory
[AIAA PAPER 83-0419] 05 p0597 A83-16702
- Dynamic behavior of turbulent flow in a widely-spaced co-axial jet diffusion flame combustor
[AIAA PAPER 83-0575] 05 p0637 A83-16800
- Panetal jets. II - A problem of hypersustentation --- upper surface blowing
06 p0713 A83-19412
- Jet flow of an ideal liquid past a flexible shell
06 p0760 A83-19430
- Investigation of the dynamics of charged particles in the dispersion of a reaction jet in conditions of orbital flight
06 p0724 A83-19558
- Shock-tube investigation of jet flows from slotted and wedge-shaped nozzles --- for gasdynamic lasers
06 p0767 A83-19565

Velocity field characteristics of a swirling flow combustor
[AIAA PAPER 83-0314] 06 p0761 A83-19586

Experimental and theoretical studies on the relationship between engine exhaust and the surrounding flow field --- German thesis 06 p0714 A83-19618

The shape of low Reynolds number jets
07 p0926 A83-20527

Structure of a premixed concentric jet flame at main flame blow-off 08 p1056 A83-22065

Prediction of turbulent mixing in confined co-axial reacting jets 08 p1088 A83-23191

On the interaction of a sound pulse with the shear layer of an axisymmetric jet. II - Heated jets
09 p1340 A83-23704

Visualization of multijet impingement flow
09 p1198 A83-24652

Buoyant plane jets in thermally stratified media
[ASME PAPER 82-WA/HT-57] 10 p1413 A83-25696

Analysis of the effect of heated jet flow on the far field radiation from a noise source
[ASME PAPER 82-WA/NCA-4] 10 p1472 A83-25697

Near field pressure fluctuations of an elliptic jet
[AIAA PAPER 83-0663] 10 p1472 A83-25901

Some new results on edge-tone oscillations in high-speed subsonic jets
[AIAA PAPER 83-0665] 10 p1473 A83-25902

Scattering of an acoustic field by a free jet shear layer
[AIAA PAPER 83-0698] 10 p1474 A83-25918

A model of the excitation of large scale fluctuations in a shear layer
[AIAA PAPER 83-0724] 10 p1475 A83-25935

Cylindrical resonators --- shock wave production in jet nozzles 10 p1380 A83-26162

Efficiency of combined jet cooling of a plate in conditions of complex heat transfer 10 p1417 A83-26254

Prediction of the trajectory of triple jets in a uniform crossflow 10 p1418 A83-26629

Axially symmetric jet flows 11 p1564 A83-26975

Lagrangian pressure fluctuations in a jet
11 p1566 A83-27423

Use of an equation for the transport of the energy of turbulent pulsations to calculate two-phase jets
11 p1567 A83-27707

Turbulence measurements in wall jets along strongly concave surfaces 11 p1567 A83-27861

Sound generation by instability waves in a low Mach number jet
[AIAA PAPER 83-0661] 11 p1650 A83-28001

Direct measurement of sound from large scale structures in jet flows
[AIAA PAPER 83-0662] 11 p1653 A83-28197

Estimation of the vortex ratio and Karman constant for vortices 11 p1570 A83-28553

A theoretical prediction of the fluid buckling frequency
13 p1839 A83-30108

The effect of nonequilibrium on the expansion of CO₂ issuing into a rarefied medium 13 p1842 A83-30679

Computation of two-dimensional jet interaction flow field
[AIAA PAPER 83-1546] 14 p1971 A83-32769

Ablation of carbonaceous materials in a hydrogen-helium arc-jet flow
[AIAA PAPER 83-1561] 14 p1998 A83-32778

Turbulent flow induced by a jet in a cavity-measurements and 3D numerical simulation 15 p2155 A83-33666

Three-dimensional film cooling on a flat plate with tangential multi-jets 15 p2156 A83-33774

The distribution of the disperse fraction of a polydisperse jet injected into a gas flow 15 p2161 A83-34472

The thermal mechanism of barrier destruction by a transonic jet of rocket propellant combustion products
15 p2172 A83-34473

Solution of the problem of flow past a permeable plate with separation of jets 15 p2162 A83-35316

A study of a supersonic three-dimensional jet flow in a duct 16 p2289 A83-35718

Investigations of particle-grid turbulence
16 p2354 A83-36957

Aerodynamic studies on swirled coaxial jets from nozzles with divergent quarls 17 p2504 A83-37398

A study of the distribution of the noise source strengths in coaxial double jet 17 p2578 A83-37570

A study of the concentration field of a round jet by a quantitative visualization method
17 p2507 A83-38065

Surface pressures induced on a flat plate with in-line and side-by-side dual jet configurations
[AIAA PAPER 83-1849] 17 p2456 A83-38677

A study on the fluctuation concentration field in a turbulent jet 18 p2687 A83-40336

The principles governing the formation of circulation zones in the wake of mechanical and jet screens in confined flows 19 p2794 A83-42147

Pressure measurements of coaxial jet of high mean-velocity ratio 20 p2969 A83-42348

Instabilities in the slit-jet flow field 20 p2984 A83-43096

Note on the axisymmetric sonic jet 20 p2930 A83-43123

A general solution to the problem of jet flow past a wedge 20 p2931 A83-43520

Speckle velocimetry study of vortex pairing in a low-Re unexcited jet 21 p3128 A83-43928

An investigation of the Mach disc and the Riemann wave formation in impulsive jets 21 p3132 A83-44947

Diffusion of heat as a passive contaminant in a slightly pulsating jet 22 p3283 A83-46450

The preferred-mode coherent structure in the near field of an axisymmetric jet with and without excitation
22 p3283 A83-46451

Bell-shaped jet flow into a vacuum and interference effects with affected surfaces 22 p3261 A83-46486

Penetration and break-up behaviour of a discrete liquid jet in a cross flowing airstream - A further study
[ASME PAPER 83-GT-170] 23 p3448 A83-47971

Annular jets of different diameter ratios
23 p3449 A83-48142

Isothermal predictions of recirculating turbulent flowfields of confined dual coaxial jets behind an axisymmetric bluff body
[ASME PAPER 83-FE-14] 23 p3450 A83-48232

Interaction of a jet issuing from a body with a supersonic rarefied-gas counterflow 23 p3400 A83-48666

Spinning modes on axisymmetric jets. I
24 p3578 A83-49469

Smoke wire visualization of the external region of a two dimensional jet 24 p3585 A83-49822

JET FUELS

U JET ENGINE FUELS

JET IMPINGEMENT

Friction and heat transfer from plates to normally-incident axisymmetric turbulent jets
02 p0170 A83-11874

Heat transfer and microstructure of the boundary layer in the vicinity of the stagnation point of a jet flowing over a baffle 02 p0170 A83-11875

Oblique impingement of a round jet on a plane surface
03 p0278 A83-13145

Experimental study of a four-jet impingement flow using visualization techniques --- with applications to high performance VTOL aircraft
[AIAA PAPER 83-0171] 05 p0633 A83-16568

Calculation of the dispersal of a layer of granular material by a supersonic gas jet 05 p0639 A83-17407

The standoff distance of a compression shock upon impingement of an underexpanded jet onto a spherical baffle 05 p0590 A83-17419

An approach to calculating the flow following impingement of an underexpanded jet onto an infinite planar baffle 05 p0590 A83-17420

The impingement of a jet, in its initial formation stage, on a planar baffle 05 p0590 A83-17421

Visualization of heat transfer from arrays of impinging jets 05 p0640 A83-17702

A numerical study of the lateral interaction between an axisymmetric jet issuing into vacuum and an obstacle
06 p0760 A83-19431

Atomization of impinging liquid jets in a supersonic crossflow
[AD-A130714] 07 p0924 A83-19806

Flames with impinging jets 07 p0882 A83-21423

Two-dimensional flow impinging obliquely on a moving plane wall 08 p1083 A83-21867

Inviscid axisymmetric jet impingement with recirculating stagnation regions 08 p1042 A83-22130

Visualization of multijet impingement flow
09 p1198 A83-24652

An analysis of the thermal entrainment effect on jet impingement heat transfer
[ASME PAPER 82-WA/HT-54] 10 p1413 A83-25694

A numerical and experimental investigation of turbulent heat transport of an axisymmetric jet impinging on a flat plate
[ASME PAPER 82-WA/HT-55] 10 p1413 A83-25695

Analysis of jet-airframe interaction noise
[AIAA PAPER 83-0783] 10 p1376 A83-25964

On discrete tones generated by an impinging underexpanded rectangular jet
[AIAA PAPER 83-0729] 10 p1478 A83-26919

Improved Stirling engine performance using jet impingement 11 p1588 A83-27288

Investigation of the length and wave structure of the gasdynamic part in straight and spreading gas jets
11 p1567 A83-27718

Rain erosion damage in brittle materials
11 p1551 A83-28439

Analytical model of jet shielding --- aircraft noise reduction 12 p1777 A83-28958

The impact of compressible liquids
13 p1843 A83-31078

Loads and pressures due to underexpanded jets impinging on wedges 16 p2288 A83-35619

Stagnation point heat transfer for jet impingement to a plane surface 19 p2842 A83-40879

The effect of viscosity on flow in the circulation region in front of a plane obstacle perpendicular to the axis of an underexpanded supersonic jet
19 p2790 A83-41254

An experimental study of the impingement of a supersonic annular jet on an obstacle
19 p2790 A83-41260

Cooling of a rotating disk by means of an impinging jet
20 p2978 A83-42739

Experimental investigation of heat transfer by a single- and a triple-row round jets impinging on semi-cylindrical concave surfaces 20 p2929 A83-42740

Cross flow influence upon impingement convective heat transfer in circular arrays of jets - A general correlation
20 p2978 A83-42741

Heat transfer and flow characteristics of jets impinging on a concave hemispherical plate
20 p2979 A83-42743

Heat transfer augmentation in an axisymmetric impinging jet
20 p2979 A83-42744

Effect of semi-confinement on impingement heat transfer 20 p2979 A83-42746

Heat transfer from a turbulent, swirling, impinging jet
20 p2979 A83-42747

The effect of ordered structure of turbulence on momentum, heat and mass transfer of impinging round jets 20 p2984 A83-43020

A critical study of the erosion of an aluminum alloy by solid spherical particles at normal impingement
21 p3112 A83-44375

An experimental investigation into the effect of changes in the geometry of a slot nozzle on the heat transfer characteristics of an impinging air jet
21 p3131 A83-44851

Unsteady structures of a separated three-dimensional turbulent boundary layer 22 p3285 A83-47017

Heat transfer characteristics for jet array impingement with initial crossflow
[ASME PAPER 83-GT-28] 23 p3393 A83-47891

Characteristics of the ground vortex developed by various V/STOL jets at forward speeds
[AIAA PAPER 83-2494] 24 p3545 A83-49585

JET LAG

Effects of travel across time zones /jet-lag/ on exercise capacity and performance 07 p0977 A83-20782

JET MIXING FLOW

Flow instability and turbulence
03 p0317 A83-14454

Visualization study of the axisymmetric mixing layer of a high Reynolds number jet 03 p0320 A83-14482

Resonant entrainment of a confined pulsed jet
04 p0478 A83-16139

Jet trajectories and surface pressures induced on a body of revolution with various dual jet configurations
[AIAA PAPER 83-0080] 05 p0579 A83-16508

Experimental study of a four-jet impingement flow using visualization techniques --- with applications to high performance VTOL aircraft
[AIAA PAPER 83-0171] 05 p0633 A83-16568

Interaction of a pair of curved wall jets after a circular cylinder
[AIAA PAPER 83-0290] 05 p0584 A83-16632

Interactive phenomena in supersonic jet mixing problems
[AIAA PAPER 83-0288] 05 p0588 A83-16826

Mixing in jet flames by laser Rayleigh scattering
[AIAA PAPER 83-0403] 05 p0612 A83-16827

Calculation of parameters of a near wake produced by injection of an annular jet into the base region
05 p0590 A83-17424

On the deformation of the rectangular turbulent jet cross-section 05 p0640 A83-17703

Measurements of reactive recirculating jet mixing in a combustor 07 p0924 A83-19819

Counter-current jet combustion of a hydrocarbon fuel in air 07 p0882 A83-21422

An experimental investigation of the dispersion of a gas jet in a coflowing stream of air 08 p1042 A83-23215

Principles governing the mixing of transverse jets
09 p1196 A83-23439

Investigation of the flow in a jet produced by two nozzles 09 p1197 A83-24045

Viscous stability of compressible axisymmetric jets
09 p1341 A83-24651

Experimental study of jet mixing mechanisms in a model secondary combustor 09 p1198 A83-24664

Eddy viscosity in axisymmetric swirling jets
09 p1263 A83-25025

- On the shock cell structure and noise of supersonic jets
[AIAA PAPER 83-0703] 10 p1474 A83-25923
- Flight effects on jet mixing noise - Scaling laws predicted for single jets from flight simulation data
[AIAA PAPER 83-0748] 10 p1476 A83-25950
- Flight effects on jet noise sources investigated by model experiments in the DNW
[AIAA PAPER 83-0752] 10 p1476 A83-25951
- Regular structures in a plane triple jet
10 p1418 A83-26627
- Investigation of the optical inhomogeneities of the active medium of a fast-flow CO₂ laser with mixing
10 p1433 A83-26677
- Shock-capturing parabolized Navier-Stokes model /SCIPVIS/ for the analysis of turbulent underexpanded jets
[AIAA PAPER 83-0704] 10 p1418 A83-26916
- Coherent structures in rectangular jets
11 p1565 A83-27418
- Turbofan mixer nozzle flowfield - A benchmark experimental study
11 p1525 A83-27419
- Penetration into a supersonic flow of a jet injected through a convex cylindrical surface
11 p1526 A83-27722
- Effect of initial conditions on constant pressure mixing between two turbulent streams
11 p1567 A83-27875
- Experimental study of a gas film in a tube
11 p1568 A83-28371
- Experimental investigation of multiple jets in a cross-flow
[AIAA PAPER 83-1545] 14 p1971 A83-32768
- Profile losses during the release of air onto the surface of nozzle vanes
16 p2288 A83-35590
- The relationship between the aerodynamic and acoustic characteristics of coaxial jets
16 p2408 A83-35712
- Edge tones in high-speed flows and their application to multiple-jet mixing
16 p2408 A83-36077
- Perspectives on the mixing of a row of jets with a confined crossflow
[AIAA PAPER 83-1200] 16 p2352 A83-36276
- Experiments in dilution jet mixing
[AIAA PAPER 83-1201] 16 p2352 A83-36277
- An experimental study of downstream mixing CO₂ laser
[AIAA PAPER 83-1703] 17 p2513 A83-37200
- An integral model for confined axisymmetric turbulent jet mixing
[AIAA PAPER 83-1742] 18 p2680 A83-39098
- The cold locking of the duct of a gas-liquid mixer by burning fuel jets
18 p2663 A83-39168
- An analysis of the axisymmetric turbulent buoyant jet
20 p2973 A83-42685
- An experimental study of the interaction between two hypersonic wakes
20 p2931 A83-43521
- The effect of forcing on the mixing-layer region of a round jet
22 p3283 A83-46452
- Instability and coherent structures in jet flames
22 p3266 A83-46458
- Measured velocity fluctuations inside the mixing layer of a supersonic jet
22 p3249 A83-46468
- Statistical characteristics of velocity, concentration, mass transport, and momentum transport for coaxial jet mixing in a confined duct
[ASME PAPER 83-GT-39] 23 p3447 A83-47899
- Mixing and fuel atomisation effects on premixed combustion performance
[ASME PAPER 83-GT-55] 23 p3407 A83-47911
- Temperature profile development in turbulent mixing of coolant jets with a confined hot cross flow
[ASME PAPER 83-GT-220] 23 p3448 A83-48019
- Effectiveness measurements for a cooling film disrupted by a single jet
[ASME PAPER 83-GT-250] 23 p3397 A83-48037
- Multiple jet mixing in a rectangular duct - Centre-plane behaviour
[ASME PAPER 83-FE-35] 23 p3399 A83-48238
- Analytical description of a hypersonic gas jet flowing into a medium at rest or into a supersonic wake
23 p3400 A83-48673
- Alternating-triangular difference scheme for solving the Navier-Stokes equations
24 p3576 A83-48946
- On the organized motion of a turbulent plane jet
24 p3577 A83-49464
- JET NOISE**
U JET AIRCRAFT NOISE
- JET NOZZLES**
Permissible model sizes for measurements in free-jet supersonic wind tunnels
02 p0132 A83-13000
- Nozzle design yielding interferometrically flat fluid jets for use in single-mode dye lasers
03 p0332 A83-14164
- Porous-plug flowfield mechanisms for reducing supersonic jet noise
[AIAA PAPER 83-0774] 10 p1378 A83-25959
- Optimization of the jet cooling of a rotating disk
19 p2844 A83-41567
- JET PILOTS**
U AIRCRAFT PILOTS
- JET PROPULSION**
The Talos propulsion system
02 p0148 A83-12857
- Flight/propulsion control system integration
[AIAA PAPER 83-1238] 16 p2308 A83-36301
- Jet-propulsion of subsonic bodies with jet total-head equal to free stream's
[AIAA PAPER 83-1790] 17 p2469 A83-38630
- JET PUMPS**
Upgrading vortex amplifier performance by matched ejectors
11 p1568 A83-28175
- JET STAR AIRCRAFT**
U C-140 AIRCRAFT
- JET STREAMS (METEOROLOGY)**
An analysis of the LFM-11 simulations of the Presidents' Day Cyclone, February 18-19, 1979
03 p0368 A83-14442
- Aerodynamic platform comparison for jet-stream electricity generation
04 p0507 A83-16102
- On the rotary wing concept for jet stream electricity generation
04 p0507 A83-16111
- Airborne radar altimeter measurements of geostrophic and ageostrophic winds over irregular topography
05 p0668 A83-17447
- A newly found jet in north Kenya /Turkana Channel/
06 p0792 A83-18473
- A subsynoptic-scale kinetic energy analysis of the Red River Valley tornado outbreak /AVE-SESAME I/ --- Atmospheric Variability Experiment - Severe Environmental Storms and Mesoscale Experiment
08 p1140 A83-22298
- Numerical simulation of nonlinear jet streak adjustment
08 p1140 A83-22300
- The instability of the gravity-inertia wave and its relation to low-level jet and heavy rainfall
09 p1311 A83-23889
- The causes of the origin of mesojets and the calculation of the wind velocity at their axes in narrow zones of warm fronts
09 p1315 A83-24936
- Relationships among the stratospheric and tropospheric zonal flows and the Southern Oscillation
10 p1450 A83-25387
- Forecasting foehn winds at Anchorage, Alaska
13 p1888 A83-30566
- Relative humidity distribution in the vicinity of the warm conveyor belt
13 p1889 A83-30574
- The interactive role of subsynoptic scale jet streak and planetary boundary layer adjustments in organizing an apparently isolated convective complex
13 p1890 A83-30585
- Ageostrophic winds and vertical motion fields accompanying upper level jet streak propagation during the Red River Valley tornado outbreak
13 p1890 A83-30587
- Barotropic instability of the polar night jet stream
16 p2385 A83-35477
- A three-dimensional planetary boundary layer model for the somali jet
16 p2386 A83-35482
- Charney's problem for baroclinic instability applied to barotropic instability
16 p2387 A83-35492
- A simple Lagrangian forecast system with aviation forecast potential
17 p2550 A83-38727
- JET THRUST**
The measurement of impulsive forces on a wind tunnel model with a conventional strain gage balance
01 p0014 A83-11069
- Progress towards a theory of jet flap thrust recovery
[AIAA PAPER 83-0079] 06 p0717 A83-19579
- Ion sensor signal fluctuations during spacecraft jet engine operation
17 p2481 A83-37467
- Design of reaction jet attitude control systems for flexible spacecraft
17 p2479 A83-37471
- Plume/flowfield jet interaction effects on the Space Shuttle Orbiter during entry
18 p2646 A83-40009
- Accommodation of practical constraints by a linear programming jet select --- for Space Shuttle
[AIAA PAPER 83-2209] 19 p2815 A83-41693
- JET VANES**
Aerodynamics propulsion and longitudinal control requirements for a tilt-nacelle V/STOL with control vanes submerged in the nacelle slipstream
[AIAA PAPER 83-2513] 23 p3404 A83-48357
- JETAVATORS**
U GUIDE VANES
- JETS**
In situ acceleration in extragalactic radio jets
03 p0423 A83-14185
- Jet activity in the Seyfert galaxy MKN 335
18 p2777 A83-39779
- JETTISONING**
An analysis of the fatality rate data from 'jettison-canopy' and 'through-the-canopy' ejections from automated airborne escape systems
04 p0443 A83-15403
- Preliminary generalized thoughts concerning jettisoned vs through-the-canopy ejection escape systems
04 p0444 A83-15406
- Ground contamination by fuel jettisoned from aircraft in flight
[AD-A128451] 09 p1294 A83-24041
- JFET**
Application of JFets to low background focal planes in space
03 p0308 A83-13456
- Ionizing radiation response of GaAs JFETs and DCLF circuits
05 p0626 A83-17503
- Dependence of normally-off GaAs JFET performance on device structure
05 p0631 A83-17756
- Signal processing and compensation electronics for junction field-effect transistor /JFET/ focal plane arrays
08 p1081 A83-22606
- Hybrid packaging approach to improved low-noise operation of photovoltaic InSb detectors
14 p2015 A83-31981
- Computer-aided design of infrared detector preamplifiers having switched feedback resistors
22 p3292 A83-46604
- JIMSPHERE BALLOONS**
Information retrieval from wide-band meteorological data - An example
17 p2552 A83-38758
- JITTER**
U VIBRATION
- JOBS**
U TASKS
- JOINTS (ANATOMY)**
NT ELBOW (ANATOMY)
NT KNEE (ANATOMY)
NT WRIST
- A comparative analysis of the movement of traumatized and healthy extremities during running on a treadmill
01 p0083 A83-10521
- The active and passive flexibility of athletes of various specialties
01 p0083 A83-10523
- The treatment of trauma of the locomotor system in athletes /Study of the work of the athletic clinic for trauma in Austria/
01 p0084 A83-11385
- Histological and histochemical investigations of the locomotor system during general hypoxia
03 p0375 A83-13640
- Vibratory behavior of the lumbo-sacral joint after ablation of the pulposus nucleus
14 p2063 A83-32459
- JOINTS (JUNCTIONS)**
NT BUTT JOINTS
NT LAP JOINTS
NT METAL JOINTS
NT RIVETED JOINTS
NT SEAMS (JOINTS)
NT SPOT WELDS
NT WELDED JOINTS
- Hollow section joints --- Thesis
02 p0190 A83-11945
- On the workspace of mechanical manipulators
[ASME PAPER 82-DET-127] 02 p0187 A83-12781
- Optimal cooling of cross-ply composite laminates and adhesive joints
[ASME PAPER 82-WA/APM-24] 04 p0455 A83-15679
- Systematic development of constant velocity joints - A contribution to methodical designing --- German thesis
04 p0487 A83-15848
- Mechanism of interfacial bond failure
04 p0463 A83-15873
- An equation for bolt clampup relaxation in transient environments
05 p0611 A83-16935
- Joining of components moulded in carbon fibre-reinforced thermoplastics
06 p0724 A83-17963
- Scattering at rectangular-to-rectangular waveguide junctions
06 p0748 A83-18775
- The design of bonded structure repairs
09 p1243 A83-23329
- Experimental study of junctions of dielectric strip waveguides in the millimeter-wave range
09 p1253 A83-23471
- Strength of mechanically fastened composite joints
10 p1439 A83-25880
- On the analysis of adhesive joints in fiber reinforced composite plates and shells
11 p1591 A83-27430
- An approach to the analysis of the compliance of threaded connections in creep
11 p1598 A83-28502
- The strength of S0115M glass ceramic and its joints made through optical contact
11 p1551 A83-28511
- Design, fabrication and test of graphite/polyimide composite joints and attachments
[AIAA 83-0907] 12 p1739 A83-29763
- The fracture toughness of interlayers in joints with layers of different moduli under static tension
14 p2030 A83-32384

- Surface roughness effects on the stress analysis of adhesive joints 14 p2032 A83-32843
- Calculation of the local compliance of elements of a multiple-row double-shear bolt joint 17 p2518 A83-37256
- The use of the moire method to study the local compliance of the joined element of a double-shear bolt joint 17 p2518 A83-37270
- Interaction of a sunk bolt with parts of a single-shear joint in conditions of radial tension 17 p2520 A83-37517
- Utilization of the dynamic characteristics of a structure to evaluate its technological state --- dynamic structural analysis of caissons 18 p2698 A83-39510
- Fatigue of composite bolted joints under dual load levels 18 p2703 A83-40158
- Strength tests of CFRP joint assembly models for tailplane structure 18 p2703 A83-40159
- The comparison of the results of service-spectrum tests with the help of the relative Miner rule --- fatigue life analysis of aircraft structures 18 p2696 A83-40471
- A moment solution for waveguide junction problems 19 p2837 A83-41083
- 2000 W mean-power X-band waveguide junction circulator using a composite turnstile resonator 20 p2966 A83-42370
- Analysis and filtering applications of two newly proposed waveguide-coaxial line junctions 20 p2967 A83-42611
- The effect of composite prebond moisture on adhesive-bonded CFRP-CFRP joints 20 p2947 A83-42807
- Kinematics of robot wrists 20 p2959 A83-43110
- An approach for the generation of kinematic chains with multiple joints 21 p3147 A83-44030
- Pin joints in composites 21 p3151 A83-44053
- Fracture toughness of composite adherend adhesive joints under mixed mode I and III loading 21 p3115 A83-44121
- Effects of anomalous rotor joints on turbomachine dynamics [ASME PAPER 83-GT-175] 23 p3464 A83-47974
- Brazing of silicon nitride 23 p3437 A83-48286
- Selection and development of numerical methods for studying the stress-strain state in cases involving connections with a guaranteed interference fit 24 p3595 A83-49903
- JOSEPHSON JUNCTIONS**
- Superconductive behavior of a multiconnected Josephson network in a periodically varying magnetic field of two frequency components 01 p0109 A83-10632
- Fluxon propagation in Josephson junction transmission lines coupled by resistive networks 01 p0036 A83-10639
- Ac Josephson effect in small-area superconducting tunnel junctions at 604 GHz 01 p0039 A83-10995
- Logic delays of 5-micron resistor coupled Josephson logic 01 p0039 A83-10996
- Electrical properties of an input-output cable for Josephson applications 02 p0168 A83-12815
- An SIS receiver for the 3 mm wavelength range --- Superconductor Insulator Superconductor 04 p0472 A83-15811
- Current-waveform dependence of punchthrough probability in a Josephson tunnel junction 04 p0473 A83-16072
- Effect of trapped magnetic flux on the threshold curves of three-junction superconducting quantum interference devices 04 p0473 A83-16073
- A high-sensitivity millimeter-wave radiometer with a Josephson detector 06 p0819 A83-18802
- Photon-assisted tunneling at 246 and 604 GHz in small-area superconducting tunnel junctions 07 p0999 A83-19995
- Intermittency in Josephson junctions 07 p0918 A83-19996
- A symmetrical three-junction superconducting quantum interference device 07 p0921 A83-20755
- Voltage and current expressions for a two-junction superconducting interferometer 08 p1093 A83-22340
- Coherent behavior of 2N-Josephson junction closed loop 08 p1081 A83-22769
- Josephson technology special purpose systolic architecture signal processing application 08 p1153 A83-22802
- Response of a selective receiver with a Josephson detector to microwave signals with different spectra 09 p1252 A83-23466
- Study of tunnel junctions in niobium films for use in microwave receivers 09 p1254 A83-23995
- Synchronization effects in a submillimeter Josephson self-oscillator 10 p1409 A83-25812
- Josephson-junction mm-wave mixer 10 p1410 A83-25892

- Fabrication and Josephson behavior of high-Tc superconductor-normal-superconductor microbridges 10 p1410 A83-25988
- A consistent model for 1/f-noise in thin-film devices such as bolometers, Josephson junctions and SQUIDs 11 p1562 A83-28074
- Direct-coupled Josephson exclusively or gate with a high gain and a wide margin 11 p1563 A83-28615
- Superconducting current injection transistor 13 p1832 A83-30354
- Subharmonic generation in Josephson junction fluxon oscillators biased on Fiske steps 13 p1832 A83-30355
- Sub-10 ps high-gain direct coupled Josephson logic gate 13 p1837 A83-31764
- All-refractory Josephson logic circuits 15 p2150 A83-33888
- Josephson-junction circuit analysis via integral manifolds 15 p2151 A83-33928
- Flux-flow type Josephson oscillator for millimeter and submillimeter wave region 16 p2345 A83-35445
- Dynamics of accelerated Josephson junctions 16 p2345 A83-35515
- Absolute measurement at 1 THz of the optical coupling of a F.I.R. conical antenna with a Josephson detector 17 p2511 A83-37759
- Allowance for the skin effect in a superconductor-semiconductor-superconductor d structure 17 p2499 A83-38487
- High speed logic operations of all refractory Josephson integrated circuits 18 p2677 A83-40068
- High-precision test of the universality of the Josephson voltage-frequency relation 19 p2837 A83-40959
- A superconducting tunnel junction receiver for 230 GHz 19 p2838 A83-41091
- Sensitivity of a wide-band far-IR receiver using a Josephson self-oscillator mixer 21 p3125 A83-44387
- Simulation of the noise rise in three-photon Josephson parametric amplifiers 21 p3127 A83-45501
- The mechanisms of flicker noise in Josephson junctions 22 p3276 A83-45673
- Solitons in solids 22 p3354 A83-45894
- Nb3Al/oxide/Pb Josephson tunnel junctions fabricated using a CF4 cleaning process 22 p3279 A83-46740
- Random instability in Josephson junctions 22 p3279 A83-46786
- Microwave properties of superconducting tunnel junctions during quasiparticle tunneling 24 p3572 A83-48865
- High-resolution imaging of inhomogeneities in superconducting tunnel junctions by scanning with a modulated electron beam 24 p3636 A83-49757
- JOUKOWSKI TRANSFORMATION**
- Unsteady flows about a Joukowski airfoil in the presence of moving vortices [AIAA PAPER 83-0129] 05 p0580 A83-16542
- Bow wave patterns 14 p2012 A83-32990
- JOULE HEATING**
- U OHMIC DISSIPATION
- U RESISTANCE HEATING
- JOULE-THOMSON EFFECT**
- Miniature J-T refrigerators using adsorption compressors 20 p2960 A83-43231
- JOURNAL BEARINGS**
- Dynamics of rotor bearing systems supported by floating ring bearings [ASME PAPER 81-LUB-37] 02 p0186 A83-11938
- Characteristics of an oil squeeze film 02 p0186 A83-11939
- A sensitivity analysis of squeeze-film bearings 02 p0186 A83-11941
- An experimental investigation of the vaporous/gaseous cavity characteristics of an eccentric journal bearing [ASLE PREPRINT 82-LC-3A-1] 03 p0333 A83-13230
- Estimating the severity of shaft vibrations within fluid film journal bearings [ASME PAPER 82-LUB-1] 03 p0335 A83-13502
- Overall characteristics of bearings lubricated with ferrofluids [ASME PAPER 82-LUB-14] 03 p0335 A83-13508
- High-speed motion picture camera experiments of cavitation in dynamically loaded journal bearings [ASME PAPER 82-LUB-18] 03 p0335 A83-13509
- Analysis of gas-lubricated foil journal bearings [ASME PAPER 82-LUB-40] 03 p0336 A83-13519
- A note on rotor-bearing stability 09 p1274 A83-23706
- Frequency effects in tilting-pad journal bearing dynamic coefficients 12 p1732 A83-29125
- High-speed motion picture camera experiments of cavitation in dynamically loaded journal bearings [ASME PAPER 82-LUB-18] 18 p2695 A83-39944
- High-speed floating-ring bearing test and analysis [ASLE PREPRINT 83-AM-3E-2] 20 p2999 A83-43337

- An investigation into the effect of side-plate clearance in an uncentralized squeeze-film damper [ASME PAPER 83-GT-176] 23 p3464 A83-47975
- Gas bearings. II - Design data for centrally loaded partial arc journal bearings 23 p3466 A83-48155
- JOURNALS (DOCUMENTS)**
- U PERIODICALS
- JOURNALS (SHAFTS)**
- U SHAFTS (MACHINE ELEMENTS)
- JP-4 JET FUEL**
- Flight testing with hot JP-4 fuel --- in helicopter suction fuel systems 09 p1208 A83-24831
- JUMPERS**
- Selection and prediction of the athletic results of young female long-jumpers 03 p0382 A83-14353
- JUNCTION DIODES**
- NT MIM DIODES
- Theory and experiments on open circuit voltage decay of p-n junction diodes with arbitrary base width, including the effects of built-in drift field in the base and recombinations in the emitter 04 p0473 A83-16088
- Electron transport in GaAs n+ / -p / -n / + / submicron diodes 05 p0624 A83-17296
- Experimental results on junction charge-coupled devices 06 p0752 A83-18760
- Long wavelength Pb1-x/Sn/x/Te homostructure diode lasers having a gallium-doped cladding layer 07 p0937 A83-21369
- Unified analysis of the bulk unipolar diode 09 p1255 A83-24492
- Integrated fin-line components and subsystems at 60 and 94 GHz 10 p1409 A83-25806
- A reevaluation of the meaning of capacitance plots for Schottky-barrier-type diodes 11 p1564 A83-28712
- Analysis and modeling of 'two-gap' coaxial line rectangular waveguide junctions 13 p1831 A83-30233
- Photovoltaically active p layers of amorphous silicon 13 p1870 A83-30352
- Post-hydrogenated CVD amorphous silicon p-n diodes for photovoltaic applications 14 p2005 A83-32285
- Double-injection currents and the field effect in p(+)nn(+) silicon-on-sapphire diodes 16 p2346 A83-35946
- Ultrafast GaAs microwave PIN diode 17 p2500 A83-38883
- SEM-EBIC and traveling light spot diffusion length measurements - Normally irradiated charge-collecting diode 18 p2678 A83-40371
- Electrical diagnostics of the amplifier operation and a feasibility of signal registration on the basis of the voltage saturation effect in junction laser diodes 19 p2852 A83-40941
- JUNCTION FIELD EFFECT TRANSISTORS**
- U JFET
- JUNCTION TRANSISTORS**
- NT JFET
- High-power field effect transistors in low-frequency and high-frequency power amplifiers 01 p0038 A83-10802
- Ion-implanted s lateral PNP transistors 05 p0624 A83-17288
- The characterization of transistor electrical overstress failure probability density functions 05 p0625 A83-17477
- An improved bipolar junction transistor model for electrical and radiation effects 05 p0626 A83-17488
- High-voltage two-dimensional simulations of permeable base transistors 09 p1256 A83-24684
- Development of a measurement technique for qualitative analysis of MOS transistors using Kuhn's method for MOS varactors --- German thesis 11 p1564 A83-28644
- Superconducting current injection transistor 13 p1832 A83-30354
- Establishment of the steady state during the switching on of a high-power high-voltage transistor 17 p2499 A83-38496
- JUNCTIONS**
- Equivalent circuit of a coaxial-waveguide junction 04 p0471 A83-15732
- JUNGLES**
- U TROPICAL REGIONS
- JUPITER (PLANET)**
- Planetary magnetospheres 02 p0264 A83-12181
- Improvement of the theories of Jupiter and Saturn by harmonic analysis 02 p0247 A83-12533
- Three characteristic parameters of orbits of Hilda-type asteroids 02 p0247 A83-12544
- Decametric emission of Jupiter and solar activity 02 p0268 A83-12860
- Tidal heating of Io and orbital evolution of the Jovian satellites 03 p0401 A83-13302
- Poynting-Robertson drag and orbital resonance 03 p0407 A83-13839
- On the nature of S II emission from Jupiter's hot plasma torus 04 p0569 A83-15642

- Galileo Atmospheric Entry Probe System - Design, development, and test
[AIAA PAPER 83-0098] 05 p0605 A83-16520
- By Jupiter: Odysseys to a giant --- Book
05 p0704 A83-17118
- Formation of Jovian decametric S bursts by modulated electron streams 05 p0705 A83-17387
- Pre-discovery encounters between short-period comets and Jupiter estimated by a Keplerian approximation
05 p0695 A83-17831
- Occultations of Jupiter by the moon in 1983
06 p0817 A83-18065
- Identification of radio emission from the Io flux tube
06 p0848 A83-18315
- Perturbations by Jupiter of the particles ejected from Comet Lexell 06 p0816 A83-18529
- Influence of interplanetary magnetic field sector boundary passages on Jovian decametric radio bursts
07 p1036 A83-21587
- The planet Jupiter in 1979-1980 - The observers and their works 08 p1188 A83-22050
- Jupiter --- Book 09 p1366 A83-24900
- The C-12/C-13 ratio in Jupiter from the Voyager infrared investigation 10 p1518 A83-25515
- Coordinate systems --- of Jupiter 10 p1497 A83-26624
- Investigation of encounters of Comet Chernykh /1978 IV/ with Jupiter in 1978-1981 and with Saturn in 1981-1984 11 p1674 A83-28052
- A second order Jupiter-Saturn planetary theory. I
11 p1685 A83-28381
- Families of asymmetric periodic solutions of the restricted problem of three bodies for the sun-Jupiter mass ratio and their relationship with the symmetric families.
12 p1786 A83-29104
- Computation of Jupiter interior models from gravitational inversion theory 15 p2275 A83-34720
- Amalthea - Implications of the temperature observed by Voyager 15 p2275 A83-34724
- A second order Jupiter-Saturn planetary theory
16 p2439 A83-36787
- The Io-control of Jupiter's decametric radiation - The Alfven wave model 17 p2620 A83-38115
- Energetic ion acceleration and transport in the upstream region of Jupiter - Voyager 1 and 2 17 p2621 A83-38117
- Return to Jupiter - Project Galileo 18 p2644 A83-40344
- The source location of certain Jovian decametric radio emissions 20 p3078 A83-42408
- Velocities of ejection of comets by Jupiter and Saturn 20 p3061 A83-43414
- A mechanism of formation for the Kirkwood gaps
22 p3376 A83-47089
- A catalogue of Jovian radio observations from January 1980 to December 1981 24 p3672 A83-49318
- High precision spectropolarimetry of stars and planets. II Spectropolarimetry of Jupiter and Saturn 24 p3643 A83-49354
- The planet Jupiter in 1980-1981 24 p3673 A83-49449
- A new type of decametric radio emission from Jupiter 24 p3673 A83-49631
- Observations of Jupiter with the CERGA astrolabe (February 1980-May 1981) 24 p3645 A83-49843
- ### JUPITER ATMOSPHERE
- Solutions to the equations for corotating magnetospheric convection 02 p0263 A83-11602
- Investigation of the flux of Jupiter electrons with energy not less than 40 keV by the Mars-7 interplanetary probe 02 p0263 A83-11715
- Copernicus measurement of the Jovian Lyman-alpha emission and its aeronomical significance 02 p0264 A83-12142
- The abundances of CH₄, CH₃D, NH₃, and PH₃ in the troposphere of Jupiter derived from high-resolution 1100-1200/cm spectra 02 p0264 A83-12143
- Thermal- and plasma-induced molecular redistribution on the icy satellites 03 p0133 A83-13831
- The tropospheric gas composition of Jupiter's north equatorial belt /NH₃, PH₃, CH₃D, GeH₄, H₂O/ and the Jovian D/H isotopic ratio 04 p0569 A83-15643
- Io's surface - Its phase composition and influence on Io's atmosphere and Jupiter's magnetosphere 04 p0571 A83-16245
- Emissions from neutrals and ions in the Jovian magnetosphere 04 p0572 A83-16247
- On the C/H and D/H ratios in the atmospheres of Jupiter and Saturn 05 p0703 A83-16959
- Motion in the interiors and atmospheres of Jupiter and Saturn - Scale analysis, anelastic equations, barotropic stability criterion 05 p0703 A83-16960
- Airborne spectroscopy of Jupiter in the 100- to 300/cm region - Global properties of ammonia gas and ice haze 05 p0703 A83-16961
- The effect of ammonia ice on the outgoing thermal radiance from the atmosphere of Jupiter 05 p0703 A83-16962
- Observations of Jupiter's distant magnetotail and wake
[AD-A123812] 05 p0704 A83-17384
- Thin, rotating plasma disks 06 p0847 A83-18277
- Photochemistry of NH₃, CH₄ and PH₃ - Possible applications to the Jovian planets 06 p0801 A83-19403
- The Voyager mission and the origin of life - Selected references 06 p0801 A83-19409
- The hydrogen to helium ratio in Jupiter and Saturn 06 p0849 A83-19465
- Galileo atmospheric entry probe mission description [AIAA PAPER 83-0100] 06 p0722 A83-19580
- Departure from corotation of the Io plasma torus - Local plasma production 07 p1028 A83-20190
- Gold's hypothesis and the energetics of the Jovian magnetosphere 07 p1029 A83-20410
- Measurements of stratospheric ethane in the Jovian South Polar Region from infrared heterodyne spectroscopy of the nu₉ band near 12 microns 07 p1031 A83-21151
- Temporal variation of the Jovian H I Lyman-alpha emission /1979-1982/ 07 p1031 A83-21158
- A theory of Jovian decameter radiation 07 p1036 A83-21505
- Photochemistry of acetylene at 1849 A 08 p1053 A83-22217
- The abundance of water on Jupiter from the Voyager IRIS data at 5 microns 08 p1189 A83-22932
- Lightning activity on Jupiter 08 p1189 A83-22933
- Effects of differential rotation on the gravitational figures of Jupiter and Saturn 08 p1189 A83-22935
- Jovian modulation of interplanetary electrons as observed with Voyagers 1 and 2 09 p1365 A83-23754
- A model of mean zonal flows in the major planets 10 p1517 A83-25415
- Further observations of 8-micron polar brightenings of Jupiter 10 p1518 A83-25516
- An analysis of the reflection spectrum of Jupiter from 1500 A to 1740 A 10 p1518 A83-25736
- Physics of the Jovian magnetosphere --- Book 10 p1519 A83-26611
- Jupiter's magnetic field and magnetosphere 10 p1519 A83-26612
- Ionosphere --- of Jupiter 10 p1519 A83-26613
- The low-energy plasma in the Jovian magnetosphere 10 p1519 A83-26614
- Low-energy particle population --- in Jupiter magnetosphere 10 p1519 A83-26615
- High-energy particles --- in Jovian magnetosphere 10 p1519 A83-26616
- Spectrophotometric studies of the Io Torus 10 p1519 A83-26617
- Phenomenology of magnetospheric radio emissions 10 p1519 A83-26618
- Plasma waves in the Jovian magnetosphere 10 p1519 A83-26619
- Theories of radio emissions and plasma waves --- in Jupiter magnetosphere 10 p1520 A83-26620
- Magnetospheric models --- Jovian phenomena 10 p1520 A83-26621
- Plasma distribution and flow --- in Jovian magnetosphere 10 p1520 A83-26622
- Microscopic plasma processes in the Jovian magnetosphere 10 p1520 A83-26623
- Alfven wave propagation in the Io plasma torus 11 p1685 A83-28305
- Cosmological implications of helium and deuterium abundances on Jupiter and Saturn 11 p1686 A83-28388
- Experimental study of the pure rotational S₁ line of the H₂-He spectrum induced by an absorption defect collision due to collisional interference effects 12 p1778 A83-29390
- Narrowband electromagnetic emissions from Jupiter's magnetosphere 12 p1799 A83-29707
- Kelvin-Helmholtz instability and the Jovian Great Red Spot 13 p1960 A83-30797
- Rocket detection of ultraviolet emission from neutral oxygen and sulfur in the IO Torus 13 p1962 A83-31452
- A simple model of the distant Jovian tail with magnetic flux loss 13 p1962 A83-31662
- Near-infrared mapping spectrometer for investigation of Jupiter and its satellites 14 p1983 A83-32000
- Observed departure of the Io plasma torus from rigid corotation with Jupiter 14 p2113 A83-33233
- On the nature of the interaction of the Jovian magnetosphere with the icy Galilean satellites 15 p2273 A83-33930
- HCN formation on Jupiter - The coupled photochemistry of ammonia and Acetylene 15 p2275 A83-34718
- Study of the deep cloud structure in the equatorial region of Jupiter from Voyager infrared and visible data 15 p2275 A83-34719
- Reconnection in the Jovian magnetosphere 15 p2275 A83-34730
- Physics of the Jovian and Saturnian magnetospheres Highlights of a conference held at the Applied Physics Laboratory, the Johns Hopkins University, October 22-24, 1981 16 p2437 A83-36622
- Energetic oxygen and sulfur ions in the Jovian magnetosphere and their contribution to the auroral excitation 17 p2618 A83-37580
- Turbulence analysis of the Jovian upstream 'wave' phenomenon 17 p2618 A83-37584
- Planetary radio astronomy from Voyager 17 p2620 A83-38108
- Synchrotron radiation as a probe of the inner magnetosphere of Jupiter 17 p2620 A83-38110
- Force balance in the magnetospheres of Jupiter and Saturn 17 p2620 A83-38114
- The Jovian magnetosphere 17 p2622 A83-38291
- Plasma waves in planetary magnetospheres 17 p2542 A83-38298
- Dynamo region and the equatorial electrojet in the Jovian atmosphere 17 p2623 A83-38517
- Nonequilibrium radiative heating during outer planet atmospheric entry 18 p2687 A83-40022
- Planetary lightning - Earth, Jupiter, and Venus 18 p2780 A83-40328
- Ion cyclotron waves in the Io plasma torus - Polarization reversal of whistler mode noise 19 p2922 A83-41130
- A test of self-organization hypothesis in Jovian and Saturnian wind systems 20 p3077 A83-42337
- Electron precipitation and related aeronomy of the Jovian thermosphere and ionosphere 20 p3077 A83-42407
- Terrestrial versus Jovian VLF chorus - A comparative study 20 p3078 A83-42409
- Escape and ionization of atomic oxygen from Io 20 p3078 A83-43078
- Electromagnetic ion-cyclotron instability in the multi-ion Jovian magnetosphere 20 p3079 A83-43192
- On the detectability of H₂S in Jupiter 21 p3239 A83-44087
- Sloping convection in the laboratory and in the atmospheres of Jupiter and Saturn 21 p3240 A83-44233
- A static structural model of the outer magnetosphere of Jupiter 21 p3240 A83-44286
- Detonation propulsion experiments and theory --- for spacecraft in high pressure planetary atmospheres 21 p3105 A83-45585
- Charged particle distributions in Jupiter's magnetosphere 22 p3384 A83-46028
- The detection of X rays from Jupiter 22 p3387 A83-47037
- The Jovian spectrum in the 3-micron window 22 p3388 A83-47082
- Formation and photochemistry of methylamine in Jupiter's atmosphere 22 p3388 A83-47083
- The reaction NH₂ + PH₃ yields NH₃ + PH₂ - Absolute rate constant measurement and implication for NH₃ and PH₃ photochemistry in the atmosphere of Jupiter 24 p3672 A83-49343
- The planet Jupiter in 1980-1981 24 p3673 A83-49449
- ### JUPITER PROBES
- NT GALILEO PROBE
- NT GALILEO SPACECRAFT
- Galileo - Mission to Jupiter 02 p0263 A83-11793
- Observations of Jupiter's distant magnetotail and wake
[AD-A123812] 05 p0704 A83-17384
- Voyager orbit determination at Jupiter 10 p1381 A83-26259
- Charge-coupled device (CCD) television camera for NASA's Galileo mission to Jupiter 14 p1983 A83-32024
- Nonequilibrium radiative heating of an ablating Jovian entry probe 20 p2930 A83-43452
- Two classes of volcanic plumes on Io 21 p3239 A83-44081
- ### JUPITER RED SPOT
- The planet Jupiter in 1979-1980 - The observers and their works 08 p1188 A83-22050
- Long-lived eddies in the laboratory and in the atmospheres of Jupiter and Saturn 10 p1517 A83-25444
- Kelvin-Helmholtz instability and the Jovian Great Red Spot 13 p1960 A83-30797
- ### JUPITER RINGS
- The dynamics of planetary rings 02 p0246 A83-12185
- The rings of Jupiter 04 p0570 A83-16227

- The adiabatic motion of charged dust grains in rotating magnetospheres --- and for ring systems of Jupiter and Saturn 06 p0847 A83-18276
- Pioneer 11 observations of trapped particle absorption by the Jovian ring and the satellites 1979, J1, J2, and J3 06 p0847 A83-18280
- Planetary rings 06 p0849 A83-19464
- Resonances and rings in the solar system 07 p1005 A83-20408
- Lorentz forces on the dust in Jupiter's ring 17 p2619 A83-37586
- Electromagnetic effects on planetary rings 17 p2621 A83-38119
- Collisions in self-gravitating clouds of planetesimals 20 p3079 A83-43588

JUPITER SATELLITES

- NT AMALTHEA
- NT CALLISTO
- NT EUROPA
- NT GALILEAN SATELLITES
- NT GANYMEDE
- NT IO
- Rheology of ices - A key to the tectonics of the ice moons of Jupiter and Saturn 01 p0129 A83-11497
- The satellites of Jupiter and Saturn 02 p0264 A83-12191
- Satellites of Jupiter --- Book 04 p0569 A83-16226
- The outer satellites of Jupiter 04 p0570 A83-16230
- Origin and evolution of the Jupiter satellite system 04 p0572 A83-16249
- Mass-radius relationships in icy satellites after Voyager 05 p0703 A83-16958
- Jupiter --- Book 09 p1366 A83-24900
- Determination of the mass of Jupiter from perturbations of the orbit of Comet P/Wolf in its sphere of action in 1922 10 p1498 A83-26797
- Near-infrared mapping spectrometer for investigation of Jupiter and its satellites 14 p1983 A83-32000
- The Jovian satellites J VI and J VII - Ephemerides for the years 1981-1990 14 p2112 A83-33065
- The gravitational escape/capture of planetary satellites 24 p3646 A83-49891

K

K BAND

- U EXTREMELY HIGH FREQUENCIES

K LINES

- Ca II K2V spectral features and their relation to small-scale photospheric magnetic fields 02 p0270 A83-12573
- A search for resonance polarization in stars with enhanced Ca II H and K emission 06 p0821 A83-19062
- K-alpha and K-beta spectra from M-shell-ionized ions produced in a vacuum spark 10 p1485 A83-25410
- Brightness oscillations of the sun's chromosphere in K and H-alpha 10 p1521 A83-25494
- The dependence of H-alpha on chromospheric activity in G and K main-sequence stars 10 p1516 A83-26759
- HR 7578 - A K dwarf double-lined spectroscopic binary with peculiar abundances 13 p1951 A83-31422
- A study of shapes of Ca II chromospheric emissions in late type stars 13 p1955 A83-31655
- The Mg II h and k lines in Vega 13 p1959 A83-31742
- OSO-8 observations of a quiescent prominence - A comparison of Lyman-alpha with theoretical intensities 13 p1966 A83-31756
- Fluorescent excitation of photospheric Fe K-alpha emission during solar flares 15 p2284 A83-35218
- The Ca II K emission from the sun as a star. I - Observational parameters 16 p2440 A83-36668
- Catalog of profiles and equivalent widths of the Ca II K line in the spectra of metallic-line stars 17 p2589 A83-37654
- X-ray spectra from H-, He- and Li-like iron ions in a vacuum spark plasma 20 p3049 A83-42339
- The Ca II K emission from the sun as a star. II - The plage emission profile 20 p3080 A83-42382
- Spatially resolved K-alpha spectra of two-structure plasmas in a vacuum spark 21 p3215 A83-45487
- Stellar activity and calcium emission variability 23 p3521 A83-47492
- RS CVn stars - Chromospheric phenomena 23 p3522 A83-47512
- Interpretation of the soft X-ray spectra from Hinotori --- Japanese satellite data 23 p3532 A83-47667
- A model of a quiescent prominence on the basis of studying the K Ca(+) line fine structure 23 p3535 A83-47706
- Enhanced polarization in the Ca II K line of the Be star Kappa Dra 24 p3660 A83-49385

KA BAND

- U EXTREMELY HIGH FREQUENCIES

KALMAN FILTERS

- Software optimization of a Kalman filter for an AP-120B array processor 01 p0091 A83-11111
- Sensor-independent target state estimator design and evaluation 01 p0096 A83-11193
- A time-invariant state estimator for continuous time systems 02 p0229 A83-11853
- A program for satellite-orbit determination - An application to the case of earth-observation satellites [IAF PAPER 82-301] 03 p0283 A83-14400
- Optimal interpolation and the Kalman filter --- for analysis of numerical weather predictions 03 p0365 A83-14409
- Determination of aerodynamic coefficients for a re-entry body by means of an extended Kalman filter 04 p0451 A83-15544
- Design of stabilizing controller with incomplete state data for linear stochastic system with multiplicative noise 04 p0527 A83-15923
- A mathematical model for computer image tracking 04 p0528 A83-16030
- Adaptive control of a class of linear stochastic systems with continuous and discrete unknown parameters 04 p0528 A83-16150
- Inertial navigation and optimal filtering --- Russian book 05 p0680 A83-17123
- Simple tracking filters - Position and velocity measurements 06 p0753 A83-19027
- Variable dimension filter for maneuvering target tracking 06 p0803 A83-19033
- A new square root filtering algorithm 07 p0985 A83-21020
- Real time estimation of ship motions using Kalman filtering techniques 08 p1158 A83-22720
- Self-adaptive filters for the integration of navigation data 09 p1204 A83-23374
- Bearings-only passive ranging using Kalman-Bucy and Moore-Penrose methods 09 p1266 A83-23543
- The impact of filtering on maritime and flight operations 09 p1215 A83-24373
- A comparison between the pseudomeasurement and extended Kalman observers 09 p1328 A83-24715
- Estimation and identification of two dimensional images 09 p1328 A83-24718
- A duality principle for state estimation with partially noise corrupted measurements 09 p1330 A83-24746
- Robust control/estimator design by frequency-shaped cost functionals 09 p1333 A83-24797
- Self-adaptive filters for the integration of navigation data 09 p1335 A83-24866
- Flight tests of integrated navigation by least squares adjustment 09 p1202 A83-24871
- Decoupled Kalman filters for phased array radar tracking 10 p1462 A83-26260
- Estimation and prediction for maneuvering target trajectories 10 p1373 A83-26261
- Multiconfiguration Kalman filter design for high-performance GPS navigation 10 p1373 A83-26262
- Nonlinear Kalman filtering techniques for terrain-aided navigation 10 p1373 A83-26263
- Application of multiple model estimation to a recursive terrain height correlation system 10 p1374 A83-26264
- An integrated multisensor aircraft track recovery system for remote sensing 10 p1374 A83-26266
- Bathymetric and oceanographic applications of Kalman filtering techniques 10 p1452 A83-26267
- Measurement of instantaneous flow rate through estimation of velocity profiles 10 p1417 A83-26268
- Features of the microprocessor implementation of algorithms of the space-time processing of signals and noise in radio-electronic systems 10 p1460 A83-26956
- Rapid interference suppression using a Kalman filter technique 11 p1554 A83-27906
- Terrain profile matching for missile guidance 11 p1527 A83-28164
- Understanding Kalman filters - How to extract the maximum information from imperfect measurement 11 p1648 A83-28167
- The extended Kalman filter and its use in estimating aerodynamic derivatives 11 p1531 A83-28183
- Integrated GPS, DLMS, and radar altimeter measurements for improved terrain determination 12 p1700 A83-29212
- Identification of helicopter rotor dynamic models [AIAA 83-0988] 12 p1702 A83-29866
- Efficient square root algorithm for measurement update in Kalman filtering 13 p1910 A83-30156
- Stochastic independent modal-space control of distributed-parameter systems 13 p1911 A83-31249

- A duality principle for state estimation with partially noise-corrupted measurements 14 p2074 A83-31929

- Observability, eigenvalues, and Kalman filtering 14 p2076 A83-33134

- A method of two-dimensional filter image with a nonseparable autocovariance function 15 p2220 A83-33520

- Meteorological data simulation using Kalman filter estimation model 16 p2390 A83-36496

- Estimation enhancement by trajectory modulation for homing missiles 17 p2461 A83-37135

- Nonlinear generalized likelihood ratio algorithms for maneuver detection and estimation 17 p2461 A83-37136

- Attitude measurement and estimation of solar observation satellites 17 p2478 A83-37451

- Kalman filter formulations for transfer alignment of strapdown inertial units 18 p2739 A83-40303

- New target models for homing missile guidance [AIAA PAPER 83-2166] 19 p2795 A83-41662

- Adaptive control for large space structures [AIAA PAPER 83-2246] 19 p2816 A83-41722

- Open-loop residuals and alternate trajectories as a means of validating IMU calibration and alignment performance [AIAA PAPER 83-2252] 19 p2811 A83-41727

- Reconstruction of the shuttle reentry air data parameters using a linearized Kalman filter [AIAA PAPER 83-2097] 19 p2810 A83-41926

- Filtering flight data prior to aerodynamic system identification [AIAA PAPER 83-2098] 19 p2798 A83-41928

- Two applications of thermal network correction techniques 20 p2982 A83-42780

- Estimation of parameters in models for Cesium beam atomic clocks 20 p2990 A83-42944

- Estimating time from atomic clocks 20 p2990 A83-42945

- Estimation and identification of two-dimensional images 20 p2991 A83-43404

- Airborne radar tracking system based on optimal filtering theory 20 p2932 A83-43696

- A 'current' statistical model and adaptive tracking algorithm for maneuvering targets 20 p3040 A83-43697

- Consistency and robustness of PDAF for target tracking in cluttered environments --- Probabilistic Data Association Filter 21 p3194 A83-44370

- Introduction to random signal analysis and Kalman filtering --- Book 21 p3197 A83-45143

- A Kalman filter algorithm for terminal-area navigation with sensors of moderate accuracy 21 p3090 A83-45460

- Adaptive Kalman filter for tracking maneuvering targets 21 p3197 A83-45474

- Post-flight compensation for a master navigator error 22 p3253 A83-46966

- Comparison of simple position resets and Kalman filter position updates for correcting inertial navigation system errors 22 p3253 A83-46967

- Suboptimal stochastic control with compensators of reduced size for discrete-time non-stationary systems [ONERA, TP NO. 1983-57] 23 p3501 A83-48179

- Comparative analysis of the efficiency of practical realizations of the Kalman algorithm --- for microwave landing systems 23 p3406 A83-48518

- Integrated navigation systems for aircraft 23 p3402 A83-48735

- An adaptive robustizing approach to Kalman filtering 24 p3621 A83-49924

KAPITZA RESISTANCE

- Cryogenic heat transfer - He-4 Kapitza conductances including phase change effects 20 p2971 A83-42660

KAPTON (TRADEMARK)

- Electrical conductivity and discharge in spacecraft thermal control dielectrics 05 p0618 A83-17491

- A summary of spacecraft charging results 23 p3423 A83-48129

KARHUNEN-LOEVE EXPANSION

- Landsat images multitemporal analysis 01 p0063 A83-10055

- Method of main components in nondestructive testing. II Signal detection and estimation 02 p0188 A83-12160

- Recognition of vector signals in a coordinate domain 13 p1910 A83-30727

KARMAN VORTEX STREET

- Flow behavior and heat transfer around a circular cylinder at high blockage ratios 03 p0315 A83-13344

- Some dynamical properties of vortex streets in Saturn's atmosphere from analyses of Voyager images 22 p3387 A83-46880

Vortex pairing in a Karman vortex street
24 p3580 A83-49821

KC-130 AIRCRAFT
U C-130 AIRCRAFT

KC-135 AIRCRAFT
U C-135 AIRCRAFT

KEELS
How to improve air cushion vehicle performance with VUMP equipped wave-forming keels --- Vent-pump
15 p2242 A83-34855

KELVIN-HELMHOLTZ INSTABILITY
Structure and dynamics of supersonic jets
01 p0126 A83-10946
Helical wave and K-H instability in Type I comet tails. I
- Waves of infinitesimal amplitude in incompressible plasma
06 p0832 A83-18850
Kelvin-Helmholtz instability at the magnetopause. I -
Solution for compressible plasmas. II - Energy flux into the magnetosphere
07 p0966 A83-21511
Inertial effects of the gas motion upon the linear and nonlinear waves in Kelvin-Helmholtz flow
08 p1083 A83-21813
On the role of instabilities in unsteady-beam models of extended radio sources
09 p1362 A83-24982
Sunspots and physics of magnetic flux tubes overstability and Kelvin-Helmholtz instability in a magnetic field
12 p1799 A83-29066
Kelvin-Helmholtz instability and the Jovian Great Red Spot
13 p1960 A83-30797
Parallel electric fields and shear instabilities --- in magnetosphere
15 p2195 A83-33934
Effects of the Kelvin-Helmholtz surface instability on supersonic jets --- in galactic structure
15 p2267 A83-34621
Effect of the Coriolis force and slowly varying flow on the Kelvin-Helmholtz instability
15 p2161 A83-34783
Nonlinear Kelvin-Helmholtz magnetohydrodynamic instability of a rotating plasma
15 p2236 A83-34784
Kelvin-Hemholtz instability in relativistic mechanics
16 p2427 A83-35715
A numerical study of the instability of a tangential velocity discontinuity in compressible gases
16 p2350 A83-35716
On the relevance of the MHD approach to study the Kelvin-Helmholtz instability of the terrestrial magnetopause
16 p2376 A83-35785
Scalloped disk galaxies - A Kelvin-Helmholtz instability?
19 p2918 A83-41618
On the effect of oblique disturbances on Kelvin-Helmholtz instability at magnetospheric boundary layers and in solar wind
20 p3023 A83-43152
A discrete vortex simulation of Kelvin-Helmholtz instability
20 p2987 A83-43453
Kelvin-Helmholtz instability in boundary layer regions of the plasma sheet during magnetospheric substorm recovery
21 p3171 A83-44291
Kelvin-Holmholtz instabilities in a sheared compressible plasma --- plasma physics
21 p3233 A83-44757
Stabilization of tangential shear instability in shallow water with 'supersonic' fluid flow
22 p3285 A83-46939
Determination of physical parameters in extragalactic radio jets from large scale, small amplitude oscillations
23 p3518 A83-47432
The MHD Kelvin-Helmholtz instability in the solar photosphere
24 p3675 A83-50103

KENYA
Refugee settlements and vegetation change - A multistage Landsat data analysis of a semi-arid region in Kenya
09 p1286 A83-24560

KEPLER LAWS
On spinor equations of motion and their 'possible integrals'
01 p0017 A83-10262
Orbital eccentricity in a logarithmic potential
02 p0249 A83-12924
Diffusion of Keplerian motions by a stochastic force. II
- Lorentz scattering of interplanetary dusts
03 p0429 A83-14784
Comments on Aksnes' intermediary --- in theory of artificial satellite orbits
04 p0452 A83-16358
Pre-discovery encounters between short-period comets and Jupiter estimated by a Keplerian approximation
05 p0695 A83-17831
An analytic solution to the classical two-body problem with drag
06 p0720 A83-17990
An empirical initial estimate for the solution of Kepler's equation
07 p0868 A83-21427
The modified Encke method --- for orbit calculation
11 p1672 A83-27884
The KS-transformation in hypercomplex form
12 p1786 A83-29103
The reduction to the rotation for planar perturbed Keplerian systems
12 p1787 A83-29114
Stability criteria in many-body systems. V - On the totality of possible hierarchical general four-body systems
12 p1787 A83-29117

A Keplerian method to estimate perturbations in the restricted three-body problem
16 p2426 A83-36785
Stability and integrability in the planar general three-body problem
18 p2757 A83-39606
Kepler and two-body problems in bimetric Machian gravitation
18 p2763 A83-40625
A methodology for aerodecelerating entry trajectory analysis
[AIAA PAPER 83-2096]
19 p2810 A83-41925

KERATITIS
The stimulating effect of a helium-neon laser in acute inflammatory processes of the eye
03 p0378 A83-13603

KERNEL FUNCTIONS
Asymptotic error behavior in the Gaussian quadrature procedure --- German thesis
01 p0101 A83-10166
An integral equation connected with the Jacobi polynomials
09 p1336 A83-24371
Eigenfunctions of an integral operator generated by a logarithmic kernel on two intervals and their application to contact problems
11 p1596 A83-28462
Kernel estimates as a basis for general particle methods in hydrodynamics
12 p1724 A83-29617
A natural interpolation formula for Cauchy-type singular integral equations with generalized kernels
12 p1772 A83-29643
Supersonic three-dimensional oscillatory piecewise continuous kernel function method --- for planar supersonic wing study
19 p2789 A83-41043
A Chebyshev expansion of singular integral equations with a logarithmic kernel
21 p3198 A83-45523

KEROGEN
Isotopic composition of carbonaceous-chondrite kerogen Evidence for an interstellar origin of organic matter in meteorites
24 p3673 A83-50173

KEROSENE
Investigation of slurry fuel performance for use in a ramjet propulsor
07 p0902 A83-21014
Degradation and characterization of antimisting kerosene
09 p1242 A83-24035
Shock initiated ignition in heptane-oxygen-argon mixtures
10 p1391 A83-26198
The properties of fuel fractions obtained by the hydrogenation of Kansk-Achinsk coal
10 p1401 A83-26920
Effective generalized conductivity of three-phase cellular systems --- with kerosene-air-water fuel mixture example
12 p1775 A83-29270
Future U.S. jet fuels - A refiner's viewpoint
13 p1826 A83-30187
Feasibility of a full-scale degrader for antimisting kerosene
[AIAA PAPER 83-1137]
16 p2339 A83-36240
Testing of antimisting kerosene in the DC-10/KC-10 fuel system simulator
[SAE PAPER 821485]
17 p2492 A83-38004

KERR EFFECTS
Optical Kerr effect in fiber gyroscopes - Effects of nonmonochromatic sources
07 p0930 A83-20800
Propagation in media with Raman-type nonlinearity
Polarization states of the waves and gains
14 p2024 A83-32445

KERR ELECTROOPTICAL EFFECT
Source statistics and the Kerr effect in fiber-optic gyroscopes
02 p0176 A83-11570
Electro-optic shutter devices utilizing lead lanthanum zirconate titanate /PLZT/ ceramic wafers
08 p1098 A83-22565
Coherent phenomena involved in the time-resolved optical Kerr effect
14 p2026 A83-33430
Transient behavior of Kerr-like phase conjugators - The inverse problem
15 p2228 A83-33527
Efficient femtosecond optical Kerr shutter
21 p3208 A83-45477
Generation and amplification of ultrashort laser pulses and applications to electron trapping in amorphous media
22 p3299 A83-46683

KERR MAGNETOOPTICAL EFFECT
Material and electromagnetic sources of the Kerr-Newman geometry --- of collapsed rotating star
23 p3525 A83-47602
Experimental investigation of the characteristics of magnetic mirrors at a wavelength of 1.15 micron --- for laser gyroscopes
23 p3459 A83-48493

KETONES
NT ACETONE
Polyetheretherketone matrix composites
09 p1221 A83-23605

KEVLAR (TRADEMARK)
The thermal conductivity of Kevlar fibre-reinforced composites
02 p0149 A83-11667
A production engineers view of advanced composite materials
02 p0149 A83-11800

KILOMETRIC WAVES
A study into the degradation of nylon, Kevlar and polyester fabrics when exposed to varying amounts of ultra violet in the laboratory and in natural environment and the effects of varying degrees of heat on the degradation of these fabrics
04 p0463 A83-15439
Space radiation effects on structural composites
[AIAA PAPER 83-0591]
05 p0610 A83-16808
Relation of interfacial adhesion in Kevlar/epoxy systems to surface characterization and composite performance
08 p1055 A83-22716
Accelerated aging studies of low density /hydrocarbon/ resin systems
09 p1222 A83-23646
Transverse moisture sensitivity of aramid/epoxy composites
10 p1388 A83-25626
Thermal degradation of aramids. I - Pyrolysis/gas chromatography/mass spectrometry of poly(1,3-phenylene isophthalamide/ and poly(1,4-phenylene terephthalamide/
11 p1543 A83-28199
Thermal degradation of aramids. II - Pyrolysis/gas chromatography/mass spectrometry of some model compounds of poly(1,3-phenylene isophthalamide/ and poly(1,4-phenylene terephthalamide/
11 p1551 A83-28200
Drop weight impact testing of laminates reinforced with Kevlar aramid fibers, E-glass, and graphite
12 p1711 A83-29891
First design details of the all-composite Lear Fan
13 p1806 A83-30829
Static fatigue life of Kevlar aramid/epoxy pressure vessels at room and elevated temperatures
[AIAA PAPER 83-1328]
16 p2324 A83-36342
Matrix/fiber interface effects on Kevlar 49 pressure vessel performance --- for rocket engine cases
18 p2701 A83-40018
Inelastic deformation of certain high-modulus reinforcing fibers
18 p2649 A83-40102
Impact damage tolerance of composites reinforced with Kevlar aramid fibers
18 p2656 A83-40214
Swelling of Kevlar 49/epoxy and S2-glass/epoxy composites
18 p2657 A83-40228
Vibro-punching Kevlar aramid and carbon fiber reinforced composites
18 p2661 A83-40284
Kevlar aramid as a fiber reinforcement with emphasis on aircraft
18 p2661 A83-40286
Unresolved stress analysis problems in Kevlar composite pressure vessels --- helically wound solid rocket motor cases
22 p3305 A83-46308
Photochemical ageing of Kevlar 49
22 p3270 A83-46708
The effect of moisture on the fatigue resistance of an aramid/epoxy composite
22 p3265 A83-46904
Creep of Kevlar 49 fibre and a Kevlar 49-cement composite
24 p3554 A83-50066

KEYING
NT FREQUENCY SHIFT KEYING
NT PHASE SHIFT KEYING
Evaluation of alternative alphanumeric keying logics
02 p0225 A83-12087

KIDNEY DISEASES
Systemic and renal hemodynamics in hypertension
19 p2881 A83-41429
The mathematical selection of information criteria for the differential diagnosis of renovascular hypertonia and hypertension
19 p2881 A83-41436
The direct electrical stimulation of the upper urinary tract in case of ureteroliths in flight crew personnel
24 p3618 A83-49071

KIDNEYS
The effect of clonidine on the central and renal hemodynamics of individuals with hypertension during the administration of orthostatic probes --- side effects of antihypertensive treatments
05 p0674 A83-17198
The role of the kidneys in the pharmacokinetics of novocainamide
07 p0975 A83-20989
The role of the kidneys and extrarenal mechanisms in the regulation of the concentration of sodium in the blood plasma of rats during the intravenous injection of a hypertonic solution of sodium chloride
08 p1145 A83-22115
Alterations in glomerular and tubular dynamics during simulated weightlessness
11 p1636 A83-27795
Prostaglandins of the renal vascular bed during arterial hypertension of various etiologies
19 p2881 A83-41437

KILOMETRIC WAVES
Auroral hiss, Z mode radiation, and auroral kilometric radiation in the polar magnetosphere - DE 1 observations
[AD-A125914]
06 p0784 A83-18302
Computer simulation of auroral kilometric radiation
15 p2202 A83-34738
Observational evidence of Z and L-O mode waves as the origin of auroral kilometric radiation from the Jikiken (EXOS-B) satellite
20 p3018 A83-42411

- Spectral characteristics of radio noise at low and medium frequencies in the Antarctic topside ionosphere
22 p3330 A83-46507
Auroral kilometric radiation induced by double layers
23 p3481 A83-47624

KIMBERLITE

- U BIOTITE
U PERIDOTITE

KINEMATIC EQUATIONS

- Mechanism case studies VI
[ASME PAPER 82-DET-47] 02 p0187 A83-12772
Magnetohydrodynamic interaction between convection and imposed magnetic field in Boussinesq fluid
09 p1357 A83-23861
Robot motion: Planning and control --- Book
15 p2172 A83-33695
A comparison of two types of atmospheric transport models Use of observed winds versus dynamically predicted winds
18 p2722 A83-39134
The calculation of robot dynamics using articulated-body inertias
20 p2959 A83-43109

KINEMATICS**NT BODY KINEMATICS**

- An extension of classical shell theory - The influence of thickness strains and cross-sectional warping
01 p0059 A83-10575
Relativistic kinematics for motions faster than light
01 p0124 A83-10705
Tooth profile analysis of circular-cut, spiral-bevel gears [ASME PAPER 82-DET-79] 02 p0187 A83-12776
Kinematics of ring-shaped nebulae in the LMC. II - The radial velocity field of N 185 03 p0429 A83-14790
Stationary magnetic field in a periodic flow
04 p0537 A83-15883
Kinematics of a multi-dimensional shock of arbitrary strength in an ideal gas 05 p0642 A83-17846
On exactness of the kinematical approach in the structural shakedown and limit analysis
06 p0778 A83-19325
Radial velocities and kinematics in star systems of the Milky Way 06 p0846 A83-19533
Type II supernovae photospheres and distances
08 p1177 A83-21838
Kinematic and kinetic parameters as information feedback in the acquisition of man-machine skills
10 p1458 A83-26338
On the kinematic control of the motion of a vessel with an ideal heavy fluid 11 p1649 A83-28468
Diagnosis of weather events via kinematic analysis
13 p1888 A83-30572
Kinematic structure of planetary nebulae. I - The highly evolved nebula Abell 30. II - The Eskimo, NGC 2392
15 p2265 A83-34594
Kinematics, dynamics and structure of the Milky Way; Proceedings of the Workshop on the Milky Way, Vancouver, British Columbia, Canada, May 17-19, 1982
18 p2767 A83-39626
Kinematics of molecular clouds - Evidence for agglomeration in spiral arms 18 p2769 A83-39646
The kinematics of orographic airflow during Sierra storms 18 p2729 A83-40037
The large-scale circulation and heat sources over the Tibetan Plateau and surrounding areas during the early summer of 1979. I - Precipitation and kinematic analyses
20 p3029 A83-42502
Kinematics of robot wrists 20 p2959 A83-43110
Kinematics --- Book 21 p3200 A83-45138
Nonlinear shell dynamics - Intrinsic and semi-intrinsic approaches 23 p3468 A83-47592
Morphology and kinematics of planetary nebulae
24 p3638 A83-49129
Distribution and motions of atomic hydrogen in lenticular galaxies 24 p3655 A83-49219
Kinematic modelling of NGC 3379
24 p3641 A83-49251
Exact formulas for calculations concerned with proper motions 24 p3644 A83-49602

KINESTHESIA

- The threshold of the kinesthetic sensitivity in the vertical posture 04 p0522 A83-15783
The effect of dangerous motions on kinesthesia
05 p0672 A83-17152
Information in optical flows induced by curved paths of observation --- by monocular moving observer
09 p1324 A83-24093

KINETIC ENERGY

- Scanning delay generator for measurement of kinetic decays using laser-induced fluorescence techniques
02 p0181 A83-12823
Some recent developments in the theory of premixed turbulent flames 03 p0319 A83-14472
Efficiency improved turboprop
05 p0596 A83-16491
[AIAA PAPER 83-0059]
Physical conditions in H II/OH maser regions
06 p0825 A83-18088

- Global-scale weekly and monthly energetics during January and February 1979 06 p0790 A83-18259
Defect forces, defect couples and path integrals --- J integral study of crack propagation stability
08 p1115 A83-21656
Numerical calculations of turbulent heat transfer downstream of a rearward-facing step
08 p1089 A83-23199
Spectral study of wintertime kinetic energy of the Northern Hemisphere in the troposphere
11 p1633 A83-28085
A study of energy conversion in the wave number domain 11 p1619 A83-28341
A study of turbulent energy over complex terrain (state, 1978) 12 p1757 A83-29127
Improving the Eddy Kinetic Energy model for planetary boundary layer description 12 p1758 A83-29129
Collisional forcing of raindrop oscillations
13 p1893 A83-31042
The effect of velocity distribution in a bunch on the efficiency of kinetic-energy extraction in a klystron
14 p2003 A83-32115
The energetics of the general circulation of the atmosphere in southern hemisphere during the IGY. II - The cycle of the energetics of the atmosphere in southern hemisphere 14 p2056 A83-32401
Kinematics and correlation of the surface wind field in the South Atlantic Bight 14 p2059 A83-33079
Energy dependence of the O(-) transfer reactions of O3(-) and CO3(-) with NO and SO2
14 p1991 A83-33103
A model for the turbulent energy spectrum
14 p2013 A83-33385
Eddy kinetic energy in the North Atlantic from surface drifters 15 p2207 A83-33492
Kinetic effects on trace element partitioning
15 p2274 A83-34498
Encounters of binaries. I - Equal energies
15 p2265 A83-34596
The critical energy density and the inelasticity coefficient for asteroidal catastrophic collisions
15 p2250 A83-35029
Nonlinear baroclinic instability - An approach based on Serrin's energy method 16 p2385 A83-35472
Studies of collision interactions and kinetic energy distribution of eV recoil ions inside Penning traps
16 p2409 A83-35631
Enhancement of charge-transfer reaction rate constants by vibrational excitation at kinetic energies below 1 eV
16 p2327 A83-36522
Dislocation kinetics and the formation of deformation bands 17 p2522 A83-38383
The Hamilton-Jacobi equation and its complementary form 18 p2741 A83-39148
A simple scheme for daytime estimates of the surface fluxes from routine weather data
18 p2724 A83-39675
Large-scale energy transformations in the high latitudes of the Northern Hemisphere 18 p2728 A83-40026
Corotating pressure waves without fast streams in the solar wind 20 p3080 A83-42401
A nonlinear kinetic energy principle for two-dimensional collision-free plasmas 21 p3209 A83-43940
Multiple scales for modelling turbulent flows. I - A multiple scales model for the kinetic energy of the turbulence and variance of a passive scalar 21 p3129 A83-44460
A new look at the energy cycle --- in atmosphere
22 p3341 A83-46848
Oceanic turbulence - Big bangs or continuous creation? 22 p3344 A83-46909
The energy exchange between the baroclinic and barotropic components of atmospheric flow in the tropics during the FGGE summer 23 p3490 A83-47407
Estimated energy and momentum input to the interstellar medium for several external galaxies
23 p3519 A83-47448
Turbulent kinetic energy balance in a conical diffuser
24 p3579 A83-49805

KINETIC EQUATIONS

- NT HELMHOLTZ VORTICITY EQUATION
NT HYDRODYNAMIC EQUATIONS
NT KINEMATIC EQUATIONS
The kinetics of charged particles in the polar ionosphere 01 p0071 A83-10595
The distribution of stars around a black hole - Numerical solution of the kinetic equation with collisions
01 p0125 A83-10932
A relativistic gas in a gravitational field
03 p0417 A83-13527
Kinetics of the isotropic expansion of a homogeneous electron-photon plasma 03 p0397 A83-13535
Equations for the dynamics of a vibrationally nonequilibrium gas under conditions of anharmonicity in the molecular vibrations 04 p0544 A83-15775

- The thermodynamic basis of a dynamic method for investigating relaxation processes
06 p0815 A83-18002
Third-order optical nonlinearity induced by effective mass gradient in heterostructures
07 p0994 A83-21364
[AD-A130018]
Application of modified BGK-equations to the calculation of the shock wave structure in Xe-He mixtures
08 p1083 A83-21817
Global solutions of nonstationary kinetic equations
09 p1350 A83-24322
A kinetic equation for the correlation functions of a quantum system interacting with a Gaussian thermostat
09 p1350 A83-25080
Kinetic description of a dynamically coupled free-electron-and molecular gas laser
11 p1584 A83-28239
Kinetic equations and an analysis of the stability of irradiated matter 13 p1927 A83-30008
Calculation of the kinetic coefficients for a moderately dense gas 13 p1932 A83-30657
A quasi-classical kinetic equation for molecular gases with polar molecules 13 p1933 A83-30674
Approximate method of solving the kinetic equation for moderately dense gases near a boundary temperature jump in a binary mixture 13 p1933 A83-31467
A kinetic model of the polar wind with a Landau collision integral 14 p2054 A83-33028
MHD turbulence via extended Burgers' equation
15 p2235 A83-34544
An approximate method for solving a kinetic equation for moderately dense gases near a boundary - The slip of a binary mixture 16 p2350 A83-35711
Invariant transformations of kinetic equations
23 p3512 A83-47176
Relativistic kinetic equation for inelastically interacting particles in a gravitational field 24 p3636 A83-49062
- KINETIC FRICTION**
NT SLIDING FRICTION
Some features of the spatial structure of the Arctic Ocean ice cover in connection with turbulent friction and geostrophic capture of tide waves
01 p0077 A83-10833
Dynamical friction on extended objects --- during gravitational interaction with non-colliding particles
07 p1023 A83-21205
Subsonic motion of the edge of a shear shift with friction along an interface between elastic materials
19 p2858 A83-41214
- KINETIC HEATING**
NT AERODYNAMIC HEATING
NT SHOCK HEATING
Heat transfer with bubble formation - Results of the TEXUS IIIb experiment 02 p0138 A83-12998
- KINETIC THEORY**
NT CHAPMAN-ENSKOG THEORY
NT MIXING LENGTH FLOW THEORY
NT TRANSPORT THEORY
NO infrared radiation in the upper atmosphere
02 p0204 A83-11967
Picosecond amplification and kinetic studies of XeCl
02 p0184 A83-12272
A bimodal Maxwellian distribution as the equilibrium solution of the two-particle regime
03 p0399 A83-13117
Kinetic analysis of evaporation and condensation in a vapor-gas mixture 03 p0315 A83-13118
A kinetic description of the Rayleigh scattering of light in dense gases 06 p0815 A83-19184
Investigation of the vibrational temperature kinetics in a TEA CO2 laser 07 p0934 A83-20113
Interpretation of auroral radar experiments using a kinetic theory of the two-stream instability
07 p0961 A83-20373
General frequency gyrokinetics
07 p0997 A83-20540
Modern exospheric theories and their observational relevance --- kinetic theory 07 p1031 A83-20839
The mathematical kinetics of reacting gases --- Russian book 09 p1227 A83-25220
Kinetic theory of evaporation and condensation for a cylindrical condensed phase 10 p1490 A83-25784
The effects of segregation on the kinetics of intergranular cavity growth under creep conditions
10 p1396 A83-25862
Theory of a nonwiggler collective free electron laser in uniform magnetic field 10 p1427 A83-26011
Fluctuation-dissipation relations in the scattering problem and the method of fluctuations in the kinetic theory of gases 10 p1490 A83-26246
Solar wind theory 11 p1687 A83-27381
Kinetic model of a structural suspension of particles in a gas 11 p1665 A83-27715
Gas-kinetic magnetic resonance in N2 and CO gases
11 p1654 A83-28062

Kinetic theory of phase space vortices and double layers 11 p1660 A83-28248
 Generation of lower hybrid waves by inhomogeneous electron streams --- with application to wave turbulence in auroral zone and solar corona 11 p1617 A83-28313
 A kinetic model for a fine anhydrous aerosol in the troposphere 13 p1873 A83-30027
 Analytical methods for solving the Boltzmann equation 13 p1932 A83-30652
 Demonstration and generalization of the Boltzmann kinetic theory 13 p1932 A83-30654
 On the kinetic theory of dense gases 13 p1932 A83-30656
 The problem of boundary conditions in the kinetic theory of gases 13 p1932 A83-30661
 The kinetic theory of gas mixtures 13 p1932 A83-30666
 Certain aspects of the kinetic theory of reacting gases and its applications to relaxation aerodynamics 13 p1932 A83-30667
 The use of kinetic theory for describing disperse media 13 p1933 A83-30670
 Theory of thermophoresis of moderately large aerosol particles 13 p1933 A83-30820
 Mesoscopic kinetic theory 13 p1933 A83-30960
 Non-Maxwellian electrons in a laser produced sodium plasma 13 p1926 A83-31061
 Kinetic theory of a free-electron laser amplifier with guide magnetic field 13 p1853 A83-31113
 Evaporation and condensation on two parallel plates at finite Reynolds numbers 14 p2094 A83-33379
 A kinetic cross-field streaming instability 14 p2087 A83-33387
 Kinetic theory of the anomalous electrical conductivity of a turbulent plasma 16 p2417 A83-39637
 The kinetic theory of electromagnetic processes 17 p2575 A83-37165
 Theory of electron-hole kinetics in amorphous semiconductors under illumination - Application to solar cells 17 p2584 A83-38213
 Kinetic theory for plasmas with non-Abelian interactions 19 p2901 A83-40965
 The kinetic theory of H₂ dissociation --- in interstellar molecular clouds 19 p2918 A83-41624
 Generation of static magnetic fields by a test charge in a plasma with an electron temperature anisotropy 21 p3210 A83-44129
 Kinetic description of a relativistic plasma with a one-dimensional momentum distribution in initial state 21 p3212 A83-44495
 H-theorem and trend to equilibrium in the kinetic theory of gases 21 p3220 A83-44942
 Boltzmann equation on a lattice global solution for non-Maxwellian gases 21 p3220 A83-44944
 The H-theorem and the Onsager principle for the steady Boltzmann equation 21 p3220 A83-45221
 Self-consistent kinetic theory for the Lorentz gas 22 p3366 A83-45938
 Observation of self-binding turbulent fluctuations in simulation plasma and their relevance to plasma kinetic theories 22 p3361 A83-46009
 Kinetic theory of transport processes in partially ionized gases --- Thesis 22 p3366 A83-46696

KINETICS
 NT ELECTROKINETICS
 NT KINETIC ENERGY
 NT NEWTON THEORY
 NT REACTION KINETICS
 NT VARIABLE MASS SYSTEMS
 On a stationary solution for the motion of a rigid body about a fixed point under the influence of a Newtonian force field 07 p0988 A83-20200
 Recrystallization of a nickel-base superalloy - Kinetics and microstructural development 15 p2138 A83-34132
 On the choice of boundary conditions for the matching of kinetic to hydrodynamic polar wind models 16 p2376 A83-35787
 The effect of the kinetics of erythrocyte destruction on the dynamic behavior of the erythropoiesis system 16 p2395 A83-36805

KINOFORM
 Kinoform filter for an incoherent optical processor 10 p1424 A83-26862

KIRCHHOFF LAW OF RADIATION
 Possible generalization of the Kirchhoff approximation in problems of wave diffraction by transparent inhomogeneous objects 23 p3504 A83-48484

KIRCHHOFF-HELMHOLTZ FLOW
 U PIPE FLOW

KIRCHHOFF-HUYGENS PRINCIPLE
 U DIFFRACTION
 U WAVE PROPAGATION

KITE BALLOONS
 U TETHERED BALLOONS

KLEIN-GORDON EQUATION

Single-particle problem concerning the motion of a relativistic particle in a static electric field 01 p0104 A83-11349
 Exact solutions of relativistic wave equations --- Russian book 07 p0989 A83-20378
 Large-parameter asymptotics of the solution of the Fock-Klein-Gordon equation in the case of a discontinuous initial condition 09 p1339 A83-24318
 The scattering of waves described by the Klein-Gordon equation by an inclined half-plane 13 p1913 A83-30082

The connection between partial differential equations soluble by inverse scattering and ordinary differential equations of Painlevé type 14 p2078 A83-32836

KLYSTRONS

An estimate of the maximum modulation bands of an electron beam by means of systems of noncoupled resonators 04 p0469 A83-15137
 Small-signal gain of the TOK amplifier --- Transverse Optical Klystron 04 p0535 A83-15949
 A relativistic-electron-beam klystron 05 p0630 A83-17597
 Results of the efficiency optimization of multicavity klystrons 06 p0755 A83-19364
 Calculation of the frequency spectrum of an electron beam in a klystron with premodulation 07 p0921 A83-20855
 Simulation and study of efficiency-optimized interaction processes in multicavity klystrons 09 p1252 A83-23463

Modern multistage depressed collectors - A review 09 p1254 A83-24025
 Generalized description of harmonic generation in a transverse optical klystron 10 p1427 A83-26007
 Gain and efficiency of a stimulated Cherenkov optical klystron 10 p1428 A83-26020
 A comparison of meteorological Doppler radars with magnetron and klystron transmitters 11 p1624 A83-27006

Microwave contactless technique for photoconductivity measurements 11 p1573 A83-27980
 Theoretical analysis of the possibilities of an open-cavity klystron 13 p1833 A83-30710
 Two-cavity klystron uses single-cavity tuning 13 p1835 A83-30913

Optical klystron spontaneous emission and gain --- as undulator for free electron laser 13 p1852 A83-31106
 TOK-transverse optical klystron and converter physics and figures 13 p1856 A83-31136
 Free-electron coherent relativistic scatterer for UV generation 13 p1856 A83-31137
 The effect of velocity distribution in a bunch on the efficiency of kinetic-energy extraction in a klystron 14 p2003 A83-32115

Bernstein mode quasi-optical gyroklystron [AD-A130124] 17 p2497 A83-37760

KNEE (ANATOMY)

Knee-ligament loading properties as influenced by gravity. I - Junction with bone of 3-G rodents 02 p0223 A83-12407
 The change of the contralateral reflex effects on the background of the Jendrassik technique 12 p1766 A83-29319

KNIGHT SHIFT

U NUCLEAR MAGNETIC RESONANCE

KNOOP HARDNESS

Controlled flaws in ceramics - A comparison of Knoop and Vickers indentation 08 p1070 A83-22193

KNOWLEDGE

NT PARADOXES

KNUDSEN FLOW

Heat transport in porous cometary nuclei 04 p0551 A83-15369
 Photophoretic force on particles for low Knudsen number 06 p0786 A83-18586
 Theory of electrostatic probes under intermediate collisional conditions 07 p0995 A83-20063
 Kinetic theory of evaporation and condensation for a cylindrical condensed phase 10 p1490 A83-25784
 Asymmetries in evaporation and condensation Knudsen layer problems 13 p1840 A83-30110
 Hydrodynamic equations for partially ionized multicomponent gas mixtures with higher approximations to the transport coefficients 13 p1925 A83-30653
 Flow of a gas mixture near a catalytic surface 13 p1932 A83-30669
 Knudsen layer characteristics for a highly cooled blunt body in hypersonic rarefied flow [AIAA PAPER 83-1424] 14 p1970 A83-32703
 An asymptotic method for solving the Boltzmann equation for low Knudsen numbers 17 p2585 A83-38096

A method for obtaining closed-form systems of equations for macroparameters of distribution functions in the case of small Knudsen numbers 18 p2751 A83-39493
 Measurements of the conduction of heat in water vapor, nitrogen and mixtures of these gases in an extended temperature range 20 p2972 A83-42671
 The Knudsen ion layer problem in the theory of the collisionless sheath 21 p3212 A83-44356
 Flow past a sphere at low Mach and Knudsen numbers 24 p3544 A83-48931
 Flow of a gas mixture in a cylindrical channel at intermediate Knudsen numbers 24 p3576 A83-48940

KNUDSEN NUMBER

U KNUDSEN FLOW

KNURLING

Automated knurl inspection for rockets 12 p1733 A83-29374

KOHOUTEK COMET

On the CN(0,0) spectrum of comet Kohoutek 1973 XII 14 p2101 A83-33286
 Neutral cometary atmospheres. IV - Brightness profiles in the inner coma of comet Kohoutek 1973 XII 20 p3059 A83-42463

KOLMOGOROFF THEORY

Solution to the backward-Kolmogorov equation for a nonstationary oscillation problem 04 p0531 A83-15697

Estimation of convergence speed in the second uniform limit theorem of Kolmogoroff 04 p0530 A83-16410
 Generalized solutions of the inverse Kolmogoroff equation, corresponding to the stochastic Navier-Stokes system 05 p0638 A83-17136

On the analytic treatment of non-integrable difference equations 06 p0805 A83-18327
 Kolmogorov unstable stellar oscillations 11 p1689 A83-27650
 Dome induced image motion --- in astronomical telescopes 13 p1920 A83-30999

The dependence of the Kolmogorov entropy of mappings on coordinate systems 18 p2740 A83-39001
 Hydrodynamic and turbulent motions in the galactic disk 18 p2775 A83-39755
 New representation of Navier-Stokes equations governing self-similar homogeneous turbulence 20 p2970 A83-42648

Variational approach to the closure problem of turbulence theory 21 p3128 A83-43931
 Statistical solutions to Navier-Stokes system and Euler's systems 21 p3131 A83-44658
 Estimation of the Kolmogorov entropy from a chaotic signal 24 p3623 A83-48849
 The application of the Kolmogoroff-Feller equation to problems of stellar dynamics 24 p3650 A83-48930

KOLMOGOROFF-SMIRNOFF TEST

The Wolf 630 moving group of stars 21 p3234 A83-44760
 A modified Kolmogorov-Smirnov test for Weibull distributions with unknown location and scale parameters 23 p3467 A83-47619

KOREA

A study of early Korean rockets (1377-1600) [IAF PAPER 83-291] 23 p3540 A83-47331

KORTEWEG-DEVRIES EQUATION

Poisson brackets compatible with algebraic geometry and Korteweg-de Vries dynamics over a set of finite-gap potentials 02 p0232 A83-11651
 Collisions between two solitary waves. II - A numerical study 03 p0315 A83-13249
 Horizontally propagating solitary waves in the upper atmosphere 04 p0509 A83-15723
 Growth rates of bending KdV solitons 06 p0812 A83-18917
 Moving frames and prolongation algebras 07 p0988 A83-21043
 Simple relationship between the geometric and Hamiltonian representations of integrable nonlinear equations 09 p1339 A83-24325
 On the inverse scattering and direct linearizing transforms for the Kadomtsev-Petviashvili equation 09 p1340 A83-25283

The emergence of solitons of the Korteweg-de Vries equation from arbitrary initial conditions 10 p1471 A83-25464

An explicit finite-difference scheme with exact conservation properties 12 p1772 A83-29624
 Nonlinear electron Landau damping of ion-acoustic solitons 13 p1923 A83-30115
 Asymptotic behavior of solutions of the Cauchy problem for a KdV-type system for large times 13 p1914 A83-31346

Convergence of Galerkin approximations for the Korteweg-de Vries equation 13 p1912 A83-31360

- Experimental determination of the velocity and width of plane ion-acoustic solitons propagating in a plasma
14 p2086 A83-32423
- The connection between partial differential equations soluble by inverse scattering and ordinary differential equations of Painlevé type
14 p2078 A83-32836
- The small dispersion limit of the Korteweg-de Vries equation. I
14 p2078 A83-32850
- Formation of ion-acoustic double layers
17 p2581 A83-37037
- Completeness of derivatives of squared Schrödinger eigenfunctions and explicit solutions of the linearized KdV equation
17 p2572 A83-38464
- On the Stokes wave in shallow water - Perspective in the context of spectral-transform theory
17 p2577 A83-38938
- Nonlinear Fourier analysis of localized wave fields described by the Korteweg-de Vries equation
17 p2577 A83-38939
- Theoretical and numerical methods for the nonlinear Fourier analysis of shallow-water wave data
17 p2577 A83-38940
- On Korteweg-de Vries and drift-wave turbulence
17 p2577 A83-38953
- A new method for the numerical solution of nonlinear evolutionary equations
19 p2895 A83-40995
- Nonlinear dispersive systems - Theory and examples
19 p2893 A83-41023
- Solitary waves induced by boundary motion
21 p3199 A83-43826
- Nonlinear lattice and soliton theory
22 p3353 A83-45696
- The small dispersion limit of the Korteweg-de Vries equation. II
22 p3353 A83-47092
- Soliton and nonlinear wave equations --- Book
23 p3503 A83-47574
- Exact k-spectrum for the KdV equation - Application to drift wave turbulence
24 p3633 A83-49752

KP INDEX

- The geoeffectiveness of the meridional component of the large-scale magnetic field of the sun
02 p0210 A83-12442
- Relation of the B sub z component of the interplanetary magnetic field to the generation of the semi-annual wave in Kp-indices
11 p1616 A83-28106
- Milestone Hill incoherent scatter observations of auroral convection over Lambda = 60-75 deg. III - Average patterns versus Kp
17 p2537 A83-37576
- Systematics of the equatorward diffuse auroral boundary
17 p2538 A83-37595
- Dependence of ionospheric drift speed on geomagnetic activity
17 p2495 A83-38544
- Correlation of cosmic-ray intensity with geomagnetic Kp index and solar-magnetic-field reversal
17 p2630 A83-38868
- A statistical study of the relation between solar flare and geomagnetic disturbance for 1966-1978
21 p3172 A83-44526

KRAMERS-KRONIG FORMULA

- On wave propagation in random particulate composites
23 p3428 A83-48095

KREBS CYCLE

- The morphological characteristics of the myons of the masticatory muscle of mammals and humans
07 p0975 A83-20990

KREEP

- KREEP glass and the exotic provenance and formation of polymict breccia 66055
04 p0560 A83-15341
- Rock 67015 - A feldspathic fragmental breccia with KREEP-rich melt clasts
07 p1033 A83-21299

KRONCKER PRODUCT

U ORTHOGONALITY

KRYPTON

- Investigation of the ionization relaxation of shock-wave heated krypton with an HCN laser interferometer --- German thesis
04 p0536 A83-15842
- Absorption of HCN-laser rays with inverse bremsstrahlung in a krypton atom field --- German thesis
06 p0811 A83-18520
- Number density of the 5s states during the ionisation relaxation of shock heated krypton
10 p1479 A83-26176
- Photoionisation of krypton atoms in 'strong' electric fields
11 p1653 A83-27512
- Formation of highly excited Ar and Kr atoms in the case of asymmetric charge transfer of Ar(+) and Kr(+) ions with rare-gas atoms
13 p1915 A83-30019
- Short wavelength laser calculations for electron pumping in neon-like krypton (Kr XXVII)
13 p1857 A83-31377
- Kinetics of formation of krypton-halogen atom exciplexes in electron beam irradiated gases
16 p2358 A83-35436
- Electron-beam-induced emission of KrXe(+)
24 p3589 A83-49613

KRYPTON FLUORIDE LASERS

- Wide aperture self-sustained discharge KrF and XeCl lasers
01 p0055 A83-10984
- Kinetic studies of KrF2/asterisk/ in electron-beam excited mixtures
06 p0766 A83-18953
- An UV-preionized KrF excimer laser with an output energy of 0.42 J
06 p0766 A83-19143
- Theoretical analysis of electron-beam-excited KrF laser performance - New F2 concentration optimization
07 p0938 A83-21599
- Generation of 35.5-nm coherent radiation
10 p1429 A83-26115
- Phase conjugate reflection of KrF laser radiation
11 p1582 A83-27599
- High-power KrF laser transmission through optical fibers and its application to the triggering of gas switches
16 p2357 A83-35427
- Electrically triggered multimodule KrF laser system with narrow-linewidth output
18 p2692 A83-39092
- Simultaneous ultraviolet laser triggering of two multimegavolt gas switches
18 p2677 A83-40059
- Laser induced damage in the ultraviolet
21 p3145 A83-44831
- Narrow-linewidth gain and saturation measurements of a KrF discharge laser
24 p3587 A83-48906

KU BAND

U SUPERHIGH FREQUENCIES

KUIPER AIRBORNE OBSERVATORY

U C-141 AIRCRAFT

KUTTA-JOUKOWSKI CONDITION

- Low frequency flows through an array of airfoils
09 p1196 A83-23703
- A model of the excitation of large scale fluctuations in a shear layer
10 p1475 A83-25935
- [AIAA PAPER 83-0724]
10 p1446 A83-26628
- Aerodynamic loads on a Darrieus rotor blade
10 p1446 A83-26628
- Unsteady Kutta condition of a plunging airfoil
22 p3248 A83-46438
- Considerations of the vorticity fields on wings
22 p3249 A83-46465

L

L BAND

U ULTRAHIGH FREQUENCIES

L-SAT

- The ESA Large Telecommunications Satellite Programme and its projections into the future
04 p0466 A83-15665

L-1011 AIRCRAFT

- The use of modal control to minimize errors in the analytical reconstruction of flight control sensor signals
01 p0013 A83-11210
- Wake vortex attenuation flight tests - A status report
02 p0134 A83-11806
- Fault isolation methodology for the L-1011 digital avionic flight control system
09 p1209 A83-24427
- Static and damage tolerance tests of an advanced composite vertical fin for L-1011 aircraft
12 p1701 A83-29780
- Four-dimensional flight management using colour CRT displays
21 p3091 A83-44689

LABORATORIES

- NT ENGINE TESTING LABORATORIES
NT ENVIRONMENTAL LABORATORIES
NT LONG DURATION EXPOSURE FACILITY
NT MANNED ORBITAL LABORATORIES
NT SPACE LABORATORIES
- Laboratory facility for testing electric-vehicle batteries
Test rig for simulating duty cycles with different discharge modes
16 p2371 A83-35554

LABORATORY EQUIPMENT

- NT IMAGE FURNACES
Mathematical model of beam intensity dispersion at the detector plane in a molecular-beam apparatus
08 p1163 A83-23226
- Versatile curved crystal spectrometer for laboratory extended X-ray absorption fine structure measurements
08 p1105 A83-23227
- Design and experiences with a laboratory Stirling cycle machine
11 p1588 A83-27284

LABYRINTH

- NT COCHLEA
NT VESTIBULES
- The diagnosis of latent vestibular disorders in patients with otosclerosis
07 p0978 A83-20877
- The role of the osmolality of the blood serum in the pathogenesis of Meniere's disease
15 p2211 A83-34423
- Necrotic epitympanitis complicated by paresis of the facial nerve and labyrinthitis
16 p2399 A83-36815
- Early ultrastructural changes in the auditory labyrinth of frogs produced by the action of pulsed ultrasound
18 p2731 A83-39497

LABYRINTH SEALS

- Experimental study of the air flow through labyrinth seal
16 p2361 A83-35860
- A study of the gas-dynamic efficiency of the labyrinth seals of gas-turbine engines with a profiled stator wall
19 p2801 A83-42153

LACTATES

- Lactate accumulation relative to the anaerobic and respiratory compensation thresholds
13 p1901 A83-30451
- Blood lactate threshold in some well-trained ischemic heart disease patients
13 p1902 A83-30452
- Human frontal sweat rate and lactate concentration during heat exposure and exercise
13 p1903 A83-30468
- Anaerobic threshold, blood lactate, and muscle metabolites in progressive exercise
13 p1905 A83-30503
- The effect of alimentary alkalemia on the maximum duration of anaerobic work and the concentration of lactate in the muscles and blood
16 p2398 A83-35906
- Thiol-catalyzed formation of lactate and glyceralate from glyceraldehyde --- significance in molecular evolution
20 p3036 A83-42398
- Lactate in human skeletal muscle after 10 and 30 s of supramaximal exercise
20 p3034 A83-43479

LACTIC ACID

- Blood osmolality in vitro - Dependence on P(CO2), lactic acid concentration, and O2 saturation
13 p1902 A83-30459

LAG (DELAY)

U TIME LAG

LAGEOS (SATELLITE)

- Early experience with a highly mobile Lageos ranging system --- satellite tracking
01 p0019 A83-10023
- A refined gravity model from Lageos /GEM-L2/
03 p0358 A83-13549
- Effects of the earth-reflected sunlight on the orbit of the LAGEOS satellite
07 p0868 A83-21204
- Relative lateration across the Los Angeles basin using a satellite laser ranging system
07 p0952 A83-21524
- Secular variation of earth's gravitational harmonic J2 coefficient from Lageos and nontidal acceleration of earth rotation
17 p2545 A83-38597
- On filtering and compressing LAGEOS laser range data
19 p2860 A83-41558
- Constraint on deep mantle viscosity from Lageos acceleration data
20 p3028 A83-43557
- Deformation of the Australian plate - Preliminary findings from laser ranging to the LAGEOS satellite
22 p3317 A83-46363

LAGRANGE COORDINATES

- On certain motions of a system of three Lagrange gyroscopes
09 p1337 A83-23558
- Sufficient conditions of the stability of the regular precessions of a system of n Lagrange gyroscopes
09 p1337 A83-23562
- On the stabilization of an unbalanced Lagrange gyroscope at rest
09 p1337 A83-23563
- Calculation of ephemerides for libration points
09 p1355 A83-25282

LAGRANGE EQUATIONS OF MOTION

U EULER-LAGRANGE EQUATION

LAGRANGE MULTIPLIERS

- Nonlinear program based optimization of boost and buck-boost converter designs
01 p0040 A83-11016
- Combined penalty multiplier optimization methods to enforce integral invariants conservation --- for shallow water equations
23 p3489 A83-47397

LAGRANGIAN EQUILIBRIUM POINTS

- On a theorem of stability for a homogeneous potential
03 p0387 A83-13411
- Hermitian gravity and supergravity
12 p1774 A83-29029
- Hamiltonian structure of the theory of gravity with R + T(2) type of Lagrangian
12 p1775 A83-29043
- A search for objects near the earth-moon Lagrangian points
13 p1939 A83-31206
- The motion of a stationary satellite in the neighbourhood of the equilibrium points of a central potential perturbed by the J(2) term
17 p2472 A83-38941
- Non-Einsteinian gravitational Lagrangians assuring cosmological solutions without collapse
22 p3380 A83-46753
- Cases of integrability of equations for the inertial motion of two bodies connected by means of a spherical joint
23 p3504 A83-48453

LAGUERRE FUNCTIONS

Soliton and algebraic equation

- 14 p2077 A83-32509

LAKE ICE

NT ICE FLOES

- The brightness temperature of sea ice and fresh-water ice in the frequency range 500 MHz to 37 GHz
22 p3313 A83-46205

LAKE MICHIGAN

- Lake-effect disturbances over Lake Michigan - Some numerical results 03 p0368 A83-14439
 Numerical simulation of land-breeze-induced snowbands along the western shore of Lake Michigan 06 p0791 A83-18461

LAKE ONTARIO

- Use of chromaticity in remote measurements of water quality 14 p2035 A83-32615

LAKES

- NT GREAT LAKES (NORTH AMERICA)
 NT GREAT SALT LAKE (UT)
 NT LAKE MICHIGAN
 NT LAKE ONTARIO
 Definition of alteration belts in the Walker Lake, Nevada-California 1 deg x 2 deg quadrangle --- remote sensing maps for mineral exploration 01 p0062 A83-10033
 Surficial geology mapping from Landsat-Kaminak Lake, N.W.T. 03 p0348 A83-14268
 Temporary lakes and salt plains in the high plateaus of the Andes /Bolivia/ - A continuing survey of periodic hydrologic phenomena using the geostationary satellite GOES-EST 03 p0360 A83-14574
 Use of Landsat data to predict the trophic state of Minnesota lakes 07 p0952 A83-21432
 Landsat-data for distributed hydrological models 08 p1127 A83-21934
 Automatic mapping of lakes for small-scale maps using digital Landsat Imagery 08 p1129 A83-21969
 Developing lake sampling strategies with existing Landsat data 17 p2531 A83-38353

LALLEMAND CAMERAS

- An electronic camera with a remotely controlled shutter at the primary focus of the 3.60 m C.F.H. telescope 06 p0822 A83-19192

LAMB WAVES

- Optical probing of resonant ultrasonic scattering from machined flaws in plates 04 p0492 A83-15208
 Lamb pulse observed in nature 18 p2717 A83-39800
 A Lamb wave voltage sensor 23 p3454 A83-47627

LAMBERT SURFACE

- Lambertian analysis of mirrors and Fresnel lenses for solar concentration 14 p2043 A83-32271
 Point spread functions in imaging a Lambert surface from zenith through a thin scattering layer 20 p3011 A83-42964

LAME WAVE EQUATIONS

- On the numerical construction of ellipsoidal wave functions 07 p0987 A83-20512

LAMELLA (METALLURGY)

- Control of microstructures of (alpha + beta)-titanium alloys 15 p2140 A83-34797
 Stress field related to dislocation arrangements observed in the phase boundary of a lamellar in-situ composite 18 p2667 A83-40257

LAMINA

U LAYERS

LAMINAR BOUNDARY LAYER

- Transient extinction of counter flow diffusion flame 01 p0022 A83-10497
 The effects of Reynolds number and pressure gradient on the transitional spot in a laminar boundary layer 01 p0047 A83-10896
 Fluid injection to a laminar boundary layer with variable wall mass and heat flux [ASME PAPER 82-HT-61] 02 p0173 A83-12801
 Laminar and turbulent boundary layers on moving, nonisothermal continuous flat surfaces 03 p0316 A83-13486
 On the spreading of a turbulent spot in the absence of a pressure gradient 03 p0321 A83-14578
 Asymptotic solutions of the laminar boundary-layer equations 03 p0323 A83-14675
 On the disputes about open separation --- in three dimensional flow [AIAA PAPER 83-0296] 05 p0634 A83-16636
 A new transformation and method of solution of laminar boundary layer equations 06 p0756 A83-18152
 A new multifold series general solution of the steady, laminar boundary layers. I - Theory of the multifold series expansion. II - Application theory of the Euler transformation 07 p0925 A83-20278
 Correlation of Preston tube data with laminar skin friction 08 p1084 A83-22134
 Accurate solutions for laminar and turbulent boundary layers at very large pressure gradient parameters 08 p1089 A83-23195
 Numerical study on flow behaviour and heat transfer in the vicinity of starting point of transpiration 08 p1090 A83-23206
 Low Reynolds number flow between interrupted flat plates 09 p1259 A83-23878

- Shock induced unsteady flat plate boundary layers and transitions 10 p1414 A83-26147
 The boundary layer behind a shock wave incident on a leading edge 10 p1372 A83-26148
 Stability limits and transition times of wave-induced wall boundary layers 10 p1415 A83-26151
 Exact solution of the thermal boundary-layer equations for an arbitrary heat-flux distribution on a surface in a flow 10 p1417 A83-26253
 Unsteady boundary layer with self-induced pressure near a rapidly heated section of the surface of a flat plate in supersonic flow 11 p1527 A83-28536
 The conjugate heat-transfer problem of a controlled laminar boundary layer in a magnetic field 12 p1781 A83-29265
 Asymptotics of solutions of the Orr-Sommerfeld equation describing unstable oscillations at large Reynolds numbers 13 p1839 A83-30091
 Decay of streamwise vorticity downstream of a three-dimensional protuberance 14 p1971 A83-32983
 Turbulent spots, wave packets, and growth 14 p2013 A83-33378
 Theoretical studies of boundary layers --- Russian book 15 p2158 A83-34163
 The evolution of Tollmien-Schlichting waves near a leading edge. II - Numerical determination of amplitudes. 16 p2348 A83-35346
 The effect of acoustic perturbations on the flow structure in a boundary layer with an unfavorable pressure gradient 16 p2289 A83-35705
 Unsteady nonsimilar laminar boundary-layer flows with heat and mass transfer 17 p2501 A83-37024
 An approximate calculation of laminar boundary layer flow of an incompressible fluid 17 p2501 A83-37049
 Experimental studies of the boundary layer on an airfoil at low Reynolds numbers [AIAA PAPER 83-1671] 17 p2444 A83-37181
 Three-dimensional skewed shock wave laminar boundary layer interaction at Mach 2.25 [AIAA PAPER 83-1755] 17 p2446 A83-37228
 The stability of a laminar boundary layer on an elastic surface 17 p2505 A83-37510
 The effect of a sudden change in the motion of a plate surface on flow in a laminar boundary layer in supersonic flow 17 p2450 A83-37634
 Laminar boundary layer stability experiments on a cone at Mach 8. I - Sharp cone [AIAA PAPER 83-1761] 18 p2633 A83-39264
 Holographic measurement of transition and turbulent bursting in supersonic axisymmetric boundary layers [AIAA PAPER 83-1724] 18 p2633 A83-39269
 An interacting boundary layer model for cascades [AIAA PAPER 83-1915] 18 p2635 A83-39372
 Laminar boundary layers behind detonation waves 18 p2684 A83-39450
 Subsonic laminar separation at the breaking point of an airfoil 19 p2790 A83-41216
 Nonsimilar laminar incompressible boundary layer flow over a rotating sphere 19 p2843 A83-41542
 The possibility of a quick determination of the onset of turbulence in a laminar boundary layer 19 p2791 A83-41578
 A class of exact solutions of the laminar-boundary-layer equations 19 p2845 A83-41892
 Features of the effect of admixtures on the characteristics of a region perturbed by a body moving at hypersonic velocity 19 p2792 A83-41893
 Heat transfer characteristics and boundary layer development about heating and cooling rotating blunt bodies at supersonic speeds 20 p2929 A83-42710
 Flow and heat transfer past a semi-infinite vertical plate with oscillating plate temperature 20 p2977 A83-42720
 Generalization of results of experimental and numerical studies of heat transfer in flows with increased external turbulence on the bases of two-parameter models of turbulence 20 p2977 A83-42724
 Coefficients for the combined heat- and momentum-transfer in laminar and turbulent boundary layers 20 p2977 A83-42728
 The two-dimensional laminar wake with initial asymmetry 20 p2930 A83-43454
 Application of unsteady laminar triple-deck theory to viscous-inviscid interactions from an oscillating flap in supersonic and subsonic flow 21 p3086 A83-44457
 Heat and mass transfer toward bluff bodies 21 p3133 A83-45348
 Prediction of boundary-layer characteristics of an oscillating airfoil 22 p3248 A83-46435
 Finite-difference solutions for laminar boundary layer flows with separation 22 p3249 A83-46459
 Calculation of a laminar-turbulent two-dimensional turbine blade boundary layer including surface curvature effects 22 p3249 A83-46464

- Rotating compressible flow over an infinite disk 23 p3446 A83-47590
 Boundary layer and loss measurements on the rotor of an axial-flow turbine [ASME PAPER 83-GT-4] 23 p3392 A83-47878
 A light test of laminar flow control leading-edge systems [AIAA PAPER 83-2508] 23 p3404 A83-48356
 The effect of injection in the boundary layer on supersonic flow past an oscillating cone 23 p3400 A83-48654
 Design integration of laminar flow control for transport aircraft [AIAA PAPER 83-2440] 24 p3547 A83-49577
 Calculation of a boundary layer with phase transformations --- oxygen condensation at cooled surface 24 p3579 A83-49661
- LAMINAR BOUNDARY LAYER SEPARATION**
 U LAMINAR BOUNDARY LAYER
- LAMINAR FLAMES**
 U FLAMES
 U LAMINAR FLOW
- LAMINAR FLOW**
 NT HARTMANN FLOW
 NT STRATIFIED FLOW
 Heat transfer by laminar forced flow against a rotating disk 01 p0044 A83-10227
 The use of forced Rayleigh scattering to study laminar and turbulent flows 02 p0169 A83-11855
 The development of jets in stratified fluids 02 p0169 A83-11860
 Compressible second-order boundary layers for three-dimensional stagnation point flows with mass transfer 02 p0170 A83-12049
 Finite analytic numerical solution of axisymmetric Navier-Stokes and energy equations [ASME PAPER 82-HT-42] 02 p0172 A83-12795
 Natural convection heat transfer between eccentric horizontal cylinders [ASME PAPER 82-HT-43] 02 p0172 A83-12796
 Finite-element simulation of natural convection in three-dimensional enclosures [ASME PAPER 82-HT-71] 02 p0173 A83-12803
 Finite element, stream function-vorticity solution of steady laminar natural convection 02 p0173 A83-12903
 Spectral method solutions for some laminar channel flows with separation 03 p0315 A83-13138
 Laminar and turbulent natural convection in the annulus between horizontal concentric cylinders 03 p0315 A83-13485
 Transient lubricating films with inertia [ASME PAPER 82-LUB-12] 03 p0335 A83-13507
 Eigenvalue problems on infinite intervals 03 p0387 A83-13569
 Combustion of a layer of fuel in a flow of oxidizer over its surface 03 p0295 A83-14058
 Modified gauge for time-resolved skin-friction measurements 03 p0329 A83-14172
 Experiments on the role of amplitude and phase modulations during transition to turbulence 03 p0321 A83-14576
 Flame quenching by turbulence 03 p0295 A83-14848
 Boundary-layer diffusion on a plate with inhomogeneous chemical properties 03 p0323 A83-14900
 Streamwise corner flow with wall suction 04 p0442 A83-15279
 Laminar flow of vapor flux in the condensation region of heat tubes 04 p0477 A83-15864
 Laminar free convection on a vertical nonisothermal plate under strong injection 04 p0478 A83-16164
 Developments in the NASA transport aircraft laminar flow program [AIAA PAPER 83-0090] 05 p0579 A83-16514
 Laminar viscous flow-field prediction of Shuttle-like vehicle aerodynamics [AIAA PAPER 83-0211] 05 p0581 A83-16586
 Aerodynamic features of turbulent flames [AIAA PAPER 83-0470] 05 p0636 A83-16737
 Calculation of the pressure distribution and streamline pattern around a ring wing using finite difference methods [AIAA PAPER 83-0645] 05 p0588 A83-16812
 Water tunnel construction for continuous mode flow visualization [AIAA PAPER 83-0657] 05 p0599 A83-16821
 The calculation of some laminar flows using various discretisation schemes 05 p0642 A83-17900
 Parameters controlling the spacing of streamwise vortices on concave walls [AIAA PAPER 83-0380] 05 p0591 A83-17924
 Field observations of stratified atmospheric flow above an obstacle 06 p0788 A83-18237

Longitudinal-dispersion calculations in laminar flows by statistical analysis of molecular motions 06 p0758 A83-19019

Experimental study of the structure of the turbulent thermal boundary layer in laminarized flows developed in strong favorable pressure gradients 06 p0759 A83-19156

Application of Gyarmati's variational principle to laminar stagnation flow problem 06 p0760 A83-19400

The turbulent motions of a fluid in a closed region in a strong magnetic field 06 p0814 A83-19555

The interaction of a two-dimensional jet with three-dimensional perturbations 06 p0760 A83-19564

Application of the finite-element method to one-dimensional flame propagation problems 07 p0878 A83-19818

Laminar burning velocities of hydrogen-air and hydrogen-air-steam flames 07 p0878 A83-19837

The mechanism of lean limit flame extinction 07 p0879 A83-19841

Numerical study of a confined premixed laminar flame - Oscillatory propagation and wall quenching 07 p0879 A83-19842

Temperature measurements in a radially symmetric flame using holographic interferometry 07 p0879 A83-19845

An experimental study of the stationary propagation of a flame in a tube under conditions of weightlessness 07 p0868 A83-19957

A numerical analysis of flow using streamline coordinates - The case of two-dimensional steady incompressible flow 07 p0925 A83-20277

Numerical calculation of the laminar flow in the inlet of the axial sealing gap of radial-flow compressors 07 p0864 A83-21339

On certain aspects of three-dimensional instability of parallel flows 07 p0927 A83-21353

Numerical studies of laminar flame propagation in spherical bombs 08 p1056 A83-22139

Lift-off characteristics of turbulent jet diffusion flames 08 p1056 A83-22140

Evaluation of total body heat transfer in hypersonic flow 08 p1042 A83-22150

NO₂ formation in laminar flames 08 p1057 A83-22397

Numerical methods in laminar and turbulent flow; Proceedings of the Second International Conference, Venice, Italy, July 13-16, 1981 08 p1087 A83-23176

Hypersonic viscous flows in a streamline coordinate system 08 p1090 A83-23205

An experimental investigation of the dispersion of a gas jet in a coflowing stream of air 08 p1042 A83-23215

Laterally converging flow. I - Mean flow. II - Temporal wall shear stress 09 p1262 A83-24418

Computation of hypersonic viscous flow over a body with mass transfer and/or spin 09 p1198 A83-24878

Theory of laminar flames --- Book 09 p1227 A83-24946

Flow through rotating straight pipes of a circular cross section 10 p1413 A83-25780

Sensitivity analysis for premixed, laminar, steady state flames 10 p1390 A83-25898

Measurement of dynamic pressure in shock tube by streak photography 10 p1421 A83-26135

Visualization studies of a shear driven three-dimensional recirculating flow 11 p1565 A83-27411

Development of finite-amplitude disturbances in a Poiseuille flow 11 p1566 A83-27706

Strained premixed laminar flames under nonadiabatic conditions 11 p1546 A83-28599

Mixed laminar convection on a vertical surface under conditions of strong injection 11 p1571 A83-28799

The three-dimensional laminar asymptotic boundary layer with suction 12 p1721 A83-28847

Induced drag of a slender wing in a nonuniform stream 12 p1696 A83-28970

Computation of steady laminar flow over a circular cylinder with third-order boundary conditions 12 p1725 A83-29664

Driven cavity flows by efficient numerical techniques 12 p1726 A83-29669

Velocity measurements in an axisymmetric laminar flow using an optical technique of visualization in coherent light 12 p1726 A83-29704

Flow in curved pipes 13 p1843 A83-31086

Viscous shock-layer flowfield analysis by an explicit-implicit method [AIAA PAPER 83-1423] 14 p1970 A83-32702

Viscous real gas flowfields about three dimensional configurations [AIAA PAPER 83-1511] 14 p1970 A83-32748

A simple model for carbon monoxide in laminar and turbulent hydrocarbon diffusion flames 14 p1990 A83-32939

In-situ optical measurement of additive effects on particulates in a sooting diffusion flame 14 p1991 A83-32943

Laminar compressible flow between close rotating disks - An asymptotic and numerical study 15 p2157 A83-33869

Numerical methods in laminar flame propagation; Proceedings of the Workshop, Aachen, West Germany, October 12-14, 1981 15 p2131 A83-34026

Discussion of test problem A --- numerical solutions of laminar flame propagation 15 p2131 A83-34027

Discussion of test problem B --- numerical methods in flame propagation 15 p2132 A83-34031

Results of a study of several transport algorithms for premixed, laminar steady-state flames 15 p2132 A83-34033

Toward the formulation of a global local equilibrium kinetics model for laminar hydrocarbon flames 15 p2132 A83-34035

Time-dependent simulation of flames in hydrogen-oxygen-nitrogen mixtures 15 p2132 A83-34036

Mechanism of flame propagation in hydrogen-air and methane-air systems 15 p2132 A83-34037

An effective numerical technique for entry length laminar convective heat transfer in vertical and horizontal ducts of any cross section 15 p2160 A83-34258

Laminar, natural convection heat transfer in a horizontal gap, bounded by an elliptic and A circular cylinder 15 p2160 A83-34260

Mass, heat, and momentum transfer in laminar and turbulent pipe flow with vaporization of a liquid film 15 p2161 A83-34266

Numerical study of transient laminar combustion in boundary layer flow 15 p2161 A83-34267

Laminar natural convection from a horizontal plate and the influence of plate-edge extensions 16 p2348 A83-35337

Calculation of flow past a small projection directed toward the flow 16 p2288 A83-35531

Free and induced oscillations in Poiseuille flow 16 p2349 A83-35642

Calculation of a laminar flow of a compressible gas in plane curvilinear ducts with heat transfer 16 p2349 A83-35701

Group combustion of liquid fuel sprays [AIAA PAPER 83-0150] 16 p2326 A83-36044

Numerical solution of the problem of flame propagation by the use of the random element method [AIAA PAPER 83-0600] 16 p2326 A83-36062

Influence of laminar flame speed on the blowoff velocity of bluff-body stabilized flames [AIAA PAPER 83-1327] 16 p2326 A83-36341

Analysis of turbulent diffusion flames using unique relationships from laminar flame calculations [AIAA PAPER 83-1364] 16 p2326 A83-36360

Natural laminar flow data from full-scale flight and wind-tunnel experiments 16 p2296 A83-36409

Heat transfer performance of ceramic regenerator matrices with sine-duct shaped passages 16 p2353 A83-36592

Stability of relativistic laminar flow equilibria for electrons drifting in crossed fields 17 p2496 A83-37042

Transonic flow at the break point of a profile with a free streamline 17 p2448 A83-37527

The effect of the geometrical parameters of an air intake with a central body on drag relative to the fluid streamline in the case when there is an incompressible-gas flow around it 17 p2448 A83-37531

Numerical model for dynamic and thermal developments of a pulsed laminar ducted flow 17 p2506 A83-37867

Plane flow past an air-supported soft cylindrical shell 17 p2522 A83-38099

The prediction of compressible, laminar viscous flows using a time-marching control volume and multigrid technique [AIAA PAPER 83-1896] 18 p2682 A83-39360

Global PNS solutions for laminar and turbulent flow --- Parabolized Navier-Stokes equations around boattail, flat plate and NACA 0012 airfoil geometries [AIAA PAPER 83-1911] 18 p2635 A83-39369

Prediction of laminar separated flows using the partially parabolized Navier-Stokes equations [AIAA PAPER 83-1954] 18 p2682 A83-39397

Annular squeeze films with inertial effects 18 p2695 A83-39942

The application of the matched-asymptotic-expansion method to two-dimensional laminar flows with finite separated regions --- German thesis 19 p2844 A83-41810

Gas flow through rotameters 19 p2849 A83-41870

The effect of the wave injection of a fluid jet into a gas cross-stream 19 p2794 A83-42155

Study of 2-D laminar separated flow using unsteady incompressible Navier-Stokes equations 20 p2969 A83-42530

Numerical simulation of laminar natural convection in shallow inclined enclosures 20 p2973 A83-42680

Modification of the turbulent temperature field in strongly heated air flows 20 p2977 A83-42726

Natural, mixed and forced convection in a vertical channel with asymmetric uniform heating 20 p2979 A83-42750

Laminar flow in the interior of a rotating hollow sphere as it is set in motion 20 p2983 A83-43010

Vapor flow reversal in the condensation zone of a simulated flat-plate heat pipe 20 p2984 A83-43023

The laminar unsteady flow of a viscous fluid away from a plane stagnation point 20 p2985 A83-43102

Flight investigation of natural laminar flow on the Bellanca Skyrocket II [SAE PAPER 830717] 20 p2933 A83-43326

An interferometric investigation of separated forced convection in laminar flow past cavities 20 p2986 A83-43360

Flow characteristics in the curved rectangular channels Visualization of secondary flow 21 p3129 A83-44064

The effect of boundary absorption on longitudinal dispersion in steady laminar flows 21 p3130 A83-44466

The preferred-mode coherent structure in the near field of an axisymmetric jet with and without excitation 22 p3283 A83-46451

A numerical method to solve the steady-state Navier-Stokes equations for natural convection in enclosures 22 p3284 A83-46472

Numerical computation of laminar steady-state inlet-aperture flow and the evolving flow after an embankment 22 p3284 A83-46493

Vortices, stability, and turbulence 22 p3285 A83-46718

Effect of crossflow on the vortex-layer-type three-dimensional flow separation 22 p3250 A83-47018

Boundary layers on bodies of revolution spinning in axial flows 22 p3286 A83-47023

Inertia effects of the dynamics of a disk levitated by incompressible laminar fluid flow [ASME PAPER 83-GT-149] 23 p3464 A83-47968

Chemical equilibrium laminar or turbulent three-dimensional viscous shock-layer flows 23 p3398 A83-48133

An experimental study of the effects of gravity on flame spread in high oxygen concentration environments 23 p3430 A83-48158

Numerical modeling of ethylene oxidation in laminar flames 23 p3430 A83-48159

Laminar flow in the entrance region of elliptical ducts [ASME PAPER 83-FE-1] 23 p3449 A83-48226

Prediction of sudden expansion flows using the boundary-layer equations [ASME PAPER 83-FE-11] 23 p3450 A83-48230

Unified approach to the solution of problems of unsteady laminar flow in long pipes [ASME PAPER 83-APM-2] 23 p3451 A83-48240

Noise generated by airfoil profiles placed in a uniform laminar flow 24 p3625 A83-49463

Flow of a dipolar fluid due to suddenly accelerated flat plate 24 p3581 A83-50149

LAMINAR FLOW AIRFOILS

Subsonic laminar separation at the breaking point of an airfoil 19 p2790 A83-41216

LAMINAR FLOW CONTROL

U BOUNDARY LAYER CONTROL
U LAMINAR BOUNDARY LAYER

LAMINAR HEAT TRANSFER

Effect of aspect ratio on heat transfer in shallow enclosures [ASME PAPER 82-HT-44] 02 p0172 A83-12797

Mixed convection over a horizontal heated flat plate [ASME PAPER 82-HT-75] 02 p0173 A83-12804

Generalized laminar heat transfer from the surface of a rotating disk 03 p0323 A83-14673

Integral method to thermally developing laminar flow in a duct subjected to external radiation and convection [AIAA PAPER 83-0529] 05 p0637 A83-16768

Combined / radiative-convective/ heat transfer from laminar and turbulent radiating flows in cooled ducts 06 p0759 A83-19160

Numerical calculation of pressure loss and forced convective heat transfer in rotating channels of arbitrary rectangular cross section 08 p1083 A83-21634

An integral method in laminar film condensation of plane and axisymmetric bodies 08 p1083 A83-21893

Analysis of viscous dissipation effect on thermal entrance heat transfer in laminar pipe flows with convective boundary conditions 08 p1086 A83-23123

- Momentum and heat transfer in power-law fluid flow over two-dimensional or axisymmetrical bodies 08 p1087 A83-23143
- Laminar natural convection along vertical corners and rectangular channels 08 p1090 A83-23208
- The conjugate heat-transfer problem of a controlled laminar boundary layer in a magnetic field 12 p1781 A83-29265
- Optimization of heat transfer in an incompressible-fluid boundary layer with allowance for the heat-balance equation 12 p1723 A83-29279
- Calculation of equilibrium temperature on a profile with variable heat capacity 12 p1783 A83-29290
- Parametric method for solving problems of heat transfer for the film flow of a fluid 13 p1838 A83-30045
- Experimental aerodynamic heating to simulated Shuttle tiles [AIAA PAPER 83-1536] 14 p2011 A83-32764
- Analysis of STS-2 experimental heating rates and transition data 15 p2125 A83-33732
- Combined free and forced laminar convection in a vertical channel 15 p2160 A83-34257
- An effective numerical technique for entry length laminar convective heat transfer in vertical and horizontal ducts of any cross section 15 p2160 A83-34258
- Laminar flow heat transfer with axial conduction in a circular tube - A finite difference solution 15 p2160 A83-34262
- Solution of the equations of an unsteady boundary layer 16 p2349 A83-35533
- Buoyancy effect on heat transfer in forced channel flows 20 p2971 A83-42661
- Natural convection with volumetric energy sources in a fluid bounded by a spherical segment 20 p2972 A83-42676
- Convective heat transfer from laminar and turbulent premixed flames 20 p2979 A83-42748
- The effect of Prandtl number on heat transfer from an isothermal rotating disk with blowing at the wall 24 p3578 A83-49574
- LAMINAR JETS**
- U JET FLOW
- U LAMINAR FLOW
- LAMINAR MIXING**
- Influence of hydrodynamics and diffusion upon the stability limits of laminar premixed flames 04 p0457 A83-16261
- Flowfield experiments on a DF chemical laser 07 p0932 A83-19815
- Solution of burner-stabilized premixed laminar flames by boundary value methods 12 p1712 A83-29642
- Calculation of laminar premixed and diffusion flames with fast chemical reaction using a self-consistent method 15 p2132 A83-34269
- Three dimensional disturbances propagated from a tunnel side wall to a mixing layer 24 p3580 A83-49831
- LAMINAR WAKES**
- An experimental investigation of wake edge tones [AIAA PAPER 83-0741] 10 p1476 A83-25944
- Measurements of nonlinear interactions during natural transition of a symmetric wake 17 p2501 A83-37029
- The two-dimensional laminar wake with initial asymmetry 20 p2930 A83-43454
- The effect of heat release and injection on the structure of a laminar hypersonic flow behind a body 23 p3399 A83-48534
- On the asymptotic structure of interaction in a laminar axisymmetric wake 23 p3451 A83-48653
- LAMINATED MATERIALS**
- U LAMINATES
- LAMINATES**
- A study of the stressed state of inhomogeneous cylindrical shells 01 p0059 A83-10679
- Axisymmetric thermoplastic state of layered shells on the basis of the theory of small-curvature processes 01 p0059 A83-10680
- Analysis of simply supported multilayer trapeziform plates 01 p0059 A83-10685
- Fracture of fatigue-loaded composite laminates 02 p0149 A83-12013
- Moving cracks in layered composites 02 p0190 A83-12048
- Fatigue of graphite/epoxy /0/90/45/-45/s laminates under dual stress levels 02 p0149 A83-12060
- Nonlinear matrix failure criterion for fiber-reinforced composite materials 02 p0150 A83-12062
- Survey of recent research in the analysis of composite plates 02 p0191 A83-12065
- Small transverse vibrations of circular laminate plates 02 p0191 A83-12334
- Elastoplastic behavior of a fiber laminate 02 p0150 A83-12340
- The effect of a longitudinal delamination in a laminate cylindrical shell on the critical external pressure 02 p0192 A83-12360
- Dynamic instability of suddenly heated angle-ply laminated composite cylindrical shells 02 p0194 A83-12742
- Nonlinear analysis of axially-loaded laminated cylindrical shells 02 p0194 A83-12743
- An energy theory for postbuckling of composite plates under combined loading 02 p0195 A83-12758
- A comprehensive theory for planar bending of composite laminates 02 p0195 A83-12760
- Dynamic finite element model for laminated structures 02 p0195 A83-12761
- Simple calculations for the stability of soft, thin-walled mandrels during filament winding [ASME PAPER 82-PPV-1] 02 p0195 A83-12767
- An experimental and analytical study of the dynamic response of a linkage fabricated from a unidirectional fiber-reinforced composite laminate [ASME PAPER 82-DET-67] 02 p0187 A83-12775
- Residual stress measurement of laminated anisotropic plate by strain gauge method 02 p0197 A83-13067
- A unifying strain criterion for fracture of fibrous composite laminates 03 p0291 A83-13340
- A numerical solution for layered solid contact problems with application to bearings [ASME PAPER 82-LUB-8] 03 p0335 A83-13505
- Rheological characterization of epoxy prepreg resins 03 p0302 A83-13563
- Experimental mechanics of fiber reinforced composite materials --- Book 03 p0341 A83-14117
- Interaction of cylindrical eddy-current transducers with a multilayered spherical product 03 p0338 A83-14294
- Calculation of the stresses on the free edges in symmetric composite plates with or without a hole - Comparison with experiment [ONERA, TP NO. 1982-97] 03 p0342 A83-14544
- Fractographic studies of graphite/epoxy fatigue specimens 03 p0292 A83-14554
- An investigation of cumulative damage development in quasi-isotropic graphite/epoxy laminates 03 p0292 A83-14555
- Effects of moisture, residual thermal curing stresses, and mechanical load on the damage development in quasi-isotropic laminates 03 p0292 A83-14556
- Stiffness-reduction mechanisms in composite laminates 03 p0292 A83-14558
- The dependence of transverse cracking and delamination on ply thickness in graphite/epoxy laminates 03 p0292 A83-14559
- Characterization of delamination onset and growth in a composite laminate 03 p0293 A83-14560
- Compression fatigue behavior of composites in the presence of delaminations 03 p0293 A83-14562
- Effect of stacking sequence on damage propagation and failure modes in composite laminates 03 p0293 A83-14563
- Damage mechanism and life prediction of graphite/epoxy composites 03 p0293 A83-14564
- Fracture toughness of high-strength laminate sheets containing plastic layers of high elastic modulus 03 p0293 A83-14728
- Analysis of process stresses in SiC-Si two-layer disks 03 p0302 A83-14735
- Finite element analysis of plates with nonlinear properties 04 p0495 A83-15018
- Fatigue lifetime predictions from ultrasonically detected laminar defects in a graphite-epoxy composite 04 p0454 A83-15180
- Optimal cooling of cross-ply composite laminates and adhesive joints [ASME PAPER 82-WA/APM-24] 04 p0455 A83-15679
- Plasticity analysis of laminated composite plates [ASME PAPER 82-WA/APM-11] 04 p0498 A83-15680
- Plane-strain surface waves in a laminated composite [ASME PAPER 82-WA/APM-21] 04 p0498 A83-15681
- Wave propagation in a unidirectional composite in comparison with that in a layered elastic body 04 p0455 A83-16397
- Three-dimensional analysis of /0/90/s and /90/0/s laminates with a central circular hole 05 p0653 A83-16933
- An equation for bolt clampup relaxation in transient environments 05 p0611 A83-16935
- Evaluation of finite-element software packages for stress analysis of laminated composites 05 p0678 A83-16936
- An analysis of impact failure modes for fiber-reinforced composite laminates by using fault tree 05 p0611 A83-17104
- Effect of transverse direction strain on fracture of notched 0 deg/90 deg GRP laminate under biaxial fatigue 05 p0611 A83-17105
- A finite element formulation for multilayered and thick plates 05 p0655 A83-17737
- Dynamic coefficient of a two-layered thick beam with imperfect bonding 06 p0774 A83-18396
- Love waves in orthotropic periodically layered composites 06 p0725 A83-18510
- Longitudinal elastic wave propagation in laminated composites with bonds 06 p0776 A83-19147
- Bending vibrational behavior of laminated rotors --- German thesis 06 p0769 A83-19620
- Delamination in graphite/epoxy laminates 07 p0875 A83-20437
- Knitted fabrics in fiber reinforced structural composites 07 p0876 A83-20470
- The effect of matrix strain limitations on composite design allowables 07 p0877 A83-20495
- Computer-aided design of complex composite material systems and structures 07 p0877 A83-20498
- On the buckling and vibration of antisymmetric angle-ply laminated circular cylindrical shells 07 p0946 A83-20639
- Tensile fatigue of carbon fiber reinforced plastics 07 p0877 A83-20924
- Variation of in-plane elastic constants in material design of composite laminates 07 p0949 A83-21623
- Impact fatigue strength and reliability for fiber reinforced epoxy resin laminates subjected to repeated impact loads 07 p0877 A83-21624
- Fracture analyses of angle-ply laminates 08 p1054 A83-21729
- Vibrations of layered shells with transverse shear and rotatory inertia effects 08 p1120 A83-21808
- A note on specially orthotropic laminates 08 p1121 A83-21821
- Pure plastic bending of sheet laminates under plane strain condition 08 p1122 A83-21991
- A unit for combined inspection of large multilayer parts of composite polymer materials 08 p1113 A83-22401
- Note on the postbuckling analysis of cross-ply laminated plates with elastically restrained edges and initial curvatures 08 p1123 A83-22414
- Graphite/epoxy material characteristics and design techniques for airborne instrument application 08 p1055 A83-22595
- Experimental study on cut-off phenomenon for layered composite 09 p1276 A83-23330
- Fabrication of aircraft components using prepried broadgoods layed-up in the flat and subsequently formed - Cost benefits and resource utilization enhancements 09 p1195 A83-23602
- Fracture tough composites - The effect of toughened matrices on the mechanical performance of carbon fiber reinforced laminates 09 p1222 A83-23642
- Surface notches in composites 09 p1223 A83-23931
- Stress singularities in laminated composites 09 p1223 A83-23939
- The relationship of stiffness changes in composite laminates to fracture-related damage mechanisms 09 p1223 A83-23940
- Post-crazing analysis of glass-epoxy laminates 09 p1223 A83-23941
- Strength of layered composite cylindrical shells under dynamic loading 09 p1224 A83-23946
- Comparative evaluation of shear test methods for composites 09 p1224 A83-23948
- Experimental determination of flaw shapes and stress intensity distributions - Conditions for application to composite materials 09 p1224 A83-23949
- Optimally discretized finite elements for boundary-layer stresses in composite laminates 09 p1281 A83-24671
- Geometrically nonlinear transient analysis of laminated composite plates 09 p1281 A83-24672
- Structural deformation model of spatially reinforced composites 09 p1282 A83-25107
- An effective dispersion theory for layered composites 10 p1441 A83-26441
- Steady-state point-source excitation of a laminated composite 10 p1441 A83-26442
- Delamination buckling and growth in laminates [ASME PAPER 83-APM-3] 10 p1441 A83-26445
- Deformations of anisotropic layered materials 10 p1442 A83-26818
- Viscoelastic effects in buckling of laminated plates subjected to hygrothermal conditions 11 p1591 A83-27428
- A finite element method for construction of dynamical theories of layered plates 11 p1591 A83-27429
- Geometrically nonlinear analysis of layered composite shells 11 p1591 A83-27431
- Three-dimensional finite-element analysis of layered composite plates 11 p1591 A83-27432
- A theory for transverse cracks in composite laminates 11 p1591 A83-27435

On the nature of stress singularities in anisotropic layered composites 11 p1592 A83-27437

Edge effects in composites by moire interferometry 11 p1594 A83-28076

Global-local laminate variational model 11 p1544 A83-28409

Nonlinear bending of bimodular-material plates 11 p1544 A83-28410

The development of a theory for the bending of layered plates with essentially different layer characteristics 11 p1598 A83-28508

Tensile stress-strain behavior of hybrid composite laminates 12 p1709 A83-28900

The stability of inhomogeneous cylindrical shells --- Russian book 12 p1735 A83-29339

The prediction of material damping of laminated composites 12 p1709 A83-29396

Fracture behavior of hybrid composite laminates [AIAA 83-0804] 12 p1710 A83-29736

A theory for stress analysis of composite laminates [AIAA 83-0833] 12 p1737 A83-29742

Delamination-based compression residual-strength prediction model for composites [AIAA 83-0872] 12 p1738 A83-29756

Stability of imperfect laminated cylinders - A comparison between theory and experiment [AIAA 83-0874] 12 p1738 A83-29758

Buckling behavior and imperfection sensitivity of composite panels [AIAA 83-0877] 12 p1739 A83-29761

Buckling of anisotropic laminated cylindrical plates [AIAA 83-0979] 12 p1740 A83-29786

Vibration and flutter of advanced composite lifting surfaces [AIAA 83-0961] 12 p1744 A83-29861

Analysis of progressive damage in thin circular laminates due to static-equivalent impact loads [AIAA 83-0997] 12 p1711 A83-29872

Large-amplitude vibration of laminated composite plates of arbitrary shape [AIAA 83-1035] 12 p1745 A83-29880

Drop weight impact testing of laminates reinforced with Kevlar aramid fibers, E-glass, and graphite 12 p1711 A83-29891

Variational methods in elasticity and in elastoplasticity for multilayered structures --- French thesis 12 p1747 A83-29947

Uniform and graded multilayers as X-ray optical elements 13 p1845 A83-30212

Optimum design of multilayer panels on the basis of a vector of quality criteria 13 p1866 A83-30309

A study of the possibility of producing multilayer materials based on titanium 13 p1816 A83-30700

Numerical solution of problems of the statics of layered shells of revolution in a refined formulation 13 p1867 A83-30720

Singularity of contact-edge stress in laminated composites under uniform extension 13 p1868 A83-31620

Distributions of fatigue life and fatigue strength in notched specimens of a carbon eight-harness-satin laminate 13 p1816 A83-31621

Laminated modules with new plastic material based on an ethylene-vinylacetate copolymer --- for solar cells 14 p1986 A83-32226

Mathematical modeling of damage in unidirectional composites 14 p1986 A83-32344

Energy dissipation during the vibration of multilayer shells 14 p2031 A83-32389

Thermophysical properties data on graphite/polyimide composite materials 14 p1987 A83-33118

Environmental exposure of carbon/epoxy composite material systems 14 p1987 A83-33123

An analytic description of the kinetics of fatigue cracks in laminated composites 15 p2180 A83-35041

Generation of thermal strains in GRP. I - Effect of water on the expansion behaviour of unidirectional glass fibre-reinforced laminates. II - The origin of thermal strains in polyester cross-ply laminates 15 p2130 A83-35074

The effect of creep on the magnitude of elastic deformation in a laminated composite 16 p2323 A83-35506

Free vibrations of antisymmetric angle-ply laminated circular cylindrical panels 16 p2365 A83-35641

Standard failure criteria needed for advanced composites 16 p2324 A83-35771

The mean transverse shear in stratified anisotropic plates [ONERA, TP NO. 1983-15] 16 p2368 A83-36425

Calculation of stresses on the free edge in composite plates undergoing mechanical and thermal loading [ONERA, TP NO. 1983-20] 16 p2368 A83-36429

A 3-D finite difference solution for orthotropic laminated composites using curvilinear coordinates 16 p2369 A83-36559

Effective macroscopic description for heat conduction in periodic composites 16 p2353 A83-36593

Calculation of stresses, strains and displacements in an n-layer elastic-continuous system under the action of two complex loads uniformly distributed on circular areas 17 p2519 A83-37273

Process-induced residual thermal stresses in advanced fiber-reinforced composite laminates 17 p2483 A83-37366

Homogenization in yield design - The case of multilayered composite material 17 p2522 A83-38068

Elastic stability of plane laminates 18 p2697 A83-39422

Stress intensity factors in two bonded elastic layers containing cracks perpendicular to and on the interface. I Analysis. II - Solution and results 18 p2698 A83-39535

Diffusion in composite layers with automatic solution of the eigenvalue problem 18 p2684 A83-39848

A boundary-layer theory for the orthotropic plate 18 p2700 A83-39986

Damage tolerance evaluation of adhesively laminated titanium 18 p2666 A83-39994

The effect of fibre surface treatment on the compressive strength of CFRP laminates 18 p2651 A83-40145

Three-dimensional interlaminar stress distribution in symmetric composite laminate 18 p2702 A83-40148

Stress and strength analysis of composite laminates at delamination 18 p2651 A83-40149

An analysis of free-edge delamination in laminated composite under uniform axial strain 18 p2702 A83-40150

On fibre composites with intermittent interlaminar bonding 18 p2651 A83-40151

Factors affecting the interlaminar fracture energy of graphite/epoxy laminates 18 p2651 A83-40152

Fracture mechanics for delamination problems in composite materials 18 p2652 A83-40153

Unsymmetrically laminated composites 18 p2703 A83-40163

Analysis of elastic anisotropy in CFRP laminate beam 18 p2652 A83-40164

Stress distribution around hole of angle-ply laminates under uni-axial tension 18 p2652 A83-40166

Experimental investigation of anisotropic laminate structural behavior 18 p2652 A83-40167

Vibration characteristics of laminated composite plates 18 p2703 A83-40170

Analysis of compression failures in fibre composite laminates 18 p2653 A83-40172

In-plane tensile strength of multidirectional composite laminates 18 p2653 A83-40173

On the knee-point of cross-ply composite 18 p2653 A83-40175

Influence of the polymer matrix on the mechanical response of a unidirectional composite 18 p2653 A83-40179

Probabilistic design on strength of fiber reinforced composite laminates 18 p2654 A83-40182

Stability optimization of laminated composite plates under in-plane loads 18 p2704 A83-40185

Best angles against buckling for rectangular laminates 18 p2704 A83-40186

Coupling effect on axial compressive buckling of laminated composite cylindrical shells 18 p2704 A83-40187

The effect of the direction of shear on the buckling of laminated plates subjected to combined shear and compressive loading 18 p2704 A83-40188

Damage analysis of fibrous composites 18 p2654 A83-40189

Analysis of mechanical damage growth in notched carbon-epoxy (+ or - 45 deg) laminates 18 p2654 A83-40191

Deformation characteristics and failure modes of center-notched graphite/epoxy laminates 18 p2654 A83-40198

Statistical analysis of composite fatigue life 18 p2655 A83-40200

Distributions of fatigue life and fatigue strength in notched specimens of a carbon eight-harness-satin laminate 18 p2655 A83-40201

Compressive fatigue damage accumulation near holes in graphite/epoxy laminates 18 p2655 A83-40203

Fatigue crack growth behavior in the vicinity of interface of dissimilar materials 18 p2705 A83-40204

Effect of combination of glass mat and cloth on the fatigue properties of fibrous composite materials 18 p2655 A83-40206

Creep behaviour of carbon-epoxy (+ or - 45 deg)2s laminates 18 p2655 A83-40209

The prediction of long term viscoelastic properties of fiber reinforced plastics 18 p2655 A83-40210

Effect of time on the mechanical behavior of laminated composites 18 p2655 A83-40211

Analysis of Charpy impact failure for unidirectional fiber-reinforced composite laminates by using a computerized fault tree 18 p2655 A83-40212

Effect of defect on the behaviour of composites 18 p2656 A83-40215

The initiation of fracture in fiber-composites at elevated loading rates 18 p2656 A83-40217

Impact behaviour of quasi-isotropic CFRP laminate 18 p2656 A83-40220

Properties of composite box beams under combined impact loading 18 p2705 A83-40222

The environmental stress corrosion cracking of glass fibre reinforced polyester and epoxy composites 18 p2656 A83-40223

Origins of thermal strains in polyester laminates 18 p2657 A83-40230

On the hybrid effect and fracture mode of interlaminated hybrid composites 18 p2658 A83-40241

Analysis and evaluation of interfacial delamination energy of notched laminated composites 18 p2660 A83-40272

Fractography of carbon/epoxy angle-ply laminates 18 p2660 A83-40273

Effect of stacking sequence in cross-ply graphite/epoxy laminates on acoustic emission results 18 p2661 A83-40276

Material design of composite laminates with required in-plane elastic properties 18 p2662 A83-40292

A new method to determine the bending rigidities of anisotropic plates 18 p2662 A83-40293

Generic aspects of three-dimensional internal-damage development in fatigue-loaded composite laminates 19 p2819 A83-41035

Stress damping in viscoelastic composite laminates under uniform harmonic loading 19 p2820 A83-41599

Acoustoelectric oscillations in a bounded active stratified-periodic medium 19 p2841 A83-41820

Prestrained elastic laminates - Deformations, stability and vibrations 19 p2860 A83-41996

A modified chemical-stress crazing test method 20 p2958 A83-42545

Environmental fatigue of reinforced plastics 20 p2947 A83-42812

Post-impact fatigue performance of carbon fibre laminates with non-woven and mixed-woven layers 20 p2948 A83-42814

Experimental study on compressive properties of sheets and plates and shapes 20 p2957 A83-43693

Polar-scan - A nondestructive test method for the inspection of layer orientation and stacking order in advanced fiber composites 21 p3148 A83-43828

Sensitivity of X-ray computer tomography in the inspection of thin layers, glued joints, cracks, laminations, and coatings 21 p3149 A83-43877

Moisture and temperature effects on the instability of cylindrical composite panels 21 p3105 A83-43968

Residual stresses and their effects in composite laminates 21 p3105 A83-44045

Peculiarities in stress solutions in laminated composites 21 p3105 A83-44047

Biilinear failure analysis of fiber composite laminates 21 p3106 A83-44049

Wave propagation in a graphite/epoxy laminate 21 p3151 A83-44050

Acoustic emission from graphite/epoxy composite laminates with special reference to delamination 21 p3106 A83-44126

Compression fatigue behaviour of notched composite laminates 21 p3106 A83-44334

A comparative analysis of certain versions of shear models in problems regarding the equilibrium and vibration of multilayer plates 21 p3155 A83-44723

Finite element analysis of 3-ply laminated conical shell for flutter 21 p3160 A83-45052

Control of composite cure processes 21 p3119 A83-45067

Void formation and transport during composite laminate processing - An initial model framework 21 p3107 A83-45070

Characterization of quick-cure and vacuum-bag cure composites 21 p3119 A83-45073

Out-of-plane deformation of balanced and symmetric composites as measured by holographic interferometry 21 p3108 A83-45153

Electroelasticity relationships for multilayer piezoceramic shells with layer polarization in the thickness direction 21 p3163 A83-45365

Low-velocity impact response of laminated plates 21 p3164 A83-45589

Resonance phenomena in multiple-boundary periodic metal-dielectric systems 22 p3277 A83-45676

Laser-driven shock-wave propagation in pure and layered targets 22 p3361 A83-45937

Characterization of the matrix glass transition in carbon-epoxy laminates using the CSD test geometry --- centro-symmetric deformation 22 p3262 A83-46282

Control of composite cure processes 22 p3262 A83-46284

Observation of damage growth in compressively loaded laminates 22 p3264 A83-46810

Numerical solution of problems in the mechanics of a deformable inhomogeneous solid 23 p3468 A83-47177

A singular hybrid finite element analysis of boundary-layer stresses in composite laminates 23 p3470 A83-48098

A numerical solution to boundary-value thermoelasticity problems for multilayer hollow cylinders 23 p3471 A83-48247

Contact stiffness of layered cylindrical shells. I - An analytical solution to the problem in the axisymmetrical case 23 p3472 A83-48439

ARALL (aramid-fiber-reinforced aluminum laminate) - A new hybrid composite with exceptional fatigue-resistance properties 23 p3428 A83-48500

Polymer laminate structures --- electrical properties 24 p3552 A83-48779

Nonlinear flexural vibrations of initially deflected cross-ply laminated plates with elastically restrained edges 24 p3591 A83-48894

The Fourier method in problems of the mechanics of layered media with nontraditional contact conditions 24 p3593 A83-49040

Global transverse shear in laminated composite plates [ONERA, TP NO. 1983-110] 24 p3593 A83-49421

A three-dimensional nonlinear analysis of cross-ply rectangular composite plates 24 p3593 A83-49439

An analysis of nonstationary processes resulting from the nonaxisymmetric loading of multiple-layer finite cylinders 24 p3595 A83-49901

Statistical analysis of multiple fracture in 0 deg/90 deg/0 deg glass fibre/epoxy resin laminates 24 p3554 A83-50064

Wrinkling phenomenon in structures. I - Model formulations 24 p3596 A83-50123

LAMINATIONS

U LAMINATES

LAMPS

U LUMINAIRES

LAMPS PROGRAM

U LIGHT AIRBORNE MULTIPURPOSE SYSTEM

LAND

NT ARID LANDS

NT CASCADE RANGE (CA-OR-WA)

NT COASTAL PLAINS

NT DESERTS

NT FARMLANDS

NT FLOOD PLAINS

NT GOBI DESERT

NT GRASSLANDS

NT ISTHMUSES

NT LIBYAN DESERT

NT MARSHLANDS

NT NATIONAL PARKS

NT PARKS

NT PLAINS

NT RANGELANDS

NT SAHARA DESERT (AFRICA)

NT WETLANDS

LAND ICE

Methane - The record in polar ice cores 03 p0357 A83-13539

Predicting permafrost conditions with infrared sensing techniques 03 p0348 A83-14264

A time-dependent ice sheet model - Preliminary results 03 p0359 A83-14505

A one-dimensional model of the atmosphere considered as a climatic system block comprising the ocean, the atmosphere, and the ice cover 03 p0371 A83-14826

Electrical properties of frozen ground at VHF near Point Barrow, Alaska 03 p0352 A83-14858

The thermal physics of glaciers --- Russian book 05 p0657 A83-17132

Surface elevation contours of Greenland and Antarctic ice sheets 09 p1305 A83-24286

Slope-induced errors in radar altimetry over continental ice sheets 09 p1305 A83-24289

A comparison between the calculated and measured characteristics of an advection fog and a stratus over ice 09 p1316 A83-25229

The application of aerial techniques in geocryological explorations --- Russian book 16 p2370 A83-36446

ERS-1 - An ice and ocean monitoring mission 20 p2938 A83-42826

Simple energy balance model resolving the seasons and the continents - Application to the astronomical theory of the ice ages 20 p3021 A83-42841

The scattering of radio waves by ice covers 20 p3010 A83-42872

Mathematical model of the glaciers-ocean-atmosphere system 24 p3610 A83-49556

LAND MANAGEMENT

Application of Landsat imagery to flood control and management of agricultural land - A case study of northern India 03 p0345 A83-14233

The possibilities of using aerospace remote sensing techniques in the North Sahelian regions of Africa 08 p1128 A83-21963

Photointerpretation for land use planning --- using digital terrain models 08 p1129 A83-21966

Joint U.S.-Mexican activities in arid land management and desertification control 09 p1284 A83-24531

Urban encroachment on agricultural land 09 p1285 A83-24544

Remote sensing in range management - An approach for practical application in development 09 p1285 A83-24545

Applying Landsat and ancillary data to arid land inventories - A case study 09 p1285 A83-24546

The development of a land image-based resource information system /LIBRIS/ and its application to the assessment and monitoring of Australian arid rangelands 09 p1286 A83-24547

Assessment and management of land and water resources in drought prone areas from satellite derived data - An Indian example 09 p1290 A83-24611

The utility of Landsat for monitoring the ephemeral water and herbage resources of arid lands - An example of rangeland management in the Channel Country of Australia 09 p1290 A83-24614

Causes and effects of increasing aridity in Northwest Bangladesh 09 p1291 A83-24628

Remote sensing and regional land management; Conference, Universite de Picardie, Amiens, France, October 26, 27, 1981, Reports 11 p1600 A83-28144

Remote sensing techniques for monitoring and managing irrigated lands 15 p2181 A83-33564

A holistic approach to the monitoring of land cover changes in Sri Lanka using intermediate remote sensing techniques 15 p2181 A83-33565

A review of current Australian work on the application of Landsat to land transformation processes 15 p2182 A83-33569

Some aspects of large-scale land transformation due to urbanization and agricultural development in recent Japan 15 p2182 A83-33570

Land use systems and their impact on environment - An attempt at a classification 15 p2182 A83-33576

Utilization of remote sensing in wetland management 15 p2184 A83-34814

A framework for analysis of temporal and spatial patterns of land use changes in Michigan's coastal zone 15 p2186 A83-34835

Matching remote sensing technology to operational requirements for land resource management in Canada 15 p2187 A83-35278

Comparing digital data processing techniques for surface mine and reclamation monitoring 17 p2530 A83-38337

Investigation of signs of erosion of agricultural lands on the basis of aerial and space remote sensing data (using the southwestern spurs of the Gissar ridge as an example) 24 p3598 A83-48935

LAND MOBILE SATELLITE SERVICE

Elimination of false-locking in long loop phase-locked receivers 03 p0312 A83-13868

Interactive systems analysis of four structural concepts for a Land Mobile Satellite System [AIAA PAPER 83-0219] 05 p0606 A83-16590

Comparative analysis of large antenna spacecraft using the ideas system [AIAA 83-0798] 12 p1707 A83-29731

Uplink coarse acquisition for a mobile user satellite system 19 p2833 A83-41404

Need for, and financial feasibility of, satellite-aided land mobile communications 19 p2834 A83-41415

Technical feasibility of satellite-aided land mobile radio 19 p2834 A83-41416

Satellite-aided land mobile communications system implementation considerations 19 p2834 A83-41417

Feasibility of international transport communications system 19 p2834 A83-41418

Concepts of 2.6/2.5 GHz mobile satellite communication system 19 p2834 A83-41419

Weight and structural analysis of four structural concepts for a land mobile satellite system [SAWE PAPER 1456] 20 p2945 A83-43737

A transportable satellite earth station for television outside broadcast contributions 23 p3442 A83-47652

LAND USE**NT RURAL LAND USE**

Ongoing microwave remote sensing-activities for land applications in Germany 01 p0020 A83-10083

Analyzing and mapping regional land use trends by combining Landsat and topographic data 01 p0066 A83-10119

Future land remote sensing data and services - A commercial perspective 02 p0244 A83-11933

Operational land cover type mapping in Ontario by Landsat based digital analysis and map production 03 p0345 A83-14230

A procedure to overlay thematic map and dominion land survey system data to geometrically-corrected Landsat images and its application to agricultural land use studies in western Canada 03 p0345 A83-14231

Land use/land cover mapping from enhanced Landsat imagery of the eastern provinces of the People's Republic of China 03 p0346 A83-14241

Vegetation and human impact mapping for the management of the sunshine area, Canadian Rocky Mountains 03 p0346 A83-14242

Bank erosion and flood plain studies of the Annapolis River - An application of remote sensing data 03 p0348 A83-14262

Office automation in resource-management - The future is now --- agricultural land use map dissemination 03 p0348 A83-14269

Investigating the possibility of producing a land-use map for Cuba on the basis of space imagery 03 p0350 A83-14305

Monitoring recent changes in extent of natural forests in Kenya using remote sensing techniques 08 p1127 A83-21940

Renewal of land use data base with the aid of remote sensing 08 p1128 A83-21952

The development of a sampling procedure for urban land use mapping from aerial photographs - A study in Calabar, Nigeria 08 p1172 A83-21960

Multitemporal remote sensing of land use in the Sahelian region of Africa by Meteosat 1 08 p1128 A83-21961

Study of the biophysical land cover of the French national parks 08 p1128 A83-21962

Some problems of computer-assisted mapping of land use from Landsat data - The Hong Kong case 08 p1128 A83-21965

Photointerpretation for land use planning --- using digital terrain models 08 p1129 A83-21966

Low cost monitoring of land use and soil erosion in the humid tropics - An application of aerial photography 08 p1129 A83-21967

Monitoring of seasonal and yearly land-use changes on aerial photography and Landsat imagery - A case study in the Yemen Arab Republic 09 p1285 A83-24538

Reclamation of salt-affected soils in California 09 p1285 A83-24539

Urban expansion in the Nile River Valley and Delta 09 p1351 A83-24575

Use of remote sensing techniques to study geothermal resources in arid and semi-arid zones in Chile 09 p1288 A83-24577

Application of multispectral aerial photography in land use and land cover mapping of a part of El Fayoum depression northwestern Egypt 09 p1289 A83-24593

Monitoring land use and land use appropriateness in the central Sudan - A combination of Landsat data and statistical analysis of climatic data 09 p1290 A83-24608

A land use survey of Northwest Somalia as interpreted from Landsat imagery 09 p1290 A83-24619

Land use mapping from Landsat imagery applied to central Tunisia 09 p1291 A83-24620

A noninteractive procedure for land-use determination 10 p1443 A83-25642

Remote sensing and regional land management; Conference, Universite de Picardie, Amiens, France, October 26, 27, 1981, Reports 11 p1600 A83-28144

Remote sensing and cartography for soil use in Algeria: Comparative study of the interpretation of analog imagery /aerial photographs/ and of data treatment of digitized versions of the same images and spacial imagery - Application to the mouth of the Isser wadi /coastal Kabylie/ - Algeria 11 p1600 A83-28146

Land use mapping in lower Chaozia 11 p1601 A83-28147

Regional land use research with multitemporal classification - On an image of Thailand 11 p1601 A83-28149

Issues surrounding the commercialization of civil land remote sensing from space 12 p1783 A83-22915

Remote sensing as a means for units of landscape in forest regions - Applications to the Ambazac Mountains (Limousin, France) 14 p2034 A83-32170

Remote sensing in Picardie: The arrangement of structures The use of Landsat satellite data 14 p2034 A83-32171

Remote sensing and regional arrangement in the Nord-Pas de Calais region 14 p2034 A83-32172

Spectral signatures obtained from Landsat digital data for forest vegetation and land-use mapping in India

14 p2036 A83-33350

Land development, tall buildings and airport operations

[AIAA PAPER 83-1581] 14 p1978 A83-33353

Study of land transformation processes from space and ground observations; Proceedings of the Symposium, Ottawa, Canada, May 16-June 2, 1982

15 p2181 A83-33551

The first decade of regular observation of land transformation from space

15 p2181 A83-33552

Some aspects of land transformation in the western Mediterranean desert of Egypt

15 p2181 A83-33553

Mapping recent agricultural developments in China from satellite data

15 p2181 A83-33562

Canadian Landsat studies for monitoring agricultural intensification and urbanization - A summary

15 p2182 A83-33566

The evolution of land use over a 10 year period in France Results and methodology

15 p2182 A83-33568

Some aspects of large-scale land transformation due to urbanization and agricultural development in recent Japan

15 p2182 A83-33570

A study of land transformation processes after the atomic bombing damage in Hiroshima

15 p2182 A83-33572

Land use - A study of the Regional Center for Remote Sensing at Quagadougou --- Upper Volta

15 p2182 A83-33574

Land use systems and their impact on environment - An attempt at a classification

15 p2182 A83-33576

Land remote sensing in the 1980's

15 p2241 A83-34802

Employing Landsat MSS data in land use mapping - Observations and considerations

15 p2184 A83-34804

Integration of Landsat RBV and MSS imagery to produce land use maps of Soviet cities --- Return Beam Vidicon

15 p2241 A83-34805

Urban land use classification using synthetic aperture radar

15 p2184 A83-34808

The role of change data in a land use and land cover map updating program

15 p2184 A83-34811

Urban change detection procedures using Landsat digital data

15 p2241 A83-34815

Evaluation of land cover change detection techniques using Landsat MSS data

15 p2184 A83-34816

Hierarchical modeling for image classification

15 p2185 A83-34820

Forest management applications of Landsat data in a geographic information system

15 p2185 A83-34823

The development and application of a county-level geographic data base

15 p2186 A83-34828

Combining land use data acquired from Landsat with soil map data using an information system

15 p2186 A83-34833

A framework for analysis of temporal and spatial patterns of land use changes in Michigan's coastal zone

15 p2186 A83-34835

Oregon's Statewide Landuse Inventory - Remote sensing input to geographic information systems

15 p2187 A83-34844

Urban land use classification using synthetic aperture radar

15 p2187 A83-35279

Geological exploration and landuse using Landsat data, Sierra Leone, West Africa

17 p2527 A83-38137

Mapping snow and ice and other land cover categories in south-central Alaska

17 p2532 A83-38355

Delineation of selected urban features utilizing single date and multitemporal Landsat data - A comparative analysis

17 p2586 A83-38356

Survey and analysis of present or potential environmental impact sites in Woburn, Massachusetts

17 p2536 A83-38359

Utilization of Landsat data to monitor deforestation of Kenya's Mau Forest

17 p2534 A83-38461

Global vegetation and land use - New high-resolution data bases for climate studies

18 p2706 A83-39141

Classification of present-day landscapes on the basis of space imagery

18 p2706 A83-40586

Comparison of land use structures from multitemporal remote sensing satellite data

20 p3011 A83-43138

Effect of differences in categories dispersion patterns on digital image classification results

22 p3308 A83-46118

Improved landuse classification through principal component analysis based on category statistics and synthetic variables

22 p3308 A83-46119

The use of the Space Shuttle for land remote sensing

22 p3259 A83-46146

Multispectral observations of agricultural fields in the Kiskoore test-area

22 p3310 A83-46161

Application of remotely sensed data for the assessment of landscape ecology

22 p3311 A83-46164

Satellite image processing for a small country - The

Hungarian case

[IAF PAPER 83-123] 23 p3475 A83-47280

LANDAU DAMPING

Observation of guided ULF-waves correlated with auroral particle precipitation theoretically explained by negative Landau damping

03 p0357 A83-13298

On uniform limits in the propagation of electromagnetic waves in a hot plasma

06 p0812 A83-18820

Influence of gyroradius and dissipation on the Alfvén wave continuum

07 p0997 A83-20538

Nonlinear electron Landau damping of ion-acoustic solitons

13 p1923 A83-30115

Nonlinear Landau damping phenomenon in a strongly turbulent plasma

13 p1924 A83-30414

A kinetic model of the polar wind with a Landau collision integral

14 p2054 A83-33028

Cyclotron absorption of finite-amplitude waves

16 p2417 A83-36932

Nonlinear Landau damping of a whistler in a current-carrying plasma

17 p2583 A83-38209

The role of non-linear Landau damping in cosmic ray shock acceleration

17 p2609 A83-38421

Electron acceleration by Landau resonance with whistler mode wave packets

20 p3024 A83-43185

Effect of nonlinear Landau damping on long time behaviour of modulational instability of Langmuir wave

24 p3631 A83-48818

LANDAU FACTOR

Cyclotron emission in strongly magnetized plasmas

03 p0429 A83-14795

Electrostatic bursts generated by electrons in Landau resonance with whistler mode chorus

11 p1617 A83-28311

Inversion of hot carriers in Landau levels

20 p3051 A83-42279

Study of the autoionising states of the hydrogen atom in intense magnetic fields by the complex coordinate coupled-channel formalism

23 p3506 A83-48576

Radiative and thermal widths of Landau-excited hydrogen atoms in very strong magnetic fields

23 p3527 A83-48578

LANDAU-GINZBURG EQUATIONS

The thermoelectric effect in superconductors

01 p0109 A83-10820

LANDFORMS

NT ALPS MOUNTAINS (EUROPE)

NT ANDES MOUNTAINS (SOUTH AMERICA)

NT BERMUDA

NT CALDERAS

NT CAPES (LANDFORMS)

NT CASCADE RANGE (CA-OR-WA)

NT COLUMBIA RIVER BASIN (ID-OR-WA)

NT CONES (VOLCANOES)

NT CUBA

NT DELTAS

NT DUNES

NT ESCARPMENTS

NT GREENLAND

NT HIMALAYAS

NT INDONESIA

NT ISLANDS

NT ISTHMUSES

NT JAMAICA

NT JAPAN

NT MALAGASY REPUBLIC

NT MARS VOLCANOES

NT MISSISSIPPI DELTA (LA)

NT MOUNTAINS

NT PACIFIC ISLANDS

NT PLATEAUS

NT PYRENEES MOUNTAINS (EUROPE)

NT RIVER BASINS

NT SALT BEDS

NT STRUCTURAL BASINS

NT TIDAL FLATS

NT VOLCANOES

NT WADIS

NT WATERSHEDS

Morphometric consistency with the

Hausdorff-Besicovich dimension

02 p0203 A83-11844

Predicting forest land attributes from aerial photo interpretation variables

03 p0347 A83-14259

Relict drainages, conical hills, and the eolian veneer in southwest Egypt - Applications to Mars

04 p0566 A83-15567

Ice sculpture in the Martian outflow channels

04 p0566 A83-15568

Numerical modeling of diurnal convergence oscillations above sloping terrain

10 p1450 A83-25385

3D statistics of landforms from single air-photos - A hypothesis

11 p1601 A83-28172

How continents break up

16 p2377 A83-36020

LANDING

NT AIRCRAFT LANDING

NT CRASH LANDING

NT LUNAR LANDING

NT PLANETARY LANDING

NT SKID LANDINGS

NT SOFT LANDING

NT SPACECRAFT LANDING

NT VERTICAL LANDING

NT WATER LANDING

Handling qualities criteria for STOL flight path control for approach and landing

[AIAA PAPER 83-2106] 19 p2806 A83-41935

LANDING AIDS

NT AIRPORT LIGHTS

NT ALL-WEATHER LANDING SYSTEMS

NT APPROACH INDICATORS

NT ARRESTING GEAR

NT AUTOMATIC LANDING CONTROL

NT DISCRETE ADDRESS BEACON SYSTEM

NT INSTRUMENT LANDING SYSTEMS

NT LANDING INSTRUMENTS

NT MICROWAVE LANDING SYSTEMS

Helmet mounted display symbology for helicopter landing on small ships

04 p0448 A83-16134

Lidar system for visibility monitoring

14 p2019 A83-32449

Simulated fan-beam radar imagery --- use in assessing aircraft approach-to-landing paths

18 p2675 A83-40302

A new generation of navigation and landing aids for aviation

23 p3401 A83-47188

LANDING GEAR

Hydromechanical dynamics of aircraft landing gear

06 p0717 A83-18925

Serviceability evaluation of advanced composite F-14A main-landing-gear-strut doors and overwing fairings

07 p0861 A83-20480

Investigation of landing gear alternatives for high performance aircraft

09 p1202 A83-24030

Aircraft vehicle equipment improvements via microprocessors

[SAE PAPER 820868] 10 p1375 A83-25767

Motion of the ski runners of an aircraft on soil. I

12 p1701 A83-29281

Landing gear design handbook

13 p1805 A83-30143

Measuring and processing of undercarriage loading spectra of the L-39 aircraft

13 p1805 A83-30513

The response of aircraft to pulse excitation

15 p2122 A83-34312

From new technology development to operational usefulness B-36, B-58, F-111/FB-111

[AIAA PAPER 83-1046] 16 p2287 A83-36459

A crack growth fatigue life under spectrum loading

20 p3009 A83-43692

Safe structures for future aircraft

22 p3254 A83-46350

LANDING INSTRUMENTS

NT APPROACH INDICATORS

Improvement of the measurement system for the survey of class-II ILS installations

21 p3090 A83-45401

LANDING LOADS

Measuring and processing of undercarriage loading spectra of the L-39 aircraft

13 p1805 A83-30513

LANDING MODULES

Method of the complex postflight ballistic analysis of the descent trajectories of Venera-type descent modules

09 p1212 A83-25032

The automatic interplanetary probes Venera-13 and Venera-14

14 p1979 A83-31951

Analysis of the descent trajectories of the Venera-13 and Venera-14 descent modules in the atmosphere of the planet

14 p1979 A83-31953

Continuation of the TV study of the Venus surface from descent modules

14 p1983 A83-31955

The first color panoramic pictures of the Venus surface transmitted by the Venera 13, 14 probes

14 p2014 A83-31956

Investigation of the characteristics of the Venus stratosphere from acceleration measurements during the braking of the Venera-13 and Venera-14 probes

14 p2110 A83-31959

LANDING SIMULATION

Optical information for descent in flight simulation

01 p0085 A83-11137

Perception of position by the pilot in the case of computer-generated external visual scene displays for a landing approach --- German book

03 p0383 A83-14111

Pilot judgements of distance, height and glide slope angle from computer generated landing scenes

04 p0524 A83-16327

Assessment of

The learning behaviour of trainee pilots during aircraft-landing - A simulator study 07 p0981 A83-19662

Realistic 'feel' in flight simulators is based on precise control loading 08 p1048 A83-23240

Simulation evaluation of flight controls and display concepts for VTOL shipboard operations [AIAA PAPER 83-2173] 19 p2789 A83-41668

Application of Monte-Carlo techniques to the 757/767 autoland dispersion analysis by simulation [AIAA PAPER 83-2193] 19 p2802 A83-41678

Carrier landing simulation results of precision flight path controllers in manual and automatic approach [AIAA PAPER 83-2072] 19 p2796 A83-41909

Features of the physical simulation of the landing of the Venera-9 - Venera-14 descent modules 21 p3103 A83-45279

Mathematical modeling and experimental study of the landing of the Venera 9-14 probes on deformable soils 21 p3095 A83-45280

Evaluation of control and display configurations for helicopter shipboard operations [AIAA PAPER 83-2486] 23 p3405 A83-48346

LANDING SITES

NT LUNAR LANDING SITES

Panoramas of the Venera-13 and Venera-14 landing sites /A preliminary analysis/ 09 p1367 A83-25276

Analysis of the panoramas of the Venera 13 and Venera 14 landing sites 12 p1798 A83-29484

Microseisms at the Venera 13 and Venera 14 landing sites 12 p1799 A83-29487

Summary of preliminary results of the Venera 13 and Venera 14 missions 17 p2616 A83-37406

Panorama of Venera 9 and 10 landing sites 17 p2616 A83-37409

LANDING SPEED

Instantaneous, predictable balloon system descent from high altitude 18 p2640 A83-39808

LANDING SYSTEMS

U LANDING AIDS

LANDMARKS

Intelligent control of tactical target cueing --- by subsonic flight vehicles 02 p0133 A83-12879

Geopositioning accuracy of an autonomous navigation system using landmarks 17 p2474 A83-37107

LANDSAT C

U LANDSAT 3

LANDSAT D PRIME

LandSAT-D - An end-to-end data system 19 p2813 A83-41339

LANDSAT SATELLITES

NT LANDSAT D PRIME

NT LANDSAT 2

NT LANDSAT 3

NT LANDSAT 4

Exploration for fractured petroleum reservoirs using radar/Landsat merge combinations 01 p0062 A83-10031

Rock type discrimination techniques using Landsat and Seasat image data 01 p0063 A83-10057

Wetland mapping with imaging radar 01 p0063 A83-10072

LandSAT monitoring of Desert Locust breeding grounds in Africa, the Near East and Southwest Asia 01 p0065 A83-10097

A comparison of unsupervised classification procedures on Landsat MSS data for an area of complex surface conditions in Basilicata, Southern Italy 02 p0198 A83-12037

Atmospheric effects on radiation reflected from soil and vegetation as measured by orbital sensors using various scanning directions 02 p0198 A83-12315

Background reflectance effects in Landsat data 02 p0199 A83-12602

Contribution of Landsat imagery to the study of volcanic structures 02 p0211 A83-12641

Landsat observations of Mount St. Helens 02 p0199 A83-12671

Operational land cover type mapping in Ontario by Landsat based digital analysis and map production 03 p0345 A83-14230

A procedure to overlay thematic map and dominion land survey system data to geometrically-corrected Landsat images and its application to agricultural land use studies in western Canada 03 p0345 A83-14231

Toward an operational, satellite-based, wetland monitoring program for the Fraser River Estuary, British Columbia 03 p0345 A83-14234

Monitoring revision requirements for Canadian maps 03 p0346 A83-14237

Land use/land cover mapping from enhanced Landsat imagery of the eastern provinces of the People's Republic of China 03 p0346 A83-14241

Application of Landsat imagery to natural resources management in Sierra Leone, West Africa 03 p0347 A83-14247

Digital colour enhancement of Landsat data for mapping vegetation of barrenground caribou winter range in northern Manitoba 03 p0347 A83-14249

Integration of Landsat imagery into a program for aerial surveying of deer populations in Alberta 03 p0347 A83-14252

Landsat-based forest mapping in Ontario north of latitude 52 deg north 03 p0347 A83-14253

Multitemporal analysis of Landsat data for forest cutover mapping - A trial of two procedures 03 p0347 A83-14254

Landsat for resource evaluation and management in the Alberta foothills 03 p0347 A83-14256

Landsat for delineation and mapping of saline soils in dryland areas in southern Alberta 03 p0348 A83-14261

Colour Landsat images and mosaics - Basic tools in areal and ecological differentiation in Canada 03 p0348 A83-14265

A national Landsat collection and a proposal for a library of Landsat images 03 p0348 A83-14270

An experimental Landsat Quicklook System for Alaska 03 p0348 A83-14271

Definition and potential of geocoded satellite imagery products 03 p0349 A83-14272

A refined destripping procedure for Landsat MSS data products 03 p0349 A83-14281

Investigation of altitude determination program for Landsat image processing 03 p0289 A83-14282

Reference quicklook images for monitor of Landsat image data acquisition 03 p0349 A83-14286

A study of atmospheric diffusion from the Landsat imagery 03 p0350 A83-14504

Evaluating the effectiveness of Landsat data as a tool for locating buried pre-glacial valleys in eastern South Dakota 03 p0351 A83-14667

Preparation of a sediment map of the North Frisian shoal areas on the basis of Landsat imagery 03 p0352 A83-14945

The use of large-area spectral data in wheat yield estimation 05 p0657 A83-16910

Geomorphological mapping using Landsat imagery - A case study in Argentina 05 p0657 A83-17841

American photoreconnaissance satellites 06 p0722 A83-19413

The application of forest classification from Landsat data as a basis for natural hydrocarbon emission estimation and photochemical oxidant model simulations in southeastern Virginia 07 p0957 A83-19848

Use of Landsat data to predict the trophic state of Minnesota lakes 07 p0952 A83-21432

Landsat multitemporal color composites 07 p0952 A83-21433

Landsat-derived land-cover classifications for locating potential Kestrel nesting habitat 07 p0952 A83-21435

Creation of new channels by photographic methods 08 p1125 A83-21913

Multidensity and its application to Landsat imagery 08 p1125 A83-21915

The utilization of SLAR and the Landsat satellites in geomorpho-pedological surveys performed in the Venezuelan Amazon - Methodology and initial results 08 p1126 A83-21924

A Spot-Landsat comparison simulation in a forested region - Ermenonville 1980 08 p1126 A83-21929

Research advances in satellite-aided crop forecasting 08 p1126 A83-21930

A Canadian approach to large region crop area estimation with Landsat 08 p1126 A83-21932

Landsat-data for distributed hydrological models 08 p1127 A83-21934

The visual interpretation of Landsat imagery - The possibilities of the utilization of Landsat imagery improved for forestry studies in tropical regions 08 p1127 A83-21935

Monitoring ecology in inaccessible areas of tropical zones by interpretation of machine processed Landsat-scenes 08 p1127 A83-21937

Satellite remote sensing over Quebec for inventory of the vegetal canopy 08 p1127 A83-21938

Prospects for multitemporal studies focusing on a forested region - Proof of clear-cutting 08 p1127 A83-21939

Tectonic elements registered on the Landsat imagery in area of Yugoslavia and their practical meaning 08 p1127 A83-21945

Overcoming urban monitoring problems with the new generation satellite sensors 08 p1172 A83-21964

Automatic mapping of lakes for small-scale maps using digital Landsat imagery 08 p1129 A83-21969

Characteristics of the detectors of multi spectral scanner /MSS/ of Landsat in space environment 09 p1219 A83-23895

Use of Seasat synthetic aperture radar and Landsat multispectral scanner subsystem data for Alaskan glaciology studies 09 p1305 A83-24287

Remote sensing of arid and semi-arid lands; Proceedings of the International Symposium on Remote Sensing of Environment, Cairo, Egypt, January 19-25, 1982. Volumes 1 & 2 09 p1284 A83-24526

Potential application of remote sensing to the study of arid and semi-arid lands in Argentina 09 p1284 A83-24529

Eolian sand bodies of the world --- classification techniques for Landsat imagery applications 09 p1284 A83-24533

Resource inventories of arid and semi-arid lands using Landsat 09 p1284 A83-24534

Landsat data in the Sahel - Their use and accuracy for small-scale soil surveys and their time and cost efficiency 09 p1285 A83-24535

Dynamic modeling of vegetation change in arid lands 09 p1285 A83-24537

Soil classification and potentials in Sinai peninsula from Landsat images 09 p1285 A83-24540

Analysis of man-induced and natural resources of an arid region in California 09 p1285 A83-24543

Applying Landsat and ancillary data to arid land inventories - A case study 09 p1285 A83-24546

Discrimination of phosphate, gypsum, limestone, halide and quartz-sand deposits in south-central Tunisia by cluster analysis of Landsat multispectral data 09 p1286 A83-24552

Monitoring of water quality and environmental changes in the Aswan High Dam reservoir from Landsat imagery 09 p1286 A83-24555

Remote sensing of coastal processes with emphasis on the Nile Delta 09 p1286 A83-24556

Approaches to desertification monitoring in the Sudan using Landsat data: A test of a geographical data base approach - Preliminary results 09 p1286 A83-24558

Landsat data for monitoring rural settlement and population A test in the Umm Ruwaba region, the Sudan 09 p1286 A83-24559

Landsat and the southward drift of Madagascar 09 p1287 A83-24562

On attaining semi-aridity of North-Bengal in Bangladesh as viewed through the Landsat imageries 09 p1287 A83-24565

Application of remote sensing data to hydrogeological purposes in the Fezzan Region-Lybia 09 p1287 A83-24566

A Landsat-based inventory procedure for the estimation of irrigated land in arid areas 09 p1287 A83-24567

Satellite monitoring of recent desertification in the Yulin region The People's Republic of China 09 p1287 A83-24569

Mapping oases and soil types from Landsat digital multispectral scanner data - Kharga Depression, Western Desert, Egypt 09 p1287 A83-24572

The imperial college multi-channel electronic image classifier and its applications to the classification of surface types by multi-spectral analysis 09 p1288 A83-24580

Sand distribution in the Kharga depression of Egypt - Observations from Landsat images 09 p1289 A83-24590

Use of Landsat multispectral scanner data in geologic mapping of the Meatiq Dome, central Eastern Desert, Egypt 09 p1289 A83-24591

Landsat as an aid in consulting projects in the Middle East and Africa some examples of applications on VBB/SWECO projects 09 p1289 A83-24592

An example of the application of a procedure for determining the extent of erosional and depositional features and rock and soil units in the Kharga Oasis Region, Egypt, using remote sensing 09 p1290 A83-24603

Land use mapping from Landsat imagery applied to central Tunisia 09 p1291 A83-24620

Estimation of the forage production of semi-and rangelands with variable tree and shrub cover using land resource satellites 09 p1291 A83-24625

Mapping built up areas using Landsat MSS digital imagery 09 p1291 A83-24629

Environmental change detection in the Nile using multitemporal Landsat imagery 09 p1291 A83-24630

The Earthnet LEDA-2 image catalogue system 11 p1666 A83-27375

Classification of Landsat data for hydrologic application, Everglades National Park 12 p1748 A83-29916

An integrated study of reservoir-induced seismicity and Landsat imagery at Lake Kariba, Africa 12 p1748 A83-29917

Remote sensing in Picardie: The arrangement of structures The use of Landsat satellite data 14 p2034 A83-32171

Remote sensing and regional arrangement in the Nord-Pas de Calais region 14 p2034 A83-32172

Landsat digital enhancements for change detection in urban environments 14 p2035 A83-32614
 Giant volcanic calderas 14 p2054 A83-33099
 The effects of additive radiance terms on ratios of Landsat data --- for mineral exploration 14 p2036 A83-33348
 The first decade of regular observation of land transformation from space 15 p2181 A83-33552
 Space platform albedo measurements as indicators of change in arid lands 15 p2181 A83-33554
 Landsat monitoring of desert vegetation growth, 1972-1979 using a plant-shadowing model 15 p2181 A83-33556
 Use of Landsat satellite data for multitemporal analysis of Landes forest lumbering. (Nezer forest test site) 15 p2181 A83-33559
 Satellite data as a basis for planning studies of infrastructure and related rural development in Atacora Province, Benin, West Africa 15 p2181 A83-33560
 A technique for mapping environmental change using digital Landsat data 15 p2181 A83-33561
 Mapping recent agricultural developments in China from satellite data 15 p2181 A83-33562
 Canadian Landsat studies for monitoring agricultural intensification and urbanization - A summary 15 p2182 A83-33566
 Canadian Landsat studies for monitoring resource development A summary 15 p2182 A83-33567
 A review of current Australian work on the application of Landsat to land transformation processes 15 p2182 A83-33569
 The evolution of the southern coastline of the Vendee (France) according to data from Landsat 1, 2, 3 and Seasat 15 p2182 A83-33578
 Causes of flood streamlines observed on Landsat images and their use as indicators of floodways 15 p2183 A83-34151
 Preparation of a 1:25000 Landsat map for assessment of burnt area on Etajima Island 15 p2183 A83-34152
 Interpretation of structural characteristics of the Taupo volcanic zone, New Zealand, from Landsat imagery 15 p2183 A83-34158
 Urban change detection procedures using Landsat digital data 15 p2241 A83-34815
 GIS information layers derived from Landsat classification --- Geographic Information Systems 15 p2185 A83-34826
 Glacial geologic interpretation of southeastern Wisconsin through diazo enhancement of Landsat multispectral imagery 15 p2186 A83-34839
 A comparative study of linear and nonlinear edge finding techniques for Landsat multispectral data 15 p2187 A83-34840
 Use of Landsat data to develop a fuels database for a wildland fire simulation model 15 p2187 A83-34847
 Using Landsat imagery interpretation for underground water prospectation around Qena Province, Egypt 15 p2187 A83-35276
 Assessing the user environment for Landsat in developing countries 15 p2187 A83-35277
 Evaluation of MSS Landsat imagery over Central Spain 17 p2527 A83-38131
 Visual thematic mapping from Landsat and collateral data in support of mineral development 17 p2527 A83-38134
 Geological exploration and landuse using Landsat data, Sierra Leone, West Africa 17 p2527 A83-38137
 The role of image processing in mineral exploration - Why stop at Landsat? 17 p2528 A83-38148
 Enhanced Landsat and HCMM imagery for mineral exploration in contrasting areas of subtropical humid and semi-arid terrain 17 p2528 A83-38150
 Remote-sensing technology applied to forest assessment in California 17 p2528 A83-38152
 Sensor data for forest policy information 17 p2530 A83-38166
 Soil vegetation inventories in Arizona 17 p2531 A83-38339
 Petroleum exploration in the western United States using Landsat imagery 17 p2531 A83-38344
 A streamflow model based on Landsat imagery for the Wasatch Mountains 17 p2531 A83-38348
 Enhanced thermal mapping with Landsat and HCMM digital data 17 p2531 A83-38351
 Multidate Landsat water quality models 17 p2531 A83-38352
 Land resources inventory assessment by Landsat image processing case study - Kano State, Nigeria (Africa) 17 p2532 A83-38354
 Delineation of selected urban features utilizing single date and multitemporal Landsat data - A comparative analysis 17 p2586 A83-38356
 Landsat image enhancement in support of seismotectonic studies in Utah 17 p2532 A83-38360

Global satellite remote sensing for energy, minerals and other resources 17 p2534 A83-38450
 Analysis of effects after typhoon 8115 in coastal area and fields in Hokkaido, Northern Japan, using Landsat MSS data 17 p2534 A83-38453
 Monitoring of water characteristic using the synchronous observation data of Landsat and NOAA 17 p2554 A83-38455
 A composite Landsat image of the United Kingdom 20 p3010 A83-42958
 Comparative experimental study on the use of original and compressed multispectral Landsat data for applied research 20 p3011 A83-42963
 The significance of a strong value-added industry to the successful commercialization of Landsat [AAS PAPER 83-185] 20 p3011 A83-43769
 Space technology - Remote sensing: The best view in town 21 p3166 A83-45604
 The application of processed Landsat imagery in photo-interpretation 22 p3308 A83-46121
 Interpretation of Landsat imagery - A case study of lineations in a part of north-western Himalaya, India 22 p3309 A83-46134
 Remote sensing of arid and semiarid rangeland 22 p3310 A83-46163
 Landsat standard family of CCT formats Europe specific problems --- Computer Compatible Tapes 22 p3311 A83-46172
 Augmenting Landsat MSS data with topographic information for enhanced registration and classification 22 p3314 A83-46229
 The thematic mapper - An overview --- Landsat-borne earth resources sensor performance 22 p3261 A83-46230
 Technology for large digital mosaics of Landsat data 22 p3318 A83-46766
 Large-area relation of Landsat MSS and NOAA-6 AVHRR spectral data to wheat yields 23 p3474 A83-47218
 Change detection using Landsat photographic imagery 23 p3474 A83-47219
 Modeling inland water quality using Landsat data 23 p3475 A83-47223
 Satellite image processing for a small country - The Hungarian case [IAF PAPER 83-123] 23 p3475 A83-47280
 Experiments on digital image data comparison --- for Landsat satellite photos 24 p3598 A83-48990

LANDSAT 2

Analysis of multitemporal Landsat 2 imagery of the Annaba zone of Algeria - April 28, 1977 and February 28, 1978 / Earthnet 20 834/ 11 p1600 A83-28145

LANDSAT 3

Spatial and radiometric resolution of the Landsat-3 RBV system --- Return Beam Vidicon 15 p2188 A83-35293

LANDSAT 4

Multispectral scanner, thematic mapper, and beyond 01 p0019 A83-10002
 The early 1981 view of Landsat-D progress 02 p0199 A83-12673
 Potentials of Landsat-D and SPOT-1 for crop identification in the maritimes 03 p0346 A83-14240
 Comparison study of future SPOT and Landsat-D satellite products from a simulation flight --- for determining spatial and spectral resolution 03 p0346 A83-14243
 Earthnet prepares for Landsat-D 05 p0603 A83-17426
 Spectral characterization of the Landsat-4 MSS sensors 16 p2370 A83-36575
 Comparison of simulated data of SPOT and Landsat-D sensors Application to an agricultural region 17 p2529 A83-38162
 Landsat-D wideband unbalanced QPSK demodulator/bit synchronizer signal conditioner 19 p2813 A83-41359
 Autonomous failure detection and correction on Landsat-4 [AIAA PAPER 83-2265] 19 p2817 A83-41735
 Production and analysis of output data products for Landsat-4 in the engineering check-out phase [AAS PAPER 83-158] 20 p3011 A83-43762
 Landsat-4 Thematic Mapper calibration and atmospheric correction [AAS PAPER 83-162] 20 p2992 A83-43763
 Landsat-D TM application to porphyry copper exploration 22 p3309 A83-46132
 Landsat-D, about to be reality 22 p3258 A83-46147
 Landsat-D thematic mapper simulator 22 p3260 A83-46148
 Mapping of deciduous forest cover using simulated Landsat-D TM data- 22 p3311 A83-46166
 Experimental results of using the GPS for Landsat 4 onboard navigation 22 p3253 A83-46963

Information extraction from thematic mapper data [IAF PAPER 83-114] 23 p3475 A83-47275

LANDSCAPE

U TERRAIN
 U TOPOGRAPHY

LANDSLIDES

Acoustic fluidization --- of dry rock landslides 10 p1519 A83-25900

LANGEVIN FORMULA

Markov-chain simulation of particle dispersion in inhomogeneous flows - The mean drift velocity induced by a gradient in Eulerian velocity variance 03 p0363 A83-13269
 Termolecular ionic recombination at high ambient gas density 16 p2414 A83-35326

LANGMUIR PROBES

U ELECTROSTATIC PROBES

LANGUAGE PROGRAMMING

A general precompiler for algebraic manipulation 12 p1768 A83-29110
 Using English as a high-level robot command language 21 p3191 A83-44080
 An attribute grammar for the semantic analysis of Ada --- Book 21 p3191 A83-45140

LANGUAGES

NT ADA (PROGRAMMING LANGUAGE)
 NT ASSEMBLY LANGUAGE
 NT BASIC (PROGRAMMING LANGUAGE)
 NT ENGLISH LANGUAGE
 NT FORTRAN
 NT HIGH LEVEL LANGUAGES
 NT ORTHOGRAPHY
 NT PASCAL (PROGRAMMING LANGUAGE)
 NT PROGRAMMING LANGUAGES
 NT WORDS (LANGUAGE)

LANTHANIDE SERIES METALS

U RARE EARTH ELEMENTS

LANTHANUM

NT LANTHANUM ISOTOPES

LANTHANUM COMPOUNDS

Particle size distribution of Ni microprecipitates in LaNi₅ used for hydrogen storage 02 p0202 A83-12295
 Electro-optic shutter devices utilizing lead lanthanum zirconate titanate /PLZT/ ceramic wafers 08 p1098 A83-22565
 Progress in the development of ternary sulfides for use from 8 to 14 microns 09 p1345 A83-24955
 A study of the hydrating kinetics of Mg-(10-20 w/o) LaNi₅ 15 p2133 A83-34867
 On some transport properties of strontium-doped lanthanum chromite ceramics 18 p2671 A83-39057
 The maser effect in a paramagnetic crystal caused by the thermal action of the spin system aided by a pulsed magnetic field 19 p2853 A83-41500

LANTHANUM ISOTOPES

5s/2/5p/4/-5s5p/5/ transitions in Cs IV, Ba V, and La VI 09 p1342 A83-24095

LANTHANUM 140

U LANTHANUM ISOTOPES

LAP JOINTS

Water-displacing organic corrosion inhibitors - Their effect on the fatigue characteristics of aluminum alloy bolted joints 02 p0148 A83-12014
 The effect of moisture and temperature on the properties of an epoxide-polyamide adhesive in relation to its performance in single lap joints 04 p0463 A83-15872
 Effect of heating time at high temperatures on the structure and properties of brazed joints 05 p0652 A83-16884
 Development of a two-directional scan tracking system with laser sensor 07 p0940 A83-20524
 Characterization of room temperature curing adhesives 09 p1237 A83-23622
 An analysis of adhesive-bonded single-lap joints [ASME PAPER 83-APM-14] 10 p1441 A83-26436
 Optimization of bonded joints [AIAA 83-0906] 12 p1739 A83-29762
 Effect of stitching on the strength of bonded composite single lap joints [AIAA 83-0969] 12 p1739 A83-29779
 Comparison of properties of joints prepared by ultrasonic welding and other means 14 p2031 A83-32586
 On improving the fatigue performance of a double-shear lap joint 15 p2180 A83-34744
 Tubular lap joints in composite cylindrical shells under external bending and shear 18 p2703 A83-40154
 Stress analysis and strength of adhesive bonded joints under bending loads 18 p2703 A83-40156
 Stress analysis of stepped-lap joints with bondline flaws 23 p3471 A83-48214

LAPLACE EQUATION

A boundary value problem for the Laplace equation with nonclassical spectral asymptotics 01 p0103 A83-11317

Expansion of planetary gravitational potential in a system of fundamental solutions of the Laplace equation 04 p0514 A83-16383

Finite element iterative techniques for determining the interface boundary between Laplace and Poisson domains - Characteristic analysis of a field effect transistor 11 p1563 A83-28417

Assessing the quality of curvilinear coordinate meshes by decomposing the Jacobian matrix 17 p2574 A83-38811

Exact solutions of certain dual integral equations and their asymptotic properties 20 p3042 A83-43374

The variation with frequency of the long-period tides 22 p3344 A83-46911

LAPLACE OPERATORS

U LAPLACE TRANSFORMATION

LAPLACE TRANSFORMATION

Image data compression with the Laplacian pyramid 01 p0098 A83-11426

Application of finite-part integrals to the singular integral equations of crack problems in plane and three-dimensional elasticity 02 p0190 A83-12001

Simplified Laplace transform inversion for unsteady surface element method [AIAA PAPER 83-0527] 05 p0638 A83-16830

Quasi-static coupled problems of thermoelasticity for cylindrical regions 06 p0775 A83-18805

Numerical operational methods for time-dependent linear problems 07 p0948 A83-21437

Eigenvalue approach to thermoelasticity 12 p1747 A83-29923

Exact solutions to the nonlinear Boltzmann equation and its models 13 p1932 A83-30655

The Laplacian pyramid as a compact image code 14 p2075 A83-32868

Impact damping and airplane towing 15 p2120 A83-33625

A z-transform theory for distributed sensing and control 15 p2222 A83-35128

LARGE AREA CROP INVENTORY EXPERIMENT

A Canadian approach to large region crop area estimation with Landsat 08 p1126 A83-21932

LARGE SCALE INTEGRATION

Test generation using binary decision diagrams 01 p0038 A83-10774

VLSI system design --- Book 01 p0038 A83-10881

Influence of LSI and VLSI technology on the design of error-correction coding systems 02 p0163 A83-11552

The Waveform Relaxation method for time-domain analysis of large scale integrated circuits 02 p0167 A83-11797

Fast LSI based on current switches --- Russian book 02 p0168 A83-12374

Residue-based image processor for very large scale integration /VLSI/ implementation 02 p0182 A83-12900

Temperature effects on failure and annealing behavior in dynamic random access memories 05 p0626 A83-17506

Total dose response of STL and I2L logic devices --- Schottky Transistor Logic 05 p0627 A83-17517

Single event upset sensitivity of low power Schottky devices 05 p0629 A83-17542

GaAs LSI-directed MESFET's with self-aligned implantation for n/+/-layer technology /SAINT/ 05 p0631 A83-17759

The effect of materials and processes on package reliability 07 p0920 A83-20473

Investigation of aspects of the design of base-crystal matrix computing devices 08 p1152 A83-22182

A large scale integration based, signal processor - Its application and possible evolution 08 p1155 A83-22811

Polyimide adhesives to reduce thermal stresses in LSI ceramic packages 09 p1237 A83-23621

Questions of the modular design of microprocessor models for problems of mathematical physics 12 p1768 A83-29350

An LSI adaptive array processor 15 p2216 A83-33887

10 ns 8 x 8 multiplier LSI using super self-aligned process technology 15 p2216 A83-33891

Fast hardware implementation of the Winograd Fourier transform algorithm 15 p2218 A83-34514

Near term perspectives of LSI implementation of on-board switching units for SS-TDMA systems 18 p2677 A83-39998

GaAs digital dynamic IC's for applications up to 10 GHz 19 p2837 A83-40793

The use of production hardware for the development of control laws --- LSI for engine control [ASME PAPER 83-GT-6] 23 p3406 A83-47879

Low-loss unidirectional SAW filters using integrated microinductors 24 p3575 A83-49996

LARGE SPACE STRUCTURES

Development of advanced composite materials and geodetic structures for future space systems 01 p0017 A83-11334

Development of dynamics and control simulation of large flexible space systems 02 p0141 A83-12456

On-orbit propulsion requirements and performance assessment of ion propulsion subsystems for future GEO large satellite missions [AIAA PAPER 82-1872] 02 p0141 A83-12460

On the analytical modeling of the nonlinear vibrations of pretensioned space structures 02 p0142 A83-12752

Design of space structure control systems using on-off thrusters [AIAA PAPER 81-1847] 04 p0453 A83-16121

The optimal projection approach to fixed-order compensation - Numerical methods and illustrative results --- for large flexible spacecraft design [AIAA PAPER 83-0303] 05 p0680 A83-16641

Effect of solar radiation disturbance on a flexible beam in orbit [AIAA PAPER 83-0431] 05 p0607 A83-16710

The construction of ten-foot long composite space tubes [AIAA PAPER 83-0644] 05 p0653 A83-16811

Large space structures, alignment, and extravehicular activities /EVA/ crew support 09 p1213 A83-23585

Ten-channel vibration sensor --- for future large flexible space structures 09 p1219 A83-23595

Orbital ring systems and Jacob's ladders. II --- large space structures for space payload transfer 09 p1210 A83-23682

Static shape determination and control for a large space antenna 09 p1328 A83-24722

Singular value analysis of deformable systems --- of flexible large space structures 09 p1216 A83-24747

Digital stochastic control of distributed-parameter systems --- large flexible space structures 09 p1216 A83-24754

Qualitative stability of large space structures with noncollocated actuators and sensors 09 p1217 A83-24756

Experimental results for active structural control --- of large space structures 09 p1217 A83-24758

Discrete Large Space Structure control system design using positivity 09 p1217 A83-24760

Aggregation of large space structure dynamics with respect to actuator and sensor influences 09 p1217 A83-24784

Reduced order modeling of large space structures via least squares estimation 09 p1217 A83-24785

The decentralized control of large flexible space structures 09 p1217 A83-24786

Closed-loop asymptotic stability and robustness conditions for large space systems with reduced-order controllers 09 p1218 A83-24819

Low cost cold plate approach for large space platforms [SAE PAPER 820843] 10 p1383 A83-25755

An application of robust servomechanisms to control of flexible structures. I - Modelling and synthesis 10 p1385 A83-26586

A sensitivity analysis of modal controller for flexible space structures 10 p1385 A83-26587

A perspective of power management for large space platforms 11 p1538 A83-27144

Space platforms 11 p1534 A83-28414

Orbital ring systems and Jacob's Ladders. III 12 p1705 A83-29457

Comparative analysis of large antenna spacecraft using the ideas system [AIAA 83-0798] 12 p1707 A83-29731

Optimization of parabolic box truss reflector structures [AIAA 83-0830] 12 p1737 A83-29739

Effective constitutive relations for the microstructure of periodic frames [AIAA 83-1006] 12 p1740 A83-29793

Thermal-structural analysis of large space structures - An assessment of recent advances [AIAA 83-1018] 12 p1741 A83-29800

Reduction of rms-error in shallow faceted large space antennas [AIAA 83-1021] 12 p1707 A83-29803

Vibration characteristics of hexagonal radial rib and hoop platforms [AIAA 83-0822] 12 p1742 A83-29819

A preliminary look at control augmented dynamic response of structures [AIAA 83-0850] 12 p1708 A83-29825

Experiments using least square lattice filters for the identification of structural dynamics [AIAA 83-0880] 12 p1742 A83-29830

Transient response of damped space systems [AIAA 83-0900] 12 p1743 A83-29840

A travelling wave approach to the dynamic analysis of large space structures [AIAA 83-0964] 12 p1744 A83-29862

System identification of large flexible structures by using simple continuum models 13 p1812 A83-29995

Experimental demonstration of static shape control --- for large space structure development 13 p1812 A83-30165

Suboptimal control of large-scale mechanical systems 13 p1910 A83-30650

Thermal control testing for low cost programs 13 p1861 A83-31188

The specialized thermal modeling of sparse structures in space [AIAA PAPER 83-1461] 14 p2031 A83-32720

Radiation exchange in large space structures and frames [AIAA PAPER 83-1462] 14 p2032 A83-32721

Dynamic qualification of spacecraft by means of modal synthesis. II 14 p1982 A83-33474

Choice of lunar materials as determined by fabrication methods 16 p2313 A83-35613

Large size multi-use platform 16 p2316 A83-35952

Benefits and costs of low thrust propulsion systems [AIAA PAPER 83-1248] 16 p2316 A83-36306

Procedures to integrate electric secondary propulsion systems to large deployable space systems [AIAA PAPER 83-1392] 16 p2322 A83-36382

Comparison of electric and chemical thruster systems for secondary propulsion on a large space system [AIAA PAPER 83-1393] 16 p2322 A83-36383

Control of robot manipulators for handling and assembly in space 16 p2402 A83-36981

A comparison of control techniques for large flexible systems 17 p2475 A83-37070

Parameter estimation and control of distributed systems with application to large deployable antennae 17 p2475 A83-37077

Number and placement of control system actuators considering possible failures --- for large space structures 17 p2476 A83-37078

Least-squares sequential parameter and state estimation for large space structures 17 p2476 A83-37079

Spillover prevention via proper synthesis/placement of actuators and sensors --- on large space structures 17 p2476 A83-37157

Lumped parameter dynamic models for large space structures with flexible and rigid parts 17 p2477 A83-37444

Progress in modelling and control of flexible spacecraft 18 p2646 A83-39094

Control of large spaceborne antenna systems with flexible booms by mechanical decoupling 18 p2646 A83-39095

Space station USA 18 p2644 A83-40341

The earth's horizon - A reference for sub arc minute attitude sensing on flexible space structures [AIAA PAPER 83-2179] 19 p2815 A83-41673

Robustness of flexible spacecraft control to actuator and sensor model errors [AIAA PAPER 83-2190] 19 p2815 A83-41676

Scale model testing for control system parameters [AIAA PAPER 82-2225] 19 p2811 A83-41705

Attitude stabilization of flexible spacecraft during stationkeeping maneuvers [AIAA PAPER 83-2226] 19 p2815 A83-41706

Dynamics and control of a Shuttle attached antenna experiment [AIAA PAPER 83-2227] 19 p2816 A83-41707

Reduced order control design benefits and costs of frequency-shaped LQG methodology --- Linear-Quadratic-Gaussian [AIAA PAPER 83-2229] 19 p2891 A83-41708

Parameter testing for lattice filter based adaptive modal control systems [AIAA PAPER 83-2245] 19 p2892 A83-41721

Adaptive control for large space structures [AIAA PAPER 83-2246] 19 p2816 A83-41722

Electro-static surface control of a large radiometer spacecraft [AIAA PAPER 83-2248] 19 p2816 A83-41724

Reliability considerations in the placement of control system components [AIAA PAPER 83-2260] 19 p2816 A83-41730

Design of reduced order optimal state estimators with applications to stochastic linear optimal regulators [AIAA PAPER 83-2277] 19 p2892 A83-41743

Reduction of large flexible spacecraft models using internal balancing theory [AIAA PAPER 83-2292] 19 p2817 A83-41751

Time domain analysis for Stability Robustness of large scale LQG regulators [AIAA PAPER 83-2293] 19 p2892 A83-41752

Robust control system design techniques for large flexible space structures having non-collocated sensors and actuators [AIAA PAPER 83-2294] 19 p2817 A83-41753

An analytical investigation of shape control of large space structures by applied temperatures 21 p3098 A83-43891

Modal cost analysis as an aid in control system design for large space structures 21 p3098 A83-44005

Control of distributed hyperbolic systems - 'What does a tokamak and a large spacecraft have in common?' 21 p3192 A83-44011

On modern modal controller for flexible space structures - A sensitivity analysis 21 p3099 A83-44032

General conditions on reduced-order control for ensuring full-order closed-loop asymptotic stability --- of large space structures 21 p3099 A83-44033

Dynamics and control of large flexible spacecraft; Proceedings of the Third Symposium, Blacksburg, VA, June 15-17, 1981 21 p3101 A83-45101

Control of a flexible satellite via elimination of observation spillover 21 p3101 A83-45103

Spillover and model error bounding techniques for large scale systems 21 p3195 A83-45104

Numerical implementation of suboptimal output feedback control for large space structures 21 p3195 A83-45105

Application of classical techniques to control of continuous systems 21 p3196 A83-45109

The control of a flexible square plate in space 21 p3101 A83-45110

Modeling and control of flexible space structures 21 p3101 A83-45111

On the rigid body motion and shape distortion evaluation for large flexible spacecraft 21 p3101 A83-45112

On adaptive regulation of flexible spacecraft 21 p3101 A83-45114

Finite element models and system identification of large space structures 21 p3196 A83-45115

An approximation technique for the control and identification of hybrid systems 21 p3196 A83-45116

Optimal positive real controllers for large space structures 21 p3102 A83-45117

Stability and robustness of control systems for large space structures 21 p3102 A83-45119

Optimal damper location in the vibration control of large space structures 21 p3102 A83-45120

Stability augmentation for large space structures by modal dashpots and modal springs 21 p3102 A83-45121

Multi-body dynamics analysis on small computers 21 p3190 A83-45123

Generalized frequency-shaped KTC and Riccati approaches for space structure control 21 p3196 A83-45128

On the uniqueness of the independent modal-space control method 21 p3102 A83-45130

An integrated approach to optimal reduced order control theory 21 p3196 A83-45131

Partitioning control of Large Space Structures 21 p3103 A83-45132

Active control of large flexible spacecraft - A new design approach based on minimum information modelling of parameter uncertainties 21 p3196 A83-45133

Model error estimation for large flexible spacecraft 21 p3103 A83-45134

Dislocated actuator/sensor positioning and feedback design for flexible structures 21 p3103 A83-45465

Identification of structural dynamics systems using least-square lattice filters --- large space structures 21 p3103 A83-45467

Closed-loop control performance sensitivity to parameter variations --- applied to orbiting large space structures 21 p3103 A83-45471

Auxiliary propulsion requirements for large space systems [AIAA PAPER 83-1217] 21 p3105 A83-45512

Launching large antennas 22 p3258 A83-45721

Large space structures 22 p3257 A83-45858

Adaptive control of a flexible beam using least square lattice filters 22 p3351 A83-46099

Experimental implementation of parameter adaptive control on a free-free beam 22 p3351 A83-46100

A Space Station experiment on large antenna assembly and measurement [IAF PAPER 83-50] 23 p3413 A83-47244

An optimal active control system with Fourier transformed states for a flexible structure in space [IAF PAPER 83-68] 23 p3421 A83-47250

Dynamic modeling of flexible spacecraft - A general program for simulation and control [IAF PAPER 83-339] 23 p3421 A83-47348

On the controllability and control law design for an orbiting large flexible antenna system [IAF PAPER 83-340] 23 p3422 A83-47349

A large deployable antenna structure for the ERS-1 satellite [IAF PAPER 83-361] 23 p3422 A83-47359

Technical issues in dynamics and control of large space structures [IAF PAPER 83-403] 23 p3422 A83-47375

A new approach to the dynamics and control analysis of a class of large flexible spacecraft [IAF PAPER 83-408] 23 p3422 A83-47376

The features of the space structures dynamic design [IAF PAPER 83-409] 23 p3423 A83-47377

Active vibration control of a cantilevered beam - A study of control actuators --- for large space structures [IAF PAPER 83-ST-11] 23 p3423 A83-47388

Remote work station concept study [IAF PAPER 83-ST-14] 23 p3415 A83-47390

Product decompositions for certain types of coordinate transformation 23 p3502 A83-48141

Large space structures raise testing challenges 24 p3551 A83-48888

LARGE SPACE TELESCOPE

A data analysis facility for the Faint Object Camera 01 p0114 A83-10143

Space Telescope - Eye on the universe 02 p0247 A83-12642

Progress report on the high resolution spectrograph for the Space Telescope 03 p0288 A83-13971

Development of a photon counting hybrid CCD digicon detector [AIAA PAPER 83-0103] 05 p0608 A83-16521

Thin mirrors for large optical telescopes 05 p0656 A83-17824

Faint-object spectrograph optical bench 07 p0872 A83-20462

Design and tolerance analysis of two null corrector designs for the Space Telescope fine guidance aspheric collimating mirror 08 p1175 A83-22871

Control technology as applied to Space Telescope 09 p1218 A83-23592

Speckle interferometry, speckle holography, speckle spectroscopy, and reconstruction of high-resolution images from space telescope data 10 p1419 A83-25833

Design and verification for Space Telescope maintenance 10 p1381 A83-26248

Space Telescope neutral buoyancy mockup - A test bed for evaluating man/system interfaces 10 p1459 A83-26304

Infrared and submillimeter astronomy from space 10 p1497 A83-26700

High voltage power electronics packaging on NASA's Space Telescope 11 p1539 A83-27155

How to achieve diffraction limited resolution with large space telescopes 11 p1656 A83-27727

The Space Telescope, a valuable contribution to astronomy 11 p1674 A83-28218

Conceptual design of a coherent optical system of modular imaging collectors (COSMIC) --- telescope array deployed by space shuttle in 1990's 13 p1938 A83-30996

Speckle interferometry and related techniques with advanced technology optical telescope 13 p1920 A83-31011

Metrology mount development and verification for a large spaceborne mirror 13 p1939 A83-31030

Space Telescope verification - Ground and in-orbit 13 p1810 A83-31195

Performance of the spectropolarimeter for the Space Telescope faint object spectrograph 14 p2096 A83-32010

Faint Object Spectrograph (FOS) calibration 14 p2017 A83-32011

Grazing incidence optics - New techniques for high sensitivity spectroscopy in the space ultraviolet 14 p2084 A83-32018

Wide Field and Planetary Camera for Space Telescope 14 p2018 A83-32025

Space telescope low scattered light camera - A model 14 p2096 A83-32026

Space Telescope pointing control 17 p2480 A83-37434

Noise characterization and minimization of a precision gyroscopic rate sensor --- for Space Telescope 17 p2482 A83-37477

Space telescope. I - Implications for astronomy 17 p2595 A83-38624

Space telescope. II - A Science Institute 19 p2906 A83-40901

Galaxies, quasars, and beyond - The Space Telescope [AAS PAPER 83-168] 20 p3063 A83-43768

Design and fabrication of the NASA 2.4-meter space telescope 22 p3357 A83-46592

A space-telescope able to see the planets and even the satellites around the nearest stars [IAF PAPER 83-222] 23 p3515 A83-47313

Precise thermal control test demonstration on simulated space telescope main ring 23 p3418 A83-48699

LARMOR RADIUS

Evolution of nonlinear Alfvén waves propagating along the magnetic field in a collisionless plasma 06 p0812 A83-18916

Drift theory of the motion of a charged particle in a high-frequency wave in the case of finite Larmor radius 07 p0998 A83-20874

Quasilinear theory of inhomogeneous magnetized plasmas 08 p1168 A83-22387

Drift waves in sheet plasmas 12 p1780 A83-29009

Hamiltonian formulation of the second-order drift equations of motion --- for charged particles in fixed electromagnetic fields in high temperature plasmas 15 p2232 A83-33781

Transition to chaos for ballooning modes stabilized by finite Larmor radius effects 23 p3511 A83-48575

The gravitational instability of a rotating plasma in the presence of finite Larmor radius, Hall currents and suspended particles 24 p3633 A83-50168

LASER ALTIMETERS

Satellite laser altimeter for measurement of ice sheet topography 01 p0021 A83-10092

Remote sensing of sea state using laser altimeters 02 p0142 A83-12316

Multicolor laser altimeter for barometric measurements over the ocean - Theoretical 22 p3259 A83-46070

Multicolor laser altimeter for barometric measurements over the ocean - Experimental 22 p3259 A83-46071

LASER ANEMOMETERS

Measurements in shear layers in transonic flows with a laser transit anemometer 01 p0003 A83-10697

Laser transit anemometer measurements with unseeded backscatter 01 p0051 A83-11057

Laser anemometry studies of a separated turbulent boundary layer in supersonic flow, using a ten-nanosecond data acquisition system 01 p0052 A83-11063

Optical methods of flow diagnostics in turbomachinery 01 p0053 A83-11076

The coincidence tracker - Electronic equipment for a time-of-flight wind-speed measurement system 02 p0177 A83-12009

Direct measurement of laser velocimeter bias errors in a turbulent flow 03 p0323 A83-13139

Instantaneous two-component laser anemometry and temperature measurements in a complex flow model combustor [AIAA PAPER 83-0334] 06 p0765 A83-19587

A laser anemometer seeding technique for combustion flows with multiple stream injection 07 p0928 A83-19843

Long-range laser anemometry - A comparative review 08 p1091 A83-21976

Comparison between probe and laser measurements at the outlet of a centrifugal impeller 10 p1421 A83-26418

Estimation regarding the feasibility of using larger distances in measurements with L2F systems in flight tests --- Laser-two-Focus 10 p1431 A83-26487

Investigation of a Laser Doppler anemometer with counter-propagating beams 11 p1574 A83-28562

Engineering applications of laser velocimetry; Proceedings of the Symposium, Phoenix, AZ, November 14-19, 1982 12 p1727 A83-28830

Laser velocimetry - Problems and opportunities 12 p1727 A83-28831

Some solutions to the problems and pitfalls of laser velocimetry in a large transonic wind tunnel 12 p1704 A83-28832

Laser anemometer using a Fabry-Perot interferometer for measuring mean velocity and turbulence intensity along the optical axis in turbomachinery 12 p1727 A83-28834

Flow measurements using a laser two-focus anemometer in a high-speed centrifugal and a multistage axial compressor 12 p1695 A83-28835

Flow measurements using a laser-2-focus velocimeter in a high-pressure ratio centrifugal impeller 12 p1695 A83-28836

Optical development and application of a two colour LDA system for the simultaneous measurement of particle size and particle velocity 12 p1721 A83-28838

Laser velocimeter measurements in highly turbulent recirculating flows 12 p1721 A83-28841

Peculiarities in measuring the velocity vector using a laser anemometer in flow through axisymmetric models 13 p1848 A83-31470

A version of a single-beam laser time-of-flight method for measuring flight velocity 17 p2510 A83-37642

DFVLR-remote slant visual range (SVR) and wind vector measuring systems 17 p2552 A83-38750

A thermistor probe for use in laser Doppler anemometry 17 p2512 A83-38861

Methods of laser Doppler anemometry --- Russian book 18 p2692 A83-40605
LDA signal discrimination in two-phase flows 21 p3140 A83-44971
Particle-sampling statistics in laser anemometers Sample-and-hold systems and saturable systems 23 p3458 A83-48120
Two focus laser velocimeter applied to measurements in an experimental centrifugal compressor [ONERA, TP NO. 1983-113] 24 p3583 A83-49424
New applications of laser velocimetry in ONERA wind-tunnels [ONERA, TP NO. 1983-114] 24 p3550 A83-49425

LASER ANNEALING
CW-laser annealed solar cells 01 p0068 A83-10638
Electrolyte electroreflectance study of laser annealing effects of the CdTe/Hg/0.8/Cd/0.2/Te/111/ system 01 p0110 A83-10992
Pulsed excimer laser annealing of ion implanted silicon - Characterization and solar cell fabrication 02 p0243 A83-12284
Laser annealing study of the grain size effect in polycrystalline silicon Schottky diodes 04 p0542 A83-16067
Total dose radiation-bias effects in laser-recrystallized SOI MOSFET's 05 p0627 A83-17510
Short time annealing --- in silicon processing 07 p0999 A83-20592
New experimental evidence of surface ripples on gallium arsenide in laser annealing 08 p1169 A83-22758
Melt dynamics of silicon-on-sapphire during pulsed laser annealing 08 p1170 A83-22764
Microscopic processes in low-power laser annealing of ion-implanted Ge 11 p1661 A83-28068
Preparation of high purity II-VI compounds by laser annealing 14 p2090 A83-32303
Status of ion-implanted silicon solar cells 14 p2005 A83-32326
Laser processing in the preparation of high efficiency polycrystalline silicon solar cells 14 p2005 A83-32329
The influence of surface texture and thermal treatment on the performance of laser-annealed silicon solar cells 14 p2045 A83-32330
Implantation of boron and boron fluoride compounds into silicon for production of solar cells 14 p2005 A83-32331
Light assisted pulsed annealing of photovoltaic silicon by microwave energy 14 p2005 A83-32338
Fabrication of GaAs-Mo-Si structures by metalorganic chemical vapor deposition and laser annealing 15 p2238 A83-33848
Optical transmission at 3.39 microns during pulsed laser annealing of silicon 15 p2238 A83-33849
Laser annealing of submicrometer NMOS test structures and devices 15 p2152 A83-34696
Structure of ion-implanted and annealed Hg(1-x)Cd(x)Te 16 p2418 A83-35439
Laser processing of silicon 16 p2420 A83-35993
Epitaxial growth of Hg(0.7)Cd(0.3)Te by laser-assisted deposition 19 p2903 A83-40741
Electrical and structural properties of pulse laser-annealed polycrystalline silicon films 20 p3054 A83-43347
CW laser-annealing behavior of Se(+)-implanted InP investigated by ellipsometry 20 p3055 A83-43603
The use of the internal friction method for studying laser-irradiated materials 21 p3115 A83-45502
Use of laser annealing to achieve low loss in Corning 7059 glass, ZnO, Si3N4, Nb2O5, and Ta2O5 optical thin film waveguides 22 p3359 A83-46647
Developments in mode-locked lasers and their applications 22 p3298 A83-46670
Radiation-proof satellite technology [IAF PAPER 83-69] 23 p3421 A83-47251
High-efficiency Si solar cells by beam processing 24 p3598 A83-48791

LASER APPLICATIONS

NT LASER CUTTING
NT LASER FUSION
NT LASER PROPULSION
Theoretical and experimental research on the formation, propagation, and use of laser-induced pressure waves --- German thesis 01 p0048 A83-10165
Performance of laser-glazed zirconia thermal barrier coatings in cyclic oxidation and corrosion burner rig tests 01 p0027 A83-10300
Photoconductivity kinetics in Cd/x/Hg/1-x/Te crystals under surface excitation 01 p0108 A83-10374
The effect of biostimulation amplification after the combined action of laser irradiation in the blue and red regions of the spectrum 01 p0078 A83-10456
A medical laser unit for continuous operation 01 p0054 A83-10559

High repetition rate, high resolution back-lit, shadow, and schlieren photography of gaseous and liquid mass-transport phenomena and flames 01 p0052 A83-11061
Subsurface-structure determination using photothermal laser-beam deflection 02 p0177 A83-12282
Suppressed turn-on laser regenerative optoelectronic amplifier 02 p0185 A83-12301
The absorption of electromagnetic radiation in an advanced propulsion system [AIAA PAPER 82-1950] 02 p0147 A83-12507
The retinal visual acuity of normal eyes 03 p0377 A83-13290
Coherent optical methods for applications in robot visual sensing [AD-A110107] 03 p0324 A83-13446
Perspectives on the use of stimulating laser therapy in ophthalmology 03 p0374 A83-13601
Concerning the so-called laser stimulation of the macula lutea and the possibility of theoretical interpretation of the mechanism of its action 03 p0378 A83-13602
The stimulating effect of a helium-neon laser in acute inflammatory processes of the eye 03 p0378 A83-13603
Stimulation laser therapy for diseases of the cornea with the irradiation of a ruby laser 03 p0378 A83-13604
The stimulating action of coagulating laser interventions in macular pathologies 03 p0378 A83-13606
A stimulating laser therapy for sclerotic and posttraumatic central dystrophies of the retina 03 p0378 A83-13607
Laser stimulation in the comprehensive therapy of central dystrophies of the retina 03 p0378 A83-13608
Integrated optics strapdown inertial system 03 p0326 A83-13755
An optical-radar model of continental aerosols --- Russian book 03 p0358 A83-13821
Lasers in the 200-400 nm region - Characteristics and applications 03 p0332 A83-13956
Display methods of laser radar data using a computer system 03 p0328 A83-14132
On the use of laser profilometry for ocean wave studies 03 p0373 A83-14502
Low-temperature refractory metal film deposition 03 p0301 A83-14936
Compensation of scanner error 04 p0482 A83-15917
Autonomous navigation for satellites using lasercom systems [AIAA PAPER 83-0428] 05 p0605 A83-16709
Mixing in jet flames by laser Rayleigh scattering [AIAA PAPER 83-0403] 05 p0612 A83-16827
Refractive thermo- and laser keratoplasty 05 p0674 A83-17208
An experimental study of the possibility of using a CO2 laser for changing the cornea refraction /A preliminary report/ 05 p0671 A83-17211
Laser treatment of open-angle glaucoma: Randomized comparative studies - Cyclotrabeculospas and trabeculoplasty 05 p0674 A83-17212
An experimental unit for investigating two-phase flows 05 p0639 A83-17410
Laser weather identifier - Present and future 05 p0668 A83-17448
Nondestructive laser method for measuring charge profiles in irradiated polymer films 05 p0618 A83-17501
A new method for the laser sounding of the atmosphere based on the reception of an echo signal by the laser 05 p0645 A83-17632
Laboratory analysis of techniques for remote sensing of estuarine parameters using laser excitation 06 p0762 A83-18583
Interaction of three coherent fields with Doppler broadened serial four-level systems - Application to four-level FIR lasers 06 p0766 A83-18907
New pulsed laser data-acquisition system 06 p0764 A83-19233
Localized metallic melting and hole boring by laser guided discharges 06 p0769 A83-19234
The picosecond laser - An instrument for scientific research 06 p0767 A83-19416
Error probabilities in lasercom PPM systems 07 p0905 A83-19705
Pulse decoding in stretched pulse laser PMM systems 07 p0905 A83-19706
Determination of grain boundary barrier height and interface states by a focused laser beam 07 p0999 A83-19992
Rapid-flow combined-action industrial CO2 laser 07 p0933 A83-20104
Induced dichroism in passive laser switches 07 p0934 A83-20111
A study on the measurement of particle size distribution with laser diffraction systems 07 p0929 A83-20286

The possibility of the acceleration of charged particles by laser radiation 07 p0935 A83-20306
Lasers in aviation --- Russian book 07 p0936 A83-20384
Fast position-sensitive shadowmeter --- utilizing nanosecond-pulse-width nitrogen laser 07 p0931 A83-21376
The evaluation of the receiver noise level of a lidar response 08 p1074 A83-21873
Military applications of coherent infrared radar 08 p1095 A83-22500
Overview of technology developments in coherent infrared radar 08 p1109 A83-22501
Laser and millimeter-wave backscatter of transmission cables 08 p1043 A83-22523
High performance image generators for reconnaissance applications 08 p1099 A83-22580
Surface magic - Making metals tougher 08 p1068 A83-22775
Towards displacement measurement in remote locations by holographic fiber optics probes 09 p1264 A83-23362
High temperature thermal strain measurement using laser speckles 09 p1264 A83-23364
Laser acceleration of particles 09 p1270 A83-23380
Optical communications and laser beam acquisition performances 09 p1245 A83-23528
Control and communication technology in laser systems; Proceedings of the Twenty-fifth Annual International Technical Symposium, San Diego, CA, August 25, 26, 1981 09 p1214 A83-23576
Laser space communication technology status 09 p1214 A83-23577
GaAs laser beacon for satellite communications 09 p1214 A83-23582
Parametric performance analysis of spaceborne laser communication systems 09 p1214 A83-23583
Acquisition, tracking, and fine pointing control of space-based laser communication systems 09 p1215 A83-23587
Precision optical encoder 09 p1267 A83-23588
Digital control system for the Lasercom Space Measurement Unit 09 p1215 A83-23589
Acquisition and tracking system for a ground-based laser communications receiver terminal 09 p1245 A83-23594
Numerical modeling of nonstationary processes during sputtering and interaction of an erosion laser flare 09 p1274 A83-23992
Lidar measurements of the atmosphere 09 p1272 A83-24644
Multiwavelength laser rate calorimetry on various infrared window materials 09 p1346 A83-24967
Regularizing the solution of the laser sounding equation of atmospheric aerosols by means of a stabilizing functional 10 p1425 A83-25567
Field investigation of techniques for remote laser sensing of oceanographic parameters 10 p1419 A83-25643
Application of digital image analysis techniques to antismisting fuel spray characterization [ASME PAPER 82-WA/HT-23] 10 p1401 A83-25690
Laser-controlled etching of chromium-doped 100 line-type GaAs 10 p1390 A83-25986
Holographic intensity correlator with a laser electron beam tube for inputting images for processing 10 p1422 A83-26467
Thermoelectric phenomena in the oxidation of vanadium by laser radiation 10 p1392 A83-26664
Determination of the aluminum content in high-purity germanium by laser multistage photoionization of atoms 10 p1432 A83-26667
Nonlinear optics of the stratosphere and the laser chemistry of ozone 10 p1449 A83-26785
A laser-based technique for the measurement of hydrogen at local areas in metals 11 p1547 A83-27331
Nonlinear optical study of interfaces --- at rough noble metal surfaces in electrolytic cells 11 p1545 A83-27510
Submicrostructures generated in semiconductors by athermal laser processing 11 p1661 A83-27561
Mechanisms of acoustic wave generation by lasers 11 p1650 A83-27563
Laser bonding of dissimilar semiconductors 11 p1560 A83-27564
Review of laser technology at M.I.T. Lincoln Laboratory 11 p1580 A83-27575
Peculiarities of laser radiation and solid aerosol interaction 11 p1612 A83-27607
Erbium glass lasers and their applications 11 p1583 A83-27620
Deep-space laser communications. I - Optical receivers probe the depths of space 11 p1535 A83-28154

Design considerations for deep-space transmitters. II - Deep-space laser communications 11 p1535 A83-28156

Flashlamp-pumped iodine monobromide laser characteristics 11 p1585 A83-28704

Improved acousto-optic modulators for CO₂ heterodyne laser systems 12 p1732 A83-29467

Laser sounding of aerosols using airborne and space facilities 12 p1755 A83-29563

Reconstruction of the profiles of atmospheric optical parameters on the basis of data from laser probing 13 p1873 A83-30028

Laser induced deposition of zinc oxide 13 p1928 A83-30335

Laser-formed connections using polyimide --- on integrated circuits 13 p1832 A83-30346

Scientific foundations of advanced technology --- Russian book on production engineering techniques 13 p1826 A83-30525

New applications of CO lasers 13 p1851 A83-30823

Interferometric control of a beam expander consisting of multiple telescopes 13 p1921 A83-31022

A survey of laser and selected optical systems for remote measurement of pollutant gas concentrations 13 p1848 A83-31595

Fresnel detour-phase circular computer generated holograms 14 p2083 A83-31948

Laser treatment of the thin surface layers of semiconductors 14 p2024 A83-32165

Gas immersion laser diffusion - A new method for making efficient Si solar cells 14 p2041 A83-32234

Grain boundary photocurrent enhancement in solar cells made by laser diffusion 14 p2046 A83-32332

Free-electron lasers and prospects of their utilization 14 p2024 A83-32592

Feasibility of laser-driven repetitively-pulsed MHD generators [AIAA PAPER 83-1442] 14 p1984 A83-32713

Surface treatments using laser, electron and ion beam processing methods 14 p2028 A83-32803

A system for spacecraft attitude determination using laser techniques 14 p1981 A83-33148

Use of a laser in the collimation of the CIDA Schmidt camera 14 p2101 A83-33293

Nondestructive airfield pavement testing using laser technology [AIAA PAPER 83-1601] 14 p1978 A83-33364

Laser polarization of accelerated protons 15 p2228 A83-33785

Optical systems of laser scanners 15 p2168 A83-33787

Lasers in aircraft construction --- Russian book 15 p2169 A83-34170

Free-electron lasers and their applications 15 p2169 A83-34398

Laser light scattering technique in the diagnostics of sprays in isothermal and burning conditions 16 p2351 A83-35825

Laser processing of silicon 16 p2420 A83-35993

Laser applications to combustion research [AIAA PAPER 83-1360] 16 p2360 A83-36358

Thermoelastic hologram for focused ultrasound 16 p2357 A83-36773

The development, performance, and potential application of the copper halide laser [AIAA PAPER 83-1702] 17 p2513 A83-37199

Laser scattering and current transport in an argon arc plasma --- German thesis 17 p2582 A83-37504

A visualization study of wakes at large distances from the wing 17 p2511 A83-37809

A prospectus on airborne laser mapping systems 17 p2530 A83-38168

Laser diagnostic methods - A summary [AIAA PAPER 83-1683] 18 p2688 A83-39100

High-speed laser visualization of detonation-sprayed particles 18 p2688 A83-39172

Use of planar laser-induced fluorescence for the study of combustion flowfields [AIAA PAPER 83-1361] 18 p2688 A83-39263

Rydberg atoms 18 p2743 A83-40003

Thin-film thickness measurements with thermal waves 18 p2689 A83-40060

Hydrogenated amorphous silicon produced by laser induced chemical vapor deposition of silane 19 p2903 A83-40743

Lasers in metallurgy; Proceedings of the Symposium, Chicago, IL, February 22-26, 1981 19 p2854 A83-41468

A laser method for investigating aerosol systems 19 p2854 A83-41588

Airborne dual laser excitation and mapping of phytoplankton photopigments in a Gulf Stream Warm Core Ring 20 p3032 A83-42210

A high-energy, laser accelerator for electrons using the inverse Cherenkov effect 20 p2994 A83-42586

Lasers and avionic integration 20 p2995 A83-42836

A real-time signal processor with high resolution using acousto-optic light deflectors and a prism 20 p3048 A83-42947

Trends in the development of the application of CO₂-lasers in Materials Technology 20 p2999 A83-43627

Technological issues in communication and control of optical systems for space applications 21 p3097 A83-44035

Process for producing laser-formed video calibration markers 21 p3136 A83-44155

Ultraviolet (UV) photochemical doping of silicon 21 p3218 A83-44817

Automatic laser photometer-polarimeter 21 p3141 A83-45310

Photodeposition of aluminum oxide and aluminum thin films 21 p3219 A83-45489

Heteroepitaxial growth of CdTe on GaAs by laser assisted deposition 21 p3219 A83-45492

Laser and laser systems reliability; Proceedings of the Conference, Los Angeles, CA, January 28, 29, 1982 22 p3296 A83-46611

Tradeoff between laser diodes and light-emitting diodes (LEDs) for the common weapon control system 22 p3278 A83-46616

Integrated optical circuits fabricated with laser-written masks 22 p3359 A83-46648

Picosecond lasers and applications; Proceedings of the Conference, Los Angeles, CA, January 26, 27, 1982 22 p3297 A83-46663

Synchronously mode-locked continuous wave dye lasers - Recent advances and applications 22 p3297 A83-46664

Picosecond transient grating generation of tunable ultrasonic waves 22 p3298 A83-46671

Picosecond fluorescence in spinach chloroplasts 22 p3346 A83-46672

Picosecond photoconductivity and its applications 22 p3298 A83-46674

Advances in picosecond optoelectronics 22 p3298 A83-46675

New developments in subpicosecond optoelectronics 22 p3298 A83-46676

Ultrafast picosecond chronography 22 p3293 A83-46679

Accurate range gating technique with mode-locked dye lasers 22 p3298 A83-46680

Acoustic wave calibration for CO₂ laser scattering experiments 23 p3461 A83-47647

Atmospheric pressure and temperature profiling using near IR differential absorption lidar 23 p3457 A83-47781

Signal averaging limitations in heterodyne- and direct-detection laser remote sensing measurements 23 p3457 A83-47789

Rayleigh and resonance sounding of the stratosphere and mesosphere 23 p3457 A83-47790

High-resolution lidar system for measuring the spatial and temporal structure of the mesospheric sodium layer 23 p3457 A83-47791

Solid-state laser sources for remote sensing 23 p3461 A83-47797

Coherent IR radar technology 23 p3442 A83-47805

Processing signals the optical way 23 p3508 A83-47821

On-line calibration technique for laser diffraction droplet sizing instruments [ASME PAPER 83-GT-232] 23 p3458 A83-48028

Laser-induced chemistry 23 p3429 A83-48082

Surface modification of materials by laser irradiation 23 p3467 A83-48427

Alloying of surface layers during laser treatment 23 p3433 A83-48430

Problems encountered in the development of 1-10-kw industrial lasers 23 p3462 A83-48431

Projects carried out by the Physics Institute of the Academy of Sciences of the USSR in the field of industrial laser development and applications 23 p3463 A83-48432

The effect of fluorescence decay time on echo-signal kinetics in the case of remote laser sounding of water bodies 23 p3493 A83-48505

Recent progress on LADA growth of HgCdTe and CdTe epitaxial layers --- laser assisted deposition 24 p3633 A83-48739

High speed read/write techniques for advanced printing and data handling; Proceedings of the Meeting, Los Angeles, CA, January 20, 21, 1983 24 p3637 A83-48996

Measurements of the concentration of carbon monoxide in the atmospheric surface layer using tunable diode lasers 24 p3583 A83-49110

Flow visualization by light sheet [ONERA, TP NO. 1983-105] 24 p3583 A83-49416

Recent applications of a laser velocimeter in the Langley 4by 7-meter Wind Tunnel 24 p3586 A83-50145

LASER BEAM DEFOCUSING

U THERMAL BLOOMING

LASER CAVITIES

Transient pulse evolution of active mode locking in an intracavity frequency-doubled laser 01 p0054 A83-10642

Low threshold InGaAsP/InP lasers with microcleaved mirrors suitable for monolithic integration 01 p0055 A83-10981

Relationship between carrier-induced index change and feedback noise in diode lasers 02 p0184 A83-12169

Influence of the active-medium inhomogeneity and of aperture stops on the output-beam parameters of a CO₂ laser 03 p0330 A83-13585

Optimal ring lasers with coupled resonators and a homogeneously broadened active medium 03 p0330 A83-13587

Novel semiconductor lasers for integrated optics 03 p0331 A83-13765

Numerical modeling of processes occurring in the cavity of a CW chemical HF laser on the basis of Navier-Stokes equations 03 p0332 A83-14061

A new numerical method for turbulent mixing of supersonic reacting flows in chemical laser cavities [ONERA, TP NO. 1982-85] 03 p0332 A83-14537

High-power individually addressable monolithic array of constricted double heterojunction large-optical-cavity lasers 03 p0333 A83-14935

Simple spectral control technique for external cavity laser transmitters 04 p0485 A83-16023

Effects of cavity length on 20 micron stripe laser waveguiding 04 p0486 A83-16221

Spatial mode discrimination and control in high-power single-mode constricted double-heterojunction large-optical-cavity diode lasers 05 p0648 A83-16942

Synchronization of lasers with intracavity second harmonic generation 05 p0648 A83-17039

Carbon monoxide laser with selective and nonselective resonators 05 p0648 A83-17048

Approximate method for calculations of unstable telescopic resonators --- carbon dioxide gasdynamic laser design 05 p0649 A83-17061

Influence of the spatial structure of the gain on the dynamic properties of a laser 05 p0650 A83-17075

Observation of bifurcation to chaos in an all-optical bistable system 05 p0686 A83-17935

Lasers with distributed feedback and reflection on the basis of cholesteric liquid crystals /CLC/ 06 p0768 A83-19572

Flowfield experiments on a DF chemical laser 07 p0932 A83-19815

Divergence of radiation from an electric-discharge CO₂ laser having an unstable resonator 07 p0934 A83-20108

Formation of a non-Gaussian intensity profile in a laser with inhomogeneous mirrors 07 p0934 A83-20110

Cherenkov parametric optical oscillations in a 'double' Fabry-Perot interferometer 07 p0934 A83-20116

Generation of continuous-wave 194-nm radiation by sum-frequency mixing in an external ring cavity 07 p0936 A83-20789

Quantum theory of laser and optical-bistability instabilities 07 p0936 A83-20790

Contribution to the construction of a submillimeter laser - Application to the characterization of various mesomorphic substances --- French thesis 07 p0937 A83-21097

Selective enhancement of the 251-micron line in an optically pumped CH₃OH laser 07 p0937 A83-21360

Pulsed visible laser flow and acoustics 08 p1108 A83-22459

Adaptive optics - Problems and prospects 08 p1109 A83-22465

Optical bistability of a CO₂ laser with intracavity saturable absorber Experiment and model 09 p1271 A83-23710

Thermal homogeneity in a closed excimer laser cavity 09 p1272 A83-24661

The laser gyro - Myth or panacea 09 p1270 A83-24858

FEL's with Bragg reflection resonators - Cyclotron autoresonance masers versus ubitrons 10 p1427 A83-26005

External cavity controlled operation of a semiconductor diode gain element in series with an optical fiber 10 p1428 A83-26025

Bistable operation of two semiconductor lasers in an external cavity - Rate-equation analysis 10 p1428 A83-26026

Laser oscillator using resonator with self-pumped phase-conjugate mirror 10 p1429 A83-26112

Semiconductor integrated etalon interference laser with a curved resonator 10 p1430 A83-26206

Use of unstable resonators in CW chemical lasers with radial flow of a gas mixture 10 p1431 A83-26652

Determination of the effective stimulated emission cross section for a neodymium laser with a selective resonator 10 p1431 A83-26653

Laser with diffraction-limited divergence and Q switching by stimulated Brillouin scattering 10 p1431 A83-26655

Influence of a nonlinear active medium on the structure of natural oscillation modes of a Fabry-Perot interferometer 10 p1433 A83-26681

High-sensitivity atmospheric gas analysis based on intracavity laser detection of scattered radiation 10 p1392 A83-26685

Resonances of the polarization of gas laser radiation under mode self-locking conditions 10 p1433 A83-26688

High-pressure NH₃-N₂ laser 10 p1434 A83-26689

Continuous-wave YAG:Nd³⁺/+/- laser with mode locking and intracavity frequency doubling 10 p1434 A83-26695

Intracavity double resonance in the CH₃OH submillimeter laser 10 p1435 A83-26879

Cavity phase shift method for high reflectance measurements 11 p1572 A83-27513

On the interpretation of interferograms of cavity turbulence --- in laser cavity medium 11 p1577 A83-27516

New types of mode locking in stimulated radiation in optical resonators 11 p1578 A83-27539

A single mode /F₂+/-asterisk color-center laser for application in optical pumping of helium 11 p1578 A83-27543

The interaction between single-mode laser radiation and sodium vapour in a Fabry-Perot etalon and a ring optical cavity 11 p1657 A83-27850

The intracavity magneto-optical modulation of the intensity of laser radiation 11 p1583 A83-27949

Gas-lens effect and cavity design of some frequency-stabilized He-Ne lasers 13 p1849 A83-30213

Operator calculation of anisotropic resonators with allowance for the optical mismatch of their elements 13 p1850 A83-30265

Runaway self-absorption in multikilowatt CO₂ lasers 13 p1850 A83-30328

High-speed direct single-frequency modulation with large tuning rate and frequency excursion in cleaved-coupled-cavity semiconductor lasers 13 p1850 A83-30332

Additional experimental results from the Stanford 3 micron FEL 13 p1852 A83-31103

The Stanford Superconducting Linear Accelerator --- for powering free electron laser 13 p1917 A83-31104

Optical mode control in the free-electron laser 13 p1854 A83-31121

The application of free-electron lasers to the transmission of energy in space 13 p1856 A83-31141

Demonstration of multilevel multichannel optical frequency shift keying (FSK) with cleaved-coupled-cavity (C3) semiconductor lasers 13 p1922 A83-31784

Intracavity second harmonic excitation under the action of an external signal on a Q-switched solid-state ring laser 14 p2023 A83-31907

Natural fluctuations in a multimode standing-wave laser 14 p2023 A83-31909

Passive mode locking in iodine photodissociation laser 14 p2023 A83-31913

High-power continuously tunable atmospheric-pressure CO₂ laser operating in the superregenerative amplification regime 14 p2023 A83-31915

Quantitative intracavity spectroscopy 14 p2052 A83-32561

An investigation of the possibilities for lowering the detection limits of elements in a graphite laser torch using the intracavity method for the registration of atomic absorption 14 p2020 A83-32826

Simultaneous determination of the spectral and temporal properties of tunable, single, picosecond pulses from a short cavity dye laser 14 p2026 A83-33409

The self-injected nonmode-locked picosecond laser 14 p2026 A83-33413

Characterization of pulsed Nd:YAG active/passive mode-locked laser 14 p2026 A83-33414

Short cavity InGaAsP/InP lasers with dielectric mirrors 14 p2027 A83-33436

New large optical cavity laser with distributed active layers 14 p2027 A83-33437

Bistability and slow oscillation in an external cavity semiconductor laser 14 p2027 A83-33440

Saturation effects in phase-conjugate lasers 15 p2167 A83-33534

Power and stability of phase-conjugate lasers 15 p2167 A83-33535

Intracavity resonant degenerate four-wave mixing - Bistability in phase conjugation 15 p2229 A83-33536

Mirrors that are electron transparent for use in free-electron-laser oscillators 15 p2167 A83-33760

Lasing characteristics of a Nd(3+):YAG laser with a long optical-fiber resonator 15 p2168 A83-33812

Integrated arrays of 1.3-micron buried-crescent lasers 15 p2168 A83-33842

Modulation intracavity laser spectroscopy, polarimetry, and interferometry 15 p2163 A83-33979

Interference irregularities in complex laser resonators 15 p2169 A83-34024

Influence of Lorentz broadening on the stability of monomode ring lasers 15 p2169 A83-34370

New scheme for ultrashort-pulsed Nd(3+):YAG laser operation A branched cavity, internally seeded regenerative amplifier 15 p2169 A83-34455

Radiation characteristics of a multimode linear Zeeman laser 15 p2170 A83-34703

Quantum theory of optical bistability. III - Atomic fluorescence in a low-Q cavity 16 p2411 A83-35659

Observation of cavity-enhanced single-atom spontaneous emission 16 p2410 A83-35746

Investigation of the temperature field in the active rod of a laser 16 p2359 A83-35939

Mode structure of a tapered-wiggler free-electron laser stable oscillator 16 p2360 A83-35960

Stable single-longitudinal-mode operation under high-speed direct modulation in cleaved-coupled-cavity GaInAsP semiconductor lasers 17 p2515 A83-38885

Laser cavity dumping using optical bistability 17 p2515 A83-38971

Disappearance of laser instabilities in a Gaussian cavity mode 17 p2515 A83-38973

Dependence of the sensitivity of intracavity laser spectroscopy on generation parameters 18 p2693 A83-40347

Interference inhomogeneities of the stacks used in laser cavities 18 p2694 A83-40403

Intracavity pumped NH₃ laser using a very small cavity 19 p2853 A83-41184

Theory of acoustooptic interaction in active resonators 19 p2854 A83-41774

Intracavity mode-locked and frequency-doubled Nd:YAG laser Pump- and mode-size effects 20 p2993 A83-42225

High-efficiency pulse compression with intracavity Raman oscillators 20 p2993 A83-42345

Optimal physical parameters for a high-power He-Ne laser 20 p2995 A83-42949

Computation of reacting flowfield with radiation interaction in chemical lasers 20 p2995 A83-43445

Superluminescent damping of relaxation resonance in the modulation response of GaAs lasers 20 p2995 A83-43592

Anisotropic Gaussian beams 20 p2995 A83-43628

Electron-diffractive mode selection in free electron lasers 20 p2995 A83-43632

Influence of transit effects on frequency resonances in gas lasers 20 p2997 A83-43799

External-cavity diode laser emitting in the middle infrared range 20 p2998 A83-43804

Self-pulsing and chaos in inhomogeneously broadened single mode lasers 21 p3143 A83-44192

Chaos in coherent two-photon processes in a ring cavity 21 p3143 A83-44196

Superfluorescence in a cavity 21 p3143 A83-44197

An external cavity diode laser sensor 21 p3136 A83-44209

Resonant modes in a dispersive cavity --- nonlinear optical effects in active interferometer 21 p3206 A83-44802

Operating characteristics of a laser with supplementary inertial negative feedback 21 p3146 A83-45387

Wavelength multiplexing of 1.31-micron InGaAsP buried crescent laser arrays 21 p3146 A83-45476

Influence of an external cavity on semiconductor laser phase noise 21 p3146 A83-45479

Twisted double-heterostructure GaAs-(AlGa)As laser 21 p3146 A83-45484

Quantum statistics of parametric oscillation 22 p3356 A83-45930

Short-cavity hydrogen-halide laser 22 p3296 A83-46086

Enhanced frequency modulation in cleaved-coupled-cavity semiconductor lasers with reduced spurious intensity modulation 22 p3299 A83-46722

Electronic wavelength tuning with semiconductor integrated etalon interference lasers 22 p3299 A83-46723

Classical derivation of the laser rate equation 22 p3300 A83-46814

Characteristics of lasers with condensed active media exhibiting linear anisotropy induced by polarized pump radiation 23 p3460 A83-47162

An experimental study of the generation parameters of a laser with a thin absorption layer in the cavity 23 p3460 A83-47163

Directionality of the radiation of a misaligned cavity with a lens-like medium 23 p3460 A83-47166

A theory for parametric wave amplification in a cavity in the approximation of a specified intensity 23 p3460 A83-47170

Fine tuning lasers by means of an intracavity interferometer enclosing an absorbing gas 23 p3461 A83-47620

Dewar design for optically pumped semiconductor ring laser 23 p3461 A83-47646

Subharmonic and chaotic bifurcation structure in optical bistability 23 p3509 A83-48320

Bandwidth-limited picosecond pulse generation in a synchronously pumped GaAs laser containing a variable absorber diode 24 p3586 A83-48783

Inhomogeneity effects in a gas laser 24 p3587 A83-48842

Observation of absorptive bistability with two-level atoms in a ring cavity 24 p3628 A83-48847

A study of the emission spectrum of a TEA CO₂ laser with an intracavity absorber 24 p3588 A83-49048

Ultrashort optical pulse generation from microwave modulated AlGaAs diode laser with Selfoc rod resonator 24 p3588 A83-49611

Generation of single longitudinal mode pulses in passively Q-switched lasers via passive pre-lasing 24 p3589 A83-49614

Self-pulsing in two-cavity optical bistability 24 p3589 A83-49617

An investigation of the kinetics of processes by the intracavity method according to the change in the intensity of lasing 24 p3589 A83-49739

Thermal defocusing (LIMP) in stable CO₂ resonators 24 p3589 A83-49835

Wideband frequency-shift keying with a spectrally bistable cleaved-coupled-cavity semiconductor laser 24 p3630 A83-49976

LASER COMMUNICATION

U OPTICAL COMMUNICATION

LASER CUTTING

Splicing of single-polarisation fibres by an optical short-pulse method 04 p0534 A83-15235

Method of raw material continuous feeding on silicon ribbon growth 14 p2090 A83-32319

The physical processes occurring during the deep penetration of metals by a laser beam 23 p3462 A83-48428

The current status and future prospects of laser cutting 23 p3467 A83-48429

LASER DAMAGE

The aging of alpha-LiIO₃ single crystals under laser irradiation 01 p0055 A83-10819

Raising damage thresholds of gradient-index antireflecting surfaces by pulsed laser irradiation 01 p0055 A83-10977

Optical damage resistance of lithium niobate waveguides 03 p0393 A83-13759

The role of physical characteristics of laser radiation in the absorption of light by heme-containing biological molecules 03 p0376 A83-14369

The mutagenic effect of laser radiation in the visible range on cultured human cells 03 p0377 A83-14890

Laser-induced damage to transparent conducting SnO₂ films at 1062 nm 07 p0936 A83-20753

Laser-induced damage and two-photon absorption measurements in CdTe 09 p1273 A83-24974

Selective and uniform laser-induced failure of antireflection-coated LiNbO₃ surfaces 10 p1429 A83-26030

Measurement of laser photoelectron image degradation at high current densities 16 p2356 A83-35989

The Brillouin-scattering method in quantum electronics and laser-induced damage 18 p2694 A83-40608

Investigation of mechanisms of damage induced in ionic crystals by pulsed nanosecond laser radiation 18 p2694 A83-40610

Investigation of processes of the bulk damage of semiconductors under the effect of pulsed infrared laser radiation 18 p2694 A83-40611

Picosecond air breakdown studies at 0.53 micron 20 p3051 A83-43598

Plastics for high-power laser applications - A review 21 p3115 A83-43861

On the nature of the accumulation effect in laser-induced damage to optical materials 21 p3203 A83-43862

LASER DOPPLER VELOCIMETERS

- Single and multiple pulse catastrophic damage in diamond-turned Cu and Ag mirrors at 10.6, 1.06, and 0.532 microns 21 p3203 A83-43863
- Picosecond damage studies at 0.5 and 1 micron --- laser induced breakdown in optical materials 21 p3203 A83-43864
- Continuous wave laser damage on optical components 21 p3142 A83-43865
- Review of laser induced damage thresholds 21 p3144 A83-44784
- Quantitative measurement of energy deposited in optical coatings 21 p3205 A83-44785
- Laser induced damage in the ultraviolet 21 p3145 A83-44831
- Picosecond laser damage mechanisms at semiconductor surfaces 22 p3298 A83-46673
- A prism reflector of anti-resonant ring configuration 24 p3586 A83-48749
- A theoretical model for multiple-pulse laser-induced damage to metal mirrors 24 p3587 A83-48911

LASER DOPPLER VELOCIMETERS

- Fibre-optic laser Doppler anemometer with Bragg frequency shift utilising polarisation-preserving single-mode fibre 02 p0177 A83-12010
- Miniature solid-state directional laser Doppler velocimeter 02 p0183 A83-13043
- Laser velocimeter for large wind tunnels 03 p0324 A83-13171
- Measuring movement with an LDV system 03 p0329 A83-14382
- Laser velocimetric analysis of the flow downstream of missile aft-bodies [ONERA, TP NO. 1982-94] 03 p0279 A83-14543
- Reduction of flow-measurement uncertainties in laser velocimeters with nonorthogonal channels [AIAA PAPER 83-0051] 05 p0642 A83-16486
- Two-component LDA measurement in a two-phase turbulent jet [AIAA PAPER 83-0052] 05 p0642 A83-16487
- A two-grating method for combined beam splitting and frequency shifting in a two-component laser-Doppler velocimeter 05 p0645 A83-17352
- Quantitative measurement of density and velocity in compressible flows using laser-induced iodine fluorescence [AIAA PAPER 83-0049] 05 p0646 A83-17903
- Laminar burning velocities of hydrogen-air and hydrogen-air-steam flames 07 p0878 A83-19837
- An experimental study of turbulent free convection boundary layer in air along a vertical plate using LDV 07 p0925 A83-20279
- An analytical and experimental comparison of the flow field of an advanced swept turboprop [AIAA PAPER 83-0189] 07 p0864 A83-21080
- Assessment of surface texture from analysis of the signal visibility of a laser Doppler anemometer 08 p1091 A83-22003
- Some aspects of measuring the structure of non-isothermal turbulence by simultaneous application of DISA's LDA and hot-wire anemometer 09 p1259 A83-23697
- Conditional sampling with a laser velocimeter --- for tone-excited jet and rotating propeller blade [AIAA PAPER 83-0756] 10 p1420 A83-25953
- Ring laser for the determination of linear velocities 10 p1433 A83-26675
- Coherent structures in rectangular jets 11 p1565 A83-27418
- Direct measurement of sound from large scale structures in jet flows [AIAA PAPER 83-0662] 11 p1653 A83-28197
- Investigation of a Laser Doppler anemometer with counterpropagating beams 11 p1574 A83-28562
- Engineering applications of laser velocimetry: Proceedings of the Symposium, Phoenix, AZ, November 14-19, 1982 12 p1727 A83-28830
- Laser velocimetry - Problems and opportunities 12 p1727 A83-28831
- A laser-Doppler velocimeter technique for in situ local measurement of dilute two-phase suspension flows 12 p1720 A83-28837
- Local velocity measurement of opaque fluid flow using laser Doppler velocimeter with optical dual fiber pickup 12 p1727 A83-28839
- An experimental verification of laser-velocimeter sampling bias and its correction 12 p1727 A83-28840
- LDV measurements near a vortex shedding strut mounted in a pipe 12 p1721 A83-28842
- Spectral analysis algorithms for the laser velocimeter - A comparative study 12 p1728 A83-28961
- A comparison of experimental and numerical results obtained for the secondary flow in a large turbine cascade 12 p1696 A83-29157
- Separation of time-averaged turbulence components by laser-induced fluorescence 13 p1839 A83-30102

- Multichannel fiber-optic Doppler velocimeters 15 p2165 A83-34884
- Energy relationships in a laser Doppler velocimeter at the subcarrier 15 p2166 A83-35173
- Aerodynamic measurements about a rotating propeller with a laser velocimeter [AIAA PAPER 83-1354] 16 p2295 A83-36355
- An assessment of flow-field simulation and measurement [AIAA PAPER 83-1721] 17 p2509 A83-37210
- A remote laser-probe system for velocity and temperature measurements 17 p2509 A83-37394
- A thermistor probe for use in laser Doppler anemometry 17 p2512 A83-38861
- New developments in the field of laser Doppler wind velocity measurements. I - Theory and experimental verification 18 p2689 A83-39988
- Supersonic-nitrogen flow-field measurements with the resonant Doppler velocimeter 18 p2689 A83-40054
- Methods of laser Doppler anemometry --- Russian book 18 p2692 A83-40605
- Laser anemometry velocity measurements in a heated turbulent flow 19 p2843 A83-41322
- Analysis of instrument errors arising in velocity measurement by an LDV based on a Fabry-Perot interferometer 19 p2849 A83-41900
- Velocity measurements in a turbulent natural convection boundary layer 20 p2973 A83-42684
- Raman anemometry, a method for component-selective velocity measurements of particles in a flow 20 p2990 A83-42950
- LDA measurements of separated flows and a simple calculation method for the drag of a sharp-edged cylinder 20 p2929 A83-43006
- Measurement of surface rheological effects on a rotating flow 20 p2986 A83-43271
- Real-time measurements of spatial velocity distribution with a laser Doppler imaging system 21 p3136 A83-44151
- Velocity and turbulence measurements in combustion systems 21 p3131 A83-44684
- Comparison of photon correlation laser Doppler anemometry data processing techniques 21 p3139 A83-44798
- Aspects of light scattering by spherical particles 21 p3207 A83-44836
- Experimental study of the effect of the polarization of scattered waves on the signal of a laser Doppler velocimeter 21 p3142 A83-45311
- Laser-induced fluorescence technique for velocity field measurements in subsonic gas flows 22 p3287 A83-45962
- Effect of wall scattering on SNR in off-axis differential-type laser Doppler velocimetry 24 p3581 A83-48747
- New developments in the field of laser-Doppler wind velocity measurements. II - LDA-system for field measurements and its application 24 p3582 A83-49023
- Precautions that have to be taken in applying LDV to combustion chambers [ONERA, TP NO. 1983-112] 24 p3583 A83-49423
- Turbulence-induced statistical bias in laser anemometry 24 p3584 A83-49811
- Three-component laser-Doppler anemometry measurements in a circular mixing tube 24 p3585 A83-49824
- A 3-D laser Doppler velocimeter for use in high-speed flows 24 p3585 A83-49825
- A three component velocity measurement in an open channel by a combination of LDA and hot film anemometry 24 p3585 A83-49826
- Space-correlation measurement of attaching jets by the new scanning laser Doppler velocimeter using a diffraction grating 24 p3585 A83-49827
- LASER DRILLING**
- Diodes formed by laser drilling and diffusion 04 p0473 A83-16090
- Effect of laser produced pinholes upon the charging characteristics of spacecraft thermal control surfaces 05 p0608 A83-17499
- Localized metallic melting and hole boring by laser guided discharges 06 p0769 A83-19234
- Metal drilling investigation by means of different high power laser radiation 07 p0940 A83-21031
- Investigation of stresses in a plate with holes made by laser drilling 11 p1598 A83-28500
- Accuracy of an optical open area ratimeter 12 p1729 A83-29147
- Laser chemical etching of vias in GaAs 21 p3142 A83-43847
- The physical processes occurring during the deep penetration of metals by a laser beam 23 p3462 A83-48428

LASER FUSION

- Shockfronts as model targets in laser-plasma interaction experiments 10 p1487 A83-26173
- The high-power iodine laser --- Book 13 p1849 A83-30135
- A soft X-ray streak camera 14 p2022 A83-33416
- An experimental study of the absorption mechanisms in laser-matter interaction at high energies - The effect of wavelength --- French thesis 15 p2232 A83-33699
- Laser wavelength effect on the thermal conductivity and ablation in plasmas created by a laser --- French thesis 15 p2232 A83-33700
- Future development of high-power solid-state laser systems 16 p2358 A83-35884
- A study of ablation by laser irradiation of plane targets at wavelengths 1.05, 0.53, and 0.35 micron 18 p2749 A83-40519

LASER GEODYNAMIC SATELLITE

U LAGEOS (SATELLITE)

LASER GYROSCOPES

- Mechanically dithered RLG at the quantum limit --- Ring Laser Gyro 01 p0053 A83-11130
- Mass-produced laser gyros 02 p0176 A83-11628
- Integrated optics elements for an optical gyro 03 p0326 A83-13763
- From the pendulum to the laser gyroscope 05 p0644 A83-16899
- The fundamental precision limit of optical gyros 06 p0763 A83-19142
- A fiber-optic gyrometer in a gravitational field 08 p1105 A83-23165
- Ring laser gyroscopes - Charge-coupled device /CCD/ readout and signal processing for high resolution applications 09 p1267 A83-23590
- Control technology as applied to Space Telescope 09 p1218 A83-23592
- The laser gyro - Myth or panacea 09 p1270 A83-24858
- Guidance and flight control demonstration in a helicopter flight environment using a laser-gyro inertial navigation system 11 p1528 A83-28779
- Performance of a Strapdown Ring Laser Gyro Tetrad Inertial Navigation System in a helicopter flight environment 11 p1528 A83-28781
- The laser gyro as a self-contained inertial navigation aid 12 p1729 A83-29208
- A lab test to find the major error sources in a laser strapdown inertial navigator 12 p1706 A83-29211
- Laser gyro for instrumentation of advanced missile guidance system testing [AIAA PAPER 83-2271] 19 p2848 A83-41737
- Errors of a three-axis unit of laser gyroscopes with common initial displacement 19 p2850 A83-42018
- Ultra-stable laser clock - Second generation 20 p2989 A83-42576
- Fibre-optic gyroscope 21 p3135 A83-44075
- Mode matching for a passive resonant ring laser gyroscope 21 p3136 A83-44157
- DINS - Lessons learned and successes achieved --- ring laser gyro Dormant Inertial Navigation System for maneuvering reentry vehicles [AAS PAPER 83-084] 21 p3097 A83-44184
- Experimental investigation of the characteristics of magnetic mirrors at a wavelength of 1.15 micron --- for laser gyroscopes 23 p3459 A83-48493
- LASER HEATING**
- Effect of electronic excitations on laser heating of a stationary plasma 01 p0107 A83-10698
- Steady-state ablation of aluminium alloys by a CO₂ laser 01 p0054 A83-10701
- Time resolved study of superelastic collisions in laser excited strontium vapor 02 p0241 A83-12399
- Titanium ignition by the emission of a CO₂ laser 03 p0299 A83-14062
- Wavefront reversal in four-wave interaction in a medium with a thermal nonlinearity 07 p0934 A83-20107
- Transition from steady-state to pulsed gas breakdown near the surface of a target subjected to laser radiation 07 p0935 A83-20124
- CO₂-laser-induced deflagration of fuel/oxygen mixtures 07 p0882 A83-20732
- The thermal-emf mechanism of the oxidation kinetics of laser-irradiated metals 09 p1272 A83-24218
- Plasma production during vaporization of materials by the radiation from a CO₂ TEA laser 10 p1486 A83-25890
- Determination of absorption coefficients in shock heated propellant mixtures for laser-heated rocket thrusters 10 p1387 A83-26170
- Silicon melt, regrowth, and amorphization velocities during pulsed laser irradiation 10 p1490 A83-26269
- Instability of surface combustion on exposure to laser radiation 10 p1433 A83-26680
- Thermal action of laser radiation on imidization 10 p1392 A83-26690

- Combustion of carbon particles, initiated by laser radiation 10 p1392 A83-26777
- The heating and vaporization of water drops under the effect of radiation in the case of inhomogeneous internal heat-evolution 10 p1434 A83-26779
- Drop explosion under the effect of intense laser radiation 10 p1434 A83-26780
- LIMP in continuously coupled unstable resonator --- Laser Induced Medium Perturbation effect in pulsed carbon dioxide laser 12 p1731 A83-29155
- Narrow optical hole burning and related effects in ruby 12 p1782 A83-29198
- RECLAS - Resonant-enhanced CARS from C2 produced by laser ablation of soot particles 13 p1844 A83-30201
- Stepwise dependence of a portion of hot molecules on the intensity of exciting radiation 13 p1850 A83-30317
- A new type of laser probe --- for surface acoustic wave beam measurement 13 p1846 A83-30334
- Direct measurement of the melt depth of silicon during laser irradiation 13 p1929 A83-30351
- Hypervelocity erosion of carbon-carbon composites by laser simulation [AIAA PAPER 83-1440] 14 p1986 A83-32711
- Laser heat treatment - The state of the art 15 p2172 A83-33770
- The laser ignition of compact mixed compositions 18 p2663 A83-39171
- Phase transitions of solid particles of small dimension in the case of laser heating 18 p2664 A83-39494
- Laser-controlled chemical etching of aluminum 18 p2693 A83-40055
- Experimental determination of vapor species from laser-ablated carbon phenolic composites 19 p2823 A83-40875
- Collisional quenching of A 2Sigma(+) OH at elevated temperatures 20 p2950 A83-42633
- Atomic fluorescence study of high temperature aerodynamic levitation 20 p2939 A83-43256
- Calculation of heating of metals by continuous laser radiation in an oxidizing atmosphere 20 p2996 A83-43780
- Temperature dependence of the absorptivity of aluminum targets at the 10.6 microns wavelength 20 p2957 A83-43785
- Interferometric determination of slow movements --- thermal dilatation measurement on laser heated semiconductor surface 21 p3139 A83-44795
- Growth and characterization of single crystal refractory oxide fibers 22 p3358 A83-46629
- Carbon dioxide laser-induced fast signals from silicon photodiodes 22 p3301 A83-46826
- Reconstruction of the intensity distribution of heating radiation from the thermal damage profile of a thin plate 23 p3460 A83-47571
- The relationship between the optical properties of scale and its growth kinetics during laser ignition and combustion of metals 24 p3566 A83-49542
- Combustion regimes with laser-induced plasma 24 p3556 A83-49782
- A class of similarity solutions for the nonlinear thermal conduction problem 24 p3581 A83-50201
- LASER INTERFEROMETRY**
- On the application of variable shear double exposure interferometer for the study of heat transfer to or from solid surfaces 01 p0051 A83-11056
- Recent development in high speed cinematographic and interferometric studies of high power laser target interaction 01 p0052 A83-11067
- A Michelson interferometer for high resolution of shot start movement using a CO2 laser 01 p0052 A83-11068
- Application of a laser interferometer skin-friction meter in complex flows 01 p0053 A83-11075
- Surface recession measurements using a projected fringe technique 01 p0053 A83-11077
- Performance of LDI in predicting density profiles of compressible boundary layers --- laser differential interferometry 01 p0053 A83-11078
- Extending the laser-specklegram technique to strain analysis of rotating components 02 p0192 A83-12514
- Interferometric measurement of the electron density in laser-matter interaction --- French thesis 03 p0398 A83-13808
- Nozzle design yielding interferometrically flat fluid jets for use in single-mode dye lasers 03 p0332 A83-14164
- The precise measurement of gravitational acceleration using a laser interferometric technique 04 p0481 A83-15275
- Investigation of the ionization relaxation of shock-wave heated krypton with an HCN laser interferometer --- German thesis 04 p0536 A83-15842
- A laser interferometer for measuring skin friction in three-dimensional flows [AIAA PAPER 83-0385] 05 p0643 A83-16685
- Laser holographic interferometry for an unsteady airfoil in dynamic stall [AIAA PAPER 83-0388] 05 p0643 A83-16688
- Laser interferometer with low-frequency phase modulation 05 p0644 A83-17066
- Adaptive optics methods in interferometry 05 p0644 A83-17073
- Light-in-flight recording - High-speed holographic motion pictures of ultrafast phenomena 07 p0928 A83-20153
- Measuring amplitude and phase of microvibrations by heterodyne speckle interferometry 07 p0930 A83-20796
- An experimental study of the Dugdale model --- relation between crack tip displacement and applied load 08 p1119 A83-21787
- An improved schlieren system and some new results on acoustically excited jets 08 p1162 A83-21806
- Diagnostics of shock tube flows by laser interferometry 08 p1083 A83-22062
- In-plane interferometric strain/displacement measurement at high temperatures 09 p1264 A83-23363
- Velocity measurements of incident and reflected shock waves in various gases and in saturated water vapour 10 p1414 A83-26139
- Semiconductor integrated etalon interference laser with a curved resonator 10 p1430 A83-26206
- High-sensitivity laser interferometer based on a multimode optical waveguide 10 p1484 A83-26659
- Laser microspeckle technique in displacement measurement near a crack tip 11 p1575 A83-28701
- Optically recording interferometer for velocity measurements with subnanosecond resolution 11 p1575 A83-28706
- A simple fibre Fabry-Perot sensor 12 p1729 A83-29189
- Speckle interferometry, a simple method for deformation analysis 12 p1735 A83-29362
- Automated laser speckle interferometry displacement contour analyzer 12 p1730 A83-29587
- Aperture analysis of laser speckle interferograms 12 p1730 A83-29588
- Double-pass oblique-incidence interferometer for the inspection of nonoptical surfaces 13 p1845 A83-30204
- Progress in absolute distance interferometry 13 p1851 A83-31019
- Group combustion models and laser diagnostic methods in sprays - A review 14 p1990 A83-32938
- Wave-front dislocations - Topological limitations for adaptive systems with phase conjugation 15 p2228 A83-33526
- Autocorrelation of ultrashort optical pulses using polarization interferometry 15 p2230 A83-33764
- Modulation intracavity laser spectroscopy, polarimetry, and interferometry 15 p2163 A83-33979
- Nonintrusive laser-based particle diagnostics [AIAA PAPER 83-1514] 15 p2165 A83-34919
- Automatic photoelectric device with a laser interferometer for measuring photographs of limbs of meridian instruments 16 p2357 A83-36863
- Measurement of an object's displacements along six coordinates by a differential laser method 18 p2690 A83-40402
- How to detect the gravitationally induced phase shift of electromagnetic waves by optical-fiber interferometry 19 p2846 A83-40967
- Holographic laser scanners for multidirectional scanning 19 p2847 A83-41100
- Measuring laser flow fields with a 64-channel heterodyne interferometer 19 p2847 A83-41102
- Recording of interferograms on normal high resolution plates using a CO2 laser at 10.6 microns 19 p2847 A83-41103
- Interferometric displacement sensing in the open atmosphere 19 p2848 A83-41177
- Film cooling effectiveness of discrete holes measured by mass transfer and laser interferometer 20 p2983 A83-43017
- Autocollimation multibeam interferometer with spatial beam separation and its use in frequency selection of laser radiation 20 p2997 A83-43790
- Laser diagnostics of a nonuniform dense plasma 21 p3211 A83-44147
- An external cavity diode laser sensor 21 p3136 A83-44209
- Sensitive all-single-mode-fiber resonant ring interferometer 21 p3136 A83-44212
- A 28 micron water-vapor laser interferometer for plasma diagnostics 21 p3144 A83-44381
- A nonintrusive laser interferometer method for measurement of skin friction 21 p3138 A83-44677
- Single mode laser spectral spread repercussion in single-mode optical fiber coherent detection systems 21 p3145 A83-44832
- Measurement of coherence of radiation from diffusely illuminated beam splitters 21 p3140 A83-44842
- Laser optical measurements of density and temperature in flowing gases 22 p3291 A83-46487
- Setting up the Sagnac experiment in a gamma-ray ring interferometer --- Russian book 23 p3453 A83-47122
- Stark widths and shifts of singly ionized silicon spectral lines 24 p3631 A83-48836
- Observation of absorptive bistability with two-level atoms in a ring cavity 24 p3628 A83-48847
- LASER MATERIALS**
- Reversible nonradiative transfer of excitation energy in a system of strongly interacting particles --- in laser materials 01 p0055 A83-10817
- B-X transitions in HgCl and HgI --- for high power UV-visible lasers 01 p0055 A83-10980
- Influence of the active-medium inhomogeneity and of aperture stops on the output-beam parameters of a CO2 laser 03 p0330 A83-13585
- Optimal ring lasers with coupled resonators and a homogeneously broadened active medium 03 p0330 A83-13587
- Energy transfer and lasing in phosphate glasses activated with chromium, ytterbium, and erbium 03 p0331 A83-13594
- Polymeric passive laser shutters 04 p0484 A83-15265
- Coherent transitional processes in the presence of standing waves 04 p0484 A83-15270
- Material parameters of In(1-x)/Ga(x)/As(y)/P(1-y) and related binaries 04 p0542 A83-16064
- A distributed-feedback tunable laser with dye-activated polymer matrices 04 p0486 A83-16325
- Spectral characteristics of the extraction of excitation energy from neodymium glass amplifiers 05 p0649 A83-17051
- Weak diffraction approximation in the theory of a ring laser with a Gaussian stop 05 p0649 A83-17053
- Using estimates of the effect of heating on the operation of a solid-state laser to select the laser parameters 05 p0651 A83-17662
- Kinetic studies of Kr2F/asterisk/ in electron-beam excited mixtures 06 p0766 A83-18953
- Phonons in Group II B-Group VI A semiconductors /Review/ 06 p0815 A83-19573
- Passively Q-switched laser utilizing concentrated Li-Nd-La phosphate glass 07 p0933 A83-20102
- Investigation of the active medium in a fast-flow closed-cycle industrial CO2 laser 07 p0933 A83-20105
- Investigation of the operation of dispersive optical components 07 p0995 A83-20115
- Propagation of interacting first and second optical harmonics in a nonlinear active medium 07 p0934 A83-20118
- Production of electronically excited bismuth in a supersonic flow 07 p0936 A83-20726
- Repetitive passive Q-switching and bistability in lasers with saturable absorbers 08 p1107 A83-22079
- Optical distortion and far field measurements for laser window materials 08 p1108 A83-22458
- Characterization of candidate laser window materials 09 p1272 A83-24971
- Actively cooled silicon mirrors --- for high energy cw lasers 09 p1346 A83-24972
- Infrared optics hot pressed from fluoride glass 09 p1239 A83-24973
- Selective and uniform laser-induced failure of antireflection-coated LiNbO3 surfaces 10 p1429 A83-26030
- Temperature dependence of the excited-state absorption of alexandrite 10 p1429 A83-26031
- Heat load limits in laser mirrors with a cooled porous backing 10 p1430 A83-26256
- Spectral composition of the radiation emitted from a concentrated LiNdLa phosphate glass laser with a Q switch made of a LiF crystal with F2/-/ centers 10 p1432 A83-26662
- Influence of a nonlinear active medium on the structure of natural oscillation modes of a Fabry-Perot interferometer 10 p1433 A83-26681
- Semiconductor lasers 11 p1576 A83-27502
- Progress in the development of color centers for stable CW tunable laser operation 11 p1578 A83-27542
- Three wavelength laser emission in Ho:YLF via sequential cascade 11 p1578 A83-27544
- Tunable visible lasers using defects in oxides 11 p1578 A83-27545
- Diatomic molecules as storage media for high energy lasers 11 p1580 A83-27573
- Optical transitions of RbMgF3:Eu(2+/-) and RbMgF3:Mn(2+/-),Eu(2+/-) 11 p1581 A83-27590

- New data on nonradiative relaxation of impurity center excitations in laser materials 11 p1581 A83-27591
- Radiationless processes and their implications for new laser materials 11 p1581 A83-27593
- Some surprising results in studies of transition-metal-doped crystals --- materials for tunable lasers 11 p1581 A83-27595
- Erbium glass lasers and their applications 11 p1583 A83-27620
- The optical properties and applications of germanium semiconductor single crystals 11 p1657 A83-28368
- Physical nature of the degradation of light emitting diodes and semiconductor lasers 13 p1849 A83-30261
- Spectroscopy of the isoelectronic nitrogen addition in epitaxial structures based on wide-band solid solutions of the system In-Ga-P-As 13 p1927 A83-30262
- Synthesis and investigation of GdScO₃ single crystals, activated by Nd(3+) ions 13 p1849 A83-30263
- Modal analysis of separate-confinement heterojunction lasers with inhomogeneous cladding layers 13 p1851 A83-30750
- Diffraction splitting of frequencies in a ring laser with a misaligned quadratically homogeneous active element 14 p2023 A83-31910
- The vibronic spectra of neodymium-doped crystals 14 p2025 A83-32830
- Ultrashort pulse propagation in saturable media - A simple physical model 14 p2025 A83-33404
- Kinetics of formation of krypton-halogen atom exciplexes in electron beam irradiated gases 16 p2358 A83-35436
- Infrared temperature tunability in GaSe, HgS, and Tl₃AsSe₃ nonlinear devices 16 p2359 A83-35954
- Cathode materials for sealed CO₂ waveguide lasers 16 p2360 A83-35962
- Temperature requirements and corrosion rates in combustion driven hydrogen fluoride supersonic diffusion lasers 19 p2850 A83-40857
- Temperature effects in AgGaS₂ nonlinear devices 21 p3143 A83-44158
- Window and mirror materials for use at 10.6 micron 21 p3144 A83-44788
- Laser induced damage in the ultraviolet 21 p3145 A83-44831
- Passive mode locking of a long pulse XeCl laser 22 p3299 A83-46724
- Neodymium laser glasses as optical media for luminescent solar concentrators 23 p3476 A83-47169
- Analysis of the spin-Hamiltonian parameters for Cr(3+) in mirror and inversion symmetry sites of alexandrite (Al_{1/2}-x/Cr_x/BeO₄) - Determination of the relative site occupancy by EPR 23 p3461 A83-47630
- A theoretical model for multiple-pulse laser-induced damage to metal mirrors 24 p3587 A83-48911
- Several generation parameters of a CO₂ gasdynamic laser with a high-temperature regenerative-heat-transfer heater of the working gas 24 p3588 A83-48936
- ### LASER MICROSCOPY
- Scanning photoacoustic microscopy /SPAM/ of Si₃N₄ ceramic test bars 04 p0463 A83-15220
- Quantitative flaw characterization by means of the Scanning Laser Acoustic Microscope /SLAM/ 04 p0493 A83-15227
- Holography at X-ray wavelengths 11 p1572 A83-27534
- Channeling contrast microscopy - Application to semiconductor structures 13 p1929 A83-31067
- ### LASER MODE LOCKING
- Perfect mode locking of solid-state lasers by a double passive modulation 01 p0054 A83-10616
- Transient pulse evolution of active mode locking in an intracavity frequency-doubled laser 01 p0054 A83-10642
- Passive mode locking of lasers with a tunable dye cell 02 p0183 A83-11561
- Frequency locking to absorption lines by wave competition in a tunable ring dye laser 02 p0185 A83-12302
- Injection-locking of TEA CO₂ lasers by an orthogonally-polarised injection source 02 p0185 A83-12400
- Gas laser mode-locking using an external acousto-optic modulator with a potential application to passive ring gyroscopes 02 p0185 A83-12589
- Continuous wave high-power, high-temperature semiconductor laser phase-locked arrays 03 p0333 A83-14932
- FM sideband injection locking of diode lasers 04 p0483 A83-15240
- Mode-locked semiconductor lasers and their spectroscopic applications 04 p0485 A83-15805
- Stable single-mode operation of a Q-switched laser by a simple resonator length control technique 04 p0485 A83-15948
- Influence of the spatial structure of the gain on the dynamic properties of a laser 05 p0650 A83-17075
- Injection-locked dye laser pumped and injected by a pulsed xenon-ion laser 06 p0767 A83-19144
- Single longitudinal mode operation of high power multiple-stripe injection lasers 06 p0767 A83-19256
- Injection locking of wide-aperture TEA CO₂ lasers 07 p0935 A83-20151
- Influence of transient absorber gratings on the pulse parameters of passively mode-locked CW dye ring lasers 07 p0937 A83-21362
- Theory of line narrowing and frequency selection in an injection locked laser 07 p0938 A83-21600
- Design of double passive modulated mode-locked lasers 08 p1107 A83-22333
- Diffraction coupled phase-locked semiconductor laser array 10 p1430 A83-26203
- Resonances of the polarization of gas laser radiation under mode self-locking conditions 10 p1433 A83-26688
- Continuous-wave YAG:Nd/3+ / laser with mode locking and intracavity frequency doubling 10 p1434 A83-26695
- Injection locking of excimer lasers 11 p1577 A83-27518
- New types of mode locking in stimulated radiation in optical resonators 11 p1578 A83-27539
- Real time monitoring of CW mode-locked dye laser pulses using a rapid-scanning autocorrelator 12 p1729 A83-29194
- Mode-locking in solid-state and semiconductor lasers --- Book 13 p1849 A83-30133
- A passive film gate for mode-locked infrared lasers 13 p1850 A83-30267
- Phase-locked (GaAl)As laser emitting 1.5 W CW per mirror 13 p1850 A83-30330
- Passive mode locking of buried heterostructure lasers with nonuniform current injection 13 p1852 A83-31057
- Microtron free-electron laser experiment 13 p1854 A83-31124
- Passive mode locking in iodine photodissociation laser 14 p2023 A83-31913
- Passive mode lockers for lasers generating at a wavelength of 1.06 micron 14 p2025 A83-32832
- Femtosecond optical pulses 14 p2025 A83-33402
- Pulse shaping in passively mode-locked ring dye lasers 14 p2025 A83-33405
- Calculation of the colliding pulse mode locking in CW dye ring lasers 14 p2026 A83-33406
- Compression mechanism of subpicosecond pulses by malachite green dye in passively mode-locked rhodamine 6G/DODCI CW dye lasers 14 p2026 A83-33407
- Single and double mode-locked ring dye lasers - Theory and experiment 14 p2026 A83-33408
- Passive mode locking of flashlamp-pumped dye lasers in the 508-583 nm range 14 p2026 A83-33411
- Spectral development of picosecond pulses of mode-locked Nd-glass lasers 14 p2026 A83-33412
- Characterization of pulsed Nd:YAG active/passive mode-locked laser 14 p2026 A83-33414
- Measurement conditions for continuously recording picosecond pump-and-probe spectrometers 14 p2022 A83-33419
- Amplitude and phase nonlinear response of bleachable dyes using picosecond excitation 14 p2026 A83-33431
- A single-block hexagonal electrooptical Q-switch 14 p2085 A83-33433
- Single-mode operation of Doppler-broadened lasers by injection locking 15 p2167 A83-33761
- Dye laser spectrum narrowing by 'double pulse' flashlamp pumping 15 p2169 A83-34369
- New scheme for ultrashort-pulsed Nd(3+):YAG laser operation A branched cavity, internally seeded regenerative amplifier 15 p2169 A83-34455
- Radiation characteristics of a multimode linear Zeeman laser 15 p2170 A83-34703
- Generation of coherent picosecond pulses using mode-locked semiconductor lasers 16 p2358 A83-35886
- Experimental and theoretical investigations of the influence of a saturation grating in an absorber on pulse generation in a passively mode-locked dye laser 16 p2359 A83-35887
- Mode selection and frequency tuning by injection in pulsed TEA-CO₂ lasers 16 p2360 A83-35963
- Microwave signal generation with injection-locked laser diodes 17 p2515 A83-38887
- Passive mode locking in the blue spectral region 17 p2515 A83-38969
- Phase-locked InGaAsP laser array with diffraction coupling 18 p2693 A83-40051
- Modulation detuning characteristics of actively mode-locked diode lasers 19 p2852 A83-40939
- Intracavity mode-locked and frequency-doubled Nd:YAG laser Pump- and mode-size effects 20 p2993 A83-42225
- Mode-locked semiconductor lasers with gateable output and electrically controllable optical absorber 20 p2995 A83-43595
- Mode locking in a fiber laser 20 p2997 A83-43798
- High resolution spectroscopy using picosecond pulse trains 21 p3140 A83-44818
- Far-field distributions of semiconductor phase-locked arrays with multiple contacts 21 p3145 A83-44953
- Generation of single-longitudinal-mode gigabit-rate optical pulses from semiconductor lasers through harmonic-frequency sinusoidal modulation 21 p3145 A83-44956
- Wavelength-discriminating photodetector for lightwave systems 21 p3208 A83-44957
- Efficient femtosecond optical Kerr shutter 21 p3208 A83-45477
- Broadly tunable mode-locked HgCdTe lasers 21 p3146 A83-45478
- Control of mutual phase locking of monolithically integrated semiconductor lasers 21 p3146 A83-45482
- Synchronously mode-locked continuous wave dye lasers - Recent advances and applications 22 p3297 A83-46664
- Subpicosecond pulses from a synchronously mode-locked traveling-wave ring dye laser 22 p3297 A83-46665
- Comparisons of traveling-wave and standing-wave operations of mode-locked continuous-wave dye lasers 22 p3297 A83-46666
- Two-photon pumped synchronously mode-locked bulk GaAs laser 22 p3298 A83-46668
- Continuous-wave mode locked Nd:YAG laser - A picosecond pump source for the future 22 p3298 A83-46669
- Developments in mode-locked lasers and their applications 22 p3298 A83-46670
- Optical switches for generation and pulse shaping of ultrashort electrical pulses 22 p3278 A83-46677
- Accurate range gating technique with mode-locked dye lasers 22 p3298 A83-46680
- Gigabit optical pulse generations in integrated lasers 22 p3298 A83-46681
- Picosecond photofragmentation experiments with a repetitively pulsed mode-locked Nd:phosphate glass laser system 22 p3266 A83-46684
- Passive mode locking of a long pulse XeCl laser 22 p3299 A83-46724
- Bistable operation of a dual-wavelength synchronously mode-locked CW dye laser 23 p3463 A83-48705
- Coupled-wave theory regarding phase-locked-array lasers 23 p3464 A83-48715
- A prism reflector of anti-resonant ring configuration 24 p3586 A83-48749
- Bandwidth-limited picosecond pulse generation in a synchronously pumped GaAs laser containing a variable absorber diode 24 p3586 A83-48783
- The generation of ultrashort laser pulses 24 p3586 A83-48801
- Ultrashort optical pulse generation from microwave modulated AlGaAs diode laser with Selfoc rod resonator 24 p3588 A83-49611
- Generation of single longitudinal mode pulses in passively Q-switched lasers via passive pre-lasing 24 p3589 A83-49614
- Optical injection locking of X-band FET oscillator using coherent mixing of GaAlAs lasers 24 p3630 A83-49991
- ### LASER MODES
- Gas discharge lasers --- Russian book 01 p0054 A83-10673
- Scaling laws for the mode purity of simple TEA CO₂ lasers 01 p0054 A83-10696
- The use of the pulse-repetition mode of a CO₂ electroionization laser for laser welding 02 p0187 A83-11957
- On spontaneous emission into guided modes with curved wavefronts 02 p0184 A83-12264
- High-power multiple-stripe injection lasers with channel guides 02 p0184 A83-12269
- Influence of quadratic pump power distribution on hole burning in neodymium lasers 02 p0185 A83-12598
- Continuous-wave garnet ring laser emitting single-mode linearly polarized radiation and intracavity second harmonic generation in LiIO₃ 03 p0330 A83-13584
- Influence of the active-medium inhomogeneity and of aperture stops on the output-beam parameters of a CO₂ laser 03 p0330 A83-13585
- Influence of an axial magnetic field on the frequency shifts in a two-mode He-Ne/CH₄ laser 03 p0331 A83-13589
- Novel semiconductor lasers for integrated optics 03 p0331 A83-13765

- High-power single-mode AlGaAs laser diodes
03 p0331 A83-13875
- Nozzle design yielding interferometrically flat fluid jets for use in single-mode dye lasers
03 p0332 A83-14164
- Improved orotron performance in the 50- to 75-GHz frequency region
03 p0314 A83-14516
- Investigations of optically pumped submillimeter wave laser modes
04 p0485 A83-15814
- Transformation of the spatial statistics of a partially coherent light beam in a nonlinear medium
04 p0485 A83-15902
- Saturation characteristics of a free-electron laser with a large undulator length
04 p0485 A83-15904
- Theory of rotating mirror Q-switching in a helical transversely excited CO₂ laser
04 p0485 A83-16056
- Single-mode lasers for optical communications
04 p0486 A83-16213
- 'Nonwaveguide'-mode semiconductor injection lasers
04 p0486 A83-16214
- Longitudinal mode competition in semiconductor lasers - Rate equations revisited
04 p0486 A83-16217
- Spatial mode discrimination and control in high-power single-mode constricted double-heterojunction large-optical-cavity diode lasers
05 p0648 A83-16942
- Polarization coupling effects in transversely excited atmospheric CO₂ lasers - Application to single axial mode operation
05 p0648 A83-16943
- Influence of lateral waveguiding properties on the longitudinal mode spectrum for semiconductor lasers
05 p0648 A83-16944
- Investigation of the mode competition in an He-Ne/CH₄ laser with independent variation of the mode spacing and spatial shift
05 p0648 A83-17046
- Weak diffraction approximation in the theory of a ring laser with a Gaussian stop
05 p0649 A83-17053
- Dye lasers --- in tunable high-power modes
05 p0650 A83-17224
- Regular and chaotic behaviour of multimode gas lasers
05 p0651 A83-17893
- High-performance single-mode AlGaAs Gaussian channel substrate planar laser diodes
06 p0765 A83-18566
- Anomalous tuning of single mode AlGaAs diode lasers
06 p0765 A83-18901
- Mode partition noise characteristics in high-speed modulated laser diodes
06 p0766 A83-18902
- Role of the conductivity of the confining layers in DH-laser spatial hole burning effects
06 p0766 A83-18903
- Stability of the horizontal transverse modes of the planar stripe lasers with deep Zn-diffusion
06 p0766 A83-19141
- Transversely excited Sr/⁺/ recombination laser
06 p0767 A83-19251
- High power single mode InGaAsP lasers fabricated by single step liquid phase epitaxy
06 p0767 A83-19254
- Rapid-flow combined-action industrial CO₂ laser
07 p0933 A83-20104
- Stimulated bremsstrahlung effect in multimode laser radiation field
07 p0934 A83-20120
- Prediction of transverse-mode selection in double heterojunction lasers by an ambipolar excess carrier diffusion solution
08 p1107 A83-22332
- Multilongitudinal mode operation in angled stripe buried heterostructure lasers
08 p1107 A83-22342
- Wavefront sensing and control aspects in a high energy laser optical train
08 p1109 A83-22467
- The measurement of the dispersion of the intensity fluctuations during the reflection of multimode laser beams in the atmosphere
09 p1273 A83-25085
- Mode effects in second harmonic generation and their uses for laser stabilization
10 p1425 A83-25404
- Influence of Doppler broadening on the stability of monomode ring lasers
10 p1425 A83-25430
- Quantum/classical mode evolution in free electron laser oscillators
10 p1426 A83-26004
- Noise and longitudinal mode characteristics of GaAl/As TS lasers with reduced facet reflectivities
10 p1429 A83-26029
- Multimode theory of free-electron laser oscillators
10 p1431 A83-26275
- Synthesis of spatial filters for investigation of the transverse mode composition of coherent radiation
10 p1432 A83-26669
- Mode structure of a DFB gas laser
11 p1578 A83-27547
- The interaction between single-mode laser radiation and sodium vapour in a Fabry-Perot etalon and a ring optical cavity
11 p1657 A83-27850
- Pulse evolution and mode selection characteristics in a TEA-CO₂ laser perturbed by injection of external radiation
12 p1731 A83-29195
- High-speed direct single-frequency modulation with large tuning rate and frequency excursion in cleaved-coupled-cavity semiconductor lasers
13 p1850 A83-30332
- Hamiltonian picture of the free-electron laser - Multimode, super mode and all that
13 p1854 A83-31120
- Optical mode control in the free-electron laser
13 p1854 A83-31121
- Resonator mode structure --- in free electron lasers
13 p1854 A83-31122
- Natural fluctuations in a multimode standing-wave laser
14 p2023 A83-31909
- A classification scheme for the light-current (L/I) characteristics of a two photon mode semiconductor laser
14 p2024 A83-32447
- Space-time and space-averaged equations for a two-mirror laser - Theory and numerical results
14 p2025 A83-32917
- Passive mode locking of flashlamp-pumped dye lasers in the 508-583 nm range
14 p2026 A83-33411
- A high-power, single-mode laser with twin-ridge-substrate structure
14 p2027 A83-33438
- Complete experimental evaluation of the carrier dependence of the refractive index from the frequency modulation spectra of single mode injection lasers
15 p2168 A83-33841
- Influence of Lorentz broadening on the stability of monomode ring lasers
15 p2169 A83-34370
- Analysis of multielement semiconductor lasers
16 p2357 A83-35428
- Theoretical investigation of the spectral properties of gas lasers
16 p2359 A83-35889
- Problems in steady-state theory of a multimode laser with a selective saturable absorber
16 p2359 A83-35896
- Mode structure of a tapered-wiggler free-electron laser stable oscillator
16 p2360 A83-35960
- Crystal growth of mode-stabilized semiconductor diode lasers by liquid-phase epitaxy
16 p2420 A83-35987
- The wavefront curvature of an optically pumped waveguide laser
17 p2514 A83-37762
- Direct amplitude modulation of short-cavity GaAs lasers up to X-band frequencies
17 p2514 A83-38042
- Beam-propagation analysis of stripe-geometry semiconductor lasers - Threshold behavior
17 p2514 A83-38043
- The design and manufacture of a prototype for absolute measurement of laser wavenumbers
17 p2511 A83-38431
- An instrument for absolute or relative measurement of wavenumbers of a continuous or pulsed laser - The sigmameter. Application to the spectroscopic study of the D lines of a series of alkaline radioactive isotopes --- French thesis
17 p2512 A83-38432
- Stable single-longitudinal-mode operation under high-speed direct modulation in cleaved-coupled-cavity GaInAsP semiconductor lasers
17 p2515 A83-38885
- Synchrotron instability for long pulses in free electron laser oscillators
17 p2515 A83-38970
- Disappearance of laser instabilities in a Gaussian cavity mode
17 p2515 A83-38973
- Photon antibunching effect and statistical properties of single-mode emission in free-electron lasers
18 p2694 A83-40411
- Anomalous longitudinal mode behavior of a deep Zn-diffused GaAs/GaAlAs laser
19 p2850 A83-40736
- Effect of an active layer thickness on lateral and longitudinal modes of a gain guiding laser with a tapered stripe structure
19 p2850 A83-40737
- On the high power limit of the laser linewidth
19 p2851 A83-40927
- Coherence properties of gain- and index-guided semiconductor lasers
19 p2851 A83-40933
- Effect of temporal nonstationarity on the spectrum of injection lasers
19 p2852 A83-40940
- Multi-mode CW dye laser
19 p2853 A83-41187
- Cylindrical Gaussian-Hermite modes in rectangular waveguide resonators --- for free electron lasers
20 p2968 A83-43375
- Electron-diffractive mode selection in free electron lasers
20 p2995 A83-43632
- Temporal and interference fringe analysis of excimer TEM₀₁ zone laser modes
21 p3142 A83-43874
- Mode matching for a passive resonant ring laser gyroscope
21 p3136 A83-44157
- Self-pulsing and chaos in inhomogeneously broadened single mode lasers
21 p3143 A83-44192
- Dynamic single-mode semiconductor lasers with a distributed reflector
21 p3144 A83-44217
- A 1.59 micron wavelength GaInAsP/InP distributed feedback laser with first-order grating on anti-meltback layer
21 p3144 A83-44500
- Operation and performance of the CW visible atomic mercury laser
21 p3145 A83-44813
- A He-Sr laser with a mean power of 3 W
21 p3147 A83-45504
- Temporal coherence characteristics of InGaAsP laser diode with single-longitudinal-mode oscillation
22 p3295 A83-45972
- Functional life testing of multimoded lasers for digital communications applications
22 p3296 A83-46614
- Narrow diffused stripe GaAs/GaAlAs lasers for high speed integrated optical transmitters
22 p3297 A83-46655
- Stability of a detuned single mode homogeneously broadened ring laser
23 p3462 A83-48319
- Longitudinal mode spectrum of GaAs injection lasers under high-frequency microwave modulation
24 p3586 A83-48780
- First-passage-time distributions and switching statistics in a bistable two-mode laser
24 p3587 A83-48840
- Picosecond spectra of gain-switched quarterwave lasers
24 p3589 A83-49612
- The amplification of a polarized signal by an anisotropic laser superregenerative amplifier in the linear mode
24 p3589 A83-49738
- The effect of the mode structure of laser radiation on the stability of lead azide
24 p3557 A83-49795

LASER OUTPUTS

- A medical laser unit for continuous operation
01 p0054 A83-10559
- Scaling laws for the mode purity of simple TEA CO₂ lasers
01 p0054 A83-10696
- Effect of electronic excitations on laser heating of a stationary plasma
01 p0107 A83-10698
- Observations of grains in the extreme ultraviolet
01 p0104 A83-10859
- A study of the excitation threshold and intensity of stimulated Raman scattering in rubidium vapor at various pump spectrum widths
01 p0055 A83-10913
- 200-MHz electrodeless discharge excitation of an XeF laser
01 p0055 A83-10982
- Wide aperture self-sustained discharge KrF and XeCl lasers
01 p0055 A83-10984
- The effect of IR radiation on generation in Gunn diodes
01 p0044 A83-11311
- Raman gain in 12-micron NH₃ lasers
02 p0183 A83-11560
- Vector polynomials orthogonal to the gradient of Zernike polynomials --- in measurement of laser beam phase
02 p0175 A83-11562
- Photon-counting statistics of pulsed light sources [AD-A124141]
02 p0175 A83-11563
- A high-power polarised coherent TE N₂ laser
02 p0183 A83-12011
- The effect of a weak axial magnetic field on a He-Cd laser
02 p0184 A83-12085
- A tunable emerald laser
02 p0184 A83-12263
- High-power multiple-stripe injection lasers with channel guides
02 p0184 A83-12269
- Dispersion-induced instability in CW laser oscillators
02 p0184 A83-12270
- Quantum statistics of light after saturated two-photon emission processes and the photon statistics of a two-photon laser
02 p0185 A83-12401
- High repetition rate mini TEA CO₂ laser using a semiconductor preionizer
02 p0185 A83-12816
- Miniature solid-state directional laser Doppler velocimeter
02 p0183 A83-13043
- Uniformity of an externally sustained steady-state volume discharge
03 p0392 A83-13196
- Atomic collisions in the presence of laser radiation - Time dependence and the asymptotic wave function [AD-A126927]
03 p0391 A83-13247
- A proposed new method for damping relaxation oscillations in laser diodes
03 p0330 A83-13560
- Kinetic processes in the HgBr/B-X//HgBr₂ dissociation laser
03 p0331 A83-13917
- Calculated threshold current of GaAs quantum well lasers
03 p0331 A83-13918
- Numerical modeling of processes occurring in the cavity of a CW chemical HF laser on the basis of Navier-Stokes equations
03 p0332 A83-14061
- Gasdynamic laser --- Book
03 p0332 A83-14100
- Simple arrangement for spatially scanning gain measurements in CW lasers
03 p0332 A83-14165
- Optical coherence effects on a fiber-sensing Fabry-Perot interferometer
03 p0330 A83-14390
- Improved orotron performance in the 50- to 75-GHz frequency region
03 p0314 A83-14516
- High quantum efficiency InGaAsP/InP lasers
03 p0333 A83-14931
- Picosecond, tunable ArF/asterisk/ excimer laser source
03 p0333 A83-14933
- Operating efficiencies in pulsed carbon dioxide lasers
03 p0333 A83-14934

High-power individually addressable monolithic array of constricted double heterojunction large-optical-cavity lasers 03 p0333 A83-14935

High-luminosity solid-state lasers 04 p0483 A83-15254

Atmospheric- and supraatmospheric-pressure CO₂ lasers with a self-maintained discharge 04 p0483 A83-15256

The angular divergence of radiation from flowing gas lasers 04 p0483 A83-15258

Control of the spatial characteristics of laser radiation based on the electro-optical effect in crystals 04 p0483 A83-15259

The optimal control of laser beams in nonlinear media 04 p0483 A83-15261

The effects of light scattering on the directivity of radiation from unstable-resonator lasers 04 p0484 A83-15266

Spectrum control of laser radiation by means of linear phase anisotropy, induced in an amplifying or absorbing medium by an external magnetic field 04 p0484 A83-15268

Two-coordinate acoustooptic Q-switch for a YAG-Nd/3+ / laser with nonpolarized radiation 04 p0484 A83-15271

The control of solid-state laser radiation by paratellurite acoustooptic devices 04 p0484 A83-15274

Spatial coherence of laser light propagating in an optical fibre 04 p0535 A83-15793

Saturation characteristics of a free-electron laser with a large undulator length 04 p0485 A83-15904

He-Ne laser generation of 1.15-1.20 microns in a hollow copper cathode 04 p0485 A83-15950

Theory of rotating mirror Q-switching in a helical transversely excited CO₂ laser 04 p0485 A83-16056

Gain, saturation, and optimization of the XeF discharge laser 04 p0485 A83-16057

Polarization control of an antireflection-coated GaAlAs laser diode by an external optical feedback 04 p0535 A83-16092

Longitudinal mode competition in semiconductor lasers - Rate equations revisited 04 p0486 A83-16217

Forward bias voltage characteristics for /GaAl/As and /GaN/ /AsP/ lasers 04 p0486 A83-16222

Alexandrite-laser performance at high temperature 05 p0647 A83-16838

A fast wave of gas-ionization in a laser beam 05 p0686 A83-16892

Catastrophic degradation level of visible and infrared GaAlAs lasers 05 p0647 A83-16941

Spatial mode discrimination and control in high-power single-mode constricted double-heterojunction large-optical-cavity diode lasers 05 p0648 A83-16942

Analysis of the energetics of a chemical oxygen-iodine laser 05 p0648 A83-17047

Investigation of a high-efficiency photodissociation laser operating in the free-lasing regime 05 p0649 A83-17054

Technological CW CO₂ laser with a nonself-sustained discharge 05 p0649 A83-17067

Influence of electron heating during recombination of copper atoms in copper halide vapor lasers on their output parameters 05 p0650 A83-17068

Two-frequency helium-neon laser in a transverse magnetic field 05 p0650 A83-17078

Pulsed high-pressure chemical HF laser with electric-discharge initiation 05 p0650 A83-17084

Investigation of preionization CO and CO₂ lasers operating in the active zone of a stationary nuclear reactor 05 p0650 A83-17085

Dye lasers --- in tunable high-power modes 05 p0650 A83-17224

Transient radiation screening of silicon devices using backside laser irradiation --- for military IIC hardness against EMP 05 p0628 A83-17527

Design of a XeF-pumped second Stokes amplifier for blue-green production in H₂ 05 p0651 A83-17877

Observation of bifurcation to chaos in an all-optical bistable system 05 p0686 A83-17935

Coherent emission from electron clusters in free-electron lasers 06 p0765 A83-17981

Photocounting statistics associated with temperature fluctuations in semiconductor lasers 06 p0765 A83-18592

Direct modulation of semiconductor injection lasers 06 p0765 A83-18762

A theoretical and experimental analysis of modulated laser fields and power spectra 06 p0766 A83-18908

Forming of ultrafast light pulses with predetermined temporal shape 06 p0766 A83-18957

An UV-preionized KrF excimer laser with an output energy of 0.42 J 06 p0766 A83-19143

Injection-locked dye laser pumped and injected by a pulsed xenon-ion laser 06 p0767 A83-19144

Transversely excited Sr/ + / recombination laser 06 p0767 A83-19251

High power single mode InGaAsP lasers fabricated by single step liquid phase epitaxy 06 p0767 A83-19254

Single longitudinal mode operation of high power multiple-stripe injection lasers 06 p0767 A83-19256

Polarized fluorescence line narrowing measurements of Nd laser glasses - Evidence of stimulated emission cross section anisotropy 06 p0767 A83-19258

The effect of the nozzle profile on the characteristics of a gas-dynamic laser 06 p0767 A83-19440

Laser switching of constant and radio-frequency signals 06 p0768 A83-19574

IR and UV laser activity in a slit-shaped copper hollow cathode --- German thesis 06 p0768 A83-19617

Flowfield experiments on a DF chemical laser 07 p0932 A83-19815

Optically pumped sodium-dimer supersonic-beam laser 07 p0933 A83-19981

Characteristics of Schottky diodes at 10.6 microns 07 p0918 A83-19988

Photon-assisted tunneling at 246 and 604 GHz in small-area superconducting tunnel junctions 07 p0999 A83-19995

Spatial, temporal, and power characteristics of a streamer CdS semiconductor laser 07 p0933 A83-20101

Influence of translational and rotational relaxation on the specific energy characteristics of a CW chemical HF laser 07 p0933 A83-20103

Light-induced drift in cascade excitation of levels --- laser effects on atomic energy levels 07 p0934 A83-20117

Stimulated bremsstrahlung effect in multimode laser radiation field 07 p0934 A83-20120

Calculation of the energy characteristics of a pulse-periodic electron-beam-controlled CO₂ laser with a cooled active mixture 07 p0935 A83-20131

New heartbeat phenomenon, and the concept of 2-D optical turbulence 07 p0935 A83-20160

Electronic beam steering of semiconductor injection lasers - A theoretical analysis 07 p0935 A83-20162

Nuclear-reactor pumped lasers excited by ion-ion neutralization 07 p0936 A83-20728

The spectrum of strong intensity fluctuations of light beams in randomly irregular media 07 p0937 A83-20875

Compact repetitively pulsed excimer laser 07 p0938 A83-21383

A sealed 100-Hz CO₂ TEA laser using high CO₂ concentrations and ambient-temperature catalysts 08 p1107 A83-21983

Wavefront distortions in power optics; Proceedings of the Meeting, San Diego, CA, August 27, 28, 1981 08 p1107 A83-22449

Phase aberrations and laser output beam quality 08 p1108 A83-22450

Limitations on the use of root-mean-square /rms/ phase to describe beam quality characteristics --- of high power lasers 08 p1108 A83-22451

Aberrations in high power laser systems 08 p1108 A83-22452

Wavefront distortion introduced by sampling with a hole grating --- high power laser beam diagnostics 08 p1108 A83-22455

Fresnel ripple mapping of water-cooled laser mirrors 08 p1108 A83-22457

Medium induced phase aberrations in continuous wave /CW/ hydrogen fluoride chemical lasers 08 p1109 A83-22460

Intracavity phase conjugation --- for high power lasers 08 p1109 A83-22463

Continuous-wave HF R-branch laser demonstration 08 p1110 A83-22637

Underwater measurements of off-axis radiance compared with various analytical treatments of the radiative transfer equation - A comment 08 p1161 A83-22673

Diode laser threshold current density and lasing wavelength as functions of active region thickness 08 p1110 A83-22751

High optical power CW operation in visible spectral range by window V-channeled substrate inner stripe lasers 08 p1110 A83-22753

Infrared calibration facilities at Newark Air Force Station 08 p1047 A83-22875

Analysis, design and construction of rare-gas halide discharge lasers 09 p1271 A83-23695

Optical bistability of a CO₂ laser with intracavity saturable absorber Experiment and model 09 p1271 A83-23710

Ferroelectric crystals for the control of laser radiation --- Russian book 09 p1271 A83-23815

Propagation model of laser beams in turbulence 09 p1271 A83-24084

Scattering of laser beams and the optical potential well for a homogeneous sphere 09 p1272 A83-24088

Single-parameter characterization of bistability in double contact injection lasers 09 p1273 A83-25285

High power pulsed FIR laser lines from CD₃OH 10 p1425 A83-25429

A self-setting attenuator for laser pulse energy stabilization 10 p1425 A83-25431

Transient response in absorptive bistability 10 p1481 A83-25433

Operating conditions of a CW water-vapour laser at 28, 47, 78, 79 and 119 microns 10 p1425 A83-25454

Efficiency of free-electron lasers with a scattered electron beam 10 p1426 A83-25791

Motion and emission of a classical relativistic particle in a nonuniform laser wave 10 p1426 A83-25884

Spectroscopy and efficiency of the /Hg-200/Br-81 and /Zn-64/I photodissociation lasers 10 p1426 A83-26003

Quantum/classical mode evolution in free electron laser oscillators 10 p1426 A83-26004

Free electron laser small signal gain measurement at 10.6 microns 10 p1427 A83-26009

Time-dependent gain and absorption in a 5 J UV preionized XeCl laser 10 p1428 A83-26024

Statistical analysis of aging-induced degradation /or lifetime/ variations in /Al, Ga/As/GaAs double-heterostructure lasers 10 p1429 A83-26028

Improvement of phase-conjugate beam fidelity in degenerate four-wave mixing by focused probe fields 10 p1429 A83-26111

Laser phase noise effects in fiber-optic signal processors with recirculating loops 10 p1429 A83-26118

High gain CO chemical laser produced in a shock tunnel 10 p1429 A83-26168

Diffraction coupled phase-locked semiconductor laser array 10 p1430 A83-26203

Semiconductor integrated etalon interference laser with a curved resonator 10 p1430 A83-26206

Photodissociation CW laser using condensation and evaporation for a closed cycle 10 p1430 A83-26235

Pumping of gas lasers by runaway-electron beams 10 p1430 A83-26241

Wedge coupling of lasers into multimode fibers 10 p1431 A83-26631

Determination of the effective stimulated emission cross section for a neodymium laser with a selective resonator 10 p1431 A83-26653

Service life of a copper bromide vapor laser 10 p1432 A83-26674

Numerical modeling of a chemical oxygen-iodine laser 10 p1433 A83-26676

Investigation of the optical inhomogeneities of the active medium of a fast-flow CO₂ laser with mixing 10 p1433 A83-26677

Problem of accurate intensity measurements in focused laser beams 10 p1433 A83-26683

Thermal defocusing and transformation of the statistics of a spatially noncoherent light beam 10 p1434 A83-26691

Unstable resonator with multiple outputs 10 p1435 A83-26880

He-Ne laser in the near infrared of the type LG-1-1.R 10 p1435 A83-26881

Paraboloid of revolution used for receiving the laser radiation, for beams not parallel to the axis of the paraboloid 10 p1435 A83-26883

Squeezed states in harmonic generation of a laser beam 10 p1435 A83-26971

XeF laser beam quality impact of pump-induced medium inhomogeneities 11 p1576 A83-27505

Analysis of the lifetime of a small volume UV preionized discharge XeCl excimer laser 11 p1576 A83-27507

High spectral brightness extreme ultraviolet generation with excimer lasers 11 p1576 A83-27508

On the interpretation of interferograms of cavity turbulence --- in laser cavity medium 11 p1577 A83-27516

Injection locking of excimer lasers 11 p1577 A83-27518

Single-axial-mode operation of a polarization-coupled stable/unstable-resonator Nd:YAG laser oscillator - Update 11 p1577 A83-27519

Cooperative effects and transverse coherence in superfluorescence 11 p1577 A83-27536

Nonperturbative calculations of the indices of refraction of multilevel systems 11 p1577 A83-27537

Cerenkov-type optical parametric oscillation in a 'double' Fabry-Perot interferometer 11 p1578 A83-27540

Advances in divalent transition-metal lasers 11 p1578 A83-27541

A single mode /F₂+/-asterisk color-center laser for application in optical pumping of helium 11 p1578 A83-27543

Three wavelength laser emission in Ho:YLF via sequential cascade 11 p1578 A83-27544

Theory on distributed feedback /DFB/ lasers including strong modulations 11 p1578 A83-27548

Submillimeter-wave laser emission in carbonyl fluoride 11 p1578 A83-27549

Theoretical spectral profiles of laser assisted Penning ionization 11 p1658 A83-27550

Wigner approach to laser-induced molecular collisions 11 p1579 A83-27551

High performance DF-CO₂ chain-reaction laser 11 p1579 A83-27572

High-power electro-ionization CO₂ - Lasers for laser technology 11 p1580 A83-27574

High efficiency infrared xenon laser excited by a U.V. preionized discharge 11 p1580 A83-27579

Corona preionization technique for CO₂ TEA lasers 11 p1580 A83-27580

Phase conjugate reflection of KrF laser radiation 11 p1582 A83-27599

Peculiarities of laser radiation refraction in the clearing process of cloud medium 11 p1632 A83-27608

Absorption and reshaping of 10.6 microns light in pure SF₆ using 1.5 ns, low-intensity incident pulses 11 p1582 A83-27610

Xe Cl laser pumped by an intense short-pulse electron beam 11 p1582 A83-27611

Improved performance and rotational spectral characteristics of a doped helical TEA CO₂ laser 11 p1583 A83-27623

Growth of emission in a far infrared laser 11 p1583 A83-27625

The intracavity magneto-optical modulation of the intensity of laser radiation 11 p1583 A83-27949

Analysis of the output signal of devices for measuring the defocusing of lenses under coherent illumination 11 p1574 A83-28498

The mechanism of the effect of striations on the output power of a helium-neon laser 11 p1584 A83-28522

CW operation of an injection ring laser 11 p1585 A83-28673

Bistable operation of a semiconductor laser 11 p1585 A83-28674

Theoretical simulation of a pulsed HF optical resonance transfer laser 11 p1585 A83-28703

Helical-flow CO₂ laser 11 p1585 A83-28705

High repetition rate operation of a N₂ waveguide laser 12 p1731 A83-29151

Resonant and nonresonant electron scattering in an inhomogeneous laser field 12 p1732 A83-29246

Investigation of the gain in a CO₂ GDL behind wedge-shaped and contoured nozzles. I - The experimental setup, the repetitively pulsed system for gain measurement 13 p1849 A83-30042

Measurement of laser beam divergence 13 p1844 A83-30202

High-power-density electron-beam-sustained laser 13 p1849 A83-30256

Performance of a laser beam wave-front sensor 13 p1845 A83-30257

Effect of outgassing on the performance of a TE CO₂ laser sealed in an acrylic chamber 13 p1849 A83-30258

Laser oscillation at 3.53 microns from Fe(2+) in n-InP:Fe 13 p1850 A83-30327

High-repetition-rate CO₂-lasers 13 p1850 A83-30645

Effects of optical irregularities in the active medium on angular divergence of a beam in a CW supersonic DF-CO₂ chemical laser 13 p1851 A83-30819

Some properties of phase-matched resonators 13 p1919 A83-30826

Bistable operation and nonuniform output in an injection heterostructure laser 13 p1851 A83-30907

Experiments with high bandwidth segmented mirrors 13 p1921 A83-31020

A high-power, narrow linewidth XeCl(asterisk) oscillator 13 p1852 A83-31058

Heavy ion beam pumped He-Ar laser 13 p1852 A83-31060

Free-electron generators of coherent radiation - /Volumes 8 & 9/ 13 p1852 A83-31101

Additional experimental results from the Stanford 3 micron FEL 13 p1852 A83-31103

Results of the first phase of the ACO storage ring laser experiment 13 p1852 A83-31105

A free-electron laser for the storage ring BESSY 13 p1853 A83-31109

U.K. free-electron laser proposal 13 p1853 A83-31110

Pulse propagation in the tapered wiggler 13 p1854 A83-31116

Millimeter-wave generation by a single-pass, Compton-regime, variable-parameter free-electron laser 13 p1854 A83-31123

The FEL-microtron activity at the C.N.E.N. Frascati Center Progress and perspectives 13 p1854 A83-31125

Experimental results from the HDL orotron - A tunable source of coherent millimeter wave radiation 13 p1855 A83-31126

Experimental study of axial magnetic field effects on the operation of a millimeter-wave free-electron laser 13 p1855 A83-31129

The effect of an axial guide field on free-electron lasers 13 p1855 A83-31130

A two-dimensional numerical model of the tapered wiggler free-electron laser 13 p1856 A83-31142

International intercomparison of laser power measurements in the visible region 13 p1856 A83-31278

Nonlinear self-consistent theory of the orotron 13 p1857 A83-31380

Effects of space charge on the performance of an orotron 13 p1857 A83-31392

Radio-frequency-excited carbon dioxide metal waveguide laser 13 p1857 A83-31457

Unpolarized EO Q-switched laser 13 p1857 A83-31458

Application of the 2-D discrete-ordinates method to multiple scattering of laser radiation 13 p1857 A83-31460

GaAs/GaAlAs active-passive-interference laser 13 p1858 A83-31768

Total radiant power measurement of laser diode by a calorimetric method 13 p1858 A83-31774

Investigation of CW operation of a GaAs laser pumped by an electron beam 14 p2022 A83-31906

Spectral characteristics of carbon monoxide laser with different isotopic compositions 14 p2023 A83-31912

Influence of a counterpressure on the operation of a CO₂ gasdynamic laser emitting of 18.4 microns 14 p2023 A83-31914

Theory of time-dependent intense-field collisional resonance fluorescence 14 p2079 A83-31925

Tunable sealed-off CW CO laser at room temperature 14 p2023 A83-31950

An investigation of the photodestruction of zinc-oxide film by means of surface-polariton spectroscopy and X-ray diffraction analysis 14 p2088 A83-32130

A ruby laser in an electron-beam field 14 p2023 A83-32133

Diffraction gyration and reversal of the wavefront of laser beams in electro-optical crystals 14 p2084 A83-32134

The gain of a solid-state gamma-ray laser 14 p2023 A83-32162

Propagation in media with Raman-type nonlinearity Polarization states of the waves and gains 14 p2024 A83-32445

A classification scheme for the light-current (L/I) characteristics of a two photon mode semiconductor laser 14 p2024 A83-32447

Free-electron lasers and prospects of their utilization 14 p2024 A83-32592

Influences of thermal effects on high power CW outputs of b-axis Nd:YAP lasers 14 p2024 A83-32596

Laser action benzimidazoles in various aggregate states 14 p2024 A83-32827

Passive mode lockers for lasers generating at a wavelength of 1.06 micron 14 p2025 A83-32832

Digital image processing of flow visualization photographs 14 p2020 A83-32906

Calculation of the diffraction of laser beams with a smooth profile of intensity variation 14 p2025 A83-33396

New large optical cavity laser with distributed active layers 14 p2027 A83-33437

A high-power, single-mode laser with twin-ridge-substrate structure 14 p2027 A83-33438

Bistability and slow oscillation in an external cavity semiconductor laser 14 p2027 A83-33440

Saturation effects in phase-conjugate lasers 15 p2167 A83-33534

Power and stability of phase-conjugate lasers 15 p2167 A83-33535

An experimental study of the absorption mechanisms in laser-matter interaction at high energies - The effect of wavelength --- French thesis 15 p2232 A83-33699

Initiation of a pulsed-beam free-electron-laser oscillator 15 p2168 A83-33796

Integrated arrays of 1.3-micron buried-crescent lasers 15 p2168 A83-33842

Continuous-wave industrial electron-beam-controlled CO laser of 10 kW output power 15 p2168 A83-33976

Quasi-continuous excitation regime of electric-discharge exciplex lasers 15 p2168 A83-33980

Properties of a gasdynamic NO₂ laser 15 p2169 A83-34023

A model for superradiance and superfluorescence in free-electron lasers 15 p2169 A83-34274

A study of the CO₂-GDL gain behind wedge-shaped and contoured nozzles. II - Measurement results. Comparison of experimental data with calculations 15 p2169 A83-34474

HF chemical laser amplification properties in homologous turbulent shear flow 15 p2170 A83-35250

Miniature 250 Hz, TEA CO₂ laser using H₂ buffered gas mixture 15 p2170 A83-35251

Analysis of multielement semiconductor lasers 16 p2357 A83-35428

Large-bore copper-vapor lasers - Kinetics and scaling issues 16 p2358 A83-35429

GaAs/(GaAl)As deep Zn-diffused channelled-substrate laser 16 p2358 A83-35454

Free-electron lasers 16 p2358 A83-35725

Measurement of the spectral-frequency and correlation parameters and characteristics of laser radiation --- Russian book 16 p2360 A83-36439

Optimization of electrically excited Xe(C yields A) laser performance 16 p2361 A83-36770

Superemission (collective spontaneous emission) of photons by atoms moving in a substance 16 p2361 A83-36966

High-power, long-pulse CO₂ laser transversely excited by a damped oscillating discharge through dielectric electrodes 17 p2513 A83-36998

The development, performance, and potential application of the copper halide laser [AIAA PAPER 83-1702] 17 p2513 A83-37199

An experimental study of downstream mixing CO₂ laser [AIAA PAPER 83-1703] 17 p2513 A83-37200

Modeling of overlap thermal blooming in smoke [AIAA PAPER 83-1719] 17 p2503 A83-37208

Performance characteristics of a transverse-flow, oxygen-iodine chemical laser in a low gas-flow velocity 17 p2513 A83-37609

Far-field characterization of diode lasers with standard vidicons 17 p2514 A83-37745

A new stabilization system for optically pumped CW far infrared lasers 17 p2514 A83-37752

The wavefront curvature of an optically pumped waveguide laser 17 p2514 A83-37762

1-W CW Zn ion laser 17 p2514 A83-38045

A two-dimensional flow model of laser supported combustion waves [AIAA PAPER 83-1718] 17 p2507 A83-38088

A kinetic model of the sustained discharge HgBr laser 17 p2514 A83-38207

The design and manufacture of a prototype for absolute measurement of laser wavenumbers 17 p2511 A83-38431

Microwave signal generation with injection-locked laser diodes 17 p2515 A83-38887

Passive mode locking in the blue spectral region 17 p2515 A83-38969

Synchrotron instability for long pulses in free electron laser oscillators 17 p2515 A83-38970

Laser cavity dumping using optical bistability 17 p2515 A83-38971

Optical bistability in four-level nonradiative dyes 17 p2515 A83-38974

Breathing, spiking and chaos in a laser with injected signal 17 p2515 A83-38975

Electrically triggered multimodule KrF laser system with narrow-linewidth output 18 p2692 A83-39092

High-order series solution for unsteady thermal blooming with crosswind 18 p2692 A83-39147

The effect of diffusion on the energy characteristics of molecular lasers 18 p2693 A83-39525

Phase-locked InGaAsP laser array with diffraction coupling 18 p2693 A83-40051

Reliability of constricted double-heterojunction AlGaAs diode lasers 18 p2693 A83-40052

Occupation fluctuation noise - A fundamental source of linewidth broadening in semiconductor lasers 18 p2693 A83-40053

Simultaneous ultraviolet laser triggering of two multimegavolt gas switches 18 p2677 A83-40059

A preliminary study of a retroreflective mirror resonator 18 p2693 A83-40345

Dependence of the sensitivity of intracavity laser spectroscopy on generation parameters 18 p2693 A83-40347

Nonlinear conversion of laser radiation in optical fibres and its applications for spectral investigation 18 p2744 A83-40351

Temperature dependence of the gain coefficient of phosphate-neodymium glass 18 p2694 A83-40404

Photon antibunching effect and statistical properties of single-mode emission in free-electron lasers 18 p2694 A83-40411

- Quantum fluctuations in the two-photon laser 18 p2694 A83-40412
- The helium-iodine laser 18 p2694 A83-40664
- Operation of an inductively ballasted helical TE-CO₂ laser 19 p2850 A83-40734
- Streak camera study of short pulse generation in an optically pumped GaAs/(GaAl)As laser 19 p2850 A83-40735
- Anomalous longitudinal mode behavior of a deep Zn-diffused GaAs/GaAlAs laser 19 p2850 A83-40736
- Effect of an active layer thickness on lateral and longitudinal modes of a gain guiding laser with a tapered stripe structure 19 p2850 A83-40737
- A YAG:Nd(3+) ring laser 19 p2850 A83-40917
- On the high power limit of the laser linewidth 19 p2851 A83-40927
- A nondestructive method for predicting laser emission wavelength from photocurrent spectra of GaAlAs double heterostructure wafers 19 p2851 A83-40930
- Models of the static and dynamic behavior of stripe geometry lasers 19 p2851 A83-40931
- Analysis of diode laser properties. II 19 p2851 A83-40934
- Effect of temporal nonstationarity on the spectrum of injection lasers 19 p2852 A83-40940
- A compact CW HCN gas laser with RF-excited discharge 19 p2852 A83-40946
- Estimation of boresight error in autoboreighting a laser beam on a point target - Influence of weak statistical fluctuations 19 p2900 A83-41094
- Light induced drift of CH₃F 19 p2853 A83-41181
- High neon pressure longitudinal copper vapour laser 19 p2853 A83-41185
- A dual-stripe phase-locked diode laser 19 p2853 A83-41288
- Increasing the transillumination capacity of a laser beam in the atmosphere 19 p2854 A83-41768
- Launching light from semiconductor lasers into plane-ended multimode optical fibers 20 p3046 A83-42220
- Accelerated precipitation of water fogs due to acoustic action of a CO₂ laser pulse 20 p3028 A83-42278
- Superfluorescence pulse shape 20 p2993 A83-42289
- Routes to chaotic output from a single-mode, dc-excited laser 20 p2994 A83-42650
- A technique for measuring energy absorption from high energy laser radiation 20 p2989 A83-42781
- Characteristics of mercurous bromide and iodide visible lasers 20 p2995 A83-43104
- XeCl excimer laser excited by longitudinal discharge 20 p2995 A83-43597
- Problem of stabilization of laser radiation parameters 20 p2996 A83-43784
- Radiative characteristics of injection lasers with short resonators 20 p2996 A83-43788
- Formation of free fluorine atoms by laser-collisional initiation of the CH₃F + F₂ reaction 20 p2997 A83-43789
- Autocollimation multibeam interferometer with spatial beam separation and its use in frequency selection of laser radiation 20 p2997 A83-43790
- Investigation of the power stability of a CW carbon monoxide laser 20 p2997 A83-43793
- Calculation of the maximum output power of a continuous-flow CO₂ laser 20 p2997 A83-43794
- determination of the rate constants used in design calculations relating to low-temperature CO₂-D₂ gasdynamic lasers 20 p2998 A83-43801
- Pulsed chemical HF laser utilizing a mixture of technical-grade C₃H₈ and SF₆ and initiated by an electric discharge 20 p2998 A83-43802
- Laser spark with a continuous channel in air 20 p2998 A83-43803
- Steady-state emission from a Y₃Al₅O₁₂:Er(3+) laser (lambda = 2.94 microns, T = 300 K) 20 p2998 A83-43806
- Experimental observation of amplification of beams by dynamic surface holograms 20 p2998 A83-43807
- Chemical laser amplifier using a photon-branched reaction in an aerosol medium 20 p2998 A83-43808
- Tunable lasers --- Russian book 21 p3142 A83-43903
- Maximum input energy for an externally sustained CO₂ laser discharge 21 p3143 A83-44144
- Lasing and fluorescent characteristics of nine, new, flashlamp-pumpable, coumarin dyes in ethanol and ethanol:water 21 p3143 A83-44193
- Tunable infrared difference-frequency generation in lithium iodate 21 p3143 A83-44194
- Chaos in coherent two-photon processes in a ring cavity 21 p3143 A83-44196
- An external cavity diode laser sensor 21 p3136 A83-44209
- Transient effects, transverse mode coupling, and diffraction in swept-gain superradiance in the nonlinear regime Evolution from the superradiant state 21 p3144 A83-44793
- Phase matching and frequency detuning effects in Brillouin enhanced four-wave mixing 21 p3144 A83-44805
- Operation and performance of the CW visible atomic mercury laser 21 p3145 A83-44813
- Picosecond continuum generation and spectroscopy 21 p3145 A83-44819
- Intelligent attenuator for laser pulse energy and power stabilization 21 p3145 A83-44833
- An increase in laser gain to free electrons by means of laser radiation from an external source 21 p3145 A83-45202
- The use of piecewise-exponential functions in transfer theory --- of chemical laser energy characteristics 21 p3146 A83-45222
- Operating characteristics of a laser with supplementary inertial negative feedback 21 p3146 A83-45387
- The electromagnetic field in a randomly inhomogeneous medium Phase-space representation 21 p3201 A83-45391
- Optical stability of narrow stripe, proton-isolated AlGaAs double heterostructure lasers with gain guiding 21 p3147 A83-45485
- Optimization of a self-terminating ionized strontium laser in a pulsed periodic mode 21 p3147 A83-45503
- A He-Sr laser with a mean power of 3 W 21 p3147 A83-45504
- Continuous laser amplification in a monomode fiber longitudinally pumped by evanescent field coupling 22 p3295 A83-45971
- Temporal coherence characteristics of InGaAsP laser diode with single-longitudinal-mode oscillation 22 p3295 A83-45972
- Study of gain, bandwidth, and tunability of a millimeter-wave free-electron laser operating in the collective regime 22 p3295 A83-46016
- Second-harmonic emission from laser-plasma interactions 22 p3363 A83-46273
- Reliability factors in gas lasers 22 p3296 A83-46612
- Carbon dioxide waveguide laser design for maximum output power at specified frequency offset 22 p3299 A83-46747
- Atmospheric-pressure electroionization CO₂ laser using CO₂-N₂-H₂O mixtures 22 p3300 A83-46785
- Gain measurements on semiconductor lasers by optical feedback from an external grating cavity 22 p3300 A83-46817
- Low-threshold semiconductor Raman laser 22 p3300 A83-46818
- Spectral quality of He-Zn II and he-cd II hollow cathode metal vapor lasers in the magnetic fields 22 p3300 A83-46820
- Modeling of the 10-micron natural laser emission from the mesospheres of Mars and Venus 22 p3387 A83-47080
- Characteristics of lasers with condensed active media exhibiting linear anisotropy induced by polarized pump radiation 23 p3460 A83-47162
- An experimental study of the generation parameters of a laser with a thin absorption layer in the cavity 23 p3460 A83-47163
- Sources of stimulated radiation using resonance electron accelerator 23 p3460 A83-47557
- Analysis of temporal-length limitations in XeCl lasers 23 p3460 A83-47605
- Vernier fringe-counting device for laser wavelength measurements 23 p3454 A83-47645
- Progress in laser sources for remote sensing 23 p3461 A83-47798
- Chaotic and periodic emission of high power solid state lasers 23 p3462 A83-48318
- Stability of a detuned single mode homogeneously broadened ring laser 23 p3462 A83-48319
- Generation of continuous-wave 243-nm radiation by sum-frequency mixing 23 p3462 A83-48321
- The physical processes occurring during the deep penetration of metals by a laser beam 23 p3462 A83-48428
- Two-dimensional Rayleigh scattering in a semi-infinite cylindrical medium exposed to a laser beam 23 p3463 A83-48650
- Fundamental linewidth in solitary, ultranarrow output PbS(1-x)Se(x) diode lasers 24 p3586 A83-48784
- Highly efficient, high-quality phase-conjugate reflection at 308 nm using stimulated Brillouin scattering 24 p3587 A83-48854
- Narrow-linewidth gain and saturation measurements of a KrF discharge laser 24 p3587 A83-48906
- Several generation parameters of a CO₂ gasdynamic laser with a high-temperature regenerative-heat-transfer heater of the working gas 24 p3588 A83-48936
- Aerosol backscattering of a laser beam 24 p3588 A83-49004
- Axial irradiance and optimum focusing of laser beams 24 p3588 A83-49015
- Elastic scattering of electrons by hydrogen atoms in a laser field 24 p3626 A83-49432
- Visible iodine and bromine laser, and coaxial discharge excited strong UV iodine laser 24 p3589 A83-49615
- Ultraviolet four-photon mixing in an multimode silica fiber Raman amplifier 24 p3589 A83-49616
- High-gain optical amplification of laser diode signal by Raman scattering in single-mode fibres 24 p3589 A83-49960
- Theory of spontaneous emission in gain-guided laser amplifiers 24 p3590 A83-49975
- Optical properties for an antireflection-coated LD optical switch 24 p3630 A83-49983

LASER PLASMA INTERACTIONS

The influence of charge transfer on ion probe measurements of laser-produced plasmas

01 p0107 A83-10693

On the distribution of second harmonic emission from a laser-produced plasma 02 p0241 A83-12082

Numerical simulation of a light-absorbing plasma at a shock front 03 p0396 A83-13177

Interferometric measurement of the electron density in laser-matter interaction --- French thesis 03 p0398 A83-13808

Subsonic radiation waves - Comparison of the theory with experiment --- in laser induced plasma discharges 05 p0687 A83-17074

Self-consistent treatment of resonance absorption in a streaming plasma 05 p0688 A83-17363

lasma fluctuations at critical density in a CO₂ laser plasma interaction 05 p0688 A83-17364

Modulation depth in the scattering spectra for a plasma in a magnetic field 06 p0811 A83-18447

Absorption of HCN-laser rays with inverse bremsstrahlung in a krypton atom field --- German thesis 06 p0811 A83-18520

Artificial microburst dielectrics produced in laser-sol interactions 07 p0994 A83-20050

Dynamics of harmonic generation in a laser plasma 07 p0995 A83-20059

Numerical modeling of optical-breakdown waves in gases 07 p0996 A83-20303

Profile steepening by resonance absorption in spherically-expanding plasmas --- density analysis 07 p0997 A83-20542

Intense X-ray emission in the interaction of a laser plasma with a solid surface 07 p0997 A83-20608

Time-resolved Thomson-scattering measurements of ion fluctuations driven by stimulated Brillouin scattering 07 p0998 A83-20816

Analysis of a class of free electron laser using a periodic static magnetic field 07 p0937 A83-20825

Observation of suprathermal electrons produced by stimulated Raman scattering processes 08 p1168 A83-22376

Gain scaling of short-wavelength plasma-recombination lasers 08 p1110 A83-22636

Laser light backscattering off an electron beam-plasma system 10 p1428 A83-26019

Shockfronts as model targets in laser-plasma interaction experiments 10 p1487 A83-26173

Stimulated Raman backscattering in the presence of ion-acoustic fluctuations 13 p1923 A83-30119

Growth and saturation of the two-plasmon decay instability 14 p2087 A83-33390

Laser wavelength effect on the thermal conductivity and ablation in plasmas created by a laser --- French thesis 15 p2232 A83-33700

Theory of transient self-focusing of a CO₂ laser pulse in a cold dense plasma 16 p2358 A83-35432

Analysis of laser light scattered by cold, dense hydrogen plasmas produced in a Z pinch 17 p2581 A83-37040

The instability of two plasmons and suprathermal electrons in the laser-matter interaction --- French thesis 17 p2583 A83-38224

Penning ionization in the field of a light wave 17 p2583 A83-38964

Intense laser self-focusing in plasmas 18 p2693 A83-40366

Unified theory of parametric excitations in magnetized plasma produced by the action of nonmonochromatic driver pump. I Modulated driver pump 18 p2748 A83-40507

Operating conditions for free-electron lasers 19 p2851 A83-40918

Second-harmonic emission from laser-plasma interactions 22 p3363 A83-46273

Generation of higher harmonics of an intense laser beam in a plasma 22 p3363 A83-46935

Magnetic surface waves in plasmas 23 p3511 A83-48621

- Simultaneous measurement of magnetic field direction and ion temperature in a plasma by collective scattering with a CO₂ laser 24 p3630 A83-48786
- Numerical study of the interaction of supersonic viscous gas jets in the presence of nonequilibrium physicochemical processes 24 p3588 A83-49122
- Bound states of electrons in a light field 24 p3589 A83-49744
- Electron temperature measurements in a HF plasma source using a 200 J Nd:glass laser 24 p3633 A83-49747

LASER PLASMAS

- C I isoelectronic sequence - Observations of 2s/m/2p/n/-2s/m-1/2p/n+1/ intersystem transitions and improved measurements for Cl XII, K XIV, Ca XV, Sc XVI, Ti XVII, and V XVIII 01 p0105 A83-10198
- Switched optoelectronic microwave load 01 p0035 A83-10295
- The influence of charge transfer on ion probe measurements of laser-produced plasmas 01 p0107 A83-10693
- Formation of the ionization state of a plasma during laser vaporization 01 p0107 A83-10818
- A calculation of supersonic radiation waves with an allowance made for the plasma motion 02 p0240 A83-11513
- Propagation of an electromagnetic beam in an inhomogeneous plasma formed during the interaction of this beam with a thin dense-gas layer 02 p0240 A83-11681
- On the distribution of second harmonic emission from a laser-produced plasma 02 p0241 A83-12082
- Millimeter wave integrated circuit devices based on optoelectronic control 03 p0310 A83-13782
- A fast wave of gas-ionization in a laser beam 05 p0686 A83-16892
- The effect of giant laser pulses on a quasi-stationary plasma torch 05 p0687 A83-16893
- Transmission cutoff accompanying remote optical breakdown of the atmosphere by CO₂ laser pulses 05 p0687 A83-17064
- Influence of radiative losses on the hydrodynamics of a laser plasma corona 05 p0687 A83-17072
- A scaling model for plasma columns produced by CO₂ laser-induced breakdown in a solenoidal field 05 p0688 A83-17368
- Time-resolved X-ray spectrometry of UV laser produced plasmas 06 p0763 A83-18954
- Gas-dynamic processes in a gas layer heated by high-intensity radiation during target acceleration 06 p0813 A83-19436
- Runaway ions in an expanding plasma 07 p0994 A83-20051
- Observation of the population inversion of O VIII levels in a laser plasma 07 p0996 A83-20126
- Time-resolved X-ray transmission grating spectrometer for studying laser-produced plasmas 07 p0928 A83-20163
- Numerical modeling of optical-breakdown waves in gases 07 p0996 A83-20303
- Electron energy transport in ion waves and its relevance to laser-produced plasmas 07 p0997 A83-20543
- New technique for measurement of upper laser level decay rates in gas laser plasmas 07 p0938 A83-21597
- Time-resolved observations of stimulated Raman scattering from laser-produced plasmas 08 p1168 A83-22390
- Ultraviolet fluorescence by optical pumping with extreme ultraviolet line radiation 08 p1110 A83-22646
- The determination of parameters of recombining laser-produced plasmas by means of X-ray spectroscopy 09 p1347 A83-23654
- Radial multi-slit coding for X-ray imaging of laser microplasmas 09 p1267 A83-23709
- Processes occurring in an erosion plasma during laser vacuum deposition of films. I - Properties of a laser erosion plasma in the inertial-expansion stage. II - Interaction of laser erosion products with the solid surface 09 p1348 A83-23991
- Numerical modeling of nonstationary processes during sputtering and interaction of an erosion laser flare 09 p1274 A83-23992
- Ablation of a solid target by laser irradiation --- German thesis 09 p1348 A83-24848
- The determination of electron density profiles from refraction measurements obtained using holographic interferometry 10 p1418 A83-25427
- Plasma production during vaporization of materials by the radiation from a CO₂ TEA laser 10 p1486 A83-25890
- Experimental study of an axial discharge in a turbulent gas flow 10 p1430 A83-26252
- Inversion of lithium-like ions with respect to the 2p state in a recombining plasma 10 p1432 A83-26666

- Rotational relaxations in a high pressure N₂ laser 10 p1435 A83-26858
- Evidence of population inversion in Li-like aluminum ions in a laser produced plasma 11 p1577 A83-27522
- Simulation of a DNP laser plasma --- Direct Nuclear Pumped 11 p1579 A83-27559
- Generation of O₂/1Delta/ by nuclear pumping --- of laser plasmas 11 p1579 A83-27560
- Temporal and spatial laser diagnostics of the laser pyrolysis of methane 11 p1545 A83-27585
- Efficient laser-induced plasma formation in alkali-metal vapors 11 p1658 A83-27587
- Amplifications of atomic fluorine, nitrogen ion and XeF lasers 11 p1582 A83-27614
- Metal vapor recombination laser research 11 p1583 A83-27618
- Spontaneous magnetization of thermal conductivity in a dispersing laser plasma 11 p1658 A83-28061
- Detection of the Z-dependence of laser-plasma corona temperature in a study of half-integer harmonic radiation 11 p1658 A83-28063
- Limitation to the accuracy of interferometrically measured electron density profiles of laser-produced plasmas 11 p1661 A83-28709
- New dielectric waveguide structure for millimetre-wave optical control 12 p1720 A83-29466
- Stimulated Brillouin scattering in an inhomogeneous plasma with broad-bandwidth thermal noise 13 p1923 A83-30120
- Expansion of a multi-ion plasma into a vacuum 13 p1924 A83-30123
- The role of plasma turbulence for wave excitation in a free-electron-laser combined with a molecular and plasma medium. 13 p1925 A83-30418
- Laser-plasma antennas, concentrators, and directional couplers for the rf range 13 p1851 A83-30910
- Plasma shifts of the Lyman lines to shorter wavelengths in C VI 13 p1926 A83-30919
- Non-Maxwellian electrons in a laser produced sodium plasma 13 p1926 A83-31061
- Measured gain for XUV plasma lasers at varying pump intensities 13 p1857 A83-31459
- Refraction and absorption in plasma atmospheres 13 p1927 A83-31573
- Spectroscopic investigation of laser-initiated low-pressure plasmas in atmospheric gases [AD-A130571] 14 p1990 A83-32916
- Observations of magnetized plasma flow through stationary background plasma 14 p2087 A83-33380
- Picosecond transient orientational and concentration gratings in germanium 14 p2093 A83-33427
- Laser wavelength effect on the thermal conductivity and ablation in plasmas created by a laser --- French thesis 15 p2232 A83-33700
- Bremsstrahlung emission in a non LTE plasma 15 p2233 A83-34139
- Observations of Stark-shifts of Lyman-alpha lines of low-Z ions in laser-produced plasmas 15 p2233 A83-34140
- Metal plasma induced by the bombardment of 308 nm excimer and 585 nm dye laser pulses at low pressure 15 p2235 A83-34368
- A reexamination of the laser supported combustion wave [AIAA PAPER 83-1444] 15 p2129 A83-34906
- Evidence of anomalous multiplet line shapes in optically thick, laser-produced plasmas 15 p2236 A83-34997
- Electron distribution function in a laser plasma 16 p2415 A83-35888
- Self-focusing of multiply charged ions of a laser plasma 17 p2582 A83-38124
- Investigation of strata in small-scale He-Ne lasers 17 p2515 A83-38488
- The energy of thermal electrons in electron beam created helium discharges 17 p2583 A83-38965
- Linear mode conversion in laser plasmas 18 p2748 A83-40511
- Harmonic generation of radiation in a steep density profile 18 p2748 A83-40512
- A study of ablation by laser irradiation of plane targets at wavelengths 1.05, 0.53, and 0.35 micron 18 p2749 A83-40519
- Unlimited electron acceleration in laser-driven plasma waves 19 p2901 A83-40969
- Local temperature of a plasma corona 20 p3049 A83-42270
- Investigation of soft X-ray population inversion in laser produced plasmas 20 p3050 A83-43176
- Effect of resonant absorption of laser-induced plasma on temporal resolved spectrum and temporal integrated spectrum 20 p3050 A83-43177
- Novel short-pulse photoionization electron source - Li (1s2s2p)4P0 deexcitation measurements in a plasma 21 p3209 A83-43885

- Effect of focusing and detection lenses on the Raman frequency spectrum in a laser plasma 21 p3210 A83-44132
- Optical properties of a laser plasma near a solid surface in a dense gas 21 p3211 A83-44146
- Laser diagnostics of a nonuniform dense plasma 21 p3211 A83-44147
- Photoionization by intense line radiation in laser-produced plasmas --- by X-ray lasers 22 p3295 A83-45946
- Second-harmonic emission from laser-plasma interactions 22 p3363 A83-46273
- Shock wave pressure enhancement using short wavelength (0.35 micron) laser irradiation 22 p3363 A83-46727
- Optical plasmatron [IAF PAPER 83-399] 23 p3509 A83-47374
- Electron temperature monitor for laser-produced plasmas 23 p3454 A83-47641
- High-speed, low-cost laser-triggered plasma shutter 23 p3461 A83-47644
- Converging shock on laser plasma - Density profiles by holographic interferometry 23 p3510 A83-48316
- The origin of line-free XUV continuum emission from laser-produced plasmas of the elements Z = 62-74 23 p3511 A83-48586
- Properties of the corona generated by the incidence of intense CO₂ laser pulses on spherical targets 24 p3631 A83-48820
- Combustion regimes with laser-induced plasma 24 p3556 A83-49782

LASER PROPULSION

- A reexamination of the laser supported combustion wave [AIAA PAPER 83-1444] 15 p2129 A83-34906
- Prediction of the flowfield in laser propulsion devices [AIAA PAPER 83-1445] 15 p2129 A83-34907
- Radiation energy receiver for laser and solar propulsion systems [AIAA PAPER 83-1207] 16 p2319 A83-36281
- Laser-driven MHD-fanjet [AIAA PAPER 83-1345] 16 p2321 A83-36350
- The influence of boundaries and electrical currents on plasma jet expansion into vacuum --- in laser thrusters [IAF PAPER 83-398] 23 p3426 A83-47373

LASER PUMPING

- Direct observation of picosecond light pulses from a pulse-current pumped semiconductor laser 01 p0054 A83-10615
- A study of the excitation threshold and intensity of stimulated Raman scattering in rubidium vapor at various pump spectrum widths 01 p0055 A83-10913
- Broadband infrared generation in liquid-bromine-core optical fibers 02 p0183 A83-11571
- Threshold of a thallium-iodide photodissociation laser operated at low pressure 04 p0485 A83-16052
- Stability of compensation regimes for nonlinear distortions of beams with any polarization 05 p0650 A83-17077
- Harmonic generation with noncollinear laser beams - Application to pulse stacking 06 p0766 A83-18958
- Injection-locked dye laser pumped and injected by a pulsed xenon-ion laser 06 p0767 A83-19144
- Nonadiabatic transitions in a three-level system subjected to a laser radiation field with a smoothly varying frequency 07 p0934 A83-20109
- Nitrogen-laser-pumped ultrashort pulse amplifier 07 p0934 A83-20114
- Amplification in a waveguide CO₂ laser employing an RF electrodeless discharge 07 p0935 A83-20129
- Theory of line narrowing and frequency selection in an injection locked laser 07 p0938 A83-21600
- New CH₃OH laser lines pumped with a fine-tuned high-power CO₂-TEA laser 08 p1107 A83-22247
- Interaction of electromagnetic waves with a moving perturbation in a stationary gas 10 p1471 A83-25648
- Laser oscillator using resonator with self-pumped phase-conjugate mirror 10 p1429 A83-26112
- Pumping of gas lasers by runaway-electron beams 10 p1430 A83-26241
- Pumping of pulsed gas lasers by bulk and sliding spark discharges 10 p1431 A83-26464
- Upconversion of laser radiation to gamma-ray energies 11 p1577 A83-27533
- Three wavelength laser emission in Ho:YLF via sequential cascade 11 p1578 A83-27544
- Laser action continuously tunable from 1.98 to 3.76 microns using F₂⁺ and lithium /F₂⁺/A centers in KI 11 p1578 A83-27546
- Radio frequency pumped infrared lasers 11 p1580 A83-27576
- Stepwise excitation - A limiting process in pulsed gas lasers 11 p1582 A83-27601
- New CW two-photon pumped and Raman FIR laser lines in /N-14/H₃ and /N-15/H₃ 11 p1583 A83-27848

Operating characteristics of a transverse-excited 16 microns CO₂ laser with profile electrodes and UV-preionization 12 p1732 A83-29408
Laser studies of electronic energy transfer in atomic copper 13 p1851 A83-30957
Design considerations of a Compton scattering free-electron laser with an axial electrical field 13 p1855 A83-31131

Gain-enhanced free-electron laser with an electromagnetic pump field 13 p1855 A83-31133
The lasing mechanism, active layer thickness, natural resonator effects, and the nature of the M and P bands of the emission spectrum of CdS pumped by a nitrogen laser - T = 4.2-420 K 14 p2023 A83-32163
FIR NH₃ cascade laser excited by a Q-switch laser 14 p2025 A83-33143

Synchronous amplification of subpicosecond pulses 14 p2025 A83-33403
Pulse shortening in dye laser side-pumped by TEA N₂ laser 14 p2026 A83-33410

Passive mode locking of flashlamp-pumped dye lasers in the 508-583 nm range 14 p2026 A83-33411
Efficient phase conjugation under parametric-feedback conditions 15 p2167 A83-33778

Dye laser spectrum narrowing by 'double pulse' flashlamp pumping 15 p2169 A83-34369
Numerical analysis of an optically pumped D₂O far infrared laser 16 p2358 A83-35430

A high power D₂O laser optimized for microsecond pulse duration 16 p2358 A83-35431
New pulsed far infrared laser lines in D₂O 16 p2359 A83-35959

Resonant transformer command charging system for high repetition rate rare-gas halide lasers 17 p2513 A83-36997

Blackbody-pumped CO₂ laser experiment [AIAA PAPER 83-1701] 17 p2513 A83-37198

Dependence of the sensitivity of intracavity laser spectroscopy on generation parameters 18 p2693 A83-40347

Observation of period doubling in an all-optical resonator containing NH₃ gas 19 p2900 A83-41156
Intracavity mode-locked and frequency-doubled Nd:YAG laser Pump- and mode-size effects 20 p2993 A83-42225

Lithium niobate laser with frequency-degenerate pumping 20 p2993 A83-42290

Optically pumped molecular laser utilizing C₂H₅Br and C₂H₅I halogen derivatives of ethane 20 p2996 A83-43779

Generation of Stokes and anti-Stokes waves initiated by two-photon additional illumination 20 p2996 A83-43782

Second-harmonic photons from the interaction of free electrons with intense laser radiation 22 p3294 A83-45929

Intense proton beam excitation of the high pressure Ar/N₂ laser 22 p3296 A83-46270

Generation of coherent far-infrared radiation using lasers 22 p3296 A83-46497

Continuous-wave mode locked Nd:YAG laser - A picosecond pump source for the future 22 p3298 A83-46669

Wideband frequency conversion in the UV by nine orders of stimulated Raman scattering in a XeCl laser pumped multimode silica fiber 22 p3299 A83-46719

Observation and assignment of torsional transitions in FIR emission from optically pumped CH₃OH 22 p3299 A83-46743

Characteristics of lasers with condensed active media exhibiting linear anisotropy induced by polarized pump radiation 23 p3460 A83-47162

Observations of self-induced Rabi oscillations in two-level atoms excited inside a resonant cavity - The ringing regime of superradiance 23 p3461 A83-47609

Relative quantum yield of I-asterisk(2P1/2) in the tunable laser UV photodissociation of i-C₃F₇I and n-C₃F₇I - Effect of temperature and exciplex emission 23 p3461 A83-47632

Picosecond light-pulses tunable from the violet to the near infrared 23 p3463 A83-48708

Visible iodine and bromine laser, and coaxial discharge excited strong UV iodine laser 24 p3589 A83-49615

LASER RADAR

U OPTICAL RADAR

LASER RANGE FINDERS

Ice-sheet dynamics by satellite laser altimetry 01 p0064 A83-10093

Noncontact visual three-dimensional ranging devices 03 p0324 A83-13448

A refined gravity model from Lageos /GEM-L2/ 03 p0358 A83-13549

Relative lateration across the Los Angeles basin using a satellite laser ranging system 07 p0952 A83-21524

A laser range finder for the dimensional control of radio telescope antennas 08 p1092 A83-22225

Multifunction CO₂ laser radar technology 08 p1045 A83-22502

Detection efficiency for large-aperture coherent laser radars 08 p1096 A83-22508

Heterodyne laser radar performance 08 p1096 A83-22511

Adaptive detection of targets in laser speckle noise 08 p1045 A83-22521

Multidimensional clustering - An application to three-dimensional /3D/ surface extraction 09 p1265 A83-23533

Precision distance measurements in and between satellites 09 p1214 A83-23586

A rangefinder for coherent detection with a CW CO₂ laser - Study and design 09 p1272 A83-24643

Improvement of the ephemerides of the inner planets and the moon using radar, laser, and meridian measurements during 1961-1980 11 p1673 A83-28044

A perspective on range finding techniques for computer vision 12 p1767 A83-28946

Studies on the Metsaehovi satellite laser ranging system --- Thesis 13 p1811 A83-30145

Comparison of earth rotation as inferred from radio interferometric, laser ranging and astrometric observations 13 p1874 A83-30218

Progress in absolute distance interferometry 13 p1851 A83-31019

DFVLR-remote slant visual range (SVR) and wind vector measuring systems 17 p2552 A83-38750

On filtering and compressing LAGEOS laser range data 19 p2860 A83-41558

The Airborne Laser Ranging System - Its capabilities and applications 19 p2848 A83-41560

Neodymium YAG laser in airborne systems 20 p2936 A83-42835

A wide-field scanning triangulation rangefinder for machine vision 20 p2991 A83-43111

The contributions of the Zentralinstitut fuer Physik der Erde to the MERIT project --- Monitor Earth-Rotation and Intercompare the Techniques of observation and analysis 20 p3022 A83-43132

Experiments in combining intensity and range edge maps 21 p3137 A83-44272

CO₂ laser rangefinders 21 p3090 A83-44812

Multicolor laser altimeter for barometric measurements over the ocean - Experimental 22 p3259 A83-46071

Laser ranging to artificial earth satellites and to the moon Present capabilities and trends 22 p3288 A83-46110

Deformation of the Australian plate - Preliminary findings from laser ranging to the LAGEOS satellite 22 p3317 A83-46363

Accurate range gating technique with mode-locked dye lasers 22 p3298 A83-46680

Tactical and atmospheric coherent laser radar technology 23 p3462 A83-47806

Determination of a chord length from laser and camera observations made on common orbital arc 23 p3421 A83-48068

Optimal conditions for determinations of polar coordinates from lunar laser ranging 23 p3483 A83-48069

LASER RANGER/TRACKER

Airborne laser ranging system for monitoring regional crustal deformation 01 p0047 A83-10024

Multifunction CO₂ NOE sensor - A status report --- Nap-Of-the-Earth 01 p0010 A83-11147

Coherent adaptive speckle tracking 08 p1097 A83-22522

Theory of tracking accuracy of laser systems 14 p2025 A83-33175

LASER SPECTROMETERS

Single-scan current-modulated tunable diode laser spectrometer of improved calibration and throughput performance 02 p0179 A83-12607

A two-channel picosecond parametric spectrometer with high temporal resolution 04 p0481 A83-15267

Royal Society, Discussion on New Techniques in Optical and Infrared Spectroscopy, London, England, April 21, 22, 1982, Proceedings 04 p0482 A83-15801

The picosecond laser - An instrument for scientific research 06 p0767 A83-19416

Atmospheric spectroscopy studies 07 p0958 A83-19972

Control of cryogenic Fourier transform spectrometer scanning mirrors 09 p1267 A83-23591

Water vapor absorption at isotopic CO₂ laser wavelengths 09 p1269 A83-24446

Tunable diode laser heterodyne spectrometer for remote observations near 8 microns 14 p2016 A83-32001

A laser spectrometer for Raman scattering 16 p2357 A83-36874

CO₂ measurements with an infrared laser spectrometer on flask samples collected at Jungfraujoch high-altitude research station (3500 meters asl) and with light aircraft up to 8000 meters over Switzerland 20 p3022 A83-42867

Optical and laser remote sensing 23 p3455 A83-47766

Remote measurement of trace gases with the JPL laser absorption spectrometer 23 p3456 A83-47771

Tunable laser heterodyne spectrometer measurements of atmospheric species 23 p3456 A83-47774

LASER SPECTROSCOPY

NT OPTOGALVANIC SPECTROSCOPY

One-photon laser spectroscopy of Rydberg series from metastable levels in calcium and strontium 01 p0105 A83-10197

Measurements of collisional broadening and the shift of argon spectral lines using a tunable diode laser 01 p0105 A83-10203

The methods and results for the laser probing of the upper atmosphere in the polar region 01 p0072 A83-10604

Spatially precise laser diagnostics for combustion 01 p0055 A83-11060

Temperature profile of a stoichiometric CH₄/N₂O flame from laser excited fluorescence measurements on OH 02 p0152 A83-12080

Concentration profiles of NH and OH in a stoichiometric CH₄/N₂O flame by laser excited fluorescence and absorption 02 p0152 A83-12081

Linewidth measurements of tunable diode lasers using heterodyne and etalon techniques 02 p0185 A83-12318

Absorption spectra of deuterated water at DF laser wavelengths 02 p0211 A83-12601

Scanning delay generator for measurement of kinetic decays using laser-induced fluorescence techniques 02 p0181 A83-12823

Measurement of the excited-atom density in a discharge in neon by laser resonance fluorescence 03 p0396 A83-13185

Absorption spectra of toxic compounds at CO₂ laser wavelengths 03 p0294 A83-13722

Spectral line inversion for sounding of stratospheric minor constituents by infrared heterodyne technique from balloon altitudes 03 p0325 A83-13723

Below room temperature measurements of the 8-12 micron water vapor continuum absorption 03 p0358 A83-13980

Precision collisional lineshapes by difference-frequency laser spectroscopy 03 p0294 A83-13982

High-resolution atmospheric spectroscopy using a diode laser heterodyne spectrometer 03 p0327 A83-13984

Atmospheric model for laser transmission in the infrared 03 p0359 A83-13990

Spatially resolved IR absorption spectroscopy by optical Stark modulation 03 p0295 A83-14376

Spectrum control of laser radiation by means of linear phase anisotropy, induced in an amplifying or absorbing medium by an external magnetic field 04 p0484 A83-15268

Shock tube diagnostics utilizing laser Raman scattering 04 p0481 A83-15287

Royal Society, Discussion on New Techniques in Optical and Infrared Spectroscopy, London, England, April 21, 22, 1982, Proceedings 04 p0482 A83-15801

Survey of lasers for spectroscopic use - Optical and ultraviolet 04 p0485 A83-15802

Critique of tunable infrared lasers 04 p0485 A83-15803

Mode-locked semiconductor lasers and their spectroscopic applications 04 p0485 A83-15805

Laser heterodyne spectroscopy 04 p0482 A83-15808

Advances in picosecond spectroscopy 04 p0456 A83-15820

Resonance structure of the photoionization cross section of atomic hydrogen in an electric field 04 p0534 A83-15903

Flow visualization in combustion gases using planar laser-induced fluorescence [AIAA PAPER 83-0405] 05 p0643 A83-16694

Investigation of the mode competition in an He-Ne/CH₄ laser with independent variation of the mode spacing and spatial shift 05 p0648 A83-17046

Feasibility of determining concentrations of atmospheric pollutants by comparative absorption using lasers having a single emission line 05 p0659 A83-17057

NO₂A₂B₂ state properties from Zeeman quantum beats 05 p0684 A83-17652

Laser absorption under saturation conditions with allowance for spectral hole burning 05 p0651 A83-17869

- 3.508 micron-HeXe-laser line absorption by formaldehyde monomer and dimer and by nitrogen dioxide monomer and dimer without and in the presence of argon 05 p0684 A83-17871
- Measurement of time dependent optical gain using frequency modulation spectroscopy 06 p0763 A83-18955
- Laser resonant optoacoustic gas-analyzer for the monitoring of trace contaminants of the atmosphere 06 p0764 A83-19183
- 2.5-THz frequency difference measurements in the visible using metal-insulator-metal diodes 06 p0764 A83-19253
- Atmospheric spectroscopy studies 07 p0958 A83-19972
- Phase-polarization laser spectroscopy 07 p0933 A83-19974
- Investigation of nonlinear absorption in H₂O vapors subjected to strong optical fields with linear and circular polarizations 07 p0991 A83-20128
- FM spectroscopy detection of stimulated Raman gain 07 p0937 A83-20798
- Influence of suspended inorganic sediment on airborne laser fluorosensor measurements 07 p0971 A83-20830
- A semiclassical study of laser-induced atomic fluorescence from Na₂, K₂ and NaK [AD-A127849] 07 p0991 A83-21051
- Contribution to the development of picosecond Raman spectroscopy and to its applications --- French thesis 07 p0882 A83-21095
- Laser optogalvanic photodetachment spectroscopy - A new technique for studying photodetachment thresholds with application to I-/I⁺ 07 p0882 A83-21190
- A study of the dynamics of UV laser photolysis of NOCl and NOBr 07 p0882 A83-21195
- Simple absolute calibration method using laser sources for pulsed spectroscopic applications in the visible and UV 07 p0932 A83-21384
- Pressure broadening of OCS in the 10 microns region 07 p0992 A83-21400
- New technique for measurement of upper laser level decay rates in gas laser plasmas 07 p0938 A83-21597
- High-performance transient absorption spectrometry on the nanosecond scale 08 p1105 A83-23228
- Single frequency scanning laser as a plasma diagnostic 08 p1111 A83-23230
- Radiative lifetimes in Fe II using selective laser excitation 09 p1341 A83-23651
- Laser-saturated fluorescence measurements of OH concentration in flames 09 p1225 A83-23749
- Infrared laser spectroscopy of molecular beams 09 p1342 A83-24146
- Laser fluorescence measurements of the OH concentration in a combustion boundary layer 09 p1226 A83-24367
- Shock-tube absorption measurements of OH using a remotely located dye laser 09 p1269 A83-24438
- Absorption of 9.6-micron CO₂ laser radiation by CO₂ at elevated temperatures 09 p1272 A83-24447
- Infrared laser optogalvanic spectroscopy of molecules 09 p1227 A83-25132
- Investigation of absorption line profiles of molecular gases by methods of laser spectroscopy 10 p1419 A83-25525
- Observation of macroscopic quantum fluctuations in stimulated Raman scattering 10 p1426 A83-25796
- Spectroscopy and efficiency of the /Hg-200/Br-81 and /Zn-64/I photodissociation lasers 10 p1426 A83-26003
- Electron spectrum measurements for a tapered-wiggler free-electron laser 10 p1428 A83-26018
- Measurements of a supersonic velocity in a nitrogen flow using inverse Raman spectroscopy 10 p1420 A83-26114
- Difference frequency laser spectroscopy of the nu₃ band of the CH₃ radical 10 p1480 A83-26451
- The rotational spectrum and hyperfine structure of the methylene radical CH₂ studied by far-infrared laser magnetic resonance spectroscopy 10 p1480 A83-26452
- The laser magnetic resonance spectrum of the nu₂ band of the methylene radical CH₂ 10 p1480 A83-26453
- Laser photofragment spectroscopy of N₂⁺/I⁺ - Evidence for predissociation of B₂Sigma⁺ u⁺ 10 p1480 A83-26455
- Propagation at 10 microns through smoke produced by atmospheric combustion of diesel fuel 10 p1447 A83-26641
- Detection of trace concentrations of H₂ in air by coherent active Raman spectroscopy 10 p1423 A83-26657
- Raman oxygen detection for combustion control and regulation 10 p1425 A83-26876
- High spectral brightness extreme ultraviolet generation with excimer lasers 11 p1576 A83-27508
- Cavity phase shift method for high reflectance measurements 11 p1572 A83-27513
- Determination of accurate dissociation limits and interatomic interactions at large internuclear distances 11 p1653 A83-27526
- Calculation of radiative transition probabilities and lifetimes 11 p1653 A83-27527
- Time-resolved infrared-ultraviolet double resonance spectroscopy of formaldehyde 11 p1653 A83-27528
- Infrared absorption spectroscopy with color center lasers 11 p1653 A83-27529
- Modeling of optical impedance spectroscopy 11 p1572 A83-27530
- Submillimeter-wave laser emission in carbonyl fluoride 11 p1578 A83-27549
- CARS-spectroscopy of UF₆ and SF₆ 11 p1654 A83-27552
- Investigations on the dynamical occupation behavior of optically excited F-centers in alkali halides by use of picosecond laser spectroscopy 11 p1579 A83-27554
- New optically pumped alkali metal dimer lasers 11 p1579 A83-27555
- Half-collision aspects of ion photofragment spectroscopy 11 p1654 A83-27584
- Sub-Doppler spectroscopy of SF₆ and OsO₄ by resonant degenerate four-wave mixing at 10.6 microns 11 p1581 A83-27598
- Minority species concentration measurements in flames using the photoacoustic and photothermal deflection technique 11 p1572 A83-27617
- Difference frequency laser spectroscopy of the nu₁ band of the HO₂ radical 11 p1655 A83-28526
- Raman spectroscopy --- Russian book 12 p1727 A83-28810
- Tunable diode laser measurements of the band strength and collision halfwidths of nitric oxide 12 p1778 A83-29149
- Resonance fluorescence and Raman line shapes produced by monochromatic laser fields - effects of branching ratio and homogeneous broadening 12 p1731 A83-29150
- CW ultraviolet saturation spectroscopy of the 6p 3P₀-9s 3S₁ transition in Mercury at 246.5 nm 12 p1778 A83-29191
- Narrow optical hole burning and related effects in ruby 12 p1782 A83-29198
- The effect of laser radiation on absorption in the far wings of spectral lines 13 p1849 A83-30084
- Biological applications of picosecond spectroscopy 13 p1845 A83-30214
- Intracavity dye-laser photothermal deflection spectroscopy 13 p1845 A83-30253
- Atomic emission spectral analysis using lasers in the monopause regime 13 p1817 A83-30260
- Inverse Lamb dip spectroscopy using microwave modulation sidebands of CO₂ laser lines 13 p1850 A83-30333
- Spatially resolved temperature measurements in a flame using laser-excited two-line atomic fluorescence and diode-array detection 13 p1817 A83-30746
- Laser induced fluorescence and absorption measurements of NO in NH₃/O₂ and CH₄/air flames 13 p1818 A83-30969
- Anti-Stokes scattering as an XUV radiation source --- for spectroscopy 13 p1818 A83-31810
- Laser techniques for spectroscopy of core-excited atomic levels 13 p1819 A83-31811
- Laser methods for the control of atmospheric gases and gases which pollute the atmosphere 14 p2052 A83-32560
- Quantitative intracavity spectroscopy 14 p2052 A83-32561
- Temperature and concentration measurements in an internal combustion engine using laser Raman spectroscopy [AIAA PAPER 83-1551] 14 p1990 A83-32772
- An investigation of the possibilities for lowering the detection limits of elements in a graphite laser torch using the intracavity method for the registration of atomic absorption 14 p2020 A83-32826
- The absorption spectrum of (C-12)D₂ in the 1.06-micron region 14 p2048 A83-32833
- Coherent anti-Stokes Raman scattering as a probe in reactive media 14 p2021 A83-33172
- Picosecond streak camera fluorimetry - A review 14 p2022 A83-33415
- Picosecond spectrochronography 14 p2022 A83-33418
- Measurement conditions for continuously recording picosecond pump-and-probe spectrometers 14 p2022 A83-33419
- Tone-burst modulated color-center-laser spectroscopy 15 p2167 A83-33758
- Laser optogalvanic detection of molecular ions 15 p2227 A83-33896
- Modulation intracavity laser spectroscopy, polarimetry, and interferometry 15 p2163 A83-33979
- Sidebands in cooperative resonance fluorescence in collections of N three-level atoms in strong excitation laser fields 15 p2169 A83-34371
- Modelling atmospheric aerosol backscatter at CO₂ laser wavelengths. I - Aerosol properties, modeling techniques, and associated problems. II - Modeled values in the atmosphere. III - Effects of changes in wavelength and ambient conditions 15 p2201 A83-34461
- Aerial testing of an N₂ laser fluorosensor system 15 p2169 A83-34467
- Photoelectrochemical and microprobe laser Raman studies of lead corrosion in sulfuric acid 15 p2133 A83-34691
- The laser-induced Schlieren effect in sodium-nitrogen mixtures [AIAA PAPER 83-1467] 15 p2165 A83-34911
- Electronically resonant CARS detection of OH [AIAA PAPER 83-1477] 15 p2133 A83-34912
- Laser tomography for simultaneous concentration and temperature measurement in reacting flows [AIAA PAPER 83-1553] 15 p2165 A83-34924
- Rayleigh thermometry with low power laser sources [AIAA PAPER 83-1554] 15 p2165 A83-34925
- Time-resolved fluorescence spectra of rotationally cooled NO₂ 16 p2408 A83-35331
- Level crossing and polarization rotation in doubly resonant third-harmonic generation in I₂ 16 p2358 A83-35658
- Excitation mechanisms for hydrogen atoms in an inverse-brush-cathode discharge 16 p2415 A83-35668
- Problems in steady-state theory of a multimode laser with a selective saturable absorber 16 p2359 A83-35896
- Measurement of the spectral-frequency and correlation parameters and characteristics of laser radiation --- Russian book 16 p2360 A83-36439
- Observation of a new electronic state of carbon monoxide using LIF on highly vibrationally excited CO(X¹Sigma⁺) 16 p2410 A83-36517
- A pulsed molecular beam for laser spectroscopy 16 p2410 A83-36554
- Determination of natural radiative lifetimes of the 5p₂ P state in Ga I and 6p₂ P state in In I using a pulsed dye laser 16 p2410 A83-36653
- Absorption measurements of H₂O at high temperatures using a CO laser 16 p2328 A83-36795
- Laser optogalvanic spectroscopy of molecules 16 p2328 A83-36974
- Laboratory simulation of tunable diode laser remote measurement of atmospheric gases using topographic targets 17 p2510 A83-37741
- Coherent Anti-Stokes Raman scattering with reflective optics Kr(+) and Ar(+) laser-excited fluorescence of CN in a flame 17 p2485 A83-37746
- Spatially resolved tunable diode-laser absorption measurements of CO using optical Stark shifting 17 p2485 A83-37747
- Simultaneous observation of rotational coherent Stokes Raman scattering and coherent anti-Stokes Raman scattering in air and nitrogen 17 p2511 A83-37943
- Single-pulse gas thermometry at low temperatures using two-photon laser-induced fluorescence in NO-N₂ mixtures 17 p2511 A83-37944
- Particle sizing in two-phase flows from scattered laser power spectra and laser attenuation 17 p2511 A83-38205
- Line strength measurements using diode lasers - The nu₂ band of H₂S 18 p2742 A83-39182
- Line broadening in multiphoton processes with a resonant intermediate transition 18 p2743 A83-39924
- Surface photoacoustic wave spectroscopy of thin films 18 p2689 A83-40058
- Dependence of the sensitivity of intracavity laser spectroscopy on generation parameters 18 p2693 A83-40347
- Investigation of superelastic electron scattering by laser-excited Ba - Experimental procedures and results 18 p2743 A83-40407
- A middle-infrared heterodyne spectrometer to be used at the Cassegrain-focus of medium-size and large astronomical telescopes 18 p2761 A83-40436
- Fluorescence measurements of OH in a turbulent flame --- A feasibility study 19 p2820 A83-40859
- Optical splitter for dynamic range enhancement of optical multichannel detectors 19 p2847 A83-41098
- Absorption of H₂S at DF laser wavelengths 19 p2852 A83-41108
- Spectroscopic laser scanning analysis of photo-induced current on a-Si solar cells 19 p2862 A83-41286

Selective nonlinear spectroscopy of inhomogeneously broadened phonon resonances in a disordered medium 20 p2993 A83-42285

Photometer for quasielastic and classical light scattering 20 p2988 A83-42295

Picosecond laser-spectroscopy measurement of hydroxyl fluorescence lifetime in flames 20 p2949 A83-42347

Dynamic measurements in gas flowfields using rotational Raman spectroscopy 20 p2950 A83-42580

Effect of resonant absorption of laser-induced plasma on temporal resolved spectrum and temporal integrated spectrum 20 p3050 A83-43177

A re-evaluation of laser heterodyne radiometer CIO measurements --- for stratospheric chemistry studies 20 p3026 A83-43209

Atomic fluorescence study of high temperature aerodynamic levitation 20 p2939 A83-43256

External-cavity diode laser emitting in the middle infrared range 20 p2998 A83-43804

Nascent NO vibrational distribution from 2485 A NO₂ photodissociation 21 p3201 A83-43959

Light scattering from gaseous nitrous oxide - Effects of correlation between molecular and intermolecular axes upon the depolarization ratio in terms of the anisotropic potential choice 21 p3204 A83-44190

Continuous wave (CW) Doppler free two-photon frequency modulated (FM) spectroscopy 21 p3139 A83-44816

High resolution spectroscopy using picosecond pulse trains 21 p3140 A83-44818

Picosecond continuum generation and spectroscopy 21 p3145 A83-44819

Picosecond spectroscopy of free complex molecules 21 p3146 A83-45335

Laser-sounding measurement of rotational temperature in a high-frequency flare discharge 21 p3215 A83-45383

Time-resolved nonlinear luminescence spectroscopy by picosecond excitation correlation 21 p3219 A83-45491

Identification of forbidden transitions in the nu-4 band of (N-14)H₃ by intracavity laser-Stark spectroscopy 22 p3355 A83-45966

New technological developments for the remote detection of atmospheric hydroxyl radicals 22 p3288 A83-46072

Frequency-doubled CO₂ lidar measurement and diode laser spectroscopy of atmospheric CO₂ 22 p3288 A83-46073

Balloon-borne diode-laser absorption spectrometer for measurements of stratospheric trace species 22 p3288 A83-46079

The collision half-width for the R(0) line of the nu3 band of methane 22 p3355 A83-46268

Developments in mode-locked lasers and their applications 22 p3298 A83-46670

Picosecond and subpicosecond luminescence in semiconductors 22 p3293 A83-46682

Generation and amplification of ultrashort laser pulses and applications to electron trapping in amorphous media 22 p3299 A83-46683

Picosecond kinetics of excited state decay processes in internally hydrogen-bonded polymer photostabilizers 22 p3269 A83-46685

Collisional broadening of nonlinear optical resonances 22 p3355 A83-46713

Assignments of optically pumped CD₃OH laser lines 22 p3299 A83-46746

Narrow output line from a distributed-feedback dye laser with broad-spectrum pumping 22 p3299 A83-46784

Laser-induced fluorescence spectroscopy for combustion diagnostics 23 p3455 A83-47656

Optical and laser remote sensing 23 p3455 A83-47766

Airborne remote sensing measurements with a pulsed CO₂ DIAL system 23 p3455 A83-47767

Differential-absorption measurements with fixed-frequency IR and UV lasers --- for pollution monitoring and control 23 p3455 A83-47768

Remote sensing of hydrazine compounds using a dual mini-TEA CO₂ laser DIAL system --- differential-absorption LIDAR 23 p3456 A83-47769

The Hull coherent DIAL programme --- differential-absorption LIDAR 23 p3456 A83-47770

Laser remote sensing measurements of atmospheric species and natural target reflectivities 23 p3456 A83-47772

Remote sensing of OH in the atmosphere using the technique of laser-induced fluorescence 23 p3457 A83-47792

Progress in laser sources for remote sensing 23 p3461 A83-47798

Review of NDRE remote sensing program and development of high pressure RF excited CO₂ waveguide lasers 23 p3462 A83-47799

Polymers in solar energy utilization 23 p3433 A83-47823

Coherent pulse propagation in the infrared on the picosecond time scale 23 p3462 A83-48314

Longitudinal Ramsey-fringe spectroscopy in a calcium beam --- for optical frequency standard 23 p3509 A83-48707

Proposal for the measuring molecular velocity vector with single-pulse coherent Raman spectroscopy 23 p3459 A83-48709

Direct observation of visibility curve of semiconductor lasers 23 p3464 A83-48721

Thermal lens spectroscopic studies of radiationless processes in NO₂ 24 p3625 A83-48796

Plasma electron density measurements by the laser-and collision-induced fluorescence method 24 p3631 A83-48819

Optogalvanic double-resonance spectroscopy in a neon discharge 24 p3631 A83-48834

Nonlinear noise fields and strongly driven atomic transitions 24 p3587 A83-48839

Atmospheric temperature measurements using a pure rotational Raman lidar 24 p3582 A83-49007

Feasibility of airborne detection of laser-induced fluorescence emissions from green terrestrial plants 24 p3598 A83-49008

A study of the emission spectrum of a TEA CO₂ laser with an intracavity absorber 24 p3588 A83-49048

An investigation of the kinetics of processes by the intracavity method according to the change in the intensity of lasing 24 p3589 A83-49739

Nonlinear plasma spectroscopy of the hydrogen Balmer-alpha line 24 p3627 A83-50196

LASER STABILITY

Self-focusing effects in free electron lasers 02 p0184 A83-12084

Relationship between carrier-induced index change and feedback noise in diode lasers 02 p0184 A83-12169

Dispersion-induced instability in CW laser oscillators 02 p0184 A83-12270

Nonlinear interaction between elliptically polarized waves in a ring gas laser in a magnetic field 03 p0316 A83-13586

Mode stabilized terrace InGaAsP lasers on semi-insulating InP 03 p0332 A83-13919

Hysteresis and stochastic phenomena in nonlinear optical systems 04 p0534 A83-15257

Gas breakdown on the surface of metallic mirrors due to radiation from a pulsed /periodic pulsed/ CO₂ laser 04 p0484 A83-15263

Ion aging effects on the dissociative-attachment instability in CO₂ lasers 04 p0484 A83-15792

Stable single-mode operation of a Q-switched laser by a simple resonator length control technique 04 p0485 A83-15948

Pulsed-power performance and stability of 880 nm GaAlAs/GaAs oxide-stripe lasers 04 p0486 A83-16215

Passive frequency stability of pulsed CO₂ lasers 05 p0647 A83-16919

Catastrophic degradation level of visible and infrared GaAlAs lasers 05 p0647 A83-16941

Approximate method for calculations of unstable telescopic resonators --- carbon dioxide gasdynamic laser design 05 p0649 A83-17061

Influence of the spatial structure of the gain on the dynamic properties of a laser 05 p0650 A83-17075

Stability of compensation regimes for nonlinear distortions of beams with any polarization 05 p0650 A83-17077

Stability of the horizontal transverse modes of the planar stripe lasers with deep Zn-diffusion 06 p0766 A83-19141

Divergence of radiation from an electric-discharge CO₂ laser having an unstable resonator 07 p0934 A83-20108

Unstable resonator misalignment in ring and linear toroidal resonators 07 p0935 A83-20159

Quantum theory of laser and optical-bistability instabilities 07 p0936 A83-20790

Frequency stabilization of GaAlAs laser using a Doppler-free spectrum of the Cs-D₂ line 07 p0938 A83-21593

Transient and stationary properties in bistable operation of a GaAs laser coupled to an external resonator 08 p1106 A83-21885

Mode-medium interactions --- high power CO₂ laser output instability 08 p1109 A83-22461

Local optical correction system --- adaptive laser beam control 08 p1109 A83-22466

Wavefront sensing and control aspects in a high energy laser optical train 08 p1109 A83-22467

Frequency-stabilized transversely excited atmospheric /TEA/ CO₂ lasers for coherent infrared radar systems 08 p1109 A83-22515

Direct frequency measurements of transitions at 520 THz /576 nm/ in iodine and 260 THz /1.15 micron/ in neon 08 p1110 A83-22633

Direct frequency measurement of the I₂-stabilized He-Ne 473-THz /633-nm/ laser 08 p1110 A83-22634

Frequency stabilization of internal-mirror He-Ne lasers 09 p1272 A83-24443

Single-parameter characterization of bistability in double contact injection lasers 09 p1273 A83-25285

Mode effects in second harmonic generation and their uses for laser stabilization 10 p1425 A83-25404

Influence of Doppler broadening on the stability of monomode ring lasers 10 p1425 A83-25430

A self-setting attenuator for laser pulse energy stabilization 10 p1425 A83-25431

Intense free electron laser harmonic generation in a longitudinal magnetic wiggler 10 p1426 A83-25792

Finite-temperature effects in free-electron lasers 10 p1427 A83-26013

Laser light backscattering off an electron beam-plasma system 10 p1428 A83-26019

External cavity controlled operation of a semiconductor diode gain element in series with an optical fiber 10 p1428 A83-26025

Bistable operation of two semiconductor lasers in an external cavity - Rate-equation analysis 10 p1428 A83-26026

Rotational nonequilibrium influences in CW HF/DF chemical lasers 10 p1429 A83-26167

Supersonic flow e-beam stabilized discharge excimer lasers 10 p1430 A83-26171

Frequency reproducibility of ring He-Ne/CH₄ lasers 10 p1433 A83-26686

Injection locking of excimer lasers 11 p1577 A83-27518

Nonlinear optical indication in frequency-stabilization systems --- for metal vapor lasers 11 p1583 A83-27955

Stabilisation of carbon dioxide lasers using the Stark effect 12 p1731 A83-29154

LIMP in continuously coupled unstable resonator --- Laser Induced Medium Perturbation effect in pulsed carbon dioxide laser 12 p1731 A83-29155

Evaluation of the light shift in a frequency standard based on Raman induced Ramsey resonance 12 p1729 A83-29192

Solid-state laser having a reflector that transmits IR and UV radiation 13 p1851 A83-30870

Bistable operation and nonuniform output in an injection heterostructure laser 13 p1851 A83-30907

Theory of a free-electron laser with gain expansion 13 p1853 A83-31111

Resonator mode structure --- in free electron lasers 13 p1854 A83-31122

Saturation of side-band instabilities in a free-electron laser 13 p1855 A83-31134

Results of international comparisons using methane-stabilized He-Ne lasers at 3.39 microns and iodine-stabilized He-Ne lasers at 633 nm 13 p1856 A83-31279

Evaluation of the thermal focal length produced in a repetitively pulsed solid-state laser 13 p1857 A83-31379

Actively coupled index-guided lasers 14 p2024 A83-32448

On a regime of the development of oscillations in a spin oscillator 14 p2025 A83-33394

The self-injected nonmode-locked picosecond laser 14 p2026 A83-33413

Power and stability of phase-conjugate lasers 15 p2167 A83-33535

Influence of Lorentz broadening on the stability of monomode ring lasers 15 p2169 A83-34370

Numerical study of overpopulation density for laser oscillation in recombining hydrogen plasmas 15 p2170 A83-34998

Natural fluctuations of the emission frequency of an He-Ne/CH₄ 3.39 micron laser 16 p2359 A83-35895

Mode structure of a tapered-wiggler free-electron laser stable oscillator 16 p2360 A83-35960

Crystal growth of mode-stabilized semiconductor diode lasers by liquid-phase epitaxy 16 p2420 A83-35987

A new stabilization system for optically pumped CW far infrared lasers 17 p2514 A83-37752

Investigation of strata in small-scale He-Ne lasers 17 p2515 A83-38488

Synchrotron instability for long pulses in free electron laser oscillators 17 p2515 A83-38970

Laser cavity dumping using optical bistability 17 p2515 A83-38971

Disappearance of laser instabilities in a Gaussian cavity mode 17 p2515 A83-38973

Optical bistability in four-level nonradiative dyes 17 p2515 A83-38974

Breathing, spiking and chaos in a laser with injected signal 17 p2515 A83-38975

- Reliability of constricted double-heterojunction AlGaAs diode lasers 18 p2693 A83-40052
- Occupation fluctuation noise - A fundamental source of linewidth broadening in semiconductor lasers 18 p2693 A83-40053
- Instabilities in inhomogeneously broadened single-mode lasers 18 p2693 A83-40346
- Room-temperature optically triggered bistability in twin-stripe lasers 18 p2693 A83-40400
- Quantum fluctuations in the two-photon laser 18 p2694 A83-40412
- Observation of changes of laser beam characteristics in aged oxide-defined narrow-stripe lasers 19 p2852 A83-40943
- Pulsed laser beam control by hot spot tracking 20 p2993 A83-42212
- New approach towards frequency stabilisation of linewidth-narrowed semiconductor lasers 20 p2994 A83-42493
- Ultra-stable laser clock - Second generation 20 p2989 A83-42576
- Routes to chaotic output from a single-mode, dc-excited laser 20 p2994 A83-42650
- Analysis of a multistable semiconductor light amplifier 20 p2994 A83-42791
- Scattering of light and acoustic disturbances in the atomic iodine laser 20 p2995 A83-42795
- Problem of stabilization of laser radiation parameters 20 p2996 A83-43784
- Investigation of the power stability of a CW carbon monoxide laser 20 p2997 A83-43793
- Noise of He-Cd laser and its suppression 21 p3143 A83-44156
- Self-pulsing and chaos in inhomogeneously broadened single mode lasers 21 p3143 A83-44192
- Intelligent attenuator for laser pulse energy and power stabilization 21 p3145 A83-44833
- Emission frequency stability in single-mode-fibre optical feedback controlled semiconductor lasers 21 p3145 A83-44954
- Operating characteristics of a laser with supplementary inertial negative feedback 21 p3146 A83-45387
- Optical stability of narrow stripe, proton-isolated AlGaAs double heterostructure lasers with gain guiding 21 p3147 A83-45485
- Diagnostic testing for evaluation of semiconductor lasers for space communications 22 p3296 A83-46613
- Spectrophon stabilization and offset tuning of a carbon dioxide waveguide laser 22 p3300 A83-46816
- Directionality of the radiation of a misaligned cavity with a lens-like medium 23 p3460 A83-47166
- Chaotic and periodic emission of high power solid state lasers 23 p3462 A83-48318
- Stability of a detuned single mode homogeneously broadened ring laser 23 p3462 A83-48319
- A study of the statistics of optical field in nonlinear media by the Monte Carlo method 23 p3463 A83-48433
- First-passage-time distributions and switching statistics in a bistable two-mode laser 24 p3587 A83-48840
- Self-pulsing in two-cavity optical bistability 24 p3589 A83-49617
- An analysis of the international comparison results of helium-neon lasers stabilized by saturated absorption in I-127 (review) 24 p3589 A83-49736
- Thermal defocusing (LIMP) in stable CO2 resonators 24 p3589 A83-49835
- LASER TARGET DESIGNATORS**
- The A6E /TRAM/ all-weather weapon system --- Target Recognition and Attack Multisensor 01 p0008 A83-11260
- The Aquila - A versatile, cost-effective military tool shows its potential 04 p0447 A83-16399
- Effects of piston and tilt errors on the performance of multiple mirror telescopes --- in laser relay systems 08 p1108 A83-22456
- LASER TARGET INTERACTIONS**
- Observations of grains in the extreme ultraviolet 01 p0104 A83-10859
- Recent development in high speed cinematographic and interferometric studies of high power laser target interaction 01 p0052 A83-11067
- A calculation of supersonic radiation waves with an allowance made for the plasma motion 02 p0240 A83-11513
- Interferometric measurement of the electron density in laser-matter interaction --- French thesis 03 p0398 A83-13808
- Titanium ignition by the emission of a CO2 laser 03 p0299 A83-14062
- The effect of giant laser pulses on a quasi-stationary plasma torch 05 p0687 A83-16893
- Reaction of metal-target vaporization to energy-flux modulation 06 p0765 A83-18445
- Gas-dynamic processes in a gas layer heated by high-intensity radiation during target acceleration 06 p0813 A83-19436
- Transition from steady-state to pulsed gas breakdown near the surface of a target subjected to laser radiation 07 p0935 A83-20124
- Concerning certain numerical models in plasma physics 07 p0996 A83-20305
- Optical orientation of a dense sodium charge-exchange target for producing polarized protons and H⁻/ ions 07 p0992 A83-20604
- Laser-generated electron emission from surfaces - Effect of the pulse shape on temperature and transient phenomena 07 p1000 A83-20749
- Laser induced structural vibration 08 p1119 A83-21803
- Overview of aero-optical phenomena --- in pulsed and continuous wave laser-target interactions 08 p1108 A83-22453
- Chemical amplification of optoacoustic signals 08 p1162 A83-23269
- Numerical method for solving radiative-transfer equations in one-dimensional problems of radiative gas-dynamics 09 p1258 A83-23568
- Ablation of a solid target by laser irradiation --- German thesis 09 p1348 A83-24848
- Plasma production during vaporization of materials by the radiation from a CO2 TEA laser 10 p1486 A83-25890
- Fluid-dynamical aspects of laser-matter interaction 10 p1416 A83-26172
- Instability of surface combustion on exposure to laser radiation 10 p1433 A83-26080
- Above threshold ionisation - Multiphoton ionization involving continuum-continuum transitions 11 p1654 A83-27557
- Optical properties of metal surfaces during laser irradiation 11 p1656 A83-27562
- Role of gas absorption in formation of fluctuations in parameters of cleared cloud medium and laser radiation 11 p1631 A83-27606
- The physics of electric-discharge CO2-lasers --- Russian book 12 p1731 A83-28815
- Narrow optical hole burning and related effects in ruby 12 p1782 A83-29198
- Diffusion mechanism of the interaction of aerosol drops and the possibility of controlling this mechanism by means of electromagnetic radiation 13 p1874 A83-30043
- Measurements of the stimulated Cerenkov interaction at optical wavelengths 13 p1856 A83-31138
- Application of the 2-D discrete-ordinates method to multiple scattering of laser radiation 13 p1857 A83-31460
- Thermal coupling on aluminum alloy surfaces in vacuum at 10.6 micrometer --- pulsed CO2 laser-duraluminum target interaction 14 p2024 A83-32712
- [AIAA PAPER 83-1441] Nonintrusive pressure measurement with laser-induced iodine fluorescence 14 p2019 A83-32724
- [AIAA PAPER 83-1468] An experimental study of the absorption mechanisms in laser-matter interaction at high energies - The effect of wavelength --- French thesis 15 p2232 A83-33699
- Collisionless dissociation of molecules due to their interaction with infrared radiation 15 p2227 A83-33984
- The instability of two plasmons and suprathermal electrons in the laser-matter interaction --- French thesis 17 p2583 A83-38224
- Surface light-induced drift of a rarefied gas 17 p2515 A83-38959
- Modification of the photoionization of hydrogen by a low-frequency laser 18 p2743 A83-40409
- A study of ablation by laser irradiation of plane targets at wavelengths 1.05, 0.53, and 0.35 micron 18 p2749 A83-40519
- Diffraction of an atomic beam by standing-wave radiation 19 p2852 A83-40966
- Pulsed laser beam control by hot spot tracking 20 p2993 A83-42212
- Temperature dependence of the absorptivity of aluminum targets at the 10.6 microns wavelength 20 p2957 A83-43785
- Effects of laser irradiation on the electrophysical properties of an indium antimonide MIS-structure interface 21 p3219 A83-45390
- Laser-driven shock-wave propagation in pure and layered targets 22 p3361 A83-45937
- Shock wave pressure enhancement using short wavelength (0.35 micron) laser irradiation 22 p3363 A83-46727
- Carbon dioxide laser-induced fast signals from silicon photodiodes 22 p3301 A83-46826
- Nonequilibrium distribution of particles with doublet levels in the infrared radiation field of a laser 23 p3460 A83-47164
- LASER TARGETS**
- Simultaneous multiple-point velocity measurements using laser-induced iodine fluorescence 05 p0646 A83-17884
- Shockfronts as model targets in laser-plasma interaction experiments 10 p1487 A83-26173
- Nonlinear energy attenuation of pulsed CO2 laser radiation in the atmospheric surface layer 10 p1434 A83-26776
- Propagation of laser radiation in water aerosol in conditions of the dispersal of this aerosol 10 p1434 A83-26778
- Numerical study of the propagation of intense laser radiation in the atmosphere 10 p1434 A83-26781
- Thermal distortions of focused laser beams in the atmosphere 10 p1434 A83-26782
- Thermal self-defocusing of laser beams in a turbulent medium 10 p1434 A83-26783
- Investigation of thermal self-defocusing of intense beams in homogeneous gas flows 10 p1435 A83-26784
- An investigation of the possibilities for lowering the detection limits of elements in a graphite laser torch using the intracavity method for the registration of atomic absorption 14 p2020 A83-32826
- Laser-modified electron scattering from a slowly ionising atom 17 p2579 A83-38366
- Estimation of boresight error in autoboresighting a laser beam on a point target - Influence of weak statistical fluctuations 19 p2900 A83-41094
- Target reflectance measurements for calibration of lidar atmospheric backscatter data 22 p3295 A83-46075
- Properties of the corona generated by the incidence of intense CO2 laser pulses on spherical targets 24 p3631 A83-48820
- LASER WEAPONS**
- War and peace in the space age 06 p0720 A83-18965
- Continuous-wave laser radiation simulation 13 p1810 A83-31193
- Pulsed laser beam control by hot spot tracking 20 p2993 A83-42212
- Simulation of hot spot tracking loops [AAS PAPER 83-007] 21 p3104 A83-44166
- LASER WELDING**
- NT BRAZING
- NT FUSION WELDING
- NT GAS WELDING
- The use of the pulse-repetition mode of a CO2 electroionization laser for laser welding 02 p0187 A83-11957
- Advances in laser and MIAB welding techniques 07 p0940 A83-20523
- Laser beam welding of aluminum alloy 5456 07 p0940 A83-20525
- Some aspects of the fluid dynamics of laser welding 08 p1112 A83-23090
- Laser welding of aluminum and aluminum alloys 12 p1733 A83-29524
- Advanced processing methods for titanium; Proceedings of the Symposium, Louisville, KY, October 13-15, 1981 15 p2134 A83-33632
- Laser welding of a titanium alloy 15 p2135 A83-33643
- Microstructures and mechanical properties of laser-welded titanium alloys 15 p2135 A83-33644
- A statistical approach to nondestructive testing of laser welds 18 p2696 A83-39997
- Improved welding penetration of a 10-kW industrial laser 21 p3146 A83-45480
- Laser treatment in mechanical engineering 23 p3466 A83-48426
- The physical processes occurring during the deep penetration of metals by a laser beam 23 p3462 A83-48428
- Laser welding of PM materials 23 p3467 A83-48724
- LASER WINDOWS**
- Wide aperture self-sustained discharge KrF and XeCl lasers 01 p0055 A83-10984
- A 10 cm aperture, high quality TEA CO2 laser 06 p0766 A83-18956
- Optical distortion and far field measurements for laser window materials 08 p1108 A83-22458
- High optical power CW operation in visible spectral range by window V-channelled substrate inner stripe lasers 08 p1110 A83-22753
- Emerging optical materials; Proceedings of the Conference, San Diego, CA, August 25, 26, 1981 09 p1345 A83-24951
- Characterization of candidate laser window materials 09 p1272 A83-24971
- Laser-induced damage and two-photon absorption measurements in CdTe 09 p1273 A83-24974
- Shock tube simulation of pulsed flow aerodynamic windows 10 p1371 A83-26138

Optics and resonator design issues for high-power free electron lasers 11 p1579 A83-27570
Thermal theory of convectively cooled mirrors, windows for CW and repetitively pulsed lasers
[AIAA PAPER 83-1720] 17 p2503 A83-37209

LASERS

NT ARGON LASERS
NT ATMOSPHERIC LASERS
NT CARBON DIOXIDE LASERS
NT CARBON MONOXIDE LASERS
NT CHEMICAL LASERS
NT CONTINUOUS WAVE LASERS
NT DF LASERS
NT DYE LASERS
NT EXCIMER LASERS
NT FREE ELECTRON LASERS
NT GALLIUM ARSENIDE LASERS
NT GAMMA RAY LASERS
NT GAS LASERS
NT GASDYNAMIC LASERS
NT GLASS LASERS
NT HCL ARGON LASERS
NT HCN LASERS
NT HELIUM-NEON LASERS
NT HF LASERS
NT HIGH POWER LASERS
NT INFRARED LASERS
NT INJECTION LASERS
NT IODINE LASERS
NT KRYPTON FLUORIDE LASERS
NT LIQUID LASERS
NT METAL VAPOR LASERS
NT NEODYMIUM LASERS
NT NITROGEN LASERS
NT NUCLEAR PUMPED LASERS
NT OPTICAL RESONATORS
NT ORGANIC LASERS
NT PLASMADYNAMIC LASERS
NT PULSED LASERS
NT Q SWITCHED LASERS
NT RAMAN LASERS
NT RARE GAS-HALIDE LASERS
NT RING LASERS
NT RUBY LASERS
NT SEMICONDUCTOR LASERS
NT SOLID STATE LASERS
NT TEA LASERS
NT TUNABLE LASERS
NT TWO-WAVELENGTH LASERS
NT ULTRASHORT PULSED LASERS
NT ULTRAVIOLET LASERS
NT WAVEGUIDE LASERS
NT X RAY LASERS
NT XENON CHLORIDE LASERS
NT XENON FLUORIDE LASERS
NT YAG LASERS

All-Union Conference on Laser Optics, 3rd, Leningrad, USSR, January 4-8, 1982, Proceedings

Applied nonlinear-optics: Second-harmonic generators and parametric light-generators --- Russian book 04 p0483 A83-15253

Fast determination of the extent of spatial and temporal coherence 05 p0650 A83-17126

Lasers '81; Proceedings of the International Conference, New Orleans, LA, December 14-18, 1981 06 p0767 A83-19191

Model of the Cerenkov laser 11 p1576 A83-27501

Investigation of the gain in a CO₂ GDL behind wedge-shaped and contoured nozzles. I - The experimental setup, the repetitively pulsed system for gain measurement 13 p1849 A83-30042

Rate equation theory of two-photon lasers 19 p2851 A83-40919

Observations of the 10-micron natural laser emission from the mesospheres of Mars and Venus 22 p3387 A83-47079

LASING

Iron diiodide photodissociation laser 02 p0184 A83-12265

Influence of quadratic pump power distribution on hole burning in neodymium lasers 02 p0185 A83-12598

Energy transfer and lasing in phosphate glasses activated with chromium, ytterbium, and erbium 03 p0331 A83-13594

An ultra-short-pulsed laser with adjustable parameters 04 p0484 A83-15264

A handbook of gasdynamic lasers --- in Russian 04 p0485 A83-15831

Methods for spectral selection in the region of the 2P_{1/2}-2P_{3/2} transition in an iodine atom under conditions of lasing in a Zeeman inhomogeneous gain profile 05 p0648 A83-17041

Spectral characteristics of neodymium-activated yttrium aluminum garnet in the ultraviolet and visible ranges 05 p0648 A83-17044

Quasi-CW lasing of a Ne-Xe-HCl mixture excited by an electric discharge 05 p0650 A83-17083

Iodine monofluoride B 3P_{1/2}+ / to X 1Sigma+ lasing from collisionally pumped states 05 p0651 A83-17653

Using estimates of the effect of heating on the operation of a solid-state laser to select the laser parameters 05 p0651 A83-17662

Investigation of a single-frequency YAG:Nd³⁺ / laser with a ring resonator 06 p0767 A83-19329

Propagation of submillimeter radiation from the output of a hollow dielectric waveguide 06 p0767 A83-19362

The picosecond laser - An instrument for scientific research 06 p0767 A83-19416

Some features of generation of spoke-shaped neodymium lasers 07 p0937 A83-20841

Contribution to the construction of a submillimeter laser - Application to the characterization of various mesomorphic substances --- French thesis 07 p0937 A83-21097

Diode laser threshold current density and lasing wavelength as functions of active region thickness 08 p1110 A83-22751

Chemical lasers --- Russian book 09 p1271 A83-23824

Motion and emission of a classical relativistic particle in a nonuniform laser wave 10 p1426 A83-25884

Quantum and quasiclassical lasing regimes 10 p1432 A83-26663

Generation of light in optical fibers made of glasses formed from rare-earth ultraphosphate crystals 10 p1432 A83-26670

Squeezed states in harmonic generation of a laser beam 10 p1435 A83-26971

XeF laser beam quality impact of pump-induced medium inhomogeneities 11 p1576 A83-27505

Transient regime and correction with adaptive optics of thermal blooming 11 p1579 A83-27553

Advances in NASA research on nuclear-pumped lasers 11 p1579 A83-27558

Laser action during the induction period of photoinitiated F₂/H₂ chain reactions 11 p1580 A83-27582

A discharge-heated calcium vapor laser 11 p1582 A83-27602

Comparison of He-Kr / + / laser oscillations in transverse and longitudinal hollow - Cathode discharges 11 p1582 A83-27603

Bistable operation of a semiconductor laser 11 p1585 A83-28674

Temporal measurement of the gain of a CuCl laser 11 p1585 A83-28702

Laser oscillation at 3.53 microns from Fe(2+) in n-InP:Fe 13 p1850 A83-30327

Thermodynamics of daylight-pumped lasers 13 p1850 A83-30749

Short wavelength laser calculations for electron pumping in neon-like krypton (Kr XXVII) 13 p1857 A83-31377

Simple and efficient preionization system for gaseous lasers 13 p1857 A83-31472

Space-time and space-averaged equations for a two-mirror laser - Theory and numerical results 14 p2025 A83-32917

Lasing characteristics of a Nd(3+):YAG laser with a long optical-fiber resonator 15 p2168 A83-33812

Laser cathode ray tube with a semiconductor double-heterostructure screen 15 p2163 A83-33921

Efficient lasing of a TEA Co₂ laser with ultraviolet preionization and utilizing unconventional transitions 15 p2168 A83-33977

Theoretical investigation of the spectral properties of gas lasers 16 p2359 A83-35889

Plasma pump sources for lasers 16 p2416 A83-35892

Possibility of operation of a chemical oxygen-iodine laser without a cooled trap 16 p2359 A83-35893

Long delay time for lasing in very narrow graded barrier single-quantum-well lasers 16 p2360 A83-36008

Resonatorless generation of a giant laser pulse 17 p2514 A83-37900

A general theory of the Raman-type free-electron laser 17 p2514 A83-38206

Calculation of optimal lasing regimes for CW supersonic electroionization CO lasers 18 p2692 A83-39516

Threshold-wavelength and threshold-temperature dependences of GaInAsP/InP lasers with frequency selective feedback operating in the 1.3- and 1.5-micron regions 18 p2693 A83-40057

Spectral characteristics of gain-guided semiconductor lasers 19 p2851 A83-40932

Reduced threshold current temperature dependence in double heterostructure lasers due to separate p-n and heterojunctions 19 p2852 A83-40938

Xenon laser action in discharge and electron-beam excited Ar-Xe mixture 19 p2853 A83-41183

Lithium niobate laser with frequency-degenerate pumping 20 p2993 A83-42290

Characteristics of mercurous bromide and iodide visible lasers 20 p2995 A83-43104

Optically pumped molecular laser utilizing C₂H₅Br and C₂H₅I halogen derivatives of ethane 20 p2996 A83-43779

Mechanism of pulse emission from high-pressure electric-discharge He-Ar, He-Kr, and He-Xe infrared lasers 20 p2996 A83-43783

Laser action in xenon pumped by pulsed beams of runaway electrons 20 p2997 A83-43800

External-cavity diode laser emitting in the middle infrared range 20 p2998 A83-43804

Tunable lasers --- Russian book 21 p3142 A83-43903

A visible free electron laser in France 21 p3143 A83-43984

Lasing and fluorescent characteristics of nine, new, flashlamp-pumpable, coumarin dyes in ethanol and ethanol:water 21 p3143 A83-44193

The lasing capacity of pyrenes in the gas phase 21 p3146 A83-45386

Lasing on the B-X band of cadmium moniodide (CdI) and (Cd-114) in a UV-preionized, transverse discharge 21 p3146 A83-45481

A He-Sr laser with a mean power of 3 W 21 p3147 A83-45504

Probabilities for transition processes crucial to Li lasers 22 p3295 A83-45945

Switching of a GaAs bistable etalon - External switching on and off, regenerative pulsations, transverse effects, and lasing 22 p3360 A83-46653

Reliability of InGaAsP/InP buried heterostructure 1.3 micron lasers 22 p3301 A83-46824

Sources of stimulated radiation using resonance electron accelerator 23 p3460 A83-47557

Analysis of temporal-length limitations in XeCl lasers 23 p3460 A83-47605

Generation of high power, very coherent radiation by interaction of a free electron laser with a molecular (or ionic) medium 23 p3463 A83-48573

Multiphoton excitation and frequency tripling in xenon 23 p3463 A83-48579

The generation of ultrashort laser pulses 24 p3586 A83-48801

LASV

U F-111 AIRCRAFT

LATCH-UP

Latchup window tests 05 p0628 A83-17526

Latchup-free Schottky-barrier CMOS 09 p1255 A83-24494

High-density and reduced latchup susceptibility CMOS technology for VLSI 19 p2837 A83-41020

Switching conditions for CMOS latch-up path with shunt resistances 21 p3124 A83-43858

LATE STARS

A further discussion on the mass loss of Mira stars 01 p0119 A83-10231

TiO band strengths in metal-rich globular clusters. V - 47 Tucanae 02 p0255 A83-12116

Observations of the first-overtone silicon monoxide bands in late-type stars 02 p0256 A83-12123

Convection in pulsating stars. I - Nonlinear hydrodynamics. II - RR Lyrae convection and stability 02 p0257 A83-12137

The infrared properties of Mira-type variables and other cool stars as determined from JHKL photometry 03 p0412 A83-13305

Two lithium-rich supergiants 03 p0421 A83-14144

Abundances in metal-poor stars. I - The globular clusters NGC 2808, NGC 3201, NGC 6397, and M 22 03 p0430 A83-14805

Abundances in metal-poor stars. II - The anomalous globular cluster Omega Centauri 04 p0550 A83-15041

Abundance of lithium in unevolved halo stars and old disk stars - Interpretation and consequences 04 p0550 A83-15043

Stokes polarimetry of main-line OH emission from stellar masers 04 p0553 A83-15617

Supergiants and the galactic metallicity gradient. I - 27 late-type supergiants in the inner-arm regions 04 p0553 A83-15623

Rotational studies of late-type stars. I - Rotational velocities of solar-type stars 04 p0553 A83-15625

Further observational evidence for a coronal boundary line in the cool star region of the H-R diagram 04 p0553 A83-15626

A comparison of observed and theoretical luminosity functions of carbon stars and late M giants 04 p0553 A83-15627

Ultraviolet and X-ray detection of the 56 Pegasi system /KO IIp + WD/ - Evidence for accretion of a cool stellar wind onto a white dwarf 04 p0553 A83-15628

The space density distribution of late-type giants in the solar neighbourhood 04 p0547 A83-15969

An unusual microwave flare with 56 second oscillations on the M dwarf L726-8 A 05 p0700 A83-17032

Studies on the spectra of K-giants. II - Abundance determinations for K-giants from very strong iron lines 06 p0827 A83-18170

The combined effect of mass loss and overshooting. I - The evolution of 35 solar mass to 100 solar mass stars during core hydrogen burning 06 p0829 A83-18543

A photometric map of interstellar reddening within 100 PC 06 p0820 A83-18863

A technique for measuring magnetic fields on solar-type stars 06 p0836 A83-19070

Photographic photometry of the eclipsing binary AD Bootes 06 p0822 A83-19173

The Cyanogen distribution of the red giants in M5 06 p0840 A83-19284

Molecular self-shielding in the outflows from late-type stars 06 p0844 A83-19496

A giant X-ray flare in the Hyades 06 p0845 A83-19525

Precise radial velocities. II - A possible detection of oscillations or running waves in Aldebaran and Arcturus 07 p1022 A83-21130

The three micron 'ice' band in grain mantles --- and their influence in interstellar extinction and polarization 07 p1024 A83-21219

Radial velocities of a random sample of K giant stars and implications concerning multiplicity among giant stars in clusters 08 p1185 A83-23084

Chromospheric activity of late-type giants and supergiants Reappearance of dynamo activity in the interior due to the spin-up of the core in evolution 08 p1185 A83-23105

Low dispersion spectrophotometry of late-type stars 09 p1353 A83-23899

Stars in late stages of evolution in close binary systems 09 p1358 A83-23904

Physical processes determining the structure of stellar chromospheres. I 09 p1358 A83-24014

RGU photometry of a southern starfield near the galactic centre /SA 158/ 09 p1354 A83-24515

Detection and BVR photometry of late type stars in the Large Magellanic cloud 09 p1355 A83-24521

Variable K-type stars in the Pleiades cluster 09 p1364 A83-25291

Discovery of an S star in the Fornax dwarf elliptical galaxy 10 p1491 A83-25353

Near infrared spectroscopy and infrared photometry of a new WC9 star 10 p1499 A83-25367

The abundance analysis of metal-poor late-type stars from a theoretical standpoint 10 p1501 A83-25578

Kinematics of the late M stars in the galactic nuclear bulge 10 p1503 A83-25721

The H I content of envelopes around evolved stars 10 p1509 A83-26377

Studies of late-type dwarfs. V - Theoretical models for lower main-sequence stars 10 p1509 A83-26382

Detection of $J = 5-4$ SiO masers in late-type stars 10 p1511 A83-26408

Periodic light variations in four pre-main-sequence K stars 10 p1513 A83-26721

Identification and properties of the M giant/X-ray system HD 154791 = 2A 1704+241 10 p1514 A83-26730

The relationship between soft X-rays and the 1640 Å feature fluxes in late-type stars 11 p1678 A83-27684

Detection of a late B star companion of the bright cluster giant c Pup equals HD 63032 11 p1679 A83-27701

The spectra of late type dwarfs and sub-dwarfs in the near ultraviolet. II - Limits to variability in MglI emission from IUE spectrophotometry 12 p1789 A83-28869

Spectral line profiles from spherical shells 12 p1789 A83-28877

Photometry of the fast-rotating late-type star W92 in NGC 2264 12 p1786 A83-29082

An H-alpha survey of southern hemisphere active chromosphere stars 13 p1951 A83-31419

Infrared speckle imaging - Improvement of the method; results on Miras and protostars 13 p1941 A83-31562

A study of shapes of Ca II chromospheric emissions in late type stars 13 p1955 A83-31655

Waves in stellar atmospheres. II - Heating of flux tubes by magnetohydrodynamic waves 13 p1955 A83-31657

Atomic and molecular hydrogen in the circumstellar envelopes of late-type stars 13 p1956 A83-31680

Photometry of the post T Tauri star HD 36705 14 p2098 A83-33058

New optical positions and proper motions of late type stars associated with SiO masers 14 p2098 A83-33061

Observation of ice mantles toward HD 29647 14 p2107 A83-33232

Narrow-band photometry in the 1-4 micron region - Calibration and applications 14 p2100 A83-33258

IUE observations of cool stars 15 p2250 A83-33585

Solar and late-type dwarfs 15 p2252 A83-33602

Coronal activity in F-, G-, and K-type stars - Relations between parameters characterizing stellar structures and X-ray emission 15 p2252 A83-33604

The magnetic field on the RS Canum Venaticorum star Lambda Andromedae 15 p2260 A83-34129

DDO photometry of the open cluster IC 4756 15 p2247 A83-34505

Rotational studies of late-type stars. III - Rotation among BY Draconis stars 15 p2268 A83-34634

Determination of the atmospheric parameters of late-type stars from low resolution spectra 16 p2432 A83-36693

A spectroscopic study of four late-type galactic WN stars The question of duplicity 17 p2588 A83-37320

Nucleosynthesis of Al-26 at low stellar temperatures 17 p2598 A83-37331

Concentrations in the local association. III - Late-type bright giants, ages and abundances 17 p2607 A83-38256

Outer atmospheres of late stars 17 p2611 A83-38556

Spectroscopic binaries near the north galactic pole paper 7: HD 107742 18 p2754 A83-39189

Magnetic heating of solar and stellar coronae 18 p2765 A83-39232

Theory of magnetic activity of late type stars 18 p2765 A83-39241

Is the SiO maser in Orion associated with a late-type star? 18 p2773 A83-39723

An analysis of the Orion SiO maser 18 p2773 A83-39724

Abundances in metal-poor stars. III - Eleven field giants 19 p2914 A83-40721

Abundances in globular cluster red giants. V - The metal-rich globular clusters 19 p2919 A83-41631

The detection of H2 in cool carbon stars 19 p2921 A83-41651

The peculiar circumstellar envelope around IRC+ 10420 20 p3065 A83-42377

Spectrum analysis of the barium stars HD 83548 and HD 65699 20 p3065 A83-42384

The H2O/OH maser 342.01+0.25 - A case of supernova-induced star formation? 20 p3066 A83-42394

The Wolf 630 moving group of stars 21 p3234 A83-44760

A catalogue of late-type supergiant stars in the Small Magellanic Cloud 21 p3226 A83-44981

Radial velocities of bright southern stars. III - Late-type standard stars at 12 Å/mm 21 p3226 A83-44983

Rotational studies of late-type stars. II - Ages of solar-type stars and the rotational history of the sun 22 p3377 A83-46256

VRI photometry - An addendum 22 p3373 A83-46403

HR 4912 - A variable of the old-disk population 22 p3374 A83-46412

Spectroscopy of six Wolf-Rayet stars - The latest and faintest 22 p3374 A83-46416

The Al I-cyanogen correlation in the spectra of globular cluster red giants and the origin of intracuster heavy element variations 22 p3382 A83-46992

Outer atmospheres of cool stars. XIV - A model for the chromosphere and transition region of Beta Ceti (G9.5 III) 22 p3382 A83-46995

Spots, spot-cycles, and magnetic fields of late-type dwarfs 23 p3521 A83-47487

Doppler imaging of starspots 23 p3516 A83-47513

Theory and observations of negative preflares in UV Cet stars 23 p3525 A83-47545

Basic parameters determining X-ray emission level in stars of spectral type later than F5 23 p3525 A83-47550

Four-colour uvby and H-beta photometry of A5 to G0 stars brighter than 8.3 m 24 p3642 A83-49317

Four-colour photometry of eclipsing binaries. XVII - Light curves of DM Virginis 24 p3642 A83-49320

Late type stars 24 p3662 A83-49570

Narrow-band photometry of G and K stars near the North Galactic Pole 24 p3645 A83-49851

Abundance of lithium in old dwarf stars 24 p3667 A83-50060

LATENT HEAT OF FUSION

U HEAT OF FUSION

LATERAL CONTROL

Application of matrix singular value properties for evaluating gain and phase margins of multiloop systems --- stability margins for wing flutter suppression and drone lateral attitude control 02 p0230 A83-12457

Cross-coupling between longitudinal and lateral aircraft dynamics in a spiral dive 04 p0449 A83-15312

Implicit adaptive control for a class of MIMO systems --- with application to lateral dynamics of F-8 aircraft 06 p0719 A83-19031

Subsonic rolling moments for wing roll control of a cruciform missile model 09 p1210 A83-24876

Zero PID control for bias momentum satellites --- Proportional Integral Derivative 10 p1385 A83-26584

Excessive roll damping can cause roll ratchet 13 p1808 A83-30171

A delayed pulse roll/yaw controller for a momentum biased spacecraft 17 p2478 A83-37458

Magnetic roll/way attitude control of a momentum biased near polar orbit satellite 17 p2478 A83-37459

Robustness analysis of a multiloop flight control system [AIAA PAPER 83-2189] 19 p2802 A83-41675

The use of singular value gradients and optimization techniques to design robust controllers for multiloop systems [AIAA PAPER 83-2191] 19 p2891 A83-41677

LATERAL OSCILLATION

An asymptotic solution to the equations of motion for the wobblestone --- asymmetrical spinning top dynamics 14 p2080 A83-32360

Numerical analysis of natural, coupled, longitudinal-lateral vibrations of an asymmetric aeroplane 20 p3001 A83-42334

LATERAL STABILITY

Optimal design of high speed rotating graphite/epoxy shafts 15 p2172 A83-34796

Application of maximum likelihood estimation to the identification of the stability derivatives of a wide body transport aircraft 15 p2123 A83-35121

The lateral response of an airship to turbulence [AIAA PAPER 83-1989] 17 p2459 A83-38915

F/A-18 high angle of attack departure resistant criteria for control law development 19 p2806 A83-41950

An improved method for predicting lateral-directional dynamic stability characteristics [SAE PAPER 830711] 20 p2937 A83-43321

LATERALITY

U LATERAL STABILITY

LATENCIALIZATION

U LATERAL CONTROL

LATITUDE

NT GEOMAGNETIC LATITUDE

Estimation of reddening at low galactic latitudes from the Lick galaxy counts 09 p1363 A83-24990

A determination of coupling coefficients on the basis of latitude measurements made during the 28th voyage of the research vessel Akademik Kurchatov --- cosmic ray neutron intensity analysis 10 p1523 A83-26106

The latitudinal dependence of the IMF polarity during 1975-1981 12 p1792 A83-29035

Features of the relationship between the spatial-temporal behavior of pulsations of decreasing period with magnetic activity 13 p1876 A83-30614

Latitudinal influences on the quiet daytime D-region [AD-A128591] 16 p2375 A83-35391

Ice and snow feedbacks and the latitudinal and seasonal distribution of climate sensitivity 16 p2386 A83-35489

Latitudinal distribution of ten stratospheric species deduced from simultaneous spectroscopic measurements 16 p2381 A83-36151

Time and latitude results of observations made at Merate Observatory with the astrolabe for the year 1982 19 p2910 A83-41058

Stratospheric aerosol mass and latitudinal distribution of the El Chichon eruption cloud for October 1982 22 p3333 A83-46883

El Chichon eruption cloud - Latitudinal variation of the spectral optical thickness for October 1982 22 p3333 A83-46884

LATITUDE MEASUREMENT

Results of astrolabe observations made at Paris - Time and latitude 1981 03 p0402 A83-13358

The effect of some systematic errors on the determination of time and latitude, and group corrections 05 p0693 A83-16858

Determination of the latitude of Sq focus and its relation to the electrojet variations 24 p3606 A83-49306

LATTICE IMPERFECTIONS

U CRYSTAL DEFECTS

LATTICE PARAMETERS

The relationship between the solutions to mixed dynamic problems for a continuous elastic medium and a lattice 02 p0189 A83-11655

Crosspolar levels of ring arrays in reflection at 45 deg incidence - Influence of lattice spacing 04 p0466 A83-15252

- Structure refinement of yttrium alpha-sialon from X-ray powder profile data 04 p0464 A83-15999
- Theoretical strength of a perfect nickel crystal under simple stresses 04 p0461 A83-16063
- On the prediction of lattice parameter vs. concentration for solid solutions extended by rapid quenching from the melt 07 p0887 A83-20635
- Microstructural changes and deformation mechanisms during creep of an unidirectionally solidified gamma/delta and gamma/gamma'-alpha eutectic alloy at elevated temperature 07 p0897 A83-21610
- Phase relations and ordering in the system erbia-hafnia 08 p1070 A83-22191
- Short-range stratification in Ti-Zr, Ti-Hf, and Zr-Hf alloys and lattice instability 08 p1068 A83-22783
- Estimation of the high-temperature strength of a nickel alloy on the basis of the degree of misorientation of the lattices of the matrix and strengthening phases during alloying with niobium and chromium 10 p1395 A83-25630
- Lattice parameter changes in Al_{0.39}/Ga_{0.61}/As due to O, Ge, Si, and S doping 10 p1488 A83-26059
- Decomposition of the metastable beta phase in the textured alloy VT19 11 p1550 A83-28545
- The Raman scattering of light and crystal-lattice dynamics 14 p2092 A83-33037
- Intraresonator conversion of the fields of plane wide-aperture resonators 18 p2744 A83-39515
- LATTICE VIBRATIONS**
- An antiplane problem concerning crack propagation in a lattice 04 p0497 A83-15388
- Defects and dislocations in the upper mantle /asthenosphere/ and attenuation of shear waves 09 p1301 A83-23674
- Large anisotropic vibrational correlations in A15 Nb₃Ge 13 p1929 A83-30922
- A study of the coupled and continuous vibrational states of dielectric crystals by Raman spectroscopy 14 p2092 A83-33039
- Group-theory properties of crystal vibrations with allowance for spatial symmetry 14 p2092 A83-33040
- Lattice dynamics of solid I₂ under high pressure 23 p3511 A83-47634
- LATTICES**
- Lattice implementation of some recursive parameter-estimation algorithms 10 p1461 A83-25395
- Collective behavior of magnons in superlattices 19 p2904 A83-40975
- LATTICES (MATHEMATICS)**
- NT BOOLEAN ALGEBRA
- NT BOOLEAN FUNCTIONS
- Periodic travelling waves in a non-integrable one-dimensional lattice 03 p0389 A83-13415
- The implementation of lattice calculations on the DAP --- Distributed Array Processor 12 p1768 A83-29623
- Boltzmann equation on a lattice: global solution for non-Maxwellian gases 21 p3220 A83-44944
- Classical statistical mechanics of a lattice model of superradiance 23 p3505 A83-48590
- LAUNCH COMPLEXES**
- U LAUNCHING BASES
- LAUNCH VEHICLE CONFIGURATIONS**
- Atlas and Centaur adaptation and evolution - 27 years and counting 01 p0018 A83-11483
- Liftoff ignition overpressure - A correlation --- full-scale measurements on Titan vehicle launch conditions 02 p0140 A83-13086
- Ariane uprated 14 p1980 A83-31924
- Integrating engine performance and trajectory analysis in designing future Shuttle systems [AIAA PAPER 83-1189] 16 p2316 A83-36267
- A Shuttle Derived Vehicle launch system [SAE PAPER 821342] 17 p2473 A83-37953
- Design of satellite launch vehicles 21 p3098 A83-43817
- Fully reusable launch vehicle with airbreathing booster [IAF PAPER 83-376] 23 p3419 A83-47364
- LAUNCH VEHICLES**
- NT ARIANE LAUNCH VEHICLE
- NT ATLAS CENTAUR LAUNCH VEHICLE
- NT ATLAS LAUNCH VEHICLES
- NT CENTAUR LAUNCH VEHICLE
- NT DELTA LAUNCH VEHICLE
- NT HEAVY LIFT LAUNCH VEHICLES
- NT REUSABLE LAUNCH VEHICLES
- NT SATURN 5 LAUNCH VEHICLES
- NT SINGLE STAGE TO ORBIT VEHICLES
- NT STANDARD LAUNCH VEHICLES
- NT TITAN LAUNCH VEHICLES
- NT TITAN 3 LAUNCH VEHICLE
- The evolution of launch systems during the next decade 01 p0018 A83-10433
- Soviet launchers 01 p0018 A83-10434

- U.S. launch systems evolution [AAS 82-136] 02 p0140 A83-11934
- The TRANSCOST' - Model for estimation of launch vehicle development, fabrication and operations cost [AAS 82-139] 02 p0244 A83-11935
- A Retrievable Carrier for European science and applications 04 p0452 A83-15671
- Launch-vehicle simulation for uniaxial transient vibration testing of satellites 08 p1050 A83-22374
- Istra - An air-breathing ballistic space transport vehicle for Europe [DGLR PAPER 82-075] 09 p1213 A83-24189
- A radio guidance algorithm for M Series rockets that are used to launch Japanese scientific satellites 10 p1382 A83-26593
- LOX/LH₂ propulsion system for launch vehicle upper stage. I System study 12 p1708 A83-29416
- A short cut integration scheme to determine the dynamic response of a launch vehicle with several payloads [AIAA 83-0817] 12 p1707 A83-29816
- Debris from spallation of foam insulation of cryogenic fuel tanks in space launch systems [AIAA PAPER 83-1457] 14 p1980 A83-32718
- Spin free analytic platform type guidance and control system --- for attitude control of rocket launcher 17 p2473 A83-37488
- Progression on the design of the high thrust hydrogen/oxygen engine HM60 17 p2483 A83-38335
- Design and development of advanced-composite shrouds 18 p2662 A83-40297
- A new approach for the design and analysis of On-Off reaction control systems --- for satellite launch vehicle upper stages 19 p2815 A83-40882
- Japan's expendable launch vehicles 19 p2812 A83-41373
- Beyond Percheron - Launch vehicle systems from the private sector [AAS PAPER 83-081] 21 p3096 A83-44181
- Commercial launch vehicle services 22 p3258 A83-45720
- Space transportation 22 p3258 A83-45859
- Competition in space - Government vs. industry 23 p3514 A83-47322
- Push to commercialize space runs into budget cutbacks, boondoggle charges, and fear of high risks 23 p3514 A83-47820

LAUNCHERS

- NT AIRCRAFT LAUNCHING DEVICES
- NT GUN LAUNCHERS
- NT HYPERVELOCITY LAUNCHERS
- NT MISSILE LAUNCHERS
- NT MOBILE MISSILE LAUNCHERS
- NT ROCKET CATAPULTS
- NT ROCKET LAUNCHERS
- Rail accelerator research at Lewis Research Center [AIAA PAPER 82-1938] 08 p1052 A83-22075
- An efficient system for transportation to and from earth orbit 11 p1536 A83-27347
- IRIS - A new Italian upper stage system [IAF PAPER 83-25] 23 p3419 A83-47237

LAUNCHING

- NT AIR LAUNCHING
- NT ORBITAL LAUNCHING
- NT ROCKET LAUNCHING
- NT SEA LAUNCHING
- NT SPACECRAFT LAUNCHING
- An analysis of the vertical launch phase of a missile concept [AIAA PAPER 83-0569] 05 p0603 A83-16796
- A new static-launch method for plastic balloons 18 p2642 A83-39816

LAUNCHING BASES

- NT CAPE KENNEDY LAUNCH COMPLEX
- The San Marco project - Prospects and programs 04 p0452 A83-15666
- Case for a Space Center in the Arabian Gulf 06 p0720 A83-18812
- The Baikonor cosmodrome 06 p0721 A83-19174

LAUNCHING DEVICES**U LAUNCHERS****LAUNCHING SITES**

- Launch sites around the world 01 p0017 A83-10436
- The Baikonor cosmodrome 06 p0721 A83-19174
- Payload/Shuttle integration at the Eastern Launch Site 13 p1809 A83-31177

LAVA

- A review of lava flow processes related to the formation of lunar sinuous rilles 02 p0266 A83-12640
- Io - A volcanic flow model for the hot spot emission spectrum and a thermostatic mechanism 03 p0133 A83-13833
- Homogeneity of lava flows - Chemical data for historic Mauna Loa eruptions 07 p0965 A83-21321

- Radar scatterometry of sand dunes and lava flows 22 p3313 A83-46218
- Petrologic monitoring of 1981 and 1982 eruptive products from Mount St. Helens 22 p3333 A83-46799
- Monitoring the 1980-1982 eruptions of Mount St. Helens
- Compositions and abundances of glass 22 p3333 A83-46800

LAW (JURISPRUDENCE)

- NT AIR LAW
- NT INTERNATIONAL LAW
- NT LEGAL LIABILITY
- NT SEA LAW
- NT SPACE LAW
- Breach of warranty - Rights and obligations 03 p0400 A83-13430
- Aircraft leasing practices in the United States - A few observations 09 p1351 A83-25120
- Essays in air law 22 p3368 A83-45826
- The Freedom of Information Act - Its impact on civil aviation 22 p3370 A83-45839

LAWS

- NT CHILD-LANGMUIR LAW
- NT CLOSURE LAW
- NT COFFIN-MANSON LAW
- NT CONSERVATION LAWS
- NT KEPLER LAWS
- NT KIRCHHOFF LAW OF RADIATION
- NT NEWTON-BUSEMANN LAW
- NT RADIATION LAWS
- NT SCALING LAWS
- NT STEFAN-BOLTZMANN LAW
- NT STOKES LAW OF RADIATION
- NT WEBER-FECHNER LAW

LAY-UP

- Variation of in-plane elastic constants in material design of composite laminates 07 p0949 A83-21623

LAYERS

- The internal structure of the earth and its concentric faults 13 p1880 A83-31348
- Stability of a thin local zone of irreversible deformations 24 p3592 A83-49037

LAYOUTS

- A general theory of optimal structural layouts 06 p0771 A83-18211
- A methodology for custom VLSI layout 21 p3124 A83-44099

LC CIRCUITS

- Transformer induced instability of the series resonant converter 19 p2838 A83-41152
- Experimental study of the 'Cerenkov' emission of solitons in two-dimensional LC-lattices 23 p3504 A83-48480

LDEF**U LONG DURATION EXPOSURE FACILITY****LEAD (METAL)**

- NT LEAD ISOTOPES
- Seasonal variations of Cd, Pb, Cu and Ni levels in snow from the eastern Arctic Ocean 11 p1613 A83-27673

LEAD ACID BATTERIES

- Results of chopper-controlled discharge life cycling studies on lead-acid batteries 11 p1604 A83-27183
- The lead-acid battery - Demonstrating the systems design approach to a practical electric vehicle power source 13 p1871 A83-31090
- Matching the characteristics of batteries with solar cell modules 14 p2004 A83-32220
- A comparison of procedures used in assessing the anodic corrosion of metal matrix composites and lead alloys for use in lead-acid batteries 14 p1989 A83-32626
- Photoelectrochemical and microprobe laser Raman studies of lead corrosion in sulfuric acid 15 p2133 A83-34691

LEAD ALLOYS

- Aluminum-lead antifriction alloys produced under conditions of compensation of gravitational segregation by electromagnetic forces 03 p0298 A83-13268
- A two-dimensional phase separation on the spherical surface of the metallic glass Au₅₅Pb_{22.5}Sb_{22.5} 03 p0399 A83-14937
- Wear resistance of dynamically compacted aluminum-steel and Al-steel-Pb alloy mixtures 06 p0731 A83-19089
- A comparison of procedures used in assessing the anodic corrosion of metal matrix composites and lead alloys for use in lead-acid batteries 14 p1989 A83-32626
- The influence of gravity on the solidification of monotectic and near monotectic Cu-Pb alloys 20 p2942 A83-43307
- Low gravity solidification structures in the tin-15 wt pct lead and tin-3 wt pct bismuth alloys 20 p2943 A83-43314

LEAD COMPOUNDS

NT LEAD OXIDES
NT LEAD SULFIDES
NT LEAD TELLURIDES

Unit cell parameters for a new crystalline polymorph of lead phthalocyanine and for two polymorphs of magnesium phthalocyanine 07 p1000 A83-21573
The interband Faraday effect and g-factors in Group IV A-VI A semiconductors 19 p2904 A83-40994
Tunable diode lasers and laser systems for the 3 to 30 microns infrared spectral region

22 p3297 A83-46638
The effect of the mode structure of laser radiation on the stability of lead azide 24 p3557 A83-49795

LEAD ISOTOPES

Distribution of lead and thallium in the matrix of the Allende meteorite and the extent of terrestrial lead contamination in chondrites 12 p1797 A83-29174
The radon cycle and its daughters - An application to the study of troposphere-stratosphere exchanges

13 p1883 A83-31720
U-Th-Pb in chondrites - Evidence of elemental mobilities and the singularity of primordial Pb

16 p2438 A83-36745
Pb, Sr, Nd and Hf isotopic evidence of multiple sources for Oahu, Hawaii basalts 18 p2718 A83-39957
Relationships between Pb and Pb-210 in aerosol and precipitation at a semiremote site in northern Wisconsin

20 p3014 A83-42854
Particle size distribution of n-alkanes nda Pb-210 in aerosols off the coast of Peru 20 p3028 A83-43556
Lead isotope systematics of some igneous rocks from the Egyptian Shield 22 p3332 A83-46704

LEAD OXIDES

Spectroscopic analysis of the chemiluminescence from lead oxide flames 20 p2950 A83-42579

LEAD POISONING

A hygienic evaluation of the effectiveness of ultraviolet radiation during the action of industrial poisons on the organism 03 p0375 A83-14347
The state of hepatic circulation under the combined effect of lead and electromagnetic fields

05 p0673 A83-17159

LEAD SULFIDES

A monolithic lead sulfide-silicon MOS integrated-circuit structure 06 p0752 A83-18756
Photosensitivity spectra of InAs-PbS heterojunctions 11 p1663 A83-28520

LEAD TELLURIDES

Dielectric constant and optical confinement in homostructure PbSnTe diode lasers

06 p0766 A83-18942
Solutal diffusion coefficient for liquid PbTe-SnTe 09 p1227 A83-25225

Ground based studies for the space processing of lead-tin-telluride 20 p2943 A83-43310
Galvanomagnetic and thermoelectric properties of p-Pb(1-x)Ge(x)Te in a 80-300 K temperature range 21 p3216 A83-44488

LEAD ZIRCONATE TITANATES

Electro-optic shutter devices utilizing lead lanthanum zirconate titanate /PLZT/ ceramic wafers

08 p1098 A83-22565
Advances in electro-optic shutter stereoscopic displays 08 p1098 A83-22566

Minimum/constant voltage lead lanthanum zirconate titanate /PLZT/ electro-optic shutters 08 p1099 A83-22567

LEADING EDGE FLAPS

Segmented vortex flaps [AIAA PAPER 83-0424] 05 p0585 A83-16706

Trailing edge flap influence on leading edge vortex flap aerodynamics 06 p0712 A83-18411

Application of Free Vortex Sheet theory to slender wings with leading-edge vortex flaps

[AIAA PAPER 83-1813] 17 p2454 A83-38646
Experimental and analytical investigation of the subsonic aerodynamics of slender wings with leading-edge vortex flaps

[AIAA PAPER 83-2113] 19 p2793 A83-41940
Wing loading on a 60 degree delta wing with vortex flaps

[AIAA PAPER 83-2555] 23 p3399 A83-48374

LEADING EDGE SLATS

The effect of a leading-edge slat on the dynamic stall of an oscillating airfoil [AIAA PAPER 83-2533] 23 p3399 A83-48368

LEADING EDGE SWEEP

Numerical study of flowfields about asymmetric external conical corners 03 p0277 A83-13130

An investigation of wing leading-edge vortices at supersonic speeds [AIAA PAPER 83-1816] 17 p2454 A83-38648

LEADING EDGES

NT BLUNT LEADING EDGES
NT SHARP LEADING EDGES

Numerical experiments on the leading-edge flowfield 03 p0277 A83-13131

Blunt fin-induced shock wave/turbulent boundary-layer interaction 03 p0277 A83-13132

Concerning dynamic stall --- of laminar flow near leading edges of airfoils 04 p0442 A83-15150

Oscillations of an unstable mixing layer impinging upon an edge 04 p0479 A83-16264

Aircraft icing roughness features and its effect on the icing process [AIAA PAPER 83-0111] 05 p0666 A83-16527

Space Shuttle Orbiter Leading Edge Structural Subsystem development [AIAA PAPER 83-0483] 05 p0604 A83-16744

Slender wings with leading-edge vortex separation - A challenge for panel-methods and Euler-solvers [AIAA PAPER 83-0562] 05 p0588 A83-16790

Development of a structural, bird impact resistant, de-iced wing leading edge for the de Havilland Dash 8 aircraft using fibre-reinforced composites 06 p0717 A83-18823

The stability of a preseparation boundary layer at the leading edge of a thin profile 06 p0713 A83-19432

Leading edge vortex flap aerodynamics 07 p0863 A83-21004

An experimental investigation of heat transfer near the leading edge of inclined flat plate in hypersonic flow 08 p1041 A83-22071

The evolution of Tollmien-Schlichting waves near a leading edge 09 p1261 A83-24410

Some new results on edge-tone oscillations in high-speed subsonic jets [AIAA PAPER 83-0665] 10 p1473 A83-25902

An experimental investigation of wake edge tones [AIAA PAPER 83-0741] 10 p1476 A83-25944

The boundary layer behind a shock wave incident on a leading edge 10 p1372 A83-26148

The development of intermittent turbulence on a swept attachment line including the effects of compressibility 11 p1567 A83-27872

Influence of leading-edge thrust on twisted and cambered wing design for supersonic cruise 12 p1696 A83-29018

Alleviation of the subsonic pitch-up of delta wings 14 p1969 A83-32583

Aerodynamic theory for wing with side edge passing subsonically through a gust 14 p1971 A83-32977

Recent studies at NASA-Langley of vortical flows interacting with neighboring surfaces 15 p2120 A83-33972

The evolution of Tollmien-Schlichting waves near a leading edge. II - Numerical determination of amplitudes 16 p2348 A83-35346

Prediction of stagnation flow heat transfer on turbomachinery airfoils [AIAA PAPER 83-1173] 16 p2294 A83-36259

Conical similarity of shock/boundary layer interactions generated by swept fins [AIAA PAPER 83-1756] 17 p2446 A83-37229

Experimental and computational investigation of the flow in the leading edge region of a swept wing [AIAA PAPER 83-1762] 17 p2446 A83-37233

Optimal form of the middle surface of a wing with supersonic leading edge, assuring minimum drag for a prescribed lift force and pitching moment 17 p2448 A83-37518

The impact of strakes on a vortex-flapped delta wing [AIAA PAPER 83-1814] 17 p2454 A83-38647

The leading-edge vortex trajectories of close-coupled wing-canard configurations and their breakdown characteristics [AIAA PAPER 83-1817] 17 p2455 A83-38649

On the conceptual design of supersonic cruising aircraft with subsonic wing leading edges 17 p2466 A83-38950

Computation of leading edge vortices [AIAA PAPER 83-1907] 18 p2634 A83-39366

Numerical simulation of the leading-edge separation vortex for a wing and strake-wing configuration [AIAA PAPER 83-1908] 18 p2637 A83-39408

An investigation of the breakdown of the leading edge vortices on a delta wing at high angles of attack [AIAA PAPER 83-2114] 19 p2793 A83-41941

An experimental study of the development of a supersonic zone near the leading edge of an airfoil oscillating in subsonic flow [AIAA PAPER 83-2133] 19 p2793 A83-41955

Wing modification for increased spin resistance [SAE PAPER 830720] 20 p2937 A83-43327

Unsteady transonic cascade with a subsonic leading-edge locus 21 p3088 A83-44931

Slender wings with leading edge vortex-separation 22 p3249 A83-46466

A method for three-dimensional boundary layer calculations on arbitrary bodies - Some results on aircraft wings and engine cowlings 22 p3251 A83-47031

Flow in a turbine cascade. I - Losses and leading-edge effects [ASME PAPER 83-GT-68] 23 p3395 A83-47921

Cooling airflow studies at the leading edge of a film-cooled airfoil [ASME PAPER 83-GT-82] 23 p3447 A83-47935

Drag of wings with cambered airfoils and partial leading-edge suction 23 p3398 A83-48220

A flight test of laminar flow control leading-edge systems [AIAA PAPER 83-2508] 23 p3404 A83-48356

Vortex sheet shortening in the Smith model for slender delta wings with leading-edge separation 24 p3544 A83-49025

Shuttle engine problems spark broad review 08 p1052 A83-22176

Calculating the amount of liquid penetrating through a leak into the closed cavity of a component pressure-tested in liquid 08 p1113 A83-22407

Aging of gas tight seals in single and multiconductor feedthroughs 09 p1238 A83-23632

Optical strip waveguide - A detailed analysis including leaky modes 09 p1344 A83-24096

Oil leakage and friction forces of reciprocating O-ring seals considering cavitation 13 p1859 A83-30249

Composites in the construction of the Lear Fan 2100 aircraft 12 p1710 A83-29718

Determination of horizontal tail load and hinge moment characteristics from flight data --- on Learjet Model 55 Longhorn 13 p1805 A83-30162

High speed propeller for the Lear Fan 2100 [AIAA PAPER 83-2465] 24 p3549 A83-49580

ASTRONAUT TRAINING

CONDITIONING (LEARNING)

HABITUATION (LEARNING)

TRANSFER OF TRAINING

The effect of autogenous training on the success of the flight training of students 03 p0383 A83-14500

The role of sleep in the regulation of learning and memory 04 p0522 A83-15776

The pattern of the energy characteristics of the EEG as an indicator of the effectiveness of the autogenous stimulation of work capacity 07 p0979 A83-20344

The effect of a peptide which induces 'delta sleep' and its analogues on the encephalogram of rabbits under normal conditions and during the deprivation of sleep and its effect on learning processes in rats 08 p1144 A83-22101

Effects of practice and the separation of test targets on foveal and peripheral stereoacuity 08 p1150 A83-23145

Genetic predispositions in human learning of motor actions 17 p2559 A83-38173

Modification by sulpiride, pimozide, or domperidone of apomorphine's effects on learning in hypoxic rats 21 p3183 A83-43995

Methods of increasing the tolerance of humans to acute hypoxia 23 p3496 A83-47101

Self-learning of sensor-motor control sequences 11 p1647 A83-27490

Adaptation and learning in systems of control and decision making --- Russian book 14 p2076 A83-33025

Applying stochastic control theory to robot sensing, teaching, and long term control 17 p2568 A83-37154

Adaptive manipulator control (movement learning algorithms) 22 p3352 A83-46399

FUNCTION OF DREAM SLEEP

'Unlearning' has a stabilizing effect in collective memories 18 p2738 A83-39966

Analysis and optimization of Rosenblatt-Parsen classifier with the aid of asymptotic expansions 19 p2889 A83-40898

Informational evaluation of operator activity in an ergatic system with a learning model 20 p3035 A83-43503

AIRCRAFT LEASING PRACTICES IN THE UNITED STATES - A few observations 09 p1351 A83-25120

LEAST SQUARES METHOD

The use of bicubic spline surfaces to represent aircraft wings and propellers --- German thesis
01 p0008 A83-10170

A numerical simulation of three-dimensional transonic flows of compressible perfect fluids around aircraft by use of the finite element and least squares methods
[AAAF PAPER NT 81-23] 02 p0169 A83-11779

Simulation of mid-infrared clutter rejection. I - One-dimensional LMS spatial filter and adaptive threshold algorithms
02 p0177 A83-12305

Procedure for camera calibration with image sequences
02 p0182 A83-12899

Decoupling the structural modes estimated using recursive lattice filters
03 p0386 A83-14174

Stochastic adaptive control and prediction based on a modified least squares - The general delay-colored noise case
03 p0387 A83-14596

A least-square iterative technique for solving time-domain scattering problems
04 p0530 A83-16316

Runge's theorem and far field patterns for the impedance boundary value problem in acoustic wave propagation
04 p0533 A83-16365

A Differential Dynamic Programming approach to nonlinear parameter identification
[AIAA PAPER 83-0284] 05 p0678 A83-16629

Adaptive antenna studies for HF communications
06 p0739 A83-18635

Parameters of CO₂ bands near 3.6 microns
07 p0881 A83-20164

Convergence in distribution of LMS-type adaptive parameter estimates
07 p0984 A83-20721

Steered beam and LMS interference canceler comparison
08 p1077 A83-22728

Some comments on Beck's solution of the inverse problem of heat conduction through the use of Duhamel's theorem
08 p1087 A83-23144

Bearings-only passive ranging using Kalman-Bucy and Moore-Penrose methods
09 p1266 A83-23543

A comparison between the pseudomeasurement and extended Kalman observers
09 p1328 A83-24715

Estimation and identification of two dimensional images
09 p1328 A83-24718

Convergence properties of LMS adaptive estimators with unbounded dependent inputs
09 p1330 A83-24743

A new recursive partitioned estimation algorithm derived from Extended Least Squares technique
09 p1330 A83-24744

Reduced order modeling of large space structures via least squares estimation
09 p1217 A83-24785

Flight tests of integrated navigation by least squares adjustment
09 p1202 A83-24871

1980-81 observations of Miranda - New orbit and mass of Ariel and Umbriel
10 p1491 A83-25354

Numerical conformal mapping and analytic continuation
10 p1470 A83-25875

Design of a continuous-time adaptive regulator
10 p1467 A83-26551

A design procedure for linear multi-variable feedback systems
10 p1468 A83-26564

Analysis method for Fourier transform spectroscopy
10 p1424 A83-26867

Calculation of the parameter for the quality of the least-squares fit in investigating atmospheric pollution by resonance absorption
11 p1613 A83-28204

Spectral least squares quantification of several atmospheric gases from high resolution infrared solar spectra obtained at the South Pole
12 p1752 A83-29148

Experiments using least square lattice filters for the identification of structural dynamics
[AIAA 83-0880] 12 p1742 A83-29830

System identification - On the variety and coherence in parameter- and other estimation methods --- Thesis
13 p1913 A83-30146

Performance of a fast algorithm for FIR system identification using least-squares analysis
13 p1911 A83-31725

Multi-segments approximation to a three-dimensional curved line using the least-squares locating method.
14 p2022 A83-33345

Parameter identification in a class of nonlinear systems
14 p2077 A83-33448

A method of two-dimensional filter image with a nonseparable autocovariance function
15 p2220 A83-33520

The covariance least-squares algorithm for spectral estimation of processes of short data length
15 p2163 A83-33690

Global fringe search techniques for VLBI
15 p2245 A83-33839

An adaptive filter using polynomial least squares methods
15 p2221 A83-35108

Least-squares sequential parameter and state estimation for large space structures
17 p2476 A83-37079

Real-time solution of linear least-squares estimation problem with semi-degenerate covariance
17 p2566 A83-37105

Progress in finite element techniques for transonic flows
[AIAA PAPER 83-1919] 18 p2635 A83-39375

An efficient short-arc orbit computation
19 p2814 A83-41559

Collocations and thirtieth order resonant harmonics --- for determining earth's gravitational field
20 p3023 A83-43153

An alternative view of the optimal output feedback compensator problem
21 p3195 A83-45106

Contour-based motion estimation
22 p3350 A83-46252

Combined least squares solution using terrestrial and Doppler observations
22 p3317 A83-46361

A complex algorithm for linearly constrained adaptive arrays
23 p3443 A83-47843

A brief note on the 'local least squares' stress smoothing technique
23 p3471 A83-48172

Systolic array for recursive least-squares minimisation
23 p3500 A83-48718

A least squares finite element scheme for transonic flow around harmonically oscillating airfoils
24 p3543 A83-48872

LEAVES

Characteristics of statoliths from rootcaps and coleoptiles
11 p1637 A83-27810

Gravitropic basis of leaf blade nastic curvatures
11 p1639 A83-27828

The changes in leaf reflectance of sugar maple (*Acer saccharum* Marsh) seedlings in response to heavy metal stress
15 p2209 A83-34156

The relationships between the chlorophyll concentration, LAI and reflectance of a simple vegetation canopy --- leaf area index
15 p2187 A83-35280

Diurnal variations of vegetation canopy structure
15 p2188 A83-35281

The red edge of plant leaf reflectance
15 p2188 A83-35282

Leaf water stress detection utilizing thematic mapper bands 3, 4 and 5 in soybean plants
15 p2188 A83-35283

The influence of soil salinity, growth form, and leaf moisture on the spectral radiance of *Spartina alterniflora* canopies
16 p2370 A83-35741

Red edge measurements for remotely sensing plant chlorophyll content
17 p2529 A83-38161

Scattering from a random layer of leaves in the physical optics limit
22 p3311 A83-46184

A video system to demonstrate interactions of near-infrared radiation with plant leaves
23 p3453 A83-47225

LED (DIODES)

U LIGHT EMITTING DIODES

LEE WAVES

The effects of moisture on trapped mountain lee waves
04 p0517 A83-15934

Field observations of stratified atmospheric flow above an obstacle
06 p0788 A83-18237

An analysis of three-dimensional mountain lee-waves in a stratified shear flow. II
06 p0790 A83-18256

Ship waves and lee waves
13 p1892 A83-31038

The numerical simulation of the interaction of cloud formation and lee waves
15 p2206 A83-34067

Numerical and analytical investigations of three-dimensional lee waves
17 p2553 A83-38763

LEG (ANATOMY)

NT FEET (ANATOMY)

NT KNEE (ANATOMY)

A comparative analysis of the movement of traumatized and healthy extremities during running on a treadmill
01 p0083 A83-10521

Rudder pedal force and seat relation for optimal efficiency with different leg geometry
02 p0225 A83-12255

Closed osteosynthesis and conservative therapy of fresh diaphyseal fractures of the crural bones
03 p0381 A83-14339

Isometric muscle force response of the human lower limb
06 p0797 A83-18195

Histometric indicators of the structure of the femoral and crural muscles of children, adolescents, and young men
07 p0978 A83-20991

The changes of the blood flow during longitudinal strains of the gastrocnemius muscle in cats
08 p1145 A83-22106

The distensibility of the veins of skeletal muscles during shifts in the level of hydrostatic venous pressure
08 p1145 A83-22109

The blood supply and the oxygen consumption of the gastrocnemius muscles of cats during isometric tetanus in conditions of a partial arterial occlusion
08 p1145 A83-22110

The activity of afferents during the effects of temperature on the skin of the forelegs of cats
08 p1145 A83-22114

The physiology and pathology of the venous blood circulation of the lower extremities --- Russian book
09 p1322 A83-23822

Supervisory control of a multilegged robot
11 p1648 A83-28098

The formation of an organic matrix in distractional bone regenerate and the characteristics of its mineralization during experimental crus stretching
14 p2066 A83-33338

Hemodynamic responses during prolonged sitting
17 p2558 A83-36995

LEGAL LIABILITY

Legal-political discrimination in cross-border satellite-mediated TV advertising and publicity - Review of problems
01 p0112 A83-10400

Recent developments in aviation case law
03 p0400 A83-13429

Breach of warranty - Rights and obligations
03 p0400 A83-13430

Environmental contamination in light of space law
05 p0692 A83-16973

The nuclear question and liability in space law
05 p0692 A83-16974

The Montreal Agreement of 1966 and the Malta Agreement of 1965
05 p0692 A83-16975

On the constitutionality of seizing aircraft without a hearing pursuant to Section 903/b/ of the Federal Aviation Act of 1958 - Procedural due process up in the air
07 p1002 A83-21548

Limitations on air carrier liability - An inadvertent return to common law principles
07 p1003 A83-21550

Space law in the United Nations - The work of the UN Outer Space Committee in 1982
08 p1171 A83-21897

Official liability for insufficient airworthiness - Comments in connection with a supreme-court decision
08 p1171 A83-21898

Air cargo - Liability limitations of the Warsaw Convention for loss of cargo are unenforceable in United States courts
09 p1351 A83-25121

International aspects of air traffic control liability. I
11 p1666 A83-27968

The role of insurance in United States authorization and supervision of non-governmental space activities
13 p1934 A83-31808

Two decades of space law codification
15 p2241 A83-35050

Legislative developments affecting the aviation industry 1981-1982
18 p2752 A83-39043

Aircraft crashworthiness in the United States - Some legal and technical parameters
18 p2752 A83-39044

Strict liability in military aviation cases - Should it apply?
18 p2753 A83-39045

Prime contractor/subcontractor product liability exposure under government contracts
18 p2753 A83-39693

Airline liability for the involuntary violation of immigration laws
18 p2753 A83-39694

Manufacturer's liability in international aerospace - A view from the United States
18 p2753 A83-39696

International aspects of air traffic control liability. II
19 p2907 A83-40900

Are the principles of the Warsaw Convention endangered by recent U.S. court decisions?
20 p3057 A83-43126

The implications of the United Nations Convention on International Multimodal Transport of Goods (Geneva, 1980) for International Civil Aviation
22 p3367 A83-45804

With regards to the Warsaw Convention - A bad process for false problems --- legal liability in air law
22 p3367 A83-45806

Aircraft crashworthiness and the manufacturer's tort liability in the United States
22 p3367 A83-45808

Spacecraft insurance
22 p3368 A83-45816

Some thoughts on the economic significance of limited liability in air passenger transport
22 p3369 A83-45828

Passenger liability in international carriage by air - Lines of development
22 p3369 A83-45831

Liability and insurance for damage caused by foreign aircraft to third parties on the surface - A possible new approach to an old problem
22 p3369 A83-45835

International multimodal transport - A legal labyrinth
22 p3369 A83-45837

The legal status of the aircraft commander - Ups and downs of a controversial personality in international law
22 p3370 A83-45842

Montreal Protocol - The most recent attempt to modify the Warsaw Convention 24 p3637 A83-49026

LEGENDRE CODE

U COMPUTER PROGRAMMING
U NEUTRON SCATTERING

LEGENDRE FUNCTIONS

Conditions of optimality for singular trajectories in the problem of the minimization of a curvilinear integral

06 p0805 A83-17977
Recursive formulas for determining perturbing accelerations in intermediate satellite motion

08 p1048 A83-22097
Legendre transformations and extremum principles

10 p1470 A83-25315
Local toroidal black holes that are static and axisymmetric 19 p2916 A83-41292

LEGENDRE POLYNOMIALS

U LEGENDRE FUNCTIONS

LEGENDRE TRANSFORMATION

U LEGENDRE FUNCTIONS

LEIDENFROST PHENOMENON

Theory of the Leidenfrost phenomenon 18 p2685 A83-39866

LEMMAS

U THEOREMS

LENGTH

Growth behavior of small cracks and variation of statistical crack-length distribution in corrosion fatigue 05 p0653 A83-17091

Effects of random member length errors on the accuracy and internal loads of truss antennas [AIAA 83-1019] 12 p1741 A83-29801

An examination of hot-wire length corrections 18 p2692 A83-40501

LENNARD-JONES GAS

Calculation of the kinetic coefficients for a moderately dense gas 13 p1932 A83-30657

LENS ANTENNAS

Commutating spot transmissive lens antenna 01 p0042 A83-11158

Radiation pattern computation of a spherical lens using Mie series 03 p0306 A83-14027

Bispherical constrained lens antennas 03 p0306 A83-14028

Characteristics of the cross-polarized radiation of dielectric radio lenses 04 p0466 A83-15718

Rotman lens fed multiple beam array 06 p0738 A83-18618

Some characteristics of multiple beam antennas - A review 06 p0739 A83-18624

Design considerations for millimetre wave lens antennas 07 p0913 A83-20183

Dielectric lens shaping and coma-correction zoning. I - Analysis 09 p1248 A83-23813

A coma-corrected multibeam shaped lens antenna. II - Experiments 09 p1248 A83-23814

An antenna system with a passive scatterer 11 p1558 A83-28682

A scanned antenna with an electrically controlled lens 11 p1559 A83-28684

Shaped lens antennas 15 p2146 A83-35081

A geodesic lens antenna for 360 deg azimuthal coverage 15 p2146 A83-35085

Studies on certain modified Luneberg lenses 20 p2963 A83-42369

The theory of three-dimensional bifocal antennas 22 p3271 A83-45650

Off-axis scanning of cylindrical lenses 23 p3442 A83-47831

LENS DESIGN

Light transmission optics /2nd edition/ --- Book 01 p0106 A83-10879

The image-forming properties of multiple-zone Fresnel lenses in the millimeter-wavelength range 02 p0175 A83-11539

Phase-space performances of optimized and conventional synchrotron radiation grazing incidence mirrors 02 p0237 A83-12696

Traditions of optical fabrication 02 p0237 A83-12697

Multifocal three-dimensional bootlace lenses 03 p0305 A83-14002

Null test for hyperbolic convex mirrors 06 p0809 A83-18578

Dual GRIN lens wavelength multiplexer --- Graded Refractive Index 07 p0993 A83-20831

Infrared zoom lens system for target detection 08 p1103 A83-22855

A wide-angle scanning optical antenna 09 p1246 A83-23783

Rectangular Luneburg-type lenses for integrated optics 10 p1482 A83-26117

Paraboloid of revolution used for receiving the laser radiation, for beams not parallel to the axis of the paraboloid 10 p1435 A83-26883

Analysis of the output signal of devices for measuring the defocusing of lenses under coherent illumination 11 p1574 A83-28498

The effect of aberrations on the quality of the optical Fourier transformation 13 p1918 A83-30444

Generation of off-axis aspherics --- optical surfaces for telescopes 13 p1921 A83-31015

Multisection planar focusing lenses as concentrators of solar radiation 14 p2036 A83-32047

Confocal optical feedback processing system - An improved optical design 14 p2076 A83-32903

Optimal conditions for protecting the eyes from solar radiation with vision correction 14 p2073 A83-33314

Exact analytical solution of the generalized Luneburg lens problem 15 p2230 A83-33807

Chirped grating lenses in Ti-indiffused LiNbO3 optical waveguides 21 p3207 A83-44835

Integrated optical microwave spectrum analyser (IOSA) using geodesic lenses 21 p3208 A83-44844

Double ion exchanged chirp grating lens in lithium niobate waveguides 21 p3208 A83-45483

Compact refractor telescopes for the thermal infrared 22 p3357 A83-46588

Development of a tantalum pentoxide Luneburg lens 22 p3359 A83-46644

Fabrication and performance of diffraction lenses 22 p3359 A83-46645

A method of calculating the efficiency for coupling light power from a LED into an optical fibre by use of a sphere lens 24 p3627 A83-48745

Chirped grating lenses on Nb2O5 transition waveguides 24 p3629 A83-49020

Applied optics (2nd revised edition) --- Russian book 24 p3629 A83-49411

Development of a tantalum pentoxide Luneburg lens 22 p3359 A83-46644

Fabrication and performance of diffraction lenses 22 p3359 A83-46645

A method of calculating the efficiency for coupling light power from a LED into an optical fibre by use of a sphere lens 24 p3627 A83-48745

Chirped grating lenses on Nb2O5 transition waveguides 24 p3629 A83-49020

Applied optics (2nd revised edition) --- Russian book 24 p3629 A83-49411

Development of a tantalum pentoxide Luneburg lens 22 p3359 A83-46644

Fabrication and performance of diffraction lenses 22 p3359 A83-46645

A method of calculating the efficiency for coupling light power from a LED into an optical fibre by use of a sphere lens 24 p3627 A83-48745

Chirped grating lenses on Nb2O5 transition waveguides 24 p3629 A83-49020

Applied optics (2nd revised edition) --- Russian book 24 p3629 A83-49411

Development of a tantalum pentoxide Luneburg lens 22 p3359 A83-46644

Fabrication and performance of diffraction lenses 22 p3359 A83-46645

A method of calculating the efficiency for coupling light power from a LED into an optical fibre by use of a sphere lens 24 p3627 A83-48745

Chirped grating lenses on Nb2O5 transition waveguides 24 p3629 A83-49020

Applied optics (2nd revised edition) --- Russian book 24 p3629 A83-49411

Development of a tantalum pentoxide Luneburg lens 22 p3359 A83-46644

Fabrication and performance of diffraction lenses 22 p3359 A83-46645

A method of calculating the efficiency for coupling light power from a LED into an optical fibre by use of a sphere lens 24 p3627 A83-48745

Chirped grating lenses on Nb2O5 transition waveguides 24 p3629 A83-49020

Applied optics (2nd revised edition) --- Russian book 24 p3629 A83-49411

Development of a tantalum pentoxide Luneburg lens 22 p3359 A83-46644

Fabrication and performance of diffraction lenses 22 p3359 A83-46645

A method of calculating the efficiency for coupling light power from a LED into an optical fibre by use of a sphere lens 24 p3627 A83-48745

Chirped grating lenses on Nb2O5 transition waveguides 24 p3629 A83-49020

Applied optics (2nd revised edition) --- Russian book 24 p3629 A83-49411

Development of a tantalum pentoxide Luneburg lens 22 p3359 A83-46644

Fabrication and performance of diffraction lenses 22 p3359 A83-46645

A method of calculating the efficiency for coupling light power from a LED into an optical fibre by use of a sphere lens 24 p3627 A83-48745

Chirped grating lenses on Nb2O5 transition waveguides 24 p3629 A83-49020

Applied optics (2nd revised edition) --- Russian book 24 p3629 A83-49411

Development of a tantalum pentoxide Luneburg lens 22 p3359 A83-46644

Fabrication and performance of diffraction lenses 22 p3359 A83-46645

A method of calculating the efficiency for coupling light power from a LED into an optical fibre by use of a sphere lens 24 p3627 A83-48745

Chirped grating lenses on Nb2O5 transition waveguides 24 p3629 A83-49020

Applied optics (2nd revised edition) --- Russian book 24 p3629 A83-49411

Development of a tantalum pentoxide Luneburg lens 22 p3359 A83-46644

Fabrication and performance of diffraction lenses 22 p3359 A83-46645

A method of calculating the efficiency for coupling light power from a LED into an optical fibre by use of a sphere lens 24 p3627 A83-48745

Chirped grating lenses on Nb2O5 transition waveguides 24 p3629 A83-49020

Applied optics (2nd revised edition) --- Russian book 24 p3629 A83-49411

Development of a tantalum pentoxide Luneburg lens 22 p3359 A83-46644

Fabrication and performance of diffraction lenses 22 p3359 A83-46645

A method of calculating the efficiency for coupling light power from a LED into an optical fibre by use of a sphere lens 24 p3627 A83-48745

Chirped grating lenses on Nb2O5 transition waveguides 24 p3629 A83-49020

Applied optics (2nd revised edition) --- Russian book 24 p3629 A83-49411

Development of a tantalum pentoxide Luneburg lens 22 p3359 A83-46644

Fabrication and performance of diffraction lenses 22 p3359 A83-46645

A method of calculating the efficiency for coupling light power from a LED into an optical fibre by use of a sphere lens 24 p3627 A83-48745

Chirped grating lenses on Nb2O5 transition waveguides 24 p3629 A83-49020

Applied optics (2nd revised edition) --- Russian book 24 p3629 A83-49411

Development of a tantalum pentoxide Luneburg lens 22 p3359 A83-46644

Fabrication and performance of diffraction lenses 22 p3359 A83-46645

A method of calculating the efficiency for coupling light power from a LED into an optical fibre by use of a sphere lens 24 p3627 A83-48745

Chirped grating lenses on Nb2O5 transition waveguides 24 p3629 A83-49020

Applied optics (2nd revised edition) --- Russian book 24 p3629 A83-49411

Development of a tantalum pentoxide Luneburg lens 22 p3359 A83-46644

Fabrication and performance of diffraction lenses 22 p3359 A83-46645

A method of calculating the efficiency for coupling light power from a LED into an optical fibre by use of a sphere lens 24 p3627 A83-48745

Chirped grating lenses on Nb2O5 transition waveguides 24 p3629 A83-49020

Applied optics (2nd revised edition) --- Russian book 24 p3629 A83-49411

Development of a tantalum pentoxide Luneburg lens 22 p3359 A83-46644

Fabrication and performance of diffraction lenses 22 p3359 A83-46645

A method of calculating the efficiency for coupling light power from a LED into an optical fibre by use of a sphere lens 24 p3627 A83-48745

Chirped grating lenses on Nb2O5 transition waveguides 24 p3629 A83-49020

Applied optics (2nd revised edition) --- Russian book 24 p3629 A83-49411

Development of a tantalum pentoxide Luneburg lens 22 p3359 A83-46644

Fabrication and performance of diffraction lenses 22 p3359 A83-46645

A method of calculating the efficiency for coupling light power from a LED into an optical fibre by use of a sphere lens 24 p3627 A83-48745

Chirped grating lenses on Nb2O5 transition waveguides 24 p3629 A83-49020

Applied optics (2nd revised edition) --- Russian book 24 p3629 A83-49411

Development of a tantalum pentoxide Luneburg lens 22 p3359 A83-46644

Fabrication and performance of diffraction lenses 22 p3359 A83-46645

A method of calculating the efficiency for coupling light power from a LED into an optical fibre by use of a sphere lens 24 p3627 A83-48745

Chirped grating lenses on Nb2O5 transition waveguides 24 p3629 A83-49020

Applied optics (2nd revised edition) --- Russian book 24 p3629 A83-49411

Development of a tantalum pentoxide Luneburg lens 22 p3359 A83-46644

Fabrication and performance of diffraction lenses 22 p3359 A83-46645

Vertebral lesions after pilot ejection from fighter aircraft 16 p2397 A83-35580

Unique biological aspects of radiation hazards - An overview 19 p2873 A83-40847

Vertebral lesions after pilot ejection from fighter aircraft 16 p2397 A83-35580

Unique biological aspects of radiation hazards - An overview 19 p2873 A83-40847

Vertebral lesions after pilot ejection from fighter aircraft 16 p2397 A83-35580

Unique biological aspects of radiation hazards - An overview 19 p2873 A83-40847

Vertebral lesions after pilot ejection from fighter aircraft 16 p2397 A83-35580

Unique biological aspects of radiation hazards - An overview 19 p2873 A83-40847

Vertebral lesions after pilot ejection from fighter aircraft 16 p2397 A83-35580

Unique biological aspects of radiation hazards - An overview 19 p2873 A83-40847

Vertebral lesions after pilot ejection from fighter aircraft 16 p2397 A83-35580

Unique biological aspects of radiation hazards - An overview 19 p2873 A83-40847

Vertebral lesions after pilot ejection from fighter aircraft 16 p2397 A83-35580

Unique biological aspects of radiation hazards - An overview 19 p2873 A83-40847

Vertebral lesions after pilot ejection from fighter aircraft 16 p2397 A83-35580

Unique biological aspects of radiation hazards - An overview 19 p2873 A83-40847

Vertebral lesions after pilot ejection from fighter aircraft 16 p2397 A83-35580

Unique biological aspects of radiation hazards - An overview 19 p2873 A83-40847

Vertebral lesions after pilot ejection from fighter aircraft 16 p2397 A83-35580

Unique biological aspects of radiation hazards - An overview 19 p2873 A83-40847

Vertebral lesions after pilot ejection from fighter aircraft 16 p2397 A83-35580

Unique biological aspects of radiation hazards - An overview 19 p2873 A83-40847

Vertebral lesions after pilot ejection from fighter aircraft 16 p2397 A83-35580

Unique biological aspects of radiation hazards - An overview 19 p2873 A83-40847

Vertebral lesions after pilot ejection from fighter aircraft 16 p2397 A83-35580

Unique biological aspects of radiation hazards - An overview 19 p2873 A83-40847

Vertebral lesions after pilot ejection from fighter aircraft 16 p2397 A83-35580

Unique biological aspects of radiation hazards - An overview 19 p2873 A83-40847

Vertebral lesions after pilot ejection from fighter aircraft 16 p2397 A83-35580

Unique biological aspects of radiation hazards - An overview 19 p2873 A83-40847

Vertebral lesions after pilot ejection from fighter aircraft 16 p2397 A83-35580

Unique biological aspects of radiation hazards - An overview 19 p2873 A83-40847

Vertebral lesions after pilot ejection from fighter aircraft 16 p2397 A83-35580

Unique biological aspects of radiation hazards - An overview 19 p2873 A83-40847

Vertebral lesions after pilot ejection from fighter aircraft 16 p2397 A83-35580

Unique biological aspects of radiation hazards - An overview 19 p2873 A83-40847

Vertebral lesions after pilot ejection from fighter aircraft 16 p2397 A83-35580

Unique biological aspects of radiation hazards - An overview 19 p2873 A83-40847

Vertebral lesions after pilot ejection from fighter aircraft 16 p2397 A83-35580

Unique biological aspects of radiation hazards - An overview 19 p2873 A83-40847

Vertebral lesions after pilot ejection from fighter aircraft 16 p2397 A83-35580

Unique biological aspects of radiation hazards - An overview 19 p2873 A83-40847

Vertebral lesions after pilot ejection from fighter aircraft 16 p2397 A83-35580

Unique biological aspects of radiation hazards - An overview 19 p2873 A83-40847

Vertebral lesions after pilot ejection from fighter aircraft 16 p2397 A83-35580

Unique biological aspects of radiation hazards - An overview 19 p2873 A83-40847

Vertebral lesions after pilot ejection from fighter aircraft 16 p2397 A83-35580

Unique biological aspects of radiation hazards - An overview 19 p2873 A83-40847

Vertebral lesions after pilot ejection from fighter aircraft 16 p2397 A83-35580

- Design of adaptive controllers using the method of Lyapunov functions 07 p0984 A83-19998
- Adaptive systems and time varying plants 07 p0985 A83-21164
- Robust Lyapunov stability results and adaptive systems 09 p1328 A83-24724
- Design of a multivariable model following adaptive control system 09 p1333 A83-24793
- Chaos in the semiclassical N-atom-Jaynes-Cummings model - Failure of the rotating-wave approximation 10 p1481 A83-25797
- A new method for synthesis of nonlinear parameter and state estimators for noisily disturbed processes 10 p1465 A83-26532
- On the Liapounov-Movchan stability of equilibrium of elastic orthotropic plates 11 p1593 A83-27860
- Some difficulties generated by small sinks in the numerical study of dynamical systems - Two examples 12 p1775 A83-29163
- Method of Liapunov functions in the theory of the analytical design of nonlinear controllers 13 p1910 A83-30013
- A study of the stability of nearly periodic resonance systems with respect to some of the variables 14 p2080 A83-32361
- Stability in the restricted problem of three bodies with Liapounov Characteristic Numbers 15 p2246 A83-34394
- Some necessary conditions for steepest descent controllability 17 p2566 A83-37099
- Proportional + integral + double integral adaptive laws for Liapunov MRAC --- Model Reference Adaptive Control 17 p2566 A83-37100
- Adaptive control of nonlinear self-oscillating systems using MRAS technique 17 p2568 A83-37127
- The dependence of the Kolmogorov entropy of mappings on coordinate systems 18 p2740 A83-39001
- Stability of systems - A survey 19 p2891 A83-41490
- A Liapunov theory for the existence and uniqueness of solutions to boundary value problems 20 p3042 A83-42939
- Lyapunov exponents for multidimensional orbits 20 p3043 A83-43566
- Basic methods for stability analysis of nonlinear oscillations and waves 20 p3043 A83-43670
- On the status of stability of interconnected systems 21 p3198 A83-44098
- Real-time parameter identification in a class of distributed systems using Lyapunov design method. I - Theory 24 p3620 A83-49895

LIBRARIES

- Architecture for scientific software. I - Data centralization 02 p0229 A83-12348
- A national Landsat collection and a proposal for a library of Landsat images 03 p0348 A83-14270
- The data library --- for flow data storage 13 p1934 A83-30629

LIBRATION

- Accelerometer-enhanced orbit control near the sun-earth L1 libration point [AIAA PAPER 83-0018] 05 p0601 A83-16467
- Analytical theory of the libration of the moon 08 p1190 A83-23125
- Libration points of central configurations 13 p1940 A83-31273
- Hyperion - Collisional disruption of a resonant satellite 16 p2436 A83-35739
- Secular orbit-orbit resonance between two satellites with non-zero masses 20 p3062 A83-43572
- A semi-passive procedure for librational control of communications and earth sensing satellites [IAF PAPER 83-337] 23 p3421 A83-47347
- Rotatory motion of a rigid body near libration points [IAF PAPER 83-342] 23 p3417 A83-47351

LIBRATIONAL MOTION

- Global sensitivity to velocity errors at the libration points 03 p0405 A83-13420
- Transient dynamics during the Space Shuttle based manufacture of structural components - General formulation of the problem [AIAA PAPER 83-0432] 05 p0600 A83-16711
- Periodic satellite orbits. II - Libration of the Mimas-Tethys type 06 p0817 A83-17989
- Nature of the Kirkwood gaps in the asteroid belt 08 p1176 A83-23259
- Calculation of ephemerides for libration points 09 p1355 A83-25282
- A search for objects near the earth-moon Lagrangian points 13 p1939 A83-31206
- An asymptotic solution to the equations of motion for the wobblestone --- asymmetrical spinning top dynamics 14 p2080 A83-32360

- The stability of the stationary motions of a dynamically symmetric solid at a triangular libration point 14 p1979 A83-32362
- A note on the normalized period of libration of Trojan asteroids 15 p2246 A83-34388
- Three-dimensional control of the Shuttle supported tethered satellite systems during retrieval 21 p3102 A83-45125

LIBYAN DESERT

- Application of remote sensing data to hydrogeological purposes in the Fezzan Region-Lybia 09 p1287 A83-24566

LICENSING

- Selected topics in licensing Airbus A310 [DGLR PAPER 82-042] 09 p1199 A83-24166
- Comfort criteria and/or national requirements in the issuance of a license for air service in Canada 22 p3367 A83-45807

LIDAR

- U OPTICAL RADAR

LIE GROUPS

- NT SPINOR GROUPS

- Estimating three-dimensional motion parameters of a rigid planar patch 01 p0097 A83-11419
- Moving frames and prolongation algebras 07 p0988 A83-21043
- A group-theoretic approach to discrete-time non-linear controllability 09 p1329 A83-24732
- A Lie algebraic decomposition of nonlinear systems 09 p1329 A83-24735
- The reduction to the rotation for planar perturbed Keplerian systems 12 p1787 A83-29114
- Differential-geometric methods in control theory 13 p1911 A83-31723
- Method for generating discrete soliton equations. I. II 14 p2080 A83-32517
- The unitary group and the electron correlation problem 19 p2899 A83-41872
- Asymptotic expansions and Lie algebras for some nonlinear filtering problems 20 p3040 A83-43406
- A unified treatment of some expansion procedures in perturbation theory - Lie series, Faadi Bruno operators, and Arbogast's Rule 20 p3043 A83-43576
- The Lie transformation group model of visual perception 22 p3348 A83-45947
- Lie-isotopic lifting of the special relativity for extended deformable particles 23 p3503 A83-47420
- The Lie-series method in the problem of the separation of motions in nonlinear mechanics 23 p3505 A83-48527

LIFE (BIOLOGY)

- U LIFE SCIENCES

LIFE (DURABILITY)

- NT FATIGUE LIFE
- NT SATELLITE LIFETIME
- NT SERVICE LIFE
- NT STORAGE STABILITY
- Evaluation of titanium prebond treatments by stress durability testing 07 p0886 A83-20455
- Carrier lifetimes in silicon epitaxial layers deposited on oxygen-implanted substrates 08 p1082 A83-22920
- Creep damage concepts and applications to design life prediction 09 p1233 A83-24080
- Catalyst durability evaluation for advanced gas turbine engines [ASME PAPER 82-JPGC-GT-21] 09 p1274 A83-25270
- Calculation of the durability distribution functions for structural elements with cracks 11 p1598 A83-28484
- Life estimation of an S-Glass/epoxy composite under sustained tensile loading 12 p1711 A83-29894
- Validity of the effective lifetime concept in polycrystalline silicon 14 p2088 A83-32235
- Determination of minority carrier lifetime and effective back surface recombination velocity in BSF silicon solar cells from transient measurements 15 p2191 A83-34515
- Mobility-lifetime product and interface property in amorphous silicon solar cells 16 p2418 A83-35442
- Minority carrier recombination in heavily-doped silicon 16 p2419 A83-35673
- Elemental carbon in the atmosphere - Cycle and lifetime 21 p3171 A83-44376

LIFE CYCLE COSTS

- Testability - A quantitative approach 01 p0057 A83-10756
- Design for testability /DFT/ 01 p0058 A83-10757
- A software lifecycle case study using the PRICE model 01 p0112 A83-11105
- Activity distribution analysis --- for life cycle budgeting and program management 01 p0112 A83-11154
- Life Cycle Cost analysis of standard avionics hardware and software 01 p0112 A83-11256

- The application of energy saving concepts to future fighter/attack aircraft design [AIAA PAPER 83-0092] 05 p0594 A83-16516
- Setting design goals for advanced propulsion systems [AIAA PAPER 81-1505] 08 p1045 A83-22154
- Tactical aircraft engine usage - A statistical study 09 p1206 A83-24033
- Benefits of mission profile testing 13 p1862 A83-31481
- Expected cycle life vs. depth of discharge relationships of well-behaved single cells and cell strings 14 p2046 A83-32627
- MX Launcher gas generator development 15 p2125 A83-33737
- Space station propulsion system trade study [AIAA PAPER 83-1220] 16 p2316 A83-36289
- The impact of engine usage on life cycle cost [AIAA PAPER 83-1406] 16 p2310 A83-36395
- LCC evaluation of advanced engine damage tolerance goals for a hot-section disk --- in aircraft engines [AIAA PAPER 83-1407] 16 p2310 A83-36396
- Space station automation and autonomy - Advantages and problems 17 p2476 A83-37096
- Economic evaluation of a standard product of fiber-reinforced composite material in comparison with steel 17 p2483 A83-38875
- Estimation of the life cycle costs of complex technical systems 18 p2752 A83-39990
- Availability as a function of usage profile [AIAA PAPER 83-2287] 19 p2855 A83-41747
- The cost-effectiveness of modular and single-purpose rocket boosters and worldwide trends 20 p2944 A83-42566
- The entropy of affordability 20 p3042 A83-42569
- Economic evaluation of wind energy applications for remote location power supply 20 p3056 A83-43367
- Life cycle cost applications to conceptual designs [SAWE PAPER 1479] 20 p3056 A83-43748
- MATE institutionalization --- Management of Automatic Test Equipment for weapon systems 22 p3303 A83-45823
- EAGLE/DTA - A life cycle cost model for damage tolerance assessment --- Engine/Aircraft Generalized Life cycle cost Evaluator [ASME PAPER 83-GT-76] 23 p3407 A83-47929
- Life cycle cost management - An engineer's view [AIAA PAPER 83-2451] 23 p3513 A83-48334
- Avionics built-in-test effectiveness and life cycle cost [AIAA PAPER 83-2448] 24 p3543 A83-49578

LIFE DETECTORS

- A quarantine protocol for analysis of returned extraterrestrial samples 19 p2885 A83-40830

LIFE SCIENCES

- NT EXTRATERRESTRIAL LIFE

- NT MOLECULAR BIOLOGY

- Life science research in space - The Spacelab era 03 p0375 A83-13720
- Life sciences experiments for a space platform/station [SAE PAPER 820834] 13 p1898 A83-30932
- Life science research on-board Spacelab. I - The Spacelab system 16 p2393 A83-35609
- Life science research on-board Spacelab. II - European multipurpose experimental facilities 18 p2732 A83-39968
- Life sciences and Space Research XX(1); Proceedings of the Workshops and Topical Meeting, Ottawa, Canada, May 16-June 2, 1982 19 p2871 A83-40826
- Space Station and the life sciences [AIAA PAPER 83-7089] 19 p2884 A83-42078

LIFE SPAN

- Heredity, aging, and longevity of humans 18 p2735 A83-40572
- Effects of simulated increased gravity on the rate of aging of rats - Implications for the rate of living theory of aging 21 p3183 A83-44575
- Antioxidants, metabolic rate and aging in Drosophila 21 p3183 A83-44600

LIFE SUPPORT SYSTEMS

- NT CLOSED ECOLOGICAL SYSTEMS
- NT PORTABLE LIFE SUPPORT SYSTEMS
- An atmospheric exposure chamber for small animals 01 p0086 A83-11108
- The 1981 Naval and Marine Corps aviation anthropometry survey and applications 04 p0525 A83-15414
- Environmental control and life support - Partially closed system will save big money 09 p1324 A83-24356
- Control problems in Autonomous Life Support Systems 09 p1325 A83-24764
- Space station environmental, thermal control and life support /ETCLS/ - Meeting the evolutionary growth challenge [ASME PAPER 82-WA/AERO-1] 10 p1458 A83-25676
- Spacelab ECLS follow-on-development [SAE PAPER 820848] 10 p1458 A83-25757

Spacelab ECLS current status --- Environmental Control/Life Support Subsystem [SAE PAPER 820884] 10 p1458 A83-25775

The characterization of carbon dioxide absorbing agents for life support equipment; Proceedings of the Winter Annual Meeting, Phoenix, AZ, November 14-19, 1982 11 p1644 A83-28329

Carbon dioxide scrubbing materials in life support equipment 11 p1644 A83-28330

Air revitalization compounds - A literature survey 11 p1644 A83-28332

Chemical and physical factors affecting the absorption capability of calcium hydroxide based carbon dioxide absorbents 11 p1645 A83-28333

Absorption of carbon dioxide by solid hydroxide sorbent beds in closed-loop atmospheric revitalization system 11 p1645 A83-28338

Applications of permeable membranes as carbon dioxide scrubbers 11 p1645 A83-28339

Space Station crew operations impact on ECLSS design [SAE PAPER 820839] 13 p1906 A83-30934

A flow-system comparison of the reactivities of calcium superoxide and potassium superoxide with carbon dioxide and water vapor [SAE PAPER 820873] 13 p1907 A83-30946

Space Shuttle environmental and life support system (ECLSS) [SAE PAPER 821420] 17 p2562 A83-37977

LIFETIME (DURABILITY)
U LIFE (DURABILITY)

LIFT

An asymptotic expression of lift slope of elliptic wing with high aspect ratio 01 p0002 A83-10125

A study of the effect of the transverse sweep of delta wings on their vortex structures and aerodynamic characteristics in separated flows at low subsonic velocities 04 p0442 A83-15096

Vibration of airfoils in sinusoidal oblique gust [AIAA PAPER 83-0005] 05 p0577 A83-16457

Calculation of the lift distribution and aerodynamic derivatives of quasi-static elastic aircraft 06 p0712 A83-18151

Visualization of multijet impingement flow 09 p1198 A83-24652

Investigation of possible LTA craft application to solve national economy problems 11 p1527 A83-28194

Applications of advanced upper surface blowing propulsive-lift technology [SAE PAPER 820956] 15 p2122 A83-33628

How to improve air cushion vehicle performance with VUMP equipped wave-forming keels --- Vent-pump 15 p2242 A83-34855

ACV lift air systems - More puff for less power 15 p2242 A83-34861

Determination of basic constants of satellite - Atmosphere interaction from the analysis of motion of 1974-70A 16 p2314 A83-36114

A technique to determine lift and drag polars in flight 16 p2296 A83-36913

Unsteady flow field, lift and drag measurements of impulsively started elliptic cylinder and circular-arc airfoil [AIAA PAPER 83-1711] 17 p2502 A83-37205

Wake characteristics and interactions of the canard/wing lifting surface configuration of the X-29 forward-swept wing flight demonstrator [AIAA PAPER 83-1835] 17 p2455 A83-38664

Powered lift aerodynamics of USB STOL aircraft --- Upper Surface Blowing [AIAA PAPER 83-1848] 17 p2456 A83-38676

Convergence characteristics of nonlinear vortex-lattice methods for configuration aerodynamics [AIAA PAPER 83-1882] 18 p2637 A83-39421

The aerodynamic characteristics at the mid-span of a circular cylinder with tangential blowing 18 p2684 A83-39457

The hydrodynamic forces acting on a cylinder set in motion in an impulsive manner 19 p2843 A83-41264

The lift on an aerofoil in starting flow 23 p3398 A83-48121

Experimental wing and canard jet-flap aerodynamics [AIAA PAPER 83-0081] 23 p3398 A83-48211

Problem of the motion of a thin airfoil near a wavy boundary 24 p3576 A83-48945

LIFT AUGMENTATION

Some recent applications of high-lift computational methods at Boeing 04 p0443 A83-15313

Augmentation of fighter aircraft lift and STOL capability by blowing outboard from the wing tips [AIAA PAPER 83-0078] 05 p0578 A83-16507

Trimming high lift for STOL fighters [AIAA PAPER 83-0168] 05 p0598 A83-16566

An overview of two nonlinear supersonic wing design studies [AIAA PAPER 83-0182] 11 p1527 A83-28349

Certain features of transverse flow past a cylinder with longitudinal fins 11 p1569 A83-28551

Development of advanced circulation control wing high lift airfoils [AIAA PAPER 83-1847] 17 p2456 A83-38675

Powered lift aerodynamics of USB STOL aircraft --- Upper Surface Blowing [AIAA PAPER 83-1848] 17 p2456 A83-38676

Large-scale wind-tunnel investigation of a close-coupled canard-delta-wing fighter model through high angles of attack [AIAA PAPER 83-2554] 23 p3399 A83-48373

Von Mises wing optimization [AIAA PAPER 83-2558] 23 p3405 A83-48377

LIFT COEFFICIENTS
U AERODYNAMIC COEFFICIENTS
U LIFT

LIFT DEVICES

Design, analyses, and model tests of an aeroelastically tailored lifting surface 08 p1044 A83-22155

Aerodynamic characteristics of a circulation controlled elliptical airfoil with blown jets [AIAA PAPER 83-1794] 17 p2453 A83-38633

An investigation of wing leading-edge vortices at supersonic speeds [AIAA PAPER 83-1816] 17 p2454 A83-38648

LIFT DISTRIBUTION
U FORCE DISTRIBUTION
U LIFT

LIFT DRAG RATIO

Modular asymmetric parachute for wind tunnel testing 04 p0443 A83-15322

Segmented vortex flaps [AIAA PAPER 83-0424] 05 p0585 A83-16706

Steady-state solution of the Euler equations for transonic flow 12 p1698 A83-29929

Transonic flows with viscous effects 12 p1698 A83-29935

Recent studies at NASA-Langley of vortical flows interacting with neighboring surfaces 15 p2120 A83-33972

System technology analysis of aeroassisted orbital transfer vehicles - Moderate lift/drag [AIAA PAPER 83-2108] 19 p2809 A83-41474

Aerobraking of a low L/D manned vehicle from Geo return to rendezvous with the Space Shuttle [AIAA PAPER 83-2110] 19 p2811 A83-41937

Minimum-fuel aeroassisted coplanar orbit transfer using lift-modulation [AIAA PAPER 83-2094] 20 p2944 A83-43812

Optimization of waverider configurations generated from axisymmetric conical flows 23 p3398 A83-48134

LIFT FANS

A remote augmentor lift system with a turbine bypass engine 06 p0719 A83-19595

Inlet-fan flow field computation [ASME PAPER 83-GT-41] 23 p3394 A83-47901

LIFT FORCES
U LIFT

LIFTING BODIES
NT LIFTING REENTRY VEHICLES

Extension of the lifting body theory to evolution on random trajectories at subsonic velocities 01 p0002 A83-10576

Supersonic flow around a conical fuselage of arbitrary section isolated or equipped with a delta wing with subsonic leading edges 01 p0002 A83-10579

Experimental forces and moments on cone-derived waveriders for freestream $M = 3$ to 5 02 p0132 A83-13092

Modular asymmetric parachute for wind tunnel testing 04 p0443 A83-15322

Aerodynamic investigation of closely coupled lifting surfaces with positive and negative stagger for general aviation applications [AIAA PAPER 83-0057] 05 p0578 A83-16489

Optimization of variable-altitude flyback maneuvers --- for rocket-propelled lifting vehicles [AIAA PAPER 83-0282] 05 p0594 A83-16627

Derivation and solution of the transonic integral equation for lifting flows 05 p0590 A83-17553

Slender body theory and optimization procedures for transonic lifting wing bodies [AIAA PAPER 83-0184] 05 p0591 A83-17911

Aerodynamic characteristics of polygonal lifting bodies at supersonic speeds 06 p0713 A83-19571

A finite state aerodynamic model for a lifting surface in incompressible flow 07 p0862 A83-19802

On numerical methods of subsonic lifting surface theory 07 p0864 A83-21012

Quadrature formulas for chordwise integrals of lifting surface theories 08 p1042 A83-22146

Vibration and flutter of advanced composite lifting surfaces [AIAA 83-0961] 12 p1744 A83-29861

Numerical solution of transonic wing flowfields 14 p1971 A83-32984

Certain aspects of the optimum design of hydrodynamic lifting complexes 14 p1972 A83-33002

The problem of an optimum wing of constant seaworthiness 14 p1972 A83-33003

Second approximation of quadrupole wing theory in lifting surface theory 14 p1972 A83-33004

Hypersonic flow behind a lifting body 19 p2790 A83-41206

Viscous effects on the performance of cone-derived waveriders [AIAA PAPER 83-2084] 19 p2792 A83-41918

Equivalent angle of attack for the lifting plane with linear camber-twist at low speeds 20 p2931 A83-43690

LIFTING REENTRY VEHICLES

Three-dimensional recoiling/optimal entry, with minimum heating of the vehicle 01 p0017 A83-10583

Analysis of optimal trajectories for lifting spacecraft atmospheric reentry 01 p0017 A83-10585

Shock strength modification for reduced heat transfer to lifting re-entry vehicles 10 p1372 A83-26160

Heating analysis of bent-nose biconics at high angles of attack using the parabolized Navier-Stokes equations [AIAA PAPER 83-1507] 14 p1970 A83-32744

Asset and prime - Gliding re-entry test vehicles 18 p2645 A83-39972

LIFTING ROTORS
NT BEARINGLESS ROTORS

LIFTING SURFACES
U LIFT DEVICES
U LIFTING BODIES
U SURFACES

LIGAMENTS

Knee-ligament loading properties as influenced by gravity. I - Junction with bone of 3-G rodents 02 p0223 A83-12407

LIGHT (VISIBLE RADIATION)
NT AIRGLOW
NT COHERENT LIGHT
NT DAYGLOW
NT GEOCORONAL EMISSIONS
NT LIGHT BEAMS
NT NIGHTGLOW
NT POLARIZED LIGHT
NT SKY RADIATION
NT SUNLIGHT
NT TWILIGHT GLOW
NT ZODIACAL LIGHT

Light rays in gravitating, refractive media 02 p0233 A83-12138

Solar irradiance calculations in the UV and visible using the adjoint discrete ordinates method 03 p0360 A83-14637

Photobiological aspects of the damage of cells by radiation 03 p0377 A83-14927

Theoretical and experimental investigation of high temperature insulators subjected to intense visible radiation [AIAA PAPER 83-0158] 05 p0617 A83-16562

Optical variability and radio structure of extragalactic sources - Evidence of recurrent activity 06 p0838 A83-19224

Light-induced drift in cascade excitation of levels --- laser effects on atomic energy levels 07 p0934 A83-20117

Charge-coupled device /CCD/ visible light sensor for the Teal Ruby Experiment 08 p1051 A83-22602

Broadband lamp standard for ultraviolet /UV/, visible, and infrared calibration to 6.0 microns 08 p1104 A83-22878

On the wind model of novae 09 p1363 A83-25000

Coherent versus incoherent detection for interferometry at infrared wavelengths 10 p1495 A83-25846

The extragalactic background light at 4400 A 10 p1511 A83-26400

Ultralow stationary pulses in a periodically modulated medium with an active nonlinearity --- lasers 10 p1435 A83-26954

Polyamine formation by arginine decarboxylase as a transducer of hormonal, environmental and stress stimuli in higher plants 11 p1639 A83-27830

On the light-induced drift of SF6 molecules 11 p1654 A83-28060

Supernova remnants in the Magellanic Clouds 12 p1786 A83-29092

The spectrum of the extragalactic background light 14 p2107 A83-33237

Characteristics of the diffraction of light by regular reflections of an acoustic wave 15 p2231 A83-34707

Visible light reflectance, transmittance, and absorbance of differently pigmented cotton leaves 17 p2526 A83-37622

- Preliminary results of the analysis of light refraction in the atmospheric boundary layer of Venus
19 p2923 A83-41236
- Conductivity, ion production rate, and light flashes in air under the effect of a short pulse of relativistic electrons
19 p2902 A83-41794
- Aircraft-borne lightning sensor
21 p3134 A83-43867
- A theory of the diffraction of light by shear waves in an isotropic solid dielectric
22 p3355 A83-45651
- Deflection of a phase-conjugate wave in nondegenerate four-wave mixing
23 p3509 A83-48322
- Simultaneous pulses in light and electric field from stepped leaders near ground level
24 p3610 A83-49346
- Bound states of electrons in a light field
24 p3589 A83-49744

LIGHT ABSORPTION

U ELECTROMAGNETIC ABSORPTION

LIGHT ADAPTATION

- The spatial parameters of color vision in humans
07 p0977 A83-20357
- Pupillary escape intensified by large pupillary size
15 p2211 A83-34873
- The selective sensitivity of color mechanisms of vision to spatial frequency
16 p2398 A83-35903

LIGHT AIRBORNE MULTIPURPOSE SYSTEM

- LAMPS MK III acoustic target tracker
19 p2799 A83-41533

LIGHT AIRCRAFT

- NT DO-28 AIRCRAFT
NT OH-58 HELICOPTER
NT YAK 40 AIRCRAFT
- The aviation and radioelectronic equipment of the Yak-18T aircraft --- Russian book
03 p0282 A83-13814
- An evaluation of aerodynamics modeling of spinning light airplanes
[AIAA PAPER 83-0368] 05 p0598 A83-17922
- The learning behaviour of trainee pilots during aircraft-landing - A simulator study
07 p0981 A83-19662
- Performance improvements of single-engine business airplanes by the integration of advanced technologies [DGLR PAPER 82-064] 09 p1203 A83-24178
- Experimental investigations concerning the noise produced by model propellers and propeller-driven small aircraft
[DGLR PAPER 82-068] 09 p1206 A83-24182
- A theoretical and experimental study of propeller noise
[ONERA, TP NO. 1982-122] 09 p1340 A83-24333
- Homebuilt airplanes - The sky's the limit
09 p1196 A83-25122
- Direct measurement of transmission loss of aircraft structures using the acoustic intensity approach
11 p1530 A83-28185
- Modern propellers for commuter airlines
[SAE PAPER 820719] 13 p1807 A83-30874
- Laboratory study of add-on treatments for interior noise control in light aircraft
14 p1974 A83-32581
- Performance estimation for light propeller airplanes
14 p1975 A83-32589
- Performance flight testing --- Book
15 p2122 A83-33621
- Light aircraft and sailplane structures in reinforced plastics
16 p2299 A83-36065
- Design of an aerobatic aircraft wing using advanced composite materials
[SAE PAPER 821346] 17 p2463 A83-37955
- Applications and market potentials for the light utility airship concept
[AIAA PAPER 83-1975] 17 p2443 A83-38906
- LHX system design for improved performance and affordability --- Light Helicopter
19 p2797 A83-41080
- An application of parameter identification to the oscillatory motion of an airplane at high C(L)
[AIAA PAPER 83-2067] 19 p2804 A83-41905
- A simulation study of the low-speed characteristics of a light twin with an engine-out
[AIAA PAPER 83-2128] 19 p2806 A83-41951
- Studies of light-twin wing-body interference
[SAE PAPER 830709] 20 p2930 A83-43319
- Flight investigation of natural laminar flow on the Bellanca Skyrocket II
[SAE PAPER 830717] 20 p2933 A83-43326
- Light aircraft wing structure optimization
[AIAA PAPER 83-2446] 23 p3403 A83-48332
- Von Mises wing optimization
[AIAA PAPER 83-2558] 23 p3405 A83-48377
- Ultralight aircraft safety and regulation
24 p3546 A83-48885
- Army family of light rotorcraft (LHX) concept formulation
[AIAA PAPER 83-2552] 24 p3548 A83-49592

LIGHT ALLOYS

- NT ALUMINUM ALLOYS
NT BERYLLIUM ALLOYS
NT MAGNESIUM ALLOYS
- Light alloys containing lithium --- Russian book
13 p1820 A83-30424
- Superlight alloys of magnesium-lithium-hydrogen
17 p2490 A83-38472

LIGHT AMPLIFIERS

- A high-power polarised coherent TE N2 laser
02 p0183 A83-12011
- On the gain of the free electron laser /FEL/ amplifier for a nonmonoenergetic beam
02 p0184 A83-12271
- Picosecond amplification and kinetic studies of XeCl
02 p0184 A83-12272
- Suppressed turn-on laser regenerative optoelectronic amplifier
02 p0185 A83-12301
- Small-signal gain of the TOK amplifier --- Transverse Optical Klystron
04 p0535 A83-15949
- Steady-state pulses in a laser amplifier with a delayed swept gain
05 p0647 A83-16837
- Spectral characteristics of the extraction of excitation energy from neodymium glass amplifiers
05 p0649 A83-17051
- Determination of the width of the gain profile of an iodine laser with the aid of stimulated Brillouin scattering
05 p0649 A83-17059
- Determination of the parameters of injection laser amplifiers based on GaAlAs heterostructures from superluminescence characteristics
05 p0649 A83-17060
- Amplification of light in inhomogeneous waveguides with an adjacent active medium
05 p0685 A83-17076
- Applied nonlinear-optics: Second-harmonic generators and parametric light-generators --- Russian book
05 p0650 A83-17126
- Design of a XeF-pumped second Stokes amplifier for blue-green production in H2
05 p0651 A83-17877
- Optical parametric amplification from quantum noise
05 p0651 A83-17889
- Nitrogen-laser-pumped ultrashort pulse amplifier
07 p0934 A83-20114
- Propagation of interacting first and second optical harmonics in a nonlinear active medium
07 p0934 A83-20118
- Q-switched semiconductor diode lasers
07 p0938 A83-21591
- Three-dimensional propagation in free-electron laser amplifiers
10 p1427 A83-26006
- Three-dimensional theory of free electron lasers with an axial guide field
10 p1427 A83-26010
- Theory of a nonwiggler collective free electron laser in uniform magnetic field
10 p1427 A83-26011
- Finite-temperature effects in free-electron lasers
10 p1427 A83-26013
- Results of the Los Alamos Free-Electron Laser Experiment
10 p1428 A83-26021
- Line shape parameter analysis of individual vibrational-rotational transitions in a CO2 laser amplifier
10 p1428 A83-26023
- Influence of rotational relaxation in a CO2 amplifier on the shape of a short amplified pulse
10 p1432 A83-26668
- High-resolution line-shape analyses of the pulsed cuprous chloride-laser oscillator and amplifier
10 p1435 A83-26878
- A long pulse width neodymium-doped glass rod laser amplifier with a moving input laser beam
11 p1581 A83-27592
- Amplifications of atomic fluorine, nitrogen ion and XeF lasers
11 p1582 A83-27614
- Optical bistability and nonlinear resonance in a resonant-type semiconductor laser amplifier
12 p1732 A83-29472
- Free-electron generators of coherent radiation - /Volumes 8 & 9/
13 p1852 A83-31101
- Optical klystron spontaneous emission and gain --- as undulator for free electron laser
13 p1852 A83-31106
- Status and perspectives of the FEL experiment at Brookhaven
13 p1853 A83-31107
- FEL program at the Adone storage ring
13 p1853 A83-31108
- A note on the Madey gain-spread theorem --- concerning energy change experienced by electrons in free electron laser
13 p1853 A83-31112
- Kinetic theory of a free-electron laser amplifier with guide magnetic field
13 p1853 A83-31113
- An experiment on FEL efficiency enhancement with a variable wiggler
13 p1853 A83-31114
- Comparison of noise characteristics of Fabry-Perot-type and travelling-wave-type semiconductor laser amplifiers
13 p1858 A83-31763
- High-power continuously tunable atmospheric-pressure CO2 laser operating in the superregenerative amplification regime
14 p2023 A83-31915

- Time-dependent oscillations of the gain factor during the stimulated Raman scattering of light by polaritons under nonstationary conditions
14 p2024 A83-32166
- Femtosecond optical pulses
14 p2025 A83-33402
- Synchronous amplification of subpicosecond pulses
14 p2025 A83-33403
- HF chemical laser amplification properties in homologous turbulent shear flow
15 p2170 A83-35250
- Third order autocorrelation study of amplified subpicosecond laser pulses
16 p2359 A83-35953
- Rate equation theory of two-photon lasers
19 p2851 A83-40919
- Electrical diagnostics of the amplifier operation and a feasibility of signal registration on the basis of the voltage saturation effect in junction laser diodes
19 p2852 A83-40941
- Initiation of superfluorescence in a three-level 'swept-gain' amplifier
19 p2853 A83-41178
- Small-signal gain in lethargic and conventional laser amplifiers
19 p2853 A83-41198
- Efficient backward and forward pumping CW Raman amplification for InGaAsP laser light in silica fibres
20 p2993 A83-42486
- Analysis of a multistable semiconductor light amplifier
20 p2994 A83-42791
- Monolithic integration of a double heterostructure light-emitting diode and a field-effect transistor amplifier using molecular beam grown AlGaAs/GaAs
20 p2968 A83-43596
- Formation of the spatial structure of radiation in solid-state laser systems by apodizing and hard apertures
20 p2996 A83-43786
- Gain measurements on semiconductor lasers by optical feedback from an external grating cavity
22 p3300 A83-46817
- A study of optical amplification in a double heterostructure GaAs device using the density matrix approach
22 p3301 A83-46825
- Generation of short laser pulses during coherent amplification
22 p3301 A83-46937
- High-power, subpicosecond 10-micron pulse generation
24 p3587 A83-48851
- Ultraviolet four-photon mixing in an multimode silica fiber Raman amplifier
24 p3589 A83-49616
- The amplification of a polarized signal by an anisotropic laser superregenerative amplifier in the linear mode
24 p3589 A83-49738
- Theory of spontaneous emission in gain-guided laser amplifiers
24 p3590 A83-49975
- Evanescent amplification in a single-mode optical fibre
24 p3630 A83-49980

LIGHT BEAMS

- Waveguide-type solutions for light beams with nonlocal self-defocusing in the geometric-optics approximation
01 p0054 A83-10816
- Optimum control of the wave front and time profile of optical radiation propagating in a nonlinear medium
01 p0106 A83-10902
- Vector polynomials orthogonal to the gradient of Zernike polynomials --- in measurement of laser beam phase
02 p0175 A83-11562
- Reflection properties and applications of resonant optical cavities
02 p0235 A83-11564
- Measurement of beam parameters of index-guided and gain-guided single-frequency InGaAsP injection lasers
02 p0183 A83-11982
- Subsurface-structure determination using photothermal laser-beam deflection
02 p0177 A83-12282
- Effect of particle size distribution and chlorophyll content on beam attenuation spectra
02 p0203 A83-12314
- Adaptive optics
03 p0395 A83-14928
- The optimal control of laser beams in nonlinear media
04 p0483 A83-15261
- Transformation of the spatial statistics of a partially coherent light beam in a nonlinear medium
04 p0485 A83-15902
- Test of fidelity of phase conjugation
05 p0647 A83-16841
- A fast wave of gas-ionization in a laser beam
05 p0686 A83-16892
- The propagation of a narrow modulated light beam in a scattering medium with allowance for the photon path fluctuations during multiple scattering
05 p0651 A83-17590
- The electric reactions of the cat brain to light following the section of the optic tracts
05 p0672 A83-17636
- FET photodetectors - A combined study using optical and electron-beam stimulation
05 p0631 A83-17762
- Photophoretic force on particles for low Knudsen number
06 p0786 A83-18586
- Harmonic generation with noncollinear laser beams - Application to pulse stacking
06 p0766 A83-18958
- Integral photoelasticity of cylindrical bodies with measurement of light-ray deflection
07 p0944 A83-19634

Beam aberration in phase conjugation by degenerate four-wave mixing in optical waveguides
07 p0993 A83-20152

The spectrum of strong intensity fluctuations of light beams in randomly irregular media
07 p0937 A83-20875

Phase aberrations and laser output beam quality
08 p1108 A83-22450

Limitations on the use of root-mean-square /rms/ phase to describe beam quality characteristics --- of high power lasers
08 p1108 A83-22451

Local optical correction system --- adaptive laser beam control
08 p1109 A83-22466

Absorption and lateral shift of beams incident upon lossy multilayered media
08 p1161 A83-22670

Thermal blooming of a partially coherent light beam
09 p1271 A83-23493

Optical communications and laser beam acquisition performances
09 p1245 A83-23528

Transient behavior of nonlinear thermal effects in an intense light beam in a uniform gas flow
09 p1271 A83-23988

Correlation analysis of the optical fields in optoacoustic interaction
09 p1344 A83-24001

Gaussian Schell-model sources - An example and some perspectives --- generation of directional light beams
09 p1344 A83-24083

Propagation model of laser beams in turbulence
09 p1271 A83-24084

Scattering of laser beams and the optical potential well for a homogeneous sphere
09 p1272 A83-24088

The propagation of narrow light beams in rain
09 p1273 A83-25079

The measurement of the dispersion of the intensity fluctuations during the reflection of multimode laser beams in the atmosphere
09 p1273 A83-25085

The dependence of the sharpness of an interference pattern on the quantum state of the electromagnetic field
09 p1346 A83-25092

The spectral theory of a light field
09 p1347 A83-25253

The nonstationary scattering of spatially confined and ultrashort light pulses
09 p1273 A83-25256

Methods for practical calculations of light fields under conditions of multiple scattering
09 p1347 A83-25257

Improvement of phase-conjugate beam fidelity in degenerate four-wave mixing by focused probe fields
10 p1429 A83-26111

Problem of accurate intensity measurements in focused laser beams
10 p1433 A83-26683

Thermal defocusing and transformation of the statistics of a spatially noncoherent light beam
10 p1434 A83-26691

Thermal distortions of focused laser beams in the atmosphere
10 p1434 A83-26782

Investigation of thermal self-defocusing of intense beams in homogeneous gas flows
10 p1435 A83-26784

Paraboloid of revolution used for receiving the laser radiation, for beams not parallel to the axis of the paraboloid
10 p1435 A83-26883

Propagation of intense CW-light through a strongly absorbing medium - Self-focusing and spatial ringings
11 p1576 A83-27514

Peculiarities of laser radiation and solid aerosol interaction
11 p1612 A83-27607

On the reflection of wave beams from a screen located in a nonlinear medium
11 p1657 A83-27953

Resonant and nonresonant electron scattering in an inhomogeneous laser field
12 p1732 A83-29246

The possibility of channeling a light beam in a nonlinear medium with spatially inhomogeneous amplification and absorption
12 p1732 A83-29254

Measurement of laser beam divergence
13 p1844 A83-30202

Performance of a laser beam wave-front sensor
13 p1845 A83-30257

Interferometric control of a beam expander consisting of multiple telescopes
13 p1921 A83-31022

Correction of angular displacements of optical beams
14 p2083 A83-31911

Acoustooptic excitation of surface electromagnetic waves by a light beam of finite aperture
14 p2003 A83-32119

The phase-conjugation method in adaptive systems for the shaping of light beams
14 p2024 A83-32593

The characteristics of a confined light beam in an absorptive medium having a narrow indicatrix of scattering
14 p2085 A83-32858

The phasic neuron reactions of the visual cortex to flashes of light in various conditions of stimulation
14 p2066 A83-33340

Calculation of the diffraction of laser beams with a smooth profile of intensity variation
14 p2025 A83-33396

On the nonlinear aberrations with self-deflection of a light beam in a moving medium
14 p2025 A83-33397

Receiver-aperture averaging effects for the intensity fluctuation of a beam wave in the turbulent atmosphere
15 p2168 A83-33811

The properties of focused fields --- for optical beams
15 p2147 A83-35152

Calculated transmission profile of an interference filter placed in a convergent beam under various incidence angles --- for nightglow observations
16 p2357 A83-36753

Isoplanatism with respect to the arrival angles of light rays in telescopes
16 p2426 A83-36856

Modeling of overlap thermal blooming in smoke [AIAA PAPER 83-1719]
17 p2503 A83-37208

Phenomenon of interference between two light beams propagating in optical fibers having a large path difference
17 p2580 A83-37744

Beam propagation in uniaxial anisotropic media
17 p2580 A83-38048

Method of the coherent spatial filtering of one-dimensional distortions of images using a white-light source
17 p2512 A83-38501

Surface light-induced drift of a rarefied gas
17 p2515 A83-38959

Distribution of illumination from a narrow light beam in a turbid atmosphere
17 p2515 A83-38978

On an explicit method for the numerical solution of problems of light wave propagation in nonlinear media
18 p2692 A83-39155

Light-induced effects in amorphous silicon material and devices
18 p2749 A83-39464

Nonlinear conversion of laser radiation in optical fibres and its applications for spectral investigation
18 p2744 A83-40351

SEM-EBIC and traveling light spot diffusion length measurements - Normally irradiated charge-collecting diode
18 p2678 A83-40371

A worldwide examination of solar beam-slope angle values
19 p2861 A83-40768

Self-diffraction of light waves in gyrotropic crystals
19 p2899 A83-40997

Estimation of boresight error in autoboresighting a laser beam on a point target - Influence of weak statistical fluctuations
19 p2900 A83-41094

Mode propagation of the field generated by Collett-Wolf Schell-model sources
19 p2852 A83-41176

Stark interference effects in a weak magnetic field on the 6S-7S forbidden transition of cesium
19 p2898 A83-41180

Light induced drift of CH₃F
19 p2853 A83-41181

Increasing the transillumination capacity of a laser beam in the atmosphere
19 p2854 A83-41768

Launching light from semiconductor lasers into plane-ended multimode optical fibers
20 p3046 A83-42220

Anisotropic Gaussian beams
20 p2995 A83-43628

Spectral characteristics of light wave reversal in a nondegenerate four-wave interaction in a resonant medium
20 p2996 A83-43781

Temporal and interference fringe analysis of excimer TEM01 zone laser modes
21 p3142 A83-43874

Review of laser induced damage thresholds
21 p3144 A83-44784

Modified Monte-Carlo method to evaluate multiple scattering effects on lightbeam transmission through a turbid atmosphere
21 p3144 A83-44794

Distortions of a CW light beam propagating through gas
21 p3144 A83-44804

Self-lensing and spatial ringings
21 p3144 A83-44805

Phase matching and frequency detuning effects in Brillouin enhanced four-wave mixing
21 p3144 A83-44805

Asymmetry of diffraction orders during the diffraction of light by a surface acoustic wave
22 p3277 A83-45681

Widening the energy and technological possibilities of equipment for light beam welding with the pulsed feed of arc xenon lamps
22 p3301 A83-45701

Directionality of the radiation of a misaligned cavity with a lens-like medium
23 p3460 A83-47166

Volume vector holograms with opposed reference beams
23 p3453 A83-47168

A model of the random phase screen in the problem of the thermal self-defocusing of light
23 p3462 A83-48090

Intensity fluctuations in the case of the specular reflection of light beams in the turbulent atmosphere
23 p3463 A83-48482

The beam propagation method - An analysis of its applicability --- to integrated optics
24 p3627 A83-48748

Theory of phase conjugation by degenerate four-wave mixing using spatially varying pump beams
24 p3623 A83-48978

Deflection from the incidence plane of a light beam refracted in an absorbing (amplifying) isotropic medium
24 p3629 A83-49552

LIGHT BULBS

U LUMINAIRES

LIGHT COMMUNICATION

U OPTICAL COMMUNICATION

LIGHT CURVE

Photoelectric light-curves of the eclipsing binary XY Leonis
01 p0116 A83-10236

Photographic observations of supernova 1979c in NGC 4321
01 p0116 A83-10237

Light variations in several broad-lined B stars
01 p0120 A83-10309

A preliminary report on simultaneous ultraviolet and optical observations of Lambda Eridani
01 p0121 A83-10326

The lower end of the main sequence
01 p0124 A83-10571

The light curves of RR Lyrae field stars
02 p0251 A83-11593

Ultraviolet light curves of the dwarf novae U Geminorum and VW Hydri
02 p0256 A83-12127

Infrared photometry of the X-ray binary 2A 1822-371 - A model for the ultraviolet, optical, and infrared light curve
02 p0256 A83-12128

The nature of the 1E1145.1-6141 optical counterpart
02 p0259 A83-12517

AN And - A detached eclipsing binary system with an Am primary member
02 p0260 A83-12526

The ellipsoidal light curve of VV Puppis
03 p0413 A83-13312

A possible outburst on AM Canem Venaticorum
03 p0414 A83-13335

Physical studies of asteroids. VIII - Photoelectric photometry of the asteroids 42, 48, 93, 105, 145 and 245
03 p0403 A83-13366

The light curve of the eclipsing binary system CX Cephei and the properties of the Wolf-Rayet component
03 p0418 A83-13661

A photometric study of Pluto near perihelion. I - U,B,V photometry
03 p0408 A83-13895

The hot halo subdwarf binary system HZ-22
03 p0421 A83-14145

HR 6434 and the factors limiting pulsational amplitudes of delta Scuti stars
03 p0421 A83-14150

High-energy gamma-ray light curve of PSR0531+21
03 p0409 A83-14175

The 27-day periodicity of outbursts of Comet Schwassman-Wachmann I
03 p0410 A83-14680

Classification of the results of the electrophotometry of artificial celestial bodies
03 p0286 A83-14684

A light curve of BX Pegasi
03 p0410 A83-14722

Photometric observations of CN Orionis
03 p0411 A83-14807

The dependence of asteroid lightcurves on the orientation parameters and the shapes of asteroids
03 p0435 A83-14866

Physical studies of asteroids. IX - The light curve of the M asteroid 77 Frigga
03 p0411 A83-14870

Properties of Wolf-Rayet stars in eclipsing binary systems
04 p0548 A83-14978

The six-day rotation period of 1689 Floris-Jan - A new record among slowly rotating asteroids
04 p0545 A83-15031

Frequency analyses of light and radial velocity observations of Alpha Lupi
04 p0546 A83-15049

Search for rapid variability of 53 Cam
04 p0546 A83-15110

The semi-detached binary system RZ Draconis
04 p0546 A83-15596

Photoelectric photometry of Z Herculis
04 p0547 A83-15955

Theory of the light curves of eclipsing systems with oscillating components. I
04 p0556 A83-15963

The longitudinal distribution of sunspots and the RS CVn starspot model
04 p0556 A83-15966

The light curve variations in AR Lacertae
04 p0547 A83-15970

Photoelectric observations of the eclipsing binary U Pegasi
04 p0548 A83-15973

Photoelectric photometry of asteroids 33 Polyhymnia and 386 Siegena
05 p0693 A83-16970

A new X-ray pulsar with a 67-millisecond period in the constellation Equuleus
05 p0693 A83-17008

A photometric study of the short-period eclipsing binary BW Eridani
05 p0695 A83-17817

A new light curve analysis of the eclipsing binary SX Aur
05 p0703 A83-17857

Two bright supernovae in NGC 6946 and NGC 4536
06 p0817 A83-18079

Spectra and light curves of three recent supernovae
06 p0825 A83-18080

- The unprecedented light variations of NGC 2346
06 p0829 A83-18527
- A superflare in EV Lacertae
06 p0830 A83-18783
- The period shortening of RY Sagittarii
06 p0820 A83-18864
- Rapid optical variation of the semiregular variable R
Crt
06 p0820 A83-18865
- Red variable stars. I - UBVRi photometry and photometric properties
06 p0833 A83-18866
- Theory of the light curves of eclipsing systems with oscillating components. II
06 p0834 A83-18884
- BV Dra and BW Dra - Two contact systems in one visual binary
06 p0834 A83-18889
- On the convergent solution in Kopal's iterative method of solving eclipsing binary orbits
06 p0822 A83-19164
- H2215-086 - King of the DQ Herculis stars
06 p0846 A83-19526
- Photoelectric photometry of the eclipsing binary NN Cephei
07 p1006 A83-20561
- Seasonal light curves of TY UMa - Observations and solutions
07 p1006 A83-20568
- A multicolour photometric analysis of the eclipsing binary VV Ori
07 p1006 A83-20569
- A check for the pole coordinates of asteroid 22 Kalliope
07 p1008 A83-21203
- Remarkable light changes of the active RSCVn system V 711 Tau / equals HR 1099/ during 1979-1981
07 p1009 A83-21222
- Rotation periods and lightcurves of the asteroids 136 Austria and 238 Hypatia
07 p1009 A83-21252
- An optimist's guide to supernovae
08 p1176 A83-21828
- The nature of supernovae as determined from their light curves
08 p1177 A83-21837
- Type I supernovae - Observational constraints
08 p1178 A83-21839
- Pulsational mode switching in HD 161796
08 p1184 A83-23065
- The eclipsing binary V 836 Cygni - Photometric evidence for an early evolutionary status
08 p1185 A83-23101
- Intensity and polarization line profiles in a semi-infinite Rayleigh-scattering planetary atmosphere. I - Integrated flux
08 p1190 A83-23107
- Simultaneous IR and optical light curves of 2A0311-227
08 p1176 A83-23262
- Three unusual cataclysmic variable stars
08 p1176 A83-23292
- On the wind model of novae
09 p1363 A83-25000
- The double-mode Cepheid CO Aur
10 p1499 A83-25370
- Determination of parameters of W UMa systems. IV - BV Dra, BW Dra, EM Lac, SW Lac
10 p1493 A83-25656
- Double-mode RR Lyrae variables in M15
10 p1502 A83-25709
- The light and velocity curves of classical Cepheids - Theory versus observation
10 p1510 A83-26387
- Atmospheric trajectory, orbit, and photometric light curve of the fragmented meteor No. 770533
10 p1498 A83-26902
- On the change of period and light curves of DS Aqr
10 p1516 A83-26904
- Photoelectric observations of four classical cepheids
10 p1498 A83-26905
- NGC 6067 and three cepheids
11 p1668 A83-27111
- An analysis of the small amplitude variations in the light curves of the R Coronae Borealis variables, S Apodis and UW Centauri
11 p1680 A83-28254
- Laboratory simulation of photometric light curves of the asteroids
11 p1685 A83-28378
- Physical studies of asteroids. X - Photoelectric light curves of the asteroids 219 and 512
11 p1686 A83-28384
- Light curves of four southern bright hitherto unknown eclipsing binaries
12 p1784 A83-28860
- Infrared photometry of the RS CVn binaries. I - TY Pyxidis
12 p1785 A83-28885
- Five years of photometry of Lambda Andromedae
12 p1785 A83-28995
- U, B, V light curves of CO Lacertae
12 p1792 A83-29051
- Three years of photometry of IM Pegasi - HR 8703
12 p1785 A83-29054
- Three colour photoelectric observations of the symbiotic eclipsing binary CI Cyg
12 p1786 A83-29081
- Photometry of the fast-rotating late-type star W92 in NGC 2264
12 p1786 A83-29082
- The short-period eclipsing system XY UMa - 1982 UVB light curves and a flare-like event
12 p1794 A83-29182
- A UVB photoelectric investigation of the eclipsing binary system DM Virginis
12 p1788 A83-29183
- On variations of the light curve of long-period variables
12 p1795 A83-29300
- Detailed photometry of the Cepheid AD Geminorum
12 p1789 A83-29954
- The light variation of the eclipsing variable UX Eridani
13 p1945 A83-30378
- Changes in the period of the eclipsing system AH Virginis
13 p1945 A83-30379
- AQ Leonis revisited --- electrophotometry of double-mode RR Lyrae variable
13 p1942 A83-31666
- RY Geminorum - An algol binary with moderate circumstellar emission
13 p1955 A83-31669
- Optical and IR light curves of VV Puppis
13 p1957 A83-31699
- Lightcurves and phase function of asteroid 44 Nysa during its 1979 apparition
14 p2097 A83-32601
- Pole orientation of asteroid 44 Nysa via photometric astrometry, including a discussion of the method's application and its limitations
14 p2097 A83-32602
- Worldwide photometry and lightcurve observations of 1 Ceres during the 1975-1976 apparition
14 p2097 A83-32603
- Worldwide photometry and lightcurve observations of 16 Psyche during the 1975-1976 apparition
14 p2097 A83-32604
- Asteroid rotation. IV
14 p2097 A83-32607
- UBV photometry of the minor planets 86 Semele, 521 Brixia, 53 Kalyppo and 113 Amalthea
14 p2097 A83-33052
- TV Cassiopeiae in the Utrecht photometric system
14 p2097 A83-33053
- The variability of the optical counterparts of four extragalactic radio sources
14 p2103 A83-33059
- Lightcurve synthesis of the semi-detached binaries LT Her, WX Eri, AW Cam
14 p2103 A83-33062
- Four-colour photometry of eclipsing binaries. XV B - Light curves of V Puppis
14 p2098 A83-33064
- X-ray spectra and light curves of accreting magnetic degenerate dwarfs
14 p2105 A83-33207
- On the machine computation of the orbits of eclipsing binaries
14 p2099 A83-33249
- Light curves of some periodic comets
14 p2101 A83-33287
- Orbital periods of novae before eruption
15 p2257 A83-34096
- Infrared light curves of Type I supernovae. II - Late stages
15 p2257 A83-34097
- ANS spectrophotometry - Delta Pictoris as an upper-main-sequence algol system
15 p2247 A83-34508
- Computation of the elements of eclipsing binaries from a part of their light curve. I - Spherical model
15 p2263 A83-34553
- Light-curve analysis of eclipsing variables - The interpretation of photometric observations
15 p2264 A83-34570
- An analysis of V 861 Sco. I - Light-curve synthesis
15 p2265 A83-34589
- MM Herculis - An eclipsing binary of the RS CVn
15 p2272 A83-34789
- Notes on the associated alpha-functions and related integrals --- for variable eclipsing binary star studies
15 p2249 A83-34791
- Photometric observations of PU Vulpeculae (Nova VUL 1979) in faint phases
16 p2423 A83-35682
- Light curve variation and period changes of VW Cep
16 p2428 A83-36530
- Optical photometry of massive X-ray binaries - 4U 1538-52/QV Nor
16 p2425 A83-36666
- The light curves of a freely precessing spheroidal minor planet
16 p2438 A83-36689
- 2 Pallas pole revisited
16 p2426 A83-36778
- Infrared photometry of the RS CVn binaries. II - JHKL light curves of HR 1099
17 p2587 A83-37277
- VBLUW photometry of Cepheids in the Magellanic Clouds made in 1971-1978
17 p2587 A83-37283
- Photometric observations of AC Boo
17 p2587 A83-37286
- Short-period noncontact close binary systems. I - UU Lynx
17 p2588 A83-37362
- Absolute spectrophotometry of Upsilon Sgr
17 p2589 A83-37683
- TV photometric observations of 10 extragalactic peculiar objects
17 p2589 A83-37685
- Brightness variations of the star HD 29697
17 p2590 A83-37705
- Polarimetric observations of Polar AN UMa
17 p2590 A83-37706
- Photometry of magnetic stars
18 p2755 A83-39240
- Intermediate band and (R,I) observations of long-period cepheids
18 p2757 A83-39596
- The photometric period of 39 AY Ceti
18 p2759 A83-39739
- Five years of photometry of Sigma Geminorum
18 p2759 A83-39743
- Extensive photometric study of RT Lacertae
18 p2759 A83-39751
- V1343 Aquilae (SS 433) as a double-period variable
18 p2777 A83-40477
- Variability of the Seyfert galaxy IV Zw 29, 1967-1981
18 p2763 A83-40487
- Remarkable modification of light curves for shadowing effects on irregular surfaces - The case of the asteroid 37 Fides
19 p2909 A83-40726
- Light curves and elements of AH Virginis
19 p2910 A83-41054
- The large C-type asteroids 146 Lucina and 410 Chloris, and the small S-type asteroids 152 Atala and 631 Philippina - Rotation periods and lightcurves
19 p2910 A83-41061
- Lightcurves and rotation periods for the asteroids 70 Panopaea and 235 Carolina
19 p2910 A83-41062
- Physical studies of asteroids. XI - Photoelectric observations of the asteroids 2, 161, 216 and 276
19 p2911 A83-41070
- YZ Cassiopeiae and the Utrecht photometric system
19 p2911 A83-41071
- The photometric behavior of FK Comae Berenices
20 p3064 A83-42325
- The light curve of the ZZ Ceti star G226-29
20 p3073 A83-43067
- Cygnus X-1 - Optical variation on the 294 day X-ray period
20 p3073 A83-43085
- New light curve analyses for the eclipsing binaries u Her and UV Leo
20 p3074 A83-43380
- On the variability of RZ Cephei
20 p3061 A83-43382
- HD 134518 - A main-sequence detached or a semi-detached eclipsing binary?
20 p3075 A83-43395
- Photoelectric photometry of asteroids 45, 120, 776, 804, 814, and 1982DV
21 p3222 A83-44084
- The disappearance of OH from Comet P/Encke
21 p3227 A83-44086
- BD Pavonis - A unique cataclysmic variable
21 p3229 A83-44423
- Optical photometry of massive X-ray binaries - Cen X-3/V779 Cen
21 p3229 A83-44424
- Dwarf novae: Observational results and their interpretation. III - What separates dwarf novae from novae, and what characteristics do they share?
21 p3234 A83-44929
- Electrophotometry of variable stars
21 p3225 A83-44930
- HD 164615 - A probable spotted single F type star
21 p3237 A83-45548
- A search for light-time effects in binary cepheids - AW Persei
21 p3226 A83-45551
- The spectrum of Nova Sagittarii 1982 in the transition phase
22 p3373 A83-46406
- New observations of six RV Tauri and SRd variable stars
22 p3374 A83-46414
- BD + 43 deg 1894, a mono-periodic Delta Scuti star
22 p3374 A83-46417
- Recent photometry of the central star of NGC 2346
22 p3375 A83-46578
- The rotation, color, phase coefficient, and diameter of 1915 Quetzalcoatl
22 p3388 A83-47090
- Two-spot modeling of synoptic light curves of II Peg
23 p3516 A83-47490
- The timescales of variations in continuum and hydrogen lines during stellar flares
23 p3521 A83-47498
- IUE spectra of the BY Dra/flarestar AU Mic
23 p3522 A83-47500
- X-ray observations of stellar flares
23 p3522 A83-47502
- RS CVn stars - Photospheric phenomena and rotation
23 p3522 A83-47511
- Twenty years of dedicated photometry of RS CVn at Catania Observatory
23 p3516 A83-47514
- Features of the wave-like distortion in some RS CVn binaries
23 p3522 A83-47515
- HK Lacertae
23 p3522 A83-47517
- Light curves and CA II emissions of V711 Tauri during 1981-82
23 p3522 A83-47518
- A flare-like event from the short-period system XY UMa
23 p3522 A83-47519
- The VW Cephei system
23 p3524 A83-47530
- A bright spot and a serendipitous stellar flare on the contact-binary VW Cep
23 p3524 A83-47531
- Numerical analysis of orbital period variations and a mechanism for changes in the light curve of VW Cep
23 p3524 A83-47532
- The light curve changes of VW Cephei
23 p3527 A83-48063
- Three-colour electrophotometry of Dy Peg
23 p3517 A83-48442
- Four-colour photometry of eclipsing binaries. XVI - Light curves of VV Pyxidis
24 p3642 A83-49319

- Four-colour photometry of eclipsing binaries. XVII - Light curves of DM Virginis 24 p3642 A83-49320
- Optical and X-ray observations of 2S 0921-630 24 p3660 A83-49381
- New results on symbiotic stars 24 p3662 A83-49566
- Infrared photometry of the RS CVn binaries. III - JHK light curves of UV Psc 24 p3645 A83-49841
- A photometric study of the eclipsing binary V478 Cygni 24 p3645 A83-49844
- Study of the variability of the Delta Scuti stars. VI Pulsational behaviour of HR 1392 (69 Tau). VII - The problem of stability and monop periodicity in 20 CVn 24 p3663 A83-49847
- Photometric observations - Is HZ Herculis getting darker? 24 p3649 A83-50082
- Photometric observations and elements of the eclipsing binary TT Herculis 24 p3649 A83-50090
- LIGHT DURATION**
U PULSE DURATION
- LIGHT ELEMENTS**
The cosmological relevance of light element abundances 18 p2776 A83-39772
- The origin of the light elements - A quite complex problem --- primordial abundances in universe 24 p3664 A83-50031
- Nuclear uncertainties of element yields in the big bang 24 p3665 A83-50035
- LIGHT EMISSION**
NT CATHODE GLOW
NT CATHODOLUMINESCENCE
NT CHEMILUMINESCENCE
NT ELECTROLUMINESCENCE
NT FLUORESCENCE
NT LUMINESCENCE
NT OPTICAL RESONANCE
NT PHOSPHORESCENCE
NT PHOTOLUMINESCENCE
NT RESONANCE FLUORESCENCE
NT SHOCK WAVE LUMINESCENCE
NT THERMOLUMINESCENCE
NT TRIBOLUMINESCENCE
NT X RAY FLUORESCENCE
- A possibility of detecting optical radiation from superhigh-energy extensive air showers 02 p0276 A83-11761
- Radio jets in NGC 4151 02 p0254 A83-12108
- Rocket-borne investigations of the optical emissions of the equatorial ionosphere during periods of moderate and high geomagnetic activity 03 p0356 A83-13220
- An optical emission mechanism for the Crab pulsar 03 p0419 A83-13888
- Optical bursts from 4U/MXB 1636-53 04 p0554 A83-15635
- Optical conductivity of amorphous Ta and beta-Ta films 04 p0543 A83-16079
- Two-channel rocket photometer for tracing weak optical emissions at night 06 p0723 A83-18023
- The violet emissions produced by laser excitation of Na vapor in the 570-595 nm region 06 p0808 A83-18952
- Electron-beam-pumped multicomponent semiconductor laser emitting visible radiation 07 p0935 A83-20130
- Optical and radio structure of the quasar PKS 0812 + 02 07 p1019 A83-21105
- Kinematics of the optical filaments in W50 07 p1021 A83-21121
- Space Shuttle glow observations 07 p0869 A83-21552
- Observations of optical emissions on STS-4 07 p0870 A83-21553
- Visible glow induced by spacecraft-environment interaction 07 p0870 A83-21554
- Optical emission in the radio lobes of radio galaxies. II - New observations of 21 radio lobes 08 p1175 A83-23036
- The possibility of stimulated three-photon emission in molecular media 09 p1270 A83-23492
- A mechanism to explain the generation of earthquake lights 09 p1307 A83-24696
- Size of a gamma-ray burster optical emitting region 09 p1361 A83-24697
- A high-latitude H I-cloud with optical emission 12 p1785 A83-28883
- The optical emission from the supernova remnant HB 12 p1797 A83-29955
- Optical emission from ring-shaped nebulae in the LMC 14 p2110 A83-33283
- Correlated irregular magnetic pulsations and optical emissions observed at Siple Station, Antarctica 15 p2195 A83-33936
- Analysis of gravity-wave induced instabilities and turbulence viscosity parameters from optical emissions 16 p2374 A83-35377
- The motion of spots and the flare of July 4, 1974 17 p2625 A83-37667

- Antibunching in the Franck-Hertz experiment --- subpoissonian light generation from space-charge limited electron beams colliding with atoms 19 p2900 A83-41189
- Observations of optical emissions from precipitation of energetic neutral atoms and ions from the ring current 20 p3019 A83-42424
- Variation in light intensity with height and time from subsequent lightning return strokes 20 p3030 A83-42839
- Photometric evidence of electron precipitation induced by first HOP whistlers 20 p3024 A83-43187
- Longitudinal asymmetry of the Io plasma torus 23 p3529 A83-47865

LIGHT EMITTING DIODES

- Silicon carbide blue light emitting diodes with improved external quantum efficiency 01 p0106 A83-10634
- PPS - A switch in time --- Programmable Pushbutton Switch 01 p0029 A83-11169
- Flat-panel video resolution LED display system 01 p0029 A83-11170
- Dot-matrix display light measurement and interpretation techniques --- for qualification tests techniques 01 p0011 A83-11257
- Amplification of light in inhomogeneous waveguides with an adjacent active medium 05 p0685 A83-17076
- Infrared to visible up-conversion using GaP light-emitting diodes 07 p0992 A83-19990
- Spectral tuning of shallow-junction surface-emitting light-emitting diodes /LEDs/ through gamma-ray irradiation 08 p1170 A83-22846
- Horizontal tunneling and surface band bending - An external technique for wavelength tuning of surface-emitting light-emitting diodes /LEDs/ 08 p1081 A83-22860
- Electron traps in GaAs_{1-x}P_x/Al_x alloys 10 p1488 A83-25985
- Theory of beam-induced currents in semiconductor diodes 10 p1489 A83-26212
- Ga/0.47/In/0.53/As/Al/0.48/In/0.52/As m-well LEDs emitting at 1.6 microns 11 p1664 A83-28613
- New measurement method for polarisation dispersion in single-mode fibres employing frequency-modulated optical signal 12 p1779 A83-29460
- Physical nature of the degradation of light emitting diodes and semiconductor lasers 13 p1849 A83-30261
- Single crystal growth of SiC substrate material for blue light emitting diodes 15 p2237 A83-33676
- Recent advances in the performance and reliability of InGaAsP: LED's for lightwave communication systems 15 p2229 A83-33677
- Positive feedback model of defect formation in gradually degraded GaAlAs light emitting devices 15 p2237 A83-33678
- Wavelength tuning of GaAs LED's through surface effects 15 p2149 A83-33679
- The capacitance-voltage characteristics of m-n GaN light emitting diodes --- metal-insulator-n-type semiconductor 17 p2496 A83-37649
- Monolithic integration of a double heterostructure light-emitting diode and a field-effect transistor amplifier using molecular beam grown AlGaAs/GaAs 20 p2968 A83-43596
- Optoelectronic devices based on silicon carbide p-n junctions produced by various processes 21 p3125 A83-44597
- Tradeoff between laser diodes and light-emitting diodes (LEDs) for the common weapon control system 22 p3278 A83-46616
- Proton damage in laser diodes and light-emitting diodes (LEDs) 22 p3296 A83-46618
- Reliability of fiber optic emitters 22 p3360 A83-46654
- A method of calculating the efficiency for coupling light power from a LED into an optical fibre by use of a sphere lens 24 p3627 A83-48745

LIGHT INTENSITY

U LUMINOUS INTENSITY

LIGHT IONS

- Ion whistlers in mid-latitude trough of light ions 02 p0205 A83-11999
- Effects of ion-acoustic instability on light ion beam transport in deuterium channels 22 p3362 A83-46019

LIGHT MODULATION

- Perfect mode locking of solid-state lasers by a double passive modulation 01 p0054 A83-10616
- Optical guided-wave interactions with magnetostatic waves at microwave frequencies 01 p0039 A83-10976
- Optical phase modulation in an injection locked AlGaAs semiconductor laser 02 p0184 A83-12168
- Applications of the Priz light modulator 02 p0236 A83-12307

- Development of the multiwavelength monolithic integrated fiber optics terminal 03 p0393 A83-13760
- Applications of the integrated optical light modulator 03 p0393 A83-13764
- Optical-to-optical image conversion with the liquid crystal light valve 03 p0394 A83-13776
- Silicon liquid crystal light valves for optical-data processing 03 p0394 A83-13778
- Spatially resolved IR absorption spectroscopy by optical Stark modulation 03 p0295 A83-14376
- Infrared spectrum of a single aerosol particle by photothermal modulation of structure resonances 03 p0356 A83-14379
- A spatio-temporal light modulator with a DKDP crystal in an adaptive optical system 04 p0534 A83-15262
- High-rate amplitude and frequency modulation of semiconductor lasers 04 p0486 A83-16218
- Effects of operating mode on electrooptic spatial light modulator resolution and sensitivity 05 p0684 A83-16832
- Opto-optical modulation in N-/p-methoxybenzylidene-/p-butylaniline 05 p0647 A83-16833
- An investigation of the dislocation density of a wave front in light fields having a speckle structure 05 p0647 A83-16889
- Higher-order distributed feedback and generation of light 05 p0648 A83-17049
- Prototype of an integrated-optics four-digit analog-digital converter 05 p0685 A83-17062
- Influence of the spatial structure of the gain on the dynamic properties of a laser 05 p0650 A83-17075
- The propagation of a narrow modulated light beam in a scattering medium with allowance for the photon path fluctuations during multiple scattering 05 p0651 A83-17590
- Coherent optical-fibre sensors with modulated laser sources 06 p0762 A83-18568
- Direct modulation of semiconductor injection lasers 06 p0765 A83-18762
- Mode partition noise characteristics in high-speed modulated laser diodes 06 p0766 A83-18902
- Measurement of time dependent optical gain using frequency modulation spectroscopy 06 p0763 A83-18955
- Forming of ultrafast light pulses with predetermined temporal shape 06 p0766 A83-18957
- Investigation of the operation of dispersive optical components 07 p0995 A83-20115
- Measurement of the linewidth enhancement factor alpha of semiconductor lasers 07 p0937 A83-21363
- Third-order optical nonlinearity induced by effective mass gradient in heterostructures 07 p0994 A83-21364
- [AD-A130018] 07 p0994 A83-21364
- Instabilities and chaotic behavior in a hybrid bistable system with a short delay 08 p1163 A83-21886
- Precision optical wavefront measurement 08 p1103 A83-22872
- Laser space communication technology status 09 p1214 A83-23577
- Oscillations in an acoustooptic bistable device 09 p1345 A83-24638
- The formation of the frequency-angular spectrum of the signals of linear antenna arrays using coherent optical processors based on spatial light modulators with multichannel optical addressing 09 p1345 A83-24906
- Coherent-optical processor for two-dimensional antenna arrays with a complex format of signal recording 09 p1345 A83-24920
- A shearing, modulating interferometer --- for astronomical observation 10 p1420 A83-25838
- Radiation exchange and oscillations in a pair of cavities sharing a partial reflector 10 p1482 A83-26002
- Investigation of an electrooptic modulator formed from coupled channel diffused waveguides in LiNbO₃ 10 p1483 A83-26656
- Image processing by a spatial light modulator utilizing the Pockels effect 10 p1484 A83-26658
- Determination of the amplitude-frequency characteristics of W-type fiber waveguides 10 p1484 A83-26692
- Acoustooptical device with extremely high contrast ratio 10 p1424 A83-26872
- Theory on distributed feedback /DFB/ lasers including strong modulations 11 p1578 A83-27548
- Frequency modulation spectroscopy and frequency domain optical memories 11 p1656 A83-27594
- The intracavity magneto-optical modulation of the intensity of laser radiation 11 p1583 A83-27949
- Improved acousto-optic modulators for CO₂ heterodyne laser systems 12 p1732 A83-29467
- Electro-optical light modulation in InGaAsP/InP double heterostructure diodes 13 p1918 A83-30343

Broadband guided-wave optical frequency translator using an electro-optical Bragg array 13 p1922 A83-31053

Random modulation CW lidar 13 p1857 A83-31464

Characterization of pulsed Nd:YAG active/passive mode-locked laser 14 p2026 A83-33414

Picosecond pulse response of broad-band guided-wave interferometric light modulators 14 p2085 A83-33424

Transient behavior of Kerr-like phase conjugators - The inverse problem 15 p2228 A83-33527

Fabry-Perot interferograms for amplitude and phase modulated light 15 p2163 A83-33755

Modulation intracavity laser spectroscopy, polarimetry, and interferometry 15 p2163 A83-33979

Statistics of photocounts of modulated radiation and coherence of field in optical waveguides 15 p2230 A83-33982

Electrooptical Bragg modulator based on the Ag-diffused LiTaO₃ waveguide 15 p2232 A83-34888

Traveling-wave electrooptic modulator 17 p2580 A83-37750

Microwave characteristics of an optically controlled GaAs MESFET 19 p2838 A83-41092

Optical differential-modulation correlometer for the detection of linear-FM signals in noise 19 p2900 A83-41780

Acousto-optic phase modulator for single-mode fibres 20 p3047 A83-42479

Measurement of small optically pulse-modulated reflection coefficients 20 p2986 A83-42489

Superluminescent damping of relaxation resonance in the modulation response of GaAs lasers 20 p2995 A83-43592

Two-dimensional magneto-optic spatial light modulator for signal processing 21 p3134 A83-43869

Modulation characteristics of constricted double-heterojunction AlGaAs laser diodes 21 p3144 A83-44216

Time- and frequency-domain response of directional-coupler traveling-wave optical modulators 21 p3205 A83-44223

GaAlAs p-i-n junction waveguide modulator 21 p3205 A83-44224

Design and performance of an integrated optical digital correlator 21 p3205 A83-44225

Picosecond signal sampling and multiplication by using integrated tandem light modulators 21 p3205 A83-44229

Laser pulse shaping with liquid crystals 21 p3206 A83-44792

Propagation, transverse, diffraction effects, and coherent pump dynamics in three-level superfluorescence and light control by light 21 p3144 A83-44801

Opto-optical light deflection 21 p3207 A83-44834

Generation of single-longitudinal-mode gigabit-rate optical pulses from semiconductor lasers through harmonic-frequency sinusoidal modulation 21 p3145 A83-44956

Optoacoustic transducers with intensity-modulated inputs 22 p3287 A83-45699

Heterodyne receiver on silicon - An exercise in integration 22 p3359 A83-46646

Enhanced frequency modulation in cleaved-coupled-cavity semiconductor lasers with reduced spurious intensity modulation 22 p3299 A83-46722

Generation of short laser pulses during coherent amplification 22 p3301 A83-46937

A bistable hybrid optical device using an integrated modulator with an induced dielectric channel 23 p3507 A83-47561

Waveguide light modulators using the Keldysh-Franz effect in gallium arsenide 23 p3507 A83-47570

1.5 GHz operation of an Al(x)Ga(1-x)As/GaAs modulation-doped photoconductive detector 23 p3446 A83-48712

Longitudinal mode spectrum of GaAs injection lasers under high-frequency microwave modulation 24 p3586 A83-48780

Total-internal-reflection electrooptic thin-film modulator 24 p3628 A83-48859

Fluorescent window as wavelength shifter for a polysulfide containing photoelectrochemical cell 24 p3601 A83-50183

LIGHT PRESSURE

U ILLUMINANCE

LIGHT PROBES

U LIGHT BEAMS

LIGHT SCATTERING

NT HALOS

Features of the Raman spectra of noncrystalline semiconductor compounds of the type Hg/Ga/-As/Sb/-S-I 01 p0110 A83-10847

Laser transit anemometer measurements with unseeded backscatter 01 p0051 A83-11057

The accuracy of the representation of a real scattering signal by the lidar equation 02 p0176 A83-11697

The coincidence tracker - Electronic equipment for a time-of-flight wind-speed measurement system 02 p0177 A83-12009

Normalized scattering diagram for atmospheric aerosols with Junge particle size distribution 02 p0206 A83-12304

Reflective and refractive scattering of ultraviolet radiation caused by state of the art optical grinding and polishing techniques 02 p0237 A83-12701

Interpreting the thermal properties of cometary dust 03 p0415 A83-13388

Light scattering by arbitrarily oriented cylinders 03 p0395 A83-14636

Bandwidth, scattered light, and temporal variability effects in spectral solar radiometry 03 p0370 A83-14643

Effects of cloud shape on cloud field identification 03 p0371 A83-14656

Rayleigh scattering in ZrF₄-based glasses 04 p0534 A83-15247

The effects of light scattering on the directivity of radiation from unstable-resonator lasers 04 p0484 A83-15266

Transverse photon bunching and two-photon processes in a parametric scattering field --- in image converters 04 p0482 A83-15906

The structure of cometary dust tails. II - Tail brightness profiles and dust characteristics of comet Arend-Roland, 1957 III 05 p0695 A83-16855

The Raman scattering of light by stationary waves of nonlinear polarization 05 p0684 A83-16888

Color photometry of surface features on Ganymede and Callisto 05 p0704 A83-16963

Interaction and competition between forward and backscattering in stimulated Raman scattering 05 p0649 A83-17058

Determination of the width of the gain profile of an iodine laser with the aid of stimulated Brillouin scattering 05 p0649 A83-17059

The propagation of a narrow modulated light beam in a scattering medium with allowance for the photon path fluctuations during multiple scattering 05 p0651 A83-17590

A scattering model for the zodiacal light particles 06 p0824 A83-18076

Possibility of determining the dispersed composition of a two-phase flow from small-angle light scattering 06 p0757 A83-18448

Measurement of temperature conductivity of pure fluids and binary mixtures with the aid of dynamic light scattering in the general region of the critical point --- German thesis 06 p0757 A83-18521

Effects on skylight at South Pole Station, Antarctica, by ice crystal precipitation in the atmosphere 06 p0778 A83-18585

A kinetic description of the Rayleigh scattering of light in dense gases 06 p0815 A83-19184

The inhomogeneous development of the decomposition reaction of shock-compressed homogeneous explosives 07 p0880 A83-19960

Stimulated Mandel'shtam-Brillouin scattering in a multimode glass fiber lightguide 07 p0933 A83-20046

Coherent echo spectroscopy of small liquid particles 07 p0881 A83-20112

Influence of aperture effects on the spectral structure of stimulated Raman scattering by optical phonons and polaritons in a resonator 07 p0992 A83-20119

Reversal of the wavefront of nanosecond and subnanosecond light pulses in stimulated Brillouin scattering 07 p0935 A83-20121

Stimulated Raman scattering in a multipass cell filled with CO₂ 07 p0935 A83-20125

Determination of velocity gradients with scattered light cross-correlation measurements 07 p0928 A83-20165

Study of the particulate sulfur-light scattering relationship using in situ aerosol thermal analysis 07 p0957 A83-20222

Closure hypotheses from the method of smoothing for coherent wave propagation in discrete random media 07 p0989 A83-20792

Time-resolved Thomson-scattering measurements of ion fluctuations driven by stimulated Brillouin scattering 07 p0998 A83-20816

Polarization backscatter analysis of field distributions using fiber optics 07 p0930 A83-20828

The possibilities of measuring the optical characteristics of scattering media by moving lidars 07 p0963 A83-20892

Experimental and mathematical modeling of the conditions of the seeing of objects through a turbid-medium layer --- earth atmosphere 07 p0963 A83-20893

Results of a statistical analysis of the backscattering of light with model indicatrices --- remote sensing of atmospheric aerosols 07 p0963 A83-20896

Time-resolved observations of simulated Raman scattering from laser-produced plasmas 08 p1168 A83-22390

Frequency-shift of self-trapped light --- due to decrease in resonant frequency of plasma cavity 08 p1168 A83-22391

Transverse velocity measurements using coherent lidar 08 p1096 A83-22514

Improved light-scattering cavitation nuclei classifier 08 p1106 A83-23229

Simplified calculational procedure for determining the amount of intercepted sunlight in an imaging solar concentrator 09 p1293 A83-23884

Phase function in the scattering in arbitrary higher order --- of light in planetary atmospheres 09 p1365 A83-23896

Light scattering in the reversible electrical memory effect in smectic liquid crystals 09 p1344 A83-23996

Scattering of laser beams and the optical potential well for a homogeneous sphere 09 p1272 A83-24088

Integral equation for the scattered field in the presence of a phase-conjugate mirror 09 p1344 A83-24101

The brightening effect during nonlinear light scattering by static optical inhomogeneities 09 p1345 A83-24217

Light scattering in polycrystalline materials 09 p1346 A83-24969

Spectroscopic measurements of the 'additional absorbing mass' in total and partial cloudiness 09 p1316 A83-25055

The calculation of the spectral characteristics of the scattering of light by seawater 09 p1320 A83-25057

The reconstruction of images scattered in an inhomogeneous medium --- Russian book 09 p1270 A83-25224

Light propagation in a disperse medium --- Russian book 09 p1346 A83-25251

Important trends in the modern theory for the scattering and absorption of radiation by individual particles 09 p1339 A83-25252

The scattering of light in an inhomogeneous atmosphere 09 p1364 A83-25254

Topics in the theory of radiative transfer in horizontally inhomogeneous media --- scattering of sunlight in clouds 09 p1317 A83-25255

The nonstationary scattering of spatially confined and ultrashort light pulses 09 p1273 A83-25256

Methods for practical calculations of light fields under conditions of multiple scattering 09 p1347 A83-25257

The development of numerical methods for solving the radiative transfer equation 09 p1340 A83-25258

Inverse problems in the laser probing of atmospheric aerosols 09 p1309 A83-25261

Laser with diffraction-limited divergence and Q switching by stimulated Brillouin scattering 10 p1431 A83-26655

Tuning characteristics of multistage stimulated Raman scattering by polaritons in a layer of an LiIO₃ crystal 10 p1432 A83-26671

Ring laser for the determination of linear velocities 10 p1433 A83-26675

High-sensitivity atmospheric gas analysis based on intracavity laser detection of scattered radiation 10 p1392 A83-26685

CARS-spectroscopy of UF₆ and SF₆ 11 p1654 A83-27552

Elastic light-scattering Mueller-matrix photopolarimetry 11 p1572 A83-27566

Investigation of domains of validity of approximation methods in forward light scattering from long absorbing cylinders 11 p1657 A83-27845

Theory of the interaction of counterpropagating waves in a nonlinear cubic medium 11 p1583 A83-27954

Amplification of the mean intensity of backscattering in a turbulent atmosphere 11 p1632 A83-27957

On the size, shape, and orientation of noctilucent cloud particles 11 p1616 A83-28094

Investigation of a Laser Doppler anemometer with counterpropagating beams 11 p1574 A83-28562

Raman spectroscopy --- Russian book 12 p1727 A83-28810

Optical development and application of a two colour LDA system for the simultaneous measurement of particle size and particle velocity 12 p1721 A83-28838

Study of dynamical effects using phase conjugation of light waves 12 p1729 A83-29167

Solar rotation results at Mount Wilson 13 p1963 A83-29988

Stimulated Brillouin scattering in an inhomogeneous plasma with broad-bandwidth thermal noise 13 p1923 A83-30120

- Expansion of a multi-ion plasma into a vacuum
13 p1924 A83-30123
- Radiation pressure and 360 deg scattering diagrams for infinite cylinders
13 p1829 A83-30748
- Fluctuation and scattering properties of RF sputtered glass thin film optical waveguides
13 p1919 A83-30781
- Scattering and mode conversion of guided modes in an optical slab waveguide caused by a cylindrical of arbitrary cross section shape
13 p1919 A83-30782
- Application of the 2-D discrete-ordinates method to multiple scattering of laser radiation
13 p1857 A83-31460
- High spectral resolution lidar system with atomic blocking filters for measuring atmospheric parameters [AD-A129929]
13 p1857 A83-31463
- Anti-Stokes scattering as an XUV radiation source --- for spectroscopy
13 p1818 A83-31810
- Scattering of light by an intense saturating pulse in a resonance medium
14 p2078 A83-31901
- Space telescope low scattered light camera - A model
14 p2096 A83-32026
- An investigation of the effect of polarizing radiation, scattered by an optically inhomogeneous layer, on the quality of its holographic image
14 p2019 A83-32126
- The polarization control of tone-transmission brightness in a holographic image of light-scattering surfaces and layers
14 p2019 A83-32132
- Time-dependent oscillations of the gain factor during the stimulated Raman scattering of light by polaritons under nonstationary conditions
14 p2024 A83-32166
- Simultaneous determination of complex refractive index and size distribution of airborne and water-suspended particles from light scattering measurements
14 p2052 A83-32440
- Frequency-angular diffusion of intense quiescent radiation
14 p2024 A83-32617
- The matrix coefficient for the brightness of radiation reflected by a semi-infinite absorptive medium with a greatly extended indicatrix of scattering
14 p2085 A83-32857
- The characteristics of a confined light beam in an absorptive medium having a narrow indicatrix of scattering
14 p2085 A83-32858
- The Raman scattering of light and crystal-lattice dynamics
14 p2092 A83-33037
- Raman scattering of light during phase transitions in crystals
14 p2092 A83-33038
- Real-time holography and wave-front conjugation by stimulated scattering
15 p2229 A83-33529
- Numerical study of phase conjugation in stimulated Brillouin scattering from an optical waveguide
15 p2229 A83-33530
- Coherent anti-Stokes Raman scattering in thin-film dielectric waveguides
15 p2230 A83-33756
- High-efficiency laser-pulse compression by stimulated Brillouin scattering
15 p2167 A83-33759
- Inverse problems of lidar sensing of the atmosphere --- Book
15 p2195 A83-33768
- Diffraction of light by a perfectly conducting biaxial periodic surface
15 p2231 A83-34367
- Time-dependent aureole about a source in a multiple-scattering medium --- for solar blind UV communication and warning systems
15 p2201 A83-34458
- Modelling atmospheric aerosol backscatter at CO₂ laser wavelengths. I - Aerosol properties, modeling techniques, and associated problems. II - Modeled values in the atmosphere. III - Effects of changes in wavelength and ambient conditions
15 p2201 A83-34461
- Scattering phase matrix comparison for randomly hexagonal cylinders and spheroids
15 p2226 A83-34463
- Elements of the theory of light scattering and optical radar --- Russian book
15 p2170 A83-34573
- Passage of a pulsed optical signal through an absorbing medium with strongly anisotropic scattering
15 p2231 A83-34705
- Increasing backscattered light from the stratospheric aerosol layer after Mt. El Chichon eruption - Laser radar measurement at Nagoya (35 deg N, 137 deg E)
15 p2202 A83-34728
- The derivation of Halley parameters from observations
15 p2273 A83-35018
- Comparison of Monte Carlo calculations with observations of light scattering in finite clouds
16 p2387 A83-35491
- Formation of fine dust on Saturn's rings as suggested by the presence of spokes
16 p2436 A83-35732
- Twilight observations from a balloon gondola - Preliminary results
16 p2376 A83-35788
- Laser light scattering technique in the diagnostics of sprays in isothermal and burning conditions
16 p2351 A83-35825
- Theory of backward Rayleigh scattering in polarization-maintaining single-mode fibers and its application to polarization optical time domain reflectometry
16 p2412 A83-35967
- Rayleigh scattering in fluoride glass optical fibres
16 p2412 A83-36480
- Calculation of the inversion curves by the Monte Carlo method --- for ozone attenuation coefficient determination
16 p2392 A83-36849
- A laser spectrometer for Raman scattering
16 p2357 A83-36874
- Analysis of laser light scattered by cold, dense hydrogen plasmas produced in a Z pinch
17 p2581 A83-37040
- Redistribution - Why half a collision is better than a whole one --- spectra of scattered light from perturbed atomic system
17 p2484 A83-37075
- Solar scattered radiation measurements by Venus probes
17 p2617 A83-37420
- Laser scattering and current transport in an argon arc plasma --- German thesis
17 p2582 A83-37504
- Coherent Anti-Stokes Raman scattering with reflective optics
17 p2485 A83-37742
- A general theory of the Raman-type free-electron laser
17 p2514 A83-38039
- Distribution of illumination from a narrow light beam in a turbid atmosphere
17 p2515 A83-38978
- Novel mirror telescope for prominences
18 p2755 A83-39225
- A point source of light in an absorbing and scattering plane layer --- interstellar extinction of stellar radiation
18 p2766 A83-39486
- Scattered visible and ultraviolet solar radiation from condensed attitude control jet plumes
18 p2648 A83-40015
- The problem of the scattering of light by a horizontally inhomogeneous cloud
18 p2730 A83-40081
- The Brillouin-scattering method in quantum electronics and laser-induced damage
18 p2694 A83-40608
- Investigation of Brillouin light scattering in crystals and glasses with application to problems of quantum electronics and fiber optics
18 p2694 A83-40609
- Experimental study of launched ion-acoustic waves in a plasma using continuous wave CO₂ laser scattering
19 p2902 A83-41309
- Effects of the El Chichon volcanic cloud in the stratosphere on the intensity of light from the sky
20 p3028 A83-42209
- Particle size distributions from forward scattered light using the Chahine inversion scheme
20 p3046 A83-42213
- Simultaneous determination of refractive index and size of spherical dielectric particles from light scattering data
20 p3046 A83-42214
- Scattering from a V-shaped groove in the resonance domain --- optical measurement for comparison with theoretical prediction
20 p3046 A83-42215
- Techniques for measuring radiance in sea and air
20 p2988 A83-42216
- Photometer for quasielastic and classical light scattering
20 p2988 A83-42295
- A search for the Sunyaev-Zel'dovich effect at millimeter wavelengths --- cosmic background photon energy increase due to Compton scattering by high temperature galactic cluster plasma electrons
20 p3082 A83-42467
- Performance degradation due to stimulated Raman scattering in wavelength-division-multiplexed optical-fiber systems
20 p3047 A83-42492
- Scattering of light and acoustic disturbances in the atomic iodine laser
20 p2995 A83-42795
- Determination of Mode I stress intensity factors in surface-flawed plates by scattered-light photoelasticity
20 p3002 A83-42833
- Point spread functions in imaging a Lambert surface from zenith through a thin scattering layer
20 p3011 A83-42964
- Out of ecliptic zodiacal cloud profile
20 p3081 A83-43158
- Fraunhofer diffraction by ice crystals suspended in the atmosphere
20 p3028 A83-43465
- Light scattering from gaseous nitrous oxide - Effects of correlation between molecular and intermolecular axes upon the depolarization ratio in terms of the anisotropic potential choice
21 p3204 A83-44190
- Measurement of axially nonsymmetrical refractive-index distribution of a single-mode fiber by a multidirectional scattering-pattern method
21 p3204 A83-44201
- Modified Monte-Carlo method to evaluate multiple scattering effects on lightbeam transmission through a turbid atmosphere
21 p3144 A83-44794
- The generation of picosecond pulses of stimulated combination scattering light in an external resonator
21 p3145 A83-45203
- Experimental study of the effect of the polarization of scattered waves on the signal of a laser Doppler velocimeter
21 p3142 A83-45311
- Resonance Raman scattering of light and characteristics of the formation of low-temperature luminescence in anthracene crystals
21 p3219 A83-45337
- Operating characteristics of a laser with supplementary inertial negative feedback
21 p3146 A83-45387
- Scattering and mode conversion of guided modes by an arbitrary cross-sectional cylindrical object in an optical slab waveguide
22 p3355 A83-45729
- Rayleigh backscattering in a fiber gyroscope with limited coherence sources
22 p3287 A83-45730
- Enhanced Raman scattering from silicon microstructure
22 p3356 A83-45968
- Calculation of surface-scattered optical fields in designing optical scanning devices
22 p3357 A83-46335
- Pulse compression by stimulated Brillouin scattering
22 p3297 A83-46630
- Use of laser annealing to achieve low loss in Corning 7059 glass, ZnO, Si₃N₄, Nb₂O₅, and Ta₂O₅ optical thin film waveguides
22 p3359 A83-46647
- Wideband frequency conversion in the UV by nine orders of stimulated Raman scattering in a XeCl laser pumped multimode silica fiber
22 p3299 A83-46719
- Refractive index and size distribution of aerosols as estimated from light scattering measurements
22 p3334 A83-46947
- Diffuse light near Zeta Orionis and the Horsehead nebula, and anomalous extinction of HD 37903, as measured with the ANS
23 p3516 A83-47441
- Rayleigh backscattering theory for single-mode optical fibers
23 p3508 A83-47584
- Acoustic wave calibration for CO₂ laser scattering experiments
23 p3461 A83-47647
- Coherent light scattering from ruby dressed with RF photons
23 p3462 A83-48323
- Apportioning light extinction coefficients to chemical species in atmospheric aerosol
23 p3479 A83-48689
- Effect of wall scattering on SNR in off-axis differential-type laser Doppler velocimetry
24 p3581 A83-48747
- Transient stimulated Raman scattering of femtosecond laser pulses
24 p3586 A83-48782
- Simultaneous measurement of magnetic field direction and ion temperature in a plasma by collective scattering with a CO₂ laser
24 p3630 A83-48786
- Quantum theory of laser-radiation scattering by electrons in magnetic fields
24 p3587 A83-48841
- Highly efficient, high-quality phase-conjugate reflection at 308 nm using stimulated Brillouin scattering
24 p3587 A83-48854
- Aerosol backscattering of a laser beam
24 p3588 A83-49004
- Light scattering by randomly oriented cubes and parallelepipeds --- for interpretation of observed data from planetary atmospheres
24 p3671 A83-49009
- Monte Carlo estimation of polarization in reflection nebulae
24 p3659 A83-49375
- Multiple scattering in the reflection nebula NGC 1999 and the nature of interstellar dust
24 p3659 A83-49376
- ### LIGHT SCATTERING METERS
- Measurement of angle resolved light scattering from optical surfaces in the 75 to 750 eV range
02 p0239 A83-12716
- Aspects of light scattering by spherical particles
21 p3207 A83-44836
- ### LIGHT SOURCES
- Photon-counting statistics of pulsed light sources [AD-A124141]
02 p0175 A83-11563
- Optical components and systems for synchrotron radiation - An introduction
02 p0237 A83-12692
- Intensity-dependent nonreciprocal phase shift in fiber-optic gyroscopes for light sources with low coherence
05 p0643 A83-16842
- Simple absolute calibration method using laser sources for pulsed spectroscopic applications in the visible and UV
07 p0932 A83-21384
- Bright light sources from shock deceleration of hypersonic plasma streams in dense gases
13 p1926 A83-30827
- Collection efficiency of a spectrograph for distributed sources
16 p2357 A83-36762
- Limit of concentration for cylindrical concentrators under extended light sources --- parabolic solar collectors
21 p3167 A83-44149
- Fiber-optic gyroscopes with broad-band sources
21 p3136 A83-44210
- GaAs optoelectronic integrated light sources
21 p3125 A83-44226
- Estimation of the angular position of an optical source whose emission is received by a photodetector array
22 p3355 A83-45691

- Nonlinear optics with a diode-laser light source 22 p3356 A83-45963
- Infrared synchrotron radiation from electron storage rings 22 p3355 A83-46842
- Sources of stimulated radiation using resonance electron accelerator 23 p3460 A83-47557
- High efficiency mid-IR generation by Raman down conversion in liquid nitrogen 24 p3587 A83-48907
- LIGHT SPEED**
- Relativistic kinematics for motions faster than light 01 p0124 A83-10705
- An estimate of the effects of light travel times in the optical jets of SS433 16 p2428 A83-36537
- Lie-isotopic lifting of the special relativity for extended deformable particles 23 p3503 A83-47420
- LIGHT TRANSMISSION**
- NT HALOS
- NT LIGHT SCATTERING
- Transmission characteristics of a pulsed laser beam in natural sea-water - Determination of the attenuation coefficients in the 415-660 nm spectral range 01 p0054 A83-10695
- Light transmission optics /2nd edition/ --- Book 01 p0106 A83-10879
- Low loss poly/methyl methacrylate-d5/ core optical fibers 01 p0106 A83-10985
- Investigation of the multimode interference of surface optical waves in a microwaveguide interferometer 02 p0175 A83-11528
- A comparison of lightwave, microwave, and coaxial transmission technologies 02 p0164 A83-12165
- Transport of solar energy with optical fibres 03 p0354 A83-13698
- Switching of reflection of light at nonlinear interfaces 03 p0394 A83-13793
- Ultraviolet measurements, methods and production 03 p0394 A83-13968
- Atmospheric transmission; Proceedings of the Meeting, Washington, DC, April 21, 22, 1981 03 p0344 A83-13976
- An optical device for path-averaged measurements of Cn2 03 p0364 A83-13977
- REALTRAN - Real-time implementation of atmospheric-transmittance codes 03 p0359 A83-13989
- High-resolution lower atmospheric transmission predictions over long paths 03 p0359 A83-13991
- Drop-size distribution of fog droplets determined from transmission measurements in the 0.53-10.1-microns wavelength range 03 p0365 A83-14378
- Atmospheric turbulence simulation cell for optical propagation experiment [ONERA, TP NO. 1982-84] 03 p0330 A83-14536
- Optical absorption above the optical gap of amorphous silicon hydride 04 p0541 A83-15520
- Spatial coherence of laser light propagating in an optical fibre 04 p0535 A83-15793
- The transmission to space of the light produced by lightning in the clouds of Venus 05 p0704 A83-16967
- Propagation and conversion of light waves in corrugated waveguide structures 05 p0685 A83-17081
- The propagation of a narrow modulated light beam in a scattering medium with allowance for the photon path fluctuations during multiple scattering 05 p0651 A83-17590
- A comparative study of the light transmission, acoustic emission, and thermal effects of a glass-reinforced plastic under mechanical loads 06 p0725 A83-18519
- Propagation of interacting first and second optical harmonics in a nonlinear active medium 07 p0934 A83-20118
- Closure hypotheses from the method of smoothing for coherent wave propagation in discrete random media 07 p0989 A83-20792
- Diffraction of a surface optical wave in an optical slab waveguide by a surface acoustic wave /SAW/ 07 p0993 A83-20856
- The optical scalar equations in the presence of a refractive medium 07 p1023 A83-21142
- Obscuration by helicopter-produced snow clouds 08 p1043 A83-22357
- Effects of piston and tilt errors on the performance of multiple mirror telescopes --- in laser relay systems 08 p1108 A83-22456
- New methods for optical, quasi-optical, acoustic and electromagnetic synthesis; Proceedings of the Meeting, San Diego, CA, August 25, 26, 1981 08 p1161 A83-22468
- Atmospheric propagation effects on coherent laser radars 08 p1096 A83-22509
- Measurements of infrared and visible extinction in adverse weather 08 p1140 A83-22546
- Measurements of the phase function of natural particles 08 p1076 A83-22547
- Assessment of operational techniques for estimating visible spectrum contrast transmittance 08 p1098 A83-22548
- Experimental measurements of turbulence induced beam spread and wander at 1.06, 3.8, and 10.6 microns 08 p1110 A83-22562
- Light transport in planar luminescent solar concentrators - The role of DCM self-absorption --- 4-dicyano-methylene-2-methyl-6-p-dimethyl H-pyran 08 p1130 A83-22619
- Laser transmissometer calibration of long-path atmospheric transmission measurements 08 p1104 A83-22889
- Propagation model of laser beams in turbulence 09 p1271 A83-24084
- Inner-scale size effect on the scintillations of light in the turbulent atmosphere 09 p1344 A83-24086
- The brightening effect during nonlinear light scattering by static optical inhomogeneities 09 p1345 A83-24217
- Light propagation in a disperse medium --- Russian book 09 p1346 A83-25251
- Coherence and interferometry through optical fibers --- of stellar interferometers 10 p1482 A83-25847
- Propagation of laser radiation in water aerosol in conditions of the dispersal of this aerosol 10 p1434 A83-26778
- Numerical study of the propagation of intense laser radiation in the atmosphere 10 p1434 A83-26781
- Modeling propagation of coherent optical pulses through molecular vapor 11 p1577 A83-27535
- Single mode fiber isolator in toroidal configuration 11 p1656 A83-27565
- Fluctuations of optical radiation on an inclined path 11 p1556 A83-27944
- Study of dynamical effects using phase conjugation of light waves 12 p1729 A83-29167
- Experiments with high bandwidth segmented mirrors 13 p1921 A83-31020
- Unpolarized EO Q-switched laser 13 p1857 A83-31458
- An experimental study of atmospheric optical transmission 13 p1830 A83-31724
- A thermo-optical method for the formation of lightguide channels 14 p2084 A83-32122
- Effect of turbulent boundary layer flow on optical transmission [AIAA PAPER 83-1524] 14 p2085 A83-32755
- Ultrashort pulse propagation in saturable media - A simple physical model 14 p2025 A83-33404
- Nonideal phase-conjugate resonators - A canonical operator analysis 15 p2229 A83-33533
- Fine-structure transitions occurring in collisional redistribution of light 15 p2227 A83-33795
- Optical transmission at 3.39 microns during pulsed laser annealing of silicon 15 p2238 A83-33849
- Parametric interaction and backward wave oscillation in stimulated Compton scattering 15 p2169 A83-34372
- Variational approach to nonlinear pulse propagation in optical fibers 16 p2411 A83-35660
- Tensorial rank of gravitational theories in flat space-time 16 p2407 A83-36553
- Distribution of illumination from a narrow light beam in a turbid atmosphere 17 p2515 A83-38978
- On an explicit method for the numerical solution of problems of light wave propagation in nonlinear media 18 p2692 A83-39155
- Image transmission through a turbulent medium using a point reflector and four-wave mixing in BSO crystal --- Bismuth Silicon Oxide 19 p2847 A83-41107
- Mode propagation of the field generated by Collett-Wolf Schell-model sources 19 p2852 A83-41176
- Optical bistability 20 p3048 A83-42624
- Problem of stabilization of laser radiation parameters 20 p2996 A83-43784
- Theory of self-induced transparency without the approximation of slowly varying amplitudes and phases 20 p2996 A83-43787
- Distortions of a CW light beam propagating through gas Self-lensing and spatial ringings 21 p3144 A83-44804
- Polarisation-mode dispersion as a bandwidth-limiting factor in a long-haul single-mode optical-transmission system 21 p3208 A83-44964
- The reconstruction of meteorological parameters from intra-atmospheric measurements of the optical refraction of cosmic sources 22 p3338 A83-45634
- Optical wave propagation in form-birefringent media and waveguides 22 p3356 A83-45732
- Filamentation instability in magneto plasmas 22 p3362 A83-46013
- Optical amplitude and polarization multistability in a nonlinear interferometer 22 p3360 A83-46790
- Properties of light transmission across an ultrasound beam with strong acoustooptical interaction 23 p3507 A83-47562
- Effects of atmospheric obscurants on the propagation of optical/IR radiation 23 p3442 A83-47785
- The beam propagation method - An analysis of its applicability --- to integrated optics 24 p3627 A83-48748
- Wave propagation in random media - A comparison of two theories 24 p3623 A83-48979
- Factorization of the transfer matrix for symmetrical optical systems 24 p3628 A83-48980
- LIGHT TRANSPORT AIRCRAFT**
- Unconventional commuter configurations - A design investigation [SAE PAPER 830710] 20 p2933 A83-43320
- Design consideration for lighting modern commercial aircraft [SAE PAPER 830712] 20 p2933 A83-43322
- Fail-operational DAFCs for business/commuter aircraft --- Digital Automatic Flight Control System [SAE PAPER 830714] 20 p2937 A83-43324
- LIGHT VALVES**
- Dynamic optical cross-correlator using a liquid crystal light valve for real time data input 21 p3207 A83-44827
- LIGHT-CONE EXPANSION**
- The cosmological problem as initial value problem on the observer's past light cone - Observations 23 p3526 A83-48059
- LIGHTHILL METHOD**
- Linear approximation of the reflection of a shock wave from a concave wall 05 p0639 A83-17414
- The pseudo sound contribution to the pressure field under a turbulent boundary layer [AIAA PAPER 83-0755] 11 p1652 A83-28020
- Airfoil generation with a desktop computer using Lighthill's exact inverse method [AIAA PAPER 83-1867] 18 p2632 A83-39096
- LIGHTING**
- U ILLUMINATING
- LIGHTING EQUIPMENT**
- NT AIRCRAFT LIGHTS
- NT AIRPORT LIGHTS
- NT ARC LAMPS
- NT FLASH LAMPS
- NT LUMINAIRES
- NT MERCURY LAMPS
- NT XENON LAMPS
- Aircraft electrical equipment --- Russian book 05 p0597 A83-17125
- Design consideration for lighting modern commercial aircraft [SAE PAPER 830712] 20 p2933 A83-43322
- LIGHTNING**
- NT BALL LIGHTNING
- In-flight lightning data measurement system for fleet application - Flight test results 01 p0009 A83-11087
- Associated lightning discharges 03 p0364 A83-13540
- The effect of polarization on radar detection of lightning 03 p0364 A83-13541
- A comparison of lightning electromagnetic fields with the nuclear electromagnetic pulse in the frequency range 10 to the 4th to 10 to the 7th Hz 03 p0344 A83-14550
- Charge deposition on ice particles by positive streamers 04 p0518 A83-16018
- Acoustics of thunder - A quasilinear model for tortuous lightning 04 p0519 A83-16315
- The transmission to space of the light produced by lightning in the clouds of Venus 05 p0704 A83-16967
- Lightning leader characteristics in the Thunderstorm Research International Program /TRIP/ 07 p0960 A83-20218
- Lightning and surface rainfall during Florida thunderstorms 07 p0969 A83-20219
- On the characteristics of some radiation fields from lightning and their possible origin in positive ground flashes 07 p0960 A83-20220
- Comparison of Venusian lightning observations 07 p1030 A83-20620
- Role of various charging mechanisms in thundercloud electrification 08 p1140 A83-22316
- Electrification of convective clouds 08 p1140 A83-22317
- Some scientific objectives of a satellite-borne lightning mapper 08 p1141 A83-22702
- Observations of optical lightning emissions from above thunderstorms using U-2 aircraft 08 p1141 A83-22703
- Photographs of lightning from the Space Shuttle 08 p1141 A83-22705
- Lightning activity on Jupiter 08 p1189 A83-22933

The microwave radiation of lightning and thunderstorm atmospheric processes 09 p1310 A83-23392

Progress in the large-scale determination and analysis of thunderstorm activity with the aid of atmospheric measurements 09 p1310 A83-23403

Experiences with two new lightning localization devices 09 p1310 A83-23405

Lightning propagation and flash density in squall lines as determined with radar 09 p1314 A83-24276

Controlled stimulation of magnetospheric electrons by radio waves Experimental model for lightning effects 09 p1309 A83-25288

A 4-quadrant lightning detector 11 p1571 A83-27009

Velocity structures in electrically active thunderstorms 11 p1625 A83-27014

Return-stroke electromagnetic fields of oblique lightning channels 11 p1632 A83-27970

Various features of VLF waves generated by lightning discharge 11 p1619 A83-28429

Integrating non-first order automated meteorological observations into national weather forecasting and analysis programs 13 p1891 A83-30593

Acoustic and electric signals from lightning 13 p1892 A83-30899

Deductions concerning accumulations of electrified particles in thunderclouds based on electric field changes associated with lightning 13 p1892 A83-30904

Evidence for a low-altitude origin of lightning on Venus 13 p1961 A83-31212

Nitrogen fixation by lightning activity in a thunderstorm 15 p2197 A83-34039

In situ aircraft measurements of enhanced levels of N₂O associated with thunderstorm lightning 15 p2199 A83-34222

Radar cross section of a lightning element modeled as a plasma cylinder 16 p2383 A83-35412

Oscillating bipolar electric field changes due to close lightning return strokes 16 p2383 A83-35413

Effects of propagation on the rise times and the initial peaks of radiation fields from return strokes 16 p2341 A83-35415

Saturn's electrostatic discharges - Could lightning be the cause? 16 p2436 A83-35734

Lightning research from space 16 p2422 A83-35778

Lightning and precipitation in a small multicellular thunderstorm 16 p2390 A83-36155

The electrical activity of the atmosphere of Venus 17 p2617 A83-37418

Cloud electrification --- during thunderstorms 17 p2547 A83-38315

Lightning --- research in U.S. 17 p2547 A83-38316

The LLP lightning locating system --- Lightning Location and Protection 17 p2549 A83-38720

Planetary lightning - Earth, Jupiter, and Venus 18 p2780 A83-40328

Experiment of artificial lightning triggered with rocket 18 p2731 A83-40335

Optical signature of Venus lightning as seen from space 19 p2922 A83-40789

On the origin of whistlers 20 p3016 A83-42306

Induced currents at the resonant frequency in the Rocket Triggered Lightning Investigation 20 p3030 A83-42534

Variation in light intensity with height and time from subsequent lightning return strokes 20 p3030 A83-42839

Observations of severe in-flight environments on airplane composite structural components 20 p2933 A83-43330

Aircraft-borne lightning sensor 21 p3134 A83-43867

Theoretical and experimental studies of the electromagnetic coupling mechanisms between aircraft and consecutive lightning strikes, both direct and nearby [ONERA, TP NO. 1983-44] 21 p3089 A83-44318

Hypotheses on the physical mechanisms of VHF-UHF radiation from lightning [ONERA, TP NO. 1983-45] 21 p3178 A83-44319

The 300 MHz electromagnetic radiation and electrostatic field associated with lightning discharges [ONERA, TP NO. 1983-46] 21 p3178 A83-44320

The estimate of probability distribution of the dominant frequencies for the lightning during an eclipse of the sun 21 p3179 A83-44587

The global distribution of thunderstorm activity observed by the Ionosphere Sounding Satellite (ISS-b) 21 p3182 A83-45451

Global distribution of atmospheric radio noise derived from the global distribution of lightning activity 21 p3178 A83-45454

The lightning current 22 p3339 A83-45878

Whistlers --- in earth ionosphere and magnetosphere 22 p3325 A83-45886

Lightning detection from space 22 p3259 A83-45887

Lightning within planetary atmospheres 22 p3384 A83-45888

Instrumentation --- for atmospheric analysis 22 p3287 A83-45890

Acoustic radiations from lightning 22 p3339 A83-45891

Lightning, auroras, nocturnal lights, and related luminous phenomena: A catalog of geophysical anomalies -- Book 22 p3325 A83-45913

Global distribution of atmospheric radio noise derived from distribution of lightning activity 22 p3275 A83-46918

Laboratory simulation of Venusian lightning 23 p3529 A83-47863

UHF interferometric imaging of lightning [ONERA, TP NO. 1983-55] 23 p3492 A83-48177

A contribution to the analysis of triggered lightning - First results obtained during the trip 82 experiment [ONERA, TP NO. 1983-56] 23 p3492 A83-48178

A systematic characterization of the effects of atmospheric electricity on the operational conditions of aircraft [ONERA, TP NO. 1983-59] 23 p3400 A83-48180

The peak electromagnetic power radiated by electrified return strokes 24 p3610 A83-49335

Positive cloud to ground lightning return strokes 24 p3610 A83-49336

Simultaneous pulses in light and electric field from stepped leaders near ground level 24 p3610 A83-49346

The optical power radiated by lightning return strokes 24 p3610 A83-49347

Holographic device for rectilinear surface discharge visualization [ONERA, TP NO. 1983-104] 24 p3583 A83-49415

LIGHTNING SUPPRESSION

Methods for minimizing the effects of lightning transients on aircraft electrical systems 01 p0009 A83-11088

LIGHTS

U LUMINAIRES

LIKELIHOOD RATIO

Data-adaptive detection of a weak signal 14 p2002 A83-33136

Application of the Generalized Likelihood Ratio algorithm to maneuver detection and estimation 17 p2567 A83-37120

LIMB BRIGHTENING

Further observations of 8-micron polar brightenings of Jupiter 10 p1518 A83-25516

Observation of the flare of 12 June 1982 by Norikura coronagraph and Hinotori 23 p3533 A83-47676

LIMB DARKENING

Observation of global 160-min infrared /differential/ intensity variation of the sun 11 p1688 A83-27628

The electrophotometry of Saturn. I - The distribution of brightness over the equatorial regions in the spectral range of 0.3-0.6 micron 14 p2095 A83-31837

Limb darkening of meteorites and asteroids 14 p2112 A83-32605

Infrared limb-darkening effects for the earth-atmosphere system [AIAA PAPER 83-0161] 16 p2377 A83-36045

New information on Saturn and its rings from multi-frequency VLA data 17 p2620 A83-38111

YZ Cassiopeiae and the Utrecht photometric system 19 p2911 A83-41071

Photometric observations - Is HZ Herculis getting darker? 24 p3649 A83-50082

LIMBS (ANATOMY)

NT ARM (ANATOMY)

NT ELBOW (ANATOMY)

NT FEET (ANATOMY)

NT FINGERS

NT FOREARM

NT HAND (ANATOMY)

NT KNEE (ANATOMY)

NT LEG (ANATOMY)

Preliminary generalized thoughts concerning ejection flail phenomena 04 p0443 A83-15404

Age-related patterns of lateral movement preferences 05 p0673 A83-17156

A comparison of limb plethysmograph systems proposed for use on the Space Shuttle 06 p0799 A83-18187

Effect of suspension hypokinesia/hypodynamia on glucocorticoid receptor levels in rat hindlimb muscles 11 p1640 A83-27836

Evaluation of the response of rat skeletal muscle to a model of weightlessness 11 p1640 A83-27837

Transducers for ultrasonic limb plethysmography 14 p2072 A83-32694

LIME

U CALCIUM OXIDES

LIMITATIONS

U CONSTRAINTS

LIMITER CIRCUITS

Phase-locked loops with limiter phase detectors in the presence of noise 03 p0312 A83-13860

Hard limiter performance as a polarity detector for extremely polluted signals --- in Ioran C navigation systems 06 p0716 A83-19026

A limiter for high-power millimeter-wave systems 10 p1409 A83-25821

Doppler signal processing using IF limiting 11 p1626 A83-27025

Design concepts and performance characteristics of a high performance linear/digital shunt regulator 11 p1559 A83-27134

Problems associated with correlation-loop adaptive antennas employing hard limiting 11 p1554 A83-27910

Millimeter wave high power solid state limiter 11 p1563 A83-28590

The technology of metal semiconductor contacts - Application to the manufacture of microwave modulators and limiters on GaAs --- French thesis 12 p1720 A83-29948

Performance of digital implementations of an adaptive processor 14 p2007 A83-33127

Performance of a microwave amplitude limiter using GaAs MESFET 15 p2149 A83-33522

LIMITS (MATHEMATICS)

Existence of a generalized solution in thermoelasticity with two relaxation times. I 06 p0775 A83-18807

Limiting density of matter as a universal law of nature 13 p1947 A83-30798

The small dispersion limit of the Korteweg-de Vries equation. I 14 p2078 A83-32850

Representations of intervals and optimal error bounds 20 p3041 A83-42500

The small dispersion limit of the Korteweg-de Vries equation. II 22 p3353 A83-47092

LIMNOLOGY

Automatic mapping of lakes for small-scale maps using digital Landsat Imagery 08 p1129 A83-21969

Lake-effect snow storms on Lake Michigan, USA 09 p1312 A83-23956

Analysis on the spatial distribution of water quality and pollution sources of a shallow lake by digital image processing 09 p1290 A83-24613

Automatic classification of Lake Qarun water by digital processing of Landsat MSS data 09 p1291 A83-24624

Numerical simulation of the airflow over Lake Michigan for a major lake-effect snow event 10 p1451 A83-25392

Canadian Landsat studies for monitoring hydrologic conditions and coastal environments - A summary 15 p2183 A83-33579

Characterization of lake water quality parameters with airborne multispectral scanner data - Flathead Lake, Montana 17 p2531 A83-38350

LINE OF SIGHT

The frequency of cloud-free viewing intervals [AIAA PAPER 83-0441] 05 p0666 A83-16715

Sodar echoes and line of sight microwave propagation 06 p0736 A83-18349

The interstellar medium near the sun. III - Detailed analysis of the line of sight to lambda24 Scorpii 06 p0840 A83-19281

Reflection effect in close binaries. II - Distribution of emergent radiation from the irradiated component along the line of sight 18 p2764 A83-39188

Line of sight reconstruction for faster homing guidance [AIAA PAPER 83-2170] 19 p2796 A83-41666

Direct conversion of LOS acceleration data to vertical gravity anomalies - A new approach --- Line Of Sight 20 p3062 A83-43587

LINE OF SIGHT COMMUNICATION

Measurement of wind across a microwave line-of-sight propagation path 15 p2207 A83-35289

Microwave radio meteorology - Seasonal fading distributions 16 p2383 A83-35411

A statistical model of multipath fading on a space diversity radio channel 19 p2830 A83-41372

Performance of adaptive equalization for staggered QPSK and QPR over frequency-selective LOS microwave channels --- Quadrature Partial Response 19 p2831 A83-41377

A comparative study of scintillation analysis over two line-of-sight paths at 6.7 GHz and 7.6 GHz 23 p3443 A83-47834

Rain-induced amplitude scintillation on 8.2 km line-of-sight path at 30 GHz 24 p3571 A83-50120

LINE SHAPE

Off-axis effects in a mosaic Michelson interferometer [AD-A123678] 02 p0179 A83-12609

Precision collisional lineshapes by difference-frequency laser spectroscopy 03 p0294 A83-13982

Proton NMR line shapes in ZrHx 07 p0991 A83-21063

- Kinematics of the optical filaments in W50
07 p1021 A83-21121
- Effect of the stratospheric medium temperature on strong lines observed in the far infrared region
07 p0965 A83-21399
- High-resolution line-shape analyses of the pulsed cuprous chloride-laser oscillator and amplifier
10 p1435 A83-26878
- Resonance fluorescence and Raman line shapes produced by monochromatic laser fields - effects of branching ratio and homogeneous broadening
12 p1731 A83-29150
- Emission-line profiles for selected planetary nebulae and symbiotic stars, V1016 Cygni, and HM Sagittae
12 p1797 A83-29959
- A statistical analysis of Na I D1 profile fluctuations at the center of the solar disk. I - Data reduction and resolvable velocities
13 p1963 A83-29981
- The identification of orientation at the threshold of line detectors
13 p1900 A83-30429
- The interaction between detectors of line orientations
13 p1900 A83-30430
- Spatial adaptation and line detectors
13 p1900 A83-30431
- Evidence of anomalous multiplet line shapes in optically thick, laser-produced plasmas
15 p2236 A83-34997
- A galaxy with a 3.2×2.2 sq kpc H II region surrounding its nucleus
16 p2431 A83-36671
- Influence of an external cavity on semiconductor laser phase noise
21 p3146 A83-45479
- Fundamental linewidth in solitary, ultranarrow output PbS(1-x)Se(x) diode lasers
24 p3586 A83-48784
- Broad emission lines of QSOs are consistent with rotating supermassive stars
24 p3670 A83-50112
- LINE SPECTRA**
- NT BALMER SERIES
- NT D LINES
- NT ELECTRONIC SPECTRA
- NT FRAUNHOFER LINES
- NT H ALPHA LINE
- NT H BETA LINE
- NT H LINES
- NT K LINES
- NT LYMAN SPECTRA
- NT PASCHEN SERIES
- NT RYDBERG SERIES
- Measurements of collisional broadening and the shift of argon spectral lines using a tunable diode laser
01 p0105 A83-10203
- Luminosity classification of Be stars by Balmer line narrow band photometry
01 p0120 A83-10307
- Spectroscopic study of Pleione in 1977-1979 --- Be star
01 p0121 A83-10324
- Recent changes of the Be star HD 58050
01 p0121 A83-10328
- Determination of the inclination of rotational axes and rotational velocity from the line profiles of rotating stars
01 p0122 A83-10337
- Detection of the 1400 Å absorption in the ultraviolet spectrum of the DA white dwarf LB 3303
02 p0253 A83-11614
- The interstellar absorption-line spectrum of Mu Ophiuchi
02 p0256 A83-12124
- The ultraviolet continuous and emission-line spectra of the Herbig-Haro objects HH 2 and HH 1
02 p0256 A83-12125
- Photospheric spectrum line asymmetries and wavelength shifts
02 p0258 A83-12178
- Spectral line transfer effects in Lambdameter measurements of solar short-period oscillations
02 p0269 A83-12528
- Detection and study of secondary structures in some planetary nebulae
02 p0247 A83-12545
- Impulsive brightenings and velocity transients in prominences. I - Large events
02 p0270 A83-12577
- Two-line atomic fluorescence temperature measurement in flames - An experimental study
02 p0179 A83-12608
- The Lyman-alpha emission-line profiles in high-redshift QSOs
03 p0413 A83-13323
- TAURUS: A wide-field imaging Fabry-Perot spectrometer for astronomy
03 p0401 A83-13324
- GX 1+4: pulse period measurement and detection of phase-variable iron line emission
03 p0402 A83-13330
- The mid-ultraviolet spectrum of Epsilon Aurigae
03 p0415 A83-13362
- Spectral line inversion for sounding of stratospheric minor constituents by infrared heterodyne technique from balloon altitudes
03 p0325 A83-13723
- Electron collision strengths for the far-infrared lines of O III --- in Milky Way Galaxy
03 p0419 A83-13933
- Dielectronic satellite spectra for highly-charged helium-like ions. VII - Calcium spectra: Theory and comparison with SMM observations
03 p0420 A83-13948
- Two Cr II multiplets around 1430 Å appearing in absorption in the spectrum of a solar active region
03 p0436 A83-13952
- Effects of excitation mechanism on linewidth parameters of conventional vacuum ultraviolet /VUV/ discharge line sources
03 p0392 A83-13957
- [AD-A112052]
- Broad line region clouds and the absorbing material in NGC 4151
03 p0423 A83-14189
- Diffuse galactic gamma-ray line emission from nucleosynthetic Fe-60, Al-26, and Na-22 - Preliminary limits from HEAO 3
03 p0439 A83-14210
- Empirical NLTE analyses of solar spectral lines. III - Iron lines versus LTE models of the photosphere
03 p0437 A83-14797
- Detection of the /8,8/ and /9,9/ absorption lines of ammonia - The hot molecular cloud toward Sgr B2
03 p0438 A83-14806
- The detection of extranuclear emission lines in the Seyfert galaxies Mk10 and Mk79
03 p0430 A83-14811
- Proposed Mg V, Fe XIV and forbidden Fe XVII line identifications in the EUV solar spectrum
03 p0438 A83-14907
- Shifts of spectral lines emitted from stars
03 p0431 A83-14947
- Coma quasars
04 p0551 A83-15603
- The H II regions of Messier 8
04 p0552 A83-15615
- On the systematics of line ratios along the helium isoelectronic sequence
04 p0554 A83-15645
- Forbidden line emission from highly ionized atoms in tokamak plasmas
04 p0538 A83-16060
- Intensities, half-widths and shapes of spectral lines in the fundamental band of CO at low temperatures
04 p0534 A83-16436
- On the distribution of interstellar gas in the galactic halo
05 p0698 A83-16996
- The helium 10830 Å line in early-type stars - An atlas of Fabry-Perot scans
05 p0698 A83-17003
- Second-order escape probability approximations in radiative transfer
05 p0699 A83-17016
- Line positions and strengths in the H2 quadrupole spectrum
05 p0700 A83-17024
- Detection of H/C-17/O plus in Sagittarius B2
05 p0700 A83-17034
- The Seyfert 1 galaxy NGC 4593. I - Variability of the UV spectrum and physical conditions in the broad line emitting region
06 p0826 A83-18161
- Studies on the spectra of K-giants. II - Abundance determinations for K-giants from very strong iron lines
06 p0827 A83-18170
- Coronal line intensities for ions with fine-structured ground states - Si X
06 p0854 A83-18532
- The analysis of Fe XIV 5303 coronal emission-line polarization measurements
06 p0854 A83-18535
- Near infrared spectroscopy of W 51 IRS-2
06 p0818 A83-18541
- The asymmetry of photospheric absorption lines. I - An analysis of mean solar line profiles
06 p0854 A83-18547
- Simultaneous spectroscopy and photometry of RW Aurigae
06 p0830 A83-18785
- Spectrophotometry of the nucleus of the galaxy Arakelyan 144
06 p0831 A83-18792
- Supplements to the identification of CN lines in the solar spectrum in the wavelength range of 4145-4190 Å - Weak lines not listed in Rowland's Tables of 1966
06 p0854 A83-18846
- H I observations of high-luminosity elliptical galaxies
06 p0819 A83-18853
- A simple /and unexpected/ experimental law relating to the number of weak lines in a complex spectrum
06 p0813 A83-19001
- Detection of the secondary star in the eclipsing cataclysmic variable AC Cancri
06 p0821 A83-19063
- Line identifications in the spectrum of HR 1100
06 p0821 A83-19068
- Circumstellar material around rapidly rotating B stars. I - Nonemission-line stars
06 p0836 A83-19071
- Spectral observations of M 82
06 p0822 A83-19204
- Gamma ray lines from solar flares and cosmic transients
07 p1011 A83-20020
- Parameters of CO2 bands near 3.6 microns
07 p0881 A83-20164
- Effects of volume averaging on the line spectra of vertical velocity from multiple-Doppler radar observations
07 p0969 A83-20807
- The use of precision oscillator strengths as a means for obtaining large numbers of moderately accurate gf-values --- spectral line intensity
07 p0991 A83-20926
- Further ultraviolet observations of interstellar gas associated with the supernova remnant S 147
07 p1017 A83-20931
- Theoretical quasar emission-line profiles. I - Curve-of-growth effects on observed profiles
07 p1019 A83-21104
- Pulsational mode-typing in line profile variables. V - Multimodes and 'moving shells' in Nu Eridani and other Beta Cephei stars
07 p1022 A83-21132
- A feature in the X-ray spectrum of Cygnus X-1 - A possible positron annihilation line
07 p1022 A83-21136
- Simultaneous ultraviolet line and hard X-ray bursts in the impulsive phase of solar flares
07 p1038 A83-21148
- Observations of the 145.5 micron O I forbidden emission line in the Orion Nebula
07 p1023 A83-21155
- Empirical NLTE analyses of solar spectral lines. IV - The Fe I curve of growth --- nonlocal thermodynamic equilibrium
07 p1023 A83-21207
- Observations of emission line galaxies. I - The Seyfert-1 galaxies Mkn 1040, Mkn 1044
07 p1008 A83-21216
- Properties of amorphous H2O ice and origin of the 3.1-micron absorption
07 p1024 A83-21224
- On the errors of the Kurucz-Peytremann Fe I oscillator strengths
07 p1024 A83-21226
- Profiles and shifts of the Cl 5052-Å line in the granulation spectrum --- of sun
07 p1038 A83-21239
- The asymmetry of photospheric absorption lines. II - The asymmetry of medium-strong Fe I lines in quiet and active regions of the sun
07 p1038 A83-21243
- Frequency stabilization of GaAlAs laser using a Doppler-free spectrum of the Cs-D2 line
07 p0938 A83-21593
- X-ray spectroscopy and imagery of supernova remnants with the Einstein Observatory
08 p1179 A83-21854
- A survey of ultraviolet interstellar absorption lines
08 p1175 A83-22748
- Interstellar absorption toward HD 14633
08 p1183 A83-23051
- Evidence of non-LTE in photospheric lines of G and K giants
08 p1185 A83-23087
- Intensity and polarization line profiles in a semi-infinite Rayleigh-scattering planetary atmosphere. I - Integrated flux
08 p1190 A83-23107
- Density-dependent Si XII dielectronic satellite spectra
09 p1347 A83-23655
- Observations of HF-enhanced plasma line with a 46.8-MHz radar and reinterpretation of previous observations with the 430-MHz radar
09 p1303 A83-23764
- Orbital elements for the double-line spectroscopic binaries HD 104451 and HD 141458
09 p1358 A83-24021
- Observation of higher lines of NO gamma/0, 0/ band O12 branch using two-photon excitation
09 p1341 A83-24094
- The Hubble sequence of masses
09 p1359 A83-24454
- On the nature of the /intermittent/ emission line star LkH-alpha 324
09 p1361 A83-24478
- Emission-line spectra of H II regions - Dependence on metal abundances in the atmosphere of the ionizing star and in the nebular gas
09 p1361 A83-24482
- Observations of M42 in the O III 52 and 88-micron forbidden lines, the O I 63-micron forbidden line, and the N III 57-micron forbidden line
09 p1362 A83-24977
- Transition probabilities for forbidden lines in the 3p4 configuration. III --- in astrophysics
09 p1362 A83-24986
- IUE observations of W UMa-type stars
09 p1364 A83-25005
- Near infrared observations of O stars
09 p1356 A83-25292
- High spectral resolution observations of forbidden S II lines in the planetary nebula IC 418 at the CES spectrograph
09 p1356 A83-25294
- The diffuse interstellar medium and the CES --- Coude Echelle Spectrograph
09 p1365 A83-25299
- A spectrographic study of the Beta Cephei star 16 Lacertae
10 p1491 A83-25366
- Six-centimeter H2CO observations - Envelopes of dark clouds
10 p1499 A83-25373
- K-alpha and K-beta spectra from M-shell-ionized ions produced in a vacuum spark
10 p1485 A83-25410
- Investigation of absorption line profiles of molecular gases by methods of laser spectroscopy
10 p1419 A83-25525
- H1340 no. 10 - A high-redshift QSO with very narrow emission lines
10 p1501 A83-25579
- Prominent ultraviolet emission lines from Type 1 Seyfert galaxies
10 p1493 A83-25703
- IUE observations of E1405-451 - A new AM Herculis type cataclysmic variable
10 p1505 A83-25744
- A large-amplitude photometric periodicity on a T Tauri star
10 p1494 A83-25745

The formation of permitted and forbidden lines in quasars 10 p1507 A83-26233

Why are broad emission lines seen in Seyfert galaxies and not in BL Lacertae objects 10 p1507 A83-26355

Formation of the Cl I line at 1351 Å in the solar chromosphere 10 p1522 A83-26396

Line positions and strengths in the /001/, /110/, and /030/ bands of HDO 10 p1481 A83-26877

The changes of spectral line contours of P Cygni 10 p1517 A83-26947

X-ray and optical studies of emission-line Markarian galaxies 11 p1668 A83-27103

IUE observations of the high velocity symbiotic star AG Draconis during active phase 11 p1678 A83-27694

Arc measurements of FeII transition probabilities 12 p1789 A83-28863

The use of derivative techniques in astronomical spectroscopy 12 p1786 A83-29080

The redshift distribution of quasar absorption lines and its origin 12 p1795 A83-29353

Spectral ranges for determining the concentration of hydrogen bromide and hydrogen fluoride in the earth's atmosphere 13 p1872 A83-30036

Analysis of additional absorption components of MgII lines in Algol in terms of a model of gas stream 13 p1955 A83-31668

A survey of formaldehyde in the Cepheus OB3 molecular cloud 13 p1958 A83-31709

On the Baldwin effect in optically-selected quasars 13 p1943 A83-31711

Solar corona photoelectric photometer using mica etalons 14 p2096 A83-32031

The lasing mechanism, active layer thickness, natural resonator effects, and the nature of the M and P bands of the emission spectrum of CdS pumped by a nitrogen laser - T = 4.2-420 K 14 p2023 A83-32163

Measurement of absorption line intensities with VUV monochromators 14 p2021 A83-32913

Infrared heterodyne spectroscopy of seven gases in the vicinity of chlorine monoxide lines 14 p1990 A83-32915

An extensive galactic search for conformer II glycine 14 p2073 A83-33191

High-velocity, asymmetric Doppler shifts of the X-ray emission lines of Cassiopeia A 14 p2104 A83-33193

On the constancy of spectral-line bisectors --- for cool stars 14 p2110 A83-33463

On the intensity ratio of emission lines of Na I D1 to D2 in prominences 15 p2278 A83-34280

New absolute spectroscopic measurement of the solar equatorial rotation rate 15 p2281 A83-34308

Interstellar Ca II and Na I line profiles towards halo OB stars 15 p2264 A83-34585

The structure of bright-rimmed molecular clouds 15 p2267 A83-34625

The interpretation of observations of weak molecular lines on the sun 15 p2282 A83-34768

A generalized method for deriving mass-loss rates - The first order moment of unsaturated P Cygni line profiles 15 p2272 A83-34780

Absorption and emission line profile coefficients of multilevel atoms. I - Atomic profile coefficients. II Velocity-averaged profile coefficients 15 p2227 A83-34991

Improved Ar(II) transition probabilities 15 p2236 A83-34993

Nitrogen-, oxygen-, and air-broadened widths and relative intensities of N2O lines near 2450 per cm 15 p2228 A83-34996

Stark shift trends in homologous ions 16 p2414 A83-35327

The synthetic method in radiative transfer theory 16 p2427 A83-35614

Transition probability of the Si III 189.2-nm intersystem line 16 p2427 A83-35657

Solar flare soft X-ray spectra from the Hinotori. I - Iron line spectra and their time variations of seven X-class flares. 16 p2439 A83-35678

Line radiation from a hot, optically thin plasma - Collision strengths and emissivities --- in stellar atmospheres 16 p2416 A83-35974

Observations of the MG II lambda 2800 spectral region in broad absorption line quasars 16 p2431 A83-36661

A matrix photodiode array to measure Doppler shifts of solar spectral lines 16 p2425 A83-36664

Observations of the iron emission lines in the X-ray spectrum of the supernova remnant Cassiopeia A 16 p2431 A83-36673

Profiles and intensity ratios of the C IV lambda 1548, 1550 emission lines in planetary nebulae 16 p2433 A83-36706

Redistribution - Why half a collision is better than a whole one --- spectra of scattered light from perturbed atomic system 17 p2484 A83-37075

Solar emission lines near 12 microns 17 p2624 A83-37350

Couderadial velocities of Zeta Herculis 17 p2589 A83-37370

The double-lined spectroscopic binary HD28475 17 p2589 A83-37371

The change in the physical conditions of the spots in the active region McMath 14943 during the period from September 12 to September 19, 1977 17 p2625 A83-37665

Submillimeter detection of stratospheric OH and further line assignments in the stratospheric emission spectrum 17 p2540 A83-37764

Empirical improvement in accuracy of atomic oscillator strengths calculated by Kurucz and Peytremann --- of relevance to model stellar atmospheres 17 p2606 A83-38240

Radio recombination lines and the distance to quasars 17 p2608 A83-38401

The strength of the C IV 1550 Å resonance lines in planetary nebulae 17 p2608 A83-38413

Line profiles and a model of the envelope of the type II supernova SN 1970g 17 p2611 A83-38557

Mapping of chemical elements on the surfaces of Ap stars. I Solution of the inverse problem of finding local profiles of spectral lines 17 p2611 A83-38558

Effect of search lines on emission and absorption redshift distribution of QSOs 17 p2611 A83-38587

The novalike star TT Arietis - A binary system with conical accretion? 17 p2614 A83-38843

Polarization in spectral lines. I - A unifying theoretical approach. II - A classification scheme for solar observations --- of solar active regions 18 p2780 A83-39017

Are plasma satellites present among chromospheric lines? 18 p2780 A83-39019

Origin of the weakening of EUV emission lines formed in the chromosphere-corona transition zone 18 p2781 A83-39020

Visibility of facular fields in Mg I b-lines 18 p2781 A83-39025

Type I noise storms and the structure of the extreme ultraviolet corona 18 p2782 A83-39035

CO 1-0 band isotopic lines as intensity standards 18 p2742 A83-39176

Line strength measurements using diode lasers - The nu2 band of H2S 18 p2742 A83-39182

Sensitivity of ozone retrievals in limb-viewing experiments to errors in line-width parameters 18 p2664 A83-39183

Intensity and polarization line profiles in a semi-infinite Rayleigh-scattering planetary atmosphere. II - Variations of equivalent width over the disk 18 p2779 A83-39190

Gamma-ray spectroscopy - Status and prospects 18 p2647 A83-39294

Changes in interstellar atomic abundances from the galactic plane to the halo 18 p2768 A83-39630

Millimeter-wavelength lines from the Orion plateau source 18 p2772 A83-39709

Far-infrared CO line emission from Orion-KL 18 p2772 A83-39712

Maser sources in the Orion-KL region 18 p2772 A83-39713

Coronal index of solar activity. IV - Years 1964-1970 18 p2785 A83-39978

B-alpha and Ne II line spectroscopy in the vicinity of the galactic center source IRS 16 19 p2908 A83-40685

Theory of spontaneous-emission line shape in an ideal cavity 19 p2898 A83-41155

Dense cores in dark clouds. IV - HC5N observations 19 p2919 A83-41626

Computer measurement of line strengths with application to the methane spectrum 19 p2820 A83-41868

AFGL atmospheric absorption line parameters compilation - 1982 edition 20 p3016 A83-42207

Rapid variations in forbidden emission line profiles in a Seyfert 2 galaxy 20 p3065 A83-42329

Stark-shifts of the He II spectral lines 20 p3049 A83-42340

Detection of CH3OH J = 5 to 4 lines around 242 GHz from OMC-1 20 p3067 A83-42446

Time-dependent scattering in resonance lines 20 p3044 A83-42458

The influence of waves on line formation in stellar atmospheres 20 p3075 A83-43383

Spectrophotometric studies of star HD 157978 20 p3062 A83-43651

The distribution of absorption lines in QSO spectra 21 p3232 A83-44731

The effect of hyperfine structure on stellar abundance analysis 21 p3233 A83-44752

The space density and spectroscopic properties of a new sample of emission-line galaxies 21 p3235 A83-45532

Shifts of hydrogen lines from electron collisions in dense plasmas 22 p3361 A83-45931

Remote sensing by IR heterodyne spectroscopy 22 p3260 A83-46078

The solar O III spectrum. II - Longer wavelengths, line widths, and the He II Lyman alpha radiation field 22 p3388 A83-46263

Early-type high-velocity stars in the solar neighborhood. III - Radial velocities, rotation indices, and line-strength indices for southern candidates 22 p3373 A83-46383

VRI photometry - An addendum 22 p3373 A83-46403

Sk-71 deg 34 - A new Wolf-Rayet star in the Large Magellanic Cloud 22 p3374 A83-46411

Measurement of relative oscillator strengths for Ti I. III Weak transitions from levels a3F(3, 4) (0.02 eV, 0.05 eV), a5F(1-5) (0.81 eV-0.85 eV), a1D(2) (0.90 eV), a3P(0-3) (1.05 eV-1.07 eV) with solar analysis --- for spectrum analysis of cool stars 22 p3388 A83-46538

Narrow output line from a distributed-feedback dye laser with broad-spectrum pumping 22 p3299 A83-46784

The magnetic field of the NGC 2024 molecular cloud - Detection of OH line Zeeman splitting 23 p3518 A83-47431

Observations of H-beta and He II lambda 4686 lines in the spectra of flares of UV Cet-type stars 23 p3521 A83-47497

Possible origins for the 12 microns emission lines in the solar spectrum 23 p3530 A83-47508

Doppler imaging of starspots 23 p3516 A83-47513

Gamma-ray lines and neutrons from solar flares 23 p3535 A83-47698

Characteristics of gamma-ray line flares as observed in hard X-ray emissions and other phenomena 23 p3535 A83-47699

Line profile analysis of an active region corona observed successively at the east and west limb 23 p3536 A83-47708

Calculation of coronal line intensities for boron-like ions 23 p3536 A83-47721

Strong coupling effects on plasma lineshapes and Thomson scattering signals 23 p3511 A83-48585

On the effect of temperature fluctuations on line intensities --- from stellar atmospheres 23 p3528 A83-48648

Infrared emission lines in planetary nebulae 24 p3639 A83-49133

Relative intensities of hydrogen lines in the spectra of quasars and the nuclei of Seyfert galaxies 24 p3653 A83-49164

Ca XVII line ratios in solar flares 24 p3674 A83-49356

Hyperfine structure measurements for lines of astrophysical interest in Mn I 24 p3658 A83-49364

Enhanced polarization in the Ca II K line of the Be star Kappa Dra 24 p3660 A83-49385

Active galactic nuclei - IUE results on continuum, emission and absorption lines 24 p3661 A83-49559

Oscillator strengths of lines of ionized titanium and chromium --- in solar atmosphere 24 p3674 A83-49633

Detection of the 3.46 cm line of interstellar He-3(+) (He-3(+)/H(+)) ratios 24 p3667 A83-50062

LINEAMENT

U STRUCTURAL PROPERTIES (GEOLOGY)

LINEAR ACCELERATORS

Investigation of a slow-wave structure of ring-bar type --- for high power traveling wave tubes in linear accelerators 09 p1252 A83-23453

The Stanford Superconducting Linear Accelerator --- for powering free electron laser 13 p1917 A83-31104

Optical pulse evolution in the Stanford free-electron laser and in a tapered wiggler 13 p1854 A83-31117

Computer simulation study of multiple germanium gamma-ray sensor arrays 18 p2756 A83-39295

Flying railway - A means for orbital transfer [IAF PAPER 83-390] 23 p3415 A83-47370

LINEAR AMPLIFIERS

Improving the power-added efficiency of FET amplifiers operating with varying-envelope signals 10 p1410 A83-26340

A new baseband linearizer for more efficient utilization of earth station amplifiers used for QPSK transmission 11 p1556 A83-28130

Improvement of signal-to-noise ratio in a combination of a linear and a nonlinear amplifier 13 p1834 A83-30784

A fluidic/pneumatic interface amplifier 17 p2501 A83-37117

LINEAR ARRAYS

- NT MULTISPECTRAL LINEAR ARRAYS
NT YAGI ANTENNAS
- An automated mapping satellite system / Mapsat/
01 p0066 A83-10715
- Optimal beamforming for a linear array antenna
01 p0032 A83-11159
- A note on utilizing far-field phase information
01 p0034 A83-11375
- On an index for array optimization and the discrete prolate spheroidal functions
01 p0034 A83-11379
- Statistics of the polarization structure of oblique-sounding signals in the aperture of a linear antenna array
02 p0162 A83-11542
- Resolution of monochromatic signal sources using a simple receiving antenna array
02 p0164 A83-11985
- Conceptual design and requirements of a pushbroom focal plane
03 p0325 A83-13729
- 1.0 to 2.5 micrometer short wavelength infrared /SWIR/ linear array technology for low background applications
03 p0326 A83-13739
- A wide-band omnidirectional vertical shaped-beam collinear array
03 p0307 A83-14038
- Simultaneous detection, resolution, and measurement of the parameters of signals on a noise background at the output of an antenna array - Synthesis of the algorithm
04 p0467 A83-15737
- The suppression of the interference signal in a band of frequencies by means of an adaptive array
04 p0467 A83-15753
- Design and development of an omnidirectional antenna with a collinear array of slots
05 p0622 A83-17343
- 'Super-suppression' of side lobes in linear arrays
06 p0737 A83-18604
- Difference patterns of antenna arrays
06 p0749 A83-19358
- The use of a two-dimensional fast Fourier transformation algorithm for processing information from a linear antenna array
06 p0749 A83-19359
- New doubly orthogonal functions and their application to pattern synthesis --- in antenna design
07 p0913 A83-20071
- A pole-zero modeling approach to linear array synthesis. I - The unconstrained solution
07 p0913 A83-20368
- Dynamic programming in problems of the synthesis of multichannel phasing devices
07 p0921 A83-20881
- Analysis of a linear array taking into account satellite-sensor performances and a digital terrain model
08 p1124 A83-21904
- Integrating 128-element linear imager for the 1 to 5 microns region
08 p1100 A83-22601
- Operation and applications of linear pyroelectric arrays
08 p1101 A83-22611
- An analog open-loop adaptive-array antenna system
08 p1077 A83-22733
- An algebraic approach to superresolution array processing
08 p1158 A83-22735
- Estimating the angles of arrival of multiple plane waves
08 p1158 A83-22736
- Coherent behavior of 2N-Josephson junction closed loop
08 p1081 A83-22769
- Solid-state Shuttle-launched meteorological sensor
08 p1052 A83-22852
- Development and evaluation of integrated infrared arrays for astronomical applications
08 p1052 A83-22858
- Improved pattern synthesis for equispaced linear arrays
09 p1246 A83-23691
- Hydraulics of a channel with a linear jet array --- heat transfer coefficient enhancement by transpiration cooling
09 p1260 A83-24049
- The formation of the frequency-angular spectrum of the signals of linear antenna arrays using coherent optical processors based on spatial light modulators with multichannel optical addressing
09 p1345 A83-24906
- Experimental linear phased array with partial adaptivity
11 p1555 A83-27918
- A quasi-optimum algorithm for measuring the amplitudes and phases of signals at the outputs of the elements of a receive array antenna operating in an inhomogeneous medium
11 p1555 A83-27936
- An analytical method for calculating the parameters of a linear phased-array antenna
11 p1559 A83-28688
- Microstrip linear array with polarisation control
12 p1719 A83-29439
- The effect of errors in the amplitude-phase distribution of a linear antenna on its scattering coefficient
13 p1828 A83-30282
- Conceptual design of a coherent optical system of modular imaging collectors (COSMIC) --- telescope array deployed by space shuttle in 1990's
13 p1938 A83-30996

- Coherent optical system of modular imaging collectors (COSMIC) telescope array - Astronomical goals and preliminary image reconstruction results
13 p1920 A83-30997
- InSb charge-injection device array performance
14 p2015 A83-31979
- Near-infrared linear array spectrometer for space applications
14 p2016 A83-31999
- Almost-periodic linear arrays
14 p2002 A83-33469
- Small array illuminations for pattern nulling with sidelobe level control
15 p2146 A83-35083
- Matching networks in linear phased arrays
17 p2497 A83-37791
- Prediction of adaptive array performance
19 p2826 A83-41145
- Parallel architectures for computing cyclic convolutions
20 p3037 A83-43679
- Broadband adaptive array processing
20 p2965 A83-43682
- Solid-state sensors for the 1990's
22 p3260 A83-46153

LINEAR CIRCUITS

- Linear digital phase-locked loops using integrators in a pulse frequency-modulation system
02 p0166 A83-11556
- CIECA - Application to current programmed switching Dc-Dc converters --- Current Injection Equivalent Circuit Approach
06 p0753 A83-19028
- Design concepts and performance characteristics of a high performance linear/digital shunt regulator
11 p1559 A83-27134
- Nuclear radiation effects on linear circuits (Reference diode, operational amplifier)
14 p2006 A83-32417
- Detection of constant signals in skewed noise
15 p2222 A83-35137
- The synthesis of linear electric and electronic networks (the method of state variables) --- Russian book
21 p3126 A83-45046

LINEAR ENERGY TRANSFER (LET)

- Factors which determine the differences in the biological effectiveness of ionizing radiation with various physical characteristics
06 p0796 A83-19376
- Cataractogenesis from high-LET radiation and the Casarett model
19 p2873 A83-40848

LINEAR EQUATIONS

- Solution of operator equations by the method of multiparametric regularization
01 p0102 A83-11262
- Solvability of boundary value problems for linear and quasi-linear B-elliptic equations
02 p0231 A83-11637
- Linear systems of ordinary differential equations
02 p0231 A83-11640
- Fully-parallel relaxation algebraic operations for optical computers
02 p0236 A83-12398
- Analysis of global expansion methods: Weakly asymptotically diagonal systems --- Book
03 p0387 A83-13500
- On optimal integration methods for Volterra integral equations of the first kind
03 p0387 A83-13572
- The first boundary value problem for the linearized Navier-Stokes equations
03 p0316 A83-13694
- On preconditioned iterative methods for elliptic partial differential equations
03 p0388 A83-14084
- Adapting iterative algorithms developed for symmetric systems to nonsymmetric systems
03 p0388 A83-14088
- Linear/nonlinear behavior in unsteady transonic aerodynamics
04 p0442 A83-15280
- The induced radiation of linear oscillators in a spatially inhomogeneous variable field
06 p0750 A83-18142
- The effect of the force structure on the stability of a linear system
06 p0806 A83-19550
- Equations of the linear theory of shells with slowly varying curvatures
07 p0947 A83-21086
- Numerical operational methods for time-dependent linear problems
07 p0948 A83-21437
- Linear functional differential equations as semigroups on product spaces
08 p1156 A83-22025
- Organization of the solution of systems of linear algebraic equations in pipeline computing systems
08 p1154 A83-22185
- Solution of systems of linear equations with a sparse matrix --- for geodesy, photogrammetry and navigation
08 p1159 A83-22789
- Implementation of cellular arrays --- of computing elements for linear algebraic equations
08 p1153 A83-22805
- The representation of a matricant of a linearized system of differential equations of motion in a field of forces possessing potential
09 p1338 A83-23865
- On linear perturbations in generalized Einstein space
09 p1359 A83-24203
- Boundary solutions for the linear theory of structures and the generalization of the work theorem
09 p1280 A83-24510

- The perturbation method in application to shells with random imperfections
09 p1282 A83-25102
- On the inverse scattering and direct linearizing transforms for the Kadomtsev-Petviashvili equation
09 p1340 A83-25283
- High-gain tracking systems incorporating Lur'e plants with multiple switching nonlinearities
10 p1463 A83-26506
- Linear analysis by the finite element method of the dynamics of axisymmetric structures subjected to arbitrary loads
10 p1442 A83-26819
- Elastic-plastic boundary element analysis as a linear complementarity problem
11 p1593 A83-27774
- Numerical experiments involving Galerkin and collocation methods for linear integral equations of the first kind
12 p1771 A83-29098
- The use of the Walsh transformation to solve systems of linear differential equations with variable coefficients
12 p1771 A83-29344
- Stability of periodic solutions under stochastic perturbations
12 p1771 A83-29599
- Conjugate gradient method for the solution of linear equations - Application to molecular electronic structure calculations
12 p1778 A83-29640
- On an iterative method with fictitious unknowns
13 p1912 A83-30076
- Linear and nonlinear instability theory of a noble gas MHD generator --- Thesis
13 p1924 A83-30150
- Thresholds for the onset of fluid and magnetofluid turbulence
13 p1840 A83-30413
- Behavior of the roots of the dispersion equation in linear TWT theory
13 p1833 A83-30709
- An efficient parallel algorithm for the solution of large sparse linear matrix equations
13 p1908 A83-32790
- A computational study of finite element methods for second order linear two-point boundary value problems
13 p1912 A83-31362
- The stability of motion with respect to some of the variables under continuous perturbations
14 p2079 A83-32357
- Algebra related to the N-soliton solution of the Benjamin-Ono equation
14 p2077 A83-32508
- On the Benjamin-Ono equation-method for exact solution
14 p2077 A83-32513
- Stabilizability of multidimensional discrete systems in cases of complete and incomplete information
14 p2076 A83-32964
- The use of the asymptotic method of short-time space for solving systems of differential and algebraic equations
14 p2078 A83-33010
- Linear isotropic elasticity with body forces
15 p2173 A83-33856
- Parallel solution of finite element equations
16 p2403 A83-36721
- Triangular system solutions on an optical systolic processor
16 p2403 A83-36752
- On the question of using the method of false perturbations in astronomical practice
16 p2427 A83-36862
- On the application of the fast Fourier transform in simulation problems
16 p2406 A83-36905
- Linear conversion of magnetogravity waves in an exponential atmosphere
16 p2434 A83-36931
- Determination of higher order accelerations by a functional method
17 p2575 A83-37023
- Shock waves and reaction-diffusion equations --- Book
17 p2575 A83-37162
- Estimation of the value of the small parameter in a linear singularly perturbed system of differential equations
17 p2571 A83-38074
- Oscillation properties of solutions of second order elliptic equations
17 p2572 A83-38466
- Comparison of fast iterative methods for symmetric systems
18 p2739 A83-39255
- Necessary and sufficient conditions of the convergence asynchronous iterative computational processes when solving systems of linear algebraic equations
19 p2888 A83-41420
- Basic methods for stability analysis of nonlinear oscillations and waves
20 p3043 A83-43670
- Suboptimality and stability of linear distributed parameter systems with finite-dimensional controllers
21 p3196 A83-45136
- A method for solving a system of equations discretized in problems of electrodynamics --- for multi-discrete element antennas
22 p3272 A83-45693
- Solution of linear equations with a symmetrically skyline-stored nonsymmetric matrix
24 p3620 A83-49438
- A modification of Potter's method for diagonal matrices with common unknown
24 p3593 A83-49440
- A linear test algorithm of pattern recognition
24 p3620 A83-49538
- Dynamics of a mobile tank partially filled with liquid Equations of motion and their linearization
24 p3581 A83-50124

LINEAR FILTERS

NT KALMAN FILTERS

NT REDUCED ORDER FILTERS

Optimization of the input signal of a linear filter, maximizing the signal/noise ratio

02 p0162 A83-11530
Image restoration - A linear stochastic filtering approach --- Thesis 02 p0176 A83-11900
An introduction to adaptive signal processing 02 p0163 A83-11914

The separation of wave fronts by rectification of the Choleski factor in their cross spectral matrix 04 p0465 A83-15075

The accuracy, stability, and filtering properties of a linear pulsed phase-locked loop system for tracking the rate of Doppler shift changes 04 p0467 A83-15752

Fast algorithms for linear prediction and system identification filters with linear phase 05 p0680 A83-16914

Optimal adaptive smoothing in correlated noise conditions 07 p0984 A83-20000

Second-order convergence analysis of stochastic adaptive linear filtering 07 p0985 A83-20723

Optimization and filtering of linear systems of finite dimension by hierarchical calculation --- French thesis 08 p1156 A83-22089

Restoration of bilinearly distorted images. I - Finite impulse response linear digital filtering 08 p1101 A83-22672

The design of high-order active RC filters --- Russian book 09 p1254 A83-23827

Control of coupled bilinear stochastic systems 10 p1466 A83-26543

Recursive computation of linear prediction filter coefficients for 2-D spectral analysis 11 p1648 A83-28614

Autocorrelation compression filter for radio pulses with linear frequency modulation 13 p1829 A83-30729

Accuracy of the linear filtering of a narrow-band Gaussian signal from a mixture with Markovian Gaussian correlation noise and white noise 17 p2494 A83-38498

Filtering of semitransparent cloud cover 18 p2692 A83-40597

Multigigahertz-bandwidth linear-frequency-modulated filters using a superconductive stripline 19 p2836 A83-40747

Optimal linear receiver filters for binary digital signals 19 p2839 A83-41348

Reconstruction of the shuttle reentry air data parameters using a linearized Kalman filter [AIAA PAPER 83-2097] 19 p2810 A83-41926

LINEAR INTEGRATED CIRCUITS

NT OPERATIONAL AMPLIFIERS

An examination of background noise in analog integrated circuits and components --- French thesis 02 p0166 A83-11765

LINEAR POLARIZATION

The Hanle effect and the diagnostics of turbulent magnetic fields in the solar atmosphere 02 p0269 A83-12572

Continuous-wave garnet ring laser emitting single-mode linearly polarized radiation and intracavity second harmonic generation in LiIO₃ 03 p0330 A83-13584

The calibration of a radio-independent search for BL Lac objects 03 p0408 A83-13929

Birefringence variation with temperature in elliptically clad single-mode fibers 03 p0395 A83-14386

UBV-polarimetry of the X-ray binaries HD 77581 /4U 0900-40/, HD 153919 /4U 1700-37/ and of HD 152667 03 p0410 A83-14766

Non-LTE resonance line polarization with partial redistribution effects --- In solar spectra 03 p0437 A83-14783

On interstellar linear polarization and grain growth 04 p0549 A83-15026

Radio structures of Seyfert galaxies. IV - Jets in NGC 1068 and NGC 4151 05 p0697 A83-16985

The polarization of supernova light - A measure of deviation from spherical symmetry 05 p0699 A83-17015

Polarisation preserving single-mode-fibre coupler 06 p0809 A83-18570

Polarization of early-type stars in Norma 06 p0820 A83-18861

A search for resonance polarization in stars with enhanced Ca II H and K emission 06 p0821 A83-19062

Infrared excesses of stars with intrinsic polarization 06 p0838 A83-19227

Investigation of nonlinear absorption in H₂O vapors subjected to strong optical fields with linear and circular polarizations 07 p0991 A83-20128

Depolarization of 19-GHz signals --- from satellite beacons 07 p0871 A83-20552

The rotation measures of radio sources in selected celestial zones - The Perseus arm window 07 p1006 A83-20571

Asymptotic solution of the transfer equation for linearly polarized X-ray and gamma radiation 07 p1026 A83-21264

Doppler-free polarization spectroscopy of diatomic molecules in flame reactions 08 p1056 A83-21884

Propagation constants for linearly polarized modes of arbitrarily shaped optical fibers or dielectric waveguides 08 p1166 A83-22639

Impact linear polarization observed in a UV chromospheric line during a solar flare 08 p1191 A83-23071

Opacity effects at radio wavelengths in the quasar 1308+326 10 p1504 A83-25737

The polarization of Seyfert galaxies 10 p1496 A83-26356

The polarization of millimeter-wave emission lines in dense interstellar clouds 10 p1513 A83-26713

Polarization of interstellar radio-frequency lines and magnetic field direction 10 p1513 A83-26714

Conductive flux in flaring solar chromospheres deduced from the linear polarization observations 11 p1691 A83-27685

Linear polarization observations in selected celestial zones The anticentre region 12 p1784 A83-28867

Coherent scattering in the solar spectrum - Survey of linear polarization in the range 3165-4230 Å 12 p1799 A83-28871

Linear polarization variations of six T Tauri stars 13 p1941 A83-31557

New polarization measurements of HD 183143, HD 204827, and Cyg OB 2 Sch. No. 12 13 p1943 A83-31757

Measurement of unambiguous rotation measures of extragalactic sources 14 p2098 A83-33063

A beam waveguide linearly polarized KU band feed system 15 p2146 A83-35079

New advances in wide band dual polarization antenna elements for EW applications 15 p2121 A83-35087

Evidence for evolving elongated pulsar beams 16 p2431 A83-36660

Polarimetric observations of white dwarf stars 17 p2589 A83-37684

Effects of rectangular boundaries in a linearly polarized wiggler free electron laser [AIAA PAPER 83-1729] 17 p2514 A83-38090

SAW convolvers using the transverse-horizontal bilinear field 17 p2500 A83-38877

Stellar and interstellar magnetic fields 18 p2765 A83-39236

The magnetic intensification mechanism and its relevance for the study of stellar activity 18 p2765 A83-39239

High-order azimuthal modes in the open resonator 18 p2679 A83-40392

High-resolution polarization images of Crab Nebula with a charge-coupled device camera 20 p3059 A83-42330

Optical polarimetry of broad-line radio galaxies 20 p3059 A83-42435

Fabrication of polarization-maintaining and absorption-reducing fibers 21 p3204 A83-44203

Polarization of interstellar molecular radiofrequency absorption lines 22 p3376 A83-45633

Differences in two linear like-polarized SAR images at same frequency 22 p3310 A83-46138

Linear polarization observations in selected celestial zones The Gum nebula area 22 p3372 A83-46264

Electronographic polarimetry - The Durham polarimeter 22 p3291 A83-46562

Flux density and linear polarization measurements of variable radio sources at 9.00 mm (33.5 GHz) 22 p3380 A83-46575

Microphysical interpretation of multi-parameter radar measurements in rain. I - Interpretation of polarization measurements and estimation of raindrop shapes. II Estimation of raindrop distribution parameters by combined dual-wavelength and polarization measurements 22 p3341 A83-46855

Interstellar polarization, grain growth, and alignment 22 p3381 A83-46985

Reflection of a linearly polarized plane wave from a lossless stratified mirror in the presence of a phase-conjugate mirror 23 p3508 A83-47587

Conductive flux in the chromosphere derived from line linear polarization observation 23 p3532 A83-47670

Analytic treatment of polarization by arbitrary scattering mechanisms in circumstellar envelopes. II - Binary stars 24 p3658 A83-49361

Broadband linear polarization from magnetized stellar atmospheres. II - The influence of damping on net spectral line polarization 24 p3663 A83-49838

Fabrication of polarisation-maintaining (3 x 3) single-mode-fibre couplers 24 p3630 A83-49971

LINEAR PREDICTION

A time-invariant state estimator for continuous time systems 02 p0229 A83-11853

Adaptive optical processor 02 p0178 A83-12592

An improved model for isolated word recognition 04 p0529 A83-16324

Fast algorithms for linear prediction and system identification filters with linear phase 05 p0680 A83-16914

Limitations in the use of linear system theory for the prediction of hardened-MOS device response in space satellite environments 05 p0630 A83-17546

Discrimination of speech and high-speed data using an adaptive predictor for DSI application --- Digital Speech Interpolation 07 p0910 A83-19756

Adaptive filter with a time-domain implementation using correlation cancellation loops 07 p0993 A83-20158

SNR enhancement of narrowband signals in colored noise using adaptive predictors 09 p1327 A83-24703

Direct adaptive pole placement with application to nonminimum phase systems 09 p1329 A83-24728

A family of special purpose microprogrammable digital signal processor IC's in an LPC vocoder system 10 p1410 A83-26124

A practical method for sensor selection in linear estimation --- applied to inertial navigation systems 10 p1465 A83-26531

Recursive computation of linear prediction filter coefficients for 2-D spectral analysis 11 p1648 A83-28614

Real-time solution of linear least-squares estimation problem with semi-degenerate covariance 17 p2566 A83-37105

LINEAR PROGRAMMING

Operational planning of the process of earth survey by satellites 03 p0350 A83-14314

Design with several eigenvalue constraints by finite elements and linear programming 08 p1122 A83-22411

A linear programming approach for multivariable feedback control with inequality constraints 09 p1326 A83-23689

A linear programming approach for multivariable feedback control with inequality constraints 09 p1328 A83-24720

A computational technique for optimizing correction weights and axial location of balance planes of rotating shafts 11 p1589 A83-28121

Design for minimum stress concentration by finite elements and linear programming 14 p2033 A83-33111

Linear models in nonlinear control systems --- Russian book 19 p2889 A83-40990

Accommodation of practical constraints by a linear programming jet select --- for Space Shuttle [AIAA PAPER 83-2209] 19 p2815 A83-41693

Scale-free models of elliptical galaxies 24 p3641 A83-49249

LINEAR SYSTEMS

On the definiteness of quadratic forms subject to linear constraints 01 p0101 A83-10252

Relative stability test for continuous and sampled-data control systems using the generalised sign matrix 01 p0094 A83-10291

Low-sensitivity observer-compensator design for two-dimensional digital systems 01 p0094 A83-10292

Suggestions for optimal regulation of linear systems using approximation methods --- German thesis 01 p0094 A83-10472

Identification of bilinear systems using relay feedback 01 p0095 A83-10800

A discrete model reference adaptive control system for a plant with input amplitude constraints 01 p0095 A83-10956

Computation of the zeros and zero directions of linear multivariable systems 01 p0095 A83-10961

Transmission matrix approach to variable-rate sampled-data systems 01 p0095 A83-11132

A general scheme for signal restoration with application to picture processing 01 p0099 A83-11453

Wiener estimator for inversion of linear operators and superresolution 01 p0099 A83-11454

Model reference adaptive control of bilinear systems 02 p0229 A83-11789

Pole placement and order reduction in two-time-scale control systems through Riccati iteration 02 p0229 A83-11838

A time-invariant state estimator for continuous time systems 02 p0229 A83-11853

Feedback control of linear multivariable systems with uncertain description in the frequency domain 02 p0230 A83-12550

Block-indexed solution of very large linear equation systems with symmetric DBBF coefficient matrix --- Double Bounded Band Form 02 p0228 A83-12839

Linear phase-locked loop theory for cyclostationary input disturbances 03 p0311 A83-13854

The ltpack package for large sparse linear systems 03 p0385 A83-14082

An empirical investigation of methods for nonsymmetric linear systems 03 p0385 A83-14091

Bounded error adaptive control 03 p0386 A83-14589

Stable model reference adaptive control in the presence of bounded disturbances 03 p0386 A83-14590

Transfer function matrix description of decentralized fixed modes 03 p0386 A83-14591

On optimal nonlinear feedback regulation of linear plants 03 p0387 A83-14597

Computation of a degree of controllability via system discretization --- with application to flexible spacecraft control 03 p0287 A83-14844

Optimal discrete control of a linear plant 04 p0527 A83-15922

Design of stabilizing controller with incomplete state data for linear stochastic system with multiplicative noise 04 p0527 A83-15923

Adaptive ultimately optimal control of linear stochastic object in correlated noise conditions 04 p0527 A83-15924

Dispersion relations for hot electrons 04 p0542 A83-16066

Improved design technique for uncertain multiple-input-multiple-output feedback systems 04 p0528 A83-16148

Uncertain multiple-input-multiple-output systems with internal variable feedback 04 p0528 A83-16149

Adaptive control of a class of linear stochastic systems with continuous and discrete unknown parameters 04 p0528 A83-16150

Quantitative feedback theory 04 p0528 A83-16185

Principal gains and phases - insensitive robustness measures for assessing the closed-loop stability property 04 p0529 A83-16186

Stability margins of diagonally perturbed multivariable feedback systems 04 p0529 A83-16188

Multivariable stability-margin optimisation with decoupling and output regulation 04 p0529 A83-16191

Robust control strategy for a linear time-invariant multivariable sampled-data servomechanism problem 04 p0529 A83-16192

State variable representation of a class of linear shift-variant systems 05 p0680 A83-16911

Discrete model reference adaptive control of non-minimum phase systems 05 p0681 A83-17582

Adaptive control and optimal input design - A realistic approach 05 p0681 A83-17584

The design and control of linear bidirectional stepping motors - Application to machine tools --- French thesis 06 p0750 A83-18495

Angles of multivariable root loci [LIDS-P-1147] 06 p0803 A83-19320

Time suboptimal feedback control of high order linear systems 06 p0803 A83-19389

A geometric approach to stabilization by output feedback 06 p0804 A83-19390

Generic pole assignment using dynamic output feedback 06 p0804 A83-19391

On the minimality of feedback realizations 06 p0804 A83-19392

Estimate of the transient conduction of heat in materials with linear thermal properties based on the solution for constant properties 06 p0760 A83-19399

An algorithm for identifying multi-input, multi-output linear dynamical systems based on the maximum likelihood method 06 p0804 A83-19568

Spectroscopic study of the mechanism of the linear electrooptic effect 06 p0810 A83-19575

Global transformations of nonlinear systems 07 p0984 A83-20719

Equations for the angles of arrival and departure for multivariable root loci using frequency-domain methods 07 p0985 A83-20724

Design of linear systems with saturating linear control and bounded states 07 p0985 A83-20725

The problem of guaranteeing robust disturbance rejection in linear multivariable feedback systems 07 p0985 A83-21161

Pole placement in multi-input systems via elementary transformations 07 p0985 A83-21162

Design of an adaptive observer and its application to an adaptive pole placement controller 07 p0985 A83-21163

Synthesis of feedback systems for specified time domain insensitivity to interaction induced plant ignorance 07 p0985 A83-21165

Covariance analysis of oscillatory systems under combined periodic and random forced vibrations 08 p1160 A83-21862

A new multiple-model adaptive filter for continuous-time

stochastic distributed parameter systems 08 p1156 A83-22073

Optimization and filtering of linear systems of finite dimension by hierarchical calculation --- French thesis 08 p1156 A83-22089

The dynamic braking of a linear induction motor at a variable speed 08 p1080 A83-22224

Strictly observable linear systems 08 p1157 A83-22241

Bootstrap algorithms for parameter and smoothing state estimation 08 p1158 A83-22732

Matrix triangulation by systolic arrays 08 p1152 A83-22797

On the recursive identification of multivariable state space models 08 p1159 A83-23174

Suboptimal control of discrete stochastic amplitude constrained systems 09 p1326 A83-23687

Deadbeat error control of discrete multivariable systems 09 p1326 A83-23688

The stability of linear multivariable systems 09 p1326 A83-23690

Model reference adaptive control of large structural systems 09 p1327 A83-24433

Robust Lyapunov stability results and adaptive systems 09 p1328 A83-24724

Filtering for piecewise linear drift and observation 09 p1330 A83-24740

Minimal Pade model reduction of multivariable systems 09 p1330 A83-24748

Model reduction of discrete time-variable systems via balancing 09 p1330 A83-24749

On matrix reductions by unimodular transformations 09 p1330 A83-24750

Minimal polynomial bases for the dual spaces of rational vector spaces with applications to realization theory 09 p1331 A83-24751

Suboptimal LQG-design via balanced realizations --- Linear Quadratic Gaussian regulators 09 p1331 A83-24752

Stochastic control of randomly varying systems 09 p1331 A83-24770

A note on word length and memory requirements in digital control 09 p1332 A83-24775

Model adaptive dual control of MIMO stochastic systems 09 p1332 A83-24777

The Total Synthesis Problem of linear multivariable control. II - Unity feedback and the design morphism 09 p1332 A83-24782

A constructive method for stabilizing linear systems with time delays 09 p1332 A83-24783

Multivariable adaptive pole placement 09 p1333 A83-24790

Necessary and sufficient conditions for regulation of linear systems 09 p1333 A83-24794

On the relation between stable matrix fraction factorizations and regulable realizations of linear systems over rings 09 p1333 A83-24795

An adaptive servomechanism control strategy for a single-input single-output linear discrete system 09 p1334 A83-24803

On spectrum placement for linear time invariant delay systems 09 p1334 A83-24808

Design of multivariable optimal control systems using asymptotic root loci 09 p1335 A83-24814

Near insensitivity of linear feedback systems 09 p1335 A83-24817

Linear cascade codes --- Russian book 09 p1335 A83-25099

Time suboptimal feedback control design through coordinate transformation 10 p1461 A83-25396

The design of optimal output regulators for linear multivariable systems with constant disturbances 10 p1461 A83-25400

Multivariable system compensation [ASME PAPER 82-WA/DSC-19] 10 p1462 A83-25682

Optimal adaptive control of linear-quadratic-Gaussian systems 10 p1462 A83-25996

A new class of stabilizing controllers for uncertain dynamical systems 10 p1462 A83-25997

An economical algorithm of adaptive control of a multidimensional static plant 10 p1462 A83-26068

A linear theory for pretwisted elastic beams [ASME PAPER 83-APM-9] 10 p1441 A83-26439

Approximation of multivariable linear systems with impulse response and autocorrelation sequences 10 p1463 A83-26502

On a method for reconstructing inaccessible state variables using time delays 10 p1463 A83-26508

On the compensation in linear feedback control systems - Transfer functions attainable by realizable linear compensation 10 p1464 A83-26519

The manipulation of interaction effects in multivariable feedback systems 10 p1465 A83-26525

D-decomposition in the space of feedback gains for arbitrary pole regions 10 p1465 A83-26526

New results for the joint input-output identification method 10 p1466 A83-26537

Control of coupled bilinear stochastic systems 10 p1466 A83-26543

Generalized observations control in problems of stochastic optimization 10 p1466 A83-26545

Optimal cyclostationary control - A parameter-optimization frequency-domain approach 10 p1467 A83-26546

Design of a continuous-time adaptive regulator 10 p1467 A83-26551

Adaptive identification and control of linear MIMO discrete systems in a noisy environment 10 p1467 A83-26552

Model reference invariant control for a class of unknown multivariable plants 10 p1468 A83-26558

A new solution to parameter adaptive estimation of random processes 10 p1468 A83-26561

An adaptive observer with exponential rate of convergence for single-input single-output linear systems 10 p1468 A83-26562

A design procedure for linear multi-variable feedback systems 10 p1468 A83-26564

Frequency domain structure for disturbance rejection 10 p1468 A83-26565

Algebraic and topological aspects of the servo problem for lumped linear systems 10 p1469 A83-26567

Scalar output feedback in linear multivariable systems 10 p1469 A83-26568

Perfect and subperfect regulation in linear multivariable control systems 10 p1469 A83-26569

The linear servomechanism with non-unity feedback 10 p1469 A83-26570

Feedback, optimal sensitivity, and plant uncertainty via multiplicative seminorms 10 p1469 A83-26572

Structural optimality of linear optimal control 10 p1469 A83-26573

On the design of linear time-invariant robust controller 10 p1469 A83-26574

Robust control of tracking problem with internal stability for linear structured system 10 p1469 A83-26575

Chained aggregation - A geometric analysis --- of large scale systems 10 p1469 A83-26576

Results of the simulation of an adaptive nonparametric linear classifier of polarization-shift-keyed signals 10 p1407 A83-26939

Investigation of types of root loci of Fourth-order linear and linearized systems --- automatic pilot control system 11 p1647 A83-27448

The control of linear multivariable systems in the presence of harmonic disturbances 12 p1769 A83-28845

Frequency-domain identification of transmission-zero locations of linear multivariable plants 12 p1769 A83-29469

Robust controller design for linear dynamic systems using approximate models 12 p1770 A83-29521

Multivariable system theory and design --- Book 12 p1770 A83-29536

On a method of frozen coefficients in the synthesis of linear controllers 13 p1910 A83-30079

Controller design for linear multivariable feedback systems with stable plants, using optimization with inequality constraints 14 p2074 A83-31926

A model reference adaptive control system for discrete bilinear systems 14 p2074 A83-31931

A study of the stability of nearly periodic resonance systems with respect to some of the variables 14 p2080 A83-32361

Mathematical models of pulsed noise 14 p2001 A83-32483

A linear model of the general coordinates of the functional condition of a human operator, and their calculation and interpretation 14 p2072 A83-32956

Stabilization of linear dynamic systems 14 p2076 A83-33007

Control of stochastic systems with Markov interrupted observations 14 p2076 A83-33131

Nondegenerative conditions and physical realizability of multivariable linear feedback systems 14 p2077 A83-33157

Linear dynamic output feedback - Invariants and stability [AD-A129968] 14 p2077 A83-33447

Inverse problem of three-dimensional elasticity 15 p2178 A83-34434

On the decoupling of linear systems into single input-multiple output subsystems 15 p2221 A83-35110

Feedback stabilization and control of linear neutral systems 15 p2222 A83-35119

Some results on stability and stabilization of systems with retardation 15 p2222 A83-35127

A z-transform theory for distributed sensing and control 15 p2222 A83-35128

Interactive fine-tuning of linear-quadratic governors by selective and direct action on the poles of the control system [ONERA, TP NO. 1983-21] 16 p2404 A83-36430

Dynamic properties of linear vibration-isolation systems --- Russian book 16 p2362 A83-36440

Symmetric linear systems - An application of algebraic systems theory 16 p2405 A83-36454

Reconstructable states of linear multivariable systems with unknown inputs 16 p2405 A83-36456

Equations of a dynamic object when its properties are represented by a response to a prescribed action 16 p2405 A83-36901

A Z-domain controller design method for sampled-data systems having feedback dynamics 17 p2565 A83-37083

Effects of noise on the accurate identification of a vibrating system 17 p2565 A83-37084

A recursive algorithm by using eigenvector method for identifying multivariable linear time-invariant systems 17 p2565 A83-37086

Nonparametric identification of weighting function by orthogonal series method 17 p2565 A83-37087

An adaptive identifier for discrete-time linear systems 17 p2565 A83-37088

Theory of design using nonlinear transformations 17 p2565 A83-37091

Minimum information stochastic modelling of linear systems with a class of parameter uncertainties 17 p2566 A83-37106

Parametric failure detection and estimation in linear systems 17 p2567 A83-37122

Fundamental issues in guidance and control of uncertain systems 17 p2568 A83-37132

Quadratic weight adjustment for the enhancement of feedback properties 17 p2568 A83-37138

Asymptotic expansions of singularly perturbed Chandrasekhar type of equations 17 p2571 A83-37146

Asymptotic unbounded root loci - Formulas and computation 17 p2571 A83-37548

Singularly perturbed systems with low sensitivity to model reduction 17 p2570 A83-38030

An optimal design approach for the robust controller problem 17 p2570 A83-38818

On model-following using measured output feedback 17 p2570 A83-38820

A synthesis theory for a class of saturating systems --- in feedback control 17 p2570 A83-38821

The immersion under feedback of a multidimensional discrete-time non-linear system into a linear system 17 p2570 A83-38823

Fast suboptimal state-space self-tuner for linear stochastic multivariable systems 18 p2738 A83-40069

Linear ill-posed problems with random errors in the data 19 p2889 A83-40987

A new approach to exact model-matching with applications to aircraft systems 19 p2890 A83-41477

Discrete control scheme design for multi input multi output systems 19 p2890 A83-41478

A generalised moment method for the simplification of multivariable systems 19 p2890 A83-41486

The use of structural properties in multivariable model reduction and control system design 19 p2890 A83-41487

Maximum likelihood estimation of stochastic model parameters for inertial systems and components [AIAA PAPER 83-2249] 19 p2892 A83-41725

Analysis of the controllability property in linear control systems with parameters 20 p3039 A83-42920

Limit-optimal control of linear stochastic plants 20 p3039 A83-42921

Application of projectors to the numerical search for a minimax 20 p3041 A83-42924

Optimal nearly singular estimation of continuous linear stationary uniform rank systems 20 p3040 A83-43618

Discrete models for linear multivariable systems 20 p3040 A83-43619

Model reduction by cost decomposition - Implications of coordinate selection 21 p3192 A83-44003

Selecting measurements and controls in log problems 21 p3192 A83-44004

Identification of a system containing multi-valued nonlinearity 21 p3192 A83-44006

On stabilizing uncertain systems 21 p3192 A83-44008

Finite-dimensional discrete-time control of linear distributed parameter systems 21 p3192 A83-44009

Information induced multimodel solutions in multiple decisionmaker problems 21 p3198 A83-44100

Optimal instrumental-variable methods for identification of multivariable linear systems 21 p3194 A83-44369

An alternative view of the optimal output feedback compensator problem 21 p3195 A83-45106

Structural properties of the linear-quadratic stochastic control problem 22 p3351 A83-46091

Nested bases of invariants for minimal realizations of finite matrix sequences 22 p3351 A83-46094

Linear feedback decoupling - Transfer function analysis 22 p3351 A83-46365

Global adaptive pole placement - Detailed analysis of a first-order system 22 p3351 A83-46368

Model reference adaptive control of system having purely deterministic disturbances 22 p3351 A83-46369

On asymptotically stabilizing feedback control of bilinear systems 22 p3352 A83-46370

The use of structural properties in linear multivariable control system design --- Thesis 22 p3352 A83-46690

Angular points of the boundaries of domains of attainability --- for dynamic control of linear systems 23 p3501 A83-48528

Asymptotic behavior of the closed loop poles of linear optimal multivariable systems 23 p3502 A83-48676

Variational approach by means of adjoint systems to structural optimization and sensitivity analysis. I - Variation of material parameters within fixed domain 23 p3474 A83-48696

Tuning of a multivariable discrete time PI controller for unknown systems 24 p3620 A83-49894

Reduced-order observers for linear multivariable systems with disturbance and tracking signal accommodation 24 p3620 A83-49896

Stability analysis of adaptively controlled systems subject to bounded disturbances 24 p3621 A83-49921

Characterization of equilibrium sets for bilinear systems with feedback control 24 p3621 A83-49923

LINEAR TRANSFORMATIONS

Equilibrium points of the Riccati equation - Geometric structure 09 p1329 A83-24736

Riccati transformations in the back-and-forth shooting method for solving two-point boundary-value problems 10 p1465 A83-26524

A method of designing 2-D digital filters with quadrantal symmetry 10 p1412 A83-26887

Propagation and transformation of short radio waves in magnetospheric waveguides 12 p1753 A83-29251

LINEAR VIBRATION

Low and middle frequencies in highly heterogeneous structures 08 p1122 A83-22057

Medium frequency linear vibrations of anisotropic elastic structures 09 p1278 A83-23680

Sensitivity of the solutions of the equation of the linear vibrations of a membrane to changes of the coefficients of the equation 09 p1282 A83-25021

Optimal design of linear and nonlinear vibration absorbers for damped systems [ASME PAPER 81-DET-83] 11 p1594 A83-28123

Periodically forced linear oscillator with impacts - Chaos and long-period motions 20 p3042 A83-42649

Reanalysis and design in structural dynamics 21 p3151 A83-44031

LINEARITY

NT COLLINEARITY

Linearity in solid state microwave voltage tuned oscillators 09 p1255 A83-24350

An accurate scalar potential finite element method for linear, two-dimensional magnetostatics problems 16 p2406 A83-35645

LINEARIZATION

Analog computer simulation of a Duffing oscillator and comparison with statistical linearization 02 p0233 A83-12869

Measurability analysis of the linearized gravitational field 06 p0806 A83-19448

Completeness of derivatives of squared Schroedinger eigenfunctions and explicit solutions of the linearized KdV equation 17 p2572 A83-38464

The paralleling of algorithms for the simulation of nonlinear systems of large dimensionality 19 p2888 A83-41422

The development of a comprehensive two-dimensional linearized airfoil theory 20 p2928 A83-42529

Equivalent linearization for continuous dynamical systems [ASME PAPER 83-APM-30] 23 p3503 A83-48241

LINERS

U LININGS

LINES (GEOMETRY)

NT CHORDS (GEOMETRY)

NT GEODESIC LINES

Using program transformations to derive lind-drawing algorithms 11 p1646 A83-27121

Hidden line elimination in projected grid surfaces 11 p1646 A83-27122

A hidden line elimination method for curved surfaces 20 p3036 A83-42797

The use of the method of lines in 3-D fracture mechanics analyses with application to compact tension specimens 21 p3158 A83-44911

LINES OF FORCE

A comparison of different solar magnetic field extrapolation procedures 03 p0438 A83-14909

Penetration of geomagnetic pulsations from one polar cap to the other 05 p0663 A83-17616

On reconnection and plasmoids in the geomagnetic tail 07 p0966 A83-21512

Solitary waves and double layers on auroral field lines 07 p0966 A83-21517

Numerical simulation of a current sheet in the vicinity of the magnetic zero line 14 p2086 A83-32530

Magnetic reconnection - A problem of general physical and astrophysical interest, with special implications in solar

physics 15 p2277 A83-33584

Poleward migration of the magnetic neutral line and the reversal of the polar fields on the sun. I - Period 1945-1981 18 p2781 A83-39031

Asymmetries in Stokes profiles of magnetic lines - A linear analysis in terms of velocity gradients --- in solar atmosphere active regions 23 p3536 A83-47720

LING-TEMCO-VOUGHT AIRCRAFT

NT A-7 AIRCRAFT

NT F-8 AIRCRAFT

LINGUISTICS

NT SEMANTICS

NT SYNTAX

NT WORDS (LANGUAGE)

A linguistic concept for the advancement of structured programming --- German thesis 11 p1647 A83-28662

LININGS

NT ROCKET LININGS

Nonlinear structural and life analyses of a combustor liner 02 p0195 A83-12764

Small gas turbine combustor study - Combustor liner evaluation [AIAA PAPER 83-0337] 05 p0596 A83-16663

Eigensolutions for liners in uniform mean flow ducts 07 p0990 A83-19810

Sound attenuation in ducts with lined walls of non-uniform acoustic impedance 08 p1162 A83-22074

An experimental investigation of sound radiation from a duct with a circumferentially varying liner [AIAA PAPER 83-0712] 10 p1475 A83-25928

An evaluation of circumferentially segmented duct liners [AIAA PAPER 83-0732] 10 p1475 A83-25939

Friction drag and other design parameters for acoustic face sheets --- for aircraft noise reduction [AIAA PAPER 83-0780] 10 p1477 A83-25962

The design and flight test of an engine inlet bulk acoustic liner [AIAA PAPER 83-0781] 10 p1378 A83-25963

Optimization of acoustic liners by the hybrid finite element-integral approach [AIAA PAPER 83-0670] 10 p1478 A83-26917

Effect of sound absorbing wall linings on aerodynamic forces of a subsonic vibrating cascade 14 p2081 A83-33372

LINKAGES

Mechanism case studies VI [ASME PAPER 82-DET-47] 02 p0187 A83-12772

An experimental and analytical study of the dynamic response of a linkage fabricated from a unidirectional fiber-reinforced composite laminate [ASME PAPER 82-DET-67] 02 p0187 A83-12775

The dynamics of spatial linked quadrangle chains 20 p2999 A83-42986

LIQVILVE EQUATIONS

Demonstration and generalization of the Boltzmann kinetic theory 13 p1932 A83-30654

LIQVILVE THEOREM

Theorems of stability in geometry and analysis --- Russian book 21 p3199 A83-43905

LIPID METABOLISM

Concerning the interrelationship between protein, fat, and carbohydrate metabolisms 01 p0081 A83-10560

Metabolism during hypodynamia --- Russian book 02 p0221 A83-11950

Relative content of cholesterol and the microviscosity of serum apo-B-containing lipoproteins of mammals 03 p0376 A83-14372

The inhibitory effect of linoleic acid hydroperoxide on the activity of superoxide dismutase --- radioprotective substance 03 p0377 A83-14887

The effect of mechanical asphyxiation on lipid peroxidation processes in the rat brain 05 p0670 A83-17185

The effect of xenogenous cerebrospinal fluid on the course of experimental hypercholesterolemia 05 p0670 A83-17187

The phospholipid composition of blood platelets in healthy individuals and in individuals with diabetes mellitus 05 p0674 A83-17205

Metabolic effects of facial cooling in exercise 06 p0796 A83-18190

The content of phosphoglycerides in Rhodotulula rubra in three of its phenotypes as influenced by the lunar environment during the flight of Apollo 16 06 p0794 A83-18369

The effect of a magnetic field on the patterns of the frequency changes and the content of serotonin in the isolated heart of frogs 07 p0974 A83-20968

The acceleration of lipid peroxidation by the action of electromagnetic radiation of the millimeter range 08 p1146 A83-23024

Biochemical changes in rat liver after 18.5 days of spaceflight (41566) 12 p1763 A83-29546

A study of the fatty acid composition of the major brain 14 p2065 A83-33316

The phospholipid composition of various tissues of rats in dehydration conditions 16 p2395 A83-36829

The effect of low-frequency acoustic vibrations on the

phospholipid composition of the whole blood and some tissues of animals 17 p2556 A83-38187
The effect of disorders of lipid metabolism on the rheological properties of blood in patients with ischemic heart disease 18 p2735 A83-40548
Disorders of lipid metabolism in the testes during emotion and painful stress 18 p2733 A83-40564
Effects of acute moderate-intensity exercise on carnitine metabolism in men and women 20 p3034 A83-43484

Oxidant- and lipid-induced pulmonary vasoconstriction mediated by arachidonic acid metabolites 22 p3346 A83-45997

The effect of hypokinesia on lipid metabolism in adipose tissue [IAF PAPER 83-189] 23 p3494 A83-47305

The action of palmitate on the energy coupling in mitochondria of the skeletal muscles and liver 24 p3617 A83-49546

LIPIDS

NT LIPOPROTEINS

The implantation of sarcoplasmic reticulum membranes in a planar lipid membrane 03 p0375 A83-14359
The effect of 8-methoxypsoralen and UV radiation on the electric stability of liposome membranes 03 p0375 A83-14360

Optical determination of the thickness of an inhomogeneous membrane --- lipid layer reflectance measurement 03 p0376 A83-14371

The lipid balance of technical flight personnel between 50 and 55 years old in commercial and civil aviation 06 p0798 A83-18340

Lipids in aerosols from the tropical North Pacific - Temporal variability 07 p0960 A83-20214

Degradation of the phospholipids of the outer and inner membranes of mitochondria under exposure to low temperature 07 p0974 A83-20844

A device for the formation and investigation of spherical artificial phospholipid membranes 13 p1895 A83-30305

The effect of roughness on the optical parameters and capacitance of bilayer lipid membranes 13 p1895 A83-30404

The interaction of plasma lipoproteins with bilateral lipid membranes - The role of the surface charge 13 p1895 A83-30405

The relationship of the properties of model and natural channel permeability in biological membranes 13 p1896 A83-30411

The circadian rhythm of liver phospholipids in normal golden hamsters and in those with opisthorchiasis 15 p2211 A83-34963

Computer simulation of the main gel-fluid phase transition of lipid bilayers 20 p3033 A83-42639

Cholesterol esters increase the permeability of lecithin bilayer membranes 21 p3184 A83-45223

Computer modeling of membrane structures and the distribution of admixture particles in a lipid bilayer 21 p3184 A83-45224

Chemistry of lipids --- Russian book 23 p3427 A83-47147

LIPOPROTEINS

Antibodies to streptococcal lipoproteinase in the blood of healthy persons 01 p0083 A83-10554
Relative content of cholesterol and the microviscosity of serum apo-B-containing lipoproteins of mammals 03 p0376 A83-14372

High density lipoprotein /HDL/ finding in young airline pilots 08 p1147 A83-22953

The interaction of plasma lipoproteins with bilateral lipid membranes - The role of the surface charge 13 p1895 A83-30405

Exercise training, sex hormones, and lipoprotein relationships in men 13 p1903 A83-30487

The effect of thyroxin on the concentration of lipoproteins of various densities in the blood serum of rats 17 p2556 A83-38075

The metabolism of lipoproteins in conditions of experimental hyperthyrosis 17 p2556 A83-38125

Physiological mechanisms of the regulation of lipoprotein biosynthesis in the liver during physical loading and in various phases of the recovery period 18 p2733 A83-40563

A new detailed lipidogram - Methods and clinical applications 22 p3347 A83-45766

LIQUEFACTION

The effect of parasitic refrigeration on the efficiency of magnetic liquefiers 11 p1552 A83-27212

On the mathematical simulation of non-equilibrium cloud condensation rates 15 p2205 A83-34061

Helium liquefier cycles with saturated vapor compression 20 p2960 A83-43225

LIQUEFIED GASES

NT LIQUID HELIUM

NT LIQUID HELIUM 2

NT LIQUID HYDROGEN

NT LIQUID NITROGEN

NT LIQUID OXYGEN

Vibrational relaxation of gaseous CO/v - 1/ and N2/v

- 1/ from 300 K to liquid temperatures - A comparison with liquid state relaxation 10 p1389 A83-25563

LIQUID ATOMIZATION

Break-up and droplet formation of slurry jets

[AIAA PAPER 83-0067] 05 p0632 A83-16499

Instability and atomization of a liquid layer adjacent to a gas stream [AIAA PAPER 83-0339] 05 p0635 A83-16665

Transverse jet break-up and atomization with rapid vaporization along the trajectory [AIAA PAPER 83-0419] 05 p0597 A83-16702

The effect of the wave injection of a fluid jet into a gas cross-stream 19 p2794 A83-42155

Mixing and fuel atomisation effects on premixed combustion performance [ASME PAPER 83-GT-55] 23 p3407 A83-47911

LIQUID BEARINGS

A sensitivity analysis of squeeze-film bearings 02 p0186 A83-11941

Dynamic behavior of fluid bearings - Linear and nonlinear study --- French thesis 11 p1589 A83-28631

Effects of fluid inertia and viscoelasticity on the one-dimensional squeeze-film bearing [ASLE PREPRINT 83-AM-3E-1, 20 p2999 A83-43336

LIQUID BREATHING

Liquid ventilation in dogs - An apparatus for normobaric and hyperbaric studies 13 p1898 A83-30510

LIQUID CHROMATOGRAPHY

HPLC evaluation of MY 720 II --- High Performance Liquid Chromatography-tetraglycidylated methylenedianiline used in epoxy graphite composites 07 p0875 A83-20441

Separation of lower carbonyl compounds as their 2,4-dinitrophenylhydrazones by high-performance liquid chromatography and analytical application from jet engine exhaust 10 p1388 A83-26087

Quality assurance of graphite/epoxy by high-performance liquid chromatography 21 p3149 A83-45066

LIQUID COOLED REACTORS

NT EXPERIMENTAL BREEDER REACTOR 2

LIQUID COOLING

NT FILM COOLING

Fresnel ripple mapping of water-cooled laser mirrors 08 p1108 A83-22457

Study of + Gz protection given by an anti 'G' suit worn on top of a liquid cooled suit 09 p1324 A83-24003

Increasing summer peak power with aquifer storage 11 p1609 A83-27313

Heat transfer during the film boiling of liquids under conditions of free convection 11 p1570 A83-28555

Cooling liquid He-3 to around 100 micro-K 14 p1999 A83-31921

Computation of the three-dimensional unsteady thermal field in a cooled mirror by a finite difference explicit method 15 p2159 A83-34247

Development and application of a liquid-cooled V-8 piston engine for general aviation aircraft [AIAA PAPER 83-1342] 16 p2309 A83-36347

The application of a liquid-cooled V-8 piston engine to general aviation aircraft [SAE PAPER 821446] 17 p2468 A83-37994

Flow reversal in turbulent mixed convection 20 p2980 A83-42756

Study of the accelerated cooling of a very hot wall with a forced flow of subcooled liquid in film boiling regime 20 p2981 A83-42772

The cooling power of He-3/He-4 dilution refrigerators 20 p2960 A83-43227

An investigation into the effect of coolant flow on the vibration characteristics of hollow blades conveying fluid [ASME PAPER 83-GT-217] 23 p3470 A83-48017

LIQUID CRYSTALS

Photoconductor-liquid crystal photosensitive structures --- for optoelectronic information processing 02 p0235 A83-12197

Optical bistability in nematic films utilizing self-focusing of light 02 p0236 A83-12278

Optical-to-optical image conversion with the liquid crystal light valve 03 p0394 A83-13776

Silicon liquid crystal light valves for optical-data processing 03 p0394 A83-13778

Opto-optical modulation in N-/p-methoxybenzylidene/p-butylaniline 05 p0647 A83-16833

Optical bistability and self-oscillation of a nonlinear Fabry-Perot interferometer filled with a nematic-liquid-crystal film 05 p0685 A83-17882

Lasers with distributed feedback and reflection on the basis of cholesteric liquid crystals /CLC/ 06 p0768 A83-19572

Switchable coaxial optical coupler using a liquid crystal mixture 07 p0994 A83-21361

Quantitative geometric characterization of two-dimensional flaws via liquid crystals thermography 08 p1113 A83-22409

Liquid crystals as large aperture waveplates and circular polarizers 08 p1166 A83-22571

Dynamic spatial filter for optical signal processing using a liquid crystal light valve 08 p1166 A83-22809

Light scattering in the reversible electrical memory effect in smectic liquid crystals 09 p1344 A83-23996

Theory and experiment on optical bistability in a Fabry-Perot interferometer with an intracavity nematic liquid-crystal film 16 p2411 A83-35666

Heat evolution investigated by a liquid crystal film technique during fracture in metals 16 p2330 A83-35978

Freedericksz transition in a nematic liquid crystal under the action of the field of the standing light wave --- in nonlinear Fabry-Perot resonator 19 p2900 A83-41190

The effect of liquid crystals on the lubricating properties of mineral oils 19 p2824 A83-41975

Laser pulse shaping with liquid crystals 21 p3206 A83-44792

Optical memory with twisted nematic liquid crystal (TNLC) devices 21 p3206 A83-44806

Dynamic optical cross-correlator using a liquid crystal light valve for real time data input 21 p3207 A83-44827

Optically induced Freedericksz transition and bistability in a nematic liquid crystal 24 p3628 A83-48843

LIQUID DROPS

U DROPS (LIQUIDS)

LIQUID FILLED SHELLS

The damping of the elastic vibrations of structures with liquids 04 p0487 A83-15391

On the natural frequencies and modes of beams loaded by sloshing liquids 04 p0501 A83-16340

Rotating finite liquid systems under zero-gravity 06 p0759 A83-19247

Jet flow of an ideal liquid past a flexible shell 06 p0760 A83-19430

Numerical calculation of the translational forced oscillations of a sloshing liquid in axially symmetric tanks 07 p0926 A83-21003

A liquid-filled projectile simulator 08 p1106 A83-23297

The quasi-static stability loss in a rotating cylindrical shell containing a liquid 09 p1281 A83-25013

Determination of the natural frequencies and vibration modes of liquids in vessels of arbitrary shapes 09 p1263 A83-25015

Collapse by ponding of shells --- stability analysis 11 p1594 A83-28411

An analysis of the transient processes of the interaction between elastic bodies of revolution and a fluid 11 p1596 A83-28456

On the kinematic control of the motion of a vessel with an ideal heavy fluid 11 p1649 A83-28468

The propagation of small perturbations in a system consisting of a prestressed compressed solid body and a viscous compressible fluid 11 p1597 A83-28474

The stationary motions of a liquid-filled solid suspended on a string 11 p1650 A83-28772

Experimental study of the generation of Goertler vortices in an unsteady boundary layer 12 p1724 A83-29444

Angular motion of a spinning projectile with a viscous liquid payload 17 p2470 A83-37067

Liquid payload roll moment induced by a spinning and coning projectile [AIAA PAPER 83-2142] 19 p2811 A83-41964

Flight data on liquid-filled shell for spin-up instabilities [AIAA PAPER 83-2143] 19 p2811 A83-41965

Bubble motion in a rotating liquid body --- ground based tests for space shuttle experiments 20 p2940 A83-43272

Direct method for investigating the dynamics of liquid-filled bodies 24 p3624 A83-49672

Deformation of a cylindrical shell during an explosion in the vicinity of a concentrated explosive charge 24 p3595 A83-49905

Dynamics of a mobile tank partially filled with liquid Equations of motion and their linearization 24 p3581 A83-50124

LIQUID FLOW

NT OPEN CHANNEL FLOW

NT WATER FLOW

Resin flow during the cure of fiber reinforced composites 08 p1054 A83-21822

Determination of the cavitation boundary in liquid flows through constricting devices 09 p1258 A83-23432

A study of the processes involved in the filling of pipelines with liquid 09 p1258 A83-23444

Determination of amplitude-frequency response of thermoacoustic oscillations in a liquid at supercritical pressures 09 p1260 A83-24050

Turbine meters for liquid measurement 09 p1270 A83-25143

Film flow of a liquid on a convergent-nozzle surface 11 p1568 A83-28372

Instability in the film boiling of a moving liquid 11 p1570 A83-28556

The generation of electric currents by the turbulent flow of dielectric liquids. I - Long pipes 12 p1722 A83-29089

The impact of compressible liquids 13 p1843 A83-31078

- Two parametric flow measurement in gas-liquid two-phase flow 20 p2981 A83-42773
- Liquid materials and flow processes in reduced gravity 20 p2940 A83-43268
- Steady thermocapillary flows and their stability 20 p2986 A83-43270
- Surface tension driven flow in glass melts and model fluids 20 p2941 A83-43284
- Numerical method for the study of the planar unsteady-state flow of compressible viscous liquids 21 p3132 A83-45000

LIQUID FUELS

- NT AIRCRAFT FUELS
- NT AUTOMOBILE FUELS
- NT CRYOGENIC ROCKET PROPELLANTS
- NT DIESEL FUELS
- NT GASOLINE
- NT HYDROCARBON FUELS
- NT HYDROGEN FUELS
- NT HYPERGOLIC ROCKET PROPELLANTS
- NT JET ENGINE FUELS
- NT KEROGEN
- NT KEROSENE
- NT LIQUID HYDROGEN
- NT LIQUID ROCKET PROPELLANTS
- NT MONOPROPELLANTS
- NT SLURRY PROPELLANTS
- A carbon-13 and proton nuclear magnetic resonance study of some experimental referee broadened-specification /ERBS/ turbine fuels 01 p0028 A83-11482
- Observation of vapor generation preceding the ignition of liquid n-decane and l-decene by CO₂ laser radiation 02 p0152 A83-13094
- Liquid fuel spray ignition predictions for JP-10 04 p0464 A83-16113
- Prediction of liquid fuel spray capture by v-gutter downstream of plain orifice injector under uniform cross air-flow [AIAA PAPER 83-0153] 05 p0596 A83-16559
- Trajectory with diffusion method for predicting the fuel distribution in a transverse stream [AIAA PAPER 83-0336] 05 p0596 A83-16662
- Investigation of a dual inlet side dump combustor using liquid fuel injection [AIAA PAPER 83-0420] 05 p0609 A83-16703
- The ignition of a drop of fuel behind the front of a shock wave 07 p0901 A83-19961
- Fuel for future transport aircraft 07 p0901 A83-20082
- Spray combustion processes - A review [ASME PAPER 82-WA/HT-86] 10 p1390 A83-25691
- On the loss of stability of detonation waves in long heterogeneous-explosive charges 13 p1843 A83-31372
- Group combustion models and laser diagnostic methods in sprays - A review 14 p1990 A83-32938
- Mass, heat, and momentum transfer in laminar and turbulent pipe flow with vaporization of a liquid film 15 p2161 A83-34266
- A relationship between the flash point, boiling point and the lean limit of flammability of liquid fuels 16 p2325 A83-35791
- Combustion instability in liquid fuel ramjets 16 p2303 A83-35804
- Further study on the prediction of liquid fuel spray capture by v-gutter downstream of a plain orifice injector under uniform cross air flow 16 p2351 A83-35810
- Further studies on the prediction of spray evaporation rates --- for aircraft fuels 16 p2338 A83-35811
- Group combustion of liquid fuel sprays [AIAA PAPER 83-0150] 16 p2326 A83-36044
- Thermal stability of alternative aircraft fuels [AIAA PAPER 83-1143] 16 p2339 A83-36243
- Liquid fuel cyclone combustors for gas turbine applications [AIAA PAPER 83-1205] 16 p2361 A83-36280
- Droplet heating and vaporization at high Reynolds and Peclet numbers [AIAA PAPER 83-1706] 17 p2502 A83-37203
- Operation of an aircraft engine using liquefied methane fuel 20 p2927 A83-43239
- Hydrodynamics and heat transfer in sphere assemblages Cylindrical cell models 21 p3131 A83-44928
- Testing of a full-scale staged combustor operating with a synthetic liquid fuel [ASME PAPER 83-GT-27] 23 p3464 A83-47890
- Experimental investigation of fuel distribution in a transverse stream [ASME PAPER 83-GT-207] 23 p3410 A83-48008

- LIQUID HELIUM**
- NT LIQUID HELIUM 2
- Statistical mechanics of dilute liquid mixtures of He-3 in He-4 05 p0691 A83-17228
- Cooling liquid He-3 to around 100 micro-K 14 p1999 A83-31921
- Thermal conductance of pressed contacts at liquid helium temperatures [AIAA PAPER 83-1436] 14 p2010 A83-32708
- High resolution acoustic microscopy in superfluid helium 14 p2022 A83-33443
- Quantized evaporation from liquid helium 20 p3044 A83-42167
- Cryogenic heat transfer - He-4 Kapitza conductances including phase change effects 20 p2971 A83-42660
- Superfluid helium (He - II) film boiling on vertical heat transfer surfaces 20 p2981 A83-42763
- Critical heat flux in flow boiling of helium 20 p2981 A83-42769
- A computer model for transient heat transfer to liquid helium 20 p2985 A83-43222
- Transient heat transfer in superfluid helium 20 p2986 A83-43223
- Helium liquefier cycles with saturated vapor compression 20 p2960 A83-43225
- The cooling power of He-3/He-4 dilution refrigerators 20 p2960 A83-43227
- Single shot demountable self-contained He-3 refrigerator 20 p2960 A83-43230
- Sub-Kelvin temperatures in space 20 p2961 A83-43232
- Performance of a superfluid helium facility for Spacelab payloads 20 p2961 A83-43243
- Integrating and testing the thermal model of the German Infrared Laboratory (GIRL) 20 p2961 A83-43244
- Superfluid-supercritical helium tradeoff analysis for the Shuttle Infrared Telescope Facility (SIRTF) 20 p2962 A83-43245
- Orbital performance of a one-year lifetime superfluid helium dewar based on ground testing and computer modelling 20 p2962 A83-43247
- Top-off procedure for space-bound superfluid helium cryostats 20 p2962 A83-43248

LIQUID HELIUM 2

- Improved active phase separator for He II space cooling systems 20 p2962 A83-43246

LIQUID HYDROGEN

- Fuel for future transport aircraft 07 p0901 A83-20082
- Is LH2 the high cost option for aircraft fuel 11 p1552 A83-27215
- Cryogenic fluid management experiment trunnion fatigue verification [AIAA PAPER 83-0911] 14 p1982 A83-32782
- A parametric study of thermally augmented O₂/H₂ rocket engines [AIAA PAPER 83-1258] 16 p2319 A83-36312
- The performance and application of high speed long life LH₂ hybrid bearings for reusable rocket engine turbomachinery [AIAA PAPER 83-1389] 16 p2362 A83-36379
- Critical fields of liquid superconducting metallic hydrogen 16 p2421 A83-36991
- Model of a cryogenic liquid-hydrogen pipeline for an airport ground distribution system 20 p3013 A83-43641
- An airline view of LH₂ as a fuel for commercial aircraft 23 p3440 A83-48598

LIQUID INJECTION

- NT WATER INJECTION
- The effect of transverse injection on steady liquid flows between a rotating and a stationary porous disk 04 p0480 A83-16389
- Effects of properties and location in the plume on droplet diameter for injection in a supersonic stream 16 p2351 A83-36080
- Penetration and breakup of slurry jets in a supersonic stream 16 p2352 A83-36094
- Aerodynamic-wave break-up of liquid sheets in swirling airflows and combustor modules [AIAA PAPER 83-1204] 21 p3133 A83-45511
- Penetration and break-up behaviour of a discrete liquid jet in a cross flowing airstream - A further study [ASME PAPER 83-GT-170] 23 p3448 A83-47971
- Instabilities of a cylindrical liquid sheet in the presence of two gaseous flows 24 p3578 A83-49647

LIQUID LASERS

- Intracavity double resonance in the CH₃OH submillimeter laser 10 p1435 A83-26879
- Broadband infrared generation by stimulated Raman scattering in liquid filled fibers 22 p3297 A83-46631

LIQUID MERCURY**U MERCURY (METAL)****LIQUID METAL COOLED REACTORS****NT EXPERIMENTAL BREEDER REACTOR 2****LIQUID METALS****NT MERCURY (METAL)**

- Radiant heating tests of several liquid metal heat-pipe sandwich panels [AIAA PAPER 83-0319] 05 p0635 A83-16649
- The thermal diffusion and heat conduction of solid and liquid titanium 06 p0727 A83-17982
- A study of the structure of liquid aluminum-silicon alloys I - Hypoeutectic and eutectic melts 07 p0890 A83-20916
- The effect of soldering on the characteristics of heat

- pipes with a liquid-metal heat-transfer agent 09 p1258 A83-23449
- A theory for the formation of closed shrinkage cavities during alloy solidification in large volumes 09 p1229 A83-23519
- Direct contact droplet heat exchangers for thermal management in space 11 p1564 A83-27137
- Computer simulation of transient energy storage in a packed-bed of iron spheres with liquid-metal through-flow by numerical inversion of Laplace transforms 11 p1610 A83-27320
- The specific heat of liquid cesium at temperatures up to 2000 K and pressures up to 12 MPa 11 p1550 A83-28558
- Thermal convection instability of liquid metals of magneto-hydrodynamics 12 p1780 A83-29053
- The effect of electromagnetic forces on the hydrodynamics of a melt in the process of high-frequency floating zone melting 12 p1782 A83-29269
- Oriented crystallization of metals in the presence of electric current 13 p1822 A83-30906
- A study of the structure of liquid aluminum-silicon alloys. II - Hypereutectic melts 15 p2141 A83-35308
- Liquid-metal flows and magnetohydrodynamics; Beersheba International Seminar on Magneto-hydrodynamic Flows and Turbulence, 3rd, University of the Negev, Beersheba, Israel, March 23-27, 1981, Technical Papers --- Book 16 p2416 A83-36451

- Ordered pairing in liquid metallic hydrogen 19 p2899 A83-41867
- The time of formation of liquid metal into spheres during the passage into weightlessness 19 p2807 A83-42004
- Heat capacities of liquid metals above 1500 K 20 p2954 A83-43255
- The calculation of transport phenomena in electromagnetically levitated metal droplets 20 p2963 A83-43273
- Studies of liquid metal surfaces using Auger spectroscopy 20 p2942 A83-43301
- Directional solidification of alloys in systems containing a liquid miscibility gap 20 p2942 A83-43305
- A study of the coalescence process inside the miscibility gap in Zn-Bi alloys 20 p2942 A83-43306
- Strong spherical two-phase blowoff of liquid metals into vacuum 21 p3220 A83-43395
- Metallic infiltration of reaction bonded silicon nitride 23 p3436 A83-48285
- Oxidation of high alloyed steels 24 p3563 A83-49494

LIQUID NITROGEN

- Experimental study of flash boiling in liquid nitrogen [AIAA PAPER 83-1378] 16 p2341 A83-36369
- The effect of the real properties of a carrier vapor on the evaporation time of a drop 17 p2506 A83-37814
- High efficiency mid-IR generation by Raman down conversion in liquid nitrogen 24 p3587 A83-48907

LIQUID OXYGEN

- A parametric study of thermally augmented O₂/H₂ rocket engines [AIAA PAPER 83-1258] 16 p2319 A83-36312
- Dynamic response of the LE-5 rocket engine liquid oxygen pump [AIAA PAPER 83-1385] 16 p2321 A83-36375
- LOX/hydrocarbon injector performance [AIAA PAPER 83-1390] 16 p2322 A83-36380
- Potential for catastrophic rupture of large liquid oxygen storage tanks 20 p2961 A83-43238
- Analysis of spiral-groove face seals for liquid oxygen [ASLE PREPRINT 83-AM-4B-2] 20 p2999 A83-43339
- Dynamic response of a centrifugal liquid oxygen rocket pump [ASME PAPER 83-FE-24] 23 p3426 A83-48235

LIQUID PHASE EPITAXY

- Raman scattering characterization of Ga_{1-x}Al_x/As/GaAs heterojunctions - Epilayer and interface 02 p0243 A83-12289
- Epitaxial HgCdTe/CdTe photodiodes for the 1 to 3 micron spectral region 03 p0309 A83-13737
- Liquid encapsulated Czochralski growth of low dislocation GaAs 03 p0399 A83-13784
- HgCdTe liquid phase epitaxy - An overview 03 p0399 A83-13787
- Mode stabilized terrace InGaAsP lasers on semi-insulating InP 03 p0332 A83-13919
- High power single mode InGaAsP lasers fabricated by single step liquid phase epitaxy 06 p0767 A83-19254
- Mercury pressure-induced LPE growth of HgCdTe 07 p0998 A83-19899
- Long wavelength Pb_{1-x}Sn_x/Te homostructure diode lasers having a gallium-doped cladding layer 07 p0937 A83-21369
- Enhanced indium phosphide substrate protection for liquid phase epitaxy growth of indium-gallium-arsenide-phosphide double heterostructure lasers 08 p1107 A83-22331
- Lattice parameter changes in Al_{0.39}Ga_{0.61}/As due to O, Ge, Si, and S doping 10 p1488 A83-26059

- A study of impurities and traps in liquid phase epitaxial InP in relation to melt prebaking
- 10 p1488 A83-26063
- InGaAsP photodiodes 15 p2150 A83-33680
- Liquid phase epitaxial growth of ZnSnP₂ on GaAs 15 p2238 A83-34697
- Very low threshold InGaAsP mesa laser 16 p2359 A83-35955
- Crystal growth of mode-stabilized semiconductor diode lasers by liquid-phase epitaxy 16 p2420 A83-35987
- Accumulation mode Ga(0.47)In(0.53)As insulated gate field-effect transistors 19 p2836 A83-40746
- The design and manufacture of a GaAs solar cell by liquid phase epitaxy --- French thesis 19 p2862 A83-41813
- Resistivity and mobility of GaP at 300 K 20 p3054 A83-43358
- Measurement of compositional inhomogeneity of liquid phase epitaxial InGaPAs 20 p3055 A83-43602
- High-resistivity greater than 10 to the 5th ohm/cm InP layers by liquid phase epitaxy 20 p3055 A83-43604
- A new Faraday rotator using a thick Gd:YIG film grown by liquid-phase epitaxy and its applications to an optical isolator and optical switch 21 p3205 A83-44228
- Liquid phase growth of epitaxial Ni and Co silicides 21 p3219 A83-45494
- pAl(x)Ga(1-x)AspGaAs-nGaAs heterostructure concentrator photocells synthesized by liquid-gas-phase epitaxy 22 p3366 A83-46787
- LIQUID PHASES**
- Broadband infrared generation in liquid-bromine-core optical fibers 02 p0183 A83-11571
- Changes in the volume of Al-Zn compacts during liquid-phase sintering 02 p0159 A83-13027
- Controlling the structure of hard alloys and other heterophase materials produced by liquid-phase sintering. II - Optimum design principles for hard alloys 02 p0159 A83-13029
- The effect of heat treatment on element redistribution between the phase components of W-Ni-Fe alloy 02 p0159 A83-13032
- Effect of liquid phase decomposition on fuel droplet distribution function [AIAA PAPER 83-0069] 05 p0632 A83-16501
- Liquid phase thermochemical energy conversion systems - An application of Diels-Alder chemistry 05 p0658 A83-17149
- A study of inter-phase exchange laws in spray combustion modeling [AIAA PAPER 83-0152] 05 p0613 A83-17910
- Liquid phase sintering and infiltration of some nickel base alloys produced by P/M techniques 06 p0730 A83-19080
- Producing coatings in the presence of the liquid phase 07 p0888 A83-20687
- Enthalpies of formation of liquid aluminum-silicon alloys 09 p1229 A83-23518
- Solutal diffusion coefficient for liquid PbTe-SnTe 09 p1227 A83-25225
- A dual focus fiber optic anemometer for measurements in wet steam 10 p1422 A83-26422
- The dependence of ice formation on the evolution of the liquid phase 15 p2204 A83-34052
- Anomalous backscattering of optical radiation in a stratified solution 20 p2993 A83-42280
- Experimental observation of the thermocapillary driven motion of bubbles in a molten glass under low gravity conditions 20 p2941 A83-43283
- Aqueous-phase source of formic acid in clouds 20 p3028 A83-43555
- Liquid phase sintering of tungsten 21 p3111 A83-44337
- Liquid phase sintering 23 p3435 A83-48265
- The unexpectedly high solubility of water in cryogenic liquids 24 p3570 A83-50114
- LIQUID PROPELLANT ROCKET ENGINES**
- NT HYDRAZINE ENGINES
- NT HYDROGEN OXYGEN ENGINES
- NT RL-10 ENGINES
- NT SPACE SHUTTLE MAIN ENGINE
- The reliability of the engines of flying vehicles --- Russian book 03 p0289 A83-13813
- The shy eccentric who fathered the rocket 03 p0439 A83-14049
- A study of mesospheric rocket contrails and clouds produced by liquid-fueled rockets 03 p0290 A83-14518
- Model studies of the dynamic characteristics of the pumps and turbines of liquid propellant rocket engines in transition regimes 08 p1052 A83-22660
- Liquid-rocket propulsion technology 11 p1543 A83-28693
- Liquid rocket propulsion: An evaluation of our national capability - An AIAA position paper 12 p1708 A83-29534
- Experimental investigation of bipropellant exhaust plume flowfield, heating, and contamination, and comparison with the CONTAM computer model predictions [AIAA PAPER 83-1447] 14 p1984 A83-32715
- Effects of tripropellant engines on earth-to-orbit vehicles [AIAA PAPER 83-1187] 16 p2318 A83-36265
- Anane 4 liquid boosters and first stage propulsion system [AIAA PAPER 83-1192] 16 p2319 A83-36268
- Analytical prediction capability for a spacecraft bipropellant propulsion system [AIAA PAPER 83-1222] 16 p2319 A83-36290
- Monomethylhydrazine versus hydrazine fuels - Test results using flight qualified 100 LBF and 5 LBF bipropellant engine configurations [AIAA PAPER 83-1257] 16 p2340 A83-36311
- Double perforated plate as a capillary barrier --- in liquid propellant propulsion systems in low-G environment [AIAA PAPER 83-1379] 16 p2317 A83-36370
- Suction performance of high speed cryogenic inducers [AIAA PAPER 83-1387] 16 p2321 A83-36377
- Chemical orbit transfer vehicles - Options for the future [IAF PAPER 83-11] 23 p3418 A83-47231
- Liquid propellant rocket development by the U.S. Navy during World War II [IAF PAPER 83-298] 23 p3425 A83-47333
- Peculiarities of start regime organisation in stage combustion cycle liquid rocket engines [IAF PAPER 83-373] 23 p3426 A83-47363
- State-space analysis of the dynamic characteristics of a variable thrust liquid propellant rocket engine [IAF PAPER 83-ST-06] 23 p3426 A83-47385
- A mathematical model for the dynamics of liquid-propellant rocket engines 24 p3552 A83-48928
- LIQUID ROCKET PROPELLANTS**
- NT CRYOGENIC ROCKET PROPELLANTS
- NT HYPERGOLIC ROCKET PROPELLANTS
- NT MONOPROPELLANTS
- NT SLURRY PROPELLANTS
- The centenary of Robert Hutchings Goddard, 1862-1982 02 p0276 A83-12646
- Liquid-rocket propulsion technology 11 p1543 A83-28693
- Effects of tripropellant engines on earth-to-orbit vehicles [AIAA PAPER 83-1187] 16 p2318 A83-36265
- Experimental exhaust plume analysis with MBB 10 N thruster --- Bipropellant for US/German Galileo spacecraft propulsion [AIAA PAPER 83-1259] 16 p2320 A83-36313
- Development of a toroidal tank for missile applications [AIAA PAPER 83-1657] 16 p2317 A83-36402
- LIQUID ROTATION**
- U ROTATING LIQUIDS
- LIQUID SLOSHING**
- On the damping effect of sloshing fluid on flexible rotor systems [ASME PAPER 82-DET-140] 02 p0196 A83-12783
- On the natural frequencies and modes of beams loaded by sloshing liquids 04 p0501 A83-16340
- Numerical calculation of the translational forced oscillations of a sloshing liquid in axially symmetric tanks 07 p0926 A83-21003
- On the kinematic control of the motion of a vessel with an ideal heavy fluid 11 p1649 A83-28468
- Potential function and problems of oscillations of an exponentially stratified fluid 13 p1838 A83-30011
- Normal oscillations of an ideal compressible fluid in rotating elastic vessels 13 p1838 A83-30012
- Parametric excitation of oscillations in a liquid flowing out of a container 16 p2350 A83-35717
- A minicomputer finite elements program for microgravity hydroelastic analysis --- of spacecraft flexible propellant tanks 16 p2317 A83-36499
- The effects of propellant motion on a spinning satellite with vanned tanks [AIAA PAPER 83-2262] 19 p2816 A83-41732
- Flight data on liquid-filled shell for spin-up instabilities [AIAA PAPER 83-2143] 19 p2811 A83-41965
- Energy dissipation due to liquid slosh in spinning spacecraft 21 p3102 A83-45124
- Liquid surface oscillations induced by temperature fluctuation 24 p3576 A83-49024
- Direct method for investigating the dynamics of liquid-filled bodies 24 p3624 A83-49672
- The effect of the intensity of pressure pulses on the splashing of a liquid in a vessel 24 p3579 A83-49673
- LIQUID SURFACES**
- NT MENISCI
- Velocity distribution due to thermal Marangoni effect in a liquid column 01 p0044 A83-10123
- New heartbeats phenomenon, and the concept of 2-D optical turbulence 07 p0935 A83-20160
- Coupled oscillations of a solidly rotating liquid bridge --- under reduced gravity 11 p1531 A83-27342
- Free-surface oscillations of a liquid in a cylindrical container under longitudinal vibrations 11 p1569 A83-28458
- Transient thermal Marangoni convection in a liquid bridge 13 p1844 A83-31625
- Liquid surface oscillations in a viscous liquid column induced by temperature fluctuations 13 p1844 A83-31800
- Surface oscillation due to Marangoni-effect in a freely floating sphere 23 p3451 A83-48498
- Direct method for investigating the dynamics of liquid-filled bodies 24 p3624 A83-49672
- LIQUID WASTES**
- NT WASTE WATER
- LIQUID-GAS MIXTURES**
- NT AEROSOLS
- NT FOG
- The dynamic stability of a liquid-gas oscillatory system under the effect of vibration 03 p0341 A83-14075
- Rarefaction shock wave near the critical liquid-vapour point 08 p1086 A83-23089
- Shock propagation in liquid-gas media 10 p1417 A83-26194
- The cold locking of the duct of a gas-liquid mixer by burning fuel jets 18 p2663 A83-39168
- The influence of undissolved gas on the magnitude of hydraulic shock during the filling of a pipeline 24 p3579 A83-49654
- The ignition of a vapor bubble in a liquid 24 p3556 A83-49774
- LIQUID-LIQUID INTERFACES**
- Motion of a droplet in a nonisothermal flow 05 p0639 A83-17411
- Deformation of a drop in a viscous flow and conditions for the existence of the equilibrium form of the drop 06 p0758 A83-19122
- Admissibility criteria for propagating phase boundaries in a van der Waals fluid 10 p1490 A83-26773
- Thermal imaging system with a two-phase ternary mixture of liquids 14 p2014 A83-31947
- Marangoni effects under electric fields 18 p2686 A83-39911
- Natural damped frequencies of an infinitely long column of immiscible viscous liquids 19 p2841 A83-40800
- LIQUID-SOLID INTERFACES**
- Osmosis in composite materials 01 p0022 A83-10240
- An implicit formulation for the one-dimensional two-phase multi-interface Stefan Problem [ASME PAPER 82-HT-21] 02 p0171 A83-12787
- An interdigital transducer for ultrasonic nondestructive testing 03 p0327 A83-13921
- The effect of liquid media on the strength of an aluminum-matrix composite 04 p0455 A83-15394
- A study of the corrosion activity of the fuselage condensate of passenger aircraft 04 p0445 A83-15398
- Collision between an evaporating drop and a hot wall 04 p0478 A83-16166
- Design of a 13% efficient n-GaAs 1-x/P/x/ semiconductor-liquid junction solar cell 05 p0658 A83-17801
- Startup conditions of alkali-metal vaporization from rectangular channels --- in heat pipes 06 p0756 A83-18446
- The combustion of substances with a liquid reaction layer 07 p0880 A83-19953
- Semiconductor electrodes. XLVII - A-C impedance technique for evaluating surface state properties of n-Mo Te2 in acetonitrile solutions containing various redox couples 07 p0999 A83-20588
- Free energy loss during the breakdown of liquid films 08 p1087 A83-23141
- Finite-element methods for steady solidification problems 09 p1338 A83-23723
- A coupled ice-ocean model of upwelling in the marginal ice zone 10 p1452 A83-26348
- Motion of a circular cylinder in a rectangular channel 11 p1567 A83-27720
- An analysis of the transient processes of the interaction between elastic bodies of revolution and a fluid 11 p1596 A83-28456
- The effect of initial stresses on the back wave in the system prestressed compressible cylinder-liquid 11 p1596 A83-28457
- Free-surface oscillations of a liquid in a cylindrical container under longitudinal vibrations 11 p1569 A83-28458
- An analysis of the thermal state of plane channels with allowance for the mutual influence of the processes in the wall and in the fluid 11 p1570 A83-28796
- Acoustical speckle interferometry 12 p1730 A83-29586
- Hydrogen in pure aluminum solidified unidirectionally 13 p1824 A83-31601
- Heat release during the interphase interaction of titanium with an NiMn melt 14 p1993 A83-32595
- Overview of D.C. casting --- Direct-Chill solid-liquid interface shape prediction using heat transfer models 14 p1995 A83-32878
- Connectivity methods for free boundary problems - 2 phase heat flow 15 p2159 A83-34238
- Submersion of a disk into a compressible fluid at an angle to the free surface 16 p2350 A83-35714

On waves of general type propagating at the interface between an elastic half-space and a liquid 16 p2369 A83-36549

Growth rate dependence of the interface distribution coefficient in the system Ge-Ga 16 p2421 A83-36714

Effect of heat transfer of melt/solid interface shape and solute segregation in Edge-Defined Film-Fed growth - Finite element analysis 16 p2354 A83-36715

Determination of the charging current of a plate in an aerosol flow when a liquid film is separated from its surface 17 p2503 A83-37266

Solution of problems in the dynamics of noncircular cylindrical shells in a liquid 17 p2521 A83-37573

The dependence of the shape and stability of captive rotating drops on multiple parameters 17 p2507 A83-38615

The breaking of axisymmetric slender liquid bridges 18 p2680 A83-39206

Theory of the Leidenfrost phenomenon 18 p2685 A83-39866

Melt temperature fluctuations - Causes and response of the solidification front --- in low gravity environments 18 p2643 A83-39895

Morphological and convective instabilities during solidification 18 p2686 A83-39902

Solid/liquid interface instability - Limits and morphological aspects in microgravity conditions 18 p2643 A83-39904

An effective numerical method in phase change problems with temperature dependent thermal properties 20 p2971 A83-42670

Liquid-solid contact and its relationship to improved film boiling heat transfer rates 20 p2980 A83-42761

Subcooled film boiling and the behavior of vapor film on a horizontal wire and a sphere 20 p2981 A83-42764

Study of the accelerated cooling of a very hot wall with a forced flow of subcooled liquid in film boiling regime 20 p2981 A83-42772

Finite element analysis of the effect of a non-planar solid-liquid interface on the lateral solute segregation during unidirectional solidification 20 p2943 A83-43312

The spreading of a viscous fluid on a horizontal surface 20 p2987 A83-43515

The direct method of solving the problem concerning the combined three-dimensional motions of the system solid-liquid 23 p3504 A83-48473

Nonaxisymmetric equilibrium shapes of a drop on a plane 23 p3452 A83-48670

A model relating ultrasonic scattering measurements through liquid-solid interfaces to unbounded medium scattering amplitudes 24 p3625 A83-48975

Transient Workman-Reynolds freezing potentials --- at ice-water interfaces causing thunderstorm electrification and aircraft static 24 p3610 A83-49337

LIQUID-VAPOR EQUILIBRIUM

Equation of state and phase equilibrium curve for liquid-vapor systems 02 p0243 A83-11657

The phase realignment of clouds 19 p2868 A83-41583

New approach for analysis and prediction of liquid-vapor coexistence densities including the critical region 20 p3055 A83-43236

Nucleation theory - Is replacement free energy needed? --- error analysis of capillary approximation 20 p3056 A83-43287

LIQUID-VAPOR INTERFACES

Methods for calculating the stabilization limits of a flame of inhomogeneous mixtures using a bluff body 02 p0136 A83-11512

Capillary priming characteristics of a high capacity dual passage heat pipe [ASME PAPER 82-HT-14] 02 p0171 A83-12784

Investigation of intermittent phenomena in two phase boundary layer 03 p0319 A83-14473

Use of thermocapillary migration in a controllable heat valve 04 p0477 A83-16093

Instability and atomization of a liquid layer adjacent to a gas stream [AIAA PAPER 83-0339] 05 p0635 A83-16665

The liquid-gas interface in grooved face seals 06 p0768 A83-18048

Pnming considerations of heat pipes in zero-G 06 p0757 A83-18454

Vibration effects in bodies containing a gas-liquid medium 06 p0760 A83-19547

Inertial effects of the gas motion upon the linear and nonlinear waves in Kelvin-Helmholtz flow 08 p1083 A83-21813

Sulfur-dioxide/water equilibria between 0 and 50 C - An examination of data at low concentrations 09 p1298 A83-25195

Asymmetries in evaporation and condensation Knudsen layer problems 13 p1840 A83-30110

Fluid flow in the contact line region of a mixture of alkanes - 98 percent hexane and 2 percent octane [AIAA PAPER 83-1528] 14 p2011 A83-32759

Vapor/droplet coupling and the mist flow (OTEC)

cycle 15 p2189 A83-33992

Gas-liquid interface behaviour in a pulse-tube thruster --- in hydrofoils and surface effect ships [AIAA PAPER 83-1278] 16 p2362 A83-36320

First-order wetting transition at a liquid-vapor interface 16 p2327 A83-36523

The effect of the real properties of a carrier vapor on the evaporation time of a drop 17 p2506 A83-37814

Nonstationary pressure waves in various types of flow of a vapor-liquid medium 19 p2843 A83-41270

Film condensation in a tube with counter current vapor flow 20 p2969 A83-42535

Instabilities of dynamic thermocapillary liquid layers. I Convective instabilities 20 p2985 A83-43098

LIQUIDS

NT CRYOGENIC FLUIDS

NT CRYOGENIC ROCKET PROPELLANTS

NT FERMI LIQUIDS

NT FERROFLUIDS

NT HYDRAULIC FLUIDS

NT HYPERGOLIC ROCKET PROPELLANTS

NT LIQUEFIED GASES

NT LIQUID FUELS

NT LIQUID HELIUM

NT LIQUID HYDROGEN

NT LIQUID METALS

NT LIQUID NITROGEN

NT LIQUID OXYGEN

NT LIQUID ROCKET PROPELLANTS

NT MERCURY (METAL)

NT MONOPROPELLANTS

NT ORGANIC LIQUIDS

NT ROTATING LIQUIDS

NT SLURRY PROPELLANTS

Spectroscopy of molecular rotation in gases and liquids --- Russian book 03 p0392 A83-13816

The effect of changes in the turbulent flow structure of the unsteady heat transfer during the heating of gases and liquids in pipes 04 p0478 A83-16163

The dielectric properties of liquids in the submillimeter range 08 p1082 A83-23151

Possibility of observing stimulated thermal scattering of sound 10 p1477 A83-26287

Mechanisms of acoustic wave generation by lasers 11 p1650 A83-27563

On the electrokinetic energy conversion in liquid mixtures 11 p1612 A83-28069

Van der Waals picture of liquids, solids, and phase transformations 13 p1933 A83-31199

Autothermal reforming of aliphatic and aromatic hydrocarbon liquids 20 p2946 A83-42955

Nonlinear theory for acoustic beams --- Russian book 21 p3201 A83-45028

Experimental study of the thermal explosion of liquids --- Thesis 22 p3267 A83-46695

A pulsating detonation front 24 p3557 A83-49799

LIQUIDUS

Elevation of liquidus temperature in a gel-derived Na2O-SiO2 glass 08 p1070 A83-22194

Solidus and liquidus temperatures and mineralogies for anhydrous garnet-lherzolite to 15 GPa 17 p2546 A83-38698

LITERATURE

NT BIOGRAPHY

NT DOCUMENTATION

The initial manifestations of the defects of blood supply to the brain /Review of the literature/ 03 p0380 A83-13642

Heat transfer - A review of 1981 literature 05 p0682 A83-17701

The physics of strength and plasticity: A systematic index of the major literature in Russian and in foreign languages 1970-1975. Number 2 - Current and special topics in the plastic deformation of materials --- Russian book 09 p1231 A83-23925

Review of prior work in high-speed machining --- of metals and alloys 15 p2171 A83-33646

Survey of usage of technical report components to establish their most effective organization 15 p2239 A83-34800

Physiological and hygienic aspects of artificial heat adaptation (Review of the literature) 16 p2397 A83-35596

Interstellar travel and communication bibliography - 1982 update 18 p2754 A83-39610

LITHERGOLIC PROPELLANTS

U HYBRID PROPELLANTS

LITHIUM

NT LITHIUM ISOTOPES

Electron impact cross sections for the 2,2P state excitation of lithium 03 p0391 A83-13225

Two lithium-rich supergiants 03 p0421 A83-14144

Abundance of lithium in unevolved halo stars and old disk stars - Interpretation and consequences 04 p0550 A83-15043

Secondary lithium cells employing vanadium tungsten oxide positive electrodes 07 p0953 A83-19902

Stored chemical energy propulsion system for underwater applications [AIAA PAPER 81-1601] 08 p1132 A83-23132

A lithium electrode with a zinc substrate for secondary batteries 10 p1446 A83-26057

Lithium cycling in polymethoxymethane solvents --- for use in batteries 10 p1390 A83-26058

Pulsed optical-optical double resonance spectroscopy of the gerade excited states of 7Li2 11 p1653 A83-27524

Hydrogen and lithium atoms in a strong electric field 13 p1915 A83-30266

A spectrophotometric investigation of the lithium star Xi Boo A 17 p2590 A83-37702

Radiative recombination of the ground state of lithium-like ions 17 p2578 A83-37934

Modeling of interaction of artificially released lithium with the earth's bow shock 19 p2864 A83-41114

Lithium abundance and age spread in the Pleiades 20 p3072 A83-43059

Probabilities for transition processes crucial to Li lasers 22 p3295 A83-45945

Lithium in stone meteorites and stony irons 22 p3385 A83-46374

The effect of the dispersion medium on the properties of complex Li lubricants 23 p3439 A83-48545

Rydberg atoms in 'circular' states 24 p3626 A83-49293

International Meeting on Lithium Batteries, Rome, Italy, April 27-29, 1982 24 p3600 A83-49932

The reactivity of organic electrolytes with lithium Mechanistic aspects 24 p3558 A83-49934

Film forming reaction at the lithium/electrolyte interface 24 p3558 A83-49935

Surface films on lithium in acetonitrile-sulphur dioxide solutions 24 p3558 A83-49937

Polarization of the lithium electrode in sulflury chloride solutions 24 p3558 A83-49939

Mechanistic studies of oxide electrodes reversibly incorporating Li(+) ions 24 p3558 A83-49941

Electrochemical method for studying the reversibility of the lithium intercalation in secondary batteries 24 p3600 A83-49942

Chromium oxides as cathodes for lithium cells 24 p3600 A83-49943

Behaviour of various cathode materials for nonaqueous lithium cells 24 p3600 A83-49944

Li-AgBi(CrO4)2 - A new highly reliable lithium battery for long service life applications 24 p3600 A83-49945

A reversible graphite-lithium negative electrode for electrochemical generators 24 p3558 A83-49946

Interfacial conduction in lithium iodide containing inert oxides 24 p3558 A83-49947

A pre-testable low temperature lithium thermal battery 24 p3600 A83-49949

The cycling behaviour and stability of the lithium electrode in propylene carbonate and acetonitrile electrolytes 24 p3600 A83-49950

Galvanostatic cycling of vanadium oxide (V6O13) in a nonaqueous secondary lithium cell 24 p3601 A83-49952

The anodic passivation of lithium 24 p3558 A83-49956

Optimization of the vanadium oxide (V6O13) electrode in a nonaqueous secondary lithium cell 24 p3601 A83-49958

Abundance of lithium in old dwarf stars 24 p3667 A83-50060

LITHIUM ALLOYS

Effect of defect structure upon the mechanical behavior of beta-LiAl through dislocation damping and hardness studies 04 p0460 A83-16002

The influence of grain structure on the ductility of the Al-Cu-Li-Mn-Cd alloy 2004 04 p0460 A83-16004

Texture and grain boundary strengthening in hot rolled magnesium - 12.5 at.% lithium alloy 05 p0616 A83-17951

Superplasticity in Al-Li based alloys 11 p1548 A83-28224

Properties and application benefits of low density aluminum alloys [AIAA 83-0981] 12 p1715 A83-29788

Light alloys containing lithium --- Russian book 13 p1820 A83-30424

The effect of cold deformation during rolling on the mechanical properties of sheets and foil of magnesium-lithium alloys 13 p1821 A83-30699

A study of coalescence processes in Al - 2.8 pct Li alloy 13 p1821 A83-30739

Aluminum-lithium alloys 14 p1995 A83-32876

Casting problems specific to aluminum-lithium alloys 14 p2028 A83-32879

Al-Li-X alloys - An overview 14 p1995 A83-32880

A perspective on the development of aluminum-lithium alloys 14 p1996 A83-32881

Microstructural characteristics of Al-Li alloys 14 p1996 A83-32882

Relationship between microstructure and mechanical properties of aluminum-lithium-magnesium alloys 14 p1996 A83-32883

Alloying additions and property modification in aluminum-lithium - X systems 14 p1996 A83-32884

Microstructure and deformation of rapidly solidified Al-3Li

- alloys containing incoherent dispersoids
14 p1996 A83-32885
- Toughness and ductility of aluminum-lithium alloys prepared by powder metallurgy and ingot metallurgy
14 p1996 A83-32886
- The design and mechanical properties of rapidly solidified Al-Li-X alloys
14 p1996 A83-32887
- A comparison of microstructure and tensile properties of P/M and I/M Al-Li-X alloys --- Powder Metallurgy and Ingot Metallurgy
14 p1996 A83-32888
- The effect of microstructure and moisture on the low cycle fatigue and fatigue crack propagation of two Al-Li-X alloys
14 p1996 A83-32889
- Microstructure, deformation, and corrosion-fatigue behavior of a rapidly solidified Al-Li-Cu-Mn alloy
14 p1996 A83-32890
- The influence of microstructure on the corrosion of Al-Li, Al-Li-Mn, Al-Li-Mg and Al-Li-Cu alloys in 3.5 percent NaCl solution
14 p1997 A83-32892
- HVEM in situ deformation of Al-Li-X alloys --- High Voltage Electron Microscope
14 p1997 A83-32948
- Comparison of microstructure and mechanical properties of Al-Li-X alloys made by conventional and by powder-metallurgy procedures
15 p2136 A83-33959
- Lithium alloy-thionyl chloride cells - Performance and safety aspects
15 p2192 A83-34694
- Heat treatment, microstructure and mechanical property correlations in Al-Li-Cu and Al-Li-Mg PM alloys
17 p2489 A83-37850
- Development of Al-Li-X alloys using rapidly solidified powders
17 p2489 A83-37851
- Superlight alloys of magnesium-lithium-hydrogen
17 p2490 A83-38472
- The effect of structural transformations on the properties of the aluminum alloy VAD23
20 p2955 A83-43494
- LITHIUM ALUMINUM HYDRIDES**
Structure and spectra of H₂O in hydrated beta-alumina
09 p1227 A83-25212
- Hydration of lithium beta-alumina
09 p1227 A83-25213
- LITHIUM CHLORIDES**
Sources of pressure in lithium thionyl chloride batteries
02 p0202 A83-12054
- Qualification testing of large lithium-thionyl chloride batteries for US Air Force Minuteman extended survival power
11 p1539 A83-27191
- LITHIUM COMPOUNDS**
NT LITHIUM ALUMINUM HYDRIDES
NT LITHIUM CHLORIDES
NT LITHIUM FLUORIDES
NT LITHIUM HYDROXIDES
NT LITHIUM IODATES
NT LITHIUM NIOBATES
NT LITHIUM OXIDES
NT LITHIUM PERCHLORATES
NT LITHIUM SULFATES
- Conductivity of the mixed organic electrolyte containing propylene carbonate and 1,2-dimethoxyethane --- for lithium cells
07 p0880 A83-19889
- Lithium cycling behavior in 2-methyltetrahydrofuran with alcohol additives --- in lithium batteries
07 p0880 A83-19890
- The effect of the melt heat treatment time on the properties of lithium lubricants with additives
10 p1401 A83-26921
- The electrochemistry of molten lithium chlorate and its possible use with lithium in a battery
11 p1546 A83-28296
- Photogalvanic currents in reduced crystals of lithium tantalate
13 p1930 A83-31303
- Electrooptical Bragg modulator based on the Ag-diffused LiTaO₃ waveguide
15 p2232 A83-34888
- Determining the characteristics of Ag:LiTaO₃ diffused optical waveguides
22 p3360 A83-46788
- Study of a lithium-lithium propionate electrode in propylene carbonate
24 p3558 A83-49927
- LITHIUM FLUORIDES**
Spectral diversity crystalline fluoride lasers
11 p1581 A83-27588
- Pulsed gain and thermal lensing of Nd:LiYF₄
14 p2025 A83-33401
- Vacuum-ultraviolet refractive index of LiF and MgF₂ in the temperature range 80-300 K
21 p3203 A83-43875
- LITHIUM HYDRIDES**
NT LITHIUM ALUMINUM HYDRIDES
LITHIUM HYDROXIDES
Carbon dioxide absorption dynamics of lithium hydroxide
11 p1645 A83-28334
- Lithium hydroxide as a CO₂ scrubber in closed circuit breathing apparatus
11 p1645 A83-28335
- LITHIUM IODATES**
The aging of alpha-LiIO₃ single crystals under laser irradiation
01 p0055 A83-10819
- Continuous-wave garnet ring laser emitting single-mode linearly polarized radiation and intracavity second harmonic generation in LiIO₃
03 p0330 A83-13584
- Influence of aperture effects on the spectral structure of stimulated Raman scattering by optical phonons and

- polaritons in a resonator
07 p0992 A83-20119
- Tuning characteristics of multistage Stimulated Raman scattering by polaritons in a layer of an LiO₃ crystal
10 p1432 A83-26671
- Tunable infrared difference-frequency generation in lithium iodate
21 p3143 A83-44194

LITHIUM ISOTOPES

- The interstellar lithium abundance
24 p3667 A83-50061

LITHIUM NIOBATES

- Electro-optic-waveguide frequency translator in LiNbO₃ fabricated by proton exchange
02 p0235 A83-11566
- Electrical and acoustical crosstalk in integrated optical strip waveguide devices
02 p0168 A83-13044
- Optical damage resistance of lithium niobate waveguides
03 p0393 A83-13759
- Asymmetry of conductivity along the polarization axis in ferroelectric crystals
04 p0542 A83-15885
- Prototype of an integrated-optics four-digit analog-digital converter
05 p0685 A83-17062
- Bulk wave Bragg cells with 1 GHz bandwidth
06 p0753 A83-18935
- Frequency doubling in a LiNbO₃ thin film deposited on sapphire
07 p0993 A83-20730
- Semiconductor surface characterization using transverse acoustoelectric voltage versus voltage measurements
07 p0921 A83-20752
- Low-loss LiNbO₃ waveguide bends with coherent coupling
07 p0993 A83-20799
- Sputtering of Al₂O₃ and LiNbO₃ in the electronic stopping region
07 p0901 A83-21057
- Surface acoustic wave parametric oscillation in Si/LiNbO₃ substrate
08 p1081 A83-22622
- Selective and uniform laser-induced failure of antireflection-coated LiNbO₃ surfaces
10 p1429 A83-26030
- Rectangular Luneburg-type lenses for integrated optics
10 p1482 A83-26117
- hotodeposition of Ti and application to direct writing of Ti:LiNbO₃ waveguides
10 p1483 A83-26205
- Investigation of an electrooptic modulator formed from coupled channel diffused waveguides in LiNbO₃
10 p1483 A83-26656
- The effect of the anisotropy of thermophysical and elastic properties on the thermal stresses in profiled sapphire and lithium niobate single crystals
11 p1662 A83-28358
- The growth of lithium niobate ribbons using Stepanov's method
11 p1663 A83-28365
- Proton-exchanged optical waveguides in Y-cut lithium niobate
11 p1657 A83-28611
- Vacuum annealing effects in lithium niobate
12 p1782 A83-29170
- Optical second-harmonic generation in a thin-film waveguide without control of film thickness
12 p1731 A83-29190
- Blocking oscillation of optical bistable devices using dc drift phenomena of LiNbO₃ waveguide
13 p1922 A83-31059
- A single-block hexagonal electrooptical Q-switch
14 p0285 A83-33433
- Efficient SAW convolver with 30 microsec integration time
16 p2346 A83-36002
- Traveling-wave electrooptic modulator
17 p2580 A83-37750
- SAW convolvers using the transverse-horizontal bilinear field
17 p2500 A83-38877
- Comparison of guided-wave interferometric modulators fabricated on LiNbO₃ via Ti diffusion and proton exchange
18 p2744 A83-40050
- Electro-optic X-switch using single-mode Ti:LiNbO₃ channel waveguides
18 p2744 A83-40396
- Lithium niobate laser with frequency-degenerate pumping
20 p2993 A83-42290
- Integrated optical polariser on LiNbO₃:Ti channel waveguides using proton exchange
20 p3047 A83-42483
- Polarization characteristics of LiNbO₃ channel waveguide directional couplers
21 p3205 A83-44221
- Design and performance of an integrated optical digital correlator
21 p3205 A83-44225
- Picosecond signal sampling and multiplication by using integrated tandem light modulators
21 p3205 A83-44229
- Chirped grating lenses in Ti-indiffused LiNbO₃ optical waveguides
21 p3207 A83-44835
- Double ion exchanged chirp grating lens in lithium niobate waveguides
21 p3208 A83-45483
- Fabrication and performance of diffraction lenses
22 p3359 A83-46645
- Progress on electro-optic integrated optic devices
22 p3360 A83-46650
- Electro-optic branching-waveguide switch with low drive voltage
24 p3628 A83-48855
- Total-internal-reflection electrooptic thin-film modulator
24 p3628 A83-48859

LITHIUM OXIDES

- Fabrication of optical waveguides in LiNbO₃ and LiTaO₃

- crystals by ion irradiation
13 p1919 A83-30824

LITHIUM PERCHLORATES

- Physical-chemical transformations in mixtures of lithium perchlorate with finely dispersed metals under shock compression
24 p3557 A83-49788

LITHIUM SULFATES

- The use of a lithium sulfate pulse pressure transducer in a gasdynamic experiment
07 p0928 A83-19959

LITHIUM SULFUR BATTERIES

- Pelletized lithium-metal sulphide cells. I - A selective review
01 p0068 A83-10791
- Pelletized lithium-metal sulphide cells. II - Some operating characteristics of pelletized LiAl-FeS cells
01 p0068 A83-10792
- Investigation and production control of Li/SO₂ cells by the galvanostatic pulse method
01 p0068 A83-10796
- Characterization of ether electrolytes for rechargeable lithium cells
02 p0152 A83-12052
- Sources of pressure in lithium thionyl chloride batteries
02 p0202 A83-12054
- Spectroscopic studies of the hazards of Li/SOCl₂ batteries during anode-limited cell reversal
02 p0202 A83-12056
- Defects and disorder in the fast-ion electrode lithium-aluminum
02 p0154 A83-12057
- Status cells - A demonstration of performance reproducibility, capacity retention, and cycle life for LiAl/FeS cells
04 p0506 A83-15868
- Morphological studies on the Li-Al electrode in fused salt electrolytes --- in Li-Al/FeS cells
07 p0879 A83-19877
- Effective conductivities of a positive electrode in an Li-Al/FeS cell at different states of charge
07 p0952 A83-19878
- Self-discharge behavior of engineering-scale LiAl/FeS cells
07 p0952 A83-19879
- Electrochemical behavior of Li₂S in fused LiCl-KCl electrolytes --- in redox cells
07 p0879 A83-19886
- Construction of reference electrodes for long-term testing of compact Li-Al/FeS cells
07 p0953 A83-19900
- Reactions of FeS₂, CoS₂, and NiS₂ electrodes in molten LiCl-KCl electrolytes
07 p0881 A83-20578
- Lithium-metal sulfide cells and battery development progress at Eagle-Picher Industries
11 p1602 A83-27165
- Development of a tubular LiAl/FeS cell battery
11 p1603 A83-27166
- Relaxation-phenomena in LiAl/FeS-cells
11 p1603 A83-27167
- Flexible ceramic powder separators for molten salt electrolyte galvanic cells
11 p1603 A83-27168
- Comparison of Na/S and LiAl/FeS batteries
11 p1603 A83-27169
- Design considerations for a lithium-aluminum/iron sulfide electric vehicle battery
11 p1603 A83-27173
- Performance of a 10-cell LiAl/metal sulfide battery
11 p1603 A83-27174
- Abuse resistant high rate lithium/thionyl chloride cells
11 p1604 A83-27180
- Lithium-thionyl chloride battery safety
11 p1604 A83-27181
- Spectroscopic evidence for the formation of polysulfide species during charging of an Li-Al/S couple
11 p1546 A83-28298
- Elastomeric binders for electrodes --- in secondary lithium cells
14 p1998 A83-32638
- Rechargeable Li/Li(1+x)VSO₄ cells
14 p2047 A83-32645
- Lithium alloy-thionyl chloride cells - Performance and safety aspects
15 p2192 A83-34694
- Statistical analysis of lithium iron sulfide status cell cycle life and failure mode
20 p3013 A83-43419
- A possible mechanism for the reduction of voltage delay in the Li/SOCl₂ system via cyanoacrylate coatings on lithium
24 p3599 A83-49929
- Electrical conductivity of the Li₂SO₄-Li₂CO₃ system
24 p3558 A83-49930
- Raman spectroscopic studies of the structure of electrolytes used in the Li/SOCl₂ battery
24 p3558 A83-49936
- Electrochemistry of a nonaqueous lithium/sulfur cell
24 p3600 A83-49938
- Li/SOCl₂ cells for high temperature applications
24 p3600 A83-49940
- Characterization of the chemistry at the anode and cathode in the Li/SO₂ battery system
24 p3600 A83-49948
- Galvanostatic cycling of lithium-titanium disulphide cells in propylene carbonate and propylene carbonate-acetonitrile electrolytes
24 p3558 A83-49951
- High temperature batteries with a solid sulphate electrolyte
24 p3601 A83-49955

LITHIUM 4**U LITHIUM ISOTOPES****LITHIUM 6****U LITHIUM ISOTOPES**

LITHOGRAPHY

NT PHOTOLITHOGRAPHY
Ultraviolet and X-ray lithography 03 p0313 A83-13962
0.15 micron channel-length MOSFET's fabricated using e-beam lithography 05 p0624 A83-17297
Ralicon anodes fabricated by electron beam lithography for image photon counting detectors 11 p1553 A83-27754
Developing a technology base for advanced devices and circuits 17 p2496 A83-37057
GaAs microwave devices and circuits with submicron electron-beam defined features 17 p2496 A83-37059
Small-radii curved rib waveguides in GaAs/GaAlAs using electron-beam lithography 21 p3205 A83-44222

LITHOLOGY

Petrography and mineralogy of two basalts and olivine-pyroxene-spinel fragments in achondrite EETA79001 04 p0563 A83-15362
A simulation model supporting HCMM investigation on geological objectives --- heat capacity mapping mission 15 p2188 A83-35287
Effect of a Hadean terrestrial magma ocean on crust and mantle evolution 16 p2381 A83-36598
Cryolithogenesis --- Russian book 21 p3169 A83-43919
Lithologic mapping using solar infrared 22 p3309 A83-46129
Petrogenesis of the Elephant Moraine A79001 meteorite
Multiple magma pulses on the shergottite parent body 24 p3671 A83-48810

LITHOSPHERE

NT EARTH CORE
NT EARTH CRUST
NT EARTH MANTLE
NT EARTH SURFACE
Heavy element fission products on earth --- Russian book 02 p0204 A83-11923
Lithospheric flexure at fracture zones 02 p0212 A83-12870
Convective thinning of the lithosphere - A mechanism for the initiation of continental rifting 02 p0212 A83-12871
Mechanisms for lithospheric heat transport on Venus
Implications for tectonic style and volcanism 02 p0268 A83-13102
Constraints on the expansion of Ganymede and the thickness of the lithosphere 04 p0560 A83-15334
Astronomic geology - Its subject and general problems 04 p0502 A83-15400
Thick shell tectonics on one-plate planets - Applications to Mars 04 p0564 A83-15552
Evolution of the Tharsis province of Mars - The importance of heterogeneous lithospheric thickness and volcanic construction 04 p0565 A83-15555
The role of lithospheric stress in the support of the Tharsis rise 04 p0565 A83-15557
Vertical movements following a dip-slip earthquake 07 p0958 A83-20094
Critique of 'Elastic thickness of the Venus lithosphere estimated from topography and gravity' by A. Cazenave and K. Dominh 07 p1028 A83-20099
P/n/ velocity and cooling of the continental lithosphere --- upper mantle compression waves in North America 07 p0961 A83-20227
A discussion of world-wide measurements of tidal gravity with respect to oceanic interactions, lithosphere heterogeneities, earth's flattening and inertial forces 07 p0963 A83-20973
Thermal stresses in planetary elastic lithospheres 07 p1032 A83-21292
Thermal parameters of the oceanic lithosphere estimated from geoid height data 08 p1144 A83-22363
Continental lithospheric thickness and deglaciation induced true polar wander 09 p1305 A83-24337
Viscosity of the lithosphere of Enceladus 10 p1518 A83-25514
The driving mechanism of plate tectonics - Relation to age of the lithosphere at trenches 12 p1748 A83-28910
The global stress field in the lithosphere obtained from the satellite gravitational harmonics 12 p1752 A83-29222
The interior of Venus and Tectonic implications 17 p2166 A83-37411
Thick plate flexure --- for lithospheric models of Mars and earth 17 p2540 A83-38055
Global tectonics and metallogeny - Deep roots of some ore-controlling fracture zones: A possible relation to small-scale convective cells at the base of the lithosphere? 17 p2529 A83-38153
Electromagnetic induction studies --- of earth lithosphere and asthenosphere 17 p2543 A83-38311
On a new type of rotation-tectonic lines in the earth's lithosphere 18 p2715 A83-39533
Constraints on rift thermal processes from heat flow and uplift 19 p2867 A83-41857

Long-term thermo-mechanical properties of the continental lithosphere 20 p3017 A83-42333
Age dependence of oceanic intraplate seismicity and implications for lithospheric evolution 21 p3169 A83-43824
Uppermantle anisotropy and the oceanic lithosphere 22 p3333 A83-46878
Constraints on the structure of the Himalaya from an analysis of gravity anomalies and a flexural model of the lithosphere 23 p3482 A83-47811
Hot spot heat transfer - Its application to Venus and implications to Venus and earth 23 p3528 A83-47812

LITTORAL CURRENTS

U COASTAL CURRENTS

LIVER

The effect of a normoxic helium-oxygen gas mixture on the consumption of oxygen by the tissues of the liver and lungs in white rats 01 p0078 A83-10489
Heart and liver energetics in mountain voles of the genus *Microtus juldaschi-caruthersi* /mammalia/ 02 p0219 A83-11661
Dependence of the structural lability of the outer membrane of liver mitochondria on the age and sex of rats 03 p0375 A83-14358
The state of hepatic circulation under the combined effect of lead and electromagnetic fields 05 p0673 A83-17159
The condition of the metabolism of the brain and liver during the experimental application of a microwave field of nonthermal intensities 05 p0669 A83-17166
Histochemical changes in muscles and liver during physical loads and overheating /experimental investigation/ 05 p0669 A83-17174
The functional characteristics of the immune response stimulators circulating in the blood in a toxic affection of the liver 05 p0670 A83-17182
A P-31 NMR study of the metabolism of phosphorus-containing compounds in the livers of mice in conditions of stress 08 p1146 A83-23023
Biochemical changes in rat liver after 18.5 days of spaceflight (41566) 12 p1763 A83-29546
The role of the middle hypothalamus structures in the regulation of the glucose content in the blood and the glycogen content in the liver 13 p1895 A83-30304
The changes in the liver and muscles due to the effect of physical exercise during overheating in different water regimes 14 p2061 A83-31974
An investigation of DNA synthesis in the liver of irradiated and serotonin-treated rats following the removal of the cycloheximide block 14 p2061 A83-32053
The early changes in the activation of nucleoside diphosphatekinase in the brain and liver of rats following total-body gamma-irradiation at an absolutely lethal dose 14 p2062 A83-32062
The effect of pyridoxine, riboflavin, and glutamic acid on the activity of lysosomal hydrolases in the liver and blood serum of rats during traumatic stress 14 p2066 A83-33330
The circadian rhythm of liver phospholipids in normal golden hamsters and in those with opisthorchiasis 15 p2211 A83-34963
The turnover of mitochondrial proteins in the livers of rats of various ages 15 p2211 A83-34964
The hypertrophy of cells and hyperplasia of ultrastructures in spleen parenchyma of mice as a consequence of acute stress 16 p2395 A83-36833
Changes in the liver of white rats under the influence of low temperatures 17 p2556 A83-38198
Physiological mechanisms of the regulation of lipoprotein biosynthesis in the liver during physical loading and in various phases of the recovery period 18 p2733 A83-40563
The dependence of the topography of the hepatic veins on the external form of the liver, its sizes, and age 18 p2736 A83-40583
The effect of electrostimulation of the hypothalamus on the methylation of DNA from the livers of rats 19 p2876 A83-41844

LIXISCOPES
A small, battery-operated fluoroscopic system
Lixiscope with X-ray generator 16 p2355 A83-35761

LOAD DISTRIBUTION (FORCES)
Load distribution on deformed wings in supersonic flow 01 p0002 A83-10180
An analysis of an Euler-Bernoulli beam-column with arbitrary initial crookedness by transfer matrix methods 02 p0195 A83-12757
Development of analytical and experimental techniques for determining store airload distributions 02 p0132 A83-13077
Vortex theory for hovering rotors 03 p0278 A83-13144
A creep type strategy used for tracing the load path in elastoplastic post buckling analysis 04 p0494 A83-15009
Force distribution in a shell loaded tangentially along a circle 04 p0500 A83-16049
Dynamic coefficient of a two-layered thick beam with imperfect bonding 06 p0774 A83-18396

LOAD TESTS

Post-yield deflections of elastic-plastic beams under uniformly increasing loads 08 p1114 A83-21631
Elliptic plate with clamped edge 08 p1122 A83-22046
Plotting and investigating the loading curves of mechanical systems --- toroidal shells 09 p1279 A83-23867
A Saint-Venant principle for nonlinear elasticity 09 p1279 A83-24134
Linear analysis by the finite element method of the dynamics of axisymmetric structures subjected to arbitrary loads 10 p1442 A83-26819
The use of multiple coordinate systems to form stiffness matrices of thin-walled structures on the basis of hybrid computational schemes 12 p1735 A83-29283
On the determination of the load-carrying capacity of the glass-plastic propeller blade of an aircraft 12 p1703 A83-29294
The structure of trailing vortices generated by model rotor blades 12 p1696 A83-29404
Nondestructive airfield pavement testing using laser technology 14 p1978 A83-33364
[AIAA PAPER 83-1601] Linear isotropic elasticity with body forces 15 p2173 A83-33856
Subsonic steady motion of a uniform load over the surface of a thermoelastic half space 15 p2175 A83-34243
A thermoelastic contact problem concerning the bending of a band with allowance for its deformability in the thickness direction 19 p2859 A83-41572
The elastic solution of the dynamic elastic-plastic response of a circular plate 21 p3151 A83-44104
Nonlinear vibrations of a clamped rectangular plate with initial deflection and initial edge displacement. I - Theory 21 p3153 A83-44622
Concentrated body force loading of an elastically bridged penny shaped flaw in a unidirectional fibre reinforced composite 21 p3156 A83-44893
Probability distributions for the strength of composite materials. IV - Localized load-sharing with tapering 21 p3159 A83-44926
Stress analysis of stepped-lap joints with bondline flaws 23 p3471 A83-48214
Integral-equation solution for half planes bonded together or in contact and containing internal cracks or holes 23 p3473 A83-48495
On dynamics and stability of continuous systems subjected to a distributed moving load 23 p3473 A83-48496

LOAD FACTORS
U LOADS (FORCES)

LOAD TESTING MACHINES
Load insensitive electro-hydraulic servo system 06 p0769 A83-18924
Automated testing systems with hydraulic force excitation /review/ 08 p1074 A83-22632
A machine for the mechanical testing of polymers in a three-dimensional stressed state 16 p2364 A83-35513
The use of various ultrasonic systems for fatigue testing 16 p2367 A83-36183
High-temperature bending tests on powder metallurgy materials during exploratory studies 17 p2484 A83-38873
Precision bending apparatus for high temperature measurement 19 p2819 A83-41289
A loading device for the creation of mixed mode in fracture mechanics 21 p3158 A83-44919
Experimental study of the dynamic loading of metal disks 21 p3161 A83-45152
A semi-automated in-plane loader for materials testing ... of fiber reinforced composites 21 p3108 A83-45162

LOAD TESTS
Hollow section joints --- Thesis 02 p0190 A83-11945
Some observations on creep crack growth 02 p0190 A83-12043
One-dimensional isentropic compression measurements of multiply loaded polymethylmethacrylate 02 p0191 A83-12280
The load-carrying capacity of hollow composite rods in torsion 02 p0192 A83-12364
The lubrication of the roller-rib contacts of a radial cylindrical roller bearing carrying thrust load [ASLE PREPRINT 82-LC-3C-1] 03 p0334 A83-13238
New high-strength aluminum alloy V95och 03 p0296 A83-13251
A comparison of the geometry dependence of several nonlinear fracture toughness parameters 03 p0298 A83-13339
The effect of load ratio on fatigue crack growth in T8-A1-1Mo-1V 03 p0298 A83-13342
Compression fatigue behavior of composites in the presence of delaminations 03 p0293 A83-14562
Dynamic crack-tip stresses under stress wave loading

- A comparison of theory and experiment
03 p0343 A83-14820
- The effect of microstructure and environment on the crack growth behavior of Inconel 718 alloy at 650 C under fatigue, creep and combined loading
04 p0458 A83-14999
- A mode solution for the finite deflections of a circular plate loaded impulsively
04 p0500 A83-16199
- Decrease in closure and delay of fatigue crack growth in plane strain
04 p0501 A83-16258
- Some properties of foamed material-aluminum composites
05 p0611 A83-17108
- Stable and unstable crack growth in sintered and infiltrated P/M steels
06 p0730 A83-19084
- Composite drapability - A too often ignored impacting cost characteristic
07 p0875 A83-20438
- Fatigue crack front shape and its effect on fracture toughness measurements
07 p0886 A83-20519
- Comparison of impact testing on Charpy V-notch specimens and WOL-1X-specimens
08 p1058 A83-21672
- Criterion for crack instability under short pulse loads
08 p1116 A83-21674
- The relationship of compliance changes during fatigue loading to the fracture of composite materials
08 p1054 A83-21682
- Shear bands and fracture in crystalline polymers
08 p1069 A83-21697
- Stress biaxiality effects on slow crack growth in polymethylmethacrylate
08 p1069 A83-21723
- Creep fracture behavior of austenitic stainless steels from 550 to 800 C
08 p1062 A83-21746
- Residual stress effects on fracture toughness measurements
08 p1064 A83-21791
- Deflections of elastic-plastic hyperstatic beams under cyclic loading
08 p1120 A83-21810
- Dynamic stability boundaries for a sinusoidal shallow arch under pulse loads
08 p1122 A83-22148
- Study on composite flywheels for energy storage
08 p1131 A83-22701
- Mechanical behavior of thick filament-wound composites tested in transverse compression
09 p1221 A83-23606
- Evaluation of the P2 and PAA treatments --- sulfuric acid-ferric sulfate etching and phosphoric acid anodizing
09 p1238 A83-23627
- Dynamic impact tests of radiated and temperature conditioned elastomers
09 p1238 A83-23628
- Advanced methods for damage analysis in graphite-epoxy composites
09 p1222 A83-23648
- Equation of state for reinforced plastic materials subjected to mechanical and thermal loading with the account taken of damage and physical-chemical transformations
09 p1224 A83-23945
- Comparative evaluation of shear test methods for composites
09 p1224 A83-23948
- Fracture test methods
10 p1392 A83-25319
- Experimental study of the T-criterion in ductile fractures
11 p1596 A83-28445
- A recommended procedure for determining the strain rate sensitivity in superplasticity --- of metal alloys
12 p1714 A83-29721
- Stability of imperfect laminated cylinders - A comparison between theory and experiment
[AIAA 83-0874] 12 p1738 A83-29758
- Design, fabrication and test of graphite/polyimide composite joints and attachments
[AIAA 83-0907] 12 p1739 A83-29763
- On the dynamic response and collapse of slender guyed booms for space application
[AIAA 83-0821] 12 p1742 A83-29818
- Measuring and processing of undercargue loading spectra of the L-39 aircraft
13 p1805 A83-30513
- Engineering property comparisons of 7050-T73651, 7010-T7651 and 7010-T73651 aluminum alloy plate
14 p1992 A83-32340
- Modelling of fracture process zones and singularity dominated zones
14 p2029 A83-32341
- Fatigue crack closure after overload
14 p2031 A83-32660
- Fracture characterization of a random fiber composite material
14 p1988 A83-33296
- Canadian forces tracker aircraft full-scale fatigue test at the National Aeronautical Establishment
15 p2122 A83-33548
- The ductile fracture of metals - A microstructural viewpoint
15 p2138 A83-34131
- Numerical determination of the parameters of Krupkowski's function for a torsion test taking into consideration the strain hardening ranges
15 p2140 A83-35066
- Some experimental verification of predicted load-carrying capacities of contacting pairs
15 p2172 A83-35249
- The fracture of composites with allowance for the effects of temperature and humidity
16 p2323 A83-35508
- A tensile testing technique for fibre-reinforced composites at impact rates of strain
16 p2324 A83-35981
- Corrosion fatigue crack propagation
16 p2330 A83-36162
- Effects of high frequency loading on materials
16 p2331 A83-36181
- On life behavior under spectrum loading --- effects of cumulative damage in structures
16 p2368 A83-36503
- Crack closure studies under constant amplitude loading
16 p2333 A83-36508
- Micromechanisms of fatigue crack growth retardation following overloads
18 p2699 A83-39540
- Secondary loading of I-spar caps due to shear deformation of the web
18 p2700 A83-39991
- An experimental study of the thermal cycling of composite materials with disperse reinforcement
18 p2649 A83-40104
- Impact behaviour of quasi-isotropic CFRP laminate
18 p2656 A83-40220
- Long term strength of glass reinforced plastics
18 p2656 A83-40224
- A new method to determine the bending rigidities of anisotropic plates
18 p2662 A83-40293
- Photoelastic analysis of the behaviour of curved fibers in composite
18 p2662 A83-40300
- Creep crack growth behavior of several structural alloys --- superalloys
18 p2669 A83-40636
- Elastoplastic double-wall shells under complex nonisothermal loading
19 p2859 A83-41603
- The effect of grain size on fatigue growth of short cracks
20 p2954 A83-43346
- Determination of the initial loss of stability of shells by the shadow moiré method
20 p3008 A83-43623
- Appliance for fatigue tests of materials with symmetrical and asymmetrical loading
20 p2992 A83-43624
- Pin joints in composites
21 p3151 A83-44053
- Fracture toughness tests on an aluminum alloy using a chevron notch bend specimen
21 p3113 A83-44899
- A probabilistic treatment of brittle fracture under nonmonotonically increasing stresses
21 p3159 A83-44923
- Plane-stress fracture testing of finite sheets under biaxial loads
21 p3161 A83-45161
- A semi-automated in-plane loader for materials testing --- of fiber reinforced composites
21 p3108 A83-45162
- Characterization of the matrix glass transition in carbon-epoxy laminates using the CSD test geometry --- centro-symmetric deformation
22 p3262 A83-46282
- Contact stresses at ceramic interfaces
23 p3438 A83-48302
- Theory for saturation stress difference in torsion versus other types of deformation at low temperatures
23 p3473 A83-48601
- A simplified procedure for predicting the performance of inherently compensated aerostatic thrust bearings
24 p3590 A83-48823
- Characteristics of brittle fracture under general combined modes including those under bi-axial tensile loads
24 p3594 A83-49866
- Determination of anisotropy during the analysis of the long-term strength under conditions of plane stressed state
24 p3596 A83-49912
- LOADING FORCES**
U LOADS (FORCES)
- LOADING MOMENTS**
Vibration and radiation of a shell of revolution under circumferential loading
23 p3472 A83-48468
- LOADING RATE**
Susceptibility of a pseudo-alpha titanium alloy to cyclic damage in the frequency range from 33 Hz to 10 KHz
02 p0156 A83-12329
- DSO-series devices for fatigue testing under repeated impact and harmonic loading with various cycle ratios
02 p0191 A83-12342
- Fracture modes of inelastic materials as a function of loading rate and temperature, and associated fracture criteria
02 p0192 A83-12354
- Quantitative analysis of delayed fracture observed in stress rate tests on brittle materials
03 p0290 A83-13686
- A new method for optimal design of structures
06 p0773 A83-18229
- Experimental determination of high loading rate effects on fracture toughness of aluminum alloys
08 p1058 A83-21673
- A technique for measuring crack length and load in compact fracture mechanics specimens using strain gauges
08 p1118 A83-21763
- Estimation of the cyclic fatigue life of parts subjected to complex loading patterns --- for compressor disks and turbine wheels in aircraft engines
09 p1228 A83-23502
- A study of the effect of the cycle ratio on the fatigue of titanium alloys under high-frequency loading
09 p1228 A83-23503
- Nonuniform loading of shells by ponderomotive forces
09 p1277 A83-23505
- The initiation of fracture in fiber-composites at elevated loading rates
18 p2656 A83-40217
- Load-shedding techniques for fatigue-threshold determination
21 p3161 A83-45149
- LOADING WAVES**
U ELASTIC WAVES
U LOADS (FORCES)
- LOADS (FORCES)**
NT AERODYNAMIC LOADS
NT AXIAL COMPRESSION LOADS
NT AXIAL LOADS
NT BLAST LOADS
NT COMPRESSION LOADS
NT CRITICAL LOADING
NT CYCLIC LOADS
NT DYNAMIC LOADS
NT EDGE LOADING
NT GUST LOADS
NT IMPACT LOADS
NT LANDING LOADS
NT RANDOM LOADS
NT ROLLING CONTACT LOADS
NT SHOCK LOADS
NT STATIC LOADS
NT THRUST LOADS
NT TRANSIENT LOADS
NT VIBRATORY LOADS
NT WING LOADING
- The lubrication of roller bearing ribs - Hydrodynamic approach
01 p0056 A83-10225
- A study of the creep of thin-walled shells under nonstationary loading
01 p0059 A83-10681
- Analysis of simply supported multilayer trapeziform plates
01 p0059 A83-10685
- Key curve analysis of crack-growth-resistance curves
02 p0190 A83-12041
- Moving cracks in layered composites
02 p0190 A83-12048
- Rudder pedal force and seat relation for optimal efficiency with different leg geometry
02 p0225 A83-12255
- Recent advances in reduction methods for instability analysis of structures
02 p0193 A83-12738
- Cracked shells under skew-symmetric loading --- Reissner theory
03 p0338 A83-13125
- Test with graded physical load on bicycle-ergometer and treadmill in patients with chronic ischemic heart disease
03 p0381 A83-14346
- The effect of two sided surface roughness on ultra-thin gas films
06 p0769 A83-18390
- Crack separation energy rates for inclined cracks in an elastic-plastic material
06 p0774 A83-18479
- The exact form of caustics in mixed-mode fracture - A comparison with approximate solutions
07 p0948 A83-21342
- Regularities of similarity and fatigue damage accumulation under irregular loading
08 p1118 A83-21737
- The applicability of the theory of small elastoplastic deformations in the case of simple loading
09 p1280 A83-24237
- Crystal elasticity --- mechanical behavior under loading
10 p1392 A83-25311
- The interface crack behavior in dissimilar anisotropic composites under mixed-mode loading
[ASME PAPER 83-APM-7] 10 p1441 A83-26444
- The association between cancellous architecture and loading in bone - An optical data analytic view
11 p1636 A83-27786
- A contribution to the solution of axisymmetric thermoelastic notch problems using the boundary integral equation method --- German thesis
11 p1599 A83-28646
- Creation and checking of load transformation matrices for modally coupled systems using the acceleration method with recursive equations
12 p1742 A83-29815
- Thermoelasticity of ideal fibre-reinforced materials
16 p2324 A83-35775
- On life behavior under spectrum loading --- effects of cumulative damage in structures
16 p2368 A83-36503
- Method for the formation of design schemes for calculating load-bearing structures
17 p2518 A83-37254
- Application of a modified scheme of the method of characteristics to calculate the propagation of a plane loading-wave
18 p2698 A83-39503
- Effect of non-uniform pressure on the extension of an external crack
21 p3157 A83-44898
- Postbuckling behavior of inelastic inextensional rings under external pressure
[ASME PAPER 83-WA/APM-4] 23 p3468 A83-47593
- Effects of crack growth on the load-displacement characteristics of precracked specimens under bending
24 p3594 A83-49864
- Termination of processes of finite plastic deformations of incomplete toroidal shells
24 p3596 A83-50122
- LOCALIZATION**
U POSITION (LOCATION)

LOCATION			
U POSITION (LOCATION)			
LOGI			
Investigation of types of root loci of Fourth-order linear and linearized systems --- automatic pilot control system	11	p1647	A83-27448
LOCKHEED AIRCRAFT			
NT C-5 AIRCRAFT			
NT C-130 AIRCRAFT			
NT C-140 AIRCRAFT			
NT C-141 AIRCRAFT			
NT F-104 AIRCRAFT			
NT L-1011 AIRCRAFT			
NT P-3 AIRCRAFT			
NT U-2 AIRCRAFT			
Model and full-scale studies of the exhaust noise from a bypass engine in flight			
[AIAA PAPER 83-0751]	11	p1531	A83-28019
Airspeed calibrations on a stretch YC-141B aircraft	14	p1975	A83-32931
Certification of the Lockheed 1011-500 active control system	22	p3255	A83-45850
LOCKHEED C-5 AIRCRAFT			
U C-5 AIRCRAFT			
LOCKHEED U-2 AIRCRAFT			
U U-2 AIRCRAFT			
LOCKING			
NT LASER MODE LOCKING			
LOCOMOTION			
NT WALKING			
Age-related patterns of lateral movement preferences	05	p0673	A83-17156
Control of the constrained planar simple inverted pendulum	10	p1461	A83-25397
The role of suprachiasmatic nuclei of the anterior hypothalamus in the organization of the circadian rhythms of locomotor activity in rats	14	p2063	A83-32564
The use of a combined pressure and medication treatment for the rehabilitation and recovery of the functions of the locomotor system	14	p2070	A83-33307
The structure of the microtubule organizational centers in a comparative evolutionary aspect	14	p2065	A83-33318
Rhythms in the range of 4.5-12 Hz of the background EEG from the visual and sensorimotor cortex in rats under different patterns of locomotor activity	19	p2876	A83-41565
LOCOMOTIVES			
A systems analysis comparing conventional and hydrogen powered rail locomotives	11	p1667	A83-27213
Economic aspects of advanced coal-fired gas turbine locomotives			
[ASME PAPER 83-GT-241]	23	p3514	A83-48031
The coal-fired gas turbine locomotive - A new look			
[ASME PAPER 83-GT-242]	23	p3466	A83-48032
LOCUSTS			
Landsat monitoring of Desert Locust breeding grounds in Africa, the Near East and Southwest Asia	01	p0065	A83-10097
Identification and monitoring of Australian plague locust habitats from Landsat	14	p2035	A83-32610
LOG PERIODIC ANTENNAS			
Analysis of the loop-coupled log-periodic dipole array	10	p1405	A83-26831
A network formulation for phased arrays - Application to log-periodic arrays of monopoles on curved surfaces	15	p2121	A83-35090
Natural oscillations in a log-periodic chain of oscillators	18	p2676	A83-39526
A frequency-independent parabolic log-periodic phased-array antenna	22	p3272	A83-45686
Design of the log-periodic feed of a reflector antenna	24	p3570	A83-49269
LOG SPIRAL ANTENNAS			
Low frequency performance of hemispherical coverage conical log-spiral antennas	06	p0722	A83-18654
Experimental investigation on a method of lowering the silhouette of conical log-spiral antenna	10	p1406	A83-26843
Radiation characteristics of a plane logarithmic spiral on a magnetized-plasma layer	13	p1828	A83-30284
Determination of the effect of losses in the dielectric substrate on the radiation of a plane logarithmic spiral with a screen	13	p1828	A83-30715
Multimode planar spiral for DF applications	15	p2121	A83-35089
LOGARITHMS			
Orbital eccentricity in a logarithmic potential	02	p0249	A83-12924
Statistics of the logarithmic flare index	06	p0856	A83-19171
A one-dimensional logarithmic criterion for the evaluation of multiparametric systems	06	p0803	A83-19176
Fast realisation of 2-D digital filters using logarithmic number systems	16	p2404	A83-36012
A new binary logarithm-based computing system			

LOGIC CIRCUITS			
NT THRESHOLD GATES			
Gigabit logic - A review	01	p0035	A83-10293
A test pattern generation technique for detection of digital circuits	01	p0038	A83-10773
Application of static Automatic Test Program Generators /ATPG/ to dynamic circuitry	01	p0038	A83-10775
Demonstration of a figure of merit for inherent testability	01	p0050	A83-10790
Logic delays of 5-micron resistor coupled Josephson logic	01	p0039	A83-10996
An automatic test generation system for complex digital logic	01	p0042	A83-11230
Fast LSI based on current switches --- Russian book	02	p0168	A83-12374
Integrated optical logic devices	03	p0392	A83-13756
Current-waveform dependence of punchthrough probability in a Josephson tunnel junction	04	p0473	A83-16072
From state machines to temporal logic - Specification methods for protocol standards --- of computer communication networks	05	p0621	A83-17270
Geometrical considerations in the transient ionization testing of digital logic circuits	05	p0628	A83-17528
Dependence of normally-off GaAs JFET performance on device structure	05	p0631	A83-17756
Addressing and control of high-speed logic circuits with picosecond light pulses	07	p0921	A83-20793
Circuit analysis, logic simulation, and design verification for VLSI	07	p0923	A83-21539
Fast low-power driver and Schmitt trigger using GaAs MESFET and tunnel diode	10	p1411	A83-26886
A new design method for m-out-of-n TSC checkers --- Totally Self-Checking for codes	13	p1908	A83-30791
Gigabit logic bipolar technology advanced super self-aligned process technology	13	p1837	A83-31761
The effects of nuclear radiation on integrated circuits	14	p2005	A83-32416
Optical logic array processor using shadowgrams	15	p2230	A83-33808
All-refractory Josephson logic circuits	15	p2150	A83-33888
On testing stuck-open faults in CMOS combinational circuits	15	p2153	A83-35141
A deductive method for the simulation of faults in Programmable Logic Arrays	15	p2218	A83-35142
NORA - A racefree dynamic CMOS technique for pipelined logic structures	19	p2887	A83-40790
Reduction method for verifying the correctness of parallel algorithms of logic control	19	p2893	A83-42021
Integrated optical logic devices	22	p3359	A83-46649
LOGIC DESIGN			
VLSI system design --- Book	01	p0038	A83-10881
Systolic cellular logic - Inexpensive parallel image processors	01	p0089	A83-11438
Design guidelines for the testability of microprocessor based logic designs	02	p0227	A83-11906
Evaluation of alternative alphanumeric keying logics	02	p0225	A83-12087
PICCOLO logic for a picture database computer and its implementation	02	p0228	A83-12248
CAD system for VLSI in Japan	07	p0924	A83-21543
Basic conceptions of the external software system for programmable logic controllers	09	p1325	A83-24244
Facilities of the formal description of the semantics of input languages for the automated logic design of digital systems	09	p1325	A83-24245
Design and implementation of the Delft Image Processor DIP-1 --- Thesis	11	p1575	A83-28641
Comments on 'Silicon MESFET digital circuit techniques'	15	p2151	A83-33895
Fail safe logic design	16	p2345	A83-35555
On the theory of program synthesis	19	p2888	A83-41992
A new method of VLSI conform design for MOS cells	20	p2967	A83-43026
Infinite-valued logic in problems of cybernetics --- Russian book	21	p3192	A83-43910
A new binary logarithm-based computing system	24	p3619	A83-48999
LOGIC NETWORKS			
U LOGIC CIRCUITS			
LOGICAL ELEMENTS			
Integrated optical logic devices	03	p0392	A83-13756
Realization of an InSb bistable device as an optical AND gate and its use to measure carrier recombination times	06	p0810	A83-19252
General principles for the reliability analysis of systems of logical redundancy in multivalued structures	08	p1113	A83-22121
Sub-10 ps high-gain direct coupled Josephson logic			

gate	13	p1837	A83-31764
A probability of logical-dynamical systems with random structural changes	14	p2075	A83-32573
Switching characteristics of logic gates addressed by picosecond light pulses	14	p2008	A83-33422
Converters of the levels of logical elements --- Russian book	15	p2152	A83-34174
Human thinking and the computer processing of information	16	p2402	A83-36825
Principles for the adaptation of logical integrating computing structures for the implementation of fuzzy algorithm	16	p2403	A83-36902
High-speed logic at 300 K with self-aligned submicrometer-gate GaAs MESFET's	19	p2837	A83-41019
Bi-linear logico-dynamic model for a controlled process	20	p3039	A83-42917
Integrated optical logic devices	22	p3359	A83-46649
LOGISTICS			
NT SPACE LOGISTICS			
United States Air Force tactical reconnaissance - An analysis and commentary	08	p1041	A83-22574
Instability and irregular behavior of coupled logistic equations	22	p3354	A83-45934
Depot level repairability, maintainability, and supportability of advanced composites	23	p3404	A83-48360
[AIAA PAPER 83-2516]			
LOGISTICS MANAGEMENT			
Integrated CNI avionics logistics considerations	01	p0103	A83-11157
Designing for supportability and cost effectiveness	24	p3543	A83-49586
[AIAA PAPER 83-2499]			
LOMONOSOV CURRENT			
Synoptic oscillations of the currents in the FGGE Atlantic equatorial test-region	09	p1320	A83-24941
LONG DURATION EXPOSURE FACILITY			
Fiber optic experiment for the Shuttle long-duration exposure facility	08	p1166	A83-22491
LDEF - Chemical and isotopic measurements of micrometeoroids by SIMS --- Secondary Ion Mass Spectroscopy from Long Duration Exposure Facility	15	p2129	A83-35031
Improvement of a large analytical model using test data	19	p2856	A83-40870
LONG DURATION SPACE FLIGHT			
Mission to Mars: Plans and concepts for the first manned landing --- Book	03	p0434	A83-14048
Problems of psychophylaxis in prolonged manned space flights	08	p1151	A83-22989
Human capabilities: Long residence - An uncharted field	09	p1325	A83-24359
The interstellar solar sail - Optimization and further analyses	12	p1708	A83-29452
Comets and interstellar travel	12	p1784	A83-29453
The 211-day mission on Salyut-7 is completed	13	p1808	A83-30322
Life sciences experiments for a space platform/station	13	p1898	A83-30932
[SAE PAPER 820834]			
Application of the turbo-refrigerator to long-term cryogenic storage	13	p1812	A83-30935
[SAE PAPER 820841]			
An integrated regenerative air revitalization system for spacecraft	13	p1907	A83-30937
[SAE PAPER 820846]			
SOYCHMBR-1 - A model designed for the study of plant growth in a closed chamber	13	p1899	A83-30941
[SAE PAPER 820853]			
Late skin damage in rabbits and monkeys after exposure to particulate radiations	19	p2873	A83-40849
Planning for long term control of Space Station	21	p3096	A83-44175
[AAS PAPER 83-062]			
Mass-, time-, and energy - Characteristics of the interstellar flights during the long proper time of astronauts	23	p3415	A83-47328
[IAF PAPER 83-284]			
Generation of trajectories by multiple planetary swingbys	23	p3417	A83-47342
[IAF PAPER 83-326]			
LONG RANGE WEATHER FORECASTING			
Provision of ice information to icebreaker-transport vessels in the Arctic	01	p0077	A83-10827
A comparison of long-range predictions from Hough and statistical interpolation analyses	03	p0365	A83-14408
Predictability of quasi-geostrophic planetary waves in global and hemispheric domains	03	p0366	A83-14417
Seasonal climatic sources of heat in the North Atlantic	03	p0373	A83-14833
Fine mesh models in the U.K. Meteorological Office	04	p0519	A83-16157
El Chichon climate effect estimated	06	p0786	A83-18815
Fuzzy differential equations and their possible use in meteorology	09	p1316	A83-25145
The improvement of atmospheric predictability by using			

- a history 16 p2385 A83-35475
 Fitting a linear autoregressive model for long-range forecasting 16 p2388 A83-36030
 Three-dimensional teleconnections in the zonally asymmetric height field during the Northern Hemisphere winter 16 p2390 A83-36490
 The problem of the predictability of the atmosphere and certain questions relating to the hydrodynamic theory of long-term weather prediction 19 p2867 A83-41580

LONG TERM EFFECTS

- Long-term variation of Be stars on the color-magnitude diagram 01 p0120 A83-10308
 Causal relationship between pulsar long-term intensity variations and the interstellar medium 01 p0126 A83-10948
 Long term storage of cryogens in space 01 p0029 A83-11487
 The 11-year variation of the western drift of the magnetic center of the earth 02 p0211 A83-12455
 The effects of humidity on fatigue due to shear stress in unidirectional composites - Attempts at interpretation and a summing up [ONERA, TP NO. 1982-98] 03 p0292 A83-14546
 The role of catechol-o-methyltransferase in catecholamine transformations in the hypothalamus of rats at long-term intervals after irradiation 03 p0377 A83-14886
 Long-period atmospheric waves excited by a periodic source 04 p0515 A83-15055
 The long-term consequences of combined radiation damage 05 p0675 A83-17696
 Quasi-biennial cyclicity as a parametric phenomenon in the climatic system 06 p0788 A83-17994
 An empirical investigation of climate sensitivity 06 p0788 A83-17995
 Surface marking variations of selected areas on Mars 06 p0848 A83-18546
 Climatic fluctuations due to deep ocean circulation 07 p0969 A83-20299
 Large-scale changes in North Pacific and North American weather patterns in recent decades 08 p1139 A83-22289
 A comparative analysis of certain characteristics of the long-term softening of heat-resistant and refractory metals 09 p1228 A83-23504
 Causes and effects of increasing aridity in Northwest Bangladesh 09 p1291 A83-24628
 Effect of long-term exposure at elevated temperatures on the structure and properties of a Nimonic PE 16 superalloy 10 p1393 A83-25419
 Life estimation of an S-Glass/epoxy composite under sustained tensile loading 12 p1711 A83-29894
 Multiyear characteristics of the circulation in the lower thermosphere over parts of Central Asia 13 p1873 A83-30032
 The contribution of volcanoes to the global atmospheric sulfur budget 13 p1877 A83-30886
 Evolution of the orbits of the Andromedids meteoroid shower 13 p1940 A83-31313
 Measurement of changes in Sahelian surface cover using Landsat albedo images 15 p2181 A83-33555
 The characteristics of thermoregulation and blood circulation during prolonged exposure to low temperature 16 p2398 A83-35912
 Solar, geomagnetic and long term effects on thermospheric neutral kinetic temperatures at midlatitude 16 p2378 A83-36121
 The effect of ship noise on sailors during prolonged sea voyages 17 p2560 A83-38192
 Solar cycle and long term changes in the solar wind 17 p2627 A83-38287
 Instrumental effects on the sunshine record 18 p2727 A83-39888
 The geologic record of climatic change 18 p2730 A83-40327
 The effect of long-acting nitrates on hemodynamic indicators in patients with acute myocardial infarcts 18 p2736 A83-40580
 Fluid and electrolyte homeostasis during prolonged exercise at altitude 20 p3034 A83-43481
 Handgrip and general muscular strength and endurance during prolonged bedrest with isometric and isotonic leg exercise training 21 p3186 A83-43990
 The long-term strength of metals in a complex stressed state 21 p3114 A83-45318
 On the temporal increase of tropospheric CH₄ 24 p3607 A83-49333
- LONG WAVE RADIATION**
 Observations of the Coma Cluster of galaxies /A 1656/ at frequency 102.5 MHz 06 p0838 A83-19218
 The method of multiply reflected waves in the problem of the propagation of electromagnetic waves in regular waveguides /Review/ 09 p1250 A83-25076
 An examination of a technique for estimating the longwave radiation budget from satellite radiance observations 12 p1760 A83-29680
 Method for determining the electrical properties of the underlying surface on inhomogeneous paths from measurements of the fields of VLF radio stations 14 p2050 A83-31882

The response of a spectral general circulation model to refinements in radiative processes 16 p2384 A83-35462

- Propagation of VLF radio waves at high latitudes --- Russian book 18 p2720 A83-40603
 A method to measure the daytime long wave radiation 20 p3028 A83-43466
 Long-wave acoustic flowmeter 24 p3586 A83-49925

LONG WAVES (METEOROLOGY)**U PLANETARY WAVES****LONGITUDE**

- Regional variations of equatorial electrojet parameters 08 p1134 A83-22308
 Preferred longitudes of sunspot groups and high-speed solar wind streams - Evidence for a 'solar memory' 23 p3535 A83-47704

LONGITUDINAL CONTROL

- Experiment control in problems of minimax estimation --- for aircraft longitudinal control 01 p0094 A83-10455
 Intelligence allocation and digital control for automated guideway transit systems 01 p0112 A83-11036
 Piloting techniques on the backside --- of drag curve 05 p0598 A83-16927
 Nonlinear observers for evaluating the state variables of the longitudinal motion of an aircraft --- German thesis 06 p0719 A83-19622
 Investigation of the longitudinal motion of a flight vehicle by the method of the separation of motions 07 p0867 A83-20144
 Application of vector performance optimization to a robust control loop design for a fighter aircraft 07 p0867 A83-21160
 A unifying framework for longitudinal flying qualities criteria 09 p1209 A83-24429
 The definition of short-period flying qualities characteristics via equivalent systems 14 p1977 A83-32578
 Longitudinal control and a new spacing policy for automated transit vehicles 17 p2586 A83-37101
 Pilot modeling and closed-loop analysis of flexible aircraft in the pitch tracking task [AIAA PAPER 83-2231] 19 p2803 A83-41709
 MIMO controller design for longitudinal decoupled aircraft motion --- Multi-Input/Multi-Output [AIAA PAPER 83-2274] 19 p2804 A83-41740
 New flying qualities criteria for relaxed static longitudinal stability [AIAA PAPER 83-2104] 19 p2806 A83-41933
 Aerodynamics propulsion and longitudinal control requirements for a tilt-nacelle V/STOL with control vanes submerged in the nacelle slipstream [AIAA PAPER 83-2513] 23 p3404 A83-48357
- LONGITUDINAL STABILITY**
 Effects of control saturation on the command response of statically unstable aircraft [AIAA PAPER 83-0065] 05 p0598 A83-16497
 Trimming high lift for STOL fighters [AIAA PAPER 83-0168] 05 p0598 A83-16566
 Effects of large oscillation amplitude on axisymmetric vehicle longitudinal static and dynamic stability in hypersonic flow [AIAA PAPER 83-0215] 05 p0581 A83-16587
 Investigation of the longitudinal motion of a flight vehicle by the method of the separation of motions 07 p0867 A83-20144
 Study on longitudinal dynamic characteristics of pilot-airplane system - Approach to the method for studying PIO problem --- Pilot-Induced Oscillation 10 p1379 A83-26762
 Use of flight test results to improve the flying qualities simulation of the B-52H weapon system trainer [AIAA PAPER 83-1091] 16 p2300 A83-36215
 Suggested changes in large aircraft flying qualities criteria [AIAA PAPER 83-2071] 19 p2805 A83-41908
- LONGITUDINAL WAVES**
NT PLANE WAVES
 Periodic travelling waves in a non-integrable one-dimensional lattice 03 p0389 A83-13415
 Nonlinear interaction of longitudinal-transverse acoustic waves in a circular cylinder 04 p0532 A83-15076
 A resonance method for measurement of longitudinal and transverse ultrasonic wave velocities and their attenuations 04 p0492 A83-15217
 Longitudinal vortices imbedded in turbulent boundary layers [AIAA PAPER 83-0378] 05 p0635 A83-16682
 On the longitudinal vibrations of tapered bars 08 p1115 A83-21636
 Experimental study on cut-off phenomenon for layered composite 09 p1276 A83-23330
 Local admittance measurement in forced longitudinal wave motors --- propellant combustion in solid rocket engines [AIAA PAPER 83-0579] 09 p1220 A83-24150

The excitation of longitudinal waves in an inhomogeneous plasma by two pumping waves 09 p1349 A83-25173

- The focusing of longitudinal waves during the diffraction of plane electromagnetic waves by a plasma cylinder and sphere 09 p1349 A83-25174
 A study of the propagation modes and velocities of axisymmetrical waves in an orthotropic hollow cylinder 11 p1596 A83-28453
 Fluctuations of the parameters of the longitudinal waves of an electric field in a turbulent-plasma flow 12 p1780 A83-29259
 The effect of longitudinal waves on the input conductance of a ring aperture antenna 12 p1780 A83-29261
 An experimental investigation of pass bands and stop bands in two periodic particulate composites 18 p2649 A83-39556
 Generation of single longitudinal mode pulses in passively Q-switched lasers via passive pre-lasing 24 p3589 A83-49614

LONGSHORE CURRENTS**U COASTAL CURRENTS****LOOK ANGLES (TRACKING)**

Maximum-likelihood receiver for low-angle tracking radar. II - The nonsymmetric case 02 p0163 A83-11554

LOOP ANTENNAS

- A generalized 'polarity-type' Costas loop for tracking MPSK signals 03 p0312 A83-13859
 Analysis of VOR antenna radiation patterns 06 p0735 A83-18348
 The crow's-nest antenna - A spatial array in theory and experiment 06 p0737 A83-18606
 High gain and broad band Yagi-Uda array antenna composed of twin-delta loops 06 p0743 A83-18680
 The loop antenna with a cylindrical core - Theory and experiment 10 p1405 A83-26826
 Radiation from an Alford loop antenna in two-component warm plasma --- on Ariel-3 satellite 17 p2495 A83-38543
 Loop antennas for directive transmission into a material half space 22 p3274 A83-46527

LORAN**NT LORAN C****LORAN C**

- Timing a LORAN-C chain 02 p0133 A83-12225
 Use of aerial photography with Loran C positioning to map offshore surface currents 03 p0372 A83-14093
 Loran-C RNAV - The best near-term solution to air operations in northeastern North America 06 p0716 A83-18822
 Hard limiter performance as a polarity detector for extremely polluted signals --- in Loran C navigation systems 06 p0716 A83-19026
 Uncertainties regarding the transmission of time and frequency 09 p1336 A83-23401
 Flight test evaluation of Loran-C in Alaska 22 p3252 A83-46955
 Improved system reliability through master independent operation --- for Loran C 22 p3252 A83-46956

LORENTZ CONTRACTION

- Influence of Lorentz broadening on the stability of monomode ring lasers 15 p2169 A83-34370
 The standard of length in the theory of relativity and Ehrenfest paradox 15 p2225 A83-34413
 Lorentz factor of particles emitting in pulsars 17 p2608 A83-38403

LORENTZ FORCE

- The effect of displacing the center of a protective sphere on the oscillations of a body acted upon by Lorentz forces under conditions of resonance --- stability of rotating electrostatically protected satellite under resonant vibration 04 p0452 A83-15772
 Nonlinear resonances in the problem of the motion of a body near the center of mass when acted upon by Lorentz forces 09 p1212 A83-24486
 Lorentz forces on the dust in Jupiter's ring 17 p2619 A83-37586
 Theory and applications of electromagnetic levitation 20 p2962 A83-43259
 Registration of transition X-radiation at gamma - 1000-10,000 by the photon-counting method 20 p2991 A83-43535

LORENTZ GAS

- Self-consistent kinetic theory for the Lorentz gas 22 p3366 A83-45938

LORENTZ TRANSFORMATIONS

- Nonlinear systems that are gyrostat superpositions 02 p0232 A83-11953
 Dipole-field sums and Lorentz factors for orthorhombic lattices, and implications for polarizable molecules 05 p0690 A83-17226
 Conformal hyperbolicity of Lorentzian warped products 06 p0841 A83-19445
 An introduction to tensor calculus, relativity and cosmology /3rd edition/ --- Book 07 p0988 A83-19675
 Some applications of transformation to the processes of strong radiation in plasmas 15 p2235 A83-34493

On a nonlinear and Lorentz-invariant version of
Newtonian gravitation 18 p2741 A83-39197

LOSSES
Generation of a train of laser pulses by partially switching
off the resonator losses 05 p0650 A83-17071
Coherence loss and delay observation error in
very-long-baseline interferometry 22 p3376 A83-46919

LOSSLESS EQUIPMENT
An ideal six-port network consisting of a matched
reciprocal lossless five-port and a perfect directional
coupler 13 p1831 A83-30231
Parameters of lossless transmission lines with spherical
T-waves 14 p2003 A83-32107
Magnetostatic waves with complex wavenumbers in a
lossless ferrite film 15 p2153 A83-35163

LOSSLESS MATERIALS
Radiation patterns of interfacial dipole antennas
02 p0165 A83-12631
Gyrotropic waveguides --- Book 05 p0625 A83-17373
On the existence of branch points in the eigenvalues
of the electric field integral equation operator in the
complex frequency plane 09 p1253 A83-23787
High frequency scattering by a thin lossless dielectric
slab 09 p1247 A83-23790
Optical constants of some commercial microwave
materials between 90 and 1200 GHz 20 p3047 A83-42365

LOSSY MEDIA
Radiation from a charge moving in a lossy waveguide
01 p0036 A83-10419
Practical problems in the time-domain probing of lossy
dielectric media 01 p0034 A83-11372
Plane wave scattering by a thick lossy dielectric
half-plane 06 p0805 A83-18714
Absorption and lateral shift of beams incident upon lossy
multilayered media 08 p1161 A83-22670
Scattering and absorption characteristics of lossy
dielectric objects exposed to the near fields of aperture
sources --- of electromagnetic radiation 09 p1324 A83-23791
Finite-element solution of three-dimensional
electromagnetic problems 11 p1560 A83-27893
Wave resistance and energy losses in a cylindrical
slotted line 14 p2003 A83-32106
Numerical calculations of low-frequency TE fields in
arbitrarily shaped inhomogeneous lossy dielectric
cylinders 16 p2407 A83-35407
An iterative extended boundary condition method for
solving the absorption characteristics of lossy dielectric
objects of large aspect ratios --- under exposure to incident
plane wave radiation 21 p3189 A83-43833
The reflection and transmission of electromagnetic
waves from the lossy plasma moving parallel to the
interface 21 p3213 A83-44527
Wide-band chain-type divider-summatoms based on
quarter-wave lossy couplers 22 p3277 A83-45679

LOST WAX PROCESS
U INVESTMENT CASTING

LOUDNESS
The functional asymmetry of the brain and the direct
subjective evaluation of loudness 01 p0085 A83-10503
Differential loudness sensitivity, the strength of the
nervous system, and the psychophysiological scale of
loudness 16 p2399 A83-36821

LOVE WAVES
Love waves in orthotropic periodically layered
composites 06 p0725 A83-18510
Coupling of Love waves with the bulk elastic waves in
the substrate --- for microwave applications 16 p2344 A83-35433
On the applicability of the Kirchhoff-Love hypothesis to
the elastoplastic calculation of nonuniformly heated
shells 18 p2698 A83-39507
Love surface waves in regularly layered isotropic
composites 18 p2701 A83-40113
SH waves in composite media under initial stresses
24 p3597 A83-50134

LOW ALLOY STEELS
U HIGH STRENGTH STEELS

LOW ALTITUDE
Configuration design of a closed-loop,
pseudogravitational, environmental research facility in low
earth orbit [AIAA PAPER 83-0651] 05 p0607 A83-16817
Particle and wave observations of low-altitude
ionospheric ion acceleration events 06 p0784 A83-18303
Scattering of radiation by particles in low-altitude
plumes 09 p1220 A83-24893
Radar propagation at low altitudes --- Book 09 p1250 A83-24897
An onboard navigator for the extremely low-altitude
satellite utilizing accelerometers 13 p1812 A83-30167
Evidence for a low-altitude origin of lightning on Venus

Very low altitude remote sensing of the water quality
of rivers 16 p2370 A83-36574

LOW ASPECT RATIO
Experiments on natural convection heat transfer in low
aspect ratio enclosures 07 p0924 A83-19822

LOW ASPECT RATIO WINGS
NT DELTA WINGS
NT TRAPEZOIDAL WINGS
Approximate calculation of the aerodynamic
characteristics of a cylindrical body of small aspect ratio
in an incompressible flow 12 p1696 A83-29287
Concerning a type of separated flow on a rectangular
wing of small aspect ratio 17 p2447 A83-37260
The effect of the blunting of the leading edges on the
characteristics of separated flow past delta wings of low
aspect ratio 17 p2449 A83-37551
Parametric investigation of the strength and mass of
low-aspect-ratio wings by the plate-analogy method 17 p2521 A83-37569
Subsonic compressible-gas separated flow past a
low-aspect-ratio wing 17 p2450 A83-37626
Algorithmic mass-factoring of finite element model
analyses [SAWE PAPER 1451] 20 p3009 A83-43733

LOW CARBON STEELS
Mode II fatigue crack growth in aluminum alloys and
mild steel 08 p1063 A83-21759
An experimental investigation of the internal methane
pressure in hydrogen attack 14 p1994 A83-32682
Tool wear during taper turning 15 p2172 A83-35241
The effect of titanium on creep strength in 2.25 pct Cr-1
pct Mo steels 18 p2669 A83-40634
Use of S/N-sensors for measuring the fatigue damage
of materials 20 p2992 A83-43563
The use of the internal friction method for studying
laser-irradiated materials 21 p3115 A83-45502

LOW COST
Unaided tactical guidance flight test results 01 p0005 A83-11140
Trends in radar signal processing 02 p0163 A83-11917
The next generation - The Stencil S45 ejection seat
development program 04 p0446 A83-15440
The 'Flying Peanut' - Revolutionary design promises high
performance 04 p0447 A83-16400
Low cost planetary science missions [AIAA PAPER 83-0518] 05 p0600 A83-16763
Low-cost, focused-science Mars mission [AIAA PAPER 83-0519] 05 p0600 A83-16764
Low cost fabrication of sheet structure using a new beta
titanium alloy, Ti-15V-3Cr-3Al-3Sn 07 p0886 A83-20469
Hardware systems design of an airborne video
bandwidth compressor 08 p1099 A83-22585
Fabrication of thin glass mirrors on alnico magnets 08 p1112 A83-22866
Low cost cold plate approach for large space
platforms [SAE PAPER 820843] 10 p1383 A83-25755
Flight testing the Low Cost Inertial Guidance System 12 p1700 A83-29210
Thermal control testing for low cost programs 13 p1861 A83-31188
Low-cost digital random vibration control (DRV)C
technology demonstration 13 p1862 A83-31488
Low cost random vibration testing 13 p1863 A83-31489
Low cost modular designs for photovoltaic array fields 14 p2039 A83-32208
A detailed package of digital codes specially developed
for the array design 14 p2074 A83-32210
Low-cost solar array progress and plans 14 p2040 A83-32225
Advanced photovoltaic devices 14 p2042 A83-32259
Low cost processes for cast silicon solar cells 14 p2045 A83-32313
Polycrystalline silicon solar cells utilizing an integral
screen printing technique 14 p2045 A83-32314
Solar grade floating-zone silicon 14 p2045 A83-32316
Fast silicon-sheet growth with the supported-web
method 14 p2091 A83-32321
Recent developments in multi-wire fixed abrasive slicing
technique (FAST) --- for low cost silicon wafer production
from ingots 14 p2027 A83-32322
Use of tin oxide as an inexpensive antireflection coating
for p on n polycrystalline silicon solar cells 15 p2189 A83-33918
The growth and characterization of epitaxial solar cells
on resolidified metallurgical-grade silicon 16 p2420 A83-35986
The application of low-cost demonstrators for
advanced fighter technology evaluation [AIAA PAPER 83-1052] 16 p2300 A83-36462
Low cost antenna pointing system --- with computerized
control for transmission from aircraft to satellite 20 p3038 A83-42575
A family of small low cost gas turbines for unmanned

LOW GRAVITY MANUFACTURING
vehicle systems 20 p2936 A83-42616
Development of low cost RPVs under Indian
conditions 20 p2934 A83-43701
Low cost expendable turbojet engines 20 p2937 A83-43711
Low cost and high performance antireflective (AR)
coatings for solar cells 22 p3319 A83-46586

LOW DENSITY GASES
U RAREFIED GASES

LOW DENSITY MATERIALS
Some properties of foamed material-aluminum
composites 05 p0611 A83-17108
Properties and application benefits of low density
aluminum alloys [AIAA 83-0981] 12 p1715 A83-29788

LOW DENSITY WIND TUNNELS
A study of hypersonic low-density gas flows in
low-pressure blowdown wind tunnels using pressure
tanks 13 p1804 A83-30680

LOW FREQUENCIES
NT VERY LOW FREQUENCIES
Inverse scattering for an exterior Dirichlet problem ---
due to metallic cylinder 01 p0104 A83-10494
Crosspolarisation in scattering at low frequencies 02 p0163 A83-11553
An examination of background noise in analog integrated
circuits and components --- French thesis 02 p0166 A83-11765
The pathological and anatomical characteristics of
experimental myocardial infarction under the effect of
electromagnetic fields of low frequencies and low
strengths 02 p0221 A83-11888
The reaction of a biological system to adequate or weak
low-frequency electromagnetic fields 02 p0221 A83-11889
Ionospheric ELF radio signal generation due to LF
and/or MF radio transmissions. I - Experimental results 02 p0205 A83-12015
Ionospheric ELF radio signal generation due to LF
and/or MF radio transmissions. II - Interpretation 02 p0205 A83-12016
Laser interferometer with low-frequency phase
modulation 05 p0644 A83-17066
Observations of upstream ions and low-frequency waves
on ISEE 3 06 p0782 A83-18284
Charged particle behavior in low-frequency geomagnetic
pulsations. III - Spin phase dependence 06 p0783 A83-18291
Low-frequency radio observations of the emission
nebula NGC 2264 06 p0832 A83-18833
On the spectra of type-III solar radio bursts observed
at low frequencies 06 p0855 A83-19136
Two-phase frequency-conversion type spectrum
analyzer for low-frequency noise measurement 07 p0929 A83-20547
The low-frequency limit of the application of ferrite
circulators 10 p1412 A83-26940
The low-frequency electromagnetic field in the Venus
atmosphere - Evidence from Venera 13 and Venera 14 12 p1798 A83-29483
Low frequency dielectric relaxation in boracites 12 p1709 A83-29555
Detection of pulsars PSR 1133 + 16 and PSR 2045-16
at low radio frequencies 14 p2108 A83-33268
Low-frequency unsteadiness of a reattaching turbulent
shear layer 15 p2155 A83-33663
A hygienic evaluation of the combined effect of
infrasound and low-frequency noise on the auditory and
vestibular analyzer of compressor operators 15 p2212 A83-34932
Calculation of ionospheric conductivity profiles by
inverting VLF/LF reflection data. I - Isotropic
propagation 16 p2341 A83-35419
Turbulent absorption of lower hybrid waves due to
scattering by low frequency fluctuations --- in plasma 21 p3211 A83-44346
Low-frequency measurement of the spectrum of the
cosmic background radiation 21 p3245 A83-45200
Low frequency radio noise 22 p3273 A83-45881
Theory of low frequency wave propagation 22 p3273 A83-45889
Frequency splitting in stria bursts - Possible roles of
low-frequency waves --- in solar radio emission 23 p3537 A83-47731
Low-frequency noise in GaAs current limiters 23 p3446 A83-48607

LOW FREQUENCY BANDS
NT VERY LOW FREQUENCIES

LOW GRAVITY
U REDUCED GRAVITY

LOW GRAVITY MANUFACTURING
The effect of zero gravity on the structure and properties
of alloys with special physical properties 01 p0015 A83-10386
MLR - A Shuttle experiment 01 p0016 A83-10464
Preparation of dispersed alloys under micro-gravity
conditions 01 p0016 A83-11326
Protein single crystal growth in a microgravity field 02 p0138 A83-12996
Measurement of the concentration-dependence of

interdiffusion coefficients in fused salts --- in microgravity environments 02 p0138 A83-12997
 Rotating finite liquid systems under zero-gravity 06 p0759 A83-19247
 Interface and transport phenomena in space conditions. I - Transport phenomena 07 p0924 A83-19660
 Crystallization of copper under zero-g conditions 09 p1229 A83-23520
 Investigation of the features of formation of crystalline structures grown in conditions of microgravity 11 p1661 A83-27447
 New opportunities in space - Research in microgravity 15 p2123 A83-33544
 Numerical analysis of heat and mass transfer processes during directional solidification in weightlessness 20 p2939 A83-42893
 Influence of gravity driven convection on the directional solidification of Bi/MnBi eutectic composites 20 p2942 A83-43302
 Solidification of hypermonotectic Al-In alloys under microgravity conditions 20 p2942 A83-43304
 Brazing under microgravity in a resistance heated furnace 20 p2943 A83-43313
 Low gravity solidification structures in the tin-15 wt pct lead and tin-3 wt pct bismuth alloys 20 p2943 A83-43314
 Materials processing in the reduced-gravity environment of space 22 p3257 A83-45895
 Surface oscillation due to Marangoni-effect in a freely floating sphere 23 p3451 A83-48498

LOW INTENSITY X RAY IMAGING SCOPE

U LIXISCOPEs

LOW LATITUDES

U TROPICAL REGIONS

LOW LEVEL TURBULENCE

Formation of the low-level jet under an inversion 03 p0369 A83-14449
 Airborne operation of an infrared low-level wind shear prediction system 06 p0791 A83-18412
 The dependence of wave parameters on the velocity of wind, the duration of its action, and the acceleration in the theory of weakly turbulent wind waves 14 p2059 A83-32859
 Dynamics of the Venera 13 and 14 descent modules 19 p2809 A83-41239

LOW MASS

U MASS

LOW MOLECULAR WEIGHTS

A comparison of the neural and immunological modulator properties of low molecular weight neuropeptides 01 p0080 A83-10551
 A general diagram for estimating pore size of ultrafiltration and reverse osmosis membranes 02 p0151 A83-11841

LOW NOISE

Monolithic GaAs FET low-noise amplifiers for X-band applications 03 p0308 A83-13441
 1.0 to 2.5 micrometer short wavelength infrared /SWIR/ linear array technology for low background applications 03 p0326 A83-13739
 FIR filter structures having low sensitivity and roundoff noise 05 p0623 A83-16913
 Quarter micron low noise GaAs FET's 05 p0624 A83-17293
 0.5 micron GaAs FET for low-noise circuits for Orbital Test Satellite reception 09 p1252 A83-23396
 Practical design of 2-4 GHz low intermodulation distortion GaAs FET amplifiers with flat gain response and low noise figure 09 p1255 A83-24348
 V-band low-noise integrated circuit receiver --- for space communication systems 10 p1382 A83-25807
 Si Impatts exhibit low noise at mm-waves 11 p1562 A83-28157
 A low-noise GaAs FET preamplifier for 21 GHz satellite earth terminals 11 p1563 A83-28591
 Hybrid packaging approach to improved low-noise operation of photovoltaic InSb detectors 14 p2015 A83-31981
 Optimization of charge-coupled device (CCD) imager performance for astronomy 14 p2015 A83-31987
 Low noise spectrometer for the daily measurement of solar chromospheric flux 14 p2017 A83-32007
 A low-noise low input impedance amplifier for magnetic measurements of nerve action currents 14 p2020 A83-32798
 Low-noise, low power dissipation GaAs monolithic broad-band amplifiers 14 p2008 A83-33459
 Practical low-noise quasparticle receiver for 80-100 GHz 17 p2500 A83-38890
 A theory of noise in GaAs FET microwave oscillators and its experimental verification 20 p2968 A83-43349
 Submicron GaAs microwave FET's with low parasitic gate and source resistances 21 p3123 A83-43848
 Radio-frequency amplified based on a dc superconducting quantum interference device 24 p3572 A83-48795
 30 GHz band low noise receiver for 30/20 GHz single-conversion transponder 24 p3570 A83-49857

LOW PASS FILTERS

A-878

Direct form expansion of the transfer function for a digital Butterworth low-pass filter 05 p0623 A83-16916
 Frequency limitations and optimal step size for the two-point central difference derivative algorithm with applications to human eye movement data 10 p1460 A83-26650
 Band-reject filters suppress second harmonics 11 p1562 A83-28161
 System matrices of wave-digital filter related by similarity transformations 13 p1838 A83-31781
 Novel synthesis method of microwave integrated low-pass filters 21 p3127 A83-45414

LOW PRESSURE

NT CYCLOGENESIS

NT HIGH ALTITUDE PRESSURE

An approximate method for calculating the ultraviolet radiation of diatomic molecules at low pressures 09 p1342 A83-24231
 Orographic trough or low in the Alpine region /and their effect on weather in the CSR/ 11 p1633 A83-28114
 Enhanced HgBr(B2Sigma+ - X2Sigma -) emission at low pressures --- blue-green laser 13 p1852 A83-31062
 Gain anisotropy in low-pressure chemical lasers 13 p1857 A83-31456
 The critical angles of shock-wave collision in porous media in the low-pressure region 14 p1992 A83-32095
 Low pressure nitrided-oxide as a thin gate dielectric for MOSFET's 14 p2006 A83-32640
 On the mechanism for the development of polar lows 16 p2386 A83-35480
 Details of low latitude medium range numerical weather prediction using a global spectral model. I - Formation of a monsoon depression 20 p3031 A83-43458
 Energy distribution functions of electrons in low-temperature helium-neon plasma at low pressures 24 p3632 A83-49113
 Effect of oxygen pressure on the high temperature oxidation of Ni-Cr alloys 24 p3562 A83-49489

LOW PRESSURE CHAMBERS

U VACUUM CHAMBERS

LOW REYNOLDS NUMBER

Nonlinear problem of heat and mass transfer to a particle in a gas flow at low Reynolds numbers 04 p0477 A83-15876
 An experimental investigation of the low Reynolds number performance of the Lissaman 7769 airfoil [AIAA PAPER 83-0647] 05 p0588 A83-16814
 Boundary-layer development on circular cylinders 06 p0756 A83-18235
 The shape of low Reynolds number jets 07 p0926 A83-20527
 Flow in a differentially rotated cylindrical drop at low Reynolds number 08 p1086 A83-23093
 Low Reynolds number flow between interrupted flat plates 09 p1259 A83-23878
 Study of a circular jet at low Reynolds numbers and with impact on a wall --- French thesis 13 p1840 A83-30127
 Direct simulation of homogeneous turbulence at low Reynolds numbers 13 p1841 A83-30640
 Low-Reynolds-number airfoils 13 p1804 A83-31082
 Low Reynolds number shear flow along an elliptic hole in a wall 14 p2009 A83-32522
 Experimental studies of the boundary layer on an airfoil at low Reynolds numbers [AIAA PAPER 83-1671] 17 p2444 A83-37181
 On an experimental possibility of investigating the hydrodynamic interaction of particles at low Reynolds numbers 17 p2505 A83-37556
 Boundary layer characteristics of the Miley airfoil at low Reynolds numbers [AIAA PAPER 83-1795] 17 p2453 A83-38634
 Effect of low Reynolds number turbulence amplification on the Galileo probe flowfield 18 p2645 A83-40023
 Numerical study of heat transfer system with staggered array of vertical flat plates used at low Reynolds number 20 p2980 A83-42755
 Low-Reynolds-number flow past a cylindrical body 20 p2985 A83-43103
 The influence of free-stream disturbances on low Reynolds number airfoil experiments 21 p3088 A83-44676
 Low Reynolds number flow heat exchangers; Proceedings of the Fourth Advanced Study Institute, Ankara, Turkey, July 13-24, 1981 21 p3133 A83-45099
 An experimental study of low Reynolds number turbulent circular jet flow [ASME PAPER 83-FE-36] 23 p3451 A83-48239
 The standing vortex behind a disk normal to uniform flow at small Reynolds number 24 p3577 A83-49468

LOW SPEED

Measurements and visualizations of unsteady flow /low speed/ [AAAF PAPER NT 81-14] 02 p0176 A83-11774

NASA low-speed centrifugal compressor for fundamental research [AIAA PAPER 83-1351] 16 p2312 A83-36353
 A method for predicting low-speed aerodynamic characteristics of transport aircraft [AIAA PAPER 83-1845] 17 p2456 A83-38673
 Equivalent angle of attack for the lifting plane with linear camber-twist at low speeds 20 p2931 A83-43690
 Low speed performance of a supersonic axisymmetric mixed compression inlet with auxiliary inlets [AIAA PAPER 83-1414] 21 p3088 A83-45516

LOW SPEED WIND TUNNELS

NT SUBSONIC WIND TUNNELS

Development and trial of a rotary balance for the 3 M low speed wind tunnels of West Germany 01 p0015 A83-11082
 Low-speed investigation of the maneuver capability of supersonic fighter wings [AIAA PAPER 83-0426] 05 p0585 A83-16708
 Experimental investigation of the confluent boundary layer of a multielement low speed airfoil [AIAA PAPER 83-0566] 05 p0588 A83-16793
 A new surface-streamline flow-visualization technique 06 p0763 A83-19016
 A wind tunnel for unsteady turbulent shear flows - Design and flow calculation 07 p0867 A83-19664
 An experimental investigation of turbulent wake behind 'S'-shaped profiles 07 p0926 A83-20502
 Flat spin of slender bodies at high angles of attack 09 p1210 A83-24879
 Cryogenic wind tunnels for high Reynolds number testing 14 p1977 A83-32175
 Low-speed aerodynamic characteristics of a generic forward-swept-wing aircraft [SAE PAPER 821467] 17 p2451 A83-37998
 Local heat transfer rates from two adjacent spheres in turbulent axisymmetric flow 20 p2976 A83-42719
 The use of resistance strain gages for measurements in a low-speed wind tunnel 20 p2993 A83-43814
 Something about to improve the accuracy of testing in low speed wind tunnel 21 p3093 A83-44571
 Boundary layer and loss measurements on the rotor of an axial-flow turbine [ASME PAPER 83-GT-4] 23 p3392 A83-47878
 Exploratory low-speed wind-tunnel investigation of advanced commuter configurations including an over-the-wing propeller design [AIAA PAPER 83-2531] 24 p3548 A83-49590

LOW TEMPERATURE

The nucleation mechanism during the low-temperature decomposition of ammonium perchlorate 05 p0620 A83-17142
 Degradation of the phospholipids of the outer and inner membranes of mitochondria under exposure to low temperature 07 p0974 A83-20844
 Response of irradiated optical waveguides at low temperatures 08 p1165 A83-22480
 The results of an investigation of the intermittent effects of low temperature on the human body 09 p1322 A83-23973
 Vibrational relaxation of gaseous CO/v = 1/ and N2/v = 1/ from 300 K to liquid temperatures - A comparison with liquid state relaxation 10 p1389 A83-25563
 Resistive force acting on a microscopic particle in a low-temperature plasma jet 10 p1487 A83-26251
 Ultrastructural changes of acinar cells of the pancreas due to the effects of cold 14 p2066 A83-33329
 The plastic zone and growth of fatigue cracks in magnesium MA12 alloy at room and low temperatures 15 p2140 A83-34741
 Changes in the liver of white rats under the influence of low temperatures 17 p2556 A83-38198
 Establishment of the optimal irradiance of man at low ambient temperatures in the workplace 17 p2561 A83-38929
 Low temperature hot corrosion 20 p2953 A83-42252
 Low temperature operation of an S2 laser using radio frequency simmer discharges 20 p2994 A83-42794
 Low-temperature oxygen diffusion in alpha titanium characterized by Auger sputter profiling 21 p3113 A83-44608
 Low temperature selective absorber research --- coatings for solar energy devices 22 p3319 A83-46581

LOW TEMPERATURE ENVIRONMENTS

Heat conduction of inert gases at low temperatures 04 p0544 A83-16168
 A low-temperature chamber for calibrating thermal radiation detectors 07 p0902 A83-20965
 Cold-induced losses in loose-sheath fiber-optic cables 08 p1165 A83-22484
 Observation of ice aggregation at temperatures near -50 C 24 p3612 A83-49699

LOW TEMPERATURE PHYSICS

Hot electrons in a GaAs heterolayer at low temperature 01 p0109 A83-10626
 Thermophysical properties of materials at low temperatures: A handbook /2nd revised and enlarged edition/ 05 p0610 A83-17129

- Cooling liquid He-3 to around 100 micro-K
14 p1999 A83-31921
- Progress in low temperature physics. Volume 8
15 p2224 A83-33610
- Electrical conductivity of a low-temperature two-dimensional medium
20 p3051 A83-42273
- Vacuum-ultraviolet refractive index of LiF and MgF2 in the temperature range 80-300 K
21 p3203 A83-43875
- A two-beam interferometer for dispersive reflection spectroscopy of solids in the far infrared at temperatures between 4 and 300K
21 p3137 A83-44388
- The use of superconductivity in magnetic measurements --- Russian book
21 p3141 A83-45015

LOW TEMPERATURE PLASMAS**U COLD PLASMAS****LOW TEMPERATURE TESTS**

Solar cell performance at low illumination and temperature for deep-space applications
01 p0068 A83-10662

Method for measuring specific heats in intense magnetic fields at low temperatures using capacitance thermometry
02 p0180 A83-12813

Low temperature /650 to 700 C/ burner rig testing
02 p0158 A83-12835

Feasibility study on strain gauge balances for cryogenic wind tunnels at ONERA
[ONERA, TP NO. 1982-87]
03 p0282 A83-14539

Simple double diaphragm press for diamond anvil cells at low temperatures
06 p0735 A83-19235

The effect of primer-adhesive compatibility on adhesive peel strength at low temperature
07 p0898 A83-20448

On the controlling parameters for fatigue-crack threshold at low homologous temperatures
07 p0887 A83-20636

An instrument for studying the thermophysical properties of solids at low temperatures
07 p0931 A83-20961

Low temperature oxidation of SiC
08 p1072 A83-22259

The low-temperature behavior of the direct volt-ampere characteristics of Schottky-barrier diodes
09 p1255 A83-24211

The effect of prior elastic-plastic cyclic deformation on the mechanical characteristics of 1201 alloy at cryogenic temperatures
11 p1550 A83-28517

Low-temperature studies of plasticity and strength /instruments, techniques, and methods/ --- Russian book
12 p1729 A83-29328

Low temperature fatigue fracture of metals and alloys
13 p1824 A83-31585

InSb charge-injection device array performance
14 p2015 A83-31979

Delay times in Si MOSFETs in the 4.2-400 K temperature range
14 p2007 A83-32674

Mechanical tests of structural alloys at cryogenic temperatures
14 p1997 A83-33012

A study of the short-term strength of structural materials under static loading --- of metal alloys at cryogenic temperatures
14 p1997 A83-33013

The use of the acoustic emission method for studying the strength and ductility of materials at low temperatures
14 p1997 A83-33014

The resistance of structural materials to fracture during impact bending
14 p2033 A83-33015

A study of the temperature dependence of the mechanical characteristics of structural alloys under impact tension
14 p1997 A83-33016

A study of the elastic characteristics of structural alloys over a wide temperature range
14 p1998 A83-33017

A study of the low-cycle fatigue of the structural alloys for cryogenic applications
14 p1998 A83-33018

A study of the fatigue of structural alloys under repeated static loading with superposed vibration
14 p1998 A83-33019

A study of the high-cycle fatigue of materials under plane cantilever bending
14 p1998 A83-33020

High-frequency fatigue testing of structural steels and alloys at 77 K
14 p1998 A83-33021

Elastic properties and fracture behavior of graphite/polyimide composites at extreme temperatures
14 p1987 A83-33119

Changes in the yield stress of nickel in the low-temperature region due to magnetic field variation
19 p2822 A83-41979

Materials at low temperatures --- Book
21 p3114 A83-45098

A pre-testable low temperature lithium thermal battery
24 p3600 A83-49949

spacecraft
[AIAA PAPER 83-1305]
16 p2320 A83-36330

High and low thrust acceleration
24 p3551 A83-49625

LOW THRUST PROPULSION
NT ELECTROMAGNETIC PROPULSION
NT ELECTROSTATIC PROPULSION
NT ION PROPULSION
NT MAN OPERATED PROPULSION SYSTEMS
NT PLASMA PROPULSION
NT SOLAR ELECTRIC PROPULSION
NT SOLAR PROPULSION
NT SOLAR THERMAL PROPULSION

Linearized transfer between inclined circular orbits using low-thrust blow down propulsion system
[AIAA PAPER 83-0194]
05 p0602 A83-16579

Simplified power processing for ion-thruster subsystems
18 p2648 A83-39271

Losses in the combustion chamber of low-thrust engines
19 p2818 A83-42142

Bell-shaped jet flow into a vacuum and interference effects with affected surfaces
22 p3261 A83-46486

Complex optimization of engine systems for spacecraft control --- Russian book on low thrust propulsion control
23 p3427 A83-48248

LOW TURBULENCE
Unified approach to weak turbulence
15 p2239 A83-34543

LOW VELOCITY
U LOW SPEED

LOW VISIBILITY
Information requirements for pilot supervision of automatic landing in low visibility conditions
04 p0524 A83-16129

Tracking of obscured targets via generalized correlation measures
09 p1266 A83-23542

Guidance control systems for aircraft on airport surfaces
[AIAA PAPER 83-1579]
16 p2297 A83-36953

Instrument-approach technique for poor-visibility landings
19 p2795 A83-41228

LOW VOLTAGE
The changes in the nerve and cardiac activity in animals of various ages during the application of electromagnetic fields of low frequency and low voltage
02 p0220 A83-11884

A low-voltage alterable EEPROM with Metal-Oxide-Nitride-Oxide-Semiconductor /MONOS/ structures
09 p1255 A83-24495

Electro-optic branching-waveguide switch with low drive voltage
24 p3628 A83-48855

LOWER ATMOSPHERE
NT BIOSPHERE
NT OZONOSPHERE
NT TROPOSPHERE

Airglow at a height below 40 km in the vacuum ultraviolet
03 p0356 A83-13216

Infrasound of cosmic origin in the atmosphere
07 p0962 A83-20606

NASA multipurpose airborne DIAL system and measurements of ozone and aerosol profiles --- Differential Absorption Lidar
08 p1101 A83-22615

Sulfur trioxide in the lower atmosphere of Venus
10 p1518 A83-25505

The interplanetary magnetic field and the earth's lower atmosphere
11 p1634 A83-28744

Investigation of remote sensing possibilities of the lower atmosphere in the microwave range and some aspects of statistical data use
15 p2180 A83-35291

On the mechanism of the effect of solar corpuscular radiation on the circulation of the lower atmosphere
18 p2724 A83-39489

Acetonitrile in the atmosphere
20 p3026 A83-43208

A theoretical study of small amplitude waves in the Martian lower atmosphere and a comparison made with those on earth
21 p3240 A83-44240

Relationship between thermal-radiation characteristics and concentrations of trace gases in different layers of the atmosphere
23 p3488 A83-47160

Infrasonic and internal gravity waves in the atmosphere during large fires
23 p3485 A83-48503

A study of multiple stable layers in the nocturnal lower atmosphere
23 p3492 A83-48732

LOWER BODY NEGATIVE PRESSURE
The physiological mechanisms responsible for an increase in muscular efficiency under local decompression
05 p0669 A83-17153

Cardiovascular and endocrine effects of gravitational stresses /LBNP/ - The influence of angiotensin-converting enzyme inhibition with captopril
11 p1642 A83-27798

The observation of influence on the characteristics of cardiovascular response during bed rest
21 p3187 A83-44517

LOWER CALIFORNIA (MEXICO)
Fire mosaics in southern California and northern Baja California
09 p1292 A83-25287

LOWER IONOSPHERE

NT D REGION

Electron density profiles in the nighttime high-latitude lower ionosphere, artificially disturbed by high-power radio waves
02 p0209 A83-12425

Combined mass spectrometric composition measurements of positive and negative ions in the lower ionosphere. I - Positive ions
05 p0665 A83-17786

VLF/ELF radiation from the ionospheric dynamo current system modulated by powerful HF signals
09 p1300 A83-23311

ELF and VLF wave generation by modulated HF heating of the current carrying lower ionosphere
09 p1300 A83-23312

The variations in the spectrum of electron-density inhomogeneities in the lower ionosphere under the effect of high-power electromagnetic radiation
09 p1301 A83-23478

The effects of the interplanetary magnetic field in the lower ionosphere at middle latitudes
11 p1620 A83-28742

An investigation of the winter anomaly in Czechoslovakia (Survey) --- radio wave absorption in lower ionosphere
19 p2866 A83-41589

The effect of motions of the ionospheric plasma on the formation of artificial periodic inhomogeneities
19 p2866 A83-41803

Reflection of radio waves from an artificial ionized region
21 p3174 A83-45231

The effect of disturbances of lower ionospheric parameters by powerful radio waves on partially reflected signals
21 p3121 A83-45344

Schumann resonances --- earth surface-ionosphere cavity resonator
22 p3325 A83-45880

Standing wave patterns in VLF hiss
22 p3326 A83-46044

LOX (OXYGEN)
U LIQUID OXYGEN

LOX-HYDROGEN ENGINES
U HYDROGEN OXYGEN ENGINES

LRC CIRCUITS
U RLC CIRCUITS

LSI
U LARGE SCALE INTEGRATION

LST
U LARGE SPACE TELESCOPE

LUBRICANT TESTS

The use of powdered metals as antifricton additions to plastic lubricants
01 p0027 A83-10459

The mechanism of the dissipation of elastic energy by a lubricant layer
02 p0186 A83-11647

Development of an oxidation-wear-coupled test for the evaluation of lubricants
[ASLE PREPRINT 82-LC-1D-2]
03 p0302 A83-13232

Wear and friction of high-temperature self-lubricating composites
[ASLE PREPRINT 82-LC-2B-2]
03 p0334 A83-13234

Friction oxidation characteristics
[ASLE PREPRINT 82-LC-3B-2]
03 p0334 A83-13236

Thick film formation by zinc dialkylthiophosphates
06 p0734 A83-18200

The effect of the surrounding medium on the wear of solid lubricants
07 p0898 A83-20325

A general-purpose oil for ground-based gas-turbine engines
14 p1998 A83-32076

The effect of the soap cation on the anticuff and antiwear properties of lubricant greases
14 p1998 A83-32079

Evaluation of the thermal and oxidation stability of synthetic lubricants using a derivatograph
14 p1998 A83-32080

The stability of oils in aviation systems
15 p2142 A83-34499

Effects of MoS2 concentration on friction
15 p2143 A83-35244

The effect of the dispersion medium on the properties of complex Li lubricants
23 p3439 A83-48545

Surface interaction of lubricant greases
23 p3439 A83-48546

Determination of the thermal stability of oils by pyrolytic gas chromatography
23 p3439 A83-48547

Effect of molecular weight distribution of mineral oils on life of thrust ball bearings
24 p3590 A83-48924

LUBRICANTS

NT GAS LUBRICANTS

NT HIGH TEMPERATURE LUBRICANTS

NT LUBRICATING OILS

NT SOLID LUBRICANTS

Dynamics of rotor bearing systems supported by floating ring bearings
[ASME PAPER 81-LUB-37]
02 p0186 A83-11938

Theory of lubrication with ferrofluids - Application to short bearings
[ASME PAPER 81-LUB-39]
02 p0186 A83-11940

Morphological and frictional behavior of sputtered MoS2 films
02 p0160 A83-12652

Transient lubricating films with inertia

- [ASME PAPER 82-LUB-12] 03 p0335 A83-13507
Lubrication: A practical guide to lubricant selection ---
Book 03 p0337 A83-14043
Evaluation of fretting corrosion by means of a new device
for the control of oscillation amplitude
05 p0652 A83-17255
Microscopic aspects of the effect of friction reducers
at the lubrication limit --- French thesis
11 p1590 A83-28663
A three-dimensional analysis of thermohydrodynamic
performance of sector-shaped, tilting-pad thrust bearings
[ASME PAPER 82-LUB-3] 18 p2695 A83-39943

LUBRICATING OILS

- A study on thermal behavior of large seal-ring
[ASME PAPER 81-LUB-27] 02 p0186 A83-11937
Characteristics of an oil squeeze film
02 p0186 A83-11939
On the mechanism of lubrication by tricresylphosphate
/TCP/ - The coefficient of friction as a function of
temperature for TCP on M-50 steel
[ASLE PREPRINT 82-LC-4C-1] 03 p0333 A83-13228

- An experimental investigation of the vaporous/gaseous
cavity characteristics of an eccentric journal bearing
[ASLE PREPRINT 82-LC-3A-1] 03 p0333 A83-13230

- Development of an oxidation-wear-coupled test for the
evaluation of lubricants
[ASLE PREPRINT 82-LC-1D-2] 03 p0302 A83-13232

- The effect of metal composition on the adsorption of
zinc di-isopropylthiophosphate
[ASLE PREPRINT 82-LC-4C-2] 03 p0302 A83-13242

- New developments in synthetic oils
05 p0617 A83-16879
The effect of the melt heat treatment time on the
properties of lithium lubricants with additives
10 p1401 A83-26921

- Optimization of the oil-change period for aircraft systems
and units
10 p1401 A83-26922
Lubrication mechanism of solid lubricants in oils
[ASME PAPER 81-LUB-50] 13 p1859 A83-30248
Oil leakage and friction forces of reciprocating O-ring
seals considering cavitation
13 p1859 A83-30249
A general-purpose oil for ground-based gas-turbine
engines
14 p1998 A83-32076
Evaluation of the thermal and oxidation stability of
synthetic lubricants using a derivatograph
14 p1998 A83-32080

- The stability of oils in aviation systems
15 p2142 A83-34499
The effect of liquid crystals on the lubricating properties
of mineral oils
19 p2824 A83-41975
Synthetic basestocks for partial synthetic motor oils
[ASLE PREPRINT 83-AM-2B-1] 20 p2958 A83-43335

- Final evaluation of multi-viscosity oils designed for
aircraft reciprocating engines
[SAE PAPER 830707] 21 p3116 A83-44685

LUBRICATION

- NT BOUNDARY LUBRICATION
NT SELF LUBRICATION
NT SPACECRAFT LUBRICATION

- The lubrication of roller bearing ribs - Hydrodynamic
approach
01 p0056 A83-10225
Non-Newtonian lubrication theory for rough surfaces -
Application to rigid and elastic rollers
01 p0056 A83-10499

- The nature of wear debris generated during lubricated
wear-in
[ASLE PREPRINT 82-LC-3B-1] 03 p0334 A83-13235

- The lubrication of the roller-rib contacts of a radial
cylindrical roller bearing carrying thrust load
[ASLE PREPRINT 82-LC-3C-1] 03 p0334 A83-13238

- Elastohydrodynamic lubrication of finite line contacts
[ASME PAPER 82-LUB-4] 03 p0335 A83-13503

- An experimental investigation of the stability of externally
pressurized gas-lubricated porous thrust bearings
[ASME PAPER 82-LUB-38] 03 p0336 A83-13517

- Dynamic analysis of turbulent annular seals based on
Hirs' lubrication equation
[ASME PAPER 82-LUB-41] 03 p0336 A83-13520

- Surface roughness effects in hydrodynamic lubrication
- The flow factor method
[ASME PAPER 82-LUB-45] 03 p0337 A83-13523

- Lubrication: A practical guide to lubricant selection ---
Book 03 p0337 A83-14043

- Micropolar squeeze films between rough rectangular
plates
06 p0768 A83-18062

- A study on characteristics of surface-restriction
compensated gas bearing with T-shaped grooves
07 p0939 A83-20293

- Theoretical and applied problems of the friction, wear
and lubrication of machines --- Russian book
07 p0939 A83-20320

- Slip measurement in an angular contact ball bearing

- [ASME PAPER 81-LUB-33] 13 p1858 A83-30243
Effect of inlet shear heating due to sliding on
elastohydrodynamic film thickness
13 p1858 A83-30244

- Experimental investigation of the effect of system rigidity
on wear and friction-induced vibrations
[ASME PAPER 81-LUB-3] 13 p1858 A83-30246

- Lubrication mechanism of solid lubricants in oils
[ASME PAPER 81-LUB-50] 13 p1859 A83-30248

- Analysis of externally pressurized gas-lubricated conical
bearings
16 p2363 A83-36941

- Externally pressurized magnetohydrodynamic bearings
under a non-uniform magnetic field
16 p2363 A83-36942

- Meeting on Tribology - In Theory and Practice: Wear -
Lifetime - Economics, Essen, West Germany, September
28, 29, 1982, Reports
17 p2517 A83-38223

- Effects of fluid inertia and viscoelasticity on the
one-dimensional squeeze-film bearing
[ASLE PREPRINT 83-AM-3E-1] 20 p2999 A83-43336

LUBRICATION SYSTEMS

- Full-flow debris monitoring and fine filtration for
helicopter propulsion systems
09 p1208 A83-24838

- Optimization of the oil-change period for aircraft systems
and units
10 p1401 A83-26922

- Simulation of advanced engine lubrication and rotor
dynamics systems - Rig design and fabrication
[AIAA PAPER 83-1133] 16 p2306 A83-36238

- Feasibility of dry lubrication for limited-duty gas turbine
engines
[AIAA PAPER 83-1130] 16 p2362 A83-36405

LUCITE (TRADEMARK)

- U POLYMETHYL METHACRYLATE

LUDER BANDS

- U PLASTIC DEFORMATION

- U YIELD POINT

LUGS

- Fracture mechanics deliberation of lugs
16 p2368 A83-36515
Fatigue crack growth of a corner crack in an attachment
lug
21 p3158 A83-44920

LUMBAR REGION

- Some considerations on lumbar pains and diseases of
the intervertebral disk to civilian aircrewmembers
08 p1148 A83-22974

- Quantitative histochemistry of rat lumbar vertebrae
following spaceflight
21 p3184 A83-44864

LUMBERING AREAS

- U FORESTS

LUMINAIRES

- NT AIRCRAFT LIGHTS

- NT AIRPORT LIGHTS

- NT ARC LAMPS

- NT FLASH LAMPS

- NT MERCURY LAMPS

- NT XENON LAMPS

- Application of light polarization technique to the
generalized line-reversal method for gaseous temperature
measurements
02 p0181 A83-12814

- Broadband lamp standard for ultraviolet /UV/, visible,
and infrared calibration to 6.0 microns
08 p1104 A83-22878

LUMINANCE

- Some perceptual effects of differential luminance
induced by the use of a monocular head-up display
10 p1456 A83-26305

- Method of calculating the expected background
luminance from the moon for planning astronomical
observations
15 p2244 A83-33788

- Representation of spatial spectrum in terms of the
density of luminance differences
18 p2739 A83-40401

- The roles of contour and luminance distribution in
determining perceived centers within shapes
22 p3349 A83-45956

LUMINESCENCE

- NT CATHODE GLOW

- NT CATHODOLUMINESCENCE

- NT CHEMILUMINESCENCE

- NT ELECTROLUMINESCENCE

- NT FLUORESCENCE

- NT OPTICAL RESONANCE

- NT PHOSPHORESCENCE

- NT PHOTOLUMINESCENCE

- NT RESONANCE FLUORESCENCE

- NT SHOCK WAVE LUMINESCENCE

- NT THERMOLUMINESCENCE

- NT TRIBOLUMINESCENCE

- NT X RAY FLUORESCENCE

- Luminescence spectra of stripe-geometry laser
heterostructures in GaAs-Al_x/Ga_{1-x}/As
02 p0183 A83-11695

- Luminescent solar concentrators - A review
03 p0353 A83-13581

- Simultaneous luminescent assessment of the
phagocytic and bactericidal functions of the macrophages
and neutrophils of human skin exudate
03 p0381 A83-14336

- Luminescence fatigue and light-induced electron spin
resonance in amorphous silicon-hydrogen alloys
04 p0541 A83-15514

- Hot-electron luminescence in aged electrodeposited
CdSe liquid-junction solar cell
05 p0658 A83-16946

- Determination of the parameters of injection laser
amplifiers based on GaAlAs heterostructures from
superluminescence characteristics
05 p0649 A83-17060

- Generation of holes during the disintegration of
dislocations and mechanoluminescence of metals
08 p1170 A83-22781

- Submicrostructures generated in semiconductors by
athermal laser processing
11 p1661 A83-27561

- Experimental investigation of the glow of certain
fragments observed in cometary spectra
11 p1679 A83-27887

- Efficiency of luminescence in luminescent solar
concentrators
13 p1870 A83-30205

- Luminescent solar concentrators as bifacial captors
15 p2192 A83-34669

- Diagrammatic analysis of third order nonlinear optical
processes
16 p2412 A83-35968

- Modification of the local interstellar gas properties in
the heliospheric interface
16 p2432 A83-36681

- Transparent high surface area porous supports as new
materials for luminescent solar concentrators
16 p2371 A83-36739

- The effect of external factors (heat treatment,
deformation, and irradiation) on the luminescence of GaAs
(review)
21 p3217 A83-44593

- Luminescence of strong exciton transitions
21 p3219 A83-45336

- Time-resolved nonlinear luminescence spectroscopy by
picosecond excitation correlation
21 p3219 A83-45491

- Neodymium laser glasses as optical media for
luminescent solar concentrators
23 p3476 A83-47169

- Use of the Fraunhofer line discriminator (FLD) for remote
sensing of materials stimulated to luminescence by the
sun
23 p3458 A83-47793

LUMINESCENT INTENSITY

- U LUMINOUS INTENSITY

LUMINOSITY

- NT STELLAR LUMINOSITY

- Evolution of the cluster X-ray luminosity function slope
02 p0254 A83-12101

- On the neutrino luminosity from a type II supernova
02 p0257 A83-12147

- Luminosity limits for funnels in thick accretion discs
03 p0414 A83-13325

- Inference of nebular density and luminosity structure
from polarization maps
03 p0414 A83-13328

- Luminosity classification of galaxies in the revised
Shapley-Ames Catalog
03 p0409 A83-14136

- A spectroscopic method for determining the luminosities
of spiral galaxies and estimating their stellar population
04 p0551 A83-15601

- Low surface brightness spiral galaxies. I - Neutral
hydrogen content and location in the infrared Fisher-Tully
diagram
04 p0552 A83-15610

- H I observations of high-luminosity elliptical galaxies
06 p0819 A83-18853

- A study of the two-dimensional luminosity distribution
of NGC 3379
06 p0833 A83-18855

- Isolated triplets of galaxies: Virial mass - Luminosity
ratios
06 p0836 A83-19201

- On the possibility of gas being swept out of a galaxy
under the influence of the radiation pressure of an active
nucleus
06 p0838 A83-19223

- Optical studies of H I-rich southern galaxies. II - The
low-visibility spiral NGC 1079
07 p1010 A83-19856

- The observational consequences of an intrinsic burst
luminosity distribution
07 p1011 A83-20011

- An optimal procedure for non-parametric elimination of
observational cutoff bias in complete samples --- of
celestial objects
09 p1354 A83-24477

- Can C IV emission be used as a luminosity indicator
--- of quasars
09 p1362 A83-24987

- The composite UV emission spectrum of Seyfert 1
galaxies
10 p1500 A83-25486

- The cosmological evolution and luminosity function of
X-ray selected active galactic nuclei
10 p1510 A83-26399

- Comptonization effects in spherical accretion onto black
holes
10 p1515 A83-26739

- The statistics of gravitational lenses - Apparent
changes in the luminosity function of distant sources due
to passage of light through a single galaxy
13 p1949 A83-31403

- On the Baldwin effect in optically-selected quasars
13 p1943 A83-31711

- Auroral X-ray and luminosity pulsations and microbursts
measured during February 25, 1974 SAMBO-1 balloon
flight
13 p1883 A83-31718

- X-ray studies of quasars with the Einstein Observatory
III The 3CR sample
14 p2104 A83-33183

- Effects of galaxy collisions on the structure and evolution
of galaxy clusters. I - Mass and luminosity functions and

background light 15 p2255 A83-34078
On the nature of two gamma bursts with spectral evolutions observed by the KONUS experiment 15 p2286 A83-34123
Some properties of radio galaxies in clusters 15 p2261 A83-34495
An infrared luminosity function for star-forming molecular clouds 15 p2264 A83-34584
Analysis of complete quasar samples to obtain parameters of luminosity and evolution functions 15 p2266 A83-34615
Quasar evolution derived from the Palomar bright quasar survey and other complete quasar surveys 17 p2596 A83-37302
Posterior probability of the deceleration parameter q sub 0 from quasars provided with a luminosity indicator 18 p2764 A83-39194
NGC 3200 - Is this what our Galaxy is like? 18 p2771 A83-39672
The variation of radio luminosity with epoch and its effect on the angular diameter-redshift relation 19 p2917 A83-41605
A search for X-ray emission from optically quiet, compact radio sources 19 p2918 A83-41613
The X-ray luminosity function of very rich clusters and the luminosity-richness relation 20 p3070 A83-43037
The relationship between the X-ray and optical luminosities for QSOs 20 p3071 A83-43045
Luminosity distribution in galaxies. II - A study of accidental and systematic errors with application to NGC 3379 21 p3222 A83-44118
Super-Eddington luminosity characteristics of active galactic nuclei 21 p3230 A83-44439
High-resolution optical observations of NGC 3379. I - An analysis of previous data 21 p3225 A83-44980
Optical variability, absolute luminosity, and the Hubble diagram for QSOs 21 p3235 A83-45527
A deep survey of galaxies 22 p3372 A83-46377
Luminosity function of high-redshift quasars 22 p3376 A83-46975
The trivariate (radio, optical, X-ray) luminosity function of cD galaxies. I - New Westerbork observations of 22 cD galaxies and Einstein observations of A 1918 and A 2317. II - The fuelling of radio sources 23 p3518 A83-47437
Formation of rings and lenses --- in disk galaxies 24 p3657 A83-49245

LUMINOUS FLUX DENSITY U LUMINOUS INTENSITY

LUMINOUS INTENSITY
NT ILLUMINANCE
NT LUMINANCE
Application of a computer controlled intensity registering procedure to the spectral region at 4430 Å 01 p0116 A83-10268
Measurements of intensities and self- and foreign-gas-broadened half-widths of spectral lines in the CO fundamental band 02 p0234 A83-11574
Accurate frequency and intensity measurements of the infrared spectra of atmospheric molecules 03 p0294 A83-13981
High-luminosity solid-state lasers 04 p0483 A83-15254
The population of localized states and the photoconductivity of disordered systems 04 p0542 A83-15920
Luminosity evolution of QSOs 05 p0695 A83-16856
Formation of a non-Gaussian intensity profile in a laser with inhomogeneous mirrors 07 p0934 A83-20110
The spectrum of strong intensity fluctuations of light beams in randomly irregular media 07 p0937 A83-20875
Ratio of the intensities of 5577-Å and 4278-Å auroral emissions in proton and electron polar-auroras 07 p0964 A83-21183
Noise of semiconductor lasers with external feedback 09 p1270 A83-23378
Transient behavior of nonlinear thermal effects in an intense light beam in a uniform gas flow 09 p1271 A83-23988
The brightening effect during nonlinear light scattering by static optical inhomogeneities 09 p1345 A83-24217
Problem of accurate intensity measurements in focused laser beams 10 p1433 A83-26683
Interaction between high-intensity arbitrarily polarized radiation and molecules under collisional relaxation conditions 10 p1480 A83-26684
The intracavity magneto-optical modulation of the intensity of laser radiation 11 p1583 A83-27949
Amplification of the mean intensity of backscattering in a turbulent atmosphere 11 p1632 A83-27957
New dielectric waveguide structure for millimetre-wave optical control 12 p1720 A83-29466
The effect of an intermittent-light frequency on the quantum yield of chlorophyll photosynthesis 13 p1895 A83-30406
Intensity variations and ratios of (9-4) and (7-3) hydroxyl

bands in nightglow at Poona 13 p1882 A83-31632
Calculations of the intensity of a partially coherent optical beam in a turbulent atmosphere 14 p2023 A83-31908
Direct intensity microphotometer 14 p2019 A83-32396
The characteristics of a confined light beam in an absorptive medium having a narrow indicatrix of scattering 14 p2085 A83-32858
Visible signatures of the multi-step transition to a beam-plasma-dicharge 15 p2234 A83-34195
Simultaneous CARS and luminosity measurements in a bluff-body combustor [AIAA PAPER 83-1481] 15 p2134 A83-34915
The effect of prolonged illumination of the retina of a rabbit with monochromatic light on its functional condition 15 p2210 A83-34936
The properties of focused fields --- for optical beams 15 p2147 A83-35152
Surface photometry of edge-on galaxies. III - Luminosity distributions in eight galaxies 16 p2422 A83-35676
X-ray emission from the Pleiades cluster 16 p2424 A83-36540
The induction of circadian rhythm by light impulses - The dependence on illumination and duration of the impulse 16 p2395 A83-36808
Vinal mass and luminosity of the Virgo cluster of galaxies 17 p2602 A83-37881
Energy model of image formation by an optical system 17 p2580 A83-38480
The effect of light soaking on the low temperature photoconductivity of hydrogenated amorphous silicon 18 p2749 A83-39470
Balloon-borne imagery of the solar granulation. IV - The centre-to-limb variation of the intensity fluctuations 19 p2924 A83-40725
Initiation of superfluorescence in a three-level 'swept-gain' amplifier 19 p2853 A83-41178
Variation in light intensity with height and time from subsequent lightning return strokes 20 p3030 A83-42839
Mathematical models of the readaptation of the human visual analyzer following short light flashes 23 p3497 A83-47111
Reconstruction of the intensity distribution of heating radiation from the thermal damage profile of a thin plate 23 p3460 A83-47571
Calculation of coronal line intensities for boron-like ions 23 p3536 A83-47721
Intensity estimation from pixel data --- for stellar and galactic magnitude determination 24 p3648 A83-50013

LUMPED PARAMETER SYSTEMS

A review and assessment of methods for prediction of the dynamic stability of air cushions 01 p0112 A83-11038
An optimization technique for lumped-distributed two ports 07 p0922 A83-21528
A scheme of feedback compensation for CMG gimbal compliance, using multiple rate sensors --- Control Moment Gyroscope [ASME PAPER 82-WA/DSC-10] 10 p1419 A83-25681
Algebraic and topological aspects of the servo problem for lumped linear systems 10 p1469 A83-26567
Lumped parameter dynamic models for large space structures with flexible and rigid parts 17 p2477 A83-37444
Nonlinear lumped circuit model of GaAs MESFET 20 p2968 A83-43354

LUNA LUNAR PROBES

U LUNIK LUNAR PROBES

LUNAR ALBEDO

Correlation between albedo and polarization properties of the moon /heterogeneity of the relative porosity of the surface of the western part of the visible hemisphere/ 03 p0133 A83-13667
Correlation between albedo and polarization characteristics of the moon - Application of digital image processing 07 p1031 A83-21271

LUNAR BASES

Recent advances in lunar base simulation [IAF PAPER 83-237] 23 p3414 A83-47319

LUNAR CINEMATOGRAPHY

U LUNAR PHOTOGRAPHY

LUNAR COMMUNICATION

Autonomous navigation using lunar beacons [AIAA PAPER 83-0351] 16 p2315 A83-36052

LUNAR COMPOSITION

NT LUNAR CORE

A roentgenographic and X-ray-diffraction investigation of plagioclases of the lunar regolith returned by the Luna 16, Luna 20, and Luna 24 probes 03 p0432 A83-13525
Analysis of crater distribution in mare units on the lunar far side 03 p0435 A83-14869
The mare basalt magma source region and mare basalt magma genesis 04 p0559 A83-15331
Further efforts to limit lunar internal temperatures from electrical conductivity determinations

04 p0560 A83-15337
Comparison of thermal history of orthopyroxenes between lunar norites 78236, 72255, and diogenites 04 p0560 A83-15339
The Apollo 15 yellow impact glasses - Chemistry, petrology, and exotic origin 04 p0560 A83-15342
The Apollo 14 regolith - Chemistry of cores 14210/14211 and 14220 and soils 14141, 14148, and 14149 04 p0561 A83-15349
Comparative geochemistry of Apollo 16 surface soils and samples from cores 64002 and 60002 through 60007 04 p0561 A83-15351
Low temperature volatilization on the moon 04 p0562 A83-15352
The isotopic composition of primordial xenon 05 p0706 A83-17461
Constraints on the size of the moon's core 06 p0847 A83-18176
Cooling rates for glass containing lunar compositions 07 p1035 A83-21324
The isotopic composition of solar flare noble gases 10 p1522 A83-26397
Uranium in rock fragments from the lunar soil 17 p2619 A83-37817
Hydrogen in Luna-24 regolith 18 p2779 A83-39534
Lunar utilization --- materials resources and cislunar transportation considerations for space industrialization 22 p3257 A83-45857
Origin of lunar meteorite ALHA 81005 - Clues from the presence of terrae clasts and a very low-titanium mare basalt clast 22 p3385 A83-46862
Evidence of endogenic processes on the surface of lunar regolith particles 24 p3671 A83-48953
Petrology and chemistry of two 'large' granite clasts from the moon 24 p3673 A83-50172

LUNAR CORE

Constraints on the size of the moon's core 06 p0847 A83-18176
Probing the lunar interior 08 p1190 A83-23251

LUNAR CRATERS

Analysis of crater distribution in mare units on the lunar far side 03 p0435 A83-14869
Morphological characteristics of lunar craters with moderate depth/diameter ratio II - d/D between 0.12 and 0.15 03 p0435 A83-14871
Volumetric analysis of complex lunar craters
Implications for basin ring formation 04 p0560 A83-15333
Subcrater lithification of polymict regolith breccias 04 p0560 A83-15340
Interpreting the cratering record - Mercury to Ganymede and Callisto 04 p0570 A83-16234
The history of meteoritic bombardment in the early stage of the evolution of planetary bodies - Models and observational data 05 p0706 A83-17474
Geochemical studies of feldspathic fragmental breccias and the nature of North Ray Crater ejecta 07 p1033 A83-21300
The Manicouagan impact structure - An analysis of its original dimensions and form 07 p0950 A83-21315
Acoustic fluidization and the scale dependence of impact crater morphology 07 p1034 A83-21317
Optical investigations of the moon and spectrophotometric standards 09 p1367 A83-25278
Large-scale impact cratering on the terrestrial planets 15 p2277 A83-35033
Palisa catena - Small volcano chains in the western part of the central highlands 16 p2438 A83-36779
Linear crater chains - Indication of a volcanic organ 16 p2439 A83-36786
Applicability of the slow-denudation model to young craters and craters with viscous relaxation on the moon 17 p2615 A83-37015
The morphometric index - The profile characteristic of a crater in the process of denudation 17 p2615 A83-37016
Relief of the far side of the moon under the path of the Zond-8 probe 17 p2615 A83-37017

LUNAR CRUST

Accumulus growth of anorthosite at the base of the lunar crust 04 p0559 A83-15328
A partially molten magma ocean model 07 p1031 A83-21286
The magma ocean from the Fra Mauro shoreline - An overview of the Apollo 14 crust 07 p1032 A83-21294
Petrology and comparative thermal and mechanical histories of clasts in breccia 62236 07 p1033 A83-21298
Lunar magnetism, polar displacements and primeval satellites in the earth-moon system 21 p3241 A83-45055

LUNAR DUST

A model for the accumulation of solar wind radiation damage effects in lunar dust grains, based on recent results concerning implantation and erosion effects 07 p1033 A83-21305
The biological activity of lunar soil from Mare Fecunditatis during intratracheal injection 16 p2394 A83-35924

LUNAR ECHOES

A lunar radio interferometer 03 p0407 A83-13671

LUNAR ECLIPSES

OH airglow phenomena during the 5-6 July 1982 total lunar eclipse 22 p3328 A83-46082

LUNAR EFFECTS

NT LUNAR GRAVITATIONAL EFFECTS

NT LUNAR TIDES

LUNAR EVOLUTION

Could the earth's core and moon have formed at the same time 03 p0432 A83-13548

The mare basalt magma source region and mare basalt magma genesis 04 p0559 A83-15331

The Apollo 15 yellow impact glasses - Chemistry, petrology, and exotic origin 04 p0560 A83-15342

The history of meteoritic bombardment in the early stage of the evolution of planetary bodies - Models and observational data 05 p0706 A83-17474

The origin of the moon - A reappraisal 06 p0849 A83-19467

Stratigraphy and structural evolution of southern Mare Serenitatis - A reinterpretation based on Apollo Lunar Sounder Experiment data 07 p1029 A83-20240

Volcanism and magnetism of the moon 07 p1031 A83-20933

A partially molten magma ocean model 07 p1031 A83-21286

Thermal stresses in planetary elastic lithospheres 07 p1032 A83-21292

Magnetic dipole moment estimates for an ancient lunar dynamo 07 p1032 A83-21293

Subdivision of the Mg-suite noritic rocks into Mg-gabbroanorites and Mg-norites 07 p1032 A83-21295

A review of lunar paleointensity data and implications for the origin of lunar magnetism 07 p1033 A83-21302

The evolution of the moon - A finite element approach 11 p1686 A83-28385

Grabens, basin tectonics, and the maximum total expansion of the moon 12 p1799 A83-29965

Lunar palaeomagnetism and its implications 15 p2276 A83-35004

A review of lunar paleointensity data 15 p2276 A83-35005

Linear crater chains - Indication of a volcanic organ 16 p2439 A83-36786

Problems of the internal structure of the moon 17 p2614 A83-37002

Applicability of the slow-denudation model to young craters and craters with viscous relaxation on the moon 17 p2615 A83-37015

The morphometric index - The profile characteristic of a crater in the process of denudation 17 p2615 A83-37016

Origin of the moon - Capture by gas drag of the earth's primordial atmosphere 20 p3079 A83-43590

Regolith breccia Allan Hills A81005 - Evidence of lunar origin, and petrography of pristine and nonpristine clasts 22 p3385 A83-46861

Regolith breccia Allan Hills A81005 - Evidence of lunar origin, and petrography of pristine and nonpristine clasts 22 p3385 A83-46861

Regolith breccia Allan Hills A81005 - Evidence of lunar origin, and petrography of pristine and nonpristine clasts 22 p3385 A83-46861

Regolith breccia Allan Hills A81005 - Evidence of lunar origin, and petrography of pristine and nonpristine clasts 22 p3385 A83-46861

Regolith breccia Allan Hills A81005 - Evidence of lunar origin, and petrography of pristine and nonpristine clasts 22 p3385 A83-46861

Regolith breccia Allan Hills A81005 - Evidence of lunar origin, and petrography of pristine and nonpristine clasts 22 p3385 A83-46861

Regolith breccia Allan Hills A81005 - Evidence of lunar origin, and petrography of pristine and nonpristine clasts 22 p3385 A83-46861

Regolith breccia Allan Hills A81005 - Evidence of lunar origin, and petrography of pristine and nonpristine clasts 22 p3385 A83-46861

Regolith breccia Allan Hills A81005 - Evidence of lunar origin, and petrography of pristine and nonpristine clasts 22 p3385 A83-46861

Regolith breccia Allan Hills A81005 - Evidence of lunar origin, and petrography of pristine and nonpristine clasts 22 p3385 A83-46861

Regolith breccia Allan Hills A81005 - Evidence of lunar origin, and petrography of pristine and nonpristine clasts 22 p3385 A83-46861

Regolith breccia Allan Hills A81005 - Evidence of lunar origin, and petrography of pristine and nonpristine clasts 22 p3385 A83-46861

Regolith breccia Allan Hills A81005 - Evidence of lunar origin, and petrography of pristine and nonpristine clasts 22 p3385 A83-46861

Regolith breccia Allan Hills A81005 - Evidence of lunar origin, and petrography of pristine and nonpristine clasts 22 p3385 A83-46861

Regolith breccia Allan Hills A81005 - Evidence of lunar origin, and petrography of pristine and nonpristine clasts 22 p3385 A83-46861

Regolith breccia Allan Hills A81005 - Evidence of lunar origin, and petrography of pristine and nonpristine clasts 22 p3385 A83-46861

Regolith breccia Allan Hills A81005 - Evidence of lunar origin, and petrography of pristine and nonpristine clasts 22 p3385 A83-46861

Regolith breccia Allan Hills A81005 - Evidence of lunar origin, and petrography of pristine and nonpristine clasts 22 p3385 A83-46861

Regolith breccia Allan Hills A81005 - Evidence of lunar origin, and petrography of pristine and nonpristine clasts 22 p3385 A83-46861

Regolith breccia Allan Hills A81005 - Evidence of lunar origin, and petrography of pristine and nonpristine clasts 22 p3385 A83-46861

Regolith breccia Allan Hills A81005 - Evidence of lunar origin, and petrography of pristine and nonpristine clasts 22 p3385 A83-46861

Regolith breccia Allan Hills A81005 - Evidence of lunar origin, and petrography of pristine and nonpristine clasts 22 p3385 A83-46861

Regolith breccia Allan Hills A81005 - Evidence of lunar origin, and petrography of pristine and nonpristine clasts 22 p3385 A83-46861

Regolith breccia Allan Hills A81005 - Evidence of lunar origin, and petrography of pristine and nonpristine clasts 22 p3385 A83-46861

Regolith breccia Allan Hills A81005 - Evidence of lunar origin, and petrography of pristine and nonpristine clasts 22 p3385 A83-46861

Sixth foray for pristine nonmare rocks and an assessment of the diversity of lunar anorthosites 07 p1032 A83-21296

Rock 67015 - A feldspathic fragmental breccia with KREEP-rich melt clasts 07 p1033 A83-21299

Beginning and end of lunar mare volcanism 11 p1686 A83-28392

Geological mapping of the moon 17 p2615 A83-37012

The lunar regolith - Chemistry, mineralogy, and petrology 17 p2621 A83-38226

The geology of the terrestrial planets 17 p2622 A83-38269

A correlation between large-scale asymmetry of the moon and the foci of moonquakes 20 p3079 A83-43585

A correlation between large-scale asymmetry of the moon and the foci of moonquakes 20 p3079 A83-43585

A correlation between large-scale asymmetry of the moon and the foci of moonquakes 20 p3079 A83-43585

A correlation between large-scale asymmetry of the moon and the foci of moonquakes 20 p3079 A83-43585

A correlation between large-scale asymmetry of the moon and the foci of moonquakes 20 p3079 A83-43585

A correlation between large-scale asymmetry of the moon and the foci of moonquakes 20 p3079 A83-43585

A correlation between large-scale asymmetry of the moon and the foci of moonquakes 20 p3079 A83-43585

A correlation between large-scale asymmetry of the moon and the foci of moonquakes 20 p3079 A83-43585

A correlation between large-scale asymmetry of the moon and the foci of moonquakes 20 p3079 A83-43585

A correlation between large-scale asymmetry of the moon and the foci of moonquakes 20 p3079 A83-43585

A correlation between large-scale asymmetry of the moon and the foci of moonquakes 20 p3079 A83-43585

A correlation between large-scale asymmetry of the moon and the foci of moonquakes 20 p3079 A83-43585

A correlation between large-scale asymmetry of the moon and the foci of moonquakes 20 p3079 A83-43585

A correlation between large-scale asymmetry of the moon and the foci of moonquakes 20 p3079 A83-43585

A correlation between large-scale asymmetry of the moon and the foci of moonquakes 20 p3079 A83-43585

A correlation between large-scale asymmetry of the moon and the foci of moonquakes 20 p3079 A83-43585

A correlation between large-scale asymmetry of the moon and the foci of moonquakes 20 p3079 A83-43585

A correlation between large-scale asymmetry of the moon and the foci of moonquakes 20 p3079 A83-43585

A correlation between large-scale asymmetry of the moon and the foci of moonquakes 20 p3079 A83-43585

A correlation between large-scale asymmetry of the moon and the foci of moonquakes 20 p3079 A83-43585

A correlation between large-scale asymmetry of the moon and the foci of moonquakes 20 p3079 A83-43585

A correlation between large-scale asymmetry of the moon and the foci of moonquakes 20 p3079 A83-43585

A correlation between large-scale asymmetry of the moon and the foci of moonquakes 20 p3079 A83-43585

A correlation between large-scale asymmetry of the moon and the foci of moonquakes 20 p3079 A83-43585

A correlation between large-scale asymmetry of the moon and the foci of moonquakes 20 p3079 A83-43585

A correlation between large-scale asymmetry of the moon and the foci of moonquakes 20 p3079 A83-43585

A correlation between large-scale asymmetry of the moon and the foci of moonquakes 20 p3079 A83-43585

A correlation between large-scale asymmetry of the moon and the foci of moonquakes 20 p3079 A83-43585

A correlation between large-scale asymmetry of the moon and the foci of moonquakes 20 p3079 A83-43585

A correlation between large-scale asymmetry of the moon and the foci of moonquakes 20 p3079 A83-43585

A correlation between large-scale asymmetry of the moon and the foci of moonquakes 20 p3079 A83-43585

A correlation between large-scale asymmetry of the moon and the foci of moonquakes 20 p3079 A83-43585

A correlation between large-scale asymmetry of the moon and the foci of moonquakes 20 p3079 A83-43585

A correlation between large-scale asymmetry of the moon and the foci of moonquakes 20 p3079 A83-43585

A correlation between large-scale asymmetry of the moon and the foci of moonquakes 20 p3079 A83-43585

A correlation between large-scale asymmetry of the moon and the foci of moonquakes 20 p3079 A83-43585

A correlation between large-scale asymmetry of the moon and the foci of moonquakes 20 p3079 A83-43585

A correlation between large-scale asymmetry of the moon and the foci of moonquakes 20 p3079 A83-43585

A correlation between large-scale asymmetry of the moon and the foci of moonquakes 20 p3079 A83-43585

A correlation between large-scale asymmetry of the moon and the foci of moonquakes 20 p3079 A83-43585

A correlation between large-scale asymmetry of the moon and the foci of moonquakes 20 p3079 A83-43585

A correlation between large-scale asymmetry of the moon and the foci of moonquakes 20 p3079 A83-43585

A correlation between large-scale asymmetry of the moon and the foci of moonquakes 20 p3079 A83-43585

A correlation between large-scale asymmetry of the moon and the foci of moonquakes 20 p3079 A83-43585

A correlation between large-scale asymmetry of the moon and the foci of moonquakes 20 p3079 A83-43585

planets 17 p2614 A83-37008

The lunar figure and problems in the development of planimetric and topographic bases for lunar maps 17 p2614 A83-37009

Problems of the thematic mapping of the moon 17 p2615 A83-37010

Representation of the surface and gravitational field of the moon on maps 17 p2615 A83-37011

Geological mapping of the moon 17 p2615 A83-37012

Features of the compilation of structural-morphological maps of the moon 17 p2615 A83-37013

On the mineralogical mapping of the lunar surface 17 p2615 A83-37014

Relief of the far side of the moon under the path of the Zond-8 probe 17 p2615 A83-37017

The possibility of mapping the porosity index and the determinant of lunar-rock types 17 p2615 A83-37018

Application of computers for the mapping of photogrammetric parameters --- for planet and satellite surfaces 17 p2615 A83-37019

Means and methods of refining the planimetric and topographic bases of lunar maps 17 p2615 A83-37020

Thematic mapping of the moon 24 p3671 A83-48943

Thematic mapping of the moon 24 p3671 A83-48943

Thematic mapping of the moon 24 p3671 A83-48943

Thematic mapping of the moon 24 p3671 A83-48943

Thematic mapping of the moon 24 p3671 A83-48943

Thematic mapping of the moon 24 p3671 A83-48943

Thematic mapping of the moon 24 p3671 A83-48943

Thematic mapping of the moon 24 p3671 A83-48943

Thematic mapping of the moon 24 p3671 A83-48943

Thematic mapping of the moon 24 p3671 A83-48943

Thematic mapping of the moon 24 p3671 A83-48943

Thematic mapping of the moon 24 p3671 A83-48943

Thematic mapping of the moon 24 p3671 A83-48943

Thematic mapping of the moon 24 p3671 A83-48943

Thematic mapping of the moon 24 p3671 A83-48943

Thematic mapping of the moon 24 p3671 A83-48943

Thematic mapping of the moon 24 p3671 A83-48943

Thematic mapping of the moon 24 p3671 A83-48943

Thematic mapping of the moon 24 p3671 A83-48943

Thematic mapping of the moon 24 p3671 A83-48943

Thematic mapping of the moon 24 p3671 A83-48943

Thematic mapping of the moon 24 p3671 A83-48943

Thematic mapping of the moon 24 p3671 A83-48943

Thematic mapping of the moon 24 p3671 A83-48943

Thematic mapping of the moon 24 p3671 A83-48943

Thematic mapping of the moon 24 p3671 A83-48943

Thematic mapping of the moon 24 p3671 A83-48943

Thematic mapping of the moon 24 p3671 A83-48943

Thematic mapping of the moon 24 p3671 A83-48943

Thematic mapping of the moon 24 p3671 A83-48943

Thematic mapping of the moon 24 p3671 A83-48943

Thematic mapping of the moon 24 p3671 A83-48943

Thematic mapping of the moon 24 p3671 A83-48943

Thematic mapping of the moon 24 p3671 A83-48943

Thematic mapping of the moon 24 p3671 A83-48943

Thematic mapping of the moon 24 p3671 A83-48943

Thematic mapping of the moon 24 p3671 A83-48943

Thematic mapping of the moon 24 p3671 A83-48943

Thematic mapping of the moon 24 p3671 A83-48943

Thematic mapping of the moon 24 p3671 A83-48943

NT LUNIK 20 LUNAR PROBE
 Characteristics of a dual mission concept for intensive study of moon and Mars or moon and asteroids [AIAA PAPER 83-0349] 05 p0601 A83-17920

LUNAR PROGRAMS
 NT APOLLO PROJECT

LUNAR RADIATION
 Thermoluminescence of the lunar surface 06 p0848 A83-18474
 Method of calculating the expected background lumiance from the moon for planning astronomical observations 15 p2244 A83-33788

LUNAR RANGEFINDING
 Improvement of the ephemerides of the inner planets and the moon using radar, laser, and meridian measurements during 1961-1980 11 p1673 A83-28044
 Optimal conditions for determinations of polar coordinates from lunar laser ranging 23 p3483 A83-48069

LUNAR ROCKS
 NT KREEP
 Iron metal production in silicate melts through the direct reduction of Fe/II/ by Ti/III/, Cr/II/, and Eu/II/ --- in lunar basalts 02 p0267 A83-12846
 Effects of fractional crystallization and cumulus processes on mineral composition trends of some lunar and terrestrial rock series 04 p0559 A83-15332
 Comparison of thermal history of orthopyroxenes between lunar nortes 78236, 72255, and diogenites 04 p0560 A83-15339
 Subcrater lithification of polymict regolith breccias 04 p0560 A83-15340
 KREEP glass and the exotic provenance and formation of polymict breccia 66055 04 p0560 A83-15341
 Ferromagnetic resonance intensity - A rapid method for determining lunar glass bead origin 04 p0561 A83-15344
 Petrologic variations in Apollo 16 surface soils 04 p0561 A83-15345
 Modal petrology of six soils from Apollo 16 double drive tube core 64002 04 p0561 A83-15346
 Adsorption and excess fission Xe - Adsorption of Xe on vacuum crushed minerals 04 p0564 A83-15376
 Lunar and Planetary Science Conference, 13th, Houston, TX, March 15-19, 1982, Proceedings. Part 2 07 p1031 A83-21281
 Magnetic dipole moment estimates for an ancient lunar dynamo 07 p1032 A83-21293
 Sixth foray for pristine nonmare rocks and an assessment of the diversity of lunar anorthositic 07 p1032 A83-21296
 Petrological and thermal histories of a lunar breccia 73217 as inferred from pyroxene crystallization sequences, exsolution phenomena, and pyroxene geothermometry 07 p1033 A83-21297
 Petrology and comparative thermal and mechanical histories of clasts in breccia 62236 07 p1033 A83-21298
 Rock 67015 - A feldspathic fragmental breccia with KREEP-rich melt clasts 07 p1033 A83-21299
 Geochemical studies of feldspathic fragmental breccias and the nature of North Ray Crater ejecta 07 p1033 A83-21300
 The role of phosphorus in lunar samples - A chemical study 07 p1033 A83-21303
 Cooling rates for glass containing lunar compositions 07 p1035 A83-21324
 Probing the lunar interior 08 p1190 A83-23251
 A lunar meteorite and maybe some from Mars 11 p1686 A83-28768
 Structural features of two-phase clinopyroxene from the Luna-24 regolith 13 p1960 A83-30088
 Choice of lunar materials as determined by fabrication methods 16 p2313 A83-35613
 The possibility of mapping the porosity index and the determinant of lunar-rock types 17 p2615 A83-37018
 Studies of the content and the distribution of uranium of lunar mare basaltic fragments taken by Apollo 17 21 p3240 A83-44503
 The discovery and initial characterization of Allan Hills 81005 - The first lunar meteorite 22 p3385 A83-46860
 Regolith breccia Allan Hills A81005 - Evidence of lunar origin, and petrography of pristine and nonpristine clasts 22 p3385 A83-46861
 Petrology of ALHA 81005, the first lunar meteorite 22 p3385 A83-46863
 ALHA 81005 - Moon, Mars, petrography, and Giordano Bruno 22 p3385 A83-46864
 Meteorite ALHA 81005 - Petrology of a new lunar highland sample 22 p3385 A83-46865
 Oxygen and silicon isotopes in ALHA 81005 22 p3386 A83-46866
 Trapped noble gases indicate lunar origin for Antarctic meteorite 22 p3386 A83-46867
 Ferromagnetic resonance and magnetic properties of ALHA 81005 22 p3386 A83-46869
 Thermoluminescence and nuclear particle tracks in

ALHA-81005 Evidence for a brief transit time 22 p3386 A83-46870
 Possible lunar source areas of meteorite ALHA 81005
 Geochemical remote sensing information 22 p3386 A83-46871
 Antarctic meteorite ALHA 81005 - A piece from the ancient lunar crust 22 p3386 A83-46872
 Siderophile, lithophile and mobile trace elements in the lunar meteorite Allan Hills 81005 22 p3386 A83-46873
 Alha 81005 meteorite - Chemical evidence for lunar highland origin 22 p3386 A83-46874
 Antarctic meteorite ALHA81005 - Not just another lunar anorthositic norite 22 p3386 A83-46875
 Compositional implications regarding the lunar origin of the ALHA 81005 meteorite 22 p3386 A83-46876
 Composition of bulk samples and a possible pristine clast from Allan Hills A81005 22 p3387 A83-46877
 Al-Sm-Eu-Sr systematics of eucrites and moon rocks
 Implications for planetary bulk compositions 24 p3672 A83-49348
 Petrology and chemistry of two 'large' granite clasts from the moon 24 p3673 A83-50172

LUNAR ROTATION
 Analytical theory of the libration of the moon 08 p1190 A83-23125
 A search for objects near the earth-moon Lagrangian points 13 p1939 A83-31206
 Accuracy of the external orientation of a selenodetic coordinate system 16 p2439 A83-36860

LUNAR SATELLITES
 NT LUNAR ORBITER
 The mechanics of an anchored lunar satellite 03 p0283 A83-13215

LUNAR SCATTERING
 U DIFFUSE RADIATION

LUNAR SEISMOGRAPHS
 Apollo lunar seismic experiment - Final summary 04 p0560 A83-15338

LUNAR SHADOW
 Low temperature volatilization on the moon 04 p0562 A83-15352

LUNAR SOIL
 NT LUNAR DUST
 Ferromagnetic resonance g-factor measurement on LUNA 20 soil 03 p0432 A83-13297
 Color differences and chemical abundances in lunar soils 03 p0432 A83-13367
 Correlation between albedo and polarization properties of the moon /heterogeneity of the relative porosity of the surface of the western part of the visible hemisphere/ 03 p0133 A83-13667
 Adcumulus growth of anorthosite at the base of the lunar crust 04 p0559 A83-15328
 Subcrater lithification of polymict regolith breccias 04 p0560 A83-15340
 Chemistry and phase relations of VLT volcanic glasses from Apollo 14 and Apollo 17 --- Very Low Titanium 04 p0561 A83-15343
 Ferromagnetic resonance intensity - A rapid method for determining lunar glass bead origin 04 p0561 A83-15344
 Petrologic variations in Apollo 16 surface soils 04 p0561 A83-15345
 Modal petrology of six soils from Apollo 16 double drive tube core 64002 04 p0561 A83-15346
 The Apennine Front core 15007/8 - Irradiational and depositional history 04 p0561 A83-15347
 The Apollo 14 regolith - Petrology of cores 14210/14211 and 14220 and soils 14141, 14148, and 14149 04 p0561 A83-15348
 The Apollo 14 regolith - Chemistry of cores 14210/14211 and 14220 and soils 14141, 14148, and 14149 04 p0561 A83-15349
 Lunar regolith - Petrology of the less than 10 micron fraction 04 p0561 A83-15350
 Comparative geochemistry of Apollo 16 surface soils and samples from cores 64002 and 60002 through 60007 04 p0561 A83-15351
 Low temperature volatilization on the moon 04 p0562 A83-15352
 Synthesis of molecules by irradiation in silicates --- in lunar soil 04 p0564 A83-15373
 Fractionation of mineral species by electrophoresis 07 p1029 A83-20235
 Decrease of the solar flare/solar wind flux ratio in the past several aeons deduced from solar neon and tracks in lunar soil plagioclases 07 p1033 A83-21304
 Radiation history of lunar microbreccias and lithic chondrules from Weston meteorite by track data 07 p1034 A83-21310
 Advanced alloys and metal/ceramic composites from lunar source materials 11 p1531 A83-27345
 Sulphur content and sulphur isotope composition of orange and black glasses in Apollo 17 drive tube 74002/1 15 p2274 A83-34497
 The biological activity of lunar soil from Mare Fecunditatis during intratracheal injection 16 p2394 A83-35924
 Uranium in rock fragments from the lunar soil

17 p2619 A83-37817
 The lunar regolith - Chemistry, mineralogy, and petrology 17 p2621 A83-38226
 Hydrogen in Luna-24 regolith 18 p2779 A83-39534
 A method for the identification and elimination of contamination during carbon isotopic analyses of extraterrestrial samples 22 p3385 A83-46375

LUNAR SPACECRAFT
 NT APOLLO SPACECRAFT
 NT LUNAR ORBITER
 NT LUNAR PROBES
 NT LUNAR SATELLITES
 NT LUNIK LUNAR PROBES
 NT LUNIK 20 LUNAR PROBE

LUNAR SURFACE
 A review of lava flow processes related to the formation of lunar sinuous rilles 02 p0266 A83-12640
 Color differences and chemical abundances in lunar soils 03 p0432 A83-13367
 A colorimetric mapping of the moon's surface in the 0.62-0.95-micron spectral region 03 p0432 A83-13368
 Analysis of crater distribution in mare units on the lunar far side 03 p0435 A83-14869
 Volumetric analysis of complex lunar craters
 Implications for basin ring formation 04 p0560 A83-15333
 Comparative geochemistry of Apollo 16 surface soils and samples from cores 64002 and 60002 through 60007 04 p0561 A83-15351
 Low temperature volatilization on the moon 04 p0562 A83-15352
 Thermoluminescence of the lunar surface 06 p0848 A83-18474
 Correlation between albedo and polarization characteristics of the moon - Application of digital image processing 07 p1031 A83-21271
 Thorium concentrations in the lunar surface. IV - Deconvolution of the Mare Imbrium, Aristarchus, and adjacent regions 07 p1032 A83-21287
 The lunar nearside highlands - Evidence of resurfacing 07 p1032 A83-21288
 Thermal stresses in planetary elastic lithospheres 07 p1032 A83-21292
 Effects of subsurface volume scattering on the lunar microwave brightness temperature spectrum 08 p1189 A83-22941
 Optical investigations of the moon and spectrophotometric standards 09 p1367 A83-25278
 Problem of the global asymmetry of the lunar sphere 09 p1367 A83-25279
 Results of an analysis of space photographs of the moon magnified to a scale of 1:500,000 13 p1961 A83-31100
 Calculation of the electrostatic field strength above the lunar surface covered by a hydrogen monolayer 15 p2276 A83-34770
 A critical analysis of the results of treatment of heliometric observations of the moon 15 p2276 A83-34771
 A review of lunar paleointensity data 15 p2276 A83-35005
 Should we make products on the moon? 16 p2313 A83-35774
 Palisa catena - Small volcano chains in the western part of the central highlands 16 p2438 A83-36779
 Variances and correlations of errors of rectangular coordinates of selenodetic reference points 16 p2439 A83-36859
 Accuracy of the external orientation of a selenodetic coordinate system 16 p2439 A83-36860
 Determination of the orientation angles of a selenodetic coordinate system on the basis of photographic positional observations of the moon 16 p2439 A83-36861
 General-survey mapping of the moon 17 p2614 A83-37004
 Representation of the surface and gravitational field of the moon on maps 17 p2615 A83-37011
 On the mineralogical mapping of the lunar surface 17 p2615 A83-37014
 The possibility of mapping the porosity index and the determinant of lunar-rock types 17 p2615 A83-37018
 Application of computers for the mapping of photogrammetric parameters --- for planet and satellite surfaces 17 p2615 A83-37019
 The lunar regolith - Chemistry, mineralogy, and petrology 17 p2621 A83-38226
 Tectonic evolution of Mercury - Comparison with the moon 21 p3241 A83-44668
 Evidence of endogenic processes on the surface of lunar regolith particles 24 p3671 A83-48953

LUNAR TEMPERATURE
 Further efforts to limit lunar internal temperatures from electrical conductivity determinations 04 p0560 A83-15337
 Low temperature volatilization on the moon 04 p0562 A83-15352
 Petrological and thermal histories of a lunar breccia 73217 as inferred from pyroxene crystallization sequences,

exsolution phenomena, and pyroxene geothermometry
07 p1033 A83-21297

LUNAR TIDES

Solar and lunar seasonal variations in the American sector
08 p1133 A83-22302

Interpretation of seasonal variations of S and L --- solar and lunar geomagnetic variations
08 p1133 A83-22303

Sq and L currents in the ionosphere --- solar quiet and lunar tidal effects on ionospheric and geomagnetic variations
08 p1134 A83-22307

Effect of the equatorial counter-electrojet in the Indian region on the geomagnetic solar and lunar daily variations
08 p1134 A83-22310

The lunar semi-diurnal tide observed by stratospheric sounding units on the TIROS-N series of satellites
09 p1307 A83-24689

Lunar modulations of the equatorial electrojet
17 p2544 A83-38373

Lunar-solar periodicities of large earthquakes in southern California
18 p2718 A83-39956

Tidal evolution of the earth-moon system during the resonant excitation of tides in the world ocean
24 p3608 A83-49528

LUNAR TOPOGRAPHY

The lunar nearside highlands - Evidence of resurfacing
07 p1032 A83-21288

Remote sensing for planetary topographic mapping
17 p2623 A83-38437

LUNAR TRAJECTORIES

NT EARTH-MOON TRAJECTORIES
NT MOON-EARTH TRAJECTORIES

LUNEBERG LENSES

U RADAR CORNER REFLECTORS

LUNG MORPHOLOGY

The pathological anatomy of shock lung
01 p0081 A83-11390

Significance of the measurement of colloidal-oncotic and hydrostatic pressures in lung capillaries for the diagnosis of edema of the lungs
05 p0673 A83-17177

The surfactant system of the lungs in experimental papain-induced emphysema
05 p0670 A83-17188

The response of the surfactant system and the air-blood barrier of the lungs to overall acute hypothermia
07 p0974 A83-20977

The content of water in the lungs of a healthy individual
08 p1147 A83-22779

Regional gas distributions and single-breath washout curves in head-down position
13 p1903 A83-30469

Breathing He-O₂ shifts the lung pressure-volume curve of the dog
13 p1897 A83-30479

The ultrastructural bases of pulmonary edema in patients with myocardial infarction
15 p2213 A83-34956

Hypoxic constriction of alveolar and extra-alveolar vessels in isolated pig lungs
17 p2555 A83-36994

Morphofunctional changes of the lymphoid tissue of the respiratory organs following the administration of gamma-globulin
18 p2733 A83-40582

Responses of the lung periphery to 1.0 ppm ozone
22 p3346 A83-45990

Effects of ozone on peripheral lung reactivity
22 p3346 A83-45991

LUNGS

The effect of a normoxic helium-oxygen gas mixture on the consumption of oxygen by the tissues of the liver and lungs in white rats
01 p0078 A83-10489

Oxygen toxicity
02 p0222 A83-12261

The role of the lung in the formation of the rheological properties of the blood
05 p0670 A83-17183

Surfactant homeostasis in the rat lung during swimming exercise
05 p0671 A83-17330

Attenuation of hypoxic pulmonary vasoconstriction by pulsatile flow in dog lungs
05 p0673 A83-17336

Role of lung surfactant in cerebral decompression sickness
06 p0793 A83-18188

The effect of adrenalectomy and hydrocortisone on the carbohydrate metabolism in the lungs and myocardium during chronic hypoxia
07 p0972 A83-19922

Endotoxin protects against hyperoxic alterations in lung endothelial cell metabolism
13 p1896 A83-30453

Hypoxic pulmonary hypertension in the mast cell-deficient mouse
13 p1897 A83-30485

An ultrasonic investigation of the blood flow in various parts of the vascular bed of the lungs of cats
15 p2211 A83-34966

The biological activity of lunar soil from Mare Fecunditatis during intratracheal injection
16 p2394 A83-35924

LUNIK LUNAR PROBES

NT LUNIK 20 LUNAR PROBE

A roentgenographic and X-ray-diffraction investigation of plagioclases of the lunar regolith returned by the Luna 16, Luna 20, and Luna 24 probes
03 p0432 A83-13525

Structural features of two-phase clinopyroxene from the Luna-24 regolith
13 p1960 A83-30088

Hydrogen in Luna-24 regolith
18 p2779 A83-39534

LUNIK 20 LUNAR PROBE

Ferromagnetic resonance g-factor measurement on LUNA 20 soil
03 p0432 A83-13297

LUTETIUM

NT LUTETIUM ISOTOPES

LUTETIUM ISOTOPES

Lu-176 - Cosmic clock and stellar thermometer
03 p0425 A83-14209

Importance of the Lu-Hf isotopic system in studies of planetary chronology and chemical evolution
08 p1190 A83-22996

LUTETIUM 176

U LUTETIUM ISOTOPES

LYAPUNOV FUNCTIONS

U LIAPUNOV FUNCTIONS

LYMAN ALPHA RADIATION

Copernicus measurement of the Jovian Lyman-alpha emission and its aeronomic significance
02 p0264 A83-12142

Determination of the parameters of the interstellar wind from observations of the Lyman-alpha background at large distances from the sun
03 p0412 A83-13210

The Lyman-alpha emission-line profiles in high-redshift QSOs
03 p0413 A83-13323

Ultraviolet spectroscopy of comae
03 p0416 A83-13394

Ly-alpha absorption at a high velocity in NGC1275
03 p0411 A83-14923

On the distribution of interstellar gas in the galactic halo
05 p0698 A83-16996

Detection of auroral hydrogen Lyman-alpha emission from Uranus
05 p0704 A83-17037

Can planetary nebulae rotate
06 p0832 A83-18842

Altitude profile of H in the atmosphere of Venus from Lyman alpha observations of Venera 11 and Venera 12 and origin of the hot exospheric component
07 p1029 A83-20612

An attempt to determine stellar Lyman-alpha emission-line fluxes for F stars with different metal abundances
07 p1022 A83-21131

Temporal variation of the Jovian H I Lyman-alpha emission /1979-1982/
07 p1031 A83-21158

Lyman-alpha observations of comets West 1976 VI and P d'Arrest 1976 XI with Copernicus
08 p1175 A83-23058

Daytime mesospheric temperatures over the low-latitude station Thumba derived from rocket-borne solar Lyman-alpha absorption measurements
09 p1307 A83-24691

High-resolution spectroscopy of selected absorption lines toward quasi-stellar objects. I - Lyman-alpha toward PHL 957
10 p1512 A83-26703

PKS 0119-046 and the origin of infalling absorption-line systems in quasars
10 p1515 A83-26747

Generation and application of coherent radiation at Lyman-alpha
11 p1583 A83-27619

Relation of absorption of radio waves to solar X-rays and to Lyman-alpha radiation at the time of low solar and geomagnetic activity
11 p1616 A83-28110

A statistical study of the Lyman-alpha absorption lines of nine quasars
12 p1795 A83-29352

On the role of solar Lyman alpha radiation in radio-wave absorption in the D-region
12 p1753 A83-29406

OSO-8 observations of a quiescent prominence - A comparison of Lyman-alpha with theoretical intensities
13 p1966 A83-31756

The aeronomic dissociation of water vapor by solar H Lyman-alpha radiation
15 p2196 A83-33947

Physical properties of the intergalactic medium and the Lyman-alpha absorbing clouds
15 p2259 A83-34118

Observations of Stark-shifts of Lyman-alpha lines of low-Z ions in laser-produced plasmas
15 p2233 A83-34140

The Lyman-alpha absorption anomaly in satellite occultation measurements as a tracer for some thermospheric composition variations
16 p2378 A83-36117

Variability of the Lyman alpha flux with solar activity
17 p2625 A83-37601

The location of material producing Lyman-limit discontinuities in QSO spectra
17 p2607 A83-38251

The Lyman alpha line in solar prominences
18 p2781 A83-39027

Experience related to the employment of a highly sensitive humidity probe with miniature humidity sensor on a barium fluoride basis - Comparison with a Lyman alpha-hygrometer
18 p2723 A83-39260

Geocoronal imaging with Dynamics Explorer - A first look
19 p2864 A83-41116

Common Lyman-alpha absorption lines in the triple QSO PG 1115 + 08
22 p3376 A83-45626

The solar O III spectrum. II - Longer wavelengths, line widths, and the He II Lyman alpha radiation field
22 p3388 A83-46263

H I Lyman-alpha in the sun - The effects of partial redistribution in the line wings
22 p3389 A83-47001

Transfer of H I Lyman-alpha radiation in optically thick media
24 p3674 A83-49632

LYMAN SPECTRA

Plasma shifts of the Lyman lines to shorter wavelengths in C VI
13 p1926 A83-30919

On the N2 Lyman-Birge-Hopfield band nightglow
15 p2196 A83-33946

Observations of Stark-shifts of Lyman-alpha lines of low-Z ions in laser-produced plasmas
15 p2233 A83-34140

Broadening of Lyman lines of hydrogen and hydrogen ions by low-frequency fields in dense plasmas
16 p2415 A83-35662

Radiative excitation and the intensities of radio recombination lines
16 p2429 A83-36627

Hydrogen line ratios of low redshift QSO's
16 p2430 A83-36658

The spectral features in the microwave background spectrum due to energy release in the early universe
19 p2914 A83-40707

Evidence of hourly variations in the deuterium Lyman line profiles toward Epsilon Persei
20 p3065 A83-42389

LYMPH

NT LYMPHOCYTES

The arterial vascular bed of the human mesenteric lymph nodes
03 p0380 A83-13644

The molecular mechanisms of the interphase death of lymphoid cells. VI - A low molecular weight DNA fraction in the products of the degradation of the chromatin of irradiated rat thymus
03 p0377 A83-14883

Physiological aspects of lymphology
04 p0523 A83-15788

The content of endogenous serotonin in the lymph organs of rats during the adaptation to high-altitudes and the pattern of radiation sickness
11 p1641 A83-28763

The changes in the chromosome pattern of mouse lymphosarcoma cells during prolonged irradiation
14 p2061 A83-32054

The response of the lymph and blood coagulation systems to gamma-radiation at high altitudes
14 p2062 A83-32064

Morphofunctional changes of the lymphoid tissue of the respiratory organs following the administration of gamma-globulin
18 p2733 A83-40582

LYMPHOCYTES

An increase in the effectiveness of the transplantation of allogenic bone marrow
01 p0080 A83-10547

The distribution of functionally different cells in immunocompetent organs after an injection of haloperidol
01 p0080 A83-10550

The role of Fc-receptors of lymphocytes, macrophages, and other mammalian cells during the immune processes
01 p0082 A83-11406

Cytochemical labeling and morphological characterization of lymphocyte subpopulations in health and disease
03 p0381 A83-14332

The changes in the T and B immune systems in sailors during prolonged voyages
13 p1906 A83-30950

The mechanism of the degradation of chromatin in the thymocytes of irradiated rats. VI - The postirradiation changes in the activity of poly(ADP-ribose)-polymerase
14 p2061 A83-32052

The effect of T and B lymphocytes on the phagocytotic activity of polymorphonuclear neutrophils in the peripheral blood of humans
14 p2070 A83-33333

Coping and immunosuppression - Inescapable but not escapable shock suppresses lymphocyte proliferation
19 p2873 A83-40905

The mechanism of the secondary postirradiation degradation of DNA in thymocytes of irradiated rats. I - The substrate specificity of alkaline endonuclease
19 p2874 A83-41003

The reaction of the human lymphocyte chromosome to graded doses of neutrons during irradiation in vitro
19 p2874 A83-41006

'Pseudonormal' thymocytes - A peculiar reaction of lymphoid elements of the thymus cortex to high doses of ionizing radiation
19 p2874 A83-41016

The effect of microwave radiation on several parameters of cellular immunity in conditions of chronic exposure
23 p3495 A83-48207

The effect of a constant magnetic field and gamma-radiation on the hereditary structure of somatic cells - The effect of the combination of a constant magnetic field and ionizing radiation on the blood lymphocytes of humans in vitro
23 p3498 A83-48210

LYOPHILS

U COLLOIDS

LYRAE CONSTELLATION

On the problem of the chemical composition of Beta Lyrae
01 p0121 A83-10329

Concentrations in the local association. I - The southern concentrations NGC 2516, IC 2602, Centaurus-Lupus and upper Scorpius --- young star clusters in Galaxy
17 p2593 A83-38255

LYSOZYME

The effect of physical exercise on changes of lysozyme in the blood of athletes
01 p0084 A83-11388

The effect of physical loads on the lysosome apparatus of neutrophilic leukocytes of the peripheral blood
08 p1145 A83-22105

IAA

DOMESTIC & FOREIGN

